ENCYCLOPEDIA OF CHROMATOGRAPHY

Third Edition

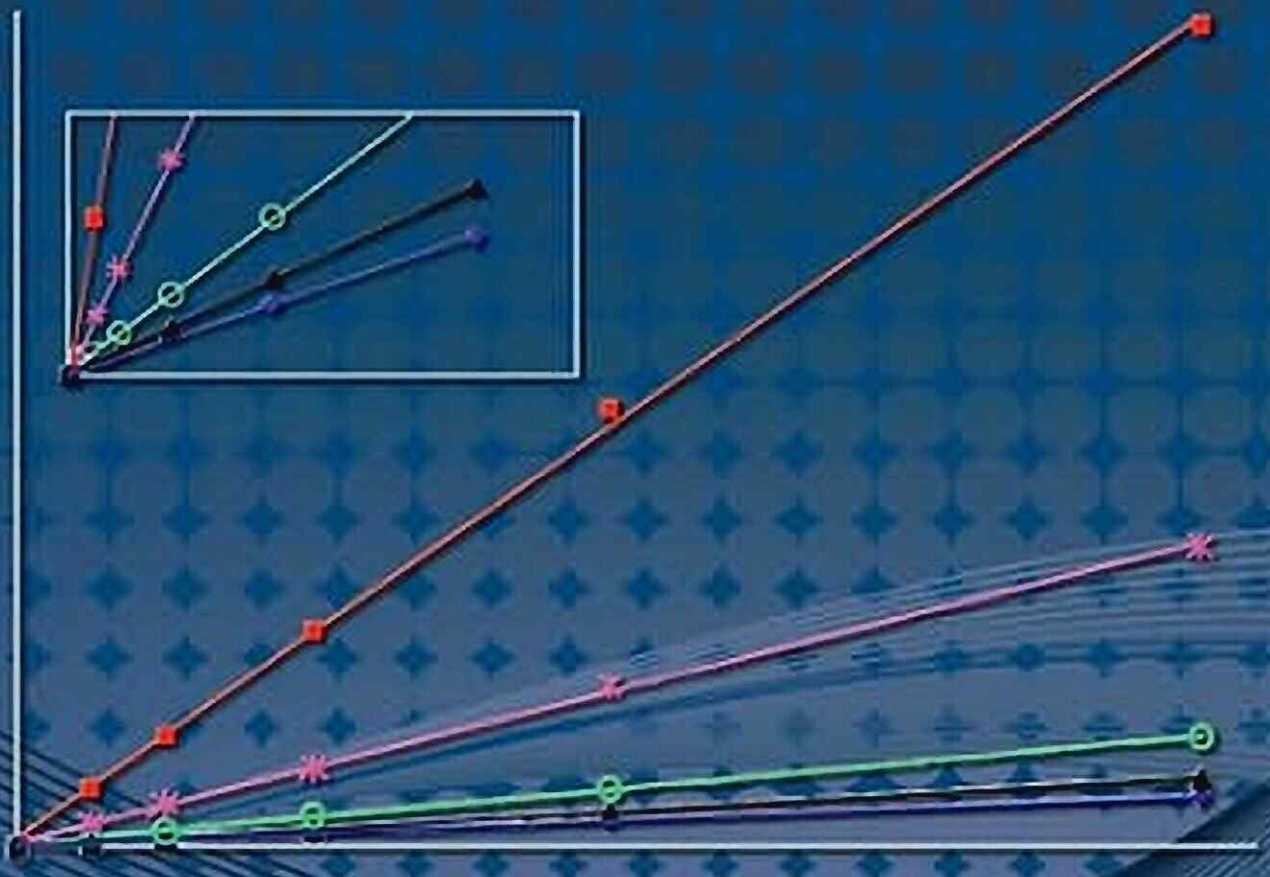

EDITED BY

JACK CAZES

CRC Press
Taylor & Francis Group

ENCYCLOPEDIA OF
CHROMATOGRAPHY

Third Edition

VOLUME I, II, and III

Encyclopedias from Taylor & Francis Group

Agriculture Titles

Dekker Agropedia Collection (Eight Volume Set)
ISBN: 978-0-8247-2194-7 Cat. No.: DK803X

Encyclopedia of Agricultural, Food, and Biological Engineering
Edited by Dennis R. Heldman
ISBN: 978-0-8247-0938-9 Cat. No.: DK9381

Encyclopedia of Animal Science
Edited by Wilson G. Pond and Alan Bell
ISBN: 978-0-8247-5496-9 Cat. No.: DK2206

Encyclopedia of Pest Management
Edited by David Pimentel
ISBN: 978-0-8247-0632-6 Cat. No.: DK6323

Encyclopedia of Pest Management, Volume II
Edited by David Pimentel
ISBN: 978-1-4200-5361-6 Cat. No.: 53612

Encyclopedia of Plant and Crop Science
Edited by Robert M. Goodman
ISBN: 978-0-8247-0944-0 Cat. No.: DK1190

Encyclopedia of Soil Science, Second Edition (Two Volume Set)
Edited by Rattan Lal
ISBN: 978-0-8493-3830-4 Cat. No.: DK830X

Encyclopedia of Water Science, Second Edition (Two Volume Set)
Edited by Stanley W. Trimble
ISBN: 978-0-8493-9627-4 Cat. No.: DK9627

Chemistry Titles

Encyclopedia of Chromatography, Third Edition (Three Volume Set)
Edited by Jack Cazes
ISBN: 978-1-4200-8459-7 Cat. No.: 84593

Encyclopedia of Supramolecular Chemistry (Two Volume Set)
Edited by Jerry L. Atwood and Jonathan W. Steed
ISBN: 978-0-8247-5056-5 Cat. No.: DK056X

Encyclopedia of Surface and Colloid Science, Second Edition (Eight Volume Set)
Edited by P. Somasundaran
ISBN: 978-0-8493-9615-1 Cat. No.: DK9615

Engineering Titles

Encyclopedia of Chemical Processing (Five Volume Set)
Edited by Sunggyu Lee
ISBN: 978-0-8247-5563-8 Cat. No.: DK2243

Encyclopedia of Corrosion Technology, Second Edition
Edited by Philip A. Schweitzer, P.E.
ISBN: 978-0-8247-4878-4 Cat. No.: DK1295

Encyclopedia of Energy Engineering and Technology (Three Volume Set)
Edited by Barney L. Capehart
ISBN: 978-0-8493-3653-9 Cat. No.: DK653X

Dekker Encyclopedia of Nanoscience and Nanotechnology, Second Edition (Six Volume Set)
Edited by Cristian I. Contescu and Karol Putyera
ISBN: 978-0-8493-9639-7 Cat. No.: DK9639

Encyclopedia of Optical Engineering (Three Volume Set)
Edited by Ronald G. Driggers
ISBN: 978-0-8247-0940-2 Cat. No.: DK9403

Business Titles

Encyclopedia of Library and Information Science, Third Edition (Seven Volume Set)
Edited by Marcia J. Bates and Mary Niles Maack
ISBN: 978-0-8493-9712-7 Cat. No.: DK9712

Encyclopedia of Public Administration and Public Policy, Second Edition (Three Volume Set)
Edited by Evan M. Berman
ISBN: 978-0-4200-5275-6 Cat. No.: AU5275

Encyclopedia of Wireless and Mobile Communications (Three Volume Set)
Edited by Borko Furht
ISBN: 978-0-4200-4326-6 Cat. No.: AU4326

These titles are available both in print and online. To order, visit:
www.crcpress.com
Telephone: 1-800-272-7737
Fax: 1-800-374-3401
E-Mail: orders@taylorandfrancis.com

ENCYCLOPEDIA OF
CHROMATOGRAPHY

Third Edition

VOLUME I, II, and III

EDITED BY

JACK CAZES

CRC Press
Taylor & Francis Group
Boca Raton London New York

CRC Press is an imprint of the
Taylor & Francis Group, an **informa** business

Encyclopedia of Chromatography
Third Edition

Volume I
Pages 1–828
Absorbance through Extra

Encyclopedia of Chromatography
Third Edition

Volume II
Pages 829–1636
Fast through Open

Encyclopedia of Chromatography
Third Edition

Volume III
Pages 1637–2457
Optical through Zone

CRC Press
Taylor & Francis Group
6000 Broken Sound Parkway NW, Suite 300
Boca Raton, FL 33487-2742

CRC Press is an imprint of Taylor & Francis Group, an Informa business

No claim to original U.S. Government works

Printed in the United States of America on acid-free paper
10 9 8 7 6 5 4 3 2 1

International Standard Book Number: 978-1-4200-8459-7 (Hardback)

Library of Congress Cataloging-in-Publication Data

Encyclopedia of chromatography / editor, Jack Cazes. -- 3rd ed.
p. cm.
Includes bibliographical references and index.
ISBN 978-1-4200-8459-7 (hardcover : alk. paper)
1. Chromatographic analysis--Encyclopedias. I. Cazes, Jack, 1934- II. Title.

QD79.C4E63 2010
543'.803--dc22 2009031443

Visit the Taylor & Francis Web site at
http://www.taylorandfrancis.com

and the CRC Press Web site at
http://www.crcpress.com

This work is dedicated to my lovely grandchildren,
Matthew, Monica, Brett, and Evan,
the shining lights of my life,
and to my wife, Eleanor,
who has stood by my side
and made this ambitious project possible

Contributors

Concepción Abad / *Department of Biochemistry and Molecular Biology, University of Valencia, Valencia, Spain*
Maged S. Abdel-Kader / *Department of Pharmacognosy, King Saud University, Riyadh, Saudi Arabia*
Mohamed Abdel-Rehim / *Research and Development, AstraZeneca, Södertälje, and Department of Chemistry, Karlstad University, Karlstad, Sweden*
Hassan Y. Aboul-Enein / *Pharmaceutical and Medicinal Chemistry Department, Pharmaceutical and Drug Industries Research Division, National Research Center, Dokki, Cairo, Egypt*
Manuel Acosta / *Department of Plant Biology (Plant Physiology), University of Murcia, Murcia, Spain*
Ibrahim A. Al-Duraibi / *Pharmaceutical Analysis Laboratory, King Faisal Specialist Hospital and Research Center, Riyadh, Saudi Arabia*
Serge Alex / *Center for Chemical Process Studies of Quebec (CEPROCQ), Montreal, Quebec, Canada*
Imran Ali / *Department of Chemistry, Jamia Millia Islamia (A Central University), New Delhi, India*
Abdul-Rahman A. Al-Majed / *Department of Pharmaceutical Chemistry, King Saud University, Riyadh, Saudi Arabia*
Maria de Fatima Alpendurada / *Faculty of Pharmacy, University of Porto, Porto, Portugal*
Juan G. Alvarez / *Department of Obstetrics and Gynecology, Beth Israel Deaconess Medical Center, Boston, Massachusetts, U.S.A.*
P.B. Andrade / *Requimte, Department of Pharmacognosy, Faculty of Pharmacy, University of Porto, Porto, Portugal*
Victor P. Andreev / *Institute for Analytical Instrumentation, Russian Academy of Sciences, St. Petersburg, Russia*
M.J. Arín / *Analytical Chemistry, Department of Applied Chemistry and Physics, University of León, León, Spain*
Marino B. Arnao / *Department of Plant Biology (Plant Physiology), University of Murcia, Murcia, Spain*
Christine M. Aurigemma / *Pfizer Global Research and Development, Pfizer Inc., La Jolla, California, U.S.A.*
Yoshinobu Baba / *Department of Medicinal Chemistry, University of Tokushima, Tokushima, Japan*
M.A. Bagool / *Wockhardt Research Centre, Aurangabad, India*
Eunmi Ban / *Research Institute of Pharmaceutical Sciences, Seoul National University, Seoul, South Korea*
James J. Bao / *Advanced Medicine Inc., San Francisco, California, U.S.A.*
M.A. Barbirato / *Chromatography Laboratory, University of São Paulo, São Carlos, Brazil*
Csaba Barta / *Novartis Agricultural Discovery Institute, Inc., San Diego, California, U.S.A.*
M. Barut / *BIA Separations d.o.o., Ljubljana, Slovenia*

I. Bataille / *Galilee Institute, University of North Paris, Villetaneuse, France*
Maria Bathori / *Department of Pharmacognosy, University of Szeged, Szeged, Hungary*
S. Battu / *Analytical Chemistry and Bromatology Laboratory, University of Limoges, Limoges, France*
Ronald Beckett / *Water Studies Centre, Monash University, Melbourne, Victoria, Australia*
Eva Benicka / *Institute of Analytical Chemistry, Slovak University of Technology, Bratislava, Slovakia*
A. Berecka / *Department of Medicinal Chemistry, Medical University of Lublin, Lublin, Poland*
Philippe J. Berny / *Toxicology Unit, National Veterinary School of Lyon, Marcy L'Etoile, France*
Alain Berthod / *Laboratory of Analytical Sciences, University of Lyon I, Villeurbanne, France*
Clayton B'Hymer / *National Institute for Occupational Safety and Health, Centers for Disease Control and Prevention, U.S. Department of Health and Human Services, Cincinnati, Ohio, U.S.A.*
Peng-Yu Bi / *College of Science, Beijing University of Chemical Technology, Beijing, China*
Jacques Bodennec / *Department of Biological Chemistry, Weizmann Institute of Science, Rehovot, Israel*
Pierina Sueli Bonato / *Faculty of Pharmaceutical Sciences of Ribeirão Preto, University of São Paulo, Ribeirão Preto, Brazil*
Frederic Bonfils / *French Agricultural Research Center for International Development (CIRAD-CP), Montpellier, France*
Evropi Botsoglou / *Laboratory of Hygiene of Foods of Animal Origin, Department of Veterinary Medicine, University of Thessaly, Karditsa, Greece*
Nikolas A. Botsoglou / *Laboratories of Nutrition, Faculty of Veterinary Medicine, Aristotle University of Thessaloniki, Thessaloniki, Greece*
Natasa Brajenovic / *Institute for Medical Research and Occupational Health, Zagreb, Croatia*
E. Brandsteterova / *Department of Analytical Chemistry, Slovak Technical University, Bratislava, Slovakia*
Michael Breslav / *Johnson & Johnson Pharmaceutical Research and Development, LLC, Spring House, Pennsylvania, U.S.A.*
Silvia H.G. Brondi / *Embrapa Livestock Southeast, São Carlos, Brazil*
Yefim Brun / *Waters Corporation, Milford, Massachusetts, U.S.A.*
Christopher E. Bunker / *Propulsion Directorate, Air Force Research Laboratory, Wright-Patterson Air Force Base, Ohio, U.S.A.*
Jean-Pierre Busnel / *Physical Chemistry of Material Polymers, University of Main, Le Mans, France*
S. Bilal Butt / *Central Analytical Facility Division, Pakistan Institute of Nuclear Science and Technology, Islamabad, Pakistan*
Yong Cai / *Department of Chemistry, Florida International University, Miami, Florida, U.S.A.*
Agustín Campos / *Institute of Materials Science, University of Valencia, Valencia, Spain*
Antonio Cano / *Department of Plant Biology (Plant Physiology), University of Murcia, Murcia, Spain*
Ping Cao / *Biology Department, Tularik, Inc., South San Francisco, California, U.S.A.*
Wenjie Cao / *Huntsman Polymers Corp., Odessa, Texas, U.S.A.*
Philippe Cardot / *Analytical Chemistry and Bromatology Laboratory, University of Limoges, Limoges, France*
Susana Casal / *Requimte, Bromatology Service, Faculty of Pharmacy, University of Porto, Porto, Portugal*

M. Caude / *Analytical Chemistry Department, City of Paris Industrial Physics and Chemistry Higher Educational Institution (ESPCI), Paris, France*
Teresa Cecchi / *Department of Chemical Science, University of Camerino (UNICAM), Camerino, Italy*
Zhikuan Chai / *Research Center for Eco-Environmental Sciences, Chinese Academy of Sciences, Beijing, China*
Jeffrey J. Chalmers / *Department of Chemical and Biomolecular Engineering, Ohio State University, Columbus, Ohio, U.S.A.*
Huan-Tsung Chang / *Department of Chemistry, National Taiwan University, Taipei, Taiwan*
Bezhan Chankvetadze / *Department of Physical and Analytical Chemistry and Molecular Recognition and Separation Science Laboratory, School of Exact and Natural Sciences, Tbilisi State University, Tbilisi, Georgia*
C. Char / *French Agricultural Research Center for International Development (CIRAD-CP), Montpellier, France*
Kenneth L. Cheever / *National Institute for Occupational Safety and Health, Centers for Disease Control and Prevention, U.S. Department of Health and Human Services, Cincinnati, Ohio, U.S.A.*
Bailin Chen / *Department of Chemistry, University of Kentucky, Lexington, Kentucky, U.S.A.*
Sarah S. Chen / *Analytical Science, GlaxoSmithKline, King of Prussia, Pennsylvania, U.S.A.*
Oscar Chiantore / *Department of Inorganic, Physical, and Material Chemistry, University of Torino, Torino, Italy*
Tai-Chia Chiu / *Department of Chemistry, National Taiwan University, Taipei, Taiwan*
Josef Chmelík / *Institute of Analytical Chemistry, Academy of Sciences of the Czech Republic, Prague, Czech Republic*
Du Young Choi / *Center for Advanced Bioseparation Technology and Department of Chemical Engineering, Inha University, Incheon, South Korea*
Irena Choma / *Department of Chemical Physics, Marie Curie-Sklodowska University, Lublin, Poland*
Christodoulos Christodoulis / *Department of Chemical and Physical Examinations, Forensic Science Division, Hellenic Police Headquarter, Athens, Greece*
Witold Ciesielski / *Department of Instrumental Analysis, University of Łódź, Łódź, Poland*
Gabriela Cimpan / *Sirius Analytical Instruments Ltd., East Sussex, U.K.*
Alessandra Cincinelli / *Department of Chemistry, University of Florence (UNIFI), Florence, Italy*
Christa L. Colyer / *Department of Chemistry, Wake Forest University, Winston-Salem, North Carolina, U.S.A.*
Danilo Corradini / *Institute of Chromatography, Rome, Italy*
Tibor Cserháti / *Institute of Chemistry, Chemical Research Center, Hungarian Academy of Sciences, Budapest, Hungary*
James Curry / *Senior Scientist, Research and Development, R.P. Scherer North America, St. Petersburg, Florida, U.S.A.*
S.-L. Da / *Department of Chemistry, Wuhan University, Wuhan, China*
José Almiro da Paixão / *Department of Nutrition, Center of Health Sciences, Federal University of Pernambuco, Recife, Brazil*
Victor David / *Department of Analytical Chemistry, University of Bucharest, Bucharest, Romania*
Cristiane Masetto de Gaitani / *Faculty of Pharmaceutical Sciences of Ribeirão Preto, University of São Paulo, Ribeirão Preto, Brazil*
M. de Moraes / *Chromatography Laboratory, University of São Paulo, São Carlos, Brazil*

Melgardt M. de Villiers / *School of Pharmacy, University of Wisconsin, Madison, Wisconsin, U.S.A.*
Yulin Deng / *Neuropsychiatry Research Unit, University of Saskatchewan, Saskatoon, Saskatchewan, Canada*
Yves Denizot / *Immunology Laboratory, University of Limoges, Limoges, France*
A.A. Deo / *Wockhardt Research Centre, Aurangabad, India*
M.T. Diez / *Analytical Chemistry, Department of Applied Chemistry and Physics, University of León, León, Spain*
N. Dimov / *Chemical Pharmaceutical Research Institute (NIHFI), Bulgarian Pharmaceutical Group Ltd., Sofia, Bulgaria*
Hui-Ru Dong / *College of Science, Beijing University of Chemical Technology, Beijing, China*
Vasile I. Dorneanu / *Analytical Chemistry Department, Grigore T. Popa University of Medicine and Pharmacy, Iasi, Romania*
Qizhen Du / *Institute of Food and Biological Engineering, Zhejiang Gongshang University, Hangzhou, China*
N.M. Edwards / *Grain Research Laboratory, Canadian Grain Commission, Winnipeg, Manitoba, Canada*
Jahangir Emrani / *Department of Civil and Environmental Engineering, North Carolina A & T State University, Greensboro, North Carolina, U.S.A.*
William P. Farrell / *Pfizer Global Research and Development, Pfizer Inc., La Jolla, California, U.S.A.*
Petr S. Fedotov / *Vernadsky Institute of Geochemistry and Analytical Chemistry, Russian Academy of Sciences, Moscow, Russia*
Y.-Q. Feng / *Department of Chemistry, Wuhan University, Wuhan, China*
I.M.P.L.V.O. Ferreira / *Service of Bromatologia, Pharmacy College, University of Porto, Porto, Portugal*
Sam J. Ferrito / *Analytical Services Department, Cooper Power Systems, Franksville, Wisconsin, U.S.A.*
John C. Ford / *Department of Chemistry, Indiana University of Pennsylvania, Indiana, Pennsylvania, U.S.A.*
Esther Forgács / *Institute of Chemistry, Chemical Research Center, Hungarian Academy of Sciences, Budapest, Hungary*
George M. Frame II / *Wadsworth Laboratory, New York State Department of Health, Albany, New York, U.S.A.*
Kenneth G. Furton / *Department of Chemistry, International Forensic Research Institute (IFRI), Miami, Florida, U.S.A.*
M.C. García-Alvarez-Coque / *Department of Analytical Chemistry, University of Valencia, Valencia, Spain*
J.C. Garcia-Glez / *Physical Chemistry Department, University of León, León, Spain*
Rosa Garcia-Lopera / *Institute of Materials Science, University of Valencia, Valencia, Spain*
Dimitrios Gavril / *Physical Chemistry Laboratory, Department of Chemistry, University of Patras, Patras, Greece*
Barbara Gawdzik / *Faculty of Chemistry, MCS University, Lublin, Poland*
Kalliopi A. Georga / *Laboratory of Analytical Chemistry, Chemistry Department, Aristotle University of Thessaloniki, Thessaloniki, Greece*
Árpád Gerstner / *Novartis Agricultural Discovery Institute, Inc., San Diego, California, U.S.A.*
H.G. Gika / *Laboratory of Analytical Chemistry, Chemistry Department, Aristotle University of Thessaloniki, Thessaloniki, Greece*

Michel Girard / *Bureau of Biologics and Radiopharmaceuticals, Health Canada, Ottawa, Ontario, Canada*
Ivan Gitsov / *College of Environmental Science and Forestry, State University of New York, Syracuse, New York, U.S.A.*
Kazimierz Glowniak / *Department of Pharmacognosy, Medical University of Lublin, Lublin, Poland*
Simion Gocan / *Department of Analytical Chemistry, Babes-Bolyai University, Cluj-Napoca, Romania*
Karen M. Gooding / *Eli Lilly and Company, Indianapolis, Indiana, U.S.A.*
Tomomi Goto / *Aichi Prefectural Institute of Public Health, Nagoya, Japan*
Mohan Gownder / *Huntsman Polymers Corp., Odessa, Texas, U.S.A.*
Henryk Grajek / *Institute of Chemistry, Military University of Technology, Warsaw, Poland*
Susan V. Greene / *Ethyl Petroleum Additives Corp., Richmond, Virginia, U.S.A.*
Nelu Grinberg / *Analytical Research Department, Merck Research Laboratories, Rahway, New Jersey, U.S.A.*
A. Gumieniczek / *Department of Medicinal Chemistry, Medical University of Lublin, Lublin, Poland*
András Guttman / *Diversa Company, San Diego, California, U.S.A.*
David S. Hage / *Department of Chemistry, University of Nebraska-Lincoln, Lincoln, Nebraska, U.S.A.*
J.E. Haky / *Department of Chemistry and Biochemistry, Florida Atlantic University, Boca Raton, Florida, U.S.A.*
Susana Maria Halpine / *STArt! teaching Science Through Art, Playa del Rey, California, U.S.A.*
Jamel S. Hamada / *Southern Regional Research Center, Agricultural Research Service, U.S. Department of Agriculture (USDA-ARS), New Orleans, Louisiana, U.S.A.*
Toshihiko Hanai / *Health Research Foundation, Pasteur Institut, Kyoto, Japan*
Martin Hassellöv / *Department of Chemistry, Analytical and Marine Chemistry, Göteborg University, Göteborg, Sweden*
Mohamed M. Hefnawy / *Department of Pharmaceutical Chemistry, King Saud University, Riyadh, Saudi Arabia*
Michael P. Henry / *Advanced Technology Center, Beckman Coulter, Inc., Fullerton, California, U.S.A.*
Tatsuya Higashi / *Division of Pharmaceutical Sciences, Graduate School of Natural Science and Technology, Kanazawa University, Kanazawa, Japan*
Chuichi Hirayama / *Department of Applied Chemistry and Biochemistry, Kumamoto University, Kumamoto, Japan*
H. Hopkała / *Department of Medicinal Chemistry, Medical University of Lublin, Lublin, Poland*
Y.-L. Hu / *Department of Chemistry, Wuhan University, Wuhan, China*
Chih-Ching Huang / *Department of Chemistry, National Taiwan University, Taipei, Taiwan*
W. Jeffrey Hurst / *Hershey Foods Technical Center, Hershey, Pennsylvania, U.S.A.*
Robert J. Hurtubise / *Department of Chemistry, University of Wyoming, Laramie, Wyoming, U.S.A.*
Christine Hürzeler / *Postnova Analytics, Munich, Germany*
Radovan Hynek / *Department of Biochemistry and Microbiology, Institute of Chemical Technology, Prague, Czech Republic*
Hirotaka Ihara / *Department of Applied Chemistry and Biochemistry, Kumamoto University, Kumamoto, Japan*

Gunawan Indrayanto / *Faculty of Pharmacy, Airlangga University, Surabaya, Indonesia*
Haleem J. Issaq / *National Cancer Institute at Frederick (NCI-Frederick), National Institutes of Health (NIH), Frederick, Maryland, U.S.A.*
Rie Ito / *Department of Analytical Chemistry, Faculty of Pharmaceutical Sciences, Hoshi University, Tokyo, Japan*
Yoichiro Ito / *National Heart, Lung, and Blood Institute (NHLBI), National Institutes of Health (NIH), Bethesda, Maryland, U.S.A.*
Yuko Ito / *Aichi Prefectural Institute of Public Health, Nagoya, Japan*
Yusuke Iwasaki / *Department of Analytical Chemistry, Faculty of Pharmaceutical Sciences, Hoshi University, Tokyo, Japan*
Eshwar Jagerdeo / *Federal Bureau of Investigation Laboratory, Quantico, Virginia, U.S.A.*
Josef Janca / *Department of Chemistry, University of La Rochelle, La Rochelle, France*
J. Jancar / *BIA Separations d.o.o., Ljubljana, Slovenia*
Pavel Jandera / *Department of Analytical Chemistry, University of Pardubice, Pardubice, Czech Republic*
A. Jardy / *Analytical Chemistry Department, City of Paris Industrial Physics and Chemistry Higher Educational Institution (ESPCI), Paris, France*
Dennis R. Jenke / *Technology Resources Division, Baxter Healthcare Corporation, Round Lake, Illinois, U.S.A.*
Alfonso Jiménez / *Department of Analytical Chemistry, Nutrition and Food Sciences, University of Alicante, Alicante, Spain*
Kiyokatsu Jinno / *Department of Materials Science, Toyohashi University, Toyohashi, Japan*
Harald John / *Bundeswehr Institute of Pharmacology and Toxicology, Munich, Germany*
Brian Jones / *Selerity Technologies, Inc., Salt Lake City, Utah, U.S.A.*
Krzysztof Kaczmarski / *Faculty of Chemistry, Technical University of Rzeszów, Rzeszów, Poland*
Adnan A. Kadi / *Department of Pharmaceutical Chemistry, King Saud University, Riyadh, Saudi Arabia*
Huba Kalász / *Department of Pharmacology and Pharmacotherapy, Semmelweis University of Medicine, Budapest, Hungary*
John Kapolos / *Department of Agricultural Products Technology, Technological Educational Institute of Kalamata, Kalamata, Greece*
George Karaiskakis / *Physical Chemistry Laboratory, Department of Chemistry, University of Patras, Patras, Greece*
Jan Kás / *Department of Biochemistry and Microbiology, Institute of Chemical Technology, Prague, Czech Republic*
Galina Kassalainen / *Department of Chemistry and Geochemistry, Colorado School of Mines, Golden, Colorado, U.S.A.*
Sindy Kayillo / *Center for Biostructural and Biomolecular Research, University of Western Sydney, Sydney, New South Wales, Australia*
Sarah Kazmi / *Department of Chemistry, Northeastern University, Boston, Massachusetts, U.S.A.*
Ernst Kenndler / *Institute for Analytical Chemistry, University of Vienna, Vienna, Austria*
Eileen Kennedy / *Novartis Crop Protection, Inc., Greensboro, North Carolina, U.S.A.*
Tabrez A. Khan / *Department of Chemistry, Jamia Millia Islamia (A Central University), New Delhi, India*
Yuriko Kiba / *Department of Medicinal Chemistry, University of Tokushima, Tokushima, Japan*
Peter Kilz / *Polymer Standards Service GmbH, Mainz, Germany*

Chong-Kook Kim / *Research Institute of Pharmaceutical Sciences, Seoul National University, Seoul, and Department of Pharmaceutical Engineering, Inje University, Gyeongnam, Korea*
Peter T. Kissinger / *Chairman and CEO, Bioanalytical Systems, Inc., West Lafayette, Indiana, U.S.A.*
Eiichi Kitazume / *Faculty of Humanities and Social Sciences, Iwate University, Iwate, Japan*
Thorsten Klein / *Postnova Analytics, Munich, Germany*
Oliver Klett / *Institute of Chemistry, Uppsala University, Uppsala, Sweden*
Athanasia Koliadima / *Physical Chemistry Laboratory, Department of Chemistry, University of Patras, Patras, Greece*
B.L. Kolte / *Department of Chemical Technology, Dr. Babasaheb Ambedkar Marathwada University, Aurangabad, India*
Fumio Kondo / *Aichi Prefectural Institute of Public Health, Nagoya, Japan*
Vadim L. Kononenko / *Institute of Biochemical Physics, Russian Academy of Sciences, Moscow, Russia*
Teresa Kowalska / *Institute of Chemistry, Silesian University, Katowice, Poland*
Anna Kozak / *Department of Biochemistry and Microbiology, Institute of Chemical Technology, Prague, Czech Republic*
Ira S. Krull / *Department of Chemistry, Northeastern University, Boston, Massachusetts, U.S.A.*
Ján Krupcik / *Institute of Analytical Chemistry, Slovak University of Technology, Bratislava, Slovakia*
Svetlana Kulevanova / *Institute of Pharmacognosy, Faculty of Pharmacy, Sts. Cyril and Methodius University, Skopje, Republic of Macedonia*
Silvia Lacorte / *Department of Environmental Chemistry, Chemical and Environmental Research Institute of Barcelona (IIQAB), Barcelona, Spain*
Vaishali Soneji Lafita / *Abbott Laboratories, Inc., Abbott Park, Illinois, U.S.A.*
Fernando M. Lanças / *Institute of Chemistry of São Carlos (USP), University of São Paulo, São Carlos, Brazil*
James P. Landers / *Department of Chemistry, University of Virginia, Charlottesville, Virginia, U.S.A.*
David Y.W. Lee / *McLean Hospital, Harvard Medical School, Belmont, Massachusetts, U.S.A.*
Seungho Lee / *Department of Chemistry, Hannam University, Taejon, Korea*
Jozef Lehotay / *Institute of Analytical Chemistry, Slovak University of Technology, Bratislava, Slovakia*
Luciano Lepri / *Department of Chemistry, University of Florence (UNIFI), Florence, Italy*
James Lesec / *National Center for Scientific Research (CNRS), City of Paris Industrial Physics and Chemistry Higher Educational Institution (ESPCI), Paris, France*
Vera Leshchinskaya / *Bristol-Myers Squibb Co., Princeton, New Jersey, U.S.A.*
Chenchen Li / *College of Chemistry and Molecular Engineering, Peking University, Beijing, China*
Wilna Liebenberg / *Research Institute for Industrial Pharmacy, North-West University, Potchefstroom, South Africa*
Xiuli Lin / *Department of Chemistry, Wake Forest University, Winston-Salem, North Carolina, U.S.A.*
Cheng-Ming Liu / *Department of Medical Technology, Institute of Biomedical Technology, Taipei Medical University, Taipei, Taiwan*
Huwei Liu / *Institute of Analytical Chemistry, Peking University, Beijing, China*
Rosario LoBrutto / *Merck Research Laboratories, Rahway, New Jersey, U.S.A.*

E.S.M. Lutz / *Bioanalytical Chemistry Department, AstraZeneca R&D Mölndal, Mölndal, Sweden*
Ying Ma / *National Heart, Lung, and Blood Institute (NHLBI), National Institutes of Health (NIH), Bethesda, Maryland, U.S.A.*
Mohamed E. Mahmoud / *Medical Chemistry Department, King Abdullaziz University, Jeddah, Saudi Arabia*
Edward Malawer / *International Specialty Products, Wayne, New Jersey, U.S.A.*
Abul K. Mallik / *Department of Applied Chemistry and Biochemistry, Kumamoto University, Kumamoto, Japan*
P. Manesiotis / *Department of Materials Science, University of Patras, Patras, Greece*
M.L. Marín / *Department of Analytical Chemistry, University of Alicante, Alicante, Spain*
Wojciech Markowski / *Department of Inorganic and Analytical Chemistry, Medical University of Lublin, Lublin, Poland*
J. Martin-Villacorta / *Physical Chemistry Department, University of León, León, Spain*
C. Marutoiu / *Department of Chemistry, Lucian Blaga University of Sibiu, Sibiu, Romania*
T. Maryutina / *Vernadsky Institute of Geochemistry and Analytical Chemistry, Russian Academy of Sciences, Moscow, Russia*
Kazuhiro Matsuda / *Pharmacology Division, National Cancer Center Research Institute, Tokyo, Japan*
Sachie Matsuda / *Department of Dermatology, Horikiri Central Hospital, Tokyo, Japan*
Kiichi Matsuhisa / *Asahikawa National College of Technology, Asahikawa, Japan*
Maria T. Matyska / *Department of Chemistry, San Jose State University, San Jose, California, U.S.A.*
Andrei Medvedovici / *Department of Analytical Chemistry, University of Bucharest, Bucharest, Romania*
Gregorio R. Meira / *National Scientific and Technical Research Council (CONICET), Santa Fe, Argentina*
R. Mendez / *Physical Chemistry Department, University of León, León, Spain*
Raniero Mendichi / *Institute of Macromolecular Chemistry, National Research Council (CNR), Milan, Italy*
Jean-Michel Menet / *Aventis Pharma, Vitry-sur-Seine, France*
Damián Mericko / *Institute of Analytical Chemistry, Slovak University of Technology, Bratislava, Slovakia*
Rajmund Michalski / *Institute of Environmental Engineering, Polish Academy of Science, Zabrze, Poland*
Ivan Miksík / *Institute of Physiology, Academy of Sciences of the Czech Republic, Prague, Czech Republic*
Toshiaki Miura / *College of Medical Technology, Hokkaido University, Sapporo, Japan*
Emi Miyamoto / *Department of Health Science, Kochi Women's University, Kochi, Japan*
N. Montes / *Physical Chemistry Department, University of León, León, Spain*
Myeong Hee Moon / *Department of Chemistry, Kangnung National University, Kangnung, South Korea*
J.J.S. Moreira / *Chromatography Laboratory, University of São Paulo, São Carlos, Brazil*
Sadao Mori / *PAC Research Institute, Mie University, Nagoya, Japan*
Mark Moskovitz / *Dynamic Adsorbents, Inc., Atlanta, Georgia, U.S.A.*
Tomasz Mroczek / *Department of Pharmacognosy, Medical University of Lublin, Lublin, Poland*
Muhammad Mulja / *Faculty of Pharmacy, Airlangga University, Surabaya, Indonesia*

D. Muller / *Galilee Institute, University of North Paris, Villetaneuse, France*
Subra Muralidharan / *Chemistry Department, Western Michigan University, Kalamazoo, Michigan, U.S.A.*
Roy A. Musil / *Althea Technologies, Inc., San Diego, California, U.S.A.*
Ron Myers / *Wyatt Technology Corp., Santa Barbara, California, U.S.A.*
Noh-Hong Myoung / *Seoul Metropolitan Government, Institute of Health and Environment, Seoul, South Korea*
Monica J.S. Nadler / *Beth Israel Deaconess Medical Center, Harvard Medical School, Boston, Massachusetts, U.S.A.*
Tim Nadler / *Applied Biosystems, Inc., Framingham, Massachusetts, U.S.A.*
Shoji Nagaoka / *Kumamoto Industrial Research Institute, Kumamoto, Japan*
Hiroyuki Nakazawa / *Department of Analytical Chemistry, Faculty of Pharmaceutical Sciences, Hoshi University, Tokyo, Japan*
A. Negro / *Analytical Chemistry Section, Faculty of Biological and Environmental Sciences, University of León, León, Spain*
Tuan Q. Nguyen / *Department of Materials Science, Polymer Laboratory, Swiss Federal Institute of Technology, Lanne, Switzerland*
Boryana Nikolova-Damyanova / *Institute of Organic Chemistry, Bulgarian Academy of Sciences, Sofia, Bulgaria*
Tadashi Nishio / *Division of Pharmaceutical Sciences, Graduate School of Natural Science and Technology, Kanazawa University, Kanazawa, Japan*
Hisao Oka / *Food-Related Chemistry, Laboratory of Chemistry, Aichi Prefectural Institute of Public Health, Nagoya, Japan*
Beatriz Oliveira / *Requimte, Bromatology Service, Faculty of Pharmacy, University of Porto, Porto, Portugal*
Jerzy Oszczudlowski / *Institute of Chemistry, Jan Kochanowski University, Kielce, Poland*
Koji Otsuka / *Department of Material Science, Himeji Institute of Technology, Hyogo, Japan*
Anders Palm / *Cell and Molecular Biology, Astra Zeneca, Lund, Sweden*
Irene Panderi / *School of Pharmacy, Division of Pharmaceutical Chemistry, University of Athens, Athens, Greece*
Ioannis N. Papadoyannis / *Laboratory of Analytical Chemistry, Chemistry Department, Aristotle University of Thessaloniki, Thessaloniki, Greece*
Elias Papapanagiotou / *Laboratories of Food Hygiene, Faculty of Veterinary Medicine, Aristotle University of Thessaloniki, Thessaloniki, Greece*
D.M. Pereira / *Requimte, Department of Pharmacognosy, Faculty of Pharmacy, University of Porto, Porto, Portugal*
Joseph J. Pesek / *Department of Chemistry, San Jose State University, San Jose, California, U.S.A.*
Terry M. Phillips / *Ultramicro Analytical Immunochemistry Resource (UAIR), DBEPS, ORS, OD, National Institutes of Health, Bethesda, Maryland, U.S.A.*
Aleš Podgornik / *BIA Separations d.o.o., Ljubljana, Slovenia*
Valquíria Aparecida Polisel Jabor / *Faculty of Pharmaceutical Sciences of Ribeirão Preto, University of São Paulo, Ribeirão Preto, Brazil*
Stanisław Popiel / *Institute of Chemistry, Military University of Technology, Warsaw, Poland*
Iolanda Porcar / *Institute of Materials Science, University of Valencia, Valencia, Spain*
Jacques Portoukalian / *Laboratory of Tumor Glycobiology, University Claude Bernard Lyon I, Oullins, France*

M. Soledad Prats Moya / *Department of Analytical Chemistry, Nutrition and Food Sciences, University of Alicante, Alicante, Spain*
K.R. Preston / *Grain Research Laboratory, Canadian Grain Commission, Winnipeg, Manitoba, Canada*
Wojciech Prus / *School of Technology and the Arts in Bielsko-Biała, Bielsko-Biała, Poland*
Waraporn Putalun / *Graduate School of Pharmaceutical Sciences, Kyushu University, Fukuoka, Japan*
Alina Pyka / *Department of Analytical Chemistry, Medical University of Silesia, Sosnowiec, Poland*
Javier Quagliano / *Organic Synthesis Division, Argentine R&D Institute for the Defense (CITEFA), Buenos Aires, Argentina*
Rashid Nazir Qureshi / *Central Analytical Facility Division, Pakistan Institute of Nuclear Science and Technology, Islamabad, Pakistan*
B. Rabanal / *Analytical Chemistry Section, Faculty of Biological and Environmental Sciences, University of León, León, Spain*
Fred M. Rabel / *EMD Chemicals, Inc., Gibbstown, New Jersey, U.S.A.*
Abdul Rahman / *Assessment Service Unit, Airlangga University, Surabaya, Indonesia*
M. Mizanur Rahman / *Department of Applied Chemistry and Biochemistry, Kumamoto University, Kumamoto, Japan*
P.R. Vasudeva Rao / *Chemistry Group, Indira Gandhi Center for Atomic Research (IGCAR), Kalpakkam, India*
Chitra K. Ratnayake / *Advanced Technology Center, Beckman Coulter, Inc., Fullerton, California, U.S.A.*
B.B. Raut / *Department of Chemical Technology, Dr. Babasaheb Ambedkar Marathwada University, Aurangabad, India*
Jetse C. Reijenga / *Department of Chemical Engineering and Chemistry, Eindhoven University of Technology, Eindhoven, The Netherlands*
Pierluigi Reschiglian / *Department of Chemistry "G. Ciamician", University of Bologna, Bologna, Italy*
J.A. Resines / *Department of Teaching General, Specific and Theory of Education, University of León, León, Spain*
Mark P. Richards / *Livestock and Poultry Sciences Institute (LPSI), Agricultural Research Service, U.S. Department of Agriculture (USDA-ARS), Beltsville, Maryland, U.S.A.*
Anna Rigol / *Department of Analytical Chemistry, University of Barcelona, Barcelona, Spain*
M.-C. Rolet-Menet / *Analytical Chemistry Laboratory, Unit of Formation and Research (UFR) of Pharmaceutical and Biological Sciences, Paris, France*
Kyung Ho Row / *Center for Advanced Bioseparation Technology and Department of Chemical Engineering, Inha University, Incheon, South Korea*
Jan K. Rozylo / *Department of Adsorption Chromatography and Planar Chromatography, Marie Curie-Sklodowska University, Lublin, Poland*
M.J. Ruiz-Angel / *Department of Analytical Chemistry, University of Valencia, Valencia, Spain*
Roxana A. Ruseckaite / *Research Institute of Material Science and Technology (INTEMA), University of Mar del Plata, Mar del Plata, Argentina*
Koichi Saito / *Department of Analytical Chemistry, Faculty of Pharmaceutical Sciences, Hoshi University, Tokyo, Japan*
Jirí Sajdok / *Department of Biochemistry and Microbiology, Institute of Chemical Technology, Prague, Czech Republic*
Mieczysław Sajewicz / *Institute of Chemistry, Silesian University, Katowice, Poland*

Peter Sajonz / *Merck Research Laboratories, Rahway, New Jersey, U.S.A.*
Masayo Sakata / *Department of Applied Chemistry and Biochemistry, Kumamoto University, Kumamoto, Japan*
Victoria F. Samanidou / *Laboratory of Analytical Chemistry, Chemistry Department, Aristotle University of Thessaloniki, Thessaloniki, Greece*
Mária Sasvári-Székely / *Department of Pharmacology and Pharmacotherapy, Semmelweis University of Medicine, Budapest, Hungary*
Wes Schafer / *Merck Research Laboratories, Rahway, New Jersey, U.S.A.*
John E. Schiel / *Department of Chemistry, University of Nebraska-Lincoln, Lincoln, Nebraska, U.S.A.*
Martin E. Schimpf / *Chemistry Department, Boise State University, Boise, Idaho, U.S.A.*
Oliver Schmitz / *Division of Molecular Toxicology, German Cancer Research Center, Heidelberg, Germany*
Raymond P.W. Scott / *Scientific Detectors Ltd., Banbury, Oxfordshire, U.K.*
Stephen L. Secreast / *Pharmaceutical Sciences, Pharmacia Corporation, Kalamazoo, Michigan, U.S.A.*
H. Seegulum / *Department of Chemistry and Biochemistry, Florida Atlantic University, Boca Raton, Florida, U.S.A.*
Adriana Segall / *Pharmacy and Biochemistry Faculty, University of Buenos Aires, Buenos Aires, Argentina*
Larry Senak / *International Specialty Products, Wayne, New Jersey, U.S.A.*
Vince Serignese / *Pharmaceutical Analysis Laboratory, King Faisal Specialist Hospital and Research Center, Riyadh, Saudi Arabia*
Joanne Severs / *Bayer Pharmaceuticals, Berkeley, California, U.S.A.*
R. Andrew Shalliker / *Center for Biostructural and Biomolecular Research, University of Western Sydney, Sydney, New South Wales, Australia*
Joseph Sherma / *Department of Chemistry, Lafayette College, Easton, Pennsylvania, U.S.A.*
Yoichi Shibusawa / *Division of Pharmaceutical and Biomedical Analysis, School of Pharmacy, Tokyo University of Pharmacy and Life Science, Tokyo, Japan*
Zak K. Shihabi / *Department of Pathology, Wake Forest University, Winston-Salem, North Carolina, U.S.A.*
Kazutake Shimada / *Division of Pharmaceutical Sciences, Graduate School of Natural Science and Technology, Kanazawa University, Kanazawa, Japan*
D.B. Shinde / *Department of Chemical Technology, Dr. Babasaheb Ambedkar Marathwada University, Aurangabad, India*
Kazufusa Shinomiya / *College of Pharmacy, Nihon University, Chiba, Japan*
Yukihiro Shoyama / *Graduate School of Pharmaceutical Sciences, Kyushu University, Fukuoka, Japan*
Atsuomi Shundo / *Department of Applied Chemistry and Biochemistry, Kumamoto University, Kumamoto, Japan*
Maria Victoria Silva Elipe / *Analytical Research and Development Department, AMGEN, Thousand Oaks, California, U.S.A.*
N. Sivaraman / *Chemistry Group, Indira Gandhi Center for Atomic Research (IGCAR), Kalpakkam, India*
Piotr Słomkiewicz / *Institute of Chemistry, Jan Kochanowski University, Kielce, Poland*
Edward Soczewinski / *Department of Inorganic and Analytical Chemistry, Medical University of Lublin, Lublin, Poland*

M.L. Soran / *National Institute of Research and Development for Isotopic and Molecular Technology, Cluj-Napoca, Romania*
Adrian Florin I. Spac / *Department of Chemistry, Grigore T. Popa University of Medicine and Pharmacy, Iasi, Romania*
Boris Ya. Spivakov / *Vernadsky Institute of Geochemistry and Analytical Chemistry, Russian Academy of Sciences, Moscow, Russia*
Fernanda C. Spoljaric / *Chemical Institute of São Carlos, University of São Paulo, São Carlos, Brazil*
T.G. Srinivasan / *Chemistry Group, Indira Gandhi Center for Atomic Research (IGCAR), Kalpakkam, India*
Trajce Stafilov / *Institute of Chemistry, Faculty of Science, Sts. Cyril and Methodius University, Skopje, Republic of Macedonia*
Raluca-Ioana Stefan / *Chemistry Department, University of Pretoria, Pretoria, South Africa*
Marina Stefova / *Institute of Chemistry, Faculty of Science, Sts. Cyril and Methodius University, Skopje, Republic of Macedonia*
Susan G. Stevenson / *Grain Research Laboratory, Canadian Grain Commission, Winnipeg, Manitoba, Canada*
A. Strancar / *BIA Separations d.o.o., Ljubljana, Slovenia*
Richard C. Striebich / *University of Dayton Research Institute, Dayton, Ohio, U.S.A.*
Andre M. Striegel / *Department of Chemistry, Florida State University, Tallahassee, Florida, U.S.A.*
Suciati / *Faculty of Pharmacy, Airlangga University, Surabaya, Indonesia*
Ian A. Sutherland / *Brunel Institute for Bioengineering, Brunel University, Uxbridge, Middlesex, U.K.*
Dorota Szydlowska / *Department of Chemistry, Warsaw University, Warsaw, Poland*
Makoto Takafuji / *Department of Applied Chemistry and Biochemistry, Kumamoto University, Kumamoto, Japan*
Hiroyuki Tanaka / *Graduate School of Pharmaceutical Sciences, Kyushu University, Fukuoka, Japan*
Naohiro Tateda / *Asahikawa National College of Technology, Asahikawa, Japan*
M.C.H. Tavares / *Chromatography Laboratory, University of São Paulo, São Carlos, Brazil*
D.A. Teifer / *Department of Chemistry and Biochemistry, Florida Atlantic University, Boca Raton, Florida, U.S.A.*
Shigeru Terabe / *Department of Material Science, Himeji Institute of Technology, Hyogo, Japan*
Iwao Teraoka / *Department of Chemistry, Polytechnic University, Brooklyn, New York, U.S.A.*
Gerald J. Terfloth / *Research and Development Division, SmithKline Beecham Pharmaceuticals, King of Prussia, Pennsylvania, U.S.A.*
Richard Thede / *Institute of Chemistry and Biochemistry, University of Greifswald, Greifswald, Germany*
Georgios A. Theodoridis / *Laboratory of Analytical Chemistry, Chemistry Department, Aristotle University of Thessaloniki, Thessaloniki, Greece*
Richard Thompson / *Analytical Research Department, Merck Research Laboratories, Rahway, New Jersey, U.S.A.*
J.R. Torres-Lapasio / *Department of Analytical Chemistry, University of Valencia, Valencia, Spain*
Niem Tri / *Water Studies Centre, Monash University, Melbourne, Victoria, Australia*
Marek Trojanowicz / *Department of Chemistry, Warsaw University, Warsaw, Poland*

Anna Tsantili-Kakoulidou / *Department of Pharmaceutical Chemistry, University of Athens, Athens, Greece*
Anant Vailaya / *Merck Research Laboratories, Rahway, New Jersey, U.S.A.*
P. Valentão / *Requimte, Department of Pharmacognosy, Faculty of Pharmacy, University of Porto, Porto, Portugal*
Jacobus F. van Staden / *Chemistry Department, University of Pretoria, Pretoria, South Africa*
Jorge R. Vega / *National Scientific and Technical Research Council (CONICET), Santa Fe, Argentina*
Manuel C. Ventura / *Pfizer Global Research and Development, Pfizer Inc., La Jolla, California, U.S.A.*
J. Vial / *Analytical Chemistry Department, City of Paris Industrial Physics and Chemistry Higher Educational Institution (ESPCI), Paris, France*
Nikolay Vladimirov / *Research Center, Hercules Inc., Wilmington, Delaware, U.S.A.*
Frank von der Kammer / *Department for Environmental Science and Technology, Technical University of Hamburg-Harburg, Hamburg, Germany*
Monika Waksmundzka-Hajnos / *Department of Inorganic Chemistry, Medical University of Lublin, Lublin, Poland*
Qin-Sun Wang / *National Key Laboratory of Elemento-Organic Chemistry, Nankai University, Tianjin, China*
Tao Wang / *Merck Research Laboratories, Rahway, New Jersey, U.S.A.*
Fumio Watanabe / *Department of Health Science, Kochi Women's University, Kochi, Japan*
Teresa Wawrzynowicz / *Department of Inorganic and Analytical Chemistry, Medical University of Lublin, Lublin, Poland*
Robert Weinberger / *CE Technologies, Inc., Chappaqua, New York, U.S.A.*
Adrian Weisz / *Office of Cosmetics and Colors, Center for Food Safety and Applied Nutrition, U.S. Food and Drug Administration (USFDA), Washington, District of Columbia, U.S.A.*
Jaroslaw Widelski / *Department of Pharmacognosy, Medical University of Lublin, Lublin, Poland*
P. Stephen Williams / *Department of Biomedical Engineering, Cleveland Clinic Foundation, Cleveland, Ohio, U.S.A.*
S. Kim Ratanathanawong Williams / *Department of Chemistry and Geochemistry, Colorado School of Mines, Golden, Colorado, U.S.A.*
Zygfryd Witkiewicz / *Institute of Chemistry, Jan Kochanowski University, Kielce, Poland*
Gary Witman / *Dynamic Adsorbents, Inc., Atlanta, Georgia, U.S.A.*
Philip Wood / *Brunel Institute for Bioengineering, Brunel University, Uxbridge, Middlesex, U.K.*
Chi-san Wu / *International Specialty Products, Wayne, New Jersey, U.S.A.*
Philip J. Wyatt / *Wyatt Technology Corp., Santa Barbara, California, U.S.A.*
Feng Xu / *Department of Medicinal Chemistry, University of Tokushima, Tokushima, Japan*
Akio Yanagida / *Division of Pharmaceutical and Biomedical Analysis, School of Pharmacy, Tokyo University of Pharmacy and Life Sciences, Tokyo, Japan*
Fuquan Yang / *National Heart, Lung, and Blood Institute (NHLBI), National Institutes of Health (NIH), Bethesda, Maryland, U.S.A.*
Xia Yang / *Institute of Analytical Chemistry, Peking University, Beijing, China*
Yiwen Yang / *Department of Chemical and Biochemical Engineering, Zhejiang University, Hangzhou, China*

Yu Yang / *Department of Chemistry, East Carolina University, Greenville, North Carolina, U.S.A.*
L.M. Yuan / *Department of Chemistry, Yunnan Normal University, Kunming, China*
Mochammad Yuwono / *Faculty of Pharmacy, Airlangga University, Surabaya, Indonesia*
Robert Zakrzewski / *Department of Instrumental Analysis, University of Łódz, Łódz, Poland*
Maciej Zborowski / *Department of Biomedical Engineering, Cleveland Clinic Foundation, Cleveland, Ohio, U.S.A.*
Igor G. Zenkevich / *Chemical Research Institute, St. Petersburg State University, St. Petersburg, Russia*
Ji-Feng Zhang / *Massachusetts Institute of Technology, Cambridge, Massachusetts, U.S.A.*
L. Zhang / *National Key Laboratory of Elemento-Organic Chemistry, Nankai University, Tianjin, China*
Lifeng Zhang / *Environmental Technology Institute, Innovation Centre (NTU), Singapore*
Weihua Zhang / *Department of Chemistry, Florida International University, Miami, Florida, U.S.A.*
Xi-Chun Zhou / *Department of Chemistry, Cambridge University, Cambridge, U.K.*
Wenshan Zhuang / *Taro Pharmaceuticals, Inc., Brampton, Ontario, Canada*
A. Ziakova-Caniova / *Department of Analytical Chemistry, Slovak Technical University, Bratislava, Slovakia*
Anastasia Zotou / *Laboratory of Analytical Chemistry, Chemistry Department, Aristotle University of Thessaloniki, Thessaloniki, Greece*

Contents

Volume I

Volume I (*cont'd.*)

Volume I (*cont'd.*)

Volume II

Volume II (*cont'd.*)

Volume II (*cont'd.*)

Volume III

Volume III (*cont'd.*)

Volume III (*cont'd.*)

Topical Table of Contents

Affinity Chromatography

Amino Acids/Peptides/Proteins

Basic Theory/Definitions

Biomedical

Biomedical (*cont'd.*)

CCC (Countercurrent Chromatography)

CE/CEC, and Related Techniques

CE/CEC, and Related Techniques (*cont'd.*)

Chiral Techniques

Derivatization

Detection/Detectors

Detection/Detectors (*cont'd.*)

FFF (Field-Flow Fractionation)

GC (Gas Chromatography)

GC (Gas Chromatography) (*cont'd.*)

Gradient/Programmed Techniques

HPLC

HPLC (*cont'd.*)

Multidimensional Techniques

Natural Products

Pharmaceuticals

Polymers and Additives

Preparative Chromatography

Sampling Techniques

SEC/GPC (Size Exclusion/Gel Permeation)

SFC/SFE (Supercritical Fluid Techniques)

Solvents/Mobile Phases

Solvents/Mobile Phases (*cont'd.*)

Stationary Phases, Columns

TLC (Thin Layer Chromatography)

TLC (Thin Layer Chromatography) (*cont'd.*)

Vitamins

Foreword

The collection of techniques known as chromatography may be the world's most prevalent and useful analytical methodology. In the pharmaceutical industry alone, HPLC is the second most prevalent instrument, after the pH meter. Thus, it is not surprising that the *Encyclopedia of Chromatography* is one of the most authoritative and best-selling scientific encyclopedias that have been published. This *Third Edition* is a three-volume set containing over 500 entries. The entries vary from the short and concise definition of terms to more extensive tomes on specific methods, background, optimization, practice, and theory. The majority of the entries have been updated and there are over 100 new entries. Many of these were edited and reviewed after being published online. Hence, the *Third Edition* contains the very latest information on this most important analytical technique, in addition to all relevant background material.

Given the size and extent of coverage of the *Encyclopedia of Chromatography*, *Third Edition*, a considerable effort was made by the Editor, Dr. Jack Cazes, to make sure the information is crisp, clear, and easy to access. Indeed, in response to reader feedback, there are two tables of contents: one in alphabetical order and the other by category of chromatography. This encyclopedia contains essential information for both the novice and the experienced scientist. If you don't have access to an entire university library and considerable excess time, then the *Encyclopedia of Chromatography*, *Third Edition*, is essential.

Prof. Daniel W. Armstrong, Ph.D.
University of Texas at Arlington, Arlington, Texas, U.S.A.

February 6, 2009

Foreword

Years ago, it was said that the difference between scientific research done in academia and that done in industry or government was that those involved in the former had lots of time but little money, while those involved in the latter had little time but lots of money. As the economic and technological realities of the twenty-first century unfold, it has become clear that such differences are no longer operative. In whatever setting it is performed, the goal of scientific research must be to give accurate information in the shortest possible time at the least possible expense. Recent advances in chromatography research have been consistent with this goal.

Since the publication of the first full edition of the *Encyclopedia of Chromatography* eight years ago, a myriad of existing methods have been improved and numerous new methods have been developed that achieve the goal of reducing both time and costs. Additionally, limits of detection have been reduced to previously unimaginable levels and new applications of chromatographic techniques have emerged in areas as diverse as chemical biology, materials science, and nanotechnology. As the first decade of this century comes to an end, it is therefore fitting that this new revised and updated edition be published.

While retaining the basic information on the theory and practice of all the realms of chromatographic science in the first edition, this new version includes updated material on all the advances that have occurred in the past several years. Therefore, it is a useful resource both for novices who are interested in learning basic chromatographic techniques and for experienced experts who are exploring new methods and applications. Most of all, this encyclopedia will stimulate the imagination and creativity of all who read it, thereby assisting in the progression of new advances that will surely come in the next decade and beyond.

Prof. Jerome E. Haky, Ph.D.
Florida Atlantic University, Boca Raton, Florida, U.S.A.

February 9, 2009

Preface for the Third Edition

The thoroughly revised and expanded third edition of the *Encyclopedia of Chromatography* is an authoritative source of information for practitioners and researchers in chemistry, biology, physics, engineering, and materials science. It is a quick reference source and a clear guide to specific chromatographic techniques and theory, providing a basic introduction to the science and technology of the method, as well as leading key references dealing with the theory and methodology for analysis of specific chemicals and applications in industry.

The third edition provides an abundance of updated topics, applications, and references from the literature, many discussions on emerging technologies and applications in chromatography, including numerous tables and figures to illustrate and clarify technical points presented in the entries—showcasing modern applications and instrumentation in use today—and detailed discussions on the methodology, with authoritative coverage of the instrumentation and theoretical aspects of chromatography.

The third edition will doubtless continue to serve as a valuable, reader-friendly reference for all practitioners of analytical chemistry and materials science, as well as for those who employ chromatographic methods for analysis of complex mixtures of substances.

Acronyms

AAS	Atomic Absorption Spectrometry
ACE	Affinity Capillary Electrophoresis
ADC (A/D)	Analog to Digital Converter
AES	Atomic Emission Spectroscopy
AMD	Automated Multiple Development
ANOVA	Analysis of Variance (a statistical term)
APCI	Atmospheric Pressure Chemical Ionization
APPI	Atmospheric Pressure Photo-Ionization
BGE	Background Electrolyte
BHT	Butylated Hydroxytoluene
CAE	Capillary Array Electrophoresis
CCC	Countercurrent Chromatography
CCD	Charge Coupled Device
CD	Compact Disk
CD	Cyclodextrin
CE	Capillary Electrophoresis
CEC	Capillary Electrochromatography
CF-FAB	Continuous-Flow Fast Atom Bombardment
CGE	Capillary Gel Electrophoresis
CIEF	Capillary Isoelectric Focusing
CITP	Capillary Isotachophoresis
CPC	Coil Planet Centrifuge or Centrifugal Partition Chromatography
CPU	Central Processing Unit
CSF	Cerebrospinal Fluid
CSP	Chiral Stationary Phase
CTAB	Hexadecyltrimethylammonium Bromide
CV	Coefficient of Variation
CZE	Capillary Zone Electrophoresis
DAD	Diode-Array Detection
DELFIA	Dissociation-Enhanced Lanthanide Fluoroimmunoassay
DHPLC	Denaturing High-Performance Liquid Chromatography
DNA	Desoxyribonucleic Acid
DOC	Dissolved Organic Carbon
DVD	Digital Video Disk
ECD	Electrochemical Detector or Electron Capture Detector
EDXRF	Energy-Dispersive X-ray Fluorescence
EI-MS	Electron Impact Mass Spectrometry
ELISA	Enzyme-Linked Immunosorbent Assay
ELSD	Evaporative Light Scattering Detector
EMIT	Enzyme Multiplied Immunoassay Technique
EOF	Electro-osmotic Flow
EPS	Extra-cellular Polymeric Secretions
ESI	Electrospray Ionization
FAAS	Flame Atomic Absorption Spectrometry
FFF	Field-Flow Fractionation
FID	Flame Ionization Detection (Detector)
FlFFF	Flow Field-Flow Fractionation
FPLC	Fast Protein Liquid Chromatography
FTIR	Fourier Transform Infrared
GC	Gas Chromatography
GFC	Gel Filtration Chromatography
GI	Gastrointestinal
GLC	Gas Liquid Chromatography
HIC	Hydrophobic Interaction Chromatography
HIV	Human Immunodeficiency Virus
HPLC	High-Performance Liquid Chromatography
HPSEC	High-Performance Size-Exclusion Chromatography
HPTLC	High-Performance Thin-Layer Chromatography
HSCCC	High-Speed Countercurrent Chromatography
HTAB	Hexadecyltrimethylammonium Bromide
ICP	Inductively Coupled Plasma
ICP-MS	Inductively Coupled Plasma-Mass Spectrometry
IEC	Ion-Exchange Chromatography
IEF	Isoelectric Focusing
γ-IFN	Gamma Interferon
IgG	Immunoglobulin G
IMAC	Immobilized Metal Affinity Chromatography; Immobilized Ion Metal Affinity Chromatography
I/O	Input/Output
IR	Infrared
IRMA	Immuno-Radiometric Assay
LC	Liquid Chromatography
LC-FTIR	Liquid Chromatography-Fourier Transform Infrared
LCD	Liquid Crystal Display
LIF	Laser-Induced Fluorescence
LIMS	Laboratory Information Management System
LLE	Liquid–Liquid Extraction
LOD	Limit of Detection
LOQ	Limit of Quantitation
LSER	Linear Solvation Energy Relationship
MALDI	Matrix-Assisted Laser Desorption Ionization
MALLS	Multiangle Laser Light Scattering
MDLC	Multidimensional Liquid Chromatography

MEEKC	Microemulsion Electrokinetic Chromatography
MEKC	Micellar Electrokinetic Chromatography
MEPS	Microextraction in a Packed Syringe
MFFF	Magnetic Field-Flow Fractionation
MIBK	Methyl Isobutyl Ketone
MIP	Molecularly Imprinted Polymer
MIP-OES	Microwave Induced Plasma Optical Emission Spectroscopy
MISP	Molecularly Imprinted Stationary Phase
pMMA	Poly-methylmethacrylate
MS	Mass Spectrometry
MSPD	Matrix Solid-Phase Dispersion
MTase	Methyl Transferase
MW	Molecular Weight
NACE	Non-Aqueous Capillary Electrophoresis
NARP	Non-Aqueous Reverse Phase
NIC	Network Interface Card
NIR	Near Infrared
NMR	Nuclear Magnetic Resonance
NSAID	Non-Steroidal Anti-Inflammatory Drug
OD	Optical Density
OPTLC	Over-Pressured Thin-Layer Chromatography
PAD	Pulsed Amperometric Detection
PAH	Polynuclear Aromatic Hydrocarbon
PAS	Photoacoustic Spectroscopy
PCB	Polychlorinated Biphenyl
PCR	Polymerase Chain Reaction
PDA	Photodiode Array
PITC (PTC)	Phenyl Isothiocyanate
PIXE	Proton-Induced X-ray Emission
RNA	Ribonucleic Acid
RP-HPLC	Reverse-Phase HPLC
RRHT	Rapid Resolution High Throughput
RRLC	Rapid Resolution Liquid Chromatography
RSD	Relative Standard Deviation
SATP	Salicylideneamino-2-thiophenol
SCSI	Small Computer System Interface
SD	Standard Deviation
SdFFF	Sedimentation Field-Flow Fractionation
SEC	Size-Exclusion Chromatography
SELDI	Surface-Enhanced Laser Desorption Ionization
SEM	Scanning Electron Microscopy
SFC	Supercritical Fluid Chromatography
SFE	Supercritical Fluid Extraction
SIMS	Secondary Ion Mass Spectrometry
SPE	Solid-Phase Extraction
SPME	Solid-Phase Microextraction
TB	Tuberculosis
TFA	Trifluoroacetic Acid
THF	Tetrahydrofuran
TLC	Thin-Layer Chromatography
TOC	Total Organic Carbon
TOF-MS	Time-of-Flight-Mass Spectrometry
TSP	Thermospray
UV	Ultraviolet
VIS, Vis	Visible
XPS	X-ray Photoelectron Spectroscopy

About the Editor

Jack Cazes is a world-renowned expert and consultant in chromatography and analytical instrumentation and is a Visiting Scholar at Florida Atlantic University, Boca Raton, Florida. The author, co-author, and editor of numerous books and research papers in these disciplines, he is Editor of the *Journal of Liquid Chromatography & Related Technologies, Instrumentation Science & Technology, Preparative Biochemistry & Biotechnology, and Journal of Immunoassay and Immunochemistry*, and the Editor of the *Chromatographic Science Series* books *and* the *Encyclopedia of Chromatography*.

Dr. Cazes has been at the forefront of liquid chromatography for over 45 years, during which time he pioneered the development of liquid chromatography. Dr. Cazes was previously Professor-in-Charge of the ACS Short Course and the ACS Audio Course on Gel Permeation Chromatography, and has taught organic chemistry at Rutgers University and Queens College (CUNY) and a special topics graduate-level course at Florida Atlantic University.

He was CEO of Sanki Laboratories, a company that developed and manufactured instruments for Centrifugal Partition Chromatography.

Dr. Cazes is a member Emeritus of the American Chemical Society and is featured in *Who's Who and American Men of Science*.

Absorbance Detection in CE

Robert Weinberger
CE Technologies, Inc., Chappaqua, New York, U.S.A.

INTRODUCTION

Most forms of detection in high-performance capillary electrophoresis (HPCE) employ on-capillary detection. Exceptions are techniques that use a sheath flow such as laser-induced fluorescence[1] and electrospray ionization mass spectrometry.[2]

In high-performance liquid chromatography (HPLC), postcolumn detection is generally used. This means that all solutes are traveling at the same velocity when they pass through the detector flow cell. In HPCE with on-capillary detection, the velocity of the solute determines the residence time in the flow cell. This means that slowly migrating solutes spend more time in the optical path and thus accumulate more area counts.[3]

Because peak areas are used for quantitative determinations, the areas must be normalized when quantitating without standards. Quantitation without standards is often used when determining impurity profiles in pharmaceuticals, chiral impurities, and certain DNA applications. The correction is made by normalizing (dividing) the raw peak area by the migration time. When a matching standard is used, it is unnecessary to perform this correction. If the migration times are not reproducible, the correction may help, but it is better to correct the situation causing this problem.

LIMITS OF DETECTION

The limit of detection (LOD) of a system can be defined in two ways: the concentration limit of detection (CLOD) and the mass limit of detection (MLOD). The CLOD of a typical peptide is about 1 μg/ml using absorbance detection at 200 nm. If 10 nl are injected, this translates to an MLOD of 10 pg at three times the baseline noise. The MLOD illustrates the measuring capability of the instrument. The more important parameter is the CLOD, which relates to the sample itself. The CLOD for HPCE is relatively poor, whereas the MLOD is quite good, especially when compared to HPLC. In HPLC, the injection size can be 1000 times greater compared to HPCE.

The CLOD can be calculated using Beer's Law:

$$\text{CLOD} = \frac{A}{ab} = \frac{5 \times 10^{-5}}{(5000)(5 \times 10)^{-3}} = 2 \times 10^{-6}\,M \quad (1)$$

where A is the absorbance (AU), a is the molar absorptivity (AU/cm/M), b is the capillary diameter or optical path length (cm), and CLOD is the concentration (M). The noise of a good detector is typically 5×10^{-5} AU. A modest chromophore has a molar absorptivity of 5000. Then in a 50 μm inner diameter (I.D.) capillary, a CLOD of 2×10^{-6} M is obtained at a signal-to-noise (S/N) ratio of 1, assuming no other sources of band broadening.

DETECTOR LINEAR DYNAMIC RANGE

The noise level of the best detectors is about 5×10^{-5} AU. Using a 50 μm I.D. capillary, the maximum signal that can be obtained while yielding reasonable peak shape is 5×10^{-1} AU. This provides a linear dynamic range of about 10^4. This can be improved somewhat through the use of an extended path-length flow cell. In any event, if the background absorbance of the electrolyte is high, the noise of the system will increase regardless of the flow cell utilized.

CLASSES OF ABSORBANCE DETECTORS

Ultraviolet/visible absorption detection is the most common technique found in HPCE. Several types of absorption detectors are available on commercial instrumentation, including the following:

1. Fixed-wavelength detector using mercury, zinc, or cadmium lamps with wavelength selection by filters.
2. Variable-wavelength detector using a deuterium or tungsten lamp with wavelength selection by a monochromator.
3. Filter photometer using a deuterium lamp with wavelength selection by filters.
4. Scanning ultraviolet (UV) detector.
5. Photodiode array detector.

Each of these absorption detectors have certain attributes that are useful in HPCE. Multiwavelength detectors such as the photodiode array or scanning UV detector are valuable because spectral as well as electrophoretic information can be displayed. The filter photometer is invaluable for low-UV detection. The use of the 185 nm mercury line becomes practical in HPCE with phosphate buffers

because the short optical path length minimizes the background absorption.

Photoacoustic, thermo-optical, or photothermal detectors have been reported in the literature.[4] These detectors measure the non-radiative return of the excited molecule to the ground state. Although these can be quite sensitive, it is unlikely that they will be used in commercial instrumentation.

OPTIMIZATION OF DETECTOR WAVELENGTH

Because of the short optical path length defined by the capillary, the optimal detection wavelength is frequently much lower into the UV compared to HPLC. In HPCE with a variable-wavelength absorption detector, the optimal S/N ratio for peptides is found at 200 nm. To optimize the detector wavelength, it is best to plot the S/N ratio at various wavelengths. The optimal S/N is then easily selected.

EXTENDED PATH-LENGTH CAPILLARIES

Increasing the optical path length of the capillary window should increase S/N simply as a result of Beer's Law. This has been achieved using a z cell (LC Packings, San Francisco California, U.S.A.),[5] bubble cell (Agilent Technologies, Wilmington, Delaware, U.S.A.), or a high-sensitivity cell (Agilent Technologies). Both the z cell and bubble cell are integral to the capillary. The high-sensitivity cell comes in three parts: an inlet capillary, an outlet capillary, and the cell body. Careful assembly permits the use of this cell without current leakage. The bubble cell provides approximately a threefold improvement in sensitivity using a 50 μm capillary, whereas the z cell or high-sensitivity cell improves things by an order of magnitude. This holds true only when the background electrolyte (BGE) has low absorbance at the monitoring wavelength.

INDIRECT ABSORBANCE DETECTION

To determine ions that do not absorb in the UV, indirect detection is often utilized.[6] In this technique, a UV-absorbing reagent of the same charge (a co-ion) as the solutes is added to the BGE. The reagent elevates the baseline, and when non-absorbing solute ions are present, they displace the additive. As the separated ions migrate past the detector window, they are measured as negative peaks relative to the high baseline. For anions, additives such as trimellitic acid, phthalic acid, or chromate ions are used at 2–10 m*M* concentrations. For cations, creatinine, imidazole, or copper(II) are often used. Other buffer materials are either not used or added in only small amounts to avoid interfering with the detection process.

It is best to match the mobility of the reagent to the average mobilities of the solutes to minimize electrodispersion, which causes band broadening.[7] When anions are determined, a cationic surfactant is added to the BGE to slow or even reverse the electro-osmotic flow (EOF). When the EOF is reversed, both electrophoresis and electro-osmosis move in the same direction. Anion separations are performed using reversed polarity.

Indirect detection is used to determine simple ions such as chloride, sulfate, sodium, and potassium. The technique is also applicable to aliphatic amines, aliphatic carboxylic acids, and simple sugars.[8]

REFERENCES

1. Cheng, Y.F.; Dovichi, N.J. Fluorescence detection in capillary electrophoresis. SPIE **1988**, *910*, 111.
2. Huang, E.C.; Wachs, T.; Conboy, J.J.; Henion, J.D. Atmospheric pressure chemical ionization: Detection. Anal. Chem. **1990**, *62*, 713–724.
3. Huang, X.; Coleman, W.F.; Zare, R.N. Analysis of factors causing peak broadening in capillary zone electrophoresis. J. Chromatogr. **1989**, *480*, 95–100.
4. Saz, J.M.; Diez-Masa, J.C. Thermo-optical spectroscopy: New and sensitive schemes for detection in capillary separation techniques. J. Liq. Chromatogr. Relat. Technol. **1994**, *17* (3), 499.
5. Chervet, J.P.; van Soest, R.E.J.; Ursem, M. Z-shaped flow cell for UV detection in capillary electrophoresis. J. Chromatogr. **1991**, *543*, 439.
6. Jandik, P.; Jones, W.R.; Weston, A.; Brown, P.R. Violet diode laser for metal ion determination by capillary electrophoresis-laser induced fluorescence. LC-GC **1991**, *9*, 634.
7. Weinberger, R. Am. Lab. **1996**, *28*, 24.
8. Xu, X.; Kok, W.T.; Poppe, H. Capillary electrophoresis using air and helium as cooling fluids. J. Chromatogr. A, **1995**, *716*, 231.

Acids: Derivatization for GC Analysis

Igor G. Zenkevich
Chemical Research Institute, St. Petersburg State University, St. Petersburg, Russia

Abstract
The class *acids* includes various types of chemical compounds with active hydrogen atoms usually having $pK_a < 7$. The most important group of organic acids is the compounds with carboxyl fragment –COOH. The simplest monofunctional carboxylic acids retain their boiling points at standard atmospheric pressure without undergoing decomposition and, hence, can be analyzed directly by gas chromatography (GC). However, owing to the high polarities of carboxyl compounds, these compounds yield broad non-symmetrical chromatographic peaks on non-polar phases, which leads to poor detection limits and unsatisfactory reproducibility of their retention indices. The application of polar polyethylene glycols for analysis of free carboxylic acid is restricted by less thermal stability of such phases. The general approach in the (GC) analysis of acids is their derivatization, preferably esterification with the formation of alkyl or silyl esters. Many types of polyfunctional carboxylic acids (hydroxy-, mercapto-, amino-, etc.) cannot be analyzed in free, underivatized form owing to non-volatility and/or absence of thermal stability. These features are the principal reasons for the conversion of carboxylic acids into less polar derivatives without active hydrogen atoms in their molecules before their GC analysis.

INTRODUCTION

The class *acids* includes various types of chemical compounds with active hydrogen atoms usually having $pK_a < 7$. The most important group of organic acids is the compounds with carbonyl fragment $-CO_2H$. Some other compounds can be classified not only as O acids (e.g., hydroxamic acids, $-CONHOH \rightleftharpoons -C(OH)=NOH$), but also as C–H acids [with the presence of structural fragments $-CH(NO_2)_2$, $-CH(CN)_2$, $-CHF_2$, etc.]. Well-known compounds belonging to this class that can be subjected to GC analysis are semivolatile fatty acids of triglycerides and lipids,[1] numerous non-volatile polyfunctional biogenic compounds (including phenol carboxylic acids like gallic, vanillic, syringic), plant hormones (gibberellins), different acidic herbicides (e.g., 2,4-D, 2,4,5-T, MCPB, MCPA, fenoprop, haloxyfop), and many other substances. Strong inorganic acids like volatile hydrogen halides (HHal) and non-volatile H_2SO_4, H_3PO_4 can be objects of GC analysis too.

The simplest monofunctional carboxylic acids retain their boiling points at standard atmospheric pressure without undergoing decomposition and, hence, can be analyzed directly by GC. However, owing to the relatively high polarities of carbonyl compounds, a typical problem of their GC analysis with standard non-polar phases is the non-linear sorption isotherm. As a result, these compounds yield broad non-symmetrical peaks, which lead to poor detection limits and unsatisfactory reproducibility of their retention indices. The recommended stationary phases for direct analysis of free carboxylic acids are polar polyethylene glycols (Carbowax 20M, DBWax, SP-1000, FFAP, etc.). However, these phases have lower thermal stability as compared with polydimethyl siloxanes (~225–250°C vs. 300–350°C). This implies that the upper limit of the retention index (RI) is not more than 2500–3000 i.u. for these polar phases. High homologues of monocarboxylic acids cannot be eluted within this RI window (this is confirmed by the absence of RI data for palmitic acid, $C_{15}H_{31}CO_2H$, on the mentioned type of polar phases). Owing to this, thermally stable polar cyanoalkyl polysiloxanes (OV-225, OV-275, etc.) are preferable for direct analysis of carboxylic acids.

Large standard deviations of RIs of arenecarboxylic acids (benzoic, phenylacetic, etc.) on standard non-polar phases are explained by the high asymmetry of their chromatographic peaks. This effect cannot be eliminated by the use of inert chromatographic systems, special techniques of injection, or the application of modern WCOT columns. It depends on the typical non-linear sorption isotherm *polar sorbate–non-polar phase* and, hence, the conversion of these polar analytes into less polar derivatives is strongly recommended.

Some aliphatic dicarboxylic acids can also be distilled without decomposition under reduced pressures. Their direct GC analysis is at least theoretically possible. However, there have been very few successful attempts as these analytes require *on-column* injection of samples and chromatographic systems that are extremely inert. Most polyfunctional carboxylic acids (hydroxy, mercapto, amino, etc.) cannot be analyzed in free, underivatized form because they are non-volatile and/or lack thermal stability. That is why these carboxylic acids are converted into less polar derivatives without active hydrogen atoms before their GC analysis is undertaken.

The pH of samples containing acids should not be more than their pK_a values, i.e., not less than 4–4.5 for organic

Table 1 The comparison of key physicochemical and chromatographic properties of some aliphatic and aromatic carboxylic acids.

Acid	pK_a	T_b, °C	$RI_{non\text{-}polar}$	RI_{polar}
Acetic	4.75	118	638 ± 10	1428 ± 30
Palmitic	4.9	351.5	1966 ± 7	No data
Benzoic	4.2	250	1201 ± 24	2387 ± 15
Phenylacetic	4.2	266	1290 ± 44	No data

carboxylic acids, as non-volatile salts might be formed with organic or inorganic bases. Any attempts to analyze these salts by increasing the temperature of the injector and GC column usually lead to their thermal decomposition and should be avoided.

METHODS OF ACID DERIVATIZATION

The common method for derivatizing is by carboxylic acids their esterification with the formation of alkyl (arylalkyl, halogenated alkyl) or silyl esters:[2–5]

$$XCO_2H + RY \rightarrow XCO_2R + YH$$
$$XCO_2H + ZSi(CH_3)_3 \rightarrow XCO_2Si(CH_3)_3 + ZH$$

Some of the most widely used reagents for the esterification of acids are listed in Table 2. The general method for the silylation of mono- and polyfunctional carboxylic acids by forming for trimethylsilyl (TMS)[6,7] or the more stable *tert*-butyldimethylsilyl (TBDMS)[8,9] derivatives is similar to that for the silylation of other hydroxy-containing compounds (see *Hydroxy Compounds: Derivatization for GC Analysis*, p. 1165).

Table 2 Physicochemical and gas chromatographic properties of some alkylating derivatization reagents for carboxylic acids.

Reagent	Abbreviation	MW	T_b, °C	$RI_{non\text{-}polar}$	By-products ($RI_{non\text{-}polar}$)
Methanol/BCl_3, BF_3, HCl, DCC, etc.	—	32	64.6	381 ± 15	H_2O
Diazomethane (in diethyl ether solution)	—	42	–23	None (unstable)	N_2
Methyl iodide/DMFA, K_2CO_3	—	142	42.8	515 ± 7	CH_3OH (381 ± 15)
Dimethyl sulfate/base	—	126	188.5	853 ± 22	CH_3OH (381 ± 15)
1-Iodopropane/DMFA, K_2CO_3	—	170	102	711 ± 11	C_3H_7OH (552 ± 13), $(C_3H_7)_2O$ (680 ± 6)
2-Bromopropane	—	122	59.4	571 ± 5	*iso*-C_3H_7OH (486 ± 9), (*iso*-$C_3H_7)_2O$ (598 ± 5)
Ethyl orthoformate	—	148	145	870 ± 9	C_2H_5OH (452 ± 18)
Diethyl carbonate	—	118	126	761 ± 4	CO_2, C_2H_5OH (452 ± 18)
Methyl chloroformate	—	94	71	582 ± 17	CH_3OH (381 ± 15)
Ethyl chloroformate	—	108	—	640 ± 12	C_2H_5OH (452 ± 18)
Butyl chloroformate	—	136	—	832 ± 10	C_4H_9OH (658 ± 12)
Pentafluorobenzyl bromide	PFB-Br	260	174–175	991 ± 11[a]	$C_6F_5CH_2OH$ (934 ± 16)[a]
3,5-*bis*-Trifluoromethylbenzyl bromide	BTB-Br	306	—	1103 ± 9[a]	$(CF_3)_2C_6H_3CH_2OH$ (1046 ± 15)[a]
Tetramethylammonium hydroxide (25% aqueous solution)	TMAH	74	—	Non-volatile	$(CH_3)_3N$ (418 ± 9)
Trimethylanilinium hydroxide (0.2 *M* methanol solution)	TMPAH	136	—	Non-volatile	$C_6H_5N(CH_3)_2$ (1065 ± 9)
3,5-*bis*-Trifluoromethylbenzyl dimethylanilinium fluoride	BTBDMA-F	258	—	Non-volatile	$(CF_3)_2C_6H_3CH_2N(CH_3)_2$, $C_6H_5N(CH_3)_2$ (1065 ± 9)
2-Bromoacetophenone (phenacyl bromide)	—	198	260	1321 ± 4	$C6H_5COCH_2OH$ (1118)[a]
Dimethylformamide dimethylacetal	DMF-DMA	119	107–108	726 ± 4	$(CH_3)_2NCHO$ (749 ± 16), CH_3OH (381 ± 15)
Dimethylformamide diethylacetal	DMF-DEA	147	134–136	826[a]	$(CH_3)_2NCHO$ (749 ± 16), C_2H_5OH (452 ± 18)

[a]Estimated RI values.

In general, the simplest methyl esters of carboxylic acids are more stable to hydrolysis than are TMS-esters and, hence, they are the preferable derivatives for GC analysis.[10,11] The commonly available esterification reagents are the corresponding alcohols, ROH, themselves. Different esters have been used as the analytical derivatives of carboxylic acids: Me, Et, Pr, *iso*-Pr, isomeric Bu (excluding *tert*-Bu esters owing to their poorer synthetic yields), and so forth. This method requires an excess of dry alcohol and acid catalysis by BCl_3, BF_3, CH_3COCl, $SOCl_2$, etc. Otherwise, the alcohol used might become saturated with gaseous HCl, which must then be removed by heating the reaction mixtures after completion of the reaction. However, instead of easily volatile acid catalysts, completely non-volatile acids like H_2SO_4 can be used in this reaction.[12]

The treatment of polyfunctional acids by alcohols in the presence of strong inorganic acids as catalysts can simultaneously be accompanied by the derivatization of other functional groups. For example, carbonyl groups in ketocarboxylic acids are converted into dialkylketal fragments in the presence of in ketocarboxylic acids.[13,14]

Also, 2-chloroethyl ($RCO_2CH_2CH_2Cl$), 2,2,2-trifluoroethyl ($RCO_2CH_2CF_3$), 2,2,2-trichloroethyl ($RCO_2CH_2CCl_3$), and hexafluoroisopropyl esters [$RCO_2CH(CF_3)_2$] can be synthesized for GC analysis with selective detection in a similar manner. Instead of acids, some other reagents, namely, 1,1′-carbonyldiimidazole (I) and 1,3-dicyclohexylcarbodiimide (DCC, II), are recommended, as catalysts for this reaction.

The application of any additive reagents usually leads to the appearance of additional peaks on the chromatograms [including the peaks of by-products, e.g., imidazole from (I), $RI_{non\text{-}polar}$ 1072 ± 17], which must be reliably identified and excluded from data interpretation. The by-product from compound (II)—1,3-dicyclohexylurea—is non-volatile for GC analysis.

Another class of esterification reagents are halogenated compounds (alkyl iodides, substituted benzyl,[15] and phenacyl bromides), which need basic media for their reaction [K_2CO_3 or DMFA (dimethyl formamide) is normally used for the neutralization of HHal as acid by-product]. For methylation of carboxylic acids, some tetra-substituted ammonium hydroxides or halides can be used, e.g., tetramethylammonium hydroxide (in aqueous solutions) or trimethylanilinium hydroxide (in methanol solution). The intermediate ammonium carboxylates are thermally unstable and produce methyl alkanoates when the reaction mixtures are heated or when the carboxylates are introduced into the hot injector of the gas chromatograph (flash or on-column methylation):

$$RCO_2H + XNMe_3^+OH^{\&} \rightarrow [RCO_2^{\&}XNMe_3^+] \rightarrow RCO_2Me + XNMe_2 (X = Me, Ph, PhCH_2)$$

The possible by-products of these reactions are the corresponding amines (Me_3N, $PhNMe_2$). A similar method has been proposed for the butylation of organic acids.[16] Besides tetra-substituted ammonium hydroxides, more *exotic* reagents, e.g., trimethylsulfonium hydroxide, $(CH_3)_3S^+ OH^-$, in methanol solution, were recommended as the donors of methyl groups.[17]

If the appearance of any volatile by-products is undesirable, carboxylic acids can be methylated by diazomethane (CH_2N_2) (the single gaseous by-product is N_2). This reagent (*warning*: highly volatile and toxic) should by synthesized by the alkaline cleavage of *N*-methyl-*N*-nitrosourea, *N*-methyl-*N*-nitrosotoluenesulfamide, or (latest recommendations) *N*-methyl-*N*′-nitro-*N*-nitrosoguanidine (MNNG); however, owing to its low boiling point (–23C) it can be used only in diethyl ether solutions prepared immediately before use.

In the absence of acid catalysis, diazomethane reacts only with carboxylic acids (pK_a 4–5) and phenols (pK_a 9–10), but has no influence on aliphatic OH groups. Besides CH_2N_2, some more complex diazocompounds (diazoethane, diazotoluene) have been recommended for the synthesis of ethyl and benzyl esters, respectively. For the synthesis of benzyl (or substituted benzyl) esters, some special reagents have also been proposed, e.g., *N*,*N*′-dicyclohexyl-*O*-benzylurea and 1-(4-methylphenyl)-3-benzyltriazene.

However, reactive diazocompounds are not very selective as compared to carboxy groups, and the formation of numerous artifacts has been reported. For example, the reaction of sorbic (2,4-hexadienoic) acid with CH_2N_2 besides leading to the formation of methyl ester, methylated homologues (the result of interaction of diazomethane through the C–H bonds), and two isomeric 2-pyrazolines,[18] which makes this mode inappropriate in practice.

The esterification of carboxylic acids can also be accomplished using synthetic equivalents of acetals of alkanols $RCH(OR')_2$ (by acid catalysis), *ortho*-esters $RC(OR')_3$ (by acid catalysis), and dialkylcarbonates $CO(OR)_2$ (by base catalysis). A series of bifunctional reagents of this type—dimethylformamide dialkylacetals $(CH_3)_2N–CH(OR')_2$—are available at present. These compounds also react with primary amino groups, that is used in derivatization of amino acids for GC analysis (Fig. 1).

A *sandwich* injection technique (flash methylation) can also be used for derivatization. It implies the injection of the sample and reagent in the same syringe into the gas chromatographic column, e.g., successively placed 1 μl of derivatization reagent, 1 μl of pyridine with internal standard, and 1 μl of the solution of analytes in the same solvent.

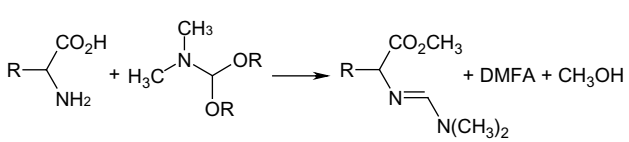

Fig. 1 One-step derivatization of amino acids by dimethylformamide dialkylacetals.

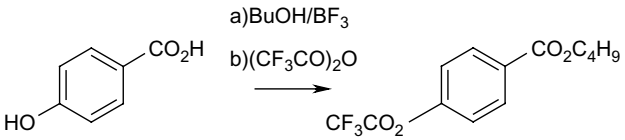

Fig. 2 Two-step derivatization of hydroxyarenecarboxylic acids.

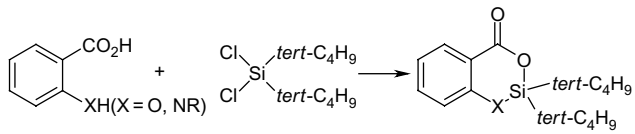

Fig. 4 One-step derivatization of hydroxy- or aminoarenecarboxylic acids by dichlorosilane reagents.

Alkyl chloroformates, $ClCO_2R$ (R = Me, Et, Bu), have been proposed as convenient alkylation reagents for carboxylic acids:[19]

$$RCO_2H + ClCO_2R' + B \rightarrow RCO_2R' + CO_2 + BH^+Cl$$

Two-stage single-pot derivatization of carboxylic acids (with intermediate formation of chloroanhydrides with thionyl chloride followed by their conversion into amides) was recommended preferably for HPLC analysis, but the simplest dialkylamides and even anilides[20] are volatile enough for GC analysis also (the mixture of Ph_3P and CCl_4, instead of $SOCl_2$, can be used in this reaction). Moreover, the same procedure is used for the synthesis of diastereomeric derivatives of enantiomeric carboxylic acids (see below):

$$RCO_2H + SOCl_2 + B \rightarrow RCOCl + SO_2 + BH^+Cl^-$$
$$RCOCl + R'R''NH + B \rightarrow RCONR'R'' + BH^+Cl^-$$

Derivatives of carboxylic acids such as amides are relatively stable to hydrolysis and can exist in aqueous solutions, at least at pH $\approx$ 7. However, the important modification of this reaction, namely rapid one-step formation of amides in aqueous media at room temperature, has been proposed only in 2007.[21] Besides the selected amine, 2,2,2-trifluoroethylamine hydrochloride (TFEA), special catalyst should be used: ethyl-[3-(dimethylamino)propyl]carbodiimide, C_2H_5–N=C=N–$(CH_2)_3$–$N(CH_3)_2$ (EDC, used as hydrochloride also).

The reactivities of carboxy and hydroxy groups in the polyfunctional hydroxy carboxylic acids are different. This indicates the possibility of an independent two-stage derivatization of these compounds (Fig. 2).

If these functional groups are located in *vic* (aliphatic series) or *ortho* positions (substitutes arenecarboxylic acids), methyl, butyl, or phenyl boronic acids are convenient reagents for their one-step derivatization with the formation of cyclic methyl(butyl, phenyl) boronates (Fig. 3).

A similar method for simultaneous derivatization of two functional groups is the formation of cyclic silylene derivatives for the same types of compounds (Fig. 4).[22]

A special type of carbonyl group derivatization is aimed at GC–MS determination of C=C double-bond positions in unsaturated long-chain acids. The analytical derivatives for the solution of this problem are nitrogen-containing heterocycles. These compounds can be synthesized by high-temperature condensation of carboxylic acids with 2-amino-2-methyl-1-propanol (2-substituted 4,4-dimethyloxazolines), 2-aminophenol (2-substituted benzoxazoles), and so forth (Fig. 5).

This reaction is so important in the analytical practice of carboxylic acids that their 4,4-dimethyloxazoline derivatives have been denoted with special abbreviations: DMOX derivatives. They have been used for a long time, but the optimization of reaction conditions, namely by in situ activation of carboxyl group, remains the actual problem up to the present. Numerous additional reagents have been proposed for these purposes, including those utilized in peptide syntheses: 2-chloro- and/or 2-bromo-1-methylpyridinium iodide (CMPI, BMPI), benzotriazol-1-yl-*N*-oxy-*tris*(dimethylamino)phosphonium hexachlorophosphate (BOP), and so forth. The latest recommendations permit us to carry out one-pot direct synthesis of amides and oxazolines with the use of such reagents as *bis*(2-methoxyethyl)aminosulfur trifluoride (Deoxo-Fluor) or diethylaminosulfur trifluoride (DAST).[23] Both of these compounds of general formula R_2NSF_3 belong to the group of fluorinating reagents and convert carboxylic acids in situ into more

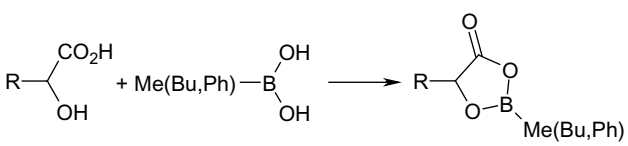

Fig. 3 One-step derivatization of α-hydroxyalkanecarboxylic acids by substituted boronic acids.

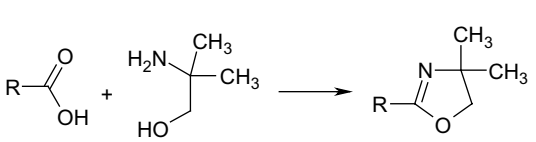

Fig. 5 An example of the formation of oxazoline derivatives from carboxylic acids.

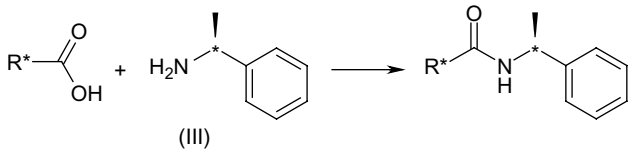

Fig. 6 An example of the formation of diastereomeric amides from chiral carboxylic acids and (S)-α-methylbenzenemethanamine.

reactive acyl fluorides, followed by their interaction with amino alcohols.

Methyl esters of carboxylic acids can be used for the formation of oxazolines, but this also requires the heating of reaction mixtures up to 180°C[24] and, hence, seems less convenient in analytical practice.

GC separation of enantiomeric carboxylic acids on non-chiral phases is based on the formation of their esters or amides with optically active alcohols (e.g., stereochemically pure (–)-menthol), or amines [(*S*)-α-methylbenzenemethaneamine, III], usually through the intermediate chloroanhydrides. These diastereomeric products are not as volatile as other acid derivatives, but, owing to the presence of two chiral centers (*) in the molecule, can be separated on non-chiral phases (Fig. 6).

A problem closely related to the derivatization of free carboxylic acids is the determination of their composition in biogenic triglycerides, lipids, and so forth. The sample preparation includes the re-esterification (preferably with formation of methyl esters) of these compounds in acidic ($MeOH/CH_3COCl$, $MeOH/BF_3$, etc.) or basic [MeOH/MeONa, $(MeO)_2SO_2$/NaOH, etc.] media. Methyl esters of fatty acids are a group of compounds well characterized by both standard mass spectra and GC retention indices on standard phases. The combination of these analytical parameters facilitates their reliable identification. Moreover, as the variety of biogenic carboxylic acids is very large,[1] it is important to mention the possibility of the theoretical prediction of their retention indices with the use of contemporary methods of chemometrics.[25] For the determination of the positions of C=C double bonds in the carbon skeleton of unsaturated fatty acids, different adducts with specific mass spectrometric fragmentation are recommended.[26]

Numerous derivatives of polyfunctional carboxylic acids important for analytical practice are characterized by GC RIs and mass spectra. As an example of this information, the data for 3 compounds from 136 known natural gibberellins are presented in Table 3. Commonly accepted

Table 3 An example of analytical data for some gibberellins (methyl ester TMS-ethers).

Gibberellin	Structural formula	$RI_{non\text{-}polar}$	$MW/(m/z)^{100}$
A2	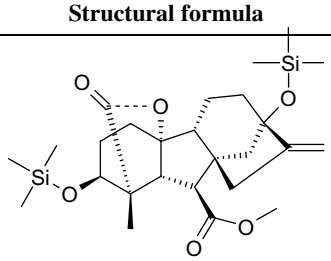	2,741	508/130
A61	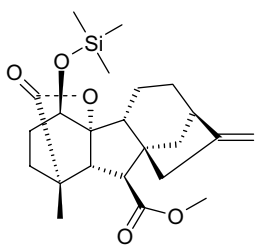	2,409	418/296
A106	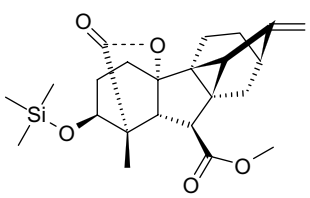	2,421	416/282

Table 4 Gas chromatographic retention indices of volatile TMS derivatives of some inorganic acids.

Anion	TMS derivative	$RI_{non\text{-}polar}$
Borate	$B(OTMS)_3$	1,010
Carbonate	$CO(OTMS)_2$	1,048
Phosphite	$P(OTMS)_3$	1,115
Sulfate	$SO_2(OTMS)_2$	1,148
Arsenite	$As(OTMS)_3$	1,149
Phosphate	$PO(OTMS)_3$	1,273
Vanadate	$VO(OTMS)_3$	1,301
Arsenate	$AsO(OTMS)_3$	1,353

derivatives of these compounds are the methyl esters of TMS-ethers.[27] Even restricted GC–MS information (namely, molecular weight (MW), mass number of maximal peak in mass spectrum, $(m/z)^{100}$, and GC RI) is enough for reliable identification of all analogues of this group.

The general method for GC analysis of anions of inorganic acids is their silylation. The values of the retention indices on standard non-polar phases are known for TMS derivatives of the most important among them[4] (Table 4).

CONCLUSIONS

Both strong inorganic and weak organic acids usually need derivatization prior to GC analysis. The existence of active hydrogen atoms in the molecules explains the significant contribution of ionic structures, which are responsible for the high polarity and low volatility of these substances.

Most universal methods of derivatization of acids are silylation (TMS or TBDMS) and alkylation (the simplest methyl esters with minimal retention parameters are preferable among all possible derivatives). Other methods involve an auxiliary predetermination and can be recommended for the solution of special analytical problems.

REFERENCES

1. Fatty acids. http://www.cyberlipid.org/fa/acid0001.htm (accessed September 2008).
2. Blau, K.; King, G.S., Eds. *Handbook of Derivatives for Chromatography*; John Wiley & Sons: Chichester. U.K., 1978; 576.
3. Knapp, D.R. *Handbook of Analytical Derivatization Reactions*; John Wiley & Sons: New York, 1979; 741.
4. Drozd, J. Chemical derivatization in gas chromatography. In *Journal of Chromatography Library*; Elsevier: Amsterdam, 1981; Vol. 19, 232.
5. Blau, K.; Halket, J.M., Eds. *Handbook of Derivatives for Chromatography*, 2nd Ed.; John Wiley & Sons: New York, 1993; 369.
6. Wurth, C.; Kumps, A.; Mardens, Y. Urinary organic acids: Retention indices on two capillary GC columns. J. Chromatogr. **1989**, *491*, 186–192.
7. Lefevere, M.F.; Verkaeghe, B.J.; Declerk, D.H.; Van Bocxlaer, J.F.; De Leenheer, A.P.; De Sagher, R.M. Metabolic profiling of urinary organic acids by single and multicolumn capillary gas chromatography. J. Chromatogr. Sci. **1989**, *27* (1), 23–29.
8. Rodriguez, I.; Quintana, J.B.; Carpinteiro, J.; Carro, A.M.; Lorenzo, R.A.; Cela, R. Determination of acidic drugs in sewage water by GC–MS as *tert*-butyl dimethylsilyl derivatives. J. Chromatogr. A, **2003**, *985*, 265–274.
9. Crouholm, T.; Norsten, C. Gas chromatography–mass spectrometry of carboxylic acids in tissues as their *tert*-butyl dimethylsilyl derivatives. J. Chromatogr. B, **1985**, *344*, 1–9.
10. Gonzales, G.; Ventura, R.; Smith, A.K.; De la Torre, R.; Segura, J. Determination of nonsteroidal anti-inflammatory drugs in equine plasma and urine by gas chromatography–mass spectrometry. J. Chromatogr. A, **1996**, *719*, 251–264.
11. Nilsson, T.; Baglio, D.; Galdo-Miquez, I.; Madsen, O.J.; Facchetti, S. Derivatization/solid-phase microextraction followed by GC–MS for the analysis of phenoxy acid herbicides in aqueous samples. J. Chromatogr. A, **1998**, *826*, 211–216.
12. Xiao, J.B. Identification of organic acids and quantification of dicarboxylic acids in Bayer process liquors by GC–MS. Chromatographia **2007**, *65* (3/4), 185–190.
13. Li, Y.-C.; Yu, J.Z. Simultaneous determination of mono- and dicarboxylic acids, omega-Oxo-carboxylic acids, midchain ketocarboxylic acids, and aldehydes in atmospheric aerosol samples. Environ. Sci. Technol. **2005**, *39*, 7616–7624.
14. Wang, H.; Kawamura, K.; Ho, K.F.; Lee, S.C. Low molecular weight dicarboxylic acids, ketoacids, and dicarbonyls in the fine particles from a roadway tunnel: Possible secondary production from the precursors. Environ. Sci. Technol. **2006**, *40*, 6255–6260.
15. Gabelish, C.L.; Crisp, P.; Schneider, R.P. Simultaneous determination of chlorophenols, chlorobenzenes and chlorobenzoates in microbial solutions using pentafluorobenzyl bromide derivatization and analysis by GC with electron capture detection. J. Chromatogr. A, **1996**, *749*, 165–171.
16. Burke, D.G.; Halpern, B. Quaternary ammonium salts for butylation and mass spectral identification of volatile organic acids. Anal. Chem. **1983**, *55* (6), 822–826.
17. Zapf, A.; Stan, H.-J. GC analysis of organic acids and phenols using on-line methylation with trimethylsulfonium hydroxide and PTV solvent split large volume

injection. J. High Resolut. Chromatogr. **1999**, *22* (2), 83–88.
18. http://userpage.chemie.fu-berlin.de/~tlehmann/krebs/files_diazoalkanes.pdf (accessed September 2008).
19. Butz, S.; Stan, H.-J. Determination of chlorophenoxy and other acidic herbicide residues in ground water by capillary GC of their alkyl esters formed by rapid derivatization using various chloroformates. J. Chromatogr. **1993**, *643*, 227–238.
20. Umeh, E.O. Separation and determination of low molecular weight straight chain C_1–C_8 carboxylic acids by gas chromatography of their anilide derivatives. J. Chromatogr. **1970**, *51*, 147–154.
21. Ford, Q.L.; Burns, J.M.; Ferry, J.L. Aqueous in situ derivatization of carboxylic acids by an ionic carbodiimide and 2,2,2-trifluoroethylamine for electron-capture detection. J. Chromatogr. A, **2007**, *1145*, 241–245.
22. Brooks, C.J.W.; Cole, W.T. Cyclic di-*tert*-butylsilylene derivatives of substituted salicylic acids and related compounds. A study by gas chromatography–mass spectrometry. J. Chromatogr. **1988**, *441*, 13–29.
23. Kangani, C.O.; Kelley, D.E. One pot synthesis of amides or oxazolines from carboxylic acids using Deoxo-Fluor reagent. Tetrahedron Lett. **2005**, *46* (51), 8917–8920.
24. Fay, L.; Richli, U. Location of double bonds in polyunsaturated fatty acids by GC–MS after 4,4-dimethyloxazoline derivatization. J. Chromatogr. **1991**, *541*, 89–98.
25. Farkas, O.; Zenkevich, I.G.; Stout, F.; Kalivas, J.H.; Heberger, K. Prediction of retention indices for identification of fatty acids methyl esters. J. Chromatogr. A, **2008**, *1198–1199*, 188–195.
26. http://www.lipidlibrary.co.uk/ms/ms04/index.htm (accessed September 2008).
27. http://www.plant-hormones.info/gainfo.asp?ID= (accessed September 2008).

Adsorption Chromatography

Robert J. Hurtubise
Department of Chemistry, University of Wyoming, Laramie, Wyoming, U.S.A.

INTRODUCTION

In essence, the original chromatographic technique was adsorption chromatography. It is frequently referred to as liquid–solid chromatography. Tswett developed the technique around 1900 and demonstrated its use by separating plant pigments. Open-column chromatography is a classical form of this type of chromatography, and the open-bed version is called thin-layer chromatography (TLC).

Adsorption chromatography is one of the more popular modern high-performance liquid chromatography (HPLC) techniques today. However, open-column chromatography and TLC are still widely used.[1] The adsorbents (stationary phases) used are silica, alumina, and carbon. Although some bonded phases have been considered to come under adsorption chromatography, these bonded phases will not be discussed. By far, silica and alumina are more widely used than carbon. The mobile phases employed are less polar than the stationary phases, and they usually consist of a signal or binary solvent system. However, ternary and quaternary solvent combinations have been used.

Adsorption chromatography has been employed to separate a very wide range of samples. Most organic samples are readily handled by this form of chromatography. However, very polar samples and ionic samples usually do not give very good separation results. Nevertheless, some highly polar multifunctional compounds can be separated by adsorption chromatography. Compounds and materials that are not very soluble in water or water–organic solvents are usually more effectively separated by adsorption chromatography compared to reversed-phase liquid chromatography.

When one has an interest in the separation of different types of compound, silica or alumina, with the appropriate mobile phase, can readily accomplish this. Also, isomer separation frequently can easily be accomplished with adsorption chromatography; for example, 5,6-benzoquinoline can be separated from 7,8-benzoquinoline with silica as the stationary phase and 2-propanol : hexane (1 : 99). This separation is difficult with reversed-phase liquid chromatography.[1]

STATIONARY PHASES

Silica is the most widely used stationary phase in adsorption chromatography.[2] However, the extensive work of Snyder[3] involved investigations with both silica and alumina. Much of Snyder's earlier work was with alumina. Even though the surface structures of the two adsorbents have distinct differences, they are sufficiently similar. Thus, many of the fundamental principles developed for alumina are applicable to silica. The general elution order for these two adsorbents is as follows:[1] saturated hydrocarbons (small retention time), olefins, aromatic hydrocarbons, aromatic hydrocarbons ≈ organic halides, sulfides, ethers, nitrocompounds, esters ≈ aldehydes ≈ ketones, alcohols ≈ amines, sulfones, sulfoxide, amides, carboxylic acids (long retention time). There are several reasons why silica is more widely used than alumina. Some of these are that a higher sample loading is permitted, fewer unwanted reactions occur during separation, and a wider range of chromatographic forms of silica are available.

Chromatographic silicas are amorphous and porous and they can be prepared in a wide range of surface areas and average pore diameters. The hydroxyl groups in silica are attached to silicon, and the hydroxyl groups are mainly either free or hydrogen-bonded. To understand some of the details of the chromatographic processes with silica, it is necessary to have a good understanding of the different types of hydroxyl groups in the adsorbent.[1,3] Chromatographic alumina is usually γ-alumina. Three specific adsorption sites are found in alumina: (a) acidic, (b) basic, and (c) electronacceptor sites. It is difficult to state specifically the exact nature of the adsorption sites. However, it has been postulated that the adsorption sites are exposed aluminum atoms, strained Al–O bonds, or cationic sites.[4] Table 1 gives some of the properties of silica and alumina.

The adsorbent water content is particularly important in adsorption chromatography. Without the deactivation of strong adsorption sites with water, non-reproducible retention times will be obtained, or irreversible adsorption of solutes can occur. Prior to using an adsorbent for open-column chromatography, the adsorbent is dried, a specified amount of water is added to the adsorbent, and then the adsorbent is allowed to stand for 8–16 hr to permit the equilibration of water.[3,4] If one is using a high-performance column, it is a good idea to consider adding water to the mobile phase to deactivate the stronger adsorption sites on the adsorbent. Some of the benefits are less variation in retention times, partial compensation for lot-to-lot differences in the adsorbent, and reduced band tailing.[1] However, there can be some problems in

Table 1 Some adsorbents used in adsorption chromatography.

Type	Name	Form	Average particle area size (μm)	Surface area (m^2/g)
Silica[a]	BioSil A	Bulk	2–10	400
	μPorasil	Column	10	400+
Silica[b]	Hypersil	Bulk	5–7	200
	Zobax Sil	Bulk or column	6	350
Alumina[a]	ICN Al-N	Bulk	3–7, 7–12	200
	MicroPak Al	Bulk or column	5, 10	79
Alumina[b]	Spherisorb AY	—	5, 10, 20	95

[a]Irregular
[b]Spherical
Source: From Adsorption chromatography, in J. Chromatogr. A.[11]

adding water to the mobile phase, such as how much water to add to the mobile phase for optimum performance. Snyder and Kirkland[1] have discussed several of these aspects in detail.

MOBILE PHASES

To vary sample retention, it is necessary to change the mobile-phase composition. Thus, the mobile phase plays a major role in adsorption chromatography. In fact, the mobile phase can give tremendous changes in sample retention characteristics. Solvent strength controls the capacity factor's values of all the sample bands. A solvent strength parameter (ε^0), which has been widely used over the years, can be employed quantitatively for silica and alumina. The solvent strength parameter is defined as the adsorption energy of the solvent on the adsorbent per unit area of solvent.[1,3] Table 2 gives the solvent strength values for selected solvents that have been used in adsorption chromatography. The smaller values of ε^0 indicate weaker solvents, whereas the larger values of ε^0 indicate stronger solvents. The solvents listed in Table 2 are single solvents. Normally, solvents are selected by mixing two solvents with large differences in their ε^0 values, which would permit a continuous change in the solvent strength of the binary solvent mixture. Thus, some specific combination of the two solvents would provide the appropriate solvent strength. In adsorption chromatography, the solvent strength increases with solvent polarity, and the solvent strength is used to obtain the proper capacity factor values, usually in the range of 1–5 or 1–10. It should be realized that the solvent strength does not vary linearly over a wide range of solvent compositions, and several guidelines and equations that allow one to calculate the solvent strength of binary solvents have been developed for acquiring the correct solvent strength in adsorption chromatography.[1,3] However, it frequently happens that the solvent strength is such that all of the solutes are not separated in a sample. Thus, one needs to consider solvent selectivity, which is discussed below.

Table 2 Selected solvents used in adsorption chromatography.

	Solvent strength (ε^0)	
	Silica	**Alumina**
Solvent		
n-Hexane	0.01	0.01
1-Chlorobutane	0.20	0.26
Chloroform	0.26	0.40
Isopropyl ether	0.34	0.28
Ethyl acetate	0.38	0.58
Tetrahydrofuran	0.44	0.57
Acetonitrile	0.50	0.65

Source: From Adsorption chromatography, in J. Chromatogr. A.[11]

To change the solvent selectivity, the solvent strength is held constant and the composition of the mobile phase is varied. It should be realized that because the solvent strength is directly related to the polarity of the solvent and polarity is the total of the dispersion, dipole, hydrogen-bonding, and dielectric interactions of the sample and solvent, one would not expect that solvent strength alone could be used to fine-tune a separation. A trial-and-error approach can be employed by using different solvents of equal ε^0. However, there are some guidelines that have been developed that permit improved selectivity. These are the "B-concentration" rule and the "hydrogen-bonding" rule.[1] In general, with the B-concentration rule, the largest change in selectivity is obtained when a very dilute or a very concentrated solution of B (stronger solvent) in a weak solvent (A) is used. The hydrogen-bonding rule states that any change in the mobile phase that results in a change in hydrogen-bonding between sample and mobile-phase molecules usually results in a large change in selectivity. A more comprehensive means for improving selectivity is the solvent-selectivity triangle.[1,5] The solvent-selectivity triangle classifies solvents according to their relative dipole moments, basic properties, and acidic properties. For example, if an initial chromatographic experiment does not separate all the components with a binary mobile phase, then the solvent-selectivity triangle can be used to choose another solvent for the binary system that has properties that are very different than one of the

solvents in the original solvent system. A useful publication that discusses the properties of numerous solvents and also considers many chromatographic applications is Ref.[6]

MECHANISTIC ASPECTS IN ADSORPTION CHROMATOGRAPHY

Models for the interactions of solutes in adsorption chromatography have been discussed extensively in the literature.[7–9] Only the interactions with silica and alumina will be considered here. However, various modifications to the models for the previous two adsorbents have been applied to modern high-performance columns (e.g., amino-silica and cyano-silica). The interactions in adsorption chromatography can be very complex. The model that has emerged which describes many of the interactions is the displacement model developed by Snyder.[1,3,4,7,8] Generally, retention is assumed to occur by a displacement process. For example, an adsorbing solute molecule X displaces n molecules of previously adsorbed mobile-phase molecules M:[8]

$$X_n + nM_a \rightleftharpoons X_a + nM_n$$

The subscripts n and a in the above equation represent a molecule in a non-sorbed and adsorbed phase, respectively. In other words, retention in adsorption chromatography involves a competition between sample and solvent molecules for sites on the adsorbent surface. A variety of interaction energies are involved, and the various energy terms have been described in the literature.[7,8] One fundamental equation that has been derived from the displacement model is

$$\log\left(\frac{k_1}{k_2}\right) = \alpha' A_S(\varepsilon_2 - \varepsilon_1)$$

where k_1 and k_2 are the capacity factors of a solute in two different mobile phases, α' is the surface activity of the adsorbent (relative to a standard adsorbent), A_S is the cross-sectional area of the solute on the adsorbent surface, ε_1 and ε_2 are the solvent strengths of the two different mobile phases. This equation is valid in situations where the solute and solvent molecules are considered non-localizing. This condition is fulfilled with non-polar or moderately polar solutes and mobile phases. If one is dealing with multisolvent mobile phases, the solvent strength of those solvents can be related to the solvent strengths of the pure solvents in the solvent system. The equations for calculating solvents strengths for multisolvent mobile phases have been discussed in the literature.[8]

As the polarities of the solute and solvent molecules increase, the interactions of these molecules become much stronger with the adsorbent, and they adsorb with localization. The net result is that the fundamental equation for adsorption chromatography with relatively non-polar solutes and solvents has to be modified. Several localization effects have been elucidated, and the modified equations that take these factors into consideration are rather complex.[7,8,10] Nevertheless, the equations provide a very important framework in understanding the complexities of adsorption chromatography and in selecting mobile phases and stationary phases for the separation of solutes.

APPLICATIONS

There have been thousands of articles published on the application of adsorption chromatography over the decades. Today, adsorption chromatography is used around the world in all areas of chemistry, environmental problem solving, medical research, and so forth. Only a few examples will be discussed in this section. Gogou et al.[11] developed methods for the determination of organic molecular markers in marine aerosols and sediment. They used a one-step flash chromatography compoundclass fractionation method to isolate compound-class fractions. Then, they employed GC/MS and/or GC/flame ionization detection analysis of the fractions. The key adsorption chromatographic step prior to the GC was the one-step flash chromatography. For example, an organic extract of marine aerosol or sediment was applied on the top of a 30×0.7 cm column containing 1.5 g of silica. The following solvent systems were used to elute the different compound classes: (a) 15 ml of *n*-hexane (aliphatics); (b) 15 ml toluene : *n*-hexane (5.6 : 9.4) (polycyclic aromatic hydrocarbons and nitropolycyclic aromatic hydrocarbons); (c) 15 ml *n*-hexane: methylene chloride (7.5 : 7.5) (carbonyl compounds); (d) 20 ml ethyl acetate: *n*-hexane (8 : 12) (*n*-alkanols and sterols); (e) 20 ml (4%, v/v) pure formic acid in methanol (free fatty acids). This example illustrates very well how adsorption chromatography can be used for compound-class separation.

Hanson and Unger[12] have discussed the application of non-porous silica particles in HPLC. Non-porous silica packings can be used for the rapid chromatographic analysis of biomolecules because the particles lack pore diffusion and have very effective mass-transfer capabilities. Several of the advantages of non-porous silica are maximum surface accessibility, controlled topography of ligands, better preservation of biological activity caused by shorter residence times on the column, fast column regeneration, less solvent consumption, and less susceptibility to compression during packing. The very low external surface area of the non-porous supports is a disadvantage because it gives considerably lower capacity compared with porous materials. This drawback is

counterbalanced partially by the high-packing density compared to porous silica. The smooth surface of the non-porous silica offers better biocompatibility relative to porous silica. Well-defined non-porous silicas are now commercially available.

REFERENCES

1. Snyder, L.R.; Kirkland, J.J. *Introduction to Modern Liquid Chromatography,* 2nd Ed.; John Wiley & Sons: New York, 1979.
2. Knox, J.H. *High-Performance Liquid Chromatography*; Ed.; Edinburgh University Press: Edinburgh, 1980.
3. Snyder, L.R. *Principles of Adsorption Chromatography*; Marcel Dekker, Inc.: New York, 1968.
4. Snyder, L.R. *Chromatography: A Laboratory Handbook of Chromatographic and Electrophoretic Methods,* 3rd Ed.; Heftmann, E., Ed.; Van Nostrand Reinhold: New York, 1975, 46–76.
5. Snyder, L.R.; Glajch, J.L.; Kirkland, J.J. *Practical HPLC Method Development*; John Wiley & Sons: New York, 1988, 36–39.
6. Sadek, P.C. *The HPLC Solvent Guide*; John Wiley & Sons: New York, 1996.
7. Snyder, L.R.; Poppe, H. Mechanism of solute retention in liquidsolid chromatography and the role of the mobile phase in affecting separation: competition versus "sorption." J. Chromatogr. **1980**, *184*, 363.
8. Snyder, L.R. *High-Performance Liquid Chromatography*; Horvath, C., Ed.; Academic Press: New York, 1983, Vol. 3, 157–223.
9. Scott, R.P.W.; Kucera, P. Liquid chromatography theory. J. Chromatogr. **1979**, *171*, 37.
10. Snyder, L.R.; Glajch, J.L. Solven strength of multicomponent mobile phases in liquidsolid chromatograph: Further study of different mobile phases and silica as adsorbent. J. Chromatogr. **1982**, *248*, 165.
11. Gogou, A.I.; Apostolaki, M.; Stephanou, E.G. J. Adsorption chromatography. J. Chromatogr. A, **1998**, *799*, 215.
12. Hanson, M.; Unger, K.K. Adsorption chromatography. LC-GC **1997**, *15*, 364.

Adsorption Studies by FFF

Niem Tri
Ronald Beckett
Water Studies Centre, Monash University, Melbourne, Victoria, Australia

INTRODUCTION

Adsorption is an important process in many industrial, biological, and environmental systems. One compelling reason to study adsorption phenomena is because an understanding of colloid stability depends on the availability of adequate theories of adsorption from solution and of the structure and behavior of adsorbed layers. Another example is the adsorption of pollutants, such as metals, toxic organic compounds, and nutrients, onto fine particles and their consequent transport and fate, which has great environmental implications. Often, these systems are quite complex and it is often favorable to separate these into specific size for subsequent study.

BACKGROUND INFORMATION

A new technique able to separate such complex mixtures is field-flow fractionation.[1–3] Field-flow fractionation (FFF) is easily adaptable to a large choice of field forces (such as gravitational, centrifugal, fluid cross-flows, electrical, magnetic and thermal fields or gradients) to effect high-resolution separations. Although the first uses for FFF were for sizing of polymer and colloidal samples, recent advances have demonstrated that well-designed FFF experiments can be used in adsorption studies.[4,5]

Although the theory of FFF for the characterization and fractionation of polymers and colloids has been outlined elsewhere, two important features of FFF need to be emphasized here. The first is the versatility of FFF, which is partly due to the diverse range of operating fields that may be used and the fact that each field is capable of delivering different information about a colloidal sample. For example, an electrical field separates particles on the basis of both size and charge, whereas a centrifugal field (sedimentation FFF) separates particles on the basis of buoyant mass (i.e., size and density). The second important feature is that this information can usually be measured directly from the retention data using rigorous theory. This is in contrast to most forms of chromatography (size-exclusion chromatography exempted), where the retention time of a given component must be identified by running standards.

In 1991, both Beckett et al.,[4] and Li and Caldwell[5] published articles demonstrating novel but powerful uses for sedimentation FFF in probing the characteristics of adsorbed layers or films on colloidal particles. Beckett et al., article demonstrated that it is possible to measure the mass of an adsorbed coating down to a few attograms (10^{-18} g), which translates to a mean coating thickness of human γ-globulin, ovalbumin, RNA, and cortisone ranging from 0.1 to 20 nm. A discussion of the theory and details of the experiment is beyond the scope of this entry. However, it is possible to appreciate how such high sensitivities arise by considering the linear approximation of retention time, t_r, of an eluting particle in sedimentation FFF with the field-induced force on the particle, F.

$$t_r = t_0 \frac{Fw}{6kT} \tag{1}$$

where w is the thickness of the channel (typically 100–500 μm), k is the Boltzmann constant, and T is the temperature in Kelvin. F is the force on the individual particle and is the product of the applied field and the buoyant mass of the particle (relative mass of the particle in the surrounding liquid medium).

The highest sensitivity of retention time to changes in the surface coating was found to occur when the density of the core particle was equal to that of the surrounding medium (i.e., the buoyant mass diminishes to zero and no retention is observed for the bare particle). If a thin film of a much denser material is adsorbed onto the particles, then the small increment in mass due to the adsorbed film causes a significant change in the particle's buoyant mass (see Fig. 1a). Consequently, the force felt by the particle is now sufficient to effect retention by an observable amount. Incidentally, analogous behavior is also possible if the coatings are less dense than the carrier liquid. If the diameter of the bare particle is known (from independent experiments) so that the surface area can be estimated, then it is also possible to calculate the thickness of the adsorbed film, provided the density of the film is the same as the bulk density of the material being adsorbed (i.e., no solvation of the adsorbed layer). In some systems, it may be possible to alter the solvent density to match the core particle density by the addition of sucrose or other density modifiers to the FFF carrier solution.

Using the above approach with experimental results from centrifugal FFF, adsorption isotherms were constructed by

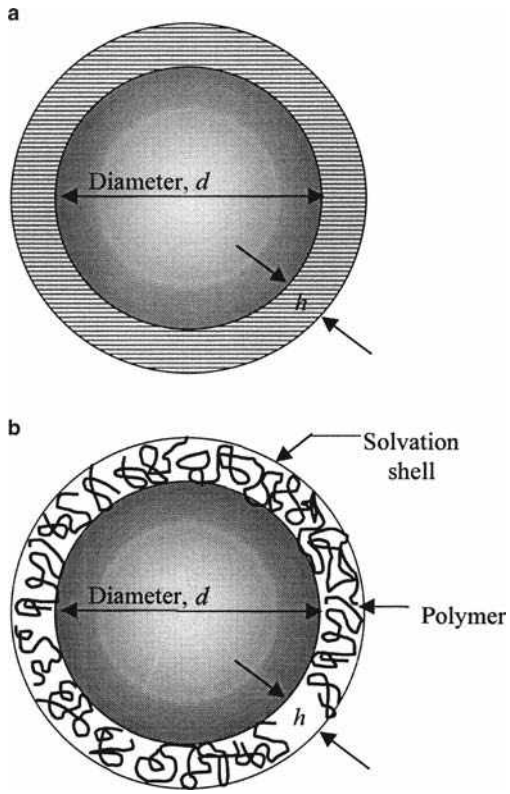

Fig. 1 Schematic representation of the adsorption complex proposed by (a) Beckett et al.,[4] showing the core particle with a dense non-hydrated adsorbed film and by (b) Li and Caldwell[5] showing the core particle with an adsorbed polymer and the associated solvation shell.

directly measuring the mass of adsorbate deposited onto the polymer latex particle surface at different solution concentrations. It was found that for human globulin and ovalbumin adsorbates, Langmuir isotherms were obtained. The measured limiting adsorption density was found to agree with values measured using conventional solution uptake techniques.

The model used in the above studies ignores the departure from the bulk density of the adsorbate brought about by the interaction of the two interfaces. Li and Caldwell's article addresses this issue by introducing a three-component model consisting of a core particle, a flexible macromolecular substance with affinity toward the particle, and a solvation shell (see Fig. 1b).

In this model, the buoyant mass is then the sum of the buoyant mass of the three components, assuming that these are independent of the mass of solvent occupied in the solvation shell. Thus, the mass of the adsorbed shell can be calculated if information about the mass and density of the core particle and the density of the macromolecule and solvent are known. Photon correlation spectroscopy, electron microscopy, flow FFF, or other sizing techniques can readily provide some independent information on the physical or hydrodynamic particle size, and pycnometry can be used to measure the densities of the colloidal suspension, polymer solution, and pure liquid.

The above measurements were combined to estimate the mass of the polymer coating, a surface coverage density, and the solvated layer thickness. These results showed good agreement with the adsorption data derived from conventional polymer radiolabeling experiments.

Another approach for utilizing FFF techniques in the study of adsorption processes is to use the following general protocol:

1. Expose the suspension to the adsorbate.
2. Run the sample through an FFF separation and collect fractions at designated elution volume intervals corresponding to specific size ranges.
3. Analyze the size fractions for the amount of adsorbate.

It must be emphasized that only strongly adsorbed material will be retained on the particles as the sample is constantly washed by the carrier solution during the FFF separation. Unless adsorbent is added to the carrier, these experiments will not represent the reversible equilibrium adsorption situation.

This approach was first outlined by Beckett et al.,[6] where radiolabeled pollutants (^{32}P as orthophosphate, ^{14}C in atrazine, and glyphosate) were adsorbed to two Australian river colloid samples. Sedimentation FFF was used to fractionate the samples and the radioactivity of each fraction was measured. From this, it was possible to generate a surface adsorption density distribution (SADD) across the size range of the sample. The SADD is a plot of the amount of compound adsorbed per unit particle surface area as a function of the particle size. It was shown that the adsorption density was not always constant, indicating perhaps a change in particle mineralogy, surface chemistry, shape, or texture as a function of particle size.

The above method is currently being extended to use other sensitive analytical techniques such as inductively coupled plasma–mass spectrometry (ICP–MS), graphite furnace atomic absorption (GFAAS), and inductively coupled plasma–atomic emission spectrophotometry (ICP–AES). With multielement techniques, it is not only possible to measure the amount adsorbed but changes in the particle composition with size can be monitored,[7] which is most useful in interpreting the adsorption results.[8] Hassellov et al.,[9] showed that using sedimentation FFF coupled to ICP–MS, it was possible to study both the major elements Al, Si, Fe, and Mn but also the Cs, Cd, Cu, Pb, Zn, and La. It was shown that it was possible to distinguish between the weaker and stronger binding sites as well as between different adsorption and ion-exchange mechanisms.

In electrical FFF, samples are separated on the basis of surface charge and even minute amount of adsorbate will

significantly be reflected in electrical FFF data, as demonstrated by Dunkel et al.[10] However, this technique is severely limited by the generation of polarization products at the channel wall due to the applied voltages.

In conclusion, the versatility and power of FFF are not restricted to its ability to effect high-resolution separations and sizing of particles and macromolecules. FFF can also be used to probe the surface properties of colloidal samples. Such studies have great potential to provide detailed insight into the nature of adsorption phenomena.

REFERENCES

1. Caldwell, K.D. Field-flow fractionation. Anal. Chem. **1988**, *60*, 959A.
2. Giddings, J.C. Field-flow fractionation: Analysis of macromolecular, colloidal, and particulate materials. Science **1993**, *260*, 1456.
3. Beckett, R.; Hart, B.T. *Environmental Particles*; Buffle, J., van Leeuwen, H.P., Eds.; Lewis Publishers, 1993; Vol. 2, 165–205.
4. Beckett, R.; Ho, Y.; Jiang, Y.; Giddings, J.C. Measurement of mass and thickness of adsorbed films on colloidal particles by sedimentation field-flow fractionation. Langmuir **1991**, *7*, 2040.
5. Li, J.-T.; Caldwell, K.D. Sedimentation field flow fractionation in the determination of surface concentration of adsorbed materials. Langmuir **1991**, *7*, 2034.
6. Beckett, R.; Hotchin, D.M.; Hart, B.T. Use of field-flow fractionation to study pollutant—colloid interactions. J. Chromatogr. **1990**, *517*, 435.
7. Ranville, J.F.; Shanks, F.; Morrison, R.J.F.; Harris, P.; Doss, F.; Beckett, R. Development of sedimentation field-flow fractionation-inductively coupled plasma mass-spectrometry for the characterization of environmental colloids. Anal. Chem. Acta **1999**, *381*, 315.
8. Vanberkel, J.; Beckett, R. Estimating the effect of particle surface coatings on the adsorption of orthophosphate using sedimentation field-flow fractionation. J. Liq. Chromatogr. Relat. Technol. **1997**, *20*, 2647.
9. Hassellov, M.; Lyven, B.; Beckett, R. Sedimentation field-flow fractionation coupled online to inductively coupled plasma mass spectrometry—new possibilities for studies of trace metal adsorption onto natural colloids. Environ. Sci. Technol. **1999**, *33*, 4528.
10. Dunkel, M.; Tri, N.; Beckett, R.; Caldwell, K.D. Electrical field-flow fractionation: A tool for characterization of colloidal adsorption complexes. J. Micro. Separ. **1997**, *9* (3), 177.

Affinity Chromatography

David S. Hage
Department of Chemistry, University of Nebraska-Lincoln, Lincoln, Nebraska, U.S.A.

Abstract
The history and basic principles of affinity chromatography are discussed in this entry. Affinity chromatography is a liquid chromatographic technique that uses a biologically related agent as a ligand for the purification or analysis of sample components. Affinity chromatography is a valuable tool in areas such as biochemistry, biotechnology, pharmaceutical science, clinical chemistry, and environmental testing, where it has been used for both the purification and analysis of compounds in complex sample mixtures. The various components of an affinity chromatographic method, including the types of affinity ligands, support materials, immobilization methods, and application or elution conditions that are employed in this technique, are discussed in this entry. Several specific types of affinity chromatography, including bioaffinity chromatography, immunoaffinity chromatography, lectin affinity chromatography, dye–ligand affinity chromatography, immobilized metal-ion affinity chromatography (IMAC), boronate affinity chromatography, weak affinity chromatography, and analytical affinity chromatography, are also described.

INTRODUCTION

Affinity chromatography is a liquid chromatographic technique that uses a biologically related agent as a stationary phase for the purification or analysis of sample components.[1,2] The retention of solutes in this method is based on the specific reversible interactions that occur in many biological systems, such as the binding of an enzyme with a substrate or of an antibody with an antigen. These interactions are exploited in affinity chromatography by placing one of a pair of interacting molecules onto or within a solid support and using this immobilized agent as a stationary phase. This immobilized agent is known as the *affinity ligand* and is what gives an affinity column the ability to bind to particular compounds in a sample.[2]

Affinity chromatography is a valuable tool in areas such as biochemistry, proteomics, pharmaceutical science, clinical chemistry, and environmental testing, where it has been used for both the purification and analysis of compounds in complex sample mixtures.[3–11] The strong and relatively specific binding that characterizes many affinity ligands allows solutes to be measured or purified by these ligands with little or no interference from other sample components. Often the solute of interest can be isolated in one or two steps, with purification yields of one hundred to several thousandfold being common.[3,6,7] This entry will first examine the history of affinity chromatography and the different ways in which affinity chromatography is performed. The various features of an affinity chromatographic method, including the types of affinity ligands, support materials, immobilization methods, and application or elution conditions that are employed in this technique, will then be discussed. Several specific types of affinity chromatography will be described next.

HISTORY OF AFFINITY CHROMATOGRAPHY

The earliest known use of affinity chromatography was in 1910 when Emil Starkenstein examined the binding of insoluble starch to the enzyme α-amylase.[12] Similar work with starch and other insoluble ligands (acting as both binding agents and supports) was conducted in the 1920s through the 1940s. Most of these early studies involved the use of affinity supports for the purification of enzymes. However, work on the selective purification of antibodies with biological ligands through the use of immunoprecipitation also began at this time.[2]

In the 1940s and 1950s, synthetic techniques became available for placing a broader range of ligands on insoluble materials that could be used as supports. These efforts began by employing solids that contained a non-covalently adsorbed layer of ligand, followed later by the development of methods for chemically bonding a ligand to solid supports. A covalent technique for ligand attachment to a support was first used by Landsteiner and van der Sheer in 1936, when they adapted the diazo-coupling technique to attach a number of haptens to a material based on chicken erythrocyte stroma.[13] Another significant development in this area occurred in 1951, when Campbell and coworkers used an activated form of cellulose (*p*-aminobenzylcellulose) for immobilizing the protein serum albumin, which was then employed in the isolation of antialbumin antibodies from rabbit serum.[14]

The modern era of affinity chromatography began in the late 1960s with the creation of beaded agarose supports by Hjerten[15] and the use of the cyanogen bromide immobilization method by Axen, Porath, and Ernback.[16] These two methods were combined in 1968 by Cuatrecasas, Wilchek, and Anfinsen to create immobilized nuclease inhibitor columns. These columns were then used for purifying the enzymes staphylococcal nuclease, α-chymotrypsin, and carboxypeptidase A. It was at this time that the name *affinity chromatography* was first used to describe this separation technique.[17] This was followed by a significant increase in the use of affinity chromatography in the 1970s up to the present time, with over 1000 entries per year appearing on this method.[2–7]

AFFINITY CHROMATOGRAPHY: METHODS

The most common method for performing affinity chromatography is to use a step gradient for elution, as shown in Fig. 1. This approach involves injecting a sample onto the affinity column in the presence of a mobile phase that has the right pH and solvent composition for solute–ligand binding. This solvent, which represents the weak mobile phase of the affinity column, is called the *application buffer*. In the presence of this buffer, compounds that are complementary to the affinity ligand bind as the sample is carried through the column by the application buffer. However, because of the high selectivity of the solute–ligand interaction, the other sample components tend to pass through the column without being retained. After the non-retained components have been completely washed from the column, the retained solutes can be eluted by applying a solvent that displaces them from the column or that promotes dissociation of the solute–ligand complex. The second solvent represents the strong mobile phase for the column and is known as the *elution buffer*. As the solutes of interest elute from the column, they are either measured or collected for later use. The column is then regenerated by re-equilibrating it with the application buffer before the injection of the next sample.[3,7]

Even though the *step gradient*, or *on/off*, *elution method* is the most common way of performing affinity chromatography, it is possible to use affinity methods under isocratic conditions. Isocratic elution can be employed if the retention of a solute is sufficiently weak to allow elution on the minute-to-hour timescale and if the kinetics for binding and dissociation with the ligand are fast enough to allow a large number of solute–ligand interactions to occur as the solute travels through the column. This approach is called *weak affinity chromatography* and is best performed if a solute binds to the ligand with an association equilibrium constant less than or equal to about 10^4–10^6 M^{-1}.[18–20]

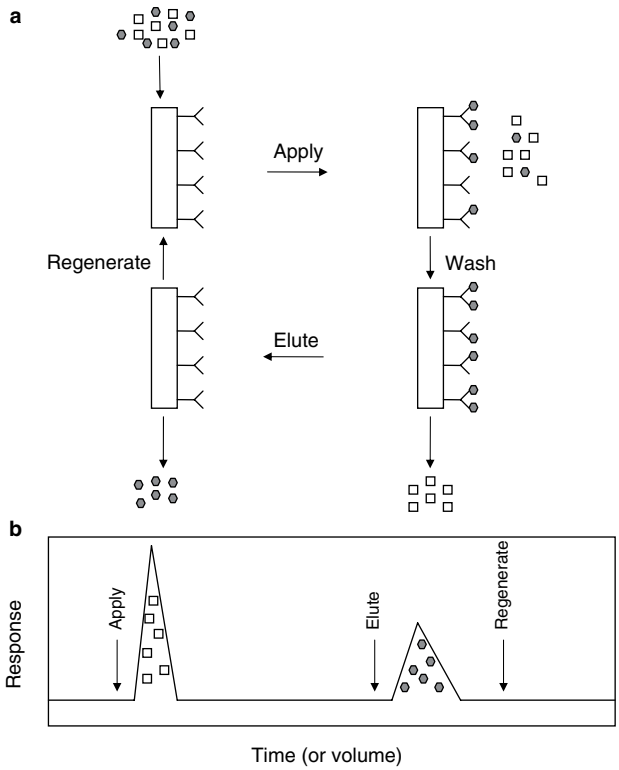

Fig. 1 a, Typical separation scheme and b, chromatogram for affinity chromatography. The filled circles represent the test analyte and the open squares represent other non-retained sample components.

TYPES OF AFFINITY LIGANDS

The most important factor that determines the success of any affinity separation is the type of ligand that is used within the column. A number of ligands that are commonly used in affinity chromatography are listed in Table 1. Most of these ligands are of biological origin, but a wide range of natural and synthetic molecules of non-biological origin have also been used in affinity separations. Regardless of their origin, all of these ligands can be placed into one of two categories: high-specificity ligands or general ligands.[2,6,7]

The term *high-specificity ligand* refers to a compound that binds to only one or a few closely related molecules. This type of ligand is used in affinity separations where the goal is to analyze or purify a specific solute. Examples include antibodies (for binding antigens), substrates or inhibitors (for separating enzymes), and single-stranded nucleic acids (for the retention of a complementary sequence). As this list suggests, most high-specificity ligands tend to be of biological origin. High-specificity ligands also tend to have large association equilibrium constants for their targets.

General, or *group-specific*, *ligands* are agents that bind to a family or class of related targets. These ligands are

Table 1 Common ligands used in affinity chromatography.

Type of ligand	Examples of retained targets
High-specificity ligands	
Antibodies	Drugs, hormones, peptides, proteins, viruses
Enzyme inhibitors and cofactors	Enzymes
Nucleic acids	Complementary nucleic acid strands and DNA/RNA-binding proteins
General ligands	
Lectins	Small sugars, polysaccharides, glycoproteins, and glycolipids
Protein A and protein G	Intact antibodies/immunoglobulins and F_c fragments
Boronates	Catechols and compounds that contain sugar residues, such as polysaccharides and glycoproteins
Synthetic dyes	Dehydrogenases, kinases, and various proteins
Metal chelates	Metal-binding amino acids, peptides, or proteins

used when the goal is to isolate a class of structurally related compounds. General ligands can be of either biological or non-biological origin and include agents such as protein A or protein G, lectins, boronates, biomimetic dyes, and immobilized metal chelates. This class of ligands usually exhibits weaker binding for targets than is seen with high-specificity ligands. However, some general ligands like protein A and protein G do have association equilibrium constants that rival those of high-specificity ligands.

SUPPORT MATERIALS

Another important factor to consider in affinity chromatography is the material used to hold the ligand within the column. Ideally, this support should have low non-specific binding for sample components, it should be easy to modify for ligand attachment, and it should be stable under the flow rate, pressure, and solvent conditions that will be employed in the analysis or purification of samples. Depending on what type of support material is being used, affinity chromatography can be characterized as being either a low- or a high-performance technique.[7,21,22]

In *low-performance* (or *column*) *affinity chromatography*, the support is usually a large-diameter, non-rigid material, such as a carbohydrate-based gel, or one of several synthetic organic-based polymers. The low back pressures that are produced by these supports means that these materials can often be operated under gravity flow or with a peristaltic pump, making them relatively simple and inexpensive to use for affinity purification or sample pretreatment. Disadvantages of these materials include their slow mass transfer properties and their limited stabilities at high flow rates and pressures. These factors tend to limit the direct use of these supports in analytical applications, where both rapid and efficient separations are usually desired.[7,21]

High-performance affinity chromatography (*HPAC*) is characterized by a support that consists of small, rigid particles that are capable of withstanding high flow rates and/or pressures.[7,21,22] Examples of affinity supports that are suitable for work under these conditions include modified silica or glass, azalactone beads, and hydroxylated polystyrene media. The stability and efficiency of these supports allows them to be used with standard high-performance liquid chromatography (HPLC) equipment. Although the need for HPLC instrumentation does make HPAC more expensive to perform than low-performance affinity chromatography, the better speed and precision of HPAC makes it the method of choice for many analytical applications.

Although porous, particulate materials like agarose, polymethacrylate, and silica are used in most current applications of affinity chromatography, there are several other types of supports that have recently become available for affinity separations.[21] Materials that fall in this category include non-porous supports, membranes, flow-through beads, continuous beds, and expanded bed particles. The good mass transfer properties of non-porous beads with diameters of 1–3 μm make them appealing for fast analytical or micropreparative separations, as well as for quantitative studies of affinity interactions. Similar properties are obtained using flow-through beads or continuous beds. An example is the use of monolithic supports with affinity ligands in a method known as affinity monolith chromatography (AMC).[23] The flat geometry and shallow bed depth of affinity membranes allow their use at high flow rates, making them well suited for capturing proteins from dilute feed streams. Similarly, the presence of low back pressures makes expanded bed particles attractive for use in isolating proteins from cell culture samples while allowing solid contaminants like cells and cell debris to pass through, thereby avoiding column clogging.[21]

IMMOBILIZATION METHODS

An additional factor to consider in affinity chromatography is the way in which the ligand is attached to the solid

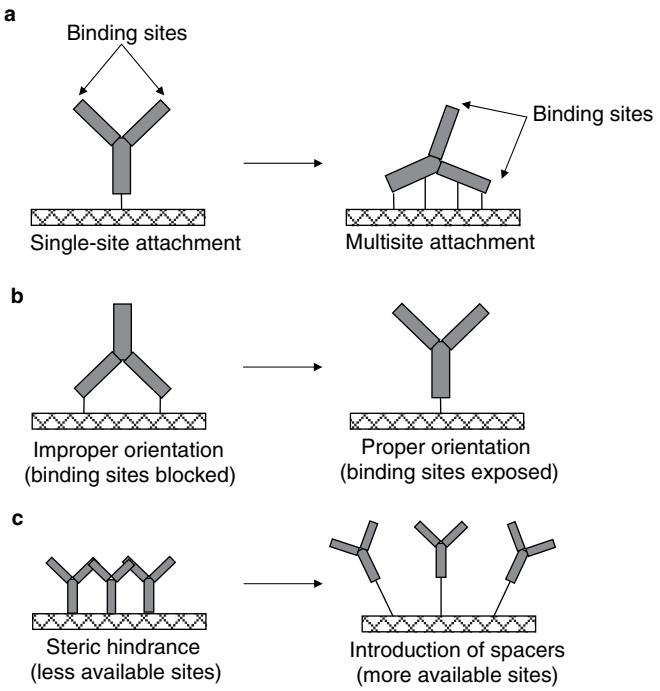

Fig. 2 Common immobilization effects during the coupling of affinity ligands to solid supports.
Source: From Immobilization methods for affinity chromatography, in *Handbook of Affinity Chromatography*.[24]

support, or the *immobilization method*. For a ligand that is a protein or peptide, immobilization generally involves coupling the ligand through free amine, carboxylic acid, or sulfhydryl residues in its structure. Immobilization of a ligand through other functional sites is also possible (e.g., the use of aldehyde groups produced by mild oxidation of the carbohydrate chains on a glycoprotein). All covalent immobilization methods involve at least two steps: 1) an *activation step*, in which the support is converted to a form that can be chemically attached to the ligand; and 2) a *coupling step*, in which the affinity ligand is attached to the activated support.[7,24] Occasionally, a third step is necessary to remove remaining activated groups and to minimize non-specific binding to the final support.[24]

The method by which an affinity ligand is immobilized is important because it can affect the actual or apparent activity of the final affinity column.[7,24] If the correct procedure is not used, a decrease in ligand activity can result from multisite attachment, improper orientation, or steric hindrance (Fig. 2). *Multisite attachment* refers to the coupling of a ligand to the support through more than one functional group, which can lead to distortion of the active region in a ligand and a loss of activity. This effect can be avoided by using a support with a limited number of activated sites or by using a method that couples through groups that are present in only a few places in the structure of the ligand. *Improper orientation* can lead to a loss in activity by coupling the ligand to the support through its active region; this effect can be minimized by coupling through functional groups that are distant from the active region. *Steric hindrance* refers to the loss of ligand activity due to the presence of a nearby support or neighboring ligands that interfere with solute binding. This effect can be avoided through the use of a spacer arm or by using supports that contain a relatively low coverage of the ligand.[7,24]

It is possible to place an affinity ligand within a column through means other than covalent immobilization.[24] The simplest of these alternative approaches is to use physical adsorption of the ligand onto a surface through ionic or non-specific interactions. In addition, a ligand can be held non-covalently on a column by means of a secondary ligand. A common example of the latter technique is the use of immobilized protein A or protein G to adsorb antibodies for use in immunoaffinity chromatography.[25,26] It is also possible to entrap or encapsulate a ligand within a support if the size of the entrapped ligand is larger than the pores of the support material (e.g., as occurs in the use of sol gels for protein entrapment).[24] Finally, there are instances in which the ligand itself can be used as both the support and stationary phases. Insoluble starch was used as both the support and the ligand for isolation of the enzyme amylase when affinity chromatography was first used.[12]

APPLICATION AND ELUTION CONDITIONS

The effect of application and elution buffers must be taken into consideration in affinity chromatography. Most application buffers in affinity chromatography are solvents that mimic the pH, ionic strength, and polarity experienced by the solute and ligand in their natural environment. These conditions give the solute its highest

association equilibrium constant for the ligand and, thus, its highest degree of retention on the column. The application buffer should be chosen so that it minimizes non-specific binding due to other sample components.[20]

Elution conditions in affinity chromatography are usually chosen so that they promote either the fast or gentle removal of solute from the column. The two most common approaches used for this purpose are *biospecific elution* and *non-specific elution*.[7,20] Biospecific elution is based on the addition of a competing agent that gently displaces a solute from the column. This type of elution is done by adding an agent that either competes with the ligand for the target solute (i.e., *normal role elution*) or competes with the target solute for binding sites on the ligand (i.e., *reversed role elution*). Although it is a gentle method, biospecific elution does result in long elution times and broad solute peaks that can be difficult to detect and measure. Non-specific elution uses a solvent that directly promotes weak solute–ligand binding. For instance, non-specific elution is carried out by changing the pH, ionic strength, or polarity of the mobile phase or by adding a denaturing agent or chaotropic substance to the elution buffer. Non-specific elution tends to be much faster than biospecific elution and results in sharper peaks that help provide lower limits of detection. However, care must be exercised when utilizing non-specific elution to avoid using a buffer that is too harsh and may cause denaturation of the target solute or a loss of ligand activity.

TYPES OF AFFINITY CHROMATOGRAPHY

There are many types of affinity chromatography that are in common use. *Bioaffinity chromatography* is the broadest category and includes any affinity separation method that uses a biological molecule as the ligand.[4–7,27] *Immunoaffinity chromatography* (*IAC*) is a special subcategory of bioaffinity chromatography in which the affinity ligand is an antibody or antibody-related agent.[25,26,28] This combination creates a highly specific method that is ideal for use in affinity purification or in analytical methods that involve complex samples. *Immunoextraction* is a subcategory of IAC in which an affinity column is used to isolate compounds from a sample before analysis by a second method. IAC can also be used to monitor the elution of analytes from other columns, giving rise to a scheme known as *postcolumn immunodetection*.[25,28,29]

Another common type of bioaffinity method is a technique that uses bacterial cell wall proteins like protein A or protein G for antibody purification. This approach is sometimes categorized as a subset of immunoaffinity chromatography but it is more appropriate to consider it under bioaffinity methods.[26–29] In *lectin affinity chromatography*, another type of bioaffinity chromatography, immobilized lectins like concanavalin A or wheat germ agglutinin are used for binding to targets that contain certain sugar residues.[27] Additional types of bioaffinity chromatography are those that make use of ligands that are enzymes, inhibitors, cofactors, nucleic acids, hormones, or cell receptors.[4–7,27] Examples of these methods include *receptor affinity chromatography*[30] and *DNA affinity chromatography*,[31] the latter of which can include the use of aptamers as binding agents.[32,33]

There are many types of affinity chromatography that use ligands that are of non-biological origin. For instance, the closely related methods of *dye–ligand affinity chromatography* and *biomimetic affinity chromatography* can use an immobilized synthetic dye (e.g., Fig. 3) to mimic a target that will bind to the active site of a protein or enzyme, making these methods popular tools for enzyme and protein purification.[32–35] *Immobilized metal-ion affinity chromatography* (*IMAC*) is an affinity technique in which the ligand is a metal ion that is complexed with an immobilized chelating agent.[36–38] IMAC is used to separate proteins and peptides that contain amino acids with electron donor groups and has become a popular tool for isolating recombinant proteins that contain histidine tags.[38] *Boronate affinity chromatography* employs boronic acid or a boronate as the affinity ligand. Boronate-related ligands are useful in binding to targets that contain *cis*-diol groups, such as catecholamines and glycoproteins.[39,40]

There are a number of other chromatographic methods that are closely related to traditional affinity chromatography. For instance, affinity chromatography can be adapted as a tool for studying solute–ligand interactions. This application is known as *analytical affinity chromatography*, *quantitative affinity chromatography*, or *biointeraction*

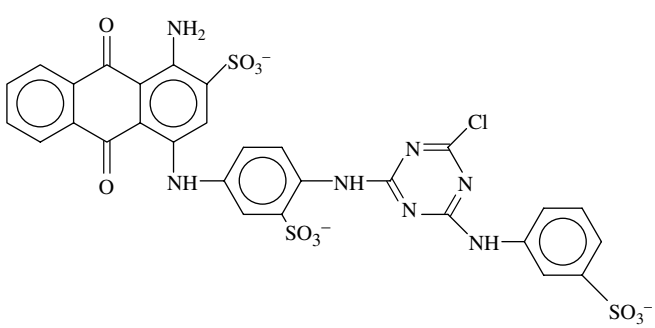

Fig. 3 Cibacron Blue 3GA, a triazine dye that is commonly used as a ligand for protein and enzyme purification in the method of dye–ligand affinity chromatography.

chromatography.[41–44] Methods that have been developed for this field can be used to acquire information regarding the equilibrium and rate constants for biological interactions, as well as the number and type of binding sites that are involved in these interactions. This method can also be used to examine the competition between two solutes for binding sites on a ligand (as is common in *frontal affinity chromatography*)[45] and to study both direct and allosteric effects during such competition.[41–43]

Other methods that are related to affinity chromatography include *hydrophobic interaction chromatography* (*HIC*) and *thiophilic adsorption*.[2,7] HIC is based on the interactions of proteins, peptides, and nucleic acids with short non-polar chains, such as those that were originally used as spacer arms on affinity supports. Thiophilic adsorption, also known as *covalent* or *chemisorption chromatography*, makes use of immobilized thiol groups for solute retention. Applications of this method include the analysis of sulfhydryl-containing peptides or proteins and mercurated polynucleotides.

Many types of *chiral liquid chromatography* can be considered affinity methods because they are based on binding agents that are of biological origin. Examples include columns that use cyclodextrins or immobilized proteins for chiral separations.[27,46,47] The growing use of molecularly imprinted polymers as stationary phases can also be considered to be a subset of affinity chromatography, because such materials are designed to mimic the multiple interactions and selectivity that are characteristic of many biological ligands.[48,49] Another area of growth in recent years has been the combined use of affinity columns (e.g., those containing antibodies) with other analytical methods, such as mass spectrometry,[42,45,50] liquid chromatography,[25,29,42] or capillary electrophoresis.[25,51]

CONCLUSION

In summary, affinity chromatography is a selective separation method that has numerous applications in the purification and analysis of compounds, especially targets that are related to biological systems. The wide variety of available ligands makes it possible to design affinity separations for a large range of target compounds. Some of these ligands are of biological origin while others are man-made. It is also possible to perform affinity chromatography with support materials that allow its use as either a preparative tool or an analytical method. In addition, affinity chromatography can be used as a tool to study biological interactions. These features have made affinity methods valuable in a number of fields, including biotechnology, biochemistry, clinical analysis, pharmaceutical science, and environmental testing. In recent years there has been considerable improvement in the use of affinity chromatography in combination with other methods, such as mass spectrometry and capillary electrophoresis.

REFERENCES

1. Ettre, L. Nomenclature for chromatography. Pure Appl. Chem. **1993**, *65*, 819–872.
2. Hage, D.S.; Ruhn, P.F. An introduction to affinity chromatography. In *Handbook of Affinity Chromatography*, 2nd Ed.; Hage, D.S., Ed.; Taylor & Francis: New York, 2006; Chapter 1.
3. Hage, D.S., Ed. *Handbook of Affinity Chromatography*, 2nd Ed.; Taylor & Francis: New York, 2006.
4. Turkova, J. *Affinity Chromatography*; Amsterdam: Elsevier, 1978.
5. Scouten, W.H. *Affinity Chromatography: Bioselective Adsorption on Inert Matrices*; Wiley: New York, 1981.
6. Parikh, I.; Cuatrecasas, P. Affinity chromatography. Chem. Eng. News **1985**, *63*, 17–29.
7. Walters, R.R. Affinity chromatography. Anal. Chem. **1985**, *57*, 1099A–1114A.
8. Lee, W.-C.; Lee, K.H. Applications of affinity chromatography in proteomics. Anal. Biochem. **2004**, *324*, 1–10.
9. Wolfe, C.A.C.; Clarke, W.; Hage, D.S. Affinity methods in clinical and pharmaceutical analysis. In *Handbook of Affinity Chromatography*, 2nd Ed.; Hage, D.S., Ed.; Taylor & Francis: New York, 2006; Chapter 17.
10. Jordan, N.; Krull, I.S. Affinity chromatography in biotechnology. In *Handbook of Affinity Chromatography*, 2nd Ed.; Hage, D.S., Ed.; Taylor & Francis: New York, 2006; Chapter 4.
11. Nelson, M.A.; Hage, D.S. Environmental analysis by affinity chromatography. In *Handbook of Affinity Chromatography*, 2nd Ed.; Hage, D.S., Ed.; Taylor & Francis: New York, 2006; Chapter 19.
12. Starkenstein, E. Ferment action and the influence upon it of neutral salts. Biochem. Z. **1910**, *24*, 210–218.
13. Landsteiner, K.; van der Scheer, J. Cross reactions of immune sera to azoproteins. J. Exp. Med. **1936**, *63*, 325–339.
14. Campbell, D.H.; Luescher, E.; Lerman, L.S. Immunologic adsorbents. I. Isolation of antibody by means of a cellulose-protein antigen. Proc. Natl. Acad. Sci. U.S.A. **1951**, *37*, 575–578.
15. Hjerten, S. The preparation of agarose spheres for chromatography of molecules and particles. Biochem. Biophys. Acta **1964**, *79*, 393–398.
16. Axen, R.; Porath, J.; Ernback, S. Chemical coupling of peptides and proteins to polysaccharides by means of cyanogen halides. Nature **1967**, *214*, 1302–1304.
17. Cuatrecasas, P.; Wilchek, M.; Anfinsen, C.B. Selective enzyme purification by affinity chromatography. Proc. Natl. Acad. Sci. U.S.A. **1968**, *68*, 636–643.
18. Wang, W.T.; Kumlien, J.; Ohlson, S.; Lundblad, A.; Zopf, D. Analysis of a glucose-containing tetrasaccharide by high-performance liquid affinity chromatography. Anal. Biochem. **1989**, *182*, 48–53.
19. Standh, M.; Andersson, H.S.; Ohlson, S. Weak affinity chromatography. In *Affinity Chromatography*; Bailon, P.; Ehrlich, G.K.; Fung, W.J.; Berthold, W., Eds.; Humana Press: Totowa, NJ, 2000; Chapter 2.
20. Hage, D.S.; Xuan, H.; Nelson, M.A. Application and elution in affinity chromatography. In *Handbook of Affinity Chromatography*, 2nd Ed.; Hage, D.S., Ed.; Taylor & Francis: New York, 2006; Chapter 4.

21. Gustavsson, P.E.; Larson, P.O. Support materials for affinity chromatography. In *Handbook of Affinity Chromatography*, 2nd Ed.; Hage, D.S., Ed.; Taylor & Francis: New York, 2006; Chapter 2.
22. Ohlson, S.; Hansson, L.; Larsson, P.O.; Mosbach, K. High-performance liquid affinity chromatography (HPLAC) and its applications to the separation of enzymes and antigens. FEBS Lett. **1978**, *93*, 5–9.
23. Mallik, R.; Hage, D.S. Affinity monolith chromatography. J. Sep. Sci. **2006**, *29*, 1686–1704.
24. Kim, H.S.; Hage, D.S. Immobilization methods for affinity chromatography. In *Handbook of Affinity Chromatography*, 2nd Ed.; Hage, D.S., Ed.; Taylor & Francis: New York, 2006; Chapter 3.
25. Hage, D.S. Survey of recent advances in analytical applications of immunoaffinity chromatography. J. Chromatogr. B, **1998**, *715*, 3–28.
26. Phillips, T.M. High performance immunoaffinity chromatography: An introduction. LC Mag. **1985**, *3*, 962–972.
27. Hage, D.S.; Bian, M.; Burks, R.; Karle, E.; Ohnmacht, O.; Wa, C. Bioaffinity chromatography. In *Handbook of Affinity Chromatography*, 2nd Ed.; Hage, D.S., Ed.; Taylor & Francis: New York, 2006; Chapter 5.
28. Hage, D.S.; Phillips, T.M. Immunoaffinity chromatography. In *Handbook of Affinity Chromatography*, 2nd Ed.; Hage, D.S., Ed.; Taylor & Francis: New York, 2006; Chapter 6.
29. Hage, D.S.; Nelson, M.A. Chromatographic immunoassays. Anal. Chem. **2001**, *73*, 198A–205A.
30. Bailon, P.; Nachman-Clewner, M.; Spence, C.L.; Ehrlich, G.K. Receptor-affinity chromatography. In *Handbook of Affinity Chromatography*, 2nd Ed.; Hage, D.S., Ed.; Taylor & Francis: New York, 2006; Chapter 16.
31. Moxley, R.A.; Oak, S.; Gadgil, H.; Jarrett, H.W. DNA affinity chromatography. In *Handbook of Affinity Chromatography*, 2nd Ed.; Hage, D.S., Ed.; Taylor & Francis: New York, 2006; Chapter 7.
32. Labrou, N.E.; Mazitsos, K.; Clonis, Y.D. Dye-ligand and biomimetic affinity chromatography. In *Handbook of Affinity Chromatography*, 2nd Ed.; Hage, D.S., Ed.; Taylor & Francis: New York, 2006; Chapter 9.
33. Peyrin, E. Aptamers as ligands for affinity chromatography and capillary electrophoresis. In *Aptamer Handbook*; Klussman, S., Ed.; Wiley-VCH: Weinheim, Germany, 2006; 324–342.
34. Labrou, N.E.; Clonis, Y.D. Immobilized synthetic dyes in affinity chromatography. In *Theory and Practice of Biochromatography*; Vijayalakshmi, M.A., Ed.; Taylor & Francis: London, 2002; 335–351.
35. Clonis, Y.D. Affinity chromatography matures as bioinformatic and combinatorial tools develop. J. Chromatogr. A, **2006**, *1101*, 1–24.
36. Porath, J.; Carlsson, J.; Olsson, I.; Belfrage, B. Metal chelate affinity chromatography, a new approach to protein fraction. Nature **1975**, *258*, 598–599.
37. Chage, G.S. Twenty-five years of immobilized metal ion affinity chromatography: Past, present and future. J. Biochem. Biophys. Methods **2001**, *49*, 313–334.
38. Todorova, D.; Vijayalakshmi, M.A. Immobilized metal-ion affinity chromatography. In *Handbook of Affinity Chromatography*, 2nd Ed.; Hage, D.S., Ed.; Taylor & Francis: New York, 2006; Chapter 10.
39. Liu, X.-C.; Scouten, W.H. Boronate affinity chromatography. In *Affinity Chromatography*; Bailon, P.; Ehrlich, G.K.; Fung, W.J., Berthold, W., Eds.; Humana Press: Totowa, NJ, 2000; 119–128.
40. Liu, X.-C.; Scouten, W.H. Boronate affinity chromatography. In *Handbook of Affinity Chromatography*, 2nd Ed.; Hage, D.S., Ed.; Taylor & Francis: New York, 2006; Chapter 8.
41. Chaiken, I.M., Ed. *Analytical Affinity Chromatography*; CRC Press: Boca Raton, FL, 1987.
42. Hage, D.S.; Tweed, S.A. Recent advances in chromatographic and electrophoretic methods for the study of drug–protein interactions. J. Chromatogr. B, **1997**, *699*, 499–525.
43. Hage, D.S.; Chen, J. Quantitative affinity chromatography: Practical aspects. In *Handbook of Affinity Chromatography*, 2nd Ed.; Hage, D.S., Ed.; Taylor & Francis: New York, 2006; Chapter 22.
44. Winzor, D.J. Quantitative affinity chromatography: Recent theoretical developments. In *Handbook of Affinity Chromatography*, 2nd Ed.; Hage, D.S., Ed.; Taylor & Francis: New York, 2006; Chapter 23.
45. Schriemer, D.C. Biosensor alternative: Frontal affinity chromatography. Anal. Chem. **2004**, *76*, 440A–448A.
46. Patel, S.; Wainer, I.W.; Lough, W.J. Affinity-based chiral stationary phases. In *Handbook of Affinity Chromatography*, 2nd Ed.; Hage, D.S., Ed.; Taylor & Francis: New York, 2006; Chapter 21.
47. Allenmark, S. *Chromatographic Enantioseparation: Methods and Applications*, 2nd Ed.; Ellis Horwood: New York, 1991.
48. Sellergren, B. *Molecularly Imprinted Polymers: Man-Made Mimics of Antibodies and Their Applications in Analytical Chemistry*; Elsevier: Amsterdam, 2001.
49. Haupt, K. Molecularly imprinted polymers: artificial receptors for affinity separations. In *Handbook of Affinity Chromatography*, 2nd Ed.; Hage, D.S., Ed.; Taylor & Francis: New York, 2006; Chapter 30.
50. Briscoe, C.J.; Clarke, W.; Hage, D.S. Affinity mass spectrometry. In *Handbook of Affinity Chromatography*, 2nd Ed.; Hage, D.S., Ed.; Taylor & Francis: New York, 2006; Chapter 27.
51. Heegaard, N.H.H.; Schou, C. Affinity ligands in capillary electrophoresis. In *Handbook of Affinity Chromatography*, 2nd Ed.; Hage, D.S., Ed.; Taylor & Francis: New York, 2006; Chapter 26.

Affinity Chromatography: Molecularly Imprinted Polymers

P. Manesiotis
Department of Materials Science, University of Patras, Patras, Greece

Georgios A. Theodoridis
Laboratory of Analytical Chemistry, Chemistry Department, Aristotle University of Thessaloniki, Thessaloniki, Greece

Abstract
Since the first reports in the early 1970s, molecular imprinting has evolved as a powerful technique with a variety of applications, ranging from trace analysis and sample pre-concentration to molecularly imprinted sensing devices and online extraction systems. In this entry, the authors outline the principles of molecular imprinting and the main approaches toward synthesis of such materials and discuss their most common applications, including the use of imprinted polymers for the recognition of biological macromolecules, as potential alternative media for affinity chromatography stationary phases.

INTRODUCTION

Molecular imprinting, in a primitive form, was first presented by Polyakov in 1931 when he attributed the differences he observed in the pore structure of silica to the differences in size and shape of the solvent used, namely benzene, toluene, or xylene. Several years later, in 1949, Dickey prepared silica gels in the presence of different dyes that showed selectivity for the latter over similar compounds. Wulff and coworkers were the first to report molecular imprinting in organic polymers in 1972, introducing the so-called covalent technique. Finally, Mosbach and coworkers, in 1981, reported on a "host-guest" polymerization used for the imprinting of dyes, thus introducing the non-covalent approach. Since the foundations of molecular imprinting technology were laid, it has evolved as an elegant technique for the generation of synthetic media with predetermined selectivity, the latter being a major parameter in separation science. Optimization of a chromatographic separation is often based on the enhancement of the selectivity of the separation system for a given analyte. This optimization procedure can aim at: 1) mobile-phase composition; 2) stationary phase choice; and 3) simultaneous optimization of both mobile and stationary phases. The first approach was for years (and still remains, but to a lesser extent) the subject of extensive research and development. Recent years, however, have seen tremendous increase in the drive toward the optimization of the selectivity of the chromatographic stationary phase. Affinity chromatography utilizing immobilized antibodies, receptors, or other proteinaceous recognition elements is an important development in contemporary separation science.

Molecular imprinting is now established as a powerful technique for producing artificial receptors. The drive toward selective stationary phases is indicated by the more than 4500 published papers and 500 filed patents related to molecular imprinting, since the mid-1990s. The imprinting process is based on the production of a polymeric network in the presence of a template molecule. The latter is subsequently removed from the polymer, thus leaving an active site, a "cavity" exhibiting molecular recognition toward the template molecule. Such cavities are complementary to the template molecule in terms of stereochemistry, shape, and chemical interactions. When at a later stage, a sample containing the template is administered to the polymer, selective binding of the template molecule will occur (Fig. 1). Such polymers are called molecularly imprinted polymers (MIPs) and have been used in separations, binding assays, sensors, and catalysis.

MOLECULAR IMPRINTING—PRINCIPLES

The principal idea behind MIP synthesis is the generation of solution state complexes between the template ligand in hand and appropriate functional monomers, followed by subsequent "freezing" of these complexes by copolymerization of the above with an excess of a cross-linking monomer. These monomer–template complexes are stabilized by non-covalent interactions, reversible covalent interactions, or metal ion-mediated interactions. The types of interactions that are usually exploited in molecular imprinting are: 1) cleavable covalent bonds; 2) π–π interactions; 3) hydrogen bonds; 4) hydrophobic van der Waals interactions; 5) crown-ether/cyclodextrin type interactions; 6) metal–ligand

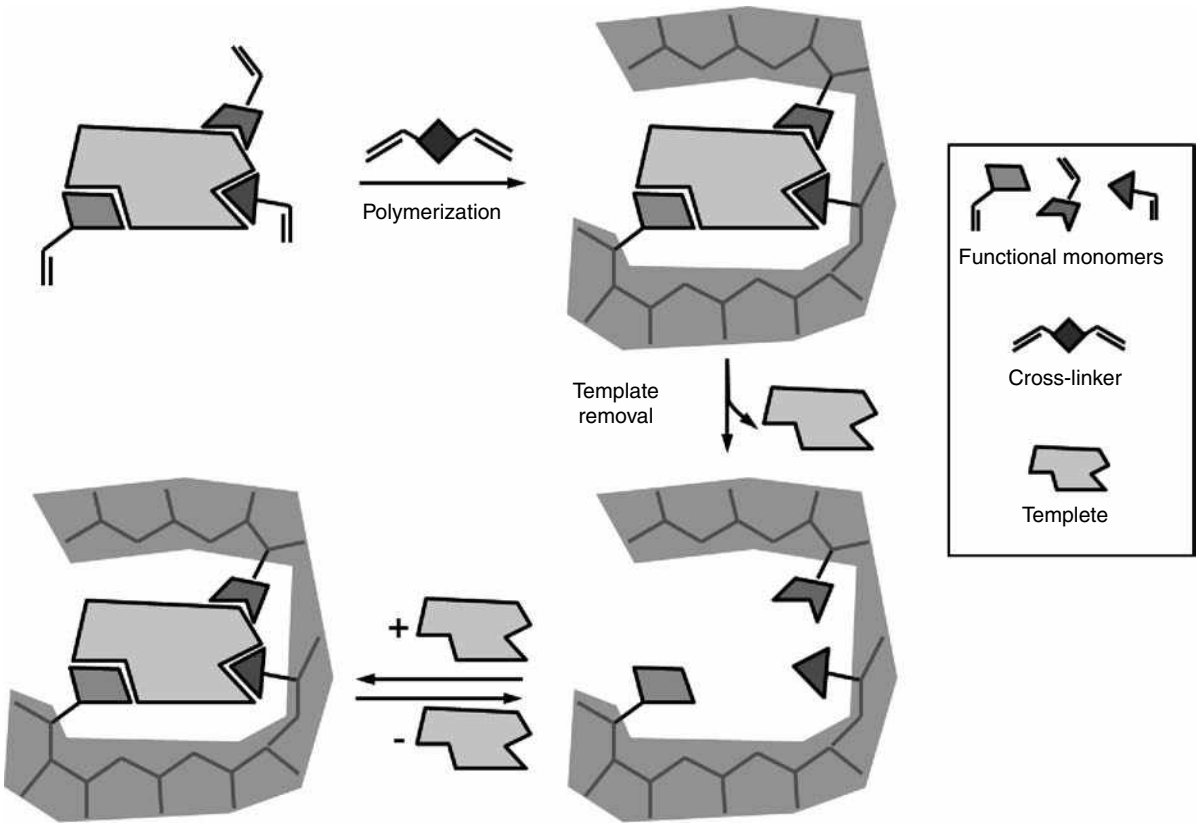

Fig. 1 Schematic representation of the imprinting process.

bonds; and 7) ionic forces. The imprinting effect is maximized when the template interacts with more than one binding site and when the interactions involved have directional or spatial determination.

NON-COVALENT APPROACH

The non-covalent or "self-assembly" approach was pioneered by K. Mosbach and coworkers and is now the most widely applied mode in molecular imprinting. The template is mixed with monomers and cross-linkers in an appropriate solvent. In this prepolymerization mixture, complexes of the template with the monomers are formed as a result of polar interactions such as hydrogen bonds, ionic interactions, van der Waals forces, etc. The strength of these interactions and the resulting complexes is of vital importance for the templating effect in the final polymer. Hence, "selective" interactions, such as the spatially determined hydrogen bonds, are preferred in contrast to more generic forces (hydrophobic interactions, van der Waals forces). Aprotic solvents allow polar interactions (hydrogen bonds) and are usually chosen, provided that they can dissolve the template molecule and the monomers. On the contrary, polar protic solvents suppress the formation of hydrogen bonds, whereas they promote hydrophobic and ionic interactions between the template and the monomers. Typical polymerization solvents are chloroform, acetonitrile, and tetrahydrofuran. Protic solvents like methanol have found limited use in specific cases. The role of the solvent is not only to provide the environment for the polymerization reaction, but also to produce a porous structure in the resulting polymer. Meso-/macroporous structure is necessary to ensure reasonable operating flow and pressure in liquid chromatographic applications and, most of all, good accessibility to the imprinted binding sites. Hence, the choice of the polymerization solvent determines the rigidity and the pore size of the MIP.

Monomers used for non-covalent molecular imprinting include methacrylic acid (MAA), 2- and 4-vinylpyridine (2- and 4-VP), trifluoromethacrylic acid (TFMAA), acrylamide and 2-hydroxyethyl methacrylate (HEMA). Ethyleneglycol dimethacrylate (EGDMA) is the most common cross-linker whereas divinylbenzene (DVB) and trimethylolpropane trimethacrylate (TRIM) have been used to a lesser extent. The cross-linker is added in excess concentrations (up to 80–90% of the molar ratio in the polymerization mixture), in order to obtain a rigid, highly dense polymeric network. This enables the imprinted sites to retain their shape and size and tolerate different environments, "resisting" shrinkage and swelling. Most researchers base their work on the above-mentioned monomers or combinations of them (cocktail of

monomers). In this approach, the formation of the template–monomer complex is expected to occur via selected functionalities of the corresponding molecules. Lately, the development of novel monomers specific for a given template has opened new ways in molecular imprinting. To achieve this, existing monomers are modified or totally new entities are prepared, aiming at a multipoint association with the template molecule. It is expected that such complexes will be stronger and more specific for the template molecule, thus the resulting MIP will exhibit higher affinity/avidity toward the template.

COVALENT AND SEMICOVALENT APPROACH

Covalent imprinting was first described in 1972 by G. Wulff and coworkers as a method of manufacturing enzyme analogue built polymers. This work is considered by many researchers as a major breakthrough, the actual initiation of molecular imprinting. In covalent imprinting, the template molecule is modified in order to incorporate a polymerizable functional group in it. Typically the template is bound to an appropriate monomer by labile covalent bonds. The monomers frequently used are 4-vinylphenylboronic acid and 4-vinylbenzylamine. During polymerization, the template is fixed in spatial arrangement within the polymer network. To recover the polymer, the labile bonds are cleaved, releasing the active binding sites.

The advantage of this technique is the predetermined stoichiometry between the template and the functional monomer. As a result covalent imprinting results in a high density of well-defined sites. Disadvantages of this approach is the synthetic effort that is required to come up with specific bonds that will tolerate the polymerization conditions and additionally can be easily cleaved in order to recover the template and free the active sites. Rebinding occurs by the formation of either covalent bonds or by formation of other types of interactions, as in the non-covalent approach. In the first case, an additional drawback is the slow kinetics of bond formation. The latter method of covalent imprinting with non-covalent rebinding, so-called semicovalent imprinting, is an ingenious hybrid technique that combines attractive features of the two modes. The template molecule is bound to the functional monomer via a sacrificing spacer (e.g., a carbonate ester). Following polymerization, the ester is cleaved with the loss of CO_2, leaving the functional monomer in appropriate position for interaction with the template.

SYNTHESIS OF MOLECULARLY IMPRINTED POLYMERS

After the template–monomer complexes have been formed in the prepolymerization solution, an azo initiator (e.g., azo-*N,N′*-bis-isobutyronitrile, AIBN) is added in the polymerization mixture. Free radical polymerization is initiated by heating at 40–60°C or photochemical homolysis by UV radiation (0–15°C). MIPs prepared at lower temperatures (0°C) by photopolymerization have been found to exhibit better molecular recognition due to the destabilizing effect of elevated temperatures to the monomer–template complexes.

Polymerization is allowed to take place for 10–24 hr. Next, the polymer is further processed in order to extract the template molecule and remove unreacted components from the polymer matrix. This step is of great importance for the successful future use of the MIP. Typical extraction solvents are mixtures of protic solvents with acids (e.g., methanol with 10% acetic acid). Such mixtures suppress polymer–template interactions and extract the template from the polymer core almost quantitatively. Soxhlet extraction, extensive washing, or alternative acid–base washing are the main experimental protocols used. Quantitative removal of the template is essential for two reasons: 1) the more template is removed, the higher the number of active sites revealed in the MIP and 2) it has been repeatedly reported that leakage or so-called bleeding of the remaining template from the MIP may occur. In such a case, even a minimal amount of template added as an artifact in a sample may interfere with the results of the analysis to a great extent. An elegant solution to this problem is the utilization of an analyte analogue, a "dummy template," during polymerization. By this approach even if leakage of the "dummy template" occurs, this will not interfere with the analysis, provided a separation step capable of separating the two analogue molecules is used.

Bulk polymerization is the dominant synthetic method in molecular imprinting. Polymerization occurs in sealed tubes resulting to a rigid highly cross-linked polymeric monolith exhibiting macroporous and mesoporous structure. Following template removal, the polymer is processed by grinding and sieving in order to reduce the size of the polymer particles. Grinding is performed manually by mortar and pestle or in a mechanical mill and results in irregularly shaped particles and a large quantity of fine particles ($<$20 μm). Extreme care should be taken during the removal of fine particles as they may severely hinder further analytical work by blocking the frits or tubing and thus building high pressure. Fines, however, may be used ideally for binding assays. Typically, MIP particles of 25–36 μm are used as a chromatographic material in high-performance liquid chromatography (HPLC) columns; 50–100 μm particles are used for solid-phase extraction media. Depending on the care taken during grinding and sieving about 50–60% of the produced MIPs are recovered for use as chromatographic material.

Alternative polymerization methods such as suspension polymerization, dispersion polymerization, and precipitation polymerization have been shown to produce spherical particles of a determined size; however, their use is limited.

Finally, the production of monolithic polymeric imprinted materials is a straightforward method of producing MIP rods inside a stainless-steel or a PEEK column and has drawn significant interest in the past few years.

MIPs AS CHROMATOGRAPHIC MEDIA

The use of MIPs as chromatographic stationary phases is their most studied application. This method is in fact the best way to rapidly and efficiently validate the performance of a developed MIP. To achieve this, the MIP is packed in an HPLC column and retention characteristics of the template and/or analogue molecules are collected in various selected mobile phases. From the collected data, useful parameters such as capacity factor, imprinting factor, and peak asymmetry are calculated and used to evaluate polymer affinity, cross-selectivity, and other features of the MIP.

Another attractive usage of MIPs is as chiral stationary phases (CSPs). Molecular imprinting offers a very efficient way of producing receptors against an enantiomer within a stationary phase. A major advantage of the use of MIPs is the predetermined selectivity. Hence, by preparing an MIP against an optically pure *R*-template, chiral separations of remarkable selectivity are easily achieved. The *R*-enantiomer will preferentially bind to the MIP and thus elute late, whereas the *S*-enantiomer will elute much earlier. Pharmaceuticals were the majority of the template molecules studied, given that the pharmaceutical industry's needs in chiral separations are still massive. MIP-based chiral separations of various types of drugs, peptides, protected amino acids, alkaloids, and other chiral compounds exhibited enantio-selectivities higher than conventional CSPs. "Enantio-polishing" is a useful application in that direction. In this approach, a synthetic product is assayed in an MIP-based CSP manufactured against an enantiomer. Optical impurities elute fast, leading to a purification of the desired enantiomer.

Despite these attractive features, MIP-based CSPs exhibit limitations, the dominant being the heterogeneity of the active binding sites. During the polymerization process active sites of high and lower affinity are both produced. High-affinity sites are produced where the best-defined interactions occur; sites of one-point interaction or other sites in the polymer network that exhibit non-selective interaction are responsible for lower affinity. This heterogeneity may result in peak asymmetry and tailing, and greatly decrease separation efficiency. As a result, multibinding site adsorption isotherms are typically observed for the template molecule. Another limitation of MIPs is capacity, which is in general lower than for other CSPs. Finally, the achievement of molecular recognition in an aqueous environment remains a challenge for MIP technologies. This challenge however, is to be exploited not only in chiral separations but also in sensing, catalysis, and any other application area. The use of tailored "designer" monomers specifically binding to the template in hand has shown significant promise to overcome these limitations.

Apart from HPLC, MIPs have also been used as media for capillary electrochromatography (CEC) and thin-layer chromatography (TLC). CEC is a hybrid separation technique that utilizes a stationary phase as in liquid chromatography and an electro-osmotic flow (EOF) as in capillary electrophoresis (CE). MIPs have been successfully employed as stationary phases of predetermined selectivity for CEC. In fact, high efficiency of CEC may potentially overcome the efficiency problems encountered with MIP chromatographic media. Mass transfer and kinetic limitations in MIP-based liquid chromatography could be addressed by the enhanced flow dynamics of CEC. A problem to be overcome is the introduction and immobilization of the polymer particles in packed capillaries. Usual techniques are the employment of a plug of polyacrylamide as a retaining frit or fusion of the silica capillary at both ends of the polymer bed to create a porous silica frit. Alternatively, in situ polymerization is used to produce monolithic MIP rods inside the column or coating of the inner walls of the capillary with thin-imprinted polymeric films. Additional obstacles include the known problems of capillary techniques: the need for increased sensitivity and column/polymer's capacity.

To conclude, MIP technology has to overcome important issues such as the need for a significant amount of template molecule, the production of particles of reproducible size and shape, and the tedious grinding–sieving process in order to provide a viable and pragmatic alternative for the large-scale production of materials to be widely used as stationary phases in either electrochromatography or conventional liquid chromatography. Alternative polymerization protocols, such as precipitation polymerization, which overcome the need for mechanical processing of the material postsynthesis, have recently been successfully employed in molecular imprinting protocols.

MIPs IN EXTRACTION AND SAMPLE PRETREATMENT

The use of MIPs as media for selective solid-phase extraction (SPE) is the application area closest to viable completion and product commercialization. This combination is abbreviated either as MI–SPE or as MIP–SPE and is the most successful application of MIPs so far. SPE is now an established technique for sample preparation due to its advantages as compared to other extraction methods: ease and simplicity, automation capability, reduced consumption of organic solvents, and choice between several stationary phases (C8, C18, CN, NH_2, Ph, ion exchange, mixed mode, etc.). These generic phases are the first choice for the development of a number of SPE protocols since

they offer high capacity, interaction with a wide range of analytes, and good reproducibility. The mechanism involved in extraction is the same that governs chromatographic analysis; thus it is rather easily conceived, controlled, and optimized. This conventional mechanism may also be considered as a drawback; therefore in many cases the need for alternative separation mechanisms of higher selectivity is evident.

Extraction mechanisms that take advantage of molecular recognition interactions (immuno-extraction and MI–SPE) are increasingly being developed to cover this need. Advantages of MIPs vs. immunoaffinity sorbents are the low cost and ease of preparation, the elimination of the biological receptor (and thus the long and tedious immunization experiments), the robustness and long life of the MIP, and the compatibility with elevated temperatures, organic solvents, and environments of increased ionic strength.

MI–SPE has been applied in either online or off-line mode for several analytes. In the first case, the MIP is packed as an HPLC precolumn. Column switching and pulsed elution modes are employed in online MI–SPE. An advantage of this design is the automation capability and the direct coupling to HPLC or other separation modes. Despite these advantages, the off-line mode is the most common practice and has been applied successfully to bio and environmental and food analysis.

There are some critical issues to be taken into consideration for the successful application of MI–SPE. Sample loading may occur in conditions of molecular recognition. In this case the entrapment of the analytes is selective and the following elution will provide an enriched sample to be further analyzed. Usually this selective adsorption/entrapment occurs in the polymerization solvent. It is theorized that by mimicking the conditions of polymerization, the assembly of the template–monomers complex will recur between the MIP and the template. Therefore it is expected and has also been found experimentally that molecular recognition and selective retention of the template is enhanced in the polymerization solvent.

A second strategy is the entrapment of the analytes by non-selective sorption on the MIP. Usually this is achieved by loading in aqueous environment and trapping by hydrophobic interactions. Next, a selective washing step removes unwanted matrix compounds from the SPE cartridge, whereas it facilitates selective binding of the analyte on the MIP. Finally, a selective desorption/elution solvent step obstructs hydrogen bonds or other such specific interactions and recovers the analyte. This mode employs additional extraction steps, but offers the advantage of straightforward application of aqueous samples (biofluids or environmental samples). The two modes of analyte trapping mentioned above could be easily understood by chromatographers as binding in the two chromatographic modes: normal phase for selective binding and reversed phase for non-selective binding–selective desorption. Fig. 2 depicts the operation principles of off-line MIP–SPE.

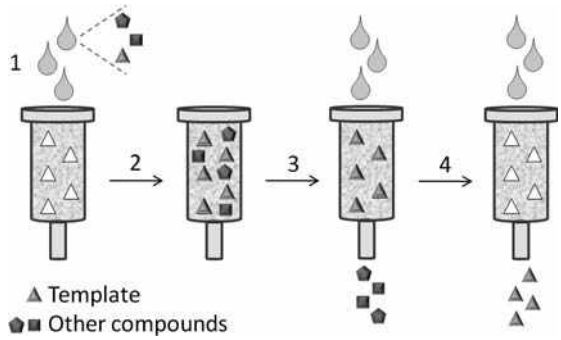

Fig. 2 Off-line application of MIP–SPE: 1, sample loading; 2, dry column; 3, wash out unwanted components; 4, elute selectively bound compounds.

MIPs IN SENSORS AND BINDING ASSAYS

MIPs are ideal media to be used in sensing devices. Typically, sensors include a substrate-selective element (a receptor or an enzyme) immobilized on an appropriate surface (a membrane or an electrode). Binding of a ligand causes a signal, which is translated by an appropriate transducer to a quantitative response. MIPs provide inherent molecular recognition properties with no need for tedious chemical modifications. Therefore it is not surprising that various sensors have been developed utilizing MIPs as the recognition element; quartz crystal microbalance, acoustic, piezoelectric odor, luminescent, fiber optics, electrochemical, conductometric, and surface plasmon resonance sensors have been used in the analysis of a diversifying range of analytes: polyaromatic hydrocarbons, propranolol, nitrate, pesticides, nerve agents, caffeine, nucleotides, fluorescent-labeled amino acids, chloramphenicol, cholesterol, and many others. The methods have been applied to the analysis of different samples and matrices (biological, environmental, and so forth). Molecular imprinting may prove a smooth way toward the effective and straightforward production of sensors. Virtually any low molecular mass compound can be imprinted. Lately, larger entities such as proteins, bacteria, and living cells were targeted by MIP-based sensors, increasing dramatically the applicability and prospects of MIP technologies.

MIPs have also been used alternatively to biological receptors in competitive binding assays. The assay principle is the same as in known biological assays such as radioimmunoassay (RIA) or enzyme-linked immunosorbent assay (ELISA), but instead of antibodies MIPs are utilized. The method is often called molecularly imprinted assay (MIA). Typically, in MIA methods a marker

molecule (a labeled analyte analogue) is incubated together with the sample and the MIPs. Analyte and marker molecules compete for the binding sites of the polymer. Provided that the number of polymer's binding sites is limited and within an optimum range of the assay, the amount of marker bound on the polymer will depend on the amount of analyte in the sample. Hence, in samples rich in analyte molecules the marker will not bind in the polymer. In contrast, in samples with no or minimal quantities of analyte, the lot of the marker molecule will bind on the MIP. MIA protocols have been developed so far mostly in heterogeneous format, meaning that a separation step follows in order to separate the MIP particles from the sample. Marker molecules are often radiolabeled, but lately fluorescence tagging tends to substitute radioassays.

The advantages of using MIPs instead of antibodies in binding assays are the same attractive features that drive the utilization of MIPs as affinity chromatographic media: ease of preparation, lower cost, tolerance to extreme chemical and thermal conditions, no need for animal immunization, and long shelf life. For example, MIA protocols employ organic solvents offering an attractive alternative to conventional immunoassays. Additionally, MIPs have been found to provide affinity/avidity and cross-reactivity comparable to antibodies.

IMPRINTING LARGER BIOMOLECULES

Although imprinting of low-molecular-weight compounds has evolved to a significant extent with great achievements as discussed so far, imprinting of larger molecules, such as biological macromolecules, has remained underdeveloped. This is mainly due to the accessibility limitation of conventional MIP formulations. Recent years have seen a significant drive to overcome this limitation by means of novel ingenious approaches, most important of which are surface and epitope imprinting. In the first case, the macromolecule of interest, usually a protein, is attached reversibly to a surface that will not compromise its integrity and conformation, and an MIP is synthesized above the protein layer. Removal of the binding surface and the template results in an imprinted surface with cavities complementary to the protein of interest (Fig. 3). However, this approach is characterized by low selectivity and high cross-reactivity, due to the variety of different interactions between the protein and the functional monomer, and low capacity.

Hence, building on this approach, part of the protein of interest, an epitope, has been surface imprinted, instead of the whole, and the resulting binding sites were successfully used to capture the whole protein by recognition of the imprinted part (Fig. 4). In both cases, silica beads, membrane pores, or nanowire surfaces have been used as sacrificial supports and were easily removed by dissolution after polymerization occurred.

CONCLUDING REMARKS

Molecular imprinting technologies have found a niche in separation science. MIPs offer a good alternative to proteinaceous receptors and have been successfully used in affinity-based separations. Furthermore, the polymeric nature of the MIPs bears attractive features for applications that could not be achieved by antibodies or enzymes: gas chromatography, solid phase microextraction, and so forth. The amount of fundamental research and application labor that has been invested in MIP technologies combined with the emergence of a number of spin-off companies developing commercial products has led to the recent appearance of MIPs in chemical catalogs available for purchase.

The number of research groups working in the field is expanding; thus significant advances are made and new targets are aimed at. Imprinting in aqueous environment, imprinting of large biomolecules, imprinting in different formats, and implementation of existing recognition elements (e.g., cyclodextrins) are some of the areas where

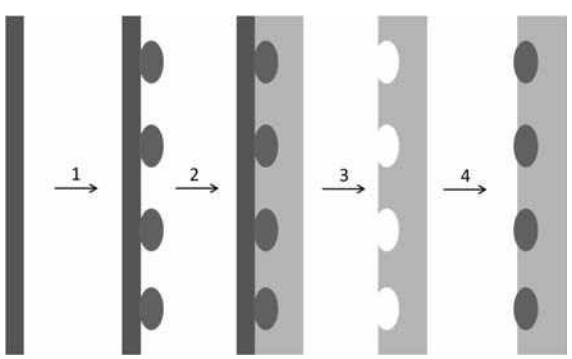

Fig. 3 Schematic representation of surface imprinting of a protein: 1, protein immobilization on the surface; 2, surface polymerization; 3, removal of initial surface and template; 4, protein rebinding.

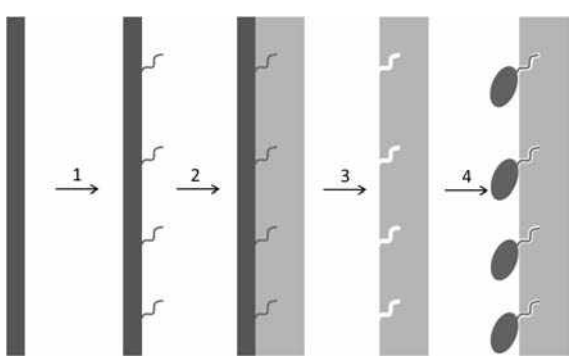

Fig. 4 Schematic representation of epitope imprinting: 1, epitope attachment on the surface; 2, surface imprinting of the epitope; 3, removal of the initial surface and template; 4, binding of the epitope-containing protein.

striking developments are expected. Parallel to these developments, antibody/receptor technologies spread out and become more robust. Techniques like solid phase peptide synthesis, recombinant protein technologies, and antibody engineering expand continuously. Taking into account the rapid growth in biotechnology and immunology, a central role of molecular recognition technologies is seen in many scientific disciplines: analytical chemistry, medicinal chemistry, drug and gene delivery, synthetic catalysis, and proteome research. In that direction MIPs could serve as a powerful tool complementary and/or alternative to biological receptors.

BIBLIOGRAPHY

1. Sellergren B. *Molecularly Imprinted Polymers*; Elsevier: Amsterdam, 2000.
2. Bartsch, R.A.; Maeda M. Molecular and Ionic Recognition with Imprinted Polymers. ACS Symposium Series, No. 703, American Chemical Society, 1998.
3. Yan, M.; Ramström, O., Eds.; *Molecularly Imprinted Polymers: Science and Technology*; New York: Marcer Dekker/CRC Press, 2005.
4. Owens, P.K.; Karlsson, L.; Lutz, E.S.M.; Andersson, L.I. Molecular imprinting for bio- and pharmaceutical analysis. TRAC Trends Anal. Chem. **1999**, *18* (3), 146–154.
5. Dickert, F.L.; Hayden, O. Molecular imprinting in chemical sensing. TRAC Trends Anal. Chem. **1999**, *18* (3), 192–199.
6. Haupt, K.; Mosbach, K. Plastic antibodies: Developments and applications. Trends Biotechnol. **1998**, *16* (11), 468–475.
7. Wulff, G. Molecular imprinting in crosslinked polymers—The role of the binding sites. Mol. Cryst. Liq. Cryst. Sci. Technol. Section A. Mol. Cryst. Liq. Cryst. **1996**, *276*, 1–6.
8. Wulff, G. Molecular imprinting in crosslinked materials with the aid of molecular templates—a way towards artificial antibodies. Angew. Chemie. **1995**, *34*, 1812–1832.
9. Ansell, R.J.; Ramstrom, O.; Mosbach, K. Towards artificial antibodies prepared by molecular imprinting. Clin. Chem. **1996**, *42* (9), 1506–1512.
10. Andersson, L.I. Molecular imprinting for drug bioanalysis—A review on the application of imprinted polymers to solid-phase extraction and binding assay. J. Chromatogr. B, **2000**, *739* (1), 163–173.
11. Asanuma, H.; Hishiya, T.; Komiyama, M. Tailor-made receptors by molecular imprinting. Adv. Mater. **2000**, *12* (14), 1019–1030.
12. Andersson, L.I. Molecular imprinting: Developments and applications in the analytical chemistry field. J. Chromatogr. B, **2000**, *745* (1), 3–13.
13. Sellergren, B.; Andersson, L.I. Application of imprinted synthetic polymers in binding assay development. Methods: A Companion to Methods Enzymol. **2000**, *22* (1), 92–106.
14. Lanza, F.; Sellergren, B. The application of molecular imprinting technology to solid phase extraction. Chromatographia **2001**, *53* (11/12), 599–611.
15. Stevenson, D. Molecular imprinted polymers for solid-phase extraction. TRAC Trends Anal. Chem. **1999**, *18* (3), 154–158.
16. Valano, P.T.; Remcho, V.T. Highly selective separations by capillary electrochromatography: Molecular imprint polymer sorbents. J. Chromatogr. A, **2000**, *887*, 125–135.
17. Whitcombe, M.J.; Rodriguez, M.E.; Villar, P.; Vulfson, E.N. A new method for the introduction of recognition site functionality into polymers prepared by molecular imprinting: Synthesis and characterization of polymeric receptors for cholesterol. J. Am. Chem. Soc. **1995**, *117* (27), 7105–7111.
18. Ge, Y.; Turner, A.P.F. Too large to fit? Recent developments in macromolecular imprinting. Trends Biotechnol. **2008**, *26* (4), 218–224.
19. Wang, J.F.; Cormack, P.A.G.; Sherrington, D.C.; Khoshdel, E. Monodisperse, molecularly imprinted polymer microspheres prepared *via* precipitation polymerisation for affinity separation applications. Angew. Chem. Int. Ed. **2003**, *42* (43), 5336–5338.
20. Theodoridis, G.; Manesiotis, P. A selective solid phase extraction sorbent for caffeine made by molecular imprinting. J. Chromatogr. A, **2002**, *948*, 163–169.
21. Manesiotis, P.; Hall, A.J.; Emgenbroich, M.; Quaglia, M.; de Lorenzi, E.; Sellergren, B. An enantioselective imprinted receptor for Z-glutamate exhibiting a binding induced color change. Chem. Commun. **2004**, 2278–2279.
22. Hall, A.J.; Manesiotis, P.; Emgenbroich, M.; Quaglia, M.; de Lorenzi, E.; Sellergren, B. Urea host monomers for stoichiometric molecular imprinting of oxyanions. J. Org. Chem. **2005**, *70*, 1732–1736.
23. Manesiotis, P.; Hall, A.J.; Courtois, J.; Irgum, K.; Sellergren, B. An artificial riboflavin receptor prepared by a template analogue imprinting strategy. Angew. Chem. Int. Ed. **2005**, *44*, 3902–3906.
24. Vlatakis, G; Andersson, L.I.; Mueller, R.; Mosbach, K. Drug assay using antibody mimics made by molecular imprinting. Nature **1993**, *361* (6413), 645–647.

Affinity Chromatography: Spacer Groups

Terry M. Phillips
Ultramicro Analytical Immunochemistry Resource (UAIR), DBEPS, ORS, OD, National Institutes of Health, Bethesda, Maryland, U.S.A.

INTRODUCTION

A major problem arising in both affinity and immunoaffinity chromatography is the inefficiency of analyte recovery as a result of steric hindrance between the ligand (capture molecule) support and the analyte (molecule to be isolated), resulting in reduced or no recovery. This situation commonly occurs when low molecular weight ligands, such as pharmaceutical drugs, enzyme substrates, or receptor-binding ligands, are employed as the immobilized capture molecules. An accepted approach to rectify this situation is the employment of an accessory molecule or spacer arm to extend the capture molecule or ligand from the support surface.

USE OF SPACER ARMS

As a result of the popularity of affinity and immunoaffinity separation procedures, supports incorporating suitable spacer arms are commercially available (Table 1). The addition of even a short (4–6 carbon atoms) spacer arm will often ensure adequate clearance of the ligand from the support surface. This gives the analyte (molecule to be isolated) adequate access to the immobilized ligand.

A spacer molecule should be employed in cases where ligand attachment lies in close proximity to the analyte-binding site and interferes with analyte–ligand binding. In such cases, the length of the spacer arm is crucial and must be determined empirically, with six to eight carbon atoms often being the most successful. The spacer should be hydrophilic and not bind proteins nonspecifically, either because of its hydrophobicity or its charge. Some activation chemistries will automatically insert a suitable spacer between the support and the ligand, e.g., bis-oxirane, although the simplest technique for introducing a spacer arm is to directly derivatize a long carbon chain onto the surface itself. Many supports can be modified to accept a suitable carbon-based spacer arm and a convenient approach is to condense the spacer onto the support surface using carbodiimides. During the coupling stage, the carbodiimide reacts with carboxyl groups to form *O*-cylisourea at pH 4–5. The activated carboxyl group then condenses with an amino group on the support surface to form a peptide-bond-generating urea, a by-product that has to be removed from the reaction mixture. Two water-soluble carbodiimides are commercially available: 1-ethyl-3-(3-ethylamino-propyl) carbodiimide (EDC) or 1-cyclohexyl-3-(2-morpholinoethyl) carbodiimide metho-*p*-toluene sulfonate (CMC). Both of these agents have been successfully used to couple spacer arms to any support that has free amino groups.

Spacer arms can be attached directly to the support surface by linking them to reactive side chains present on the support itself, the ligand being attached to a reactive group positioned at the end of the spacer farthest away from the support surface. Pimplikar and Reithmeier[1] described a technique for the affinity isolation of a specific protein from solubilized erythrocyte ghosts using hydrophilic spacer arms of four or greater atoms in length. The support was prepared by reacting 4-acetamido-4′-*iso*-thiocyanostilbene-2,2′-disulfonate with Affi-Gel 102. The incorporation of the spacer arm was found to be essential for protein binding, removing steric hindrance of the support and allowing the protein to bind via its stilbene disulfonate-binding site. In a similar manner, Ivanov et al.[2] covalently immobilized the small blood group B antigenic molecule, trisaccharide-beta-aminopropyl glycoside, to poly-*N*-(2-hydroxyethyl) acrylamide-modified porous glass. This affinity support was then used to isolate anti-blood group B monoclonal antibodies. The incorporation of a short (4–6 atom) spacer arm was found to be essential in order to project the affinity ligand away from the support surface.

Table 1 Commercially available support spacer arm molecules.

Hexamethylenediamine
Aminocaproic acid
N-hydroxysuccinimide
Arylsulfonate
Bis-oxiran
3,3′-Diaminodipropylamine
Hydroxyalkyl
Long-chain hydrazine biotin

REFERENCES

1. Pimplikar, S.W.; Reithmeier, R.A. Affinity chromatography of band 3, the anion transport protien of erythrocyte membranes. J. Biol. Chem. **1986**, *261*, 9770–9778.
2. Ivanov, A.E.; Bovin, N.V.; Korchagina, E.Yu.; Zubov, V.P. Favourable biospecific reactivity of blood group B antigenic trisaccharide chemically to poly-N-(2-hydroxyethyl)acrylamide-coated porous glass. Biomed. Chromatogr. **1992**, *6*, 39–42.

BIBLIOGRAPHY

1. Matejtschuk, P. *Affinity Separations*; IRL Press at Oxford University Press: Oxford, U.K., 1997.
2. Mohr, P.; Pommerening, K. *Affinity Chromatography: Practical and Theoretic Aspects*; Marcel Dekker, Inc.: New York, 1985.
3. Phillips, T.M. *Analytical Techniques in Immunochemistry*; Marcel Dekker, Inc.: New York, 1992; 40–74; Chapter 3.

Affinity Chromatography: Weak

David S. Hage
Department of Chemistry, University of Nebraska-Lincoln, Lincoln, Nebraska, U.S.A.

Abstract
The general principles of weak affinity chromatography (WAC) are discussed in this entry. WAC is a subset of affinity chromatography that makes use of weak interactions for the separation or analysis of chemicals. These conditions create a situation in which isocratic elution can be used to pass an analyte through the column. The theory of WAC is discussed and examples are given of ligands that can be used in this technique. Examples of applications that have made use of WAC are also presented.

INTRODUCTION

Weak affinity chromatography (WAC) is a subset of affinity chromatography that makes use of weak interactions for the separation or analysis of chemicals.[1–4] This method is also referred to as *dynamic affinity chromatography*. Like traditional affinity chromatography, this is a liquid chromatographic technique that uses a selective binding agent as the stationary phase. This agent, which is known as the affinity ligand, might be a biological substance like a serum protein, a lectin, a low affinity antibody, or a carbohydrate.[1–10] The affinity ligand might also be a substance that mimics a biological system or uses specific interactions for retention, such as is found for certain dyes, biomimetic ligands, and boronates.[11–16]

Traditional affinity chromatography generally makes use of the on-off mode of elution. In this mode, a ligand with strong binding for the solute of interest is placed within the column.[4] A sample containing this solute is then injected onto this column in the presence of a mobile phase, known as the application buffer, which has a pH, ionic strength, and solvent composition that provide for strong and essentially irreversible solute–ligand binding. After non-retained sample components in this buffer have been washed from the column, a second solvent is applied for elution of the retained compounds. This second solvent is known as the elution buffer and acts to dissociate the retained substances from the affinity ligand by either disrupting their interactions with this stationary phase or displacing them with another chemical that binds to the ligand or analyte. This is usually performed with a step gradient, but other types of gradient elution schemes can also be used.

A different elution approach is used in WAC. In this case, a ligand is used within the column that has only weak-to-moderate binding to the target solutes. This approach involves the use of a system that has an association equilibrium constant of 10^5–10^6 M^{-1} or lower, as well as relatively fast association and disassociation kinetics. Under these conditions, a solute can take part in many binding and dissociation events with the ligand as it passes through the column. This also makes it possible for a solute to elute in the presence of the original application buffer, eliminating the need for a separate elution buffer. This process is usually conducted under isocratic conditions rather than with gradient elution.[1–4]

THEORY OF WAC

For a simple 1:1 interaction between an injected analyte (A) and an immobilized affinity ligand (L), the following equations can be used to describe the binding that occurs between A and L within an affinity column:

$$A + L \overset{K_a}{\rightleftharpoons} A - L \tag{1}$$

$$K_a = \frac{k_a}{k_d} = \frac{\{A - L\}}{[A]\{L\}} \tag{2}$$

In this equation, K_a is the association equilibrium constant for the binding of A with L, k_a is the association rate constant for this reaction, and k_d is the corresponding dissociation rate constant. The terms [A], {L}, and {A–L} represent the concentration of the analyte in a solution at equilibrium and the surface concentrations of the ligand and analyte–ligand complex under these same conditions.[4]

The reaction between the analyte and the ligand in this system can also be related to the retention of A on an affinity column that is operated under linear elution conditions (i.e., when a small amount of analyte is injected).

$$k = \frac{(t_R - t_M)}{t_M} \quad (3)$$

In this relationship, t_R is the average retention time measured for the analyte in the mobile phase and t_M is the void time of the system (i.e., the observed elution time for a totally non-retained solute).

The retention factor for an analyte can also be related to its association equilibrium constant with the immobilized ligand in the affinity column. This is shown in Eq. 4,

$$k = \frac{K_a\, m_L}{V_M} \quad (4)$$

where m_L is the moles of active ligand in column, V_M is the column void volume, and the combined term m_L/V_M is the phase ratio (i.e., the relative amount of stationary phase vs. mobile phase in the column). According to Eq. 4, the retention factor for an analyte on an affinity column will depend on two factors. The first of these is the strength of analyte–ligand binding in the mobile phase, as represented by the association equilibrium constant. The second is the relative concentration of active ligand within the column, as represented by the binding capacity or phase ratio (m_L/V_M). An increase in either or these two factors will cause a proportional increase in a solute's retention factor, as well as in its retention time and retention volume.[4,17]

Many biological ligands have moderate-to-large equilibrium constants for their target solutes under physiological conditions. This gives these ligands strong retention and long elution times when they are used in affinity columns under normal sample application conditions. For instance, a typical polyclonal antibody with an association equilibrium constant of 10^8–$10^{10}\ M^{-1}$ for a target compound will give a retention factor of 100–10,000 when this antibody is present at a concentration of $10^{-6}\ M$ in an affinity column. This level of retention is much higher than the optimum range of $k = 1$–20 that should ideally be present for work under isocratic conditions. This is the reason why step changes in the mobile phase or gradients are usually required for elution with such columns. However, with a weaker ligand it is possible to use isocratic elution. As an example, a ligand with an association constant of $10^6\ M^{-1}$ for an analyte will give a retention factor of $k = 1$ when this ligand is present at an effective concentration of $10^{-6}\ M$ in an affinity column, or $k = 10$ when the ligand is present at a concentration of $10^{-5}\ M$.[4]

APPLICATIONS OF WAC

All binding agents used in affinity chromatography can be placed into one of two categories. These are high-specificity ligands and general, or group-specific, ligands. High-specificity ligands bind to only one or a few closely related molecules. These tend to be biological compounds (e.g., antibodies) with large association equilibrium constants and high retention for their solutes. As a result, they are usually not used in WAC because they require step or gradient elution to dissociate their adsorbed solutes. It is possible for certain types of antibodies to be used as ligands in WAC if they have relatively weak binding for a target.[1–3,17–19] For instance, monoclonal antibodies with association equilibrium constants of 10^2–$10^4\ M^{-1}$ for carbohydrates have been used in several studies examining the theory and behavior of WAC (see Fig. 1).

General ligands are agents that bind to a family or class of related molecules. These ligands can be of either biological or non-biological origin. Examples include lectins, triazine dyes, serum proteins, boronates, and cyclodextrins (see Fig. 2). These ligands tend to have lower association constants than high-specificity ligands, making them more useful for work in WAC.[5–16] There are, however, some exceptions to this. Two examples of exceptions are protein A and protein G, which are general ligands commonly used in antibody isolation and which have association equilibrium constants of 10^7–$10^8\ M^{-1}$ for some types of antibodies.[5]

Two other types of biological ligands that can be used in WAC are enzymes and lectins.[5,9] As an example, the enzyme α-chymotrypsin has weak interactions with many of its inhibitors, which has allowed the separation of these inhibitors under isocratic conditions on an immobilized α-chymotrypsin column. Lectins are non-immune system proteins that bind carbohydrates with low-to-moderate association constants, allowing these agents to be used

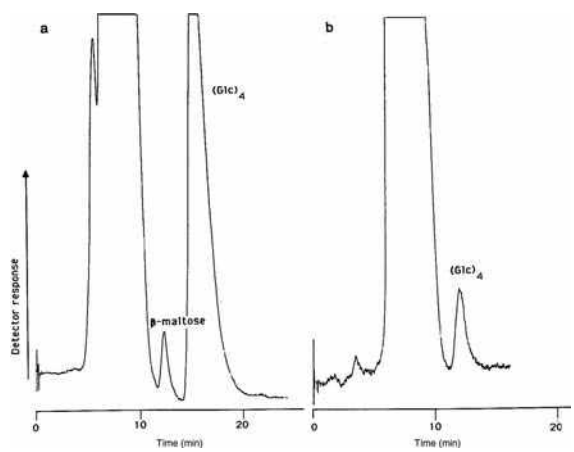

Fig. 1 Analysis of the oligosaccharide $(Glc)_4$ in (a) human urine and (b) serum by weak affinity chromatography. The affinity column was 5 × 100 mm I.D. and contained immobilized monoclonal antibodies against $(Glc)_4$. Elution was carried out under isocratic conditions at a flow rate of 0.2 ml/min using a pH 7.5, 0.02 *M* phosphate buffer that contained 0.1 *M* sodium sulfate.
Source: From Weak affinity chromatography, in *Handbook of Affinity Chromatography*.[3]

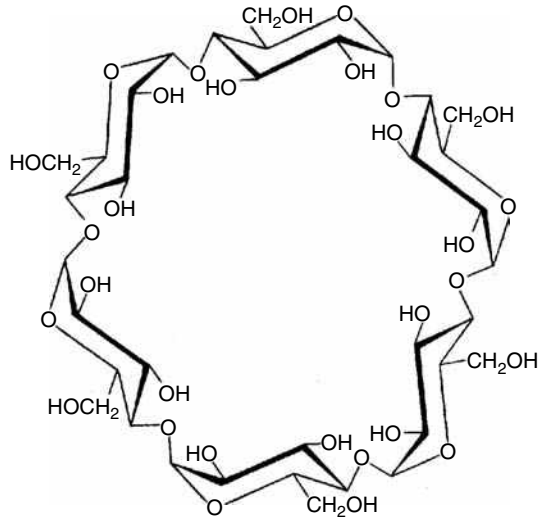

Fig. 2 Structure of α-cyclodextrin.

as affinity ligands under isocratic conditions. Wheat germ agglutinin has been used in an affinity column under such conditions for separating *N*-acetyl derivatives of mono-, di-, tri-, and tetrasaccharides.[7] Lectins have also been used as ligands for WAC coupled with mass spectrometry in proteomic studies examining protein modifications that involve O-linked *N*-acetyloglucosamine residues.[20]

Additional biological ligands that have been used in weak affinity separations include human serum albumin, bovine serum albumin, α_1-acid glycoprotein, and β-cyclodextrin.[5,9,10] These ligands have been particularly useful as chiral stationary phases for the separation of drugs and other agents (Fig. 3).[9] It is common with these immobilized ligands to use a mobile phase that contains a small amount of an organic modifier or a displacing agent to reduce analyte retention times and improve peak shapes. These ligands can also be used under physiological conditions as tools for studying the interactions with such binding agents in the body.

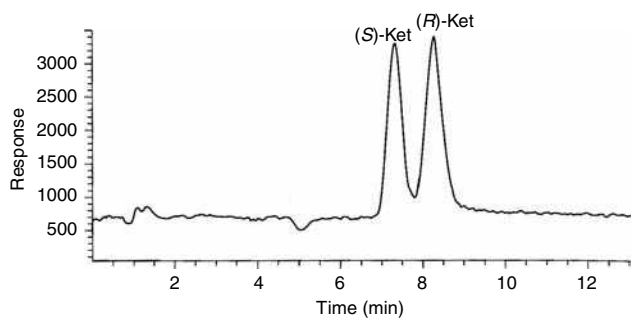

Fig. 3 Separation and determination of the enantiomers of ketamine in human plasma by using weak affinity chromatography and a column containing α_1-acid glycoprotein as the stationary phase with detection by mass spectrometry.
Source: From Affinity-based chiral stationary phases, in *Handbook of Affinity Chromatography*.[9]

Several non-biological ligands can be utilized in WAC, such as those used in *dye–ligand affinity chromatography*.[11–13] In this method, a synthetic triazine or a triphenylmethane dye acts as the immobilized ligand. *Biomimetic affinity chromatography* is a closely related method that can also be used in WAC. This uses a ligand that has been designed or selected to mimic the binding of a substance to a natural ligand. Synthetic dyes produced by combinatorial techniques might be utilized for this purpose, as well as binding agents that have been created through phage display or ribosome libraries.[11]

Boronic acid and its derivatives are another class of non-biological ligands that have weak binding and are often used under isocratic conditions. These are used in the method of *boronate affinity chromatography*, which makes use of the ability of such ligands to form covalent bonds with compounds that contain *cis*-diol groups. Such a property has made boronate ligands useful for the purification and analysis of many compounds that contain sugar residues, such as polysaccharides, glycoproteins, ribonucleic acids, and catecholamines.[14–16]

CONCLUSION

WAC involves the use of ligands in affinity chromatography that have relatively weak interactions with their target compounds. This feature allows the affinity column to be used under isocratic conditions. Ligands that have been used in WAC methods have included biological agents such as monoclonal antibodies, serum proteins, lectins, and carbohydrates such as cyclodextrins.[1–3,5–16,18–20] Additional binding agents such as dyes, biomimetic ligands, and boronates have also been used for this purpose.[11–16] This range of ligands has made WAC useful in applications that have ranged from chiral separations to proteomics and the study of solute–protein interactions in the body.[1–3,5–16,20]

REFERENCES

1. Ohlson, S.; Lundblad, A.; Zopf, D. Novel approach to affinity chromatography using "weak" monoclonal antibodies. Anal. Biochem. **1988**, *169*, 204–208.
2. Strandh, M.; Andersson, H.S.; Ohlson, S. Weak affinity chromatography. In *Methods in Molecular Biology*; Bailon, P., Ehrlich, G.K., Fung, W.-J., Berthold, W., Eds.; Humana Press: Totowa, NJ, 2000; Chapter 2.
3. Ohlson, S.; Zopf, D. Weak affinity chromatography. In *Handbook of Affinity Chromatography*; Kline, T., Ed.; Marcel Dekker; New York, 1993; Chapter 11.
4. Hage, D.S.; Xuan, H.; Nelson, M.A. Application and elution in affinity chromatography. In *Handbook of Affinity Chromatography*, 2nd Ed.; Hage, D.S., Ed.; Taylor & Francis: New York, 2006; Chapter 4.

5. Hage, D.S.; Bian, M.; Burks, R.; Karle, E.; Ohnmacht, O.; Wa, C. Bioaffinity chromatography. In *Handbook of Affinity Chromatography*, 2nd Ed.; Hage, D.S., Ed.; Taylor & Francis: New York, 2006; Chapter 5.
6. Hage, D.S. Chromatographic and electrophoretic studies of protein binding to chiral solutes. J. Chromatogr. A, **2001**, *906*, 459–481.
7. Ohlson, S.; Bergstrom, M.; Leickt, L.; Zopf, D. Weak affinity chromatography of small saccharides with immobilized wheat germ agglutinin and its application to monitoring of carbohydrate transferase activity. Bioseparation **1998**, *7*, 101–105.
8. Hage, D.S. Affinity chromatography: A review of clinical applications. Clin. Chem. **1999**, *24*, 593–615.
9. Patel, S.; Wainer, I.W.; Lough, W.J. Affinity-based chiral stationary phases. In *Handbook of Affinity Chromatography*, 2nd Ed.; Hage, D.S., Ed.; Taylor & Francis: New York, 2006; Chapter 21.
10. Allenmark, S. *Chromatographic Enantioseparation: Methods and Applications*, 2nd Ed.; Ellis Horwood: New York, 1991.
11. Labrou, N.E.; Mazitsos, K.; Clonis, Y.D. Dye–ligand and biomimetic affinity chromatography. In *Handbook of Affinity Chromatography*, 2nd Ed.; Hage, D.S., Ed.; Taylor & Francis: New York, 2006; Chapter 9.
12. Labrou, N.E.; Clonis, Y.D. Immobilized synthetic dyes in affinity chromatography. In *Theory and Practice of Biochromatography*; Vijayalakshmi, M.A., Ed.; Taylor & Francis: London, 2002; 335–351.
13. Clonis, Y.D. Affinity chromatography matures as bioinformatic and combinatorial tools develop. J. Chromatogr. A, **2006**, *1101*, 1–24.
14. Liu, X.C.; Scouten, W.H. Boronate affinity chromatography. In *Affinity Chromatography*; Bailon, P., Ehrlich, G.K., Fung, W.J., Berthold, W., Eds.; Humana Press: Totowa, NJ, 2000; 119–128.
15. Liu, X.-C.; Scouten, W.H. Boronate affinity chromatography. In *Handbook of Affinity Chromatography*, 2nd Ed.; Hage, D.S., Ed.; Taylor & Francis: New York, 2006; Chapter 8.
16. Benes, M.J.; Stambergova, A.; Scouten, W.H. Affinity chromatography with immobilized benzeneboronates. In *Molecular Interactions in Bioseparations*; Ngo, T.T., Ed.; Plenum Press: New York, 1993; 313–322.
17. Wikstroem, M.; Ohlson, S. Computer simulation of weak affinity chromatography. J. Chromatogr. **1992**, *597*, 83–92.
18. Bergstrom, M.; Ohlson, S. Use of perfusion supports in weak affinity chromatography. Intl. J. BioChromatogr. **2001**, *6*, 163–172.
19. Engstroem, H.A.; Johansson, R.; Koch-Schmidt, P.; Gregorius, K.; Ohlson, S.; Bergstrom, M. Evaluation of a glucose sensing antibody using weak affinity chromatography. Biomed. Chromatogr. **2008**, *22*, 272–277.
20. Vosseller, K.; Trinidad, J.C.; Chalkley, R.J.; Specht, C.G.; Thalhammer, A.; Lynn, A.J.; Snedecor, J.O.; Guan, S.; Medzihradszky, K.F.; Maltby, D.A.; Schoepfer, R.; Burlingame, A.L. *O*-Linked *N*-acetylglucosamine proteomics of postsynaptic density preparations using lectin weak affinity chromatography and mass spectrometry. Mol. Cell. Proteomics **2006**, *5*, 923–934.

Alcoholic Beverages: GC Analysis

Fernando M. Lanças
Institute of Chemistry of São Carlos (USP), University of São Paulo, São Carlos, Brazil

M. de Moraes
Chromatography Laboratory, University of São Paulo, São Carlos, Brazil

INTRODUCTION

Alcoholic beverages have been consumed by a significant range of worldwide population since the beginning of civilization until the present time. Therefore, there should be a great interest on consumption of beverages quality and, consequently, the usage of a suitable analytical technique to verify and control this desirable quality.

Alcoholic beverages are classified, in a general way, in fermented beverages (such as beer, wine, sake, etc.) and distilled ones (vodka, whisky, aguardente, tequila, cognac, liquors, etc.). The main volatile substances present in most alcoholic beverages belongs to the following chemical classes: alcohols (including ethanol, methanol, isobutanol, 3-methyl butan-2-ol, etc.), esters (such as ethyl acetate, methyl acetate, ethyl isobutyrate, isoamyl acetate, etc.), aldehydes (propanal, isobutanal, acetal, furfural, etc.), acids (acetic acid, propionic acid, butyric acid, etc.), and ketones (acetone, diacetyl, etc.).

Some of the substances are of greater concern than the others due to its relative quantities or to its flavored characteristic.[1] As an example, ethanol is the major compound in the group of alcohols being responsible for the formation of various other substances, such as acetaldehyde, resulting from ethanol oxidation, and it is the most abundant of the carbonylic compounds in distilled beverages. For the same reason, acetic acid is the major compound within its group, the carboxylic acids. Fusel alcohols (e.g., 1-propanol and 3-methyl butan-2-ol) as well as ethanol are also important substances in the alcohols group contributing to the flavor of distilled beverages because their odor is very distinctive and characteristic. There is an enormous variety of substances in small concentrations belonging to the esters group. Even so, ethyl acetate corresponds to more than 50% of the esters within this group.

These compounds are responsible to important characteristics as smell and taste, in which the large fraction of these substances originates from fermentation or during beverages storage.[1]

Because gas chromatography (GC) is an analytical technique in which separation and identification of volatile compounds occurs, it might be considered the best technique for this kind of sample.[2]

ANALYSIS BY GC

Analysis of alcoholic beverages by GC have as their main objectives to investigate flavoring compounds and contaminants which might be intentional or occasional. Whereas the former ones (the flavors) are analyzed to control their favorable characteristics to the beverage, the adulterants have to be controlled due to their deleterious contribution. Adulteration includes the addition of certain compounds to enhance a desirable flavor. Because these compounds are usually added as a racemic mixture, their presence can be verified using a suitable chiral column for enantiomer separation.[3] On the other hand, occasional contaminants are substances originating in small quantities during beverage production and might be carcinogenic. The main source might be raw materials like grape, sugar-cane, and so forth contaminated with pesticides[4] or as a result of the fermentation process itself.[5,6]

Comments in each major part of the GC instrumentation as used for beverage analysis are presented.

SAMPLE INTRODUCTION

Distilled Beverages

Generally, samples are injected in the chromatographic system without any dilution or pretreatment step, using the split mode (i.e., with sample division), which is suitable for the analysis of the major compounds in beverages.When the objective of analysis is the determination of compounds present in small quantities (μg/L), some extraction and/or concentration step is necessary, followed by the sample injection in the splitless mode (without sample division). This last sample introduction mode is usually combined with extraction techniques such as liquid–liquid extraction (LLE), solid-phase extraction (SPE),[4] and solid-phase microextraction (SPME).[7,8]

Fermented Beverages

Sample introduction is basically the same compared to the distilled one. Nevertheless, in many complex samples

(i.e., some kind of wines), it is not advisable to inject them into the chromatograph without a pretreatment step.

Recently, SPME has provided many improvements as the cleanup step of complex samples, particularly for the analysis of volatile compounds by *headspace* techniques.[8] SPME is a solventless extraction and concentration technique which has advantages as a simple and economic technique that reduces health hazards and environmental issues.

COLUMNS

Until 1960, all commercial chromatographic columns were packed in wide-bore tubing and separations had low resolution and low efficiency, taking a long time for a run to be completed. Since then, there have been significant improvements with the introduction of wall-coated open tubular (WCOT) columns, whose inner diameter was smaller than the packed ones are coated with a thin film of the liquid phase.[9]

When capillary fused-silica columns arose, a large number of separations of complex samples have obtained success as a result of the higher number of plates (about 30 times over the packed columns in average).

Despite the efficient separations, it has been noticed that some low-boiling compounds of alcoholic beverages coeluted because of the use of a polar stationary phase. This column separates mainly based on the boiling temperatures of chemical substances, but separation becomes very difficult if there are some compounds with similar boiling temperatures. A polar stationary phase like poly(ethylene glycol) (PEG) is a better choice for this sort of problem because these separations are based on compound structures. In all cases, cross-linked or immobilized phases are recommended because they are more thermolabile and also resistant to most solvents. This is particularly important when splitless injection is used in combination with PEG-type phases because otherwise a severe column bleeding might be observed after ~220°C.

Detection Systems

The flame ionization detector (FID) is one of the most commonly used detectors in beverage analysis by GC, as it is suitable to most groups of compounds investigated in alcoholic beverages.[9] This occurs because almost all compounds of interest in such samples are able to burn in the flame, forming ions and producing a potential difference measured by a collector electrode.

In trace analysis of contaminant substances, one can use specific detectors for certain compounds, such as a nitrogen–phosphorus detector (NPD), thus gaining detection ability for nitrogenated and phosphorylated compounds; the electron-capture detector (ECD) shows excellent

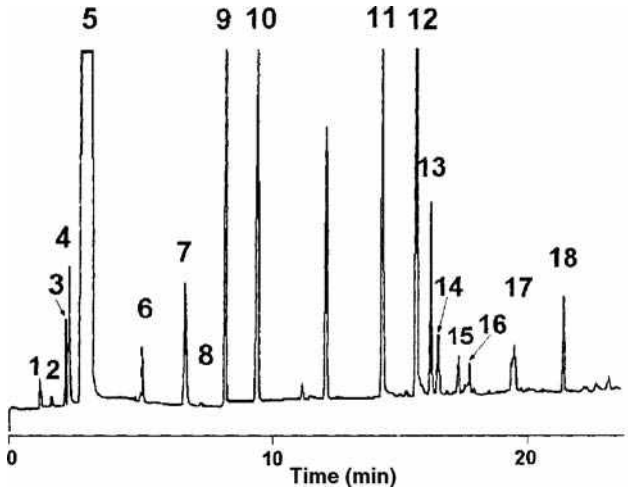

Fig. 1 GC analysis of white wine sample by fused-silica column poly(ethylene glycol) type (15.00 m × 0.53 mm × 1.00 μm). Chromatographic conditions: carrier gas: hydrogen (3.6 ml/min); column temperature: 40°C (4 min) → 8°C/min → 270°C; injector port temperature: 250°C; detector temperature: 300°C. Identity of the selected peaks: (1) acetaldehyde, (2) acetone, (3) ethyl acetate, (4) ethanol, (5) ethanol, (6) propanol, (7) isoamyl acetate, (8) *n*-butanol, (9) heptanone, (10) isoamyl alcohol, (11) acetic acid, (12) propionic acid, (13) isobutyric acid, (14) 2,3 butanediol, (15) 1,2 propanediol, (16) butyric acid, (17) isovaleric acid, (18) valeric acid.

performance for chlorinated substances and the flame photometric detector (FPD) is the most widely used for sulfur-containing compounds.

GC–mass spectrometry (MS) combination has become one of the most important coupling in analytical chemistry used for the confirmation of results obtained by other detectors.[9] This technique is based on the fragmentation of the molecules that arrives into the detector. Ion formation occurs and they are separated by the mass/charge (*m/z*) ratio generally detected by a electron multiplier. Quantitative analysis can be realized through the single-ion monitoring (SIM) mode, where some characteristic ions are selected and monitored increasing the detection sensibility and selectivity. Another qualitative technique, GC–sniffing[10] is very much used for flavor analysis, despite discordance among researchers. In this case, the volatile substances from a extract are separated by GC, and as they leave the equipment through a specially designed orifice, a trained analyst is able to smell some of the substances and tentatively identify them (Fig. 1).

More than 500 compounds have been found in concentrated flavor extracts in distilled beverages.[1] For this reason, there is an obvious necessity to find and optimize analytical techniques capable of investigating and to keep trading control of the alcoholic beverages. Among them, GC has been far from any other preferred tool for the analysis of alcoholic beverages.

ACKNOWLEDGMENTS

Professor Lanças wishes to express his acknowledgments to FAPESP (Fundação de Amparo à Pesquisa do Estado de São Paulo), CNPQ (Conselho Nacional de Desenvolvimento Científico e Tecnológico), and CAPES (Coordenação de Aperfeiçoamento e Pessoal de Nível Superior) for financial support to our laboratory and a fellowship to Marcelo de Moraes.

REFERENCES

1. Nykänen, L.; Nykänen, I. Distilled beverages. In *Volatiles Compounds in Foods and Beverages*; Maarse, H., Ed.; Marcel Dekker, Inc.: New York, 1991, 547–580.
2. Lanças, F.M.; Galhiane, M.S. Fast routine analysis of light components of alcoholic beverage using large bore open tubular fused silica column. Bol. Soc. Chil. Quim. **1993**, *38*, 177.
3. König, W.A. New developments in enantiomer separation by capillary gas chromatography. In *Analysis of Volatiles Methods, Applications*; Schreier, P., Ed.; Berlin, 1984, 77–91.
4. Kaufmann, A. Fully automated determination of pesticides in wine. J. AOAC Int. **1997**, *80* (6), 1302.
5. Lawrence, J.F.; Page, B.D.; Conacher, B.S. The formation and determination of ethyl carbamate in alcoholic beverages. Adv. Environ. Sci. Technol. **1990**, *23*, 457.
6. Shiomi, K. Determination of acetaldehyde, acetal and other volatile congeners in alcoholic beverages. J. High Resol. Chromatogr. **1991**, *14* (2), 136.
7. Pawliszyn, J. *Solid Phase Microextraction—Theory and Practice*; Ed.; Wiley–VCH: New York, 1997, 1–247.
8. Garcia, D.; de la, C.; Reichenächer, M.; Danzer, K.; Hurlbeck, C.; Bartzsch, C.; Feller, K.H. Analysis of wine bouquet components using headspace solid phase micro extraction–capillary gas chromatography. J. High Resol. Chromatogr. **1998**, *21* (7), 373.
9. Smith, R.M. *Gas and Liquid Chromatography in Analytical Chemistry*; Smith, R.M., Ed.; John Wiley & Sons: London, 1988, 1–401.
10. Abbott, N.; Etievant, P.; Langlois, D.; Lesschaeve, I.; Issanchou, S. Evaluation of the representativeness of the odor of beer extracts prior to analysis by GC eluate sniffing. J. Agric. Food Chem. **1993**, *41* (5), 777.

Alkaloids: CCC Separation

Fuquan Yang
Yoichiro Ito
National Heart, Lung, and Blood Institute (NHLBI), National Institutes of Health (NIH), Bethesda, Maryland, U.S.A.

INTRODUCTION

Alkaloids are an important class of compounds that have pharmacological effects on various tissues and organs of humans and other animal species. More than 16,000 are known and most are derived from higher plants. Alkaloids have also been isolated from microorganisms, from marine organisms such as algae, dinoflagellates, and puffer fish, as well as from terrestrial animals, such as insects, salamanders, and toads.

Pelletier[1] defines an alkaloid as "a cyclic compound containing nitrogen in a negative oxidation state which is of limited distribution in living organisms." This definition includes both alkaloids with nitrogen as part of a heterocyclic system and the many exceptions with extracyclic bound nitrogen. From the viewpoint of analytical chemistry, the most important trait of alkaloids is their basicity, arising from a heterocyclic tertiary nitrogen atom. Many alkaloids are complex components which are biosynthetically derived from various amino acids, such as phenylalanine, tyrosine, tryptophan, ornithine, and lysine. The biogenesis of alkaloids is used for their classification, as this is directly linked with their molecular skeleton, e.g., the two largest groups are indole alkaloids and isoquinoline alkaloids. Other important groups are tropane alkaloids, pyridine, and pyrrolizidine alkaloids. In the past 10 years, there has been an increasing interest in the isolation and determination of alkaloids in plant materials, in pharmaceutical products, and in other samples of biological interest. Currently, much work is being carried out to discover new alkaloid molecules for different applications, such as new antiviral and antitumor treatments. So the separation and analysis of alkaloids are of great importance.[2,3] But the problem is that extensive tailing and irreversible adsorption may occur due to the interaction between the basic alkaloids and acidic silanol groups when alkaloids are separated by conventional column chromatography with silica gel or chemically bonded C_{18} on silica as the stationary phase.

OVERVIEW

Countercurrent chromatography (CCC), as a support-free liquid–liquid partition chromatographic separation technique, eliminates various complications such as irreversible adsorption loss, denaturation of sample, tailing of solute peaks, contamination, etc. that sometimes arise from the interaction between solute molecules and the solid support matrix present in most other chromatographic methods. Countercurrent chromatography utilizes an immiscible two-phase solvent system, one phase as the stationary phase and the other as the mobile phase. The chromatographic process in CCC is based on the partition of a solute between the stationary and mobile phases. The partition coefficient (K), being one of the most important parameter in CCC, is defined as the ratio of the concentration of a solute in the stationary phase (C_s) to that in the mobile phase (C_m). In the past, various CCC systems, such as droplet CCC, rotation locular CCC, and centrifugal partition chromatography, have been used for the final or partial separation of alkaloids from a crude sample. The high-speed CCC (HSCCC) technique developed in the early 1980s[4] improved in both the partition efficiency and separation speed, and has been successfully applied to the separation of alkaloids.

pH-Zone-refining CCC was developed for the large-scale separation of ionizable compounds, including alkaloids and organic acids in the mid-1990s by Ito.[5,6] It uses a retainer base (or acid) in the stationary phase to retain the solutes in the column and an eluter acid (or base) to elute the solutes according to their pK_a values and hydrophobicities, and produces a succession of highly concentrated rectangular solute peaks with minimum overlap while impurities are concentrated at the peak boundaries. This technique has been successfully used for large-scale separation of alkaloids.

SEPARATION OF ALKALOIDS BY STANDARD COUNTERCURRENT CHROMATOGRAPHY

The standard CCC separation is solely based on the difference in the partition coefficients of solutes between the two phases of a solvent system. Most alkaloids have basic properties with pK_a values ranging from 6 to 12, but usually 7 to 9. Although the free base is soluble only in organic solvents, protonation of the nitrogen in the free base usually results in a water-soluble compound. This behavior serves as the basis for the selective extraction or isolation of alkaloids by liquid–liquid partitioning

processes. On the other hand, quaternary alkaloids are poorly soluble in organic solvents, but they are soluble in water, regardless of its pH.

Generally, a systematic search for the two-phase solvent systems for CCC is focused on the hydrophobicity of the solvent system for providing a proper range of partition coefficients of solutes. For the separation of ionizable compounds such as alkaloids, however, an additional adjustment is required with respect to the pH and ionic strength of the solvent system.

Halogen-containing organic solvents, such as chloroform and dichloromethane, have been widely used in alkaloid separation because of their relatively strong proton-donor character. The chloroform-containing, two-phase solvent systems (chloroform–aqueous phosphate or citrated buffer and chloroform–methanol–dilute inorganic acid) have been widely used for the separation of alkaloids by CCC (Table 1).

Cai et al. first used a chloroform–0.07 *M* sodium phosphate buffer (pH 6.4–6.5) solvent system for the separation of matrine and oxymatrine from *Sophora flavescens*, atropine, scopolamine, and hyoscyamine from *Datura mete* L. by HSCCC.[7] Cooper et al. successfully used chloroform–0.2 *M* potassium phosphate buffer with an

Table 1 Separation of alkaloids by CCC.

Alkaloids	Source	Two-phase solvent system	Instrument
Matrine and oxymatrine	*Sophora flavescens*	$CHCl_3$–0.07 *M* sodium phosphate (pH 6.4) (1 : 1)	HSCCC
Atropine, scopolamine, hyoscyamine	*Datura mete*	$CHCl_3$–0.07 *M* sodium phosphate (pH 6.5) (1 : 1)	HSCCC
Cephalotaxus alkaloids	*Cephalotaxus fortunei*	$CHCl_3$–0.07 *M* sodium phosphate–0.04 *M* citric acid (pH 5.0) (1 : 1)	HSCCC
Pyrrolizidine alkaloids	*Amsinckia tessellata*, etc.	$CHCl_3$–0.2 *M* potassium phosphate (pH 7.4, 6.0, 5.6, 5.0) (1 : 1)	HSCCC
Pentacyclic aromatic alkaloid	*Amphicarpa meridiana*	$CHCl_3$–MeOH–5% HCl (5 : 5 : 3)	HSCCC
Flavonoid alkaloids	*Buchenavia capitata*	$CHCl_3$–MeOH–0.5% HCl (5 : 5 : 3)	Sanki CPC
Isoquinoline alkaloids	*Ancistrocladus abbreviatus*	$CHCl_3$–MeOH–0.5% HBr (5 : 5 : 3)	HSCCC
Naphthyltetrahydroisoquinoline alkaloids	*Ancistrocladus korupensis*	$CHCl_3$–MeOH–0.5% HBr (5 : 5 : 3)	CPC
Aporphine alkaloids	*Dehaasia triandra*	$CHCl_3$–MeOH–0.5% HAc (5 : 5 : 3)	HSCCC
Naphthylisoquinoline alkaloids	*Ancistrocladus robertsoniorum*	$CHCl_3$–MeOH–0.1 *M* HCl (5 : 5 : 3)	HSCCC
Isoquinoline alkaloids	*Coptis chinensis*	$CHCl_3$–MeOH–0.2 *M* HCl (4 : 1.5 : 2)	HSCCC
Diterpenoid alkaloids	*Aconitum sinomontanum*	$CHCl_3$–MeOH–0.3/0.2 *M* HCl (4 : 1.5 : 2)	HSCCC
Pyrrolizidine alkaloids	*Symphytum officinale*	*n*-C_6H_{14}–EtOH–MeOH–0.05% TFA (5 : 5 : 5 : 5)	HSCCC
β-Carboline alkaloids	*Pachypellina* sp.	*n*-C_6H_{14}–MeCN–CH_2Cl_2 (10 : 7 : 3)	HSCCC
Vinca alkaloids	*Vinca rosea*	*n*-C_6H_{14}–EtOH–H_2O (6 : 5 : 5)	HSCCC
Isoquinoline alkaloids	*Stephania tetrandra*	*n*-C_6H_{14}–EtOAc–MeOH–H_2O (3 : 7 : 5 : 5), (1 : 1 : 1 : 1)	HSCCC
Diterpenoid alkaloids	*Consolida ambigua*	C_6H_6–$CHCl_3$–MeOH–H_2O (5 : 5 : 7 : 2)	CPC
Pyrroloquinoline alkaloids	*Bazella* sp.	*n*-C_6H_{14}–$CHCl_3$–MeOH–H_2O (4 : 7 : 4 :3), (2 : 7 : 6 : 3); $CHCl_3$-*i*-Pr_2NH–MeOH–H_2O (7 : 1 : 6 : 4)	HSCCC
Pyrroloquinoline alkaloids	*Bazella* sp.	*n*-C_7H_{16}–$CHCl_3$–MeOH–H_2O (2 : 7 : 6 : 3), *n*-C_7H_{16}–EtOAc–$CHCl_3$–MeOH–H_2O (4 : 7 : 4 : 3)	HSCCC
Acridine alkaloids	*Dercitus* sp. and *Stellatta* sp.	CH_2Cl_2–MeOH–H_2O (5 : 5 : 3)	HSCCC
Quinoline alkaloids	*Camptotheca acuminata*	CCl_4–$CHCl_3$–MeOH–H_2O (2 : 2 : 3 : 1), CH_2Cl_2–$CHCl_3$–MeOH–H_2O (5 : 3 : 1)	HSCCC
Ergot alkaloids	*Stipa robusta*	$CHCl_3$–MeOH–H_2O (5 : 4 : 3)	HSCCC
Benzylisoquinoline alkaloids	*Anisocycla cymosa*	$CHCl_3$–MeOH–H_2O (10 : 10 : 1)	HSCCC
Imidazole alkaloids	*Discodermia polydiscus*	$CHCl_3$–MeOH–H_2O (5 : 10 : 6)	HSCCC
bis-Indole alkaloid	*Strychnos guianensis*	EtOAc–MeOH–H_2O (4 : 1 : 3)	HSCCC
Indole alkaloids	*Strychnos usambarensis*	*n*-BuOH–0.1 *M* NaCl (1 : 1)	HSCCC
Indole alkaloids	*Venezuelan curare*	*n*-BuOH–Me_2CO–H_2O (8 : 1 : 10)	HSCCC

optimum pH value of each at 5.0, 5.6, 6.0, and 7.4 for the separation of pyrrolizidine alkaloids from various sources of *Senecio douglasii* var. *longilobus*, *Trichodesma incanum*, *Symphytum* spp. and *Amsinckia tessellata*, respectively.[8]

A two-phase solvent system composed of chloroform–methanol–dilute inorganic acid has been used for the separation of a variety of alkaloids including isoquinoline alkaloids, naphthyl-tetrahydroisoquinoline alkaloids, flavonoid alkaloids, pentacyclic aromatic alkaloids, diterpenoid alkaloids, aporphine alkaloids, etc. The following example illustrates a typical systematic solvent selection for the separation of palmatine, berberine, epiberberine, and coptisine from the crude alkaloids of *Coptis chinensis* Franch by analytical HSCCC.[9] In Fig. 1, nine chromatograms are arranged in such a way that the effects of the concentration of HCl (0.3–0.1 *M*) and the relative volumes of methanol (4 : 3 : 2–4 : 1.5 : 2, v/v) on the separation of alkaloids from *C. chinensis* Franch are each readily observed. As the concentration of HCl is reduced from 0.3 to 0.1 *M* in the solvent system, the retention time of alkaloids and their peak resolution are increased. A similar effect is also produced by decreasing the relative volumes of methanol in the solvent system from 4 : 3 : 2 to 4 : 1.5 : 2). Among those, the solvent system composed of $CHCl_3$–MeOH–0.2 *M* HCl (4 : 1.5 : 2) produced the best separation of all four major alkaloids components. The optimum solvent system thus obtained led to the successful separation of alkaloids from *C. chinensis* Franch by preparative HSCCC. A similar method was also used for the separation of diterpenoid alkaloids, including lappaconitine, ranaconitine, *N*-deacetyllappaconitine, and *N*-deacetylranaconitine from *Aconitum sinomontanum*.[10]

More than 10 kinds of neutral two-phase solvent systems have been successfully used for the separation of alkaloids by CCC.[11] Most of the alkaloids from marine sponge—including acridine, pyrroloquinoline, imidazole, β-carboline alkaloids, etc.—were separated with neutral two-phase solvent systems by HSCCC in the final or middle step of separation (Table 1).

SEPARATION OF ALKALOIDS BY H-ZONE-REFINING COUNTERCURRENT CHROMATOGRAPHY

Fig. 2 shows a typical separation of 3 g of three alkaloids from a crude extract of *Crinum moorei* using a binary

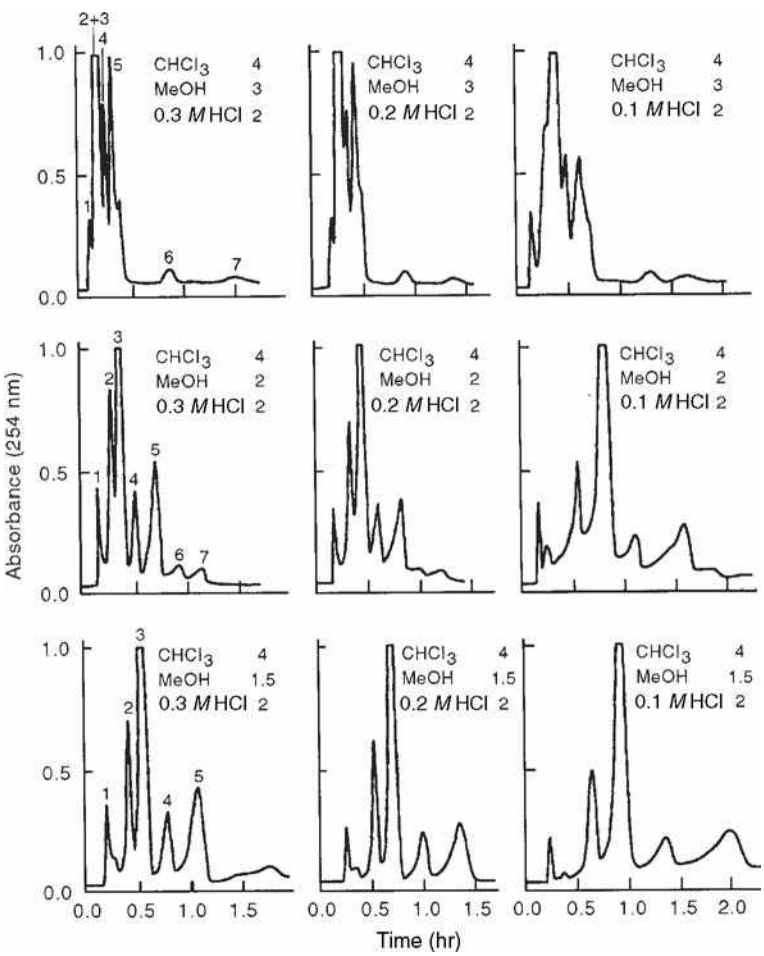

Fig. 1 Chromatograms of the crude alkaloids from *C. chinensis* Franch by analytical HSCCC. Nine chromatograms are arranged in such a way that the effects of methanol and HCl concentrations on the alkaloid separation are each clearly visualized. Experimental conditions: apparatus: analytical HSCCC instrument equipped with a multilayer coil of 0.85 mm I.D. and 30 ml capacity; sample: 2.5 mg of crude alkaloid extract of *C. chinensis* Franch; solvent system: shown above each chromatogram; mobile phase: lower organic phase; flow rate: 1 ml/min; revolution: 1500 rpm. Retention of the stationary phase was as follows: $CHCl_3$–MeOH–(0.1–0.3 *M* HCl) (4 : 3 : 2), 77%; $CHCl_3$–MeOH–(0.1–0.3 *M* HCl) (4 : 2 : 2), 80%; and $CHCl_3$–MeOH–(0.1–0.3 *M* HCl) (4 : 1.5 : 2), 77%.

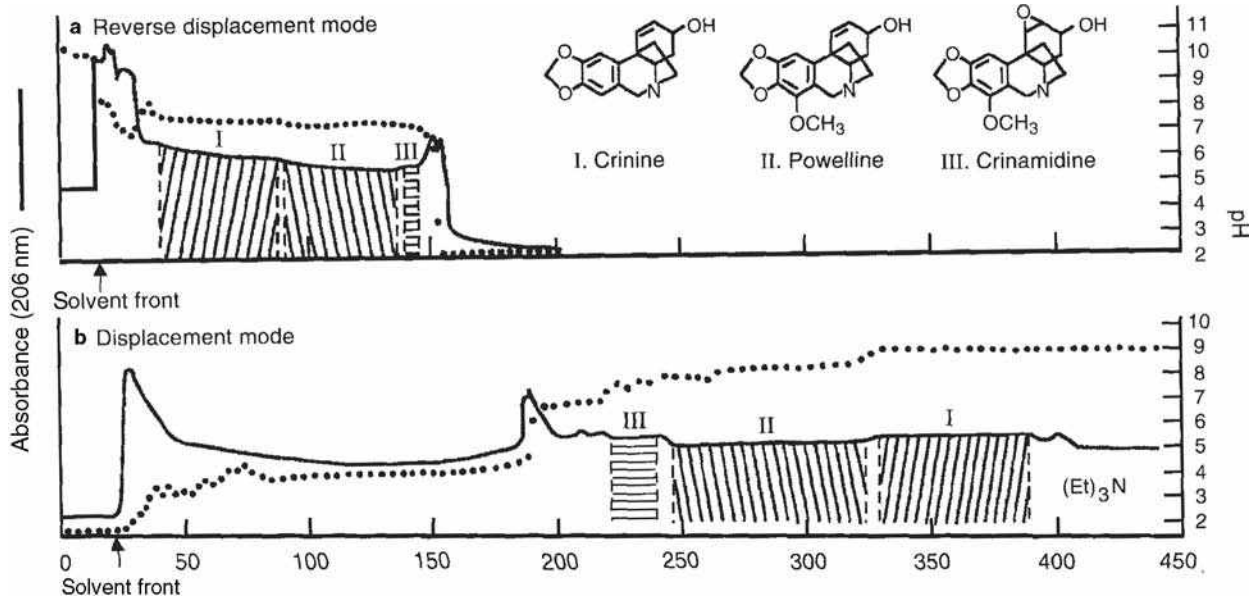

Fig. 2 Chromatograms of the crude alkaloid extract of *Crinum moorei* obtained by pH-zone-refining CCC. Experimental conditions were as follows: apparatus: high-speed CCC centrifuge equipped with a multiplayer coil of 1.6 mm I.D. and about 300 ml capacity; solvent system: methyl-*tert*-butyl ether–water; stationary phase: (a) upper phase (5 m*M* triethylamine) and (b) lower phase (10 m*M* HCl); mobile phase: (a) lower phase (5 m*M* HCl) and (b) upper phase (10 m*M* triethylamine); flow rate: 3.3 ml/min; sample: crude alkaloid extract of *C. moorei*, 3 g dissolved in 30 ml of each phase; revolution: (a) 800 rpm (600 rpm until 66 ml of mobile phase was eluted) and (b) 600 rpm throughout.

solvent system composed of methyl-*tert*-butyl ether–water where triethylamine (5–10 m*M*) was added to the organic phase and HCl (5–10 m*M*) was added to the aqueous phase.[12] In Fig. 2a, where the aqueous phase was used as the mobile phase and HCl as the eluter, the alkaloids were eluted as HCl salts, while in Fig. 2b, where the organic phase is used as mobile phase and triethylamine as the eluter, the alkaloids were eluted as free bases. The same binary solvent system was also used for the separation of alkaloids from the root of *S. flavescens* Ait.[13] In order to increase the solubility of the alkaloids in methyl-*tert*-butyl ether–water solvent system, this solvent system was modified to methyl-*tert*-butyl ether–tetrahydrofuran–water (2 : 2 : 3, v/v), while triethylamine (10 m*M*) was added to the upper organic stationary phase as a retainer and hydrochloric acid (10 m*M*) to the aqueous mobile phase as an eluter. This solvent system was applied to the separation of diterpenoid alkaloids from a crude prepurified sample containing lappaconitine at about 90% purity. Up to 10.5 g of the sample loading yielded 9.0 g of lappaconitine at a high purity of over 99% as determined by HPLC.[14] As most alkaloids have a high solubility in chloroform, a binary solvent system composed of chloroform–water is suitable for a large-scale preparative separation when 18–24 m*M* HCl was added to the aqueous stationary phase as a retainer and 0.1% triethylamine (TEA) to the organic mobile phase as an eluter. This system was successfully used for the separation of berberine chloride, canadaline, canadine, β-hydrastine, and isocorypalmine from a methanolic extract of Goldenseal by pH-zone-refining CCC.[15] The separation of alkaloids by pH-zone-refining CCC is summarized in Table 2.

Table 2 Separation of alkaloids by pH-zone-refining CCC.

Alkaloids	Source	Solvent systems[a]	Retainer[b]	Eluter[c]
Amaryllis alkaloids	*Crinum moorei*	M*t*BE–H_2O (1 : 1)	TEA (5 m*M*/SP)	HCl (5 m*M*/MP)
		M*t*BE–H_2O (1 : 1)	HCl (10 m*M*/SP)	TEA (10 m*M*/MP)
Vinca alkaloids	*Vinca minor*	M*t*BE–H_2O (1 : 1)	TEA (5 m*M*/SP)	HCl (5 m*M*/MP)
Matrine, sophocarpine	*Sophora flavescens*	M*t*BE–H_2O (1 : 1)	TEA (10 m*M*/SP)	HCl (5–0 m*M*/MP)
Diterpenoid alkaloids	*Aconitum sinomontanum*	M*t*BE–THF–H_2O (2 : 2 :7 : 3)	TEA (10 m*M*/SP)	HCl (10 m*M*/MP)
Isoquinoline alkaloids	*Hydrastis canadensis rhizomes*	$CHCl_3$–H_2O (1 : 1)	18–24 m*M* HCl	TEA (0.1%/MP)

[a]M*t*BE = methyl-*tert*-butyl ether; THF = tetrahydrofuran.
[b]TEA = triethylamine; SP = stationary phase.
[c]MP = mobile phase.

CONCLUSIONS

Countercurrent chromatography overcomes all of the problems caused by solid support matrix present in most other chromatographic methods. Countercurrent chromatography can purify alkaloids with high recovery and reproducibility.

pH-Zone-refining CCC extends the preparative capacity of HSCCC and provides many important advantages over the conventional CCC method, including an over 10-fold increase in sample loading capacity, high concentration of fractions with very high purity, concentration of minor impurities, etc.

REFERENCES

1. Pelletier, S.W., Ed.; *Alkaloids: Chemical and Biological Perspective*; John Wiley: New York, 1983; Vol. 1–6.
2. Muzquiz, M. Alkaloids/gas chromatography. In *Encyclopedia of Separation Science*; Wilson, I.D., Adlard, E.R., Cooke, M., Poole, C.F., Eds.; Academic Press: New York, 1938–1949; Vol. 5.
3. Verpoorte, R. Alkaloids/liquid chromatography. In *Encyclopedia of Separation Science*; Wilson, I.D., Adlard, E.R., Cooke, M., Poole, C.F., Eds.; Academic Press: New York, 1949–1956; Vol. 5.
4. Ito, Y. High-speed countercurrent chromatography. CRC Crit. Rev. Anal. Chem. **1986**, *17* (1), 65–143.
5. Ito, Y. pH-peak-focusing and pH-zone-refining countercurrent chromatography. In *High-Speed Countercurrent Chromatography*; Ito, Y., Conway, W.D., Eds.; John Wiley: New York, 1996; 121–175.
6. Ito, Y.; Ma, Y. pH-zone-refining countercurrent chromatography. J. Chromatogr. A, **1996**, *753* (1), 1–36.
7. Cai, D.G.; Gu, M.J.; Zhang, J.D.; Zhu, G.P.; Zhang, T.Y.; Li, N.; Ito, Y. Separation of alkaloids from *Datura mete* L. and *Sophora flavescens* Ait by high-speed countercurrent chromatography. J. Liq. Chromatogr. **1990**, *13* (12), 2399–2408.
8. Cooper, R.A.; Bowers, R.J.; Beckham, C.J.; Huxtable, R.J. Preparative separation of pyrrolizidine alkaloids by high-speed countercurrent chromatography. J. Chromatogr. A, **1996**, *732* (1), 43–50.
9. Yang, F.Q.; Zhang, T.Y.; Zhang, R.; Ito, Y. Application of analytical and preparative high-speed countercurrent chromatography for separation of alkaloids from *Coptis chinensis* Franch. J. Chromatogr. A, **1998**, *829* (1–2), 137–141.
10. Yang, F.Q.; Ito, Y. Preparative separation of lappaconitine, ranaconitine, *N*-deacetyllappaconitine and *N*-deacetylranaconitine from crude alkaloids of sample *Aconitum sinomontanum* Nakai by high-speed countercurrent chromatography. J. Chromatogr. A, **2002**, *943* (2), 219–225.
11. Marston, A.; Hostettmann, K. Countercurrent chromatography as a preparative tool applications and perspectives. J. Chromatogr. A, **1994**, *658* (2), 315–341.
12. Ma, Y.; Ito, Y.; Sokoloski, E.; Fales, H.M. Separation of alkaloids by pH-zone-refining countercurrent chromatography. J. Chromatogr. A, **1994**, *685* (2), 259–262.
13. Yang, F.Q.; Quan, J.; Zhang, T.Y.; Ito, Y. Preparative separation of alkaloids from the root of *Sophora flavescens* Ait by pH-zone-refining countercurrent chromatography. J. Chromatogr. A, **1998**, *822* (2), 316–320.
14. Yang, F.Q.; Ito, Y. pH-Zone-refining countercurrent chromatography of lappaconitine from *Aconitum sinomontanum* Nakai: I. Separation of prepurified extract. J. Chromatogr. A, **2001**, *923* (1–2), 281–285.
15. Chadwick, L.R.; Wu, C.D.; Kinghorn, A.D. Isolation of alkaloids from goldenseal (*Hydrastis canadensis rhizomes*) using pH-zone-refining countercurrent chromatography. J. Liq. Chromatogr. Relat. Technol. **2001**, *24* (16), 2445–2453.

Alumina-Based Supports for LC

Esther Forgács
Tibor Cserháti
Institute of Chemistry, Chemical Research Center, Hungarian Academy of Sciences, Budapest, Hungary

INTRODUCTION

Various liquid chromatography (LC) techniques offer a unique possibility for the separation and quantitative determination of a large variety of organic, metalloorganic, and inorganic compounds with highly similar molecular structures. These methods are indispensable in medical practice and research, pharmaceutical chemistry, food science and technology, environmental pollution control, legislation procedures, etc. The rapid development of the theory of the retention processes in chromatography have made it obvious that the efficient separation of various compounds (selection of the best separation method, support and mobile phase, and any other parameter influencing the efficacy) requires a profound knowledge of the impact of molecular characteristics of solutes, stationary and mobile phases, and their interplay at the molecular level on retention. The expert application of such knowledge will highly facilitate the rational design of optimal separation methods. As the chemistry and physicochemistry of the surface of the support determines the retention characteristics of stationary phases, physical methods such as nuclear magnetic resonance (NMR), Fourier transform infrared (FTIR), etc. have been frequently used to study the stationary phases in LC.

The overwhelming majority of LC separations are carried out in silica or in silica-based, reversed-phase (mainly octadecylsilica, ODS) stationary phases. Although the retention characteristics of silica and surface-modified silica supports are excellent, and they can be used for the successful separation of a wide variety of solutes, they also have some drawbacks. Thus, the acidic character of the free silanol groups exert a considerable impact on the retention behavior of both silica and silica-based supports; basic solutes are more strongly bonded onto the silica surface than neutral or acidic substances, resulting in unpredictable retention behavior. Moreover, silica and silica derivatives are not stable at alkaline pHs, making the separation of strongly basic compounds difficult. The objectives of the newest developments in LC are the development and practical application of more stable supports than silica and modified silicas, with different separation capacities (alumina, zirconia, titania, mixed oxides, and their modified derivatives, porous graphitized carbon, various polymer supports, etc.). Although these new supports show excellent separation characteristics, they are not well known, not frequently used, and the molecular basis of retention has not been elucidated in detail.

The objectives of this entry are the enumeration and critical evaluation of the recent results obtained in the assessment of the relationship between the physicochemical characteristics and retention behavior of a wide variety of solutes on alumina stationary phases and the elucidation of the efficacy of various multivariate mathematical–statistical methods for the quantitative description of such relationships.

ALUMINA

Alumina offers another alternative to silica because of its inherent higher pH stability. However, in contrast to its extensive use as a medium in column chromatography for purification purposes, or for separations in the normal-phase mode, there are still relatively few reports concerning alumina-based materials in the reversed-phase mode.

The chromatographic aspects of the surface characteristics of alumina stationary phases have not been studied as profoundly as zirconia supports; however, the presence of hydroxyl and oxide ions on the surface has been reported.[1]

Crystalline alumina may exist in various forms; the τ-form is generally used in chromatography. Alumina strongly adsorbs water molecules, as depicted in Fig. 1. The two different hydroxyl groups show acidic or alkaline properties, resulting in amphoteric characteristics and ion exchange behavior of the alumina surface, as demonstrated in Fig. 2.[2] It has been further shown that the simultaneous interaction of pH, the composition of buffer and that of the mobile phase modifier governs the retention on alumina surfaces in ion exchange chromatography.[3,4] The good separation characteristics of alumina stationary phase were exploited, not only in the ion-exchange mode, but also in the adsorption (direct phase) chromatographic mode. Alumina supports have been frequently used in thin-layer chromatography (TLC), and the separation of inorganic and organometallic solutes on alumina layers was reviewed.[5] Non-ionic surfactants (α-(1,1,3,3-tetramethylbutyl)phenyl ethylene oxide oligomers) were also

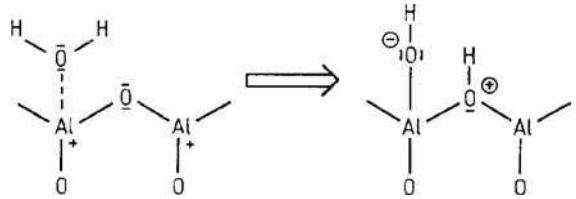

Fig. 1 Chemisorption of water on bare alumina.
Source: From The use of organic modifiers in ion exchange chromatography on alumina. The separation of basic drugs, in Chromatographia.[2]

separated on alumina layers using *n*-hexane mixed with ethyl acetate, dioxane, and tetrahydrofurane (THF), and the data were evaluated by spectral mapping technique. Surfactants were separated according to the number of ethylene oxide groups in the molecule; surfactants with longer ethylene oxide chain were eluted later. This finding indicates that the polar ethylene oxide units turn toward the stationary phase and that they are bonded to the adsorption sites on the alumina surface. Calculations proved that the solvent strength of THF was the highest, followed by dioxane and ethyl acetate. The selectivity of ethyl acetate differed considerably from the selectivities of THF and dioxane.[6] Other nonionic surfactants (nonylphenyl[7] and tetrabutylphenyl[8] ethyleneoxide oligomers) were

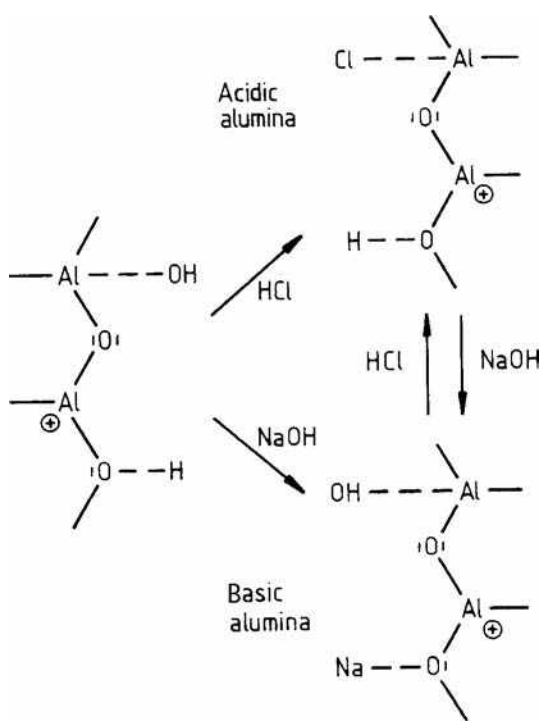

Fig. 2 Surface behavior of alumina in basic and acidic media, respectively.
Source: From The use of organic modifiers in ion exchange chromatography on alumina. The separation of basic drugs, in Chromatographia.[2]

successfully separated on an alumina HPLC column using *n*-hexane-ethyl acetate mixtures as mobile phases. Significant linear correlations were found between the molecular parameters of the solutes and their retention characteristics:

$$\log k_0' = 3.61 + (0.37 \pm 0.03)n_e \quad r = 0.9911 \tag{1}$$

$$b = 3.54 + (1.18 \pm 0.03)n_e \quad r = 0.9991 \tag{2}$$

where k_0' is the capacity factor of nonylphenyl ethyleneoxide oligomer surfactants, extrapolated to zero concentration of ethyl acetate in the mobile phase; b is the slope value of the linear relationship between the log k' values of surfactants and the concentration of ethyl acetate in the eluent $\pm$ standard deviation; and n_e is the number of ethylene oxide groups per molecule.

$$\log k_0' = 3.41 + (0.36 \pm 0.01)n_e + (0.13 \pm 0.03)\text{PI} \quad F = 217.65 \tag{3}$$

$$b = 3.56 + (0.78 \pm 0.07)n_e + (0.52 \pm 0.13)\text{PI} \quad F = 64.65 \tag{4}$$

where PI characterizes the position of the butyl substituents, other symbols are the same as in Eqs. 1 and 2.

The data entirely support the previous conclusions concerning the retention mechanism of surfactants on alumina. Moreover, Eqs. 3 and 4 indicate that alumina is an excellent support for the separation of tetrabutylphenyl ethylene oxide oligomers according to the number of ethylene oxide groups and the position of the alkyl substituents in one run. The efficiency of alumina support for the separation of positional isomers was also established with HPLC–mass spectrometry (HPLC–MS).[9]

MODIFIED ALUMINA

Polymers have also been used for the coating of alumina. Thus, maleic acid adsorbed onto the alumina surface was, in situ, polymerized with 1-octadecene and cross-linked with 1,4-divinylbenzene.[10] It was assumed that the polymer forms a monolayer on the alumina, forming a reversed-phase surface. This assumption was substantiated by results showing that the retention order of model compounds was the same as on an ODS column. The lower separation capacity of the new stationary phase was tentatively explained by the lower surface porosity of alumina. Principal component analysis was employed for the elucidation of the relationship between the retention behavior of non-homologous series of solutes on polybutadiene (PBD)-coated alumina and their physicochemical parameters.[11] Calculations revealed significant relationships

between the capacity factor extrapolated to pure water (k_w') and the physicochemical parameters:

$$\log k_w' = 0.052 + 0.208(\log P) \quad (5)$$

$n = 21;\ s = 0.279;\ r = 0.9711;\ F = 314$

$$\log k_w' = 1.618 + 0.089\text{bonrefr } 2.505\text{delta} \quad (6)$$

$n = 21;\ s = 0.500;\ r = 0.9090;\ F = 42.8$

$$\log k_w' = 1.272 + 0.089\text{bonrefr } 2.648\text{delta } 0.598\text{ind} \quad (7)$$

$n = 21$; $s = 0.394$; $r = 0.9476$; $F = 49.8$ where $\log P$ is the hydrophobicity, "bondrefr" is the molecular refractivity, "delta" is the submolecular polarity parameter, "ind" indicator variable (0 for heterocyclics and 1 for benzene derivatives). Calculations indicated that PBD-coated alumina behaves as an RP stationary phase, the bulkiness and the polarity of the solute significantly influencing the retention. The separation efficiency of PBD-coated alumina was compared with those of other stationary phases for the analysis of *Catharanthus* alkaloids. It was established that the pH of the mobile phase, the concentration and type of the organic modifier, and the presence of salt simultaneously influence the retention. In this special case, the efficiency of PBD-coated alumina was inferior to that of ODS.[12] The retention characteristics of polyethylene-coated alumina (PE-Alu) have been studied in detail using various non-ionic surfactants as model compounds.[13] It was found that PE-Alu behaves as an RP stationary phase and separates the surfactants according to the character of the hydrophobic moiety. The relationship between the physicochemical descriptors of 25 aromatic solutes and their retention on PE-coated silica (PE-Si) and PE-Alu was elucidated by stepwise regression analysis.[14]

$$\log k_{\text{PE-Alu}}' = 0.144(\pm 0.092) + 0.9325(\pm 0.0505)\log k_{\text{PE-Si}}' \quad (8)$$

$n = 25;\ r = 0.968;\ s = 0.333;\ F = 340$

$$\log k_{\text{PE-Alu}}' = 1.474(\pm 0.376) + 0.5976(\pm 0.2990)R_2 + 0.9162(\pm 0.3025)\pi_2{}^{*}0.8279(\pm 0.2624) \times \sum \beta_2{}^{\text{H}} + 3.206(\pm 0.304)V_x \quad (9)$$

$n = 24;\ r = 0.958;\ s = 0.397;\ F = 53$

$$\log k_{\text{PE-Si}}' = 1.670(\pm 0.373)0.9167(\pm 0.2120)\pi_2{}^{*} + 3.842(\pm 0.267)V_x \quad (10)$$

$n = 24;\ r = 0.956;\ s = 0.398$

$$\log k_{\text{PE-Alu}}' = 2.122(\pm 0.549)2.068(\pm 0.798)\delta_{\max} + 0.3283(\pm 0.0897)\mu + 0.00940(\pm 0.00111)V_{\text{aq}} \quad (11)$$

$n = 25;\ r = 0.926;\ s = 0.525;\ F = 42$

$$\log k_{\text{PE-Si}}' = 2.401(\pm 0.456)2.424(\pm 0.662)\delta_{\max} + 0.2821(\pm 0.0746)\mu + 0.01057(\pm 0.00092)V_{\text{aq}} \quad (12)$$

$n = 25$; $r = 0.953$; $s = 0.436$; $F = 69$ where μ is the total dipole moment, $\delta_{\max}$ is the maximum electron excess charge (electron deficiency) on an atom in the solute molecule, V_{aq} is the solvent (water) accessible molecular volume. Calculations proved that both stationary phases behave as RP supports, with the retention strength of PE-Si being higher. The retention can be successfully related to the molecular parameters included in the calculations.

The differences observed may be attributed to free silanol groups on the silica surface not covered by the polyethylene coating.

Various synthetic methods were developed for the covalent binding of hydrophobic ligands to the surface of alumina.[15,16] These methods generally resulted in real RP stationary phases with higher pH stability than the silica-based stationary phase. The retention of 33 commercial pesticides was determined on OD alumina, ODS, and on alumina support.[17] Stepwise regression analysis proved that the retention of pesticides on OD alumina does not significantly depend on the lipophilicity of pesticides determined on a silica-based RP support. This discrepancy was tentatively explained by the different binding characteristics of the adsorption centers on the surfaces of silica and alumina not covered by the hydrophobic ligand. Using another set of solutes, the similarities of the retention order on both OD alumina and ODS was observed.[18]

The spectral mapping technique, combined with cluster analysis and non-linear mapping, was used for the comparison of the retention behaviors of RP silica and RP alumina columns using tributylphenol ethylene oxide oligomers as model compounds.[19] The columns included in the experiments were C_1, C_2, C_6, C_8, and C_{18} silica, Pe-Si, alumina, and C_{18} alumina. The retention strengths of RP-HPLC columns showed considerable variations, the strongest and the weakest being C_{18} silica and PE-Si, respectively. The retention strength of alkyl-modified silicas depended linearly on the carbon load. The two-dimensional selectivity map and the cluster dendogram of the column selectivities are depicted in Figs. 3 and 4, respectively. From the results, it is clear that both the strength and the selectivity of retention show high variations. C_1, PE-Si, and PE-Alu exhibited similar retention selectivity.

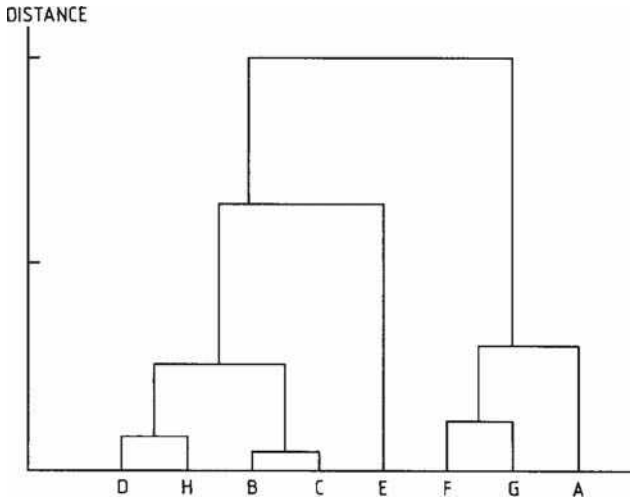

Fig. 3 Two-dimensional non-linear selectivity map of reversed-phase HPLC columns. Number of iterations: 377. Maximum error: 2.1×10^{-3}. (A) C_1 silica; (B) C_2 silica; (C) C_6 silica; (D) C_8 silica; (E) C_{18} silica; (F) polyethylene coated silica; (G) polyethylene-coated alumina; (H) C_{18} alumina.
Source: From Determination of retention behaviour of some non-ionic surfactants on reversed-phase high-performance liquid chromatography supports by spectral mapping in combination with cluster analysis or non-linear mapping, in J. Chromatogr. A.[19]

This result may be attributed to the fact that polyethylene chains lie parallel to the surface of the support, with the end groups being anchored to the polar adsorption centers. According to this model, only the surface of the polyethylene coating pointing toward the mobile phase is available to the solutes in the mobile phase. This apolar polymeric layer is similar in thickness to the C_1 coating but differs markedly from the longer alkyl chains that are more or less immersed in the mobile phase and are providing more CH_2 groups for the binding of apolar solutes. The conclusions drawn from the two-dimensional non-linear mapping and cluster analysis are similar, suggesting that both methods can be used for the reduction of the dimensionality of a multidimensional spectral map.

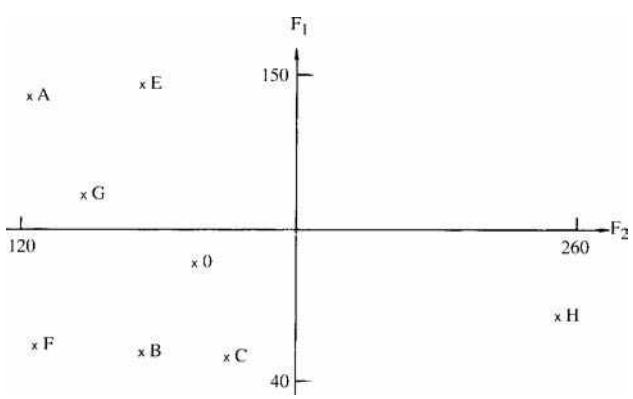

Fig. 4 Cluster dendogram of RP-HPLC columns. For symbols, see Fig. 3.
Source: From Determination of retention behaviour of some non-ionic surfactants on reversed-phase high-performance liquid chromatography supports by spectral mapping in combination with cluster analysis or non-linear mapping, in J. Chromatogr. A.[19]

CONCLUSIONS

The development of new non-silica-based stationary phases was mainly motivated by the poor stability of silica and modified silicas at extreme pH values. It was shown that alumina supports can be used successfully for the solution of a wide variety of analytical problems concerning the separation of natural products, pharmaceuticals, and xenobiotics at any mobile phase pH. Moreover, alumina shows different retention characteristics than silica (i.e., it shows higher separation capacity for positional isomers). The data may facilitate not only the solution of various practical separation problems in LC, but will also promote a better understanding of the underlying physicochemical principles governing retention.

REFERENCES

1. Snyder, L.R. Separability of aromatic isomers on alumina: Mechanism of adsorption. J. Phys. Chem. **1962**, *72*, 489–492.
2. Laurent, C.; Billiet, H.A.H.; de Galan, L. The use of organic modifiers in ion exchange chromatography on alumina. The separation of basic drugs. Chromatographia **1983**, *17*, 253–258.
3. Laurent, C.; Billiet, H.A.H.; de Galan, L. On the use of alumina in HPLC aqueous mobile phases at extreme pH. Chromatographia **1983**, *17*, 394–398.
4. Laurent, C.; Billiet, H.A.H.; de Galan, L.; Byutenhuys, F.A.; van der Maeden, F.P.B. High-performance liquid chromatography of proteins on alumina. J. Chromatogr. **1984**, *287*, 45–49.
5. Ahmad, J. The use of alumina as stationary phase for thin layer chromatography of inorganic and organometallic compounds. JPC, J. Planar Chromatogr.-Mod. TLC **1996**, *9*, 236–239.
6. Szilagyi, A.; Forgács, E.; Cserháti, T. Separation of non-ionic surfactants according to the length of the ethylene oxide chain on alumina layers. Toxicol. Environ. Chem. **1998**, *65*, 95–102.
7. Forgács, E.; Cserháti, T. Retention behavior of nonylphenyl ethyleneoxide oligomers on an alumina high-performance liquid chromatographic column. Fresenius J. Anal. Chem. **1995**, *351*, 688–689.
8. Forgács, E.; Cserháti, T. Retention behaviour of tributylphenol ethylene oxide oligomers on an alumina high

performance liquid chromatographic column. J. Chromatogr. **1994**, *661*, 239–243.

9. Kòsa, A.; Dòbo, A.; Vèkey, K.; Forgács, E. Separation and identification of nonylphenylethylene oxide oligomers by high-performance liquid chromatography with UV and mass spectrometric detection. J. Chromatogr. A, **1998**, *819*, 297–302.
10. Mao, Y.; Fung, B.M. Use of alumina with anchored polymer coating as packing material for reversed-phase high performance liquid chromatography. J. Chromatogr. A, **1997**, *790*, 9–15.
11. Kaliszan, R.; Osmialowski, K. Correlation between chemical structure of non-congeneric solutes and their retention on polybutadiene-coated alumina. J. Chromatogr. **1990**, *506*, 3–16.
12. Theodoridis, G.; Papadoyannis, I.N.; Hermans-Lokkerbol, A.; Verpoorte, R. A study of the behaviour of some new column materials in the chromatographic analysis of *Catharanthus* alkaloids. Chromatographia **1997**, *45*, 52–57.
13. Forgács, E. Comparison of reversed-phase chromatographic systems with principal component and cluster analysis. Anal. Chim. Acta **1994**, *296*, 235.
14. Cserháti, T.; Forgács, E.; Payer, K.; Haber, P.; Kaliszan, R.; Nasal, A. Quantitative structure–retention relationships in separation mechanism studies on polyethylene-coated silica and alumina stationary phases. LC-GC Int. **1998**, *11*, 240.
15. Pesek, J.J.; Lin, H.-D. Evaluation of synthetic procedures for the chemical modification of alumina for HPLC. Chromatographia **1989**, *28*, 565–574.
16. Pesek, J.J.; Sandoval, E., Jr.; Su, M. New alumina-based stationary phases for high-performance liquid chromatography. J. Chromatogr. **1993**, *630*, 95–103.
17. Cserháti, T.; Forgács, E. Separation of pesticides on an octadecyl-coated alumina column. Fresenius J. Anal. Chem. **1997**, *358*, 558–560.
18. Haky, J.E.; Vemulapalli, S.; Wieserman, L.F. Comparison of octadecyl-bonded alumina and silica for reversed-phase high performance liquid chromatography. J. Chromatogr. **1990**, *505*, 307–318.
19. Forgács, E.; Cserháti, T. Determination of retention behaviour of some non-ionic surfactants on reversed-phase high-performance liquid chromatography supports by spectral mapping in combination with cluster analysis or non-linear mapping. J. Chromatogr. A, **1996**, *722*, 281–287.

Amines, Amino Acids, Amides and Imides: Derivatization for GC Analysis

Igor G. Zenkevich
Chemical Research Institute, St. Petersburg State University, St. Petersburg, Russia

Abstract

The amines are an extensive class of organic compounds of general formula RNH_2 (primary), RR′NH (secondary), and RR′R″N (tertiary). The chemical and chromatographic properties of these compounds are determined by the presence of a basic functional group and active hydrogen atom(s) in the molecule. Amides are derivatives of carboxylic acids with structural fragments –CO–N < , > PO–N <, or $–SO_2^-$ N, while imides have two acyl fragments connected through a nitrogen atom, e.g., –CO–NR–CO–, or –CO–NR–SO_2^-. The compounds with structural fragment > C=N–, "imines", have the trivial name "Schiff bases." As these compounds have no active hydrogen atoms, they need no derivatization and, moreover, they themselves are the derivatives of both amines and carbonyl compounds.

The simplest members of the amine class usually are volatile enough for their direct gas chromatography (GC) analysis. Nevertheless, the principal reason for the derivatization of amines and related compounds is the high sensitivity of amino compounds to various chemical agents. Among the multitude of organic substances, only amines in acidic media reversibly form nonvolatile salts, which can make their GC analysis impossible. Besides that, these compounds are very sensitive to the action of various electrophilic reagents; their exhaustive alkylation gives nonvolatile quaternized ammonium salts, which cannot be restored to the initial analytes. Finally, amino compounds are easily oxidized. Owing to the above-mentioned facts, the principal goal of derivatization of amines and related substances is to protect these compounds from chemical transformations prior to GC analysis by their conversion to more stable derivatives.

INTRODUCTION

Amides are an extensive class of organic compounds of general formula RNH_2 (primary), RR′NH (secondary), and RR′R″N (tertiary). Their chemical and chromatographic properties are determined by the presence of a basic functional group and (for *prim* and *sec* amines) active hydrogen atoms in the molecule. The basicity is very different for aliphatic amines (pK_a 10.5 ± 0.8) and substituted anilines (pK_a 4.9 ± 0.3) owing to the p–π conjugation N–Ar. Amides are derivatives of carboxylic acids with structural fragments -CO–N<, >PO–N<, or $–SO_2–$N< (including cyclic structures), while imides have two acyl fragments connected through a nitrogen atom, e.g., –CO–NR–CO–, as in the molecule of saccharine. Some other groups of nitrogen-containing compounds should also be mentioned here: compounds with structural fragment >C = N– (the so-called Schiff bases), which also have the synonym *imines*. As the last-mentioned compounds have no active hydrogen atoms they need no derivatization, and, moreover, they themselves are the derivatives of both amines and carbonyl compounds.

The simplest members of the amine class are usually volatile enough for direct gas chromatography (GC) analysis. For example, the comparison of simple tertiary amines with the structurally analogous isoalkanes indicates that both the boiling point at atmospheric pressure and the gas chromatographic retention indices (RIs) for the tertiary amines are slightly lower (!) than for the corresponding alkanes (Table 1).

A similar comparison of physicochemical and chromatographic properties of amides (first, the primary amines, $RCONH_2$) indicates that these compounds are highly polar, the polarity exceeding that of the corresponding carboxylic acids, RCO_2H. This is because of the high polarity of the CO–NH bond, which is reflected by the dipole moments (μ): about 1.7 D for acids and ~3.7 D for amides. Moreover, the difference in the boiling point (T_b) of simplest amides and acids exceeds 100°C. The measure of chromatographic polarity is the difference in RI in the standard polar and non-polar

Table 1 Comparison of physicochemical (boiling points) and chromatographic (retention indices) properties of some tertiary amines and structurally related alkanes.

Compound	T_b, °C	$RI_{non\text{-}polar}$
tert-Amine R_3N		
Et_3N	89.4	677 ± 8
Pr_3N	156.5	933 ± 8
Hydrocarbon analog R_3CH		
Et_3CH	93.4	687 ± 3
Pr_3CH	157.5	936 ± 15

Table 2 Comparison of physicochemical (boiling points) and chromatographic (retention indices on non-polar and polar phases) properties of some carboxylic acids and their primary amides.

Acid	Tb, °C	$RI_{non\text{-}polar}$	RI_{polar}	Amide	Tb, °C	$RI_{non\text{-}polar}$	RI_{polar}
CH_3CO_2H	118	638 ± 10	1428 ± 30	CH_3CONH_2	221	711 ± 19	1759 ± 26
$C_2H_5CO_2H$	141	725 ± 18	1524 ± 23	$C_2H_5CONH_2$	222	808 ± 6	1815 ± 12

phases (ΔRI): about 800 i.u. for acids and above 1000 i.u. for amides (Table 2).

However, high polarity is not the principal reason why amines and related compounds can be derivatized easily. More important is the high sensitivity of amino compounds to various chemical agents. Among the multitude of organic substances, only amines in acidic media form non-volatile salts, which can make their GC analysis impossible. Of course, these salts can be recovered as free bases by treating them with other (more basic) amines or with excess of ammonia.[1] Besides, these compounds are very sensitive to various electrophilic reagents; their exhaustive alkylation yields non-volatile quaternized ammonium salts $(R_4N)^+X^-$, which cannot be restored to the initial analytes by the action of bases. Owing to their non-volatility, these salts cannot be the objects of GC analysis, but their injection into hot parts of chromatographic systems can lead to the formation of some volatile products (artifacts). Also, some of the amino compounds are easily oxidized. Hence, the principal goal of derivatization of amines and related substances is to protect these compounds from chemical transformations prior to GC analysis by converting them to more stable derivatives.

Also, as per the general principles of derivatization, when other polar functional groups with active hydrogen atoms are present in molecules, the derivatization of one or (better) all of them becomes necessary. This is typical in the case of amino acids, which exist in the form of inner-molecular salts $RCH(NH_3^+)CO_2^-$ in the solid state.

Table 3 Physicochemical and gas chromatographic properties of some derivatization reagents for acylation of amino compounds.

Reagent	Abbreviation	MW	T_b, °C (P)	$RI_{non\text{-}polar}$	By-products ($RI_{non\text{-}polar}$)
Acetic anhydride	—	102	139.6	706 ± 9	CH_3CO_2H (638 ± 10)
Trifluoroacetic anhydride	TFAA	210	39–40	515 ± 6	CF_3CO_2H (744 ± 6)
Pentafluoropropionic anhydride	PFPA	310	70–72	606 ± 6[a]	$C_2F_5CO_2H$ (781 ± 12)
Heptafluorobutyric anhydride	HFBA	410	109–111	745 ± 4[a]	$C_3F_7CO_2H$ (863 ± 16)
bis-Trifluoroacetyl methylamine	MBTFA	223	120–122	773 ± 16[a]	$CF_3CONHCH_3$ (540)
N-Trifluoroacetyl imidazole	TFAI	164	137–138	830 ± 21[a]	Imidazole (1072 ± 17)
Chloroacetic anhydride	—	170	203	1116 ± 18[a]	ClH_2CO_2H (864 ± 10)
Dichloroacetic anhydride	—	238	214–216	1248 ± 14[a]	Cl_2CHCO_2H (1048 ± 23)
Trichloroacetic anhydride	—	306	222–224	1471 ± 27[a]	CCl_3CO_2H (1270[a])
Benzoyl chloride	—	140	197–198	1046 ± 9	$C_6H_5CO_2H$ (1201 ± 24)
Pentafluorobenzoyl chloride	PFB-Cl	230	158–159	922 ± 14[a]	$C_6F_5CO_2H$ (no data)
Chlorodifluoroacetic anhydride	—	242	92–93	679 ± 8[a]	$ClCF_2CO_2H$ (793)
Acetyl chloride	—	78	51.8	542 ± 7	CH_3CO_2H (638 ± 10)
Chloroacetyl chloride	—	112	106.1	622 ± 8	$ClCH_2CO_2H$ (864 ± 3)
Dichloroacetyl chloride	—	146	107–108	726 ± 19[a]	Cl_2CHCO_2H (1048 ± 23)
Trichloroacetyl chloride	—	180	118	778 ± 15	CCl_3CO_2H (1270[a])
Pivaloyl anhydride	—	186	192–193	1053 ± 31[a]	$(CH_3)_3CO_2H$ (804)
Methyl chloroformate	—	94	71	586 ± 16	CH_3OH (348 ± 12)
Ethyl chloroformate	—	108	93	652 ± 17	C_2H_5OH (452 ± 18)
Propyl chloroformate	—	122	105–106	718 ± 13	C_3H_7OH (552 ± 13)
Chloromethyl chloroformate	—	128	107–108	714 ± 23[a]	—
2-Fluoroethyl chloroformate	—	126	131–135	—	FCH_2CH_2OH (494 ± 9)
2,2,2-Trichloroethyl chloroformate	—	210	171–172	976 ± 18[a]	CCl_3CH_2OH (850 ± 7)
Diethyl pyrocarbonate	DEPC	162	93–94(18)	—	CO_2, C_2H_5OH (452 ± 18)

[a]Estimated RI values.

Table 4 Physicochemical and gas chromatographic properties of some carbonyl reagents and their analogs used for derivatization of amino compounds.

Reagent	Abbreviation	MW	T_b, °C	$RI_{non\text{-}polar}$
Acetone	—	58	56.2	472 ± 12
Pentafluorobenzaldehyde	—	196	166–168	943 ± 22[a]
Thiophen-2-carboxaldehyde	—	112	198	966 ± 9
Carbon disulfide	—	76	46.3	530 ± 9
Methyl isothiocyanate[b]	—	73	118	689 ± 16
Phenyl isothiocyanate[b]	—	135	219–221	1163 ± 7
Dimethyl formamide dimethyl acetal	DMF-DMA	119	106	726 ± 4
Dimethyl formamide diethyl acetal	DMF-DEA	147	134–136	826 ± 5[a]

[a]Estimated RI values.
[b]Only for derivatization of amino acids; with monofunctional amines non-volatile thiocarbamoyl derivatives can be formed.

DERIVATIZATION OF AMINES

The principal methods of amino compound derivatization for GC analysis include the following types of chemical reactions:[2–5]

- Acylation: $RR'NH + R''COX + B \rightarrow RR'NCOR'' + BH^+X^-$
- Formation of Schiff bases (only for primary amines): $RNH_2 + R'R''CO \rightarrow RN = CR'R'' + H_2O$
- Alkylation: $RR'NH + R''X + B \rightarrow RR'NR'' + BH^+X^-$
- Silylation: $RR'NH + XSi(CH_3)_3 \rightarrow RR'NSi(CH_3)_3 + XH$

Acylation is the most common method as amides are preferred over other kinds of derivatives. Their basicity is significantly less than that of amines and, hence, the pH of samples indicates that the influence is not as strong as on initial amines. Schiff bases and especially *N*-trimethylsilyl (TMS) derivatives are sensitive to postreaction hydrolysis.

A number of recommended acylating reagents are listed in Table 3, and they belong to two classes of chemicals: anhydrides (X = OCOR″) and chloroanhydrides (X = Cl). The most widely used among them are acetic, trifluoroacetic (TFA), pentafluoropropanoic (PFP), and heptafluorobutanoic (HFB) anhydrides, as well as pentafluorobenzoyl chloride (PFB-Cl).[6] The by-products of acylation in all cases are acids; these reactions need basic media (additives of pyridine or tertiary amines) to prevent the formation of non-volatile salts from the analytes. The technique of derivatization is extremely simple: sample mixtures are allowed to stand with acylating reagents for some minutes prior to analysis.

The anhydrides and chloroanhydrides of chlorinated acetic acids and PFB-Cl (electrophoric reagents) are used for the synthesis of chlorinated amides for GC analysis with selective detectors [e.g., electron-capture detector (ECD)]. Diethylpyrocarbonate converts primary and secondary amines (including NH_3) into *N*-substituted carbamates:

$$RR'NH + O(CO_2C_2H_5)_2 \rightarrow RR'NCO_2C_2H_5 + CO_2 + C_2H_5OH$$

The next group of derivatization reactions is the formation of Schiff bases from primary amines with carbonyl compounds. Some recommended reagents are listed in Table 4. Aromatic aldehydes (including pentafluorobenzaldehyde as electrophoric reagent[7]) are much more reactive in this condensation as compared with ketones and aliphatic compounds (of the latter, only low-boiling acetone and cyclohexanone have been used in GC practice). The synthetic analogs, primarily acetals and ketals, of carbonyl compounds can be made to react with amines. Thus dimethylformamide dialkylacetals, $(CH_3)_2N–CH(OR)_2$, react with primary amines, $R'NH_2$ forming *N*-dimethylaminomethylene derivatives, $R'–N = CH–N(CH_3)_2$. As long as these reagents catalyze the esterification of carboxyl groups, they can be used for single-stage derivatization of amino acids (see below).

Table 5 Comparison of retention indices for *N*-trimethylsilyl derivatives of simplest primary amines and corresponding isothiocyanates.

R	$RI_{non\text{-}polar}$ [$RNHSi(CH_3)_3$]	$RI_{non\text{-}polar}$ (RNCS)
Me	689 ± 21	689 ± 16
Et	756 ± 11	736 ± 5

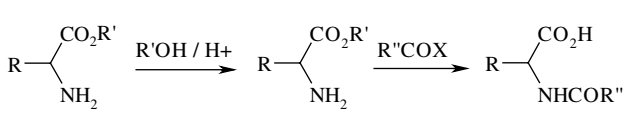

Fig. 1 "Classical" two-step scheme for derivatization of amino acids.

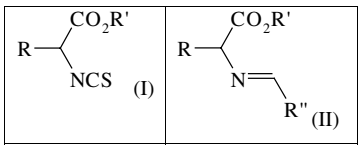

Fig. 2 Some alternative to *N*-acylated derivatives of amino acids.

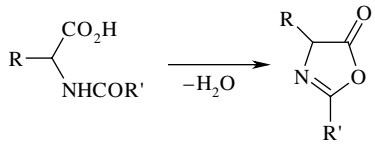

Fig. 4 Dehydration of *N*-acyl derivatives of amino acids with formation of azlactones.

Carbon disulfide as the thio-analog of carbonyl compounds reacts with primary amines, resulting in the formation of alkyl isothiocyanates, which have slightly lower RIs than those of other derivatives of primary amines, including *N*-trimethylsilylated amines (Table 5). The sole product of this reaction is gaseous hydrogen sulfide:

$$RNH_2 + CS_2 \rightarrow RNCS + H_2S$$

The alkylation of amines was a highly popular method of derivatization in peptide chemistry before the practice of contemporary mass spectrometric techniques for the analysis of non-volatile compounds. Direct alkylation of amines by alkyl halides (Hoffman reaction) can finally lead to non-volatile ammonium salts and, hence, other *soft* reagents should be used. For example, exhaustive methylation without quaternization can be provided by the mixtures $CH_2O/NaBH_4/(H^+)$ or CH_2O/formic acid.

At present silylation of amines is a well-investigated,[8] but relatively rarely used, method for their derivatization owing to the facile hydrolysis of the resultant *N*-TMS compounds. It leads to the formation, in the reaction mixtures, of both *mono*-(RNHTMS) and *bis*-[RN(TMS)$_2$] derivatives. This multiplicity of products from the same precursor presents some difficulties in data interpretation. The *N*-(*tert*-butyldimethylsilyl) (TBDMS) derivatives are more resistant to hydrolysis, and their formation is unambiguous (only *N*-monosubstituted compounds are formed) because of steric reasons.[9–11] It is interesting to note that one of the numerous silylating agents (see Table 3 in *Hydroxy Compounds: Derivatization for GC Analysis*, p. 1165)—trimethylsilyl imidazole—possesses a unique selectivity, because it is inert in relation to amines.

Some special derivatization methods are recommended for amines for optimizing their determination in dilute water samples, especially in combination with preconcentration of analytes. This explains the choice of conversion of primary aromatic amines by iodine into the corresponding iodoarenes:[12]

$$ArNH_2 + 1.5I_2 \rightarrow ArI + 2HI + 0.5N_2$$

In the example of amines it is interesting to note an *exotic* derivatization reaction, where a single reagent provides double functionalization of the protected group by different structural fragments. This reagent is trimethylsilylketene, $(CH_3)_3Si–CH = C = O$, which reacts with primary amines giving their TMS-acetyl derivatives:[13]

$$RNH_2 + Me_3SiCHCO \rightarrow [R - N(COCH_3) - SiMe_3] \rightarrow R - N = C(CH_3) - OSiMe_3$$

Because there were no obvious advantages, this method was not modified; however, it illustrates the specific chemical properties of an interesting reagent.

Tertiary amines have no active hydrogen atoms, and their derivatization is not required in the generally accepted sense. The reactions of these compounds do not imply the substitution of active hydrogen atoms, but the cleavage of N–C bonds. If necessary (for GC analysis with selective detectors), N–CH_3 bonds can be cleaved by chloroformates:

$$R'R''N - CH_3 + CCl_3CH_2OCOCl \rightarrow R'RN - CO_2CH_2CCl_3$$

DERIVATIZATION OF AMINO ACIDS

Mixtures of amino acids, R–CH(NH_2)CO_2H, produced by the hydrolysis of polypeptides are important for chromatographic analysis. Some dozens of methods have been proposed for derivatization of these compounds for their GC

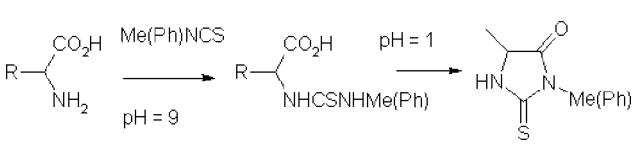

Fig. 3 Formation of *N*-carbamoyl derivatives of amino acids, followed by their cyclization to phenylthiohydantoines.

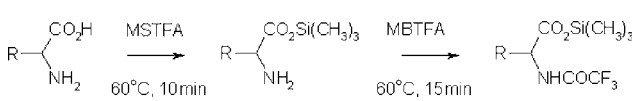

Fig. 5 Two-stage *O*-silylation-*N*-acylation of amino acids.

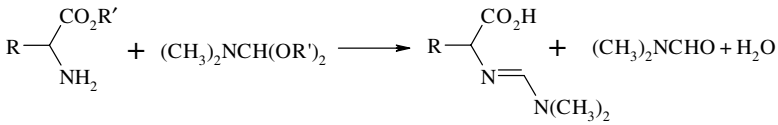

Fig. 6 One step formation of *N*-dimethylaminomethylene derivatives of amino acids *O*-esters.

determination. The most widely used can be subdivided into two types:

1. Separate derivatization of functional groups CO_2H and NH_2 by different reagents.
2. Protection of both groups by only one reagent.

Typical derivatives of the first type are the various esters (Me, Et, Pr, *iso*-Pr, Bu, *iso*-Bu, *sec*-Bu, Am, *iso*-Am, etc.) of *N*-acyl (acetyl, TFA, PFP, HFB, etc.) amino acids. The butyl esters of *N*-TFA amino acids owing to the frequency of their use even have a special abbreviation: TAB derivatives. The two-stage process includes the esterification of amino acids by an excess of the corresponding alcohol in the presence of HCl and, after the evaporation of volatile compounds, the treatment of the non-volatile hydrochlorides of alkyl esters by acylating reagents (Fig. 1).

Some variations of this process are known. Instead of *N*-acylation, intermediate esters can be treated with CS_2/Et_3N and CH_3OCOCl, which leads to the formation of 2-alkoxycarbonyl isothiocyanates (I), or with carbonyl compounds, which leads to formation of Schiff bases (II, see Fig. 2), but the analytical advantages of these derivatives are not obvious.

Similar *N*-acyl-*O*-alkyl derivatives can also be used for GC analysis of the simplest oligopeptides (at least dipeptides and tripeptides). The GC analysis of oligopeptides involving multistep sequences including their reduction into polyaminoalcohols by $LiAlH_4$, followed by their secondary derivatization, is outdated.

A typical example of single-stage derivatization of amino acids is based on their reaction with methyl or phenyl isothiocyanates with the formation of 3-methyl (phenyl) thiohydantoins. The optimal analytical method for the analysis of semivolatile organic compounds of this class is RP HPLC, but derivatives of the simplest amino acids can be objects of GC analysis as well (Fig. 3).

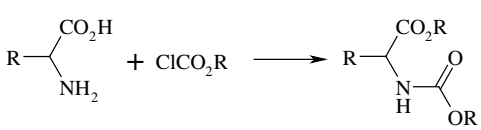

Fig. 7 One-step derivatization of both carboxy and amino groups of amino acids in reaction with chloroformates.

The stable non-volatile intermediate phenyl thiocarbamoyl derivatives are formed in basic media and can be analyzed directly only by RP HPLC. Their cyclization into thiohydantoins requires acid catalysis. This mode of derivatization is an important supplement to the Edman's method of *N*-terminated sequencing of polypeptides. Before GC analysis, all thiohydantoins can be further converted into *N*-TFA or enol-*O*-TMS derivatives, which increases the selectivity of their determination in complex matrices.

N-acylated amino acids in the presence of water-coupling reagents [dicyclohexylcarbodiimide (DCC) or an excess of trifluoroacetic anhydride] form other cyclic derivatives—so-called azolactones (2,4-disubstituted oxazolin-5-ones) (Fig. 4).

The known disadvantage of TMS derivatives of amino acids is the easy postreaction hydrolysis of N–Si bonds in the formed derivatives, which leads to uncertainty regarding the formed products. At the same time, silylation of carboxylic acids is the most popular method for their derivatization (see *Acids: Derivatization for GC Analysis*, p. 3). Hence, it seems reasonable to combine the silylation of CO_2H groups in amino acids with the formation of other derivatives of amino groups, e.g., amides. This method of derivatization was realized only in 2007.[14] The first step is the formation of *O*-TMS derivatives under mild conditions (with MSTFA as reagent), followed by trifluoroacetylation of amino groups by MBTFA (Fig. 5).

One of the most popular methods of single-stage amino acid derivatization at present is their conversion into *N*,*O*(*S*)-*tert*-butyldimethylsilyl (TBDMS) derivatives by the treatment of *tert*-butyldimethylsilyl trifluoroacetamide (MTBSTFA) or its *N*-methyl analog.[9–11,15] Another method was proposed at the beginning of the 1970s and is based on amino acid interaction with dimethylformamide dialkylacetals, $(CH_3)_2NCH(OR')_2$ (R = Me, Et, Pr, *iso*-Pr, Bu, Am), with the formation of

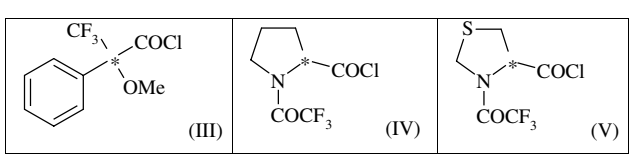

Fig. 8 Some examples of chiral reagents used for separation of chiral amines in the form of diastereomers.

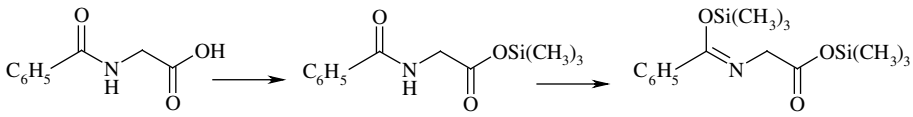

Fig. 9 Consequent formation of mono- and *bis*-TMS derivatives from *N*-acylated amino acids.

N-dimethylaminomethylene derivatives of amino acids alkyl esters (Fig. 6).[16]

An alternative method for the simultaneous derivatization of both carboxylic and amino fragments in amino acids known since the 1990s implies the interaction of these analytes with chloroformates. It leads to the esterification of carboxy groups together with the formation of *N*-ethoxycarbonyl derivatives (Fig. 7).[17]

The GC separation of enantiomeric D- and L-amino acids with non-chiral phases needs their conversion into diastereomeric derivatives. The second chiral center in the molecule [asterisk (*) in Fig. 8] arises after their *O*-esterification by stereochemically pure alcohols [(*R*)- or (*S*)-2-butanol, 2-pentanol, pinacolol, menthol, etc.] or acylation of NH_2 groups by chiral reagents, e.g., α-methoxy-α-trifluoromethylphenylacetyl chloride [MTPAC (III)],[18] *N*-trifluoroacetyl-L-prolyl chloride [*N*-TFA-L-Pro-Cl (IV)], or the corresponding anhydride[19] *N*-trifluoroacetylthiazolidine-4-carbonyl chloride (V).

DERIVATIZATION OF AMIDES AND IMIDES

The derivatization methods available for amides and imides is not so vast as for other classes of amino compounds (remember that numerous amides themselves are used as the target analytical derivatives of amino compounds). The active hydrogen atoms in the structural fragments –CO–NH– or SO_2–NH– are rather acidic and, hence, sometimes the recommended acetyl or TFA derivatives of these compounds (with additional acidic protection groups) are unstable with respect to hydrolysis.

Trimethylsilyl derivatives of amides seem to be more appropriate for GC analysis.[20] However, the molecules of amides contain two nucleophilic centers (*N* and *O*) and, depending on their chemical origin, they can form *N*-TMS or *O*-TMS derivatives. The latter prevails in the case of arylamides, like *N*-aroyl amides [e.g., *N*-benzoyl glycine (hippuric acid)], owing to the formation of conjugate systems (usually both *mono*- and *bis*-TMS derivatives are registered on the chromatograms) (Fig. 9).

The preferable derivatization method for amides is their exhaustive alkylation (e.g., methylation), because permethylated amides and imides are volatile enough for GC analysis. This can be illustrated by the retention data of methylated derivatives of the simplest diamide, namely urea, $CO(NH_2)_2$. Both the initial compound and its mono and two dimethyl homologues cannot be analyzed by GC owing to their non-volatility (contain active hydrogen atoms). The RI of trimethyl urea (one active hydrogen) on standard non-polar polydimethyl siloxanes is 976 ± 28, whereas for tetramethyl urea it is 956 ± 5 (see the better interlaboratory reproducibility of the latter RI value as compared with the previous one).

The exhaustive methylation of amides can be realized with rather high yields by their reactions with dimethyl sulfate in the presence of bases [(*iso*-Pr)$_2$NEt],[21] by CH_3I in acetone solution, with CH_3I in the presence of K_2CO_3 or (less convenient) LiH in DMSO (high-boiling solvent), in heterophase *water–organic solvent* systems (together with the extraction of derivatives from matrices), and directly in the injector of a gas chromatograph (flash methylation) by $PhNMe_3^+OH^-$ (TMPAH). These modes of derivatization precede the GC determination of numerous diuretics (acetazolamide, ethacrinic acid, clopamide, etc.),[22] some barbiturates and their metabolites, xanthines (theophylline, theobromine), different urea and carbamate pesticides (monuron, fenuron, linuron, and their metabolites), and so forth.

CONCLUSIONS

The main reason for the derivatization of amines and related compounds is their chemical lability. Compared with other classes of organic compounds, only amines can reversibly form non-volatile salts with acids. Besides, these compounds are very sensitive to the action of electrophilic reagents, which can irreversibly convert amines into non-volatile ammonium salts. This explains the necessity for derivatization of different amines to prevent chemical transformation of analytes prior to their GC analysis.

REFERENCES

1. Nagase, M. Conversion of amines from their salts into free bases with ammonia. Bunseki Kagaku **1980**, *29* (5), 293–297 (in Japanese).
2. Blau, K.; King, G.S., Eds.; *Handbook of Derivatives for Chromatography*; John Wiley & Sons: Chichester, U.K., 1978; 576.

3. Knapp, D.R. *Handbook of Analytical Derivatization Reactions*; John Wiley & Sons: New York, 1979; 741.
4. Drozd, J. Chemical derivatization in gas chromatography. In *Journal of Chromatography Library*; Elsevier: Amsterdam, 1981; Vol. 19, 232.
5. Blau, K.; Halket, J.M., Eds.; *Handbook of Derivatives for Chromatography*, 2nd Ed.; John Wiley & Sons: New York, 1993; 369.
6. Jia, M.; Wu, W.W.; Yost, M.G.; Chadik, P.A.; Stacpoole, P.W.; Henderson, G.N. Simultaneous determination of trace levels of nine haloacetic acids in biological samples as their pentafluorobenzyl derivatives by gas chromatography/tandem mass spectrometry in electron capture negative ion chemical ionization mode. Anal. Chem. **2003**, *75*, 4065–4080.
7. Avery, M.J.; Junk, G.A. Gas chromatographic/mass spectrometric determination of water soluble primary amines as their pentafluorobenzaldehyde imines. Anal. Chem. **1985**, *57* (4), 790–792.
8. Iwase, H.; Takeuchi, Y.; Murai, A. Gas chromatography—mass spectrometry of TMS derivatives of amines. Chem. Pharm. Bull. **1979**, *27* (4), 1009–1014.
9. Biermann, C.J.; Kinoshita, C.M.; Marlett, J.A.; Steele, R.D. Analysis of amino acids as *tert*-butyldimethylsilyl derivatives by gas chromatography. J. Chromatogr. **1986**, *357*, 330–334.
10. Mawhinney, T.P.; Robinett, R.S.R.; Atalay, A.; Madson, M.A. Analysis of amino acids as their *tert*-butyldimethylsilyl derivatives by gas–liquid chromatography and mass spectrometry. J. Chromatogr. **1986**, *358*, 231–242.
11. Chaves das Neves, H.T.; Vasconcelos, A.M.P. Capillary gas chromatography of amino acids, including asparagines and glutamine: Sensitive gas chromatographic–mass spectrometric and selected ion monitoring gas chromatographic–mass spectrometric detection of the *N*,*O*(*S*)-*tert*-butyldimethylsilyl derivatives. J. Chromatogr. **1987**, *392*, 249–258.
12. Schmidt, T.C.; Less, M.; Haas, R.; VanLow, E.; Steinbach, K.; Stork, G. Gas chromatographic determination of aromatic amines in water samples after solid phase extraction and derivatization with iodine. J. Chromatogr. A, **1998**, *810*, 161–172.
13. Coutts, R.T.; Jones, G.R.; Benderly, A.; Mac, A.L.C. A note on the synthesis and gas chromatographic mass spectrometric properties of *N*-(trimethylsilyl)acetates of amphetamine and analogs. J. Chromatogr. Sci. **1979**, *17* (6), 350–352.
14. Yoon, H.-R. Two step derivatization for the analyses of organic amino acids and glycines on filter paper plasma by GC-MS/SIM. Arch. Pharm. Res. **2007**, *30* (3), 387–395.
15. Paik, M.-J.; Kim, K.-R. Sequential ethoxycarbonylation, methoximation and *tert*-butyldimethylsilylation for simultaneous determination of amino acids and carboxylic acids by dual column gas chromatography. J. Chromatogr. A, **2004**, *1034*, 13–23.
16. Horman, L.; Hesfold, F.J. Amino acid mixture analysis by mass spectrometry in the form of their dimethylaminomethylene methyl esters. Biomed. Mass Spectrom. **1974**, *1* (2), 115–119.
17. Husek, P.; Liebich, H.M. Organic acid profiling by direct treatment of deproteinized plasma with ethyl chloroformate. J. Chromatogr. B, **1994**, *656*, 37–43.
18. Allen, D.A.; Tomaso, A.E.; Priest, O.P.; Hindson, D.F.; Hurlburt, J.L. Mosher amides: Determining the absolute stereochemistry of optically-active amines. J. Chem. Educ. **2008**, *85* (5), 698–700.
19. Adams, J.D.; Woolf, T.F.; Trevor, A.J.; Williams, L.R.; Castagnoli, N. Derivatization of chiral amines with (*S*,*S*)-*N*-trifluoroacetylproline anhydride for GC estimation of enantiomeric composition. J. Pharm. Sci. **1982**, *71* (6), 658–661.
20. Gee, A.J.; Groen, L.A.; Johnson, M.E. Determination of fatty acid amides as trimethylsilyl derivatives by gas chromatography with mass spectrometric detection. J. Chromatogr. A, **1999**, *849*, 541–552.
21. Nazareth, A.; Joppich, M.; Pauthani, A.; Fisher, D.; Giese, R.W. Alkylation with dialkyl sulfate and ethyl-diisopropyl amine. J. Chromatogr. **1985**, *319*, 382–386.
22. Carreras, D.; Imas, C.; Navajas, R.; Garcia, M.A.; Rodrigues, C.; Rodrigues, A.F.; Cortes, R. Comparison of derivatization procedures for the determination of diuretics in urine by GC-MS. J. Chromatogr. A, **1994**, *683*, 195–202.

Amino Acids and Derivatives: TLC Analysis

Luciano Lepri
Alessandra Cincinelli
Department of Chemistry, University of Florence (UNIFI), Florence, Italy

Abstract
The best operative conditions to separate the 20 natural amino acids by using a wide variety of commercially available stationary phases used both in normal and in reversed-phase chromatography and by two-dimensional (2D) chromatography technique are described. Resolution of amino acids derivatives, which play a fundamental role in the peptide and protein sequence structures, is also reported.

INTRODUCTION

Amino acids are carboxylic acids in which a hydrogen atom in the side chain (usually on the α-carbon) has been replaced by an amino group. Hence, they are amphoteric. In weak acid solution, the carboxyl group of a neutral amino acid (with one amino group and one carboxyl group) is dissociated, and the amino group binds a proton to give a dipolar ion (zwitterion). The pH at which the concentration of the dipolar ion is maximum is called the isoelectric point (pI), which is calculated using the relation

$$\mathrm{p}I = \frac{1}{2}(\mathrm{p}K_1 + \mathrm{p}K_2)$$

where pK_1 and pK_2 refer to the dissociation of the carboxyl group and the protonated amino group, respectively (most neutral aliphatic amino acids with a non-polar side chain have pI 6.0, which corresponds to pK_{a1} 2.3 and pK_{a2} 9.7).

Amino acids constitute the basic units of all proteins. The number of α-amino acids obtained from various proteins is about 40, but only 20 are present, in varying amounts, in all proteins. Thin-layer chromatography (TLC) is one of the most promising separation methods for these compounds, for which gas chromatographic (GC) analysis is not suitable.

PREPARATION OF TEST SOLUTIONS

Amino acids should be as free from impurities as possible, since they exhibit a pronounced capacity for binding metal ions. The analysis of amino acids in natural fluids or extracts requires the removal of interfering compounds prior to chromatographic separation, in order to prevent tailing and deformation of the spots (e.g., high salt concentrations are found in urine samples and hydrolysates of proteins or peptides).

Salts can be conveniently removed by passing the sample through a cation-exchange resin column. Free amino acids from sanguine plasma can be obtained after centrifugation of the suspension resulting from the addition of a $Na_3(PW_{12}O_{40})$ solution to the samples for removing proteins.

Enrichment of amino acids in urine (10 ml) can be performed by extracting the lyophilized sample with 1 ml of a methanol–1 *M* HCl mixture (4:1 v/v) and applying an aliquot of supernatant liquid to the plate after centrifugation.

Multivitamin syrups and energy drinks are diluted with an appropriate aqueous–alcoholic mixture (80% ethanol), and the resulting solution is applied to plates for the determination of taurine and lysine.

CHROMATOGRAPHIC TECHNIQUES FOR AMINO ACID SEPARATION

Untreated Amino Acids

Standard solutions of amino acids are usually prepared in water or in aqueous–alcoholic solvents (70% ethanol), with the addition of hydrochloric acid (0.1 *M*) for the dissolution of relatively insoluble amino acids (e.g., tyrosine and cystine). Detection is generally performed with ninhydrin reagent by heating the plates at about 100°C for 5–10 min. After color development with the ninhydrin, treatment of the layer with a complex-forming cation (e.g., Cu^{II}, Cd^{II}, Ni^{II}) causes the color to change from blue to red and increases color fastness considerably. More specific coloration of amino acids can be achieved by adding bases such as collidine and cyclohexylamine to the detecting agent solution, or by using 4-hydroxybenzaldehyde–ninhydrin as spray reagent. For the location of tryptophan and its

derivatives, a 1% solution of *p*-dimethylaminobenzaldehyde in ethanol–hydrochloric acid (1:1 v/v) can be used.

Distinguishable and stable colors of amino acids can be obtained by spraying first with 0.25% 2,3-dichloro-1,4-naphthaquinone and, successively, with 0.4% isatin in ethanol and heating at 110°C for 10 min.

Amino acids have been separated on layers of a wide variety of inorganic and organic adsorbents, ion exchangers, and impregnated plates. The two most commonly used adsorbents are silica gel and cellulose.

Separation on Silica Gel and Cellulose Layers

It is interesting to note that by using neutral eluents such as ethanol or *n*-propanol–water, the acidic amino acids (e.g., Glu, Asp) travel much faster on silica gel than basic amino acids (e.g., Lys, Arg, His), which, indeed, show very small R_f values. The difference is likely due to cation exchange between the protonated amino groups of basic amino acids and the acidic groups present on silica gel. The strong retention observed for these compounds when eluting with acidic solvents (Table 1) confirms this hypothesis. A similar phenomenon is also observed on cellulose plates and may be for the cellulose carboxyl groups.

Furthermore, it is seen that the presence of a hydroxyl group in the molecule does not necessarily reduce the R_f value, as the chromatographic behavior of serine with respect to glycine on layers of silica gel and cellulose shows (Table 1). Some of the numerous eluents that have been used for the separation of amino acids on silica gel are acetone–water–acetic acid–formic acid (50:15:12:3), ethylacetate–pyridine–acetic acid–water (30:20:6:11), 96% ethanol–water–diethylamine (70:29:1), chloroform–formic acid (20:1), chloroform–methanol (9:1), isopropanol–5% ammonia (7:3), and phenol–0.06 *M* borate buffer pH 9.30 (9:1). On cellulose plates, ethylacetate–pyridine–acetic acid–water (5:5:1:3), *n*-butanol–acetic acid–water (4:1:1 and 10:3:9), *n*-butanol–acetone–acetic acid–water (35:35:7:23), *n*-butanol–acetone–ammonia–water (20:20:4:1), collidine–*n*–butanol–acetone–water (2:10:10:5), phenol–methanol–water (7:10:3), ethanol–acetic acid–water (2:1:2), and cyclohexanol–acetone–diethylamine–water (10:5:2:5) have also been used as eluents.

Recently, amino acids used in medical practice as drugs for parenteral and per os feeding, in cattle breeding, and in poultry raising were separated and determined on silica plates.[1] Quantitative determination of serine, threonine, phenylalanine, tryptophan, lysine, ornithine, arginine, valine, and leucine was effected by videodensitometric scanning after selection of the optimum conditions for visualization of the spots on chromatograms by using the plate-immersion technique.

Separation efficiency can be increased by multiple developments or two-dimensional (2D) chromatography.

Table 1 R_f values of the 20 common amino acids in different experimental conditions (ascending technique).

Amino acid and abbreviation	Silica gel G[a]	Microcrystalline cellulose[b]	Fixion 50-X8 (Na+)[c]	Silanized silica gel + 4% HDBS[d]	p*I*
Glycine (Gly)	18	15	56	83	6.0
Alanine (Ala)	22	29	51	74	6.0
Serine (Ser)	18	16	67	85	5.7
Threonine (Thr)	20	21	67	83	6.5
Leucine (Leu)	44	64	22	26	6.0
Isoleucine (Ile)	43	60	28	31	6.1
Valine (Val)	32	48	43	54	6.0
Methionine (Met)	35	23	28	42	5.8
Cysteine (Cys)	7	3	56	–	5.0
Proline (Pro)	14	34	–	63	6.3
Phenylalanine (Phe)	43	55	14	21	5.5
Tyrosine (Tyr)	41	36	12	45	5.7
Tryptophan (Trp)	47	36	2	13	5.9
Aspartic acid (Asp)	17	15	72	86	3.0
Asparagine (Asn)	14	–	–	85	5.4
Glutamic acid (Glu)	24	27	35	83	3.2
Glutamine (Gln)	15	–	–	–	5.7
Arginine (Arg)	6	11	2	28	10.8
Histidine (His)	5	7	11	40	7.6
Lysine (Lys)	3	7	8	47	9.8

[a]Eluent: *n*-butanol–acetic acid–water (80 + 20 + 20 v/v/v).
[b]Eluent: 2-butanol–acetic acid–water (3:1:1 v/v/v).
[c]Eluent: 84 g citric acid + 16 g NaOH + 5.8 g NaCl + 54 g ethylene glycol + 4 ml concentrated HCl (pH = 3.3).
[d]Eluent: 0.5 *M* HCl + 1 *M* CH_3COOH in 30% methanol (pH = 0.7).

Several solvent systems are suitable for 2D separation, and the combination of chloroform–methanol–17% ammonium hydroxide (40 + 40 + 20) and phenol–water (75 + 25) separates all protein amino acids, except leucine and isoleucine, on silica plates.

Multiple development techniques [unidimensional multiple development (UMD) and incremental multiple development (IMD)] were also used to separate the components of a reference solution of amino acids in blood plasma on cellulose plates eluted with acetonitrile–water (8:2 v/v).[2]

Separation on Ion Exchangers and Impregnated Plates

Cellulose ion exchangers (e.g., diethylaminoethyl cellulose) and ion-exchange resins have been widely used as stationary phases for TLC separation of untreated amino acids. Fixion 50-X8 commercial plates, which contain Dowex 50-X8 type resin, have been tested on both Na^+ and H^+ forms for 30 amino acids, and the results obtained for the 20 common protein amino acids are reported in Table 1. The isomer pair of leucine and isoleucine is well separated by this method. In addition, the hydroxyl group notably increases the R_f values owing to the hydrophobic properties of the resin, and the pairs serine/glycine and threonine/alanine can be resolved.

Many studies have focused on impregnated plates. The methods used for impregnation depend on whether the plates are homemade or commercially available. In the first case, the impregnation reagent is usually added to a slurry of the adsorbent, whereas ready-to-use plates are dipped in the solution of the reagent.

The resolution of amino acids has been affected by using different metal ions as impregnating agents at various concentrations. On silica gel impregnated with Ni^{II} salts, the results indicate a predominant role of the partitioning phenomenon when eluting with acidic aqueous and non-aqueous solutions (e.g., *n*-butanol–acetic acid–water and *n*-butanol–acetic acid–chloroform in the 3:1:1 v/v/v ratio). The impregnation of silanized silica gel with 4% dodecylbenzenesulfonic acid (HDBS) solution on both homemade and ready-to-use plates is particularly useful in resolving amino acids.[3] The parameters affecting the retention of amino acids on these layers are the type of adsorbent, the concentration and properties of the impregnating agent, the percentage and kind of organic modifier, pH, and the ionic strength of the eluent.

The data in Table 1 show that complete resolution of basic amino acids (Arg, His, Lys) and of neutral amino acids that differ in their side-chain carbon atom number (i.e., Gly, Ala, Met, Val, Leu, and Ile) is possible on homemade plates of silanized silica gel (C_2) impregnated with a 4% solution of HDBS in 95% ethanol. More compact spots can be obtained on RP-18 ready-to-use plates dipped in the same solution of the surfactant agent.

RESOLUTION OF AMINO ACID DERIVATIVES

The identification of N-terminal amino acids in peptides and proteins is of considerable practical importance because it constitutes an essential step in the process of sequential analysis of peptide structures. Many N-amino acid derivatives have been proposed for this purpose and the ones most commonly studied by TLC are 2,4-dinitrophenyl (DNP)- and 5-dimethylaminonaphthalene-1-sulfonyl (dansyl, Dns)-amino acids, and 3-phenyl-2-thiohydantoins (PTH-amino acids). Recently, 4-(dimethylamino)azobenzene-4′-isothiocyanate (DABITC) and phenyl-isothiocyanate (PITC) have also been investigated as derivatizing agents of amino acids.

DNP-Amino Acids

The dinitrophenylation of amino acids, peptides, and proteins and their separation by 1D and 2D TLC have been reviewed by Rosmus and Deyl.[4]

DNP-amino acids are divided into those that are ether extractable and those that remain in the aqueous phase. Water-soluble α-DNP-Arg, α-DNP-His, ε-DNP-Lys, bis-DNP-His, *O*-DNP-Tyr, DNP-cysteic acid ($CySO_3H$), and DNP-cystine $(Cys)_2$ have been identified on silica gel plates in the *n*-propanol–34% ammonia (7:3 v/v) system. Although separation of DNP-Arg and ε-DNP-Lys is incomplete (R_f values 0.43 and 0.44, respectively), both of them can be detected because of the color difference produced in the ninhydrin reaction.

Ether-soluble DNP-amino acids have been investigated by 1D and 2D chromatography. The latter technique offers the possibility of almost complete separation of the two groups of derivatives.

The yellow color of DNP-amino acids deepens upon exposure to ammonia vapor, and it is sufficiently intense for visualizing even 0.1 μg. The detection limit is lower (about 0.02 μg) under UV light (360 nm with dried plates and 254 nm with wet ones), but it increases for 2D chromatography (about 0.5 μg). At present, the applications of DNP-amino acids are limited.

PTH-Amino Acids

The formation of PTH-amino acids by the Edman degradation[5] of peptides and proteins or by successive modifications of the method constitutes the most commonly used technique for the study of the structure of biologically active polypeptides today. Identification of PTH-amino acids in mixtures may be successfully achieved by TLC. Quantitative determination is based on UV adsorption (detection limit: 0.1 μg at 270 nm). An alternative is offered by the chlorine/toluidine test, which is very useful since the minimal amount required for detection is about 0.5 μg.

When 1D chromatography on alumina, polyamide, and silica gel is used, difficulties are encountered in resolving Leu/Ile and Glu/Asp pairs as well as other combinations

of PTH-amino acids (e.g., Phe/Val/Met/Thr). The most common solvents used on polyamide plates are *n*-heptane–*n*-butanol–acetic acid (40:30:9), toluene–*n*-pentane–acetic acid (60:30:35), ethylene chloride–acetic acid (90:16), and ethylacetate–*n*-butanol–acetic acid (35:10:1), and those employed on silica gel are *n*-heptane–methylene chloride–propionic acid (45:25:30), xylene–methanol (80:10), chloroform–ethanol (98:2), chloroform–ethanol–methanol (89.25:0.75:10), chloroform–*n*-butylacetate (90:10), diisopropyl ether–ethanol (95:5), methylene chloride–ethanol–acetic acid (90:8:2), *n*-hexane–*n*-butanol (29:1), *n*-hexane–*n*-butylacetate (4:1), pyridine–benzene (2.5:20), methanol–carbon tetrachloride (1:20), and acetone–methylene dichloride (0.3:8). The complete resolution of specific mixtures is possible with 2D chromatography by the use of certain solvent systems mentioned.

The characteristic colors of PTH-amino acids following ninhydrin spray and the colored spots observed under UV light on polyamide plates containing fluorescent additives are very useful in identifying those amino acids that have nearly identical R_f values. TLC of PTH-amino acids has been reviewed by Rosmus and Deyl.[4]

Dns-Amino Acids

Dansylation in 0.2 *M* sodium bicarbonate solution is widely used for the identification of N-terminal amino acids in proteins, and it is the most sensitive method for the quantitative determination of amino acids, since dansyl derivatives are highly fluorescent under a UV lamp (254 nm). Much research has focused on silica gel and polyamide plates using both 1D and 2D chromatography.

No solvent system resolves all the Dns-amino acids by 1D chromatography. Also, 2D chromatography requires more than two runs for a complete resolution. The eluents most commonly used on polyamide layers are benzene–acetic acid (9:1), toluene–acetic acid (9:1), toluene–ethanol–acetic acid (17:1:2), water–formic acid (200:3), water–ethanol–ammonium hydroxide (17:2:1 and 14:15:1), ethylacetate–ethanol–ammonium hydroxide (20:5:1), *n*-heptane–*n*-butanol–acetic acid (3:3:1), chlorobenzene–acetic acid (9:1), and ethylacetate–acetic acid–methanol (20:1:1). On silica plates, acetone–isopropanol–25% aqueous ammonia (9:7:1), chloroform–benzyl alcohol–ethyl acetate–acetic acid (6:4:5:0.2), chloroform–ethyl acetate–acetic acid (38:4:2.8 or 24:4:5), and dichloromethane–methanol–propionic acid (21:3:2) are used.

A widely employed chromatographic system is the one based on polyamide plates eluted with water–formic acid (200:3 v/v) in the first direction and benzene–acetic acid (9:1 v/v) in the second direction. A third run with 1 *M* ammonia–ethanol (1:1 v/v) or ethylacetate–acetic acid–methanol (20:1:1 v/v/v) in the direction of solvent 2 resolves especially basic Dns-amino acids or Glu/Asp and Thr/Ser pairs.

DABTH-Amino Acids

These compounds are obtained in acid medium via dimethylaminoazobenzenethiocarbamyl (DABTC) derivatives formed by the reaction in basic medium of DABITC with the primary amino group of N-terminal amino acids in peptides. The color differences among DABITC, DABTC derivatives, and dimethylaminoazobenzenethiohydantoin (DABTH)-amino acids facilitate identification on TLC. These derivatives are colored compounds and, because of their stability and sensitivity, are usually used for qualitative and quantitative analyses of amino compounds such as amino acids and amines.

All DABTH-amino acids, except the Leu/Ile pair, can be separated by 2D chromatography on layers of polyamide, with water–acetic acid (2:1 v/v) and toluene–*n*-hexane–acetic acid (2:1:1 v/v/v) being solvents 1 and 2, respectively. Resolution of the DABTH-Leu/Dns-Ile pair on polyamide is possible with formic acid–ethanol (10:9 v/v) and on silica plates using chloroform–ethanol (100:3 v/v) as eluent.

PTC-Amino Acids

Phenylthiocarbamyl (PTC) derivatives[6] were obtained at pH 12 by in situ reaction for 15 min or in a tube of phenylisothiocyanate with the amino group of amino acids and separated on silica gel 60 F_{254} and RP-18 F_{254} plates with 2D and 1D chromatography, respectively.

In normal-phase chromatography the 2D technique was used to resolve two mixtures of 10 and 11 PTC-amino acids, by eluting with ethanol–chloroform (2:1 v/v) in the first direction and methanol–dioxane–chloroform (1:1:1 v/v/v) in the second direction.

The PITC zone does not interfere with the spots of amino acids since the derivatizing agent migrates toward the solvent front in such experimental conditions

Detection was performed by exposing the plates sprayed with a sodium azide and starch solution to iodine vapor. White spots on a violet-gray background appeared.

In reversed-phase chromatography, the separations of three mixtures of seven PTC- amino acids were effected by eluting with acetonitrile–4% sodium azide + 2% starch solution (pH = 6.5) (2:8 v/v).

Detection was effected by exposing the plates to iodine vapor for 5 sec. The groups of PTC-Leu, PTC-Ile, and PTC-Phe were not resolved. PITC remains near origin.

Cbo AND BOC-AMINO ACIDS

Carbobenzoxy (Cbo) and *tert*-butyloxycarbonyl (BOC) amino acids are very useful in the synthesis of peptides, and consequently their separation from each other and from unreacted components used in their preparation is

very important. For this separation, various mixtures of *n*-butanol–acetic acid–5% ammonium hydroxide and of *n*-butanol–acetic acid–pyridine with or without the addition of water have been used on silica gel.

The BOC-amino acids give a negative ninhydrin test; however, if the plates are heated at 130°C for 25 min and immediately sprayed with a 0.25% solution of ninhydrin in butanol, a positive test is obtained.

RESOLUTION OF ENANTIOMERIC AMINO ACID AND THEIR DERIVATIVES

Amino acids are optically active and the separation of the enantiomeric pairs is an important objective. (The topic is discussed in the entry *Enantiomeric Separations by TLC*.)

REFERENCES

1. Krasikov, V.D.; Malakhova, I.I.; Degterev, E.V.; Tyaglov, B.V. Planar chromatography of free industrial amino acids. J. Planar Chromatogr. -Mod. TLC **2004**, *17*, 113–122.
2. Flieger, J.; Tatarczak, M.; Szumilo, H. Multiple development HPTLC analysis of amino acids on cellulose layers. J. Planar Chromatogr. -Mod. TLC **2006**, *19*, 161–166.
3. Lepri, L.; Desideri, P.G.; Heimler, D. Reversed-phase and soap-thin-layer chromatography of amino acids. J. Chromatogr. **1980**, *195*, 65–73; J. Chromatogr. **1981**, *209*, 312–315.
4. Rosmus, J.; Deyl, Z. The methods for identification of N-terminal amino acids in peptides and proteins. Part B. J. Chromatogr. **1970**, *70*, 221–339.
5. Edman, P. Method for determination of the amino acid sequence in peptides. Acta Chem. Scand. **1950**, *4*, 283–293.
6. Kaźmierczak, D.; Ciesielski, W.; Zakrzewski, R. Separation of amino acids as phenyl thiocarbamyl derivatives by normal- and reversed-phase thin-layer chromatography. J. Planar Chromatogr. -Mod. TLC **2005**, *18*, 427–431.

BIBLIOGRAPHY

1. Bhushan, R.; Martens, J. Amino acids and their derivatives. In *Handbook of Thin-Layer Chromatography*, Sherma, J.; Fried B., Eds.; Marcel Dekker: New York, 1996; Vol. 71, pp. 389–425.

Amino Acids, Peptides, and Proteins: CE Analysis

Danilo Corradini
Institute of Chromatography, Rome, Italy

INTRODUCTION

Amino acids, peptides, and proteins are analyzed by a variety of modes of capillary electrophoresis (CE) which employ the same instrumentation, but are different in the mechanism of separation. A fundamental aspect of each mode of CE is the composition of the electrolyte solution. Depending on the specific mode of CE, the electrolyte solution can consist of either a continuous or a discontinuous system. In continuous systems, the composition of the electrolyte solution is constant along the capillary tube, whereas in discontinuous systems, it is varied along the migration path.

Capillary zone electrophoresis (CZE), micellar capillary electrokinetic chromatography (MECC), capillary gel electrophoresis (CGE), and affinity capillary electrophoresis (ACE) are CE modes using continuous electrolyte solution systems. In CZE, the velocity of migration is proportional to the electrophoretic mobilities of the analytes, which depends on their effective charge-to-hydrodynamic radius ratios. CZE appears to be the simplest and, probably, the most commonly employed mode of CE for the separation of amino acids, peptides, and proteins. Nevertheless, the molecular complexity of peptides and proteins and the multifunctional character of amino acids require particular attention in selecting the capillary tube and the composition of the electrolyte solution employed for the separations of these analytes by CZE.

DISCUSSION

The various functional groups of amino acids, peptides, and proteins can interact with a variety of active sites on the inner surface of fused-silica capillaries, giving rise to peak broadening and asymmetry, irreproducible migration times, low mass recovery, and, in some cases, irreversible adsorption. The detrimental effects of these undesirable interactions are usually more challenging in analyzing proteins than peptides or amino acids, owing to the generally more complex molecular structures of the larger polypeptides. One of the earliest, and still more adopted, strategy to preclude the interactions of peptides and proteins with the wall of bare fused-silica capillaries is the chemical coating of the inner surface of the capillary tube with neutral hydrophilic moieties.[1] The chemical coating has the effect of deactivating the silanol groups by either converting them to inert hydrophilic moieties or by shielding all the active interacting groups on the capillary wall. A variety of alkylsilane, carbohydrate, and neutral polymers can be covalently bonded to the silica capillary wall by silane derivatization.[2] Polyacrylamide (PA), poly(ethylene glycol) (PEG), poly(ethylene oxide) (PEO), and polyvinylpyrrolidone (PVP) can be successfully anchored onto the capillary surface treated with several different silanes, including 3-(methacryloxy)-propyltrimethoxysilane, 3-glycidoxypropyltrimethoxysilane, trimethoxyallylsilane, and chlorodimethyloctylsilane. Alternatively, a polymer can be adsorbed onto the capillary wall and then cross-linked in situ. Other procedures are based on simultaneous coupling and cross-linking. Alternative materials to fused silica such as polytetrafluorethylene (Teflon) and poly(methyl methacrylate) (PMMA) hollow fibers has found limited application.

The deactivation of the silanol groups can also be achieved by the dynamic coating of the inner wall by flushing the capillary tube with a solution containing a coating agent. A number of neutral or charged polymers with the property of being strongly adsorbed at the interface between the capillary wall and the electrolyte solution are employed for the dynamic coating of bare fused-silica capillaries. Modified cellulose and other linear or branched neutral polymers may adsorb at the interface between the capillary wall and the electrolyte solution with the main consequence of increasing the local viscosity in the electric double layer and masking the silanol groups and other active sites on the capillary surface. This results in lowering or suppressing the electro-osmotic flow and in reducing the interactions with the capillary wall.

Polymeric polyamines are also strongly adsorbed in the compact region of the electric double layer as a combination of multisite electrostatic and hydrophobic interactions. The adsorption results in masking the silanol groups and the other adsorption active sites on the capillary wall and in altering the electroosmotic flow, which is lowered and, in most cases, reversed from cathodic to anodic. One of the most widely employed polyamine coating agents is polybrene (or hexadimetrine bromide), a linear hydrophobic polyquaternary amine polymer of the ionene type.[3] Alternative choices are polydimethyldiallylammonium

chloride, another linear polyquaternary amine polymer, and polyethylenimine (PEI). Very promising is the efficient dynamic coating obtained with ethylenediamine-derivatized spherical polystyrene nanoparticles of 50–100 nm diameter, which can be successively converted to a more hydrophilic diol coating by in situ derivatization of the free amino groups with 2,3-epoxy-1-propanol.[4]

In most cases, the electrolyte solution employed in CZE consists of a buffer in aqueous media. Although all buffers can maintain the pH of the electrolyte solution constant and can serve as background electrolytes, they are not equally meritorious in CZE. The chemical nature of the buffer system can be responsible for poor efficiency, asymmetric peaks, and other untoward phenomena arising from the interactions of its components with the sample. In addition, the composition of the electrolyte solution can strongly influence sample solubility and detection, native conformation, molecular aggregation, electrophoretic mobility, and electroosmotic flow. Consequently, selecting the proper composition of the electrolyte solution is of paramount importance in optimizing the separation of amino acids, peptides, and proteins in CZE. The proper selection of a buffer requires evaluating the physical–chemical properties of all components of the buffer system, including buffering capacity, conductivity, and compatibility with the detection system and with the sample.

Non-buffering additives are currently incorporated into the electrolyte solution to enhance solubility, break aggregation, modulate selectivity, improve resolution, and allow detection, which is particularly challenging for amino acids and short peptides. In addition, a large number of amino compounds, including monovalent amines, amino sugars, diaminoalkanes, polyamines, and short-chain alkylammonio quaternary salts are successfully employed as additives for the electrolyte solution to aid in minimizing interactions of peptides and proteins with the capillary wall in bare fused-silica capillaries. Other additives effective at preventing the interactions of proteins, peptides, and amino acids with the capillary wall include neutral polymers, zwitterions, and a variety of ionic and non-ionic surfactants.[5] Less effective at preventing these untoward interactions are strategies using electrolyte solutions at extreme pH values, whether acidic, to suppress the silanol dissociation, or alkaline, to have both the analytes and the capillary wall negatively charged.

Selectivity in CZE is based on differences in the electrophoretic mobilities of the analytes, which depends on their effective charge-to-hydrodynamic radius ratios. This implies that selectivity is strongly affected by the pH of the electrolyte solution and by any interaction of the analyte with the components of the electrolyte solution which may affect its charge and/or hydrodynamic radius.

Additives can improve selectivity by interacting specifically, or to different extents, with the components of the sample. Most of the additives employed in amino acid, peptide, and protein CZE are amino modifiers, zwitterions, anionic or cationic ion-pairing agents, inclusion complexants (only for amino acids and short peptides), organic solvents, and denaturing agents.

The capability of several compounds to ion-pair with amino acids, peptides, and proteins is the basis for their selection as effective additives for modulating the selectivities of these analytes in CZE.[5] Selective ion-pair formation is expected to enlarge differences in the effective charge-to-hydrodynamic radius ratio of these analytes, leading to enhanced differences in their electrophoretic mobilities, which determine improved selectivity. Several diaminoalkanes, including 1,4-diaminobutane (putrescine), 1,5-diaminopentane (cadaverine), 1,3-diaminopropane, and *N*,*N*,*N*′,*N*′-tetramethyl-1,3-butanediamine (TMBD) can be successfully employed as additives for modulating the selectivity of peptides and proteins (Figs. 1 and 2). Moreover, several anions, such as phosphate, citrate, and borate, which are components of the buffer solutions employed as the background electrolyte, may also act as ion-pairing agents influencing the electrophoretic mobilities of amino acids, peptides, and proteins and, hence, selectivity and resolution. Other cationic ion-pairing agents include the ionic polymers polydimethyldiallylammonium chloride and polybrene, whereas myoinositol hexakis-(dihydrogen phosphate), commonly known as phytic acid, is an interesting example of a polyanionic ion-pairing agent.

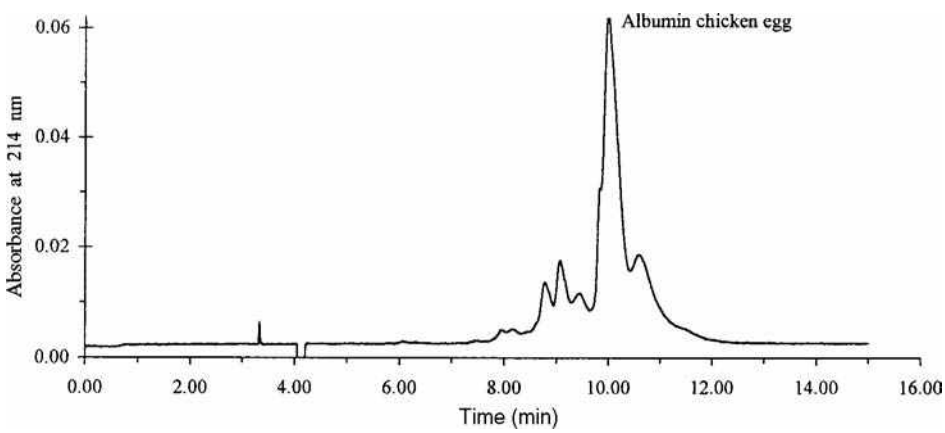

Fig. 1 Detection of microheterogeneity of albumin chicken egg by capillary zone electrophoresis. Capillary, bare fused-silica (50 μm × 37 cm, 30 cm to the detector); electrolyte solution, 25 m*M* Tris-glycine buffer containing 0.5% (v/v) Tween-20 and 2.0 m*M* putrescine; applied voltage, 20 kV; UV detection at the cathodic end.

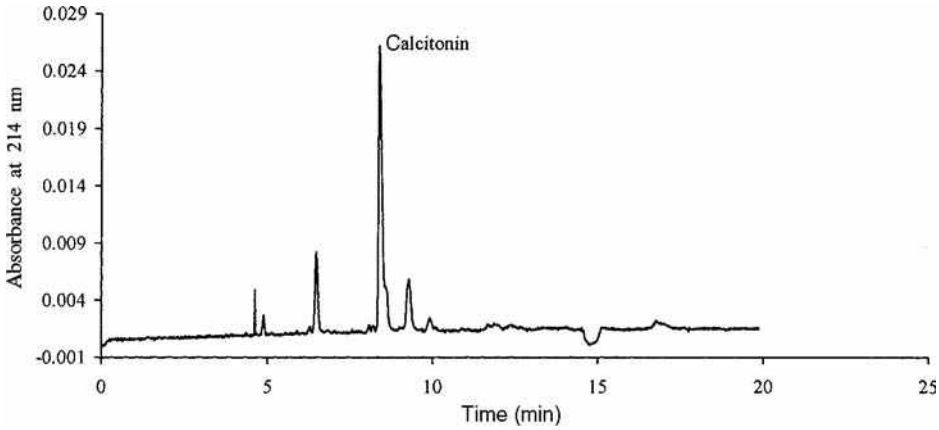

Fig. 2 Separation of impurities from a sample of synthetic human calcitonin for therapeutic use by CZE. Capillary, bare fused-silica (50 μm × 37 cm, 30 cm to the detector); electrolyte solution, 40 m*M* *N*,*N*,*N*′,*N*′-tetramethyl-1,3-butanediamine (TMBD), titrated to pH 6.5 with phosphoric acid; applied voltage, 15 kV; UV detection at the cathodic end.

Surfactants have been investigated extensively in CE for the separation of both charged and neutral molecules using a technique based on the partitioning of the analyte molecules between the hydrophobic micelles formed by the surfactant and the electrolyte solution, which is termed micellar electrokinetic capillary chromatography (MECC or MEKC). This technique is widely used for the analysis of a variety of peptides and amino acids,[6] but it is less popular for protein analysis.[7] The limited applications of MECC to protein analysis may be attributed to several factors, including the strong interactions between the hydrophobic moieties on the protein molecules and the micelles, the inability of large proteins to penetrate into the micelles, and the binding of the monomeric surfactant to the proteins. The result is that, even though the surfactant concentration in the electrolyte solution exceeds the critical micelle concentration, the protein–surfactant complexes are likely to be not subjected to partitioning in the micelles, as do amino acids, peptides, and other smaller molecules.

However, surfactants incorporated into the electrolyte solution at concentrations below their critical micelle concentration (CMC) may act as hydrophobic selectors to modulate the electrophoretic selectivity of hydrophobic peptides and proteins. The binding of ionic or zwitterionic surfactant molecules to peptides and proteins alters both the hydrodynamic (Stokes) radius and the effective charges of these analytes. This causes a variation in the electrophoretic mobility, which is directly proportional to the effective charge and inversely proportional to the Stokes radius. Variations of the charge-to-hydrodynamic radius ratios are also induced by the binding of non-ionic surfactants to peptide or protein molecules. The binding of the surfactant molecules to peptides and proteins may vary with the surfactant species and its concentration, and it is influenced by the experimental conditions such as pH, ionic strength, and temperature of the electrolyte solution. Surfactants may bind to samples, either to the same extent [e.g., protein–sodium dodecyl sulfate (SDS) complexes], or to a different degree, which can enlarge differences in the electrophoretic mobilities of the separands.

In CGE, the separation is based on a size-dependent mechanism similar to that operating in polyacrylamide gel electrophoresis (PAGE), employing as the sieving matrix either entangled polymer solutions or gel-filled capillaries.[8] This CE mode is particularly suitable for analyzing protein complexes with SDS. The separation mechanism is based on the assumption that fully denatured proteins hydrophobically bind a constant amount of SDS (1.4 g of SDS per 1 g of protein), resulting in complexes of approximately constant charge-to-mass ratios and, consequently, identical electrophoretic mobilities. Therefore, in a sieving medium, protein–SDS complexes migrate proportionally to their effective molecular radii and, thus, to the protein molecular weight. Consequently, SDS–CGE can be used to estimate the apparent molecular masses of proteins, using calibration procedures similar to those employed in SDS–PAGE.

Continuous electrolyte solution systems are also employed in ACE,[9] where the separation depends on the biospecific interaction between the analyte of interest and a specific selector or ligand. The molecules with bioaffinity for the analyte (the selector or ligand) can be incorporated into the electrolyte solution or can be immobilized, either to an insoluble polymer filled into the capillary or to a portion of the capillary wall. ACE is a useful and sensitive tool for measuring the binding constant of ligands to proteins and characterizing molecular properties of peptides and proteins by analyzing biospecific interactions. Examples of biospecific interactions currently investigated by ACE include molecular recognition between proteins or peptides and low-molecular-mass receptors, antigen–antibody complexes, lectin–sugar interactions, and enzyme–substrate complexes. ACE is also employed for the chiral separation of amino acids using a protein as the chiral selector.

Enantiomeric separations of amino acids and short peptides are performed using either a direct or the indirect approach.[10] The indirect approach employs chiral reagents for diasteromer formation and their subsequent

separation by various modes of CE. The direct approach uses a variety of chiral selectors that are incorporated into the electrolyte solution. Chiral selectors are optically pure compounds bearing at least one functional group with a chiral center (usually represented by an asymmetric carbon atom) which allows sterically selective interactions with the two enantiomers. Among others, cyclodextrins (CDs) are the most widely chiral selectors used as additives in chiral CE. These are cyclic polysaccharides built up from D-(+)-glucopyranose units linked by α-(1,4) bonds, whose structure is similar to a truncated cone. Substitution of the hydroxyl groups of the CDs results in new chiral selectors which exhibit improved solubility in aqueous solutions and different chiral selectivity. Other chiral selectors include crown ethers, chiral dicarboxylic acids, macrocyclic antibiotics, chiral calixarenes, ligand-exchange complexes, and natural and semisynthetic linear polysaccharides. Chiral selectors are also commonly employed in combination with ionic and non-ionic surfactants for enantiomeric separations of amino acids and peptides by MECC.

In discontinuous systems, the composition of the electrolyte solution is varied along the migration path with the purpose of changing one or more parameters responsible for the electrophoretic mobilities of the analytes. The discontinuous electrolyte solution systems employed in capillary isoelectric focusing (CIEF) have the function of generating a pH gradient inside the capillary tube in order to separate peptides and proteins according to their isoelectric points.[11] Each analyte migrates inside the capillary until it reaches the zone with the local pH value corresponding to its isoelectric point, where it stops moving as a result of the neutralized charge and consequent annihilated electrophoretic mobility. CIEF is successfully employed for the resolution of isoenzymes, to measure the isoelectric point (p*I*) of peptides and proteins, for the analysis of recombinant protein formulation, hemoglobins, human serum, and plasma proteins. Discontinuous electrolyte solution systems are also employed in capillary isotachophoresis (CITP), where the analytes migrate as discrete zones with an identical velocity between a leading and a terminating electrolyte solution having different electrophoretic mobilities. CITP finds large applications as an online preconcentration technique prior to CZE, MECC, and CGE. It is also employed for the analysis of serum and plasma proteins and amino acids.[12]

The majority of amino acids and short peptides have no, or only negligible, UV absorbance. Detection of these analytes often requires chemical derivatization using reagents bearing UV or fluorescence chromophores. High detection sensitivity, reaching the attomolar (10^{-21}) mass detection limit can be obtained using fluorescence labeling procedures in combination with laser-induced fluorescence detection.[13] A variety of fluorescence and UV labeling reagents are currently employed, including *O*-phthaldehyde (OPA), fluorescein isothiocyanate (FITC), 1-dimethylaminonaphthalene-5-sulfonyl chloride (dansyl chloride), 4-phenylspiro[furan-2(3H)-1′ phthalene (fluorescamine), and naphthalene dicarboxaldehyde (NDA). However, derivatization may reduce the charge-to-hydrodynamic radius ratio differences between analytes, making separations difficult to achieve. In addition, precolumn derivatization is not suitable for large peptides and proteins, due to the formation of multilabeled products. These problems can be overcome using postcolumn derivatization procedures.

Another, very attractive alternative is indirect UV detection.[14] This indirect detection procedure makes use of a UV-absorbing compound (or "probe"), having the same charge as the analytes, that is incorporated into the electrolyte solution. Displacement of the probe by the migrating analyte generates a region where the concentration of the UV-absorbing species is less than that in the bulk electrolyte solution, causing a variation in the detector signal. In the indirect UV detection technique, the composition of the electrolyte solution is of critical importance, because it dictates separation performance and detection sensitivity.

Probes currently employed in the indirect UV detection of amino acids include *p*-aminosalicylic acid, benzoic acid, phthalic acid, sodium chromate, 4-(*N*,*N*′-dimethylamino)-benzoic acid, 1,2,4,-benzenetricarboxylic acid (trimellitic acid), 1,2,4,5-benzenetetracarboxylic acid (pyromellitic acid), and quinine sulfate. Several of these probes are employed in combination with metal cations and cationic surfactants, which are incorporated into the electrolyte solution as modifiers of the electro-osmotic flow.

Coupling mass spectrometry (MS) to CE provides detection and identification of amino acids, peptides, and proteins based on the accurate determination of their molecular masses.[15] The most critical part of coupling MS to CE is the interface technique employed to transfer the sample components from the CE capillary column into the vacuum of the MS. Electrospray ionization (ESI) is the dominant interface which allows a direct coupling under atmospheric pressure conditions. Another distinguishing features of this "soft" ionization technique when applied to the analysis of peptides and proteins is the generation of a series of multiple charged, intact ions. These ions are represented in the mass spectrum as a sequence of peaks, the ion of each peak differing by one unit of charge from those of adjacent neighbors in the sequence. The molecular mass is obtained by computation of the measured mass-to-charge ratios for the protonated proteins using a "deconvolution algorithm" that transforms the multiplicity of mass-to-charge ratio signals into a single peak on a real mass scale. Obtaining multiple charged ions is actually advantageous, as it allows the analysis of proteins up to 100–150 KDa using mass spectrometers with an upper mass limit of 1500–4000 amu.

Concentration detection limits in CE/MS with the ESI interface are similar to those with UV detection. Sample sensitivity can be improved by using ion-trapping or time-of-flight (TOF) mass spectrometers. MS analysis can also

be performed off-line, after appropriate sample collection, using plasma desorption–mass spectrometry (PD–MS) or matrix-assisted laser desorption–mass spectrometry (MALDI–MS).

REFERENCES

1. Hjerten, S. Free zone electrophoresis. Chromatogr. Rev. **1967**, *9*, 122–219.
2. Rodriguez, I.; Li, S.F.Y. Surface deactivation in protein and peptide analysis by capillary electrophoresis. Anal. Chim. Acta **1999**, *383*, 1.
3. Wiktorowicz, J.E.; Colburn, J.C. Separation of cationic proteins via charge reversal in capillary elextrophoresis. Electrophoresis **1990**, *11*, 769–773.
4. Kleindiest, G.; Huber, C.G.; Gjerde, D.T.; Yengoyan, L.; Bonn, G.K. Capillary electrophoresis of peptides and proteins in fused silica capillaries coated with derivatized polystyrene nanoparticles. Electrophoresis **1998**, *19*, 262.
5. Corradini, D. Buffer additives other than the surfactant sodium dodecyl sulfate for protein separations by capillary electrophoresis. J. Chromatogr. B, **1997**, *699*, 221.
6. Muijselaar, P.G.; Otsuka, K.; Terabe, S. Micelles as pseudostationary phases in micellar electrokinetic chromatography. J. Chromatogr. A, **1998**, *780*, 41.
7. Strege, M.A.; Lagu, A.L. Micellar electrokinetic chromatography of proteins. J. Chromatogr. A, **1997**, *780*, 285.
8. Guttman, A. Capillary sodium dodecyl sulfate-gel electrophoresis of proteins. Electrophoresis **1996**, *17*, 1333.
9. Kajiwara, H. Affinity capillary electrophoresis of proteins and peptides. Anal. Chim. Acta **1999**, *383*, 61.
10. Wan, H.; Blomberg, L.G. Chiral separation of amino acids and peptides by capillary electrophoresis. J. Chromatogr. A, **2000**, *875*, 43.
11. Rodriguez-Diaz, R.; Wehr, T.; Zhu, M. Capillary isoelectric focusing. Electrophoresis **1997**, *18*, 2134.
12. Gebauer, P.; Bocek, P. Recent application and developments of capillary isotachophoresis. Electrophoresis **1997**, *18*, 2154.
13. Swinney, K.; Bornhop, D.J. Detection in capillary electrophoresis. Electrophoresis **2000**, *21*, 1239.
14. Hjerten, S.; Elenbring, K.; Kilar, F.; Liao, J.-L.; Chen, A.J.C.; Siebert, C.J.; Zhu, M.-D. Carrier-free zone electrophoresis, displacement electrophoresis and isoelectric focusing in a high-performance electrophoresis apparatus. J. Chromatogr. **1987**, *403*, 47.
15. Smith, R.D.; Loo, J.A.; Barinaga, C.J.; Edmonds, C.G.; Udseth, H.R. Capillary zone electrophoresis and isotachophoresis- mass spectrometry of polypeptides and proteins based upon an electrospray ionization interface. J. Chromatogr. **1989**, *480*, 211.

Amino Acids: HPLC Analysis

Ioannis N. Papadoyannis
Georgios A. Theodoridis
Laboratory of Analytical Chemistry, Chemistry Department, Aristotle University of Thessaloniki, Thessaloniki, Greece

INTRODUCTION

Amino acids are small organic molecules that posses both an amino and a carboxyl group. Amino acids occur in nature in a multitude of biological forms, either free or conjugated to various types of compounds, or as the building blocks of proteins. The amino acids that occur in proteins are named α-amino acids and have the empirical formula $RCH(NH_2)COOH$. Only 20 amino acids are used in nature for the biosynthesis of the proteins, because only 20 amino acids are coded by the nucleic acids.

DISCUSSION

Amino acids show acid–base properties, which are strongly dependent on the varying R groups present in each molecule. The varying R groups of individual amino acids are responsible for specific properties: polarity, hydrophilicity–hydrophobicity.[1,2] Hence, the 20 α-amino acids could be categorized in the 4 distinct groups listed in Table 1.

Their dipolar (zwitterionic) behavior is a fundamental factor in any separation approach. At low pH, amino acids exist in their cationic form with both amino and carboxyl groups protonated. The ampholyte form appears at a pH of 6–7, whereas at higher values, amino acids are in their anionic form (carboxyl group dissociated). Another important parameter is that all α-amino acids (with the exception of Gly) are asymmetrical molecules exhibiting optical isomerization (L being the isomer found in nature). As can be seen in Table 1, amino acids are actually small [molecular weight (MW) ranging from 75 to 204] molecules, exhibiting pronounced differences in polarity and a few chromophoric moieties.

The determination of amino acids in various samples is a usual task in many research, industrial, quality control, and service laboratories. Hence, there is a substantial interest in the HPLC analysis of amino acids from many diverse areas like biochemistry, biotechnology, food quality control, diagnostic services, neuro-chemistry/biology, and so forth. As a result, the separation of amino acids is probably the most extensively studied and best developed chromatographic separation in biological sciences. The most known system is the separation on a cation-exchange column and postcolumn derivatization with ninhydrin, which was described in 1951 by Moore and Stein. With this approach, a sulfonated polystyrene column achieved a separation of the 20 naturally occurring amino acids within approximately 6 hr; modifications of the original protocol enhanced color stabilization of the derivatives and enabled the application of the method in various real samples. Since then, immense developments in instrumentation, column technologies, and automation established high-performance liquid chromatography (HPLC) as the dominant separation technique in chemical analysis. Numerous published reports described the HPLC analysis of amino acids in a great variety of samples. To no surprise, a two-volume handbook is entirely devoted to HPLC for the separation of amino acids, peptides and proteins.[3] Many of the initial reports employed soft resins or ion exchangers such as polystyrene or cellulose as stationary phases. These materials show some disadvantages (e.g., compaction under pressure, reduced porosity, and wide particle size distribution). The last decades' developments in manufacturing silica-based materials resulted in the domination of reversed-phase (RP) silica-based packing in liquid chromatography. As a result, RP-HPLC is, at present, widely used for the separation of amino acids, because it offers high resolution, short analysis time, ease in handling combined with low cost, and environmental impact per analysis circle.

In ligand-exchange chromatography (LEC), the separation of analytes is due to the exchange of ligands from the mobile phase with other ligands coordinated to metal ions immobilized on a stationary phase. LEC has been used successfully for the resolution of free amino acids, amino acid derivatives, and for enantiomeric resolution of racemic mixtures.[3]

Apart from ninhydrin, many other derivatization reagents have been used; both precolumn and postcolumn derivatization modes have been extensively employed.[3–5] Derivatization procedures offer significant advantages in both separation and detection aspects and, thus, will be discussed in further detail. The rest of the entry will be divided into two sections: separation of underivatized amino acids, where the determination of free amino acids and postcolumn derivatization procedures are described; and separation of derivatized amino acids, where precolumn derivatization approaches are discussed.

	Amino acid	Structure at pH 6-7	MW	pK_a
Hydrophobic Aminoacids (Non-polar R)	Alanine Ala	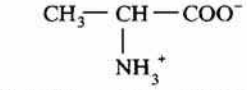	89	2.35, 9.69
	Leucine Leu		131	2.36, 9.60
	Isoleucine Ile	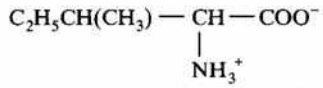	131	2.36, 9.68
	Valine Val	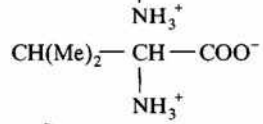	117	2.36, 9.68
	Proline Pro	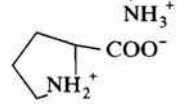	115	1.99, 10.60
	Methionine Met	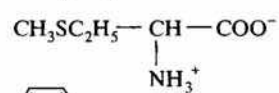	149	2.28, 9.21
	Phenylalanine Phe	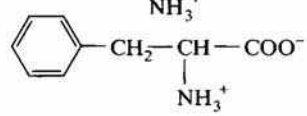	165	1.83, 9.13
	Tryptophan Trp	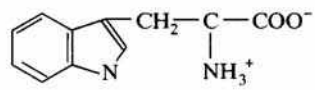	204	2.38, 9.39
Hydrophilic Aminoacids (Not Charged R)	Glycine Gly	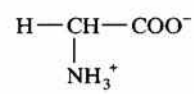	75	2.34, 9.6
	Serine Ser	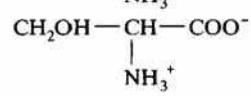	105	2.21, 9.15
	Threonine Thr	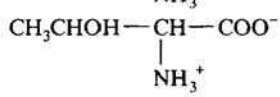	119	2.63. 10.43
	Cysteine Cys	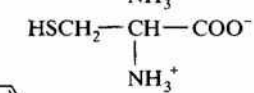	121	1.71, 10.78
	Tyrosine Tyr	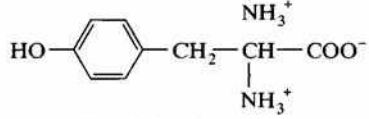	181	2.20, 9.11
	Glutamine Gln	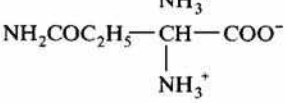	146	2.17, 9.13
	Asparagine Asn	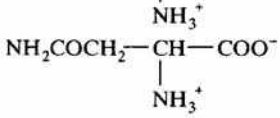	132	2.02, 8.8
Acidic Aminoacids	Aspartic Acid Asp	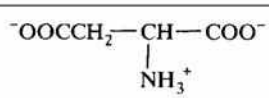	133	2.09, 3.86, 9.86
	Glutamic Acid Glu	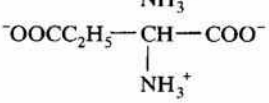	147	2.19, 4.25, 9.67

(Continued)

	Amino acid	Structure at pH 6-7	MW	pK_a
Basic Aminoacids	Lysine Lys	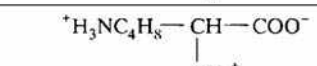	133	2.18, 8.95, 10.53
	Arginine Arg	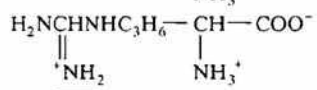	133	2.17, 9.04, 12.48
	Histidine His	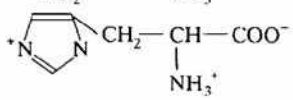	155	1.82, 8.95, 10.53

SEPARATION OF UNDERIVATIZED AMINO ACIDS

The differing solubilities, polarities, and acid–base properties of free amino acids have been exploited in their separation by partition chromatography, ion-exchange chromatography, and electrophoresis. For example, the elution order obtained from a polystyrene ion-exchange resin with an acidic mobile phase corresponds to the amino acid classification depicted in Table 1: Acidic amino acids are eluted early, neutral between, and basic amino acids later. In this case, ionic interactions between the sample and the stationary phase are the driving force for the separation of the groups. However, hydrophobic van der Waals and π–π aromatic interactions are responsible for the separation of amino acids within the groups.[3]

The dominant stationary phase in HPLC is modified silica and, to be more specific, octadecyl silica (ODS). It should be pointed out that there could be great differences between various types of ODS materials or even between different batches of the same material. Carbon load, free silanol content, endcapping, type of silica, and coupling chemistry to the C_{18} moiety, not to mention the several physical characteristics of the packing material all involve the behavior of an ODS column. However, a rather safe generalization is that, in such material, hydrophobic interactions are a dominant mechanism of separation.[3–7]

In typical ODS materials, polar amino acids are very weakly retained on column; thus, they are insufficiently resolved. In contrast, non-polar amino acids are stronger retained and adequately separated. To overcome the poor resolution of polar amino acids, two strategies are the most promising:

1. Derivatization (as discussed in the next section).
2. Modification of the mobile phase with the addition of ion-pairing reagents.

Alkyl sulfates/sulfonates added to the mobile phase form a micellar layer interacting with both the stationary phase and the amino acids (which under these conditions are protonated). A mixed mechanism (ion-pairing and dynamic ion exchange) is observed. Furthermore, the ion-pairing reagent masks underivatized silanols of the ODS material, reducing non-specific unwanted interactions. Sodium dodecyl sulfate (SDS) is the most often used ion-pairing reagent. Gradient elution is often required to achieve reasonable analysis time for non-polar amino acids. Despite the above-mentioned advantages, ion-pairing shows some disadvantages, such as irreproducibility (especially in gradient runs), long equilibration times, and difficulties in ultraviolet (UV) detection.

Another possibility is the use of alternative stationary phases. A strong trend of the last decade is the employment of specialty phases in challenging and complex separations. Thus, newer C_8, NH_2, CN, mixed mode phases (materials incorporating both ion exchange and reversed-phase moieties), new polymeric phases, and zirconia-based materials offer attractive stationary-phase selectivities.

POSTCOLUMN DERIVATIZATION

The non-derivatized amino acids, following their chromatographic separation, can either be directly detected as free amino acids, online derivatized, or by postcolumn derivatization. Derivatization with ninhydrin, the classical amino acid analysis, was the first reported postcolumn derivatization method. Modern postcolumn derivatization protocols employ sophisticated instrumentation and achieve high resolution and sensitivity. In such configurations, derivatization occurs in a reaction coil placed between the analytical column and the detector. Additional pumps and valves are required; thus, such systems typically run fully automated and controlled by a computer. The major disadvantages of postcolumn derivatization are the need for sophisticated and complex instrumentation and the band broadening occuring in the reactor. *O*-phthaldialdehyde (OPT) is the most common reagent in postcolumn derivatization. OPT reacts with primary amino acids under basic conditions, forming a fluorescent derivative (OPA derivative) that allows detection at femtomole levels. Disadvantages of OPA derivatization are the instability of the resultant derivatives and the fact that secondary amino acids are not detected.

If no derivatization takes place, detection is preferably accomplished by UV at a low wavelength (200–210 nm) in order to enhance detection sensitivity. However, detection selectivity is sacrificed at such low wavelengths. Electrochemical detection, when applied to the analysis

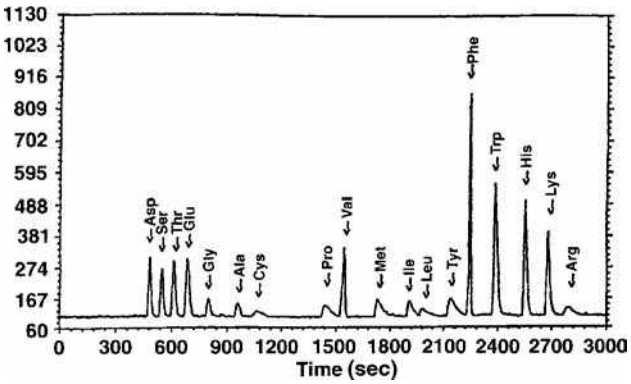

Fig. 1 HPLC analysis of 18 common amino acids. Conditions: stationary phase: CS-10 cation exchange; mobile phase: gradient of aqueous 0.01% TFA and ammonium acetate; detection at the ELSD.
Source: From Amino acid analysis of peptides using HPLC with evaporative light scattering detection, in J. Liq. Chromatogr. Relat. Technol.[11]

of free amino acids, offers higher selectivity but suffers from a small linearity range. Furthermore, most amino acids (with the excepion of tryptophan, tyrosine, and cysteine) are not intrinsically electrochemically active within the current useful potential range.[5] Lately, the development of the evaporative light-scattering detector (ELSD) offers an attractive alternative for the determination of non-derivatized amino acids (Fig. 1).

SEPARATION OF DERIVATIZED AMINO ACIDS

Precolumn derivatization is the generally accepted approach for the determination of amino acids, because it offers significant advantages: increased detection sensitivity, enhanced selectivity, enhanced resolution, and limited needs for sophisticated instrumentation (in contrast with postcolumn derivatization techniques).

In modern instrument configurations, derivatization can take place in a conventional autosampler; the resultant derivatives are separated on the analytical column. Detection limits at the femtomole level are achieved, and the resolution of polar amino acids is greatly enhanced.

The most common derivatization reagents are as follows:

- Dimethylamino azobenzene isothiocyanate (DABITC).
- 4-(Dimethylamino)azobenzene-4-sulfonyl chloride (dabsyl chloride or DABS-Cl) [dabsyl derivatives].
- 1-*N*-*N*-Dimethylaminonaphthalene-5-sulfonyl chloride [dansyl derivatives].
- Fluorodinitrobenzene (DNP derivatives).
- Fluorescamine.
- 9-Fluorenylmethyl chloroformate (FMOC-Cl).
- 4-Chloro-7-nitro-2,1,3-benzoxadiazole (NBD-Cl).
- Phenylisothiocyanate (PITC) [phenylthiohydantoin (PTH) derivatives].
- Methylisothiocyanate (MITC) [methylthiohydantoin (MTH) derivatives].

Fig. 2 illustrates the structure of the product resulting from the derivatization of an amino acid with the above-mentioned reagents. Mixtures of derivatives with the most commonly used reagents (dansyl, DNP, PTH) are readily provided in kits, to be directly used as reference standards in HPLC analysis.

Phenylthiohydantoin derivatization offers a special value because it is actually performed during Edman degradation, the sequencing technique mostly used for the determination of the primary structure of proteins and peptides. PTH derivatives are separated in many different stationary phases, in either normal- or reversed-phase mode and are mostly detected at 254 nm.[8–9] Using radiolabeled proteins, sequencing of proteins down to the 1–100 pmol range can be achieved. The formed derivatives are basic and thus interact strongly with base silica materials. RP separations are mostly carried out in acidic conditions with the addition of appropriate buffers (sodium acetate mostly, but also phosphate, perchlorate, etc). Failings of PTH derivatization are the lengthy procedure and the higher detection limits obtained (compared to fluorescent derivatives). Potent advantages of the method are its robustness and reproducibility, and the extensive research literature that covers any possible requirement. An alternative to PTH is MTH derivatization, a method well suited for solid-phase sequencing.[3]

Dimethylamino azobenzene isothiocyanate microsequencing results in red–orange derivatives, which exhibit their absorbance maximum at 420 nm with $\varepsilon = 47.000$, in other words offering threefold higher sensitivity compared to PTH derivatives. DABITC derivatives are separated in C_8 or C_{18} columns in acidic environment, within 20 min.

Dabsyl chloride is an alternative to DABITC as a derivatization reagent to be used for manual sequencing. Dabsyl chloride reacts with primary and secondary amino acids forming red–orange derivatives that are stable for months. The method offers excellent sensitivity, ease, and speed of preparation and high-resolution capabilities. However, it suffers from interferences with ammonia present in biological samples. Furthermore, it results in a relatively reduced column lifetime due to the utilization of excess of Dabsyl chloride.[9]

The dansyl derivatization has been extensively studied to label α- or ε-amino groups. DNS derivatives are formed within 2 min and are detected by either UV or fluorescence. A typical example of a separation of dansyl amino acids is illustrated in Fig. 3.

The FMOC derivatization offers high fluorescent detection sensitivity, but it requires an extraction step to remove unreacted FMOC and by-products. This step is a potential cause of analyte losses. Furthermore, it not suitable for

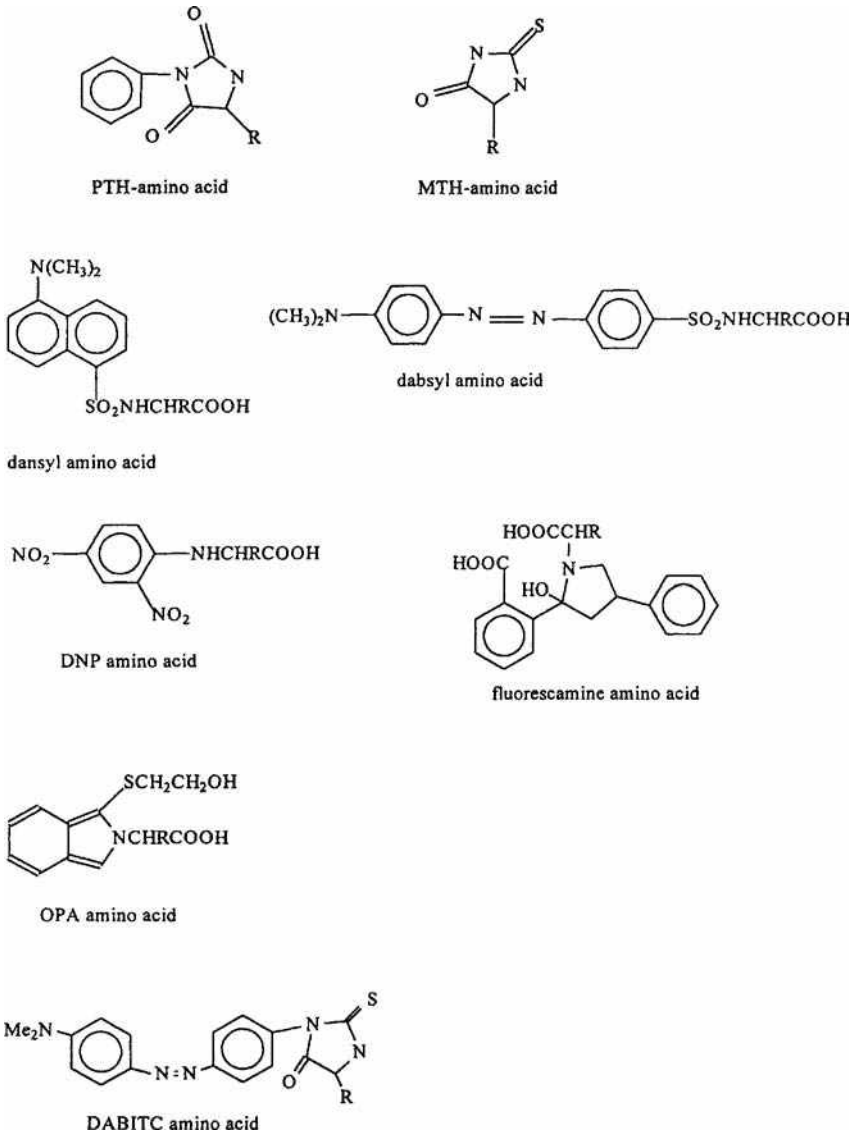

Fig. 2 Structures of the most common amino acid derivatives.

Trp and Cys, because the corresponding derivatives exhibit a lower response due to intramolecular quenching of fluorescence.

The DNP derivatives are analyzed either in normal or reversed phase. Disadvantages of this method are the lower detection sensitivity (60 times less sensitive compared to dabsyl detection) and the lower separation resolution. However, this approach has proven useful for the determination of lysine in food materials.

Finally, the incorporation of an electroactive functionality into a chromatographic label is an attractive alternative for the HPLC of amino acids. Reagents like p–*N* and *N*-dimethylaminosothiocyanate have been used to facilitate amperometric detection of the derivatives.

CHIRAL SEPARATION OF AMINO ACIDS

The importance of chirality has rapidly evolved the last decade. Both analytical and preparative separations are needed for biochemical, pharmaceutical, and alimentary purposes. Amino acids are asymmetrical molecules. L is the form appearing in proteins; however the D form is also present in nature. Enantiomeric separation of amino acids has been achieved in various stationary phases, such as polystyrene and polyacrylamide to which chiral ligands were covalently bound. Metal ions, in conjunction with chiral ligands, have also been utilized in the mobile phase in the reversed-phase and ligand-exchange mode. Novel stationary chiral phases developed for enantiomeric analysis incorporate chiral ligands (e.g., cyclodextrins or even amino acids) immobilized on silica. Generally, L-amino acid-bonded phases retain L-amino acids stronger than the D species.[3,5,10]

Recently, a strong trend in molecular recognition is the development of molecular imprinting polymers (MIP). MIPs have been used as synthetic antibodies in immunoassays and biosensors, but also as catalysts and separation media (employed both in analysis and extraction). One of

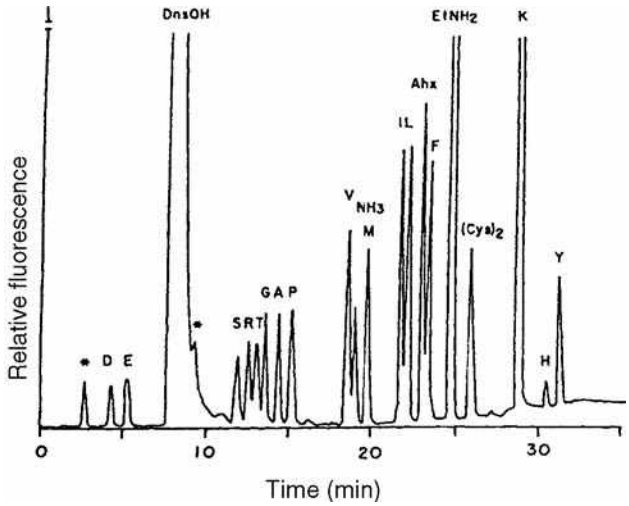

Fig. 3 RP–HPLC analysis of a mixture of dansyl amino acids. Conditions: stationary phase: 4 μm Nova Pak C_{18}; mobile phase: gradient of methanol and tetrahydrofuran versus aqueous phosphate buffer; detection in a fluorescent detector; excitation 338 nm, emission 455 nm. Amino acids are abbreviated by the one-letter system.
Source: From A practical approach to improve the resolution of dansyl amino acids by high-performance liquid chromatography, in J. Liq. Chromatogr. Relat. Technol.[12]

the first applications of MIPs in separations was the enantiomeric separation of amino acids derivatives.

CONCLUSIONS

High-performance liquid chromatography, when compared to other instrumental methods [thin-layer chromatography (TLC), gas chromatography (GC), automated amino acid analyzer], offers significant advantages in the analysis of amino acids: high resolution, high sensitivity, low cost, time saving (one-third of the analysis time of an amino acid analyzer), and a multivariate optimization scheme offering versatility and flexibility. Furthermore, optimization of HPLC determination enables the practitioner to overcome typical problems of other methods (e.g., the well-known interferences of ammonia in amino acid analyzer). An additional advantage of HPLC is its direct compatibility with mass spectrometry. The widespread use of liquid chromatography–mass spectrometry (LC–MS) in proteomic analysis, which at present utilizes state of the art mass spectrometers (e.g., matrix-assisted laser desorption ionization–time-of-flight—mass spectrometry), is seen as a potent future trend.

The variety of instrumentation and experimental conditions (columns, buffers, organic modifiers, derivatization procedures, etc.) reported in the vast literature may hinder the novice from pinpointing the best method to use. The choice of the appropriate method depends on the specific needs of each analytical problem and the nature of the sample to be analyzed. Aspects such as specificity and speed of the derivatization reaction should always be considered. Furthermore, in such multivariate dynamic systems, precision, accuracy, and linearity of the chosen method is a very important factor. The practitioner should carefully follow the developed protocol; the use of automated systems, especially in derivatization procedures, could greatly enhance the reproducibility of the method.

REFERENCES

1. Silverman, L.M.; Christenson, R.H. Amino acids and proteins. *Fundamentals of Clinical Chemistry*, 4th Ed.; Burtis, C.A., Ashwood, E.R., Eds.; Saunders: Philadelphia, 1996.
2. Matthews, C.K.; van Holde, K.E. *Biochemistry*, 2nd Ed.; Benjamin-Cummings: Menlo Park, CA, 1995; 129–214.
3. Hancock, W.S., Ed.; *CRC Handbook of HPLC for the Separation of Amino Acids, Peptides and Proteins*; CRC Press: Boca Raton, FL, 1984.
4. Hancock, W.S.; Sparrow, J.T. *HPLC of Biological Compounds*; Marcel Dekker, Inc.: New York, 1984; 187–207.
5. Papadoyannis, I.N. HPLC in the analysis of amino acids. In *HPLC in Clinical Chemistry*; Marcel Dekker, Inc.: New York, 1990; 97–154.
6. Kamp, R.M. High sensitivity amino acid analysis. In *Protein Structure Analysis*; Kamp, R.M. Choli-Papadopoulou, T., Wittman-Liebold, B., Eds.; Springer-Verlag: Berlin, 1997.
7. Lottspeich, F.; Hernschen, A. Amino acids, peptides, proteins. In *HPLC in Biochemistry*; Hernschen, A. Hupe, K.P. Lottspeich, F., Voelter, W., Eds.; VCH Weinheim: 1985.
8. Waterfield, M.D.; Scrace, G.; Totty, N. Analysis of phenylthiohydantoin amino acids. In *Practical Protein Chemistry—A Handbook*; Darbre, A., Ed.; John Wiley & Sons: Chichester, 1986.
9. Bergman, T.; Carlquist, M.; Jornvall, H. Amino acid analysis by high performance liquid chromatography of phenylthiocarbamyl derivatives, and amino acid analysis using DABS-Cl precolumn derivatization method, R. Knecht and J. Y. Chang. In *Advanced Methods in Protein Microsequence Analysis*; Wittmann-Liebold, B. Salnikow, J., Erdmann, V.A., Eds.; Springer-Verlag: Berlin, 1986.
10. Vollenbroich, D.; Krause, K. Quantitative analysis of D- and L-amino acids by HPLC. In *Protein Structure Analysis*; Kamp, R.M. Choli-Papadopoulou, T., Wittman-Liebold, B., Eds.; Springer-Verlag: Berlin, 1997.
11. Petterson, J.; Lorenz, L.J.; Risley, D.S.; Sanmann, B.J. Amino acid analysis of peptides using HPLC with evaporative light scattering detection. J. Liquid Chromatogr. Relat. Technol. **1999**, *22*, 1009.
12. Martins, A.R.; Padovan, A.F. A practical approach to improve the resolution of dansyl amino acids by high-performance liquid chromatography. J. Liquid Chromatogr. Relat. Technol. **1999**, *19* (3), 467.

Amino Acids: HPLC Analysis Advanced Techniques

Susana Maria Halpine
STArt! teaching Science Through Art, Playa del Rey, California, U.S.A.

INTRODUCTION

Amino acid analysis (AAA) is a classic analytical technique that characterizes proteins and peptides based on the composition of their constituent amino acids.[1,2] It provides qualitative identification and is essential for the accurate quantification of proteinaceous materials.

Amino acid analysis is widely applied in research, clinical facilities, and industry. It is a fundamental technique in biotechnology, used to determine the concentration of peptide solutions, to confirm protein binding in antibody conjugates, and for end-terminal analysis following enzymatic digestion. Clinical applications include diagnosing metabolic disorders in newborns. In industry, it is used for quality control of products ranging from animal feed to protein pharmaceuticals.

The analysis of a polypeptide typically involves four steps: hydrolysis (or deproteination with physiological samples), separation, derivatization, and detection. Hydrolysis breaks the peptide bonds and releases free amino acids, which are then separated by side-group using column chromatography. Derivatization with a chromogenic reagent enhances the separation and spectral properties of the amino acids, and is required for sensitive detection. A data processing system compares the resulting chromatogram, based on peak area or peak height, to a calibrated standard (Fig. 1a). The results, expressed as mole percent and micrograms of residue per sample, determine the percentage composition of each amino acid as well as the total amount of protein in the sample. Unknown proteins may be identified by comparing their amino acid composition with those in protein databases. Successful identification of unknown proteins may be achieved using internet search programs.[3]

Other techniques, such as capillary electrophoresis (CE) and matrix-assisted laser desorption ionization (MALDI) mass spectrometry, provide qualitative analyses–often with greater speed and sensitivity.[1] Nevertheless, AAA by high-performance liquid chromatography (HPLC) complements other structural analysis techniques, such as peptide sequencing, and remains indispensable for quantifying the composition and absolute content of proteinaceous materials.[2]

PEPTIDE HYDROLYSIS

Acid hydrolysis of proteins and peptides yields 16 of the 20 DNA-coded amino acids; tryptophan is destroyed, cysteine recovery is unreliable, and asparagine and glutamine are converted to aspartic acid and glutamic acid, respectively.[1,2,4,5] Furthermore, some side-groups, such as the hydroxyl in serine, promote the breakdown of the residue, while aliphatic amino acids such as valine and leucine, protected by stearic hindrance, require longer hydrolysis time. This variation in yield can be overcome by hydrolyzing samples for 24, 48, and 72 hr and extrapolating the results to zero time point.

Conventional hydrolysis exposes the polypeptide to 6 *M* HCl under vacuum at 110°C for 20–24 hr. Protective agents, such as 0.1% phenol, are added to improve recovery. Gas-phase hydrolysis, in which the acid is delivered as a vapor, gives comparable results to liquid-phase hydrolysis. Additionally, the gas phase minimizes acid contaminants and allows parallel hydrolysis of standards and samples within the same chamber.

The reaction rate doubles with every 10°C increase, so that hydrolysis at 145°C for 4 hr gives results comparable to those from the conventional method. Microwave hydrolysis reduces analysis time to 30–45 min. Alternative hydrolysis agents include methane sulfonic acid, which often gives better recovery but is non-volatile, and alkaline hydrolysis, used in the analysis of tryptophan, proteoglycans, and proteolipids.

Careful sample preparation and handling during the hydrolysis step are critical for maintaining accurate and reproducible results.[1,2,4–6] Salts, metal ions, and other buffer components remaining in a sample may accelerate hydrolysis, producing unreliable quantification. The Maillard reaction between amino acids and carbohydrates results in colored condensation products (humin) and decreased yield.[7] Routine method calibration with proteins and amino acid standards, use of an internal standard (1 nmol norleucine is used for sensitive analysis), and control blanks are strongly recommended, along with steps to minimize background contaminants (Fig. 1b). Attention to housekeeping details, such as cleaning glassware and baking in a muffle furnace, can minimize background contaminants. The practical limit for high sensitivity hydrolysis is 10–50 ng of sample; below this amount, background contaminants and losses during hydrolysis begin to play a larger role.

DERIVATIZING REAGENTS FOR ANALYSIS OF AMINO ACIDS BY HPLC

The first automated analyzer was developed by Moore, Stein, Spackman, and Hamilton in the 1950s. Hydrolysates

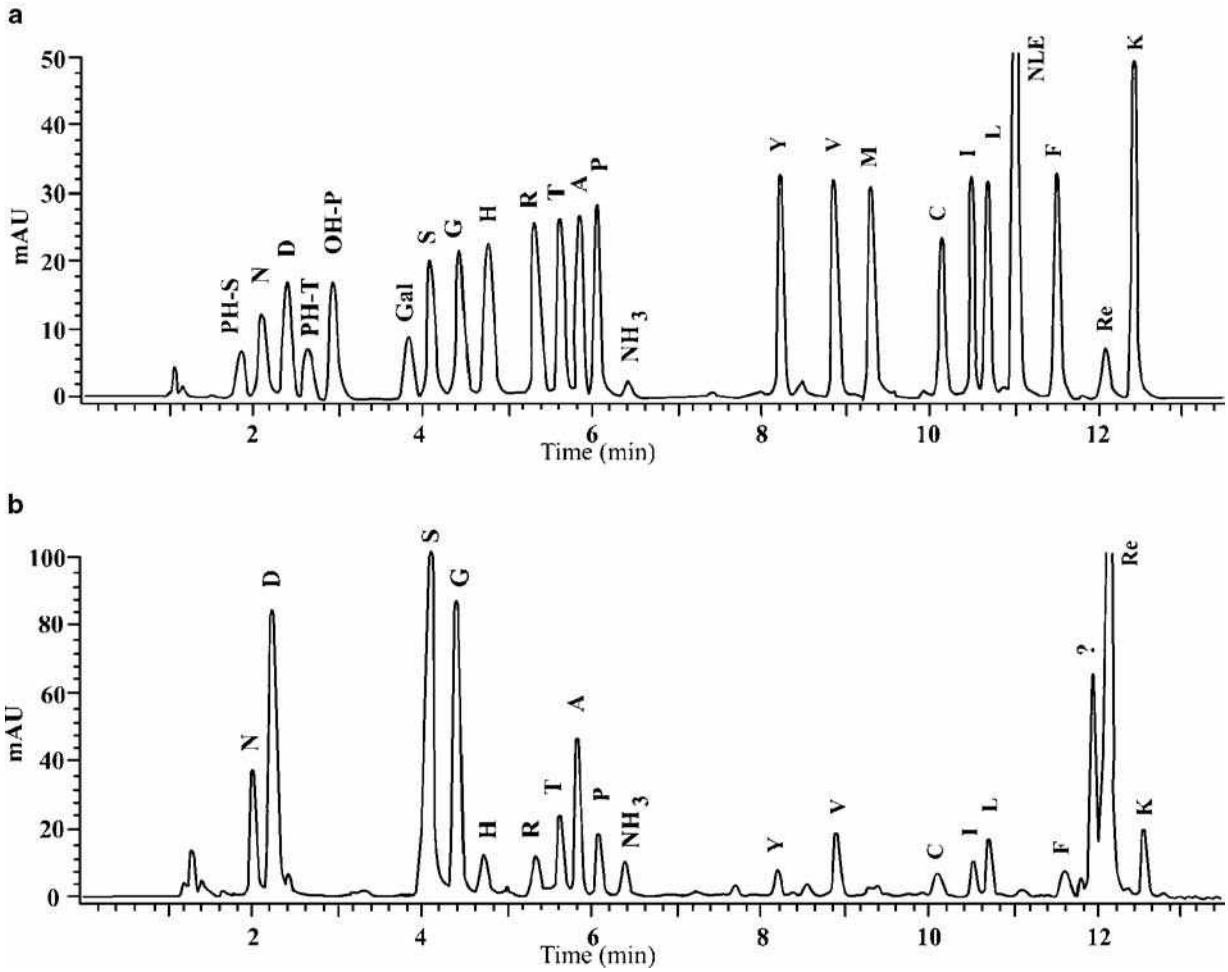

Fig. 1 A, PTC-amino acid standard (200 pmol), including phosphoserine (PH-S), aspartate (N), glutamate (D), phosphothreonine (PH-T), hydroxyproline (OH-P), galactosamine (Gal), serine (S), glycine (G), histidine (H), arginine (R), threonine (T), alanine (A), proline (P), tyrosine (Y), valine (V), methionine (M), cysteine (C), isoleucine (I), leucine (L), norleucine (NLE, 1 nmol internal standard), phenylalanine (F), excess reagent (Re), and lysine (K). B, Analysis of a human fingerprint, taken up from a watch glass using a mixture of water and ethanol.

Source: Courtesy of the National Gallery of Art and the Andrew W. Mellon Foundation.

were separated on an ion-exchange column, followed by postcolumn reaction with ninhydrin. Although this system remains the standard method, especially for physiological amino acids, its major drawback is low sensitivity, typically at the nanomole level. Several methods have since been developed offering high sensitivity and faster analyses without sacrificing reproducibility.[1–5,7–9] The choice of an optimal derivative technique depends on factors such as specific application requirements, sample size, sample preparation time, and equipment maintenance.[10] Amino acid derivatives based on ultraviolet (UV) light detection provide accurate analysis at the picomole level and derivatives requiring fluorescence detection are accurate at the femtomole level.

Amino acids react with many reagents to form stable derivatives and strong chromophores (Table 1). Derivatization can precede (precolumn) or follow (in-line postcolumn) the chromatographic separation. Both pre- and postcolumn systems are currently employed: ninhydrin and phenylisothiocyanate (PITC) analyzers are widely used, while 6-aminoquinolyl-*N*-hydroxysuccinimidyl carbamate (AQC), *O*-phthalaldehyde (OPA), and OPA/9, fluorenylmethylchloro-formate (FMOC) systems provide the highest sensitivity.

Postcolumn systems typically use cation-exchange columns with either sodium citrate (for hydrolysates) or lithium citrate (for physiological samples) as the mobile phase. Contaminating salts and detergents are better tolerated because the samples are "cleaned up" before reaction with the reagent. The additional pump for the reagent, however, may lead to sample dilution, peak broadening, baseline fluctuations, and longer analysis time (30–90 min). Fluorescent reagents are compatible with a wider range of buffers, but the buffers must be amine-free if used with precolumn methods.

Since the 1980s, precolumn derivatization methods have gained wider acceptance due to simpler preparation,

Table 1 Amino acid derivatization reagents.

Reagent	Chromophore	Detection limit	Separation time	Drawbacks	Advantages
AQC (6-aminoquinolyl-*N*-hyfroxysuccinimidyl carnamate)	Fluorescent (ex. 245 nm, em. 395 nm); UV 245 nm	160 fmol	35–50 min precolumn	Quaternary gradient elution required for complex, non-hydrolysate samples	Tolerates salts and detergents, rapid reaction, stable product, good reagent separation, high sensitivity and accurancy
Dansyl chloride(4-*N*, *N*-dimethylaminoazobenzene-4′-sulfonyl chloride)	Visible 436 nm	Low fmol	18–44 min precolumn	Multiple products, critical concentration	Stable product, good separation, high sensitivity
Dansyl chloride (5,*N*, *N*-dimethylaminonaphthalene-1-sulfonyl chloride)	Fluorescent (ex. 360–385 nm, em. 460–495 nm); UV 254 nm	Low pmol	60–90 min	Multiple products, critical concentration, difficult separation leads to long separation time	Stable product
Fluorescamine(4-phenyl-spiro[furan-2(3H), 1′-phthalan]-3,3′-dione)	Fluorescent (ex. 390 nm, em. 475 nm)	20–100 pmol	30–90 min postcolumn	Secondary amine pretreatment, critical concentraion, may give background interference	Rapid reaction, stable product, good reagent separation
FMOC (9-fluorenylmethylchloro formate)	Fluorescent (ex. 265 nm,1 pmol em, 320 nm); UV 265 nm	1 pmol	20–45 min precolumn	Multiple products, extraction of excess reagent	Stable product, used with OPA for detection of secondary amine
Ninhydrin (triketohydrindene hydrate)	Primary amine (440 nm), secondary amine (570 nm)	100 pmol	30 min postcolumn	Low sensitivity and resolution	Good reproducibility
OPA (*O*-phthalaldehyde)	Fluorescent (ex. 340 nm, em. 455 nm	50 fmol	90 min postcolumn, 17–35 precolumn	Secondary amine pretreatment, slow reaction, unstable derivative, background interference	Good reagent separation, high sensitivity and reproducibility with automated system
PITC (phenylisothiocyanate)	UV 254 nm	1 pmol	15–27 min precolumn	Salt interference, requires refrigeration, excess reagent removed under vacuum	Ease of use, flexibility, good separation, reproducibility enhanced with automation

Adapted from Cooper, Packer, & Williams[1] and Smith.[2]

faster analyses, and better resolution. The separation on reversed-phase C-8 or C-18 columns typically requires low-UV mobile phases, such as sodium phosphate or sodium acetate buffers, with acetonitrile or methanol as organic solvent. Separation times range from 15 to 50 min.

IMPROVED RECOVERY OF SENSITIVE AMINO ACIDS

Cysteine and tryptophan require special treatment for quantitative analysis.[1,11] Cystine/cysteine can be determined using three equally successful methods: oxidation, alkylation, and disulfide exchange. Oxidation to cysteic acid is commonly carried out by pretreatment with performic acid. Alkylation using pretreatment with 4-vinylpyridine or iodoacetate produces piridylethylcysteine (PEC) and carboxymethylcysteine (CMC), respectively. Disulfide exchange is achieved by adding reagents such as dithiodipropionic acid, dithiodiglycolic acid, or dimethylsulfoxide (DMSO) to the HCl during hydrolysis. The latter treatment offers ease of use as well as accurate yields.

The superior approach to tryptophan analysis involves the addition of dodecanethiol to HCl, especially when combined with automatic vapor-phase hydrolysis. Alternative hydrolysis agents such as methane sulfonic acid, mercaptoethanesulfonic acid, or thioglycolic acid can produce 90% or greater yields. Acid hydrolysis additives and alkaline hydrolysis using 4.2 *M* NaOH are also used with varying results.

Qualitative analysis of glycopeptides and phosphoamino acids is achieved through a separate, partial hydrolysis with 6 N HCl acid at 110°C for 1 and 1.5 hr, respectively.[1,12] Separation of cysteine, tryptophan, and amino sugars requires minimal chromatographic adjustments; phosphoamino acid separation is straightforward using reversed phase but cumbersome using ion exchange.

ANALYSIS OF FREE AND MODIFIED AMINO ACIDS

Blood, urine, and cerebrospinal and other physiological fluids contain a great number of post-translationally modified amino acids (approximately 170 have been studied to date) and in a wider range of concentrations than protein hydrolysates.[1,13,14] Additionally, plant sources produce about 500 non-protein amino acids, and in geological samples, highly unusual amino acids may indicate extraterrestrial origin.[15,16]

Although the free amino acids in these samples do not require hydrolysis, blood plasma and cerebrospinal fluid must be deproteinated before analysis. Otherwise, proteins may bind irreversibly to ion-exchange columns, resulting in loss of resolution. Furthermore, any peptide hydrolases must be inactivated. For ion-exchange analysates, a protein precipitant is added before centrifugation. Sulfosalicylic acid, a common precipitating agent, is added in solid form to avoid sample dilution. For reversed-phase analysates, ultrafiltration, SEC, or organic solvent extraction is recommended. Samples with low protein and high amino acid concentrations, such as urine and amniotic fluid, need only to be diluted before analysis.

Precolumn derivatives are more tolerant of lipid-rich samples.[1] Changing the guard column routinely is recommended to avoid column buildup, especially for reversed-phase systems.

AMINO ACID RACEMIZATION ANALYSIS

L-Amino acid enantiomers are the most prevalent in nature. However, D-forms are increasingly found in living organisms, fossils, and extraterrestrial samples. D-Amino acids resulting from post-translational modifications now appear to be fundamental components of bacterial cell walls and microbial antibiotics.[2]

Racemization, the interconversion of amino acid enantiomers, occurs slowly in biological and geological systems. The rate increases with extreme pH values, high temperature, and high-ionic strength. Rates also vary between amino acids: At 25°C, the racemization half-life of serine is about 400 yr, while that of isoleucine is 40,000 yr. Enantiomer analysis is used to confirm bioactivity of synthetic peptides and for geological dating.[1,2,7,16]

Hydrolysis itself accelerates racemization. Shorter acid exposure at higher temperatures, such as 160°C for 1 hr, decreases racemization by about 50% compared to conventional hydrolysis. Liquid-phase methanesulfonic acid, gas-phase microwave, conventional, and gas-phase microwave hydrolysis produce progressively higher rates of racemization. Additional phenol, however, significantly reduces racemization during microwave hydrolysis.[4]

The three general approaches to enantiomer separation entail a chiral stationary phase, a chiral mobile phase, or a chiral reagent. Tandem columns, with reversed and chiral stationary phases, were used to separate 18 D–L pairs of phenylthiocarbamyl (PTC)-amino acids in 150 min. OPA-amino acid enantiomers have been separated on both ion-exchange and reversed-phase columns using a sodium acetate buffer with an L-proline-cupric acetate additive. Chiral reagents, such as Marphey's reagent and OPA/IBLC (*N*-isobutyryl-L-cysteine), were successfully used for racemization analysis within 80 min.

CONCLUSIONS

Amino acid analysis continues to be an essential tool in protein chemistry. It has been described as "deceptively

difficult": Accurate results require attention to sophisticated instrumentation, sample handling, and consideration of the chemistry of specific amino acids under investigation.[17] When the "art and practice" are carefully addressed, however, AAA provides a fundamental understanding of peptides and proteins unmatched by other techniques.[6]

ACKNOWLEDGMENT

The author would like to thank Drs. Steven Birken, Chun-Hsien Huang, Stacy C. Marsella, and Conceicao Minetti for their proofreading assistance.

REFERENCES

1. Cooper, C., Packer, N., Williams, K., Eds.; *Amino Acid Analysis Protocols*; Humana Press: Totowa, NJ, 2001.
2. Smith, B.J., Ed.; *Protein Sequencing Protocols*; Humana Press: Totowa, NJ, 2003, 111–194.
3. Schegg, K.M.; Denslow, N.D.; Andersen, T.T.; Bao, Y.; Cohen, S.A.; Mahrenholz, A.M.; Mann, K. Quantitation and identification of proteins by amino acid analysis: ABRF-96AAA collaborative trial. In *Techniques in Protein Chemistry,* 8th Ed.; Marshak, D.R., Ed.; Academic Press: San Diego, CA, 1997, 207–216.
4. Fountoulakis, M.; Lahm, H.-W. Hydrolysis and amino acid composition analysis of proteins. J. Chromatogr. A, **1998**, *826*, 109–134.
5. Fini, C., Floridi, A., Finelli, V.N., Wittman-Liebold, B., Eds.; *Laboratory Methodology in Biochemistry, Amino Acid Analysis and Protein Sequencing*; CRC Press: Boca Raton, FL, 1990.
6. West, K.A.; Hulmes, J.D.; Crabb, J.W. Amino acid analysis tutorial: Improving the art and practice of amino acid analysis. In *The Association of Biomolecular Resource Facilities (ABRF) Annual Meeting: Biomolecular Techniques*; San Francisco, CA, March 30–April 2, 1996, www.abrf.org/ResearchGroups/AminoAcidAnalysis/EPosters/Archive/1c.html
7. Barrett, G.C., Ed.; *Chemistry and Biochemistry of Amino Acids*; Chapman and Hall: London, 1985.
8. Tarr, G.E.; Paxton, R.J.; Pan, Y.C.E.; Ericsson, L.H.; Crabb, J.W. Amino acid analysis 1990: The third collaborative study from the Association of Biomolecular Resource Facilities (ABRF). In *Techniques in Protein Chemistry,* 2nd Ed.; Villafranca, J.J., Ed.; Academic Press: San Diego, CA, 1991, 139–150.
9. Hancock, W.S., Ed.; *CRC Handbook of HPLC for the Separation of Amino Acids, Peptides, and Proteins*; CRC Press: Boca Raton, FL, 1984, Vol. I.
10. Chin, D. 2004 AAA Roundtable Summary. In *ABRF Amino Acid Analysis Research Group*, www.abrf.org/ResearchGroups/AminoAcidAnalysis/EPosters/Chin_RT_Summary.pdf (accessed September 2004).
11. Strydom, D.J.; Andersen, T.T.; Apostol, I.; Fox, J.W.; Paxton, R.J.; Crabb, J.W. Cysteine and tryptophan amino acid analysis of ABRF92-AAA. In *Techniques in Protein Chemistry,* 4th Ed.; Hogue Angeletti, R., Ed.; Academic Press: San Diego, CA, 1993, 279–288.
12. Yuksel, K.U.; Andersen, T.T.; Apostol, I.; Fox, J.W.; Crabb, J.W.; Paxton, R.J.; Strydom, D.J. Amino acid analysis of phospho-peptides: ABRF-93AAA. In *Techniques in Protein Chemistry,* 5th Ed.; Crabb, J., Ed.; Academic Press: San Diego, CA, 1994, 231–240.
13. Haynes, P.A.; Sheumack, D.; Greig, L.G.; Kibby, J.; Redwood, J.W. Applications of automated amino acid analysis using 9-fluorenylmethyl chloroformate. J. Chromatogr. **1991**, *588*, 107–114.
14. Gibson, M. Amino acid analysis by HPLC/ninhydrin and tandem mass spectrometry detection. In *ABRF Amino Acid Analysis Research Group*, http://www.abrf.org/ResearchGroups/AminoAcidAnalysis/EPosters/Gibson_MS.pdf (accessed September 2004).
15. Rosenthal, G. *Plant Nonprotein Amino and Imino Acids: Biological, Biochemical, and Toxicological Properties*; Academic Press: New York, 1982.
16. Hare, P.E.; Hoering, T.C.; King, K., Eds. *Biogeochemistry of Amino Acids*; John Wiley and Sons: New York, 1980.
17. Andersen, T.T. Practical amino acid analysis. In *ABRF Amino Acid Analysis Research Group; 1995*, www.abrf.org/ABRFNews/1994/September1994/sep94-practicalaaa.html (accessed September 2004).

Analyte–Analyte Interactions: TLC Band Formation

Krzysztof Kaczmarski
Faculty of Chemistry, Technical University of Rzeszów, Rzeszów, Poland

Mieczysław Sajewicz
Institute of Chemistry, Silesian University, Katowice, Poland

Wojciech Prus
School of Technology and the Arts in Bielsko-Biała, Bielsko-Biała, Poland

Teresa Kowalska
Institute of Chemistry, Silesian University, Katowice, Poland

INTRODUCTION

Chromatographic separations are mainly used for analytical purposes and, as such, are termed analytical chromatography. Chromatography, however, is gaining increasing importance as a tool that enables isolation of preparative amounts of the desired substances. Such "preparative chromatography" is usually achieved with liquid chromatography (LC) and high-performance liquid chromatography (HPLC), but also occasionally with thin-layer chromatography (TLC).

Each separation occurs because of the different interactions of each species with a sorbent. To describe the partitioning process, knowledge of the isotherm involved is needed. In analytical chromatography, the concentration of a species in an analyzed sample is very low, so description of the retention process typically requires knowledge of the slope of the isotherm when the concentration is zero.

When chromatography is used in the preparative mode, the entire dependence of the equilibrium on the concentrations of adsorbed and non-adsorbed solute must be established. The equilibrium isotherm is usually non-linear and analysis of such isotherms is a necessary prerequisite to enable prediction of the retention mechanism.

OVERVIEW

Physicochemical description of retention processes in liquid chromatography (planar chromatography included) is far from complete and, therefore, new endeavors are regularly undertaken to improve existing retention models and/or to introduce the new ones. The excessive simplicity of already established retention models in planar chromatography is—among other reasons—because some types of intermolecular interaction in the chromatographic systems are disregarded. For example, none of the validated models focusing on prediction of solute retention takes into consideration so-called "lateral interactions," the term used to denote self-association of solute molecules.

The aim of this report is to give insight into the role of lateral interactions in TLC band formation.

THEORY OF CHROMATOGRAPHIC BAND FORMATION

Study of the mechanism of adsorption in TLC is more difficult than in column liquid chromatography. The nonlinear isotherm model in TLC can be designed in a qualitative way only, after investigation of chromatographic band shape and of the concentration distribution within this band; phenomena characteristic of TLC band formation can also have a major effect on the mechanism of retention.

Transfer Mechanism in TLC

In TLC, as most frequently practiced, transfer of mobile phase through the thin layer is induced by capillary flow. Solvents or solvent mixtures contained in the chromatographic chamber enter capillaries in the solid bed, attempting to reduce both their free surface area and their free energy. The free-energy gain ΔE_m of a solvent entering a capillary is given by the relationship:

$$\Delta E_m = -\frac{2\gamma V_n}{r} \quad (1)$$

where γ is the free surface tension, V_n denotes the molar volume of the solvent, and r is the capillary radius.

From Eq. l, it follows that the capillary radius r has a very important effect on capillary flow; a smaller radius leads to more efficient flow. The methods used for preparation of commercial stationary phases and supports cannot ensure all pores are of equal, ideal diameter; this results in side effects that contribute to the broadening of chromatographic spots. Other mechanisms of spot broadening are described below.

Broadening of Chromatographic Bands as a Result of Eddy Diffusion and Resistance to Mass Transfer

The most characteristic feature of chromatographic bands is that the longer the development time and the greater the distance from the start, the greater become their surface areas. This phenomenon is not restricted to planar chromatography—it occurs in all chromatographic techniques. Band broadening arises as a result of eddy and molecular diffusion, the effects of mass transfer, and the mechanism of solute retention.

Eddy diffusion of solute molecules is induced by the uneven diameter of the stationary phase or support capillaries, which automatically results in uneven mobile phase flow rate through the solid bed. Some solute molecules are thus displaced more quickly than the average rate of displacement of the solute, whereas others are retarded.

Molecular diffusion is the regular diffusion in the mobile phase, the driving force of each dissolving process and, therefore, needs no further explanation.

The effects of mass transfer are different in the stationary and mobile phases. The resistance to mass transfer in the mobile phase varies with the reciprocals of mobile phase velocity and the diffusivity of the species. The resistance to mass transfer inside the stationary phase varies with the reciprocal of diffusivity and is proportional to the radius of the adsorbent granules attached to the chromatography plate, or the structural complexity of the internal pores in chromatographic paper. For both types of mass-transfer resistance, band stretching is proportional in each direction, as measured from the geometrical spot center, and increases in magnitude the greater the resistance.

All the aforementioned phenomena, which contribute jointly to spot broadening, are used to be described as the effective diffusion. Effective diffusion is a convenient notion, which, apart from being concise and informative, emphasizes that all the contributory phenomena occur simultaneously.

Broadening of Chromatographic Bands as a Result of the Mechanism of Retention

Mechanisms of solute retention, which are also responsible for spot broadening, differ from one chromatographic technique to another, and their role in this process is far less simple than that of diffusion and mass transfer. Use of densitometric detection has, however, furnished insight into concentration profiles across the chromatographic band, enabling estimation of the role of solute retention in peak broadening and prediction of the retention mechanism. Fig. 1 shows three examples of such concentration profiles in the absence of mass overload.

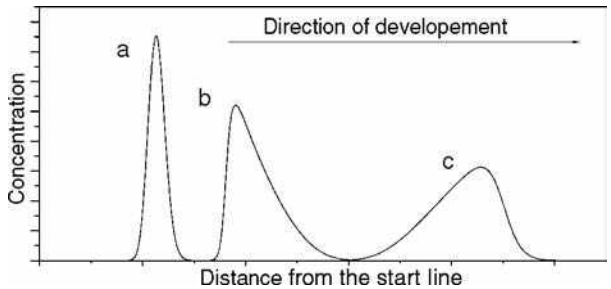

Fig. 1 Three examples of concentration profiles along the chromatographic stationary phase bed: a, symmetrical without tailing; b, skewed with tailing toward the mobile-phase front; and c, skewed with tailing toward the origin.

Numerous efforts have been made to describe the band broadening effect and the formation of the concentration profiles. The most interesting models are those that consider band broadening as a two-dimensional process.

Two models of two-dimensional band broadening were established by Belenky et al.[1,2] and by Mierzejewski.[3] In these models, non-linearity of the adsorption isotherm was neglected so that elliptical spots only, with symmetrically distributed concentration (as shown in Fig. 1a), could be modeled. We will now focus our attention on the effect of the adsorption mechanism on the concentration profiles of chromatographic bands.

ADSORPTION EQUILIBRIUM ISOTHERMS

Isotherm models reflect interactions between active sites on the sorbent surface and the adsorbed species and, simultaneously, interactions occurring exclusively among the adsorbed species. The dependence of isotherm shapes on concentration profiles in TLC is fully analogous to relationships between HPLC peak profiles and the isotherm models, which have been discussed in depth by Guiochon et al.[4]

Let us briefly recall several chromatographic models and analyze the correspondence between concentration profiles and types of isotherm. The simplest isotherm model is furnished by Henry's law.

$$q = HC \tag{2}$$

where q is the concentration of the adsorbed species, H is Henry's constant, and C is the concentration in the mobile phase. This isotherm is also called the linear isotherm, and

concentration profiles obtained with its aid are similar to that shown in Fig. 1a. It should be stressed that, for the linear isotherm, peak broadening results from eddy diffusion and from resistance of the mass transfer only; it does not depend on Henry's constant. In practice, such concentration profiles are observed only for analyte concentrations that are low enough for the equilibrium isotherm to be regarded as linear.

One of the simplest non-linear isotherm models is the Langmuir model.

$$q = \frac{q_s KC}{1 + KC} \tag{3}$$

where q_s is the saturation capacity and K the equilibrium constant. To make use of this isotherm, ideality of the liquid mixture and of the adsorbed phase must be assumed. Concentration profiles obtained with the aid of this isotherm are similar to that presented in Fig. 1c. The larger the equilibrium constant, the more stretched is the concentration tail (and the chromatographic band).

More complicated models take into account lateral interaction between the adsorbed molecules. One of these models was designed by Fowler and Guggenheim.[5] It assumes ideal adsorption on a set of the localized sites, with weak interactions among molecules adsorbed on neighboring sites. It also assumes that the energy of interactions between two adsorbed molecules is so small that the principle of random distribution of the adsorbed molecules on the sorbent surface is not significantly affected. For liquid–solid equilibria, the Fowler and Guggenheim isotherm is empirically extended and written in the form:

$$KC = \frac{\theta}{1 - \theta} e^{-\chi\theta} \tag{4}$$

where χ denotes the empirical interaction energy between two molecules adsorbed on nearest-neighbor sites, and θ is the degree of the surface coverage. For $\chi = 0$, the Fowler–Guggenheim isotherm simply becomes the Langmuir isotherm.

Another model, which takes into account lateral interaction and surface heterogeneity, is the Fowler–Guggenheim–Jovanovic isotherm.[6]

$$\theta = 1 - e^{-(aCe^{\chi\theta})^{\nu}} \tag{5}$$

where a is a constant and χ a heterogeneity term.

The next model, which assumes single-component localized monolayer adsorption with specific lateral interactions among all the adsorbed molecules, is the Kiselev model.[7–9] The final equation of this model is

$$\frac{\theta}{(1 - \theta)C} = \frac{K}{(1 - KK_a(1 - \theta)C)^2} \tag{6}$$

where $\theta = q/q_s$, K is the equilibrium constant for adsorption of analyte on active sites, and K_a is the association constant.

All these isotherms can generate the concentration profiles presented in Fig. 1b. The more pronounced the tailing, the stronger the lateral interactions. The concentration profiles presented in Fig. 1b could also be obtained if the adsorbed species formed multilayer structures.[10,11]

Multilayer isotherm models can be derived from the equations:

$$K_1 C(q_s - q_1 - q_2 - q_3 - \cdots - q_n) - q_1 = 0 \tag{7}$$

$$K_2 C q_1 - q_2 = 0 \tag{8}$$

$$K_3 C q_2 - q_3 = 0 \tag{9}$$

$$K_n C q_{n-1} - q_n = 0 \tag{10}$$

where the first equation describes the equilibrium between free active sites and adsorbed species, and subsequent equations depict equilibria between adjacent analyte layers. It is usually assumed that $K_2 = K_3 = \ldots = K_n = K_a$. This set of equations (i.e., Eqs. 7–10) results in the isotherm:

$$q = q_s \frac{KC(1 + 2K_p C + 3(K_p C)^2 \cdots)}{1 + KC + KCK_p C + KC(K_p C)^2 \cdots} \tag{11}$$

The Retention Model

Qualitative modeling of the experimentally observed densitometric profiles for any given adsorption isotherm has been presented in Refs.[11,12] on the basis of the model:

$$\frac{\partial C}{\partial t} + w\frac{\partial C}{\partial x} + \Phi\frac{\partial q}{\partial t} = D_x\frac{\partial^2 C}{\partial x^2} + D_y\frac{\partial^2 C}{\partial y^2} \tag{12}$$

with the assumed boundary conditions:

$$\frac{\partial C}{\partial x}\Big|_{x=0,x=x1} = \frac{\partial C}{\partial y}\Big|_{y=0,y=y1} = 0 \tag{13}$$

where Eq. 12 represents the differential mass balance for the mobile phase and the solid state, w is the average mobile-phase flow rate, C and q are, respectively, the concentrations (mol dm^{-3}) of the analyte in the mobile phase and on the sorbent surface, D_x and D_y are, respectively, the effective diffusion coefficients lengthwise (x) and in the direction perpendicular to this direction (y), Φ is the so-called phase ratio, and $x1$ and $y1$ are the plate length and width, respectively. It was assumed that at time $t = 0$,

analyte is concentrated in a rectangular spot at the start of the chromatogram.

The Role of Intermolecular Interactions: Multilayer Adsorption

When low-molecular–weight carboxylic acids are chromatographed on cellulose powder with a non-polar mobile phase, the densitograms obtained are similar to those presented in Fig. 2. Carboxylic acids form associative multimers by hydrogen bonding because of the presence of the negatively polarized oxygen atom from the carbonyl group and the positively polarized hydrogen atom from the hydroxyl group. Direct contact of these cyclic acidic dimers with a sorbent results in forced cleavage of most of the dimeric rings (e.g., because of inevitable intermolecular interactions by hydrogen bonding with hydroxyl groups of the cellulose), thus considerably shifting the equilibrium of self-association toward linear associative multimers.

The tendency of carboxylic acid analytes to form associative multimers can also be viewed as multilayer adsorption. Analysis of the concentration profiles presented in Fig. 2 reveals that for low concentrations of the analyte, peaks a and b are similar to the band profiles simulated by use of the Langmuir isotherm, whereas peaks c–f resemble profiles obtained by use of the anti-Langmuir isotherm (tailing toward the front of the chromatogram is more pronounced than tailing toward the start of the chromatogram.)

More spectacular results are obtained with some alcohols. Figs. 3 and 4 depict the densitometric profiles for 5-phenyl-1-pentanol chromatographed on Whatman No. 3 and Whatman No. 1 chromatography papers.

In this instance, very steep concentration profiles toward the start of the chromatogram are obtained; this is

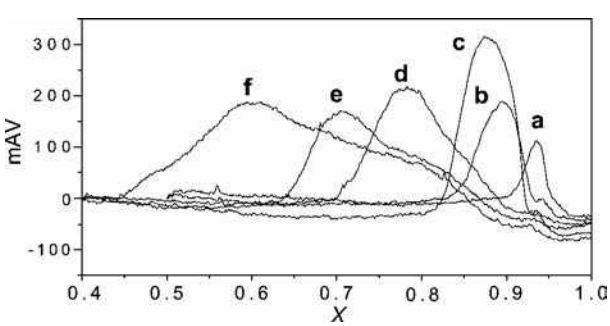

Fig. 2 Concentration profiles of 4-phenylbutyric acid on microcrystalline cellulose at 15°C with decalin as mobile phase. Concentrations of the analyte solutions in 2-propanol were (a) 0.1, (b) 0.2, (c) 0.3, (d) 0.4, (e) 0.5, and (f) 1.0 *M*. The volumes of sample applied were 3 μl.
Source: From Densitometric acquisition of concentration profiles in planar chromatography and its possible shortcomings. Part 1.4-Phenylbutyric acid as an analyte, in Acta Chromatogr.[13]

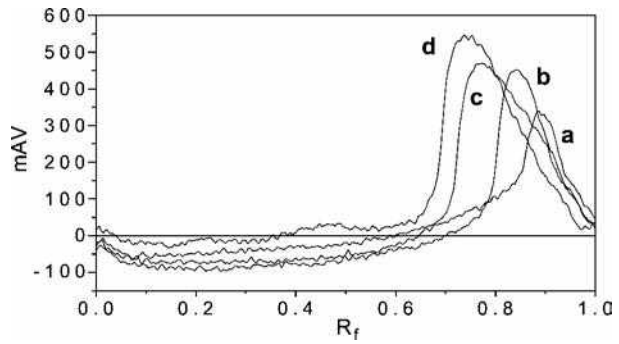

Fig. 3 Concentration profiles of 5-phenyl-1-pentanol obtained on Whatman No. 3 chromatography paper at ambient temperature with *n*-octane as mobile phase. Concentrations of the analyte solutions in 2-propanol were (a) 0.5, (b) 1.0, (c) 1.5, and (d) 2.0 *M*. The volumes of sample applied were 5 μl.
Source: From Densitometric comparison of the performance of Stahl-type and sandwich-type planar chromatographic chambers, in J. Liq. Chromatogr. Relat. Technol.[14]

indisputably indicative of some kind of interaction among the adsorbed molecules. The concentration profiles presented in Figs. 2–4 can be obtained theoretically from the model given by Eqs. 12 and 13 combined with the isotherm (Eq. 11), assuming three-layer adsorption as a maximum.

As an example, qualitative reproduction of the experimental concentration profiles shown in Figs. 3 and 4 is given in Fig. 5. The Eq. 11 constants of the adsorption isotherm, the mobile phase velocity, and effective diffusion coefficients were chosen to reproduce the shapes of the lengthwise cross sections of the chromatographic bands obtained in the experimental densitograms.

The calculations presented in graphical form in Fig. 5 were performed for $q_s = 1.5$, $K = 0.5$, $K_p = 5$, $w = 0.3$ cm/min,

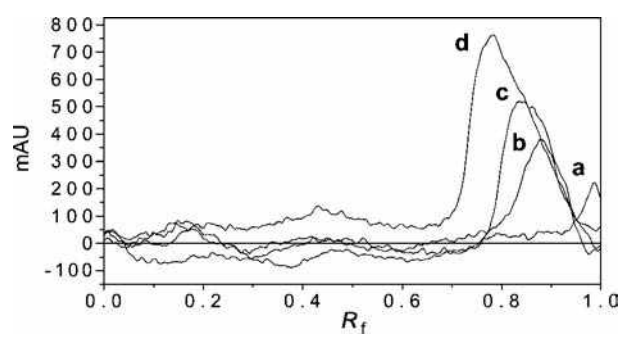

Fig. 4 Concentration profiles of 5-phenyl-1-pentanol obtained on Whatman No. 1 chromatography paper at ambient temperature with *n*-octane as mobile phase. Concentrations of the analyte solutions in 2-propanol were (a) 0.25, (b) 0.50, (c) 0.75, and (d) 1.0 *M*. The volumes of sample applied were 5 μl.
Source: From Densitometric comparison of the performance of Stahl-type and sandwich-type planar chromatographic chambers, in J. Liq. Chromatogr. Relat. Technol.[14]

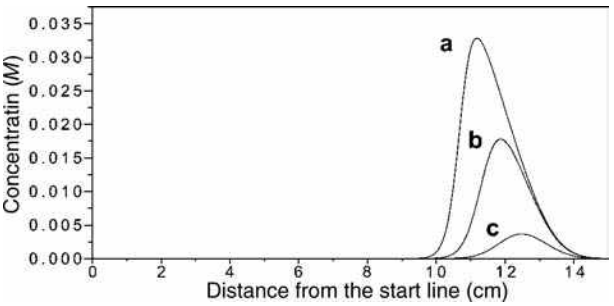

Fig. 5 The lengthwise cross section of the simulated chromatogram for a hypothetical alcohol or acid, according to the model given by Eqs. 12 and 13 in conjunction with the isotherm given by Eq. 11. Concentrations of the applied solutions were (a) 1.0, (b) 0.5, and (c) 0.1 *M*.

$D_x = 0.007$ cm^2/min, and an initial spot length of 0.06 cm. The phase ratio Φ was assumed to be 0.25.

From Fig. 5, it is apparent that the adsorption fronts are considerably less steep than the desorption fronts, and that the adsorption fronts simulated for different initial concentrations of the spots overlap. Similar behavior is apparent in the typical experimental densitograms, given in Figs. 3 and 4. In all these densitograms, the adsorption fronts for the different concentrations of acid also overlap.

CONCLUSIONS

Satisfactory qualitative agreement between experimental and theoretical concentration profiles for polar analytes suggests their retention is substantially affected by lateral interactions, which are probably even more complex than is assumed in this isotherm model. Overlapping of the adsorption fronts can be explained solely on the basis of the lateral interactions among the adsorbed molecules.

REFERENCES

1. Belenky, B.G.; Nesterov, V.V.; Gankina, E.S.; Smirnov, M.M. A dynamic theory of thin layer chromatography. J. Chromatogr. **1967**, *31*, 360–368.
2. Belenky, B.G.; Nesterov, V.V.; Smirnov, M.M. Theory of thin-layer chromatography. I. Differential equation of thin-layer chromatography and its solution (in Russian). Zh. Fiz. Khim. **1968**, *42*, 1484–1489.
3. Mierzejewski, J.M. The mechanism of spot formation in flat chromatographic systems. I. Model of fluctuation of substance concentration on spots in paper and thin layer chromatography. Chem. Anal. (Warsaw) **1975**, *20*, 77–89.
4. Guiochon, G.; Shirazi, S.G.; Katti, A.M. *Fundamentals of Preparative and Nonlinear Chromatography*; Academic Press: Boston, MA, 1994.
5. Fowler, R.H.; Guggenheim, E.A. *Statistical Thermodynamics*; Cambridge University Press: Cambridge, UK, 1960.
6. Quinones, I.; Guiochon, G. Extension of a Jovanovic–Freundlich isotherm model to multicomponent adsorption on heterogeneous surfaces. J. Chromatogr. A, **1998**, *796*, 15–40.
7. Berezin, G.I.; Kiselev, A.V. Adsorbate–adsorbate association on a homogenous surface of a nonspecific adsorbate. J. Colloid Interface Sci. **1972**, *38*, 227–233.
8. Berezin, G.I.; Kiselev, A.V.; Sagatelyan, R.T.; Sinitsyn, V.A. Thermodynamic evaluation of the state of the benzene and ethanol on a homogenous surface of a nonspecific adsorbent. J. Colloid Interface Sci. **1972**, *38*, 335–340.
9. Quinones, I.; Guiochon, G. Isotherm models for localized monolayers with lateral interactions. Application to single-component and competitive adsorption data obtained in RP/HPLC. Langmuir **1996**, *12*, 5433–5443.
10. Wang, C.-H.; Hwang, B.J. A general adsorption isotherm considering multi-layer adsorption and heterogeneity of adsorbent. Chem. Eng. Sci. **2000**, *55*, 4311–4321.
11. Kaczmarski, K.; Prus, W.; Dobosz, C.; Bojda, P.; Kowalska, T. The role of lateral analyte–analyte interactions in the process of TLC band formation. II. Dicarboxylic acids as the test analytes. J. Liq. Chromatogr. Relat. Technol. **2002**, *25*, 1469–1482.
12. Prus, W.; Kaczmarski, K.; Tyrpień, K.; Borys, M.; Kowalska, T. The role of the lateral analyte–analyte interactions in the process of TLC band formation. J. Liq. Chromatogr. Relat. Technol. **2001**, *24*, 1381–1396.
13. Kaczmarski, K.; Sajewicz, M.; Pieniak, A.; Piętka, R.; Kowalska, T. Densitometric acquisition of concentration profiles in planar chromatography and its possible shortcomings. Part 1. 4-Phenylbutyric acid as an analyte. Acta Chromatogr. **2004**, *14*, 5–15.
14. Sajewicz, M.; Pieniak, A.; Piętka, R.; Kaczmarski, K.; Kowalska, T. Densitometric comparison of the performance of Stahl-type and sandwich-type planar chromatographic chambers. J. Liq. Chromatogr. Relat. Technol. **2004**.

Antibiotics: CCC Separation

M.-C. Rolet-Menet
Analytical Chemistry Laboratory, Unit of Formation and Research (UFR) of Pharmaceutical and Biological Sciences, Paris, France

INTRODUCTION

Antibiotics are chemical compounds made either by living organisms or by chemical synthesis. They have the property to inhibit, in small amounts, some vital processes of viruses, micro-organisms (such as bacteria and fungi), and certain cells of multicellular organisms (cancerous cells, parasitic cells, etc.). The development of antibiotics made by micro-organisms requires isolation and purification of the desired compound from a complicated matrix such as a fermentation broth. These bioactive microbial metabolites are often produced in very small quantities and have to be removed from other secondary metabolites and non-metabolized media ingredients. Antibiotics are normally biosynthesized as mixtures of closely related congeners and many are labile molecules, thus requiring mild separation techniques with a high resolution capacity. Although recent advances in high-performance liquid chromatography (HPLC) technology using sophisticated equipment and refined adsorbents greatly facilitate the isolation of antibiotics, some drawbacks remain, related to various complications arising from the use of a solid support, such as adsorptive loss, deactivation, and contamination. Moreover, HPLC purification always requires sample preparation, prepurification, concentration, etc. Liquid–liquid partition techniques and particularly countercurrent chromatography (CCC) are suitable for the separation of antibiotics because they utilize a separation column free of solid support matrix, made of Teflon® channels or tubes. Raw material can be injected into the column without any previous sample treatment, which simplifies the purification procedure.

ANTIBIOTICS

Antibiotics differ widely in their polarities because their chemical structures are very variable. They are synthesized by various living materials like bacterial strains (such as *Streptomyces*[1] and *Bacillus*) and marine sponges. Oka et al.,[2] have gathered antibiotics purified by CCC from crude extract and fermentation broth. They have shown that CCC can be successfully applied to the separation of macrolides and of various other antibiotics, including various peptide antibiotics, which are strongly adsorbed to silanol groups on the silica gel used in the stationary phase in HPLC. Several CCC types are used, such as droplet CCC (DCCC)[3] and the more recent X-axis CCC, foam CCC, centrifugal partition chromatography (CPC), high-speed CCC (HSCCC), and Quattro CCC (QCCC). This discussion focuses on the separation of macrolides and polypeptide antibiotics by CCC.

Several separations of macrolide and polypeptide antibiotics by CCC are reported in the literature. Macrolides are heterosides in which the aglycone is a cyclic macrolactone with at least 14 atoms. They act by stopping protein synthesis. Polypeptide antibiotics are frequently cyclic molecules. They act by disorganizing the protein structure of the bacterial membrane. Figs. 1–5 show the structure of several molecules the purification of which is described subsequently. Sporaviridins[4] are produced by *Kutzneria viridogrisea*. They are very polar, water-soluble, basic glycoside antibiotics (Fig. 1). They consist of six components; each has a 34-membered lactone, seven monosaccharide units, a pentasaccharide (viridopentaose), and two monosaccharides. They are active against Gram-positive bacteria, acid-fast bacteria, and *Trichophyton*. WAP-8294A[5] complex (Fig. 2) is produced by *Lysobacter* sp. and consists of at least 19 closely related and very polar components. WAP-8294A2 is present as the major component and A1 and A4 are minor components. They show strong activity against Gram-positive bacteria, including methicillin-resistant *Staphylococcus aureus* (MRSA) and vancomycin-resistant enterococci. Ivermectins B1[6] are derived from avermectins B1, the natural fermentation products of *Streptomyces avermitilis*. The avermectins B1 have double bonds between carbon atoms 22 and 23, whereas the ivermectins B1 have single bonds in these positions (Fig. 3A). They have intermediate polarity. The ivermectins B1 are a mixture of two major homologs, ivermectins B1a (>80%) and ivermectins B1b (< 20%), but a crude ivermectin complex also contains various minor components. Ivermectins B1 are broad-spectrum antiparasitic agents used against *Onchocerca volvulus* in human medicine and for food animals such as cattle, swine, and horse. The bryostatins have been isolated from the marine bryozoan *Bugula neritina*[7] (Fig. 3B). They are macrolides with intermediate polarity. They show significant activity against lymphocytic leukemia in vitro, with ED_{50} values from 0.33 to 1.4 μg/ml, respectively. Ascomycin and related compounds[8] (Fig. 4) are macrolide antibiotics with intermediary polarity.

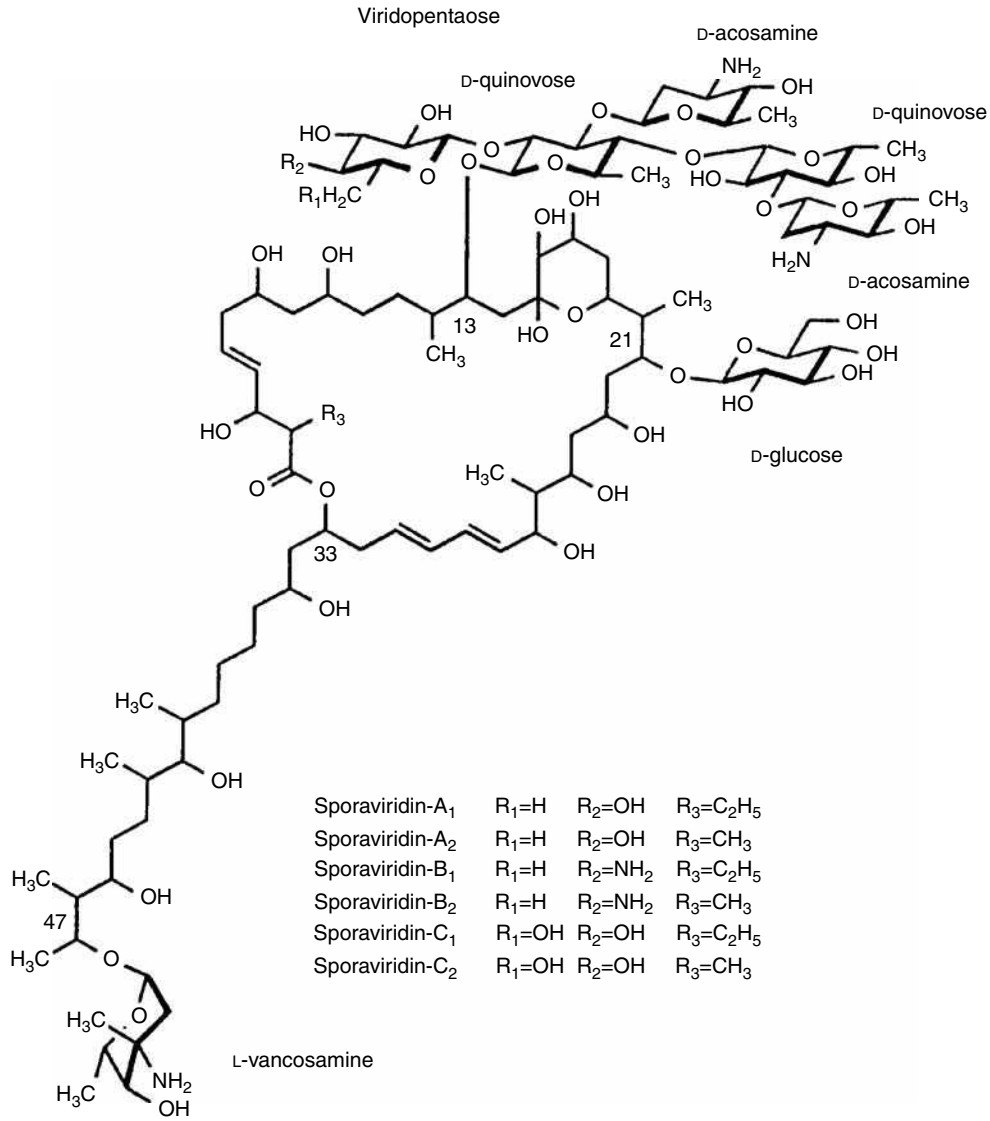

Fig. 1 Chemical structure of sporaviridins.

They have been identified from *Streptomyces tsukubaensis* and *S. hygroscopicus* and are reported as immunosuppressants with higher potency than cyclosporin A.

Finally, bacitracins[9] are peptide antibiotics produced by *Bacillus subtilis* and *Bacillus licheniformis*. Over 20 components are contained in the bacitracin complex medium, among which the major active components are bacitracin A and F (Fig. 5). They exhibit inhibitory activity against Gram-positive bacteria and are among the most commonly used antibiotics as animal feed additives.

SOLVENT SYSTEM

The polarity of the above-mentioned molecules is very variable according to the saccharide unit number contained in the chemical formula. Several procedures to choose a solvent system are described in the literature. Usual solvent systems are biphasic and made of three solvents, two of which are non-miscible. If the polarities of the solutes are known, the classification established by Ito[2] can be taken as a first approach. He classified solvent systems into three groups according to their suitability for non-polar molecules ("non-polar" systems, based on *n*-hexane), intermediate polarity molecules ("intermediary" system, based on chloroform), and polar molecules ("polar" system, based on *n*-butanol). The molecule must have a high solubility in one of the two non-miscible solvents. The addition of a third solvent enables a better adjustment of the partition coefficients (K). Oka, Oka, and Ito[10] propose a choice of various solvent systems to purify antibiotics. They have to fulfill various criteria. The settling time of the solvent system should be shorter than 30 sec to ensure satisfactory retention of the stationary phase. The partition coefficient of the target compounds should be close to 1, and the separation factor (α) between the compounds

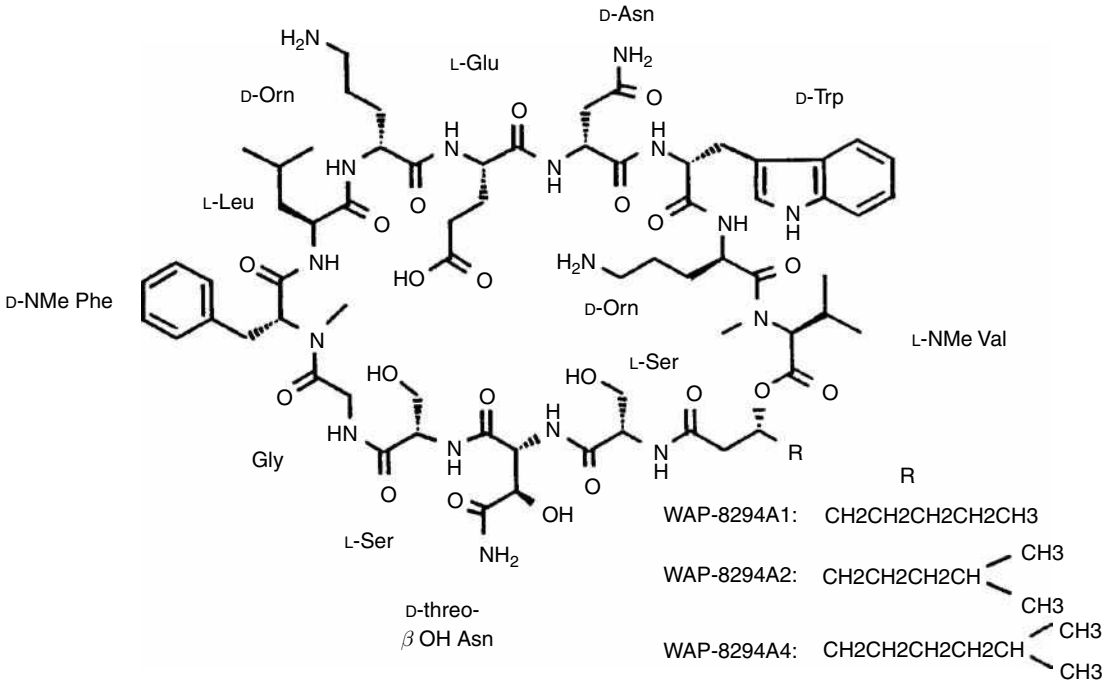

Fig. 2 Chemical structure of WAP-8294A complex.

should be larger than 1.5. Two series of solvent systems can provide an ideal range of K values for a variety of samples: *n*-hexane–ethylacetate–*n*-butanol–methanol–water and chloroform–methanol–water. These solvent series cover a wide range of hydrophobicity continuously from the non-polar *n*-hexane–methanol–water system to the more polar *n*-butanol–water system. To select the solvent system, Wang-Fan et al.[8] measured the solubility of macrolides in a series of common solvents, where the polarities were ranked with dielectric constants. The partition coefficients of solutes were compared in various ternary solvent systems selected according to the solubility studies. A ternary solvent system was selected based on suitable partition coefficients of the antibiotics. Finally, in the further optimization of composition proportions, the quaternary solvent systems showed the best solvent selectivities by giving the most prominent differences of partition coefficient.

COUNTERCURRENT CHROMATOGRAPHY FOR PURIFICATION OF ANTIBIOTICS

Several CCC devices are commonly used to purify antibiotics, such as the rotating coil instruments particularly used in HSCCC and the cartridge instruments used in CPC. A chapter of this encyclopedia is entirely devoted to the various CCC devices, so that only some indications about performances of CCC as compared to preparative HPLC are given here.

Menet and Thiébaut[11] have compared the performances of CCC and preparative HPLC regarding the separation of two antibiotics *X* and *Y*. The CCC apparatus used was a centrifugal partition chromatograph (CPC, Sanki* LLN) of 250 ml internal volume. For the purpose, classical parameters of preparative scale chromatography were calculated: experimental duration, including the sample preparation and separation time; solvent consumption, including the volume of the mobile phase, the stationary phase, and the injection solvent; and purity of the purest fraction in *Y*. The parameter "purity in *Y*" was chosen because *Y* is the solute that is the most difficult to purify because of its physical properties (particularly hydrophobicity), which are close to those of the main impurities. The hourly yield (g/hr) is defined as the ratio of the recovered quantity to the experimental duration. The volumic yield (g/L) is defined as the ratio of the recovered quantity to the solvent consumption. Table 1 summarizes the results of separations of *Y* by CCC and preparative HPLC. The solvent volume consumption is the volume of the stationary and mobile phases in CCC or the volume of the mobile phase used in HPLC and the samples. The injected sample in CCC was not prepurified to concentrate it in *Y* from 7% to 25%. So the injected quantity in *Y* in CCC is lower (0.28 g, as against 1.59 g in preparative HPLC). For similar volumic yields, i.e., 0.20 g/L in CCC and 0.15 g/L in preparative HPLC, the enrichment in *Y* is higher with CCC than with preparative HPLC. Indeed, starting from a crude extract at 7% in *Y* with CCC or from 25% in *Y* extract with preparative HPLC leads to the same 95% highest purity. These results demonstrate the advantage of CCC in directly purifying crude extracts. Moreover, no preliminary purification of the extract is required, in contrast to preparative HPLC, which requires a 1 day enrichment of the crude extract from 7% to 25% in *Y*.

A

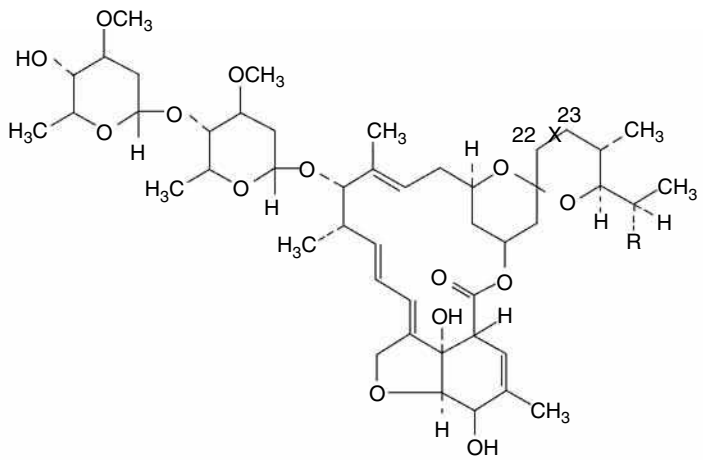

	R	–C_{22}–X–C_{23}–
Ivermectin B1a	C_2H_5	–CH_2–CH_2–
Ivermectin B1b	CH_3	–CH_2–CH_2–
Avermectin B1a	C_2H_5	–CH=CH–
Avermectin B1b	CH_3	–CH=CH–

B

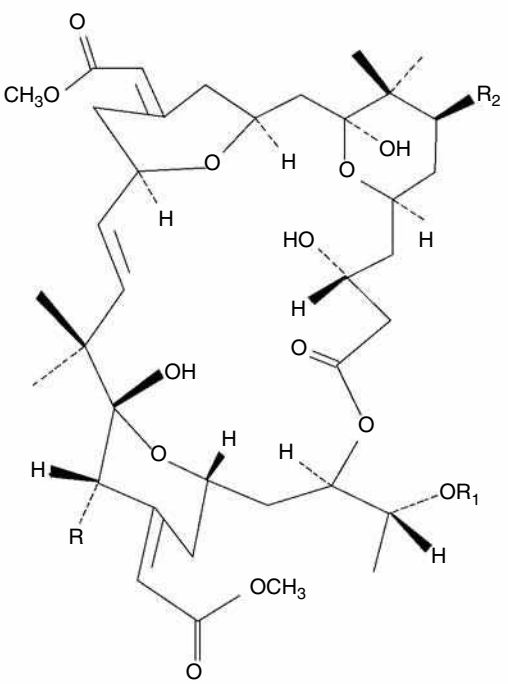

STRUCTURE	R	R_1	R_2	
1	B	H	A	Bryostatin 1
2	B	H	OH	Bryostatin 2
4	D	H	C	Bryostatin 4
5	A	H	C	Bryostatin 5
6	A	H	D	Bryostatin 6
7	A	H	A	Bryostatin 7
8	D	H	D	Bryostatin 8
9	D	H	A	Bryostatin 9
10	H	H	C	Bryostatin 10
11	H	H	A	Bryostatin 11
12	B	H	D	Bryostatin 12
13	H	H	D	Bryostatin 13
14	OH	H	C	Bryostatin 14
14a	A	A	C	
15	E	H	A	Bryostatin 15

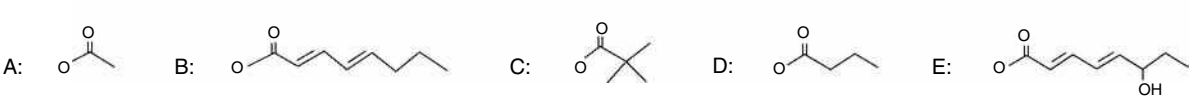

Fig. 3 Chemical structure of ivermectins (A) and bryostatins (B).

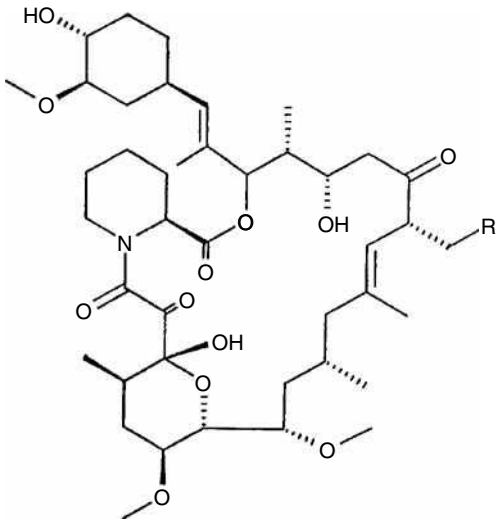

Ascomycin R = Me

FK-506 R = CH=CH$_2$

Fig. 4 Chemical structures of ascomycin and derivatives.

EXAMPLES OF PURIFICATION

Separation of Sporaviridins[4]

The chemical structures of sporaviridins are described in Fig. 1. They are only soluble in polar solvents such as water, methanol, and *n*-butanol. Therefore, a two-phase solvent system containing *n*-butanol was examined. A non-polar solvent such as diethyl ether was added to the *n*-butanol–water system to decrease the solubility of molecules in *n*-butanol and to obtain partition coefficients close to 1. The partition coefficients *K* are defined as the ratio of the solute concentration in the upper phase (butanol rich) to its concentration in the lower one (water rich).

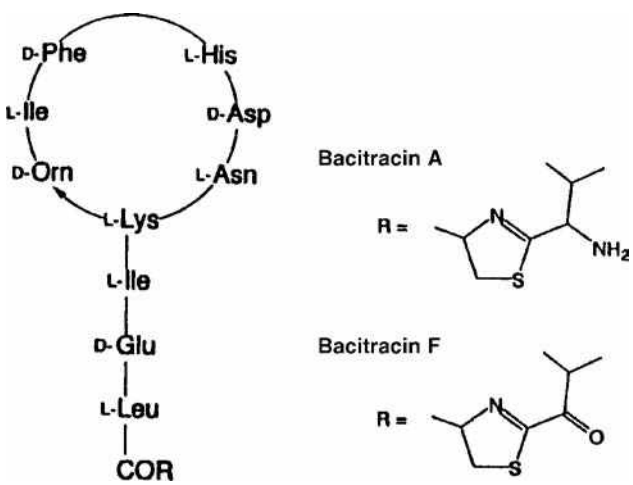

Fig. 5 Chemical structure of bacitracins.

Table 1 Comparison of CCC and HPLC performances.

	CCC	HPLC
Crude extract purity in *Y* (%)	7	25
Injected quantity of *Y* (g)	0.28	1.59
Experiment duration (hr)	6.2	2.2[a]
Solvent volume consumption (L)	1.4	10.8
Purity of the purest fraction in *Y*	>95%	>95%
Hourly yield (g/hr)	0.035	0.72
Volumic yield (g/L)	0.20	0.15

[a]1 hr for column equilibration at 90 ml/min flow rate +1 hr for separation.

A two-phase solvent system of *n*-butanol–diethylether–water (10 : 4 : 12, v/v/v) was selected because it allows one to obtain the almost equally dispersed partition coefficients among six components (C2, B2, A2, C1, B1, A1). The preparative separation of six components from sporaviridin complex by HSCCC was performed in 3.5 hr (500 ml elution volume). The six components were eluted in the order of their partition coefficients, yielding pure components A1 (1.4 mg), A2 (0.6 mg), B1 (0.7 mg), B2 (0.5 mg), C1 (1.1 mg), and C2 (1.4 mg) from 15 mg of the sporaviridin complex.

Separation of the Main Components of WAP-8294A Complex[5]

The chemical structures of WAP-8294A complex are described in Fig. 2. The structure of WAP- 8294A2 has been elucidated as a cyclic depsipeptide with a molecular mass of 1561. High-speed CCC (type J apparatus, total capacity 300 ml) was applied to the separation of the main components of the WAP-8294A complex. Due to the high polarity of these compounds, a hydrophilic two-phase solvent system composed of *n*-butanol–ethylacetate–aqueous 0.005 M trifluoroacetic acid (1.25 : 3.75 : 5, v/v/v) was used, providing a suitable range of partition coefficient values. The preparative separation of six components from the WAP-8294A complex was performed in 13.3 hr, with the lower phase as mobile phase at 0.5 ml/min. Pure fractions (1–6 mg) were obtained from 25 mg of WAP-8294A complex.

Separation of Ivermectins[6]

These molecules have an intermediary polarity (Fig. 3A). A two-phase solvent system composed of *n*-hexane, ethyl acetate, methanol, and water was selected. In this case, the partition coefficients *K* are defined as the ratio of the solute concentration in the upper phase to its concentration in the lower one. A solvent mixture of *n*-hexane–ethylacetate–methanol–water (19 : 1 : 10 : 10, v/v/v/v) yielded the best *K* values; from 0 to 3.25 mg of crude ivermectin was separated in 4.0 hr. This separation

yielded 18.7 mg of 99.0% pure ivermectin B1a, 1.0 mg of 96.0% pure ivermectin B1b, and 0.3 mg of 98.0% pure avermectin B1a.

Separation of Bryostatins[7]

An amount of 906.5 g of lymphocytic leukemia cell line active fraction was obtained by extraction from 1000 kg of *Bugula neritina*. Further purification was performed with HSCCC. Bryostatins have intermediary polarity, so that *n*-hexane–ethylacetate–methanol–water (3 : 7 : 5 : 5, v/v/v/v) was employed with the upper layer as mobile phase and lower layer as stationary phase. By this technique, from 300 mg to 3 mg of seven bryostatins have been isolated, including a new molecule, bryostatin 14 (Fig. 3B).

Separation of Ascomycin and Analogs[8,12]

Ascomycin and derivatives (Fig. 4) were purified by QCCC. The QCCC apparatus has four coils that are wound tightly on two separate bobbins on one rotor, each bobbin containing two concentrically wound coils. Optimization of solvent systems was based on solubility studies and measurements of partition coefficients for FK-506 and ascomycin. Hexane–*tert*-butylmethylether–methanol–water (1 : 3 : 6 : 5; v/v/v/v) showed the best solvent selectivity. Baseline separation of 25 mg of FK-506 and 50 mg of ascomycin was achieved in 6 hr.

Separation of Bacitracins[9]

Bacitracin complex (Fig. 5) was purified by foam CCC. The column design for foam CCC consists of a Teflon® tube. Simultaneous introduction of N_2 and the liquid phase through the respective flow tube produces a countercurrent between the gas and the liquid phase through the coil. The sample mixture injected through the middle portion of the column is separated according to the foaming capability: The foam active components travel through the coil with the gas phase and elute through the foam collection line, whereas the rest of components move with the liquid phase and elute through the liquid collection line.

After experiment, fractions from the foam and liquid outlets are collected and analyzed. The elution curve of bacitracin components from the foam outlet shows three major peaks, and the one from the liquid outlet, one peak. HPLC analysis of the fractions clearly indicates that the bacitracin components are separated in the order of hydrophobicity of the molecules in the foam fractions, and in increasing order of their hydrophilicity in the liquid fractions.

CONCLUSIONS

High-speed CCC successfully achieves preparative scale separations and purifications of numerous antibiotics from crude extracts. Moreover, the sample is directly analyzed without preliminary purification of the extract, as is required in preparative HPLC.

REFERENCES

1. Brill, G.M.; McAlpine, J.B.; Hochlowski, J.-E. Use of coil planet centrifuge in the isolation of antibiotics. J. Liq. Chromatogr. **1985**, *8* (12), 2259–2280.
2. Oka, H.; Harada, K.-I.; Ito, Y.; Ito, Y. Separation of antibiotics by counter-current chromatography. J. Chromatogr. A, **1998**, *812*, 35–52.
3. Hostettmann, K.; Appolonia, C.; Domon, B.; Hostettmann, M. Droplet countercurrent chromatography—new applications in natural products chemistry. J. Liq. Chromatogr. **1984**, *7*, 231–242.
4. Harada, K.-I.; Kimura, I.; Yoshikawa, A.; Suzuki, M.; Nakazawa, H.; Hattori, S.; Ito, Y. Structural investigation of the antibiotic sporaviridin. XV. Preparative scale separation of sporaviridin components. J. Liq. Chromatogr. **1990**, *13*, 2373–2388.
5. Harada, K.-I.; Suzuki, M.; Kato, A.; Fujii, K.; Oka, H.; Ito, Y. Separation of WAP-8294A components, a novel anti-methicillin-resistant *Staphylococcus aureus* antibiotic, using high-speed counter-current chromatography. J. Chromatogr. A, **2001**, *932*, 75–81.
6. Oka, H.; Ikai, Y.; Hayakawa, J.; Harada, K.-I.; Suzuki, M.; Shimizu, A.; Hayashi, T.; Takeba, K.; Nakazawa, H.; Ito, Y. Separation of ivermectin components by high-speed counter-current chromatography. J. Chromatogr. A, **1996**, *723*, 61–68.
7. Pettit, G.R.; Gao, F.; Sengupta, D.; Coll, J.-C.; Herald, C.L.; Doubek, D.L.; Schmidt, J.M.; Van Camp, J.-R.; Rudloe, J.J.; Nieman, R.A. Isolation and structure of bryostatins 14 and 15. Tetrahedron **1991**, *47* (22), 3601–3610.
8. Wang-Fan, W.; Kusters, E.; Lohse, O.; Mak, C.P.; Wang, Y. Application of centrifugal counter-current chromatography to the separation of macrolide antibiotic analogues. I. Selection of solvent systems based on solubility and partition coefficient investigations. J. Chromatogr. A, **1999**, *864*, 69–76.
9. Oka, H.; Harada, K.-I.; Suzuki, M.; Nakazawa, N.; Ito, Y. Foam counter-current chromatography of bacitracin. I. Batch separation with nitrogen and water free of additives. J. Chromatogr. A, **1989**, *482*, 197–205.
10. Oka, F.; Oka, H.; Ito, Y. Systematic search for suitable two-phase solvent systems for high-speed counter-current chromatography. J. Chromatogr. A, **1991**, *538*, 99–108.
11. Menet, M.-C.; Thiébaut, D. Preparative purification of antibiotics for comparing hydrostatic and hydrodynamic mode counter-current chromatography and preparative high-performance liquid chromatography. J. Chromatogr. A, **1999**, *831*, 203–216.
12. Wang-Fan, W.; Kusters, E.; Mak, C.-P.; Wang, Y. Application of coil centrifugal counter-current chromatography to the separation of macrolide antibiotic analogues. III. Effects of flow-rate, mass load and rotation speed on the peak resolution. J. Chromatogr. A, **2001**, *925* (1–2), 139–149.

Antibiotics: TLC Analysis

Irena Choma
Department of Chemical Physics, Marie Curie-Sklodowska University, Lublin, Poland

INTRODUCTION

Antibiotics are an extremely important class of human and veterinary drugs. Chemically, they constitute a widely diverse group with different functions and ways of operation. They can be derived from living organisms or obtained synthetically. Nowadays, the term "antibiotics" is often extended to so-called chemotherapeutics, such as the sulfonamides and quinolones. However, all of them exhibit antibacterial properties, i.e., either inhibit the growth of or kill bacteria.

Antibiotics are used both in human and veterinary medicine as well as in animal husbandry. They enable prevention and control of many bacterial diseases. However, there are many side effects connected with their use, such as: toxicity, allergies, or intestinal disorder. Additionally, overuse and misuse of these drugs can lead to the emergence of antibiotic resistant bacteria. Analysis of antibiotics embraces their determination in pharmaceuticals, body fluids, feed, and food. The most popular analytical methods are the chromatographic techniques. Thin-layer chromatography (TLC) is usually used as a screening method preceding high-performance liquid chromatography (HPLC) analysis, but there are also many examples of quantitative TLC analysis. TLC is also applied in the purification of newly discovered antibiotics, analysis of antibiotic metabolites and impurities, search for new biologically active compounds, and studying interactions and retention behavior of antibiotics. Antibiotics can be also applied as stationary or mobile-phase additives for chiral separations.

BACKGROUND INFORMATION

Penicillin, the first natural antibiotic, produced by genus *Penicillium*, discovered in 1928 by Fleming, and sulfonamides, the first chemotherapeutic agents, discovered in the 1930s, start a long list of presently known antibiotics. Beside β-lactams (penicillins and cephalosporins) and sulfonamides, the list includes aminoglycosides, macrolides, tetracyclines, quinolones, peptides, polyether ionophores, rifamycins, lincosamides, coumarins, nitroheterocycles, amphenicols, and others.

In principle, antibiotics should eradicate pathogenic bacteria in the host organism without causing significant damage to it. Nevertheless, most antibiotics are toxic, some of them even highly so. The toxicity of antibiotics for humans is not only due to medical treatment but also due to absorption of those drugs through contaminated food. In modern agricultural practice, antibiotics are administered to animals both for treatment of diseases and for prophylaxis as well as to promote growth as feed or water additives. All of this results in the appearance of unsafe antibiotic residues or their metabolites in edible products, e.g., milk, eggs, and meat. Some of them, like penicillins, can cause allergic reactions in sensitive individuals. Therefore, monitoring antibiotic residues should be an important task for government authorities.

There are many analytical methods for determining antibiotics in pharmaceuticals, body fluids, and food. They can be based on microbiological, immunochemical, and physicochemical principles. The most popular methods belonging to the latter group are chromatographic ones, mainly liquid chromatography, including HPLC and TLC.[1,2]

HPLC offers high sensitivity and separation efficiencies. However, it requires sophisticated equipment and is expensive. Usually, before HPLC analysis, tedious sample pretreatment is necessary, such as protein precipitation, ultrafiltration, partitioning, metal chelate affinity chromatography (MCAC), matrix solid-phase dispersion (MSPD), or solid-phase extraction (SPE). Generally, the sample clean-up procedures used before TLC separation are the same as for HPLC. Still, they can be strongly limited in the case of screening TLC or when plates with concentrating zones are applied.

TLC is cheaper and less complicated than HPLC, provides high sample throughput, and usually requires limited sample pretreatment. However, the method is generally less sensitive and selective and gives poor resolution. Some of these problems can be solved by high-performance TLC (HPTLC) or forced flow planar chromatography (FFPC), i.e., rotation planar chromatography (RPC), overpressured-layer chromatography (OPLC), and electro-planar chromatography (EPC). Lower detection limits can also be achieved using an autosampler for injection, applying special techniques of development and densitometry as a detection method, or/and spraying the plate after development with appropriate reagents. There is also a possibility of coupling TLC with autoradiography, mass spectrometry (MS) or Fourier-transform infrared (FTIR). Then, TLC can reach selectivity, sensitivity, and resolution close to those of HPLC.

TLC stripped of the above-mentioned attributes may still serve as a screening method, i.e., one that establishes the presence or absence of antibiotics above a defined level

of concentration. Screening TLC methods show sensitivity similar to microbiological assays, which are the most popular screening methods, applied for controlling antibiotic residues in food in many countries. TLC/bioautography (TLC/B) is one of the TLC screening methods. The developed TLC plates are placed on or dipped in a bacterial growth medium seeded with an appropriate bacterial strain. The location of zones of growth inhibition gives information about antibiotic residues.[3,4]

In relation to the extremely diverse nature of antibiotics, a variety of different separation and detection modes are used in analytical practice. Characteristics in brief and some general rules of separation for the most popular classes of antibiotics are presented below.

PENICILLINS

The basic structure of penicillins is a thiazolidine ring linked to a β-lactam ring to form 6-aminopenicillanic acid, the so called "penicillin nucleus" (Fig. 1). This acid, obtained from *Penicillium chrysogenum* cultures, is a precursor for semisynthetic penicillins (ampicillin, amoxicillin, oxacillin, cloxacillin, dicloxacillin, and methicillin) produced by attaching different side chains to the "nucleus." Benzylpenicillin (penicillin G) and phenoxymethylpenicillin (penicillin V) are the naturally occurring penicillins.

The most widely used stationary phase for analysis of penicillins is silica gel, but silanized silica, cyano-silica, silica gel impregnated with tricaprylmethylammonium chloride, cellulose, and alumina plates are also employed. It is advantageous to add acetic acid to the mobile-phase and/or spotting acetic acid before the sample injection in order to avoid the decomposition of β-lactams on silica gel. Mobile phases in reversed-phase (RP) systems usually contain pH 5–6 buffer and organic solvent(s).[5] The most popular detection methods are bioautography and UV densitometry, often coupled with spraying with proper reagents. A review paper on chromatographic analysis of penicillins in animal tissues, included TLC, was written by Boison.[6]

CEPHALOSPORINS

Cephalosporins are derived from natural cephalosporin C produced by *Cephalosporium acremonium*. Chemically,

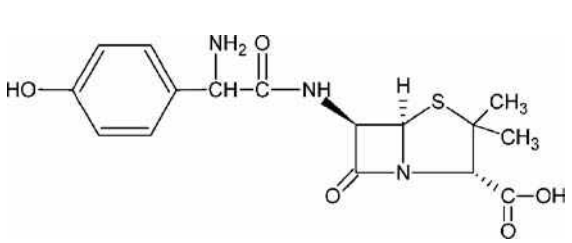

Fig. 1 Amoxicillin.

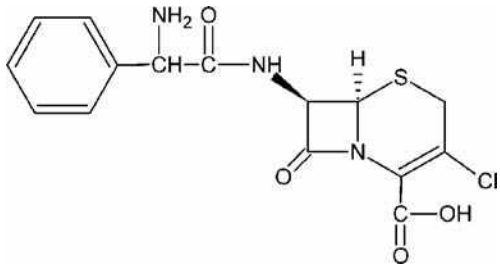

Fig. 2 Cefaclor.

they are derivatives of 7-aminocephalosporanic acid (cephem nucleus) (Fig. 2). Cephalosporins are closely related to penicillins and exhibit the same mechanisms of action, i.e., they inhibit bacterial cell wall synthesis and are used mainly for treating staphylococcal and streptococcal infections in patients who cannot use penicillins. They are commonly divided into three classes differing in the spectrum and toxicity. Cephalosporins can be analyzed by both normal-phase (NP) and RP TLC; however, more efficient separation is obtained on silanized gel than on bore silica gel.[7,8] Silica gel is sometimes impregnated with Na_2EDTA, tricaprylmethylammonium chloride, transition metal ions, or hydrocarbon. Inorganic ion exchangers (e.g., stannic oxide) or silica gel mixed with an exchanger (e.g., with Mg/Al layered double hydroxide) can be also used as stationary phases for cephalosporin analysis. The mobile phases are polar and similar to those used for penicillins. Acetic acid or acetates are very often components of solvents for NP TLC, and ammonium acetate/acetic acid buffer for RP TLC. All cephalosporins can be detected at 254 nm. Applying reagents such as ninhydrin, iodoplatinate, chloroplatinic acid, or iodine vapor can lower the detection limit. An alternative to UV detection is bioautography with, for instance, *Neisseria catarrhalis*.

AMINOGLYCOSIDES

Aminoglycosides consist of two or more amino sugars joined via glycoside linkage to a hexose nucleus (Fig. 3). Streptomycin was isolated in 1943 from *Streptomyces griseus*; then others were discovered in different *Streptomyces* strains. Aminoglycosides are particularly active against aerobic microorganisms and against the tubercle bacillus, but because of their potential ototoxicity and nephrotoxicity, they should be carefully administered. Aminoglycosides, due to their extremely polar, hydrophilic character, are analyzed mostly on silica gel, but C-18 plates can also be used. Polar organic solvents (methanol, acetone, chloroform) mixed with 25% aqueous ammonia are the most popular mobile phases. Because the majority of aminoglycosides lack UV absorption, they must be derivatized by spraying or dipping after development

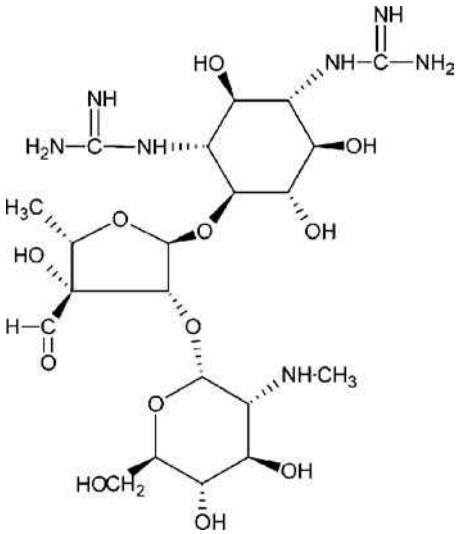

Fig. 3 Streptomycin.

with fluorescamine, vanillin, or ninhydrin solutions. They can be also detected by charring, treating with iodine vapor, or derivatization with 4-chloro-7-nitrobenzo-2-oxa-1,3-diazole (NBD-Cl) or with a mixture of diphenylboronic anhydride and salicylaldehyde. Bioautography with *Bacillus subtilis*, *Sarcina lutea*, and *Mycobacterium phlei* is also possible. Recently, a thorough review on aminoglycoside analysis appeared, embracing, among other methods, also TLC.[9]

MACROLIDES

Macrolides are bacteriostatic antibiotics composed of a macrocyclic lactone ring with one or more deoxy sugars attached to it (Fig. 4). The main representative of the class, erythromycin, was discovered in 1952 as a metabolic product of *Streptomyces erythreus*. Now, erythromycin experiences its renaissance because of its high activity against many dangerous bacteria such as *Campylobacter* and *Legionella*. The macrolide antibiotics group is still being expanded due to the search for macrolides with pharmacokinetic properties better than those of erythromycin. The separation of macrolides is performed on silica gel, kieselguhr, cellulose, and RP layers.[10] Silica gel and polar-mobile phases are extremely frequently applied, usually with the addition of methanol, ethanol, ammonia, sodium, or ammonium acetate. Because of the absence of chromophore groups, bioautography, derivatization, as well as charring are used, the last mainly by spraying with acid solutions (e.g., anisaldehyde/sulfuric acid/ethanol) and heating.

TETRACYCLINES

Tetracyclines, consisting of the octahydronaphthacene skeleton, are "broad-spectrum" antibiotics produced by *Streptomyces* or obtained semisynthetically (Fig. 5). They can be separated by both RP and NP TLC. Cellulose, kieselguhr, cyano-silica, or silica gel impregnated with EDTA or Na_2EDTA can be used. The last one is the most popular stationary phase in tetracycline analysis. Impregnation is necessary due to the very strong interaction of tetracyclines with hydroxyl groups and metal impurities. Also mobile phases, for both RP and NP TLC, should contain chelating agents such as Na_2EDTA, citric acid, or oxalic acid. Tetracyclines are amphoteric; thus, adjusting the pH of the mobile phases is very essential for their good separation. Tetracyclines give fluorescent spots, which can be detected by UV lamp, fixed at 366 nm or by densitometry. Spraying with reagents, for instance, with Fast Violet B Salt solution, provides lower detection levels. Tetracyclines can also be detected by MS (TLC/FAB/MS, TLC/MALDI/MS) as well as by bioautography. Many TLC separation methods are described in the review on the analysis of tetracyclines in food.[11]

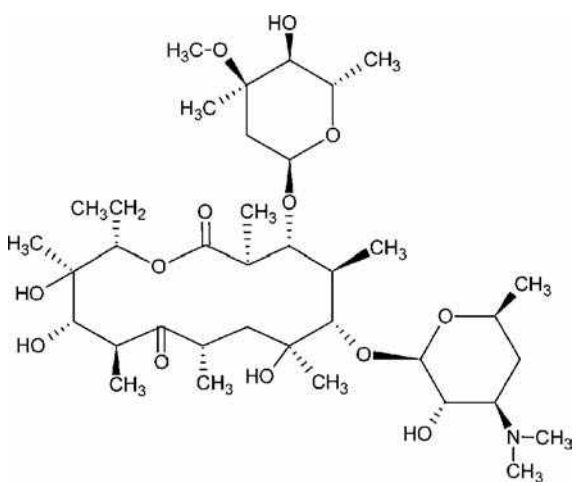

Fig. 4 Erythromycin.

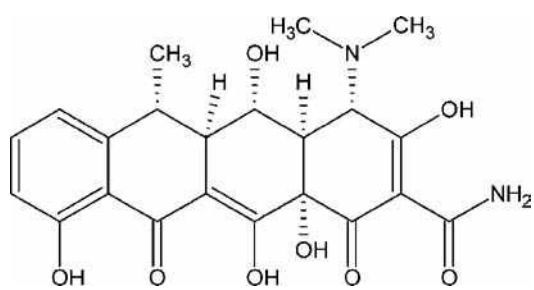

Fig. 5 Doxycycline.

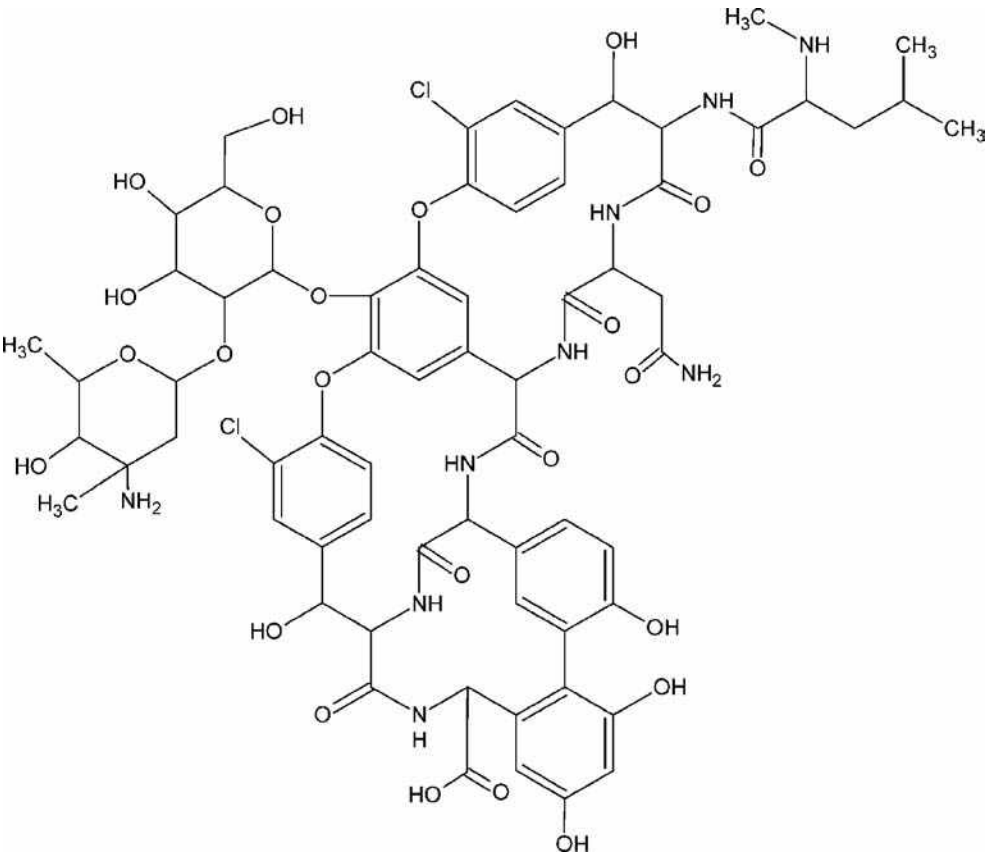

Fig. 6 Vancomycin.

MACROCYCLIC ANTIBIOTICS

Peptides

Peptide antibiotics are composed of a peptide chain of amino acids D and L covalently linked to other moieties (Fig. 6). Most peptides are toxic and have poor pharmacokinetic properties. Peptide antibiotics are difficult to analyze in biological and food samples, as they are similar to matrix components. They can be separated on silica gel, amino silica gel, polyamide, modified cellulose, and silanized silica gel plates.[12] A variety of mobile phases are applied, from simple ones like chloroform/methanol to multicomponent ones like *n*-butanol/butyl acetate/methanol/acetic acid/water. Bioautographic detection can be employed with *Bacillus subtilis* and *Mycobacterium smegmatis* as well as fluorescence densitometry or densitometry after spraying the plate with reagents such as ninhydrin or Fluram®.

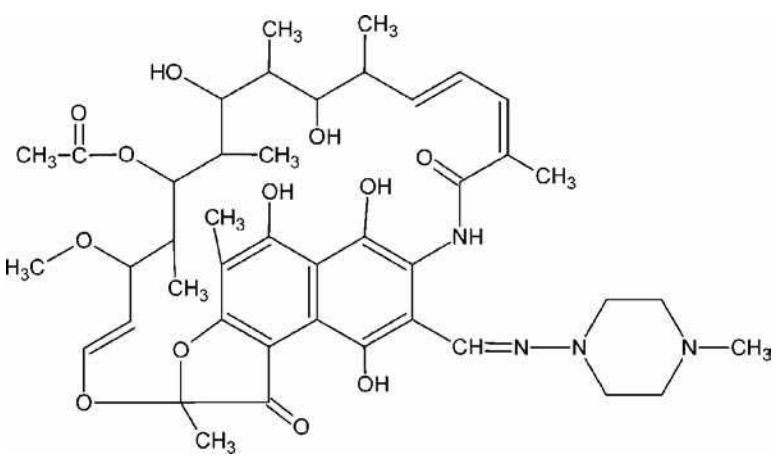

Fig. 7 Rifamycin.

Rifamycins

Rifamycins (ansamycins) are structurally similar macrocyclic antibiotics, produced by *Streptomyces mediterranei*. Their characteristic "ansa" structure consists of aromatic rings spanned by an aliphatic bridge (Fig. 7). Rifamycins are active against Gram-positive bacteria and are mainly used in treating tuberculosis. They can be analyzed using silica gel, polyamide, diphenyl, or C-18 plates and various mobile-phase systems from neat organic solvents, through binary non-aqueous solvents, to binary aqueous–organic solvents.[12] Rifamycins are colored compounds and do not require special detection methods.

POLYETHERS

Polyether or ionophore antibiotics, mainly produced by *Streptomyces* species, consist of cyclic ethers, a single carboxylic group, and several hydroxyl groups (Fig. 8). They are widely used anticoccidiosis agents for poultry. The main members of this class are salinomycin, monensin, narasin, and lasalocid. They can be analyzed on both silica gel and RP-18 plates with mixed organic phases. After derivatization with fluorescent pyrenacyl esters, they can be detected fluorodensitometrically at 360 nm. TLC/B with *Bacillus subtilis* can be used too.[13] There is also an example of coupling TLC with flame ionization detection.

AMPHENICOLS

Chloramphenicol is a highly effective broad-spectrum antibiotic originally isolated from *Streptomyces venezuelae* (Fig. 9). Nowadays, chloramphenicol is banned within the United States and the EC because it is believed to cause aplastic anemia. Other members of the amphenicol group are thiamphenicol and the recent one, florphenicol. These three antibiotics show strong UV absorption and can be determined directly, without any derivatization at 254 or 280 nm. Usually silica-gel plates and simple organic or aqueous–organic solvents are used.[14]

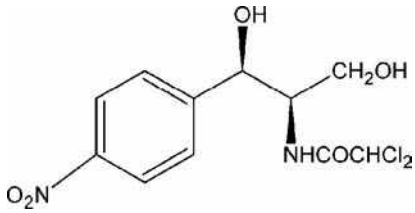

Fig. 9 Chloramphenicol.

SULFONAMIDES

Sulfonamide drugs are bacteriostatic synthetic compounds, the first chemotherapeutics used in human medicine. The progenitor of the class was a red azo dye, 2,4-diaminobenzene-4′-sulfonamide, called prontosil rubrum. The sulfonamides include sulfanilamide (4-amino-benzenesulfonamide) and numerous compounds related to it (Fig. 10).

Sulfonamide drugs are mainly used in veterinary practice and as growth promoters. They are used in the treatment of human infections to a lesser extent because they are toxic and some patients are hypersensitive to them.

Sulfonamides can be analyzed both by NP TLC (on silica gel, alumina, polyamide, and Florisil® layers) and by RP TLC (on silanized silica, RP-2, RP-8, and RP-18 layers).[15] Some sulfonamides have been separated by TLC on silica or polyamide impregnated with metal salts. Both aqueous and non-aqueous eluents are applied. Detection of sulfonamides can be performed on fluorescence layers at 254 nm and after derivatization with, for instance, fluorescamine solution at 366 nm.

NITROFURANS

Nitrofuran drugs are synthetic broad-spectrum chemotherapeutic agents, derivatives of nitrofuran (Fig. 11). Their application in human medicine is limited to some infections (e.g., nitrofurantoin is applied in treating urinary tract infections) or to external use. In veterinary practice, they are used as growth promoters and to prevent and treat diseases in poultry and swine.

Nitrofurans can be separated in NP systems on silica gel and can be detected as colored spots after spraying the plate with pyridine and illuminating with UV light at 366 nm.[16]

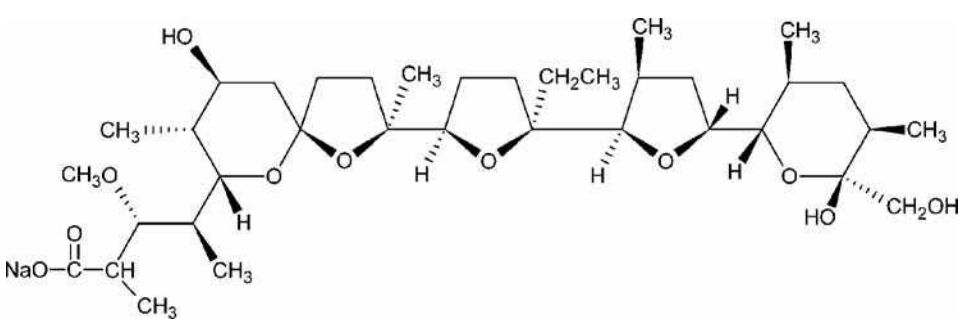

Fig. 8 Monensin.

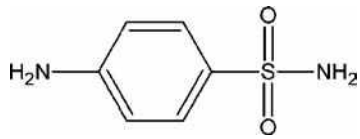

Fig. 10 Sulfanilamide.

QUINOLONES

Nalidixic acid, discovered serendipitously in 1962, was the first member of this class, though of rather minor importance. In the 1980s, synthetic fluoroquinolones were developed and became valid antibiotics with broad spectrum and of good tolerance (Fig. 12). Quinolones are polar, mostly amphoteric compounds. They are usually analyzed on silica gel plates, preferably impregnated with Na_2EDTA or K_2HPO_4 to avoid strong adsorption. Multicomponent organic-mobile phases are employed, usually with the addition of aqueous solutions of ammonia or acids to control pH. Micellar TLC with a cetyl trimethylammonium bromide/sodium dodecyl sulfate mixture as mobile phase and polyamide as stationary phase can also be applied. Densitometry or fluorescence densitometry is a detection method of choice, sometimes preceded by postchromatographic derivatization. Bioautographic detection can also be applied.[4]

ANALYSIS OF ANTIBIOTICS BELONGING TO VARIOUS CLASSES

The analysis of antibiotics belonging to various classes is much more complicated than the analysis of members of one group only. Generally, it is necessary to divide the analyzed antibiotics preliminarily into subgroups. This can be achieved by developing the plate with different mobile phases or using gradient elution.[17] Different stationary phases are sometimes used for different antibiotic classes.[18] It is also possible to use one plate and one mobile phase but various modes of detection for different groups of antibiotics or to combine various modes of development with various modes of detection.[19] Bioautography is very often applied in the multiclass screening.[20] Scanning densitometry at different wavelengths on a hydrocarbon-impregnated silica gel HPTLC plate without solvent elution for direct quantification of many different classes of antibiotics is also described.[21]

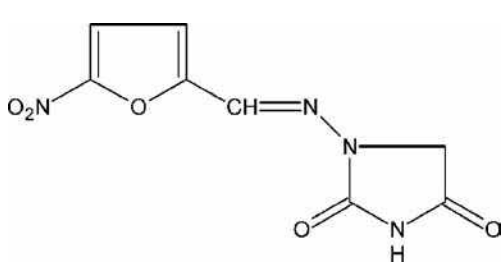

Fig. 11 Nitrofurantoin.

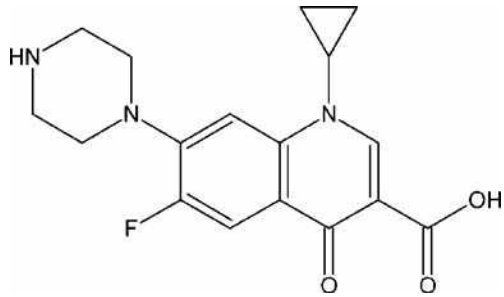

Fig. 12 Ciprofloxacin.

OTHER APPLICATIONS

Beside typical antibiotic analysis, focused on the separation of antibiotics belonging to one or various classes, there are many examples of diverse TLC applications such as the following:

1. Purity control of antibiotics.
2. Examining the stability and breakdown products of antibiotics in solutions and dosage forms.[22]
3. Analysis of antibiotic metabolites.
4. Separation of antibiotic derivatives, obtained in the process of searching for new antibiotics.
5. Purification of newly discovered antibiotics before further testing. Antimicrobial substances are isolated from culture broths or plants and purified by preparative TLC on silica-gel plates.
6. Chemical and biomolecular–chemical screening. Chemical screening is a systematic approach in the search for new biologically active compounds in extracts from microorganisms or plants. Their chromatographic parameters calculated from the TLC plate as well as their chemical reactivity toward staining reagents allow one to obtain a picture of a microbial metabolite pattern (fingerprint). Biomolecular–chemical screening combines the chemical screening strategy with binding behavior toward DNA.[23]
7. Studying interactions of antibiotics with biological matrices. The interactions of the antibiotics with various compounds, cell membranes, and proteins present in biological matrices modify the biological efficacy and stability of the drugs. The interaction of 13 antibiotics with human serum albumin (HSA) was studied by charge-transfer RP TLC in neutral, acidic, basic, and ionic conditions and the relative strength of interaction was calculated.[24]
8. Applying some antibiotics as stationary or mobile-phase additives for chiral separations. The macrocyclic antibiotics (ansamycins, glycopeptides, and

polypeptides) can be used as chiral selectors in TLC. They can be used both as mobile-phase additives (e.g., vancomycin) and for impregnation of TLC silica plates (e.g., erythromycin or vancomycin) for the separation of chiral compounds.[25]

9. Studying the retention behavior of antibiotics, e.g., determining the hydrophobicity parameters of antibiotics by RP TLC.

CONCLUSIONS

TLC is generally less sensitive and gives worse separation than HPLC. However, it predominates over HPLC in at least two aspects: It allows for the analysis of many samples at the same time, and it requires limited sample pretreatment. These features are very important in the analysis of antibiotics, which usually concerns controlling their level in many complicated matrices such as blood, urine, dietary products, and pharmaceuticals. Thus, TLC can be a very useful screening method preceding HPLC analysis. Nevertheless, there are also many examples of analytical applications of TLC, which can achieve selectivity and sensitivity comparable with those characteristic of HPLC. The future of the analytical option in antibiotic analysis is connected with progress in detection and the development of FFPC methods.

REFERENCES

1. Chromatography of antibiotics. J. Chromatogr. A, **1998**, 812 (1+2).
2. Choma, I. Antibiotics. In *Handbook of Thin-Layer Chromatography, Revised and Expanded,* 3rd Ed.; Sherma, J.; Fried, B., Eds.; Marcel Dekker Inc.: New York, 2003; 417–444.
3. Botz, L.; Nagy, S.; Kocsis, B. Detection of microbiologically active compounds. In *Planar Chromatography,* 1st Ed.; Nyiredy, Sz, Ed.; Springer: Budapest, 2001; 489–516.
4. Choma, I.; Choma, A.; Komaniecka, I.; Pilorz, K.; Staszczuk, K. Semiquantitative estimation of enrofloxacin and ciprofloxacin by thin-layer chromatography–direct bioautography. J. Liquid Chromatogr. **2004**, *27* (13), 2071–2085.
5. Hendrickx, S.; Roets, E.; Hoogmartens, J.; Vanderhaeghe, H. Identification of penicillins by thin-layer chromatography. J. Chromatogr. **1984**, *291*, 211–218.
6. Boison, J.O. Chromatographic methods of analysis of penicillins in food–animal tissues and their significance in regulatory programs for residue reduction and avoidance. J. Chromatogr. **1992**, *624*, 171–194 (review).
7. Quintens, I.; Eykens, J.; Roets, E.; Hoogmartens, J. Identification of cephalosporins by thin layer chromatography and color reaction. J. Planar Chromatogr.-Mod. TLC **1993**, *6*, 181–186.
8. Tuzimski, T. Two-dimensional thin layer chromatography of eight cephalosporins on silica gel layers. J. Planar Chromatogr.-Mod. TLC **2004**, *17*, 46–50.
9. Stead, D.A. Current methodologies for the analysis of aminoglycosides. J. Chromatogr. B, **2000**, *747*, 69–93 (review).
10. Kanfer, I.; Skinner, M.F.; Walker, R.B. Analysis of macrolide antibiotics. J. Chromatogr. A, **1998**, *812*, 255–286 (review).
11. Oka, H.; Ito, Y.; Matsumoto, H. Chromatographic analysis of tetracycline antibiotics in foods. J. Chromatogr. A, **2000**, *882*, 109–133 (review).
12. Nowakowska, J.; Halkiewicz, J.; Lukasiak, J.W. TLC determination of selected macrocyclic antibiotics using normal and reversed phases. Chromatographia **2002**, *56*, 367–373.
13. VanderKop, P.A.; MacNeil, J.D. Separation and detection of monensin, lasalocid and salinomycin by thin-layer chromatography/bioautography. J. Chromatogr. **1990**, *508*, 386–390.
14. Freimüller, S.; Horsch, Ph.; Andris, D.; Zerbe, O.; Altorfer, H. Formation mechanism of solvent induced artefact arising from chromatographic purity testing of γ-irradiated chloramphenicol. Chromatographia **2001**, *53*, 323–325.
15. Bieganowska, M.L.; Doraczyńska-Szopa, A.D.; Petruczynik, A. The retention behavior of some sulfonamides on different thin layer plates. J. Planar Chromatogr.-Mod. TLC **1993**, *6*, 121–128.
16. Abjean, J.P. Qualitative screening for nitrofuran residues in food by planar chromatography. J. Planar Chromatogr.-Mod. TLC **1993**, *6*, 319–320.
17. Krzek, J.; Kwiecień, A.; Starek, M.; Kierszniewska, A.; Rzeszutko, W. Identification and determination of oxytetracycline, tiamulin, lincomycin, and spectinomycin in veterinary preparations by thin-layer chromatography/densitometry. J. AOAC Int. **2000**, *83*, 1502–1506.
18. Vega, M.; Garcia, G.; Saelzer, R.; Villegas, R. HPTLC analysis of antibiotics in fish feed. J. Planar Chromatogr.-Mod. TLC **1994**, *7*, 159–162.
19. Abjean, J.P. Planar chromatography for the multiclass, multiresidue screening of chloramphenicol, nitrofuran, and sulfonamide residues in pork and beef. J. AOAC Int. **1997**, *80*, 737–740.
20. Gafner, J.L. Identification and semiquantitative estimation of antibiotics added to complete feeds, premixes, and concentrates. J. AOAC Int. **1999**, *82*, 1–8.
21. Dhanesar, S.C.J. Quantitation of antibiotics by densitometry on a hydrocarbon-impregnated silica gel HPTLC plate. Part V: Quantitation and evaluation of several classes of antibiotics. J. Planar Chromatogr.-Mod. TLC **1999**, *12*, 280–287.
22. Liang, Y.; Denton, M.B.; Bates, R.B. Stability studies of tetracycline in methanol solution. J. Chromatogr. A, **1998**, *827*, 45–55.
23. Maul, C.; Sattler, I.; Zerlin, M.; Hinze, C.; Koch, C.; Maier, A.; Grabley, S.; Thiericke, R. Biomolecular–chemical screening: A novel screening approach for the discovery of biologically active secondary metabolites—III. New DNA-binding metabolites. J. Antibiot. **1999**, *52*, 1124–1134.
24. Cserháti, T.; Forgács, E. Study of the binding of antibiotics to human serum albumin by charge-transfer chromatography. J. Chromatogr. A, **1997**, *776*, 31–36.
25. Ward, T.J.; Farris, A.B., III. Chiral separations using the macrocyclic antibiotics: A review. J. Chromatogr. A, **2001**, *906*, 73–89.

Antidiabetic Drugs: HPLC/TLC Determination

A. Gumieniczek
H. Hopkała
A. Berecka
Department of Medicinal Chemistry, Medical University of Lublin, Lublin, Poland

INTRODUCTION

A review of some chromatographic methods for determination of new oral antidiabetic drugs is presented: gliclazide, glimepiride, and glipizide from sulfonylureas; nateglinide and repaglinide from glinides; and pioglitazone and rosiglitazone from glitazones. This entry describes the selected methods for the analysis of these important drugs in pharmaceuticals and in biological materials. Two chromatographic techniques [High-performance liquid chromatography (HPLC), Thin-layer chromatography (TLC)] and various pretreatment modes are described. Sensitivities, linearities, and specificities of the presented methods are compared. The selected methods for determination of potential impurities in bulk drug substances and metabolites of the drugs in biological samples are described. Stability data concerning the mentioned drugs are also presented. Finally, suitable methods for separation of the drugs as well as their isomers (enantiomers and diastereoisomers) are presented.

DETERMINATION OF ANTIDIABETIC DRUGS

Currently, sulfonylureas are the oral agents most commonly used for the treatment of type II diabetes mellitus. They act by binding to receptors located on the membranes of beta cells of the islets of Langerhans. Binding of the ligand and receptor is followed by closure of the K^+-ATP channel, influx of Ca^{2+}, and depolarization of the cell membrane. These events induce degranulation of insulin-containing vesicles and are followed by a hypoglycemic effect.[1] In the past few decades, several generations of sulfonylureas have been developed for common use. Gliclazide (I), glimepiride (II), and glipizide (III) are the principal representatives from the latest generation.

Nateglinide (IV) and repaglinide (V) represent a new class of insulin secretagogues, chemically unrelated to sulfonylureas. Both nateglinide and repaglinide act by stimulating insulin secretion from the beta cells, but they bind to sites distinct from the sulfonylureas' binding sites. Importantly, insulin release takes place only in the presence of glucose. Therefore, they are highly physiologic mealtime glucose regulators.[1,2]

The advent of thiazolidinediones, pioglitazone (VI), and rosiglitazone (VII), which ameliorate insulin resistance and normalize blood glucose level, has revolutionized the treatment of type II diabetes mellitus. Their mechanism of action is quite different from that of established antidiabetic drugs. These compounds are high affinity ligands of peroxisome proliferator receptor gamma, a member of the nuclear receptor superfamily, which controls the expression of genes involved in lipid and carbohydrate metabolism.[2] Chemical structures of the mentioned antidiabetic drugs are presented in Fig. 1.

In addition to being the latest and most commonly prescribed drugs, the hypoglycemic agents selected for this review are more pharmacologically potent. Consequently, they are prescribed at low dosages. Because of the low drug levels in both plasma and urine, analytical methods for detection and quantification of these drugs must be very specific and sensitive. Chromatography plays a major role in the study of their pharmacokinetics in animals and humans. It is also applied for detection and quantification of potential impurities in bulk drug substances, and to determine the ratio of optically active enantiomers and diastereoisomers.

HPLC ANALYSIS

Determination of Sulfonylureas

Among the mentioned drugs, sulfonylureas are the compounds that are more extensively investigated. Some methods were elaborated for determination of gliclazide in human plasma, as a routine assay or to evaluate the bioequivalence of different formulations of the drug. The method of Park et al.,[3] with a semimicrochromatographic column, is fast and requires only a small amount of mobile phase, with a reasonable limit of quantification. The intraday and interday precision values are less than 5.9% and 8%, respectively. This HPLC method, with UV detection, is suitable for clinical monitoring and for pharmacokinetic study of the drug. The method of Igaki et al.[4] includes derivatization of gliclazide with 7-fluoro-4-nitro-benzene-1,3-diazole and fluorimetric detection. However, this method is not more sensitive

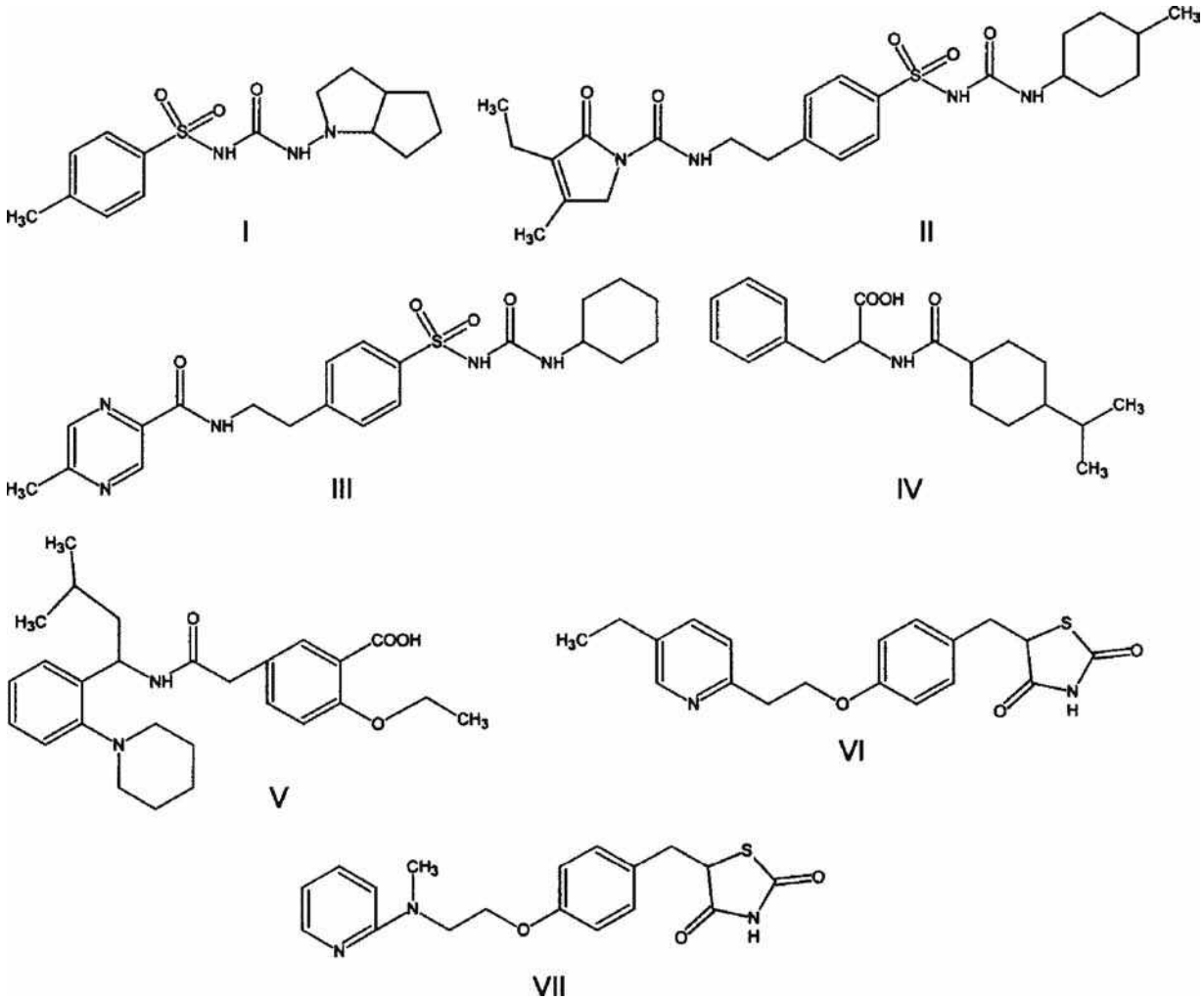

Fig. 1 (I) Chemical structures of gliclazide; (II) glimepiride; (III) glipizide; (IV) nateglinide; (V) repaglinide; (VI) pioglitazone; and (VII) rosiglitazone.

than HPLC–UV measurement. Rouini, Mohajer, and Tahami[5] described a simple assay of gliclazide, which needs a small sample volume (100 μl of serum) and minimal sample work-up. This method has many advantages such as increased sensitivity, high resolution, and economic aspects.

A sensitive method for quantitation of glimepiride in human plasma was established using electrospray ionization tandem mass spectrometry (ESI/MS/MS). Detection of glimepiride is accurate and precise with a quantitation limit of 0.1 ng/ml. This method was successfully applied to a pharmacokinetic study of glimepiride. No interferences of the analytes were observed because of high selectivity of the MS/MS technique.[6] The method of Song et al.[7] is also sufficiently sensitive, with a quantification limit lower than the minimum concentration recommended for plasma samples obtained after the administration of 2 mg glimepiride. This study indicates a reliable stability of glimepiride under the experimental conditions. The drug can remain in an autosampler for at least 24 hr, without showing significant loss in the quantified values. The analyte is also stable in plasma for three cycles of freeze-thaw, when stored at −20°C and thawed to room temperature.

A stress testing of drug substance can help to identify the likely degradation products and to provide important information on drug stability. Consequently, it can be a fundamental contribution to development and validation of stability indicating analytical methods. These methods can be used in quality monitoring of pharmaceutical products. Kovaríková et al. elaborated the study for determination of glimepiride in the presence of its degradation products. After acid hydrolysis, two additional peaks were detected, while alkaline conditions led to decomposition of glimepiride into three degradation products. Degradation of glimepiride in the solution of hydrogen peroxide resulted in formation

of two major peaks. The novelty of this work is based on the description of an analytical procedure that is suitable for monitoring the purity of glimepiride.[8]

The method of Emilsson was elaborated for determination of glipizide in plasma and urine. The utility of this assay for pharmacokinetic study is demonstrated by determining the drug in the samples from a diabetic subject receiving 5 mg of glipizide. The interassay precision is about 10%.[9] The method of Lin, Deasi-Krieger, and Shum was developed and validated for determining the fraction of free glipizide in plasma using equilibrium dialysis and tandem mass spectrometry. Equilibrium dialysis is frequently used to study protein binding and to determine free analyte in biological samples. The accurate determination of free (unbound) drug in plasma is essential for therapeutic monitoring of drugs. It is well known that only the unbound drug is available for distribution, elimination, and pharmacodynamic interaction with receptors. In the mentioned method, the intra-assay and interassay precision values are lower than 9% and 10%, respectively. Glipizide is stable throughout the equilibrium dialysis (37°C) up to six hours. The analytes are also stable when stock solutions of glipizide are stored at a temperature 4°C for one month, or at room temperature for six hours.[10]

Among these eight studies concerning sulfonylureas, six deal with plasma or serum,[3–7,10] and one study is performed on plasma and urine.[9] A study not dealing with biological samples is applied to a methanolic solution of glimepiride.[8] Most of the authors use solvent/buffered solutions as mobile phases in isocratic mode.[3,5,6,8,9] Solvent/unbuffered water or water may also be used.[4,10] The more frequently chosen columns are the C_{18} cartridges.[3,4,6–9] However, C_8 and phenyl cartridges may also be used.[5,10] Ultraviolet absorbance detection is commonly used, but in some cases MS/MS[6,10] or fluorescence detectors[4] are preferred.

Chromatographic techniques require various procedures to isolate the drugs from biological matrices. In the reviewed methods, two distinct approaches are applied: liquid–liquid extraction and direct injection into a chromatographic system. Diethyl ether and ethyl acetate,[6] chloroform,[3,4] toluene,[5] benzene,[9] methyl *t*-butyl ether, and *n*-butyl chloride[10] are used as solvents to obtain recoveries well over 80% for all considered compounds. However, manual sample preparation can be labor and time intensive. Therefore, direct injection is used as a highly automated methodology.[7] The direct injection of complex samples, however, may lead to contamination of columns, thereby impairing their performance. Contamination often persists, even when a precolumn is used to protect the analytical column. A summary of these chromatographic methods for determination of sulfonylureas is presented in Table 1.

Determination of Glinides

The method of Meng et al.[11] can be used for the quality control, stability study, and validity term of nateglinide tablets. In the linear range 0.2–2 μg/ml, the precision is 0.98%. The method of Ono, Matsuda, and Kanno[12] was elaborated for determining nateglinide and its seven metabolites in plasma and urine. However, this method requires an expensive column switching equipment.

A simple, precise, and rapid HPLC method was developed for determination of repaglinide in pharmaceutical dosage forms.[13] In this method, the intraday and interday precision values are 1.01% and 1.15%, respectively. The high efficacy of repaglinide is reflected in the low therapeutic dose of ~2 mg, which requires very sensitive assay for determination of its pharmacokinetics. The paper of Greischel et al.[14] describes a fully automated HPLC assay of repaglinide in plasma with electrochemical detection. The method was validated and applied to a routine analysis of therapeutic plasma levels of the drug. In this method, the interassay precision is 9.2% in 30 ng/ml. Repaglinide is stable in plasma at −20°C for at least six weeks, which is sufficient time for storage between blood sampling and analysis. It is also stable in plasma for over 24 hr at 30°C. A summary of these HPLC methods is shown in Table 2.

Determination of Glitazones

An HPLC method was elaborated for the purity assay of pioglitazone in tablets. This method is capable of detecting all process related compounds that may be present at trace levels in a finished product. This method is very useful for process monitoring during the production of pioglitazone. The relative standard deviation values of assay and recovery of impurities are below 1.0% and 2.7%, respectively. Accelerated degradation studies were also performed to demonstrate validity of the method. The samples of pioglitazone refluxed with HCl, subjected to high temperature or exposed to UV light, did not give any degradation products. The sample refluxed with NaOH completely decomposed to several degradation products.[15]

Some methods are adequate for determination of pioglitazone and its metabolites in biological material.[16,17] It is very important for interpretation of the results, as three of the metabolites of pioglitazone are pharmacologically active. Owing to the large differences in polarity between the parent compound and metabolites of pioglitazone, it is difficult to obtain high extraction recoveries for all of them. Thus, the emphasis is placed on the parent compound and the three active metabolites.[16] The method of Lin et al.[17] was validated for accuracy, precision, sensitivity, specificity, and reproducibility according to the Food and Drug Administration guidelines for bioanalytical methods, over the concentration range of pioglitazone 0.5–2000 ng/ml. Samples of pioglitazone remain stable for at least five

Table 1 HPLC methods for gliclazide (I), glimepiride (II) and glipizide (III).

Refs.	Matrix	Drug	Extraction (v/v)	Column	Mobile phase (v/v)	Flow rate (ml/min)	Detection method	Detection limit linearity range (μg/ml)	Recovery (%)
[3]	Plasma	I	Chloroform	SemimicroCapcell Pak C1UG120 2 × 1.5 mm, 5 μm 26°C	MeCN-isopropanol-40 m*M* KH_2PO_4 at pH 4.6 (40 : 10 : 50)	0.22	UV 229	0.1–10	84–87
[4]	Serum	I	Chloroform	Finepak SIL C1810 μm	MeCN-H_2O (60 : 40)	1.0	Fluorescence 470/534	0.1	n.a.
[5]	Serum	I	Toluene	Techsphere C8 150 × 3.9, 3 μm	MeCN-H_2O (45 : 55, pH 3.0)	0.9	UV 230	30000	84.5
[6]	Plasma	II	Diethyl ether–ethyl acetate (1 : 1)	C18	MeCN-5 m*M* ammonium acetate (60 : 40, pH 3.0)	n.a.	ESI/MS/MS	100	n.a.
[7]	Plasma	II	Online Capcell Pak MF Ph1 (10 × 4 mm)	Capcell Pak MG C18 250 × 1.5 mm, 5 μm 30°C	MeCN-10 m*M* KH_2PO_4 with 0.04% triethylamine (52 : 48, pH 2.8)	0.1–0.5	UV 228	10000	99.0
[8]	Bulk	II	MeOH	Purospher RP-18 250 × 4.6, 5 μm	MeCN-0.03 *M* phosphate buffer at pH 3.5 (48 : 52)	1.0	UV 228	20–300	98–103
[9]	Plasma urine	III	Benzene	Spherisorb ODS	MeCN-0.01 *M* phosphate buffer at pH 3.5 (35 : 65)	n.a.	UV 275	5000	n.a.
[10]	Plasma	III	Methyl *t*-butyl ether-*n*-butyl chloride (1 : 1)	Zorbax SB Phenyl 150 × 2.1 mm, 5 μm	H_2O-10 m*M* ammonium acetate and 0.02% TFA (50 : 50)	0.3	MS/MS	1000	80–82

n.a., data not available.

Table 2 HPLC methods for determination of nateglinide (IV) and repaglinide (V).

Refs.	Matrix	Drug	Extraction (v/v)	Column	Mobile phase (v/v)	Flow rate (ml/min)	Detection method	Detection limit linearity range (μg/ml)	Recovery (%)
[11]	Tablets	IV	n.a.	Kromasil C18 250 × 4.6, 5 μm 30°C	MeOH-H_2O (67 : 33, pH 6.5)	1.0	UV 210	0.2–2.0	99.6
[12]	Plasma urine	IV	SPE	ODS 250 × 4.6 mm, 5 μm	a) MeCN-0.05 *M* phosphate buffer at pH 6.6 (20 : 80) b) MeCN-EtOH-0.05 *M* phosphate buffer at pH 6.6 (32 : 6 : 62) 50°C	1.0	UV 210	0.1–10	88.0
[13]	Tablets	V	MeOH	RP-18 150 × 4.6 mm, 5 μm 30°C	MeOH-0.1% triethylamine (50 : 50, pH 7.0)	1.0	UV 235	0.1–0.5	102.7
[14]	Plasma	V	Online SPE Perisorb RP-2 (17 × 4.6 mm) ODS-Hypersil (5 μm)	LiChrospher RP-18 125 × 4mm, 5 μm	a) MeOH-MeCN-dioxane (68 : 24 : 8) b) 3 g KH_2PO_4 with 0.5 g $LiClO_4$ in 1 L of H_2O at pH 2.7	1.0	Amperometric 1.04 V	5000	98.8

n.a., data not available.

months when stored at −20°C. Extracted analytes are stable in mobile phase at an ambient temperature for 24 hr. Stock solutions of pioglitazone are also stable at 4°C for one month or at room temperature for six hours.[17]

The paper of Muxlow, Fowles, and Russell[18] describes a fully automated method for the quantitative analysis of rosiglitazone in plasma using online dialysis. Similarly, the method of Lin et al. describes a procedure employing equilibrium dialysis for separation of unbound rosiglitazone from plasma for simultaneous quantitation of the unbound and total drug. This is very important because rosiglitazone is known to be highly protein bound, mainly to serum albumin. For highly protein bound drugs, fluctuations in the free fraction can impact the interpretation of the total drug measurement. In the above method, interassay precision is less than 7.6% and intra-assay precision less than 8.9%. The method is linear in the range 1–2000 ng/ml.[10]

Because rosiglitazone is a fluorescent compound, the method with a fluorescence detector is presented with excitation at 247 nm and emission at 367 nm. The low limit of quantitation of rosiglitazone in plasma is 3 ng/ml. The interassay and intra-assay precision values are better than 10% at all concentrations.[18]

The method of Radhakrishna, Satyanarayana, and Satyanarayana was elaborated for determination of rosiglitazone and its related impurities in pharmaceutical formulations. The described method is linear over a range of 0.45–10 μg/ml for related impurities and 180–910 μg/ml for rosiglitazone. Precision values for determination of the drug and related compounds are below 1.0% and 3.6%, respectively. The samples of rosiglitazone refluxed with HCl, subjected to high temperature, and exposed to UV light gave small additional peaks. But the samples refluxed with NaOH or H_2O_2 were mostly converted to degraded products. The developed method was found to be selective, sensitive, and precise for determination of rosiglitazone and their process related impurities. Photodiode array detection (DAD) was used as evidence of the method specificity and to evaluate the homogeneity of the rosiglitazone peak.[19]

Among these six studies concerning glitazones, four deals with plasma or serum[10,16–18] and two with tablets.[15,19] As mobile phases, solvent/buffered solutions, solvent/unbuffered water, or water in isocratic mode are used. Two distinct approaches are applied to isolate the drugs from biological matrices: liquid–liquid extraction and solid-phase extraction (SPE). Solvents used to extract the drugs include methyl *t*-butyl ether and *n*-butyl chloride.[10,17] With the exception of two papers, in which serum extracts are chromatographed on C_8[16] and phenyl columns,[10] all other reviewed methods use C_{18} cartridges.

The HPLC techniques are capable of detecting most of the reported compounds using UV absorbance detection, although DAD detection provides more information in detecting some unknown peaks.[15,19] In the method of Zhong and Williams,[16] by using the wavelength 269 nm for pioglitazone and its metabolites, some interferences from human serum were eliminated. However, MS/MS detection can serve as a more reliable tool for determination of pioglitazone and its metabolites in human serum.[10,17] A summary of these chromatographic methods is shown in Table 3.

Separation of Oral Antidiabetics

The paper of Ho et al.[20] describes a convenient method for separation and simultaneous detection of 10 antidiabetic drugs, including gliclazide, glimepiride, glipizide, nateglinide, repaglinide, pioglitazone, and rosiglitazone in plasma and urine by LC–MS/MS with gradient programming. The compounds were isolated from the biological matrix by a simple liquid–liquid extraction with 1,2-dichloroethane. Confirmation of these drugs can be readily achieved by comparing the product-ion mass spectra, as well as the retention times, with those of their corresponding standards. The interday precision for the peak areas is about 20–30%. The targeted antidiabetics can be easily detected in plasma and urine at a concentration of 10 ng/ml. This method is clearly described in Table 4.

Determination of Enantiomers and Diastereoisomers

In the pharmaceutical industry, separation of enantiomers has been a field of growing interest because they often display quite different pharmacological activities and toxicity profiles. Resolution of enantiomers by liquid chromatography is very frequently used for determining the optical purity and for obtaining individual enantiomers of the drugs.

Only the D-enantiomer of nateglinide is approved to be used in clinical treatment because it is much more potent than the L-enantiomer. Some works were developed for determination of the L-enantiomer in bulk drug substance of nateglinide. The assay of Cao et al.[21] allows the accurate and precise measurement of D-nateglinide and its enantiomer during pharmacokinetic studies in humans. The interday precision values for both enantiomers in plasma and urine are about 7% and 10%, respectively.

Repaglinide has one asymmetric center. It is used for the treatment as a pure enantiomer because only the (+) form is active. Therefore, it is necessary to monitor the purity of the bulk drug substance to keep the level of inactive enantiomer under control. However, the method described in the literature is not adequate for selective determination of repaglinide enantiomers.[13,14]

Some authors propose HPLC methods for selective determination of *trans*-glimepiride and its *cis*-isomer impurity. The method of Wei et al.[22] can be applied to the assay of the *cis*-isomer of glimepiride in bulk drug substance and glimepiride tablets.

Table 3 HPLC methods for determination of pioglitazone (VI), rosiglitazone (VII).

Refs.	Matrix	Drug	Extraction (v/v)	Column	Mobile phase (v/v)	Flow rate (ml/min)	Detection method	Detection limit linearity range (μg/ml)	Recovery (%)
[15]	Tablets	VI	0.1% H_3PO_4–MeCN (1 : 1)	Symmetry C18 250 × 4.6 mm, 5 μm	MeCN-10 m*M* KH_2PO_4 (50 : 50, pH 6.0)	1.0	DAD	0.08	99–102
[16]	Serum	VI	SPE C18	Zorbax RX-C8 250 × 4.6, 5 μm	MeCN-H_2O (40 : 60) with acetic acid at pH 5.5	1.2	UV 269	20–2000	93–98
[17]	Plasma	VI	Methyl *t*-butyl ether-*n*- butyl chloride (1 : 1)	MetaChem Polaris C18 A 50 × 2 mm, 3 μm	MeCN-H_2O (60 : 40) with 10 m*M* ammonium acetate and 0.02% trifluoroacetic acid	0.2	MS/MS	5000	63–71
[18]	Plasma	VII	Online dialysis	Novapak C18 100 × 5 mm, 4 μm	MeCN-0.01 *M* ammonium acetate at pH 8.0 (35 : 65)	1.0	Fluorescence 247/367	3000	66.3
[10]	Plasma	VII	Methyl *t*-butyl ether-*n*- butyl chloride (1 : 1)	Zorbax SB-Phenyl 150 × 2.1 mm, 5 μm	MeCN-10 m*M* ammonium acetate with 0.02% TFA (50 : 50)	0.3	MS/MS	1000	73–78
[19]	Tablets	VII	Mobile phase	Symmetry C18 250 × 4.6, 5 μm	MeCN-0.025 *M* phosphate buffer at pH 6.2 (50 : 50)	1.0	DAD	180–910	95–102

n.a., data not available.

Table 4 HPLC methods for separation of all drugs, their enantiomers and diastereoisomers.

Refs.	Matrix	Drug	Extraction (v/v)	Column	Mobile phase (v/v)	Flow rate (ml/min)	Detection method	Detection limit linearity range (μg/ml)	Recovery (%)
[20]	Plasma urine	I–VII	1,2-dichloroethane	Supelcosil LC-8-DB 100 × 2.2, 3 μm 30°C	a) H_2O with 10 m*M* ammonium formate at pH 3.0 b) MeOH	2.0	MS	1000	46–62
[21]	Plasma urine	IV	n.a.	Chiralcel OD-R 250 × 4.6 mm, 10 μm	MeCN-0.05 *M* $NaClO_4$ (70 : 30, pH 2.2)	0.4	UV 214	D-0.02 L-0.08	n.a.
[22]	Bulk	II	n.a.	Zorbax SB C18 250 × 4.6 mm, 5 μm	MeOH-0.05 *M* ammonium acetate at pH 3.8 (68 : 32)	1.0	UV 230	n.a.	n.a.

n.a., data not available.

Table 5 Summary of the reviewed TLC methods.

Refs.	Matrix	Drug	Support	Mobile phase (v/v)	Detection	Linearity range (μg/ml)
[23]	Bulk	IV,VI, VII	Silica gel 60 F_{254} RP-18 F_{254}	Chloroform–ethyl acetate–acetic acid (5 : 5 : 0.1) MeCN-phosphate buffer at pH 4.4 (5 : 5)	UV 254	—
[24]	Tablets	VI	HPTLC CN F_{254}	1,4-Dioxane-phosphate buffer at pH 4.4 (5 : 5)	UV 266	40–240
[25]	Tablets	VII	HPTLC Silica gel 60 F_{254}	Chloroform–ethyl acetate-25% NH_4OH (5 : 5 : 0.1)	UV 240	20–100

These methods concerning the separation studies are presented in Table 4.

TLC ANALYSIS

Thin-layer chromatography can be successfully applied to separate the compounds, closely related in chemical structure, or used in combination therapy, as well as the metabolites from biological samples. Thin-layer chromatography may also be used to control the chemical purity of the compounds and to predict the HPLC behavior of the drugs and related metabolites. High performance TLC (HPTLC) can be used as an effective quantitative alternative to other chromatographic techniques. Its accuracy and precision are satisfactory for routine use in a pharmaceutical analysis.

The chromatographic behavior of repaglinide, pioglitazone and rosiglitazone, among four other antidiabetic drugs, was investigated on silica gel and RP-18 adsorbents. In the reversed-phase (RP) technique, the effects of different organic modifiers and pH of the buffers on the drugs retention were examined. For separation of these drugs, RP chromatography on RP-18 adsorbent was more effective than use of a normal phase technique on silica gel.[23] The TLC separation of repaglinide, pioglitazone, and rosiglitazone on cyanopropyl plates with mixtures comprising 1,4-dioxane with phosphate buffers was also elaborated. Finally, the best chromatographic conditions were applied for quantitative determination of pioglitazone in tablets. In this method, precision validated by replicate analyses of standard solutions is 4.99% and 2.57% for the lowest and the highest calibration levels, respectively.[24]

A simple, rapid HPTLC method was developed for determination of repaglinide in tablets. The effect of pH, temperature, and UV light on degradation of repaglinide was also investigated. No evidence of degradation was observed for samples subjected to alkaline and heat conditions, whereas the chromatograms of samples subjected to acid hydrolysis contained two additional peaks. Because this method can effectively separate the drug from its degradation products, it can be used as a stability-indicating procedure.[25] A summary of the reviewed TLC methods is shown in Table 5.

CONCLUSIONS

Because of their therapeutic advantages, the above-discussed oral antidiabetic drugs are more and more frequently used in therapy and are extensively examined by analytical procedures. Especially, the methods for pharmacokinetic studies and for quantification of potential impurities in bulk drug substances are continually being developed. Most favored, in terms of a number of publications, are the HPLC techniques, although TLC methods are also represented. In HPLC, a RP technique with C_{18} columns is more prevalent than the alternative phases. Isolation steps are almost evenly distributed between conventional liquid–liquid extraction and SPE procedures. The UV detection can serve as a reliable tool for determination of most of these antidiabetics. However, new prospects are represented by the MS/MS detection. Sensitive and automated HPLC techniques with column switching are also more and more frequently applied.

The TLC methods show higher interest in more recent publications. This technique may be used as an alternative quantitative procedure, especially in quality monitoring of pharmaceutical products.

REFERENCES

1. Perffetti, R. Novel sulfonylurea and non-sulfonylurea drugs to promote the secretion of insulin. TEM **2000**, *11* (6), 218–223.
2. Fuchtenbusch, M.; Standl, E.; Schatz, H. Clinical efficacy of new thiazolidinediones and glinides in the treatment of type 2 diabetes mellitus. Exp. Clin. Endocrinol. Diabetes **2000**, *108* (3), 151–163.

3. Park, J.Y.; Kim, K.A.; Kim, S.L.; Park, P.W. Quantification of gliclazide by semi-micro high-performance liquid chromatography: Application to a bioequivalence study of two formulations in healthy subjects. J. Pharm. Biomed. Anal. **2004**, *35* (4), 943–949.
4. Igaki, A.; Kobayashi, K.; Kimura, M.; Sakoguchi, T.; Matsuoka, A. Determination of serum sulfonylureas by high-performance liquid chromatography with fluorimetric detection. J. Chromatogr. **1989**, *493* (1), 222–229.
5. Rouini, M.R.; Mohajer, A.; Tahami, M.H. A simple and sensitive HPLC method for determination of gliclazide in human serum. J. Chromatogr. B, **2003**, *785* (2), 383–386.
6. Kim, H.; Chang, K.Y.; Lee, H.J.; Han, S.B. Determination of glimepiride in human plasma by liquid chromatography-electrospray ionization tandem mass spectrometry. Bull. Korean Chem. Soc. **2004**, *25* (1), 109–114.
7. Song, Y.K.; Maeng, J.E.; Hwang, H.R.; Park, J.S.; Kim, B.C.; Kim, J.K.; Kim, C.K. Determination of glimepiride in human plasma using semi-microbore high-performance liquid chromatography with column switching. J. Chromatogr. B, **2004**, *810* (1), 143–149.
8. Kovaríková, P.; Klimes, J.; Dohnal, J.; Tisovská, L. HPLC study of glimepiride under hydrolytic stress conditions. J. Pharm. Biomed. Anal. **2004**, *36* (1), 205–209.
9. Emilsson, H. High-performance liquid chromatographic determination of glipizide in human plasma and urine. J. Chromatogr. **1987**, *421* (2), 319–326.
10. Lin, Z.J.; Deasi-Krieger, D.D.; Shum, L. Simultaneous determination of glipizide and rosiglitazone unbound drug concentrations in plasma by equilibrium dialysis and liquid chromatography-tandem mass spectrometry. J. Chromatogr. B, **2004**, *801* (2), 265–272.
11. Meng, Q.; Yin, J.; Wang, E.; Yang, S. Content determination of nateglinide by RP-HPLC. Yaowu Fenxi Zazhi **2003**, *23* (5), 370–372.
12. Ono, I.; Matsuda, K.; Kanno, S. Determination of N-(trans-4-isopropylcyclohexanecarbonyl)-D-phenylalanine and its metabolites in human plasma and urine by column-switching high performance liquid chromatography with ultraviolet detection. J. Chromatogr. B, **1997**, *692* (2), 397–404.
13. Gandhimathi, M.; Ravi, T.K.; Renu, S.K. Determination of repaglinide in pharmaceutical formulations by HPLC with UV detection. Anal. Sci. **2003**, *19* (12), 1675–1677.
14. Greischel, A.; Beschke, K.; Rapp, H.; Roth, W. Quantitation of the new hypoglycaemic agent AG-EE 388 ZW in human plasma by automated high-performance liquid chromatography with electrochemical detection. J. Chromatogr. **1991**, *568* (1), 246–252.
15. Radhakrishna, T.; Rao, S.; Reddy, G.O. Determination of pioglitazone hydrochloride in bulk and pharmaceuticals by HPLC and MEKC methods. J. Pharm. Biomed. Anal. **2002**, *29* (4), 593–607.
16. Zhong, W.Z.; Williams, M.G. Simultaneous quantitation of pioglitazone and its metabolites in human serum by liquid chromatography and solid phase extraction. J. Pharm. Biomed. Anal. **1996**, *14* (4), 465–473.
17. Lin, Z.J.; Ji, W.; Desai-Krieger, D.; Shum, L. Simultaneous determination of pioglitazone and its two active metabolites in human plasma by LC-MS/MS. J. Pharm. Biomed. Anal. **2003**, *33* (1), 101–108.
18. Muxlow, A.M.; Fowles, S.; Russell, P. Automated high-performance liquid chromatography method for the determination of rosiglitazone in human plasma. J. Chromatogr. B, **2001**, *752* (1), 77–84.
19. Radhakrishna, T.; Satyanarayana, J.; Satyanarayana, A. LC determination of rosiglitazone in bulk and pharmaceutical formulation. J. Pharm. Biomed. Anal. **2002**, *29* (5), 873–880.
20. Ho, E.N.M.; Yiu, K.C.H.; Wan, T.S.M.; Stewart, B.D.; Watkins, K.L. Detection of anti-diabetics in equine plasma and urine by liquid chromatography-tandem mass spectrometry. J. Chromatogr. B, **2004**, *811* (1), 65–73.
21. Cao, G.; Hu, X.; Yan, X.; Yin, Q.; Song, Y. Determination of nateglinide enantiomer in human plasma and urine by HPLC. Yaowu Fenxi Zazhi **2001**, *21* (6), 404–407.
22. Wei, J.; Sun, Z.R.; Ma, J.Z.; Xie, J.W. Separation and determination of the isomer of glimepiride using HPLC. Guangpu Shiyanshi **2004**, *21* (1), 150–152.
23. Gumieniczek, A.; Hopkała, H.; Berecka, A.; Kowalczuk, D. Normal and reversed-phase thin-layer chromatography of seven oral antidiabetic agents. J. Planar Chromatogr. -Mod. TLC **2003**, *16* (4), 271–279.
24. Gumieniczek, A.; Hopkała, H.; Berecka, A. Reversed-phase thin-layer chromatography of three new oral antidiabetics and densitometric determination of pioglitazone. J. Liq. Chromatogr. Relat. Technol. **2004**, *27* (13), 2057–2070.
25. Gumieniczek, A.; Berecka, A.; Hopkała, H. Quantitative analysis of repaglinide in tablets by reversed-phase thin-layer chromatography with densitometric UV detection. J. Planar Chromatogr. -Mod. TLC. **2005**, *18*, 159–163.

Antioxidant Activity: Measurement by HPLC

Marino B. Arnao
Manuel Acosta
Antonio Cano
Department of Plant Biology (Plant Physiology), University of Murcia, Murcia, Spain

INTRODUCTION

The determination of antioxidant activity (capacity or potential) of diverse biological samples is generally based on the inhibition of a particular reaction in the presence of antioxidants. The most commonly used methods are those involving chromogenic compounds of a radical nature: the presence of antioxidant leads to the disappearance of these radical chromogens. They are either photometric or fluorimetric and can comprise kinetic or end-point measurements. Recently, there has been increasing interest in the adaptation of these methods for online determinations using liquid chromatography (LC). In this entry, we present the adaptation to high-performance liquid chromatography (HPLC) of our methods for the determination of the antioxidant activity in a range of samples. Advantages and disadvantages of these methods are discussed.

A biological antioxidant is a compound that protects biological systems against the potentially harmful effects of processes or reactions that cause excessive oxidation. Hydrophilic compounds, such as vitamin C, thiols, and flavonoids, as well as lipophilic compounds, such as vitamin E, vitamin A, carotenoids, and ubiquinols, are the best-known natural antioxidants. Many of these compounds are of special interest due to their ability to reduce the hazard caused by reactive oxygen and nitrogen species (ROS and RNS, some are free radicals), and have been associated with lowered risks of cardiovascular diseases and other illnesses related to oxidative stress.[1] Practically all the above-mentioned compounds are obtained through the ingestion of plant products such as fruits and vegetables, nuts, flours, vegetable oils, drinks, and infusions, taken fresh or as processed foodstuffs.[2] A common property of these compounds is their antioxidant activity. The activity of an antioxidant is determined by:

1. Its chemical reactivity as an electron or hydrogen donor in reducing the free radical.
2. The fate of the resulting antioxidant-derived radical and its ability to stabilize and delocalize the unpaired electron.
3. Its reactivity with other antioxidants present.

Thus, antioxidant activity is a parameter that permits quantification of the capacity of a compound (natural or artificial) and/or a biological sample (from a wide range of sources) to scavenge free radicals in a specific reaction medium.[1,3,4]

METHODS TO MEASURE ANTIOXIDANT ACTIVITY

Antioxidant activity can be measured in a number of different ways. The most commonly used methods are those in which a chromogenic radical compound is used to simulate ROS and RNS; it is the presence of antioxidants that provokes the disappearance of these chromogenic radicals, as shown in the reaction model given in Scheme 1. In order for this method to be effective, it is necessary to obtain synthetic metastable radicals that can easily be detected by photometric or fluorimetric techniques. Nevertheless, different strategies for the quantification of antioxidant activity have been utilized: e.g., decoloration or inhibition assays. Details of these strategies and commonly used methods have been presented and reviewed elsewhere.[3,4]

When chromogenic radicals are used to determine antioxidant activity, the simplest method is to:

1. Dissolve the radical chromogen in the appropriate medium.
2. Add antioxidant.
3. Measure the loss of radical chromogen photometrically by observing the decrease in absorbance at a fixed time.
4. Correlate the decrease observed in a dose–response curve with a standard antioxidant (e.g., trolox, ascorbic acid), expressing the antioxidant activity as equivalents of standard antioxidant, a well-established parameter in this respect being Trolox Equivalent Antioxidant Capacity (TEAC).[3]

2,2′-Azino-bis-(3-ethylbenzthiazoline-6-sulfonic acid (ABTS) (Fig. 1) and α,α′-diphenyl-β-picrylhydrazyl radical (DPPH) are the two most commonly used synthetic compounds in antioxidant activity determinations. ABTS, when oxidized by the removal of one electron, generates a metastable radical. The ABTS radical cation ($ABTS^{\cdot+}$) has a characteristic absorption spectrum with maxima at 411,

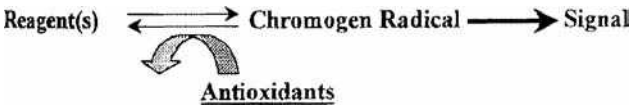

Scheme 1 Reaction model of antioxidant activity determination using chromogenic radicals.

414, 730, and 873 nm (Fig. 1), with extinction coefficients of 31 and 13 m*M*/cm at 414 and 730 nm, respectively.[5] In the reaction between $ABTS^{\cdot+}$ and antioxidants, the radical is neutralized by the addition of one electron (see the reaction presented in Scheme 1. This leads to the disappearance of the $ABTS^{+}$, which can be estimated by the decrease in absorbance (virtually any wavelength between 400 and 900 nm can be selected to avoid exogenous absorption interferences). Generally, $ABTS^{\cdot+}$ is generated directly from its precursor in aqueous media by a chemical reaction (e.g., manganese dioxide, ABAP, potassium persulfate) or by an enzymatic reaction (e.g., peroxidase, hemoglobin, met-myoglobin).[5]

Recently, we have developed a method based on $ABTS^{+}$ generated by horseradish peroxidase (HRP) that permits the evaluation of the antioxidant activity of pure compounds and plant-derived samples.[6] The method is easy, accurate, and fast to apply and presents numerous advantages because it avoids undesirable side reactions, does not require high temperatures to generate ABTS radicals, and allows for antioxidant activity to be studied over a wide range of pH values. This method is capable of determining both hydrophilic (in buffered media) antioxidant activity (HAA) and lipophilic (in organic media) antioxidant activity (LAA).[5] In the second case,

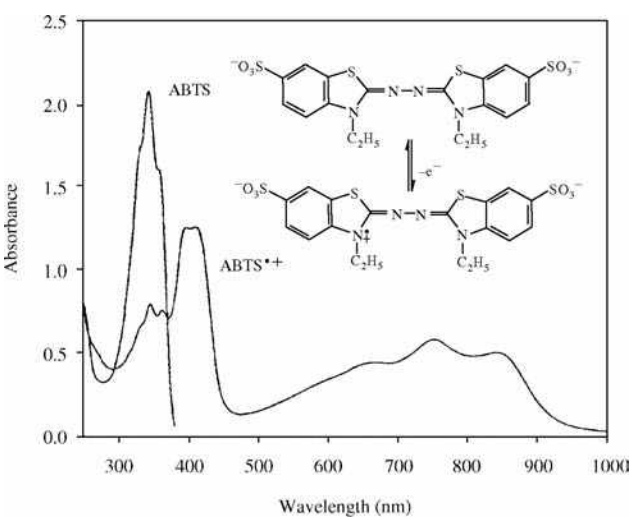

Fig. 1 Spectral characteristics of ABTS and its oxidation products, the ABTS radical ($ABTS^{\cdot+}$), showing absorbance of up to 1000 nm. The chemical structures show the nitrogen-centered radical cation of $ABTS^{\cdot+}$.

$ABTS^{\cdot+}$ is generated directly in ethanolic medium by HRP, which is a powerful oxidizing biocatalyst that can act in non-aqueous media—a capacity that has been widely used in biotechnological applications. Thus, it is possible to estimate the antioxidant activity of both antioxidant types in the same sample (HAA and LAA). The antioxidant capacities of natural compounds, such as ascorbic acid, glutathione, cysteine, phenolic compounds (resveratrol, gallic acid, ferulic acid, quercetin, etc.), or synthetic antioxidants, such as BHT, BHA, or trolox (a structural analog of vitamin E), have been estimated, as well those of plant extracts or samples from other sources. Different applications of the method have determined antioxidant activity in a range of foodstuffs.[7] The $ABTS^{\cdot+}$ chromogen used in our method has been compared with another widely used radical chromogen, $DPPH^{\cdot}$; it was concluded that in the determination of the antioxidant potential of citrus and wine samples, the $DPPH^{\cdot}$ method could significantly underestimate TEAC by up to 36% compared to $ABTS^{\cdot+}$.[8] Also, we have applied the method to study the total antioxidant activity of different vegetable soups, obtaining relevant data on the relative contribution of hydrophilic (ascorbic acid and phenols) and lipophilic (carotenoids) components to their total antioxidant activity.[9] On the other hand, our methods have been used in animal physiological studies on changes in the plasma antioxidant status caused by the hormone melatonin in rats[10] and by other authors on the effect of "in vivo" oxidant stress in the rat aorta.[11]

Under our assay conditions, $ABTS^{\cdot+}$ generation progresses quickly and only 1–5 min is necessary to reach maximum absorbance. This is a decisive factor in the easy and rapid application of the assay with minimal reagent manipulation. In contrast, other assays that use $ABTS^{\cdot+}$ to measure the activity of lipophilic antioxidants have certain drawbacks, among which are: lengthy time (up to 16 hr) to chemically generate and stabilize $ABTS^{\cdot+}$ via potassium persulfate;[12] a previous filtration step when manganese dioxide is used; or, in the case of the assay that uses ABAP, high temperatures (45–60°C) that tend to affect $ABTS^{\cdot+}$ stability. The advantage of enzymatic $ABTS^{\cdot+}$ generation, as opposed to chemical generation, is that the reaction can be controlled by the amount of H_2O_2 added, while the exceptional qualities of HRP in $ABTS^{\cdot+}$ generation is an important feature in both the aqueous and the organic system.[5–6] The most significant limiting factor in this type of strategy is the fact that the $ABTS^{\cdot+}$ must be stable during the analysis; we were able to optimize the conditions to ensure >99% stability. During optimization, it was verified that the concentration ratio between radical ($ABTS^{\cdot+}$) and substrate (ABTS) is a determining factor for the stability of $ABTS^{\cdot+}$, although pH and temperature are also important elements. With respect to the sensitivity of these methods, the calibration using L-ascorbic acid presented a detection limit of 0.15 nmol and a quantification limit of 0.38 nmol. For

lipophilic antioxidants, limit of detection (LOD) of 0.08 and limit of quantitation (LOQ) of 0.28 nmol of trolox were obtained. The LOD and LOQ of similar values were obtained for α-tocopherol and β-carotene.

ANTIOXIDANT ACTIVITY BY HPLC

The possibility of automating antioxidant activity determination and applying it to a large number of samples was an interesting objective. Previously, we have adapted our method as a microassay using a microplate reader to determine total antioxidant activity.[5] Recently, other authors have adapted radical chromogenic tests into methods that combine the advantages of rapid and sensitive chromogen radical assays with HPLC separation for the online determination of radical scavenging components in complex mixtures. Specifically, the $DPPH^{\cdot}$ method and the method of Rice-Evans, which uses $ABTS^{\cdot+}$ generated chemically with potassium persulfate, have been adapted as such.[13–14] Nonetheless, the chemical generation of $ABTS^{\cdot+}$ via potassium persulfate required 16–17 hr to complete. Our methods resulted in faster and better controlled generation of stable ABTS radical because $ABTS^{\cdot+}$ was generated enzymatically in only 2–5 min, with perfect control over the amount of $ABTS^{\cdot+}$ formed and its stability (ABTS/$ABTS^{\cdot+}$ ratios).[6] The speedy generation of $ABTS^{\cdot+}$ permitted quick acquisition of the absorbance value desired in the detector by the addition of aliquots of H_2O_2 to the ABTS solution.

The adaptation of the $ABTS^{\cdot+}$ method as an online test required that the chromogen radical should be stable for sufficient time in different solvents to permit the utilization of isocratic or gradient elution programs. The online reaction time between $ABTS^{\cdot+}$ and potential antioxidants was an additional potential limiting factor.

For online measurement of the antioxidant activity of samples using LC, it is first necessary to consider the basic equipment required. Thus, the determination of antioxidant activities in separate components of samples by HPLC in a postcolumn reaction of analytes with preformed $ABTS^{\cdot+}$ requires at least:

1. Two pumps, one for the mobile-phase solutions and another for the preformed $ABTS^{\cdot+}$ solution. A pulse dampener is recommended to minimize pulse oscillations.
2. A sample injector.
3. The chromatography column.
4. A reaction coil of adequate length to give the desired reaction time.
5. A UV–Visible (UV–Vis) detector.
6. An integration system (software) for data analysis.

Fig. 2 shows a schematic diagram of the equipment used in this study. In this case, because only one diode array detector was available, two injections of the sample were necessary: one to obtain the UV profile (at 250 nm) and another for the antioxidant activity profile at 600 nm (negative peaks). If two UV–Vis detectors had been used, only one injection would have been required to obtain the dual-HPLC profile but the chromatograms must be time-normalized.

In this type of analysis, a dual-HPLC profile was obtained. The UV profile (injection one) was of interest because all the main components of biological samples are absorbed in this wavelength range. The second injection detected absorbance changes at 600 nm or higher (see absorption spectrum of $ABTS^{\cdot+}$ in Fig. 1) to give the antioxidant activity profile. The photodiode array detector additionally recorded the absorption spectra of peaks and, consequently, could also provide data on the possible chemical nature of the analyzed compounds. The HPLC-ABTS method can be used to characterize hydrophilic (ascorbic acid, phenolic compounds, organic acids, etc.) or lipophilic antioxidants (trolox, a synthetic standard antioxidant analog of vitamin E or carotenoids such as β-carotene, lycopene, xanthophylls, etc.). Using standard antioxidants, the dual-HPLC profile as shown in Fig. 3 could be obtained. In Fig. 3A, the upper chromatogram (trolox detected at 250 nm) and the lower chromatogram

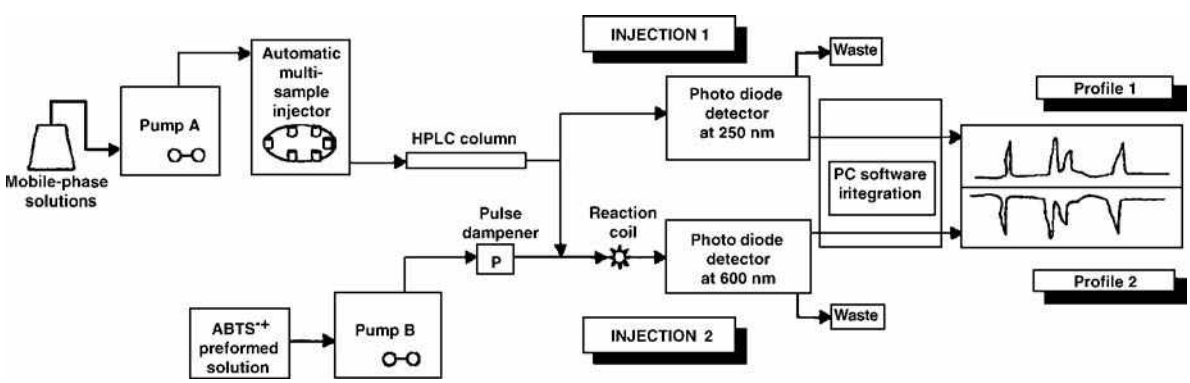

Fig. 2 Instrumental scheme for the determination of antioxidant activities by HPLC using $ABTS^{\cdot+}$ as chromogenic radical.

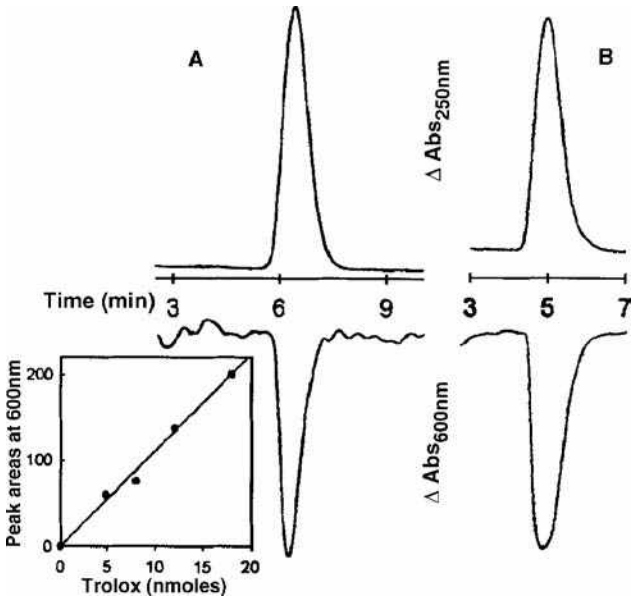

Fig. 3 Dual-HPLC plots of two antioxidants: trolox and resveratrol. Upper chromatograms show UV profiles registered at 250 nm and lower chromatograms $ABTS^{\cdot+}$ scavenging (antioxidant activity) profiles registered at 600 nm (negative peak). In (A), trolox was detected with a retention time of 6.2 min. Inset: Calibration curve of scavenging activity (peak areas at 600 nm) for different amounts of trolox. In (B), resveratrol was detected at 5.0 min.

(the scavenging activity of trolox vs. $ABTS^{\cdot+}$ measured at 600 nm) were correlated. A calibration curve relating the antioxidant concentration and the signal (600 nm, as peak areas) was obtained and used as standard to express all data as TEAC. Generally, a known amount of trolox was injected into HPLC in any chromatographic conditions (to analyze hydrophilic or lipophilic compounds) to quantify its antioxidant activity and obtain the calibration curve. Thus, antioxidant activity was calculated from the sum of the peak areas of the chromatogram profile at 600 nm (negative peaks) and expressed as trolox equivalents (TEAC) using the previously mentioned calibration curves. An example of another important antioxidant (resveratrol) is shown in Fig. 3B.

Another significant aspect was the stability of the radical chromogen $ABTS^{\cdot+}$ in different solvents, in isocratic or gradient elution programs. We found that in the mobile phases used in our determinations (saline solutions and mixtures of organic solvents in different proportions), the observed fall was less than 0.01 expressed as $-\Delta Abs_{730nm}/min$.[15] This stability is high enough to obtain accurate data, approximately 10 times greater than the data reported in Ref.[14]

It was very important to guarantee at least 1 min of online reaction time between $ABTS^{\cdot+}$ and the antioxidants because fast antioxidants, such as trolox or ascorbic acid, reacted with $ABTS^{\cdot+}$ almost immediately, but other antioxidants required more time. In our case, trolox and ascorbic acid presented TEAC values of 1.0 and 0.99, respectively, using the HPLC–ABTS method (Table 1); similar values were obtained using the ABTS end-point method or the method of Rice-Evans.[3,6] In the method of Koleva et al.,[14] ascorbic acid presented time dependence: at 30 sec, 60% of TEAC was expressed. In our system, and to guarantee sufficient online reaction time, a stainless steel reaction coil of 1 ml volume (2.5 m × 0.7 mm I.D.) coupled to a pump was connected to the chromatographic system (between the column and the diode detector) (Fig. 2). Thus, using a suitable elution program (0.5–0.7 ml/min of mobile phases) and introducing between 0.3 and 0.5 ml/min of the preformed $ABTS^{\cdot+}$ (0.2 m*M*), a total online reaction time of 1 min was obtained.

Table 1 Antioxidant activities of different compounds determined by the HPLC–ABTS and by the end-point method.

	Antioxidant activity (TEAC)	
Compound	**HPLC-ABTS method**	**End-point method**
L-Ascorbic acid	0.99	1.0
Trolox	1.0	1.0
Ferulic acid	0.87	1.94
Gallic acid	1.39	3.02
Resveratrol	1.32	2.34
Quercetin	2.83	4.30

Source: From Methods to measure the antioxidant activity in plant material. A comparative discussion, in Free. Radic. Res.[4]

Under these conditions, a study of the antioxidant potential of pure compounds could be carried out. Table 1 shows the values of antioxidant activity (expressed as TEAC) of different compounds of interest, determined by the online method (HPLC–ABTS method) and compared with the values obtained by our conventional photometric end-point method.[6] As can be observed, the two most important standard antioxidants, trolox and ascorbic acid, presented similar TEAC using either method. Thus, either can be used as reference to express antioxidant activity, except that trolox has the advantage because it can be used in both hydrophilic and lipophilic assays. The TEAC values of phenolic compounds were underestimated by approximately half when the HPLC–ABTS method was used as compared to the end-point method. This was due to the different reactivities of antioxidants with $ABTS^{\cdot+}$, and because, unfortunately, the time dependence of online scavenging activity determinations made it very difficult to obtain the total reaction for the slowest antioxidants resulting in a partial estimation of this activity. Nevertheless, the HPLC–ABTS method provided important additional information in the form of correlation between the different peaks of a sample and their antioxidant activities.

The HPLC–ABTS has been used in a study on the HAA and the LAA of fresh citrus and tomato juices.[15] The data

obtained showed a good correlation between vitamin C content and HAA and slight underestimations of LAA. We are currently applying this method to different plant materials with the aim of finding out which compounds apport significant antioxidant properties to the foodstuffs studied.

CONCLUSIONS

Determinations of antioxidant activity are widely used in phytochemistry, nutrition, food chemistry, clinical chemistry, as well as in human, animal, and plant physiology, etc. Methods adapted to HPLC have appeared only recently but can be expected to have multiple applications in the future. $ABTS^{\cdot+}$ is an excellent metastable chromogen for the detection and quantification of the HAA and LAA of biological samples. Thus, using a simple photometer (end-point method),[6] a microplate reader (multisample titration method),[5] or HPLC equipment, a broad range of possibilities are available for the characterization of diverse samples (animal- or plant-derived). Some applications of special interest could include:

1. Characterization of biological samples (e.g., plant extracts, foods).
2. Studies on the changes in the antioxidant activity of material during industrial or postharvest processing (e.g., thermal processes, Maillard reactions, and cold storage of foods, etc.).
3. The search for new natural antioxidants of vegetable or marine origin.
4. Clinical determinations.

ACKNOWLEDGMENTS

This work was supported by the Instituto Nacional de Investigación y Tecnología Agraria y Alimentaria (I.N.I.A., ministerio de Ciencia y Tecnología, Spain) project CAL00-062 and by the project PI-9/00759/FS/01 (Fundación Séneca, Murcia, Spain). A. Cano has a grant from the Fundación Séneca of the Comunidad Autónoma de Murcia (Spain). The authors wish to thank A.N.P. Hiner for checking the draft of this manuscript.

REFERENCES

1. Halliwell, B.; Gutteridge, J.M.C. *Free Radicals in Biology and Medicine*; 3rd Ed.; Halliwell, B., Gutteridge, J.M.C., Eds.; Oxford University Press: New York, 2000.
2. Mackerras, D. Antioxidants and health. Fruits and vegetables or supplements? Food Aust. **1995**, *47*, S3–S23.
3. Rice-Evans, C.A.; Miller, N.J. Total antioxidant status in plasma and body fluids. Methods Enzymol. **1994**, *234*, 279–293.
4. Arnao, M.B.; Cano, A.; Acosta, M. Methods to measure the antioxidant activity in plant material. A comparative discussion. Free Radic. Res. **1999**, *31*, S89–S96.
5. Cano, A.; Acosta, M.; Arnao, M.B. A method to measure antioxidant activity in organic media: Application to lipophilic vitamins. Red. Rep. **2000**, *5*, 365–370.
6. Cano, A.; Hernández-Ruiz, J.; García-Cánovas, F.; Acosta, M.; Arnao, M.B. An end-point method for estimation of the total antioxidant activity in plant material. Phytochem. Anal. **1998**, *9*, 196–202.
7. Arnao, M.B.; Cano, A.; Acosta, M. Total antioxidant activity in plant material and its interest in food technology. Rec. Res. Dev. Agric. Food Chem. **1998**, *2*, 893–905.
8. Arnao, M.B. Some methodological problems in the determination of antioxidant activity using chromogen radicals: A practical case. Trends Food Sci. Technol. **2000**, *11*, 419–421.
9. Arnao, M.B.; Cano, A.; Acosta, M. The hydrophilic and lipophilic contribution to total antioxidant activity. Food Chem. **2001**, *73*, 239–244.
10. Plaza, F.; Arnao, M.; Zamora, S.; Madrid, J.; Rol de Lama, M. Validación de un microensayo con $ABTS^{\cdot+}$ para cuantificar la contribución de la melatonina al estatus antioxidante total del plasma de rata. Nutr. Hosp. **2001**, *16*, 202.
11. Laight, D.W.; Gunnarsson, P.T.; Kaw, A.V.; Anggard, E.E.; Carrier, M.J. Physiological microassay of plasma total antioxidant status in a model of endothelial dysfunction in the rat following experimental oxidant stress in vivo. Environ. Toxicol. Pharmacol. **1999**, *7*, 27–31.
12. Re, R.; Pellegrini, N.; Proteggente, A.; Pannala, A.; Yang, M.; Rice-Evans, C.A. Antioxidant activity applying an improved ABTS radical cation decolorization assay. Free Radic. Biol. Med. **1999**, *26*, 1231–1237.
13. Koleva, I.I.; Niederländer, H.A.G.; van Beek, T.A. An on-line HPLC method for detection of radical scavenging compounds in complex mixtures. Anal. Chem. **2000**, *72*, 2323–2328.
14. Koleva, I.I.; Niederlander, H.A.G.; van Beek, T.A. Application of ABTS radical cation for selective on-line detection of radical scavengers in HPLC eluates. Anal. Chem. **2001**, *73*, 3373–3381.
15. Cano, A.; Alcaraz, O.; Acosta, M.; Arnao, M. On-line antioxidant activity determination: Comparison of hydrophilic and lipophilic antioxidant activity using the $ABTS^{\cdot+}$ assay. Red. Rep. **2002**, *7*, 103–109.

Antiretroviral Drugs

Melgardt M. de Villiers
School of Pharmacy, University of Wisconsin, Madison, Wisconsin, U.S.A.

Wilna Liebenberg
Research Institute for Industrial Pharmacy, North-West University, Potchefstroom, South Africa

INTRODUCTION

When seeking chromatographic analytical methods for anti-retroviral drugs (ARVs), the approved methods published in national and international pharmacopoeias such as the United States Pharmacopeia,[1] British Pharmacopoeia,[2] European Pharmacopoeia,[3] and Japanese Pharmacopoeia[4] should be considered first. However, methods of analysis for many of the newer ARVs are not listed in these pharmacopoeias. In addition, when ARVs are combined into a single dosage form, or administered together, the analytical methods for single entities frequently do not apply. Since different classes of ARVs act at different stages of the HIV life cycle, combination of several (typically three or four) ARVs is usually more effective. Combination therapy is therefore known as highly active anti-retroviral therapy (HAART).[5] The preferred initial regimens are either: Efavirenz + Lamivudine or Emtricitabine + Zidovudine or Tenofovir; or Lopinavir boosted with Ritonavir + Zidovudine + Lamivudine or Emtricitabine.[6]

ARVs are broadly classified by the phase of the retrovirus life cycle that the drug inhibits. There are thus five broad classifications of ARVs retroviral drugs in development, though only the first three classes currently have licensed examples:[6]

1. Reverse transcriptase inhibitors (RTIs) target construction of viral DNA by inhibiting activity of reverse transcriptase. There are two subtypes of RTIs, nucleoside-analogue RTIs and non-nucleoside-analogue RTIs. Nucleoside/nucleotide analogues include: Abacavir, Didanosine, Emtricitabine, Lamivudine, Stavudine, Tenofovir, Zalcitabine (production discontinued), and Zidovudine. Non-nucleoside Reverse Transcriptase Inhibitors include: Delavirdine, Efavirenz, and Nevirapine.
2. Protease inhibitors (PIs) target viral assembly by inhibiting the activity of protease. Protease inhibitors include: Amprenavir, Atazanavir, Fosamprenavir, Indinavir, Lopinavir/Ritonavir, Nelfinavir, Ritonavir, Saquinavir, and Tipranavir.
3. Fusion inhibitors block HIV from fusing with a cell's membrane to enter and infect it. An example of a drug in this class is Enfuvirtide.
4. Integrase inhibitors inhibit the enzyme integrase, which is responsible for integration of viral DNA into the DNA of the infected cell.
5. Entry inhibitors block HIV-1 from the host cell by binding CCR5, a molecule on the viral membrane termed a co-receptor that HIV-1 normally uses for entry into the cell.

In Table 1, chromatographic methods of analysis for ARVs taken from pharmacopoeial and other reports are summarized. These methods represent tested analytical methods for determining the drugs, alone or in combination, using mainly high-performance liquid chromatography (HPLC) analysis with or without sample preparation. These methods can be used for analyzing the drugs in pharmaceutical dosage forms or biological fluids.

CONCLUSION

Although there are analytical methods for some ARV drugs available in official compendia because of the constant introduction of newer drugs and with the move toward combination therapy, it is difficult to quickly find these methods. This report is an attempt to summarize these methods, thereby providing a single source of published HPLC methods.

REFERENCES

1. United States Pharmacopeial Convention. *The United States Pharmacopeia,* Rockville, MD, 28, 2005.
2. The British Pharmacopoeia; The Stationary Office: London, 2007.
3. European Pharmacopoeia EP 5th Ed. European Pharmacopoeia Commission, EDQM, Strasbourg, France, 2005.
4. Japanese Pharmacopoeia, 14th Ed.; Ministry of Health, Labour, and Welfare: Tokyo, Japan, 2000.
5. Robbins, G.K.; De Gruttola, V.; Shafer, R.W.; Smeaton, L.M.; Snyder, S.W.; Pettinelli, C.; Dube, M.P.; Fischl, M.A.; Pollard, R.B. et al. Comparison of sequential three-drug regimens as initial therapy for HIV-1 infection. N. Engl. J. Med. **2003**, *349* (24), 2293–2303.

Table 1 Conditions for the chromatographic analysis of anti-retroviral drugs.

Drug	Analysis method	Refs.
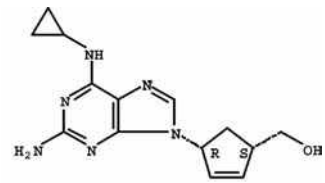 Abacavir	Mobile phase: Methanol : acetonitrile: 0.015 *M* KH_2PO_4 (36:2.6:61.4, v/v/v) adjusted to pH 6.9 with 5 N NaOH. Chromatographic system: The separation was carried out at ambient temperature on a reversed-phase Waters Spherisorb ODSI column (250 × 4.6 mm, 5 μm particle size). The chromatographic separation was performed isocratically. The UV detector was set at a wavelength of 284 nm. An injection volume of 20 μl was used. Ketoprofen was used as an internal standard. The retention times were 5.49 min for abacavir and 9.15 min for ketoprofen in the mobile phase, 5.46 min for abacavir and 9.24 min for ketoprofen in serum samples	[7]
	The standards and samples were chromatographed on a Kromasil octadecyl column at room temperature. Each set of study samples assayed with mobile phase containing 25 m*M* ammonium acetate buffer (pH 4.0 with acetic acid)–methanol (95:5, v/v) initially, and a linear gradient of acetonitrile increasing from 0% to 50% over 30 min. A 10 min HPLC column re-equilibration time followed each individual analysis. The mobile-phase flow rate 0.7 ml/min, and the total run time for each was 40 min. The analytes were quantitated following UV detection at 295 nm	[8]
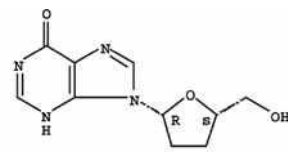 Didanosine	For the analysis of didanosine in drug substance and formulated products, tablets chromatography is carried out on a pre-packed, Lichrospher 100 Rp-8 (5.0 μm, 250 mm × 4.0 mm) column using 0.01 *M* sodium acetate solution : methanol (85:15, v/v) adjusted to pH 6.5 with acetic acid as mobile phase at a flow rate of 1.5 ml/min and a 248 nm detection. The assay was linear over the concentration range of 50–150 μg/ml ($R \approx 0.999$). The method was validated for accuracy and precision	[9]
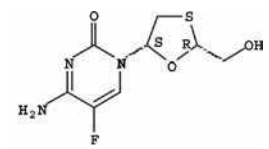 Emtricitabine	Separation of emtricitabine (FTC) enantiomers using an amylose *tris*[(*S*)-1-phenylethylcarbamate] coated onto APS-Nucleosil (7 μm particle size, 500 Å pore size, 20% w/w, 15 × 0.46 cm I.D.) chiral column under polar organic elution mode. Good enantioselectivity ($\alpha = 1.9$) with excellent enantioresolution (RS = 3.3) was achieved by the use of methanol with 0.02% of triethylamine acetate as mobile phase. The method allows the accurate determination of as low as 0.2% of each enantiomer as an impurity. The validated method proved to be reliable and sensitive for the quantification of both enantiomers as impurity in different batches of emtricitabine and b-D-(+)-FTC	[10]
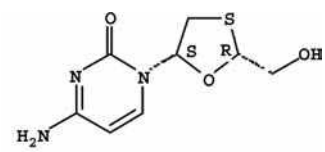 Lamivudine	Mobile phase: A filtered and degassed mixture of 0.025 *M* ammonium acetate solution (pH of 3.8 ± 0.2 adjusted with acetic acid) and methanol (95:5). Make adjustments if necessary. Chromatographic system: The liquid chromatograph must be equipped with a 277 nm detector and a 4.6 mm × 25 cm, C_{18} column. Flow rate 1.0 ml/min. Column temperature maintained at 35°C. The resolution, *R*, between lamivudine and lamivudine diastereomer is not less than 1.5 with the relative retention times about 1.0 for lamivudine and 0.9 for lamivudine diastereomer. The relative standard deviation for replicate injections must not be more than 2.0%	[1]
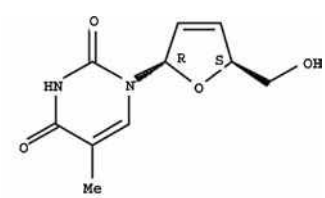 Stavudine	Mobile phase: A filtered and degassed mixture of 0.01 *M* ammonium acetate and acetonitrile (95:5). Chromatographic system: A liquid chromatograph equipped with a 254 nm detector and a 4.6 mm × 3.3 cm, C_{18} column that contains 3 μm packing. Flow rate about 0.7 ml/min. The retention time of the stavudine peak is between 2.8 and 5.0 min; the column efficiency is not less than 800 theoretical plates; the tailing factor is less than or equal to 1.6–1.8; and the relative standard deviation for replicate injections is not more than 2.0%	[1]
	This method is also used for the analysis of the drug in tablets after employing a resolution solution prepared by dissolving accurately weighed quantities of thymine and thymidine in water, diluted with water to obtain a solution having a known concentration of 0.1 μg/ml of each component. The resolution, *R*, between thymine and thymidine is not less than 2.0, and thymine is resolved from the void volume	
	For the analysis of stavudine in solution, a mobile phase composed of two solutions is recommended. Solution A: A filtered and degassed mixture of 25 m*M* ammonium acetate and methanol (94:6). Solution B: A filtered and degassed mixture of 25 m*M* ammonium acetate and methanol (1:1). Chromatographic system: A liquid chromatograph equipped with a 268 nm detector and a 4.6 mm × 3.3 cm C_{18}column and a 4 mm × 20 mm C_{18} guard column. The flow rate is about 1 ml/min. The chromatograph is programed so that from 0 to 12 min, 100% of Solution A is eluted.	

(Continued)

Table 1 Conditions for the chromatographic analysis of anti-retroviral drugs. *(Continued)*

Drug	Analysis method	Refs.
	Then by a step gradient, the mobile phase is changed to 100% Solution B. From 12.1 to 17 min, 100% Solution B is eluted. From 17 to 17.1 min, the mobile phase is changed back to 100% Solution A. From 17.1 to 35 min, the chromatograph is recalibrated with 100% Solution A. Using the resolution solution used for the analysis of tablets, the resolution, *R*, between thymine and thymidine is not less than 8.4. The column efficiency is not less than 2000 theoretical plates; the tailing factor for the stavudine peak is not more than 2; and the relative standard deviation for replicate injections is not more than 2.0%	[1]
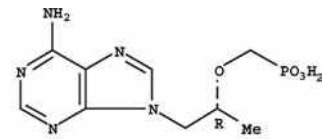 Tenofovir	This method combines a solid–liquid extraction procedure with a reversed-phase HPLC system. The system requires a mobile phase containing Na_2HPO_4 buffer, tetrabutylammonium hydrogen sulfate, and acetonitrile for different elutions through a C_{18} column with UV detection. The method proved to be accurate, precise, and linear between 10 and 4,000 ng/ml. The method was applied to determine trough levels of tenofovir in 11 HIV-infected patients and for pharmacokinetic studies in HIV-infected patients with renal failure	[11]
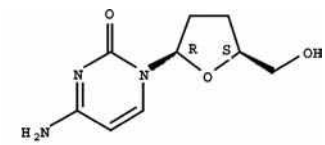 Zalcitabine	Mobile phase: A filtered and degassed mixture of phosphate buffer (6.8 g of monobasic potassium phosphate and 8.7 g of dibasic potassium phosphate in 2000 ml of water adjusted with dilute phosphoric acid or potassium hydroxide solution to a pH of 6.8 $\pm$ 0.05) and acetonitrile (97:3). Make adjustments if necessary. Chromatographic system: A liquid chromatograph equipped with a 270 nm detector and a 4.6 mm $\times$ 15 cm, C_{18} column. Flow rate is about 1 ml/min. The tailing factor for the zalcitabine peak is not greater than 1.5, and the relative standard deviation is not more than 2.0%. The resolution, *R*, between zalcitabine and a zalcitabine related compound is not less than 2	[1]
	The drug in tablets requires the following chromatographic conditions. Mobile phase: A filtered and degassed mixture of buffer solution and acetonitrile (85:15). The buffer solution is composed of 3.4g of monobasic potassium phosphate in sufficient water to make 1 L adjusted with phosphoric acid to a pH of 2.2. Chromatographic system: A liquid chromatograph is equipped with a 280 nm detector, a precolumn C_{18} cartridge and a 4.6 mm $\times$ 25 cm analytical C_{18} column that contains 5 μm packing. A flow rate of about 1.5 ml/min. The resolution, *R*, between the zalcitabine and zalcitabine related compound A peaks is not less than 1.1, and the tailing factor for the zalcitabine peak is not more than 1.5. The relative standard deviation for replicate injections is not more than 2%	[1]
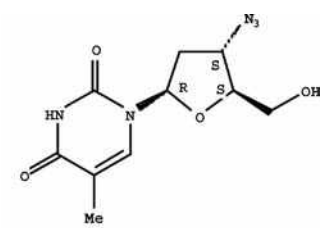 Zidovudine	Mobile phase: A filtered and degassed mixture of water and methanol (80:20). Make adjustments if necessary. Chromatographic system: A liquid chromatograph equipped with a 265 nm detector and a 4.0 mm $\times$ 25 cm C_{18} column and a 3.2 mm $\times$ 1.5 cm C_{18} guard column. The flow rate is about 1.0 ml/min. The relative retention times are about 0.25 for zidovudine related compound C (thymine), 1.0 for zidovudine, and 1.17 for zidovudine related compound B (3′-chloro-3′-deoxythymidine); the resolution, *R*, between zidovudine and zidovudine related compound B is not less than 1.4; the tailing factor is not more than 1.5; and the relative standard deviation for replicate injections is not more than 2.0%. In the USP, this method is also used for the analysis of the drug in injections and capsules	[1]
	For the analysis of zidovudine in oral solutions, the mobile phase is a filtered and degassed mixture of 0.040 *M* sodium acetate, methanol, acetonitrile, and glacial acetic acid (900:90:10:2). Chromatographic system: A liquid chromatograph equipped with a 240 nm detector and a 4.0 mm $\times$ 12.5 cm C_{18} column. The flow rate is about 1.0 ml/min. The relative retention times are about 0.12 for zidovudine related compound C (thymine) and 1.0 for zidovudine; the resolution, *R*, between zidovudine and zidovudine related compound C (thymine) is not less than 4.0; the tailing factor is not more than 2.0; and the relative standard deviation for replicate injections is not more than 2.0%	[1]

(Continued)

Table 1 Conditions for the chromatographic analysis of anti-retroviral drugs. *(Continued)*

Drug	Analysis method	Refs.
	For the analysis of zidovudine in tablets, the mobile phase suggested in the USP is 3.0 g of sodium acetate and 1.3 g of sodium 1-octanesulfonate in 900 ml of water. Add 90 ml of methanol and 40 ml of acetonitrile, and mix. Adjust with glacial acetic acid to a pH of 5.3, filter, and degas. Chromatographic system: A liquid chromatograph equipped with a 265 nm detector and a 4.6 mm × 15 cm C_{18} column. The flow rate is about 1.3 ml/min. The resolution, *R*, between zidovudine and a peak having a relative retention time of about 1.2 is not less than 2.5; the tailing factor for the zidovudine peak is not more than 2.0; and the relative standard deviation for replicate injections is not more than 2.0%	[1]
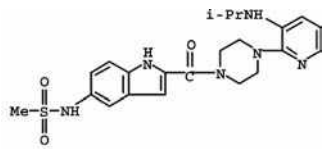 Delavirdine	Mobile phase: A mixture of 10 m*M* potassium phosphate buffer, pH 6.0, with acetonitrile (2 : 1). The chromatographic system: Separation was affected on a Zorbax SB CN, 150 × 4.6 mm I.D., 5 μm analytical column along with a RP-CN 15 × 3.2 mm I.D., 7 μm precolumn. The column effluent was monitored using a Waters Model 470 scanning fluorescence detector operated with 18 nm slit widths at 302 nm excitation and 425 nm emission. Typical injection intervals were about 11 min at a flow rate of 1.5 ml/min. Retention times were approximately 3 min for the metabolite, 7.5 min for the internal standard, and 9 min for delavirdine. Typical system performance was approximately 10,000 plates/m for the metabolite, 19,000 plates/m for the internal standard, and 31,000 plates/m for delavirdine with a minimum resolution of 1.7 between the internal standard and delavirdine	[12]
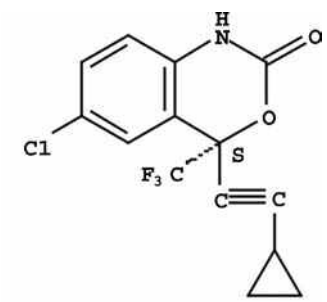 Efavirenz	Mobile phase: A mixture of 10 m*M* phosphate buffer pH 2.4 (adjusted with 1 N HCl) and acetonitrile (55:45, v/v). Chromatographic system: The analytical column was a C_{18}, 150 × 4.6 mm I.D., 5 μm particle size (Lichrospher 100 RP-18e) protected by a compatible guard column. The UV detector was set at 245 nm. 20 μl samples were injected and the chromatogram was run for 10 min at a flow rate of 2.4 ml/min at ambient temperature	[13]
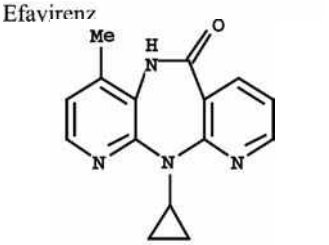 Nevirapine	Mobile phase: A filtered and degassed mixture of 0.025 *M* ammonium phosphate buffer (pH about 5) and acetonitrile (4:1). Chromatographic system: A liquid chromatograph equipped with a 220 nm detector and a 4.6 mm × 15 cm column that contains 5 μm packing L60 (spherical, porous silica gel, 3 or 5 μm in diameter, the surface of which has been covalently modified with palmitamidopropyl groups and endcapped with acetamidopropyl groups to a ligand density of about 6 μmol/m^2). The flow rate is about 1 ml/min. The column temperature is maintained at 35°C. The relative retention times are about 0.7 for nevirapine related compound B, 1.0 for nevirapine, 1.5 for nevirapine related compound A, and 2.8 for nevirapine impurity C. The resolution, *R*, between nevirapine related compound B and nevirapine is not less than 5.0; and the resolution between nevirapine and nevirapine related compound A is not less than 7.4. The relative standard deviation for replicate injections is not more than 2.0%	[1]
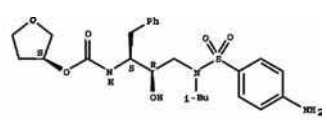 Amprenavir	Amprenavir concentrations in plasma and other solutions can be measured by HPLC with separation on a C_{18} column after liquid–liquid extraction from alkaline plasma and UV detection at 210 nm. First, amprenavir was extracted with diethylether from 0.2 ml of plasma after adding pH 9 buffer and 6,7-dimethyl-2,3-di-(2-pyridyl)-quinoxaline (internal standard from Sigma Aldrich Chemicals). Dry residues were dissolved in 100 μl of the mobile phase and 30 μl was injected onto the C_{18} column. The mobile phase consisted of water/acetonitrile/sodium hydroxide/orthophosphoric acid/triethylamine (650/350/0.9/0.7/0.5, v/v) and the flow rate was 1.2 ml/min. The HPLC system consisted of a Licrocart 125-4 mm column (licrospher phase 100 RP-18 encapped 5 μm, Merck)	[14]

(Continued)

Table 1 Conditions for the chromatographic analysis of anti-retroviral drugs. *(Continued)*

Drug	Analysis method	Refs.
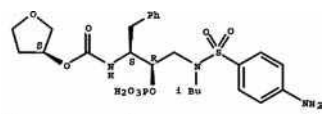 Fosamprenavir	Fosamprenavir is an oral prodrug of the protease inhibitor amprenavir, with a reduced daily dose. Since this is a prodrug, any analysis in biological fluids would be measuring amprenavir. Therefore, HPLC methods as described for amprenavir would apply	
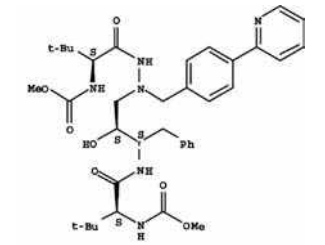 Atazanavir	Solid phase extraction: After viral inactivation by heat (60°C for 60 min), plasma (600 μl) with clozapine (internal standard) is diluted 1 + 1 with phosphate buffer pH 7 and subjected to an SPE on a C_{18} cartridge. Matrix components are eliminated with 2 × 500 μl of a solution of 0.1% H_3PO_4 neutralized with NaOH to pH 7. ATV is eluted with 3 × 500 μl MeOH. The resulting eluate is evaporated under nitrogen at room temperature and is reconstituted in 100 μl MeOH/H_2O 50/50. A 40 μl volume is injected onto a Nucleosil 100, 5 μm C_{18} AB column. Atazanavir is analyzed by UV detection at 201 nm using a gradient elution program with solvents constituted of MeCN and phosphate buffer adjusted to pH 5.14. The mobile phase also contains 0.02% sodium heptanesulfonate, enabling an excellent separation of ATV from the other HIV protease inhibitors (PIs) and the non-nucleoside reverse transcriptase inhibitors (NNRTIs). The calibration curves are linear up to 10 μg/ml, with a lower limit of quantification of 0.2 μg/ml	[15]
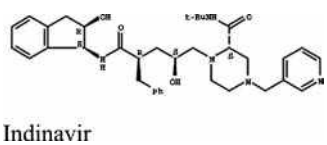 Indinavir	Mobile phase: A filtered and degassed mixture of dibutylammonium phosphate buffer and acetonitrile (11:9). The dibutylammonium phosphate buffer is prepared by transferring 20 ml of dibutyl ammonium phosphate to 1,000 ml of water and adjusting the H 6.5 ± 0.05. Chromatographic system: A liquid chromatograph equipped with a 260 nm detector and a 4.6 mm × 25 cm C_8 column that contains 5 μm packing. The flow rate is about 1.0 ml/min. The column temperature is maintained at 40°C. The column efficiency is not less than 4,000 theoretical plates; the tailing factor is less than 2.0; and the relative standard deviation for replicate injections is not more than 1.0%	[1]
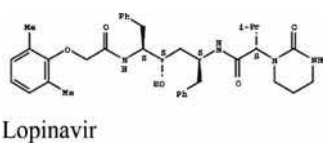 Lopinavir	Sample preparation: After viral inactivation by heat (60°C for 60 min), plasma (600 μl), with clozapine added as internal standard, is diluted 1 + 1 with phosphate buffer pH 7 and subjected to a solid-phase extraction (SPE) on a C_{18} cartridge. Matrix components are eliminated with 2 × 500 μl of a solution of 0.1% H_3PO_4 neutralized with NaOH to pH 7. Lopinavir is eluted with 3 × 500 μl MeOH. The resulting eluate is evaporated under nitrogen at room temperature and is reconstituted in 100 ml MeOH 50%. A 40 μl volume is injected onto a Nucleosil 100, 5 μm C_{18} column. The drug is analyzed separately using a gradient elution program with solvents constituted of MeCN and phosphate buffer adjusted to pH 5.07 and containing 0.02% sodium heptanesulfonate. Lopinavir is detected by UV at 201 nm. The calibration curves are linear up to 10 μg/ml. This method can also be used to analyze nevirapine with detection at 282 nm. With slight adjustments, this HPLC method can be used for the simultaneous assay of amprenavir, ritonavir, indinavir, saquinavir, nelfinavir, and efavirenz.[17]	[16, 17]
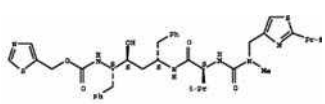 Ritonavir	Mobile phase: A mixture of acetonitrile, methanol, and 0.01 *M* tetramethylammonium perchlorate in 0.1% aqueous trifluoroacetic acid (40:5:55, v/v/v), at a constant flow rate of 1.0 ml/min at ambient temperature. Chromatographic system: Separation was accomplished on an ODS-AQ column 5 cm × 4.0 mm I.D., 3 μm particle size; similar separation could be achieved on a 5 cm × 4.6 mm, 3 μm ODS-2 column. The detector was operated at a wavelength of 205 nm. Standard curves were linear ($r > 0.9998$) over the concentration range 0.01–15 μg/ml with both inter- and intra-day coefficients of variation typically less than 5%	[18]
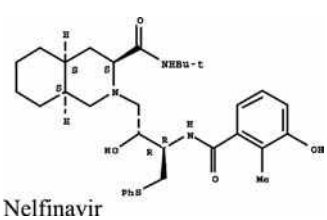 Nelfinavir	Mobile phase: A mixture of acetonitrile (MeCN) and 25 m*M* monobasic ammonium phosphate (containing 25 m*M* triethylamine, pH 3.4 with phosphate acid) (40:60, v/v) was delivered at a flow rate of 1.0 ml/min with detection at 210 nm. Chromatographic system: A CN chromatographic column (250 × 4.6 mm, 5 μm) was used for the separation at 40°C. The injection volume was 10 μl	[19]

(Continued)

Table 1 Conditions for the chromatographic analysis of anti-retroviral drugs. *(Continued)*

Drug	Analysis method	Refs.
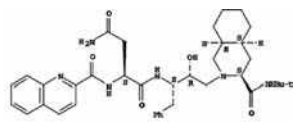 Saquinavir	Mobile phase: A filtered and degassed mixture of triethylamine phosphate solution, tetrahydrofuran, and acetonitrile (14:5:1). Chromatographic system: A liquid chromatograph equipped with a 210 nm detector and a 4.6 mm × 25 cm C_{18} column. The column temperature is maintained at 20°C, and the flow rate is about 1 ml/min. The relative retention times are about 0.89 for saquinavir related compound A and 1.0 for saquinavir; and the resolution, *R*, between saquinavir related compound A and saquinavir is not less than 1.5. The column efficiency is not less than 500 theoretical plates; and the relative standard deviation for replicate injections is not more than 2.0%. This method is also used to assay saquinavir in capsules	[1]
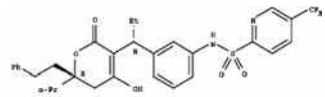 Tipranavir	An HPLC method previously described for the assay of amprenavir, ritonavir, indinavir, saquinavir, nelfinavir, lopinavir, atazanavir, nevirapine, and efavirenz can be also conveniently applied, with minor gradient program adjustment, for the determination of tipranavir in human plasma, by off-line SPE followed by HPLC coupled with UV–diode array detection (DAD).[15–17] Using this method, tipranavir is analyzed by UV detection at 201 nm using a gradient elution program constituted of MeCN and phosphate buffer adjusted to pH 5.12 and containing 0.02% sodium heptanesulfonate on a Nucleosil C_{18} AB column. Calibration curves are linear up to 75 μg/ml, with a lower limit of quantification of 0.125 μg/ml	[20]
Enfuvirtide: a 36 length protein sequence	Chromatographic system: The HPLC system used to assay used a Fluorimetric detector (excitation 280 nm, emission 350 nm). Chromatographic separation was performed by a Luna 5μ C18 column (150 × 4.6 mm I.D.) Phenomenex (CA) protected by a SecurityGuard with C_{18} (4.0 × 3.0 mm I.D.) precolumn Phenomenex (CA) at 35 °C. Analysis was performed with a gradient using a mobile phase composed of buffer A (water + 0.1% TFA + 0.5% arginine HCl) and buffer B (acetonitrile: water [70:30] + 0.1% TFA + 0.5% arginine HCl). The method showed lower limits of detection and quantification (LOD = 32 ng/ml, LOQ = 78 ng/ml), lower intra-day (RSD% 1.25–2.95) and inter-day (RSD% 1.75–4.69) coefficients of variation, greater recovery (>100%), lower duration (16 min)	[21]
Combination of nine ARVs: indinavir, saquinavir, ritonavir, amprenavir, lopinavir, delavirdine, efavirenz, elfinavir, and its M8 metabolite	Mobile phase: Separation was facilitated via gradient elution at 1.5 ml/min flow rate. The mobile phase consisted of (A) 25 m*M* potassium phosphate buffer, pH 3.1; (B) acetonitrile; and (C) methanol according to a specific program that allows linear adjustments in a 40 min run time. Chromatographic system: Analytes were isolated from plasma using tert-butyl methyl ether and separation was achieved via reversed-phase liquid chromatography on a C_8 column (5 μm, 25 cm × 4.6 mm I.D.) with a gradient mobile phase. A Discovery C (2 cm × 4 mm I.D., 5 μm) in-line guard column was used to extend the life of the analytical column. Detection at 210 nm provided adequate sensitivity. Limit of quantification is 50 ng/ml and all analytes demonstrated linearity across 50–10,000 ng/ml from a single 200 ml plasma sample	[22]
Combination of 16 ARVs: seven HIV protease inhibitors (amprenavir, atazanavir, indinavir, lopinavir, nelfinavir, ritonavir, and saquinavir), seven nucleoside reverse transcriptase inhibitors (abacavir, didanosine, emtricitabine, lamivudine, stavudine, zalcitabine, and zidovudine), and two non-nucleoside reverse transcriptase inhibitors (efavirenz and nevirapine)	Sample preparation: Automated solid-phase extraction with Oasis HLB Cartridge 1 cc (divinylbenzene and *N*-vinylpyrrolidone) and evaporation in a water bath under nitrogen stream. The extracted samples were reconstituted with 100 μl methanol. Mobile phase: The mobile phase is composed of solution A (0.01 *M* KH_2PO_4) and B (acetonitrile). Both solutions were degassed by purging with helium. The mobile phase was delivered by a linear gradient at 1.0 ml/min. The injection volume was 20 μl. Chromatographic system: Twenty microliters of extracted samples were injected into an HPLC–UV system. Separation was performed at 24.0°C on an analytical C_{18} Symmetry™ column (250 mm × 4.6 mm I.D.) with a particle size of 5.0 μm equipped with a guard column (20 × 3.9 mm I.D.) filled with the same packing material. The total run time for a single analysis was 35 min, the anti-HIV drugs were detected by UV at 240 and 260 nm. The calibration curves were linear up to 10 μg/ml. The absolute recovery ranged between 88% and 120%	[23]

6. The U.S. Department of Health and Human Services, A Pocket Guide to Adult HIV/AIDS Treatment. January 2005 edition. Washington, DC.
7. Oezkan, Y.; Savaser, A.; Oezkan, S.A. Simple and reliable HPLC method of abacavir determination in pharmaceuticals, human serum and drug dissolution studies from tablets. J. Liq. Chromatogr. Relat. Technol. **2005**, *28* (3), 423–437.
8. Ravitch, J.R.; Moseley, C.G. High-performance liquid chromatographic assay for abacavir and its two major metabolites in human urine and cerebrospinal fluid. J. Chromatogr. B, **2001**, *762* (2), 165–173.
9. Cavalcanti de Oliveira, A.M.; Loewen, T.C.R.; Cabral, L.M.; dos Santos, E.M.; Rodrigues, C.R.; Castro, H.C.; dos Santos, T.C. Development and validation of a HPLC-UV method for the determination in didanosine tablets. J. Pharm. Biomed. Anal. **2005**, *38* (4), 751–756.
10. Cass, Q.B.; Watanabe, C.S.F.; Rabi, J.A.; Bottari, P.Q.; Costa, M.R.; Nascimento, R.M.; Cruz, J.E.D.; Ronald, R.C. Polysaccharide-based chiral phase under polar organic mode of elution in the determination of the enantiomeric purity of emtricitabine an anti-HIV analogue nucleoside. J. Pharm. Biomed. Anal. **2003**, *33* (4), 581–587.
11. Sentenac, S.; Fernandez, C.; Thuillier, A.; Lechat, P.; Aymard, G. Sensitive determination of tenofovir in human plasma samples using reversed-phase liquid chromatography. J. Chromatogr. B, **2003**, *793* (2), 317–324.
12. Staton, B.A.; Johnson, M.G.; Friis, J.M.; Adams, W.J. Simple, rapid and sensitive high-performance liquid chromatographic determination of delavirdine and its N-desisopropyl metabolite in human plasma. J. Chromtogr. B, **1995**, *668* (1), 99–106.
13. Ramachandran, G.; Kumar, A.K.H.; Swaminathan, S.; Venkatesan, P.; Kumaraswami, V.; Greenblatt, D.J. Simple and rapid liquid chromatography method for determination of efavirenz in plasma. J. Chromatogr. B, **2006**, *835* (1–2), 131–135.
14. Barrail, A.; Le Tiec, C.; Paci-Bonaventure, S.; Furlan, V.; Vincent, I.; Taburet, A. Determination of amprenavir total and unbound concentrations in plasma by high-performance liquid chromatography and ultrafiltration. Ther. Drug Mon. **2006**, *28* (1), 89–94.
15. Colombo, S.; Guignard, N.; Marzolini, C.; Telenti, A.; Biollaz, J.; Decosterd, L.A. Determination of the new HIV-protease inhibitor atazanavir by liquid chromatography after solid-phase extraction. J. Chromatogr. B, **2004**, *810* (1), 25–34.
16. Marzolini, C.; Beguin, A.; Telenti, A.; Schreyer, A.; Buclin, T.; Biollaz, J.; Decosterd, L.A. Determination of lopinavir and nevirapine by high-performance liquid chromatography after solid-phase extraction: Application for the assessment of their transplacental passage at delivery. J. Chromatogr. B, **2002**, *774* (2), 127–140.
17. Marzolini, C.; Telenti, A.; Buclin, T.; Biollaz, J.; Decosterd, L.A. Simultaneous determination of the HIV protease inhibitors indinavir, amprenavir, saquinavir, ritonavir, nelfinavir and the non-nucleoside reverse transcriptase inhibitor efavirenz by high-performance liquid chromatography after solid-phase extraction. J. Chromatogr. B, **2000**, *740* (1), 43–58.
18. Marsh, K.C.; Eiden, E.; McDonald, E. Determination of ritonavir, a new HIV protease inhibitor, in biological samples using reversed-phase high-performance liquid chromatography. J. Chromatogr. B, **1997**, *704* (1+2), 307–313.
19. Jing, Q.; Shen, Y.; Tang, Y.; Ren, F.; Yu, X.; Hou, Z. Determination of nelfinavir mesylate as bulk drug and in pharmaceutical dosage form by stability indicating HPLC. J. Pharm. Biomed. Anal. **2006**, *41* (3), 1065–1069.
20. Colombo, S.; Beguin, A.; Marzolini, C.; Telenti, A.; Biollaz, J.; Decosterd, L.A. Determination of the novel non-peptidic HIV-protease inhibitor tipranavir by HPLC-UV after solid-phase extraction. J. Chromatogr. B, **2006**, *832* (1), 138–143.
21. D'Avolio, A.; Sciandra, M.; de Requena, D.G.; Ibanez, A.; Bonora, S.; Di Perri, G. An improved HPLC fluorimetric method for the determination of enfuvirtide plasma levels in HIV-infected patients. Ther. Drug Mon. **2006**, *28* (1), 110–115.
22. Turner, M.L.; Reed-Walker, K.; King, J.R.; Acosta, E.P. Simultaneous determination of nine antiretroviral compounds in human plasma using liquid chromatography. J. Chromatogr. B, **2003**, *784* (2), 331–341.
23. Notari, S.; Bocedi, A.; Ippolito, G.; Narciso, P.; Pucillo, L.P.; Tossini, G.; Donnorso, R.P.; Gasparrini, F.; Ascenzi, P. Simultaneous determination of 16 anti-HIV drugs in human plasma by high-performance liquid chromatography. J. Chromatogr. B, **2006**, *831* (1–2), 258–266.

Anti-Tuberculosis Drugs

Melgardt M. de Villiers
School of Pharmacy, University of Wisconsin, Madison, Wisconsin, U.S.A.

INTRODUCTION

The four drugs commonly used to treat tuberculosis are rifampin, isoniazid, pyrazinamide, and ethambutol hydrochloride (Fig. 1).[1] Although the drugs are used alone, the WHO recommends the four-drug fixed-dose combination (4FDC) tablet containing rifampicin 150 mg, isoniazid 75 mg, pyrazinamide 400 mg, and ethambutol (hydrochloride) 275 mg, as well as 3FDC (rifampin, isoniazid, and pyrazinamide) and 2FDC combination tablets for treating drug-resistant tuberculosis.[2,3] The combination of all four drugs in one tablet simplifies the treatment and management of drug supply, and may prevent the emergence of drug resistance.[3,4]

The official methods used to analyze these drugs alone or in drug products are published in several pharmacopoeias[5,8,9] and starting with the USP 25 onwards not only monographs for the individual drugs but also the fixed-dose combination products including the 4FDC tablets have been established, which require high-performance liquid chromatography (HPLC) for analysis of the drug substances to establish purity and also to measure the drugs in dissolution samples.[5] Similar HPLC methods are also used to measure the drugs in the fixed dose combination (FDC) products during stability testing and to monitor plasma concentrations of the drugs in biological fluids.[7,9–11]

In this report, the major chromatographic methods used for the analysis of anti-tuberculosis drugs, alone or in combination, in pharmaceutical products and biological fluids are summarized.

RIFAMPIN

The USP states that rifampin raw material contains not less than 95.0% and not more than 103.0% of $C_{43}H_{58}N_4O_{12}$, calculated on the dried basis.[5] When formulated into capsules and suspensions, it must contain not less than 90.0% and not more than 110.0% of the labeled amount, injections between 90.0% and 115%, FDC products containing isoniazid between 90% and 130%, and 3FDC and 4FDC products between 90.0% and 110.0%. The higher maximum concentration allowed when combined with isoniazid is because when present together rifampin and isoniazid (H) interact with each other, especially when moisture is present, to form isonicotinyl hydrazone.[12] This reduces the bioavailability of rifampin in an FDC combination product containing isoniazid. Therefore, accurate analysis of rifampin in the presence of isoniazid is very important.

According to the USP for the HPLC analysis of rifampin, the liquid chromatograph must be equipped with a 254 nm detector and a 4.6 mm × 10 cm column that contains 5 μm totally porous silica particles with chemically bonded octylsilane (C_8, L7).[5] The flow rate is about 1.5 ml/min. The mobile phase is a suitable mixture of water, acetonitrile, phosphate buffer (136.1 g of monobasic potassium phosphate in about 500 ml of water, to which 6.3 ml of phosphoric acid is added, before it is diluted with water to 1000 ml), 1.0 *M* citric acid, and 0.5 *M* sodium perchlorate (510 : 350 : 100 : 20 : 20), which is filtered through a suitable filter of 0.7 μm or finer porosity, and then degassed. Separately inject equal volumes (about 50 μl) of the rifampin standard solutions and assay preparations into the chromatograph, record the chromatograms, and measure the area responses for the major peaks. The relative retention times are about 0.6 for rifampin quinone (main degradation product) and 1.0 for rifampin. The quantity, in mg, of rifampin ($C_{43}H_{58}N_4O_{12}$) in the standard sample solutions are calculated on the dried basis, of rifampin in the standard preparation, using the area responses of the rifampin peaks obtained from the assay preparation and the standard preparation, respectively.[5] The resolution, *R*, between the rifampin quinone and rifampin peaks is not less than 4.0. The column efficiency determined from the rifampin peak is not less than 1000 theoretical plates, and the relative standard deviation for replicate injections is not more than 1.0%. Samples should be preserved in tight, light-resistant containers, protected from excessive heat. Stock solutions of reference standards should be used within 5 hr of preparation, while stock test solutions should be used within 2 hr. Final dilutions should be prepared immediately prior to injection into the chromatograph. The USP also requires a related substances test for rifampin where a test and diluted test preparation are injected into the chromatograph, the chromatograms recorded, and the responses for all of the peaks measured.[5] Then, the percentage of each related substance is calculated by the formula:

$$r_{Ti}/(r_D + 0.01\Sigma r_{Ti})$$

in which r_{Ti} is the area of the peak of the individual related substance in the chromatogram obtained from the test

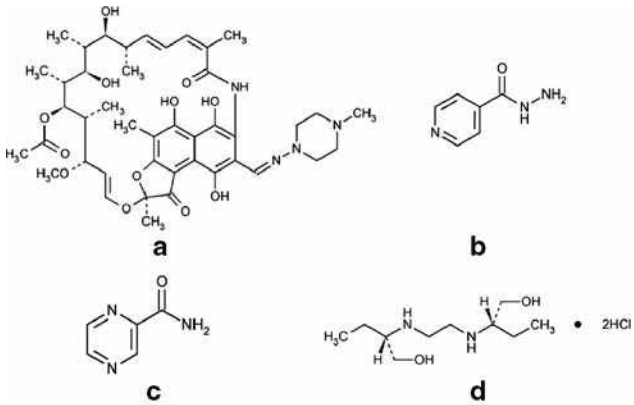

Fig. 1 (a) Rifampin (Rifamycin, 3-[[(4-methyl-1-piperazinyl)-imino]methyl]-, 5,6,9,17,19,21-Hexahydroxy-23-methoxy-2,4,12,16,18,20,22-heptamethyl-8-[*N*-(4-methyl-1-piperazinyl)formimidoyl]-2,7-(epoxypentadeca[1,11,13]trienimino)naphtho[2,1-*b*]furan-1,11-(2*H*)-dione 21-acetate, [*13292-46-1*]). $C_{43}H_{58}N_4O_{12}$, MW = 822.94. (b) Isoniazid (4-Pyridinecarboxylic acid, hydrazide, isonicotinic acid hydrazide, [54-85-3]). $C_6H_7N_3O$, MW = 137.14. (c) Pyrazinamide (Pyrazinecarboxamide, Pyrazinecarboxamide, [*98-96-4*]). $C_5H_5N_3O$, MW = 123.11. (d) Ethambutol hydrochloride (1-Butanol, 2,2′-(1,2-ethanediyldiimino)bis-, dihydrochloride, [*S*-(*R**,*R**)]-, (+)-2,2′-(Ethylenediimino)-di-1-butanol dihydrochloride, [*1070-11-7*]. $C_{10}H_{24}N_2O_2{\cdot}2HCl$, MW = 277.23.

preparation, r_D is the area of the rifampin peak in the chromatogram obtained from the dilute test preparation, and Σr_{Ti} is the sum of the areas of all of the peaks of the related substances obtained in the chromatogram of the test preparation. To comply, not more than 1.5% of rifampin quinone and not more than 1.0% of any other individual related substance can be present. In total, not more than 3.5% of all individual related substances, other than rifampin quinone, having retention times of up to 3 in relation to the retention time of rifampin can be present.

ISONIAZID

According to the USP, isoniazid contains not less than 98.0% and not more than 102.0% of $C_6H_7N_3O$, calculated on the dried basis.[5] Injections and tablets must contain between 90.0% and 110.0% of the drug while isoniazid syrups must contain in each 100 ml, not less than 0.93 g and not more than 1.10 g of isoniazid ($C_6H_7N_3O$). To determine this, a liquid chromatograph equipped with a 254 nm detector and a 4.6 mm × 25 cm column packed with porous silica or ceramic microparticles, 3–10 mm in diameter, chemically bonded to octadecyl silane (C_{18}, L1) is used. The mobile phase is made up by dissolving 4.4 g of docusate sodium in 600 ml of methanol, adding 400 ml of water, and adjusting the pH to 2.5 with 2 N sulfuric acid. The flow rate is about 1.5 ml/min. For the assay, separately inject equal volumes (about 10 μl) of the standard preparations and the assay preparations into the chromatograph, record the chromatograms, and measure the responses for the major peaks. The quantity, in mg, of $C_6H_7N_3O$ is then calculated from the peak responses of isoniazid obtained from the assay preparation and the standard preparation, respectively.[5] For this method to be accurate, the column efficiency determined from the isoniazid peak must not be less than 1800 theoretical plates; the tailing factor for the isoniazid peak not more than 2.0; and the relative standard deviation for replicate injections not more than 2.0%. For isoniazid tablets, most pharmacopoeias also require a content uniformity test.[5–7] Although this test requires the use of a spectrophotometer with absorbance at 263 nm, the accuracy of the test can be improved by using the HPLC method. Isoniazid powder and solutions of the drug must be preserved in tight, light-resistant containers and should be stored at 25°C, with excursions permitted between 15°C and 30°C.

PYRAZINAMIDE

According to the USP, pyrazinamide powder contains not less than 99.0% and not more than 101.0% of $C_5H_5N_3O$, calculated on the anhydrous basis.[5] This is determined using a titration method. This is a tedious and difficult method to perform accurately for the drug in products owing to the interference of excipients. Therefore, the assay method of pyrazinamide in tablets requires HPLC analysis to ensure that these tablets contain not less than 93.0% and not more than 107.0% of the labeled amount of pyrazinamide ($C_5H_5N_3O$).

This method requires using a liquid chromatograph equipped with a 270 nm detector and a 3.9 mm × 15 cm C_{18} column, a filtered and degassed mobile phase composed of 10 ml acetonitrile mixed with 1 L of a pH 8.0 phosphate buffer adjusted with phosphoric acid to a pH of 3.0, and a flow rate should be about 1 ml/min.[5] Separately inject equal volumes (about 20 μl) of standard and test solutions into the chromatograph, record the chromatograms, and measure the responses for the major peaks. Then calculate the quantity, in mg, of pyrazinamide ($C_5H_5N_3O$) in the tablets using the peak responses obtained from the test and the standard solutions, respectively. The column efficiency is not less than 2500 theoretical plates; and the tailing factor for the pyrazinamide peak is not more than 1.3. To determine the stability of pyrazinamide in a product, a system suitability test on a cooled solution prepared by transferring 1 ml of hydrochloric acid to a 5 ml volumetric flask, diluting with a standard solution, and then keeping it on a boiling water bath for 5 min, can be performed. The system suitability solution is chromatographed and the peak responses recorded. To comply, the relative retention times are about 0.45 for pyrazinoic acid

and 1.0 for pyrazinamide; and the resolution, *R*, between pyrazinamide and pyrazinoic acid is not less than 6.0.

ETHAMBUTOL HCL

Most pharmacopoeias specify that ethambutol hydrochloride contains not less than 98.0% and not more than 100.5% of $C_{10}H_{24}N_2O_2 \cdot 2HCl$, calculated on the dried basis. Pharmaceutical products such as tablets must contain not less than 95.0% and not more than 105.0% of the labeled amount.[5–7] As for pyrazinamide, the main pharmacopoeial assay method for ethambutol is a titration method.[5] However, an HPLC method is used for the assay of ethambutol HCl in tablets.[5] This method requires that a liquid chromatograph equipped with a 200-nm detector and a 4.6 mm × 15 cm base-deactivated column that contains 5 μm porous silica particles, 3–10 μm in diameter, with chemically bonded nitrile groups (CN, L10) is used. The mobile phase is a mixture of 1.0 ml of triethylamine and 1 L of water, adjusted with phosphoric acid to a pH of 7.0. The flow rate is about 1.0 ml/min. Separately inject equal volumes (about 50 μl) of standard preparations and the assay preparations into the chromatograph, record the chromatograms, and measure the responses for the major peaks and calculate the quantity, in mg, of ethambutol hydrochloride present in the tablets from the peak responses obtained from the assay preparation and the standard preparation, respectively. The tailing factor must not be more than 2.0, and the relative standard deviation for replicate injections not more than 2.0%.

The international pharmacopoeia recently also published an HPLC assay for ethambutol combined with isoniazid and pyrazinamide using a stainless steel C_{18} column (15 cm × 4.6 mm).[7] The mobile phase for this method is a solution prepared as follows: dissolve 50 g ammonium acetate and 0.2 g copper(II) acetate in 1000 ml of water and adjusted to pH 5.0 with glacial acetic acid. 940 ml of this solution is mixed with 60 ml methanol. The HPLC is operated at a flow rate of 2.0 ml/min. The detector is an ultraviolet spectrophotometer set at a wavelength of about 270 nm and 20 μl of the solutions are injected. The assay is not valid unless the resolution between the isoniazid peak (the peak with the shorter retention time) and the ethambutol hydrochloride peak is at least 10 (see Fig. 2) and the resolution between the isoniazid and pyrazinamide peaks is at least 2. The relative standard deviation for the peak areas of isoniazid, pyrazinamide, and ethambutol hydrochloride, eluting in this order, is less than 2.0%.

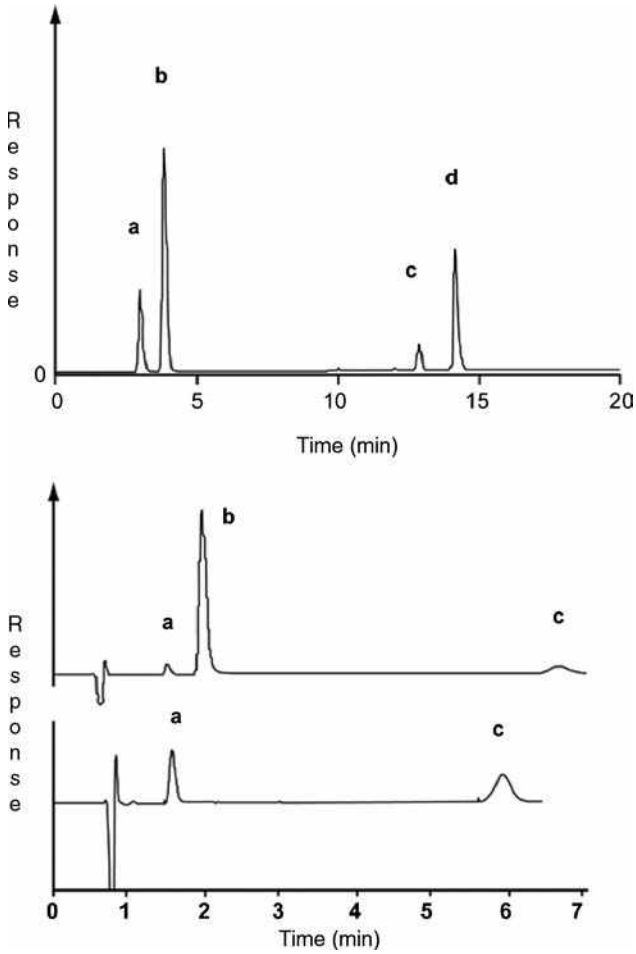

Fig. 2 Top: USP HPLC analysis of a 4FDC tablet showing the chromatograms of a, isoniazid; b, pyrazinamide; c, isonicotinyl hydrazone of 3-formylrifamycin; d, rifampin. Bottom: chromatogram of a, isoniazid, b, pyrazinamide, and c, ethambutol HCl. Adapted from United States Pharmacopeial Convention,[5] WHO,[7] and Lacroix et al.[13]

2FDC PRODUCTS—RIFAMPIN AND ISONIAZID

Most pharmacopoeias require that 2FDC products that contain at least 300 mg of rifampin and 150 mg of isoniazid shall not contain less than 90.0% and not more than 130.0% of the labeled amount of rifampin ($C_{43}H_{58}N_4O_{12}$) and not less than 90.0% and not more than 110.0% of the labeled amount of isoniazid ($C_6H_7N_3O$).[5,6] To ensure stability, these products must be preserved in tight, light-resistant containers, and avoid exposure to excessive heat.

A quick TLC identification test for the drugs in these products require that a portion of the content of a capsule tablet, equivalent to about 120 mg of rifampin, is transferred to a suitable flask, 20 ml of methanol added, and shaking for several minutes.[5] The suspension is passed through a filter having a 1 μm or finer porosity, discarding the first few ml of the filtrate. Then a volume of the filtrate is diluted with an equal volume of acetone, and mixed. A standard solution is prepared by dissolving a quantity of rifampin reference standard in methanol to obtain a

solution containing 6 mg/ml. Add an equal volume of acetone, and mix. Similarly, dissolve a quantity of isoniazid reference standard in methanol to obtain a solution containing 2.5 mg/ml. Add an equal volume of acetone, and mix. Apply 2 μl of the test solution and each of the relevant standard solutions to a suitable thin-layer chromatographic plate coated with a 0.25 mm layer of chromatographic silica gel. Place the plate in a presaturated chromatographic chamber containing the developing solvent solution (a mixture of acetone and glacial acetic acid, 100 : 1) and develop the chromatogram until the solvent front has moved about three-fourths of the length of the plate. Remove the plate from the developing chamber, mark the solvent front, and allow the solvent to evaporate. Locate the spots on the plate by examination under short-wavelength UV light. The R_f value of each principal spot in the chromatogram of the test solution corresponds to that of the principal spot in the chromatogram obtained from each relevant standard solution as appropriate for the labeled active ingredient.

The drugs in this combination product can also be assayed using an HPLC equipped with a 238 nm detector and a 4.6 mm × 25 cm base-deactivated C_{18} column with 5 μm packing. The flow rate is about 1.5 ml/min. The mobile phase consists of variable mixtures (see Table 1) of two solutions. Solution A: a filtered and degassed mixture of buffer solution and acetonitrile (96 : 4). The buffer solution is prepared by dissolving 1.4 g of dibasic sodium phosphate in 1 L of water, and adjusting with phosphoric acid to a pH of 6.8. Solution B: a filtered and degassed mixture of acetonitrile and the buffer solution (55 : 45). Standard solutions are prepared in a mixture of the buffer solution and methanol (96 : 4) so that the solutions contain rifampin and isoniazid reference standards in known concentrations of about 0.16 and 0.08 mg/ml, respectively. Assay preparations are prepared by taking the contents of not fewer than 10 capsules or tablets, mixing it, and transferring an accurately weighed portion of the powder, equivalent to about 16 mg rifampin and 8 mg of isoniazid, to a 100 ml volumetric flask, adding about 90 ml of the buffer solution, sonicating the solution for about 10 min, allowing it to equilibrate to room temperature, diluting it with buffer solution to volume and then analyzing it. These solutions must be used within 2 hr.[5]

Table 1 Conditions for the programmed change in mobile phase composition for the gradient elution of rifampin and isoniazid at a flow rate of about 1.5 ml/min.

Time (min)	Solution A	Solution B	Elution
0	100	0	Equilibration
0–5	100	0	Isocratic
5–6	100 → 0	0 → 100	Linear gradient
6–15	0	100	Isocratic

Source: From United States Pharmacopeial Convention, Rockville.[5]

For the actual HPLC assay, equal volumes (about 20 μl) of the standard preparations and the assay preparations are injected into the chromatograph, the chromatograms recorded, and the peak responses measured. From the peak responses of the standard versus the assay preparations, the quantity, in mg, of rifampin ($C_{43}H_{58}N_4O_{12}$) and isoniazid ($C_6H_7N_3O$) in the product is calculated. If the assay is performed correctly, the relative retention times are about 2.6 and 1.0 for rifampin and isoniazid, respectively; the column efficiency is not less than 50,000 and not less than 6000 theoretical plates for rifampin and isoniazid, respectively; the tailing factors are not more than 2.0; and the relative standard deviation for replicate injections is not more than 2.0%.

During dissolution testing, the amount of rifampin ($C_{43}H_{58}N_4O_{12}$) dissolved is determined from absorbances at the wavelength of maximum absorbance at about 475 nm of standard and test solutions. However, the amount of isoniazid ($C_6H_7N_3O$) dissolved is measured by HPLC. The liquid chromatograph is equipped with a 254 nm detector and a 4.0 mm × 30 cm C_{18} column (10 μm packing) and the flow rate is about 1.5 ml/min. The mobile phase is a filtered and degassed mixture of water, phosphate buffer solution, and methanol (850 : 100 : 50). Equal volumes (about 50 μl) of standard solutions and test solutions are injected into the chromatograph, the chromatograms recorded, and the responses for the isoniazid peaks measured. The capsules or tablets comply with the dissolution specification if not less than 75% (Q) of the labeled amount of rifampin and not less than 80% (Q) of the labeled amount of isoniazid are dissolved in 45 min.

3FDC PRODUCTS—RIFAMPIN, ISONIAZID, AND PYRAZINAMIDE

Rifampin, isoniazid, and pyrazinamide tablets combination products are available as tablets or capsules that must contain not less than 90.0% and not more than 110.0% of the labeled amounts of rifampin ($C_{43}H_{58}N_4O_{12}$), isoniazid ($C_6H_7N_3O$), and pyrazinamide ($C_5H_5N_3O$).[5–7] To maintain this stability, the products and raw materials must be preserved in tight, light-resistant containers at controlled room temperature. The TLC identification test for 3FDC products is similar as that for 2FDC combinations. For these products, the spots in the chromatograms of test solutions are compared with those of standard solutions of the three drugs.

The HPLC method used to assay the 2FDC products is also used for determining the drug content of 3FDC products.[5] Standard solutions are prepared by dissolving accurately weighed quantities of rifampin, isoniazid, and pyrazinamide reference standards in a mixture of buffer solution and methanol (96 : 4) to obtain a solution having known concentrations of about 0.16, 0.08, and 0.43 mg/ml, respectively. These solutions should be used within 10 min. The test solutions are prepared by weighing and

finely powdering not fewer than 20 tablets. Transfer an accurately weighed quantity of the powder, equivalent to about 8 mg of isoniazid, to a 100 ml volumetric flask, and add about 90 ml of buffer solution, sonicate for about 10 min, allow to equilibrate to room temperature, dilute with the buffer solution to volume, and mix. These solutions must be used within 2 hr.[5] Then separately inject equal volumes (about 20 μl) of the standard and test solutions into the chromatograph, record the chromatograms, and measure the peak responses. Calculate the quantities, in mg, of rifampin ($C_{43}H_{58}N_4O_{12}$), isoniazid ($C_6H_7N_3O$), and pyrazinamide ($C_5H_5N_3O$) in the product from the differences in the peak responses obtained from the standard and test solutions, respectively (see Fig. 2). The method complies to pharmacopoeial standards if the relative retention times are about 1.8, 0.7, and 1.0 for rifampin, isoniazid, and pyrazinamide, respectively; the resolution, *R*, between isoniazid and pyrazinamide is not less than 4; the column efficiency is not less than 50,000, not less than 6,000, and not less than 10,000 theoretical plates for rifampin, isoniazid, and pyrazinamide, respectively; the tailing factor is not more than 2.0; and the relative standard deviation for replicate injections is not more than 2.0%.[5–7]

In test solutions obtained during dissolution testing, the amount of rifampin present is determined spectrophotometrically at 475 nm. This method corresponds with that for rifampin in 2FDC products. The tablets comply with the dissolution specification if not less than 80% (*Q*) of the labeled amount of rifampin ($C_{43}H_{58}N_4O_{12}$) is dissolved in 30 min.[5] The amounts of isoniazid and pyrazinamide in dissolution test samples are determined by HPLC. This is done by preparing a filtered and degassed mobile phase composed of a mixture of water, 1 *M* monobasic potassium phosphate, and acetonitrile (860 : 100 : 40). This mobile phase is pumped at a flow rate of 1 ml/min on a liquid chromatograph that is equipped with a 254 nm detector and a 4.6 mm × 30 cm column that contains a multifunctional support, which consists of a high purity, 60 Å, spherical silica substrate that has been bonded with a cationic exchanger, sulfonic acid functionality in addition to a conventional reversed phase C_8 functionality (L44). Prior to the analysis of dissolution test samples, a system suitability test must be performed using a system suitability solution. This is a solution prepared by transferring 10 ml of a 0.125 mg/ml isonicotinic acid in the dissolution medium and 4 ml of the standard stock solution to a 100 ml volumetric flask containing 15 ml of 1 *M* dibasic potassium phosphate, which is then diluted with mobile phase to volume.[5]

Chromatograph this system suitability solution, the standard solutions, and dissolution test samples by separately injecting equal volumes (about 50 μl) of the solutions into the chromatograph, record the chromatograms, and measure the areas for the major peaks. For the system suitability solution, the relative retention times are about 0.7 for isonicotinic acid, 1.0 for pyrazinamide, and 1.8 for isoniazid; and the resolution, *R*, between isonicotinic acid and pyrazinamide is not less than 2.5 and between pyrazinamide and isoniazid not less than 4.0. In addition, the relative standard deviations determined from the pyrazinamide and isoniazid responses in all the solutions for replicate injections are not more than 1.5%. For 3FDC products to satisfy the dissolution criteria not less than 80% (*Q*) of the labeled amount of isoniazid ($C_6H_7N_3O$) and not less than 75% of the labeled amount of pyrazinamide ($C_5H_5N_3O$) are dissolved in 30 min.

4FDC PRODUCTS—RIFAMPIN, ISONIAZID, PYRAZINAMIDE, AND ETHAMBUTOL HCL

These products contain rifampin, isoniazid, pyrazinamide, and ethambutol hydrochloride in a single dosage form such as tablets or capsules. Such a product must contain not less than 90.0% and not more than 110.0% of the labeled amounts of rifampin ($C_{43}H_{58}N_4O_{12}$), isoniazid ($C_6H_7N_3O$), pyrazinamide ($C_5H_5N_3O$), and ethambutol hydrochloride ($C_{10}H_{24}N_2O_2 \cdot 2HCl$).[5] The products and raw materials must be preserved in tight, light-resistant containers, and stored at controlled room temperature. For the identification of rifampin, isoniazid, and pyrazinamide in these products, the same TLC method as for 3FDC products are used. While for ethambutol, the WHO prescribes the following semi-quantitative TLC method. TLC aluminum sheets precoated with silica gel 60 F254 are spotted with methanol solutions containing ethambutol, together with different mixtures of combinations of ethambutol hydrochloride, isoniazid, pyrazinamide, and rifampicin, 1.5 cm from the bottom of silica plates with a 3 μl capillary pipette. The plates are developed in a development chamber previously saturated with a freshly prepared mixture of methanol and concentrated ammonium hydroxide, the plates are then placed in the development chamber together with an iodine–potassium iodide solution, allowed to dry and the size and intensity of the spots measured and R_f values calculated. The R_f value of ethambutol hydrochloride is about 0.15.

The USP method to assay the ingredients in 4FDC products utilizes two HPLC methods.[5] The first is the method used for 3FDC products to determine the amounts of rifampin, isoniazid, and pyrazinamide described above and the second is a method to assay ethambutol HCl in tablets described earlier (Fig. 2). The analysis method for ethambutol complies with pharmacopoeial standards if the tailing factor is not more than 3; and the relative standard deviation for replicate injections is not more than 2.0%.[5] For ethambutol, in addition to the HPLC analysis, a flourometric test for aminobutanol is also required. This method determines the relative fluorescence intensities of test and standard solutions in 1 cm cells, with a suitable fluorometer, at about 485 nm, with the excitation wavelength at about 385 nm. The fluorescence intensity of the solution obtained from the test solution is not greater than the difference between the intensities of the two solutions (not

more than 1.0%). As mentioned under the subheading for ethambutol HCl in the International Pharmacopoeia, another HPLC method for isoniazid, pyrazinamide, and ethambutol HCl in 4FDC products is described (see Fig. 2).[7]

For dissolution samples, the amounts of rifampin ($C_{43}H_{58}N_4O_{12}$), isoniazid ($C_6H_7N_3O$), pyrazinamide ($C_5H_5N_3O$), and ethambutol hydrochloride ($C_{10}H_{24}N_2O_2{\cdot}2HCl$) dissolved in filtered portions of the solution under test are determined using the same procedures set forth in the HPLC assay for rifampin, isoniazid, and pyrazinamide and the assay for ethambutol hydrochloride described above.[5] The 4FDC tablet or capsule complies with the dissolution specification if not less than 75% (Q) of the labeled amounts of $C_{43}H_{58}N_4O_{12}$, $C_6H_7N_3O$, $C_5H_5N_3O$, and $C_{10}H_{24}N_2O_2{\cdot}2HCl$ is dissolved in 45 min.

CONCLUSION

The treatment of tuberculosis still largely relies on the use of rifampin, isoniazid, pyrazinamide, and ethambutol HCl. Although the chromatographic analysis of these drugs is well established, the recently notified USP gradient HPLC method for quantitative determination of rifampicin, isoniazid, and pyrazinamide in fixed-dose combination (FDC) formulations has enhanced our analytical capability to ensure the quality of these products.

However, this method is still being evaluated to determine its ability to resolve major degradation products of rifampicin, viz. 3-formylrifamycin, rifampicin *N*-oxide, 25-desacetyl rifampicin, rifampicin quinone, and the newly reported isonicotinyl hydrazone, an interaction product of 3-formylrifamycin and isoniazid, first observations show that although the requirements of theoretical plates listed in the given method are not always met and although the resolving power of the method was sometimes dependent on the make of the column used, this method gave reliable results when small modifications were made to the buffer: organic modifier ratio of solution B or the flow rate was decreased.[14]

Together with the HPLC method published by the WHO for isoniazid, pyrazinamide, and ethambutol HCl in 4FDC products, these methods provide the ability to assay these drugs in almost any pharmaceutical or biological matrix. This means that for the major drugs used for treating tuberculosis, well-established chromatographic methods, approved by the major regulatory agencies, exist. It also shows that chromatographic, especially HPLC, methods are favored for the analysis of anti-tuberculosis drugs in both pharmaceutical products and biological fluids because of their proven reliability and ease of use.[15]

REFERENCES

1. Enarson, D.A. Conquering tuberculosis: Dream or reality? Int. J. Tuberc. Lung Dis. **2002**, *6*, 369–370.
2. World Health Organization, The use of essential drugs. Ninth report of the WHO Expert Committee (including the revised Model List of Essential Drugs). WHO Technical Report Series No. 895 WHO: Geneva, 2000.
3. Stop, T.B.; World Health Organization, Frequently asked questions about the 4-drug fixed-dose combination tablet recommended by the World Health Organization for treating tuberculosis. WHO/CDS/STB/2002.18 WHO: Geneva, September 2002.
4. Blomberg, B.; Spinaci, S.; Fourie, B.; Laing, R. The rationale for recommending fixed-dose combination tablets for treatment of tuberculosis. Bull. World Health Organ. **2001**, *79* (1), 61–68.
5. United States Pharmacopeial Convention; The United States Pharmacopeia: Rockville, MD, 2001; Vol. 25, 1534–1535.
6. European Pharmacopoeia, EP5th; European Pharmacopoeia Commission, EDQM: Strasbourg, France 2005.
7. WHO. International pharmacopoeia monograph on rifampicin, isoniazid, pyrazinamide and ethambutol hydrochloride tablets. Working document QAS/04.097 rev Oct 05. Quality Assurance & Safety: Medicines (QSM), Department of Essential Drugs and Medicines Policy (EDM). WHO: Geneva, October, 2005.
8. Unsalan, S.; Sancar, M.; Bekce, B.; Clark, P.M.; Karagoz, T.; Izzettin, F.V.; Rollas, S. Therapeutic monitoring of isoniazid, pyrazinamide and rifampicin in tuberculosis patients using LC. Chromatographia **2005**, *61* (11–12), 595–598.
9. Agrawal, S.; Panchagnula, R. In vitro evaluation of fixed dose combination tablets of anti-tuberculosis drugs after real time storage at ambient conditions. Pharmazie **2004**, *59* (10), 782–785.
10. Espinosa-Mansilla, A.; Acedo-Valenzuela, M.I.; Munoz-de-la-Pena, A.; Canada, F.C.; Salinas-Lopez, F. Determination of antitubercular drugs in urine and pharmaceuticals by LC using a gradient flow combined with programmed diode-array photometric detection. Talanta **2002**, *58* (2), 273–280.
11. Zhen, Q.P.; Chen, P.; Fen, J.L.; Lai, T.B. High-performance liquid-chromatographic determination of anti-tuberculosis drugs in human body fluids. J. Liq. Chromatogr. Relat. Technol. **1997**, *20* (3), 459–469.
12. Mariappan, T.T.; Jindal, K.C.; Singh, S. Overestimation of rifampicin during colorimetric analysis of anti-tuberculosis products containing isoniazid due to formation of isonicotinyl hydrazone. J. Pharm. Biomed. Anal. **2004**, *36* (4), 905–908.
13. Lacroix, C.; Cerutti, F.; Nouveau, J.; Menager, S.; Lafont, O. Determination of ethambutol in plasma by liquid chromatography and ultra-violet spectrophotometric detection. J. Chrom. B: Biomed. Appl. **1987**, *59* (1), 85–94.
14. Mohan, B; Sharda, N.; Singh, S. Evaluation of the recently reported USP gradient HPLC method for analysis of anti-tuberculosis drugs for its ability to resolve degradation products of rifampicin. J. Pharm. Biomed. Anal. **2003**, *31* (3), 607–612.
15. Singh, S.; Mohan, B. A pilot stability study on four-drug fixed-dose combination anti-tuberculosis products. Int. J. Tuberc. Lung Dis. **2003**, *7* (3), 298–303.

Applied Voltage: Mobility, Selectivity, and Resolution in CE

Jetse C. Reijenga
Department of Chemical Engineering and Chemistry, Eindhoven University of Technology, Eindhoven, The Netherlands

INTRODUCTION

Generally, migration times t_m in capillary electrophoresis (CE) are inversely proportional to the applied voltage.

DISCUSSION

In terms of analysis time, the voltage should, therefore, be as large as possible:

$$t_m \cong \frac{1}{V}$$

Under conditions optimized for limited power dissipation, effective mobilities and selectivities (defined as effective mobility ratios) are independent of the applied voltage.

Efficiency is also determined by the applied voltage, but in a much more complicated manner (see *Band Broadening in CE*, p. 144). If efficiency is limited by diffusion, a higher voltage also leads to a higher efficiency. Limitations are due to insulation properties and heat dissipation. Voltages larger than 30 kV should always be avoided because of danger of sparking and leaking currents, even more so in cases of significant atmospheric humidity. Excessive heat dissipation leads to an average temperature increase inside the capillary, which can be reduced by forced cooling. What cannot be reduced is the contribution of heat dissipation to band broadening. This can only be reduced by a lower conductivity, a lower current density, or a smaller inner diameter (see *Band Broadening in CE*, p. 144). In the case of diffusion-limited efficiency, the efficiency (as given by the plate number) is directly proportional to the applied voltage:

$$N \cong V$$

The ultimate criterion for quality of separation is the resolution R, given by the following relationship:

$$R = \frac{\Delta t_m}{4\sigma}$$

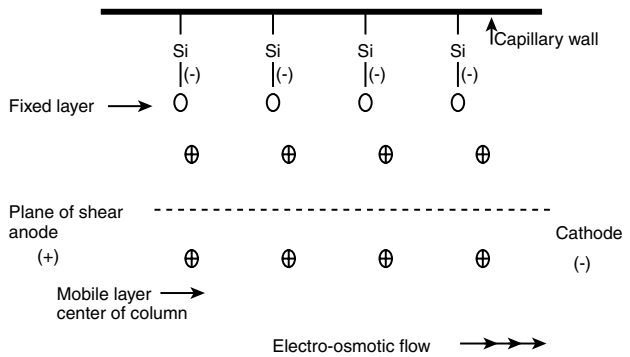

Fig. 1 Analysis of a mixture of weak anions at three different voltages. Suppressed EOF in a 400 mm capillary with negative inlet polarity. *Note*: The time axis is logarithmic.

With the definition of plate number, it follows that $R \cong \sqrt{V}$.

Fig. 1 shows a computer simulation of the resolution and analysis time of a mixture of anions at 5, 10 and 25 kV. In order to better visualize the effect on resolution, a logarithmic x axis was chosen.

BIBLIOGRAPHY

1. Hjertén, S. Free zone electrophoresis. Chromatogr. Rev. **1967**, *9* (2), 122. Publication Types Review MeSH Terms Blood Protein Electrophoresis.
2. Jorgenson, J.W.; Lucaks, K.D. Capillary zone electrophoresis. Science **1983**, *222*, 266.
3. Li, S.F.Y. In *Capillary Electrophoresis—Principles, Practice and Applications*; Elsevier: Amsterdam, 1992.
4. Reijenga, J.C.; Kenndler, E. Computational simulation of migration and dispersion in free capillary zone electrophoresis, part I, Description of the theoretical model. J. Chromatogr. A, **1994**, *659* (2), 403.
5. Reijenga, J.C.; Kenndler, E. Computational simulation of migration and dispersion in free capillary zone electrophoresis, part II, Results of simulation and comparison with measurements. J. Chromatogr. A, **1994**, *659* (2), 417.

Argon Detector

Raymond P.W. Scott
Scientific Detectors Ltd., Banbury, Oxfordshire, U.K.

INTRODUCTION

The argon detector was the first of a family of detectors developed by Lovelock[1] in the late 1950s; its function is quite unique. The outer octet of electrons in the noble gases is complete and, as a consequence, collisions between argon atoms and electrons are perfectly elastic. Thus, if a high potential is set up between two electrodes in argon and ionization is initiated by a suitable radioactive source, electrons will be accelerated toward the anode and will not be impeded by energy absorbed from collisions with argon atoms. However, if the potential of the anode is high enough, the electrons will eventually develop sufficient kinetic energy that, on collision with an argon atom, energy can be absorbed and a *metastable* atom can be produced. A metastable atom carries *no* charge but adsorbs its energy from collision with a high-energy electron by the displacement of an electron to an outer orbit. This gives the metastable atom an energy of about 11.6 electron volts. Now 11.6 V is sufficient to ionize most organic molecules. Hence, collision between a metastable argon atom and an organic molecule will result in the outer electron of the metastable atom collapsing back to its original orbit, followed by the expulsion of an electron from the organic molecule. The electrons produced by this process are collected at the anode, generating a large increase in anode current. However, when an ion is produced by collision between a metastable atom and an organic molecule, the electron, simultaneously produced, is immediately accelerated toward the anode. This results in a further increase in metastable atoms and a consequent increase in the ionization of the organic molecules. This cascade effect, unless controlled, results in an exponential increase in ion current with solute concentration.

The relationship between the ionization current and the concentration of vapor was deduced by Lovelock[2,3] to be

$$I = \frac{CA(x + y) + Bx}{CA\{1 - a\exp[b(V - 1)]\} + B}$$

where A, B, a, and b are constants, V is the applied potential, x is the primary electron concentration, and y is the initial concentration of metastable atoms. The rapid increase in current with increasing vapor concentration, as predicted by the equation, is controlled by the use of a high impedance in series with detector power supply. As the current increases, more volts are dropped across the resistance, and less are applied to the detector electrodes.

THE SIMPLE OR MACRO ARGON DETECTOR SENSOR

A diagram of the macro argon detector sensor is shown in Fig. 1. The cylindrical body is usually made of stainless steel and the insulator made of polytetrafluoroethylene (PTFE) or for high-temperature operation, a suitable ceramic. The very first argon detector sensors used a tractor sparking plug as the electrode, the ceramic seal being a very efficient insulator at high temperatures.

Inside the main cavity of the original sensor was a strontium-90 source contained in silver foil. The surface layer on the foil that contained the radioactive material had to be very thin or the β particles would not be able to leave the surface. This tenuous layer protecting the radioactive material is rather vulnerable to mechanical abrasion, which could result in radioactive contamination (strontium-90 has now been replaced by ^{63}Ni). The radioactive strength of the source was about 10 mCu which for strontium-90 can be considered a *hot* source. The source had to be inserted under properly protected conditions. The decay of strontium-90 occurs in two stages, each stage emitting a β particle producing the stable atom of zirconium-90:

$$\underset{\text{half-life 25 year}}{^{90}\text{Sr}} \xrightarrow[0.6\ \text{MeV}]{\varepsilon} \underset{\text{half-life 60 h}}{^{90}\text{Y}} \xrightarrow[2.5\ \text{MeV}]{\varepsilon} \underset{\text{stable}}{^{90}\text{Zr}}$$

The electrons produced by the radioactive source were accelerated under a potential that ranged from 800 to 2000 V, depending on the size of the sensor and the position of the electrodes. The signal is taken across a $1 \times 10^8\ \Omega$ resistor, and as the standing current from the ionization of the argon is about $2 \times 10^{-8}\ \Lambda$, there is a standing voltage of 2 V across it that requires "backing off."

In a typical detector, the primary current is about 10^{11} electrons/s. Taking the charge on the electron as 1.6×10^{-19} C, this gives a current of $1.6 \times 10^{-8}\ \Lambda$. According to Lovelock,[1] if each of these electrons can generate 10,000 metastables on the way to the electrode, the steady-state concentration of metastables will be about 10^{10} per milliliter (this assumes a life span for the

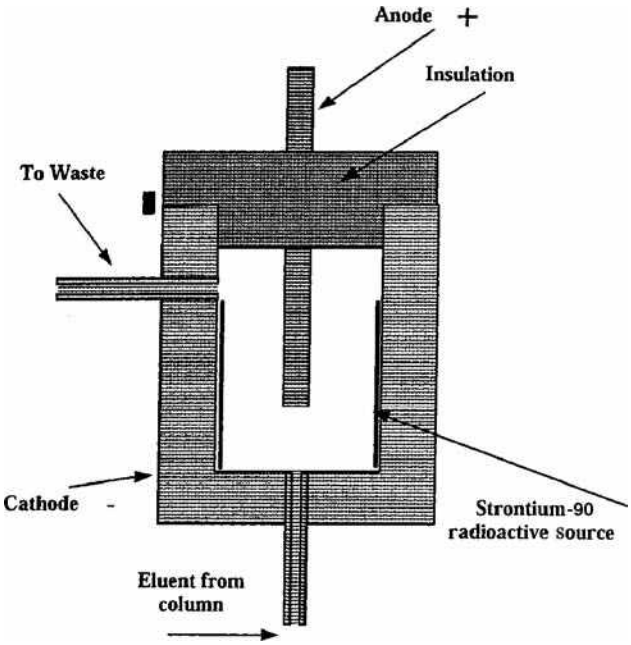

Fig. 1 The macro argon detector.

metastables of about 10^{-5} sec at NTP). From the kinetic theory of gases, it can be calculated that the probability of collision between a metastable atom and an organic molecule will be about 1.6 : 1. This would lead to a very high ionization efficiency and Lovelock claims that in the more advanced sensors ionization efficiencies of 10% have been achieved.

The minimum detectable concentration of a well-designed argon detector is about an order of magnitude higher than the flame ionization detection (FID) (i.e., 4×10^{-13} g/ml). Although the argon detector is a very sensitive detector and can achieve ionization efficiencies of greater than 0.5%, the detector was not popular, largely because it was not linear over more than two orders of magnitude of concentration ($0.98 < r > 1.02$) and its response was not predictable. In practice, nearly all organic vapors and most inorganic vapors have ionization potentials of less than 11.6 eV and thus are detected. The short list of substances that are not detected include and fluorocarbons. The compounds methane, ethane, acetonitrile, and propionitrile have ionization potentials well above 11.6 eV; nevertheless, they do provide a slight response between 1% and 10% of that for other compounds. The poor response to acetonitrile makes this substance a convenient solvent in which to dissolve the sample before injection on the column. It is also interesting to note that the inorganic gases H_2S, NO, NO_2, NH_3, PH_3, BF_3, and many others respond normally in the argon detector. As these are the type of substances that are important in environmental contamination, it is surprising that the argon detector, with its very high sensitivity for these substances, has not been reexamined for use in environmental analysis.

REFERENCES

1. Lovelock, J.E. *Gas Chromatography*; Scott, R.P.W. Butterworths Scientific: London, 1960; 9.
2. Lovelock, J.E. A sensitive detector for gas chromatography. J. Chromatogr. **1958**, *1*, 35.
3. Lovelock, J.E. Measurement of low vapour concentrations by collision with excited rare gas atoms. Nature (London) **1958**, *181* (4621), 1460.

BIBLIOGRAPHY

1. Scott, R.P.W. *Chromatographic Detectors*; Marcel Dekker, Inc.: New York, 1996.
2. Scott, R.P.W. *Introduction to Gas Chromatography*; Marcel Dekker, Inc.: New York, 1998.

Aromatic Diamidines: Electrophoresis and HPLC Analysis

A. Negro
B. Rabanal
Analytical Chemistry Section, Faculty of Biological and Environmental Sciences, University of León, León, Spain

INTRODUCTION

High-performance liquid chromatography (HPLC) can be considered to have been established by Ettre and Horvath.[1] The popularity of HPLC may be explained by the versatility of this technique, which can be used to separate and quantify large or small; polar, non-polar, or inorganic; and chiral or achiral molecules. In addition, its methods are easily automated, increasing the number of analyses that can be performed in a given time, improving accuracy and precision, as well as reducing costs. It was around 1960 that HPLC achieved its peak growth. This can be attributed, in large part, to its widespread acceptance by the pharmaceutical industry.

Electrophoresis is an analytical technique that was first introduced by Tiselius[2] in 1937. Thirty-five years ago, Hjertén[3] showed that it was possible to carry out electrophoretic separations in a 300.0 μm glass tube and to detect the separation of compounds by ultraviolet absorption. Capillary electrophoresis (CE) did not become popular until 1981, when Jorgenson and Lukacs[4] published work in which they demonstrated the simplicity of the instrumental setup required and the high-resolving power of CE. The results shown were astonishing: sharp narrow peaks, 400,000 theoretical plates per meter (compared with 10,000 theoretical plates per meter of HPLC), and short analysis times. Galery introduced the first commercial instrument in 1988. There are excellent reviews of CE, among which should be mentioned are the ones done by Kuhr, Isaaq, or Camilleri. These look at the increasing number of applications and future prospects.

CAPILLARY ELECTROPHORESIS

CE has had considerable success over the last 20 years. Gas chromatography (GC) and HPLC[1] are still the dominant techniques. However, CE has several distinct advantages over other separation techniques.[5–7] One advantage CE has, relative to HPLC, is its simplicity and applicability for the separation of widely differing substances, such as organic molecules, inorganic ions, and so on, using the same instrument and, in most cases, the same capillary, while changing only the composition of the buffer used. This cannot be said with regard to any other separation techniques. In addition, CE offers the highest resolving power.

The aim of the work reported here was to study how changes in the principal parameters for each technique affect the separation processes when analyzing a series of aromatic diamidines, and, based on the results obtained, to establish comparisons between the two analytical techniques.

The aromatic diamidines are compounds of considerable pharmaceutical interest. This is, among others, for the following reasons: they have a strong antiprotozoan action and participate in the metabolism and transport of polyamines, inhibiting, for instance, *S*-adenosyl-L-methionine decarboxylase (SAMDC). Therefore, because this route is closely linked to cell proliferation processes, aromatic diamidines can slow down or prevent the growth of tumors.[8–10] The substances used in this work are as follows:[11,12]

1. Pentamidine: 4,4′-[1,5-pentanediyl *bis*(oxy)]*bis*-benzenecarboximidamide.
2. Stilbamidine: 4,4′-(1,2-ethenediyl)*bis*-benzenecarboximidamide.
3. DAPI: 4′,6-diamidino-2-(4-amidinophenyl)indole dilactate.
4. Propamidine: 4,4′-[1,3-propanediylbis(oxy)*bis*-benzenecarboximidamide.
5. Hydroxystilbamidine: 4-[2-[4-(aminoiminomethyl) phenyl]ethenyl]-3-hydroxybenzene-carboximidamide.
6. Phenamidine: 4,4′-diamidinodiphenylether.
7. Diampron: 3,3′-diamidinocarbanilide.
8. Berenil: 4,4′-diamidinodiazoamino benzene.
9. Dibromopropamidine: 2′,2″-dibromo-4′,4″-diamidino-1,3-diphenoxypropane.

EXPERIMENTAL TECHNIQUES

Chemicals and Reagents

Pentamidine isethionate salt, berenil diaceturate salt, and DAPI dihydrochloride salt were obtained from Sigma-Aldrich Química SA (Madrid, Spain). Diampron isethionate

salt, hydroxystilbamidine isethionate salt, propamidine isethionate salt, dibromopropamidine isethionate salt, phenamidine isethionate salt, and stilbamidine isethionate salt were generously donated by Rhône Poulenc Rorer (Dagenham, U.K.). The ion-pairing reagents, pentane sulphonate, hexane sulphonate, heptane sulphonate, octane sulphonate, and decane sulphonate sodium salts were supplied by Sigma-Aldrich Química SA. Methanol of HPLC grade and other chemicals of analytical grade were supplied by Merck (Darmstadt, Germany). The water used was purified with a Milli-Q system purchased from Millipore (Bedford, Massachusetts, U.S.A.).

Chromatographic System

The HPLC system comprised a Beckman 116 programable solvent pump with a Beckman 168 photodiode detector—this was checked and data were processed with the Gold Nouveau software system (Beckman Coulter, Palo Alto, California, U.S.A.) and a Beckman 507 automatic injector with a 100.0 μl loop and a heating chamber for the columns. Analyses were carried out with an Ultrasphere ODS column (5.00 μm particle size, 15.0 cm × 4.60 mm I.D.) purchased from Beckman Coulter. A guard column (2.00 cm × 2.00 mm I.D.), packed with Sperisorb RP-18 (30.0–40.0 μm pellicular), was supplied by Upchurch Scientific (Oak Harbor, Washington, U.S.A.).

Electrophoretic System

The CE system consisted of a P/ACE System 2100 high-performance CE apparatus (Beckman Coulter, Fullerton, California, U.S.A.). An untreated, fused silica capillary tube (Beckman Coulter) was used, with dimensions of 75.0 μm I.D., $L_t = 57.0$ cm, and $L_d = 50.0$ cm, enclosed in a liquid-cooled cassette. Detection was performed with a UV-Vis detector ($\lambda = 200.0$ nm). Equipment was checked and data were processed with the Beckman P/ACE Station V 1.2 software (Beckman Coulter).

RESULTS AND DISCUSSION

To carry out a comparison of HPLC and CE, the effects of varying the parameters common to the two techniques with the greatest impact on the separation processes were evaluated. These were: pH of the mobile phase and electrolytes, buffer concentration, and temperature, with the gathered data compared in each case.

As these are separation techniques based on radically differing physical principles, it is evident that there are certain parameters, specific to a given technique, that have a strong influence over the separation process in only one of the two and are not comparable. In HPLC, there is the influence of concentration and chain length of the ion-pairing reagent and the methanol percentage; in CE, there is influence of the choice of electrolyte, length of the capillary, and voltage applied. Variations in these parameters were also taken into account because they provide extremely useful information for making an overall comparison of the two techniques.

Parameters Common to HPLC and CE

Influence of pH in the mobile phase

The pH value is the parameter with the greatest impact on the separation of ionizable molecules. To keep aromatic diamidines ionized, it is necessary to work at very low pH levels, in the range 3.00–4.50, as the diamidine groups twice present in each molecule confer on them a strongly basic character ($pK_a = 13.86$).[13] To determine the influence of pH in HPLC, five diamidines were analyzed using a mobile phase consisting of 25.0 m*M* citrate buffer, 45.0% methanol, and 4.00 m*M* octane sulphonate sodium salt, at a temperature (T) of 30.0°C and at pH values of 3.00, 3.25, and 3.70. The chromatograms obtained are shown in Fig. 1. It can be observed that, as pH increases, retention times are noticeably shortened for all the substances, with no significant variations being noted in resolution. The influence of pH in CE[14] was studied by using 25.0 m*M* citrate buffer at $T = 30.0$°C, 14.0 kV voltage, and pH levels of 3.50, 3.70, and 4.25. Fig. 1 shows that a drop in pH does not bring with it any large change in migration times, but it does produce a significant variation in resolution. It may be observed that a good separation of all nine diamidines is possible only at pH = 3.70. For all the substances, it can be noted that the times required for analyses using CE are around half those in HPLC and that efficiency is much greater in all cases with CE than it is with HPLC, with good resolution. The most appropriate pH levels for the analyses of these substances in aqueous solutions and in the serum and urine are very similar with the two techniques because both require the molecules to be strongly ionized.

Influence of buffer concentration

For HPLC, it has been decided that the preferred buffer is citrate; it was necessary to establish the most suitable concentration. To study this influence, five diamidines were analyzed using a mobile phase consisting of 45.0% methanol, 4.00 m*M* octane sulphonate, and citrate buffer at various concentrations of 15.0, 25.0, and 35.0 m*M*, with $T = 30.0$°C and pH = 3.25 in all cases. In Fig. 2, we see the results obtained. A change from 25.0 to 35.0 m*M* barely affects retention times for any of the substances, but a drop from 25.0 to 15.0 m*M* decreases retention times by almost 30.0% in every case.

With CE, citrate buffer was also selected as the electrolyte for the study, and all nine diamidines were analyzed by using an electrolyte composed of citrate buffer at pH = 3.70,

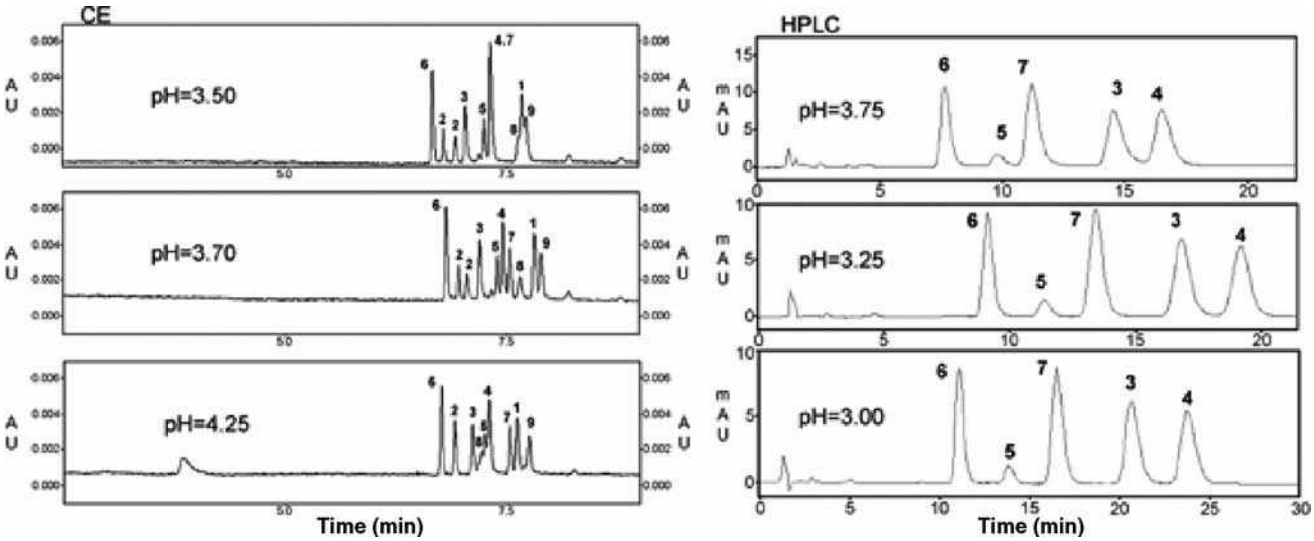

Fig. 1 Influence of pH in HPLC and CE. In HPLC, this effect was studied using a mobile phase consisting of 25.0 m*M* citrate buffer, 45.0% methanol, $T = 30.0°C$, 4.00 m*M* sodium octane sulphonate, and pH levels of 3.00, 3.25, and 3.75. In CE, a 25.0 m*M* citrate buffer electrolyte was used; pH values were 3.50, 3.70, and 4.25, and the voltage was 14.0 kV.

$T = 30.0°C$, and 14.0 kV voltage, at various concentrations (10.0, 25.0, and 40.0 m*M*), to determine which was the most appropriate. The results obtained are presented in Fig. 2. It can be seen that when concentrations go down to 10.0 m*M*, migration times are greatly reduced, but resolution also falls considerably; at 25.0 m*M*, resolution starts to be acceptable, and, at 40.0 m*M*, a good compromise between migration times and resolution is achieved. Comparison of the variations in buffer concentration in HPLC and CE allows one to conclude that, in both cases, a decrease in the concentration of the buffer reduces the time required for analyses. This reduction is much more striking in the case of CE and, in every instance, analysis times with CE are on the order of half of what they are with HPLC. Consequently, efficiency is much higher for all the compounds with CE than with HPLC, whereas resolution is good in both.

Influence of temperature

To study the effects of temperature in the analysis of these diamidines by means of HPLC, we used a mobile phase composed of 25.0 m*M* citrate buffer, with pH = 3.25,

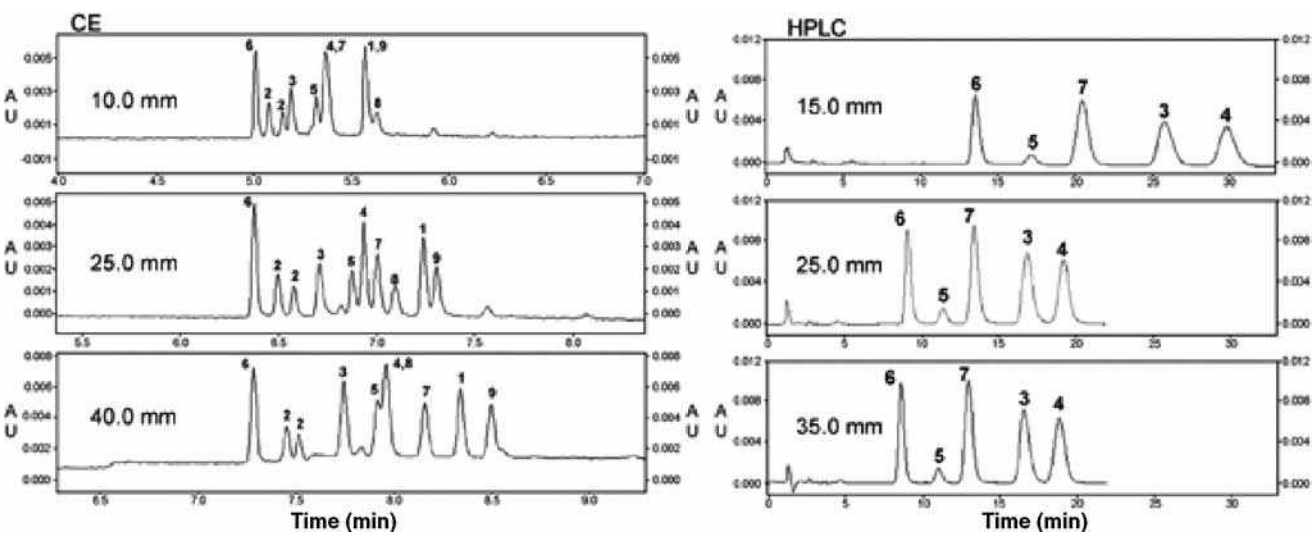

Fig. 2 Influence of buffer concentration in HPLC and CE. In HPLC, this effect was studied using a mobile phase consisting of citrate buffer at concentrations of 15.0, 25.0, and 35.0 m*M*, with 45.0% methanol, 4.00 m*M* sodium octane sulphonate, and pH = 3.25. In CE, a citrate buffer electrolyte was used at concentrations of 10.0, 25.0, and 40.0 m*M*, with pH = 3.70, voltage, 14.0 kV and $T = 30.0°C$.

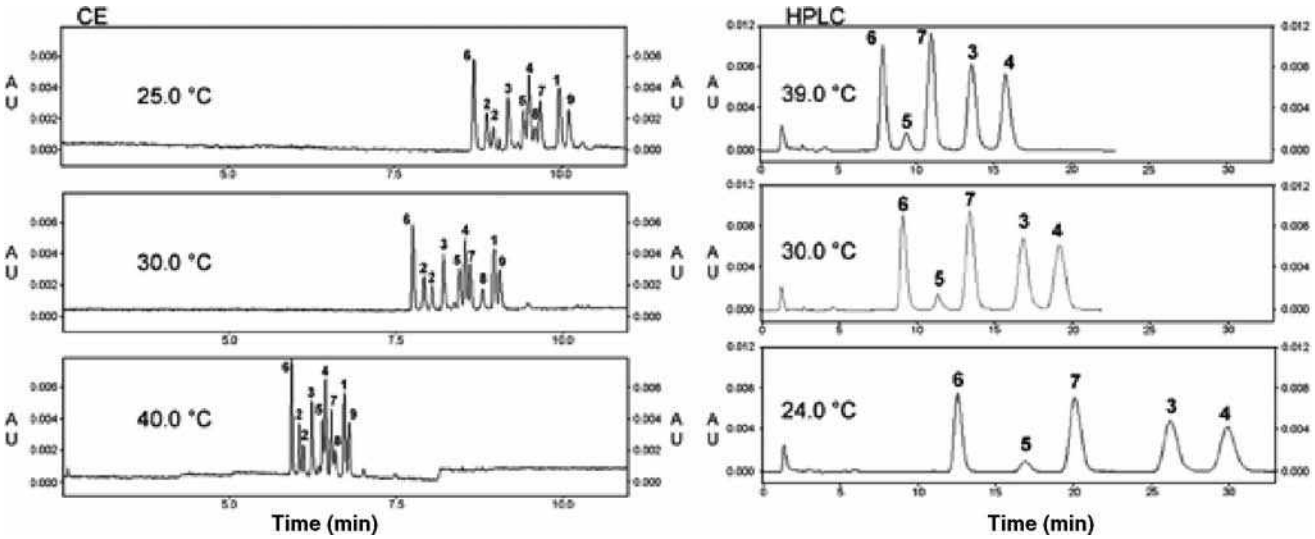

Fig. 3 Influence of temperature in HPLC and CE. In HPLC, this effect was studied using a mobile phase consisting of 25.0 m*M* citrate buffer, 45.0% methanol, 4.00 m*M* sodium octane sulphonate, pH = 3.25, and $T = 24.0°C$, 30.0°C, and 39.0°C. In CE, the electrolyte used was 25.0 m*M* citrate buffer, with pH = 3.70, 14.0 kV voltage, and $T = 25.0°C$, 30.0°C, and 40.0°C.

45.0% methanol, and 4.00 m*M* octane sulphonate, at three different temperatures: 24.0°C, 30.0°C, and 39.0°C. It may be noted in Fig. 3 that increasing the temperature causes a notable drop in retention times, whereas resolution remains at very good levels.

The temperature at which CE is carried out has to be selected carefully because this is one of the most influential parameters in the CE process.[15] Precise temperature control during the CE process is of great importance in achieving good separation selectivity and, above all, good reproducibility.[16,17] To study temperature variation in CE, an electrolyte composed of 25.0 m*M* citrate buffer, with pH = 3.70 and 14.0 kV voltage, was used at temperatures of 25.0°C, 30.0°C, and 40.0°C. Fig. 3 shows that an increase in temperature causes a drastic reduction in migration times, but also reduces resolution excessively, causing serious problems for separation from 30.0°C onward.

If CE and HPLC at 30.0°C are compared, it will be noted, as in all previous cases, that CE has much shorter analysis times than HPLC and that efficiency is much higher with CE than with HPLC, with good resolution being attained in both.

Parameters Exclusive to HPLC

Influence of concentration and chain length of the ion pair-forming agent

A technique often used in the analysis of ionic molecules is the formation of ion pairs[18] because this permits the separation of substances that are too ionized to separate by means of adsorption–partition methods, but are too insoluble in water to be analyzed through ion exchange techniques.[19] The pH of the mobile phase must be adjusted to ensure that the molecules are totally ionized and can combine with the ion pair-forming agent through the counterion. The substances most often used to form ion pairs are alkyl-sulphonate salts of varying chain length. In this work, several reagents of this type were evaluated, having chain lengths ranging from 5 to 10 carbons; the influence of the concentration of each was also investigated to determine which was the most suitable.

The effects of sulphonate salt concentration and chain length on the retention factor (k') were studied by measuring k', using only berenil as the diamidine, with a mobile phase consisting of 25.0 m*M* citrate buffer, pH = 3.25, 45.0% methanol, $T = 30.0°C$, with pentane sulphonate, hexane sulphonate, heptane sulphonate, octane sulphonate, and decane sulphonate sodium salts at concentrations of 0.00, 1.00, 2.00, 3.00, 4.00, 5.00, 6.00, 9.00, and 12.00 m*M*. The resultant data are shown in Fig. 4, where it may be observed that retention times and hence k' increase as the concentration of the ion pair-forming agent increases. This increase is much more pronounced when reagents with longer chain lengths are used.

Influence of methanol content

Two solvents were initially evaluated as organic modifiers for the mobile phase, these being acetonitrile and methanol. Methanol was finally selected, principally because of its greater solubility with respect to ion-forming reagents.

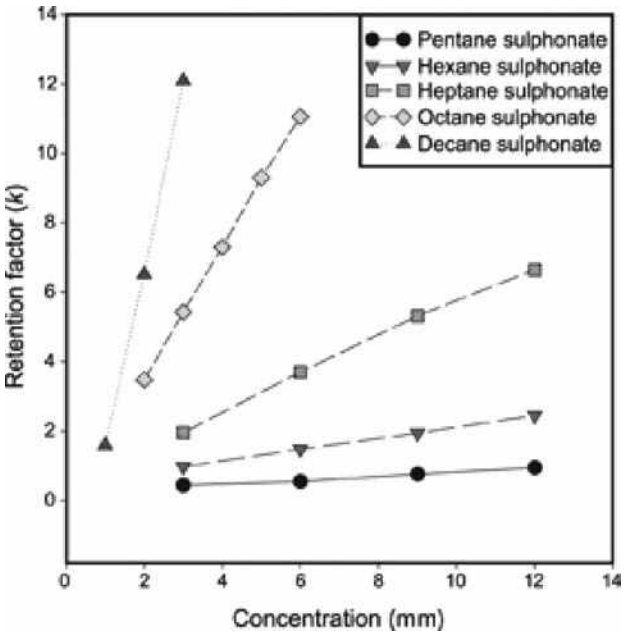

Fig. 4 Influence of concentration and chain length of the ion pair-forming agent in HPLC. This effect was studied using a mobile phase consisting of 25.0 m*M* citrate buffer, 45.0% methanol, and pH = 3.25, containing pentane sulphonate, hexane sulphonate, heptane sulphonate, octane sulphonate, and decane sulphonate sodium salts at concentrations of 0.00, 1.00, 2.00, 3.00, 4.00, 5.00, 6.00, 9.00, and 12.0 m*M*.

The effect of methanol percentage in the mobile phase on retention times was studied by using a mobile phase consisting of 25.0 m*M* citrate buffer, pH = 3.25, $T = 30.0°C$, and 4.00 m*M* octane sulphonate and methanol at 42.0%, 45.0%, and 50.0%. Fig. 5 shows that, with increasing percentages of methanol, retention times drop considerably and resolution decreases, but up to 50.0% methanol, this remains within acceptable limits.

Parameters Exclusive to CE

Selection of electrolyte

With a view to selecting the most suitable electrolyte for CE,[20,21] all the diamidines under study were analyzed by using various buffers (phosphate, acetate, and citrate), all at 25.0 m*M*, pH = 3.70, $T = 30.0°C$, and 14.0 kV voltage, as shown in Fig. 6. Only citrate gave useful values of resolution and efficiency for all the diamidines, together with migration times that were adequate for the kind of analysis they intended to optimize. Hence, citrate was also chosen for all the CE works.

Length of capillary

The length of the capillary is directly related to the electric field, efficiency, resolution,[22] and amount of sample loaded. An increase from 50.0 to 70.0 cm, up to the detector (from 57.0 to 77.0 cm overall dimension) in the length of the capillary, causes the quantity of sample loaded to be reduced by approximately 26.0% and the strength of the field to be generated when applying the same potential drops by approximately the same amount (Table 1). To study the influence of the length of the capillary on

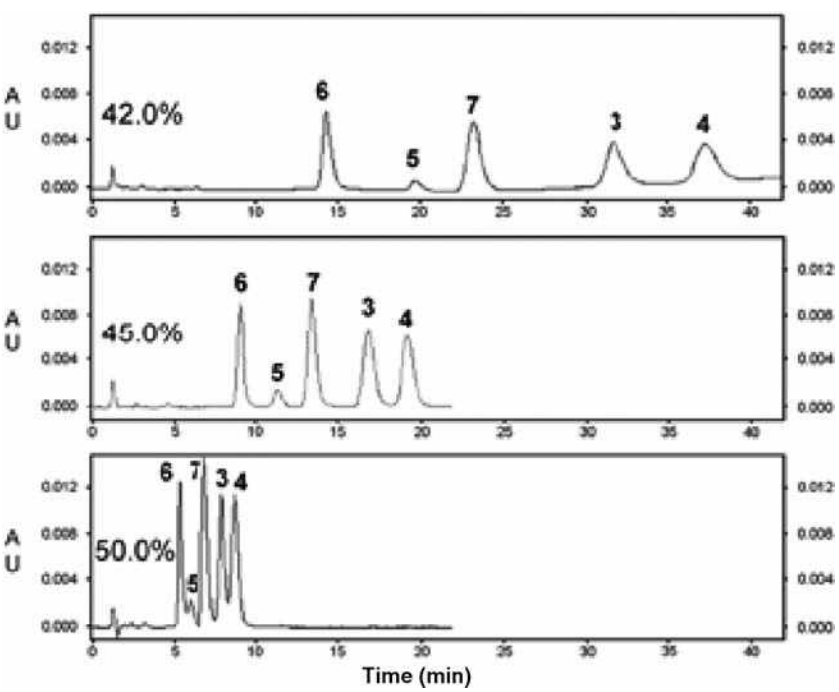

Fig. 5 Influence of methanol content in HPLC. This effect was studied using a mobile phase consisting of 25.0 m*M* citrate buffer, pH = 3.25, $T = 30.0°C$, 4.00 m*M* octane sulphonate, and 42.0%, 45.0%, and 50.0% methanol.

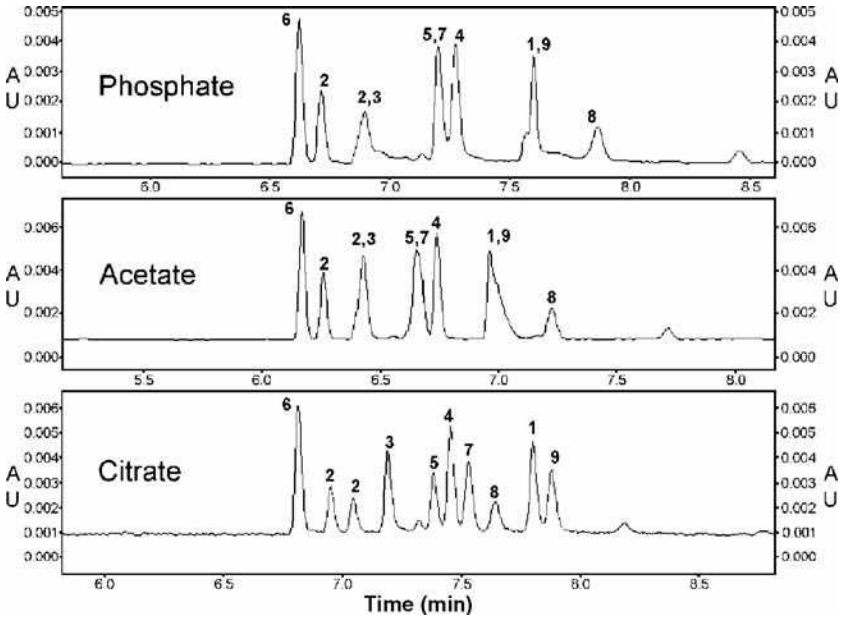

Fig. 6 Selection of electrolyte in CE. Electropherograms of nine diamidines using phosphate, acetate, and citrate electrolytes (25.0 m*M*), pH = 3.70, $T = 30.0°C$, and 14.0 kV voltage.

migration times, the following conditions were used: capillary, 75.0 μm I.D.; lengths, 50.0 and 70.0 cm to the detector (57.0 and 77.0 cm overall length); electrolyte, 25.0 m*M* citrate buffer; pH = 3.70; $T = 30.0°C$; and voltage, 14.0 kV. Fig. 7 shows that as the length is increased from 50.0 to 70.0 cm, migration times are virtually doubled and a striking improvement in efficiency is achieved (i.e., an increase of between 10.0% and 15.0% in the number of theoretical plates), with good resolution.

Voltage applied

The voltage applied is one of the factors of greatest influence in a CE experiment because almost all the parameters governing separation are related to this voltage. The analysis time is inversely proportional to the applied voltage because of, among other things, the higher electroosomotic flow (EOF). An increase in the voltage also brings with it a growth in Joule heating[15,16] and, if this is not effectively eliminated, it may cause variations in resistance, pH, viscosity of the electrolyte, and so on, thus rendering the analysis impossible to reproduce. With a view to optimizing the voltage, the Ohm's law plot of intensity against voltage must be kept in mind. The maximum efficiency in electrophoretic separation is attained at the point where this plot begins to deviate from linearity.[23] In the work reported here, this occurred from 24.0 kV upward, and, when this value was exceeded, a pronounced decrease in efficiency occurred.[24] In Fig. 8, the effects mentioned above can be readily seen; between the electropherogram at 8.00 kV and its counterpart at 14.0 kV, a clear increase in efficiency is observed, with resolution remaining at acceptable levels. On the other hand, in the electropherogram taken at 26.0 kV, outside the limits of linearity under Ohm's law, there is a complete loss of the improvements in both resolution and efficiency produced by higher voltage. This work was carried out using 25.0 m*M* citrate electrolyte, pH = 3.70, and $T = 30.0°C$, at voltages of 8.00, 14.0, and 26.0 kV.

CONCLUSIONS

A detailed study was undertaken of each of the parameters affecting the process of separation analysis in HPLC and CE for nine aromatic diamidines. The results obtained are noted and discussed; in the tables,

Table 1 Effect of capillary length on the volume of sample loaded and strength of the electric field.

Length of capillary (cm)	Volume injected (nl)	Capillary occupied by the injection (mm)	Percentage of capillary occupied	Analyte loaded (ng)	Strength of electric field (V/cm)
77.0	21.77	4.92	0.70	8.80	181.0
57.0	29.41	6.65	1.33	147.0	245.0

Capillary, 75.0 μm I.D.; overall lengths, 77.0 and 57.0 cm (70.0 and 50.0 cm to the detector); electrolyte, 25.0 m*M* citrate buffer; pH = 3.70; voltage, 14.0 kV; $T = 30.0°C$; injection under pressure for 5.00 sec.

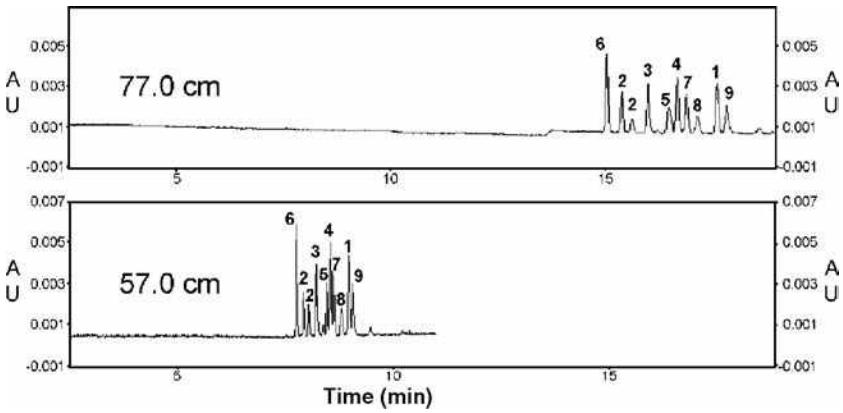

Fig. 7 Influence of capillary length in CE. Capillary, 75.0 μm I.D.; lengths, 50.0 and 70.0 cm to detector (57.0 and 77.0 cm overall); electrolyte, 25.0 m*M* citrate buffer; pH = 3.70; $T = 30.0°C$; and voltage, 14.0 kV.

comparative features of the two techniques that emerge from the data collected are recorded.

Performance of HPLC and CE in the Separation of Aromatic Diamidines

The data emerging from this work allow the selection of the optimum conditions for the analysis of each substance in aqueous solution, serum, and urine. For HPLC, they are: 25.0 m*M* citrate buffer, pH = 3.25, 45.0% methanol, column Ultrasphere ODS (5.00 μm particle size, 15.0 cm × 4.60 mm I.D.), 1.00 ml/min flow, and $T = 30.0°C$. The following features depend on the specific substance under analysis: pentamidine, 4.00 m*M* hexane sulphonate, λ = 265.0 nm; stilbamidine, 4.00 m*M* octane sulphonate, λ = 330.0 nm; DAPI, 8.00 m*M* heptane sulphonate, λ = 350.0 nm; propamidine, 6.00 m*M* heptane sulphonate, λ = 265.0 nm; hydroxystilbamidine, 4.00 m*M* octane sulphonate, λ = 350.0 nm; phenamidine, 4.00 m*M* octane sulphonate, λ = 265.0 nm; diampron, 4.00 m*M* octane sulphonate, λ = 254.0 nm; berenil, 4.00 m*M* octane sulphonate, λ = 370.0 nm; and dibromopropamidine, 3.00 m*M* hexane sulphonate, λ = 265.0 nm.

For CE, the optimum values were: overall length of capillary, 57.0 cm (50.0 cm to the detector); 75.0 μm I.D.; electrolyte, 25.0 m*M* citrate; pH = 3.70, injection under pressure for 5.00 sec; voltage, 14.0 kV; $T = 30.0°C$; and λ = 200.0 nm.

Analyses by means of HPLC and CE were carried out under these conditions for all the compounds, and comparative data for the two techniques are summarized in Table 2. The efficiency of CE is two orders of magnitude greater than HPLC for all the substances analyzed. The limits of detection (LOD) for HPLC are much lower than in

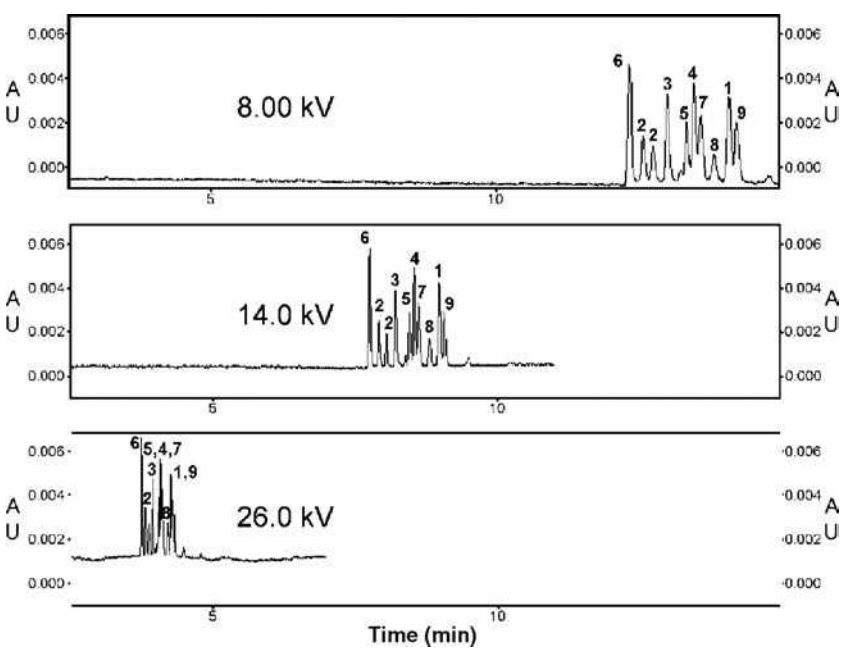

Fig. 8 Influence of variations in voltage in CE. Electrolyte, 25.0 m*M* citrate buffer; pH = 3.70; $T = 30.0°C$, and voltages, 8.00, 14.0, and 26.0 kV.

Table 2 Performance of HPLC and CE in separation of aromatic diamidines.

	HPLC	CE
Detection limit (ng/ml)		
Pentamidine	20.00	300.0
Stilbamidine	10.00	300.0
DAPI	5.00	300.0
Propamidine	30.00	200.0
Hydroxystilbamidine	15.00	400.0
Phenamidine	20.00	150.0
Diampron	10.00	300.0
Berenil	60.00	500.0
Dibromopropamidine	40.00	600.0
Precision (% CV)		
Pentamidine	1.09	3.04
Stilbamidine	1.03	1.68
DAPI	1.16	2.88
Propamidine	1.53	2.37
Hydroxystilbamidine	0.70	3.73
Phenamidine	0.70	3.52
Diampron	0.97	2.43
Berenil	0.85	1.55
Dibromopropamidine	1.36	5.30
Efficiency (theoretical plates)		
Pentamidine	2.22×10^3	2.92×10^5
Stilbamidine	3.91×10^3	3.04×10^5
DAPI	4.60×10^3	2.93×10^5
Propamidine	3.19×10^3	2.92×10^5
Hydroxystilbamidine	3.87×10^3	2.79×10^5
Phenamidine	3.65×10^3	3.06×10^5
Diampron	4.57×10^3	2.78×10^5
Berenil	3.17×10^3	2.43×10^5
Dibromopropamidine	2.63×10^3	2.46×10^5

Table 4 Schematic table of the advantages of HPLC and CE.

	HPLC	CE
Versatility	+++	++++
Speed of optimization of methods	++	++++
Stabilization time	++	++++
Analysis time	++	+++
Sensitivity	+++	++
Reproducibility of times	+++	++
Reproducibility of areas	+++	++
Precision	+++	++
Efficiency	++	++++
Amplitude of linear range	++++	++
Resolution capacity	++	++++
Interferences in complex samples	++	++++
Sample preparation	++	++++
Sample volume	++	++++
Application at pilot scale	++++	+
Automatization	+++	++++
Price of reagents and other consumables	++	++++

CE, there being some cases, such as DAPI, where the detection limit is 60 times lower with HPLC than with CE. Values for precision are significantly better with HPLC than with CE.

Operational Differences Between HPLC and CE

Table 3 shows some of the differences in working practices between HPLC and CE.

Advantages of HPLC and CE

To summarize the work reported here, there is a schematic presentation of views on the advantages and drawbacks of each technique in Table 4.

Table 3 Operational differences between HPLC and CE.

	HPLC	CE
Quantity of sample introduced into the system	10.0–1000.0 μl	1.00–50.0 nl
Size of the detector cell	8.00–12.0 mm^3	0.015 mm^3
Detection wavelength	Generally from 230.0 nm upward	Possible to use wavelengths down to 185.0 nm
Interference	All components of the sample must pass through the detector	Possible to stop the analysis once the substance of interest has been detected
Flow	0.50–2.00 ml/min	Few microliters per minute
Equipment stabilization time	Requires balancing of the column with different timings before reliable results are obtained	Analysis can be carried out almost immediately after connection of equipment

REFERENCES

1. Ettre, L.S.; Horvath, C. Foundations of modern liquid chromatography. Anal. Chem. **1975**, *47*, 422A.
2. Tiselius, A. A new apparatus for electrophoretic analysis of colloidal mixtures. Faraday Soc. **1937**, *33*, 524–531.
3. Hjertén, S. Free zone electrophoresis. Chromatogr. Rev. **1967**, *9*, 122–239.
4. Jorgenson, J.; Lukacs, K.D. Zone electrophoresis in open tubular glass capillaries. Anal. Chem. **1981**, *53*, 1298–1302.
5. Kuhr, W.G. Capillary electrophoresis. Anal. Chem. (Fund. Rev.) **1990**, *62*, 403R.
6. Issaq, H.J. Thirty-five years of capillary electrophoresis: Advances and perspectives. J. Liq. Chromatogr. Relat. Technol. **2002**, *25* (8), 1153–1170.
7. Camilleri, P. *Capillary Electrophoresis, Theories and Practice*, 2nd Ed.; CRC Press: Boca Raton, FL, 1997; 1–22.
8. Grasilli, E.; Bettuzi, S.; Monti, D.; Ingletti, M.C.; Franceschi, C.; Corty, A. Studies on the relationship between cell proliferation and cell death: Opposite patterns of SGP-2 and ornithine decarboxylase mRNA accumulation in PHA-stimulated human lymphocytes. Biochem. Biophys. Res. Commun. **1991**, *59*, 180.
9. Pegg, A.E. Recent advances in the biochemistry of polyamines in eukaryotes. Biochem. J. **1986**, *234*, 249.
10. Pegg, A.E. Polyamine metabolism and its importance in neoplastic growth and a target for chemotherapy. Cancer Res. **1988**, *48*, 759.
11. Rabanal, B.; Merino, G.; Negro, A. Determination by capillary zone electrophoresis of berenil, phenamidine, diampron and dibromopropamidine in serum and urine. J. Chromatogr. B, **2000**, *738*, 293–303.
12. Rabanal, B.; Negro, A. Study of nine aromatic diamidines designed to optimize their analysis by HPLC. J. Liq. Chromatogr. **2003**, *26* (20), 3499–3512.
13. Charton, M. The application of the Hammett equation to amidines. J. Org. Chem. **1965**, *30*, 969.
14. Bocek, P.; Deml, M.; Gebaner, P.; Dolnik, V. *Analytical Isotachophoresis*; VCH: Weinheim, 1988.
15. Rush, R.S.; Cohen, A.S.; Karger, B.L. Influence of column temperature on the electrophoretic behavior of myoglobin and α-lactalbumin in high-performance capillary electrophoresis. Anal. Chem. **1991**, *63*, 1346–1350.
16. Nelson, R.J.; Paulus, A.; Cohen, A.S.; Guttman, A.; Karger, B.L. Use of Peltier thermoelectric devices control column temperature in high performance capillary electrophoresis. J. Chromatogr. B, **1989**, *480*, 111–127.
17. Sepaniak, M.J.; Cole, R.O. Column efficiency in micellar electrokinetic chromatography. Anal. Chem. **1987**, *59*, 472–476.
18. Eksborg, S.; Lagerstom, P.; Modin, R.; Schill, G. Ion pair chromatography of organic compounds. J. Chromatogr. A, **1973**, *83*, 99–110.
19. Braithwaite, A.; Smith, F.J. *Chromatographic Methods*, 5th Ed.; Blackie Academic and Professional, 1996.
20. Issaq, H.J.; Atamna, I.Z.; Muschik, G.M.; Janini, G.M. The effect of electric field strength, buffer type and concentration on separation parameters in capillary zone electrophoresis. Chromatographia **1991**, *32*, 155–161.
21. Nashabeh, W.; El Rassi, Z. Capillary zone electrophoresis of pyridylamino derivatives of maltooligosaccharides. J. Chromatogr. **1990**, *514*, 57–64.
22. Cohen, A.S.; Paulus, A.; Karger, B.L. High performance capillary electrophoresis using open tubes and gels. Chromatographia **1987**, *24*, 15–24.
23. Beckers, J.L.; Everaests, F.M. Isotachophoresis with two leading ions and migration behaviour in capillary zone electrophoresis: II. Migration behaviour in capillary zone electrophoresis. J. Chromatogr. A, **1990**, *508*, 19–26.
24. McLaughlin, G.M.; Nolau, J.A.; Lindahl, J.L.; Palmieri, R.H.; Anderson, K.N.; Morris, S.C.; Morrison, J.A.; Bronzert, T.J. Pharmaceutical drug separations by HPCE: Practical guidelines. J. Chromatogr. **1992**, *15* (6&7), 961–1021.

Asymmetric FFF in Biotechnology

Christine Hürzeler
Thorsten Klein
Postnova Analytics, Munich, Germany

INTRODUCTION

The research and development in the fields of biochemistry, biotechnology, microbiology, and genetic engineering are fast-growing areas in science and industry. Chromatography, electrophoresis, and ultra-centrifugation are the most common separation methods used in these fields. However, even these efficient and widespread analytical methods cannot cover all applications. In this entry, asymmetric flow field-flow fractionation (AF4) is introduced as a powerful analytical separation technique for the characterization of biopolymers and bioparticles. Asymmetric flow field-flow fractionation (FFF) can close the gap between analyzing small and medium-sized molecules/particles [analytical methods: high-performance liquid chromatography (HPLC), gel filtration chromatography (GFC), etc.] on the one hand and large particles (analytical methods: sedimentation, centrifugation) on the other hand,[1,2] whereas HPLC and GFC are overlapping with asymmetric field-flow fractionation in the lower separation ranges.

The first publication about FFF by Giddings[3] appeared in 1966. From this point, FFF was developed in different directions and, in the following years, various subtechniques of FFF emerged. Well-known FFF subtechniques are sedimentation FFF, thermal FFF, electric FFF, and flow FFF. Each method has its own advantages and gives a different point of view of the examined sample systems. Using sedimentation FFF shows new insights about the size and density of the analytes, thermal FFF gives new information about the chemical composition and the size of the polymers/particles, and electric FFF separates on the basis of different charges. Flow FFF, and especially asymmetric flow FFF (the most powerful version of flow FFF) is the most universal FFF method, because it separates strictly on the basis of the diffusion coefficient (size or molecular weight) 2, and it has the broadest separation range of all the FFF methods. It is usable for a large number of applications in the fields of biotechnology, pharmacology, and genetic engineering.

SEPARATION PRINCIPLE OF ASYMMETRIC FLOW FIELD-FLOW FRACTIONATION

All FFF methods work on the same principle and use a special, very flat separation channel without a stationary phase. The separation channel is used instead of the column, which is needed in chromatography. Inside the channel, a parabolic flow is generated, and perpendicular to this parabolic flow, another force is created. In principle, the FFF methods only differ in the nature of this perpendicular force.

The separation channel in AF4 is approximately 30 cm long, 2 cm wide, and between 100 and 500 μm thick. A carrier flow which forms a laminar flow profile streams through the channel. In contrast to the other FFF methods, there is no external force, but the carrier flow is split into two partial flows inside the channel. One partial flow is led to the channel outlet and, afterward, to the detection systems. The other partial flow, called the cross-flow, is pumped out of the channel through the bottom of the channel. In the AF4, the bottom of the separation channel is limited through a special membrane and the top is made of an impermeable plate (glass, stainless steel, etc.). The separation force, therefore, is generated internally, directly inside the channel, and not by an externally applied force.

Under the impact of the cross-flow, the biopolymers/particles are forced in the direction of the membrane. To ensure that the analytes do not pass through the membrane, different pore sizes can be used. In this way, the analytes can be selectively rejected and it is possible to remove low-molecular compounds before the separation. The analytes' diffusion back from this membrane is counteracted by the cross-flow, where, after a time, a dynamic equilibrium is established. The medium equilibrium height for smaller sized analytes is located higher in the channel than for the larger analytes. The smaller sized analytes are traveling in the faster velocity lines of the laminar channel flow and will be eluted first. As a result, fractograms, which show size separation of the fractions, are obtained as an analog to the chromatograms from HPLC or GFC.

APPLICATIONS OF AF4 ASYMMETRIC FLOW FIELD-FLOW FRACTIONATION IN BIOTECHNOLOGY

In addition to widespread applications in the field of polymer and material science or environmental research, AF4 can be used in bioanalytics, especially for the characterization of proteins, protein aggregates, polymeric

proteins, cells, cell organelles, viruses, liposomes, and various other bioparticles and biopolymers.

Cells and Viruses

The advantage of AF4, in contrast to chromatography, is the capability to separate bioparticles and biopoylmers which usually stick onto chromatography columns. They are more or less filtered out (removed) by the stationary phase. Various applications using AF4 for the separation of shear-force sensitive bioparticles with high molecular weight and size have been reported in the literature. They deal with the efficient and fast separation of viruses[4,5], and bacteria.[5] Litzen and Wahlund[4] discuss the investigation of a virus (STNV) with AF4 and the separation of the viral aggregates. Litzen and Wahlund[5] report the separation of a virus (CPMV) together with different other proteins (BSA, Mab). They also present the characterization of bacillus *streptococcus faecalis* and its aggregates using AF4.

Proteins/Antibodies/DNA

The separation of proteins with AF4 has been demonstrated a number of times. For example, the fractionation of ferritin,[7] of HSA and BSA,[8] and of Mab,[8] including their various aggregates, were published. Asymmetric flow FFF is especially suitable for the separation and characterization of large and sensitive proteins and their aggregates because it is fast and gentle and aqueous solvents can be used that achieve maximum bioactivity of the isolated proteins and antibodies. Furthermore, even very large and sticky proteins can be analyzed because of the relatively low surface area and the separation in the absence a stationary phase. Nearly independent of the nature of the bioparticles, AF4 separates by size (diffusion coefficient). Therefore, DNA, RNA, and plasmids can be separated quickly and gently, together with proteins. Kirkland et al.[6] deal with this issue and present the AF4 separation of a mixture of cytochrome-*c*, BSA, ferritin, and plasmid DNA.

Artificial Polymeric Proteins

In addition to the characterization of well-known protein substances (serum proteins, aggregates, antibodies, etc.), AF4 is also a very promising separation/characterization technique for a new class of artificially made polymeric proteins from therapeutic/diagnostic applications, such as poly-streptavidin and polymeric hemoglobin (personal communication of the authors). These proteins usually have very high molecular weights and huge molecular sizes, and they are difficult to analyze by conventional GFC and related techniques. Very often, these proteins are also sticky and show adsorptive effects on the column material. Using AF4 without a stationary phase and without size-exclusion limit, these polymeric proteins can be readily separated and characterized. The application shown in Fig. 1 was done using an AF4 system (HRFFF 10,000 series, Postnova Analytics) and ultraviolet (UV) detection at 210 nm.

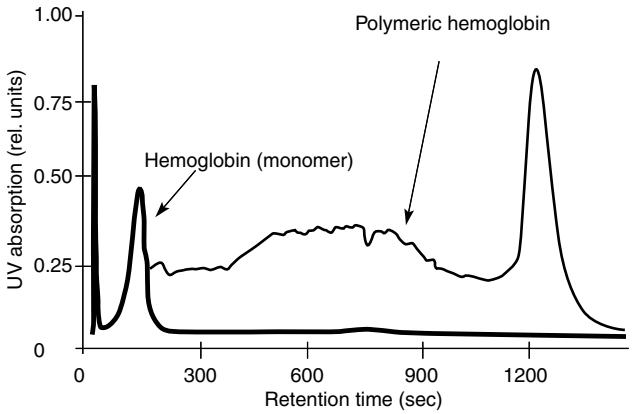

Fig. 1 Pig hemoglobin separated with AF4 and UV detection.

CONCLUSIONS

Asymmetric flow FFF is a new member in the FFF familiy of separation technologies; it is a powerful characterization technique, especially suited for the separation of large and complex biopolymers and bioparticles. Asymmetric flow FFF has many of the general benefits of FFF; it adds on several additional characteristics. In particular, these characteristics are as follows:

1. No sample preparation, or only limited sample preparation necessary.
2. Possibility of direct injection of unprepared samples.
3. Large accessible size molecular-weight range, no size-exclusion limit.
4. Very gentle separation conditions in the absence of a stationary phase.
5. Weak or no shear forces inside the flow channel.
6. Rapid analysis times, generally faster than GFC.
7. Fewer sample interactions during separation because of small surface area.
8. On-line sample concentration/large volume injection possible.
9. Gentle and flexible because it uses a wide range of eluents/buffers/detectors.
10. AF4 is a useful analytical tool, and when the limitations of the technology (e.g., sample interactions with membrane or the sample dilution during separation)

are carefully observed, samples can be characterized where other analytical technologies fail or only yield limited information.

REFERENCES

1. Klein, T. Chemisch–physikalische Charakterisierung von schwermetallhaltigen Hydrokolloiden in natürlichen aquatischen Systemen mit Ultrafiltration und Flow-FFF. *Diploma thesis*; TU-Munich, 1995.
2. Klein, T. Entwicklung und Anwendung einer Asymmetrischen Fluß-Feldflußfraktionierung zur Charakterisierung von Hydrosolen. *Ph.D. thesis*; TU-Munich, 1998.
3. Giddings, J.C. A new separation concept based on a coupling of concentration and flow nonuniformities. J. Sep. Sci. **1966**, *1*, 123.
4. Litzen, A.; Wahlund, K.G. Zone broadening and dilution in rectangular and trapezoidal asymmetrical flow field-flow fractionation channels. Anal. Chem. **1991**, *63*, 1001.
5. Litzen, A.; Wahlund, K.G. Effects of temparature, carrier composition and sample load in asymmetrical flow field-flow fractionation. J. Chromatogr. **1991**, *548*, 393.
6. Kirkland, J.J.; Dilks, C.H.; Rementer, S.W.; Yau, W.W. Asymmetric-channel flow field-flow fractionation with exponential force-field programming. J. Chromatogr. **1992**, *593*, 339.
7. Tank, C.; Antonietti, M. Characterization of water-soluble polymers and aqueous colloids with asymmetrical flow field-flow fractionation. Macromol. Chem. Phys. **1996**, *197*, 2943.
8. Litzen, A.; Walter, J.K.; Krischollek, H.; Wahlund, K.G. Separation and quantitation of monoclonal antibody aggregates by asymmetrical flow field-flow fractionation and comparison to gel permeation chromatography. Anal. Biochem. **1993**, *212*, 169.

Atomic Emission Detector for GC

Stanisław Popiel
Institute of Chemistry, Military University of Technology, Warsaw, Poland

Zygfryd Witkiewicz
Institute of Chemistry, Jan Kochanowski University, Kielce, Poland

INTRODUCTION

The gas chromatograph (GC) is one of the most popular analytical devices used in laboratories throughout the world. A reason for this is, among others, that devices being a combination of a GC and a mass spectrometer (MS), infra red and atomic emission spectrometers (AES) have been constructed to offer distinct advantages over other approaches to chemical analysis of complex mixtures. Owing to the combination of a chromatograph and a spectrometer, it is much easier to identify components of mixtures separated in a chromatographic column than was previously possible with commonly employed detectors.

GC–AES

A system comprising a GC and an AES (GC–AES) was first reported in 1965.[1] Because of the application of microwave-induced plasma (MIP) in AES, detection limits in the pg/sec range were achieved for several elements, but the selectivity against carbon was very poor. The first commercially available GC–MIP–AES device was introduced in 1978, but its production was soon abandoned.[2]

In 1989, Hewlett-Packard introduced a modernized and totally automated atomic emission detector (AED) connected with a GC equipped with a capillary column. At present, two names are used for the device: GC–AED and (less frequently) GC–AES.[3] The device utilizes a microwave-induced helium plasma for decomposition and excitation of analyzed compounds, and a photodiode array (PDA) for light emission measurement. The GC–AED may be used alone or in conjunction with GC–MS, and the situation allows for more effective use of both devices together than separately.[4]

Principle of Operation

The principle of operation of AED is based on measurement of wavelength and intensity of light emitted by the excited atoms formed by decomposition of molecules of chromatographed chemical compounds. Constituents of the mixture, separated in a capillary column, are passed into a microwave-powered, high-temperature helium plasma. This is why helium must be used as a carrier gas in GC–AED. Helium plasma-introduced compounds are decomposed into elements. Atoms or ions of these elements become excited to higher energy levels. Then, returning to their base states, they emit light with wavelengths characteristic for individual elements. To increase the detector's efficiency, after the column but before the plasma cavity, small quantities of reagent gases are added to helium. The kind of utilized reagent gas depends on the elements of analyzed chemical compounds to be detected (Table 1).

The light emitted by atoms of individual elements that formed a compound leaving a chromatographic column is focused by an optical lens onto a holographic grid. Here, it is separated into components of various wavelengths and detected by a PDA in the range from 171 nm (oxygen) through 837 nm (chlorine) with a precision of 0.004 nm. A rotating holographic grating is an important element of the optics. It varies the elemental light spectrum covered by the fixed-position PDA. Algorithms of applied computer software provide automatic wavelength calibration, automatic focus, and measurements of intensity, wavelength, and line width. Detection of an elemental emission line and its spectral background makes use of numerous simultaneous signals from the PDA. These signals are combined into pairs and the resulting portions of the chromatogram in the form of essential signals and the background is registered separately. As a result of this, the elements' selectivity can be improved after sample analysis has been completed. Detection selectivity for most elements is very high. As light emitted by carbon or hydrogen is registered as chromatograms of these elements, the detector is universal for organic compounds. When light emitted by another element is registered, the detector is specific for that element.

The signals generated by the PDA for particular elements are registered by a computer as chromatographic files. Following a single sample injection, it is possible to obtain one to six elemental chromatograms. Two of these can be displayed on a computer screen in real time, and the rest are stored in the computer memory. After separation of the mixture components is completed, chromatograms of all elements forming these components can be printed. Fig. 1 presents a schematic representation of the AED.

Table 1 Elemental properties and reagent gases that may be used for analysis.

Element	Emission wavelength (nm)	Limit of detection (pg/sec)	Reagent gases	Makeup flow (ml/min)	Dynamic range
Carbon	179	10	O_2, H_2	35	1,000
	193	0.5	O_2, H_2	35	10,000
	248	6.5	O_2, H_2	180	10,000
	264	200	O_2, H_2	180	1,000
	496	20	O_2	35	30,000
	834	50	O_2	35	1,000
Hydrogen	486	2	O_2	35	6,000
	656	0.5	O_2	180	5,000
Oxygen	171	50	H_2 and (10% CH_4 + 90% N_2)	35	5,000
Nitrogen	174	7	O_2, H_2	35	10,000
	388	20	O_2, H_2, CH_4	180	1,000
Sulfur	181	1	O_2, H_2	35	10,000
Iodine	183	10	O_2, H_2	35	5,000
	206	20	O_2, H_2	35	5,000
Arsenic	189	3	H_2	180	1,000
Selenium	196	4	H_2	180	1,000
Tellurium	208	10	H_2	180	1,000
Antimony	218	5	H_2	180	1,000
Boron	250	20	O_2	180	1,000
Silicon	252	1	O_2, H_2	180	—
Mercury	254	0.5	O_2, H_2	180	1,000
Manganese	259	2	O_2, H_2	180	1,000
Lead	261	2	O_2, H_2	180	1,000
	406	1	O_2, H_2	180	1,000
Germanium	265	10	O_2, H_2	180	1,000
Tin	271	2	O_2, H_2	180	1,000
	301	1	O_2, H_2	180	1,000
	303	1	O_2, H_2	180	1,000
	326	1	O_2, H_2	180	1,000
Vanadium	292	4	O_2, H_2	180	1,000
Nickel	301	0.8	O_2, H_2	180	1,000
Iron	302	0.05	O_2, H_2	180	1,000
Chlorine	479	15	O_2	35	20,000
	837	15	O_2	35	20,000
Bromine	478	20	O_2	35	4,000
	827	20	O_2	35	4,000
Fluorine	690	20	H_2	35	2,000
Carbon-13	177	10	O_2, H_2	35	1,000
Nitrogen-15	420	3.5	O_2, H_2, CH_4	35	1,000
Deuterium	656	1	O_2	180	4,000

A GC–AED system is characterized with resolution capacity characteristic of capillary chromatography and high selectivity characteristic of atomic emission spectrometry. Theoretically, the AED is useful for detection of all elements except helium. Practically, commercially available GC–AED devices allow detection of 26 elements, including many metals and three isotopes: deuterium, C-13 carbon, and N-15 nitrogen.

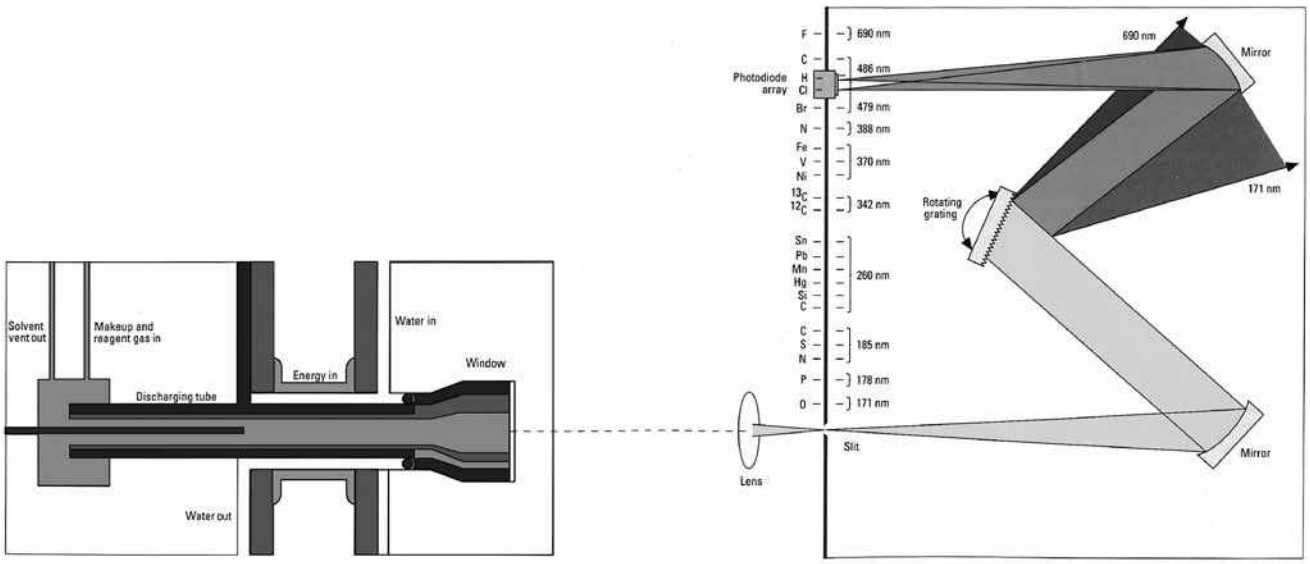

Fig. 1 Schematic diagram of AED.

Limits of detection for individual elements depend on the intensity of a particular emission line of each element—some elements can be detected with several light emission lines. In many cases, limits of detection achieved with GC–AED are at lower concentration levels than for other GC detectors. For a particular element, light emission intensity is proportional to the number of the element's atoms in a molecule of an analyzed compound; also, it is proportional to the concentration of the compound in an analyzed sample. Measuring emitted light intensity, it is possible to determine quantity of the element in a sample and to calculate the number of the element's atoms in molecules of particular compounds present in an analyzed sample.

Detector signal magnitude for an individual element is almost compound independent. The phenomenon of compound independence is used in quantitative analysis and also for identification of unknown compounds. In quantitative analysis, content of a given element in a particular compound is determined using a calibration graph for the same element, but present in various compounds in known amounts. It is then possible to perform quantitative analysis of compounds without standards of those compounds.

A direct result of a compound-independent elemental signal is the ability to measure elemental mole ratios (EMR) in analyzed compounds. For unknown compounds, the AED response in separate elemental channels for the compound is compared with the response to one or several standards. With computer software, first the EMR for known standards and then the empirical formula for an unknown compound are determined. Compound-independent calibration saves much time and cost for analysts, for it is possible to avoid using costly, and sometimes hazardous, standards.[5–9] Table 1 presents elements that can be detected and quantitatively assayed with AED, their limits of detection, wavelengths of their emissions, types of added reagent gases, and dynamic ranges of the detector signal.

Owing to a relatively low 193 carbon emission line limit of detection, it is possible for an AED to detect organic compounds at lower concentration levels compared to a flame ionization detector. Halides are detected at similar concentration levels as with an electron capture detector. AED is, however, less vulnerable to contaminations present in a sample; it also allows determination of fluorine, chlorine, bromine, and iodine. Most elements are detected in quantities ranging from several to dozens of pg/sec. The AED's sensitivity for oxygen is relatively low, however. This is manifested by the fact that the AED's oxygen detection limit in organic compounds reaches relatively high values (~50 pg/sec); one should remember, however, that it is the only detector capable of any oxygen detection in organic compounds. Owing to its high detectability and specificity toward many elements, GC–AED may be applied for analysis of environmental pollution, in the chemical industry, petroleum chemistry, pharmaceutical, cosmetic, and food industries, and in numerous other sectors where chromatographic analyses are used. GC–AED is particularly useful for analysis of organic compounds containing heteroatoms, including organometallic compounds. The method is also used for postsynthetic analysis of drugs and for monitoring them in a patient's organs, for analysis of polychlorinated biphenyls, halide derivatives of other hydrocarbons, pesticides, and other environmental pollutants such as mercury, tin, and lead compounds, and

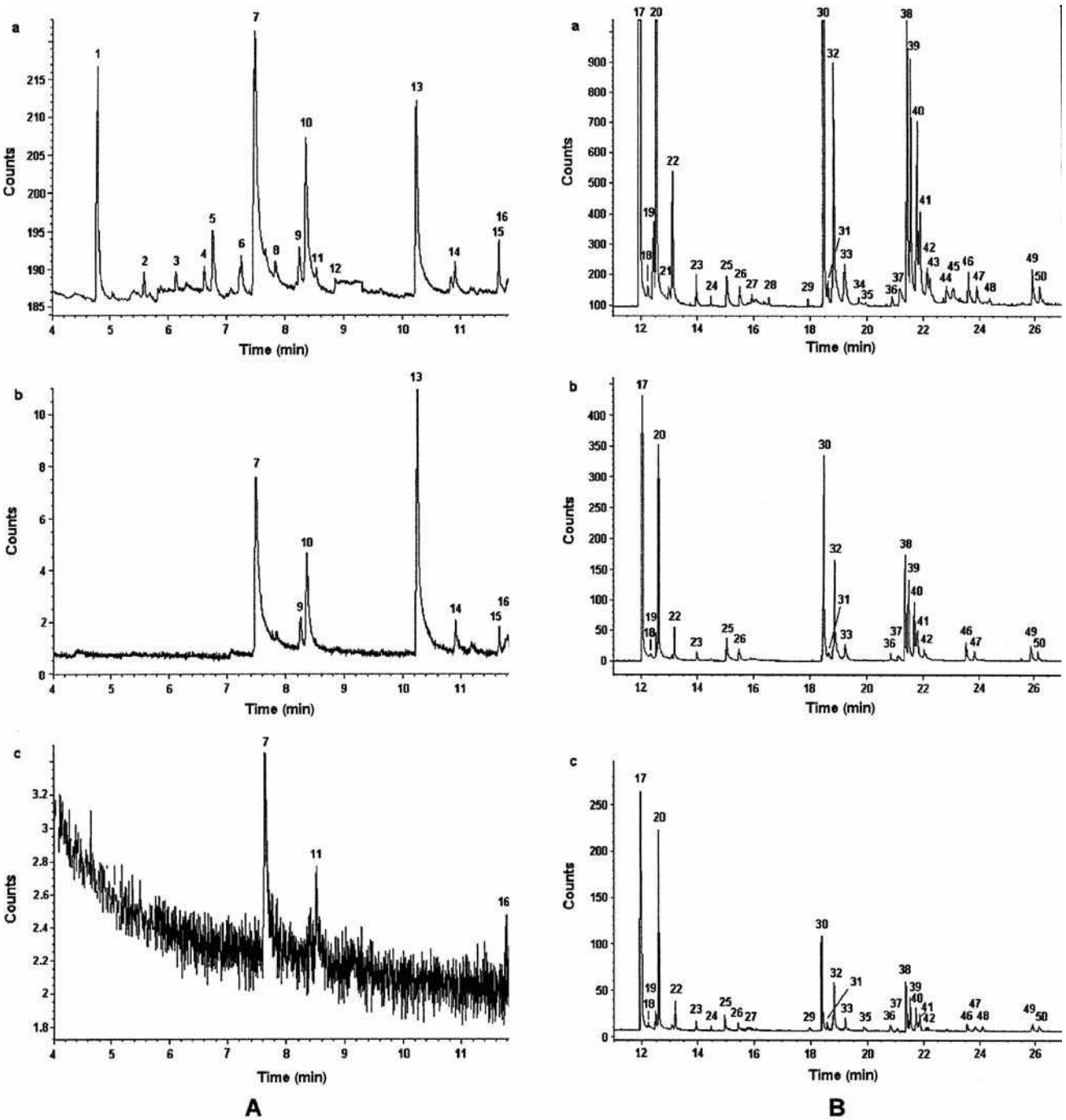

Fig. 2 A, The element chromatograms of a sample of the yperite block obtained by GC–AED on channel: (a) carbon, C-193 nm; (b) sulfur, S-181 nm; and (c) chlorine, Cl-479 nm, split ratio 20 : 1. B, The second part of the element chromatograms of a sample of the yperite block obtained by GC–AED on channel: (a) carbon, C-193 nm; (b) sulfur, S-181 nm; and (c) chlorine, Cl-479 nm, split ratio 60 : 1.

also of warfare agents. With GC–AED, it is possible to detect sulfur, nitrogen, oxygen, and lead compounds in petrochemical products.

Sample chromatograms obtained from GC–AED analysis of a sample collected from a block of yperite fished from the Baltic Sea are presented in Fig. 2.[10]

CONCLUSIONS

- GC connected with AES is a powerful technique for versatile, highly sensitive and selective analysis of heteroatoms (including metallic ones) containing compounds.

- Detector signal magnitude for individual element is almost compound-independent. The phenomenon is used in quantitative analysis and for determination of empirical formulas of unknown compounds. Contents of a given element in a particular compound can be determined using calibration graph for the same element but present in different compounds.
- Owing to a relatively low 193 carbon emission line limit of detection it is possible to detect organic compounds on five times lower concentration level comparing to flame ionization detector. Halides are detected on similar concentration levels as in electron capture detector. AED is ten times more sensitive for sulfur, with more linearity, than flame photometric detector.
- GC–MS and GC–AED can complement each other making the identification of analyzed compounds much easier and much sure than using them separately.

REFERENCES

1. McCormack, A.J.; Tong, S.C.; Cooke, W.D. Sensitive selective gas chromatography detector based on emission spectrometry of organic compounds. Anal. Chem. **1965**, *37*, 1470.
2. Uden, P.C., Ed.; *Element Specific Chromatographic Detection by Atomic Emission Spectroscopy*; American Chemical Society: Washington, DC, 1992.
3. van Stee, L.L.P.; Brinkman, U.A.Th. Gas chromatography with atomic emission detection: A powerful technique. Trends. Anal. Chem. **2002**, *21*, 618.
4. Olson, N.L.; Carrel, R.; Cummings, R.K.; Rieck, R. Gas chromatography with atomic emission detection for pesticide screening and confirmation. LC-GC **1994**, *12*, 142.
5. Wylie, P.L.; Sullivan, J.J.; Quimby, B.D. An investigation of gas chromatography with atomic emission detection for the determination of empirical formulas. HRC & CC **1990**, *13*, 499.
6. Pedersen-Bjergaard, S.; Asp, T.N.; Greibrokk, T. Factors affecting C : H and C : N ratios determined by gas chromatography coupled with atomic emission detection. HRC & CC **1992**, *15*, 89.
7. Sullivan, J.J.; Quimby, B.D. Detection of C, H, N, and O in capillary gas chromatography by atomic emission. HRC & CC **1989**, *12*, 282.
8. Janak, K.; Colmsjö, A.; Östman, C. Quantitative analysis using gas chromatography with atomic emission detection. J. Chromatogr. Sci. **1995**, *33*, 611.
9. Pedersen-Bjegard, S.; Greibrokk, T. N-, O- and P-selective on-column atomic emission detection in capillary gas chromatography. J. Chromatogr. A, **1994**, *686*, 109.
10. Mazurek, M.; Witkiewicz, Z.; Popiel, S.; Śliwakowski, M. Capillary gas chromatography–atomic emission spectroscopy–mass spectrometry analysis of sulphur mustard and transformation products in a block recovered from the Baltic Sea. J. Chromatogr. A, **2001**, *919*, 133.

Band Broadening in CE

Jetse C. Reijenga
Department of Chemical Engineering and Chemistry, Eindhoven University of Technology, Eindhoven, The Netherlands

INTRODUCTION

As in chromatography, band broadening in capillary electrophoresis (CE) is determined by a number of instrumental and sample parameters and has a negative effect on detectability, due to dilution. Also, as in chromatographic techniques, the user can minimize some, but not all, of the parameters contributing to band broadening. In CE, injection and detection are generally on-column, so that band broadening is limited to on-column effects. As will be shown, several effects are similar in chromatography; others are specific for CE and, in particular, for the potential gradient as a driving force. General equations for CE in open systems are given where the relative contribution of electro-osmosis is given by the electromigration factor f_{em}, given by

$$f_{em} = \frac{\mu_{eff}}{\mu_{eff} + \mu_{EOF}}$$

in which is the effective mobility and μ_{EOF} is the electro-osmotic flow mobility. This electromigration factor is unity for systems with suppressed electro-osmatic flow (EOF).

The band-broadening contributions can be described in the form of a plate-height equation, where one usually assumes, as in chromatography, mutual independence of terms.

INJECTION

Band broadening due to injection is naturally proportional to the injection volume, relative to the capillary volume, but, in contrast to chromatography, sample stacking or destacking may decrease or respectively increase the injection band broadening thus defined. Without stacking or destacking, the following plateheight term can be used:

$$H_{inj} = \frac{\delta_{inj}^2}{12L_d}$$

in which δ_{inj} is the length in the capillary of the sample plug and L_d is the length of the capillary to the detector. Naturally, the above relationship can be rewritten in terms of sample and capillary volume, which are in the order of 10 nl and 1 μl, respectively.

DIFFUSION

As in chromatography, the effect of diffusion on band broadening is generally pronounced. It is directly proportional to the diffusion coefficient and the residence time between injection and detection. This effect can, consequently, be reduced by increasing the voltage, or by increasing the EOF, in cases where cations are analyzed at positive inlet polarity, where it further shortens the analysis times.The effect is less at lower temperatures (as the diffusion coefficient decreases approximately 2.5% per degree Celsius of temperature drop), but most significantly decreases with increasing molecular mass of the sample component.

$$H_{diff} = \frac{2Dt_m}{L_d}$$

in which L_d is the capillary length to the detector, D is the diffusion coefficient, and t_m is the migration time. Substituting the diffusion coefficient, using the Nernst-Einstein relation, yields

$$H_{diff} = \frac{2RTf_{em}}{z_{eff}EF}$$

in which R is the gas constant, T is the temperature, z_{eff} is the overall effective charge of the sample ion, E is the electric field strength, and F is the Faraday constant. In this relationship, z_{eff} and E, by definition, have opposite signs for negative values of f_{em} only.

DETECTION

The detector time constant and detector cell volume are both involved.The slit width along the length of the capillary is proportional to the latter. A value of 200 mm for the slit width in the case of 10^5 plates in a 370 mm capillary has negligible contribution to band broadening:

$$H_{slit} = \frac{\delta_{det}^2}{12L_d}$$

where δ_{det} is the detector slit width along the capillary axis. In cases of diode array detection, larger slit widths are

usually applied; this reduces the noise level but may affect the peak shape at high plate numbers ($>10^5$).

The contribution of the detector time constant τ is modeled by the following relation:

$$H_\tau = L_d \left(\frac{\tau}{t_m}\right)^2$$

A detector time constant τ of 0.2 sec is generally safe.

THERMAL EFFECTS

In cases of a relatively high current density, power dissipation in the capillary may result in significant radial temperature profiles. The plate-height contribution is given by

$$H_{\text{ther}} = \frac{f_T^2 \kappa^2 E^5 R_i^6 z_{\text{eff}} F f_{\text{em}}}{1536 R T \lambda_s^2}$$

where f_T is the temperature coefficient for conductivity, κ is the specific conductivity of the buffer, E is the electric field strength, R_i is the capillary inner diameter, and λ_s is the thermal conductivity of the solution.

As the effective mobility increases with the temperature at approximately 2.5% per degree, radial mobility differences may accumulate to significant bandbroadening effects. The effect increases with increasing current density and capillary inner diameter. In a 75 μm inner diameter capillary, a power dissipation of 1–2 W/m is generally safe. This value is calculated by multiplying the voltage and the current and dividing by the capillary length. Under these conditions, the radial temperature profile in the capillary is less than 0.5°C and the contribution to peak broadening negligible. In the case of higher conductivity buffers (e.g., a pH 3 phosphate buffer), the power dissipation and temperature profile can be 10 times higher and the effect on peak broadening significant. It should be emphasized that more effective cooling has no effect on thermal band broadening; the only effect is decreased averaged temperature inside the capillary.

ELECTRO-OSMOTIC EFFECTS

Electro-osmosis in open systems is generally considered not to contribute to peak broadening. In hydrodynamically closed systems with non-suppressed electro-osmosis, or in cases of axially different electro-osmotic regimes, however, a considerable contribution may result. The corresponding plate-height term is

$$H_{\text{EOF}} = \frac{R_i^2 \zeta^2 \varepsilon^2 z_{\text{eff}} E F}{24 R T \eta^2 \mu_{\text{eff}}^2}$$

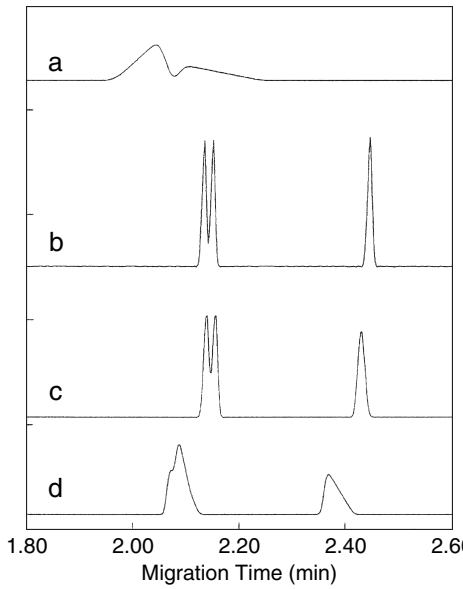

Fig. 1 Electrophoretic bandbroadening effects of benzoates as sample. Destacking trace (a) (1 m*M* sample in 1 m*M* buffer), stacking trace (b) (0.01 m*M* sample in 25 m*M* buffer), and trace (c) (1 m*M* sample in 25 m*M* buffer) and peak triangulation trace (d) (1 m*M* sample in 25 m*M* chloride buffer).

where ε is the dielectric constant and η is the local viscosity of the buffer at the plane of shear. This relationship shows that, in closed systems, the ζ-potential should be close to zero and that a viscosity increase near the capillary wall will be advantageous.

ELECTROPHORETIC EFFECTS

Peak broadening due to electrophoretic effects are generally proportional to the conductivity (and thus the ionic strength) of the sample solution, relative to that of the buffer. This effect is readily understood when considering that in the case of a high sample concentration, the electric field strength (and, consequently, the linear velocities) in the sample plug are much lower than in the adjacent buffer. Due to this, a dilution (destacking) of the sample occurs.This is illustrated in curve a in Fig. 1—the separation of a concentrated 1 m*M* solution benzenesulfonic, *p*-toluene sulfonic, and benzoic acid, dissolved in a buffer of 1 m*M* propionic acid/Tris to pH 8.

Alternatively, when injecting a low-conductivity (diluted, 0.01 m*M*) sample in a 25 m*M* buffer of same composition (curve b in Fig. 1–100 times amplified with respect to the others), the local field strength in the sample compartment is higher than in the adjacent buffer, resulting in a rapid focusing of ionic material at the sample-buffer interface (stacking), and resulting in very sharp sample injection plugs and high plate counts. This stacking takes

place during the first second after switching on the high voltage. It may thus be advantageous to inject a larger volume of a more diluted sample for better efficiency. Choosing a higher conductivity buffer also enhances the effect, where one has to consider that this may result in more pronounced band broadening due to other effects. Curve c in Fig. 1 shows that in such a high-conductivity buffer, even the 1 m*M* sample is separated to reasonable extent.

Peak symmetry is another important issue. Generally, capillary zone electrophoresis peaks are non-Gaussian and show non-symmetry.This peak triangulation increases with increasing concentration overload. It is also proportional to the difference in effective mobility of the sample ion and the coion in the buffer. For instance, analyzing the same 1 m*M* sample mixture in a buffer consisting of, for example, 25 m*M* chloride/Tris to pH 8 will give triangular peaks (curve d in Fig. 1) because the effective mobility of benzoic acid is much lower than that of the buffer anion chloride: The buffer co-ion is not properly tuned to the sample component mobilities.

BIBLIOGRAPHY

1. Giddings, J.C. *Treatise on Analytical Chemistry*; Kolthoff, I.M., Elving, P.J., Eds.; John Wiley & Sons: New York, 1981; Part I, Vol. 5.
2. Hjertén, S. Free zone electrophoresis. Chromatogr. Rev. **1967**, *9* (2), 122.
3. Jorgenson, J.W.; Lukacs, K.D. Capillary zone electrophoresis. Science **1983**, *222* (4621), 266.
4. Kenndler, E. Effect of electroosmotic flow on selectivity, efficiency, and resolution in capillary zone electrophoresis expressed by the dimensionless reduced mobility. J. Capillary Electrophoresis **1996**, *3* (4), 191.
5. Reijenga, J.C.; Kenndler, E. Computational simulation of migration and dispersion in free capillary zone electrophoresis, Part I, Description of the theoretical model. J. Chromatogr. A, **1994**, *659*, 403.
6. Reijenga, J.C.; Kenndler, E. Computational simulation of migration and dispersion in free capillary zone electrophoresis, part II, Results of simulation and comparison with measurements. J. Chromatogr. A, **1994**, *659*, 417.
7. Virtanen, R. Acta Polytech. Scand. **1974**, *123*, 1.

Band Broadening in GPC/SEC

Gregorio R. Meira
Jorge R. Vega
National Scientific and Technical Research Council (CONICET), Santa Fe, Argentina

INTRODUCTION

In ideal size exclusion chromatography (SEC), fractionation is exclusively by hydrodynamic volume. Unfortunately, perfect SEC fractionation is impossible due to the presence of secondary fractionations and band broadening (BB). Secondary fractionations result from physicochemical interactions between the polymer, the solvent, and the column packing[1] and are not discussed further. Band broadening is mainly due to axial dispersion in the columns, while other broadening sources include column end-fitting effects, finite injection volumes, finite detection cell volumes, and laminar flow profiles in the capillaries.[2,3] Mathematical models have been developed that describe the detailed fractionation processes in SEC. Their aim is to estimate the chromatograms from a priori knowledge of the molar mass distribution (MMD), the polymer–solvent–matrix interactions, the column characteristics, and the flow conditions.[4–7] Unfortunately, these complex models have not been applied so far for BB correction, and therefore they are not discussed further.

If a broad and smooth chromatogram is obtained with modern high-resolution columns, the BB effect is generally negligible, and no specific corrections are required. In contrast, corrections for BB may be important when analyzing: 1) narrow chromatograms of half-widths close to those of monodisperse samples appearing at similar elution volumes; and 2) broad but multimodal chromatograms, with sharp elbows and/or narrow peaks.

First, consider the simpler case of a mass-sensitive detector (typically, a differential refractometer, DR) in combination with a molar mass calibration (in turn, obtained from narrow standards of the analyzed polymer). Due to BB (and even in the simpler case of analyzing a linear homopolymer), a whole distribution of hydrodynamic volumes (and therefore of molar masses) is instantaneously present in the DR cell. This establishes that the mass chromatogram $w(V)$ (i.e., the instantaneous mass w vs. the elution time or elution volume V) is a broadened version of a hypothetically true (or corrected) mass chromatogram $w^c(V)$, as follows:[8]

$$w(V) = \int_0^\infty g(V, \overline{V}) w^c(\overline{V}) \mathrm{d}\overline{V} \qquad (1)$$

where $g(V, \overline{V})$ is the (in general, non-uniform) BB (or spreading) function and $\overline{V}$ is a dummy integration variable that represents an average retention volume. At each $\overline{V}$, a different individual $g(V)$ function is defined. For any symmetrical $g(V)$ function, its $\overline{V}$ value is unambiguously assigned at its maximum (or mode). For skewed $g(V)$ functions, however, the average retention volume could be assigned at the mode, the mean, or any other measure of central tendency. This ambiguity in the origin of asymmetrical BB functions is still an unresolved question regarding the specification of $g(V, \overline{V})$. For uniform (or retention volume invariant) BB functions, Eq. 1 reduces to a simple convolution integral.

The molar mass calibration is normally expressed as $\log M(V)$. This calibration is obtained from narrow standards, by associating a set of average molar masses to a set of average retention volumes. If this association is carried out correctly, then the calibration is essentially unaffected by BB. When the MMD is estimated from a (broadened) mass chromatogram $w(V)$ and an unbiased (or "true") molar mass calibration $\log M(V)$, then the distribution is broader than real, the number-averaged molar mass ($\overline{M}_n$) is underestimated, and the weight-averaged molar mass ($\overline{M}_w$) is overestimated. The direct correction procedure for these biases is as follows: 1) From the knowledge of $w(V)$ and $g(V, \overline{V})$, calculate $w^c(V)$ by inversion of Eq. 1; and 2) from $w^c(V)$ and $\log M(V)$, obtain the unbiased MMD $w^c(\log M)$.

If the analyzed polymer is strictly monodisperse (both in hydrodynamic volume and in molar mass), then the corrected chromatogram $w^c(V)$ is an impulsive function, and the mass chromatogram is a direct measure of the BB function at the given $\overline{V}$. Thus, the global $g(V, \overline{V})$ could be obtained by interpolation, from a set of monodisperse (or uniform) standards. Unfortunately, uniform standards are only available for low molar masses (e.g., a pure solvent) and for some water-soluble biopolymers. "Almost" uniform standards have been produced by fractionating narrow (synthetic) standards through temperature-gradient interaction chromatography, and their chromatograms have been adequately fit with exponentially modified Gaussian (EMG) functions.[9] Inside the linear calibration range, these functions are quite uniform but skewed, with exponential decay (or tailing) toward the higher elution

volumes. However, when approaching the limit of total exclusion, the BB function becomes narrower and more skewed, and cannot be well approximated by an EMG.[9] Even for a "linear" calibration, resolution in SEC falls exponentially with increasing molar mass,[10] while the BB function remains essentially uniform.[9] For this reason, the effects of BB are particularly serious at the higher molar masses.

Apart from the use of uniform (or almost uniform) standards, other methods for determining the BB function have been developed. For example, by assuming a uniform and Gaussian BB function with a linear molar mass calibration, it is possible to use the mass and molar mass chromatograms for simultaneously estimating the standard deviation of the BB function and the calibration coefficients.[11,12] Alternatively, if the shape of the MMD is known (e.g., it is a Poisson distribution on a linear molar mass axis), then the BB function can be estimated from the difference between the (mass or molar mass) chromatogram and its theoretical prediction in the absence of BB.[13] Finally, the BB function can be theoretically predicted from a representative fractionation model.[4,7] Unfortunately, however, this approach is so far unfeasible due to the difficulty in determining the associated physicochemical parameters.

Consider the BB problem when molar mass sensitive detectors are employed. First, let us analyze the ideal case of a chromatograph fit with perfect detectors and not exhibiting BB, secondary fractionations, or interdetector volumes. In this case, the instantaneous MMD is strictly uniform, and any molar mass detector type would provide the same result:[14]

$$M(V) = K_{\mathrm{LS}} \frac{{s_{\mathrm{LS}}}^{\mathrm{c}}(V)}{w^{\mathrm{c}}(V)} = K_{\mathrm{IV}} \left[\frac{{s_{\mathrm{IV}}}^{\mathrm{c}}(V)}{w^{\mathrm{c}}(V)}\right]^{1/a} = K_{\mathrm{OS}} \frac{w^{\mathrm{c}}(V)}{{s_{\mathrm{OS}}}^{\mathrm{c}}(V)} \tag{2}$$

where ${s_{\mathrm{LS}}}^{\mathrm{c}}(V)$, ${s_{\mathrm{IV}}}^{\mathrm{c}}(V)$, and ${s_{\mathrm{OS}}}^{\mathrm{c}}(V)$ are respectively the "true," "corrected," or unbroadened chromatograms obtained from a light-scattering (LS) detector, a specific viscosity (IV) detector, and a (still under development) colligative-property osmometer (OS) detector; a is the Mark–Houwink–Sakurada exponent at the given measuring conditions; and K_{LS}, K_{IV}, and K_{OS} are calibration constants. Eq. 2 provides an unbiased (or MMD-independent) molar mass calibration log $M(V)$ that, in principle, is identical to that determined from uniform standards in a real chromatograph with BB.

The signal-to-noise ratios are generally poor at the chromatogram tails; for this reason, the signal ratios of Eq. 2 are only precise in the mid-chromatogram region. Also, the molar mass sensitive sensor is normally connected in series with the DR, and this shows that the molar mass signal slightly leads the mass signal. To correct for this bias (and independent of BB), the LS signal must be adequately shifted toward higher retention volumes prior to calculating any quality variable (e.g., the molar masses of Eq. 2).

The BB mainly occurs in the fractionation columns, and (to a first approximation) one can neglect the extra broadening introduced by the injector, the detector cells, and the interdetector capillaries. In this case, any generic chromatogram $s_k(V)$ is broadened by a common BB function $g(V, \overline{V})$ as follows:[15,16]

$$s_k(V) = K_k \int_{{V_1}^{\mathrm{c}}}^{{V_2}^{\mathrm{c}}} g(V, \overline{V}) {s_k}^{\mathrm{c}}(\overline{V}) \mathrm{d}\overline{V} \quad (k = \mathrm{DR}, \mathrm{LS}, \mathrm{IV}, \mathrm{OS}) \tag{3}$$

Note that Eq. 3 reduces to Eq. 1 for $K_{\mathrm{DR}} = 1$, $s_{\mathrm{DR}} \equiv w$, and ${s_{\mathrm{DR}}}^{\mathrm{c}} \equiv w^{\mathrm{c}}$. The instantaneous weight-, viscosity-, and number-averaged molar masses [$M_{\mathrm{w}}(V)$, $M_{\mathrm{v}}(V)$, and $M_{\mathrm{n}}(V)$, respectively] are obtained from the signal ratios:[14,17,18]

$$M_{\mathrm{w}}(V) = K_{\mathrm{LS}} \frac{s_{\mathrm{LS}}(V)}{w(V)}; \quad M_{\mathrm{v}}(V) = K_{\mathrm{IV}} \left[\frac{s_{\mathrm{IV}}(V)}{w(V)}\right]^{1/a}; \quad M_{\mathrm{n}}(V) = K_{\mathrm{OS}} \frac{w(V)}{s_{\mathrm{OS}}(V)} \quad [M_{\mathrm{w}}(V) \geq M_{\mathrm{v}}(V) \geq M_{\mathrm{n}}(V)] \tag{4}$$

Unlike $M(V)$ of Eq. 2, $M_{\mathrm{w}}(V)$, $M_{\mathrm{v}}(V)$, and $M_{\mathrm{n}}(V)$ now depend on the analyzed MMD; therefore, log $M_{\mathrm{w}}(V)$, log $M_{\mathrm{v}}(V)$, and log $M_{\mathrm{n}}(V)$ can be thought of as "biased" or ad hoc molar mass calibrations. Even if log $M_{\mathrm{w}}(V)$, log $M_{\mathrm{v}}(V)$, and log $M_{\mathrm{n}}(V)$ were perfectly accurate, the MMDs directly derived from the (broadened) mass chromatogram and any of such calibrations are distorted with respect to the true w^{c}(log M). In spite of BB, if an instantaneous variable is accurately estimated, then its corresponding global variable is also exact. Thus, the MMD represented by w(log M_{w}) produces an exact global $\overline{M}_w$ but an overestimated global $\overline{M}_n$, while the MMD represented by w(log M_{n}) produces an exact global $\overline{M}_n$ but an underestimated $\overline{M}_w$. In both cases, the global polydispersity is underestimated.[19,20] The previous observation is generalized to any other global average obtained from multidetection SEC. For example, if an instantaneous copolymer composition is accurately calculated from a signals ratio, then the global composition will also be accurate, in spite of BB.[21]

The correction for BB in SEC is still a matter of active research, and a "state of the art" review has recently been published.[14] At present, the authors are participating in an IUPAC project entitled "Data Treatment in the Size Exclusion Chromatography of Polymers"; one of the project objectives is the evaluation and standardization of existing BB correction techniques. Thus, the present article can be considered a first contribution toward that aim.

CORRECTION FOR MASS CHROMATOGRAMS WITH INDEPENDENT CALIBRATIONS

Consider the direct inversion of Eq. 1, i.e., the calculation of $w^c(V)$ from the knowledge of $w(V)$ and $g(V, \overline{V})$. First, let us transform Eq. 1 into the following equivalent discrete expression:

$$\mathbf{w} = \mathbf{G}\mathbf{w}^c \tag{5}$$

where $\mathbf{w}$ is an $(m \times 1)$-column vector containing the heights of $w(V)$ sampled at regular ΔV intervals in the elution volumes range $[V_1–V_m]$; $\mathbf{w}^c$ is a $(p \times 1)$-column vector containing the heights of $w^c(V)$ calculated at the same elution volumes but in the narrower range $[\overline{V}_1 - \overline{V}_p]$; and $\mathbf{G}$ is an $(m \times p)$ rectangular matrix representing $g(V, \overline{V})$ in the range $[\overline{V}_1 - \overline{V}_p]$. A typical sampling interval is $\Delta V = 0.1$ ml.

Specification of Matrix G[22]

For a successful inversion of Eq. 5, it is important to adequately define matrix $\mathbf{G}$. First, it is recommendable to adjust $g(V, \overline{V})$ with a continuous analytical expression, and then to calculate the heights of the individual $g(V)$ functions from that expression. Many analytical functions (e.g., a Gaussian distribution) never strictly drop to zero, and this would produce "full" $\mathbf{G}$ matrixes with positive and non-zero elements. Instead, it is preferable to set to 0 all of the "almost-null" elements of $\mathbf{G}$ (e.g., those smaller than 1% of the maximum). Also, choose $\mathbf{G}$ of minimal dimensions, in the sense that: 1) its p columns must strictly cover the range of the corrected chromatogram $[\overline{V}_1 - \overline{V}_p]$; and 2) its m rows must strictly cover the range of the measured chromatogram $[V_1–V_m]$.[22] Since, in general, the BB functions are skewed and non-uniform, it is convenient to specify each individual $g(V)$ to contain $(c + 1 + d)$ non-zero points, where c and d are the number of points before and after $\overline{V}$, respectively. Thus, the number of columns of $\mathbf{G}$ results: $p = m - c - d$, and the matrix is defined as follows:

$$\mathbf{G} = \begin{bmatrix} g(V_1,\overline{V}_1) & \cdots & 0 & \ddots & 0 \\ \vdots & \ddots & 0 & & \vdots \\ g(V_{c+1},\overline{V}_1) & & g(V_j,\overline{V}_j) & & \\ \vdots & \ddots & \vdots & \ddots & 0 \\ g(V_{c+1+d},\overline{V}_1) & & g(V_{c+j},\overline{V}_j) & & g(V_p,\overline{V}_p) \\ 0 & \ddots & \vdots & \ddots & \vdots \\ \vdots & & g(V_{c+j+d},\overline{V}_j) & & g(V_{c+p},\overline{V}_p) \\ & & 0 & \ddots & \vdots \\ 0 & \cdots & 0 & \cdots & g(V_m,\overline{V}_p) \end{bmatrix} \quad (m > p) \tag{6}$$

where each jth column of $\mathbf{G}$ contains $(c + 1 + d)$ non-zero heights of the discrete $g(V)$, with $\overline{V}_j = V_1 + (c + j - 1)\Delta V$. Note that by adopting $\overline{V}$ at the mode of $g(V)$, in each column, the largest element is c rows below the corresponding (j, j) "diagonal" element.

The direct inversion of Eq. 5 through, for example, the pseudoinverse $\hat{\mathbf{w}}^c = [\mathbf{G}^T\mathbf{G}]^{-1}\mathbf{G}^T\mathbf{w}$ (where "^" indicates estimated value) is not recommended because the square matrix $[\mathbf{G}^T\mathbf{G}]$ is generally ill-conditioned, and this produces highly oscillatory solutions with negative peaks. The propagation of errors is determined by: 1) the condition number of $\mathbf{G}^T\mathbf{G}$ (i.e., the ratio between the largest and the smallest eigenvalue of $\mathbf{G}^T\mathbf{G}$); and 2) the type and amplitude of the noise that contaminates $w(V)$.

In what follows, several BB correction techniques are presented and evaluated. To illustrate the effect of BB on the MMD, a molar mass calibration is adopted. The evaluated techniques are classified into two groups: 1) Methods I–III, which numerically invert Eq. 1 prior to calculating the MMD; and 2) Methods IV and V, which (avoiding the numerical inversion) calculate the corrected MMD in a single step. Methods I–III are more general, in the sense that they admit non-uniform and skewed BB functions. In contrast, Methods IV and V are strictly applicable to Gaussian chromatograms with Gaussian BB functions. Methods I–III have been developed to improve the (highly oscillatory) solution of the direct pseudoinverse, but at the cost of requiring an algorithm adjustment. The solutions of Methods I–III normally involve a trade-off between an excessively "rich" corrected chromatogram (with high-frequency oscillations and negative peaks) and an excessively smoothened solution (where some of the high-frequency components of the corrected chromatogram are lost).

Method I: Difference Function[23]

This iterative procedure was originally presented as Method 1 by Ishige, Lee, and Hamielec[23] and is based on the following recursive equation:

$$\Delta_i\mathbf{w} = \Delta_{i-1}\mathbf{w} - \mathbf{G}\,\Delta_{i-1}\mathbf{w}; \quad \text{with} \quad \Delta_0\mathbf{w} = \mathbf{w} \quad (i = 1, 2, \ldots) \tag{7a}$$

where i is the iteration step. After a few r iterations, $\Delta_i\mathbf{w}$ tends to almost zero, and at that point the corrected chromatogram is obtained from

$$\hat{\mathbf{w}}^c = \sum_{i=1}^{r} \Delta_i\mathbf{w} \tag{7b}$$

Method II: Singular Value Decomposition[24]

The final expression of this least-squares estimation procedure is

$$\hat{\mathbf{w}}^{c} = \sum_{k=1}^{r} \frac{\mathbf{u}_k{}^{T}\mathbf{w}}{\sigma_k}\mathbf{v}_k \quad (r \le p)$$
$$(\sigma_1 \ge \sigma_2 \ge \cdots \ge \sigma_r \ge \cdots \ge \sigma_p \ge 0) \tag{8}$$

where $\mathbf{u}_k$ and $\mathbf{v}_k$ are the eigenvectors of $\mathbf{G}\mathbf{G}^{T}$ and $\mathbf{G}^{T}\mathbf{G}$, respectively; σ_k are the singular values[24] of $\mathbf{G}$; and p is the (full) rank of $\mathbf{G}$. In Eq. 8, the number of "effective" summation terms is limited to r. The reason for discarding the lower σ_k's is to avoid amplifying the measurement noise. The lowest admissible σ_r is selected to slightly exceed the inverse of the lowest signal-to-noise ratio (normally encountered at the chromatogram tails).

Method III: Kalman Filter[25]

This fast and effective digital algorithm is based on a linear stochastic model that is equivalent to Eq. 1. The theoretical background is beyond the scope of the present article, and some knowledge on basic Kalman filtering theory is necessary for an adequate adjustment of the algorithm.[24–26] The adjustment involves estimating the variances of the measurement noise and of the expected solution.

Method IV: Rotation of the Linear Calibration[27]

Several (rather restrictive) conditions are here imposed: 1) The true mass chromatogram $w^{c}(V)$ is Gaussian (for example, because it corresponds to a Wesslau MMD and a linear calibration); 2) the BB function is uniform and Gaussian; and 3) the molar mass calibration is linear. Under these conditions, the ad hoc calibrations log $M_w(V)$, log $M_v(V)$, and log $M_n(V)$ are all linear and rotated counterclockwise with respect to the unbiased linear calibration log $M(V)$.[20,27,28] For a non-Gaussian chromatogram, the ad hoc calibrations are generally non-linear but less steep than log $M(V)$.[19,22,29] The method aims at recuperating unbiased estimates of the global averages $\overline{M}_n$ and $\overline{M}_w$ from an "effective" linear molar mass calibration defined by $M(V)|_{IV} = D_1'\exp(-D_2'V)$, with[27]

$$D_1' = D_1 \exp\left\{\frac{D_2\sigma_g{}^2[D_2(\sigma_w{}^2 - \sigma_g{}^2) - 2\overline{V}]}{2\sigma_w{}^2}\right\} \tag{9a}$$

$$D_2' = D_2 \exp\left(1 - \frac{\sigma_g{}^2}{\sigma_w{}^2}\right) \tag{9b}$$

where $\sigma_g{}^2$ and $\sigma_w{}^2$ are the variances of $g(V)$ and $w(V)$, respectively; and $\overline{V}$ is the retention volume of the chromatogram peak. Even though the method is strictly applicable to Gaussian chromatograms, it will be tested here on a non-Gaussian chromatogram (but still satisfying the other requirements of a linear calibration and a uniform and Gaussian BB).

Method V: Approximate "Analytical" Solution[30]

This approach is again based on the following (rather strict) assumptions: 1) The BB function is Gaussian (but generally non-uniform), of variance $\sigma_g{}^2(V)$; and 2) at each retention volume, the integrand of Eq. 1 can be approximated by the product of the measured chromatogram $w(V)$ and a Gaussian "correction" function of variance $\sigma_0{}^2(V)$ and averages $\overline{V}(V)$. The molar mass calibration may be non-linear, and is given by $M(V) = D_1(V)\exp[-D_2(V)V]$. The corrected chromatogram is obtained from

$$\hat{w}^{c}(V) = w(V)\left[\frac{\sigma_g(V)}{\sigma_0(V)}\right]\exp\left[-\frac{[V - \overline{V}(V)]^2}{2\sigma_0{}^2(V)}\right] \tag{10a}$$

with

$$\overline{V}(V) = V + \frac{1}{D_2(V)} \times \ln\left\{\frac{w[V + D_2(V)\sigma_g{}^2(V)]}{\sqrt{w[V - D_2(V)\sigma_g{}^2(V)]w[V + D_2(V)\sigma_g{}^2(V)]}}\right\} \tag{10b}$$

$$\sigma_0{}^2(V) = \sigma^2(V) + \frac{1}{D_2{}^2(V)} \times \ln\left\{\frac{w[V - D_2(V)\sigma_g{}^2(V)]w[V + D_2(V)\sigma_g{}^2(V)]}{w^2(V)}\right\} \tag{10c}$$

Evaluation Example

Correction methods are normally evaluated on numerical examples. This is because their real (or true) solutions are a priori known, and therefore the quality of their recuperations is properly quantified. In contrast, in real measurements, the true corrected chromatograms (and/or the true MMDs) are never exactly known. Consider, in what follows, a synthetic example that has been previously attempted on several occasions.[25,31–33]

The raw data are the corrected chromatogram $w^{c}(V)$ of Fig. 1A, the (uniform) broadening function $g(V)$ of Fig. 1A, and the linear calibration log $M(V)$ of Fig. 1B. By convolution of $w^{c}(V)$ and $g(V)$, a noise-free "measurement" was first obtained. Then, this noise-free function was rounded to the last integer;[33] this procedure is equivalent to adding a zero-mean random noise of uniform probability distribution in the range ±0.5. The resulting "chromatogram" is $w(V)$ of Fig. 1A. Note that the multimodality of $w^{c}(V)$ is lost in $w(V)$.

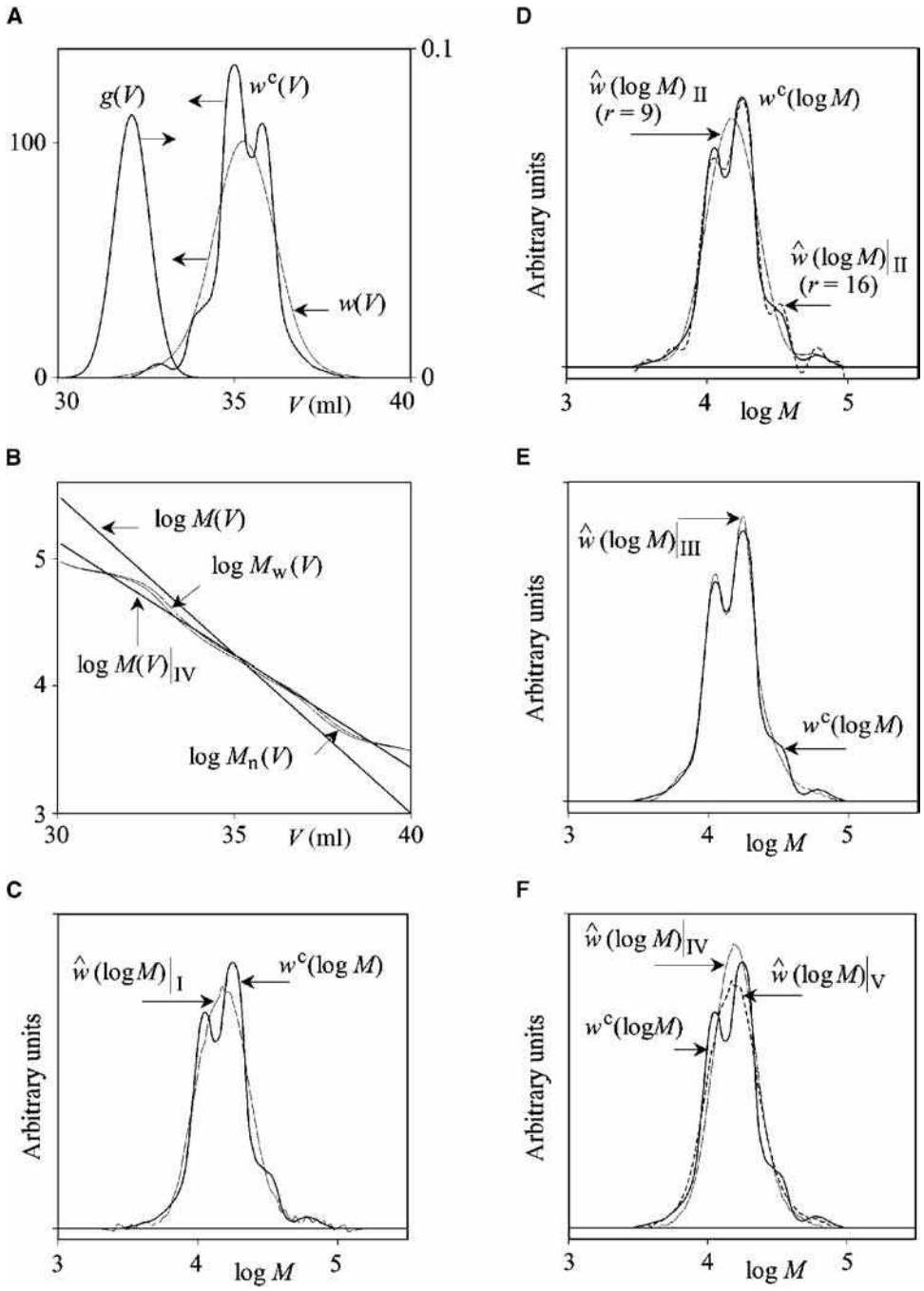

Fig. 1 Simulated example of DR detection and molar mass calibration. A) "True" mass chromatogram $w^c(V)$; uniform BB function $g(V)$; and resulting "measured" chromatogram $w(V)$. B) "True" molar mass calibration log $M(V)$; rotated "effective" calibration according to Method IV[27] log $M(V)|_{IV}$; and ad hoc calibrations assuming perfect molar mass sensors log $M_n(V)$ and log $M_w(V)$. C–F) Comparison between the true MMD $w^c(\log M)$ and its estimates according to Methods I,[23] II,[24] III,[25] IV,[27] and V,[30] respectively.

This example is particularly demanding because $w^c(V)$ is multipeaked, and the variance of $w^c(V)$ is similar to that of $g(V)$.

In previous publications,[25,31–33] only the ability of several inversion algorithms was evaluated, but not the effect of BB on the MMD. Here, the methods are compared on the basis of their performance in recuperating the true MMD. From log $M(V)$ and $w^c(V)$, the true MMD $w^c(\log M)$ of Figs. 1C–F is obtained. The aim is to estimate $w^c(\log M)$ from $w(V)$, $g(V)$, and log $M(V)$. Note that the selection of a uniform and Gaussian BB is not an impediment to adequately evaluating the (more comprehensive) Methods I–III.

In Fig. 1C–F, the MMDs recuperated through Methods I–V are compared with the real distribution; Table 1

presents the real and estimated average molar masses and polydispersities. In Method I, the best results were found after only 4 iterations (Fig. 1C). In Method II, the signal-to-noise ratio at the chromatogram tails suggested truncation of the summation of Eq. 8 at $r = 16$ (while the full rank of $\mathbf{G}$ is $p = 61$). The resulting solution exhibits a negative oscillation (Fig. 1D); and for comparison, the less "rich" solution with $r = 9$ is also presented. The Kalman filter of Method III was adjusted as follows: 1) The measurement noise variance was assumed time invariant, and estimated from the baseline noise; and 2) the solution variance was assumed time varying, and estimated by simply squaring the measured chromatogram heights (Fig. 1E). For Method IV, the "effective" linear calibration was calculated through Eq. 9, and is presented in Fig. 1B. In Method V, it was verified that (for a linear calibration) the solution becomes almost independent of $D_2(V)$.[30] The solutions of Methods IV and V are shown in Fig. 1F.

In relation to Methods IV and V, the instantaneous MMDs were simulated with the aim of calculating the (noise-free) calibrations $\log M_n(V)$ and $\log M_w(V)$ (Fig. 1B). These functions were obtained from the (noise-free or non-truncated) mass chromatogram in order to illustrate their "true" shapes in the complete range of the measured chromatogram. The resulting ad hoc calibrations are non-linear, generally less steep than $\log M(V)$, and close to the "effective" linear calibration $\log M(V)|_{IV}$ (Fig. 1B).

The following is observed. Only Method III (and to a lesser extent Method II with $r = 16$) was capable of recuperating the fine details of the true MMD, while all the other techniques yielded unimodal solutions. Methods III and II considerably improve the highly oscillatory direct pseudoinverse solution (not presented here for space reasons). The recuperated average molar masses of Table 1 are in all cases quite acceptable.

CORRECTION METHODS FOR MOLAR MASS SENSITIVE DETECTORS

Now, we wish to determine an unbiased MMD from measurements of mass and molar mass sensitive detectors. Rewrite Eq. 3 as follows:

$$\mathbf{s}_k = K_k \mathbf{G} \mathbf{s}_k^{\,c} \quad (k = \text{DR, LS, IV, OS}) \tag{11}$$

where $\mathbf{s}_k$ is an $(m \times 1)$-column vector containing the non-zero heights of $s_k(V)$, sampled at regular ΔV intervals; $\mathbf{s}_k^{\,c}$ is a $(p \times 1)$-column vector containing the non-zero heights of $s_k^{\,c}(V)$; and $\mathbf{G}$ is the $(m \times p)$ rectangular matrix of Eq. 6.

Inversion Methods

Two methods are described.[15,22] They both aim at correcting the raw chromatograms for BB prior to calculating the MMD, and are strictly applicable to linear homopolymers. Netopilík[15] proposed an iterative procedure for simultaneously estimating the MMD and the standard deviation of a uniform and Gaussian BB function (σ_g). The procedure is as follows: 1) Select a σ_g value; 2) estimate $w^c(V)$ and $s_k^{\,c}(V)$ by inversion of Eqs. 1 and 3, respectively; 3) use Eq. 2 for estimating a molar mass calibration $\log \widehat{M}(V)$; and 4) iterate until the slope of $\log \widehat{M}(V)$ coincides with that of an (independently determined) molar mass calibration. The method was theoretically tested on a narrow Schulz–Zimm MMD; while the original distribution was well recuperated, the standard deviation differed considerably from its original value.[15]

More recently, Vega and Meira[22] proposed a numerical method that does not impose any restriction on the shapes of the MMD or the BB function, and only implies a linear calibration in the range of the measured chromatograms. This last requirement is generally satisfied (especially if the MMD is narrow), and it is also easily verified from an independent calibration with narrow standards. The method is as follows: 1) Estimate $w^c(V)$ and $s_k^{\,c}(V)$ by inversion of Eqs. 1 and 3, respectively; 2) calculate an unbiased molar mass calibration $\log \widehat{M}(V)$ through Eq. 2, and use its mid-chromatogram region to adjust a linear calibration $\log \widehat{M}_{lin.}(V)$; and 3) from $\hat{w}^c(V)$ and $\log \widehat{M}_{lin.}(V)$ estimate the unbiased MMD $\hat{w}^c(\log \widehat{M}_{lin.})$.[22] Note the following: a) Any of the previously described Methods I–III can be used for solving step 1; b) by extrapolating a linear calibration toward the chromatogram tails, the technique also solves the problem of an oscillatory ad hoc calibration; and c) the resulting $\log \widehat{M}_{lin.}(V)$ can be verified with an independent calibration with narrow standards of the analyzed polymer.

Table 1 Simulated example that assumes a mass chromatogram, a linear calibration, and a Gaussian BB function: "true" and recuperated average molar masses.

	"True" values	Without BB correction	Correction method no.					
				II				
			I ($i = 4$)	($r = 9$)	($r = 16$)	III	IV	V
$\overline{M}_n$	13 975	13 464	14 029	13 993	14 033	14 084	14 871	14 038
$\overline{M}_w$	17 342	18 041	17 315	17 310	17 313	17 156	17 224	17 335
$\overline{M}_w/\overline{M}_n$	1.241	1.340	1.234	1.237	1.234	1.218	1.158	1.235

Reconsider the numerical example of Vega and Meira.[22] The basic raw data are: 1) the "true" or corrected mass chromatogram $w^c(V)$ of Fig. 2A; 2) the molar mass calibration $\log M(V)$ of Fig. 2C; and 3) the non-uniform and skewed broadening function $g(V, \overline{V})$ of Fig. 2A. All of these functions are discrete, with their heights sampled every $\Delta V = 0.1$ ml. The true mass chromatogram contains $p = 70$ non-zero points in the range

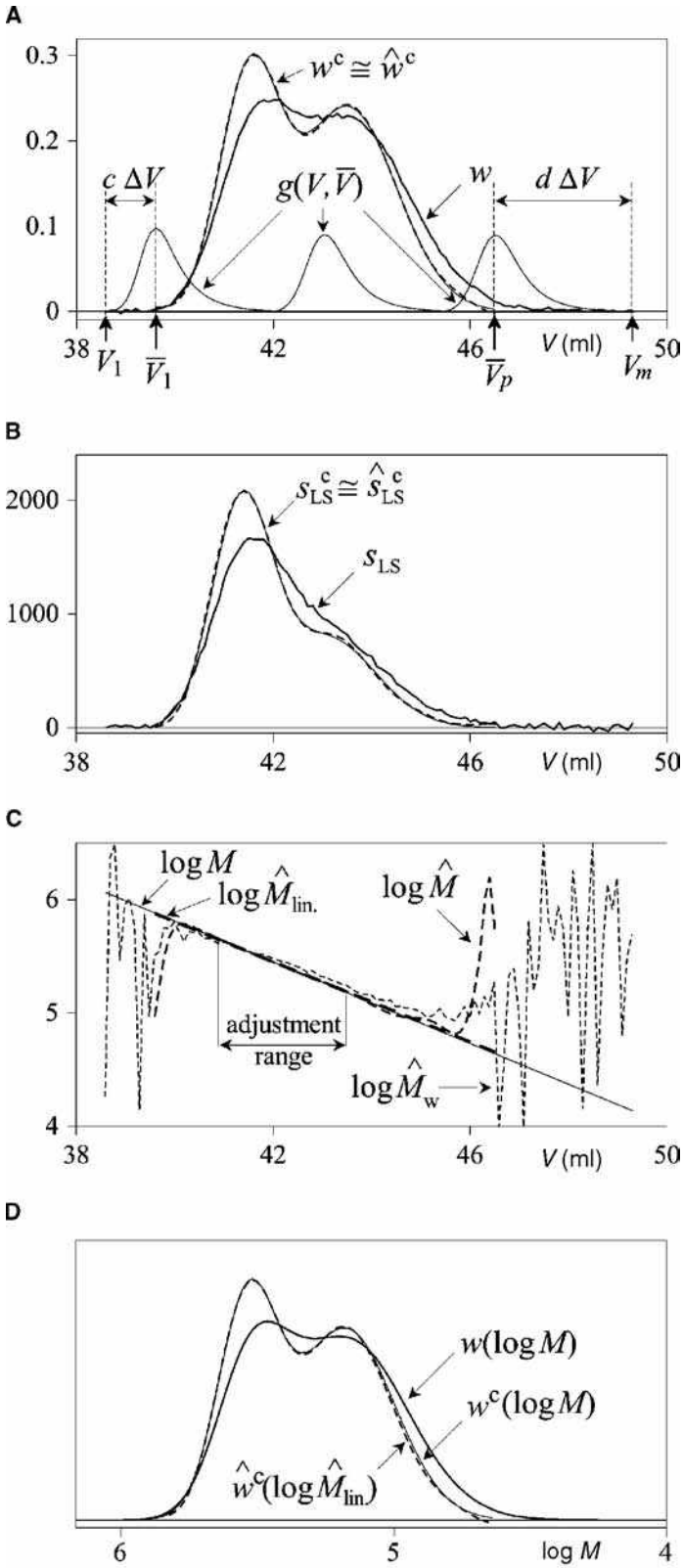

Fig. 2 Simulated example of DR/LS detection (after Ref. 22). A) "True" and "measured" mass chromatograms [$w^c(V)$, $w(V)$]; three samples of the BB function $g(V, \overline{V})$; and estimated corrected chromatogram [$\hat{w}^c(V)$]. B) "True" and "measured" molar mass chromatograms [$s_{LS}{}^c(V)$, $s_{LS}(V)$]; and estimated corrected molar mass chromatogram $\hat{s}_{LS}{}^c(V)$. C) Unbiased linear calibration [$\log M(V)$]; estimated ad hoc calibration [$\log \widehat{M}_w(V)$]; estimated unbiased calibration [$\log \widehat{M}(V)$], and estimated linear unbiased calibration [$\log \widehat{M}_{lin.}(V)$]. D) "True" MMD [$w^c(\log M)$]; MMD estimate obtained from $w(V)$ and $\log M(V)$ [$w(\log M)$]; and MMD estimate obtained from $\hat{w}^c(V)$ and $\log \widehat{M}_{lin.}(V)$ [$\hat{w}^c(\log \widehat{M}_{lin.})$].

Table 2 Simulated example for molar mass sensitive detectors: "true" and recuperated average molar masses from several MMDs.

MMD	$\overline{M}_n$	$\overline{M}_w$	$\overline{M}_w/\overline{M}_n$
$w^c(\log M)$[a]	182 000	242 000	1.33
$w(\log M)$[b]	160 000	224 000	1.40
$w(\log M_n)$[c]	182 000	233 000	1.28
$w(\log M_w)$[d]	191 000	242 000	1.27
$\hat{w}^c(\log \hat{M}_{lin.})$[e]	185 000	243 000	1.31

[a]"True" base distribution (Fig. 2D).
[b]Based on the linear calibration, without BB correction (Fig. 2D).
[c]Obtained from DR/OS detection, without BB correction.
[d]Obtained from DR/LS detection, without BB correction.
[e]Obtained from DR/LS detection, with BB correction (Fig. 2D).

$[\overline{V}_1 - \overline{V}_p]$, and it is presented in Fig. 2A. Then, the "true" molar mass chromatogram was calculated by assuming the relationship: $s_{LS}{}^c(V) = 0.02[M(V)w^c(V)]$ (Fig. 2B).

From $w^c(V)$ and $\log M(V)$, the "true" MMD $w^c(\log M)$ of Fig. 2D was obtained, and its average molar masses are shown in the second row of Table 2. The $\log M$ values of Fig. 2D vertically correspond (through the linear calibration) with the V values of Figs. 2A–C.

The non-uniform $g(V, \overline{V})$ is represented by an EMG of constant skewness, variable standard deviation, and $\overline{V}$ averages adopted at the peaks of the individual $g(V)$ functions. Each $g(V)$ exhibits 39 non-zero points (with $c = 10$ points before the maximum and $d = 28$ points after the maximum). In Fig. 2A, only the two limiting and one intermediate $g(V)$ functions are presented. The (noise-free) mass and molar mass chromatograms were calculated through Eqs. (1) and (3). Then, the "measured" chromatograms $w(V)$ and $s_{LS}(V)$ of Figs. 2A,B were obtained by adding a zero-mean Gaussian noise to the noise-free chromatograms. The broadened chromatograms contain $m = 70 + 39 - 1$ non-zero points. From $w(V)$ and $\log M(V)$, the (broadened) MMD $w(\log M)$ of Fig. 2A was obtained; its average molar masses are given in the third row of Table 2. Both averages are underestimated, while the global polydispersity is overestimated. The underestimation of the average molar masses is a result of having adopted the $\overline{V}$ averages at the maxima of skewed $g(V)$ functions.

At each retention volume of $w(V)$, the instantaneous MMDs in the detector cells were calculated by considering the contributions (toward that V) of all the hypothetical molecular species in the distribution, as determined by the discrete $w^c(V)$. From such instantaneous distributions, the ad hoc non-linear calibrations $\log M_n(V)$ and $\log M_w(V)$ were calculated.[22] From $w(V)$, $\log M_n(V)$, and $\log M_w(V)$, the MMD estimates $w(\log M_n)$ and $w(\log M_w)$ were obtained; their averages are presented in Table 2. As expected, $w(\log M_n)$ accurately estimates $\overline{M}_n$ but underestimates $\overline{M}_w$, while $w(\log M_w)$ accurately estimates $\overline{M}_w$ but overestimates $\overline{M}_n$. Thus, the global polydispersity is underestimated in both cases.

In a standard data treatment without BB correction, $M_w(V)$ would have been directly estimated from $\hat{M}_w(V) = s_{LS}(V)/[0.02w(V)]$. Due to the measurement noise, the resulting $\log \hat{M}_w(V)$ of Fig. 2C is oscillatory at the chromatogram tails, and these oscillations make it impossible to recuperate an MMD.

The proposed procedure was applied to the noisy chromatograms $w(V)$ and $s_{LS}(V)$. The dimension of $\mathbf{G}$ is $(m \times p) = (108 \times 70)$; the inversions were carried out through the singular value decomposition expression of Eq. 8. The algorithm was adjusted with the criterion of producing smooth solutions with minimal negative peaks, yielding $r = 14$ for the mass chromatogram and $r = 12$ for the molar mass chromatogram. The final estimates were $\hat{w}^c(V)$ and $\hat{s}_{LS}{}^c(V)$ of Fig. 2A,B. These functions are smooth and almost coincident with the true $w^c(V)$ and $s_{LS}{}^c(V)$.

The resulting (unbiased) calibration of Fig. 2C, $\log \hat{M}(V)$, almost overlaps the "true" $\log M(V)$ in the mid-chromatogram region, while it diverges at the tails. The linear calibration $\log \hat{M}_{lin.}(V)$ was obtained from the points of $\log \hat{M}(V)$ contained in the "adjustment range" of Fig. 2C. Finally, the unbiased distribution $\hat{w}^c(\log \hat{M}_{lin.})$ of Fig. 2D was obtained from $\hat{w}^c(V)$ and $\log \hat{M}_{lin.}(V)$. This distribution is smooth and close to the "true" $w_c(\log M)$. Accordingly, the estimated average molar masses are very close to the real values (Table 2).

Direct Calculation of the Corrected MMD

The interdetector volume compensation generally involves shifting the (leading) molar mass signal toward higher elution volumes. Independent of this compensation, a BB correction procedure has been proposed, which calculates the MMD in a single step by appropriately reducing the normal interdetector volume shift.[34] The procedure is equivalent to rotating the linear molar mass calibration counterclockwise.[28,35,36] Therefore, it is based on the following (rather strict) assumptions: 1) Both the (uniform) BB function and the measured mass chromatogram are Gaussian functions of (known) standard deviations σ_g and σ_w, respectively; 2) the calibration is linear and given by $M(V) = D_1 \exp(-D_2 V)$; and 3) the interdetector volume introduces a pure signal shift, but no additional BB. In the case of an LS/DR combination, the LS signal must suffer a (secondary) shift that involves a small reduction in the normal lag. This secondary lag reduction is given by

$$\Delta V_{LS} = \sigma_{w^c}(\sigma_w - \sigma_{w^c})D_2 \tag{12a}$$

with

$$\sigma_{w^c} = (\sigma_w{}^2 - \sigma_g{}^2)^{1/2} \tag{12b}$$

where σ_{w^c} is the standard deviation of the corrected chromatogram.

The commercially available molar mass sensitive detectors do include a correction for BB in their software. Unfortunately, the applied correction procedures are not fully disclosed, but they seem to involve an interdetector volume readjustment. For example, the Viscotek™ Model 200 detector combines a DR in parallel with a specific viscometer. First, the (mass and molar mass) chromatograms of several narrow standards must be measured to determine the interdetector volume and a (uniform EMG) BB function. Then, the MMD is corrected for BB in an unspecified manner. Similarly, Wyatt Corp. has recently introduced a patented BB correction procedure for their triple-detector system (multiangle LS, DR, and specific viscosity sensors).

CONCLUSIONS

Band broadening correction in SEC is still not a totally resolved issue, even when the MMD of a linear homopolymer is determined with a mass detector and a molar mass calibration. Fortunately, modern SEC columns are highly efficient, and the correction for BB is mainly limited to the case of narrowly distributed polymers. Even in the presence of BB, if an instantaneous quality variable is accurately measured, its corresponding global average will also be accurate.

Numerical inversion techniques aim at correcting the raw chromatograms prior to determining the MMD or any other polymer quality characteristics. Their main advantage is that they admit arbitrary shapes for the chromatograms or the BB function. Their disadvantage, however, is the ill-posedness of numerical inversions, which amplify the measurement noise. With molar mass sensitive detectors, two independent inversions are required prior to calculation of the molar masses. From the comparison of Methods I–III, Method II (a singular value decomposition technique) has shown a good compromise between a reasonably good solution and a relatively simple adjustment procedure. To improve the ill-conditioned nature of the numerical inversions, it is important to set to zero all the ultra-low elements of the BB matrix (normally placed at its upper-right and lower-left corners).

The techniques that avoid numerical inversions, correct the MMDs in a single step, and are based on either: 1) rotating the linear calibration (when only a mass chromatogram and a linear calibration are available); or 2) modifying the interdetector volume shift (when molar mass sensitive detectors are employed). Their main advantage is that they produce smooth and unique solutions. Their limitation, however, is that they produce only approximate solutions.

In general, the BB function seems to be moderately uniform in the linear calibration range, but definitely skewed toward the higher retention volumes. Its determination is only simple for low molar masses. In general, the BB function would be simpler to specify if the manufacturers of narrow standards provided the true MMDs of their samples.

A proper correction for BB and other sources of error seems essential for quantitative determinations in SEC. The following developments are expected in the future: 1) simpler techniques for determining the BB function; 2) a validation of several BB algorithms on real experimental data; and 3) a standardization of the "best" BB correction procedures (possibly, a trade-off between accuracy and simplicity).

ACKNOWLEDGMENTS

This work was carried out in the framework of Project 2003-023-2-G.Meira (IUPAC): "Data Treatment in the Size Exclusion Chromatography of Polymers," http://www.iupac.org/projects/2003/2003-023-2-400.html. Also, we are grateful for the financial support received from the following Argentine institutions: CONICET, Universidad Nacional del Litoral, and SECyT.

REFERENCES

1. Berek, D.; Marcinka, K. Gel chromatography. In *Separation Methods*; Deyl, Z., Ed.; Elsevier: Amsterdam, 1984; 271–299.
2. Hupe, K.; Jonker, R.; Rozing, G. Determination of band-spreading in high-performance liquid chromatographic instruments. J. Chromatogr. **1984**, *285*, 253–265.
3. Wyatt, P. Mean square radius of molecules and secondary instrumental broadening. J. Chromatogr. **1993**, *648*, 27–32.
4. Potschka, M. Mechanism of size-exclusion chromatography. I. Role of convection and obstructed diffusion in size-exclusion chromatography. J. Chromatogr. **1993**, *648*, 41–69.
5. Netopilík, M. Relations between the separation coefficient, longitudinal displacement and peak broadening in size exclusion chromatography of macromolecules. J. Chromatogr. A, **2002**, *978*, 109–117.
6. Dondi, F.; Cavazzini, A.; Remelli, M.; Felinger, A.; Martin, M. Stochastic theory of size exclusion chromatography by the characteristic function approach. J. Chromatogr. A, **2002**, *943*, 185–207.
7. Pasti, L.; Dondi, F.; van Hulst, M.; Schoenmakers, P.; Martin, M.; Felinger, A. Experimental validation of the stochastic theory of size exclusion chromatography: Retention on single and coupled columns. Chromatographia **2003**, *57* (Suppl.), S171–S186.
8. Tung, L. Method of calculating molecular weight distribution function from gel permeation chromatograms. III. Application of the method. J. Appl. Polym. Sci. **1966**, *10*, 1271–1283.
9. Busnel, J.P.; Foucault, F.; Denis, L.; Lee, W.; Chang, T. Investigation and interpretation of band broadening in size

exclusion chromatography. J. Chromatogr. A, **2001**, *930*, 61–71.
10. Belenkii, B.; Vilenchik, L. General theory of chromatography. In *Modern Liquid Chromatography of Macromolecules*; Journal of Chromatography Library; Elsevier: Amsterdam, 1983; Vol. 25, 1–67.
11. Lederer, K.; Imrich-Schwarz, G.; Dunky, M. Simultaneous calibration of separation and axial dispersion in size exclusion chromatography coupled with light scattering. J. Appl. Polym. Sci. **1986**, *32*, 4751–4760.
12. Billiani, J.; Rois, G.; Lederer, K. A new procedure for simultaneous calibration of separation and axial dispersion in SEC. Chromatographia **1988**, *26*, 372–376.
13. Schnöll-Bitai, I. The direct determination of axial dispersion in size exclusion chromatography based on Poissonian chain length distributions. Chromatographia **2003**, *58*, 375–380.
14. Baumgarten, J.; Busnel, J.; Meira, G. Band broadening in size exclusion chromatography of polymers. State of the art and some novel solutions. J. Liq. Chromatogr. Relat. Technol. **2002**, *25* (13–15), 1967–2001.
15. Netopilík, M. Correction for axial dispersion in gel permeation chromatography with a detector of molar masses. Polym. Bull. **1982**, *7*, 575–582.
16. Hamielec, A. Correction for axial dispersion. In *Steric Exclusion Liquid Chromatography of Polymers*; Janča, J., Ed.; Chromatographic Science Marcel Dekker, Inc.: New York, 1984; 25 117–160.
17. Jackson, C.; Barth, H. Molecular weight sensitive detectors for size exclusion chromatography. In *Handbook of Size Exclusion Chromatography and Related Techniques*; 2nd Ed.; Chromatographic Science Series; Wu, Ch., Ed.; Marcel Dekker, Inc.: New York, 2004; Vol. 91, 99–138.
18. Lehmann, U.; Köhler, W.; Albrecht, W. SEC absolute molar mass detection by online membrane osmometry. Macromolecules **1996**, *29*, 3212–3215.
19. Prougenes, P.; Berek, D.; Meira, G. Size exclusion chromatography of polymers with molar mass detection. Computer simulation study on instrumental broadening biases and proposed correction method. Polymer **1998**, *40*, 117–124.
20. Netopilík, M. Effect of local polydispersity in size exclusion chromatography with dual detection. J. Chromatogr. A, **1998**, *793*, 21–30.
21. Meira, G.; Vega, J. Characterization of copolymers by size exclusion chromatography. In *Handbook of Size Exclusion Chromatography and Related Techniques*; 2nd Ed.; Chromatographic Science Series; Wu, Ch., Ed.; Marcel Dekker, Inc.: New York, 2004; Vol. 91, 139–156.
22. Vega, J.; Meira, G. SEC of simple polymers with molar mass detection in presence of instrumental broadening. Computer simulation study on the calculation of unbiased molecular weight distribution. J. Liq. Chromatogr. Relat. Technol. **2001**, *24* (7), 901–919.
23. Ishige, T.; Lee, S.; Hamielec, A. Solution of Tung's axial dispersion equation by numerical techniques. J. Appl. Polym. Sci. **1971**, *15*, 1607–1622.
24. Mendel, J. Least-squares estimation: Singular-value decomposition. In *Lessons in Estimation Theory for Signal Processing, Communications, and Control*; Prentice Hall: New Jersey, 1995; 44–57.
25. Alba, D.; Meira, G. Inverse optimal filtering method for the instrumental broadening in SEC. J. Liq. Chromatogr. **1984**, *7*, 2833–2862.
26. Felinger, A. Signal enhancement. In *Data Analysis and Signal Processing in Chromatography*; Data Handling in Science and Technology; Elsevier: Amsterdam, 1998; Vol. 21, 143–181.
27. Jackson, C.; Yau, W. Computer simulation study of size exclusion chromatography with simultaneous viscometry and light scattering measurements. J. Chromatogr. **1993**, *645*, 209–217.
28. Netopilík, M. Combined effect of interdetector volume and peak spreading in size exclusion chromatography with dual detection. Polymer **1997**, *38*, 127–130.
29. Yau, W.; Stoklosa, H.; Bly, D. Calibration and molecular weight calculations in GPC using a new practical method for dispersion correction—GPCV2. J. Appl. Polym. Sci. **1977**, *21*, 1911–1920.
30. Hamielec, A.; Ederer, H.; Ebert, K. Size exclusion chromatography of complex polymers. Generalized analytical corrections for imperfect resolution. J. Liq. Chromatogr. **1981**, *4*, 1697–1707.
31. Chang, K.; Huang, R. A new method for calculating and correcting molecular weight distributions from permeation chromatography. J. Appl. Polym. Sci. **1969**, *13*, 1459–1471.
32. Gugliotta, L.; Alba, D.; Meira, G. Correction for instrumental broadening in SEC through a stochastic matrix approach based on Wiener filtering theory. In *Detection and Data Analysis in Size Exclusion Chromatography*; ACS Symposium Series No. 352; Provder, T., Ed.; American Chemical Society: Washington, 1987; 287–298.
33. Gugliotta, L.; Vega, J.; Meira, G. Instrumental broadening correction in size exclusion chromatography. Comparison of several deconvolution techniques. J. Liq. Chromatogr. **1990**, *13*, 1671–1708.
34. Jackson, C. Evaluation of the "effective volume shift" method for axial dispersion corrections in multi-detector size exclusion chromatography. Polymer **1999**, *40*, 3735–3742.
35. Cheung, P.; Lew, R.; Balke, S.; Mourey, T. SEC–viscometer detector systems. II. Resolution correction and determination of interdetector volume. J. Appl. Polym. Sci. **1993**, *47*, 1701–1706.
36. Netopilík, M. Effect of interdetector peak broadening and volume in size exclusion chromatography with dual viscometric-concentration detection. J. Chromatogr. A, **1998**, *809*, 1–11.

Band Broadening in SEC

Jean-Pierre Busnel
Physical Chemistry of Material Polymers, University of Main, Le Mans, France

INTRODUCTION

In classical chromatography, band broadening (BB), which defines the shape of the chromatogram of a pure solute, is one of the factors limiting the resolution, but individual peaks are generally observable and the discussion of BB extent is direct. In size-exclusion chromatography (SEC), the situation is more complex, as we observe, generally, only the envelope of a large number of individual peaks (Fig. 1). Imperfect resolution and its consequences on results cannot be directly observed. A few years after the pioneer publication on SEC by Moore,[1] Tung[2] presented the general mathematical problem of band-broadening correction (BBC). Until 1975, a number of simplified procedures have been proposed in order to compensate for the limited resolution of columns. After 1975, a spectacular increase in column resolution rendered the problem less important, but, recently, there is a growing interest in BBC as SEC users intend to obtain more and more detailed information on molecular-weight distributions (MWDs) and not only average MW values. For this reason, this discussion is separated into three parts:

- Experimental determination of extent of BB.
- Interpretation of BB processes.
- Correction methods for BB.

Experimental Determination of the Extent of Broad-Banding

It is useful to choose a solute which is really eluted by a size-exclusion process, without adsorption or any additional interaction phenomena which might modify the shape of the peak. The most trivial method is to analyze the shape of a low-MW pure substance. This is usually used to determine the number of theoretical plates, $N = (V_r/\sigma)^2$ where V_r is the retention volume (volume at peak top) and σ is the standard deviation. σ can be computed from the weighing of each data point of the peak or can be estimated from the width at 10% maximum height ($\sigma = W_{0.1}/4.3$).

For this reason, when using tetrahydrofuran (THF) as eluent and styrene/DVB gels, methanol or toluene are not good candidates; octadecane is preferred. For aqueous SEC, saccharose is the classical standard.

For polymers, a number of authors have claimed that the peak width increases as the MW increases, but to discuss BB for polymers, several precautions are required. First, it is necessary to be sure that the injected solution is sufficiently dilute to prevent any viscous effect. (Practically no viscous effect is observable, even for narrow standards when $[\eta]C < 0.1$; for flexible polymers, this corresponds roughly to a concentration <1 mg/ml for MWs up to 500,000; for a higher MW, it is necessary to reduce the concentration.) Then, the real difficulty is to analyze very narrow standards for which polymolecularity is sufficiently low, so as not to participate in the peak width, or at least which polymolecularity is very precisely known.

Commercial indications on standards are in progress, but suppliers rarely guarantee the exact value for $I_p = M_w/M_n$. A tendency is to guarantee that I_p is lower than a given value, but that is not sufficient for precise BB study. Usual values for medium MW standards are $I_p < 1.03$ and $I_p < 1.05$ for high MW standards; the situation is worse for aqueous SEC with values around 1.1.

Recently, possibilities appeared with the results from thermal gradient interaction chromatography (TGIC).[3] That method has a much better resolution than SEC and allows a very precise determination of I_p. It is even possible to use it for a preparative scale to obtain extremely narrow standards, but, until now, it is only available for organic-soluble standards.

With all these precautions and when using modern columns, it clearly appears that peaks are not Gaussian, but systematically skewed. New computing facilities allow one to analyze more precisely such peaks by various functions. The best results seems to be obtained by exponentially modified gaussian (EMG) functions,[4] which are the convolution of a Gaussian dispersion and an exponential decay. In that case, two parameters define the shape of the peak s and t, which allow quantitative mapping of BB characteristics for further correction. Generally, σ and τ are constant or admit a limited increase with MW for samples eluted well after the void volume. However, a dramatic increase of σ and τ occurs near the total exclusion volume.[5]

BAND-BROADENING INTERPRETATION

As previously indicated, this discussion is organized for chromatograms from very narrow polymer standards for which we can consider that the effect of molecular weight

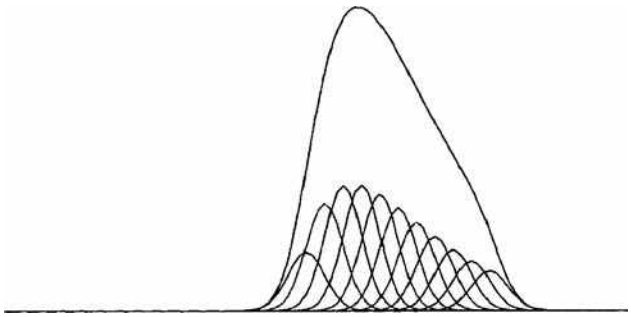

Fig. 1 Example of imperfect resolution: 10 peaks, $R = 0.25$ between neighbors.

distribution is negligible and for which the unique separation process is size exclusion. With these limitations, the contribution to band broadening is conveniently separated into extra column effects, eddy dispersion, static dispersion, and mass transfer. In the most classical chromatographic interpretation, extra-column effects are not discussed and the three other contributions are considered as Gaussian, so there is simply the addition of their variances. The number of theoretical plates is defined as $N = (V_e/\sigma)^2$ and the influence of υ, the linear velocity of the eluent, is summarized by the so-called Van Deemter equation:

$$H = \frac{L}{N} = a + \frac{b}{\upsilon} + c\upsilon$$

This classical interpretation is not sufficient, as experimental results clearly indicate that there is peak skewing; for this reason, it is useful to study each contribution separately.

Static Dispersion

This classical contribution corresponds to the diffusion of the sample along the axis of the column by Brownian motion during the time t_0 spent in the interstitial volume. That spreading effect is Gaussian and its standard deviation σ is related to D, the diffusion coefficient of the solute: $\sigma = (2Dt_0)^{1/2}$. In classical operating conditions in modern LC, that contribution is generally a minor one, due to the use of relatively high flow rate. In SEC, the diffusion coefficients of polymers are very low and that contribution becomes negligible.

Extra-Column Effects

Generally, these effects are not discussed in detail, considering it is only necessary to select a chromatographic apparatus with a proper design to render these effects negligible. Recent results indicate that this situation tends to be different for macromolecular solutes. Using a chromatographic apparatus for which the column is replaced by tubings of various lengths, the end of elution is characterized by an exponential decay, the time of which is dependent not only on geometry but also strongly increases for high-MW solutes. The explanation is related to the more or less rapid averaging of radial positions of the solute in a cylindrical tube. In the case of high-molecular-weight solutes, the diffusion coefficient is small. Solute molecules which enter near the center of the tube stay in the high-velocity zone and those which enter near the walls stay in low velocity zones; this introduces skewing which is much more important than for low-molecular-weight solutes.

Eddy Dispersion

This contribution is related to the variety of channels available for any solute molecule throughout the elution process. These channels are defined by the interstitial volume between the beads of the column package, so they correspond to a variety of shapes and flow velocities. This produces a distribution in elution time which is classically considered as Gaussian and weakly depends on flow rate. As a rule of thumb, the theoretical plate height corresponding to this effect can be considered as being equal to the bead diameter of the packing for well-packed columns.

More detailed results take into account a "wall effect" to explain why elution profiles are skewed, even for non-retained solutes in modern columns. Detailed experimental results were recently presented by Farkas and Guiochon[6] on the radial distribution of flow velocity using local multichannel detection devices. On average, the flow velocity is very homogeneous in the center of the column, but, inevitably, it becomes lower near the walls. Similarly, the peak shape from a local microdetector situated near the wall is clearly distorted and skewed compared with that of a similar detector situated near the center of the column.

Mass Transfer

The simple model of a theoretical plate, which is simply the affirmation of the existence of N successive equilibrium steps, is not satisfactory, as it assumes a Gaussian spreading.

To obtain more realistic information, it is necessary to discuss the rate of exchange between the interstitial volume and pores.[7] Potschka[8] proposed taking into account the competition between diffusion and convection in the special situation of "perfusion chromatography," where very large pores exist inside the beads, which allow some distribution of the solute by convection.

Recently, a model has been proposed for which pores are simply long cylinders and time of residence corresponds to a one-dimension Brownian motion.[5] Exact mathematical expressions are available for describing that process[9] and the distribution of such time of residence is highly skewed. Additionally, for each solute

molecule, the number of visited pores obeys a Poisson distribution, and when the average number of visits becomes small, the distribution of elution time becomes wider and more skewed. That explains, precisely, why strong peak distortion is observed for samples eluted near the total exclusion limit.

Band-Broadening Correction

As first stated by Tung, the general starting point is that the experimental chromatogram $H(V)$ (from a concentration detector) is the convolution of $g(V, V_r)$, the spreading function defining the elution of a single species with a peak apex position of V_r, and $w(V_r)\,dV_r$, the weight fraction of species which peak apex, is between V_r and $V_r + dV_r$:

$$H(V) = \int_{V_1}^{V_2} g(V, V_r) w(V_r) dV_r$$

In any case, a second step consists of converting $w(V_r)$ into $w(M)$ by defining a calibration curve which correlates M and V_r.

As there is only a finite number of data points and, with some instrumental noise, generally such an inversion problem is ill-defined, the stability of the values of $w(V_r)$ depends on the algorithm which is used. Among the huge number of articles treating such problems, a review by Meira and coworkers[10] gives useful information on the mathematical aspects and a detailed review by Hamielec[11] presents a variety of instrumental situations, from the simplest one (constant Gaussian spreading function and simple concentration detector) to the most complex (general spreading function, multidetection).

To take into account experimental evidence which clearly indicates systematic skewing, this discussion will no longer concern methods limited to Gaussian spreading functions.

SIMPLEST SITUATION: CONSTANT SPREADING FUNCTION, LINEAR CALIBRATION CURVE, SINGLE CONCENTRATION DETECTOR

This situation corresponds to a useful approximation in many cases, and it is almost strictly exact when the sample has a narrow MWD. From the chromatogram of an ideal isomolecular sample, considering that it is defined by a set of h_i values equidistant on the elution volume axis, classical summations give the uncorrected molecular-weight values:

$$M_{n_{\text{uncorrected}}} = \frac{\Sigma h_i}{\Sigma (h_i / M_i)} \quad \text{and} \quad M_{w_{\text{uncorrected}}} = \frac{\Sigma (h_i M_i)}{\Sigma h_i}$$

and the peak apex position gives the real molecular weight: M_{peak}.

Therefore, two correction factors exist for M_n and M_w:

$$K_n = \frac{M_{\text{peak}}}{M_{n_{\text{uncorrected}}}} \quad \text{and} \quad K_w = \frac{M_{peak}}{M_{w_{\text{uncorrected}}}}$$

For any other isomolecular sample analyzed on the same system, the change is simply a shift along the elution volume axis and each value M_i is multiplied by the same factor. Thus, the correction factors are unchanged. Finally, any broad MW sample analyzed on the same system is the addition of a set of isomolecular species; therefore, when summing, there is factorization of the correction factors and

$$M_{n_{\text{corrected}}} = K_n M_{n_{\text{uncorrected}}}$$
$$M_{w_{\text{corrected}}} = K_w M_{w_{\text{uncorrected}}}$$

This very simple BBC can always be used, at least to give a preliminary indication of the extent of BB. When using extremely narrow standards, as obtained by preparative TGIC, the result is accurate; more easily, it is possible to set the correction factors between two limits: lower one using data from a low-MW pure chemical and a higher limit using data from an imperfect narrow standard.

GENERAL SITUATION: SPREADING FUNCTION DEPENDS ON ELUTION VOLUME AND CALIBRATION CURVE IS NOT LINEAR, SINGLE CONCENTRATION DETECTOR

In such cases, as stated by Meira and coworkers,[10] the quality of results depends on computational refinements. It is necessary to add specific constraints related to the chromatographic problem: rejection of negative values or unrealistic fluctuations in the weight distribution. The normal way is to invert the large matrix defining the spreading function for any position on the elution volume scale. With modern computational facilities, that becomes easy, but it is still not trivial to obtain stable results, and proper filtering processes are useful.

Good results can be obtained by using a more direct iterative method which can be briefly presented: n equidistant values are chosen on the elution volume scale; let us note these values as V_i (typically, n can be 200). Any sample is arbitrarily defined as the sum of n isomolecular species, whose positions at the peak apex are V_j. For each peak j, n values of heights h_{ij} for each V_i value are computed, normalizing the surface (the peak shape is defined by interpolation from experimental BB data).

The chromatogram corresponding to the sample is defined by a set of n H_i values at positions V_i.

To define the weight distribution of the sample, it is simply necessary to adjust a set of w_i values until the summation converges toward the experimental H_i values.

For the first attempt, $w_i = H_i$. This gives, by addition, a chromatogram ($H1_i$). Then, $w_i = w_i{*}H_i/H1_i$; that gives $H2_i$ and so on until convergence.

The method is reasonably efficient. Stable convergence is observed except for very large samples for which the problem is too severely ill-conditioned. Applying it to narrow PS standards allows one to find, again, the true polymolecularity index.

MULTIDETECTION PROBLEM

The aim of multidetection, especially LS/DRI coupling, is to find a useful calibration curve directly from the sample data and without external information from standards. A crude calibration curve is obtained by plotting, on a semilogarithmic scale, the instantaneous weight average M_{wi} values for each data point at elution volume V_i. At this point, correction for BB is rarely used, as the accuracy of the calibration curve is generally poor and does not justify sophisticated corrections. Additionally, for complex polymers (blends, copolymers, branched polymers, etc.), a variety of molecular weights are eluted at the same position, even in the absence of band broadening,[12] so it is still very difficult to propose a general solution for the problem and results are available only for simplified situations. Normally, it would be necessary to find the exact weight distribution w_i as in the preceding paragraph, simply using the DRI signal; then, it becomes possible to adjust the calibration curve until the calculated M_{wi} values converge toward the experimental set of M_{wi} values.

CONCLUSIONS

Band broadening in SEC has several specific aspects, compared with other chromatographic processes. Solutes may have very low diffusion coefficients and that introduces additional tailing due the imperfect averaging of radial positions all along the tubing. Mass transfer can be described from Brownian motion properties, and for samples eluted near total exclusion volume, as the number of visited pores become small, this introduces a significant increase of skewing and a very important loss of resolution.

For correcting band broadening, the main difficulty is in obtaining precise mapping of the spreading function of the system. Normally, this needs very high quality standards and TGIC offers new possibilities in that area. Computational techniques are now sufficiently efficient to solve the general inversion problem associated with band-broadening correction, but it still needs some precautions to obtain stable results without artificial oscillations. Finally, as corrections become very important and unstable near total exclusion volume, it remains very imprudent to interpret data when part of the sample is totally excluded. It is better to first find a well-adapted column set, able to efficiently fractionate the whole sample.

REFERENCES

1. Moore, J.C. Gel permeation chromatography. I. A new method for molecular weight distribution of high polymers. J. Polym. Sci. A-2 **1964**, *835*.
2. Tung, L.H. Method of calculating molecular weight distribution function from gel. J. Appl. Polym. Sci. **1966**, *10*, 375.
3. Lee, W.; Lee, H.C.; Park, T.; Chang, T.; Chang, J.Y. Temperature gradient interaction chromatography of low molecular weight polystyrene. Polymer **1999**, *40*, 7227.
4. Jeansonne, M.S.; Foley, J.P. Review of the exponentially modified gaussian (emg) function since 1983. J. Chromatogr. Sci. **1991**, *29* (6), 258.
5. Busnel, J.-P.; Foucault, F.; Denis, L.; Lee, W.; Chang, T. Investigation and interpretation of band broadening in size exclusion chromatography. J. Chromatogr. A, **2001**, *930* (1–2), 61–71.
6. Farkas, T.; Guiochon, G. Contribution of the radial distribution of the flow velocity to band broadening in HPLC columns. Anal. Chem. **1997**, *69*, 4592.
7. Kim, D.H.; Johnson, A.F. *Size Exclusion Chromatography*; Provder, T.; ACS Symposium Series American Chemical Society: Washington, DC, 1984; 245.
8. Potschka, M. Role of convection and obstructed diffusion in size-exclusion chromatography. J. Chromatogr. **1993**, *648*, 41.
9. Karatzas, I.; Shreve, S. *Brownian Motion and Stochastic Calculus*; Springer-Verlag: New York, 1991.
10. Gugliotta, L.M.; Vega, J.R.; Meira, G.R. Instrumental broadening correction in size exclusion chromatography, comparison of several deconvolution techniques. J. Liq. Chromatogr. Relat. Techol. **1990**, *13* (4), 1671.
11. Hamielec, A.E. *Steric Exclusion Liquid Chromatography of Polymers*; Janca, J., Ed.; Marcel Dekker, Inc.: New York, 1984; 117–160.
12. Radke, W.; Simon, P.F.W.; Muller, A.H.E. Estimation of number-average molecular weights of copolymers by gel permeation chromatography. Macromolecules **1996**, *29* (14), 4926–4930.

Barbiturates: CE Analysis

Chenchen Li
College of Chemistry and Molecular Engineering, Peking University, Beijing, China

Huwei Liu
Institute of Analytical Chemistry, Peking University, Beijing, China

INTRODUCTION

Capillary electrophoresis (CE) is becoming a popular analytical tool for determining drugs because of its simplicity, high speed, and high efficiency. The present review studies different modes of CE used in the determination and chiral separation of barbiturates, as well as current developments in sample preparation for barbiturates in biological fluids. The comparison of different modes of CE with other separation approaches is also discussed.

BARBITURATES

Barbiturates, derivatives of barbituric acid, are found in a variety of pharmaceuticals, such as sedatives, hypnotics, and antiepileptics. However, their levels in body fluids have to be regulated within a narrow therapeutic window to avoid toxicity. Therefore determination of barbiturates in serum, plasma, and urine is important for investigation of intoxication, therapeutic drug monitoring, and pharmacokinetic and metabolic studies. Hence, many instrumental approaches for the analysis of barbiturates in body fluids, including immunoassays[1] and chromatographic methods, such as gas chromatography (GC),[2] gas chromatography/mass spectrometry (GC/MS),[3] and high-performence liquid chromatography (HPLC),[4–6] have been developed. Immunological techniques offer high performance, speed of analysis, and sensitivity. However, they are not specific enough to distinguish a single compound because barbiturates interfere with each other. Chromatographic methods have been applied for the determination of all common barbiturates, even while they require time-consuming sample pretreatment and are characterized by a low sample throughput.[7]

In recent years, CE has been successfully applied in the field of biochemical and analytical chemistry. It has been found to be attractive for pharmaceutical analysis because of its advantages related to excellent separation efficiency, high mass sensitivity, minimal use of samples and solvents, and the possibility of using different direct and indirect detection systems. This review focuses on analytical assays for barbiturates by CE.

SAMPLE PREPARATION FOR BARBITURATES IN BODY FLUIDS

Sample preparation is important here because matrices of biological fluids are so complicated that interfering signals are likely to appear in typical separation-based determinations. Among various sample preparation techniques, there are two major approaches combined with CE: liquid–liquid extraction (LLE) and solid-phase extraction (SPE) [or solid-phase microextraction (SPME)].

Liquid–Liquid Extraction

LLE with chloroform from acidified serum is widely executed[7–11] after the method of Shiu and Nemoto.[12] However, chloroform is of great toxicity and is not suitable for routine use. LLE with pentane at pH 6.4[7] was investigated for feasibility with seven barbiturates and was found to be specific for thiopental—an important barbiturate being used for anaesthetic medication and treatment of head trauma with severe brain injury. Comparing acetonitrile deproteinization with chloroform deproteinization, Shihabi demonstrated the feasibility of acetonitrile for extraction of pentobarbital. However, electropherograms obtained by extraction with chloroform are more sensitive and cleaner.[9] Wu et al.[10] used LLE with ether for extraction from serum, and chloroform for extraction from urine. They obtained recoveries of six barbiturates from 86.6% to 118%.

Solid-Phase Extraction and Solid-Phase Microextraction

Although LLE is useful, it is being replaced by SPE or SPME because LLE is a time-consuming and laborious process that involves consumption of large volumes of organic solvents. The use of SPE for subsequent analysis is achieved in one step, and the results have shown that this is a reproducible, safe, convenient, and time-saving alternative to LLE. Most SPE applications use disposable cartridges or columns packed with C_{18}-bonded silica, which is the most classic packing for this technique.[7,10,11,13,15] Moreover, SPME is based on partition equilibrium of target compounds between the sample matrices and a polymeric

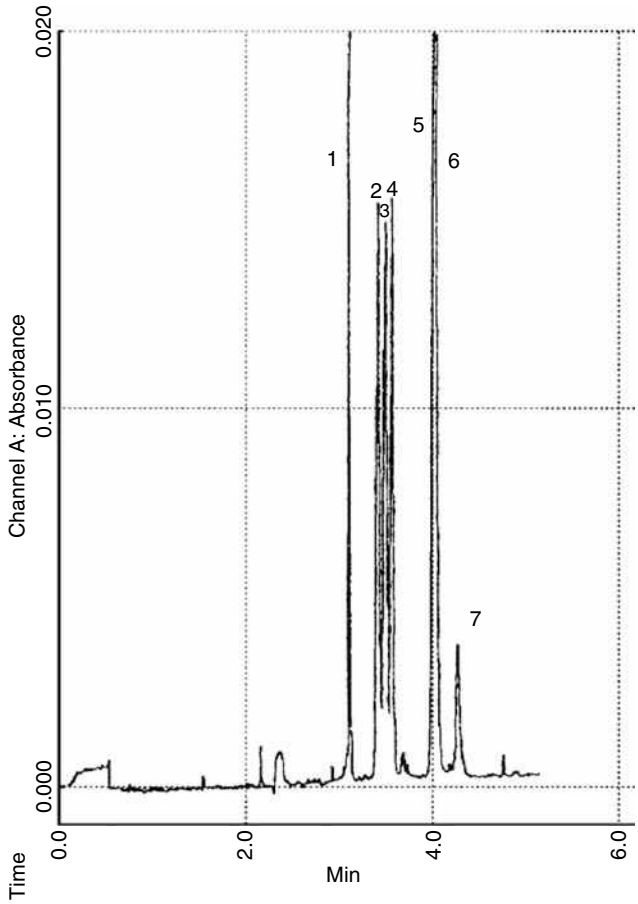

Fig. 1 Separation of different barbiturates using a 500 mmol/L borate buffer, pH 8.5. 1, Internal standard; 2, pentobarbital; 3, secobarbital; 4, amobarbital; 5, phenobarbital; 6, butabarbital; and 7, contamination.

stationary phase, such as plasticized poly vinyl chloride (PVC),[14] which is coated onto a fused silica fiber.

Among these techniques, the SPME device is reported to be the easiest to construct and it performs very reliably. Thus alkaline or neutral compounds are expected not to be extracted or backextracted, and will not interfere with analysis of barbiturates. Barbiturate concentrations of 0.1–0.3 ppm in urine and about 1 ppm in serum can be determined.[14,16]

CAPILLARY ELECTROPHORETIC MODES OF OPERATION

Capillary zone electrophoresis (CZE) and micellar electrokinectic chromatography (MEKC) are the most common CE modes used in determining barbiturates. We will discuss them separately.

Analysis by Capillary Zone Electrophoresis

In CZE, the separation mechanism is based on differences in the charge/mass ratios of ionic analytes. An electric field is applied to the capillary filled with a running buffer, and cations go to the cathode, whereas anions migrate to the anode. But because of the electro-osmotic flow (EOF) of the buffer, which is the driving force of CE, all analytes will move in the direction of EOF (usually toward the negative electrode as the inner surface of fused silica capillary is negatively charged). Although barbiturates are negatively charged at high pH, their migration velocities are close to each other and their separations by CZE are more or less insufficient. A separation of some common barbiturates using a 500 mmol/L borate buffer (pH 8.5) and an applied voltage of 11 kV is illustrated in Fig. 1.[9] The phenobarbital peak was not resolved from butabarbital. Boone et al.[17] improved separation performance by using a 90 mmol/L borate buffer (pH 8.5) and an applied voltage of 30 kV. It was found that an applied voltage of 30 kV resulted in faster separations and a better resolution compared to lower voltages. In addition, the Tapso–Tris buffer has a higher buffering capacity but lower conductivity. Baseline separation of 10 barbiturates and eight benzoates was achieved in a 50 m*M* Tapso–Tris buffer system.[14] Recently, Delinsky et al.[15] completely resolved barbiturates from meconium

Table 1 Running conditions of MEKC for determination of barbiturates.

Analytes	Running buffer	Refs.
Barbital, allobarbital, phenobarbital, butalbital, thiopental, amobarbital, and pentobarbital	50 m*M* SDS, 9 m*M* $Na_2B_4O_7$, 15 m*M* $Na_2H_2PO_4$ (pH 7.8)	[7]
Barbital, phenobarbital, methyl phenobarbital, amobarbital, thiopental, pentobarbital, and secobarbital	100 mmol/L SDS:100 mmol/L $Na_2H_2PO_4$: MeOH : H_2O (70 : 15 : 5 : 10)	[10]
Seven barbiturates and 14 benzodiazepines	100 m*M* borate, 10 m*M* SDS, and 5 *M* urea (pH 8.5)	[11]
Heptabarbital, hexobarbital, pentobarbital, butalbital, and phenobarbital	30 mmol/L SDS, 30 mmol/L borate (pH 9.3), with 200 ml/L acetonitrile	[13]
Twenty-five barbiturates	50 m*M* SDS, 20 m*M* phosphate (pH 8.4)	[17]

Table 2 Comparison of CZE and MEKC for determining barbiturates.

	CZE	MEKC
Total analysis time	No more than 10 min	About 15 min
Separation efficiencies	High	High
Analytical window	Relatively small window because of the resemblance of the chemical structures and the p*K* values of the barbiturates[17]	Provides a significantly increased analytical window
Resolution	Some barbiturates interfere with each other	Improved
Pretreatment process	Complex and time-consuming (unsatisfied resolution with LLE)	Both LLE and SPE produce good results

in a 150 m*M* Tris running buffer after sample preparation by SPE.

Analysis by MEKC

MEKC is another CE method based on the differences between interactions of analytes with micelles present in the separation buffer, which can easily separate both charged solutes and neutral solutes with either hydrophobic or hydrophilic properties. Micelles are formed by adding a surfactant [at a concentration above its critical micelle concentration (CMC)] to the separation buffer, and act as the so-called pseudo-stationary phase. The most striking observation is the resolution of MEKC,

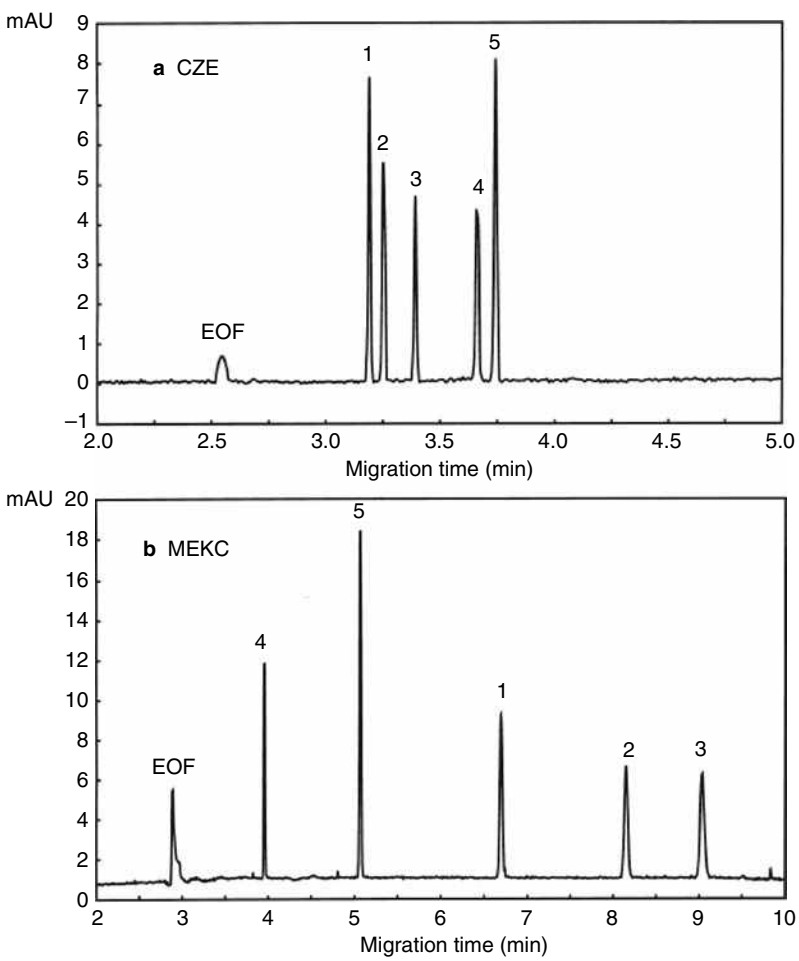

Fig. 2 Electropherograms of the separation of five barbiturate standards using a, CZE and b, MEKC. Peaks: 1, hexobarbital; 2, methohexital; 3, secobarbital; 4, barbital; and 5, phenobarbital.

which is more likely to separate complex mixtures than CZE. Because of their similar migration velocities, barbiturates are most commonly investigated in the MEKC mode.[7,8,10–13,16–19] There are various buffers and modifiers that can be selected and combined in MEKC to optimize separation; some typical examples are summarized in Table 1.

COMPARISON OF CZE AND MEKC

A comparison of the CZE and MEKC modes for determining barbiturates is summarized in Table 2.

Fig. 2[17] shows electropherograms of a mixture of five barbiturate standards; it can be observed that the addition of micelles in MEKC clearly resulted in a different separation mechanism, reflected in various changes in elution order, compared to CZE. The migration behavior in MEKC depends largely on the hydrophobic interaction of the analytes with the micelles. Hydrophobic components are more solubilized in the micelles, resulting in a slower migration compared to less hydrophobic compounds.

OPTIMIZATION OF SEPARATION

Various types of coated capillaries have been applied to the CE separation of barbiturates for improvement of separation selectivity and efficiency.[11,20,21] Jinno et al. reported a series of investigations on polyacrylamide (PAA) and AA-co-IPAAM-coated columns in both CZE and MEKC modes. By the use of PAA coating for the capillary, EOF was sufficiently eliminated, leading to a shorter analysis time and better resolution.[11,20] In addition, the elution order of barbiturates partly changed because of the hydrophobic nature of PAA. It must be noted that a non-cross-linked copolymer containing IPAAM had thermosensitive properties, and elution order was different at elevated temperatures when compared with that at ambient temperature,[21] as illustrated in Fig. 3.

In CE, the use of a reproducible identification parameter is very important because it influences identification power (IP). Boone et al.[17] used μ_{eff} and μ_{eff}^{c} instead of migration times to enhance reproducibility, to reduce the upward trend of RSD with increasing migration time, and to correct for outliers.

CHIRAL SEPARATION OF BARBITURATES

Chiral separation is one of the major outstanding advantages for CE compared to other separation techniques. As enantiomers have identical electrophoretic mobilities, some chiral complexing reagents, called chiral selectors, must be added to the separation buffer to form diastereomeric complexes in dynamic equilibrium. One of the most

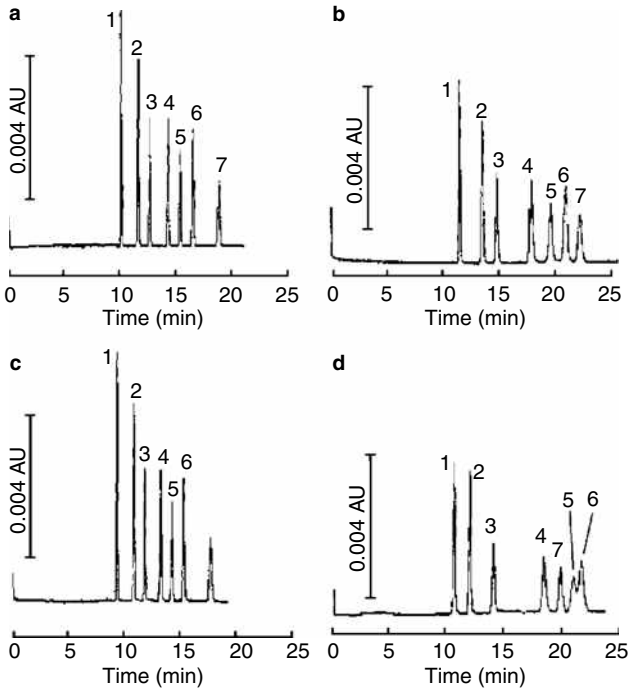

Fig. 3 Separation of barbital by the use of a capillary coated with (a and c) 10% T PAA and (b and d) 10% T poly (AA-co-IPAAM) containing 85% IPAAM. Experiments were carried out at (a and b) ambient temperature or (c and d) elevated temperature. Conditions: capillary column, 50 cm × 0.075 mm I.D. (25 cm effective length); buffer, 100 m*M* Tris–150 m*M* boric acid (pH 8.3); field strength, 300 V/cm; injection, electromigration for 5 sec at the side of cathode. Peak identification: 1, phenobarbital; 2, barbital; 3, mephobarbital; 4, amobarbital; 5, secobarbital; 6, pentobarbital; 7, metharbital.

versatile techniques for achieving chiral recognition is the addition of cyclodextrins (CDs). It is reported that determination of (*R*)-secobarbital and (*S*)-secobarbital from serum was achieved by addition of hydroxypropyl-γ-cyclodextrin (HP-γ-CD)[16] or hydroxypropyl-β-cyclodextrin (HP-β-CD)[18] in the running buffer. Fig. 4 illustrates a typical electropherogram of pentobarbital and secobarbital enantiomers, separated by HP-β-CD. Conradl and Vogt et al.[22] investigated the separation of (*R*)-thiopental and (*S*)-thiopental, and (*R*)-phenobarbital and (*S*)-phenobarbital by using α-CD and β-CD as chiral selectors, separately. They found out that the enantiomers of thiopental were not separated by β-CD, whereas cyclobarbital enantiomers were separated by both α-CD and β-CD. It is assumed that the size of the cavity of β-CD allows the side chain of thiopental, with the asymmetric carbon atom, to penetrate completely. Therefore the formation of stereoselective complexes is unlikely. In the case of α-CD, the C_5 substituents of thiopental are optimal in size and structure to fit into the cavity whereas; for cyclobarbital, a partial inclusion of the cyclohexene ring or the methyl

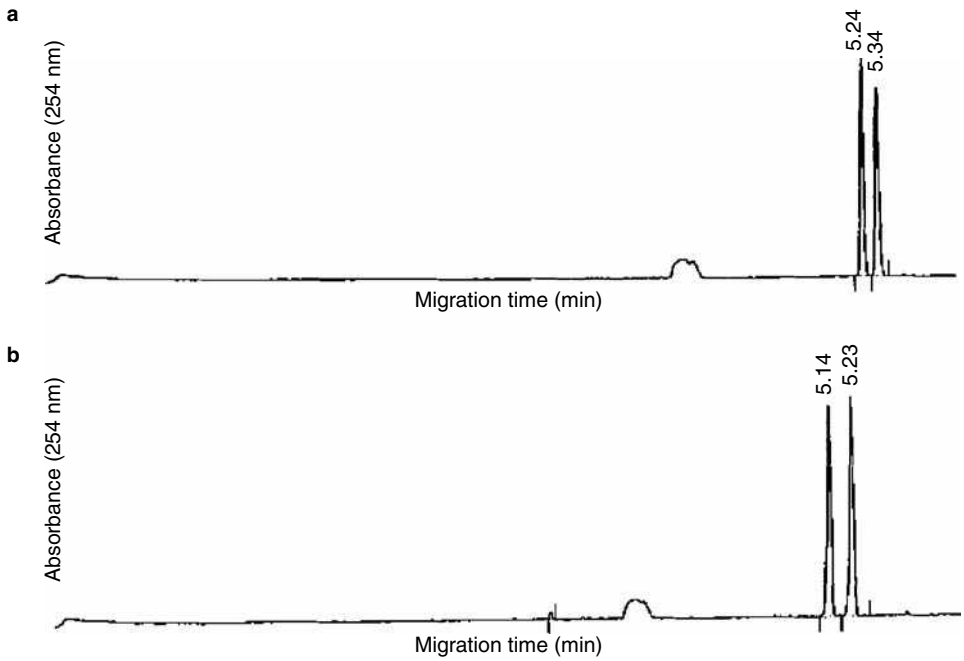

Fig. 4 Typical electropherograms of enantiomers of A, pentobarbital and B, secobarbital on a 57 cm × 75 μm I.D. fused silica capillary. The run buffer contained 40 m*M* HP-β-CD in 20 m*M* ammonium acetate buffer (pH 9.0) with detection at 254 nm. The capillary was thermostated at 25°C and the run voltage was set to 15 kV.

group at the C_5 of the heterocycle into the cavity is probable. However, the separation of cyclobarbital with low α-CD concentration was less efficient.

COMPARISON OF CE, GC, AND LC

LC, GC, and CE are three typical analytical separation approaches used to determine barbiturates. The advantages and disadvantages of the three techniques are summarized in Table 3.

CONCLUSIONS

CE offers fast analysis, low consumable expenses, ease of operation, high separation efficiency, and selectivity. Now, CE has undoubtedly become an attractive technique for the determination and therapeutic monitoring of barbiturates and other drugs, and it is becoming more and more important in biological and toxicological analyses. It was also indicated that CE has a good potential for systematic toxicological analysis (STA).[17]

At present, the coupling of CE to MS is attractive because it facilitates the identification of analytes and

Table 3 Comparative study of three techniques to determine barbiturates.

Techniques	Advantages	Disadvantages
GC	High sensitivity and selectivity	Inadequate for polar, thermolabile, and low-volatility analytes
	Coupled with MS for the identification of unknowns	High consumption of expensive, high-purity gases
LC	Application to all organic solutes in spite of volatility or thermal stability	Insufficient separation selectivity and efficiency
	Both mobile and stationary phase compositions are variables	Related long analysis time
		Large amounts of expensive and toxic organic solvents used as mobile phase, such as acetonitrile[5] and methanol.[6]
CE	High separation efficiency	Inadequate detection limit
	Small consumption of expensive reagents and toxic solvents	Lack of highly selective detectors

improves detection sensitivity. Combining CE with fluorescence detection greatly improves the sensitivity and selectivity for determining proteins and other biological molecules. Future trends of CE will be used to develop more coupling methods to combine CE with highly selective detectors and to achieve miniaturization and automation for extremely fast, easy, and real-time determination in pharmaceutical and biological analyses.

REFERENCES

1. Colbert, D.L.; Smith, D.S.; Landon, J.; Sidki, A.M. Single-reagent polarization fluoroimmunoassay for barbiturates in urine. Clin. Chem. **1984**, *30*, 1765.
2. Berry, D.J. Gas chromatographic analysis of the commonly prescribed barbiturates at therapeutic and overdose levels in plasma and urine. J. Chromatogr. **1973**, *86*, 89.
3. Soo, V.A.; Bergert, R.J.; Deutsch, D.G. Screening and quantification of hypnotic sedatives in serum by capillary gas chromatography with a nitrogen-phosphorus detector, and confirmation by capillary gas chromatography–mass spectrometry. Clin. Chem. **1986**, *32*, 325.
4. Elisabeth, I.; Rene, S.; Dieter, J. Screening for drugs in clinical toxicology by high-performance liquid chromatography: Identification of barbiturates by post-column ionization and detection by a multiplex photodiode array spectrophotometer. J. Chromatogr. **1988**, *428*, 369.
5. Feng, C.L.; Liu, Y.T.; Luo, Y. HPLC-DAD analysis of thirteen soporific sedative drugs in human blood. Acta Pharm. Sin. **1995**, *30* (12), 914–919.
6. Coppa, G.; Testa, R.; Gambini, A.M.; Testa, I.; Tocchini, M.; Bonfigli, A.R. Fast, simple and cost-effective determination of thiopental in human plasma by a new HPLC technique. Clin. Chim. Acta **2001**, *305*, 41–45.
7. Thormann, W.; Meier, P.; Marcolli, C.; Binder, F. Analysis of barbiturates in human serum and urine by high-performance capillary electrophoresis-micellar electrokinetic capillary chromatography with on-column multi-wavelength detection. J. Chromatogr. **1991**, *545*, 445–460.
8. Meier, P.; Thormann, W. Determination of thiopental in human serum and plasma by high-performance capillary electrophoresis-micellar electrokinetic chromatography. J. Chromatogr. **1991**, *559*, 505–513.
9. Shihabi, Z.K. Serum pentobarbital assay by capillary electrophoresis. J. Liq. Chromatogr. **1993**, *16* (9/10), 2059–2068.
10. Wu, H.; Guan, F.; Luo, Y. Determination of barbiturates in human plasma and urine by high performance capillary electrophoresis. Yaowu Fenxi Zazhi **1996**, *16* (5), 316–321.
11. Jinno, K.; Han, Y.; Sawada, H.; Taniguchi, M. Capillary electrophoretic separation of toxic drugs using a polyacrylamide-coated capillary. Chromatographia **1997**, *46* (5/6), 309.
12. Shiu, G.K.; Nemoto, E.M. Simple, rapid and sensitive reversed-phase high-performance liquid chromatographic method for thiopental and pentobarbital determination in plasma and brain tissue. J. Chromatogr. **1982**, *227*, 207.
13. Evenson, M.A.; Wilktorowicz, J.E. Automated capillary electrophoresis applied to therapeutic drug monitoring. Clin. Chem. **1992**, *38* (9), 1847–1852.
14. Li, S.; Weber, S.G. Determination of barbiturates by solid-phase microextraction and capillary electrophoresis. Anal. Chem. **1997**, *69*, 1217–1222.
15. Delinsky, D.C.; Srinivasan, K.; Solomon, H.M.; Bartlett, M.G. Simultaneous capillary electrophoresis determination of barbiturates from meconium. J. Liq. Chromatogr. Relat. Technol. **2002**, *25* (1), 113–123.
16. Srinivasan, K.; Zhang, W.; Bartlett, M.G. Rapid simultaneous capillary electrophoretic determination of (R)- and (S)-secobarbital from serum and prediction of hydroxypropyl-γ-cyclodextrin—secobarbital stereoselective interaction using molecular mechanics simulation. J. Chromatogr. Sci. **1998**, *36*, 85–90.
17. Boone, C.M.; Franke, J.-P.; de Zeeuw, R.A.; Ensing, K. Evaluation of capillary electrophoretic techniques towards systematic toxicological analysis. J. Chromatogr. A, **1999**, *838*, 259–272.
18. Srinivasan, K.; Bartlett, M.G. Comparison of cyclodextrin-barbiturate noncovalent complexes using electrospray ionization mass spectrometry and capillary electrophoresis. Rapid Commun. Mass Spectrom. **2000**, *14*, 624–632.
19. Wu, H.; Guan, F.; Luo, Y. A universal strategy for systematic optimization of high performance capillary electrophoretic separation. Chin. J. Anal. Chem. **1996**, *24* (10), 1117–1122.
20. Jinno, K.; Han, Y.; Sawada, H. Analysis of toxic drugs by capillary electrophoresis using polyacrylamide-coated columns. Electrophoresis **1997**, *18* (2), 284–286.
21. Sawada, H.; Jinno, K. Capillary electrophoretic separation of structurally similar solutes in noncross-linked poly(acrylamide-*co*-*N*-isopropylacrylamide) solution. Electrophoresis **1997**, *18* (11), 2030–2035.
22. Conradl, S.; Vogt, C. Separation of enantiomeric barbiturates by capillary electrophoresis using a cyclodextrin-containing run buffer. J. Chem. Educ. **1997**, *74* (9), 1122–1125.

β-Lactam Antibiotics: Effect of Temperature and Mobile Phase Composition on RP/HPLC Separation

J. Martin-Villacorta
R. Mendez
N. Montes
J.C. Garcia-Glez
Physical Chemistry Department, University of León, León, Spain

INTRODUCTION

In previous papers,[1,2] we reported the effect of column temperature on resolution in reversed-phase high-performance liquid chromatography (RP-HPLC) to separate various β-lactams (penicillins and cephalosporins) from a single sample. In this work we describe the effect of column temperature and volume fraction of an organic solvent on resolution in the isocratic elution conditions of some β-lactam antibiotics.

Mobile phase composition and column temperature are two important experimental parameters that can be altered when a mixture of several compounds is to be separated.[3–5]

The relationships between capacity factor, k', and organic modifier concentration in the mobile phase, and the effect of the column temperature on k' for the antibiotics studied have been used to define k' as a function of T and V (volume fraction) on the basis of a small number of experimental measurements for a given combination of column, organic solvent, and type of antibiotic. From calculated values of k', resolution values, R_S, may be estimated for adjacent band-pairs under all conditions. The method developed enables the optimization of RP-HPLC separations of the β-lactam antibiotics in the absence of difficult theoretical calculations, using a small number of experimental data, including the influence of the organic solvent in the mobile phase (isopropanol) and the column temperature.

INSTRUMENTS

The HPLC system consisted of a Model 600E multisolvent delivery system equipped with a heated column compartment, a Model 484 variable-wavelength detector, and a Model 745B computing integrator, all from Waters Assoc., Inc., Milford, Massachusstts, U.S.A. The chromatograph was equipped with a Spherisorb ODS column (10 μm particle size, 25 cm × 4.6 mm I.D.).

CHROMATOGRAPHIC PROCEDURE

The mobile phases used to separate the compounds were acetate buffer (pH 5.00, 0.1 *M*)/isopropanol, 96.5/3.5, 95/5, 93/7, and 90/10 (v/v). A precolumn (3 cm × 4.6 mm I.D.), packed with the same packing materials, was used to guard the main column. The detector was set at 254 nm. The flow rate of the mobile phase was 1.0 ml/min. The column dead time, t_0, was measured by injecting methanol.

RESULTS AND DISCUSSION

The mixture of β-lactams was chromatographed at each of five column temperatures from 20°C to 60°C, and at four different volume fractions of isopropanol in mobile phase, from 0.035 to 0.1. Fig. 1A shows chromatograms with the volume fraction of isopropanol ranging from 0.035 to 0.1 at a constant column temperature (30°C). Fig. 1B shows the chromatograms obtained for each column temperature at 0.05 volume fraction of isopropanol. As one can see, a marked effect is produced for both parameters on the chromatographic behavior of each antibiotic.

Capacity Factor as a Function of Volume Fraction of Isopropanol in the Mobile Phase

The volume fraction (V) of organic solvent in the mobile phase is one of the most important parameters controlling capacity factor in RP-HPLC. Many reported studies[6–10] show that, for a given solute and separation temperature, T, the relationship between capacity factor (k') and the volume fraction (V), or the eluent concentration, can be expressed as follows:

$$k' = aV^{-b} \tag{1}$$

where a and b are constants.

For all antibiotics, the plots of log k' vs. log V gave straight lines for all temperatures, with a correlation of 0.9992 or greater (Fig. 2a). As one can see, there are different slopes, which may probably be ascribed to different separation mechanisms.

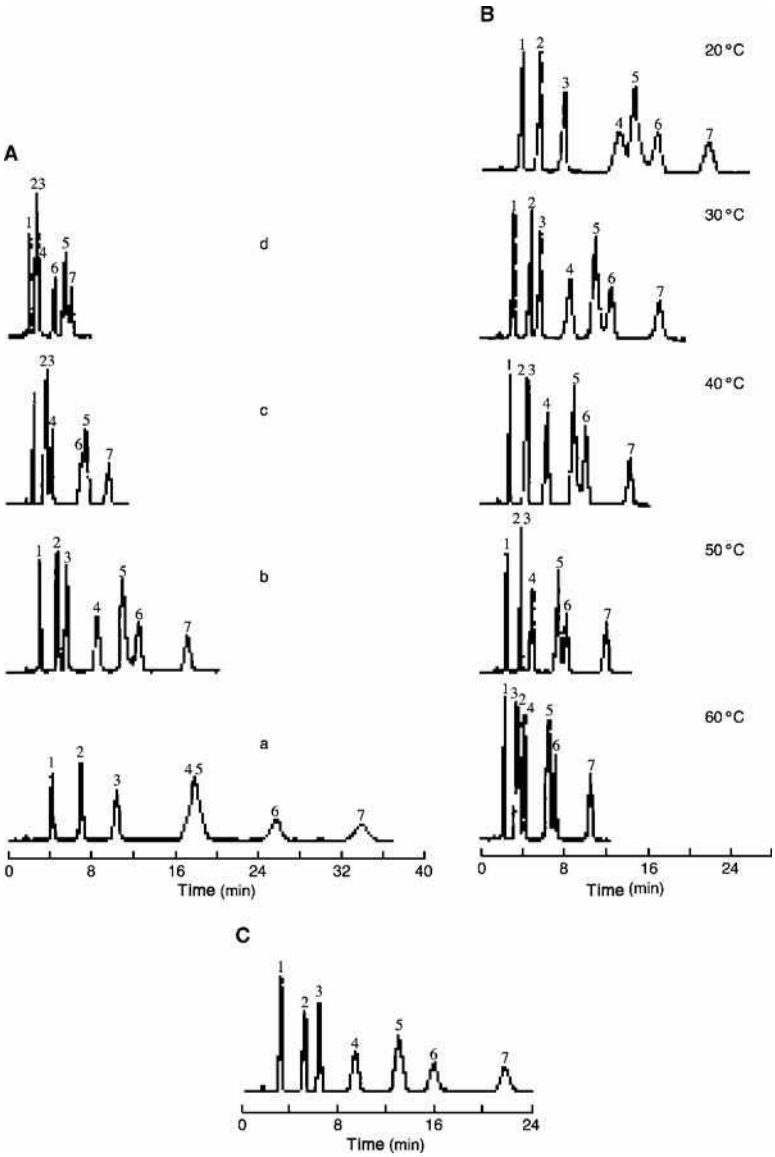

Fig. 1 A, Effect of changing isopropanol volume fraction in the mobile phase on the elution profiles of cefonicid (1), cefaclor (2), cephazolin (3), cefodizime (4), cephaloridine (5), cephamandole (6), and cephalotin (7), using a mobile phase of 0.1 *M* acetate buffer (pH 5.00)/isopropanol (v/v) $a = (96.5/3.5)$, $b = (95/5)$, $c = (93/7)$, and $d = (90/10)$ at a column temperature of 30°C. B, Effect of column temperature on the elution profiles of cephalosporins studied [numbering as in (A)], using a mobile phase of 0.1 *M* acetate buffer (pH 5.00)/isopropanol (95/5) (v/v). C, Isocratic elution profile under optimal conditions. Mobile phase 0.1 *M* acetate buffer (pH 5.00)/isopropanol (95.4/4.6) (v/v), column temperature, 32°C, numbering as in (A).

Table 1 lists constants a and b, calculated from the intercepts and the slopes, respectively, by means of a least-squares method. The slopes for 1, 2, and 7 were found to be slightly affected by the column temperature, especially the slope for 1 (Cefonicid).

Capacity Factor as a Function of Column Temperature

Fig. 1B shows five chromatograms for the mixture of β-lactams, obtained at different temperatures. As one can see, the retention time of each antibiotic increased strongly as the column temperature was increased from 20°C to 60°C.

The dependence of the capacity factor on temperature is given by the Van't Hoff equation:

$$\ln k' = -H^\circ/RT + S^\circ/R + \phi \qquad (2)$$

where R is the gas constant, ΔH° and ΔS° are the enthalpy and entropy changes, respectively, associated with the solute retention process. The parameter ϕ is the phase ratio and T is the absolute temperature.

Fig. 2b shows a van't Hoff plot for each antibiotic. It can be seen that the lines generated from the $\ln k'$ of each compound at different temperatures are linear with a correlation coefficient of 0.995 or greater. The linearity of the plots supports the assumption that single sorption mechanisms are operative for each antibiotic. As for β-lactams and other compounds,[2,11,12] the slopes of these lines were not all the same, as one might expect if the effect of temperature was generalized.

For all antibiotics, the values of enthalpy change are negative, which indicates that the transfer of antibiotic from the mobile phase to sorption sites is favored.

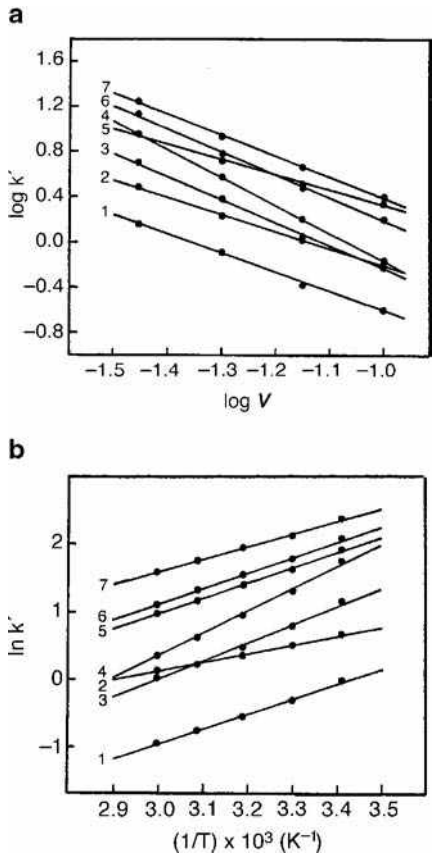

Fig. 2 a, Effect of isopropanol volume fraction (V) in mobile phase on the capacity factor (k') at 30°C. Mobile phases as in Fig. 1B and numbering as in Fig. 1A. B, Effect of column temperature on the capacity factor (k'). Mobile phase as in Fig. 1B and numbering as in Fig. 1A.

Determination of Capacity Factor for Any Value of Volume Fraction of Isopropanol and Column Temperature

Following the methodology developed by Gant et al.,[3] it is possible to obtain the values for the capacity factor ($k_{T,V}'$) for any value of volume fraction of isopropanol and any column temperature. In this methodology, a standard state is defined by a temperature (T_S) and mobile phase composition (V_S). In the present study, $T_S = 20°C$ (293.3 K) and $V_S = 0.035$. The standard state value of k' for the solute in question is k_{T_s},V_s'.

From Eq. 1, we can write:

$$\log k_{T_S,V}' = \log k_{T_S,V_S}' - b(\log V - \log V_S) \quad (3)$$

where $k_{T,V}'$ is the capacity factor for a value of V and the temperature T_S.

From Eq. 2, we can write at any value of T and V:

$$\log k_{T,V}' = \log k_{T_S,V}' - c(1/T_S - 1/T) \quad (4)$$

where $k_{T,V}'$ is the capacity factor for any value of T and V, and the parameter c varies with the β-lactam and with mobile phase composition.

According to Eqs. 3 and 4, the temperature coefficient c must be of the form:

$$c = d - e \log V \quad (5)$$

where d and e are constant for a given β-lactam and system.

Using Eqs. 3, 4, and 5, it is possible to calculate the capacity factor $k_{T,V}'$ for any value of T and V, after determining the values of b and c from these equations and the experimental data. The parameter c used for each volume fraction of isopropanol is determined from Eq. 5, using the constants d and e previously determined by plotting experimental c values vs. log V. Table 2 compares the experimental and calculated values of the capacity factor, k', for the antibiotic studied, experimental k' values being predicted generally with good agreement.

EFFECT OF ELUTION CONDITIONS ON RESOLUTION

The conventional equation to evaluate the effect of elution conditions on resolution (R_S) is:

$$R_S = 1/4\sqrt{N}(k'/1 + k')(\alpha - 1/\alpha) \quad (6)$$

Table 1 Values of constants a and b in Eq. 1 at different column temperatures.

	Column temperature (°C)									
	20		30		40		50		60	
Cephalosporin	b	$a \times 10^3$	b	$a \times 10^3$	b	$a \times 10^3$	b	$a \times 10^3$	b	$a \times 10^3$
1	1.43	13.9	1.67	5.07	1.82	2.48	2.18	0.665	2.24	0.472
2	1.41	29.5	1.49	20.0	1.55	14.1	1.52	13.4	1.65	7.86
3	2.01	7.86	2.03	5.23	1.99	4.23	2.20	1.71	2.14	1.60
4	2.50	3.22	2.46	2.29	2.48	1.54	2.71	0.559	2.70	0.410
5	1.24	163.7	1.35	92.6	1.36	68.7	1.33	60.3	1.42	37.6
6	1.96	22.8	2.03	14.1	2.03	10.4	2.04	8.25	2.20	4.30
7	1.74	59.5	1.86	33.0	1.87	25.9	2.02	13.7	1.99	12.6

Table 2 Experimental vs. calculated capacity factor (k') values for cephalosporins studied at different temperatures.

	Temperature (°C)									
	20		30		40		50		60	
Cephalosporin	Experimental	Calculated	Experimental	Calculated	Experimental	Calculated	Experimental	Calculated	Experimental	Calculated
1	1.01	1.01	0.75	0.79	0.58	0.62	0.47	0.49	0.39	0.38
2	2.03	2.03	1.69	1.75	1.46	1.51	1.26	1.30	1.14	1.12
3	3.36	3.33	2.23	2.46	1.63	1.82	1.26	1.34	1.01	0.99
4	6.31	5.52	3.75	3.85	2.60	2.69	1.87	1.88	1.42	1.31
5	7.03	6.78	5.21	5.33	4.00	4.18	3.23	3.29	2.69	2.58
6	8.34	8.05	6.03	6.33	4.66	4.98	3.73	3.92	3.08	3.08
7	11.1	10.9	8.58	8.94	7.00	7.30	5.85	5.96	4.98	4.86

Volume fraction of isopropanol $V = 0.05$.
Numbering as in Table 1.

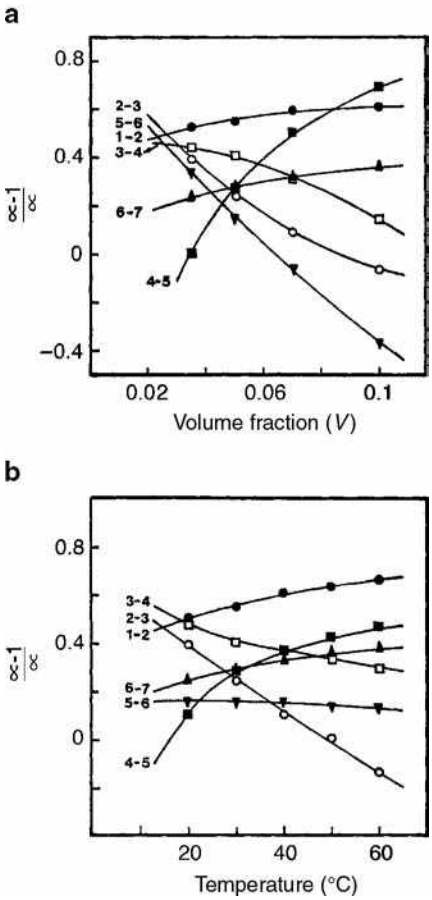

Fig. 3 a, Effect of column temperature on the selectivity factor ($\alpha - 1/\alpha$) of the six pairs of sequentially resolved peaks. Mobile phase as in Fig. 1B and numbering as in Fig. 1A. b, Effect of isopropanol volume fraction (V) in mobile phase on the selectivity factor ($\alpha - 1/\alpha$) of the six pairs of sequentially resolved peaks at 30°C. Mobile phases and numbering as in Fig. 1B and numbering as in Fig. 1A.

Here, N is the plate number, α is the selectivity factor (defined as k_2'/k_1'), where k_1' and k_2' are the capacity factors for bands 1 and 2, and k' is the average capacity factor of k_1' and k_2'. The three factors, α, N, and k', control the resolution. It is assumed that the three terms of Eq. 6 are approximately independent, which allows their separate optimization. The resolution equation Eq. 6 must be applied to each of the adjacent band-pairs considered.

As one can see in Fig. 1B, the band broadening of any peak appearing at a fixed retention time decreases as the temperature increases; accordingly, the N value increases with increasing temperature. A linear relationship was obtained for the plot of N vs. T: $N = 24.7\ T - 6560$ (T has the dimension of absolute temperature) with a correlation coefficient of 0.991. The N value is practically independent of the volume fraction of isopropanol for the β-lactam studied.

In general, the contribution of $k'/1 + k'$ terms to R_S is approximately constant as long as k' is not small. As the selectivity factor (α) is of greater concern in Eq. 6, the separate optimization of the influence of the temperature and mobile phase composition in values is in many cases a good criterion for establishing the elution conditions of the separation.

Fig. 3 shows the influence of temperature and isopropanol volume fraction in the term: ($\alpha - 1/\alpha$). There are examples of different situations: for pairs 5–6 and 4–5, the ($\alpha - 1/\alpha$) term is markedly influenced by the isopropanol volume fraction; the column temperature also exerts an important influence on this term for pairs 2–3 and 4–5. It is interesting to note that both parameters (T and V) have important and similar effects on pairs 4–5 and 2–3 in this resolution term. For these cases, both parameters can be used to obtain a better resolution. Fig. 1C shows an elution profile under optimal elution conditions.

CONCLUSIONS

The present work demonstrates that there is linear relationship between the log k′ and both the log V (volume fraction of organic solvent in the mobile phase) and the reciprocal of the absolute temperature. Therefore, it is possible with a small number of initial experimental data of the capacity factor (k') to predict k' for each cephalosporin as a function of T and V, which reveals the optimal elution conditions for the isocratic separation of a mixture of cephalosporins.

REFERENCES

1. Martín-Villacorta, J.; Méndez, R.; Negro, A. Effect of temperature on HPLC separation of penicillins. J. Liq. Chromatogr. **1988**, *11* (8), 1707.
2. Martín-Villacorta, J.; Méndez, R. Effect of temperature and mobile phase composition on RP-HPLC separation of cephalosporins. J. Liq. Chromatogr. **1990**, *13* (16), 3269.
3. Gant, J.R.; Dolan, J.W.; Snyder, L.R. Systematic approach to optimizing resolution in reversed-phase liquid chromatography, with emphasis on the role of temperature. J. Chromatogr. **1979**, *185*, 153.
4. Baba, Y.; Yoza, N.; Ohashi, S. Effect of column temperature on high-performance liquid chromatographic behaviour of inorganic polyphosphates: I. Isocratic ion- exchange chromatography. J. Chromatogr. **1985**, *348*, 27.
5. Atamna, I.; Gruska, E. Optimization by isochronal analysis: II. Changes in mobile phase velocity and temperature, and in mobile phase composition and temperature. J. Chromatogr. **1986**, *355*, 41.

6. Rothbart, H.L.; Weymouth, J.W.; Rieman, W., III Separation of the oligophoshates. Talanta **1964**, *11*, 33.
7. Ohashi, S. Chromatography of phosphorous oxoacids. Pure Appl. Chem. **1975**, *44*, 415.
8. Ohashi, S.; Tsuji, N.; Ueno, Y.; Takeshita, M.; Muto, M. Elution peak positions of linear phosphates in gradient elution chromatography with an anion-exchange resin. J. Chromatogr. **1970**, *50*, 349.
9. Nakamura, T.; Kimura, M.; Waki, H.; Ohashi, S. The pH dependence of anion exchange chromatographic separation of tri- and tetraphosphate anions. Bull. Chem. Soc. Jpn. **1971**, *44*, 1302.
10. Schoenmakers, P.J.; Billiet, H.A.H.; Tijssen, R.; de Galan, L. Gradient selection in reversed-phase liquid chromatography. J. Chromatogr. **1978**, *149*, 519.
11. Chemielowiec, J.; Sawatzky, H. Entropy dominated high performance liquid chromatographic separations of polynuclear aromatic hydrocarbons. Temperature as a separation parameter. J. Chromatogr. Sci. **1979**, *17*, 245.
12. Diasio, R.B.; Wilburn, M.E. Effect of subambient column temperature on resolution of fluorouracyl metabolites in reversed-phase high performance liquid chromatography. J. Chromatogr. Sci. **1979**, *17*, 565.

Bile Acids: TLC Analysis

Alina Pyka
Department of Analytical Chemistry, Medical University of Silesia, Sosnowiec, Poland

Abstract
The separations and the detections of selected bile acids such as: cholic acid (C), glycocholic acid (GC), glycolithocholic acid (GLC), deoxycholic acid (DC), chenodeoxycholic acid (CDC), glycodeoxycholic acid (GDC), and lithocholic acid (LC) by using normal-phase thin-layer chromatography (NP-TLC), reversed-phase thin-layer chromatography (RP-TLC), and densitometry have been discussed. The chromatographic lipophilicity parameters (R_{MW} and φ_0) were compared both with measured ($\log P_{exp}$) and calculated partition coefficients ($A\log P_S$, $IA\log P$, $\log P_{Kowwin}$, $x\log P$, $C\log P$, $\log P_{Rekker}$) for selected bile acids. The significance of structural descriptors in quantitative structure-property relationships (QSPR), quantitative structure-retention relationships (QSRR), and quantitative structure-activity relationships (QSAR) of selected bile acids has been also discussed.

INTRODUCTION

Bile acids fulfill many important functions; e.g., they facilitate digestion and absorption of fat, vitamins soluble in fat (A, E, D, and K), and cholesterol. Glycocholic (GC) and taurocholic acids emulsify hydrophobic substances which are present in the aqueous environment of the alimentary tract by reducing surface tension. Bile acids, as distinct from GC and taurocholic acids, activate the liver to produce bile; thus, they are used as cholagogues. Beef bile, which is used as a cholagogic agent, can be a source of cholic acid (C), deoxycholic acid (DC), chenodeoxycholic acid (CDC), ursodeoxycholic acid, and lithocholic acid (LC). Of all above-mentioned acids, CDC and ursodeoxycholic acid—which quite well dissolve gallstones at longer application—play a special role. CDC is generally used in the case of lithiasis caused by radiolucent cholesterol stones, whereas ursodeoxycholic acid is usually used to dissolve uncalcified gallstones, both in preserved secretory function of the gallbladder and for reflux gastritis. Numerous pharmaceutical preparations contain CDC and ursodeoxycholic acid, whereas C is generally used in the form of its sodium, magnesium, or calcium salt or in a methamine mixture.[1]

Respective ketocholanic acids, which are absent from bile, can be obtained from C, DC, and LC by oxidation of secondary alcoholic groups (dehydrogenation). Dehydrocholic acid, used both in a free and conjugated form (of sodium salt), is about 10 times less toxic than C. Dehydrocholic acid activates production of bile, speeds up its flow, and facilitates resorption of fat because it intensifies the activity of pancreatic lipase. Bile acids are well absorbed from the alimentary tract; next, they enter the blood stream and then activate liver cells to produce bile. However, bile acids are strongly toxic compounds, and their overdose leads to degeneration of cardiac muscle or lesions of the liver and kidneys. Additionally, bile acids became quite important initial material for the half synthesis of steroidal hormones.

Bile acids are the object of wide investigations because of their biological properties. High-performance liquid chromatography (HPLC), thin-layer chromatography (TLC), and gas chromatography are the principal techniques used for qualitative and quantitative investigations of bile acids. Analysis of bile acid by chromatographic techniques is the subject of many scientific publications.[1–24] Scalia[2] presented a review of the methods available for the separation of bile acids. TLC, gas chromatography, and HPLC techniques and combined detection systems for the determination of bile acids were critically evaluated, and their advantages and disadvantages were discussed.[2] Gaica et al.[3] separated C and 14 of its synthetic derivatives by using their TLC behavior in six reversed-phase systems and three normal-phase systems. Four different adsorbents were used, namely RP-18 silica, CN-silica, polyacrylonitrile adsorbent, and unmodified silica gel. Reversed-phase chromatography was performed with water–organic modifiers (methanol, dioxane, or acetone) as mobile phases in various volume compositions. However, normal-phase chromatography was performed with petroleum–acetone, chloroform–methanol, and ethyl acetate–toluene as mobile phases. Results obtained by Gaica et al. indicate that the different normal- and reversed-phase systems employed can be successfully used for separation of the substances examined. The selectivity of the RP systems is significantly better, because RP-18 silica gel, combined with mobile phases containing 65–70% methanol or 50–60% dioxane in water, can be recommended as the most suitable chromatographic system for these compounds.[3] Zarzycki, Wierzbowska, and Lamparczyk[4] studied the influence of temperature on retention and separation of cholesterol and bile acids

(taurodeoxycholic acid–sodium salt, GC, GC–sodium salt, glycodeoxycholic acid (GDC), GDC–sodium salt, C, C–sodium salt, CDC, CDC–sodium salt, and LC), using reversed-phase thin-layer chromatography (RP-TLC). As mobile phases, methanol–water mixtures of various volume compositions were used. Chromatographic experiments were performed using vapor-saturated chambers at temperatures ranging from 5°C to 60°C. In the higher temperature region, excellent separations (excepting DC and CDC) were obtained. The separation studies of multicomponent mixtures have shown that the degree of separation in the high-temperature region can be increased due to an improvement of the efficiency of the chromatographic system.[4] Earlier, Rivass-Nass and Müllner[5] evaluated the influence of temperature, ionic strength, and apparent pH of the eluent (rather than its composition) on the thin-layer chromatographic separation of sodium salts of selected bile acids. This study indicates that the overall effect of temperature on bile acid separation is dependent upon the eluent used. Reducing the running temperature is, however, strongly recommended, as this leads to an improvement not only of band shape and intensity, but also of resolution. Variation of the apparent pH and of the overall ionic strength should be carefully considered, especially if reversed-phase supports are used.[5]

Pyka and Dołowy published manuscripts which concern investigations of chromatographic separations by use of TLC, lipophilicity and application of structural descriptors in quantitative structure-activity relationships (QSAR), quantitative structure-property relationships (QSPR), and quantitative structure-retention relationships (QSRR) analysis of selected bile acids [C, GC, GDC, CDC, DC, LC, and glycolithocholic acid (GLC)].[1,6–9,11–22] In this entry, the most important results of these investigations will be presented and discussed.

SEPARATION OF SELECTED BILE ACIDS[6–16]

Separation of Bile Acids by Normal-Phase Thin Layer Chromatography (NP-TLC) on Unmodified Silica Gel and Mixtures of Silica Gel and Kieselguhr at Room Temperature[6–11]

The optimum conditions of the separations of the selected bile acids were determined: C, GC, GLC, DC, CDC, GDC, and LC by using TLC on aluminum plates which have been precoated with silica gel 60 (E. Merck, #1.05553), silica gel $60F_{254}$ (E. Merck, #1.05554), or mixtures of silica gel 60 and Kieselguhr F_{254} (E. Merck, #1.05567), as well as on glass plates precoated with silica gel $60F_{254}$ without a concentration zone (E. Merck, #1.05715) and with a concentration zone (E. Merck, #1.11798) using *n*-hexane–ethyl acetate–acetic acid in various volume compositions as mobile phases[7–9] and on aluminum plates precoated with silica gel $60F_{254}$ (E. Merck, #1.05554) using *n*-heptane–ethyl acetate–acetic acid in various volume compositions as mobile phases.[6] Chromatographic separations of studied bile acids were characterized using R_F, as well as separation factors ΔR_F and R_S. Separation factors R_S were determined by use the visual method. Table 1 presents the data, which allows an estimation of the usefulness of the examined stationary phases and mobile phases (*n*-hexane–ethyl acetate–acetic acid) in different volume compositions for the separation of all the investigated bile acids. Separation of each investigated pair of bile acids is satisfactory when $\Delta R_F \geq 0.05$ and $R_S > 1$. An optimum separation for other chromatographic adsorbents was obtained by use of one-dimensional (1-D) development at 18°C and *n*-hexane–ethyl acetate–acetic acid mobile phases in the following volume compositions: 20:20:5 and 22:22:5 on glass plates precoated with silica gel $60F_{254}$ (E. Merck, #1.05715); 22:21:5 and 25:20:8 on aluminum plates precoated with silica gel $60F_{254}$ (#1.05554); 20:20:5, 22:21:5, 22:22:5, and 25:20:8 on aluminum plates precoated with silica gel 60 (#1.05553); and 20:20:5 on glass plates precoated with silica gel $60F_{254}$ with concentration zone (#1.11798).[7,8] Fig. 1 presents a densitogram of bile acids separated on an aluminum plate precoated with silica gel $60F_{254}$ (#1.05554) by using the mobile phase *n*-hexane–ethyl acetate–acetic acid in volume composition 22:21:5.[10]

When aluminum plates precoated with the mixture of silica gel 60 and Kieselguhr F_{254} (#1.05567) were used, the selection of mobile phases depended on the kind of bile acids which are being separated. The mobile phase 25:20:8 (v/v/v) allows separation of all pairs of bile acids, with the exception of the pair of LC and DC. Using mobile phases in other volume compositions can separate the pair of LC and DC. In this case—the separation on the silica gel 60 and Kieselguhr F_{254} mixture—the biggest problem was to

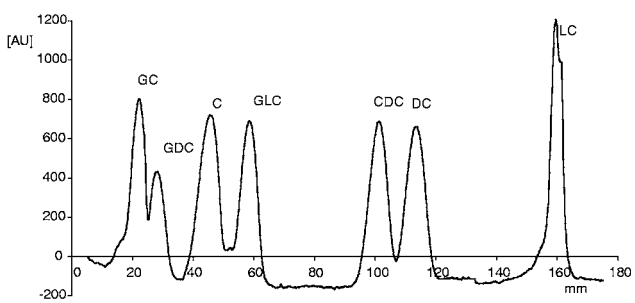

Fig. 1 Densitometric profiles obtained for the investigated bile acids on aluminum plate precoated with silica gel $60F_{254}$ (E. Merck, #1.05554) using *n*-hexane–ethyl acetate–acetic acid (22:21:5, v/v). Glycocholic acid (GC), glycodeoxycholic acid (GDC), cholic acid (C), glycolithocholic acid (GLC), chenodeoxycholic acid (CDC), deoxycholic acid (DC), lithocholic acid (LC). (Camag densitometer; wavelength $\lambda = 250$ nm; slit dimensions: 6×0.2 mm; scanning speed: 40 nm/sec).
Source: From Pyka, A., unpublished data.[10]

separate GLC and C. Separation of these acids was possible only by using a mobile phase in volume composition 25:20:8.[8]

The mobile phase *n*-hexane–ethyl acetate–acetic acid in a volume composition of 25:20:5 (v/v/v) is not optimal for separating all seven bile acids on aluminum plates precoated with silica gel 60 (#1.05553). However, when this mobile phase is used, the difference between R_F values of C and GLC is 0.05, but the R_S of this pair of bile acids is smaller than 1 ($R_{S(C/GLC)} = 0.96$; see Table 1). To obtain complete separation of the seven examined bile acids on aluminum plates precoated with silica gel 60 (#1.05553), a two-dimensional (2-D) technique was used. The first development used the mobile phase *n*-hexane–ethyl acetate–acetic acid in a volume composition of 25:20:5. Chloroform–*n*-butanol–acetic acid–water (2:32:2:2, v/v/v/v) as mobile phase was used for the second development. The scheme of the chromatogram of separated bile acids with the use of a 2-D technique is presented in Fig. 2. The chromatogram indicates that, under these conditions, all the bile acids studied were completely separated. Better separation for C and GLC was obtained.[7]

Similar analyses were also used to compare the separations of studied bile acids. Both analyses showed that on the plates precoated with silica gel, the biggest problem was to separate GC from GDC. In the case of the separation on the silica gel 60 and Kieselguhr F_{254} mixture, the biggest problem was to separate C from GLC. The obtained results indicate that similar analysis can be an alternative method of the estimation of chromatographic separations of studied acids.[9]

The separations of these bile acids on silica gel 60 with concentrating zone (E. Merck, #1.11845) and by use of *n*-hexane–ethyl acetate–acetic acid and *n*-hexane–ethyl acetate–methanol–acetic acid in different volume compositions were also investigated.[11] It was affirmed that *n*-hexane–ethyl acetate–methanol–acetic acid mobile phase in the volume composition 20:20:5:2 is optimum for the separation of the investigated bile acids. Densitometric analysis of the examined bile acids after the detection by use of methanolic solution of sulfuric acid was performed. Densitometric scanning was then performed at multi wavelength in the range of 380–460 nm, with wavelength change at every step 20 nm. A three-dimensional (3-D) densitogram of investigated substances at different wavelengths (380, 400, 420, 440, and 460 nm) is presented in Fig. 3. The resolution of peaks for the studied pairs of compounds were calculated by the use visual method $R_{S(c)}$ and by densitometric methods ($R_{S(b)}$, $R_{S(h)}$, and $R_{S(a)}$). It was affirmed that $R_{S(b)}$, $R_{S(h)}$, and $R_{S(a)}$ values calculated on the basis of the densitograms are considerably lower than the $R_{S(c)}$ values calculated using the visual method on the basis of the chromatograms. This shows that R_S values can be correctly marked exclusively on the basis of the densitograms. The scientific literature data indicate that at R_S values higher than 1.5 we can expect the complete separation of the neighboring compounds on the

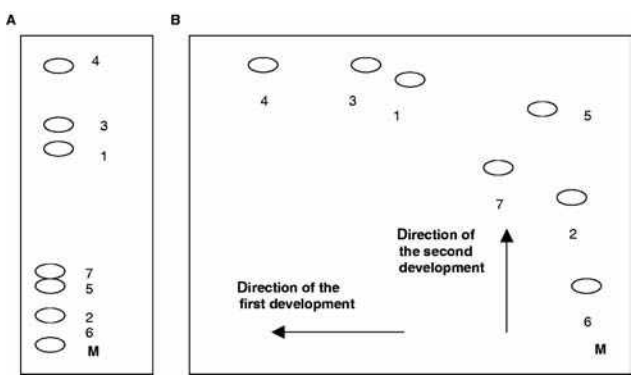

Fig. 2 The 1-D (A) and 2-D (B) chromatograms of the mixture of the seven bile acids investigated on thin-layer chromatography (TLC) silica gel 60 (E. Merck, #1.05553). I. Eluent: *n*-hexane–ethyl acetate–acetic acid (25:20:5, v/v). II. Eluent: chloroform–*n*-butanol–acetic acid–water (2:32:2:2, v/v); M represents bile acids mixture where 1 indicates chenodeoxycholic acid, 2 glycodeoxycholic acid, 3 deoxycholic acid, 4 lithocholic acid, 5 cholic acid, 6 glycocholic acid, and 7 glycolithocholic acid.
Source: From Separation of selected bile acids by TLC. II. One-dimensional and two-dimensional TLC, in J. Liq. Chromatogr. Relat. Technol. Marcel Dekker, Inc.[7]

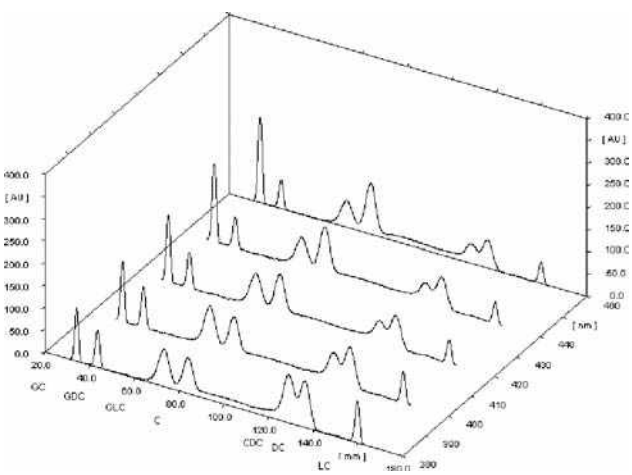

Fig. 3 The densitograms of bile acids investigated (C, cholic acid; GC, glycocholic acid; GLC, glycolithocholic acid; DC, deoxycholic acid; CDC, chenodeoxycholic acid; GDC, glycodeoxycholic acid; LC, lithocholic acid) at wavelengths 380, 400, 420, 440, and 460 nm after their separation using a *n*-hexane–ethyl acetate–methanol–acetic acid, 20:20:5:2 (v/v/v/v) as mobile phase and after the application of sulfuric acid in methanol (1:19, v/v; the plate was immersed in dipping the solution of sulfuric acid for 15 sec, and it was then heated to 90°C for 20 min) as visualizing reagent.
Source: From TLC of selected bile acids: Detection and separation, in J. Liq. Chromatogr. Relat. Technol.[11]

Table 1 Separation factors (ΔR_F and R_S) of selected bile acids separated with the mobile phase *n*-hexane–ethyl acetate–acetic acid in different volume compositions (v/v/v) on different stationary phases.

	Chromatographic plates									
	1		2		3		4		5	
***n*-Hexane–ethyl acetate–acetic acid**	$\Delta R_F \geq 0.05$	$R_S > 1$	$\Delta R_F \geq 0.05$	$R_S > 1$	$\Delta R_F \geq 0.05$	$R_S > 1$	$\Delta R_F \geq 0.05$	$R_S > 1$	$\Delta R_F \geq 0.05$	$R_S > 1$
20:20:5	+[a]	+[a]	−	+	+	+	−	−	+	+
22:20:5	−[b]	−[b]	−	−	−	−	−	−	−	+
22:21:5	−	+	+	+	+	+	−	−	−	+
22:22:5	+	+	−	−	+	+	−	−	−	+
25:20:2	−	−	−	−	−	−	−	−	−	−
25:20:5	−	−	−	+	+	−	−	−	−	+
25:20:8	−	−	+	+	+	+	−	−	−	−

Note: 1 = Glass plates precoated with silica gel 60F_{254} (#1.05715); 2 = aluminum plates precoated with silica gel 60F_{254} (#1.05554); 3 = aluminum plates precoated with silica gel 60 (#1.05553); 4 = aluminum plates precoated with the mixture of silica gel 60 and Kieselguhr F_{254} (#1.05567); 5 = glass plates precoated with silica gel 60F_{254} with concentrating zone (#1.11798).

[a]$\Delta R_F \geq 0.05$ or $R_S > 1$ for all investigated bile acids.

[b]$\Delta R_F \geq 0.05$ or $R_S > 1$ not for all investigated bile acids.

Source: From Separation of selected bile acids by TLC. III. Separation on various stationary phases, in J. Liq. Chromatogr. Relat. Technol.[8]

densitograms. It was shown that resolutions $R_{S(b)}$, $R_{S(h)}$, and $R_{S(a)}$ value larger than 1.5 were obtained at all analyzed wavelengths for the studied pairs of substances GC/GDC, GDC/GLC, C/CDC, and DC/LC. These conditions did not provide for the complete separation of the pair of substances GLC/C and CDC/DC. The characteristics of the obtained densitometric bands were also presented. Characteristic of the chromatographic band was realized using the densitometric method by determination of peak height, peak area, and the angle (β) between the tangents at the inflection points to the curves of the densitometric peak. From the obtained data, it is apparent that the band of GC has the lowest numerical value of angle β. It shows that band of GC is compact in spite of its large area. However, the heights and areas of chromatographic band obtained at different wavelengths have differentiated values. The densitometric bands with the largest area were obtained at wavelengths in the neighborhood of absorption maximum (λ_{max}) for particular substances investigated. It was affirmed that analysis of chromatographic bands was not by visual but by their densitometric characteristic, which is a supplementary element of the separation effect evaluation. Each visual evaluation is subjective and a little precise in relation to the densitometric method. Only the densitometric method can be used for the objective evaluation of the separation effect and characteristic of particular chromatographic bands.[11]

SEPARATION OF BILE ACIDS BY NORMAL PHASE HIGH-PERFORMANCE THIN-LAYER CHROMATOGRAPHY (NP-HPTLC) ON CYANO- AND DIOL-MODIFIED SILICA GEL AT ROOM TEMPERATURE[12]

The optimum conditions were determined for the separations of selected bile acids such as C, GC, GLC, DC, CDC, GDC, and LC by high-performance TLC on glass plates precoated with modified silica layers, using *n*-hexane–ethyl acetate–acetic acid in the following volume compositions: (a) 49:49:2, 47.5:47.5:5, and 37.5:37.5:25 in the case of CNF_{254} plates (E. Merck, #1.12571); (b) 48.7:48.7:2.6, 47.5:47.5:5, 45:45:10, 42:42:16, 40:40:20, and 37.5:37.5:25 in the case of $DiolF_{254}$ plates (E. Merck, #1.05636). Generally, in applied chromatographic conditions, the adsorption of the studied bile acids increases in the following order: LC, DC, CDC, GLC, C, GDC, and GC. On CNF_{254} plates, when the above-mentioned mobile phase in volume composition 37.5:37.5:25 was used, GC separated very well from GLC ($\Delta R_{F(GC/GLC)} = 0.09$, $R_{S(GC/GLC)} = 2.12$). However, weak separation was observed for other pairs of bile acids. The mobile phase in the volume composition 47.5:47.5:5 allowed separation of the following pairs of neighboring bile acids: GC/GDC, GDC/C, and DC/LC, while the mobile phase in the volume composition 49:49:2 separates almost all pairs of bile acids except for CDC/DC. Thus, it can be concluded that the application of the mobile phase *n*-hexane–ethyl acetate–acetic acid on cyano-modified silica gel plates hinders the separation of CDC from DC.[12] However, these conditions facilitate the separation of GC from GDC when compared to their separations on non-modified silica gel and a mixture of silica gel 60 and Kieselguhr F_{254}.[8,9] However, it was concluded that on $DiolF_{254}$-modified silica gel plates at 18°C and by using the above-mentioned mobile phase in the volume composition 42:42:16, the optimal separation of all examined bile acids was obtained ($\Delta R_F \geq 0.05$ and $R_S > 1$ for all pairs of neighboring bile acids). When the mobile phase in the volume composition 45:45:10 was applied, very good separations were obtained for almost all examined bile acids except for GLC and CDC ($\Delta R_{F(GLC/CDC} = 0.08$, $R_{S(GLC/CDC)} = 1.00$).[12]

Table 2 presents the R_F values and separation factors, ΔR_F and R_S, of bile acids examined at 18°C on cyano-modified silica gel CNF_{254} (#1.12571) and diol-modified silica gel $DiolF_{254}$ (#1.05636), and developed by using the mobile phase *n*-hexane–ethyl acetate–acetic acid in volume compositions 49:49:2 and 42:42:16, respectively.[12]

SEPARATION OF BILE ACIDS BY NP-TLC ON UNMODIFIED SILICA GEL AND MIXTURE OF SILICA GEL AND KIESELGUHR AT 40°C[13]

An attempt was made to determine the influence of temperature on bile separation using adsorption TLC on aluminum plates precoated with silica gel 60 (E. Merck, #1.05553), silica gel $60F_{254}$ (E. Merck, #1.05554), or the mixture of silica gel 60 and Kieselguhr F_{254} (E. Merck, #1.05567); as well as on glass plates precoated with silica gel $60F_{254}$ without concentrating zone (E. Merck, #1.05715) and with concentrating zone (E. Merck, #1.11798). The mobile phase *n*-hexane–ethyl acetate–acetic acid was used as a mobile phase in the volume compositions for which the complete separation of examined bile acids was not obtained at 18°C.[6–9] The chromatographic plates were developed with the use of the above-mentioned mobile phases at 40°C. It was observed that temperatures at 18°C and 40°C influence the effect of separation of selected bile acids. The right choice of temperature can improve the separation of some bile acids; it also causes a change of their relative positions on aluminum plates precoated with the mixture of silica gel 60 and Kieselguhr F_{254} (#1.05567). Generally, it can be stated that the temperature of 40°C improves the separation of GC from GDC on silica plates (#1.05715, #1.11798, #1.05554, and #1.05553). However, under the above-mentioned conditions, a problem concerning the separation of CDC from DC arises. For example, the development of investigated bile acids at 18°C on glass plates precoated with silica gel $60F_{254}$ without concentration zone (#1.05715), using *n*-hexane–ethyl acetate–acetic acid in a volume composition 22:20:5, leads to complete

Table 2 The R_F values and separation factors ΔR_F and R_S of bile acids examined at 18°C on cyano-modified silica gel CNF_{254} (#1.12571) and diol-modified silica gel $DiolF_{254}$ (#1.05636) and developed by using mobile phase: *n*-hexane–ethyl acetate–acetic acid in volume compositions 49:49:2 and 42:42:16, respectively.

	CNF_{254} plates (#1.12571)			$DiolF_{254}$ plates (#1.05636)		
	n-Hexane–ethyl acetate–acetic acid; v/v/v			*n*-Hexane–ethyl acetate–acetic acid; v/v/v		
	49:49:2			42:42:16		
Pair of acids	R_F	ΔR_F	R_S	R_F	ΔR_F	R_S
Glycocholic acid (GC)/glycodeoxycholic acid (GDC)	0.06/0.38	0.32	7.71	0.07/0.39	0.32	5.68
GDC/cholic acid (C)	0.38/0.64	0.26	4.00	0.39/0.49	0.10	1.80
C/glycolithocholic acid (GLC)	0.64/0.76	0.12	2.00	0.49/0.74	0.25	4.67
GLC/chenodeoxycholic acid (CDC)	0.76/0.88	0.12	2.50	0.74/0.82	0.08	2.00
CDC/deoxycholic acid (DC)	0.88/0.91	0.03	0.67	0.82/0.87	0.05	1.33
DC/lithocholic acid (LC)	0.91/0.99	0.08	3.11	0.87/0.96	0.09	3.56

Source: From Separation of selected bile acids by TLC. VI. Separation on cyano- and diol-modified silica layers, in J. Liq. Chromatogr. Relat. Technol.[12]

separation of almost all neighboring pairs of the studied bile acids, except for the pair GC and GDC ($\Delta R_{F(GC/GDC)} = 0.03$, $R_{S(GC/GDC)} = 1.00$). The separation of the pair GC and GDC improves at 40°C ($\Delta R_{F(GC/GDC)} = 0.07$, $R_{S(GC/GDC)} = 1.82$), but the separation of CDC and DC deteriorates at 40°C ($\Delta R_{F(CDC/DC)} = 0.05$, $R_{S(CDC/DC)} = 0.90$) compared to separation at 18°C ($\Delta R_{F(CDC/DC)} = 0.10$, $R_{S(CDC/DC)} = 1.46$).[13]

In the case of the separation on silica gel 60 and Kieselguhr F_{254} mixture at 18°C, the biggest problem was to separate C from GLC. Unfortunately, increasing the temperature to 40°C does not improve the separation of the above-mentioned pair of acids.[13]

SEPARATION OF BILE ACIDS BY NP-TLC ON SILICA GEL IMPREGNATED WITH SELECTED CATIONS[14,15]

To separate bile acids (LC, DC, CDC, GLC, C, GDC, and GC) using adsorption TLC at 18°C, the glass plates precoated with silica gel $60F_{254}$ (#1.05715) were impregnated with 1%, 2.5%, and 5% aqueous solutions of the following salts: $CuSO_4$, $MnSO_4$, $NiSO_4$, and $FeSO_4$. The mixtures of *n*-hexane–ethyl acetate–acetic acid in the volume compositions 22:20:5, 25:20:2, 25:20:5, and 25:20:8 were used as mobile phases.[14,15] These mobile phases were not effective for the separation of bile acids on non-impregnated silica gel $60F_{254}$ plates at 18°C.[8,9] The total number of experimental combinations regarding the impregnation of applied stationary and mobile phases used to separate bile acids was 48. The plates impregnated with the cations whose application resulted in $\Delta R_F \geq 0.05$ and $R_S > 1$ for all pairs of neighboring bile acids were considered the most effective for bile acid separation. All pairs of studied bile acids were separated on plates impregnated with the following aqueous solutions of inorganic salts:

- 1% $CuSO_4$, 2.5% $CuSO_4$, 5% $CuSO_4$, 2.5% $MnSO_4$, 1% $NiSO_4$, 2.5% $FeSO_4$, and 5% $FeSO_4$ with a mobile phase in volume composition 25:20:5 (v/v/v).
- 1% $CuSO_4$, 5% $CuSO_4$, 1% $NiSO_4$, 5% $NiSO_4$, 1% $FeSO_4$, 5% $FeSO_4$ with a mobile phase in volume composition 25:20:8 (v/v/v).
- 1% $CuSO_4$, 2.5% $CuSO_4$, 2.5% $MnSO_4$, and 5% $FeSO_4$ with a mobile phase in volume composition 22:20:5 (v/v/v).

The comparison of the selected values of separation factors ΔR_F and R_S of bile acids examined on glass plates with non-impregnated silica gel $60F_{254}$ (#1.05715) and silica gel $60F_{254}$ (#1.05715) impregnated with selected salts of inorganic acids developed by using mobile phase *n*-hexane–ethyl acetate–acetic acid is presented in Table 3.[7–9,14] It was observed that impregnation of silica gel $60F_{254}$ on glass plates with aqueous solutions of $CuSO_4$, $MnSO_4$, $NiSO_4$, and $FeSO_4$ facilitated the separation of GC from GDC and also C from GLC, which separated more poorly using NP-TLC on non-impregnated silica gel at 18°C.

Dołowy also separated selected bile acids on silica gel 60 (E. Merck, #1.05553) and on silica gel $60F_{254}$ (E. Merck, #1.05554) aluminum plates impregnated with Cu(II), Ni(II), Fe(II), and Mn(II) cations.[15]

SEPARATION OF BILE ACIDS BY REVERSED-PHASE HIGH-PERFORMANCE THIN-LAYER CHROMATOGRAPHY (RP-HPTLC) ON RP2, RP18, RP18W, AND CNF_{254} PLATES[16]

The examined bile acids (LC, DC, CDC, GLC, C, GDC, and GC) were separated on the chromatographic plates

Table 3 The comparison of the selected values of separation factors ΔR_F and R_S of bile acids examined on glass plates with non-impregnated silica gel $60F_{254}$ (#1.05715) and silica gel $60F_{254}$ (#1.05715) impregnated with selected salts of inorganic acids developed by using mobile phase *n*-hexane–ethyl acetate–acetic acid in suitable volume composition.

	Non-impregnated silica gel $60F_{254}$ (#1.05715)					
	***n*-Hexane–ethyl acetate–acetic acid; v/v/v**					
	22:20:5		**25:20:5**		**25:20:8**	
Pair of acids	ΔR_F	R_S	ΔR_F	R_S	ΔR_F	R_S
Glycocholic acid (GC)/glycodeoxycholic acid (GDC)	0.03	1.00	0.04	1.44	0.07	2.24
GDC/cholic acid (C)	0.13	3.04	0.12	3.40	0.22	6.10
C/glycolithocholic acid (GLC)	0.07	1.63	0.04	0.96	0.03	1.00
GLC/chenodeoxycholic acid (CDC)	0.30	5.12	0.29	6.72	0.35	8.91
CDC/deoxycholic acid (DC)	0.10	1.46	0.07	1.52	0.09	1.71
DC/lithocholic acid (LC)	0.29	6.38	0.25	6.73	0.17	5.75
	Impregnated silica gel $60F_{254}$ (#1.05715) with					
	2.5% $CuSO_4$		**2.5% $FeSO_4$**		**5% $NiSO_4$**	
	***n*-Hexane–ethyl acetate–acetic acid; v/v/v**					
	22:20:5		**25:20:5**		**25:20:8**	
	ΔR_F	R_S	ΔR_F	R_S	ΔR_F	R_S
GC/GDC	0.17	2.42	0.08	2.09	0.18	3.33
GDC/cholic acid (C)	0.20	2.67	0.08	1.59	0.21	3.16
C/glycolithocholic acid (GLC)	0.22	3.43	0.18	2.73	0.26	3.80
GLC/chenodeoxycholic acid (CDC)	0.14	2.52	0.12	1.89	0.10	1.65
CDC/deoxycholic acid (DC)	0.06	1.06	0.10	1.65	0.08	1.53
DC/lithocholic acid (LC)	0.13	3.50	0.29	7.00	0.12	4.60

Adapted from Pyka & Dołowy [7–9] and Pyka, Dołowy, & Gurak.[14]

RP18W (Merck, #1.14296), RP2 (Merck, #1.13726), and CNF_{254} (Merck, #1.12571), using methanol–water, dioxane–water, acetone–water, and organic mixture (methanol–acetonitrile, 50:50, v/v)–water as mobile phases; as well as on RP18W (Merck, #1.14296) and RP18 (Merck, #1.05914), using acetonitrile–phosphate buffer (V) in different compositions as mobile phases. None of the applied chromatographic conditions enabled complete separation of all bile acids. Complete separation ($\Delta R_F \geq 0.05$ and $R_S > 1$) was obtained for four or five pairs among six pairs of the investigated bile acids. Five neighboring pairs of bile acids—LC/DC ($\Delta R_{F(LC/DC)} = 0.10$, $R_{S(LC/DC)} = 1.38$), CDC/GLC ($\Delta R_{F(CDC/GLC)} = 0.08$, $R_{S(CDC/GLC)} = 1.56$), GLC/C ($\Delta R_{F(GLC/C)} = 0.08$, $R_{S(GLC/C)} = 1.04$), C/GDC ($\Delta R_{F(C/GDC)} = 0.12$, $R_{S(C/GDC)} = 1.38$), and GDC/GC ($\Delta R_{F(GDC/GC} = 0.09$, $R_{S(GDC/GC)} = 1.23$)—were separated only when CNF_{254} plates and the mobile phase acetone–water, 50:50 (v/v) were used. The biggest problem was how to separate DC from CDC. These bile acids were separated only on RP2 plates by using methanol–water, 65:35 (v/v) as the mobile phase ($\Delta R_{F(DC/CDC)} = 0.07$, $R_{S(DC/CDC)} = 1.26$).[16]

Selected bile acids (LC, DC, CDC, GLC, C, GDC, and GC) were separated by NP-TLC and RP-HPTLC. Two hundred forty-one combinations, which included changes of mobile and stationary phases (non-modified and modified adsorbents) as well as the influence of temperature on separation were examined using NP-TLC. One hundred sixty-one combinations, which included the changes of mobile and stationary phases, were examined using RP-HPTLC. It was stated that only some conditions of NP-TLC made possible separation of all neighboring pairs of bile acids.[6–16]

LIPOPHILICITIES OF SELECTED BILE ACIDS[17–20]

Lipophilicity of bile acids was investigated by RP-HPTLC on RP2, RP18, RP18W, and CNF_{254} plates using a water–organic modifier (methanol, acetonitrile, dioxane, acetone) in different volume proportions, which were varied in steps of 5% (v/v) from 35% to 80% (v/v), as mobile phases. Regular retention behavior was observed for each solute on investigated layers. The R_M values of the investigated acids were decreased with increasing fraction volume of organic modifier in the mobile phase. Because the R_M values were extrapolated to zero concentration of organic modifier in the mobile phase (R_{MW}), in accordance with the Soczewinski–Wachtmeister equation, $R_M = R_{MW} - S\varphi$ (where R_M is the value of the examined substance by content φ of volume fraction of organic modifier in mobile

Table 4 Selected R_{MW} and φ_0 lipophilicity parameters and the values of experimental partition coefficients and partition coefficients calculated by using different theoretical methods.

Acid	$R_{MW(RP18W(m))}$	$R_{MW(RP2(or))}$	$\varphi_{0(RP18W(m))}$	$\varphi_{0(RP2(or))}$	logP_{exp}	AlogPs	*IA* log*P*	*C* log*P*	logP_{Kowwin}	*x* log*P*	logP_{Rekker}
Lithocholic acid (LC)	4.552	3.871	0.920	0.773	—	4.38	5.31	6.60	6.19	6.57	7.41
Deoxycholic acid (DC)	3.683	3.346	0.874	0.720	3.50	3.30	3.26	4.51	5.06	5.76	6.26
Chenodeoxycholic acid (CDC)	3.626	3.421	0.879	0.722	3.00	3.01	3.68	4.51	5.06	4.91	6.26
Glycolithocholic acid (GLC)	3.129	3.207	0.858	0.708	—	3.71	4.11	5.89	5.08	5.75	6.88
Cholic acid (C)	2.736	2.441	0.825	0.665	2.02	2.26	2.12	2.43	3.52	4.09	4.39
Glycodeoxycholic acid (GDC)	2.591	2.307	0.816	0.656	2.25	2.69	2.40	3.80	3.95	4.93	5.00
Glycocholic acid (GC)	1.888	1.828	0.745	0.582	1.65	1.70	1.09	1.71	2.41	3.27	3.15

Note: Mobile phases: m = methanol–water; or = organic mixture (acetonitrile + methanol, 50:50, v/v)–water.
Adapted from Pyka & Dołowy [17–19] and Pyka, Dołowy, & Gurak.[20]

phase, R_{MW} is the theoretical value of R_M of analyte extrapolated to zero concentration of organic modifier in mobile phase, S is the slope of the regression curve, and φ is the volume fraction of organic modifier in the mobile phase). It was found that the values of lipophilicity parameters of R_{MW} obtained by using RP-HPTLC depend linearly on the slope of the regression curve S. Therefore, the parameters of lipophilicity φ_0 were also calculated for studied bile acids. The lipophilic parameters R_{MW} and φ_0 values indicate that the investigated bile acids may be listed in order of decreasing lipophilicity as follows: LC > DC ≈ CDC ≈ GLC > C ≈ GDC > GC. Lipophilic parameters (R_{MW} and φ_0) were compared both with measured (logP_{exp}) and with calculated partition coefficients (*A*logP_S, *IA*log*P*, logP_{Kowwin}, *x*log*P*, C log*P*, logP_{Rekker}). The best agreement was affirmed between R_{MW} values and experimental partition coefficients (logP_{exp}). It was observed that partition coefficients obtained by using different methods (*A*logP_S, *IA*og*P*, *C*log*P*, logP_{Kowwin}, *x*log*P*, and logP_{Rekker}) for respective bile acids differ from each other in several cases. The most compatibility of absolute experimental values log*P* was found with the following:

- *A*logP_S and *IA*log*P* for DC, CDC, and GDC.
- *A*logP_S, *IA*log*P*, and *C*log*P* for C.
- *A*logP_S and *C*log*P* for GC.

The R_{MW} values for LC and GLC are most similar to the *A*logP_S.

Generally, it was stated that the most significant correlation was found between the values of R_{MW} and φ_0 lipophilic parameters and logP_{Kowwin} calculated from atom/fragmental contribution values. *IA*log*P* correlates with the above-mentioned lipophilic parameters slightly worse than logP_{Kowwin} does ($r > 0.90$). It was found that chromatographic parameter of lipophilicity R_{MW} may be an alternative method of lipophilicity determination for examined bile acids. Selected R_{MW} and φ_0 lipophilicity parameters and the values of experimental *n*-octanol–water partition coefficients and partition coefficients calculated by using different theoretical methods are presented in Table 4.[17–20]

APPLICATION OF STRUCTURAL DESCRIPTORS IN QSPR, QSRR, AND QSAR OF SELECTED BILE ACIDS[1,21,22]

Selected topological indices based on adjacency matrix (Gutman (M^{ν}), Randic [$^0\chi^{\nu}$, $^1\chi^{\nu}$ and $^2\chi^{\nu}$], and Pyka χ_{012}), distance matrix (Wiener (W) and Pyka [A, ^{0}B, ^{1}B, and C]), the electrotopological states ($SdO_{(acid)}$, $SsOH_{(acid)}$, $SsOH_{(aliph)}$ $SdO_{(amid)}$ and SsNH) were calculated. Correlation between selected physicochemical properties; i.e., molar mass (M_W), molar refraction (R_m), molar volume (V_m), parachor (P), refraction index (I_r), density (d), lipophilicity parameter (R_{MW} and φ_0), and obtained structural descriptions, was found.[1] Different possibilities of application of the structural descriptors to calculate certain physicochemical data of examined bile acids (QSPR)—depending on examined physicochemical properties—were found. The structural descriptions are not useful for calculating the density (d) of the examined bile acids. Substance density, especially the densities of liquids, not only changes with mass and structure; but, to a large extent, also depends on molecular interaction. Regression equations for respective physicochemical properties with the greatest correlation coefficients were found with the following structural descriptors:[1]

Table 5 Absorption maximum of investigated bile acids after separation on silica gel 60 and after the application of sulfuric acid and phosphomolybdic acid as visualizing reagents.

	λ_{max} (nm)	
	After application of visualizing reagent	
Bile acid	Sulfuric acid[a] (color of spot on light beige background)	Phosphomolybdic acid[b] (color of spot on yellow/green background)
Glycocholic acid (GC)	458 (gray/green)	346 (navy blue)
Glycodeoxycholic acid (GDC)	393 (gray/blue)	345 (navy blue)
Glycolithocholic acid (GLC)	397 (gray)	346 (navy blue)
Cholic acid (C)	457 (green)	346 (navy blue)
Chenodeoxycholic acid (CDC)	379 (gray)	347 (navy blue)
Deoxycholic acid (DC)	386 (green)	350 (navy blue)
Lithocholic acid (LC)	380 (gray)	350 (navy blue)

[a]Sulfuric acid in methanol in volume composition 1:19; the plate was immersed in dipping solution of sulfuric acid for 15 sec, and it was then heated to 90°C for 20 min;
[b]10% phosphomolybdic acid in ethanol; after spraying by phosphomolybdic acid solution, the plate was heated at 120°C for 20 min.
Source: From TLC of selected bile acids: Detection and separation, in J. Liq. Chromatogr. Relat. Technol.[11]

- For molar mass (M_W) with Wiener index (W) and with indices based on adjacency matrix M^{ν} and ${}^{0}\chi^{\nu}$ ($r > 0.98$).
- For molar refraction (R_m) with indices based on distance matrix W and A and adjacency matrix: ${}^{0}\chi^{\nu}$, ${}^{1}\chi^{\nu}$, and χ_{012} ($r > 0.99$).
- For molar volume (V_m) with index based on distance matrix ${}^{1}B$ and electrotopological states: $SdO_{(acid)}$ and $SsOH_{(acid)}$ ($r > 0.99$).
- For parachor (P) with indices based on distance matrix W and A and distance matrix: ${}^{0}\chi^{\nu}$, ${}^{1}\chi^{\nu}$, and χ_{012} ($r > 0.99$).
- For refraction index (I_r) with electrotopological states $SsOH_{(aliph)}$ and SsOH ($r > 0.98$).

Calculated structural descriptors were also used to determine linear relationships between lipophilicity R_{MW} or φ_0, determined for the 12 chromatographic systems studied,[17–20] or theoretical values of partition coefficients ($A\log P_S$, $I\log P$, $C\log P$, $\log P_{Kowwin}$, $x\log P$, and $\log P_{Rekker}$) or experimental values determined by the classical method ($\log P_{exp}$), and the respective structural descriptors.[21] It was stated that only two structural descriptors; i.e., the Gutman index (M^{ν}) and the Pyka index (C), are best for QSAR analysis of selected bile acids.

Structural descriptors can be used for the estimation of chromatographic separation of studied bile acids (QSRR), but only for optimal conditions of their separations. It was found that among all descriptors, only the values of topological index C change inversely proportionally to the R_F values and directly proportionally to the R_M values of examined bile acids. Thus, only the topological index C was used for determining the regression equations, which allowed calculation of R_F and R_M values of studied bile acids. The topological index C made it possible to obtain linear or quadratic equations. Generally, it was found that the regression equations which describe the relationships $R_F = f(C)$ have higher values of correlation coefficients than the relationship $R_M = f(C)$. Greater compatibility between calculated and real R_F values than between calculated and real (experimental) R_M values was stated. Therefore, the topological index C is more suitable for R_F calculation of examined bile acids than for R_M calculation.[1,22]

DETECTION OF BILE ACIDS

Spots of bile acids can be visualized by spraying the chromatographic plate with an anisaldehyde–sulfuric acid reagent (solution of 8 ml sulfuric acid, 0.5 ml anisaldehyde, 10 ml acetic acid, and 85 ml methanol),[23] a solution of antimony (III) chloride (Carr Price reagent) in chloroform (1:5, w/v),[23] a manganese (II) chloride–sulfuric acid reagent [solution of 0.2 g manganese (II) chloride, 30 ml water, 30 ml methanol, and 2 ml sulfuric acid],[23] or a 10% or 50% water solution of sulfuric acid and then heating until the spots became visible.[3,18] Bile acids can be also detected by dipping plates into 10% of phosphomolybdic acid in ethanol and then heating for 20 min at 120°C[18,23] or by spraying the plates with a 1% solution of phosphomolybdic acid in 2-propanol and then heating at 120°C for 5–10 min.[4] Wardas and Jedrzejczak[24] separated selected free and conjugated

bile acids by NP-TLC. Eleven visualizing agents were used for detection of these investigated bile acids. The best results of detection of bile acids were obtained with bromocresol blue.[24]

The solutions of sulfuric acid in methanol in different volume compositions were also used to detect investigated bile acids.[11] Chromatographic plates with separated bile acids were dipped in particular sulfuric acid solutions and then heated at temperature from 60°C to 120°C for times ranging from 2 to 45 min. The best detection conditions for high signal intensity [AU] of the separated bile acid spots were determined. Particularly robust and sensitive detection of investigated bile acids separated was observed using the solution of sulfuric acid in methanol in the volume composition 1:19 and for temperature equal to 90°C and heating for 20 min. However, phosphomolybdic acid was used as the comparative visualizing reagent for the detection of studied bile acids in these investigations. The absorption maximum of separated bile acids on silica gel 60 (E. Merck, #1.11845) with concentrating zone after application of methanolic solution of sulfuric acid in volume composition 1:19 and heating at 90°C for 20 min and of phosphomolybdic acid as visualizing reagents are presented in Table 5. Colors of chromatographic spots of separated bile acids are also presented in Table 5. It was affirmed, that the resolution $R_{S(c)}$ values obtained by the visual method are better for separated bile acids after their optimal detection using sulfuric acid in relation to the detection by the use of phosphomolybdic acid. Moreover, it was affirmed that the background of a chromatogram after detection with phosphomolybdic acid is heterogeneous, which is the cause of appearance of large noises on densitograms. Therefore phosphomolybdic acid as visualizing reagent in under conditions can be used only for qualitative or semi-quantitative investigations of investigated bile acids. Particularly robust and sensitive detection of investigated bile acids separated was observed using the solution of sulfuric acid in methanol in the volume composition 1:19 and for temperature equal to 90°C and heating for 20 min.[11] Chromatographic bands of bile acids on the densitogram after the use of spray solution of phosphomolybdic acid in methanol were irregular.[25] Therefore, this way of the detection of bile acids cannot be recommended. Regular chromatographic bands of bile acids on the densitogram were obtained after the use of dipping water solution of sulfuric acid.[11]

ACKNOWLEDGMENT

This research was financed by the Ministry of Science and Information Society Technologies by resources reserved for science in the years 2005–2008 as research project No. 3 T09A 155 29.

REFERENCES

1. Pyka, A.; Dołowy, M. Application of structural descriptors for the evaluation of some physicochemical properties of selected bile acids. Acta Pol. Pharm.—Drug Res. **2004**, *61*, 407–413.
2. Scalia, S. Bile acids separation. J. Chromatogr. B, **1995**, *671*, 299–317.
3. Gaica, S.B.; Opsenica, D.M.; Šolaja, B.A.; Tešić, Ž.Lj.; Milojković-Opsenica, D.M. The retention behavior of some cholic acid derivatives on different adsorbents. J. Planar Chromatogr.-Mod. TLC **2002**, *15* (4), 299–305.
4. Zarzycki, P.K.; Wierzbowska, M.; Lamparczyk, H. Retention and separation studies of cholesterol and bile acids using thermostated thin-layer chromatography. J. Chromatogr. A, **1999**, *857*, 255–262.
5. Rivass-Nass, A.; Müllner, S. The influence of critical parameters on TLC separation of bile acids. J. Planar Chromatogr. -Mod. TLC **1994**, *7* (4), 278–285.
6. Pyka, A.; Dołowy, M. Separation of selected bile acids by TLC. I. J. Liq. Chromatogr. Relat. Technol. **2003**, *26* (7), 1095–1108.
7. Pyka, A.; Dołowy M. Separation of selected bile acids by TLC. II. One-dimensional and two-dimensional TLC. J. Liq. Chromatogr. Relat. Technol. **2004**, *27* (13), 2031–2038.
8. Pyka, A.; Dołowy, M. Separation of selected bile acids by TLC. III. Separation on various stationary phases. J. Liq. Chromatogr. Relat. Technol. **2004**, *27* (16), 2613–2623.
9. Pyka, A.; Dołowy, M. Separation of selected bile acids by TLC. IV. Comparison of separation of studied bile acids by the use of cluster analysis. J. Liq. Chromatogr. Relat. Technol. **2004**, *27* (19), 2987–2995.
10. Pyka, A., unpublished data.
11. Pyka, A. TLC of selected bile acids: Detection and separation. J. Liq. Chromatogr. Relat. Technol. **2008**, *31*, 1373–1385.
12. Pyka, A.; Dołowy, M. Separation of selected bile acids by TLC. VI. Separation on cyano- and diol-modified silica layers. J. Liq. Chromatogr. Relat. Technol. **2005**, *28* (9), 1383–1392.
13. Pyka, A.; Dołowy, M.; Gurak, D. Separation of selected bile acids by TLC. V. Influence of temperature on the separation. J. Liq. Chromatogr. Relat. Technol. **2005**, *28* (4), 631–640.
14. Pyka, A.; Dołowy, M.; Gurak, D. Separation of selected bile acids by TLC. VIII. Separation on silica gel $60F_{254}$ glass plates impregnated with Cu(II), Ni(II), Fe(II) and Mn(II) cations. J. Liq. Chromatogr. Relat. Technol. **2005**, *28* (14), 2273–2284.
15. Dołowy, M. Separation of selected bile acids by TLC. IX. Separation on silica gel 60 and silica gel $60F_{254}$ aluminum plates impregnated with Cu(II), Ni(II), Fe(II) and Mn(II) cations. J. Liq. Chromatogr. Relat. Technol. **2007**, *30*, 405–418.
16. Pyka, A.; Dołowy, M. Separation of selected bile acids by TLC. VII. Separation by reversed partition high performance thin layer chromatography, J. Liq. Chromatogr. Relat. Technol. **2005**, *28* (10), 1573–1581.

17. Pyka, A.; Dołowy, M. Lipophilicity of selected bile acids determined by TLC method. I. J. Liq. Chromatogr. Relat. Technol. **2003**, *26* (16), 2741–2750.
18. Pyka, A.; Dołowy, M. Lipophilicity of selected bile acids as determined by TLC. II. Investigations on RP18W stationary phase. J. Liq. Chromatogr. Relat. Technol. **2005**, *28* (2), 297–311.
19. Pyka, A.; Dołowy, M. Lipophilicity of selected bile acids as determined by TLC. III. Investigations on RP2 stationary phase. J. Liq. Chromatogr. Relat. Technol. **2005**, *28* (11), 1765–1775.
20. Pyka, A.; Dołowy, M.; Gurak, D. Lipophilicity of selected bile acids as determined by TLC. IV. Investigations on CN stationary phase. J. Liq. Chromatogr. Relat. Technol. **2005**, *28* (17), 2705–2717.
21. Pyka, A.; Dołowy, M. Use of selected structural descriptors for evaluation of the lipophilicity of bile acids investigated by RP HPTLC. J. Planar Chromatogr. -Mod. TLC **2005**, *18* (4), 465–470.
22. Dolowy, M. Application of selected topological indices to predict retention parameters of selected bile acids separated on modified TLC plates. Acta Pol. Pharm.—Drug Res. **2008**, *65*, 51–57.
23. Jork, H.; Funk, W.; Fischer, W.; Wimmer, H. *Dünnschicht-Chromatographie, Reagenzien und Nachweismethoden*, *Physicalische ind Chemische Nachweismethoden: Grundlagen, Reagenzien I*; VCH, Weinheim, Germany, 1989; Vol. 1a, pp. 43, 195, 206, 331, 342, 376.
24. Wardas, W.; Jedrzejczak, M. New visualizing agents for selected bile acids in TLC. Chem. Anal. (Warsaw) **1995**, *40*, 73–79.
25. Zarzycki, P.K.; Bartoszuk, M.A.; Radziwon, A.I. Optimization of TLC detection by phosphomolybdic acid staining for robust quantification of cholesterol and bile acids. J. Planar Chromatogr. -Mod. TLC **2006**, *19* (10), 52–57.

Binding Constants: Affinity Chromatography Determination

David S. Hage
John E. Schiel
Department of Chemistry, University of Nebraska-Lincoln, Lincoln, Nebraska, U.S.A.

Abstract
The use of affinity chromatography for the determination of binding constants is described in this entry. Approaches such as zonal elution, frontal analysis, and free fraction measurements can be utilized in affinity chromatography to obtain information on the extent and nature of solute–ligand binding. Information on the kinetics of solute–ligand binding can also be obtained through a variety of methods, such as band-broadening measurements, peak profiling, peak fitting, split-peak studies, and peak decay analysis. Advantages of using affinity chromatography for this type of work include the simplicity of this approach, its good precision and accuracy, and its ability to reuse the same ligand preparation for multiple studies.

INTRODUCTION

Numerous interactions within cells and the body are characterized by the specific binding that occurs between two or more molecules. Examples include the binding of hormones with hormone receptors, drugs with enzymes or receptors, antibodies with antigens, and small solutes with transport proteins. The study of these interactions is important in determining the role they play in biological systems. Because of this, there have been many methods developed to characterize such reactions. One of these approaches is affinity chromatography.

Affinity chromatography is a liquid chromatographic technique that makes use of an immobilized ligand, usually of biological origin, for the separation or analysis of chemicals within a sample. However, it is also possible to use affinity chromatography as a tool for studying the interactions between the ligand and injected solutes. This application is known as *quantitative affinity chromatography*, *analytical affinity chromatography*, or *biointeraction chromatography*.

Some advantages in using affinity chromatography to study biological interactions include the relative simplicity of this approach as well as its good precision, accuracy, and ability to use the same ligand preparation for multiple studies. The last feature creates a situation in which only a relatively small amount of ligand is needed for a large number of studies, which in turn helps provide good precision by minimizing run-to-run variations. Other advantages include the ease with which affinity methods can be automated, especially when used in high-performance liquid chromatography (HPLC) (giving a method known as *high-performance affinity chromatography*, or *HPAC*), and the relatively short periods of time that are required with such systems for binding studies (i.e., often 5–15 min per analysis). The continuous washing of the immobilized ligand by the application of the solvent is another advantage as this process minimizes the effects produced by soluble contaminants in the initial ligand preparation.

ZONAL ELUTION

The method of zonal elution is one of the most common techniques used in affinity chromatography to examine biological interactions.[1–5] An example of this method is shown in Fig. 1.[6] In its usual form, zonal elution involves the application of a small amount of analyte (in the absence or presence of a competing agent) to a column that contains an immobilized ligand. The retention of the analyte in this case will depend on how strongly the analyte and competing agent bind to the ligand and on the amount of ligand that is in the column. This makes it possible to measure the equilibrium constants for these binding processes by examining the change in analyte retention as the competing agent's concentration is varied.

Zonal elution was first used in affinity chromatography in 1974 for the quantitative analysis of biological interactions. This work was performed by Dunn and Chaiken, who examined the retention of staphylococcal nuclease on a low-performance column containing immobilized thymidine-5′-phosphate-3′-aminophenylphosphate.[1] By the late 1980s and early 1990s, reports that used this approach with HPLC also began to appear. Zonal elution and affinity chromatography have since been used to examine numerous systems, including the binding of drugs with transport proteins or receptors, lectins with sugars, enzymes with inhibitors, and hormones with hormone-binding proteins.[2–5]

Zonal elution has been used in various ways to obtain information on the binding of solutes to a ligand. These methods include not only measurements of the degree and affinity of solute–ligand binding but also studies examining changes in binding with variations in the mobile phase composition or temperature and experiments that consider

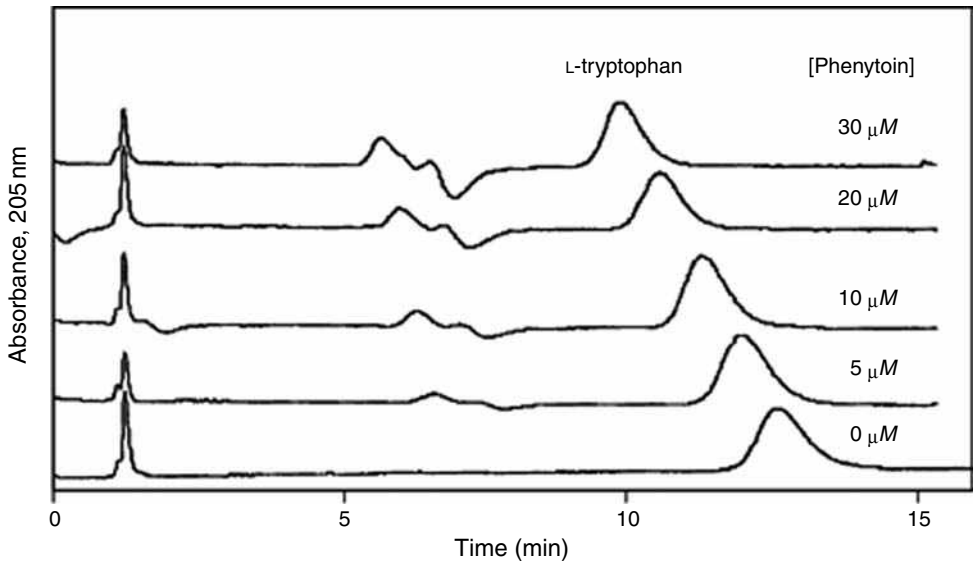

Fig. 1 Zonal elution studies for the injection of L-tryptophan onto an immobilized human serum albumin column in the presence of various concentrations of phenytoin as a mobile phase additive.
Source: From Studies of phenytoin binding to human serum albumin by high-performance affinity chromatography, in J. Chromatogr. B.[6]

how alterations in solute or ligand structure affect these interactions. Each of these applications relies on the fact that the retention observed for an injected analyte is a direct measure of the strength of binding of the analyte to the ligand within the column. This idea is described by Eq. 1, which shows how the overall retention factor (k) for an analyte is related to the moles of binding sites in the column (m_L) and to the association equilibrium constants for the analyte at each of these sites.[3]

$$k = \frac{(K_{a1}\ n_1 + \ldots\ K_{an}\ n_n)m_L}{V_M} \quad (1)$$

In Eq. 1, V_M is the column void volume; the association equilibrium constants for the analyte at the individual sites are given by the terms K_{a1} through K_{an}, while the fraction of each type of site in the column is given by the terms n_1 through n_n. From this equation, it can be seen that a change in the strength of binding, the number of binding sites, or the relative distribution of these sites can result in a shift in analyte retention.

One way zonal elution has been employed in quantitative studies of solute–ligand interactions is as a means to measure the average extent of binding that occurs between a solute and immobilized ligand.[3] This approach is based on the fact that the retention factor, when measured at true equilibrium, is equal to the fraction of an injected solute that is bound to the ligand (b) divided by the fraction of solute that remains free in the mobile phase (f), or $k = b/f$. The relative binding of two solutes can also be compared by using zonal elution and by taking the ratio of their retention factors on the same affinity column. According to Eq. 1, if both solutes have a single common binding site on the ligand, the ratio of their retention factors should equal the ratio of their association constants at this site. However, caution must be exercised when using this approach with solutes that have multisite binding or slightly different binding regions on a ligand, because these regions and sites may have different susceptibilities to a loss of activity during ligand immobilization.[7]

The second and most common use for zonal elution and affinity chromatography in the examination of biological interactions has been in competition and displacement studies. This work is performed by injecting the analyte while a fixed concentration of a potential competing agent is passed through the column in the mobile phase. It is relatively easy in such an experiment to determine whether two compounds interact as they bind to the same immobilized ligand. However, to obtain further information on this interaction (e.g., the nature of this competition and the number of sites that are involved), it is necessary to compare the zonal elution data to the response expected for various models, as given in Eq. 2 for a system with 1:1 competition between an injected analyte (A) and a competing agent (I).

$$k = \frac{K_{a,A}\ m_L}{V_M\left(1 + K_{a,I}\ [I]\right)}$$

or

$$\frac{1}{k} = \frac{K_{a,I}\ [I]\ V_M}{K_{a,A} m_L} + \frac{V_M}{K_{a,A} m_L} \quad (2)$$

Similar equations can be derived for other systems, such as those involving multiple binding sites or both the soluble

and immobilized forms of a ligand.[2–5] In Eq. 2, $K_{a,A}$ and $K_{a,I}$ are the association equilibrium constants for the binding of the ligand to the analyte and competing agent at their site of competition. The term [I] is the concentration of I that is being applied to the column in the mobile phase, m_L is the moles of common binding sites on the immobilized ligand for A and I, and k is the retention factor measured for A. In this case, the values of the association constants $K_{a,A}$ and/or $K_{a,I}$ can be obtained by examining how the retention factor for A changes as [I] is varied.

A third way zonal elution and affinity chromatography can be used is to consider how changes in the reaction conditions affect solute–ligand binding. For instance, these factors can be examined by varying the pH, ionic strength, or general content of the mobile phase.[4] This information can be valuable in determining the relative contributions of various forces to the formation and stabilization of a solute–ligand complex. As an example, changing the pH can affect the interactions between a ligand and solute by altering their conformations, net charges, or coulombic interactions. An increase in ionic strength tends to decrease coulombic interactions through a shielding effect, but may also cause an increase in non-polar solute adsorption. Adjusting the solvent polarity by adding a small amount of organic modifier can alter solute–ligand binding by disrupting non-polar interactions or by causing a change in solute and ligand structure.[4,8]

Temperature is another factor that can be varied during zonal elution studies. For instance, Eq. 3 can be used for a system with 1:1 binding

$$\ln k = -\left(\frac{\Delta H}{RT}\right) + \frac{\Delta S}{R} + \ln\left(\frac{m_L}{V_M}\right) \quad (3)$$

where T is the absolute temperature at which the retention factor is measured, R is the gas law constant, ΔH is the change in enthalpy for the reaction, ΔS is the change in entropy, and other terms are as defined previously. If it is known that there is no temperature dependence in the number of binding sites (m_L) for a ligand, the slope of a linear plot of ln k versus $1/T$ can be used to determine the value of ΔH for a solute–ligand system.[9]

Another application of zonal elution in affinity chromatography is its use in determining the location and structures of binding regions on a ligand. If it is known that one agent interacts with a specific site on a ligand, competition studies with this agent can be used to determine if other compounds bind at the same site. Another approach for learning about binding sites is to study how a change in the structure of a solute or ligand will affect their interactions. This is the principle behind the use of zonal elution to develop a *quantitative structure–retention relationship* (*QSRR*). This method involves measuring the retention factors on an affinity column for a large set of structurally related compounds under constant temperature and mobile phase conditions. The resulting data are then compared to factors that describe various structural features of the solutes.[10,11] A complementary approach is to use zonal elution to investigate how solute retention changes as alterations are made to binding sites on a ligand, as has been performed in work with modified proteins and protein fragments.[4,12,13]

FRONTAL ANALYSIS

An alternative approach for equilibrium constant measurements in affinity chromatography is to use frontal analysis. This method is sometimes known as *frontal affinity chromatography* (*FAC*). In this technique, a solution containing a known concentration of the analyte is continuously applied to an affinity column at a fixed flow rate (Fig. 2). As the analyte binds to the immobilized ligand, the ligand

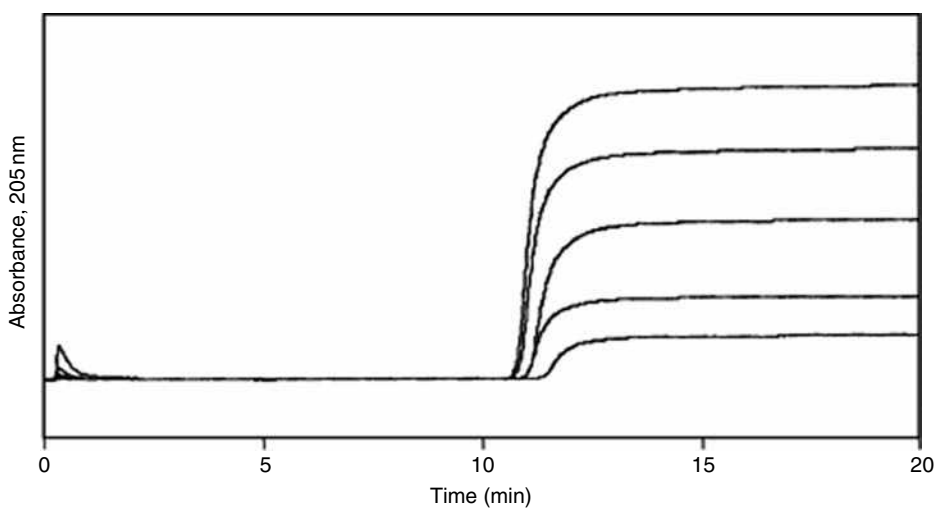

Fig. 2 Frontal analysis studies for the binding of phenytoin to immobilized human serum albumin at applied analyte concentrations (bottom-to-top) of 5, 10, 20, 30, and 40 μM.
Source: From Studies of phenytoin binding to human serum albumin by high-performance affinity chromatography, in J. Chromatogr. B.[6]

becomes saturated and the amount of analyte eluting from the column gradually increases. This forms a characteristic breakthrough curve. The volume of analyte solution or moles of applied analyte that is required to reach the mean position of this breakthrough curve is then measured. If the association and the dissociation kinetics are fast, the mean position of this curve can be related to the concentration of the applied solute, the amount of ligand in the column, and the association equilibrium constants for solute–ligand binding. Frontal analysis experiments have been used to examine such systems as drug–protein binding, antibody–antigen interactions, and enzyme–inhibitor interactions.[3–5]

A simple example of a frontal analysis system is one where an applied analyte binds to a single type of immobilized ligand site. In this situation, Eq. 4 can be used to relate the total moles of active binding sites in the column (m_L) to the apparent moles of analyte ($m_{L,app}$) that are required to reach the mean position of the breakthrough curve at a given concentration of applied analyte [A].

$$m_{L,app} = \frac{K_{a,A} m_L [A]}{1 + K_{a,A}[A]}$$

or

$$\frac{1}{m_{L,app}} = \frac{1}{K_{a,A}\ m_L\ [A]} + \frac{1}{m_L} \quad (4)$$

As defined earlier, $K_{a,A}$ is the association equilibrium constant for the binding of the analyte to the ligand. In this case, the value of $K_{a,A}$ can be determined by calculating the ratio of the intercept to the slope in the second form of Eq. 4, and $1/m_L$ can be obtained from the inverse of the intercept. Similar relationships can be derived for cases in which there is more than one type of binding site or in which both a competing agent and solute are applied simultaneously to the column.

A second application of frontal analysis has been as a tool to examine the competition between solutes for an immobilized ligand.[14–16] This is carried out in a manner similar to that described for zonal elution, in which the change in analyte retention is measured as a function of the competing agent's concentration in the mobile phase. In frontal analysis, direct competition between the analyte and competing agent leads to a smaller breakthrough time for the analyte as the competing agent's level is increased. Positive and negative allosteric effects can also be observed, which lead to a shift to higher and lower breakthrough times, respectively, with an increase in the competing agent's concentration. The same technique can be used to examine how temperature, pH, ionic strength, or solvent polarity might affect solute–ligand binding.[3] Like zonal elution, frontal analysis can be used to examine the binding of solutes to modified proteins to provide information on the nature of solute–ligand binding sites.[12,17]

Another application of frontal analysis is its use in affinity chromatography for screening mixtures of compounds for any targets that might bind to a given immobilized ligand.[18,19] The use of these tools with mass spectrometry (MS), leading to an approach known as *frontal affinity chromatography–mass spectrometry* (*FAC–MS*), is of particular interest.[19] In this approach, a mixture of analytes is passed through the affinity column and the individual analytes bind to the ligand based on their affinity for this agent. Selective detection at the characteristic mass-to-charge (m/z) value for each analyte makes it possible to generate separate breakthrough curves for each of these compounds. This information is then used to evaluate and rank the relative affinity of each compound in the mixture for the ligand in the affinity column.[18]

One disadvantage of frontal analysis is that it often requires a relatively large amount of analyte for study. However, this requirement can be minimized through the use of small-scale columns.[19] Frontal analysis is advantageous in that it provides information on both the association constant for a solute and its total number of binding sites in a column. This feature makes frontal analysis the method of choice for high accuracy in equilibrium measurements, because the resulting association constants are essentially independent of the number of binding sites in the column.

FREE FRACTION ANALYSIS

Another recent method employed for solute–ligand studies is chromatographic *free fraction analysis*. This uses small columns with antibodies that bind the solute of interest and are capable of extracting this solute in very short periods of time (i.e., 80–200 msec). With such a column it is possible to isolate the non-bound fraction of a solute from a solution in which most of this compound is bound to a soluble ligand, even when dissociation of the solute from this ligand occurs on the timescale of a few seconds. This approach can be used to examine the binding of *R*- and *S*-warfarin with human serum albumin (HSA) in solution, in which antiwarfarin antibodies were used to extract free warfarin fractions in less than 180 msec.[20] The same general approach was used to measure the free fractions of L-thyroxine and phenytoin in serum samples and in the presence of HSA.[21,22] The advantages of this approach are its speed and the ability to study the binding of solutes with ligands directly in solution.[20–22]

BAND-BROADENING MEASUREMENTS AND PEAK PROFILING

Another group of methods in quantitative affinity chromatography are those that examine the kinetics of biological interactions. Band-broadening measurements (also known as the *isocratic method* or *plate height method*) represent

one such approach. This is a modification of the zonal elution method in which the widths of the eluting peaks are measured along with their retention times. Systems that have been studied with this method include the binding of lectins with sugars, the interactions of drugs and amino acids with serum albumin, and the kinetics of protein-based chiral stationary phases.[2,23,24]

This type of experiment involves injecting a small amount of analyte onto an affinity column while carefully monitoring the retention time and width of the eluting peak. These injections are performed at several flow rates on both the affinity column and on a column of the same size that contains an identical support but with no immobilized ligand present. This control column is needed to correct for any band broadening that occurs due to processes other than the binding and dissociation of analyte from the immobilized ligand. By using plots of the peak widths (or plate heights) for the affinity and control columns, it is possible to determine the value of the dissociation rate constant for the analyte–ligand interaction. An example of such a study is given in Fig. 3.

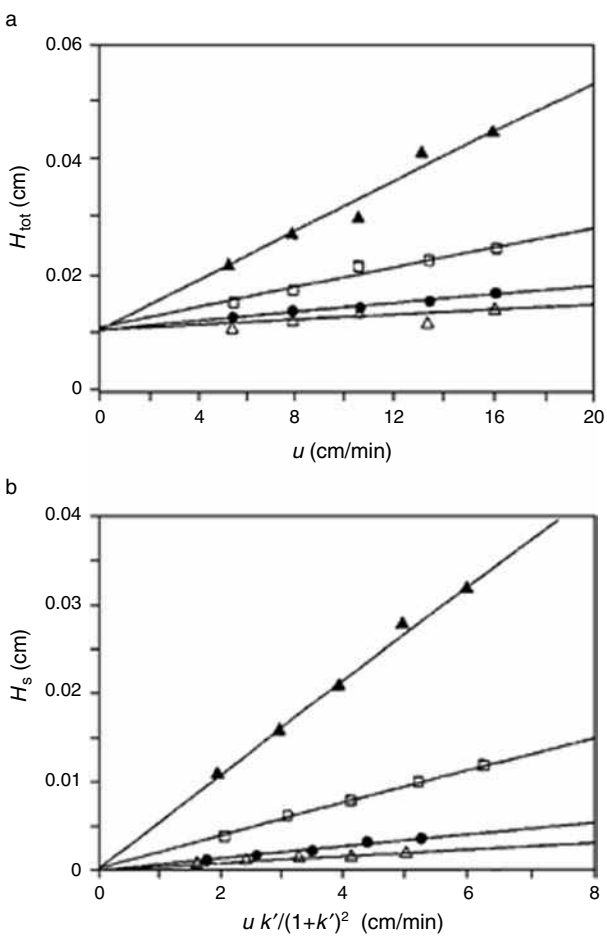

Fig. 3 Typical plots of (a) total plate height (H_{tot}) and (b) the plate height contribution due to stationary phase mass transfer (H_s) for injections of D-tryptophan at various flow rates onto an immobilized human serum albumin column. Symbols: u, linear velocity; k', retention factor.

Source: From Effect of mobile phase composition on the binding kinetics of chiral solutes on a protein-based high-performance liquid chromatography column: Interactions of D- and L-tryptophan with immobilized human serum albumin, in J. Chromatogr. A.[24]

An approach that is closely related to the plate height method is the technique of *peak profiling*. This approach was first suggested in 1975 by Denizot and Delaage.[25] In this method, measurements of the retention time for an analyte (t_R) and the elution time of a non-retained solute (t_M) are made on the same column. These elution times are then used with variances observed for the peaks of the analyte (σ_R^2) and non-retained species (σ_M^2) to calculate the apparent dissociation rate constant ($k_{d,app}$), as is demonstrated in Eq. 5.[25]

$$k_{d,app} = \frac{2\,t_M^2\,(t_R - t_M)}{\sigma_R^2\,t_M^2 - \sigma_M^2\,t_R^2} \tag{5}$$

Although this method is relatively simple and fast to perform, the use of Eq. 5 does assume that other band-broadening processes are the same for the non-retained and retained species. This assumption can create errors if significant peak broadening due to stagnant mobile phase mass transfer is present. In this situation, conditions that minimize the contribution of these other effects must be used,[26] or an alternative form of the peak profiling method can be utilized in which corrections are made for these other contributions to band broadening.[27]

PEAK FITTING METHODS

Some methods for obtaining kinetic information by affinity chromatography fit experimental elution data to empirical equations that can be used to describe profiles for a given set of application conditions. For instance, this approach has been used with zonal elution data obtained under non-linear elution conditions by using the following function.[28,29]

$$y = \frac{a_0}{a_3}\left[1 - \exp\left(\frac{-a_3}{a_2}\right)\right]\ \frac{\sqrt{\frac{a_1}{x}}\,I_1\left(\frac{2\sqrt{a_1 x}}{a_2}\right)\exp\left(\frac{-x-a_1}{a_2}\right)}{1 - T\left(\frac{a_1}{a_2},\frac{x}{a_2}\right)\left[1 - \exp\left(\frac{-a_3}{a_2}\right)\right]} \tag{6}$$

In this equation, y is the intensity of the measured signal, x is the reduced retention time, T is a switching function, and I_1 is a modified Bessel function. The terms a_0 through a_3 are the best-fit parameters used to estimate the value of the rate constants and equilibrium constant for the analyte–ligand interaction. This method has been employed in studying pNp–mannoside binding to immobilized concanavalin A[28] and the binding of various inhibitors to

immobilized nicotinic acetylcholine receptor membrane affinity columns.[30,31]

The kinetics of biological interactions have also been examined by fitting profiles generated when using frontal analysis and affinity chromatography. Many of the models and expressions that are used for this purpose are based on the initial work of Thomas.[29] This model gives an apparent rate constant for analyte binding to the column, in which it is assumed that mass transfer is infinitely fast and analyte adsorption is described by second-order Langmuir kinetics based on interaction at a single type of homogeneous ligand-binding site.[29,32,33]

SPLIT-PEAK EFFECT

Another way in which kinetic information can be obtained by affinity chromatography is the *split-peak method*.[2,34] This is based on an effect that occurs when the injection of a single solute gives rise to two peaks: the first representing a non-retained fraction and the second representing the retained solute. This effect can be observed even when only a small amount of analyte is injected and is the result of slow adsorption kinetics and/or slow mass transfer of analyte within the column (Fig. 4). Such an effect can occur in any type of chromatography but is most common in affinity columns because of their smaller size, their lower amount of binding sites, and the slower association rates of affinity ligands compared to other types of stationary phases.

Split-peak measurements can be performed by injecting a small amount of analyte onto an affinity column at various flow rates. A plot of the inverse negative log of the measured free fraction is then made versus flow rate. The slope of this graph is related to the adsorption kinetics and mass transfer rates within the column. If the system is known to have adsorption-limited retention, or if the mass transfer rates are known, then the association rate constant for analyte binding can be determined. This approach has the advantages of being fast to perform and potentially has greater accuracy and precision than band-broadening measurements. Its disadvantages are that it requires fairly specialized operating conditions that may not be suitable for all analytes. Examples of biological systems that have been examined by the split-peak method include the binding of protein A and protein G to immunoglobulins, and the binding of antibodies with antigens.[2,34–36]

PEAK DECAY METHOD

The *peak decay method* can also be used in affinity chromatography to examine the kinetics of an analyte–ligand interaction.[2,37] This technique is performed by first equilibrating and saturating a small affinity column with a solution that contains the analyte of interest or an easily detected analogue of this analyte. The column is then quickly switched to a mobile phase in which the analyte is not present. The release of the bound analyte is monitored over time, resulting in a decay curve. This decay is related to the dissociation rate of the analyte and the mass transfer kinetics within the column. If the mass transfer rate is known or is fast compared to analyte dissociation, the decay curve can be used to provide the dissociation rate constant for the analyte from the immobilized ligand. Systems studied with this approach include the dissociation of drugs from transport proteins and the dissociation of sugars from immobilized lectins.

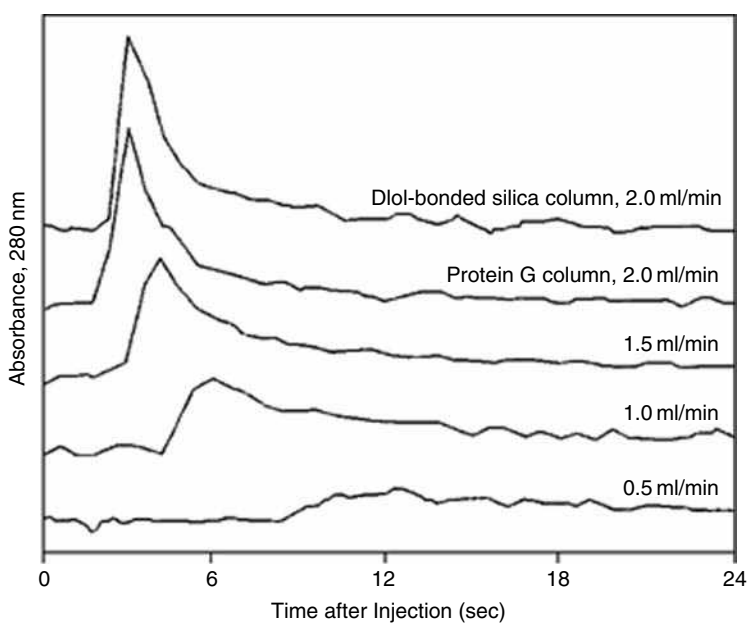

Fig. 4 Non-retained (or split-peak) fractions observed for injections of rabbit immunoglobulin G onto an immobilized protein G column at various flow rates.
Source: From Non-linear elution effects in split-peak chromatography. II. Role of ligand heterogeneity in solute binding to columns with adsorption-limited kinetics, in J. Chromatogr. A.[35]

CONCLUSION

It has been shown that there are a variety of ways in which information on solute–ligand binding can be obtained by affinity chromatography. Zonal elution, frontal analysis, and free fraction analysis are the approaches that have been developed for such studies. With these methods, information can be obtained on the extent of solute–ligand binding, binding affinity and stoichiometry, and the structure of binding sites. Kinetics information can also be obtained through a variety of methods, including band-broadening measurements, peak profiling, peak fitting methods, split-peak studies, and peak decay analysis.

REFERENCES

1. Dunn, B.M.; Chaiken, I.M. Quantitative affinity chromatography. Determination of binding constants by elution with competitive inhibitors. Proc. Natl. Acad. Sci. U.S.A. **1974**, *71*, 2382–2385.
2. Chaiken, I.M., Ed. *Analytical Affinity Chromatography*; CRC Press: Boca Raton, FL, 1987.
3. Hage, D.S.; Tweed, S.A. Recent advances in chromatographic and electrophoretic methods for the study of drug–protein interactions. J. Chromatogr. B, **1997**, *699*, 499–525.
4. Hage, D.S.; Chen, J. Quantitative affinity chromatography: Practical aspects. In *Handbook of Affinity Chromatography*, 2nd Ed.; Hage, D.S., Ed.; Taylor & Francis: New York, 2006; Chapter 22.
5. Winzor, D.J. Quantitative affinity chromatography: Recent theoretical developments. In *Handbook of Affinity Chromatography*, 2nd Ed.; Hage, D.S., Ed.; Taylor & Francis: New York, 2006; Chapter 23.
6. Chen, J.; Ohnmacht, C.; Hage, D.S. Studies of phenytoin binding to human serum albumin by high-performance affinity chromatography. J. Chromatogr. B, **2004**, *809*, 137–145.
7. Loun, B.; Hage, D.S. Characterization of thyroxine–albumin binding using high-performance affinity chromatography. I. Interactions at the warfarin and indole sites of albumin. J. Chromatogr. **1992**, *579*, 225–235.
8. Allenmark, S. *Chromatographic Enantioseparation: Methods and Applications*, 2nd Ed.; Ellis Horwood: New York, 1991; Chapter 7.
9. Yang, J.; Hage, D.S. Role of binding capacity versus binding strength in the separation of chiral compounds on protein-based high-performance liquid chromatography columns. Interactions of D- and L-tryptophan with human serum albumin. J. Chromatogr. A, **1996**, *725*, 273–285.
10. Kaliszan, R.; Noctor, T.A.G.; Wainer, I.W. Stereochemical aspects of benzodiazepine binding to human serum albumin. II. Quantitative relationships between structure and enantioselective retention in high performance liquid affinity chromatography. Mol. Pharmacol. **1992**, *42*, 512–517.
11. Wainer, I.W. Enantioselective high-performance liquid affinity chromatography as a probe of ligand–biopolymer interactions: An overview of a different use for high-performance liquid chromatographic chiral stationary phases. J. Chromatogr. A, **1994**, *666*, 221–234.
12. Chattopadhyay, A.; Tian, T.; Kortum, L.; Hage, D.S. Development of tryptophan-modified human serum albumin columns for site-specific studies of drug–protein interactions by high-performance affinity chromatography. J. Chromatogr. B, **1998**, *715*, 183–190.
13. Haginaka, J.; Kanasugi, N. Enantioselectivity of bovine serum albumin-bonded columns produced with isolated protein fragments. II. Characterization of protein fragments and chiral binding sites. J. Chromatogr. A, **1997**, *769*, 215–223.
14. Kasai, K.; Ishii, S. Affinity chromatography of trypsin and related enzymes. I. Preparation and characteristics of an affinity adsorbent containing tryptic peptides from protamine as ligands. J. Biochem. Tokyo **1975**, *78*, 653–662.
15. Nakano, N.I.; Oshio, T.; Fujimoto, Y.; Amiya, T. Study of drug–protein binding by affinity chromatography: Interaction of bovine serum albumin and salicylic acid. J. Pharmaceut. Sci. **1978**, *67*, 1005–1008.
16. Lagercrantz, C.; Larsson, T.; Karlsson, H. Binding of some fatty acids and drugs to immobilized bovine serum albumin studied by column affinity chromatography. Anal. Biochem. **1979**, *99*, 352–364.
17. Nakano, N.I.; Shimamori, Y.; Yamaguchi, S. Mutual displacement interactions in the binding of two drugs to human serum albumin by frontal affinity chromatography. J. Chromatogr. **1980**, *188*, 347–356.
18. Schriemer, D.C. Biosensor alternative: Frontal affinity chromatography. Anal. Chem. **2004**, *76*, 440A–448A.
19. Schriemer, D.C.; Bundle, D.R.; Li, L.; Hindsgaul, O. Microscale frontal affinity chromatography with mass spectrometric detection: A new method for the screening of compound libraries. Angewandte Chemie Intl. Ed. **1998**, *37*, 3383–3387.
20. Clarke, W.; Chowdhuri, A.R.; Hage, D.S. Analysis of free drug fractions by ultrafast immunoaffinity chromatography. Anal. Chem. **2001**, *73*, 2157–2164.
21. Clarke, W.; Schiel, J.E.; Moser, A.; Hage, D.S. Analysis of free hormone fractions by an ultrafast immunoextraction/displacement immunoassay: Studies using free thyroxine as a model system. Anal. Chem. **2005**, *77*, 1859–1866.
22. Ohnmacht, C.M.; Schiel, J.E.; Hage, D.S. Analysis of free drug fractions using near infrared fluorescent labels and an ultrafast immunoextraction/displacement assay. Anal. Chem. **2006**, *78*, 7547–7556.
23. Loun, B.; Hage, D.S. Chiral separation mechanisms in protein-based HPLC columns. 2. Kinetic studies of (R)- and (S)-warfarin binding to immobilized human serum albumin. Anal. Chem. **1996**, *68*, 1218–1225.
24. Yang, J.; Hage, D.S. Effect of mobile phase composition on the binding kinetics of chiral solutes on a protein-based high-performance liquid chromatography column: Interactions of D- and L-tryptophan with immobilized human serum albumin. J. Chromatogr. A, **1997**, *766*, 15–25.
25. Denizot, F.C.; Delaage, M.S. Statistical theory of chromatography: New outlooks for affinity chromatography. Proc. Natl. Acad. Sci. U.S.A. **1975**, *72*, 4840–4843.

26. Talbert, A.M.; Tranter, G.E.; Holmes, E.; Francis, P.L. Determination of drug–plasma protein binding kinetics and equilibria by chromatographic profiling: Exemplification of the method using L-tryptophan and albumin. Anal. Chem. **2002**, *74*, 446–452.
27. Schiel, J.E.; Ohnmacht, C.M.; Hage, D.S. Rapid measurement of drug–protein dissociation rates by high performance affinity chromatography and peak profiling. submitted.
28. Wade, J.L.; Bergold, A.F.; Carr, P.W. Theoretical description of nonlinear chromatography, with applications to physicochemical measurements in affinity chromatography and implications for preparative-scale separations. Anal. Chem. **1987**, *59*, 1286–1295.
29. Thomas, H.C. Heterogeneous ion exchange in a flowing system. J. Am. Chem. Soc. **1944**, *66*, 1664–1665.
30. Moaddel, R.; Wainer, I.W. Conformational mobility of immobilized proteins. J. Pharm. Biomed. Anal. **2007**, *43*, 399–406.
31. Jozwiak, K.; Haginaka, J.; Moaddel, R.; Wainer, I.W. Displacement and nonlinear chromatographic techniques in the investigation of interaction of noncompetitive inhibitors with an immobilized a3b4 nicotinic acetylcholine receptor liquid chromatographic stationary phase. Anal. Chem. **2002**, *74*, 4618–4624.
32. Golshan-Shirazi, S.; Guichon, G. Comparison of the various kinetic models of non-linear chromatography. J. Chromatogr. **1992**, *603*, 1–11.
33. Mao, Q.M.; Johnston, A.; Prince, J.G.; Hearn, M.T.W. High-performance liquid chromatography of amino acids peptides and proteins. CXII. Predicting the performance of non-porous particles in affinity chromatography of proteins. J. Chromatogr. **1991**, *548*, 147–163.
34. Hage, D.S.; Walters, R.R.; Hethcote, H.W. Split-peak affinity chromatographic studies of the immobilization-dependent adsorption kinetics of protein A. Anal. Chem. **1986**, *58*, 274–279.
35. Rollag, J.G.; Hage, D.S. Non-linear elution effects in split-peak chromatography. II. Role of ligand heterogeneity in solute binding to columns with adsorption-limited kinetics. J. Chromatogr. A, **1998**, *795*, 185–198.
36. Hage, D.S.; Thomas, D.S.; Beck, M.S. Theory of a sequential addition competitive binding immunoassay based on high-performance immunoaffinity chromatography. Anal. Chem. **1993**, *65*, 1622–1630.
37. Moore, R.M.; Walters, R.R. Peak-decay method for the measurement of dissociation rate constants by high-performance affinity chromatography. J. Chromatogr. **1987**, *384*, 91–103.

Binding Molecules via –SH Groups

Terry M. Phillips
Ultramicro Analytical Immunochemistry Resource (UAIR), DBEPS, ORS, OD, National Institutes of Health, Bethesda, Maryland, U.S.A.

INTRODUCTION

A prerequisite for producing a good affinity support is a firm, stable attachment of the ligand to the surface of the support. There are numerous linkage chemistries available for performing this task, and although the most popular approach is a reaction between the reactive side groups on the support and a primary amine on the ligand, there are a number of supports that can perform similar attachments through free thiol or sulfhydryl groups.

METHODOLOGY

Supports containing maleimide reactive side groups are specific for free sulfhydryl groups present in the ligand when the reaction is performed at pH 6.5–7.0. At pH 7.0, the interaction of maleimides with sulfhydryl groups is approximately a 1000-fold faster than with amine groups. The stable thioether linkage formed between the maleimide support and the sulfhydryl group on the ligand cannot be easily cleaved under physiological conditions, therefore ensuring a stable affinity matrix. Immobilization of sulfhydryl-containing molecules can also be achieved using either α-haloacetyl or pyridyl sulfide cross-linking agents. The α-haloacetyl cross-linkers [i.e., *N*-succinimidyl(4-iodoacetyl)aminobenzoate] contain an iodacetyl group that is able to react with sulfhydryl groups present in the ligand at physiological pH. During this reaction, the nucleophilic substitution of iodine with a thiol takes place, producing a stable thioether linkage. However, a shortcoming of this approach is that the α-haloacetyls interact with other amino acids, especially when a shortage or absence of free sulfhydryl groups exists. Linkage of pyridyl disulfides with aliphatic thiols at pH 4.0–5.0 produces a disulfide bond with the release of pyridine-2-thione as a by-product of the reaction. A disadvantage of this approach is the acidic pH of the reaction, which is essential for optimal linkage. The reaction can be performed at physiological pH, but under these conditions, the reaction is extremely slow.

Ligand immobilization through sulfhydryl groups can be advantageous due to its ability to be site-directed. Additionally, depending upon the linkage, the ligand–support can be cleavable, allowing the same support to be reused. However, many useful affinity ligands do not possess free sulfhydryl groups and in such cases, free sulfhydryl groups can be engineered into the ligand via a series of commercially available reagents. Traut's reagent (2-iminothiolane) is the most common, although *N*-succinimidyl *S*-acetylthioacetate (SATA), dithio-*bis*-maleimidoethane (DTME), and *N*-succinimidyl-3-(2-pyridyldithio)-propionate (SPDP)[1] can also be used (Fig. 1). Traut's reagent reacts with primary amines present in the ligand introducing exposed sulfhydryl groups for further coupling reactions.

Chrisey, Lee, and O'Ferrall[2] describe an interesting use of sulfhydryl-mediated immobilization for binding thiol-modified DNA. A hetero-bifunctional cross-linker bearing both thiol and amino reactive groups was used to immobilize thiol-modified DNA oligomers to self-assembled monolayer silane films on fused silica and oxidized silicon substrates. The advantage of this approach

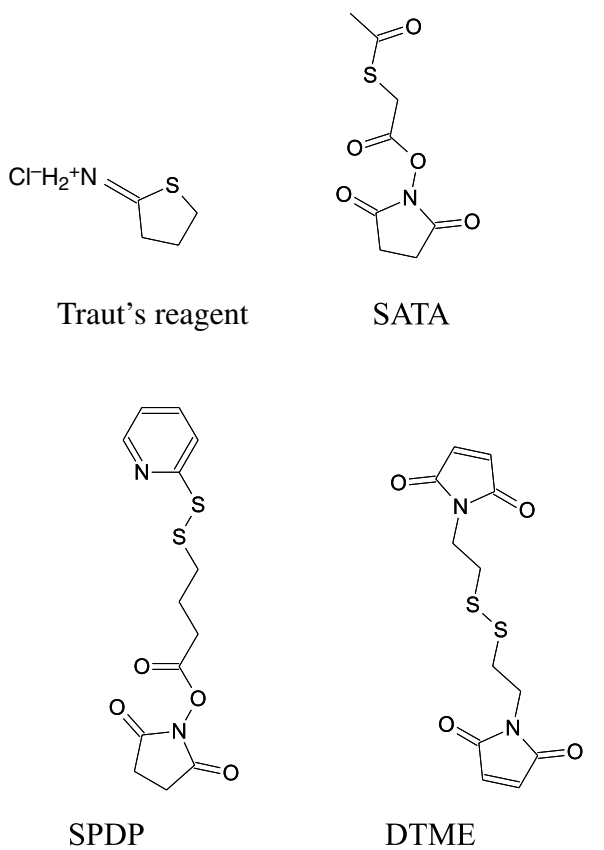

Fig. 1 Chemical structures of commercially available reagents for introducing sulfhydryl groups into molecules.

was the use of site-directed immobilization to ensure the correct orientation of the DNA molecule.

ANTIBODY IMMOBILIZATION

Cleaving disulfide bonds already present in the ligand can also generate free sulfhydryl groups. The classic example of this approach is the digestion of the IgG antibody molecule to produce two monovalent, reactive Fab fragments each containing a free sulfhydryl group. In this case, reduction of the disulfide bridge (holding the two Fab arms together) is achieved using Cleland's reagent (dithiothreitol—DTT). Each Fab is then attached to free thiol groups present on the support by reforming a disulfide bond.[3–5] Free thiol groups can be condensed into silane-activated surfaces via sulfosuccinimidyl-4-(*N*-maleimidomethyl)-cyclohexane-1-carboxylate (sulfo-SMCC) or *N*-(β-maleimidopropyloxy) succinimide ester (BMPS). The advantage of this approach is that not only is a covalent linkage formed but also the linkage helps to orient the antigen receptor of the Fab away from the support matrix.

REFERENCES

1. Carlsson, J.; Drevin, H.; Axen, R. Protein thiolation and reversible protein–protein conjugation. *N*-Succinimidyl 3-(2-pyridyldithio)propionate, a new heterobifunctional reagent. Biochem. J. **1978**, *173*, 723.
2. Chrisey, L.A.; Lee, G.U.; O'Ferrall, C.E. Covalent attachment of synthetic DNA to self-assembled monolayer films. Nucleic Acids Res. **1996**, *24*, 3031.
3. Phillips, T.M. Determination of in situ tissue neuropeptides by capillary immunoelectrophores. Anal. Chim. Acta. **1998**, *372*, 209.
4. Karyakin, A.A.; Presnova, G.V.; Rubtsova, M.Y.; Egorov, A.M. Oriented immobilization of antibodies onto the gold surfaces via their native thiol groups. Anal. Chem. **2000**, *72*, 3805.
5. Phillips, T.M.; Smith, P. Analysis of intracellular regulatory proteins by immunoaffinity capillary electrophoresis coupled with laser-induced fluorescence detection. Biomed. Chromatogr. **2003**, *17*, 182.

BIBLIOGRAPHY

1. Hermanson, G.T.; Mallia, A.K.; Smith, P.K. *Immobilized Affinity Ligand Techniques*; Academic Press: New York, 1992.
2. Lundblad, R.L. *Techniques in Protein Modification*; CRC Press: Boca Raton, FL, 1995.
3. Phillips, T.M.; Dickens, B.F. *Affinity and Immunoaffinity Purification Techniques*; BioTechniques Books, Eaton Publishing: Natick, MA, 2000.
4. Wong, S.S. *Chemistry of Protein Conjugation and Cross-linking*; CRC Press: Boca Raton, FL, 1991.

Bioanalysis: Silica- and Polymer-Based Monolithic Columns

Mohamed Abdel-Rehim
Research and Development, AstraZeneca, Södertälje, and Department of Chemistry, Karlstad University, Karlstad, Sweden

Eshwar Jagerdeo
Federal Bureau of Investigation Laboratory, Quantico, Virginia, U.S.A.

Abstract
There has been significantly more interest over the past decade in what is now termed *monolithic*. This is not because the current column technology is unsatisfactory, but monolithic material has opened up a new avenue for separation and has a significant impact on just about all analytical procedures. The use of this material for high-performance liquid chromatography (HPLC), ion chromatography (IC), and capillary electrochromatography (CEC) is finally taking hold, being provided commercially by manufacturers. Similarly, the increase in applications has proved that this material is finally becoming mainstream. The goal of this entry is to provide an overview of silica- and polymer-based monolithic material, with a special focus on how the material is being used in the manufacture of analytical columns. A comparison of silica- and polymer-based monolithic columns is made with an emphasis on their differences and similarity. Key applications are presented as a reference to highlight how the monolithic columns are being used for high-throughput drugs and metabolites, ion chromatographic separation, and proteomics.

INTRODUCTION

The introduction of a monolithic column might be a new approach or paradigm shift in how chromatography is done, but high-performance liquid chromatography (HPLC) has been very successful for decades. HPLC analysis has addressed issues encountered daily in the field of biochemistry and analytical chemistry by separation of mixtures, identification and quantitation of the individual component in the mixtures. HPLC utilizes a column that holds a packing material, a pump that moves the mobile phase(s) through the packed column, and a detector to determine the component in the mixture.[1] At the "center" of the entire HPLC procedure is the column (packed, porous material), through which the mobile phase passes. The choice of the packing material and mobile phase is made in such a way that the sample components equilibrate rapidly between the liquid and the solid phase (Fig. 1). For this process to work, the analytes should be exchanged rapidly and frequently between the mobile phase and the column material.[2] This approach leads to high column efficiency. The prerequisite for this fast equilibrium and high efficiency is fast mass transfer and the surface area of the column material must be large.

The search for the perfect chromatography began over a century ago with the work of the Russian botanist Michael Tswett,[1] who used column liquid chromatography in which the stationary phase was a solid adsorbent and the mobile phase was a liquid. The major breakthrough that would eventually lead to many of the developments of modern-day chromatography came from the work of Martin and Synge.[3] Packing material with a smaller particle size is necessary to achieve the necessary efficiency in today's chromatography. However, since particle size has an inverse squared dependence on column pressure, all particle-based chromatographic columns are limited by pressure. To overcome this hurdle, a new approach to column technology was necessary, and it was found with the development of monolithic columns.[4] The first appearance of the word monolith appeared in a publication in 1993, which describes the material as a single mass of material.[5] This term has taken hold and has provided the field of chromatography with a new and promising approach to analysis.

Several different monolithic supports are described in the literature, going back several decades. They have been synthesized from different chemicals to form silica,[6–9] acrylamide,[10–13] styrene and methacrylate,[14–16] and methacrylate[17–19] monoliths. Generally, the different types of monolithic material synthesized over the years can be subdivided into two classes: 1) silica-based and 2) polymer-based monoliths. The monolithic column that is manufactured can be viewed as a single piece of porous material. The bed of the polymer-based monolithic column resembles that of a loose packing of spherical particles with a wide size distribution. However, the silica monolith is more of a fractal morphology showing a bimodal pore size (mesopores and macropores) distribution (Fig. 2). The pores of the columns are highly interconnected to form an integrated network of channels. The mesopores, about

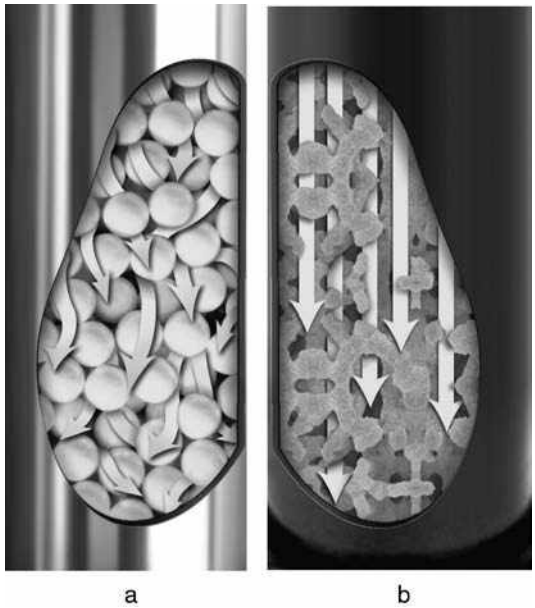

Fig. 1 Mobile phase flow through particle-based column (a) and a monolithic column (b).
Source: Reproduced with permission from Phenomenex.

13–25 nm in size, form the intraparticle network that gives access to the large surface area of the stationary phase primarily responsible for retention and column efficiency. The macropores with a size of 1 μm are the channels that the mobile phase percolates. As a result of the pores, monolithic columns operate at a significantly reduced back pressure. As reported by Cabrera,[9] the reduced pressure permits flow rates as high as 1–9 ml/min, which is not possible with typical particle columns (Fig. 3).

In the 1990s there was great interest in using monoliths for liquid chromatography (LC) or capillary electrochromatography (CEC), with extensive research devoted to developing a robust and reliable commercially available product. Siouffi[20] listed four approaches taken by researchers in creating the perfect monolith:

1. Formation of a silica-based network.
2. A polymer-based monolith from an organic monomer with additives.
3. Fusing the porous particulate in a capillary by the sintering process.
4. Organic hybrid materials.

If we can use the number of applications and published papers as a measure of success, silica- and polymer-based monoliths are certainly the winner. In part, this has come about as a result of industry getting involved and making the product available on a mass scale. The introduction of the first commercially available product, the Chromolith™ from Merck KGaA (Darmstadt, Germany), saw the beginning of a new routine chromatographic media.

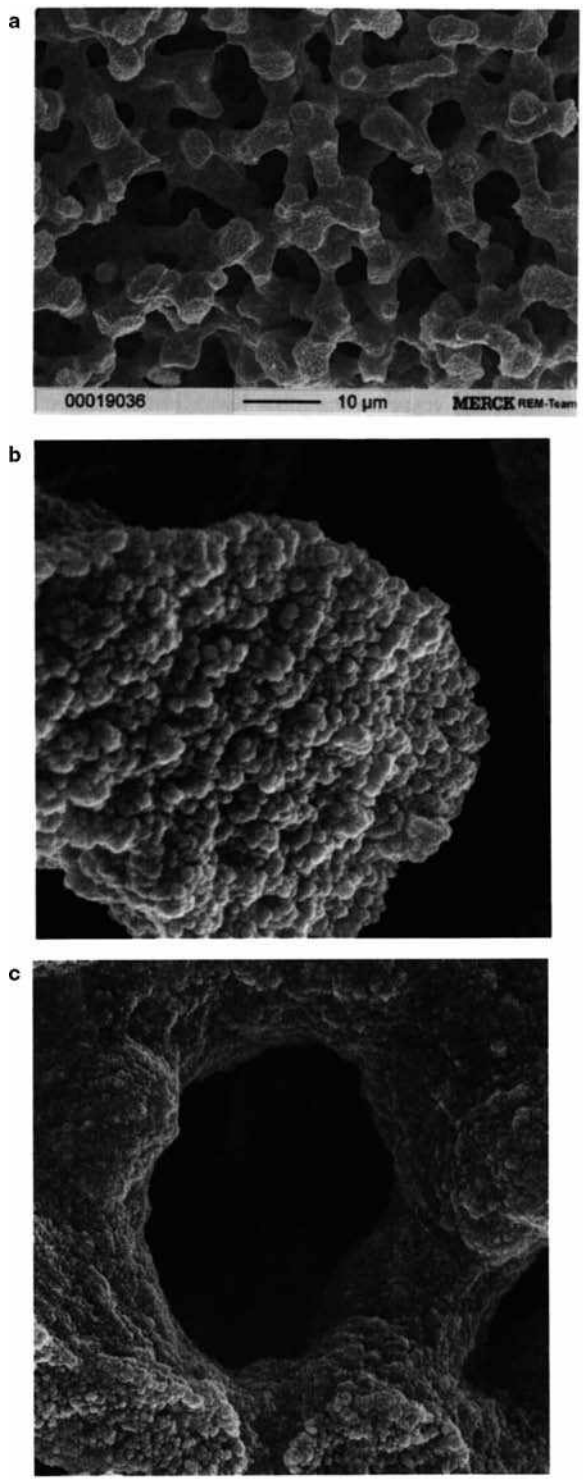

Fig. 2 SEM image of the porous structure of the monolithic column (a), image showing the mesoporous structure (b), and the macropores of the monolithic material (c).
Source: From Applications of silica-based monolithic HPLC columns, in J. Sep. Sci [9]; with permission from Wiley and the author.

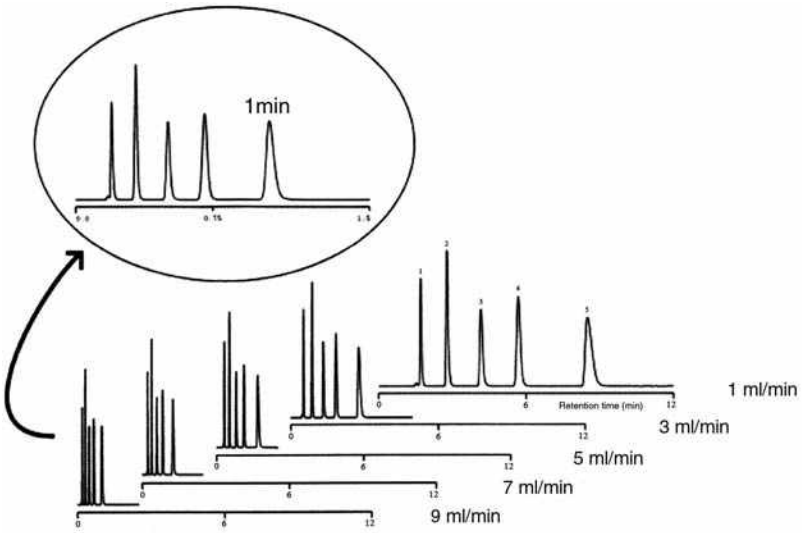

Fig. 3 The separation of a set of five compounds on a monolithic silica column with different flow rates.
Source: From Applications of silica-based monolithic HPLC columns, in J. Sep. Sci [9]; with permission from Wiley and the author.

The aim of this entry is to provide an overview of the monolithic phases that are most commonly or widely used (silica- and polymer-bases) in chromatography. In describing these materials, the focus will be on highlighting the differences between the phases and finally providing key applications to demonstrate the use of material.

SILICA-BASED MONOLITHS

This type of monolithic column was first reported by Tanaka et al.[6–8] It uses a new sol-gel process developed by Nakanishi and Soga that was based on the hydrolysis and polycondensation of alkoxy silicon derivatives [e.g., tetramethoxysilane (TMOS) or tetraethyloxysilane (TEOS) in the presence of polyethylene oxide (PO)].[21–26] They described the procedure enabling control of the bimodal pore size that is critical in the manufacture of successful analytical columns. Generally, the silica-based monoliths are prepared through a two-step process, the first step being a sol-gel mechanism overlapping the spinodal phase transition. This process determines the mesopore size and diameter. The second step is a solvent exchange with the material to carve out the silica skeleton of the mesopores. The uniform structure of the monolithic material with regular spacing and size of pores provides a surface area that is much larger than polymer-based monoliths.

In the preparation of this material, the silicon derivative is dissolved in a solvent with an aqueous solution (acid or base), which reacts to produce a gel material.[2,20] The pore size, distribution, and mechanical properties of the gel can be controlled with an additive. In the case of Nakanishi and Soga, they used polyacrylic acid and later changed to PO. By adjusting the concentration of TMOS or PO, they were able to control the pore size distribution or to produce a matrix of different degrees of strength. After preparation, the silica monolithic material has to undergo an aging and drying process. This is a critical stage in making a successful silica monolithic column and special care has to taken. Aging in a solution tends to increase the stiffness and strength of the gel. As reported by Nakanishi et al.,[27] aging the gel in the presence of a basic solution with heat treatment has an influence on the size and distribution of the mesopores. The temperature also influences the rate of formation of the pores and its network distribution. Drying of the monolith is as important as the aging process, as poor drying could lead to cracking or shrinkage of the material. The shrinkage and possible cracking of the monolithic material is a much more serious problem in the preparation of normal size HPLC columns. Nevertheless, cracking of the monolithic material could make the material unusable for chromatography. Shrinking upon drying causes the material to be separated from the column wall, thereby creating a void space. The void space would create a nonuniform flow across the column, the mobile phase tending to bypass the monolithic pores for the void space. Minakuchi et al. have demonstrated a fall of almost 2 mm after drying.[8] The drying process is very slow and takes place under an inert gas. For large HPLC columns, this process can take as long as 1 month.

Cladding the monolithic material is the last process to make a successful chromatographic column. The preparation process for monolithic silica rods was first patented in Japan and later in the United States.[24–26] Although other academic research groups have been working on monolithics, the difficulty (drying and cladding) described above has created an opportunity for industry to bring this material to market. Moreover, most of these groups have focused their interest in developing in situ preparation of capillary monolithic columns based on the work of Nakanishi et al. because of the difficulty of encasing the monolithic rods.

Although capillary columns are used in analytical chemistry, a large percentage of the columns in use today are still the conventional HPLC columns (2–4.6 mm). This has created a great opportunity for Merck KGaA, which has independently developed a process for the manufacture of monolithic columns (Chromolith) with the work of Cabrera et al. and has patented it.[16] Certainly with the gradual developments in analysis by LC/MS, Merck KGaA (http://www.Merck.de) has made available the Chromolith CapRod® (150 × 0.1 mm). Likewise, Phenomenex (http://www.phenomenex.com) has developed its line of monolithic columns (Onyx™) based on the same technology as Merck KGaA. The Onyx monolithic columns are available both in the conventional (100 × 4.6 mm) and in the capillary (150 × 0.1 mm) form.

POLYMER-BASED MONOLITHS

Hjerten and coworkers first introduced this type of monolithic column, based on polyacrylamide, in the early 1990s.[10–13] This process was further enhanced by the work of Svec and Frechet, which demonstrated the in situ copolymerization of glycidyl methacrylate and ethylene dimethacrylate.[14,17–19] As a result of these developments, a unique branch of monolithic column technology was developed. Creating this form of monolithic material requires a mold or tube that is sealed at one end, filled with the polymerization mixture, and then sealed at the other end. The polymerization is initiated by either heat or ultraviolet light. A wide variety of material have been used as the mold such as poly(ether-ether-ketone) (PEEK), fused silica capillary, or stainless steel. This process is an exothermic reaction and the heat must be controlled in order to produce a homogeneous porous structure. The polymerization comprises monomers, initiator, and porogenic solvent. Guiochon[2] has highlighted the fact that polymer-based monolithic columns can be classified based on the monomers used in the preparation. As stated by Svec,[28] the versatility of these preparation techniques was demonstrated by the use of hydrophilic (2-hydroxyethyl methacrylate, methacrylamide, methylenebisacrylamide), hydrophobic (styrene, divinylbenzene, butyl methacrylate, ethylene dimethacrylate), ionizable (vinylsulfonic acid, 2-acrylamido-2-methyl-propanesulfonic acid), and tailor-made (norbone-2-ene, 1,4,4a,5,8,8a-hexahydro-1,4,5,8-exo, endo-dimethanonapthalene) monomers.

As detailed by Guiochon,[2] the preparation of a successful polymer base column can be broken down into three steps:

1. Treating the wall of the column.
2. Polymerization of the suitable mixture of reagents.
3. Modifying the surface chemistry of the polymeric bed.

Treating the wall of the column is critical because it helps the synthesized polymer to adhere to it. This is done by treating the wall with a monomer that binds with the mixture of monomers used in making the monolith. This step is important because it enables the monolith to adhere to the wall of the mold and void any space that may be created. Since this polymerization is an in situ process, it avoids the problem of cladding that is encountered in silica-based monoliths.

The second step is the polymerization, which, in the case of hydrophilic gels, includes a monomer, a catalyst (*N*,*N*,*N*,*N*-tetramethylethylenediamine). The precipitation takes place under: 1) a high ion strength solution or 2) porogen (dextran or polyethylene glycol). For the hydrophobic gels, the reagents are the selected monomers, a catalyst [azobisisobutyronitrile or 2,2-azobis(iosbutyronitrile)], and a porogen (propanol, butanediol, cyclohexanol, dodecanol), or a mixture of porogens. After the precipitation of the polymer, the last step is modification of the surface chemistry to suit one's needs for separation. These modifications allow the column of cation or anion, reverse phase, hydrophobic, or chiral to be made.

COMPARSION OF SILCA- AND POLYMER-BASED MONOLITHICS

Overall, both silica- and polymer-based monolithic materials have their place in chromatography. However, there are differences between these monolithic materials. An awareness of these differences could provide the end user with the knowledge to make an educated decision. In describing the difference, reference will be made to the conventional particulate HPLC columns. The mesoporous structure of the silica monolithic columns is more homogeneously spaced and sized and, as a result, provides a much larger surface area than the polymeric columns. The columns sold by manufacturers have macropores and mesopores of 2 μm and 13 nm, respectively, which give them a total porosity greater than 80% and a surface area of 300 m^2/g.[2] The monolithic columns sold are equivalent to a 3 μm particulate silica column in terms of efficiency and equivalent to a 7–15 μm particle with respect to permeability. Capillary silica monolithic columns are manufactured to have 1.3 μm mesopores and, when compared to silica columns, are equivalent to a 2–2.5 μm particulate column and permeability of 5 μm HPLC columns.[9]

However, the silica-based monolithic produces a more uniform and reproducible skeleton than the polymer-based monolithic. It has several shortcomings such as:

1. pH stability;
2. improper aging;
3. proneness to cracking and shrinkage during the drying process;

4. a potential problem when cladding the monolithic material.

At pH > 8, the silica dissolves, resulting in poor reproducibility, poor efficiency, and high back pressure. Improper aging of the silica gel under an uncontrolled temperature can result in poor size and distribution of the mesopores. Drying of the monolith is just as important as the aging process, because poor drying could lead to cracking or shrinkage of the material. The shrinkage and possible cracking of the monolithic material is a much more serious problem in the preparation of normal size HPLC columns. Moreover, cladding of a silica-based monolithic column is a difficult process and it is not easily done in an academic environment. In spite of the difficulties, silica produces a more uniform and reproducible structure than most polymers.

Not all of the above problems are encountered in the manufacture of a polymer-based column as it is an in situ process that can be done in a single step. Furthermore, the polymer-based columns can be tailored by modifying the surface chemistry to perform a wide variety of analytical separation. In addition, this type of material is stable over a wide pH range. Separation that cannot be performed over pH > 8 can be accomplished with this material.

If the number of publications is a sign of the success of both these materials, the future is bright and these materials have sealed their place in chromatography. Overall, monoliths show better mass transfer at higher flow rates than particulate columns, while maintaining high efficiency.[29] At high flow rates monoliths do not produce the large back pressure seen with particle-based columns. As a result, monolithic columns can be use in fast HPLC systems for high-throughput analysis.

KEY APPLICATIONS

Since the invention of silica- and polymer-based monolithic columns, users have been finding new applications for this material (Table 1). These applications are not driven because monoliths are a new material; they are driven by a direct need or void that was present for a long time in chromatography. Sample preparation and analysis have been the limiting factor in overall sample analysis time. The main driving force in using monolithic columns in chromatography is the speed of analysis. Chromatography can now be done with flow rates from 1 to 9 ml/min, while still maintaining the necessary resolution. Many applications have compared the conventional particulate columns with the new monolithic columns. They range from direct plasma analysis, drugs of abuse, food additives, proteins and peptides, inorganic ions, and high-throughput bioanalytical separations. Overall, based on what they report in their publications, the authors are satisfied with the durability and reproducibility of the columns.

DIRECT PLASMA AND HIGH-THROUGHPUT BIOANALYSIS OF DRUGS AND METABOLITES

The demand for high sensitivity and high-throughput bioanalytical methods is substantial in the discovery process for pharmaceutical drugs. High-resolution chromatography coupled to a mass spectrometer is well suited for this type of analysis because it is viewed as an orthogonal technique that is selective and provides structural information. Hsieh et al.[30] reported rapid analysis of clozapine and 12 test compounds with an analysis time of 1.3 min. The chromatography was done on a Chromolith SpeedROD, RP-18e, with over 200 plasma injections done on the column, and was reported to have excellent reproducibility and recovery of greater than 90%.

Likewise, toxicokinetic or pharmacokinetic studies revealed the drug-like characteristics of new chemical entities by measuring the plasma time concentration profiles of preclinical species. For these methods, it is important to have rapid, selective, and sensitive bioanalytical methods capable of quantitatively determining the new chemical entities and major metabolites in biological fluids. Here Zang et al.[31] developed a rapid SPE/LC/MS/MS method for Indiplon, Verapamil, and six test compounds using a Chromolith SpeedROD, RP-18e, with a gradient mobile phase for a total analysis time of 2.80 min. A total of 300 direct plasma injections were made without any noticeable change in system performance. Similarly, three other high-throughput analyses were published showing an analysis time of <3 min. One of them demonstrated a total of 600 plasma analyses with flow rates as high as 6 ml/min within an overnight run.[32–39] CEC coupled to a mass spectrometer as a microanalysis technique has higher separation efficiency, shorter analytical times, and lower sample and solvent consumption when compared to LC/MS. Here Lu et al.[40] described an analysis of narcotics from urine using a capillary silica-based monolithic column. Likewise, Wei et al.[41] and Fan et al.[42] described an in-tube solid-phase microextraction of four amphetamines and methylxanthine from biological fluids. This extraction procedure is preferable since it uses a convective mass transfer in a monolithic column as against the diffusion mass transfer mechanism used in conventional liquid-phase-coated capillaries. Using this mechanism, the extraction is completed within a shorter time.

ION CHROMATOGRAPHY SEPARATIONS

Ion chromatography (IC) has cemented its position as an integral part of analytical chemistry for the analysis of inorganic and biological ion analysis. IC operates on a principle similar to that of HPLC (a pump, injector, column, and detector), but the main difference is that the entire flow path is constructed with a metal-free material. The principle

Table 1 Applications of monolithic columns in bioanalysis.

Sample	Column	Detector	Mobile phase	Comments	Refs.
13 Drugs in plasma high-throughput analysis	Chromolith SpeedROD, RP-18e (4.6 50 mm)	API 3000	Acetonitrile/4 m*M* ammonium acetate	Recovery > 90% efficiencies > 36,000 1.2–8 ml/min	[30]
8 Drugs in plasma high-throughput analysis	Chromolith SpeedROD, RP-18e (4.6 × 50 mm)	API 4000	Acetonitrile and water with 0.1% formic acid	3–4 ml/min	[31]
4 Drugs in plasma high-throughput analysis	Chromolith SpeedROD, RP-18e (4.6 × 50 mm)	Quattro Ultima	Acetonitrile and water with ammonium acetate	6 ml/min 600 analysis with 12 hr	[32]
3 Drugs in plasma high-throughput analysis	Chromolith SpeedROD, RP-18e (4.6 × 50 mm)	API 3000	Methanol and water with 0.1% formic acid	1–5 ml/min	[33]
Vitamin C	Onyx C18 (4.6 × 100 mm)	UV detector	30 n*M* potassium phosphate buffer/acetonitrile	2.5 ml/min Runtime 3 min.	[34]
Cytochrome markers 5 marker substrates	Chromolith SpeedROD, RP-18e (4.6 × 50 mm)	API 3000	Acetonitrile and water with 1% formic acid.	2.5 ml/min Runtime 1.4 min	[35]
Antidepressant (5 drugs) high-throughput analysis	Chromolith SpeedROD, RP-18e (4.6 × 50 mm)	API 4000	8 m*M* ammonium acetate and acetonitrile	5 ml/min Runtime 1 min	[36]
Famotidine histamine antagonist	Chromolith SpeedROD, RP-18e (4.6 × 100 mm)	UV detector	0.03 *M* phosphate buffer and acetonitrile	1.5 ml/min Runtime 8 min	[37]
Rifampicin (5 drugs) Antibiotic	Chromolith SpeedROD, RP-18e (4.6 × 100 mm)	UV detector	Phosphate buffer, methanol, and acetonitrile	2 ml/min Runtime 11 min	[38]
Drugs and metabolites 16 Illicit drugs	Chromolith SpeedROD, RP-18e (4.6 × 100 mm)	Bruker ion trap	Methanol and water	Runtime 30 min	[39]
Narcotics (5 analytes)	Home-made (56 cm × 100 μm)	Agilent MS	65% Acetonitrile/20 mmol/L ammonium acetate, pH 6.0	Runtime 10 min	[40]
Amphetamines (4 analytes)	Home-made (15 cm × 50 μm)	UV detector	0.1 *M* disodium hydrogen phosphate (pH 4.5) and 20% methanol (v/v)	Runtime 10 min	[41]
Methylxanthine (4 analytes)	Home-made (20 cm × 0.25 mm)	UV detector	70% 0.05 mol/L ammonium acetate, pH 4.5% and 30% methanol	Runtime 12 min	[42]
Inorganic ions (7 analytes)	RP-18e (4.6 × 25 mm)	ELCD detector	6 and 9 m*M* 4-cyanophenol at pH 7.3–7.4	Runtime 2 min	[46]
Inorganic ions (7 analytes)	Home-made (30 cm × 250 μm)	Conductivity or UV	Acetate or hydroxide	Runtime <2 min	[47]
Inorganic ions (7 analytes)	Home-made (10 cm × 75 μm)	UV detector	Tris/perchlorate	Runtime 90 sec	[48]
Inorganic ions (5 analytes)	Home-made (15 cm × 250 μm)	UV detection	10 m*M* copper sulfate	Runtime depends on the flow rate	[49]
Protein	10 cm × 20 μm 10 cm × 50 μm	LTQ-FTMS	Acetonitrile and water with 0.1% formic acid	Na	[50]
Protein	15 × 100 μm	QSTAR XL/ MS	Acetonitrile and water with 0.1% formic acid	Na	[51]
Protein	4.6 × 0.6 cm	UV detector	0.1% TFA in water/0.1% TFA in acetonitrile	Na	[52]

of IC includes ion interaction, ion exchange chromatography, and ion exclusion chromatography. The application of monoliths to IC has evolved over the years to affect every facet of our lives. Svec[43] has provided an in-depth review of polymer monoliths in liquid capillary chromatography and their application. Likewise, Josic, Buchacher, and Jungbauer[44] have provided an excellent review of the use of ion exchange chromatography for the separation of proteins and polynucleotides. The main reason ion exchange columns were made is for biological analysis. However, because of the speed of analysis, monolithic columns have been used for small ion analysis.

The area of focus for the use of monolithics in IC has been in post column modification. Here an ion interaction reagent or a surfactant coating can be applied to a reversed-phase column and as a result make it a column applicable to ion chromatography. Chambers, Glenn, and Lucy[45] give an excellent summary of all the surfactants used on monolithic columns, the column, eluent, detector used, and the analyte analyzed. Furthermore, this entry addresses surfactants used for anion and cation exchange chromatography. Pelletier and Lucy[46] described a fast ion exchange separation of seven analytes (iodate, chloride, nitrate, bromide, nitrate, phosphate, and sulfate) in 2 min at 2 ml/min using a silica-based column coated with the surfactant didodecyldimethylammonium bromide. Although surfactant coatings are very popular and widely used, the instability of the coating has driven the development of new technology. An electrostatically bound latex coating (or covalently bonding a reagent material) directly to the monolithic material is becoming popular. Zakaria et al.[47] described a procedure for the analysis of seven inorganic anions using latex-coated monolithic polymeric phases in less than 2 min. Likewise, Hutchinson et al.[48] described a procedure for the analysis of seven inorganic anions in 90 sec using a sulfonated methacrylate monolithic with quaternary ammonium latex particles. Ueki et al.[49] described a procedure for cation exchange analysis using a sulfonated glycidyl methacrylate and ethylene dimethacrylate monolithic column.

PROTEIN AND PEPTIDE ANALYSIS

The analysis of proteins falls under the umbrella of proteomics. For years, the field of proteomics relied on two-dimensional polyacrylamide gel electrophoresis for the separation of complex protein mixtures. With the drive to produce methods with more selective and structural methods, HPLC with new column technology combined with the mass spectrometer has revolutionized the analysis of proteins. The quality and quantity of information generated by this approach has given rise to a new field called bioinformatics. The use of monolithic material has made a significant contribution to this field and appears to be promising. Zhang et al.[50] described an LC/MS procedure for the analysis of peptides as large as 10 kDa using a narrow-bore poly(styrene-divinylbenzene) monolithic column. The authors show approximately 30% higher separation than for packed columns and a high recovery of large peptides. Callanan et al.[51] described a convective interaction media disk (short columns) with a phase that has a high-binding capacity for large molecules. The authors describe procedures using anion and cation exchanges or affinity ligands for the separation of complex biological mixtures. The LC/MS/MS procedure was used for the identification of proteins. Hjerten et al.[52] described the synthesis of monolithic column using piperazine diacrylamide, methylacrylamide, and allyl glycidyl ether. The column bed was covalently bonded with non-polar ligands and polar substance. These columns were used to separate proteins.

CONCLUSION

Within last decade, monolithic materials (silica and polymeric) have evolved into products that have a significant impact on a large number of fields in analytical chemistry. If one had to identify one feature that this material has provided for chromatography, it would be the ability to perform analysis at a high flow rate and still maintain the required resolution. The high flow rate has a significant influence in high-throughput analysis. With the wide variety of options available in making a monolithic column, one can "tailor" a specific column for a class of compounds. Looking ahead, as more analysis is carried out using mass spectrometry, the future holds great promise for the field of proteomics. In addition, more progress in the polymeric monolithic columns will be required. In the future, new monolithic columns with different range of selectivity, high loadability, improved pH stability, and improved longevity are required.

REFERENCES

1. Lough, W.J; Wainer, I.W. *High Performance Liquid Chromatography*; Blackie Academic & Professional, Chapman and Hall: Glasgow, UK, 1995; 5–14.
2. Guiochon, G. Monolithic columns in high-performance liquid chromatography. J. Chromatogr. A, **2007**, *1168*, 101–168.
3. Martin, A.J.P.; Synge, R.L.M. A new form of chromatogram employing two liquid phases. J. Biochem. **1941**, *35*, 1358.

4. Smith, J.H.; McNair, H.M. Fast HPLC with a silica-based monolithic ODS column, J. Chromatogr. Sci. **2003**, *41*, 209–214.
5. Noel, R.; Sanderson, A.; Spark, L. *Cellulosics: Materials for Selective Separations and Other Technologies*; Horwood: New York, 1993; 17–24.
6. Minakuchi, H.; Nakanishi, K.; Soga, N.; Ishizuka, N.; Tanaka, N. Octadecylsilylated porous silica rods as separation media for reversed-phase liquid chromatography. Anal. Chem. **1996**, *68*, 3498–3501.
7. Nakanishi, K.; Minakuchi, H.; Soga, N.; Tanaka, N. Double pore silica gel monolith applied to liquid chromatography. J. Sol-Gel Sci. Technol. **1997**, *8*, 547–552.
8. Minakuchi, H.; Nakanishi, K.; Soga, N.; Ishizuka, N.; Tanaka, N. Effect of skeleton size on the performance of octadecylsilylated continuous porous columns in reversed-phase liquid chromatography. J. Chromatogr. A, **1997**, *762*, 135–146.
9. Cabrera, K. Applications of silica-based monolithic HPLC columns. J. Sep. Sci. **2004**, *27*, 843–852.
10. Hjerten, S.; Liao, J-L.; Zhang, R. High performance liquid chromatography on continuous polymer beds. J. Chromatogr. **1989**, *473*, 273–275.
11. Hjerten, S.; Mosbach, R. "Molecular-Sieve" chromatography of proteins on columns of cross-linked polyacrylamide. Anal. Biochem. **1962**, *3*, 109–118.
12. Hjerten, S.; Yao, K. High-performance liquid chromatography of macromolecules agarose and its derivatives. J. Chromatogr. **1981**, *215*, 317–322.
13. Yao, K.; Hjerten, S. Gradient and isocratic high-performance liquid chromatography of proteins on a new agarose-based anion exchanger. J. Chromatogr. **1987**, *385*, 87–98.
14. Wang, Q.C.; Svec, F.; Frechet, J.M.J. Macroporous polymeric stationary-phase rod as continuous separation medium for reverse-phase chromatography. J. Anal. Chem. **1993**, *65*, 2243–2248.
15. Gusev, I.; Huang, X.; Horvath, C. Capillary columns with in situ formed porous monolithic packing for micro high-performance liquid chromatography and capillary electrochromatography. J. Chromatogr. A, **1999**, *855*, 273–290.
16. Zhang, S.H.; Zhang, J.; Horvath, C. Rapid separation of peptides and proteins by isocratic capillary electrochromatography at elevated temperatures. J. Chromatogr. A, **2001**, *914*, 189–200.
17. Tennikova, T.B.; Belenkil, B.G.; Svec, F. High performance membrane chromatography: A novel method of protein separation. J. Liq. Chromatogr. **1990**, *13*, 63–70.
18. Svec, F.; Frechet, J.M. Continuous rods of macroporous polymer as high performance liquid chromatography separation media. Anal. Chem. **1992**, *64*, 820–822.
19. Sykora, D.; Svec, F.; Frechet, J.M.J. Separation of oligonucleotides on novel monolithic columns with ion-exchange functional surfaces. J. Chromatogr. A, **1999**, *852*, 297–304.
20. Siouffi, A.M. Silica gel-based monoliths prepared by the sol-gel method: Facts and figures. J. Chromatogr. A, **2003**, *1000*, 801–818.
21. Nakanishi, K.; Soga, N. Phase separation in gelling silica-organic polymer solution: System containing poly(sodium styrenesulfonate). J. Am. Ceram. Soc. **1991**, *74*, 2518–2530.
22. Nakanishi, K.; Soga, N. Phase separation in silica sol-gel system containing polyacrylic acid. I. Gel formation behavior and effect of solvent composition. J. Non. Cryst. Sol. **1992**, *139*, 1–13.
23. Nakanishi, K.; Soga, N. Phase separation in silica sol-gel system containing polyacrylic acid. II. Effects of molecular weight and temperature. J. Non. Cryst. Sol. **1992**, *139*, 14–24.
24. Nakanishi, K.; Soga, N., Inorganic Porous Column, Japanese patent, 5–200, 392, 1993.
25. Nakanishi, K.; Soga, N., Production of Inorganic Porous Body, Japanese patent, 5–208, 642, 1993.
26. Nakanishi, K.; Soga, N. Inorganic Porous Material and Process for Making Same, U.S. patent, 5,624,875, 1997.
27. Nakanishi, K.; Minakuchi, H.; Soga, N.; Tanaka, N. Structure design of double-pore silica and its applications to HPLC. J. Sol-Gel Sci. Technol. **1998**, *13*, 163–169.
28. Svec, F. Organic polymer monoliths as stationary phases for capillary HPLC. J. Sep. Sci. **2004**, *27*, 1419–1430.
29. McCalley, D.V. Comparison of conventional microparticulate and a monolithic reversed-phase column for high-efficiency fast liquid chromatography of basic compounds. J. Chromatogr. A, **2002**, *965*, 51–64.
30. Hsieh, Y.; Wang, G.; Wang, Y.; Chackalamannil, S.; Korfmacher, W. Direct plasma analysis of drug compounds using monolithic column liquid chromatography and tandem mass spectrometry. Anal. Chem. **2003**, *75*, 1812–1818.
31. Zang, X.; Luo, R.; Song, N.; Chen, T.K.; Bozigian, H. A novel on-line solid phase extraction approach integrated with a monolithic column and tandem mass spectrometry for direct plasma analysis of multiple drugs and metabolites. Rapid Commun. Mass. Spectrom. **2005**, *19*, 3259–3268.
32. Wu, J.-T.; Zeng, H.; Debg, Y.; Unger, S.E. High-speed liquid chromatography/tandem mass spectrometry using a monolithic column for high-throughput bioanalysis. Rapid Commun. Mass Spectrom. **2001**, *15*, 1113–1119.
33. Zhou, S.; Zhou, H.; Larson, M.; Miller, D.L.; Mao, D.; Jiang, X.; Naidong, W. High-throughput biological sample analysis using on-line turbulent flow extraction combined with monolithic liquid chromatography/tandem mass spectrometry. Rapid Commun. Mass Spectrom. **2005**, *19*, 2144–2150.
34. Walker, P.G.; Gordon, S.L.; Bennan, R.X.; Hancock, R.D. A high-throughput monolithic HPLC method for rapid vitamin C phenotyping of berry fruit. Phytochem. Anal. **2006**, *17*, 284–290.
35. Chen, Y.-L.; Junga, H.; Jiang, X.; Naidong, W. Simultaneous determination of theophylline, tolbutamide, mephenytoin, debrisoquin, and dapsone in human plasma using high-speed gradient liquid chromatography/tandem mass spectrometry on a silica-based monolithic column. J. Sep. Sci. **2003**, *26*, 1509–1519.
36. Boges, V.; Yang, E.; Dunn, J.; Henion, J. High-throughput liquid chromatography—tandem mass spectrometry determination of bupropion and its metabolites in human, mouse and rat plasma using a monolithic column. J. Chromatogr. B, **2004**, *804*, 277–287.
37. Zarghi, A.; Shafaati, A.; Foroutan, S.M.; Khoddam, A. Development of a rapid HPLC method for determination of famotidine in human plasma using a monolithic column. J. Pharm. Biomed. Anal. **2005**, *39*, 677–680.

38. Liu, J.; Sun, J.; Zhang, W.; Gao, K.; He, Z. HPLC determination of rifampicin and related compounds in pharmaceuticals using monolithic column. J. Pharm. Biomed. Anal. **2008**, *46*, 405–409.
39. Bones, J.; Macka, M.; Paull, B. Evaluation of monolithic and sub 2 μm particle packed columns for the rapid screening for illicit drugs—Application to the determination of drug contamination on Irish euro banknotes. Analyst **2007**, *132*, 208–217.
40. Lu, M.; Zhang, L.; Feng, Q.; Xia, S.; Chi, Y.; Tong, P.; Chen, G. Pressure-assisted capillary electrochromatography with electrospray ionization–mass spectrometry based on silica-based monolithic column for rapid analysis of narcotics. Electrophoresis **2008**, *29*, 936–943.
41. Wei, F.; Fan, Y.; Zhang, M.; Feng, Y. Poly(methacrylic acid-ethylene glycol dimethacrylate) monolith in-tube solid-phase microextraction applied to simultaneous analysis of some amphetamine derivatives in urine by capillary zone electrophoresis. Electrophoresis **2005**, *26*, 3141–3150.
42. Fan, Y.; Feng, Y.; Da, S.; Shi, Z. Poly(methacrylic acid-ethylene glycol dimethacrylate) monolithic capillary for in-tube solid phase microextraction coupled to high performance liquid chromatography and its application to determination of basic drugs in human serum. Analytica Chimica Acta **2004**, *523*, 251–258.
43. Svec, F. Preparation and HPLC applications of rigid macroporous organic polymer monoliths. J. Sep. Sci. **2004**, *27*, 747–766.
44. Josic, D.; Buchacher, A.; Jungbauer, A. Monoliths as stationary phases for separation of proteins and polynucleotides and anzymatic conversion. J. Chromatogr. B **2001**, *752*, 191–205.
45. Chambers, S.D.; Glenn, K.M.; Lucy, C.A. Development in ion chromatography using monolithic columns. J. Sep. Sci. **2007**, *30*, 1628–1645.
46. Pelletier, S.; Lucy, C.A. Achieving rapid low-pressure ion chromatography separations on short silica-based monolithic columns. J. Chromatogr. A, **2006**, *1118*, 12–18.
47. Zakaria, P.; Hutchinson, J.P.; Avdalovic, N.; Liu, Y.; Haddad, P.R. Latex-coated polymeric monolithic ion-exchange stationary phases. 2. Micro-ion chromatography. Anal. Chem. **2005**, *77*, 417–423.
48. Hutchinson, J.P.; Zakaria, P.; Bowie, A.R.; Macka, M.; Avdalovic, N.; Haddad, P.R. Latex-coated polymeric monolithic ion-exchange stationary phases. 1. Anion-exchange capillary electrochromatography and in-line sample preconcentration in capillary electrophoresis. Anal. Chem. **2005**, *77*, 407–416.
49. Ueki, Y.; Umemura, T.; Li, J.; Odake, T.; Tsunoda, K. Preparation and application of methacrylate-based cation-exchange monolithic columns for capillary ion chromatography. Anal. Chem. **2004**, *76*, 7007–7012.
50. Zhang; J.; Wu, S.; Kim, J.; Karger, B.L. Ultratrace liquid chromatography/mass spectrometry analysis of large peptides with post-translational modifications using narrow-bore poly(styrene-divinylbenzene) monolithic columns and extended range proteomic analysis. J. Chromatogr A, **2007**, *1154*, 295–307.
51. Rucevic, M.; Clifton, J.G.; Huang, F.; Li, X.; Callanan, H.; Hixson, D.C.; Josic, D.J. Chromatogr. A, **2006**, *1123*, 199–204.
52. Hjerten, S.; Nakazato, K.; Mohammad, J.; Eaker, D. Reversed-phase chromatography of proteins and peptides on compressed continuous beds. Chromatographia **1993**, *37*, 287–294.

Biological Fluids: Glucuronides from LC/MS

Adnan A. Kadi
Mohamed M. Hefnawy
Department of Pharmaceutical Chemistry, King Saud University, Riyadh, Saudi Arabia

Abstract
The use of liquid chromatography–mass spectrometry (LC–MS) in the direct analysis and detection of glucuronide conjugates from biological fluids is described. The analysis of labile drug metabolism-conjugated molecules such as glucuronides has traditionally been carried out indirectly by enzymatic hydrolysis and subsequent analysis of the released parent compound. This approach suffered a number of disadvantages, which makes direct analysis desirable. With the advent of softer LC–MS ionization techniques, e.g., electrospray ionization (ESI), direct analysis of conjugated glucuronides has increasingly become possible. A review of recent literature shows various examples of this approach.

INTRODUCTION

Glucuronidation is a major detoxification pathway for many endogenous and exogenous materials, converting them into generally inactive water-soluble molecules, which can be easily excreted through urine. For some compounds, however, glucuronidation may be a bioactivation process that can lead to compounds that are more active than the parent drug, e.g., morphine-6-glucuronide,[1–3] or to compounds that are more toxic, e.g., compounds capable of forming acyl glucuronides[4] such as all *trans*-retinoic acid or valproic acid glucuronides.[5] Glucuronidation is considered the most important phase II metabolism pathway in mammals owing in large part to the abundance of glucuronic acid in the liver and the wide diversity of structurally unrelated compounds that can be the substrates for the reaction. Glucuronidation involves the conjugation of (D)-glucuronic acid, transferred from the endogenous material uridine-5′-diphosphoglucuronic acid (UDPGA), to a xenobiotic molecule with nucleophilic functional groups such as alcohols, phenols, carboxylic acids, amines, imides, activated methylenes, and sulfhydryl groups.[6] The conjugation process is catalyzed by UDP-glucuronosyltransferase (UGT).[7] Compounds with these functional groups give rise to conjugated β-(D)-glucuronides. Although alpha (α) anomers of the glucuronide conjugates can be chemically synthesized, biosynthesized glucuronides are invariably of the beta (β) configuration.

Traditionally, analysis of phase II metabolism conjugates, e.g., glucuronides, was carried out indirectly by first subjecting the glucuronide conjugate to appropriate enzymatic hydrolysis (β-glucuronidase) or acid hydrolysis prior to analyzing the released metabolite. While this method has been in use for a long time, it suffers certain drawbacks. First, the method is time-consuming owing to the needed sample pretreatment and subsequent sample extraction and preparation for analysis. Second, accurate quantitative analysis cannot be achieved because hydrolysis is often incomplete and some conjugated materials may still remain, even after enzymatic or acid hydrolysis. Moreover, contaminants that may be present in the enzymatic hydrolysis mixture might interfere with the identification of the aglycone.[8] Third, in the case of phase II metabolites that are actually clinically active, e.g., morphine glucuronide, it is desirable to have the intact molecule analyzed rather than the hydrolyzed drug. This can aid in the accurate quantification of the active metabolite and therefore gives a better idea about the extent to which it contributes to the parent drug's biological activity. Fourth, it is known that phase II conjugation of some drug molecules gives rise to isomers as a result of the creation of an asymmetric center. Such isomers cannot be distinguished if the traditional enzymatic or acid hydrolysis methods are used to liberate the parent drug prior to analysis. Thus, direct analysis of phase II conjugated molecules presents a clear advantage in its ability to overcome the shortcomings of the traditional methods of analysis. It is important to understand the different methods used in the liquid chromatography–mass spectrometry (LC–MS) analysis of phase II conjugated metabolites along with their respective strengths and/or weaknesses.

LC–MS

LC–MS and, in particular, tandem mass spectrometry (LC–MS/MS) techniques, offer a number of experiments for the determination of conjugated materials such as glucuronides from biological fluids.[9,10] In LC–MS instruments, the typical analyzer used (e.g., quadrupole) analyzes ions that are sampled to the MS vacuum and generates molecular weight information that is, in most cases, limited to the parent ion. In drug metabolism research, where often

the structures of metabolites are unknown, the molecular weight information alone is not sufficient for structural elucidation, and more information about the structure is needed. In tandem mass spectrometry, two analyzers are used instead of a single one. The first analyzer would analyze the ions coming from the MS source; the ions are then passed into a collision chamber where energy is applied to cause fragmentation, and the fragments are passed to the second analyzer where they can be analyzed. This yields more detailed structural information as not only the molecular weight will be known, but the fragmentation pattern of the molecule, which can aid in the overall identification and characterization process of an unknown metabolite, can be determined as well. While the triple quadrupole (QQQ) tandem MS is the most common type, newer instruments are available that combine a quadrupole analyzer with a time-of-flight analyzer for more powerful structural elucidation capabilities. QQQ mass analyzers are the instruments used most often in LC–MS/MS studies of drug metabolism.

With a QQQ instrument it is possible to scan for ions of interest using one of three modes, namely, precursor ion scan, constant neutral loss scan, and product ion scan.[11] These powerful methods can provide a great deal of information about the structure of an unknown metabolite. In the precursor ion scan mode, the metabolite is identified by determining whether it contains a portion of the unaltered parent compound. Thus, one does not need to know the exact structure of the metabolite of interest and only needs some knowledge of the fragmentation pattern of the parent compound. With glucuronide conjugates, this mode can be used by predicting precursor ion fragments of the aglycone. For example, a precursor ion scan for *m*/*z* 166, which is a fragment of the protonated parent molecule epothilone B, enabled the identification of a new metabolite for the drug.[12] In constant neutral loss scans, one looks for an expected loss of a particular molecular weight from a molecule. In the case of conjugated metabolites, such as glucuronides, neutral loss targeted is usually 176 Da, which represents the loss of a glucuronic acid moiety from the parent compound. An example would be a 176 Da loss from the drug entacapone molecule,[13] which indicated the formation of a glucuronide conjugate of the drug. This mode does not require any knowledge of the structure or fragmentation patterns of the parent compound. Unlike the first two methods, which are used for the detection of metabolites, product ion scan is intended for structure characterization. A product ion scan experiment is performed by first selecting a candidate ion to undergo further fragmentation. This information is obtained from previous knowledge of the metabolism pattern of the parent compound, as well as from the above-mentioned precursor ion and neutral loss scans. The candidate ion is subjected to an extra round of fragmentation, where it enters a trap containing an inert gas such as argon. Collision with the gas molecules will induce dissociation of the product ion and, thus, will give rise to fragments that can be detected and analyzed. This results in a series of fragment masses each of which corresponds to a part of the unknown molecule. The analysis of the combined fragmentations can lead to structure elucidation. For example, the methylated metabolite of dobutamine (*m*/*z* 316), containing a characteristic product ion at *m*/*z* 151, was identified using this technique.[14]

Selected reaction monitoring (SRM), sometimes referred to as multiple reaction monitoring (MRM), is a technique that can be utilized in the quantitative determination of drugs and metabolites, e.g., glucuronides, by tandem mass spectrometry from biological matrices. In this technique, a single ion is selected, often representing the parent compound, and the fragmentation of this ion to another known ion is monitored. This transition from parent to daughter ion is unique to every compound under the experimental conditions used and can be used for quantitatively determining any compound in the analyzed matrix. The tandem MS approach is a valuable technique for the analysis and identification of drug metabolites, e.g., glucuronides.

Scientific publications documenting the use of LC–MS for the direct analysis of glucuronide conjugates have become abundant in recent years. In the last decade or so, over 100 papers have been published on the subject. In most of the studies it has been emphasized that glucuronide conjugates are being detected directly using LC–MS techniques without the need for extensive sample preparation or hydrolysis of the conjugated compound prior to determining the unconjugated precursor. Selected xenobiotic compounds for which LC–MS studies were conducted for the analysis of glucuronide conjugates are shown in Table 1. This includes therapeutic agents, investigative drugs, and a host of other xenobiotics. The *O*-glucuronide conjugates were the most commonly analyzed, which is consistent with *O*-glucuronides being the most commonly formed glucuronide conjugates. Among the *O*-glucuronides analyzed, the majority were phenolic glucuronides, followed by acyl and hydroxy glucuronides. The *N*-glucuronides studied were formed from aromatic and aliphatic amines. Based on the diversity of the glucuronide conjugates analyzed in the reviewed literature, it is possible to conclude that LC–MS analysis can be effectively conducted for a wide spectrum of glucuronidated xenobiotics with good sensitivity and reproducibility.

CITED EXAMPLES

The LC–MS analyses documented in the reviewed literature include both in vivo and in vitro studies. In in vivo studies, conditions represented various biological matrices including plasma, urine, bile, and feces. In vitro studies, LC–MS analyses were conducted for glucuronides obtained using recombinant UGT,[21,46] liver microsomes,[28] brain microsomes,[47] hepatocytes,[24] and liver slices.[48] In most of the experiments, electrospray ionization–MS (ESI–MS) was the ionization

Table 1 Selected compounds of which glucuronide conjugates have been analyzed by LC–MS.

Xenobiotic compound	LC–MS ionization interface	Type of glucuronide	Refs.
Entacapone	APCI, ESI, APPI	*O*-glucuronides	[14]
Dobutamine	APCI, ESI, APPI	*O*- and *N*-glucuronides	[14]
Estriol	ESI	*O*-glucuronides	[15]
Apomorphine	APCI, ESI, APPI	*O*-glucuronide	[14]
Retigabine	ESI	*N*-glucuronides	[16]
N-(3,5-dichlorophenyl)succinimide	ESI	*O*-glucuronide	[17]
Olanzapine	ESI	*N*-glucuronide	[18]
Testosterone	ESI	*O*-glucuronide	[19]
Citalopram	ESI	*Acyl*- and *N*-glucuronides	[20]
AZT	ESI	*O*-glucuronide	[21]
Propranolol	ESI	*O*-glucuronide	[22]
Nandrolone	ESI	*O*-glucuronides	[23]
Leukotriene B4	ESI	*O*-glucuronide	[24]
cis- and *trans*-Resveratrol	ESI	*O*-glucuronide	[25]
Kaempferol	ESI	*O*-glucuronide	[26]
Quercetin	ESI	*O*-glucuronide	[27]
Luteolin	ESI	*O*-glucuronide	[27]
1-Hydroxypyrene	ESI	*O*-glucuronide	[28]
5,6-Dimethylxanthenone-4-acetic acid (DMXAA)	ESI, APCI	*Acyl*-glucuronide	[29]
Ketobemidone	ESI	*O*-glucuronide	[30]
2,4-Dienevalproic acid	ESI	*Acyl*-glucuronide	[31]
Desmethylnaproxen	ESI	*Acyl*- and *O*-glucuronides	[32]
2-Phenylpropionic acid	ESI	*Acyl*-glucuronide	[33]
Styrene	ESI	*O*-glucuronide	[34]
Phenytoin	ESI	*O*-glucuronide	[35]
7-Ethoxycoumarin	ESI	*O*-glucuronide	[36]
Oleuropein	ESI	*O*-glucuronide	[37]
Acetaminophen	APCI	*O*-glucuronide	[38]
Etoposide	ESI	*O*-glucuronide	[39]
11-nor-Δ(9)-Carboxy-tetrahydrocannabinol	ESI	*Acyl*-glucuronide	[40]
1-Bromopropane	ESI	*O*-glucuronide	[41]
KR-32570	ESI	*O*-glucuronide	[42]
JNJ-10198409	ESI	*N*-glucuronide	[43]
Muraglitazar	ESI	*O*-glucuronide	[44]
Ezetimibe	APCI	*O*-glucuronide	[45]

interface of choice for the analysis of conjugated glucuronides. Although the choice of the LC–MS interface is governed by the nature of the analyte, various studies have documented the preference for ESI over atmospheric pressure chemical ionization (APCI) for the analysis of polar, non-volatile, and thermolabile molecules such as glucuronide conjugates. This is mainly because of the milder ionization conditions employed by ESI in comparison with APCI. APCI experiments are carried out at temperatures that can be high enough to cause the decomposition of molecules having easily cleavable bonds such as sugar and sulfate conjugates. This results in a decrease in the concentrations of the intact analyte available for detection and, consequently, decreased sensitivity of the method. Nevertheless, APCI modes can be successfully used for the analysis of glucuronide conjugates. Some studies have reported that negative-ion modes are better suited for the analysis of polar anionic species such as glucuronide and sulfate conjugates. It has been observed that negative-ion mode is the most commonly used one for ionization in both ESI and APCI.

Mobile-phase additives are known to play an important role in the efficient separation of chromatographic peaks in LC–MS. Mobile-phase additives used for LC–MS studies are most often volatile molecules that can be easily evaporated in the LC–MS interface to prevent ionization suppression and/or detection contamination. The most commonly used mobile-phase additives in LC–MS analysis are the small organic acids, acetic and formic acids, together with their ammonium salts. Trifluoroacetic acid (TFA) is also widely used in LC–MS analysis despite reports of ionization suppression in the ESI mode. Some studies suggest that the drawback of TFA use can be overcome for some neutral analytes by using minute concentrations of the acid in the mobile phase.[49] A number of studies presented here used TFA as the mobile-phase additive, and in all those instances, ESI was the ionization interface. However, formic acid was the additive most commonly used, followed closely by TFA and then by the ammonium salts of both formic and acetic acid. The type of glucuronide conjugate (*O* vs. *N*) did not appear to influence the type of mobile-phase additive used.

Novel applications of LC–MS methodologies in the analysis of glucuronide conjugates of some drugs have been documented. The 4-vinylphenol glucuronide conjugate of styrene has been recognized as a metabolite of styrene; however, it had never been determined as the intact glucuronide until Manini et al.[34] reported the direct determination of this glucuronide conjugate as the intact glucuronide by LC–MS. Ohta et al.[38] reported the use of an LC–APCI–MS method for the determination of acetaminophen glucuronide; however, the authors encountered difficulty in the direct ionization of the glucuronide. Therefore, derivatization of the carboxyl group to the methyl ester was necessary to obtain satisfactory ionization. Skopp and Potsch[40] looked at the stability over time and at various temperatures of 11-nor-Δ9-carboxy-tetrahydrocannabinol glucuronide in plasma and urine by direct LC–MS/MS analysis of the conjugate. Liu et al.[50] used a novel approach for the elucidation of the structure of a carbamoyl-linked glucuronide conjugate of an investigational compound with the help of online hydrogen/deuterium exchange in LC–MS/MS. This was possible by the use of deuterium oxide (D_2O), instead of water, as a mobile-phase component to facilitate structure elucidation carried out with LC–MS techniques. The actual structure of the investigational compound was not revealed by the author, but was given the general representation outlined in Fig. 1. The amine group in the compound carries two exchangeable hydrogen atoms and the glucuronic acid moiety contains four exchangeable hydrogen atoms. Upon formation of a carbamoyl of the amine group followed by phase II conjugation with glucuronic acid, the total number of exchangeable hydrogen atoms was 4, and the conjugate showed a protonated molecular ion peak of *m/z* 429 as opposed to the ion peak at *m/z* 423 that results when water is used instead of deuterium oxide. The authors concluded that this experiment coupled with tandem mass spectrometry could be a very useful tool to facilitate identification of glucuronides and other metabolic products.

Dalgaard and Larsen[20] investigated the formation of glucuronide conjugates of citalopram, a potent selective serotonin uptake inhibitor. The acyl and quaternary ammonium glucuronides of citalopram, which had been previously unreported, were successfully detected in positive-ion ESI. The authors allude to the fact that acyl glucuronides are difficult to analyze under conventional enzymatic hydrolysis methods owing to their instability, and that using LC–MS techniques, these types of glucuronides can be detected. Although determining the site of glucuronidation is not possible based on LC–MS studies alone, Cui and Harvison[17] reported that LC–MS, when coupled with chemical derivatization, could be used for determining the site of glucuronidation within a xenobiotic compound. The authors described a novel glucuronide conjugate of a metabolite of the nephrotoxicant *N*-(3,5-dichlorophenyl)succinimide. The metabolite, *N*-(3,5-dichlorophenyl)-2-hydroxysuccinamic acid (NDPSA),

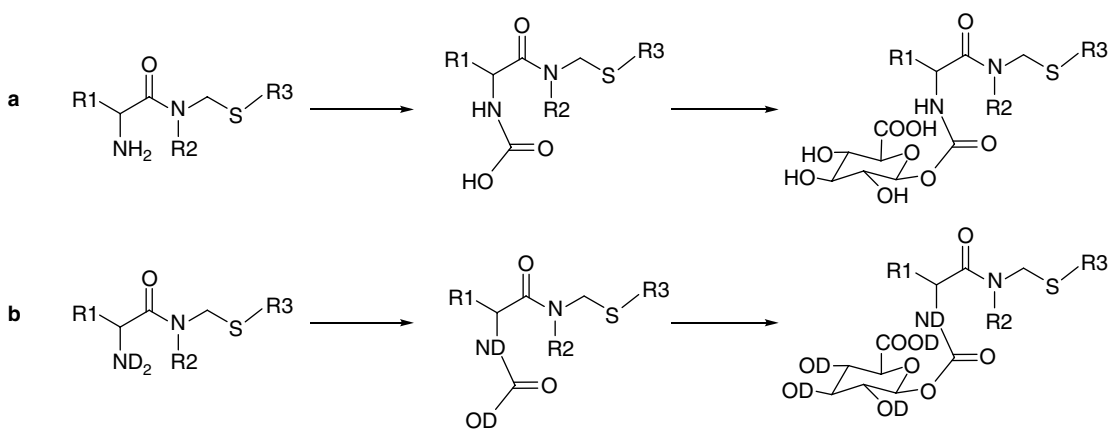

Fig. 1 Structures of the carbamoyl metabolites and their glucuronides (a) using water as a mobile-phase component and (b) using deuterium oxide as a mobile-phase component.

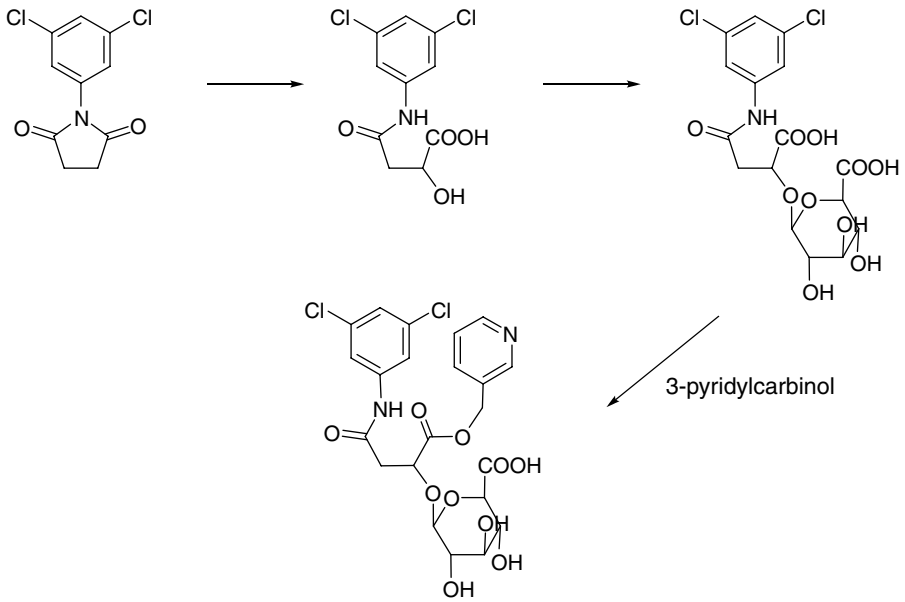

Fig. 2 Derivatization of *N*(3,5-dichlorophenyl)-2-hydroxysuccinamic acid metabolite.

contained two possible sites for glucuronidation, namely, an aliphatic hydroxy group and a carboxylic acid moiety. To determine which site was glucuronidated, the authors derivatized the glucuronide conjugate with 3-pyridylcarbinol. Based on molecular ion peaks obtained from positive-ion ESI studies of the derivatized compound, the authors were able to determine that glucuronidation indeed took place at the alcoholic hydroxyl group, rather than at the carboxylic acid group (Fig. 2).

More recently, LC–MS has been used to analyze glucuronic acid conjugates of the industrial chemical 1-bromopropane from plasma and urine of rats and mice after inhalation and intravenous injection.[41] The method demonstrates the sensitivity of LC–MS when applied to the analysis of glucuronic acid conjugates. Lin, Lee, and Chuang[51] reported on a method using positive-ion LC–ESI–MS for the analysis of the Chinese medicinal preparation Gan-Lu-Yin. Two of the components analyzed were glucuronic acid conjugates, namely oroxylin A-7-*O*-glucuronide and wogonin-7-*O*-glucuronide. The method was sensitive and accurate enough to detect the glucuronic acid conjugates, with no need for hydrolysis. Glucuronic acid-conjugated metabolites of a new Na^+/H^+ reversible-exchange inhibitor, [5-(2-methoxy-5-chlorophenyl)furan-2-ylcarbonyl]guanidine, for the treatment of ischemia have been recently analyzed by Kim et al.[42] The metabolites were formed from human liver microsomes on incubation with UDPGA and nicotinamide adenine dinucleotide phosphate (NADPH).

CONCLUSION

LC–MS techniques have been shown to be very useful for the direct analysis of glucuronide conjugates of xenobiotic molecules in biological fluids, as well as in in vitro metabolism studies. As new techniques are developed and tested, especially in the fields of sample introduction, chromatography front end, and the amount of liquid introduced into the MS analyzer, and as the volume of literature available describing the use of LC–MS grows rapidly, it will not be surprising if LC–MS procedures assume a leading place, or be the method of choice, in the analysis of glucuronic acid and other phase II conjugated metabolites of xenobiotics.

REFERENCES

1. Morland, J.; Jones, B.L.; Palomares, M.L.; Alkana, R.L. Morphine-6-glucuronide: A potent stimulator of locomotor activity in mice. Life Sci. **1994**, *55*, L163–L168.
2. Osborne, R.; Thompson, P.; Joel, S.; Trew, D.; Patel, N.; Slevin, M. The analgesic activity of morphine-6-glucuronide. Brit. J. Clin. Pharmacol. **1992,** *34*, 130–138.
3. Osborne, R.; Joel, S.; Trew, D.; Slevin, M. Analgesic activity of morphine-6-glucuronide. Lancet **1988**, *1*, 828.
4. Bailey, M.J.; Dickinson, R.G. Acyl glucuronide reactivity in perspective: Biological consequences. Chem. Biol. Interact. **2003**, *145*, 117–137.
5. Ritter, J.K. Roles of glucuronidation and UDP-glucuronosyltransferases in xenobiotic bioactivation reactions. Chem. Biol. Interact. **2000**, *129*, 171–193.
6. Radominska-Pandya, A.; Czernik, P.J.; Little, J.M.; Battaglia, E.; Mackenzie, P.I. Structural and functional studies of UDP-glucuronosyltransferases. Drug Metab. Rev. **1999**, *31*, 817–899.
7. King, C.D.; Rios, G.R.; Green, M.D.; Tephly, T.R. UDP-glucuronosyltransferases. Curr. Drug Metab. **2000**, *1*, 143–161.
8. Bowers, L.D. Direct measurement of steroid sulfate and glucuronide conjugates with high-performance liquid

chromatography–mass spectrometry. J. Chromatogr. B. Biomed. Appl. **1996**, *687*, 61–68.
9. Gao, S.; Zhang, Z.P.; Karnes, H.T. Sensitivity enhancement in liquid chromatography/atmospheric pressure ionization mass spectrometry using derivatization and mobile phase additives. J. Chromatogr. B. Analyt. Technol. Biomed. Life Sci. **2005**, *825*, 98–110.
10. Kostiainen, R.; Kotiaho. T.; Kuuranne. T.; Auriola, S. Liquid chromatography/atmospheric pressure ionization–mass spectrometry in drug metabolism studies. J. Mass Spectrom. **2003**, *38*, 357–372.
11. Schwartz, J.C.; Wade, A.P.; Enke, C.G.; Cooks, R.G. Systematic delineation of scan modes in multidimensional mass spectrometry. Anal. Chem. **1990**, *62*, 1809–1818.
12. Blum, W.; Aichholz, R.; Ramstein, P.; Kuhnol, J.; Bruggen, J.; O'Reilly, T.; Florsheimer, A. In vivo metabolism of epothilone B in tumor-bearing nude mice: Identification of three new epothilone B metabolites by capillary high-pressure liquid chromatography/mass spectrometry/tandem mass spectrometry. Rapid Commun. Mass Spectrom. **2001**, *15*, 41–49.
13. Keski-Hynnila, H.; Luukkanen, L.; Taskinen, J.; Kostiainen, R. Mass spectrometric and tandem mass spectrometric behavior of nitrocatechol glucuronides: A comparison of atmospheric pressure chemical ionization and electrospray ionization. J. Am. Soc. Mass Spectrom. **1999**, *10*, 537–545.
14. Keski-Hynnila, H.; Kurkela, M.; Elovaara, E.; Antonio, L.; Magdalou, J.; Luukkanen, L.; Taskinen, J.; Kostiainen, R. Comparison of electrospray, atmospheric pressure chemical ionization, and atmospheric pressure photoionization in the identification of apomorphine, dobutamine, and entacapone phase II metabolites in biological samples. Anal. Chem. **2002**, *74*, 3449–3457.
15. Yang, Y.J.; Lee, J.; Choi, M.H.; Chung, B.C. Direct determination of estriol 3- and 16-glucuronides in pregnancy urine by column-switching liquid chromatography with electrospray tandem mass spectrometry. Biomed. Chromatogr. **2003**, *17*, 219–225.
16. McNeilly, P.J.; Torchin, C.D.; Anderson, L.W.; Kapetanovic, I.M.; Kupferberg, H.J.; Strong, J.M. In vitro glucuronidation of D-23129, a new anticonvulsant, by human liver microsomes and liver slices. Xenobiotica **1997**, *27*, 431–441.
17. Cui, D.; Harvison, P.J. Determination of the site of glucuronidation in an *N*-(3,5-dichlorophenyl)succinimide metabolite by electrospray ionization tandem mass spectrometry following derivatization to picolinyl esters. Rapid Commun. Mass Spectrom. **2000**, *14*, 1985–1990.
18. Kassahun, K.; Mattiuz, E.; Nyhart, , Jr. E.; Obermeyer, B.; Gillespie, T.; Murphy, A.; Goodwin, R.M.; Tupper, D.; Callaghan, J.T.; Lemberger, L. Disposition and biotransformation of the antipsychotic agent olanzapine in humans. Drug Metab. Dispos. **1997**, *25*, 81–93.
19. Kuuranne, T.; Vahermo, M.; Leinonen, A.; Kostianen, R. Electrospray and atmospheric pressure chemical ionization tandem mass spectrometric behavior of eight anabolic steroid glucuronides. J. Am. Soc. Mass Spectrom. **2000**, *11*, 722–730.
20. Dalgaard, L.; Larsen, C. Metabolism and excretion of citalopram in man: Identification of *O*-acyl- and *N*-glucuronides. Xenobiotica **1999**, *29*, 1033–1041.
21. Barbier, O.; Turgeon, D.; Girard, C.; Green, M.D.; Tephly, T.R.; Hum, D.W.; Belanger, A. 3′-Azido-3′-deoxythimidine (AZT) is glucuronidated by human UDP-glucuronosyltransferase 2B7 (UGT2B7). Drug Metab. Dispos. **2000**, *28*, 497–502.
22. Beaudry, F.; Yves Le Blanc, J.C.; Coutu, M.; Ramier, I.; Moreau, J.P.; Brown, N.K. Metabolite profiling study of propranolol in rat using LC/MS/MS analysis. Biomed. Chromatogr. **1999**, *13*, 363–369.
23. Kuuranne, T.; Aitio, O.; Vahermo, M.; Elovaara, E.; Kostiainen, R. Enzyme-assisted synthesis and structure characterization of glucuronide conjugates of methyltestosterone (17 alpha-methylandrost-4-en-17 beta-ol-3-one) and nandrolone (estr-4-en-17 beta-ol-3-one) metabolites. Bioconjug. Chem. **2002**, *13*, 194–199.
24. Wheelan, P.; Hankin, J.A.; Bilir. B.; Guenette. D.; Murphy, R.C. Metabolic transformations of leukotriene B4 in primary cultures of human hepatocytes. J. Pharmacol. Exp. Ther. **1999**, *288*, 326–334.
25. Aumont, V.; Krisa, S.; Battaglia, E.; Netter, P.; Richard, T.; Merillon, J.M.; Magdalou, J.; Sabolovic, N. Regioselective and stereospecific glucuronidation of *trans*- and *cis*-resveratrol in human. Arch. Biochem. Biophys. **2001**, *393*, 281–289.
26. Oliveira, E.J.; Watson, D.G. In vitro glucuronidation of kaempferol and quercetin by human UGT-1A9 microsomes. FEBS Lett. **2000**, *471*, 1–6.
27. Boersma, M.G.; van der, W.H.; Bogaards, J.; Boeren, S.; Vervoort, J.; Cnubben, N.H.; van Iersel, M.L.; Bladeren, P.J.; Rietjens, I.M. Regioselectivity of phase II metabolism of luteolin and quercetin by UDP-glucuronosyl transferases. Chem. Res. Toxicol. **2002**, *15*, 662–670.
28. Luukkanen, L.; Mikkola, J.; Forsman, T.; Taavitsainen, P.; Taskinen, J.; Elovaara, E. Glucuronidation of 1-hydroxypyrene by human liver microsomes and human UDP-glucuronosyltransferases UGT1A6, UGT1A7, and UGT1A9: Development of a high-sensitivity glucuronidation assay for human tissue. Drug Metab. Dispos. **2001**, *29*, 1096–1101.
29. Zhou, S.F.; Paxton, J.W.; Tingle, M.D.; Kestell, P.K.; Jameson, M.B.; Thompson, P.I.; Baguley, B.C. Identification and reactivity of the major metabolite (beta-1-glucuronide) of the anti-tumour agent 5,6-dimethylxanthenone-4-acetic acid (DMXAA) in humans. Xenobiotica **2001**, *31*, 277–293.
30. Sundstrom, I.; Bondesson, U.; Hedeland, M. Identification of phase I and phase II metabolites of ketobemidone in patient urine using liquid chromatography-electrospray tandem mass spectrometry. J. Chromatogr. B. Biomed. Sci. Appl. **2001**, *763*, 121–131.
31. Tang, W.; Abbott, F.S. Bioactivation of a toxic metabolite of valproic acid, (E)-2-propyl-2,4-pentadienoic acid, via glucuronidation. *LC/MS/MS characterization of the GSH-glucuronide diconjugates*. Chem. Res. Toxicol. **1996**, *9*, 517–526.
32. Jaggi, R.; Addison, R.S.; King, A.R.; Suthers, B.D.; Dickinson, R.G. Conjugation of desmethylnaproxen in the rat—A novel acyl glucuronide-sulfate diconjugate as a major biliary metabolite. Drug Metab. Dispos. **2002**, *30*, 161–166.
33. Li, C.; Benet, L.Z.; Grillo, M.P. Studies on the chemical reactivity of 2-phenylpropionic acid 1-*O*-acyl glucuronide

and *S*-acyl-CoA thioester metabolites. Chem. Res. Toxicol. **2002**, *15*, 1309–1317.
34. Manini, P.; Andreoli, R.; Poli, D.; De Palma, G.; Mutti, A.; Niessen, W.M. Liquid chromatography/electrospray tandem mass spectrometry characterization of styrene metabolism in man and in rat. Rapid Commun. Mass Spectrom. **2002**, *16*, 2239–2248.
35. Nakajima, M.; Sakata, N.; Ohashi, N.; Kume, T.; Yokoi, T. Involvement of multiple UDP-glucuronosyltransferase 1A isoforms in glucuronidation of 5-(4′-hydroxyphenyl)-5-phenylhydantoin in human liver microsomes. Drug Metab. Dispos. **2002**, *30*, 1250–1256.
36. Fisher, M.B.; Jackson, D.; Kaerner, A.; Wrighton, S.A.; Borel, A.G. Characterization by liquid chromatography–nuclear magnetic resonance spectroscopy and liquid chromatography–mass spectrometry of two coupled oxidative-conjugative metabolic pathways for 7-ethoxycoumarin in human liver microsomes treated with alamethicin. Drug Metab. Dispos. **2002**, *30*, 270–275.
37. Del Boccio, P.; Di Deo, A.; De Curtis, A.; Celli, N.; Iacoviello, L.; Rotilio, D. Liquid chromatography–tandem mass spectrometry analysis of oleuropein and its metabolite hydroxytyrosol in rat plasma and urine after oral administration. J. Chromatogr. B. Analyt. Technol. Biomed. Life Sci. **2003**, *785*, 47–56.
38. Ohta, M.; Kawakami, N.; Yamato, S.; Shimada, K. Analysis of acetaminophen glucuronide conjugate accompanied by adduct ion production by liquid chromatography-atmospheric pressure chemical ionization–mass spectrometry. J. Pharm. Biomed. Anal. **2003**, *30*, 1759–1764.
39. Watanabe, Y.; Nakajima, M.; Ohashi, N.; Kume, T.; Yokoi, T. Glucuronidation of etoposide in human liver microsomes is specifically catalyzed by UDP-glucuronosyltransferase 1A1. Drug Metab. Dispos. **2003**, *31*, 589–595.
40. Skopp, G.; Potsch, L. Stability of 11-nor-delta(9)-carboxy-tetrahydrocannabinol glucuronide in plasma and urine assessed by liquid chromatography–tandem mass spectrometry. Clin. Chem. **2002**, *48*, 301–306.
41. Garner, C.E.; Sumner, S.C.; Davis, J.G.; Burgess, J.P.; Yueh, Y.; Demeter, J.; Zhan, Q. Valentine, J.; Jeffcoat, A.R.; Burka, L.T.; Mathews, J.M. Metabolism and disposition of 1-bromopropane in rats and mice following inhalation or intravenous administration. Toxicol. Appl. Pharmacol. **2006**, *215* (1), 23–36.
42. Kim, H.; Kang, S.; Kim, H.; Yoon, Y.J.; Cha, E.Y.; Lee, H.S.; Kim, J.H.; Yea, S.S.; Lee, S.S.; Shin, J.G.; Liu, K.H. In vitro metabolism of a new cardioprotective agent, KR-32570, in human liver microsomes. Rapid Commun. Mass Spectrom. **2006**, *20*, 837–843.
43. Yan, Z.; Caldwell, G.W.; Gauthier, D.; Leo, G.C.; Mei, J.; Chih, H.Y.; Jones, W.J.; Masucci, J.A.; Tuman, R.W.; Galemmo, R.J.; Johnson, D.L. *N*-Glucuronidation of the PDGF receptor tyrosine kinase inhibitor 6,7-(dimethoxy-2,4-dihydroindeno[1,2-c]pyrazol-3-yl)-(3-fluoro-phenyl)-amine by Human UDP-glucuronosyltransferases. Drug Metab. Dispos. **2006**, *34* (11), 1880–1886.
44. Zhang, D.; Zhang, H.; Aranibar, A.; Hanson, R.; Huang, Y.; Cheng, P.T.; Wu, S.; Bonacorsi, S.; Zhu, M.; Swaminathan, A.; Humphreys, W.G. Structural elucidation of human oxidative metabolites of muraglitazar: Use of microbial bioreactors in the biosynthesis of metabolite standards. Drug Metab. Dispos. **2006**, *34*, 267–280.
45. Oswald, S.; Scheuch, E.; Cascorbi, I.; Siegmund, W. A LC–MS/MS method to quantify the novel cholesterol-lowering drug ezetimibe in human serum, urine and feces in healthy subjects genotyped for SLCO1B1. J. Chromatogr. B. Analyt. Technol. Biomed. Life Sci. **2006**, *830*, 143–150.
46. Doerge, D.R.; Chang, H.C.; Churchwell, M.I.; Holder, C.L. Analysis of soy isoflavone conjugation in vitro and in human blood using liquid chromatography–mass spectrometry. Drug Metab. Dispos. **2000**, *28*, 298–307.
47. El Bacha, R.S.; Leclerc, S.; Netter, P.; Magdalou, J.; Minn, A. Glucuronidation of apomorphine. Life Sci. **2000**, *67*, 1735–1745.
48. Swart, P.J.; Oelen, W.E.; Bruins, A.P.; Tepper, P.G.; de Zeeuw, R.A. Determination of the dopamine D2 agonist N-0923 and its major metabolites in perfused rat livers by HPLC-UV-atmospheric pressure ionization mass spectrometry. J. Anal. Toxicol. **1994**, *18*, 71–77.
49. Marwah, A.; Marwah, P.; Lardy, H. Analysis of ergosteroids. VIII: enhancement of signal response of neutral steroidal compounds in liquid chromatographic-electrospray ionization mass spectrometric analysis by mobile phase additives. J. Chromatogr. A, **2002**, *964*, 137–151.
50. Liu, D.Q.; Hop, C.E.; Beconi, M.G.; Mao, A.; Chiu, S.H. Use of on-line hydrogen/deuterium exchange to facilitate metabolite identification. Rapid Commun. Mass Spectrom. **2001**, *15*, 1832–1839.
51. Lin, I.H.; Lee, M.C.; Chuang, W.C. Application of LC/MS and ICP/MS for establishing the fingerprint spectrum of the traditional Chinese medicinal preparation Gan-Lu-Yin. J. Sep. Sci. **2006**, *29*, 172–179.

Biological Fluids: Micro-Bore Column-Switching HPLC Determination of Drugs

Eunmi Ban
Research Institute of Pharmaceutical Sciences, Seoul National University, Seoul, South Korea

Chong-Kook Kim
Research Institute of Pharmaceutical Sciences, Seoul National University, Seoul, and Department of Pharmaceutical Engineering, Inje University, Gyeongnam, Korea

Abstract
As pharmaceutical and clinical industries are developing, various sensitive and simple analytical methods have been developed for the analysis of drugs and metabolites including endogenous compounds in biological fluids. Among these developing methods, column switching system has been mainly used to obtain a more simple pretreatment step and a more sensitive result. Column switching system can be used for determent analytes in complex biological matrix by direct injection of biological fluids or by only simple sample treatment such as a filtration step. Specially, large volume injection of sample is possible without any interference and results in significant increase of sensitivity when column switching system is connected to a microbore column. Therefore, column switching system with microbore column is applied to various analytical systems such as HPLC and mass spectrometry for the analysis of trace compounds in biological fluids. In this entry, the application of column switching system with microbore column for sample cleanup and sample enrichment for the analysis of trace compounds in various biological fluids is presented.

INTRODUCTION

High-performance liquid chromatography (HPLC) has advanced to become one of the most widely used analytical techniques since its commercial introduction in 1968. The significance of HPLC arises from its rapid resolving power and applicability to a wide range of sample types. In pharmaceutical and clinical study, HPLC is one of the most important techniques for the separation and determination of drugs and their metabolites in body fluids. Specially, the use of HPLC with mass spectrometry (MS) instead of UV and fluorescence as a detector is significantly increasing for the analysis of substances in biological matrices (plasma, blood, urine, and tissue). However, the analysis of drugs and their metabolites or endogenous compounds in biological fluids by HPLC regardless of the kind of detector is usually laborious, because of the large number of substances present; moreover, the compounds of interest are often present at low concentrations in the samples. Therefore, to improve the sensitivity and specificity, both sample pretreatment and enrichment of the investigated compounds are carried out using sample preparation step and microbore column. Between these things, sample pretreatment is the most common method to obtain high specificity and sensitivity in bioanalytical area. In general, the selective separation and concentration of compounds for biological matrix can be achieved using procedures such as liquid–liquid extraction, liquid–solid extraction, centrifugation, precipitation, and derivatization. These sample pretreatment steps are time-consuming and often result in poor recovery and reproducibility, despite the speed and accuracy of HPLC analytical techniques. Another approach to obtain more high sensitivity and resolution is the use of microbore analytical column with smaller inner diameter instead of the conventional column. Microbore column has inner diameters ranging from 1.0 to 2.1 mm and they offer some significant advantages over conventional columns. First, the use of microbore column has potential for considerable saving in mobile-phase consumption. Second, the sensitivity has 5–21 times higher value than that obtained by conventional column. Fig. 1 shows that the detection response of the microbore increases approximately twentyfold that of an analytical column with the same mass load on both a conventional analytical column (4.6 mm i.d.) and a microbore column (1.0 mm i.d.). In addition to these advantages, microbore columns are attractive for trace analysis where sample quantities may be limited, and where conventional detector system that can accommodate only small volumes of column eluent would be useful. In HPLC–MS system, flow rates of 5–10 and 50–200 μl min^{-1} were generally applied with electrospray ionization (ESI)

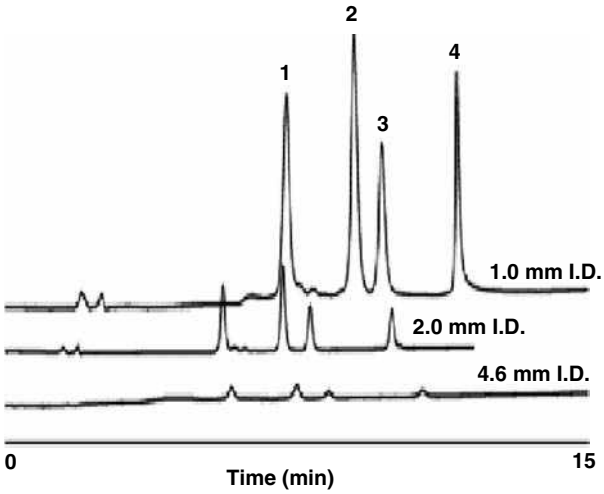

Fig. 1 Separation of peptides on RP-C_{18} column of various inner diameters.

and pneumatically assisted ESI techniques, respectively.[1] As a result, the use of narrow or microbore column is common in HPLC–MS. However, microbore column has a disadvantage that the concentration sensitivity is no higher than that of conventional column because of the limited injection volume. Therefore, a solution for the problems of these microbore column and pretreatment steps is needed and column-switching devices are well suited to such problems.

COLUMN-SWITCHING HPLC WITH MICROBORE COLUMN

The term column switching in liquid chromatography is used if two or more columns are connected to form a network. Column switching is a technique that changes the direction of flow of the mobile phase by valves, so the effluent from a primary column passes to a secondary column for a defined period of time as illustrated in Fig. 2. The objectives of column switching are to increase the chromatographic resolution and selectivity, to enrich trace amounts of sample, to protect sensitive detectors such as electrochemical detectors from contamination by coextractives, to prevent destabilization of the chromatographic equilibrium of the column by coextractives, and to achieve further objectives or a combination of

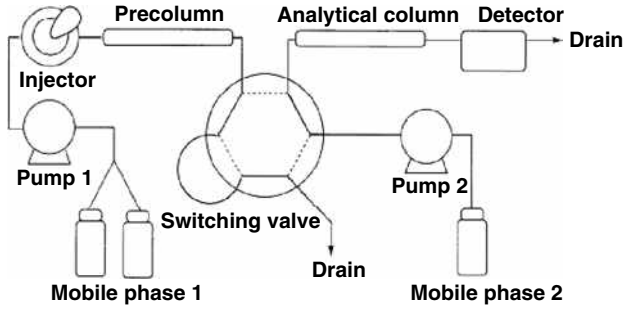

Fig. 2 A schematic diagram of a column-switching system.

several objectives within one chromatographic network. Integration of HPLC with column switching has led to the quantification of a number of compounds. This system has some advantages for the determination of drugs in biological fluids. First, this system can minimize the use of sample and the loss of sample by sample pretreatment. Second, for detection specificity, little or no baseline interference is observed because the cleanup is excellent. Third, analytical column can be used for thousands of injections. Fourth, drug recoveries in excess of 95% are often observed with high reproducibility without using an internal standard. These results indicate that it is possible to have a high-throughput analysis in clinical and pharmaceutical areas. This technology has been successfully applied to the analysis of various drugs in biological fluids using various detectors such as MS, UV, and fluorescence. Especially, in recent years, the use of column switching has been reported to be very useful in conjunction with MS detectors. In the column-switching system, switching valves are used to remove aqueous eluents used in the cleanup and separation steps. After that, the trapped analytes are eluted in a suitable solvent for HPLC–MS,[2, 3] HPLC–UV, or fluorescence. In addition, the fully automated HPLC system with precolumn sample enrichment is always not needed for additional standard compounds. Yeon et al.[4] achieved accurate and precise analysis of cilostazol in plasma without any pretreatment and internal standard.

An example of the separation steps by a column-switching system is explained:[5] in order to determine the switching time, first, a biological sample containing methamphetamine (MA) was injected on a precolumn and detected using the primary mobile phase, as illustrated in Fig. 3A, and then the time program for the column-switching system was set up as given in Table 1. Two columns containing packings with

Table 1 Time schedule of column switching for the analysis of methamphetamine (MA) enantiomers in urine.

Time after injection (min)	Switching valve position	Precolumn	Analytical column
0.0–4.0	1	Sample loading and cleanup	(Re)conditioning
4.0–6.0	2	Analytes transfer	Analytes transfer, separation
6.0–24	1	Reconditioning, next injection	Separation

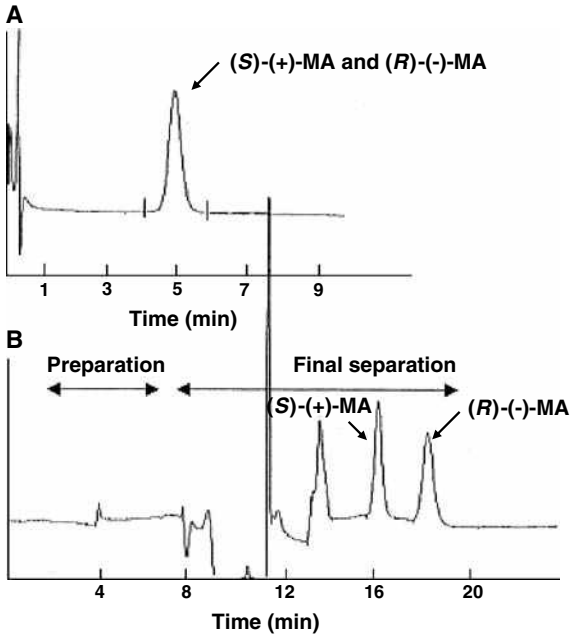

Fig. 3 Profile of separation methamphetamine enantiomer (A) in precolumn and (B) analytical column.

different column selectivities are connected in series through a six-port valve and these columns were controlled according to the time program. At position 1 of the switching valve, the primary mobile phase flushes impurities and analytes with weak retention from the precolumn. After rotating the switching valve into position 2, the secondary mobile phase with a higher elution power than the primary mobile phase elutes the analytes from the precolumn onto the analytical column. After the transfer of analytes is completed, the valve is rotated back. The analytes are separated at the secondary mobile phase and analytical column. At the same time, the primary column is reconditioned with the primary mobile phase. Fig. 3B shows typical chromatograms of plasma sample processed using column-switching system. Fig. 4 shows the reaction of the sample and mobile phase according to the time program.

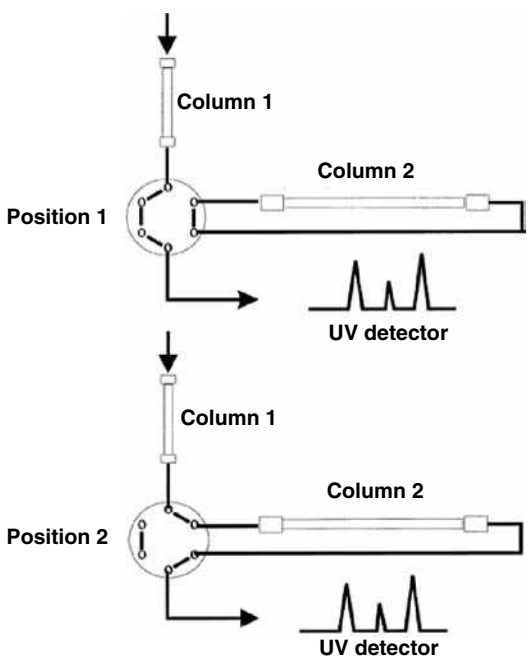

Fig. 4 A change of mobile phase and sample flow according to the valve position in the column-switching system.

COLUMN-SWITCHING HPLC SYSTEM CONFIGURATION

In order to determine optimal analysis condition for the analysis of drugs in biological fluids using column-switching HPLC system, the choice of separation media is critical to effective analysis of analytes in biological fluids. Precolumn and mobile phases are an important separation media to achieve cleanup and preconcentration in column-switching HPLC system. In most cases, short precolumns are preferable because the duration of the flushing needed to remove undesirable matrix components is minimized. And particle sizes in the 10–40 μm range provide suitable stability and loading capacity, for the majority of the applications. Peak compression can be best obtained if the analytes are introduced into a precolumn in a solvent with low elution strength.

APPLICATIONS OF COLUMN-SWITCHING HPLC WITH MICROBORE COLUMN

There have been thousands of articles published on the application of column-switching HPLC method. Today, column-switching HPLC method is being used around the world in all areas of chemistry, environmental problem solving, medical research, and so forth. In clinical and pharmaceutical analysis, column switching has been mainly applied to online sample cleanup and trace enrichment using microbore analytical column. Examples of column-switching HPLC method not discussed in any detail are presented in Table 2.

Sample Cleanup

Probably the most important application of column switching is sample cleanup, which is based on the use of multicolumn chromatography and can induce an increase in selectivity. The principle of column switching for sample cleanup is to trap, in a primary column or precolumn, the fraction of the sample that contains the analytes. The compounds of the biological matrix are eluted to waste, whereas the cut of effluent containing the analytes is diverted to the secondary column or analytical column, where they are separated for the identification and/or quantification. The

Table 2 Analysis of drugs in biological fluids using column-switching HPLC method.

Analytes	Matrix	Application	Refs.
Ziprasidone	Plasma	Therapeutic drug monitoring	[6]
Amisulpride	Plasma	Therapeutic drug monitoring	[7]
Naphthol	Urine	Clinical drug monitoring	[8]
Cefepime	Urine, plasma	Clinical drug monitoring	[9]
Ganciclovir	Plasma	Clinical drug monitoring	[10]
Tryptophan-related indoles	Plasma, urine	Metabolism	[11]
Triflusal	Plasma	Pharmacokinetic	[12]
Asiaticoside	Plasma, bile	Pharmacokinetic	[13]
Glimepiride	Plasma	Pharmacokinetic	[14]
Propiverine	Plasma	Pharmacokinetic	[15]
Methamphetamine	Urine	Clinical drug monitoring	[16]
lamotrigine, oxycarbazephine, 10-monohydroxycarbazephine	Serum	Clinical drug monitoring	[17]
yeast protein	Trypsin disest	Proteomics	[18]
Voriconazole	Plasma	Pharmacokinetic	[19]
Sibutramine	Plasma	Metabolism	[20]

fraction of effluents to be transferred may be eluted at the front (front-cut technique), in the middle (heart-cut technique), or at the end (end-cut technique) of the chromatogram of the primary precolumn. Zone cutting is probably one of the most useful and versatile among the entire column-switching techniques.[21] Fig. 5 shows chromatograms obtained for human plasma spiked with 100 ng/ml of paraquat in a separation column by zone cutting after the paraquat was separated from the plasma in the precolumn.[22] Also, column-switching configuration is a powerful technique for the stereoselective analysis of drugs in biological fluids. In this case, a various chiral stationary phases (CSP) with different chiral selectors, such as cyclodextrins,[23] cellulose derivatives,[24] proteins,[25] and antibiotics,[26] have been successfully coupled to extraction precolumns. A typical application is a CSP packed with human serum albumin as selector coupled to a LiChrospher RP-18 ADS for the determination of ketoprofen enantiomers in human plasma.[25] Biological samples are injected onto the extraction support with a phosphate buffer and, after the extraction step, analytes are flushed to the chiral column, with a loading mobile phase constituted of a mixture of phosphate buffer, propanol, and octanoic acid. Walhagen and Edholm[27] reported the isolation of terbutalin, metoprolol, oxazepam, bipivacaine, and metroprolol enantiomers in plasma. Other applications using column-switching HPLC method for the analysis of drugs including endogenous material in biological fluids have been reported in the literature. They deal with the efficient and simple analysis of a drug in biological fluid without any pretreatment step. However, centrifugation, dilution, filtration, prior off-line extraction, and protein precipitation are used as a sample

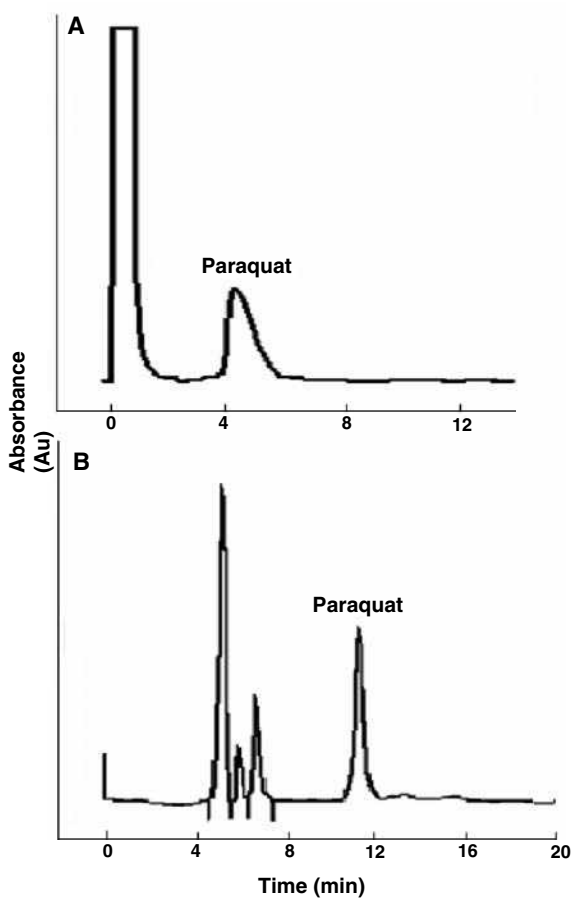

Fig. 5 Typical chromatogram of (A) precolumn matrix elution profile and (B) sample in analytical column after injection of human blood plasma spiked with 100 ng/ml of paraquat.

treatment technique before injection into the switching system to increase precolumn lifetime. The system based on the sample treatment technique was applied to the determination of baclofen in plasma.[28] Zinc sulfate solution and acetonitrile were used to precipitate protein. After centrifugation, the analyte was analyzed using column-switching HPLC system with microbore column. Precolumn and analytical column were C_8 and C_{18} stationary phase with 5 μm particle, respectively.

Sample cleanup in HPLC–MS system

As mentioned in the previous section, the application and investigation of the column-switching technique connected to an HPLC–MS system have witnessed tremendous growth due to the increase in HPLC–MS system applications in the pharmaceutical and clinical area. Recently, in the case of an HPLC–MS system with column switching, a lot of researches were mainly focused on online sample pretreatment such as online solid-phase extraction technique[29–31] and direct injection after filtration[32–34] in order to accompany high-throughput analysis by reduced sample pretreatment and analysis time. HPLC combined with MS detection played a key role in accelerating the sample throughput and providing outstanding sensitivity. In addition, the use of a column with a microbore is common for a low flow rate and for allowing sensitivity improvement. However, the absence of selectivity, which speeds up the analytical process, can become an important limitation. Indeed, the coelution of analytes and interfering substances in biological matrices can modify the MS response of the target molecules. Therefore, during method development, special attention has to be paid to remove interfering substances in biological sample using sample pretreatment. Biotransformation products can also disturb the quantitative determination of analytes in biological materials by HPLC–MS. Analysis of isomeric compounds has to be performed considering interference between each isomeric compound because of their similar physicochemical properties. Therefore, despite high MS selectivity, chromatographic separation remains essential. The coupling of an analytical column and another column for the extraction of sample using column-switching configuration appears as a suitable alternative in HPLC–MS system.

Sample Enrichment

Column switching suggests an alternative method to increase sensitivity as well as simple sample pretreatment. In a column-switching system, increase of sensitivity is based on the fact that the components will be retained in a narrow zone on the top of the column when a large volume of sample is pumped through the column. Koenigabauer et al. analyzed diazepam in serum using column-switching HPLC method with microbore column.[35] This research showed that the concentration sensitivity increased 1500 times with a 1 ml injection volume of highly dilute aqueous paraben solutions. The optimization of the chromatographic conditions should include careful choice of the type of precolumn (dimensions and packing), eluent conditions, and system design, to obtain good recovery and minimum peak broadening of the compounds of interest. The best enrichment factors can be achieved by back-flush configuration. The back-flush techniques reverse the flow of the primary column, so the analytes retained at the head of the precolumn are directly transferred to the analytical column. The precolumn can also be back-flushed to remove the components of the matrix that are strongly retained, after the fraction of interest has been eluted.[36] The back-flush configuration also minimizes peak broadening. Nielson permits samples up to 50 ml to be directly injected without significant loss of resolution although microbore separation column is used.[37] A lot of papers have demonstrated the separation of trace materials in biological fluids by large volume injection using a column-switching system. Furthermore, column-switching systems are often used, after conventional off-line cleanup or preconcentration of the samples, to improve sensitivity and the analytical separation. Kim et al.[38] have reported the determination of cetirizine in plasma using liquid–liquid extraction and column switching. After samples were extracted with dichloromethane, the extracted samples were injected on a short C_8 precolumn and cetirizine and the internal standard were transferred to the analytical microbore column. Then, the analytes were analyzed with the mobile phase containing acetonitrile and phosphate buffer (pH 2.8). The recovery was found to be higher than 80%. The analyte could be detected with detection limit 10 ng/ml (using 210 μl injection). Therefore, trace material in biological fluids can be analyzed with high sensitivity and specificity.

CONCLUSION

Here we presented column-switching HPLC system with microbore column. This system has many desirable features for performing the separation and identification by combining the valve configurations described for the specified transfer techniques. The use of column-switching system offers highly specific and sensitive results with both high speed and precision. Especially it is well suited to the analysis of samples requiring significant sample cleanup and concentration to improve selectivity and sensitivity in HPLC–UV and fluorescence as well as HPLC–MS system. Thus, column-switching HPLC with microbore column analysis has become a powerful technique in pharmaceutical and clinical areas.

REFERENCES

1. Niessen, W.M.A. State-of-the-art in liquid chromatography–mass spectrometry. J. Chromatogr. A, **1999**, *856* (1), 179–197.
2. Walhagen, A.; Edholm, L.E.; Heeremans, C.E.M.; Van Der Hoeven, R.A.M.; Niessen, W.M.A.; Tjaden, U.R.; Van Der Greef, J. Coupled column chromatography—mass spectrometry: Thermospray liquid chromatography—Mass spectrometric and liquid chromatography—tandem mass spectrometric analysis of metoprolol enantiomers in plasma using phase-system switching. J. Chromatogr. **1989**, *474* (1), 257–263.
3. Asakawa, N.; Ohe, H.; Tsuno, M.; Nezu, Y.; Yoshida, Y.; Sato, T. Liquid chromatography–mass spectrometry system using column-switching techniques. J. Chromatogr. A, **1991**, *239*, 231–241.
4. Yeon, K.J.; Park, Y.J.; Park, K.M.; Park, J.S.; Ban, E.; Kim, M.K.; Kim, Y.B.; Kim, C.K. High performance liquid chromatographic analysis of cilostazol in human plasma with on–line column switching. J. Liq. Chromatogr. Rel. Technol. **2005**, *28*, 109–120.
5. Makino, Y.; Suzuki, A.; Ogawa, T.; Shirota, O. Direct determination of methamphetamine enantiomers in urine by liquid chromatography with a strong cation-exchange precolumn and phenyl-β-cyclodextrin-bonded semi-microcolumn. J. Chromatogr. B, **1999**, *729* (1–2), 97–101.
6. Sachse, J.; Hartter, S.; Hiemke, C. Automated determination of ziprasidone by HPLC with column switching and spectrophotometric detection. Ther. Drug Monit. **2005**, *27*, 158–162.
7. Sachse, J.; Hartter, S.; Weigmann, H.; Hiemke, C. Automated determination of amisulpride by liquid chromatography with column switching and spectrophotometric detection. J. Chromatogr. B, **2003**, *784*, 405–410.
8. Preuss, R.; Angerer, J. Simultaneous determination of 1- and 2-naphthol in human urine using on-line clean-up column-switching liquid chromatography–fluorescence detection. J. Chromatogr. B, **2004**, *801*, 307–316.
9. Cherti, N.; Kinowski, J.M.; Lefrant, J.Y.; Bressolle, F. High-performance liquid chromatographic determination of cefepime in human plasma and in urine and dialysis fluid using a column-switching technique. J. Chromatogr. B, **2001**, *754*, 377–386.
10. Chu, F.; Kiang, C.H.; Sung, M.L.; Huang, B.; Reeve, R.L.; Tarnowski, T. A rapid, sensitive HPLC method for the determination of ganciclovir in human plasma and serum. J. Pharm. Biomed. Anal. **1999**, *21*, 657–667.
11. Kema, I.P.; Meijer, W.G.; Meiborg, G.; Ooms, B.; Willemse, P.H.; de Vries, E.G. Profiling of tryptophan-related plasma indoles in patients with carcinoid tumors by automated, on-line, solid-phase extraction and HPLC with fluorescence detection. Clin. Chem. **2001**, *47*, 1811–1820.
12. Park, J.-S.; Park, K.-M.; Kim, C.-K. Determination of triflusal in human plasma by high performance liquid chromatography with automated column switching system. J. Liq. Chromatogr. Rel. Technol. **2000**, *26*, 2513–2524.
13. Baek, M.; Rho, Y.S.; Kim, D.H. Column-switching high-performance liquid chromatographic assay for determination of asiaticoside in rat plasma and bile with ultraviolet absorbance detection. J. Chromatogr. B, **1999**, *732*, 357–363.
14. Song, Y.-K.; Maeng, J.-E.; Hwang, H.-R.; Park, J.-S.; Kim, B.-C.; Kim, J.-K.; Kim, C.-K. Determination of glimepiride in human plasma using semi-microbore high performance liquid chromatography with column switching. J. Chromatogr. B, **2004**, *810*, 143–149.
15. Ban, E.; Meang, J.-E.; Woo, J. S.; Kim, C.-K. Sensitive column-switching high-performance liquid chromatography method for determination of propiverine in human plasma. J. Chromatogr. B, **2006**, *831*, 230–235.
16. Kumihashi, M.; Ameno, K.; Shibayama, T.; Suga, K.; Miyauchi, H.; Jamal, M.; Wang, W.; Uekita, I.; Ijiri, I. Simultaneous determination of methamphetamine and its metabolite, amphetamine, in urine using a high performance liquid chromatography column-switching method. J. Chromatogr. B, **2007**, *845*, 180–183.
17. Haen, E.; Greiner, C. Development of a simple column-switching high performance liquid chromatography (HPLC) method for rapid and simultaneous routine serum monitoring of lamotrigine, oxcarbazephine and 10-monohydroxycarbazephine (MHD). J. Chromatogr. B, **2007**, *854*, 338–344.
18. Wang, F.; Jiang, X.; Feng, Shun.; Tian, R.; Jiang, X.; Han, G.; Liu, H.; Ye, M.; Zou, H. Automated injection of uncleaned samples using a ten-port switching valve and strong cation-exchange trap column for proteome analysis. J. Chromatogr. A, **2007**, *1171*, 56–62.
19. Nakagawa, S.; Suzuki, R.; Yamazaki, R.; Kusuhara, Y.; Mistumoto, S.; Kobayashi, H.; Shimoeda, S.; Ohta, S.; Yamato, S. Determination of the antifungal agent voriconazole in human plasma using a simple column-switching high-performance liquid chromatography and its application to a pharmacokinetic study. Chem. Pharm. Bull. **2008**, *56* (3), 328–331.
20. Um, S.Y.; Kim, K.-B.; Kim, S.H.; Ju, Y.C.; Lee, H.Y.; Choi, K.H.; Chung, M.W. Determination of the active metabolites of sibutramine in rat serum using column-switching HPLC. J. Sep. Sci. **2008**, 31, 2820–2826.
21. Little, C.J.; Tomkins, D.J.; Sthel, O. Frei, R.W.; Werkhoven-Goewie, C.E. Applications of a microprocessor-controlled valve-switching unit for automated sample cleanup and trace enrichment in high-performance liquid chromatography. J. Chromatogr. A, **1983**, *264*, 183–196.
22. Brunetto, M.R.; Morales, A.R.; Gallignani, M.; Burguera, J.L.; Burguera, M. Determination of paraquat in human blood plasma using reverse-phase ion-pair high-performance liquid chromatography with direct sample injection. Talanta **2003**, *59*, 913–921.
23. Capka, V.; Xu, Y. Simultaneous determination of enantiomers of structurally related anticholinergic analogs in human serum by liquid chromatography–electrospray ionization mass spectrometry with on-line sample cleanup. J. Chromatogr. B, **2001**, *762* (2), 181–192.
24. Ceccato, A.; Boulanger, B.; Chiap, P.; Hubert, P.; Crommen, J. Simultaneous determination of methylphenobarbital enantiomers and phenobarbital in human plasma by on-line coupling of an achiral precolumn to a chiral liquid chromatographic column. J. Chromatogr. A, **1998**, *819* (1–2), 143–153.

25. Baeyens, W.R.G.; Van Der Weken, G.; Haustraete, I.; Aboul-Enein, H.Y.; Corveleyn, S.; Remon, J.P.; Garcia-Campana, A.M.; Deprez, P. Application of the restricted-access precolumn packing material alkyl-diol silica in a column-switching system for the determination of ketoprofen enantiomers in horse plasma. J. Chromatogr. A, **2000**, *871* (1–2), 153–161.
26. Mis'anova, C.; Sterfancova, A. Comparison of two different approaches of sample pretreatment for stereoselective determination of (*R,S*)-propranolol in human plasma. J. Trace Microprobe Tech. **2001**, *19* (1), 163–170.
27. Walhagen, A.; Edholm, L.E. Coupled-column chromatography on immobilized protein phases for direct separation and determination of drug enantiomers in plasma. J. Chromatogr. A, **1989**, *473*, 371–379.
28. Ban, E; Park, J.S.; Kim, C.K. Semi-microbore HPLC for the determination of baclofen in human plasma using column switching. J. Liq. Chromatogr. Relat. Technol. **2005**, *28* (19), 109–120.
29. Ye, X.; Tao, L.J.; Needham, L.L.; Calafat, A.M. Automated o-line column-switching HPLC-MS/MS method for measuring environmental phenols and parabens in serum. Talanta **2008**, *76* (4), 865–871.
30. Korecka, M.; Solari, S.G.; Shaw, L.M. Sensitive, high throughput HPLC-MS/MS method with on-line sample clean-up for everolimus measurement. Ther. Drug Monit. **2006**, *28* (4), 484–490.
31. Xu, R.N.; Fan, L.; Rieser, M.J.; El-Shourbagy, T.A. Recent advances in high-throughput quantitative bioanalysis by LC–MS/MS. J. Pharm. Biomed. Anal. **2007**, *44*, 342–355.
32. Zhang, J.; Musson, D.G. Investigation of high-throughput ultrafiltration for the determination of an unbound compound in human plasma using liquid chromatography and tandem mass spectrometry with electrospray ionization. J. Chromatogr. B, **2006**, *843*, 47–56.
33. Cho, S.-H.; Jung, B.H.; Lee W.-Y.; Chung, B.C. Rapid column-switching liquid chromatography/mass spectrometric assay for DHEA-sulfate in the plasma of patients with Alzheimer's disease. Biomed. Chromatogr. **2006**, *20*, 1093–1097.
34. Kellert, M.; Wagner, S.; Lutz, U.; Lutz, W.K. Biomarkers of furan exposure by metabolic profiling of rat urine with liquid chromatography–tandem mass spectrometry and principal component analysis. Chem. Res. Toxicol. **2008**, *21*, 761–768.
35. Koenigabauer, M.J.; Assenza, S.P.; Willoughby, R.C.; Curtis, M.A. Trace analysis of diazepam in serum using microbore high-performance liquid chromatography and on-line preconcentration. J. Chromatogr. **1987**, *413*, 161–169.
36. Bargar, E.M. Application of column switching in high-performance liquid chromatographic analysis of medroxalol in plasma. J. Chromatogr. **1987**, *417*, 143–150.
37. Nielson, H. Use of enzymatic solubilization of tissues and direct injection of pre-columns of large volumes for analysing biological samples by high-performance liquid chromatography. J. Chromatogr. **1986**, *381*, 63–74.
38. Kim, C.K.; Yeon, K.J.; Ban, E.; Hyun, M.J.; Kim, J.K.; Kim, M.K.; Jin, S.E.; Park, J.S. Narrow-bore high performance liquid chromatographic method for the determination of cetirizine in human plasma using column switching. J. Pharm. Biomed. Anal. **2005**, *37*, 603–609.

Biological Samples: LC/MS Detection and Quantification of Naturally Occurring Steroids

Tatsuya Higashi
Tadashi Nishio
Kazutake Shimada
Division of Pharmaceutical Sciences, Graduate School of Natural Science and Technology, Kanazawa University, Kanazawa, Japan

INTRODUCTION

The basic steroid molecular skeleton consists of four rings of carbon atoms, perhydro-1,2-cyclopentenophenanthrene. Almost all natural steroids possess either one or more, usually two, methyl groups at "angular" positions where two rings meet. The steroids with which we are mainly concerned consist of five skeletal types, according to the number of C-atoms, i.e., estrane (C_{18}), androstane (C_{19}), pregnane (C_{21}), cholane (C_{24}), and cholestane (C_{27}). Almost all of these compounds are natural hormones or precursors. Steroid hormones, which mostly act as ligands to intracellular/nuclear receptors, can be divided into estrogens, androgens, progestogens, and corticoids, based on their functions. It is well known that an active metabolite of vitamin D_3 (9,10-secosteroid), 1α,25-dihydroxyvitamin D_3 [1,25-$(OH)_2$-D_3], also has hormonal properties via binding to its specific nuclear receptor. Bile acids (cholane) have been also recently reported to be ligands for orphan nuclear receptors (liver X receptor), and play an important part in lipid metabolism.[1] On the other hand, some oxosteroids (androstane and pregnane) have been found to be modulators of several membrane receptors in the nervous system, and such steroids are now universally referred to as neuroactive steroids.[2]

These steroids exert strong biological activities at very low concentrations (nanomolar and even picomolar) in the target tissues. A specific and sensitive method for the characterization and determination of the steroids in body fluids or tissues is necessary to elucidate the nature of the many endocrine disease processes and, thus, be useful for diagnosis and treatment. Because of their close structural similarity, metabolic versatility, and their occurrence at low concentrations in body fluids and tissues, the development of reliable analytical methods for the steroids is a challenging subject for analytical chemists. Numerous methods have been described to characterize and determine the steroids, such as immunoassay, receptor binding assay, high-performance liquid chromatography (HPLC), and gas chromatography (GC)–mass spectrometry (MS),[3,4] but each of these approaches has both advantages and disadvantages.

Among the alternative methods, liquid chromatography (LC), coupled with atmospheric pressure ionization (API), such as electrospray ionization (ESI) and atmospheric pressure chemical ionization (APCI)-MS has been used for steroid analyses owing to its specificity and versatility.[4,5] However, apart from the glucuronidated (G) and sulfated (S) metabolites and bile acids, the ionization efficiencies of most of the steroids are relatively low for ESI and APCI. Therefore, conventional LC–MS sometimes does not demonstrate the required sensitivity for the trace analysis of steroids in biological samples. Although a newly developed API technique, atmospheric pressure photoionization (APPI), has also been examined for steroids that are poorly ionizable in ESI or APCI,[6,7] this technique is, in the present state, far from the stage of practical application. To enhance the detection sensitivity, chemical derivatization,[8–10] enzymic conversion,[11] and mobile-phase additives[12,13] have been positively used for the LC–MS analysis of steroids. The electron capture APCI (ECAPCI) technique, combined with derivatization, which Blair and coworkers first put to practical use,[14] also has a significant advantage for the LC–MS of steroids.[15] A capillary LC has been examined for increasing the sensitivity.[16–18]

In this entry, the authors present an overview of the LC–MS of naturally occurring steroids in biological samples, which was published from January 2001 to June 2006. Steroids are divided into six categories, based on their structures and functions, and no attention has been paid to steroid hormones used as growth promoters of animals and used in sports doping. This entry also does not take up references on the in vitro assays for the measurement of enzyme activity using a steroid as the substrate.

GENERAL PROCEDURE

For the precise measurement of the trace levels of steroids in complex biological matrices, some pretreatment

(purification and concentration) procedures are usually applied prior to the LC–MS analysis. Most analytical methods employ deproteinization with an organic solvent and solid-phase extraction (SPE) using a disposable cartridge as the pretreatment. Liquid–liquid extraction (LLE) is also often used in place of/with a combination of SPE. To reduce the labor and the analysis time, an online extraction using a mini SPE cartridge or a short column (ex., restricted-access column), along with a column-switching technique, has been recently and widely introduced.

Reversed-phase (RP) chromatography with an octadecylsilyl column is usually employed for the separation of steroids from biological components. A conventional column (inside diameter, 4.0–4.6 mm) is used for LC–APCI-MS, whereas, because a low flow rate (0.05–0.2 ml/min) is required for ESI-MS detection, a semi-micro column (inside diameter, 1.0–2.1 mm) is usually employed in this mode. Methanol and acetonitrile are the most generally used organic modifiers for the mobile phase. In ESI-MS, acids (positive-ion mode) such as formic acid and acetic acid, bases (negative-ion mode) such as triethylamine or volatile salts (positive- and negative-ion modes) such as ammonium formate and ammonium acetate, are used as the mobile-phase additives to promote protonation or deprotonation of the analyte.

In LC–MS assays, it goes without saying that it is important to select the ionization methods (ESI, APCI or, in some cases, APPI) and ionization polarity (positive-ion or negative-ion mode) suitable for the analyte. Instrumental parameters, such as the flow rate of the nebulizer gas and desolvent gas, desolvation temperature, and electrospray capillary voltage can significantly affect the generation of ions during LC–API-MS detection and, therefore, the optimization of these parameters is a necessary part of the development of analytical methods. The use of the selected ion monitoring (SIM) and selected reaction monitoring (SRM) modes may allow for the improvement of the assay sensitivity, because it can significantly reduce background noise derived from the matrices. However, the chemical and physical properties of the analyte are the most critical parameters for superior sensitivity in the various modes of ionization. Therefore, if the required sensitivity cannot be obtained, chemical derivatization is now the most widely used procedure for increasing the sensitivity of the target analyte. That is, derivatization changes the chemical and physical properties of the analyte, resulting in its ionization efficiency (conversion of a poorly ionizable compound into a derivative that is easily detectable by API-MS). The chromatographic behavior of the analyte will also be changed after derivatization, therefore decreasing the ionization suppression related to the co-elution of the biomatrix components. That is, derivatization increases not only the sensitivity, but also the specificity.

ESTROGENS

Representative estrogens, estrone (E_1) and estradiol (E_2), are synthesized from androgenic precursors by demethylation and aromatization; these are transformed to each other by the action of 17β-hydroxysteroid dehydrogenase. Estriol (E_3) is formed via the 16α-hydroxylation of E_1, especially during the period of pregnancy. Among them, E_2 is functionally the most potent estrogen. Estrogens are metabolized by hydroxylation, at the steroid A-ring, into catechol estrogens [ex. 2- or 4-hydroxyE_1 (2- or 4-OH-E_1)] and, further, by methylation into guaiacol estrogens [ex. 2- or 4-methoxyE_1 (2- or 4-MeO-E_1) or E_1-3-methyl ether]. Estrogens are responsible for the development and maintenance of the female reproductive organs and female secondary gender characteristics. Furthermore, estrogens play an important role in bone maintenance, in the cardiovascular system, and in the central nervous system. Estrogens also have an injurious action; breast cancer and endometrium cancer are promoted by prolonged exposure to endogenous and/or synthetic estrogens or their metabolites.

The LC–MS assays of estrogens are summarized in Table 1. With a few exceptions, estrogens are analyzed using LC–MS after derivatization, due to their low ionization efficiencies in ESI or APCI and occurrence at low concentrations in biological fluids and tissues. Dansylation, which was first proposed as the derivatization of phenolic compounds for ESI by Quirke, Adams, and Van Berkel,[19] is now the reference and most practical derivatization procedure for the LC–MS analysis of estrogens.[20–22] Derivatization with *p*-toluenesulfonhydrazide is also useful to enhance the sensitivities of E_1 and its metabolites; the resulting derivatives are analyzed by ESI-MS.[23,24] When urinary glucuronidated metabolites of E_3 [E_3-3G and -16G], whose abundance is in the μg/ml range, are analyzed, derivatization is unnecessary.[25]

ANDROGENS

Androgens are an important group of C_{19} steroids, principally comprised of testosterone (T) and its active metabolite, 5α-dihydrotestosterone (DHT). In addition, androstenedione (AD) and dehydroepiandrosterone (DHEA) are usually classified as androgens, although their androgenic activity is low or negligible.

To review the androgen assays using LC–MS published during the last five years, many papers were concerned with prostate cancer (PCa) and benign prostate hyperplasia (BPH).[26–31] PCa is the most common malignancy in aged males in the United States. Because prostatic diseases usually depend on androgens, the measurement of androgens in the prostatic tissue, which is collected by a biopsy needle, is very important in the clinical field for the differential diagnosis of prostatic

Table 1 Estrogens.

Analyte	Sample treatment	LC conditions (analytical column, mobile phase, and flow rate)	MS (instrument, ionization mode, and detection)	Sensitivity	Refs.
E_2 IS: d_3-E_2	Human serum (3–5 ml) → RP-SPE → derivatization with dansyl chloride	Zorbax Eclipse XDB-C_{18} (150 × 2.1 mm I.D., Agilent Technologies), gradient (acetonitrile–water containing 0.1% acetic acid) and 0.25 ml/min	API 4000 (Applied Biosystems), positive ESI and SRM ($[M + H]^+$ → product ion)	LOD (S/N = 3): 0.6 pg	[20]
E_1 and E_2 IS: d_4-E_1 and d_5-E_2	Human serum (0.5 ml) → LLE (dichloromethane) → derivatization with dansyl chloride	Synergi 4μMax-RP C18 (150 × 2.0 mm I.D., Phenomenex), gradient (acetonitrile–water containing 0.1% formic acid) and 0.6 ml/min	API 3000 (ABI-Sciex), positive APCI and SRM ($[M + H]^+$ → product ion)	Measurable range: 12.9–2229 pg/ml (E_1) and 10.3–2205 pg/ml (E_2)	[21]
2-OH-E_1 and 4-OH-E_1 IS: d_4-2-OH-E_1 and d_4-4-OH-E_1	Human urine (10 ml) → enzymic hydrolysis → RP-SPE → derivatization with *p*-toluenesulfonhydrazide	Luna C_{18} (2) (150 × 2.0 mm I.D., Phenomenex), gradient (methanol–water containing 0.1% formic acid) and 0.2 ml/min	LCQ DECA (ThermoFinnigan), positive ESI and SIM ($[M + H]^+$)	S/N > 17: 50 pg	[23]
E_1, 2-OH-E_1, 4-OH-E_1, 16α-OH-E_1, 2-MeO-E_1, 2-OH-E_1-3-methyl ether and 16-keto-E_2 IS: d_4-E_1, d_4-2-OH-E_1, d_4-4-OH-E_1, d_3-16α-OH-E_1, d_4-2-MeO-E_1 and d_5-16-keto-E_2	Human urine (2.5 ml) → enzymic hydrolysis → RP-SPE → derivatization with *p*-toluenesulfonhydrazide	Luna C_{18} (2) (150 × 2.0 mm I.D., Phenomenex), gradient (methanol–water containing 0.1% formic acid) and 0.2 ml/min	LCQ DECA (ThermoFinnigan), positive ESI and SRM ($[M + H]^+$ → product ion)	S/N > 15: 10 pg Measurable range: 0.08–10.24 ng/ml	[24]
E_1, 2-OH-E_1, 4-OH-E_1, 16α-OH-E_1, 2-MeO-E_1, 4-MeO-E_1, 2-OH-E_1-3-methyl ether, E_2, 2-OH-E_2, 2-MeO-E_2, 4-MeO-E_2, 16-keto-E_2, E_3, 16-epi-E_3 and 17-epi-E_3 IS: d_4-E_2, d_5-2-OH-E_2, d_5-2-MeO-E_2, d_3-E_3, and d_3-16-epi-E_3	Human urine (0.5 ml) → enzymic hydrolysis → LLE (dichloromethane) → derivatization with dansyl chloride	Synergi Hydro-RP (150 × 2.0 mm I.D., Phenomenex), gradient (methanol–water containing 0.1% formic acid) and 0.2 ml/min	TSQ Quantum-AM (ThermoFinnigan), positive ESI and SRM ($[M + H]^+$ → product ion)	LOD: 250 fg Measurable range: 0.02–19.2 ng/ml	[22]
E_3-3G and E_3-16G IS: d_3-T-G	Human urine (50 μl) → filtration → column-switching technique	Capcell Pak C_{18} UG 120 (250 × 1.5 mm I.D., Shiseido Fine Chemical), acetonitrile–water containing 0.1% triethylamine and 0.1 ml/min	LCQ (ThermoFinnigan), negative ESI and SRM ($[M–H]^-$ → product ion)	LOD (S/N = 3): 10 ng/ml (E_3-3G) and 5 ng/ml (E_3-16G) Measurable range: 0.1–20 μg/ml	[25]

diseases and to evaluate the effects of therapy. However, the sample volume collected by a biopsy needle is about 10 mg, and, therefore, the prostatic androgen assay requires a very high sensitivity. Recently, the introduction of derivatization with a permanently charged reagent enabled the quantification of prostatic DHT with a 10-mg tissue sample using LC–ESI-MS–MS.[26–28] The abundance of the precursors [DHEA and 5-androstenediol (Δ^5-Adiol)] and the downstream conversion products [androsterone (A) and epiandrosterone (EpiA)] of T in biological fluids reflects the individual androgen status (balance of production and excretion), which may also be a maker of prostatic diseases. Based on this, the LC–MS assays of sulfates of the above steroids have been reported.[29–31] Glucuronides of T and DHT excreted into urine were also analyzed by LC–ESI-MS–MS.[32]

The anesthetic and anxiolytic effects of androgens, mainly T and 5α-androstane-3α,17β-diol (3α,5α-Adiol), is another hot topic; these steroids are classified now as, not only androgens, but also neuroactive steroids. The determination of the brain and circulating levels of these steroids in animal models is useful for the elucidation of their physiological roles and pharmacological effects. Based on this information, papers that deal with the determination of these steroids in the rat brain and serum/plasma are recently increasing.[35–37]

The LC–MS assays of androgens, including the above-mentioned methods, are summarized in Table 2.

PROGESTOGENS

17α-Hydroxyprogesterone (17-OH-PROG), a metabolic precursor of corticoids and androgens, is the most important parameter for diagnosing and monitoring congenital adrenal hyperplasia (CAH) caused by the 21-hydroxylase deficiency. 17-OH-PROG has been conventionally determined by immunoassay, but this method has a serious drawback, i.e., a false positive due to poor antibody specificity and interference from endogenous components, such as lipids. As an alternative method, LC–MS has recently been proposed as the analytical technique of choice for the determination of 17-OH-PROG in a dried blood spot[38–40] or serum[41] (Table 3). Methods that can simultaneously determine 17-OH-PROG, some androgens, and cortisol (F) in blood spots have been reported.[42,43]

Neuroactive steroids affect neurotransmission through their action at the membrane ion-gated and other neurotransmitter receptors.[2] Recent studies have demonstrated that pregnane-type neuroactive steroids, such as pregnenolone (PREG) and its downstream conversion products, play an important role in the homeostatic mechanisms that counteract the inhibitory effect of stress on the γ-aminobutyric acid type A receptor function and are involved in the stress-elicited disorders, such as depression. Therefore, a method for the determination of neuroactive steroids in the brains of animal models can contribute to the elucidation of their physiological roles and the development of new antipsychotic agents targeting neurosteroidogenesis. Based on this background information, the LC–MS analysis of pregnane-type neuroactive steroids has been reported, in which derivatization is employed because of the low ionization efficiencies and low concentrations of the neuroactive steroids (Table 3).[44,45]

CORTICOIDS

Corticoids are also called corticosteroids; they are physiologically divided into mineralocorticoids acting during the metabolism of electrolytes (sodium and potassium) and glucocorticoids acting during saccharometabolism, the antiinflammatory response, and the sodium pool.

Aldosterone (ALDO) is a major mineralocorticoid, and hyperaldosteronism is a recognized cause of hypertension, whereas, a low level of ALDO is observed in patients with Addison's disease. Because of its low blood concentration (picomolar–nanomolar range), ALDO has been conventionally measured by immunoassay, and no LC–MS method has been proposed during the last five years.

F (Cortisol) is a major glucocorticoid and its serum/plasma and urinary levels are good biochemical markers of several diseases, such as Cushing's syndrome. A large number of LC–MS methods have been described for the quantitative measurement of F in the serum/plasma[46–49] and urine[50–54] (Table 4). In some of these methods, the simultaneous determination of F and its inactive metabolite, cortisone (E), was done.[49,53] F and E are usually ionized by ESI[46–49,52,53,55,56] and APCI[51] operating in the positive-ion mode, but seldom in the negative-ion mode.[50,54] The level of F circulation is also considered to be a marker of stress and the salivary F assay using LC–ESI-MS–MS has been proposed.[56]

F and E are metabolized into tetrahydrocortisol (THF), allotetrahydrocortisol (ATHF), and tetrahydrocortisone (THE), respectively, and are excreted into the urine. Measurement of their urinary ratio [(THF + ATHF)/THE] is clinically important for the diagnosis of hypertension caused by the congenital absence of 11β-hydroxysteroid dehydrogenase type 2 (apparent mineralocorticoid excess). The measurement of the blood 21-deoxycortisol (21-DOF) level is useful for the diagnosis of CAH. The endogenous ratio of 6β-hydroxycortisol (6β-OH-F) and F in the urine is an index for the activity of cytochrome P450 3A4. Based on their clinical importance, the LC–MS methods for THF,

Table 2 Androgens.

Analyte	Sample treatment	LC conditions (analytical column, mobile phase, and flow rate)	MS (instrument, ionization mode, and detection)	Sensitivity	Refs.
DHT IS: d_3-^{18}O-DHT	Human prostate (5–10 mg tissue) → NaOH treatment → RP-SPE → derivatization with 2-fluoro-1-methylpyridine → RP-SPE	Docosil (100 × 2.0 mm I.D., Senshu Scientific), acetonitrile–water containing 0.05% formic acid and 0.1 ml/min	Quattro II (Micromass), positive ESI and SRM ($[M]^+$ → product ion)	LOQ: 5 pg Measurable range: 5–100 pg/tube	[26,27]
T and DHT IS: d_3-T	Human prostate (10 mg tissue) → extraction (70% methanol) → PR-SPE → derivatization with 2-hydrazino-1-methylpyridine	J'sphere ODS H-80 (150 × 2.0 mm I.D., YMC), acetonitrile–methanol-10 m*M* ammonium formate and 0.2 ml/min	API 2000 (Applied Biosystems), positive ESI and SRM ($[M]^+$ → residual $[M]^+$)	LOQ: 1.0 ng/g tissue	[28]
T	Human plasma (1 ml) → LLE (hexane-dichloromethane) → derivatization with pentafluorophenylhydrazine → LLE (hexane and HCl aq)	Luna C_{18} (250 × 4.6 mm I.D., Phenomenex), acetonitrile–water and 1 ml/min	Quattro Ultima (Micromass), ECAPCI and SRM ($[M–HF]^-$ → product ion)	LOD (S/N = 3): 24.3 fmol Measurable range: 0.1–25 ng/ml	[33]
T, DHT, 3α,5α-Adiol, E_2 IS: Dimethyl benzoyl phenyl urea	Human testicular fluid (20 μl) → LLE (diethyl ether)	X-Terra MS (150 × 2.1 mm I.D., Waters), acetonitrile–water containing 0.1% formic acid and 0.15 ml/min	Quattro (Micromass), positive ESI, SRM ($[M + H]^+$ or $[H + H–H_2O]^+$ → product ion)	Measurable range: 0.1–50 ng/ml (T), 0.02–1 ng/ml (DHT), 0.2–10 ng/ml (3α,5α-Adiol) and 0.05–2 ng/ml (E_2)	[34]
DHEA-S IS: d_2-DHEA-S	Human serum (20 μl) → zinc sulfate treatment → deproteinization (methanol–acetonitrile)	Mercury Fusion-RP (20 × 2.0 mm I.D., Phenomenex), gradient (methanol–water containing 2 m*M* ammonium acetate and 0.1% formic acid) and 0.4 ml/min	Quattro (Micromass), negative ESI, SRM ($[M–H]^-$ → product ion)	LOQ: 1 nmol/ml	[29]
Adiol-3S and DHEA-S IS: d_5-Adiol-3S and d_4-DHEA-S	Human serum (100 μl) → deproteinization (acetonitrile) → RP-SPE → wash (hexane)	Develosil ODS-HG-5 (150 × 2.0 mm I.D., Nomura Chemical), acetonitrile-5 m*M* ammonium formate, and 0.15 ml/min	LCQ (ThermoQuest), negative ESI and SRM ($[M]^-$ → residual $[M]^-$)	LOD (S/N = 5): 0.25 ng on column (Adiol-3S) Measurable range: 10–400 ng/ml (Adiol-3S) and 0.05–8 μg/ml (DHEA-S)	[30]
A-S, EpiA-S and DHEA-S IS: d_4-DHEA-S	Human serum (10 μl) → deproteinization (acetonitrile) → RP-SPE → wash (hexane)	Develosil ODS-HG-5 (150 × 2.0 mm I.D., Nomura Chemical), acetonitrile-5 m*M* ammonium formate, and 0.15 ml/min	API 2000 (Applied Biosystems), negative ESI and SIM ($[M]^-$)	Measurable range: 0.02–5 μg/ml (A-S), 0.005–1.5 μg/ml (EpiA-S) and 0.02–10 μg/ml (DHEA-S)	[31]
T-G and DHT-G IS: d_3-T-G	Human urine (50 μl) → filtration → column-switching technique	Capcell Pak C_{18} (150 × 1.0 mm I.D., Shiseido Fine Chemical), gradient (acetonitrile–water) and 0.1 ml/min	LCQ (ThermoQuest), negative ESI and SRM ($[M–H]^-$ → product ion)	LOD (S/N = 3): 0.2 ng/ml (T-G) and 3 ng/ml (DHT-G) LOQ: 1.0 ng/ml (T-G) and 10 ng/ml (DHT-G)	[32]

(Continued)

Table 2 Androgens. *(Continued)*

Analyte	Sample treatment	LC conditions (analytical column, mobile phase, and flow rate)	MS (instrument, ionization mode, and detection)	Sensitivity	Refs.
T IS: d_4-^{18}O-T	Rat plasma (50 μl) → RP-SPE → derivatization with ethoxyamine hydrochloride → acetylation → filtration	Unison UK-C8 (75 × 4.6 mm I.D., Imtakt), methanol-10 m*M* ammonium acetate and 1 ml/min	API 4000 (Applied Biosystems), positive APCI and SRM ($[M + H]^+$ → product ion)	LOQ: 0.2 ng/ml	[35]
3α,5α-Adiol IS: 6β-Hydroxy-testosterone	Rat plasma (50 μl) → LLE (methyl *t*-butyl ether)	Synergy Max-RP (50 × 2.0 mm I.D., Phenomenex), gradient (methanol–water containing 0.05% acetic acid) and 0.15 ml/min	Quattro II (Micromass), positive APCI and SRM ($[M + H]^+$ → product ion)	LOD (S/N = 2.5): 2 ng/ml Measurable range: 10–2000 ng/ml (standard addition method)	[36]
T IS: d_3-T	Rat brain (100 mg) → extraction (methanol-acetic acid) → RP-SPE → preparative NP-HPLC → derivatization with 2-hydrazino-1-methylpyridine Rat serum (50 μl) → deproteinization (methanol–acetic acid) → RP-SPE → derivatization with 2-hydrazino-1-methylpyridine	J'sphere ODS H-80 (150 × 2.0 mm I.D., YMC), acetonitrile–methanol–10 m*M* ammonium formate and 0.2 ml/min	API 2000 (Applied Biosystems), positive ESI, SRM ($[M]^+$ → residual $[M]^+$)	LOQ: 0.06 ng/g tissue (brain) and 0.06 ng/ml (serum)	[37]
3α,5α-Adiol IS: d_3-3α,5α-Adiol	Rat brain (100 mg) → extraction (methanol–acetic acid) → RP-SPE → NP-SPE → derivatization with 4-nitrobenzoyl chloride	J'sphere ODS H-80 (150 × 4.6 mm I.D., YMC), methanol–water and 1.0 ml/min	LCQ (ThermoQuest), ECAPCI, SIM ($[M]^-$)	Measurable range: 0.2–1.0 ng/g tissue	[37]

Table 3 Progestogens.

Analyte	Sample treatment	LC conditions (analytical column, mobile phase, and flow rate)	MS (instrument, ionization mode, and detection)	Sensitivity (sample volume used)	Refs.
17-OH-PROG IS: 6α-Methylprednisolone	Human whole blood (1/8 inch dried blood spot, equivalent to 12 μl whole blood) → extraction (methanol) → derivatization with Girard reagent P	5 μm C_4 (50 × 1.0 mm I.D., Vydac), acetonitrile–water and 50 μl/min	API 2000 (PE Sciex), positive ESI and SRM ($[M]^{2+}$ → product ion)	LOD (S/N = 3): 10 ng/ml Measurable range: 30–500 ng/ml	[38,39]
17-OH-PROG IS: 6α-Methylprednisolone	Human whole blood (1/8 inch dried blood spot, equivalent to 12 μl whole blood) → extraction (methanol)	Polaris C_{18} (50 × 2.0 mm I.D., MetaChem Technologies), methanol–1% acetic acid and 0.2 ml/min	API 2000 (PE Sciex), positive ESI and SRM ($[M + H]^+$ → product ion)	LOD (S/N = 3): 20 ng/ml Measurable range: 50–500 ng/ml	[40]
17-OH-PROG IS: 6α-Methylprednisolone or d_8-17-OH-PROG	Human serum (0.5 ml) → LLE (diethyl ether–ethyl acetate)	Purospher Star RP-18 (55 × 2.0 mm I.D., Merck), gradient (methanol–water) and 0.25 ml/min	API 2000 (PE Sciex), positive ESI and SRM ($[M + H]^+$ → product ion)	LOD (S/N = 3): 1 nmol/L Measurable range: 5–250 nmol/L	[41]
17-OH-PROG, AD and F IS: d_8-17-OH-PROG	Human whole blood (3/16 inch dried blood spot) → extraction (diethyl ether)	Symmetry C_{18} (50 × 2.1 mm I.D., Waters), gradient (methanol–water) and 0.25 ml/min	API 3000 (Applied Biosystems), positive ESI and SRM ($[M + H]^+$ → product ion)	Measurable range: ~160 ng/ml	[42]
17-OH-PROG, AD and T IS: d_8-17-OH-PROG, d_7-AD and d_5-T	Human serum or plasma → deproteinization (methanol–zinc sulfate) → online RP-SPE and column-switching technique	Chromolith RP-18e (100 × 4.6 mm I.D., Merck), methanol–2 m*M* ammonium acetate and 1 ml/min	API 4000 (Applied Biosystems), positive APCI and SRM ($[M + H]^+$ → product ion)	LOD (S/N = 3): 0.05 ng/ml (100 μl) LOQ: 0.1 ng/ml Measurable range: 0.1–250 ng/ml	[43]
PREG, PROG, allopregnanolone and epiallopregnanolone IS: d_4-PREG and d_8-PROG	Rat brain (5–100 mg) → extraction (methanol–acetic acid) → RP-SPE → NP-SPE → derivatization with 2-nitro-4-trifluoromethylphenylhydrazine	J'sphere ODS H-80 (150 × 4.6 mm I.D., YMC), methanol–water or acetonitrile–methanol and 1 ml/min	LCQ (ThermoQuest), ECAPCI and SIM ($[M]^-$)	LOD (S/N = 5): 19 fmol on column (PREG) and 3.2 fmol on column (PREG) LOQ: 2 ng/g tissue (PREG) and 0.5 ng/g tissue (PROG)	[44,45]

Table 4 Corticoids.

Analyte	Sample treatment	LC conditions (analytical column, mobile phase, and flow rate)	MS (instrument, ionization mode, and detection)	Sensitivity	Refs.
F IS: d_3-F	Human serum (2 ml) → RP-SPE → LLE (ethyl acetate and water)	Zorbax Eclipse XDB-C_{18} (150 × 2.1 mm I.D., Agilent Technologies), methanol–water containing 0.1% acetic acid and 0.25 ml/min	Quattro Ultima (Micromass), positive ESI, SRM ($[M + H]^+$ → product ion)	LOD (S/N = 3–5): 10 pg	[46]
F IS: d_3-F	Human serum (1 ml) → LLE (dichloromethane)	Hypersil ODS (C18) (10 × 2.1 mm I.D., Agilent Technologies), gradient (methanol–20 m*M* ammonium acetate) and 0.4 ml/min	Quattro Ultima (Micromass), positive ESI, SIM ($[M + H]^+$)	LOD (S/N = 3): 10 ng/ml	[47]
F IS: d_3-F	Human serum (0.15 ml) → deproteinization (methanol and zinc sulfate) → online RP-SPE and column-switching technique	Reprosil pur C18-AQ (125 × 2.0 mm I.D., Maisch), methanol–2 m*M* ammonium acetate and 0.4 ml/min	Quattro (Micromass), positive ESI, SRM ($[M + H]^+$ → product ion)	LOD (S/N = 4): 1 ng/ml Measurable range: 7.8–500 ng/ml	[48]
F IS: 6α-Methyl-prednisolone	Human urine (1 ml) → LLE (dichloromethane)	Purospher Star RP-18 (55 × 2.0 mm I.D., Merck), gradient (methanol–water) and 0.3 ml/min	API 2000 (Applied Biosystems), negative ESI, SRM ($[M–H]^-$ → product ion)	LOD (S/N = 3): 1 pmol/ml Measurable range: 10–400 pmol/ml	[50]
F IS: d_4-F	Human urine (0.5 ml) → RP-SPE	Eclipse XDB-C18 (75 × 4.6 mm I.D., Mac-Mod Analytical), methanol–water containing 0.03% TFA and 1.0 ml/min	TSQ 7000 (Finnigan), positive APCI, SRM ($[M + H]^+$ → product ion)	Measurable range: 5–500 ng/ml	[51]
F IS: d_2-F	Human urine (0.3 ml) → RP-SPE	Chromolith RP-18 SpeedRod (50 × 4.6 mm I.D., Merck), methanol–2 m*M* ammonium acetate containing 0.1% formic acid and 0.6 ml/min	Quattro (Micromass) positive ESI, SRM ($[M + H]^+$ → product ion)	LOD (S/N = 3): 3 pmol/ml Measurable range: 20–1000 pmol/ml	[52]
F IS: d_4-F	Human saliva (0.25 ml) → deproteinization (acetonitrile)	Genesis C_8 (20 × 2.1 mm I.D., Jones), gradient (methanol–water containing 0.5% acetic acid) and 0.2 ml/min	API 3000 (Applied Biosystems/ MDX-SCIEX), positive ESI, SRM ($[M + H]^+$ → product ion)	LOD (S/N = 3): 0.2 ng/ml Measurable range: 0.8–80 ng/ml	[56]
F and E IS: d_4-F	Human serum or plasma (0.1 ml) → LLE (methyl *t*-butyl ether)	Luna Phenyl-Hexyl (50 × 2.1 mm I.D., Phenomenex), methanol–water and 0.45 ml/min	API 3000 (Applied Biosystems/ MDX-SCIEX), positive APPI, SRM ($[M + H]^+$ → product ion)	LOD (S/N = 5): 1 ng/ml (F) and 5 ng/ml (E) Measurable range: 10–200 ng/ml	[49]
F and E IS: d_4-F	Human urine (0.5 ml) → LLE (dichloromethane)	LC-18l (33 × 4.6 mm I.D., Supelco), methanol–water and 0.2 ml/min	API 2000 (Applied Biosystems), positive ESI, SRM ($[M + H]^+$ → product ion)	Measurable range: 7–828 pmol/ml	[53]
F and E IS: d_4-F	Human adipose homogenate (0.2 g) → extraction (ethyl acetate) → LLE (heptane, and methanol–water)	Luna C18 (2) (150 × 2.0 mm I.D., Phenomenex), gradient (methanol containing 0.02% TFA–water containing 0.02% TFA) and 0.3 ml/min	Micromass Ultima Pt (Micromass), positive ESI, SRM ($[M + H]^+$ → product ion)	Measurable range: 0.6–1200 pmol/mg	[55]

THF, ATHF and THE	Human urine (1 ml) → RP-SPE	Discovery HS F5 (50 × 2.1 mm I.D., Supelco), gradient (methanol–water) and 0.25 ml/min	API 2000 (Applied Biosystems), negative ESI, SRM ($[M-H]^-$ → product ion)	LOD (S/N = 3): 0.4–0.8 pmol/ml Measurable range: 7.5–120 pmol/ml	[57]
THF, ATHF and THE	Human urine (1 ml) → RP-SPE	Luna C8 (50 × 2.0 mm I.D., Phenomenex), gradient (methanol–water containing 0.1% formic acid)	API 4000 (Applied Biosystems/MDX-SCIEX), positive ESI, SRM ($[M + H]^+$ → product ion)	Measurable range: 2.5–600 ng/ml (THF and ATHE) and 5–500 ng/ml (THE)	[58]
F and 6β-OH-F IS: 6α-Methyl-prednisolone	Human urine (0.1 ml) → online RP-SPE → column-switching technique	Symmetry Shield RP_{18} (100 × 2.1 mm I.D., Waters), gradient (methanol containing 0.1% formic acid–water containing 0.1% formic acid) and 0.3 ml/min	API 3000 (Applied Biosystems/MDX-SCIEX), negative ESI, SRM ($[M + HCOO]^-$ → product ion)	Measurable range: 2–56 ng/ml (F) and 17–300 ng/ml (6β-OH-F)	[54]
21-DOF	Human plasma (2 ml) → LLE (isooctane–ethyl acetate)	Alltima C_{18} (250 × 2.1 mm I.D., Alltima), gradient (methanol containing 0.025% TFA-water containing 0.025% TFA) and 0.2 ml/min	LCQ^{xp} (ThermoFinnigan), positive ESI, SRM ($[M + H]^+$ → product ion)	LOD: 4 pg Measurable range: 0.25–600 ng/ml	[59]
B IS: 5-Pregnen-3β-ol-20-one-16α-carbonitrile	Rat plasma (0.1 ml) → LLE (diethylether)	Zorbax-Eclipse C_8 (50 × 4.6 mm I.D., Agilent Technologies), gradient (methanol–water) and 0.8 ml/min	1100 series (Agilent Technologies), positive ESI, SIM ($[M + Na]^+$)	LOD: 9 fmol Measurable range: 2–400 pg/ml	[60]
B and 11-dehydro-corticosterone IS: E	Mouse liver homogenate (0.1 g) or adipose (0.2 g) → extraction (ethyl acetate) → LLE (heptane and methanol–water)	Symmetry C8 (150 × 2.1 mm I.D., Waters), gradient (methanol containing 0.02% TFA-water containing 0.02% TFA) and 0.3 ml/min	Micromass Ultima Pt (Micromass), positive ESI, SRM ($[M + H]^+$ → product ion)	Measurable range: 60–1200 pmol/mg (liver) and 6–600 pmol/mg (adipose)	[55]
B and 11-dehydro-corticosterone IS: E	Mouse adipose homogenate (0.2 g) → extraction (ethyl acetate) → LLE (heptane, methanol and water)	Symmetry C8 (150 × 2.1 mm I.D., Waters), gradient (methanol containing 0.02% TFA–water containing 0.02% TFA) and 0.3 ml/min	Micromass Ultima Pt (Micromass), positive ESI, SRM ($[M + H]^+$ → product ion)	Measurable range: 6–600 pmol/mg	[55]

ATHF and THE,[57,58] 21-DOF,[59] and 6β-OH-F[54] have also been reported. Corticosterone (B) is the most typical glucocorticoid in rodents, and its plasma level in the rat[60] and tissue level of the mouse[55] have been measured using LC–MS.

BILE ACIDS

Bile acids play a pivotal role in the metabolism of cholesterol and lipids. Their blood concentrations are important prognostic and diagnostic indicators of the hepatobiliary and intestinal dysfunction. The naturally occurring common bile acids are saturated C_{24} steroid carboxylic acids, including cholic acid (CA), chenodeoxycholic acid (CDCA), deoxycholic acid (DCA), lithocholic acid (LCA), and ursodeoxycholic acid (UDCA). Bile acids are conjugated in the human liver with taurine or glycine before they are secreted via the biliary canaliculi into the bile. Thus, bile acids usually have an ionic functional group and, therefore, their LC–MS assays are performed using negative ESI[61–65] (Table 5).

Bile acid CoA esters are the intermediates in the oxidative shortening of the side chain of the C_{27}-bile acids (β-oxidation) in the biosynthesis of bile acids. Therefore, the blood levels of the bile acid CoA esters and C_{27}-bile acids are good markers for the diagnosis of peroxisomal disorders, such as Zellweger syndrome. The development and clinical applications of the LC–ESI-MS methods for bile acid CoA esters[66] and C_{27}-bile acids[67] have been reported.

Recently, it was found that unconjugated bile acids (CA, CDCA, and DCA) are present at high (nmol/g tissue) levels in the rat brain cytoplasmic fraction,[64] but their functions in the central nervous system are unclear. To clarify this point, a profile analysis of the rat serum bile acids (eight common bile acids and their glycine and taurine conjugates) has been demonstrated.[65]

VITAMIN D METABOLITES

The measurements of the serum/plasma concentration of the vitamin D [vitamin D_2 (D_2) and vitamin D_3 (D_3)] metabolites are widely used for the diagnostic assessment and the follow-up of several diseases (osteoporosis, renal osteodystrophy, parathyroid gland disorders, and sarcoidosis). Although the ionization efficiencies of the vitamin D metabolites are very low in ESI or APCI, the serum/plasma 25-hydroxyvitamin D_3 [25-OH-D_3] can be measured using LC–ESI- or APCI-MS without derivatization when a relatively large volume of sample (0.1–0.2 ml) is used,[68–71] because of its relatively high serum/plasma level (10–40 ng/ml) (Table 6). Some of these methods can simultaneously determine the 25-hydroxyvitamin D_2 [25-OH-D_2] levels.[69–71] If the available sample volume is limited, a derivatization is required to measure the serum/plasma 25-OH-D_3 and 25-OH-D_2 (sample volume, 20 μl).[72,73] Cookson-type reagents rapidly and quantitatively react with vitamin D compounds to form Diels–Alder adducts, which increase their detection responses (more than 10 times) in APCI-MS. 4-[2-(6,7-Dimethoxy-4-methyl-3-oxo-3,4-dihydroquinoxalyl) ethyl]-1,2,4-triazoline-3,5-dione (DMEQTAD) and 4-(4-nitrophenyl)-1,2,4-triazoline-3,5-dione (NPTAD) were used as the derivatization reagents for the positive APCI-[72] and ECAPCI-MS detection,[73] respectively. Another Cookson-type reagent, 4-[4-(6-methoxy-2-benzoxazolyl)phenyl]-1,2,4-triazoline-3,5-dione (MBOTAD), was also used for the plasma 24,25-dihydroxyvitamin D_3 [24,25-$(OH)_2$-D_3] measurement.[74]

Because the serum/plasma concentration of the active form of vitamin D_3, 1,25-$(OH)_2$-D_3, is extremely low (30–70 pg/ml), it has been conventionally measured by a radioreceptor assay technique using the vitamin D receptor in the clinical field. Although a method has been reported for the LC–MS assay of 1,25-$(OH)_2$-D_3,[75] its applicability was proved only for the rat serum assay; this method is of less practical use in the clinical field. Even if an up-to-date mass spectrometer model is employed, it may be difficult to measure the serum/plasma 1,25-$(OH)_2$-D_3 levels with a clinically available sample volume (<1 ml).

OTHERS AND STEROID PROFILES

Oxysterols are oxidized derivatives of cholesterol (Ch) and of potential diagnostic interest because their circulating levels may reflect the cholesterol metabolism in the brain. For example, it has been reported that the plasma 24*S*-hydroxycholesterol (24-OH-Ch, cerebrosterol) is increased in Alzheimer and vascular demented patients.[76] Recently, application of LC–MS for the measurement of these sterols,[18,77] which are conventionally measured by GC–MS, has been attempted (Table 7).

Steroid profile analysis (simultaneous measurement of various types of steroids) plays an important role in the clinical evaluation of a number of common endocrine disorders in humans and animal models. LC–MS profiles of steroids in bovine adrenal cells,[78] the rat brain,[17] and human serum[7] have been reported during the past five years (Table 7).

Table 5 Bile acids.

Analyte	Sample treatment	LC conditions (analytical column, mobile phase, and flow rate)	MS (instrument, ionization mode, and detection)	Sensitivity	Refs.
UDCA, its glycine and taurine conjugates IS: 23-Nordeoxycholic acid	Human plasma (0.3 ml) → RP-SPE	Prism RP (100 × 4.6 mm I.D., ThermoHypersil), methanol-25 m*M* ammonium acetate containing 0.05% acetic acid and 1 ml/min (split rate of 1 : 5)	API 2000 (Sciex), negative ESI, SRM ($[M–H]^-$ → product ion)	Measurable range: 10–3000 ng/ml	[61]
CA, CDCA, DCA, LCA, their glycine and taurine conjugates, UDCA and its taurine conjugate	Human plasma (0.25 ml) → deproteinization (acetonitrile)	Pinnacle ODS (100 × 4.6 mm I.D., Restek), gradient (methanol-5 m*M* ammonium acetate containing 0.012% formic acid) and 1 ml/min (split rate of 1 : 20)	API 365 (Applied Biosystems-SCIEX), negative ESI, SRM ($[M–H]^-$ → product ion)	Measurable range: 0.1–100 nmol/ml	[62]
CA, CDCA, DCA, LCA, UDCA, their glycine and taurine conjugates IS: d_4-CA, d_4-CDCA, d_4-DCA, d_4-LCA, d_4-UDCA, and glycine conjugates of d_4-CA, d_4-CDCA	Human serum (0.75 ml) → RP-SPE	Uptisphere C_{18} ODB (125 × 2.0 mm I.D., Interchim), gradient (methanol containing 0.012% formic acid–10 m*M* ammonium acetate) and 0.2 ml/min	TSQ 7000 (Finnigan), negative ESI, SIM ($[M–H]^-$, unconjugates), SRM ($[M–H]^-$ → product ion, conjugates)	Measurable range: 0.12–60 nmol/ml	[63]
Dihydroxycholestanoic acid CoA ester and trihydroxycholestanoic acid CoA ester IS: d_4-CA CoA ester	Rat liver homogenate (0.1 g) → extraction (ethyl acetate) → RP-SPE	Synergi HydroRP 80A (150 × 2.0 mm I.D., Phenomenex), isopropanol–acetonitrile–water adjusted to pH 2.7 with formic acid and 0.4 ml/min	API 365 (Sciex), positive ESI, SRM ($[M + H]^+$ → product ion)	LOD: 0.1 nmol	[65]
CA, CDCA, DCA, LCA, UDCA, hydroxycholic acid, α-muricholic acid, β-muricholic acid, their glycine and taurine conjugates IS: d_2-$^{18}O_2$-CDCA and d-^{18}O-LCA	Rat serum (0.1 ml) → RP-SPE	Luna C18 (2) (150 × 2.0 mm I.D., Phenomenex), gradient (acetonitrile–methanol–20 m*M* ammonium acetate) and 0.2 ml/min	Quattro II (Micromass), negative ESI, SRM ($[M–H]^-$ → product ion)	Measurable range: 5–2000 ng/ml (CA, CDCA, DCA, UDCA, hydroxycholic acid, α-muricholic acid, β-muricholic acid, and their conjugates) and 5–500 ng/ml (LCA and its conjugate)	[66]
Dihydroxycholestanoic acid, trihydroxycholestanoic acid and their taurine conjugates IS: d_4-CA and taurine conjugate of d_4-CA	Human plasma (50 μl) → deproteinization (acetonitrile)	Alltima C_{18} (250 × 2.1 mm I.D., Alltima), gradient (ethanol–5 m*M* ammonium formate) and 0.3 ml/min	Quattro II (Micromass), negative ESI, SRM ($[M–H]^-$ → product ion, unconjugates), SIM ($[M–H]^-$, taurine conjugates)	LOD: 0.05 nmol/ml	[67]
CA, CDCA, DCA IS: d_2-$^{18}O_2$-CDCA	Rat brain (30 mg) → denaturation of protein (1.65 *M* Tris–HCl buffer containing 0.03 *M* EDTA and 7.3 *M* guanidine hydrochloride) → deproteinization (ethanol)	Inertsil ODS-2 (150 × 2.1 mm I.D., GL Science), acetonitrile-20 m*M* ammonium acetate and 0.22 ml/min	JMS-LC mate (JEOL), negative ESI, SIM ($[M–H]^-$)	LOD (S/N = 5): 5 pg	[64]

Table 6 Vitamin D metabolites.

Analyte	Sample treatment	LC conditions (analytical column, mobile phase, and flow rate)	MS (instrument, ionization mode, and detection)	Sensitivity	Refs.
25-OH-D_3 IS: d_4-25-OH-D_3	Human serum (0.2 ml) → deproteinization (acetonitrile) → online RP-SPE → column-switching technique	LiCrospher 100RP-18 (125 × 4.0 mm I.D., Merck), methanol-0.5 m*M* ammonium acetate and 0.85 ml/min	Quattro (Micromass), positive ESI and SRM ($[M + H]^+$ → product ion)	Measurable range: 7.3–182 pmol/ml	[68]
25-OH-D_2 and 25-OH-D_3 IS: d_3-Δ^9-Tetrahydro-cannabinol	Human serum (0.2 ml) → LLE (heptane)	XTerra (50 × 2.1 mm I.D., Waters), methanol–2 m*M* ammonium acetate containing 0.1% formic acid and 0.1 ml/min	Quattro (Micromass), positive ESI, SRM ($[M + H]^+$ → product ion)	LOD: 0.06 ng/ml (25-OH-D_3) and 0.09 ng/ml (25-OH-D_2)	[69]
25-OH-D_2 and 25-OH-D_3 IS: d_6-25-OH-D_3	Human plasma (0.1 ml) → deproteinization (methanol) → RP-SPE	Capcell Pak C18 UG120 (250 × 4.6 mm I.D., Shiseido Fine Chemical), methanol–water and 0.5 ml/min	API 3000 (Applied Biosystems), positive APCI and SRM ($[M + H]^+$ → product ion)	LOD (S/N = 3): 2.5 ng/ml Measurable range: 5–100 ng/ml	[70]
25-OH-D_2 and 25-OH-D_3 IS: d_6-25-OH-D_3	Human serum (0.1 ml) → deproteinization (methanol–propanol)	BDS C_8 (51 × 2.1 mm I.D., ThermoHypersil), gradient (methanol–water containing 0.05% formic acid) and 0.3 ml/min	API 3000 (Applied Biosystems), positive ESI, SRM ($[M + H]^+$ → product ion)	Measurable range: 4.0–256 pmol/ml (25-OH-D_3) and 4.95–316 pmol/ml (25-OH-D_2)	[71]
25-OH-D_2 and 25-OH-D_3 IS: 25-OH-D_4	Human plasma (20 μl) → deproteinization (acetonitrile) → LLE (ethyl acetate and water) → derivatization with DMEQTAD	J'sphere ODS H-80 (150 × 4.6 mm I.D., YMC), acetonitrile–water and 1 ml/min	LCQ (ThermoQuest), positive APCI and SRM ($[M + H]^+$ → residual $[M + H]^+$)	LOD (S/N = 3): 12.5 fmol (25-OH-D_3) and 20 fmol (25-OH-D_2) Measurable range: 0.05–1 ng/tube	[72]
25-OH-D_3 IS: 25-OH-D_4	Human plasma (20 μl) → deproteinization (acetonitrile) → LLE (ethyl acetate and water) → derivatization with NPTAD	J'sphere ODS H-80 (150 × 4.6 mm I.D., YMC), methanol–water and 1 ml/min	LCQ (ThermoQuest), ECAPCI and SRM ($[M]^-$ → residual $[M]^-$)	LOD (S/N = 3): 10 fmol, Measurable range: 0.05–1 ng/tube	[73]
24,25-$(OH)_2$-D_3 IS: d_6-24,25-$(OH)_2$-D_3	Human plasma (0.3 ml) → deproteinization (acetonitrile) → RP-SPE → silica gel column → derivatization with MBOTAD	J'sphere ODS H-80 (150 × 4.6 mm I.D., YMC), acetonitrile–water and 1 ml/min	LCQ (ThermoQuest), positive APCI and SRM ($[M + H]^+$ → residual $[M + H]^+$)	LOD (S/N = 3): 18 fmol, Measurable range: 0.05–1.2 ng/tube	[74]
1,25-$(OH)_2$-D_3 IS: d_6-1,25-$(OH)_2$-D_3	Human, rat, and pig serum (1 ml) → deproteinization (acetonitrile) → RP-SPE	Symmetry C_8 (50 × 2.1 mm I.D., Waters), gradient (methanol–2 m*M* ammonium acetate) and 0.3 ml/min	API 3000 (PE/Sciex), positive ESI and SRM ($[M + NH_4]^+$ → product ion)	Measurable range: 20–100 pg/ml	[75]

Table 7 Others and steroid profile.

Analyte	Sample treatment	LC conditions (analytical column, mobile phase, and flow rate)	MS (instrument, ionization mode, and detection)	Sensitivity	Refs.
24-OH-Ch and 27-OH-Ch IS: d_7-24-OH-Ch	Human plasma (0.5 ml) → saponification (NaOH) → RP-SPE	Nucleosil C_{18} HD (125 × 2.0 mm I.D., Machery-Nagel), methanol–acetonitrile–10 m*M* ammonium acetate buffer and 0.25 ml/min	TSQ 7000 (ThermoQuest), positive APCI and SIM ($[M + H–H_2O]^+$ or $[M + H–2H_2O]^+$)	LOQ: 40 ng/ml (24-OH-Ch) and 25 ng/ml (27-OH-Ch)	[77]
Various hydoxy-cholesterol	Rat brain (100 mg) → ethanol extraction → anion-exchange column (Lipidex DEAP) → NP-mini-column → oxidation with cholesterol oxidase → derivatization with Girard reagent P	PepMap C18 (150 × 0.18 mm I.D., Dionex), gradient (methanol–water containing 0.1% fomic acid) and 1 μl/min	Q-TOF Global (Micromass), positive ESI and MS or MS–MS (not quantitative analysis)	LOD: sub-pg	[18]
ALDO, F, E, DOC, PREG and PROG IS: d_2-F and d_2-E	Bovine adrenal cell culture medium → LLE (ethyl acetate)	Kromasil (250 × 2.0 mm I.D., Eka Chemical), gradient (methanol–water) and 0.25 ml/min	1100 series (Agilent), positive ESI, SIM ($[M + Na]^+$)	LOD (S/N = 3): 2 pg on column [except for PREG (10 pg on column)] Measurable range: 5–1000 pg [except for PREG (25–5000 pg)]	[78]
DHEA, PREG, PROG, T, pregnanolone, allopregnanolone, epipregnanolone and epiallopregnanolone, IS: d_4-DHEA and $^{13}C_2$-PROG	Rat brain (50–300 mg) → extraction (ethanol) → RP-SPE → cation exchange column (SP-LH-20) → anion exchange column (Lipidex-DEAP) → derivatization with hydroxylammonium chloride → RP-SPE → cation exchange column (SP-LH-20)	Genesis C18 (350 × 0.1 mm I.D., Jones Chromatography), gradient (methanol–water containing 10 m*M* ammonium acetate) and 0.2–0.3 μl/min	AutoSpec-OATOFFPD, Quattro Ultima or Quattro Micro (Micromass), positive ESI and SRM ($[M + H]^+$ → product ion) or precursor ion scan	LOD (S/N = 10); 1.5 pg (DHEA, PREG, allopregnanolone), 3 pg (PROG) and 1 pg (T)	[17]
E_2, E_3, DHEA, DHEA-S, AD, T, PROG, 17-OH-PROG, F and 11-DOF IS: d_4-E_2, d_2-E_3, d_2-DHEA, d_7-AD, d_2-T, d_8-PROG, d_8-17-OH-PROG, d_4-F and d_2-11-DOF	Human serum (760 μl) → deproteinization (acetonitrile) → column-switching technique	LC-18-DB (33 × 3.0 mm I.D., Supelco), gradient (methanol–water) and 0.5 ml/min	API 3000 (Applied Biosystems), positive APPI and SRM ($[M + H]^+$ → product ion)	LOD: 100 pg/ml	[7]

REFERENCES

1. Tu, H.; Okamoto, A.Y.; Shan, B. FXR, a bile acid receptor and biological sensor. Trends Cardiovasc. Med. **2000**, *10* (1), 30–35.
2. Baulieu, E.E.; Robel, P.; Schumacher, M. Neurosteroids: Beginning of the story. Int. Rev. Neurobiol. **2001**, *46*, 1–32.
3. Andrew, R. Clinical measurement of steroid metabolism. Best Pract. Res. Clin. Endocrinol. Metab. **2001**, *15* (1), 1–16.
4. Shimada, K.; Mitamura, K.; Higashi, T. Gas chromatography and high-performance liquid chromatography of natural steroids. J. Chromatogr. A, **2001**, *935* (1–2), 141–172.
5. Ma, Y.-C.; Kim, H.-Y. Determination of steroids by liquid chromatography/mass spectrometry. J. Am. Soc. Mass Spectrom. **1997**, *8* (9), 1010–1020.
6. Leinonen, A.; Kuuranne, T.; Kostiainen, R. Liquid chromatography/mass spectrometry in anabolic steroid analysis—optimization and comparison of three ionization techniques: Electrospray ionization, atmospheric pressure chemical ionization and atmospheric pressure photoionization. J. Mass Spectrom. **2002**, *37* (7), 693–698.
7. Guo, T.; Chan, M.; Soldin, S.J. Steroid profiles using liquid chromatography–tandem mass spectrometry with atmospheric pressure photoionization source. Arch. Pathol. Lab. Med. **2004**, *128* (4), 469–175.
8. Griffiths, W.J.; Liu, S.; Alvelius, G.; Sjövall, J. Derivatisation for the characterisation of neutral oxosteroids by electrospray and matrix-assisted laser desorption/ionization tandem mass spectrometry: The Girard P derivative. Rapid Commun. Mass Spectrom. **2003**, *17* (9), 924–935.
9. Higashi, T.; Shimada, K. Derivatization of neutral steroids to enhance their detection characteristics in liquid chromatography–mass spectrometry. Anal. Bioanal. Chem. **2004**, *378* (4), 875–882.
10. Higashi, T.; Yamauchi, A.; Shimada, K. 2-Hydrazino-1-methylpyridine: A highly sensitive derivatization reagent for oxosteroids in liquid chromatography–electrospray ionization-mass spectrometry. J. Chromatogr. B, **2005**, *825* (2), 214–222.
11. Higashi, T.; Takayama, N.; Shimada, K. Enzymic conversion of 3β-hydroxy-5-ene-steroids and their sulfates to 3-oxo-4-ene-steroids for increasing sensitivity in LC–APCI-MS. J. Pharm. Biomed. Anal. **2005**, *39* (3–4), 718–723.
12. Marwah, A.; Marwah, P.; Lardy, H. Analysis of ergosteroids VIII: Enhancement of signal response on neutral steroidal compounds in liquid chromatographic–electrospray ionization mass spectrometric analysis by mobile phase additive. J. Chromatogr. A, **2002**, *964* (1–2), 137–151.
13. Goto, T.; Shibata, A.; Iida, T.; Mano, N.; Goto, J. Sensitive mass spectrometric detection of neutral bile acid metabolites. Formation of adducts with an organic anion in atmospheric pressure chemical ionization. Rapid Commun. Mass Spectrom. **2004**, *18* (19), 2360–2364.
14. Singh, G.; Gutierrez, A.; Xu, K.; Blair, I.A. Liquid chromatography/electron capture atmospheric pressure chemical ionization/mass spectrometry: Analysis of pentafluorobenzyl derivatives of biomolecules and drugs in the attomole range. Anal. Chem. **2000**, *72* (14), 3007–3013.
15. Higashi, T.; Takido, N.; Yamauchi, A.; Shimada, K. Electron-capturing derivatization of neutral steroids for increasing sensitivity in liquid chromatography/negative atmospheric pressure chemical ionization-mass spectrometry. Anal. Sci. **2002**, *18* (12), 1301–1307.
16. Liu, S.; Griffiths, W.J.; Sjövall, J. Capillary liquid chromatography/electrospray mass spectrometry for analysis of steroid sulfate in biological samples. Anal. Chem. **2003**, *75* (4), 791–797.
17. Liu, S.; Sjövall, J.; Griffiths, W.J. Neurosteroids in rat brain: Extraction, isolation, and analysis by nanoscale liquid chromatography–electrospray mass spectrometry. Anal. Chem. **2003**, *75* (21), 5835–5846.
18. Griffiths, W.J.; Wang, Y.; Alvelius, G.; Liu, S.; Bodin, K.; Sjövall, J. Analysis of oxysterols by electrospray tandem mass spectrometry. J. Am. Soc. Mass Spectrom. **2006**, *17* (3), 341–362.
19. Quirke, J.M.E.; Adams, C.L.; Van Berkel, G.J. Chemical derivatization for electrospray ionization mass spectrometry. 1. Alkyl halides, alcohols, phenols, thiols, and amines. Anal. Chem. **1994**, *66* (8), 1302–1315.
20. Tai, S.S.; Welch, M.J. Development and evaluation of a reference measurement procedure for the determination of estradiol-17β in human serum using isotope-dilution liquid chromatography–tandem mass spectrometry. Anal. Chem. **2005**, *77* (19), 6359–6363.
21. Nelson, R.E.; Grebe, S.K.; Okane, D.J.; Singh, R.J. Liquid chromatography–tandem mass spectrometry assay for simultaneous measurement of estradiol and estrone in human plasma. Clin. Chem. **2004**, *50* (2), 373–384.
22. Xu, X.; Veenstra, T.D.; Fox, S.D.; Roman, J.M.; Issaq, H.J.; Falk, R.; Saavedra, J.E.; Keefer, L.K.; Ziegler, R.G. Measuring fifteen endogenous estrogens simultaneously in human urine by high-performance liquid chromatography–mass spectrometry. Anal. Chem. **2005**, *77* (20), 6646–6654.
23. Xu, X.; Ziegler, R.G.; Waterhouse, D.J.; Saavedra, J.E.; Keefer, L.K. Stable isotope dilution high-performance liquid chromatography–electrospray ionization mass spectrometry method for endogenous 2- and 4-hydroxyestrones in human urine. J. Chromatogr. B, **2002**, *780* (2), 315–330.
24. Xu, X.; Keefer, L.K.; Waterhouse, D.J.; Saavedra, J.E.; Veenstra, T.D.; Ziegler, R.G. Measuring seven endogenous ketolic estrogens simultaneously in human urine by high-performance liquid chromatography–mass spectrometry. Anal. Chem. **2004**, *76* (19), 5829–5836.
25. Yang, Y.J.; Lee, J.; Choi, M.H.; Chung, B.C. Direct determination of estriol 3- and 16-glucuronides in pregnancy urine by column-switching liquid chromatography with electrospray tandem mass spectrometry. Biomed. Chromatogr. **2003**, *17* (14), 219–225.
26. Nakagawa, Y.; Hashimoto, Y. Polar derivatization of 5α-dihydrotestosterone and sensitive analysis by semimicro-LC/ESI-MS. J. Mass Spectrom. Spc. Jpn. **2002**, *50* (6), 330–336.

27. Nishiyama, T.; Hashimoto, Y.; Takahashi, K. The influence of androgen deprivation therapy on dihydrotestosterone levels in the prostatic tissue of patients with prostate cancer. Clin. Cancer Res. **2004**, *10* (21), 7121–7126.
28. Higashi, T.; Yamauchi, A.; Shimada, K.; Koh, E.; Mizokami, A.; Namiki, M. Determination of prostatic androgens in 10 mg of tissue using liquid chromatography–tandem mass spectrometry with charged derivatization. Anal. Bioanal. Chem. **2005**, *382* (2), 1035–1043.
29. Chadwick, C.A.; Owen, L.J.; Keevil, B.G. Development of a method for the measurement of dehydroepiandrosterone sulphate by liquid chromatography–tandem mass spectrometry. Ann. Clin. Biochem. **2005**, *42* (Pt 6), 468–474.
30. Mitamura, K.; Nagaoka, Y.; Shimada, K.; Honma, S.; Namiki, M.; Koh, E.; Mizokami, A. Simultaneous determination of androstenediol 3-sulfate and dehydroepiandrosterone sulfate in human plasma using isotope diluted liquid chromatography–electrospray ionization-mass spectrometry. J. Chromatogr. B, **2003**, *796* (1), 121–130.
31. Mitamura, K.; Nagaoka, Y.; Shimada, K.; Honma, S.; Namiki, M.; Koh, E.; Mizokami, A. Determination of sulfates of androsterone and epiandrosterone in human serum using isotope diluted liquid chromatography–electrospray ionization-mass spectrometry. Biomed. Chromatogr. **2005**, *19* (10), 796–801.
32. Chol, M.H.; Kim, J.N.; Chung, B.C. Rapid HPLC-electrospray tandem mass spectrometric assay for urinary testosterone and dihydrotestosterone glucuronides from patients with benign prostate hyperplasia. Clin. Chem. **2003**, *49* (2), 322–325.
33. Sheen, J.F.; Her, G.R. Application of pentafluorophenylhydrazine derivative to the analysis of nabumetone and testosterone in human plasma by liquid chromatography-atmospheric pressure chemical ionization-tandem mass spectrometry. Anal. Bioanal. Chem. **2004**, *380* (7–8), 891–897.
34. Zhao, M.; Baker, S.D.; Yan, X.; Zhao, Y.; Wright, W.W.; Zirkin, B.R.; Jarow, J.P. Simultaneous determination of steroid composition of human testicular fluid using liquid chromatography–tandem mass spectrometry. Steroids **2004**, *69* (11–12), 721–726.
35. Niwa, M.; Watanabe, N.; Ochiai, H.; Yamashita, K. Determination of testosterone concentrations in rat plasma using liquid chromatography–atmospheric pressure chemical ionization mass spectrometry combined with ethyl oxime and acetyl ester derivatization. J. Chromatogr. B, **2005**, *824* (1–2), 258–266.
36. Reddy, D.S.; Venkatarangan, L.; Chien, B.; Ramu, K. A high-performance liquid chromatography–tandem mass spectrometry assay of the androgenic neurosteroid 3α-androstanediol (5α-androstane-3α,17β-diol) in plasma. Steroids **2005**, *70* (13), 879–885.
37. Higashi, T.; Ninomiya, Y.; Iwaki, N.; Yamauchi, A.; Takayama, N.; Shimada, K. Studies on neurosteroids XVIII. LC–MS analysis of changes in rat brain and serum testosterone levels induced by immobilization stress and ethanol administration. Steroids **2006**, *71* (7), 609–617.
38. Lai, C.-C.; Tsai, C.-H.; Tsai, F.-J.; Lee, C.-C.; Lin, W.-D. Rapid monitoring assay of congenital adrenal hyperplasia with microbore high-performance liquid chromatography/electrospray ionization tandem mass spectrometry from dried blood spots. Rapid Commun. Mass Spectrom. **2001**, *15* (22), 2145–2151.
39. Lai, C.-C.; Tsai, C.-H.; Tsai, F.-J.; Wu, J.-Y.; Lin, W.-D.; Lee, C.-C. Monitoring of congenital adrenal hyperplasia by microbore HPLC–electrospray ionization tandem mass spectrometry of dried blood spots. Clin. Chem. **2002**, *48* (2), 354–356.
40. Lai, C.-C.; Tsai, C.-H.; Tsai, F.-J.; Wu, J.-Y.; Lin, W.-D.; Lee, C.-C. Rapid screening assay of congenital adrenal hyperplasia by measuring 17α-hydroxyprogesterone with high-performance liquid chromatography/electrospray ionization tandem mass spectrometry from dried blood spot. J. Clin. Lab. Anal. **2002**, *16* (2), 20–25.
41. Turpeinen, U.; Itkonen, O.; Ahola, L.; Stenman, U.H. Determination of 17α-hydroxyprogesterone in serum by liquid chromatography-tandem mass spectrometry and immunoassay. Scand. J. Clin. Lab. Invest. **2005**, *65* (1), 3–12.
42. Lacey, J.M.; Minutti, C.Z.; Magera, M.J.; Tauscher, A.L.; Casetta, B.; McCann, M.; Lymp, J.; Hahn, S.H.; Rinaldo, P.; Matern, D. Improved specificity of newborn screening for congenital adrenal hyperplasia by second-tier steroid profiling using tandem mass spectrometry. Clin. Chem. **2004**, *50* (3), 621–625.
43. Rauh, M.; Groschl, M.; Rasher, W.; Dorr, H.G. Automated, fast and sensitive quantification of 17α-hydroxyprogesterone, androstenedione and testosterone by tandem mass spectrometry with on-line extraction. Steroids **2006**, *71* (6), 450–458.
44. Higashi, T.; Takido, N.; Shimada, K. Detection and characterization of 20-oxosteroids in rat brains using LC-electron capture APCI-MS after derivatization with 2-nitro-4-trifluoromethylphenylhydrazine. Analyst **2003**, *128* (2), 130–133.
45. Higashi, T.; Takido, N.; Shimada, K. Studies on neurosteroids XVII. Analysis of stress-induced changes in neurosteroid levels in rat brains using liquid chromatography-electron capture atmospheric pressure chemical ionization-mass spectrometry. Steroids **2005**, *70* (1), 1–11.
46. Tai, S.S.; Welch, M.J. Development and evaluation of a candidate reference method for the determination of total cortisol in human serum using isotope dilution liquid chromatography/mass spectrometry and liquid chromatography/tandem mass spectrometry. Anal. Chem. **2004**, *76* (4), 1008–1014.
47. Jung, P.G.; Kim, B.; Park, S.R.; So, H.Y.; Shi, L.H.; Kim, Y. Determination of serum cortisol using isotope dilution–liquid chromatography–mass spectrometry as a candidate reference method. Anal. Bioanal. Chem. **2004**, *380* (5–6), 782–788.
48. Vogeser, M.; Briegel, J.; Jacob, K. Determination of serum cortisol by isotope-dilution liquid-chromatography electrospray ionization tandem mass spectrometry with on-line extraction. Clin. Chem. Lab. Med. **2001**, *39* (10), 944–947.
49. Kushnir, M.M.; Neilson, R.; Roberts, W.L.; Rockwood, A.L. Cortisol and cortisone analysis in serum and plasma by atmospheric pressure photoionization tandem mass spectrometry. Clin. Biochem. **2004**, *37* (5), 357–362.
50. Turpeinen, U.; Stenman, U.H. Determination of urinary free cortisol by liquid chromatography–tandem mass

spectrometry. Scand. J. Clin. Lab. Invest. **2003**, *63* (2), 143–150.
51. Nassar, A.E.; Varshney, N.; Getek, T.; Cheng, L. Quantitative analysis of hydrocortisone in human urine using a high-performance liquid chromatographic–tandem mass spectrometric–atmospheric-pressure chemical ionization method. J. Chromatogr. Sci. **2001**, *39* (2), 59–64.
52. McCann, S.J.; Gillingwater, S.; Keevil, B.G. Measurement of urinary free cortisol using liquid chromatography–tandem mass spectrometry: Comparison with the urine adapted ACS:180 serum cortisol chemiluminescent immunoassay and development of a new reference range. Ann. Clin. Biochem. **2005**, *42* (2), 112–118.
53. Taylor, R.L.; Machacek, D.; Singh, R.J. Validation of a high-throughput liquid chromatography–tandem mass spectrometry method for urinary cortisol and cortisone. Clin. Chem. **2002**, *48* (9), 1511–1519.
54. Barrett, Y.C.; Akinsanya, B.; Chang, S.Y.; Vesterqvist, O. Automated on-line SPE LC–MS/MS method to quantitate 6beta-hydroxycortisol and cortisol in human urine: Use of the 6beta-hydroxycortisol to cortisol ratio as an indicator of CYP3A4 activity. J. Chromatogr. B, **2005**, *821* (2), 159–165.
55. Ronquist-Nii, Y.; Edlund, P.O. Determination of corticosteroids in tissue samples by liquid chromatography–tandem mass spectrometry. J. Pharm. Biomed. Anal. **2005**, *37* (2), 341–350.
56. Jonsson, B.A.; Malmberg, B.; Amilon, A.; Helene Garde, A.; Orbaek, P. Determination of cortisol in human saliva using liquid chromatography–electrospray tandem mass spectrometry. J. Chromatogr. B, **2003**, *784* (1), 63–68.
57. Turpeinen, U.; Markkanen, H.; Sane, T.; Hamalainen, E. Determination of free tetrahydrocortisol and tetrahydrocortisone ratio in urine by liquid chromatography–tandem mass spectrometry. Scand. J. Clin. Lab. Invest. **2006**, *66* (2), 147–159.
58. Raffaelli, A.; Saba, A.; Vignali, E.; Marcocci, C.; Salvadori, P. Direct determination of the ratio of tetrahydrocortisol + allotetrahydrocortisol to tetrahydrocortisone in urine by LC–MS–MS. J. Chromatogr. B, **2006**, *830* (2), 278–285.
59. Cristoni, S.; Cuccato, D.; Sciannamblo, M.; Bernardi, L.R.; Biunno, I.; Gerthoux, P.; Russo, G.; Weber, G.; Mora, S. Analysis of 21-deoxycortisol, a marker of congenital adrenal hyperplasia, in blood by atmospheric pressure chemical ionization and electrospray ionization using multiple reaction monitoring. Rapid. Commun. Mass Spectrom. **2004**, *18* (1), 77–82.
60. Marwah, A.; Marwah, P.; Lardy, H. Liquid chromatography–electrospray ionization mass spectrometric analysis of corticosterone in rat plasma using selected ion monitoring. J. Chromatogr. B, **2001**, *757* (2), 333–342.
61. Tessier, E.; Neirinck, L.; Zhu, Z. High-performance liquid chromatographic mass spectrometric method for the determination of ursodeoxycholic acid and its glycine and taurine conjugates in human plasma. J. Chromatogr. B, **2003**, *798* (2), 295–302.
62. Tagliacozzi, D.; Mozzi, A.F.; Casetta, B.; Bertucci, P.; Bernardini, S.; Di, I.C.; Urbani, A.; Federici, G. Quantitative analysis of bile acids in human plasma by liquid chromatography–electrospray tandem mass spectrometry: A simple and rapid one-step method. Clin. Chem. Lab. Med. **2003**, *41* (12), 1633–1641.
63. Burkard, I.; von Eckardstein, A.; Rentsch, K.M. Differentiated quantification of human bile acids in serum by high-performance liquid chromatography–tandem mass spectrometry. J. Chromatogr. B, **2005**, *826* (1–2), 147–159.
64. Ando, M.; Kaneko, T.; Watanabe, R.; Kikuchi, S.; Goto, T.; Iida, T.; Hishinuma, T.; Mano, N.; Goto, J. High sensitive analysis of rat serum bile acid by liquid chromatography/electrospray ionization tandem mass spectrometry. J. Pharm. Biomed. Anal. **2006**, *40* (5), 1179–1186.
65. Gan-Schreier, H.; Okun, J.G.; Kohlmueller, D.; Langhans, C.D.; Peters, V.; Ten Brink, H.J.; Verhoeven, N.M.; Jakobs, C.; Voelkl, A.; Hoffmann, G.F. Measurement of bile acid CoA esters by high-performance liquid chromatography–electrospray ionization tandem mass spectrometry (HPLC–ESI–MS/MS). J. Mass Spectrom. **2005**, *40* (7), 882–889.
66. Ferdinandusse, S.; Overmars, H.; Denis, S.; Waterham, H.R.; Wanders, R.J.; Vreken, P. Plasma analysis of di- and trihydroxycholestanoic acid diastereomers in peroxisomal α-methylacyl-CoA racemase deficiency. J. Lipid Res. **2001**, *42* (1), 137–141.
67. Mano, N.; Goto, T.; Uchida, M.; Nishimura, K.; Ando, M.; Kobayashi, N.; Goto, J. Presence of protein-bound unconjugated bile acid in the cytoplasmic fraction of rat brain. J. Lipid Res. **2004**, *45* (2), 295–300.
68. Vogeser, M.; Kyriatsoulis, A.; Huber, E.; Kobold, U. Candidate reference method for the quantification of circulating 25-hydroxyvitamin D_3 by liquid chromatography–tandem mass spectrometry. Clin. Chem. **2004**, *50* (8), 1415–1417.
69. Saenger, A.K.; Laha, T.J.; Bremner, D.E.; Sadrzadeh, S.M. Quantification of serum 25-hydroxyvitamin D_2 and D_3 using HPLC–tandem mass spectrometry and examination of reference intervals for diagnosis of vitamin D deficiency. Am. J. Clin. Pathol. **2006**, *125* (6), 914–920.
70. Tsugawa, N.; Suhara, Y.; Kamao, M.; Okano, T. Determination of 25-hydroxyvitamin D in human plasma using high-performance liquid chromatography–tandem mass spectrometry. Anal. Chem. **2005**, *77* (9), 3001–3007.
71. Maunsell, Z.; Wright, D.J.; Rainbow, S.J. Routine isotope-dilution liquid chromatography–tandem mass spectrometry assay for simultaneous measurement of the 25-hydroxy metabolites of vitamins D_2 and D_3. Clin. Chem. **2005**, *51* (9), 1683–1690.
72. Higashi, T.; Awada, D.; Shimada, K. Simultaneous determination of 25-hydroxyvitamin D_2 and 25-hydroxyvitamin D_3 in human plasma by liquid chromatography–tandem mass spectrometry employing derivatization with a Cookson-type reagent. Biol. Pharm. Bull. **2001**, *24* (7), 738–743.
73. Higashi, T.; Yamauchi, A.; Shimada, K. Application of 4-(4-nitrophenyl)-1,2,4-triazoline-3,5-dione to analysis of 25-hydroxyvitamin D_3 in human plasma by liquid chromatography/electron capture atmospheric pressure chemical ionization–mass spectrometry. Anal. Sci. **2003**, *19* (6), 941–943.

74. Higashi, T.; Awada, D.; Shimada, K. Determination of 24,25-dihydroxyvitamin D_3 in human plasma using liquid chromatography–mass spectrometry after derivatization with a Cookson-type reagent. Biomed. Chromatogr. **2001**, *15* (2), 133–140.
75. Kissmeyer, A.M.; Sonne, K. Sensitive analysis of 1α,25-dihydroxyvitamin D_3 in biological fluids by liquid chromatography–tandem mass spectrometry. J. Chromatogr. A, **2001**, *935* (1–2), 93–103.
76. Lütjohann, D.; Papassotiropoulos, A.; Björkhem, I.; Locatelli, S.; Bagli, M.; Oehring, R.D.; Schlegel, U.; Jessen, F.; Rao, M.L.; von Bergmann, K.; Heun, R. Plasma 24S-hydroxycholesterol (cerebrosterol) is increased in Alzheimer and vascular demented patients. J. Lipid Res. **2000**, *41* (2), 195–198.
77. Burkard, I.; Rentsch, K.M.; von Eckardstein, A. Determination of 24S- and 27-hydroxycholesterol in plasma by high-performance liquid chromatography-mass spectrometry. J. Lipid Res. **2004**, *45* (4), 776–781.
78. Nithipatikom, K.; Holmes, B.B.; Isbell, M.A.; Hanke, C.J.; Gomez-Sanchez, C.E.; Campbell, W.B. Measurement of steroid synthesis in zona glomerulosa cell by liquid chromatography–electrospray ionization-mass spectrometry: inhibition by nitric oxide. Anal. Biochem. **2005**, *337* (2), 203–210.

Bioluminescence: Detection in TLC

Joseph Sherma
Department of Chemistry, Lafayette College, Easton, Pennsylvania, U.S.A.

Abstract
Toxicity screening of complex mixtures using the bioluminescent bacteria *Vibrio fischeri* following separation on a thin-layer chromatography (TLC) or high-performance thin-layer chromatography (HPTLC) plate is described. A commercial kit, Bioluminex™, is available for the method.

BIOLUMINESCENCE DETECTION

Physical, chemical, and biological, or bioactivity-based methods are used to detect zones in thin-layer chromatography (TLC) after the development of the plate with the mobile phase.[1] Advantages of combining TLC with a bioassay are high specificity and reduced interference of the matrix leading to less need for sample cleanup;[2] high sensitivity, with detection limits typically in the subnanogram to picogram range; and the identification of separated toxic compounds, degradation products, and metabolites based on chromatographic retention (R_f values), physical detection, and specific biological activity related to the test system.

Biological detection methods for microbiologically active compounds have been classified as diffusion methods, dilution methods, and bioautography.[3] The principle of direct bioautography is that a suspension of a microorganism growing in a suitable medium is applied to a developed TLC plate after drying; incubation of the plate with the microbes at optimum humidity and temperature allows growth of the bacteria; and, by use of a specific dye, live cells can be visualized because, for example, dehydrogenases from living microorganisms convert a tetrazolium salt into intensely colored formazan.[4] This entry will be limited to a description of TLC in combination with bioluminescence detection, in which antibacterial compounds are detected as dark zones against a luminescent layer background instead of as colorless zones against a colored layer background in bioautography. Bioluminescence–TLC is increasingly being used because of the commercial availability of a reagent kit, detection device, and supporting accessory instruments to standardize the method and provide the optimum results.

PRINCIPLES OF TLC–BIOLUMINESCENCE COUPLING

The technology for bioactivity screening by TLC–bioluminescence direct coupling was developed by Bayer AG (Leverkusen, Germany) and published in 1996.[5] The method is based on the change in emission by luminescent microorganisms in the presence of bioactive substances, which provides an effective way to detect toxic compounds on a TLC plate. The combination of TLC separation technology with the biospecific sensing ability of living cells represents a novel screening tool for targeting bioactive compounds in complex samples. In the published study,[5] the TLC–bioluminescence technique proved to be superior to a high-performance liquid chromatography (HPLC)–bioluminescence method.

After TLC separation and evaporation of the mobile phase, the plate is coated with a bioluminescent solution of the non-pathogenic marine organism *Vibrio fischeri* by dipping. *V. fischeri* emits light as a product of cellular respiration. As *V. fischeri* cells reach a critical cellular density, the bioluminescence catalyst, luciferase, is expressed. Luciferase, in the presence of oxygen, catalyzes an oxidation reaction that releases excess energy in the form of light. Toxic substances on the layer are selectively identified as dark zones (inhibited bacteria) on a luminescent background (viable bacteria). The degree of toxicity is proportional to the luminescence inhibition. The results occur within seconds and last until the plate dries. Results can be documented by video imaging with a charge coupled device (CCD) camera inside a dark box or by X-ray filming. The detection approach of bioluminescence is similar to classical fluorescence quenching detection in which compounds that contain aromatic rings or multiple bonds absorb 254 nm light from a UV source and appear as dark zones against a bright background when layers impregnated with a fluorescent phosphor (F_{254} layers) are used. Because a TLC plate is used only once, less purified samples can be tolerated, as compared with column chromatography, in which strongly retained impurities from a previous sample can be eluted and can interfere with later samples injected onto the column.

HPTLC–BIOLUMINESCENCE WITH THE BIOLUMINIZER®

In modern TLC–bioluminescence analysis, an HPTLC plate is used instead of a TLC plate in order to achieve greater resolution and speed. The sample is separated by HPTLC, and the plate is subsequently immersed in the luminescent bacterial suspension (*V. fischeri*; Bioluminex™ assay kit from ChromaDex, Irvine, California, U.S.A.). After an incubation time for completion of the reaction, all zones with inhibitory or toxic effects appear as black zones and those with stimulatory effect as lighter zones in the chromatograms on the plate, which is photographed by the Camag (Muttenz, Switzerland) BioLuminizer® (Fig. 1), a dark box imaging system employing a high-resolution cooled CCD camera with 16-bit data acquisition carried out for a specified time period. The BioLuminizer was developed specifically to accumulate the light signal from HPTLC plates for bioluminescence-based effect-directed analysis (EDA). The BioLuminizer has a holder that enables exact plate positioning (to 0.1 mm) and an optimized compartment that resists plate dryout and keeps the bacteria moist and luminescent for hours, leading to predictable bioluminescence activity for consistent results. EDA, combining HPTLC with direct bioluminescence, is a practical alternative to complex target analysis and provides a fast, low-cost means of demonstrating biological activity in cases where many unknown substances are present, such as environmental samples. The time and effort required to examine structures or isolate substances can be restricted to a few relevant substances. By using HPTLC to separate the test sample into individual substances, the possibility of antagonistic or synergistic effects leading to false results that can occur with classic cuvette tests are eliminated. Detection levels are typically in the picomole range. Inhibition values can be determined by special software for quantification of luminescence inhibition. In addition to bioluminescent bacteria, HPTLC–EDA has proven effective for other types of bioassays, such as acetylcholinesterase inhibition, penicillin, and *Bacillus subtilis*, as well as for genotoxicity tests such as umu (*Salmonella thyphimurium*) and yeast estrogen screen (YES).

Fig. 1 BioLuminizer® detection system for bioactive compounds.
Source: Photograph supplied by Camag, Muttenz, Switzerland.

Typically, the plate is dipped for 2 sec into the luminescent bacteria in the Bioluminex assay. Instead of manual dipping, this step can be carried out more reproducibly using the Camag Chromatogram Immersion device or Desaga TLC Dip-Fix (Desaga products are supplied by Sarstedt, Inc., Newton, North Carolina, U.S.A.),[6] which offer uniform vertical speed of immersion and withdrawal for selectable time periods. The dipping devices are also useful for prewashing the HPTLC plates to remove layer impurities before sample application. For highest resolution, samples can be applied bandwise with an automated instrument such as the Camag Linomat 5 or Desaga HPTLC-Applicator As 30.[7] Ascending chromatogram development is usually carried out in a traditional rectangular glass chamber such as the ridged-bottom twin-trough chamber,[8] but improved reproducibility can be achieved by using the Camag Automatic Developing Chamber or Desaga TLC-MAT automatic chamber,[6] which control chromatographic conditions such as saturation, layer activity, and drying; the highest-resolution separations can be performed by automated multiple development (AMD).[9] Chromatograms can be photographed under white light (colored zones detected), 254 nm (fluorescence-quenched zones), or 366 nm UV light (fluorescent zones) using a Desaga Digital Documentation System DD 50, ChromaDoc-IT Imaging System (Analtech, Newark, Delaware, U.S.A.), or Camag Digistore-2 Documentation System.[6] The light-quenching zones can be quantified based on their scan areas compared to standard zones measured with a slit-scanning densitometer such as the TLC Scanner 3 or Desaga CD 60,[6,10] or using image analysis software available with the three documentation systems mentioned above. These accessory instruments improve the methodology and complement the analytical information generated by the Bioluminex.

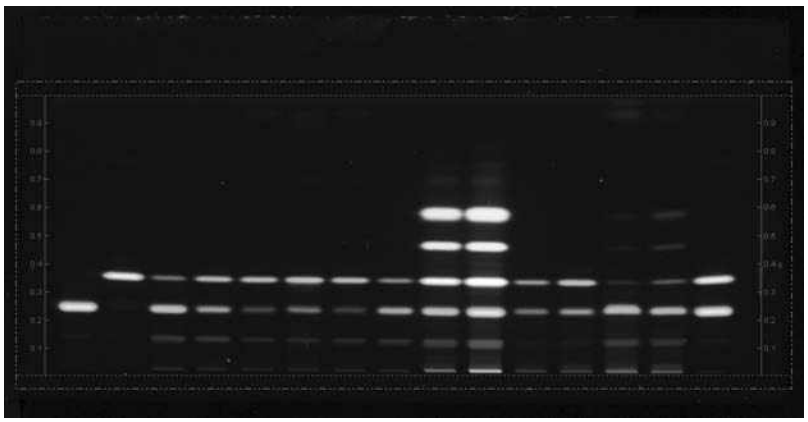

Fig. 2 Detection of berberine alkaloids by their green-to-yellow fluorescence under 366 nm UV light using a Digistore-2 Documentation System and by the Bioluminex assay. Lane numbers: 1, palmatine; 2, berberine; 3–8, *Mahonia* sp.; 9–10, *Coptis chinensis*; 11–12, *Phellodendron chinensis*; 13–14, *Tinospora* sp.; 15, palmatine plus berberine. Chromatographic conditions: HPTLC silica gel $60F_{254}$ Merck plate, toluene–ethyl acetate–methanol–isopropanol–water (60:30:20:15:3) mobile phase, 1 μl test and standard solutions applied, development in a twin-trough chamber.
Source: Photograph supplied by Camag, Muttenz, Switzerland.

APPLICATIONS OF TLC–BIOLUMINESCENCE ANALYSIS

Application areas suggested by ChromaDex[11] are natural biological and chemical toxins, chemical contaminants and pollutants, identification of potential biological activity (antimicrobiological screening), raw material identity testing, simultaneous chemical and biological profiling, parallel processing of up to 22 samples, and qualitative and quantitative analysis. Specific applications offered by ChromaDex are mycotoxin in corn; strychnine in infant formula; carbaryl insecticide in wine; fingerprint of *Capsicum annuum* in cayenne; and steroid As (III) and the herbicide metolachlor in tap water. For these applications, images of chromatograms are presented by ChromaDex. Other applications of TLC–bioluminescence described by Bayer[12] are toxicity profiling of wastewater over a 15 day period, analysis of natural product extracts, detection of tea seed oil residual, quantification of toxicity by toxicity equivalents based on calibration with 4-nitrophenol, United States Pharmacopeia (USP) method for *Matricaria chamomilla* detection using bioluminescence and anisaldehyde/366 nm, analysis of kava kava, and toxicity in process water.

Specific applications for the HPTLC-BioLuminizer method offered by Camag[13] are the following: analysis of wastewater containing X-ray contrast media for oxidation products produced by irradiation with UV light; toxicity screening for environmental applications; risk assessment and monitoring of drinking water, wastewater, and natural attenuation processes; detection of toxins and chemical adulterants in foodstuffs, beverages, and cosmetics; identification of biological activity in natural product extracts; determination of the biological activity of berberine-containing drugs (Figs. 2 and 3); determination of pesticides, heavy metals, organic pollutants, pharmaceuticals, and mycotoxins in a variety of complex matrices; and bioactivity-based analysis of irradiated sunscreens.

CONCLUSION

TLC or HPTLC combined with bioluminescence detection is an important method for the EDA of bioactive zones on the layer. Bioluminescent bacteria can be used or other types of bioassays can be carried out. A system incorporating *V. fischeri*, HPTLC, and detection with a CCD camera

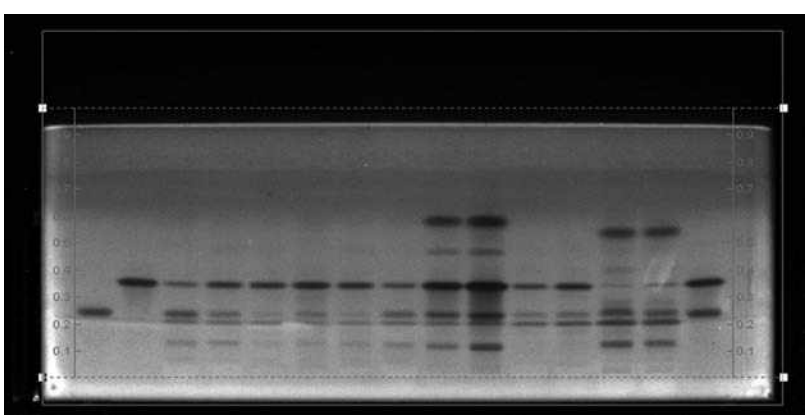

Fig. 3 HPTLC bioluminescence image of the same plate as in Fig. 2. Note that the different numbers of zones in the chromatograms detected in some of the lanes by the two methods provide complementary information on the samples.
Source: Photograph supplied by Camag, Muttenz, Switzerland.

in a dark box (BioLuminizer) is available from Camag. Various accessory HPTLC instruments can be incorporated to obtain improved results and additional analytical information. Key advantages are the avoidance of tedious single-compound screening, rapid response time and fast results, absence of false results due to antagonistic effects/interferences, detection in the picomole range, high sample throughput due to parallel analysis of multiple samples on one plate, low cost, and possibility of further investigation of toxic zones.

REFERENCES

1. Sherma, J. Detection of TLC zones. In *Encyclopedia of Chromatography*, 3rd Ed.; J. Cazes, Ed.; Taylor & Francis: New York, 2010; 581–587.
2. Sherma, J. Sample Preparation for TLC. In *Encyclopedia of Chromatography*; 3rd Ed.; J. Cazes, Ed.; Taylor & Francis: New York, 2010; 2111–2115.
3. Botz, L.; Nagy, S.; Kocsis, B. Detection of microbiologically active compounds. In *Planar Chromatography-A Retrospective for the Third Millennium*; Springer Scientific Publisher: Budapest, Hungary, 2001; 489–516.
4. Tyihak, E.; Mincsovics, E.; Katay, G.; Kiraly-Veghely, Z.; Moricz, A.M.; Ott, P.G. BioArena: An unlimited possibility of biochemical interactions in the adsorbent layer after chromatographic separation. J. Planar Chromatogr. -Mod. TLC **2008**, *21*, 15–20.
5. Eberz, G.; Rast, H.G.; Burger, K.; Kreiss, W.; Weisemann, C. Bioactivity screening by chromatography-bioluminescence coupling. Chromatographia **1996**, *43*, 5–9.
6. Sherma, J. Field guide to instrumentation: Instrumentation for modern thin layer chromatography. J. AOAC Intl., **2008**, *91*, 51A–58A.
7. Sherma, J. Sample Application in TLC. In *Encyclopedia of Chromatography*; 3rd Ed.; J. Cazes, Ed.; Taylor & Francis: New York, 2010; 2053–2057.
8. Verbitski, S.M.; Gourdin, G.T.; Ikenouye, L.M.; McChesney, J.D. Rapid screening of complex mixtures by thin layer chromatography-bioluminescence. Am. Biotechnol. Lab. **2006**, *24* (9), 40–42.
9. Sherma, J. Modern thin layer chromatographic pesticide analysis using automated multiple development. J. AOAC Intl. **1992**, *75*, 15–17.
10. Sherma, J. Optical Quantification or Densitometry in TLC. In *Encyclopedia of Chromatography*; 3rd Ed; J. Cazes, Ed.; Taylor & Francis: New York, 2010; 1640–1647.
11. http://www.chromadex.com (accessed March 15, 2008).
12. http://www.hptlc.com/berlin/2006pdf/pdf11am/HPTLC_2006_kreiss.pdf (accessed March 15, 2008).
13. http://www.camag.ch (accessed May 2008).

Biomarkers and Metabolites: HPLC/MS Analysis

Clayton B'Hymer
Kenneth L. Cheever
National Institute for Occupational Safety and Health, Centers for Disease Control and Prevention, U.S. Department of Health and Human Services, Cincinnati, Ohio, U.S.A.

Abstract
High-performance liquid chromatography–mass spectrometry (HPLC–MS) is a powerful analytical technique widely used in recent years for the analysis of biomarkers and metabolites. Biomarker determination and quantification, whether metabolic or adducted biomolecules, are commonly used to evaluate exposure and support biomonitoring research, especially in the area of occupational exposure and health. Some of the common problems and strategies of HPLC–MS biomarker analysis involve matrix effects, the use of isotope-labeled internal standard compounds, and sample cleanup; usually all of these factors must be evaluated within the development phase of an analysis procedure. Specific examples of biomarker analysis using HPLC–MS include acrylamide, aromatic compounds, and 1-bromopropane, and these examples are discussed in detail.

INTRODUCTION

A biomarker can be described as a substance from an organism that can be measured from a biological sample and can reflect *either* exposure, the effect of exposure or susceptibility to exposure. Biomarkers can be specific molecular, cellular, genetic, or protein changes resulting from environmental conditions including exposure to toxicants. Molecular biomarkers of chemical exposure, such as from an environmental toxicant, are commonly metabolites, protein adducts, or DNA adducts derived from the parent chemical. Developments in analytical chemistry have considerably improved the capability to detect biomarkers; thus, individual human exposure to occupational or environmental contaminants can be characterized by the measurement of the sampled biological media collected. Metabolites, adducted molecules, or residues from adducted proteins can be detected and quantified by means of modern analytical techniques using high-performance liquid chromatography (HPLC) and utilizing the detection capability of mass spectrometry (MS). Although other separation techniques have been employed for metabolite detection or the monitoring of biomarkers, HPLC offers the advantage of requiring only the solubility of the analyte and its inherent separation reliability. MS offers an ideal detection system for analyte specificity, excellent sensitivity, and reasonably low detection limits. The application of HPLC–MS in biomonitoring analysis for specific metabolites or adducted molecules is extensive, and HPLC–MS has often been used in the support of industrial hygiene studies and environmental risk assessments. The determination of biomarkers by HPLC–MS and examples of applications of this technique to occupational exposures will be the focus of this entry.

BACKGROUND ON BIOMONITORING AND BIOMARKERS

Biomonitoring generally refers to the periodic measurement of a biomarker to assess the internal dose and the health or health risk associated with exposure to a chemical. Biomonitoring or the monitoring of biomarkers has been used extensively during the past decade. The analysis of biomarkers of metabolic pathways for dysfunction has been used by both the scientific and the medical community for the determination of overall health or for use in health assessment. Biomarkers might indicate histopathologic changes, immunotoxicity, adverse biochemical alterations, and endocrine alterations. Monitoring of biomarkers, as well as the closely related field of metabolomics (the profiling of an organism's metabolites), has gained greater interest in recent years owing to the advances in analytical instrumentation and techniques. The hyphenated technique of combining liquid chromatography with MS detection is of major importance in biomarker research, and it can be considered the standard technique for biomarker identification and analysis.

The best review of the role of biomarkers in monitoring exposures to chemicals has been described by Watson and Mutti[1] and will not be repeated here in detail. Fig. 1 displays the general relation of events, such as exposure and biomarker classification.[2,3] The type of biomarkers with which this entry is concerned can generally be categorized as biomarkers of exposure, although metabolic changes can be detected by HPLC–MS and thus be a biomarker of effect. Biomarkers of susceptibility are outside the scope of this discussion and are related to effect-modifying factors, which include both genetic and

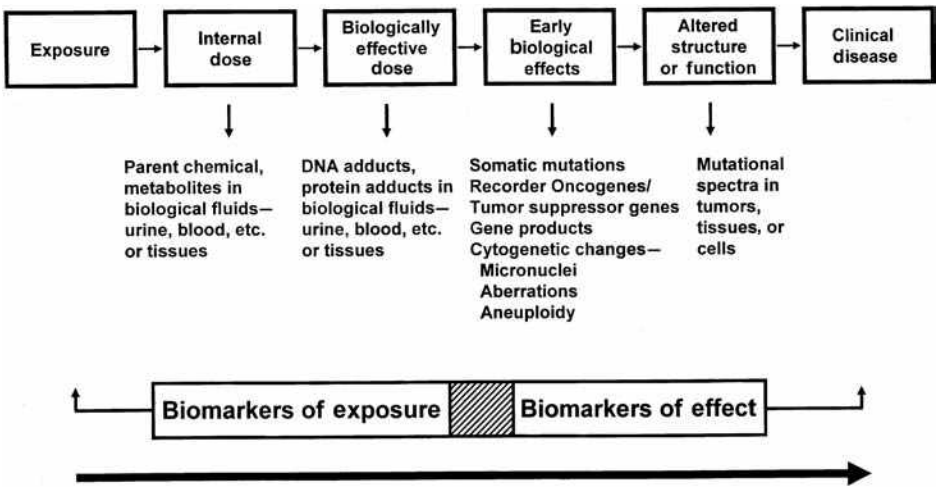

Fig. 1 The relation of events and biomarker classification.
Adapted from Watson & Mutti,[1] Albertini,[2] and Manini, Andreoli, & Niessen.[3]

acquired conditions. As the term implies, biomarkers of exposure are those related to exposure and the internal levels of some agent or chemical. Biomarkers of effect are those markers related to an early biological effect or altered structural function within an organism including any measurable biochemical or other physiological alteration that would be recognized as a potential impairment to health. In environmental or occupational health biomarker research, the major focus of interest has been on biomarkers of exposure. Parent chemicals, their metabolites, and the residues of adducted molecules are those biomarkers of exposure that can be detected and measured by HPLC–MS.[3–5] Common popular biomarker research has included various industrial chemicals, metals, pesticides, polycyclic aromatic hydrocarbons (PAHs), phthalates, acrylamide, benzene, and toluene, as well as biomarkers from tobacco smoke including cotinine, a metabolite of nicotine.

A good, well-chosen biomarker of exposure should have several qualities. One is it should be specific for the exposure of interest; some metabolites are common to multiple chemical substances and may not be a suitably specific biomarker. Even a small quantity of the biomarker should be easily detectable; therefore, high sensitivity is important. Also, the biomarker should be associated with exposure. Ideally, biomarkers should provide good predictive value to a specific health status and have reference values in the population if possible. Low overall analysis expense is another desirable characteristic of biomarker analysis for use in biomonitoring. The availability of suitable economical reference standards, as well as low-cost sample preparation, is an important consideration for extensive studies. This also implies that the analytical measurement procedure for the biomarker should have high throughput capability. Finally, measurements by non-invasive techniques are desirable. Urine-based biomarkers, either parent compounds or metabolites, are widely used in biomarker research today. Blood drawing is most often needed for the determination of macromolecular adducts such as protein adducts.

HPLC–MS

General Capabilities and Advantages

HPLC has many advantages and strengths as a separation technique. One is that solubility is the main requirement for sample introduction, unlike in gas chromatography (GC) where sample volatility is required. HPLC can avoid complicated derivatization procedures necessary for GC analysis of compounds that are not normally volatile. Thermal decomposition of analytes is also avoided by the use of HPLC, a requirement for many metabolic or protein-related biomarkers. Another important advantage of HPLC as a separation technique is in the general reproducibility and ruggedness of the procedure. Capillary electrophoresis (CE) has many unique separation qualities, including high plate number in the separation of analytes and electrophoretic separation of analytes, but it lacks the general ruggedness and reproducibility of HPLC. Also, CE is not as easily adaptable to interfaces with MS as is HPLC. This has made HPLC the preferred separation technique for metabolite analysis. The separation capabilities of HPLC with respect to urinary metabolites have been described by Waybright et al.[6] Reversed-phase HPLC is the most common mode of chromatography in metabolite and biomarker analysis. Small molecules require a C8 or a C18 stationary phase for good retention; larger molecules or proteins would typically require a C4 phase. Efficient chromatography of acidic metabolites often requires the use of buffered mobile phases, whereas retention of conjugated metabolites can be accomplished by ion-pair reversed-phase chromatographic systems. Gradient elution by increasing the organic modifier can greatly improve analyte resolution and reduce elution times for

well-retained analytes. In general, buffers used with the MS detector are chosen for their volatility and compatibility with the ionization source as well as chromatographic considerations.

MS detection has many strengths for use with HPLC, which have been described in the literature.[7,8] Tandem mass spectrometric (MS/MS) detection is considered the method of choice for the quantitative determination of metabolites in biological fluids.[8] MS possesses high sensitivity and also adds a higher degree of specificity (the ability of a technique to accurately measure the analyte in the presence of all potential sample components) to the detection technique. Limitations owing to low sensitivity and selectivity of UV detection can be overcome by more extensive sample cleanup and sample preconcentration, but MS offers overall method simplification by reducing those procedural steps. Unlike other forms of detection, MS measures specific mass-to-charge ratios of ions from the analytes, adding to method specificity. Therefore, HPLC–MS and HPLC–MS/MS can eliminate the numerous interferences typical of a sample derived from a biological matrix. Sample treatment is less complicated; moreover, the probability of having interfering components coeluting with analytes and having ions with the same mass-to-charge ratio is reduced. The MS detector also offers the possibility of identification of unknown compounds from fragmentation patterns; other HPLC detectors, such as UV, conductivity, fluorescence, or refractive index, lack that capability. The mass spectrometer may be considered as the instrument closest to the ideal universal HPLC detector. The only disadvantages of HPLC–MS are the high instrument cost and the requirement of highly qualified personnel to operate the mass spectrometer.

Mass Spectrometer

The basic function of the mass spectrometer is to measure the mass-to-charge ratios of analyte ions, and the various designs of mass spectrometers have been described in detail in the literature.[7,9] The HPLC–MS system has four main components consisting of a sample inlet, an ion source, a mass analyzer, and finally an ion detector. The sample introduction system vaporizes the HPLC column effluent. The ion source produces ions from the neutral analyte molecules in the vapor phase. Several designs of ion sources have been used over the past years including electrospray ionization (ESI), atmospheric pressure chemical ionization (APCI), thermospray ionization (TSP), continuous flow fast atom bombardment (FAB), and atmospheric pressure photoionization (APPI). The inductively coupled plasma (ICP) is a *hard* ionization source and is used specifically for the detection of metals and metals in adducts or in organometallic compounds. Generally, ICP–MS is used for elemental speciation analysis with HPLC, which has been described elsewhere in the literature[10] and will not be covered here. In recent years, ESI has become the most common ion source in HPLC–MS analysis of biomarkers, with the APCI source a close second. The third component of a mass spectrometer, the mass analyzer, separates the formed ions according to their mass-to-charge ratio (m/z ratio). The most widely used analyzer design is the quadrupole (or multipole) analyzer used either as a single stage or as a triple quadrupole combined with a soft ionization technique. In the triple quadrupole design with additional soft ionization, MS/MS can be accomplished. Other analyzer types, such as the time of flight (TOF), have been coupled to HPLC. The TOF analyzer has been used mainly for the analysis of proteins and other macromolecules. Magnetic sector design has been used when there was a need for high mass resolution capability or improved sensitivity. Ion trap has also been in common use with HPLC for the analysis of metabolites and biomarkers. Finally, the last component of the MS is the ion detector, which is necessary to record the separated ions. Multipliers are the most frequently used detectors in HPLC–MS commercial instruments.

Capabilities of the Common MS Ion Sources

The two most common ion sources for HPLC–MS determination and measurement of metabolites and biomarkers are ESI and APCI. Both have certain advantages. The ESI technique was invented by Nobel Prize winner John Fenn in 1992 and has become the ion source of choice for most HPLC–MS work. This technique has rapidly displaced TSP and continuous flow FAB in most HPLC–MS commercial systems. In ESI, the effluent from the HPLC system is passed through a small capillary or jet held at a high electrical potential (2000–5000 V). This results in electrostatic nebulization of the liquid. During desolvation of the droplets, the electric field increases in strength at the diminishing droplet surface and leads to the ejection of charged analyte ions upon final evaporation. The ESI source is a gentle ionization technique and does not cause thermal degradation as significant as that caused by other ion sources. It also exhibits a high level and efficiency of ionization, which leads to a high level of MS sensitivity. Finally, ESI can form multiple ions, which lower the m/z ratio of analytes, thus permitting the analysis of high molecular weight molecules typical of biological samples.

In APCI, the effluent from the HPLC is heated and sprayed with a high flow of nitrogen from a nebulizer, which generates an aerosol. This aerosol is subjected to a corona discharge to form ions of the sample components. In APCI, the ionization is in the gas phase, unlike ionization from the liquid phase in ESI. The APCI source allows improved analysis of non-polar and medium polar volatile compounds.

Mass Analyzer

The most common mass analyzer used in HPLC–MS analysis of metabolites is some variation of the quadrupole. A quadrupole consists of four parallel rods that utilize an oscillating electric field to select ions passing through the radio frequency field generated by the quadrupole. Many modern instruments actually use hexapoles and octapoles; they have a compact geometry using more rods, but operate under the same principle as the *quadrupole* and are often referred to as quadrupoles. In MS/MS, a *triple quadrupole* (TQ) mass spectrometer is used, which consists of three sets of quadrupoles that can either transmit all ions or function as a mass filter allowing ions of a specific *m*/*z* ratio to pass. The middle quadrupole of the TQ often serves as a collision cell and thus produces daughter ions to be filtered by the last quadrupole. Also, the ion trap in MS can be used for accumulation, fragmentation, and ejection of selected ions, thus allowing the analysis of molecular and daughter ions. These common mass analyzers have been described in detail elsewhere in the literature.[7,9]

COMMON PROBLEMS AND STRATEGIES OF HPLC–MS BIOMARKER ANALYSIS

The accurate determination of metabolites or biomarkers from complex biological samples, including biological fluids such as whole blood, plasma, urine, or extracts from tissue or structures such as fingernails, hair, or skin scrapings poses a complex set of problems for the analytical chemist. Some of these problems have been described in detail in the literature.[8,11] Although there is a common perception that the use of HPLC–MS, and especially HPLC–MS/MS, practically guarantees method specificity, in actual practice the quantitative determination of biomarkers from biological fluids has several pitfalls. Common possible problems include ion suppression or ion enhancement caused by the sample matrix and interferences from other metabolites within the sample. Ion effects have been reviewed in detail elsewhere[12] and will be summarized here. Matrix components may affect the response of the target analyte, either by reducing the efficiency of ionization and the MS response signal or sometimes by increasing or enhancing the signal. Hence, the assessment and elimination of any matrix effects from biological samples during the method development process is needed. Samples of biological origin generally contain hundreds or even thousands of components over a wide range of structural types and concentrations. Many of these components have variable or unknown MS responses, and most are unknown prior to the analysis.

Several strategies are generally incorporated into HPLC–MS method design and development to counter matrix effect problems. When the analytes are known, stable isotope-labeled internal standards (isotope dilution) can be used to counter matrix effects on ionization. Deuterated or carbon-13 analogues of the analytes can be spiked into the biological samples to counter or eliminate such effects. In the case of validated methods, the quality control or assurance samples can be prepared by spiking blank biological matrix samples with known concentrations of the analyte within the method's validated analyte concentration range. Also, the use of pooled urine samples from unexposed subjects represents the most widely used strategy to construct external calibration curves, which reduce the matrix effects found in biological samples. Finally, the importance of initial sample cleanup and good chromatographic separation cannot be overstated. Removal of inorganic salts from a sample matrix can reduce ion suppression of the ESI source. Liquid–liquid extraction (LLE) and solid-phase extraction (SPE) are commonly used for the sample cleanup of biological matrices. Also, the use of chromatographic gradients to increase the separation of sample components[6] can reduce the probability of the coelution of possible interferences.

APPLICATIONS OF HPLC–MS IN BIOMARKER ANALYSIS

As was mentioned in the previous section, HPLC–MS is widely used for the determination of biomarkers. Three specific applications of biomarker analysis using HPLC–MS are described in additional detail; they are acrylamide, common aromatic compounds such as toluene and benzene, and, finally, 1-bromopropane. These are common compounds found in general and work environments and are of interest for human exposure studies and health risk assessment.

Acrylamide

Acrylamide is a common industrial substance with many applications including its use as a polymerizing agent in grouts and in the preparation of laboratory gels for electrophoresis. Applications of the polymer form of acrylamide include water treatment, soil stabilization, and paper manufacture. Low levels of acrylamide have been detected in baked, fried, and roasted foods, largely derived from heat-induced Maillard reaction between asparagine and the carbonyl group of reducing sugars such as glucose during the process of cooking.[13] Acrylamide is a potent neurotoxicant in humans and is also a probable human carcinogen that makes exposure a concern for human health. The accepted metabolic scheme for acrylamide has been described in the literature[14] and is displayed in Fig. 2. Acrylamide forms several mercapturic acid metabolites that are useful urinary biomarkers in both animals and man. *N*-acetyl-*S*-(2-carbamoylethyl)cysteine (NACEC), acrylamide's primary urinary metabolite in both animals

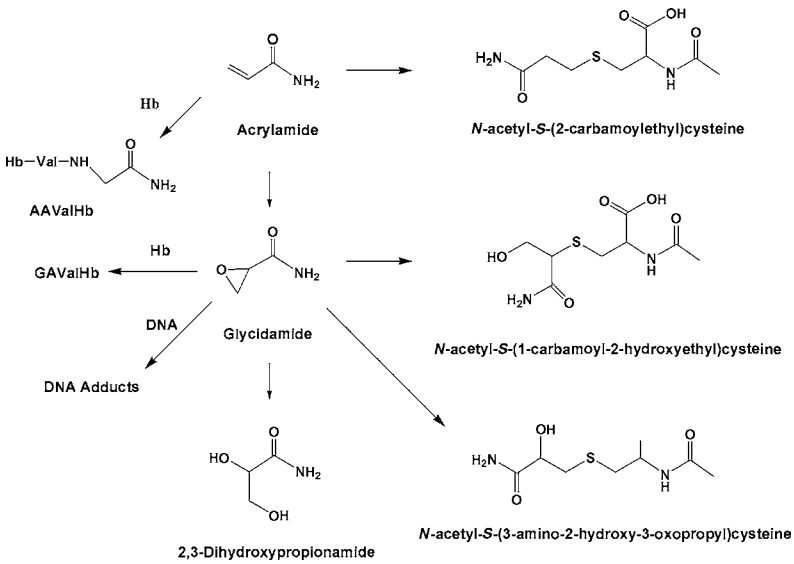

Fig. 2 A simplified metabolic scheme for acrylamide. *N*-acetyl-*S*-(2-carbamoylethyl)cysteine (NACEC) is the primary metabolite and is under study as a biomarker for acrylamide exposure.

and man, is formed by glutathione conjugation.[14–16] This is a first-order conjugation and is catalyzed by hepatic glutathione-*S*-transferase (GST). The other metabolic path, with glycidamide as an intermediate, leads to two other mercapturic acids, 2,3-dihydroxypropionamide as well as glycidamide–valine–hemoglobin adduct and DNA adducts. The glycidamide intermediate metabolite is also considered a toxicant. Formation of glycidamide from acrylamide is catalyzed by cytochrome P450; the two mercapturic acid metabolites of glycidamide, *N*-acetyl-*S*-(1-carbamoyl-2-hydroxyethyl)cysteine and *N*-acetyl-*S*-(3-amino-2-hydroxy-3-oxopropyl)cysteine, are GST catalyzed and are quantitatively minor metabolites. Both acrylamide and glycidamide react with proteins such as hemoglobin or albumin. Specifically, acrylamide reacts with the *N*-terminal valine amino acid of hemoglobin; the *N*-(2-carbamoylethyl)valine adducts are considered a biomarker of long-term acrylamide exposure.

The two main routes of biomarker analysis for acrylamide exposure involve the determination of either the valine adduct in hemoglobin or the urinary mercapturic acid metabolites.[14–16] The acrylamide–valine levels in hemoglobin are measured by hemolysis of the erythrocytes using a modified Edman degradation usually with pentafluorophenyl-isothiocyanate derivatization. This analysis is commonly performed by GC–MS[14] and will not be described in any further detail here. The mercapturic acid metabolites are commonly determined by HPLC–MS or HPLC–MS/MS.[14–16] The urinary NACEC metabolite has been determined using HPLC–MS in this laboratory; the metabolite was extracted from human urine by means of mixed-mode SPE, as has been reported in the literature by others.[16] Both the parent acrylamide and the NACEC metabolite were chromatographed using gradient reversed-phase HPLC. The chromatogram of a 10 μl injection prepared from spiked urine sample containing acrylamide, NACEC, and a deuterated analogue of NACEC is shown in Fig. 3. Specifically, a Phenomenex Synergi^{TM} 4 μ Hydro-RP 80 A (Torrance, California, U.S.A.) column with dimensions of 250 × 3 mm (I.D.) was used with a mobile phase consisting of 2/98/0.05% acetonitrile/water/formic acid held initially for 3 min, followed by a linear gradient for 15 min, and finishing with a mobile-phase composition of 80/20/0.05% acetonitrile/water/formic acid. The mobile-phase flow rate was 0.4 ml/min. The detector

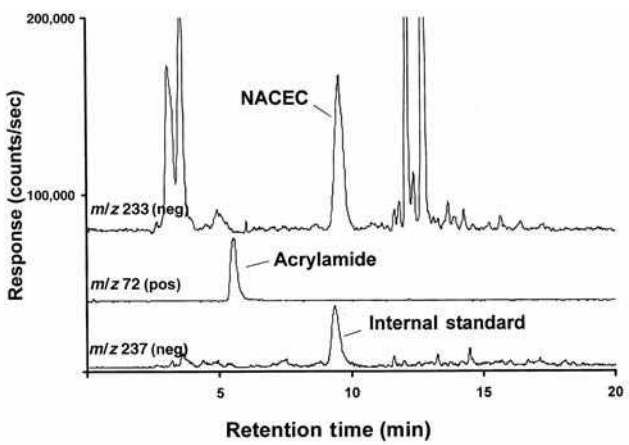

Fig. 3 The HPLC–MS chromatogram of a spiked urine sample containing acrylamide and the metabolite NACEC. Single-ion monitoring (SIM) at *m/z* 233 (negative mode) was used for NACEC, *m/z* 237 (negative mode) was used for the deuterated internal standard, and *m/z* 72 (positive mode) was used for the parent acrylamide. The urine sample was spiked at the 5 μg/ml level of acrylamide and NACEC and 2 μg/ml of the deuterated internal standard. For the chromatographic conditions used see the text or B'Hymer & Cheever.

Source: From Evaluation of extraction conditions and use of HPLC–MS for the simultaneous determination of acrylamide and its primary metabolite, *N*-acetyl-*S*-(2-carbamoylethyl)cysteine, in human urine, in J. Liq. Chromatogr. Relat. Technol. [17]

used was an Agilent Technologies (Palo Alto, California, U.S.A.) single lens (SL) mass selective detector (MSD) equipped with an ESI interface. Single-ion monitoring was used for quantification of the analytes; *m/z* 72 positive ion mode was used for the parent acrylamide, *m/z* 233 negative ion mode for NACEC, and *m/z* 237 negative ion mode was used for the deuterated NACEC internal standard. The use of a deuterated analogue of the metabolite of interest as the internal standard, a form of isotope dilution, is a common strategy in HPLC–MS biomarker analysis. The chromatographic system described was unique for acrylamide biomarker analysis in that both the parent acrylamide and its primary metabolite, NACEC, could be accurately determined simultaneously.[17] Other chromatographic systems that determined all the mercapturic acid metabolites of acrylamide have been described elsewhere.[14–16] As acrylamide is a potential carcinogen, these types of HPLC–MS methods have important applications in acrylamide biomarker research. The Urban et al.[14] study evaluated these metabolites with the dosimetry of acrylamide in smokers and non-smokers. Fennell et al.[15] used the mercapturic acid metabolites of acrylamide to study the kinetics of their elimination from urine in humans.

Common Aromatic Industrial Compounds

Toluene and benzene, as well as xylenes, are fairly common solvents encountered in the modern environment. These solvents are aromatic hydrocarbons frequently used as industrial chemicals. All are components of gasoline fuels, and our modern motor vehicle-based society represents one of the main emission sources. Benzene can also be released by several combustion reactions and can be found in tobacco smoke as well as in many consumer products. Benzene is a known human cancer hazard, and the hematotoxicity of benzene has been well elucidated during the past two decades. The acute internal dose of these aromatic compounds can be estimated by determining the amount of parent compound in blood, breath, or urine; however, the use of sensitive HPLC–MS procedures for measuring urinary metabolites has also been commonly reported in the literature.[18–21] Table 1 displays some of

Table 1 Structures and mass spectrometric behavior of phase I and II metabolites of some important aromatic industrial chemicals.

Parent compound	Metabolite[a]	Phase[b]	Structure	Ion mode	Ion,[c] *m/z*
Benzene	t,t-Muconic acid	I	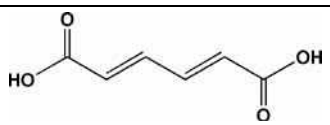	Negative	141
	S-PMA	II	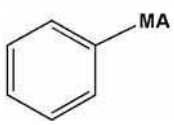	Negative	238
Toluene	Hippuric acid	I	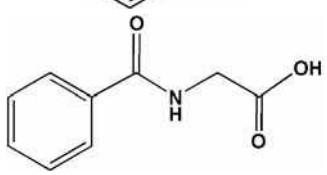	Negative	178
	BMA	II	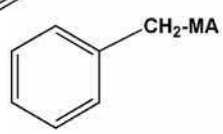	Negative	252
Xylene	MBAs	II	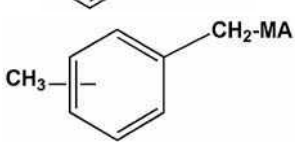	Negative	266
	DMPMAs	II	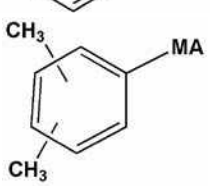	Negative	266

[a]Abbreviations: *S*-PMA, *S*-phenylmercapturic acid; BMA, benzylmercapturic acid; MBAs, methylbenzylmercapturic acids; DMPMAs, dimethylphenylmercapturic acids.
[b]Phase I (carboxylic acid) metabolites or phase II (mercapturic acid) metabolites.
[c]$[M - H]^-$ for negative ion mode.
Adapted from Manini, Andreoli, & Niessen.[3]

the metabolites of benzene, toluene, and xylene, many of which have been used as biomarkers of exposure. Phenol and its conjugates are the main biotransformation products for benzene; however, these compounds are not suitable as specific biomarkers for benzene because they are the products of other chemicals. Two other minor urinary benzene metabolites, *S*-phenylmercapturic acid (*S*-PMA) and *trans*,*trans*-muconic acid (see Table 1), are considered more suitable as specific biomarkers, and they are the better choice for biomonitoring studies. Similarly, the corresponding mercapturic acids of toluene, *S*-benzylmercapturic acid, and those of xylene are important biomarkers for these compounds (see Table 1).

Maestri et al.[18] describe an HPLC–MS method for the determination of urinary *S*-PMA acid. Sample cleanup and extraction utilized SPE C18 cartridges. The HPLC separation was performed on a reversed-phase column; specifically, a Waters (Milford, Massachusetts, U.S.A.) Symmetry C18 column (150 × 3 mm, 3.5 μm) was used with gradient elution by means of a methanol/water/acetic acid mobile phase. The MS detector was a single quadrupole design from Waters, the ZQ MS. Again, as in most methods described, an isotopic analogue of the target analyte was used as the internal standard; [^{13}C6]*S*-PMA was used in this case. Single-ion monitoring (ESI-negative mode) was used for quantitation of *S*-PMA; *S*-PMA molecular ions *m*/*z* 238 for *S*-PMA and *m*/*z* 244 for the internal standard were used. In a similar procedure developed by Li et al.[21] using a deuterated [^{2}H5] analogue of *S*-PMA as the internal standard, improved sensitivity with HPLC–MS/MS for the measurement of *S*-PMA was reported. Daughter ions *m*/*z* 109 for *S*-PMA and *m*/*z* 114 for the deuterated internal standard were used in this study.[21]

In an extensive study described by Manini, Andreoli, and Mutti,[19] both HPLC–MS and HPLC–MS/MS were used to develop methods to determine the metabolic biomarkers for numerous industrial chemicals including benzene and toluene. Either ESI or APCI was used as appropriate for each type of sample. The experimental evidence produced during this study demonstrated the need for carefully addressing the matrix effect of biological samples. Matrix effects were recorded not only for the type of sample matrix but also for individual subjects. The use of isotopically labeled internal standards is important for developing accurate HPLC–MS biomarker methods. This study also clearly showed the potential of HPLC–MS and HPLC–MS/MS in the determination of traditional biomarkers, as well as their possible use in metabolism studies aimed at investigating new and minor metabolic routes. The use of a methodology based on HPLC–MS for monitoring biomarkers from common industrial chemical exposure has been clearly demonstrated and will continue to grow in importance in the near future.

1-Bromopropane

1-Bromopropane (BP) is a widely used industrial solvent that has replaced many ozone-depleting chlorofluorocarbons. Applications of BP include metal and electronics, as a solvent in adhesive coatings and aerosol propellants. BP has been reported to cause central neurological and peripheral neuropathy disorders in workers and reproductive or hematopoietic problems in rats.[22] The metabolism of BP has been described in the literature,[23,24] and a simplified and condensed scheme is displayed in Fig. 4. Potential biomarkers for the evaluation of BP exposure, including urinary bromide, GC/electron capture detector (ECD) analysis of BP in breath, and GC–MS or HPLC–MS), analysis of BP metabolites, have been tried with varying degrees of success.[25] Several mercapturic acid metabolites in the urine of humans or animals have been suggested as biomarkers of exposure even though the majority of administered BP is exhaled or eliminated unchanged in the urine.[23] Although information on BP metabolism is somewhat limited, *N*-acetyl-*S*-(*n*-propyl)cysteine and *N*-acetyl-*S*-(2-hydroxyethyl)cysteine (i.e., 2-hydroxymercapturic acid or 2-HMA) are the

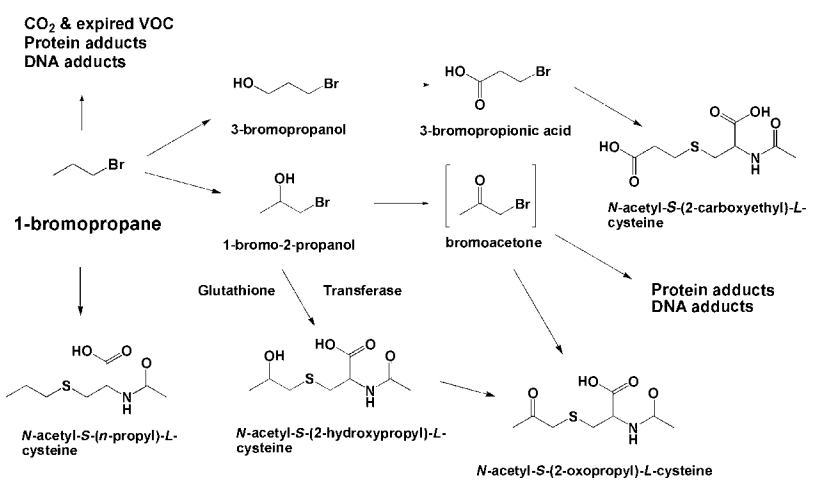

Fig. 4 A simplified metabolic scheme for 1-bromopropane. *N*-acetyl-*S*-(*n*-propyl)cysteine is a major metabolite and under study as a biomarker for 1-bromopropane exposure.

major metabolites in animals.[22] Other mercapturic acid metabolites have been reported for BP but several, including 2-HMA, *N*-acetyl-*S*-(2-carboxyethyl)cysteine, and *N*-acetyl-*S*-(2-oxopropyl)cysteine, are metabolites of related compounds and are not suitable as specific biomarkers of BP. *N*-acetyl-*S*-(*n*-propyl)cysteine is formed by glutathione conjugation; this metabolite may be further oxidized to the sulfoxide analogue, but this mercapturic acid oxide is not a major urinary metabolite. The other metabolic path, via P450 oxidation, may be important for low-level BP exposure with detectable amounts of bromide ion and 2-HMA found in the urine. However, with increasing exposure *N*-acetyl-*S*-(*n*-propyl)cysteine appears to be a likely biomarker candidate. The formation of reactive intermediates such as bromoacetone that would form DNA and protein adducts has been proposed[23] (see Fig. 4). In addition to non-specific biomarkers of BP exposure such as bromide ion, valine adducts from isolated hemoglobin or urinary *N*-acetyl-*S*-(*n*-propyl)cysteine have been considered possible biomarkers. The BP–valine adduct levels can be measured by high-resolution GC–MS. The modified Edman degradation of purified globin and the derivatization of valine adducts are expensive and time-consuming procedures, which would be most applicable to the detection of long-term exposures; it will not be described in further detail here.

Although mercapturic acids can be analyzed using GC–MS, derivatization would be required; however, *N*-acetyl-*S*-(*n*-propyl)cysteine can be more readily analyzed using HPLC–MS. The urinary *N*-acetyl-*S*-(*n*-propyl)cysteine metabolite of bromopropane has been determined in this laboratory, and a typical HPLC–MS chromatogram from this work is displayed in Fig. 5. Specifically, the metabolite was extracted from human urine using C18 reversed-phase SPE. Both *N*-acetyl-*S*-(*n*-propyl)cysteine and [d_7]-*N*-acetyl-*S*-(*n*-propyl)cysteine, the internal standard, were chromatographed using a Phenomenex Aqua 3 μm C18 125A column with dimensions of 150 × 2 mm (I.D.). A 10 min linear gradient (85:15 H_2O:MeOH 0.1% acetic acid to 100% MeOH 0.1% acetic acid) was used at a constant flow rate of 0.3 ml/min. The detector used was an Agilent Technologies 1100 SL mass spectrometer (MSD) equipped with an ESI interface. Single-ion (negative mode) monitoring was used for quantification of the analytes; *m/z* 204 was used for *N*-acetyl-*S*-(*n*-propyl)cysteine and *m/z* 211 was used for the [d_7]-*N*-acetyl-*S*-(*n*-propyl)cysteine internal standard (see Fig. 5). This specific example has important applications within this laboratory. These mercapturic acid metabolites are specific to 1-BP exposure. Worker exposure studies using total urinary bromide measurements[25] have been done; however, total urinary bromide is not specific and can be affected by diet. Therefore, the HPLC–MS methodology described, which measures the specific biomarkers of 1-BP, will obviously lead to more accurate human exposure assessment and improved industrial hygiene studies in the future.

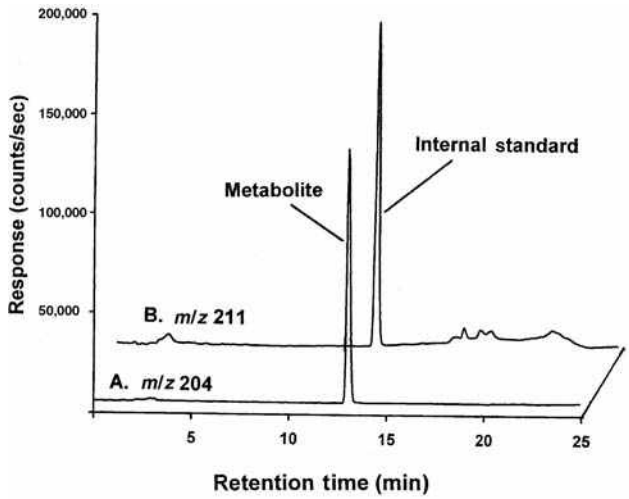

Fig. 5 The HPLC–MS chromatogram of a spiked urine sample containing the 1-bromopropane metabolite *N*-acetyl-*S*-(*n*-propyl)-cysteine (5 μg) and [d_7]-*N*-acetyl-*S*-(*n*-propyl)cysteine internal standard (10 μg). Single-ion monitoring (SIM) at *m/z* 204 (negative mode) was used for *N*-acetyl-*S*-(*n*-propyl)cysteine (A) and *m/z* 211 (negative mode) was used the deuterated internal standard (B). See the text for the chromatographic conditions used.

CONCLUSIONS

For biomarker and metabolite analysis HPLC–MS is a vital technique in biomonitoring and has been growing rapidly in the past decade. The inherent advantages of the mass spectrometer as a detector with high sensitivity and analyte specificity, combined with HPLC, make HPLC–MS one of the most valuable techniques for biomonitoring, metabolomics, and related bioanalytical fields. As more powerful commercial instrumentation becomes available at lower cost for the user, biomonitoring research will have continued rapid growth in the near future. For a more detailed description of HPLC–MS applications in occupational toxicology see Manini, Andreoli, and Niessen,[3] which provides a comprehensive review of biomarker and metabolite analysis for many common industrial chemicals.

ACKNOWLEDGMENTS

The authors would like to thank Gayle DeBord, Dennis Lynch, Jeanette Krause, Robert Chaplin, Anne Vonderheide, Nathan Coker, and Jonathan Doorn for their assistance in the editing and proofreading of this manuscript.

DISCLAIMERS

The findings and conclusions in this entry are those of the authors and do not necessarily represent the views of the

National Institute for Occupational Safety and Health (NIOSH). Mention of company names and/or products does not constitute endorsement by NIOSH.

REFERENCES

1. Watson, W.P.; Mutti, A. Role of biomarkers in monitoring exposures to chemicals: present position, future prospects. Biomarkers **2004**, *9*, 211–242.
2. Albertini, R.J. Developing sustainable studies on environmental health. Mutat. Res. **2001**, *480–481*, 317–331.
3. Manini, P.; Andreoli, R.; Niessen, W.M.A. Liquid chromatography–mass spectrometry in occupational toxicology: A novel approach to study of biotransformation of industrial chemicals. J. Chromatogr. A, **2004**, *1058*, 21–37.
4. Koc, H.; Swenberg, J.A. Applications of mass spectrometry for quantitation of DNA adducts. J. Chromatogr. B, **2002**, *778*, 323–343.
5. Törnqvist, M.; Fred, C.; Haglund, J.; Helleberg, H.; Paulsson, B.; Rydberg, P. Protein adducts: Quantitative and qualitative aspects of their formation, analysis and applications. J. Chromatogr. B, **2002**, *778*, 279–308.
6. Waybright, T.J.; Van, Q.N.; Muschik, G.M.; Conrads, T.P.; Veenstra, T.D.; Issaq, H.J. LC–MS in metabolomics: Optimization of experimental conditions for the analysis of metabolites in human urine. J. Liq. Chromatogr. Rel. Technol. **2006**, *29*, 2475–2497.
7. Goodlett, D.R.; Gale, D.C.; Guiles, S.; Crowther, J.B. Mass spectrometry in pharmaceutical analysis. In *Encyclopedia of Analytical Chemistry: Applications, Theory and Instrumentation*, Meyers, R.A. Ed.; John Wiley & Sons: Chichester, England, 2000; Vol. 8, 7209–7278.
8. Matuszewski, B.K.; Constanzer, M.L.; Chavez-Eng, C.M. Strategies for the assessment of matrix effect in quantitative bioanalytical methods based on HPLC–MS/MS. Anal. Chem. **2003**, *75*, 3019–3030.
9. Pramanik, B.N.; Ganguly, A.K.; Gross, M.L., Eds.; *Applied Electrospray Mass Spectrometry*; Marcel Dekker: New York, 2002.
10. B'Hymer, C.; Brisbin, J.A.; Sutton, K.L.; Caruso, J.A. New approaches for elemental speciation using plasma mass spectrometry. Am. Lab. **2000**, *32*, 17–14.
11. Sangster, T.; Major, H.; Plumb, R.; Wilson, A.J.; Wilson, I.D. A pragmatic and readily implemented quality control strategy for HPLC–MS and GC–MS-based metabonomic analysis. Analyst **2006**, *131*, 1075–1078.
12. Annesley, T.M. Ion suppression in mass spectrometry. Clin. Chem. **2003**, *49*, 1041–1044.
13. Zyzak, D.V.; Sanders, R.A.; Stojanovic, M.; Tallmadge, D.H.; Eberhart, B.L.; Ewald, D.K.; Gruber, D.C.; Morsch, T.R.; Strothers, M.A.; Rizzi, G.P.; Villagran, M.D. Acrylamide formation mechanism in heated foods. J. Agric. Food Chem. **2003**, *51*, 4782–4787.
14. Urban, M.; Kavvadias, D.; Riedel, K.; Scherer, G. Urinary mercapturic acids and a hemoglobin adduct for the dosimetry of acrylamide exposure in smokers and nonsmokers. Inhalation Tox. **2006**, *18*, 831–839.
15. Fennell, T.R.; Sumner, S.C.J.; Snyder, R.W.; Burgess, J.; Friedman, M.A. Kinetics of elimination of urinary metabolites of acrylamide in humans. Toxicol. Sci. **2006**, *93*, 256–267.
16. Boettcher, M.I.; Bolt, H.M.; Drexler, H.; Angerer, J. Excretion of mercapturic acids of acrylamide and glycidamide in human urine after single oral administration of deuterium-labeled acrylamide. Arch. Toxicol. **2006**, *80*, 55–61.
17. B'Hymer, C.; Cheever, K.L. Evaluation of extraction conditions and use of HPLC–MS for the simultaneous determination of acrylamide and its primary metabolite, *N*-acetyl-*S*-(2-carbamoylethyl)cysteine, in human urine. J. Liq. Chromatogr. Rel. Technol. **2007**, *30*, 1303–1316.
18. Maestri, L.; Negri, S.; Ferrari, M.; Ghittori, S.; Imbriani, M. Determination of urinary S-phenylmercapturic acid, as a specific metabolite of benzene, by liquid chromatography/single quadrupole mass spectrometry. Rapid Commun. Mass Spectrom. **2005**, *19*, 1139–1144.
19. Manini, P.; Andreoli, R.; Mutti, A. Application of liquid chromatography–mass spectrometry to biomonitoring of exposure to industrial chemicals. Toxicol. Lett. **2006**, *162*, 202–210.
20. Marchese, S.; Cruini, R.; Gentili, A.; Perret, D.; Rocca, L.M. Simultaneous determination of urinary metabolites of benzene, toluene, xylene and styrene using high-performance liquid chromatography/hybrid quadrupole time-of-flight mass spectrometry. Rapid Commun. Mass Spectrom. **2004**, *18*, 265–272.
21. Li, Y.; Li, A.C.; Shi, H.; Junga, H.; Jiang, X.; Naidong, W.; Lauterbach, J.H. Determination of S-phenylmercapturic acid in human urine using an automated sample extraction and fast liquid chromatography–tandem mass spectrometric method. Biomed. Chromatogr. **2006**, *20*, 597–604.
22. Ishihara, G. Neuro-reproductive toxicities of 1-bromopropane and 2-bromopropane. Int. Arch. Occup. Environ. Health **2005**, *78*, 79–96.
23. Jones, A.R.; Walsh, D.A. The oxidative metabolism of 1-bromopropane in the rat. Xenobiotica **1979**, *9*, 763–772.
24. Garner, C.E.; Sumner, S.C.J.; Davis, J.G.; Burgess, J.P.; Yueh, Y.; Demeter, J.; Zhan, Q.; Valentine, J.; Jeffcoat, A.R.; Burka, L.T.; Mathews, J.M. Metabolism and disposition of 1-bromopropane in rats and mice following inhalation or intravenous administration. Toxicol. Appl. Pharmacol. **2006**, *215*, 23–36.
25. Hanley, K.W.; Petersen, M.; Curwin, B.D.; Sanderson, W.T. Urinary bromide and breathing zone concentrations of 1-bromoporpane from workers exposed to flexible foam spray adhesives. Ann. Occup. Hyg. **2006**, *50*, 599–607.

Biopharmaceuticals: CE Analysis

Michel Girard
Bureau of Biologics and Radiopharmaceuticals, Health Canada, Ottawa, Ontario, Canada

INTRODUCTION

Capillary electrophoresis (CE) has rapidly established itself as one of the most versatile techniques for the analysis of biomolecules. In addition to providing exceptional separation efficiencies, it offers substantial advantages over conventional slab-gel electrophoretic techniques, namely, fast separation times, automation, reproducibility, and quantitative capabilities. Furthermore, owing to the different mechanisms by which products are separated in CE, data generated are generally complementary to those obtained by high-performance liquid chromatography (HPLC), thus allowing for more complete product characterization. CE methods can be successfully validated with respect to well-established analytical criteria (e.g., precision, accuracy, reproducibility, and linearity), making them a source of reliable information. These considerations are of key importance to the pharmaceutical industry in adopting CE as a frontline analytical technique for product characterization to meet the specific requirements associated with the manufacturing and testing of therapeutic substances.

Therapeutic biological compounds are collectively referred to as biopharmaceuticals and include recombinant proteins, monoclonal and polyclonal antibodies, antisense oligonucleotides, therapeutic genes, and recombinant and DNA vaccines. Although the majority of products on the market to date are proteins and antibodies, the first antisense oligonucleotide therapeutic, fomivirsen sodium, was approved in 1998 in the United States. Several other antisense and DNA-based products are being actively developed. Historically, biopharmaceuticals were obtained from biological sources, whether of human, animal, plant, or cellular origin, in the form of crude extracts or partially purified components of extracts. Because of the highly complex nature of these mixtures, only minimal physicochemical characterization could be carried out and product evaluation was generally based on biological response or surrogate bioassays. While a few traditional products remain in use today, newer production methods based on recombinant DNA or hybridoma technology are now being used for the large scale production of biopharmaceuticals. These developments have been paralleled by major advances in biomolecular separation and purification techniques and, consequently, have resulted in improvements in product development leading to the preparation of more consistent products with purity levels approaching those of conventional, small-molecule pharmaceuticals. A number of important therapeutics are produced in this manner. This is the case for somatropin human growth hormone (HGH), insulin, erythropoietin (EPO), several interferons (IFN-α, -β, and -γ), and hepatitis B vaccine, to name just a few. These products are currently used for diseases not otherwise well treated with small-molecule pharmaceuticals.

Despite these advances, the characterization of biopharmaceuticals remains a challenge. The inherent structural complexity of the therapeutic substance and the potential presence of numerous process- and product-related impurities and contaminants in the final product complicate the analysis. In addition, biological activity determination is still often performed using costly and imprecise animal testing. Nevertheless, the regulatory approval of biopharmaceuticals is based in part upon a comprehensive chemistry and manufacturing submission with a strong emphasis on high resolution analytical methodologies. The determination of the quality of a product through the verification of product identity, strength, stability, and consistency of manufacture and the quantitative evaluation of impurities and contaminants are of prime importance. Therefore, the establishment of more precise and selective methods of analysis is highly relevant to the pharmaceutical and regulatory sectors.

COMMON CE SEPARATION MODES FOR BIOPHARMACEUTICALS

There are several CE modes, based on different separation mechanisms, that, alone or in combination, are commonly used for the analysis of biopharmaceuticals (Table 1). Capillary zone electrophoresis (CZE) is the simplest and most commonly used CE mode for the analysis of peptides and proteins, including glycoproteins and monoclonal antibodies (MABs). In this mode, analytes migrate in a free solution according to their effective charge-to-size ratio. In capillary gel electrophoresis (CGE), analytes are separated according to their size through gel matrices by a molecular sieving mechanism analogous to that of polyacrylamide gel electrophoresis (PAGE). In capillary isoelectric focusing (CIEF), a stable pH gradient is formed inside the capillary and analytes migrate until they reach the pH equal to their isoelectric point (p*I*), at which time the net charge and mobility are zero and the analytes stop migrating. In micellar electrokinetic chromatography (MEKC),

Table 1 CE separation modes for the characterization of biopharmaceuticals.

Mode	Separation mechanism	Applications
CZE	Charge-to-size ratio	Proteins, peptides Glycoproteins MABs Peptide mapping Monosaccharides, oligosaccharides
CIEF	Isoelectric point (p*I*)	Proteins, peptides Glycoproteins MABs Isoelectric point determination Peptide mapping
CGE	Size	Protein MW determination Aggregates Oligonucleotides, DNA fragments Polysaccharides
MEKC	Partition	Proteins, peptides Peptide mapping Monosaccharides, oligosaccharides

analytes interact with micelles formed by adding surfactants to the running buffer at concentrations above the critical micelle concentration. The separation mechanism involves partition of the analyte between the micelle and the electrolyte.

PRODUCT CHARACTERIZATION

The characterization of biopharmaceuticals involves carrying out tests to demonstrate that a given product meets established criteria and that it remains safe and efficacious. There is a wide range of physicochemical methods that are frequently used for comprehensive characterization. Methods used include, among others, electrophoresis, HPLC, mass spectrometry (MS), UV spectrophotometry, nuclear magnetic resonance, sequencing, and amino acid analysis. CE is particularly well suited for the characterization of complex biomolecules, especially with regards to product identity and for assessing product heterogeneity arising from translational and post-translational modifications, degradation, or genetic variation. These considerations are particularly important for biopharmaceuticals, since they are inherently labile substances, especially when placed under non-physiological conditions. Consequently, the formation of impurities may occur throughout the manufacturing process and during the shelf life of the product.

Proteins are particularly susceptible to modification and degradation through a variety of pathways, leading to the formation of several types of variants. Some of the more commonly encountered pathways include deamidation, oxidation, dimerization/aggregation, peptide bond cleavage through proteolysis or hydrolysis, N- or C-terminal truncation, and disulfide scrambling (Table 2). These transformations have a significant impact on the physicochemical properties of the molecule by altering its size, charge, mass, hydrophobicity, or conformation. For example, deamidation leads to the formation of a more acidic variant from the transformation of the amide side chain in asparagine or glutamine residues into a carboxylic acid functional group. Furthermore, degradation may occur at more than one residue, a situation that leads to the formation of complex mixtures. Consequently, the choice of a separation mode or detection system depends mainly on an in-depth evaluation of the physicochemical properties of the product under study, that is, hydrophobicity, isoelectric point, size, post-translational modifications, and susceptibility to degradation/aggregation or conformational stability, and on the type of information required.

In the following sections, an overview of the use of CE for the characterization of selected classes of biopharmaceuticals is presented. The emphasis is placed on the relationship between the test performed and its intended purpose, that is, in terms of its usefulness for product identity or product purity determination.

In-Process Monitoring

CE has widespread applications in the biopharmaceutical industry owing, in large part, to the rapidity with which methods can be developed and to its versatility by virtue of the wide range of separation modes available. Besides its use in the development, quality control, and batch release stages,[1] CE is also commonly applied for in-process monitoring.[2] Manufacturing processes using recombinant DNA technology involve, as a first step, the large scale production of the desired protein in a suitable expression system

Table 2 Common protein modification and degradation pathways.

Pathways	Reaction	Reaction site
Deamidation	—$CONH_2$ → —COOH	Asn, Gln
Isomerization	Asn/Asp → isoAsp	Asn, Asp
Oxidation	—SR → —SOR, —SO_2R	Met
	—SH → —SS—	Cys
Dimerization/aggregation	Electrostatic, covalent, noncovalent bond formation	Various
Peptide bond proteolysis/hydrolysis	—CONH— → —COOH + NH_2^-	Various
N-, C-terminal truncation	Peptide bond cleavage	Various
Disulfide scrambling	R—SS—R′ → R—SS—R″	Disulfide bridge (—SS—)

through fermentation or cell cultivation. Experimental conditions are critical at this stage for ensuring the production of the required substance. As such, the detection of the product or its precursor at this early stage of the manufacturing process clearly confers an economic benefit. Conventional gel electrophoretic techniques cannot be readily applied since they are labor intensive and require considerable periods of time (e.g., staining/destaining procedures). CE methods have a clear advantage in these situations by providing fast analysis, sometimes in less than 5 min. In addition, apart from enabling the confirmation of the identity of the substance, they can provide a quantitative assessment of the process. Methods based on CZE, CGE, and CIEF are commonly used for the characterization of the product in fermentation broth or cell cultivation and during the various purification steps. Optimization includes attaining maximal separation of the reference compounds, such as the intact product or the pro-product, because the presence of impurities lowers resolution and selectivity.

Product Identity

One of the critical aspects to be considered during the manufacturing of any drug is product identity. While in itself it does not fulfill all of the requirements for a safe and effective drug, product identity testing provides assurance that the product generated is that which is intended and offers a measure of the consistency of the manufacturing process. CE-based methods are applied to confirm the product identity of biopharmaceuticals. Approaches usually involve the comparison of the property of the substrate to that of a pre-established, well-characterized reference standard with demonstrated quality, efficacy, and safety. In some instances, primary reference standards are available from official organizations such as the World Health Organization, the European Pharmacopoeia (EP), or the United States Pharmacopeia (USP). These preparations are established through international collaborative studies and are generally intended for use in the characterization of in-house reference standards. Aside from performing a simple identity test involving comigration of the substrate with the reference standard, a number of methods have been devised to provide qualitative and quantitative information with respect to specific structural features of the molecule such as primary sequence, molecular weight or size, and carbohydrate or isoform profile and distribution.

Peptide mapping is one of the most powerful tools for the identification of proteins and has been successfully adapted to CE.[3] It involves the cleavage of the amino acid chain at specific sites, using proteases or chemical reagents, to generate a mixture of smaller peptides. Different proteins generate different peptides after digestion, and separation of these peptides leads to a characteristic map or "fingerprint" of that protein. The analysis of peptide digests is generally carried out by CZE, where products are separated based on differences in charge-to-mass ratios. Peptide mapping by CZE is generally considered an orthogonal technique to HPLC. Peptide mapping by CZE is usually faster than by HPLC and typically provides greater resolution of a larger number of peptides. For instance, highly hydrophilic peptides are often poorly resolved or elute in the column dead volume by reversed phase HPLC. In CZE, these peptides migrate according to their charge-to-size ratio and are typically resolved. By contrast, peptides with similar net charges are not separated by CZE, and, in such cases, MEKC provides a useful alternative. The peptide map serves as a fingerprint of the substrate that, when compared to that of a reference standard, enables confirmation of the identity. Alternatively, it allows the detection and identification of amino acid and peptide modifications, which are indicative of the presence of product variants. In addition, it may be used to confirm the presence and position of disulfide bridges and glycosylation sites. Besides its application to simple proteins, peptide mapping by CZE can be particularly useful for the characterization of MABs.[4]

Several important therapeutic proteins are glycoproteins [e.g., EPO and tissue plasminogen (tPA)] that exist as mixtures of closely related species that differ in their glycosylation patterns (glycoforms). These differences are often the result of both compositional and sequence variations of the glycan chains. Moreover, the biological activity of glycoproteins is frequently linked to the presence of these carbohydrates, and, consequently, the characterization of glycoprotein microheterogeneity represents one of the more challenging tasks in identity testing. Several

CE approaches, based mostly on CZE and CIEF, have been devised.[5] For the frequently encountered sialoglycoproteins (i.e., sialic acid-containing glycoproteins), the analysis of the glycoform profile can be performed on the intact glycoprotein or on the glycopeptides obtained after the enzymatic digestion of the polypeptide chain. Alternatively, the analysis of the oligosaccharide profile can be performed following the chemical or enzymatic release of the glycan chains from the polypeptide backbone. In both cases, the profile obtained is an indication of the varying number of sialic acid residues on the oligosaccharide chains.

Carbohydrate analysis is essential to fully characterize a glycoprotein. CE methods are used for the analysis of the monosaccharide composition resulting from hydrolysis of the glycosylation chains. In those cases, monosaccharides must be derivatized with reagents such as 1-aminopyrene-3,6,8-trisulfonate (APTS) to provide both a readily ionizable group and a detectable chromophore. APTS has been used successfully for the derivatization of both oligosaccharides and monosaccharides and, coupled with CE/laser induced fluorescence (LIF), provides high sensitivity quantitative information with increased resolving power.

CE is a valuable tool for the confirmation of the structural integrity of biopharmaceuticals in final drug formulations.[6,7] Finished products generally contain low amounts of the active ingredient since the therapeutic effect can usually be achieved at low concentrations. In turn, formulations of low concentration proteins usually require the addition of large amounts of excipients to enhance product stability and to prevent nonspecific adsorption. Usual excipients include inorganic salts, amino acids, sugars, surfactants (e.g., polysorbate), and other proteins [e.g., human serum albumin (HSA)]. Typically, isotonic salt preparations are produced as most of these products are injectables and consequently high salt concentrations are present. Furthermore, many of these excipients may be present simultaneously, leading to complex mixtures. Such mixtures can interfere with traditional assay methodologies like HPLC or slab-gel electrophoresis. CZE is well suited for the direct analysis of products containing high salt concentrations, since conditions using highly concentrated buffer solutions increase the efficiency by contributing to the focusing effect. Fig. 1 shows the comparison of electropherograms obtained by reversed-polarity CZE[6] for a sample of formulated EPO-α (top trace) and a sample of its unformulated drug substance (bottom trace). Both traces show qualitatively similar glycoform profiles, a good indication of the structural integrity of the formulated product. These conditions also provide satisfactory results for assaying of the active ingredient and for quantitation of the glycoforms in the finished product.

In addition to other size-based analytical techniques such as size-exclusion HPLC or slab gel electrophoresis, CGE can be adequately used for the determination of a protein's apparent molecular weight.[8] Denaturing conditions are usually employed whereby sodium dodecyl sulfate (SDS)–protein complexes are formed with net overall negative charges that are proportional to their masses. These complexes migrate through the gel-filled capillary, acting as a sieving medium, in order of increasing molecular weight. The mobility of the substrate is used to estimate the molecular weight from a pre-established calibration plot of log molecular mass vs. mobility prepared from a series of protein standards of known molecular mass. CGE separation of SDS–proteins has the advantage over SDS–PAGE of giving higher resolution and requiring shorter analysis time. Oligonucleotides and DNA size determination is also achieved by CGE.[9] In these cases, the sieving matrix is required to separate the individual components since they have nearly identical charge-to-size ratios. Similarly, CIEF is used to determine the p*I* of a protein by interpolation from a p*I* calibration plot generated from a series of protein standards with known isoelectric points.[10]

Several MABs have been prepared for therapeutic purposes. They are among the most complex protein-based molecules, consisting of several light and heavy polypeptide chains, joined by multiple disulfide bridges, and containing a number of glycosylation sites of varying sequences and arrangements. Typically, MABs are very large molecules with molecular weights around 150,000 Da, a feature that, when combined with their structural complexity, makes high resolution chromatographic methods for the analysis of the intact molecule of little value. However, CE approaches have been highly successful for their characterization.[11] While all of the major CE separation modes have been applied, CIEF and CGE are particularly useful techniques. For instance, the high resolution achieved in CIEF allows monitoring of the profile of charge isoforms resulting from differential C-terminal processing (at lysine or arginine), a situation that frequently occurs in mammalian cell-derived products. CGE analysis under denaturing conditions has been used to estimate MAB molecular weight as well as the presence of aggregates. When performed under denaturing and reducing conditions, CGE provides an effective way to monitor the light and heavy chains that make up the typical antibody structure.

With the recent progress made on mass spectrometric ionization modes, large biomolecules can now be readily analyzed. The most widely used ionization mode for proteins and peptides characterization is electrospray ionization (ESI).[12] Molecular weights can be readily determined for large proteins with accuracies in the range of ±0.01–0.05%. The ESI method is sensitive, presently requiring samples in the 100 fmol–10 pmol range for proteins. As a result, the coupling of CE to MS provides an extremely powerful tool for the unambiguous structural confirmation or identification of biomolecules. A widely used approach consists in the analysis of intact proteins, which enables the determination of exact molecular

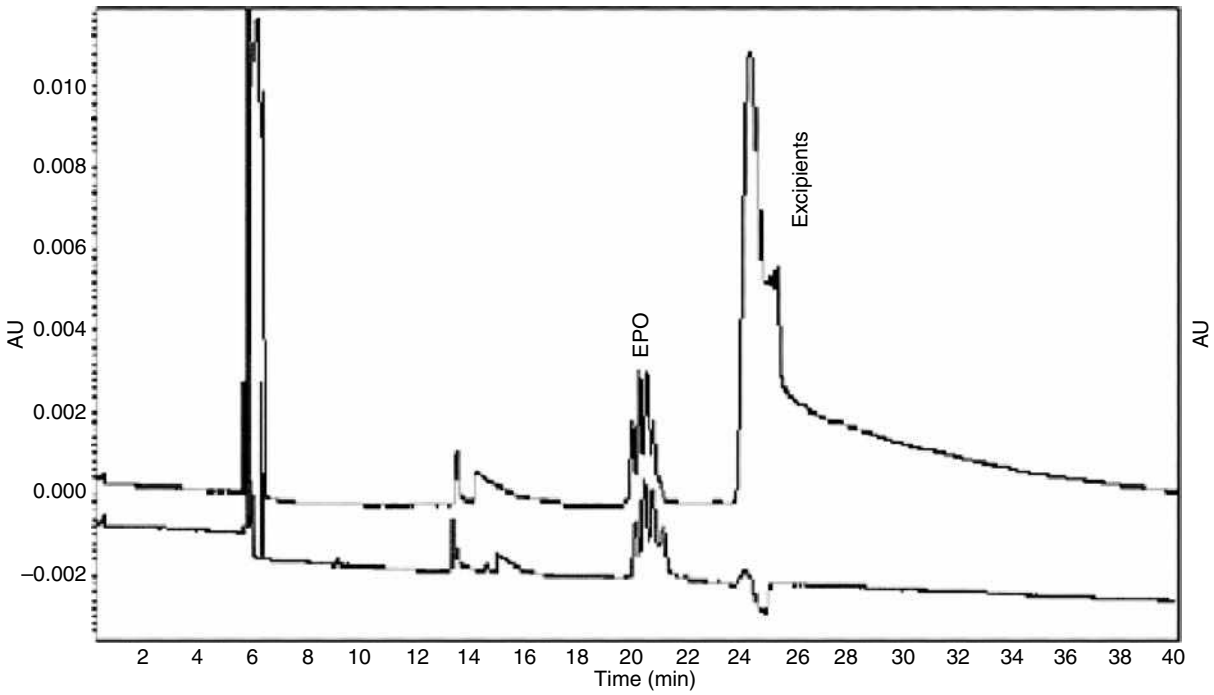

Fig. 1 Analysis of samples of EPO-α by reversed-polarity CZE: drug substance sample containing 8000 IU/ml (bottom trace) and drug product sample 10,000 IU/ml (top trace). Conditions were similar to those reported previously:[6] eCAP amine capillary (50 μm × 50 cm, 40 cm effective length); electrolyte: 200 m*M* sodium dihydrogen phosphate/1 m*M* nickel chloride, adjusted to pH 4.0 with acetic acid; 8 kV; UV detection at 200 nm.

weights. However, little or no fragmentation results from ESI and, as a consequence, no information on the sequence is obtained. An alternative, and more commonly used, approach for protein identification by MS is peptide mapping. In this approach, the peptide fragments separated by CE are analyzed by MS to determine their respective molecular weight. The protein is then identified through a database search from which two or more of the separated peptides can be matched to the predicted ones. In some cases, it may be necessary to obtain sequence information for a given peptide in order to ascertain its identity. This can be accomplished by using CE/MS/MS.

Product Purity

Purity determination is an essential component of the assessment of the quality of any drug. However, the purity determination of biopharmaceuticals is not as straightforward as that of small-molecule pharmaceuticals, since biopharmaceuticals are structurally complex and have a wide range of potential impurities. Approaches usually involve the judicious choice of a combination of methods that enable the detection and quantitation of impurities from which an overall purity assessment can be derived. As mentioned previously, proteins undergo degradation or modification through a number of pathways. Most of the more common variants encountered in protein preparations can be detected by CE methods.[13] The high efficiency and quantitative properties of CGE can be used to detect nondissociable aggregates and clipped forms in proteins. This separation mode also provides an effective means to monitor the presence of deletion sequences in oligonucleotides.[14] The separation and detection of charge variants such as deamidation products and clipped forms resulting from the proteolytic cleavage of the polypeptide chain are readily amenable using CE methods. In particular, CZE has proven to be highly effective for simple proteins having no carbohydrate-mediated heterogeneity present. The high efficiency of CZE, in some cases, allows the resolution of multiple charge variants, such as occur in HGH,[15] to be accomplished in a single run (Fig. 2). The coupling of CE to high sensitivity detection devices such as LIF detectors provides substantial enhancement of the detection limits of impurities.[16]

REGULATORY CONSIDERATIONS

CE is now recognized as a mature technique alongside HPLC and other modern analytical techniques. A harmonized general monograph[17] that presents both theoretical and practical considerations of the technique has been recently adopted by the Pharmacopoeial Discussion Group (PDG) for implementation into the USP, the

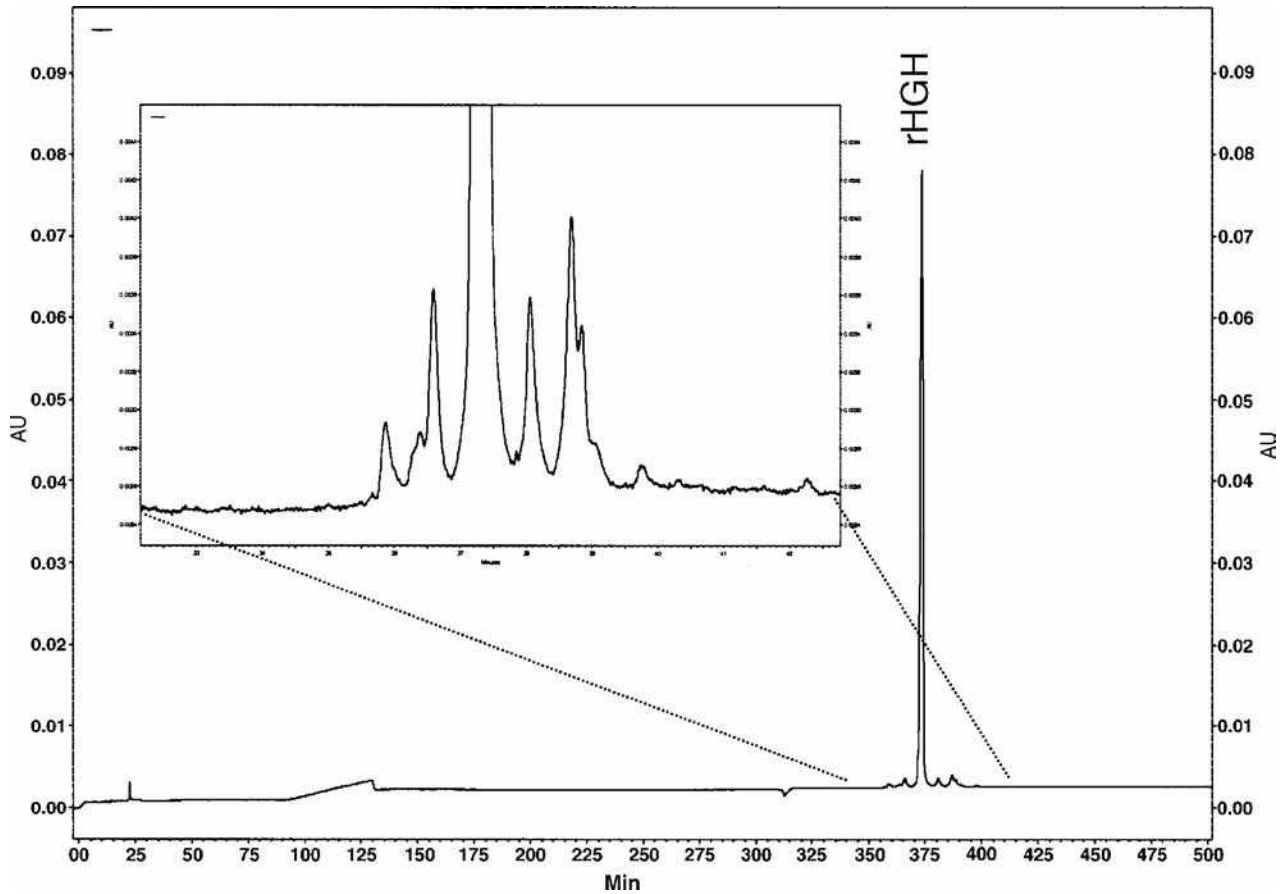

Fig. 2 Analysis of a sample of somatropin (recombinant HGH) by CZE. Inset: enlarged view showing the separation of impurities. Conditions were similar to those reported previously:[15] bare fused silica capillary (50 μm × 100 cm, 90 cm effective length); electrolyte: 0.1 *M* diammonium hydrogen phosphate, adjusted to pH 6.0 with phosphoric acid; 20 kV; UV detection at 200 nm.

Japanese Pharmacopoeia (JP), and the EP. In addition, a CZE method is currently used as an identification test for EPO concentrated solution in the EP.[18] This represents the first example of the use of CE for the monitoring of a biopharmaceutical by an official method. A second example is in the final stage of implementation and involves the determination by CZE of charge variants in somatropin preparations.[19] This test, which was found to provide more precise quantitative data, will replace the current isoelectric focusing method.

Regulatory agencies around the world are seeing an increasing number of drug manufacturers that include CE methods in drug submissions. While most regulatory agencies recognize the applicability of CE for biopharmaceuticals, they require the methods to be validated based on well-established parameters that include accuracy, precision, specificity, limit of detection, limit of quantitation, linearity, and range. There is considerable guidance available for the validation of analytical methods. The International Conference on Harmonisation (ICH) has published guidelines that refer specifically to biopharmaceuticals: Q6B—Specifications: Test Procedures and Acceptance Criteria for Biotechnological/Biological Products; Q5C: Quality of Biotechnological Products: Stability Testing of Biotechnological/Biological Products; Q5E: Comparability of Biotechnological/Biological Products Subject to Changes in Their Manufacturing Process; Q2A: Text on Validation of Analytical Procedures; Q2B: Validation of Analytical Procedures: Methodology. Guidelines are available on the ICH website.[20]

CONCLUSIONS

The use of CE has become an integral part of the study of biopharmaceuticals, especially for the monitoring of product identity and purity. It is a powerful technique that, in many instances, is superior to the more conventional electrophoretic techniques and complementary to the widely used high resolution chromatographic techniques. It is

particularly well suited to the study of complex mixtures of biomolecules such as glycoproteins and MABs.

REFERENCES

1. Chen, A.B.; Canova-Davis, E. Capillary electrophoresis in the development of recombinant protein pharmaceuticals. Chromatographia **2001**, *53* (Suppl.), S7–S17.
2. Klyushnichenko, V. Capillary electrophoresis in the analysis and monitoring of biotechnological processes. Meth. Mol. Biol. **2004**, *276*, 77–120.
3. Rickard, E.C.; Towns, J.K. The use of capillary electrophoresis for peptide mapping of proteins. In *New Methods in Peptide Mapping for the Characterization of Proteins*; Hancock, W.S., Ed.; CRC Press: New York, 1996; 97–118.
4. Liu, J.; Zhao, H.; Volk, K.J.; Klohr, S.E.; Kerns, E.H.; Lee, M.S. Analysis of monoclonal antibody and immunoconjugate digests by capillary electrophoresis and capillary liquid chromatography. J. Chromatogr. A, **1996**, *735*, 357–366.
5. Kakehi, K.; Honda, S. Analysis of glycoproteins, glycopeptides and glycoprotein-derived oligosaccharides by high performance capillary electrophoresis. J. Chromatogr. A, **1996**, *220*, 377–393.
6. Bietlot, H.P.; Girard, M. Analysis of recombinant human erythropoietin in drug formulations by high performance capillary electrophoresis. J. Chromatogr. A, **1997**, *759*, 177–184.
7. Park, S.S.; Cate, A.; Chang, B.S. Use of capillary electrophoresis to determine the dilute protein concentration in formulations containing interfering excipients. Chromatographia **2001**, *53* (Suppl.), S34–S38.
8. Ma, S.; Nashabeh, W. Analysis of protein therapeutics by capillary electrophoresis. Chromatographia **2001**, *53* (Suppl.), S75–S89.
9. Karger, B.L.; Foret, F.; Berka, J. Capillary electrophoresis with polymer matrices: DNA and protein separation and analysis. Meth. Enzymol. **1996**, *271*, 293–319.
10. Wehr, T.; Rodriguez-Diaz, R.; Zhu, M. Recent advances in capillary isoelectric focusing. Chromatographia **2001**, *53* (Suppl.), S45–S58.
11. Krull, I.S.; Liu, X.; Dai, J.; Gendreau, C.; Li, G. HPCE methods for the identification and quantitation of antibodies, their conjugates and complexes. J. Pharm. Biomed. Anal. **1997**, *16*, 377–393.
12. Severs, J.C.; Smith, R.D. Capillary electrophoresis–electrospray ionization mass spectrometry. In *Electrospray Ionization Mass Spectrometry*; Cole, R.B., Ed.; John Wiley & Sons: New York, 1997; 343–382.
13. Teshima, G.; Wu, S.-L. Capillary electrophoresis analysis of recombinant proteins. Meth. Enzymol. **1996**, *271*, 264–293.
14. Srivatsa, G.S.; Pourmand, R.; Winters, S. Use of capillary electrophoresis for concentration analysis of phosphorothioate oligonucleotides. Meth. Mol. Biol. **2001**, *162*, 371–376.
15. Dupin, P.; Galinou, F.; Bayol, A. Analysis of recombinant human growth hormone and its related impurities by capillary electrophoresis. J. Chromatogr. A, **1995**, *707*, 396–400.
16. Lee, T.T.; Lillard, S.J.; Yeung, E.S. Screening and characterization of biopharmaceuticals by highperformance capillary electrophoresis with laser-induced native fluorescence detection. Electrophoresis **1993**, *14*, 429–438.
17. *European Pharmacopoeia*, 5th Ed.; 2005; 74–79 (Chapter 2.2.47).
18. *European Pharmacopoeia*, 5th Ed.; 2005; 1528–1532 (01/2005:1316).
19. Draft monograph for comment. Pharmeuropa **2004**, *16* (1), 72–73.
20. International Conference on Harmonisation, http://www.ich.org/ (accessed September 2004).

Biopolymers and Pharmaceuticals: CEC

Ira S. Krull
Sarah Kazmi
Department of Chemistry, Northeastern University, Boston, Massachusetts, U.S.A.

INTRODUCTION

Capillary electrochromatography (CEC) has grown considerably over the past few years, due to the developments in column technology and the appearance of several articles demonstrating the high efficiencies possible with this technique.[1] The literature has shown that there can be numerous applications for this technology, which was not possible with the earlier separation methods.

CEC Technique

Tsuda published an article that discussed the CEC technique in detail.[2] The technique itself is a derivative of high-performance capillary electrophoresis (HPCE) and high-performance liquid chromatography (HPLC), where the separations are performed using fused-silica tubes of 50–100 μm inner diameter (I.D.), that are packed with either a monolithic packing or small (3 μm or smaller) silica-based particles.[3–5] The packing is similar to the conventional HPLC; however, the mobile phase is driven by electro-osmosis, which results from the electric field applied across the capillary rather than by pressurized flow. The mobile phase is made up of aqueous buffers and organic modifiers [e.g., (ACN)]. An electro-osmotic flow (EOF) of up to 3 mm/sec can be generated. It is a plug flow, where the linear velocity is independent of the channel width and there is no column back-pressure.[4] Partitioning or adsorption of the neutral analyte occurs in the same way as in HPLC. The analytes are separated while moving through the column with the EOF. Charged solutes have additional electrophoretic mobility in the applied electric field; therefore, the separation occurs by electrophoresis and partitioning. The selectivity in analysis of the charged analytes is increased by electromigration of the sample molecules. The flat flow profile results in a more efficient radial mass transport compared to the parabolic laminar flow in pressure-driven LC, and this results in a significant enhancement in separation performance and shorter analysis times.[1,5,6] The capillaries can be made shorter to offer the same plate count as HPLC, therefore reducing the back-pressure. The packing material is smaller compared to HPLC, so with the high electric fields, the efficiency of this technique is very high (up to about 500,000 plates/m),[1] the peaks are sharp, the resolution is high, and the process is highly selective. An article by Angus et al.[7] demonstrated the separation efficiencies of 200,000–260,000 plates/m that were obtained by CEC and were reproducible from column to column for structurally related, polar neutral compounds of pharmaceutical relevance. The sample capacity in CEC is 10–100 times higher than that of capillary electrophoresis (CE), and this means that more sample volume can be placed on the CEC column to give better sensitivity. The high capacity comes from the high column loadability that results from the stationary phase's retentive mechanism.[8] The absence of additives and predominantly organic mobile phases make CEC better suited for use in mass spectrometry (MS). In fact, non-aqueous CEC is already being practiced by analysts.[8] A recent article by Hansen and Helboe gives a detailed study of the possibility of using CEC to replace gradients or ion-pairing reagents. The group optimized the separation of six nucleotides using a background analyte consisting of 5 m*M* acetic acid, 3 m*M* triethylamine (TEA), and 98% acetonitrile and a C_{18} 3 μm column. This was accomplished in half the time taken for a similar separation in HPLC.[9]

A variation of gradient CEC is pressurized-flow CEC or PEC (pressurized flow electrochromatography). A pump forms the gradient and then allows part of this pressurized flow to pump the mobile phase through the packed bed. In this way, one can perform isocratic or gradient CEC with part of the mobile-phase driving force being pumped, part electrophoretic and part electro-osmotic flows.[1,8,10]

Detection of Biomolecules and Pharmaceuticals in CEC

There are many different types of detectors used for pharmaceutical applications in CEC. They vary from indicating just the presence of a sample [fluorescence (FL)], to giving some qualitative information about a sample [photodiode array UV/Vis detection (PDA)], to absolute sample determination of the analyte (MS). The methods can be on-column, off-column, and end-column. With on-column, the solutes are detected while still on the capillary, in off-column, the solute is transported from the outlet of the capillary to the detector, and end-column is done with the

detector placed right at the end of the capillary. Some modes of detection used in CEC are as follows:

1. UV/Vis absorbance detection is widely used in CE Absorptivity depends on the chromophore (light-absorbing part) of the solute, the wavelength of the incident light, and the pH and composition of the run buffer. A photodetector measures light intensities and the detector electronics convert this into absorbance.[11]
2. Fluorescence detection is based on the fact that, when light energy strikes a molecule, some of that energy may be given off as heat and some as light. Depending on the electronic transitions within a molecule, the light given off may be fluorescent or phosphorescent.[12] Fluorescence occurs when an electron drops from an excited singlet to the ground state, as opposed to phosphorescence, which occurs when an electron's transition is from an excited triplet to the ground state.
3. LIF detection, such as argon ion, helium–cadmium,[5] and helium–argon lasers, can be used for this detection method. The criterion for choosing the laser is that the wavelength should be at or near the excitation maxima for the solute to be determined. The higher the power of the laser, the higher the intensity and the peak height and the laser's ability to focus the beam to a small spot.
4. MS detection[4] is the only detector that has high sensitivity and selectivity and can be used universally, thus, the increased interest in interfacing this technology with CEC compared to other detection methods. It can detect all solutes that have a molecular weight within the mass range of the MS. In the selected ion-monitoring mode, it detects only solutes of a given mass, and in the total ion chromatogram mode, it detects all the solutes within a given mass range.

Current applications of CEC use on-column UV or laser-induced fluorescence detection; however, for UV, the path length is quite short, which limits sensitivity, although bubble, Z-shaped, and high-sensitivity cells have helped to improve detection limits. However, UV and fluorescence are only good for samples that fluoresce and absorb light or are amenable to derivatization with fluorescing or absorbing chromophores. These detectors impose difficult cell volumes and sample size limits if high separation efficiencies are to be realized, and they are very expensive. All of these drawbacks are non-existent for MS techniques, which are expensive but provide more structural information and high sensitivity and appear to have the greatest overall potential.[8]

According to an issue of LC/GC,[10] combining CEC with detection techniques such as MS, MS/MS, and inductively coupled plasma (ICP)-MS are easier to accomplish, as the flow rates are at nanoliter per minute levels. Analysts must add makeup solvent after the capillary separation for certain ionization methods, and, because it is added later, users can select solvents that are more compatible with the detection technique. CEC mobile phases have a high organic solvent content that is more amenable to MS. Also, the low CEC flow rates means less maintenance and downtime for MS source cleaning.

In the references to the application of CEC to biopolymers, most of the work discusses CEC–electrospray ionization (ESI)/MS, much less to direct CEC-UV/FL methods. However, much of the work has evolved from the use of commercially available, prepacked capillaries, such as C_{18} or ion exchange or a mixed mode containing both ion exchange and reversed phase (RP). There are very few articles that have actually attempted to develop new phases specifically for biopolymers.

When using MS, the actual CEC conditions never really need to be fully optimized because the MS accomplishes the additional resolution and specific identification, as needed. The specific mobile-phase conditions in CEC/MS may be quite different than for CEC-UV/FL or HPLC, and thus optimization of CEC/MS conditions will be somewhat different than for CEC-UV/FL. This would include, just as for LC/MS, the use of volatile organic solvents and organic buffers, low flow rates, no void volumes, or loss of resolution in the CEC/MS interface and the usual interfacing requirements already developed and optimized for CE/MS.[10,13–23]

Few descriptions of quantitation have been reported so far. Most of the literature is qualitative by nature, simply demonstrating suitable, if not fully optimized, experimental conditions that provide evidence of the presence of certain biopolymers and their high resolution from other components in that particular sample. Absolute quantitation and validation needs to be developed and fully optimized for CEC, to become a more valuable and applicable separation mode for biopolymers.

SEPARATION OF PROTEINS

Capillary electrochromatography can accomplish high plate counts, as mentioned earlier; this means a high peak capacity (number of peaks that can be fitted into a typical separation time for a given length of column), therefore highly complex materials can be separated. The implication of better peak capacities is a better resolution of the peaks in a complex analyte. Because of the frequent overlap of peaks due to components in a complex sample, it is difficult to demonstrate peak purity with other methods. It is possible in CEC to quantitatively determine the presence of a particular analyte. CEC techniques have produced the separation of the enantiomers of amino acids.[24–27] This is done with limited use of solvents, buffer additives, salts, organics, chiral species, packing materials, and total time

of analysis. Other groups have successfully utilized gradient elution to separate mixtures of dansylated amino acid mixtures on the ODS (octadecylsilane) stationary phase.[24] Also, microprocessor control of pressure flow and voltage, automated sample injection, automated data collection, automated capillary switching, and the ability to interface with a variety of detection instrumentation make CEC an appealing technique for protein separation and peptide mapping.

Proteins and peptides are water-soluble complex molecules that are composed of amino acids linked by peptidic and disulfide bonds. Proteins are really just larger peptides of higher molecular weight, and antibodies are larger proteins of specific conformations, shape, size and immunogenicity, together with antigenic recognition properties.[28–31] The type, number, and sequence of amino acids in the chain determine the chemical characteristics of a peptide. The amino acid sequence determines the electrophoretic properties of the peptide. In addition to the amine terminus of the sequence, the amine and the guanidine residues of lysine and arginine are the main carriers of the positive charges, and the negative charge contribution is associated with the carboxylic acid terminus and the acidic groups of the aspartic and glutamic acids. The isoelectric and isoionic points of the peptide are their important characteristics in electrophoresis. These points are similar in peptides but not identical; the isoelectric point is determined by the given aqueous medium, whereas the isoionic point is related to the interactions with protons. The relation of the electrophoretic mobility of the peptides and their relative molecular weight is described by Offord'sequation:

$$\mu_{\text{rel}} = \frac{Z}{[\sqrt[3]{(M^2)}]}$$

where μ_{rel} is the relative mobility, Z is the total net charge, and M is the molar mass in gram per mole. Calculation of the net charge cannot be done easily from the pK values of the acidic and basic groups for large peptides, but additional factors such as conformational differences, primary sequence, chirality, and so forth need to be considered.

The popular methods of analysis of proteins currently are HPLC, HPCE, and MS. However, due to the complexity of proteins, LC approaches show a single, broad, ragged peak, which indicates that the method is unable to resolve the individual species.[1] In CEC, the success of the protein separation requires that the capillary packing material meet certain properties. Depending on the ionic characteristics of the biopolymers, pH-dependent "ideal" packings would be either RP or ion-exchange chromatography (IEC) or a combination of both.[1,32–46] There are several references that detail the possible application of SEC packings in CEC, but these have mainly been applied to synthetic organic polymers and much less to biopolymers.[47–50] Regardless of which packing is actually utilized, it should contain a stationary (bonded, not coated) phase that can successfully interact with the biopolymers, as in RP-HPLC, and prevent any unwanted silanol interactions with the underlying silica or ionic sites. It must also provide additional or programable EOF, besides that from the uncoated fused-silica capillary walls. Perhaps an ideal packing would combine a cationic-exchange material (cationic-exchange chromatography (CIEC) together with RP, in order to allow separations based on RP (hydrophobicity) alone, a combination of RP and IEC, or just IEC alone, mobile phase (buffer) dependent. Also, that packing, be it single or mixed mode, should prevent unwanted biopolymer (e.g., peptide amino groups) interaction with the support, such as amine–silanol hydrogen-bonding in RP-HPLC for amine containing analytes (e.g., pharmaceuticals, peptides, and proteins). Additional articles on open tubular CEC (OT-CEC) applications, where a coating is applied on the inner surface of the capillary as in capillary GC have appeared.[51–54] There are articles on packed-bed CEC, where there is a real packing in the capillary.[55,56] Also, then there are methods that employ just CEC, without any additional, pressure-driven flow,[38,39] as well as pressurized CEC or PEC, with additional pressurized flow.[4,51–53] There is also electro-HPLC that utilizes gradient elution with an applied voltage, but it is mainly conventional HPLC with some voltage applied sporadically or continuously during the HPLC separation.[54]

CEC OF BIOPOLYMERS (PROTEINS, PEPTIDES, AND ANTIBODIES)

The majority of the applications of CEC for biopolymers have dealt with peptides, of varying sizes and complexity, utilizing different modes of CEC (OT–CEC, conventional isocratic CEC, gradient CEC, PEC, and others). The following accounts are listed according to the work of different authors in the field.

Palm and Novotny applied the polymeric gel beds (monoliths) for peptide resolutions in CEC.[5] The peptide separation used the above packing beds with 29% as the ligand. Additional CEC conditions are indicated in Fig. 1, which depicts the separation of a series of tyrosine-containing peptides, with detection at 270–280 nm. In this particular study, peptide elution patterns were very sensitive to changes in pH and ACN concentrations. A gradient elution technique, not employed here, would have been more appropriate for such samples of peptides having small differences in their constitution. Attempts to elute protein samples were unsuccessful with these particular gel matrices, perhaps due to the high hydrophobicity of the packings.[5]

Euerby et al. reported the separation of an *N*-methylated, C- and N-protected tetrapeptide from its non-methylated analog (Fig. 2).[38] These separations utilized a Spherisorb ODS-1, 3 μm packing material, without pressure-driven flow (true CEC using a commercially

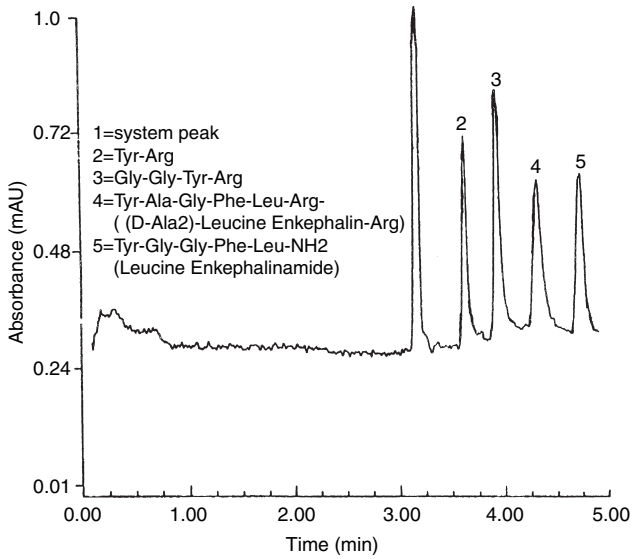

Fig. 1 Isocratic electrochromatography of peptides in a capillary filled with a macroporous polyacrylamide–polyethylene glycol matrix, derivatized with a C_{12} ligand (29%) and containing acrylic acid. Conditions: mobile phase, 47% acetonitrile in a buffer; voltage, 22.5 kV (900 V/cm), 7 μm; sample concentration, 4–10 mg/ml; detection, UV absorbance at 270 nm; other conditions are described in Ref.5

Source: From Macroporous polyacrylamide/poly(ethylene glycol) matrixes as stationary phases in capillary electrochromatography, in Anal. Chem.[5]

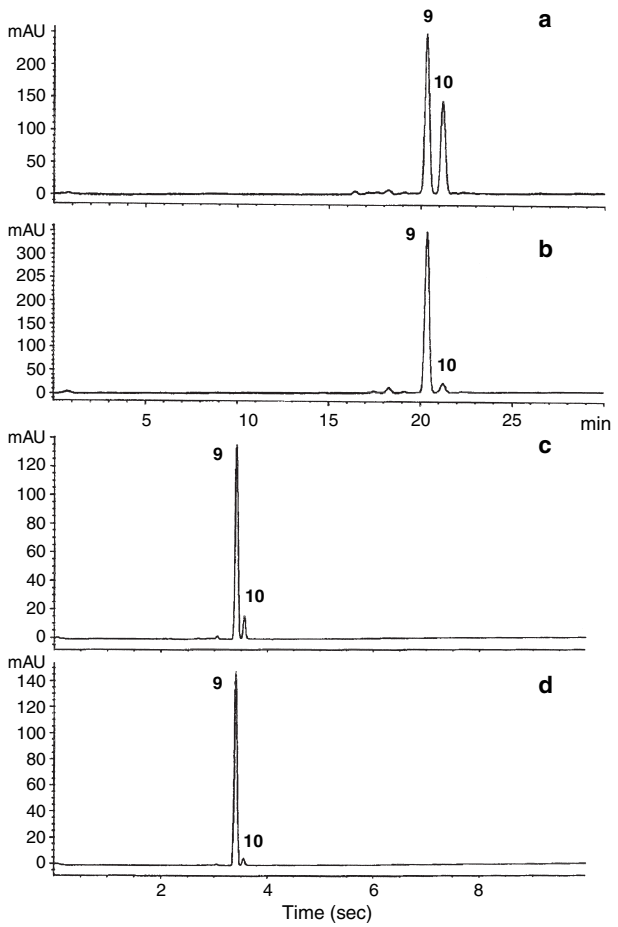

Fig. 2 Separation of synthetic, protected tetrapeptide intermediates: (9) *N*-methyl C- and N-protected tetrapeptide; (10) non-*N*-methyl C- and N-protected tetrapeptide. The structures of these compounds is proprietary information and consequently cannot be disclosed. Detection wavelength of 210 nm with a 10 nm bandwidth and a 1 sec rise time. Electrochromatography was performed on a 250 mm × 50 μm I.D. spherisorb ODS-1 packed capillary using an ACN-Tris (50 mmol/L, pH 7.8) buffer 80:20 v/v mobile phase, capillary temperature of 15°C, and an electrokinetic injection of 5 kV/15 sec. a, Synthetic mixture of protected tetrapeptides 9 and 10. Efficiency values of 124,000 and 131,000 plates/m were obtained for analytes 9 and 10, respectively. b, Chromatogram of synthetically prepared 9, the presence of residual non-methylated tetrapeptide (10) can be seen. c, Chromatogram of synthetically prepared 9, spiked with 10% of the non-methylated tetrapeptide (10). Efficiency values of 83,000 and 101,000 plates/m were obtained for analytes 9 and 10, respectively. d, Chromatogram of synthetically prepared 9, the presence of residual non-methylated tetrapeptide (10) can be clearly seen at the 3% level. Additional conditions are indicated in Ref.38.

Source: From Applications of capillary electrochromatography in pharmaceutical analysis, in J. Micro. Separ.[38]

available CE instrument), and an ACN buffer. Using non-optimized, non-pressurized CEC conditions (non-PEC, non-pressure-driven CEC), separation of the two tetrapeptides could be achieved in a run time of 21 min with efficiency values of 124,000 and 131,000 plates/m. In comparison, when a pressurized CE (buffer reservoirs and capillary were pressurized, with pressure-driven flow of buffer) system was used, separation of the components was achieved within 3.5 min. According to Euerby et al. the separation of these two peptides using a pressure-driven HPLC gradient analysis took 30 min and gave comparable peak area results. Although this study illustrated the improved efficiency of both non-pressurized CEC and pressurized CEC over HPLC, no reasonable conclusions can be drawn from this work.

The attempts that have been made to utilize true chemometric optimization of operating conditions in CEC are unclear in most of the studies done utilizing CEC. This has been done for many years in GC and HPLC, as well as in CE, but there are no obvious articles that have appeared which have utilized true chemometric software approaches to optimization in CEC.[57–59] It is not clear that any true method optimization has been performed or what analytical figures of merit were used to define an optimized set of conditions for biopolymer analysis by CEC. It is also unclear as to why a specific stationary phase (packing) was finally selected as the optimal support in these particular CEC applications for biopolymers. In the future, it is hoped that more sophisticated optimization routines, especially computerized chemometrics (expert systems, theoretical software, or simplex/optiplex routines) will be employed from start to finish.

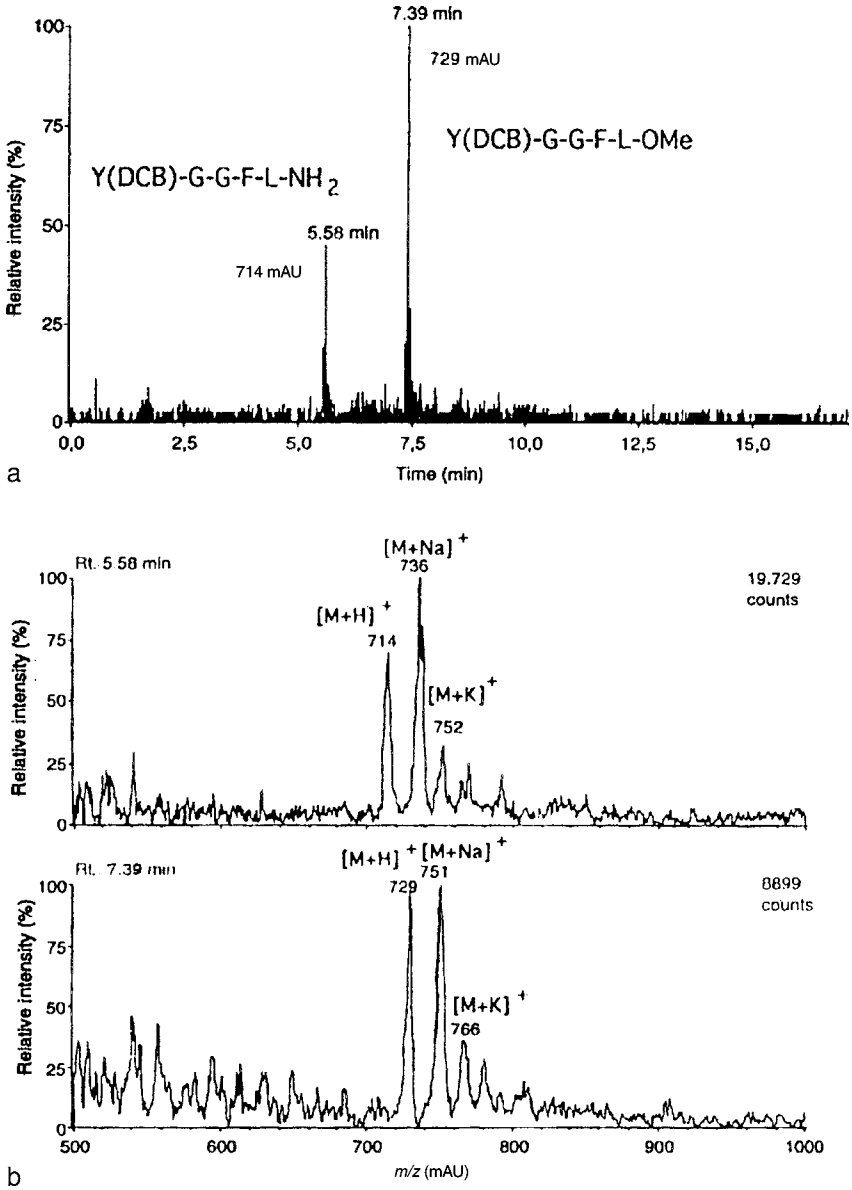

Fig. 3 Interfacing of pressure-driven CEC (PEC) for the separation of two simple peptides, enkephalin methyl ester (5.58 min) and enkephalin amide (7.39 min). (a) Extracted mass chromatogram of *m/z* 714 and 729 for the online peptide separation. Specific operating conditions are indicated in Ref. 4. (b) Mass spectra taken from the chromatographic peaks in (a), illustrating true M_r and the presence of M + H, M + Na, and M + K cations at appropriate *m/z* (amu) values.

Source: From Capillary electrochromatography-electrospray mass spectrometry: A microanalysis technique, in Anal. Chem.[4]; with permission of the authors and the American Chemical Society.

The coupling of ESI and MS with a pressurized CEC system (PEC) has been shown to separate peptides.[4] This particular study of Schmeer et al. utilized a commercial RP silica gel, Gromsil ODS-2, 1.5 mm packing material, already utilized in capillary HPLC for peptide separations. It was never made perfectly clear why this particular packing material was selected or why PEC was selected for MS interfacing over conventional, isocratic CEC conditions. It is possible that the EOF alone with this packing material was insufficient to elute all peptides in a reasonable time frame and, thus, pressurized flow was introduced. No gradient elution PEC was demonstrated in this particular study. A mixture of enkephalin methyl ester and enkephalin amide was separated using the packed capillary column (Fig. 3a and b. The coupling of these two methods showed enhanced sensitivity and detectability. Like the Euerby study, this offered little insight into the capabilities of CEC to separate peptides; however, the study does provide a nice example of a peptide separation based on chromatographic and electrophoretic separation mechanisms, probably occurring simultaneously. This report also described the ability of easily interfacing CEC and PEC with ESI/MS.

The coupling of an MS with CEC or PEC provides several advantages. With the capillary columns of 100 mm inner diameter (I.D.), flow rates of 1–2 L/min are obtained, which are ideal for electrospray MS.[4] No interface like a liquid sheath flow is required and the sintered silica gel frits allow direct coupling of the packed capillary columns without additional transfer capillaries. The spray is therefore formed directly at the outlet side of the column. Verheij et al. carried out the first coupling of a

pseudoelectrochromatography system to a fast-atom bombardment (FAB)-MS in 1991.[6] However, this required transfer capillaries that caused a loss in efficiency, which was also a problem with other experimentations with this technique.

Lubman's group published several papers on the PEC/MS system.[51–54] RP open tubular columns (RP-OTC), which were prepared by a sol–gel process, were coated with an amine that enhanced the EOF in an acidic buffer solution and reduced the non-specific adsorption between the peptides and the column wall. A six-peptide mixture was separated to baseline within 3 min using this system coupled to an online ion-trap storage–time-of-flight mass spectrometer (ITS–TOF-MS). A full-range mass detection speed of 8 Hz was used in all these experiments, which was rapid to maintain the high efficiency and ultrafast separation. A high-quality total ion chromatogram could be obtained with only a couple of femtomoles of peptide samples, due to the high-duty cycle of the MS and the column path-length-independent and concentration-sensitive feature of the ESI process. The concentration limit of detection was also improved to about 1×10^{-6} *M* because of the preconcentration capability of the RP-CEC. A tryptic digest of horse myoglobin was successfully separated within 6 minon the gradient CEC system. The use of the MS increased the resolving power of this system by clearly identifying the coeluting components.

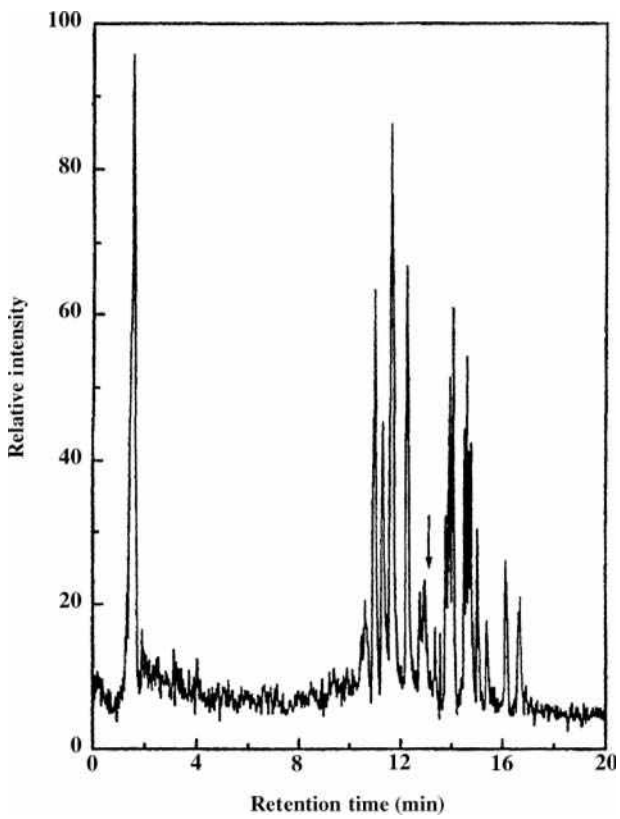

Fig. 4 The total ion chromatography (TIC) of the separation of a tryptic digest of chicken ovalbumin with a sample injection amount of 12 pmol corresponding to the original protein.[52] Column length, 6 cm. Conditions: 20 min, 0–40% acetonitrile gradient: 1000 V applied voltage with a 40-bar supplementary pressure.
Source: From Open-tubular capillary electrochromatography with an online Ion trap storage/reflectron time-of-flight mass detector for ultrafast peptide mixture analysis, in Anal. Chem.[52]; with permission of the authors and the American Chemical Society.

Another article by Wu et al.[52] dealt with a PEC coupled to an ion-trap storage/reflectron TOF-MS (RTOF-MS) for the analysis of peptide mixtures and protein digests. Taking advantage of the EOF, a high separation efficiency has been achieved in PEC due to a relatively flat flow profile and the use of smaller packing materials. With columns only 6 cm long, a tryptic digest of bovine cytochrome-c was successfully separated in about 14 min by properly tuning the applied voltage and the supplementary pressure. A relatively complex protein digest (tryptic digest) of chicken albumin gave 20 peaks (resolved) in the total ion current chromatogram in 17 min (Fig. 4). The sample concentrations were also on the order of about 1×10^{-5} *M*. The detector increased the resolving power of PEC by unambiguously identifying coeluting components. The CEC was directly interfaced to the MS via an ESI, which provided the molecular-weight information of the protein digest products and structural information via MS/MS (Table 1). The device uses a quadrupole ion trap as a front-end storage device, which converts a continuous electrospray beam for TOF analysis. The storage property of the ion trap provides ion integration for low-intensity signals, whereas the non-scanning property of the TOF-MS provides high sensitivity. A description of the MS is provided in an article by Wu et al.[54] According to an article by Verheij et al., problems that were encountered earlier, like formation of bubbles, have been overcome by using liquid junctions to apply the electric field over the column.[60]

A recent review article by the Lubman group points out that there are some serious advantages in using an open tubular column (OTC) for CEC as compared with packed-bed CEC.[54] OTCs with inner diameters around 10 μm have been found to have a smaller plate height when compared to packed columns. This is due to the lack of band-broadening effects associated with the presence of packing materials and end-column frits. OTC capillaries do not require end frits. High concentration sensitivity is another advantage of OTCs, as columns with very small dimensions are used. The small diameters of OTCs allow for the use of a higher voltage in CEC, without significant Joule heating. OTCs can also often provide more rapid separations than packed columns, by eliminating intraparticle diffusion, which is an important elimination for ultrafast separations in packed columns. However, there are some grave difficulties involved in using OTCs, perhaps because of the real difficulties with sample injection and detection. The injection volume of OTCs is in the low nanoliter or even picoliter range. The very small inner

Table 1 Comparison of calculated and measured tryptic peptides of chicken ovalbumin from PEC/MS.

No.	Tryptic peptides	Calculated mass[a]	Determined mass[1–2][a,b]	Sequence
1	1–16	1709.0	1709.6	GSIGAASMEFCFDVFK
4, 5	47–55	1080.2	1079.7	DSTRTQINK
5	51–55	602.7	602.9	TQINK
6, 7	56–61	781.0	781.4	VVRFDK
7	59–61	408.5	408.4	FDK
10	105–110	779.8	780.1	IYAEER
11	111–122	1465.8	1466.3	YPILPEYLQCVK
12	123–126	579.7	579.7	ELYR
13	127–142	1687.8	1687.5	GGLEPINFQTAADQAR
16	182–186	631.7	631.6	GLWEK
16, 17	182–189	996.1	995.9	GLWEKAFK
17	187–189	364.4	364.5	AFK
18	190–199	1209.3	1209.0	DEDTQAMPFR
20	219–226	821.9	821.7	VASMASEK
21	227–228	277.4	277.6	MK
23	264–276	1581.7	1581.3	LTEWTSSNVMEER
24, 25	277–279	405.5	405.4	KIK
26	280–284	646.8	646.8	VYLPR
26, 27	280–286	924.2	924.4	VYLPRMK
27, 28	285–290	813.0	813.1	MKMEEK
28	287–290	535.6	535.5	MEEK
30	323–339	1773.9	1774.2	ISQAVHAAHAEINEAGR
31	340–359	2009.1	2008.5	EVVGSAEAGVDAASVSEEFR
32	360–369	1190.4	1190.2	ADHPFLFCIK
33	370–381	1345.6	1345.3	HIATNAVLFFGR
33, 34	370–385	1750.1	1749.5	HIATNAVLFFGRCVSP
34	382–385	404.5	404.4	CVSP

[a]Average masses.
[b]Average of all charge states observed.
Source: From Open-tubular capillary electrochromatography with an online Ion trap storage/reflectron time-of-flight mass detector for ultrafast peptide mixture analysis, in Anal. Chem.[52] ; reproduced with permission of the authors and the American Chemical Society.

diameters of most OTCs make optical detection difficult, but they are very compatible with a concentration-sensitive detection method, such as ESI–IT–TOF-MS. With peptide mixtures, however, gradient elution CEC, with or without pressure-driven flow, is almost required over isocratic or step-gradient methods, because small changes in the mobile phase composition results in large changes in peptide retention times.

In a later study, Pesek et al. reported the separation of other proteins using a diol stationary phase.[61–64] The use of a diol stationary phase should result in a surface that is more hydrophilic than a typical alkyl-bonded moiety, like C_{18} or C_8. The overall results showed significant variations in retention times due to differences in solute-bonded phase interactions. Other factors, such as pH, could also influence this interaction, due to its influence on charge and protein conformations. Combining all these factors in the separation of peptides and proteins provides an experimentalist with many decisions to be made in the optimized experimental conditions to be used. Other chemical modifications of etched fused silica need to be studied in order to provide a better understanding of their interactions with proteins and peptides, as well as other classes of biopolymers.

CONCLUSIONS

At the present time, although there are several applications of CEC/PEC to biopolymer classes, these are to be considered only preliminary and not necessarily fully optimized in all possible parameters. At times, significant improvements in peak shape, plate counts, resolutions, efficiency, and the time of analysis can be realized.

However, final optimizations of these separations have not been realized or possible. Some workers have utilized pressurized flow to solve the problems of obtaining reasonable EOF without silanol–analyte interaction; however, this does not solve the problem. It just forces the analyte to elute and approaches electro-HPLC, rather than true CEC. There are real differences between electro-HPLC, PEC, and CEC that need to be recognized. There does not, in general, seem to have been any serious attempt to utilize any chemometric software approaches in CEC/PEC for biopolymer separation optimizations or rationale for doing so. At this time, packings are simply used because they were on the shelf in a laboratory or commercially available and not necessarily because they were really the best for protein–peptide separations in PEC/CEC. There remains a need for research-oriented column choices from commercial vendors to avoid the need to pack capillaries in-house with commercial HPLC supports.

REFERENCES

1. Krull, I.S.; Mistry, K.; Stevenson, R. CEC '98: the state-of-the-art. Am. Lab. August, **1998**, *16A*.
2. Tsuda, T. Electrochromatography using high applied voltage. Anal. Chem. **1987**, *59*, 521.
3. Olivares, J.A.; Nguyen, N.T.; Yonker, C.R.; Smith, R.D. On-line mass spectrometric detection for capillary zone electrophoresis. Anal. Chem. **1987**, *59*, 1230.
4. Schmeer, K.; Behnke, B.; Bayer, E. Capillary electrochromatography–electrospray mass spectrometry: A microanalysis technique. Anal. Chem. **1995**, *67*, 3656.
5. Palm, A.; Novotny, M.V. Macroporous polyacrylamide/poly(ethylene glycol) matrices as stationary phases in capillary electrochromatography. Anal. Chem. **1997**, *69*, 4499.
6. Verheij, E.R.; Tjaden, U.R.; Niessen, W.A.M.; van der Greef, J. Pseudo-electrochromatography–mass spectrometry: A new alternative. J. Chromatogr. **1991**, *554*, 339.
7. Angus, P.D.A.; Victorino, E.; Payne, K.M.; Demarest, C.W.; Catalano, T.; Stobaugh, J.F. Method development in pharmaceutical analysis employing capillary electrochromatography. Electrophoresis **1998**, *19*, 2073.
8. Majors, R.E. Perspectives on the present and future of capillary electrochromatography. LC–GC Mag. **1998**, *16* (2), 96.
9. Hansen, S.H.; Helboe, T. Separation of nucleosides using capillary electrochromatography. J. Chromatogr. A, **1999**, *836*, 315.
10. Landers, J.P., Ed.; *CRC Handbook of Capillary Electrophoresis—Principles, Methods, and Applications*; 2nd Ed.; CRC Press: Boca Raton, FL, 1997.
11. Baker, D.R. *Capillary Electrophoresis*; Techniques in Analytical Chemistry Series; John Wiley & Sons: New York, 1995.
12. Hercules, D.M. *Fluorescence and Phosphorescence Analysis: Principles and Applications*; Interscience: New York, 1966; 19.
13. Cunico, R.L.; Gooding, K.M.; Wehr, T. *Basic HPLC and CE of Biomolecules*; Bay Bioanalytical Laboratory: Richmond, CA, 1998.
14. Horvath, Cs., Nikelly, J.G., Eds.; *Analytical Biotechnology: Capillary Electrophoresis and Chromatography*; ACS Symposium Series; American Chemical Society: Washington, DC, 1990; Vol. 434.
15. Li, S.F.Y. *Capillary Electrophoresis: Principles, Practice and Applications*; Elsevier Science: Amsterdam, 1992.
16. Grossman, P.D., Colburn, J.C., Eds.; *Capillary Electrophoresis—Theory and Practice*; Academic Press: San Diego, CA, 1992.
17. Righetti, P.G., Ed.; *Capillary Electrophoresis in Analytical Biotechnology*; CRC Series in Analytical Biotechnology; CRC Press: Boca Raton, FL, 1996.
18. Camilleri, P., Ed.; *Capillary Electrophoresis: Theory and Practice*; CRC Press: Boca Raton, FL, 1993.
19. Mosher, R.A.; Thormann, W. *The Dynamics of Electrophoresis*; VCH: Weinhein, 1992, Chap. 7.
20. Altria, K.D.; Rogan, M.M. *Introduction to Quantitative Applications of Capillary Electrophoresis in Pharmaceutical Analysis, A Primer*; Beckman Instruments, Inc.: Fullerton, CA, 1995.
21. Weinberger, R.; Lombardi, R. *Method Development, Optimization and Troubleshooting for High Performance Capillary Electrophoresis*; Simon and Schuster Custom Publishing: Needham Heights, MA, 1997.
22. Karger, B.L., Hancock, Wm., Eds.; *High Resolution Separation and Analysis of Biological Macromolecules*; Methods in Enzymology Series, Part A, Fundamentals Academic Press: San Diego, CA, 1996; Vol. 270.
23. Altria, K.D., Ed.; *Capillary Electrophoresis Guidebook, Principles, Operation and Applications*; Methods in Molecular Biology; Humana Press: Totowa, NJ, 1996.
24. Lurie, I.S.; Meyers, R.P.; Conver, T.S. Capillary Electrochromatography of cannabinoids. Anal. Chem. **1998**, *70*, 3255.
25. Sandra, P.; Dermaux, A.; Ferraz, V.; Dittman, M.M.; Rozing, G. Analysis of triglycerides by capillary electrochromatography. J. Micro. Separ. **1997**, *9* (5), 409–419.
26. Dermaux, A.; Sandra, P.; Ksir, M.; Zarrouck, K.F.F. Analysis of the triglycerides and the free and derivatized fatty acids in fish oil by capillary electrochromatography. J. High Resolut. Chromatogr. **1998**, *21*, 545.
27. Kitagawa, S.; Tsuji, A.; Watanabe, H.; Nakshima, M.; Tsuda, T. Pressurized flow-drive capillary electrochromatography using ion exchange resins. J. Micro. Separ. **1997**, *9* (5), 347–356.
28. Mazzeo, J.R.; Krull, I.S. *Capillary Electrophoresis—Technology*; Guzman, N., Ed.; Marcel Dekker, Inc.: New York, 1993, Chap. 29.
29. Mazzeo, J.R.; Martineau, J.; Krull, I.S. *CRC Handbook of Capillary Electrophoresis: Principles, Methods, and Applications*; Landers, J.P., Ed.; CRC Press: Boca Raton, FL, 1994, Chap. 18.
30. Liu, X.; Sosic, Z.; Krull, I.S. Capillary isoelectric focusing as a tool in the examination of antibodies, peptides and proteins of pharmaceutical interest. J. Chromatogr. B, **1996**, *735*, 165.

31. Krull, I.S.; Dai, J.; Gendreau, C.; Li, G. HPCE methods for the identification and quantitation of antibodies, their conjugates and complexes. J. Pharm. Biomed. Anal. **1997**, *16*, 377.
32. Capillary Electrochromatography, Symposium, San Francisco, CA, organized by the California Separations Science Society, San Francisco, August 1997.
33. Royal Society of Chemistry Analytical Division, Northeast Region, Chromatography and Electrophoresis Group Symposium on New Developments and Applications in Electrochromatography, University of Bradford, Bradford, U.K., December, 3, 1997.
34. Tsuda, T., Ed.; *Electric Field Applications in Chromatography, Industrial and Chemical Processes*; VCH: Weinheim, 1995.
35. Dittmann, M.M.; Weinand, K.; Bek, F.; Rozing, G.P. LC/GC Mag. **1995**, *13* (10), 800.
36. Dittmann, M.M.; Rozing, G.P. Capillary electrochromatography—a high-efficiency micro-separation technique. J. Chromatogr. A, **1996**, *744*, 63.
37. Ross, G.; Dittmann, M.; Bek, F.; Rozing, G. Capillary electrochromatography: enhancement of LC separation in packed capillary columns by means of electrically driven mobile phases. Am. Lab. March, **1996**, 34.
38. Euerby, M.R.; Gilligan, D.; Johnson, C.M.; Roulin, S.C.P.; Myers, P.; Bartle, K.D. Applications of capillary electrochromatography in pharmaceutical analysis. J. Micro. Separ. **1997**, *9* (5), 373–372.
39. Euerby, M.R.; Johnson, C.M.; Bartle, K.D.; Myers, P.; Roulin, S.C.P. Capillary electrochromatography in the pharmaceutical industry. Practical reality or fantasy? Anal. Commun. **1996**, *33*, 403.
40. Robson, M.M.; Cikalo, M.G.; Myers, P.; Euerby, M.R.; Bartle, K.D. Capillary electrochromatography: A review. J. Micro. Separ. **1997**, *9* (5), 357–372.
41. Miwaya, J.H.; Alesandro, M.S. LC/GC Mag. **1998**, *16* (1), 36.
42. Majors, R.E. LC/GC Mag. **1998**, *16* (1), 12.
43. Grant, I.H. *Capillary Electrochromatography*; Methods in Molecular Biology; Altria, K.D., Ed.; Humana Press: Totowa, NJ, 1996; Vol. 52, Chap. 15.
44. Euerby, M.R.; Johnson, C.M.; Bartle, K.D. LC/GC Int. **1998**, 39.
45. Cikalo, M.G.; Bartle, K.D.; Robson, M.M.; Myers, P.; Euerby, M.R. Capillary electrochromatography. Analyst **1998**, *123*, 87R.
46. Wei, W.; Luo, G.; Yan, C. Am. Lab. **1998**, 20C.
47. Peters, E.C.; Lewandowsk, K.; Petro, M.; Frechet, J.M.J.; Svec, F. J.M.J. Anal. Commun. 1998, 35,83 a "Molded" Rigid Monolithic Capillary Column. In *HPLC 98*; St. Louis, MO, 1998.
48. Peters, E.C.; Lewandowski, K.; Petro, M.; Svec, F.; Frechet, J.M.J. Chiral electrochromatography with a "molded" rigid monolithic capillary column. Anal. Commun. **1998**, *35*, 83.
49. Peters, E.C.; Petro, M.; Svec, F.; Frechet, J.M.J. Molded rigid polymer monoliths as separation media for capillary electrochromatography. Anal. Chem. **1997**, *69*, 3646.
50. Venema, E.; Kraak, J.C.; Poppe, H.; Tijssen, R. Electrically driven capillary size exclusion chromatography. Chromatographia **1998**, *48* (5/6), 347.
51. Wu, J.T.; Huang, P.; Li, M.X.; Qian, M.G.; Lubman, D.M. Open-tubular capillary electrochromatography with an online ion trap storage/reflectron time-of-flight mass detector for ultrafast peptide mixture analysis. Anal. Chem. **1997**, *69* (3), 320–326.
52. Wu, J.T.; Huang, P.; Li, M.X.; Qian, M.G.; Lubman, D.M. Open-tubular capillary electrochromatography with an online Ion trap storage/reflectron time-of-flight mass detector for ultrafast peptide mixture analysis. Protein digest analysis by pressurized capillary electrochromatography using an ion trap storage/reflectron time-of-flight mass detector. Anal. Chem. **1997**, *69* (3), 320–326.
53. Wu, J.T.; Huang, P.; Li, M.X.; Qian, M.G.; Lubman, D.M. Open-tubular capillary electrochromatography with an online Ion trap storage/reflectron time-of-flight mass detector for ultrafast peptide mixture analysis. Anal. Chem. **1997**, *69* (3), 320–326.
54. Wu, J.T.; Huang, P.; Li, M.X.; Qian, M.G.; Lubman, D.M. On-line analysis by capillary separations interfaced to an ion trap storage/reflectron time-of-flight mass spectrometer. J. Chomatogr. A, **1998**, *794*, 377.
55. Yang, C.; El Rassi, Z. Capillary electrochromatography of derivatized mono- and oligosaccharides. Electrophoresis **1998**, *19*, 2061.
56. Zhang, M.; El Rassi, Z. Capillary electrochromatography with novel stationary phases. I. Preparation and characterization of octadecylsulfonated silica. Electrophoresis **1998**, *19*, 2068.
57. Bopp, R.J.; Wozniak, T.J.; Anliker, S.L.; Palmer, J. Pharmaceutical and biomedical applications of liquid chromatography. *Progress in Pharmaceutical and Biomedical Analysis*; Riley, C.M, Lough, W.J., Wainer, I.W., Eds.; Pergamon/Elsevier Science: Amsterdam, 1994; Vol. 1, Chap. 10.
58. Dolan, J.W.; Snyder, L.R. Liquid chromatography expert systems: a modular approach. Am. Lab. May, **1990**, 50.
59. Snyder, L.R.; Kirkland, J.J.; Glajch, J.L. *Practical HPLC Method Development*, 2nd Ed.; John Wiley & Sons: New York, 1997; Chap. 10.
60. Verheij, E.R.; Tjaden, U.R.; Niessen, W.A.M.; van der Greef, J. Development of an instrumental configuration for pseudo-electrochromatography–electrospray mass spectrometry. J. Chromatogr. **1995**, *712*, 201.
61. Pesek, J.J.; Matyska, M.T.; Sandoval, J.E.; Williamsen, E.J. Synthesis, characterization and applications of hydride-based surface materials for HPLC, HPCE and electrochromatography. J. Liq. Chromatogr. Relat. Technol. **1996**, *19* (17/18), 2843.
62. Pesek, J.J.; Matyska, M.T.; Mauskar, L. Separation of proteins and peptides by capillary electrochromatography in diol- and octadecyl-modified etched capillaries. J. Chromatogr. A, **1997**, *763*, 307.
63. Pesek, J.J.; Matyska, M.T. Electrochromatography in chemically modified etched fused-silica capillaries. J. Chromatogr. A, **1996**, *736*, 255.
64. Pesek, J.J.; Matyska, M.T. Separation of tetracyclines by high-performance capillary electrophoresis and capillary electrochromatography. J. Chromatogr. A, **1996**, *736*, 313.

Biopolymers: CZE Analysis

Feng Xu
Yoshinobu Baba
Department of Medicinal Chemistry, University of Tokushima, Tokushima, Japan

INTRODUCTION

Since Jorgenson and Lukacs[1] separated peptides in 1981 using free zone electrophoresis in glass capillaries, capillary electrophoresis (CE) has become a highly efficient technique for the separation of biopolymers such as proteins, peptides, carbohydrates, and DNA. Free solution CE, or capillary zone electrophoresis (CZE), is an electrophoresis in free homogeneous solution.[2,3] Charged solutes are simply separated on the basis of the solute charge-to-mass (*m/z*) ratio, applied electric field, and the pH and ionic strength of the background electrolyte (BGE).

Separation of DNA is generally conducted by capillary gel electrophoresis (CGE), in which gel or polymer solutions act as sieving media, rather than by CZE, because each DNA has the same *m/z* ratio. The CZE separation of DNA can only be achieved by using some special modifications to break the charge-to-mass symmetry through either trapping analytes into sodium dodecyl sulfate (SDS) micelles or labeling analytes with large and weakly charged molecules at the DNA fragment ends (end-labeled free-solution electrophoresis).[4] Separation of DNA is not covered here. Interested readers are referred to our previous entries,[5,6] dealing with DNA size separation and sequencing, in the *Encyclopedia of Chromatography*. Here we concentrate on the CZE separations of three kinds of biopolymers (proteins, peptides, and carbohydrates), including the factors influencing the separations and the promising development of CZE in microchip and capillary array platforms.

PROTEINS AND PEPTIDES

Proteins are key participants in all biological activities. Peptides, generally shorter than proteins, have important biological functions, as hormones, neurotransmitters, etc. Owing to the similarity in structure, the general principles of the separations of proteins and peptides are alike. A semiempirical relation exists between mobility, charge, and size of a peptide or protein:

$$\mu = A\frac{q}{M^p} + B$$

where μ is mobility, q is charge, M is molecular mass, A and B denote empirical constants, and p varies from 1/3 to 2/3 as a function of the pH and ionic strength of BGE, and shape of peptides and proteins, etc. For a protein, the most difficult part is estimation of the charge.[7]

Sample Preconcentration

The CZE of a low concentration protein or peptide requires preconcentration of the sample before analysis, either off-line or online. Preconcentration is commonly performed by using solid-phase packing material at the inlet end of the capillary and is based on chromatographic or electrophoretic principle. Solid-phase extraction (SPE) on C_{18} or C_8 cartridges can be online connected to CZE and the concentrated non-specific analytes are released by an organic solvent (e.g., acetonitrile).[8] Alternatively, specific analytes can be concentrated by the use of antibody-containing cartridges and enzyme-immobilized microreactors. Desalting is important in protein processing. Microdialysis sampling can be used for the desalting of samples prior to introduction into electrospray ionization/mass spectrometry (ESI/MS). Capillary isoelectric focusing (CIEF), with slow ramping of voltage, can achieve online desalting of proteins in cerebrospinal fluid. Head column stacking has a long history and is now a popular technique in which the injected sample is simply dissolved in water and is focused at the interface between the sample plug and separation buffer, as a result of different mobilities in the two solutions. Capillary isotachophoresis (CITP) can also be utilized to achieve on-column sample preconcentration. The sample is introduced as a plug between a leading electrolyte, which has a higher mobility than the sample, and a trailing electrolyte, which has a lower mobility than the sample. After applying the voltage, the sample components are focused as a concentrated band. Very large sample zones can be accommodated by isotachophoresis to enhance the limit of detection (LOD).[9]

Detection

Peptide bonds enable proteins and peptides to be directly detected by ultraviolet (UV) radiation, at 200–220 nm, where the absorption is proportional to the number of peptide bonds. Sometimes, detection is performed around

254 or 280 nm, where proteins have modest absorbance in the presence of aromatic residues. However, the sensitivity of UV detection is relatively poor (to μM). Several commercially available Z-type cells and bubble-shaped cells can help, somewhat, in improving the sensitivity.

Laser-induced fluorescence (LIF) produces low LOD and a wide dynamic range. Native fluorescence of proteins is primarily associated with emission from tryptophan and tyrosine, between 300 and 400 nm. Proteins are easy to derivatize with a fluorescent reagent prior to electrophoresis. Postcolumn derivatization can be performed in sheath flow systems where the sheath flow cell acts as a postseparation labeling reactor. To avoid the formation of a mixture of multiply labeled products for originally single species, some special procedures utilizing Edman degradation chemistry or fluorescein isothiocyanate (FITC) labeling at lower than normal derivatization buffer pH have been developed. Noncovalent labeling is performed with dyes that interact with proteins, either by H bonding or through hydrophobic interactions. The sensitivity of LIF approaches the absolute LOD of a single molecule. A number of fluorescent dyes are widely used,[10] such as fluorescamine, 1-anilinonaphthalene-8-sulfonic acid, 4,4′-dianilino-1,1′-binaphthyl-5,5′-disulfonic acid, 2-(*p*-toluidino)naphthene-6-sulfonic acid, 3-(2-furoyl)quinoline-2-carboxaldehyde, naphthalene-2,3-dicarboxaldehyde, 4-chloro-7-nitrobenzofurazan, 4-fluro-7-nitrobenzofurazan, *O*-phthaldialdehyde-2-mercaptoethanol, and 3-(4-carboxybenzoyl)-2-quinolinecarboxaldehyde, etc.

Mass spectrometric detection has come into frequent use, as it provides significant information relating to the solute structure. Protein analysis using CZE/MS has been applied to abundant proteins in a single cell after the single intact cell was introduced into a separation capillary and after being lyzed. On the other hand, ESI/MS is a soft ionization technique that can form molecular ions. Online ESI detection requires an external interface and volatile buffers to avoid contamination of the ionization chamber. Proteins can also be off-line identified by matrix-assisted laser desorption ionization/time-of-flight mass spectrometry (MALDI/TOF/MS), in which the matrix utilizes a low-molecular-weight organic acid that absorbs laser light and dissipates the energy in such a way that protein is evaporated, usually in a single protonated form. Time of flight has an advantage of having no upper mass-to-charge limit.

Coatings and Additives

The interaction of proteins with the negative charges of the ionized silanol groups on the inner capillary wall should be overcome prior to separation. The interaction results in peak tailing, poor resolution, unstable electro-osmotic flow (EOF), and sample adsorption loss. A variety of approaches have been developed to overcome this problem, including the use of extreme buffer pH, coated capillaries, and additives in BGE.

The simplest way is to use extreme buffer pH, i.e., either a low pH at which the dissociation of silanol groups is suppressed so as to prevent their electrostatic interactions with positively charged polypeptides, or an alkaline pH that is at least two units above the isoelectric point of an analyzed polypeptide, which leads to electrostatic repulsion between the negatively charged polypeptide and the negatively charged silanol groups on the capillary wall. Unfortunately, even proteins that behave as anions still have a positively charged section on their surface that can interact with the capillary wall. In addition, more extreme pHs may denature proteins.

Static wall coatings are usually made by reacting the capillary wall with a small bifunctional reagent, which is then used to bind a polymer to the wall. The polymer is usually prepared in situ. γ-methacryloxypropyltrimethoxysilane is a classical bifunctional reagent, while polyacrylamide is a frequently used polymer for coatings. A variety of polymer coatings can be anchored onto capillaries, such as polystyrene, polybrene, polyvinyl alcohol, polyethyleneimine, polyethylene glycerol, polyvinylpyrrolidone, polyethylene oxide, and nonionic surfactant coatings. Hydrophilic coating, epoxy-poly(-dimethylacrylamide), can separate proteins over the range of pH 4–10 with the recovery of both cationic and anionic proteins over 90%.

Dynamic wall coatings are replaceable. There are two kinds of dynamic coatings: One is performed by introducing a neutral polymer to the BGE, and the other is performed by adding ions to the BGE. The neutral polymers not only shield capillary wall from interactions with solutes, but also increase the viscosity in the electric double layer and reduce EOF. Various cellulose derivatives and other hydrophilic polymers, such as polyvinyl alcohol, polyethyleneoxide, hydroxyethyl cellulose, copolymer of hydroxypropylcellulose and hydroxyethylmethacrylate, and polysaccharide guaran, have been used for this purpose. Ionic (mainly cationic) additives titrate the negative charge of the capillary wall so that the EOF is decreased, neutralized, or even reversed. Polyionic species reduce the pH dependence of the EOF if, for example, the coating contains sulfonic acid groups that are fully ionized over a wide pH range. One can also add, to the BGE,[11,12] oligoamines such as putrescine, spermine, and tetraethylene pentamine, cationic surfactants such as cetyltrimethylammonium bromide (CTAB) and didodecyldimethylammonium bromide (DDAB), high concentration of anionic surfactants such as SDS, zwitterionic phospholipids such as 1,2-dilauroyl-*sn*-phosphatidylcholine, high concentration of alkali salts and phytic acid, other compounds such as cyclodextrins, etc. A mixture of cationic and anionic fluorosurfactants produces efficient separations of acidic and basic proteins in a single run at neutral pH. Zwitterionic surfactants are typically superior to the non-ionogenic ones. The protein interactions with the capillary wall are inversely proportional to the critical micellar concentration (CMC) of surfactants.

In addition to reducing the adsorption, the dynamic additives also play important roles in selectivity enhancement. pH is an important option for protein and peptide separation. An increase in the buffer ionic strength can increase the resolution. Any ion that displays a preferential affinity with the peptides has a potential modifying effect on the selectivity. The addition of organic modifiers, e.g., methanol, ethanol, and acetonitrile, in the BGE, can induce different solvation of the peptide chains and modify the migration order and selectivity of peptides. For separation of very hydrophobic proteins, e.g., lipoproteins, surfactants can act as buffer additives to improve solubilization.

Using amphoteric, isoelectric buffers at pH close to their isoelectric points (p*I*), at which the electrolytes have a net charge of zero, is an efficient way to decrease the BGE conductivity and apply extremely high field strength. Thus the separation time can be reduced to the order of a few minutes, and high resolution is achieved as a result of minimal diffusion-driven peak spreading. Several acidic isoelectric buffers, such as cysteic acid (p*I*: 1.85), iminodiacetic acid (p*I*: 2.23), aspartic acid (p*I*: 2.77), and glutamic acid (p*I*: 3.22), all at 50 m*M* concentration,[13] have been used in CZE separation of proteins and peptides. Fig. 1 shows a decrease of total running time from 70 to 12 min when using an isoelectric solution.

CARBOHYDRATES

Carbohydrates are the third most important class of biopolymers, next to proteins and DNA. However, their analyses by CZE are still in infancy because of the complexity and diversity of their structures. In terms of ionization ability, carbohydrates may be divided into acidic and weakly ionizable classes. Acidic carbohydrates are negatively charged at neutral pH and can be conveniently separated. Weakly ionizable carbohydrates are neutral at mild pH, but deprotonate at extremely basic condition (e.g., pH $>$ 12).

Underivatized Carbohydrates

The borate buffer is the most effective buffer for the CZE separation of native (and derivatized) carbohydrates. Borate complexes with adjacent hydroxyl groups on carbohydrates to form a negatively charged complex, which has a 2- to 20-fold increased UV absorbance at 195 nm.[9] The stability of sugar–borate complexes increases with increasing pH and borate concentration, and depends on the number and configuration of the hydroxyl groups. The presence of a surfactant (e.g., tetrabutylammonium) in a borate buffer also enhances the solute selectivity by interacting with anionic borate–sugar complexes. Saccharides, e.g., sucrose, glucose, fructose, etc. can also be separated by chelating with Cu^{2+} present in the BGE. Elevated temperature up to 60°C facilitates the enhancement of resolution and efficiency.

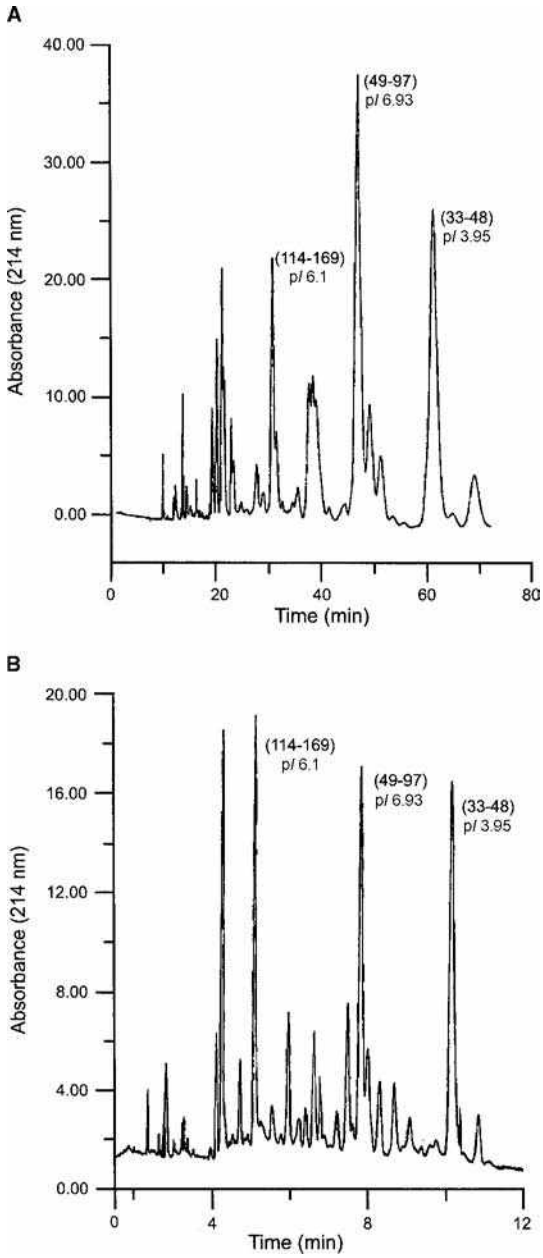

Fig. 1 CZE of tryptic digests of β-casein in 100 mm I.D. × 37 cm capillary. A, BGE: 80 m*M* phosphate buffer, pH 2.0; injection: 0.5 p.s.i. for 3 sec; applied field strength: 110 V/cm. The three major peaks are: 1) p*I* 6.1, fragment β-CN (114–169); 2) p*I* 6.93, fragment β-CN (49–97); and 3) p*I* 3.95, fragment β-CN (33–48). Note that the total running time is 70 min. B, BGE: 50 m*M* isoelectric aspartic acid (pH = p*I* = 2.77) added with 0.5% hydroxyethyl cellulose (HEC) (M_n 27,000 Da) and 5% trifluoroethanol; applied field strength: 600 V/cm.
Source: From Capillary electrophoresis of peptides in isoelectric buffers, in J. Chromatogr. A.[13]

Underivatized carbohydrates are mainly detected using low-wavelength UV (at 190–200 nm), indirect UV, or indirect LIF. The indirect method is based on the physical displacement of analytes with the added chromophoric or

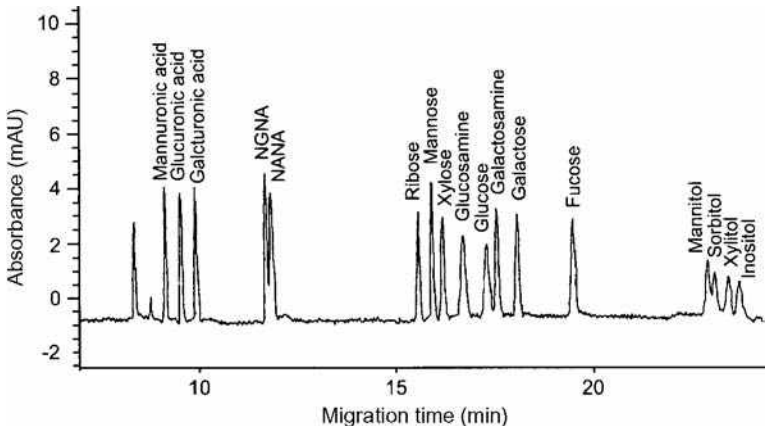

Fig. 2 Capillary zone electrophoresis of saccharides (1 m*M* each) standard mixture. Capillary: Fused silica, 50 μm I.D. × 80.5 cm (72 cm effective length); BGE: 20 m*M* 2,6-pyridinedicarboxylic acid (PDC) and 0.5 m*M* CTAB, pH 12.1; voltage: −25 kV. The signal wavelength was set at 350 nm with a reference at 275 nm.
Source: From Simultaneous determination of monosaccharides in glycoproteins by capillary electrophoresis, in Anal. Biochem.[14]

flurophoric compounds in the BGE. Indirect UV detection, using sorbic acid as both carrier electrolyte and chromophore, and employing high pH to achieve ionization of saccharides, permits the analysis of underivatized saccharides in low concentration. Fig. 2 shows the separation of underivatized acidic, neutral, and amino sugars and sugar alcohols by CZE-indirect UV.[14] Capillary electrophoresis-pulsed amperometric detection (CE/PAD) in the analysis of oligosaccharides derived from glycopeptides provides structural information through simply modulating the detection potentials. Refractive index detection is a universal detection and is also useful for oligosaccharide analysis. However, the detection limit is rather poor.

Derivatized Carbohydrates

Derivatization provides the advantage of incorporating chromophoric or fluorophoric functions into carbohydrates to achieve highly sensitive detection. Electromigration can also be achieved by derivatization of neutral saccharides with reagents possessing ionizable functions. Derivatization of the reducing aldehyde and/or keto groups present in carbohydrates can be performed by reductive amination and condensation reaction.

The reaction of reductive amination is based on the reducing end of a saccharide reacting with the primary amino group of a chromophoric or fluorophoric reagent to form a Schiff base that is subsequently reduced to a stable secondary amine. For example, in the reductive amination of malto-oligosaccharides, 8-aminonaphthalene-1,3,6-trisulfonic acid (ANTS) introduces both electric charge and fluorescence to the saccharides.[15] The products are ionized at a pH as low as 2.5, allowing CZE of carbohydrates under conditions where both EOF and adsorption to the internal capillary wall are negligible, even in the absence of any coating. Aminobenzoic acid and related compounds have the merit to react with both ketoses and aldoses of oligosaccharides in less than 15 min at 90°C. Such fast reactions could be compatible with the CE separation speed. Other conventional fluorophores for carbohydrate labeling include 8-aminopyrene-1,3,6-trisulfonate (APTS), 7-amino-4-methylcoumarin, 3-(4-carboxybenzoyl)-2-quinolinecarboxaldehyde, 2-aminobenzamide, 4-aminobenzoate, 4-aminobenzonitrile, etc.

The derivatization of aldehydes in reducing carbohydrates can also be performed by a condensation reaction between the active hydrogens of 1-phenyl-3-methyl-5-pyrazolone (PMP) and the aldehyde functionality under slightly basic condition. The formed *bis*-PMP derivatives can be separated by CZE and detected by UV absorbance.[16] Oligosaccharides can also be separated as complexes with a variety of compounds, including acetate, molybdate, germanate, stannate, arsenite, wolframate, vanadate, and tellurate of various alkali and alkaline earth metal ions. In a BGE containing calcium, barium, or strontium acetate, a mixture of PMP-derivatized reducing carbohydrates such as arabinose, ribose, galactose, glucose, and mannose was fully resolved.[16]

Glycoprotein analysis requires both protein and glycan identification. CE/LIF is widely used in the fingerprinting of fluorescently labeled glycans and in detection differences in maps of the oligosaccharides released from glycoproteins. The analysis of the complete composition of saccharides occurring in glycoproteins can be performed by separating the hydrolyzed sugars using CZE. Useful information about the glycoprotein structure can be obtained by combining CZE with MALDI-MS and ESI–MS. The techniques are well suited for the sensitive determination of the degree of heterogeneity, the site of glycosylation in a protein, and the composition and branching patterns of *N*- and *O*-linked glycans.

CONCLUSIONS

CZE, with its automation, simplicity, and rapid method development, is an attractive choice for biopolymer separation. Future methodological advances include

novel capillary wall coatings, specific buffer additives, effective sample preconcentration, and highly sensitive detection. At the same time, CZE development will move toward two promising directions: High-throughput and ultrafast separations (in seconds not minutes). Previously, CZE was a sequential technique, which allowed analysis of one sample per analysis. One remedy to this problem is the use of the capillary array electrophoresis (CAE) technique. Array instruments use 100 or more capillaries in parallel, with the laser excited fluorescence signals from each channel simultaneously recorded, e.g., by a charge-coupled device (CCD) array. Another remedy for fast analysis is the use of microchip-based CE devices. All operations, e.g., sample manipulation, separation, and detection, are performed on the microstructures of the chips. The short sample injecting plug, essentially zero dead volume intersections, and high field strength result in extremely rapid and high efficient separation.[17] The advantage of microfabricated devices is also the potential of producing arrays of separation channels for high-throughput applications in a single run. After solving some technical problems, the microchip-based separations are expected to become a highly powerful tool in future separations of biopolymers.

REFERENCES

1. Jorgenson, J.W.; Lukacs, K.D. Zone electrophoresis in open-tubular glass capillaries. Anal. Chem. **1981**, *53* (8), 1298–1302.
2. Righetti, P.G., Ed.; *Capillary Electrophoresis in Analytical Biotechnology*; CRC Press: Boca Raton, FL, 1996.
3. Camilleri, P., Ed.; *Capillary Electrophoresis—Theory and Practice;* New Directions in Organic and Biological Chemistry Series; CRC Press: Boca Raton, FL, 1997.
4. Heller, C.; Slater, G.W.; Mayer, P.; Dovichi, N.; Pinto, D.; Viovy, J.-L.; Drouin, G. Free-solution electrophoresis of DNA. J. Chromatogr. A, **1998**, *806* (1), 113–221.
5. Xu, F.; Baba, Y. DNA sequencing: CE. In *Encyclopedia of Chromatography*, 3rd Ed.; Cazes, J., Ed.; Taylor & Francis: New York, 2010; 626–633.
6. Xu, F.; Kiba, Y.; Baba, Y. Nucleic acids, oligonucleotides, and DNA: CE. In *Encyclopedia of Chromatography*, 3rd Ed.; Cazes, J., Ed.; Taylor & Francis: New York, 2010; 1606–1615.
7. Kašička, V. Recent advances in capillary electrophoresis of peptides. Electrophoresis **2001**, *22* (19), 4139–4162.
8. Dolník, V.; Hutterer, K.M. Capillary electrophoresis of proteins 1999–2001. Electrophoresis **2001**, *22* (19), 4163–4178.
9. Krylov, S.N.; Dovichi, N.J. Capillary electrophoresis for the analysis of biopolymers. Anal. Chem. **2000**, *72* (12), 111R–128R.
10. Bardelmeijer, H.A.; Waterval, J.C.M.; Lingeman, H.; van't Hof, R.; Bult, A.; Underberg, W.J.M. Pre-, on-, and post-column derivatization in capillary electrophoresis. Electrophoresis **1997**, *18* (12–13), 2214–2227.
11. Tabuchi, M.; Baba, Y. A separation carrier in high-speed proteome analysis by capillary electrophoresis. Electrophoresis **2001**, *22* (16), 3449–3457.
12. Cunliffe, J.M.; Baryla, N.E.; Lucy, C.A. Phospholipid bilayer coatings for the separation of proteins in capillary electrophoresis. Anal. Chem. **2002**, *74* (4), 776–783.
13. Righetti, P.G.; Nembri, F. Capillary electrophoresis of peptides in isoelectric buffers. J. Chromatogr. A, **1997**, *772* (1–2), 203–211.
14. Soga, T.; Heiger, D.N. Simultaneous determination of monosaccharides in glycoproteins by capillary electrophoresis. Anal. Biochem. **1998**, *261* (1), 73–78.
15. El Rassi, Z. Recent developments in capillary electrophoresis and capillary electrochromatography of carbohydrate species. Electrophoresis **1999**, *20* (15–16), 3134–3144.
16. Honda, S.; Yamamoto, K.; Suzuki, S.; Ueda, M.; Kakehi, K. High-performance capillary zone electrophoresis of carbohydrates in the presence of alkaline earth metal ions. J. Chromatogr. **1991**, *588* (1–2), 327–333.
17. Effenhauser, C.S.; Bruin, G.J.M.; Paulus, A. Integrated chip-based capillary electrophoresis. Electrophoresis **1997**, *18* (12–13), 2203–2213.

Biopolymers: Separations

Masayo Sakata
Chuichi Hirayama
Department of Applied Chemistry and Biochemistry, Kumamoto University, Kumamoto, Japan

INTRODUCTION

Endotoxin [lipopolysaccharides (LPSs)] is an integral part of the outer cellular membrane of Gram-negative bacteria and is responsible for organization and stability. In the biotechnology industry, Gram-negative bacteria are widely used to produce recombinant DNA products such as peptides and proteins. Thus these products are always contaminated with LPS. Such contaminants have to be removed from drugs and fluids before use in injections, because their potent biological activities cause pyrogenic reactions.

To achieve selective removal of LPS from final biological products, such as proteins and protective antigens, it is necessary to consider not only the chemical and physical structures of LPS, but also those of the adsorbents and proteins, as well as the solution conditions. In physiological solutions, LPS aggregates form supramolecular assemblies (M_w: 4×10^5 to 1×10^6) with phosphate groups as the head group and exhibit a net-negative charge because of their phosphate groups. However, as proteins may release LPS monomers from the aggregates, we assume that LPS aggregates comprise a wide range of molecular sizes, with M_w from 2×10^4 to 1×10^6 in physiological solutions. On the other hand, the molecular weights of proteins are generally about 1×10^4 to 5×10^5. Therefore, it is extremely difficult to separate LPS from protein solely by size-separation methods, such as size-exclusion chromatography (SEC) and ultrafiltration. Various procedures of LPS removal, such as ion-exchange membrane, ultrafiltration, and extraction, have been developed for pharmaproteins. These procedures, however, are unsatisfactory with respect to selectivity, adsorption capacity, and protein recovery.

For the removal of LPS from final solutions of bioproducts, selective adsorption has proven to be the most effective technique. Therefore considerable effort is being put into the development of adsorbents capable of retaining high LPS selectivity under physiological conditions (ionic strength of $\mu = 0.05$–0.2, neutral pH). Recently, numerous cationic polymer adsorbents have been developed for removing LPS from protein solutions. This entry will elucidate the chromatographic properties of various LPS adsorbents and will describe recent findings concerning methods for eliminating LPS from protein solutions using the adsorption technique.

CHROMATOGRAPHIC MATRICES WITH POLYCATIONIC LIGANDS

Lipopolysaccharide is an amphipathic substance[1–3] that has both an anionic region (the phosphoric acid groups) and a hydrophobic region (the lipophilic groups). From this point of view, an LPS-selective ligand should have, not only cationic properties, but also hydrophobic properties.[4–6] Fig. 1 shows structures of various cationic substances that are suitable as LPS-selective ligands. Through immobilization of polymyxin B on CNBr-activated Sepharose, Issekutz[7] created a polymyxin–Sepharose adsorbent for selective removal of LPS. This adsorbent is now commercially available. Although the polymyxin–Sepharose columns showed high LPS-adsorbing activity, protein losses during passage through the column have been noted (20% loss of BSA in Ref.[8]). This is due to the ionic interaction between the cationic region of the polymyxin B and the net-negatively charged proteins at low-ionic strengths. Furthermore, polymyxin B is not suitable as a ligand for LPS removal from a solution for intravenous injection because it could escape from the column and would be physiologically active in solution. If any polymyxin is to be released into a solution, it would be physiologically active. Poly(ethyleneimine) (PEI)-immobilized cellulose fibers have been prepared by Morimoto et al.[9] and the PEI fibers showed significant LPS-adsorbing capacity under physiological conditions (neutral and ionic strength of $\mu = 0.1$–0.2). In a more recent publication, poly(ε-lysine) (PL) was covalently immobilized onto cellulose spherical particles and used for selective adsorption of LPS from protein solutions.[10] In addition, the PL (degree of polymerization: 35, pK_a: 7.6) (Chisso)[11] produced by *Streptomyces albulus*, which has become commercially available as a safe food preservative, is more suitable as a ligand than is polymyxin B. The high LPS adsorption of chromatographic matrices having polycationic ligands, such as polymyxin B, PEI, or PL, is

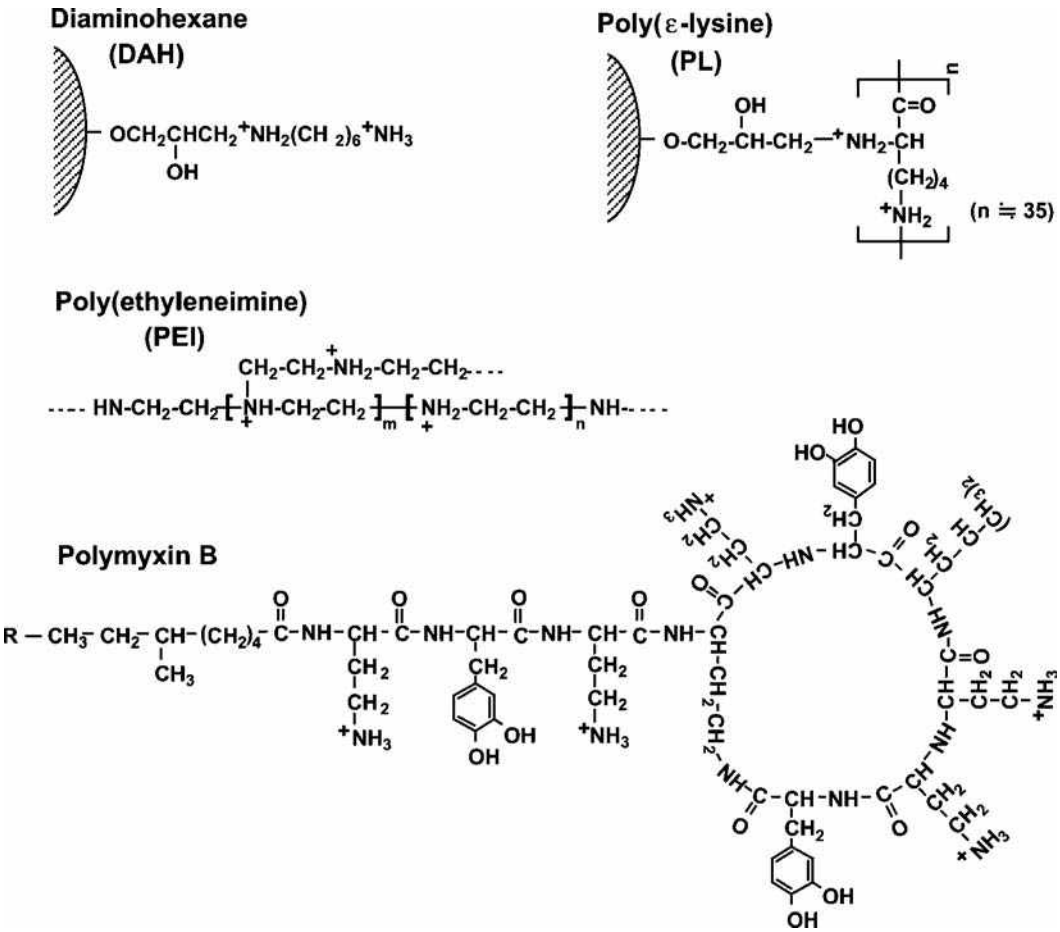

Fig. 1 Structure of LPS-selective ligands. Sepharose and cellulose particles are used as the matrix.

possibly due to the simultaneous effects of the cationic properties of the ligand and its hydrophobic properties.

EFFECTS OF VARIOUS FACTORS ON THE SEPARATION OF BIOPOLYMERS BY POLYCATIONIC ADSORBENTS

Effect of Pore Size of the Adsorbent on LPS Selectivity

To achieve the selective removal of LPS, it is important to determine the adsorbing activity of proteins. Table 1 shows the effect of the adsorbent pore size (molecular mass exclusion of polysaccharide, M_{lim})[12] on the adsorption of cellular products (biorelated polymers). The various PL-immobilized cellulose particles (PL cellulose) with pore sizes of M_{lim} 2×10^3 to $>2 \times 10^6$ were used as adsorbents. Lipopolysaccharide, DNA, and RNA, which are anionic biorelated polymers with phosphoric acid groups, were adsorbed very well by all the adsorbents. By contrast, the adsorption of protein was more dependent on the M_{lim} of the adsorbent than its anion-exchange capacity (AEC). The adsorption of bovine serum albumin (BSA) (M_w 6.9×10^4), an acidic protein, increased from 5% to 68% with an increase in the M_{lim} from 2×10^3 to 1×10^4. The adsorption of γ-globulin (M_w 1.6×10^5), a hydrophobic protein, increased from 2% to 22% with an increase in the M_{lim} from 1×10^4 to $>2 \times 10^6$. Polymyxin–Sepharose with large pore size ($M_{lim} > 2 \times 10^6$) also adsorbed BSA (78%) and γ-globulin (26%), as shown in Table 1. Very little of the other neutral or basic proteins adsorbed onto the adsorbents under similar conditions. As a result, only when the PL cellulose (10^3), with a M_{lim} of 2×10^3 and AEC of 0.6 meq/g, was used as the adsorbent at pH 7.0 and ionic strength of $\mu = 0.05$ were LPS and DNA selectively well adsorbed.

The results reported in Table 1 show that the adsorption of protein was caused, mainly, by the entry of the protein into the pores of the adsorbent. This indicates that both BSA and γ-globulin can readily penetrate into a particle with an M_{lim} of $> 2 \times 10^6$, but cannot penetrate into a particle with 2×10^3 (M_{lim}). On the other hand, it would also appear that LPS aggregates are not able to enter the pores of the adsorbents with 2×10^3 (M_{lim}) because their molecular weights (4×10^5 to

Table 1 Effect of adsorbent's pore size on adsorption of a bio-related polymer.

			Adsorption[a] (%)			
			PL-cellulose (10^3)[b]	PL-cellulose (10^4)[c]	PL-cellulose (10^6)[d]	Polymyxin–sepharose[e]
		AEC[f] (meq/g):	0.6	0.8	0.6	0.2
Cellular product	(p*I*)	*Pore size* (M_{lim})[g]:	2×10^3	1×10^4	$>2 \times 10^6$	$>2 \times 10^6$
Ovalbumin	4.6		2	65	85	75
BSA	4.9		5	68	82	78
Myoglobin	6.8		<1	<1	<1	<1
γ-Globulin	7.4		2	2	22	26
Lysozyme	11.0		<1	<1	<1	<1
DNA (salmon spermary)			99	99	99	99
RNA (yeast)			98	99	99	99
LPS (*E. coli* O111 : B4)			91	98	99	99
LPS (*E. coli* UKT-B)			89	96	99	99

[a]The adsorption of a cellular product was determined using a batchwise method with 0.3 ml of wet adsorbent and 2 ml of a sample solution (100 μg/ml, pH 7.0, ionic strength of $\mu = 0.05$).
[b]Poly(ε-lysine)-immobilized Cellufine-GC-15.[10]
[c]Poly(ε-lysine)-immobilized Cellufine-GC-700.[10]
[d]Poly(ε-lysine)-immobilized Cellufine-CPC.[10]
[e]Detixi-Gel.[7]
[f]Anion-exchange capacity of the adsorbent.
[g]Value deduced as molecular weight of polysaccharide.[12]

1×10^6)[13] are significantly larger than the M_{lim} of the adsorbent. Many of the standard LPS molecules (*Escherichia coli* O111:B4 and UKT-B), however, were well adsorbed even by the adsorbent with an M_{lim} of 2×10^3, as shown in Table 1. We previously reported[13] that the LPS molecules were adsorbed by aminated poly (γ-methyl L-glutamate) particles not only into the pores of the particles but also on their surfaces. Poly(ε-lysine)-immobilized cellulose particles have similar characteristics.

Effect of Degree of Ligand Polymerization on Adsorption of Biopolymer

For selective removal of LPS from a protein solution, it is also necessary to select the ligand of the adsorbent. Fig. 2 shows the effects of a buffer's ionic strength and pH on the adsorption of LPS by diaminohexane-(DAH), PL-, or PEI-immobilized cellulose particles. Diaminohexane monomer (M_w: 116), PL (degree of polymerization: 35, M_w: 4.0×10^3), and PEI (degree of polymerization: 1600, M_w: 7×10^4) were used respectively as adsorbent ligands, and cellulose particles with M_{lim} 2×10^3 (Cellufine GC-15) were used as the matrix. As shown in Fig. 2a, the higher the ionic strength of the buffer the lower the LPS-adsorbing activity of the adsorbent. Both PEI cellulose and PL cellulose always showed a greater LPS-adsorbing activity (99% to 82%) at a wide range of ionic strengths ($\mu = 0.05$–0.8). The adsorbing activity of DAH cellulose decreased markedly when the ionic strength was increased to 0.2 or higher.

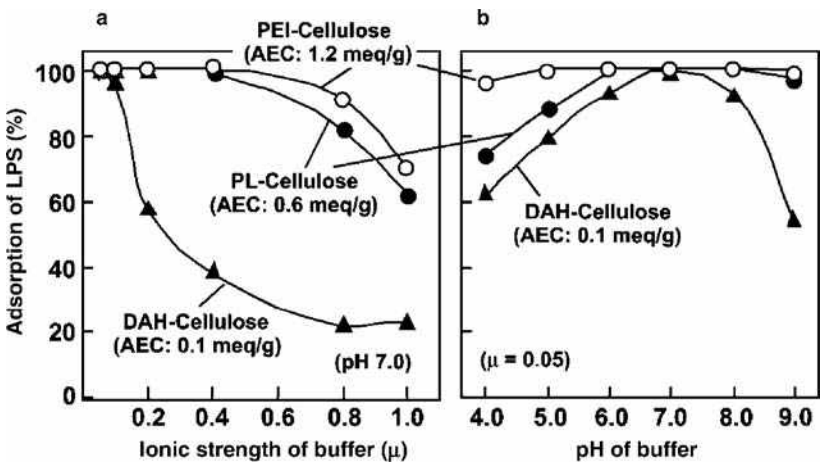

Fig. 2 Effects of a buffer's (a) ionic strength and (b) pH on the adsorption of LPS by various aminated cellulose adsorbents. The adsorption of LPS was determined using a batchwise method with 0.2 g of the wet adsorbent and 2 ml of a LPS (*E. coli* O111:B4, 1000 ng/ml) solution. Adsorbent and AEC of adsorbent: PEI-cellulose = poly(ethyleneimine)-immobilized Cellufine-GC15 (AEC:1.2 meq/g); PL-cellulose = poly(ε-lysine)-immobilized Cellufine-GC15 (AEC:0.6 meq/g); DAH-cellulose = diamino hexane-immobilized Cellufine-GC15 (AEC: 0.2 meq/g). M_{lim} of adsorbent: 2×10^3.

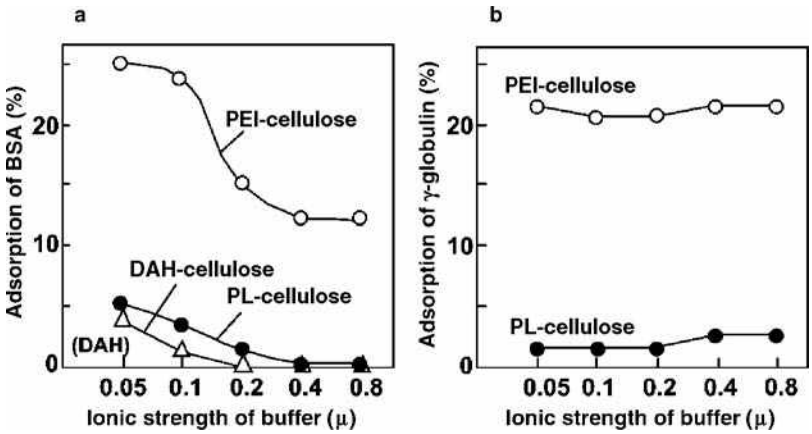

Fig. 3 Effect of a buffer's ionic strength on the adsorption of (a) BSA and (b) γ-globulin by various aminated cellulose adsorbents reported in Fig. 2. The adsorption of protein was determined using a batchwise method with 0.2 g of the wet adsorbent and 2 ml of a protein (100 μg/ml) solution.

Fig. 2b shows the effect of pH on the adsorption of LPS by various aminated cellulose adsorbents. The larger the molecular weight (polymerization degree) of an adsorbent's ligand the higher the LPS-adsorbing activity of the adsorbent. Over a wide pH range of 4.0–9.0 and at an ionic strength of $\mu = 0.05$, PEI cellulose (AEC:1.2 meq/g), with the largest polymerization degree of ligand, always showed the highest LPS-adsorbing activity (>98%). Poly(ε-lysine)-immobilized cellulose (AEC:0.6 meq/g) also showed a high activity (>97%) over a pH range from 6.0 to 9.0, although it decreased from 99% to 75% as the pH decreased from 6.0 to 4.0. On the other hand, DAH cellulose (AEC: 0.1 meq/g) showed high-adsorbing activity only at pH 7.0.

Fig. 3a and b shows the effect of a buffer's ionic strength on adsorption of BSA and γ-globulin, respectively, by aminated cellulose adsorbents. The stronger the ionic strength the lower the BSA-adsorbing activity of the adsorbent (Fig. 3a). By contrast, adsorption of BSA and γ-globulin is independent of ionic strength (Fig. 3b). Poly(ethyleneimine)-immobilized cellulose showed the highest adsorption of each protein among the three adsorbents.

From these results (Table 1, Figs. 2 and 3), we assumed that the adsorbing activity of aminated-cellulose adsorbents for biopolymers was induced by the simultaneous effects of their cationic properties and hydrophobic or other properties. The charge of LPS is anionic at pH values greater than its pK_a (pK_1 = 1.3[14]). The charge of BSA is also anionic at pH values greater than 4.9 (its pI). The adsorption of LPS and BSA increased with increasing AEC content of the adsorbent (Figs. 2 and 3). It is also dependent on the ionic strength and pH values (Fig. 2a and b, respectively). These results suggest that aminated-cellulose adsorbents adsorb LPS and BSA mainly by ionic interaction. On the other hand, the ionic interaction of the adsorbent with γ-globulin (pI: 7.4) is not induced at pH 7.0, as the charge of the protein is cationic at a pH under its pI value. γ-Globulin is a weakly hydrophobic protein. Its adsorption was independent of ionic strength and increased with an increase in the hydrophobicity (ligand-polymerization degree) of the adsorbent (Fig. 3b). Hou and Zaniewski[15] also reported that a hydrophobic bond was formed between LPS and the polymeric affinity matrix. These findings suggest the participation of hydrophobic binding. Furthermore, as shown in Table 1, polycation-immobilized cellulose adsorbents bind more strongly with LPS than protein. This is because the pK_a of the phosphate residues of LPS is lower than the pI of protein (pI: 4.6–11.0), and, probably, because the LPS is adsorbed by the adsorbent through its multipoint attachment onto the polycation chain of the adsorbent surface.

CHROMATOGRAPHIC RESULTS FOR SELECTIVE LPS REMOVAL

For selective LPS removal, it is necessary not only to select the ligand of the adsorbent, but also to control the conditions of the buffer (pH and ionic strength). The effect of ionic strength on the selective adsorption of LPS from a BSA-containing solution by various aminated cellulose adsorbents (M_{lim} 2×10^3) was examined (results are shown in Fig. 4a–c). A BSA solution, 500 μg/ml of BSA and 100 ng/ml of standard LPS, was used as a sample solution. The LPS-adsorbing activity of DAH cellulose decreased remarkably with an increase in the ionic strength. The DAH cellulose selectively adsorbed LPS only at $\mu = 0.05$ (Fig. 4a). Poly(ethyleneimine)-immobilized cellulose showed adsorbing activities for both LPS and BSA over a wide ionic strength, from $\mu = 0.05$ to 0.8 (Fig. 4c). It cannot therefore selectively adsorb LPS from the BSA solution at all ionic strengths. By contrast, PL cellulose selectively adsorbed LPS in the solution at ionic strengths of $\mu = 0.05$ to 0.4 and pH 7.0, without adsorption of BSA (Fig. 4b). The residual concentrations

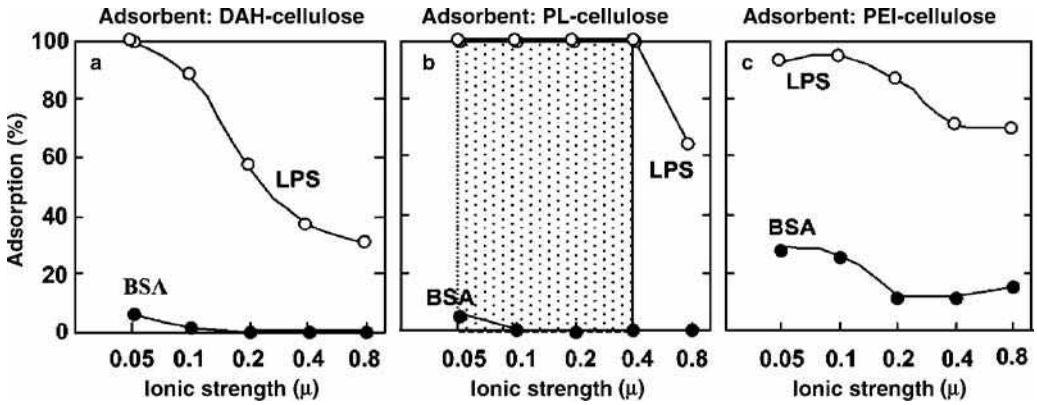

Fig. 4 Effects of ionic strength on selective adsorption of LPS from a BSA solution containing LPS by the various aminated cellulose adsorbents reported in Fig. 2. The selective adsorption of LPS was determined by a batchwise method with 0.2 g of the wet adsorbent and 2 ml of a sample solution [BSA: 500 μg/ml, LPS (*E. coli* O111:B4): 100 ng/ml, pH 7.0, and ionic strength of $\mu = 0.05$–0.8].

of LPS after treatment were less than 100 pg/ml [1 endotoxin unit (EU)/ml] and each BSA recovery was over 95%.[10] The threshold level for intravenous application is set to 5 EU per kg body weight per hour by all pharmacopoeias.[2] The PL-cellulose adsorbent was able to remove LPS from a BSA solution to a level below 1 EU/ml.

As regards the adsorbing capacity of LPS, the cationic polymers with large pore sizes show a greater capacity, because of the entry of LPS molecules into the large pores. We have already reported[10] that PL cellulose with $M_{lim} > 2 \times 10^6$ can reduce the concentration of LPS to 0.1 EU/ml or under in a LPS solution, at a neutral pH and $\mu = 0.05$–0.4. As shown in Table 1, Polymyxin B-Sepharose ($M_{lim} > 2 \times 10^6$) and PL cellulose (10^6) ($M_{lim} > 2 \times 10^6$) readily removed LPS from lysozyme and myoglobin solutions at pH 7 without a loss of protein. This is because the ionic interaction of the adsorbent with lysozyme (p*I*: 11.0) and myoglobin (p*I*: 6.8) is not induced at pH 7.0. Thus the cationic polymer particles having a large pore size are suitable as an adsorbent for removal of LPS from bioproducts (p*I*: 7.0–11.0) containing large quantities of LPS, such as a crude antigen solution originating from a Gram-negative bacterium.

CONCLUSIONS

The present results suggest that PL-cellulose spherical particles can reduce the concentrations of natural LPS to 1 EU/ml or lower in drugs and fluids used for intravenous injection, at a neutral pH and ionic strengths of $\mu = 0.05$–0.4. These processes did not affect the recovery, even of acidic proteins such as BSA. The high LPS-adsorbing activity of the PL cellulose is possibly due to the cationic properties of the ligand and its suitable hydrophobic properties. The high LPS selectivity of the particles with small pore size is due to the size-exclusion effects on protein molecules. By contrast, that of the particles with large pore sizes is due to the decreases in ionic interactions for net-negative charged proteins, which arise when the buffer's ionic strength is adjusted to 0.2 or stronger.

For practical application, ease of regeneration is very important. The PL-cellulose spherical particles can be completely regenerated by frontal chromatography with 0.2 *M* sodium hydroxide followed by 2.0 *M* sodium chloride.[10] Their stable structures, even under extreme pH values, are due to their –CHNH– bonds. Of course, the development of even better adsorbents should be pursued, by continuing this search for materials. To achieve selective removal of LPS, it is important to not only select a suitable ligand, but also to adjust the pore size of the matrix.

REFERENCES

1. Vaara, M.; Nikaido, H. Outer Membrane Organization. In *Handbook of Endotoxin*; Rietschel, E.T., Ed.; Elsevier: Amsterdam, 1984; Vol. 1, 1–45.
2. Hirayama, C.; Sakata, M.; Ihara, H.; Ohkuma, K.; Iwatsuki, M. Effect of the pore size of an animated poly(γ-methyl L-glutamate) adsorbent on selective removal of endotoxin. Anal. Sci. **1992**, *8*, 805–810.
3. Li, L.; Luo, R.G. Protein concentration effect on protein-lipopolysaccharide (LPS) binding and endotoxin removal. Biotechnol. Lett. **1997**, *19*, 135–138.
4. Petsch, D.; Anspach, F.B. Endotoxin removal from protein solutions. J. Biotechnol. **2000**, *79*, 97–119.
5. Minobe, S.; Watanabe, T.; Sato, T.; Tosa, T.; Chibata, I. Preparation of adsorbents for pyrogen adsorption. J. Chromatogr. **1982**, *248*, 401–408.

6. Matsumae, H.; Minobe, S.; Kindan, K.; Watanabe, T.; Tosa, T. Specific removal of endotoxin from protein solutions by immobilized histidine. Biotechnol. Appl. Biochem. **1990**, *12*, 129–140.
7. Issekutz, A.C. Removal of gram-negative endotoxin from solutions by affinity chromatography. J. Immunol. Methods **1983**, *61*, 275–281.
8. Anspach, F.B.; Kilbeck, O. Removal of endotoxins by affinity sorbents. J. Chromatogr. A, **1995**, *711*, 81–92.
9. Morimoto, S.; Sakata, M.; Iwata, T.; Esaki, A.; Hirayama, C. Preparations and applications of polyethyleneimine-immobilized cellulose fibers for endotoxin removal. Polym. J. **1995**, *27*, 831–839.
10. Todokoro, M.; Sakata, M.; Matama, S.; Kunitake, M.; Ohkuma, K.; Hirayama, C. Pore-size controlled and poly(ε-lysine)-immobilized cellulose spherical particles for removal of lipopolysaccharides. J. Liq. Chromatogr. Relat. Technol. **2002**, *25* (4), 601–614.
11. Shima, S.; Sakaki, H. Poly-L-lysine produced by *Streptomyces*: Part III. Chemical studies. Agric. Biol. Chem. **1981**, *45* (11), 2503–2508.
12. Hirayama, C.; Ihara, H.; Nagaoka, S.; Furusawa, H.; Tsuruta, S. Regulation of pore-size distribution of poly(γ-methyl L-glutamate) spheres as a gel permeation chromatography packings. Polym. J. **1990**, *22* (7), 614–619.
13. Hirayama, C.; Sakata, M.; Ihara, H.; Ohkuma, K.; Iwatsuki, M. Effect of pore size of an aminated poly(γ-methyl L-glutamate) adsorbent on the selective removal of endotoxin. Anal. Sci. **1992**, *8*, 805–810.
14. Hou, K.C.; Zaniewski, R. Depyrogenation by endotoxin removal with positively charged depth filter cartridge. J. Parenter. Sci. Technol. **1990**, *44*, 204–209.
15. Hou, K.C.; Zaniewski, R. The effect of hydrophobic interaction on endotoxin adsorption by polymeric affinity matrix. Biochem. Biophys. Acta **1991**, *1073*, 149–154.

Biotic Dicarboxylic Acids: CCC Separation with Polar Two-Phase Solvent Systems Using a Cross-Axis Coil Planet Centrifuge

Kazufusa Shinomiya
College of Pharmacy, Nihon University, Chiba, Japan

Yoichiro Ito
National Heart, Lung, and Blood Institute (NHLBI), National Institutes of Health (NIH), Bethesda, Maryland, U.S.A.

INTRODUCTION

Among various types of countercurrent chromatographic instruments developed in the past, the cross-axis coil planet centrifuge (cross-axis CPC) is one of the most useful systems for separation of numerous kinds of natural and synthetic products.[1–3]

The cross-axis CPC produces a unique mode of planetary motion, such that the column holder rotates about its horizontal axis while revolving around the vertical axis of the centrifuge.[4,5] This motion provides satisfactory retention of the stationary phase for viscous, low-interfacial tension, two-phase solvent systems, such as aqueous–aqueous polymer phase systems. Our previous studies demonstrated that the cross-axis CPC equipped with a pair of multiplayer coils or eccentric coil assemblies in the off-center position was very useful for the separation of proteins with polyethylene glycol-potassium phosphate solvent systems.[6–8] The apparatus is also useful for the separation of highly polar compounds such as sugars,[9] hippuric acid, and related compounds,[10] which require the use of polar two-phase solvent systems.

This entry illustrates the separation of biotic dicarboxylic acids using the cross-axis CPC with eccentric coil assemblies.[11]

CCC APPARATUS AND SEPARATION COLUMNS

The cross-axis CPC produces a synchronous planetary motion of the column holder, which rotates about its horizontal axis and simultaneously revolves around the vertical axis of the apparatus at the same angular velocity. In the $X - 1.5L$ type of the apparatus, the column holder was mounted at an off-center position ($X = 10$ cm and $L = 15$ cm), which provides efficient mixing of the two-phase solvent systems and stable retention of the stationary phase in the coiled column.

The separation column was prepared using a pair of eccentric coil assemblies, which were made by winding a 1 mm I.D. polytetrafluoroethylene (PTFE) tubing onto 7.6 cm long, 5 mm O.D. nylon pipes forming a series of tight left-handed coils. A set of these coil units was symmetrically arranged around the holder hub of 7.6 cm diameter in such a way that the axis of each coil unit is parallel to the axis of the holder. A pair of eccentric coil assemblies was mounted on the rotary frame, one on each side, and serially connected with a flow tube.

CCC SEPARATION OF DICARBOXYLIC ACIDS

The chemical structures of eight typical biotic dicarboxylic acids are shown in Fig. 1. They are extremely hydrophilic and require a specific reaction for detection using the color-producing reagent such as 2-nitrophenylhydrazine hydrochloride.[12–13]

Fig. 2 illustrates the partition coefficient (K) values for these dicarboxylic acid samples in the polar two-phase solvent systems composed of methyl *t*-butyl ether (MBE)/1-butanol/acetonitrile (ACN)/aqueous 0.1% trifluoroacetic acid (TFA), at various volume ratios. K values of the organic acids decreased as the hydrophobicity of the solvent system was increased, except for fumaric acid, which showed high K values regardless of the phase composition.

Fig. 3 illustrates the CCC chromatograms of dicarboxylic acids obtained with the above solvent system. In Fig. 3A, maleic acid and fumaric acid are separated at a volume ratio of 1 : 0 : 0 : 1, which is used for the separation of aromatic acids such as hippuric acid.[10] Using a more polar solvent system, at a volume ratio of 2 : 0 : 2 : 3, tartaric acid, succinic acid, and fumaric acid were well resolved by the lower aqueous mobile phase, as shown in Fig. 3B.

Fig. 4 illustrates a chromatogram of oxalic acid, malonic acid, and succinic acid obtained using the most polar

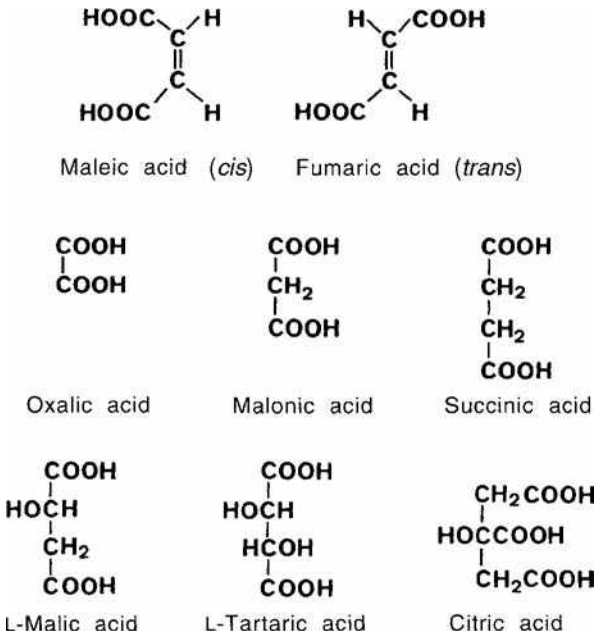

Fig. 1 Chemical structures of polar organic acids.

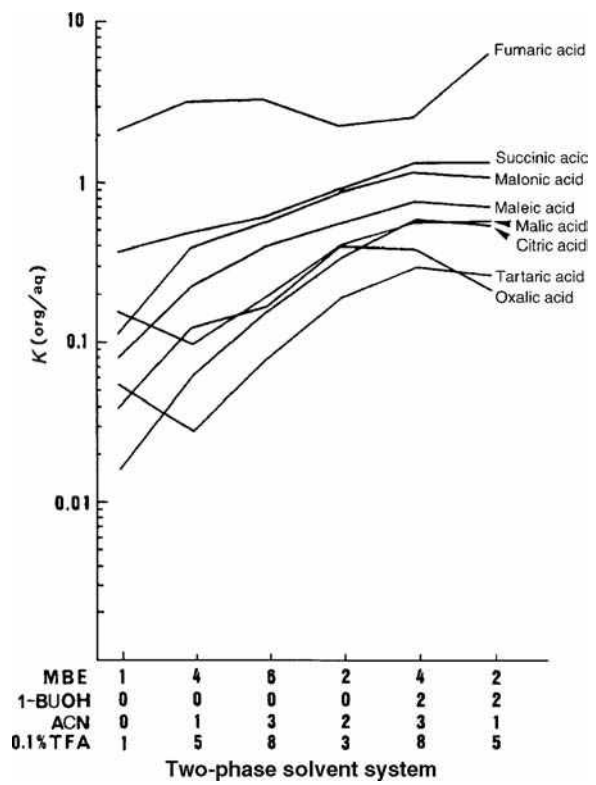

Fig. 2 Partition coefficients (K org/aq) of polar organic acids in methyl t-butyl ether/1-butanol/acetonitrile/aqueous 0.1% trifluoroacetic acid system. K is expressed by solute concentration in the organic phase divided by that in the aqueous phase. MBE = methyl t-butyl ether; 1-BuOH = 1-butanol; AcN = acetonitrile; TFA = trifluoroacetic acid.

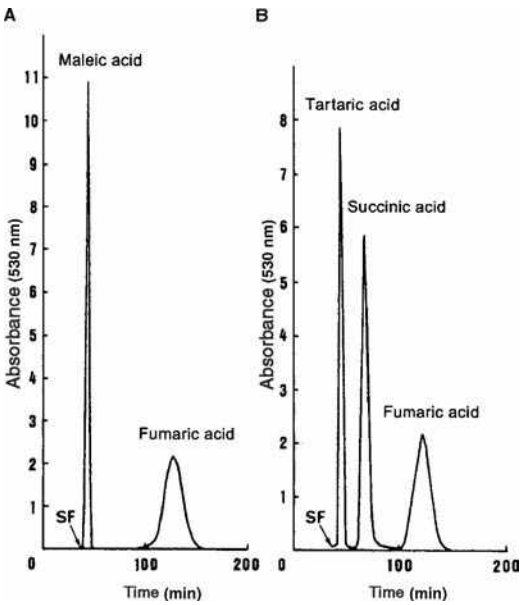

Fig. 3 CCC separation of polar organic acids by cross-axis CPC. Experimental conditions: apparatus, cross-axis CPC equipped with a pair of eccentric coil assemblies, 1 mm I.D. and 26.5 ml total column capacity; sample, (A) maleic acid (3 mg) and fumaric acid (3 mg); (B) tartaric acid (5 mg), succinic acid (5 mg), and fumaric acid (2.5 mg); solvent system, methyl t-butyl ether/1-butanol/acetonitrile/aqueous 0.1% trifluoroacetic acid (A) (1 : 0 : 0 : 1); (B) (2 : 0 : 2 : 3); mobile phase, lower phase; flow rate, 0.4 ml/min; revolution, 800 rpm. SF = solvent front.

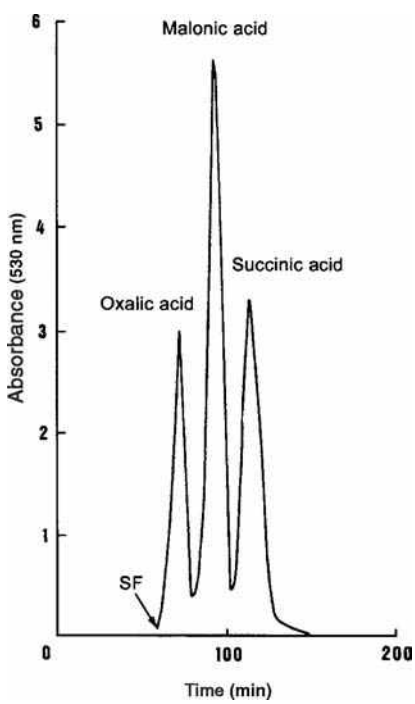

Fig. 4 CCC separation of oxalic acid, malonic acid, and succinic acid by cross-axis CPC. Experimental conditions: sample, 3 mg each; solvent system, 1-butanol/water; flow rate, 0.25 ml/min. For other experimental conditions, see the Fig. 3 caption. SF = solvent front.

binary solvent system, composed of 1-butanol/water. All components were well resolved from each other and eluted within 2.3 hr, using the lower-aqueous phase as the mobile phase.

As described above, various polar organic acids, such as dicarboxylic acids, can be separated with polar two-phase solvent systems, using the cross-axis CPC equipped with a pair of eccentric coil assemblies mounted in the off-center position.

REFERENCES

1. Mandava, N.B., Ito, Y., Eds.; *Countercurrent Chromatography: Theory and Practice*; Marcel Dekker: New York, 1988.
2. Conway, W.D. *Countercurrent Chromatography: Apparatus, Theory and Applications*; VCH: New York, 1990.
3. Ito, Y., Conway, W.D., Eds.; *High-Speed Countercurrent Chromatography*; Wiley-Interscience: New York, 1996.
4. Ito, Y. Cross-axis synchronous flow-through coil planet centrifuge free of rotary seals for preparative countercurrent chromatography. Part I: Apparatus and analysis of acceleration. Sep. Sci. Technol. **1987**, *22*, 1971.
5. Ito, Y. Cross-axis synchronous flow-through coil planet centrifuge free of rotary seals for preparative countercurrent chromatography. Part II: Studies on phase distribution and partition efficiency in coaxial coils. Sep. Sci. Technol. **1987**, *22*, 1989.
6. Shinomiya, K.; Menet, J.-M.; Fales, H.M.; Ito, Y. Studies on a new cross-axis coil planet centrifuge for performing counter-current chromatography. I. Design of the apparatus, retention of the stationary phase, and efficiency in the separation of proteins. J. Chromatogr. **1993**, *644*, 215.
7. Shinomiya, K.; Inokuchi, N.; Gnabre, J.N.; Muto, M.; Kabasawa, Y.; Fales, H.M.; Ito, Y. Countercurrent chromatographic analysis of ovalalbumin obtained from various sources using the cross-axis coil planet centrifuge. J. Chromatogr. A, **1996**, *724*, 179.
8. Shinomiya, K.; Muto, M.; Kabasawa, Y.; Fales, H.M.; Ito, Y. Protein separation by improved cross-axis coil planet centrifuge with eccentric coil assemblies. J. Liq. Chromatogr. Relat. Technol. **1996**, *19*, 415.
9. Shinomiya, K.; Kabasawa, Y.; Ito, Y. Countercurrent chromatographic separation of sugars and their p-nitrophenyl derivatives by cross-axis coil planet centrifuge. J. Liq. Chromatogr. Relat. Technol. **1999**, *22*, 579.
10. Shinomiya, K.; Sasaki, Y.; Shibusawa, Y.; Kishinami, K.; Kabasawa, Y.; Ito, Y. Countercurrent chromatographic separation of hippuric acid and related compounds using cross-axis coil planet centrifuge with eccentric coil assemblies. J. Liq. Chromatogr. Relat. Technol. **2000**, *23*, 1575.
11. Shinomiya, K.; Kabasawa, Y.; Ito, Y. Countercurrent chromatographic separation of biotic dicarboxylic acids with polar two-phase solvent systems using cross-axis coil planet centrifuge. J. Liq. Chromatogr. Relat. Technol. **2001**, *24*, 2625.
12. Horikawa, R.; Tanimura, T. Spectrophotometric determination of carboxylic acids with 2-nitrophenylhydrazine in aqueous solution. Anal. Lett. **1982**, *15*, 1629.
13. Shinomiya, K.; Ochiai, H.; Suzuki, H.; Koshiishi, I.; Imanari, T. Simple method for determination of urinary mucopolysaccharides. Bunseki Kagaku **1986**, *35*, T29.

Body Fluids: CE Analysis of Drugs

Pierina Sueli Bonato
Cristiane Masetto de Gaitani
Valquíria Aparecida Polisel Jabor
Faculty of Pharmaceutical Sciences of Ribeirão Preto, University of São Paulo, Ribeirão Preto, Brazil

Abstract
The demand for analytical methods suitable for accurate and reproducible determination of drugs and metabolites in biological samples has increased significantly in the past few years. High-performance liquid chromatography (HPLC) is the most important technique used for this purpose, but electromigration techniques represent a powerful alternative. We discuss here some fundamental aspects of capillary electrophoresis (CE) and related electrokinetic separation techniques applied to the analysis of drugs and metabolites in biological samples. In addition, recent developments in these techniques and important aspects that could be addressed to obtain reliable methods for bioanalysis are also discussed.

INTRODUCTION

The demand for analytical methods suitable for accurate and reproducible determination of drugs and their metabolites in biological samples has increased significantly during recent years, as the data obtained in this kind of analysis are essential for drug discovery, modern drug therapy, diagnosis, clinical and forensic toxicology, and for assessment of drug abuse.[1] High-performance liquid chromatography (HPLC) has been the main technique used for this purpose, but capillary electrophoresis (CE) and related techniques have begun to be explored extensively. Several review papers have appeared in recent literature.[2–6] In addition, routine CE methods have been successfully submitted to regulatory authorities, including the US Food and Drug Administration.[7]

CE has several advantages for the analysis of drugs in biological samples. High separation efficiency is the most important one, allowing the resolution of compounds with similar structures and preventing the interference of matrix compounds, metabolites, and other coadministered drugs. Due to the several separation mechanisms that are possible, CE is a versatile technique; it has been considered complementary to HPLC. For instance, CE is particularly attractive for the analysis of polar and/or basic drugs and their metabolites, including phase II metabolites such as glucoronides, sulfates, etc. that are not easily analyzed by chromatographic techniques. The simplicity of the instrumentation, the relatively easy method development, the speed of the analysis, the small amounts of samples (nanoliters), reduced operational costs, and the production of minimal amounts of waste, mostly of an aqueous buffer, are also important characteristics of this technique for biomedical applications. Owing to the limited sample volume analyzed and the short optical path length available when employing on-capillary detection, CE is characterized by relatively poor limits of detection. To minimize the impact of this feature, several approaches have been used, such as the use of more sensitive detection systems and concentration of the analyte by a suitable sample extraction procedure from the matrix or by online enrichment.[8]

We discuss here some fundamental aspects of CE and related electrokinetic separation techniques applied to the analysis of drugs and metabolites in biological samples. In addition, recent developments in these techniques and important aspects that could be addressed to obtain reliable methods for bioanalysis are also discussed.

ELECTROKINETIC TECHNIQUES FOR THE ANALYSIS OF DRUGS AND METABOLITES IN BODY FLUIDS

Free-solution capillary electrophoresis (FSCE) is the major technique used for drug analysis, considering the fact that many drugs have acidic or basic groups that allow them to analyzed as charged molecules. In this technique, the capillary is filled with a buffer solution and the separation is based on the different electrophoretic mobilities of the solutes. Separation of both anionic and cationic solutes is possible, owing to electro-osmotic flow (EOF). The pH of the buffer has a major influence on selectivity, but other factors such as buffer concentration, additives, etc. should also be considered during method development.[9]

Encyclopedia of Chromatography, Third Edition DOI: 10.1081/E-ECHR3-120045251

If the separation is not possible by FSCE, or if neutral drugs are to be analyzed, micellar electrokinetic capillary chromatography (MEKC) should be considered. In this case, a charged surfactant is added to the running buffer at a concentration above its critical micellar concentration; sodium dodecyl sulfate (SDS) is the main surfactant employed for this purpose. Neutral solutes partition with these micelles and their separation are based on their hydrophobic character. Charged solutes could also interact with the charged micelles. In addition to buffer type, concentration, and pH (typically between 7 and 10 for SDS), other parameters such as type and concentration of the surfactant, presence of organic solvent, urea, cyclodextrin or other additives, temperature, etc. should also be optimized.[9] Microemulsion electrokinetic chromatography (MEEKC) has recently appeared as a complementary technique to MEKC. In this case, the solutes interact with an oil droplet instead of a micelle.[10]

During recent years, there has been an increasing interest in using new electromigration technology for the analysis of drugs in biological samples. Capillary electrochromatography (CEC) is a hybrid technique that combines the advantages of CE with those of HPLC. It is similar to CE, as the separation is carried out in a capillary and the driving force for analyte movement is the EOF, resulting in reduced solvent consumption and high efficiency. The CEC also has features in common with HPLC, owing to the use of a stationary phase, providing additional selectivity and allowing the resolution of compounds not resolved by CE. Generally, the columns used in CEC have been classified into three types: packed, open-tubular, and continuous-bed or monolithic columns.[11] The major drawbacks associated with packed capillaries originate from the presence of frits, which retain the particles inside the column and can be responsible for bubble formation and zones of heterogeneities inside the packed capillary. These problems can be overcome by the use of monolithic stationary phases that eliminate the necessity for frits.[12] Monolithic stationary phases can be based on inorganic or organic polymers. The inorganic based monolithic phases are prepared by the sol–gel process whereas the monolithic phases based on organic polymers are generally made by in situ polymerization of monomers, cross-linkers, and porogens. Due to characteristics such as good permeability, high stability, fast mass transfer, and ease of modification, monolithic materials have been intensively used for both CEC and capillary liquid chromatography.

The use of organic solvents as the electrolyte medium is a relatively recent development in CE. Typically, the electrolytes are prepared in 100% organic solvents such as methanol or acetonitrile. The use of non-aqueous solvents affects the solvation of the charged molecules and also their pK_a values, providing additional selectivity to that obtained under aqueous conditions. Selectivity can also be altered by the use of additives such as ion-pair reagents, cyclodextrin, etc. Non-aqueous CE has also proved to be a powerful tool when the analyte has solubility and/or stability problems in aqueous solutions.[13]

Another direction in the development of electromigration techniques is the use of microchip technology. Microfabricated chips have advantages compared to conventional capillaries. They are disposable, rugged, and inexpensive. In addition, these systems can offer enhanced performance in terms of fast response and increased analysis speed. Through the use of chips with several separation microchannels, greater improvement in analysis speed is easily achieved. However, the applications of on-chip CE an on-chip CEC have centered on protein and DNA analysis.[13,14,15]

DETECTION

Detection in electromigration techniques is normally carried out by UV detection. In spite of its widespread use, UV detection offers limited concentration sensitivity for CE and related techniques, owing to the extremely short optical path lengths afforded by the small inner diameters of the capillaries. To maximize sensitivity, detection is often performed at low wavelengths such as 200 nm or using an extended light path (bubble cell) or high sensitivity cells.[16,17]

In addition to UV detection, two other more sensitive and selective detection systems have attracted attention for the analysis of drugs and metabolites in biological samples: laser-induced fluorescence (LIF) and mass spectrometry (MS). A powerful detection system is that which is based on LIF. The LIF detection provides extremely high mass sensitivity, but it is only applicable to some analytes that absorb in the 325 nm (helium–cadmium) or 488 nm (argon) region, as lasers are only commercially available for these wavelengths. Derivatization with fluorescent tags is an alternative for non-fluorescent species.[16,17]

The development of electrospray ionization–mass spectrometry (ESI–MS) has had a dramatic impact on the practice of bioanalytical chemistry by providing great selectivity and more sensitivity, thereby reducing, significantly, the time necessary for method development. ESI–MS has been successfully coupled to HPLC and, more recently, to CE and CEC systems.[18] The advantages of the system providing either selectivity/sensitivity or additional information for structural elucidation have increased the interest in this technique for biomedical applications. However, interfacing CE or CEC systems to MS is a difficult task due to limitations on the composition of the background electrolyte that could be used in the separation; in addition, the flow rates required to maintain a stable electrospray could only be supplied under conditions giving a maximized

EOF. The use of a flowing sheath liquid was offered as a solution to these problems and this design is most commonly used in commercial interfaces.[19]

SOME IMPORTANT ASPECTS FOR THE ANALYSIS OF DRUGS AND METABOLITES IN BODY FLUIDS

Sample Preparation and Concentration

When the concentration of the analyte is high enough, small amounts of biological samples such as serum, plasma, urine, etc., can be directly injected into the capillary, mainly when using MEKC, owing to the use of surfactants that solubilize proteins. However, the analysis of high-ionic-strength matrices can result in bandspreading, while proteins can be adsorbed onto the capillary walls, affecting reproducibility of the analysis.

To avoid the problems related to proteins and high salt concentration and also to obtain the detection of analytes usually present in the nanogram per milliliter range, some kind of sample preparation is frequently used. Conventional off-line sample preparation techniques such as protein precipitation, liquid–liquid extraction, and solid-phase extraction (SPE) have been used for sample preparation in several procedures described in the literature.[20] The main disadvantage of these off-line preconcentration methods is the inefficient use of the concentrated sample, because usually less than 1% of it is injected into the capillary. Regarding this aspect, solid-phase extraction has the advantage of easy automation; online SPE coupled to CE systems seems to be very attractive.[21] This technique is usually carried out using a short-length capillary packed with appropriate adsorbent material connected to the separation capillary.

Solid-phase microextraction (SPME)[20] and membrane microextraction[22] are new and very attractive sample preparation techniques because of low, or no, requirement of organic solvent. In SPME, a fiber coated with a stationary phase is used as the extraction medium. After extraction, the analytes could be desorbed into a suitable eluent and analyzed by CE. Membrane extractions have been performed using several systems. The most interesting one is based on the use of a hollow fiber. In this case, the hollow fiber is impregnated with an organic solvent and filled with an acceptor phase. When an aqueous solution is used as the acceptor phase, it can be directly analyzed by the CE system. Online extraction using these techniques is also possible. They are still less frequently used for the analysis of drugs in biological samples, but the interest in them has increased.

As pointed out previously, the lack of sensitivity in CE is the major concern when this technique is applied to the analysis of drugs in biological samples. One way to improve the sensitivity is to concentrate a large volume of sample introduced in the capillary (>5% of the capillary volume) using stacking techniques.[23] The simplest and most extensively used sample stacking effect is obtained by dissolving the extraction residue sample in diluted running buffer solution or in water. The stacking effect can also be observed when the sample is dissolved in acetonitrile or acetonitrile–water mixtures because of its low conductivity that can cause some stacking because of the high field strength. The stacking effect could also be obtained by injecting a small plug of water or other low conductivity solvent before the sample is injected electrokinetically, a procedure named field-amplified sample injection or head-column field-amplified sample stacking.[23]

Qualitative Aspects of CE-based Methods

As in related chromatographic methods, qualitative analysis is performed by comparing retention data and by using additional techniques. Migration times in CE are less reproducible than retention times (HPLC), owing to effects of analysis parameters on electro-osmosis and electrophoretic mobility. The use of internal markers has reduced the relative standard deviation (RSD) to acceptable values. The adsorption of proteins and other sample components onto the capillary wall also results in migration time variations. These retained compounds can be removed using a washing procedure between analyses. Another way to decrease protein adsorption onto the capillary is the use of dynamically or permanently coated capillaries. Capillaries coated with polyvinyl alcohol, cellulose derivatives, and polyacrylamide have been used.[8]

Another factor that can result in migration time variation is buffer electrolysis (buffer depletion). Several approaches have been used to reduce buffer depletion, such as the use of high concentration buffers with optimum buffer capacity, replenishment, changing the vials after a certain number of analyses, etc. During method development, buffer depletion should be investigated before the method is submitted to a validation procedure.[8]

Identification by comparing migration times (sometimes spiking the sample with a standard) is only suitable for non-complex samples and when the available information for the sample is enough for the analyst to have a certain degree of confidence. For really unknown samples, the confirmation of sample identity can be obtained using information from a diode array detector and MS detection.[13]

Quantitative Aspects of CE-based Methods

The quantification of drugs and metabolites in biological samples is performed by comparing peak areas or, less frequently, peak height of the analytes in the unknown sample with those obtained in quality control samples prepared by spiking the same matrix with known amounts of the analytes. The reproducibility of areas is mainly dependent on the volume of sample injected, which can

be affected by the temperature in hydrodynamic injection owing to changes in buffer viscosity. When using electrokinetic injection, the amount of sample introduced into the capillary depends on the EOF and the electrophoretic mobility of the analyte. Therefore, factors affecting the EOF, such as temperature, ionic strength, buffer composition, and pH will affect the precision of the sample volume introduced into the capillary. In addition, the amount of sample injected also depends on the sample composition as well as on the properties of the analytes.[24]

Advances in the development of equipment (better control of temperature and better injection systems) and the use of an internal standard to correct errors owing to sample preparation and injection have reduced the impact of injection variation on the final precision of the method.

The results obtained when analyzing a real sample using a specific analytical method can only be acceptable if the method is submitted to a reliable validation process. Method validation is particularly important for the analysis of drugs and metabolites in biological samples, as the results are used to adjust drug dosage [therapeutic drug monitoring (TDM)], to establish pharmacokinetics, metabolism, bioavailability, and stability parameters (accepted by health official authorities when a new drug is under the registration process), and for legal applications (forensic toxicology).

The most important parameters in method validation for bioanalysis applications are linearity, precision, accuracy, selectivity, and limits of detection and quantification. In addition to these parameters, other method properties should also be evaluated, such as recovery to establish the efficiency of the method used for sample preparation, sample stability to evaluate the period allowed for sample storage, and robustness.[25–26]

To evaluate the linearity of the method, drug-free matrix samples are spiked with known amounts of the drug. A minimum of five to eight calibration standards is required, including the concentration established as the quantification limit. Peak area is frequently used to establish the linear relationship between detector response and concentration because it is less influenced by peak distortion at high concentrations, which sometimes results in non-linear calibration curves when using peak height. In addition, peak area can be corrected (peak area/migration time ratio), avoiding any influence of drift of migration times.

The precision of a bioanalytical method is a measure of the random error and is defined as the agreement between replicate measurements of the same sample. It is expressed as an RSD. Precision can be evaluated by analyzing replicate samples on the same day (repeatability or within-day precision) or on different days (intermediate precision or between-day precision). The accuracy is defined as the agreement between the measured value and the true value. Accuracy is determined using reference samples, when available, or spiking a blank matrix with known amounts of the analyte and considering this value as the real concentration. Values lower than 15% for both precision and accuracy are considered acceptable for the analysis of drugs and metabolites in biological samples.

The sensitivity of the method is evaluated by the limit of detection and quantification. In general, there are no specific criteria for the limit of detection, but for bioanalysis purposes, the limit of quantification is established for the concentration with precision and accuracy lower than 20%. Limits of detection and quantification obtained in CE with UV detection are generally higher than in HPLC, owing to the small optical path in the detection window and injected volumes. As discussed previously, by using preconcentration procedures (off-line sample preparation and/or stacking sample injection techniques) and a more sensitive detection system, particularly LIF and MS detection, suitable detection or quantification limits could be obtained for the application of the methods to the analysis of real samples.

Selectivity is evaluated by analyzing the blank matrix and commonly used drugs and/or metabolites under the same conditions as developed for the analysis of the drug. Reproducibility in migration times is essential to evaluate the selectivity of the method. As peak width depends on the injected amount, the effects of sample overload must be investigated. Another way to validate the specificity is to assess peak purity using diode array or MS detection.

For robustness testing, several parameters are evaluated which are expected to vary slightly during routine use, such as age of the analytical solutions, buffer pH, temperature, rinse cycles, etc. It is important to observe the influence of all of these parameters on migration times, resolution of critical peak pairs, efficiencies, and peak areas.

Stability data are required to show that the concentration of the analyte in the sample at the time of analysis corresponds to the concentration of the analyte at the time of sampling. The stability test is carried out by evaluating the stability of standard solutions and the analyte in the biological sample and in the processed sample.

APPLICATIONS

Enantioselective Analysis of Drugs and Metabolites

Considering that a large number of drugs are chiral and used as racemic mixtures, and that the enantiomers may have very different pharmacokinetic and pharmacodynamic properties, there is an increased interest in the production of chiral drugs as single enantiomers as well as in the evaluation of the stereoselective properties of drugs that have already been used as racemates. This new trend has resulted in an increase in the demand for enantioselective methods for the analysis of chiral drugs and metabolites in biological fluids to permit pharmacokinetic and

metabolic studies. The main advantages of CE for the enantioselective analysis of chiral drugs are the extremely high efficiency, instrumentation simplicity, low sample and reagent consumption, and speed in method development and analysis. Although chiral CE separations can be carried out in different modes, FSCE, EKC, and, more recently, CEC are the most widely used methods. The separation of enantiomers by FSCE and EKC is possible by the addition of chiral selectors to the running buffer. The most common chiral selectors are cyclodextrins and their derivatives. In CEC, the capillary is packed or coated with a chiral stationary phase. The most common application of chiral CE is in the chiral purity testing of drug substance material, but the number of applications involving the analysis of the enantiomers in biological fluids has grown rapidly in recent years.[27]

Pharmacokinetics and Metabolic Studies

Emphasis has recently been placed on the importance of performing well-designed pharmacokinetics–pharmacodynamic, as well as metabolic studies, as early as possible in the process of new drug development. Advantages of this approach include greater efficiency in establishing effective dosage regimens, increased understanding of drug action, and identification of metabolites and their pharmacological activity. In addition, the influence of age, disease, sex, and genetic and other factors on drug disposition must also be evaluated, including the drugs already marketed, to make them safer. The high resolving power of the electrophoretic techniques, including for phase II metabolites, is the main advantage for pharmacokinetic and metabolic studies. The low requirement of sample volume is also very attractive for certain studies such as investigations involving pediatric patients. Unfortunately, the low concentration sensitivity of CE with UV detection has limited its application in this area. The use of LIF and MS detection seems to be the appropriate direction for the evolution of applications of CE in pharmacokinetic studies. MS detection is also important for the identification of unknown metabolites in in vitro and in vivo metabolism studies.[6]

Forensic Applications

CE is also useful in forensic toxicology laboratories to screen urine for drugs of abuse such as opiates, barbiturates, benzodiazepines, amphetamines, morphine, etc. and also for screening postmortem fluids for illicit drugs or elevated levels of legal drugs. When coupled to MS, CE is a powerful tool in the confirmation of positive results.[4]

CONCLUSIONS

Electromigration techniques represent a powerful alternative to the well-established HPLC based methods for the analysis of drugs and their metabolites in biological samples, with the advantages of high resolution power, low cost, low-waste production, short analysis time, and easy method development. The general direction of developments for CE is toward ultrafast separations using microchip technologies, high-efficiency analysis employing narrow capillaries, and high-throughput analyses using array systems. In addition, coupled systems, mainly CE–MS or CEC–MS, will be routinely used for the separation and identification of complex mixtures in the near future. Among these, the use of electrophoretic techniques coupled to MS detections seems to be the logical further step for the analysis of drugs in biological fluids.

REFERENCES

1. Srinivas, N.R. Changing need for bioanalysis during drug development. Biomed. Chromatogr. **2008**, *22*, 235–243.
2. Lloyd, D.K. Capillary electrophoresis analysis of biofluids with a focus on less commonly analyzed matrices. J. Chromatogr. B, **2008**, *866*, 154–166.
3. Sniehotta, M.; Schiffer, E.; Zürbig, P.; Novak, J.; Mischak, H. CE—A multifunctional application for clinical diagnosis. Electrophoresis **2007**, *28*, 1407–1417.
4. Tagliaro, F.; Bortolotti, F.; Pascali, J.P. Current role of capillary electrophoretic/electrokinetic techniques in forensic toxicology. Anal. Bioanal. Chem. **2007**, *388*, 1359–1364.
5. Amundsen, L.K.; Sirén, H. Immunoaffinity CE in clinical analysis of body fluids and tissues. Electrophoresis **2007**, *28*, 99–113.
6. Sung, W.-C.; Chen, S.-H. Pharmacokinetic applications of capillary electrophoresis: A review on recent progress. Electrophoresis **2006**, *27*, 257–265.
7. Altria, K.D.; Elder, D. Overview of the status and applications of capillary electrophoresis to the analysis of small molecules. J. Chromatogr. A, **2004**, *1023*, 1–14.
8. Bonato, P.S. Recent advances in the determination of enantiomeric drugs and their metabolites in biological fluids by capillary electrophoresis mediated microanalysis. Electrophoresis **2003**, *24*, 4078–4094.
9. Suntornsuk, L. Capillary electrophoresis in pharmaceutical analysis: A survey on recent applications. J. Chromatogr. Sci. **2007**, *45*, 559–577.
10. McEvoy, E.; Marsh, A.; Altria, K.; Donegan, S.; Power, J. Recent advances in the development and application of microemulsion EKC. Electrophoresis **2007**, *28*, 193–207.
11. Ou, J.; Dong, J.; Dong, X.; Yu, Z.; Ye, M.; Zou, H. Recent progress in polar stationary phases for CEC. Electrophoresis **2007**, *28*, 148–163.
12. Zhu, G.; Zhang, L.; Yuan, H.; Liang, Z.; Zhang, W.; Zhang, Y. Recent development of monolithic materials as matrices in microcolumn separation systems. J. Sep. Sci. **2007**, *30*, 792–803.

13. Varenne, A.; Descroix, S. Recent strategies to improve resolution in capillary Electrophoresis—A review. Anal. Chim. Acta **2008**, *628*, 9–23.
14. Peng, Y.; Pallandre, A.; Tran, N.T.; Taverna, M. Recent innovations in protein separation on microchips by electrophoretic methods. Electrophoresis **2008**, *29*, 157–178.
15. Chen, L.; Manz, A.; Day, P.J.R. Total nucleic acid analysis integrated on microfluidic devices. Lab Chip **2007**, *7*, 1413–1423.
16. Swinney, K.; Bornhop, D.J. Detection in capillary electrophoresis. Electrophoresis **2000**, *21*, 1239–1250.
17. Hempel, G. Strategies to improve the sensitivity in capillary electrophoresis for the analysis of drugs in biological fluids. Electrophoresis **2000**, *21*, 691–698.
18. Nesbitt, C.A.; Zhang, H.; Yeung, K.K.-C. Recent applications of capillary electrophoresis–mass spectrometry (CE–MS): CE performing functions beyond separation. Anal. Chim. Acta **2008**, *627*, 3–24.
19. Maxwell, E.J.; Chen, D.D.Y. Twenty years of interface development for capillary electrophoresis–electrospray ionization–mass spectrometry. Anal Chim. Acta **2008**, *627*, 25–33.
20. Wille, S.M.R.; Lambert, W.E.E. Recent developments in extraction procedures relevant to analytical toxicology. Anal. Bioanal. Chem. **2007**, *388*, 1381–1391.
21. Tempels, F.W.A.; Underberg, W.J.M.; Somsen, G.W.; de Jong, G.J. Design and applications of coupled SPE–CE. Electrophoresis **2008**, *29*, 108–128.
22. Lee, J.; Lee, H.K.; Rasmussen, K.E.; Pedersen-Bjergaard, S. Environmental and bioanalytical applications of hollow fiber membrane liquid-phase microextraction: A review. Anal. Chim. Acta **2008**, *624*, 253–268.
23. Simpson Jr., S.L.; Quirino, J.P.; Terabe, S. On-line sample preconcentration in capillary electrophoresis. Fundamentals and applications. J. Chromatogr. A, **2008**, *1184*, 504–541.
24. Mayer, B.X. How to increase precision in capillary electrophoresis. J. Chromatogr. A, **2001**, *907*, 21–37.
25. http://www.fda.gov/cder/guidance/4252fnl.htm. Guidance for industry. Bioanalytical method validation (accessed November 2008).
26. Viswanathan, C.T.; Bansal, S.; Booth, B.; DeStefano, A.J.; Rose, M.J.; Sailstad, J.; Shah, V.P.; Skelly, J.P.; Swann, P.G.; Weiner, R. Quantitative bioanalytical methods validation and implementation: Best practices for chromatographic and ligand binding assays. Pharm. Res. **2007**, *24*, 1962–1973.
27. Gübitz, G.; Schmid, M.G. Chiral separation by capillary electromigration techniques. J. Chromatogr. A, **2008**, *1204*, 140–156.

Bonded Phases in HPLC

Joseph J. Pesek
Maria T. Matyska
Department of Chemistry, San Jose State University, San Jose, California, U.S.A.

INTRODUCTION

The development of chemically bonded stationary phases is one of the major factors that lead to the growth of high-performance liquid chromatography (HPLC) and is responsible for its importance as a separation technique.

HISTORICAL BACKGROUND

In its earliest form, gravity flow moved the mobile phase through the column which was generally packed with a solid adsorbent such as silica or alumina. In a few instances, a high-molecular-weight liquid was coated on the solid particle to provide different types of selectivity. Under these circumstances, the column was similar to those used in gas chromatography (GC), where a liquid stationary phase was held in place by physical forces alone. In GC, the requirement for the stationary phase to remain in place for a long time is low volatility. In liquid chromatography (LC), the requirement for durability is insolubility in the mobile phase. However, with the development of reliable high-pressure pumps that could produce stable flow rates for long periods of time, immiscibility with the mobile phase is not sufficient. At the pressures used to force solvents through most packed HPLC columns (from tens to a few hundred atmospheres), the shear forces developed at the interface between the stationary and the mobile phases are high enough to remove even insoluble liquids from the surface of the solid support. The stationary phase then is forced out of the column as an insoluble droplet. Removal of the stationary phase from a chromatography column is usually referred to as "column bleed." Therefore, it was necessary to develop a means of fixing the stationary phase on the solid support through a chemical bond. If the chemical bond between the surface of the solid support and the compound used as the stationary phase is stable under the experimental conditions of the HPLC experiment (temperature and mobile-phase composition), then column bleed will be avoided.

Fortunately, the most common support material used in LC experiments was silica. The chemistry of silica had been investigated for many years so a considerable amount of information was available about possible reactions on its surface. Silica can be considered as a polymer of silicic acid (H_2SiO_3). The terminal groups of the polymer located on the surface of the solid are hydroxide groups. These Si–OH functions are referred to as silanols. Because they come from an acid precursor, they are acidic themselves and generally have a pK_a near 5. This value is variable, depending on other constituents in the silica matrix such as metals. The structure of silica, including its major chemical features, are shown in Fig. 1. The polymeric unit consists of a series of siloxane bonds (–Si–O–Si–) that are slightly hydrophobic in nature. What is generally regarded as the most prominent feature on the surface is the silanol group, as indicated earlier. In a few cases, a single silicon atom will have two hydroxyl groups, which is called a geminal silanol. The silanols exist in two forms. First, they can be independent of other entities around them and are thus referred to as free or isolated silanols. If they are close enough to interact with a neighboring silanol, then these moieties become hydrogen-bonded or associated silanols. All forms of silanol are polar hydrophilic species. The relative number of free versus hydrogen-bonded silanols also has an influence on the pK_a value of the silica. Finally, because of the polar and hydrogen-bonding characteristics of the silanols, water is strongly adsorbed to the surface. This water is not easily removed, even at prolonged heating above 100°C. It is this complex matrix that must undergo a chemical reaction in order to attach a moiety to the surface as a stationary phase. According to the findings of early investigations on the reactivity of silica, it was determined that the silanol groups were the site of chemical modification on the surface.

The concept of attaching an organic moiety as a stationary phase to a silica surface was first applied in packed-column GC. The rationale for developing these materials was to prevent column bleed at the high temperatures required for some separations in GC. As long as the chemical bond was stable, the organic moiety would remain fixed to the surface. Some of the reactions utilized for the attachment of organic compounds in the synthesis of bonded stationary phases were originally developed for the modification of ordinary glass surfaces. Therefore, it was known that most of these modified surfaces were reasonably temperature stable and should be applicable to the bonding of organic groups onto the porous silica particles used as supports in chromatography.

The first reaction used for the modification of porous silica in chromatography involves an alcohol as the organic

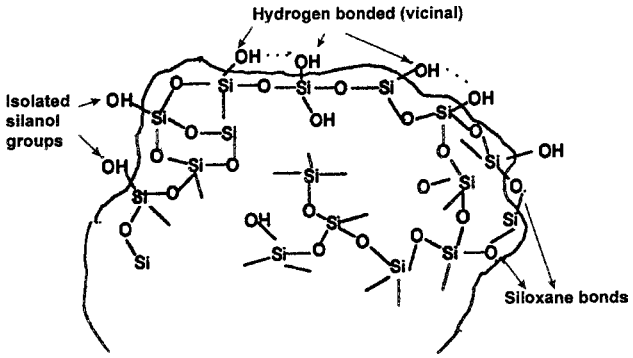

Fig. 1 Structure of silica showing the surface chemical features.

species. This process is referred to as an esterification reaction. This may seem like incorrect nomenclature in order to describe the chemical process taking place between the silianol (Si–OH) and the organic compound (R–OH). However, the OH of the silanol is an acidic species, so the reaction taking place involves an acid and an alcohol, which, in typical organic chemistry nomenclature, is an esterification. The chemical reaction is illustrated in Fig. 2. The product of this reaction can be used as a stationary phase in GC because the material is thermally stable up to temperatures of approximately 300°C. However, the Si–O–C bond that exists between the surface and the bonded moiety is hydrolytically unstable in the presence of relatively small amounts of water. Therefore, these materials cannot be used for stationary phases in LC, where water comprises even a small fraction of the mobile phase.

The second reaction shown in Fig. 2 is the most common means used for the modification of silica surfaces. This method is referred to as organosilanization. Within this general reaction scheme, there are two possible approaches, as shown in Fig. 2. The first possibility involves the use of an organosilane reagent (RR′R′SiX) with only a single reactive group (X). The substituents on the silicon atom are as follows: X is a halide, most often Cl, methoxy or ethoxy; R is the organic moiety giving the surface the desired properties (i.e., hydrophobic, hydrophilic, ionic, etc.), and R′ is a small organic group, typically methyl. This reaction leads to a single siloxane bond between the reagent and the surface. Because of the single point of attachment of the reagent, the resulting bonded material is referred to as a monomeric phase. The second approach to organosilanization involves a reagent with the general formula $RSiX_3$. The substituents on the silicon atom in this reagent are defined as above. The basic difference between the approaches (as shown in Fig. 2) is that the reagent with three reactive groups results in bonding to the surface as well as cross-linking among adjacent bonded moieties and is referred to as a polymeric phase. This cross-linking effect provides extra stability to the bonded moiety but is less reproducible than the monomeric method. The one-step organosilanization procedure

REACTION TYPE	REACTION	SURFACE LINKAGES
ESTERIFICATION	$Si\text{-}OH + R\text{-}OH \rightarrow Si\text{-}OR + H_2O$	Si - O - C
ORGANOSILANE	$Si\text{-}OH + X\text{-}SiR'_2R \rightarrow Si\text{-}O\text{-}SiR'_2R + HX$ $\equiv Si\text{-}OH + X_3Si\text{-}R \rightarrow \equiv Si\text{-}O\text{-}Si(\equiv)_2\text{-}R + 3HX$	Si - O - Si - C
CHLORINATION FOLLOWED BY REACTION OF GRIGNARD REAGENTS OR ORGANOLITHIUM COMPOUNDS	$Si\text{-}OH + SOCl_2 \xrightarrow{\text{Toluene}} Si\text{-}Cl + SO_2 + HCl$ a). $Si\text{-}Cl + BrMgR \rightarrow Si\text{-}R + MgClBr$ or b). $Si\text{-}Cl + Li\text{-}R \rightarrow Si\text{-}R + LiCl$	Si - C
a). TES SILANIZATION	a). $\equiv Si\text{-}OH + \equiv Si\text{-}OH + \equiv Si\text{-}OH \rightarrow \equiv Si\text{-}O\text{-}Si(\equiv)_2\text{-}H$	a). Si - H monolayer
b). HYDROSILATION	b). $Si\text{-}H + CH_2 = CH\text{-}R \xrightarrow{\text{Catalyst}} Si\text{-}CH_2\text{-}CH_2\text{-}R$	b). Si - C

Fig. 2 Reactions for the modification of silica surfaces.

is relatively easy and the modification of the surface can be done by stirring the reagent continuously with the porous silica support. The reaction mixture is heated for about 1–2 hr, then the reagent solution is removed, usually by centrifugation and/or filtration. The bonded phase is then washed with several solvents and dried under vacuum to remove as much of the rinse solutions as possible. Organosilanization accounts for virtually all of the commercially available chemically bonded stationary phases.

Another method that has been reported for the modification of silica supports is based on a chlorination/organometalation two-step reaction sequence. This process is also depicted in Fig. 2. In the first step, the silanols on the porous silica surface are converted to chlorides via a reaction with thionyl chloride. This step must be done under extremely dry conditions because the presence of any water results in the reversal of the reaction with hydroxyl replacing the chloride (Si–Cl), resulting in the regeneration of silanols (Si–OH). If the chlorinated material can be preserved (usually done in a closed vessel purged with a dry gas like nitrogen), then an organic group can be attached to the surface via a Grignard reaction or an organolithium reaction. The main advantage of this process is that it produces a very stable silicon–carbon linkage at the surface. However, the stringent reaction conditions for the first step and the possibility of forming salts that could affect chromatographic properties as by-products in the second reaction have resulted in relatively little commercial use of this process.

The final method shown in Fig. 2 involves, first, silanization of the silica surface, followed by attachment of the organic group through a hydrosilation reaction. In the first step, the use of triethoxysilane under controlled conditions results in a monolayer of the cross-linked reagent being deposited on the surface. This reaction results in the replacement of hydroxides by hydrides. In the second step, an organic moiety is attached to the surface via the hydride moiety by a hydrosilation reaction using a catalyst such as hexachloroplatinic acid (Speier's catalyst), but other transition metal complexes or a free-radical initiator have been reported as well. This process also results in a silicon–carbon bond at the surface, does not require dry conditions (water is required as a catalyst in the first step), and is applicable to a variety of unsaturated functional groups in the hydrosilation reaction, although terminal olefins are the most common. The silanization/hydrosilation method also has seen limited commercial utilization to date.

In all of the reactions described, the choice of the organic moiety on the reagent (R group) determines the properties of the material as a stationary phase. Therefore, selection of a hydrophobic moiety where R is typically an alkyl group leads to a stationary phase that selectively retains non-polar analytes. These materials are typically used in reversed-phase chromatography. If the organic moiety contains a polar functional group such as amine, cyano, or diol, then the stationary phase selectively retains polar compounds. These materials are typically used in normal-phase chromatography.

The bonding of the organic group on the surface results in the replacement of silanols whose adsorptive properties are strong, especially for bases, and often non-reproducible. Although it is impossible to replace all silanols, the remaining Si–OH groups are often shielded from solutes by the steric hindrance of the bonded organic moiety. In many cases though, some silanols are accessible to typical solutes. In order to inhibit the interaction between analytes and residual silanols, the bonded phase is subjected to an additional reaction referred to as endcapping. In this case, a small organosilane, often trimethylchlorosilane, penetrates into the spaces between the bonded groups to react with the most accessible silanols. This process generally greatly reduces or eliminates solute interactions with silanols.

After the bonded phase is prepared, it must be packed into a column, usually a stainless-steel tube. In order for the material to form a uniform bed of high density that will not form voids after prolonged use, the packing process must be done under high pressure (>500 atm). The stationary phase is mixed with a solvent of approximately the same density as silica, so that a slurry is formed. This slurry is then forced into the column at high pressure with another solvent, usually methanol. After packing, most stationary phases require several hours of conditioning, with the mobile phase passing through the column at normal flow rates, before actual chromatographic analysis can begin.

BIBLIOGRAPHY

1. Iler, R.K. *The Chemistry of Silica*; John Wiley & Sons: New York, 1979.
2. Marciniec, B. *Comprehensive Handbook on Hydrosilylation*; Pergamon Press: Oxford, 1992.
3. Nawrocki, J. Silica surface controversies, strong adsorption sites, their blockage and removal. Part I. Chromatographia **1991**, *31* (3–4), 177.
4. Nawrocki, J. Silica surface controversies, strong adsorption sites, their blockage and removal. Part II. Chromatographia **1991**, *31* (3–4), 193.
5. Pesek, J.J.; Matyska, M.T. Methods for the modification and characterization of oxide surfaces. Interf. Sci. **1997**, *5* (2–3), 103.
6. Pesek, J.J.; Matyska, M.T.; Sandoval, J.E.; Williamsen, E.J. Synthesis, characterization and applications of hydride-based surface materials for HPLC, HPCE and electrochromatography. J. Liq. Chromatogr. Relat. Technol. **1996**, *19* (17/18), 2843.
7. Unger, K.K. *Porous Silica*; Elsevier: Amsterdam, 1979.
8. Vansant, E.F.; Van Der Voort, P.; Vrancken, K.C. *Characterization and Chemical Modification of Silica*; Elsevier: Amsterdam, 1995.

Buffer Systems in CE

Robert Weinberger
CE Technologies, Inc., Chappaqua, New York, U.S.A.

INTRODUCTION

The solution contained within the capillary in which the separation occurs is known as the background electrolyte (BGE), carrier electrolyte, or, simply, the buffer. The BGE always contains a buffer because pH control is the most important parameter in electrophoresis. The pH may affect the charge and thus the mobility of an ionizable solute. The electro-osmotic flow (EOF) is also affected by the buffer pH. Table 1 contains a list of buffers that may prove useful in high-performance capillary electrophoresis (HPCE). As will be seen later, only a few of these buffers are necessary for most separations.

Other reagents, known as additives, are often added to the BGE to adjust selectivity (secondary equilibrium), modify the EOF, maintain solubility, and reduce the adherence of the solute or sample matrix components to the capillary wall. Table 2 provides these applications, along with some of the commonly used reagents.

BUFFERS

The selection of the appropriate buffer is usually straightforward. For acids, start with a borate buffer (pH 9.3), and for bases, a phosphate buffer (pH 2.5). These two buffer systems, along with the appropriate additives will work well for most applications. Both buffers have good buffer capacity and the ultraviolet (UV) absorbance of each is low. If bases are not soluble in phosphate buffer, acetate buffer (pH 4) may be more effective. Higher pHs may be required for basic proteins to avoid solute adherence to the capillary wall. If pH 7 is desired, the phosphate buffer works well at that pH. If necessary, the buffer pH can be fine-tuned using a mobility plot.

Alternative buffer systems include zwitterions and dual-buffering reagents. Zwitterionic buffers such as bicine, tricine, N-cyclohexyl-3-aminopropanesulfonic acid (CAPS), morpholino ethane sulfonic acid (MES) and Tris may be useful for protein and peptide separations. An advantage of a zwitterionic buffer is low conductivity when the buffer pH is adjusted to its pI. There is little buffer capacity when the pK_a and pI are separated by more than 2 pH units. When the pI and pK_a are close together, the buffer is known as an isoelectric buffer.[1]

Selection of the appropriate counterion is also important. Lithium ion has the lowest mobility of the alkali earth metals. Its use provides for a low-conductivity buffer. Sodium salts are used more frequently due to purity and availability. It makes little sense to ever use a potassium salt. Dual-buffering systems with low-mobility ions and counterions (Tris-phosphate, Tris-borate, aminomethyl-propanediol–cacodylic acid) are effective in minimizing buffer conductivity. These buffers are often used in the slab–gel, where low conductivity is particularly important.

The buffer concentration plays an important role in the separation. Typical buffer concentrations range from 20 to 150 mM. At the higher buffer concentrations, the production of heat may require the use of lower field strength or smaller-diameter capillaries (25 μm instead of 50 μm). An Ohm's law plot is used to select the appropriate voltage. The advantages of high-concentration buffers include improved peak shape, fewer wall effects, and increased sample stacking.

Low-concentration buffers (less that 20 mM) provide the fastest separations because solute mobility and EOF is inversely proportional to the square root of the buffer concentration. Because the conductivity of a dilute buffer is low, a high electric field strength can be used as well. Problems with low-concentration buffers are loading capacity, wall effects, and poor stacking. Sawtooth-shaped peaks from a process known as electrodispersion may occur whenever the solute concentration approaches the BGE concentration. It also becomes more likely that proteins will adhere to the capillary wall when the buffer concentration is low. Ionic-strength-mediated sample stacking relies on a high-conductivity BGE and a low-conductivity sample.[2] This important process is less effective at low buffer concentrations. When indirect detection is employed, the buffer (indirect detection reagent) concentration must be kept low to optimize sensitivity.[3] Sawtooth peaks are often observed when this technique is used.

It is important to refresh the BGE reservoirs frequently to avoid a process known as buffer depletion.[4] Electrolysis at the respective electrodes produces protons and hydroxide ions. This can cause pH changes in the buffer reservoirs.

High-pH buffers (>pH 11) are used for certain small ion separations and for the separation of carbohydrates using indirect detection. Adsorption of carbon dioxide can cause the buffer pH to decline. It is best to use small containers filled to the top when storing these buffers.

Encyclopedia of Chromatography, Third Edition DOI: 10.1081/E-ECHR3-120039896

Table 1 Buffers for HPCE.

Buffer	pK_a	Buffer	pK_a
Aspartate	1.99	DIPSO	7.5
Phosphate	2.14, 7.10, 13.3	HEPES	7.51
Citrate	3.12, 4.76, 6.40	TAPSO	7.58
β-Alanine	3.55	HEPPSO	7.9
Formate	3.75	EPPS	7.9
Lactate	3.85	POPSO	7.9
Acetate	4.76	DEB	7.91
Creatinine	4.89	Tricine	8.05
MES	6.13	GLYGLY	8.2
ACES	6.75	Bicine	8.25
MOPSO	6.79	TAPS	8.4
BES	7.16	Borate	9.14
MOPS	7.2	CHES	9.55
TES	7.45	CAPS	10.4

BUFFER ADDITIVES

Secondary Equilibrium

If two solutes are inseparable based on pH alone, secondary equilibrium can be employed to effect a separation. The following equilibrium expressions can be written.[5]

$$A^+ + R \overset{K_A}{\rightleftharpoons} A^+R \quad (1)$$

$$B^+ + R \overset{K_B}{\rightleftharpoons} B^+R \quad (2)$$

If the equilibrium is pushed too far to the left, no separation can occur because A^+ and B^+ are inseparable. When the reagent interacts with the solute, the mobility decreases because the neutral reagent contributes mass without charge. However, if the equilibrium is pushed too far to the right, no separation occurs because A^+R and B^+R are inseparable. Separation only occurs when two conditions are met:

1. K_A does not equal K_B.
2. The equilibrium is not pushed to either extreme.

The next feature to consider is the charge of the reagent and solute. To separate charged solutes, the reagent can be charged or neutral. When the solute is neutral, the reagent must be charged.

Micelles and cyclodextrins are the most common reagents used for this technique. Micellar capillary electrokinetic chromatography (MECC) or MEKC is generally used for the separation of small molecules.[6] Sodium dodecyl sulfate at concentrations from 20 to 150 m*M* in conjunction with 20 m*M* borate buffer (pH 9.3) or phosphate buffer (pH 7.0) represent the most common operating conditions. The mechanism of separation is related to reversed-phase liquid chromatography (LC), at least for neutral solutes. Organic solvents such as 5–20% methanol or acetonitrile are useful to modify selectivity when there is too much "retention" in the system. Alternative surfactants such as bile salts (sodium cholate), cationic surfactants (cetyltrimethylammonium bromide), non-ionic surfactants (polyoxyethylene-23-lauryl ether), and alkyl glucosides can be used as well.

Cyclodextrins (CD) are frequently used for chiral recognition,[7] although they are quite useful for achiral applications as well. Many classes have been used including native, functionalized, sulfobutylether, and highly sulfated CDs. The latter two are generally most effective for chiral and structural isomer separations. The typical CD concentrations range from 1 to 20 m*M* in 20–50 m*M* of borate (pH 9.3) or phosphate buffer (pH 2.5). Other reagents useful for chiral recognition include macrocyclic antibiotics, bile salts, chiral surfactants, non-cyclic oligosaccharides and polysaccharides, and crown ethers.

Additional reagents useful for secondary equilibrium include borate buffer for carbohydrates, chelating agents for transition metals, ion-pair reagents for acids and bases, transition metals for proteins and peptides, silver ion for alkenes, and Mg^{2+} for nucleosides.

Electro-Osmotic Flow Control

The control of EOF is critical to the migration time precision of the separation. Among the factors affecting the EOF are buffer pH, buffer concentration, buffer viscosity, temperature, organic modifiers, cationic surfactants or protonated amines, polymer additives, field strength, and the nature of the capillary surface.

Table 2 Buffer additives.

Purpose	Reagent	Mechanism
Modify mobility	Borate	Complex with carbohydrates, diols
	Calixarenes	Inclusion complex
	Chelating agents	Complex formation with metals
	Crown ethers	Inclusion complex
	Cyclodextrins	Inclusion complex
	Dendrimers	Inclusion complex
	Macrocyclic antibiotics	Inclusion complex
	Organic solvents	Solvation
	Sulfonic acids	Ion-pair formation
	Surfactants	Micelle interaction
	Transition metals	Complex formation
	Quaternary amines	Ion-pair formation
Modify EOF	Cationic surfactant	Dynamic coating, EOF reversal
	Linear polymers	Dynamic coating
	Organic solvents	Affects viscosity
Reduce wall effects	Cationic surfactant	Dynamic coating, EOF reversal
	Linear polymers	Dynamic coating
Polyamines		Covers silanols
Maintain solubility	Organic solvents	Hydrophobicity
	Urea	"Iceberg effect"

At pH 2.5, the EOF is approximately 10^{-5} $cm^2/V/s$ in 50 m*M* buffer. At pH 7, it is an order of magnitude higher. The EOF is inversely proportional to BGE viscosity and is proportional to temperature, up until the point where heat dissipation is inadequate. Organic modifiers such as methanol decrease the EOF because hydro-organic mixtures have higher viscosity compared to water alone. Acetonitrile does not strongly affect the EOF. Polymer additives such as methylcellulose derivatives increase viscosity as well as coat the capillary wall.

Cationic surfactants and protonated polyamines may reverse the direction of the EOF as they impart a positive charge on the capillary wall. This technique is used to prevent wall interactions with cationic proteins. Changing the direction of the EOF is important in anion analysis where comigration of anions and the EOF is required. Otherwise, highly mobile anions such as chloride migrate toward the anode, whereas lower mobility anions are swept by the EOF toward the cathode.

A new series of reagents (CElixir, MicroSOLV, Long Branch, New Jersey, U.S.A.) have been shown to dramatically stabilize the EOF, resulting in highly reproducible run-to-run and capillary-to-capillary migration times.[8] First, a capillary is treated as usual with 0.1*N* sodium hydroxide, followed by a rinse with a polycation solution. Then, a second layer consisting of a polyanion in a buffer at the desired pH is flushed through the capillary. Replicate runs are virtually superimposible, yielding reproducibility seldom found in HPCE. The reagents have been shown to work best for bases below at a pH below the pK_a.

Maintaining Solubility

All solutes and matrix components must remain in solution for an effective separation to occur. In aqueous systems, surfactants and urea are the most useful reagents. Organic solvents can be used as well, but this is less desirable because of evaporation. It can be difficult to separate solutes with widely different solubilities in a single run. In some cases, non-aqueous separations are necessary.

Reducing Wall Effects

Wall effects, or the adherence of material to the bare silica capillary wall, has been a difficult problem since the early days of HPCE, particularly for large molecules such as proteins. Small molecules can have, at most, one point of attachment to the wall and the kinetics of adsorption/desorption are rapid. Large molecules can have multiple points of attachment resulting in slow kinetics. Several solutions have been proposed, including the use of: (a) extreme-pH buffers; (b) high-concentration buffers; (c) amine modifiers; (d) dynamically coated capillaries; and (e) treated or functionalized capillaries.

In the first case, it was recognized that if the buffer pH is greater that 2 units above the protein, the anionic protein

would be repelled from the anionic capillary wall.[9] At a pH < 2, the capillary wall is neutral and does not attract the cationic protein. The problem with this approach is that a wide range of pHs are not available for use and separations of similar proteins may not occur. For high-p*I* proteins such as histones, a buffer pH of 13 is required. The conductivity and UV background of such an electrolyte is too high to be generally applicable.

The use of high-concentration buffers is effective in reducing wall effects. This includes electrolytes containing up to 250 m*M* added salt. The problem with this approach is the high conductivity of the BGE. This requires a reduction in field strength resulting in lengthy separations. Zwitterionic buffers titrated to their p*I* can be used as well at concentrations approaching 1 *M*. At that concentration, it is important to select a reagent with low UV absorption.

The latter three cases are most commonly employed to reduce wall effects. In the third case, amine modifiers such as polyamines are added to the BGE at concentrations ranging from 1 to 60 m*M*.[10] These reagents coat the free silanols and reduce wall interactions. Now, any pH electrolyte can be employed. Diaminobutane, otherwise known as putrecein, is the preferred reagent because it is less volatile compared to diaminopropane. Monovalent amines such as triethanolamine are not as effective in this regard.

Dynamically coated capillaries (case d) are often used to reduce wall effects.[11] The mechanism of charge reversal is as follows. Ion-pair formation between the cationic head group of the surfactant and the anionic silanol group naturally occurs. The hydrophobic surfactant tail extending into the bulk solution is poorly solvated by water. The molecular need for solvation is satisfied by binding to the tail of another surfactant molecule. The cationic head group of the second surfactant molecule now extends into the bulk solution. The capillary wall becomes positively charged and the EOF is directed toward the anode. Separations are performed using the reversed-polarity mode (inlet side negative). Following this approach, a buffer pH is selected that is below the p*I* of the target protein. The cationic protein is now repelled from the cationic wall.

When coated capillaries are employed (case e), conventional buffers without additives to reduce wall effects are used. Urea and/or organic solvents can be added to aid solubility. Reagents for secondary equilibrium can be used as well. It is best to operate at a pH below 8 to maximize the stability of the often labile coating material. Coated capillaries are also used simply to eliminate the EOF in some applications.

REFERENCES

1. Righetti, P.G.; Gelfi, C.; Perego, M.; Stoyanov, A.V.; Bossi, A. Capillary zone electrophoresis of oligonucleotides and peptides in isoelectric buffers: Theory and methodology. Electrophoresis **1997**, *18*, 2145.
2. Burgi, D.; Chien, R.-L. Optimization in sample stacking for high-performance capillary electrophoresis. Anal. Chem. **1991**, *63*, 2042.
3. Jandik, P.; Jones, W.R.; Weston, A.; Brown, P.R. LC GC **1991**, *9*, 634.
4. Macka, M.; Andersson, P.; Haddad, P.R. Changes in electrolyte pH due to electrolysis during capillary zone electrophoresis. Anal. Chem. **1998**, *70*, 743.
5. Wren, S.A.C.; Rowe, R.C. Theoretical aspects of chiral separation in capillary electrophoresis: I. Initial evaluation of a model. J. Chromatogr. **1992**, *603*, 235.
6. Nishi, H.; Terabe, S. Micellar electrokinetic chromatography perspectives in drug analysis. J. Chromatogr. A, **1996**, *735*, 3.
7. Chankvetadze, B. *Capillary Electrophoresis in Chiral Analysis*; John Wiley & Sons: Chichester, 1997.
8. Weinberger, R. Am. Lab. **1999**, *31*, 59.
9. Lauer, H.H.; McManigill, D. Capillary zone electrophoresis of proteins in untreated fused silica tubing. Anal. Chem. **1986**, *58*, 166.
10. Bullock, J.A.; Yuan, L.-C. Free solution capillary electrophoresis of basic proteins in uncoated fused silica capillary tubing. J. Microcol. Separ. **1991**, *3*(3), 241–248.
11. Wiktorowicz, J.E.; Colburn, J.C. Separation of cationic proteins via charge reversal in capillary electrophoresis. Electrophoresis **1990**, *11*, 769.

Buffer Type and Concentration: Mobility, Selectivity, and Resolution in CE

Ernst Kenndler
Institute for Analytical Chemistry, University of Vienna, Vienna, Austria

INTRODUCTION

Resolution in capillary zone electrophoresis (CZE) is, as in elution chromatography, a quantity that describes the extent of the separation of two consecutively migrating compounds, *i* and *j*. It is the result of the counterplay of two effects: migration and zone dispersion. The different migration velocities of the two separands lead (at least potentially) to the separation of the sample zones. The simultaneous mixing of the samples with the background electrolyte (BGE), caused by a number of processes, results in zone broadening and counteracts separation. Both effects determine the overall degree of separation. A quantitative measure that describes this degree is the resolution a dimensionless number. It is expressed by the difference of the apex of the two peaks, on the one hand. It is of advantage not to measure this difference in an absolute scale (e.g., in seconds when the electropherogram is depicted in the time domain). In fact, a relative scale is taken, which is based on the widths of the peaks. We define the resolution as the difference in migration times, *t*, related to the peak width, taken, for example, by the mean standard deviation of the Gaussian peaks, as the scaling unit:

$$R_{ji} \equiv \frac{t_j - t_i}{2(\sigma_{t,i} + \sigma_{t,j})} \tag{1}$$

Baseline separation is achieved for two peaks with the same area when the resolution is 1.5. For peak area ratios larger than unity, the resolution must be larger.

SELECTIVITY AND EFFICIENCY

This definitional Eq. 1 is not very operative and is, thus, transformed to an expression which more clearly visualizes the dependence of the resolution on sample properties and experimental variables. The migration times are substituted for by the mobilities of the separands, and the standard deviations by the plate height, *H*, or the plate number, *N*, respectively.

The resulting resolution is then

$$R_{ji} = \frac{1}{4}\frac{\mu_i - \mu_j}{\bar{\mu}}\sqrt{\frac{L}{\bar{H}}} = \frac{1}{4}\frac{\Delta\mu}{\bar{\mu}}\sqrt{\bar{N}} \tag{2}$$

where $\bar{\mu}$, $\bar{H}$, and $\bar{N}$ are the average values; *L* is the migration distance.

The resolution consists of two terms, the selectivity term, $\Delta\mu/\bar{\mu}$, with the relative difference of the mobilities, and the efficiency term, the square root of the mean plate number. It must be pointed out that the plate height, $\bar{H}$, on which this plate number is based consists of all the contributions to peak broadening.

At this point, a differentiation should be made between two cases: the simple one, where migration is only caused by the electric force on the ionic separands, and the second, where an additional migration due to the occurrence of an electro-osmotic flow (EOF) takes place.

RESOLUTION IN ABSENCE OF EOF

Two main parameters determine the resolution: the effective mobility and the plate number. The effective mobility of a simple ion (e.g., the anion from a monovalent weak acid) is given by

$$\mu_{\text{eff}} = \frac{\mu_{\text{act}}}{1 + 10^{\text{p}K_a - \text{pH}}} \tag{3}$$

We take, here, only protolysis into consideration and do not discuss such important other equilibria such as complexation or interactions with pseudo-stationary phases. It follows from Eq. 3 that the effective mobility depends on the actual mobility (that of the fully charged particle at the ionic strength of the experiment), on the pK_a value of the analyte, and on the pH of the BGE. It follows that all these properties determine the selectivity term in the resolution.

The actual mobility depends on the following:

1. *The solvent*. There is a more or less pronounced influence of the solvent viscosity, reflected by Walden's rule. However, this rule is obeyed in rare cases; mainly in some mixed aqueous–organic solutions is an acceptable agreement found. On the other hand, in very viscous aqueous solutions of water-soluble polymers, such as poly(ethylene glycol), it was found that the actual mobility is independent of the viscosity.
2. *The size of the solvated ion*. Here, we must note that water is an excellent solvator for anions and cations

Encyclopedia of Chromatography, Third Edition DOI: 10.1081/E-ECHR3-120039897

as well, compared to most organic solvents. Only few exceptions for preferred solvation of the organic solvents are found (e.g., for Ag^+ and acetonitrile).

3. *The ionic strength of the BGE*. The dependence of the mobility on the ionic strength is expressed for simple systems (and simple ions) by the theory of Debye, Hückel, and Onsager. Without going into detail, we can state that the mobility decreases, in all cases, with increasing ionic strength of the BGE, and the decrease is more pronounced the higher the charge number of the ion.
4. *On the temperature*. In aqueous solutions, the mobility increases with temperature roughly by about 3% per degree. This is a strong effect as, for example, a temperature difference of only 5 K between the center and the wall of the separation capillary leads to a mobility difference of about 15%.

The pK_a value is also a function, mainly, of the solvent. Note that the pH scale is strongly dependent on the kind of solvent. Restricting the discussion to protolysis, it can be followed that the pH of the buffer has the most pronounced effect on the effective mobility, because the other effects change the mobility roughly in parallel for all separands. Again, it must be pointed out that other equilibria have an enormous potential to affect the effective mobility (cf. e.g., the use of cyclodextrins to introduce selectivity for the separation of enantiomers).

How is the efficiency influenced by the BGE? Peak broadening is the result of different processes in CZE occurring during migration [in addition, extracolumn effects contribute to peak width (e.g., that stemming from the width and shape of the injection zone, or the aperture of the detector cell)]. If the system behaves linearly, the individual peak variances (the second moments), are additive according to

$$\sigma_{\text{tot}}{}^2 = \Sigma\sigma_{\text{ind}}{}^2 = \sigma_{\text{extr}}{}^2 + \sigma_{\text{dif}}{}^2 + \sigma_{\text{Joule}}{}^2 + \sigma_{\text{conc}}2 + \sigma_{\text{ads}}{}^2 \quad (4)$$

where the subscripts extr, dif, Joule, conc, and ads indicate the contributions from extracolumn dispersion, longitudinal diffusion, Joule self-heating, concentration overload, and wall adsorption, respectively. All but one effect might be eliminated: The longitudinal diffusion is inevitable. Plate number expressing this contribution is dependent on the voltage, U, applied and on the charge number, z_i, of the analytes according to

$$N_i \approx 20 z_i U \quad (5)$$

at 20°C. It is obvious that the charge number depends on the pH of the BGE, as it is related to the degree of ionization. It follows that the plate number is a function of the pH as well. Thus, the resolution is influenced by the pH of the BGE twofold: via the selectivity, on the one hand, and via the plate number, on the other hand.

In conclusion, it follows for the limiting case of longitudinal diffusion as the only peak-broadening effect, that the resolution depends on the following:

- Instrumental variables: U and T.
- Analyte parameters: μ_{act} and pK_a.
- Chemical conditions determining the degree of ionization, α, or charge number z.

RESOLUTION IN PRESENCE OF EOF

The EOF brings an additional, unspecific velocity vector to the electrophoretic migration of the separands. The total migration velocity of the analyte, i, is then

$$\nu_{i,\text{tot}} = (\mu_{i,\text{eff}} + \mu_{\text{EOF}})E \quad (6)$$

Note that the mobilities are taken as signed quantities. By convention, cations have positive electrophoretic mobilities and those of anions are negative. The mobility of the EOF when directed toward the cathode has positive sign, and vice versa.

The effect of the EOF on migration time and selectivity depends on the mutual signs of the mobilities of analytes and EOF, respectively. Concerning the change in separation selectivity, we refer to the expression of the selectivity term in the resolution equation. The difference between the mobilities of the two separands, i and j, will not be influenced by the EOF. However, the mean mobility is larger for the case of comigration. This means that the selectivity term in the expression for the resolution is always reduced in this case. In practice, selectivity is lost for cation separation when the EOF is directed, as is usual in uncoated fused-silica capillaries, toward the cathode. For this reason, cationic additives are applied in the BGE to reverse the EOF direction.

The effect of the EOF on separation selectivity (in comparison with the situation without EOF) can be quantified by the so-called electromigration factor, or reduced mobility, $\mu_i{}^*$, defined as

$$\mu_i{}^* = \frac{\mu_{i,\text{eff}}}{\mu_{i,\text{eff}} + \mu_{\text{EOF}}} \quad (7)$$

The change of the selectivity term in the resolution is directly expressible by $\mu_j{}^*$. Interestingly, the effect of the EOF on the dispersion effects, expressed by the plate height H, also depends directly on μ^*. For longitudinal diffusion, Joule self-heating, and concentration overload, the variation of the plate height in the presence of the EOF is directly dependent upon this reduced mobility according to

$$H^{\text{EOF}} = H^0\mu^* \quad (8)$$

where the superscript 0 indicates the system without EOF. For wall adsorption, the corresponding effect is related to the reciprocal of μ^*.

An analysis of the effect of the EOF on the resolution brings the following result: For comigration of the analyte and EOF, the efficiency always increases and the selectivity term always decreases. As the decrease is directly proportional to μ^* but the gain in plate number is only increasing with the square root of μ^*, the resolution is always worse than without comigrating EOF.

For the case of countermigration, the situation is more complicated, because the overall effect depends on the magnitude of the mobility of analyte and that of the EOF. Roughly, it can be concluded that the resolution is increased for a given pair of analytes when the EOF is counterdirected, and it has a lower mobility than the analytes. Here, efficiency is lost, but selectivity is gained overproportionally. When the EOF mobility reaches a value that is twice as large as the analyte mobility (note that the signs of the mobilities are different), an analogous situation is found as without EOF. At mobilities of the EOF larger than twice the analyte mobility (conditions not impossible for high pH values of the BGE), resolution is worse here than without EOF, but the analysis time is shorter than in all other cases. It should be pointed out that all of these effects can be quantified by the reduced mobility defined in Eq. 7.

BIBLIOGRAPHY

1. Camillieri, P. *Capillary Electrophoresis, Theory and Practice*; CRC Press: Boca Raton, FL, 1998.
2. Giddings, J.C. Harnessing electrical forces for separation: CZE, IEF, FFF, SPLITT, and other techniques. J. Chromatogr. **1989**, *480*, 21.
3. Guzman, N.A. *Capillary Electrophoresis Technology*; Marcel Dekker, Inc.: New York, 1993.
4. Kenndler, E. Dependence of analyte separation on electroosmotic flow in capillary zone electrophoresis: Quantitative description by the reduced mobility. J. Microcol. Separ. **1998**, *10*(3), 273–279.
5. Kenndler, E. *High Performance Capillary Electrophoresis, Theory, Techniques and Applications*; Khaledi, M.G., Ed.; John Wiley & Sons: New York, 1998; Vol. 146, 25–76.
6. Landers, J.P. *Handbook of Capillary Electrophoresis*, 2nd Ed.; CRC Press: Boca Raton, FL, 1997.
7. Reijenga, J.C.; Kenndler, E. Computational simulation of migration and dispersion in free capillary zone electrophoresis, part I, Description of the theoretical model. J. Chromatogr. A, **1994**, *659*, 403.

Capacity

M. Caude
A. Jardy
Analytical Chemistry Department, City of Paris Industrial Physics and Chemistry Higher Educational Institution (ESPCI), Paris, France

INTRODUCTION

The capacity is closely related to the number of active sites of the stationary phase per volume or mass unit. Practically, there are two definitions corresponding to two different approaches to the problem. On the one hand, there is the linear capacity and, on the other, the maximum available capacity.

DISCUSSION

It is well known that when increasing the injected sample quantity, whether in volume or in concentration, peaks are distorted and/or shifted beyond a certain limit; the column is said to be overloaded. To quantify how much sample can be injected into a column without altering the resolution, it is convenient to define the column linear capacity. It is well known, for small injected quantities, that solute retention times and column efficiency are not affected by the sample size. However, above a critical sample size, a noticeable decrease in retention time and column efficiency are always observed.

Snyder has defined[1] the adsorbent linear capacity as the ratio (weight sample)/(weight stationary phase) giving a value of k' (or V_R) reduced by 10% relative to the constant k' values measured for smaller samples (Fig. 1). In Fig. 1, the adsorbent (Silica Davison) has a linear capacity close to 0.5 mg of dibenzyl per gram of silica. When the linear capacity of the column is exceeded, qualitative and quantitative analyses become much more complicated. Retention factors vary according to the injected solute quantity and the column efficiency can be tremendously decreased, entailing a degradation of resolution. Therefore, for analytical separations, it is always preferable to choose operating conditions corresponding to the linear capacity (k' and N values are constant whatever the injected sample sizes).

However, the practical interest of column linear capacity is very limited because its value varies according to various parameters: solute nature and retention and, even for the same quantity of injected solute, both the injected volume and the solute concentration of the injected solution. Thus, although widely accepted, the column linear capacity is misleading because it characterizes not only the thermodynamic nature of the chromatographic system but also the kinetic conditions (in term of column efficiency).

Consequently, it is preferable, according to Gareil et al.,[2] to define the concept of maximum available capacity C_D for a stationary phase:mass of solute entailing the saturation of the mass m of stationary phase contained in the column for given operating conditions:

$$C_D = \frac{Qs}{m} \tag{1}$$

with

$$k' = \frac{Qs}{Qm} = \frac{Qs}{V_m C_0} \tag{2}$$

The combination of Eqs. 1 and 2 gives

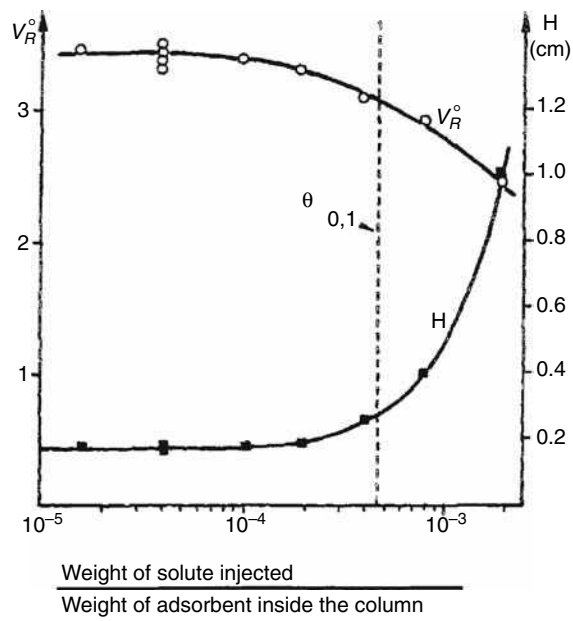

Fig. 1 Variation of the specific retention volume $V_R{}^0$ and of the height equivalent to a theoretical plate H as a function of the weight of injected solute (dibenzyl) related to the weight of adsorbent inside the column.
Source: From Column efficiency in liquid-solid adsorption chromatography. H.E.T.P. [height equivalent to a theoretical plate] values as a function of separation condition, in Anal. Chem.[1]

Encyclopedia of Chromatography, Third Edition DOI: 10.1081/E-ECHR3-120039900

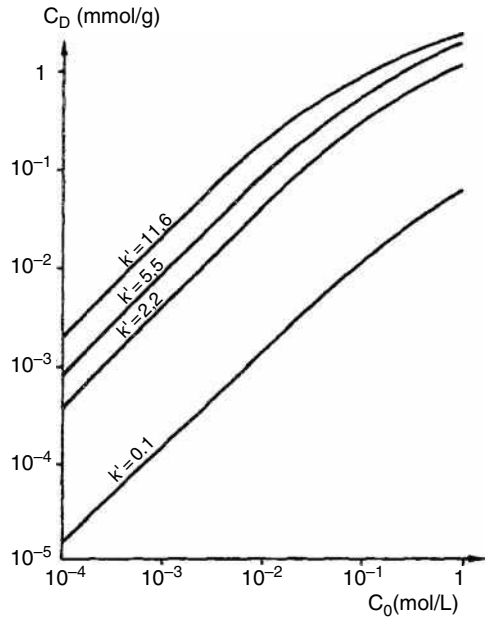

Fig. 2 Variation of the available capacity C_D as a function of the solute concentration in the module-phase C_0 (logarithm scales). In the case of RP chromatography, the stationary phase is *n*-octyl-bonded silica Lichroprep R.P.8 with 11.6% of carbon, the mobile phases are water-methanol mixtures, and the solute is phenol.

$$C_D = \frac{k' V_m C_0}{m}$$

where k' is the solute retention factor measured for an analytical injection, V_M is the mobile-phase volume contained in the column, and C_0 is the solute concentrationin the mobile phase.

Fig. 2 shows, for various retention factors, the available capacity variation versus the solution concentration in the mobile phase in (RP) chromatography. These curves, called distribution isotherms, can be divided into two parts. In the first part, a linear variation of C_D versus C_0 is observed (bilogarithm scale); in the second part, a plateau is reached. In the first part and for the same retention (k' constant), the available capacity is independent of the solute nature.

The maximum available capacity is defined as the C_D limit value when both C_0 and k' are high ($C_0 \cong 1$ mol/L, $k' \geq 10$). This value does not vary either with or k', or the solute nature (for the same family).

The maximum available capacity depends on the nature of the stationary phase:specific area for adsorption, the ion-exchange capacity for ion-exchange capacity, and the bonded rate for partition chromatography.

As a general rule, the maximum values of available capacity vary from 1.2 mmol/g (silica having a specific area close to 400 m^2/g) to 5 mEq/g for the cation exchanger (sulfonate groups).

REFERENCES

1. Snyder, L.R. Column efficiency in liquid-solid adsorption chromatography. H.E.T.P. [height equivalent to a theoretical plate] values as a function of separation conditions. Anal Chem. **1967**, *39*, 698.
2. Gareil, P.; Semerdjian, L.; Caude, M.; Rosset, R. J. High. Resolut. Chromatogr. Chromatogr. Commun. **1984**, *7*, 123.

BIBLIOGRAPHY

1. Knox, J.H., Ed.; *High Performance Liquid Chromatography*; Edinburgh University Press: Edinburgh, 1978; 27–28, 50.
2. Rosset, R.; Caude, M.; Jardy, A. *Chromatographies en phases liquide et supercritique*; Masson: Paris, 1991; 32–37.

Capillary Isoelectric Focusing

Robert Weinberger
CE Technologies, Inc., Chappaqua, New York, U.S.A.

Abstract
Capillary isoelectric focusing (CIEF) is designed to separate solutes based on their p*I*, the pH where they are electrically neutral. Because solutes do not migrate when they are neutral, the mobilization step distinguishes CIEF from other capillary electrophoretic techniques. This entry reviews the basis for CIEF including pH gradient formation, mobilization techniques, additives, and applications.

INTRODUCTION

Capillary isoelectric focusing (CIEF) employs a pH gradient developed within the capillary to separate zwitterions, usually proteins and peptides, based on each solute's p*I*. The technique is analogous to slab–gel CIEF[1] with several important differences: a) Slab–gel IEF is a non-elution process. After running the electrophoretic step, the proteins are detected by staining. CIEF is usually an elution technique. The contents of the capillary are mobilized to pass through the detector region. b) In the slab–gel, detection is by Commassie or silver staining. In CIEF, detection is by ultraviolet (UV) absorbance at 280 nm. c) In the capillary format, no gel is required because mechanical stability is provided by the rigid capillary walls. d) The field strength is at least an order of magnitude higher in the capillary format compared to the slab–gel.

The usual advantages of capillary electrophoresis apply equally to CIEF. Slab–gel IEF is extremely labor intensive and time-consuming. CIEF is simple to run, fully automated, and high speed and provides improved quantitative results compared to slab–gel IEF. This topic has been recently reviewed,[2] and is usually covered as a chapter in many high-performance capillary electrophoresis textbooks.

pH GRADIENT FORMATION

A solution containing 0.5–2.0% carrier ampholytes and 0.1–0.4% methylcellulose (1500 cP for a 2% solution) is filled into the capillary. A coated capillary is used to suppress the electro-osmotic flow (EOF) in conjunction with the methylcellulose solution. The sample (protein) concentration in the ampholyte blend is usually between 50 and 200 μg/ml. The inlet reservoir (anolyte) is filled with 10 m*M* phosphoric acid in methylcellulose solution. The outlet reservoir (catholyte) contains 20 m*M* sodium hydroxide. Higher concentrations of acid and base may be used to further stabilize the pH gradient.

The condition of the capillary immediately upon activation of the voltage is illustrated at the top of Fig. 1. In this case, the capillary is filled with a p*I* 3–10 mixture of ampholytes. Assuming the pH of the solution is 7, charges have been assigned to the individual ampholytes. The ampholyte charge dictates the direction of migration. Should any ampholyte migrate into a reservoir, the extreme pH conditions cause immediate charge reversal. Likewise, as the steady state is approached, should an ampholyte migrate into a more acidic or basic zone, charge reversal occurs as well. The result is the formation of a pH gradient as indicated at the bottom of Fig. 1. As each ampholyte approaches a pH equal to its individual p*I*, migration slows and then ceases. Because overlapping Gaussian zones of each ampholyte are formed, the gradient is smooth and linear.

The conventional pH range for CIEF is pH 3–10. Narrow-range gradients can be created by selecting custom ampholyte blends (e.g., pH 6–8). To avoid problems such as a step-gradient or the creation of water zones, the narrow-range ampholyte solution is usually supplemented with 20% pH 3–10 ampholytes. This ensures that there are sufficient ampholyte species to produce Gaussian overlaps.

The focusing step takes 2–5 min at a field strength of 500–1000 V/cm. Overfocusing causes precipitation of proteins and can damage the capillary as well. Initially, the current is high as ampholytes and proteins are highly charged. As their p*I*'s are approached, the current declines and reaches 1–4 μA when focusing is complete.

The 2:1 ratio of base:acid in the reservoirs is not coincidental. It is selected to minimize drift of the pH gradient. The pH of the anolyte must be lower than that of the most acidic ampholyte; likewise, the pH of the catholyte must be higher than the most basic ampholyte. Otherwise, ampholytes will migrate into the reservoirs and cause gradient drift. If the EOF is not reduced, a form of cathodic drift occurs as well. An exception to this is when one-step mobilization is employed.

Internal standards are always used to calibrate the pH gradient. This is important because the salt content of the

Encyclopedia of Chromatography, Third Edition DOI: 10.1081/E-ECHR3-120045233

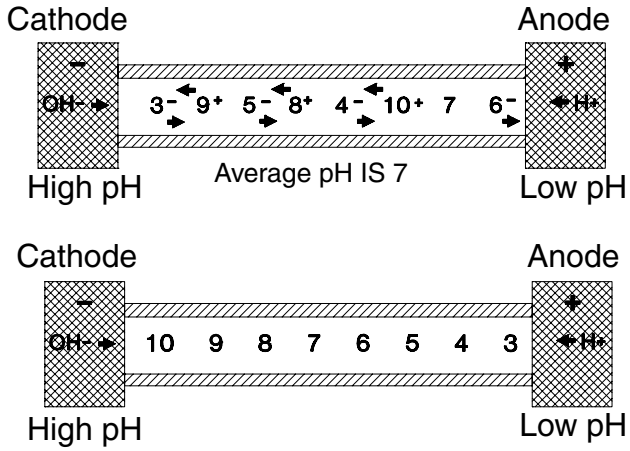

Fig. 1 Illustration of the process of pH gradient formation.

sample can compress the gradient. The ideal internal standard absorbs at a wavelength other than 280 nm. It can then be added to the ampholytes and monitored without producing interference. In this case, photodiode array detection is used for multiwavelength monitoring. Methyl red, p*I* 3.8, is ideal in this regard, but other such markers have not been identified. Aminomethylphenyl dyes are often used with monitoring at 400 nm, but they have some absorbance at 280 nm.

To prevent focused zones from reaching the blind side of the capillary past the detector, the ampholytes are either filled just prior to the detector or the reagent TEMED (*N,N,N,N*-tetramethylenediamine) is added to the blend at the appropriate concentration (0.5–2.0%). TEMED, a basic amine, then occupies that space past the detector window.

RESOLVING POWER

The resolving power, ΔpI of CIEF is described by

$$\Delta pI = 3\sqrt{\frac{D\left(\frac{dpH}{dx}\right)}{E\left(\frac{d\mu}{dpH}\right)}} \quad (1)$$

where D is the diffusion coefficient, E is the field strength, μ is the mobility of the protein, and $d\mu/dpH$ describes the mobility–pH relationship. The term dpH/dx represents the change in the buffer pH per unit of capillary length. This adjustable parameter is controlled by selecting an appropriate ampholyte pH range as well as the capillary length. Under optimal conditions, a resolution of 0.02 pH units is possible.

MOBILIZATION

There are three ways of mobilizing the contents of the capillary: a) chemical (salt) mobilization, b) electro-osmotic (one-step) mobilization, and c) hydrodynamic mobilization. Hydrodynamic mobilization is the simplest and most widely used method. Low pressure is used to evacuate the capillary with the voltage activated. Laminar band broadening is minimized by simultaneous focusing. In one-step mobilization, the EOF is reduced but not absent. If done correctly, focusing occurs prior to any proteins reaching the detector. This is the fastest method but has lower resolution and linearity compared to hydrodynamic mobilization. Salt mobilization is infrequently used today, but it produces the highest resolution at the expense of run time and gradient linearity. The mobilization step is time consuming and may reduce the overall resolution of the separation. Imaged detection permits the entire capillary to be monitored in real time.[3] The disadvantage of this technique is the requirement for a dedicated CIEF instrument that is available from only one manufacturer.

DETECTION

Because the ampholytes absorb below 250, 280 nm detection is required. It is critical to run ampholyte blanks because the reagents are not checked by the manufacturers for UV absorption at 280 nm. The limit of detection is a few micrograms per milliliter of protein and this is usually limited by the UV reagent background. Proteins that are deficient in aromatic amino acids are poorly detected. Different lots of ampholytes from various manufacturers show variation in the UV background.

The combination of CIEF and mass spectrometry is analogous to two-dimensional (2-D) electrophoresis.[4] In this case, the mass spectrometer provides the molecular-weight information instead of sodium dodecyl sulfate–polyacrylamide gel electrophoresis. This information can be obtained by online CIEF/MS[5] or by using CIEF as a micropreparative technique.[6]

For the online system, CIEF is performed conventionally in a 20 cm capillary mounted inside an electrospray probe. After focusing, the outlet reservoir (catholyte) is removed and the capillary tip set to 0.5 mm outside of the probe. A sheath liquid of 50% methanol, 49% water, and 1% acetic acid (pH 2.6) pumped with a syringe pump at 3 μl/min produces a stable electrospray. Cathodic mobilization is produced by changing the anolyte to the sheath liquid. The ampholyte ions were observed up to m/z 800 and thus did not interfere with the protein signals.

CIEF IN MICROFABRICATED SYSTEMS

Adaptation of CIEF to the microchip format can provide higher performance compared to conventional capillaries.[7] Whole channel imaging can be performed, thereby eliminating the need for mobilization. The chip can be interfaced to the mass spectrometer while maintaining the short length of the separation channel which is a distinct advantage compared to the conventional capillary.

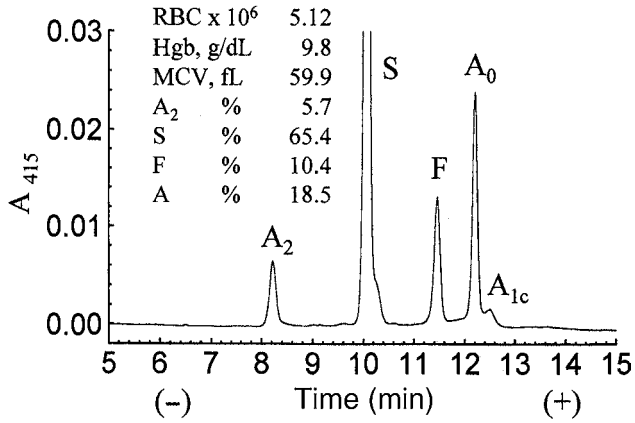

Fig. 2 Separation of hemoglobins by CIEF in blood from a patient suffering Hb *S*/β+ from thalessemia. Capillary: 27 cm (20 cm to detector) × 50 μm I.D. DB-1 (J & W Scientific); ampholytes: 2% pH 6–8:10–3 (10:1) Pharmalytes (Pharmaceia Biotech) and 0.375% methylcellulose; catholyte: 20 m*M* sodium hydroxide; anolyte: 100 m*M* phosphoric acid in 0.375% methylcellulose; focusing: 5 min at 30 kV; mobilization: low pressure (0.5 psi) for 10 min at 30 kV; detection: UV, 415 nm.
Source: From Capillary isoelectric focusing of hemoglobin variants in the pediatric clinical laboratory, in Electrophoresis.[11]

ADDITIVES FOR HYDROPHOBIC PROTEINS

The tendency of hydrophobic proteins to aggregate and precipitate is a major problem in IEF whether in the slab–gel or capillary format. The focusing power of CIEF produces an increase in solute concentration by a factor of over 200.[8] Proteins also readily precipitate as the p*I* is approached because their charge and, thus, electrostatic repulsion approach zero.

Protein precipitation is indicated first by spikes in the electropherogram followed by clogging of the capillary. Additives are required to suppress the aggregation of hydrophobic proteins to keep them in solution. Two excellent review articles describe this in detail.[9–10]

Among the reagents used to prevent aggregation are urea, non-ionic surfactants such as Brij-35, zwitterionic detergents such as sulfobetains, polyols such as ethyleneglycol, glycerol, and sorbitol or non-reducing sugars. A strategy of mixing polyols and zwitterions is often successful in dealing with solubility problems. Urea is often used to keep some monoclonal antibodies in solution.

APPLICATIONS

CIEF has been employed for separations of many proteins, recombinant proteins, monoclonal antibodies, and protein glycoforms. The most widely used method employing isoelectric focusing is the neonatal determination of hemoglobin variants for the screening of genetic disorders, including sickle cell anemia, thalassemias, and other hemoglobinopathies. Fig. 2 illustrates the separation of hemoglobins in a patient with S/β thalassemia. Eventually, this application will be performed clinically using microfabricated systems.

CONCLUSIONS

CIEF is a charge-based method that is orthogonal to ion-exchange chromatography. Of the CE methods, CIEF is more difficult to implement. The method works best on a dedicated instrument that uses whole capillary imaging instead of the classical mobilization step. The technique has gained general acceptance within the biopharmaceutical industry primarily for checking monoclonal antibody purity.

REFERENCES

1. Righetti, P.G. *Isoelectric Focusing: Theory, Methodology and Applications;* Elsevier Biomedical Press: Amsterdam, 1983.
2. Silvertand, L.H.; Torano, J.S.; van Bennekom, W.P.; de Jong, G.J. Recent developments in capillary isoelectric focusing. J. Chromatogr. A, **2008**, *1204*, 157.
3. Li, N.; Kessler, K.; Bass, L.; Zeng, D. Evaluation of the iCE280 Analyzer as a potential high-throughput tool for formulation development. J. Pharm. Biomed. Anal. **2007**, *43* (3), 963–972.
4. Tang, Q.; Harrata, A.K.; Lee, C.S. Two-dimensional analysis of recombinant *E. coli* proteins using capillary isoelectric focusing electrospray Ionization mass spectrometry. Anal. Chem. **1997**, *69*, 3177.
5. Tang, Q.; Kamel Harrata, A.; Lee, C.S. Capillary isoelectric focusing-electrospray mass spectrometry for protein analysis. Anal. Chem. **1995**, *67*, 3515.
6. Foret, F.; Muller, O.; Thorne, J.; Gotzinger, W.; Karger, B.L. Analysis of protein fractions by micropreparative capillary isoelectric focusing and matrix-assisted laser desorption time-of-flight mass spectrometry. J. Chromatogr. A, **1995**, 7*16*, 157.
7. Shimura, K.; Takahashi, K.; Koyama, Y.; Sato, K.; Kitamori, T. Isoelectric focusing in a microfluidically defined electrophoresis channel. Anal. Chem. **2008**, *80*, 3818.
8. Yowel, G.G.; Fazio, S.D.; Vivilecchia, R.V. Analysis of a recombinant granulocyte macrophage colony stimulating factor dosage form by capillary electrophoresis, capillary isoelectric focusing and high-performance liquid chromatography. J. Chromatogr. **1993**, *652*, 215.
9. Rabilloud, T. Solubilization of proteins for electrophoretic analyses. Electrophoresis **1996**, *17*, 813.
10. Rodriguez-Diaz, R.; Wehr, T.; Zhu, N. Capillary isoelectric focusing. Electrophoresis **1997**, *18*, 2134.
11. Hempe, J.M.; Granger, J.N.; Craver, R.D. Capillary isoelectric focusing of hemoglobin variants in the pediatric clinical laboratory. In *Electrophoresis*; Wiley-VCH, **1997**; Vol. 18, 1785–1795.

Capillary Isotachophoresis

Ernst Kenndler
Institute for Analytical Chemistry, University of Vienna, Vienna, Austria

INTRODUCTION

Three analytical electrophoretic techniques can be distinguished. They differ in the kind of background electrolyte (BGE) and in its arrangements. Zone electrophoresis has a uniform BGE without a gradient; in isoelectric focusing, the separation is established by the aid of a BGE forming a continuous (linear) pH gradient. In contrast, isotachophoresis (ITP) is an electrophoretic method with a stepwise gradient of the background electrolyte.

ISOTACHOPHORESIS

In ITP, samples of only one charge type are separated in the same run (i.e., either anions or cations). The BGE in ITP is selected in the way that (the anion or cation of) the leading (L) and the terminating (T) electrolyte will have a higher and a lower mobility, μ, respectively, than the analytes of interest. Thus, the prerequisite for separation by ITP is that $\mu_L > \mu_{analytes} > \mu_T$.

Consider the case that the sample ions are anions (consisting of analytes A^- and B^-), and that the ions exhibit mobilities in the sequence $\mu_L > \mu_A > \mu_B > \mu_T$. The capillary is filled with and separated by a sharp boundary, and the sample is injected between the two electrolyte zones (for simplicity, it is assumed that the counterions, Q^+, are all the same). After application of an electric field, a certain field strength is established in the zones as depicted in Fig. 1 (it is assumed that the capillary has uniform diameter). Across the individual zone, the field strength is constant, but it increases due to the decreasing mobility (and increasing electrical resistance) from L to T. Across the zone of the mixed sample (A + B) it is constant as well, with strength E_{mix}. In this zone, the two analytes A and B are moving with different migration velocities, ν, according to $\nu_A = \mu_A E_{mix}$ and $\nu_B = \mu_B E_{mix}$. Due to the higher mobility of A, this analyte moves faster here than B: $\mu_A E_{mix} > \mu_B E_{mix}$. This effect leads to the migration of ions out of the mixed zone, forming a separate zone in front with pure A^- (which is always placed behind the zone of the leading electrolyte). For B^- the analogous situation occurs; it is moving slower in the mixed zone and forms a separate zone at the rear side (but in front of T). The formation of zones of pure analyte ions (obviously with counterions, Q^+, the counterions of the leading electrolyte) is, therefore, observed. Five zones can be differentiated in this transient state: L^-, pure A^-, mixed $A^- + B^-$, pure B^-, and T^-. Due to the different mobilities, the field strength increases in this sequence. Separation takes place as long as the mixed zone exists. Finally, this zone disappears and the isotachophoretic condition is established: All zones and zone boundaries migrate with the same mean velocity ("isotachophoresis"); consequently,

$$\mu_L E_L = \mu_A E_A = \mu_B E_B = \mu_T E_T \quad (1)$$

This is the isotachophoretic condition. The conditions of electroneutrality must be fulfilled as well, which means, in the case considered, that in each zone the concentration of ions and counterions is equal. The third condition is Ohm's law, stating that (for given constant current) the product of electrical conductivity and field strength in each zone is equal. The combination of these conditions leads to the so-called regulation function (Kohlrausch), which reads in a simplified form (for monovalent strong electrolytes):

$$c_A = c_L \frac{\mu_A(\mu_L + \mu_Q)}{\mu_L(\mu_A + \mu_Q)} \quad (2)$$

It relates the concentration of a species in its own zone to the concentration of the species in the subsequent zone and, as a consequence, to the concentration of the first zone, the leading ion. It is also a function of the mobility of the ions involved: the analyte, the leading ion, and the counterion. This function allows two conclusions as follows.

As for given conditions, the mobilities in Eq. 2 are constant under ITP conditions; the concentration of the sample in its zone is constant as well. The concentration distribution is, therefore, given by a rectangular function. It follows that the temperature and the pH within the particular zone is constant, too, and changes stepwise at the boundary to the neighboring zone.

The concentration depends only on that of the leading ion; it is independent of the initial concentration in the sample. Therefore, ITP can act as an enrichment

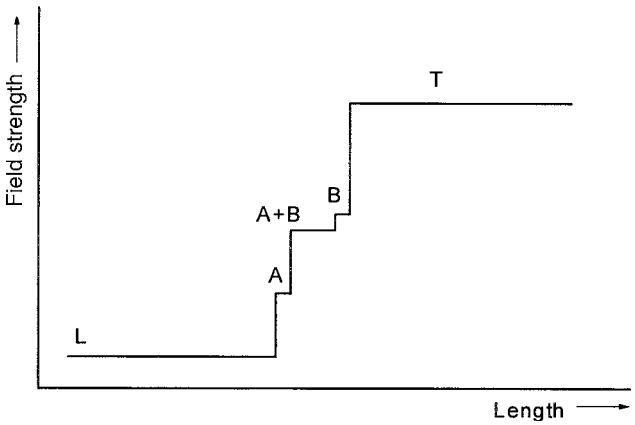

Fig. 1 Electrical field strength in the zones of the leading electrolyte, L, the sample consisting of A and B, and the termination electrolyte, T.

method, analogous to displacement chromatography and in contrast to zone electrophoresis and elution chromatography. The concentration in the steady state is adjusted to the value given in Eq. 2. If the concentration of the analyte species is lower in the initial sample, the higher steady-state concentration is established. This concentration is independent of the migration distance: there is no dilution with a BGE as there is in capillary zone electrophoresis (CZE).

The adjustment of the steady-state concentration to a certain constant value has the consequence that the zone length of an analyte depends on the amount present in the sample. Increasing the amount results in an increase of the zone length under ITP conditions. The length is, therefore, the parameter for quantitative analysis.

The stepwise gradient of the electrical field at the zone boundary is the source of the "self-sharpening" effect in ITP. When, by diffusion, an ion migrates out of its own zone, into a neighboring zone (where the field strength is higher or lower, respectively), the condition given in Eq. 1 is not fulfilled any more. Therefore, the velocity of the considered ion is either accelerated or retarded, and the ion is pushed back into its initial zone. As a consequence, the boundary between the zones remains sharp and its shape is not dependent on the migration distance.

Isotachophoresis might have several advantages compared to zone electrophoresis. The adaptation to a considerably high concentration of the sample components in their own zones in the absence of further BGE favors the use of the electrical conductivity detector. The high concentration and the long sample zone have also some advantage in combining capillary electrophoresis with, for example, MS. Also, ITP can be used as an enrichment technique prior to zone electrophoretic separation, a phenomenon that is applied routinely in sodium dodecyl sulfate–polyacrylamide gel electrophoresis using a discontinuous buffer for sample introduction, and a technique called sample stacking in CZE. In fact, both methods rely on an isotachophoretic principle.

BIBLIOGRAPHY

1. Bocek, P.; Deml, M.; Gebauer, P.; Dolnik, V. *Analytical Isotachophoresis*; VCH: Weinheim, 1988.
2. Everaerts, F.M.; Beckers, J.L.; Verheggen, T.P.E.M. *Isotachophoresis: Theory, Instrumentation, and Applications*; Elsevier: Amsterdam, 1976.
3. Mosher, R.A.; Saville, D.A.; Thormann, W. *The Dynamics of Electrophoresis*; VCH: Weinheim, 1992.

Carbohydrates: Affinity Ligands

I. Bataille
D. Muller
Galilee Institute, University of North Paris, Villetaneuse, France

INTRODUCTION

Since its conception 30 years ago, affinity chromatography has been a powerful technique to separate or purify biological compounds, but also a method to study the interactions between living systems and molecules of biological or therapeutical interest. Among these molecules, oses, polysaccharides, or more complex molecules such as glycosaminoglycans constitute a family of potential ligands.

DISCUSSION

The majority of applications of affinity chromatography has been, for quite some time, in the field of protein purification. For example, some of the most rewarding applications have been in the area of purification of hormone and drug receptors. Among these drugs, carbohydrate-based structures are well known for their biological activity (e.g., their anticoagulant or antiproliferative properties). Although some of these biological properties are widely used in medical applications, the mechanisms of action at the molecular level is not accurately determined.

An example of the use of carbohydrate-based affinity chromatography is, thus, the separation of proteins that are responsible for the action of bioactive polysaccharides or oses. The strategy consists in the immobilization of these carbohydrates on classical low- or high-pressure affinity phases. We will distinguish two types of ligands: those based on osidic structures and those prepared from glycosaminoglycans or polysaccharides.

OSIDIC LIGANDS

All osidic structures that can interact with proteins implicated in biological responses or phenomenons are, a priori, candidates as ligands in affinity chromatography. Here, we give some examples of oses which have been successfully immobilized to make selective chromatographic supports.

Sialic Acid (*N*-Acetylneuraminic Acid)

Purification of immunoglobulins G is of great interest in biological science. Among other separation methods, affinity chromatography has been used in different ways. Affinity supports were first prepared using protein A or protein G, whose affinity constants take different values according to the IgG subclasses (IgG1, 2, 3, or 4). Among interesting carbohydrates, sialic acid is known to specifically interact with IgGs. Indeed, immunoglobulins are able to react to the presence of tumoral cells. The antigens that are suspected to promote this reaction are gangliosids. Beyond a ceramide molecule, some oses are present in gangliosids, among which are included between one and three sialic acids.

The hypothesis has been made that sialic acid may lead to the formation of specific interactions with immunoglobulins G. Some workers have, thus, developed affinity supports bearing sialic acid in order to purify IgGs. Sialic acid can be extracted from swallow nests and coupled on activated coated silica. This support has been found to possess a good specificity for IgGs, in particular for the subclass IgG3.[1]

Supports prepared with sialic acid have also been used in the purification of insulin, as this sugar and *N*-acetylglucosamine have been found to take part in the interaction between insulin and its glycosylated receptor. The affinity between insulin and sialic acid-bearing supports has been found to be rather strong ($K_a \sim 10^9/M$) and the system allows the separation of beef and pig insulins,[2] which differ by only two amino acids.

N-Acetylglucosamine

N-Acetylglucosamine also shows a specific interaction with insulin. Affinity chromatography experiments have evidenced results very close to those observed in the case of sialic acid. An interesting result is that the improvement of both affinity and capacity of supports bearing both sugars.[3] These supports are supposed to more accurately mimic the structure of insulin receptor.

Mannose and Derivatives

Mannose has been immobilized in order to separate mannose-binding proteins such as mannose-binding lectin. When grafted onto agarose, it constitutes a purification step of a specific lectin that does not bind to DEAE–cellulose or Affi-gel Blue gel.[4] Another way to obtain mannose-binding lectin is to perform expanded-bed

affinity chromatography by immobilizing mannose on a DEAE Streamline support.[5] Affinity agarose supports, grafted with pentamannosyl phosphate, allowed the testing of the functionality (in terms of ligand binding) of truncated and glycosylation-deficient forms of the mannose 6-phosphate receptor from insect cells.[6] Phosphomannan affinity chromatography has been used to purify a human insulinlike growth factor II mannose 6-phosphate receptor.[7]

GLYCOSAMINOGLYCANS AND POLYSACCHARIDES

One of the most used glycosaminoglycans is heparin because of its anticoagulant properties. Other glycosaminoglycans or polysaccharides have also shown such properties; among them, sulfated dextran derivatives and naturally sulfated polysaccharides extracted from algae (fucans) will be discussed further.

Heparin

Anticoagulant properties are due to the formation of a complex between heparin and antithrombin (ATIII); heparin increases ATIII activity, inhibiting thrombin, which is responsible for the formation of the clot.[8] Although this complex is already characterized by a weak affinity, the exact mechanism of association between heparin and antithrombin is not exactly known. A multistep protocol of immobilization of heparin on silica beads permitted high-performance chromatographic phases to be obtained. Thus, it has been possible to evidence a slightly stronger affinity of heparin for antithrombin than for thrombin.

ATIII has been also used as a model protein to test a novel affinity chromatographic system: capillary affinity chromatography.[9] Separation quality has been found equivalent to that observed with classical affinity chromatography, whereas the necessary protein amount is strongly reduced to the nanogram level.

Heparin possesses an affinity for many molecules, among which is a phospholipid-binding protein, annexin V. Affinity chromatography evidenced the Ca^{2+} dependence of the binding mechanism;[10] von Willebrand factors with high and low molecular weights have been separated using their different affinities toward heparin.[11]

Heparin has been used in enzyme purification such as recombinant human mast cell tryptase. The purified enzyme is fully active.[12] Heparin-based affinity chromatography also permitted the isolation of growth factors such as basic fibroblast growth factor (bFGF). The affinity is lower when bFGF is complexed with acidic gelatin.[13] The elution of synthetic TFPI (tissue factor pathway inhibitor) peptidic fragments on immobilized heparin has allowed one to find the peptidic sequence responsible for the TFPI-heparin interaction.[14]

Heparin is able to inhibit smooth-muscle cell (SMC) proliferation in vitro. SMCs are present in blood vessel walls and may proliferate in the case of an internal injury. The antiproliferative action of heparin is due to its internalization in SMCs, which is probably mediated by membrane receptors. Heparin-based affinity chromatography of SMC membrane extracts allowed the separation of a few proteins, which could be implicated in the growth inhibition.[15]

The different actions taking place in the overall affinity mechanism of immobilized heparin for different biological compounds are not yet elucidated, but the influence of ionic strength demonstrates the important contribution of ionic interactions in this mechanism. However, the large spectrum of biological activities of heparin is also a limit for its specificity.

Other Glycosaminoglycans

Dermatan sulfate is known to specifically catalyze thrombin inhibition by the plasmatic inhibitor heparin cofactor II (HCII). Dermatan sulfate has been immobilized on a dextran- or agarose-coated silica matrix. These systems were tested as high-performance chromatographic supports for the purification of HCII from human plasma. The eluted HCII was obtained with no contamination of ATIII, the other main thrombin inhibitor.[16]

DEXTRAN DERIVATIVES

Phosphorylated dextran derivatives, called phosphodextrans, possess a strong affinity for K-vitamin-dependent coagulation factors, like factor II or prothrombin. This property was used to separate them by affinity chromatography on phosphodextrans, which interact in a similar way as phospholipids from the cell membrane.[17]

Heparinlike sulfated dextran derivatives, like carboxymethyldextran benzylamide sulfonates (CMDBS), have been immobilized on silica beads. By high-performance liquid affinity chromatography (HPLAC), they allow a good recovery of thrombin, with a yield of 80%. The affinity constant was estimated ($K_a \sim 10^5/M$) and was found superior to the value obtained between thrombin and heparin. On the contrary, the affinity of dextran derivatives for ATIII is estimated at a lower value than that of heparin.[17]

FUCANS

Fucan is a sulfated polysaccharide, naturally present in algae such as *Fucus vesiculosus* or *Ascophyllum nodosum*. Fucan is a general name for a mixture of three polysaccharides; among them, fucoidan (or homofucan) can be theoretically considered as an homopolymer of α-1,2

L-fucose-4-sulfate and has been studied as a ligand in the same way as fucan itself. Their interaction with two proteins implicated in the coagulation process (thrombin and antithrombin) has been studied and is at least partially ionic. However, the dissociation of the complex fucan–antithrombin seems to include a slower step which could be attributed to a conformation change of the fucan.[18]

Fucan was also used as ligand for HPLAC. In the same way as dextran derivatives, a good separation was obtained for thrombin, with a yield of 80%. The affinity constant was estimated in the same order as that obtained for CMDBS ($K_a \sim 10^5/M$) and superior to the value obtained for heparin.[17]

CONCLUSIONS

In this entry, we have described several uses of carbohydrate compounds as affinity ligands. These few examples clearly demonstrate the importance of such affinity supports in the separation of biological products. Affinity chromatography is also able to help in the determination of the interaction mechanisms of carbohydrate derivatives in biological reactions. This developing field of research will lead to improved quality and specificity of affinity-chromatographic phases.

REFERENCES

1. Serres, A.; Legendre, E.; Jozefonvicz, J.; Muller, D. Affinity of mouse immunoglobulin G subclasses for sialic acid derivatives immobilized on dextran-coated supports. J. Chromatogr. B, **1996**, *681*, 219.
2. Lakhiari, H.; Jozefonvicz, J.; Muller, D. Separation and purification of insulins on coated silica support functionalized with sialic acid by affinity chromatography. J. Liq. Chromatogr. Relat. Technol. **1996**, *19*, 2423.
3. Lakhiari, H. Supports de silice enrobée à ligands biospécifiques: Synthèse, caractérisation et relations structure-propriétés de séparation. Application à la purification de l'insuline et des immunoglobulines G. In *Thesis*; University Paris, 1996; 13.
4. Ooi, L.S.M.; Ang, H.X.W.; Ng, T.B.; Ooi, V.E.C. Isolation and characterization of a mannose-binding lectin from leaves of the chinese daffodil Narcissus tazetta. Biochem. Cell Biol. **1998**, *76*, 601.
5. Bertrand, O.; Cochet, S.; Cartron, J.P. Expanded bed chromatography for one-step purification of mannose binding lectin from tulip bulbs using mannose immobilized on DEAE Streamline. J. Chromatogr. A, **1998**, *822*, 19.
6. Marron-Terada, P.G.; Bollinger, K.E.; Dahms, N.M. Characterization of truncated and glycosylation deficient forms of the cation-dependent mannose 6-phosphate receptor expressed in baculovirus-infected insect cells. Biochemistry **1998**, *37*, 17, 223.
7. Costello, M.; Baxter, R.C.; Scott, C.D. Regulation of soluble insulin-like growth factor II mannose 6-phosphate receptor in human serum: Measurement by enzyme-linked immunosorbent assay. J. Clin. Endocrinol. Metab. **1999**, *84*, 611.
8. Björk, I.; Olson, S.T.; Shore, J.D. Molecular mechanisms of the accelerating effect of heparin on the reactions between antithrombin and clotting proteinases. In *Heparin, Chemical and Biological Properties, Clinical Applications*; Lane, D.A., Lindahl, U., Eds.; Edward Arnold: London, 1989; 229–255.
9. Wu, X.J.; Linhardt, R.J. Capillary affinity chromatography and affinity capillary electrophoresis of heparin binding proteins. Electrophoresis **1998**, *19*, 2650.
10. Capila, I.; Van der Noot, V.A.; Mealy, T.R.; Seaton, B.A.; et al. Interaction of heparin with annexin V. FEBS Lett. **1999**, *446*, 327.
11. Fischer, B.E.; Thomas, K.B.; Schlokat, U.; Dorner, F. Selectivity of von Willebrand factor triplet bands towards heparin binding supports structural model. Eur. J. Haematol. **1999**, *62*, 169.
12. Niles, A.L.; Maffit, M.; Haak-Frendscho, M.; Wheeless, C.J.; et al. Recombinant mast cell tryptase: Stable expression in Pichia pastoris and purification of fully active enzyme. Biotechnol. Appl. Biochem. **1998**, *28*, 125.
13. Muniruzzaman, M.; Tabata, Y.; Ikada, Y. Complexation of basic fibroblast growth factor with gelatin. J. Biomater. Sci. Polym. Ed. **1998**, *9*, 459.
14. Ye, Z.Y.; Takano, R.; Hayashi, K.; Ta, T.V.; et al. Structural requirements of human tissue factor pathway inhibitor (TFPI) and heparin for TFPI-heparin interaction. Throm. Res. **1998**, *89*, 263.
15. Clairbois, A.S.; Letourneur, D.; Muller, D.; Jozefonvicz, J. High-performance affinity chromatography for the purification of heparin-binding proteins from detergent-solubilized smooth muscle cell membranes. J. Chromatogr. B, **1998**, *706*, 55.
16. Sinninger, V.; Tapon-Bretaudière, J.; Zhou, F.L.; Bros, A.; et al. Immobilization of dermatan sulphate on a silica matrix and its possible use as an affinity chromatography support for heparin cofactor II purification. J. Chromatogr. **1991**, *539*, 289.
17. Zhou, F.L. Supports à base de silice enrobée par des polysaccharides pour chromatographie d'affinité haute performance: Préparation, caractérisation et application dans la purification de protéines. In *Thesis*; University Paris, 1990; 13.
18. Legendre, E. Etude par chromatographie d'affinité liquide haute performance des interactions entre des protéines de la coagulation et des polysaccharides sulfatés à activité anticoagulante immobilisés sur des supports de silice enrobée. In *Thesis*; University Paris, 1996; 13.

Carbohydrates: CE Analysis

Oliver Schmitz
Division of Molecular Toxicology, German Cancer Research Center, Heidelberg, Germany

INTRODUCTION

Carbohydrates play an important role in many research and industrial domains. The huge number of stereoisomers, the immense combination possibilities of carbohydrate monomers in oligosaccharides, and the lack of chromophores are the major problems in the analysis of carbohydrates. Capillary electrophoresis (CE), in its various modes of operation, has been developed as a very useful tool in the analysis of carbohydrate species such as monosaccharides and oligosaccharides, glycoproteins, and glycopeptides.

DISCUSSION

Some simple sugar mixtures, such as monosaccharides and oligosaccharides, consisting of not more than about 15 monomer units, can be separated in free solution due to their mass-to-charge ratio (*m/z*). For an increase in selectivity or for analyzing neutral carbohydrates, MEKC can be used for analysis. In this case, charged amphiphilic molecules containing both hydrophilic and hydrophobic regions (e.g., sodium dodecyl sulfate) are used as buffer surfactants.

Higher oligosaccharides or polysaccharides possess unfavorable mass-to-charge ratios, preventing their effective resolution in open tubes. The separation of these carbohydrates is possible with capillary gel electrophoresis (CGE). The analytes are selectively retarded by a sieving network (gel or polymer matrix) due to differences in their sizes and structural conformations.

Complex carbohydrates (in particular, glycoproteins) play an important role in various biological processes and in biotechnological production of glycoproteinaceous pharmaceuticals. To elucidate the relationship between bioactivity and structures of complex carbohydrates, it is necessary to determine the sites of attachment of the oligosaccharide chains to the polypeptide backbone and to characterize the oligosaccharide class (N- or O-linked, high mannose, hybrid, etc.).

For this reason, glycoproteins must first be isolated from the biological matrix by dialysis, preparative chromatography, isoelectric focusing, and so forth or by a combination of several methods. For a structural determination, degradation steps such as a site-specific proteolysis (e.g., with trypsin), removal of oligosaccharides from the polypeptide (by an enzymatic hydrolysis or hydrazine treatment), or chemical hydrolysis, yielding a monosaccharide mixture may be applied. Then, the CE can function as a powerful end method in analytical and structural glycobiology. Due to the complexity of the carbohydrate-dependent microheterogeneity of glycoproteins, several electrophoretic techniques are usually needed, in concert, to characterize the various glycoforms of a given glycoprotein.

For detection of carbohydrates in principle, ultraviolet (UV), laser-induced fluorescence, refractive index, electrochemical, amperometric, and mass spectrometric detection can be used. Mass spectrometry (MS), with its various ionization methods, has traditionally been one of the key techniques for the structural determination of proteins and carbohydrates. Fast-atom bombardment (FAB) and electrospray ionization (ESI) are the two online ionization methods used for carbohydrate analysis. The ESI principle has truly revolutionized the modern MS of biological molecules, due to its high sensitivity and ability to record large molecule entities within a relatively small-mass scale.

The refractive index detection (RID), often used in high-performance liquid chromatography (HPLC), is an interesting detection method in CE with a laser light source and a limit of detection (LOD) in the micromolar range. Electrochemical detection (ECD) and pulsed amperometric detection (PAD) of sugars are common and effective methods used in HPLC. Some recent communications show that the sensitivity of these detection methods in CE have an approximately 1000-fold better LOD than RID. Unfortunately, these detectors (RID, ECD, and PAD) are not commercially available for CE at the moment.

Indirect detection methods are a viable alternative for compounds lacking a chromophoric or a fluorophoric group. An electrolyte containing a chromophore or fluorophore allows the indirect detection of carbohydrates. This method is based on the displacement of the background electrolyte (BGE) by carbohydrates, which are dissociated in strongly alkaline electrolytes. The LOD with indirect LIF detection is in the nanometer range, but the lack of any specificity is a great disadvantage of this detection method, because all sample compounds displace the BGE and the peak identification is only possible by the migration time.

Direct UV detection is the most versatile detection method in CE and is implemented in every commercial CE system. Unfortunately, its use for carbohydrates detection is restricted because of their lack of conjugated p-electron systems and, consequently, the relatively low

extinction coefficients. Despite this fact, it is possible to detect carbohydrates with UV detection without any derivatization at 200 nm. Sensitivity and selectivity can be increased by the use of an alkaline borate buffer as the electrolyte by in situ complexation with the tetrahydroxyborate ion rather than the boric acid (Fig. 1A). The LOD is between micromolar and nanomolar. A further advantage of very high pH values (>10) is the negative charge of the carbohydrates, which are repelled by the negatively charged surface. Consequently, the surface problems in high-performance CE are much lower in carbohydrate analysis than in the analysis of proteins. Therefore, simple carbohydrates are often analyzed in uncoated fused-silica capillaries. Unlike the analysis of simple carbohydrates, for glycopeptides and glycoproteins, the use of coated capillaries such as hydroxypropylcellulose, hydroxyethylmethacrylate, polyether, or other commercially available coated fused-silica capillaries is necessary to achieve high resolution and reproducibility.

In complex matrices, the insufficient specificity at 200 nm and the low sensitivity of direct UV detection make the analysis of carbohydrates more difficult. Therefore, derivatization of carbohydrates with a suitable agents is still a preferred approach for the detection of monosaccharides and oligosaccharides. Derivatization agents like 2-aminopyridine, 8-aminonaphthalein-1,3,6-trisulfonate

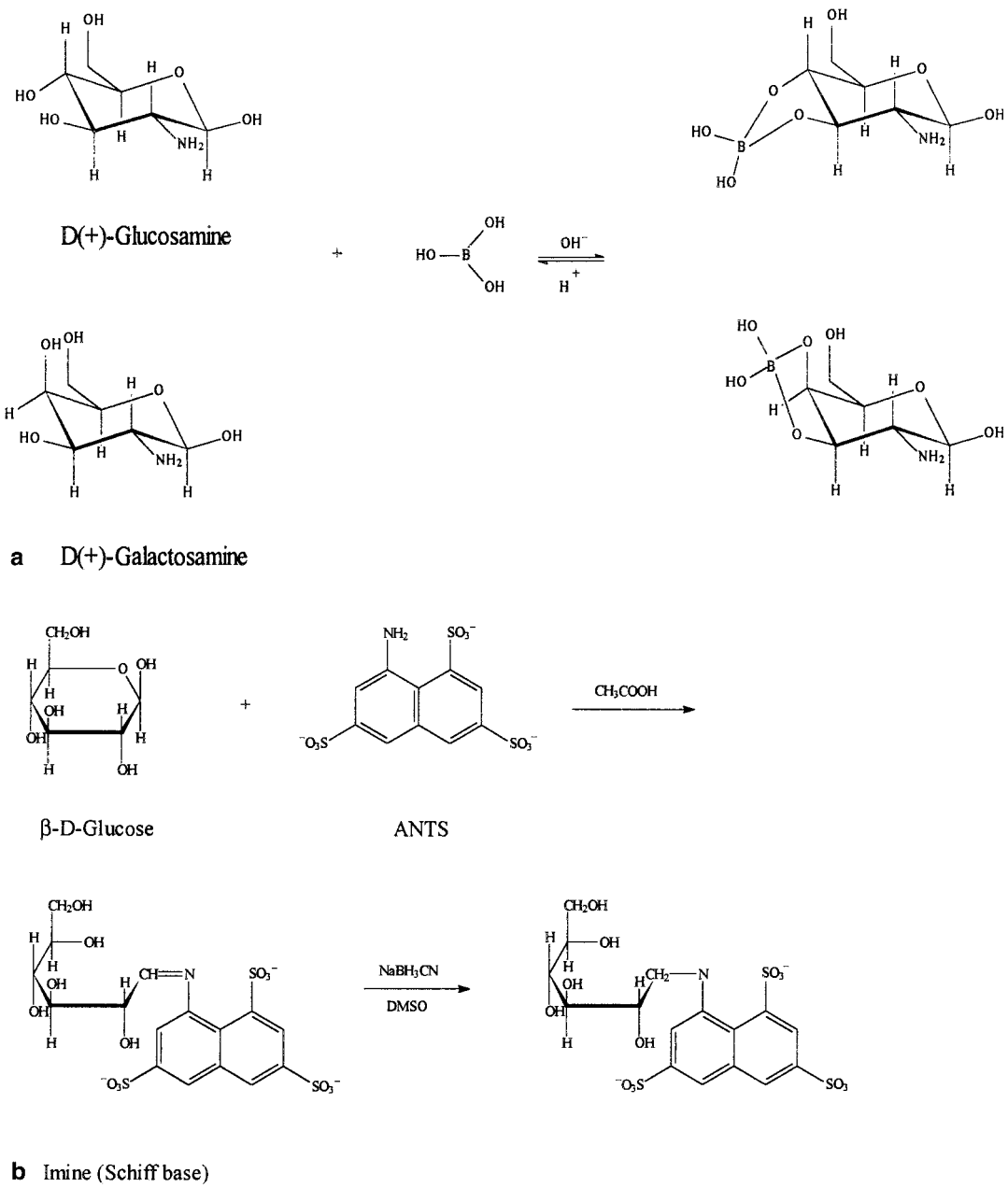

Fig. 1 Derivatization of Carbohydrates.

(ANTS) or 8-aminopyren-1,3,6-trisulfonate (APTS) can be introduced mostly by reductive amination. This reaction is based on imine formation (Schiff base) by the condensation of the aldehyde group in a carbohydrate with the amino group in a primary amine (fluorescent tag), followed by reduction to an N-substituted glycamine with a reductant like sodium cyanoborohydride (see Fig. 1b). Selection of the suitable derivatization reagent is important, because the electrophoretic migration of the carbohydrates and, therefore, the separation power is influenced by the properties of the tags. Fluorescent dyes are better suitable than UV-active derivatization reagents, because CE analysis permits the use of laser-induced-fluorescence (LIF) detection with excellent sensitivity up to the femtomolar-level.

CONCLUSIONS

CE in carbohydrate analysis has advantages in both separation and detection over other techniques of electrophoresis, as well as chromatography. It allows high efficiency (up to a few million plate numbers) and very good sensitivities (up to femtomolar). In addition, CE permits analysis by a variety of separation modes simply by changing the electrolyte (capillary zone electrophoresis, micellar electrokinetic chromatography (MEKC), capillary gel electrophoresis (CGE)).

BIBLIOGRAPHY

1. El assi, Z. Recent developments in capillary electrophoresis of carbohydrate species. Electrophoresis **1997**, *18*, 2400.
2. Grimshow, J. Analysis of glycosaminoglycans and their oligosaccharide fragments by capillary electrophoresis. Electrophoresis **1997**, *18*, 2408.
3. Linhardt, R.J.; Pervin, A. Separation of negatively charged carbohydrates by capillary electrophoresis. J. Chromatogr. **1996**, *720*, 323.
4. Novotny, M.V. Capillary electrophoresis of carbohydrates. In *High-Performance Capillary Electrophoresis*; Khaledi, M.G., Ed.; John Wiley & Sons: New York, 1998; 729–765.
5. Paulus, A.; Klockow, A. Detection of carbohydrates in capillary electrophoresis. J. Chromatogr. A, **1996**, *720*, 353.
6. Suzuki, S.; Honda, S. A tabulated review of capillary electrophoresis of carbohydrates. Electrophoresis **1998**, *19*, 2539.

Carbohydrates: Derivatization for GC Analysis

Raymond P.W. Scott
Scientific Detectors Ltd., Banbury, Oxfordshire, U.K.

INTRODUCTION

As a result of the development of special bonded phases, carbohydrates or their derivatives are usually separated by liquid chromatography (LC). However, certain carbohydrate samples are still analyzed by gas chromatography (GC) due to the inherent high efficiencies obtainable from the technique and to the associated short elution times. In addition, gas chromatography (GC)/ mass spectrometry (MS) is a particularly powerful analytical technique for carbohydrates, especially for their identification. As a consequence, appropriate derivatives must be formed to render them sufficiently volatile but still easily recognizable from their mass spectra.

DISCUSSION

It is relatively easy to form the trimethylsilyl derivatives, employing standard silyl reagents such as trimethylchlorsilane or hexamethyltrisilazane, and the reactions normally can be made to proceed to completion. However, there is a major problem associated with the derivatization of natural sugars which arises from the formation of anomers and the pyranose–furanose interconversion. Reducing sugars in solution (e.g., glucose) exist as an equilibrium mixture of anomers. Consequently, each sugar produces five tautomeric forms—two pyranose, two furanose, and one open-chain form. In general, all the anomers can be separated by GC. This autoconversion can be minimized by mild and rapid derivatization. Equilibrium mixtures are to be expected from reducing sugars isolated from natural products.

Mixtures of hexamethyltrisilazane and trimethylchlorsilane are frequently used to derivatize sugars. Pure sugars (e.g., glucose, mannose, and xylose) can be readily derivatized using a mixture of hexamethyltrisilazane : trimethylchlorsilane : pyridine (2:1:10 v/v/v), giving single GC peaks; however, if the proportion of trimethylchlorsilane is doubled, small amounts of the anomeric forins are observed. One disadvantage of this procedure is the formation of an ammonium chloride precipitate, which, if injected directly onto the column, can cause column contamination and eventually column blockage. The formation of ammonium chloride can be avoided by extracting the derivative into hexane or by the use of an alternative derivatizing agent.

N,*O*-Bistrimethylsilyltrifluoroacetamide, usually combined with trimethylchlorosilane (10:1, v/v) is also a popular derivatizing agent for carbohydrates and the reaction mixture can be injected directly onto the column without fear of column contamination. The formation of anomers can also be avoided by preparing the alditols by treating with sodium borohydride. The alditols can then be separated after derivatizing with trimethylchlorosilane, a procedure that is considered preferable to the preparation of their acetates. The rapid preparation of trimethylsilylalidtols using trimethylsilylimidazole in pyridine mixtures at room temperature has the advantage over other methods, which require longer reaction times and higher temperatures. The use of silylaldolnitrile derivatives has been reported for the separation of aldoses. The sugars are reacted with hydroxylamine-*O*-sulfonic acid to form aldonitriles which are then silanated with *N*,*O*-bistrimethylsilyltrifluoroacetamide : pyridine (1:1 v/v). The silylaldonitrile derivatives are readily separated on open tubular columns.

Another silanization procedure for the derivatization of carbohydrates is the formation of trimethylsilyl oximes. The methyloxime is heated with hexarnethyldisilazane : trifluoroacetic anhydride (9:1 v/v) for 1 hr at 100°C. Anthrone *O*-glucoside is an important ingredient in skin care cosmetics and can be fully silylated by reaction with *N*,*O*-bistrimethylsilylacetamide : acetonitrile mixture (1:1 v/v) for 1 hr at 90°C, and subsequently separated by GC.

CONCLUSIONS

Acetylation and the use of trifluoroacetates, originally the more popular derivatives for the separation of carbohydrates by GC, are still used on occasion, but the various silanization methods are, today, the most common and considered the most effective for GC carbohydrate analysis.

BIBLIOGRAPHY

1. Blau, K., Halket, J., Eds.; *Handbook of Derivatives for Chromatography*; John Wiley and Sons: New York, 1993.
2. Grant, D.W. *Capillary Gas Chromatography*; John Wiley and Sons: New York, 1996.
3. Scott, R.P.W. *Introduction to Analytical Gas Chromatography*; Marcel Dekker, Inc.: New York, 1998.
4. Scott, R.P.W. *Techniques of Chromatography*; Marcel Dekker, Inc.: New York, 1995.

Carbohydrates: HPLC Analysis

Juan G. Alvarez
Department of Obstetrics and Gynecology, Beth Israel Deaconess Medical Center, Boston, Massachusetts, U.S.A.

INTRODUCTION

Carbohydrates are widely distributed molecules in biological systems and pharmaceutical products, not only in free form but also in conjugated form. Because they are present in various forms and there are isomers and analogs, the separation of carbohydrates involves more difficult problems than those of proteins or nucleic acids. Difficulties are also found in detection, especially in biochemical and biomedical analyses due to their low abundance and the fact that photometric and fluorimetric methods cannot be applied directly because of the lack of chromophores and fluorophores.

Analysis of carbohydrates in body fluids by high-performance liquid chromatography (HPLC) using anion-exchange columns was first reported in the 1970s.[1–5] This method has been greatly improved by the use of packing materials of fine, spherical particles and by the development of photometric and fluorimetric postcolumn labeling systems for sensitive detection. Honda et al. established rapid automated methods for microanalysis of aldoses,[6] uronic acids,[7] and sialic acids using a Hitachi 2633 anion-exchange resin and a photometric and fluorimetric postcolumn labeling system with 2-cyanoacetamide. Alditols[8] were fluorescence labeled by the use of sequential periodate oxidation and the Hantzsch reaction. Microanalysis of aminosugars was successful when their borate complexes were separated in the cation-exchange mode and detected by fluorescence generated either by the reaction with 2-cyanoacetamide[9] or by the Hantzsch reaction.[10] All these methods are suitable for routine analysis of clinical samples because of their speed of analysis and high sensitivity.

The United States Food and Drug Administration and the regulatory agencies in other countries require that pharmaceutical products be tested for composition to verify their identity, strength, quality, and purity. Recently, attention has been given to inactive ingredients as well as active ingredients. Some of these ingredients are non-chromophoric and cannot be detected by absorbance. Some non-chromophoric ingredients, such as carbohydrates, glycols, sugar, alcohols, amines, and sulfur-containing compounds, can be oxidized and, therefore, can be detected using amperometric detection. This detection method is specific for those analytes that can be oxidized at the selected potential, leaving all other non-oxidizable compounds transparent.[11] Amperometric detection is a powerful detection technique with a broad linear range and very low detection limits.

This review outlines current chromatographic methods utilized in the analysis of carbohydrates in biological systems and pharmaceutical products.

ANALYSIS OF CARBOHYDRATES BY PARTITION HPLC

Partition HPLC is an important type of chromatography for the analysis of monosaccharides and oligosaccharides. Analysis in this mode has the advantages that it requires a shorter analysis time and gives sharper peaks than anion-exchange chromatography of borate complexes, although it has the drawback of low sensitivity, as detection is usually performed by refractometry. Generally, silica gel whose silanol groups are substituted by alkyl or aminoalkyl groups is used as the stationary phase. HPLC separations using such a stationary phase has been applied successfully to separate oligosaccharides liberated from glycoproteins with hydrazine or borohydride in alkali, permitting quick separation within 60 min.[12–14] Previously, such oligosaccharides were separated and purified by tedious procedures involving gel permeation chromatography on Bio-Gel P-2 or P-4, paper chromatography, and paper electrophoresis. However, modified silica, especially amine-modified silica, has difficulties in durability, being unsuitable for routine analysis.

ANALYSIS OF CARBOHYDRATES BY ANION-EXCHANGE HPLC

The introduction in the 1980s by Honda and Suzuki[15] of the anion-exchange resin resulted in a significant improvement in the separation of carbohydrates by HPLC using the partition mode. Honda and Suzuki, using this mode, established analytical conditions common to aldoses, amino sugars, and sialic acids. Aldoses in the intact state, amino acids as their *N*-acetates, and sialic acids as *N*-acylmannosamines were separated on a column of a proton-formed, sulfonated styrene–divinylbenzene copolymer and detected by measuring absorption at 280 nm after postcolumn labeling with 2-cyanoacetamide.

Postcolumn labeling is a characteristic feature of carbohydrate analysis in which no direct physical methods are available for sensitive detection. Many labeling methods have hitherto been developed. The methods with phenol in

sulfuric acid,[16] orcinol in sulfuric acid,[17] anthrone in sulfuric acid,[18] tetrazolium blue in alkali,[19] copper(II)-2-2′-bicinchonitate,[20] and 2-cyanoacetamide[21] are used for photometric detection. The methods with 2-cyanoacetamide,[6] ethylenediamine,[22] ethanolamine,[23] taurine,[24] and arginine[25] are used for fluorimetric detection. Some labeling methods for electrochemical detection were reported by Honda and Suzuki in 1984.[26,27]

Quantification of Carbohydrates by Anion-Exchange HPLC and Amperometric Detection

Two main columns are used in the analysis of carbohydrates by amperometric detection: the CarboPac™ PA10 and the CarboPac MA1 anion-exchange columns. The CarboPac PA10 column packing consists of a non-porous, highly cross-linked polystyrene–divinylbenzene substrate agglomerated with 460 nm-diameter latex. The MicroBead™ latex is functionalized with quaternary ammonium ions, which create a thin surface-rich anion-exchange site. The packing is specifically designed to have a high selectivity for carbohydrates. The PA10 has an anion-exchange capacity of approximately 100 μEq/column.

The CarboPac MA1 resin is composed of a polystyrene–divinylbenzene polymeric core. The surface is grafted with quaternary ammonium anion-exchange functional groups. Its macroporous structure provides an extremely high anion-exchange capacity of 1450 μEq/column. The CarboPac MA1 column is designed specifically for sugar alcohol and glycol separations. The PA10 but not the MA1 is compatible with eluents containing organic solvents, which can be used to clean these columns.

The equipment used for the analysis of carbohydrates by anion exchange and amperometric detection include a Dionex DX-500 system consisting of a GP40 gradient pump, an ED40 electrochemical detector, a LC30 chromatography oven, and a PeakNet chromatography workstation. A gold electrode is used for both column applications. The flow rate used for the PA10 column is 1.5 ml/min and 0.4 ml/min for the MA1. Injection volumes are typically 10 μl and the oven temperature 30°C. Eluent components include water and 200 m*M* sodium hydroxide for the PA10 column and water and 480 m*M* sodium hydroxide for the MA1 column. Eluent concentration for the PA10 column starts at 91% water/9% 200 m*M* sodium hydroxide for up to 11 min, 100% 200 m*M* sodium hydroxide from 11.1 to 17.6 min, and 91% water/9% 200 m*M* sodium hydroxide from 17.7 to 40.0 min. Eluent concentration for the MA1 column system starts at 52% water/48% 480 m*M* sodium hydroxide and is maintained for up to 60 min.

Table 1 shows the separation of alcohols (2,3-butanediol, ethanol, methanol), glycols (glycerol), alditols (erythritol, arabitol, sorbitol, galactitol, mannitol), and carbohydrates (rhamnose, arabinose, glucose, galactose, lactose, sucrose, raffinose, maltose) using a CarboPac MA1 column set with 480 m*M* sodium hydroxide eluent flowing at 0.4 ml/min. The alcohols, sugar alcohols (alditols), glycols, and carbohydrates are well resolved. Maltose elutes at about 60 min.

Table 1 Separation of carbohydrates, alditols, alcohols, and glycols using a CarboPac MA1 column and pulsed amperometry.

Analyte	Retention time (min)
2,3-Butanediol	7.4
Ethanol	7.6
Methanol	7.8
Glycerol	9.0
Erythritol	10.1
Rhamnose	13.4
Arabitol	14.2
Sorbitol	16.3
Galactitol	18.0
Mannitol	19.5
Arabinose	21.8
Glucose	23.3
Galactose	27.4
Lactose	29.7
Ribose	32.0
Sucrose	46.5
Raffinose	52.9
Maltose	61.2

REFERENCES

1. Jolley, R.L.; Scott, C.D. Preliminary results from high-resolution analyses of ultraviolet- absorbing and carbohydrate constituents in several pathologic body fluids. Clin. Chem. **1970**, *16*, 687.
2. Butts, W.C.; Jolley, R.L. Gas-chromatographic identification of urinary carbohydrates isolated by anion-exchange chromatography. Clin. Chem. **1970**, *16*, 722.
3. Katz, S.; Dinsmore, S.R.; Pitt, W.W., Jr. A small, automated high-resolution analyzer for detemination of carbohydrates in body fluids. Clin. Chem. **1971**, *17*, 731.
4. Scott, C.D.; Chilcote, D.D.; Katz, S.; Pitt, W.W., Jr. Advances in the application of high resolution liquid chromatography to the separation of complex biological mixtures. J. Chromatogr. Sci. **1973**, *11*, 96.
5. Young, D.S.; Epley, J.A.; Goldman, P. Influence of a chemically defined diet on the composition of serum and urine. Clin. Chem. **1971**, *17*, 765.
6. Honda, S.; Takahashi, M.; Kakehi, K.; Ganno, S. Rapid, automated analysis of monosaccharides by high-performance anion-exchange chromatography of borate complexes with flurimetric detection using 2-cynoacetamide. Anal. Biochem. **1981**, *112*, 130.
7. Honda, S.; Suzuki, S.; Takahashi, M.; Kakehi, K.; Ganno, S. Automated analysis of uronic acids by high-performance liquid chromatography with photometric and fluorimetric

postcolumn labeling using 2-cyanoacetamide. Anal. Biochem. **1983**, *134*, 34.
8. Honda, S.; Takahashi, M.; Shimada, S.; Kakehi, K.; Ganno, S. Automated analysis of alditols by anion-exchange chromatography with photometric and fluorimetric postcolumn derivatization. Anal. Biochem. **1983**, *128*, 429.
9. Honda, S.; Konishi, T.; Suzuki, S.; Takahashi, M.; Kakehi, K.; Ganno, S. Automated analysis of hexosamines by high-performance liquid chromatography with photometric and fluorimetric postcolumn labeling using 2-cyanoacetamide. Anal. Biochem. **1983**, *134*, 483.
10. Honda, S.; Konishi, T.; Suzuki, S.; Kakehi, K.; Ganno, S. Sensitive monitoring of hexosamines in high-performance liquid chromatography by fluorimetric postcolumn labelling using the 2,4-pentanedione-formaldehyde system. J. Chromatogr. **1983**, *281*, 340.
11. Rocklin, R.D. Detection in ion chromatography. J. Chromatogr. **1991**, *546*, 175.
12. Mellis, S.J.; Baenziger, J.U. Separation of neutral oligosaccharides by high-performance liquid chromatography. Anal. Biochem. **1981**, *114*, 276.
13. Dua, V.K.; Bush, C.A. Identification and fractionation of human milk oligosaccharides by proton-nuclear magnetic resonance spectroscopy and reverse-phase high-performance liquid chromatography. Anal. Biochem. **1983**, *133*, 1.
14. Dua, V.K.; Bush, C.A. Resolution of some glycopeptides of hen ovalbumin by reverse-phase high-pressure liquid chromatography. Anal. Biochem. **1984**, *137*, 33.
15. Honda, S.; Suzuki, S. Common conditions for high-performance liquid chromatographic microdetermination of aldoses, hexosamines, and sialic acids in glycoproteins. Anal. Biochem. **1984**, *142*, 167.
16. Simatupang, M.H. Hochdruckflssigkeitschromatographische Trennungen von Kohlenhydraten mit einem colorimetrischen Nachweisverfahren. J. Chromatogr. **1979**, *180*, 177.
17. Smith, D.F.; Zopf, D.A.; Ginsburg, V. Fractionation of sialyl oligosaccharides of human milk by ion-exchange chromatography. Anal. Biochem. **1978**, *85*, 602.
18. Kramer, K.J.; Speirs, R.D.; Childs, C.N. A method for separation of trehalose from insect hemolymph. Anal. Biochem. **1978**, *86*, 692.
19. Mopper, K.; Degens, E.T. A new chromatographic sugar autoanalyzer with a sensitivity of 10-10 moles. Anal. Biochem. **1972**, *45*, 147.
20. Mopper, K.; Gindler, E.M. A new noncorrosive dye reagent for automatic sugar chromatography. Anal. Biochem. **1973**, *56*, 440.
21. Honda, S.; Matsuda, Y.; Takahashi, M.; Kakehi, K.; Ganno, S. Fluorimetric determination of reducing carbohydrates with 2-cyanoacetamide and application to automated analysis of carbohydrates as borate complexes. Anal. Chem. **1980**, *55*, 1079.
22. Mopper, K.; Dawson, R.; Liebezeit, G.; Hansen, H.P. Borate complex ion exchange chromatography with fluorimetric detection for determination of saccharide ethylenediamine. Anal. Chem. **1980**, *52*, 2018.
23. Kato, T.; Kinoshita, T. Fluorometric detection and determination of carbohydrates by high-performance liquid chromatography using ethanolamine. Anal. Biochem. **1980**, *106*, 238.
24. Kato, T.; Kinoshita, T. Fluorometric analysis of biological materials. I. A fluorophotometric determination of carbohydrates using taurine and borate. Chem. Pharm. Bull. **1978**, *26* (4), 1291.
25. Mikami, H.; Ishida, Y. Post-column fluorometric detection of reducing sugars in high-performance liquid chromatography using arginine. Bunseki Kagaku **1983**, *32*, E207.
26. Rocklin, R.D.; Pohl, C.A. Determination of carbohydrates by anion exchange chromatography with pulsed amperometric detection. J. Liquid Chromatogr. Relat. Technol. **1983**, *6* (9), 1577.
27. Honda, S.; Konishi, T.; Suzuki, S. Electrochemical detection of reducing carbohydrates in high-performance liquid chromatography after post-column derivatization with 2-cyanoacetamide. J. Chromatogr. **1984**, *299*, 245.

Carbonyls: Derivatization for GC Analysis

Igor G. Zenkevich
Chemical Research Institute, St. Petersburg State University, St. Petersburg, Russia

Abstract
The carbonyl group in aldehydes (RCHO) and ketones (RCOR′) is one of the frequently encountered functionalities in the composition of organic compounds. This group has no active hydrogen atoms, excluding the cases of high content of enols for β-dicarbonyl compounds (β-diketones, esters of β-ketocarboxylic acids, etc.); hence the simplest carbonyl compounds are volatile enough to be analyzed with gas chromatography (GC) in their native forms. Nevertheless, if any other polar groups are present in the molecules of analytes, the conversion of all of them into less polar fragments is recommended. The most important type of organic reactions used in derivatization of carbonyl compounds is condensation with different nucleophilic reagents having primary amino groups, i.e., -NH_2 (aryl hydrazines, *O*-alkyl hydroxylamines, etc.).

INTRODUCTION

The carbonyl group in aldehydes (RCHO) and ketones (RCOR′) is one of the frequently encountered functional groups in organic compounds. This group has no active hydrogen atoms, excluding the enol tautomers in β-dicarbonyl compounds (β-diketones, esters of β-ketocarboxylic acids, etc.). In these cases enol tautomers are stabilized by intramolecular hydrogen bond, as it is shown in Fig. 1.

The carbonyl fragment is present in more complex functional groups like carboxyl (–COOH) in organic acids or (–CO–NRR′) in amides. Owing to the different chemical properties, these classes of carbonyl compounds are considered independently.

One of the general objectives of derivatization is to replace active hydrogen atoms in different functional groups by less polar fragments (see *Derivatization of Analytes: General Aspects*, p. 562). However, in accordance with this aim, the derivatization of monofunctional carbonyl compounds is not an obligatory stage of sample preparation before gas chromatography (GC) analysis. Nevertheless, the main reasons for their derivatization are the following:

1. The simple aldehydes and ketones are slightly polar low boiling substances with small retention indices (RIs) both on standard non-polar and on polar stationary phases (Table 1).

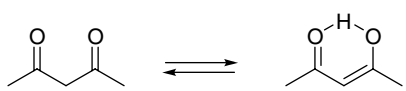

Fig. 1 Appearance of active hydrogen atoms in the molecules of β-diketones in a result of keto-enol tautomerism.

From these data it is easy to conclude that RIs of both aldehydes and ketones exceed these parameters for *n*-alkanes with the same number of carbon atoms only at 176 ± 5 retention index units (i.u.) on standard non-polar phases. This small ΔRI value indicates that these compounds belong to the group of only slightly polar chemicals. At the same time, the average difference of RIs of carbonyl compounds on standard polar polyethylene glycols and non-polar polydimethyl siloxanes is 293 ± 15 (aldehydes) and 282 ± 39 (ketones), which is only slightly more than, for example, the corresponding ΔRI value for alkyl-substituted arenes (246 ± 30) (they are not classified as polar compounds).[1]

However, in the numerous GC analytical procedures, the first part of chromatograms very often can be overloaded by intense poorly resolved peaks of auxiliary compounds (solvents, by-products, etc.). The optimization of the determination of target carbonyl compounds usually needs the "replacement" of their analytical signals into less "populated" areas of chromatograms (the

Table 1 Retention indices of simplest aliphatic aldehydes and ketones on standard non-polar and polar phases.

Compound	$RI_{non\text{-}polar}$	RI_{polar}
Aldehyde		
Ethanal	369 ± 7	701 ± 14
Propanal	479 ± 9	794 ± 9
Ketone		
Acetone	472 ± 12	820 ± 14
2-Butanone	578 ± 12	907 ± 14

Table 2 Comparison of dipole moments of structurally related alkanals, 1-alkanols, and alkanecarboxylic acids.

Compound	μ, D	Compound	μ, D
Ethanal	2.7	Propanal	2.6
Ethanol	1.7	1-Propanol	1.7
Acetic acid	1.7	Propionic acid	1.7

derivatives with retention parameters that exceed those for initial analytes).

At the same time it is interesting to note one paradox connected with the term "polarity." If we consider such characteristics of polarity as dipole moment (D), commonly accepted in chemistry, we should conclude that simplest carbonyl compounds (RCHO) are more polar as corresponding aliphatic alcohols (RCH_2OH) and, moreover, carboxylic acids (RCO_2H) (Table 2). Hence, it is not the dipole moment, but just the presence of active hydrogen atoms in the molecules of alcohols and carboxylic acids that is responsible for the chromatographic polarity of analytes and in that sense polarity in organic chemistry and chromatography are not equivalent to each other.

However, instead of interpretation of a term as ambiguous as polarity, it is better to bear in mind the structural features of molecules of analytes (presence or absence of functional groups with active hydrogen atoms).

2. The simplest monofunctional compounds with active hydrogens in the functional groups OH, NH_2, and so forth are typically volatile enough for their direct GC determination. However, the presence of any additional polar fragments (including C═O) in the molecules makes GC analysis of these compounds difficult, and they usually need derivatization of one or (better) both polar functional groups. Thus, in many cases, the necessity of derivatization of the carbonyl fragment in polyfunctional compounds is a secondary procedure that is required because of the presence of other functional groups.

   More importantly, some silylating reagents used for protection of functional groups with active hydrogen atoms can react with carbonyl fragments with the formation of trimethylsilyl (TMS) derivatives of enols. If such unpredictable mode of derivatization is undesirable, all carbonyl fragments should be protected before silylation, for example, by conversion into alkoxyimino groups (alkyl ethers of oximes, see below).
3. Both aliphatic and aromatic aldehydes are compounds that are easily oxidized even by atmospheric oxygen dissolved in the liquid samples. Hence, one of the aims of their derivatization is to prevent the oxidation of analytes.

METHODS OF DERIVATIZATION OF CARBONYL COMPOUNDS

Some methods for derivatizing carbonyl compounds have been known in "classical" organic chemistry since the 19th century. Their predestination was the identification of such compounds by simple comparison of melting points of purified solid derivatives with reference data. These derivatives are, for example, semicarbazones $RR'C{=}NNHCONH_2$, thiosemicarbazones $RR'C{=}NNHCSNH_2$, 2,4-dinitrophenyl hydrazones $RR'C{=}NNHC_6H_3(NO_2)_2$, and so forth. However, most of these derivatives are not volatile for their direct GC analysis owing to the presence of active hydrogen atoms. The convenient derivatives for GC determination should include not more than one of these atoms (as in monosubstituted aryl hydrazones) or they need to be free of them (*O*-alkyl or *O*-benzyl ethers of oximes).[2–6] The oximes themselves can be synthesized by the reaction of carbonyl compounds with hydroxylamine, but they are usually used in GC practice in the form of *O*-TMS ethers.

$$RR'CO + H_2NNHAr \rightarrow RR'C = NNHAr$$
$$RR'CO + H_2N - OR'' \rightarrow RR'C = N - OR''$$
$$RR'CO + H_2NOH \rightarrow RR'C = NOH \rightarrow RR'C = N - OSi(CH_3)_3$$

Formation of 2,4-dinitrophenylhydrazones of carbonyl compounds is a "popular" method for their derivatization. However, owing to low volatility of these derivatives, their reversed-phase high-performance liquid chromatography (HPLC) analysis seems more preferable than GC analysis.[7]

Other types of carbonyl derivatives are acetals or ketals, including their thio- and aza-analogues, preferably cyclic 1,3-dioxolanes, 1,3-oxothiolanes, or thiazolidines. The last method of derivatization with 2-aminoethanethiol has been proposed for sampling and GC determination of volatile aliphatic aldehydes (see Fig. 2).[8]

All the above-mentioned processes are classified as reactions of condensation. Hence, in all cases, the target derivatives are theoretically the sole components of reaction mixtures and no other detectable by-products excluding water (which has no influence on the results of GC analysis) are formed. However, some features of these reactions should be mentioned:

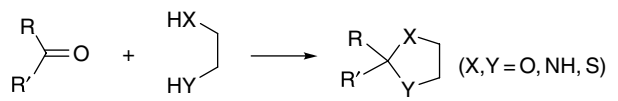

Fig. 2 Derivatization of carbonyl compounds with formation of heterocyclic products.

Table 3 Statistically processed differences of GC retention indices (ΔRIs) between products of some derivatization reactions and initial carbonyl compounds on standard non-polar phases.

Scheme of reaction	ΔMW	ΔRI
$RR'CO \rightarrow RR'C{=}NNHCH_3$	28	229 ± 23
$ArRCO \rightarrow ArRC{=}NNHCH_3$	28	320 ± 30
$RR'CO \rightarrow RR'C{=}NN(CH_3)_2$	42	302 ± 20
$RR'CO \rightarrow RR'C{=}NNHC_2H_5$	42	345 ± 16
$RR'CO \rightarrow RR'C{=}NNHC_6H_5$	90	858 ± 22
$ROH \rightarrow ROSi(CH_3)_3$ (for comparison)	72	119 ± 18

1. Some reagents, especially aryl hydrazines in the form of free bases, are slightly oxidized compounds. Their salts with inorganic acids are more stable, but even in this case, the presence of any oxidizers in the reaction mixtures must be prevented. Nevertheless, in practice, these mixtures very often contain some oxidation by-products (e.g., $ArNH_2$, ArOH, ArH). Usually, it is not difficult to obtain their chromatographic peaks, because all of them have lower retention parameters than that for initial reagents and, moreover, all target derivatives.
2. The condensation reaction of considered type can be characterized by statistically processed differences of RIs of products and initial substrates.[9] This additive scheme mode permits us to estimate these analytical parameters for any new derivatives of monocarbonyl compounds of standard non-polar polydimethyl siloxanes. For the simplest reaction scheme A + L → B + M, we have the following ΔRI = RI(B) – RI(A) values [ΔMW = MW(B) – MW(A)] (Table 3):

   This set of ΔRI values illustrates that the simplest alkyl hydrazones (methyl, ethyl, dimethyl, etc.) have appropriate GC retention parameters and theoretically can be recommended as the derivatives of carbonyl compounds. But in real analytical practice, these hydrazones are not used because of their low yields for aliphatic ketones.
3. All considered condensation reactions have some anomalies for the α,β-unsaturated carbonyl compounds. Most reagents with active hydrogen atoms can react not only with carbonyl groups, but also with polarized conjugated C=C double bond (absence of regioselectivity). As a result of this feature, three products instead of the estimated one target derivative (pair of *syn*- and *anti*-isomers) can be formed in the reactions of α,β-unsaturated carbonyl compounds with *O*-alkyl hydroxylamines, like it is illustrated by scheme presented in Fig. 3.[10]

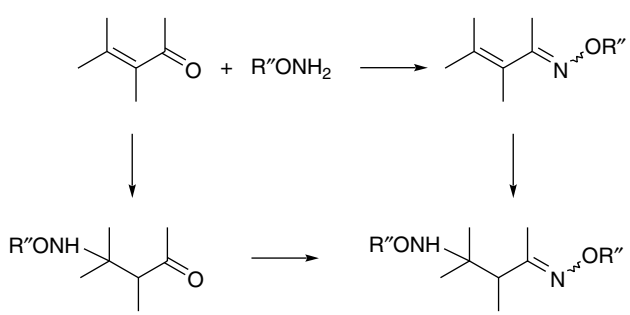

Fig. 3 Anomalous interaction of α,β-unsaturated carbonyl compounds with *O*-alkyl hydroxylamines.

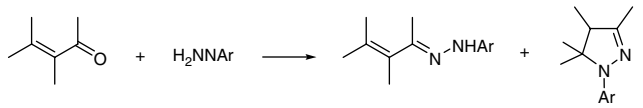

Fig. 4 Formation of two alternative products in the reaction of α,β-unsaturated carbonyl compounds with aryl hydrazines.

The relative ratio of these products depends on the excess of derivatization reagent and pH of reaction mixtures. The chemical origin of products of the reaction of aryl hydrazines with unsaturated carbonyl compounds depends on the same factors and, moreover, on the order of component mixing (it exerts influence on the current pH of reaction media). Thus, 2-pyrazolines have resulted in some cases as the predominant products instead of hydrazones (see scheme in Fig. 4).

The formation of different products means that the quantitative yields of each of them are not enough, as is necessary for GC analysis of derivatives. It is quite probable that the same anomalies can take place in the reactions of unsaturated carbonyls with other reagents. This fact is reflected by the small number of published RI data for the derivatives of these compounds and it explains the necessity to search for new types of derivatization reactions for them.

Both *O*-ethers of oximes and some disubstituted hydrazones of asymmetrical carbonyl compounds exist in two isomeric structures with slightly different GC retention parameters (Fig. 5).

Hence, most of these derivatives give two analytical signals on the chromatograms. *Anti*-isomers typically

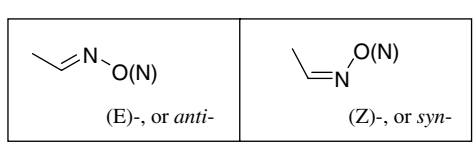

Fig. 5 *Syn-anti* isomerism of *O*-alkyl ethers of oximes (hydrazones).

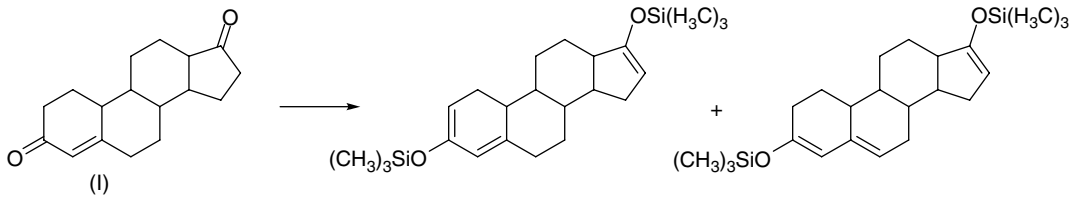

Fig. 6 Formation of two silylation products from androst-5-en-3,17-dione.

are more stable and their peaks prevail over those of the *syn*-forms. If the assignment of these two peaks to the isomeric compounds is not obvious, in accordance with the usual chromatographic practice they can be marked by symbols #1 and #2 (in order of chromatographic elution). The same duplication of analytical signals takes place, for example, during RP HPLC analysis of 2,4-dinitriphenylhydrazones (2,4-DNPHs).

The condensation reaction of carbonyl compounds with halogen-containing derivatization chemicals (so-called electroforic reagents like pentafluorophenyl hydrazine, 2,4,6-trichlorophenyl hydrazines)[11] and, especially, pentafluorobenzyl hydroxylamine (PFBHA)[12–14] that has been considered can provide the possibility of their selective GC determination with electron capture detectors. For GC analysis of monosaccharides (an important group of hydroxy carbonyl compounds), many combinations of derivatization reagents have been proposed, but most of them are based on the conversion of carbonyl group into hydroxyimino (>C=NOH) with following silylation, and alkoxy (methoxy)imino (>C=NOR).[15]

For polyfunctional organic compounds, the condensation reactions of carbonyls considered should be combined with different derivatization of other functional groups. The "standard" method for the derivatization of hydroxysteroids for GC analysis is their two-stage treatment by *O*-methyl hydroxylamine, followed by silylation of OH groups. The resulting trimethylsilylated methyl oxime derivatives (MO-TMS) of compounds of this class are well characterized by standard mass spectra and GC RIs on standard non-polar phases for their identification. The use of most active silylating agents permits us to exclude the stage of *O*-methyl oxime formation, as long as ketosteroids can form the enol-TMS ethers. For example, androst-5-en-3,17-dione (I, no hydroxyl groups present in the molecule) after silylation by MSTFA/AcOK or ethyl (trimethylsilyl)acetate [$(CH_3)_3SiCH_2CO_2C_2H_5$] forms the *bis*-*O*-TMS derivative of *bis*-enol.[16] The enolization of the carbonyl group in the third position in similar structures can lead to the formation of a conjugate system of C=C double bonds in enol not only in positions 2,4, but also in positions 3,5 (see Fig. 6). These isomeric TMS-enol derivatives have different retention parameters[17] that should be kept in mind during interpretation of the results (duplication of analytical signals for the single precursor). Because of the presence of p-π-(d) conjugated systems C=C–O–(Si), these enol-TMS derivatives indicate intense signals of the molecular ions in their mass spectra.

To minimize the risk of accessory reactions during silylation of α,β-unsaturated carbonyl compounds and, hence, the uncertainty in the structures of derivatives, some original recommendations have been proposed. One of them implies the use of mixed reagent MSTFA + I_2, that provides silylation of carbonyl enols accomplished by entering of *N*-containing fragment from TMS-carrier in the α-position of carbonyl compound in the result of nucleophilic substitution (it is recommended just for steroidal 3-ketones with C=C double bond in the position 4).[18] However, this proposition remains discussible at first in respect of the yield of the derivatization and regioselectivity of the reaction.

Sometimes the products of carbonyl compounds silylation are not TMS-enols, but *bis*-TMS derivatives of hydrated carbonyls, $RR'C=O \leftrightarrows RR'C(OH)_2 \rightarrow RR'C(OTMS)_2$.[19] More unpredictable products can be formed during silylation of α-ketocarboxylic acids. For example, ketomalonic acid (II) besides the normal *bis*-TMS ester gives an unusual TMS derivative of the enol-hydrate form[20] (see Fig. 7).

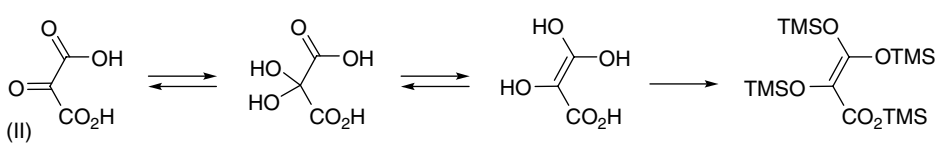

Fig. 7 Example of unusual silylation of ketomalonic acid with formation of tetrakis-TMS derivative instead of normal *bis*-TMS ester.

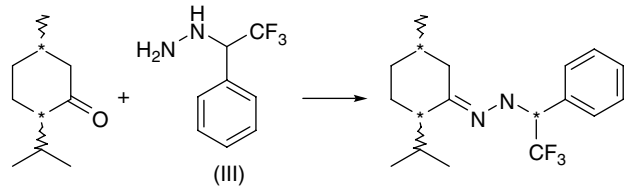

Fig. 8 Example of formation diastereomeric derivatives from chiral carbonyl compound and derivatization reagent.

The formation of volatile acetals or ketals from carbonyl compounds requires acid catalysis and (sometimes) the presence of water-coupling reagents. This reaction accomplishes alkylation of carboxyl groups when ketocarboxylic acids are derivatized by this method.[21,22] The conversion of aliphatic aldehydes into dimethyl acetals only slightly increases the retention parameters of analytes ($\Delta RI = 189 \pm 17$). Cyclic ethylene derivatives (1,3-dioxolanes, $\Delta RI = 212 \pm 23$ for acyclic carbonyl compounds) are more resistant to hydrolysis and used in GC practice preferably. Their important advantage for gas chromatography–mass spectrometry (GC–MS) analysis is the very specific fragmentation of molecular ions with the loss of substituents R and R′ in the second position of the cycle (see Fig. 3) and the formation of daughter ions $[M\text{-}R]^+$ and $[M\text{-}R']^+$, which gives useful information for the determination of the initial carbonyl compound structure. The use of 2-aminoethanethiol instead of ethylene glycol in this reaction leads to the formation of thiazolidines, which indicate intense signals of molecular ions in mass spectra. It is noteworthy that the latter reagent (solid substance with high melting point) contains two polar functional groups (NH_2 and SH) with active hydrogen atoms in the molecule and its GC analysis without derivatization is impossible.

The GC separation of chiral carbonyl compounds (at first natural terpenoids) on the non-chiral phases can be carried out in accordance with the same principles as those for enantiomers of other classes. Their conversion to diastereomers by reaction with chiral derivatization reagents is necessary. An example is the reaction of stereochemically pure α-trifluoromethylbenzyl hydrazine (III) with isomeric menthones; symbol (*) in the Fig. 8 means the chiral center in the molecule.

Principal physicochemical and gas chromatographic properties of some reagents for derivatization of carbonyl compounds are summarized in Table 4.

Table 4 Physicochemical and gas chromatographic properties of some reagents for derivatization of carbonyl compounds.

Reagent	Abbreviation	MW	T_b, °C (m.p., °C)	$RI_{non\text{-}polar}$
Phenyl hydrazine	—	108	244	1157 ± 11
Pentafluorophenyl hydrazine	PFPH	198	(74–75)	1164 ± 16
2,4,6-Trichlorophenyl hydrazine	TCPH	210	(141–143)	1654[a]
2,4-Dinitrophenyl hydrazine	2,4-DNPH	198	(200.5–202.5)	—
N-Aminopiperidine	—	100	146	859 ± 14
O-Methyl hydroxylamine	—	47	47 (148[b])	—
O-Ethyl hydroxylamine	—	61	68 (130–133[b])	—
O-Pentafluorobenzyl hydroxylamine	PFBHA, Florox	213	227 (subl)	1068 ± 12
Hydroxylamine (with following silylation of oximes)	—	33	(151[b])	ND[c]
Ethylene glycol/(H^+), $CuSO_4$	—	62	108.8	726 ± 28
rac-2,3-Butanediol	—	90	181	824 ± 32
Ethanolamine	—	61	171	698 ± 46
2-Mercaptoethanol	—	78	158	725 ± 9
2-Mercaptoethyl amine (cysteamine)	—	77	(95–97) (67[b])	—
Silylating reagents (for synthesis of TMS-ethers of enols)	See table in *Hydroxy Compounds: Derivatization for GC Analysis*			

[a]Estimated RI values.
[b]Melting point of hydrochloride.
[c]ND: reagent is not detected.

CONCLUSIONS

Monofunctional carbonyl compounds belong to the group of slightly polar organic substances and typically need no derivatization prior to GC analysis. However, the carbonyl functional group is one of the most encountered fragments in the composition of organic compounds. In accordance with general principles of derivatization, all the polar groups present in molecules should be transformed into less polar fragments having no active hydrogen atoms. Following this concept, numerous methods have been proposed for the derivatization at first of polyfunctional carbonyl compounds.

Some special methods for derivatization of simple low boiling aldehydes and ketones are used for the "displacement" of their analytical signals into less "populated" parts of chromatograms. It increases the resulting selectivity for determining target analytes.

REFERENCES

1. Zenkevich, I.G. Chemometrics characterization of the differences of GC retention indices on standard polar and nonpolar phases as the criterion of group identification of organic compounds. Rus. J. Anal. Chem. **2003**, *58* (2), 119–129.
2. Blau, K.; King, G.S., Eds.; *Handbook of Derivatives for Chromatography*; John Wiley & Sons: Chichester. U.K., 1978; 576.
3. Knapp, D.R. *Handbook of Analytical Derivatization Reactions*; John Wiley & Sons: New York, 1979; 741.
4. Drozd, J. *Chemical Derivatization in Gas Chromatography*. In *Journal of Chromatography Library*; Elsevier: Amsterdam, 1981; Vol. 19, 232.
5. Blau, K.; Halket, J.M., Eds.; *Handbook of Derivatives for Chromatography*, 2nd Ed.; John Wiley & Sons: New York, 1993; 369.
6. Levine, S.R.; Harvey, T.M.; Waeghe, T.J.; Shapiro, R.H. *O*-Alkyloxime derivatives for GC–MS and GC determination of aldehydes. Anal. Chem. **1981**, *53* (6), 805–809.
7. Chi, Y.; Feng, Y.; Wen, S.; Lu, H.; Yu, Z.; Zhang, W.; Sheng, G.; Fu, J. Determination of carbonyl compounds in the atmosphere by DNPH derivatization and LC-ESI–MS/MS detection. Talanta **2007**, *72*, 539–545.
8. Yasuhara, A.; Shibamoto, T. Determination of volatile aldehydes in the headspace of heated food oils by derivatization with 2-aminoethanethiol. J. Chromatogr. **1991**, *547*, 291–298.
9. Zenkevich, I.G. Chromatographic characterization of organic reactions by additivity of GC retention parameters of reagents and products. Rus. J. Org. Chem. **1992**, *29* (9), 1827–1840.
10. Zenkevich, I.G., Artsybasheva, Yu, P.; Ioffe, B.V. Application of alkoxyamines for derivatization of carbonyl compounds in gas chromatography–mass spectrometry. Rus. J. Anal. Chem. **1989**, *25* (3), 487–492.
11. Lehmpuhl, D.W.; Birks, J.W. New gas chromatographic electron capture detection method for the determination of atmospheric aldehydes and ketones based on cartridge sampling and derivatization with 2,4,6-trichlorophenyl hydrazine. J. Chromatogr. A, **1996**, *740*, 71–81.
12. Biondi, P.A.; Mauca, F.; Negri, A.; Secchi, C.; Montana, N. Gas chromatographic analysis of neutral monosaccharides as their *O*-pentafluorobenzyloxime derivatives. J. Chromatogr. **1987**, *411*, 275–284.
13. Bao, M.L.; Pantani, F.; Griffini, P.; Burrini, D.; Santianni, D.; Barbieri, K. Determination of carbonyl compounds in water by derivatization–solid phase microextraction and gas chromatographic analysis. J. Chromatogr. A, **1998**, *809*, 75–87.
14. Schmarr, H.-G.; Sang, W.; Ganβ, S.; Fischer, U.; Kopp, B.; Schulz, C.; Potouridis, T. Analysis of aldehydes via SPME with on-fiber derivatization to their *O*-(2,3,4,5,6-pentafluorobenzyl)oxime derivatives and comprehensive 2D-GC–MS. J. Sep. Sci. **2008**, *31*, 1–8.
15. Robards, K.; Whitelaw, M. Chromatography of monosaccharides and disaccharides. J. Chromatogr. **1986**, *373*, 81–110.
16. Gleisch, H. The use of different silylating agents for structure analysis of steroids. J. Chromatogr. **1974**, *91*, 407–412.
17. Iida, T.; Hikosaka, M.; Goto, J.; Nambara, T. Capillary gas chromatographic behavior of *tert*-hydroxylated steroids by trialkylsilylation. J. Chromatogr. A, **2001**, *937*, 97–105.
18. Maume, D.; Le Bizee, B.; Marchand, P.; Montrade, M.-P.; Andre, F. *N*-Methyl-*N*-alkylsilyltrifluoroacetamide – I_2 as a new derivatization reagent for anabolic steroid control. Analyst **1998**, *123*, 2645–2648.
19. Little, J.L. Artifacts in trimethylsilyl derivatization reactions and ways to avoid them. J. Chromatogr. A, **1999**, *844*, 1–22, http://users.chartertn.net/slittle/files/silyl.pdf (accessed September 2008).
20. Lee, B.J.; Yanamandra, K.; Thurmon, T.F. Quantitative estimation of organic analytes with a capillary column. Am. Clin. Lab. **2002**, *5*, 30–34.
21. Li, Y.-C.; Yu, J.Z. Simultaneous determination of mono- and dicarboxylic acids, omega-Oxo-carboxylic acids, midchain ketocarboxylic acids, and aldehydes in atmospheric aerosol samples. Environ. Sci. Technol. **2005**, *39*, 7616–7624.
22. Wang, H.; Kawamura, K.; Ho, K.F.; Lee, S.C. Low molecular weight dicarboxylic acids, ketoacids, and dicarbonyls in the fine particles from a roadway tunnel: Possible secondary production from the precursors. Environ. Sci. Technol. **2006**, *40*, 6255–6260.

Catalysts: Reversed-Flow GC

Dimitrios Gavril
Physical Chemistry Laboratory, Department of Chemistry, University of Patras, Patras, Greece

Abstract
Reversed-flow gas chromatography (RF-GC) has been used to study the kinetics of surface-catalyzed reactions and the nature of the active sites. RF-GC is technically very simple and it is combined with a mathematical analysis that gives the possibility for the estimation of various physicochemical parameters related to catalyst characterization in a simple experiment under conditions compatible with the operation of real catalysts. The experimental findings of RF-GC for the oxidation of CO over well-studied silica-supported platinum–rhodium bimetallic catalysts are in agreement with the results of other workers using different techniques ascertaining that RF-GC methodologies can be used for the characterization of various solids with simplicity and accuracy.

INTRODUCTION

During the last four decades, various chemical reactions concerning processes of technological and environmental interest have been related to the development of catalysts. Catalyst characterization is a necessary step and it usually involves activity tests and investigation of the kinetics of the related reactions as well as of the nature of the active sites.

Diffusion, adsorption, and surface reaction are closely interconnected in heterogeneous catalysis characterization studies. Chromatographic separation is a physicochemical process also based on diffusion, adsorption as well as liquid dissolution. Based on the broadening factors embraced by the van Deemter equation, precise and accurate physicochemical measurements have been made by gas chromatography, using relatively cheap instrumentation and a very simple experimental setup.

Reversed-flow gas chromatography (RF-GC) is another gas chromatographic technique based on the perturbation of the carrier gas flow, which has been utilized for the measurement of physicochemical parameters. The fundamental difference of RF-GC from classic GC is the use of a T-form system of chromatographic columns (sampling and diffusion columns) placed perpendicularly one in the middle of the other. The carrier gas flows continuously through the sampling column, while it is stagnant in the diffusion column. The solid catalyst under study is placed either near the injection point at the closed end of the diffusion column, for experiments under *non-steady-state* conditions, or at the middle of the sampling column, for experiments under *steady-state* conditions, as is shown in Fig. 1. The fact that the solid material is under investigation also classifies RF-GC as an inverse gas chromatographic (IGC) methodology. The reversing of the carrier gas flow for short time intervals results in extra chromatographic peaks on the continuous concentration–time curve. Thus, a repeated sampling of the physicochemical phenomena occurring into the diffusion column is achieved, and by using appropriate mathematical analysis the values of the relevant physicochemical quantities are determined.

EXPERIMENTAL

The experimental setup of RF-GC for the study of catalytic processes has been presented elsewhere,[1–21] and it is very simple. It comprises of a conventional gas chromatograph equipped with the appropriate detector (e.g., flame ionization, thermal conductivity) depending on the reactant(s) and product(s). A separation column L' can also be incorporated in the GC oven. The separation column can be filled with the appropriate material for the separation of the reactants and products and it can be heated at the same or at a temperature different from that of the sampling cell. The "sampling cell" is formed by the sampling column $l' + l$ and the diffusion column L, which is connected perpendicularly to the middle of the sampling column. The ends D_1 and D_2 of the sampling column are connected through a four-port valve, to the carrier gas inlet and the detector, as shown in Fig. 1.

When flow perturbations are performed, negative and positive abrupt fronts appear in the chromatogram, forming the so-called *sampling peaks* like those shown in Fig. 2.[1] The volumetric carrier gas flow rate does not affect the physicochemical phenomena occurring in the diffusion column, but affects only the speed of the sampling procedure.

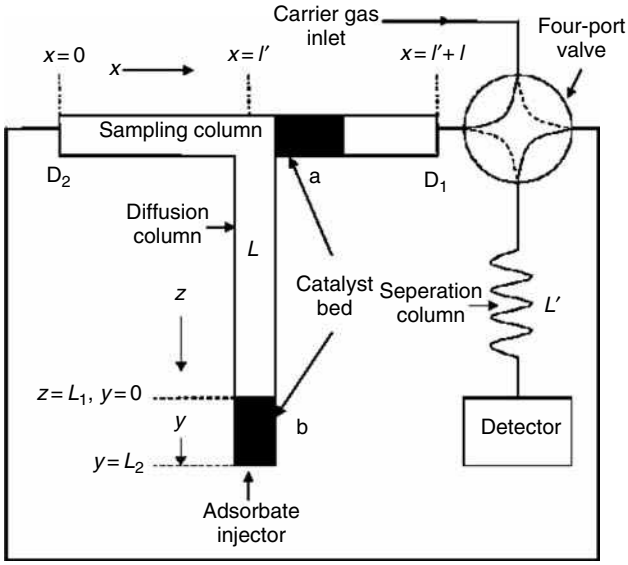

Fig. 1 Experimental setup used from RF-GC for the characterization of solid catalysts: a) Under steady-state conditions, with catalyst bed being put at a short length of sampling column *l*, near the junction of diffusion and sampling columns; b) Under non-steady-state conditions, with catalytic bed being put at the top of diffusion column *L*.

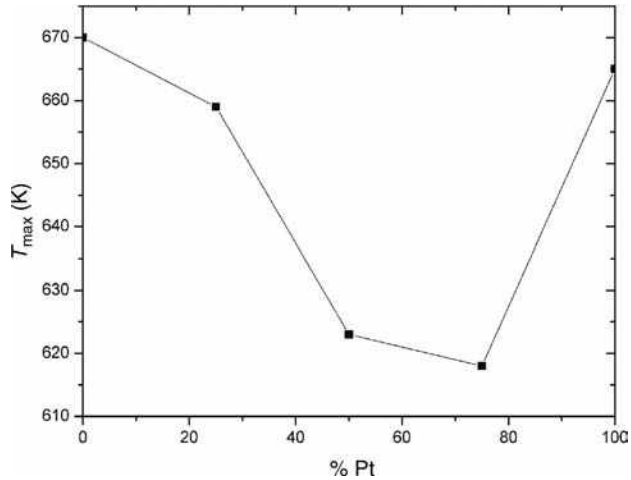

Fig. 2 Characteristic temperatures of maximum activity [T_{max}(K)] for the oxidation of CO, over Pt–Rh alloy catalysts against the catalyst Pt content (% Pt).
Source: From Gas chromatographic kinetic study of carbon monoxide oxidation over platinum–rhodium catalysts, in J. Chromatogr. A.[3]

THEORETICAL

The sampling peaks are predicted theoretically by the "chromatographic sampling equation," describing the concentration–time curve of the sampling peaks created by the flow reversals. The area or the height H, of the sampling peaks is proportional to the concentration of the substance under study at the junction $x = l'$ of the sampling cell at time t from the beginning of the experiment. If ln H is plotted against time t for each solute, the so-called diffusion band, is obtained. An example is shown in Fig. 3.[1]

Under Steady-State Conditions

By placing the catalyst bed at a short length of the sampling column l near the junction of the diffusion and sampling column (cf. Fig. 1), the catalytic behavior under steady-state conditions can be studied. In this case, time-dependent fractional conversions X_t are determined from the heights or the areas of the sampling peaks obtained after each flow reversal, and overall conversions X can be calculated from the total areas of the diffusion bands corresponding to reactants and products.[1]

Under Non-Steady-State Conditions

The catalytic behavior under non-steady-state conditions can be studied by placing the catalyst bed at a short length at the entrance of the diffusion column L (cf. Fig. 1). In this case not only conversions but also a large number of physicochemical parameters related to the interaction of the studied catalyst with the injected adsorbate can be determined. The whole treatment of experimental data is based on the fact that the heights of the "sampling peaks" are described by a clear function of time comprising the sum of 2–4 exponentials.

$$H^{1/M} = \sum_i A_i \exp(B_i t) \tag{1}$$

where H is the height of the experimentally obtained chromatographic peaks, M the response factor of the detector, and t the time from the beginning of the experiment. Eq. 1 is not an a priori assumption, but results from the solution of the mathematical model. The values of the pre-exponential factors A_i and the corresponding coefficients of time B_i are easily and accurately determined from the chromatogram by PC programmes of non-linear least-squares regression (cf. Appendix of Ref. 13).

The experimental pairs H, t are the variables of Eq. 1. By introducing them into the data lines of the GWBASIC program as given in Appendix of Ref. 12, together with other easily obtained quantities required by the input lines (such as the geometric details of the diffusion column, mass and porosity of the catalyst bed, solute amount as well as its diffusion coefficient in the carrier gas, and the carrier gas flow rate), the various physicochemical parameters related to the studied catalyst are calculated.

POTENTIAL OF THE METHODOLOGY AND INDICATIVE RESULTS

RF-GC methodologies have been utilized for the investigation of various catalytic processes and a large amount of physicochemical quantities related to the kinetics of the elementary steps (adsorption, desorption, surface reaction) and the nature of the active sites have been determined. These parameters are summarized as follows:

1. Time-dependent, X_t, and overall, X, conversions, either under steady- or non-steady-state conditions.[1,2,17,21]
2. Adsorption, k_1, desorption, k_{-1}, and surface reaction, k_2, rate constants and the respective activation energies, E_a.[3,4,5,15]
3. Local adsorption energies, ε, local adsorption isotherms, $\theta(p, T,\varepsilon)$, local monolayer capacities, c^*_{max}, and adsorption energy distribution functions, $f(\varepsilon)$, for the adsorption of gases on heterogeneous surfaces circumventing altogether the integral equation:[6,7]

$$\theta(p,T) = \int_0^\infty \theta(\varepsilon,p,T) f(\varepsilon) d\varepsilon \qquad (2)$$

where (p,T) is the overall experimental adsorption isotherm.

4. The energy of the lateral molecular interactions on heterogeneous surfaces in a time-resolved procedure.[8,12,18,19]
5. Surface diffusion coefficients for physically adsorbed or chemisorbed species on heterogeneous surfaces in a time-resolved procedure.[9,20]
6. Standard free energy of adsorption and its probability density function over time, together with the geometrical mean of the London parts of the total surface free energy $(\gamma_1^L\gamma_2^L)^{\frac{1}{2}}$ of the adsorbed probe and the solid surface, accompanied by the relevant probability density functions over time.[10,11]
7. Investigation of the nature of the various groups of active sites of solid catalysts.[12,18,19]
8. Study of the competition between mass transfer and kinetics of solid catalysts.[14]
9. Adsorption entropy, Gibbs free energy, and enthalpy for the adsorption of gases on heterogeneous surfaces.[16]

The question naturally arising is how reliable are the physicochemical quantities determined by means of RF-GC. For this reason, the adsorption of CO, O_2, and CO_2 as well as the oxidation of CO have been studied over well-studied silica-supported Pt–Rh bimetallic catalysts. Indicative conclusions extracted by using RF-GC, which are in agreement with the observation of other techniques, are the following:

Table 1 Rate constants for the adsorption (k_1), desorption (k_{-1}), and disproportionation reaction (k_2) of carbon monoxide over a Pt/SiO_2 catalyst, determined by reversed-flow gas chromatography, at various temperatures.

T(K)	10^1k_1(sec^{-1})	10^4k_{-1}(sec^{-1})	10^4k_2(sec^{-1})
555.0	1.33	6.09	2.80
573.6	1.41	6.48	2.91
595.7	1.59	6.76	3.62
615.6	1.63	6.85	4.04
633.6	1.86	7.34	4.13
643.2	1.84	7.63	3.78
657.7	1.83	7.82	3.95
673.2	1.98	8.23	4.00
692.3	2.13	8.74	4.15
707.5	2.27	9.29	4.58
723.7	2.68	9.62	4.53

Source: From Gas chromatographic kinetic study of carbon monoxide oxidation over platinum–rhodium catalysts, in J. Chromatogr. A.[5]

a. The experimental data for carbon monoxide adsorption over the studied catalysts (in the absence of oxygen in the carrier gas), at temperatures higher than 300°C, suggest that the adsorption of CO is a dissociative process.[2,4]
b. There is a characteristic temperature of maximum catalytic activity, T_{max}, for every bimetallic catalyst. The temperatures found by RF-GC are very close to those found for the same catalysts by using different techniques.[1–4]
c. The bimetallic catalysts exhibit higher catalytic activity at lower temperatures in comparison to pure Pt and Rh ones, as shown in Fig. 2. Other workers have also observed this synergism for Pt–Rh bimetallic catalysts.[1–4]
d. The rate constants found by the RF-GC technique, as those in Table 1, are very close to those determined experimentally by the frequency response method[2,4,5] for the adsorption of CO on Pt/SiO_2.
e. The values of the estimated activation energies for CO-dissociative adsorption, shown in Table 2, are low. Low activation energy values are indicative of

Table 2 Activation energies (kJ/mol) corresponding to the adsorption, E_{a1}, desorption, E_{a-1} and disproportionation reaction, E_{a2}, of carbon monoxide over silica supported Pt, Rh, and $Pt_{0.50}$–$Rh_{0.50}$ alloy catalysts.

% Rh	E_{a1}(kJ mol^{-1})	E_{a-1}(kJ mol^{-1})	E_{a2}(kJ mol^{-1})
0	13.1 ± 1.2	9.4 ± 0.6	8.4 ± 1.3
50	18.2 ± 2.6	12.6 ± 1.7	–
100	19.4 ± 6.5	11.9 ± 2.2	3.8 ± 1.0

Source: From Study of CO dissociative adsorption over Pt and Rh catalysts by inverse gas chromatography, in Chromatographia.[2]

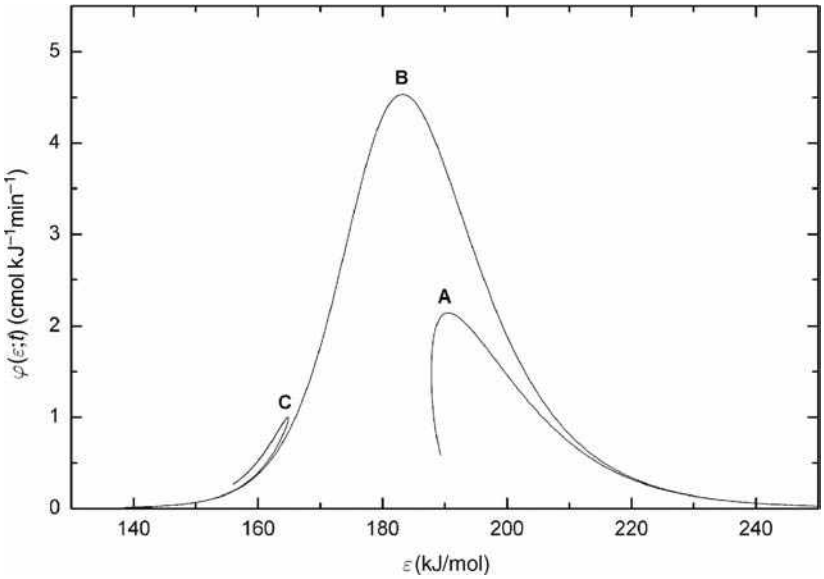

Fig. 3 Variation of the energy distribution function, $\varphi(\varepsilon;t)$ (cmol/kJ/mol), Vs. the local adsorption energy, ε(kJ/mol), for the adsorption of carbon monoxide on a bimetallic silica supported $Pt_{0.25}$–$Rh_{0.75}$ catalyst, at 698 K.
Source: From Gas chromatographic kinetic study of carbon monoxide oxidation over platinum–rhodium catalysts, in J. Chromatogr. A.[12]

corrugated surfaces. From the difference noticed in the energy barriers, it is also concluded that CO adsorption is the rate-determining step for CO-dissociative adsorption, followed by the dissociation step. These findings suggest a precursor-mediated mechanism for CO-dissociative adsorption.[2]

f. The nature of the different groups of active sites for the catalytic oxidation of CO has also been investigated from the experimentally determined energy distribution functions. The existence of three groups of active sites is observed as is shown in Figs. 3 and 4,[12] which is also expected from thermal desorption spectroscopy (TDS) for the adsorption of CO over group VIII noble metals.

Group A active sites correspond to β states of TDS, arising from CO-dissociative adsorption. The topography of these active sites is random, as the values of the lateral interaction energy, β, are negative. The B and C groups of active sites shown in our plots correspond to α states of TDS. They are characterized by positive values of β, which means that they have a patchwise topography. Group C active sites correspond to higher β values, in comparison with B group active sites. They are indicative of CO island formation. The experimental results also explain the superior activity of the $Pt_{0.25} + Rh_{0.75}$ alloy catalyst (synergism) as a result not only of its capacity to adsorb higher amount of carbon monoxide at lower temperatures, but also due to the fact that this catalyst is characterized by a more random topography in contrast with the other studied silica supported pure Pt and Rh catalysts.

The utilization of RF-GC methodologies has been extended in the study of the surface properties of various solids and related processes. Novel methodologies of RF-GC have been developed for the study of the competition between mass transfer and kinetics[14] as well as to measure the adsorption entropy.[16] It should be noted that in contrast with other IGC methods, which determine the standard entropy at zero surface coverage, the present method operates over a wide range of surface coverage taking into account not only the adsorbate–adsorbent interaction, but also the adsorbate–adsorbate interaction.

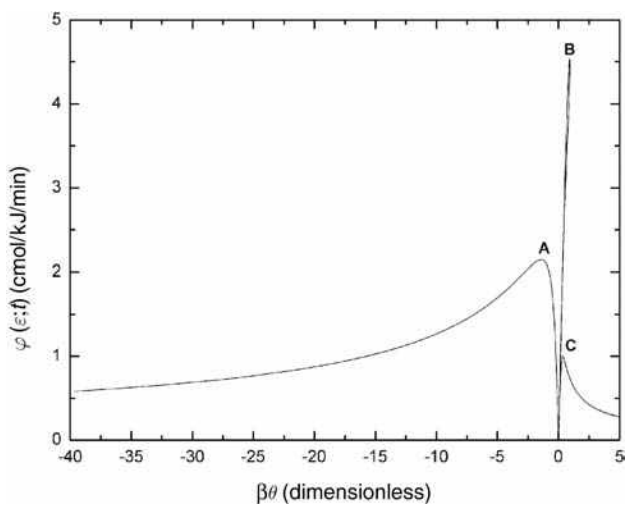

Fig. 4 Energy distribution function, $\varphi(\varepsilon;t)$ (cmol/kJ/mol/), against the dimensionless product of the lateral interaction energy (β) and the local isotherm $(\theta)\beta\theta$, for carbon monoxide adsorption over a bimetallic $Pt_{0.25}$–$Rh_{0.75}$ silica supported catalyst, at 698 K.
Source: From Gas chromatographic kinetic study of carbon monoxide oxidation over platinum–rhodium catalysts, in J. Chromatogr. A.[12]

Moreover, in recent works the effect of the presence of hydrogen on the adsorptive behavior of monometallic Rh, bimetallic Pt–Rh/SiO_2,[13,15,18] and Au/γ–Al_2O_3 catalysts[17,19,21] was studied, since the selective CO oxidation (SCO) in a rich hydrogen atmosphere is a process of great technological and environmental interest, as it is related to the development of proton exchange membrane (PEM) fuel cells.

CO adsorption, being an elementary step of SCO, was studied over silica-supported monometallic Rh and $Rh_{0.50}$ + $Pt_{0.50}$ alloy catalysts, under various atmospheres ranging from 25% to 75% H_2.[15] The variation of the experimentally determined rate constants and the activation energies against the nature of the used catalyst (monometallic or alloy) and the amount of hydrogen in the carrier gas gives useful information about the selectivity as well as the activity of SCO. At low temperatures and under H_2-rich conditions, compatible with the operation of PEM fuel cells, the activity of the monometallic and the alloy catalysts is expected to be similar; however, the selectivity of $Rh_{0.50}$ + $Pt_{0.50}$ alloy catalyst is expected to be higher, making the Pt–Rh alloy catalyst a better candidate for CO-preferential oxidation. The determined desorption barriers were in any case much lower than the respective activation energies found for CO desorption in the absence of hydrogen, indicating H_2-induced desorption, which explains the observed in the literature rate enhancement of SCO oxidation.

Then, the effect of hydrogen in the "topography" of the active sites related to CO adsorption was studied on a silica-supported Rh catalyst, at 90°C.[18] It was found that the topography of the catalyst in the absence of hydrogen consists of both random and islands of CO bound over chemisorbed CO molecules. In contrast, under H_2-rich conditions, the topography observed was almost entirely patchwise ascribed to long-range lateral attractions between adsorbate molecules as shown in Fig. 5.[18] In excess of hydrogen, CO adsorption is shifted at higher lateral attractions values, β, which correspond to weaker adsorbate–adsorbent interactions and lower surface coverage. This provides an indication of a H_2-induced desorption, which can be attributed to the formation of an H–CO complex desorbing from the catalyst surface below the temperature required for CO desorption, in the absence of H_2, and could explain the well-known in the literature enhancement of SCO rate by H_2.

Recently, new findings giving further information on the mechanism of CO oxidation over γ-alumina-supported nanoparticle-sized gold catalysts were found, utilizing, among other techniques, RF-GC[17,21]: 1) CO_2 formation, increasing with rising temperature, was observed in the absence of hydrogen and oxygen pointing to a model of active sites consisting of an ensemble of metallic Au atoms and a cationic Au with a hydroxyl group; 2) at high temperatures (>200°C) in excess of H_2, reversed water gas shift (RWGS) reaction results in CO_2 consumption toward CO and H_2O formation; 3) hydrogen strongly influences the interaction of CO on Au/γ–Al_2O_3, by weakening the CO adsorption. The presence of hydrogen plays an important role in both decreasing the strength of CO bonding and preventing deactivation and regeneration.

The study of the nature of the active sites related to CO adsorption over Au/γ–Al_2O_3 both in the presence and in the absence of hydrogen in a wide temperature range has revealed[19] the following: 1) higher amounts of CO can be bound on the catalyst active sites, at conditions compatible with the operation of PEM-FCs; 2) at rising temperatures, catalyst adsorptive capacity decreases while the degree of surface heterogeneity increases since new groups of active sites appear, both in the presence and in the absence of hydrogen; 3) the experimentally observed high activity of Au/γ–Al_2O_3 for SCO at ambient temperatures can be explained as a consequence of weaker CO bonding over metallic Au active sites in comparison to stronger CO bonding taking place at active sites located on γ-Al_2O_3 support, which is related to deactivation.

CONCLUSIONS

The usual IGC, in which the stationary phase is the main object of investigation, is a classical elution method that neglects the mass transfer phenomena; it does not take into account the sorption effect and is also influenced by the carrier gas flow. In contrast to the integration method, the new methodology of RF-GC, although being an IGC technique, is a differential method not depending either on retention times and net retention volumes or on broadening factors and statistical moments of the elution bands.

The RF-GC methodology is technically very simple and it is combined with mathematical analysis for estimating various physicochemical parameters related to solid catalysts' characterization in a simple experiment under conditions compatible with the operation of real catalysts. The experimentally determined kinetic quantities are not only consistent with the results of other techniques but they can also give important information about the mechanism of the relevant processes, the nature of the active sites, and the topography of the heterogeneous surfaces. The utilization of RF-GC methodologies can be extended to the study of the surface properties of various solids of technological and environmental interest.

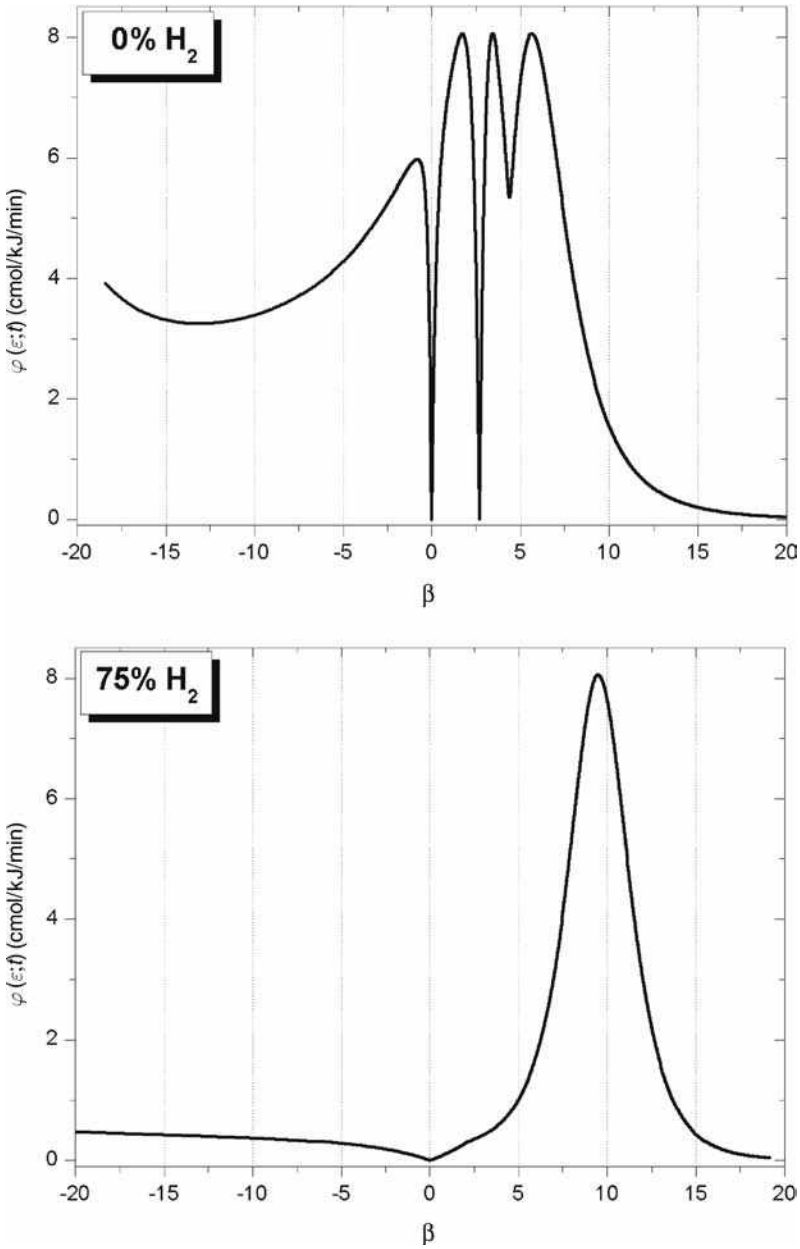

Fig. 5 Comparative study of the energy distribution functions $\varphi(\varepsilon;t)$ against the lateral interaction energy β, for CO adsorption on Rh/SiO_2 catalysts, at 90°C, in the absence of hydrogen (0% H_2) and in excess of hydrogen (75% H_2).

REFERENCES

1. Gavril, D. Reversed flow gas chromatography: A tool for instantaneous monitoring of the concentrations of reactants and products in heterogeneous catalytic processes. J. Liq. Chromatogr. Rel. Technol. **2002**, *25*, 2079–2099.
2. Gavril, D.; Loukopoulos, V.; Karaiskakis, G. Study of CO dissociative adsorption over Pt and Rh catalysts by inverse gas chromatography. Chromatographia **2004**, *59*, 721–729.
3. Gavril, D.; Katsanos, N.A.; Karaiskakis, G. Gas chromatographic kinetic study of carbon monoxide oxidation over platinum–rhodium catalysts. J. Chromatogr. A, **1999**, *852*, 507–523.
4. Gavril, D.; Koliadima, A.; Karaiskakis, G. Adsorption studies of gases on Pt–Rh bimetallic catalysts by reversed flow gas chromatography. Langmuir **1999**, *15*, 3798–3806.
5. Gavril, D.; Katsanos, N.A.; Karaiskakis, G. Gas chromatographic kinetic study of carbon monoxide oxidation over platinum–rhodium catalysts. J. Chromatogr. A, **1999**, *852*, 507–523.
6. Katsanos, N.A.; Iliopoulou, E.; Roubani-Kalantzopoulou, F.; Kalogirou, E. Probability density function for adsorption energies over time on heterogeneous surfaces by inverse gas chromatography. J. Phys. Chem. B, **1999**, *103*, 10228–10233.
7. Gavril, D. An inverse gas chromatographic tool for the experimental measurement of local adsorption isotherms, Instrum. Sci. Technol. **2002**, *30*, 397–413.
8. Katsanos, N.A.; Roubani-Kalantzopoulou, F.; Iliopoulou, E.; Vassiotis, I.; Siokos, V.; Vrahatis, M.N.; Plagianakos, V.P. Lateral molecular interaction on heterogeneous surfaces experimentally measured. Colloid Surf. A, **2002**, *201*, 173–180.

9. Katsanos, N.A.; Gavril, D.; Karaiskakis, G. Time–resolved determination of surface diffusion coefficients for physically adsorbed or chemisorbed species on heterogeneous surfaces, by inverse gas chromatography. J. Chromatogr. A, **2003**, *983*, 177–193.
10. Katsanos, N.A.; Gavril, D.; Kapolos J.; Karaiskakis, G. Surface energy of solid catalysts measured by inverse gas chromatography. J. Colloid Interf. Sci. **2003**, *270*, 455–461.
11. Margariti, S.; Katsanos, N.A.; Roubani-Kalantzopoulou, F. Time distribution of surface energy on heterogeneous surfaces by inverse gas chromatography. Colloid Surf. A, **2003**, *226*, 55–67.
12. Gavril, D.; Nieuwenhuys, B.E. Investigation of the surface heterogeneity of solids from reversed flow inverse gas chromatography. J. Chromatogr. A, **2004**, *1045*, 161–172.
13. Loukopoulos, V.; Gavril, D.; Karaiskakis, G. An inverse gas chromatographic instrumentation for the study of carbon monoxide's adsorption on Rh/SiO_2, under hydrogen-rich conditions. Instrum. Sci. Technol. **2003**, *31*, 165–181.
14. Loukopoulos, V.; Gavril, D.; Karaiskakis, G.; Katsanos, N.A. Gas chromatographic investigation of the competition between mass transfer and kinetics on a solid catalyst. J. Chromatogr. A, **2004**, *1051*, 55–73.
15. Gavril, D.; Loukopoulos, V.; Georgaka, A.; Gabriel, A.; Karaiskakis, G. Inverse gas chromatographic investigation of the effect of hydrogen in carbon monoxide adsorption over silica supported Rh and Pt–Rh alloy catalysts, under hydrogen-rich conditions. J. Chromatogr. A, **2005**, *1087*, 158–168.
16. Katsanos, N.A.; Kapolos, J.; Gavril, D. Bakaoukas, N.; Loukopoulos, V.; Koliadima, A.; Karaiskakis, G. Time distribution of adsorption entropy of gases on heterogeneous surfaces by inverse gas chromatography. J. Chromatogr. A, **2006**, *1127*, 221–227.
17. Gavril, D.; Georgaka, A.; Loukopoulos, V.; Karaiskakis, G.; Nieuwenhuys, B. On the mechanism of selective CO oxidation on nanosized $Au/\gamma–Al_2O_3$ catalysts. Gold Bull. **2006**, *39(4)*, 192–199.
18. Gavril, D.; Georgaka, A.; Loukopoulos, V.; Karaiskakis, G. Inverse gas chromatographic investigation of the active sites related to CO adsorption over Rh/SiO_2 catalysts in excess of hydrogen. J. Chromatogr. A, **2007**, *1160*, 289–298.
19. Gavril, D.; Georgaka, A.; Loukopoulos, V.; Karaiskakis, G. Gas chromatographic investigation of the effects of hydrogen and temperature on the nature of the active sites related to CO adsorption on nanosized $Au/\gamma–Al_2O_3$. J. Chromatogr. A, **2007**, *1164*, 271–280.
20. Gavril, D.; Khan, R.A. Inverse gas chromatographic study of the factors affecting surface diffusivity of gases over heterogeneous solids. Instrum. Sci. Technol. **2008**, *36*, 1–15.
21. Georgaka, A.; Gavril, D.; Loukopoulos, V.; Karaiskakis, G.; Nieuwenhuys, B. H_2 and CO_2 coadsorption effects in CO adsorption over nanosized $Au/\gamma–Al_2O_3$ catalysts, J. Chromatogr. A, **2008**, *1205*, 128–136.

CCC/MS

Hisao Oka
Food-Related Chemistry, Laboratory of Chemistry, Aichi Prefectural Institute of Public Health, Nagoya, Japan

Yoichiro Ito
National Heart, Lung, and Blood Institute (NHLBI), National Institutes of Health (NIH), Bethesda, Maryland, U.S.A.

INTRODUCTION

Countercurrent chromatography (CCC) is a unique liquid–liquid partition technique which does not require the use of a solid support,[1–5] hence eliminating various complications associated with conventional LC, such as tailing of solute peaks, adsorptive sample loss and deactivation, contamination, and so forth. Since 1970, the CCC technology has advanced in various directions, including preparative and trace analysis, dual CCC, foam CCC, and, more recently, partition of macromolecules with polymerphase systems. However, most of these methods were only suitable for preparative applications due to relatively long separation times required. In order to fully explore the potential of CCC, efforts have been made to develop analytical high-speed CCC (HSCCC) by designing a miniature multilayer coil planet centrifuge; interfacing analytical HSCCC to a mass spectrometer (HSCCC/MS) began in the late 1980s.

Integration of the high-purity eluate of HSCCC with a low detection limit of MS has led to the identification of a number of natural products, as shown in Table 1.[6–10]

Various HSCCC/MS techniques and their applications are described herein.

INTERFACING HSCCC TO THERMOSPRAY MS

HSCCC/thermospray (TSP) MS was initiated using an analytical HSCCC apparatus of a 5-cm revolution radius, equipped with a 0.85 mm inner diameter (I.D.) polytetrafluoroethylene (PTFE) column at 2000 rpm.[6–8] Directly interfacing HSCCC to the MS produced, however, a problem in that the high back-pressure generated by the TSP vaporizer often damaged the HSCCC column. To overcome this problem, an additional high-performance liquid chromatography (HPLC) pump was inserted at the interface junction between HSCCC and MS to protect the column against high back-pressures. The effluent from the HSCCC column (0.8 ml/min) was introduced into the HPLC pump through a zero-dead-volume tee fitted with a reservoir supplying extra solvent or venting excess solvent from the HSCCC system. The effluent from the HPLC pump, after being mixed with 0.3 *M* ammonium acetate at a rate of 0.3 ml/min, was introduced into the TSP interface. This system has been successfully applied to the analyses of alkaloids,[6] triterpenoic acids,[7] and lignans[8] from plant natural products, thereby providing useful structural information. However, a large dead space in the pump at the interface junction adversely affected the resulting chromatogram, as evidenced by loss of a minor peak when HSCCC/UV and HSCCC/TSP–MS total ion current (TIC) chromatograms of plant alkaloids were compared.

In the subsequently developed techniques, the HSCCC effluent is directly introduced into the MS to preserve the peak resolution. Direct HSCCC/MS techniques have many advantages over the HSCCC/TSP method as follows:

1. High enrichment of sample in the ion source
2. High yield of sample reaching the MS
3. No peak broadening
4. High applicability to non-volatile samples

Various types of HSCCC/MS have been developed using frit fast-atom bombardment (FAB) including continuous flow (CF) FAB, frit electron ionization (EI), frit chemical ionization (CI), TSP, atmospheric pressure chemical ionization (APCI), and electrospray ionization (ESI). Each interface has its specific features. Among those, frit MS and ESI are particularly suitable for directly interfacing to HSCCC, because they generate low back-pressures of approximately 2 kg/cm^2, which is only one-tenth of that produced by TSP.

INTERFACING OF HSCCC TO FRIT EI, CI, AND FAB–MS

In our laboratory, separations were conducted by newly developed HSCCC-4000 with a 2.5 cm revolution radius, equipped with a 0.3 mm or 0.55 mm I.D. multilayer coil at a maximum revolution speed of 4000 rpm.[9] The system produced an excellent partition efficiency at a flow rate ranging between 0.1 and 0.2 ml/min, whereas the suitable

Table 1 Summary of previously reported HSCCC/MS conditions.

Sample	Column	Column capacity (ml)	Revolutional speed (rpm)	Solvent system	Mobile phase	Flow rate (ml/min)	Retention of stationary phase (%)	Ionization	Refs.
Alkaloids	0.85 mm PTFE tube	38	1,500	*n*-Hexane–ethanol–water (6 : 5 : 5)	Lower phase	0.7	—	Thermospray	[6]
Triterpenoic acids	0.85 mm PTFE tube	38	1,500	*n*-Hexane–ethanol–water (6 : 5 : 5)	Lower phase	0.7	—	Thermospray	[7]
Lignans	0.85 mm PTFE tube	38	1,500	*n*-Hexane–ethanol–water (6 : 5 : 5)	Lower phase	0.7	—	Thermospray	[8]
Indole auxins	0.3 mm PTFE tube	7	4,000	*n*-Hexane–ethyl acetate–methanol–water (1 : 1 : 1 : 1)	Lower phase	0.2	27.2	Frit–EI	[9]
Mycinamicins	0.3 mm PTFE tube	7	4,000	*n*-Hexane–ethyl acetate–methanol–8% ammonia (1 : 1 : 1 : 1)	Lower phase	0.1	40.4	Frit–CI	[9]
Colistins	0.55 mm PTFE tube	6	4,000	*n*-Butanol–0.04 *M* TFA (1 : 1)	Lower phase	0.16	34.3	Frit–FAB	[9]
Erythromycins	0.85 mm PTFE tube	17	1,200	Ethyl acetate–methanol–water (4 : 7 : 4 : 3)	Lower phase	0.8	—	Electrospray	[10]
Didemnins	0.85 mm PTFE tube	17	1,200	Ethyl acetate–methanol–water (1 : 4 : 1 : 4)	Lower phase	0.8	—	Electrospray	[10]

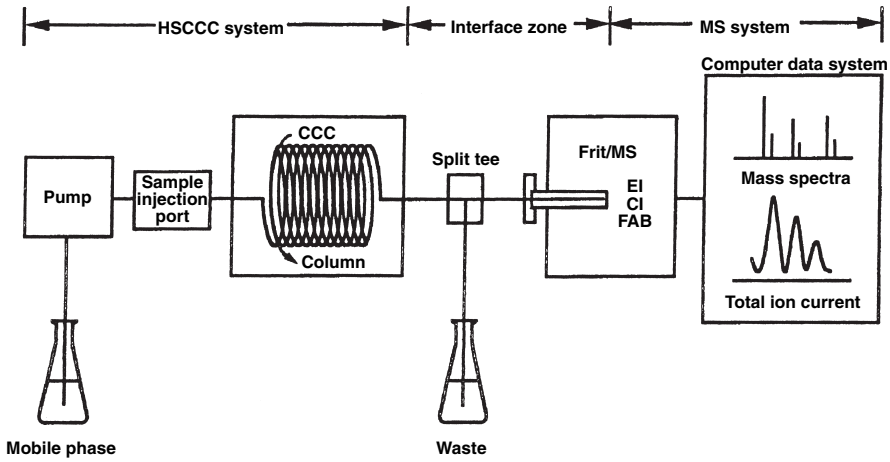

Fig. 1 HSCCC/frit MS system.

flow rate for HSCCC/frit MS is between 1 and 5 μl/min. Therefore, the effluent of the HSCCC column was introduced into the MS through a splitting tee which was adjusted to a split ratio of 1 : 40 to meet the above requirement. A 0.06 mm I.D. fused-silica tube was led to the MS and a 0.5 mm I.D. stainless-steel tube was connected to the HSCCC column. The other side of the fused-silica tube extended deeply into the stainless-steel tube to receive a small portion of the effluent from the HSCCC column, and the rest of the effluent was discarded through a 0.1 mm I.D. PTFE tube. The split ratio of the effluent depended on the flow rate of the effluent and the length of the 0.1 mm I.D. tube. For adjusting the split ratio at 40 : 1, a 2-cm length of the 0.1 mm I.D. tube was needed. Fig. 1 shows the HSCCC/MS system, including an HPLC pump, sample injection port, HSCCC/4000, the split tee, and mass spectrometer.[9]

In order to demonstrate the potential of HSCCC/frit MS, indole auxins, mycinamicins (macrolide antibiotics), and colistin complex (peptide antibiotics) were analyzed under HSCCC–frit, EI, CI, and FAB–MS conditions.

Three indole auxins, including indole-3-acetamide (IA, MW: 174), indole-3-acetic acid (IAA, MW: 175), and indole-3-butyric acid (IBA, MW: 203) were analyzed under frit EI–MS conditions. In comparison of a TIC with a UV chromatogram, both showed similar chromatographic resolution with excellent theoretical plate numbers ranging from 12,000 to 5500. The results indicate that MS interfacing does not adversely affect chromatographic resolution. In frit EI–MS, the mobile phase behaves like a reagent gas in CI–MS. Both molecular ions and protonated molecules appear in all mass spectra and these data are very useful for the estimation of the molecular weight. Common fragment ions originating from the indole nuclei are found at *m/z* 116 and 130.

A mixture of mycinamicins was analyzed under HSCCC/frit CI–MS conditions. Mycinamicins consist of six components, mycinamicins I to VI, and isolated mycinamicins IV (MN-IV, MW: 695) and V (MN-V, MW: 711) were used. The structural difference is derived from the hydroxyl group at C-14. These antibiotics were detected under CI conditions, but a reagent gas such as methane, isobutane, or ammonia was not introduced, because the mobile phase behaves like a reagent gas, as described earlier. Both UV and TIC chromatograms showed similar efficiencies, indicating that the MS interfacing does not affect peak resolution, as demonstrated in the analysis of indole auxins. An applicability of this HSCCC/MS system to less volatile compounds was examined under frit FAB–MS conditions.

A peptide antibiotic colistin complex consisting of two major components of colistins A (CL-A, MW: 1168) and B (CL-B, MW: 1154) is difficult to ionize by CI and EI–MS. For HSCCC analysis of these polar compounds, a wider column of 0.55 mm I.D. (instead of 0.3 mm I.D.) was used to achieve satisfactory retention of the stationary phase for a polar *n*-butanol–trifluoroacetic acid (TFA) solvent system. In addition, for obtaining FAB mass spectra, it is necessary to introduce a sample with an appropriate matrix such as glycerol, thioglycerol, and *m*-nitrobenzyl alcohol into the FAB–MS ion source. In the present study, glycerol was added as a matrix to the mobile phase at a concentration of 1%. Although a two-phase solvent system containing glycerol was the first trial for a HSCCC study, similarly satisfactory results were obtained in both retention and separation efficiency. Because of the use of a wider column with a viscous *n*-butanol–aqueous TFA solvent system, the separation was less efficient compared with those obtained from the above two experiments, but the peaks corresponding to CL-A and CL-B were clearly resolved. Mass chromatograms at individual protonated molecules showed symmetrical peaks without a significant loss of peak resolution due to MS interfacing. In all spectra, protonated molecules appeared well above the chemical noise to indicate the molecular weights. These experiments demonstrated that the present HSCCC/frit MS system including EI, CI, and FAB is very potent and is applicable to various

analytes having a broad range of polarity. For a non-volatile, thermally labile and/or polar compound, HSCCC–frit FAB is most suitable, whereas both HSCCC–frit EI and CI can be effectively used for a relatively non-polar compound.

INTERFACING HSCCC TO ESI–MS

The experiment was carried out using a small analytical coiled column (17 ml) at 1200 rpm. The effluent from the CCC column at 800 μl/min was split at a 1 : 7 ratio to introduce the smaller portion of the effluent into ESI–MS using a tee adaptor, as described earlier.

The performance of HSCCC–ESI–MS was evaluated by analyzing erythromycins and didemnins.[10] Because erythromycins (macrolide antibiotics) show weak UV absorbance and cannot be detected easily with a conventional UV detector, mass spectrometric detection is a very useful technique for analysis of these antibiotics. A mixture of erythromycin A (Er-A, MW: 733), erythromycin estolate (Er-E, MW: 789), and erythromycin ethyl succinate (Er-S, MW: 789) was analyzed using HSCCC–ESI–MS with a two-phase solvent system composed of *n*-hexane–ethyl acetate–methanol–water (4 : 7 : 4 : 3). TIC showed, clearly, four peaks corresponding to Er-A, Er-E, Er-S, and an unknown substance. The mass spectra of Er-E and Er-S gave $[M + H]^+$ at *m/z* 862 and 789 and $[M + H - H_2O]^+$ at *m/z* 844 and 772, respectively. In the mass spectrum of Er-A, $[M + H - H_2O]^+$ was observed at *m/z* 761; however, no $[M + H]$ was given. The mass spectrum of the unknown peak indicated that it consists of two components with molecular weights of 843 and 772, which correspond to dehydrated Er-S and Er-E, respectively.

Didemnin A (Did-A, MW: 942) is one of the main components of didemnins (cyclic depsipeptides) and is a precursor for synthesis of other didemnins which exhibit antiviral, antitumor, and immunosuppressive activities. Therefore, its purification is very important in the field of pharmaceutical science. However, largescale purification of Did-A using conventional LC is difficult due to the presence of nordidemnin A (Nordid-A), which contaminates the target fraction. HSCCC–ESI–MS has been successfully applied to the separation and detection of didemnins. Three peaks were observed on TIC corresponding to didemnins A and B and nordidemnin A. Their mass spectra gave only protonated molecules without fragmentation. The first eluted peak was didemnin B, which gave $[M + H]^+$ and $[M + Na]^+$ at *m/z* 1112 and 1134, respectively. Did-A appeared as the second peak with $[M + H]^+$ at *m/z* 943 and $[M + Na]^+$ at *m/z* 965. The third peak was Nordid-A, showing $[M + H]^+$ at *m/z* 929 and $[M + Na]^+$ at *m/z* 951. The results indicated that Did-A can be isolated by HSCCC.

FUTURE PROSPECTS

HSCCC/MS has many desirable features for performing the separation and identification of natural and synthetic products, because it eliminates various complications arising from the use of solid support and offers a powerful identification capacity of MS with its low detection limit. We believe that the combination of these two methods, HSCCC–MS, has great a potential for screening, identification, and structural characterization of natural products and will contribute to a rapid advance in natural products chemistry.

REFERENCES

1. Mandava, N.B., Ito, Y., Eds.; *Countercurrent Chromatography: Theory and Practice*; Marcel Dekker, Inc.: New York, 1988.
2. Conway, W.D. *Countercurrent Chromatography: Apparatus, Theory and Applications*; VCH: New York, 1990.
3. Foucault, A., Ed.; *Centrifugal Partition Chromatography*; Marcel Dekker, Inc.: New York, 1995.
4. Ito, Y.; Conway, W.D. High-speed countercurrent chromatography. CRC Crit. Rev. Anal. Chem. **1986**, *17* (1), 65.
5. Ito, Y., Conway, W.D., Eds.; *High-Speed Countercurrent Chromatography*; Wiley–Interscience: New York, 1996.
6. Lee, Y.-W.; Voyksner, R.D.; Fang, Q.-C.; Cook, C.E.; Ito, Y. Application of countercurrent chromatography/thermospray mass spectrometry for the analysis of natural products. J. Liquid Chromatogr. Related. Technol. **1988**, *11* (1), 153.
7. Lee, Y.-W.; Pack, T.W.; Voyksner, R.D.; Fang, Q.-C.; Ito, Y. Application of high speed countercurrent chromatography/thermospray mass spectrometry for the analysis of bio-active triterpenoic acids from Boswellia Carterh. J. Liquid Chromatogr. Related. Technol. **1990**, *13* (12), 2389.
8. Lee, Y.-W.; Voyksner, R.D.; Pack, T.W.; Cook, E.; Fang, Q.-C.; Ito, Y. Application of countercurrent chromatography/thermospray mass spectrometry for the identification of bioactive lignans from plant natural products. Anal. Chem. **1990**, *62*, 244–248.
9. Oka, H.; Ikai, Y.; Kawamura, N.; Hayakawa, J.; Harada, K.-I.; Murata, H.; Suzuki, M. Direct interfacing of high-speed countercurrent chromatography to frit electron ionization, chemical ionization, and fast atom bombardment mass spectrometry. Anal. Chem. **1991**, *63*, 2861–2865.
10. Kong, Z.; Rinehart, K.L.; Milberg, R.M.; Conway, W.D. Application of high-speed countercurrent chromatography/electrospray ionization mass spectrometry (HSCCC/ESIMS) in natural products Chemistry. J. Liquid Chromatogr. Relat. Technol. **1998**, *21* (1–2), 65.

CCC: Instrumentation

Yoichiro Ito
National Heart, Lung, and Blood Institute (NHLBI), National Institutes of Health (NIH), Bethesda, Maryland, U.S.A.

INTRODUCTION

Countercurrent chromatography (CCC) is a support-free liquid–liquid partition system where solutes are partitioned between the mobile and stationary liquid phases in an open column space. The instrumentation, therefore, requires a unique approach for achieving both retention of the stationary phase and high partition efficiency in the absence of a solid support. The variety of existing CCC systems may be divided into two classes,[1] i.e., hydrostatic and hydrodynamic equilibrium systems. The principle of each system can be illustrated by a simple coil, as shown in Fig. 1.

TWO BASIC CCC SYSTEMS

The basic hydrostatic equilibrium system (Fig. 1, left) utilizes a stationary coil. The mobile phase is introduced at the inlet of the coil, which has been filled with the stationary phase. The mobile phase then displaces the stationary phase completely on one side of the coil (dead space), but only partially displaces it on the other side due to the effect of gravity. This process continues until the mobile phase elutes from the coil. Once this hydrostatic equilibrium state is established throughout the column, the mobile phase only displaces the same phase while leaving the stationary phase permanently in the coil. Consequently, the solutes locally introduced at the inlet of the coil are subjected to a continuous partition process between two phases at each helical turn and separated according to their partition coefficients in the absence of a solid support.

The basic hydrodynamic equilibrium system (Fig. 1, right) uses a rotating coil, which generates an Archimedean screw effect, whereby all objects of different densities in the coil are driven toward one end, conventionally called "head," the other end being the tail. The mobile phase introduced through the head of the coil is mixed with the stationary phase to establish hydrodynamic equilibrium, with a portion of the stationary phase retained in each turn of the coil. This process continues until the mobile phase elutes from the tail of the coil. After hydrodynamic equilibrium is established throughout the coil, the mobile phase displaces only the same phase while leaving the other phase stationary in the coil. Consequently, solutes introduced locally at the head of the coil are subjected to an efficient partition process between the two phases and separated according to their partition coefficients.

Each basic system has its specific advantages as well as disadvantages. The hydrostatic system provides stable retention of the stationary phase but has relatively low partition efficiency due to the limited degree of mixing. The hydrodynamic system, on the other hand, has a high partition efficiency in a short elution time, but the retention of the stationary phase tends to become unstable due to violent mixing, often resulting in emulsification and extensive carryover of the stationary phase.

DEVELOPMENT OF HYDROSTATIC CCC SYSTEMS

In the early 1970s, the hydrostatic system was quickly developed into several efficient CCC schemes, as shown in Fig. 2.[2] The development has been done by utilizing unit gravity (Fig. 2, top) or centrifugal force (Fig. 2, bottom).

In droplet CCC, which utilizes unit gravity, one side of the coil (Fig. 1, left), entirely occupied by the mobile phase, is reduced to a fine flow tube, while the other side of the coil is replaced by a straight tubular column. The column is first filled with the stationary phase and the mobile phase is introduced into the column in a proper direction so that it forms a string of droplets in the stationary phase by the effect of gravity. The system necessitates the formation of droplets, which limits the choice of solvent system. In order to allow more universal application of solvent systems, a locular column was devised by inserting centrally perforated disks into the tube at regular intervals to form a number of compartments called "locules." The locular column is held at an angle and rotated along its axis to mix the two phases in each locule. As in droplet CCC, the lower phase is eluted from the upper end of the locular column and the upper phase from the lower end for better retention of the stationary phase.

In the toroidal coil CCC (helix CCC) system, operated under a centrifugal force, the dimensions of the coil are reduced (Fig. 2, lower left). The coil is mounted around the periphery of a centrifuge bowl so that the stable, radially acting centrifugal force field retains the stationary phase,

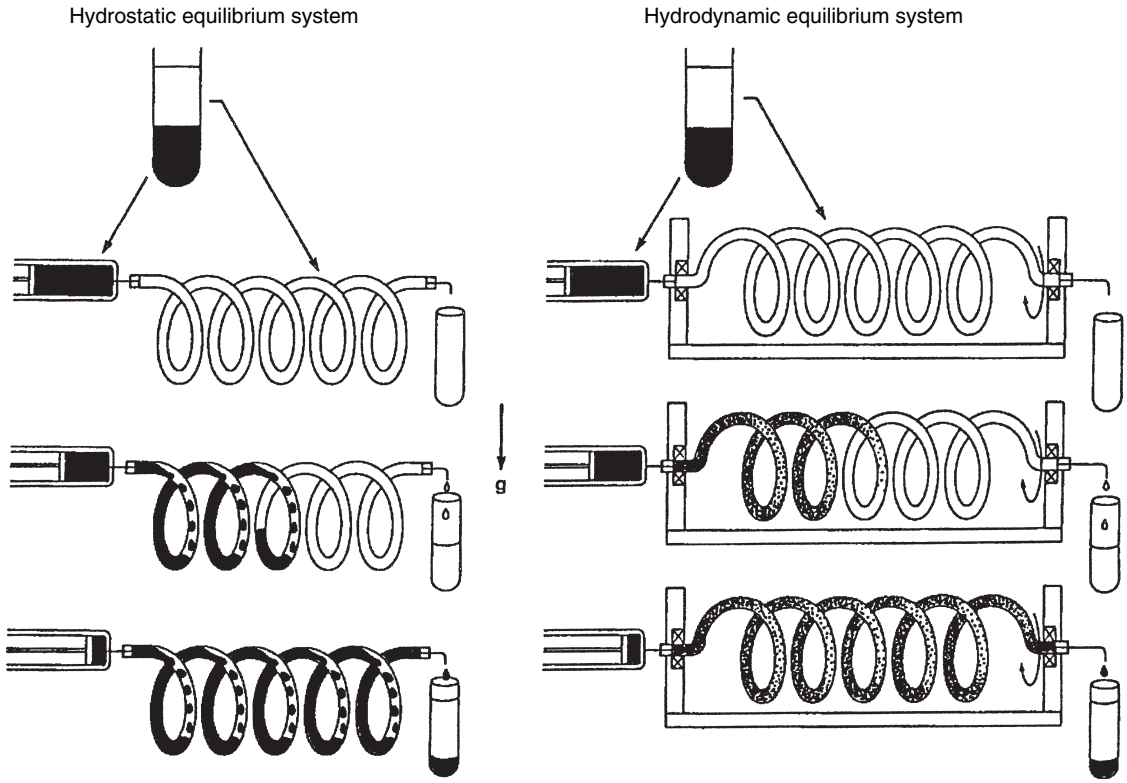

Fig. 1 Two basic CCC systems: hydrostatic equilibrium system (left) and hydrodynamic equilibrium system (right).

either upper or lower, on one side of the coil, as in the basic hydrostatic system (Fig. 1, left). The effective column capacity and retention of the stationary phase can be increased by replacing the coil with a locular column arrangement (centrifugal partition chromatography).

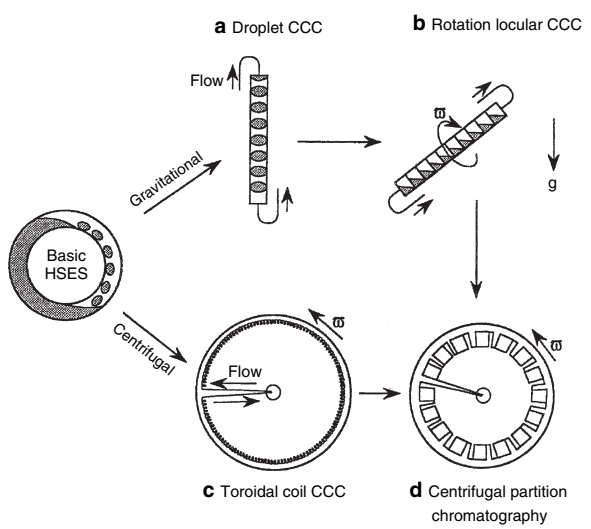

Fig. 2 Development of hydrostatic CCC systems.

INSTRUMENTATION OF HYDROSTATIC CCC SYSTEMS

Helix CCC (Toroidal Coil CCC)

Fig. 3A shows the design of the original helix CCC centrifuge rotor. A long helical column (typically 0.2–0.3 mm I.D. × 40 m length coiled onto a 0.85 mm xdO.D. tube making ~8000 turns) is accommodated around the periphery of the rotor. The mobile phase is introduced into the coil from a rotating syringe mounted at the center of the rotor, while the effluent from the outlet of the coil is collected through a rotary seal at the upper end of the syringe plunger. The system has a high partition efficiency of several thousand theoretical plates.[3]

The above original design has been improved using a seal-free centrifuge system based on non-planetary motion (Fig. 5, bottom middle). Fig. 3B shows a cross-sectional view of the seal-free toroidal coil centrifuge. A long helical tube is accommodated around the periphery of the column holder. The seal-free (non-planetary) motion of the column is achieved by a set of four miter gears: When the motor drives the gear box with a pair of toothed pulleys and a toothed belt, a pair of idler miter gears, engaged with the stationary miter gear at the bottom, rotate about their own axis at the same speed in a revolving gear box. This motion is further conveyed to the top miter gear, which is directly

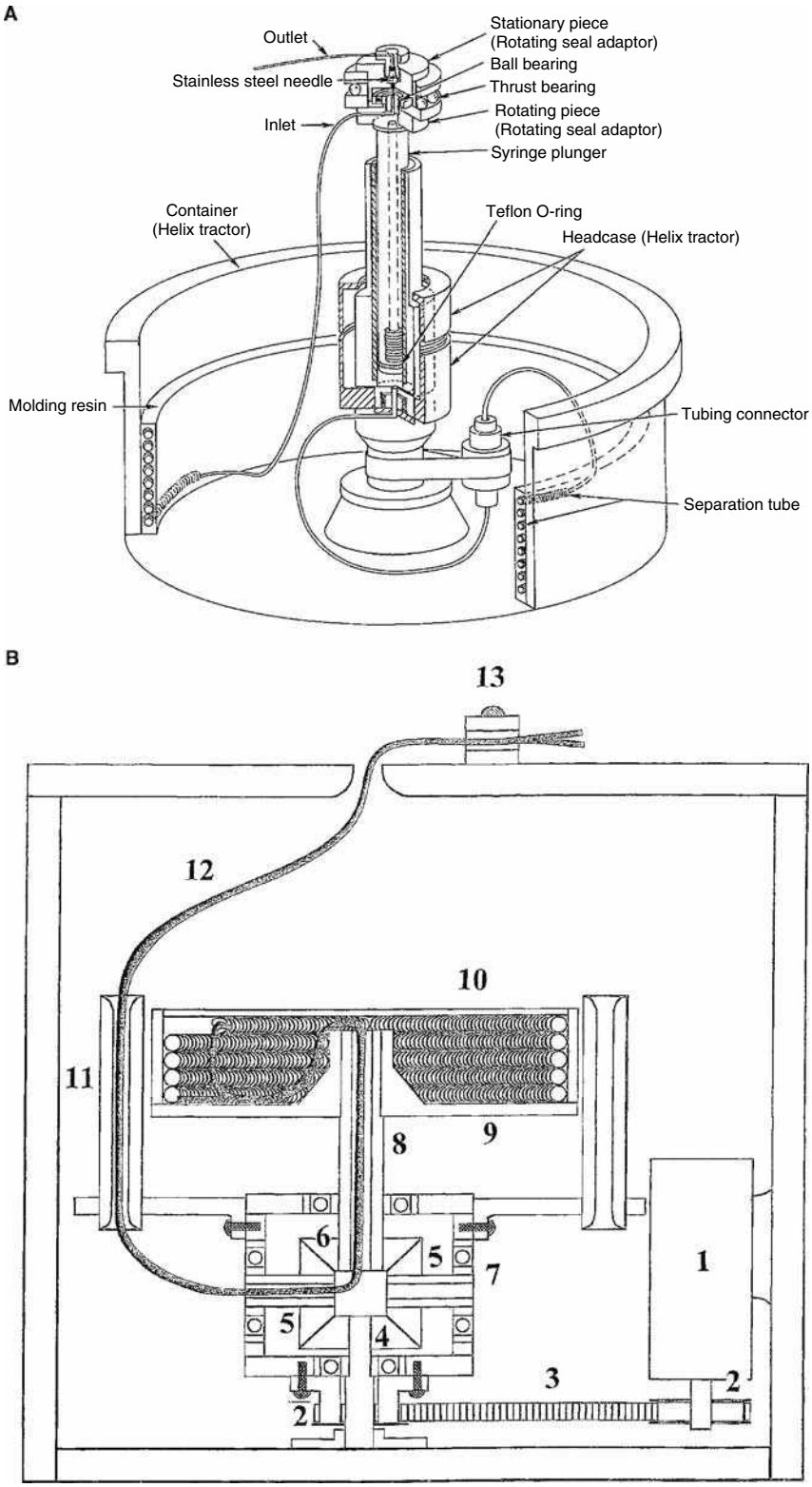

Fig. 3 Design of helix CCC (toroidal coil CCC) apparatus. A, Schematic drawing of centrifuge head of original helix CCC apparatus; B, cross-sectional view of advanced design of helix CCC equipped with seal-free flow-through device. 1, Motor; 2, toothed pulleys; 3, toothed belt; 4, stationary miter gear; 5, horizontal idler miter gear; 6, inverted upper miter gear mounted at bottom of column holder shaft (8); 7, gear box; 9, column holder; 10, coiled separation column; 11, hollow tube support; 12, flow tubes; and 13, clamps.

mounted at the lower end of the column holder shaft. Consequently, the column holder rotates at double the speed of an ordinary flow-through centrifuge system but without the need for the conventional rotary seal device. A pair of flow tubes from the coiled column pass through the holder shaft downward, through the horizontal shaft of an idler miter gear, and then through the vertical tube support (left) to exit the system at the center of the centrifuge cover, where they are tightly fixed with a pair of clamps, as indicated in the diagram. Because of the

near-symmetrical arrangement of the design, the system is well balanced and the column can be rotated at a high speed up to 2000 rpm, while the elution can be performed through its seal-free flow-through system to eliminate complications, such as leakage of solvent and cross-contamination of solutes, that are often caused by the use of a conventional rotary seal device.[4]

Centrifugal Partition Chromatography

Fig. 4 schematically shows a design of the centrifugal partition chromatographic system (see Fig. 2). The separation disk has a series of partition chambers connected by narrow ducts. The disk is rotated up to 2000 rpm. The flow-through system is made by a pair of rotary seals, which can maintain leak-free elution up to 60 bar (~ 800 psi), although the seals should be kept clean. The system is computerized and the operation is programed as in an high-performance liquid chromatography (HPLC) system.[5]

DEVELOPMENT OF HYDRODYNAMIC CCC SYSTEMS

The performance of the basic hydrodynamic CCC system (Fig. 1, right) is remarkably improved by rotating the coil in a centrifugal force field, i.e., by applying a planetary motion to the coil. During the 1970s, a series of flow-through centrifuge schemes has been developed for performing CCC. In these centrifuge systems, the use of the conventional rotary seal devise is eliminated, since it leads to various complications such as leakage, clogging, and cross-contamination. These seal-less flow-through centrifuge schemes are divided into three classes: synchronous, non-planetary, and non-synchronous, according to the mode of planetary motion (Fig. 5).

In type I synchronous planetary motion (Fig. 5, upper left), a vertical holder revolves around the central axis of the centrifuge while it counter-rotates around its own axis at the same angular velocity. This counter-rotation of the holder unwinds the twist of the tube bundle caused by revolution, thus eliminating the need for the rotary seal. This principle works well for the rest of the synchronous schemes with tilted (types I-L and I-X), horizontal (types L and X), inversely tilted (types J-L and J-X), and even inverted orientation (type J) of the holder. When a holder of type I is moved to the center of the centrifuge, the counter-rotation of the holder cancels out the revolution effect, resulting in no rotation (Fig. 5, upper center). In contrast, when this shift is applied to type J planetary motion, the rotation of the holder is added to the revolution, resulting in the rotation of the holder at doubled speed, while the tube bundle revolves around the holder to unwind the twisting (Fig. 5, bottom center). This non-planetary scheme is a transitional form to non-synchronous planetary motion. On the basis of the non-planetary scheme, the holder is again shifted toward the periphery to undergo a synchronous planetary motion. Since the net revolution

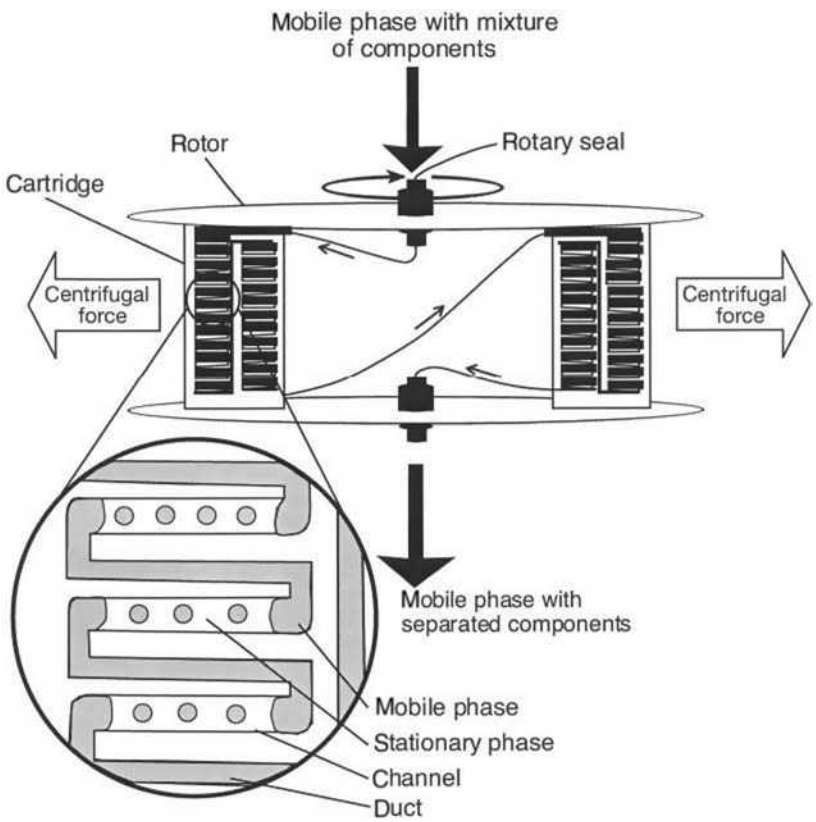

Fig. 4 Design of centrifugal partition chromatography.

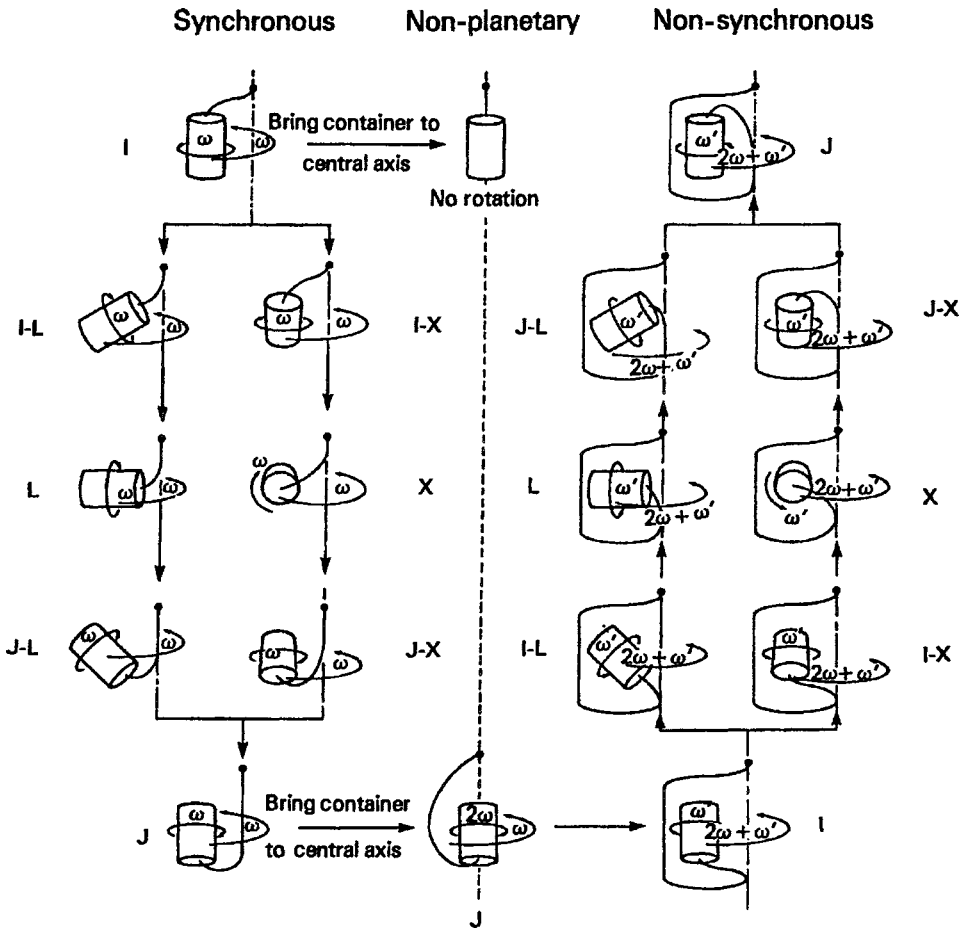

Fig. 5 Series of seal-less flow-through centrifuge systems for performing CCC.

speed of the coil is the sum of the non-planetary and synchronous planetary motions, the ratio of the rotation and revolution becomes freely adjustable.

Several useful CCC systems have been developed from these centrifuge schemes. The non-planetary scheme has been used for toroidal coil CCC,[4,6] centrifugal precipitation chromatography,[7,8] and online apheresis in blood banks.[9,10] The non-synchronous scheme has been applied to the partitioning of cells with polymer phase systems and also to cell elutriation with physiological solutions.[11,12] The type J synchronous scheme has been further developed into a highly efficient CCC system called high-speed CCC.[13,14]

Development of High-Speed Countercurrent Chromatography (HSCCC)

The development of HSCCC was initiated by the discovery that when type J planetary motion is applied to an end-closed coil coaxially mounted on a holder (Fig. 6A), the two solvent phases are completely separated in such a way that one phase occupies the head side and the other phase the tail side of the coil.

This bilateral hydrodynamic distribution can be utilized for performing CCC, as illustrated in Fig. 6B, where each of the coils is schematically shown as a straight tube to indicate the overall distribution of the two phases. The top coil shows the bilateral distribution of the two phases as mentioned above, with the white phase occupying the head side and the black phase the tail side. This hydrodynamic distribution of the two phases can be utilized for performing CCC. In the middle diagram, the upper coil is filled with the white phase and the black phase is introduced from the head end. The mobile black phase then rapidly travels through the coil, leaving a large volume of the white phase stationary in the coil. Similarly, the lower coil is filled with the black phase and the white phase is introduced from the tail end. The mobile white phase then travels through the coil, leaving a large volume of the black phase stationary in the coil. In either case, solutes locally injected at the inlet of the coil are efficiently partitioned between the two phases and quickly eluted from the coil in the order of their partition coefficients, thus yielding high partition efficiency in a short elution time.

The present system also permits simultaneous introduction of the two phases through the respective terminals, as illustrated in the bottom coil. This dual countercurrent

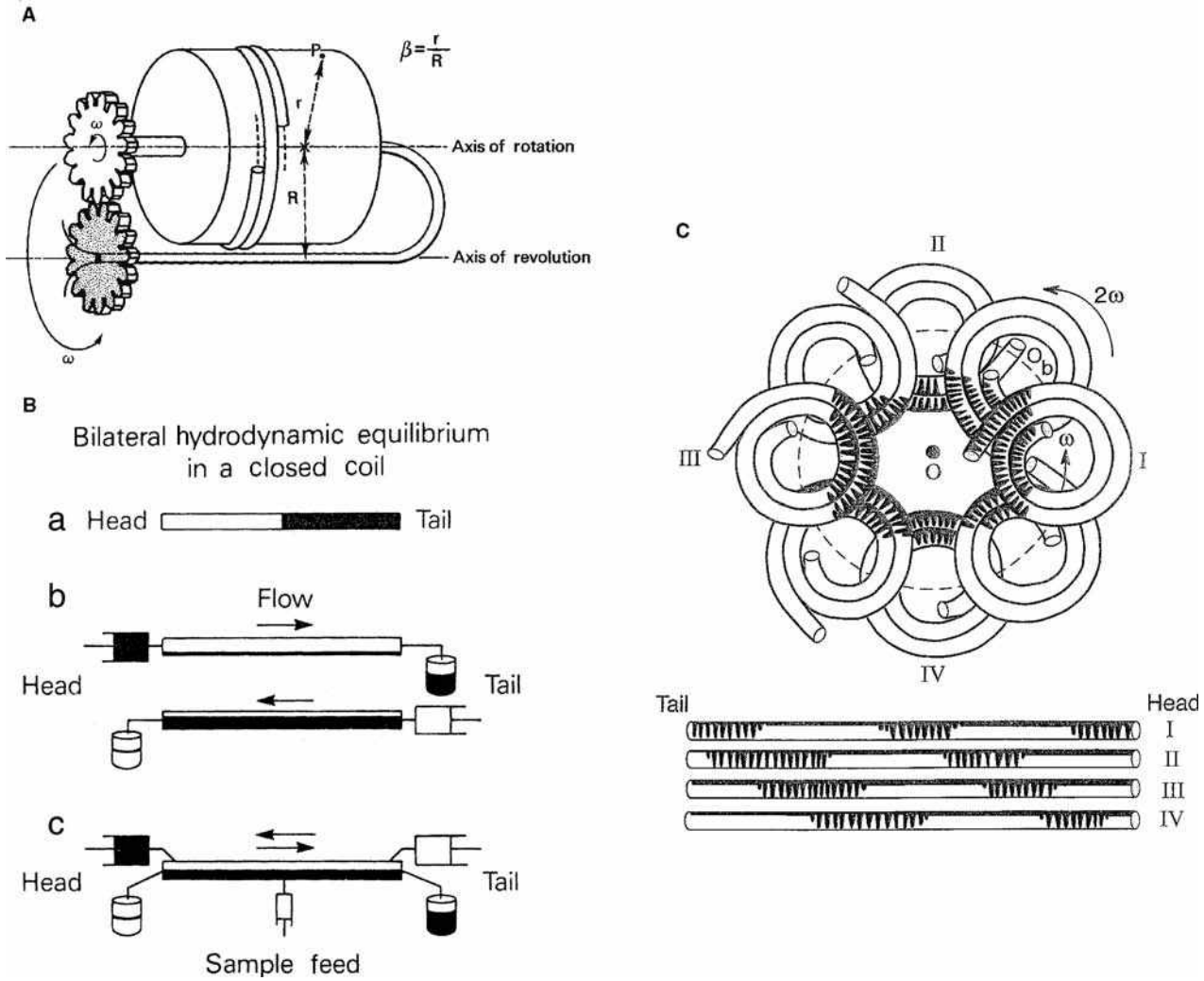

Fig. 6 Principle and mechanism of high-speed CCC. A, Coaxial coil orientation on holder of type J coil planet centrifuge; B, mechanism of high-speed CCC; and C, distribution of mixing and settling zones in spiral column undergoing type J synchronous planetary motion.

operation requires an additional flow tube at each terminal to collect the effluent, and if desired, a sample injection port is created at the middle portion of the coil. This system has been effectively applied to foam CCC[15,16] and dual CCC.[17]

The hydrodynamic motion of the two solvent phases in the rotating spiral column has been observed under stroboscopic illumination (Fig. 6C). As shown in the upper diagram, the spiral column is divided into two areas, a mixing zone near the center of the centrifuge and a settling zone in the rest of the area. The lower diagram shows the motion of the mixing zone by stretching the spiral column from position I to IV. It demonstrates that the mixing zones travel through the spiral column at a rate of one round per revolution. This implies high efficiency of this system: Solutes present in any portion in the column are subjected to an efficient partition cycle of repeating mixing and settling at an enormously high frequency (13 cycles/sec at 800 rpm of column revolution).

INSTRUMENTATION OF HYDRODYNAMIC CCC SYSTEMS

Type J HSCCC

Fig. 7A shows a cross-sectional view of the original design of the HSCCC centrifuge.[18] The rotary frame holds a large multilayer coil holder and a counterweight mass symmetrically to balance the centrifuge system. Twist-free type J synchronous planetary motion is provided by coupling a pair of identical gears, the planetary gear mounted on the column holder flange and the

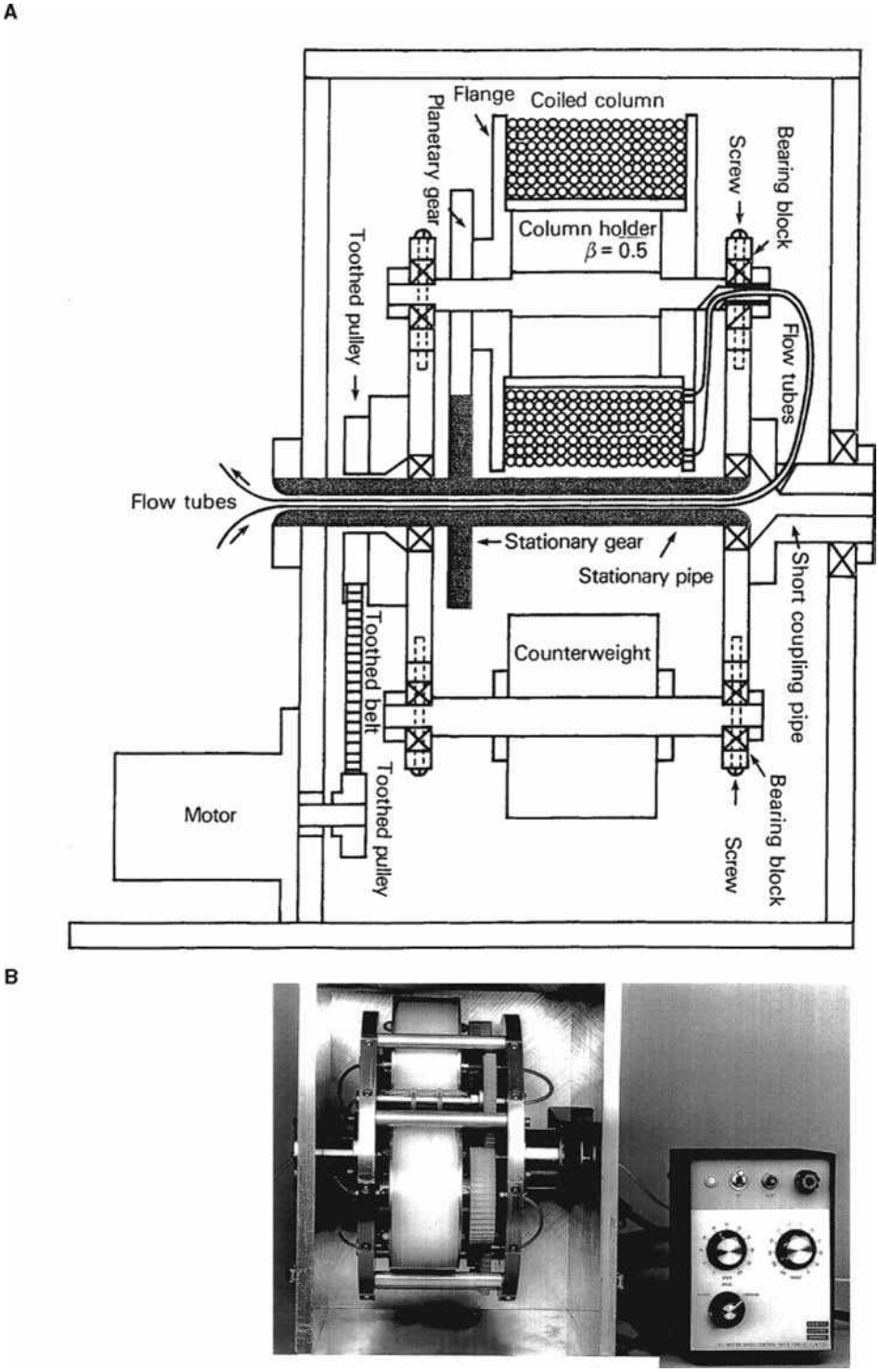

Fig. 7 Design of high-speed CCC apparatus. A, Original multilayer coil planet centrifuge: cross-sectional view through center of apparatus; B, photograph of most advanced prototype of high-speed CCC centrifuge equipped with a set of three multilayer coils connected in series.

stationary sun gear (shaded) on the centrifuge axis. The flow tubes from the separation column first pass through the center of the holder and then, forming an arch, enter the central stationary pipe (shaded) via a side hole made in the short rotary shaft (right). These tubes can maintain their integrity for many runs when protected with a short segment of Tygon tubing to avoid direct contact with metal parts.

Later, the above original design was improved by eliminating the counterweight mass and arranging two to three identical columns symmetrically around the rotary frame. Fig. 7B shows the most advanced form of high-speed CCC centrifuge, equipped with a set of three multilayer coil separation columns. All three columns are serially connected with flow tubes through a counter-rotation hollow pipe to prevent twisting.

This type J high-speed CCC system equipped with the multilayer coil separation column can separate a variety of natural and synthetic products with high partition efficiency using organic–aqueous two-phase solvent systems. The system, however, fails to retain a satisfactory amount of stationary phase in low interfacial aqueous–aqueous polymer phase systems due to intensive emulsification.

Cross-Axis Coil Planet Centrifuge (X-Axis CPC)

In this CCC system, the column holder revolves around the vertical axis of the centrifuge while it rotates about its horizontal axis at the same angular velocity.[19] This second HSCCC system is based on a hybrid between type *L* and *X* synchronous systems (Fig. 5), and it leads to bilateral hydrodynamic distribution of the two phases in an end-closed coaxial multilayer coil as in the type J HSCCC (Fig. 6B). However, in contrast to type J synchronous planetary motion, the centrifugal vectors fluctuate in a three-dimensional space where one component steadily acts across the diameter of the tube to stabilize the retention of the stationary phase. This stabilizing effect becomes greater as the hybrid approaches the type *L* synchronous system, while the phase-mixing effect is reduced. The optimum column position for separating proteins with a polyethylene glycol (PEG) and potassium phosphate system is at around $L/X = 1.5$ (Fig. 8), where X is the distance from the axis of the holder to the central axis of the centrifuge and L the length of column shift from the center along the rotary shaft. For highly viscous and very low interfacial tension polymer phase systems such as dextran/PEG, $L/X = 3$ provides satisfactory retention of the stationary phase. Fig. 8 shows a cross-sectional view through the horizontal plane of the *X*-axis CPC ($L/X = 1.5$). A pair of column holders is mounted symmetrically around the rotary frame. When the motor (not shown) drives the rotary frame around the centrifuge axis, a pair of horizontal miter gears engaged with a stationary sun gear (center) rotates about their own axes on the rotating frame. This motion is further conveyed to each column holder by coupling with a pair of pulleys, one at the end of the gear shaft and the other mounted on the flange of the column holder, with a toothed belt. The flow tubes leading from each holder, as indicated in the diagram, are not twisted when they are supported at the center of the centrifuge cover. These tubes maintain their integrity for many runs when lubricated with grease and protected with a short sheath of Tygon tubing to prevent direct contact with metal parts. This apparatus has been successfully used for the purification of various kinds of proteins with PEG/potassium phosphate systems.

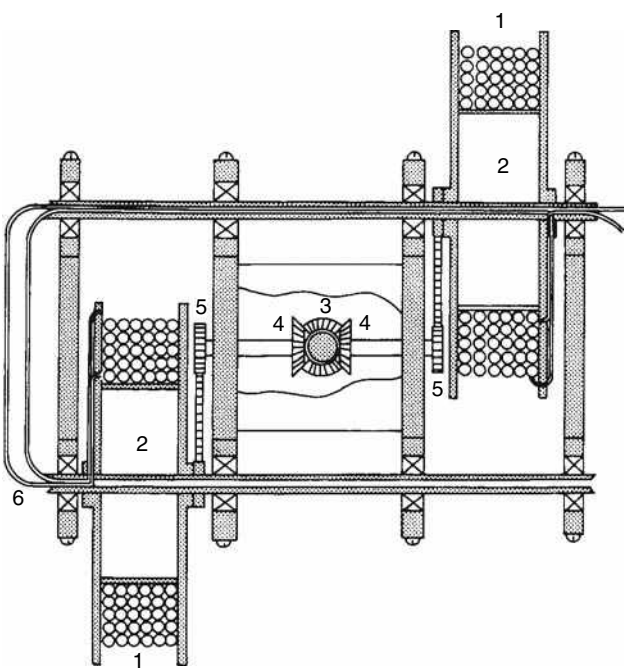

Fig. 8 Cross-sectional view through central horizontal plane of 1.5*L*/*X* cross-axis coil planet centrifuge. 1, Multilayer coil separation column; 2, column holder; 3, stationary miter gear; 4, horizontal miter gears each equipped with toothed pulley; 5, at peripheral end; and 6, flow tubes.

REFERENCES

1. Ito, Y. Countercurrent chromatography (minireview). J. Biophys. Biochem. Meth. **1980**, *3*, 77–87.
2. Ito, Y. Recent advances in countercurrent chromatography (review). J. Chromatogr. **1991**, *538*, 3–25.
3. Ito, Y.; Bowman, R.L. Countercurrent chromatography: Liquid–liquid partition chromatography without solid support. Science **1970**, *167*, 281–283.
4. Matsuda, K.; Matsuda, S.; Ito, Y. Toroidal coil countercurrent chromatography. Achievement of high resolution by optimizing flow-rate, rotation speed, sample volume and tube length. J. Chromatogr. A, **1998**, *808*, 95–104.
5. Marchal, L.; Foucault, A.P.; Patissier, G.; Rosant, J.-M.; Legrand, J. Centrifugal partition chromatography: An engineering approach. In *Countercurrent Chromatography: The Support-Free Liquid Stationary Phase*; Berthod, A., Ed.; Elsevier: New York, 2002; 115–157, Chapter 5.
6. Ito, Y.; Bowman, R.L. Countercurrent chromatography with flow-through centrifuge without rotating seals. Anal. Biochem. **1978**, *85*, 614–617.
7. Ito, Y. Centrifugal precipitation chromatography applied to fractionation of proteins with ammonium sulfate. J. Liq. Chromatogr. Relat. Technol. **1999**, *22*, 2825–2836.
8. Ito, Y. Centrifugal precipitation chromatography: Principle, apparatus and optimization of key parameters for protein fractionation by ammonium sulfate precipitation. Anal. Biochem. **2000**, *277* (1), 143–153.

9. Ito, Y.; Suaudeau, J.; Bowman, R.L. New flow-through centrifuge without rotating seals applied to plasmapheresis. Science **1975**, *189*, 999–1000.
10. Ito, Y. Sealless continuous flow centrifuge. In *Apheresis: Principles and Practice*; McLeod, B., Price, T.H., Drew, M.J., Eds.; AABB Press: Bethesda, MD, 1997; 9–13.
11. Ito, Y.; Blamblett, G.T.; Bhatnagar, R.; Huberman, M.; Leive, L.; Cullinane, L.M.; Groves, W. Improved non-synchronous flow-through coil planet centrifuge without rotating seals. Principle and application. Sep. Sci. Technol. **1983**, *18*, 33–48.
12. Okada, T.; Metcalf, D.D.; Ito, Y. Purification of mast cells with an improved non-synchronous flow-through coil planet centrifuge. Int. Arch. Allergy Immunol. **1996**, *109*, 376–382.
13. Ito, Y. High-speed countercurrent chromatography. CRC Crit. Rev. Anal. Chem. **1986**, *17*, 65–143.
14. Ito, Y., Conway, W.D., Eds.; *High-speed Countercurrent Chromatography*; Wiley Interscience: New York, 1996.
15. Ito, Y. Foam countercurrent chromatography based on dual countercurrent system. J. Liq. Chromatogr. **1985**, *8*, 2131–2152.
16. Oka, H. Foam countercurrent chromatography. In *High-Speed Countercurrent Chromatography*; Ito, Y., Conway, W.D., Eds.; Wiley Interscience: New York, 1996; 107–120, Chapter 5.
17. Lee, Y.W. Dual countercurrent chromatography. In *High-Speed Countercurrent Chromatography*; Ito, Y., Conway, W.D., Eds.; Wiley Interscience: New York, 1996; 93–104, Chapter 5.
18. Ito, Y.; Sandlin, J.L.; Bowers, W.G. High-speed preparative countercurrent chromatography (CCC) with a coil planet centrifuge. J. Chromatogr. **1982**, *244*, 247–257.
19. Ito, Y.; Menet, J.-M. Coil planet centrifuges for high-speed countercurrent chromatography. In *Countercurrent Chromatography*; Menet, J.-M., Thiébaut, D., Eds.; Marcel Dekker: New York, 1999; 87–119, Chapter 3.

CCC: Solvent Systems

T. Maryutina
Boris Ya. Spivakov
Vernadsky Institute of Geochemistry and Analytical Chemistry, Russian Academy of Sciences, Moscow, Russia

INTRODUCTION

Countercurrent chromatography (CCC) has been mainly developed and used for preparative and analytical separations of organic and bio-organic substances.[1] The studies of the last several years have shown that the technique can be applied to analytical and radiochemical separation, preconcentration, and purification of inorganic substances in solutions on a laboratory scale by the use of various two-phase liquid systems.[2] Success in CCC separation depends on choosing a two-phase solvent system that provides the proper partition coefficient values for the compounds to be separated and satisfactory retention of the stationary phase. The number of potentially suitable CCC solvent systems can be so great that it may be difficult to select the most proper one.

DISCUSSION

Recent studies have made it possible to classify water-organic solvent systems in CCC for separation of organic substances on the basis of the liquid-phase density difference, the solvent polarity, and other parameters from the point of view of stationary-phase retention in a CCC column.[1,3–9] Ito[1] classified some liquid systems as hydrophobic (such as heptane–water or chloroform–water), intermediate (chloroform–acetic acid–water and *n*-butanol–water) and hydrophilic (such as *n*-butanol–acetic acid–water) according to the hydrophobicity of the non-aqueous phase. Thirteen two-phase solvent systems were evaluated for relative polarity by using Reichardt's dye to measure solvachromatic shifts and using the solubility of index compounds.[6]

However, the systems for inorganic separations are very different from those for organic separations, as, in most cases, they contain a complexing (extracting) reagent (ligand) in the organic phase and mineral salts and/or acids or bases in the aqueous phase. Thus, the complexation process, its rate, and the masstransfer rate can play a significant role in the separation process.[9] There are three important criteria for choosing a two-phase liquid system.

First, the systems must be composed of two immiscible phases. Each solvent mixture should be thoroughly equilibrated in a separatory funnel at room temperature and the two phases separated after the two clear phases have been formed. When the nature of the organic sample to be separated is known, one may find a suitable solvent system by searching the literature for solvent systems that have been successfully applied to similar compounds.[1,3–8] In the case of organic-aqueous two-phase systems, the organic phase consists of one solvent or of a mixture of different solvents. Various non-aqueous–non-aqueous two-phase solvent systems have been used for separation of non-polar compounds and/or compounds that are unstable in aqueous solutions. Separation of macromolecules and cell particles can be performed with a variety of aqueous–aqueous polymer-phase systems. Among the various polymer-phase systems available, the following two types are the most versatile for performing CCC.[1,8] Poly (ethylene glycol) (PEG)–potassium phosphate systems provide a convenient means of adjusting the partition coefficient of macromolecules by changing the molecular weight of PEG and/or the pH of the phosphate buffer. The PEG 6000–Dextran 500 systems provide a physiological environment, suitable for separation of mammalian cells by optimizing osmolarity and pH with electrolytes.

For preconcentration and separation of inorganic species, a stationary phase containing extracting reagents of different types (cation-exchange, anion-exchange, and neutral) in an organic solvent should be usually applied.[2,9–12] The mobile-phase components should not interfere with the subsequent analysis. Solutions of inorganic acids and their salts are most often used.The mobile phase may also contain specific complexing agents, which can bind one or several elements under separation.

Second, one of the phases (stationary one) must be retained in the rotating column to a required extent. The most important factor, which determines the separation efficiency and peak resolution for both organic and inorganic compounds, is the ratio of the stationary-phase volume retained in a column to the total column volume. The volume of the stationary phase retained in the column depends on various factors, such as the physical properties of the two-phase solvent system, flow rate of the mobile phase, and applied centrifugal force field. In droplet CCC, where the separation is performed in a stationary column, a large density

difference between the stationary solvent phases becomes the predominant factor for the retention of the stationary phase. In other CCC schemes, various types of two-phase solvent systems can be used under optimized experimental conditions. The influence of planetary centrifuge parameters and operation conditions on the stationary-phase retention have been well studied for some simple two-phase liquid systems consisting of water and one or two organic solvents.[1,3–8]

According to Ito's classifications,[1,3] hydrophobic organic phases are easily retained by all types of CCC apparatus. Intermediate solvent systems involve a more hydrophilic organic phase. Their tendency to evolve, after mixing, to a more stable emulsion than the hydrophobic systems decreases the retention of stationary phase. The hydrophilic two-phase systems containing a polar phase are even less retained in the column.

However, the addition of extracting reagents and mineral salts to a two-phase system (in case of inorganic separations) can strongly affect the physicochemical properties of liquid systems and, consequently, their hydrodynamic behavior and S_f value. Varying concentrations of the system constituents used for inorganic separation allows selective changing of a certain physicochemical parameter (interfacial tension γ, density difference between two liquid phases $\Delta\rho$ and viscosity of the organic stationary phase η_{org}). The type of the solvent may often have a great effect on the stationary-phase retention and, consequently, on the chromatographic process. The correlations between the physicochemical parameters of the complex liquid systems under investigation and their behavior in coiled columns are described in detail.[10] The composition and physicochemical properties of the organic phase in inorganic analysis were modified by adding an extracting reagent [e.g., di-2-ethylhexylphosphoric acid (D2EHPA), tri-*n*-butyl phosphate, trioctylamine].[2,10] The density and viscosity of the organic phase were varied by changing the amount of reagents in the stationary phase. For example, a small addition (5%) of D2EHPA in an organic solvent (*n*-decane, *n*-hexane, chloroform, and carbon tetrachloride) leads to a considerable increase in the factor in the organic solvent—$(NH_4)_2SO_4$—water systems (from 0 to 0.73 in the case of carbon tetrachloride).[10]

Third, the stationary phase should permit separate elution of the substances into the mobile phase and the selectivity toward samples of interest has to be sufficient to lead to separations with good resolution. The selectivity of solvent systems can be estimated by determination of the partition coefficients for each substance. The batch partition coefficients D^{bat} are calculated as the ratio of the component concentration in the organic phase to that in the aqueous phase. The dynamic partition coefficients of compounds are determined from an experimental elution curve.[7] Several solvent systems for organic separation were investigated.[4–8] The most efficient evolution usually occurs when the value of the partition coefficient is equal 1. However, in some CCC schemes, the best results are obtained with lower partition coefficient values of 0.3–0.5.[1,4]

CONCLUSIONS

In inorganic analysis with the use of CCC, the stationary phase should provide preconcentration of the elements to be determined, if necessary. It should be noted that the element elution depends on the operation conditions for the planetary centrifuge, which influence the quantity of the stationary phase in the column. A chromatographic peak shifts to left and narrows if the volume of the stationary phase lowers (all the other factors being the same).[2] The reagent concentration in the organic solvent also affects the elution curve shape and, therefore, the dynamic partition coefficient values. An increase of the reagent concentration in the organic phase leads to higher partition coefficients for the elements, and a better separation is achieved. However, a rather large volume of the mobile phase can be required for the elution of elements from the column.

The composition of the mobile phase also has an influence on the partition coefficients of inorganic substances and the separation efficiency. Concentrations of the mobile-phase constituents should provide partition coefficient values needed for the enrichment or separation of components under investigation. If a step-elution mode is used, partition coefficients higher than 10 and less than 0.1 are favorable for the enrichment of components into the stationary phase and their recovery into the mobile phase, respectively. Chemical kinetics factors may also play an important role in the separation of inorganic species by CCC.[9] It has been shown that the values of masstransfer coefficients determine the type of elution (isocratic or step), which is necessary for the element separation. The data on batch extraction (mass-transfer coefficients and partition coefficients) and parameters of chromatographic peaks (half-widths) can be interrelated by some empirical expressions.[9] The application of CCC in inorganic analysis looks promising because various two-phase liquid systems, providing the separation of a variety of inorganic species, may be used for the separation of trace elements.

REFERENCES

1. Ito, Y. *Countercurrent Chromatography. Theory and Practice*; Mandava, N.B., Ito, Y., Eds.; Marcel Dekker, Inc.: New York, 1988.

2. Ya. Spivakov, B.; Maryutina, T.A.; Fedotov, P.S.; Ignatova, S.N. *Metal-Ion Separation and Preconcentration: Progress and Opportunities*; Bond, A.N. Dietz, M.L., Rodgers, R.D., Eds.; American Chemical Society: Washington, DC, 1999; 333–347.
3. Conway, W.D. *Countercurrent Chromatography. Apparatus, Theory and Applications*; VCH: New York, 1990.
4. Berthod, A.; Schmitt, N. Waterorganic solvent systems in countercurrent chromatography: Liquid stationary phase retention and solvent polarity. Talanta **1993**, *40*, 1489.
5. Menet, J.-M.; Thiebaut, D.; Rosset, R.; Wesfreid, J.E.; Martin, M. Classification of countercurrent chromatography solvent systems on the basis of the capillary wavelength. Anal. Chem. **1994**, *66* (1), 168.
6. Abbott, T.P.; Kleiman, R. Solvent selection guide for counter-current chromatography. J. Chromatogr. **1991**, *538*, 109.
7. Drogue, S.; Rolet, M.-C.; Thiebaut, D.; Rosset, R. Separation of pristinamycins by high-speed counter-current chromatography I. Selection of solvent system and preliminary preparative studies. J. Chromatogr. **1992**, *593*, 363.
8. Foucault, A.P.; Chevolot, L. Counter-current chromatography: Instrumentation, solvent selection and some recent applications to natural product purification. J. Chromatogr. A, **1998**, *808*, 3.
9. Fedotov, P.S.; Maryutina, T.A.; Pichugin, A.A.; Spivakov, B.Ya. Russ. J. Inorg. Chem. **1993**, *38*, 1878.
10. Matyutina, T.A.; Ignatova, S.N.; Fedotov, P.S.; Spivakov, B.Ya.; Thiebaut, D. Influence of composition and some physico-chemical properties of two-phase liquid systems on the stationary phase retention in a coil planet centrifuge. J. Liq. Chromatogr. Relat. Technol. **1998**, *21* (1), 19.
11. Kitazume, E.; Bhatnagar, M.; Ito, Y. Separation of rare earth elements by high-speed counter-current chromatography. J. Chromatogr. **1991**, *538*, 133.
12. Zolotov, Yu.A.; Spivakov, B.Ya.; Maryutina, T.A.; Bashlov, V.L.; Pavlenko, I.V. Partition countercurrent chromatography in inorganic analysis. Fresenius Anal. Chem. **1989**, *335* (8), 938.

CE

Joseph J. Pesek
Maria T. Matyska
Department of Chemistry, San Jose State University, San Jose, California, U.S.A.

INTRODUCTION

Electrophoresis has been used as a separation technique for decades, particularly by biochemists, in the open-bed format. In this mode, a layer of a gel is formed on a flat-bed support which is in contact with an electrolyte and two electrodes are situated at either end of the open slab. The sample is placed at one end of the separation medium, and when voltage is applied, the molecules migrate through the gel by electrophoresis. The components in the sample are separated based on their differences in electrophoretic mobility. The electrophoretic mobility is controlled by molecular parameters such as charge, size, and shape. After the electric field is turned off, the separation is evaluated by spraying the plate with a dye and the bands of the sample components become visible, similar to the detection format used in paper or thin-layer chromatography.

DISCUSSION

Although the basic principle was conceived many years ago, the practical development of electrophoresis experiments in a closed or tubular format was only begun a little more than a decade ago. The main problem of the closed system is that the application of high voltages leads to the generation of Joule heat as current flows through the electrolyte solution. The heat generated can often cause sample decomposition or, more frequently, result in a large increase in molecular diffusion, leading to zone broadening that obliterates the separation between adjacent bands. Therefore, for these experiments to work in a tubular format, it is necessary to use capillary tubes with diameters of 100 μm or less in most cases. The answer to overcoming the Joule heat problem is to use fused-silica tubes, similar to those developed for capillary gas chromatography but having a smaller internal diameter. A second advantage of the fused-silica capillary is that it is suitable for direct online detection because it is optically transparent to ultraviolet (UV) and visible light. Typical dimensions for the capillary under experimental conditions are an outer diameter (O.D.) of ~375 μm, an inner diameter (I.D.) of 50–100 μm, and an overall length of 50–100 cm. To protect the fragile fused-silica tube, the capillary is coated with an external layer of polyimide, allowing it to be flexible and manipulated into a variety of instrumental geometries. A detection window can be made by removing a small amount of the protective coating.

The fused-silica surface also provides another mechanism, electro-osmosis, which drives solutes through the tube under the influence of an electric field. The principle of electro-osmotic flow (EOF) is illustrated in Fig. 1. The inner wall of the capillary contains silanol groups on the surface that become ionized as the pH is raised above about 3.0. This creates an electrical double layer in the presence of an applied electric field so that the positively charged species of the buffer which are surrounded by a hydrated layer carry solvent toward the cathode (negatively charged electrode). This results in a net movement of solvent toward the cathode that will carry solutes in the same direction as if the solvent were pumped through the capillary. This electrically driven solvent pumping mechanism results in a flat flow profile in contrast to the laminar one (parabolic) obtained from mechanical pumps such as those used in high-performance liquid chromatography (HPLC). However, EOF is uniform throughout the capillary and does not depend on any solute properties. All solutes are affected by EOF uniformly and this process does not contribute to the separation mechanism. Therefore, only differences in electrophoretic velocity are responsible for the separation of charged compounds in a fused-silica capillary in the presence of an applied electric field. In fact, EOF is detrimental to the separation process because it moves positively charged species through the capillary faster, thus allowing less time for differences in electrophoretic velocity to separate two species with similar mobilities. This effect can be described mathematically by the following equation:

$$v_{tot} = v_{ep} + v_{EOF}$$

where v_{tot} is the total velocity of the charged species, v_{ep} is the electrophoretic velocity of that species, and v_{EOF} is the electro-osmotic velocity. In a typical experiment, sample migration rates through the capillary are as follows: cationic species > neutral compounds > anionic species. Because both cationic and anionic compounds can have different electrophoretic mobilities, they can be separated within the capillary. However, neutral species are carried through the capillary only by EOF, so these compounds will all migrate at the same rate and, therefore, cannot by separated by capillary electrophoresis (CE).

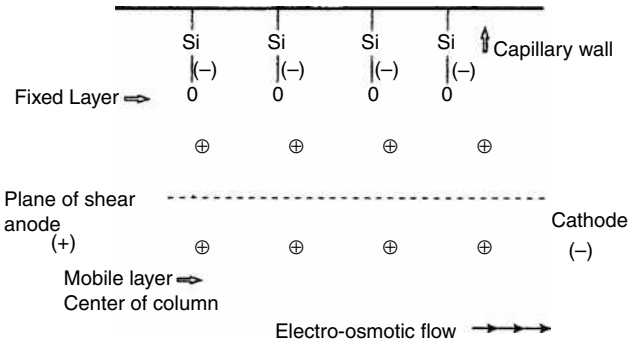

Fig. 1 Principle of electro-osmotic flow.

The basic apparatus necessary for a CE system is shown in Fig. 2. The instrument must have the following components: power supply, electrodes (anode and cathode), vials for electrodes and buffers, separation capillary, detector, and data system or recorder (not shown). The function of each of these components is as follows:

- Power Supply. This device supplies the high voltage to the system. Typically, experiments are run at several kilovolts up to 30 kV or more. Most power supplies will also have an ammeter to measure the current flowing through the system.
- Electrodes. These components are generally platinum wires which serve as the contact point between the liquid (buffer solutions) in the system and the high-voltage power supply. An inert metal is desirable to avoid an electrochemical reaction or excessive fouling of the electrode surface that would disrupt current flow in the system.
- Buffer Reservoirs. These containers hold the buffer solution that provides for a complete electrical circuit through the capillary and connection to the high-voltage supply. Due to EOF as described earlier, the vials also serve as reservoirs to maintain electroneutrality in the system.

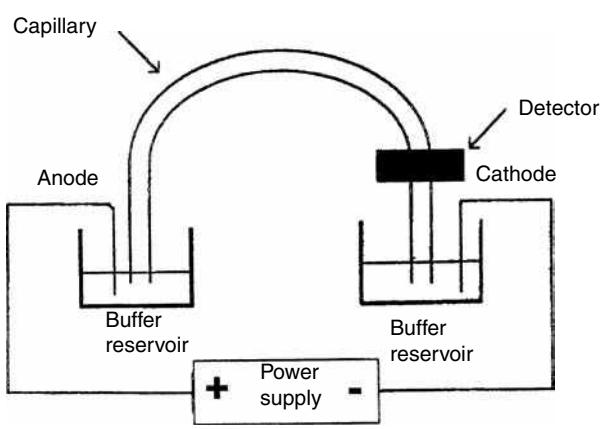

Fig. 2 Basic apparatus for capillary electrophoresis.

- Separation Capillary. The fused-silica capillary tube is the focal point in the instrument because sample separation takes place here. The length is typically 50–100 cm and the ends are placed in the buffer reservoirs. The capillary is filled with the running buffer before the analysis begins.
- Detector. This device measures a property of the solute in order to determine when each compound has passed through a significant portion of the capillary to the detection window. The detector is not placed at the end of the capillary, as this part of the tube must be in the buffer solution. Solute properties most often used for detection are absorbance and fluorescence, although CE can also be coupled to a mass spectrometer.
- Data System/Recorder. The simplest device for output is an ordinary recorder. However, an integrator will provide more information about the peaks (time and area). The most sophisticated apparatus is a computer, which can be used to process and evaluate the data. The computer can also be used to control the operations of the instrument.

The sample can be introduced into the capillary by several methods. The simplest approach is to remove the end of the capillary from the anode buffer reservoir and place it in the sample vial that has been elevated slightly above the level of the cathode buffer container. Gravity flow for several seconds will move some of the sample in the separation capillary. Another approach is to place the anode end of the capillary into the sample vial and apply pressure to the analyte solution. The next method involves placing the anode end of the capillary in the sample vial and applying a vacuum to the cathodic side of the capillary to draw solution into the tube. The previous three means of sample introduction are referred to as hydrodynamic modes of injection. The last method involves placing the anodic end of the capillary in the sample vial and applying a low voltage for several seconds. This approach is referred to as electrokinetic injection.

Information about the analyte can be qualitative and/or quantitative, with the data resembling a chromatogram. The output from the recorder/integrator/data system is in the form of peaks which are indicated by a time (migration time) from the start of the experiment. The migration time is analogous to the retention time in a chromatographic separation and provides qualitative information by comparison to a known compound under identical experimental conditions. Because the majority of detection in CE is by spectroscopic means, the area under the peak is proportional to the concentration. Therefore, quantitative information can be obtained by making a calibration curve from a plot of peak area vs. concentration.

Even though CE is a relatively simple method, several formats exist that allow for analyses of different types of samples or to take advantage of certain solute properties. The primary modes of CE are as follows:

- Capillary Zone Electrophoresis. The most fundamental approach that involves the use of a fused-silica capillary placed between the two buffer vials so that separation of the sample component occurs after an electric field (voltage) is applied to the system. Separation of the analytes is based on differences in electrophoretic mobility. Only charged compounds, both large and small, can be separated in this format.
- Capillary Gel Electrophoresis. In this mode, molecules are separated according to size as they migrate through a polymer matrix. The polymer can be in solution, physically coated on the capillary wall, or chemically bonded to the capillary wall. This mode is primarily used for the separation of large molecules like proteins, peptides, and DNA species.
- Capillary Isoelectric Focusing. In this approach, the capillary contains a pH gradient. When the sample is introduced and voltage is applied, it migrates to the point in the capillary where it has zero net charge (isoelectric point). The analytes are removed from the capillary by adding a salt to one of the reservoirs and then applying voltage again. The solutes will then migrate past the detector, with the time being related to its position in the capillary.
- Capillary Isotachophoresis. In isotachophoresis, the capillary is first filled with a buffer of higher mobility than any of the solutes, then the sample, and, finally, a second buffer with lower mobility than any of the analytes. Separation occurs in the zone formed between the two electrolytes.
- Micellar Electrokinetic Capillary Chromatography. Surfactants that form micelles in solution are added to the buffer in the capillary. When the solute is injected, it partitions itself between the buffer and the micelle. Migration of the solute depends on the amount of time it spends in the micelle vs. the time it spends in the buffer. Therefore, the separation of analytes occurs due to differences in the partition coefficient between the two phases, much like in a chromatographic process.

CONCLUSION

CE is still an emerging technology. Rapid development is occurring in separation capillaries, detector technology, and applications.

BIBLIOGRAPHY

1. Altria, K.D. *Capillary Electrophoresis Guidebook: Principles, Operation and Applications*; Humana Press: Totowa, NJ, 1996.
2. Camilleri, P. *Capillary Electrophoresis: Theory and Practice*; CRC Press: Boca Raton, FL, 1998.
3. Hjerten, S. Methods Enzymol. **1996**, *270*, 296.
4. Landers, J.P. *Handbook of Capillary Electrophoresis,* 2nd Ed.; CRC Press: Boca Raton, FL, 1997.
5. Lunte, S.M.; Radzik, D.M. *Pharmaceutical and Biomedical Applications of Capillary Electrophoresis*; Pergammon: Oxford, 1996.
6. Parves, H.; Candy, P.; Parvez, S.; Roland-Gosselin, P. *Capillary Electrophoresis in Biotechnology and Environmental Analysis*; VSP: Utrecht, 1997.
7. Righetti, P.G. *Capillary Electrophoresis in Analytical Biotechnology*; CRC Press: Boca Raton, FL, 1996.

CE in Nonaqueous Media

Ernst Kenndler
Institute for Analytical Chemistry, University of Vienna, Vienna, Austria

INTRODUCTION

Organic solvents are used in capillary electrophoresis (CE) for several reasons:

1. To increase the solubility of lipophilic analytes.
2. To affect the actual mobilities of the analytes (those of the fully charged species at the ionic strength of the solution).
3. To change the pK values of the analytes.
4. To influence the magnitude of the electro-osmotic flow.
5. To influence the equilibrium constant of association reactions between analytes and additives (e.g., for the adjustment of the degree of complexation; an important example is the separation of chiral compounds by the use of cyclodextrins).
6. In some rare cases, to allow homoconjunction or heteroconjugation of the analytes with other species present and, thus, enable separation. For such interactions, a low dielectric constant of the solvent is a prerequisite.

APPLICATION OF NONAQUEOUS SOLVENTS

The organic solvents are applied in many cases in order to enhance the separation selectivity by changing the effective mobilities of the analytes. They are either applied as pure solvents, or as nonaqueous mixtures, or as constituents of mixed aqueous–organic systems. Solvents used for CE, as described in the literature, are methanol, ethanol, propanol, acetonitrile, tetrahydrofuran, formamide, *N*-methylformamide, *N*,*N*-dimethylformamide, *N*,*N*-dimethylacetamide, dimethylsulfoxide, acetone, ethylacetate, and 2,2,2- trifluoroethanol.

Organic solvents have relevance in many fields of application: for the separation of inorganic ions, organic anions and cations, pharmaceuticals and drugs, amino acids, peptides, and proteins.

There are some practical restrictions for the use of organic solvents:

1. Many organic solvents have a significant ultraviolet (UV) absorbance in the range of wavelengths that are normally also used for the detection of the analytes. This property leads to a poor signal-to-noise ratio or limits the applicability to solutes with UV absorbances at a higher wavelength.
2. Many electrolytes cannot be used as buffers, due to their low solubilities in organic solvents.
3. The low dielectric constant of solvents suppresses ion dissociation and favors ion-pair formation.
4. Important physicochemical properties (e.g., ionization constants of weak acids and bases) are often not known, which leads to a more or less random experimental approach for the optimization of the resolution.
5. In this context, it should be mentioned that the clear determination of the pH scale in these solvents is not a straightforward task, which may introduce a certain inaccuracy for the description of the experimental conditions. As this aspect is not adequately considered in many articles on CE in nonaqueous solvents, it is discussed here in more detail.

ACIDITY SCALES IN ORGANIC SOLVENTS

When investigating the effect of organic solvents on the pK_a of an acid, the significance of the pH scale in this solvent must be questioned. We base such scales on the measurement of the activity of the solvated proton. We define the activity, a_i, of a particle, i, the proton in the case of interest, by the difference between the chemical potential, ω_i in the given and in a standard state (indicated by superscript 0)

$$\omega_i = \omega_i^{\,0} + RT \ln a_i$$

In practice, we therefore differentiate a number of acidity scales: the standard, the conventional, the operational, and the absolute (thermodynamic) scale.

STANDARD ACIDITY SCALE

The standard state might be chosen in various ways (e.g., as the state at infinitely diluted solution). The resulting standard acidity scale is characterized by the activity of the proton solvated by the given solvent, HS, according to

$$\mathrm{pH} = -\log a_{\mathrm{SH}_2^1} \qquad (1)$$

The range of this scale is defined by the ionic product of the solvent, pK_{HS}.

Measurements in the standard acidity scale are carried out in cells without liquid junctions (e.g., with the following setup: $Pt/H_2/HCl$ in SH/AgCl/Ag). It is assumed, here, that the activities of the solvated proton and the counterion, chloride, are equal. In this case, the electromotive force (emf) of the cell can be expressed by

$$E = E_S^0 - \frac{RT}{F}\ln a_{SH_2} - a_{Cl^-} = E_S^0 - \frac{2RT}{F}\ln\left(c_{HCl}\gamma_{HCl}\right) \quad (2)$$

where is c_{HCl} the concentration γ_{HCl} and is the mean activity coefficient of HCl. $E_S{}^0$ is the standard potential of the silver chloride electrode in the given solvent, S, after extrapolation of the measured emf to zero ionic strength. Rearrangement leads to the expression of the pH in the standard scale:

$$\mathrm{pH} = -\frac{(E - E_S^0)F}{2.3RT} + \log c_{Cl^-} + \log \gamma_{Cl^-} \quad (3)$$

CONVENTIONAL ACIDITY SCALE

The standard acidity scale, although well defined theoretically, has the limitation in practice that only the mean activity coefficient, but not the single-ion activity coefficient, is thermodynamically assessible. The single-ion coefficient depends on the composition of the solution as well. One way to circumvent this problem would be to have a defined value of the activity coefficient for one selected ion. Given that, all other activity coefficients could be obtained from the activity coefficients of the particular electrolytes and that special single-ion coefficient. The value of this selected coefficient could be used, then, as the base of the conventional acidity scale. This single-ion activity coefficient is derived for chloride by the Debye–Hückel theory. This choice is made by convention, initially proposed for aqueous solutions; it is accepted also for other amphiprotic, polar solvents. Note that the measurements of the proton activity are carried out in cells without liquid junction.

OPERATIONAL ACIDITY SCALE

Due to the disadvantage of working with cells without liquid junctions, in practice the operational scale uses buffer solutions with known conventional pH for the calibration of cells with liquid junction [e.g., the convenient glass electrode (with the calomel or silver electrode, respectively, as reference)]. After calibration of the measuring cell (with a buffer of known conventional pH), the acidities of unknown samples can be measured in the same solvent. It is clear that for the standard buffers used, the conventional and the operational pH are identical. However, we cannot assume such an identity for the unknown samples. This is because the activities and the mobilities of the different ionic species might change the potential on the boundary with all liquid junctions (even without taking effect of the non-electrolytes into account).

ABSOLUTE (THERMODYNAMIC) SCALE AND MEDIUM EFFECT

This scale, in fact, would allow comparing the basicities of the different solvents in a general way. It is based on the question of the chemical potential of the proton (as a single-ion species) in water, W, and the organic solvent, S. Taking the hypothetical 1 *M* solution as the standard state, the chemical potential is given, according to Eq. 1, as

$$\omega_{H^+} = \omega_{H^+}^0 + RT\ln m_{H^+} + RT\ln\gamma_{H^+} \quad (4)$$

where *m* is the molal concentration. The so-called medium effect on the proton is given by

$$\ln {}_W\gamma_{H^+} - \ln {}_S\gamma_{H^-} = \ln\left(\frac{{}_W\gamma_{H^-}}{{}_S\gamma_{H^+}}\right) = \ln {}_m\gamma_{H^+} = \frac{{}_S\omega_{H^+}^0 - {}_W\omega_{H^+}^0}{RT} \quad (5)$$

${}_m\gamma_{H^+}$ is named the transfer activity coefficient. The medium effect is proportional to the reversible work of transfer of 1 mol of protons in water to the solvent, S (in both solutions at infinite dilution). If the medium effect is negative, the proton is more stable in the solvent, S. It is, thus, an unequivocal measure of the basicity of the solvent, compared to water, as it allows us to establish a universal pH scale due to

$$-\log {}_W a_{H^+} = -\log {}_S a_{H^+} - -\log {}_m a_{H^+} \quad (6)$$

It is a serious drawback that it is not possible to determine the transfer activity coefficient of the proton (or of any other single-ion species) directly by thermodynamic methods, because only the values for both the proton and its counterion are obtained. Therefore, approximation methods are used to separate the medium effect on the proton. One is based on the simple *sphere-in-continuum* model of Born, calculating the electrostatic contribution of the Gibb's free energy of transfer. This approach is clearly too weak, because it does not consider solvation effects. Different extrathermodynamic approximation methods, unfortunately, lead not only to different values of the medium effect but also to different signs in some cases. Some examples are given in the following: ${}_m\gamma_{H^+}$ for methanol +1.7 (standard deviation 0.4); ethanol +2.5 (1.8), *n*-butanol +2.3 (2.0), dimethyl

sulfoxide −3.6 (2.0), acetonitrile + 4.3 (1.5), formic acid +7.9 (1.7), NH_3 −16. From these data, it can be seen that methanol has about the same basicity as water; the other alcohols are less basic, as is acetonitrile. Dimethyl sulfoxide, on the other hand, is more basic than water. However, the basicity of the solvent is not the only property that is important for the change of the p*K* values of weak acids in comparison to water. The stabilization of the other particles that are present in the acido-basic equilibrium is decisive as well.

BIBLIOGRAPHY

1. Bates, R.G. Medium effect and pH in non-aqueous and mixed solvents. In *Determination of pH, Theory and Practice*; John Wiley & Sons: New York, 1973; 211–253.
2. Covington, A.K.; Dickinson, T. Introduction and solvent properties. In *Physical Chemistry of Organic Solvents Systems*; Covington, A.K., Dickinson, T., Eds.; Plenum Press: London, 1973; 1–23.
3. Kolthoff, I.M.; Chantooni, M.K. General introduction to acid–base equilibria in non-aqueous organic solvents. In *Treatise on Analytical Chemistry, Part I, Theory and Practice*; Kolthoff, I.M., Elving, P.J., Eds.; John Wiley & Sons: New York, 1979; 239–301.
4. Popov, A.P.; Caruso, H. Amphiprotic solvents. In *Treatise on Analytical Chemistry, Part I, Theory and Practice*; Kolthoff, I.M., Elving, P.J., Eds.; John Wiley & Sons: New York, 1979; 303–347.
5. Sarmini, K.; Kenndler, E. Ionization constants of weak acids and bases in organic solvents. J. Biophys. Biochem. Methods **1999**, *38*, 123.
6. Sarmini, K.; Kenndler, E. Influence of organic solvents on the separation selectivity of capillary electrophoresis. J. Chromatogr. A, **1997**, *792*, 3.

CE on Chips

Christa L. Colyer
Department of Chemistry, Wake Forest University, Winston-Salem, North Carolina, U.S.A.

INTRODUCTION

It is no wonder that capillary electrophoresis (CE) has evolved into one of the premier separation techniques in use today, due to its extremely high efficiencies, fast analysis times, reduced sample and reagent consumption, and vast array of operating modes. The transposition of CE methods from conventional capillaries to channels on planar chip substrates is a more recent phenomenon and has been driven by several factors, including, but not limited to, the need for ever-more sensitive and selective assays, the need to manipulate increasingly smaller samples, and the desire to process many samples in parallel.[1] Perhaps of greater significance to the rapid development of this important field, however, is its amenability to the assimilation of multiple components of an assay—beyond simple separation of analytes—into a single, fully integrated device. The promise of the "lab-on-a-chip," although seemingly ambitious in concept, is clearly attainable, and microchip capillary electrophoresis (μ-chip CE) has quickly established itself as one of the most fundamental constituents of such systems.

One of the first published demonstrations of capillary electrophoresis on a chip appeared in 1992, when Harrison et al. separated a mixture of fluorescein and calcein.[2] Although separation efficiencies and analysis times in this pioneering work did not represent significant improvements over those achievable by way of conventional CE, this work demonstrated the feasibility of miniaturizing a chemical analysis system involving electrokinetic phenomena for sample injection, separation, and solvent pumping. Within 2 years of the appearance of this seminal paper, analysis times on the order of seconds and even milliseconds had been demonstrated with similar μ-chip systems, and efficiencies in excess of 100,000 theoretical plates were routinely obtained. Subsequently, the integration of other functionalities, such as sample manipulations and chemical reactions, alongside the CE separation, has vaulted CE-on-a-chip to new heights.

CHIP FABRICATION TECHNOLOGY

The evolution of CE on a chip has directly benefited from the tremendous advances in semiconductor microfabrication technologies that have taken place over the past two decades. Although semiconducting substrates are not ideally suited to CE applications due to the high voltages applied for separation and fluid manipulation, many of the established semiconductor microfabrication techniques can be modified for the insulating glass or quartz substrates most commonly encountered in μ-chip CE. Here, the name μ-chip refers to the channel dimensions as opposed to the actual substrate dimensions, which commonly are on the order of 0.5 mm thick and anywhere from 3 to 10 cm in length and width (or diameter for circular substrates).

In many cases, standard photolithographic and wetetching techniques are employed in the manufacture of CE chips. To begin, the clean glass or quartz substrate is uniformly coated with sequential thin layers of chromium/gold and positive photoresist by sputtercoating and spin-coating methods, respectively. The design for the CE channel structure is then transferred to the substrate by exposure of the photoresist to ultraviolet (UV) light through a photomask of the channel pattern. After photoresist development, a series of wet etches are employed, first to remove the metal etch mask and, second, to etch the channels into the substrate. Channels created in this fashion are trapezoidal in profile due to the isotropic etching of amorphous materials. Typical channel dimensions range from 5 to 40 μm deep and 20 to 100 μm wide (at half the channel depth). Residual photoresist and metal film are stripped from the etched substrate prior to thermal bonding of a cover plate, thereby forming closed channels suitable for electrophoresis. Access to the channels is most commonly gained through holes drilled in the cover plate prior to bonding.

Capillary electrophoresis chips so created are quite rugged due to the monolithic nature of their structure, and they can withstand applied voltages in the same range (up to 30 kV) as those commonly encountered in conventional CE. In addition, they offer greater heat dissipation than conventional CE capillaries, thereby allowing for operation under conditions of higher power. Although quartz substrates have superior optical properties relative to their glass counterparts, both present an optically flat surface for detection schemes, which is a definite advantage over the curvature inherent to conventional capillary walls. As well, the void volumes associated with channel intersections on-chip are virtually non-existent. Despite their many advantages, these chips are time-consuming and expensive to fabricate. As such, alternative methods for CE chip fabrication are being developed, such as the creation of channels in polymeric materials by casting, molding, and

imprinting techniques. The success of these methods will rely, in part, on the concomitant development of suitable surface modification procedures to successfully manage channel wall properties.

INJECTION ON CHIPS

Clever chip design permits the integration of the sample injector directly on the chip, thereby combining injection and separation functions by default on a single substrate. Most commonly, the injector is fashioned as a simple cross or "double-T" arrangement of etched channels, as shown in Fig. 1. One branch of this cross serves as the sample channel, and the other serves as the separation channel. Fluid flow is manipulated through this cross, just as with all other fluid manipulations on chip, by control of electrokinetic phenomena: electrophoresis and electro-osmosis. By first applying the appropriate voltage between the sample and sample waste reservoirs (Fig. 1a), the sample solution crosses the separation channel, filling the double-T intersection. Consequently, injection volumes are defined by the injector geometry. Typical sample plug volumes and lengths are on the order of about 10–100 pl and 50–200 μm, respectively. Provided the injection field strength and time are sufficient to ensure that the least mobile sample component has moved through the channel intersection, this method results in an unbiased injection, with all sample components represented in the intersection volume according to their original proportions. Having thus formed a sample plug, the voltage is switched so as to generate electro-osmotic flow EOF along the separation channel (Fig. 1b), sweeping the sample plug out of the

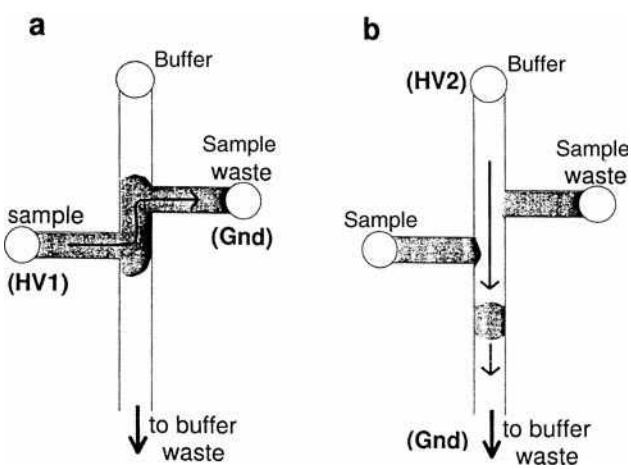

Fig. 1 Illustration of a μ-chip CE sample injector. Injection consists of (a) sample loading across the separation channel by application of a high voltage (HV1) across the sample and sample waste reservoirs, followed by (b) mobilization of the sample plug along the separation channel by application of HV2 across the buffer and buffer waste reservoirs.

double-T injector and initiating separation along the second branch of the injector. This branch—the separation channel—typically ranges from 1 to 10 cm in length. Further control of sample plug size and shape and prevention of sample leakage can be effected by carefully controlling voltages applied to all four arms of the cross simultaneously during injection and separation phases.

DETECTION ON CHIPS

It is not surprising that the requirements for detection on chips are very stringent, especially given the extremely small sample sizes discussed earlier. This need for sensitivity, along with the optically flat chip surface, makes laser-induced fluorescence (LIF) detection a natural choice; consequently, LIF detection on chips is the most widespread of all detection types. However, because relatively few analytes are natively fluorescent, LIF detection necessitates the development of selective and sensitive labeling strategies for each assay. Other detection methods, such as UV-Vis absorption, chemiluminescence, and electrochemical, are less commonly encountered in chip CE, but they have been successfully demonstrated. Recently, the ability to generate an electrospray from the edge of a CE chip[3] has spawned a flurry of additional work in the area of electrospray ionization–mass spectrometry (ESI–MS) detection for CE chips. This promises to be a particularly powerful and exciting advance, as both quantitative and qualitative information can be provided simultaneously by this method of detection.

BEYOND CE: SAMPLE MANIPULATIONS

The most fundamental purpose of a CE chip is, of course, the separation and subsequent detection of analytes within a manifold of micromachined channels on a miniaturized substrate. This separation may take place as a result of basic electrokinetic phenomena or it may be enhanced or assisted by implementation of any one of various other separation techniques, such as isotachophoresis, micellar electrokinetic chromatography, isoelectric focusing, or capillary gel electrophoresis, all of which have been successfully demonstrated on-chip. However, the feature that truly distinguishes μ-chip CE from its conventional capillary counterpart is not its separative ability but, rather, its facility to integrate other functions onto the chip alongside the separation. This has already been discussed with respect to the sample injector and it is equally applicable to various sample preparation techniques. For example, controlled sample dilution, achieved by mixing buffer and sample streams directly on-chip, was first shown by Harrison et al.[4] By increasing the voltage applied to a buffer reservoir while holding the voltage applied to a fluorescein dye sample reservoir constant, a controlled

decrease in fluorescence intensity, corresponding to increasingly greater dilutions of the fluorescein, was observed downstream at the detector.

Preconcentration is another commonly encountered sample pretreatment method that has been successfully integrated onto a CE chip. Ramsey and coworkers incorporated a porous membrane structure into a microfabricated injection valve, enabling electrokinetic concentration of DNA samples using homogeneous buffer conditions.[5] Sample preconcentration in non-homogeneous buffer systems—a technique known as sample stacking—has also been achieved on-chip.[6]

Filtration is yet another pretreatment technique commonly encountered in CE. The reduced dimensions of fluid channels on chip substrates make the need for solution filtration all the more critical in this work. Until very recently, filtration was exclusively conducted "off-line" (i.e., before the sample and/or buffer solution was ever introduced to the chip). However, Regnier and coworkers recently micromachined solvent and reagent filters into quartz substrates using deep reactive ion etching.[7] Flow through these microfabricated lateral percolation filters was driven by EOF, thus making them compatible with other fluidic processes in a chip CE system. The on-chip filters were shown to be capable of removing a variety of particulate materials, ranging from dust to cells. Surface fouling and loss of cationic proteins from analyte streams were minimized by applying a polyacrylamide coating to the filter surfaces. Hence, these selected examples of the transposition of some traditional sample pretreatment methods onto chip substrates and their compatibility with on-chip CE separations illustrate the potential for achieving a fully integrated lab-on-a-chip.

BEYOND CE: CHEMICAL REACTIONS ON CHIP

Full functionality of these chips cannot be realized by the integration of sample pretreatment, injection, and separation methods alone. Additionally, the ability to carry out chemical reactions on-chip must be included in the list of integrated functions in order to extend the utility of these systems. Indeed, a wide variety of on-chip chemical reactions coupled to CE separations have been successfully demonstrated, including fluorescent derivatization, digestion of DNA and proteins, affinity-type reactions, and the polymerase chain reaction (PCR) for DNA amplification. The first of these reactions is necessitated by the laser-induced fluorescence detection schemes commonly used with CE chips. Because few analytes are natively fluorescent, it is often necessary to either (a) react the analyte with a fluorescent tag prior to separation (preseparation or precolumn labeling) or (b) separate the analyte first, followed by reaction of the separated zones with a derivatizing agent (postseparation or postcolumn labeling). The former, although leading to greater sensitivity, often suffers from increased band broadening and reduced separation efficiencies. The latter, although leading to higher efficiencies, offers reduced sensitivity and requires very fast labeling kinetics. Preseparation and postseparation labeling schemes were the first reactions demonstrated in conjunction with CE separations on chip substrates. Although the initial on-chip reactors suffered from inefficient mixing, and therefore inefficient reactions, improvements in channel structures and geometries along with optimization of solution conditions soon led to satisfactory results. The geometry of one such "second-generation" CE reactor chip is shown in Fig. 2, along with the electropherogram generated by postseparation labeling of amino acids with *O*-phthaldialdehyde (OPA). Despite the fact that the amino acids, once separated, had to mix and react with OPA in order to be rendered fluorescent, their corresponding peaks remained as sharp and well-defined as the peak obtained

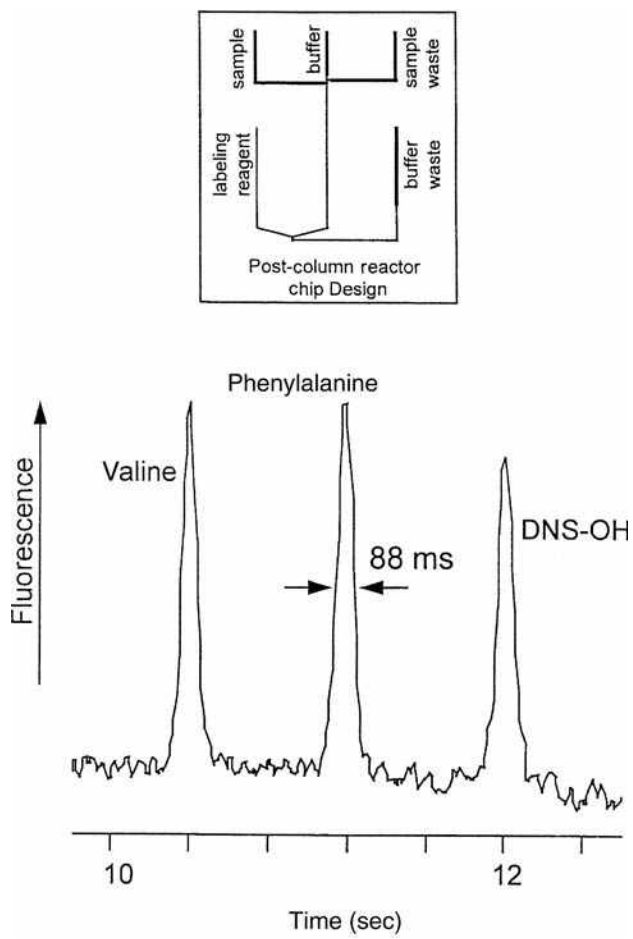

Fig. 2 Electrokinetically driven on-chip reaction in a CE-based system. Postseparation labeling of amino acids with OPA. Sample contained 200 μm each of phenylalanine and valine, and 10 μm of hydrolyzed dansyl chloride. The postcolumn reactor chip design is shown in the inset.
Source: From Clinical potential of microchip capillary electrophoresis systems, in Electrophoresis.[13]

for hydrolyzed dansylchloride (DNS–OH), which did not react with OPA.[8]

The products of digestion reactions involving either protein or DNA substrates are conveniently separated and detected by CE on a chip. Improvements in digestion product assays should, therefore, be realized by marrying the digestion reaction and separation on a single chip. Jacobson and Ramsey demonstrated one such marriage by fabricating a chip device capable of both digesting a DNA sample with a restriction enzyme and separating the resulting DNA fragments using electrophoresis in a sieving matrix. Subsequent detection of the DNA restriction fragments was achieved by way of LIF using an intercalating dye that was introduced to the fragments on-chip.[9] In some cases, the products of a digestion reaction may not, in themselves, be of interest, but, rather, they may be used to determine information about the digestion enzyme itself. In one such chip assay, the reaction kinetics for the enzyme β-galactosidase were determined using resorufin β-D-galactopyranoside, a substrate that is hydrolyzed to resorufin, a fluorescent product.[10] Precise concentrations of substrate, enzyme, and inhibitor (phenylethyl β-D-thiogalactoside) were mixed on-chip, and the entire integrated assay was conducted in a 20 min period using only 120 pg of enzyme and 7.5 ng of substrate. Thus, the facility to perform digestion reactions directly on chip prior to separation and detection of digestion products necessarily improves the efficiency of these assay methods and represents a powerful new tool in the area of biochemical analysis.

Affinity-type reactions, which involve an analyte's affinity for a conjugate molecule, such as antibody–antigen interactions, form an important part of biochemical research. CE on a chip provides for the separation of complexes of the analyte with its conjugate from uncomplexed reagents. However, the ability to carry out the reaction between the analyte and its conjugate to form a complex directly on-chip, in conjunction with electrophoretic separation, is an important advance, and many examples of such on-chip affinity reactions exist. In one such example, Chiem and Harrison presented a μ-chip CE device capable of functioning as a complete immunoreactor for the determination of serum theophylline, a therapeutic drug for asthma treatment.[11] In this competitive immunoassay, a serum sample containing theophylline was mixed, directly on the chip, with fluorescently labeled theophylline tracer prior to introducing a limited amount of anti-theophylline antibody, also on-chip. The products of this immunoassay were subsequently separated by electrophoresis and detected by LIF on-chip. As the concentration of theophylline in the serum increased, this competitive assay led to an increase in signal for free, labeled theophylline and a corresponding decrease in signal for the labeled theophylline–antibody complex. Total analysis time, including on-chip reagent mixing, reaction, separation, and detection, was 150 sec per sample, demonstrating one of the obvious advantages (along with reduced reagent consumption and increased sensitivity) of being able to conduct reactions on-chip alongside CE separations and other functions.

Another important reaction that has found a place on CE chips is the PCR, which is used to amplify DNA and which is critical to high-throughput genetic analyses. With the demonstrated ability of CE chips to integrate chemical reactions alongside high-speed separations, it is perhaps not surprising that μ-chip devices capable of genetic analysis would be fabricated. For example, a single monolithic chip capable of PCR amplification of up to four DNA samples, followed by product analysis has been demonstrated.[12] Integrated onto this chip are the facilities to thermally lyse cells to release DNA, standard PCR protocols to amplify DNA, gel electrophoresis to separate PCR products, intercalation of a fluorescent dye into PCR products, and detection of labeled products by LIF. The level of sophistication in a device such as this clearly illustrates the reality of the lab-on-a-chip concept: A concept that is founded upon the many advantages of μ-chip CE.

CONCLUSIONS AND FUTURE DIRECTIONS

The advantages typically associated with capillary electrophoresis, such as reduced sample and reagent consumption, reduced analysis time, and increased separation efficiency, are augmented when the CE system is transposed to a chip substrate. More importantly, however, μ-chip CE offers the further advantage of integrating analytical processes beyond separation. Sample preparation, injection, reaction, and detection can be seamlessly tied to the electrophoretic separation stage of the analysis. The monolithic CE chips capable of separation coupled to some of these other analytical steps are precursors to the ultimate "lab-on-a-chip," which promises high-throughput sensitive analyses with minimal user intervention. Applications of such devices in biochemical, clinical, forensic, and environmental analyses are seemingly unlimited. However, several challenges remain despite the great promise of these devices. In order to fully realize the advantages offered by the microfluidics regime of the chip, methods of addressing these microvolumes and of interfacing them to the macroscale world beyond the chip must be carefully managed. Although chip fabrication techniques are now well established, they are by no means accessible to the majority of analysts. Fabrication processes that rely less heavily on high-tech processing facilities must be developed or, more realistically, the chips themselves must be made available inexpensively and in a variety of application designs for all potential users. Miniaturization or careful arrangement of the apparatus accompanying the CE chip, including power supplies, detection components, and computer controllers, into a compact and robust system must be considered in order to take full advantage of the chip's

inherently small size. Finally, true parallel processing facilities must be routinely developed on single chips in order to increase sample throughput and increase the applicability of these systems to large-scale analytical problems. These challenges, although formidable, are worthy of solutions in order to successfully build labs-on-a-chip around the cornerstone of CE on a chip.

REFERENCES

1. Jacobson, S.C.; Ramsey, J.M. *High-Performance Capillary Electrophoresis*; Khaledi, M., Ed.; John Wiley & Sons: New York, 1998; 613–633.
2. Harrison, D.J.; Manz, A.; Fan, Z.; Lüdi, H.; Widmer, H.M. Capillary electrophoresis and sample injection systems integrated on a planar glass chip. Anal. Chem. **1992**, *64* (17), 1926–1932.
3. Ramsey, R.S.; Ramsey, J.M. Generating electrospray from microchip devices using electroosmotic pumping. Anal. Chem. **1997**, *69* (6), 1174–1178.
4. Harrison, D.J.; Fluri, K.; Seiler, K.; Fan, Z.; Effenhauser, C.S.; Manz, A. Micromachining a miniaturized capillary electrophoresis-based chemical analysis system on a chip. Science **1993**, *261* (5123), 895.
5. Khandurina, J.; Jacobson, S.C.; Waters, L.C.; Foote, R.S.; Ramsey, J.M. Microfabricated porous membrane structure for sample concentration and electrophoretic analysis. Anal. Chem. **1999**, *71* (9), 1815–1819.
6. Jacobson, S.C.; Ramsey, J.M. Microchip electrophoresis with sample stacking. Electrophoresis **1995**, *16* (1), 481–486.
7. He, B.; Tan, L.; Regnier, F. Microfabricated filters for microfluidic analytical systems. Anal. Chem. **1999**, *71* (7), 1464–1468.
8. Fluri, K.; Fitzpatrick, G.; Chiem, N.; Harrison, D.J. Integrated capillary electrophoresis devices with an efficient postcolumn reactor in planar quartz and glass chips. Anal. Chem. **1996**, *68* (23), 4285–4290.
9. Jacobson, S.C.; Ramsey, J.M. Integrated microdevice for DNA restriction fragment analysis. Anal. Chem. **1996**, *68* (5), 720–723.
10. Hadd, A.G.; Raymond, D.E.; Halliwell, J.W.; Jacobson, S.C.; Ramsey, J.M. Microchip device for performing enzyme assays. Anal. Chem. **1997**, *69* (17), 3407–3412.
11. Chiem, N.H.; Harrison, D. Microchip systems for immunoassay: An integrated immunoreactor with electrophoretic separation for serum theophylline determination. J. Clin. Chem. **1998**, *44*, 591.
12. Waters, L.C.; Jacobson, S.C.; Kroutchinina, N.; Khandurina, J.; Foote, R.S.; Ramsey, J.M. Multiple sample PCR amplification and electrophoretic analysis on a microchip. Anal. Chem. **1998**, *70* (24), 5172–5176.
13. Colyer, C.L.; Tang, T.; Chiem, N.; Harrison, D.J. Clinical potential of microchip capillary electrophoresis systems. Electrophoresis **1997**, *18* (10), 1733.

CE/MS: Large Molecule Applications

Ping Cao
Biology Department, Tularik, Inc., South San Francisco, California, U.S.A.

INTRODUCTION

Capillary electrophoresis (CE) is a modern analytical technique which permits rapid and efficient separation of charged components present in small-sample volumes. Separation occurs due to differences in electrophoretic mobilities of ions inside small capillaries. The impetus for CE method developments focused primarily on the separation of larger biopolymers such as polypeptides, proteins, oligonucleotides, DNA, RNA, and oligosaccharides.[1] Mass Spectrometry (MS) has long been recognized as the most selective and broadly applicable detector for analytical separations. Currently, electrospray ionization (ESI) serves as the most common interface between CE and MS. Generation of multiply-charged species with an ESI extends the applicability of conventional mass analyzers of limited mass-to-charge (m/z) ranges to molecular mass and structure determination of larger biopolymers. CE/MS combines the advantages of CE and MS so that information on both high efficiency and molecular masses and/or fragmentation can be obtained in one analysis. This entry focuses on larger-molecular analysis by online CE/MS interfaced via ESI sources.[2,3] However, CE/MS using continuous-flow – fast atom bombardment (CF–FAB) sources employing either "liquid-junction" or "coaxial" interfaces and several off-line CE/MS combination should be noted.

When ESI–MS is employed as detector, the proper choice of a suitable electrolyte system is essential to both a successful CE separation and good quality ESI mass spectra. Even though a wide range of CE buffers were successfully electrosprayed when the liquid-junction and sheath flow CE/MS interfaces were employed since the low CE effluent flow is effectively diluted by a much large volume of sheath liquid;[4] the best detector response is produced by volatile electrolyte systems at the lowest practical concentration and ion strength and by minimizing other non-volatile and charge-carrying components. Volatile reagents like ammonium acetate (pH 3.5–5.5) or formate (pH 2.5–5; both adjustable to high pH) and ammonium bicarbonate have been proven to be well suited for CE/ESI/MS.

Due to the inherent tendency to adsorb strongly to the inner walls of the fused-silica capillary, the analysis of proteins and peptides by CE has presented unique challenges to the analyst because this phenomenon gives rise to substantial peak broading and loss of separation efficiency. Successful separations of proteins and peptides by CE involve efficient suppression of adsorption to the fused-silica wall. Basically, there are two approaches to prevent protein adsorption: modification of the fused-silica surface by dynamic or static coating or by performing analysis under experimental conditions that minimize adsorption.[5] The static coating capillary is preferred under CE/ESI/MS analysis of large molecules because the CE buffer composition is simplified. This entry is meant only to provide the reader with a description of most common approaches taken to analyze large molecules, especially polypeptides and proteins, by CE/ESI/MS.

LARGE-MOLECULE ANALYSIS OF CE/MS BY NEUTRAL CAPILLARY

Because there is no ionizable groups of the coating in the neutral capillary, the interaction between charged molecules with ionic capillary surface is eliminated. Also, the electro-osmotic flow (EOF) of a neutral capillary is eliminated. However, a continuous and adequate flow of the buffer solution toward the CE capillary outlet is an important factor for routine and reproducible CE/ESI/MS analysis; in order to maintain a stable ESI operation, some low pressure applied to the CE capillary inlet is usually needed, especially when the sheathless interface is employed. The disadvantage of the pressure-assisted CE/ESI/MS is the loss of some resolution because the flat flow profile of the EOF is partially replaced by the laminar flow profile of the pressure-driven system. A typical neutral capillary is a linear polyacrylamide (LPA)-treated capillary. Karger and coworkers[6] used mixtures of model proteins, a coaxial sheath flow ESI interface, and a 75 μm inner diameter (I.D.), 360 μm outer diameter (O.D.), 50 cm-long LPA-coated capillary to evaluate CE/MS, capillary isotachophoresis (CITP)–MS, and the on-column combination of CITP/CE/MS. In the CE/MS experimental, 0.02 M 6-aminohexanoic acid + acetic acid (pH 4.4) was employed and a 18 kV constant voltage was applied during the experiment. Seven model proteins were well resolved. They showed that the sample concentration necessary to obtain a reliable full-scan spectrum was in the range of 10^{-5} M. However, by proper selection of the running buffers, they demonstrated that the on-column combination of both CITP and capillary zone electrophoresis (CZE) can improve the concentration detection limits for a full-scan CE/MS analysis to approximately 10^{-7} M.

LARGE-MOLECULE ANALYSIS OF CE/MS BY A POSITIVELY CHARGED CAPILLARY

To help overcome adsorption, positively charged coatings have been employed for the separation of positively charged solutes. In this approach, positively charged proteins are electrostatically repelled from the positively charged capillary inner wall. Two examples of such coatings are aminopropyltrimethoxysilane (APS) and polybrene, a cationic polymer. These coatings reverse the charge at the column–buffer interface and, thus, the direction of the EOF compared to uncoated capillaries.

The CE/MS analysis of the venom of the snake *Dendroaspis polylepis polylepis*, the black mamba, is reported by Tomer and coworkers.[7] A VG 12-250 quadrupole equipped with a Vestec ESI source (coaxial sheath flow interface) was employed for this experiment. The sheath fluid was a 50 : 50 methanol : 3% aqueous acetic acid solution. The CE voltage was set at −30 kV during the analysis and the ESI needle was held at +3 kV. The CE running buffer used was 0.01 *M* acetic acid at pH 3.5. The APS column was flushed with buffer solution for 10 min prior to sample analysis. The snake venom was dissolved in water at a concentration of 1 mg/ml and 50 nl of the analyte solution was injected into the column. They demonstrated the existence of at least 70 proteins from this venom.

One interesting example of intact protein analysis was described by Smith and coworkers.[8] They used the high sensitivity and mass accuracy of a Fourier transform ion cyclotron resonance (FTICR) MS detector to analyze hemoglobin α and β in a single human erythrocyte. Human erythrocytes were obtained from the plasma of a healthy adult male. A small drop of blood diluted with saline solution (pH 7.4) was placed on a microscope slide. With the help of a stereomicroscope and a micromanipulator, the etched terminus of the CE capillary was positioned within a few microns of the cell to be injected. Following electro-osmotic injection of the cell, the end of the CE capillary was placed in a vial containing the CE running buffer (10 m*M* acetic acid, pH 3.4), and the cell membrane was lysed via osmotic shock from the running buffer and the cellular contents of the cell released for subsequent CE separation and mass analysis. A 1 m APS column and a sheathless interface employing a gold-coated capillary with −30 kV CE separation and +3.8 kV ESI voltage were used for this study. They demonstrated that adequate sensitivity needed to characterize the hemoglobin from a single human erythrocyte (~450 μmol) and mass spectra with average mass resolution in excess of 45,000 (full width at half-maximum) were obtained for both the α- and β-chain of hemoglobin. Fig. 1 shows the mass spectra obtained from this experiment.

In order to overcome the bubble formation associated with the sheathless CE/MS interface and quick degradation of the coated capillary, Moini et al.[9] introduced hydroquinone (HQ) as a buffer additive to suppress the bubbles formed due to the electrochemical oxidation of the CE buffer at the outlet electrode. The oxidation of water ($2H_2O(l) \leftrightarrow O_2\ (g) + 4H^+\ 4e$) was replaced with that of more easily oxidized HQ (hydroquinone ↔ *p*-benzoquinone + $2H^+ + 2e$). Formation of *p*-benzoquinone, other than the formation of oxygen gas, effectively suppresses gas bubble formation. The APS-coated capillaries and 10 m*M* acetic acid CE running buffer containing 10 or 20 m*M* HQ were used for the experiments. The CE outlet/ESI electrode was maintained at +2 kV and the CEinlet electrode was held at −30 kV. Tryptic digest of cytochrome-*c* and hemoglobin were used as model proteins. They demonstrated that the combination of the in-capillary electrode sheathless interface using a platinum wire, HQ as a buffer additive, and

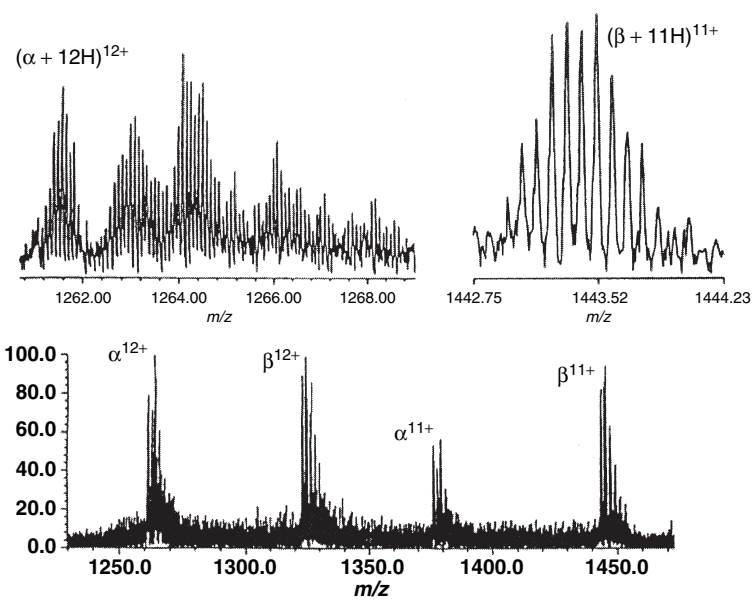

Fig. 1 Mass spectra obtained from CE/MS analysis of a single human erythrocyte using an FTICR mass analyzer.

Source: From The charaterization of snake venoms using capillary electrophoresis in conjuction with electrospray mass spectronetry: Black Mambas, in Electrophoresis.[7]

pressure programming at the CE inlet provides a rugged high-efficiency setup for analysis of peptide mixtures.

Because the concentration limits of detection of CE are often inadequate for most practical applications (approximately 10^{-6} *M*), several analyte concentration techniques have been developed, including combining CITP with CE, transient isotachophoresis (TITP) in a single capillary, analyte stacking, and field amplification. Such electrophoretic techniques have extended the applicability of CE for the analysis of dilute analyte solutions. Chromatographic online sample concentration has been achieved by using an extraction cartridge which contains a bed of reversed-phase packing[10] or a membrane[11] with properties. Accumulated analyte on the cartridge can be prewashed to remove salts and buffers that are not suited for CE separation or ESI operation. Figeys and Aebersold[12] designed the solid-phase extraction (SPE)/CE/MS/MS system which consists of a small cartridge C_{18} of extraction material immobilized in a Teflon sleeve. Solutions of peptide mixtures typically derived by proteolysis of gel-separated proteins were forced through the capillary by applying positive pressure at the inlet and the peptides were concentrated on the SPE device. After equilibration with an electrophoresis buffer compatible with ESI, eluted peptides were separated by CE and analyzed by ESI/MS. A detection limit of 400 αmol tryptic digest of bovine serum albumin (20 μl of solution at a concentration of 20 αmol/μl was applied) was achieved in the ion trap mass spectrometer-based system. This method was successfully applied to the identification of yeast proteins separated by two-dimensional gel electrophoresis.

Applications of CE/MS to large molecules are progressing rapidly. As biology enters an era of large-scale systematic analysis of biological systems as a consequence of genome sequencing projects, rapid and sensitive identifications of large-scale (proteomewide) proteins that constitute a biological system is essential. CE/MS with its high separation efficiency, rapid separation, and economy of sample size is complementary to microcolumn high-performance liquid chromatography (μHPLC)/MS. In addition, high-resolution, multiple-dimensional separations become increasingly attractive. HPLC/CE/MS, affinity CE/MS, capillary microreactor on line with CE/MS, and microchip based separations will be used in a broad range of future applications.

REFERENCES

1. Kuhr, W.G.; Monnig, C.A. Capillary electrophoresis. Anal. Chem. **1992**, *64*, 389.
2. Smith, R.D.; Udseth, H.R. *Pharmaceutical and Biomedical Applications of Capillary Electrophoresis*; Elsevier Science: New York, 1996; 229–276.
3. Banks, J.F. Recent advances in capillary electrophoresis/electrospray/mass spectrometry. Electrophoresis **1997**, *18*, 2255.
4. Smith, R.D.; Loo, J.A.; Edmonds, C.G.; Barinaga, C.J.; Udseth, H.R. New developments in biochemical mass spectrometry: Electrospray ionization. Anal. Chem. **1992**, *62*, 882.
5. Thibault, P.; Dovichi, N.J. *Capillary Electrophoresis (Theory and Practice)*; 2nd ed.; CRC Press: Boca Raton, FL, 1998; 23–90.
6. Thompson, T.J.; Foret, F.; Vouros, P.; Karger, B.L. Capillary electrophoresis/electrospray ionization mass spectrometry: Improvement of protein detection limits using on-column transient isotachophoretic sample reconcentration. Anal. Chem. **1993**, *65*, 900.
7. Perkins, J.R.; Parker, C.E.; Tomer, K.B. The characterization of snake venoms using capillary electrophoresis in conjunction with electrospray mass spectrometry: Black Mambas. Electrophoresis **1993**, *14*, 458.
8. Hofstadler, S.A.; Severs, J.C.; Smith, R.D. Rapid Commun. Mass Spectros **1996**, *10*, 919.
9. Moini, M.; Cao, P.; Bard, A.J. Hydroquinone as a buffer additive for suppression of bubbles formed by electrochemical oxidation of the CE buffer at the outlet electrode in capillary electrophoresis/electrospray ionization-mass spectrometry. Anal. Chem. **1999**, *71*, 1658–1661.
10. Figeys, D.; Aebersold, R. Electrophoresis **1998**, *19*, 885.
11. Tomlinson, A.J.; Benson, L.M.; Guzman, N.A.; Naylor, S. Preconcentration and microreaction technology on-line with capillary electrophoresis. J. Chromatogr **1996**, *744*, 3.
12. Figeys, D.; Aebersold, R. Electrophoresis **1997**, *18*, 360.

CE: ICP/MS

Clayton B'Hymer
National Institute for Occupational Safety and Health, Centers for Disease Control and Prevention, U.S. Department of Health and Human Services, Cincinnati, Ohio, U.S.A.

INTRODUCTION

Capillary electrophoresis (CE) has many well-known advantages including low-sample-volume requirements, high plate number (i.e., peak efficiency), the ability to separate positive, neutral, and negatively charged species in a single run, and, when properly developed, relatively short analysis times. The ability of CE to separate ionic multispecies and to have low operational costs makes the technique superior in certain specific applications to conventional high-performance liquid chromatography (HPLC). The inductively coupled plasma-mass spectrometer (ICP–MS) has the advantages of possessing low detection limits for the majority of the chemical elements. The ICP–MS detector has other additional positive attributes including linearity over a wide dynamic range, multielement detection capability, and the ability to perform isotopic analysis. Also, the ICP–MS is known to have minimal matrix-effect problems when compared to other detection systems. Sample matrix-effect problems are further reduced in CE–ICP–MS analysis owing to the small sample size and flow rates associated with CE. With all of these strong points, CE–ICP–MS is a rapidly growing hyphenated technique; the separation capability of CE is combined with the highly sensitive, element-specific detection system of ICP–MS.

HISTORICAL BACKGROUND AND USE

The first research papers describing CE–ICP–MS were written in 1995 by the Olesik, Lopez-Avila, and Barnes research groups.[1–3] The coupling of the ICP–MS detector with CE and HPLC has become the dominant analysis technique for elemental speciation analysis. Elemental speciation analysis is defined as the separation, identification, and quantification of the different chemical forms (organometallic and inorganic) and oxidation states of specific elements in a given sample. Information on elemental speciation in clinical and environmental material is vital in the study of mechanisms of element transport within living as well as environmental systems, elemental bioavailability, metabolic pathways within living organisms, and toxicology.

THE FUNDAMENTALS OF CAPILLARY ELECTROPHORESIS–INDUCTIVELY COUPLED PLASMA–MS

The Inductively Coupled Plasma–MS Detector

MS has established itself as the detection system of choice for CE of trace metals and metalloids, as well as their chemical species. The ICP–MS has dominated CE analysis methods in recent years. The ICP–MS differs from the more commonly used electrospray or ion-spray mass spectrometer method of ion generation. The electrospray MS can be described as using a "soft" ion source; that is, structural information can be obtained from molecular fragments. The ICP-MS is a "hard" ion source; that is, the plasma generally operates at an approximate temperature of 8000 K. Under these conditions, the ICP generates ions of elements and a few polyatomic ions. The ICP–MS has been well documented since its early development by both the Houk[4] and Gray[5] research groups over 20 years ago. A diagram of a typical commercial ICP–MS detector is shown in Fig. 1. The inductively coupled plasma is formed from a flow of gas, typically argon, through a series of concentric tubes made of quartz called the torch. The ICP torch is surrounded by a copper load coil. The load coil is connected to a radio-frequency generator, which operates between 27 and 40 MHz at a power of 700–1500 W.[6] This induces an oscillating magnetic field near the exit of the torch. A plasma is formed while a spark is applied to the flowing gas stream to form gaseous ions. The free electrons created during this process are accelerated by the magnetic field and bombard other gas atoms; this causes further ionization and produces the plasma. Sample introduction into the plasma is via a carrier argon gas flow through the central tube of the ICP torch. Liquid samples are nebulized into an aerosol before being carried into the ICP torch, a function performed by a nebulizer and spray chamber. The nebulizer produces the aerosol, and the spray chamber separates and removes the large droplets from the aerosol to form a more uniform mist. Once the fine aerosol sample reaches the plasma, vaporization, atomization, and ionization of the analyte to element ions occur almost simultaneously. Coolant and auxiliary gas are added to the ICP torch to keep the quartz

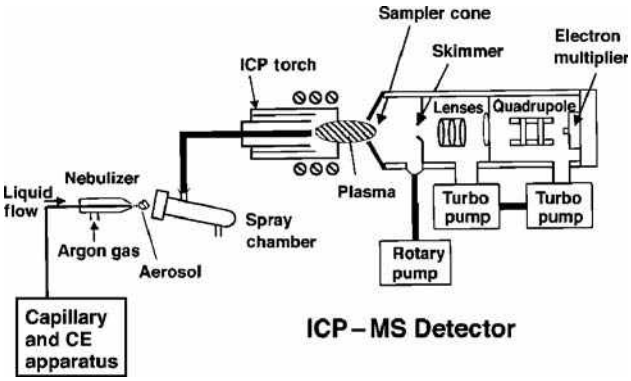

Fig. 1 The ICP–MS used as a detector for HPLC. The liquid sample passes through the capillary into a nebulizer where it is changed into an aerosol. The aerosol passes through a spray chamber and into the plasma. The analytes pass into the mass spectrometer. The CE interface is not in detail in this figure.

from melting and to provide a tangential flow of gas, which serves to center and stabilize the plasma.

Beyond the ICP torch are the sampler and skimmer cones of a typical mass spectrometer (Fig. 1). Ions generated from the sample pass through the aperture of the cones into low-pressure chambers. Ion lenses, which are actually a series of electrodes, are used to "focus" the ion path, before reaching the quadrupole mass analyzer. Ions of only one mass-to-charge ratio are transmitted at a time and impacted onto an electron multiplier detector. The electron pulse is amplified and this signal is then recorded by the instrument's data system. The diagram in Fig. 1 displays a quadrupole mass analyzer, but other spectrometers have been used with CE including scanning instruments such as the double-focusing and sector-field mass detectors, and for fast separations of multielement mixtures of chemical species, the time-of-flight (TOF) MS.

Alternative plasmas have been occasionally used for elemental speciation analysis, including the microwave-induced plasma (MIP), which has been reviewed in Ref.[7] and the low-power helium plasma. Both of these plasma sources have the advantage of reduced gas and power consumption over the traditional ICP; however, the use of these plasmas with interfaces with CE has been very infrequent and does not warrant further discussion in this entry. The MIP has been occasionally used with low flow rate liquid sample introduction. The low-power helium plasma has generally only been used with GC interfaces; their low-power levels are generally not capable of properly vaporizing and ionizing a liquid aerosol.

Interfacing Capillary Electrophoresis to the Inductively Coupled Plasma–MS

Overview of design considerations

The main design challenge of CE–ICP–MS is in the actual interface. In the typical practice of CE, a fused silica capillary filled with a buffer has both ends submerged or in physical contact with two buffer reservoirs. Electrodes placed in the buffer reservoir provide the application of a high electrical potential through the capillary. When attempting to interface CE to an ICP–MS, several problems need to be overcome. One is that CE has an extremely low flow rate (approximately 1 μl/min or less). This requires the use of a low liquid flow nebulizer to be used in the interface. A low liquid flow rate nebulizer is required that maintains a high transport efficiency and delivers a large quantity of analyte to the plasma. The ICP–MS detector sensitivity is based on mass of the analytes, not concentration of the solution. Because CE injection volumes are low, high transport efficiency by the nebulizer is vital to reduce analyte loss to the MS detector. The second problem with CE–ICP–MS interfacing is that an electrical connection must be maintained to the end of the fused silica capillary, yet the capillary must still introduce the CE buffer flow into the nebulizer and produce a uniform aerosol for the analysis system. This problem has been solved by various designs, which usually involves the addition of a "make-up" buffer or sheath electrolyte added near the end of the fused silica capillary. Interfacing CE with ICP–MS has the advantage of requiring a low liquid flow rate, and therefore places a small demand on the desolvation and solvent load capacity of the inductively coupled plasma. This makes a more stable plasma less subject to long-term signal drift over the course of several CE runs. Two other design considerations of a CE–ICP–MS interface are countering or minimizing laminar flow through the capillary generated by the operation of the nebulizer[8] and minimizing band broadening for the separation of analytes. There are various strategies in reducing laminar flow through the electrophoretic capillary, and band broadening is minimized through geometry considerations in the design of the CE–ICP–MS interface. These points will be discussed in further detail in this entry.

The nebulizer

A basic understanding of the nebulizer function and the types of nebulizers is necessary to successfully interface CE to the ICP-MS. Nebulization, as previously described, is the process to form an aerosol, i.e., to suspend a liquid sample into a gas in the form of a cloud of droplets. The quality of any nebulizer is based on many different parameters including mean droplet diameter, droplet size distribution, span of droplet size distribution, droplet number density, and droplet mean velocity. There are numerous nebulizers commercially available for the use with ICP-MS systems, and their detailed description can be found elsewhere.[9,10] Pneumatic designs, both concentric and cross flow, are the most popular for CE interfaces with the occasional use of the ultrasonic nebulizer (USN). Fig. 2 shows some typical nebulizers. The pneumatic nebulizer is either a concentric design (Fig. 2A), where both

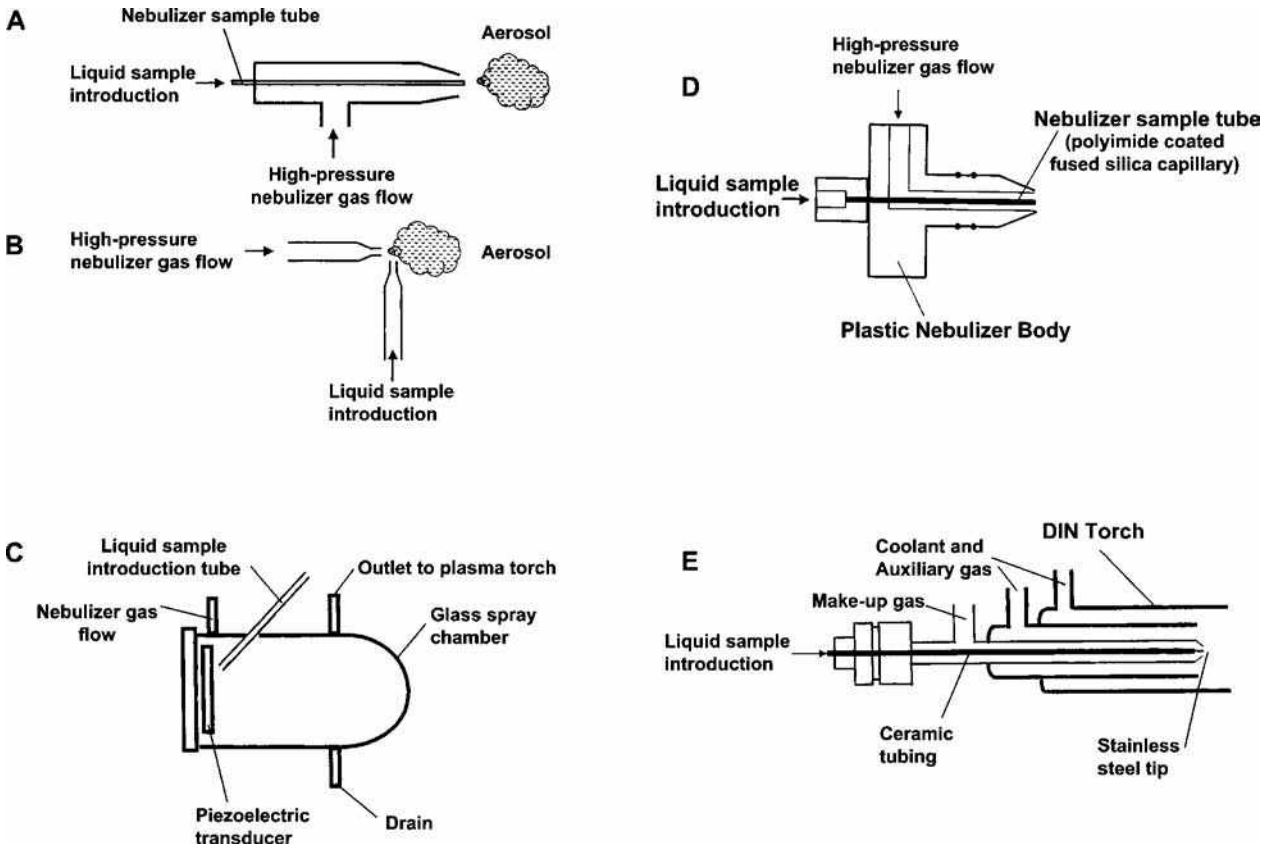

Fig. 2 A, The concentric nebulizer; B, The cross-flow nebulizer; C, The ultrasonic nebulizer (USN); D, The microconcentric nebulizer (MCN) by CETAC. The body of this nebulizer is made of plastic; and E, The direct injection nebulizer (DIN).

the gas stream and the liquid flow in the same direction or the cross-flow design (Fig. 2B), where the gas stream is at a right angle to liquid flow. Gas flowing past the tip of the liquid sample introduction tube generates the aerosol. The ultrasonic nebulizer (Fig. 2C) consists of a piezoelectric transducer and a liquid sample introduction tube. Liquid flow over the transducer plate forms a thin film and is nebulized by the high-frequency mechanical vibrations from the transducer.

There are several concentric-like pneumatic low liquid flow nebulizers commercially available that are often used in the construction of CE–ICP–MS interfaces. The Meinhard high-efficiency nebulizer (HEN) (Meinhard Glass Products, Golden, Colorado) is a variation of the concentric nebulizer that has smaller internal dimensions and is specifically designed to operate at low liquid flow rates. A very similar nebulizer is also commercially available and is known as the MicroMist nebulizer (Glass Expansion Pty. Ltd., Victoria, Australia). Another low-flow commercial nebulizer, the Microconcentric Nebulizer (MCN) (CETAC Technologies, Inc., Omaha, Nebraska, U.S.A.), has been used with liquid flow rates down to 10–30 μl/min. The MCN is also concentric in nature, but it differs from both the Meinhard and MicroMist in having its outer body constructed of plastic instead of glass. Also, the MCN has its inner sample tube made of fused silica capillary tube, not drawn glass (Fig. 2D). All three of these commercial nebulizers have comparable analyte transport efficiencies.

Although there has been limited use with CE interfaces, the direct injection nebulizer (DIN) was first described by Shum et al.[11] and later used by Liu et al.[2] for CE (Fig. 2E). In this design, the nebulizer introduces the sample very near the plasma inside the ICP torch and eliminates the spray chamber assembly. Close to 100% analyte transport efficiency can theoretically be obtained with the DIN, but the nebulizer is restricted to very low-liquid flow rate and thus is well matched to CE interfacing. This design does induce local plasma cooling due the lack of desolvation and detection limits are only slightly improved over other nebulizer designs.[12]

Specific capillary electrophoresis interface designs

The CE–ICP–MS interface based on the sheath-flow (make-up buffer) and pneumatic concentric nebulizers described by Lu et al.[3] is the most widely used CE–ICP–MS interface, and it has also been applied to electrospray MS interfaces.[13] The sheath-flow or make-up buffer acts to complete electrical connection to the exit end of the electrophoretic capillary; grounding is achieved by having a metal tube or metal "tee" near the connection to the

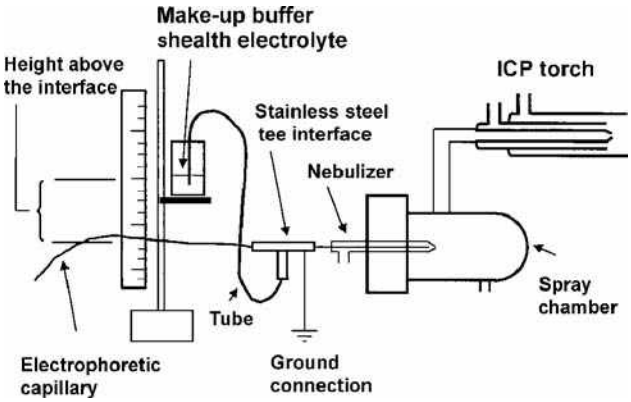

Fig. 3 A typical self-aspirating CE–ICP–MS interface. The make-up buffer/sheath electrolyte reservoir is positioned above the interface to provide the correct pressure and flow of buffer to the pneumatic nebulizer.

nebulizer (Fig. 3) or by coating the capillary with silver[1] (Fig. 4). The second function of the sheath flow is to compensate for the suction effect. Low pressure created near the tip of the pneumatic nebulizer by the flow gas of the operating nebulizer can induce laminar flow through the electrophoretic capillary. This can impair separation of analytes. Sheath flow can be introduced into the nebulizers by either self-aspiration with gravity siphoning control or by a pumping system. These strategies involve the precise addition of a sheath or make-up buffer to the nebulizer to prevent the degradation of the CE separation profile of the analytes. In the self-aspiration designs, the sheath flow is automatic, although adjustments to height of the sheath buffer reservoir (Fig. 3) can be used to optimize flow and separation to the nebulizer–CE interface. When a pumping system is used, the flow rate must be optimized to obtain the desired separation by reducing laminar flow through the capillary.

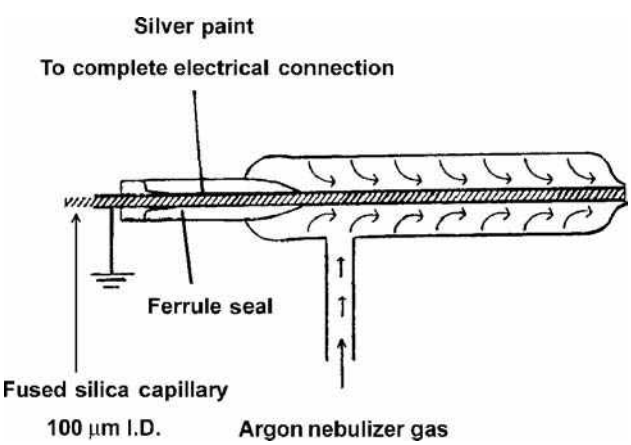

Fig. 4 Interface of an electrophoresis capillary and the concentric nebulizer. Silver paint was used to complete the electrical connection. **Source:** From Capillary electrophoresis inductively-coupled plasma spectrometry for rapid elemental speciation, in Anal. Chem.[1]; with permission of the American Chemical Society.

The use of controlled sheath-flow/make-up buffer rates to give equivalent CE/MS and CE–UV electopherograms was reported by Day et al.[14] It has also been reported that the sheath flow should be kept low and just compensate for laminar flow through the electrophoretic capillary.[8] This minimizes dead volume and band broadening of the CE separation. Precise pumping of a make-up buffer was demonstrated by Kinzer et al.[8] and later by Sutton et al.[15] The use of sol–gel frits near the exit tip of the electrophoretic capillary has been reported to reduce laminar flow effects and reduce the sheath flow.[16] Other important design and optimization considerations exit for the sheath-flow/make-up buffer interfaces. The positioning of the electrophoretic capillary into a concentric nebulizer is critical in these designs. Placement of the exit tip of the capillary close to the tip of the nebulizer can increase the "suction effect" and cause greater laminar flow to be generated through the capillary. Placement too far back from the tip of the nebulizer may induce greater band broadening from the extra dead volume. There has been some arguments about dilution effects of the sheath flow; that is, the sheath-flow lowers sensitivity of the MS detector from dilution of the analytes. The use of a sheath flow does not cause a decrease in sensitivity because of dilution, but actually because of a decrease in analyte transport efficiency through the spray chamber to the plasma. Large liquid flow rates generally have less-efficient analyte transport, droplet sizes, and distribution change so that the analyte loss is greater out the spray chamber drain. Generally, the sheath flow rate can be kept low and the low liquid flow nebulizers commercially available have high analyte transport efficiency, making loss of sensitivity minimal. Finally, if the sheath-flow/make-up buffer is different from the run buffer, changes to the separation will obviously occur. Creation of a pH gradient across the electrophoretic capillary or isoelectric focusing from the use of a mismatch of the run and make-up buffer may cause undesirable results with the analyte separation.

Another less often used, but successful, technique to counter laminar flow in pneumatic-based nebulizer CE–ICP-MS interfaces is by the application of negative buffer reservoir pressure. This approach was first demonstrated by Lu et al.[3] and later by Taylor et al.[17] A matching mechanical counterbalance to the pneumatic nebulizer's suction was used in both of these interfaces. The theoretical advantage of non-sheath-flow system is that sensitivity of the CE–ICP–MS system is not reduced by dilution by the make-up buffer. Olesik et al.[1] originally described a sheathless pneumatic interface, but the main flaw in the design was the increased liquid flow through the electrophoretic capillary owing to the suction or Bernoulli effect of the operating nebulizer. The electro-osmotic flow of this CE system was measured at 0.05 μl/min, while the natural aspiration rate of the nebulizer vacuum was measured to be 2 μl/min. Some degradation of the separation of analytes

was noted, but the high plate number of CE and the selective detection capability of MS allowed this to be a useful separation. Another problem encountered in some sheathless interfaces is the loss of electrical connectivity of the electrophoretic capillary.

Finally, other nebulizers have been used in CE–ICP–MS interfaces. In an interface developed by the Barnes research group[18] using the ultrasonic nebulizer, the ground connection was provided by a make-up buffer/sheath-flow electrolyte. The separations obtained with the USN were demonstrated by Barnes' group to be superior to those obtained using a concentric pneumatic nebulizer in their study. Kirlew et al.[19] reported the comparison of a "home-made" ultrasonic nebulizer and a CETAC USN in CE–ICP–MS interfaces. Again, a make-up buffer was used, added to the system via a concentric capillary outside the electrophoretic capillary. In another work by Kirlew and Caruso,[20] an oscillating capillary nebulizer (OCN), which is a variation of the pneumatic concentric nebulizer built from flexible capillary tubes, was used in an interface. The OCN has had little application in CE interfaces, owing to its generally lower sensitivity performance when compared to other pneumatic nebulizers used with ICP–MS detection.[21] The DIN, previously described in "The Nebulizer," was used by Liu et al.[2] in a CE interface. The electrophoretic capillary was directly inserted through the central sample introduction capillary of the DIN. A platinum grounding electrode was positioned into a three-port connector. This connector contained the DIN sample introduction capillary as well as a make-up buffer flow. These alternative nebulizers have been successfully used in CE interfaces, but the pneumatic designs dominate the interface systems reported in the literature.

One last CE–ICP interface worthy of mention that is specific for the determination of elements capable of forming volatile compounds is by the use of a hydride generation system. Hydride generation followed by a gas–liquid separator in CE interfaces has been reviewed.[22] This technique has a drawback, because only arsenic, tin, lead, antimony, bismuth, germanium, selenium, and tellurium are capable of forming gaseous hydrides at room temperature. Hydride generation allows for the introduction of analyte species into the inductively coupled plasma nearly quantitatively; that is, the transport efficiency is nearly 100% percent less some loss by venting in the gas–liquid separator or other inefficiencies within the interface/sampling tube design to the plasma. In theory, detection limits are lower. In practice, hydride generation of the analytes may occur at different rates and the extra complexity and expense of the interface make these systems less useful as compared to the direct sample introduction systems previously described.

APPLICATIONS IN SAMPLE ANALYSIS

As mentioned in the Introduction, the main application of CE–ICP–MS is in the field generally known as elemental speciation analysis. There are a number of good reviews on elemental speciation CE advances including use MS detection; the two most recent were by Kannamkumarath et al.[23] and Timerbaev.[24] Work performed in this relatively young technique is very extensive, and only a few examples will be cited in this entry.

Speciation analysis of arsenic and selenium is very active in the recent literature. The toxicity of arsenic varies widely and is dependent on the specific compound present. Arsenic in its various forms is also widely distributed in the environment and the food that human eats. Speciation of arsenic in human depends both on the form of the arsenic taken in and the metabolism within the body. Inorganic arsenic, in the forms of arsenite (As^{III}) and arsenate (As^{V}), is highly toxic. The common organic forms of arsenic have varying degrees of toxicity. Monomethylarsonic acid [MMA^{v}, $CH_3AsO(OH)_2$] and dimethylarsinic acid [DMA^{v}, $(CH_3)_2AsO(OH)$] exhibit a toxicity factor of 1 in 400 that of the inorganic forms. Arsenobetaine [$(CH_3)_3As^{+}CH_2COO^{-}$] and arsenocholine [$(CH_3)_3As^{+}CH_2CH_2O^{-}$] are commonly found in seafood and are relatively non-toxic. A variety of arsenic compounds are currently used as antifungal agents, herbicides, and pharmaceuticals; they are also used in semiconductor processing and there was an extensive use in pesticides before the invention of the more advanced organophophorus compounds. Thus the literature is filled with arsenic speciation analysis of food, the environment, and biological systems. Selenium has also been widely studied for many of the same reasons. Selenium intake in the human diet is essential, but excess intake can cause toxic reactions. A variety of selenium-containing species are present in the environment, natural foods, and food supplements.

In a previously mentioned work by Kirlew et al.,[19] electrophoretic separations of Se^{IV}, Se^{VI}, As^{III}, As^{V}, and dimethylarsinic acid were performed using various ultrasonic nebulizer (USN) interfaces. Using the optimized CE interface conditions and a borate run buffer at pH 8, a separation was accomplished within 10 min. Electrokinetic injections gave better sensitivities for the analytes as compared to hydrostatic sample injection. In the Kirlew study, arsenate and selenite ions had very similar migration times, but these analytes were easily resolved by the multielement capability of the ICP–MS detector. An electropherogram of this work is shown in Fig. 5. In an application to field samples, Van Holderbeke et al.[25] investigated arsenic speciation in three different sample matrices: drinking water, human urine, and soil leachate. All were run under basic conditions with 20 m*M* borate buffer (pH 9.40) and in the presence of cationic surfactant as the osmotic flow modifier (OFM) supplied by Waters Associates (Milford, Massachusetts, U.S.A.). The separation of As^{v}, monomethylarsonic acid, dimethylarsinic acid, monomethylarsonic acid, arsenite As^{III}, arsenobetaine, and arsenocholine was obtained. Electropherograms from the Van Holderbeke study are shown in Fig. 6.

Capillary electrophoresis has been extensively used to separate biological molecules. Therefore it was only a

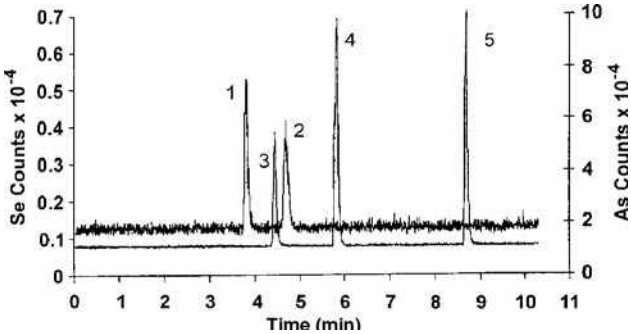

Fig. 5 Electropherogram of a mixed anion standard. Hydrodynamic injection (15 cm, 120 sec, 39.1 nl) with sodium borate buffer at pH 8. Peak 1: 3.2 ppm selenate; peak 2: 3.6 ppm selenite; peak 3: 1.9 ppm arenate; peak 4: 4.4 ppm DMA; peak 5: 4.7 ppm arsenite.
Source: From An evaluation of ultrasonic nebulizers as interfaces for capillary electrophoresis of inorganic anions and cations with inductively coupled plasma mass spectrometric detection, in Spectrochim. Acta Part B.[19] with permission of Elsevier Science.

natural extension that CE has been used for the analysis of metalloproteins and metal binding with other macromolecules. Also, the use of CE with the ICP–MS detector has been used in many studies reported in the literature. Metallothioneins are involved in metabolism and detoxification of several trace metals; thus the ability to monitor metallothioneins by CE–ICP–MS is of great importance. In a study of standard solutions of metallothionein I and ferritin, B'Hymer et al.[16] used various geometrical configurations of a microconcentric nebulizer to obtain different electropherograms. A run buffer of 15 m*M* Tris (hydroxymethyl) aminomethane adjusted to pH 6.8 by the addition of HCl was used at a potential of 15 kV. An example electropherogram is shown in Fig. 7. The MS detector has the advantage of being capable of simultaneous monitoring of various elements, thus resolving the relative quantities of cadmium, copper, and zinc bound to the metallothionein. Ferritin was clearly resolved from the iron signal.

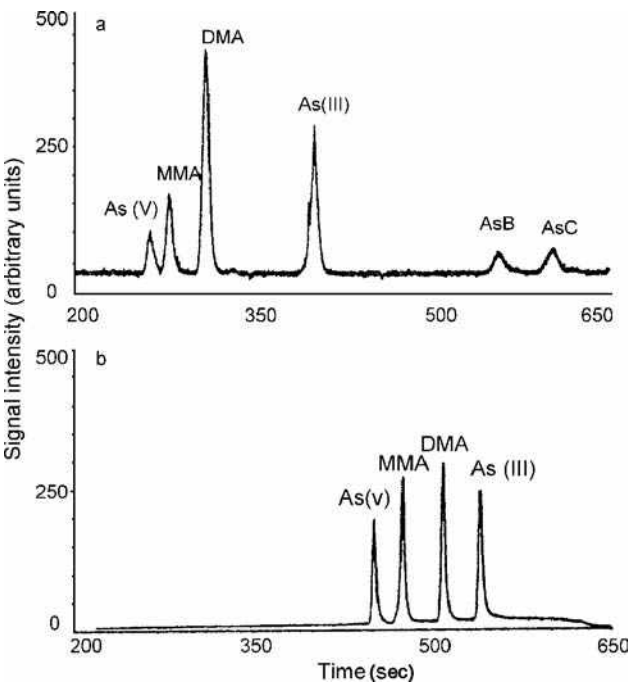

Fig. 6 a, Electropherogram showing the separation of As^V, MMA, DMA, As^{III} AsB, and AsC, obtained with CE–ICP–MS before optimization. b, Electropherogram of approximately 20 μg/L As^V, MMA, DMA, and As^{III} obtained after optimization of the CE–ICP–MS system. Conditions: 20 m*M* borate (pH 9.4), 2% OFM, 75 μm (I.D.) capillary, total length 88 cm, 5 kPA for 40 sec plus 5 sec post injection, –25 kV.
Source: From Speciation of six arsenic compounds using capillary electrophoresis inductively coupled plasma mass spectrometry, in J. Anal. At. Spectrom.[25] with permission of the Royal Society of Chemistry.

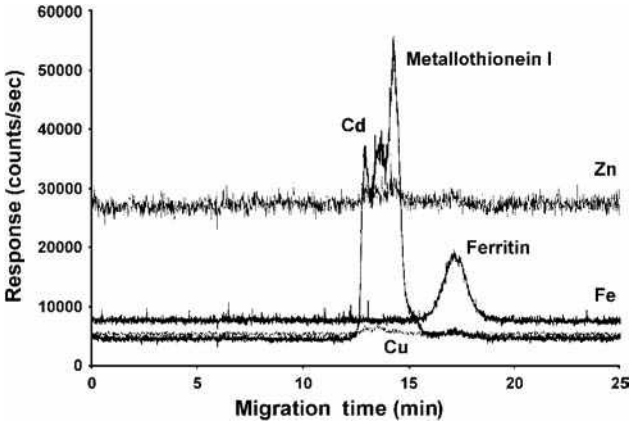

Fig. 7 Electropherogram showing separation of metallothionein I and ferritin. Zinc (mass 64) response at top and copper (mass 65) showed low signals for metallothionein. Cadmium (mass 114) showed a good response for metallothionein, and iron (mass 54) showed a good response for ferritin. This electropherogram was run using a run buffer of 15 m*M* Tris (hydroxymethyl) aminoethane (pH 6.8) at 15 kV, and the make-up buffer reservoir was positioned 2.5 cm above the MicroMist nebulizer.
Source: From Evaluation of a microconcentric nebulizer and its suction effect in a capillary electrophoresis interface with inductively coupled plasma mass spectrometry, in Appl. Spectrosc.[16]

CONCLUSIONS

The advantages of CE coupled with those of the ICP–MS detector will certainly allow this relatively young hyphenated technique to grow in the areas of elemental speciation and the analysis of environmental and biological samples. It is doubtful that CE will replace HPLC; however, CE will certainly compliment the other more traditional separation techniques owing to its separation being based on a physical rather than chemical partitioning. The ability of CE to use an extensive variety of electrolyte/buffer solutions so that specific chemical species of interest can be maintained during the course of a separation is another advantage.

The improvement in the mass spectrometer will of course lead to better detection limits and capabilities. Again, the low-flow pneumatic nebulizer will probably continue to lead the work performed in building CE–ICP–MS interfaces. Also, the current selection of commercial low-flow nebulizer will aid in the construction and use of interfaces. Finally, two books worthy of further reading are Akbar Montaser's *Inductively Coupled Plasma Mass Spectrometry* (Wiley-VCH, New York, 1998) and Joseph A. Caruso et al.'s *Elemental Speciation—New Approaches for Trace Elemental Analysis*, *Comprehensive Analytical Chemistry XXXIII* (Elsevier Science, Amsterdam, The Netherlands, 2000). Specific chapters were cited in this entry, but both books comprise other chapters containing a wealth of information about capillary electrophoresis–inductively coupled plasma-mass spectrometry.

REFERENCES

1. Olesik, J.W.; Kinzer, J.A.; Olesik, S.V. Capillary electrophoresis inductively-coupled plasma spectrometry for rapid elemental speciation. Anal. Chem. **1995**, *67*, 1–12.
2. Liu, Y.; Lopez-Avila, V.; Zhu, J.J.; Weiderin, D.R.; Beckert, W.F. Capillary electrophoresis coupled online with inductively-coupled plasma-mass spectrometry for elemental speciation. Anal. Chem. **1995**, *67*, 2020–2025.
3. Lu, Q.; Bird, S.M.; Barnes, R.M. Interface for capillary electrophoresis and inductively-coupled plasma-mass spectrometry. Anal. Chem. **1995**, *67*, 2949–2956.
4. Houk, R.S.; Fassel, V.A.; Flesch, G.D.; Svec, H.L.; Gray, L.A.; Taylor, C.E. Inductively coupled argon plasma as an ion-source for mass-spectrometric determination of trace-elements. Anal. Chem. **1980**, *52*, 2283–2289.
5. Date, A.R.; Gray, A.L. Plasma source-mass spectrometry using an inductively coupled plasma and a high-resolution quadrupole mass filter. Analyst **1981**, *106*, 1255–1267.
6. Hill, S.J., Ed.; *Inductively Coupled Plasma Spectroscopy and Its Applications*; Sheffield Academic Press: Sheffield, England, 1999.
7. Olson, L.K.; Caruso, J.A. The helium microwave-induced plasma—An alternative ion-source for plasma-mass spectrometry. Spectrochim. Acta. Part B, **1994**, *49*, 7–30.
8. Kinzer, J.A.; Olesik, J.W.; Olesik, S.V. Effect of laminar flow in capillary electrophoresis: Model and experimental results on controlling analysis time and resolution with inductively coupled plasma mass spectrometry detection. Anal. Chem. **1996**, *68*, 3250–3257.
9. Montaser, A.; Minich, M.G.; McLean, J.A.; Liu, H.; Caruso, J.A.; Mcleod, C.W. Sample introduction in ICPMS. In *Inductively Coupled Plasma Mass Spectrometry*; Montaser, A., Ed.; Wiley-VCH: New York, 1998; 1–47.
10. B'Hymer, C.; Caruso, J.A. Nebulizer sample introduction for elemental speciation. In *Elemental Speciation—New Approaches for Trace Elemental Analysis, Comprehensive Analytical Chemistry XXXIII*; Caruso, J.A. Sutton, K.L.M., Ackley, K.L., Eds.; Elsevier Science: Amsterdam, The Netherlands, 2000; 211–224.
11. Shum, S.C.K.; Neddersen, R.; Houk, R.S. Elemental speciation by liquid chromatography inductively coupled plasma mass-spectrometry with direct injection nebulization. Analyst **1992**, *117*, 577–582.
12. Shum, S.C.K.; Pang, H-M.; Houk, R.S. Speciation of mercury and lead compounds by microbore column liquid-chromatography inductively coupled plasma-mass spectrometry with direct injection nebulization. Anal. Chem. **1992**, *64*, 2444–2450.
13. Smith, R.D.; Barinaga, C.J.; Udseth, H.R. Improved electrospray ionization interface for capillary zone electrophoresis-mass spectrometry. Anal. Chem. **1988**, *60*, 1948–1952.
14. Day, J.A.; Sutton, K.L.; Soman, R.S.; Caruso, J.A. A comparison of capillary electrophoresis using indirect UV absorbance and ICP-MS detection with a self-aspirating nebulizer interface. Analyst **2000**, *125*, 819–823.
15. Sutton, K.L.; B'Hymer, C.; Caruso, J.A. UV absorbance and inductively coupled plasma spectrometric detection for capillary electrophoresis—A comparison of detection modes and interface designs. J. Anal. At. Spectrom. **1998**, *13*, 885–891.
16. B'Hymer; Day, J.A.; Caruso, J.A. Evaluation of a microconcentric nebulizer and its suction effect in a capillary electrophoresis interface with inductively coupled plasma-mass spectrometry. Appl. Spectrosc. **2000**, *54*, 1040–1046.
17. Taylor, K.A.; Sharp, B.L.; Lewis, D.J.; Crews, H.M. Design and characterisation of a microconcentric nebuliser interface for capillary electrophoresis—Inductively coupled plasma mass spectrometry. J. Anal. At. Spectrom. **1998**, *13*, 1095–1100.
18. Lu, Q.; Barnes, R.M. Evaluation of an ultrasonic nebulizer interface for capillary electrophoresis and inductively coupled plasma mass spectrometry. Microchem. J. **1996**, *54*, 129–143.
19. Kirlew, P.W.; Caruso, J.A.; Castillano, M.T.M. An evaluation of ultrasonic nebulizers as interfaces for capillary electrophoresis of inorganic anions and cations with inductively coupled plasma mass spectrometric detection. Spectrochim. Acta Part B, **1998**, *53*, 221–237.
20. Kirlew, P.W.; Caruso, J.A. Investigation of a modified oscillating capillary nebulizer design as an interface for CE–ICP-MS. Appl. Spectrosc. **1998**, *52*, 770–772.
21. B'Hymer, C.; Sutton, K.L.; Caruso, J.A. A comparison of four nebulizer/spray chamber interfaces for the high performance liquid chromatographic separation of arsenic compounds using ICP-MS detection. J. Anal. At. Spectrom. **1998**, *13*, 855–858.
22. Taylor, A.; Branch, S.; Fisher, A.; Halls, D.; White, M. Atomic spectrometry update. Clinical and biological materials, foods and beverages. J. Anal. At. Spectrom. **2001**, *16*, 421–446.
23. Kannamkumarath, S.; Wrobel, K.; Wrobel, K.; B'Hymer, C.; Caruso, J.A. Capillary electrophoresis-inductively coupled plasma-mass spectrometry: An attractive complementary technique for elemental speciation analysis. J. Chromatogr. A, **2002**, *975*, 245.
24. Timerbaev, A.R. Recent advances in capillary electrophoresis of inorganic ions. Electrophoresis **2002**, *23*, 3884–3906.
25. Van Hoderbeke, M.; Zhao, Y.; Vanhaecke, F.; Moens, L.; Dams, R.; Sndra, P. Speciation of six arsenic compounds using capillary electrophoresis inductively coupled plasma mass spectrometry. J. Anal. At. Spectrom. **1999**, *14*, 229–234.

CEC

Michael P. Henry
Chitra K. Ratnayake
Advanced Technology Center, Beckman Coulter, Inc., Fullerton, California, U.S.A.

INTRODUCTION

Capillary electrochromatography (CEC) is a technique in which a high direct voltage is applied, during analysis, across the ends of a capillary containing a solid stationary phase and a liquid mobile phase. It is thus a blend of high-performance liquid chromatography (HPLC) and capillary electrophoresis (CE).

Typically, fused silica capillaries are used with internal diameters of about 100 μm. Applied voltages of up to 30 kV are common. Mobile phases include low ionic strength aqueous buffer/organic solvent mixtures similar to those used in HPLC. Stationary phases generally consist of the same types of particulate materials as those employed in HPLC, although monolithic packings and surface-modified open tubular columns are gaining in popularity. Stationary phases of any kind usually extend only a portion of the way along the capillary, with particulate materials being held in place with small frits at either end of the packed region. Most CEC columns suffer from a degree of fragility due to the harm caused to the fused silica by the process of installing these two frits. Monolithic and wall-modified open tubular columns do not require frits and so offer an advantage here. Most instrumentation available for CEC is the same as that used for CE. Special capillary columns with a variety of dimensions and packing types are available. All sample classes that can be separated by HPLC can be separated by CEC and a great deal of work has been done to accumulate applications for this technique. There is still some controversy surrounding the immediate future of this technique, since certain technical challenges remain.

The objective of this entry is a clear understanding of the basic concepts, history, instrumentation, applications, and future prospects for CEC.

TECHNIQUE OVERVIEW AND SEPARATION MECHANISMS

The technique and features of CEC are invariably compared to those of HPLC and CE. Krull et al.[1] have published a useful table comparing the three methods, and this is shown in Table 1 with some changes. It can be seen that there are advantages of CEC over, for example, HPLC (efficiency, solvent consumption, and cost per run). On the other hand, HPLC has advantages over CEC (engineering, status of theory, frit integrity), not the least of which is the familiarity of the former and its integration into thousands of validated analyses.

CEC is a technique in which a high direct voltage is applied across the ends of a capillary containing a solid stationary phase and a liquid mobile phase. The mobile phase is driven by the mechanism of electro-osmosis from one buffer vial through the stationary phase, through an unpacked region in the capillary, and finally into a second buffer vial (Fig. 1). A liquid sample is injected from a third vial (sample vial) onto the packed column by means of a brief application of either a lower voltage or pressure. The mobile phase in the buffer vial is again driven through the column at the elution voltage, bringing about the formation of flow-derived zones of separated sample components along the packed bed. Eventually the zones elute from the packed region of the column and pass by a window in the capillary that is adjacent to a detection/data system.

Elution voltages up to 30 kV are normal, and injection voltages from 2 to 5 kV for several seconds are used. Typically, the capillary is made of high electrical resistance fused silica coated with polyimide to improve flexibility. The capillary internal diameter (I.D.) may have values from 5 to 200 μm, and the total length 20–60 cm. The small capillary I.D. is important to minimize Joule heating effects, which depend in part upon the current generated within the mobile phase. The polyimide coating is UV-opaque, and so a short cylindrical piece is removed from the capillary forming a window that is transparent to radiation down to about 190 nm wavelength.

The interior surface of the unmodified capillary is typically negatively charged due to the presence of deprotonated acidic silanol groups. Mobile cations adjacent to this surface are drawn through an electric field towards the cathode and, in the process, drag the mobile phase against the forces of viscosity towards that electrode. This mechanism electro-osmotic flow (EOF) of mobilizing the solution through the capillary results in the generation of an almost flat radial flow velocity profile across the interior, thereby substantially reducing a source of zone broadening.[1a] Sample component zones are therefore generally much narrower in CEC than in HPLC (where flow is generated hydrodynamically) and this leads directly to improved chromatographic resolution of mixture components.

As the mobile phase moves through the capillary containing the sorbent under the effect of this electro-osmotic

Table 1 Features of CEC compared with HPLC and CE.

Feature	CEC	HPLC	CE
Sample types (without additives[a])	Non-polar, polar, ionized	Non-polar, polar, ionized	Ionized
Available theoretical plates	100,000–700,000	<50,000	200,000
Peak capacity	100+	About 50	About 100
Mechanical complexity	Simple	Complex	Simple
Compatibility with MS	Better than CE	Good	Limited
Mass detection limit	Slightly better than HPLC	Good	Often inadequate
Ease of operation	Difficult	Easy	Easy
Solvent consumption	<1% of HPLC	100 L/year	<1% of HPLC
pH operating range	2–11	2–14	2–11
Frits	An experimental problem only with particle-packed columns	Not a problem	Not applicable
Purchase price (US$)	30,000–50,000	20,000–50,000	30,000–50,000
Cost per run (US$, no labor)	0.02	2.00	0.04

[a]Such as surfactants, polymers.
Source: From *Capillary Electrochromatography and Pressurized Flow Capillary Electrochromatography: An Introduction.*[1]

flow, sample components partition between the two phases in sorption and diffusive mechanisms characteristic of -liquid chromatography (LC). Ions in the sample move both under the influence of EOF and by their added attraction towards the oppositely charged electrode (electrophoresis). Uncharged components, on the other hand, move only under the influence of EOF Thus, sample components in general separate by chromatographic and sometimes electrophoretic processes.

Typical mobile phases[1b] are aqueous buffer/organic mixtures, similar to those used in HPLC. Stationary phases[1c] are generally the same as those used in HPLC and are most often particulate in nature, although monolithic (single piece) bonded phases[1d] are also used. In addition, open tubular CEC is possible, in which an adsorptive layer is formed on, or deposited onto, the interior surface of the capillary.[1e] The first generally require end frits, whereas the last do not need frits to maintain column integrity. Actual packed lengths typically range from 10 to 20 cm or in some cases may fill the entire length of the capillary.

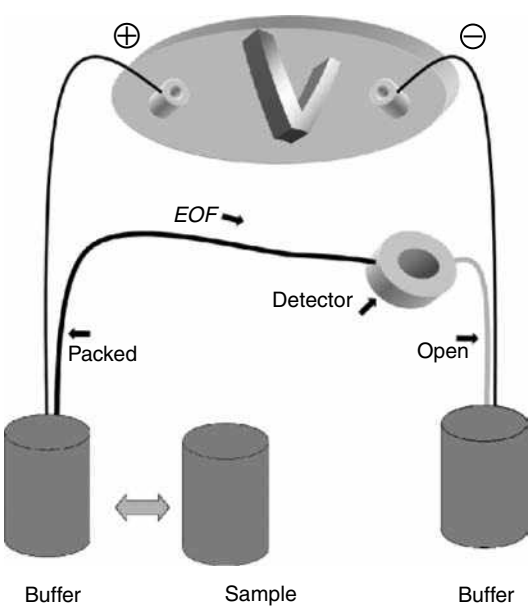

Fig. 1 Schematic illustration of a typical instrument for CEC.

All sample classes that can be separated by HPLC can be separated by CEC (see section on "Applications"). Dipping the capillary inlet into a separate vial containing the sample in solution and applying an injection voltage for a brief time accomplish sampling. The capillary inlet is then moved back to the inlet buffer vial and elution is commenced at the (normally) higher voltage.

Samples are detected by the same techniques as those used in HPLC and CE. The uses of on-column detection with UV-Vis spectrophotometers and lasers and postcolumn detection with mass spectrometers are well established.[1f] Instruments used for CEC are generally the same as those used for CE and consequently have capabilities for full automation of analysis and data processing of the results.

Two books on CEC have been published in the third millennium.[1a–f,2]

HISTORY

Pretorius, Hopkins, and Schieke[3] were among the first investigators to carry out packed column LC in a tangential electric field as a feasible alternative to using pressure. Their 1 mm I.D. quartz columns filled with 75–125 μm silica particles gave reduced plate heights of about 3 by CEC vs. the pressure mode values of about 8.

The advantages of electrochromatography, however, were not to be realized until the technology needed to create narrow capillaries (< 200 μm I.D.), stable frits, and sensitive detection systems had matured. Thus, in 1981, Jorgenson and Lukacs[4] carried out experiments in CEC using an instrument (see schematic in Fig. 1) whose basic design is still used today. Besides acting as a combined injector, separation medium, and flow cell, their column could also be used in the CE, CEC, and micro-LC modes. However, the fused silica capillaries (170 μm I.D.) drawn in their labs, packed with 10 μm particles and operated in neat acetonitrile, gave rather modest improvements in efficiency over standard liquid chromatographic techniques, with reduced plate heights of no less than 1.9. These disappointing results, coupled with an admission of the technical difficulty of using this technique, led these authors to conclude that CEC would only be useful in wider bore (several centimeters) preparative scale processes, a suggestion also made by Pretorius, Hopkins, and Schieke.[3]

Then, in 1991, Knox and Grant,[5] working carefully with 3 and 5 μm particles, showed that it was practical to achieve reduced plate heights of less than 1 in the CEC mode. These results confirmed their strongly optimistic view of the future of this technique, and a few years later, interest in CEC accelerated rapidly.

Over the past decade, CEC has become incorporated into the research and development programs of many universities and industrial organizations.[6] Progress has been made in the areas of column construction, column packing, general instrumentation, mobile phase optimization, applications, and method development.[1a–f] The elucidation of the physicochemical and electrochemical properties of CEC systems and the determination of their influence on the entire analysis is ongoing[7] and adds a fascinating dimension to the study of this technique.

OPERATIONAL LIMITS

Knox and Grant[5] have placed a general maximum limit of 200 μm on the I.D. of capillaries used in CEC in order to avoid problems with excessive internal heating, which harms column efficiency in aqueous/organic solutions. In principle, however, wider bore tubes can be used, provided the current and field strength are kept low, or the thermal conductivity of the system is kept high. Currents in general should be kept below 50 μA and field strengths held below 1000 V/cm. At higher field strengths and currents, outgassing of mobile phases can be a problem. This is often reduced in frequency if both ends of the capillary are pressurized. Most commercially available instruments have this capability. Bubbles are also a problem at higher temperatures; so cooling of the capillary is recommended.

CEC in mobile phases containing organic solvents in any proportion is possible, provided the electrical double layer is formed with appropriate dissolved salts[3] in non-aqueous cases.

The ionic strength of most conventional buffers, such as phosphate, acetate, or borate, needs to be kept within the range 0.002–0.05 *M*, but care needs to be taken with the lower concentration to avoid buffer capacity depletion due to hydrolysis. Zwitterionic buffers such as morpholino ethane sulfonic acid (MES) (whose electrical conductivity is low) can be used in the range 0.01–0.1 *M* without undue heating problems, provided field strength and aqueous content are kept low and the capillary is cooled.

Since there are few or no pressure gradients generated within a CEC column, long packed capillaries containing very small particles are possible, but the longer columns mean slower chromatography and equilibration. Generally, columns in CEC are no longer than 60 cm. Times of analyses may be reduced by increasing flow rates. This is generally accomplished by increasing the applied voltage, while remaining within the limits mentioned above. Alternatively, one may increase the electroosmotic flow rate by increasing pH or decreasing the amount of organic solvent (if any) in the mobile phase. All these changes (in flow rate, voltage, pH, and solvent), however, may cause simultaneous and undesirable shifts in resolution among the peaks of interest.

In some cases, hydrodynamic pressure may be exerted upon the inlet end of the capillary in order to increase the speed of analysis. This generally amounts to just 100 psi, and so improvements are not often seen for conventionally packed columns. However, many types of monolithic and open tubular columns are sufficiently permeable to allow significant increases in flow rates when these low inlet pressures are used.[8] A disadvantage of using applied pressure in this fashion is that efficiency is reduced due to the intrusion of a parabolic radial flow profile into the capillary.

INSTRUMENTATION

Creative solutions to practical problems abound in the evolution of instruments designed to carry out CEC. The graphite electrodes, quartz tubing, glass wool frits, and on-column pressure injection of Pretorius, Hopkins, and Schieke[3] gave way to Jorgenson and Lukacs's[4] fused silica tubing, sintered frits, and electrokinetic injection. Commercially developed automated instruments designed for CE, whose appearance in 1988[9] followed these last authors' breakthrough research, have been used for most applications in CEC. Modern instruments therefore consist of the column, a cooling system, a detector, a voltage controller, an autosampler, and a data processor.

In-capillary optical focusing of UV, visible, and laser radiation has largely solved the problems of detection.[10] In-column (through the packing) detection of appropriate analytes by laser-induced fluorescence has improved

general efficiency by avoiding the deterioration of peak shape that often occurs as the analyte zone passes through the outlet frit.[10] Mass spectrometers are also used for detection and identification in CEC since the low flow rates are compatible with the sampling kinetics required by these instruments.[1]

Columns for modern CEC have been prepared using standard HPLC particles, from 0.5 to 10 μm diameter, bearing C18, phenyl, C8, C6, C4, CN, amino, sulfo, and other functional groups and a variety of chiral polymers such as proteins and polysaccharides.[11] In situ sintered silica-based frits are most often used in these columns,[12] which are generally slurry-packed at high pressures. Several types of so-called monolithic (single piece) columns have been developed,[13,14] which dispense with frits, while generally maintaining high efficiency. Open tubular columns are becoming very popular, and many versions exist.[1]

Companies that have instruments suitable for CEC include Agilent Technologies, Beckman Coulter Inc., Prince Technologies, Unimicro Technologies, Micro-Tech Scientific, and Capital HPLC. More information on commercialized products for CEC can be found in Buyers' Guides to chromatographic instruments and accessories, such as the LC–gas chromatography (GC) North America publication, which is issued yearly in August.

APPLICATIONS

In 1998, Dadoo et al.[10] succeeded in achieving near baseline resolution of five polynuclear aromatic hydrocarbons over a 1 sec interval by CEC (Fig. 2). These high speeds were obtained from a combination of factors including a modest column length (6.5 cm), a high column plate number (13,000 plates) associated with 1.5 μm non-porous C18 particles, and a high voltage (28 kV). Although this separation is one of the fastest achieved in a liquid phase, higher column plate numbers have been obtained. Smith and Evans[15] report values of greater than 8 million plates per meter for the analysis of tricyclic antidepressants on 3 μm sulfopropyl bonded silica. These values are clearly due to a focusing effect within the column, and further work on this phenomenon has been done.[16] Dadoo et al.[10] have produced CEC columns that generate plate numbers of about 700,000 per meter when peaks were detected before they passed through the outlet column frit. These results illustrate how closely practical achievements in CEC have now approached predicted theoretical performance maxima.

Fu et al.[17] have prepared CEC columns from the highly efficient, strong cation exchange material PolySULFOETHYL A for the purpose of separating basic pharmaceuticals in human serum. This is a relatively rare example of the use of an ion exchanger to chromatograph positive organic ions. Fig. 3 shows the high quality of the capillary electrochromatogram achieved.

McKeown, Euerby, and Lomax[18] have made a detailed assessment of silica-based reversed-phase materials for the analysis of basic compounds. Walhagen et al.[19] have

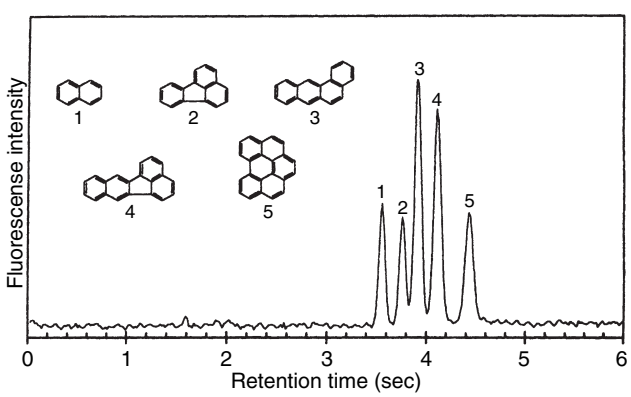

Fig. 2 Electrochromatogram of naphthalene 1, fluoranthene 2, benz[*a*]anthracene 3, benzo[*k*]fluoranthene 4, and benzo [*ghi*]perylene 5, using 1.5 μm non-porous ODS particles. Column dimensions: 100 μm I.D. × 6.5 cm packed length (10 cm total length). Mobile phase: 70% acetonitrile in a 2 m*M* Tris solution. Applied voltage for separation: 28 kV. Injection: electrokinetic at 5 kV for 2 sec.
Source: From Advances in capillary electrocromotography: Rapid and high-efficiancy separation of PAHs, in Anal. Chem.[10]

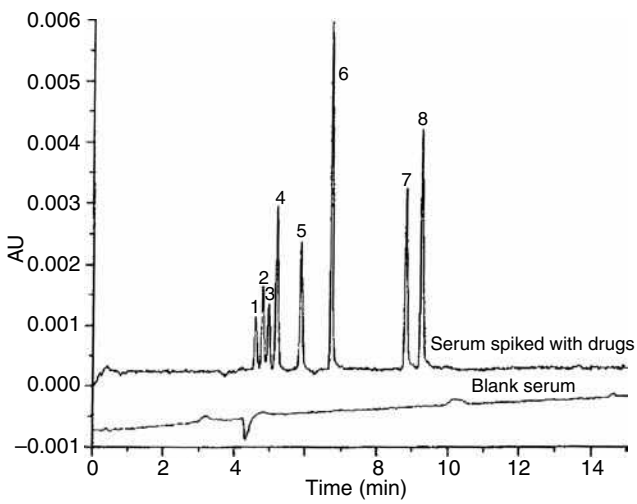

Fig. 3 Hydrophilic interaction CEC separation of basic drugs spiked in human serum. Column: fused-silica capillary, 27 cm (20 cm packed with 5 μm, 300 Å PolySULFOETHYL A particles). Mobile phase: 80% v/v acetonitrile in 100 m*M* TEAP buffer. TEAP buffer at pH 2.8. Applied voltage: 10 kV. Injection: 0.5 psi for 90 sec. Temperature: 25°C. Detection: UV at 214 nm. Concentration of drugs: 40 μg/ml. Solutes: 1, amobarbital; 2, phenobarbital; 3, barbital; 4, caffeine; 5, sulfanilamide; 6, theophylline; 7, 2,4-dimethylquinoline; 8, propranolol.
Source: From Determination of basic pharmaceuticals in human serum by hydrophilic interaction capilary electrochromatography, in Electrophoresis.[17]

investigated the nature of the forces controlling the selectivity of peptides. Kang, Wistuba, and Schurig[20] have reviewed progress in chiral separations. A widely applicable cationic/hydrophobic monolithic column has been investigated by Bedair and El Rassi[21] for the high-speed separation of proteins, pesticides, and amino acid derivatives.

Most chemical classes have been separated and analyzed by CEC.[11] These include many classes of pharmaceuticals, environmental chemicals, explosives, natural products, drugs of abuse, polypeptides, oligosaccharides, nucleosides and their bases, and polynucleotides. Applications of CEC, such as the review by Eeltink, Rozing, and Kok in *Electrophoresis*,[22] may be found in other journals such as the *Journal of Chromatography*, *Biomedical Chromatography*, *Chromatographia,* and the *Journal of Separation Science*. Access to the literature of CEC in general is readily achieved through several user-friendly websites.[23–25]

PROBLEMS, ISSUES, AND FUTURE PROSPECTS

Fundamental theory of CEC that will provide a better understanding of mechanisms of separation is being developed. In particular, the work of Rathore and Horváth[7] in elucidating the electrical properties of packed columns is particularly interesting. Technological issues that remain to be addressed include the difficulty of dealing with bubble formation and the fragility of conventional columns due to the aggressive frit-forming methods currently used. Monolithic columns[13,14] and open tubular columns[26] appear to have advantages in this regard.

Majors[6] has compiled the results of his *Perspectives* survey of 14 leading separation scientists with an interest in CEC. As expected, there is a wide divergence in the opinions of these leaders with regard to the current issues and future prospects for CEC. Few, however, underestimate the current technological difficulties in column manufacture, the reproducibility of chromatographic and electroosmotic properties of the packed capillary, and the short-term problems of competing with HPLC or CE. But the majority of scientists interviewed believe that, as with any new technique, these problems will be overcome and that CEC will become a routine method of analysis in time.

On the other hand, the future of CEC may lie with the exciting developments in microfabrication described by Regnier[27] where capillaries here are open channels 1.5 μm wide and 4.5 cm long and can achieve efficiencies of 800,000 plates per meter.

CONCLUSIONS

This entry has been a brief introduction to the technique of CEC. It is a technique in which a high voltage is applied across the ends of a capillary containing a solid stationary phase and a liquid mobile phase. Aspects of the method that were described included a brief overview of the technique, elements of the history of its development, the normal operational limits, aspects of modern instrumentation, a summary of selected applications, and future prospects for the development of CEC.

The future of the technique appears assured,[6] although the progress in moving it from the interesting stage to its use alongside the mature HPLC and CE has been quite slow. Fundamental theory of CEC continues to be developed. Several technological issues remain to be addressed, including the difficulty of dealing with bubble formation and the fragility of conventional columns. Monolithic and open tubular columns appear to have advantages in this regard.

REFERENCES

1. Krull, I.S.; Stevenson, R.L.; Mistry, K.; Swartz, M.E. *Capillary Electrochromatography and Pressurized Flow Capillary Electrochromatography: An Introduction*, 1st Ed.; HNB Publishing: New York, 2000; (a) 10–11; (b) 60–67; (c) 34–40; (d) 49–53; (e) 53–55; (f) 81–85.
2. Bartle, K.D., Myers, P., Eds.; *Capillary Electrochromatography*, 1st Ed.; RSC Chromatography Monographs Royal Society of Chemistry: Cambridge, 2001.
3. Pretorius, V.; Hopkins, B.J.; Schieke, J.D. Electro-osmosis: a new concept for high speed liquid chromatography. J. Chromatogr. **1974**, *99*, 23–30.
4. Jorgenson, J.W.; Lukacs, K.D. High resolution separations based on electrophoresis and electro-osmosis. J. Chromatogr. **1981**, *218*, 209–216.
5. Knox, J.H.; Grant, I. Electrochromatography in packed tubes using 1.5 to 50-micron silica gels and ODS bonded silica gels. Chromatographia **1991**, *32* (7–8), 317–327.
6. Majors, R.E. Perspectives on the present and future of capillary electrochromatography. LC/GC **1998**, *16*, 96–110.
7. Rathore, A.S.; Horváth, Cs. Axial non-uniformities and flow in columns for capillary electrochromatography. Anal. Chem. **1998**, *70*, 3069–3077.
8. Ratnayake, C.K.; Oh, C.S.; Henry, M.P. Characteristics of particle-loaded monolithic sol-gel columns for capillary electrochromatography. I. Structural, electrical and band-broadening properties. J. Chromatogr. A. **2000**, *887*, 277–285.
9. Weinberger, R. The evolution of capillary electrophoresis: Past, present, and future. Am. Lab. **2002**, *34* (10), 32–40.
10. Dadoo, R.; Zare, R.N.; Yan, C.; Anex, D.S. Advances in capillary electrochromatography: Rapid and high-efficiency separations of PAHs. Anal. Chem. **1998**, *70*, 4787–4792.
11. Altria, K.D.; Smith, N.W.; Turnbull, C.H. A review of the current status of capillary electrochromatography technology and applications. Chromatographia **1997**, *46*, 664–674.
12. Dittman, M.M.; Rozing, G.P.; Ross, G.; Adam, T.; Unger, K.K. Advances in capillary electrochromatography. J. Capillary Electrophor. **1997**, *5*, 201–212.
13. Svec, F.; Peters, E.C.; Sykora, D.; Yu, C.; Fréchet, J.M.J. Monolithic stationary phases for capillary electrochromatography based on synthetic polymers: Design and

applications. J. High Resolution Chromatogr. **2000**, *23* (1), 3–18.
14. Ratnayake, C.K.; Oh, C.S.; Henry, M.P. Particle loaded monolithic sol-gel columns for capillary electrochromatography: A new dimension for high-performance liquid chromatography. J. High Resolution Chromatogr. **2000**, *23* (1), 81–88.
15. Smith, N.W.; Evans, M.B. The efficient analysis of neutral and highly polar pharmaceutical compounds using reversed-phase and ion-exchange electrochromatography. Chromatographia **1995**, *41*, 197–203.
16. Euerby, M.R.; Gilligan, D.; Johnson, C.M.; Roulin, S.C.P.; Myers, P.; Bartle, K.D. Applications of capillary electrochromatography in pharmaceutical analysis. J. Microcol. Sep. **1997**, *9*, 373–387.
17. Fu, H.; Jin, W.; Xiao, H.; Xie, C.; Guo, B.; Zou, H. Determination of basic pharmaceuticals in human serum by hydrophilic interaction capillary electrochromatography. Electrophoresis **2004**, *25*, 600–606.
18. McKeown, A.P.; Euerby, M.R.; Lomax, H. Assessment of silica-based reversed-phase materials for the analysis of a range of basic analytes by capillary electrochromatography. J. Sep. Sci. **2002**, *25* (15–17), 1257–1268.
19. Walhagen, K.; Huber, M.I.; Hennessy, T.P.; Hearn, M.T.W. On the nature of the forces controlling selectivity in the high performance capillary electrochromatographic separation of peptides. Peptide Sci. **2003**, *71* (4), 429–453.
20. Kang, J.; Wistuba, D.; Schurig, V. Recent progress in enantiomeric separation by capillary electrochromatography. Electrophoresis **2002**, *23* (22–23), 4005–4021.
21. Bedair, M.; El Rassi, Z. Capillary electrochromatography with monolithic stationary phases III. Evaluation of the electrochromatographic retention of neutral and charged solutes on cationic stearyl-acrylate monolith and the separation of water soluble proteins and membrane proteins. J. Chromatogr. A. **2003**, *1013*, 47–56.
22. Eeltink, S.; Rozing, G.P.; Kok, W.Th. Recent applications in capillary electrochromatography. Electrophoresis **2003**, *24* (22–23), 3935–3961.
23. http://www3.interscience.wiley.com (Search CEC) (accessed October 2004).
24. http://www.separationsnow.com (Search CEC) (accessed October 2004).
25. http://www.ceexchange.com/nowjune2004.php (accessed October 2004).
26. Pesek, J.J.; Matyska, M.T.; Dawson, G.B.; Chen, J.I.-C.; Boysen, R.I.; Hearn, M.T.W. Open-tubular electrochromatographic characterization of synthetic peptides. Electrophoresis **2004**, *25*, 1211–1218.
27. Regnier, F.E. Microfabricated monolith columns for liquid chromatography. Sculpting supports for liquid chromatography. J. High Resolution Chromatogr. **2000**, *23* (1), 19–26.

Cell Sorting: Sedimentation FFF: A Cellulomics Concept

Philippe Cardot
Analytical Chemistry and Bromatology Laboratory, University of Limoges, Limoges, France

Yves Denizot
Immunology Laboratory, University of Limoges, Limoges, France

S. Battu
Analytical Chemistry and Bromatology Laboratory, University of Limoges, Limoges, France

INTRODUCTION

Sedimentation field-flow fractionation (SdFFF) is an efficient, analytical/preparative-scale, cell sorting device, in particular, if coupled with sophisticated cellular characterization techniques, devices, or methods, including flow cytometry (FC). Cell population, by analogy with "polymers," appears very polydisperse and disperses in many dimensions, which may not be essentially biophysical (size, shape, density, and rigidity), but also functional (cell cycle, protein expression, and differentiation stage). Cell sample pretreatment has a unique goal, which is to provide a sterile and viable cell suspension at an appropriate concentration (1–10 million cells/ml). A particular elution mode, made possible in cell purification by exploiting complex hydrodynamic forces, is usually described as a "Hyperlayer." This elution mode exploits slight differences in physical characteristics of the cell (size, shape, density, rigidity, and surface characteristics); trends are opened to their association with complete functional cell characteristics analyses. It is shown that cells can be eluted, in some examples, according to functional parameters (cell cycle and differentiation stage), and that correlations may exist between functional parameters and the physical ones. If a given cell population is considered, considerable information provided by the separation and the complete physical and functional analyses allows one to define, characterize, and produce a new type of cell subpopulation. Such separation/characterization process for cells can be described as "cellulomics," by analogy with what is done for proteins of gene systems, keeping in mind the concept that the cell is the "fundamental and unique" localization and production factory of any gene and protein.

BACKGROUND

The last decades have shown considerable development of a large panel of cell-sorting techniques.[1–5] SdFFF, such as elutriation or centrifugation methods, belongs to the group of "physical methods," comparisons of which have already been assessed.[1] In the present report, we will focus on the specific features of cell elution in FFF and on the necessity of coupling such a physical separation/purification system with detectors of high functional specificity. Cell sorting with FFF emerged in the scientific literature in the early 1980s of the last century. A pioneering report was published in 1984 by Caldwell et al.[6] in which most of the separation rules and methodologies were described. At difference with all other species, cell sorting with FFF success was proved essential by using sedimentation subtechniques that required specific instrumentation and methodological setups. Systematic instrumentation development, allowing separation of living species in sterile conditions for further use, was initiated in the late 1990s in our laboratory.[7,8]

It must be noted here that the main objective of cell separation in FFF is not only analytical, but also preparative. The main goal is strongly linked to the possibility not only to characterize as completely as possible the cell subpopulation, but to provide or produce new living cell subpopulations for any use. It is essential to keep these cells in surviving condition. Therefore considerable attention must be given to characterize a potential subpopulation, and to define and control their survival. However, if non-stable subpopulations are recovered, cinematic studies of their properties must be developed in terms of "time or age"-dependent characteristic modifications. To be clear, cells are eluted at a given stage; they are characterized or used at that stage, in whatever way they can be cultivated, maintained in survival, and evolved to other critical stages (the must be characterized) where they can be functionally used. Such complex receiver-oriented characteristic (ROC) separation/characterization step can de described as "cellulomics."

In this report, specific instrumentation of SdFFF for cell sorting will be described. The interest and potential of the "Steric Hyperlayer"[6,9] elution mode for cell sorting will be discussed, keeping in mind basic rules for physically or functionally oriented separation development. By analogy

with polymers, experimentally driven definitions, descriptions, and characterizations of cell populations will be provided, leading to an information matrix described as "cell population multipolydispersity."[1]

A particular paragraph is devoted to some specific requirements for FFF cell sorting, such as sample preparation or separator poisoning. The battery of cell population or cell subpopulation characterization methods will be described with an FFF-dependent classification: physical methods compared to functional ones. Finally, experimental correlations between functional and physical cell characteristics lead to the isolation of very specific populations, thereby opening the field of "cellulomics." In this report, it is assumed that readers have a basic knowledge of separation sciences, in particular, in chromatography and FFF.

PRINCIPLE OF SdFFF AND INSTRUMENTATION

The FFF family encompasses a broad array of subtechniques; however, FFF techniques have in common the design of a channel, generally parallelepiped and often described as "ribbonlike," in which the critical dimensions are: 1) thickness, usually lower than 300 μm; 2) length, between 20 and 100 cm; and 3) breadth, from 0.5 to 2 cm; with 4) tapered channel ends. An external field acts on the great surface of the ribbon to achieve flow rate-dependent separations (Hyperlayer elution mode for micron-sized species). SdFFF techniques can be divided into two groups. The first uses simple gravity or gravity fractions [i.e., gravitational/subgravitational FFF (GrFFF/GFFF)]; the second uses the multigravity field created by centrifugation generically described as SdFFF. With common associated devices (injection, flow, and detection devices), their instrumental design and setup are completely different. The GFFF separator is very simple to set up and does not require more specific skills than a simple "exploration desire," whereas SdFFF is much more complex to set up and requires long-term know-how in the absence of commercially available devices devoted to cell sorting.

INSTRUMENTATION

Instrumentation for cell sorting can be very simple, using GFFF devices as described by our group,[10–13] or by others.[14–16] A complete technical instrumentation has been also described.[17] The key parameter is the material used to construct the channel walls, which must be as "inert" as possible if considered against the cellular materials or their media (protein clotting). Media or sample-derived wall treatment may occur when changing, considerably, elution conditions. Such goal is empirically well assessed in the biological technology using materials of various "biocompatible" polymers. Therefore it is only necessary to choose as an appropriate material the one compatible with FFF instrumentation (low deformation under sealing pressure). It must be noticed here that some materials can be appropriate for some cell groups and be completely unusable for others, which requires a versatile instrumentation.

In SdFFF, the same strategy is employed with materials tested in GFFF, with the only price that sealing and deformability linked with centrifugation rate must be controlled. However, one particular point must be taken into account in SdFFF; long connection tubings are necessary and they must be chosen to be "biocompatible" and with appropriate inner diameter. This point is highly critical. Diameters that are too narrow may induce shear forces, destroying selective parts of the sample; too large diameters induce non-column band spreading, thereby limiting resolution. Channel dimensions and tubing choices must be chosen in the light of the sample and of the separation goals. Unfortunately, only a few laboratories exert an instrumental effort to define and construct biocompatible SdFFF systems.[18–20]

ELUTION MODE

Cells are in the 3–40 μm diameter range; channel thicknesses ranging from 70 to 250 μm are commonly used, depending on elution selectivity requirements. Therefore cell size cannot be ignored in the light of the channel thickness leading to an experimentally developed elution mode described as "Steric Hyperlayer."[6,9] Again, in the light of the preceding paragraph, a "pure steric elution mode" must be avoided as possibly generating high particle–wall interactions, these being so far determined essentially on an experimental basis. Therefore elution conditions must meet the hypotheses developed in the Hyperlayer condition. As such, model cells are focused on different stream lines by the double and opposite actions of the external field and of forces generated by the cell in motion and described generically under the term of lift forces, driving the cell into an equilibrium position in the channel thickness. The lifting force characteristics are complex, were described for the first time by Ho and Leal,[21] and were developed on a theoretical basis for FFF by Martin and Williams.[22] Experimental proofs were given for cell sorting by Caldwell et al.[6] If little is known about the kinetics of this focusing process using retention ratio analysis, it is simplified in the determination of an average "equilibrium" position in the channel thickness of the cells eluted at a given retention ratio by a position(s) in the channel thickness given by the following equation:

$$R = \frac{3s}{w} \tag{1}$$

where R is the measured retention ratio, s is the distance between the average particle gravity center and the accumulation wall, and w is the channel thickness. The calculated s value does not describe the real distance at equilibrium, but can be considered an accurate evaluation of it, assuming that: 1) in identical experimental conditions, kinematics in the channel thickness of particles of analogous size, shape, and density is analogous; 2) flow injection reduces particle–wall interactions that are negligible; and 3) lifting forces are so intense that no particle–wall retardation effects occur. If s is greater than the cell greater radius, then elution is considered as a Hyperlayer. Therefore it is essential to obtain for cells an average position that is much larger than the cell radius; this ensures that cells have a low probability to interact with channel walls. Such considerations lead to a concept applied by Battu et al.[19,20] for cell sorting—the "safety Hyperlayer" elution mode in which cell recovery is maximum in the case of flow-established injections. Depending on the elution conditions (channel dimensions, external field intensity, and flow rate), it is, so far, possible to state that, for spherical particles of identical density, the elution order is size-dependent, with the larger ones being eluted first. It is also, so far, possible to assess that, at identical sizes, spherical particles are eluted according to their mass, with the least dense being eluted first. More complex situations arise if, as in the case of cells, the population presents independent size and density distributions.

There is a particular injection mode, described often as "stop flow" or primary relaxation step, in FFF. Suspensions are inserted in the channel under an external field, then the flow is stopped for a given time (stop flow time and primary relaxation time) and flow is reestablished for elution. This particular injection procedure is specific for FFF separations[6,23] and increases selectivity considerably, even in the case of the "Hyperlayer" elution mode. Historically, this was set up because of instrumental considerations, where the inlet tubing emerged at the depletion wall.[6,10,23] Simple instrumentation modification involving, in contrast, the accumulation wall made it possible to avoid such procedure driving the species into a geometric location in the channel thickness close to the accumulation wall.[7,8,11–13,18–20] If, experimentally, such modification was successful using a channel of reduced thickness, complex injection hydrodynamics occurs if the channels are thicker than 100 μm. Considerably reducing the "stop flow time," or even avoiding it, is essential if cell sorting strategies are considered. Very little is known in terms of cell–channel interactions (even with biocompatible materials) and the stop flow procedure may be at the origin of (reversible or not) cell sticking, leading either to cell destruction (which may be selective) or cell differentiation by simple contact (stem cells). From injection to injection, the wall structure at the injection zone may be completely altered (modified), leading to analysis or

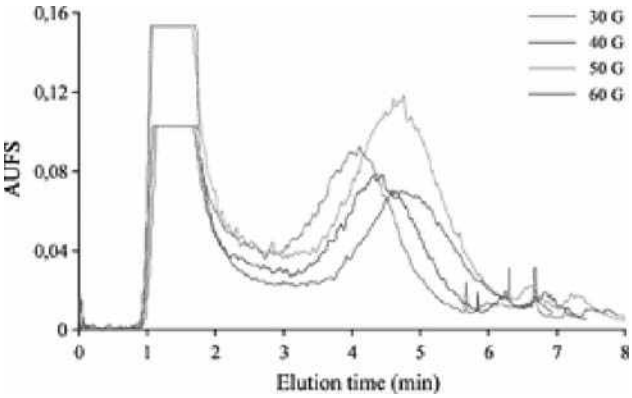

Fig. 1 Cell sorting with FFF.

separation biases. Therefore a price must be paid in terms of separation power to reduce these possible interactions. Limiting separation power by using systematic flow-established injections is essential if cell subpopulation integrity maintenance is required (cell differentiation process); in these conditions, the probability that any cell of the sample will interact with the walls is reduced—a process also limited by the kinetics (whose characteristics are not known) of the Hyperlayer focalization. As collateral consequences of flow injection, separation times are considerably reduced, recovery is enhanced, and channel poisoning is reduced. Fig. 1 shows the fractograms obtained in such conditions in the case of a mixture of ES cells and fibroblasts whose biological properties were analyzed.[7] Low-intensity spikes at the end of every fractogram signifies field stop and a low reversible release of trapped material, which may not necessarily be made of cells only.

Mouse E14 ES cells were routinely grown onto a monolayer of mitomycin-treated primary embryonic mouse fibroblasts as a source of cytokines and growth factors. The medium consisted of DMEM with 15% fetal calf serum (Gibco, Cergy Pontoise, France), 100 U/ml penicillin, 100 μg/ml streptomycin, 1 μM α-mercaptoethanol, and 10^3 U/ml leukemia-inhibitory factor (LIF; Gibco). ES cells were grown at 37°C in a humidified chamber with 10% CO_2. ES cells were recovered with trypsin treatment for SdFFF experiments or subcultures. The SdFFF separation device used in this study includes a separation channel, which consisted of two $870 \times 30 \times 2$ mm polystyrene plates, separated by a Mylar spacer in which the channel ($785 \times 10 \times 0.125$ mm with two V-shaped ends of 70 mm) was carved. Inlet and outlet were 0.254 mm I.D. Peek tubing (Upchurch Scientific, Oak Harbour, Washington, U.S.A.) was directly screwed into the accumulation wall. Then, polystyrene plates and Mylar spacers were sealed onto a centrifuge basket. The channel–rotor axis distance was measured at r (13.8 cm). Cleaning and decontamination procedures have been described in a previous report.[3] The elution signal was recorded at 254 nm.

MULTIPOLYDISPERSITY: PHYSICAL/ FUNCTIONAL AND DETECTION REQUIREMENTS

A First-Order Definition of Multipolydispersity: Example of Mass Distribution

This concept has already been defined for cell sorting.[1] To precisely know the physical characteristics of cell populations, let us imagine a simple bidimensional one where cells are spherical and rigid, and show independent size and density distribution. According to the Steric Hyperlayer mode, with some subpopulations, coelution is possible, generating a need for size or mass detectors. Therefore granulometric or mass measurements appearing at the outlet (online/off-line) are essential in terms of separation developments.

Fig. 2 shows a theoretical bidimentional polydispersity (size and density). The bidimensional Gaussian distribution is shown in Fig. 2a, where (*S*) is the size axis, (*D*) is the density, and *C* represents the number of particles. If such a sample is eluted according to the Hyperlayer elution mode, a broad fractogram is observed, as shown in Fig. 2b. From such a fractogram, every fraction corresponds to particles of different sizes and densities, as qualitatively shown in Fig. 2c. The front of the peak is associated with particles that are very different from the ones at the tail. It is possible to imagine granulometric detection all along the fractogram profile, as shown in Fig. 2d. If the density distribution coinvolved with the size distribution is considered, every fraction is associated with a particular particle size distribution (PSD). It is essential to note that, in the simulation considered here, density distribution is not disperse enough to invert or modify the "size-dependent Hyperlayer elution order," where the biggest and most polydisperse particles elute first. It is now interesting to determine this PSD in the density distributions.

GRANULOMETRIC PATTERNS AND DENSITY DISTRIBUTION

It may be possible to discriminate density vs. size if a single particle mass detector were available for micron-sized species. In the absence of such a detector, only indirect information is affordable, exploring the consequences of the Hyperlayer elution mode. From the above-described bidimentional population (size and density), the Hyperlayer mode allows us to draw iso-density and iso-size retention patterns. Such information coinvolved with the PSD permits the determination of the density distribution envelope of the fractions considered, as shown in Fig. 3. Graph a shows the iso-retention pattern of the population. It is observed that, at

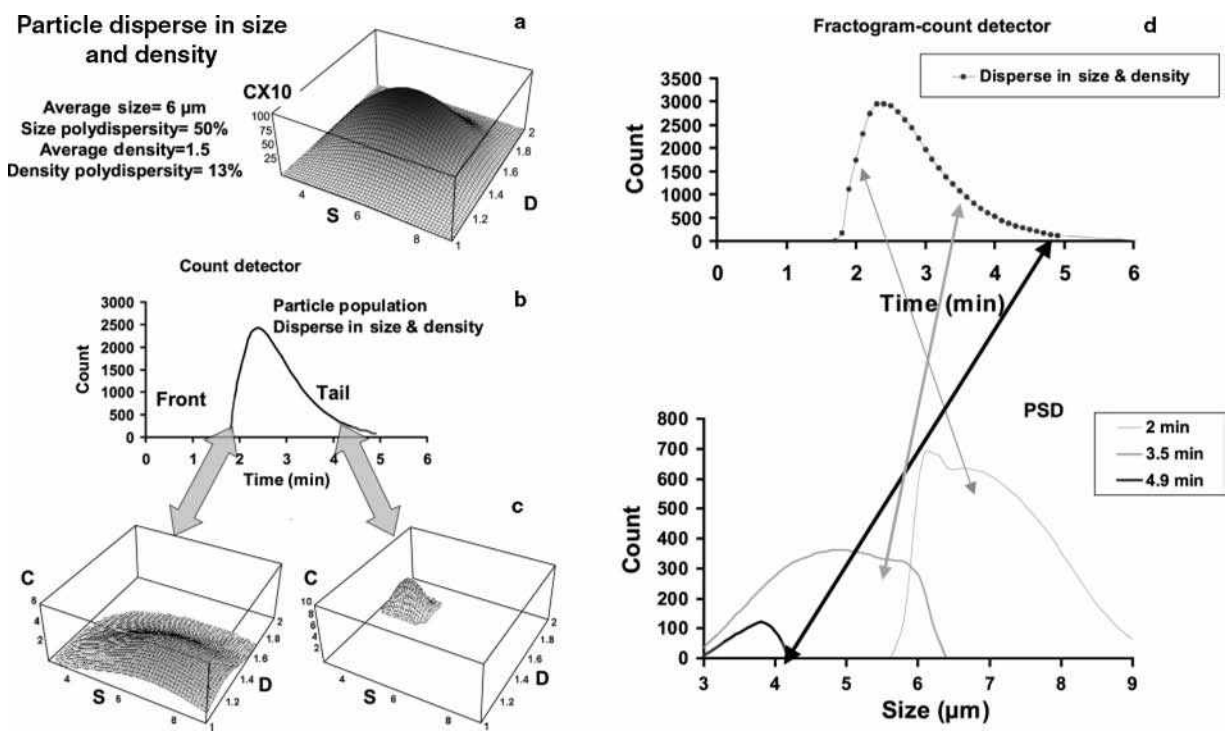

Fig. 2 The multipolydispersity concept: a bidimensional example (size and density distribution). Graph (a) represents the convolution if size and density distribution simulated by a bidimensional Gaussian. Fractogram (b) shows the elution profile obtained in the use of an ideal Steric Hyperlayer elution mode whose channel dimensions, external field, and carrier flow rate are chosen to produce discriminating separations on both size and density. Graph (c) shows bidimensional population pattern composing the fronting and tailing zones of the fractogram. The same fractogram is shown on graph (d), with simulation of fraction collection or granulometric detector time constant with three examples of PSD obtained.

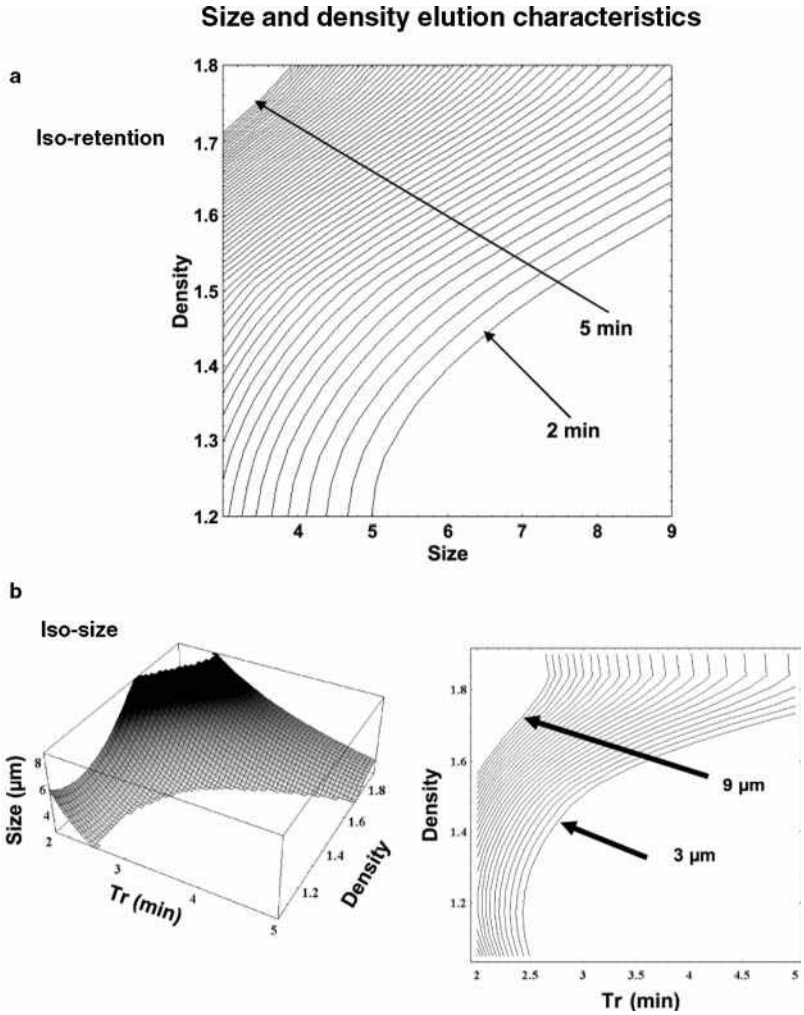

Fig. 3 a, Granulometric pattern and b, density distribution. Particle characteristics are described in Fig. 2.

the peak front, a PSD ranging from 5 to 9 µm is obtained, with light small particles (5 µm, 1.2 density) and heavy big ones (9 µm, 1.6 density). It is tempting to complicate such a chart in three dimensions, as shown in Fig. 3b, to draw an isosize retention chart as a function of density, whose bidimensional projection may be easier to read. Therefore it is observed that 3 µm particles (as well as 9 µm ones) are eluted at very different retention times, depending on their densities. It can be concluded that, in the light of what is known so far from the "Hyperlayer" elution mode, PSD obtained during elution can be linked to other dimensions (density, shape, and rigidity). Therefore it appears that large optimization processes are opened to understand the discriminating effects of channel dimensions, fields, and flow rates on a multipolydisperse population.

HIGHER ORDERS: PHYSICAL AND FUNCTIONAL

If it is relatively easy to adapt offline/online granulometric detectors allowing PSD at every retention time; only very few cell-specific characterization devices are available, with the preferred one being FC.[24] FC's versatility is impressive, allowing particle counting as well as a series of particle characteristics and distribution measurements using light diffusion principles and/or fluorescence.[24] If used in its simplest mode, count histogram vs. diffused light leads to sophisticated information. When a single particle passes in front of a laser beam, the scattered (or emitted fluorescence) light generates a signal proportional to the studied parameter of that particle. If the collected light is at a large angle [90°, side scattering (SS)] from the incident laser beam, the signal is a complex function of the particle refractive index, composition, and surface characteristics.[24,25] If the diffused light is collected at low angles[24–26] [10°, forward scattering (FS)], diffraction predominates and the signal is a function of the particle volume described by the Mie law.[27] Therefore a multidimensional detection allowing population or subpopulation discrimination, whose pattern (fingerprint) can be associated with FFF retention properties, is made possible. Other detection methods can be used with specific functional properties (surface receptors and cell content), as already described by our group.[7,28,29] Every sample or collected fraction (during FFF elution) can be, as a consequence,

described by a battery of information—some being possibly calibrated, and some others looked at only from a qualitative or comparative point of view.

SPECIFIC REQUIREMENTS

Suspension

It is essential to prepare single cell suspensions, which exist naturally in very few cases (cultured cells such as HeLa, Hel, and blood cells). In most critical cases (solid tumors, tissues, and neural cells), a preliminary step is necessary and classically requires transformation of the tissue in suspension. Two methods are used: the first is mechanical,[30] whereas the second requires enzymatic action.[30] It is essential to obtain a monocell suspension, whose characteristics have to be controlled by FC. Once this suspension is obtained, another critical parameter is its concentration; blood cells can be injected in a highly concentrated suspension, whereas neural ones must be inserted into the FFF system highly diluted, requiring large injection volumes. So far, no prediction rules have been established and the technique requires experience-based empirical knowledge.

FFF Device

Channel walls are assumed to be biocompatible, but so is the carrier phase, which can be added with specific surfactants to avoid aggregation during separations: so far, bovine serum albumin (BSA)[11–13] (and, recently, cholic acid) appeared to be more stable and at least as efficient.[31] Such precautions must be associated with systematic recovery measurements—a multidimensional concept associated with the detector pattern, and a comparison of the crude sample with every collected fraction.

Operating Conditions

A flow injection of appropriate cell number sometimes requires adapting the injection volume. In terms of elution, it is essential to observe or follow the safety Hyperlayer requirements that have been already defined. In this order, with the help of the granulometric detector, it is possible to determine the average sizes of cells eluting in the front and the tail of the fractogram, and to calculate, by means of the (S) position, their average position in the channel thickness; by experience, a useful recovery is found if the elution conditions (field and flow) drive to an average position in the channel thickness (s) at, at least, 0.75 times the diameter.

Poisoning/Cleaning

Cell suspensions are often introduced into the SdFFF separator in their cultivation media; these complex solutions encompass proteinaceous hydrophilic compounds as well as hydrophobic ones. It has been also observed that cell recovery may reach 90% in optimized conditions with either a reversible trapping (released at field stopped) or an irreversible one, leading to the release of cellular material that may interact irreversibly with channel walls, thereby leading to surface modifications. Using a biocompatible carrier phase may generate local bacterial growth, either at the channel surface or within the channel; some workers use some toxic cellular killing compounds (e.g., sodium azide).[32] The experimenter must be warned about the toxicity, even at low concentration, of such compounds not only as far as the sample is concerned, but also the experimenter. With experience, it appears that channel poisoning is progressive, with constant recovery reduction, as well as baseline and noise evolution. Therefore there is a need to regularly clean the channel over the life of the separator. This procedure is relatively easy and must be performed in three steps: channel wall regeneration, which destroys sorbed proteins or biological compounds such as membranes or genetic materials; sterilization of the channel by means of an appropriate cocktail involving hypochlorite and ethanol; and rinsing of the separator with sterile mobile phase to completely wash the channel.

The effectiveness of instrument design and setup to reduce cell–accumulation wall interactions was demonstrated, first, by the recovery of cells in the corresponding elution peak (>70%). Second, it was shown by conservation of cell viability, which was, after SdFFF elution, similar to that of the control population. Finally, reduction of interactions was partially demonstrated by a very low cell release peak, which was observed at the end of the fractogram when channel rotation was stopped and the mean gravity was equal to zero (external field applied = 1g; Fig. 4); such procedure is not possible in GFFF. This residual signal corresponded to reversible cell sticking due to weak interactions between cells and the accumulation wall.[7,11–14] Cells or cellular materials can be released from the accumulation wall under the effect of the mobile phase flowing in the absence of channel rotation. However, irreversible cell trapping is due to strong cell–channel interaction and cannot be reversed under these conditions. This phenomenon cannot be observed on the fractogram and leads to channel poisoning, requiring routine channel wall regeneration procedures. For this purpose, cleaning cocktails used in FC or clinical instrumentation appear to be very effective.

These poisonings can be overcome by systematically performed cleaning and decontamination procedures.[19,20,28,29] Some experiments (not published) have shown that the absence of effective and systematic channel cleaning has led to many problems, in particular, an increase in apoptosis of separated cells, even though elution conditions were set up to enhance the "Hyperlayer" mode because the small portion of

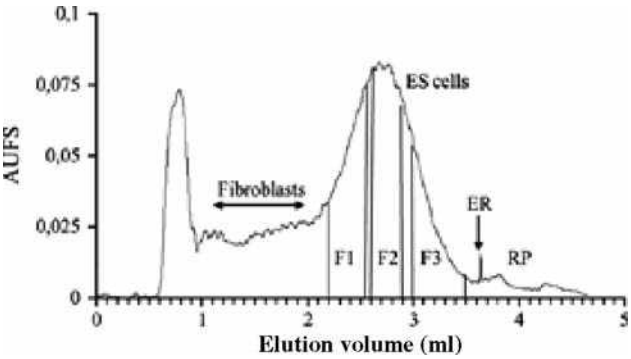

Fig. 4 Optimized SdFFF fractogram of ES Cells. Representative fractogram of ES cell suspensions after SdFFF elution. Elution conditions: Flow injection of 100 μl of ES suspension; flow rate, 0.6 ml/min (sterile PBS, pH 7.4); and external multigravitational field, 40 (0.1 g; spectrophotometric detection at 254 nm). Fractions were collected as follows: PF1, 3 min 40 sec/4 min 15 sec; PF2, 4 min 20 sec/4 min 50 sec; PF3, 5 min 0 sec/5 min 50 sec. ER corresponds to the end of channel rotation. In this case, the mean externally applied field strength was equal to zero gravity; thus RP, a residual signal, corresponds to the release peak of reversible cell accumulation wall sticking.

definitively trapped cell die released apoptotic signals into the separator, which could activate apoptosis in freshly separated cells.

The different steps and instrument setups used for cleaning and decontamination have been extensively described.[19,20,28,29] The cleaning procedure is based on the use of osmotic shock and injection of deproteinizing agent. The use of polystyrene plates and BSA-free mobile phase has simplified the previous steps;[10–13] it is now performed as an end-of-day cleaning–decontamination procedure. First, phosphate-buffered saline (PBS; pH 7.4) was replaced by flushing the entire system with sterile distilled water at a high flow rate. Second, the entire SdFFF device was flushed at 0.8 ml/min for 30 min with a protein cleaning agent (CLENZ; Beckman Coulter, Fullerton, California, U.S.A.). The system was rinsed with sterile distilled water for 1 hr at 0.8 ml/min. Then, the entire SdFFF device was flushed at 0.8 ml/min for 30 min with a 3–4°C sodium hypochlorite solution. The system was rinsed with sterile distilled water for 2 hr at 1 ml/min. The system was then ready to use by replacing the sterile water with sterile PBS. By implementing this cleaning–decontamination procedure, the same channel can be used for analysis of various cell populations without sample cross-contamination and microorganism proliferation.

FROM PHYSICAL/FUNCTIONAL TO BIOLOGICAL, AN EMPIRICAL EXPERIENCE: THE CONCEPT OF "CELLULOMICS"

ES mice embryonic stem cells are an important tool for the generation of transgenic and gene modified mice. We report the effectiveness of an SdFFF cell sorter to provide, from a crude ES cell preparation, a purified ES cell fraction with the highest in vivo developmental potential, to prepare mice chimeras having a high percentage of chimerism.

By taking advantage of biophysical properties (size, density, and shape), SdFFF sorts viable cells without labeling of any kind. SdFFF has a great potential with major biomedical applications, including hematology, neuroscience, cancer research, microorganism analysis, and molecular biology.[8,19,20,30] Embryonic stem cells are used in studies of gene disruption and transgenesis by using their ability to colonize the germline after introduction into blastocysts. Major limitations are the time required to obtain germline transmission, which sometimes required numerous experiments. ES cell suspensions are a mixture of cells at various stages of proliferation; heterogeneity within cells arises during culture with respect to their in vivo developmental potential. We tested the effectiveness of SdFFF to provide, from crude ES cells, an enriched cell fraction with the highest in vivo developmental potential, to prepare chimeras having a high percentage of chimerism,[7] as shown in Fig. 5.

E14 ES cell cultures and the SdFFF device were used as previously described.[7,33] The optimal elution conditions (Hyperlayer mode[34]) were: flow injection 1.5×10^5 cells/0.1 ml, flow rate 0.6 ml/min, mobile phase PBS pH 7.4, external multigravitational field strength 40.0 ± 0.1 g, and spectrophotometric detection $\lambda = 254$ nm. Three cell fractions were collected as shown in Fig. 4: F_1: 3 min 40 sec/4 min 15 sec; F_2: 4 min 20 sec/4 min 50 sec; F_3: 5 min/5 min 50 sec. Fractionated ES cells were stained with propidium iodide and analyzed for DNA cell status using an XL.2 flow cytometer (Beckman Coulter). The percentage of G_0/G_1 cells was higher in F_3 as compared with F_1 and F_2. The percentage of $Ki67^+$ cells (a protein expressed in all phases of the cell cycle, except G_0 and early G_1)[5] confirmed results with propidium iodide. Thus because F_2 and F_3 cells had the highest and lowest in vitro clonogenicity, respectively, 10 cells from these fractions were injected into C57 Bl/6 blastocysts to derive somatic chimeras. The frequency of chimeras obtained was similar (9 of 37 injected blastocysts). In contrast, a higher degree ($p < 0.02$, Mann–Whitney U-test) of color coat chimerism was obtained with F_3 ($87 \pm 5\%$) compared to F_2 ($63 \pm 9\%$). A germline transmission was obtained for all four F_3 males within 3 months as compared with one of four F_2 males after 6 months.

These results clearly show that SdFFF can sort, in a few minutes, the most convenient ES cell population to generate chimeras having the highest ability to colonize the germline. This result is, in particular, based on its newly described capacity to sort cells by their position in the cell cycle. In conclusion, SdFFF is of great interest to improve transgenesis and might also have further interesting applications for human gene therapy.

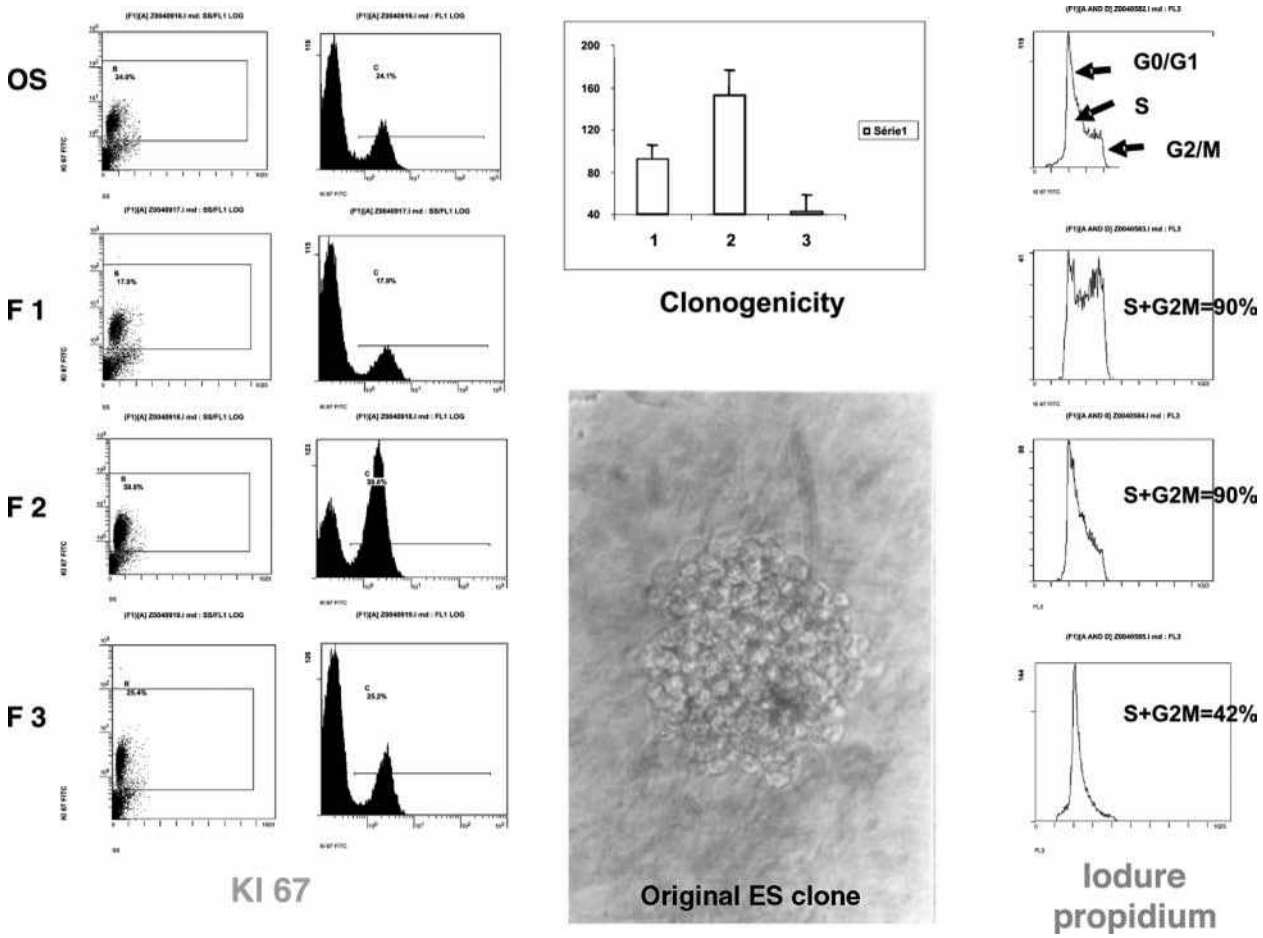

Fig. 5 ES cells, eluted as shown in Fig. 4, are characterized according to functional parameters described in the text: Bidimensional cytometric map of FS and fluorescence (Ki67). Right: Monodimensional propidium iodine fluorescence. Top center: Clonogenicity activities of the three collected fractions of Fig. 4. Bottom center: Microscopic image of ES cell clone.

CONCLUSIONS

The major difficulty in the development of FFF methodologies and instrumentations is linked to the complexity of correlating elution mode hypotheses (Hyperlayer) with experimental proofs, which depends essentially upon physical properties of the cellular material, such as size, density, shape, rigidity, and cellular viscosity, which are of greatest interest if the "physical point of view" is considered. This point of view is historical and is linked to the wide experience of FFF practitioners with latex or silica, micron-sized species, or starch granules, or others. There are some examples dealing with cellular materials (e.g., red blood cells[10] or yeast[35]) where elution is correlated with the above-described physical properties; in these cases, "cellulomics" concepts are relatively simple.

More delicate are the situations where experimentally obtained functional properties, such as specific receptor presence or cell-dependent cycle elution, are the essential ROC and define the goal or the results of the separations. There is, as a consequence, a considerable task in understanding the very different origins of such links, where physics meets or generates biological results of interest, leading to the wide domain of "cellulomics."

The main general consideration that can be stated so far is: 1) the smoothness of the separations; 2) the absence of cell prelabeling; and 3) the development of biocompatible instrumentation, which allows subpopulation lineage to be produced, which are not only usable for fundamental studies such as differentiation pathways or apoptosis studies, but also for transplantation or genetic engineering. One must have in mind that the cell is definitively the place, home, and native localization of genes and proteins. The possibility of rapid, non-destructive separation, purification, and characterization of cells (cellulomics) opens fabulous dimensions for proteomics and genomics.

REFERENCES

1. Lucas, A.; Lepage, F.; Cardot, Ph. *Field Flow Fractionation Handbook*; Shimpf, M.E., Caldwell, K., Giddings, J.C., Eds.; Wiley-Interscience: New York, 2000; 471.

2. Lutz, M.P.; Geadick, G.; Hartmann, W. Large-scale cell separation by centrifugal elutriation. Anal. Biochem. **1992**, *200*, 376.
3. Axen, R.; Porath, J.; Ernback, S. Chemical coupling of peptides and proteins to polysaccharides by means of cyanogen halides. Nature **1967**, *214*, 1302.
4. Hansen, E.; Hanning, K. Electrophoretic separation of lymphoid cells. Methods Enzymol. **1984**, *108*, 180.
5. Sharpe, P.T. *Laboratory Techniques in Biochemistry and Molecular Biology*; Burdon, R.H., Knippenberg, P.H., Eds.; Elsevier: Amsterdam, 1988; Vol. 18, 208.
6. Caldwell, K.D.; Cheng, Z.Q.; Hradecky, P.; Giddings, J.C. Separation of human and animal cells by steric field-flow fractionation. Cell Biophys. **1984**, *6*, 233.
7. Guglielmi, L.; Battu, S.; Le Bert, M.; Faucher, J.L.; Cardot, P.J.P.; Denizot, Y. Mouse embryonic stem cell sorting for the generation of transgenic mice by sedimentation field-flow fractionation. Anal. Chem. **2004**, *76* (6), 1580.
8. Lautrette, C.; Cardot, P.J.P.; Vermot-Desroches, C.; Wijdenes, J.; Jauberteau, M.O.; Battu, S. Sedimentation field flow fractionation purification of immature neural cells from a human tumor neuroblastoma cell line. J. Chromatogr. B, **2003**, *791* (1–2), 149.
9. Williams, P.S.; Koch, T.; Giddings, J.C. Characterization of near-wall hydrodynamic lift forces using sedimentation field-flow fractionation. Chem. Eng. Commun. **1992**, *111*, 121.
10. Cardot, P.J.; Gerota, J.; Martin, M. Separation of living red blood cells by gravitational field-flow fractionation. J. Chromatogr. **1991**, *568* (1), 93.
11. Merino-Dugay, A.; Cardot, P.J.; Czok, M.; Guernet, M.; Andreux, J.P. Monitoring of an experimental red blood cell pathology with gravitational field-flow fractionation. J. Chromatogr. **1992**, *579* (1), 73–83.
12. Andreux, J.P.; Merino, A.; Renard, M.; Forestier, F.; Cardot, P. Exp. Hematol. **1993**, *21* (2), 326–330.
13. Bernard, A.; Paulet, B.; Colin, V.; Cardot, P.J.P. Red blood cell separations by gravitational field-flow fractionation: Instrumentation and applications. TrAC, Trends Anal. Chem. **1995**, *14* (6), 266–273.
14. Sanz, R.; Galceran, M.T.; Puignou, L. Determination of viable yeast cells by gravitational field-flow fractionation with fluorescence detection. Biotechnol. Prog. **2004**, *20* (2), 613–618.
15. Urbankova, E.; Vacek, A.; Novakova, N.; Matulik, F.; Chmelik, J. Investigation of red blood cell fractionation by gravitational field-flow fractionation. J. Chromatogr. **1992**, *583* (1), 27–34.
16. Urbankova, E.; Vacek, A.; Chmelik, J. Micropreparation of hemopoietic stem cells from the mouse bone marrow suspension by gravitational field-flow fractionation. J. Chromatogr. B. Biomed. Sci. Appl. **1996**, *687* (2), 449–452.
17. Cardot, P.; Chianea, T.; Battu, S. Sedimentation Field-Flow Fractionation of Living Cells. In *Encyclopedia of Chromatography*, 1st Ed.; Cazes, J., Ed.; Marcel Dekker, Inc.: New York, 2002; 742–746.
18. Metreau, J.M.; Gallet, S.; Cardot, P.J.; Le Maire, V.; Dumas, F.; Hernvann, A.; Loric, S. Sedimentation field-flow fractionation of cellular species. Anal. Biochem. **1997**, *251* (2), 178.
19. Battu, S.; Delebasse, S.; Bosgiraud, C.; Cardot, P.J. Sedimentation field-flow fractionation device cleaning, decontamination and sterilization procedures for cellular analysis. J. Chromatogr. B, **2001**, *751* (1), 131.
20. Battu, S.; Cook-Moreau, J.; Cardot, P.J.P. Sedimentation field-flow fractionation: Methodological basis and applications for cell sorting. J. Liq. Chromatogr. & Relat. Technol. **2002**, *25* (13–15), 2193–2210.
21. Ho, P.B.; Leal, L.G. Inertial migration of rigid spheres in twodimensional unidirectional flows. J. Fluid Mech. **1974**, *65*, 365.
22. Martin, M.; Williams, P.S. *Theoretical Advances in Chromatography and Related Separation Techniques*; NATO ASI Series; Dondi, F., Guiochon, G., Eds.; Kluwer Academic Publishers: London, 1991; Vol. 383, 513.
23. Lee, S.H.; Myers, M.N.; Giddings, J.C. Hydrodynamic relaxation using stopless flow injection in split inlet sedimentation field-flow fractionation. Anal. Chem. Nov. 1, **1989**, *61* (21), 2439–2444.
24. Cram, L. Flow cytometry, an overview. Methods Cell Sci. **2002**, *24* (1–3), 1.
25. Papa, S.; Zamai, L.; Cecchini, T.; Del Grande, P.; Vitale, M. Cell cycle analysis in flow cytometry: Use of BrdU labelling and side scatter for the detection of the different cell cycle phases. Cytotechnology **1991**, *5* (Suppl. 1), 103–106.
26. Petriz, J.; Tugues, D.; Garcia-Lopez, J. Relevance of forward scatter and side scatter in aneuploidy detection by flow cytometry. J. Eur. Soc. Anal. Cell. Pathol. **1996**, *10* (3).
27. Adams, J.M. Light extinction photometer for measurement of particle sizes in polydispersions. Rev. Sci. Instrum. **1968**, *39* (11), 1748–1751.
28. Cardot, P.; Battu, S.; Simon, A.; Delage, C. Hyphenation of sedimentation field flow fractionation with flow cytometry. J. Chromatogr. B, **2002**, *768* (2), 285–295.
29. Sanz, R.; Cardot, P.; Battu, S.; Galceran, M.T. Steric-hyperlayer sedimentation field flow fractionation and flow cytometry analysis applied to the study of *Saccharomyces cerevisiae*. Anal. Chem. **2002**, *74* (17), 4496–4504.
30. Battu, S.; Elyaman, W.; Hugon, J.; Cardot, P.J. Cortical cell elution by sedimentation field-flow fractionation. Biochim. Biophys. Acta **2001**, *1528* (2–3), 89.
31. Reschiglian, P.; Zattoni, A.; Roda, B.; Cinque, L.; Melucci, D.; Min, B.R.; Moon, M.H. Hyperlayer hollow-fiber flow field-flow fractionation of cells. J. Chromatogr. A, **2003**, *985*, 519–529.
32. Hofstetter-Kuhn, S.; Rosler, T.; Ehrat, M.; Widmer, H.M. Characterization of yeast cultivations by steric sedimentation field-flow fractionation. Anal. Biochem. **1992**, *206*, 300–308.
33. Giddings, J.C. *Field-Flow Fractionation Handbook*; Schimpf, M.E. Caldwell, K., Giddings, J.C., Eds.; Wiley-Interscience: New York, 2000.
34. Pinaud, E. Localization of the 3′ IgH locus elements that effect long-distance regulation of class switch recombination. Immunity **2001**, *15*, 187–199.
35. Sanz, R.; Puignou, L.; Reschiglian, P.; Galceran, M.T. Gravitational field-flow fractionation for the characterisation of active dry wine yeast. J. Chromatogr. A, **2001**, *919* (2), 339–347.

Cells: Affinity Chromatography

Terry M. Phillips
Ultramicro Analytical Immunochemistry Resource (UAIR), DBEPS, ORS, OD, National Institutes of Health, Bethesda, Maryland, U.S.A.

INTRODUCTION

Affinity cell separation techniques are based on similar principles to those described in procedures for the isolation of molecules and are used to quickly and efficiently isolate specific cell types from heterogeneous cellular suspensions. The procedure (Fig. 1) involves making a single cell suspension and passing it through a column packed with a support to which a selective molecule (ligand) has been immobilized. As the cells pass over the immobilized ligand-coated support (Fig. 1a), the ligand interacts with specific molecules on the cell surface, thus capturing the cell of interest (Fig. 1b). This cell is retained by the ligand-coated support, while non-reactive cells are washed through the column. Finally, the captured cell is released (Fig. 1c) by disrupting the bond between the ligand and its selected molecule, allowing a homogeneous population of cells to be harvested.

METHODOLOGY

Although affinity chromatography of cells is essentially performed in a manner similar to other affinity techniques, it is commonly used for both negative and positive selection. Negative selection removes specific cell types from the sample population, whereas positive selection isolates a single cell type from the sample. In the latter situation, the selected cells are recovered by elution from the immobilized ligand, thus yielding an enriched population. However, unlike molecules, cells are often quite delicate, and care must be exercised when choosing the chromatographic support and the method of retrieval. The support matrix must exhibit minimal non-specific cell adhesion but be sufficiently porous to allow cells to pass through without physically trapping them or creating undue sheer forces likely to cause cell injury or death. Usually the support matrices of choice are loosely packed fibers, large pore cross-linked dextrans or agarose and large plastic or glass beads. Immunologists have long used the relatively non-specific affinity of charged nylon wool to fractionate lymphocytes into different subpopulations. Such separations are achieved because certain subpopulations of lymphocytes express an affinity for the charged fibers while others do not. This negative selection process has been used to prepare pure suspensions of T-lymphocytes for many years, but has recently been replaced by the more selective antibody-mediated or immunoaffinity procedures. The use of immobilized ligands on magnetic beads has gained popularity, especially when employing immobilized lectins or antibodies as the capture ligand.[1,2]

AFFINITY LIGANDS

Plant lectins are some of the most popular ligands for affinity cell separations. These molecules express selective

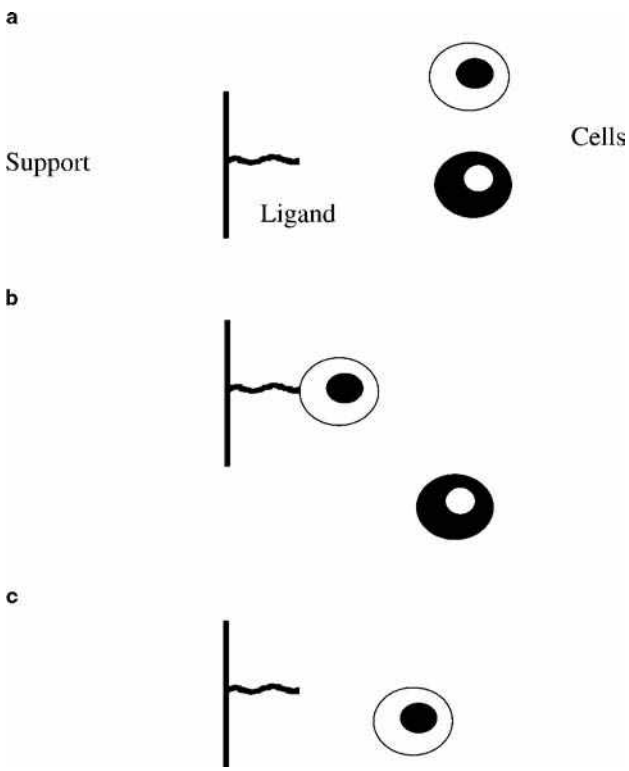

Fig. 1 Affinity isolation of specific cells. (a) A cell suspension containing the cell of interest (clear cytoplasm) and another cell type (dark cytoplasm) are passed over the support bearing a selective ligand immobilized to its surface. (b) The ligand interacts, with the surface molecules on the cell of interest, thus capturing it. The other cell type is not bound and passes through the column. (c) The bound cell is released by the addition of an elution agent to the running buffer of the column. This agent competes or disrupts the interaction between the ligand and the cell thus releasing the cell. The free cell is now washed through the column and harvested.

Table 1 Lectins and their reactive sugar moieties.

Common name	Latin name	Reactive sugar residues
Castor bean RCA_{120}	*Ricinus communis*	β-D-Galactosyl
Fava bean	*Vicia faba*	D-Mannose D-Glucose
Gorse UEA I UEA II	*Ulex europaeus*	α-L-Fucose *N*,*N*′-Diacetylchitobiose
Jacalin	*Artocarpus integrifolia*	α-D-Galactosyl β-(1,3)-*n*-Acetyl galactosamine
Concanavalin A	*Canavalia ensiformis*	α-D-Mannosyl α-D-Glucosyl
Jequirity bean	*Abrus precatorius*	α-D-Galactose
Lentil	*Lens culinaris*	α-D-Mannosyl α-D-Glucosyl
Mistletoe	*Viscum album*	β-D-Galactosyl
Mung bean	*Vigna radiata*	α-D-Galactosyl
Osage orange	*Maclura pomifera*	α-D-Galactosyl *N*-Acetyl-D-galactosaminyl
Pea	*Pisum sativum*	α-D-Glucosyl α-D-Mannosyl
Peanut	*Arachis hypogaea*	β-D-Galactosyl
Pokeweed	*Phytolacca americana*	*N*-Acetyl-β-D-glucosamine oligomers
Snowdrop	*Galanthus nivalis*	Non-reducing terminal end of α-D-mannosyl
Soybean	*Glycine max*	*N*-Acetyl-D-galactosamine
Wheat germ	*Triticum vulgaris*	*N*-Acetyl-β-D-glucosaminyl *N*-Acetyl-β-D-glucosamine oligomers

affinities for certain sugar moieties often present on cell surfaces (Table 1), different lectins being used as selective agents for specific sugars. Whitehurst, Day, and Gengozian[3] found that the lectin *Pisum sativum* agglutinin could bind feline B-lymphocytes much more readily than T-lymphocytes and used lectin-coated supports to obtain pure subpopulations of T-lymphocytes by negative selection. Additionally, the retained cells were recovered by elution from the immobilized lectin with a suitable sugar. Lectins are efficient ligands for cell selection, but in many cases, their interaction with the selected cell surface molecule is highly stable and efficient, requiring mechanical agitation of the packing before recovery of the cells can be achieved. Pereira and Kabat[4] have reported the use of lectins immobilized to Sephadex or Sepharose beads for the isolation of erythrocytes.

Another useful ligand is protein A, which is a protein derived from the wall of certain *Staphylococcus* species of bacteria. This reagent binds selected classes of IgG immunoglobulin via their Fc or tail portion, making it an excellent ligand for binding immunoglobulins attached to cell surfaces, making it an ideal general-purpose reagent. Ghetie, Mota, and Sjoquist[5] demonstrated that protein A-coated Sepharose beads were useful for cell separation following initial incubation of the cells with IgG antibodies directed against specific cell surface markers. Surface IgG-bearing mouse spleen cells were pretreated with rabbit antibodies to mouse IgG prior to passage over the protein A-coated support. The cells of interest were then isolated by positive selection chromatography.

In addition to bacterial proteins, other binding proteins such as chicken egg white avidin have become popular reagents for affinity chromatography. These supports work on the principle that immobilized avidin binds biotin, which can be chemically attached to a variety of ligands including antibodies. Tassi et al.[6] used a column with an avidin-coated polyacrylamide support to bind and retain cells marked with biotinylated antibodies. Human bone marrow samples were incubated with monoclonal mouse antibodies directed against the surface marker CD34, followed by a second incubation with biotinylated goat anti-mouse immunoglobulins. Binding of the biotin to the avidin support effectively isolated the antibody-coated cells.

A wide variety of immobilized antigens, chemicals, and receptor molecules have been used effectively for affinity cell chromatography. Sepharose beads coated

with thyroglobulin have been used to separate thyroid follicular and parafollicular cells, while immobilized insulin on Sepharose beads has been used to isolate adipocytes by affinity chromatography. Dvorak, Gipps, and Kidson[7] reported the successful retrieval of a 95% pure fraction of chick embryonic neuronal cells using an affinity chromatography approach utilizing α-bungarotoxin immobilized to Sepharose beads.

Tlaskalova-Hogenova et al.[8] demonstrated the usefulness of affinity cell chromatography to isolate T- and B-lymphocytes from human tissues. These authors describe comparative studies on three popular approaches to the isolation of lymphocyte subpopulations, namely nylon wool columns, immunoaffinity cell panning (a batch technique using antibodies immobilized to the bottom of culture dishes), and immunoaffinity using anti-human immunoglobulins attached to Sephron (hydroxyethylmethacrylate) or Sepharose supports. These studies clearly indicate that the selectiveness of immobilized antibodies was superior for isolating defined subpopulations of cells.

Immobilized antibody ligands or immunoaffinity chromatography is now the approach of choice for cell separation procedures. Kondorosi, Nagy, and Denes[9] prepared columns packed with a support coated with non-immune rat immunoglobulin and used these columns to isolate cells expressing surface Fc or immunoglobulin receptors, while van Overveld et al.[10] used anti-human IgE-coated Sepharose beads as an immunoaffinity chromatography step when fractionating human mast cells from lung tissue.

ELUTION TECHNIQUES

The elution agent used to recover affinity-selected cells must be carefully chosen. It must be able to either disrupt the binding of the ligand to the cell surface molecule or compete with the cell molecule for ligand binding. In many cases, such as lectin affinity chromatography, the elution agent is easy to select—it is usually a higher concentration of the sugar to which the ligand binds. Elution agents for other techniques such as immunoaffinity are harder to select. Harsh acid or alkaline conditions, although efficient at breaking antibody–antigen binding, are usually detrimental to cell membranes. Elution in these cases is often achieved using mild acids or mild chaotropic ion elution (Table 2).

Table 2 Elution buffers suitable for cell affinity chromatography.

Acids
0.33 *M* Citric acid
0.15 *M* Formic acid
Chaotropic ions
1–3.0 *M* Sodium and potassium thiocyanate
0.9 *M* Sodium chloride
0.5–1.5 *M* Iodine
Competition agents
Various sugars as competition agents for lectin binding (see Table 1)
Antigens for competition binding in immunoaffinity matrices

REFERENCES

1. Putnam, D.D.; Namasivayam, V.; Burns, M.A. Cell affinity separations using magnetical stabilized fluidized beds: Erythrocyte subpopulation fractionation utilization a lectin-magnetite support. Biotechnol. Bioeng. **2003**, *81*, 650.
2. Vroemen, M.; Weidner, N. Purification of Schwann cells by selection of p75 low affinity nerve growth factor receptor expressing cells from adult peripheral nerve. J. Neurosci. Meth. **2003**, *124*, 135.
3. Whitehurst, C.E.; Day, N.K.; Gengozian, N. A method of purifying feline T lymphocytes from peripheral blood using the plant lectin from *Pisum sativum*. J. Immunol. Meth. **1994**, *175*, 189.
4. Pereira, M.E.; Kabat, E.A. A versatile immunoadsorbent capable of binding lectins of various specificities and its use for the separation of cell populations. J. Cell Biol. **1979**, *82*, 185.
5. Ghetie, V.; Mota, G.; Sjoquist, J. Separation of cell by affinity chromatography on SpA-sepharose 6MB. J. Immunol. Meth. **1978**, *21*, 133.
6. Tassi, C.; Fortuna, A.; Bontadini, A.; Lemoli, R.M.; Gobbi, M.; Tazzari, P.L. CD34 or S313 positive cells selection by avidin-biotin immunoadsorption. Haematologica **1991**, *76* (Suppl 1.), 41.
7. Dvorak, D.J.; Gipps, E.; Kidson, C. Isolation of specific neurones by affinity methods. Nature **1978**, *271*, 564.
8. Tlaskalova-Hogenova, H.; Vetvicka, V.; Pospisil, M.; Fornusek, L.; Prokesova, L.; Coupek, J.; Frydrychova, A.; Kopecek, J.; Fiebig, H.; Brochier, J. Separation of human lymphoid cells by affinity chromatography and cell surface labelling by hydroxyethyl methacrylate particles using monoclonal antibodies. J. Chromatogr. **1986**, *376*, 401.
9. Kondorosi, E.; Nagy, J.; Denes, G. Optimal conditions for the separation of rat T lymphocytes on anti-immunoglobulin–immunoglobulin affinity columns. J. Immunol. Meth. **1977**, *16*, 1.
10. van Overveld, F.J.; Terpstra, G.K.; Bruijnzeel, P.L.; Raaijmakers, J.A.; Kreukniet, J. The isolation of human lung mast cells by affinity chromatography. Scand. J. Immunol. **1988**, *27*, 1.

BIBLIOGRAPHY

1. Phillips, T.M.; Dickens, B.F. *Affinity and Immunoaffinity Purification Techniques*; BioTechniques Books Eaton Press: Natick, MA, 2000.
2. Sharma, S.K.; Mahendroo, P.P. Affinity chromatography of cells and cell membranes. J. Chromatogr. **1980**, *184*, 471.

Centrifugal Precipitation Chromatography

Yoichiro Ito
National Heart, Lung, and Blood Institute (NHLBI), National Institutes of Health (NIH), Bethesda, Maryland, U.S.A.

Abstract
Centrifugal precipitation chromatogram performs purification of proteins and other macromolecules according to their solubility in suitable precipitants such as ammonium sulfate (AS) and ethanol. It has been successfully applied to separation of a variety of macromolecules including human serum albumin (HSA), γ-globulin, recombinant ketosteroid isomerase (rKSI), carotenoid cleavage enzymes, RNA, plasmid DNA, and polysaccharides. The method can single out a target compound by ligand-affinity or immunoaffinity separation. It has been demonstrated that the sample size can be increased up to 100 mg using a separation column consisting of convoluted tubing with a dialysis tubing insert.

INTRODUCTION

For many years, proteins have been fractionated with ammonium sulfate (AS) by stepwise precipitation. In this conventional procedure, an increasing amount of AS is added to the protein solution and the precipitates are removed by centrifugation in each step. Recently, "centrifugal precipitation chromatography"[1–3] has been developed to replace the tedious manual procedure. This novel chromatographic system is capable of internally generating a concentration gradient of AS through a long separation channel under a centrifugal force field. Proteins introduced into the channel are exposed to a gradually increasing AS concentration and finally precipitated at different locations according to their solubility in the AS solution. Then, the AS concentration in the upper channel is gradually reduced so that the AS concentration gradient in the lower channel is proportionally decreased. This manipulation causes the precipitated proteins to be redissolved and eluted out by repeating precipitation and dissolution along the channel. As in liquid chromatography (LC), the effluent is continuously monitored with a UV monitor and fractionated in test tubes using a fraction collector.

PRINCIPLE AND DESIGN OF THE APPARATUS

The principle and unique design of the separation column is shown in Fig. 1 and Figs. 2 and 3, respectively. In Fig. 1, a pair of separation channels is partitioned by a dialysis membrane. A concentrated (C) AS solution is introduced through the upper channel at a high flow rate (V) from the right, whereas water is fed into the lower channel from the left at a much lower rate (v). This countercurrent flow of the two liquids through the channels results in AS transfer from the upper channel to the lower channel at every point, as shown by arrows across the membrane. Because the AS transfer rate through the membrane is proportional to the difference in AS concentration between the two channels, an exponential gradient of AS concentration (c) is formed through the lower channel. The system allows manipulation of the AS concentration in this gradient by modifying the AS concentration in the upper channel as described earlier. The separation column is fabricated from a pair of plastic disks (high-density polyethylene, 13.5 cm in diameter and 1.5 cm thick) equipped with mutually mirror-imaged spiral grooves (1.5 mm wide, 2 mm deep, and ~200 cm long), as shown in Fig. 2a. On both sides of the spiral groove in the lower disk (right), a pair of circular grooves is made to set O-rings to provide a perfect seal. A regenerated cellulose membrane with desirable pore size (MWCO 6000–8000 or 12,000–14,000) is cut in a doughnut shape as shown in Fig. 2a bottom and placed over the spiral groove between the two O-rings. Then the two disks are put together and tightly pressed between two metal plates with a number of screws (Fig. 2b). The capacity of each channel is about 5 ml. This column assembly is mounted on a seal-less continuous flow centrifuge, which allows continuous elution through the rotating column without the use of a conventional rotary seal device. Fig. 2c schematically illustrates the entire elution system of the present chromatographic system. Two sets of pumps are used, one (upper right) for pumping AS solution at a high rate, and the other (upper left) for eluting buffer solution and protein samples at a lower rate. The total of four flow tubes leading from these two pumps are bundled together and clamped at the top of the seal-less continuous flow centrifuge to reach the column assembly as illustrated. As mentioned above, these flow lines are twist free as the column rotates around the central axis of the centrifuge. Consequently, the system eliminates various complications such as leakage, clogging, and cross-contamination, which often arise from the use of the conventional rotary seal device for multiple flow lines. Fig. 3 shows a cross-sectional view through the central axis of the centrifuge.

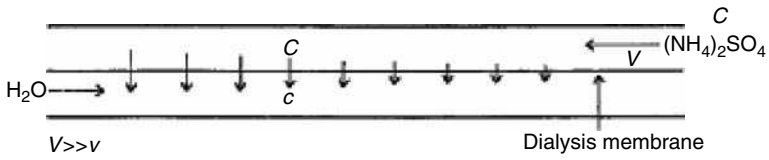

Fig. 1 Principle of the present method.

BASIC STUDIES

A series of experiments was conducted to study the AS transfer rate through the dialysis membrane by pumping a concentrated AS solution into the upper channel at 1 ml/min and water into the lower channel at varied flow rates ranging from 1 to 0.1 ml/min without sample injection. In these experiments, the AS input concentration into the upper channel and the AS output concentration from the lower channel were compared. The rate of AS transfer rose, as expected, with decrease of flow rate through the water channel, and at a flow rate of 0.1 ml/min the AS concentration collected through the lower channel reached nearly 100% that of the AS input in the upper channel. While AS diffuses from the upper channel toward the lower channel, water in the lower channel is absorbed into the upper channel. This water transfer rate is estimated by comparing input and output flow rates through the water channel. At an input rate of 0.1 ml/min, the outlet flow was decreased to one-fourth of the input rate, indicating that the separated fractions would be eluted in a highly concentrated state. Generating an AS concentration gradient and concentrating fractions are the two unique capabilities of the

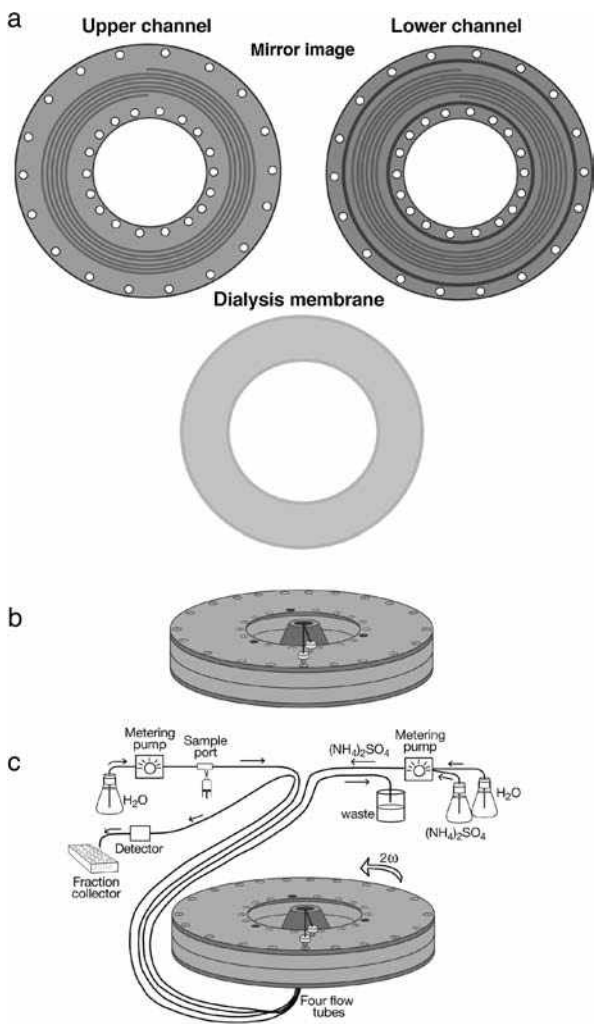

Fig. 2 Design of the separation column assembly; and schematic illustration of the entire elution system of centrifugal precipitation chromatography. a, Upper and lower disks and dialysis membrane; b, Separation disk assembly; c, Elution system for centrifugal precipitation chromatography.

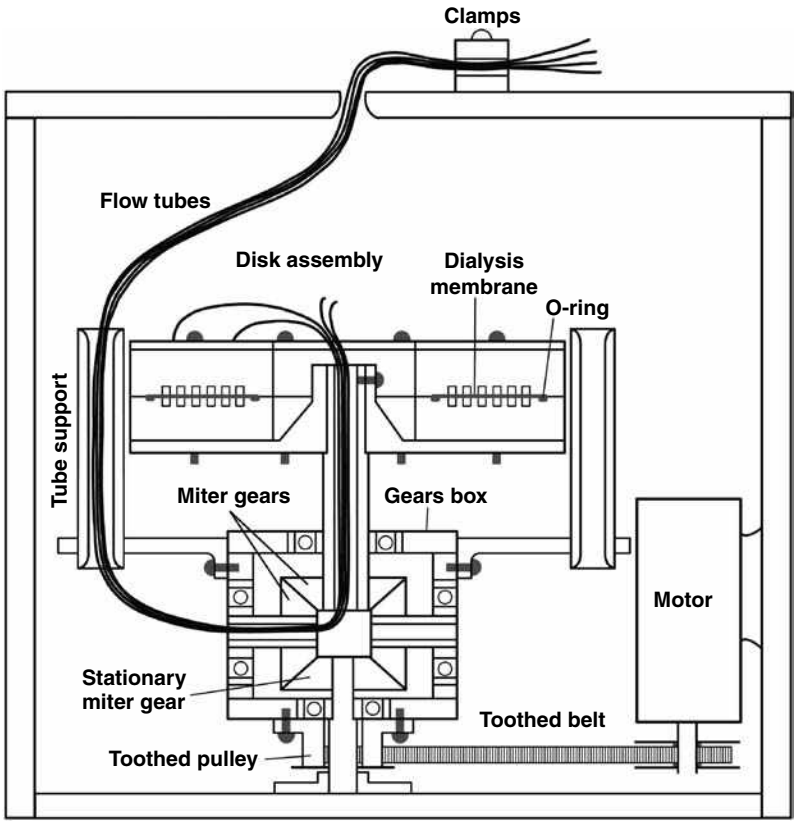

Fig. 3 Cross-sectional view through the central axis of the apparatus.

present system, which can be effectively utilized for the fractionation of proteins.

APPLICATIONS

Separation of Serum Proteins

Fig. 4 illustrates serum protein separation by centrifugal precipitation chromatography: the chromatographic tracing of the elution curve in Fig. 4A and sodium dodecyl sulfate–polyacrylamide gel electrophoresis (SDS–PAGE) analysis of separated fractions in Fig. 4B. In this example, 100 μl of normal human serum (pooled) was diluted to 1 ml and introduced into the separation channel. The experiment was initiated by filling both upper and lower channels with 75% AS solution followed by sample charge into the lower channel through the sample loop. After the separation column assembly was rotated at 2000 rpm, the upper channel was eluted with 75% AS solution at a flow rate of 1 ml/min,

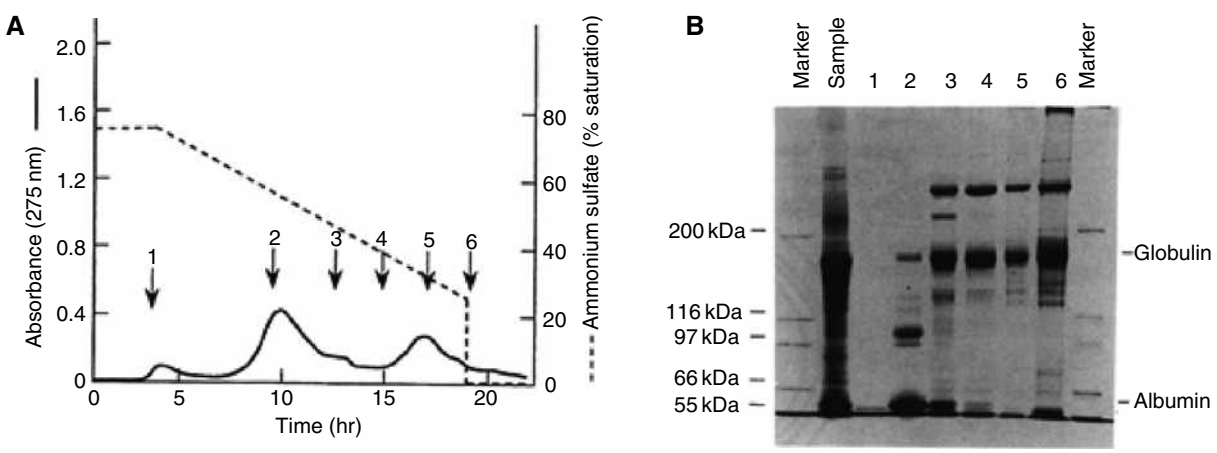

Fig. 4 Separation of human serum proteins by centrifugal precipitation chromatography. A, Elution curve; B, SDS–PAGE analysis of separated fractions.

while the lower channel was eluted with 50 m*M* potassium phosphate at 0.06 ml/min. After 4 hr of elution, the AS concentration in the upper channel was linearly decreased down to 25%, as indicated in the chromatogram. The effluent from the lower channel was continuously monitored with a UV monitor (LKB Uvicord S) at 275 nm and fractionated into test tubes using a fraction collector (LKB Ultrorac), while the AS solution eluted from the upper channel was discarded. The chromatogram (Fig. 4A) produced two major peaks, one at AS saturation at 60–50% and the other at 35–30%. The SDS–PAGE analysis of peak fractions (Fig. 4B) revealed that the first peak represents albumin (MW 68,000) and the second peak, γ-globulin (MW 160,000).

Separation of Antimast Cell Antibody

The present method was applied to purification of monoclonal antibody against human mast cells from the supernatant of culture media (hybridoma). The sample solution was prepared from 45 ml of hybridoma culture supernatant by adding AS at 60% saturation followed by centrifugation to precipitate the target protein, and the concentrated suspension (2 ml) was injected into the separation column. Fig. 5 illustrates the precipitation chromatogram, which shows three peaks, the first peak corresponding to calf serum albumin initially added to the culture medium, the second peak to IgM, and the third peak to γ-globulin. Using the fluorescent labeling technique with secondary antibodies, strong activity was found in the IgM fraction that produced a high activity of over 10 times that in the original supernatant, as indicated in the diagram. Monoclonal antibodies (IgG) present in ascitic fluids were similarly separated by the present method.

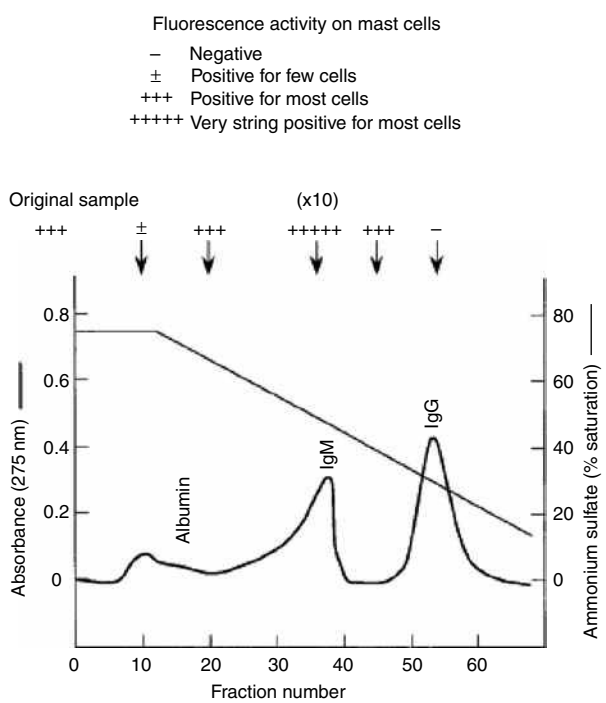

Fig. 5 Purification of monoclonal antibody from cell culture supernatant by centrifugal precipitation chromatography.

Separation of Recombinant Ketosteroid Isomerase Using Affinity Ligand

Crude *Escherichia coli* lysate containing a recombinant ketosteroid isomerase (rKSI) was fractionated with and without an affinity ligand estradiol-PEG5000. Fig. 6a and b show the results without the ligand. The chromatogram shows the first peak mostly consisting of a mixture of low-molecular-weight compounds and the second peak consisting of a mixture of proteins including the target rKSI, as shown in SDS–PAGE analysis of fractions in Fig. 6b. Fig. 6c and d show the results obtained by adding the affinity ligand to the sample solution under otherwise identical conditions. The addition of the ligand in the sample solution produced a remarkable change in the chromatogram. The second peak become smaller and a new small peak appeared later, which was followed by a large peak of the affinity ligand. The SDS–PAGE analysis revealed that the third small peak (fraction 7) mainly consisted of rKSI forming dimers and tetramers due to its high concentration, while no protein band was detected in the fourth peak (fraction 8). Although the rKSI fractions thus obtained also contain high-molecular-weight compounds, they can be eliminated by pretreating the sample solution by adding AS at 40% followed by centrifugation. The supernatant is then used as the sample solution after adding the ligand. The present method also works well to detect a minute amount of KSI present in *E. coli* mutant strain.

Immunoaffinity Separation of Human Serum albumin

This method uses an antibody to purify an antigen by precipitating the complex followed by dissociating the antigen with a releasing reagent.[4] The antibody is added to the sample solution to form an antigen-antibody complex that is precipitated at a low AS concentration of 35% saturation in the column. After most of the other proteins are eluted out from the column, a releasing agent is added to the AS channel to dissociate the antigen from the complexes which is then harvested from the column. The antibody still remaining in the column is recovered by elution with water through AS channel. Fig. 7 illustrates an example of the present method using a rabbit polyclonal antibody to purify human serum albumin (HSA).

In addition to the above examples, the present system has been successfully applied to the fractionation of various samples, including minor protein components (less than 1% of total proteins) from a crude rabbit reticulocyte lysate containing a large amount of

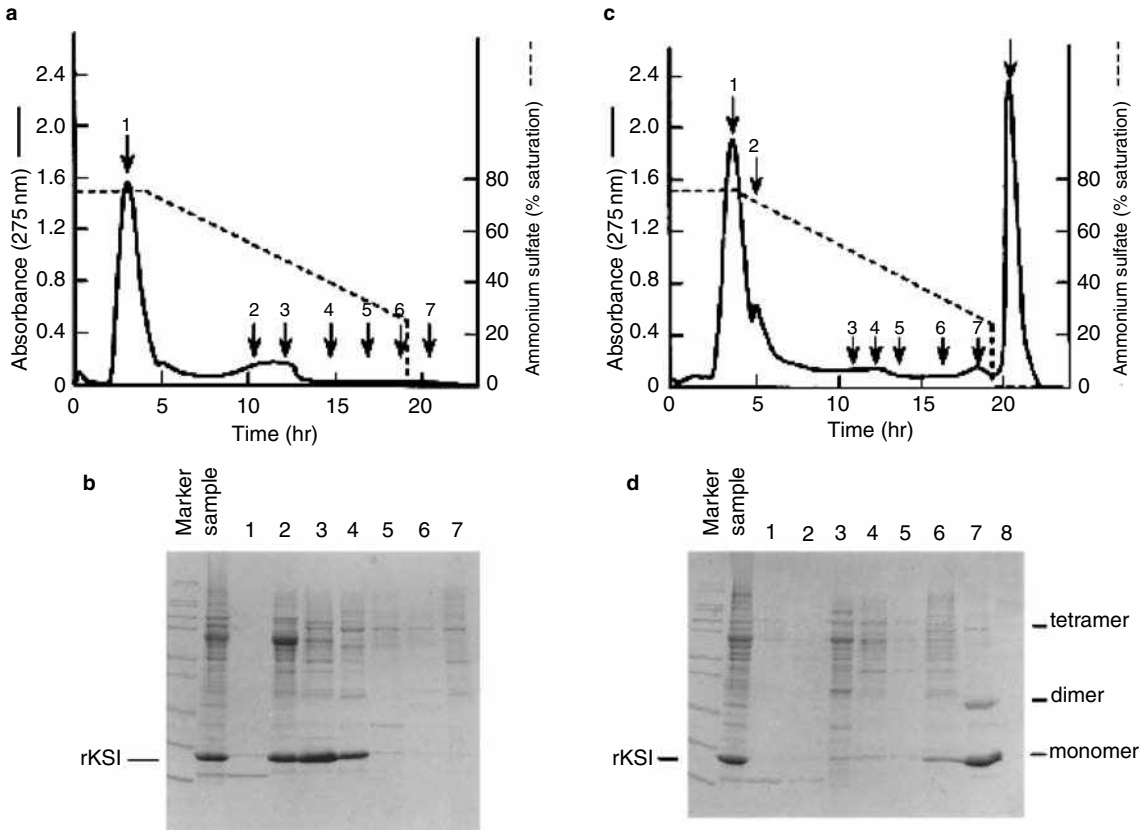

Fig. 6 Purification of recombinant ketosteroid isomerase (rKSI) by affinity ligand. a, Centrifugal precipitation chromatogram of rKSI obtained without affinity ligand; b, SDS–PAGE analysis of fractions obtained from a. above; c, Centrifugal precipitation chromatogram of rKSI obtained with an affinity ligand (estradiol-PEG5000) added to the sample solution; d, SDS–PAGE analysis of fractions obtained from c. above.

hemoglobin,[1–3] protein–polyethylene glycol conjugates,[3,5] carotenoid cleavage enzymes by ethanol gradient,[6] dextran by ethanol gradient,[7] polysaccharide fragments by ethanol gradient;[8] plasmid DNA, RNA, and proteins using cationic surfactant CTAB containing NaCl and NH_4Cl,[9] etc.

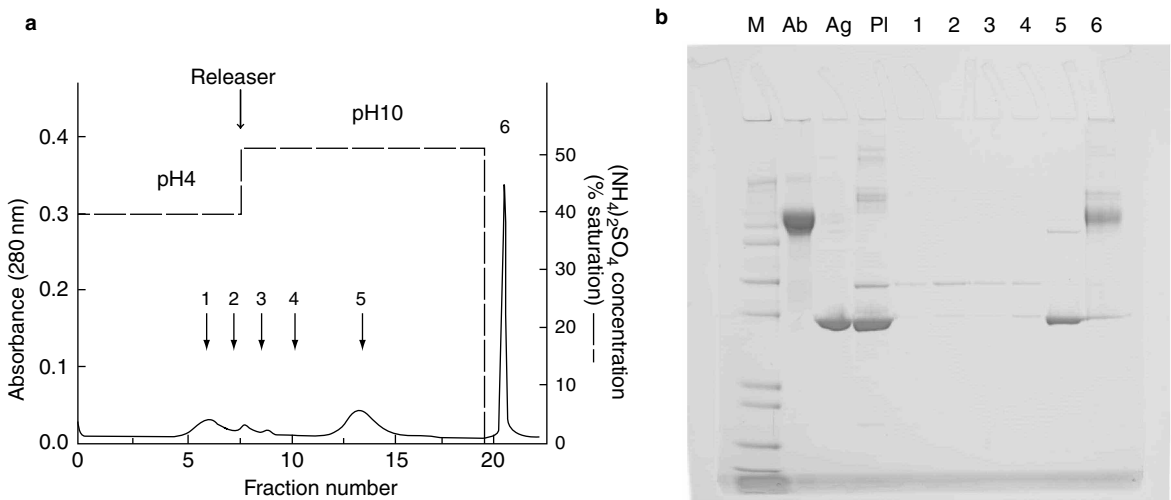

Fig. 7 Purification of human serum albumin (HSA) human blood plasma by immunoaffinity centrifugal precipitation chromatography. a, Immunoaffinity precipitation chromatogram; b, SDS–PAGE analysis of collected fractions. Sample: human blood plasma 20 μl mixed with 2 mg of rabbit anti-HSA polyclonal antibody (Sigma). The releasing solution: 0.5 *M* glycine in 50% saturated AS at pH 10 and after HSA was harvested, the antibody was recovered by pumping water at 1 ml/min through AS channel. Water channel flow rate: 0.03 ml/min throughout; rotation: 2000 rpm: Gel: precasted tris-glycine gel (invitrogen). M: marker; Ab: antibody; Ag: antigen; Pl: plasma.

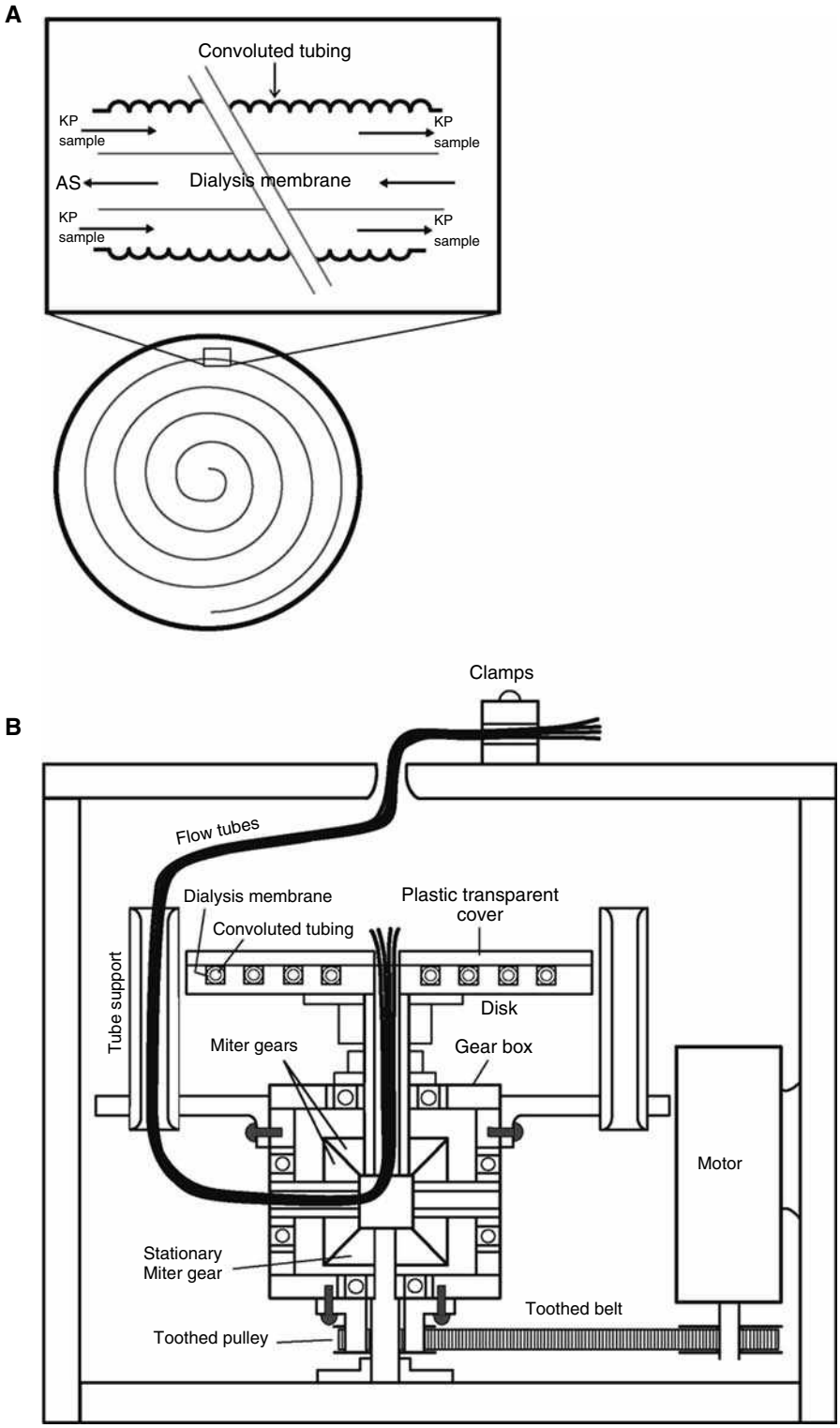

Fig. 8 Preparative centrifugal precipitation chromatograph. A, Column design: a dialysis tubing (3 mm I.D.) is inserted into convoluted tubing (5.7 mm I.D. and 2.2 m length). B, Cross-sectional view through the apparatus. The convoluted tubing is accommodated in a spiral groove of the centrifuge head.

Centrifugal precipitation chromatography can produce highly purified protein fractions because the proteins are refined by repetitive precipitation and dissolution. The method has the following advantages over the conventional manual procedure: The method is programmed and automated; the fractions are almost free of small molecules, which are dialyzed through the membrane or otherwise quickly eluted out from the channel; non-charged macromolecules such as polysaccharides are washed out while charged biopolymers

such as DNA and RNA may also be separated according to their solubility in AS solution; the method may be amenable for micro-scale to large-scale fractionation by designing the separation column in suitable dimensions.

PREPARATIVE SCHEME

Recently, the sample loading capacity of the method was improved by a new column design, which uses dialysis membrane inserted into convoluted Teflon tubing (Fig. 8A).[10] The column is snugly accommodated in a spiral groove of the rotary plate of the centrifuge (Fig. 8B). The AS solution is introduced through the dialysis tubing (membrane channel), while the phosphate buffer is eluted through the outside of the dialysis membrane (tubing channel) in the opposite direction. In this way, precipitated protein molecules can be retained more stably on the inner wall of the convolution tubing. A sample mixture containing 50 mg each of HSA and γ-globulin was separated by either stepwise or linear gradient elution of AS solution through the membrane channel.

REFERENCES

1. Ito, Y. Centrifugal precipitation chromatography applied to fractionation of proteins with ammonium sulfate. J. Liq. Chromatogr. Relat. Technol. **1999**, *22* (18), 2825–2836.
2. Ito, Y. Centrifugal precipitation chromatography: Principle, apparatus, and optimization of key parameters for protein fractionation by ammonium sulfate precipitation. Anal. Biochem. **2000**, *277*, 143–153.
3. Ito, Y. Centrifugal precipitation chromatography: Novel fractionation method for biopolymers, based on their solubility. J. Liq. Chromatogr. Relat. Technol. **2002**, *25*, 2039–2064.
4. Qi, L.; Ito, Y. Immunoaffinity centrifugal precipitation chromatography. J. Chromatogr. A, **2007**, *1151*, 121–125.
5. Sookkumnerd, T.; Hsu, J.T.; Ito, Y. Purification of peg-protein conjugates by centrifugal precipitation chromatography. J. Liq. Chromatogr. Relat. Technol. **2000**, *23*, 1973–1979.
6. Baldermann, S.; Fleischmann, P.; Watanabe, N.; Fales, H.M.; Winterhalter, P.; Ito, Y. Centrifugal Precipitation Chromatography—A Powerful Technique for the Isolation of Active Carotenoid Cleavage Enzymes from *Camellia sinensis*, Presented at the CCC2008 meeting, July 26–29, 2008. J. Chromatogr. A, **2009**, *216*, 4263–4267.
7. Yang, F.-Q.; Ito, Y. A novel method of fractionation of dextran by centrifugal precipitation chromatography. Anal. Chem. **2002**, *74*, 440–445.
8. Shinomiya K.; Kabasawa, Y.; Toida, T.; Imanari, T.; Ito, Y. Separation of chondroitin sulfate and hyaluronic acid fragments. J. Chromatogr. A, **2001**, *922*, 365–369.
9. Tomanee, P.; Hsu, J.T.; Ito, Y. Fractionation of protein, RNA and plasmid DNA in centrifugal precipitation chromatography using cationic surfactant CTAB containing inorganic salts NaCl and NH_4Cl. Biotechnol. Bioeng. **2004**, *88* (1), 52–59.
10. Ng, V.; Yu, H.; Ito, Y. Preparative centrifugal precipitation chromatography using dialysis membrane inserted into convoluted tubing. J. Liq. Chromatogr. Relat. Technol. **2005**, *28*, 2061–2070.

Channeling and Column Voids

Eileen Kennedy
Novartis Crop Protection, Inc., Greensboro, North Carolina, U.S.A.

INTRODUCTION

Channeling can occur when voids that are created in the packing material of a column cause the mobile phase and accompanying solutes to move more rapidly than the average flow velocity. The most common result of channeling is band broadening and, occasionally, elution of peak doublets.

DISCUSSION

Column voids can develop in a poorly packed column from settling of the packing material or by erosion of the packed bed. In a properly packed column, voids can develop gradually over time or suddenly as the result of pressure surges. A void that forms in the inlet of a column may lead to poor peak shape, including severe band tailing, band fronting, or even peak doubling for every peak in the chromatogram. Filling the column inlet with the same or equivalent column packing can sometimes reduce voids. For this type of repair, the column should be held in a vertical position while the inlet frit is removed. The void will be evident as either settling of the packing material or as holes in the column surface. The new packing should be slurried with an appropriate mobile phase and packed into the column void with a flat spatula. Once the top of the new packing is level with the column end, a new inlet frit can be added and the end fitting reinstalled. The column should then be reconnected to the liquid chromatography (LC) system and conditioned with the mobile phase at a fairly high flow rate to help settle the new column bed. After filling the void, the packing bed will generally be more stable if the repaired column is operated with the direction of flow reversed from the original direction. This repair procedure can be used to extend column life; however, it should be noted that the plate number of the repaired column would be, at best, only 80–90% of the original column. Columns that develop voids over time are often near the end of their useful life spans and in some cases it may be more cost efficient to discard such a column rather than to repair it.

BIBLIOGRAPHY

1. Dolan, J.W.; Snyder, L.R. *Troubleshooting LC Systems*; Humana Press: Totowa, NJ, 1989.
2. Majors, R.E. The care and feeding of modern HPLC columns. LC–GC **1998**, *16*, 900.

Chemical Warfare Agent Degradation Products: HPLC/MS Analysis

Clayton B'Hymer
Kenneth L. Cheever
National Institute for Occupational Safety and Health, Centers for Disease Control and Prevention, U.S. Department of Health and Human Services, Cincinnati, Ohio, U.S.A.

Abstract
High-performance liquid chromatography–mass spectrometry (HPLC–MS) has become a commonly used analytical technique for the analysis of chemical warfare agent (CWA) degradation products. This area of research has gained greater importance in recent years. Most CWAs are not persistent and degrade in the open environment. The degradation products are usually polar or ionic; thus, HPLC is considered an ideal separation technique. MS detection offers a sensitive and specific means for quantitative analysis for these compounds. Some of the common designs and strategies of HPLC–MS are discussed as well as the common analytical challenges. Also, specific examples of HPLC–MS applications involving screening procedures are reviewed and described. These procedures utilized both reversed-phase and ion-pair reversed-phase HPLC to separate several alkyl methylphosphonic acids, which are the degradation products of nerve agents.

INTRODUCTION

Many chemical warfare agents (CWAs) are not persistent, that is, they readily degrade or hydrolyze in the general environment with the only exceptions being some of the mustard agents. This has led to a need to analytically detect and quantitate the levels of CWA degradation products in soil, surface waters, or contaminated surfaces. Many CWAs, as well as some of their degradation products, have low polarity or are volatile; thus, much of the past analysis methodology was based on gas chromatography (GC). However, the majority of CWA degradation products are polar and non-volatile. High-performance liquid chromatography (HPLC) allows for the analysis of a broader range of compounds from low polarity to ionic. Also, HPLC techniques require only the solubility of the target analyte, whereas GC requires volatility and thermal stability of the analyte or chemical derivative of an analyte. The main limitation with HPLC analysis has been in applicable detection systems. The majority of important CWA degradation products are without chromophores or fluorophores, which makes their detection by ultraviolet absorbance or fluorescence impossible. Although many other types of HPLC detectors have been used for CWA degradation products, mass spectrometry (MS) has offered the greatest potential owing to its inherent advantages of high sensitivity and analyte specificity. Specificity, or the lack of interferences, is very important because of the general complexity of sample matrices encountered from environmental samples. HPLC–MS analysis of CWA degradation products has experienced significant growth in recent years and has seen numerous applications reported in the literature. This entry will report and summarize the current literature and discuss a few applications of HPLC–MS analysis of CWA degradation products.

BACKGROUND AND DEGRADATION PRODUCTS

Increases in terrorist activity around the world during the twenty-first century, as well as increases in the development and use of CWAs by third world nations, have led to a high demand for improved methods for the analysis of the active agents and their degradation products. The sophistication of weapons used by terrorists as well as the frequency of terrorist attacks has dramatically risen in recent years. The 1995 release of the nerve agent sarin in the Tokyo subway resulted in the death of 12 people; approximately 5000 were injured or exposed.[1,2] The 2001 use of anthrax in the U.S. Postal system resulted in six deaths from respiratory anthrax infections. Also, the need for better methodology was spurred by the convention of the prohibition of the development, production, stockpiling, and use of chemical weapons and on their destruction.[3] This convention came into force in 1997 and analytical methods were needed in verification of its fulfillment. Most nations in the world, with the exceptions of some Mideastern countries and North Korea, have agreed to the convention which eliminates the use and stockpiling of CWAs.

Most CWAs are not persistent in the environment; they generally undergo a variety of abiotic and biotic

degradation mechanisms. Munro et al.[4] have described the degradation pathways and reviewed the general toxicity of the major CWA degradation products. Most CWAs have the characteristic of being highly reactive to nucleophiles, particularly with water present in the environment. The analysis of biological or environmental residues for hydrolysis degradation products is, therefore, an important part of CWA analysis. Handheld or field-deployable detectors are useful in many settings for CWA or degradation product analysis, but most portable instruments lack both sensitivity and specificity of laboratory-based instrumental techniques.[5] The most frequently used technique for the analysis of CWAs or their degradation products is GC–MS.[6] However, GC–MS is not suitable for the direct analysis of the polar and non-volatile CWA hydrolysis products. Many of these compounds require sample derivatization before introducing them into a GC, and they frequently require a significant sample preparation scheme.[6] These reasons, as well as those mentioned in the introduction, make HPLC–MS the preferred methodology for the analysis of CWA degradation products.

The main exception to low persistence of CWAs is sulfur mustard, which maintains a high degree of stability. Most of this discussion will refer to the chemical agent bis(2-chloroethyl) sulfide (HD) (Table 1), which is the pure form. Older munitions and the older manufacturing process of mustard gas contain up to 40% bis[2-(2-chloroethylthio)ethyl] ether (HT) and a variety of contaminants and impurities. Although volatilization in an open environment is significant for HD, the primary fate mechanism of stored or buried sulfur mustard is hydrolysis.[4] HD is more stable in seawater than in freshwater owing to the high concentration of chloride in seawater.[7] The final hydrolysis product is thiodiglycol (TDG), which may occur by either of the two degradation routes depending on the availability of water. Fortunately, TDG has relatively low toxicity, and it has been easily analyzed by HPLC–MS.[8]

The nitrogen mustards belong to the same vesicant or blister agents like sulfur mustard. Nitrogen mustards were developed in the 1930s[9] and were never stockpiled on a large scale in the U.S. chemical warfare inventory. The three nitrogen mustards are bis(2-chloroethyl)ethylamine (HN1), bis(2-chloroethyl)methylamine (HN2), and tris (2-chloroethyl)amine (HN3) (Table 1). On the basis of susceptibility to hydrolysis and volatility, HN3 is environmentally persistent, whereas HN1 and HN2 are considered moderately persistent. The primary degradation fate process in either water or soil is hydrolysis; weakly alkaline conditions enhance the hydrolysis of the nitrogen mustards. The major degradation products of HN1 are diethanolamine (DEA) and *N*-ethyldiethanolamine (EDEA). Correspondingly, the major degradation product of HN2 is methyldiethanolamine (MDEA) and triethanolamine (TEA) for HN3. These compounds have been analyzed by HPLC–MS;[10] however, they represent more of an analytical challenge. DEA and TEA are frequently used in common consumer and industrial products including soaps, detergents, cosmetics, and textiles. DEA is also used as liquid detergent for emulsion paints, a dispersing

Table 1 Structures of the mustard agents and their major degradation products.

CW compound	Abbreviation	CW structure	Major degradation product(s)	Degradation product abbreviation	Degradation product structure
Sulfur mustard					
bis(2-Chloroethyl) sulfide	HD	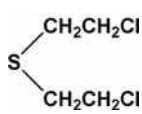	Thiodiglycol	TDG	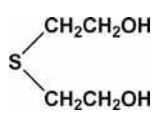
Nitrogen mustards					
bis(2-Chloroethyl) ethylamine	HN1	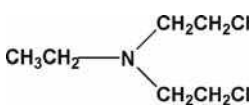	Ethyldiethanolamine	EDEA	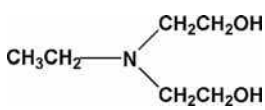
			Diethanolamine	DEA	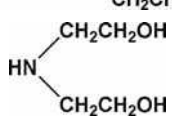
bis(2-Chloroethyl) methyl amine	HN2	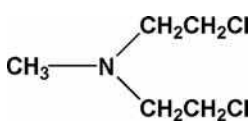	Methyldiethanolamine	MDEA	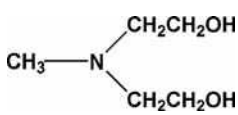
tris (2-Chloroethyl) amine	HN3	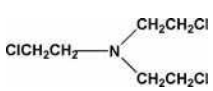	Triethanolamine	TEA	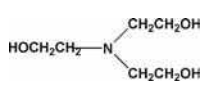

agent, and is often found as a component in metal-cutting fluids. EDEA is also used in detergents and MDEA is used as a catalyst for polyurethane foams and as a pH control agent in various formulations. These rather innocuous uses of ethanolamines can lead to false positives for nitrogen mustard agent degradation products from environmentally collected samples.

The nerve agents represent the most toxic and probably the most feared CWAs. Chemically, the nerve agents are alkyl phosphonic acid esters which elicit toxicity by the specific irreversible inhibition of the enzyme cholinesterase resulting in the accumulation of acetylcholine. The accumulation of acetylcholine results in continuous stimulation of the nervous system and eventual failure of the vital autonomic body functions after a lethal exposure level to the nerve agent. The nerve agents are subdivided into two classes, the V agents and the G agents (Table 2). *O*-ethyl-*S*-[2-(diethylamino)ethyl] methylphosphonothioate (VX) is among the most lethal substances ever produced by man and is a persistent nerve agent on surfaces as well as possessing the slowest hydrolysis rate. *O*-isobutyl-*S*-[2-(diethylamino)] methylphosphonothioate (Russian VX or RVX) is chemically very similar. The G agents include ethyl phosphorodimethylamidocyanidate (tabun, GA); isopropyl methylphosphonofluoridate (sarin, GB); pinacolyl methylphosphonofluoridate (soman, GD); and cyclohexyl methylphosphonofluoridate (cyclosarin, GF). The G agents are volatile and present a vapor hazard, but in turn, dissipate more quickly in the open environment. The G agents are also more susceptible to hydrolysis than the V agents. All the nerve agents can act by dermal, oral, or inhalation routes of exposure. The anticholinesterase mechanism of action of these organophosphonic acids is due to the oxo group (=O) and is influenced by the presence of alkyl substituents in the molecular structure. Thus, many of the initial degradation products of these compounds may retain some anticholinesterase activity and toxicity, but hydrolysis of one or more alkyl ester bonds results in the generally non-toxic alkyl methylphosphonic acids. The final degradation product of GB, GD, and GF is methylphosphonic acid (MPA), although isopropyl methylphosphonic acid (iPrMPA) is an intermediate degradation product of GB; pinacolyl methylphosphonic acid (PinMPA) is an intermediate degradation product of GD; and cyclohexyl methylphosphonic acid (CHMPA) is the corresponding intermediate product of GF. MPA is, however, fairly stable in the environment. GA hydrolyzes to ethylphosphoryl cyanidate and dimethylamine under acidic conditions; GA hydrolyzes ultimately to phosphoric acid, cyanide, and dimethylamine at neutral or basic pH conditions with *O*-ethyl *N,N*-dimethylamidophosphoric acid (EDMAPA) as an intermediate. VX also has two hydrolysis pathways. At pH values of less than 6 and greater than 10, the main signature degradation product is ethyl methylphosphonic acid (EMPA). EMPA can continue to degrade to MPA. At a pH range between 7 and 10, VX will degrade to *S*-(2-diisopropylaminoethyl) methyl phosphonothioate (EA 2192). EA 2192 is highly soluble in water and is not readily found in soil, but remains toxic and is relatively stable in water. RVX initially degrades to isobutyl methylphosphonic acid (iBuMPA) and finally to MPA. MPA is, therefore, a common degradation product for GB, GD, VX, and RVX, and it is a common target analyte for most HPLC–MS methods.

Other CWAs and their degradation products have been actively analyzed, reported, and reviewed in the literature,[1,2,4] but will not be described in further detail. Additional vesicants include the chlorovinylarsines (Lewisites) which are complex mixtures of several related compounds. The third class of CWAs, the blood agents, interferes with the oxygen transport capability of blood and thus causes death by suffocation. The primary blood agent used during World War I was hydrogen cyanide. Finally, a fourth class of CWAs, incapacitating agents, has generally non-lethal physiological effects such as vomiting or mental disorientation. The compound 3-quinuclidinyl benzilate (BZ) is an example of a modern incapacitant which causes mental disorientation. This discussion will remain focused on the analysis of degradation products of the nerve and mustard agents.

HPLC–MS

General Advantages

The general advantages of HPLC for use as a separation technique for chemical warfare degradation products have been mentioned. Since the degradation products are generally water-soluble and polar, HPLC can be used directly unlike GC which would require a more complicated derivatization procedure to make the analytes volatile for chromatographic analysis. Generally, reversed-phase HPLC has been used for CW degradation product analysis although some ion-pair reversed-phase HPLC procedures have been applied. Some of these applications will be discussed in detail later. MS has much strength for use with HPLC; MS possesses high sensitivity and adds a higher degree of specificity, the ability of a technique to accurately measure the analyte in the presence of all potential sample matrix components without interference. Since the CW degradation products would be tested in environmental samples, test method specificity is a very important analytical trait. Also, as in the case of the MPAs, the lack of UV absorbance and fluorescence makes direct MS detection the preferred technique. Earlier HPLC methods using derivatization with *b*-bromophenacyl bromide to provide a UV chromophore have been reported,[11] but the use of MS detection eliminates a derivatization step to the analysis procedure. Another added benefit in avoiding chemical derivatization is that preliminary interpretation of

Table 2 Structures of the nerve agents and their major degradation products.

CW compound	Abbreviation	CW structure	Major degradation product(s)	Degradation product abbreviation	Degradation product structure
V agents					
O-ethyl-*S*-[2-(diethylamino) ethyl] methylphosphonothioate	VX	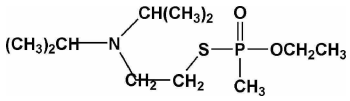	Ethyl methylphosphonic acid(pH <6 and >10)	EMPA	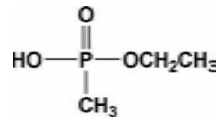
			S-[2-(diisopropylamino)ethyl] methylphosphonothioate (pH 7–10)	EA 2192	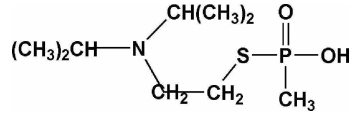
			Methylphosphonic acid	MPA	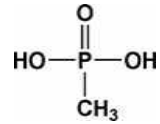
O-isobutyl-*S*-[2-(diethylamino) ethyl]methylphosphonothioate	Russian VX or RVX	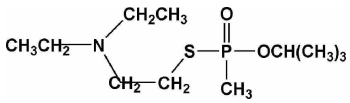	Isobutyl methylphosphonic acid	iBuMPA	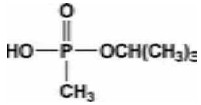
			Methylphosphonic acid	MPA	see above
G agents					
Ethyl phosphorodimethylamidocyanidate	Tabun/GA	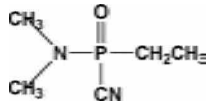	Ethylphosphoryl cyanidate (low pH)	EPC	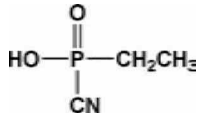
			Dimethylamine (low pH) Phosphoric acid, cyanide, dimethylamine (high pH)	DEA	$(CH_3)_2NH$ H_3PO_4, CN^-, $(CH_3)_2NH$
Isopropyl methylphosphonofluoridate	Sarin/GB	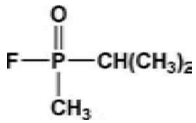	Isopropyl methylphosphonic acid	iPrMPA	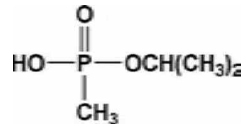
			Methylphosphonic acid	MPA	see above
Pinacolyl methylphosphonofluoridate	Soman/GD	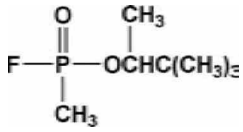	Pinacolyl methylphosphonic acid	PinMPA	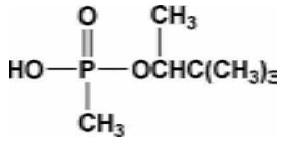
			Methylphosphonic acid	MPA	see above
Cyclohexyl methylphosphonofluoridate	Cyclosarin/ GF	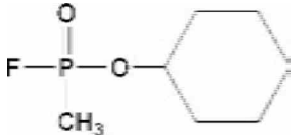	Cyclohexyl methylphosphonic acid	CHMPA	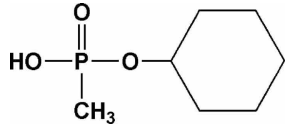

fragmentation, in the case of unknowns, is much simpler with the underivatized analytes.

The Mass Spectrometer and Its Various Designs

The various designs of the mass spectrometers have been described in detail in the literature,[12–14] and its basic function is to measure the mass-to-charge ratios (*m*/*z* ratio) of analyte ions. The HPLC–MS system has four main components, consisting of a sample introduction system or inlet, an ion source, a mass analyzer, and an ion detector. The sample introduction system vaporizes the HPLC column effluent. This can be simple as a nebulizer, which have been described in the literature.[14] The other three components of the mass spectrometer will be described in further detail.

The ion source creates analyte ions from the neutral species in the vapor phase. Several designs of ion sources have been used for CWA degradation product analysis in recent years including thermospray ionization (TSP),[15] atmospheric pressure chemical ionization (APCI),[16,17] and electrospray ionization (ESI).[18] These "soft" ionization techniques generally produce $[M–H]^-$ or $[M+H]^+$ fragments for the alkyl phosphonic acids and some other CWA degradation products. The inductively coupled plasma (ICP) is a "hard" ionization source and has been described in the literature.[19] HPLC–ICP–MS has been reported for the detection of alkyl phosphonic acids.[20] In recent years, ESI has become the most common ion source in HPLC–MS analysis in general with the APCI source a close second. The thermospray source has fallen out of favor in HPLC–MS systems since the introduction of ESI.

ESI is commonly used as an ion source for HPLC–MS. The ESI technique was invented by Nobel Prize winner John Fenn in 1992. ESI has rapidly displaced the older TSP and continuous flow fast atom bombardment (FAB) sources for most commercial HPLC–MS systems. In ESI, the HPLC effluent is passed through a small capillary jet or nebulizer held at a high electrical potential (2000–5000 V) along with a nitrogen flow. This results in electrostatic nebulization of the liquid. During desolvation of the aerosol droplets, the electric field increases strength at the diminishing droplet surface under vacuum; this process leads to the ejection of charged analyte ions upon final evaporation. The ESI source is a "soft" ionization technique and does not cause as significant thermal degradation when compared to the other ion sources. ESI also has a high level of ionization efficiency which leads to high MS sensitivity for the analyte ion, which is an advantage for the detection of trace levels of CWA degradation products.

In APCI, the HPLC effluent is heated and sprayed with a high flow of nitrogen from a nebulizer, which generates an aerosol. This aerosol is subjected to a corona discharge to form ions of the sample analytes. In APCI, the ionization occurs in the gas phase, unlike ESI which occurs in the liquid phase. The APCI source allows for improved analysis of non-polar and medium-polar analyte compounds as compared to the ESI source.

In ICP, the plasma is formed from a flow of gas, usually argon, through a quartz torch. The quartz plasma torch is typically constructed of concentric tubes and is surrounded by a copper load coil. The load coil is connected to the radio frequency generator and power (~1000–1500 W) is directed into the coil. This induces an oscillating magnetic field near the end of the torch and a plasma is formed while a spark is applied to the flowing gas stream. Sample introduction is by means of a carrier argon gas flow through the central tube in the quartz torch. Liquid samples are nebulized into an aerosol before being carried into the plasma torch; a function performed by a nebulizer. Once a sample analyte is exposed to the 8000 K plasma, vaporization, atomization, and ionization of the analyte occurs almost simultaneously. The ICP source is known as a "hard" ionization source, that is, the analytes are reduced to atomic ions. Until recently, the specific analysis of phosphorus from alkyl phosphonic acids by ICP–MS was limited because of its high first ionization potential (10.5 eV) and polyatomic interferences produced by the ICP technique.[21] Recent developments in collision/reaction cell technology with ICP–MS have allowed for the analysis of phosphorus and other elements prone to isobaric and polyatomic interferences through removal by collisional dissociation.[22] The only chromatographic limitation of the ICP is that methanol is the preferred organic modifier. Acetonitrile-based mobile phases will cause sooting of the MS sampler cone and should be avoided.[19]

The third component of a mass spectrometer, the mass analyzer, separates the formed ions according to their *m*/*z* ratios. The most widely used analyzer design is the quadrupole (or multipole) analyzer, used as either a single stage or a triple quadrupole (TQ) combined with a soft ionization technique. In the TQ design, with additional soft ionization such as a collision gas, tandem MS can be accomplished. A quadrupole consists of four parallel rods, which utilize an oscillating electric field to select ions passing through a radio frequency field generated by the quadrupole. Many modern instruments actually use hexapoles or octapoles; they have a more compact geometry using more rods, but operate under the same principle as the "quadrupole" described previously. Many of these multipoles are referred to as a quadrupole. In tandem MS, a TQ mass spectrometer consists of three sets of quadrupoles that transmit ions or function as a mass filter. The middle quadrupole of the TQ serves as a collision cell and produces daughter ions to be filtered by the last quadrupole. Other mass analyzer types, such as the time of flight (TOF), have been coupled to HPLC. The ion trap is another commonly used design in HPLC–MS, since the "trap" can be used to accumulate, fragment, and then eject selected ions. All of these common mass analyzers have been described in detail elsewhere in the literature.[12,13]

The last component of the MS is the ion detector, which is necessary to record the separated ions. Multipliers are the most frequently used detectors for commercial HPLC–MS instruments and ion detectors have been described in detail in the literature.[12,13]

COMMON STRATEGIES OF HPLC–MS IN CWA DEGRADATION PRODUCT ANALYSIS

The accurate determination of CWA degradation products from surface water, soil, or wipe samples from various surfaces creates an interesting challenge for the analytical chemist. Although there is a common perception that the use of HPLC–MS, and especially HPLC–MS/MS, practically guarantees method specificity, in practice this may not be the actual case. Common problems include ion suppression caused by the sample matrix effects and interference from other components encountered from environmental sampling. Several strategies are generally incorporated into HPLC–MS method design and development to counter matrix problems. Stable isotope-labeled internal standards (isotope dilution), such as deuterated or carbon-13 analogues, can be used to counter matrix effects. The importance of initial sample cleanup and good chromatographic separation cannot be overstated. Removal of inorganic salts from a sample matrix can reduce ion suppression of the ESI source. Liquid–liquid extraction (LLE) or solid-phase extraction (SPE) can be used for sample cleanup of environmental samples. The use of chromatographic gradients to increase the separation of sample analytes or components can reduce the probability of possible interferences.

Strategies to optimize chromatographic conditions to the MS ion source employed must be considered. Black and Read[23] noted that a considerable improvement in sensitivity was obtained by using formic acid instead of trifluoroacetic acid (TFA) in the mobile phase of a reversed-phase HPLC system when using ESI as the ionization source for the analysis of alkyl phosphonic acids. Zhou and Hamburger[24] reported that formic acid enhances the formation of $[M+H]^+$ ions for a range of compounds when using ESI–MS and have given a detailed discussion of the factors involved. As with all HPLC–MS, only volatile buffers and acids are compatible with the MS detector.

APPLICATIONS OF HPLC–MS IN CWA DEGRADATION PRODUCT ANALYSIS

Black's research[6,16,23,25] has included extensive work in the analysis of CWA degradation products. In one study, the separation of the major alkyl phosphonic acids was accomplished using gradient reversed-phase HPLC.[23]

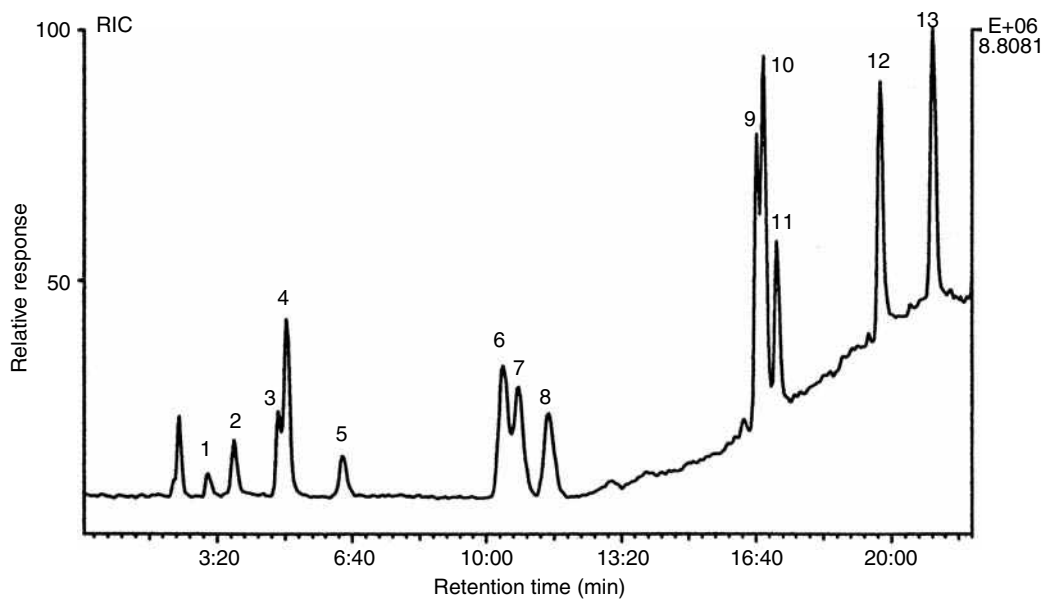

Fig. 1 HPLC–ESP–MS reconstructed (total) ion chromatogram from a standard mixture of alkyl phosphonic acids at a concentration of 1 μg/ml each: 1) methylphosphonic acid (MPA); 2) ethylphosphonic acid (EPA); 3) methyl ethylphosphonic acid (MEPA); 4) ethyl methylphosphonic acid (EMPA); 5) *n*-propylphosphonic acid (*n*PrPA); 6) ethyl ethylphosphonic acid (EEAP); 7) isopropyl methylphosphonic acid (iPrMPA); 8) *n*-propyl methylphosphonic acid (*n*PrMPA); 9) isopropyl ethylphosphonic acid (iPrEPA); 10) *n*-propyl ethylphosphonic acid (*n*PrEPA); 11) isobutyl methylphosphonic acid (iBuMPA); 12) cyclohexyl methylphosphonic acid (CHMPA); 13) pinacolyl methylphosphonic acid (PinMPA).
Source: From Analysis of degradation products of organophosphorus chemical warfare agents and related compounds by liquid chromatography–mass spectrometry using electrospray and atmospheric pressure chemical ionisation, in J. Chromatogr. A.[23]

An example reconstructed (total) ion chromatogram from this study which demonstrates the separation of alkyl phosphonic acids is shown in Fig. 1. The chromatographic conditions included the use of a 5 μm particle C_8/C_{18} mixed-phase column (Hichrom, Theale, U.K.) with dimensions of 150 × 2.1 mm. Optimum ESI sensitivity was obtained with 0.1% formic acid in water (mobile phase A) and 0.1% formic acid in methanol (mobile phase B). The elution gradient was 5% B (0–5 min), 5–80% B (5–15 min), and hold 80% B at a flow rate of 0.2 ml/min. Injection volume was 5 μl. Ions *m/z* 97, 111, 125, 139, 153, 181, and 179 were monitored (Finnigan TSQ700 MS, Thermo Electron Corporation, San Jose California, U.S.A.) for the various target alkyl phosphonic acid analytes (see compounds listed in Fig. 1 caption). This method was essentially designed as a rapid screening procedure of aqueous samples or extracts and avoided extensive sample pretreatment or concentration. Black and Read[23] noted that the avoidance of derivatization not only made a simpler sample preparation scheme, but also made preliminary interpretation of fragmentation, in the case of unknowns, much less complicated than with derivatized analytes. Other interesting results were reported from this study. ESI was compared to APCI and found to be approximately twice as sensitive for the alkyl phosphonic acids. Formic acid was found to improve sensitivity when using ESI by nearly an order of magnitude over a similar mobile phase using TFA as the acid modifier. This study indicated that HPLC–MS could not completely displace GC–MS with respect to the hydrolysis products for the nerve agents since some GC-based methods have superior sensitivity and limits of detection.[23]

In a study by Richardson, Baki, and Caruso,[20] reversed-phase ion-pairing HPLC was used in conjunction with the ICP–MS to separate and detect EMPA, iPrMPA, and MPA. Phosphorus-31 was monitored for the ICP–MS detector and a collision cell was used to minimize interference from nitrogen polyatomic species formed in the plasma. ICP–MS is generally noted in its ability to obtain high sensitivity and very low detection limits. A chromatogram showing the separation of MPA, EMPA, and iPrMPA, respectively, using reversed-phase ion-pair HPLC is shown in Fig. 2. Chromatographic conditions included the use of a 5 μm C_8 column (Alltima C8, Alltech Associates, Deerfield, Illinois, U.S.A.) with dimensions of 150 × 3.2 mm. The isocratic mobile phase consisted of 2/98 (v/v) methanol/water made 50 m*M* in ammonium acetate (apparent pH 4.85) and 5 m*M* myristyl trimethylammonium bromide as the ion-pair reagent. The flow rate was 0.5 ml/min and the injection volume was 100 μl. Isotope $^{31}P^+$ and polyatomic $^{47}PO^+$ were monitored by the MS (Agilent 7500ce, Agilent Technologies, Tokyo, Japan), and the He collision cell was optimized before each experiment. This study also included an investigation into the use of complex samples; river water, tap water, topsoil, and potting soil were spiked with the three target analytes.

Chromatographic separation methods for various CWA degradation products have been devised and used within this laboratory. As part of a current study, an HPLC–MS/MS method employing ESI as the source was developed to allow for the trace analysis of environmental water samples or surface wipe samples for specific degradation products of organophosphate (OP) nerve agents. Specifically, the target analytes were MPA, EMPA, EDMAPA (a short-lived intermediate degradation product of GA), iPrMPA, PinMPA, and diisopropyl methylphosphonic acid (DiPrMPA, an impurity of production grade GB). Two gradient reversed-phase systems were employed; one utilized formic acid as the acid modifier and the other was an ion-pair system using heptafluorobutyric acid (HFBA). Example chromatograms of these two systems are displayed in Figs. 3 and 4. For the formic acid system, an Atlantis dC18 125A column with dimensions of 150 × 3.0 mm I.D. (Waters Corporation, Milford, Massachusetts, U.S.A.) was used. The mobile-phase composition consisted of 0.1% (v/v) formic acid in water (mobile phase A) and 0.1% (v/v) formic acid in acetonitrile (mobile phase B). The gradient elution program was 100% mobile phase A for 4 min followed by a linear ramp of 0–95% mobile phase B in 7 min and then a hold at 95% mobile phase B. The flow rate was constant at 0.3 ml/min with a sample injection volume of 5 μl. The Atlantis column is noted for its ability to run 100% aqueous initially for gradients, and a reasonable retention of MPA was obtained as is shown in Fig. 3. For the second ion-pair

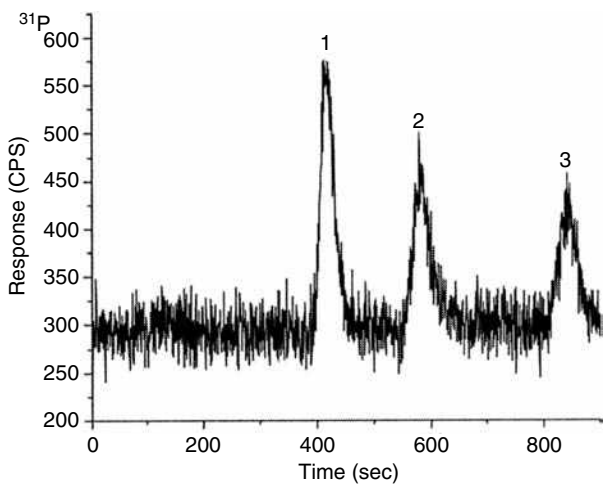

Fig. 2 HPLC–ICP–MS single ion monitoring (SIM) from a standard mixture of three alkyl phosphonic acids at a concentration of 100 ng/ml each: 1) methylphosphonic acid (MPA); 2) ethyl methylphosphonic acid (EMPA); 3) isopropyl methylphosphonic acid (iPrMPA).
Source: From Reversed phase ion-pairing HPLC–ICP–MS for analysis of organophosphorus chemical warfare agent degradation products, in J. Anal. At. Spectrom.[20]

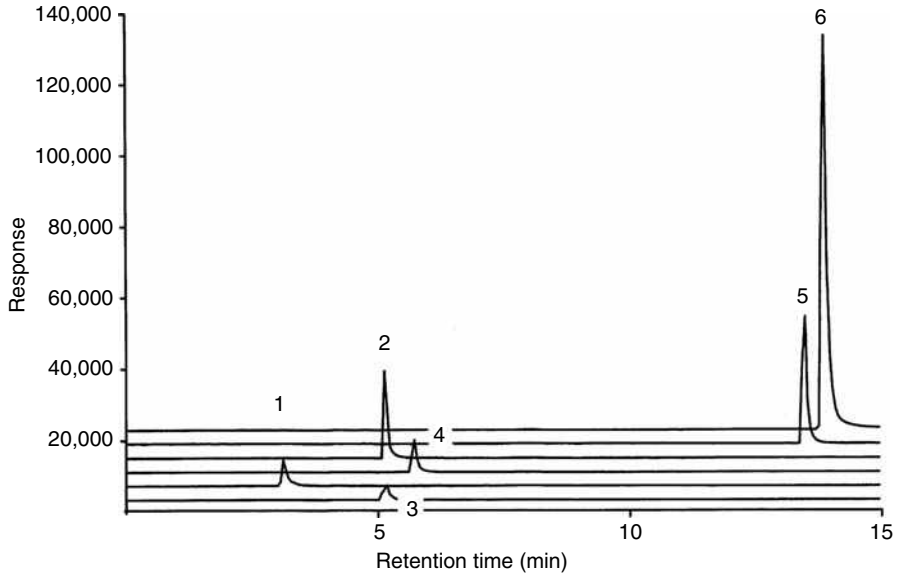

Fig. 3 Reversed-phase HPLC–MS/MS chromatogram using formic acid in the mobile phase and an Atlantis dC18 column. The standard mixture of alkyl phosphonic acids with a concentration of 10 μg/ml each was detected using multiple reaction monitoring (MRM): 1) methylphosphonic acid (MPA, *m/z* 96.8→78.7); 2) ethyl methylphosphonic acid (EMPA, *m/z* 125→96.8); 3) *O*-ethyl *N,N*-dimethylamidophosphoric acid (EDMAPA, *m/z* 154.2→126); 4) isopropyl methylphosphonic acid (iPrMPA, *m/z* 139.1→96.8); 5) pinacolyl methylphosphonic acid (PinMPA, *m/z* 181.3→96.8); 6) diisopropyl methylphosphonic acid (DiPrMPA, *m/z* 181.3→139.1). See the text for further chromatographic details and the MS/MS conditions used.

chromatographic system, a Zorbax SB-Aq 3.5 μm column (Agilent Technologies, Palo Alto, California, U.S.A.) with dimensions of 150 × 3 mm I.D. was used. The mobile-phase composition consisted of 0.1% (v/v) HFBA in water (mobile phase A) and 0.1% (v/v) in acetonitrile (mobile phase B). The gradient elution program was 100% mobile phase A for 3 min followed by a linear ramp of 0–95% mobile phase B in 6 min and then a hold at 95% mobile phase B. The flow rate was constant at 0.3 ml/min with a sample injection volume of 5 μl. Both chromatographic systems used an Agilent Model 6410A Triple Quad MS/MS detector equipped with an ESI interface operated in positive mode using multiple reaction monitoring (MRM); the ions monitored are listed in the captions of Figs. 3 and 4. Both systems can be used for quantitative measurements using isotopically labeled analogues of the analytes which are not shown in the chromatograms displayed.

This study showed some interesting results. Formic acid appeared to have slightly better sensitivity over HFBA; the response of DiPrMPA was roughly double in the formic acid system over the ion-pair system. This result is similar to what Black and Read[23] noted during their comparison of formic acid and TFA mobile phases for the analysis of nerve agent degradation products. MPA and some of the other analytes were not as suppressed by HFBA using the ESI interface, but generally all the analytes had lower responses. Also, the Atlantis dC18 column produced more symmetrical peaks than the ion-pair system and showed less peak tailing (Figs. 3 and 4). Both chromatographic systems could be used for a general screening

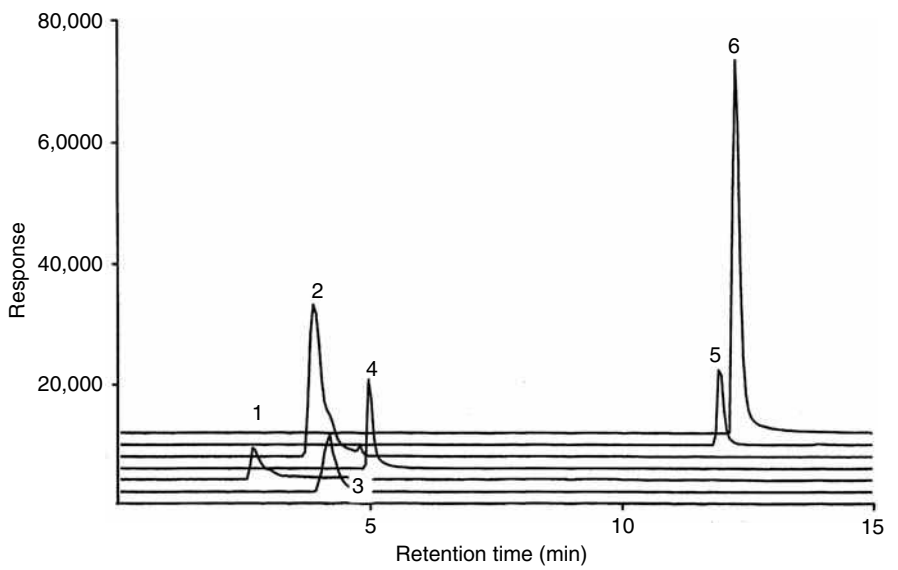

Fig. 4 Ion-pair reversed-phase HPLC–MS/MS chromatogram using heptafluorobutyric acid (HFBA) as the ion-pair reagent in the mobile phase and a Zorbax SB-Aq column. The standard mixture of alkyl phosphonic acids with a concentration of 10 μg/ml each was detected using MRM: 1) MPA (*m/z* 96.8→78.7); 2) EMPA (*m/z* 125→96.8); 3) EDMAPA (*m/z* 154.2→126); 4) iPrMPA (*m/z* 139.1→96.8); 5) PinMPA (*m/z* 181.3→96.8); 6) DiPrMPA (*m/z* 181.3→139.1). See the text for further chromatographic details and the MS/MS conditions used.

procedure for a variety of nerve agent degradation products as well as other CWAs. For example, *N*-ethyl diethanolamine (EDEA, *m/z* 134→116) from the agent HN1 had a retention time of 4 min and TDG (*m/z* 123→105) from the agent HD had a retention time of 5 min using the described formic acid HPLC conditions; thus, this methodology can easily be applied to general screening analysis for a variety of CWA degradation products and has greater versatility than just for the analysis of alkyl methylphosphonic acids.

CONCLUSIONS

HPLC–MS CWA degradation product analysis is a vital technique for use in general enforcement of the chemical warfare treaty and the continued threat of sophisticated world terrorism of the twenty-first century. The inherent advantages of the mass spectrometer with analyte specificity, high sensitivity, and a wide dynamic range of detection, combined with HPLC, makes HPLC–MS a valuable analytical tool for use in CWA degradation product analysis methods for many years to come. HPLC–MS has been demonstrated by various researchers to be useful in rapid screening for the degradation products of OP agents, as well as other agents, particularly when minimum sample pretreatment and preliminary interpretation of fragmentation, in the case of unknowns, is simplified over derivatized analytes.

ACKNOWLEDGMENTS

The authors would like to acknowledge the support of the U.S. Environmental Protection Agency for providing one of the HPLC columns and some of the reagents used in this work. The authors would also like to thank Dennis Lynch, Galye DeBord, Anne Vonderheide, Jeanette Krause, and Nathan Coker for their help in reviewing, editing, and correcting this manuscript.

DISCLAIMERS

The findings and conclusions in this report are those of the authors and do not necessarily represent the views of the National Institute for Occupational Safety and Health (NIOSH) or the Centers for Disease Control and Prevention (CDC). Mention of company names and/or products does not constitute endorsement by NIOSH.

REFERENCES

1. Hooijschuur, E.W.J.; Kientz, C.E.; Brinkman, U.A.Th. Analytical separation techniques for the determination of chemical warfare agents. J. Chromatogr. A, **2002**, *982*, 177–200.
2. Papouskova, B.; Bednar, P.; Bartak, P.; Frycak, P.; Sevcik, J.; Stransky, Z.; Lemr, K. Utilisation of separation methods in the analysis of chemical warfare agents. J. Sep. Sci. **2006**, *29*, 1531–1538.
3. The Convention on the Prohibition of the Development, Production, Stockpiling and Use of Chemical Weapons and on Their Destruction, Organisation for the Prohibition of Chemical Weapons (OPCW), The Hague 1994 (http://www.opcw.org).
4. Munro, N.B.; Talmage, S.S.; Griffin, G.D.; Waters, L.C.; Watson, A.P.; King, J.F.; Hauschild, V. The sources, fate and toxicity of chemical warfare agent degradation products. Environ. Health Perspect. **1999**, *107*, 933–974.
5. Hill, H.H.; Martin, J.S. Conventional analytical methods for chemical warfare agents. Pure Appl. Chem. **2002**, *74*, 2281–2291.
6. Black, R.M.; Muir, G. Derivatisation reactions in the chromatographic analysis of chemical warfare agents and their degradation products. J. Chromatogr. A, **2003**, *1000*, 253–281.
7. Epstein, J.; Rosenblatt, D.H.; Gallacio, A.; McTeague, W.F. Summary report on a data base for predicting consequences of chemical disposal operations. EASP 1200–12, Edgewood Arsenal, Maryland, Department of the Army Headquarters, 1973.
8. Rohrbaugh, D.K.; Yang, Y.C. Liquid chromatography electrospray mass spectrometry of mustard-related sulfonium ions. J. Mass Spectrom. **1997**, *11*, 1247–1252.
9. Ward, K. The chlorinated ethylamines: A new type of vesicant. J. Am. Chem. Soc. **1935**, *57*, 914–916.
10. Chua, H.-C.; Lee, H.-S.; Sng, M.-T. Screening of nitrogen mustards and their degradation products in water and decontamination solution by liquid chromatography–mass spectrometry. J. Chromatogr. A, **2006**, *1102*, 214–223.
11. Bossle, P.C.; Martin, J.J.; Sarver, E.W.; Sommer, H.Z. High-performance liquid chromatography analysis of alkyl methylphosphonic acids by derivatization. J. Chromatogr. **1983**, *267*, 209–212.
12. Goodlett, D.R.; Gale, D.C.; Guiles, S.; Crowther, J.B. Mass spectrometry in pharmaceutical analysis. In *Encyclopedia of Analytical Chemistry: Applications, Theory and Instrumentation*; Meyers, R.A. Ed.; John Wiley & Sons: Chichester, England, 2000; Vol. 8, 7209–7278.
13. Pramanik, B.N.; Ganguly, A.K.; Gross, M.L., Eds; *Applied Electrospray Mass Spectrometry*; Marcel Dekker: New York, 2002.
14. Caruso, J.A.; Sutton, K.L.; Ackley, K.L., Eds; *Elemental Speciation, New Approaches for Trace Elemental Analysis, Wilson & Wilson's Comprehensive Analytical Chemistry XXXIII*; Elsevier Science, Amsterdam: The Netherlands, 2000.
15. Wils, E.R.J.; Hulst, A.G. Determination of organophosphorous acids by thermospray liquid chromatography–mass spectrometry. J. Chromatogr. **1988**, *454*, 261–272.
16. Black, R.M.; Read, R.W. Application of liquid chromatography—atmospheric pressure chemical ionisation mass spectrometry, and tandem mass spectrometry, to the analysis and identification of degradation products of chemical warfare agents. J. Chromatogr. A, **1997**, *759*, 79–92.

17. Mercier, J.P.; Morin, Ph.; Dreux, M.; Tambute, A. Liquid chromatography analysis of phosphonic acids on porous graphitic carbon stationary phase with evaporative light-scattering and mass spectrometry detection. J. Chromatogr. A, **1999**, *849*, 197–207.
18. Rohrbaugh, D.K.; Yang, Y.-C. Liquid chromatography/electrospray mass spectrometry of mustard-related sulfonium ions. J. Mass Spectrom. **1997**, *32*, 1247–1252.
19. B'Hymer, C.; Brisbin, J.A.; Sutton, K.L.; Caruso, J.A. New approaches for elemental speciation using plasma mass spectrometry. Am. Lab. **2000**, *32*, 17–32.
20. Richardson, D.D.; Baki, B.M.; Caruso, J.A. Reversed phase ion-pairing HPLC–ICP–MS for analysis of organophosphorus chemical warfare agent degradation products. J. Anal. At. Spectrom. **2006**, *21*, 396–403.
21. Stalikas, C.D.; Konidari, C.N. Analytical methods to determine phosphonic and amino acid group-containing pesticides. J. Chromatogr. A, **2001**, *907*, 1–19.
22. Bandura, D.R.; Baranov, V.I.; Tanner, S.D. Reaction chemistry and collisional processes in multipole devices for resolving isobaric interferences in ICP–MS. Fresenius J. Anal. Chem. **2001**, *370*, 454–470.
23. Black, R.M.; Read, W.R. Analysis of degradation products of organophosphorus chemical warfare agents and related compounds by liquid chromatography—mass spectrometry using electrospray and atmospheric pressure chemical ionisation. J. Chromatogr. A, **1998**, *794*, 233–244.
24. Zhou, S.; Hamburger, M. Effects of solvent composition on molecular ion response in electrospray mass spectrometry: Investigation of the ionization processes. Rapid Commun. Mass Spectrom. **1995**, *9*, 1516–1521.
25. Read, R.W.; Black, R.M. Rapid screening procedures for the hydrolysis products of chemical warfare agents using positive and negative ion liquid chromatography–mass spectrometry with atmospheric pressure chemical ionisation. J. Chromatogr. **1999**, *862*, 169–177.

Chemical Warfare Agents: GC Analysis

Stanisław Popiel
Institute of Chemistry, Military University of Technology, Warsaw, Poland

Zygfryd Witkiewicz
Institute of Chemistry, Jan Kochanowski University, Kielce, Poland

INTRODUCTION

Chemical warfare agents (CWA) are still an element of equipment of some countries' military forces.[1] Thus, their usage in military conflicts and for acts of terror cannot be excluded, despite the existence of the Convention on the prohibition of the development, production, stockpiling, and use of chemical weapons and their destruction.[2] The Convention provides measures for checking compliance of their provisions. Those measures include (among others): CWA, substrates for their production, and degradation products analysis. Chemical warfare agents analyses performed by inspectors of the Organisation for Prohibition of Chemical Weapons in CWA stockpiles and places of their destruction are presently the most important. Necessity for CWA analysis in the battlefield or following their use by terrorists cannot be, however, excluded.

Chemical warfare agents are mainly organic compounds and, as is the case with many other organic compounds, chromatography is the best method for their analysis. Gas chromatography (GC) is mainly used for the CWA analysis, although liquid column and thin-layer chromatography are also used for this purpose.[3,4] GC is characterized by high detectability and speed and possibility of continuous operation even in field conditions. It is possible to identify CWAs in complex mixtures, even at very low quantities—e.g., picograms and lower.

The particular CWAs differ considerably in their physicochemical properties—e.g., polarity and boiling point, which are important in chromatographic analysis. The formulae and basic physicochemical properties of CWAs are provided in Table 1.

COLLECTION AND SAMPLE PREPARATION FOR CWA ANALYSIS

The collected samples should have the qualitative and quantitative composition representative of the original analyzed material. This should be observed both during the isolation of analytes from their matrix and during their preparation.

Chemical warfare agents samples from the atmosphere are taken mainly through adsorption or absorption. The absorption method consists of passing the polluted air through a solvent or mixture in which the chemical agents dissolve or through the solution of a reagent with which the chemical agents form derivatives. Solvent cooling fosters common dissolution. Samples collected this way may often be analyzed without additional concentration. If concentration is required, solvent evaporation or extraction with a solvent other than that used for absorption is applied. Other extraction methods, including solvent-free techniques (often utilized for liquid samples), may also be used.

Adsorption is an important means of collecting CWA samples from the atmosphere. Adsorption tubes filled, among others, with activated carbon, silica gel, and porous polymers are used for this purpose. A properly selected adsorbent allows for selective analyte adsorption. A chemical agent adsorbed onto a small quantity of adsorbent in a large gas volume (e.g., 50 L) becomes concentrated. In order to transfer it into a solution, analyte desorption is performed with use of a solvent or by direct heating in a thermal desorber, constituting an integral part of a GC.

In cases where chemical agent concentrations in the atmosphere are sufficiently high for direct analysis, they are collected into Tedlar sampling bags. Metal or glass containers usage is not recommended due to the possibility of irreversible chemical agents adsorption to their walls.

Aerosols are collected with filters made of glass fibres, with pores up to 5 μm, and next dissolved in a proper solvent or solvent mixture. Chemical warfare agents or their degradation products, which are dissolved in water or other solvents, are extracted by liquid–liquid extraction (LLE), solid-phase extraction (SPE), solid-phase microextraction (SPME), and stirr bar sorptive extraction (SBSE) methods. Head space (HS) analysis is also employed. In the case of the SPE method, XAD-4 and XAD-2 resins are frequently used.

For analysis of some CWA and their degradation products, it is favorable to transform them into their derivatives.[5] An interesting concept of combining extraction and derivatization was realized using XAD-2 resin impregnated with pentafluorobenzyl bromide. This method may be useful in the analysis of degradation products of organophosphorus warfare agents contained in water.[6]

Table 1 Nomenclature and physicochemical characteristics of selected chemical warfare agents (CWA).

Chemical name [CAS number]	Common name/ Chemical formula	Abbreviation	Class schedule no.	Structure	Molecular weight	m.p.,°C/ b.p.,°C
Isopropyl methylphosphonofluoridate [107-44-8]	Sarin $C_4H_{10}FO_2P$	GB	Nerve agent 1.A.1	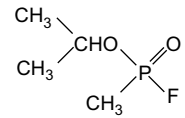	140.1	–54/151.5
Pinacolyl methylphosphonofluoridate [96-64-0]	Soman $C_7H_{16}FO_2P$	GD	Nerve agent 1.A.1	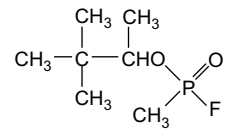	182.1	–80/167
Cyclohexyl methylphosphonofluoridate [74192-15-7]	Cyclosarin $C_7H_{14}FO_2P$	GF	Nerve agent 1.A.1	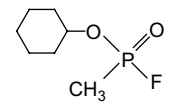	180.2	–30/239
Ethyl *N*,*N*′-dimethylphosphoroamidocyanidate [77-81-6]	Tabun $C_5H_{11}N_2O_2P$	GA	Nerve agent 1.A.2	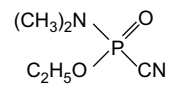	162.1	–50/230
O-ethyl, S-2-diisopropylaminoethyl methylphosphonothiolate [50782-69-9]	VX $C_7H_{18}NO_2PS$	VX	Nerve agent 1.A.3	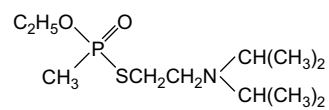	267.3	–30/>300
Diisopropyl phosphorofluoridate [55-91-4]	DFP $C_6H_{14}FO_3P$	PF-3	Nerve agent —	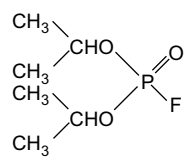	184.2	–82/183
Bis-(2-chloroethyl)sulfide [505-60-2]	Sulfur mustard; Yperite $C_4H_8Cl_2S$	H, HD	Vesicant 1.A.4	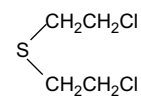	159.1	14.5/217
1,2-Bis-(2-chloroethylthio)ethane [3563-36-8]	Sesquimustard $C_6H_{12}Cl_2S_2$	Q	Vesicant 1.A.4	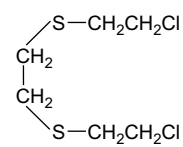	219.2	56.6/140 (2 *Torr*)
Bis-(2-chloroethylthioethyl)ether [63918-89-8]	O-mustard $C_8H_{16}Cl_2OS_2$	T	Vesicant 1.A.4	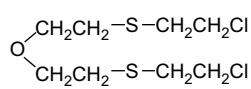	263.3	10/120 (0.2 *Torr*)

Table 1 Nomenclature and physicochemical characteristics of selected chemical warfare agents (CWA). *(Continued)*

Chemical name [CAS number]	Common name/ Chemical formula	Abbreviation	Class schedule no.	Structure	Molecular weight	m.p.,°C/ b.p.,°C
2-Chlorovinyldichloroarsine [541-25-3]	Lewisite $C_2H_2AsCl_3$	L	Vesicant 1.A.5	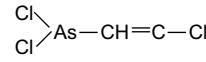	207.3	–2.4/196.6
Tris-(2-chloroethyl)amine [555-77-1]	Nitrogen Mustard $C_6H_{12}Cl_3N$	HN-3	Vesicant 1.A.6	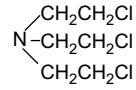	204.5	–4/235
O,*O*-Diethyl S-[2-(diethylamino)ethylo] phosphorothiolate [78-53-5]	Amiton $C_{10}H_{24}NO_3PS$	VG	Nerve agent 2.A.1	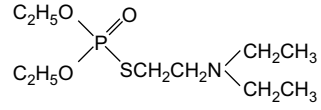	237.3	—/80 (0.01 *Torr*)
3-Quinuclidinyl benzilate [6581-06-2]	BZ $C_{21}H_{23}NO_3$	BZ	Physicochemical 2.A.3	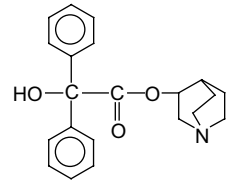	337.4	165/320
Carbonyl dichloride [75-44-5]	Phosgene CCl_2O	CG	Choking agent 3.A.1	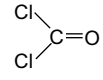	98.92	–128/7.8
Cyanogen chloride [506-77-4]	ClCN	CK	Blood agent 3.A.2	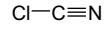	61.47	–6.9/12.8
Hydrogen cyanide (HCN) [74-90-8]	Prussic acid HCN	AC	Blood agent 3.A.3	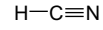	27.03	–13.3/25.5

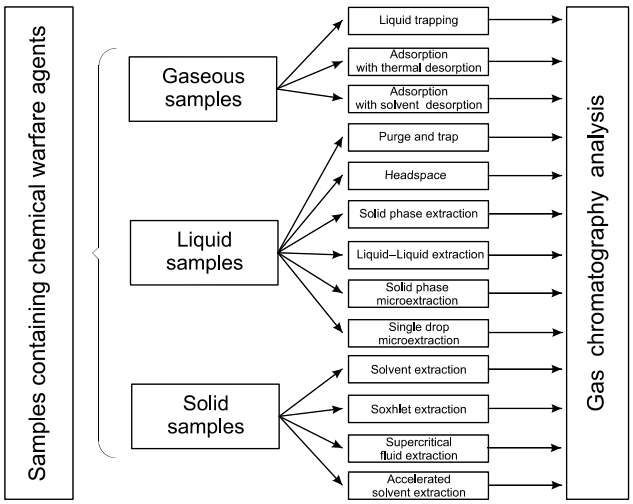

Fig. 1 Methods of sampling and sample preparation for GC analysis of CWAs.

In order to enrich samples containing trace amounts of the CWAs, lyophilization is sometimes applied. In a different procedure, an organic solvent is added to the water and, after freezing out ice, the organic phase is physically removed.

Most methods of collecting and preparing samples of contaminated soil are rather complex. They are predominantly useful only with respect to chemically stable CWA that are resistant to degradation reactions occurring in the environment. The common method of isolating CWAs to be analyzed from soil is their extraction with organic solvents, preceded by wetting of the soil with water. The volatile and medium volatile substances may be isolated from soil by evaporation. The evaporated CWAs are introduced to a chromatographic column directly or after their concentration.

Supercritical fluid extraction may be useful for extraction CWAs or products of their destruction—e.g., for alkyl alkylphosphonofluoridates and dialkyl alkylphosphonates from painted surfaces.[7]

Chemical warfare agents are usually isolated from vegetable materials by the homogenization and extraction of the toxic substances in a Soxhlet apparatus with a mixture of organic solvents.

The contamination of humans and animals is usually determined by analyzing body fluids, such as urine, plasma, or blood. The isolation of CWAs or their metabolites is usually performed by LLE, SPE, or SPME. If tissues are to be analyzed, the CWAs are extracted after homogenization with water.

Examples of sampling and sample preparation procedures for GC analysis of materials contaminated with CWA are shown in Fig. 1.

GENERAL PROBLEMS OF CWA ANALYSIS BY GAS CHROMATOGRAPHY

Gas chromatography is a proper method for analysis of CWAs whose vapor pressures are high enough or if they can be transferred into the gaseous state without decomposition. The properties of only a few CWAs, mainly arsenic containing substances, are not proper for direct GC analysis. Such chemical agents, especially the products of their decomposition and metabolites, including organophosphorus agents and vesicants, are analyzed after their derivatization.[5]

Packed and capillary columns are suitable for chemical agent analysis. Chemical warfare agents are mostly polar, so in packed columns, silanized supports are most often used—mainly Chromosorbs W and G and Gas-Chrom Q and P. The majority of analyses are performed using capillary columns, especially the fused silica types.

Stationary phases SE-52 and OV-1 are considered to be among the best for CWA analysis. They do not react with chemical agents and have high thermal stability. SE-54, DB-1, DB-5, and FFAP are also recommended, especially for use in the analysis of organophosphorus compounds, vesicants, and irritants. OV-1701 may be used for analyzing DFP and SE-54 for hydrogen cyanide (HCN), cyanogen chloride, and phosgene.

A good way to introduce CWA samples into a chromatographic column is to inject a sample into the column directly. By applying direct injection, the thermal decomposition of some compounds, e.g., VX, is avoided. When using a glass injector, it is important to note that during the analysis of some agents, e.g., soman, adsorption onto the active surface of the glass injector may occur. Strongly adsorbed phosgene and HCN may undergo decomposition, so the use of deactivated injection systems is essential.

DETECTORS FOR CWA ANALYSIS

Many detectors have been used in the analysis of CWA. Among them, selective detectors are especially recommended because they facilitate, considerably, the identification of chemical agents. They are useful for detecting agents that contain elements to which the molecules of these detectors are particularly sensitive. The following detectors can be employed for analysis of the following chemical agents: electron capture detector (ECD) for agents containing halogens; flame-photometric detector (FPD) for agents containing sulphur and phosphorus; nitrogen-phosphorus detector (NPD) for agents containing nitrogen and phosphorus; and alkali flame-ionization detector-AFID (alkali thermionic detector-ATD) for organophosphorus agents.

The flame-ionization detector (FID) and thermal conductivity detector (TCD) are rarely used in CWA analyses due to their relatively low sensitivity and selectivity. Sometimes, combining two detectors may be useful—e.g., FID–AFID, FID–ECD, FID–FPD, and ECD–AFID. Such combinations facilitate the identification of agents separated in one or two chromatographic columns.

Currently, instruments consisting of a GC and a spectrometer are very often employed. Mass spectrometry (MS), atomic emission spectrometry (AES), and infrared spectrometry with Fourier transformation (FTIR) are commonly used in this case.[8,9]

The most often used apparatus for CWA analysis is GC–MS.[4,10] Such a device is very useful for rapid analysis of trace amounts of chemical agents present in a complex mixture. The mass spectra recorded for the components of the mixture are compared with those contained in a computer database, and on this basis, the particular substances are reliably identified. The detectability of these instruments is very good. It is possible to detect organophosphorus agents at the level of 10^{-12}–10^{-13} g and even lower.

In some cases, the identification of chemical agents with GC–MS may be difficult. In those cases, analysis with GC–AED (atomic emission detector) may be of assistance. This device makes elemental analysis of chemical agents separated in the chromatographic column possible. The quantitative assay of elements in a given chemical compound allows determination of its molecular formula. Analysis of the same samples with GC–MS and GC–AED allows much more certain identification of chemical agents than the utilization of any of those instruments separately.

Using ordinary detectors (e.g., FID, TCD, ECD, NPD), the identification of particular chemical agents is usually performed by comparing the retention indices of the substances being identified and the standard agent measured on at least two columns containing stationary phases of different polarities. Under isothermal conditions, the Kovats indices are applied and, under temperature programing, the equation of Van den Dool and Kratz is applied.[11–13]

THE SPECIFICITY OF ANALYSIS OF PARTICULAR GROUPS OF CHEMICAL AGENTS

Due to the high toxicity of organophosphorus chemical agents, their detection requires detectors characterized by high detectability. The presence of phosphorus in molecules of those chemical agents enables satisfactory detectability with FPD, ATD, and AED. Analysis of organophosphorus chemical agents is not difficult, but an analysis of polar products of their degradation is not easy and is frequently performed following their derivatization, consisting of the conversion of hydroxyl groups to their methyl esters using diazomethane or to trimethylsilyl (TMS) esters using *N*,*O*-bis (trimethylsilyl) trifluoroacetamide (BSTFA) or BSTFA +1% trimethylsilyl chloride (TMSCl).[5]

Organophosphorus chemical agents are often mixtures of isomers. It is possible to separate, chromatographically, four stereoisomers of soman and enantiomers of sarin and tabun using short capillary columns packed with chiral stationary phases. They may also be separated in columns packed with Triton X-305 and DC-550 phases. The analysis of isomers is particularly important when studying organophosphorus chemical agents' transformations in living organisms.

Among vesicants, the majority of analyses apply to sulfur mustard (yperite), and much less to lewisite. After yperite was used in the Iraq–Iran war, this agent was analyzed in the munition, water, soil, and body fluids of contaminated soldiers. Numerous products of yperite's decomposition were also analyzed. In a lump of sulphur mustard taken from the sea approximately 50 years after it sank, approximately 40 other chemical compounds have were detected.[9,14] Those been probably impurities of the yperite and products of its degradation. GC–MS is frequently used for analysis of those chemical agents, but FPD and ECD may also be used.

Lewisite may be analyzed indirectly. In the course of action of sodium hydroxide on lewisite present in water, acetylene is released, which is easy to chromatographically analyze. This method allows detection of lewisite in water at concentration levels down to $10^{-8\%}$. The derivatization of lewisite with thiol reagent makes it possible to detect it using the FPD.[5]

Irritants are used as vapors or aerosols. The most important irritants are chloroacetophenone (CN), chloropicrin (PS), *O*-chlorobenzylidenemalonodinitrile (CS), camite (CA), dibenzo[bf]-1-4-oxazepine (CR), and adamsite (DM). Because of the presence of halogens in the molecules of these chemical agents, the ECD is commonly used for their detection. This detector allows detection of tear agents at the nanogram and subnanogram levels. Nitrogen-phosphorus detector is also suitable for the analysis of agents containing nitrogen in their molecules.

GC–MS instruments allow the rapid analysis of irritant agents with good detectability and reliable identification. Using such instruments, it is possible to determine CN, CS, and CR at concentrations lower than 1 ng/ml.

Chloropicrin is often analyzed by GC–MS and GC with ECD, as it is used as a component of plant protection agents and as a monitoring substance for testing filtration equipment. Analysis of PS in water by headspace analysis or extraction with *n*-heptane is often applied.

Chloroacetophenone and CS may be analyzed using Carbowax 20 *M* and other polar stationary phases. Packed columns filled with squalane or silicone phases, or capillary columns containing DB-5, OV-1, SE-30, or OV-17 phases are used for PS assay.

As with other organic arsenical chemical agents, DM analysis is difficult. Their detectability is not good[15] and derivatization may facilitate their analysis.[16] Adamsite degradation products may be analyzed with capillary columns containing SE-52 or OV-1 phases.

At present, HCN, cyanogen chloride, and phosgene are of less importance as CWAs, but the agents were used in battle in the past. Presently, they are of industrial

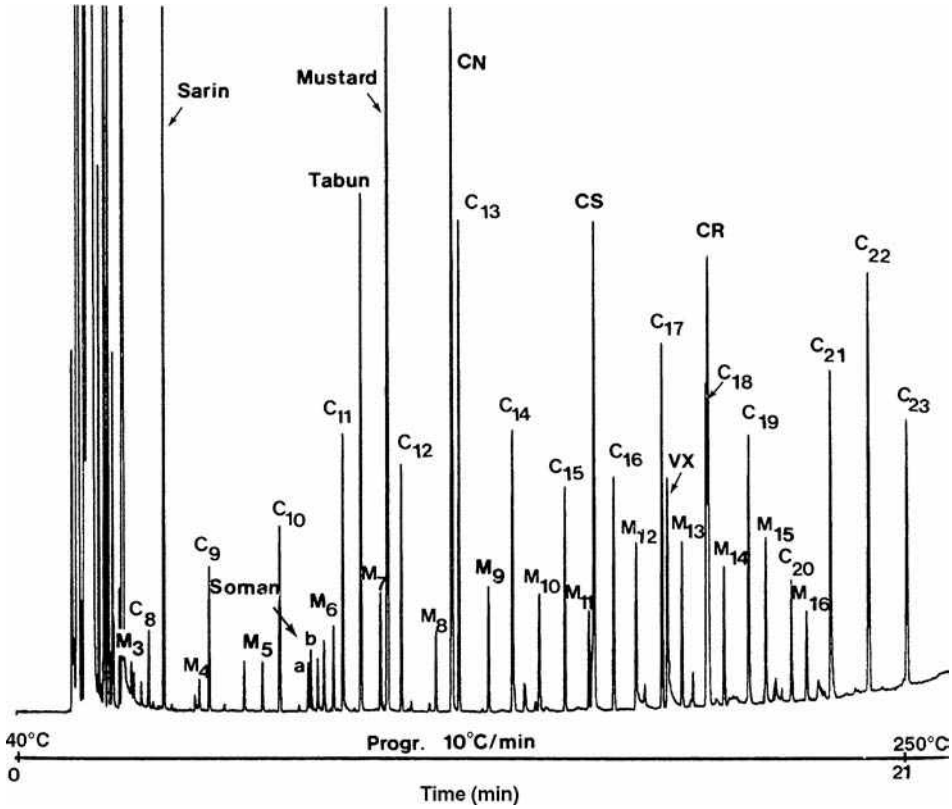

Fig. 2 Separation of chemical warfare agents and the C and M standard series mixture by GC with temperature programing. Conditions: 30 m × 0.33 mm I.D. fused-silica capillary column with 0.25 μm film of DB-5; carrier gas, helium at a flow rate of 2 ml/min; detection, flame-ionization detector (FID).
Source: From Elsevier. Effect of variations in gas chromatographic conditions on the linear retention indices of selected chemical warfare agents, in J. Chromatogr.[12]

significance (especially phosgene), and, in case of a tank or a reactor breakdown, they may cause intoxication, including fatal results.

Glass and metal containers are not recommended for collection of HCN samples; this is due to adsorption of the compound onto the walls of such containers. Good results are achieved when HCN is adsorbed onto porous materials, from which it can be desorbed with a solvent or by using thermal methods. For HCN detection in biological samples (e.g., in blood), a HS analysis method may be applied. Hydrogen cyanide detectability with a thermionic nitrogen detector may reach 1 pg in a sample.

In the analysis of HCN in mixtures of inorganic gases, medium polarity and polar stationary phases in packed and capillary columns (SE-52, SE-54), as well as Porapaks (e.g., QS) and Chromosorb 104, may be used.

After derivatization of HCN with chlorinating agents—e.g., chloramine T—cyanogen chloride is obtained. Following dissolution of cyanogen chloride in ethylacetate, toluene, or hexane, it can be determined by GC with ECD. This method was used for the determination of HCN in tobacco smoke. The amount of HCN in one cigarette was found to exceed 50 ng.[3]

The GC analysis of phosgene is difficult due to its high reactivity. At low concentration, it decomposes completely, even on contact with active surfaces. This is the reason that some parts of a GC should be made of inert materials (e.g., polytetrafluoroethylene or glass). Using ECD, phosgene may be determined at the 1–2 ppb level. Derivatization of phosgene with nucleophilic regents, e.g., amines, is the recommended solution.[17]

Liquid stationary phases (e.g., didecyl phthalate, E-301) are mainly used for phosgene analyses, but adsorbents may be used, as well. An example of a CWA chromatogram is given in Fig. 2.

CONCLUSION

Thanks to GC, it is possible to rapidly analyze CWA in complex mixtures with good detectability and sensitivity in air, water, soil, plants, and animal organisms. There are instruments which may be used in automatic air control systems. In the military, instruments consisting of GC and MS are applied for CWA analysis in air and water under field conditions. Portable and pocket chromatographs are also known.[18]

REFERENCES

1. Croddy, E.; Perez-Armendariz, C.; Hart, J. *Chemical and Biological Warfare*; Copernicus Book: New York, 2001.
2. Convention on the Prohibition of the Development, Production. Stockpiling and Use of Chemical Weapons and their Destruction; Technical Secretariat of the Organization for Prohibition of Chemical Weapons: The Hague, 1997.

3. Witkiewicz, Z.; Mazurek, M.; Szulc, J. Chromatographic analysis of chemical warfare agents. J. Chromatogr. **1990**, *503* (2), 293–357.
4. Hooijschuur, E.W.J.; Kientz, C.E.; Brinkman, U.A.Th. Analytical separation techniques for the determination of chemical warfare agents. J. Chromatogr. A, **2002**, *982* (2), 177–200.
5. Black, R.M.; Muir, B. Derivatization reactions in the chromatographic analysis of chemical warfare agents and their degradation products. J. Chromatogr. A, **2003**, *1000* (1–2), 253–281.
6. Rosenfeld, J.M.; Mureika-Russel, M.; Phatak, A. Macroreticular resin XAD-2 as a catalyst for the simultaneous extraction and derivatization of organic acids from water. J. Chromatogr. **1984**, *283*, 127–135.
7. Chaudot, X.; Tambute, A.; Caude, M. Comparison of supercritical fluid extraction with solvent sonication for chemical warfare agent determination in alkyd painted plates. J. High Resolut. Chromatogr. **1998**, *21* (8), 457–463.
8. Soderstrom, M.T.; Bjork, H.; Hakkinen, V.M.A.; Kostiainen, O.; Kuitunen, M.-L.; Rautio, M. Identification of compounds relevant to the chemical weapons convention using selective gas chromatography detectors, gas chromatography-mass spectrometry and gas chromatography-Fourier transform infrared spectroscopy in an international trial proficiency test. J. Chromatogr. A, **1996**, *742* (1–2), 191–203.
9. Mazurek, M.; Witkiewicz, Z.; Popiel, S.; Śliwakowski, M. Capillary gas chromatography-atomic emission spectroscopy-mass spectrometry analysis of sulphur mustard and transformation products in a block recovered from the Baltic Sea. J. Chromatogr. A, **2001**, *919* (1), 133–145.
10. Kientz, Ch.E. Chromatography and mass spectrometry of chemical warfare agents, toxins and related compounds: State of the art and future prospects. J. Chromatogr. A, **1998**, *814* (1–2), 1–23.
11. Hancock, J.R.; Peters, P.R. Retention index monitoring of compounds of chemical defence interest using thermal desorption gas chromatography. J. Chromatogr. **1991**, *538* (2), 249–257.
12. Kokko, M. Effect of variations in gas chromatographic conditions on the linear retention indices of selected chemical warfare agents. J. Chromatogr. **1993**, *630* (1–2), 231–249.
13. Huber, J.F.K.; Kendler, E.; Reich, G.; Hack, W.; Wolf, J. Optimal selection of gas chromatographic columns for the analytical control of chemical warfare agents by application of information theory to retention data. Anal. Chem. **1993**, *65* (20), 2903–2906.
14. Mazurek, M.; Witkiewicz, Z.; Śliwakowski, M. Analysis of the yperite block fished up from the Baltic Sea. J. Planar Chromatogr. **2000**, *13* (5), 359–364.
15. Haas, R.; Krippendorf, A. Determination of chemical warfare agents in soil and material samples: Gas chromatographic analysis of phenylarsenic compounds (Sternutators). Environ. Sci. Pollut. Res. **1997**, *4* (3), 123–124.
16. Schoene, K.; Bruckert, H.-J.; Jurling, H.; Steinhanses, J. Derivatization of 10-chloro-5,10-dihydrophenarsazine (Adamsite) for gas chromatographic analysis. J. Chromatogr. A, **1996**, *719* (2), 401–409.
17. Schoene, K.; Bruckert, H.-J.; Steinhanses, J. Derivatization of acylating gases and vapours on the sorbent tube and gas-chromatographic analysis of the products by atomic-emission and mass-spectrometric detection. Fresenius' J. Anal. Chem. **1993**, *345* (11), 688–694.
18. Smith, A.; Jackson Lepage, C.R.; Koch, D. Detection of gas-phase chemical warfare agents using field-portable gas chromatography-mass spectrometry systems: Instrument and sampling strategy considerations. Trends Anal. Chem. **2004**, *23* (4), 296–306.

Chemical Warfare Agents: TLC Analysis

Javier Quagliano
Organic Synthesis Division, Argentine R&D Institute for the Defense (CITEFA), Buenos Aires, Argentina

Zygfryd Witkiewicz
Institute of Chemistry, Jan Kochanowski University, Kielce, Poland

Stanisław Popiel
Institute of Chemistry, Military University of Technology, Warsaw, Poland

Abstract
In this entry, advances in thin-layer chromatography (TLC) of chemical warfare agents (CWA) are reviewed. Procedures for the separation and identification of CWA occurring alone or in the presence of related compounds, such as nerve agents in organophosphorous pesticides, are described. Analysis of blister agents (vesicants) and their differentiation, irritants (CS, CN, and CA), and mixtures of irritants and nerve agents are discussed. Solvents for running the TLC plates, reagents, and conditions for development of the plates are described in detail. Two-dimensional overpressured TLC (OPLC) used for the separation and identification of nerve agents in the presence of organophosphorous pesticides proved to be an adequate technique for detecting very low concentrations of these compounds.

INTRODUCTION

Chemical warfare agents (CWA), commonly used during World War I, were also produced for possible use during World War II; however, they were not used in the battlefield during the latter war. Only hydrogen cyanide was used for killing prisoners held in German death camps, e.g., in Auschwitz. Despite existing proof that a war was fought without the use of CWA, these agents were industrially produced after World War II. Those were used on a local scale, and still remain in the stores of some armies. Therefore, use of CWA cannot be ruled out in local armed conflicts. Also, there have been instances of CWA use by terrorists.[1]

The international community revoked the development, production, storage, and usage of CWA with a Chemical Weapons Convention (CWC), which came into force in 1997. One of the basic tasks foreseen by the Convention is the destruction of CWA stocks owned by member states of the Convention. Inspectors of the Organization for the Prohibition of Chemical Weapons (OPCW), monitoring observance of provisions of the Convention, perform analyses of chemical substances that could potentially be CWA. Analyses of various substances are also performed in places where the use of chemical warfare is suspected. One of the analytical methods used for the detection and determination of precursors for the production of CWA, CWA themselves, and their decomposition products is thin-layer chromatography (TLC).

Currently, gas chromatography (GC), including GC–mass spectrometry (GC–MS), is the main method used for CWA analysis.[2,3,4] High-performance liquid chromatography with MS (HPLC–MS) is another popular method frequently used for that purpose. These analytical methods are very efficient but are expensive and require some complex apparatuses.

TLC is a relatively simple and cheap analytical method, although increasingly elaborate devices are used in it, and it is a fully instrumental method. High selectivity, good detectability of analytes, and reliability of the analysis, even if a relatively simple equipment is used, make the method applicable not only for stationary laboratories, but also for mobile field laboratories.

GENERAL CHARACTERISTICS OF TLC AS A CWA ANALYSIS METHOD

A TLC analysis can be performed right at the site of occurrence of suspicious chemicals, checking, for example, 34–40 samples in 4–5 hr. The analysis provides information on the presence or absence of the chemicals of interest, and dubious samples can be further analyzed using other chromatographic techniques, such as GC–MS. Analysis using TLC is particularly recommended if numerous samples of unknown origin have to be analyzed. Therefore, in some armies, including the Polish army, TLC apparatuses and procedures have been and are still used for CWA analysis in field laboratories.

For TLC analyses, the samples should be in the form of a solution. If the analyzed material is located on a chemical

reactor wall, the surface of a contaminated equipment, or the remains of a missile, the surface is wiped with cloth or polyester and the chemical substance is extracted with a proper solvent, e.g., dichloromethane, hexane, or acetone. Also samples of soil and water are extracted with solvents. These extracts can be concentrated, if necessary.

Extracts thus obtained are applied onto a chromatographic plate covered by a thin layer of adsorbent (volume 1–5 μl). Silica gel is most frequently used as an adsorbent, and aluminum oxide is used less frequently. Components of the sample mixture are separated by developing a chromatogram using a single or mixed mobile phase characterized by appropriate polarity and elution force. After development of a chromatogram, colorless components are transformed into colored chemicals by spraying the chromatographic plate with the solution of an appropriate reactant. Positive color reactions can occur immediately, after some time (depending on the quantity of analyte), or only after the plate is heated up. Detectability limit of TLC is usually between 10^{-6} and 10^{-9} g per spot, and of HPTLC, between 10^{-9} and 10^{-12} g.

Sample components on the plate are identified by comparing the obtained colors with a specific standard. To increase the reliability of identification, several reactants can be used, which yield products of various colors characteristic of a given CWA.

Apart from the color of the analyte, the delay factor of a given spot with respect to the front end of the mobile phase (R_F) can also form the basis for identification. Value of the measured delay factor is then compared to the corresponding value of this factor for a standard.

In cases where a toxic substance occurs alone, without any admixtures, it can be detected on a chromatographic plate without developing a chromatogram. A drop analysis is performed using one or more reactants that provide colored products with the detected (identified) substance.

Besides the visualization of components on a chromatogram realized by their transition to colored chemicals, other visualization methods also are used, e.g., irradiation with UV light. After irradiation of a developed chromatogram, spots invisible in visible light can become fluorescent, or the background fluorescence of the plate surface can get extinguished. Components of a single sample can be detected and identified on a single plate using various methods.

TLC is used for qualitative, semiquantitative, and quantitative analyses. Precise, accurate and repeatable results of quantitative analysis are achieved using densitometers. In this method, spot chromatograms can be transformed into peak chromatograms and absorption spectra of the analytes can be registered. These spectra are used for the identification of analyzed substances. Detailed description of TLC as an analytical method is presented, among others, in a monograph edited by Nyiredy.[5]

Some examples of the analysis of individual groups of CWA using TLC are provided below.

ANALYSIS OF ORGANOPHOSPHOROUS COMPOUNDS

Combination of mixture components separation using HPTLC with enzymatic visualization is a very good method for the analysis of organic phosphorous compounds. This method is characterized by low detectability thresholds. Organic phosphorous compounds are inhibitors of the enzymes cholinesterase or acetylcholinesterase.[6,7] Therefore, their detection on a plate is limited to finding those places on a chromatogram, where the enzyme was applied. For example, analysis of sarin, soman, tabun, and VN_1 is performed using a plate covered by a layer of silica gel and diatomaceous earth, and a mobile phase containing hexane, pyridine, and dioxane (7:2:1). After the plate is dried, it is sprayed with aqueous solution of an enzyme (cholinesterase), and after 5 min, with a mixture of β-naphthol acetate and diazo-*o*-dianisidine in aqueous alcohol solution. White spots contrasting on an intense violet gel appear in those places where organic phosphorous toxic compounds are located. This visualization method allows the detection of 10 ng of an organic phosphorous compound per spot. Under the conditions described above, VN_1 appeared as two spots of isomers: thiolic and thionic.

Enzymatic reaction can be used for the analysis of not only organic phosphorous chemical agents, but also organic phosphorous pesticides and carbamates, as these compounds also inhibit cholinesterase, and can occur together with CWA in field conditions. Therefore, methods have been developed for differentiating cholinesterase-blocking pesticides and organic phosphorous CWA.[8] Ten insecticides and soman and VX were separated on a plate with silica gel. A mixture of dichloroethane and ethyl acetate (9:1) was used as the mobile phase. Analyzed chemicals were identified with selective reactions. Total time of the analysis did not exceed 30 min.

Enzymatic visualization of organic phosphorous warfare agents (sarin, soman, tabun, and VX) and organic phosphorous pesticides (diazinon, dichlorvos, chlorfenvinphos, fenitrothion, and phosalone) uses 4-methylumbelliferone esters as reagents. The performance of the enzymatic reaction on a chromatographic plate was estimated by the measurement of fluorescence of the reaction product 4-methylubelliferone. The results of this reaction were compared with those of another reaction where indoxyl acetate was used. Using this procedure it was possible to determine sarin, soman, and tabun at the level of a dozen picograms per spot and VX as well as pesticides from the individual nanograms to their dozens per spot.[9]

Two-dimensional overpressured TLC (OPLC) has been used for the separation and quantitative densitometric

analysis of organophosphorous warfare agents in the presence of 22 pesticides.[10] The CWA were tabun, sarin, soman, DFP, and VX, and the pesticides belonged to the groups of organochlorine (5), organophosphorus (13), carbamate (2), and carbamide (2) compounds. The optimum composition of the mixed eluents was established using the PRISMA model. The chromatograms were developed to a distance of 6 cm in the first direction with diisopropyl ether/benzene/tetrahydrofuran/*n*-hexane (10:7:5:11, v/v) and to a distance of 6 cm in the second direction with tetrahydrofuran/*n*-hexane (2:3, v/v). Three spray reagents were used for visualization of the analyzed compounds: Reagent A was a solution of cholinoesterase in borate buffer; reagent B was a solution of butyrylthiocholine iodide and Michler's hydrol; and reagent C was a saturated solution of cobaltic chloride in acetone. After evaporation of the mobile phase, the plate was sprayed with reagent A, placed in an oven at 37°C for up to 15 min, and then sprayed successively with reagents B and C. The presence of the analytes was revealed as blue spots on a white background. The detectability was 1.3 pg for tabun and 48 ng for VX, and it was possible to determine the organophosphorous warfare agents quantitatively in the range of 15 pg to 100 ng (JPC 4).

It was found that the presence of metal ions in the enzymatic visual reagent leads to a decrease in the detection limit of organophosphorous compounds to the level of 10^{-12} g per spot. The best results were obtained for Co^{2+}; the results were slightly worse for Mg^{2+} ions.[11,12]

DFP can be determined using a highly sensitive nonenzymatic method, after its visualization in a reaction with 2,4-dinitrophenol (DNP) and 2,4,6-trinitrophenol (TNP).[13] Spots—brown (DNP) or orange (TNP)—disappeared within several minutes. Restaining could be achieved by spraying the plate with NaOH solution. Determinability of DFP was between 1 and 2 nmol per spot.

ANALYSIS OF BLISTER AGENTS (VESICANTS)

This group of CA includes mustards and arsenic compounds, especially lewisites. Various reagents were used for the visualization of sulfur and nitrogen mustards. A group reagent for sulfur and nitrogen mustards can be 4,4′-nitrobenzylpyridine, which forms blue-colored products with mustards. Sulfur mustards can be differentiated from nitrogen mustards by spraying the plates with Cu-3,3′-dimethoxybenzidine. These reagents allow the detection of mustards at a level of micrograms per spot.[14] Also, a biochemical method was used for the development of thin-layer chromatograms of compounds having cytotoxic activity. This method allowed determination of sulfur mustards at the level of a single microgram.

Munawalli and Pannel[15] analyzed sulfur mustard and its metabolites in biological fluids using TLC. Very good separation of these substances was achieved using a two-component mixture of chloroform and methanol (10:1) and chloroform and acetylnitrile (5:1) for the development of chromatograms. Visualization of the chromatograms was achieved using 1% $KMnO_4$ solution in 6% Na_2CO_3 and 7% 4,4′-*p*-nitrobenzylpyridine solution in acetone. Heating of the plate for 15 min at 70°C and exposure to ammonia vapors caused the formation of blue stains in places where sulfur mustard was present. This method allowed the detection of less than 0.05 μg of yperite per spot.

A significant amount of CWA, mostly sulfur mustard, was sunk in the Baltic Sea after World War II.[16,17] The analysis of a yperite block retrieved from the Baltic Sea in 1997 was performed using HPTLC and OPLC.[18] Using of two-dimensional elution, it was possible to detect from 13 to 22 different compounds in the samples from the block. The detected compounds were identified by GC–MS. Sulfur mustard was found to be the major component of the yperite block. It was determined at a limit of detection of 20 ng per spot. The maximum quantity of sulfur mustard in the analyzed samples did not exceed 26%. Plates with silica gel were used for analysis. The following mobile phases were used: for development in one direction toluene/dichloromethane/*n*-propanol/*n*-hexane (25:25:1:50, v/v) and for development in the second direction diisopropyl ether/chloroform/*n*-hexane (1:1:3, v/v). The chromatograms were visualized by spraying with a reagent containing 4,4′-bis(diethylamino)benzophenone and mercury(II)chloride in ethanol. Better separation results for the components of a mixture and in shorter time were achieved using OPLC, as compared to HPTLC. It is interesting to note that even after staying for approximately 50 years in marine water, the block contained significant amounts of yperite.

The group of necrosis-inducing CWA also includes primary, secondary, and tertiary arsines. These chemical compounds were also analyzed using TLC. Separation of mixtures of these arsines is not difficult, and they can be visualized using Michler's thioketone, iodine, dithizone, and a metacresol purple dye. Using the last reagent it is possible to detect lewisite at the level of 0.05 μg per spot.[19]

ANALYSIS OF IRRITANTS

Chemicals belonging to this group differ in polarity, which requires an appropriate mobile phase on the one hand, and favors their separation on the other. Good separation of a mixture of CS, CA, and CN can be achieved using 5% chloroform in benzene as a mobile phase. Developing the chromatogram with quinone solution yields a yellow CA spot and a blue CS spot. Following additional spraying with 5% NaOH solution, a brown CN spot appears.

DM and diphenylcyanoarsine can be separated using 20% acetone in chloroform and visualized with a solution of 3,3′-dimethoxybenzidine, copper acetate, and 50% H_2SO_4, which yields an orange spot.

CA, CS, and CN present in a single sample become separated when a chromatogram is developed using a mixture of toluene and dichloroethane (1:1). After a plate is sprayed with thiourea and 3,3′-dimethoxybenzidine solution, yellow CA, beige CS, and brown-violet CN spots are obtained. Detectability of these substances is approximately 1 μg per spot.

A mixture of CA, CS, and CN can be using chloroform as a mobile phase. Dragendorff reagent or $KMnO_4$ solution can be used for development. Separation takes place according to the following order of increasing R_F values: CA < CN < CS.

ANALYSIS OF MIXTURES CONTAINING CWA BELONGING TO PARTICULAR GROUPS

In the analysis of a blend of 12 organic phosphorous compounds, necrosis-inducing compounds, and irritants using an enzymatic reaction, besides the spots corresponding to organic phosphorous compounds, spots corresponding to lacrimators CS and CN also appear. Spots of these agents overlap the spots of sarin and soman, and therefore analysis of such a blend should be carried out in two chromatographic systems. In the first one a mixture of *n*-hexane, dioxane, and pyridine (1:1:2) can be used as a mobile phase. Developing the chromatogram using an enzymatic reaction leads to the appearance of GB, GA, GD, VN_1, CS, and CN spots, and spraying the chromatogram with Tollens' reagent leads to the appearance of mustard, CA, CS, CN, and DM spots. In a second system, using dichloroethane and ethyl acetate (7:3) as a mobile phase, separation of CS, CN, DM, and GB as well as GA can be achieved. In this system, R_F values for lacrimators and organic phosphorous toxic agents were clearly different. Chromatogram can be visualized using an enzymatic reaction. Preliminary spraying of the plate with I_2 solution in chloroform increases the sharpness of the silhouettes of spots and makes the visualization of adamsite possible.

Analysis of sulfur mustard can be performed when the compound is contained in a blend of organic phosphorous and/or organic chlorine insecticides.[20] Identification of sulfur mustard was possible by the application of a mobile phase that ensured its good separation from pesticides. For yperite R_F value was high, and for the other components of the blend it was low. Mustard spot was visualized using a selective reagent, e.g., an iodineplatinate ion $[PtJ_6]^{2-}$. This allowed the detection of yperite at the submicrogram level.

CONCLUSIONS

Presented data concerning CWA analysis using TLC method indicate that there are numerous procedures for the separation, identification, and determination of CWA. Analysis using TLC is possible even when CWA are present in mixtures, containing other substances, that can be present in environmental samples. Analyses can be carried out in the mobile laboratories many armies are equipped with.

Although no new methods of CWA analysis have been published recently, analysis methods for chemical compounds similar to CWA by using TLC are being developed. A procedure intended for the analysis of organic phosphorous pesticides described by Hamada and Wintersteiger could be used for the analysis of organic phosphorous toxic agents.[21]

For the analysis of organic phosphorous compounds in human serum after acute poisoning, the procedure proposed by Futagami et al.[22] may be used. They applied HPTLC for the detection of 25 commonly used organic phosphorous insecticides in human serum. These organophosphates were separated on plates with three different separating systems within 6–18 min and detected by means of UV radiation and coloring reactions.

Not only common TLC, but also some of the more advanced techniques can be used for CWA analysis. For example, a combination of TLC with flame ionization detection was suggested for the analysis of phosphorous and sulfur compounds.[23]

Chromatographic plates used for typical TLC analysis of CWA can be used for preliminary, rapid detection of CWA. Chromatograms are not developed in that case, but tested samples in the form of a solution are applied over a layer of adsorbent and then wetted with solutions of appropriate reagents. Appearance of characteristic green spots indicates the presence of a toxic agent in the tested sample.[24]

REFERENCES

1. Croddy, E.; Clarisa P.-A.; Hart, J. *Chemical and Biological Warfare*; Springer Verlag: New York, 2002.
2. Carrick, W.A.; Cooper, D.B.; Muir, B. Retrospective identification of chemical warfare agents by high-temperature automatic thermal desorption–gas chromatography–mass spectrometry. J. Chromatogr. A, **2001**, *925*, 241.
3. Hooijschuur, E.W.J.; Kientz, C.E.; Brinkman, U.A.Th. Chromatography and mass spectrometry of chemical warfare agents, toxins and related compounds: state of the art and future prospects. J. Chromatogr. A, **1998**, *814*, 1–23.
4. D'Agostino, P.A.; Chenier, C.L. *Analysis of Chemical Warfare Agents: General Overview*, LC–MS Review, In – House LC–ESI–MS Methods and Open Literature

Bibliography, Technical Report; DRDC Suffield TR: Canada, 2006; 1–86.

5. Nyiredy, Sz., Ed.; *Planar Chromatography*; Springer Scientific Publisher: Budapest, 2001.
6. Mendoza, C.E. Thin layer chromatography and enzyme analytical techniques. J. Chromatogr. **1973**, *78*, 29.
7. Akerman, W.P. Thin layer chromatography and detection of organophosphorus. J. Chromatogr. **1973**, *78*, 39.
8. Stachlewska-Wróblowa, A. Separation and identification of a group of toxic substances by-thin layer chromatography. Biul. WAT, **1984**, 385–387, 45.
9. Popiel, S.; Witkiewicz, Z.; Kapała, A.; Kwaśny, M. Thin-layer chromatography and enzymatic analysis of phosphor-organic compounds using 4-methylumbelliferone esters. Chem. Anal. **1998**, *43*, 733–742.
10. Mazurek, M.; Witkiewicz, Z. The analysis of organophosphorus warfare agents in the presence of pesticides by overpressured thin layer chromatography. J. Planar Chromatogr., **1991**, *4*, 379–384.
11. Mazurek, M.; Witkiewicz, Z. Chem. Anal. **1995**, *40*, 531.
12. Mazurek, M.; Witkiewicz, Z. Visualization with thin layer chromatography of inhibitory effect on enzymes. Polish patent, Pl 162454, 1993.
13. Jacobson, K.; Patchornik, A. Visual methods for the nanomolar detection of electrophilic reagents. J. Biochem. Biophys. Methods **1983**, *8*, 213.
14. Sass, S.; Stutz, M.H. Thin-layer chromatography of some sulfur and nitrogen mustards. J. Chromatogr. **1981**, *213*, 173.
15. Munawalli, S.; Pannell, M. J. Chromatogr. **1988**, *437*, 423.
16. Report on Chemical Munitions Dumped in the Baltic Sea, Report to the 16th Meeting of the Helsinki Commission, 8–11 March 1994, HELCOM CHEMU.
17. Kaffka, A.V., Ed.; *Sea-Dumped Chemical Weapons: Aspects, Problems and Solutions*, Kluwer: Dordrecht, 1996.
18. Mazurek, M.; Witkiewicz, Z.; Śliwakowski, M. Analysis of the yiperite block fished up from the Baltic Sea. J. Planar Chromatogr. **2000**, *13*, 359.
19. Stachlewska-Wróblowa, A. Thin layer chromatography identification of arsines. Chem. Anal. **1979**, *24*, 1061.
20. Appler, B.; Christmann, K. Detection of β,β′-dichloroethyl sulphide on thin-layer chromatograms. J. Chromatogr. **1983**, *264*, 445.
21. Hamada, M.; Wintersteiger, R. Fluorescence screening of organophosphorus pesticides in water by an enzyme inhibition procedure on TLC plates. J. Planar Chromatogr. Modern TLC, **2003**, *16*, 4.
22. Futagami, K.; Narazaki, C.; Kataoka, Y.; Shuto, H.; Oishi, R. Application of high-performance thin-layer chromatography for the detection of organophosphorus insecticides in human serum after acute poisoning. J. Chromatogr. B, **1997**, *704*, 369.
23. Ogasawara, M.; Tsuruta, K.; Arao, S. Frame photometric detector for thin-layer chromatography. J. Chromatogr. A, **2002**, *973*, 151.
24. Microspot test methods and field test kit for on-site inspections of chemical agents. Patent U.S.A. 5935862, August 10, 1990.

Chemometrics

Tibor Cserháti
Esther Forgács
Institute of Chemistry, Chemical Research Center, Hungarian Academy of Sciences, Budapest, Hungary

INTRODUCTION

During the last few decades, one of the major advances in chromatography has been the development and commercialization of automated chromatographic instruments. The output of retention data per unit of time has been considerably increased, and the evaluation of large data matrices, containing large amounts of chromatographic information (i.e., retention parameters of a homologous or non-homologous series of solutes, measured on various stationary and mobile phases), is no longer possible without the application of high-speed computers and a wide variety of chemometric techniques. These methods allow the simultaneous evaluation of an almost unlimited amount of data, highly facilitating the clarification of both practical and theoretical problems. These chemometric procedures have been extensively employed in chromatography for the identification of the basic factors influencing retention and separation; for the comparison of various stationary and mobile phases; for the assessment of the relationship between molecular structure and retention behavior [quantitative structure–retention relationship, (QSRR)]; for the elucidation of correlations between retention behavior and biological activity; etc. As each chemometric procedure generally highlights only one, or only a few features of the chromatographic problem under analysis, the concurrent application of more than one technique is rather a rule than an exception.

The objectives of this entry are the enumeration, brief description, and critical evaluation of the recent results obtained in the application of various chemometric techniques in chromatography, and the comparison of the efficacy of various methods for the quantitative description of a wide variety of chromatographic processes. Fundamentals of chemometrics are discussed to an extent to facilitate the understanding of the principles at the application level.[1]

CHEMOMETRIC METHODS IN CHROMATOGRAPHY

Linear Regression Analyses

Linear and various multiple linear regression analysis techniques have been developed for the elucidation of the relationship between one dependent and one or more independent variables.[2] Because of their simplicity and excellent predictive power, they have been successfully applied in various fields of chromatography, such as gas–liquid chromatography (GLC), thin-layer chromatography (TLC), and high-performance liquid chromatography (HPLC).

Linear regression analysis with one independent variable

This simple technique can be employed in the case when the dependence of one parameter (dependent variable, Y) on another parameter (independent variable, X) has to be verified:

$$Y = a + bX \tag{1}$$

The result contains the intercept (a) values, an indicator of the amount of Y when X is equal to zero; slope (b) values measuring the change of Y at unit change of X; and the regression coefficient (r), an indicator of the extent of fit of equation to the experimental data, which serves for the determination of the significance level of the correlation and for the calculation of the variance of Y explained by X. Because of the restricted number of independent variables, the method found is only limited in applications in chromatography. It has been employed for the calculation of the dependence of the retention of one solute and the temperature of a column in GLC, and the concentration of one component in the mobile phase in TLC and HPLC. Furthermore, it can be used for the comparison of the separation characteristics of two (and no more) chromatographic systems. The log k'_o values of commercial pesticides, measured on alumina and on octadecyl-coated alumina columns, have been compared with this technique. They have been used for the calculation of the dependence of retention on the number of ethylenoxide groups of oligomeric non-ionic surfactants on a porous graphitized carbon column; for the study of the effect of salt and pH on the hydrophobicity parameters of surfactant; for the assessment of the relationship between the retention and the hydrophobic surface area of nonylphenyl ethylene oxide oligomers on a polyethylene-coated zirconia HPLC column; for the determination of congenericity of a set of 2,4-dihydroxythiobenzanilide derivatives by reversed-phase (RP) HPLC; etc.

Linear regression analysis with more than one independent variable (multiple linear regression analysis)

When the relationship between one dependent variable and more than one independent variables has to be calculated, Eq. 1 must be modified accordingly:

$$Y = a + b_1X_1 \ldots + b_iX_i \ldots + b_kX_k \quad (2)$$

In this instance, the r value is suitable only for the calculation of the variance of Y, explained by the X values; consequently, for the establishment of the significance level of the correlation, the F value has to be calculated and compared with the tabulated data. The path coefficients (normalized slope values) indicate the relative impact of the individual X values independent of their original dimensions. Because of the possibility to include more variables in the equation, the application field of multiple linear regression is more extended than that of simple linear regression analysis. Thus, it has been recently employed for the investigation of the molecular mechanism of separation, for the classification of modern stationary phases, for structure–retention relationship study in HPLC and in GLC, for the elucidation of the correlation between retention and biological activity, and for the study of the retention mechanism in adsorption and RP TLC. The method found further applications in the study of the effect of cyclodextrins and cyclodextrin derivatives on the retention characteristics of a wide variety of bioactive compounds such as steroidal drugs, in the prediction of chromatographic properties of organophosphorous insecticides, and those of polychlorinated biphenyls in GLC.

Stepwise Regression Analysis

Stepwise regression analysis can be also used when the relationship between one dependent variable and more than one independent variables has to be assessed. In the common multiple linear regression analysis, the presence of independent variables exerting no significant influence on the change of dependent variable considerably decreases the significance level of the equation. Stepwise regression analysis automatically eliminates from the selected equation the dependent variables having no significant impact on the dependent variable, thereby increasing the reliability of calculation. The final form of the results of stepwise regression analysis is similar to Eqs. 1 or 2, depending on the number of independent variables selected by the method. Because of its versatility and simplicity, the method has been frequently used in chromatography. It has found application in the study of the retention behavior of ethylene oxide surfactants and dansylated amino acids in adsorption and RP TLC, in the elucidation of the relative impact of various molecular parameters on the retention in adsorption and RP HPLC and GLC, in the determination of the molecular parameters significantly influencing the interaction of antibiotics with sodium dodecyl sulfate measured by TLC, in the evaluation of the stability of pigments of paprika (*Capsicum annuum*) measured by HPLC, and in the determination of the relative impact of HPLC conditions on the retention behavior.

Partial Least Squares (PLS) Regression

When the independent variables are highly interrelated, the application of traditional methods for the calculation of linear regressions may cause biased and unreliable results. PLS has been developed for the prevention of errors originating from such intercorrelations. PLS has not been frequently employed in the analysis of chromatographic retention data; it has been only used in GLC for the study of the retention behavior of oxo compounds, in HPLC for the QSRR of chalcones, and in RP HPLC for the QSRR study of antimicrobial hydrazides.

Free–Wilson and Fujita–Ban Analysis

These special cases of multiple linear regression analysis have been developed for the determination of the impact of individual molecular substructures (independent variables) on one dependent variable. Both techniques are similar; yet, the Free–Wilson method considers the retention of the unsubstituted analyte as base, while Fujita–Ban analysis uses the less substituted molecule as reference. These procedures have not been frequently employed in chromatography; only their application in QSRR studies in RP TLC and HPLC have been reported.

Canonical Correlation Analysis (CCA)

CCA can be considered as a special case of multiple linear regression analysis, when the relationship between minimally more than one dependent variable (matrix I) and minimally more than one independent variable (matrix II) has to be elucidated. CCA acalculates the relationships between matrices I and II by extracting theoretical factors which explain the maximum of variance of the matrix with the lower number of variables. However, it can be employed only in the instances when the number of dependent variables is lower than that of independent variables. The maximal number of equations selected by CCA is equal to the number of columns in the smaller set of data. The results consist of the standard and weighted canonical coefficients (they are similar to the b values and path coefficients of Eq. 2), of the r values related to the ratio of variance explained by the equations, and of the X (Greek Chi) value, indicating the fitness of equation to the experimental data. Despite its evident benefits, the technique has not been frequently employed for the analysis of chromatographic data. It has been applied for the elucidation of the relationship between the retention parameters of ring-substituted aniline derivatives determined on

various HPLC columns (smaller matrix) and their calculated physicochemical parameters (larger matrix), for the study of the relationship between the physicochemical parameters of steroidal drugs and their retention characteristics in HPLC, and for the assessment of the correlation between the physicochemical parameters of tetrazolium salts and their retention behavior in various TLC systems.

Multivariate Mathematical–Statistical Methods

The prerequisite of the application of the regression analytical methods discussed above is that one or more chromatographic parameters have to be considered as being the dependent variables. However, when the simultaneous relationships among more retention parameters, or more retention parameters and more physicochemical parameters of a given set of analytes have to be elucidated, the linear regression methods cannot be employed. A considerable number of multivariate methods have been developed to overcome the disadvantages of regression analyses.[3] Various multivariate mathematical–statistical methods have been successfully employed for the elucidation of the relationship between the retention parameters and the structural descriptors of solutes for the comparison of more than two stationary phases, for the prediction of solute retention, for the assessment of the correlation between retention characteristics and biological activity, etc. As the information content of the mathematical–statistical methods considerably depends on the mode of calculation, the character of the problem to be elucidated limits, to some extent, the choice of the method.

Principal Component Analysis (PCA)

PCA can be used when the inherent relationships between the columns and rows of a data matrix have to be determined without one (stepwise regression analysis) or more (CCA) being the selected dependent variables. PCA is a versatile and easy-to-use multivariate mathemathical–statistical method. It has been developed to contribute to the extraction of maximal information from large data matrices containing numerous columns and rows. PCA makes possible the elucidation of the relationship between the columns and rows of any data matrix without being one the dependent variable. PCA is a so-called projection method representing the original data in smaller dimensions. It calculates the correlations between the columns of the data matrix and classifies the variables according to the coefficients of correlation. The results of PCA generally contain the so-called eigenvalues which are related to the relative importance of the principal components calculated by PCA, the variance explained by the individual PCs, and the contributions (impacts) of the columns and rows of the original matrix to the principal component loadings and variables, respectively. Unfortunately, PCA does not define the principal components as concrete physical or physicochemical entities; it only indicates its mathematical possibility. Calculating linear regression between the principal component loadings and the chromatographic parameters and physicochemical characteristics may help the determination of the concrete constitution of principal components. Stepwise regression analysis is especially adequate to carry out such types of calculations.

Because of its simplicity, PCA has been frequently used in many fields of up-to-date chromatographic research. Thus, PCA has been employed for the evaluation of molecular lipophilicity, for QSRR studies, for the testing of the authenticity of edible oils, for the determination of the botanical origin of cinnamon, for the differentiation of Spanish white wines, for the characterization of RP supports, for the assessment of the relationship between molecular structure and retention behavior, etc. The method has found further applications in the classification of chili powders according to the distribution of pigments separated by TLC, in the determination of the molecular parameters of peptides and barbituric acid derivatives showing a significant impact on their retention on porous graphitized carbon column, in QSRR study of pesticide retention on polyethylene-coated silica column, in the study of the retention characteristics of titanium dioxide and polyethylene-coated titanium dioxide stationary phases, in the comparison of alumina stationary phases in TLC and HPLC, in the elucidation of the relationship between the retention of environmental pollutants on an alumina HPLC column and their physicochemical parameters, and in the study of the energy of interaction between commercial pesticides and a non-ionic surfactant by GLC.

Spectral Mapping (SPM) Technique

The calculation methods discussed above classify the chromatographic systems (stationary and mobile phases) or solute molecules while simultaneously taking into consideration the retention strength and retention selectivity; thus, it cannot be applied when the separation of the strength and selectivity of the effect is required. SPM, another multivariate mathematical–statistical method, overcomes this difficulty.[4]

The SPM divides the information into two matrices using the logarithm of the data in the original matrix. The first one is a vector containing so-called potency values proportional to the overall effect; that is, it is a quantitative measure of the effect. The second matrix (selectivity map) contains the information related to the spectrum of activity, i.e., the qualitative characteristics of the effect. SPM first calculates the logarithm of the members of the original data matrix, facilitating the evaluation of the final plots in terms of log ratios. Subsequently, SPM subtracts the corresponding column-mean and row-mean from each logarithmic element of the matrix calculating potency values. The source of variation remaining in the centered data set can be evaluated graphically (selectivity map). This elegant and versatile calculation method has been used in chromatography for

the characterization of stationary phases in TLC and HPLC, for the separation of the solvent strength and selectivity on a cyclodextrin-coated HPLC column using monoamine oxidase inhibitory drugs as solutes, for the investigation of the complex interaction between anticancer drugs and cyclodextrin derivatives, for the determination of the influence of storage conditions on pigments analyzed by HPLC, for the comparison of polymer-coated HPLC columns, and for the optimization of the microwave-assisted extraction of pigments for HPLC analysis.

Cluster Analysis (CA) and Non-linear Mapping (NLM) Technique

Although both the PCA and the SPM techniques reduce the number of variables, the resulting matrices of PC loadings and variables and the spectral map are still multidimensional. The plot of PC loadings in the first vs. the second principal component has been frequently used for the evaluation of the similarities and differences among the observations. This method takes into consideration only the variance explained in the first two principal components and entirely ignores the impact of variances explained by the other principal components on the distribution of the matrix elements. The use of this approximation is only justified when the first two principal components explain the overwhelming majority of variance, which is not probable in the case of large original data matrices. As the evaluation of the distribution of data points in the multidimensional space is extremely difficult, calculation methods were developed for the reduction of the dimensionality of the matrices to one (CA) or to two (NLM). These methods can also be employed for the reduction of the dimensionality of the original data matrices before any other mathematical–statistical evaluation. CA has been employed for the elucidation of the retention behavior of anti-hypoxia drugs in adsorption TLC, that of barbituric acid derivatives and anti-inflammatory drugs in HPLC, for the classification of pharmaceutical substances according to their retention data, for the prediction of retention of phoshoramidate derivatives, etc.

However, both CA and NLM take into consideration the positive and negative sign of the coefficient of correlation and carry out the calculation accordingly. Therefore, the highly but negatively correlated points are far away on the maps and on the cluster dendograms in the same manner as the points that are not correlated. This procedure leads to correct assumptions in the case when the scientist is interested only in the positive correlations among variables and observations. To evaluate precisely the relationships between the points without taking into consideration the positive or negative character of the correlation, it is advisable to carry out the calculations with the absolute values of PC loadings and variables. The validity of this experimental approximation has been proven in the evaluation of the interaction of non-steroidal anti-inflammatory drugs with a model protein studied by HPLC, and the parallel application of the original PC loadings and their absolute values in the data reduction techniques has been proposed. This procedure has been successfully used for the study of the effect of carboxymethyl-β-cyclodextrin on the hydrophobicity parameters of steroidal drugs measured by TLC, and for the assessment of the binding characteristics of environmental pollutants to the wheat protein, gliadin, investigated by HPLC.

The distances between the elements on the cluster dendograms and NL maps are a quantitative measure of similarity: Smaller distances indicate greater similarity. However, the fact that the differences among the elements are significant or not cannot be established on the traditional NL map or on the cluster dendogram. A graphical approximation has been developed for the inclusion of standard deviation in the NL maps and cluster dendograms. The data matrix for PCA has been composed from the main values of the matrix elements, the mean values minus twice their standard deviation, and the mean values plus twice their standard deviation. PCA has been carried out, and the cluster dendograms and NL maps have been calculated. A circle can be formed from the mean values and the mean value $\pm$ two standard deviations on the NL map, the center of the circle being the mean, and the radius of the circle being represented by the mean $\pm$ two standard deviations. It was assumed that the differences between the elements on the map are significant at the 95% significance level when the circles do not overlap. It was further assumed that the mean value and mean value $\pm$ two standard deviations of the matrix elements are close to each other (form a triad) on the cluster dendogram when they significantly differ from the others. The method has been employed for the classification of paprika (*C. annuum*) powders according to their pigment composition as determined by HPLC and for the comparison of HPLC and TLC systems.

Miscellaneous Multivariate Methods

The chemometric methods discussed above have found widespread applications in chromatography, and many theoretical and practical chromatographers have become familiar with these techniques and have applied them successfully. However, other less well-known methods have also found applicability in the analysis of chromatographic retention data. Thus, canonical variate analysis has been applied in pyrolysis GC/MS,[5] artificial neural network for the prediction of GLC retention indices, and factor analysis for the study of the retention behavior of *N*-benzylideneaniline derivatives.[6]

CONCLUSIONS

The examples enumerated above prove conclusively that chemometric techniques can be effectively employed for the elucidation of a large number of problems in

chromatography, connected with the accurate and precise evaluation of large data matrices.

These methods allow not only the classification and clustering of any set of chromatographic systems but also exact determination of the relationship between the characteristics (physicochemical parameters or molecular substructures) of solutes and their retention behavior. It can be further concluded that chemometry considerably promotes a more profound understanding of the basic processes underlying chromatographic separations, increasing, in this manner, the efficiency (reliability, rapidity, etc.) of the methods.

REFERENCES

1. Cserháti, T.; Forgács, E. Use of multivariate mathematical statistical methods for the evaluation of retention data matrices. In *Advances in Chromatography*; Brown, P.R., Grushka, E., Eds.; Marcel Dekker, Inc.: New York, 1996; Vol. 36, 1–63.
2. Mager, H. *Moderne Regressions analyse*; Salle, Sauerlander: Frankfurt am Main, Germany, 1982.
3. Mardia, K.V.; Kent, J.T.; Bibby, J.M. Multivariate Analysis; Academic Press: London, 1979.
4. Levi, P.J. Spectral map analysis. Factorial analysis of contrast, especially from log ratios. Chemometr. Intell. Lab. Syst. **1989**, *5*, 105–116.
5. Kochanowski, B.K.; Morgan, S.L. Forensic discrimination of automotive paint samples using pyrolysis–gas chromatography–mass spectrometry with multivariate statistics. J. Chromatogr. Sci. **2000**, *38*, 100–108.
6. Ounnar, S.; Righezza, M.; Chretien, J.R. Factor analysis in normal phase liquid chromatography of *N*-benzylideneanilides. J. Liq. Chromatogr. Relat. Technol. **1998**, *20*, 2017–2037.

BIBLIOGRAPHY

1. Acuna-Cueva, R.; Hueso-Urena, F.; Cabeza, N.A.J.; Jimenez-Pulido, S.B.; Moreno-Carretero, M.N.; Martos, J.M.M. Quantitative structure–capillary column gas chromatographic retention time relationships for natural sterols (trimethylsilyl esters) from olive oil. J. Am. Chem. Soc. **2000**, *77*, 627–630.
2. Al-Haj, M.A.; Kaliszan, R.; Nasal, A. Test analytes for studies of the molecular mechanism of chromatographic separations by quantitative structure–retention relationships. Anal. Chem. **1999**, *71*, 2976–2985.
3. Andrisano, V.; Bertucci, C.; Cavrini, V.; Recatini, M.; Cavalli, A.; Veroli, L.; Felix, G.; Wainer, I.W. Stereoselective binding of 2,3-substituted 3-hyroxypropionic acids on an immobilized human serum albumin chiral stationary phase. Stereo-chemical characterisation and quantitative structure–retention relationship study. J. Chromatogr. A, **2000**, *876*, 75–86.
4. Dillon, W.R. *Multivariate Analysis*; John Wiley and Sons: New York, 1984; 213–254.
5. Geladi, P.; Kowlski, B.R. Partial least-squares regression: A tutorial. Anal. Chim. Acta **1986**, *185*, 1–17.
6. Gozalbes, R.; de Julián-Ortiz, J.; Antón-Fos, G.M.; Galvez-Alvarez, J.; Garcia-Domenech, R. Prediction of chromatographic properties of organophosphorous insecticides by molecular connectivity. Chromatographia **2000**, *51*, 331–337.
7. Hamoir, T.; Cuaste Sanchez, F.; Bourguignon, B.; Massart, D.L. Spectral mapping analysis: A method for the characterization of stationary phases. J. Chromatogr. Sci. **1994**, *32*, 488–498.
8. Heberger, K.; Gorgenyi, M. Principal component analysis of Kovats indices for carbonyl compounds in capillary gas chromatography. J. Chromatogr. A, **1999**, *845*, 21–31.
9. Ivaniuc, O.; Ivanciuc, T.; Cabrol-Bass, D.; Balaban, A.T.; Com, D.L. Spectral mapping analysis: A method for the comparison of weighting schemes for molecular graph descriptors. Application in quantitative structure–retention relationship models for alkylphenols in gas–liquid chromatography. J. Chem. Inf. Comput. Sci. **2000**, *40*, 732–743.
10. Jozwiak, K.; Szumilo, H.; Senczyna, B.; Niewiadomy, A. RP-HPLC as a tool for determining the congenericity of a set of 2,4-dihydroxythiobenzanilide derivatives. Chromatographia **2000**, *52*, 159–161.
11. Kaliszan, R.; van Straaten, M.A.; Markuszewski, M.; Cramers, C.A.; Claessens, H.A. Molecular mechanism of retention in reversed-phase high-performance liquid chromatography and classification of modern stationary phases by using quantitative structure–retention relationships. J. Chromatogr. A, **1999**, *855*, 455–480.
12. Monatana, M.P.; Pappano, N.B.; Debattista, N.B.; Raba, J.; Luco, J.M. High-performance liquid chromatography of chalcones. Quantitative structure–activity relationship using partial least squares (PLS) modeling. Chromatographia **2000**, *51*, 727–735.
13. Sammon, J.W., Jr. A nonlinear mapping for data structure analysis. IEEE Trans. Comput. **1969**, *C18*, 401–407.

Chiral CCC

Ying Ma
Yoichiro Ito
National Heart, Lung, and Blood Institute (NHLBI), National Institutes of Health (NIH), Bethesda, Maryland, U.S.A.

INTRODUCTION

Countercurrent chromatography (CCC) can be used for the separation of a variety of enantiomers by adding a chiral selector to the liquid stationary phase.[1,2] The method is free of complications arising from the use of a solid support and also eliminates the procedure of chemically bonding the chiral selector to a solid support as in conventional chiral chromatography.

In the past, various CCC systems, such as droplet CCC, rotation locular CCC (RLCCC), and centrifugal partition chromatography (CPC), have been used for the separation of chiral compounds. None of those techniques, however, is considered satisfactory for preparative purposes in terms of sample size, resolution, and/or separation time. In the early 1980s, the high-speed CCC (HSCCC) technique improved both the partition efficiency and separation time and has been successfully applied to the separation of racemates using a Pirkle-type chiral selector. Both analytical (milligram) and preparative (gram) separations can be performed simply by adjusting the amount of chiral selector in the liquid stationary phase in the standard separation column. A large-scale separation of enantiomers can also be performed by pH-zone-refining CCC, a recently developed preparative CCC technique for the separation of ionized compounds.[3] One of the important advantages of the CCC technique over the conventional chiral chromatography is that the method allows computation of the formation constant of the chiral-selector complex, one of the most important parameters for studies of the mechanism of enantioselectivity.[4]

STANDARD HIGH-SPEED CCC TECHNIQUE IN CHIRAL SEPARATION

The separations are performed using a commercial high-speed CCC centrifuge equipped with a multilayer coil separation column(s). The column is first entirely filled with the stationary phase that contains the desired amount of chiral selector (CS). In order to prevent the contamination of CS in the eluted fractions, some amount of the CS-free stationary phase should be left at the end of the column, typically at about 10% of the total column capacity. After the sample solution is injected through the sample port, the mobile phase is pumped into the column while the column is rotated. Separation can be carried out by the successive injection of samples without renewing the stationary phase containing the chiral selector in the column.

Figure 1 shows the separation of four pairs of DNB–amino acid enantiomers by the standard CCC technique using a two phase solvent system composed of hexane–ethyl acetate–methanol–10 m*M* HCl and *N*-dodecanoyl-L-3,5-dimethylanilide as a CS which is almost entirely partitioned into the organic stationary phase ($K > 100$) due to its high hydrophobicity. All analytes are well resolved in 1–3 hr. The CS used in this separation is similar to the chiral stationary phase which has been introduced by Pirkle et al. for the high-performance liquid chromatography (HPLC) separation of racemic DNB–amino acid *t*-butylamide. A hydrophobic *N*-dodecanoyl group is connected to the CS molecule for retaining the CS in the organic stationary phase.

The effect of CS concentration in the stationary phase was investigated.[1] As the CS concentration is increased, the separation factor and peak resolution are also increased.[5] The result clearly indicates an important technical strategy: The best peak resolution is attained by saturating the CS in the stationary phase in a given column, where the resolution is further improved by using a longer and/or wider-bore coiled column, which can hold greater amounts of CS in the stationary phase.

The preparative capability of the present system is demonstrated in the separation of DNB–leucine enantiomers by varying the CS concentration in the stationary phase. The sample loading capacity is found to be determined mainly by the CS concentration or total amount of CS in the stationary phase; that is, the higher the CS concentration in the stationary phase, the greater the peak resolution and sample loading capacity. Consequently, the standard HSCCC column can be used for both analytical and preparative separations simply by adjusting the amount of CS in the stationary phase.

pH-ZONE-REFINING CCC FOR CHIRAL SEPARATION

pH-Zone-refining CCC is a powerful preparative technique that yields a succession of highly concentrated

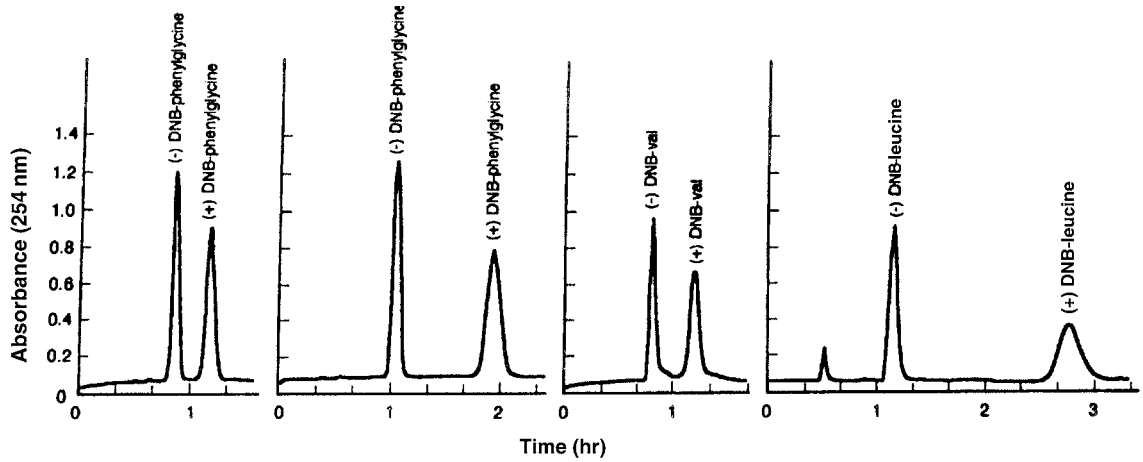

Fig. 1 Separation of four pairs of (±)-DNB–amino acids by the standard analytical HSCCC technique with a CS (*N*-dodecanoyl-L-proline-3,5-dimethylanilide) in the stationary phase.

rectangular solute peaks with minimum overlap where impurities are concentrated at the peak boundaries (see *pH-Peak-Focusing pH-Zone-Refining CCC*, p. 1808). This technique was applied to the resolution of DNB–amino acid racemates using a binary two-phase solvent system composed of methyl *t*-butyl ether–water where trifluoroacetic acid (retainer) and CS were added to the organic stationary phase and ammonia (eluter) to the aqueous mobile phase. Figure 2 shows a typical chromatogram obtained by pH-zone-refining CCC. The pH of the fraction (dotted line) revealed that the peak was evenly divided into two pH zones, each corresponding to a pure enantiomeric species with a sharp transition. Compared with the standard CCC technique, the pH-zone-refining CCC technique allows separation of large amounts in a shorter elution time.

In both techniques, leakage of the chiral selector into the elute can be completely eliminated by filling the outlet of the column with a proper amount of the CS-free stationary phase so as to absorb the chiral selector leaking into the flowing mobile phase.

ADVANTAGES

Countercurrent chromatography can be applied to the separation of enantiomers by adding a suitable chiral selector to the liquid stationary phase by analogy to binding the

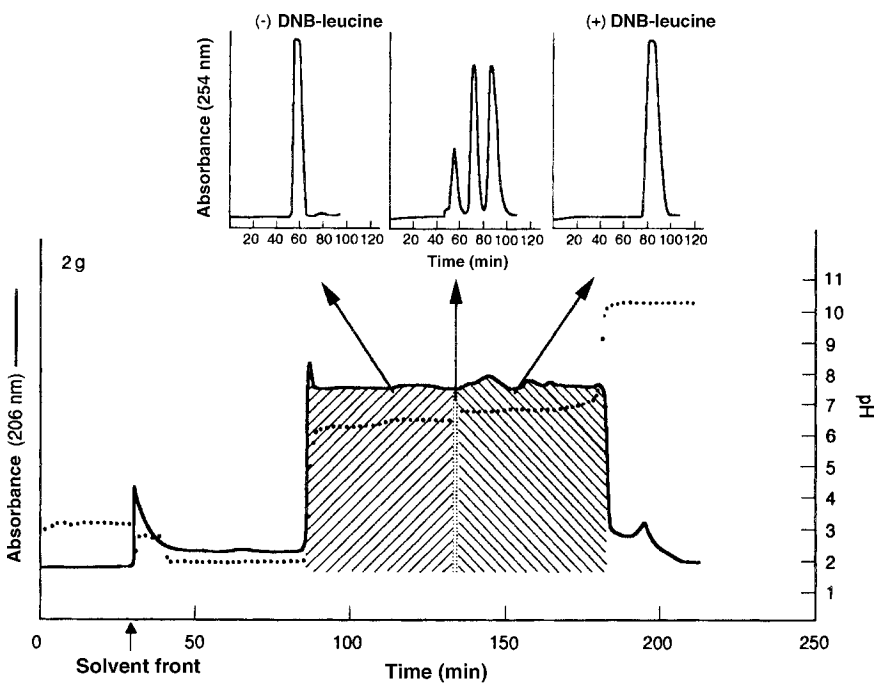

Fig. 2 pH-Zone-refining CCC separation of 2 g (±) DNB–leucine using the same HSCCC centrifuge with a CS (*N*-dodecanoyl-L-proline-3,5-dimethylanilide) in the stationary phase.

CS to the solid support in conventional chiral chromatography. The HSCCC technique has the following advantages over the conventional chromatography technique:

1. The method permits repetitive use of the same column for a variety of chiral separations by choosing appropriate CSs.
2. Both analytical and preparative separations can be performed with a standard CCC column by adjusting the amount of CS in the liquid stationary phase, and the method is cost-effective, especially for large-scale preparative separations.
3. The separation factor and peak resolution can be improved simply by increasing the concentration of CS in the stationary phase.
4. The method is very useful for the investigation of the enantioselectivity of CS including determination of the formation constant and separation factor.
5. pH-Zone-refining CCC can be applied for gram-quantity separation in a short elution time.

REFERENCES

1. Ma, Y.; Ito, Y. Chiral separation by high-speed countercurrent chromatography. Anal. Chem. **1995**, *67*, 3069.
2. Ma, Y.; Ito, Y.; Foucault, A. Resolution of gram quantities of racemates by high-speed CCC. J. Chromatogr. A, **1995**, *704*, 75.
3. Ito, Y.; Ma, Y. pH-Zone-refining countercurrent chromatography. J. Chromatogr. A, **1996**, *753*, 1.
4. Ma, Y.; Ito, Y.; Berthod, A. A chromatographic method for measuring K_f of enantiomer–chiral selector complexes. J. Liquid Chromatogr. **1999**, *22* (19), 2945.
5. Ma, Y.; Ito, Y. Affinity CCC using a ligand in the stationary phase. Anal. Chem. **1996**, *68*, 1207.

Chiral Chromatography by Subcritical and SFC

Gerald J. Terfloth
Research and Development Division, SmithKline Beecham Pharmaceuticals, King of Prussia, Pennsylvania, U.S.A.

INTRODUCTION

The intrinsic physical properties of supercritical fluids—increased diffusivity and reduced viscosity—when compared to "normal" liquid phases make sub-/supercritical fluid chromatography a very attractive technology when short cycle times are required. Chiral sub-/supercritical fluid chromatography typically is carried out using packed columns (pSFC) that frequently are identical in mechanical construction to the ones used in traditional high-performance liquid chromatography (HPLC). It should be noted, though, that capillary columns coated or packed with a chiral stationary phase (CSP) have been used for the separation of racemic mixtures. The direct separation of racemic mixtures by chromatographic means can be effected by using a CSP or chiral mobile phase additives. Both techniques have been used successfully in HPLC and pSFC. The use of chiral pSFC is not limited to analytical applications. The relative ease of solvent removal and recycling, typically carbon dioxide modified with a polar organic solvent such as methanol, makes pSFC a very attractive tool for preparative separations. Equipment for laboratory- and industrial-scale pSFC in traditional discontinuous batch-chromatography mode as well as continuous simulated moving bed (SMB) mode has been developed and is commercially available. pSFC can be used as an orthogonal method when techniques such as reversed-phase HPLC, capillary electrophoresis, or capillary electrochromatography provide insufficient or ambiguous results.

CHARACTERISTICS AND ADVANTAGES OF SUBCRITICAL AND SUPERCRITICAL FLUIDS

The advantages of using supercritical mobile phases in chromatography were recognized in the 1950s by Klesper et al.,[1] among others.[2] Carbon dioxide is the most frequently used supercritical mobile phase due to its moderate critical temperature and pressure, almost complete chemical inertness, safety, and low cost. Virtually all chiral pSFC separations published have used carbon dioxide as the primary mobile phase component. Compared to most commonly used organic solvents, it is environmentally friendly. The reduced viscosity of carbon dioxide-based mobile phases, typically one order of magnitude less than that of water (0.93 cP at 20°C), allows for efficient chromatography at higher flow rates. In addition, diffusion coefficients of compounds dissolved in supercritical mobile phases are about one order of magnitude larger than in traditional aqueous and organic mobile phases [D_M(naphthalene): 0.97×10^{-4} cm^2/sec in CO_2 at 25°C, 171 bar, 0.90 g/cm]. This directly translates to higher efficiency of the separation due to improved mass transfer.

The first chiral separation using pSFC was published by Caude and colleagues[3] in 1985. pSFC resembles HPLC. Selectivity in a chromatographic system stems from different interactions of the components of a mixture with mobile phase and stationary phase.[4] Characteristics and choice of the stationary phase are described in the "Method Development" section. In pSFC, the composition of the mobile phase, especially for chiral separations, is almost always more important than its density for controlling retention and selectivity. Chiral separations are often carried out at $T < T_c$ using liquid modified carbon dioxide. However, high linear velocity and low pressure drop typically associated with supercritical fluids are retained with near critical liquids. Adjusting pressure and temperature can control the density of the sub-/supercritical mobile phase. Binary or ternary mobile phases are commonly used.[5] Modifiers, such as alcohols, and additives, such as acids and bases, extend the polarity range available to the practitioner.

A typical pSFC instrument, at first glance, is designed like an HPLC system. The major differences are encountered at the pump, the column oven, and downstream of the column. pSFC is best carried out using pumps in a flow-control mode. A regulator mounted downstream of the column and ultraviolet (UV)/visible detector controls the pressure drop in the chromatographic system. Detection is not limited to UV. If pure carbon dioxide is used as the mobile phase, an easy-to-use, sensitive, and stable universal detector such as the FID can be employed. Other detection techniques are FTIR and evaporative light scattering detection (ELSD), or hyphenated techniques such as pSFC/MS and pSFC/NMR. Temperature control of mobile phase and column is achieved by a column oven allowing for operation under cryogenic conditions and/or from ambient temperature to 150°C. Capillary column supercritical fluid chromatography (cSFC), though, resembles gas chromatography (GC) at high pressures, with the pressure (density) programming

taking the place of temperature programming in GC. Typical operating temperatures are up to 100°C.

METHOD DEVELOPMENT

Mechanistic considerations, e.g., the extensive work published on brush-type phases, or the practitioner's experience might help to select a CSP for initial work.[6] Scouting for the best CSP/mobile phase combination can be automated by using automated solvent and column switching. More than 100 different CSPs have been reported in the literature to date. Stationary phases for chiral pSFC have been prepared from the chiral pool by modifying small molecules like amino acids or alkaloids, by the derivatization of polymers such as carbohydrates, or by bonding of macrocycles. Also, synthetic selectors such as the brush-type ("Pirkle") phases, helical poly(meth)acrylates, polysiloxanes and polysiloxane copolymers, and chiral selectors physically coated on graphite surfaces have been used as stationary phases.

Generally accepted starting conditions are summarized in Table 1. Typically, alkanol-modified carbon dioxide is used as the mobile phase. Depending on the nature of the analyte, acids or bases can be added to the modifier for controlling ionization of stationary phase and analyte. If partial selectivity is observed after the first injection, it is advisable to first adjust the modifier concentration. If the peak shape is not satisfactory, then the addition of 0.1% trifluoroacetic acid or acetic acid for acidic compounds or 0.1% diethylamine or triethylamine for basic compounds to the modifier can bring about an improvement. In case the selectivity cannot be improved by the previous measures, decreasing the operating temperature can result in the desired separation. Although many chiral separations improve as the temperature is reduced, this does not occur in all cases. The temperature dependence of the selectivity does not necessarily follow the van't Hoff equation ($\ln \alpha \propto 1/T$), as one might expect based on experience with other chromatographic techniques. Stringham and Blackwell,[7] who have reported several examples of entropically driven separations, studied the effects of temperature in detail. In the temperature range between –10, 70 (T_{iso}), and 190°C, a reversal of elution order for the enantiomers of a chlorophenylamide was observed on an (*S*,*S*) -Whelk-O 1 CSP using 10% ethanol in carbon dioxide at a pressure of 300 bar. The potential for reversing the elution order can be valuable if just one enantiomer of the CSP affecting the separation is available. If all of the above adjustments should fail, a different CSP should be investigated. Due to the low viscosity of carbon dioxide-based mobile phases, multiple columns can be coupled. This provides the opportunity to increase chemical selectivity for the analysis of complex samples by coupling an initial achiral column with a chiral column.[8] Also, the successful coupling of multiple different chiral columns has been reported.

Table 1 Initial conditions for chiral method development using modified carbon dioxide as the mobile phase.

Parameter	Unit	Value
Flow rate	ml/min	2.0
Pressure	bar	200
Temperature	°C	30
Methanol	%	5
Gradient	%/min	5
Gradient time	min	10
Injection volume	μl	5
Sample concentration	mg/ml	1
Detection	Diode array detector, 190–320 nm	

CONCLUSIONS

Analytical applications of chiral pSFC in chemical and pharmaceutical research, development, and manufacturing comprise screening of combinatorial libraries, monitoring chemical and biological transformations from the laboratory to the process scale, following stereochemical preferences of drug metabolism and pharmacokinetics, and assessing toxicology and stability of drug substance and dosage form. Preparative applications are of considerable interest because of the relative ease with which the mobile phase can be removed and recycled. This is of particular interest in the pharmaceutical environment since a small amount of the desired product can be obtained almost free of solvent quite rapidly. Recent advances in automation and separation technology now allow for a predictable scale-up of the separation from a laboratory to a production scale.

REFERENCES

1. Klesper, E.; Corwin, A.H.; Turner, D.A. High pressure gas chromatography above critical temperatures. J. Org. Chem. **1960**, *27*, 700.
2. Gere, D.R. Supercritical fluid chromatography. Science **1983**, *222*, 253–259.
3. Mourier, P.A.; Eliot, E.; Caude, M.H.; Rosset, R.H. Supercritical and subcritical fluid chromatography on a chiral stationary phase for the resolution of phosphine oxide enantiomers. Anal. Chem. **1985**, *57*, 2819–2823.
4. Ruffing, F.J.; Lux, J.A.; Schomburg, G. Chiral stationary phases for LC and SFC obtained by "polymer coating." Chromatographia **1988**, *26*, 19–28.
5. Anton, K.; Eppinger, J.; Fredriksen, L.; Francotte, E.; Berger, T.A.; Wilson, W.H. Chiral separations by packed-column super- and subcritical fluid chromatography. J. Chromatogr. **1994**, *666*, 395–401.

6. Terfloth, G. Enantioseparations in super- and subcritical fluid chromatography. J. Chromatogr. **2001**, *906*, 301–307.
7. Stringham, R.W.; Blackwell, J.A. Entropically driven chiral separations in supercritical fluid chromatography. Confirmation of isoelution temperature and reversal of elution order. Anal. Chem. **1996**, *68*, 2179–2185.
8. Phinney, K.W.; Sander, L.C.; Wise, S.A. Coupled achiral/chiral column techniques in subcritical fluid chromatography for the separation of chiral and nonchiral compounds. Anal. Chem. **1998**, *70*, 2331–2335.

BIBLIOGRAPHY

1. Anton, K.; Berger, C. *Supercritical Fluid Chromatography with Packed Columns*; Marcel Dekker, Inc.: New York, 1998.
2. Berger, T.A. *Packed Column SFC*; The Royal Society of Chemistry: Cambridge, 1995.
3. Chester, T.L.; Pinkston, J.D. Supercritical fluid and unified chromatography. Anal. Chem. **2004**, *76*, 4606–4613.
4. Chester, T.L.; Pinkston, J.D.; Raynie, D.E. Supercritical fluid chromatography and extraction. Anal. Chem. **1996**, *68*, 487–514.
5. Depta, A.; Giese, T.; Johannsen, M.; Brunner, G. Separation of stereoisomers in a simulated moving bed–supercritical fluid chromatography plant. J. Chromatogr. 1999, *865*, 175–186.
6. Gyllenhaal, O. Packed column supercritical fluid chromatography of a peroxysome proliferator-activating receptor agonist drug: Achiral and chiral purity of substance, formulation assay and its enantiomeric purity. J. Chromatogr. 2004; , *1042*, 173–180.
7. Ying, L.; Lantz, A.W.; Armstrong, D.W. High efficiency liquid and super-/subcritical fluid-based enantiomeric separations: An overview. J. Liq. Chromatogr. Relat. Technol. 2004; , *27*, 7–9.

Chiral Compounds: Separation by CE and MEKC with Cyclodextrins

Bezhan Chankvetadze
Department of Physical and Analytical Chemistry and Molecular Recognition and Separation Science Laboratory, School of Exact and Natural Sciences, Tbilisi State University, Tbilisi, Georgia

Abstract
This entry summarizes the application of cyclodextrins (CDs) for separation of enantiomers by using capillary electrophoresis (CE) [capillary electrokinetic chromatography (CEKC) and micellar electrokinetic chromatography (MEKC)]. Together with major properties of cyclodextrins as very useful chiral selectors, some mechanistic aspects of enantioseperations by using CE techniques are also emphasized.

INTRODUCTION

Cyclodextrins (CDs) and their derivatives represent a unique group of chiral selectors applicable for enantioseparations in almost all instrumental separation techniques such as gas chromatography (GC), high-performance liquid chromatography (HPLC), super/subcritical fluid chromatography (SFC), and capillary electrophoresis (CE). CDs are non-reducing, cyclic oligosaccharides produced enzymatically from starch. The most widely applied native α-, β-, and γ-CDs are constructed from six, seven, and eight glucose units bonded through 1, 4-α linkages, respectively. The inner cavity of the CDs, which is lined with hydrogen atoms and glycoside oxygen bridges is hydrophobic, which favors hydrophobic interactions between a guest and the CD host in aqueous medium. The outer CD rims are formed by the secondary 2- and 3- and the primary 6-hydroxyl groups. The location of the polar hydroxyl groups on the outer rim determines the solubility of the CDs in aqueous solutions as well as hydrogen bonding, and other polar interactions preferably in non-aqueous medium. The intramolecular hydrogen bonding between the secondary C(2) and C(3) hydroxyl groups of adjacent D-glucopyranosyl residues stabilizes the structure of the CD macrocycle.

DISCUSSION

The ability of CDs to form intermolecular complexes with other molecules was already known in the early twentieth century. These complexes are mostly of inclusion type but might also be of "external" type. Another important property of CDs is that each glucose molecule in this macrocycle contains five chiral carbon atoms, which results in a chiral recognition ability in complex formation. This property of CDs was first evidenced by Cramer in 1952.[1] Relatively easy availability from regenerable natural sources, existence in various sizes, stable structure, localized hydrophobic and hydrophilic areas, solubility in the hydrophilic solvents, ability of intermolecular complex formation, and chiral recognition ability together with their non-toxicity, transparency for UV-light, and feasibility of their modification contributed greatly to the establishment of CDs as major chiral selectors in CE and CD-modified micellar electrokinectic chromatography (CD–MEKC) separation of enantiomers.

The first applications of CDs as chiral selectors in CE were reported in capillary isotachophoresis (CITP)[2] and capillary gel electrophoresis (CGE).[3] Soon after, Fanali described the application of CDs as chiral selectors in the so-called free-solution CE[4] and Terabe used the charged CD for enantioseparations in the capillary electrokinetic chromatography (CEKC) method.[5] It seems important to note that although the experiments in CITP, CGE, CE, and CEKC are different from one another, the enantiomers in all of these techniques are mainly resolved based on the same (chromatographic) principle, i.e., a stereoselective distribution of enantiomers between two (pseudo)phases with different mobilities. Thus, enantioseparations in CE are commonly based on an electrophoretic migration principle and on a chromatographic separation principle.[6] Exceptions from this mechanism are also possible as is shown below.[6,7]

Separation of enantiomers in CE significantly differs from true electrophoretic separations that are based on the difference in charge-to-mass (size) ratio between the analyte molecules. These peculiarities need to be considered when looking at the differences between enantioseparations with uncharged and charged chiral selectors

respectively, and between enantiomer separations in capillary zone electrophoresis (CZE) and MEKC, for the evaluation of the role of the electro-osmotic flow (EOF) in enantiomer separations in CE, and so forth.

The separation of enantiomers in CE means that they reach a detection window at different periods of time after their simultaneous injection at the capillary inlet. Thus, to be separated by CE, the enantiomers must migrate with different velocities along the longitudinal axis of a separation capillary. For species possessing different charge-to-mass (size) ratios, this occurs automatically after a voltage is applied between the ends of the separation capillary. However, enantiomers do not differ from each other in terms of their effective charge-to-mass ratio in an achiral medium. Therefore, in order to achieve enantioseparations, the addition of chiral substances—the so-called chiral selectors—to the background electrolyte (BGE) is required. If a chiral selector interacts stereoselectively with enantiomers of an analyte, this secondary equilibrium can generate a velocity or mobility difference between the enantiomers of a chiral analyte ($\Delta\mu$) that can be calculated using the following equation:[8]

$$\Delta\mu = \mu_R - \mu_S = \frac{\mu_f + \mu_{cR}K_R[C]}{1 + K_R[C]} - \frac{\mu_f + \mu_{cS}K_S[C]}{1 + K_S[C]} \quad (1)$$

where μ_R and μ_S are the observed mobilities of R and S enantiomers, respectively, μ_f is the mobility of the analyte enantiomers in the non-complexed form, K_R and K_S are the complexation equilibrium constants of the R and S enantiomers with the chiral selector, μ_{cR} and μ_{cS} are the mobilities of the respective temporary diastereomeric complexes between the chiral selector and the R and S enantiomers, respectively, and [C] is the concentration of the chiral selector. As mentioned above, the mobilities of the free enantiomers in an achiral medium are equal. For many years it was assumed that the mobilities of the temporary diastereomeric associates also do not differ significantly ($\mu_{cR} = \mu_{cS}$), while the association constants of R and S enantiomers with the chiral selector may be different ($K_R \neq K_S$).

This enabled the simplification of Eq. 1 to the following equation:[8,9]

$$\Delta\mu = \frac{(\mu_f - \mu_c)(K_S - K_R)[C]}{1 + (K_R + K_S)[C] + K_R K_S[C]^2} \quad (2)$$

This simplified equation was widely used in enantiomer separations in CE and favored the establishment of the idea that no enantioseparation is possible in CE without a difference between the association constants of the two enantiomers with the chiral selector. In addition, Eq. 2 was also used to calculate the concentration of the chiral selector that will induce the maximal mobility difference between the enantiomers.[10,11]

Contrary to above-mentioned assumption, a few earlier studies indicated that the mobilities of the diastereomeric associates of two enantiomers with the chiral selector are not always equal to each other.[12,13] In 1997, a theoretical assumption was made that two enantiomers can be resolved in CE even when their association constants with the chiral selector are equal to each other ($K_R = K_S = K$).[6] The prerequisite for enantiomer separation in this particular case is the non-zero difference between the mobilities of temporary diastereomeric associates ($\mu_{cR} \neq \mu_{cS}$). Under these conditions Eq. 1 transforms to Eq. 3.[7,14]

$$\Delta\mu = \frac{K[C](\mu_{cR} - \mu_{cS})}{1 + K[C]} \quad (3)$$

The theoretical possibility of enantiomer separation even in the case of equal affinity of the enantiomers to a chiral selector is a conceptual difference between chromatographic techniques and CE.[6,7,14,15]

As shown in Eq. 2, in separations based on the difference between the affinities of the enantiomers to the chiral selector ($K_R \neq K_S$), the other necessary requirement for enantioseparation is a mobility difference between the free and the complexed analyte ($\mu_f - \mu_c \neq 0$). Otherwise, it will be impossible to generate a chiral separation based on chiral recognition. This prerequisite is not met when neutral analytes are analyzed with uncharged chiral selectors. Therefore, enantiomers of neutral chiral analytes cannot be resolved with uncharged chiral selectors in CE. However, in this particular case, an additional charged component can be added to the BGE which can assist in generating a difference between the mobilities of the analyte in its free and complexed forms. This is achieved by an achiral micellar phase in CD-modified micellar electrokinetic chromatography.[16] However, a charged CD[17] or a charged chiral micellar phase can combine both of the above-mentioned functions (chiral recognition and the mobility difference between free and complexed analyte) of a neutral CD and a micellar phase.

Depending on the experimental conditions, the EOF may contribute significantly to the mobility of analytes in CE. The EOF is considered to be a non-selective mobility and this is true but only for those separations that are based on the mobility difference of diastereomeric associates (described by Eq. 3). However, for enantioseparations based on different affinities of the enantiomers to the chiral selector, both the EOF and the electrophoretic mobility of the analyte are inherently non-enantioselective. The enantioselective analyte–selector interactions may turn both of

these mobilities into a selective transport mechanism with equal success. This is the principal difference between the roles of the EOF in true electrophoretic separations and in chiral CE separations.

The principal mechanism for separation of enantiomers in CE is enantioselective selector–analyte interactions. The enantioselectivity might be reflected in the binding constants, in the mobilities of diastereomeric associates, or in both simultaneously.

One of the important technical advantages of CE as compared to other instrumental enantioseparation techniques, apart from its extremely high peak efficiency, miniaturized size, low costs, and less environmental problems, is its high flexibility. Separation in different modes can be performed using the same instrumental setup, and it takes just a few minutes to change from one chiral selector to another, to combine two or more chiral selectors, or to vary the concentration of a chiral selector. These variations are impossible or very time-consuming in chromatographic techniques.

The number of variables available for adjustment of separations is higher in CE compared with chromatographic techniques, and these include the type and concentration of the chiral selector, pH of the BGE, concentration and type of the buffer, achiral buffer additives, capillary dimensions and nature of its inner surface, EOF, temperature, and so forth.

Owing to high theoretical plate numbers, CE makes it possible to observe even very weak (enantio) selective effects in intermolecular interactions that are not detectable using other techniques. This important advantage of CE is not yet effectively exploited for studies of noncovalent intermolecular interactions.

CDs are commercially available in various sizes (α, β, γ), carrying different functionalities, with different substitution pattern, different electric charge, and so forth. At present, β-CD and its neutral and ionic derivatives are considered to be the most suitable chiral selectors in CE. However, α- and γ-CD sometimes offer complementary chiral recognition ability to that of β-CD.[7,9,19] Among the native CDs, β-CD is characterized with the lowest solubility in aqueous solutions. Therefore, the neutral derivatives carrying alkyl and hydroxyalkyl substituents that possess a higher solubility in aqueous buffers and sometimes offer complementary chiral recognition properties are widely used as chiral selectors in CE. Among the neutral CD derivatives, single-component heptakis-(2,6-di-*O*-methyl)-β-CD, heptakis-(2,3-diacetyl)-β-CD, and heptakis-(2,3-6-tri-*O*-methyl)-β-CD generate special interest. Many

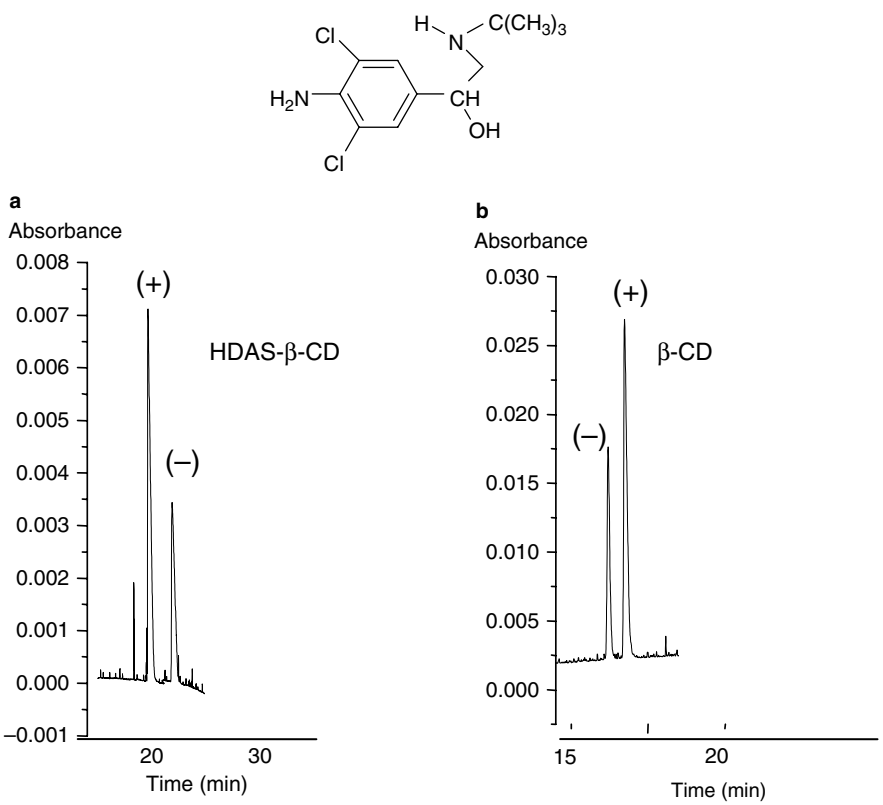

Fig. 1 Separation of enantiomers of clenbuterol (a) with heptakis-(2,3-di-*O*-acetyl)-β-CD and (b) with native β-CD.

Table 1 Enantiomer affinity pattern of selected chiral analytes to native and selectively methylated CDs.

	Chiral selector and the first-migrating enantiomer		
Analyte	**β-CD**	**DM-β-CD**	**TM-β-CD**
Aminoglutethimide	S	S	R
Brompheniramine	(−)	No separation	(+)
Chlorpheniramine	(−)	(+)	(+)
Dimethindene	S	R	R
Ephedrine	(+)	(−)	(−)
Ketoprofen	R	No separation	(S)
Metaraminol	(+)	(−)	(+)
Tetramisole	R	R	S
Verapamil	(−)	(−)	(+)

chiral compounds exhibit the opposite affinity pattern toward the last two derivatives as compared with native β-CD (Fig. 1 and Table 1). This is of practical importance when the adjustment of enantiomer migration order is desired based on the analytical challenge.[9] In addition, the elucidation of the molecular mechanisms of this phenomenon can markedly contribute to a better understanding of the nature of forces determining the binding of the chiral analytes to CDs and their enantioselective recognition.

Ionic derivatives of CDs represent another group of effective chiral selectors in CE.[6,9,17] They offer the following advantages for enantioseparations: 1) enhanced solubility in aqueous buffers; 2) self-electrophoretic mobility enabling their application also for enantioseparation of neutral analytes; 3) presence of additional functional groups for alternative and more intense intermolecular interactions; 4) their use as chiral carriers; 5) higher separation power toward enantiomers of chiral analytes carrying the opposite electric charge, which is not only due to more tight electrostatic interaction but also due to the countercurrent mobility of an analyte and a selector; 6) easier online coupling of chiral CE with mass spectrometry (MS); and so forth.

Charged CD derivatives are commercially available with cationic and anionic groups. Among cationic CDs, randomly substituted 2-hydroxypropylammonium salt of β-CD and 6-monoamino-6-monodeoxy-β-CD have been intensively studied as chiral selectors in CE.[9] Cationic CD derivatives tend to be adsorbed to the negatively charged inner surface of a fused-silica capillary and reverse the direction of EOF from the cathode to the anode. Therefore, these derivatives need to be used with capillaries having neutral or positive inner-wall coatings. The number of randomly substituted and well-characterized single-component cationic CD derivatives has increased in the last few years. Despite this, anionic derivatives of CDs are still more widely used as charged chiral selectors in CE.

Among the anionic CDs, randomly substituted carboxyalkyl, sulfoalkyl, and sulfate derivatives became commercially available earlier and played an important role in the development of chiral CE.[6,9,18] However, all randomly substituted uncharged and charged derivatives of CDs suffer from the disadvantages of being a multicomponent mixture. The individual components of these mixtures may exhibit different enantiomer-resolving properties. In rare cases, even the opposite migration order of the enantiomers has been reported depending on the degree of substitution of the charged CDs. Thus, it is extremely difficult to optimize and validate a chiral CE separation using randomly substituted derivatives of CDs. Therefore, after the introduction of various single-component sulfated CD derivatives by Vigh's group[17] these became the predominantly used anionic chiral selectors in CE.[19] These derivatives are of significance not only for the development of reproducible, validated methods in chiral CE, but also for mechanistic studies.[19]

Another important advantage of charged CD derivatives is their use as chiral carriers.[5,6,9,7,20] This enables one to mobilize a neutral analyte even in the absence of EOF and a charged analyte in the opposite direction to its electrophoretic mobility, and to suppress the mobility of an analyte in the uncomplexed form. The last offers an important advantage for the improvement of the separation factor.

Two unique advantages of chiral CE using the selector in a double function, first for the separation of enantiomers and in addition for transport of the resolved enantiomers, are illustrated in Fig. 2. The chiral compounds are the well-known former sedative drug thalidomide (TD) and its metabolites detected in the body of humans after TD administration. TD had been withdrawn from clinical practice in the 1960s due to severe toxic effects probably residing in one enantiomer, but the drug has been reapproved in 1998 as a result of its potential antileprosy, anti-HIV, anti-inflammatory, and

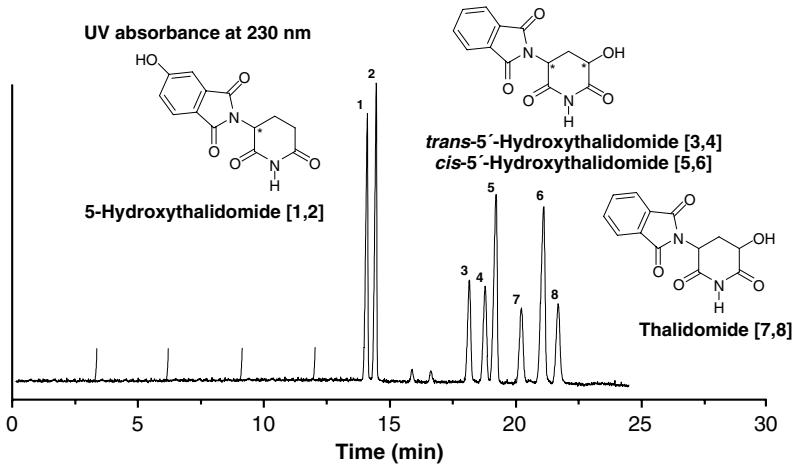

Fig. 2 Simultaneous separation and enantioseparation of thalidomide, 5-hydroxythalidomide, and 5′-hydroxythalidomide in CE using polyacrylamide-coated capillary and a mixture of 15 mg/ml sulfobutyl (4.0)-β-CD and 10 mg/ml β-CD as the chiral carrier.

antirheumatoid activity. The compounds to be separated in this particular case are uncharged and lack electrophoretic mobility. This makes separation difficult. In the separation system described in Fig. 2, the analytes are stereoselectively accelerated with one of the CDs (sulfobutyl-β-CD) and also stereoselectively but decelerated by another CD (β-CD). This, in combination with an easy variation of the CD concentration, allows one to optimize this complex separation to achieve simultaneous baseline separation and enantioseparation of all components. This example also illustrates the application of enantioselective CE separations for solving of practical biomedical problems. This seems to be one of the major application areas of chiral CE.[9]

It seems important to notice that CDs can be used for separation of enantiomers of chiral compounds by CE not only in aqueous buffers but also in non-aqueous media.[21] Contrary to the assumption that inclusion complex formation with CDs may not be favored in non-aqueous buffers, our recent studies indicate that CDs may form inclusion complexes also in non-aqueous buffers. In addition, non-inclusion type complexes of CDs are also enantioselectively formed with chiral analytes, which may lead to separation of enantiomers in CE.

CONCLUSION

CDs and their uncharged and charged derivatives are clearly established as the major chiral selectors in CE, CEKC, and MEKC (in combination with achiral surfactants). In the near future, together with the applications for solving analytical problems in chemical, agrochemical, food, environmental, and, mainly, in pharmaceutical and biomedical fields, CDs shall be used to an increasing extent for understanding the fine mechanisms of non-covalent (enantioselective) intermolecular interactions.

ACKNOWLEDGMENT

I would like to thank the Georgia National Science Foundation (GNSF) for financial support of my research in the field of microseparation techniques.

REFERENCES

1. Cramer, F. Einschluβverbindungen der Cyclodextrine. Angew. Chem. **1952**, *64*, 136.
2. Snopek, J.; Jelinek, I.; Smolkova-Keulemansova, E. Use of cyclodextrins in isotachophoresis: IV. The influence of cyclodextrins on the chiral resolution of ephedrine alkaloid enantiomers. J. Chromatogr. **1988**, *438*, 211–218.
3. Guttman, A.; Paulus, A; Cohen, A.S.; Grinberg, N.; Karger, B.L. Use of complexing agents for selective separation in high-performance capillary electrophoresis: Chiral resolution via cyclodextrins incorporated within polyacrylamide gel columns. J. Chromatogr. **1988**, *448*, 41–53.
4. Fanali, S. Separation of optical isomers by capillary zone electrophoresis based on host–guest complexation with cyclodextrins. J. Chromatogr. **1989**, *474*, 441–446.
5. Terabe, S. Electrokinetic chromatography: An interface between electrophoresis and chromatography. Trends Anal. Chem. **1989**, *8*, 129–134.
6. Chankvetadze, B. Separation selectivity in chiral capillary electrophoresis with charged selectors. J. Chromatogr. A, **1997**, *792*, 269–295.
7. Chankvetadze, B.; Blaschke, G. Enantioseparations in capillary electromigration techniques: Recent developments and future trends. J. Chromatogr. A, **2001**, *906*, 309–363.
8. Wren, A.S.; Rowe, R.C. Theoretical aspects of chiral separation in capillary electrophoresis: I. Initial evaluation of a model. J. Chromatogr. **1992**, *603*, 235–241.
9. Chankvetadze, B. *Capillary Electrophoresis in Chiral Analysis*; John Wiley & Sons: Chichester, 1997, 555.
10. Penn, S.G.; Bergstrom, E.T.; Goodall, D.M.; Loran, J.S. Capillary electrophoresis with chiral selectors: Optimization

of separation and determination of thermodynamic parameters for binding of tioconazole enantiomers to cyclodextrins. Anal. Chem. **1994**, *66*, 2866–2873.
11. Baumy, P.; Morin, P.; Dreux, M.; Viaud, M.C.; Boye, S.; Guillaumet, G.; Determination of β-cyclodextrin inclusion complex constants for 3,4-dihydro-2-*H*-1-benzopyran enantiomers by capillary electrophoresis. J. Chromatogr. A, **1995**, *707*, 311–326.
12. Schmitt, T.; Engelhardt, H. Derivatized cyclodextrins for the separation of enantiomers in capillary electrophoresis. J. High Resolut. Chromatogr. **1993**, *16*, 525–529.
13. Süβ, F.; Sänger-van de Griend, C.; Scriba, G.K.E. Migration order of dipeptide and tripeptide enantiomers in the presence of single isomer and randomly sulfated cyclodextrins as a function of pH. Electrophoresis **2003**, *24*, 1069–1076.
14. Chankvetadze, B.; Lindner, W.; Scriba, G. Enantiomer separations in capillary electrophoresis in the case of equal binding constants of the enantiomers with a chiral selector: Commentary on the feasibility of the concept. Anal. Chem. **2004**, *76*, 4256–4260.
15. Chankvetadze, B.; Enantioseparations by using capillary electrophoretic techniques: The story of 20 and a few more years. J. Chromatogr. A, **2007**, *1168*, 45–70.
16. Terabe, S.; Miyashita, Y.; Shibata, O.; Barnhart, E.R.; Alexander, L.R.; Patterson, D.G.; Karger, B.L.; Hosoya, K.; Tanaka, N. Separation of highly hydrophobic compounds by cyclodextrin-modified micellar electrokinetic chromatography. J. Chromatogr. **1990**, *516*, 23–31.
17. Vigh, Gy.; Sokolowski, A.D. Capillary electrophoretic separations of enantiomers using cyclodextrin-containing background electrolytes. Electrophoresis **1997**, *18*, 2305–2310.
18. Stalcup, A.M.; Gham, K.-H. Application of sulfated cyclodextrins to chiral separations by capillary zone electrophoresis. Anal. Chem. **1996**, *68*, 1360–1368.
19. Chankvetadze, B. Combined approach using capillary electrophoresis and NMR spectroscopy for an understanding of enantioselective recognition mechanisms by cyclodextrins. Rev. Chem. Soc. **2004**, *33*, 337–347.
20. Fillet, M.; Hubert, P.; Crommen, J. Method development strategies for the enantioseparation of drugs by capillary electrophoresis using cyclodextrins as chiral additives. Electrophoresis **1998**, *19*, 2834–2840.
21. Chankvetadze, B.; Blaschke, G. Enantioseparations using capillary electromigration techniques in non-aqueous buffers. Electrophoresis **2000**, *21*, 4159–4178.

Chiral Separations by GC

Raymond P.W. Scott
Scientific Detectors Ltd., Banbury, Oxfordshire, U.K.

INTRODUCTION

In gas chromatography (GC), chiral selectivity is controlled solely by the choice of the stationary phase and the operating temperature. Thermodynamically, it is achieved by introducing an additional entropic component to the standard free energy of distribution. This is accomplished by employing a chiral stationary phase which will have unique spatially oriented groups or atoms that allow one enantiomer to interact more closely with the molecules of the stationary phase than the other. The enantiomer that can approach more closely to the stationary phase molecules will interact more strongly (the dispersive or polar charges being nearer) and, thus, the standard enthalpy of distribution of the two enantiomers will also differ. Consequently, the Van't Hoff curves will have different slopes and intersect at a particular temperature (see *Thermodynamics of Retention in GC*, p. 2307 and *van't Hoff Curves*, p. 2406). At this temperature, the two enantiomers will coelute and, hence, temperature is an important variable that must be used to control chiral selectivity. The farther the operating temperature of the column is away from the temperature of coelution, the greater the separation ratio and the easier will be the separation (less theoretical plates, shorter column, faster analysis).

HISTORICAL BACKGROUND

The first effective chiral stationary phases for GC were the derivatized amino acids,[1] which, however, had very limited temperature stability. The first reliable GC stationary phase was introduced by Bayer and coworkers,[2] who synthesized a thermally stable, low-volatility polymer by attaching l-valine-tbutylamide to the carboxyl group of dimethylsiloxane or (2-carboxypropyl)-methylsiloxane with an amide linkage. This stationary phase was eventually made available commercially as Chirasil-Val and could be used over the temperature range of 30°C to 230°C. OV-225 (a well-established polar GC stationary phase) has also been used for the synthesis of chiral polysiloxanes, which, in this case, possess more polar characteristics than the (2-carboxypropyl)-methylsiloxane derivatives.

Although the polysiloxane phases carrying chiral peptides are still used in contemporary chiral GC, the presently popular phases are based on cyclodextrins. These materials are formed by the partial degradation of starch followed by the enzymatic coupling of the glucose units into crystalline, homogeneous, toroidal structures of different molecular sizes. The best known are the α-, β-, and γ-cyclodextrins which contain six (cyclohexamylose), seven (cycloheptamylose), and eight (cyclooctamylose) glucose units, respectively. The cyclodextrins are torus shaped macromolecules which incorporate the D(+)-glucose residues joined by α-(1-4)glycosidic linkages. The opening at the top of the torus-shaped cyclodextrin molecule has a larger circumference than that at the base. The primary hydroxyl groups are situated at the base of the torus, attached to the C_6 atoms. As they are free to rotate, they partly hinder the entrance to the base opening. The cavity size becomes larger as the number of glucose units increases. The secondary hydroxyl groups can also be derivatized to insert different interactive groups into the stationary phase. Due to the many chiral centers the cyclodextrins contain (e.g., β-cyclodextrin has 35 stereogenic centers), they exhibit high chiral selectivity and, as a consequence, are probably the most effective GC chiral stationary phases presently available.

DISCUSSION

The α-, β-, or γ-cyclodextrins that have been permethylated do not coat well onto the walls of quartz capillaries and must be dissolved in appropriate polysiloxane mixtures for stable films to be produced. In contrast, underivatized cyclodextrins can be coated directly onto the walls of the column with the usual techniques. The thermal stability of a mixed stationary phase can be improved by including some phenylpolysiloxane in the coating material. Phenylpolysiloxane also significantly inhibits any oxidation that might take place at elevated temperatures. However, unless some methylsiloxane is present the cyclodextrin may not be sufficiently soluble in the polymer matrix for successful coating.

The inherent chiral activity of the cyclodextrins can be strengthened by bonding other chirally active groups to the secondary hydroxyl groups of the cyclodextrin. Certain derivatized cyclodextrins are susceptible to degradation, on contact with water or water vapor. Consequently, all carrier gases must be completely dry and all samples that are placed on the column must also be dry.

Derivatized cyclodextrins can interact with chiral substances in a number of different ways. If, the positions 2 and 6 are alkylated (pentylated), very dispersive (hydrophobic)

centers are introduced that can strongly interact with any alkyl chains contained by the solutes. After pentylation of the 2 and 6 positions has been accomplished, the 3-position hydroxyl group can then be trifluoroacetylated. This stationary phase is widely used and it has been found that the derivatized γ-cyclodextrin is more chirally selective than the β material. It has been successfully used for the separation of both very small and very large chiral molecules. The cyclodextrin hydroxyl groups can also be made to react with pure "S" hydroxypropyl groups and then permethylated. As a result, the size selectivity of the stationary phase is reduced, but its interactive character is made more polar (hydrophilic). In general, the α or γ phases have less chiral selectivity than the β material. There are a considerable number of cyclodextrin based chiral stationary phases commercially available and, without doubt, there will be many more introduced in the future.

REFERENCES

1. Gil-Av, D.; Feibush, B.; Charles-Sigler, R. Separation of enantiomers by gas liquid chromatography with anoptically active stationary phase. Tetrahedron Lett. **1988**, 1009.
2. Frank, H.; Nicholson, G.J.; Bayer, E. Rapid gas chromatographic separation of amino acid enantiomers with a novel chiral stationary phase. J. Chromatogr. Sci. **1974**, *15* (5), 174.

BIBLIOGRAPHY

1. Beesley, T.E.; Scott, R.P.W. *Chiral Chromatography*; John Wiley & Sons: Chichester, 1998.
2. Scott, R.P.W. *Techniques of Chromatography*; Marcel Dekker, Inc.: New York, 1995.
3. Scott, R.P.W. *Introduction to Gas Chromatography*; Marcel Dekker, Inc.: New York, 1998.

Chiral Separations by HPLC

Nelu Grinberg
Richard Thompson
Analytical Research Department, Merck Research Laboratories, Rahway, New Jersey, U.S.A.

INTRODUCTION

Chirality arises in many molecules from the presence of a tetrahedral carbon with four different substituents. However, the presence of such atoms in a molecule is not a necessary condition for chirality. An object is said to be chiral if it is not superposable with its mirror image and achiral when the object and its mirror image are superposable. A chiral pair can be distinguished through their interaction with other chiral molecules to form either long-lived or transient diastereomers. Diastereomers are molecules containing two or more stereogenic (chiral) centers and having the same chemical composition and bond connectivity. They differ in stereochemistry about one or more of the chiral centers.

LONG-LIVED DIASTEREOMERS

Long-lived diastereomers are generated by chemical derivatization of the enantiomers with a chiral reagent. They may be separated subsequently by achiral means. Their formation energies have no relevance to their chromatographic separation; it is, rather, due to the difference in their solvation energies. Differences in their shape, size, or polarity will affect the energy needed to displace solvent molecules from the stationary phase.[1]

There are several characteristics of diastereomeric chiral separations (also known as indirect enantiomeric separations) that are worth mentioning. Achiral phases that are cheaper, more rugged, and widely commercially available are used. The elution order can be controlled by choice of the chirality of the derivatizing agent. This feature is useful for the analysis of trace levels of enantiomers. The separation can be designed such that the minor enantiomer is eluted first, allowing for more accurate quantitation.

Derivatization requires that the species of interest must contain a functional group that can be chemically modified. There should be no enantioselectivity of the rate of the derivatization.[2] There are several disadvantages to an indirect chromatographic chiral separation. The derivatization procedure may be complex and time-consuming and there is always a possibility of racemization during the derivatization procedure. In the case of preparative chromatography of the diastereomeric species, they have to be chemically reversed to the initial enantiomers. Fig. 1 shows the main types of derivatives formed from amines, carboxylic acids, and alcohols in reaction with chiral reagents.[3]

There are several structural considerations to achieving a diastereomeric separation. The diastereomers should possess a degree of conformational rigidity in order to maximize their physical differences. Large size differences between the groups attached to the chiral center enhance the separation in most cases. The distance between the asymmetric centers should be minimal and ideally less than three bonds. The presence of polar or polarizable groups can enhance hydrogen-bonding interactions with the stationary phase, resulting in increased resolution.

TRANSIENT DIASTEREOMERS

Objects that can distinguish between enantiomers are chiral receptors. Nature gives us plenty of examples of chiral receptors, such as enzymes and nucleic acids. There are also man-made chiral receptors such as chiral phases (CP) used in gas chromatography high-performance liquid chromatography (GC HPLC), supercritical fluid chromatography (SFC), and capillary electrophoresis (CE). The operation of a CP involves the formation of transient diastereomeric complexes between the enantiomer (selectand) and the CP (selector). They must be energetically nondegenerate in order to effect a separation. Because of their transient nature, it is usually not possible to isolate them.

There are specific criteria for the interaction between the selectand and the selector which leads to separation on a particular column:[4]

1. Strong interactions, such as p–p interactions, coordinative bonds, and hydrogen bonds between the selector and selectand
2. Close proximity of the transient bonds to the respective asymmetric carbons
3. Inhibition of free rotation of the transient bonds
4. Minimal non-contributing associative forms that do not bring the respective asymmetric centers to proximity

The diastereomeric associate between selectand and selector is formed through bonds between one or more

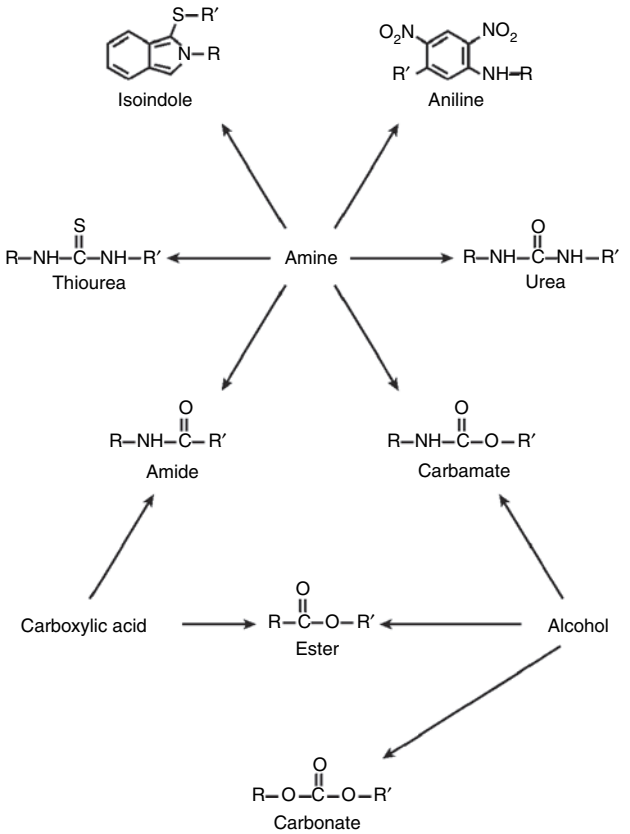

Fig. 1 Main types of derivatives formed from amines, carboxylic acids, and alcohols in reactions with chiral derivatizing reagents. **Source:** From *Chiral Liquid Chromatography.*[3]

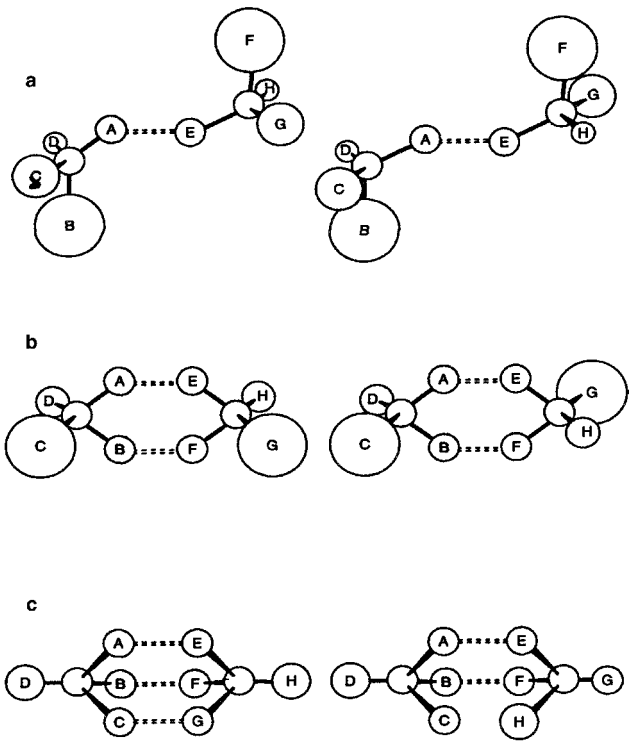

Fig. 2 Schematic representation of selectand–selector association. A dotted line represents a leading interaction between the two molecules. (a) The selectand forms a bond that involves only one substituent of its asymmetric carbon; (b) the selectand binds through two of its substituents; (c) the selectand binds through three substituents. **Source:** From Chiral separation of enantiomers via selector/selectand hydrogen bondings, in Chirality.[1]

substituents of the asymmetric carbon. These bonds are the leading selectand–selector interactions. Only when the leading bonds are formed and the asymmetric moieties of the two molecules are brought to close proximity do the secondary interactions (e.g., van der Waals, steric hindrance, dipole–dipole) become effectively involved (Fig. 2). The secondary interactions can affect the conformation and the formation energy of the diastereomeric associates. In Fig. 2a, the size, shape and polarity of the unbounded B, C, and D substituents of the selectand and their positions to the groups F, G, and H of the selector will determine the enantioselectivity of the system. One particular enantiomer of the selectands will interact more strongly with a particular selector. When the selective associate is formed through interactions A–E and B–F (Fig. 2b), enantioselectivity and elution order are determined by the effective size of unbounded groups C and D their relative positions, syn or anti, to groups G and H of the selector. In most of the cases that include hydrogen-bonding or ligand–metal complexes, the enantiomer with the larger non-bonded groups positioned syn to the selector's larger non-bonded group will elute last from the chiral column. When the selective association is formed through three leading interactions (Fig. 2c), the enantioselectivity is determined by the stereochemistry of the two enantiomers. One enantiomer in one configuration will establish three leading bonds (H bonds or a combination of H bonds and π–π interactions), whereas the other one will not.[1]

In chromatographic systems, the selectors are either added to the mobile phase [chiral mobile phases (CMP)] or are bonded to a stationary phase (e.g., silica gel) as chiral stationary phases (CSP).

CHIRAL MOBILE PHASES

In this mode of separation, active compounds that form ion pairs, metal complexes, inclusion complexes, or affinity complexes are added to the mobile phase to induce enantioselectivity to an achiral column. The addition of an active compound into the mobile phase contributes to a specific secondary chemical equilibrium with the target analyte. This affects the overall distribution of the analyte between the stationary and the mobile phases, affecting its

Table 1 Main classes of chiral additives and their applications.

Mechanism	Additive	Application	Mode of separation	Refs.
Ion pair	(+)-10-camphorsulfonic acid	Aminoalcohols, alkaloids	HPLC	[5,6]
Ion pair	Quinines	Carboxylic acids	HPLC	[7,8]
Inclusion	Dimethyl β-cyclodextrin	Aminoalcohols, carboxylic acids	CE	[9,10]
Inclusion	Crown ether	Primary amines	CE	[11]
Ligand exchange	L-Proline/Cu^{2+}	Amino acids	HPLC	[12]
Proteins	α_1-Acid glycoprotein	Hexobarbitone	CE	[13]
Antibiotics	Rifamycin	Amino acids	CE	[14]

retention and separation at the same time. The chiral mobile phase approach utilizes achiral stationary phases for the separation. Table 1 lists several common chiral additives and applications.

CHIRAL STATIONARY PHASES

Compared to CMP, the mechanism of separation on a chiral stationary phase is easier to predict, due to a much simpler system. Because the ligand is immobilized to a matrix and is not constantly pumped through the system, the detection limits for the enantiomers are much lower. Depending on the ligand immobilized to the matrix, one can have different types of interactions between the selectand and selector: metal complexes, hydrogen-bonding, inclusion, π–π interactions, and dipole interactions, as well as a combination thereof.

CHIRAL SEPARATION WHERE THE LEADING INTERACTION IS ESTABLISHED THROUGH METAL COMPLEXES (LIGAND EXCHANGE)

Chiral separation using ligand-exchange chromatography involves the reversible complexation of metal ions and chiral complexing agents. The central ion, usually Cu^{2+} or Ni^{2+} forms a bis complex with bidentates ligands. If one of the chelating ligands is anchored to a support, the CSP can form diastereomeric adsorbates with the bidentate selectand. The metal ion is held by the stationary phase through coordination to the bound ligand. If the coordination sphere of the metal is unsaturated or is occupied by weakly bound solvent molecules, it can reversibly attach different solute ligands from the mobile phase. The solute ligands are then resolved according to differences in their binding constants. Ligand exchange is possible only in systems where the interaction of the mobile ligand with the stationary phase is reversible. The coordination bonds must be kinetically labile. If the chelating ligands are amino acids and the metal is copper (II), the amine and carboxylate groups of the ligands are arranged around the metal ion in a trans configuration, forming a square planar complex. A third interaction should take place to ensure enantioselectivity. The third interaction may arise through steric hindrance or attractive or repulsive interactions between the selector and the selectand.[15,16]

CHIRAL SEPARATION WHERE THE LEADING INTERACTION IS ESTABLISHED THROUGH HYDROGEN BONDING

A hydrogen bond is formed by the interaction between the partners R–X–H and :Y–R′ according to

$$R-X-H\,1:Y-R9 \rightarrow R-X-H^{\cdots}Y-R'$$

R–X–H is the proton donor and :Y–R′ makes an electron pair available for the bridging bond. X and Y are atoms of higher electronegativity than hydrogen (e.g., C, N, P, O, S, F, Cl, Br, I). Hydrogen-bonding acceptors are the oxygen atoms in alcohols, ethers, and carbonyl compounds, as well as nitrogen atoms in amines and Nheterocycles. Hydrogen-bonding donors are hydroxy, carboxyl, and amide protons. Interactions can be modified by changing the elution conditions. The more non-polar the elution conditions, the stronger the H-bond interactions. Enantioselectivity is determined by the strength of the hydrogen bonds, which is, in turn, affected by secondary interactions such as steric hindrance or attractive or repulsive interactions between the selector and the selectand.

CHIRAL SEPARATION THROUGH CHARGE TRANSFER

Complexes formed by weak interactions of electron donors with electron-acceptor compounds are known as charge-transfer complexes. The necessary condition for the formation of a charge transfer complex is the presence of an occupied molecular orbital of sufficiently high energy in the electron-donor molecule, and the presence of a sufficiently low unoccupied orbital in the electron-acceptor molecule. Small unsaturated hydrocarbons are usually weak donors or weak acceptors. Polynuclear aromatic

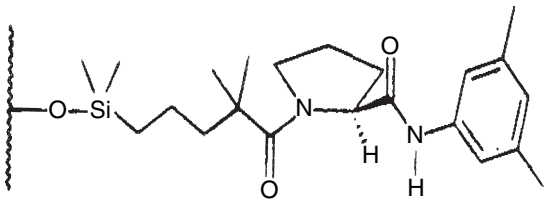

Fig. 3 The structure of the (*S*)-proline derivative chiral stationary phase.
Source: From Chiral recognition studies: Intra and intermolecular 1H{1H}-nuclear overhauser effects as effective tools in the study of bimolecular complexes, in J. Org. Chem.[18]

hydrocarbons are efficient π-donor molecules. Replacement of a hydrogen atom in the parent molecule with an electron-releasing substituent such as alkyl, alkoxy, or amino, increases the capability of the molecule to donate π-electrons. Aromatic molecules containing groups such as NO_2, Cl, C N are efficient electron acceptors. Carbonyl compounds are acceptors to aromatic hydrocarbons but are donors to bromine.

The overlapping and the orientation of the molecules in the crystal correspond to parallel planes if the bonding occurs only through π orbitals. π-donor–π-donor interactions do not occur in the same fashion because of repulsion between the π clouds. This repulsion leads to edge-to-face interactions, where weakly positive H atoms at the edge of the molecule point toward negatively charged C atoms on the faces of adjacent molecule. The dihedral ring planes are often close to perpendicular. Aromatic rings can act as hydrogenbond acceptors for the amidic proton.[17]

In general, the stability of a charge-transfer complex increases with the increase in the polarity of the solvent. To establish the enantiomeric separation under such conditions, secondary interactions must occur: namely the charge-transfer interactions have to be accompanied by hydrogen bonds and/or steric hindrance. Under these conditions, the mobile-phase conditions should be adjusted such that these interactions are achieved. Fig. 3 presents an example of a chiral stationary phase designed by Pirkle's group. This CSP allows for charge-transfer interaction with secondary interactions such as hydrogen-bonding and steric hindrance.[18]

CHIRAL SEPARATION THROUGH HOST–GUEST COMPLEXATION

Cyclodextrins and crown ethers are the main classes of compounds able to undergo host–guest complexes with a particular pair of enantiomers. Cyclodextrins (CD) are natural macrocyclic polymers of glucose that contain 6–12 D-(+)-glucopyranose units which are bound through α-1,4-glucopyranose linkages. The number of glucose

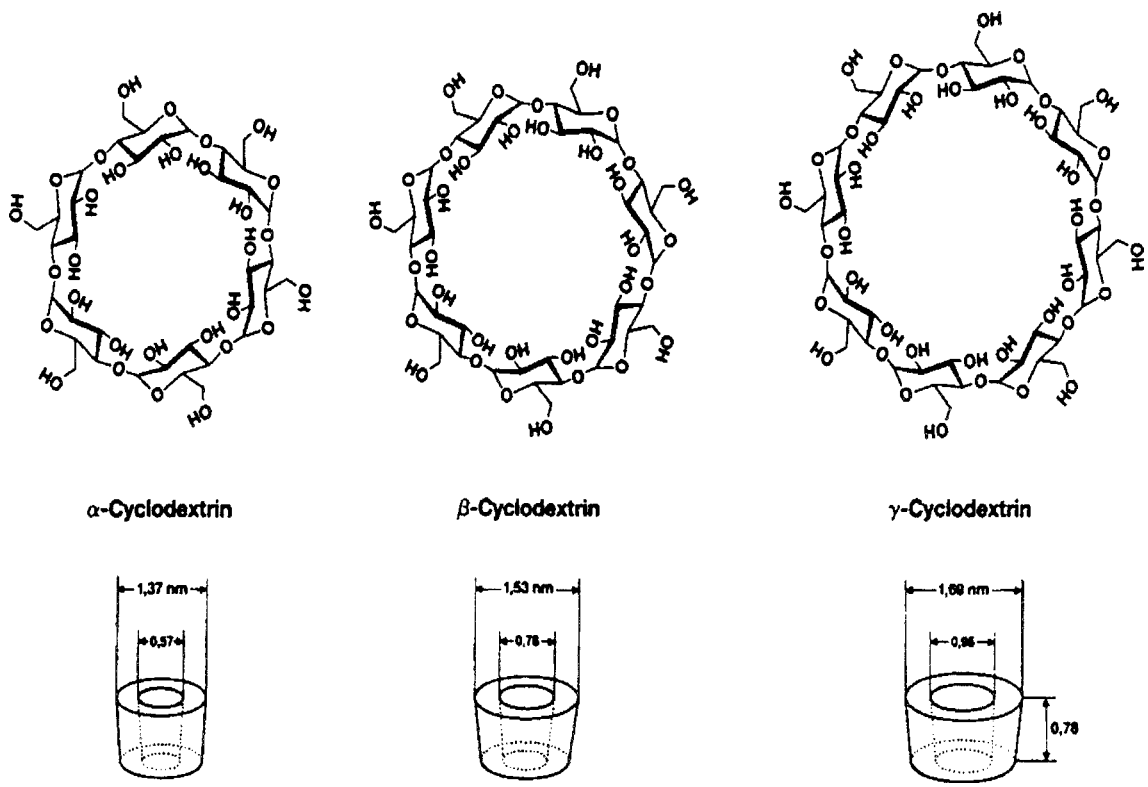

Fig. 4 Schematic representation of α-CD, β-CD, and γ-CD.
Source: From *Gas Chromatographic Enantiomer Separation with Modified Cyclodextrins.*[19]

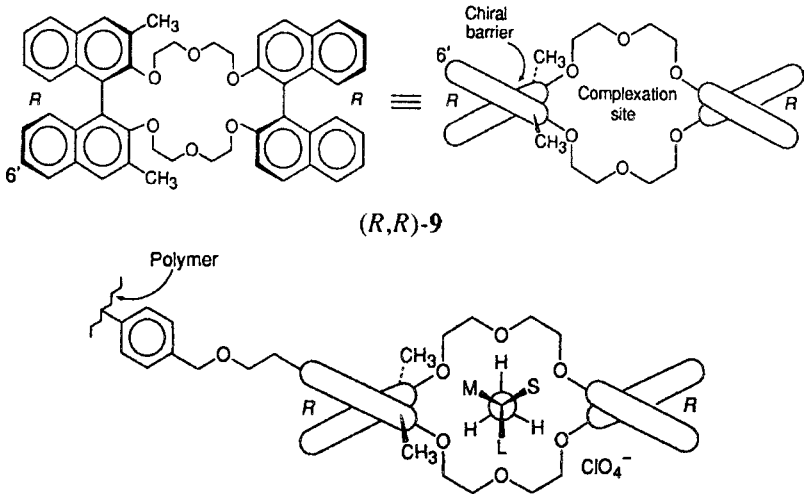

Fig. 5 Structure of the crown ether and the most stable complex.
Source: From *Container Molecules and Their Guests.*[21]

units per CD is denoted by a Greek letter: α for six, β for seven, and γ for eight (Fig. 4).[19] The inherent chirality of the CD renders them useful for chromatographic enantioseparations. In most cases, an inclusion complex is formed between the solute and the cyclodextrin cavity. The host–guest complexation is dependent on the polarity, hydrophobicity, size, and geometry of the guest, as well as the size of the internal cavity of the CD. Enantioselectivity is then determined by the fit in the cavity and by the interactions between substituents attached to or near the chiral center of the analyte and the unidirectional secondary hydroxyl groups at the mouth of the cavity. The temperature, pH, and the composition of the mobile phase influence the complexation.

Under reversed-phase conditions (RP), the presence of an organic modifier affects the binding of the guest molecule in the CD's cavity. The inclusion complex is usually strongest in water and decreases upon addition of organic modifiers. The modifier competes with the guest analyte for the cavity. Under normal-phase conditions, apolar solvents such as hexane and chloroform occupy the CD's cavity and cannot be easily displaced by the solute molecules. In these circumstances, the solute is usually restricted to interactions with the exterior of the CD. Chemical modifications of CD has opened new possibilities for enantiorecognition, widening the range of compounds that can be separated into enantiomers.[20]

Crown ethers, especially 18-crown-6 ethers, can complex not only inorganic cations but also alkylammonium compounds. The primary interactions occur between the hydrogens of the ammonium group and the oxygens of the crown ether. The introduction of bulky groups such as binaphtyl onto the exterior of the crown ether provides steric barriers and induces enantioselective interactions with the guest molecule.

The rigid binaphthyl units occupy planes that are perpendicular to the plane of the cyclic ether. One of the naphthalene rings forms a wall that extends along the sides and outward from the other face of the cyclic ether. The substituents attached at the 3-position of the naphthalene rings extend along the side or over the face of the cyclic ether. In the presence of a chiral primary amine, it forms a triple hydrogen bond with the primary ammonium cation. The same complex is formed whether the guest approaches from the top or from the bottom of the crown ether, as the crown ether has a C_2 axis of symmetry. In the complex, the large (L), medium (M), and small (S) groups attached to the asymmetric carbon of the guest must adjust themselves into two identical cavities. The L is placed in one cavity and the M and S into the other cavity. M will reside in the pocket with S against the wall for the more stable diastereomeric complex (Fig. 5).[21]

CHIRAL SEPARATION THROUGH COMBINATION OF INTERACTIONS

Included in this category are stationary phases such as biopolymers (e.g., celluloses and cellulose derivatives, proteins),[22,23] as well as macrocyclic antibiotics.[24] These stationary phases exhibit interactions with a particular enantiomer through hydrogen-bonding, charge transfer, and inclusion interactions. They proved to be very effective in resolving a wide class of racemates encompassing a variety of structures. Describing the mechanism of such separation is very challenging due to the complexity of these stationary phases. Such stationary phases can be operated under RP conditions (protein phases, cellulose phases, and macrocyclic antibiotics), as well as in the normal-phase conditions (cellulose phases and macrocyclic antibiotics). Conformational changes of biopolymers under the temperature and mobile-phase conditions can occur and they should be controlled such that the separation can be maximized.[25,26]

REFERENCES

1. Feisbush, B. Chiral separation of enantiomers via selector/selectand hydrogen bondings. Chirality **1998**, *10* (5), 382–395.
2. Lindner, W. *Chromatographic Chiral Separation*; Zieff, M., Crane, L.J., Eds.; Marcel Dekker, Inc.: New York, 1988; 91.
3. Ahnoff, M.; Einarsson, S. *Chiral Liquid Chromatography*; Lough, W.J., Ed.; Blackie and Son: Glasgow, 1989; 39.
4. Feibush, B.; Grinberg, N. *Chromatographic Chiral Separation*; Zieff, M., Crane, L.J., Eds.; Marcel Dekker, Inc.: New York, 1988; 1.
5. Pettersson, C.; Schill, G. Separation of enantiomeric amines by ion-pair chromatography. J. Chromatogr. **1981**, *204*, 179–183.
6. Pettersson, C.; Schill, G. Chiral separation of aminoalcohols by ion-pair chromatography. Chromatographia **1982**, *16*, 192.
7. Karlsson, A.; Pettersson, C. Separation of enantiomeric amines and acids using chiral ion-pair chromatography on porous graphitic carbon. Chirality **1992**, *4*, 323.
8. Pettersson, C.; No, K. Chromatographic separation of enantiomers of acids with quinine as chiral counter ion. J. Chromatogr. **1984**, *316*, 553–567.
9. Guttman, A. Novel separation scheme for capillary electrophoresis of enantiomers. Electrophoresis **1995**, *16*, 1900.
10. Guttman, A.; Cooke, N. Practical aspects in chiral separation of pharmaceuticals by capillary electrophoresis: II. Quantitative separation of naproxen enantiomers. J. Chromatogr. **1994**, *685*, 155.
11. Lin, J.-M.; Nakagama, T.; Hobo, T. Combined chiral crown ether and b-cyclodextrin for the separation of o-, m-, p-fluoro-D,L-phenylalanine by capillary gel electrophoresis. Chromatographia **1996**, *42*, 559.
12. Gil-Av, E.; Tishbee, S. Resolution of underivatized amino acids by reversed-phase chromatography. J. Am. Chem. Soc. **1980**, *102*, 5115.
13. Clar, B.; Mame, J. Resolution of chiral compounds by HPLC using mobile phase additives and a porous graphitic carbon stationary phase. J. Pharm. Biomed. Anal. **1989**, *7*, 1883.
14. Armstrong, D. Use of a macrocyclic antibiotic, rifamycin B, and indirect detection for the resolution of racemic amino alcohols by CE. Anal. Chem. **1994**, *66*, 1690.
15. Davankov, V.A. *Advances in Chromatography*; Giddings, J.C., Grushka, E., Cazes, J., Brown, P.R., Eds.; Marcel Dekker, Inc.: New York, 1980; Vol. 18, 139.
16. Davankov, V.A.; Kurganov, A.A.; Bochkov, A.S. *Advances in Chromatography*; Giddings, J.C. Grushka, E. Cazes, J., Brown, P.R., Eds.; Marcel Dekker, Inc.: New York, 1983; Vol. 22, 71.
17. Foster, R. *Organic Charge-Transfer Complexes*; Academic Press: London, 1969; 217.
18. Pirkle, W.H.; Selness, S.R. Chiral recognition studies: Intra- and intermolecular 1H{1H}-nuclear overhauser effects as effective tools in the study of bimolecular complexes. J. Org. Chem. **1995**, *60*, 3252.
19. Konig, W.L. *Gas Chromatographic Enantiomer Separation with Modified Cyclodextrins*; Hütihig Buch Verlag: Heidelberg, 1992; 4.
20. Stalcup, A.M. *A Practical Approach to Chiral Separations by Liquid Chromatography*; VCH: Weinheim, 1994; 1994.
21. Cram, D.J.; Cram, J.M. *Container Molecules and Their Guests*; Royal Society of Chemistry: London, 1994; 56.
22. Okamoto, Y.; Kaida, Y. Resolution by high-performance liquid chromatography using polysaccharide carbamates and benzoates as chiral stationary phases. J. Chromatogr. **1994**, *666*, 403.
23. Allenmark, S.G.; Anderson, S. Proteins and peptides as chiral selectors in liquid chromatography. J. Chromatogr. **1994**, *666*, 167.
24. Ekborg-Ott, K.H.; Youbang, L.; Armstrong, D.W. Highly enantioselective HPLC separations using the covalently bonded macrocyclic antibiotic, ristocetin A, chiral stationary phase. Chirality **1998**, *10*, 434.
25. Waters, M.; Sidler, D.R.; Simon, A.J.; Middaugh, C.R.; Thompson, R.; August, L.J.; Bicker, G.; Perpall, H.J.; Grinberg, N. Mechanistic aspects of chiral discrimination by surface-immobilized alpha1-acid glycoprotein. Chirality **1999**, *11* (3), 224–232.
26. O'Brien, T.; Crocker, L.; Thompson, R.; Thomson, K.; Toma, P.H.; Conlon, D.A.; Feibush, B.; Moeder, C.; Bocker, G.; Grinberg, N. Mechanistic aspects of chiral discrimination on modified cellulose. Anal. Chem. **1997**, *69*, 1999.

Chiral Separations by MEKC with Chiral Micelles

Koji Otsuka
Shigeru Terabe
Department of Material Science, Himeji Institute of Technology, Hyogo, Japan

INTRODUCTION

Since micellar electrokinetic chromatography (MEKC) was first introduced in 1984, it has become one of major separation modes in capillary electrophoresis (CE), especially owing to its applicability to the separation of neutral compounds as well as charged ones. Chiral separation is one of the major objectives of CE, as well as MEKC, and a number of successful reports on enantiomer separations by CE and MEKC has been published. In chiral separations by MEKC, the following two modes are normally employed: (a) MEKC using chiral micelles and (b) cyclodextrin (CD)-modified MEKC (CD/MEKC).

MEKC USING CHIRAL MICELLES

An ionic chiral micelle is used as a pseudo-stationary phase; it works as a chiral selector. When a pair of enantiomers is injected to the MEKC system, each enantiomer is incorporated into the chiral micelle at a certain extent determined by the micellar solubilization equilibrium. The equilibrium constant for each enantiomer is expected to be different more or less among the enantiomeric pair; that is, the degree of solubilization of each enantiomer into the chiral micelle would be different for each. Thus, the difference in the retention factor would be obtained and different migration times would occur.

CD/MEKC

An ionic achiral micelle [e.g., sodium dodecyl sulfate (SDS)] and a neutral CD are typically used as a pseudo-stationary phase and a chiral selector, respectively. When a pair of enantiomers is injected into this system, two major distribution equilibria can be considered for the solutes or enantiomers: (a) the equilibrium between the aqueous phase and the micelle (i.e., micellar solubilization) and (b) the equilibrium between the aqueous phase and CD (i.e., inclusion complex formation). Each enantiomer may have a different equilibrium constant for the inclusion complex formation among the enantiomeric pairs due to the enantioselectivity of the CD. As a result, each enantiomer exists in the aqueous phase at a different time among the enantiomeric pairs; hence, the time spent in the micelle would be varied.

In some cases, an ionic chiral micelle (e.g., a bile salt) is also used as a chiral pseudo-stationary phase with a CD. Moreover, cyclodextrin electrokinetic chromatography (CDEKC), where a CD derivative having an ionizable group is used as a chiral pseudo-stationary phase, has become popular recently since several commercially available ionic CD derivatives have appeared. Although the CDEKC technique is actually beyond the field of MEKC, it is an important method for enantiomer separation by CE.

In this section, chiral separation by MEKC with chiral micelles is mainly treated. The development of novel chiral surfactants adaptable to pseudo-stationary phases in MEKC for enantiomer separation is continuously progressing. It seems somewhat difficult for a researcher to find an appropriate mode of CE when one wants to achieve a specific enantioseparation. However, nowadays, various method development kits for chiral separation have been commercially available and some literature on the topic is also available, so that helpful information may be obtained without difficulty.

MEKC USING NATURAL CHIRAL SURFACTANTS

Bile Salts

Bile salts are natural and chiral anionic surfactants which form helical micelles of reversed micelle conformation. The first report on enantiomer separation by MEKC using bile salts was the enantioseparation of dansylated DL-amino acids (Dns-D,L-AAs) and, since then, numerous papers have been available. Nonconjugated bile salts, such as sodium cholate (SC) and sodium deoxycholate (SDC), can be used at pH > 5, whereas taurine-conjugated forms, such as sodium taurocholate (STC) and sodium taurodeoxycholate (STDC), can be used under more acidic conditions (i.e., pH > 3). Several enantiomers, such as diltiazem hydrochloride and related compounds, carboline derivatives, trimetoquinol and related compounds, binaphthyl derivatives, Dns-DL-AAs, mephenytoin and its metabolites, and 3-hydroxy-1,4-benzodiazepins have been successfully separated by MEKC with bile salts. In general, STDC is considered as the the most effective chiral selector among the bile salts used in MEKC.

The use of CDs with bile salt micelles has been also successful for enantiomer separations. For example, Dns-DL-AAs, baclofen and its analogs, mephenytoin and fenoldopam, naphthalene-2,3-dicarboxaldehyde derivatized DL-AAs (CBI-DL-AAs), diclofensine, ephedrine, nadolol, and other β-blockers, and binaphthyl-related compounds were enantioseparated by CD/MEKC with bile salts.

Digitonin and Saponins

Digitonin, which is a glycoside of digitogenin and used for the determination of cholesterol, is a naturally occurring chiral surfactant. By using digitonin with ionic micelles, such as SDS or STDC as pseudo-stationary phases, some phenylthiohydantoin-DL-AAs (PTH-DL-AAs) were enantioseparated.

On the other hand, glycyrrhizic acid (GRA) and β-escin can be employed as chiral pseudo-stationary phases in MEKC. Chiral separations of some Dns-DL-AAs and PTH-DL-AAs were achieved.

MEKC USING SYNTHETIC CHIRAL SURFACTANTS

N-Alkanoyl-L-Amino Acids

Various *N*-alkanoyl-L-amino acids, such as sodium *N*-dodecanoyl-L-valinate (SDVal), sodium *N*-dodecanoyl-L-alaninate (SDAla), sodium *N*-dodecanoyl-L-glutamate (SDGlu), *N*-dodecanoyl-L-serine (DSer), *N*-dodecanoyl-L-aspartic acid (DAsp), sodium *N*-tetradecanoyl-L-glutamate (STGlu), and sodium *N*-dodecanoyl-L-threoninate (SDThr) have been employed as synthetic chiral micelles in MEKC; several enantiomers have been successfully separated (Fig. 1). In each case, the addition of SDS, urea, and organic modifiers such as methanol or 2-propanol were essential to obtain improved peak shapes and enhanced enantioselectivity.

N-Dodecoxycarbonyl-Amino Acids

Chiral surfactants of amino acid derivatives, such as (*S*)- and (*R*)-*N*-dodecoxycarbonylvaline (DDCV) and *N*-dodecoxycarbonylproline (DDCP) are available for enantiomer separation by MEKC: Several pharmaceutical amines, benzoylated amino acid methyl ester derivatives, piperidine-2,6-dione enantiomers, and aldose enantiomers were successfully resolved. Because both enantiomeric forms of DDCV or (*S*)- and (*R*)-forms are available, we can expect that the migration order of an enantiomeric pair would be reversed.

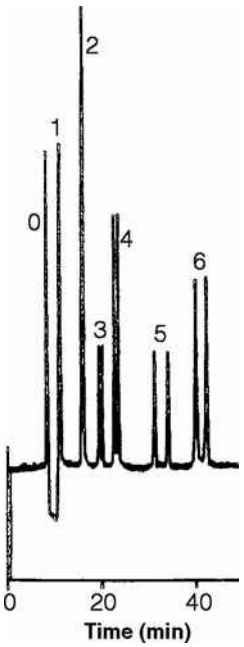

Fig. 1 Chiral separation of six PTH-DL-AAs by MEKC with SDVal. Corresponding AAs: (1) Ser, (2) Aba, (3) Nva, (4) Val, (5) Trp, (6) Nle; (0) acetonitrile. Micellar solution: 50 m*M* SDVal–30 m*M* SDS–0.5 *M* urea (pH 9.0) containing 10% (v/v) methanol; separation column: 50 μm inner diameter × 65 cm, 50 cm effective; applied voltage, 20 kV; current, 17 μA; detection wavelength, 260 nm; temperature, ambient.
Source: From Chiral separations by micellar electrokinetic chromatography with sodium *N*-dodecanoyl-valinate, in J. Chromatogr. A.[6]

Alkylglucoside Chiral Surfactants

Anionic alkylglucoside chiral surfactants, such as dodecyl β-D-glucopyranoside monophosphate and monosulfate, and sodium hexadecyl D-glucopyranoside 6-hydrogen sulfate, were used as chiral pseudostationary phases in MEKC, where several enantiomers (e.g., PTH-DL-AAs and binaphthol) were resolved.

Several neutral alkylglucoside surfactants, such as heptyl-, octyl-, nonyl-, and decyl-β-D-glucopyranosides and octylmaltopyranoside, were also employed for the enantiomer separation of phenoxy acid herbicides, Dns-DL-AAs, 1,1′-bi-2-naphthyl-2,2′-diyl hydrogen phosphate (BNP), warfarin, bupivacaine, and so forth.

Tartaric Acid-Based Surfactants

A synthesized chiral surfactant based on (*R*,*R*)-tartaric acid was used for the enantiomer separation in MEKC, where enantiomers having fused polyaromatic rings were separated easier than those having only a single aryl group.

Some PTH-DL-AAs and drug enantiomers were successfully resolved by using tartaric acid-based chiral surfactants.

Steroidal Glucoside Surfactants

Neutral steroidal glucoside surfactants, such as *N*,*N*-bis-(3-D-gluconamidopropyl)-cholamide (Big CHAP) and *N*,*N*-bis-(3-D-gluconamidopropyl)-deoxycholamide (Deoxy Big CHAP), which contain a cholic or deoxycholic acid moiety, respectively, have been introduced for use as chiral pseudo-stationary phases in MEKC. By using a borate buffer under basic conditions, these surfactant micelles could be charged via borate complexation. Some binaphthyl enantiomers, Tröger's base, phenoxy acid herbicide, and Dns-DL-AAs were enantioseparated.

MEKC USING HIGH-MOLECULAR-MASS SURFACTANTS

The use of a high-molecular-mass surfactant (HMMS) or polymerized surfactant has been recently investigated as a pseudo-stationary phase in MEKC. Because a HMMS forms a micelle with one molecule, enhanced stability and rigidity of the micelle can be obtained. Also, it is expected that the micellar size is controlled easier than with a conventional low-molecular-mass surfactant (LMMS). The first report on enantiomer separation by MEKC using a chiral HMMS appeared in 1994, where poly(sodium *N*-undecylenyl-L-valinate) [poly(L-SUV)] was used as a chiral micelle and binaphthol and laudanosine were enantioseparated. The optical resolution of 3,5-dinitrobenzoylated amino acid isopropyl esters by MEKC with poly(sodium (10-undecenoyl)-L-valinate) as well as with SDVal, SDAla, and SDThr was also reported.

As for the use of monomeric and polymeric chiral surfactants as pseudo-stationary phases for enantiomer separations in MEKC, a review article has been available.

The use of an achiral HMMS butyl acrylate/butyl methacrylate/methacrylic acid copolymer (BBMA) sodium salt was also investigated for enantiomer separations with CDs or as a CD/MEKC mode. A better enantiomeric resolution of Dns-DL-AAs was obtained by a β-CD/BBMA/MEKC system than an β-CD/SDS/MEKC system.

Polymerized dipeptide surfactants, which are derived from sodium *N*-undecylenyl-L-valine-L-leucine (L-SUVL), sodium *N*-undecylenyl-L-leucine-L-valine (L-SULV), sodium *N*-undecylenyl-L-leucine-L-leucine (L-SULL), and sodium *N*-undecylenyl-L-valine-L-valine (L-SUVV), were employed. Among these dipeptides, poly(L-SULV) showed the best enantioselectivity for the separation of 1,1′-bi-2-naphthol (BN).

BIBLIOGRAPHY

1. Camilleri, P. Chiral surfactants in micellar electrokinetic capillary chromatography. Electrophoresis **1997**, *18*, 2332.
2. Chankvetadze, B. *Capillary Electrophoresis in Chiral Analysis*; John Wiley & Sons: New York, 1997.
3. Otsuka, K.; Terabe, S. Enantiomer separation of drugs by micellar electrokinetic chromatography using chiral surfactants. J. Chromatogr. A, **2000**, *875*, 163.
4. Otsuka, K.; Terabe, S. Micellar electrokinetic chromatography. Bull. Chem. Soc. Jpn. **1998**, *71*, 2465.
5. Terabe, S.; Otsuka, K.; Nishi, H. Separation of enantiomers by capillary electrophoretic techniques. J. Chromatogr. A, **1994**, *666*, 295.
6. Otsuka, K.; Kawahara, J.; Tatekawa, K.; Terabe, S. Chiral separations by micellar electrokinetic chromatography with sodium *N*-dodecanoyl-valinate. J. Chromatogr. A, **1991**, *559*, 209.

Chlorinated Fatty Acids: Trace Analysis

Wenshan Zhuang
Taro Pharmaceuticals, Inc., Brampton, Ontario, Canada

INTRODUCTION

Many fatty acids, especially the so-called essential fatty acids, are of great nutrient importance; their chlorinated derivatives seem to have little usage in human life. Nevertheless, naturally occurring chlorinated fatty acids were found in marine animals,[1,2] though little is known about their biological functions. On the other hand, most chlorinated fatty acids found in the environment are of anthropogenic origin; they are generated as unwanted byproducts by industrial processes involving the use of chlorine-based reagents.[1,2] Their discharge into the aquatic environment and their presence in certain food products[1,2] have caused an increasing concern, because they are highly bioaccumulative and persistent in the food chain.[3] Not only do these compounds tend to be passively stored in the depot lipids of exposed animals,[1,2] but also they are actively built into cell membrane lipids.[4] Strikingly, chlorinated fatty acids were found to account for a major portion of extractable organochlorine in marine fish,[1,2] freshwater fish,[5] bivalves,[1,2] and lobster[6] that had been exposed to the waters in which chlorine bleaching effluents or municipal sewage are gathered. Although the toxicology of chlorinated fatty acids was not studied as much as that of those commonly known organochlorine compounds, e.g., chlorinated pesticides, polychlorinated biphenyls, and chlorinated dioxins, some effects on the biological properties of animal tissues and the functions of cell membranes were reported in recent years.[3,7,8]

A major difficulty with analysis of chlorinated fatty acids has been that they are usually present at levels undetectable by most chromatographic detectors. In this entry, chromatographic techniques including enrichment methods that were successfully developed and used in the analysis of these compounds in the past, mostly in the last decade, are summarized.

GAS CHROMATOGRAPHIC ANALYSIS WITHOUT PRIOR ENRICHMENT

As chlorinated fatty acids in lipid extracts cannot be separated from non-chlorinated matrix by routine cleanup techniques, because of the similarity in their chemical and physicochemical properties, chromatographic elution is often the sole effective means of separation for identification and quantitation of chlorinated fatty acids. As chlorinated fatty acids are present in biota extracts at trace levels, it is critical to have a detector that is highly specific for organochlorine. There are a range of detection techniques and specialized detectors that can be specific for chlorine or halogen: the electron capture detector (ECD); the atomic emission detector (AED); a mass spectrometer with negative ion chemical ionization (NICIMS); the selective ion monitoring (SIM) technique employed in mass spectrometry with commonly used ionization sources such as electron impact ionization, positive and negative ion chemical ionizations, and with other ionization sources such as the dissociative electron attachment (DEA) and the chemical reaction interface mass spectrometer (CRIMS); the Hall electrolytic conductivity detector (ELCD); and the halogen-specific detector (XSD^{TM}). Among these detectors, only the ELCD and XSD have been successfully used in gas chromatography (GC) for identification and quantitation of trace chlorinated fatty acid methyl esters (FAMEs) in transesterified fish lipids without resorting to prior enrichment of the analytes.[5,9–11] This is particularly desirable for quantitative analysis of trace chlorinated fatty acids in complex matrices, as enrichment processes often cause certain amount of sample loss.

Gas Chromatography/Hall Electrolytic Conductivity Detector

The ELCD can detect selectively halogen (X), nitrogen (N), or sulfur (S), depending on the instrument setup. In the X mode, GC eluate undergoes hydrogenolysis in a pyrolysis reactor, where X-containing compounds are converted to HX. This strong electrolytic species is carried into a conductivity cell and ionized in 1-propanol whose conductivity is monitored. An increase in conductivity owing to the presence of halide is translated to the response of the detector. A postreactor chemical scrubber is needed to remove HX and H_2S for ELCD operating in the N mode; otherwise the detector response to NH_3, a weak electrolyte resulting from hydrogenolysis of N-containing compounds, would be severely interfered if there is any X- or S-containing compound present in the eluate. In the S mode, air (oxygen) is used as the reaction gas, yielding an oxidative environment in the reactor in which S-containing compounds are pyrolyzed to SO_2, and a specific scrubber is employed to remove HX. Both S and N modes need a more polar solvent than does the X mode in the conductivity cell, usually methanol (capable of ionizing SO_2) for the S mode and aqueous *tert*-butyl alcohol (in which NH_3 is ionizable) for the N mode. The X-mode ELCD exhibits a very high selectivity for chlorine; one of its manufacturers proclaims that Cl/HC $> 10^6$, Cl/N $> 10^5$,

and Cl/S $> 10^5$.[12] The detection limit of ELCD, defined as the analyte amount that yields a detection response twice the noise, is about 0.25 ng of methyl dichlorooctadecanoate or 50 pg of chlorine.[9] For this compound, the reported linear range of ELCD is up to 500 ng/μl with a correlation coefficient of 0.999.[13]

Using GC/ELCD with coinjection of the synthesized reference standard, Wesén et al.[9] identified methyl 9,10-dichlorooctadecanoate in transesterified eel lipids containing 1200 ppm of Cl and quantitatively determined that the concentration of the analyte is 600 ppm.[9] In comparison, when the same sample was analyzed with GC/ECD, the detector was incapable of overcoming the interference from non-chlorinated FAMEs that were dominant components in the sample and generated a useless chromatogram.[9] In a subsequent study,[10] based on linear relationship obtained from plotting the linear retention indices vs. the carbon chain lengths of a homologous series of reference standards and of chlorinated unknowns in the eel sample with tentatively assigned carbon numbers, these researchers identified six major peaks in the GC/ELCD chromatogram as being *threo*- and *erythro*-diastereomers of methyl dichlorooctadecanoate, dichlorohexadecanoate, and dichlorotetradecanoate.

Gas Chromatography/Halogen-Specific Detector

The XSD manufactured by the OI Analytical is a GC detector that is dedicated to the selective detection of halogen-containing compounds. The detector consists of an alkali glass ceramic rod, a cathodic platinum bead attached to the bottom of the rod, an anodic platinum coil wound around the rod above the bead, and a reactor core which maintains a high temperature for the detector and serves as an auxiliary anode (Fig. 1). The working principle of the XSD roots in thermal electron emission, and negative and positive surface ionizations, whereby free electrons, anions, and cations are produced to form the emission current.[14] The detector is operated at 800–1100°C; therefore the background current is attributed largely to the thermal electron emission of the cathode. The GC effluent flowing into the heated reactor tube with the added reaction gas (air or oxygen at 20–40 ml/min) is pyrolyzed at high temperature. Halogenated compounds in the effluent are oxidized to CO_2, H_2O, and halogen atoms, which are subsequently absorbed onto the potassium-sensitized cathode surface. Negative surface ionization occurs, as the electron affinities of halogens (e.g., 3.61 eV for Cl) are higher than the work function of the sensitized cathode (2.29 eV). Detector response is noted by a sharp increase in thermal electron emission owing to a decrease of the surface's work function by halogen adsorption and also because of an increase in the local surface temperature caused by excess energy released from negative surface ionization. Potassium atoms on the cathode surface or K^+ ions arriving from the anode may react with halogen atoms or anions by impinging on them; this exothermic reaction also contributes to a rise in the local temperature. Halogen species

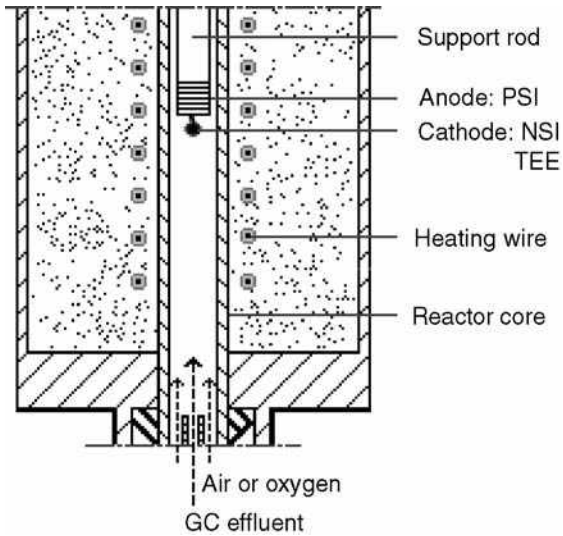

Fig. 1 A cutaway view of the core portion of XSD. PSI, positive surface ionization; NSI, negative surface ionization; TEE, thermal electron emission.[14]

(X^- and KX) are subsequently desorbed from the cathode surface into the gaseous flow moving toward the anode. The cathode surface is replenished by K^+ ions migrating from the anode in the external electric field. These cations are derived from positive surface ionization of potassium atoms on the surface of the anode, which is in contact with the potassium source (the alkali glass ceramic). It is possible that some of KX molecules desorbed from the cathode surface subsequently strike the anode surface. When this happens, KX incident on the hot surface could dissociate into K and X atoms, the former thus being recycled. The high selectivity of XSD lies in the fact that, among common elements of organic compounds such as C, H, O, N, S, and X, only halogens, formed in the heated oxidative environment, possess sufficient high electron affinities to cause significant increase in thermal electron emission. Indeed, in an evaluation of XSD for analysis of trace chlorinated FAMEs in a matrix composed of non-chlorinated FAMEs, the selectivity of Cl over C is estimated to be 10^5:1,[14] which agrees with the manufacturer's claim that Cl/HC $\geq 10^4$.[15] In addition, it was shown that under optimal conditions XSD has a detectivity, defined as being twice the peak-to-peak noise level divided by the response factor, of about 0.5 pg Cl/sec for dichloro FAMEs or detection limit of about 10 pg of methyl dichlorooctadecanoate (equivalent to 2 pg Cl), and a linearity range of up to 50-ng injection for methyl dichlorooctadecanoate (equivalent to 10 ng Cl) with an R^2 of 0.999.[14] These values are in agreement with the manufacturer's performance specifications.[15]

The XSD has found increasing use in the analysis of chlorinated compounds in biological samples.[5,11,16–18] Using GC/XSD, Zhuang et al.[5,11] identified and quantitated methyl esters of *threo*-5,6-dichlorotetradecanoic, *threo*-7,8-dichlorohexadecanoic, and *threo*-9,10-dichlorooctadecanoic

acids in transesterified lipids of filets, gonad, intestinal fat, and carcass of freshwater fish (white sucker) with the chlorine content ranging from 22 to 124 ppm. Identification was accomplished by matching the retention times of sample peaks with those of synthesized authentic reference standards and by comparing the elution behavior of configurational and positional isomers of dichloro FAMEs.[11] The work presented for the first time the unambiguous determination of chlorine positions in dichlorohexadecanoic and dichlorotetradecanoic acids present in fish lipids, thus providing analytical evidence to support the hypothesis of β-oxidative metabolism of dichlorooctadecanoic acid in fish. Quantitative analysis was based on internal standard calibration using methyl esters of *threo*-10,11-dichloroundecanoic and *threo*-10,11-dichlorononadecanoic acids as internal standards, which eluted before and after all analytes, respectively, and for which there was no chromatographic interference from samples.[5] Gustafson-Svärd et al.[16] used GC/XSD to study the incorporation, metabolism, and secretion of chlorinated fatty acids following the incubation of two human cell lines with 9,10-dichloro-octodecanoic acid.[16] The GC/XSD was also a useful tool in the enrichment of chlorinated fatty acids.[17,18]

CONFIRMATION WITH THE SECOND CHROMATOGRAPHIC COLUMN

After a chlorinated fatty acid or derivative has been identified chromatographically with the aid of the authentic reference standard, a simple approach of confirming the identification is to run the sample on a second chromatographic column, which has a very different polarity or elution mechanism. The second column of such selection greatly reduces the chance of false identification because the coelution is not likely to occur again when an unknown which is not the same compound as the reference standard does happen to coelute on the first column. Zhuang et al.[11] identified three metabolism-related dichloro FAMEs by GC/XSD with an HP-5 column (5% phenyl and 95% methyl polysiloxane), which is basically a non-polar GC column, and subsequently confirmed the identification using a DB-WAX column (polyethylene glycol), a typically polar GC column.

ENRICHMENT

Structural analysis of traces of chlorinated fatty acids in biota often requires prior enrichment or cleanup. Analysis of chlorinated pesticides and polychlorinated biphenyls can be facilitated by a simple cleanup procedure such as the sulfuric acid treatment or gel permeation chromatography with a single cutoff point to eliminate high molecular weight lipids. Owing to the similarity in chemical and physicochemical properties between analytes (chlorinated fatty acids) and matrix compounds (non-chlorinated fatty acids), conventional cleanup procedures are not applicable for the enrichment of chlorinated fatty acids that are present in complex biological matrices such as fish lipids. To deal with chlorinated fatty acids in biota samples, several successful enrichment techniques were developed.[6,10,17–21] The goal of enrichment is to maximize the degree of removal of non-chlorinated matrix compounds while minimizing the loss of chlorinated analytes.

COMPLEXATION

One of the enrichment techniques is based on complexing mechanisms, which involves the treatment of lipid sample solutions separately or consecutively with ethanol–water (1:1)-containing 25% (w/v) silver nitrate and with urea moistened with methanol.[10] Silver ions tend to interact strongly with polyunsaturated hydrocarbon chains of FAMEs to form complexes which are favorably partitioned into the polar EtOH–H_2O phase; uncomplexed FAMEs remain in the nonpolar phase (e.g., isooctane) in which the whole lipid sample was initially dissolved. Chlorinated FAMEs that do not possess polyunsaturated acyl chains are thus concentrated in the enriched samples. Urea has an interesting property: when it crystallizes in the presence of certain long-chain aliphatic molecules, it forms hexagonal prisms in such a way that a channel is created, in which the long straight carbon chain of the molecule is trapped and together forms a complex known as the urea inclusion complex. Uncomplexed lipid components can be extracted with effort by appropriate organic solvents from the urea slurry. It is known that branched, cyclic, and polyunsaturated FAMEs are too bulky to be contained in urea channels. It was assumed that the presence of bulky chlorine atoms in dichloro FAMEs would also inhibit the molecules from fitting into urea channels.[10]

In a study of transesterified eel lipids containing 1200 ppm Cl, Mu et al.[10] observed significant enrichment from each of the silver nitrate and urea treatments and also from the consecutive treatments (silver nitrate followed by urea), the latter resulting in a 30-fold increase in the ELCD response and by the appearance of new chlorinated peaks which had been undetectable prior to enrichment. Based on linear GC retention indices, column difference values, and response ratios of ELCD vs. the flame ionization detector (FID) and GC/mass spectrometry (MS), they identified additional chlorinated FAMEs in the enriched sample of the previously studied eel lipids: isomers of methyl dichlorooctadecenoate, dichlorohexadecenoate, and dichlorotetradecenoate, and isomers of methyl tetrachlorooctadecanoate and tetrachlorotetradecanoate.[19] Identification of *erythro*, *erythro*- and *threo*, *threo*-tetrachlorooctadecanoates, each present in two diastereomeric forms, was established by coinjection of the synthesized reference standards.[19] Mu et al.[10] also successfully applied the consecutive treatments to fish samples containing only 30–60 ppm Cl.

However, the effectiveness of the complexing methods depends on the fatty acid composition of the sample and thus the type and source of the sample. For instance, neither of the

above treatments was effective in enrichment of chlorinated components in transesterified lipids obtained from freshwater fish (white sucker).[17] The silver nitrate treatment was found to be unsatisfactory for enrichment of chlorinated species in transesterified lipids from the lobster digestive gland.[6]

GC with Cryogenic Trapping of Selected Eluate

A straightforward approach for enriching chlorinated fatty acids is the repeated collection of the selected narrow GC fractions corresponding to chromatographic peaks which are recorded by a halogen selective detector, such as ELCD or XSD. To maximize the degree of enrichment, GC conditions should be optimized so that there are no major non-chlorinated components (as indicated by FID) coeluting with the ELCD or XSD peaks. Using glass splitters, the GC outlet can be connected to a halogen-specific detector and to a number of separate coils of capillary tubing which are ended with shut-off valves.[20] By opening a valve, about a half of the eluate was diverted into the respective coil. The coils are cooled by dry ice and the diverted eluate is thus condensed and collected. By applying this technique to the transesterified eel lipids that contained 1200 ppm Cl, Wesén et al.[20] successfully obtained several GC fractions for GC/MS studies, in which two diastereomeric forms of methyl tetrachlorooctadecanoate were identified and the previously identified methyl *threo*-dichlorooctadecanoate was confirmed.

Thin-Layer Chromatography

One of the first techniques that have been utilized for enrichment of chlorinated fatty acids in biota lipids is thin-layer chromatography (TLC). White and Hager[21] used preparative TLC (20 cm × 20 cm plates precoated with silica gel F-254, 2.5 mm thick) to enrich chlorinated components in jellyfish lipids that contained 4.8 mg Cl/g lipid. After chromatography of the transesterified lipids with hexane–diethyl ether–acetic acid (90:10:1), 30% of the chlorine was recovered in a fraction having a R_f value of 0.22–0.38. When eel filet lipids containing 1.2 mg Cl/g lipid is studied, Mu et al.[10] used silica gel TLC with a solvent system of cyclohexane–diethyl ether (96:4) to enrich chlorinated FAMEs following consecutive treatment with silver ions and urea. A band with R_f 0.14–0.18 was found to contain the major portion of chlorinated species, among which were methyl dichlorooctadecanoate, dichlorohexadecanoate, and dichlorotetradecanoate.[10]

Florisil Column Chromatography

The presence of a hydroxyl group in FAMEs has the same effect on the GC elution time as does the incorporation of a chlorine atom into the FAMEs.[11] Thus, dichloro FAMEs were unseparated from chlorohydroxy analogs on the GC column; the same was true for the tetrachloro FAMEs and trichlorohydroxy analogs.[11,22] Heikes[22] used an absorption column that contained 60–100 mesh Florisil (magnesia–silica gel) that had been activated at 650°C, to separate chloro FAMEs from chlorohydroxy FAMEs. The former was eluted from the column by 12% ethyl ether in petroleum ether, and the latter by 20% ethyl ether in petroleum ether.

Gel Permeation Chromatography

The solute molecules according to their hydrodynamic volumes using gel permeation chromatography (GPC). Milley et al.[7] reported a reinforced enrichment process, in which transesterified lipids of lobster digestive glands containing about 50 ppm Cl were enriched for chlorinated FAMEs first by the urea treatment and then further by GPC fractionation (Sephadex LH-20). One of the GPC fractions contained a high concentration of methyl dichlorotetradecanoate and was thus identified and confirmed by GC/MS.

High-Performance Liquid Chromatography

High-performance liquid chromatography (HPLC) has been widely used for analytical separations by virtue of its high-resolution capability. This type of chromatography is characterized by wide selections of stationary and mobile phases. Although preparative HPLC columns are commercially available, enrichment can also be made with an analytical column by repeated runs from which the same HPLC fractions are pooled. Small quantities of enriched samples are usually sufficient for GC/MS studies. As chlorinated FAMEs are usually analyzed by GC, the advantage of using HPLC for enrichment is that enrichment chromatography and analysis chromatography are based on different elution mechanisms. Thus when matrix compounds coeluted with chlorinated FAME in HPLC are collected together in an HPLC fraction, the chance for a second coelution is greatly reduced in the subsequent GC analysis.[17]

After carrying out preconcentration with three sequential TLC systems, Song et al.[23] further enriched hatching factors in barnacle lipids by normal-phase HPLC fractionation on an S5w column using hexane–isopropanol–acetic acid (97:3:0.1) as the mobile phase. Each fraction was tested for hatching factor activity, and one of the most active fractions was subsequently subjected to GC/MS. Several major components were identified as being hydroxylated fatty acids, two of which happened to be chlorodihydroxy fatty acids.[23]

However, in general cases, such as analysis of chlorinated fatty acids in food and environmental samples, it is difficult to determine in which of HPLC fractions trace chlorinated components are present, because none of LC detectors are specific for chlorine. Zhuang et al.[17] devised a new enrichment approach of utilizing reversed-phase RP-HPLC for its high separation power and XSD for its high selectivity for organochlorine. In a study of white sucker lipids, to maximize the degree of enrichment of traces of chlorinated FAMEs, a gradient elution using water, methanol, acetonitrile, and cyclohexane–isopropanol (1:1) as mobile phases

was optimized so that chlorinated analytes were present in the valleys of the elution profile of matrix materials.[23] Owing to their presence at trace levels with coeluting matrix compounds, chlorinated analytes were invisible in chromatograms recorded by the photodiode-array detector (215 nm) employed in HPLC fractionation; the determination of optimal demarcation for fractionation was assisted by GC/XSD, which is capable of detecting these otherwise undetectable chlorinated analytes. As a result, the bulk of non-chlorinated matrix was removed by RP-HPLC fractionation using an ODS2 column, and target-chlorinated analytes were selectively enriched. As assessed by a universal detector (FID), on a transesterified fish lipids containing only 15 ppm Cl, chlorinated FAMEs were completely nondetectable prior to HPLC fractionation, but were present as moderate or small yet discernible peaks after the HPLC enrichment.[17] This enrichment method is efficient with good selectivity, reproducibility, and predictability.

Solid-Phase Extraction

Solid-phase extraction (SPE) offers an alternative way for enrichment of chlorinated fatty acids. Akesson-Nilsson[18] presented an aminopropyl-based SPE technique for enrichment of chlorinated FAMEs in a cell-culture medium and for previously silver nitrate and urea treated eel lipids. In this application, a 500-mg aminopropyl column was connected to a vacuum manifold and conditioned with 2 ml of hexane. After transesterified lipid samples in 0.2 ml of hexane were loaded, the column was first eluted with 6 ml of hexane and then with 4 ml of a solvent mixture made of hexane–diethyl ether–dichloromethane (89:1:10).[18] In this way, the majority of non-chlorinated FAMEs were removed in the first elution and chlorinated FAMEs enriched in the later elution.

IDENTIFICATION AND CONFIRMATION BY GC/MS FOLLOWING ENRICHMENT

Mass spectrometry coupled with chromatography is commonly used for identification and confirmation of unknowns. Mass spectrometry can offer more structural information needed for identification and confirmation, but it is less selective and less sensitive than those detectors designed specifically for organohalogen such as ELCD and XSD. Therefore, GC/MS studies often require prior enrichment of chlorinated analytes. The sensitivity of MS for trace analytes can often be enhanced dramatically by SIM and, in the case of MS/MS, by selected-reaction monitoring (SRM). Several ionization modes and reagent gases were reported for GC/MS analysis of chlorinated FAMEs in the presence of non-chlorinated matrix compounds. The objective in choosing ionization conditions is to increase sensitivity through achieving high ionization efficiency, especially for chlorinated analytes, and low degrees of fragmentation.

GC/EIMS Analysis of Methyl Esters

Electron impact (EI) is the most common ionization mode used in MS. Generally EIMS is not favored for trace analysis because of its high degree of fragmentation. Nevertheless, when enriched samples contain adequate concentrations of analytes, GC/EIMS is a convenient tool for identification.

By using GC/EIMS (70 eV) with known synthetic compounds, White and Hager[21] identified several isomers of chlorohydroxyhexadecanoic and chlorohydroxyoctadecanoic acids in a TLC-enriched jellyfish lipid sample. Song et al.[23] used GC/EIMS operated at a low electron acceleration potential (25 eV) to analyze methyl ester trimethylsilyl ether derivatives of an HPLC fraction that exhibited strong hatching factor activity. In addition to a number of trihydroxy fatty acids that were determined, two unknown GC peaks which had almost identical mass spectra were tentatively identified as being 9-chloro- and/or 11-chloro-8,12-dihydroxyeicosatetraenoic acids. GC/EIMS was also used for tentative identification of chlorinated fatty acids in transesterified fish lipids following enrichment.[10,19,20]

GC/PICIMS Analysis of Methyl Esters

Ions generated by soft ionization such as positive ion chemical ionization (PICI) are much less fragmented; thus, those characteristic ions are generally produced with sufficient intensities, which are desirable for trace analysis, especially when SIM is utilized. An additional advantage of using soft ionization is that molecular ions are usually observable. Note that only a limited number of reagent gases were found to be suitable for analysis of trace chlorinated FAMEs. In analysis of chlorinated fatty acid in food items derived from bleached flours, Heikes[24] reported the formation of significant protonated molecular ion adducts through the use of ethylene oxide (oxiran) as the reagent gas in GC/MS with PICI operated at 200°C and 45 eV. The identification of 9,10-dichloro-12-octadecenoic acid along with several other chlorinated fatty acids in these flour-containing food samples was established by matching GC retention indices and mass spectra between the test samples and the synthesized reference standards. Shortly thereafter, Sundin et al.[25] reported that PICI using ammonia as the reagent gas results in abundant ammonium adduct molecular ions $[M + NH_4]^+$ in the mass spectrum of monochloro and dichloro FAMEs. Gas chromatography equipped with ammonia-induced PICIMS was later used by them as an important tool for identification and confirmation of chlorinated FAMEs in transesterified fish lipids.[4,10,19,20] To assist the trace analysis, SIM[4,20] and high-resolution SIM[19] were also utilized.

GC/DEA–NICIMS Analysis of Methyl Esters

Negative ion chemical ionization is an attractive ionization method for analysis of trace chlorinated compounds,

because chloride ions generated can be conveniently used for detecting chlorinated unknowns in the chromatographic elution profiles of complex samples.

Curtis and Boyd[26] utilized this feature to the full by optimizing NICI conditions for achieving "hard" ionization, viz., DEA, by which chloride ions are predominantly produced from chlorinated compounds and detected by SIM at *m/z* 35 and 37. Operated in this way, NICIMS is effectively turned into a chlorine-specific GC detector with selectivity and sensitivity comparable to those of the ELCD. By using this technique, Milley et al.[6] successfully identified dichlorotetradecanoic acid in a GPC-enriched sample from lobster digestive gland lipids (but with the chlorine position remaining undetermined). The identification of this compound was supported by the mass spectrum obtained with "soft" NICI optimized for molecular anions, which resembled that of a synthesized 9,10-dichlorotetradecanoic acid.

GC/NICIMS Analysis of Pentafluorobenzyl Esters

Fatty acids and their methyl esters are ineffective in ionization under normal (soft) ionization conditions. On the other hand, the ionization efficiency can be enhanced significantly by using an appropriate derivative. Zhuang et al.[27] demonstrated striking difference between NICIMS response to pentafluorobenzyl esters and that to methyl esters or underivatized fatty acids. An additional desirable feature of NICIMS of pentafluorobenzyl esters of chlorinated fatty acids is their extreme low degrees of fragmentation: the most abundant ion (the base peak) shown in the mass spectrum is usually the quasi-molecular ion, i.e., the carboxylate anion generated upon the loss of the pentafluorobenzyl moiety from the pentafluorobenzyl ester having captured a thermal electron. Based on this feature, Zhuang et al.[27] presented a GC/NICIMS technique that is particularly useful for detecting and identifying trace chlorinated unknowns. The method consists of the following sequential steps:

1. Enriching chlorinated analytes by HPLC fractionation or other effective enrichment techniques.
2. Performing GC/NICIMS following pentafluorobenzyl esterification.
3. Locating chlorinated analytes: when available reference standards do not match in retention time with unknown chlorinated compounds, chloride ion chromatograms extracted at *m/z* 35 and 37 from full scans can utilized for locating traces of chlorinated unknowns in a total ion chromatogram (TIC) that is complicated by the presence of ions derived from non-chlorinated matrix compounds.
4. Retrieving the mass spectrum: once the location of a chlorinated unknown has been determined, the mass spectrum scanned in a narrow range of its retention time can be readily retrieved.
5. Analyzing the mass spectrum: the origins of significant ions displayed in the retrieved mass spectrum can be evaluated using ion chromatograms extracted at the *m/z* of these ions; the chromatographic peaks of those ions derived from the chlorinated unknown are expected to center at the retention time determined by chloride ion chromatograms, whereas those originating from matrix compounds are not. Furthermore, the isotopic patterns of chlorinated ions can be examined against their theoretical relative abundances.
6. Analyzing the background-subtracted mass spectrum: once matrix ions have been identified, they can be subtracted from the spectrum. The resulting spectrum provides information on the molecular identity of the chlorinated unknown; for instance, the molecular weight and the number of chlorine can be readily obtained from the quasi-molecular ions. The comparison of the background-subtracted spectrum with the spectrum of the synthesized reference standard, if available, that matches in retention time with the chlorinated unknown will establish the identification of the unknown analyte.

STRUCTURAL ANALYSIS WITH GC/EIMS FOLLOWING DMOX DERIVATIZATION

A traditional method to determine halogen positions in unknown halogenated fatty acids is dehalogenation which may be followed by ozonation, with the subsequent GC analysis of dehalogenated or ozonated products, from which the double bond position(s) and thus the chlorine position(s) can be deduced.[28] Recently, Zhuang et al.[29] presented a GC/MS technique to locate the chlorine in fatty acids containing vicinal dichloro atoms. In this method, lipid samples including chlorinated components are transformed to 4,4-dimethyloxazoline (DMOX) derivatives, which are then subjected to EIMS. It was found that DMOX derivatives of dichloro fatty acids display some distinctive EIMS features, which are characteristic of positional isomers, and fragmentation mechanisms responsible for important fragment ions and patterns are inherently related to the position of the vicinal dichloro group on the acyl chain. Furthermore, a "$144 + 14x$" rule, which facilitates mass spectral interpretation was identified: the first ion in a homologous series of characteristic chlorodienyl ions, notable by their sizeable intensity and chlorine isotope pattern, has a *m/z* equal to "$144 + 14x$," where x is a number corresponding to the location of the first of the vicinal chlorine atoms on the acyl chain.

CONCLUSIONS

A difficulty with analysis of chlorinated fatty acids has been that they are often present at levels undetectable by most chromatographic detectors. In this entry, the approaches such as gas chromatographic analysis without prior enrichment, GC/ELCD, GC/XSD, enrichment, complexation, GC with cryogenic trapping of selected eluate, TLC, florisil

column chromatography, GPC, HPLC, SPE, identification and confirmation by GC/MS following enrichment, and GC/EIMS analysis of methyl esters have been described.

REFERENCES

1. Mu, H.; Wesén, C.; Sundin, P. Trends Anal. Chem. **1997**, *16* (5), 266–274.
2. Dembitsky, V.M.; Srebnik, M. Prog. Lipid Res. **2002**, *41*, 315–367.
3. Ewald, G. Aquat. Ecosys. Health Manage **1999**, *2*, 71–80; and references cited therein.
4. Björn, H.; Sundin, P.; Wesén, C.; Mu, H.; Martinsen, K.; Kvernheim, A.L.; Skramstad, J.; Odham, G. Chlorinated fatty acids in membrane lipids of fish. Naturwissenschaften **1998**, *85* (5), 229–232.
5. Zhuang, W. Ph.D. thesis, University of Toronto, 2002; 127–133, 184–185.
6. Milley, J.E.; Boyd, R.K.; Curtis, J.U.M.; Musial, C.; Uthe, J.F. Dichloromyristic acid, a major component of organochlorine load in lobster digestive gland. Environ. Sci. Technol. **1997**, *31* (2), 535–541.
7. Vereskuns, G.; Wesén, C.; Skog, K.; Jagerstad, M. Mutat. Res. **1998**, *416* (3), 149–157.
8. Lystad, E.; Høstmark, A.T.; Jebens, E. Pharmacol. Toxicol. **2001**, *89*, 85–91.
9. Wesén, C.; Mu, H.; Kvernheim, A.L.; Larsson, P. Identification of chlorinated fatty acids in fish lipids by partitioning studies and by gas chromatography with Hall electrolytic conductivity detection. J. Chromatogr. A, **1992**, *625* (2), 257–269.
10. Mu, H.; Wesén, C.; Novák, L.; Sundin, P.; Skramstad, J.; Odham, G. Enrichment of chlorinated fatty acids in fish lipids prior to analysis by capillary gas chromatography with electrolytic conductivity detection and mass spectrometry. J. Chromatogr. A, **1996**, *731* (1–2), 225–236.
11. Zhuang, W.; McKague, B.; Reeve, D.; Carey, J. Identification and confirmation of traces of chlorinated fatty acids in fish downstream of bleached kraft pulp mills by gas chromatography with halogen-specific detection. J. Chromatogr. A, **2003**, *994* (1–2), 137–157.
12. OI analytical, http://www.oico.com/default.aspx?id=product&productID=52 (accessed November 2004).
13. Mu, H.; Wesén, C.; Odenbrand, I.; Nilsson, O.; Wahlund, K.G. Response factors of organochlorine compounds in the electrolytic conductivity detector. J. Chromatogr. A, **1999**, *849* (1), 285–292.
14. Zhuang, W.; McKague, A.B.; Reeve, D.W.; Carey, J.H. Evaluation of halogen-specific detector (XSD) for trace analysis of chlorinated fatty acids in fish. Instrum. Sci. Technol. **2005**, *33* (4), 481–507.
15. OI Analytical, http://www.oico.com/default.aspx?id=product&productID=53 (accessed November 2004).
16. Gustafson-Svärd, C.; Åkesson-Nilsson, G.; Mattsson, M.; Sundin, P.; Wesén, C. Removal of xenobiotic dichlorostearic acid from phospholipids and neutral lipids in cultured human cell lines by ß-oxidation and secretion of dichloromyristic acid. Pharmacol. Toxicol. **2001**, *89* (2), 56–64.
17. Zhuang, W.; McKague, B.; Carey, J.; Reeve, D. Enrichment of trace chlorinated species in a complex matrix of fatty acids using HPLC in conjunction with gas chromatography-halogen specific detection. J. Liq. Chromatogr. Relat. Technol. **2003**, *26* (11), 1809–1826.
18. Akesson-Nilsson, G. Isolation of chlorinated fatty acid methyl esters derived from cell-culture medium and from fish lipids by using an aminopropyl solid-phase extraction column. J. Chromatogr. A, **2003**, *996* (1–2), 173–180.
19. Mu, H.; Wesén, C.; Sundin, P.; Nilsson, E. Gas chromatographic and mass spectrometric identification of tetrachloroalkanoic and dichloroalkenoic acids in eel lipids. J. Mass Spectrom. **1996**, *31* (5), 517–526.
20. Wesén, C.; Mu, H.; Sundin, P.; Freyen, P.; Skramstad, J.; Odham, G. Gas chromatographic-mass spectrometric identification of chlorinated octadecanoic acids in eel lipids. J. Mass Spectrom. **1995**, *30* (7), 959–968.
21. White, R.H.; Hager, L.P. Occurrence of fatty acid chlorohydrins in jellyfish lipids. Biochemistry **1977**, *16* (22), 4944–4948.
22. Heikes, D.L. Procedure for supercritical fluid extraction and gas chromatographic determination of chlorinated fatty acid bleaching adducts in flour and flour-containing food items utilizing acid hydrolysis-methylation and Florisil column cleanup techniques. J. Agric. Food Chem. **1993**, *41* (11), 2034–2037.
23. Song, W.-C.; Holland, D.L.; Gibson, K.H.; Clayton, E.; Oldfield, A.Q. Identification of novel hydroxy fatty acids in the barnacle Balanus balanoides. Biochim. Biophys. Acta **1990**, *1047*, 239–246.
24. Heikes, D.L. Mass spectral identification and gas chromatographic determination of chlorinated bleaching adducts in flour-containing food items. J. Agric. Food Chem. **1992**, *40* (3), 489–491.
25. Sundin, P.; Larsson, P.; Wesén, C.; Odham, G. Biol. Mass Spectrom. **1992**, *21*, 633–641.
26. Curtis, J.U.M.; Boyd, R.K. Dissociative electron attachment negative ion mass spectrometry: A chlorine-specific detector for gas chromatography. Int. J. Mass Spectrom. Ion Proc. **1997**, 165–166, 625–639.
27. Zhuang, W.; McKague, A.B.; Reeve, D.; Carey, J.H. Identification of chlorinated fatty acids in fish by gas chromatography/mass spectrometry with negative ion chemical ionization of pentafluorobenzyl esters. J. Mass Spectrom. **2004**, *39* (1), 51–60.
28. Jones, B.A.; Tinsley, I.J.; Wilson, G.; Lowry, R.R. Toxicology of brominated fatty acids: Metabolite concentration and heart and liver changes. Lipids **1983**, *18* (4), 327–334.
29. Zhuang, W.; McKague, B.; Reeve, D. Mass spectrometric elucidation of chlorine location in dichloro fatty acids following 4,4-dimethyloxazoline derivatization, and its application to chlorinated fatty acids in fish. Int. J. Mass Spectrom. **2004**, *232* (2), 127–137.

BIBLIOGRAPHY

1. Mu, H.; Sundin, P.; Wesén, C. Halogenated fatty acids: II. Methods of determination in lipids. Trends Anal. Chem. **1997**, *16* (5), 274–286.

Chromatographic Peaks: Causes of Fronting

Ioannis N. Papadoyannis
Anastasia Zotou
Laboratory of Analytical Chemistry, Chemistry Department, Aristotle University of Thessaloniki, Thessaloniki, Greece

INTRODUCTION

Peaks with strange shapes represent one of the most vexing problems that can arise in a chromatographic laboratory. Fronting of peaks is a condition in which the front of a peak is less steep than the rear relative to the baseline. This condition results from non-ideal equilibria in the chromatographic process.

DISCUSSION

Fronting peaks, as well as tailing or other misshaped peaks, can be hard to quantitate. Some data systems have difficulty in measuring peak size accurately. As a result, the precision and/or reliability of assay methods involving fronting or other misshaped peaks is often poor when compared to good chromatography. There are a number of different causes of peak fronting, and discovering why peaks are thus misshaped and then fixing the problem can be a difficult undertaking. Fortunately, there is a systematic approach based on logical analysis plus practical fixes that have now been documented in numerous laboratories. Fronting peaks are less commonly encountered in liquid chromatography (LC), but they are readily distinguished from other peak-shape problems. Fronting peaks are the opposite of tailing peaks. Whereas tailing peaks suggest that sample retention decreases with increasing sample size or concentration, fronting peaks suggest the opposite: retention increases with larger samples. In both cases, a decrease in sample size may eliminate peak distortion. However, this is often not practical, because some minimum sample size is required for good detectability. In the case of tailing peaks, it is believed that peak distortion often arises because large samples use up some part of the stationary phase. However, the cause of fronting peaks is seldom fully understood.

Ion-pair chromatography (IPC) is more susceptible to peak fronting than other modes in LC. *Column temperature* problems can cause fronting peaks in IPC. Fig. 1 shows the separation of an antibiotic amine at ambient temperature. Repeating the separation at 45°C eliminated the fronting problem. Some studies have shown peak fronting in IPC that can be corrected by operating at a higher column temperature, whereas some other separations are best carried out at lower temperatures. The reason for this peculiar peak-shape behavior is unclear, but it may be related to the presence of reagent micelles in the mobile phase for some experimental IPC conditions. Generally, it is good practice to run ion-pair separations under thermostatted conditions, because relative retention tends to vary with temperature in IPC. Usually, narrower bands and better separation results when temperatures of 40–50°C are used for IPC.

The use of a *sample solvent other than the mobile phase* is another cause of fronting peaks in IPC. In this case, the sample should only be injected as a solution in the mobile

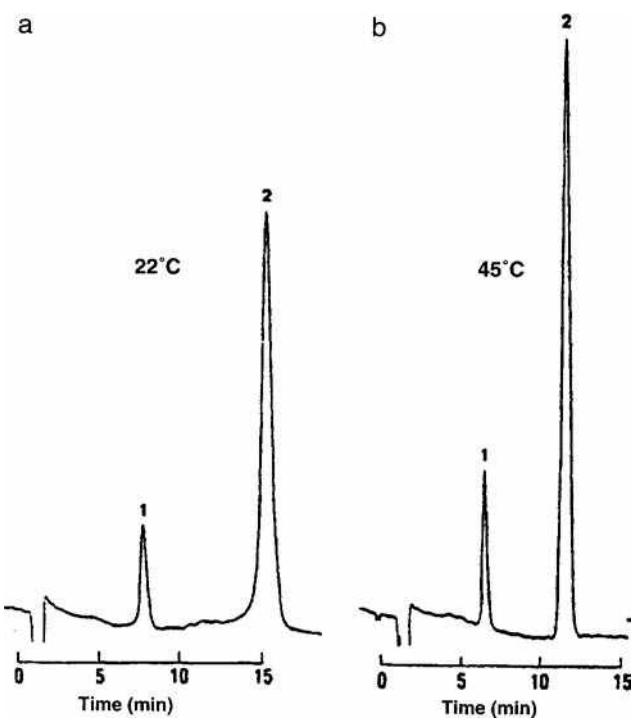

Fig. 1 Peak fronting in IPC as a function of separation temperature. Column: Zorbax C_8 mobile phase: 10 m*M* sodium dodecyl sulfate and 150 m*M* ammonium phosphate in 33% acetonitrile; pH: 6.0; flow rate: 2.0 ml/min; temperature: (a) = 22°C and (b) = 45°C. Peaks: 1 = lincomycin B; 2 = lincomycin A.
Source: From Liquid chromatographic determination of lincomycin in fermentation beers, in J. Chromatogr.[1]; Copyright © Elsevier Science. Reprinted with permission.

phase. No more than 25–50 μl of sample should be injected, if possible.

Silanol effects can adversely alter peak shape in IPC, just as in reversed-phase separations. Therefore, when separating basic (cationic) compounds, the column and mobile phase should be chosen bearing this in mind. When ion-pair reagents are used, however, silanol effects are often less important. The reason is that an anionic (acidic) reagent confers an additional negative charge on the column packing and this reduces the relative importance of sample retention by ion exchange with silanol groups. Similarly, cationic (basic) reagents are quite effective at blocking silanols because of the strong interaction between reagent and ionized silanol groups.

Still another cause of peak fronting is for the case of *anionic (acidic) sample molecules separated with higher-pH mobile phases*. For silica-based packings, the packing has an increasingly negative charge as the pH increases, and this results in the repulsion of anionic sample molecules from the pores of the packing. With larger sample sizes, however, this effect is overcome by the corresponding increase in ionic strength, caused by the sample. A remedy for this problem is to increase the ionic strength of the mobile phase, by increasing the mobile-phase buffer concentration to the range of 25–100 m*M*. It should be mentioned here that ionic or ionizable samples should never be separated with unbuffered mobile phases.

Finally, *column voids* and *blocked frits* can also cause peak fronting.

REFERENCES

1. Asmus, P.A.; Landis, J.B.; Vila, C.L. Liquid chromatographic determination of lincomycin in fermentation beers. J. Chromatogr. 1983; *264* (2), 241.

BIBLIOGRAPHY

1. Bidlingmeyer, B.A. *Practical HPLC Methodology and Applications*; John Wiley & Sons: New York, 1992; 20.
2. Dolan, J.W.; Snyder, L.R. *Troubleshooting LC Systems*; Humana Press: Totowa, NJ, 1989; 400–401.
3. Sadek, P.C.; Carr, P.W.; Bowers, L.D. Evaluation of several void-volume markers for reversed-phase HPLC. LC, Liq. Chromatogr. HPLC Mag. **1985**, *3*, 590.

Circular and Anti-Circular TLC

C. Marutoiu
Department of Chemistry, Lucian Blaga University of Sibiu, Sibiu, Romania

M.L. Soran
National Institute of Research and Development for Isotopic and Molecular Technology, Cluj-Napoca, Romania

INTRODUCTION

Thin-layer chromatography (TLC) has developed recently because of the theoretical and practical optimization of the chromatographic technique. The introduction of the commercial chromatographic plates, covered with stationary phases that have particles with controlled size and tight distribution of particle sizes (5–15 μm), was one of the reference points in modern TLC development. These new plates have given a higher efficiency and a shorter time of analysis, compared with conventional plates, when the optimum sample quantity was applied onto the stationary phase. Initially, only silica gel plates were commercially available but, in the last years, various normal and chemically modified stationary phases, including alumina, cellulose, reverse phases containing ethyl-, octyl-, octadecyl-, and diphenylsilyl radicals bonded onto silica gel have appeared. The most recent stationary phases contain a chiral layer for enantiomer separations.[1]

At the same time, with diversification of the stationary phases, various new apparatuses, like the apparatus for automatic application of spots, the chromatographic chambers for circular and anti-circular development, automatic multiple development, or development at high pressure, chambers with gradients, equipment for registering "in situ" chromatograms have appeared.[2]

The mobile phase used in TLC can migrate along the stationary phase by capillarity or by applying another external force. Depending on the movement mode of the mobile phase, various development techniques have appeared: ascending, horizontal, continuous, multiple, bidimensional, circular, and anti-circular development. The last two techniques have experienced a continuous development, especially in recent times, because of their employment in preparative applications for the separation of bioactive substances from plants.[3]

CIRCULAR AND ANTI-CIRCULAR DEVELOPMENT

Circular TLC

In circular chromatography (radial chromatography), the sample for separation is spotted in the center of a plate as a circular spot. The mobile phase is introduced in the center of the circular chromatographic plate (Fig. 1). This technique can be used with normal chromatographic plates too, but cannot be used with multi-channel plates.

The movement of the mobile phase is radial, from the center to the periphery (Fig. 1), owing to capillarity and the centrifugal force induced by rotation of the plate. The retention factor (R_F) for circular development is given by Eq. 1, which is valid only when the start position coincides with the solvent entry position, i.e., the geometrical center of the chromatographic plate:

$$R_{F(lin)} = (R_{Fcirc})^2 \tag{1}$$

In the case when the entrance of the solvent and the start positions are different (Fig. 2), the circular retention factor can be calculated with the following equation:[4]

$$R_{Fcirc} = \sqrt{\frac{z_s^2 + R_{Flin}\,(z_f^2 - z_s^2)}{z_f - z_s}} - z_s \tag{2}$$

This equation was obtained from Kaiser's equation:[5]

$$R_{Flin} = \frac{z_c^2 - z_s^2}{z_f^2 - z_s^2} \tag{3}$$

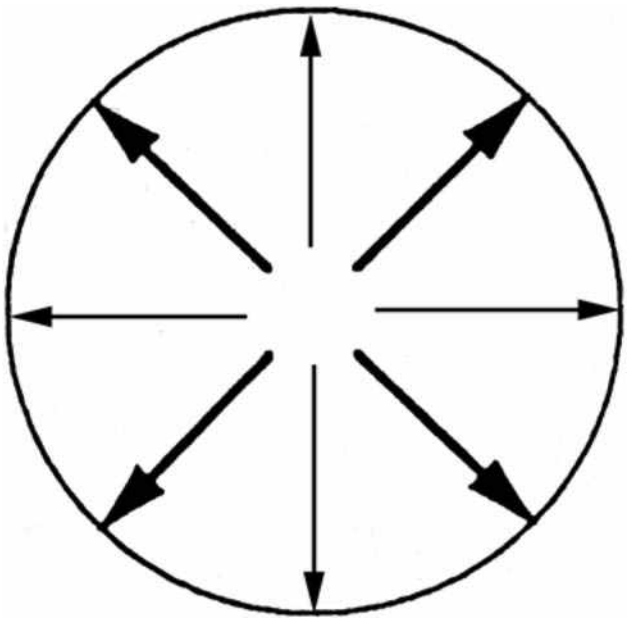

Fig. 1 Circular development.

The advantage of this technique is the improvement of resolution for compounds with low R_F, compared with linear chromatography.

One can achieve a better resolution, however, with increasing development time by modification of the circular chromatographic chamber. This modification consists of apertures made in the external part of the lid of the chamber, which leads to a continuous evaporation of the solvent. Sometimes, the solvent is continuously evaporated by heating.

By successive operations of development-drying applied to the chromatographic plate, a circular multiple development is achieved. Thus, the solvent front is multiply displaced through the chromatogram zones, achieving a concentration and deformation of the chromatographic spots. This results, in some cases, in elliptical spots or straight bands. Usually, this approach leads to an increase in resolution for compounds with R_F less than 0.5. The circular multiple development can be performed using one eluent or different eluents with various polarities, and on various lengths of development.

Anti-Circular TLC

In the case of the anti-circular technique, the chromatographic plate is placed horizontally, the sample is spotted as circles at the periphery of the plate, and the elution is performed from exterior to interior of the plate (Fig. 3).

The relationship between the retention factors in linear chromatography and anti-circular chromatography is given by the equation:

$$R_{\text{Flin}} = (R_{\text{Fanticirc}})^{0.5} \tag{4}$$

This method is advantageous for the separation of compounds with high R_F values.

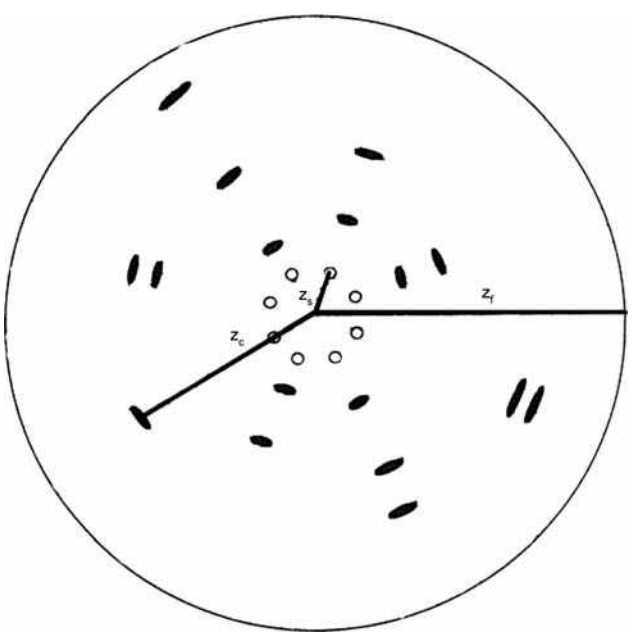

Fig. 2 Densitogram of a circular development.

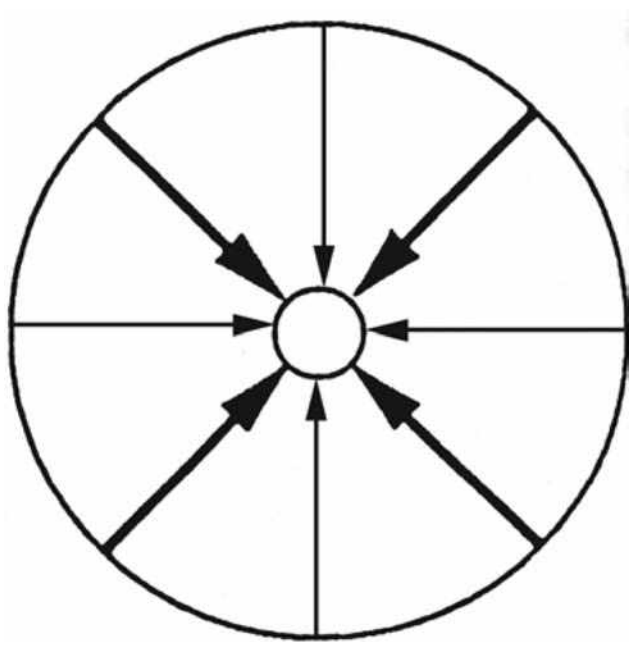

Fig. 3 Anti-circular development.

Equipment Used in Circular and Anti-Circular Chromatography

The first researchers in TLC, Ismailov and Schraiber, did not use a chamber; a vertical pipet supplied the solvent to the center of an applied sample spot. The simplest equipment for development of circular or anti-circular chromatograms in a closed system is a Petri dish containing the mobile phase and an appropriate means of transfer of mobile phase by capillary action to the chromatographic plate.[3]

The rotational circular chambers in an open system (Fig. 4) comprise a motor that rotates the chromatographic plate and a system for supplying the mobile phase, which is positioned perpendicularly to the chromatographic plate's center.

Rotation planar chromatography (RPC) uses a centrifugal force for mobile phase migration, in addition to the capillary action. The size of the vapor space above the chromatographic plate is an essential criterion in RPC methods and, based on this, the methods are classified into four basic techniques, namely normal chamber RPC (N-RPC), microchamber RPC (M-RPC), ultra-microchamber RPC (U-RPC), and column RPC (C-RPC).

Sequential RPC (S-RPC) is a special technique in which circular and anti-circular development modes are carried out sequentially in a normal chamber.

In N-RPC, the layer rotates in a stationary chromatographic chamber, whereas in M-RPC, a co-rotating chromatographic chamber is used and the vapor space is reduced. When using U-RPC, a quartz glass cover plate is placed directly on top of the layer, which almost completely eliminates the vapor space.

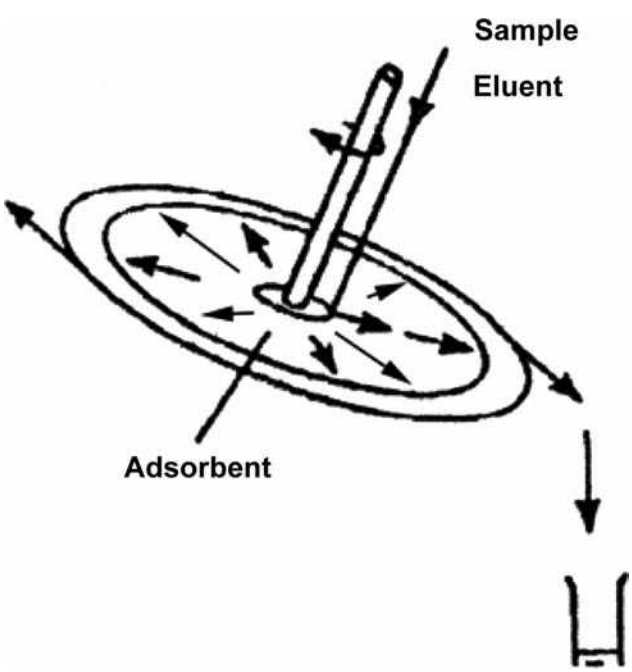

Fig. 4 Rotational chromatographic plate.

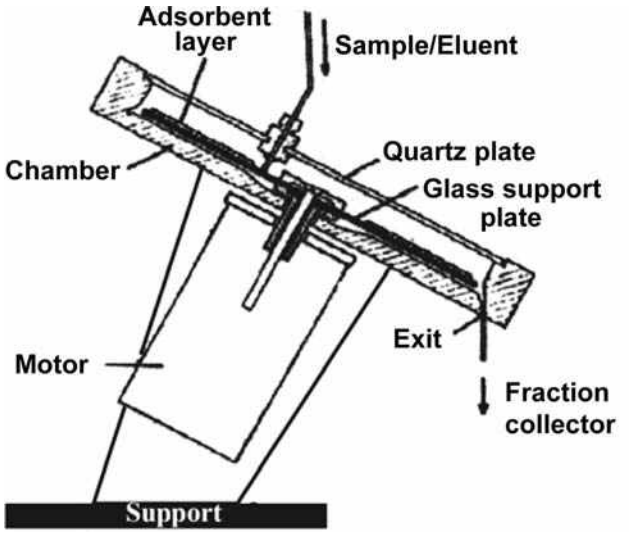

Fig. 5 Rotationally circular chromatographic chamber.

C-RPC differs from the previous three methods in that the stationary phase is placed in a closed circular chamber (planar column) and, hence, there is no vapor space. Owing to the special geometric design of the column, the volume of the stationary phase remains constant along the entire separation distance and the flow is accelerated linearly as in column chromatography.[6] The primary advantage of this design is the elimination of the extreme band broadening normally observed in all circular development techniques. As a result of its operating principle, C-RPC is only used for preparative separations.

Generally, these chambers comprise a support with a motor that rotates the circular chromatographic chamber and the chromatographic plate (Fig. 5).

The chamber is covered with a quartz glass and the mobile phase and the sample are introduced by a slide placed in the lid center of the chromatographic chamber. The mobile phase and the separated compounds are collected in a fraction collector after development.

The automatic apparatuses used for rotational circular chromatographic separations are called Chromatotron, Rotachrom, Cyclograph, and Extrachrom.

Applications of Circular Planar Chromatography

Circular planar chromatography is suitable for analytical purposes and preparative separations as well. Coumarine

from *Peucedanum polustre* (L.), iridoid glycosides, (+) catechin, and (−) epicatechin were isolated, separated, and identified by this technique for analytical purposes.[7] Circular planar chromatography was applied by Nyiredy and coworkers,[6] with success, for preparative separation of various classes of natural compounds, e.g., for peridin and β-carotene separation from *Gonyaulax polyedro* seaweed.[8]

CONCLUSIONS

The circular TLC is used for resolution increase in compounds with low R_F; the circular multiple developments are frequently used for separation of compounds with R_F less than 0.5. The anti-circular TLC is advantageous for the separation of compounds with high R_F values. The circular TLC can be performed in a closed system, on Petri dish, or in an open system, rotational circular chamber. Circular TLC was used with success for separation of bioactive compounds from plants.

REFERENCES

1. Măruţoiu, C.; Tofană, M.; Nica-Badea, D.; Popescu, A. Thin layer chromatography. In *Food Products Analysis*; Etnograph: Cluj-Napoca, 2005.
2. Ettre, L.S.; Kalász, H. LC-GC **2001**, *19*, 712.
3. Nyiredy, Sz. In *Planar Chromatography. A Retrospective View for the Third Millennium*; Nyiredy, Sz., Ed.; Springer Scientific Publisher: Budapest, 2001; 386.
4. Szabady, B. In *Planar Chromatography. A Retrospective View for the Third Millennium*; Nyiredy, Sz., Ed.; Springer Scientific Publisher: Budapest, 2001; 88.
5. Kaiser, R.E. *Einführung in die Hochdruck–Planar–Chromatographie*; Hüthig: Heidelberg, 1987.
6. Nyiredy, Sz.; Mészáros, S.Y.; Nyiredy-Mikita, K.; Dallenbach-Toelke, K.; Sticher, O. Centrifugal planar-column chromatography (CPCC): A new preparative planar technique. Part 1: Description of the method and practical aspects. J. High Resol. Chrom. **1986**, *9* (10), 605–606.
7. Vuorela, H.; Dallenbach-Tölke, K.; Hiltunen, R.; Sticher, O. J. Planar Chromatogr. -Mod. TLC **1988**, *1*, 123.
8. Pinto, E.; Catalani, L.H.; Lopes, N.P.; Di Mascio, P.; Colepicolo, P. Peridinin as the major biological carotenoid quencher of singlet oxygen in marin algae gonyaulex polyedra. Biochem. Biophys. Res. Comm. **2000**, *268*, 496.

Clinical Diagnosis by CE

Cheng-Ming Liu
Department of Medical Technology, Institute of Biomedical Technology, Taipei Medical University, Taipei, Taiwan

INTRODUCTION

The capillary electrophoresis (CE) technique has been developing since the late 1970s and early 1980s by Jorgenson and Lukacs[1] and some other investigators. This technique provides a rapid and accurate separation without the limitation of molecular size. Many instrument companies started to build a relatively sophisticated instrument for meeting the demand in the late 1980s. The first commercialized CE instrument was introduced into the market in 1989. At that time, major diagnostic reagent companies were interested in developing CE methods and reagents by using those instruments for clinical uses. So far, some routine clinical analyses, such as serum protein, myeloma protein, urinary Bence Jones protein, and hemoglobin (Hb) by CE are widely accepted by consumers. Some other specialized clinical analyses, such as nucleic acid and drug analyses, are still restricted in some clinical laboratories because of the lack of test kits and suitable software.

CLINICAL ANALYSIS

The Advanced Development Department of Beckman Instruments, Inc. (Beckman Coulter Inc., Fullerton, California, U.S.A.) began researching serum protein, myeloma protein, urinary protein, and Hb variants analysis by CE. The reason to start with those proteins as the analytes were because of their high concentrations existing either in serum or in blood. Because ultraviolet (UV) absorption has been used for protein quantitative analysis, so the concentration becomes a limitation and key factor. The results were published in Clinical Chemistry.[2] They compared the results from CE to results from the conventional methods (by gel electrophoresis) and found that they are highly similar. In serum protein analysis, the CE peaks were comparable with the results from conventional agarose gel electrophoresis in all five classical bands: albumin, alpha-1, alpha-2, beta, and gamma regions. However, CE analysis has prevailed over gel electrophoresis in terms of running time. Each run in CE, including conditioning, washing, and rinsing, required less than 10 min, as opposed to 2 hr in gel electrophoresis. High-resolution CE serum analysis was developed by the Beckman Advanced Research group in 1991.[3] Ten major serum proteins were separated, as shown in Fig. 1. Some proteins, which could not be separated by gel electrophoresis (such as C3 complement, beta lipoprotein, alpha-2 macroglobulin, alpha-1 acid glycoprotein, and prealbumin), were able to be separated by high-resolution CE analysis. These ten major proteins can give clinicians more information regarding disease status. A sharp, narrowed, outstanding peak in the gamma region usually represents myeloma protein in the serum. This "church spire-like" peak is very easy to find in the gamma region. However, the peak does not distinguish between classes and subtypes of M protein. To solve this problem, the investigators used antibodies against IgG, IgM, IgA, kappa, and lambda, each labeled with a solid phase column, separately. The patient sera were passed through the column individually, and the eluted sera were subjected to CE. The attenuated or absent peak thus reflected the class or subtype of M protein.[4] Fig. 2 is a panel of electropherograms, which represents an example of an IgGλ myeloma protein serum sample. The upper-left panel represents the whole electropherogram of patient serum. The upper-right is an overlap of two electropherograms, one before passing through the column with anti-IgG solid phase, and the other after passing through the column. Focusing on the region of immunoglobulin, the IgG peak of the second run is seen to attenuate substantially. A similar pattern is found in the antilambda column, while the remainder of the electropherograms generally overlap between the two runs. These results may indicate that the M-protein belongs to the IgG class and lambda type. Some myeloma patients may produce light-chain immunoglobulin. These proteins may be filtered through the kidney and ultimately appear in their urine (Bence Jones protein). The detection of either serum proteins or M-protein, using UV absorption (λ = 214 nm), was attempted when a small amount of undiluted urine was injected into the capillary to allow for normal spikes. The results showed a multipeaked electropherogram, with smaller protein peaks hiding among some other peaks. This renders identification of specific proteins difficult. To remove these non-protein peaks, a permeated polyacrylamide bead column was used. Large protein molecules passed through the column, while small molecules were bound by the beads. The eluted urine from the column was subjected to CE analysis, and the resulting electropherogram showed that all non-protein small molecules were retained in the column and only protein peaks

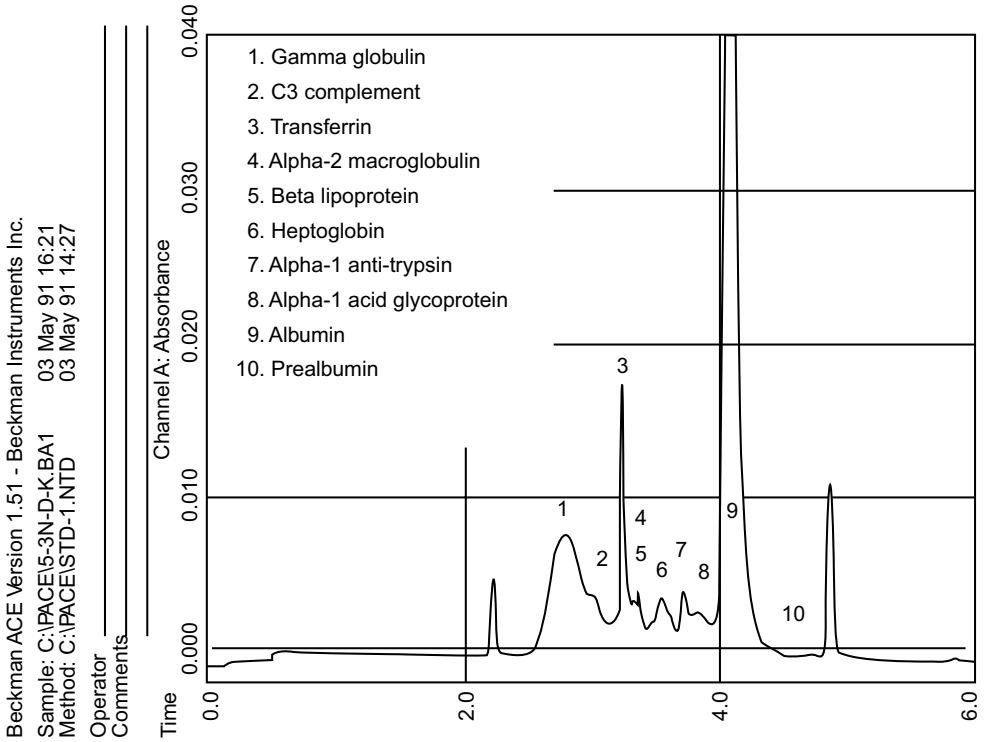

Fig. 1 The electropherogram from normal serum sample by CE. Running conditions: Fused silica capillary, 25 μm I.D. × 27 cm; detection at 214 nm; applied potential, 10 kV with Beckman Coulter proprietary running buffer. Each peak is labeled with the protein, which has been identified by both spiking and immunosubtraction methods. Two peaks without label are internal standards.

appeared, as if it was spiked or as it originally existed.[5] The first automated clinical CE instrument, Paragon CZE (capillary zone electrophoresis) 2000 (Beckman Coulter) was commercialized in the late 1990s. This automated CZE, with seven capillaries, provides reproducible and rapid serum electrophoresis. It is particularly useful in clinical laboratories that have a relatively large daily workload.

Hb is another analyte, which is easily amenable to CE analysis. This is because of its high clinical concentrations as well as its homogeneity. UV detection (absorption of 415 nm visible light) of Hb is more accurate than the dye-staining technique for protein quantitation. Hb variants such as HbS, HbC, and HbA (normal control) were subjected to CE analysis. With an optimized running buffer, the three species of Hbs were separated as three distinct peaks in the electropherogram (Fig. 3a); these results are comparable to conventional gel electrophoresis (Fig. 3b).[2]

Another clinical utility for Hb is in quantitation of HbA1c. HbA1c results from glucose binding with Hb via a non-enzymatic reaction (the Amadori rearrangement), to form a stable, glycated Hb. HbA1c is one of the best indicators for monitoring the status of diabetes control, and its clinical measurement has been recommended, by the American Diabetes Association, for patients. Glucose itself is a small, low-molecular-weight molecule, and when it is bound to Hb, the change of mobility within CE is not significantly noticeable. To solve this problem, the same group of investigators used high ionic strength running buffer, with high pH, for HbA1c analysis.[6] Fig. 4 shows that the glycated Hb was separated from non-glycated normal Hb in both a non-diabetic subject (upper panel) and in a diabetic patient (lower panel). A group of investigators in Belgium (Analis)[7] used a proprietary malic acid buffer, pH 4.5, in a preconditioned capillary tube, which was rinsed with an initiator solution and followed by a polyanion for HbA1c analysis. They found a high resolution for the HbA1c peak and some other Hb variant peaks such as HbS and HbC in the resulting electropherogram. This high-resolution Hb analytical method is very reproducible and well suited for clinical diagnostic requirements.

Single-wavelength detection is the standard method for analyte quantitative analysis. Because of the limitation of its sensitivity, a new method to overcome this problem uses a laser-induced fluorescence (LIF) approach. LIF offers high-sensitivity detection for some trace amounts of proteins or drugs in body fluids such as hormones, acute phase reactants, and drugs. The basic principle of LIF involves labeling a specific fluorochrome on either an antibody or antigen (analyte), which depends on the direct or competitive immunoassay.[8] When an analyte is bound to antibody to form a complex, the sizes and/or charges of the

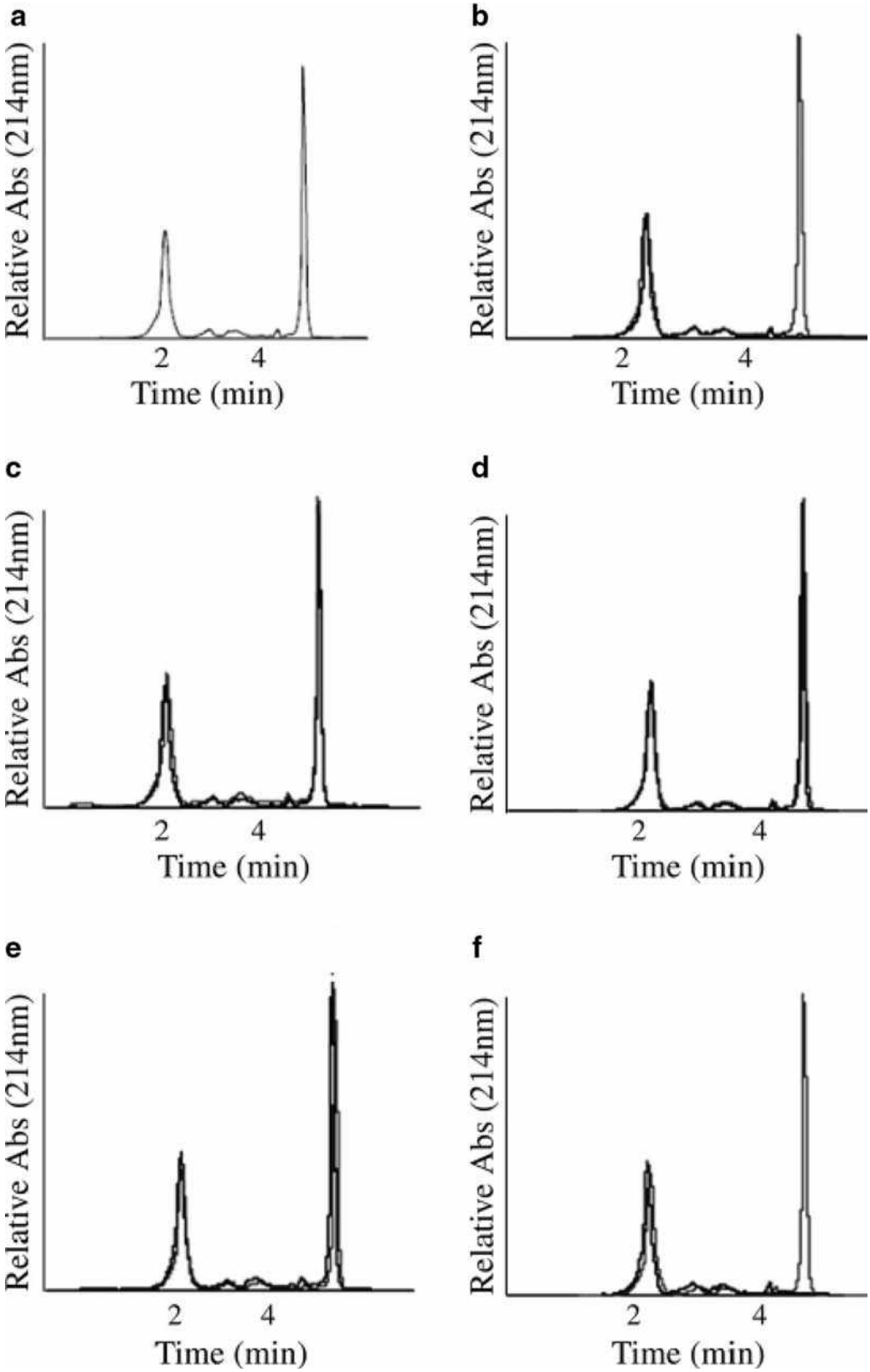

Fig. 2 Electropherograms of a myeloma patient's serum. a, Control serum protein analysis, a sharp "church spire" peak in gamma region (M protein). b, Two overlapped traces, one is before and the other (attenuated) is after incubation with solid-phase-labeled anti-IgG. c, The same processes as in (b) with solid-phase-labeled anti-IgM. d, The same processes as in (b) with solid-phase-labeled anti-IgA. e, The same processes as in (b) with solid-phase-labeled antikappa. f, The same processes as in (b) with solid-phase-labeled antilambda.

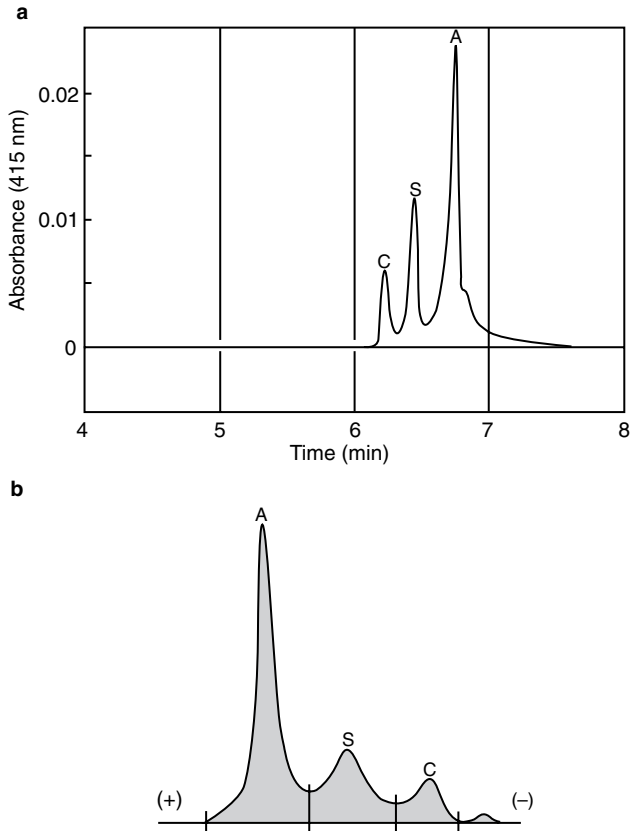

Fig. 3 Electropherogram of Hb control A, S, and C. a, Results from CE with Beckman proprietary buffer; running condition: fused-silica capillary, 75 μm (I.D.) × 27 cm; detection at 415 nm; Hb concentration is 2.5 g/L; Hb A, 65.3%; S, 23.9 and C, 10.8%. b, Results from the same sample by Acid-Hb gel with Paragon agarose gel electrophoresis system.

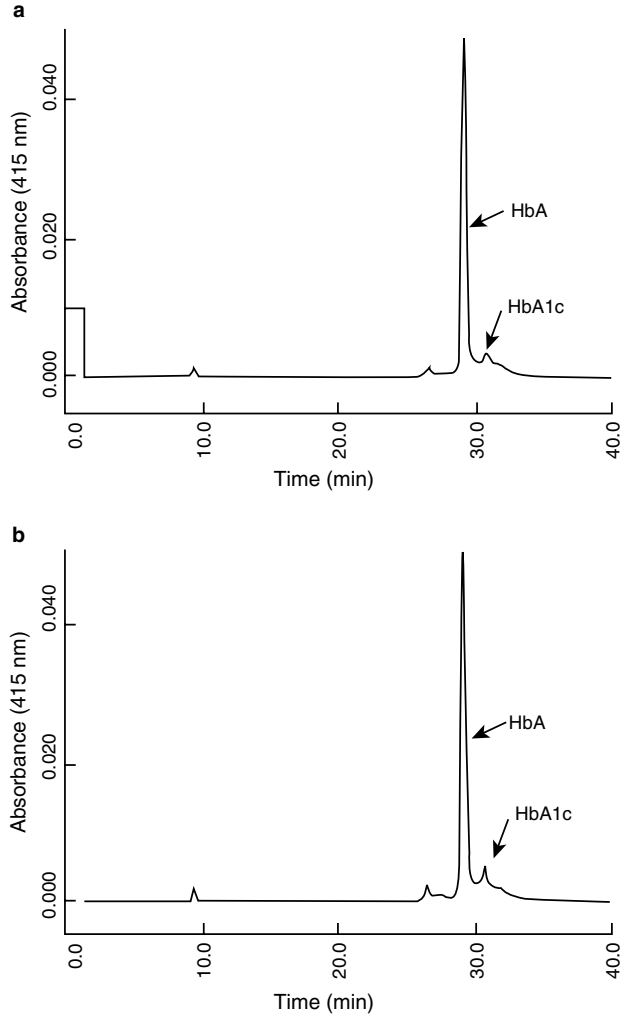

Fig. 4 Electropherograms of HbA1c. Conditions: fused-silica capillary, 25 μm (I.D.) × 27 cm; detection at 415 nm; running buffer, Beckman Coulter proprietary buffer. a, Hb from normal person. b, Hb from diabetic patient.

molecules will be changed, and the migration time will also most likely be changed. The complex peak then can be identified by its fluorescence on the antibody moiety and excited by laser; the emission light is collected and transformed to a signal by a photomultiplier tube (PMT).

Another major application of clinical CE is for DNA analysis. It includes DNA fragments analysis and DNA sequence analysis. The separation mechanism of DNA involves employing polyacrylamide-filled or agarose-filled capillaries; the different sizes of DNA fragments migrate through the pores of the gel. Hjerten[9] used 150 μm internal diameter (I.D.) gel-filled capillaries for both large- and small-molecule separations with high resolving power. Cohen, Najarian, and Karger[10] demonstrated an extremely high-resolution separation by using polyacrylamide gel, which contained sodium dodecyl sulfate; they obtained even higher resolution. The DNA fragment was amplified by using polymerase chain reaction (PCR) with fluorescent dye-labeled nucleotides. Applied Biosystems (ABI) offers the commercialized instrument, Genetic Analyzer (ABI Prism 310), which is an automated single-capillary genetic analyzer designed for a wide range of sequencing and fragment analysis applications.[11] It is very useful for rapid mapping of genetic traits leading to gene discovery and eventual diagnostic testing. Some genetic disease and neoplastic disorders[12,13] can be detected with this instrument.

In addition to aforementioned macromolecules, another area of interest is small-molecule analyses or some endogenous or exogenous compounds in biofluids and tissues, which are important for clinical diagnosis. Two capillary electrophoretic modes for small molecules analysis are CZE and micellar electrokinetic capillary chromatography (MEKC). As UV absorption detection has been used in most of cases, sample preparation is generally required. Samples are commonly from blood, serum, or urine, which may contain some macromolecules that may interfere with the UV absorption. These macromolecules such as proteins

have to be removed by either precipitation or extraction. The detection wavelength may depend upon the analyte compound's absorption maximum. Shihabi[14] used two volumes of acetonitrile mixed with one volume of serum to remove most proteins; this allows a large volume of sample to be injected into the capillary. They found some advantages of CE in drug analysis, compared with traditional high performance liquid chromatography or gas chromatography. Advantages include simplicity of sample preparation and instrumental setup, speed of analysis, high plate number of the separation, more modes for selection, and lower cost. There are two major areas for drug analysis. One is for therapeutic drug monitoring (TDM) and the other is for detection of drugs of abuse. TDM is one of the largest areas in clinical laboratory medicine, because of many drugs with narrow therapeutic windows; the other is continuous discovery of new drugs. TDM deals with the quantitation of drugs present in the serum as it relates to patient treatment and management. Many drugs such as antiepileptic drugs, immunosuppressive drugs, antiasthmatic drugs, analgesics, and antidepressants possess narrow therapeutic windows. In this regard, the precision quantitative drug analysis in serum becomes very critical. The other area for drug analysis is to detect some drugs such as cocaine, heroin, methamphetamine, lysergic acid diethylamide (LSD), and phencyclidine (PCP) that are elicited in body fluids such as urine or serum. A simple quantitative method uses CE with liquid cooling to analyze commonly seized illicit substances. Comparisons of CE quantitations with results from other laboratory techniques demonstrate the reliable adaptation of CE to the forensic laboratory.

CONCLUSIONS

Although CE is a mature analytical method in the research arena, in the clinical laboratory, it is still in its kindergarten stage. In 2001, only 13 out of 739 clinical laboratories in the U.S.A. subscribed to CAP proficiency testing for serum protein electrophoresis. To broaden the acceptance of CE in the mainstream of the clinical laboratory, the instrument companies need to develop chemical reagent kits and suitable software, with the instrument for the end user in the clinical laboratory. Because CE is still perceived as requiring a high technical expertise, precluding its use in a laboratory in which personnel are less technically adept. How to educate the laboratory personnel to convince them to understand the friendly operational procedure and efficient separation will be the future task.

REFERENCES

1. Jorgenson, J.W.; Lukacs, K.D. Zone electrophoresis in open tubular glass capillaries. Anal. Chem. **1981**, *53*, 1298–1302.
2. Chen, F.T.A.; Liu, C.M.; Hsieh, Y.-Z.; Sternberg, J.C. Capillary electrophoresis—A new clinical tool. Clin. Chem. **1991**, *37*, 14–19.
3. Liu, C.M. Clinical capillary electrophoresis on serum protein analysis. In *Feasibility and Viability Report*; Beckman Diagnostic System Group: Fullerton, California, March 28, 1992 .
4. Liu, Cheng-Ming; Wang, Hann-Ping; Chen, Fu-Tai; Klein, A.; Gerald, L.; Sternberg, J.C. Analysis of Samples by Capillary Electrophoretic Immunosubtraction. US Patent 5,228,960, July 20, 1993. Beckman and Coulter, Inc.
5. Liu, C.M.; Wang, H.P. Method of Sample Preparation for Urine Protein Analysis with CE. US Patent 5,492,834, February 20, 1996. Beckman and Coulter, Inc.
6. Keo, N.; Safarian, Z.; Liu, C.M.; Wang, H.P. Capillary Electrophoresis of Glycosylated Proteins. US Patent 5,599,433, 1997. Beckman and Coulter, Inc.
7. Doelman, C.J.A.; Siebelder, W.M.; Nijhof, W.A.; Weykamp, C.W.; Janssens, J.; Penders, T.J. Capillary electrophoresis system for hemoglobin A1c determinations evaluated. Clin. Chem. **1997**, *43* (4), 644–648.
8. Liu, C.M.; Tung, K.H.; Chang, T.H.; Chien, C.C.; Yen, M.H. Analysis of secretory immunoglobulin A in human saliva by laser-induced fluorescence capillary electrophoresis. J. Chromatogr. B, **2003**, *791*, 315–321.
9. Hjerten, S. High-performance electrophoresis: The electrophoretic counterpart of high performance liquid chromatography. J. Chromatogr. **1983**, *270*, 1–6.
10. Cohen, A.S.; Najarian, D.R.; Karger, B.L. Separation and analysis of DNA sequence reaction products by capillary electrophoresis. J. Chromatogr. **1990**, *516*, 49–60.
11. Stewart, J.E.B.; Aagaard, P.J.; Pokorak, E.G.; Polanskey, D.; Budowle, B. Evaluation of a mulicapillary electrophoresis instrument for mitochondrial DNA typing. J. Forensic Sci. **2003**, *48*, 1–9.
12. Beillard, E.; Pallisgaard, N.; van der Velden, V.H.J.; Bi, W.; Dee, R.; van der Schoot, E.; Delabesse, E.; Macintyre, E.; Gottardi, E.; Saglio, G.; Watzinger, F.; Lion, T.; van Dongen', J.J.M.; Hokland, P.; Gabert, J. Evaluation of candidate control genes for diagnosis and residual disease detection in leukemic patients using real-time quantitative reverse-transcriptase polymerase chain reaction (RQ-PCR)—a Europe against cancer program. Leukemia **2003**, *17*, 2474–2486.
13. Fallin, D.; Cohen, A.; Essioux, L.; Chumakov, I.; Blumenfeld, M.; Cohen, D.; Schork, N.J. Genetic analysis of case/control data using estimated haplotype frequencies: Application to APOE locus variation and Alzheimer's disease. Genomic Res. **2001**, *11*, 143–151.
14. Shihabi, Z.K. Sample matrix effects in capillary electrophoresis. II. Acetonitrile deproteinization. J. Chromatogr. **1993**, *652*, 471–475.

Coil Planet Centrifuges

Yoichiro Ito
National Heart, Lung, and Blood Institute (NHLBI), National Institutes of Health (NIH), Bethesda, Maryland, U.S.A.

INTRODUCTION

We have defined "coil planet centrifuge" (CPC) as a term that designates all centrifuge devices in which the coiled separation column undergoes a planetary motion, i.e., the column rotates about its own axis while revolving around the central axis of the centrifuge. Except for the original CPC, all existing CPCs are equipped with a flow-through system so that the liquid can pass through the rotating coiled column. In most of these flow-through CPCs, the use of a conventional rotary seal device is eliminated. These sealless systems are classified into two categories according to their modes of planetary motion, i.e., synchronous and non-synchronous (see *CCC: Instrumentation,* p. 327, Fig. 3). In the synchronous CPC, the coiled column rotates about its own axis during one revolution cycle, whereas in the non-synchronous CPC, the rates of rotation and revolution of the coiled column are freely adjustable. Among several different types of CPCs, the following four instruments are described below in terms of their best applications: the original CPC, the type-J CPC, the cross-axis CPC, and the non-synchronous CPC.

ORIGINAL CPC

This first CPC model was devised in an effort to improve the efficiency of lymphocyte separation which was conventionally performed in a short centrifuge tube. If a long tubing is wound into a coil and rotated in a centrifugal field, the particles present in the tube would travel through the tube from one end to the other at a rate depending on their size and density. This idea was implemented in the designs of the first device named the "CPC."[1]

Principle

Physical analysis of the motion of a particle in the rotating helical tube of a CPC has been carried out by means of a simple model is as follows.[1]

(A) We consider a tube filled with a fluid of density ρ_0 coiled into a helix of radius R, with its axis horizontal. If a spherical particle of radius a, density ρ, is placed in the tube, we can determine motion of the particle when the helix undergoes uniform rotation about its axis with angular velocity ω. As a first approximation, we neglect the lateral motion in the tube and assume that in a given turn of the coil, the particle moves on a vertical circle of radius R. The position of the particle can then be specified by the angle θ, as indicated in Fig. 1. With this approximation, the particle is acted on by only two forces, the Stokes drag

$$F_s = -6\pi a\eta R(d\theta/dt - \omega)$$

where η is the viscosity of the fluid, and the net gravitational force g tangent to the circular path

$$F_g = -(4\pi/3)a^3(\rho - \rho_0)g\sin\theta$$

The equation of motion is therefore

$$(4\pi/3)a^3\rho R(d^2\theta/dt^2) = F_s + F_g$$

and on introducing the total angle of rotation of the helix, $x = \omega t$, this can be written in the convenient form

$$d^2\theta/dx^2 + (1/\omega\tau)\{d\theta/dx - 1 + (\omega_e/\omega)\sin\theta\} = 0 \quad (1)$$

where τ is the relaxation time

$$\tau = 2\rho a^2/9\eta \quad (2)$$

and ω_e is the critical angular velocity

$$\omega_e = (2/9)\{(\rho - \rho_0)ga^2\}/\eta R = V_e/R \quad (3)$$

where V_e is the equilibrium Stokes velocity. We consider separately the motion for

$$\omega_e/\omega > 1 \quad \text{and} \quad \omega_e/\omega < 1$$

(B) $\omega_e/\omega > 1$. In this case, Eq. 1 has a singular point at $\omega_e/\omega \sin\theta = 1$, i.e., at $\theta = \theta_2 = \sin^{-1}(\omega/\omega_e)$, $0 \le \theta \le \frac{\pi}{2}$, and at $\theta = \pi - \theta_e$. The terms θ_e and $\pi - \theta_e$ are the angles at which the drag of the liquid is just balanced by the gravitational force so that the particle is at equilibrium when at rest. It is readily seen from physical considerations that the equilibrium at θ_e is stable while that at $\pi - \theta_e$ is unstable. More precisely, an analysis in the neighborhood of the singular points shows that $\pi - \theta_e$ is an unstable saddle point, while θ_e is

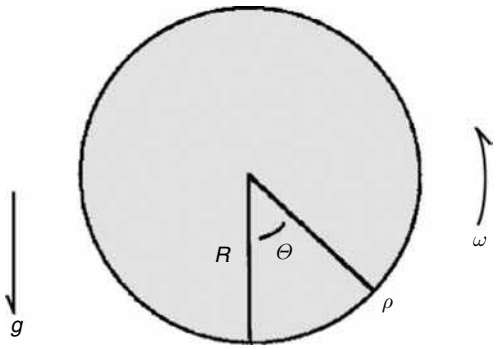

Fig. 1 The coil unit for mathematical analysis of the motion of a particle.
Adapted from The coil planet centrifuge, in Nature.[1]

a stable node if $\omega\tau \leq 1/4 \tan \theta_e$ and a stable spiral point if $\omega\tau > 1/4 \tan \theta_e$. Consequently, after a time of the order of τ, the particle will remain fixed at θ_e. Its angular velocity relative to the tube will then be

$$\omega_{rel} = \omega\{d\theta/dx - 1\} = -\omega \quad (4)$$

That is, it will spiral down the helix at a rate independent of its size and density.

(C) $\omega_e/\omega < 1$, $\omega\tau < 1$. When $\omega_e/\omega < 1$, Eq. 1 has no singular points. The character of the motion, however, depends to some extent on the size of $\omega\tau$, and we shall consider in detail only the physically interesting case $\omega\tau < 1$. It can readily be shown that within this limit, after a time of the order of τ, angular velocity of the particle adjusts itself in such a way that the inertial term, $\omega\tau\, d^2\theta/dx^2$, becomes negligible, so that Eq. 1 reduces to

$$d\theta/dx = 1 - \omega_e/\omega \ \sin \theta \quad (5)$$

The particle then always rotates in the same direction as the tube, but more slowly than the tube when $0 < \theta < \pi$ and more rapidly when $\pi < \theta < 2\pi$. The two effects, however, do not quite cancel out, and the net effect is that, again, the particle spirals down the tube in a direction opposite to that of the tube rotation.

To determine the mean angular velocity of this spiraling motion, we first calculate the time required for the particle to traverse one turn of the coil. We have from Eq. 5

$$X(2\pi) - X(0) = \int_0^{2\pi} d\theta/\{1 - (\omega_e/\omega) \sin \theta\} = 2\pi/\{1 - [(1 - \omega_e/\omega)^2]\}^{1/2}$$

The mean angular velocity of the particle relative to the tube is therefore

$$\omega_{rel} = \omega\{2\pi/[X(2\pi) - X(0)] - 1\} = -\omega\{1 - [1 - (\omega_e/\omega)^2]^{1/2}\} \quad (6)$$

which joins continuously on to the value at $\omega_e/\omega = 1$ of Eq. 4.

When ω is close to ω_e, ω_{rel} is rather insensitive to the size and density of the particle. When $\omega_e/\omega < 1$, however, Eq. 6 becomes

$$\omega_{rel} = -\omega_e^2/2\omega \quad (7)$$

so that the rate of motion down the tube is proportional to a^4 and $(\rho - \rho_0)$. Thus, when $\omega_e < \omega < 1/\tau$, the method should be quite effective in segregating particles of different size and density.

In order to apply (A)–(C) to the CPC, the value of g should be replaced by that of the centrifugal force acting on the axis of the rotating helical tube.

Design of the Original CPC

Fig. 2 shows the first commercial model of the CPC manufactured by Sanki Engineering, Ltd. (Kyoto, Japan).[1,3] The main body of the apparatus consists of three parts, each capable to rotation as a unit: coil holder (6) and interchangeable

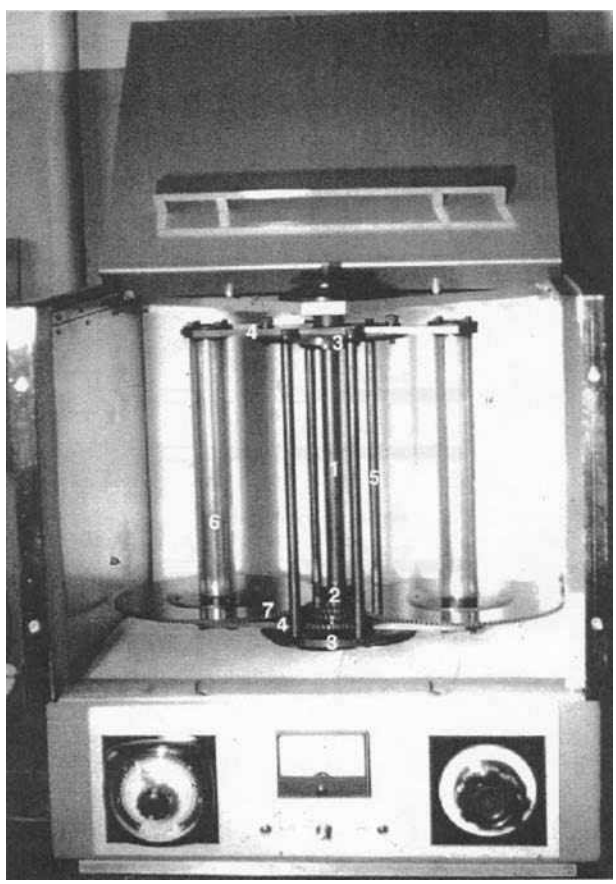

Fig. 2 The coil planet centrifuge fabricated by Sanki Engineering Ltd., Kyoto, Japan.
Source: From The coil planet centrifuge, in Nature.[1]

gear (7) (part I); frame or a pair of arms (4) and discs (3) bridged with links (5) (part II); and central shaft (1) and gear 2 which interlocks to gear 7 of part I. Simultaneous rotation of parts II and III at different angular velocities results in revolution and rotation of part I as a planet. The rotation of part I is determined by the difference in angular velocity between parts II and III and by the gear ratio between 2 and 7.

The apparatus can produce $1000 \times g$ force where the ratio between the coil rotation and revolution can be adjustable to 1/100, 1/300, or 1/500 by interchanging the planetary gears (7) at the bottom of the column holder (6). Each coil holder is equipped with six straight grooves at its periphery to accommodate six coiled tubes that are covered by a transparent vinyl sheath protector tightly fitted to the outside of the holder. Each coil is made by winding either polyethylene or Teflon tubing (typically 0.3 mm I.D.) onto a glass core (15 cm long and 6 mm diameter). After the liquid and sample are introduced into the tube, both ends of the coil are closed before loading onto the holder.

Three Different Modes of Operation

Preliminary experiments with the CPC revealed some interesting features of the apparatus. The results are summarized in Fig. 3.[1]

(I) Single medium: When the tube is filled with a single medium and a particle mixture is introduced at one end, centrifugation separates the particles according to Fig. 3. The difference in size and relative density. The method was effectively demonstrated by a model experiment using polyacrylic resin particles.[1]

(II) Two mutually miscible media (gradient method): When the tube is filled with two mutually miscible media, the heavier in one half and the lighter in the other half, centrifugation produces a density gradient. After centrifugation for some time, the gradient reaches a fairly stable state. In practice, such a stable gradient between water and isotonic saline solution can be introduced into the coil to measure osmotic fragility of erythrocytes. Erythrocytes introduced into the saline side of the coil are forced to travel through the gradient down to the point where hemolysis occurs, the distribution of hemoglobin thus formed, indicating the osmotic fragility of the sample.[2]

(III) Two mutually immiscible media CC. When two mutually immiscible media are used similarly, centrifugation forces these two media to undergo countercurrent motion, and, in the final stage, each turn of the coil is occupied by the two media nearly half and half as illustrated in Fig. 3-III. Consequently, a small amount of a sample injected beforehand at the interface of the two media, i.e., the middle portion of the tube, is distributed along the tube according to its partition coefficient. This CC method is applicable to microgram amounts of chemicals with a high efficiency that may be equivalent to near 1000 units of a Craig countercurrent distribution apparatus.

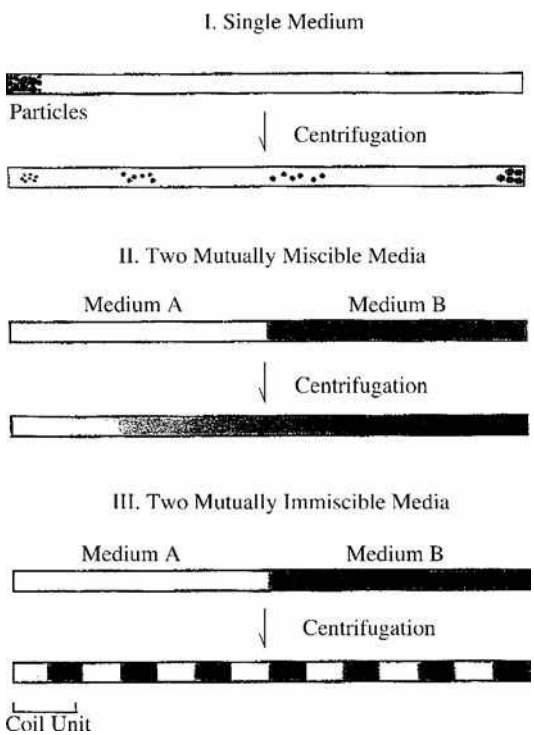

Fig. 3 The principle of three different applications of the coil planet centrifuge. All tubes are shown uncoiled before and after centrifugation.
Source: From The coil planet centrifuge, in Nature.[1]

Applications to CC

Capability of the apparatus for performing microscale CC has been demonstrated using three different samples, i.e., a mixture of dyes, agal proteins, and mammalian erythrocytes.[3]

Separation of dyes

Fig. 4a shows CC separation of four basic dyes, i.e., methyl green (MG), methylene blue (MB), neutral red (NR), and basic fuchsin using a two-phase solvent system composed of isoamylalcohol–ethanol–acetic acid-distilled water (4:2:1:5, v/v). The first coil displays the separation of the mixture, and the other coils show distribution of individual dyes to demonstrate the reproducibility of the method. The separation was performed with 6 m of 0.35 mm I.D. tubing (~300 helical turns) at relative coil rotation of 0.25 rpm at $300 \times g$ for 10 hr.

Separation of algal proteins

Phycoerythrin and phycocyanin were extracted from dried Asakusa-nori (*Porphyra tenera*) and subjected to partition with an aqueous polymer phase system (Table 1) using the above standard countercurrent method. Fig. 4b shows the results of separation, where two components are well resolved.

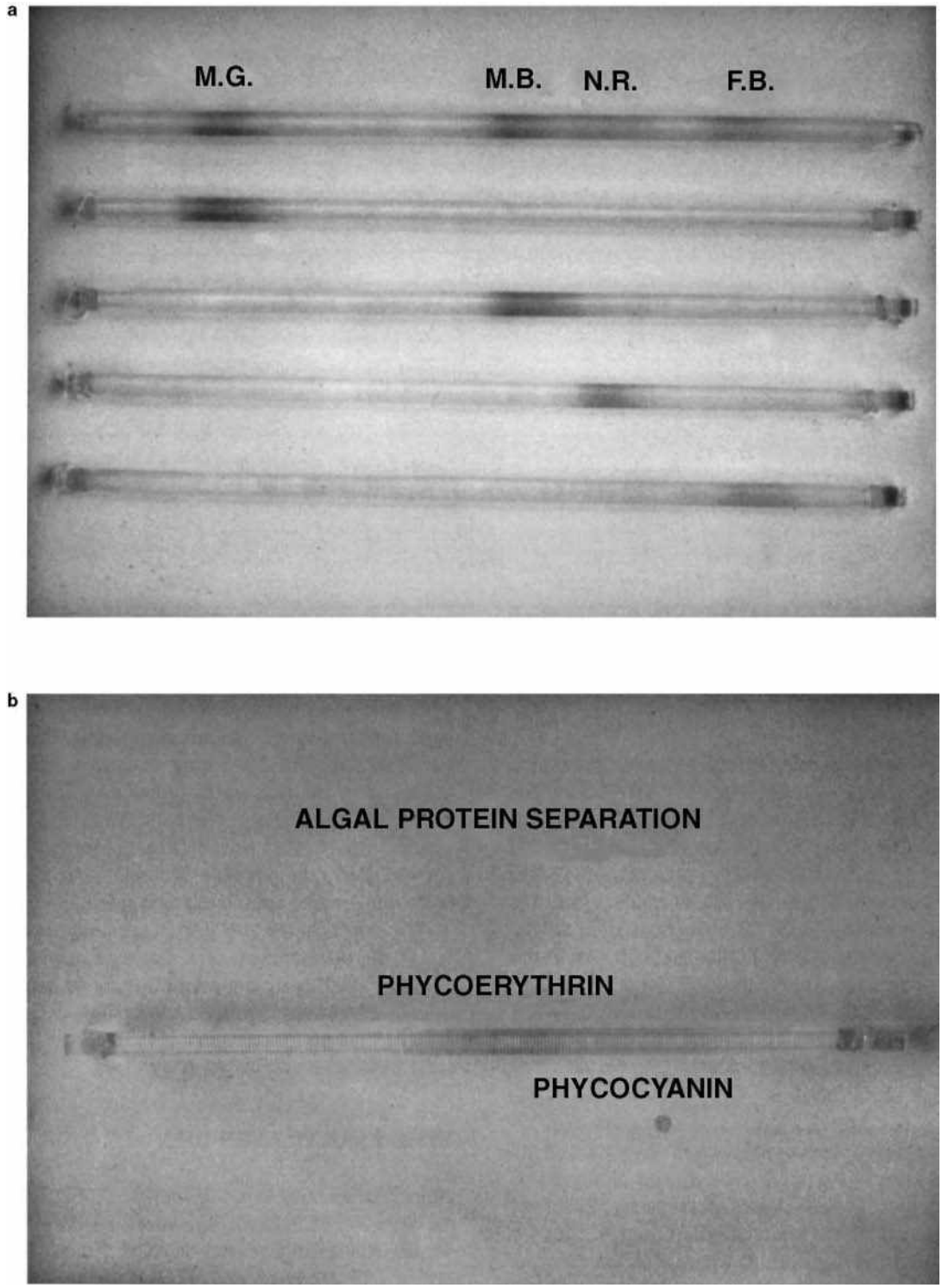

Fig. 4 Countercurrent separation of various samples by the coil planet centrifuge. a, Separation of basic dyes with an organic/aqueous two-phase solvent system. M.G.: methyl green; M.B.: methylene blue; N.R.: neutral red; F.B.; basic fuchsin. b, Solvent system consisted of isoamyl alcohol/ethanol/acetic acid/water (4:2:1:5, v/v). (c) Separation of rabbit vs. human erythorcytes.
Source: From New micro liquid–liquid partition techniques with the coil planet centrifuge, in Anal. Chem.[3]

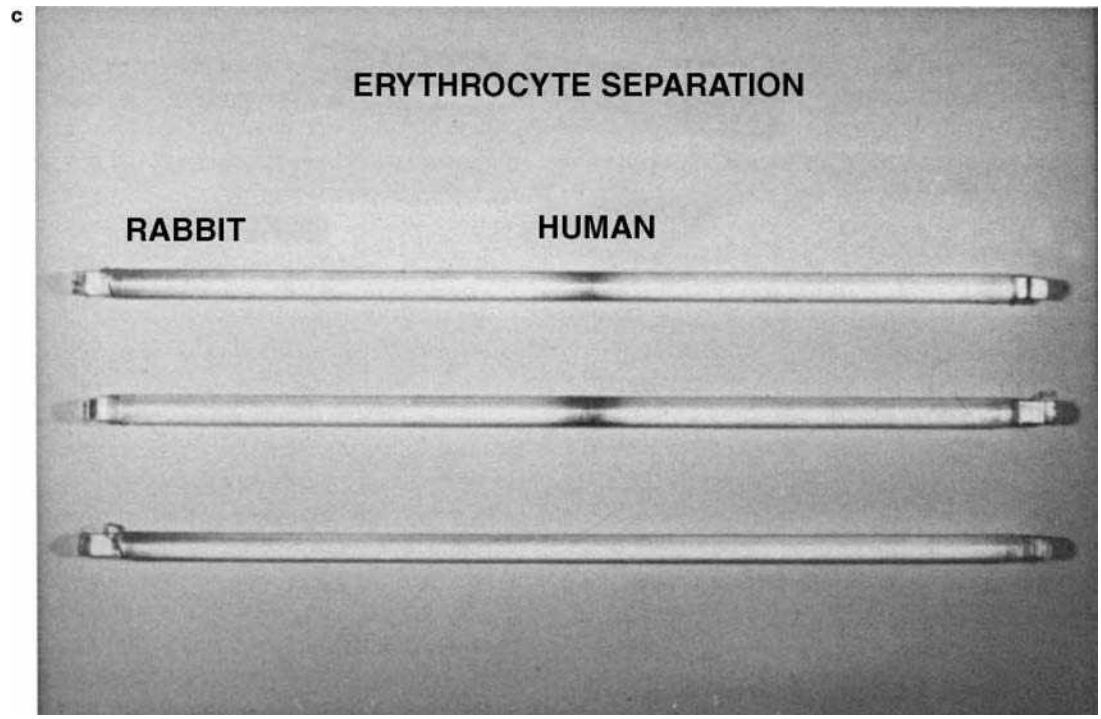

Fig. 4 (*Continued*)

Erythrocyte separation

The separation of human and rabbit erythrocytes was performed with a modified method using a gradient between a pair of polymer phase systems A and B (Table 2), where the upper phase of A and the lower phase of B were used for separation. Before charging with sample, the coil was rotated at 1500 rpm at a relative rotation of 1/100 (15 rpm) for 30 min, which produced a gradient between the two phases along the coil. Then the sample cell mixture was loaded followed by centrifugation for 1 hr. Fig. 4c shows the partition of human and rabbit erythrocytes which were completely separated along the coil.

The results of the above studies using the original CPC led to the development of a series of new CPC devices equipped with a flow-through system that permits continuous elution through the column as in other chromatographic systems.

Table 1 Polymer phase system for separation of algal proteins.

20% (w/w) Dextran 500	35.0 g
30% (w/w) PEG 8000[a]	14.7 g
0.05 *M* KH_2PO_4	10.0 ml
0.05 *M* K_2HPO_4	10.0 ml
0.22 *M* KCl	10.0 ml
H_2O	20.3 ml

Source: From New micro liquid–liquid partition techniques with the coil planet centrifuge, in Anal. Chem.[3]

Table 2 A pair of polymer phase systems for separation of erythrocytes.

System A		System B	
20% (w/w) Dextran 500	25.0 g	20% (w/w) Dextran 500	25.0 g
30% (w/w) PEG 8000[a]	13.3 g	30% (w/w) PEG 8000[a]	13.3 g
0.55 *M* NaH_2PO_4	5.0 ml	0.55 *M* NaH_2PO_4	5.0 ml
0.55 *M* Na_2HPO_4	5.0 ml	0.55 *M* Na_2HPO_4	5.0 ml
25% HSA[b]	1.0 ml	25% HSA[b]	1.0 ml
H_2O	50.7 ml	1.5 *M* NaCl	10.0 ml
		H_2O	40.7 ml

[a]PEG 8000 was labeled as PEG 6000 in early applications.
[b]HSA = human serum albumin.
Source: From New micro liquid–liquid partition techniques with the coil planet centrifuge, in Anal. Chem. [3]

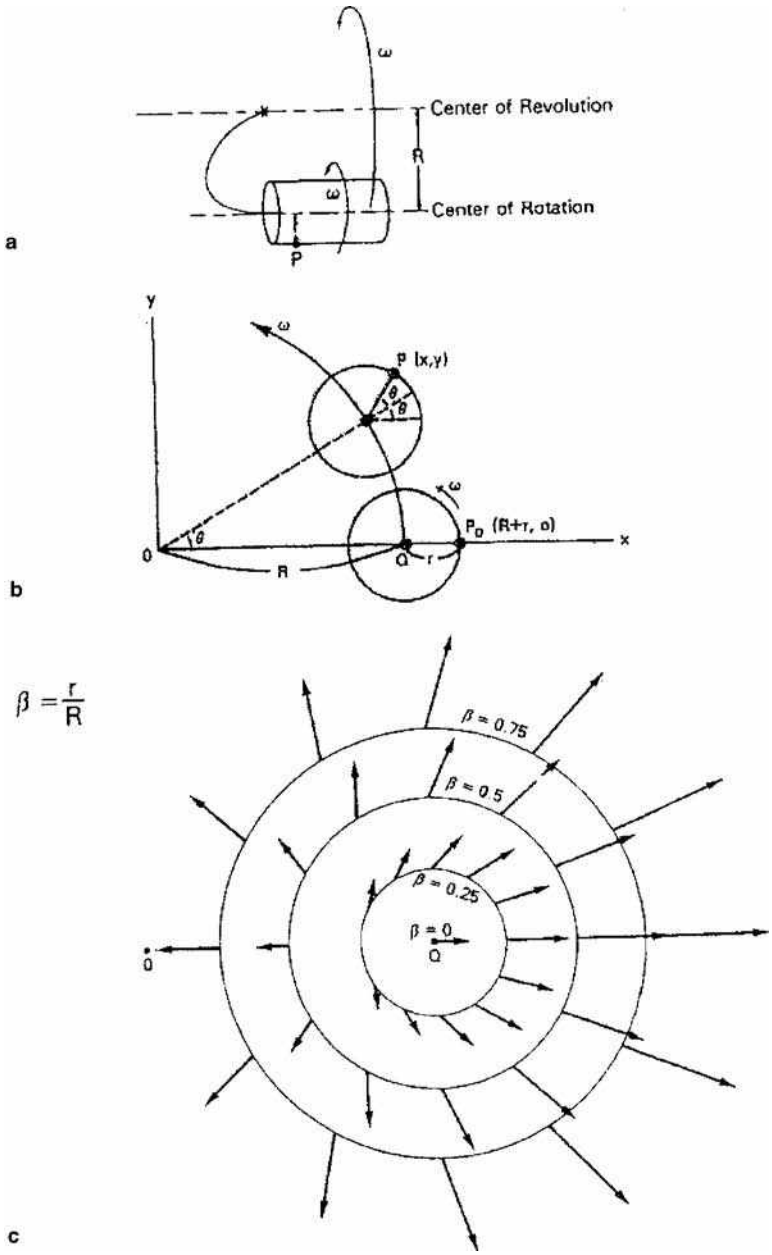

Fig. 5 Analysis of centrifugal force field for type-J planetary motion. a, Planetary motion; b, planetary motion in an *x–y* coordinate system for the analysis of centrifugal force; and c, distribution of the centrifugal vectors on the column holder.
Source: From Coil planet centrifuges for high-Speed countercurrent chromatography, in *Countercurrent Chromatography.*[12]

TYPE-J MULTILAYER CPC

Among all existing types of seal-free flow-through CPCs, the type-J CPC affords the most efficient and speedy separations or "high-speed CCC," and it has been extensively used for preparative separations of natural and synthetic products.

Mathematical Analysis of Planetary Motion

The type-J synchronous planetary motion of the coil holder is shown in Fig. 5a (see also *CCC: Instrumentation,* p. 327, Fig. 3), where the holder rotates about its own axis and simultaneously revolves around the axis of the centrifuge at the same angular velocity but in the opposite direction. Simple mathematical analysis[4] is performed using a coordinate system shown in Fig. 5b, where the center of the revolution coincides with the center of the coordinate system (point O). For convenience of analysis, the center of rotation and an arbitrary point are initially located on the *x*-axis. After the lapse of time t, the holder circles around point O by $\theta = \omega t$, while the arbitrary point circles around the axis of rotation by 2θ to reach $P(x, y)$ where

$$x = R \cos \theta + r \cos 2\theta \tag{8}$$

$$y = R \sin \theta + r \sin 2\theta \tag{9}$$

The acceleration produced by the planetary motion is then obtained from the second derivatives of Eqs. 8 and 9,

$$d^2x/dt^2 = -R\omega^2(\cos\theta + 4\beta\cos 2\theta) \quad (10)$$

$$d^2y/dt^2 = -R\omega^2(\sin\theta + 4\beta\sin 2\theta) \quad (11)$$

where $\beta = r/R$.

From Eqs. 10 and 11, two centrifugal force components, i.e., Fr (radical component) and Ft (tangential component), are computed using the following formula:

$$\mathrm{Fr} = R\omega^2(\cos\theta + 4\beta) \quad (12)$$

$$\mathrm{Ft} = R\omega^2(\sin\theta) \quad (13)$$

Fig. 5c shows the distributions of force vectors computed from Eqs. 12 and 13 at various locations on the column holder. All vectors confined in a plane perpendicular to the holder axis. As the holder rotates, both the direction and the net strength of the force vector fluctuate in such a way that the vector becomes longest at the point remote from the centrifuge axis and shortest at the point close to the central axis of the centrifuge. In most locations, the vectors are directed outwardly from the circle except for $\beta < 0.25$, where its direction is reversed at the vicinity of the center of revolution. This fluctuating centrifugal force field creates unique hydrodynamic effects on the two solvent phases in the coiled tube.

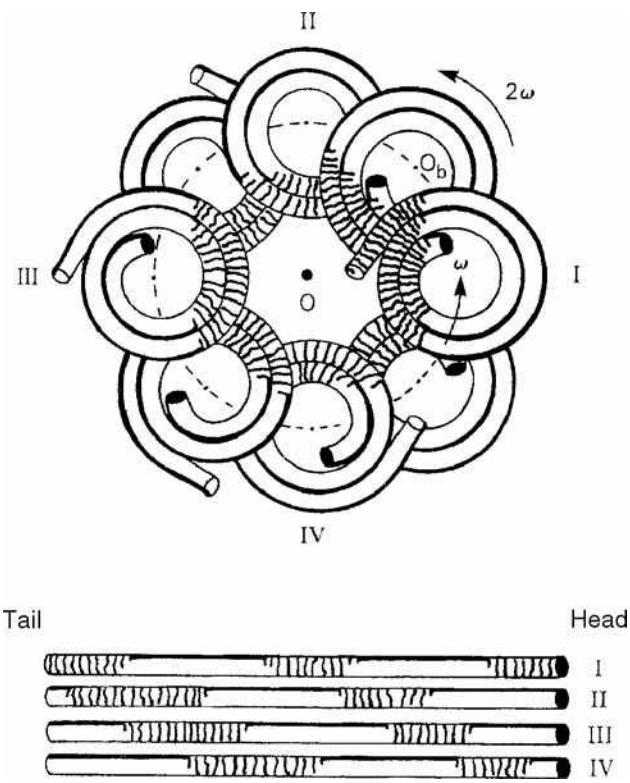

Fig. 6 Mixing and settling zones in the spiral column undergoing type-J planetary motion.
Source: From Coil planet centrifuges for high-speed countercurrent chromatography, in *Countercurrent Chromatography.*[12]

Stroboscopic Observation of Hydrodynamic Motion of Solvent Phases

Fig. 6 schematically illustrates motion of the two solvent phases in a spiral column, which is subjected to the type-J synchronous planetary motion. The upper diagram shows distribution of two solvent phases in the column observed under stroboscopic illumination. About one-fourth of the area near the center of revolution (point O) shows vigorous mixing of the two phases (mixing zone), whereas in the rest of the area, the two phases are separated by a strong centrifugal force in such a way that the lighter phase occupies the inner portion and the heavier phase occupies the outer portion of the tube. Four stretched tubes in the lower diagram illustrate the traveling pattern of the mixing zone through the spiral tube in one revolution cycle. In analogy to the motion of a wave advancing over water, the mixing zone travels one spiral turn for each revolution. This indicates that the solutes are subjected to an efficient partition process of repeating mixing and settling at a high rate of 13 times per second at 800 rpm of revolution. This accounts for the high partition efficiency of the present system, and we have called it "high-speed CCC."[4]

Design of the Apparatus

Fig. 7 shows a photograph of the most advanced model of the multilayer CPC, which holds a set of three multilayer coil separation columns symmetrically around the rotary frame.[5,6] All columns are connected in series with flow tubes which are supported by counterrotating pipes placed between the column holders. The type-J synchronous planetary motion of the holder is provided by engaging a planetary gear on the column holder with an identical stationary sun gear mounted around the central stationary shaft of the centrifuge. The counterrotation of the tube holder is effected by interlocking a pair of identical gears, one mounted on the holder and the other on the tube holder. Flow tubes from each end of the column assembly are passed through the central rotary shaft to exit the centrifuge on each side, where they are tightly affixed with a pair of clamps.

The multilayer coil separation column is prepared by winding a single piece of Teflon or Tefzel tubing around a spool-shaped column holder making multiple coiled layers between a pair of flanges. Currently, three different sets of multilayer coils are commercially available: the large preparative scale (2.6 mm I.D., ~1000 ml total capacity); the standard preparative column (1.6 mm I.D., ~320 ml total capacity); and the analytical scale (0.85 mm I.D., ~120 ml

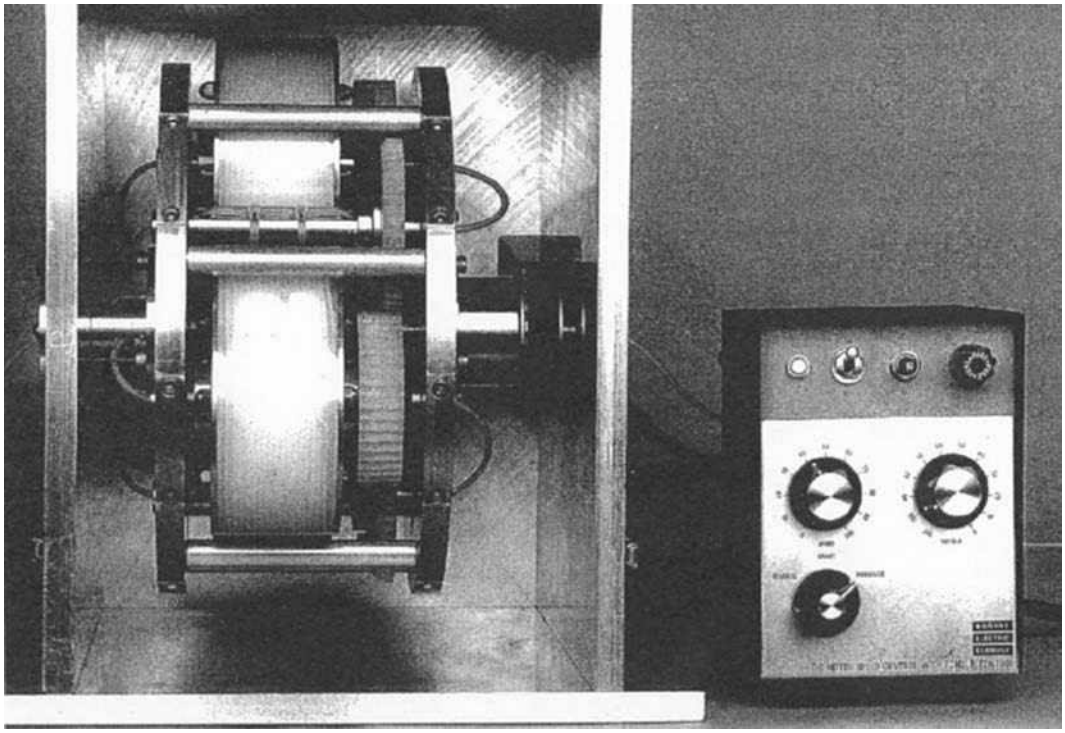

Fig. 7 Improved high-speed CCC centrifuge equipped with three column holders.
Source: From Improved high-speed countercurrent chromatograph with three multilayer coils connected in series, II. Separation of various biological samples with a semipreparative column in J. Chromatogr.[6]

capacity). The optimal revolution speed of the apparatus ranges from 800 to 1200 rpm.

Applications

Because of its rapid and high separation efficiency, the multilayer coil CPC has been extensively used for separation and purification of variety of compounds using suitable organic/aqueous solvent systems. The application also covers special CCC techniques such as peak-focusing CCC and pH-zone-refining CCC[7] (see *pH-Peak-Focusing and pH-Zone-Refining CCC*, p. 1808); chiral and affinity CCC (see *Chiral CCC*, p. 413); foam CCC[8] (see *Foam CCC*, p. 905), liquid–liquid dual CCC;[9] and CCC/MS (see *CCC/MS*, p. 323).

The method, however, fails to retain viscous, low interfacial tension polymer phase systems such as polyethylene glycol (PEG)–dextran systems[10] due to its intensive mixing effect which tends to produce emulsification, resulting in carryover of the stationary phase. This problem is largely eliminated by the cross-axis CPC described below.

CROSS-AXIS CPC

The cross-axis CPC has a specific feature in that it permits the universal use of two-phase solvent systems including aqueous–aqueous polymer phase systems which are useful for partitioning macromolecules and cell particles.[10]

Acceleration Field

The design of the cross-axis CPC is based on the hybrid between type-L and type-X planetary motions, which results in an extremely complex centrifugal force field with a three-dimensional fluctuation of force vectors during each revolution cycle of the holder. The pattern of this centrifugal force field produced by the cross-axis CPC somewhat resembles that produced by the type-J planetary motion (Fig. 5c), but it is superimposed by a force component acting in parallel to the axis of the coil holder. This additional force component acts to improve the retention of the stationary phase. This beneficial effect is greatest in type-L planetary motion and becomes smallest in the type-X planetary motion. A detailed mathematical analysis on this planetary motion is described elsewhere.[11]

Design of the Apparatus

Fig. 8 shows the general principle of various cross-axis CPCs. The geometrical parameter of the system is shown in Fig. 8a, where the orientation and planetary motion are indicated relative to the axis of the apparatus. The vertical axis of the

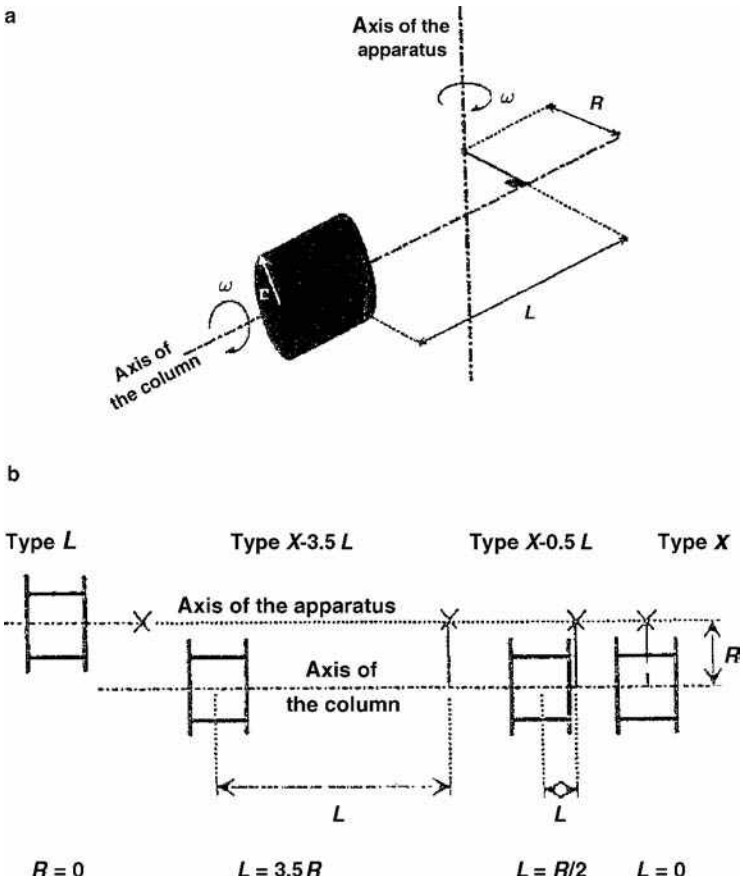

Fig. 8 General principle of various cross-axis CPCs. a, Geometrical parameters and; b, some examples of prototypes built in NIH Machine Shop. *X* type in 1987; *X*-0.5 *L* type in 1988; *X*-3.5 *L* type in 1991; and *L* type in 1992.
Source: From Coil planet centrifuges for high-Speed countercurrent chromatography, in *Countercurrent Chromatography*.[12]

apparatus and the horizontal axis of the coil are always kept perpendicular to each other at a fixed distance. The cylindrical column revolves at the central axis at the same rotational speed with which it rotates about its own axis. Three parameters displayed in Fig. 8a explain various versions of the cross-axis prototypes: r is the radius of the column holder, R is the distance between the two axis, and L is the measure of the lateral shift of the column holder along its axis. The name of a cross-axis device is based on the ratio L/R, when $R \neq 0$. Types *X* and *L* represent the limits for the column positions; type *X* involves no shifting of the column holder, while type L corresponds to an infinite shifting. Some examples of prototypes fabricated at the machine shop in the National Institutes of Health, Bethesda, MD, are shown in Fig. 8b.

The two different column designs are schematically shown in Fig. 9: The first column (multilayer coil) is used for preparative scale separations, while the second column (eccentric coil) is for analytical scale separations. The multilayer coil is prepared by winding a large Teflon tubing (2.6 mm I.D.) directly onto the holder hub in such a way that after completing each coiled layer, the tubing is directly returned to the starting point to wind the second layer over this connecting tube segment, and so on. This results in multiple coiled layers of the same handedness that are connected in series with short-tube segments as shown in Fig. 9a. The eccentric coil is prepared by winding a piece of Teflon tubing (typically 0.85 mm I.D.) onto a set of multiple short cores (~6 mm O.D.), which is arranged around the periphery of the holder hub as shown in Fig. 9b.

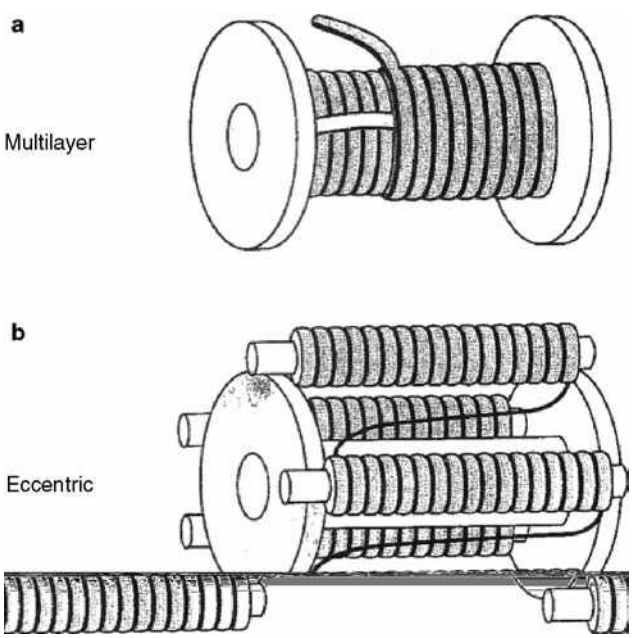

Fig. 9 Two different types of coiled columns for cross-axis CPC. Multilayer coil is for large-scale separations and eccentric coil assembly for small-scale separations.

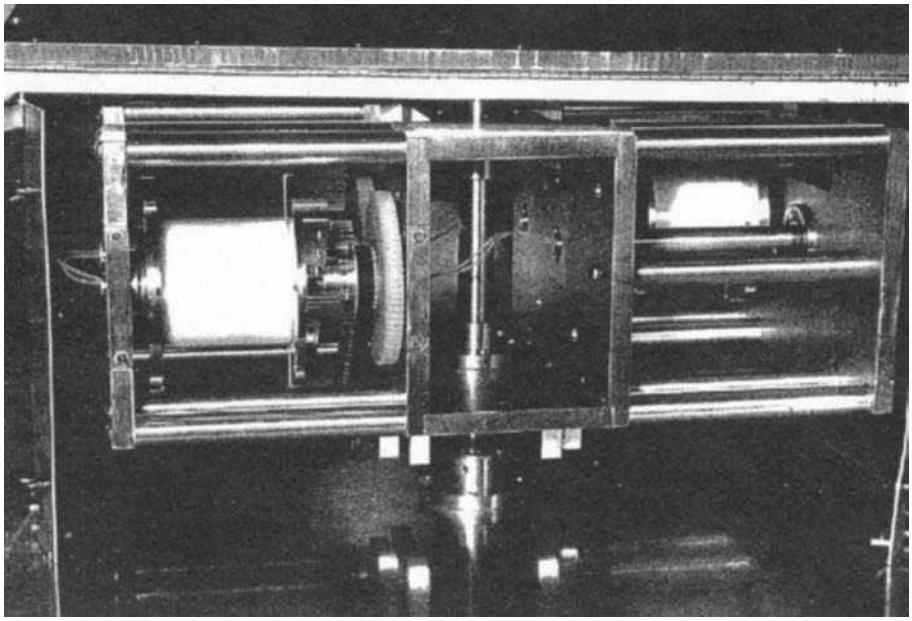

Fig. 10 Photograph of *X*-1.5 *L* and *L* prototypes. The rotary frame of the apparatus is driven by a motor (back of the apparatus) by coupling a pair of toothed pulleys one on the motor shaft and the other on the central shaft with a belt. Two cylindrical holders are mounted in the *X*-1.5 *L* or off-center position. The inlet and the outlet Teflon tubes go through the upper plate of the apparatus inside the hollow part of the central vertical axis. A circular metallic plate around the rotary frame decreases the torque by an average of 30%.
Source: From Coil planet centrifuges for high-Speed countercurrent chromatography, in *Countercurrent Chromatography*.[12]

Fig. 10 shows a photograph of a recently designed cross-axis CPC equipped with a pair of multilayer coil separation columns.[12] The column can be mounted on the rotary frame in two positions, *X*-1.5 *L* (off-center position) and *L* (central position). The off-center position is used for both organic/aqu-eous and aqueous PEG—potassium phosphate systems, while the central position is used for viscous, low interfacial tension PEG–dextran systems.

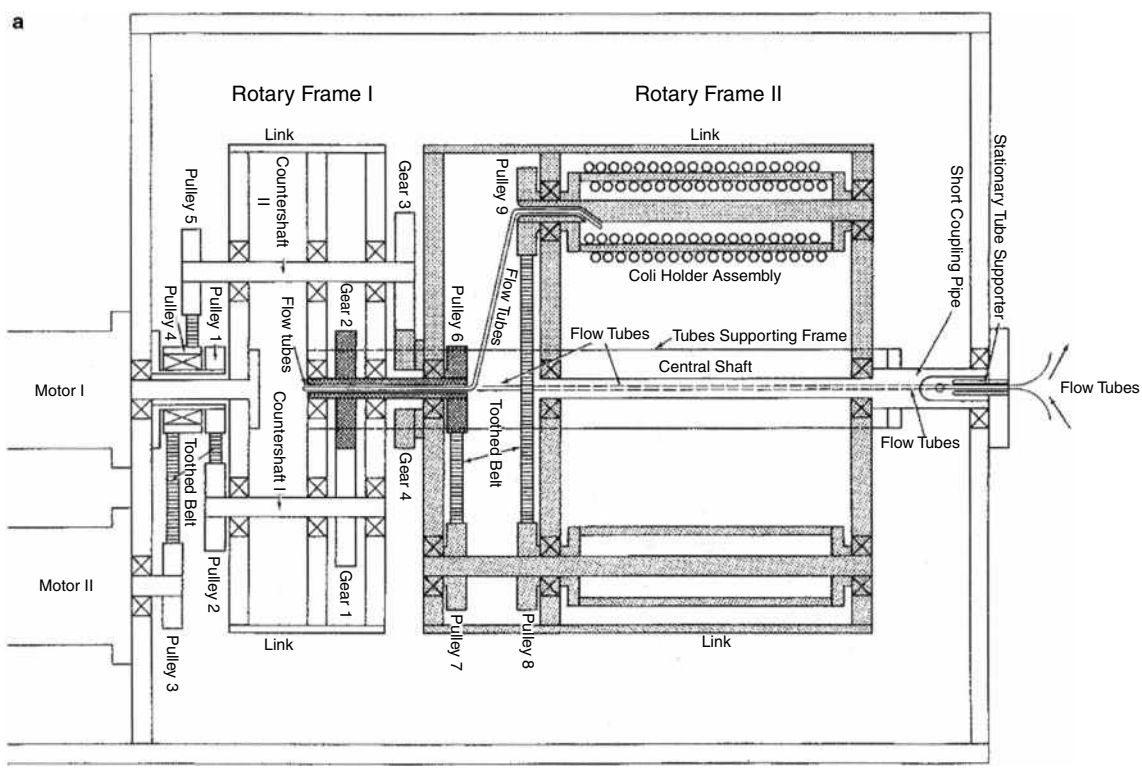

Fig. 11 Improved non-synchronous flow-through coil planet centrifuge without rotary seals. a, Cross-sectional view through the central axis of the apparatus; and b, photograph of the apparatus equipped with an eccentric coil assembly.
Source: From Improved nonsynchronous flow-through coil planet centrifuge without rotating seals, Principle and application, in Sep. Sci. Technol.[14]

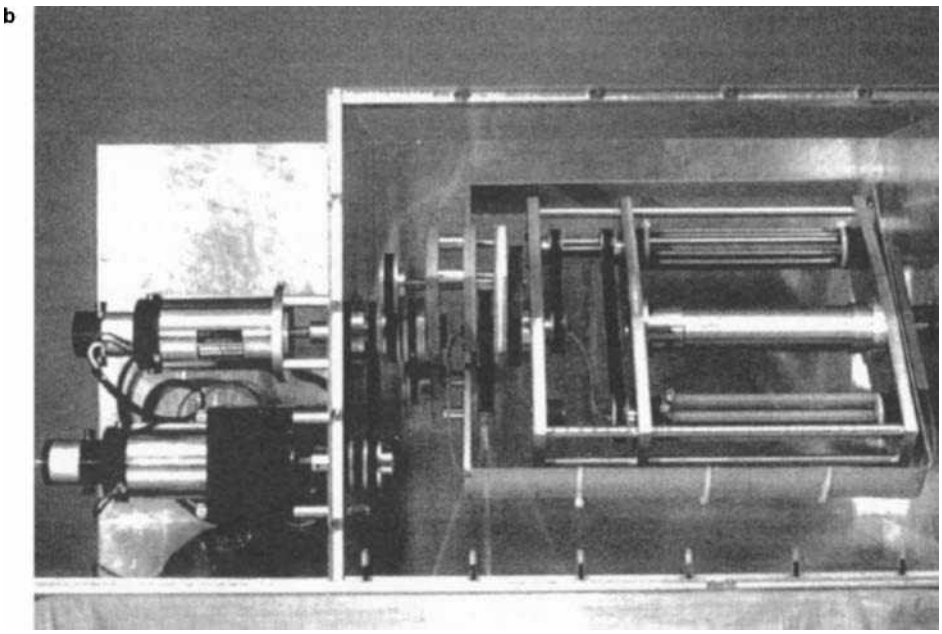

Fig. 11 (*Continued*)

Applications

Although cross-axis CPCs yield less efficient separations than the type-J multilayer CPC, they provide more stable retention of the stationary phase and are therefore useful for large-scale preparative separations with polar solvent systems. These are especially useful for the purification of proteins with aqueous–aqueous polymer phase systems composed of PEG and potassium phosphate. The cross-axis CPC has been used for the purification of various enzymes including choline esterase, ketosteroid isomerase, purine nucleoside phosphorylase, lactic acid dehydrogenase, uridine phosphorylase (see *Proteins: Cross-Axis Coil Planet Centrifuge Separation*, p. 1935).

NON-SYNCHRONOUS CPC

The non-synchronous flow-through CPC is a particular type of planetary centrifuge which allows adjustment of the rotational rate of the coiled separation column at a given revolution speed. The first prototype was equipped with a dual rotary seal for continuous elution.[13] Later, an improved model[14] was designed to eliminate the rotary seal which had become a source of complications such as leakage, contamination, and clogging.

Design Principle of the Seal-Free Non-synchronous CPC

Fig. 11a shows a cross-sectional view through the central axis of the apparatus. The rotor consists of two major rotary structures, i.e., frames I and II, which are coaxially bridged together with the center piece (dark shade).

Frame I consists of three plates rigidly linked together and directly driven by motor I. It holds three rotary elements, namely, the centerpiece (center), countershaft I (bottom), and countershaft II (top), all employing ball bearings. A pair of long arms extending symmetrically and perpendicularly from the middle plate forms the tube-supporting frame, which clears over frame II to reach the central shaft on the right side of frame II.

Frame II (light shade) consists of three pairs of arms linked together to rotate around the central shaft. It supports a pair of rotary shafts, one holding a coil holder assembly and the other the counterweight.

There are two motors, i.e., motors I and II, to drive the rotor. When motor I drives frame I, the stationary pulley 1 introduces counterrotation of pulley II through a toothed belt; therefore, countershaft I rotates at $-\omega_I$ with respect to rotating frame I. This motion is further conveyed to the centerpiece by 1:1 gearing between gears 1 and 2. Thus, the centerpiece rotates at $2\omega_I$ or at ω_I with respect to the rotating frame I. The motion of frame I also depends upon the motion of motor II.

If motor II is at rest, pulley 5 becomes stationary same with pulley 1 so that countershaft II counterrotates at ω_I as does countershaft I. This motion is similarly conveyed to the rotary arms of frame II by 1:1 gearing between gears 3 and 4, resulting in rotation of frame II at $2\omega_I$ or the same angular velocity as that of the centerpiece. Consequently, coupling of pulleys 6 to 7 and 8 to 9 with toothed belts produces no additional motion to the rotary shaft, which simply revolves with frame II at $2\omega_I$ around the central axis of the apparatus.

When motor II rotates at ω_{II}, idler pulley 4 coupled to pulley 3 on the motor shaft rotates at the same rate, which, in turn, modifies the rotational rate of pulley 5 on countershaft II. Thus, countershaft II now counter-rotates at $\omega_I - \omega_{II}$ on frame I. This motion further alters the rotational rate of frame II through 1:1 gear coupling between gears 3 and 4. Subsequently, frame II rotates at $2\omega_I - \omega_{II}$ with respect to the earth or at $-\omega_{II}$ relative to the centerpiece which always rotates at $2\omega_I$. The difference in rotational rate between frame II and the center piece is conveyed to the rotary shafts through coupling of pulleys 6 to 7 and 8 to 9. Consequently, both rotary shafts rotates at ω_{II} about their own axes while revolving around the central axis of the apparatus at $2\omega_I - \omega_{II}$. This gives the rotation/revolution ratio of the rotary shaft

$$r/R = \omega_{II}/(2\omega_I - \omega_{II}) \quad (14)$$

Therefore, any combination of revolutional and rotational speeds of the coil holder assembly can be achieved by selecting the proper values of ω_I and ω_{II}.

Coiled Column and Flow Tubes

Two different column configurations are used: a multilayer coil and an eccentric coil assembly. The multilayer coil column is prepared by winding a piece of Teflon tubing, typically 1.6 mm I.D., directly onto the holder hub ($\sim$ 2.5 cm O.D.), making multiple coiled layers as those for the type-J high-speed CCC. The eccentric coil assembly was made by winding a piece of Teflon tubing, typically 1 mm I.D., onto a set of six units of 0.68 cm O.D. stainless steel pipe in series. These coil units are arranged around the holder with their axis in parallel to the holder axis (see "Eccentric coil assembly" in Fig. 9, lower diagram). A pair of flow tubes from each end of the coiled column is first led through the hole of the rotary shaft and then pass through the opening of the centerpiece to exit at the middle portion of frame I. The flow tubes are then led along from the tube support to clear frame II and then reach the side hole of the central shaft near the right wall of the centrifuge where they are tightly held by the stationary tube supporter.

Fig. 11b shows the overall photograph of the apparatus equipped with an eccentric coil assembly. The revolution speed of the coil holder assembly is continuously adjustable up to 1000 rpm combined with any given rotational rate between 0 and 50 rpm in either direction.

Applications

The non-synchronous CPC is a most versatile centrifuge which can be applied to a variety of samples including cells, macromolecules, and small molecular weight compounds. Cell separations may be performed with a single phase such as physiological solution or culture medium[14,15] and also with PEG–dextran polymer two-phase systems.[16] DNA and RNA are partitioned with a PEG–dextran system by optimizing the pH.[14]

CONCLUSIONS

The CPC, which was originally developed for separating blood lymphocytes, has evolved into several useful instruments for separations of cells, macromolecules, and small molecular weight compounds. Among those, the type-J multilayer CPC is most extensively utilized for high-speed CCC separations of natural and synthetic products. The utility of the type-J CPC may be extended to the polymer phase separation of macromolecules and cell particles with a spiral disk assembly currently being developed in our laboratory.

ACKNOWLEDGMENT

The author is indebted to Dr. Henry M. Fales of Laboratory of Biophysical Chemistry, National Heart, Lung, and Blood Institute, National Institutes of Health, Bethesda, MD, for editing the manuscript.

REFERENCES

1. Ito, Y.; Weinstein, M.A.; Aoki, I.; Harada, R.; Kimura, E.; Nunogaki, K. The coil planet centrifuge. Nature **1966**, *212*, 985–987.
2. Harada, R.; Ito, Y.; Kimura, E. A new method of osmotic fragility test of erythrocytes with coil planet centrifuge. Jpn. J. Physiol. **1969**, *19*, 306–314.
3. Ito, Y.; Aoki, I.; Kimura, E.; Nunogaki, K.; Nunogaki, Y. New micro liquid–liquid partition techniques with the coil planet centrifuge. Anal. Chem. **1969**, *41*, 1579–1584.
4. Ito, Y. High-speed countercurrent chromatography. CRC Crit. Rev. Anal. Chem. **1986**, *17* (1), 65–143.
5. Ito, Y.; Oka, H.; Slemp, J.L. Improved high-speed countercurrent chromatograph with three multilayer coils connected in series. I. Design of the apparatus and performance of semipreparative columns in DNP amino acid separation. J. Chromatogr. **1989**, *475*, 219–227.
6. Ito, Y.; Oka, H.; Lee, Y.-W. Improved high-speed countercurrent chromatograph with three multilayer coils connected in series. II. Separation of various biological samples with a semipreparative column. J. Chromatogr. **1990**, *498*, 169–178.

7. Ito, Y.; Ma, Y. pH-zone-refining countercurrent chromatography. J. Chromatogr. A, **1996**, *753*, 1–36.
8. Ito, Y. Foam countercurrent chromatography based on dual countercurrent system. J. Liq. Chromatogr. **1985**, *8*, 2131–2152.
9. Lee, Y.-W.; Fang, Q.-C.; Cook, C.E.; Ito, Y. The application of true countercurrent chromatography in the isolation of bio-active natural products. J. Nat. Prod. **1989**, *52* (4), 706–710.
10. Albertsson, P. *Partition of Cell Particles and Macromolecules*; Wiley Interscience: New York, 1986.
11. Ito, Y.; Oka, H.; Slemp, J.L. Improved cross-axis synchronous flow-through coil planet centrifuge for performing countercurrent chromatography. I. Design of the apparatus and analysis of acceleration. J. Chromatogr. **1989**, *463*, 305–316.
12. Ito, Y.; Menet, J.-M. Coil planet centrifuges for high-Speed countercurrent chromatography. In *Countercurrent Chromatography*; Menet, J.-M., Thiebaut, D., Eds.; Marcel Dekker: New York, 1999; 87–119.
13. Ito, Y.; Carmeci, P.; Sutherland, I.A. Nonsynchronous flow-through coil planet centrifuge applied to cell separation with physiological solution. Anal. Biochem. **1979**, *94*, 249–252.
14. Ito, Y.; Bramblett, G.T.; Bhatnagar, R.; Huberman, M.; Leive, L.; Cullinane, L.M.; Groves, W. Improved non-synchronous flow-through coil planet centrifuge without rotating seals. Principle and application. Sep. Sci. Technol. **1983**, *18* (1), 33–48.
15. Okada, T.; Metcalfe, D.D.; Ito, Y. Purification of mast cells with an improved nonsynchronous flow-through coil planet centrifuge. Int. Arch. Allergy Immunol. **1996**, *109*, 376–382.
16. Leive, L.; Cullinane, M.L.; Ito, Y.; Bramblett, G.T. Countercurrent chromatographic separation of bacteria with known difference in surface lipopolysaccharide. J. Liq. Chromatogr. **1984**, *7* (2), 403–418.

Collagen: HPLC and Capillary Electromigration

Ivan Miksík
Institute of Physiology, Academy of Sciences of the Czech Republic, Prague, Czech Republic

INTRODUCTION

The term collagen covers a broad group of proteins. It is a family of extracellular matrix proteins possessing typical features—they consist of three polypeptide chains (called α-chains) and contain at least one domain composed of a repeating tripeptide sequence: -Gly-X-Y-. The protein chains are coiled together into a left-handed helix and are then wound around a common axis to form a triple helix with a shallow right-handed superhelical pitch; so, the overall structure is a rope-like rod. The typical presence of glycine at every third position is essential for this packing to a coiled-coil structure and is one of the ways to determine the presence of collagen in a tissue sample. Any amino acid other than glycine can be present in the X and Y positions, but proline is often found in the X position and 4-hydroxyproline in the Y position. 4-Hydroxyproline plays particularly an important role, because these residues are essential for the stability of the triple helix. All collagens also have non-collagenous domains.

Collagens are the most abundant proteins in the human body, constituting approximately 30% of its protein mass. At present, there are at least 28 known collagen types in vertebrates, containing a total of 42 distinct α-chains, and more than 20 additional proteins have collagen-like domains. Besides α-chains, there are also β-chains (dimers of α-chains) and γ-chains (trimers of α-chains).

The most common types of collagens occur in fibers and networks. These proteins are poorly soluble (if at all), are found in many tissues such as connective tissue, and have a slow metabolic turnover. This is the reason why they are more susceptible to some enzymatic or non-enzymatic posttranslational modifications.

Polymerized fibril-forming collagens (whether polymerized physiologically or non-physiologically) are insoluble and their solubilization is routinely performed either by mild pepsinization, in which short terminal regions containing the polymerization sites (crosslinks) are cleaved off, or by cyanogen bromide (CNBr) cleavage, which results in a limited fragmentation of the parent α-chains, as mentioned previously. Tissue collagenases split the triple-helical structure two-thirds of the way from its N-terminus; bacterial collagenases (from *Clostridium histolyticum*) are far less specific, they cleave the sequence into small fragments (mostly tripeptides) and are, therefore, of little use in structural studies.

Investigations of these proteins can either focus on their intact α-polypeptide chains or on their fragments (after cleavage). The most traditional methods for the analysis of collagens are slab gel electrophoresis (HPLC), low-pressure and high-performance liquid chromatography (HPLC), but recently capillary electromigration methods have also begun to be used.

STANDARD (LOW-PRESSURE) LIQUID CHROMATOGRAPHIC SEPARATION PROCEDURES

The application of classical (low-pressure) chromatography for the isolation of fibril-forming collagens from tissues has a long tradition and involves a large number of methods. Practically all types of chromatographic operational modes have been utilized for this purpose [for a review, see, e.g., Deyl and Adam (1989)] and frequently strategic combinations of them are used, exploiting, e.g., the presence or absence of S–S bonds in the terminal region (or along the whole molecule as is the case with collagen type III), charge, molecular size, the presence of glycosidic residues, or differences in the physicochemical properties of individual collagen species in their native and denatured forms.

The most common methods for the preparation of collagens are various extractions and precipitations or the release of protein by enzymatic hydrolysis. These methods mainly include extraction with an NaCl–phosphate buffer, acetate buffer, or acetic acid, and precipitation using various concentrations of NaCl (their usage depends on the tissue and type of collagen).

The most useful low-pressure chromatographic method for the purification of collagens is diethylaminoethyl (DEAE)-cellulose chromatography for removing co-extracted proteoglycans. Typical conditions for this form of chromatography can be as follows: the sample of collagen is dissolved in 0.2 mol/L NaCl with 0.05 mol/L Tris–HCl at pH 7.5 and fed into a DEAE-cellulose column (e.g., Whatman DE-52) which was equilibrated with the same buffer. After that, collagens are eluted with additional buffer, and proteoglycans are eluted by an increasing concentration of NaCl (1 mol/L).

Other chromatographic methods should also be mentioned: gel-permeation methods (molecular sieving), carboxymethyl (CM) cellulose chromatography, bioaffinity

chromatography (Concanavalin A, thiol-activated Sepharose, Heparin Sepharose) or zone precipitation chromatography. Cation-exchange chromatography and phosphocellulose chromatography are very popular methods (elution is carried out with an NaCl gradient).

The separation steps are most often monitored by SDS-PAGE.

HPLC AND CAPILLARY ELECTROPHORETIC METHODS

Separations of collagens must contend with the problems of achieving high resolution among poorly soluble high molecular mass proteins or a complex mixture of peptides with similar structures (glycine at every 3rd position). This task makes high demands on advanced high-performance separation methods—HPLC and capillary electrophoresis (CE).

Parent Chains

HPLC

The analysis of collagenous chains is a difficult task due to the poor solubility (hydrophobicity) of these proteins. HPLC methods are not frequently used for the separation/characterization of individual chains of a collagen type.

The reversed-phase HPLC method is a traditional method for the analysis of peptides and proteins. A good choice for the stationary phase could be a short-alkyl reversed-phase (e.g., C_4) with wide pores (30 nm). It has been shown that large pore supports give distorted peaks with small collagens and triple helical peptides, resulting in poor resolution. The formation of broad peaks has been ascribed to conformational instability of the separated solutes and slow *cis–trans* isomerization of the peptide bonds. The best sorbents of those examined were diphenyl or non-porous C_{18} reversed-phases; standard water–acetonitrile gradients were recommended as mobile phases.

For example, reversed-phase chromatography on a C_8 phase using an acetonitrile gradient in 0.1% trifluoroacetic acid was described as a suitable method for the separation of α-chains of collagen types V and XI.

Cyanopropyl bonded packing has been described as suitable for the separations of human type I–III collagens. Other stationary phases should also be mentioned: LiChrosorb Diol, TSK-SW gels and Separon HEMA 1000 Glc (a copolymer of 2-hydroxyethyl methacrylate and ethylene dimethacrylate covalently bonded with glucose). The first two phases are widely used for the separation of a number of proteins, but the use of the last phase (HEMA) is mainly used for the separation of collagens. The elution is performed by isocratic conditions with 0.2 *M* NaCl–2 *M* urea–0.05 *M* Tris/HCl (pH 7.5) as the mobile phase. This enabled the separation of α-, β-, and γ-chains of collagen type I and this method also enables the separation of a number of collagens and collagenous chains (the related molecular mass of the eluted proteins decreases with prolonged migration time).

Capillary electrophoresis

Collagen chains can be analyzed by capillary zone electrophoresis in very dilute buffers (typically 2.5 m*M* sodium borate, pH 9.2) or acidic buffers (pH∼2.5, about 25 m*M* buffer). Separation in an alkaline buffer is sensitive to overloading; the recommended buffer is sodium tetraborate. The reason for this sensitivity is probably due to the adsorption of protein onto the capillary wall.

The separation of groups of α, β, and γ can also be achieved in a phosphate buffer (at the same pH), but the resolution of individual chains (α_1 from α_2, etc.) was lost. A similar effect was observed if the background electrolyte contained a submicellar concentration of sodium dodecyl sulphate (SDS), when only the peaks of α, β, and γ fractions could be seen. At higher (supramicellar) concentrations of the negatively charged surfactant, all fractions migrated as a single broad zone. The separation of collagen chains under acidic conditions (100 m*M* phosphate buffer, pH 2.5) is possible, but again without separating tri-, di-, and monomers.

Another possibility is to use a capillary gel electrophoretic method that is nowadays a routinely and commercially available method for the determination of the molecular mass of proteins/polypeptides. This method can also be used for the separation of collagen chains and their polymers. For example, this procedure is described in the literature for the separation of collagen type I α-chains and chain polymers β (dimers), and γ (trimers), and also chain polymers of related molecular mass 300,000 and higher (typically in the study of the formation of cross-links). Besides commercially available kits, another option is to use fused-silica or polyvinylalcohol-coated capillaries filled with non-cross-linked polyacrylamide or hydroxylpropylmethylcellulose in a 50 m*M* Tris–glycine buffer (pH 8.8) or phosphate buffer (50 m*M*, pH 2.5) (Table 1).

CNBr Fragments

Analyses of the structure and modifications of the collagen molecule/chain require solubilization and fragmentation of the protein to smaller peptides. In principle, two methods can be used—non-enzymatic (chemical) or enzymatic treatment. The chemical method is cleavage by CNBr. Cyanogen bromide splits the protein molecule at specific locations—at the methionines (in this case toward the C-terminal end). In the collagen molecule, methionine is a relatively rare amino acid (some 10–20 amino acids per collagen molecule). The small number of methionine residues leads to a rather limited number of cleavage products (CNBr peptides). The profile of CNBr peptides is typical,

Table 1 Capillary electromigration methods for separation of collagens.

Collagen types	Conditions
α, β-chains (types I, II, V, IX, XI)	2.5 m*M* Sodium tetraborate buffer, pH 9.2
α, β, γ-chains (type I)	4% Non-cross-linked polyacrylamide; 50 m*M* Tris–glycine buffer, pH 8.8
α, β, γ-chains (bovine skin–type I)	Commercial CE-SDS kit (pH 8.9)
Cyanogen bromide fragments (rat tail tendon—types I and III)	25–100 m*M* Phosphate buffer, pH 2.0–2.5
CNBr fragments (rat tail tendon—types I and III)	100 m*M* Phosphate buffer, 20 m*M* heptanesulfonic acid, pH 2.5
CNBr fragments (cartilage—types I and II)	100 m*M* Phosphate buffer, pH 6; coated capillary
CNBr fragments (rat tail tendon—types I and III)	50 m*M* SDS in 50 m*M* phosphate buffer, pH 2.5
CNBr fragments (rat tail tendon—types I and III)	1% (cca 3.5 m*M*) SDS in 50 m*M* phosphate buffer, pH 2.5
CNBr fragments (rat tail tendon—types I and III)	7.5% Pluronic F127 in 10 m*M* Tris and 75 m*M* phosphate buffer, pH 2.5; 20°C
Bacterial collagenase fragments (rat tail tendon—types I and III)	100 m*M* Phosphate buffer, pH 2.5

at least for the main collagen types and, thus, provides an appropriate way to estimate the amount as well as type of collagen in a particular tissue. The nomenclature of CNBr peptides refers to the parent polypeptide chain: an α_1 polypeptide chain yields a set of α_1CB (i.e., α_1CNBr) peptides (an α_2 chain similarly yields a set of α_2CB peptides). The index, e.g., α_1CB_1, identifies a particular peptide within the set. The number in parenthesis refers to the collagen type, e.g., $\alpha_1(I)CB_1$ means a CNBr peptide of collagen type I. The number attached to each peptide at the end reflects the position of a particular fragment in the elution profile obtained after CM cellulose chromatography.

HPLC

At present, there are several methods in use for CNBr peptide analysis, with classical CM cellulose and phosphocellulose chromatography being those primarily mentioned. The disadvantage of ion-exchange chromatographic procedures is mainly due to their low selectivity, long analysis time, and poor recovery of the separated peptides. In the early 1980s, reversed-phase chromatographic procedures were introduced, which exhibited much higher selectivity and shorter analysis time. The most useful method is based on a separation using a C_{18} reversed phase in an acetonitrile gradient (0–40% acetonitrile over 90 min) containing heptafluorobutyric acid as an ion-pairing agent.

However, the most widely used method for CNBr peptides analysis today is gel electrophoretic separation, originally introduced in 1976.

Capillary electrophoresis

The main problem in separating collagenous peptides is their adhesion to the inner surface of the fused-silica capillary wall. For this reason, the separation of these peptides can only be achieved in an acidic buffer.

In the literature, the separation is carried out in a 25–100 m*M* phosphate buffer (pH from 2.0 to 2.5), applied voltage 8–25 kV (using a fused silica capillary of 70/63 cm total length/length to the detector, 75 μm I.D.). Peptides with higher-related molecular mass (over 13,500) from collagens types I and III demonstrate a linear relationship between mobility and molecular mass; however, peptides with lower related molecular mass (below 4600) do not follow this relationship. This method is also usable for the determination of collagen types I, III, and V based on their specific CNBr fragments ($\alpha_2(I)CB_4$, $\alpha_1(III)CB_2$, and $\alpha_1(V)CB_1$). The separation of lower-molecular CNBr peptides from the higher-molecular ones can be improved by adding an ion-pairing agent, heptanesulfonic acid (100 m*M*) to the separation buffer.

Another possible way to minimize the interaction of collagen with the capillary wall is the presence of a high concentration of surfactant (above the critical micellar concentration), i.e., by micellar electrokinetic chromatography (MEKC). A useful system consists of a 50 m*M* phosphate buffer (pH 2.5) with 50 m*M* SDS; this system has to be run in negative polarity mode. At low, submicellar concentrations, the separations are different and only reflect interactions between the peptides and with the capillary wall, but not the presence of SDS micelles in the background electrolyte.

A pluronic polymer, which is a triblock uncharged copolymer with the general formula $[\text{poly(ethylene oxide)}]_x[\text{poly(propylene oxide)}]_y[\text{poly(ethylene oxide)}]_x$, was also investigated for use in the separation of collagen fragments. Block (triblock) copolymers can self-assemble to form micelle structures in aqueous buffers and can also serve as thermo-responsive gels. Pluronics have many interesting features: they are soluble at low temperature and can gellify with a temperature increase, i.e., the polymer can be easily introduced into the capillaries at a lower temperature and the separation can be carried out at a

higher temperature. The 7.5% pluronic F127 (in a pH 2.5, 10 m*M* Tris, and 75 m*M* phosphate buffer at 20°C) can be used for the separation of CNBr fragments. The separation is probably a combination of the principles of MEKC and capillary gel electrophoresis (CGE), where it resembles the separation achieved by reversed-phase HPLC, but with a different elution order.

Collagenase Fragments

Specific enzymes for the cleavage of collagens are collagenases. There are two major types of collagenase—tissue (interstitial) and bacterial. Interstitial collagenase (EC 3.4.24.7) cleaves the triple helix of collagen at about three-quarters of the length of the molecule from the N-terminus (at 775Gly/Ile776 in the α-1(I)chain). Microbial collagenase, typically from *C. histolyticum*, (EC 3.4.24.3), digests native collagen in the triple helix region at the Gly-bonds where preference was shown for Gly at P3 and P1′; Pro and Ala at P2 and P2′; and hydroxyproline, Ala or Arg at P3′. Because glycine is every third amino acid in collagenous domains, the cleavage of collagen by microbial collagenase resulted in mainly short peptides and a complex mixture (theoretically up to 172 different peptides could arise from a naturally occurring mixture of collagen type I and III).

HPLC

The HPLC separation of peptides arising from the cleavage of collagen by bacterial collagenase is carried out in the "traditional" manner for peptide mapping. The column used is reversed-phase (C_{18}) with normal pore size (10 nm). The gradient used is water–methanol with trifluoroacetic acid as the ion-pairing agent.

Capillary Zone Electrophoresis

The separation of microbial collagenase' peptides (preferably tripeptides) is not a simple matter for CE; short peptides with proline in the carboxy terminus strongly adhere to the capillary wall. For this reason, both when separating collagenase and CNBr peptides, a very useful method is separation at acidic pH (2.5) using a fused silica capillary, or even the use of a modified capillary (inner surface) by dynamic coating (alkylamines added to the background electrolytes) at acidic pH (one of the best modifiers was 1,7-diaminoheptane).

The capillary electromigration methods can be also successfully used for the determination of the 1/4 and 3/4 fragments of collagens type I and II arising from cleavage by interstitial collagenase. The sensitivity can be enhanced by using a dynamic fluorescence labeling technique (argon ion 488 nm laser) with a running buffer containing 0.05% sodium dodecylsulfate and a non-covalent fluorescent dye for protein, NanoOrange. The collagen (type I or II) and both fragments can be separated and detected within a run time of 20 min by capillary gel electrophoresis using a gel buffer (pH 8.8) containing 4% polyacrylamide. The buffer was 50 m*M* AMPD-CACO (2-amino-2-methyl-1,3-propanediol-cacodylic acid) and a coated capillary was used.

Combination of HPLC and Capillary Electrophoresis

As was mentioned above, the cleavage of tissue consisting of collagen types I and III by bacterial collagenase can result in a rich mixture of peptides (theoretically up to 172 different peptides). The separation of this peptide set by only one analytical method was unsuccessful—with RP–HPLC only 45 peaks could be determined and only 65 peptides with CE. This resolution is not sufficient for the study of collagens and their posttranslational modification.

The off-line combination of both methods (CE and HPLC) improves separation—150 peaks were detected. In the first stage, the peptide mixture was separated by reversed-phase HPLC using gradient elution with a water–acetonitrile system with trifluoroacetic acid as the ion-pairing agent. The collagenous peptides were divided into a few (five or seven) fractions by HPLC. These fractions were further characterized by CE in an uncoated capillary using a phosphate buffer (100 m*M*, pH 2.5). This two-step peptide mapping with subsequent statistical evaluation (e.g., linear regression analysis) was shown to represent a reliable approach for revealing posttranslational modifications in collagen in vivo.

Coupling of HPLC and Capillary Zone Electrophoresis with Mass Spectrometry

The coupling of HPLC or capillary electrophoresis and mass spectrometry for peptide/protein analysis is a promising technique which will have a significant impact on protein research. Surprisingly, this method is only rarely used for the analysis of collagen. Because collagens are high-molecular-mass proteins, only the peptidic fragments can be analyzed by mass spectrometry.

The HPLC method uses the procedure described in the section on the separation of collagenase digest—a reversed-phase column (normal pore C_{18}) eluted by a water–acetonitrile gradient with formic acid as the additive. Alternatively, formic acid can be substituted with trifluoroacetic acid (due to its "ion-killing" properties at lower concentrations, e.g., 3 m*M*). Separation and resolution is slightly better with trifluoroacetic acid as the ion-pairing agent.

Capillary electrophoresis was carried out in a fused-silica capillary (100 cm × 75 μm I.D.) with a background electrolyte consisting of 0.25 *M* acetic acid, at an applied voltage of

20 kV. The mass spectrometer used was a quadrupole or trap (MS/MS) type. The sheath liquid used was 5 m*M* ammonium acetate/isopropanol 1:1 (v/v) at a flow-rate of 3 μl/min. This method enables the identification of typical collagenous tripeptides in the collagenase digest, as well as CNBr/trypsin and proteinase K digests.

CONCLUSION

Collagen is a broad group of the most abundant proteins in the human body that encompasses at least 28 known types in vertebrates. These proteins are poorly soluble (if at all) and, therefore, they are often split into shorter peptides by enzymatic or non-enzymatic methods before analysis. Collagenous peptides can be successfully separated by high-performance analytical methods—HPLC and CE. The HPLC methods use, most frequently, reversed-phase columns with ion-pairing. Various types of capillary electromigration methods can be used for the separation of collagens and their fragments. The main problem with capillary electrophoretic methods is adhesion of collagenous peptides to the surface of a fused-silica capillary. It can be eliminated by the use of acidic background electrolytes and/or use of surfactants in the separation medium. The high-performance method for analysis is combination of HPLC and CE. Nowadays, the high-performance approach is combination of HPLC and CE with MS.

Because collagens are highly important proteins, we can expect that studies of these proteins will be intensified in the future. For these researches we need, and we have, a broad spectrum of analytical methods. However, we can assume that new high-performance methods will be continuously developed.

ACKNOWLEDGMENTS

This work was supported by the Grant Agency of the Czech Republic, grants Nos. 203/06/1044, 203/05/2539, The Center for Heart Research 1M6798582302, and by the Research Project AV0Z50110509.

BIBLIOGRAPHY

1. Deyl, Z.; Adam, M. Separation methods for the study of collagen and treatment of collagen disorders. J. Chromatogr. **1989**, *488*, 161–197.
2. Deyl, Z.; Mikšík, I. Advanced separation methods for collagen parent α-chains, their polymers and fragments. J. Chromatogr. B, **2000**, *739*, 3–31.
3. Deyl, Z.; Mikšík, I.; Eckhardt, A. Preparative procedures and purity assessment of collagen proteins. J. Chromatogr. B, **2003**, *790*, 245–275.
4. Mikšík, I.; Sedláková, P.; Mikulíková, K.; Eckhardt, A. Capillary electromigration methods for the study of collagen. J. Chromatogr. B, **2006**, *841*, 3–13.

Colloids: Adhesion on Solid Surfaces by FFF

George Karaiskakis
Physical Chemistry Laboratory, Department of Chemistry, University of Patras, Patras, Greece

INTRODUCTION

The adhesion of colloids on solid surfaces, which is of great significance in filtration, corrosion, detergency, coatings, and so forth, depends on the total potential energy of interaction between the colloidal particles and the solid surfaces. The latter, which is the sum of the attraction potential energy and that of repulsion, depends on particle size, the Hamaker constant, the surface potential, and the Debye–Huckel reciprocal distance, which is immediately related to the ionic strength of carrier solution. With the aid of the field-flow fractionation (FFF) technique, the adhesion and detachment processes of colloidal materials on and from solid surfaces can be studied. As model samples for the adhesion of colloids on solid surfaces (e.g., Hastelloy-C), hematite (a-Fe_2O_3) and titanium dioxide (TiO_2) submicron spherical particles, as well as hydroxyapatite [$Ca_5(PO_4)_3OH$] submicron irregular particles were used. The experimental conditions favoring the adhesion process were those decreasing the surface potential of the particles through the pH and ionic strength variation, as well as increasing the effective Hamaker constant between the particles and the solid surfaces through the surface-tension variation. On the other hand, the detachment of the same colloids from the solid surfaces can be favored under the experimental conditions decreasing the potential energy of attraction and increasing the repulsion potential energy.

METHODOLOGY

FFF technology is applicable to the characterization and separation of particulate species and macromolecules. Separations in FFF take place in an open flow channel over which a field is applied perpendicular to the flow. Among the various FFF subtechniques, depending on the kind of the applied external fields, sedimentation FFF (SdFFF) is the most versatile and accurate, as it is based on simple physical phenomena that can be accurately described mathematically. SdFFF, which uses a centrifugal gravitational force field, is a flow-modified equilibrium sedimentation-separation method. Solute layers that are poorly resolved under static equilibrium sedimentation become well separated as they are eluted by the laminar flow profile in the SdFFF channel. In normal SdFFF, where the colloidal particles under study do not interact with the channel wall, the potential energy of a spherical particle, $\varphi(x)$, is related to the particle radius, a, to the density difference, $\Delta\rho$, between the particle (ρ_s) and the liquid phase (ρ), and to the sedimentation field strength expressed in acceleration, G:

$$\varphi(x) = \frac{4}{3}\pi a^3 \rho G x \tag{1}$$

where x is the coordinate position of the center of particle mass.

When the colloidal particles interact with the SdFFF channel wall, the total potential energy, φ_{tot}, of a spherical particle is given by

$$\varphi_{\text{tot}} = \frac{4}{3}\pi a^3 \Delta\rho G x + \frac{A_{132}}{6}\left[\ln\left(\frac{h+2a}{h}\right) - \frac{2a(h+a)}{h(h+a)}\right] + 16\varepsilon a\left(\frac{kT}{e}\right)^2 \tan h\left(\frac{e\psi_1}{4kT}\right)\tan h\left(\frac{e\psi_2}{4kT}\right)e^{-\kappa x} \tag{2}$$

where the second and third terms of Eq. 2 accounts for the contribution of the van der Waals attraction potential and of the double-layer repulsion potential between the particle and the wall, respectively, A_{132} is the effective Hamaker constant for media 1 and 2 interacing across medium 3, h is the separation distance between the sphere and the channel wall, e is the dielectric constant of the suspending medium, e is the electronic charge, ψ_1 and ψ_2 are the surface potentials of the particles and the solid wall, respectively, k is Boltzmann's constant, T is the absolute temperature, and κ is the Debye–Huckel reciprocal length, which is immediately related to the ionic strength, I, of the medium.

Eq. 2 shows that the total potential energy of interaction between a colloidal particle and a solid substrate is a function of the particle radius and surface potential, the ionic strength and dielectric constant of the suspending medium, the value of the effective Hamaker constant, and the temperature. Adhesion of colloidal particles on solid surfaces is increased by a decrease in the particle radius, surface potential, the dielectric constant of the medium and by an increase in the effective Hamaker constant, the ionic strength of the dispersing liquid, or the temperature. For a given particle and a medium with a known dielectric constant, the adhesion and detachment processes depend on the following three parameters:

1. The surface potential of the particles, which can be varied experimentally by various quantities one of which is the suspension pH.
2. The ionic strength of the solution, which can be varied by adding to the suspension various amounts of an indifferent electrolyte.
3. The Hamaker constant, which can be easily varied by adding to the suspending medium various amounts of a detergent. The later results in a variation of the medium surface tension.

APPLICATIONS

The critical electrolyte (KNO_3) concentrations found by SdFFF for the adhesion of a-Fe_2O_3(I) (with nominal diameter 0.148 μm), a-Fe_2O_3(II) (with nominal diameter 0.248 μm), and TiO_2 (with nominal diameter 0.298 μm) monodisperse spherical particles on the Hastelloy-C channel wall were 8×10^{-2}, 3×10^{-2}, and 3×10^{-2} *M*, respectively. The values for the same sample (a-Fe_2O_3) depend on the particle size, in accordance with the theoretical predictions, whereas the same values are identical for various samples [a-Fe_2O_3(II) and TiO_2] having different particle diameters. The latter indicates that these values depend also, apart from the size, on the sample's physicochemical properties, as is predicted by Eq. 2. The detachment of the whole number of particles of the above samples from the channel wall was succeeded by decreasing the ionic strength of the carrier solution.

The critical KNO_3 concentration for the detachment process was 3×10^{-2} *M* for the a-Fe_2O_3(I) sample and 1×10^{-2} *M* for the samples of a-Fe_2O_3(II) and TiO_2. Those obtained by SdFFF particle diameters after the detachment of the adherent particles [0.148 μm for a-Fe_2O_3(I), 0.245 μm for a-Fe_2O_3(II), and 0.302 μm for TiO_2] are in excellent agreement with the corresponding nominal particle diameters obtained by transmission electron microscopy. The desorption of all of the adherent particles was verified by the fact that no elution peak was obtained, even when the field strength was reduced to zero. A second indication for the desorption of all of the adherent material was that the sample peaks after adsorption and desorption emerge intact and without degradation.

In a second series of experiments, the adhesion and detachment processes of hydroxyapatite (HAP) polydisperse particles with number average diameter of 0.261 μm on and from the Hastelloy-C channel wall were succeeded by the variation of the suspension pH, whereas the medium's ionic strength was kept constant (10^{-3} *M* KNO_3). At a suspension pH of 6.8, the whole number of injected HAP particles was adhered at the beginning of the SdFFF channel wall, which was totally released when the pH increased to 9.7, showing that, except for the ionic strength, the pH of the suspending medium is also a principal quantity influencing the interaction energy between colloidal particles and solid surfaces. The number-average diameter of the HAP particles found by SdFFF after the detachment of the adherent particles ($d_N = 0.262$ μm) was also in good agreement with that obtained when the particles were injected into the channel with a carrier solution in which no adhesion occurs ($d_N = 0.261$ μm).

The variation of the potential energy of interaction between colloidal particles and solid surfaces can be also succeeded by the addition of a detergent to the suspending medium, which leads to a decrease in the Hamaker constant and, consequently, in the potential energy of attraction.

In conclusion, FFF is a relatively simple technique for the study of adhesion and detachment of submicrometer or supramicrometer colloidal particles on and from solid surfaces.

FUTURE DEVELOPMENTS

Looking to the future, it is reasonable to expect more experimental and theoretical work in order to quantitatively investigate the adhesion/detachment phenomena of colloids on and from solid surfaces by measuring the corresponding rate constants with the aid of FFF.

BIBLIOGRAPHY

1. Athanasopoulou, A.; Karaiskakis, G. Potential barrier gravitational field-flow fractionation based on the variation of the pH solution for the analysis of colloidal materials. Chromatographia **1996**, *43*, 369.
2. Giddings, J.C.; Myers, M.N.; Caldwell, K.D.; Fisher, S.R. *Methods of Biochemical Analysis*; Glick, D. Ed.; John Wiley & Sons: New York, 1980; Vol. 26, 79.
3. Giddings, J.C.; Karaiskakis, G.; Caldwell, K.D.; Myers, M.N. Colloid characterization by sedimentation field-flow fractionation: I. Monodisperse populations. J. Colloid Interf. Sci. **1983**, *92* (1), 66.
4. Hansen, M.E.; Giddings, J.C. Retention perturbations due to particle–wall interactions in sedimentation field-flow fractionation. Anal. Chem. **1989**, *61*, 811–819.
5. Hiemenz, P.C. *Principles of Colloid and Surface Chemistry*, Marcel Dekker, Inc.: New York, 1977.
6. Athanasopoulou, A.; Karaiskakis, G.; Travlos, A. Colloidal interactions studied by sedimentation field-flow fractionation. J. Liq. Chromatogr. Relat. Technol. **1997**, *20* (16), 2525–2541.
7. Karaiskakis, G.; Athanasopoulou, A.; Koliadima, A. Adhesion studies of colloidal materials on solid surfaces by field-flow fractionation. J. Micro. Separ. **1997**, *9*, 275.
8. Koliadima, A.; Karaiskakis, G. Potential-barrier field-flow fractionation: A versatile new separation method. J. Chromatogr. **1990**, *517*, 345–359.
9. Ruckenstein, E.; Prieve, D.C. Adsorption and desorption of particles and their chromatographic separation. AIChE J. **1976**, *22* (2), 276.

Colloids: Aggregation in FFF

Athanasia Koliadima
Physical Chemistry Laboratory, Department of Chemistry, University of Patras, Patras, Greece

INTRODUCTION

The separation of the components of complex colloidal materials is one of the most difficult challenges in separation science. Most chromatographic methods fail in the colloidal size range or, if operable, they perform poorly in terms of resolution, recovery, and reproducibility. Therefore, it is desirable to examine alternate means that might solve important colloidal separation and characterization problems encountered in working with biological, industrial, environmental, and geological materials. One of the most important colloidal processes that is generally quite difficult to characterize is the aggregation of single particles to form complexes made up of multiples of the individual particles. Aggregation is a common phenomenon for both natural and industrial colloids. The high degree of stability, which is frequently observed in colloidal systems, is a kinetic phenomenon in that the rate of aggregation of such systems may be practically zero. Thus, in studies of the colloidal state, the kinetics of aggregation are of paramount importance. Although the kinetics of aggregation can be described easily by a bimolecular equation, it is not an easy thing to do experimentally.

One technique for doing this is to count the particles microscopically. In addition to particle size limitation, this is an extraordinarily tedious procedure. Light scattering can be also used for the kinetic study of aggregation, but experimental turbidities must be interpreted in terms of the number and size of the scattering particles.

In the present work, it is shown that the field-flow fractionation (FFF) technique can be used with success to study the aggregation phenomena of colloids.

The techniques of FFF appear to be well suited to colloid analysis. The special subtechnique of sedimentation FFF (SdFFF) is particularly effective in dealing with colloidal particles in the diameter range from 0.02 to 1 μm, using the normal or Brownian mode of operation (up to 100 μm using the steric-hyperlayer mode). As a model sample for the observation of aggregate particles by SdFFF, of poly(methyl methacrylate) (PMMA) was used, whereas for the kinetic study of aggregation by SdFFF, the hydroxyapatite (HAP) sample [$Ca_5(PO_4)_3OH$] consisting of submicron irregularly shaped particles was used. The stability of HAP, which is of paramount importance in its applications, is dependent on the total potential energy of interaction between the HAP particles. The latter, which is the sum of the attraction potential energy and that of repulsion, depends on particle size, the Hamaker constant, the surface potential, and the Debye–Hückel reciprocal distance, which is immediately related to the ionic strength of carrier solution.

METHODOLOGY

FFF is a highly promising tool for the characterization of colloidal materials. It is a dynamic separation technique based on differential elution of the sample constituents by a laminar flow in a flat, ribbonlike channel according to their sensitivity to an external field applied in the perpendicular direction to that of the flow.

The total potential energy of interaction between two colloidal particles, U_{tot}, is given by the sum of the energy of interaction of the double layers, U_R, and the energy of interaction of the particles themselves due to van der Waals forces, U_A. Consequently,

$$U_{tot} = U_R + U_A \tag{1}$$

For identical spherical particles U_R and U_A are defined as follows:

$$U_R = \frac{\varepsilon r \psi_0^2}{2} \ln[1 + \exp(-\kappa H)] \quad (\kappa r \gg 1) \tag{2}$$

$$U_R = \frac{\varepsilon r \psi_0^2}{R} \exp(-\kappa H) \quad (\kappa r \ll 1) \tag{3}$$

$$U_A = -\frac{A_{212} r}{12 H} \tag{4}$$

where ε is the dielectric constant of the dispersing liquid, r is the radius of the particle, ψ_0 is the particle's surface potential, κ is the reciprocal double-layer thickness, R is the distance of the centers of the two particles, A_{212} is the effective Hamaker constant of two particles of type 2 separated by the medium of type 1, and H is the nearest distance between the surfaces of the particles.

Eqs. 2–4 show that the total potential energy of interaction between two colloidal spherical particles depends on the surface potential of the particles, the effective Hamaker constant, and the ionic strength of the suspending medium. It is known that the addition of an indifferent electrolyte can cause a colloid to undergo aggregation. Furthermore, for a particular salt, a fairly sharply defined

concentration, called "critical aggregation concentration" (CAC), is needed to induce aggregation.

The following equation gives the rate of diffusion-controlled aggregation, u_r, of spherical particles in a disperse system as a result of collisions in the absence of any energy barrier to aggregate:

$$u_r = -k_r {N_0}^2 \tag{5}$$

where k_r is the second-order rate constant for diffusion-controlled rapid aggregation and N_0 is the initial number of particles per unit volume.

In the presence of an energy barrier to aggregate, the rate of aggregation, u_s, is

$$u_s = -k_s {N_0}^2 \tag{6}$$

where k_s is the rate constant of slow aggregation in the presence of an energy barrier.

The stability ratio, w, of a dispersion is defined as the ratio of the rate constants for aggregation in the absence, k_r and the presence, k_s, of an energy barrier, respectively:

$$w = \frac{k_r}{k_s} \tag{7}$$

The aggregation process is described by the bimolecular kinetic equation

$$\frac{1}{N_i} = \frac{1}{N_0} + k_{\text{app}} t_i \tag{8}$$

where N_i is the total number of particles per unit volume at time t_i and k_{app} is the apparent rate constant for the aggregation process. The measurement of the independent kinetic units per unit volume, N_i, at different times t_i can give the rate constant for the aggregation process.

Considering that d_{N_0} and d_{N_i} are the measured number-average diameters of the particles at times $t = 0$ and t_i, respectively, Eq. 8, for polydisperse samples, gives

$${d_{N_i}}^3 = {d_{N_0}}^3 + {d_{N_0}}^3 N_0 k_{\text{app}} t_i \tag{9}$$

Eq. 9 shows that from the slope of the linear plot of the ${d_{N_i}}^3$ versus t_i, the apparent rate constant k_{app} can be determined, as the N_0 values can be found from the ratio of the total volume of the injected sample to the volume of the particle, which can be determined from the diameter calculated from the intercept of the above plot.

APPLICATIONS

The observation of a series of peaks (Fig. 1) while analyzing samples of PMMA colloidal latex spheres by SdFFF suggests that part of the latex population has aggregated into doublets, triplets, and higher-order particle clusters. The particle diameter of the latex spheres was given as 0.207 μm. The aggregation hypothesis is confirmed by retention calculations and by electron microscopy. For this purpose, narrow fractions or cuts were collected from the first five peaks as shown in Fig. 1. A fraction was also collected for the peak which appeared after the field was turned off. The individual fractions were subjected to electron microscopy and as expected, cut No. 1 yielded singlets, cut No. 2 yielded doublets, cut No. 3 yielded triplets, cut No. 4 yielded quads, cut No. 5 yielded quints, and the cut after the field was turned off yielded clusters from six individual particles.

Sedimentation field-flow fractionation was used also for the kinetic study of HAP particles' aggregation in the presence of various electrolytes to determine the rate constants for the bimolecular process of aggregation and to investigate the possible aggregation mechanisms describing the experimental data. The HAP sample contained polydisperse, irregular colloidal particles with number-average diameter $d_{\text{N}} = 0.262 \pm 0.046$ μm.

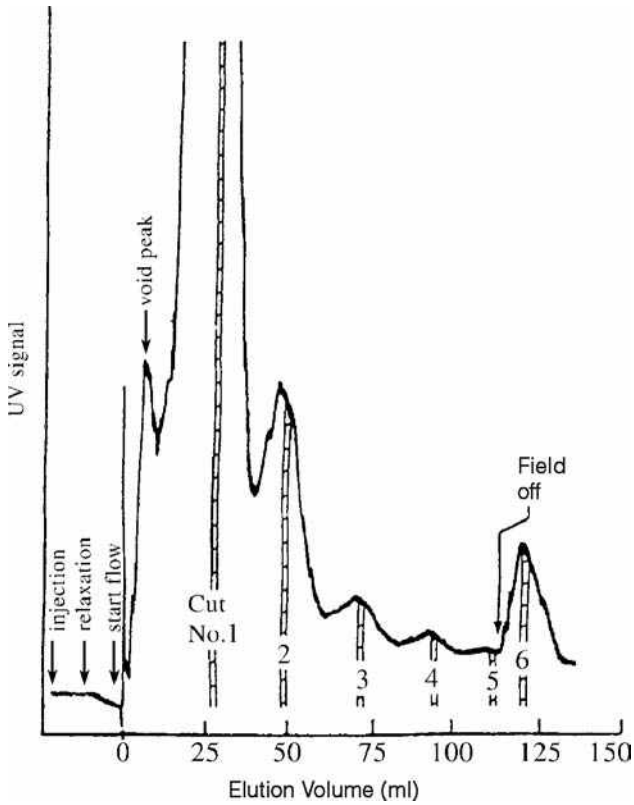

Fig. 1 SdFFF fractogram of 0.207 μm PMMA aggregate series from which six cuts were collected and analyzed by electron microscopy. Experimental conditions: field strength of 61.6 g and flow rate of 0.84 ml/min.
Source: From Resolution of colloidal latex aggregates by sedimentation field-flow fractionation, in J. Chromatogr.[1] Copyright Elsevier Science Publishers B.V.

The number-average diameter, d_N, for the HAP particles increases with the electrolyte KNO_3 concentration until the critical aggregation concentration is reached, where the d_N value remains approximately constant. The starting point of the maximum d_N corresponds to the electrolyte concentration called CAC. The last value, which depends on the electrolyte used, was found to be 1.27×10^{-2} M for the electrolyte KNO_3.

According to Eq. 9, the plot of ${d_{N_i}}^3$ versus t_i at various electrolyte concentrations determines the apparent rate constant, k_{app}, of the HAP particles' aggregation. The found k_{app} value for the aggregation of the HAP particles in the presence of 1×10^{-3} M KNO_3 is 2.5×10^{-21} cm^3/sec. It is possible to make a calculation which shows whether the value of k_{app} is determined by the rate at which two HAP particles can diffuse up to each other (diffusion control) or whether the rate of reaction is limited by other slower processes. The rate constant for the bimolecular collision (k_1) of the HAP particles, can be calculated by the Stokes–Einstein equation:

$$k_1 = \frac{8kT}{3n} \text{cm}^3/\text{sec} \tag{10}$$

where n is the viscosity of the medium. The calculated value of $k_1 = 1.1 \times 10^{-11}$ cm^3/sec is about 10 orders of magnitude greater than the value of k_{app} actually measured. So, the aggregation rates are slower than those expected if the process was simply diffusion controlled when electrostatic repulsion is absent. The latter indicates that the minimal mechanism for the aggregation process of the HAP particles would be

$$\begin{gathered} \text{Particle}_1 + \underset{2}{\text{Particle}} \underset{k_{-1}}{\overset{k_1}{\rightleftarrows}} \\ \text{Intermediate complex} \overset{k_2}{\rightleftarrows} \text{Stable aggregate} \end{gathered} \tag{11}$$

where k_{-1} is the rate constant for the dissociation of the intermediate aggregate and k_2 is the rate constant for the process representing the rate-determining step in the aggregation reaction. Because k_{app}, describing the overall process, is smaller than the calculated k_1 value, there must be rapid equilibration of the individual particles and their intermediate complexes followed by the slower step of irreversible aggregation. The stability factor, w, of HAP's particles found to be 4.4×10^9 is too high, indicating that the particles are very stable, even in the presence of significant quantity of the electrolyte KNO_3.

As a general conclusion, the FFF method can be used with success to study the aggregation process of colloidal materials.

FUTURE DEVELOPMENTS

Looking to the future, it is reasonable to expect continuous efforts to improve the theoretical predictions and more experimental work to investigate the aggregation phenomena of natural and industrial colloids.

REFERENCE

1. Jones, H.K.; Barman, B.N.; Giddings, J.C. Resolution of colloidal latex aggregates by sedimentation field-flow fractionation. J. Chromatogr. **1988**, *455*, 1–15.

BIBLIOGRAPHY

1. Athanasopoulou, A.; Karaiskakis, G.; Travlos, A. Colloidal interactions studied by sedimentation field-flow fractionation. J. Liq. Chromatogr. Related Technol. **1997**, *20*, 2525–2541.
2. Athanasopoulou, A.; Gavril, D.; Koliadima, A.; Karaiskakis, G. Study of hydroxyapatite aggregation in the presence of potassium phosphate by centrifugal sedimentation field-flow fractionation. J. Chromatogr. A, **1999**, *845*, 293.
3. Caldwell, K.D.; Nguyen, T.T.; Giddings, J.C.; Mazzone, H.M. Field-flow fractionation of alkali-liberated polyhedrosis virus from Gypsy moth (*Lymantria dispar*, L.). J. Virol. Methods **1980**, *1*, 241–256.
4. Everett, D.H. *Basic Principles of Colloid Science*; Royal Society of Chemistry Paperbacks: London, 1988.
5. Family, F., Landan, D.P., Eds.; *Kinetic of Aggregation and Gelation*; North-Holland: Amsterdam, 1984.
6. Koliadima, A. The kinetic study of aggregation of the sulphide $Cu_{0.2}Zn_{0.8}S$ particles by gravitational field-flow fractionation. J. Liq. Chromatogr. & Related Technol. **1999**, *22* (16), 2411.
7. Wittgren, B.; Borgström, J.; Piculell, L.; Wahlund, K.G. Conformational change and aggregation of kappa-carrageenan studied by flow field-flow fractionation and multiangle light scattering. Biopolymers **1998**, *45*, 85–96.

Colloids: Concentration of Dilute Samples by FFF

George Karaiskakis
Physical Chemistry Laboratory, Department of Chemistry, University of Patras, Patras, Greece

INTRODUCTION

Many colloidal systems, such as those of natural water, are too dilute to be detected by the available detection systems. Thus, a simple and accurate method for the concentration and analysis of these dilute samples should be of great significance in analytical chemistry. In the present work, two methodologies of the field-flow fractionation (FFF) technique for the concentration and analysis of dilute colloidal samples are presented. Both the conventional and potential barrier methodologies of FFF are based on the "adhesion" of the samples at the beginning of the channel wall, followed by their total removal and analysis. In the conventional sedimentation FFF (SdFFF) concentration procedure, the apparent adhesion of a dilute sample is due to its strong retention, which can be achieved by applying high field strengths and low flow rates. In the potential barrier SdFFF (PBSdFFF) concentration procedure, the true adhesion of a dilute sample is due to its reverse adsorption at the beginning of the column, which can be achieved by the appropriate adjustment of various parameters influencing the interactions between the colloidal particles and the material of the channel wall. The total release of the adherent particles is accomplished either by reducing the field strength and increasing the solvent velocity (conventional SdFFF) or by varying the potential energy of interaction between the particles and the column material—for instance, by changing the ionic strength of the carrier solution (PBSdFFF).

METHODOLOGY

FFF is a one-phase chromatographic system in which an external field or gradient replaces the stationary phase. The applied field can be of any type that interacts with the sample components and causes them to move perpendicular to the flow direction in the open channel. The most highly developed of the various FFF subtechniques is sedimentation FFF (SdFFF), in which the separations of suspended particles are performed with a single, continuously flowing mobile phase in a very thin, open channel under the influence of an external centrifugal force field.

In the normal mode of the SdFFF operation, a balance is reached between the external centrifugal field, driving the particles toward the accumulation wall, and the molecular diffusion in the opposite direction. In that case, the retention volume increases with particle diameter until steric effects dominate, at which transition point there is a foldback in elution order.

PBSdFFF which has been developed recently in our laboratory, is based either on particle size differences or on Hamaker constant, surface potential, and Debye–Hückel reciprocal distance differences.

The retention volume of a component under study, in the normal SdFFF and the PBSdFFF methodologies is a function of the following parameters:

1. SdFFF:

$$V_r = f(d,\ G,\ \Delta\rho) \tag{1}$$

2. PBSdFFF:

$$V_r = f(d,\ G,\ \Delta\rho,\ \psi_1,\ \psi_2,\ A,\ I) \tag{2}$$

where d is the particle diameter, G is the field strength expressed in acceleration, $\Delta\rho$ is the density difference between solute and solvent, ψ_1 and ψ_2 are the surface potentials of the particle and of the wall, respectively, A is the Hamaker constant, and I is the ionic strength of the carrier solution.

The conventional concentration procedure in SdFFF consists of two steps: the feeding (or concentration) and the separation (or elution) step. In the feeding step, the diluted samples are fed into the column with a small flow velocity while the channel is rotated at a high field strength to ensure the "apparent adhesion" of the total number of the colloidal particles at the beginning of the channel wall as a consequence of the particles' strong retention. In the separation step, the field is reduced and the flow rate is increased to ensure the total release and the consequence elution of the adherent dilute particles.

In PBSdFFF, the concentration step consists of feeding the column with the diluted samples at such experimental conditions, so as to decrease the repulsive component and increase the attractive component of the total potential energy of the particles under study. Because the stability of a colloid varies (increases or decreases) with a number of parameters (surface potential, Hamaker constant and ionic strength of the suspending medium), the proper adjustment of one or more of these parameters

can lead not only to the adhesion of the dilute colloidal samples, which leads to their "concentration," but also to the total release of the adherent particles during the elution step.

APPLICATIONS

Conventional SdFFF

As model samples for the verification of the conventional SdFFF as a concentration methodology monodisperse polystyrene latex beads (Dow Chemical Co.) with nominal diameters of 0.357 μm (PS1) and 0.481 μm (PS2) were used. They were either used as dispersions containing 10% solids or diluted with the carrier solution [triple-distilled water + 0.1% (v/v) detergent FL-70 from Fisher Scientific Co. + 0.02% (w/w) NaN_3] to study sample dilution effects. Diluted samples in which the amount of the polystyrene was held constant (1 μml of the 10% solids) while the volume in which it was contained was varied over a 50,000-fold range (from 1 to 50 ml of carrier solution) were introduced into the SdFFF column. During the feeding step, the flow rate was 5.8 ml/hr for the PS1 polystyrene, and 7.6 ml/hr for the polystyrene PS2, and the channel was rotated at 1800 rpm for the PS1 sample and at 1400 rpm for the PS2 sample. In the separation (elution) step, the experimental conditions for the two samples were as follows:

PS1: Field strength = 880 rpm, flow rate = 12–53 ml/hr
PS2: Field strength = 500 rpm, flow rate = 24–59 ml/hr

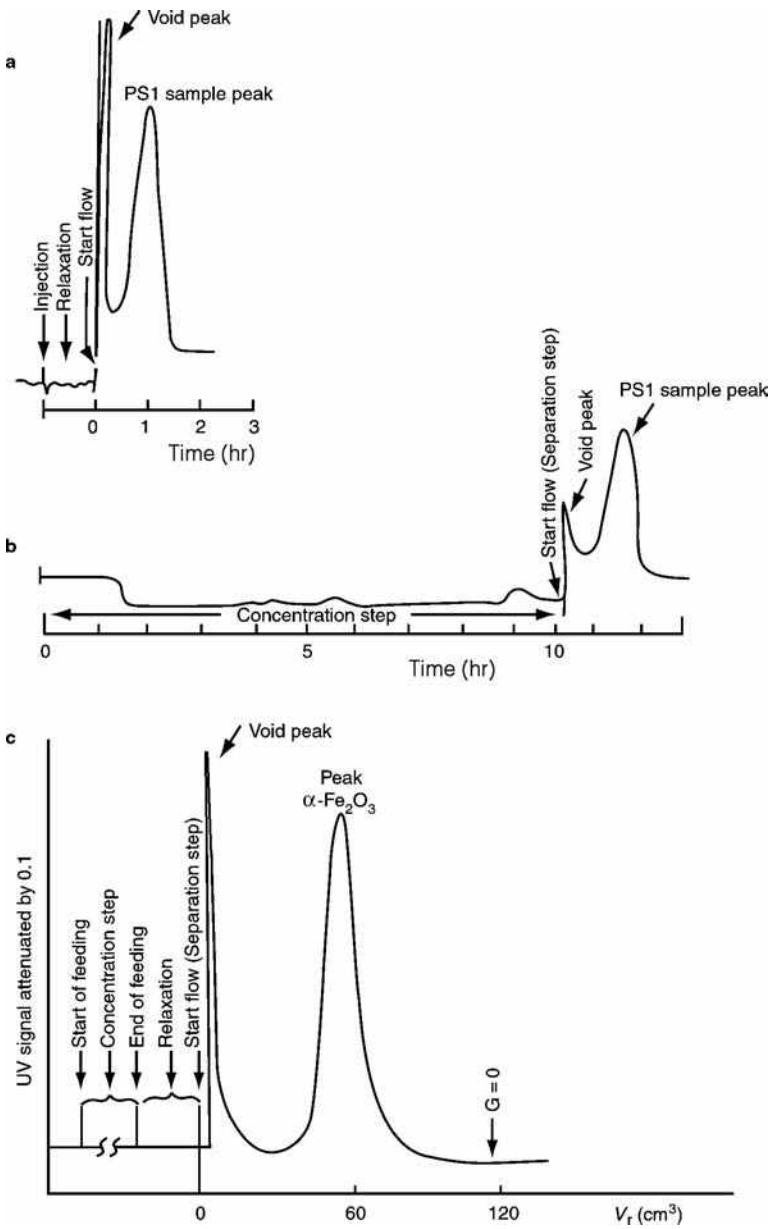

Fig. 1 Fractograms of the polystyrene latex beads of 0.357 μm (PS1) obtained by the direct injection of 1 μl of PS1 (a) and by the concentration procedure of the PS1 sample diluted in 10 ml of the carrier solution (b) using the conventional SdFFF technique, as well as of the α-Fe_2O_3 sample with nominal particle diameter of 0.271 μm diluted in 6 ml of the carrier solution obtained by the PBSdFFF concentration methodology (1c).

Fig. 1 provides a comparison of fractograms for the 0.357 μm polystyrene injected as a narrow pulse (Fig. 1a) and injected at 10 ml dilution (Fig. 1b) by the conventional SdFFF concentration procedure described previously. Fig. 1b shows that the eluted peak from the diluted sample emerges intact and without serious degradation, compared to the peak of Fig. 1a, despite the fact that the sample volume (10 ml) is over twice the channel volume (4.5 ml). The same concentration procedure was also successfully applied to the separation of the two polystyrene samples initially mixed together in a volume of 10 ml, as well as to the concentration of the colloidal particles contained in natural water samples collected from the Colorado, Green, and Price rivers in eastern Utah (U.S.A.).

As a general conclusion, the on-column concentration procedure of the conventional SdFFF method works quite successfully in dealing with highly diluted samples. Optimization, particularly higher field strengths during the concentration step, would allow higher flow rates and increased analysis speed. However, experimental confirmation would be necessary to give assurance that the particle–wall adhesion is not irreversible at higher spin rates.

Potential Barrier SdFFF

As model samples to test the validity of the PBSdFFF as a concentration procedure of diluted samples the monodisperse colloidal particles of α-Fe_2O_3 with nominal diameters of 0.271 μm were used. Diluted samples of containing 2 μl of the 10% solid, in which the volume was varied over a 10,000-fold range (from 2 to 20 ml), were introduced into the column with a carrier solution containing 0.5% (v/v) detergent FL-70 + 3×10^{-2} *M* KNO_3 to ensure the total adhesion of the particles at the beginning of the SdFFF Hastelloy-C channel wall. In the separation step, the carrier solution was changed to one containing only 0.5% (v/v) detergent FL-70 (without electrolyte) to ensure the total detachment of the adherent particles. In that case, a sample peak appeared (cf. Fig. 1c) as a consequence of the desorption of the α-Fe_2O_3 particles. The mean diameter of the particles (0.280 mm) obtained by the proposed PBSdFFF methodology for the ion_channel concentration procedure of the sample diluted in 8 ml of the carrier solution is very close to that found (0.271 μm) by the direct injection of the same particles into the channel, using a carrier in which no adsorption occurs.

As a general conclusion, one could say that the proposed PBSdFFF concentration procedure works quite successfully in dealing with highly dilute samples, separating them according to size, surface potential, and Hamaker constant. At the same time, as separation occurs, the particle sizes of the colloidal materials of the diluted mixture can be determined. The major advantage of the proposed concentration procedure is that the method can concentrate and analyze dilute mixtures of colloidal particles even of the same size but with different surface potentials and/or Hamaker constants. The method has considerable promise for the separation and characterization, in terms of particle size, of dilute complex colloidal materials, where particles are present in low concentration.

FUTURE DEVELOPMENTS

Looking to the future, we believe that the efforts of the researchers will be focused on the extension of the FFF concentration methodologies to the ranges of more dilute and complex colloidal samples, without lengthening the analysis time.

BIBLIOGRAPHY

1. Athanasopoulou, A.; Koliadima, A.; Karaiskakis, G. New methodologies of field-flow fractionation for the separation and characterization of dilute colloidal samples. Instrum. Sci. Technol. **1996**, *24* (2), 79.
2. Giddings, J.C.; Karaiskakis, G.; Caldwell, K.D. Separ. Sci. Technol. **1981**, *16* (6), 725.
3. Hiemenz, P.C. *Principles of Colloid and Surface Chemistry*; Marcel Dekker, Inc.: New York, 1977.
4. Karaiskakis, G.; Graff, K.A.; Caldwell, K.D.; Giddings, J.C. Sedimentation field-flow fractionation of colloidal particles in river water. Int. J. Environ. Anal. Chem. **1982**, *12*, 1.
5. Koliadima, A.; Karaiskakis, G. Sedimentation field-flow fractionation: A new methodology for the concentration and particle size analysis of dilute polydisperse colloidal samples. J. Liq. Chromatogr. **1988**, *11*, 2863.
6. Koliadima, A.; Karaiskakis, G. Potential-barrier field-flow fractionation, a versatile new separation method. J. Chromatogr. **1990**, *517*, 345.
7. Koliadima, A.; Karaiskakis, G. Concentration and characterization of dilute colloidal samples by potential-barrier field-flow fractionation. Chromatographia **1994**, *39*, 74.

Column Switching: Fast Analysis

Toshihiko Hanai
Health Research Foundation, Pasteur Institut, Kyoto, Japan

Abstract
Column-switching separation based on the selectivity and retention capacity of packing materials is an ideal chromatographic condition for obtaining stable, highly sensitive, and reproducible results. A column-switching system is used for trace enrichment, sample cleanup, and the so-called heart-cut, where target fractions from the first column are transferred online to a second column having different properties for further separation. The second method is also called two(multi)-dimensional chromatography. The applications are classified depending on the difference in hydrophobicity, Coulombic force, molecular size, or steric hindrance of the analytes, affinity, and enzyme reactions, and application to mass spectrophotometric analysis. Some typical examples are given from selected references.

INTRODUCTION

High-pressure and high-flow-rate separation are not ideal chromatographic conditions for obtaining stable, sensitive, and reproducible results. Gradient elution is commonly used for fast separation. The separation time in gradient elution is short, but this method requires a period of re-equilibration and, in general, is not suitable for highly sensitive detection. The column-switching method is complicated because of the instrumentation needed. Once a system is established, however, a stable, reproducible, and highly sensitive chromatography can be achieved.

A double-column amino acid analyzer is considered to have been the first column-switching instrument. Once the same sample had been applied to columns of anion- and cation-exchange resins, acidic and basic amino acids were separated in parallel and detected. The system was modified for a single injection using a switching valve.

The applications of column switching are classified into two types: the use of a short column for trace enrichment in environmental analyses and for sample cleanup in biomedical analyses; and the so-called heart-cut, where target fractions from the first column are transferred online to a second column having different properties for further separation. The second method is also called two-dimensional chromatography. The fast, two-dimensional chromatographic system is built around gas chromatography and, with the addition of a mass spectrometer, it is called three-dimensional chromatography. Enantiomeric separation and ionic separation are typical examples of heart-cut. Furthermore, the same category of compounds is continuously separated using the different retention powers of packing materials. This entry describes a methodology for preparing a successful column-switching system based on the properties of analytes.

METHODOLOGY

The success of column switching depends on the molecular properties of analytes and packing materials. A packing material can selectively separate a certain group of compounds among analytes. The selection of the packing material depends on factors of retention in chromatography. These factors are the same as the parameters of solubility such as van der Waals force, Coulombic force, and steric hindrance. Hydrogen bonding and charge-transfer interaction, such as Lewis acid–base interaction, can be treated as weak Coulombic force.[1] Applications of column-switching separation are classified as follows:

1. Dependent on the difference in hydrophobicity of analytes.
2. Dependent on the difference in Coulombic force of analytes.
3. Dependent on the molecular size of analytes.
4. Dependent on the steric hindrance of analytes.
5. Affinity and enzyme reactions.
6. Application to mass spectrophotometric analysis.

Resolution can be improved by increasing the column plate number, N, and/or the separation factor (selectivity of packing materials), α [α = the ratio of the capacity ratios (retention factors) of the two compounds]. N is the physical parameter and α is the chemical parameter for the separation.[1]

Column switching utilizes the selectivity, α, of packing materials, but not the theoretical plate number of the column. Understanding the chemistry of retention in liquid chromatography is key to preparing a column-switching system. Details on packing materials and their structures are given by Hanai.[2] A diagram of the system is shown in Fig. 1. A variety of compounds have been effectively

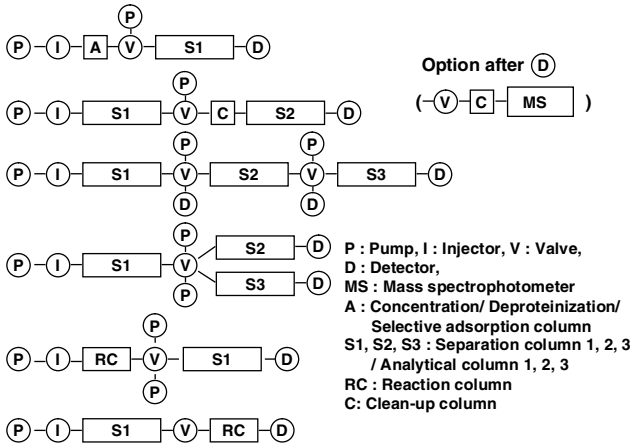

Fig. 1 Column-switching systems.

analyzed using column switching. All applications cannot be summarized in a few pages. Typical examples are given with selected references.

APPLICATIONS OF COLUMN-SWITCHING CHROMATOGRAPHY

Dependent on the Difference in Hydrophobicity of Analytes

Preconcentration on a hydrophobic cartridge is a commonly used pretreatment in trace analyses. A variety of precolumns have been used for reversed-phase liquid chromatography for prefiltration and preconcentration online. A small column for solid-phase extraction is used for the preconcentration of trace amounts of relatively hydrophobic compounds, especially in environmental analyses. Trace metals are derivatized and concentrated in a hydrophobic phase, then transferred to a separation column.[3] Peptides, drugs, and relatively hydrophobic compounds in environmental water samples were also concentrated in a hydrophobic phase and separated on a separation (analytical) column. The selection of packing material permits the selective concentration of a certain range of hydrophobic compounds. Biological samples require deproteinization before applying the sample solution for chromatographic analysis. A variety of chemicals in urine, serum, and tissues can be concentrated on hydrophobic phases after deproteinization, and then separated in an analytical column. Numerous reports have been published on the concentration of trace compounds. Some modifications to the packing materials for solid-phase extraction have been made for the direct injection of biological samples without deproteinization.

Restricted access packing materials (RAMs) have both hydrophobic and hydrophilic sites.[2] Also called internal-surface reversed-phase packing materials, RAMs have two functions: the surfaces of particles (the end groups of bonded phases) are polar to reflect the adsorption of, e.g., proteins, while the surfaces within the pores (the inner compartment of bonded phases) are relatively non-polar to support the hydrophobic adsorption of, e.g., drugs. Such a solid phase (packing material) is also called a shielded hydrophobic phase, mixed-functional phase, or dual-zone phase. This type of material can be prepared by coating proteins and cellulose. Relatively polar organic porous polymers are also used for this purpose. New bonded phases have been developed. The hydrophilic phase of the particle surface prevents the adsorption of proteins, and the hydrophobic site adsorbs hydrophobic compounds. The hydrophobicity is designed using different ligands. A column packed with inner hydrophobic packing materials is used for online prefiltration of proteins in biological samples. Relatively hydrophobic compounds are trapped inside the hydrophobic sites of the packing material and are transferred to an analytical column for further separation. Insertion of a small concentration column before the second analytical column is useful for trace analysis.

Biological samples are injected directly, and drugs and their metabolites are analyzed: for example, loxoprofen in human serum for pharmacokinetic studies;[4] propiverine in human plasma;[5] parabens, triclosan, and other environmental phenols in human milk;[6] phenols in animal feed;[7] *S*-phenylmercapturic acid and *S*-benzylmercapturic acid in urine;[8] and DNA fragments[9] and voriconazole in human plasma.[10] A longer first column is also used to purify target compounds, and the fractions are transferred to a second column for further separation of drugs in blood and urine. Baicalein, rhein, and berberine in rat plasma[11] and sulfamethoxazole and trimethoprim in whole egg[12] were analyzed using the two-column system.

The major application of column switching is sample cleanup using a small column. A combination of different hydrophobic columns in parallel permits the fast separation of a variety of hydrophobic mixtures with isocratic elution. Free amino acids are a mixture of very polar, polar, and hydrophobic amino acids. These three groups were separated in parallel using three types of hydrophobic columns by the formation of a copper complex online.[13] Very polar compounds, e.g., guanidino compounds, were also separated by reversed-phase ion-pair liquid chromatography using a very hydrophobic packing material, a carbon column.[14]

Catecholamine-related compounds—metabolites of hydrophobic aromatic amino acids—were also effectively separated using a combination of different hydrophobic packing materials.[15]

Dependent on the Difference in Coulombic Force of Analytes

The matrices of biological samples are very complicated. The selective concentration of target compounds, therefore, has been performed using ion-exchange trap columns. Sample components are separated into three groups, i.e., acidic, basic, and neutral. Further separation is carried

out using reversed-phase liquid chromatography or ion-exchange liquid chromatography with a longer ion-exchange column. Conversely, the first separation is carried out using reversed-phase liquid chromatography, and then further separation is performed by ion-exchange liquid chromatography. Utilization of ion exchangers expands the capability of a simple cleanup. Proteins[16] and peptides in human blood[17] were separated by ion exchange. Piritramide,[18] vancomycin,[19] and acidic compounds[20] in human plasma, nutrients in the presence of high chloride concentrations,[21] and inorganic selenium[22] were also analyzed using ion exchange. Ionized compounds were eluted rapidly from a reversed-phase column. A RAM column was used for direct injection of urine, and then methamphetamine and amphetamine were analyzed using ion-exchange liquid chromatography.[23] Reversed-phase ion-pair liquid chromatography was, thus, used to separate a mixture of hydrophobic and ionic compounds. The column-switching method for reversed-phase ion-pair liquid chromatography is the same as that for reversed-phase liquid chromatography. A very common application, due to Coulombic force, is sample pretreatment. Removing ionic compounds for the analysis of neutral compounds, such as saccharides, is an example. The separation of acidic and basic drugs is another example.

Dependent on the Molecular Sizes of Analytes

This approach has been applied to the separation of polymers, oligomers, and monomers. Each fraction is then further separated using a suitable separation method. One example is the separation of saccharides in exploded wood.[24] Proteins, peptides, and amino acids were analyzed, step by step, and an automated column-switching separation was studied. However, the separation of proteins does not compete with that achieved by two-dimensional electrophoresis.

A size-exclusion column is also used for sample pretreatment in biomedical analyses. Mainly, larger molecules like proteins are eluted within the exclusion limit. Then small molecules, the target molecules, are further separated by either reversed-phase liquid chromatography or ion-exchange liquid chromatography. Proteins and non-target fractions are eluted, and the target fraction is transferred to an analytical column. This system was applied to a pharmacokinetic study of omeprazole and rabeprazole,[25] and rabeprazole and its metabolites.[26] A variety of newly developed restricted access packing materials have partly replaced size-exclusion columns.

Dependent on the Steric Hindrance of Analytes

The molecular size effect is used in size-exclusion liquid chromatography. The steric effect, a difference in molecular shape, is mainly applied to normal-phase liquid chromatography. Enantiomeric separation is usually carried out with normal-phase liquid chromatography, using specially designed packing materials such as the Pirkle-type[27] and modified cyclodextrins.[28] Natural polymers having steric selectivity are also used for enantiomeric separation, using the natural form or a modified form like α-1-acid glycoprotein,[29] amylose *tris*(3,5-dimethylphenylcarbamate),[30] modified cellulose,[31] and ovomucoid.[32] Enantiomeric separation columns do not have high separation power, according to their theoretical plate number. First, the mixtures are separated using reversed-phase liquid chromatography; then the target fraction is transferred from the reversed phase to the enantiomeric separation column.

The difficulty experienced in the transfer from the reversed phase to the separation column owes to unmatched eluent components. Some technical solution is required to establish this system. When an aqueous eluent is used for the first column, a small amount of aqueous solution should be miscible in the non-aqueous eluent of the enantiomeric column. Another solution is to use a small trap column to reduce the excess aqueous solution and then back flush into an enantiomeric separation column using a suitable solvent (eluent).

Affinity and Enzymatic Reaction

Proteins attract molecules selectively. This selectivity, or affinity, is made use of after the immobilization of proteins on packing materials. Affinity is not 100% effective; therefore, affinity-based mixtures are further purified using a second column. Polyclonal antibodies,[33] monoclonal antibodies,[34] and β-cyclodextrin[35] were immobilized for specific purifications. The immobilization technique is applied to immunoassays, even if the precision of the quantitative analysis is less than that of liquid chromatography. Man-made affinity polymers, molecularly imprinted packing materials, have been developed for the selective concentration of targeted compounds. The key compounds are 17β-estradiol,[36] bisphenol,[37] atropine, propranolol, [*S*]-naproxen, and [*S*]-ibuprofen.[38] The difficulty experienced in synthesizing a suitable imprinted polymer owes to the molecular shape of the targeted compounds in the synthesis of packing materials and the extraction from the sample solution.

Quantitative analysis of enzyme reactivity is performed using an immobilized enzyme column. Given the difficulty in obtaining a relatively large amount of enzyme and retaining the enzymatic activity after the immobilization, several reaction columns are synthesized, such as monoamine oxidase,[39] β-glucuronidase,[40] lipase,[41] phenylethanol amine *N*-methyltransferase,[42] horse liver alcohol dehydrogenase,[43] and nicotinic acetylcholine receptor.[44] An enzyme column was developed for online trypsin digestion to analyze components of proteins.[45] An inorganic catalytic Pt–Rh alumina column was used to determine nitropyrene metabolites with chemiluminescence detection.[46] These online sample treatments improve the

quantitative analysis of the targeted compounds and their automated analysis.

Application to Mass Spectrometric Analysis

Mass spectrometer is a powerful tool for the identification of analytes; however, a direct free connection between liquid chromatography and mass spectrometry is not permitted. At the very least, inorganic salts should be eliminated before the use of a mass spectrometer. One approach is to collect the target fraction in a small trapped column, and then wash off the unwanted components before introduction to the mass spectrometer. Even if one uses a small column with a volatile salt, one must wash the mass chamber very often to maintain its sensitivity.

Polar compounds are separated using ion-exchange liquid chromatography; however, the inorganic salt should be eliminated before the mass spectroscopic analysis. The targeted fraction is collected on a small trap column, then the salt is removed with a volatile ion-pair reagent, and the compounds are introduced into the mass spectrometer.[47] Utilization of a miniaturized separation column with a volatile eluent and a desalting column is ideal when using a mass spectrometer as a detector.

CONCLUSION

We have seen how column switching can expedite separation of substances of interest, using techniques that take advantage of the differences in hydrophobicity, Coulombic force, molecular size, or steric hindrance of the analytes; affinity and enzymatic reactions; and the application of mass spectrophotometric analysis.

REFERENCES

1. Hanai, T. *HPLC: A Practical Guide*; Royal Society of Chemistry Cambridge, **1999**.
2. Hanai, T. Selection of chromatographic method for biological materials. In *Advanced Chromatographic and Electromigration Methods in Biosciences*; Deyl, Z., Ed.; J. Chromatogr. Library *60*, Elsevier: Amsterdam, 1998; 1–51.
3. Chen, Z.; Yang, G.-Y.; Wang, S.; Li, L.; Su, Q. Simultaneous determination of tin, nickel, lead, cadmium and mercury in tobacco and tobacco additives by microwave digestion and RP-HPLC followed by on-line column enrichment. J. Chin. Chem. Soc. **2004**, *51*, 71–77.
4. Cho, H.-Y.; Park, C.-H.; Lee, Y.-B. Direct and simultaneous analysis of loxoprofen and its diastereomeric alcohol metabolites in human serum by on-line column switching liquid chromatography and its application to a pharmacokinetic study. J. Chromatogr. B, **2006**, *835*, 27–34.
5. Ban, E.; Maeng, J.-E.; Woo, J.S.; Kim, C.-K. Sensitive column-switching high-performance liquid chromatography method for determination of propiverine in human plasma. J. Chromatogr. B, **2006**, *831*, 230–235.
6. Ye, X.; Bishop, A.M.; Needham, L.L.; Calafat, A.M. Automated on-line column-switching HPLC-MS/MS method with peak focusing for measuring parabens, triclosan, and other environmental phenols in human milk. Anal. Chim. Acta **2008**, *622*, 150–156.
7. Kawaguchi, M.; Takahashi, S.; Seshimo, F.; Sakui, N.; Okanouchi, N.; Ito, R.; Inoue, K.; Yoshimura, Y.; Izumi, S.; Makino, T.; Nakazawa, H. Determination of 4-*tert*-octylphenol and 4-nonylphenol in laboratory animal feed sample by stir bar sorptive extraction followed by liquid desorption and column-switching liquid chromatography-mass spectrometry with solid-phase extraction. J. Chromatogr. A, **2004**, *1046*, 83–88.
8. Schettgen, T.; Musiol, A.; Alt, A.; Kraus, T. Fast determination of urinary *S*-phenylmercapturic acid (*S*-PMA) and *S*-benzylmercapturic acid (*S*-BMA) by column-switching liquid chromatography-tandem mass spectrometry. J. Chromatogr. B, **2008**, *863*, 283–292.
9. Brink, A.; Lutz, U.; Voelkel, W.; Lutz, W.K. Simultaneous determination of 6-methyl-2′-deoxyguanosine, 8-oxo-7,8-dihydro-2′-deoxyguanosine, and 1,*N*6-etheno-2′-deoxyadenosine in DNA using on-line sample preparation by HPLC column switching coupled to ESI-MS/MS. J. Chromatogr. B, **2006**, *830*, 255–261.
10. Nakagawa, S.; Suzuki, R.; Yamazaki, R.; Kusuhara, Y.; Mitsumoto, S.; Kobayashi, H.; Shimoeda, S.; Ohta, S.; Yamato, S. Determination of the antifungal agent voriconazole in human plasma using a simple column-switching high-performance liquid chromatography and its application to a pharmacokinetic study. Chem. Pharm. Bull. **2008**, *56*, 328–331.
11. Yi, L.; Gao, J.-P.; Xu, X.; Dai, L. Simultaneous determination of baicalein, rhein and berberine in rat plasma by column-switching high-performance liquid chromatography. J. Chromatogr, B, **2006**, *838*, 50–55.
12. De Paula, F.C.C.R.; De Pietro, A.C.; Cass, Q.B. Simultaneous quantification of sulfamethoxazole and trimethoprinin in whole egg samples by column-switching high-performance liquid chromatography using restricted access media column for on-line sample clean-up. J. Chromatogr. A, **2008**, *1189*, 221–226.
13. Hirukawa, M.; Maeda, M.; Tsuji, A.; Hanai, T. Separation of free amino acids by reversed-phase ion-pair chromatography with column switching and isocratic elution. J. Chromatogr. **1990**, *507*, 95–101.
14. Hanai, T.; Inamoto, Y.; Inamoto, S. Chromatography of guanidino compounds. J. Chromatogr. B, **2000**, *747*, 123–138.
15. Hanai, T.; Kaneko, K.; Homma, H. Semi-micro liquid chromatography of aromatic amino acid metabolites using isocratic elution and column switching. Biomed. Chromatogr. **2002**, *16*, 420–424.
16. Pepaj, M.; Wilson, S.R.; Novotna, K.; Lundanes, E.; Greibrokk, T. Two-dimensional capillary liquid chromatography: pH gradient ion-exchange and reversed-phase chromatography for rapid separation of proteins. J. Chromatogr. A, **2006**, *1120*, 132–141.
17. Machtejevas, E.; John, H.; Wagner, K.; Standker, L.; Marko-Varga, G.; Forssmann, W.-G.; Bischoff, R.;

Unger, K.K. Automated multi-dimensional liquid chromatography: Sample preparation and identification of peptides from human blood filtrate. J. Chromatogr. B, **2004**, *803*, 121–130.
18. Kahlich, R.; Gleiter, C.H.; Laufer, S.; Kammerer, B. Quantitative determination of Piritramide in human plasma and urine by off- and on-line solid-phase extraction liquid chromatography coupled to tandem mass spectrometry. Rapid Comm. Mass Spectrom. **2006**, *20*, 275–283.
19. Saito, M.; Santa, T.; Tsunoda, M.; Hamamoto, H.; Usui, N. An automated analyzer for vancomycin in plasma samples by column-switching high-performance liquid chromatography with UV detection. Biomed. Chromatogr. **2004**, *18*, 735–738.
20. Rbeida, O.; Christiaens, B.; Hubert, Ph.; Lubda, D.; Boos, K.-S.; Crommen, J.; Chiap, P.C. Evaluation of a novel anion-exchange restricted-access sorbent for on-line sample clean-up prior to the determination of acidic compounds in plasma by liquid chromatography. J. Chromatogr. A, **2004**, *1030*, 95–102.
21. Bruno, P.; Caselli, M.; De Gennaro, G.; De Tommaso, B.; Lastella, G.; Mastrolitti, S. Determination of nutrients in the presence of high chloride concentrations by column-switching chromatography. J. Chromatogr. A, **2003**, *1003*, 133–141.
22. Gomez-Ariza, J.L.; Sanchez-Rodas, D.; Caro de la Torre, M.A.; Giraldez, I.; Morales, E. Column-switching system for selenium speciation by coupling reversed-phase and ion-exchange high-performance liquid chromatography with microwave-assisted digestion-hydride generation-atomic fluorescence spectrometry. J. Chromatogr. A, **2000**, *889*, 33–39.
23. Kumihashi, M.; Ameno, K.; Shibayama, T.; Suga, K.; Miyauchi, H.; Jamal, M.; Wang, W.; Uekita, I.; Ijiri, I. Simultaneous determination of methamphetamine and its metabolite, amphetamine, in urine using a high performance liquid chromatography column-switching method. J. Chromatogr. B, **2007**, *845*, 180–183.
24. Hanai, T. Liquid chromatography of carbohydrates. Adv. Chromatogr. **1986**, *25*, 279–307.
25. Shimizu, M.; Uno, T.; Niioka, T.; Yaui-Furukoshi, N.; Takahata, T.; Sugawara, K.; Tateishi, T. Sensitive determination of omeprazole and its two main metabolites in human plasma by column-switching high-performance liquid chromatography: Application to pharmacokinetic study in relation to CYP2C19 genotypes. J. Chromatogr. B, **2006**, *832*, 241–248.
26. Maeda, T.; Sumi, S.; Hayashi, K.; Kidouchi, K.; Owaki, T.; Togari, H.; Fujimoto, S.; Wada, Y. Automated determination of 5-fluorouracil and its metabolite in urine by high-performance liquid chromatography with column switching. J. Chromatogr. B, **1999**, *731*, 267–273.
27. Faraoni, M.; Messina, A.; Polcaro, C.M.; Aturki, Z.; Sinibaldi, M. Chiral separation of pesticides by coupled-column liquid chromatography. Application to the stereoselective degradation of fenvalerate in soil. J. Liq. Chromatogr. Rel. Technol. **2004**, *27*, 995–1012.
28. Motoyama, A.; Suzuki, A.; Shirota, O.; Namba, R. Direct determination of pindolol enantiomers in human serum by column-switching LC-MS/MS using a phenylcarbamate-β-cyclodextrin chiral column. J. Pharm. Biomed. Anal. **2002**, *28*, 97–106.
29. Whittington, D.; Sheffels, P.; Kharasch, E.D. Stereoselective determination of methadone and the primary metabolite EDDP in human plasma by automated on-line extraction and liquid chromatography mass spectrometry. J. Chromatogr. B, **2004**, *809*, 313–321.
30. Cass, Q.B.; Lima, V.V.; Oliveira, R.V.; Cassiano, N.M.; Degani, A.L.G.; Pedrazzoli, J. Enantiomeric determination of the plasma levels of omeprazole by direct plasma injection using high-performance liquid chromatography with achiral–chiral column-switching. J. Chromatogr. B, **2003**, *798*, 275–281.
31. Mitsuhashi, S.; Fukushima, T.; Arai, K.; Tomiya, M.; Santa, T.; Imai, K.; Toyo'oka, T. Development of a column-switching high-performance liquid chromatography for kynurenine enantiomers and its application to a pharmacokinetic study in rat plasma. Anal. Chim. Acta. **2007**, *587*, 60–66.
32. Boppana, V.K.; Schaefer, W.H.; Cyronak, M.J. High-performance liquid chromatographic determination of warfarin enantiomers in plasma with automated on-line sample enrichment. J. Biomed. Biophys. Meth. **2002**, *54*, 315–326.
33. Itoh, M.; Kominami, G. On-line extraction followed by high-performance liquid chromatography and radio immunoassay for a novel retinobenzoic acid, AM-80, in human plasma. J. Immunoassay Immunochem. **2001**, *22*, 213–223.
34. Holtzapple, C.K.; Stanker, L.H. Affinity selection of compounds in a fluoroquinoline chemical library by online immunoaffinity deletion coupled to column HPLC. Anal. Chem. **1998**, *70*, 4817–4821.
35. Ishimura, K.; Fukunaga, K.; Irie, T.; Uekama, K.; Ohta, T.; Nakamura, H. Application of a beta-cyclodextrin sulfate-immobilized precolumn to selective online enrichment and separation of heparin-binding proteins by column-switching high-performance liquid chromatography. J. Chromatogr. A, **1997**, *769*, 209–214.
36. Watanabe, Y.; Kubo, T.; Nishikawa, T.; Fujita, T.; Kaya, K.; Hosoya, K. Fully automated liquid chromatography-mass spectrometry determination of 17β-estradiol in river water. J. Chromatogr. A, **2006**, *1120*, 252–259.
37. Watanabe, Y.; Hosoya, K.; Tanaka, N.; Kondo, T.; Morita, M.; Kubo, T. LC/MS determination of bisphenol A in river water using a surface-modified molecular-imprinted polymer as an on-line pretreatment device. Anal. Bioanal. Chem. **2005**, *381*, 1193–1198.
38. Nakamura, M.; Ono, M.; Nakajima, T.; Ito, Y.; Aketo, T.; Haginaka, J. Uniformly sized molecular imprinted polymer for atropine and its application to the determination of atropine and scopolamine in pharmaceutical preparations containing Scopolia extract. J. Pharm. Biomed. Anal. **2005**, *37*, 231–237.
39. Markoglou, N.; Hsuesh, R.; Wainer, I.W. Immobilized enzyme reactors based upon the flavoenzymes monoamine oxidase A and B. J. Chromatogr. B, **2004**, *804*, 295–302.
40. Calleri, E.; Marrubini, G.; Massolini, G.; Lubda, D.; De Fazio, S.S.; Furlanetto, S.; Wainer, I.W.; Manzo, L.; Caccialanza, G. Development of a chromatographic bioreactor based on immobilized beta-glucuronidase on monolithic support for the determination of dextromethorphan

and dextrorphan in human urine. J. Pharm. Biomed. Anal. **2004**, *35*, 1179–1189.
41. Calleri, E.; Temporini, C.; Furlanetto, S.; Loiodice, F.; Fracchiolla, G.; Massolini, G. Lipases for biocatalysis: Development of a chromatographic bioreactor. J. Pharm. Biomed. Anal. **2003**, *32*, 715–724.
42. Markoglou, N.; Wainer, I.W. Biosynthesis in an on-line immobilized-enzyme reactor containing phenylethanolamine *N*-methyltransferase in single-enzyme and coupled-enzyme formats. J. Chromatogr. A, **2002**, *948*, 249–256.
43. Sotolongo, V.; Johnson, D.V.; Wahnon, D.; Wainer, I.W. Immobilized horse liver alcohol dehydrogenase as an online high-performance liquid chromatographic enzyme reactor for stereoselective synthesis. Chirality **1999**, *11*, 39–45.
44. Baynham, M.T.; Patel, S.; Sharvil, M.R.; Wainer, I.W. Multidimensional on-line screening for ligands to the $\alpha 3\beta 4$ neuronal nicotinic acetylcholine receptor using an immobilized nicotinic receptor liquid chromatographic stationary phase. J. Chromatogr. B, **2002**, *772*, 155–161.
45. Calleri, E.; Temporini, C.; Perani, E.; Stella, C.; Rudaz, S.; Lubda, D.; Mellerio, G.; Veuthey, J.-L.; Caccialanza, G.; Massolini, G. Development of a bioreactor based on trypsin immobilized on monolithic support for the on-line digestion and identification of proteins. J. Chromatogr. A, **2004**, *1045*, 99–109.
46. Hayakawa, K.; Lu, C.; Mizukami, S.; Toriba, A.; Tang, N. Determination of 1-nitropyrene metabolites by high-performance liquid chromatography with chemiluminescence detection. J. Chromatogr. A, **2006**, *1107*, 286–289.
47. Yoshida, H.; Mizukoshi, T.; Hirayama, K.; Miyano, H. On-line desalting-mass spectrometry system for the structural determination of hydrophilic metabolites, using a column switching technique and a volatile ion-pairing reagent. J. Chromatogr. A, **2006**, *1119*, 315–321.

Columns: CEC Measurement and Calculation of Basic Electrochemical Properties

Michael P. Henry
Chitra K. Ratnayake
Advanced Technology Center, Beckman Coulter, Inc., Fullerton, California, U.S.A.

INTRODUCTION

In general, the structures of capillary columns in capillary electrochromatography (CEC) consist of a packed region or segment and an open, unpacked length, whose electrochemical properties may differ markedly from each other. The primary difference between the packed and open segments is their electrical resistivities. Measurements of electrochemical properties of the column as a whole, however, do not give information about the individual resistivity contributions of these two segments. Resistivity of the packed segment is fundamental in determining electroosmotic and electrophoretic flow velocities (explained in the section titled "Theory"), which in turn influence the speed of analysis and chromatographic efficiency and resolution. It is, therefore, important to know specific electrochemical properties of the two major segments to control, ultimately, the chromatographic performance of the CEC system. In this entry, a method of determining certain basic individual electrochemical properties for each segment is described.

These segmental properties do, in fact, add together in various mathematical ways to give the total property value for the column as a whole. This entry also deals with how this can be determined.

THEORY

Measurement and Calculation of Segmental Electrochemical Properties

We first consider the case of an open, but buffer-filled capillary column (Type A, shown schematically in Fig. 1), which is similar to that used in capillary electrophoresis. This is typically made of polyimide-coated fused silica. Let its length be L (cm) with an interior cross-sectional area as A (cm^2). If a voltage, V (Volts), is applied across the ends of the column and the current I (Amps) is measured, the resistance, R (Ohms), of the buffer can be calculated from Ohm's law, as given in Eq. 1:

$$R = \frac{V}{I} \tag{1}$$

R is proportional to L/A and, therefore, R is $\rho L/A$, where ρ is the electrical resistivity (units of Ω cm) of the buffer solution and can be calculated from Eq. 2:

$$\rho = \frac{RA}{L} = \frac{VA}{IL} \tag{2}$$

Eq. 3 gives the electrical conductivity [σ, (1/Ω cm)] of the buffer solution:

$$\sigma = \frac{1}{\rho} \tag{3}$$

Electrical conductance [λ, (1/Ω)] of the buffer solution is given by Eq. 4:

$$\lambda = \sigma \frac{A}{L} \tag{4}$$

or, more simply, by Eq. 5:

$$\lambda = \frac{1}{R} \tag{5}$$

The field strength, E(V/cm), over the filled capillary length is calculated from Eq. 6:

$$E = \frac{V}{L} \tag{6}$$

Voltage, current, resistance, resistivity, conductivity, conductance, and field strength are some of the purely electrochemical properties of the open, buffer-filled capillary, when an emf is placed across its ends.

We next consider the case of typical CEC columns, B and C (shown schematically in Fig. 1). The columns have the same internal diameter as column A and the packed length is L_{pack} (cm), and the open length is L_{open} (cm). Columns B and C are equilibrated with the same buffer used to fill column A. A voltage (V_T, V) applied across the ends of the capillary will cause a current (I_T, A) to flow, depending upon the total column resistance (R_T, Ω) according to Ohm's law (Eq. 1). The current that flows in either the open or the packed segment of the CEC columns will be the same, because the charge will not accumulate at any point in the circuit.

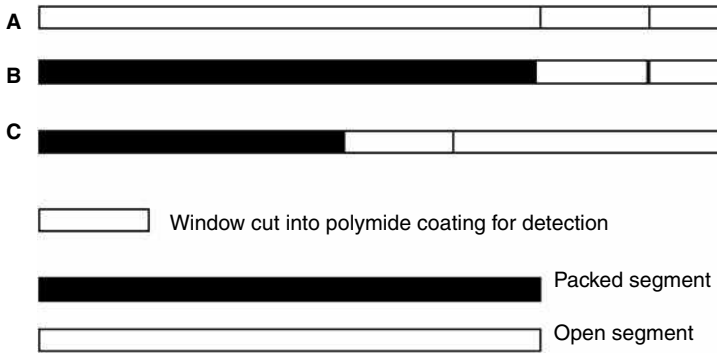

Fig. 1 Schematic diagrams of columns A–C, illustrating the locations of packed and open segments.

The total voltage drop across the capillary will be equal to the sum of the voltage drops across the packed and open segments, as shown in Eq. 7:

$$V_T = V_{open} + V_{pack} \tag{7}$$

V_{open} can be calculated from Eq. 8, where ρ_{open} is the resistivity of the buffer solution (calculated from Eq. 2) in the segment:

$$V_{open} = I_T R = \frac{I_T \rho_{open} L_{open}}{A} \tag{8}$$

Subtraction of V_{open} from V_T gives V_{pack} (Eq. 7).

Further, from Eq. 9, the resistivity of the packed segment, ρ_{pack}, can be calculated:

$$V_{pack} = \frac{I_T \rho_{pack} L_{pack}}{A} \tag{9}$$

Now that V_{open} and V_{pack} are known (Eqs. 8 and 9), the field strengths for the open and packed segments (E_{open}, E_{pack}) can be calculated from Eqs. 10 and 11:

$$E_{open} = \frac{V_{open}}{L_{open}} \tag{10}$$

$$E_{pack} = \frac{V_{pack}}{L_e} \tag{11}$$

where L_e is the "equivalent" length of the packed segment, as defined by Rathore and Horváth.[1] This parameter is the total length traveled by an unretained, neutral marker molecule, and can be calculated from Eq. 12, using electrochemical properties only, which is as follows:

$$L_e = L\left[\frac{I_{open}}{I_{pack}}\right]^{\frac{1}{2}} - L_{open} \tag{12}$$

where L is the total capillary length, and I_{open} and I_{pack} are the currents flowing through the column, in the absence and presence of packing, respectively.

Eqs. 1–12, therefore, allow the calculation of V, R, ρ, σ, λ, and E for the total column (T) and the individual open and packed segments, by the appropriate substitution of calculated values.

Linear Flow of Mobile Phase and Electric Field Strength, *E*

The axial flow of a stream of ions in an electric field formed within a capillary is generally made up of both electro-osmotic and electrophoretic components.[2] Both are directly proportional to field strength or change of voltage per centimeter. The Smoluchowski relationship[3] (Eq. 13) describes the electro-osmotic property:

$$u_{eo} = \varepsilon_o \varepsilon_r \frac{\zeta E}{\eta} \tag{13}$$

where u_{eo} is the linear velocity of the mobile phase, ε_o the permittivity of a vacuum, ε_r the dielectric constant of the buffer, ζ the zeta potential of capillary surface, E the field strength along the capillary, and η the viscosity of the mobile phase.

The linear velocity of the mobile phase is an important determinant of both speed of analysis and the chromatographic plate number, which affects peak resolution. Both are critical features of the values of chromatographic analysis.

Additivities of Segment Properties to Give Total Column Properties

Resistivities

Expressing Eq. 7 in terms of resistivities and measured parameters, we obtain the following:

$$\frac{I_T \rho_T L}{A} = \frac{I_T \rho_{open} L_{open}}{A} + \frac{I_T \rho_{pack} L_{pack}}{A} \tag{14}$$

Therefore,

$$\rho_T L = \rho_{open} L_{open} + \rho_{pack} L_{pack} \quad (15)$$

or

$$\rho_T = \rho_{open}\left(\frac{L_{open}}{L}\right) + \rho_{pack}\left(\frac{L_{pack}}{L}\right) \quad (16)$$

Thus, resistivities multiplied by the fractional length of the segment type, compared to the whole column, are additive along a column.

Resistances

Similarly, and more simply, resistances of each segment can be added as shown here:

$$V_T = I_T R_T = I_T R_{open} + I_T R_{pack} \quad (17)$$

Thus,

$$R_T = R_{open} + R_{pack} \quad (18)$$

Conductivities

As conductivity is the simple reciprocal of resistivity, substitution into Eq. 15 gives Eq. 19.

$$\frac{1}{\sigma_T} = (1/\sigma_{open})\frac{L_{open}}{L} + (1/\sigma_{pack})\frac{L_{pack}}{L} \quad (19)$$

Additivity of conductivities, therefore, occurs via the product of their reciprocals and the fractional length of segment type.

Conductances

Conductance is the simple reciprocal of resistance; therefore, Eq. 20 follows directly from Eq. 18.

$$\frac{1}{\lambda_T} = \frac{1}{\lambda_{open}} + \frac{1}{\lambda_{pack}} \quad (20)$$

Field strengths

1. With values of L_{open} and L_{pack}

$$E_T = \frac{V_T}{L} = \frac{V_{open} + V_{pack}}{L_{open} + L_{pack}} \quad (21)$$

Dividing numerator and denominator by L_{open} and putting the ratio L_{pack}/L_{open} as r,

$$E_T = \frac{E_{open} + E_{pack} r}{1 + r} \quad (22)$$

2. With values of L_{open} and L_e

Here L_{pack} is simply replaced by L_e in Eq. 22, with $r = L_e/L_{open}$

The above explanations and Eqs. 1–22 enable the calculation of many basic electrochemical properties of CEC columns. In the next section, we take data from the literature to see how the mathematics are applied to actual CEC systems.

EXPERIMENTAL DATA AND RESULTS

Ratnayake, Oh, and Henry[4] have measured currents at specific set voltages passing through CEC columns of several configurations of monolithic columns that they prepared. The three columns A (unpacked), B, and C are shown schematically in Fig. 1. The 75 μm I.D. columns were packed with 3 μm C_{18} bonded silica particles embedded in a silica gel and fitted into cartridges compatible with Beckman Coulter's P/ACE TM MDQ Capillary Electrophoresis System. The columns were equilibrated with 70/30 v/v acetonitrile/morpholino ethane sulfonic (MES) acid buffer (25 m*M*, pH 6.2).

We have used some of their data to calculate values for an expanded number of electrochemical properties of three of these columns, and the results are given in Table 1.

DISCUSSION

Column Configurations, Dimensions, and Buffers

Open and packed capillary dimensions were chosen to be the same so that Joule heating effects, if any, were similar, and column temperatures were, therefore, considered to be the same for all columns. This is an important requirement for the validity of Eqs. 8–22. The length of the packed segments was different in columns B and C to test the reproducibility of the monolithic bed preparations. The electrochemical properties in Table 1 were calculated using the same applied voltage polarity for all columns. No sample injections were needed. The choice of organic/aqueous mobile phase was made by Ratnayake, Oh, and Henry[4] in their chromatographic work such that the column functions as a standard reversed-phase packing.

Total Column Voltages, Currents, and Resistances

Similar voltages (20 kV) were applied to all columns to simplify comparisons of data. Currents were measured by

Table 1 Measured values of current, I, voltage, V, L_{open}, and L_{pack}, and calculated values of basic electrochemical properties of columns A–C.

Parameter (open) (units) (name)	Column A	Column B	Column C	Calculated	Equations
L_{open} (cm)	30	10	20	Measured	
L_{pack} (cm)	NA	21.5	10	Measured	
V_T (kV)	20	20	20	Measured	
I_T (μA) (current)	5.6	2.6	3.5	Measured	
ρ_T (Ω cm) (resistivity)	5.26×10^{-3}	11.33×10^{-3}	8.42×10^{-3}	Calculated	(2)
ρ_{open} (Ω cm) (resistivity)	5.26×10^{-3}	5.26×10^{-3}	5.26×10^{-3}	Calculated	(8)
ρ_{pack} (Ω cm) (resistivity)	NA	14.2×10^{-3}	14.7×10^{-3}	Calculated	(9)
σ_T [1/(Ω cm)] (conductivity)	1.9×10^{-4}	11.33×10^{-5}	8.42×10^{-5}	Calculated	(3)
σ_{open} [1/(Ω cm)] (conductivity)	1.9×10^{-4}	1.9×10^{-4}	1.9×10^{-4}	Calculated	(3)
σ_{pack} [1/(Ω cm)] (conductivity)	NA	7.04×10^{-4}	6.8×10^{-5}	Calculated	(3)
λ_T (1/Ω) (conductance)	0.28×10^{-9}	0.124×10^{-9}	0.175×10^{-9}	Calculated	(4) or (5)
λ_{open} (1/Ω) (conductance)	0.28×10^{-9}	0.84×10^{-9}	0.42×10^{-9}	Calculated	(4) or (5)
λ_{pack} (1/Ω) (conductance)	NA	0.14×10^{-9}	0.3×10^{-9}	Calculated	(4) or (5)
R_T (Ω) (resistance)	3.57×10^{9}	8.08×10^{9}	5.71×10^{9}	Calculated	(1)
R_{open} (Ω) (resistance)	0.28×10^{9}	0.84×10^{9}	0.42×10^{9}	Calculated	(1)
R_{pack} (Ω) (resistance)	NA	0.14×10^{9}	0.3×10^{9}	Calculated	(1)
V_{open} (kV)	20	3.09	8.33	Calculated	(8)
V_{pack} (kV)	NA	17.91	11.67	Calculated	(7)
L_e (cm) (equivalent length)	NA	36.5	17.8	Calculated	(12)
E_T[a] (V/cm) (field strength)	667	667	667	Calculated	(21)
E_T[b] (V/cm) (field strength)	667	430	529	Calculated	(21)
E_{open} (V/cm) (field strength)	667	309	417	Calculated	(10)
E_{pack} (V/cm) (field strength)	NA	491	657	Calculated	(11)

A (cm^2) $= 44 \times 10^{-6}$ cm^2.
[a]Field strength calculated using values of L_{open} and L_{pack}.
[b]Field strength calculated using values of L_e.

the instrument and total column resistance, R_T, was calculated using Ohm's law (Eq. 1). Resistance to current flow varied because of the different packed and open lengths in the three columns. The selection of a low buffer ionic strength, a zwitterionic buffer type, the presence of nonconducting acetonitrile, a small column cross-sectional area, and moderate column length contributed to the very low currents observed.)

Segmental Resistances, *R*, Resistivities, ρ, Conductivities, σ, and Conductances, λ

Resistivity (and its reciprocal, conductivity) of open segments, ρ_{open}, is assumed to be the same in all three columns. This will be true provided the composition of the buffer is the same. In principle, the resistivity of the mobile phase inside the packed segments will also be ρ_{open}.

The resistivities of the packed segments in columns B and C are very close, indicating that their preparation is quite reproducible. This property, ρ_{pack}, is, therefore, a good indicator of the reproducibility of manufacture in a commercial setting.

In qualitative terms, it can be gathered from the fact that if very small currents (I in μA) are generated from large voltages (V in kV), then column resistances must be high (R in billions of Ω) and conductances must be very low (λ in 1/nΩ). Values of resistivity (ρ in kΩ cm) and conductivity [σ in (1/mΩ cm)] are seen to be intermediate between these limits. The reason for this intermediate nature is a direct result of the configuration of the standard capillary used in CEC. In other words, the ratio of the column length to the interior cross-sectional area, L/A (1/cm) is very high, at about 450,000 to 1. Thus, when a low conductance is multiplied by this ratio, an intermediate value is obtained for conductivity. Similarly, the intermediate values of resistivity arise when the large column resistances are divided by the L/A ratio.

It can also be noted from Table 1 that conductances of both the packed and open segments are halved when their lengths are doubled.

Segment Voltages and Field Strengths

The relationship between linear velocity and field strength (Eq. 13) is analogous to the linear velocity of, for example, a stream of water under the force of gravity along an inclined plane. The steeper the plane, the faster the flow will be.

The flow of ions in the open column A is unimpeded by any solid resistance and, so, has the largest current flow (5.6 μA). Column B offers the highest resistance to current flow and has the lowest field strength in all segments and, consequently, the column generates the smallest current (2.6 μA). Column C is intermediate between A and B in field strength and current.

CONCLUSIONS

This entry is a short tutorial on the basics of electrochemistry that is applied to CEC columns. Because the typical CEC columns consist of a packed and an open segment, their individual electrochemical properties are quite different. The application of basic principles of electricity (Ohm's law) and knowledge of the lengths and cross-sectional area of the capillary are all that is necessary to calculate most of the basic electrochemical properties of the CEC column. These include voltage, V, current, I, resistance, R, resistivity, ρ, conductivity, σ, conductance, λ, and field strength, E, for each segment type and for the column as a whole. It has also been shown how the individual segment properties can be added together to produce the total column property. Voltages and resistances add simply, but other properties are more complex in the way that they add and involve reciprocal functions and ratios of segment lengths.

REFERENCES

1. Rathore, A.S.; Horváth, C.S. Axial nonuniformities and flow in columns for capillary electrochromatography. Anal. Chem. **1998**, *70*, 3069–3077.
2. Henry, M.P.; Ratnayake, C.K. CEC. In *Encyclopedia of Chromatography,* 3rd Ed.; Cazes, J., Ed.; Taylor & Francis: New York, 2010; 360–365.
3. Rice, C.L.; Whitehead, R.J. Electrokinetic flow in narrow cylindrical capillary. J. Phys. Chem. **1965**, *69*, 4017–4024.
4. Ratnayake, C.K.; Oh, C.S.; Henry, M.P. Characteristics of particle-loaded monolithic sol–gel columns for capillary electrochromatography. I. Structural, electrical and band-broadening properties. J. Chromatogr. A, **2000**, *887*, 277–285.

Columns: Resolving Power

Raymond P.W. Scott
Scientific Detectors Ltd., Banbury, Oxfordshire, U.K.

INTRODUCTION

Two solutes will be resolved if their peaks are moved apart in the column and maintained sufficiently narrow to permit them to be eluted as discrete peaks. Resolution is usually defined as the ratio of the distance between the peaks to the peak width at the points of inflection. It is generally accepted that a separation of 4σ is adequate for accurate quantitative analysis, particularly when employing peak heights measurements. It is, therefore, necessary to derive an expression for the peak width in order to equate to the peak separation.

APPLICATION

The plate theory gives an expression for the elution curve of a solute as

$$X_{m(n)} = \frac{X_0 e^{-\upsilon} \upsilon^n}{n!} \tag{1}$$

where $X_{m(n)}$ is the concentration of solute in the nth plate on elution, X_0 is the concentration placed on the first plate on injection, n is the number of plates in the column, and υ is the flow of mobile phase in plate volumes.

By differentiating and equating Eq. 1 to zero gives the following expression for the retention volume of a solute:

$$V_r = n(\upsilon_m + K\upsilon_s)$$

Now, by equating the second differential of the elution equation to zero and solving for υ, an expression for the peak width at the points of inflexion can obtained:

$$\frac{d_2\left(X_0 \frac{e^{-\upsilon}\upsilon^n}{n!}\right)}{d\upsilon^2} = X_0 e^{-\upsilon}\upsilon^n - e^{-\upsilon} n\upsilon^{n-1} - e^{-\upsilon} n\upsilon^{n-1}, \underline{\qquad +e^{-\upsilon} n(n-1)\upsilon^{n-2}} \over n!$$

Thus,

$$\frac{d_2(X_0(e^{-\upsilon}\upsilon^n/n!))}{d\upsilon^2} = X_0 \frac{e^{-\upsilon}\upsilon^{n-2}(\upsilon^2 - 2n\upsilon + n(n-1))}{n!} \tag{2}$$

Now, at the points of inflexion,

$$\frac{d_2(X_0(e^{-\upsilon}\upsilon^n/n!))}{d\upsilon^2} = 0$$

Hence,

$$\upsilon^2 - 2n\upsilon + n(n-1) = 0$$

and

$$\upsilon = \frac{2n \pm \sqrt{4n^2 - 4n(n-1)}}{2} = \frac{2n \pm \sqrt{4n}}{2} = n \pm \sqrt{n}$$

It is seen that the points of inflexion occur after $n - \sqrt{n}$ and $n + \sqrt{n}$ plate volumes of mobile phase have passed through the column. Thus, the volume of the mobile phase that has passed through the column *between* the inflexion points will be

$$n + \sqrt{n}\ n + \sqrt{n} = 2\sqrt{n} \tag{3}$$

Thus, the peak width at the points of inflexion of the elution curve will be $2\sqrt{n}$ plate volumes which, in milliliters of mobile phase, will be obtained by multiplying by the *plate volume*; that is,

$$\text{Peak width} = 2\sqrt{n}(\upsilon_m + K\upsilon_s) \tag{4}$$

The peak width at the points of inflexion of the elution curve is twice the standard deviation, and, thus, from Eq. 4, it is seen that the variance (the square of the standard deviation) is equal to n, the total number of plates in the column. Consequently, the variance of the band (σ^2) in milliliters of mobile phase is given by

$$\sigma^2 = n(\upsilon_m + K\upsilon_s)^2$$

Now,

$$V_r = n(\upsilon_m + K\upsilon_s)$$

Thus,

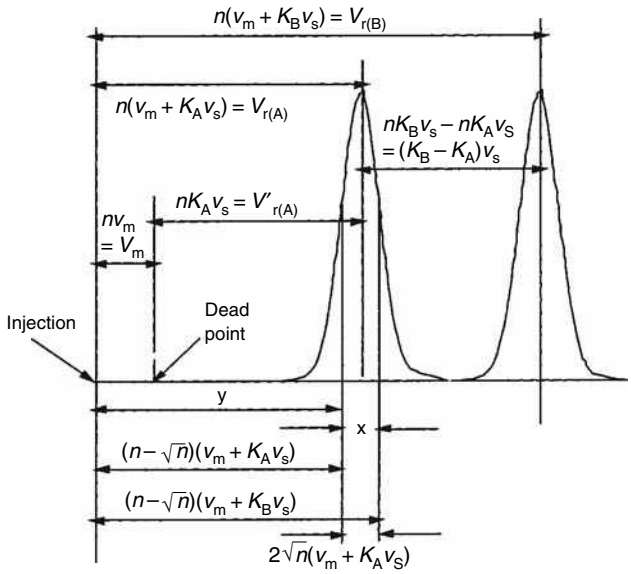

Fig. 1 A chromatogram showing two resolved solute peaks.

$$\sigma^2 = \frac{V_r{}^2}{n}$$

Let the distance between the injection point and the peak maximum (the retention distance on the chromatogram) be y cm and the peak width at the points of inflexion be x cm. If the chromatographic data are computer processed, then the equivalent retention times can be used. Then, as the retention volume is $n(\upsilon_m + K\upsilon_s)$ and twice the peak standard deviation at the points of inflexion is $2\sqrt{n}(\upsilon_m + K\upsilon_s)$ then

$$\frac{\text{Ret. distance}}{\text{Peak width}} = \frac{y}{x} = \frac{n(\upsilon_m + K\upsilon_s)}{2\sqrt{n}(\upsilon_m + K\upsilon_s)} = \frac{\sqrt{n}}{2}$$

Thus,

$$n = 4\left(\frac{y}{x}\right)^2 \tag{5}$$

Eq. 5 allows the efficiency of any solute peak, from any column, to be calculated from measurements taken directly from the chromatogram.

Consider the two peaks depicted in Fig. 1. The difference between the two peaks, for solutes A and B (see *Plate Theory*, p. 1829), measured in volume flow of mobile phase, will be

$$n(\upsilon_m + K_B\upsilon_s) - n(\upsilon_m + K_A\upsilon_s) = n(K_B + K_A)\upsilon_s \tag{6}$$

Assuming the widths of the two peaks are the same, then the peak width in volume flow of mobile phase will be

$$2\sigma = 2\sqrt{n}(\upsilon_m + K_A\upsilon_s) \tag{7}$$

where K_A is the distribution coefficient of the first of the eluted pair of solutes between the two phases. Taking the already discussed criterion that resolution is achieved when the peak maxima of the pair of solutes are 4σ apart, then

$$4\sqrt{n}(\upsilon_m + K_A\upsilon_s) = n(K_B + K_A)\upsilon_s$$

Rearranging,

$$\sqrt{n} = \frac{4(\upsilon_m + K_A\upsilon_s)}{(K_B - K_A)\upsilon_s}$$

dividing through by υ_m,

$$\sqrt{n} = \frac{4(1 + k_A{}')}{(k_B{}' - k_A{}')\upsilon_s}$$

Now, as α, the separation ratio between the two solutes, has been defined as

$$\alpha = \frac{k_B{}'}{k_A{}'}$$

then

$$\sqrt{n} = \frac{4(1 + k_A{}')}{k_A{}'(\alpha - 1)}$$

and

$$n = \left(\frac{4(1 + k_A{}')}{k_A{}'(\alpha - 1)}\right)^2 = 16\frac{(1 + k_A{}')^2}{k_A{}'^2(\alpha - 1)^2} \tag{8}$$

Eq. 8 is extremely important and was first developed by Purnell[1] in 1959. It allows the necessary efficiency to achieve a given separation to be calculated from a knowledge of the capacity factor of the first eluted peak of the pair and their separation ratio.

REFERENCE

1. Purnell, J.H. Comparison of efficiency and separating power of packed and capillary gas chromatographic columns. Nature (London) **1959**, *184* (4704), 2009.

BIBLIOGRAPHY

1. Scott, R.P.W. *Chromatographic Detectors*; Marcel Dekker, Inc.: New York, 1996.
2. Scott, R.P.W. *Introduction to Analytical Gas Chromatography*; Marcel Dekker, Inc.: New York, 1998.

Conductivity Detection in CE

Jetse C. Reijenga
Department of Chemical Engineering and Chemistry, Eindhoven University of Technology, Eindhoven, The Netherlands

INTRODUCTION

In contrast to component-specific detectors, such as ultraviolet (UV) absorbance and fluorescence, conductivity detection is a universal detection method. This means that a bulk property (conductivity) of the buffer solution is continuously measured. A migrating ionic component locally changes the conductivity and this change is monitored. As such, conductivity detection is universally sensitive because, in principle, all migrating ionic compounds show detector response, although not to the same extent.

TYPES OF CONDUCTIVITY DETECTION

Two kinds of conductivity detector are distinguished: contact detectors and contactless detectors. Both types were originally developed for isotachophoresis in 0.2–0.5-mm-inner diameter (I.D.) PTFE tubes. Contactless detectors are based on the measurement of high-frequency cell resistance and, as such, inversely proportional to the conductivity. The advantage is that electrodes do not make contact with the buffer solution and are, therefore, outside the electric field. As these types of detectors are difficult to miniaturize down to the usual 50–75 μm capillar inner diameter, their actual application in capillary electrophoresis (CE) is limited.

Contact detectors are somewhat easier to miniaturize. There are generally two subtypes: those with twin axially mounted electrodes and those with twin or quadruple radially mounted electrodes. The former can be operated in DC mode or AC mode. In the DC mode, the detector signal directly originates from the field strength between the electrodes and, given the current, is inversely proportional to the detector cell resistance. In the AC mode, both axially and radially mounted electrodes form part of a closed primary circuit of an isolation transformer, the output of which is also inversely proportional to the cell conductivity. Alternatively, the output can be linearized with respect to the conductivity.

CONDUCTIVITY DETECTOR RESPONSE

As mentioned, the detector continually measures the conductivity of the buffer solution in the capillary. If an ionic component enters the detector cell, the local conductivity will change. At first glance, one would expect the conductivity to increase, because of additional ionic material. This is a simplified and incorrect approach, however. Suppose, in a buffer consisting of 0.01 *M* potassium and 0.02 *M* acetate (pH 4.7), a 10^{-4} *M* sodium solution is analyzed. Electroneutrality requires that with an increase of the sodium concentration from zero to, in this case, initially 10^{-4} *M*, the potassium and/or charged acetate concentration cannot remain unchanged. This process is governed by the so-called Kohlrausch law. For strong ions, this equation reads

$$\Lambda = \sum_i \frac{c_i}{\mu_i}$$

in which Λ is the so-called Kohlrausch regulating function, c_i is the concentration of component i, and μ_i is the mobility of component i. Generally speaking, potassium will be partly displaced by sodium, whereas acetate will remain approximately (but not, by definition, exactly) constant. In the example given, the conductivity detector will give a negative response (see line A in Fig. 1), because potassium (with a high mobility and, hence, a higher contribution to conductivity) is, to some extent, replaced with sodium which has a ~30% lower mobility. From this example, it automatically follows that a potassium peak in a sodium acetate buffer, by contrast, will yield a positive amplitude. This makes interpretation of conductivity detector signals less straightforward.

SENSITIVITY OF CONDUCTIVITY DETECTION

A further example will illustrate aspects related to sensitivity. Suppose a 100 times more concentrated (10 m*M*) solution of ammonium is coseparated in the potassium–acetate system mentioned earlier. Naturally, ammonium will displace potassium, but as the mobilities of potassium and ammonium are almost equal, the resulting change in conductivity is minor. Sensitivity in this example is, consequently, very low (line A in Fig. 1). On the other hand, 0.005 m*M* lithium has a much lower conductivity than sodium and, consequently, shows a higher specific response (line A in Fig. 1).

Generally, one cannot expect a high sensitivity anyhow, as the background signal (originating from the buffer) is generally much higher than the eventual change

Encyclopedia of Chromatography, Third Edition DOI: 10.1081/E-ECHR3-120039929

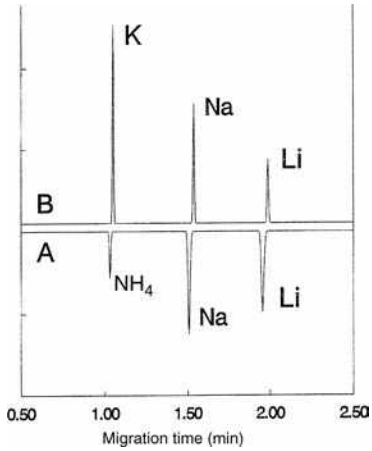

Fig. 1 Relative sensitivities in conductivity detection in CE. Trace A: sample of 10 m*M* NH_4, 0.1 m*M* Na, and 0.005 m*M* Li in a 0.01 *M* potassium–acetate buffer; trace B: sample of 0.1 m*M* each of K, Na, and Li in a 10 m*M* Tris–acetate buffer.

superimposed upon that background. One might argue that background conductivity can easily be decreased by diluting the buffer. Potential gain with this approach is very limited, because diluting the buffer below an ionic strength of 1 m*M* will lead to unacceptable loss in buffering capacity and, moreover, in severe sample overload. Another possibility to decrease the background conductivity is to use buffer components with lower mobility, such as GOOD buffers. This, however, will sooner lead to non-symmetric peaks on sample overload (peak triangulation). Using low-mobility Tris as a buffer co-ion will lead to positive peaks for 0.1 m*M* potassium, sodium, and lithium alike (line B in Fig. 1).

BIBLIOGRAPHY

1. Beckers, J.L. Isotachophoresis, some fundamental aspects. In *Thesis*; Eindhoven University of Technology, 1973.
2. Everaerts, F.M.; Beckers, J.L.; Verheggen, Th.P.E.M. *Isotachophoresis: Theory, Instrumentation and Applications*; Elsevier: Amsterdam, 1976.
3. Hjertén, S. Free zone electrophoresis. Chromatogr. Rev. **1967**, *9* (2), 122–219.
4. Kohlrausch, F. Ueber concentrations-verschiebungen durch electrolyse im innern von Lösungen und Lösungsgemischen. Ann. Phys. (Leipzig) **1897**, *62*, 209.
5. Li, S.F.Y. *Capillary Electrophoresis—Principles, Practice and Applications*; Elsevier: Amsterdam, 1992.
6. Reijenga, J.C.; Verheggen, Th.P.E.M.; Martens, J.H.P.A.; Everaerts, F.M. Buffer capacity, ionic strength and heat dissipation in capillary electrophoresis. J. Chromatogr. A, **1996**, *744*, 147.

Conductivity Detection in HPLC

Ioannis N. Papadoyannis
Victoria F. Samanidou
Laboratory of Analytical Chemistry, Chemistry Department, Aristotle University of Thessaloniki, Thessaloniki, Greece

INTRODUCTION

Conductivity detection is used to detect inorganic and organic ionic species in liquid chromatography (LC). As all ionic species are electrically conducting, conductometric detection is a universal detection technique, considered as the mainstay in high-pressure ion chromatography, in the same way as is ultraviolet (UV) detection in high-performance liquid chromatography (HPLC).

DISCUSSION

The principle of operation of a conductivity detector lies in differential measurement of mobile-phase conductivity prior to and during solute ion elution. The conductivity cell is either placed directly after an analytical column or after a suppression device required to reduce background conductivity, in order to increase the signal-to-noise ratio and, thus, sensitivity. In the first mode, known as *non-suppressed* or *single-column ion chromatography*, aromatic acid eluents are used, with low-capacity fixed-site ion exchangers and dynamically or permanently coated reversed-phase columns. In the second mode, known as *eluent-suppressed ion chromatography*, the separated ions are detected by conductance after passing through a suppression column or a membrane, to convert the solute ions to higher conducting species (e.g., hydrochloric acid in the case of chloride ions and sodium hydroxide in the case of sodium ions). In the meantime, the eluent ions are converted to a low-residual-conductivity medium such as carbonic acid or water, thus reducing background noise.

Conductance G is the ability of electrolyte solutions in an electric field applied between two electrodes to transport current by ion migration. According to Ohm's law, ohmic resistance R is given by

$$R = \frac{U}{I} \tag{1}$$

where U is the voltage (V) and I is the current intensity (A). The reciprocal of ohmic resistance is the conductance G, where

$$G = \frac{1}{R} \tag{2}$$

expressed in Siemens in the International System of Units (SI), formerly reported in the literature as mho The measured conductance of a solution is related to the inter-electrode distance d (cm) and the microscopic surface area (A) (geometric area × roughness factor) of each electrode (A is assumed identical for the two electrodes) as well as the ionic concentration, given by

$$G = \frac{kA}{d} \tag{3}$$

where k is the specific conductance or conductivity. The ratio d/A is a constant for a particular cell, referred as the cell constant K_c (cm^{-1}) and is determined by calibration. The usual measured variable in conductometry is conductivity k (S/cm)

$$k = GK_c \tag{4}$$

The conductance G (in μS) of a solution is given by

$$G = \frac{(\lambda^+ + \lambda^-)CI}{10^{-3}K_c} \tag{5}$$

where λ^+ and λ^- are limiting molar conductivities of the cation and anion, respectively, and C is the molarity and I the fraction of eluent that is ionized. If the eluent and solute are fully ionized, the conductance change accompanying solute elution is

$$\Delta G = \frac{(\lambda_s - \lambda_e)C_s}{10^{-3}K_c} \tag{6}$$

The specific conductance/conductivity k (S/cm) of salts measured by a conductivity detector is given by

$$k = \frac{(\lambda_{s+} + \lambda_{s-})C_s + (\lambda_{e+} + \lambda_{e-})C_e}{1000} = \frac{\Lambda_s C_s + \Lambda_e C_e}{1000} \tag{7}$$

where C_s and C_e are the concentration (mol/L) of the solute and eluent ions, respectively, and Λ is the molar conductivity of the electrolyte.

The change in conductance when a sample solute band passes through the detector results from replacement of some of the eluent ions by solute ions, although the total ion concentration C_{tot} remains constant:

$$C_{tot} = C_s + C_e \tag{8}$$

The background ion conductivity when $C_s = 0$ is

$$k_1 = \frac{\Lambda_e C_{\text{tot}}}{1000} \tag{9}$$

When a solute band is eluted, the ion conductivity k_2 is given by

$$k_2 = \frac{\Lambda_e C_{\text{tot}}}{1000} + \frac{(\Lambda_s - \Lambda_e)C_s}{1000} \tag{10}$$

The difference in conductivity is obtained after subtraction of the first equation from the second:

$$\Delta k = k_2 - k_1 = \frac{(\Lambda_s - \Lambda_e)C_s}{1000} \tag{11}$$

From Eq. (11), it is obvious that when a sample band is eluted, the observed difference in conductivity is proportional to the concentration of the sample solute C_s. However, the linear relation holds only for dilute solutions, as Λ is itself dependent on concentration, according to Kohlrausch's law:

$$\Lambda = \Lambda - A\sqrt{C} \tag{12}$$

where A is a constant and Λ° is the limiting molar conductivity in an infinitely dilute solution, given by the sum

$$\Lambda = \Lambda^+ + \Lambda^- \tag{13}$$

or

$$\Lambda = v_+\lambda_+ + v_-\lambda \tag{14}$$

where v_+ and v_- represent stoichiometric coefficients for the cation and anion, respectively, in the electrolyte.

Eq. 11 shows that the signal observed during solute ion elution is also proportional to the difference in limiting molar ionic conductivities between the eluent and the solute ions.

Values of limiting molar ionic conductivities for a few common ions are shown in Table 1. The data tabulated are referred to 25°C temperature. The term *limiting molar ionic conductivity* is used according to International union of pure and applied chemistry (IUPAC) recommendation, rather than the formerly used *limiting ionic equivalent conductivity*. The molar and equivalent values are interconvertible through stoichiometric coefficient z.

Conductivity is measured by applying an alternating voltage to two electrodes of various geometric shapes in a flow-through cell, which results in anion migration, as negatively charged, toward the anode (positive electrode) and cation migration, as positively charged, toward the negative electrode (cathode). An AC potential (frequency 1000–5000 Hz) is required in order to avoid electrode polarization. The cell current is measured and the solution's resistance (or more strictly the impedance) is calculated by Ohm's law. Conductance is further corrected by the conductivity cell constant, thus giving conductivity.

Table 1 Limiting molar ionic conductivities of some anions and cations at 25°C.

Anions	λ^-	Cations	λ^+
OH^-	199.1	H^+	349.6
F^-	55.4	Li^+	38.7
Cl^-	76.4	Na^+	50.1
Br^-	78.1	K^+	73.5
I^-	76.8	NH_4^+	73.5
NO_3^-	71.46	Mg^{2+}	106
NO_2^-	71.8	Cu^{2+}	107.2
SO_4^{2-}	160.0	Ca^{2+}	120
$Benzoate^-$	32.4	Sr^{2+}	118.9
$Phthalate^{2-}$	76	Ba^{2+}	127.2
$Citrate^{3-}$	168	Ethylammonium	47.2
CO_3^{2-}	138.6	Diethylammonium	42.0
$C_2O_4^{2-}$	148.2	Triethylammonium	34.3
PO_4^{3-}	207	Tetraethylammonium	32.6
CH_3COO^-	40.9	Trimethylammonium	47.2
$HCOO^-$	54.6	Tetramethylammonium	44.9

The requirements for a typical conductivity detection cell are small volume (to eliminate dispersion effects), high sensitivity, wide linear range, rapid response, and acceptable stability. The cell generally consists of a small-volume chamber (<5 μl) fitted with two or more electrodes constructed of platinum, stainless steel, or gold.

Most conductivity detectors function according to the Wheatstone Bridge principle. What is actually measured is resistance of the solution. Electronically, the electrodes are arranged in that way to constitute one arm of a Wheatstone Bridge. Eluting ions from chromatographic column subsequently enter the detector cell, leading to a change of electrical resistance and the out-of-balance signal is rectified with a precision rectifier. The DC signal is either digitized and sent to a computer data acquisition system or is passed to a potentiometric recorder, by means of a linearizing amplifier, which modifies the signal so that the output is linearly related to ion concentration. Sometimes, a variable resistance is situated in one of the other arms of the bridge and is used for zero adjustment to compensate for any signal from mobile-phase ions. As mentioned earlier, at constant voltage applied to the cell, the current will be proportional to the conductivity (Fig. 1).

The conductivity k is a characteristic property of the solution rather than a property of the cell used. It contains all the chemical information available from the measurement, such as concentration and mobilities of the ions present. Accordingly, the conductivity detector is a bulk property detector and, as such, it responds to all electrolytes present in the mobile phase as well as the solutes.

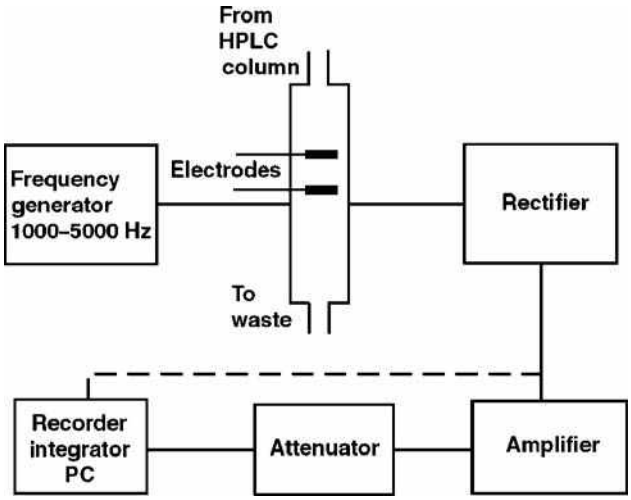

Fig. 1 Block diagram of electrical conductivity detector in HPLC.

Thus, the experimentally determined conductivity is the sum of the contributions from all ions present in the solution. The sensitivity of the conductivity detector depends on the difference between the limiting ionic conductivities of the solute and eluent ions.

The differential mode of detection is mostly effective, provided there is a significant difference in the values of the measured property between the eluent and solute ions. This difference may be either positive or negative. The former case refers to lower conductivity of the eluent ion, described as *direct detection method*, the latter to greater conductivity of the eluent ion, described as *indirect detection method* (Fig. 2).

The thermal stability of a conductivity detector is of great importance. Effective thermostating is highly required, as the temperature greatly affects the mobility of ions and, therefore, conductivity. A 0.5–3% increase of conductivity is usually expected per degree Celsius. Close temperature control is necessary to minimize background noise and maximize sensitivity; this is an especially important issue if non-suppressed eluents are used.

Typical specifications for an electrical conductivity detector are as follows: sensitivity, 5×10^{-9} g/ml; linear dynamic range, 5×10^{-9} to 1×10^{-6} g/ml; response index, 0.97–1.03.

CONCLUSIONS

Conductivity detection in HPLC or, more precisely HPIC, can be applied to ionic species, including all anions and cations of strong acids and bases (e.g., chloride, sulfate, sodium, potassium, etc.). Ions of weaker acids and bases are detected provided that the pH value of the eluent is chosen to maximize the analyte's ionization so as to increase sensitivity. The relatively simple design requirements, accuracy, and low cost contribute to its utility and popularity; thus, it is almost used in over 95% of analyses, where ion-exchange separation procedures are involved.

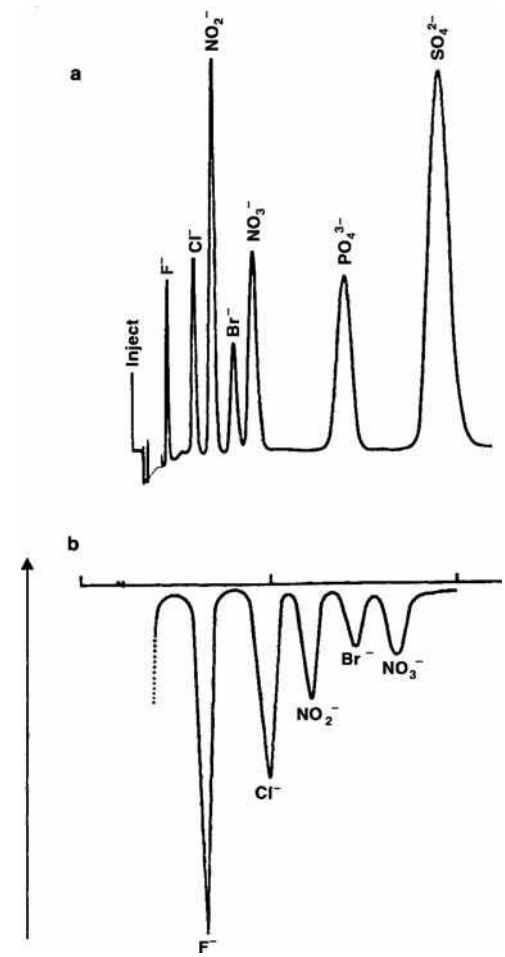

Fig. 2 Conductivity detection of anions in non-suppressed (single column) ion chromatography using an eluent of (a) low-background conductance (direct detection) and (b) high-background conductance (indirect detection). The direction of the arrow indicates the increase of conductivity.

BIBLIOGRAPHY

1. Coury, L. Conductance measurements Part I: Theory. Curr. Separ. **1999**, *18* (3), 91.
2. Papadoyannis, I.; Samanidou, V.; Zotou, A. Highly selective simultaneous determination of eight inorganic anions in drinking water by single column high pressure anion chromatography. J. Liq. Chromatogr. Relat. Technol. **1995**, *18* (7), 1383.
3. Parriott, D. *A Practical Guide to HPLC Detection*; Academic Press: San Diego, CA, 1993.
4. Schaefer, H.; Laubli, M.; Doerig, R. *Ion Chromatography*; Metrohm Monograph 50143; Metrohm AG: Herisau, 1996.
5. Scott, R. *Techniques and Practice of Chromatography*; Marcel Dekker, Inc.: New York, 1995.
6. Scott, R. *Chromatographic Detectors, Design, Function and Operation*; Marcel Dekker, Inc.: New York, 1996.
7. Tarter, J. *Ion Chromatography*; Chromatographic Science Series Marcel Dekker, Inc.: New York, 1987; Vol. 37.

Congener-Specific PCB Analysis

George M. Frame II
Wadsworth Laboratory, New York State Department of Health, Albany, New York, U.S.A.

INTRODUCTION

Polychlorinated biphenyls (PCBs) are complex mixtures of 209 possible chlorinated biphenyl molecules, referred to as congeners. There are from 3 to 46 isomers at each of the 10 possible levels of chlorination. Isomers of a given chlorination level are referred to as homologs. About 150 of these congeners appear at significant levels in commercial mixtures. These mixtures, trade named Aroclor (U.S.A.), Clophen (Germany), Kanechlor (Japan), and so forth, found use as electrical insulating fluids in transformers and capacitors and as binders for a wide variety of uncontained applications. Although their manufacture has been largely discontinued, their long-term stability, dispersion into the environment by prior uncontrolled releases, lipophilicity (resulting in biomagnification up food chains), and potential toxicity to humans and biota have sparked extensive research and the requirement for detailed analytical characterization of these mixtures.

DISCUSSION

This entry does not discuss the extensive literature on sample preparation, cleanup, and proper instrumental operation. Adsorption column chromatography and HPLC procedures find application here, and the book by Erickson[1] provides exhaustive discussions of these and of the history of PCB use and analysis. Methods for measuring total PCB content or measuring and reporting the mixtures by their commercial designation are not detailed. Congener-specific PCB analysis demands separation and quantitation either of shortlists of priority PCB congeners or of the PCB content of all chromatographic PCB peaks that can be separated in particular system(s). This latter mode is referred to as comprehensive, quantitative, congener-specific analysis (CQCS). The methods of choice for CQCS PCB analysis employ high-resolution GC (HRGC) on capillary columns with sensitive and selective detection by electron-capture detectors (ECD), selected ion monitoring-MS (MS-SIM), or full-scan, ion-trap MS (ITMS). The most complete discussion of target congeners for specific research applications is in Ref.[2] A descriptive overview of CQCS PCB analysis appears in an Analytical Chemistry A-page article,[3] and extensive reviews[4–6] provide detailed discussions and large bibliographies.

Fig. 1 summarizes PCB congener structure, nomenclature, the Ballschmiter and Zell (BZ) congener numbering system, and the relative abundances in the commercial Aroclor mixtures as a function of single-ring chlorine-substitution patterns. The BZ numbers in the matrix correspond to the chlorine-substitution positions in each ring of the biphenyl structure, which are listed along the top and right sides of the figure matrix. The abbreviated nomenclature (e.g., 234–245 = PCB #138) defines each congener by the substitution pattern in each ring, with the dash representing the bond between the two phenyl rings. Rotation about this bond is possible except in congeners with three or four chlorines in the ortho (2 or 6) positions.

In the United States, commercial mixtures were manufactured until 1977 by Monsanto under the trade name Aroclor. In the four-digit Aroclor designations (e.g., Aroclor 1242), the 12 indicates a biphenyl nucleus and the 42 the weight percentage of chlorine in the mixture. Reference to the matrix in Fig. 1 reveals congeners in black cells which never exceed 0.1 wt% in the mixtures. These "non-Aroclor" congeners are absent due to unfavored or improbable formation in the electrophilic chlorination process employed in the manufacture of Aroclors.[7] Conversely, the ring chlorine-substitution patterns giving rise to the congeners in gray cells are especially favored.

Whereas three or more *ortho*-chlorines block rotation about the ring-connecting bond, congeners with no, or only one, *ortho*-chlorine can relatively easily achieve a planar configuration (colloquially referred to as "coplanars") and may behave as isosteres (compounds with similar shape, functionality, and polarity) to 2,3,7,8-tetrachlorodibenzodioxin (TCDD). These bind significantly to the "dioxin receptor," and measurement of their concentrations can be combined with their "dioxin-like toxic equivalency factors" (TEFs) to give an estimate of a PCB mixture's "dioxin-like toxic equivalency" (TEQ).[2] Thus, one "shortlist" analysis specified by the World Health Organization (WHO) is for 12 such congeners found in commercial mixtures, namely PCBs 77, 81, 105, 114, 118, 123, 126, 156, 157, 167, 169, and 189. Although PCB 126 is generally a trace component, it has such a high TEF that it often dominates the TEQ calculation.

In the United States, the initial regulatory methods were the USEPA 8080 series. In 8080, packed column gas chromatography-electron capture detection (GC-ECD) was recommended and calibration was against Aroclor mixtures and results were reported as Aroclor

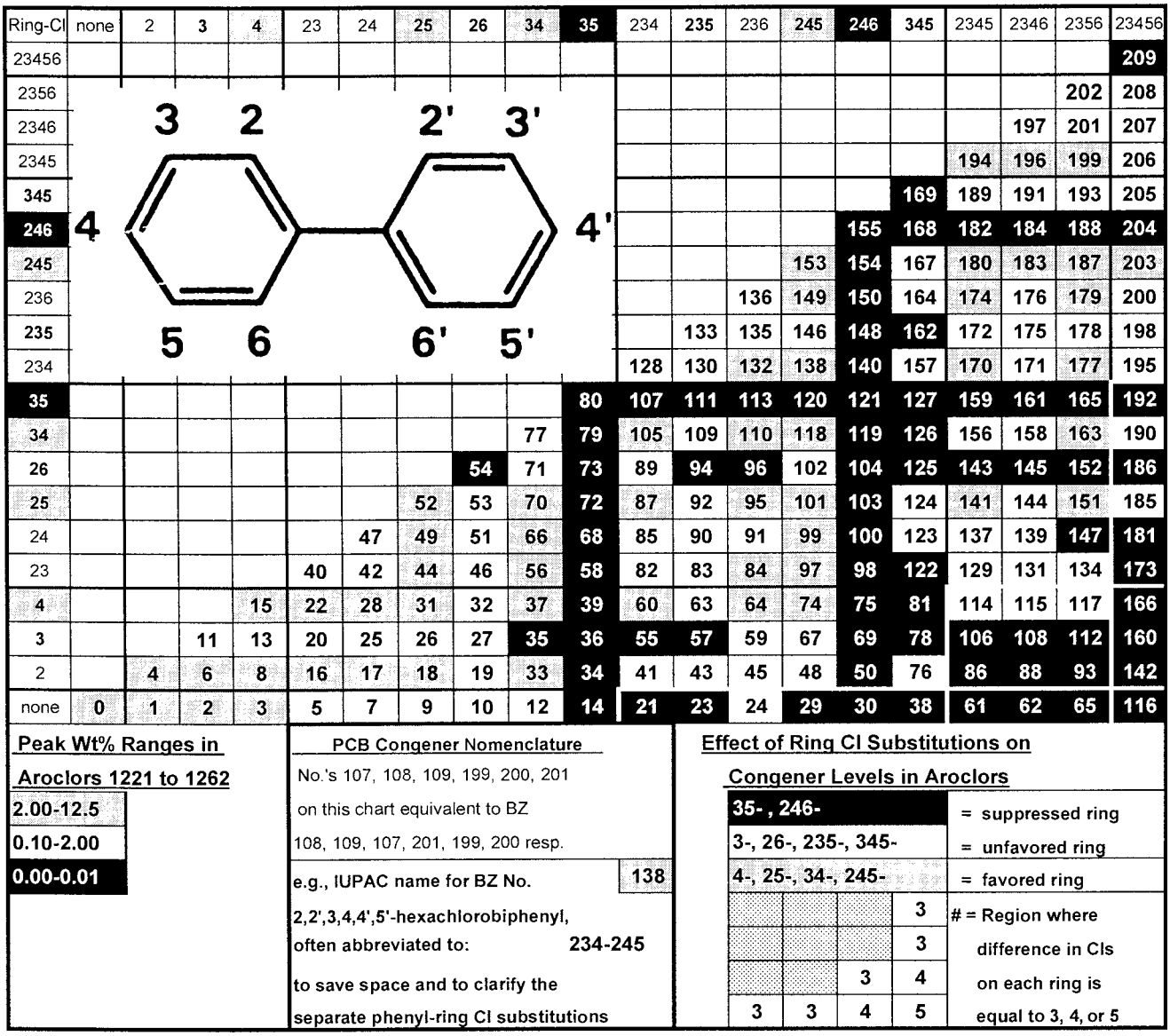

Fig. 1 PCB congener structure, nomenclature, BZ congener numbering system, and relative abundances in Aroclor mixtures.

equivalents. Method 8081 encouraged use of higher resolution capillary GC columns and MS-SIM detection, and the current version, 8082, extends this to suggest measuring some individual congeners against primary standards. An early version of CQCS analysis is EPA Method 680, which employs MS-SIM detection at the molecular ion cluster mass for each homolog level. It does not provide for actually identifying all congeners by determining their elution times and is, thus, not classified as congener-specific, but rather homolog-class-specific. It is quantitatively calibrated against an average response at each level, resulting in less precise measurement of individual congeners, but it detects and measures all PCB-containing peaks whether Aroclor derived or not. It is thus superior to the 8080 series when a PCB mixture arising from a non-Aroclor source or a substantially altered Aroclor congener distribution is encountered. In Europe, the Community Bureau of Reference (BCR) specifies measurement of a shortlist of major persistent "indicator congeners," namely PCBs 28, 52, 101, 118, 138, 153, and 180. A number of other congener shortlists are detailed in Refs.[2,3] A powerful but expensive and difficult-to-implement congener-specific PCB analysis method is USEPA Method 1668. The target list is the WHO list of coplanar PCBs with dioxin-like TEQs. The methodology is HRGC with >10,000 resolution high-resolution MS (HRMS) detection and ^{13}C-isotope dilution internal standards for all the analytes. The procedures are modeled on the well-established HRGC/HRMS USEPA Method 1613 for PCDD/Fs. The newer USEPA Method 1668 Revision A (December 1999) describes procedures for extending the analyte list to all 209 congeners that can be resolved on

either an SPB-octyl capillary column or a DB-1 (100% methyl silicone) capillary. Primary standards for all 209 congeners are distributed among five calibration solutions, which avoid any isomer coelutions on the SPB-octyl column.

No single column, nor any pair of columns, can completely separate all 209 congeners, or even the 150 or so found in Aroclors. Analysts developing CQCS or even "shortlist" congener-specific PCB analyses must select GC stationary phases capable of resolving congeners in their target list. Many analysts have employed 5% phenyl-, 95% methyl-substituted silicone polymers (e.g., DB-5) since a very similar phase was the first one for which the relative retention times for all 209 PCB congeners were published.[3] Methyl silicone phases with 50% *n*-octyl or *n*-octadecyl substituents have PCB retention characteristics similar to those of hydrocarbon columns such as Apeizon L or Apolane, but much greater stability and higher temperature limits than the latter. They permit resolution of many pairs of lower homologs, which coelute on the more polar phases. This feature is valuable for characterizing the products of dechlorination by anaerobic bacteria.[7] Phases with arylene or carborane units substituted in the silicone backbone to decrease column bleed (e.g., DB-5MS, DB-XLB, HT-8) have been found to have particularly useful congener-separation capabilities.[3,7–9] Column manufacturers Restek and SGE have subsequently modified capillary columns of this type (Rtx-PCB and HT-8-PCB, respectively) to specifically support maximal resolution of PCBs in CQCS analysis.

A database of relative retention times and coelutions for all 209 congeners on 20 different stationary phases has been published.[8] For 12 of the most useful of these phases, the elution orders of 9 solutions of all 209 congeners are available from a standard supplier, which markets these solutions (AccuStandard, New Haven, Connecticut, U.S.A.). By surveying the database, one can determine the most suitable column(s) for a particular application and can quickly establish a method component table by nine injections of the standard mixtures. This greatly facilitates the development of new CQCS PCB analyses. Tables of the weight percentages of all congeners in each of the numbered Aroclor mixtures, from which the information condensed in the figure matrix was derived, are available.[7,8] These help reduce the number of congeners that a CQCS method is required to separate when one anticipates analyzing only relatively unaltered Aroclor congener mixtures.

Prior to the availability of all 209 congeners in well-designed primary standard mixtures, much effort was expended to use structure–retention relationships on various phases to predict retention for congeners for which standards were not available.[5] In general, PCB retention times increase with chlorination level, and within chlorination levels, with less chlorine substitution in the ortho position (i.e., "coplanar PCBs" are more strongly retained). These relationships are of theoretical interest but are of less use now that accurate retention time assignments are possible with actual standards. The use of commercial mixtures such as Aroclors as quantitative secondary standards for CQCS PCB analysis is now to be discouraged,[4] as detailed studies of congener distributions show significantly different proportions among different lots.[7] In the case of Aroclor 1254, there are actually two different mixtures of radically different composition produced by totally different synthetic processes.[9]

The other major factor affecting the capability of CQCS PCB analyses is the selection of the GC detector. Initially, the ECD has been most useful for this application. It is selective for halogenated compounds, and its sensitivity is outstanding for the more chlorinated ($Cl \geq 4$) congeners. Its drawbacks are twofold: It has a limited linear range, necessitating multilevel calibration, and the relative response factors vary widely from instrument to instrument and among congeners even at the same chlorination level.[3] For mono- and dichloro-substituted congeners, it is less sensitive than the corresponding MS detectors. Other halogenated compounds such as organochlorine pesticides produce ECD responsive peaks that may interfere by coelution with certain PCB congeners. For these reasons, CQCS PCB analyses with ECD detection often employ a procedure of splitting the injected sample to two columns (each with an ECD detector) of different polarity and PCB congener elution order.[3,7] To be reported, a congener must be measured on at least one column without coelution of PCB or another interfering compound. If separately measurable on each column, the quantities found must match within a preset limit to preclude the possibility of an unexpected coeluting contaminant on one of the columns. Given the large number of congeners that may need to be measured, the data reduction algorithm for such a procedure is complex and not easily automated.

Another approach to providing a second dimension to CQCS PCB analysis is to employ much more selective mass spectrometric detection.[3,6–8] In electrospray ionization-mass spectroscopy (EI-MS), the spectra consist of a molecular ion cluster of chlorine isotope MS peaks and similar fragment ion clusters resulting from the successive loss of chlorine atoms. Congeners differing by one chlorine substituent that coelute on the GC column may often be separately quantitated by MS detection, if the more chlorinated one is not in great excess. This is because the $[M - 1Cl]^+$ fragment that interferes with the lower congener's signal is from a ^{13}C isotope peak and typically has 0.5–12% the signal level of its M^+ peak.[9] In contrast to the ECD, the sensitivity of MS-SIM or full-scan ITMS is greater for the less chlorinated congeners, as their electron affinity is lower and the positive charge of the ions is distributed over a smaller number of fragments. The linearity of the MS detectors is better than that of ECDs, and the ions monitored are more specific for PCBs and less

prone to interference from non-PCB compounds. Electron-capture detectors continue to hold the edge in absolute sensitivity (for the higher chlorinated congeners), and the dual-column/ECD detector systems are slightly less expensive than comparable bench-top, unit-mass-resolution, single-column GC/MS systems. Application to PCB analysis of more advanced (and expensive) MS detection systems, such as HRMS, MS/MS, and negative-ion MS, is described in several reviews.[4,6] Even higher throughput or more comprehensive CQCS PCB congener separations have recently been demonstrated using the latest capillary GC instrumental refinements. These are, respectively, fast GC with time-of-flight (TOF) MS detection,[10] and comprehensive 2D-GC with ECD detection.[11]

A final refinement of congener-specific PCB analysis arises from the fact that 19 of the congeners actually exist as stable enantiomeric pairs, either component of which can withstand racemization even at the elevated temperatures required to elute them from a capillary GC separation.[6] Some congeners containing either a 236- or a 2346-chlorine-substituted ring and three or more chlorines in the ortho position exist in two mirror-image forms by virtue of their inability to rotate around the bond between the two rings. These so-called atropisomers do not contain asymmetric carbon centers. They are PCB numbers 45, 84, 91, 95, 132, 135, 136, 149, 174, and 176 (containing the 236-ring), as well as PCB numbers 88, 131, 139, 144, 171, 175, 176, 183, 196, and 197 (containing the 2346-ring). They may be separated on chiral GC stationary phases, primarily those employing a family of modified cyclodextrins. A series of seven such columns have been found, which among them can achieve resolution of all 19 stable PCB atropisomers as well as separation of 11 of them from other possible coeluting PCBs if MS detection is employed.[12] Observation of PCB enantiomeric ratios significantly different from 1 is a certain indication of the action of an enzyme-mediated biological process operating on these congeners.

CONCLUSIONS

Comprehensive, quantitative, congener-specific PCB analysis requires use of high-resolution capillary GC separations, aided by selective ECD or MS detection. The availability of a range of well-documented stationary phases, complete sets of calibration and retention time standards for all 209 PCB congeners, and databases of retention data facilitates the efficient development of a CQCS assay procedure suitable for specific applications. The "holy grail" of a single system that can reliably and unambiguously identify and quantify any and all of the 209 congeners in a single run has not quite been achieved, but is being approached closely. Polychlorinated biphenyl-tailored stationary phases, fast TOF-MS detection, and comprehensive 2D-GC separations may well combine to achieve this goal.

REFERENCES

1. Erickson, M.D. *Analytical Chemistry of PCBs*; 2nd Ed.; Lewis Publishers: New York, 1997.
2. Hansen, L.G. *The Ortho Side of PCBs: Occurrence and Disposition*; Kluwer Academic: Boston, 1999.
3. Frame, G.M. Congener-specific PCB analysis. Anal. Chem. **1997**, *69*, 468A–475A.
4. Hess, P.; de Boer, J.; Cofino, W.P.; Leonards, P.E.G.; Wells, D.E. Critical review of the analysis of non- and mono-*ortho*-chlorobiphenyls. J. Chromatogr. A, **1995**, *703*, 417.
5. Larsen, B.R. HRGC separation of PCB congeners. J. High Resolut. Chromatogr. **1995**, *18*, 141.
6. Cochran, J.W.; Frame, G.M. Recent developments in the high resolution gas chromatography of polychlorinated biphenyls. J. Chromatogr. A, **1999**, *843*, 323.
7. Frame, G.M.; Cochran, J.W.; Bøwadt, S.S. Complete PCB congener distributions for 17 Aroclor mixtures determined by 3 HRGC systems optimized for comprehensive, quantitative, congener-specific analysis. J. High Resolut. Chromatogr. **1996**, *19*, 657–668.
8. Frame, G.M. A collaborative study of 209 PCB congeners and 6 Aroclors on 20 different HRGC columns: 1. Retention and coelution database, 2. Semi-quantitative Aroclor distributions. Fresenius' J. Anal. Chem. **1997**, *357*, 701–722.
9. Frame, G.M. Improved procedure for single DB-XLB column GC–MS-SIM quantitation of PCB congener distributions and characterization of two different preparations sold as "Aroclor 1254." J. High Resolut. Chromatogr. **1999**, *22*, 533–540.
10. Cochran, J.W. Fast gas chromatography–time-of-flight mass spectrometry of polychlorinated biphenyls and other environmental contaminants. J. Chromatogr. Sci. **2002**, *40*, 254–268.
11. Korytár, P.; Danielsson, C.; Leonards, P.E.G.; Haglund, P.; de Boer, J.; Brinkman, U.Th. Separation of seventeen 2,3,7,8-substituted polychlorinated dibenzo-*p*-dioxins and 12 dioxin-like polychlorinated biphenyls by comprehensive two-dimensional gas chromatography with electron-capture detection. J. Chromatogr. A, **2004**, *1038*, 189–199.
12. Wong, C.S.; Garrison, A.W. Enantiomer separation of polychlorinated biphenyl atropisomers and polychlorinated biphenyl retention behavior on modified cyclodextrin capillary gas chromatography columns. J. Chromatogr. A, **2000**, *866*, 213.

Copolymers: Composition by GPC/SEC

Sadao Mori
PAC Research Institute, Mie University, Nagoya, Japan

INTRODUCTION

Determination of the average chemical composition and polymer composition by size-exclusion chromatography (SEC) has been reported in the literature. Two different types of concentration detectors or two different absorption wavelengths of an ultraviolet or an infrared detectors are employed; the composition at each retention volume is calculated by measuring peak responses at the identical retention points of the two chromatograms.

DISCUSSION

Synthetic copolymers have both molecular-weight and chemical composition distributions and copolymer molecules of the same molecular size, which are eluted at the same retention volume in SEC, may have different molecular weights in addition to different compositions. This is because separation in SEC is achieved according to the sizes of molecules in solution, not according to their molecular weights or chemical compositions.

Molecules that appear at the same retention volume may have different compositions, so that accurate information on chemical heterogeneity cannot be obtained by SEC alone. When the chemical heterogeneity of a copolymer, as a function of molecular weight, is observed, the copolymer is said to have a heterogeneous composition, but, even though it shows constant composition over the entire range of molecular weights, it cannot be concluded that it has a homogeneous composition.[1] Nevertheless, SEC is still extremely useful in copolymer analysis, due to its rapidity, simplicity, and wide applicability.

When one of the constituents, A or B of a copolymer A–B, has an ultraviolet (UV) absorption and the other does not, a UV detector–refractive index (RI) combined detector system can be used for the determination of chemical composition or heterogeneity of the copolymer. A point-to-point composition, with respect to retention volume, is calculated from two chromatograms and a variation of composition is plotted as a function of molecular weight. The response factors of the two components in the two detectors must first be calibrated.

Let A be a constituent that has UV absorption. K_A and K_B are defined as the response factors of an RI detector for the A and B constituents, and K_A' as the response of the UV detector for A. These response factors are calculated by injecting known amounts of homopolymers A and B into the SEC dual-detector system, calculating the areas of the corresponding chromatograms, and dividing the areas by the weights of homopolymers injected as

$$F_A = K_A G_A, \quad F_B = K_B G_B, \quad F_A' = K_A' G_A$$

where F_A, F_B, and F_A' are areas of homopolymers A and B in the RI detector and of homopolymer A in the UV detector, and G_A and G_B are the weights of homopolymers A and B injected into the SEC system.

The weight fraction $W_{A,I}$ of constituent A, at each retention volume I of the chromatogram for the copolymer, is given by

$$W_{A,I} = \frac{K_B}{R_I K_A' - K_A + K_B}$$

where $R_I = F_{RI,I}/F_{UV,I}$ for the copolymer at retention volume I. Retention volume I for the RI detector is not equal to the retention volume I for the UV detector. Usually, the UV detector is connected to the column outlet and is followed by an RI detector, and the dead volume between these two detectors must be corrected. The dead volume can normally be measured by injecting a polymer sample having a narrow molecular-weight distribution and by measuring the retention difference between the two peak maxima.

Because the additivity of the RI increments of homopolymers is valid for copolymers, the additivity of the response factors is also valid:

$$K_C = W_A K_A + W_B K_B$$

where K_C is the response factor for the copolymer in the RI detector. If the response factors of one or two homopolymers that comprise a copolymer cannot be measured because of insolubility of the homopolymer(s), then this equation is employed.

Alternatively, the extrapolation of the plot of RI response factors of copolymers of known compositions can be used. An example is that the RI response for polystyrene was 2800 and that for polyacrylonitrile was 2250.

Although the values of these response factors are dependent on several parameters, the ratio of to K_A to K_B is almost constant in the same mobile phase.

An infrared detector can be used, at an appropriate wavelength, for detecting one component in copolymers or terpolymers and, thus, expand its range of applicability to copolymers analysis. Information on composition can be obtained by repeating runs, using different wavelengths to monitor different functional groups. A single-detector system is more advantageous than a dual-detector system, such as a combination of UV and RI detectors.

Instead of measuring chromatograms two or three times at different wavelengths for different functional groups, operation in a stop-and-go fashion was introduced for rapid determination of copolymer composition as a function of molecular weight.[2]

Pyrolysis gas chromatography has been widely used for copolymer analysis. This technique may offer many advantages over other detection techniques for copolymer analysis by SEC. One obvious advantage is the small sample size required. Another is the capability of application to copolymers which cannot utilize UV or IR detectors.[3]

Combination with other liquid chromatographic techniques is also reported by several workers. Orthogonal coupling of an SEC system to another high-performance liquid chromatography (HPLC) system K_B, K_A to achieve a desired cross-fractionation was proposed.[4] It was an SEC–SEC mode, using the same polystyrene column, but the mobile phase in the first system was chosen to accomplish only a hydrodynamic volume separation, and the mobile phase in the second system was chosen so as to be a thermodynamically poorer solvent for one of the monomer types in the copolymer, in order to fractionate by composition under adsorption or partition modes as well as size exclusion.

A combination of liquid adsorption chromatography with SEC has recently been developed by several workers. Poly(styrene–methyl methacrylate) copolymers were fractionated according to chemical composition by liquid adsorption chromatography and the molecular weight averages of each fraction were measured by SEC.[5,6]

REFERENCES

1. Mori, S. Comparison between size-exclusion chromatography and liquid adsorption chromatography in the determination of the chemical heterogeneity of copolymers. J. Chromatogr. **1987**, *411*, 355.
2. Mirabella, F.M., Jr.; Barrall, E.M., II; Johnson, J.F. A rapid technique for measuring copolymer composition as a function of molecular weight using gel permeation chromatography and infrared detection. J. Appl. Polym. Sci. **1975**, *19*, 2131.
3. Mori, S. Determination of the composition of copolymers as a function of molecular weight by pyrolysis gas chromatography-size-exclusion chromatography. J. Chromatogr. **1980**, *194*, 163.
4. Balke, S.T.; Patel, R.D. J. Polym. Sci. Polym. Lett. Ed. **1980**, *18* (3), 453.
5. Mori, S. Determination of chemical composition and molecular weight distributions of high-conversion styrene-methyl methacrylate copolymers by liquid adsorption and size exclusion chromatography. Anal. Chem. **1988**, *60*, 1125.
6. Mori, S. Trends Polym. Sci. **1994**, *2*, 208.

BIBLIOGRAPHY

1. Mori, S.; Barth, H.G. *Size Exclusion Chromatography*; Springer-Verlag: New York.
2. Mori, S. Copolymer analysis. In *Size Exclusion Chromatography*; Hunt, B.J., Hodling, S.R., Eds.; Blackie: Oxford, 1989.

Copolymers: Molecular Weights by GPC/SEC

Sadao Mori
PAC Research Institute, Mie University, Nagoya, Japan

INTRODUCTION

It is well known that most copolymers have both molecular weight and composition distributions and that copolymer properties are affected by both distributions. Therefore, we must know the average values of molecular weights and composition, and their distributions. These two distributions are inherently independent of each other. However, it is not easy to determine the molecular-weight distribution independently of the composition, even by modern techniques.

DISCUSSION

Size exclusion chromatography (SEC) is a rapid technique used to obtain the molecular-weight averages and the molecular-weight distributions of synthetic polymers. The objective of SEC for copolymer analysis must not only be the determination of molecular-weight averages and its distribution but also the measurement of average copolymer composition and its distribution. However, separation by SEC is achieved according to the sizes of molecules in the solution, not according to their molecular weights. Therefore, the retention volume of a copolymer molecule obtained by SEC reflects not the molecular weight, as in the case of a homopolymer, but simply the molecular size.

For example, the elution order of polystyrene (PS), poly(methyl methacrylate) (PMMA), and their copolymers [P(S–MMA)], both random and block, all having the same molecular weight are as follows: random copolymer of P(S–MMA), PS, block copolymer (MMA-S-MMA), and PMMA.[1] Copolymers having the same molecular weight but different composition are different in molecular size and elute at different retention volumes. Therefore, the accurate determination of the values of molecular-weight averages and the molecular-weight distribution for a copolymer by SEC might be limited to the case when the copolymer has the homogeneous composition across the whole range of molecular weights.

A calibration curve for a copolymer consisting of components A and B can be constructed from those for the two homopolymers A and B, if the relationships of the molecular weights and the molecular sizes of the two homopolymers are the same as their copolymer and if the size of the copolymer molecules in the solution is the sum of the sizes of the two homopolymers times the corresponding weight fractions. The molecular weight of the copolymer at retention volume I, $M_{C,I}$, is calculated using

$$\log M_{C,I} = W_{A,I} \log M_{A,I} + W_{B,I} \log M_{B,I}$$

where $M_{A,I}$ and $M_{B,I}$ are the molecular weights of homopolymers A and B, respectively, and $W_{A,I}$ and $W_{B,I}$ are the weight fractions of components A and B, respectively, in the copolymer at retention volume I. This equation was empirically postulated for block copolymers.[2]

The use of the so-called "universal calibration" is a theoretically reliable procedure for calibration. For ethylene–propylene (EP) copolymers, Mark–Houwink parameters in *O*-dichlorobenzene at 135°C are calculated as[3]

$$a_{EP} = (a_{PE} a_{pp})^{1/2}$$
$$K_{EP} = W_E K_{PE} + W_P K_{PP} - 2(K_{PE} K_{PP})^{1/2} W_E W_P$$

where W_E and W_P are the weight fractions of the ethylene and propylene units of the copolymer, respectively.

Calculated Mark–Houwink parameters for P(S–MMA) block and statistical copolymers at several compositions in tetrahydrofuran at 25°C are listed in Table 1.[4] The parameters for PS and PMMA used in the calculation are as follows:

$$PS : K = 0.682 \times 10^{-2} \mathrm{ml}/g, a = 0.766$$
$$PMMA : K = 1.28 \times 10^{-2} \mathrm{ml}/g, a = 0.69$$

If copolymer molecules and PS molecules are eluted at the same retention volume, then

$$[\mu]_C M_C = [\mu]_S M_S$$

where M_C and M_S are the molecular weights of the copolymer and PS, respectively, and $[\mu]_C$ and $[\mu]_S$ are the intrinsic viscosities of the copolymer and PS, respectively. A differential pressure viscometer can measure intrinsic viscosities for the fractions of the copolymer and PS continuously, followed by the determination of M_C of the copolymer fraction at retention volume I.

The application of a light-scattering detector in SEC does not require the construction of a calibration curve using narrow molecular-weight distribution polymers. However, this method is not generally applicable to

Table 1 Calculated Mark–Houwink parameters for P(S–MMA) block and statistical copolymers at several compositions in tetrahydrofuran at 25°C.

	Block copolymer		Statistical copolymer	
Composition (styrene wt %)	$K \times 10^2$ **(ml/g)**	a	$K \times 10^2$ **(ml/g)**	a
20	1.124	0.705	1.044	0.718
30	1.054	0.714	0.953	0.731
40	0.989	0.721	0.879	0.742
50	0.929	0.729	0.821	0.750
60	0.872	0.736	0.779	0.756
70	0.820	0.744	0.747	0.760
80	0.771	0.751	0.722	0.763

copolymers because the intensity of light scattering is a function not only of molecular weight but also of the specific refractive index (the refractive index increment) of the copolymer in the mobile phase. The refractive index increment is also a function of composition. In the case of a styrene–butyl acrylate (30 : 70) emulsion copolymer, the apparent molecular weight of the copolymer in tetrahydrofuran was only 7% lower than true one.[5] A recent study concluded that if refractive index increments of the corresponding homopolymers do not differ widely, SEC measurements combined with light scattering and concentration detectors yield good approximations to molecular weight and its distribution, even if the chemical composition distribution is very broad.[6]

REFERENCES

1. Dondos, A.; Rempp, P.; Benoit, H. Gel permeation chromatographic investigations on random and block copolymers. Macromol. Chem. **1984**, *175* (5), 1659.
2. Runyon, J.R.; Barnes, D.E.; Rudd, J.F.; Tung, L.H. Multiple detectors for molecular weight and composition analysis of copolymers by gel permeation chromatography. J. Appl. Polym. Sci. **1969**, *13*, 2359.
3. Ogawa, T.; Inaba, T. Gel permeation chromatography of ethylene-propylene copolymerization products. J. Appl. Polym. Sci. **1988**, *21*, 2979.
4. Goldwasser, J.M.; Rudin, A. Analysis of block and statistical copolymers by gel permeation chromatography: Estimation of Mark-Houwink. J. Liquid Chromatogr. Related. Technol. **1983**, *6* (13), 2433.
5. Malihi, F.B.; Kuo, C.Y.; Provder, T. Determination of the absolute molecular weight of a styrene-butyl acrylate emulsion copolymer by low-angle laser light scattering (LALLS) and GPC/LALLS. J. Appl. Polym. Sci. **1984**, *29*, 925.
6. Kratochvil, P. International Symposium on Polymer Analysis and Characterization, 1995, Abstract L14.
7. Mori, S.; Barth, H.G. *Size Exclusion Chromatography*; Chap. 12, 1999, Springer-Verlag: New York.
8. Mori, S. Copolymer analysis. In *Size Exclusion Chromatography*; Hunt, B.J., Holding, S.R., Eds.; Blackie: Oxford, 1989.

Coriolis Force in CCC

Yoichiro Ito
National Heart, Lung, and Blood Institute (NHLBI), National Institutes of Health (NIH), Bethesda, Maryland, U.S.A.

Kazufusa Shinomiya
College of Pharmacy, Nihon University, Chiba, Japan

INTRODUCTION

Coriolis force acts on a moving object on a rotating body such as the Earth or a centrifuge bowl. It was first analyzed by a French engineer and mathematician, Gaspard de Coriolis (1835).[1] The effect of the Coriolis force produced by the Earth's rotation is weak, whereas that on a rotating centrifuge is strong and easily detected. Fig. 1 illustrates the effect of Coriolis force on moving droplets in a rotating centrifuge, where the path of the sinking droplets shifts toward the direction opposite to the rotation (left); this effect is reversed for floating droplets (right).[2] Moving droplets in a rotating centrifuge have been photographed under stroboscopic illumination.[3,4] The effects of Coriolis force on countercurrent chromatography (CCC) have been demonstrated in the toroidal coil centrifuge, which uses a coiled tube mounted around the periphery of the centrifuge bowl.[2,5] When a protein mixture containing cytochrome *c*, myoglobin, and lysozyme was separated on an aqueous/aqueous polymer phase system composed of 12.5% (w/w) polyethylene glycol 1000 and 12.5% (w/w) dibasic potassium phosphate, the direction of elution through the toroidal coil had substantial effects on peak resolution, as shown in Fig. 2 and Table 1.[2,5] Since the toroidal coil separation column has a symmetrical orientation except for the handedness, the above effect is best explained on the basis of Coriolis force as follows: If the Coriolis force acts parallel to the effective coil segments (parallel orientation), the two phases form multiple droplets, which provide a broad interface area to enhance the mass transfer process, hence improving the partition efficiency (Fig. 3A). When the Coriolis force acts across the effecting coil segments, the two phases form a streaming flow, minimizing the interfacial area for mass transfer and resulting in lower partition efficiency (Fig. 3B). It is interesting to note that the above effects have not been observed during the separation of low molecular weight compounds such as dipeptides[2] and dinitrophenyl (DNP) amino acids[6] on conventional organic/aqueous two-phase solvent systems in the toroidal coil CCC centrifuge, except that at a relatively low revolution speed, the Coriolis force acting across the effective coil segments slightly improves the partition efficiency, probably due to substantially higher retention of the stationary phase.

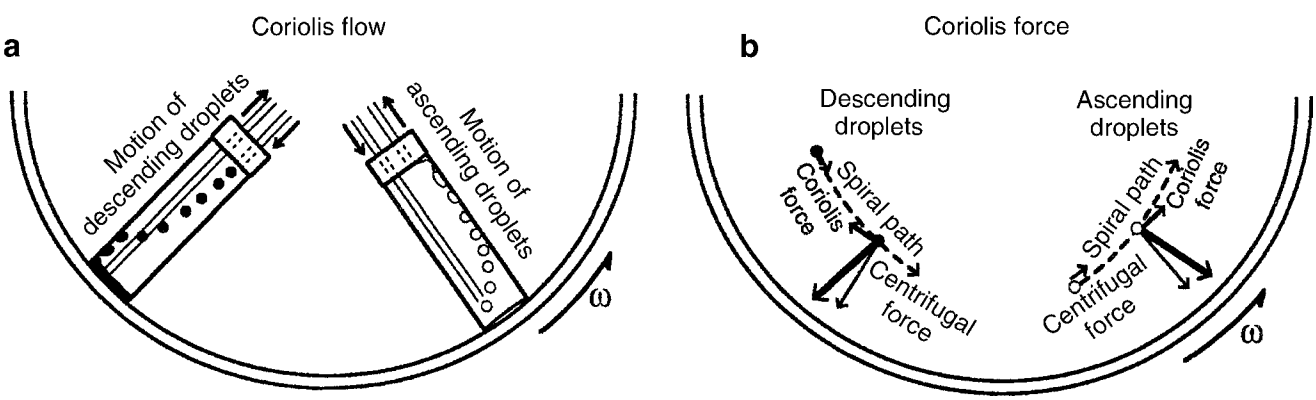

Fig. 1 Effects of Coriolis force on moving droplets in a rotating centrifuge. A. Motion of droplets in a flow through cell in a rotating centrifuge. B. Direction of Coriolis force acting on droplets on rotating centrifuge bowl.

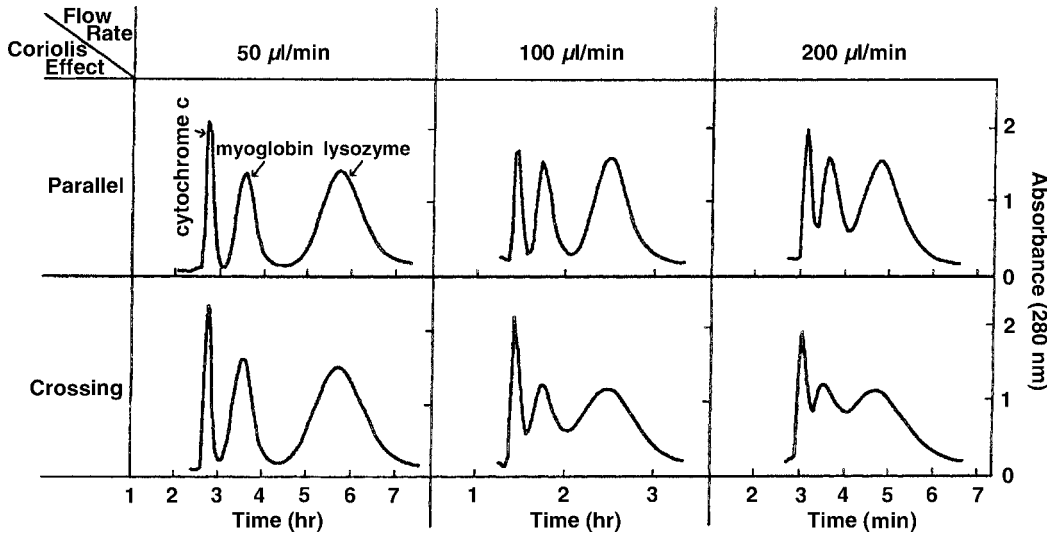

Fig. 2 Effects of Coriolis force on partition efficiency and retention of stationary phase in protein separation by toroidal coil centrifuge.

Table 1 Effects of Coriolis force on partition efficiencies of three stable proteins in toroidal coil CCC.

Flow-rate (μl/min)	Analyte peak	TP (parallel/crossing)	R_s (parallel/crossing)	Retention (%) (parallel/crossing)
50	Cytochrome *c*	1860/1490		29.2/32.0
			1.62/1.39	
	Myoglobin	365/266		
			1.66/1.40	
	Lysozyme	156/104		
100	Cytochrome *c*	1760/821		30.0/30.3
			1.27/0.86	
	Myoglobin	433/172		
			1.39/0.84	
	Lysozyme	172/63		
200	Cytochrome *c*	1296/–		22.8/21.3
			0.84/–	
	Myoglobin	330/–		
			0.92/–	
	Lysozyme	123/–		

More recently, the effect of Coriolis force was demonstrated in the separation of organic acids with organic/aqueous two-phase solvent systems in a centrifugal partition chromatograph equipped with a separation column consisting of rectangular partition compartments connected in series.[6] As shown in Fig. 4, clockwise column rotation (CW) shows substantially better peak resolution than counterclockwise column rotation (CCW), especially in the separation of *p*-methyl hippuric acid and hippuric acid (middle column) with a two-phase solvent system composed of methyl *t*-butyl ether/aqueous 0.1% trifluoroacetic acid (1 : 1, v/v). Mathematical analysis is carried out to elucidate the effect of Coriolis force on the motion of the mobile-phase droplets.[6]

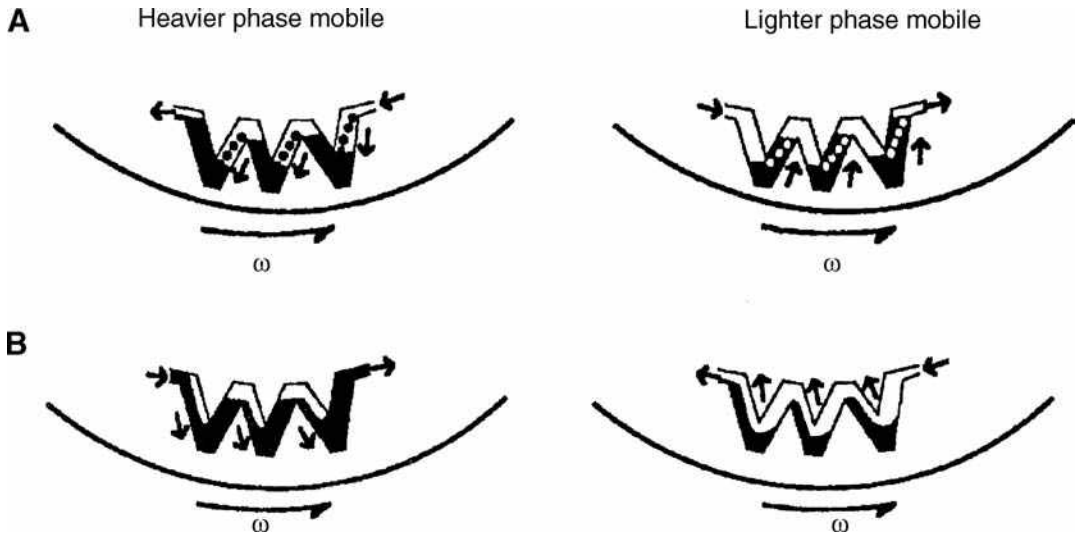

Fig. 3 Effects of Coriolis force on two-phase flow in separation coil of toroidal coil centrifuge.

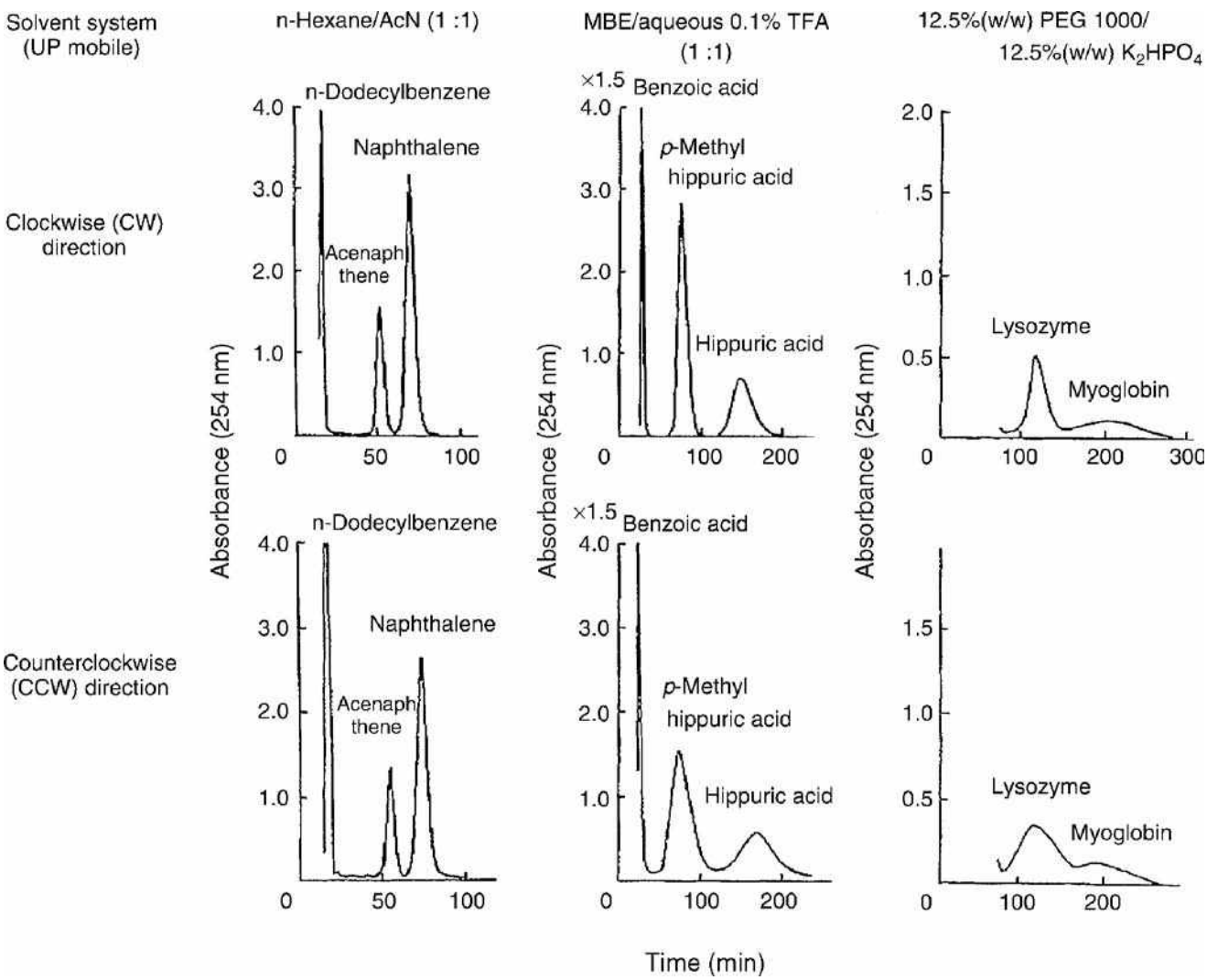

Fig. 4 Chromatograms obtained by centrifugal partition chromatography using three different two-phase solvent systems by eluting upper phase in ascending mode.

REFERENCES

1. *New Encyclopedia Britannica*; 1995; Vol. 3, 632.
2. Ito, Y.; Ma, Y. Effect of Coriolis force on countercurrent chromatography. J. Liq. Chromatogr. **1998**, *21*, 1–17.
3. Marchal, L.; Foucault, A.; Patissier, G.; Rosant, J.M.; Legrand, J. Influence of flow patterns on chromatographic efficiency in centrifugal partition chromatography. J. Chromatogr. A, **2000**, *869* (1–2), 339.
4. Morvan, A.; Foucault, A.; Patissier, G.; Rosant, J.M.; Legrand, J. J. Hydrodynamics, *in preparation.*
5. Ito, Y.; Matsuda, K.; Ma, Y.; Qi, L. Toroidal coil countercurrent chromatography. Achievement of high resolution by optimizing flow-rate, rotation speed, sample volume and tube length. J. Chromatogr. A, **1998**, *808*, 95–104.
6. Ikehata, J.; Shinomiya, K.; Kobayashi, K.; Ohshima, H.; Kitanaka, S.; Ito, Y. Effect of Coriolis force on countercurrent chromatographic separation by centrifugal partition chromatography. J. Chromatogr. A, **2004**, *1025*, 169–175.

Corrected Retention Time and Corrected Retention Volume

Raymond P.W. Scott
Scientific Detectors Ltd., Banbury, Oxfordshire, U.K.

INTRODUCTION

The corrected retention time of a solute is the elapsed time between the dead point and the peak maximum of the solute. The different properties of the chromatogram are shown in Fig. 1. The volume of mobile phase that passes through the column between the dead point and the peak maximum is called the corrected retention volume.

DISCUSSION

If the mobile phase is incompressible, as in liquid chromatography, the retention volume (as so far defined) will be the simple product of the exit flow-rate and the corrected retention time.

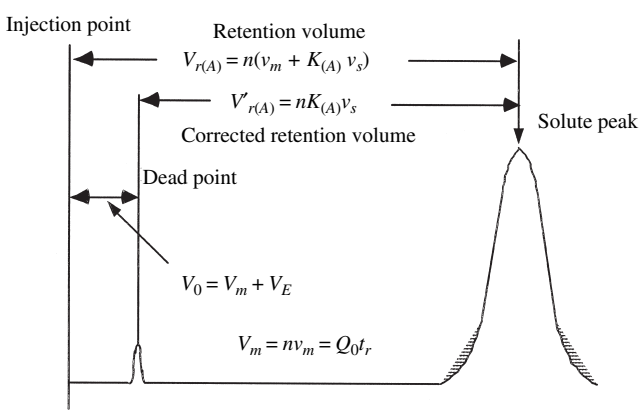

Fig. 1 Diagram depicting the retention volume, corrected retention volume, dead point, dead volume, and dead time of a chromatogram. V_0: total volume passed through the column between the point of injection and the peak maximum of a completely unretained peak; V_m: total volume of mobile phase in the column; $V_{r(A)}$: retention volume of solute A; $V_{r(A)}'$: corrected retention volume of solute A; V_E: extra column volume of mobile phase; v_m: volume of mobile phase, per theoretical plate; V_s: volume of stationary phase per theoretical plate; $K_{(A)}$: distribution coefficient of the solute between the two phases; n: number of theoretical plates in the column; Q: column flow rate measured at the exit.

If the mobile phase is compressible, the simple product of the corrected retention time and flow rate will be incorrect, and the corrected retention volume must be taken as the product of the corrected retention time and the *mean* flow rate. The true corrected retention volume has been shown to be given

$$V_r' = V_{r'}'\left(\frac{\gamma^2 - 1}{\gamma^2 - 1}\right) = Q_0 t_r' \frac{2}{3}\left(\frac{\gamma^2 - 1}{\gamma^2 - 1}\right)$$

where the symbols have the meaning defined in Fig. 1, and $V_{r'}'$ is the corrected retention volume measured at the column exit and γ is the inlet/outlet pressure ratio.

The corrected retention volume, V_r', will be the difference between the retention volume and the dead volume V_0, which, in turn, will include the actual dead volume V_m and the extra column volume V_E. Thus,

$$V_r' = V_r - (V_E + V_m)$$

The retention time can be taken as the product of the distance on the chart between the dead point and the peak maximum and the chart speed, using appropriate units. As in the case of the retention time, it can be more accurately measured with a stopwatch. Again, the most accurate method of measuring V_r' for a non-compressible mobile phase, although considered antiquated, is to attach an accurate burette to the detector exit and measure the retention volume in volume units. This is an absolute method of measurement and does not depend on the accurate calibration of the pump, chart speed, or computer acquisition level and processing.

BIBLIOGRAPHY

1. Scott, R.P.W. *Techniques and Practice of Chromatography*; Marcel Dekker, Inc.: New York, 1996.
2. Scott, R.P.W. *Liquid Chromatography Column Theory*; John Wiley & Sons: Chichester, 1992; 19.
3. Scott, R.P.W. *Introduction to Analytical Gas Chromatography*; Marcel Dekker, Inc.: New York, 1998; 77.

Coumarins: TLC Analysis

Kazimierz Glowniak
Jaroslaw Widelski
Department of Pharmacognosy, Medical University of Lublin, Lublin, Poland

INTRODUCTION

Coumarins are natural compounds that contain the characteristic benzo[α]pyrone (2H-benzopyran-2-one) moiety. They are especially abundant in Umbelliferae, Rutaceae, Leguminosae, Compositae, and other plant families. Usually the substituents are at the positions C_5, C_6, C_7, and C_8 [e.g., umbelliferone (7-hydroxycoumarin), hierniarin (7-methoxycoumarin), esculetin (6,7-dihydroxycoumarin), scopoletin (6-methoxy-7-hydroxycoumarin), and others].

In addition to simple coumarin derivatives, furano- and pyranocoumarins are also commonly encountered in the Umbelliferae and Rutaceae families. The essential chemical moiety of linear furanocoumarins consists of a 2H-furan[3.2-g]-benzo[b]pyran-2-one ring called psolaren (its derivatives include, e.g., bergapten, xanthotoxin, isopimpinelin, imperatorin, isoimperatorin, oxypeucedanin, and others). The second type of furanocoumarins (the angular type of angelicin) has a 2H-furan[2.3 h]-benzo[β]pyran-2-one structure (isobergapten, pimpinelin, sphondin). There are also both linear and angular types of pyranocoumarins. In the linear type, which is named alloxanthiletin, the 2H,8H-pyran[3.2 h]-benzo[β]pyran-2-one ring is characteristic, whereas in the angular type called seselin, the 2H,8H-pyran[2.3 h]-benzo[β]pyran-2-one moiety is typical.

THIN-LAYER CHROMATOGRAPHY

Thin-layer chromatography (TLC) is a very useful method for the separation of natural coumarins, furanocoumarins, and pyranocoumarins. Natural coumarins exhibit fluorescence properties, which they display in ultraviolet (UV) light (365 nm). Their spots can be easily detected on paper and thin-layer chromatograms without the use of any chromogenic reagents. It is often possible to recognize the structural class of coumarin from the color it displays under UV detection (Table 1). Purple fluorescence generally signifies 7-alkoxycoumarins, whereas 7-hydroxycoumarins and 5,7-dioxygenated coumarins tend to fluoresce blue. In general, furanocoumarins possess a dull yellow or ocher fluorescence, except for psolaren, sphondin, and angelicin. Spot fluorescence is more intense or its color is changed after spraying the TLC chromatogram with ammonia (Table 1).[1]

Thin-layer chromatograms can also be detected by several non-specific chromatogenic reactions:

1. 1% Aqueous solution of iron (III) chloride.
2. 1% Aqueous solution of potassium ferricyanide.
3. Diazotized sulfanilic acid and diazotized *p*-nitro-aniline.

None of these reagents is very specific for hydroxycoumarins and their confirmation should be substantiated by other methods. Exposed groups present in many natural coumarins can be detected due to their susceptibility to cleavage by acids and applied over a phosphoric acid spot on a silica TLC plate.

The linear (psolarens) and angular (angelicins) furanocoumarins can be readily differentiated with the Emerson reagent. It is also used for detection of pyranocoumarins (selinidin, pteryxin) on TLC chromatograms.

CONVENTIONAL TLC

Conventional TLC is a well-known technique, used for many years in systematic research on the coumarin content of numerous plant species, as well as for chemotaxonomic relationships between those species. Great progress in the optimization of the TLC separation process was made by the design of modern, horizontal chambers for TLC. It is a universal design offering the possibility of developing chromatograms in the space saturated or non-saturated with mobile-phase vapors. Moreover, it is possible to perform gradient elution, stepwise or continuous, or to accomplish micropreparative separation of chemical compound composites (e.g., plant extracts).[2]

Gradient elution in TLC can be obtained in several ways:[1]

1. Multizonal development: the use of multicomponent eluents that are partially separated during development (frontal chromatography), forming an eluent strength gradient along the layer.
2. Development with a strong solvent (e.g., acetone) of an adsorbent layer exposed to vapors of a less polar solvent.
3. The use of mixed layers of varying surface area and activity (compare silica and Florisil®).
4. Delivery of an eluent whose composition is varied in a continuous or stepwise manner by introducing small volumes of more polar eluent fractions (e.g., 0.2 ml).

Table 1 Chromatographic methods of coumarin identification: Fluorescence colors of coumarins under UV irradiation (365 nm).

Fluorescence color	Fluorescence color with ammonia	Coumarin or coumarin type
Blue	L. blue	7-Hydroxycoumarin
B. blue	V. blue	7-Hydroxycoumarins
Blue	B. blue	7-Hydroxy-6-alkoxycoumarins
Blue	Blue	5,7-Dialkoxycoumarins
B. blue	B. blue	6,7-Dialkoxycoumarins
Blue	Blue	6,7,8-Trialkoxycoumarins
W. blue	W. blue	5,6,7-Trialkoxycoumarins
W. blue	B. blue	7-Hydroxy-5,6-dialkoxycoumarins
Blue		Psolaren
Blue	B. blue	6-Methoxyangelicin
Blue	Green	7,8-Dihydroxycoumarin
Pink	Yellow	6-Hydroxy-7-glucosyloxycoumarin
Purple	Purple	8-Hydroxy-5-alkoxypsolarens
W. purple	Pink	6-Hydroxy-7-alkoxycoumarins
Purple	Green	Angelicin, coumestrol
Green		5-Methoxyangelicin
Green		8-Hydroxy-6,7-dimethoxycoumarin
Green	Yellow	7,8-Dihydroxy-6-methoxycoumarin
Yellow		3,4,5-Trimethoxypsolaren
Yellow		6-Hydroxy-5,7-dimethoxycoumarin
Yellow	Yellow	5-Hydroxy-6,7-dimethoxycoumarin
Yellow	Yellow	5-Hydroxypsolaren
Yellow	Yellow	5,6-Dimethoxyangelicin
Yellow	Yellow	8-Alkoxypsolarens
Yellow-green	Yellow-green	5-Alkoxypsolarens
B. yellow	B. yellow	5,8-Dialkoxypsolarens

B. = bright; V. = very bright; L. = light; W. = weak.
Source: From Coumarins, in Nat. Prod. Rep.[1]

The possibility of zonal sample dosage in equilibrium conditions (after a front of mobile phase and continuous-chromatogram development, which is provided by a horizontal "sandwich" chamber) was utilized by Glowniak, Soczewinski, and Wawrzynowicz[3] in preparative chromatography of simple coumarins and furanocoumarins found in *Archangelica* fruits, performed with a short-bed continuous development (SB-CD) technique.

The latter possibility was employed by Wawrzynowicz and Waksmundzka-Hajnos for micropreparative TLC isolation of furanocoumarins from *Archangelica*, *Pastinaca*, and *Heracleum* fruits on silica gel, silanized gel, and Florisil.

Superior coumarin compound separation with use of the described flat "sandwich" chambers is achieved with gradient chromatography on silica gel and stepwise variation of polar modifier concentrations in mobile phase, as less polar solvents (hexane, cyclohexane, toluene, or dichloromethane) and polar modifiers (acetonitrile, diisopropyl ether, ethyl acetate) are used.

Complex pyranocoumarin mixtures can be separated with the TLC technique by alternative use of two different polar adsorbents (silica gel, Florisil) and various binary and ternary eluents with different mechanisms of adsorption center effect on the molecules to be separated.[4] Improved separation can be achieved by high-performance TLC (HPTLC), which employs new, highly effective adsorbent of narrow particle size distribution, or with chemically modified surface. Because of its similarity, HPTLC is applied in designing optimal HPLC systems. Another gradient technique in coumarin compound separation is programed multiple development (PMD), also called the "reversed gradient" technique, in which chromatograms are developed to increasing distances by a sequence of eluents with decreasing polarity, with eluent evaporation after each stage.

Two-dimensional TLC (2D-TLC) is particularly effective in the case of complex extracts when one-dimensional developing yields partial separation. Moreover, it offers the possibility of modifying separation procedures when the development direction is changed.

OVERPRESSURED LAYER CHROMATOGRAPHY

The term "overpressured layer chromatography" (OPLC) was originally introduced by Tyihak, Mincsovisc, and Kalasz[5] in the late 1970s. The crucial factor is pressurized mobile-phase flow through the planar medium. Short analysis time, low solvent consumption, high resolution, and availability of online and off-line modes are the main advantages of OPLC in comparison with the classical TLC techniques. Overpressured layer chromatography was proved effective in qualitative and quantitative analysis of furanocoumarins by densitometric online detection. Overpressured layer chromatography can also be performed in two-dimensional mode (2D-OPLC). This technique was used by Harmala et al.[6] for the separation of 16 closely related coumarins from *Angelica* genus.

Long-distance OPLC is a novel form of OPLC, in which chromatograms are developed over a long distance with optimal (empiric) mobile-phase flow. Used in combination with specialized equipment designs, it produces high-performance (70,000–80,000 of theoretic plates) and excellent resolution. Botz, Nyiredy, and Sticher,[7] who initiated long-distance OPLC, proved its efficiency in the separation of eight furanocoumarin isomers and in the isolation of the furanocoumarin complex from *Peucedanum palustre* roots raw extract. This technique was used by Galand et al.[8] as well.

ROTATION PLANAR CHROMATOGRAPHY

Rotation planar chromatography (RPC), as with OPLC, is another thin-layer technique with forced eluent flow, employing a centrifugal force of a revolving rotor to move the mobile phase and separate chemical compounds. The RPC equipment can vary in chamber size, operative mode (analytical or preparative), separation type (circular, anticircular, or linear), and detection mode (off-line or online). The described technique was applied in analytical and micropreparative separation of coumarin compounds from plant extracts.

AUTOMATED MULTIPLE DEVELOPMENT

Automated multiple development (AMD), providing automatic chromatogram development and drying, is a novel form of the PMD technique. Automated multiple development as an instrumental technique can be used to perform normal-phase chromatography with solvent gradients on HPTLC plates. Most of the AMD applications use typical gradients: Starting with a very polar solvent, the polarity is varied by means of "base" solvent of medium polarity to a non-polar solvent. Instrumentation for AMD was introduced by Camag (Switzerland) and provides a means for normal-phase gradient development in HPTLC. The developing distance increases while the solvent polarity decreases. Repeated development compresses the band on the plate, resulting in increased sensitivity and resolution.[9]

CONCLUSIONS

TLC is a suitable method of separation, characterization, and quantitative evaluation for any kind of coumarin compound. Modern TLC techniques such as AMD, HPTLC, and OPLC have been in use since many years in systematic research on the coumarin content of numerous plant species, as well as for chemotaxonomic relationships between those species.

REFERENCES

1. Murray, R.D.H. Coumarins. Nat. Prod. Rep. **1989**, *6*, 591–624.
2. Soczewinski, E. Simple device for continuous thin-layer chromatography. J. Chromatogr. **1977**, *138*, 443–445.
3. Glowniak, K.; Soczewinski, E.; Wawrzynowicz, T. Optimization of chromatographic systems for the separations of components of the furocoumarin fraction of *Archangelica* fruits on a milligram scale. Chem. Anal. **1987**, *32*, 797–811.
4. Glowniak, K. Comparison of selectivity of silica and Florisil in the separation of natural pyranocoumarins. J. Chromatogr. **1991**, *552*, 453–461.
5. Tyihak, E.; Mincsovisc, E.; Kalasz, H. New planar liquid chromatographic technique: Overpressured thin-layer chromatography. J. Chromatogr. **1979**, *174*, 75–81.
6. Harmala, P.; Botz, L.; Sticher, O.; Hiltunen, R. Two-dimensional planar chromatographic separation of a complex mixture of closely related coumarins from the genus *Angelica*. J. Planar Chromatogr. **1990**, *3*, 515–520.
7. Botz, L.; Nyiredy, S.; Sticher, O. Applicability of long distance overpressured layer chromatography. J. Planar Chromatogr. **1991**, *4*, 115.
8. Galand, N.; Pothier, J.; Dollet, J.; Viel, C. OPLC and AMD, recent techniques of planar chromatography: Their interest for separation and characterisation of extractive and synthetic compounds. Fitoterapia **2002**, *73*, 121–134.
9. Gocan, S.; Cimpan, G.; Muresan, L. Automated multiple development thin layer chromatography of some plant extracts. J. Pharm. Biomed. Anal. **1995**, *14*, 1221–1227.

Counterfeit Drugs: TLC Analysis

Joseph Sherma
Department of Chemistry, Lafayette College, Easton, Pennsylvania, U.S.A.

INTRODUCTION

Counterfeit and substandard drug products and active pharmaceutical ingredients are a great problem for government regulatory agencies, pharmaceutical companies, healthcare providers, and consumers, leading to morbidity, mortality, and drug resistance. The drugs that are most counterfeited are those used to treat infections (antibiotics), malaria (e.g., artesunate), tuberculosis (TB), and HIV/AIDS. The U.S. Center for Medicine in the Public Interest has predicted that global counterfeit drug sales will reach $75 billion in 2010, a 95% increase since 2005. All countries, regardless of efforts in drug regulation, are affected by this increase, especially in the light of the ease of purchase of questionable drugs on the internet; however, developing countries are at greatest risk, so the costs of analytical screening methods are critically important. The problems caused by counterfeit medicines are described in more detail in earlier entries.[1,2]

This entry describes the three most important drug-screening methods in use at this time, for TB, macrolide antibiotics, and drugs from the World Health Organization (WHO) Essential Drug List. All of these are based on thin-layer chromatography (TLC).

OVERVIEW OF TLC METHODS

According to the WHO, counterfeit drugs are defined as mislabeled medicines manufactured with substandard safety, quality, and effectiveness. They include products with a different drug, but none of the labeled active ingredient, the correct active ingredient at the wrong level, or the correct drug and amounts in the wrong packaging. TLC is the main screening method used today to decide if a drug product meets label specifications and is legal. Drug-screening TLC methods are simple, inexpensive, selective, and semiquantitative, and they can be used in the laboratory or in the field in locations such as a port of entry, distribution center, clinic, pharmacy, or hospital. TLC can give an indication whether the active ingredient is present and its level of content, and, therefore, if the product is qualified or authorized or legal on this basis. Some related substances might also be detected and quantified. However, TLC will not detect counterfeits that have wrong active or inactive ingredients if they are not visualized by the detection method being used for the correct active drug.

SPEEDY TLC KIT

In a series of papers starting in 1989, Kenyon, Layloff, and coworkers developed simple and inexpensive TLC methods for rapid screening of counterfeit drugs that can be used either in a well-equipped laboratory or in remote areas with or without electricity and by personnel with limited technical background and training. Balances are not necessary if standard tablets of the drugs are available, the procedure can be performed safely in the open air with no hood, and estimates are made from visual inspections in daylight without electronic measurements. These entries described methods for analysis of theophylline tablets prescribed to treat respiratory disease;[3] 10 commonly used pharmaceuticals (ampicillin, benzylpenicillin, chloramphenicol, chloroquine diphosphate, estradiol cypionate, paracetamol, praziquantel, sulfamethoxazole, theophylline, and trifluoperazone HCl);[4] 13 drugs, including three on the WHO Essential Drug List;[5] and diethylene glycol/ethylene glycol in pharmaceutical elixirs.[6]

The apparatus and procedures that evolved from these earlier studies were described in detail[7] for the rapid screening of TB pharmaceuticals in underdeveloped countries in the field. The "Speedy TLC" apparatus (available from Granite Engineering, Inc., Granite City, Illinois, U.S.A.) is used for screening a single content of particular TB pharmaceuticals at a given concentration. Two reference solutions representing the upper and lower dosage limits depending on the legal specification of the drug being analyzed are spotted on the plate, 2 cm up from the bottom edge, in 3.0 μl aliquots with a sample solution representing 100% spotted between the standards. After development, the spots are examined visually under ultraviolet (UV) light and in visible light after detection by KI–iodine solution.

No analytical balance is required for sample or standard solution preparation. A sample tablet is ground to a fine powder in a small polyethylene bag, and the bag and powder are transferred to a suitable vessel (e.g., a beaker, flask, or bottle); the contents of capsules are simply emptied into a vessel. The proper volume of solvent is added, and the vessel is shaken vigorously to dissolve the powder

to prepare a concentrated solution from which the TLC sample solution is prepared by dilution.

The high reference solution, equivalent to 115% or 120% when the sample is prepared to be 100%, is prepared by dissolving a reference standard tablet containing a predetermined quantity of the drug in a fixed volume of solvent; reference tablets are formulated to dissolve completely in the solvent without grinding. The low reference solution (85.0% relative to the sample) is prepared by dilution of the high reference solution.

TLC analysis is performed using the Speedy TLC kit supplied with plastic bags, holders, and all other required accessories. Plastic-backed silica gel 60 F_{254} 5 × 10 cm sheets are required for use in the kit apparatus; the presence of fluorescent indicator in the layer is necessary for detection of drugs that quench fluorescence under 254 nm UV light. The specified mobile phases will provide the required separation for each analysis with drug R_F values between 0.2 and 0.8.

The rigid aluminum TLC frame, 10 cm plastic bag, filter paper saturator strips, aluminum developing tray, and clamp and fishhook are assembled, and the mobile phase is added. The TLC sheet is attached to the aluminum frame with the clip and lowered into the plastic bag with the fishhook. Paper clips are placed behind the sheet (between the sheet and the aluminum frame). The sheet is essentially suspended in space and is held only with the clip. The mobile phase will advance in a straight line. The sheet is allowed to stay in the bag without contacting the mobile phase for about 5 min to reach equilibrium, after which the plastic bag is pulled down to allow the mobile phase to contact the lower 1 cm of the layer. Development is carried out to within 1 cm of the top of the sheet with 15–18 ml of the mobile phase specified for the particular drug being analyzed: methanol–conc. ammonium hydroxide (25:0.38), methanol–acetone–conc. ammonium hydroxide (13:17:1), or ethyl acetate–glacial acetic acid–conc. ammonium hydroxide–water (12:12:4:4). The development bag and back-to-back aluminum trays will accommodate two sheets at a time.

The spots for all drugs can be detected, after drying the layer, under 245 nm UV light in a TLC viewing box or in an unlighted room, and/or by iodine staining. The KI–iodine staining solution is placed in a plastic bag, the sheets are immersed in the reagent, and they are then removed and the spots observed after excess reagent is evaporated. Most drugs are detectable using the iodine reagent, so this method is applicable when UV light is unavailable (e.g., absence of electricity or batteries to power a UV lamp).

After detection, visual inspection is made to assure that the sample spot size and intensity are between those of the standards. Other criteria for an acceptable drug analysis include no additional, unexplained spots in the sample and exact line up of standard and sample spots (identical R_F values).

The recipe for the KI–crystalline iodine reagent containing water, ethanol, and HCl and the preparation and use of the plastic bags are described in detail in the original paper,[7] along with drug R_F values in the three mobile phases. Experimental details are given in the paper for standard and sample preparation and TLC analysis of ethambutol hydrochloride (100 and 400 mg tablets), isoniazid (100 and 300 mg tablets), pyrazinamide (400 mg tablets), rifampin (150 mg capsules), streptomycin sulfate (200 mg/ml injectable), and various fixed combinations of two or three of these drugs.

FAST CHEMICAL IDENTIFICATION SYSTEM (FCIS)

The FCIS[8] was developed in China for determination in a drug testing laboratory of 10 macrolide antibiotics in different preparations, including erythromycin, roxithromycin, clarithromycin, azithromycin, erythromycin ethylsuccinate, midecamycin, meleumycin, kitasamycin, acetyl-kitasamycin, and acetylspiramycin. The system comprises two color reactions based on functional groups in the molecules and two TLC methods for screening of fake macrolide antibiotics after preparing test solutions by dissolving of tablet, granule, capsule powder, and dry suspension samples in absolute ethanol. For the color reactions, sulfuric acid as a common reaction of macrolides is first used to distinguish them from other types of drugs, then 14- and 16-membered macrolides are classified by potassium permanganate reactions depending on the time for loss of color in the test solution. Two TLC analyses on silica gel GF_{254} plates are used for further identification by comparison of sample and standard spots; the mobile phase is ethyl acetate–hexane–conc. ammonium hydroxide (100:15:15) for 14-membered macrolides and trichloromethane–methanol–conc. ammonium hydroxide (100:5:1) for 16-membered macrolides. Mobile phase development and spot detection with iodine vapor are carried out in closed TLC tanks. A suspected counterfeit macrolide preparation can be identified within 40 min.

MINILAB TLC SYSTEM

The main field screening method in use today is based on the portable Minilab kit, developed by the German Pharma Health Fund (GPHF).[1] The Minilab uses TLC procedures similar to those in the Speedy TLC system (above) except for crushing tablets inside aluminum foil instead of a plastic bag, development of layers and detection of spots in bottles instead of plastic bags, and detection with iodine vapor sublimed from crystals rather than KI–iodine solution. All necessary apparatus, reagents, and standards are included to test for 40 drugs on the WHO Essential Drug List (Table 1). This list features antibiotics and

Table 1 Drugs analyzed by the Minilab TLC kit.

acetylsalicylic acid	aminophylline	amodiaquine	amoxicillin
ampicillin	artemether	artesunate	cefalexin
chloramphenicol	chloroquine	ciprofloxacin	cloxacillin
cotrimoxazole	didanosine	erythromycin	ethambutol
furosemide	glibenclamide	griseofulvin	indinavir
isoniazid	lamivudine	lumefantrine	mebendazole
mefloquine	metamizole	metronidazole	nevirapine
paracetamol	Phenoxymethylpenicillin	prednisolone	primaquine
pyrazinamide	Quinine	rifampicin	salbutamol
stavudine	sulfadoxine/pyrimethamine	tetracycline	zidovudine

chemotherapeutical agents frequently used in the developing countries of the southern hemisphere, which when counterfeited can be a serious threat to patients' lives. The original Minilab TLC manual, dated 1998, and subsequent supplements (1999–2004) with detailed instructions covering analysis of the 40 drugs are available on the GPHF website.[9]

The first step in the Minilab protocol for screening counterfeit drugs is visual inspection of the product (e.g., size, shape, color) and its labeling and packaging, and comparison with a genuine example. Many fake medicines have been found at this step, but in some cases they are becoming harder to spot in this way because of an improved quality of copying the genuine packaging in the illicit manufacturing process. A dissolution and disintegration test is then carried out by dropping a tablet or capsule in warm (37°C) water contained in a 100 ml wide neck bottle and swirling periodically. Unless the product is labeled "slow release" or "enteric," it should disintegrate within 30 min, measured with a preset timer, or be suspected of being illegal.

The third stage is the use of simplified test tube color reactions for a quick check of the presence of any amount of a drug active ingredient in the sample. An example is a colorimetric field assay for artesunate based on the reaction of fast red TR salt with an alkali decomposition product of the drug to produce a distinct yellow color. Screening tests based on color reactions can be fooled by addition of another ingredient reacting the same as the active ingredient, or a small amount of the genuine pharmaceutically active substance, into the counterfeit drug product. In this case, a yes/no response is not adequate, and the method must be at least semiquantitative, like TLC.

In support of the TLC drug assays, the Minilab supplies a collection of authentic secondary standard tablets and capsules in sealed plastic tubes. The standard and the sample from a sachet or in the form of a hard gelatin capsule, soft gelatin capsule, or tablet are placed into glass bottles, and a designated volume of extraction solvent is added from a calibrated measuring pipette to prepare the stock solutions. The working solutions are prepared in 10 ml vials by appropriate dilution using pipettes. The origin and mobile phase line are marked using a soft pencil on an aluminum-backed 5×10 cm silica gel 60 F_{254} layer (called a "chromatoplate"), and disposable 2 μl glass micropipettes are used to spot the standards and sample 1.5 cm up from the bottom edge. The uniformity of the initial spots (they should be circular and evenly spaced) is checked under a 254 nm UV lamp. Layers are developed in glass jars with lids and lined with filter paper on all sides; the mobile phase is added, and after 15 min of equilibration the jar is opened and the spotted layer is quickly inserted so that the initial spots are above the mobile phase level. After development up to the marked line (about three quarters of the layer length), the chromatoplate is removed, and the mobile phase is evaporated with the help of a hotplate (a travel iron placed upside down). The spots are viewed under battery-operated 254 nm and 366 nm UV lamps. If necessary, spots not detected under UV light are detected as yellowish brown spots by placing the layer inside a capped jar containing iodine crystals and heating for about 30 sec on the hotplate. The spots detected with iodine and the spots seen under the UV lamps are marked with the soft pencil for documentation. After each analysis, all components of the kit must be thoroughly cleaned and dried and returned to the protective airtight and waterproof carrying case, and solutions must be disposed of properly.

The Minilab TLC analysis identifies the active ingredient by comparison of distance of travel (R_F value) between the sample spot and an authentic standard spotted on the same plate, and semiquantitative proof of content is made by visually comparing the color, size, and intensity between the sample spot and reference spots for each method of detection. Every drug has a detailed individual monograph for its analysis. As an example, the monograph for cotrimoxazole has the following sections: principle, equipment and reagents, preparation of the stock standard solution from the reference tablet, preparation of the 100% working standard solution (upper working limit), preparation of the 80% working standard solution (lower working limit), preparation of stock standard solution from a tablet

claiming a potency of 120 or 240 mg cotrimoxazole per unit, preparation of the working sample solution, spotting, development (including the mobile phase composition and development time), detection, example of the chromatoplate observed at 254 nm (containing four chromatograms: cotrimoxazole's upper limit representing 100% of total drug, a drug of good quality, a drug of poor quality, and cotrimoxazole's lower working limit representing 80% of total drug), observations to be made at 254 nm, observations to be made during iodine staining, and results and actions to be taken. Some drug monographs include a third detection method, e.g., anisaldehyde solution for artesunate.

A proficiency test was carried out recently to assess the performance of Minilab visual TLC quantification estimates.[10] Samples were made at 0%, 40%, and 100% from a drug reference tablet and given, unidentified, to inspectors with the Minilab protocol for quality screening. In round 1 of the proficiency test, only 3 of 28 substandard samples were correctly identified. Round 2, administered after a performance qualification test for the analytical method, showed improvement: 19 of 27 substandard drugs were correctly identified, while 5 out of 9 inspectors made the correct inference on the quality of 45 samples. In both rounds, two inspectors failed to identify substandard samples. These results show the need to have competent, well-trained users and to include a proficiency test in the Minilab screening program to obtain reliable results.

CONCLUSION

The TLC assays described here are a valuable aid in protecting patients from taking counterfeit and substandard quality medicines. They are more informative than visual inspection, dissociation tests, or simple color reaction tests, and their standardized format, ease of performance in the laboratory or in the field by persons without extensive technical training, and low cost are of great benefit to developing countries throughout the world in screening medicines used for fighting diseases such as TB and malaria. More costly analyses in a fully equipped analytical laboratory, such as infrared or mass spectrometry, electrophoresis, or high-performance column liquid chromatography,[11] are required only if the TLC-screening results are ambiguous. This application of TLC is arguably the most significantly important one being carried out in the world today.

REFERENCES

1. Jahnke, R.W.O. Counterfeit medicines and the GPHF-minilab for rapid drug quality verification. Pharm. Ind. **2004**, *66*, 1187–1193.
2. Mukhopadhyay, R. The hunt for counterfeit medicine. Anal. Chem. **2007**, *79*, 2623–2627.
3. Flinn, P.E.; Juhl, Y.H.; Layloff, T.P. A simple, inexpensive thin layer chromatography method for the analysis of theophylline tablets. Bull. World Hlth. Org. **1989**, *67*, 555–559.
4. Flinn, P.E.; Kenyon, A.S.; Layloff, T.P. A simplified TLC system for qualitative and semiquantitative analysis of pharmaceuticals. J. Liquid Chromatogr. **1992**, *15*, 1639–1653.
5. Kenyon, A.S.; Flinn, P.E.; Layloff, T.P. Rapid screening of pharmaceuticals by thin layer chromatography: Analysis of essential drugs by visual methods. J. AOAC Intl. **1995**, *78*, 41–49.
6. Kenyon, A.S.; Xiaoye, S.; Yan, W.; Har, N.W.; Prestridge, R.; Sharp, K. Simple, at-sitr detection of diethylene glycol/ethylene glycol contamination of glycerine and glycerine based raw materials by thin layer chromatography. J. AOAC Intl. **1998**, *81*, 44–50.
7. Kenyon, A.S.; Layloff, T.; Sherma, J. Rapid screening of tuberculosis pharmaceuticals by thin layer chromatography. J. Liq. Chromatogr. Relat. Technol. **2001**, *24*, 1479–1490.
8. Hu, C.-Q.; Zou, W.-B.; Hu, W.-S.; Ma, X.-K.; Yang, M.-Z.; Zhou, S.-L.; Sheng, J.-F.; Li, Y.; Cheng, S.-H.; Xue, J. Establishment of a fast chemical identification system for screening of counterfeit drugs of macrolide antibiotics. J. Pharm. Biomed. Anal. **2006**, *40*, 68–74.
9. http://www.gphf.org.
10. Risha, P.; Msuya, Z.; Ndomondo-Sigonda, Z.; Layloff, T. Proficiency testing as a tool to assess the performance of visual TLC quantitation estimates. J. AOAC Intl. **2006**, *89*, 1300–1304.
11. Sherma, J. Analysis of counterfeit drugs by thin layer chromatography. Acta Chromatogr. **2007**, *19*, 5–20.

CPC

M.-C. Rolet-Menet
Analytical Chemistry Laboratory, Unit of Formation and Research (UFR) of Pharmaceutical and Biological Sciences, Paris, France

INTRODUCTION

Centrifugal partition chromatography (CPC) is a method based on countercurrent chromatography (CCC). Separation is based on the differences in partitioning behavior of components between two immiscible liquids. Like high-performance liquid chromatography (HPLC), the phase retained in the column is called the stationary phase, and the other one, the mobile phase. In CCC, there are two modes by which to equilibrate the two immiscible phases. They depend on the characteristics of the centrifugal force field, which permits retention of the stationary phase inside the column. Devices that equilibrate the phases according to the so-called "hydrodynamic mode" were developed by Mandava and Ito.[1] They use a centrifugal force variable in intensity and direction. Alternating zones of agitation and settling of both phases are present along the column. In contrast, CPC uses a so-called "hydrostatic mode," owing to a centrifugal force constant in intensity and direction. Therefore, the mobile phase penetrates the stationary phase either by forming droplets, or by jets stuck to the channel walls, broken jets, or atomization. The more or less vigorous agitation of both phases depends on the intensity of the centrifugal force, the flow rate of the mobile phase, and the physical properties of the solvent system. Chromatographic separations obtained in hydrostatic mode are less efficient than those in the hydrodynamic one. But the retention of the stationary phase is less sensitive to the physical properties of solvents systems, such as viscosity, density, and interfacial tension. This particularity justifies the wide application field of CPC.

APPARATUS

The CPC column is made of channels engraved in plates of an inert polymer (Fig. 1), and they are connected by narrow ducts. Several plates are put together to form a cartridge. The cartridges are placed in the rotor of a centrifuge and connected to form the chromatographic column. The mobile phase enters and leaves the column via rotary seals. Since two immiscible liquids are present in the channel, the denser liquid moves away from the axis because of the centrifugal force. The less dense liquid is pushed toward the axis. The mobile phase can be either the lighter or the denser phase. In the latter case, the mobile-phase flows through the channels from the axis to the outside of the rotor. This is called the descending mode. The other case, where the mobile-phase flows toward the axis, is called the ascending mode.

Hydrostatic apparatuses are manufactured by Sanki Engineering Limited (Kyoto, Japan). They include two types of devices: The first is designed for analytical or semipreparative scale applications, and the second for scale-up at industrial scale. Centrifugal partitioning chromatograph type LLN was introduced in 1984 but is no longer available since 1992. It could be thermostatted from 15 to 35°C in an ambient temperature of 25°C. Type high-performance centrifugal partition chromatography (HPCPC) or Series 1000 supersedes type LLN. The HPCPC main frame is a 31 × 47 × 50 cm centrifuge operating in the range 0–2000 rpm; it cannot be thermoregulated. The rotor consists of two packs of six disks each, connected through a 1/16 in. tubing, and easily removable. Larger instruments have internal volumes from 1.4 to 30 L, can be used with flow rates ranging from 20 to 700 ml/min, and are custom designed for specific separation processes at a small industrial scale.

RETENTION OF STATIONARY PHASE

Before any use, the column is first filled with stationary phase and then rotated at the desired rotational speed. The mobile phase is then pumped into the cartridge at the desired flow rate and pushes out of the column a certain volume of stationary phase. Hydrostatic equilibrium is reached when the mobile phase is expelled at the column outlet. The retention of stationary phase, S_F, is defined as $S_F = V_s/V_t$, where V_s is the stationary phase volume in the column after equilibrium and V_t the total volume of the column.

The value of S_F depends on several parameters,[2,3] including the hydrodynamic properties of the channels, the centrifugal force (S_F increases to reach a maximum with the centrifugal force), the Coriolis force defined by the clockwise or counterclockwise column rotation[4] (higher retention of stationary phase is obtained with counterclockwise rotation), the mobile-phase flow rate (S_F decreases linearly with mobile-phase flow-rate), the physical properties of the solvent system (such as viscosity, density, interfacial tension), the sample volume, the sample concentration, the tensioactive properties of the

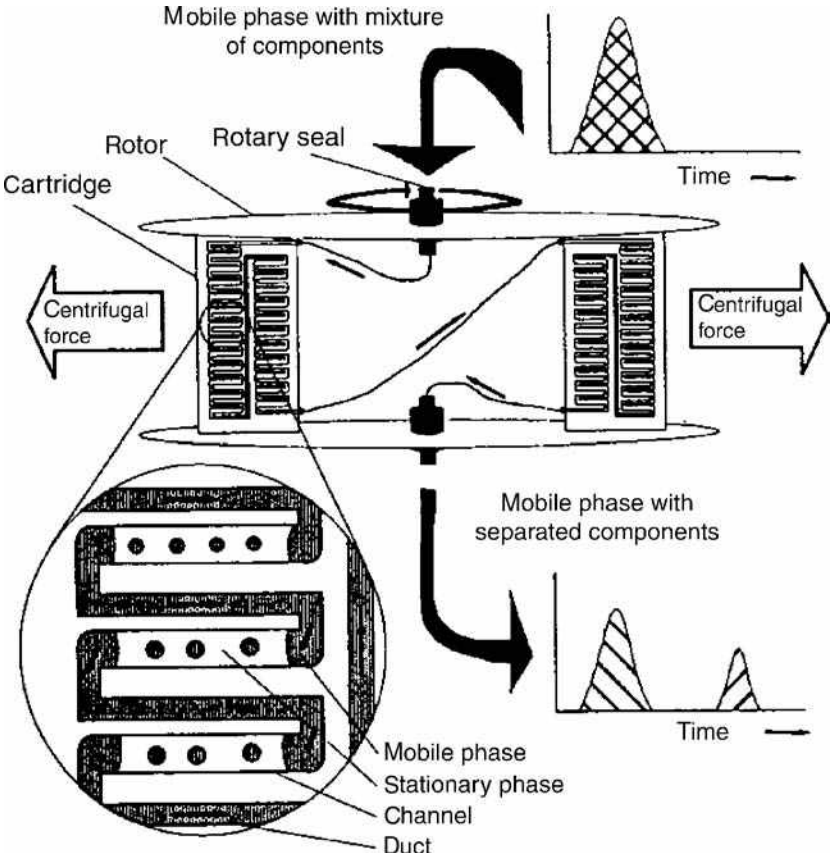

Fig. 1 Schematic representation of the CPC apparatus.
Source: From Pressure drop in centrifugal partition chromatography, in *Centrifugal Partition Chromatography*.[8]

solutes to be separated, etc. It is necessary to precisely monitor S_F because various chromatographic parameters depend on it, in particular the efficiency, the retention factor, and the resolution. Foucault[3] proposed an explanation for the variation of S_F with the various parameters described previously. He modeled the mobile phase in a channel as a droplet and applied the Stokes law, which relies on the density difference between the two phases, the viscosity of the stationary phase, and the centrifugal force. Then, he applied the Bond number derived from the capillary wavelength, which was formerly introduced for the hydrodynamic mode[5] and which relies on the density difference between the two phases, the interfacial tension, and the centrifugal force.

PRESSURE DROP

Van Buel, Van der Wielen, and Luyben[6] have proposed a model to explain the considerable pressure drop arising in the column during CPC separation. The overall pressure drop is the sum of the hydrostatic pressure drop term and the hydrodynamic pressure drop terms over the individual parts of the system. The hydrostatic contribution is caused by the difference in density between the liquids in the ducts and in the channels ($\Delta P_{stat} = nl\Delta\rho\omega^2 R$, where n is the number of channels, l the height of stationary phase in the channel, $\Delta\rho$ the density difference between the phases, ω the rotational speed, and R the average rotational radius of the cartridge). The hydrodynamic contribution (ΔP_{hydr}) is caused by the friction of the mobile phase with the walls of the channels and ducts. This latter, in a channel and a duct, is proportional to the mobile-phase density, the square of its linear velocity, the lengths of channel and duct, and the inverse of channel and duct diameter. Consequently, the overall pressure drop depends on the flow rate and rotational speed (input variables), the physical properties of the two-phase solvent system (variables), the geometry of the channels and ducts, the number of channel–duct combinations (apparatus variables), and the hold-up of stationary phase in the channel. The maximum pressure is limited by the rotary seals, which can support about 60 bars before leaking. Resolution and efficiency depend on the same variables as the pressure drop. Therefore, it is important to determine which combinations of input variables and liquid two-phases systems can be applied, with respect to the maximum pressure that can be supported by the rotary seal.

EFFICIENCY

For a symmetrical peak, Efficiency (N) in CCC can be defined as in HPLC by

$$N = 16\left(\frac{V_r}{\omega}\right)^2$$

where V_r is retention volume of the solute and ω the peak base width expressed in volume units as V_r. For an asymmetrical peak, efficiency can be defined according to the Foley–Dorsey formula

$$N = 41.7 \frac{(t_r/\omega_{0.1})^2}{(A/B) + 1.25}$$

where $\omega_{0.1}$ is the peak width at 10% of the peak height and A/B the asymmetry factor, with $A + B = \omega_{0.1}$.

Centrifugal partition chromatography apparatuses are still generally regarded as lacking efficiency (compensated by high, selectivity and S_F). The efficiency variation shows a minimum when the flow rate of the mobile phase is increased, which is the opposite of the usual HPLC Van Deemter plot. This observation has been modeled by Armstrong, Bertrand, and Berthod.[7] The mobile phase, when it comes out of the duct, flows very quickly to reach an intermediate emulsified layer and then settles in a third step before being transferred to another channel. In these conditions

$$\mathrm{In}(1 - E) = \frac{A}{F} - BF^b$$

where

$$E = \frac{C_{m,t} - C_{m,0}}{C_{m,eq} - C_{m,0}}$$

$C_{m,t}$, $C_{m,0}$ and $C_{m,eq}$ are the solute concentrations in the mobile phase at a moment t, before equilibrium, and after equilibrium, respectively, and A depends on S_F, B on the physical properties of the solvent system, and b on the solute and solvent systems. This variation is very interesting because it shows that a high-mobile-phase flow rate decreases the retention time without decreasing efficiency. However, it is observed that S_F decreases with the flow rate and the resolution R_s also decreases, as described in the following section. The flow rate of the mobile phase may be increased to lower the separation time but on condition that S_F remains adequate to maintain a sufficient R_s and consequently the quality of separation remains satisfactory.[2] Van Buel, Van der Wielen, and Luyben[8] first improved the understanding of the influence of flow patterns on the mass transfer between the two liquid phases and the chromatographic efficiency of CPC instruments. They directly visualized the mobile-phase flow through the stationary phase (in a plane parallel to the rotation axis) as a function of the rotational speed and flow rate of the mobile phase. Four main types of flow states were observed: large droplets, jets stuck along the channel walls, broken jets, and atomization. Marchal et al.[9] visualized the mobile-phase flow in a plane perpendicular to the rotation axis for different solvent systems [heptane/methanol (heptane/MeOH), chloroform/*n*-propanol/methanol/water (chloroform/*n*-ProOH/MeOH/W), heptane/chloroform/*n*-ProOH/MeOH/W, *n*-butanol/acetic acid/water (n-ButOH/acetic acid/W), aqueous two-phase systems]. They confirmed the observations of Van Buel et al. and observed deviations of jets or droplets from the radial direction caused by the Coriolis force. They correlated the chromatographic efficiency to the flow pattern observed: non-Gaussian peak corresponding to the jets stuck along the channel wall, and increase of efficiency when jets come unstuck from the walls. Increase of flow rate and rotation speed generally yielded better efficiencies.

RESOLUTION

Resolution (R_s) in CCC can be defined as in HPLC by

$$R_s = 2 \frac{V_{r2} - V_{r1}}{\omega_1 + \omega_2} = 2V_s \frac{K_2 - K_1}{\omega_1 + \omega_2}$$

where V_{r1} and V_{r2}, ω_1 and ω_2, and K_1 and K_2 are, respectively, the retention volumes, the peak base widths expressed in volume units as V_r, and the partition coefficients of the first and second eluted solutes. R_s is directly proportional to volume V_s of the stationary phase and hence on the flow rate of the mobile phase and the centrifugal force.[2,10] Resolution in CCC, as in HPLC, is governed by the Purnell relation

$$R_s = \frac{\sqrt{N}}{4} \frac{k_2'}{1 + k_2'} \frac{1 - \alpha}{\alpha}$$

where k_2' is the retention factor of the second solute and α the separation factor. N is controlled by F, the centrifugal force, S_F, and the physical properties of solvent system, k' by the nature of the solvent system (through the partition coefficient, K, and S_F), and α mainly by the solvent system. This relation shows that it is essential in CCC to control technical parameters and to judiciously choose the solvent system to separate the products. Moreover, Ikehata et al.[4] showed that partition coefficients, efficiencies, and Rs were improved by rotating the column in the clockwise direction.

SOLVENT SYSTEMS

The choice of the solvent system is the key parameter to good separation. On one hand, its physical properties define S_F, N, and R_s, on the other hand, the relative polarities of its two phases define the partition coefficients of the solutes and, as a result, the selectivities and the retention factors. The usual solvent systems are biphasic and made of three solvents, two of which are immiscible. We only give guidelines for the choice of solvent system. If the

polarities of the solutes are known, the classification established by Ito[1] can be taken as a first approach. He classified the solvent systems into three groups, according to their suitability for non-polar molecules ("non-polar" systems), intermediary polarity molecules ("intermediary" system), and polar molecules ("polar" system). The molecule must have a high solubility in one of the two immiscible solvents. The addition of a third solvent enables better adjustment of the partition coefficients. When the polarity of the solutes is not known, the Oka[11] approach uses mixtures of *n*-hexane (HEX), ethyl acetate (EtOAc), *n*-ButOH, MeOH, and water ranging from the HEX/MeOH/W (2:1:1; v/v/v) to the *n*-ButOH/W (1:1; v/v) systems and mixtures of chloroform, MeOH, and water. This solvent series covers a wide range of hydrophobicities, from the non-polar HEX/MeOH/W system to the polar *n*-ButOH/W system. Moreover, all these solvent systems are volatile and yield a desirable two-phase volume ratio of about 1. The solvent system leading to partition coefficients close to 1 is selected.

APPLICATIONS

Numerous applications using CPC are described in reference books,[1,3] covering organic and mineral solutes (Table 1). We only give key examples extracted from the CPC literature.

Polyphenols and Tannins

Open column chromatography with silica gel and alumina is not applicable to the fractionation of tannins because of their strong binding to these adsorbents, which induces extensive loss of the compounds. Such losses do not occur with CCC, as it does not use a solid stationary phase. Such molecules are very polar, so that butanol-based solvent systems can be used. Centrifugal partition chromatography is more appropriate in this case compared to hydrodynamic CCC thanks to the good retention of the stationary phase of this solvent system. Okuda, Yoshida, and Hatano[14] separated castalagin from vescalagin by using the solvent system *n*-ButOH/*n*-ProOH/W (4:1:5; v/v/v). They are diastereoisomers that differ only in the configuration of the hydroxyl group of the central carbohydrate moiety. In the same way, these authors have separated oligomeric hydrolysable macrocyclic tannins oenothein B and woodfordins by using *n*-ButOH/*n*-ProOH/W (4:1:5; v/v/v). In spite of a small structural difference (presence or absence of a galloyl group), these dimers showed a considerable difference of partition coefficients in this solvent system (0.36 for woodfordin C and 0.19 for oenothein B).

Preparative Separation of Raw Materials

One of the major applications of CPC is the purification of natural products from vegetal extracts (flowers, roots, etc.) or crude extracts from fermentation broth without previous sample preparation. Hostettmann and coworkers[12] have described many examples of isolation of natural products by CPC. Some flavonoids are, for instance, purified by using solvent systems containing chloroform, some coumarins by using solvent systems containing HEX and EtOAc, and more polar products, such as tannins, by butanol-based systems. The main interest of this technique lies, however, in the possibility to overload its column so that all the applications of semipreparative chromatography are available. For instance, Menet and Thiébaut[15] have separated 140 mg of an antibiotic from a crude extract of a fermentation broth. Some fractions of up to 95% purity were collected, while the original extract contained only 7% of the molecule of interest. They have also compared the performances of CPC, preparative LC, and hydrodynamic mode CCC. They finally showed that the solvent consumption is the lowest for CPC, while the enrichment is the best.

The pH-zone refining mode was introduced by Ito.[16] It is a variant of displacement chromatography. It is devoted to the purification of compounds whose electric charge depends on pH. For example, a mixture of free acids is injected in the organic stationary phase along with an acid stronger than all the compounds to be separated. The

Table 1 Applications in CPC.

Species	Solvents system
Polyphenols and tannins[3]	$CHCl_3$/MeOH/W (7:13:8; v/v/v), $CHCl_3$/MeOH/ *n*-ProOH/W (9:12:2:8; v/v/v/v), *n*-ButOH/*n*-ProOH/W (4:1:5; v/v/v)
Triptolide and tripdiolide[3]	HEX/EtOAc/CH_2Cl_2/MeCN/MeOH/W (12:10:3:10:5:6; v/v/v/v/v/v)
Lanthanoids[3]	HEX containing *bis*(2-ethylhexyl)phosphoric/0.1 mol/L (H, Na)Cl_2CHCOO to an appropriate pH
Flavonoids[12]	$CHCl_3$/MeOH/W (5:6:4; v/v/v)
Polyphenols[12]	C_6H_{12}/EtOAc/MeOH/W (7:8:6:6; v/v/v/v)
Tannins[12]	*n*-ButOH/*n*-ProOH/W (2:1:3; v/v/v)
Naphthoquinones[12]	HEX/MeCN/MeOH (8:5:2; v/v/v)
Retinals[12]	C_6H_6/*n*-C_5H_{12}/MeCN/MeOH (500:200:200:11; v/v/v/v)
Chiral compounds[13]	Various systems containing chiral selectors

compounds are moved along the column by pumping a basic aqueous mobile phase. Pure products are eluted from the column as salts, by contiguous rectangularly shaped peaks arranged according to the pK_a values and partition coefficients. This mode allowed a preparative isolation of indole alkaloids from *Catharanthus roseus*[17] The solvent system consisted of a mixture of methyl-*tert*-butyl ether, acetonitrile, and water. The upper organic phase was made basic with triethylamine and used as the mobile phase. The lower aqueous phase was acidified by hydrochloric acid.

log $P_{oct/water}$[18,19]

Octanol–water partition coefficients ($K_{o,w}$) have been established as the most relevant quantitative physical property correlated with biological activity. Centrifugal partition chromatography using octanol and water as the two phases is a useful alternative for providing octanol–water partition coefficients ($K_{o,w}$). It offers automation advantages compared to HPLC and the shake-flask method. Three approaches for determining $K_{o,w}$ by CPC have been described. The normal mode consists in equilibrating the CPC column according to a normal equilibrium and the overloading mode by artificially decreasing the volume of the stationary phase. $K_{o,w}$ is calculated according to the classical formula $K = k'(V_t - V_s)/V_s$ The second procedure is the dual-mode method,[20] which is based on the exchange of the role of the mobile and stationary phases during the experiment. Therefore, the determination range of partition coefficients can be extended. The third procedure, the cocurrent mode, relies on the simultaneous pumping of a mixture of a small flow of octanol and a larger flow of water to elute strongly retained compounds.

Elution Gradient[21,22]

Another way to extend the polarity range of analyzed compounds is the elution gradient. During the separation, the composition of the mobile phase is modified, while the composition of the stationary is kept constant. But in CPC, when the composition of the mobile phase is modified, the composition of the stationary phase changes. To prevent instability of the stationary phase during a gradient run, the change in stationary phase composition should be lower than 20% (v/v). Not all ternary two-phase systems are suitable for elution gradient. Foucault and Nakanishi[23] gave an overview of two-phase systems that are suitable for gradient elution.

CONCLUSIONS

Centrifugal partition chromatography is a method based on CCC. Devices equilibrate the phases according to a so-called "hydrostatic mode" owing to a centrifugal force constant in intensity and direction. So, the retention of the stationary phase is less sensitive to the physical properties of solvent systems compared to the "hydrodynamic mode." This particularity justifies the wide application field of CPC: use of *n*-But OH solvent systems, aqueous two-phase systems, and elution gradient. Moreover, the largest instruments have an internal volume from 1.4 to 30 L and are custom designed for specific separation processes at a small industrial scale. Finally, a better understanding of CPC (influence of Coriolis force) shows that the geometry of channel and duct are critical. A new CPC apparatus could take this into account.

REFERENCES

1. Mandava, B.N.; Ito, Y. Principles and instrumentation of counter current chromatography. In *Counter Current Chromatography. Theory and Practice*; Chromatographic Science Series; Mandava, B.N., Ito, Y., Eds.; Marcel Dekker, Inc.: New York, 1988; Vol. 44, 79–442.
2. Menet, J.-M.; Rolet, M.-C.; Thiébaut, D.; Rosset, R.; Ito, Y. Fundamental chromatographic parameters in countercurrent chromatography: influence of the volume of stationary phase and the flow-rate. J. Liq. Chromatogr. **1992**, *15*, 2883–2908.
3. Foucault, A.P. Theory of centrifugal partition chromatography. In *Centrifugal Partition Chromatography*; Chromatographic Science Series; Foucault, A.P., Ed.; Marcel Dekker, Inc.: New York, 1995; Vol. 68, 25–50.
4. Ikehata, J.-I.; Shinomiya, K.; Kobayashi, K.; Ohshima, H.; Kitanaka, S.; Ito, Y. Effect of Coriolis force on countercurrent chromatography separation by centrifugal partition chromatography. J. Chromatogr. A, **2004**, *1025*, 169–175.
5. Menet, J.-M.; Thiébaut, D.; Rosset, R.; Wesfreid, J.E.; Martin, M. Classification of countercurrent chromatography solvent systems on the basis of the capillary wavelength. Anal. Chem. **1994**, *66*, 168–176.
6. Van Buel, M.J.; Van der Wielen, L.A.; Luyben, K.Ch.A.M. Pressure drop in centrifugal partition chromatography. J. Chromatogr. **1997**, *773*, 1–12.
7. Armstrong, D.W.; Bertrand, G.L.; Berthod, A. Study of the origin and mechanism of band broadening and pressure drop in centrifugal partition chromatography. Anal. Chem. **1988**, *60*, 2513–2519.
8. Van Buel, M.J.; Van den Wielen, L.A.M.; Luyben, K.Ch.A.M. Pressure drop in centrifugal partition chromatography. In *Centrifugal Partition Chromatography*; Chromatographic Science Series; Foucault, A.P., Ed.; Marcel Dekker, Inc.: New York, 1995; Vol. 68, 51–69.
9. Marchal, L.; Foucault, A.; Patissier, G.; Rosant, J.M.; Legrand, J. Influence of flow patterns on chromatographic efficiency in centrifugal partition chromatography. J. Chromatogr. A, **2000**, *869*, 339–352.
10. Murayama, W.; Kobayashi, T.; Kosuge, Y.; Yano, H.; Nunogaki, Y.; Nunogaki, K. A new centrifugal countercurrent chromatograph and its applications. J. Chromatogr. A, **1982**, *239*, 643–649.

11. Oka, H.; Harada, K.-I.; Ito, Y.; Ito, Y. Separation of antibiotics by counter-current chromatography. J. Chromatogr. A, **1998**, *812*, 35–52.
12. Maillard, M.; Marston, A.; Hostettmann, K. High speed counter current chromatography of natural products. In *High-Speed Counter Current Chromatography*; Chemical Analysis; Ito, Y., Conway, W.D., Eds.; John Wiley and Sons: New York, 1995; Vol. 132, 179–218.
13. Foucault, A. Enantioseparations in counter-current chromatography and centrifugal partition chromatography. J. Chromatogr. A, **2001**, *906*, 365–378.
14. Okuda, T.; Yoshida, T.; Hatano, T. Fractionation of plant polyphenols. In *Centrifugal Partition Chromatography*; Chromatographic Science Series; Foucault, A.P., Ed.; Marcel Dekker, Inc.: New York, 1995; Vol. 68, 99–132.
15. Menet, M.-C.; Thiébaut, D. Preparative purification of antibiotics for comparing hydrostatic and hydrodynamic mode counter-current chromatography and preparative high-performance liquid chromatography. J. Chromatogr. A, **1999**, *831*, 203–216.
16. Weisz, A.; Sher, A.L.; Shinomiya, K; Fales, H.M.; Ito, Y. A new preparative-scale purification technique: pH zone-refining countercurrent chromatography. J. Am. Chem. Soc. **1994**, *116*, 704–708.
17. Renault, J.H.; Nuzillard, J.-M.; le Crorérour, G.; Thépenier, P.; Zèches-Hanrot, M.; Le Men-Olivier, L. Isolation of indole alkaloids from *Catharanthus roseus* by centrifugal partition chromatography in the pH-zone refining mode. J. Chromatogr. **1999**, *849*, 421–431.
18. Berthod, A.; Talabardon, K. Operating parameters and partition coefficient determination. In *Counter Current Chromatography*; Chromatographic Science Series; Menet, J.M., Thiébaut, D., Eds.; Marcel Dekker, Inc.: New York, 1999; 121–148.
19. Wang-Fan, W.; Kusters, E.; Mak, C.-P.; Wang, Y. Application of centrifugal counter-current chromatography to the separation of macrolide antibiotic analogues. II. Determination of partition coefficients in comparison with the shake-flask method. J. Chromatogr. A, **2000**, *23* (9), 1365–1376.
20. Bourdat-Deschamps, M.; Herrenknecht, C.; Akendengue, B.; Laurens, A.; Hocquemiller, R. Separation of protoberberine quaternary alkaloids from a crude extract of Enantia chlorantha by centrifugal partition chromatography. J. Chromatogr. A, **2004**, *1041* (1–2), 143–152.
21. Foucault, A.; Nakanishi, J.L.C. Gradient elution centrifugal partition chromatography comparison with HPLC gradients and use of ternary diagrams to build gradients. J. Liq. Chromatogr. **1990**, *13*, 3583–3602.
22. Van Buel, M.J.; Van der Wielen, L.A.M.; Luyben, K.Ch.A.M. Modelling gradient elution in centrifugal partition chromatography. J. Chromatogr. A, **1997**, *773*, 13–22.
23. Foucault, A.; Nakanishi, K. Gradient elution in centrifugal partition chromatography: use of ternary diagrams to predict stability of the stationary liquid phase and calculate the composition of initial and final phases. J. Liq. Chromatogr. **1989**, *12*, 2587–2600.

Creatinine and Purine Derivatives: Analysis by HPLC

M.J. Arín
M.T. Diez
Analytical Chemistry, Department of Applied Chemistry and Physics, University of León, León, Spain

J.A. Resines
Department of Teaching General, Specific and Theory of Education, University of León, León, Spain

Abstract
Creatinine and purine derivatives are frequently analyzed in human and veterinary clinical chemistry laboratories. We present here an overview of high-performance liquid chromatography (HPLC) and other current analytical methods, including photometric and enzymatic determinations, capillary electrophoresis (CE), and gas chromatography–mass spectrometry (GC–MS) for the measurement of these compounds.

INTRODUCTION

Creatinine and purine derivatives—allantoin, uric acid, hypoxanthine, and xanthine present in biological samples—are important analytes for diagnoses of certain types of metabolic diseases and can serve as markers for these processes. Analyses for such substances are crucial for diagnosis and the monitoring of renal diseases, metabolic disorders, and various types of tumorigenic activity. On the contrary, these compounds are very important in the field of animal nutrition, because the measurement of their urinary excretion is being used as an internal marker for microbial protein synthesis.

OVERVIEW

Creatinine is an important analyte of clinical significance that results from the irreversible, non-enzymatic dehydration and loss of phosphate from phosphocreatine (Fig. 1). Creatine is synthesized from amino acids in the kidney, liver, and pancreas. The creatine is then transported in the blood to other organs where it is synthesized into creatinine. Creatinine detection in biological fluids is a clinical test for thyroid and muscular function and for detection of myocardial infarction. Urine and serum creatinine concentrations are used to adjust the values of urinary biological indicators, and its concentrations are very useful indexes for evaluating glomerular filtration rate of the kidneys and, in general, for indicating renal function.

Allantoin is the catabolic end product of purines in most mammals. It is formed by the action of the enzyme uricase on urate. Humans and other primates lack uricase and excrete urate as the final product of purine metabolism. However, small amounts of allantoin are present in human serum. Some authors demonstrated that free radical attack on urate generates allantoin. Therefore, small amounts of allantoin detected in human serum may provide a marker of free radical activity in vivo. In humans, the allantoin to uric acid ratio in plasma increases during oxidative stress, and thus this ratio has been suggested to be an in vivo marker for oxidative stress in humans.

Uric acid is the major product of purine metabolism, and it is degraded to allantoin in most mammals by hepatic enzyme, the urate oxidase, and excreted with the urine. Hypoxanthine and xanthine are intermediates along this pathway (Fig. 2). Under normal conditions, they reflect the balance between the synthesis and breakdown of nucleotides. Levels of these compounds change in various situations (e.g., they decrease in experimental tumors), when synthesis prevails over catabolism, and are enhanced during oxidative stress and hypoxia. Uric acid is considered an important antioxidant in human adult plasma because it can directly react with free radicals. Uric acid has been employed as a biomarker of health and nutritional status. The regular measurement of its plasma and urine concentrations has important clinical utility in disease diagnoses such as gout, hyperuricemia, the Lesch–Nyhan syndrome, and the Down syndrome. Xanthines are also markers for metabolic disorders such as xanthinuria and for several central nervous system disorders such as hypoxia, hepatic encephalopathy. Nowadays in forensic toxicology the hypoxanthine levels in vitreous humor are being applied to the estimation of postmortem interval.

In ruminants, the concentration ratio of purine derivatives to creatinine (PD:C) has been widely used in metabolism studies to determine the nutrient utilization by these animals and by the ruminal microbes.

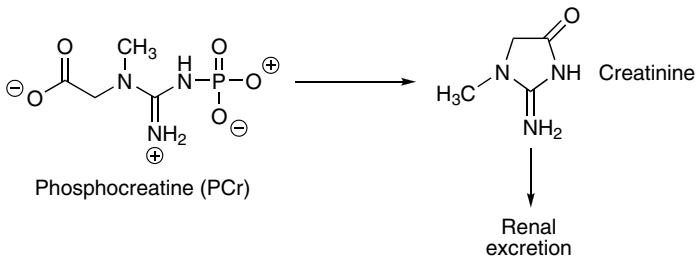

Fig. 1 Degradation of purine nucleotides and formation of purine derivatives.

SAMPLE PREPARATION

Determination of these compounds is carried out frequently in biological fluids. Analysis in urine and saliva requires previous filtration to remove cells and other particulate matter; then, the samples are diluted and directly injected onto the column. With cerebrospinal fluid, the samples are obtained by lumbar puncture; each aliquot is centrifuged and decanted before analysis. Often in plasma or serum, some form of protein removal is needed because the presence of these compounds in injected samples can cause modifications of the column and bias in chromatographic results. Protein removal can be performed by various methods, such as protein precipitation, ultrafiltration, centrifugation, liquid-phase or solid-phase extraction, and column-switching techniques. Vitreous humor samples were collected in tubes containing sodium fluoride to block the enzymes involved in glycolysis. Each sample was centrifuged and only the supernatant was used for analysis.

ANALYSIS OF CREATININE

The common spectrophotometric method for creatinine detection is based on the Jaffé reaction between creatinine and picric acid in alkaline solution to form a red-yellow complex. However, substances of endogenous and exogenous origin usually cause interference. In spite of these problems, the colorimetric method of Jaffé is still used today for the determination of creatinine in biological samples.[1] A batchwise kinetic procedure and flow injection analysis have shown the possibility to determine creatinine in human urine samples by this reaction, free from any systematic error.[2] Enzymatic methods have been reported to increase specificity/selectivity but still suffer from interferences. To avoid these problems, new analytical methods were developed. Several electroanalytical techniques, based on potentiometric or amperometric detection, are available. Potentiometric methods using several sensors and biosensors were known for the

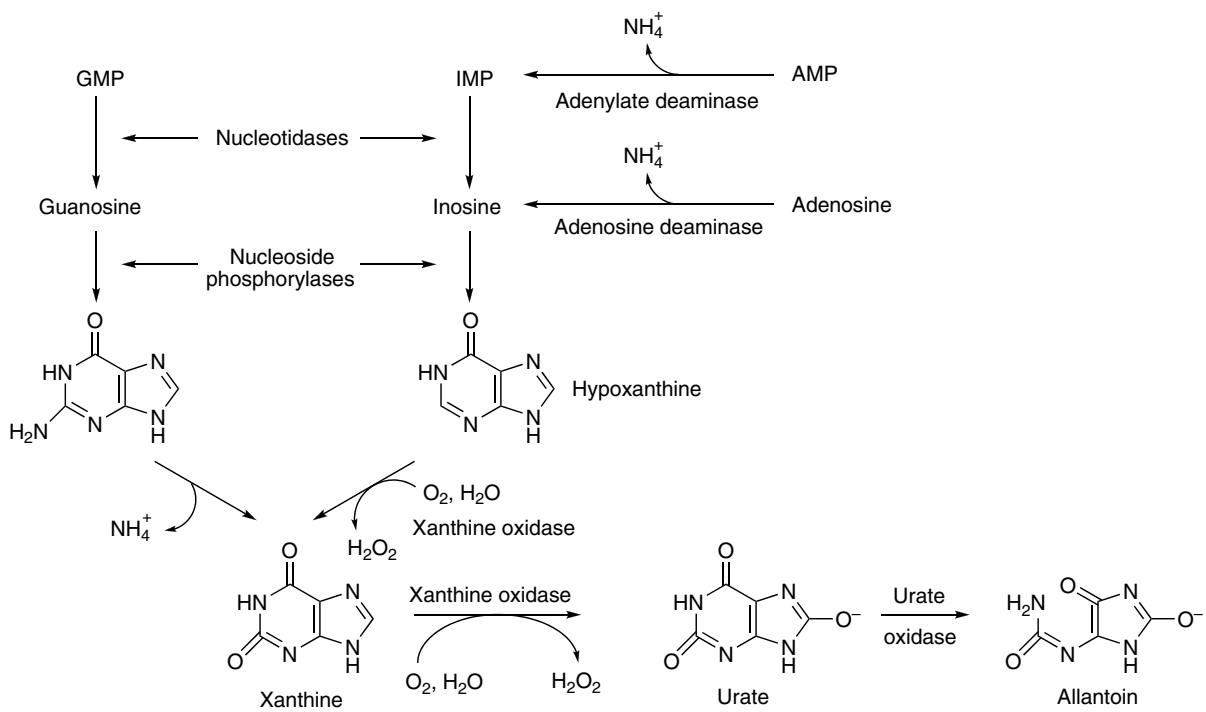

Fig. 2 Phosphocreatine metabolism.

determination of creatinine among other metabolites in biological fluids.[3–4] Capillary electrophoresis (CE), capillary zone electrophoresis (CZE), and isotope dilution–gas chromatography–mass spectrometry (ID–GC–MS),[5] proposed as a reference method, have also been used in the analysis of creatinine in human serum and urine. The advantages of CE techniques, such as a relatively short time of analysis, a usually high efficiency of resolution obtained, and a minimal amount of sample required, make electromigration techniques especially valuables in creatinine determination.[6]

Chromatographic techniques have been very useful for clinical analysis, with advantages of simultaneous measurements of different components and the elimination of interfering species. Previous reviews have been realized for the determination of creatinine.[7] High-performance liquid chromatographic (HPLC) methods include ion-exchange chromatography, reversed-phase (RP) chromatography, ion-pair chromatography, and micellar electrokinetic capillary chromatography (MEKC), and more complicated column-switching and tandem methods[8] have been described as well.

Some authors compare different methods such as electrochemical, electrophoretic, enzymatic, chromatographic, and spectrophotometric, proving that, in general, the colorimetric assays overestimated creatinine measurements.

Urinary creatinine can be analyzed by HPLC using a variety of columns. Detection methods include absorption, fluorescence after postcolumn derivatization, MS, and some other methods. The application of biosensors in HPLC could improve detection, and, in many cases, allows the detection of solutes otherwise undetectable by the common method. Review of the recent literature revealed that the method of choice for the measurement of creatinine has been RP-HPLC. C_8 and C_{18} columns and UV or electrochemical detection (ED) with isocratic elution or gradient elution were mostly used.[9]

In most cases, RP ion-pairing HPLC with UV-photometric detection was used. The advantage of this technique is the broad range of parameters that may be conveniently adjusted to optimize the separation method; they include the concentration of organic modifier in the mobile phase, the type and concentration of buffer in the mobile phase, and the type and concentration of the counterion.[10] In addition to ion-exchange methods, some authors have developed a procedure for the determination of creatinine and a wide range of amino acids that provides for fixed-site ion exchangers that eliminates the addition of ion-pairing agent in the mobile phase.[11] Creatinine has been analyzed in sera and tissues using HPLC and CE methods. Many of these determinations could also be applied to urinary creatinine analysis.

Various papers related to the simultaneous determination of creatinine and uric acid can be found in the literature. Several authors have developed CZE methods for the simultaneous analysis of these compounds in urine. The CE analysis of these renal markers offers some advantages when compared with chromatography, such as shortened separation time, reduced reagent consumption, and increased resolution. Micellar electrokinetic capillary chromatography has been applied to the simultaneous separation of creatinine and uric acid in human plasma and urine. However, chromatographic techniques are widely accepted for the determination of these compounds. Reversed-phase and ion-pair HPLC methods were applied for the simultaneous determination of these compounds in sera. These methods were consistent with the ID–GC–MS reference method. An anion-exchange HPLC-ED method using disposable electrodes has been proposed for the simultaneous determination of creatinine, uric acid, and other urinary metabolites. It requires only a small amount of urine and no sample preparation is needed. Disposable electrodes make it possible to avoid reconditioning, which are required with non-disposable electrodes.[12]

PURINE DERIVATIVES: ALLANTOIN, URIC ACID, XANTHINE, AND HYPOXANTHINE

Traditionally, oxypurines allantoin, uric acid, and, in some cases, xanthines have been analyzed in biofluids by colorimetric methods. The analysis of allantoin was based on the Rimini–Schriver reaction, in which allantoin is converted to glyoxylic acid by sequential hydrolysis under alkaline and acidic conditions, and then derivatizated with 2,4-dinitrophenylhidrazine to obtain the chromophore glyoxylate-2,4-dinitrophenylhydrazone.

The two predominant analyses of uric acid are the phosphotungstic acid (PTA) method and the uricase method. In the PTA method, urate reduces PTA to form a blue product. In the uricase analysis method, urate is oxidized by uricase oxidoreductase.

Xanthine and hypoxanthine have often been quantified colorimetrically or as uric acid following enzymatic conversion. Both approaches were problematic due to interference by compounds contained in biological fluids, whereas enzymatic conversion to uric acid has often been incomplete.

These photometric and enzymatic methods suffer from interferences by endogenous and exogenous compounds and can lead to inaccurate results. To avoid these problems, in recent years, other methods involving ED, biosensors, CZE, GC–MS, and HPLC methodology have been developed. Reversed-phase, normal-phase, ion-exchange, ion-pair, column-switching, MEKC, and size-exclusion chromatography were used for determining purine derivatives.

Different methods, mostly colorimetric and chromatographic, for the determination of allantoin have been reviewed by Chen.[13] The chromatographic procedures are mainly based on separation by HPLC using C_{18} RP columns and monitoring at wavelengths around 200 nm. Many compounds present in plasma and urine also exhibit absorbance at these

wavelengths; therefore, the detection of allantoin is not selective enough when the concentration is low (<60 μmol/L).[13] To avoid this problem, allantoin can be converted, before elution, to a derivative, which can be monitored at a more specific detection wavelength. However, allantoin is an extremely polar compound that has poor retention on C_{18} RP columns. To achieve a good separation from other polar compounds, the column length often needs to be extended. Another way to overcome the problem is the use of ion-pairing agents to slow down the elution.

For uric acid, ID–GC–MS[5] has been proposed as the candidate reference method. RP methods have been most widely employed. RP C_8 and C_{18} columns ranging from 150 to 250 mm in length and usually with an internal diameter 3.9–4.6 mm were used. Both isocratic elution and gradient elution were applied. Variable-wavelength UV or diode array detectors are the most commonly used, in the range 210–292 nm. Electrochemical and online combination of UV with ED improves the selectivity and sensitivity of analysis and decreases the probability of interfering substances being present in analyte peaks. Some methods make use of ion-exchange HPLC for the determination of uric acid and other organic compounds. In most cases, RP ion-pairing HPLC methods were used to determine uric acid in biological samples. One of these has been proposed as candidate reference method for the determination of uric acid.[14] Data obtained by this method were compared with those from ID–GC–MS using [1,3-$^{15}N_2$] uric acid as internal standard.

The main advantage of these methods is that they allow direct determination of urine samples, whereas plasma samples only need deproteinization; in addition, they offer the possibility to simultaneously determine other purine derivatives. In recent years some alternatives to HPLC involving amperometric biosensors and miniaturized CE have been proposed. The microchip CE has opened new levels in performance, functionality, and throughput.[15]

Various methods have been proposed for the simultaneous determination of uric acid and allantoin in different biological matrices. For urine samples, GC–MS was applied for the determination of both compounds.[16] However, HPLC methods are still widely accepted.

Several HPLC methods have been reported for the determination of xanthine and hypoxanthine. Different RP-HPLC methods using gradient elution and UV detection have been described to determine these metabolites and other methylated purines. To improve the determination of xanthines in urine samples, analyses were carried out with two columns—RP and anion-exchange column—connected by a column switch.[17] With this method, urinary hypoxanthine and xanthine can be measured without any sample preparation other than filtration.

Simultaneous determination of uric acid, hypoxanthine, and xanthine in different biological matrices such as urine, urinary calculi, cerebrospinal fluid, and plasma was carried out by RP-HPLC with isocratic elution and UV detection. Various analytical methods for the simultaneous determination of allantoin, uric acid, and xanthines in biological samples, such as urine, blood plasma, and serum, have been described. These procedures are mainly based on separation by HPLC using RP C_{18} columns, UV detection, and isocratic elution or gradient elution. In some cases, allantoin was converted to a derivative with a chomophoric group, but other authors avoid the disadvantages of the allantoin derivatization process.[18] The HPLC and CE methods have been compared for the determination of these compounds on plasma and atherosclerotic plaque. Comparison of results showed that CZE may have analytical performance similar, or even superior, to HPLC, especially for the determination of allantoin in biological samples.[19]

SIMULTANEOUS DETERMINATION OF CREATININE AND PURINE DERIVATIVES

Several papers can be found in the literature concerning the simultaneous determination of creatinine and uric acid or various purine metabolites; however, only a few have reported the simultaneous determination of creatinine and purine derivatives. Kochansky and Strein[20] reviewed recent developments in chromatography and CE methods for the determination of creatinine, uric acid, and xanthines in biological fluids.

RP-HPLC procedures for the determination of creatinine and purine metabolites, such as allantoin, uric acid, xanthine, and hypoxanthine in ruminant urine, were described. Chromatography was achieved with a C_{18} column under isocratic conditions, and detection at 218 nm without allantoin derivatization. The chromatographic conditions were a compromise between the sensitivity and specificity of the measurements of each analyte, analysis time, and resolution of all analyte peaks from interfering compounds.[21] This method has been improved for the simultaneous determination of allantoin, uric acid, and creatinine in cattle urine taking into account the variations in urine pH, because they could alter the retention time of analytes in RP-HPLC systems.[22] Uremic toxins creatine, creatinine, uric acid, and xanthine were simultaneously determined in human biofluids, simply after dilution, with UV detection at 200 nm. This method was compared for creatinine and uric acid with conventional routine methods and did not give significantly different results.[23]

An ion-pair HPLC method for the determination of creatinine and purine derivatives (allantoin, uric acid, and hypoxanthine in sheep urine) using allopurinol as the internal standard is described.[24] In this work, various variables were tested to optimize the simultaneous determination of these compounds, including alkyl chain length of the ion-pairing agent (C_6, C_8, and C_{10}), buffer concentration, pH, percentage of methanol of the mobile phase, and column

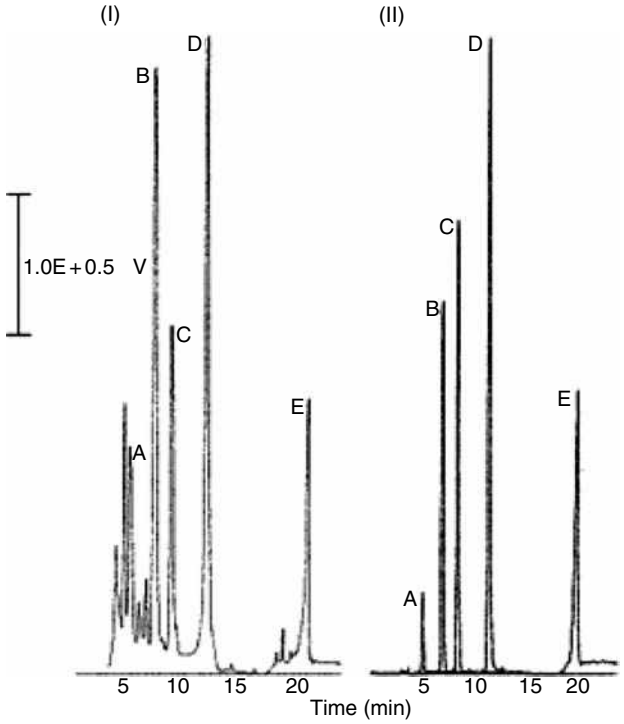

Fig. 3 (I) Chromatogram of tenfold-diluted sheep urine. (II) Chromatographic separation of standard solutions. Peaks: A, allantoin; B, uric acid; C, hypoxanthine; D, allopurinol (IS); E, creatinine.
Source: From Simultaneous measurements of creatinine and purine derivatives in ruminant's urine using ion-pair HPLC, in J. Liq. Chromatogr. Rel. Technol.[24]

temperature. The mobile-phase composition was phosphate buffer 10 m*M* with 3 m*M* 1-octanesulfonic acid, sodium salt, pH 4, mixed with methanol:eluent A (5%) and eluent B (20%). The gradient program was 0–13 min, 0–100% B, flow rate 0.5 ml/min; 13–25 min, 100–0% B, flow rate of 1.5 ml/min; re-equilibration time at 0% B, 10 min. The injection volume was 20 μl. The column temperature was set at 30°C. The chromatographic conditions adopted represented a compromise between good separation and reasonable analysis time. Fig. 3 shows the chromatograms resulting from the injection of pure standards and tenfold-diluted sheep urine sample under adopted chromatographic conditions. Under these conditions, there were no other endogenous urinary components that can interfere with the analyte peaks. This method was applied to check the validation of a new method that uses an electrochemical sensor for the determination of creatinine in urine samples. The precision and the accuracy of the results are very similar in both methods.[25]

CONCLUSIONS

HPLC, when compared to other instrumental methods, presents significant advantages in the simultaneous analysis of creatinine and purine derivatives. The variety of instrumental and experimental conditions (columns, buffers, organic modifiers, detectors, etc.) of these methods reported in the literature offer versatility and flexibility. Chromatographic conditions for these analytes are not complicated when RP columns are applied. New stationary phases with high separation power provide short analysis time. The mobile phases used are also very simple (organic–water mixtures with controlled pH); both isocratic elution and gradient elution are recommended. Different sensitivity detectors (UV, electrochemical, fluorescence, the combined techniques such as HPLC–MS and the new biosensors) are very valuable for the possible identification of all analyzed compounds. In some cases, only CE shows some advantages over HPLC, such as short analysis time, reduced reagent consumption, and increased resolution. However, detection limits are often inferior when using UV absorbance detectors.

REFERENCES

1. Chizzotti, M.L.; Valadares Filho, S.C.; Valadares, R.F.D.; Chizzotti, F.H.M.; Tedeschi, L.O. Determination of creatinine excretion and evaluation of spot urine sampling in Holstein cattle. Livestock Sci. **2008**, *113*, 218–225.
2. Campins, P.; Tortajada, L.A.; Meseger, S.; Blasco, F.; Sevillano, A.; Molins, C. Creatinine determination in urine simples by batchwise kinetic procedure and flow injection analysis using the Jaffé reaction: Chemometric study. Talanta **2001**, *55*, 1079–1089.
3. Patel, A.K.; Sharma, P.S.; Prasad, B.B. Development of a creatinine sensor based on a molecularly imprinted polymer-modified sol-gel film on graphite electrode. Electroanalysis **2008**, *20* (19), 2102–2112.
4. Chen, J.-C.; Kumar, A. S.; Chung, H.-H.; Chien, S.-H.; Kuo, M.-C.; Zen, J.-M. An enzymeless electrochemical sensor for the selective determination of creatinine in human urine. Sens. Actuators B Chem. **2006**, *115*, 473–480.
5. Thienpont, L.M.; Van Nieuwenhove, B.; Reinuer, H.; De Leenheer, A.P. Determination of reference method values by isotope dilution-gas chromatography-mass spectrometry: A five years' experience of two European Reference Laboratories. Eur. J. Clin. Chem. Clin. Biochem. **1996**, *34*, 853–860.
6. Szymanska, E.; Markuszewski, M.J.; Bodzioch, K.; Kaliszan, R. Development and validation of urinary nucleosides and creatinine assay by capillary electrophoresis with solid phase extraction. J. Pharm. Biomed. Anal. **2007**, *44*, 1118–1126.
7. Smith-Palmer, T. Separation methods applicable to urinary creatine and creatinine. J. Chromatogr. B, **2002**, *781*, 93–106.
8. Huskova, R.; Chrastina, P.; Adam, T.; Schneiderka, P. Determination of creatinine in urine by tandem mass spectrometry. Clin. Chim. Acta **2004**, *350*, 99–106.
9. Mo, Y.; Dobberpuhl, D.; Dash, A.K. A simple HPLC method with pulsed EC detection for the analysis of creatine. J. Pharm. Biomed. Anal. **2003**, *32*, 125–132.

10. Resines, J.A.; Arín, M.J.; Díez, M.T.; García del Moral, P. Ion-pair reversed-phase HPLC determination of creatinine in urine. J. Liq. Chromatogr. Rel. Technol. **1999**, *22* (16), 2503–2510.
11. Yokoyama, Y.; Horikoshi, S.; Takahashi; T.; Sato, H. Low-capacity cation-exchange chromatography of ultraviolet-absorbing urinary basic metabolites using a reversed-phase column coated with hexadecylsulfonate. J. Chromatogr. A, **2000**, *886*, 297–302.
12. Hsu, C.-T.; Lyuu, H.-J.; Yang, T.-H.; Conte, E.D.; Zen, J.-M. Profiling clinically important metabolites in human urine by an electrochemical system containing disposable electrodes. Sens. Actuators B Chem. **2006**, *113*, 22–28.
13. Chen, X.B. Determination of allantoin in biological, cosmetic and pharmaceutical samples. J. AOAC Int. **1996**, *79* (3), 628–635.
14. Kock, R.; Delvoux, B.; Tillmanns, U.; Greiling, H. A candidate reference method for the determination of uric acid in serum based on high-performance liquid chromatography, compared with an isotope dilution-gas chromatography-mass spectrometer method. J. Clin. Chem. Clin. Biochem. **1989**, *27*, 157–162.
15. Chu, Q.C., Lin, M.; Geng, C.H.; Ye, J.P. Determination on uric acid in human saliva and urine using miniaturized capillary electrophoresis with amperometric detection. Chromatographia **2007**, *65* (3/4), 179–184.
16. Chen, X.B.; Calder, A.F.; Prasitkusol, P.; Kyle, D.L.; Jayasuriya, M.C.N. Determination of 15N isotopic enrichment and concentrations of allantoin and uric acid in urine by gas chromatography/mass spectrometry. J. Mass Spectrom. **1998**, *33*, 130–137.
17. Sumi, S.; Kidouchi, K.; Ohba, S.; Wada, Y. Automated determination of hypoxanthine and xanthine in urine by high-performance liquid chromatography with column switching. J. Chromatogr. B, **1995**, *670*, 376–378.
18. Czauderna, M.; Kowalczyk, J. Quantification of allantoin, uric acid, xanthine and hypoxanthine in ovine urine by high-performance liquid chromatography and photodiode array detection. J. Chromatogr. B, **2000**, *744*, 129–138.
19. Terzuoli, L.; Porcelli, B.; Setacci, C.; Giubbolini, M.; Cinci, G.; Carlucci, F.; Pagani, R.; Marinello, E. Comparative determination of purine compounds in carotid plaque by capillary zone electrophoresis and high-performance liquid chromatography, J. Chromatogr. B, **1999**, *728*, 185–192.
20. Kochansky, C.J.; Strein, T.G. Determination of uremic toxins in biofluids: Creatinine, creatine, uric acid and xanthines. J. Chromatogr. B, **2000**, *747*, 217–227.
21. Resines, J.A., Arín, M.J.; Díez, M.T. Determination of creatinine and purine derivatives in ruminant's urine by reversed-phase high-performance liquid chromatography. J. Chromatogr. **1992**, *607*, 199–202.
22. George, S.K.; Dipu, M.T.; Mehra, U.R.; Singh, P.; Verma, A.K.; Ramgaokar, J.S. Improved HPLC method for the simultaneous determination of allantoin, uric acid and creatinine in cattle urine. J. Chromatogr. B, **2006**, *832*, 134–137.
23. Samanidou, V.F.; Metaxa, A.S.; Papadoyannis, I.N. Direct simultaneous determination of uremic toxins: Creatine, creatinine, uric acid and xanthine in human biofluids by HPLC. J. Liq. Chromatogr. Rel. Technol. **2002**, *25* (1), 43–57.
24. Del Moral, P.; Díez, M.T.; Resines, J.A.; Bravo, I.G.; Arín, M.J. Simultaneous measurements of creatinine and purine derivatives in ruminant's urine using ion-pair HPLC. J. Liq. Chromatogr. Rel. Technol. **2003**, *26* (17), 2961–2968.
25. Patel, A.K.; Sharma, P.S.; Prasad, B.B. Development of a creatinine sensor based on a molecularly imprinted polymer-modified sol-gel film on graphite electrode. Electroanalysis **2008**, *20* (19), 2102–2112.

Cyanobacterial Hepatotoxin Microcystins: Affinity Chromatography Purification

Fumio Kondo
Aichi Prefectural Institute of Public Health, Nagoya, Japan

INTRODUCTION

Freshwater cyanobacteria *Microcystis*, *Oscillatoria*, *Anabaena*, and *Nostoc* produce several types of toxins, among which the most commonly detected are the hepatotoxic peptides microcystins. The general structure of the microcystins is cyclo-(D-Ala^1-*X*^{2}-D-MeAsp^3-*Z*^{4}-Adda^5-D-Glu^6-Mdha^7), in which *X* and *Z* represent variable L-amino acids, D-MeAsp^3 is D-*erythro*-β-methylaspartic acid, Mdha is *N*-methyldehydroalanine, and Adda is the unusual C_{20} amino acid, (2*S*, 3*S*, 8*S*, 9*S*)-3-amino-9-methoxy-2,6,8-trimethyl-10-phenyldeca-4(*E*),6(*E*)-dienoic acid (Fig. 1).[1] The structural differences in the microcystins mainly depend on the variability of the two L-amino acids (denoted *X* and *Z*), and secondarily on the methylation or demethylation of D-MeAsp and/or Mdha.[1] More than 60 microcystins have been isolated from bloom samples and isolated strains of cyanobacteria.[1]

Microcystins have caused the poisoning of wild and domestic animals worldwide, and in 1996, they caused the death of 76 people in Caruaru, Brazil, which was attributed to the use of microcystin-contaminated hemodialysis water.[2] Microcystins, like the well-documented tumor promoter, okadaic acid, strongly and specifically inhibit the protein phosphatases 1 and 2A and have a tumor-promoting activity in the rat liver.[3] In addition to acute hepatotoxicity, microcystins pose problems to human health—which could result from low-level, chronic exposure to microcystins in drinking water, as suggested by the high incidence of primary liver cancer in the Qidong and Haimen regions of China.[4] In 1998, the World Health Organization (WHO) proposed a provisional guideline level of 1.0 μg/L for microcystin-LR in drinking water.[4]

OVERVIEW

In order to achieve the rapid and precise determination of microcystins in complicated matrices, a systematic procedure is seriously required. This may include screening, sample purification, identification, and quantification processes.[5] Screening is intended to rapidly check for the presence of microcystins in a small amount of sample, through sensitive and simple methods. If a sample proves positive in the screening test, it will be necessary to follow through with sample purification, identification, and quantification analyses. The purpose of sample purification is to eliminate coexisting substances by a simple operation without the loss of any analyte and, considering that the microcystin concentration may be low, it also enables the enrichment of the analyte. Octadecyl silanized (ODS) silica gel has been extensively employed for this process because it retains microcystins and allows coexisting substances to pass through.[5] A method using ODS silica gel extraction followed by a purification on silica gel has been established to effectively eliminate the coexisting substances in lake water.[6] Although this method has been successfully applied to the analysis of microcystins in lake water samples, it had several problems. The method required a large water sample (5 L) to accumulate the low level of microcystins, resulting in a laborious and time-consuming extraction process. It was also shown that less hydrophobic coexisting substances still remained even after purification on silica gel,[6] indicating that a more effective purification method is required.

Recently, an immunoaffinity purification method using antimicrocystin-LR monoclonal antibodies (named M8H5) has been developed.[7] This purification method was found to be remarkably effective in the removal of coexisting substances and in the enrichment of microcystins in samples.[7–12] This work will focus on the immunoaffinity purification methods for microcystins in lake[10] and tap water samples,[11] and the analysis methods for microcystins and their metabolites in mouse and rat livers.[7–9] It will also cover the reuse of the immunoaffinity column.[12]

IMMUNOAFFINITY COLUMN

Preparation of Immunoaffinity Column

M8H5 antimicrocystin-LR monoclonal antibodies were produced by Nagata et al. as follows:[13,14] female BALB/c mice were immunized with microcystin-LR conjugated proteins (e.g., bovine serum albumin [BSA]). The spleen cells of the immunized mice and SP2/O-Ag14 cells were

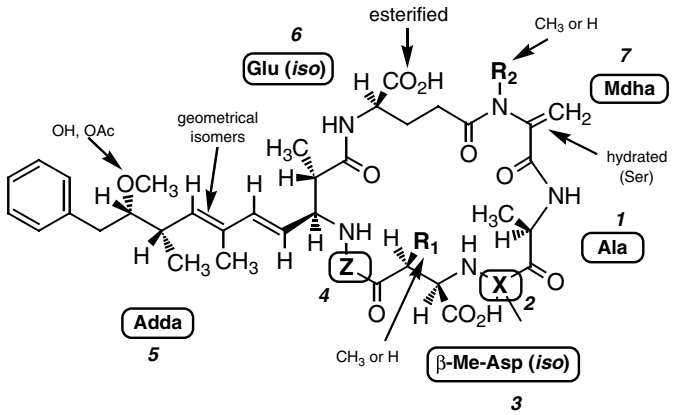

	X	Z	R_1	R_2	MW
microcystin-LA	Leu	Ala	CH_3	CH_3	909
microcystin-LR	Leu	Arg	CH_3	CH_3	994
microcystin-YR	Tyr	Arg	CH_3	CH_3	1044
microcystin-RR	Arg	Arg	CH_3	CH_3	1037
microcystin-YM	Tyr	Met	CH_3	CH_3	1019
[D-Asp^3]microcystin LR	Leu	Arg	H	CH_3	980
[Dha^7]microcystin LR	Leu	Arg	CH_3	H	980

Fig. 1 Chemical structures of microcystins.

fused with polyethylene glycol. From the serum-free cultured supernatants of the generated hybridomas, the M8H5 monoclonal antibodies were prepared by membrane ultrafiltration, ammonium sulfate, which were then finally purified using a protein G column (Pharmacia, Stockholm, Sweden). This monoclonal antibody shows extensive cross-reactivity to various microcystins and nodularin (pentapeptide sharing many common features with microcystins). Based on concentrations capable of inducing 50% inhibition of antibodies in a competitive enzyme-linked immunosorbent assay (ELISA), the cross-reactivities were 100% for microcystin-LR, 109% for microcystin-RR, 51% for [D-Asp^3]microcystin-LR, 48% for [Dha^7]microcystin-LR, 44% for microcystin-YR, 26% for microcystin-LA, and 20% for nodularin.

The antimicrocystin-LR monoclonal antibody-combined gel was prepared as follows:[7] Affi-Gel 10 (25 ml, Bio-Rad, Hercules, California, U.S.A.) was washed with distilled ice water (250 ml) and mixed with an equal volume of 10 mg/ml of M8H5 antimicrocystin-LR monoclonal antibody in phosphate buffer saline (PBS) (pH 7.4). The gel mixture was incubated at 4°C for 24 hr with gentle rocking. After the addition of 1 *M* ethanolamine hydrochloride (2.5 ml), the gel mixture was washed with distilled water (250 ml), followed by PBS (500 ml). The obtained gel cake was suspended in PBS containing 0.1% sodium azide (50 ml) and stored at 4°C. The gel mixture (0.5 ml) was transferred to a polypropylene cartridge (Muromac column; Muromachi Kagaku Kogyo Kaisha, Tokyo, Japan) when used.

Protocol for Immunoaffinity Purification

The general protocol for immunoaffinity purification of the microcystins is as follows: sample extracts dissolved in PBS are loaded onto the immunoaffinity column and passed through the column. Gravity flow is usually used. After washing with PBS and distilled water, the microcystin fraction is eluted with 100% methanol.[7,10]

Direct immunoaffinity purification of the microcystins in complicated matrices is difficult because the coexisting substances in the sample occupy the column head, so that the process ends in failure.[10] Thus preliminary semipurification is indispensable when it comes to analyzing trace amounts of microcystins in samples containing substantial amounts of coexisting substances.

DETERMINATION OF MICROCYSTINS

Lake Water

A purification method for microcystins in lake water consists of solid-phase extraction (SPE) on a Sep-Pak PS2® (styrene–divinylbenzene copolymer) or Excelpak SPE-GLF® (polymethacrylate) cartridge, followed by immunoaffinity purification.[10] A 1 L sample of lake water is filtered through a glass GF/C microfiber filter (Whatman, Maidstone, U.K.), and the filtrate is applied to a Sep-Pak PS-2 or Excelpak SPE-GLF cartridge at a flow rate of about 20 ml/min. The cartridge is washed with distilled water

(10 ml), followed by 20% methanol–water (10 ml). Finally, the eluate from the cartridge with 100% methanol (10 ml) is collected and then evaporated to dryness under reduced pressure at 35°C. The resulting residue is dissolved in PBS containing 0.1% BSA (5 ml). Bovine serum albumin is used to prevent non-specific binding of the microcystins with the immunoaffinity support Affi-Gel 10. The solution is subjected to an immunoaffinity column, which is preconditioned with PBS (5 ml), methanol (5 ml), distilled water (5 ml), and PBS containing 0.1% BSA (5 ml). After washing with PBS (5 ml) and distilled water (5 ml), the microcystin fraction is eluted with 100% methanol (10 ml). The eluate is then evaporated to dryness under reduced pressure at 35°C. The residue is dissolved in 0.5 ml of 30% methanol–water and then subjected to high-performance liquid chromatography (HPLC) with ultraviolet (UV) detection and liquid chromatography/mass spectrometry (LC/MS) analyses.

When an extract is prepared with a solid-phase extraction cartridge alone, the microcystins in lake water cannot be precisely detected because of the unstable baseline and many peaks on the chromatograms from coexisting substances (Fig. 2a). When this extract is further purified with the immunoaffinity column, the microcystin peaks are clearly detected (Fig. 2b) and effectively quantified because the coexisting substances are virtually eliminated. The recoveries from lake water (1 L) spiked with 100 ng each of microcystins-LR, -YR, and -RR are 92.2%, 89.2%, and 85.5%, respectively, with coefficients of variation of 3.3–7.6%. One of the advantages of this method is its speed; it took only 3 hr to complete the entire procedure, starting from the microcystin extraction, the immunoaffinity purification, and the quantification, whereas the previous procedures (tandem use of ODS silica gel and silica gel cartridges) took a day to complete. The detection limit for all of the three microcystins in lake water is 0.005 μg/L.

Fig. 2c shows a chromatogram of a sample taken from Lake Suwa, Japan, where water blooms occurred. Two peaks with retention times of 8.0 min (peak 1) and 17.5 min (peak 2) correspond to those of microcystins-RR and -LR, respectively, and they show the typical spectra of the respective microcystins with an absorption maximum at 238 nm (Fig. 2d), affording further confirmation.

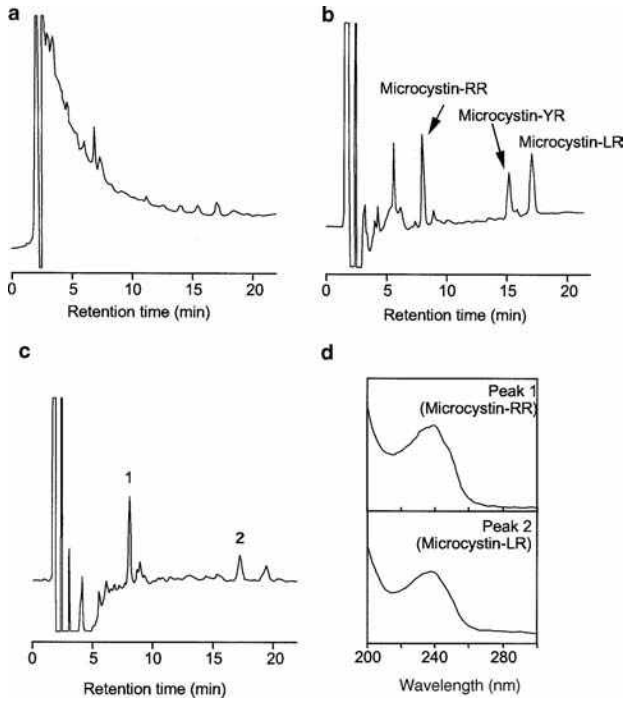

Fig. 2 HPLC analysis of lake water extracts. Microcystin-*free* lake water spiked with microcystins-LR, -YR, and -RR (100 ng each) was analyzed before (a) and after (b) purification with immunoaffinity column. (c) A water sample taken from Lake Suwa, Japan, in 1998 was analyzed after purification with the immunoaffinity column.

Tap Water and Cyanobacterial Cells

Direct purification of the microcystins in tap water with immunoaffinity columns can be achieved because the tap water contains relatively smaller amounts of coexisting substances.[11] A tap water sample is filtered through glass GF/C microfiber filters, to which a 1/10 volume of 11 × PBS is added. The sample solution is loaded onto the immunoaffinity column and passed through the column. After washing with PBS (10 ml) and distilled water (10 ml), the microcystin fraction is eluted with 100% methanol (10 ml). The eluate is evaporated to dryness and the residue is dissolved in 0.05 ml of methanol for HPLC analysis. The chromatograms of the microcystin-added tap water with immunoaffinity purification show effective elimination of the coexisting substances compared to that with the ODS cartridge (data not shown). The mean recoveries of microcystin-LR, -YR, and -RR added to tap water are 91.8%, 86.4%, and 77.3%, respectively, in the range 2.5–100 μg/L.

Microcystins in cyanobacterial cells can also be directly purified via immunoaffinity columns. A 1 L sample of lake water containing cyanobacterial cells is filtered through a glass GF/C microfiber filter (Whatman), and the cells on the filter are suspended in distilled water (10 ml). The cell containing suspension is freeze-thawed three times and then filtered through a glass GF/C microfiber filter. After the addition of a 1/10 volume of 11 × PBS, the filtrate is loaded onto the immunoaffinity column and treated in a similar manner as described above. The HPLC chromatogram shows that the peaks of microcystins-LR and -RR are clearly detected and the peaks due to the coexisting substances are almost negligible (Fig. 3a). On the other hand, the chromatogram of the same sample purified with the ODS silica gel cartridge shows that the removal of lesshydrophobic coexisting substances is insufficient, especially in a shorter retention time area (Fig. 3b).

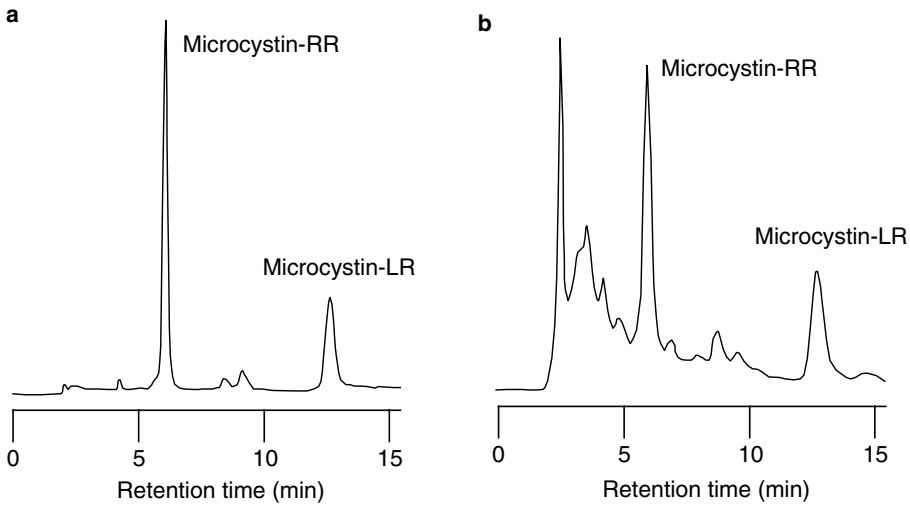

Fig. 3 HPLC analysis of cyanobacterial cells extracts. A cyanobacterial cell sample taken from Lake Suwa, Japan, in 1999 was analyzed after purification with (a) immunoaffinity column and (b) ODS silica gel cartridge.

Mouse and Rat Livers

The in vivo tissue distribution, excretion, and hepatic metabolism of microcystins have been primarily investigated using variously radiolabeled ones.[4] The amounts of the injected microcystins were too small and the amounts of the contaminants in the tissues were too large to investigate the metabolites by instrumental analysis, such as HPLC with UV detection and LC/MS. Fig. 4 shows the HPLC profiles of a cytosolic extract from mouse liver spiked with 5 μg each of microcystins-LR and -RR. When the cytosolic extract is prepared by the method described by Robinson et al.,[15] which consists of heat-denaturation, pronase digestion, and ODS silica gel treatment (Fig. 4a), the two spiked microcystins cannot be precisely analyzed because of a substantial amount of coexisting substances. When the cytosolic extract is further purified with the immunoaffinity column, the coexisting substances are effectively eliminated and the peaks of the spiked microcystins-LR and -RR are clearly detected (Fig. 4b).

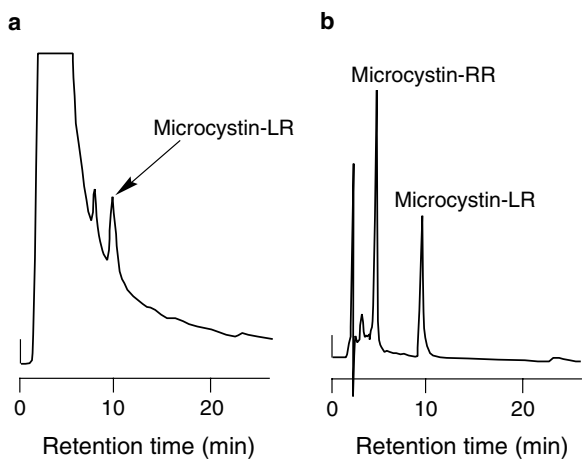

Fig. 4 HPLC analysis of a cytosolic extract from mouse liver spiked with 5 μg each of microcystins-RR and -LR. Before (a) and after (b) purification with immunoaffinity column.

The method including heat-denaturation, pronase digestion, ODS silica gel treatment, and immunoaffinity purification has been applied to the analysis of microcystins and their metabolites in hepatic cytosols from mice and rats intraperitoneally administered microcystins. A purified cytosolic extract from mouse liver at 3 hr postinjection of microcystin-RR was analyzed by Frit-FAB LC/MS. The peaks of the microcystins and related compounds can be selectively detected by monitoring the mass chromatogram at *m/z* 135, which is the characteristic ion derived from Adda, a characteristic component of microcystins.[16] The mass chromatogram shows the relatively broad peak X (Fig. 5a), which is confirmed to contain at least four peaks by using slightly modified HPLC analysis conditions. The mass spectrum of the longer retention time area of peak X shows an ion at *m/z* 1345, whose molecular weight corresponds to that of the glutathione conjugate of microcystin-RR (Fig. 5b), the thiol of GSH having been nucleophilically added to the α,β-unsaturated carbonyl of the Mdha moiety in the microcystins. The glutathione conjugate was confirmed by comparison of the retention time with that of the chemically prepared one. The mass spectrum of the shorter retention time area of peak X shows ions at *m/z* 1284, 1330, and 1459, with relatively low intensities (Fig. 5c). This area was considered to contain a conjugate of the oxidized Adda diene. The cysteine conjugate was identified in a cytosolic extract from mouse liver at 24 hr postinjection of microcystin-RR. Both the glutathione and cysteine conjugates were also identified in hepatic cytosols from the rat-administered microcystin-LR.

The immunoaffinity purification method, followed by LC/MS analysis, has also been used in other toxicological studies. When aged mice (32 weeks) were orally administered microcystin-LR at 500 μg/kg, 62% of the aged mice showed hepatic injury, whereas such changes in the liver were not found in young mice (5 weeks).[8] Upon uptake of orally administered microcystin-LR at 500 μg/kg, the

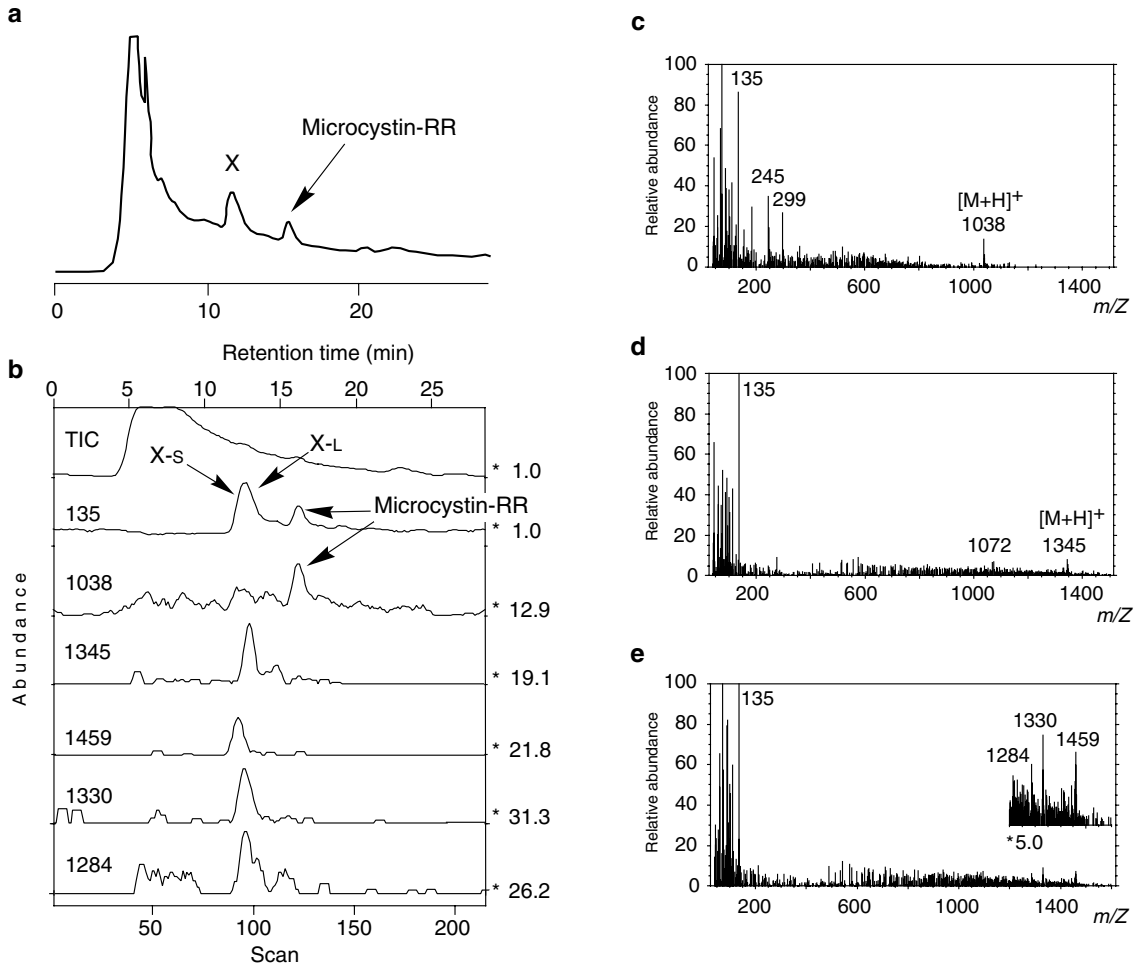

Fig. 5 Frit-FAB LC/MS analysis of a cytosolic extract from mouse liver at 3 hr postinjection of microcystin-RR. Shown are (a) simultaneously monitored UV chromatogram (238 nm), (b) total ion and mass chromatograms, (c) Frit-FAB LC/MS mass spectra of microcystin-RR, (d) longer retention time area of peak X (indicated by X-L), and (e) shorter retention time area of peak X (indicated by X-s).

toxin into the liver was confirmed by Frit-FAB LC/MS after the immunoaffinity purification. When microcystin-LR was intraperitoneally injected 100 times at 20 μg/kg into male ICR mice (5 weeks old, Charles River Japan, Atsugi, Japan) for 28 weeks, multiple hyperplastic nodules up to 5 mm in diameter were observed in every liver.[9] Microcystin-LR and its cysteine conjugate were identified from the isolated mouse livers.

REUSABLE IMMUNOAFFINITY COLUMN

Reuse of the immunoaffinity column is apparently of great value because the immunoaffinity column requires a large amount of antibodies. The immunoaffinity column using Affi-Gel 10 as the immunoaffinity support could not be repeatedly used because the applied solutions tended to stick owing to the massive bubbles produced. In order to overcome this disadvantage, a new immunoaffinity column using the immunoaffinity support Formyl-Cellulofine® has been introduced.[12] Because of the spherical shape of the immunoaffinity support Formyl-Cellulofine, the applied solutions passed through the column smoothly even when they were used repeatedly.

The purification procedure using this immunoaffinity column has been optimized as follows: After extraction with a Sep-Pak PS2 cartridge, the extract is dissolved in 25 m*M* Tris–HCl buffer (pH 7.2) containing 1 m*M* EDTA, 0.15 M sodium chloride, and 0.1% sodium azide (Tris–HCl buffer A) with 0.1% BSA (Tris–HCl buffer B) (5 ml), and the solution is loaded onto an immunoaffinity column, which is preconditioned with Tris–HCl buffer B (10 ml). After washing with Tris–HCl buffer A (10 ml) and distilled water (10 ml), the microcystin fraction is eluted with 100% dimethylformamide (DMF) (2.5 ml). The eluate is then dried on a hot block (60°C) under a constant stream of nitrogen. The residue is dissolved in 30% methanol–water (0.5 ml) and then subjected to HPLC-photodiode array (HPLC-PDA) detection and LC/MS analysis. The immunoaffinity column is regenerated by washing with Tris–HCl buffer B (10 ml) before each reuse.

Recoveries of the spiked microcystins to lake water from the first use of the column are 87–88% and 83–88% was recorded from the second and third uses. Recoveries gradually drop to 63–77% from the fourth to the fifth uses. These results indicate that the column can be repeatedly used up to three times.

CONCLUSIONS

The immunoaffinity column using antimicrocystin-LR monoclonal antibodies has proved to be an important purification tool for microcystin analysis in lake and tap water, and cyanobacterial cells and tissue samples from mice and rats. One of the advantages of the immunoaffinity purification is specificity. It enables operators to enrich the trace amounts of the microcystins and to eliminate large amounts of coexisting substances. As a result of the substantial elimination of these coexisting substances, the microcystin peaks were successfully and reliably identified with HPLC and LC/MS by excluding a few of the non-microcystin peaks that appear even after the immunoaffinity purification. On the other hand, one of the disadvantages of the analytical method using the immunoaffinity column is the requirement for large amounts of antibodies. Reuse of the immunoaffinity column is one approach to overcome this limitation. Although the immunoaffinity column for microcystins is not yet commercially available, it is believed that it will become more widely used within the next 2–3 years.

REFERENCES

1. Sivonen, K.; Jones, G. Cyanobacterial Toxins. In *Toxic Cyanobacteria in Water; a Guide to Their Public Health Consequences, Monitoring and Management*; Chorus, I., Bartram, J., Eds.; E & FN Spon: London, 1999; 41–111.
2. Carmichael, W.W.; Azevedo, S.M.F.O.; An, J.S.; Molica, R.J.R.; Jochimsen, E.M.; Lau, S.; Rinehart, K.L.; Shaw, G.R.; Eaglesham, G.K. Human fatalities from cyanobacteria: Chemical and biological evidence for cyanotoxins. Environ. Health Perspect. **2001**, *109* (7), 663–668.
3. Falconer, I.R.; Bartram, J.; Chorus, I.; Kuiper-Goodman, T.; Utkilen, H.; Burch, M.; Codd, G.A. Safe levels and safe practices. In *Toxic Cyanobacteria in Water; A Guide to Their Public Health Consequences, Monitoring and Management*; Chorus, I., Bartram, J., Eds.; E & FN Spon: London, 1999; 155–178.
4. Kuiper-Goodman, T.; Falconer, I.R.; Fitzgerald, J. Human Health Aspects. In *Toxic Cyanobacteria in Water; A Guide to Their Public Health Consequences, Monitoring and Management*; Chorus, I., Bartram, J., Eds.; E & FN Spon: London, 1999; 113–153.
5. Harada, K.-I.; Kondo, F.; Lawton, L. Laboratory analysis of cyanotoxins. In *Toxic Cyanobacteria in Water; A Guide to Their Public Health Consequences, Monitoring and Management*; Chorus, I., Bartram, J., Eds.; E & FN Spon: London, 1999; 999.
6. Tsuji, K.; Naito, S.; Kondo, F.; Watanabe, M.F.; Suzuki, S.; Nakazawa, H.; Suzuki, M.; Shimada, T.; Harada, K.-I. A clean-up method for analysis of trace amounts of microcystins in lake water. Toxicon. **1994**, *32* (10), 1251–1259.
7. Kondo, F.; Matsumoto, H.; Yamada, S.; Ishikawa, N.; Ito, E.; Nagata, S.; Ueno, Y.; Suzuki, M.; Harada, K.-I. Detection and identification of metabolites of microcystins formed in vivo in mouse and rat livers. Chem. Res. Toxicol. **1996**, *9*, 1355–1359.
8. Ito, E.; Kondo, F.; Terao, K.; Harada, K.-I. Hepatic necrosis in aged mice by oral administration of microcystin-LR. Toxicon. **1997**, *35*, 231–239.
9. Ito, E.; Kondo, F.; Harada, K.-I. Neoplastic nodular formation in mouse liver induced by repeated intraperitoneal injections of microcystin-LR. Toxicon. **1997**, *35*, 1453–1457.
10. Kondo, F.; Matsumoto, H.; Yamada, S.; Tsuji, K.; Ueno, Y.; Harada, K.-I. Immunoaffinity purification method for detection and identification of microcystins in lake water. Toxicon. **2000**, *38*, 813–823.
11. Tsutsumi, T.; Nagata, S.; Hasegawa, A.; Ueno, Y. Immunoaffinity column as clean-up tool for determination of trace amounts of microcystins in tap water. Food Chem. Toxicol. **2000**, *38*, 593–597.
12. Kondo, F.; Ito, Y.; Oka, H.; Yamada, S.; Tsuji, K.; Imokawa, M.; Niimi, Y.; Harada, K.-I.; Ueno, Y.; Miyazaki, Y. Determination of microcystins in lake water using reusable immunoaffinity column. Toxicon. **2002**, *40*, 893–899.
13. Nagata, S.; Okamoto, Y.; Inoue, T.; Ueno, Y.; Kurata, T.; Chiba, J. Identification of epitopes associated with different biological activities on the glycoprotein of vesicular stomatitis virus by use of monoclonal antibodies. Arch. Virol. **1992**, *127*, 153–168.
14. Nagata, S.; Soutome, H.; Tsutsumi, T.; Hasegawa, A.; Sekijima, M.; Sugamata, M.; Harada, K.-I.; Suganuma, M.; Ueno, Y. Novel monoclonal antibodies against microcystin and their protective activity for hepatotoxicity. Nat. Toxins. **1995**, *3*, 78–86.
15. Robinson, N.A.; Pace, J.G.; Matson, C.F.; Miura, G.A.; Lawrence, W.B. Tissue distribution, excretion and hepatic biotransformation of microcystin-LR in mice. J. Pharmacol. Exp. Ther. **1990**, *256*, 176–182.
16. Kondo, F.; Ikai, Y.; Oka, H.; Ishikawa, N.; Watanabe, M.F.; Watanabe, M.; Harada, K.; Suzuki, M. Separation and identification of microcystins in cyanobacteria by frit-fast atom bombardment liquid chromatography/mass spectrometry. Toxicon. **1992**, *30*, 227–237.

Cyclodextrins in GC

Tibor Cserháti
Institute of Chemistry, Chemical Research Center, Hungarian Academy of Sciences, Budapest, Hungary

Abstract
Cyclodextrins are cyclic oligosaccharides forming inclusion complexes with a wide variety of organic and inorganic compounds. The formation of inclusion complexes modifies the physicochemical parameters of the guest molecule, resulting in modified retention behavior. The aims of this entry are to provide a short overview of the chemistry and physicochemistry of cyclodextrins and of their application for improving separation, with special emphasis on the separation of enantiomer pairs of pharmaceuticals and environmental pollutants.

INTRODUCTION

Chromatographic methods offer an excellent possibility for the separation and quantitative determination of a considerable number of organic, metallo-organic, and even inorganic, molecules with highly similar chemical structures. These methods have found widespread application in various fields of everyday life and scientific research. Thus, they play a considerable role in medical practice and research, pharmaceutical development, food sciences and technology, environmental protection, etc.

The basis of chromatographic separation is the partition of analytes between a stationary and a mobile phase of different polarity where the stationary phase is generally solid and the mobile phase is gas or liquid. Gas chromatography (GC), a well-known and frequently applied method, uses a solid or quasi-solid stationary phase, the mobile phase generally being a neutral gas. However, the application of GC technologies is restricted to analytes, which can be volatilized and are thermostable at the temperature of the measurement.

The objectives of this entry are the compilation, brief description, and critical evaluation of the newest GC methods using native cyclodextrins (CDs) or CD derivatives as the active component of the stationary phase. Earlier results in this rapidly developing field have been previously summarized.[1]

CHEMISTRY AND PHYSICOCHEMISTRY OF CDs

CDs are cyclic, non-reducing oligosaccharides consisting of D-glucopyranose units bonded by α-1,4 linkages. They can be formed from dextrins, the products of the partial hydrolysis of starch, by the enzyme glucosyltranferase.

The main native CDs are α-, β-, and γ-CD. α-CD (Schardinger's α-dextrin, cyclomaltohexose, cyclohexaglucan, cyclohexaamilose, or C6A) is composed of six glucose units. β- and γ-CDs are formed of seven and eight glucose units, respectively. The schematic chemical structure of unsubstituted native CDs is shown in Fig. 1. Unsubstituted native CDs are crystalline non-hygroscopic substances. The sugar units adopt a $^4C_1$ conformation, orienting so that the glucose forms a toroidal conical structure. Because of the macrocyclic ring structure, CDs can form inclusion complexes with molecules or molecular substructures that fit into the CD cavity (guest molecule). The inner wall of the CD cavity is hydrophobic, facilitating the inclusion of hydrophobic guest molecules or the hydrophobic substructures of a guest molecule. The outer part is more hydrophilic, capable of polar interactions with the guest molecules or with the polar substructures of guest molecules. The main chemical and physicochemical parameters of native CDs are listed in Table 1.[2] The inclusion of complex formation modifies the physicochemical characteristics of the guest molecule (adsorption capacity, polarity, lipophilicity, etc.). As the same characteristics play a considerable role in the retention behavior of the analyte, the complexed analyte is exposed to retention parameters different from those of the non-complexed one, facilitating separation. A large number of CD derivatives were synthesized and their separation capacities and physicochemical characteristics were intensively investigated. These studies were partially motivated by the fact that the thermal stability of the native is fairly low.

CD-ASSISTED GC SEPARATIONS

Various GC methods using CDs have been used, not only for the increase of the separation efficiency, but also for the determination of the strength of interaction between CDs and a considerable number of guest molecules. The

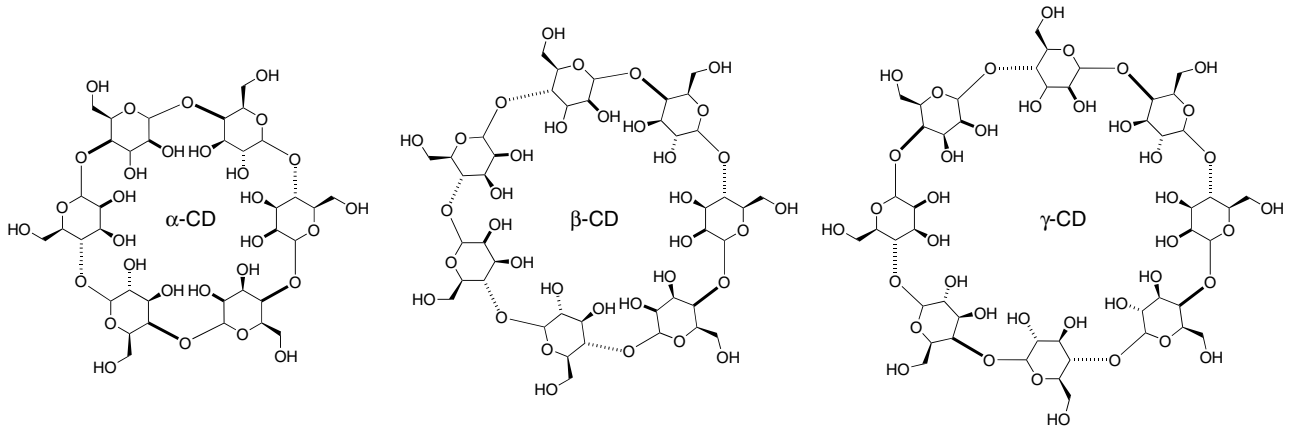

Fig. 1 Schematic structures of native α-, β-, and γ-CDs.

objectives of these investigations were the selection of the CD or CD derivative most suitable for the complexation of bioactive guest molecules or the elucidation of the molecular processes underlying inclusion complex formation. The role of CDs in separation science,[3] especially in chiral selective chromatography, has been previously reviewed[4] and discussed in detail.[5,6] A static headspace GC method and molecular modeling were employed for the study of the solubilization of chlorinated solvents by native and modified CDs. It was established that CDs effectively bind volatile pollutants.[7] Affinity capillary electrophoresis, nuclear magnetic titration, and headspace GC were applied for the measurement of the association constant between oral malodorous components and native and derivatized CDs. The binding constants are listed in Table 2. The data prove the good complexing capacity of CDs.[8]

CD-ASSISTED ENANTIOMERIC SEPARATIONS

The overwhelming majority of GC methods, employing CDs as stationary phase or as stationary phase additive, deal with the separation of optical isomers. The increasingly strong legislation regulations and the possible different biological activities of the stereoisomers motivate and promote the development and application of this type of measurement. A large variety of enantiomers was separated, including pharmaceuticals, natural products, food components, environmental pollutants.

Enantiomer Separation of Pharmaceuticals

The enantioseparation of arylpropionic non-steroidal anti-inflammatory drug methyl esters was performed with a stationary phase containing methylated and silylated-β-CD derivatives. The separation of salsolinol, levetiracetam, fluoxetine, norfluoxetine, ephedrine, methamphetamine, ephedrine type alkaloids, perfluorodiether, *N*-trifluoroacetyl-*O*-alkyl nipecotic ester, camphor, and γ-butyrolactone derivatives using different native CDs and CD derivatives were also reported.

Enantiomer Separation of Natural Compounds

The separation capacities of various stationary phases for the analysis of *R/S*-α-hydroxy fatty acid esters have been

Table 1 Chemical and physicochemical parameters of native cyclodextrins.

	α-CD	β-CD	γ-CD
Glucose units	6	7	8
Internal diameter (nm)	0.47–0.53	0.60–0.65	0.75–0.83
Depth of cavity (nm)	0.79	0.79	0.79
pK_a value	12.3	12.2	12.1
Water solubility (mg/mm, 25°C)	145	18.5	232
MW (DA)	972	1135	1297
Approximate volume of cavity (10^6 pm^3)	174	262	427
Crystal water (%, w/w)	10.2	13.2–14.5	8.13–17.7
Hydrophobic interaction	CD cavity	CD cavity	CD cavity
Hydrogen bond	Glucose–OH	Glucose–OH	Glucose–OH

Table 2 Aqueous binding constants (in units of M^{-1}) for various malodorous compounds with cyclodextrins at 22°C.

	α-CD	β-CD	γ-CD	HP-β-CD	S-α-CD	S-β-CD	CM-β-CD	Method
Acids								
Formic acid	—	—	—	—		—	—	NMR titration
Acetic acid	31.4 ± 2.9	—	—	—		—	—	NMR titration
Propionic acid	34.4 ± 4.0[a]	—	—	—		—	—	NMR titration
Butyric acid	117.1 ± 5.9[a]	120.5 ± 57.2	3.3 ± 1.1	45.5 ± 4.1		2.1 ± 1.5	1.5 ± 0.8	NMR titration
Isobutyric acid	14.5 ± 0.8	201.5 ± 2.4[a]	—	33.2 ± 3.9		2.5 ± 1.4	3.1 ± 1.0	NMR titration
Valeric acid	313.5 ± 21.0	190.6 ± 12.6	13.6 ± 1.0	100.1 ± 5.9		13.2 ± 2.7	29.7 ± 2.7	NMR titration
Isovaleric acid	35.4 ± 1.2	203.8 ± 54.2[a]	21.6 ± 3.4	144.8 ± 16.0		5.2 ± 1.2	19.0 ± 1.7	NMR titration
Lactic acid	23.2 ± 5.3	—	—	—		3.6 ± 1.1	327.3 ± 31.3	NMR titration
Succinic acid	64.3 ± 1.1	21.6 ± 16.3	6.6 ± 3.2	4.3 ± 1.3		44.4 ± 7.6	270.4 ± 25.1	NMR titration
Bases								
Ammonia	—	—	—	—		19.6 ± 4.8	2.3 ± 0.8	NMR titration
Methylamine	—	—	—	—		13.7 ± 3.8	4.8 ± 1.0	NMR titration
Cadaverine	28.9 ± 2.8	42.1 ± 2.1	11.2 ± 2.3	16.1 ± 0.2		96.0 ± 9.8	13.9 ± 1.1	NMR titration
Putrescine	32.2 ± 5.1	39.3 ± 11.6	15.2 ± 1.7	6.4 ± 0.9		82.0 ± 6.7	8.8 ± 1.2	NMR titration
Pyridine	12.7 ± 1.6	54.3 ± 1.8	19.1 ± 1.8	25.9 ± 3.1		3.5 ± 0.1	9.5 ± 0.4	NMR titration
					75.6 ± 15.8	189.7 ± 10.6	38.8 ± 3.6	ACE pH 4.5
3-Methyl pyridine	18.6 ± 1.3	32.0 ± 2.6	29.1 ± 3.2	28.0 ± 3.2		3.9 ± 0.3	10.2 ± 0.7	NMR titration
					66.1 ± 9.1	264.1 ± 11.7	27.5 ± 1.4	ACE pH 4.5
Diphenylamine	24.1 ± 2.4	216.7 ± 12.2[a]	57.4 ± 7.7[a]	248.6 ± 16.1		33.2 ± 2.9	82.7 ± 5.8	NMR titration
Neutrals								
Hydrogen sulfide	20.73 ± 0.76[a]	7.38 ± 2.20	4.98 ± 0.83	6.29 ± 0.48	1.12 ± 0.14	0.88 ± 0.07	1.65 ± 0.38	HS-GCMS
Methanethiol	23.05 ± 0.30[a]	1.70 ± 0.47	2.53 ± 0.10	1.90 ± 0.12	0.75 ± 0.13	0.18 ± 0.06	0.35 ± 0.07	HS-GCMS
Dimethyl sulfide	24.84 ± 2.19[a]	17.27 ± 3.19[a]	8.31 ± 0.45[a]	4.34 ± 0.12	0.37 ± 0.06	0.43 ± 0.03	1.57 ± 0.15	HS-GCMS
Urea	—	—	—	—		—	—	NMR titration
Phenyl acetate	6.9 ± 1.2	106.5 ± 5.3	14.0 ± 1.6	111.8 ± 7.2				NMR titration
					6.4 ± 0.6	2.6 ± 0.2	65.6 ± 5.4	ACE pH 8.5
					4.6 ± 1.8	6.0 ± 3.6	24.3 ± 8.3	ACE pH 4.5
m-Cresol	48.4 ± 2.3	124.7 ± 27.5	97.4 ± 8.2[a]	130.5 ± 13.9				NMR titration
					3.2 ± 2.4	5.9 ± 0.8	35.1 ± 2.8	ACE pH 8.5
					4.3 ± 3.7	17.9 ± 8.8	6.5 ± 2.4	ACE pH 4.5
Phenol	18.6 ± 1.3	59.6 ± 5.8	2.6 ± 1.4	52.4 ± 5.6				NMR titration

					4.4 ± 2.5	7.5 ± 0.7	29.4 ± 0.9	ACE pH 8.5
					10.7 ± 4.0	16.8 ± 9.1	23.1 ± 2.1	ACE pH 4.5
Indole	5.5 ± 0.8	166.4 ± 0.4	20.8 ± 2.0[a]	136.8 ± 8.5				NMR titration
					15.1 ± 1.4	15.6 ± 2.9	71.1 ± 1.2	ACE pH 8.5
					24.0 ± 19.8	45.4 ± 21.1	70.7 ± 17.9	ACE pH 4.5
Skatole	4.1 ± 0.6	162.3 ± 1.3	29.7 ± 2.9	171.8 ± 6.9				NMR titration
					15.5 ± 6.1	18.9 ± 1.0	72.1 ± 4.3	ACE pH 8.5
					13.9 ± 5.2	22.6 ± 4.0	86.8 ± 24.6	ACE pH 4.5
Dodecanol	142.0 ± 20.3[a]	100.7 ± 33.6[a]	80.5 ± 14.6[a]	157.6 ± 14.3		8.1 ± 2.2	25.3 ± 3.0	NMR titration
Tetradecanol	425.5 ± 71.1[a]	200.3 ± 25.0[a]	85.6 ± 7.8[a]	104.4 ± 6.9		14.5 ± 3.3	35.6 ± 2.5	NMR titration
Amino acids								
Arginine	—	—	—	—	121.6 ± 18.9	324.9 ± 93.8	—	ACE pH 9.4
	—	—	—	—	87.3 ± 18.3	151.8 ± 10.6	—	ACE pH 4.5
Lysine	—	—	—	—	167.2 ± 12.4	142.0 ± 13.7	—	ACE pH 9.4
	—	—	—	—	103.3 ± 11.9	173.6 ± 3.1	—	ACE pH 4.5
Ornithine	—	—	—	—	139.1 ± 4.8	192.2 ± 22.0	—	ACE pH 9.4
	—	—	—	—	181.8 ± 14.8	368.8 ± 24.6	—	ACE pH 4.5
Tryptophan	—	—	—	—	—	—	—	ACE pH 9.4
		—	—	—	—	49.5 ± 4.9	—	ACE pH 4.5
Citrulline	—	—	—	—	231.8 ± 24.7	1.068.6 ± 57.8	—	ACE pH 9.4
	—	—	—	—	222.1 ± 97.8	231.8 ± 24.7	—	ACE pH 4.5
Cysteine	—	—	—	—	40.3 ± 17.8	719.5 ± 37.8	—	ACE pH 9.4
	—	—	—	—	—	250.5 ± 49.1	—	ACE pH 4.5

α-CD, α-cyclodextrin; β-CD, β-cyclodextrin; γ-CD, γ-cyclodextrin; HP-β-CD, hydroxypropyl-β-cyclodextrin; S-α-CD, sulfated-α-cyclodextrin; S-β-CD, sulfated-β-cyclodextrin; CM-β-CD, carboxymethyl-β-cyclodextrin; NMR, Nuclear Magnetic Resonance; ACE, Affinity Capillary Electrophoresis; HS-GCMS, Headspace-Gas Chromatography Mass Spectrometry.
Empty cells indicate binding constant determination not performed. Extent of binding too low to be measured by the stated method.
Dashes indicate that the extent of binding is too low to be measured by the stated method.
[a]Precipitation of CD—analyte complex.
Source: From Estimation of association constants between oral malodor components and various native and derivatized cyclodextrins, in Anal. Chim. Acta.[8]

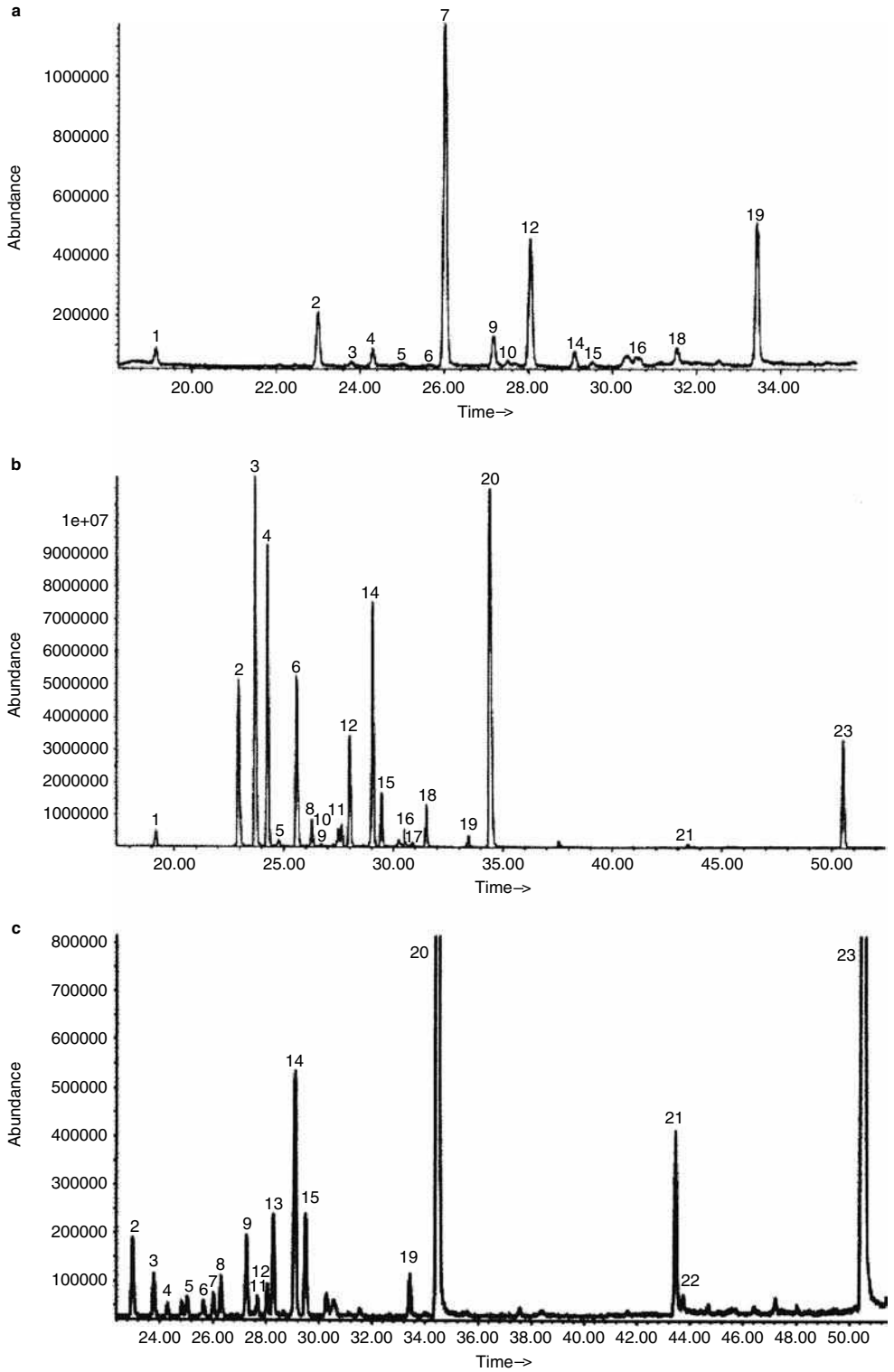

Fig. 2 Total ion chromatogram of monoterpenes present in the gaseous emission of (a) Douglas-fir, (b) Rosemary and (c) Lavender. Peaks: 1, α-Thujene; 2, (–)-α-Pinene; 3, (+) α-Pinene; 4, Myrcene; 5, Tryciclene; 6, (+)-Camphene; 7, (–)-Sabinene; 8, (–)-Camphene; 9, (+)-δ-3-Carene; 10, α-Terpinene; 11, (+)-β-Pinene; 12, (–)-β-Pinene; 13, *m*-Cymene; 14, *o*-Cymene; 15, (+)-Limonene; 16, (+)-β-Phellangrene; 17, (+)-β-Phellangrene; 18, γ-Terpinene; 19, α-Trpinolene; 20, 1,8-Cineole; 21, (–)-4-Carene; 22, (+)-4-Carene; 23, (–)-Camphor.
Source: From Analysis of enantiomeric and non-enantiomeric monoterpenes in plant emissions using portable dynamic air sampling/solid-phase microextraction (PDAS-SPME) and chiral gas chromatography/mass spectrometry, in Atm. Environ.[9]

compared. It was found that an α-CD column separated the esters with a short alkyl chain well, but was inefficient in the case of long-chain fatty acid esters. A β-CD stationary phase was applied for the successful analysis of monoterpenes, as demonstrated in Fig. 2.[9] Furan derivatives were separated on a per-*O*-methyl-β-CD column. Enantiomers of derivatized amino acids were analyzed on a stationary phase containing modified resorcinarene and β-CD. β-CD and β-CD derivatives have been further applied for the enantioseparation of monoterpenes in grapes and Scotch pines (*Pinus sylvestris*). α-CD has also found application in the separation of natural compounds. Thus, its use in monoterpenoid analysis was illustrated.[10,11]

Enantiomeric Separation of Environmental Pollutants

CD derivatives were synthesized by substituting valeryl, heptanoyl, and octanoyl groups in the 6 position of 2,3-di-*O*-pentyl-β-CD. The separation capacities of the new derivatives were tested by using 15 pairs of disubstituted benzene derivatives as analytes. The capacity factors and separation factors determined on the three stationary phases are listed in Table 3. It was concluded from the data that the separation capacity of the derivatives was markedly different; the pentyl derivative showed the best selectivity.[12] Organophosphorus pesticides were also well separated on a trimethyl-β-CD column. Because of their high toxicities, the separation possibilities of polychlorinated biphenyls have been vigorously investigated. Thus, *tert*-butylsilyl derivatives of β-CD were successfully employed for the analysis of polychlorinated biphenyls (PCB), 1,1-di(4-chlorophenyl)-2,2-dichloroethylene (DDE), and their methylsulfonyl metabolites in human adipose tissue, seal blubber, and pelican muscles. PCB atropisomers were also separated on various columns containing CD derivatives.

Two-dimensional GC was employed for the analysis of chiral PCBs in foods such as milk, cheese, and salmon.[13] A new β-CD derivative (permethylated-β-CD/hydroxy-termination silicone oil) was employed for the efficient extraction of polybrominated diphenyl ethers in soil. CDs have also been used for the analysis of toxaphene congeners. It was established that permethylated and *tert*-butyldimethylsilylated-β-CDs separate different congeners and can be applied for the study of the degradation of toxaphens. Another study applied two-dimensional GC for the successful separation of toxaphene enantiomers. It was found that the separation efficacy of β-CD containing columns showed marked differences, depending on the composition of the stationary phase. Capillary columns coated with heptakis-(2,3,6-*O*-*tert*-butyldimethylsilyl)-β-CD or octakis-(quest;2,3,6-tri-*O*-ethyl)-γ-CD were employed for the enantiomer-selective decomposition of toxaphene congeners in rats after intravenous administration. The measurement indicated the enantioselectivity of the decomposition. Other environmental pollutants, such as racemic sulfoxides, sulfinate esters, phenolic compounds, and cresol and xylene isomers, have also been analyzed by GC using various native and derivatized CDs. Interestingly, the majority of methods apply β-CD or β-CD derivatives; the use of α- and γ-CD and their derivatives is of secondary importance. CDs have been employed, not only for the enantioseparation of environmental pollutants, but also for the enhancement of the extraction efficacy.

Enantiomeric Separation of Other Compounds

The separation characteristics of the mixtures of permethylated-β-CD and heptakis-(2,6-di-*O*-pentyl-3-trifluoroacetyl)-β-CD were investigated using various organic compounds such as analytes. It was established that a synergistic effect occurs between the two CD derivatives, depending on the chemical structures of the analytes and on the ratio of the CD derivatives. Another study found a synergistic effect between the separation capacity of permethylated and perpentylated-β-CD. A gas chromatography–mass spectrometry (GC–MS) method using 2,3-di-*O*-methyl-6-*O*-*tert*-butyl-dimethylsilyl-β-CD was applied to the chiral separation of 3-hydroxyisobutyric- and 3-aminoisobutyric acids. The separation of a set of organic compounds proves the good retention capacity of CD phenyl carbamate derivatives, as illustrated in Fig. 3. The separation ability and complex stability of native α- and β-CDs were compared using a wide variety of analytes, such as dimethylnaphthalenes, α- and β-pinenes, *cis/trans* decalins, anetholes, isosafroles, (+/−)-α-pinenes, and (+/−)-camphenes. The measurements indicated that not only the stability of the inclusion complex but also the stoichiometry exerts a considerable influence on the separation. Two new enantioselective stationary phases were synthesized, i.e., heptakis(2,6-di-*O*-nonyl-3-*O*-trifluoroacetyl)-β-CD and heptakis(2,6-*O*-dodecyl-3-*O*-trifluoroacetyl)-β-CD; their separation characteristics were investigated using amines, alcohols, diols, carboxylic acids, amino acids, epoxides, halohydrocarbons, and ketones. It was proven again that the separation capacity depends on the structures of both CD derivatives and analytes. The same conclusion was drawn from the investigation of mono-ester permethylated β-CD derivatives. The application of β-CD-based chiral stationary phase for the semipreparative separation of *all-trans*-perhydrotriphenylene enantiomers in the milligram range has also been reported.

CONCLUSIONS

The development of new CD-based enantioselective stationary phases was mainly motivated by the different biological activities (both beneficial and toxic) of

Table 3 The capacity factor k and separation factor α of some racemic compounds on the three columns.

Solute	Column No.	Peak order	Temperature (°C)	Capacity	Factor k	Separation factor α
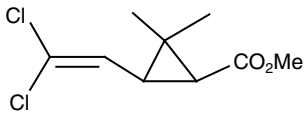 Methyl *cis*-3-(2,2-dichlorovinyl)-2,2-dimethylcyclopropanecarboxylate	1	$1R + 1S$	120	9.23	9.23	1.00
	2	$1R + 1S$	120	8.31	8.31	1.00
	3	$1R + 1S$	120	7.67	7.67	1.00
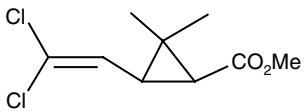 Methyl *trans*-3(2,2-dichlorovinyl)-2,2-dimethylcyclopropanecarboxylate	1	$1R$, $1S$	120	11.11	11.44	1.03
	2	$1R$, $1S$	120	9.74	9.98	1.03
	3	$1R$, $1S$	120	8.79	8.90	1.01
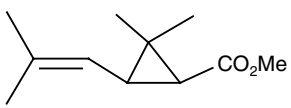 Methyl *cis*-2,2-dimethyl-3(2-methylpropenyl) cyclopropanecarboxylate	1	$1R$, $1S$	80	18.08	18.28	1.01
	2	$1R$, $1S$	80	17.22	17.45	1.01
	3	$1R + 1S$	80	14.33	14.33	1.00
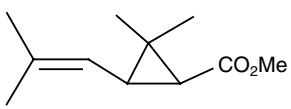 Methyl *trans*-2,2-dimethyl-3-(2-methylpropenyl) cyclopropanecarboxylate	1	$1R$, $1S$	100	8.04	8.59	1.07
	2	$1R$, $1S$	100	7.61	7.93	1.04
	3	$1R$, $1S$	100	6.63	6.74	1.02
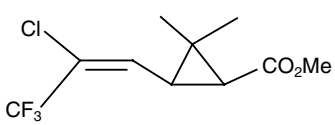 Methyl *cis*-3-(2-chloro-3,3,3-trifluoro propenyl)-2,2-dimethylcyclopropanecarboxylate	1	$1R + 1S$	100	5.73	5.73	1.00
	2	$1R + 1S$	100	5.44	5.44	1.00
	3	$1R + 1S$	100	5.19	5.19	1.00

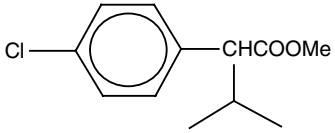

Methyl 2-(4-chlorophenyl)-3-methylbutyrate

1	$S + R$	140	11.59	11.59	1.00
2	$S + R$	140	13.04	13.04	1.00
3	$S + R$	140	21.84	21.84	1.00

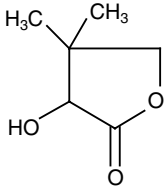

3-Hydroxy-4,4-dimethyl-dihydrofuran-2-one

1	N.D.	130	7.48	7.97	1.07
2	N.D.	120	8.74	9.21	1.05
3	N.D.	120	8.74	9.21	1.05

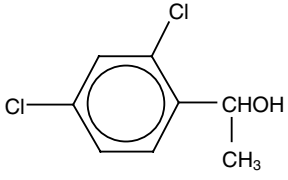

1-(2,4-Dichlorophenyl)ethanol

1	*S, R*	120	46.32	46.58	1.01
2	$S + R$	120	43.80	43.80	1.00
3	$S + R$	120	39.24	39.24	1.00

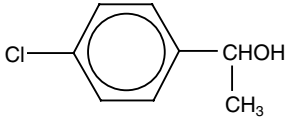

1-(2,4-Chlorophenyl)ethanol

1	$S + R$	120	21.62	21.95	1.02
2	$S + R$	120	18.88	19.07	1.01
3	$S + R$	120	16.87	16.87	1.00

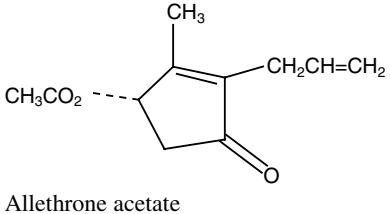

Allethrone acetate

1	*R, S*	120	24.39	24.95	1.02
2	*R, S*	120	22.79	23.25	1.02
3	*R, S*	120	20.26	20.73	1.02

(Continued)

Table 3 The capacity factor k and separation factor α of some racemic compounds on the three columns. *(Continued)*

Solute	Column No.	Peak order	Temperature (°C)	Capacity	Factor k	Separation factor α
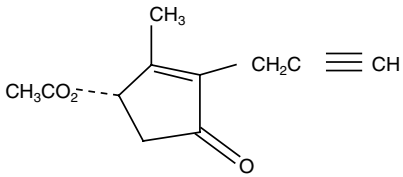 Propargyllone acetate	1	*R, S*	120	39.31	40.09	1.02
	2	*R, S*	120	36.21	36.86	1.02
	3	*R, S*	120	31.13	31.94	1.03
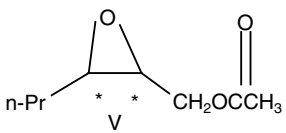 *trans*-2,3-Epoxyhexyl acetate	1	*R, S*	80	17.83	18.05	1.01
	2	$R + S$	80	16.24	16.24	1.00
	3	$R + S$	80	13.29	13.29	1.00
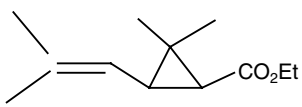 Ethyl *cis*-2,2-dimethyl-3-(2-methylpropenyl) cyclopropanecarboxylate	1	$1R + 1S$	80	25.16	25.16	1.00
	2	$1R + 1S$	80	25.71	25.71	1.00
	3	$1R + 1S$	80	24.09	24.09	1.00
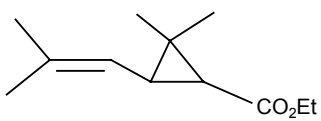 Ethyl *trans*-2,2-dimethyl-3-(2-methylpropenyl) cyclopropane-carboxylate	1	$1R + 1S$	80	28.18	28.60	1.02
	2	$1R + 1S$	80	28.06	28.61	1.02
	3	$1R + 1S$	80	25.73	25.73	1.00
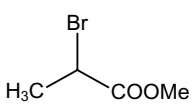 2-Bromopropionic methyl ester	1	N.D.	60	4.75	5.01	1.05
	2	N.D.	70	2.83	2.93	1.03
	3	N.D.	60	4.09	4.31	1.05

R, S or *S, R* indicates that the *R* enantiomer elutes before the *S* enantiomer or the *S* enantiomer elutes before the *R* enantiomer. $R + S$ indicates that the two enantiomers were not resolved.
N.D. indicates that the peak order was not detected.
Source: From Capillary gas chromatographic properties of three new cyclodextrin derivatives with acyl groups in the 6-position of β-cyclodextrin, in Anal. Chim. Acta.[12]

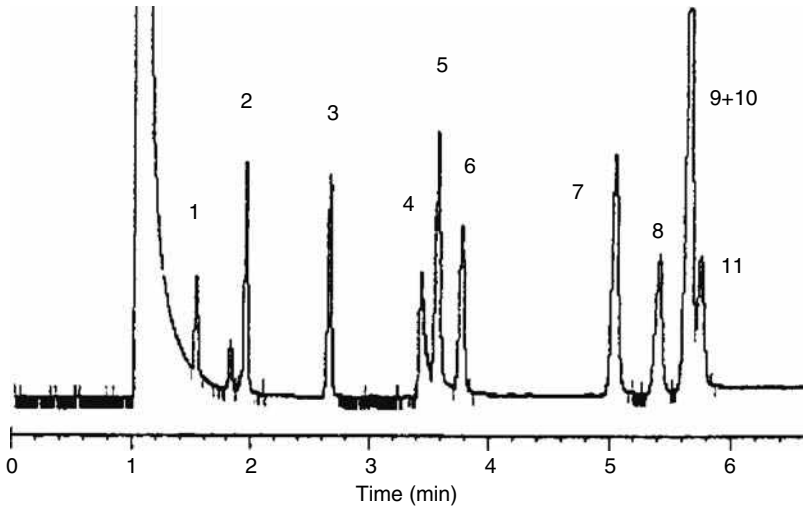

Fig. 3 Chromatogram of the Grob test mixture on Column 1. Temperature programmed from 120°C to 160°C at 4°C/min. Peaks: 1, *n*-decane; 2, *n*-undecane; 3, *n*-dodecane; 4, *n*-octanol; 5, 2,3-butanediol; 6, naphthalene; 7, *n*-tridecane; 8, 2,6-dimethylaniline; 9, *n*-tetradecane; 10, 2,6-dimethylphenol; 11, methyldecanoate.
Source: From Synthesis and properties of new cyclodextrin phenyl carbamates as capillary gas chromatography stationary phases, in Anal. Chim. Acta.[14]

many enantiomeric pairs. It was shown that native and derivatized CDs can be used successfully for the enantiomeric separation of a wide variety of enantiomer pairs. Moreover, native CDs and CD derivatives modify the retention characteristics of the GC stationary phases, resulting in improved separation parameters. The application of CDs may facilitate, not only the solution of various practical separation problems, but also the promotion of a better understanding of the underlying physicochemical principles governing both inclusion complex formation and retention.

REFERENCES

1. Cserháti, T.; Forgács, E. *Cyclodextrins in Chromatography*. The Royal Society of Chemistry: London, 2003; 11–42.
2. Szejtli, J.; Osa, T., Eds.; *Comprehensive Supramolecular Chemistry*. Cyclodextrins. Elsevier Science: New York, 1996; Vol. 3.
3. Schneiderman, E.; Stalcup, A.M. Cyclodextrins: A versatile tool in separation science. J. Chromatogr. B, **2000**, *745*, 83–102.
4. Juvancz, Z.; Szejtli, J. The role of cyclodextrins in chiral selective chromatography. TrAc Trends Anal. Chem. **2002**, *21*, 379–388.
5. Subramanian, G., Ed.; *Chiral Separation Technique: A Practical Approach*, 2nd Ed.; Wiley-VCH Weinheim: Berlin, Germany, 2001.
6. Juvancz, Z.; Seres, G. Chiral selective chromatographic analysis. In *CRC Handbook of Optical Resolutions via Diastereomeric Salt Formation*, Kozma, D., Ed.; CRC Press: Boca Raton, Florida, USA.
7. Fourmentin, S.; Outirite, M.; Blach, P.; Landy, D.; Ponchel, A.; Monflier, E.; Surpateanu, G. Solubilisation of chlorinated solvents by cyclodextrin derivatives. A study by static headspace gas chromatography and molecular modelling. J. Hazard. Mat. **2007**, *141*, 92–97.
8. Lantz, A.W.; Rodriguez, M.A.; Wetterer, S.M.; Armstrong, D.W. Estimation of association constants between oral malodor components and various native and derivatized cyclodextrins. Anal. Chim. Acta **2006**, *557*, 184–190.
9. Yassaa, N.; Williams, J. Analysis of enantiomeric and non-enantiomeric monoterpenes in plant emissions using portable dynamic air sampling/solid-phase microextraction (PDAS–SPME) and chiral gas chromatography/mass spectrometry. Atm. Environ. **2005**, *39*, 4875–4884.
10. Asztemborska, M.; Sybilska, D.; Nowakowski, R.; Perez, G. Chiral recognition ability of α-cyclodextrin with regard to some monoterpenoids under gas–liquid chromatographic conditions. J. Chromatogr. A, **2003**, *1010*, 233–242.
11. Skorka, M.; Asztemborska, M.; Yukowski, J. Thermodynamic studies of complexation and enantiorecognition processes of monoterpenoids by α- and β-cyclodextrin in gas chromatography. J. Chromatogr. A, **2005**, *1078*, 136–143.
12. Chen, G.; Shi, X. Capillary gas chromatographic properties of three new cyclodextrin derivatives with acyl groups in the 6-position of β-cyclodextrin. Anal. Chim. Acta **2003**, *498*, 39–46.
13. Bordajandi, L.; Ramos, L.R.; Gonzalez, M.J. Chiral comprehensive two-dimensional gas chromatography with electron-capture detection applied to the analysis of chiral polychlorinated biphenyls in food samples. J. Chromatogr. A, **2005**, *1078*, 128–135.
14. Shi, X.Y.; Wang, M.; Chen, G.R.; Fu, R.N.; Gu, J.L. Synthesis and properties of new cyclodextrin phenyl carbamates as capillary gas chromatography stationary phases. Anal. Chim. Acta **2001**, *445*, 221–228.

Cyclodextrins in HPLC

Tibor Cserháti
Institute of Chemistry, Chemical Research Center, Hungarian Academy of Sciences, Budapest, Hungary

Abstract
The application of cyclodextrins (CDs) in high-performance liquid chromatography (HPLC) as mobile-phase additives and components of stationary phases is briefly discussed. The advantageous separation characteristics of CDs in various HPLC technologies are demonstrated using pharmaceuticals, environmental pollutants as analytes.

INTRODUCTION

Because of the high separation power, reliability, and reproducibility, various high-performance liquid chromatographic (HPLC) methods have been extensively employed for the separation and quantitative determination of a considerable number of compounds, including pharmaceuticals, food components, environmental pollutants.

Cyclodextrins (CDs) are cyclic oligosaccharides suitable for the formation of inclusion (host–guest) complexes with many organic and inorganic compounds. The formation of inclusion complexes modifies the physicochemical characteristics of the guest molecule, resulting in different interactions with the mobile and stationary phases of the HPLC system, thereby increasing separation capacity. The complex formation influences not only the chromatographic behavior of the guest molecule, but also the solubility, uptake, decomposition rate, bioavailability, and the biological activity. These effects were demonstrated in the case of raloxifene, ketoprofene, an intestinal metabolite of ginseng saponin, pratosin hydrochloride, celecoxib, etc. The character of the various binding forces involved in the complex formation has been vigorously discussed. It has been established that, besides the decisive role of steric correspondence between the guest molecule and the dimensions of the CD cavity, hydrophobic interactive forces occur between the apolar substructures of the guest molecule and the lipophilic inner wall of the CD cavity. Moreover, the dissociable polar molecular parts pointing outside of the cavity readily interact with the polar hydroxyl groups on the outside of the cavity. These electrostatic interactions may enhance the stability of the inclusion complex. The chemistry and physicochemistry of CDs are discussed in detail in this entry. Similar to gas chromatography (GC), the overwhelming majority of the applications of CDs in HPLC deal with the separation of enantiomers. Because of their biological importance, method developments has concentrated mainly on the enantioseparation of synthetic pharmaceuticals, components of herbal medicines and food products, as well as environmental pollutants.

The aim of this work is the collection, short description, and critical survey of modern HPLC technologies applying natural CDs and various CD derivatives, both as components of the stationary phase and as additives in the mobile phase. Earlier results in the application of CDs in HPLC measurements have been previously summarized.[1]

HPLC ANALYSIS OF CYCLODEXTRINS

Because the purity of CD preparations and the character of its impurities exert a considerable influence on the complex-forming capacity, several HPLC methods were developed and successfully applied for the separation of CD mixtures. Thus, the composition of the new methylated β-CD derivatives with a low degree of substitution was investigated by matrix-assisted laser desorption/ionization mass spectrometry and HPLC, using various reversed-phase columns. Analytes were detected by evaporative light scattering detection (ELSD). Gradient elution was started at 5 vol% MeCN in distilled water and finished at 45 vol% MeCN within 40 min. The chromatograms showed good separation capacity of the HPLC system.[2]

New stationary phases were synthesized by binding substituted aromatic groups to silica. Their separation capacity was determined by using various native CDs and CD derivatives. The mobile phase for the gradient elution consisted of a mixture of MeCN, H_2O, and formic acid. CDs were detected with a refractive index detector and ELSD. The measurements indicated that the *N*-(4-nitrophenyl)-carbamide group-bonded silica was the most effective.[3]

The purity of heptakis(2,3,6-tri-*O*-methyl)-β-CD preparations was checked by reversed-phase (RP)-HPLC using the isocratic mobile phase, methanol–water 85/15, v/v. Analytes were detected by atmospheric pressure chemical ionization–mass spectrometry (APCI–MS). The measurements illustrated that the purity of the CD derivatives markedly influences the enantioselectivity of the preparation.

CYCLODEXTRINS AS MOBILE-PHASE ADDITIVES

Although CDs are generally used in the mobile phase as additives to improve separation, their application as extracting agent and sensitivity enhancer of the detection was also reported. Thus, a saturated solution of β-CD was employed for the extraction of five polycyclic aromatic hydrocarbons (PAHs) from environmental samples. The application of β-CD enhanced the efficacy of extraction and increased the sensitivity of fluorescence detection. The capacity of β-CD to enhance the sensitivity of the chemiluminscence detection of tetracyclines (oxytetracycline, tetracycline, and metacycline) has also been established.

Pharmaceuticals

A considerable number of racemic pharmaceuticals were enantioseparated by using native CDs and CD derivatives as mobile-phase additives; the optimal conditions of the enantioseparation were determined. The study of the structural features and thermodynamic parameters influencing the HPLC behavior of tolfenamic acid and ketoprofen inclusion complexes established that the decisive factor of the measurement is the entropy change in the system. The addition of β-CD to the mobile phase reduced the extent of non-specific adsorption of imipravine, desipramine, propranolol, and naproxen and enhanced the sensitivity of electrospray MS detection.[4] Norgesterol enantiomers were separated with a C_8 column using MeCN:phosphate buffer (pH 5.0, 20 m*M*) containing 25 m*M* hydroxypropyl-β-CD (HP-β-CD), 30/70, v/v. It was established that the method can be employed for the study of the stereoselectivity of the skin permeation of norgesterol. The structural isomers of madecassic acid and terminolic acid extracted from the medicinal plant *Centella asiatica* (L) Urban were separated on a C_{18} column. The mobile phase consisted of methanol:water (65/35, v/v) at pH 4. The measurements indicated that the separation efficacy increases with increasing concentration of β-CD in the mobile phase. The dependence of the retention of *S*(-)bupivacaine on the concentration of HP-β-CD in the mobile phase has been applied for the study of their interactions. Measurements were carried out on a C_{18} column using MeCN–phosphate buffer pH 7.4 (10 m*M*), 45/55, v/v. It was stated that the method can be employed for the characterization of inclusion complexes.[5]

Other Analytes

The inclusion complex formation between *trans*-resveratrol and β-CD was investigated using a C_{18} column as stationary phase and methanol–water mixtures as mobile phases. The apparent formation constants were calculated under different chromatographic conditions. The dependence of the formation constant on the concentration of methanol in the mobile phase and on the temperature of the column has been established.[6]

CYCLODEXTRINS IN STATIONARY PHASES

Pharmaceuticals

It was previously reported that a CD solution can be employed as extraction solution. Another study prepared a composite consisting of polydimethylsiloxane and β-CD and was used for stir bar sorptive extraction. It was found that the presence of β-CD increased the adsorption capacity and showed better selectivity toward polar compounds. The technique has been successfully applied for the extraction of estrogens from environmental water, bisphenol A in drinking water, and in leachate of one-off dishware. Oligo-β-CD was prepared and coupled to polyacrylate beads. This new stationary phase separated the isoflavonoid puerarin from other isoflavonoids present in the extract of *Radix puerariae* (root of the plant *Pueraria lobata*).[7] Aromatic carboxylic acid isomers and their derivatives are important metabolites of toxic compounds, drugs, and catecholamines. Their separation was performed using a β-CD-bonded phase with the s-triazine ring in the spacer. The mobile phase consisted of 4 m*M* potassium phosphate buffer and methanol (50:50, v/v). A good separation of toluic, aminobenzoic, nitrobenzoic, and hydroxybenzoic isomers was achieved. The results emphasized the importance of $\pi-\pi$ interaction and hydrogen bonding in the retention. The CD chiral stationary phases have also been employed for the enantioseparation of *cis* and *trans* nucleosides and aromatic analogues of stavudine. A β-CD capillary has been employed for the microextraction of nonsteroidal anti-inflammatory drugs (ketoprofen, fenbufen, ibuprofen) in urine. The good extraction efficacy and stability of the capillary were established. CD-based chiral stationary phases were used for the enantioseparation of furan derivatives. The retention parameters of the analytes are compiled in Table 1. It was concluded, from the data, that steric bulk, hydrogen-bonding ability, and geometry play a decisive role in the formation of inclusion complexes.[8] Similar CD-based chiral stationary phases were applied for the resolution of thioridazine enantiomers. The efficacy of a CD stationary phase to separate diastereomeric thymine derivatives has also been demonstrated, as shown in Fig. 1.[9]

Miscellaneous Analytes

Besides the separation of pharmaceuticals, CD-containing stationary phases have found application in the analysis of foods and food products, environmental pollutants, and other organic compounds. The baseline separation of lactobionic acid, sorbitol, lactose, and fructose on a β-CD phase was achieved using MeCN–sodium dihydrogen phosphate 10 m*M* (70/30, v/v) as isocratic mobile phase. Racemic 2,4-

Table 1 Retention factor of the first peak (k_1), enantioselectivity (α), and enantioresolution (R_S) of all chiral furans on the cyclobond RSP, DM, and AC CSPs.

Number	Structure	CSP	k_1	α	R_s	Mobile phase (v/v)
1	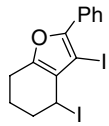	RSP	8.52	1.05	0.3	CH_3OH/H_2O = 50/50
		DM	7.59			CH_3OH/H_2O = 50/50
		AC	8.38			CH_3OH/H_2O = 50/50
2	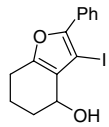	RSP	8.58	1.10	1.2	CH_3OH/H_2O = 45/55
		DM	7.46	1.23	1.9	CH_3OH/H_2O = 25/75
		AC	4.57			CH_3OH/H_2O = 40/60
3	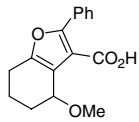	RSP	3.48			CH_3OH/H_2O = 40/60
		DM	2.03			CH_3OH/H_2O = 40/60
		AC	8.15	1.30	0.8	CH_3OH/H_2O = 60/40
4	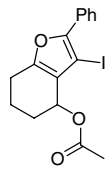	RSP	10.38	1.05	0.5	CH_3OH/H_2O = 45/55
		DM	5.13	1.13	1.2	CH_3OH/H_2O = 40/60
		AC	5.04	1.13	0.8	CH_3OH/H_2O = 40/60
5	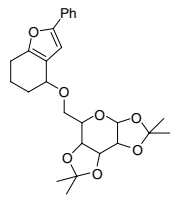	RSP	8.89			CH_3OH/H_2O = 50/50
		DM	2.12			CH_3OH/H_2O = 40/60
		AC	2.55			CH_3OH/H_2O = 50/50
6	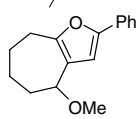	RSP	3.35			CH_3OH/H_2O = 60/40
		DM	2.72	1.48	2.6	CH_3OH/H_2O = 40/60
		AC	2.79			CH_3OH/H_2O = 50/50
7	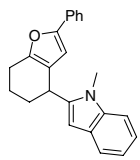	RSP	5.43	1.17	1.7	CH_3OH/H_2O = 60/40
		DM	3.94	1.35	1.6	CH_3OH/H_2O = 50/50
		AC	5.52			CH_3OH/H_2O = 50/50
8	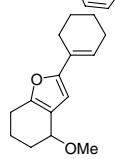	RSP	7.14			CH_3OH/H_2O = 60/40
		DM	4.08	1.29	1.9	CH_3OH/H_2O = 40/60
		AC	3.69			CH_3OH/H_2O = 50/50
9	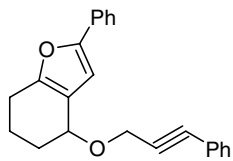	RSP	4.31	1.06	0.6	CH_3OH/H_2O = 60/40
		DM	8.75	1.10	0.4	CH_3OH/H_2O = 40/60
		AC	9.33			CH_3OH/H_2O = 50/50
10	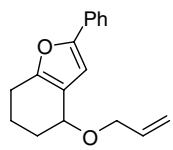	RSP	2.24			CH_3OH/H_2O = 60/40
		DM	2.52	1.32	2.0	CH_3OH/H_2O = 40/60
		AC	2.57			CH_3OH/H_2O = 50/50
11	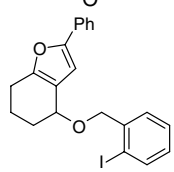	RSP	12.79			CH_3OH/H_2O = 50/50
		DM	6.96	1.26	1.0	CH_3OH/H_2O = 40/60
		AC	5.98			CH_3OH/H_2O = 50/50

(Continued)

Table 1 Retention factor of the first peak (k_1), enantioselectivity (α), and enantioresolution (R_S) of all chiral furans on the cyclobond RSP, DM, and AC CSPs. *(Continued)*

Number	Structure	CSP	k_1	α	R_s	Mobile phase (v/v)
12	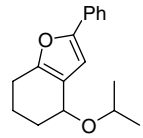	RSP	4.76	1.03	0.3	CH_3OH/H_2O = 50/50
		DM	1.57	1.34	1.7	CH_3OH/H_2O = 40/60
		AC	4.95	1.08	0.8	CH_3OH/H_2O = 40/60
13	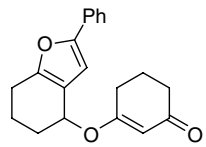	RSP	2.77			CH_3OH/H_2O = 60/40
		DM	4.06			CH_3OH/H_2O = 40/60
		AC	7.81	1.13	1.4	CH_3OH/H_2O = 40/60
14	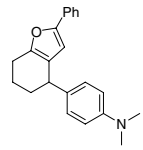	RSP	8.97	1.37	2.9	CH_3OH/H_2O = 60/40
		DM	6.28			CH_3OH/H_2O = 50/50
		AC	6.94	1.36	2.4	CH_3OH/H_2O = 50/50
15	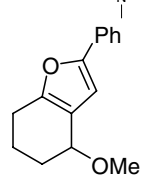	RSP	4.40	1.03	0.3	CH_3OH/H_2O = 50/50
		DM	9.57	1.28	1.7	CH_3OH/H_2O = 40/60
		AC	5.76			CH_3OH/H_2O = 40/60
16	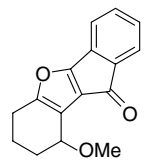	RSP	7.64	1.13	1.2	CH_3OH/H_2O = 40/60
		DM	1.66			CH_3OH/H_2O = 40/60
		AC	3.32			CH_3OH/H_2O = 40/60
17	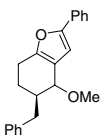	RSP	8.69	1.11	1.2	CH_3OH/H_2O = 60/40
		DM	12.60	1.10	0.6	CH_3OH/H_2O = 40/60
		AC	11.40	1.17	1.6	CH_3OH/H_2O = 40/60
18	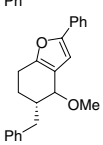	RSP	7.00			CH_3OH/H_2O = 60/40
		DM	6.95	1.55	3.1	CH_3OH/H_2O = 40/60
		AC	10.83	1.09	0.9	CH_3OH/H_2O = 40/60
19	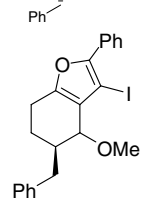	RSP	6.02	1.15	1.5	CH_3OH/H_2O = 60/40
		DM	4.50	1.27	1.2	CH_3OH/H_2O = 50/50
		AC	9.88	1.31	1.6	CH_3OH/H_2O = 40/60
20	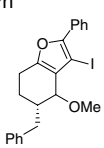	RSP	4.00			CH_3OH/H_2O = 60/40
		DM	7.37	1.22	1.0	CH_3OH/H_2O = 40/60
		AC	7.75			CH_3OH/H_2O = 40/60
21	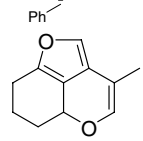	RSP	3.13	1.17	1.5	CH_3OH/H_2O = 60/40
		DM	4.64	1.34	2.8	CH_3OH/H_2O = 40/60
		AC	5.33	1.23	2.2	CH_3OH/H_2O = 40/60
22	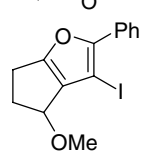	RSP	10.99	1.09	1.1	CH_3OH/H_2O = 45/55
		DM	4.09	1.28	1.7	CH_3OH/H_2O = 40/60
		AC	6.59			CH_3OH/H_2O = 40/60

(Continued)

CPC – Diode

Table 1 Retention factor of the first peak (k_1), enantioselectivity (α), and enantioresolution (R_S) of all chiral furans on the cyclobond RSP, DM, and AC CSPs. *(Continued)*

Number	Structure	CSP	k_1	α	R_s	Mobile phase (v/v)
23	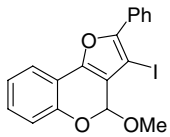	RSP	14.24	1.12	1.5	CH_3OH/H_2O = 45/55
		DM	9.57			CH_3OH/H_2O = 35/65
		AC	6.28			CH_3OH/H_2O = 40/60
24	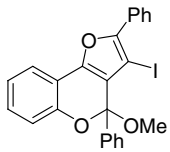	RSP	7.52			CH_3OH/H_2O = 50/50
		DM	8.26	1.11	0.6	CH_3OH/H_2O = 40/60
		AC	5.25			CH_3OH/H_2O = 50/50
25	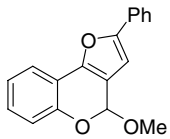	RSP	5.43	1.06	0.6	CH_3OH/H_2O = 50/50
		DM	6.99	1.15	1.2	CH_3OH/H_2O = 35/65
		AC	5.59	1.04	0.3	CH_3OH/H_2O = 40/60
26	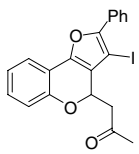	RSP	9.05	1.11	1.1	CH_3OH/H_2O = 45/55
		DM	3.71			CH_3OH/H_2O = 40/60
		AC	3.04			CH_3OH/H_2O = 50/50
27	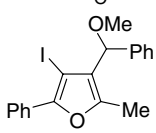	RSP	7.34			CH_3OH/H_2O = 50/50
		DM	4.83			CH_3OH/H_2O = 40/60
		AC	5.84			CH_3OH/H_2O = 40/60
28	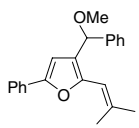	RSP	3.43			CH_3OH/H_2O = 50/50
		DM	2.28			CH_3OH/H_2O = 50/50
		AC	2.88			CH_3OH/H_2O = 50/50
29	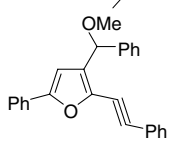	RSP	4.24	1.08	0.7	CH_3OH/H_2O = 60/40
		DM	3.86			CH_3OH/H_2O = 50/50
		AC	8.97			CH_3OH/H_2O = 50/50
30	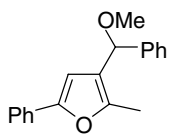	RSP	4.95	1.05	0.6	CH_3OH/H_2O = 50/50
		DM	5.78	1.10	0.8	CH_3OH/H_2O = 40/60
		AC	5.71	1.11	0.7	CH_3OH/H_2O = 40/60

[a]Separation of diastereomers.

Source: From Separation of chiral furan derivatives by liquid chromatography using cyclodextrin-based chiral stationary phases, in J. Chromatogr. A.[8]

dinitrophenyl amino acids were also separated on a β-CD-hexamethylene diisocyanate copolymer-coated zirconia stationary phase. Interestingly, a β-CD stationary phase has also been the normal-phase separation mode for the determination of polycyclic aromatic compounds. The retention factors measured on various stationary phases are compiled in Table 2. The data demonstrated that the best separation was achieved with the β-CD stationary phase.[10] Two novel β-CD derivatives were synthesized (mono-2^A-deoxyperphenylcarbamoylated β-CD and mono-2^A-azido-2^A-deoxyperacetylated β-CD) and used for the separation of a wide variety of analytes. The parameters of enantioseparation measured under reversed-phase conditions are listed in Table 3. The measurements proved again that the efficacy of enantioseparation depends on both the structure of the stationary phase and the analyte.[11] A novel stationary phase was prepared by immobilizing poly-β-CD on a silica surface. It was established that the retention behavior of monomethoxypoly (ethylene glycols) is governed by the hydrophobic interactions between the cavity of the β-CD and the lipophilic substructures of the analytes. A perphenylcarbamoylated β-CD derivative was bonded to silica particles and the enantioselectivity of this novel chiral stationary phase was tested by using racemic α-amidophosphonates as model analytes. It was assumed that hydrophobic interaction, steric effects, and π–π interaction are involved in the retention behavior.

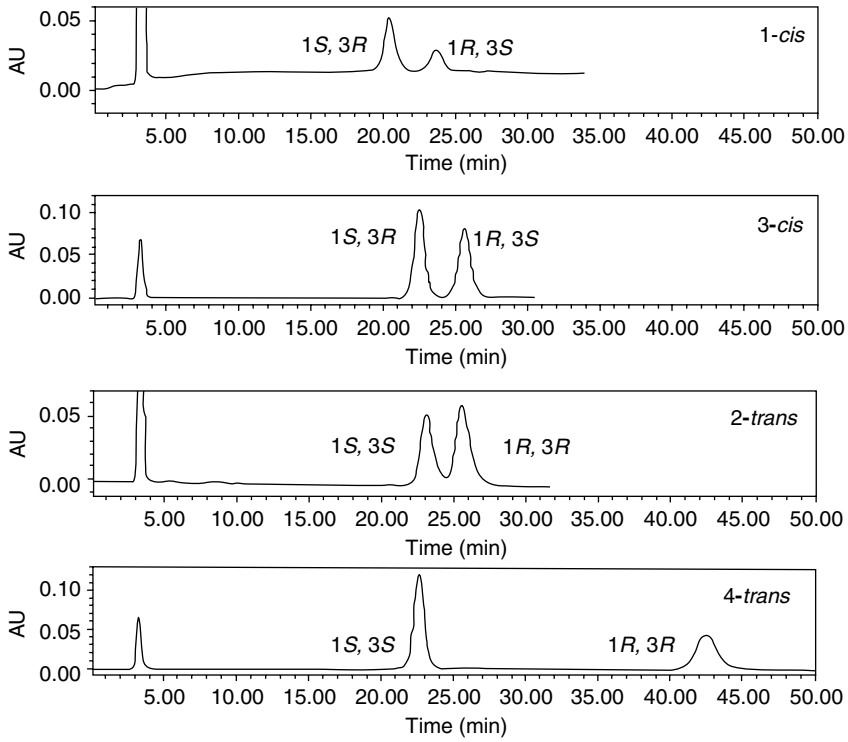

Fig. 1 Typical stacked chromatograms of the diastereomeric thymine derivatives obtained on Chiralpak AD, eluent: *n*-hexane/ethanol 80:20, 1 ml/min, 303 K, and detection at 200 nm.
Source: From Enantioseparation of *cis*- and *trans* nucleosides, aromatic analogues of stavudine, by capillary electrophoresis and high-performance liquid chromatography, in J. Chromatogr. A.[9]

Table 2 Retention factors for some polycyclic aromatic sulfur heterocycles on a β-cyclodextrin, an aminopropano, and a TCP stationary phase with cyclohexane as eluent.

	β-CD	AP	TCP
Two aromatic rings			
Benzothiophene	2.08	0.47	0.34
2-Methylbenzothiophene	1.68	0.50	0.60
3-Methylbenzothiophene	3.42	0.49	0.48
5-Methylbenzothiophene	1.60	0.52	0.52
6-Methylbenzothiophene	1.44	0.48	0.72
2,5-Dimethylbenzothiophene	1.49	0.53	0.96
2,6-Dimethylbenzothiophene	1.49	0.56	0.99
1,2,3,4-Tetrahydrodibenzothiophene	1.28	0.42	0.94
2-Dodecylbenzothiophene	0.48	0.27	0.34
Cholestano(2,3-*b*)-5,6,7,8-tetrahydronaphtho(2,1-*d*)thiophene	1.00	0.25	0.87
Three aromatic rings			
Dibenzothiophene	3.82	0.89	1.00
2-Methyldibenzothiophene	3.42	0.87	1.76
4-Methyldibenzothiophene	2.98	0.82	2.13
2,4-Dimethyldibenzothiophene	2.38	0.69	3.55
4,6-Dimethyldibenzothiophene	2.88	0.76	4.02
1,3,7-Trimethyldibenzothiophene	3.01	0.81	3.96
1,4,6-Trimethyldibenzothiophene	2.77	0.72	5.36
1,4,7-Trimethyldibenzothiophene	3.07	0.78	5.55
1,4,8-Trimethyldibenzothiophene	3.33	0.78	5.56

(Continued)

Table 2 Retention factors for some polycyclic aromatic sulfur heterocycles on a β-cyclodextrin, an aminopropano, and a TCP stationary phase with cyclohexane as eluent. *(Continued)*

	β-CD	AP	TCP
2,4,6-Trimethyldibenzothiophene	2.80	0.76	6.19
3,4,7-Trimethyldibenzothiophene	2.76	0.80	3.82
2,4-Dimethyl-6-ethyldibenzothiophene	2.44	0.69	3.97
2,3,4,7-Tetramethyldibenzothiophene	1.62	0.52	3.89
2,3,7,8-Tetramethyldibenzothiophene	3.65	0.90	5.84
2,4,6,8-Tetramethyldibenzothiophene	3.02	0.71	9.99
2-Octyldibenzothiophene	1.58	0.46	1.00
4-Octyldibenzothiophene	1.86	0.61	1.06
Naphtho(2,3-*b*)thiophene	4.32	1.17	1.76
2-(1-Naphthylethano)thiophene	3.37	1.08	0.55
3-[(4-Butylphenyl)ethano]benzo(*b*)thiophene	2.59	0.82	0.38
More than three aromatic rings			
Phenanthro(4,5-*bcd*)thiophene	5.81	1.08	2.39
Benzo(*b*)naphtho(1,2-*d*)thiophene	7.01	1.41	3.29
2-(1-Naphthalenyl)benzothiophene	4.41	1.15	0.63

For the three stationary phases here, the order of selectivity toward parent aromatic rings is in the order TCP > β-CD > AP. This might point to TCP as the more favorable phase, but retention on TCP is more sensitive to the alkylation than the other phases.

Source: From β-Cyclodextrin as a stationary phase for the group separation of polycyclic aromatic compounds in normal-phase liquid chromatography, in J. Chromatogr. A.[10]

Table 3 Enantioseparation properties between CSP 5a and SINU-PC under reversed-phase conditions.

	k'_1	k'_2	α	R_s	Columns	Conditions
Weak acids and non-protolytic racemates						
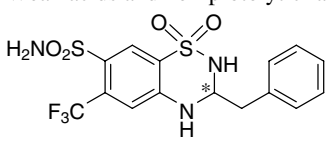	5.22	12.56	2.41	6.26	CSP 5a	III
1. Bendroflumethiazide						
	6.15	10.69	1.74	4.53	SINU-PC	
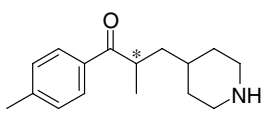	2.13	3.32	1.56	2.77	CSP 5a	I
2. Tolperisone						
	9.03	11.70	1.31	0.98	SINU-PC	
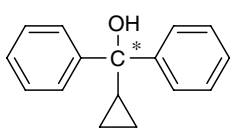	1.44	1.63	1.13	0.63	CSP 5a	I
3. Ancymidol						
	6.56	7.41	1.13	0.90	SINU-PC	
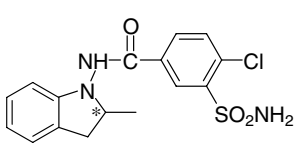	3.01	3.50	1.16	0.94	CSP 5a	I
4. Indapamide						

(Continued)

Table 3 Enantioseparation properties between CSP 5a and SINU-PC under reversed-phase conditions. *(Continued)*

	k'_1	k'_2	α	R_s	Columns	Conditions
	10.20	11.60	1.14	0.85	SINU-PC	
Antihistamines and amines						
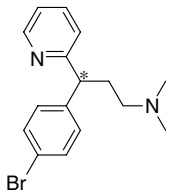	0.38	0.49	1.29	0.64	CSP 5a	I
5. Brompheniramine						
	2.06	2.43	1.18	0.84	SINU-PC	
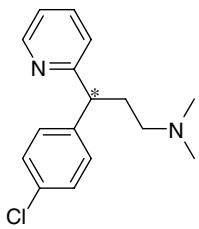	0.26	0.33	1.27	0.36	CSP 5a	I
6. Chlorpheniramine						
	1.54	1.80	1.17	0.74	SINU-PC	
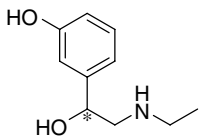	0.35	—	—	—	CSP 5a	
7. Etilefrin						
	1.00	1.51	1.51	0.81	SINU-PC	
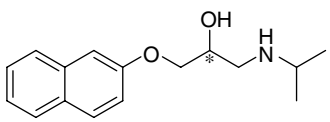	0.58	1.16	2.01	2.09	CSP 5a	
8. Propranolol						
	3.00	6.19	2.06	2.53	SINU-PC	
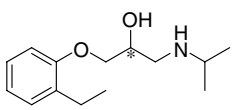	0.23	0.46	2.02	1.25	CSP 5a	
9. Alprenolol						
	1.54	2.79	1.81	2.63		
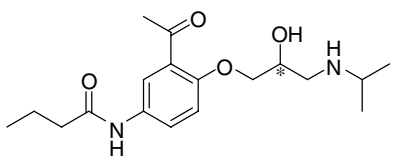	0.03	0.14	1.10	0.82	CSP 5a	I
10. Acebutolol						
	0.75	1.00	1.33	1.06	SINU-PC	
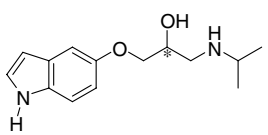	0.04	0.10	1.05	0.49	CSP 5a	I
11. Pindolol						
	0.66	0.88	1.33	0.88	SINU-PC	
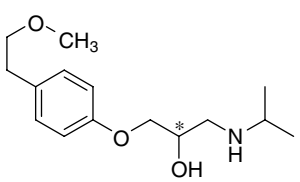	0.20	0.29	1.45	0.42	CSP 5a	I
12. Metoprolol						

(Continued)

CPC – Diode

Table 3 Enantioseparation properties between CSP 5a and SINU-PC under reversed-phase conditions. *(Continued)*

	k'_1	k'_2	α	R_s	Columns	Conditions
	1.33	—	—	—	SINU-PC	
Alkaloids						
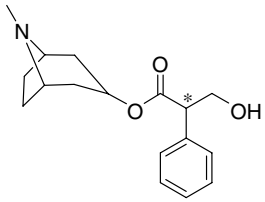	0.33	1.50	4.55	2.94	CSP 5a	I
13. Atropine						
	0.55	2.80	5.12	3.87	SINU-PC	
Flavanone compounds						
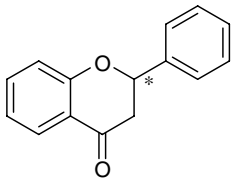	1.60	2.68	1.68	3.89	CSP 5a	II
14. Flavanone						
	8.78	14.88	1.70	4.16	SINU-PC	
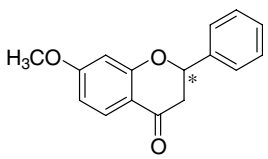	3.01	5.13	1.70	3.71	CSP 5a	II
15. 7-Methoxyflavanone						
	15.76	26.45	1.68	3.66	SINU-PC	
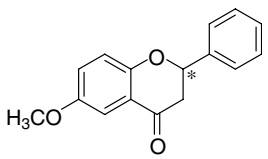	3.54	5.30	1.50	3.67	CSP 5a	II
16. 6-Methoxyflavanone						
	18.59	26.13	1.41	2.58	SINU-PC	
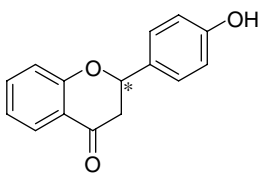	1.24	1.95	1.58	2.72	CSP 5a	II
17. 4′-Hydroxyflavanone						
	6.11	10.36	1.70	3.74	SINU-PC	
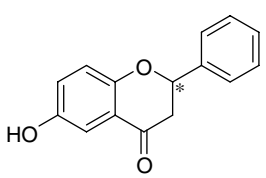	1.32	1.88	1.42	2.26	CSP 5a	II
18. 6-Hydroxyflavanone						
	5.81	7.88	1.36	2.13	SINU-PC	
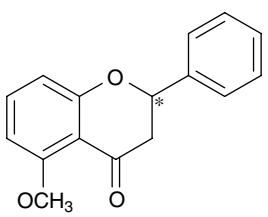	1.27	1.60	1.26	1.97	CSP 5a	II
19. 5-Methoxyflavanone						

(Continued)

Table 3 Enantioseparation properties between CSP 5a and SINU-PC under reversed-phase conditions. *(Continued)*

	k'_1	k'_2	α	R_s	Columns	Conditions
	6.32	7.99	1.26	1.86	SINU-PC	
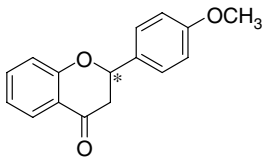	1.42	2.08	1.46	1.74	CSP 5a	II
20. 4′-Methoxyflavanone						
	5.28	8.03	1.52	2.35	SINU-PC	
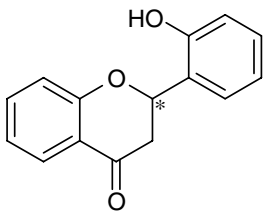	1.08	1.44	1.33	1.07	CSP 5a	II
21. 2′-Hydroxyflavanone						
	1.32	1.92	1.45	1.65	SINU-PC	

HPLC conditions: flow rate = 1.000 ml/min, detection = 254 nm, mobile phases = (I) buffer (1% TEA, pH 5.11)/methanol = 70/30; (II) water/methanol = 50/50, (III) buffer (1% TEA, pH 5.11)/acetonitrile = 70/30. (–) denotes no separation.

Source: From Synthesis and application of mono-2^A-deoxyperphenylcarbamoylated β-cyclodextrin and mono-2^A-azido-2^A-deoxyperacetylated β-cyclodextrin as chiral stationary phases for high-performance liquid chromatography, in J. Chromatogr. A.[11]

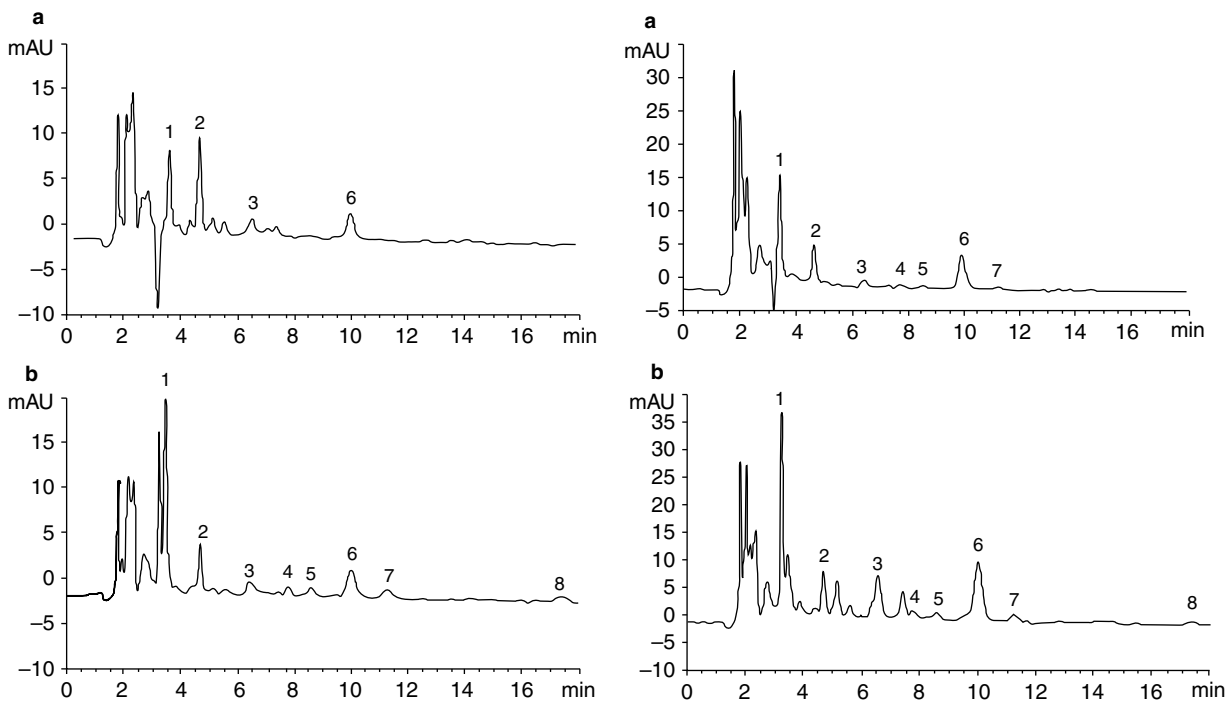

Fig. 2 *Left*: HPLC–UV chromatograms of BFRs obtained by stir bar sorptive extraction (SBSE) in (a) the original dust sample; (b) the spiked dust sample (250 μg/L BHT and 50 μg/L for each BFR were added). 1, tetrabromobisphenol (T BBPA); 2, BHT; 3, BDE-28; 4, BDE-47; 5, BDE-66; 6, BDE-100; 7, BDE-99; 8, BDE-153. *Right*: HPLC–UV chromatograms of BFRs obtained by SBSE in (a) the original dust sample; (b) the spiked dust sample (250 μg/L BHT and 45 μg/L for each BFR were added). 1, T BBPA; 2, BHT; 3, BDE-28; 4, BDE-47; 5, BDE-66; 6, BDE-100; 7, BDE-99; 8, BDE-153. BFR, brominated flame retardant; BDE-28, 2,4,4′-tribromodiphenyl ether; BDE-47, 2,2′,4,4′-tetrabromodiphenylether; BDE-66, 2,3,4,4′-tetrabromodiphenyl ether; BDE-99, 2,2′,4,4′,5-pentabromodiphenylether; BDE-100, 2,2′,4,4′,6-pentabromobromodiphenyl ether; BDE-153, 2,2′,4,4′,5,5′-hexabromodiphenylether; BHT, 2,6-di-(1,1-dimethylethyl)-4-methylphenole.

Source: From Novel combined stir bar sorptive extraction coupled with ultrasonic assisted extraction for the determination of brominated flame retardants in environmental samples using high performance liquid chromatography, in J. Chromatogr. A.[12]

A CD-modified extraction method was successfully applied for the analysis of brominated flame retardants, as illustrated in Fig. 2.[12] The enantioseparation of α-hydroxy-3-phenoxybenzeneacetonitrile and its *n*-butyl esters has also been reported and visualized in Fig. 3.[13]

CONCLUSIONS

Although native CDs show acceptable enantioselectivity toward a large number of enantiomer pairs in many HPLC systems, their separation capacity is not always enough for the baseline separation of enantiomers, which is the prerequisite for reliable quantitative analysis. To overcome this difficulty, a considerable number of CD derivatives were synthesized and their separation capacities were tested using enantiomer pairs that are not well separated by native CDs. Unfortunately, the theoretical basis of the inclusion formation of new CD derivatives and the effect of new inclusion complexes on the enantioseparation of a given isomer pair are not well understood. This type of theoretical investigation is urgently needed for further development of the application of CDs and CD derivatives in HPLC.

REFERENCES

1. Cserháti, T.; Forgács, E. *Cyclodextrins in Chromatography*; The Royal Society of Chemistry: Cambridge, 2003; 51–78.
2. Jacquet, R.; Favetta, P.; Elfakir, C.; Lafosse, M. Characterization of a new methylated β-cyclodextrin with a low degree of substitution by matrix-assisted laser desorption mass spectrometry and liquid chromatography using evaporative light scattering detection. J. Chromatogr. A, **2005**, *1083*, 106–112.
3. Szemán, J.; Csabai, K.; Kékesi, K.;, Szente, L.; Varga, G. Novel stationary phases for high performance liquid chromatography analysis of cyclodextrin derivatives. J. Chromatogr. A, **2006**, *1116*, 76–82,
4. Sun, L.; Stenken, J.A. The effect of β-cyclodextrin on liquid chromatography/electrospray-mass spectrometry analysis of hydrophobic drug molecules. J. Chromatogr. A, **2007**, *1161*, 261–268.
5. Moraes, C.M.; Abrami, P.; de Paula, E.; Braga, A.F.A.; Fraceto, L.F. Study of the interaction between S(-) bupivacaine and 2-hydroxypropyl-β-cyclodextrin. Intl. J. Pharmaceut. **2007**, *331*, 99–106.
6. López-Nicolás, J.M.; Nunez-Delicado, E.; Pérez-López, A.J.; Barrachina, A.C.; Cuadra-Crespo, P. Determination of stoichiometric coefficients and apparent formation constants for β-cyclodextrin complexes of *trans*-resveratrol using reversed-phase liquid chromatography. J. Chromatogr. A, **2006**, *1135*, 158–165.
7. Yang, L.; Zhu, Y.; Tan, T.; Janson, J.-C. Coupling oligo-β-cyclodextrin on polyacrylate beads media for separation of puerarin. Proc. Iochem. **2007**, *42*, 1075–1083.
8. Han, X.; Yao, T.; Liu, Y.; Larock, R.C.; Armstrong, D.W. Separation of chiral furan derivatives by liquid chromatography using cyclodextrin-based chiral stationary phases. J. Chromatogr. A, **2005**, *1063*, 111–120.
9. Lipka, E.; Len, C.; Rabiller, C.; Bonte, J.-P.; Vaccher, C. Enantioseparation of *cis* and *trans* nucleosides, aromatic analogues of stavudine, by capillary electrophoresis and high-performance liquid chromatography. J. Chromatogr. A, **2006**, *1132*, 141–147.
10. Panda, S.K.; Schrader, W.; Andersson, J.T. β-Cyclodextrin as a stationary phase for the group separation of polycyclic aromatic compounds in normal-phase liquid chromatography. J. Chromatogr. A, **2006**, *1122*, 88–96.
11. Poon, Y.-F.; Muderawan, I.W.; Ng, S.-C. Synthesis and application of mono-2^A-deoxyperphenylcarbamoylated β-cyclodextrin and mono-2^A-azido-2^A-deoxyperacetylated β-cyclodextrin as chiral stationary phases for high-performance liquid chromatography. J. Chromatogr. A, **2006**, *1101*, 185–197.
12. Yu, C.; Hu, B. Novel combined stir bar sorptive extraction coupled with ultrasonic assisted extraction for the determination of brominated flame retardants in environmental samples using high performance liquid chromatography. J. Chromatogr. A, **2007**, *1160*, 71–80.
13. Fadnavis, N.W.; Babu, R.L.; Sheelu, G.; Deshpande, A. Determination of enantiomeric excess of α-hydroxy-3-phenoxybenyeneacetonitrile and its *n*-butyl ester by chiral high-performance liquid chromatography. J. Chromatogr. A, **2000**, *893*, 189–193.

Dead Point: Volume or Time

Raymond P.W. Scott
Scientific Detectors Ltd., Banbury, Oxfordshire, U.K.

INTRODUCTION

The *injection point* on a chromatogram is that position where the sample is injected. The *dead point* on a chromatogram is the position of the peak maximum of a completely unretained solute. The different attributes of the chromatogram are shown in Fig. 1. The *dead time* is the elapsed time between the injection point and the dead point. The volume that passes through the column between the injection point and the dead point is called the *dead volume*.

DISCUSSION

If the mobile phase is *incompressible*, as in liquid chromatography (LC), the *dead volume* (as so far defined) will be the simple product of the *exit* flow rate and the dead time. However, in LC, where the stationary phase is a porous matrix, the dead volume can be a very ambiguous column property and requires closer inspection and a tighter definition.

If the mobile phase is compressible, the simple product of dead time and flow rate will be incorrect, and the dead volume must be taken as the product of the dead time and the *mean* flow rate. The dead volume has been shown to be given by[1]

$$V_0 = V_0' \frac{3}{2}\left(\frac{\gamma^2 - 1}{\gamma^3 - 1}\right) = Q_0 t_0 \frac{3}{2}\left(\frac{\gamma^2 - 1}{\gamma^3 - 1}\right)$$

where the symbols have the meaning defined in Fig. 1, and V_0' is the dead volume measured at the column exit and γ is the inlet/outlet pressure ratio.

The dead volume will not simply be the total volume of mobile phase in the column system (V_m) but will include extra-column dead volumes (V_E) comprising volumes involved in the sample valve, connecting tubes, and detector. If these volumes are significant, then they must be taken into account when measuring the dead volume.

There are two types of dead volume (i.e., the *dynamic* dead volume and the *thermodynamic* dead volume.[2]) The dynamic dead volume is the volume of the *moving phase* in the column and is used in kinetic studies to calculate mobile-phase velocities. In gas chromatography, both the dynamic dead volume and the thermodynamic dead volume can be taken as the difference between the dead volume and the extra-column volume. In LC, however, where a porous packing is involved, some of the mobile phase will be in pores (the *pore volume*) and some between the particles (the *interstitial volume*). In addition, some of the mobile phase in the interstitial volume which is close to the points of contact of the particles will also be stationary. The dynamic dead volume (i.e., the volume of the moving phase) is best taken as the retention volume of a relatively large inorganic salt such as potassiun nitroprusside. This salt will be excluded from the pores of the packing by ionic exclusion and will only explore the moving volumes of the mobile phase.[2] The thermodynamic dead volume will include all the mobile phase that is available to

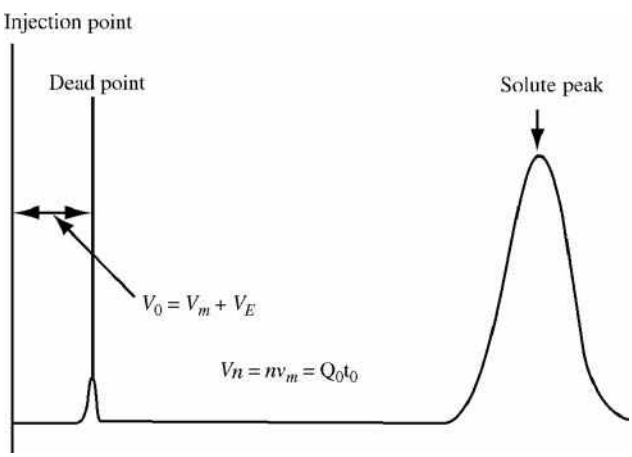

Fig. 1 Diagram depicting the dead point, dead volume, and dead time of a chromatogram. If the mobile phase is not compressible, then V_0 is the total volume passed through the column between the point of injection and the peak maximum of a completely unretained peak, V_m is the total volume of the mobile phase in the column, V_E is the extra column volume of the mobile phase, v_m is the volume of the mobile phase per theoretical plate, t_0 is the time elapsed between the time of injection and the retention time of a completely unretained peak, n is the number of theoretical plates in the column, and Q is the column flow rate measured at the exit.

the solute that is under thermodynamic examination. It is best measured as the retention volume of a solvent sample of very similar type to that of the mobile phase and of small molecular weight. If a binary solvent mixture is used (which is the more common situation), then one component of the mobile phase, in pure form, can be used to measure the thermodynamic dead volume. Careful consideration must be given to the measurement of the column dead volume when determining thermodynamic data by LC using columns packed with porous materials.

REFERENCES

1. Scott, R.P.W. *Introduction to Analytical Gas Chromatography*; Marcel Dekker, Inc.: New York, 1998; 77.
2. Alhedai, A.; Martire, D.E.; Scott, R.P.W. Column dead volume in liquid chromatography. Analyst **1989**, *114* (8), 869.

BIBLIOGRAPHY

1. Scott, R.P.W. *Liquid Chromatography Column Theory*; John Wiley & Sons: Chichester, 1992; 19.
2. Scott, R.P.W. *Techniques and Practice of Chromatography*; Marcel Dekker, Inc.: New York, 1996.

Dendrimers and Hyperbranched Polymers: GPC/SEC Analysis

Nikolay Vladimirov
Research Center, Hercules Inc., Wilmington, Delaware, U.S.A.

INTRODUCTION

Dendrimers and hyperbranched polymers are globular macromolecules having a highly branched structure, in which all bonds converge to a focal point or core, and a multiplicity of reactive chain ends. Because of the obvious similarity of their building blocks, many assume that the properties of these two families of dendritic macromolecules are almost identical and that the terms "dendrimer" and "hyperbranched polymer" can be used interchangeably. These assumptions are incorrect because only dendrimers have a precise end-group multiplicity and functionality. Furthermore, they exhibit properties totally unlike that of other families of macromolecules.

HISTORICAL BACKGROUND

Highly branched and generally irregular dendritic structures have been known for some time, being found, for example, in polysaccharides, such as amylopectin, glycogen, and some other biopolymers. In the area of synthetic structures, Flory discussed, as early as 1952, the theoretical growth of highly branched polymers obtained by the polycondensation of AB_x structures in which x is at least equal to 2. Such highly branched structures are now known as "hyperbranched polymers."

Today, regular dendrimers can only be prepared using rather tedious, multistep syntheses that require intermediate purifications. In contrast, hyperbranched polymers are easily obtained using a variety of one-pot procedures, some of which mimic, but do not truly achieve, regular dendritic growth.[1] The presence of such a large number of atoms within each dendritic or hyperbranched macromolecule permits an enormous variety of conformations with different shapes and sizes. The distribution of molecular weights focuses on the polydispersity index (M_w/M_n), and the requirements for gelation (or avoidance of gelation) when multimodal monomers are incorporated into the macromolecule. Each of these topics are discussed in Newcome's monograph.[2] Lists of reviews between 1986 and 1996 and Advances series are also given.

Buchard[3] outlined some properties of hyperbranched chains. The dilute solution properties of branched macromolecules are governed by the higher segment density found with linear chains. The dimensions appear to be shrunk when compared with linear chains of the same molar mass and composition. It is shown that the apparent shrinking has an influence also on the intrinsic viscosity and the second virial coefficient. The broad molecular-weight distribution (MWD) has a strong influence on these shrinking factors, which can be defined and used for quantitative determination of the branching density (i.e., the number of branching points in a macromolecule). Here, the branching density can be determined only by size-exclusion chromatography (SEC) in online combination with light-scattering and viscosity detectors. The technique and possibilities are discussed in detail.

DISCUSSION

Adendritic structure generally gives rise to better solubility than the corresponding linear analog. For example, aromatic polyamide dendrimers and hyperbranched polymers are soluble in amide-type solvents and even in tetrahydrofuran. Gel-permeation chromatography (GPC) was performed on a Jasco high-performance liquid chromatography (HPLC) 880PU fitted with polystyrene–divinylbenzene columns (two Shodex KD806M and KD802) and a Shodex RI-71 refractive index detector in DMF containing 0.01 mol/L of lithium bromide as an eluent. Absolute molecular weights (M_w) of 74,600, 47,800, and 36,800 were determined by light scattering using a MiniDawn apparatus (Wyatt Technology Co.) and a Shimadzu RID-6A refractive index detector. A specific refractive index increment (dn/dc) of the polymer in DMF at 690 nm was measured to be 0.216 ml/g.[4]

Standards commonly employed[5] to calibrate SEC columns do not have a well-defined size. Carefully characterized spherical solutes in the appropriate size range are therefore of considerable interest. The chromatographic behavior of carboxylated starburst dendrimers—characterized by quasi-elastic light scattering and viscometry—on a Superose SEC column was explored. Carboxylated starburst dendrimers appear to behave as non-interacting spheres during chromatography in the presence of an appropriate mobile phase. The dependence of the retention time on the solute size seems to coincide with data collected on the same column for Ficoll. Chromatography of the dendrimers yields to a remarkable correlation of the chromatographic partition coefficient with the generation number; this result is, in part, a consequence of the exponential relationship between

the generation number and the molecular volume of these dendrimers. All measurements were made in a 9:1 mixture of pH = 5.5, 0.38 *M*, which has been previously known to minimize electrostatic interactions between a variety of proteins and this stationary phase.[4]

The SEC partition coefficient[6] (K_{SEC}) was measured on a Superose 6 column for three sets of well-characterized symmetrical solutes: the compact, densely branched non-ionic polysaccharide, Ficoll; the flexible chain non-ionic polysaccharide, pullulan; and compact, anionic synthetic polymers, carboxylated starburst dendrimers. All three solutes display a congruent dependence of K_{SEC} on solute radius, *R*. In accord with a simple geometric model for SEC, all of these data conform to the same linear plot of $K_{SEC}^{1/2}$ vs. *R*. This plot reveals the behavior of non-interacting spheres on this column. The mobile phase for the first two solutes was 0.2 *M* NaH_2PO_4–Na_2HPO_4, pH 7.0. In order to ensure the suppression of electrostatic repulsive interactions between the dendrimer and the packing, the ionic strength was increased to 0.30 *M* for that solute.

The MWD[7] is derived for polymers generated by self-condensing vinyl polymerization (SCVP) of a monomer having a vinyl and an initiator group ("inimer") in the presence of multifunctional initiator. If the monomer is added slowly to the initiator solution (semibatch process), this leads to hyperbranched polymers with a multifunctional core. If monomer and initiator are mixed simultaneously (batch process), even at vinyl group conversions as high as 99%, the total MWD consists of polymers, which have grown via reactions between inimer molecules (i.e., the normal SCVP process) and those which have reacted with the initiator. Consequently, the weight distribution, $w(M)$, is bimodal. However, the *z*-distribution, $z(M)$, equivalent to the "GPC distribution," $w(\log M)$ vs. $\log M$, is unimodal. Their theoretical studies showed that the hyperbranched polymers generated from an SCVP possess a very wide MWD $M_w/M_n \cong P_n$, where P_n is the number-average degree of polymerization. The evolution of the weight-distribution and *z*-distribution curves of the total resultant polymer during the SCVP in the presence of the core moiety with $f = 10$ is given. The weight distributions become less bimodal with increasing conversion. In contrast, all *z*-distributions are unimodal.

Striegel et al.[8] employed SEC with universal calibration to determine the molecular-weight averages, distributions, intrinsic viscosities, and structural parameters of Starburst dendrimers, dextrans, and the starch-degradation polysaccharides (maltodextrins). A comparison has been made in the dilute solution behavior of dendrimers and polysaccharides with equivalent weight-average molecular weights. Intrinsic viscosities decreased in the order $[\eta_{dexstran}] > [\eta_{dextrin}] > [\eta_{dendrimer}]$. A comparison between the molecular radii obtained from SEC data and the radii from molecular dynamics studies show that Starburst dendrimers behave as θ-stars with functionality between 1 and 4. Additionally, electrospray ionization MS was employed to determine M_w, M_n, and the PD of Astromol dendrimers.

SEC experiments were carried out on a Watters 150CV$^+$ instrument (Waters Associates, Milford, Massachusetts, U.S.A.) equipped with both differential refractive index single-capillary viscometer detectors. The solvent/mobile phase was H_2O/0.02% NaN_3, at the flow rate of 1.0 ml/min. Pump, solvent, and detector compartments were maintained at 50°C. Separation occurred over a column bank consisting of three analytical columns preceded by a guard column: Shodex KB-G, KS-802, KS-803, and KB-804 (Phenomenex, Torrance, California, U.S.A.). Universal calibration was performed using a series of oligosaccharides (Sigma, St. Louis, Missouri, U.S.A.), and Pullulan Standards (American Polymer Standards, Mentor, Ohio, U.S.A., and Polymer Laboratories, Amherst, Massachusetts, U.S.A.).

The solution behavior of several generations of Starburst poly(amido amine) dendrimers, low-molecular-weight ($M_w < 60{,}000$) dextrans, and maltodextrins was also examined by SEC, using the universal calibration. For Starburst and Astramols, supplied M_w values are theoretical average molecular weights. Weight-average molecular weights for the dendrimers determined by SEC with universal calibration using oligosaccharide and polysaccharide narrow standards were slightly, albeit consistently lower than the theoretical averages. In general, the intrinsic viscosity of polymers tends to increase with increasing molecular weight (*M*), which accompanies an increase in the size of the macromolecule. Exceptions to this are the hyperbranched polymers, in which the Mark–Houwink double logarithmic $[\eta]$ vs. *M* curve passes through a minimum in the low-molecular-weight region before steadily increasing. For solutions of the dendrimers studied in their experiments, it is evident that as *M* increases, $[\eta]$ decreases. This corresponds to the molecules growing faster in density than in radial growth. Fréchet has pointed out the special situation of this class of polymers, in which their volume increases cubically and their mass increases exponentially.[9] The exponent *a* in the Mark–Houwink equation for the dendrimers is –0.2 for convergent growth for the generation studied (located in the inverted region of the Mark–Houwink plot). This value for the Starburst dendrimers is comparable to the *a* value of –0.2 for convergent-growth dendrimers, generations 3–6, studied by Mourey et al.[9] When the results from SEC are combined with those from computer modeling by comparing the ratios of geometric to hydrodynamic radii for the trifunctional Starbursts to the ratios derived for the other molecular geometries, the dendrimers appear to resemble θ-stars.

SEC[9] with a coupled molecular-weight-sensitive detection is a simple convenient method for characterizing dendrimers for which limited sample quantities are available. The polyether dendrimers increase in hydrodynamic radius approximately linearly with generation and have a characteristic maximum in viscosity. These properties

distinguish these dendrimers from completely collapsed, globular structures. The experimental data also indicate that these structures are extended to approximately two-thirds of the theoretical, fully extended length.

Puskas and Grasmüller characterized the synthesized star-branched and hyperbranched polyisobutylenes (PIBs) by SEC–light scattering in tetrahydrofuran (THF), with the *dn/dc* measured as 0.09 ml/g. The radius of gyration gave a slope of 0.3, demonstrating the formation of a star-branched polymer.[10]

Gitsov and Fréchet[11] reported the syntheses of novel linear-dendritic triblock copolymers achieved via anionic polymerization of styrene and final quenching with reactive dendrimers. For the characterization of the products in the reaction mixture, SEC with double detection was performed at 45°C on a chromatography line consisting of a 510 pump, a U6K universal injector, three Ultrastyragel columns with pore sizes 100 and 500 Å and Linear, a DRI detector M410, and a photodiode array detector M991 (all Millipore Co., Waters Chromatography Division). THF was used as the eluent at a flow rate of 1 ml/min. SEC with coupled PDA detection proves to be particularly useful in the separation and identification of all compounds in the reaction mixture. A detailed discussion can be found in Ref.[11] SEC/VISC studies show that the ABA copolymers are not entangled and undergo a transition from an extended globular form to a statistical coil when the molecular weight of their linear central block exceeds 50,000.

The solution properties of hybrid–linear dendritic polyether copolymers are investigated by SEC with coupled viscometric detection from the same authors.[12] The results obtained show that the block copolymers are able to form monomolecular and multimolecular micelles depending on the dendrimer generation and the concentration in methanol–water (good solvent for the linear blocks).

Large macromolecular assemblies and agglomerates play an important role in living matter and its artificial reproduction. AB and ABA block copolymers are convenient tools used for modeling of these processes. Usually in a specific solvent–non-solvent system, ABA triblocks form micelles with a core consisting of insoluble B blocks and a surrounding shell of A blocks that extend into the solvent phase. Two Waters/Shodex PROTEIN KW 802.5 and 804 columns were used for the aqueous SEC measurements. The columns were calibrated with 14 PEO and PEG standards. The radius of gyration was calculated from the intrinsic viscosity $[\eta]$ and Unical 4.04 software (Viscotek). The calculated values for the Mark–Houwink–Sakurada constant a are 0.583 for PEG ($K = 9.616 \times 10^{-4}$) and 0.776 for PEO ($K = 2.042 \times 10^{-4}$). They are in close agreement with the data reported for the same polymer in other aqueous mixtures (compositions).

The significant decrease in the $[\eta]$ of the copolymer solutions and the parallel decrease in R_g of the hybrid structures containing [G-4] blocks indicate that the block copolymers are undergoing intramolecular micellization. Unimolecular micelles consisting of a small, dense, dendritic core tightly surrounded by a PEO corona are formed. The influence of the size of the dendritic block was investigated with PEO7500. The solution behavior of ABA hybrid copolymers is documented. In general, materials containing more than 30 wt% of dendritic blocks are not soluble in methanol–water. However, it should be emphasized that the solubility of copolymers is also strongly influenced by the size of the dendritic block. Obviously, an optimal balance between the size of the dendrimer and the length of the linear block is required to enable the dissolution of the copolymer in the solvent composition.

Performing SEC with dual detection (DRI and viscometry) permitted application of the concept of universal calibration.

REFERENCES

1. Fréchet, J.M.J.; Hawker, C.J.; Gitsov, I.; Leon, J.W. Dendrimers and hyperbranched polymers: Two families of three dimensional macromolecules with similar but clearly distinct properties. J.M.S.-Pure Appl. Chem. A, **1996**, *33*, 1399.
2. Newcome, G.R.; Moorefield, C.N.; Vögtle, F. *Dendritic Molecules, Concepts, Syntheses, Perspectives*; VCH: Weinheim, 1996.
3. Buchard, W. Solution properties of branched macromolecules. Adv. Polym. Sci. **1999**, *143*, 113.
4. Yang, G.; Jikey, M.; Kakimoto, M. Synthesis and properties of hyperbranched aromatic polyamide. Macromolecules **1999**, *32*, 2215.
5. Dubin, P.L.; Eduards, S.L.; Kaplan, I.; Mehta, M.S.; Tomalia, D.; Xia, J. Carboxylated starburst dendrimers as calibration standards for aqueous size exclusion chromatography. Anal. Chem. **1992**, *64*, 2344.
6. Dubin, P.L.; Edwards, S.L.; Mehta, M.S.; Tomalia, D. Quantitation of non-ideal behavior in protein size-exclusion chromatography. J. Chromatogr. **1993**, *635*, 51.
7. Yan, D.; Zhou, Z.; Müller, A. Molecular weight distribution of hyperbranched polymers generated by self-condensing vinyl polymerization in the presence of a multifunctional initiator. Macromolecules **1999**, *32*, 245.
8. Strigel, A.M.; Plattner, R.D.; Willet, J.L. Dilute solution behavior of dendrimers and polysaccharides: SEC, ESI-MS, and computer modeling. Anal. Chem. **1999**, *71*, 978.
9. Mourey, T.H.; Turner, S.R.; Rubinstein, M.; Fréchet, J.M.J.; Hawker, C.J.; Wooley, K.L. The unusual behavior of dendritic macromolecules: A study of the intrinsic viscosity, density and refractiveindex increment of polyether dendrimers. Macromolecules **1992**, *25*, 2401.
10. Puskas, J.E.; Grasmüller, M. Star-branched and hyperbranched polyisobutylenes. Macromol. Symp. **1998**, *132*, 117.
11. Gitsov, I.; Fréchet, J.M.J. Novel nanoscopic architectures. Linear-hlobular ABA copolymers with polyether dendrimers as A blocks and polystyrene as B block. Macromolecules **1994**, *27* (25), 7309.
12. Gitsov, I.; Fréchet, J.M.J. Solution and solid-state properties of hybrid linear-dendritic block copolymers. Macromolecules **1993**, *26*, 6536.

Derivatization of Analytes: General Aspects

Igor G. Zenkevich
Chemical Research Institute, St. Petersburg State University, St. Petersburg, Russia

INTRODUCTION

A priori information about analytes is available for most chromatographic analyses. Depending on the amount of information available, all determinations may be classified as: 1) preferably confirmatory (determined components are known); or 2) prospective (any propositions concerning their chemical nature are very approximate). Numerous differences in the design of analytical procedures in these two cases are manifested in the features of all stages of analysis—sampling, sample preparation, analysis itself, and interpretation of results. Preferably, for procedures classified as confirmatory, the stage of sample preparation should be supplemented by chemical treatment of the sample by different reagents for the optimization of subsequent chromatographic analysis. The most widely used kind of treatment is the synthesis of various chemical derivatives of target analytes, namely derivatization.

Derivatization is a special subgroup of organic reactions used in chromatography for compounds with selected types of functional groups. Not all known reactions can be applied as methods for derivatization, because these processes should be in accordance with some specific conditions. The consideration of numerous known recommendations[1–4] permits us to underline the following most important ones:

1. The experimental operations should be as simple as possible. The mixing of sample with reagent(s) at ambient temperature, without additional treatment of the mixture, is preferable. In chromatographic practice, the time needed for the completion of the derivatization reaction may be up to 24 hr (the so-called "stay overnight"). Instead of this long time, the heating of reaction mixtures in ampoules is also permitted. Some processes (including alkylation and silylation) may be realized by injection of the reaction mixtures into the hot injector of the gas chromatography (GC) equipment.
2. The number of stages of derivatization for any functional group in organic compounds should be minimal (one or two, but no more). For multistage processes, the condition "single-pot synthesis" is necessary. Such operations as extraction or re-extraction are permitted only when the quantities of analytes are not very small or when it is necessary to isolate them from complex matrices. The large excess of derivatization reagent(s) and/or solvents should be easily removable, or have no influence on the results of the analysis. The use of high boiling solvents typically is not recommended. The possible by-products of reactions should have no influence on the results either.
3. The degree of transformation of initial compounds into products (yield, %) should be maximal and reproducible to provide for the quantitative determination of these compounds by analysis of their derivatives.
4. The chemical origin of the formed products should be strongly predictable. When a known derivatization reaction is put into practice for new compounds, this knowledge can be based on previously reported examples for the closest structural analogs of the target analytes.
5. Mutually unambiguous correspondence between the number of initial analytes and their derivatives should be assured. The optimal case for all compounds is $1 \rightarrow 1$, but numerous examples of type $1 \rightarrow 2$ are known (e.g., the derivatization of enantiomers by chiral reagents, which leads to the formation of a pair of diastereomers).[5] Similarly, the reaction of carbonyl compounds with *O*-alkoxyamines gives pairs of *syn*- and *anti*-isomers of oxime *O*-ethers, etc. All processes that lead to further uncertainty (chemical multiplication of analytical signals), such as $1 \rightarrow N$ ($N \geq 3$), are not recommended for analytical practice. In connection with this, the number of reaction by-products should be minimal.
6. The feature of structural terminology of derivatives should be noted. If the number of newly added protecting groups in the molecules is unknown for derivatives of complex polyfunctional organic compounds, they can be classified in accordance with known derivatives. For example, *N*-benzoyl glycine ($PhCONHCH_2CO_2H$) can form two trimethylsilyl (TMS) derivatives: *mono*-($PhCONHCH_2COOTMS$) and *bis*-[$PhC(OTMS) = NCH_2COOTMS$]. If precise information on their chemical origin is unavailable, both of them can be named simply "benzoylglycine TMS" or "TMS #1" and "TMS #2" in the order of chromatographic elution.

7. The foregoing remarks follow from general features of derivatization reactions. It should be noted that this method is not used for completely unknown samples, because information about the presenting analytes is needed.

In accordance with the criteria mentioned, e.g., *N*,*O*-trimethylsilyl derivatives of amino acids do not seem to be useful in analytical practice owing to the non-specific *mono*- and *bis*-silylation of primary amino groups or post-reaction hydrolysis of the resultant N–Si bonds. Even the simplest compounds of this class, $H_2N–CHR–CO_2H$, form three possible products, $H_2N–CHR–CO_2TMS$, $TMSNH–CHR–CO_2TMS$, and $(TMS)_2N–CHR–CO_2TMS$ [$TMS = Si(CH_3)_3$], with different GC retention parameters. In the case of diamino monocarboxylic acids with non-equivalent amino groups [e.g., lysine, $H_2N(CH_2)_4CH(NH_2)CO_2H$], the number of similar semi-silylated derivatives is theoretically increased up to nine.

MAIN FEATURES OF DERIVATIZATION REACTIONS

The greatest principal difference between organic reactions in general and those that can be considered chromatographic derivatization reactions is the de facto commonly accepted absence of necessity of product structure determination in the latter case. In "classical" organic chemistry, every synthesized compound must be isolated from the reaction mixture and characterized by physicochemical constants or spectral parameters for confirmation or estimation (for new objects) of its structure. Nevertheless, for the processes that have been classified as derivatization reactions, these operations are not necessary and generally not used in analytical practice. *The reaction itself is considered confirmation of the structure of the derivatives.* Of course, any exceptions to this important rule seem very dangerous and should be pronounced as special warnings for the application of any method of derivatization. Hence, in general cases, this method implies a risk in the ascribing of structures to the products formed in the chemical reactions. For new derivatives of complex organic compounds, the independent determination (or confirmation) of their structures seems desirable.

All organic reactions used for derivatization can proceed only in condensed phase, i.e., in solutions. None of these interactions are possible in gaseous media. Nevertheless, there is a special technique, flash derivatization, which involves joint (or more rarely, consecutive) injection of samples and reagents into GC equipment. It is noteworthy that in this case too, all reactions take place in the condensed phase, i.e., before evaporation of the samples. This method has been recommended for silylation, but is more often used for alkylation by a special group of chemicals—quaternized ammonium salts and hydroxides. For example, such reagents as 3,5-*bis*-(trifluoromethyl)benzyl dimethylphenylammonium fluoride have been proposed for flash conversion of hydroxy compounds (preferably phenols and carboxylic acids) into their 3,5-*bis*-(trifluoromethyl)benzyl ethers.[6]

There are many examples where well-known derivatization reactions cannot be used in specific cases owing to the absence of mutually unambiguous correspondence between initial analytes and formed derivatives. For instance, methylation by diazomethane, CH_2N_2, is not recommended for barbiturates, because of the formation of mixtures of their *N*- and/or *O*-methyl derivatives. Another example is the interaction of dimethyl disulfide with conjugate dienes,[7] which gives complex mixtures of products and indicates the absence of regioselectivity. One of the frequently used derivatization methods for carbonyl compounds [RR′CO (including the important group of ketosteroids)] is their one-step treatment by *O*-alkyl hydroxylamines ($R''ONH_2$) with the expected formation of alkyl ethers of oximes ($RR'C = NOR''$). However, this reaction has an anomaly for compounds with C = C double bonds conjugated with carbonyl groups, that is, parallel addition of reagent with active hydrogen atoms to the polarized C = C bonds (see Eq. 1 below).[8]

This means that instead of one expected product with molecular weight (MW) = $M_0 + 29$ (with *O*-methyl hydroxylamine as reagent; M_0—molecular weight of initial carbonyl compound), reaction mixtures may contain two additional products with $MW = M_0 + 47$ and $M_0 + 76$. This feature is negligible for the analysis of individual compounds, but when samples are mixtures of components of interest, the analysis becomes impossible because of the complexity of interpretation of the results.

In any case, the information about the estimated products of derivatization should be unambiguous. As an important example, it is interesting to note that for a long time, it was considered that various silylating agents could react only with compounds having active hydrogen atoms. However, only in 1999 was it shown[9] that typical reagents of this type (*N*-methyl trimethylsilyl acetamide, MSA) react with aromatic carbonyl compounds (preferably aldehydes) giving unusual products of acetamide addition to C = O bonds followed by their one- or two-step silylation. Keeping this fact in mind, it is better to name these products MSA adducts rather than TMS derivatives.

$$\begin{array}{ccc} R_2 = CR' - OR'' + CH_3ONH_2 \rightarrow & & R_2C = CR' - CR'' = NOCH_3 \\ \downarrow & & \downarrow \\ CH_3ONH - CR_2 - CHR' - COR'' & \rightarrow & CH_3ONH - CR_2 - CHR' - CR'' = NOCH_3 \end{array} \quad (1)$$

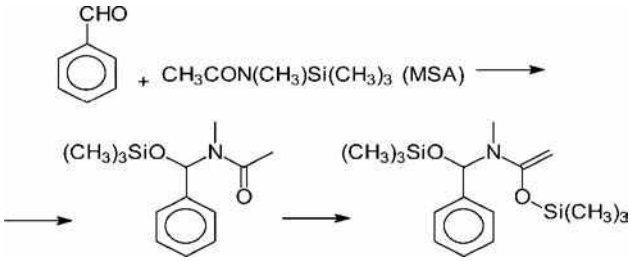

Only if the organic reaction is in accordance with all the above-mentioned criteria may it be considered a method for derivatization. Finding new appropriate processes of this type is complex and often not obvious.

One of the main, but not sole, purposes of derivatization is the transformation of non-volatile compounds into volatile derivatives. Each chromatographic method [GC, GC/mass spectrometry (MS), high-performance liquid chromatography (HPLC), capillary electrophoresis (CE), etc.] being supplemented by derivatization of analytes permits us to solve some specific problems. The principal among them are summarized briefly in Table 1; more detailed comments follow. Some of the derivatization methods mentioned can also be used in mass spectrometry, which includes no preliminary chromatographic separation of analytes,[10] but there are special derivatization techniques never used in chromatographic methods (e.g., synthesis and analysis of isotopically labeled compounds).

Most monofunctional organic compounds [including alcohols (ROH), carboxylic acids (RCO_2H), amides ($RCONH_2$), etc.] are volatile enough for direct GC analysis. Exceptions are only those compounds with high melting points (sometimes with decomposition) because of strong intermolecular interactions in their condensed phases {e.g., thiosemicarbazones ($RR'C = N–NHCSNH_2$), guanidines [$RNH–C(=NH)–NH_2$], etc.}. Ionic compounds [e.g., quaternary ammonium salts, $(R_4N)^+X^-$] are non-volatile as well. If the compounds contain two or more functional groups with active hydrogen atoms [including the case of inner molecular ionic structures such as that seen in amino acids, $RCH(NH_3^+)CO_2^-$], their volatility decreases significantly. The purpose of derivatization of all these objects is to substitute active hydrogen atoms (better in all functional groups) by covalently bonded fragments that provide more volatile products. Direct GC analysis of highly reactive compounds {free halogens, hydrogen halides, strong inorganic acids like sulfonic acid (RSO_2OH), phosphonic acid [$RPO(OH)_2$], etc.} can be accompanied by their interaction with stationary phases of chromatographic columns and they also require derivatization.

Table 1 Principal applications of derivatization in different chromatographic techniques.

Aims of derivatization	Typical examples
GC	
Transformation of non-volatile, thermally unstable, and/or highly reactive compounds into stable volatile derivatives	$ROH \rightarrow ROSiMe_3$ $ArOH \rightarrow ArOCOCF_3$ $RR'CO \rightarrow RR'C = NOCH_3$
Synthesis of derivatives for element-specific GC detectors or conversion of non-detectable compounds into suitable products for minimization of detection limit	$ROH \rightarrow ROCOCCl_3$ (ECD) $RCO_2H \rightarrow RCO_2CH_2CCl_3$ (ECD) $HCO_2H \rightarrow HCO_2CH_2C_6H_5$ (FID)
Combination with stage of sampling (preferably in environment analyses when derivatization is used as method of chemisorption)	$RCHO \rightarrow 2,4\text{-}(NO_2)_2C_6H_3–NH–N = CHR$
Separation of enantiomeric compounds on non-chiral phases after their conversion into diastereomeric derivatives	$RR'C^*HNH_2 + C_6H_5C^*H(OMe)COCl \rightarrow RR'C^*HNH–COC^*H(OMe)C_6H_5$
GC/MS	
Determination of molecular weights of compounds with $W_M \approx 0$ at electron impact ionization (synthesis of derivatives with conjugated bond and/or atom systems)	$RR'CO \rightarrow RR'C = NNH–C_6F_5$ (π–p–π conjugation system) $RNH_2 \rightarrow RN = CH–NMe_2$ (p–π conjugation system)
Increase of specificity of molecular ion fragmentation for estimation of structure of analytes (e.g., determination of C = C double bond position in carbon skeleton of molecules)	"On-site" derivatization:[11] $RCH = CHR' \rightarrow$ R–CH(SMe)–CH(SMe)–R′ "Remote-site" derivatization:[12] $RCH = CH(CH_2)_nCO_2H + H_2NCH_2CH_2OH \rightarrow$ 2-substituted oxazolines
HPLC with UV detection and CE	
Synthesis of chromogenic derivatives (with chromophores that provide adsorption within typical range of UV detection of 190–700 nm)	$C_6H_7O(OH)_5 \rightarrow C_6H_7O(OCOC_6H_5)_5$
Conversion of hydrophilic analytes into more hydrophobic derivatives	$RCH(NH_2)CO_2H \rightarrow RCH(NHCSNHC_6H_5)CO_2H$
Various chromatographic techniques	
Determination of number of functional groups with active hydrogen atoms using mixed derivatization reagents	$X(OH)_n + [(R_1CO)_2O + (R_2CO)_2O)] \rightarrow$ mixture of miscellaneous acyl derivatives

C*—chiral carbon atoms.

Table 2 Average values of differences of GC retention indices (ΔRI) for some derivatization reactions.

$\Delta MW = MW_B - MW_A$	Scheme of reaction A → B (for monofunctional compounds only)	$\Delta RI \pm s_{\Delta RI}$
14	$RCO_2H \rightarrow RCO_2Me$	–102 ± 28
14	$ArOH \rightarrow ArOMe$	–62 ± 16
28	$RCO_2H \rightarrow RCO_2Et$	–42 ± 7
28	$RR'CO \rightarrow RR'C = NNHMe$	229 ± 23
29	$ROH \rightarrow RONO$	–6 ± 27
42	$ROH \rightarrow ROCOMe$	142 ± 18
42	$ArOH \rightarrow ArOCOMe$	97 ± 20
42	$RNH_2 \rightarrow RNHCOMe$	437 ± 29
42	$ArNH_2 \rightarrow ArNHCOMe$	401 ± 7
42	$RR'CO \rightarrow RR'C = NNMe_2$	302 ± 20
72	$ROH \rightarrow ROSiMe_3$	119 ± 18
72	$RCO_2H \rightarrow RCO_2SiMe_3$	76 ± 16
96	$ROH \rightarrow ROCOCF_3$	–85 ± 24
114	$RCO_2H \rightarrow RCO_2SiMe_2$–*tert*-Bu	288 ± 29

If the initial compound A may be analyzed together with its derivative B, the comparison of their GC retention indices is a source of important information about the nature of these compounds. The average value of $\Delta RI = RI(B) - RI(A)$ may be used for the identification of both analytes and, if necessary, the reaction itself.[13] Selected ΔRI values for GC analysis on standard non-polar polydimethyl siloxanes are presented in Table 2.

GC/MS analysis completely excludes the second item (see Table 1) from the possible aims of derivatization, insofar as the mass spectrometer itself is both a universal and selective GC detector. At the same time, two new important reasons for derivatization appear in this method. The intensities of molecular ion ($M^+ \cdot$) signals are low for compounds having no structural fragments, which provides the effective delocalization of charge and unpaired electron in these ions. These fragments are conjugate bond and/or atom systems, or isolated heteroatoms with high polarizability (S, Se, I). In accordance with this regularity, *O*-TMS derivatives of alcohols in general show no $M^+ \cdot$ peaks in mass spectra, whereas for the TMS ethers of enols of carbonyl compounds ($RCH_2COR' \rightarrow RCH = CR'$–$OSiMe_3$) and TMS ethers of their oximes ($RCH = N$–$OSiMe_3$) (π–p–d conjugation systems), they are very intensive.

The determination of positions of C = C double bonds in the carbon skeletons of molecules is very often impossible owing to uncertain charge localization in molecular ions. The solution of this problem involves the conversion of unsaturated compounds into products whose molecular ions have sufficiently fixed charge localization. There are two methods by which to accomplish this localization: 1) addition of heteroatomic reagents directly to the C = C bond (the so-called "on-site" derivatization with the formation of TMS ethers of corresponding diols, adducts with dimethyl disulfide,[11] etc.); and 2) introduction or formation of nitrogen-containing heterocycles rather far from the target C = C bond[12] ("remote-site" derivatization).

The formation of new chromophores for the optimization of UV detection of analytes in HPLC involves the synthesis of derivatives with conjugate systems in the molecule. Compared with GC, there are no restrictions on the volatilities of these derivatives for HPLC analysis. They may be synthesized before analysis (precolumn derivatization) or after chromatographic separation (postcolumn derivatization, or, in other words, reaction GC). The latter technique, as a method of identification of analytes, was highly popular until the 1970s. However, at present, this approach has practically lost its significance owing to the progress of GC/MS methods. Very few new GC applications of this method have been reported during the past dozens years or so[14], but it is still used in HPLC because it permits us to combine the measurement of retention parameters of initial analytes with detection of their derivatives.[15]

The range of most convenient hydrophobicity of organic compounds for reversed-phase (RP) HPLC separation may be estimated approximately as $-1 \leq \log P \leq +5$ ($\log P$ is the logarithm of the partition coefficient of the compound being characterized in the standard solvent system 1-octanol/water). Highly hydrophilic substances with $\log P \leq -1$ need a special choice of analysis conditions, e.g., introduction of ion-pair additives into the eluents. Another approach is their conversion to more hydrophobic derivatives by the modification of functional groups with active hydrogen atoms.

The examples mentioned here for RP-HPLC analysis of monosaccharides in the form of their perbenzoates and amino acids as *N*-phenylthiocarbamoyl derivatives (Table 1) satisfy both principal criteria: introducing the chromophores into molecules of analytes (C_6H_5CO– and C_6H_5NH–CS–NH–) and optimization of their retention parameters.

Sometimes, the generally prohibited multiplication of analytical signals of derivatives may be attained artificially for the solution of special problems. For example, the treatment of polyhydroxy compounds (phenols, phenol carboxylic acids, polyamines, etc.) [$X(OH)_n$] by equimolar mixtures (1 : 1) of acylation reagents [$(R_1CO)_2O + (R_2CO)_2O$] leads to the formation of ($n + 1$) miscellaneous acyl derivatives $X(OCOR_1)_n$, $X(OCOR_1)_{n-1}(OCOR_2)$,..., $X(OCOR_2)_n$. The relative abundances of their chromatographic peaks should be close to the binomial coefficients, i.e., 1 : 1 (at $n = 1$), 1 : 2 : 1 ($n = 2$), 1 : 3 : 3 : 1 ($n = 3$), and so forth. Moreover, the differences of retention indices of all these mixed derivatives are close to each other. These two regularities permit us to determine the number of hydroxyl groups (n) in the molecules of analytes. This mode of derivatization can be realized in both HPLC[16,17] and GC[18] conditions.

Insofar as the derivatization can be considered one of the stages of sample preparation for chromatographic analysis, it can be combined with other procedures, for instance, the preconcentration of traces of analytes. For example, the yield of solid-phase extraction or microextraction of organic compounds from aqueous solutions with modified silica gels is better for more hydrophobic substances; the preliminary conversion of acidic compounds into suitable derivatives is recommended.[19]

CONCLUSIONS

Chemical derivatization as a stage of sample preparation is a widespread approach in various chromatographic and related techniques. It is used for the conversion of compounds that cannot be analyzed directly into suitable products (derivatives). The aims of this treatment of samples are very diverse and depend on the final goals of analyses as a whole. One of the most important problems to be solved using derivatization is the transformation of nonvolatile compounds into products volatile enough for GC analysis. Other aims of this method include the optimization of detection and structure evaluation of analytes.

A disadvantageous feature of derivatives of complex organic compounds can be the uncertainty in their structures. This requires their determination (or confirmation) by independent methods (MS), or the exhaustive characterization of reactions classified as those of derivatization.

REFERENCES

1. Blau, K., King, G.S., Eds.; *Handbook of Derivatives for Chromatography*; Heiden: London, 1977; 576.
2. Knapp, D.R. *Handbook of Analytical Derivatization Reactions*; John Wiley & Sons: New York, 1979; 741.
3. Drozd, J. *Chemical Derivatization in Gas Chromatography*; Journal of Chromatography Library; Elsevier: Amsterdam, 1981; Vol. 19, 232.
4. Blau, K., Halket, J.M., Eds.; *Handbook of Derivatives for Chromatography,* 2nd Ed.; John Wiley & Sons: New York, 1993; 369.
5. Allenmark, S.G. *Chromatographic Enantioseparation: Methods and Applications*; Ellis Horwood Ltd.: New York, 1988; 268.
6. Amijee, M.; Cheung, J.; Wells, R.J. Development of 3,5-*bis*-(trifluoromethyl)benzyl-dimethylphenylammonium fluoride, an efficient new on-column derivatization reagent. J. Chromatogr. A, **1996**, *738*, 57–72.
7. Vincentini, M.; Guglielmetti, G.; Gassani, G.; Tonini, C. Determination of double bond position in diunsaturated compounds by mass spectrometry of dimethyl disulfide derivatives. Anal. Chem. **1987**, *59* (7), 694–699.
8. Zenkevich, I.G.; Artsybasheva, Ju.P.; Ioffe, B.V. Application of alkoxyamines for derivatization of carbonyl compounds in gas chromatography–mass spectrometry. Zh. Org. Khim. (Russ.) **1989**, *25* (3), 487–492.
9. Little, J.L. Artifacts in trimethylsilyl derivatization reactions and ways to avoid them. J. Chromatogr. A, **1999**, *844*, 1–22.
10. Zaikin, V.G.; Mikaya, A.I. *Chemical Methods in Mass Spectromery of Organic Compounds*; (in Russian); Nauka Publ. House: Moscow, 1987; 200.
11. Buser, H.-R.; Arn, H.A.; Guerin, P.; Rauscher, S. Determination of double bond position in mono-unsaturated acetates by mass spectrometry of dimethyl disulfide adducts. Anal. Chem. **1983**, *55* (6), 818–822.
12. Yu, Q.T.; Liu, B.N.; Zhang, J.Y.; Huang, Z.H. Location of double bonds in fatty acids of fish oil and rat testis lipids. GC–MS of the oxazoline derivatives. Lipids **1989**, *24* (1), 79–83.
13. Zenkevich, I.G. Chromatographic characterization of organic reactions by additivity of GC retention parameters of reagents and products. Zh. Org. Khim. (Russ.) **1992**, *29* (9), 1827–1840.
14. Mikaia, A.I.; Trusova, E.A.; Zaikin, V.G.; Zegelman, L.A.; Urin, A.B.; Volinsky, N.P. Reaction gas chromatography/mass spectrometry. IV. Postcolumn hydrodesulfurization in capillary GC/MS as an aid in structure elucidation of cyclic sulfides within mixtures. J. High Resolut. Chromatogr. Chromatogr. Commun. **1984**, *7* (11), 625–628.
15. Vassilakis, I.; Tsipi, D.; Scoullos, N. Determination of a variety of chemical classes of pesticides in surface and ground waters by off-line solid-phase extraction, GC with ECD and NP-detection and HPLC with post-column derivatization and fluorescence detection. J. Chromatogr. A, **1998**, *823*, 49–58.
16. Zenkevich, I.G. New applications of the retention index concept in gas and high performance liquid chromatography. Fresenius J. Anal. Chem. **1999**, *365* (4), 305–309.
17. Zenkevich, I.G. Determination of the number of functional groups with active hydrogen atoms in phenols and aromatic amines by HPLC. Zh. Phys. Khim. (Russ.) **1998**, *72* (6), 1131–1136.
18. Zenkevich, I.G.; Rodin, A.A. Gas chromatographic one-step determination of the number of hydroxyl groups in polyphenols using mixed derivatization reagents. Zh. Org. Khim. (Russ.) **2002**, *5* (7), 732–736.
19. Nilsson, T.; Baglio, D.; Galdo-Miques, I.; Madsen, O.J.; Facchetti, S. Derivatization/solid-phase microextraction followed by GC–MS for the analysis of phenoxy acid herbicides in aqueous samples. J. Chromatogr. A, **1998**, *826*, 211–216.

Detection in CCC

M.-C. Rolet-Menet
Analytical Chemistry Laboratory, Unit of Formation and Research (UFR) of Pharmaceutical and Biological Sciences, Paris, France

INTRODUCTION

Detection of solutes is an essential link in the separation chain. It helps to reveal solute separation by detecting them in the column effluent, and in some cases, it could permit their characterization. These objectives are based on the various physical properties of the products.

Countercurrent chromatography (CCC) is a chromatographic method that separates solutes that are more or less retained in the column by a stationary phase (liquid in this case) and are eluted at the outlet of the column by a mobile phase. Two treatments of column effluent have been used up to now in CCC. Either the column outlet is directly connected to a detector commonly used in HPLC (online detection) or fractions of mobile phase are collected and analyzed by spectrophotometric, electrophoretic, or chromatographic methods etc. (off-line detection).

The first one is more practical and rapid to carry out. It is commonly used in analytical applications of CCC and also in preparative CCC to analyze effluent continuously and to follow the steps of the separation.

The second one is often tedious because each fraction must be analyzed. However, it is of great interest in preparative applications of CCC, especially to measure the purity of fractions and the biological activity of separated compounds and also to recover a product from one fraction or some selected fractions to resolve its chemical structure.

ON-LINE DETECTION

This type of detection can be used as such in preparative CCC to monitor separations, before the fraction collector, if any, and in analytical CCC (for instance, during the determination of log $P_{\text{octanol/water}}$).

Several detectors used in high-performance liquid chromatography (HPLC) and in supercritical fluid chromatography (SFC) can be connected to the CCC column[1] to detect solutes and thus follow separation. They can be, for instance, fluorimeters (very sensitive and used without modifications in CCC), UV–Visible spectroscopes,[1] evaporative light scattering detectors,[1,2] atomic emission spectroscopes,[3] etc. Some detectors give more information than the detection of the solute, such as structural information of separated components, as in infrared spectroscopy,[4] mass spectrometry,[5] or nuclear magnetic resonance.[6] These detectors are used either online with a collector fraction or in parallel if they are destructive.

UV Detection

The UV–Visible detector is the universal detector used in analytical and preparative CCC. It does not destroy solutes. It is used to detect organic molecules with a chromophore moiety or mineral species after formation of a complex (for instance, the rare earth elements with Arsenazo III[7]). Several problems can occur in direct UV detection, as has already been described by Oka and Ito:[8] 1) carryover of the stationary phase due to improper choice of operating conditions, with appearance of stationary phase droplets in the effluent of the column; 2) overloading of the sample, vibrations, or fluctuations of the revolution speed; 3) turbidity of the mobile phase due to difference in temperature between the column and the detection cell; or 4) gas bubbling after reduction of effluent pressure. Some of these problems can be solved by optimization of the operating conditions, better control of the temperature of the mobile phase, and addition of some length of capillary tubing or a narrow-bore tube at the outlet of the column before the detector to stabilize the effluent flow and to prevent bubble formation. The problem of stationary phase carryover (especially encountered with hydrodynamic mode CCC devices) can be solved by the addition between the column outlet and UV detector of a solvent that is miscible with both stationary and mobile phases and that allows one to obtain a monophasic liquid in the cell of the detector[1] (a common example is isopropanol).

Evaporative Light-Scattering Detection

Evaporative light-scattering detection (ELSD) involves atomization of the column effluent into a gas stream via a Venturi nebulizer, evaporation of solvents by passing it through a heated tube to yield an aerosol of non-volatile solutes, and finally measurement of the intensity of light scattered by the aerosol. After a suitable evaporation step, in the worst case of segmented or emulsified mobile phase, the column effluent should always be an aerosol of the solutes before reaching the detection cell. It can be used without modifications. For molecules without chromophore or fluorophore groups or with mobile phases with a high UV cut-off

(acetone, ethyl acetate, etc.), ELSD is useful.[1] But it cannot detect fragile or easily sublimable solutes because the nebulizate is heated. Moreover, this detection method does not preserve the solutes. To collect column effluent, a split must be installed at the outlet of the column to allow ELSD detection in a parallel direction to fraction collection with consequent loss of solutes.

Atomic Emission Spectrometry[3]

This detection mode can be used during ion separation. Kitazume et al. used a direct plasma atomic emission spectrometer (DCP, Spectra-Metrics Model SpectraSpan IIIB system with fixed-wavelength channels) for observation of the elution profile during the separation of nickel, cobalt, magnesium, and copper by CCC. For profile measurement of a single element, an analog recorder signal from the DCP was converted into a digital signal. The digital data were stored in a workstation and the elution profile was plotted. For simultaneous multielement measurement, the emission signal for each channel was integrated for 10 sec at intervals of 20 sec, and the integrated data were printed out.

Infrared Spectrometry[4]

Romanach and de Haseth have used a flow cell for liquid chromatography/Fourier transform-infrared spectrometry (LC/FT-IRS) in CCC. The main difficulty is the absorbance of the liquid-mobile phase. This problem is exacerbated in LC by low solute to solvent ratios in the eluates. In contrast, CCC leads to a high solute to solvent ratio so that it can be used with a very simple interface with a CCC column without any complex solvent removal procedures. High-sample loadings are possible by using variable path length of the IR detector (from 0.025 to 1.0 mm).

Mass Spectrometry[5]

Several interfaces have been used in CCC/MS. The first employed is the thermospray (TSP). When the column is directly coupled with TSP MS, the CCC column often breaks due to the high backpressure generated by the TSP vaporizer. In contrast, other interfaces using methods such as fast atom bombardment (FAB), electron ionization (EI), and chemical ionization (CI) have been directly connected to a CCC column without generating high backpressure. Such interfaces can be applied to analytes with broad polarity. As it is suitable to introduce effluent from the column CCC into MS only at a flow rate between 1 and 5 μl/min, the effluent is usually introduced into MS through a splitting tee, which is adjusted to an adequate ratio.

Nuclear Magnetic Resonance

Nuclear magnetic resonance (NMR) gives maximum structural information and allows measurement of the relative concentrations of eluted compounds. Spraul et al.[6] experimented with coupling of pH zone refining centrifugal partition chromatography (CPC) with NMR by using a biphasic system based on D_2O and an organic solvent.

On-line pH Monitoring

In pH zone refining, solutes are not eluted as separated peaks but as contiguous blocks of constant concentrations, so that it is highly difficult to monitor the separation by means of a UV detector. Online pH monitoring is generally used, allowing the observation of transitions between solutes, since each zone has its own pH determined by the pK_a and the solute concentration. The experiment was carried out in stop–flow mode.

OFF-LINE DETECTION

The analysis of the mobile-phase fractions collected at the outlet of the column is the oldest method used in CCC (droplet CCC and rotation locular CCC) to evaluate the quality of separation and to characterize solutes. With modern CCC methods such as CPC, CCC Type J, and

Table 1 Off-line detection.

Molecules	Fraction analysis
Schisanhenol acetate 5 and 6 of *Schisandra rubriflora*[5]	TLC
	Purity control by HPLC
Bacitracin complex[5]	Absorbance measure at 234 nm Purity control by HPLC
Dye species[5]	Mass spectrometry
Thyroid hormone derivatives[5]	UV on line at 280 nm. Gamma radioactivity measure of fractions Purity control by TLC, HPLC, and UV spectra
Cerium chloride and erbium chloride[5]	Inductively coupled plasma–atomic emission spectroscopy (ICP–AES)
Recombinant uridine phosphorylase[9]	SDS–PAGE Enzymatic activity by Magni method
Torpedo electroplax membranes[9]	Percentage of cholinergic receptor

cross axis, numerous applications have been described for preconcentration and preparative chromatography. Table 1 lists some applications described in reference books.[5,9] The type of detection used for each fraction depends on the isolated solute. They are TLC and HPLC on line with UV detector or mass spectrometer[10–12] (HPLC also enables an estimation of each fraction's purity,[13,14] a determination of fingerprints of medicinal plants,[15] etc.) for organic solutes, ICP–AES for mineral species, and polyacrylamide gel electrophoresis (PAGE) for biological molecules.[16,17] If the purity of the compound is satisfactory, a study by direct injection MS[18] and NMR[19] allows determination of its chemical structure. Biochemical tests are also available to verify the biological activity of biomolecules, which are often separated and collected in aqueous two-phase systems.[17]

CONCLUSIONS

High-speed CCC is mainly dedicated to preparative separations. Two types of detection are available: online and off-line detections. The first allows one to follow the quality of the separation. The second is suited to the analysis of fractions collected during preparative separation.

REFERENCES

1. Drogue, S.; Rolet, M.-C.; Thiébaut, D.; Rosset, R. Improvement of on-line detection in high-speed counter-current chromatography: UV absorptiometry and evaporative light-scattering detection. J. Chromatogr. A, **1991**, *538*, 91–97.
2. Bourdat-Deschamps, M.; Herrenknecht, C.; Akendengue, B.; Laurens, A.; Hocquemiller, R. Separation of protoberberine quaternary alkaloids from a crude extract of Enantia chlorantha by centrifugal partition chromatography. J. Chromatogr. A, **2004**, *1041* (1–2), 143–152.
3. Kitazume, E.; Sato, N.; Saito, Y.; Ito, Y. Separation of heavy metals by high-speed countercurrent chromatography. Anal. Chem. **1993**, *65*, 2225–2228.
4. Romanach, R.J.; de Haseth, J.A. Flow cell CCC/FT-IR spectrometry. J. Liq. Chromatogr. A, **1988**, *11* (1), 133–152.
5. Oka, H. High-speed counter current chromatography/mass spectrometry. In *High-Speed Counter Current Chromatography*; Ito, Y., Conway, W.D., Eds.; John Wiley & Sons: New York, 1995; 73–91.
6. Spraul, M.; Braumann, U.; Renault, J.-H.; Thépinier, P.; Nuzillard, J.-M. Nuclear magnetic resonance monitoring of centrifugal partition chromatography in pH-zone refining mode. J. Chromatogr. A, **1997**, *766*, 255–260.
7. Kitazume, E.; Bhatnagar, M.; Ito, Y. Separation of rare earth elements by high-speed counter-current chromatography. J. Chromatogr. A, **1991**, *538*, 133–140.
8. Oka, H.; Ito, Y. Improved method for continuous UV monitoring in high-speed counter-current chromatography. J. Chromatogr. A, **1989**, *475*, 229–235.
9. Lee, Y.W. Cross-axis counter current chromatography: A versatile technique for biotech purification. In *Counter Current Chromatography*; Menet, J.-M., Thiébaut, D., Eds.; Marcel Dekker Inc.: New York, 1999; 149–169.
10. Oka, H.; Harada, K.-I.; Suzuki, M.; Fuji, K.; Iwaya, M.; Ito, Y.; Goto, T.; Matsumoto, H.; Ito, Y. Purification of quinoline yellow components using high-speed counter-current chromatography by stepwise increasing the flow-rate of the mobile phase. J. Chromatogr. A, **2003**, *989* (2), 249–255.
11. Chen, L.-J.; Games, D.E.; Jones, J. Isolation and identification of four flavonoid constituents from the seeds of Oroxylum indicum by high-speed counter-current chromatography. J. Chromatogr. **2003**, *988* (1), 95–105.
12. Han, X.; Pathmasiri, W.; Bohlin, L.; Janson, J.-C. Isolation of high purity 1-[2′,4′-dihydroxy-3′,5′-di-(3″-methylbut-2″-enyl)-6′-methoxy]phenylethanone from Acronychia pedunculata by high-speed counter-current chromatography. J. Chromatogr. A, **2004**, *1022* (1–2), 213–216.
13. Chen, F.; Lu, H.-T.; Jiang, Y. Purification of paeoniflorin from Paeonia lactiflora by high-speed countercurrent chromatography. J. Chromatogr. A, **2004**, *1040* (2), 205–208.
14. Jiang, Y.; Lu, H.-T.; Chen, F. Preparative purification of glycyrrhizin extracted from the root of liquorice using high-speed counter-current chromatography. J. Chromatogr. A, **2004**, *1033* (1), 183–186.
15. Gu, M.; Ouyang, F.; Su, Z. Comparison of high-speed counter-current chromatography and high-performance liquid chromatography on fingerprinting of Chinese traditional medicine. J. Chromatogr. A, **2004**, *1022*, 139–144.
16. Yanagida, A.; Isozaki, M.; Shibusawa, Y.; Shindo, H.; Ito, Y. Purification of glycosyltransferase from cell-lysate of Streptococcus mutans by counter-current chromatography using aqueous polymer two-phase system. J. Chromatogr. B. & Anal. Technol. Biomed. Life Sci. **2004**, *805* (1), 155–160.
17. Shibusawa, Y.; Fujiwara, T.; Shindo, H.; Ito, Y. Purification of alcohol dehydrogenase from bovine liver crude extract by dye–ligand affinity counter-current chromatography. J. Chromatogr. B. & Anal. Technol. Biomed. Life Sci. **2004**, *799* (2), 239–244.
18. Wu, S.; Sun, C.; Cao, X.; Zhou, H.; Zhang, P.; Pan, Y. Preparative counter-current chromatography isolation of liensinine and its analogues from embryo of the seed of Nelumbo nucifera using upright coil planet centrifuge with four multiplayer coils connected in series. J. Chromatogr. A, **2004**, *1041* (1–2), 153–162.
19. Sannomiya, M.; Rodrigues, C.M.; Coelho, R.G.; dos Santos, L.C.; Hiruma-Lima, C.A.; Souza Brito, A.R.M.; Vilegas, W. Application of preparative high-speed counter-current chromatography for the separation of flavonoids from the leaves of Byrsonima crassa Niedenzu. J. Chromatogr. A, **2004**, *1035* (1), 47–51.

Detection in FFF

Martin Hassellöv
Department of Chemistry, Analytical and Marine Chemistry, Göteborg University, Göteborg, Sweden

Frank von der Kammer
Department for Environmental Science and Technology, Technical University of Hamburg-Harburg, Hamburg, Germany

INTRODUCTION

The main purpose of the detector in a field-flow fractionation (FFF) system is to quantitatively determine particle number, volume, or mass concentrations in the FFF size-sorted fractions. Consequently, a number, volume, or mass dependent size distribution of the sample can be derived from detection systems applied to FFF [e.g., (UV–Vis) fluorescence, refractive index, inductively coupled plasma ionization mass spectrometry (ICPMS)]. Further, on-line light scattering detectors can provide additional size and molecular weight distributions of the sample.

An analytical separation technique requires a detection method responding to some or all of the components eluting from the separation system. The choice of detector is determined by the demands of the sample and analysis. For FFF techniques, many of the detection systems have evolved from those used in LC techniques.

Detection can be carried out either with an online detector coupled to the eluent flow, or by collection and subsequent analysis of discrete fractions. For collected fractions, a range of analytical methods can be used, both quantitative (e.g., radioactive isotope labeling and metal analysis) and more qualitative (e.g., microscopic techniques). Online detectors suitable for coupling to the FFF channels include both non-destructive flow through cell systems and destructive analysis systems. It is often desirable to use online detection if possible since the total analysis time is much less than for discrete fraction analysis. Regardless of detector type, the dead volumes and flows in the system between the FFF channel and detector or fraction collector must be accurately determined and corrected for.

If the signal from a detector is a factor of two properties, it is possible to use another detector on line to resolve the different properties, e.g., multiangle light scattering (MALS) in combination with differential refractive index (DRI), or continuous viscosimetry + DRI. Alternatively, the two detectors may respond to two different properties of interest: In either case, it is almost as simple to acquire multiple detector signals as a single one. Multiple detectors can be arranged either in series or in parallel. A parallel detector arrangement avoids the band broadening problem encountered in the serial arrangement, where the first detector may cause significant band broadening for the second, due to the dead volume in the flow cell. For a serial detector connection, it is best to have the one with the smallest dead volume first, as long as it is not a destructive detector. Some detectors, such as DRI detectors, have restrictions regarding the maximum allowable pressure in the flow cell and must be connected last in series. For parallel coupling, the outflow from the FFF channel needs to be split to two or more detectors, and it is then essential to have control of the individual flows, since changes can induce drift in sensitivity and shifts in the dead times between the channel and detector during a run.

When choosing detector and experimental conditions, one needs to consider analyte concentration, detector sensitivity, background level, and detection limits. The maximum amount of analytes that can be injected is usually limited by sample overloading in the FFF channel (interparticle interactions), which disturbs the separation. It is necessary to have an analyte detection limit well below the overloading sample concentration to be able to quantify the peaks without too noisy a background. When using multiple detectors on line, their sensitivity may be quite different either overall or as a function of size range. An example of this is the use of a MALS detector, which has much higher sensitivity for larger particles, together with a DRI detector, which has the opposite sensitivity properties, making the small and large particle ranges difficult to cover.

OPTICAL DETECTION SYSTEMS

UV–Vis spectrophotometers are the most commonly used detectors for FFF applications mainly due to their availability, simplicity, and low cost. The majority of FFF work to date has focused on separation method development where the use of a UV–Vis detector showing the quality of the separations is sufficient. However, the quantification of the separated particles or macromolecules is not always straightforward, since the UV–Vis signal is actually a

turbidimetric measure for solid particles that is fully based on light scattering principles and an absorption measure for light-absorbing macromolecules. The absorbance contribution is only dependent on concentration, but there is a more complicated relationship involved in the light scattering signal, and both principles may be applicable if the solid particles and macromolecules are of comparable. In case of turbidity, large particles scatter light much more effectively than smaller particles, and particles with varying composition and refractive indices give rise to further complications. The correction of the detector signal according to Mie scattering theory is complicated but can often be simplified with appropriate assumptions.[1] For particles larger than 1 μm, efforts have been put into development of an absolute or standard-free quantification method using UV–Vis detection for gravitational FFF.[2] For the scattering phenomenon of nanometer sized particles, a corrective method was developed recently by evaluation of the turbidity spectrum acquired with spectral resolved UV/Diode array detector (DAD) detection.[3] In principle, the light scattering signal is dependent on particle properties such as, e.g., concentration and size, but also on the observation angle and the wavelength of the incident light. In the case of UV/DAD and fluorescence detectors, where only one fixed observation angle is available, the light scattering may be evaluated as a function of the applied wavelength. This approach was successfully applied[3] for the correction of the turbidity signal of FFF fractionated latex beads, which were smaller in size than the applied wavelength ($\lambda = 254$ nm).

The DRI detector is very common in size-exclusion chromatography (SEC) and records any change in refractive index of the sample stream relative to a reference stream. It is a general detector with the advantage of responding to almost all solutes, and it is concentration selective. The sensitivity of a DRI detector is not always the best, but new detector models offer different lengths of optical path, so that the sensitivity can be adjusted to match sample concentration. The DRI detector is not sensitive to changes in flow rate, but is highly sensitive to temperature changes. It is probably the most used detector for FFF applications after the UV detector.

Flows through fluorescence detectors are very common in LC, mainly due to the high selectivity and good signal-to-noise ratio. Only a few papers on FFF with fluorescence detectors are published, but when the analytes have suitable fluorescence properties, this is an excellent choice.

For fluorescence detectors offering excellent stray light suppression, a special mode of operation is available that turns them into simple light scattering detectors. By setting the excitation wavelength equal to the emission wavelength, the light scattered by particles is observed at 90° to the incident light. In contrast to turbidimetry in UV–Vis detectors, this is termed nephelometry and not interfered by light-absorbing substances. The problem of the dependence of the light scattering signal on sample properties other than particle concentration, such as particle size and shape, is also present with this technique.

Photon correlation spectroscopy (PCS), also called dynamic light scattering or quasielastic light scattering, correlates the short-term fluctuations of the light scattering signal to the diffusion coefficients of the sample particles. Photon correlation spectroscopy is a valuable tool in validation of FFF separations. One prerequisite of PCS is that the sample itself be at rest and show nearly no motion other than the Brownian motion of the analyte. Hence, it is too slow to be of practical use as an online detector. Recent flow-through static light scattering detectors offer a PCS option. This can only provide the PCS detection on line and "in flow" for very small macromolecules and particles, which must be present at sufficiently large concentrations. Photon correlation spectroscopy has, for example, been used for verification of the average sizes obtained from FFF theory for discrete fractions of emulsion separated using sedimentation FFF.[4]

Improvements in light scattering theory and instrumentation have been going on for decades, but the development of the MALS instrument—from the earlier low angle light scattering (LALS) technology, now incorporating up to 18 detectors measuring the scattered light at individual angles—presents a breakthrough in particle sizing. Compared to LALS instruments, multiangle detection allows more physical properties of the particles to be derived from the results. Also, the MALS instrument has higher sensitivity and is less affected by dust particles in the sample. Light scattering techniques give average values of the properties of the particle population in the sample and do not describe the property distribution of the sample, but when coupled to a particle sizing technique, such as FFF, the distributions of the different properties are derived from each size fraction.

MALS theory has been thoroughly described in several papers by Wyatt[5] and will only be mentioned briefly here. For each size fraction or batch measurement, the following applies as long as the limits of the Rayleigh–Gans–Debye approximation are fulfilled. This means that the particles are smaller than the incident light's wavelength, the refractive index is similar to that of the solvent, and no light absorption occurs:

$$\frac{Kc}{R_\theta} = \frac{1}{M_w P(\theta)} + 2A_2 c + \cdots \quad (1)$$

$$P(\theta) = 1 - a_1[2k\sin(\theta/2)]^2 + a_2[2k\sin(\theta/2)]^4 - \cdots \quad (2)$$

K is a light scattering constant including refractive index increment and wavelength of the scattering light and A_2 is the second virial coefficient. If the sample is very dilute, the second term of Eq. 1 can be neglected and the excess Rayleigh ratio, R_θ (net light scattering contribution from each component at angle θ), becomes directly proportional

to $M_wP(\theta)$. On plotting R_θ/Kc against $\sin^2(\theta/2)$, the intercept yields molecular weight (M_w) at the concentration c, and from the slope, the root mean square radius (RMS radius) can be derived. One great advantage with the MALS detector is that it does not demand calibration of the channel with reference materials. The absolute concentration of the analyte is necessary to determine the molar mass of the analyte since the signal includes a factor of concentration. The determination of the RMS radius is independent of concentration and can be achieved from the MALS signals alone. To acquire the sample concentration at each time slice, a concentration calibrated DRI detector is commonly used on line with the MALS detector. FFF/MALS/DRI is receiving much interest and attention and many applications have been developed in recent years, especially in synthetic polymer and biopolymer characterization. Thielking and Kulicke[6] have published papers on the coupling of FFF/MALS/DRI for analysis of both polystyrene particles and smaller polystyrene sulfonates (PSS). Fig. 1 shows their results of DRI derived concentration and molecular weight given from MALS data as a function of elution volume for seven PSS standards. However, for small molecules ($<$ 10 kDa), the sensitivity of the MALS detector is rather poor. The use of MALS together with FFF proved to be useful and complemented SEC/MALS techniques for polymers that could not be fractionated by SEC. After the first applications were documented,[6] several FFF subtechniques were coupled to MALS. The target analytes were mainly polysaccharides,[7] different kinds of polystyrene latex particles,[5,8] and starch polymers.[9] Nearly no characterization of natural particles using FFF/MALS is reported. Magnuson et al.[10] analyzed freshly precipitated iron oxides with FFF/MALS, and it was applied to analyze natural colloids extracted from soil.[11]

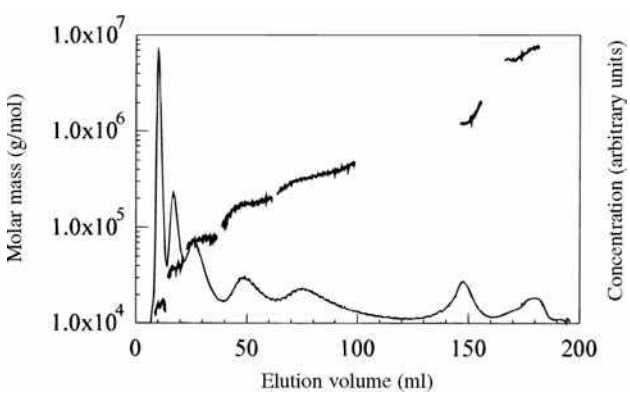

Fig. 1 Results from FlFFF/MALS/DRI analysis of seven PSS standards. Molecular weight derived from MALS data and concentration from the DRI detector.
Source: From On-line coupling of flow field-flow fractionation and multiangle laser light scattering for the characterization of macromolecules in aqueous solution as illustrated by sulfonated polystyrene samples, in Anal. Chem.[6]

The technique complements FFF ideally, since FFF provides a prefractionation to overcome limitations of MALS on broad distributed bulk samples, and MALS delivers independent molar mass and RMS radius determination.

In an evaporative light scattering detector (ELSD), the sample is nebulized, and when the solvent in the resulting droplets is evaporated, their mass content is proportional to particle mass in the sample stream. The particles are detected with a laser light scattering detector and the signal is related to their size. The ELSD has not been extensively used in FFF. Oppenheimer and Mourey[12] showed that it can be a good complement to turbidimetric detection in sedimentation FFF for particles smaller than 0.2 μm. This detector is free from the problems associated with UV detectors when applied to a broad size range or samples with differing extinction coefficients over the size range. Further, it can be used for samples lacking absorbance characteristics. Compton, Myers, and Giddings[13] presented a single particle detector for steric FFF (1–70 μm) based on light scattering of single particles flowing through the laser light path. Today, there are several other commercial flow stream particle counters available.

The continuous viscosity detector has been shown to be a good detection tool for thermal FFF analysis of polymer solutions.[14] Due to the high sample dilution in FFF, the viscosity detector response above the solvent baseline, ΔS, is only dependent on the intrinsic viscosity of every sample point, $[\eta]$, multiplied by the concentration, c, at the corresponding points:

$$\Delta S = [\eta]c \tag{3}$$

If a concentration-selective detector, such as a DRI detector, is connected on line with the viscosity detector, the ratio of the two signals yields the intrinsic viscosity distribution of the polymer sample. In polymer characterization, the intrinsic viscosity can be a property just as important as the molecular weight distribution. Furthermore, polymer intrinsic viscosity follows the Mark–Houwink relation to the molecular weight, M, where K and a are Mark–Houwink viscosity constants:

$$[\eta] = KM^a \tag{4}$$

MASS SPECTROMETRIC DETECTION SYSTEMS

The mass spectrometry (MS) detection methods covered here are mainly a selection of commonly used liquid chromatography/mass spectrometry (LC/MS) methods, some of which have been optimized for FFF techniques or could potentially be good detection tools for FFF separations.

The issue in the coupling of a liquid-based separation method to a mass spectrometer is the ion source conversion of dissolved analytes to ions in the high vacuum mass

analyzer, which for instance can be magnetic sectors, quadrupoles, ion traps, or time-of-flight (TOF) analyzers. Different ion sources give different information depending on the ionization mechanisms and will be discussed for each method below.

In most FFF separations, a moderate concentration of dispersion agent, electrolyte, or surfactant is used to improve the separations. A common feature for most MS instruments is that salt in the liquid entering the ion source leads to deterioration of the performance of the MS by lowering the signal-to-noise ratio and by condensing on surfaces inside the MS, thus continuously increasing the background level.

Today, the most frequently used LC/MS ion source is electrospray ionization (ESI), in which the sample stream ends in a narrow capillary, put on a high voltage (positive or negative). This potential, sometimes together with a sheath gas flow, gives rise to a spray of small charged droplets ($\sim$ 1 μm). When the solvent is evaporated from these droplets, electrostatic repulsion forces smaller droplets ($\sim$ 10 nm) to leave. Before entering the semivacuum region, free analytes with one or more net charges usually due to proton transfer or ion adducts (e.g., Li^+, Na^+, or NH_4^+) dominate.

Electrospray ionization is a mild ionization method, that is, almost no fragmentation of the ions occurs. It is applicable to all organic compounds involved in proton exchange or binding to ions in the gas phase, which includes almost all biomolecules and polymers. In ESI/MS, multiple charges occur with a charge distribution for all components. This charge envelope usually has maximum intensity at *m/z* about 1000 and rarely ranging beyond 2000 in *m/z*. This has the advantage that large molecules, such as peptides, DNA molecules, or polymers, can be analyzed by all common MS analyzers, but the drawback is that the resulting spectra can be complicated to interpret. For single mass molecules such as peptides, there are numerical models to deconvolute the single charge molecular weight from the ESI/MS *m/z* spectra, but for incompletely separated polymer components, the overlapping charge distributions for the individual polymer components make the interpretation complicated. ESI/MS sensitivity is dramatically reduced due to cluster formation in the presence of more than a few millimoles per liter of the salt, and surfactants can have a devastating effect on the ESI/MS spectra. Therefore, a volatile buffer should be used if possible (e.g., ammonium acetate, ammonium nitrate). ESI/MS has been used as a detector for flow field-flow fractionation (FlFFF) analysis of low molecular weight ethylene glycol polymers,[15] where the effect of different carriers on cluster formation was investigated. ESI/MS has been coupled to SEC in several applications for polymer analysis and other applications where FFF techniques can be successfully used, including proteins, neuropeptides, and DNA molecule segments. Modern ESI/MS has a broad range of flow rates from nanoliters up to a milliliter per minute.

Atmospheric pressure chemical ionization (APCI) is a method not yet applied to FFF, but could potentially be a good alternative to ESI for semivolatile analytes lacking a natural site for a charge. The analytes are evaporated and exposed to gas phase molecules ionized by a high voltage corona discharge electrode. The analytes are subsequently ionized by a charge transfer from the gas molecules. Atmospheric pressure chemical ionization has been shown to be less sensitive to buffer salts than ESI, and no fragmentation occurs in the ion source. Mainly singly charged ions are formed, making APCI less applicable to large molecules, depending on the upper range of the MS analyzer. Atmospheric pressure chemical ionization has a good flow rate compatibility (0.3–1.5 ml/min) with FFF.

Matrix assisted laser desorption ionization (MALDI) is a frequently used ionization technique, but it is rarely used as an online detector. The sample stream is applied to a target plate, and it is allowed to cocrystallize with the matrix, which is subsequently desorbed, ionized with a laser, and analyzed in the MS. MALDI/TOF has been successfully used to determine molecular weight distributions of fractions collected after thermal FFF separation of polydisperse polymers.[16] MALDI is a good ion source, due to the soft ionization with high efficiency and simple mass spectra, even for heavier molecules, since the majority carry only a single charge.

ICPMS is an ion source for elemental analysis where the analyte stream is introduced into a high-energy plasma with efficient atomization and ionization, producing almost entirely singly charged elemental ions. It has multielement capability with excellent sensitivity and has good flow rate compatibility (0.1–1.5 ml/min) with FFF techniques. ICPMS has previously been applied to sedimentation FFF for determination of major element composition in different size fractions of suspended riverine particles and soil particles in the size range 50–800 nm,[17] and recently flow FFF coupled on line to ICPMS has been used to determine elemental size distributions for over 55 elements in freshwater colloidal material (1–50 nm).[18,19] Fig. 2 shows a selection of elements and the signal from the UV detector, coupled on line before the ICPMS, from a river water sample. An interface between the FFF channel and the ICPMS was used to supply acid, to improve the performance of the nebulizer–spray chamber system, and internal standard. The interface also serves to dilute and split away about half of the salt content. The salt is necessary for the FFF separation, but harmful to the ICPMS.

DENSITY-BASED DETECTION

A continuous density detector works on the principle of a liquid flowing through an oscillating U-shaped glass tube, where the oscillating frequency is found relating the oscillations to the density of the flowing liquid. A densimetric

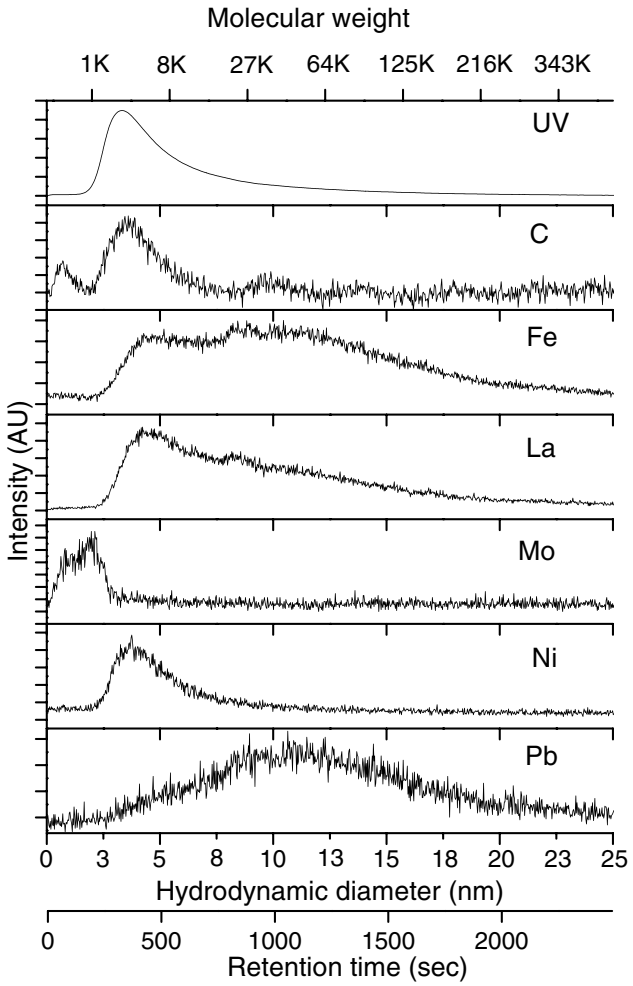

Fig. 2 Elemental size distributions of the colloidal material in a freshwater sample as given from an FlFFF coupled to ICPMS. A UV detector is placed on line prior to the ICPMS and the UV size distribution is included. The signals are plotted as a function of retention time, hydrodynamic diameter (from FFF theory), and molecular weight (from standardization with PSS standards).
Source: From Determination of continuous size and trace element distribution of colloidal material in natural water by on-line coupling of flow field-flow fractionation with ICMPS, in Anal. Chem.[18]

detector has been evaluated for sedimentation FFF,[20] and the conclusions were that it is a universal concentration-selective detector without the need for signal correction or transformation. The sensitivity is however a limiting factor, since it is dependent on the density difference between the sample and the carrier liquid. A density difference of 0.2 g ml^{-1} is sometimes sufficient, but to achieve higher sensitivity a difference up to 1.0 is desirable, making densimetric detection suitable for inorganic particles, but less appropriate for lighter organic analytes. The densimeter detector is sensitive to temperature changes, but insensitive to flow changes, making it most suitable for flow programming applications.

CONCLUSIONS

A multidetector approach is often applied in FFF since all detection systems have some advantages and limitations over some size ranges, sample types, and detection limits. For example, the most common detector, the UV–VIS, has limitations that it is selective for both absorption and turbidity but it is still widely used. Elemental analysis of FFF fractions with ICPMS has been successfully developed during recent years, but other mass spectrometric hyphenations are still very few. On-line light scattering has proven to be a very valuable system to determine molecular weight and RMS radius distributions (MALS) as well as diffusion coefficients and hydrodynamic radius (DLS).

REFERENCES

1. Yang, F.-S.; Caldwell, K.D.; Gidding, J.C. Colloid characterization by sedimentation field-flow fractionation. J. Colloid Interface Sci. **1983**, *92*, 81–91.
2. Reschiglian, P.; Melucci, D.; Zattoni, A.; Giancarlo, T. Quantitative approach to field-flow fractionation for the characterization of supermicron particles. J. Microcol. Sep. **1997**, *9*, 545–556.
3. Zattoni, A.; Loli Piccolomini, E.; Torsi, G.; Reschiglian, P. Turbidimetric detection method in flow-assisted separation of dispersed samples. Anal. Chem. **2003**, *75*, 6469–6477.
4. Caldwell, K.D.; Li, J. Emulsion characterization by the combined sedimentation field-flow fractionation–photon correlation spectroscopy methods. J. Colloid Interface Sci. **1989**, *132*, 256–268.
5. Wyatt, P.J. Submicrometer particle sizing by multiangle light scattering following fractionation. J. Colloid Interface Sci. **1998**, *197*, 9–20.
6. Thielking, H.; Kulicke, W.-M. On-line coupling of flow field-flow fractionation and multiangle laser light scattering for the characterization of macromolecules in aqueous solution as illustrated by sulfonated polystyrene samples. Anal. Chem. **1996**, *68*, 1169–1173.
7. Duval, C.; Le Cerf, D.; Picton, L.; Muller, G. Aggregation of amphiphilic pullulan derivatives evidenced by on-line flow field flow fractionation/multi-angle laser light scattering. J. Chromatogr. B, **2001**, *753*, 115–122.
8. Frankema, W.; van Bruijnsvoort, M.; Tijssen, R.; Kok, W.T. Characterisation of core-shell latexes by flow field-flow fractionation with multi-angle light scattering detection. J. Chromatogr. A, **2002**, *943*, 251–261.
9. Roger, P.; Baud, B.; Colonna, P. Characterization of starch polysaccharides by flow field-flow fractionation–multi-angle laser light scattering–differential refractometer index. J. Chromatogr. A, **2001**, *917*, 179–185.
10. Magnuson, M.L.; Lytle, D.A.; Frietch, C.M.; Kelty, C.A. Characterization of submicrometer aqueous iron III colloids formed in the presence of phosphate by sedimentation field-flow fractionation with multiangle laser light scattering detection. Anal. Chem. **2001**, *73*, 4815–4820.
11. Kammer, F.v.d.; Baborowski, M.; Friese, K. Field-flow fractionation coupled to multi-angle laser light scattering

detectors: Applicability and analytical benefits for the analysis of environmental colloids. Anal. Chim. Acta. **2005**, *552* (1–2), 166–174.
12. Oppenheimer, L.E.; Mourey, T.H. Use of an evaporative light-scattering mass detector in edimentation field-flow fractionation. J. Chromatogr. **1984**, *298*, 217–224.
13. Compton, B.J.; Myers, M.N.; Giddings, J.C. A single particle photometric detector for steric field-flow fractionation. Chem. Biomed. Environ. Instrum. **1983**, *12*, 299–317.
14. Kirkland, J.J.; Rementer, S.W.; Yau, W.W. Polymer characterization by thermal field flow fractionation with a continuous viscosity detector. J. Appl. Polym. Sci. **1989**, *38*, 1383–1395.
15. Hassellöv, H; Hulthe, G.; Lyvén, B.; Stenhagen, G. Electrospray mass spectrometry as online detector for low molecular weight polymer separations with flow field-flow fractionation. J. Liq. Chromatogr. Relat. Technol. **1997**, *20*, 2843–2856.
16. Kassalainen, G.E.; Williams, S.K.R. Coupling thermal field-flow fractionation with matrix-assisted laser desorption/ionization time-of-flight mass spectrometry for the analysis of synthetic polymers. Anal. Chem. **2003**, *75* (8), 1887–1894.
17. Taylor, H.E.; Garbarino, J.R.; Hotchin, D.M.; Beckett, R. Inductively coupled plasma-mass spectrometry as an element-specific detector for field-flow fractionation particle separation. Anal. Chem. **1992**, *64*, 5036.
18. Hassellöv, M.; Lyvén, B.; Haraldsson, C.; Sirinawin, W. Determination of continuous size and trace element distribution of colloidal material in natural water by on-line coupling of flow field-flow fractionation with ICMPS. Anal Chem. **1999**, *71*, 3497–3502.
19. Stolpe, B.; Hassellöv, M.; Andersson, K.; Turner, D.R. High resolution ICPMS as an on-line detector for flow field-flow fractionation; multi-element determination of colloidal size distributions in a natural water sample. Anal. Chim. Acta **2005**, *535* (1–2), 109–121.
20. Kirkland, J.J.; Yau, W.W. Quantitative particle-size distributions by sedimentation field-flow fractionation with densimeter detector. J. Chromatogr. **1991**, *550*, 799–809.

Detection in Ion Chromatography

Rajmund Michalski
Institute of Environmental Engineering, Polish Academy of Science, Zabrze, Poland

Abstract
Since its introduction in 1975 ion chromatography (IC) has been used in most areas of analytical and environmental chemistry. Although the conductivity detector is still the most popular, other types of detection can be applied for different analytes. These include the following methods: electrochemical (e.g., amperometric, potentiometric), photometric (UV/Vis, chemiluminescence), and spectrometric detectors used mainly in hyphenated techniques.

INTRODUCTION

Detection methods applied in ion chromatography (IC) can be divided into electrochemical and spectrometric methods. Electrochemical detection methods include conductometric, amperometric, and potentiometric methods, while spectroscopic methods include molecular techniques (UV/Vis, chemiluminescence, fluorescence, and refractive index methods), and spectroscopic techniques such as: atomic absorption spectrometry (AAS), atomic emission spectrometry (AES), inductively coupled plasma–optical emission spectrometry (ICP–OES), inductively coupled plasma–mass spectrometry (ICP–MS), and mass spectrometry (MS).[1]

The performance of ion chromatographic detectors has considerably increased over the last 30 years. The progress made so far has made them more sensitive and convenient in use, as well as increased detection selectivity.[2]

Fundamentals of detection methods used in IC have been comprehensively covered in several monographs.[3,4] Detection methods employed in IC can be divided into direct and indirect ones (Fig. 1) and taking into consideration the type of application (Table 1). Direct detection methods are those in which the eluate ions exhibit a much smaller value of the measured property than solute ions. Detection methods are called indirect if the eluate ions exhibit a much higher value of the property measured than solute ions.

CONDUCTIVITY DETECTION

The most widespread detection technique in IC is still conductometry, because electric conductivity of electrolytes is strongly dependent on concentration.

This technique has recently been simplified by the introduction of self-regenerating devices thanks to which electrolytically hydrolysis of water in the eluate stream takes place. This, in turn, produces the ions necessary for the regeneration of the suppressor, thus avoiding the need for a separate regenerant device.[5]

The principle of functioning of a conductivity detector lies in differential measurement of mobile phase conductivity both before and during solute ion elution. The conductivity cell is placed either directly next to an analytical column or after a suppressor device, which is required to reduce background conductivity, in order to increase the signal-to-noise ratio, and thus sensitivity. In IC, without eluate conductivity suppression the signal-to-noise ratio can be maximized if a low-conductivity mobile phase at a low concentration is used.

Electric conductivity usually increases with the increase of temperature, and viscosity of the solution exponentially decreases as the temperature rises.

The equivalent conductances of anions and cations are typically between 35 S cm^2/val and 80 S cm^2/val. The H^+ ion with 350 S cm^2/val and the OH^- ion with 198 S cm^2/val are the only significant exceptions. Consequently, detector signal depends not only on the solute ion concentration, but also on the equivalent conductances of both eluate cations and solute anions, and on their degree of dissociation. The degree of eluate and solute ion dissociation is determined by the pH value of the mobile phase.

A general problem in suppressed IC can be the fact that sensitivity is poor when the product of suppression exhibits a small degree of dissociation, for example in the case of very weak acid anions (e.g., silicate, cyanide).

Suppressed and non-suppressed conductivity methods of detection have a number of things in common. The things in common include the fact that in both cases electric conductivity of the analytes is measured. On the other hand, the most apparent difference is that one method uses a suppressor system while the other does not.

Table 1 Survey of the main detection methods used in ion chromatography.

Detection mode	Principle	Applications
Conductivity	Electrical conductivity	Anions and cations with pK_a or pK_b <7
Amperometry	Oxidation or reduction	Anions and cations with pK_a or pK_b >7
Direct and indirect UV/Vis	UV/Vis light absorption	UV-active anions and cations, heavy and transition metals after derivatization reaction
Fluorescence	Excitation and emission	Ammonium, amino acids, and primary amines after postcolumn derivatization
Refractive index	Change in refractive index	Anions and cations at higher concentrations
ICP-AES, ICP-MS	Atomic emission	Hyphenation techniques for selective and sensitive metal analysis
MS	ESI	Hyphenation technique for structural characterization of organic anions and cations

The use of suppressed conductivity detection is limited when high-capacity ion-exchange columns are used; the concentrations of hydroxide- or carbonate-based eluates needed for reasonable elution times would be too high for continuously working membrane suppressors.

Conductivity detection can be applied to ionic species including all anions and cations of strong acids and bases (e.g., fluoride, chloride, nitrite, nitrate, phosphate, sulfate, sodium, potassium, magnesium, calcium, and ammonia). Ions of weaker acids and bases can be detected provided the pH value of the eluate is chosen to maximize the ionization of analytes in order to increase sensitivity. The relatively simple construction and operation, accuracy and low cost contribute to its utility; thus, it is used in over 95% of the analytes, where ion-exchange separation procedures are involved.[6]

AMPEROMETRIC AND POTENTIOMETRIC DETECTIONS

Amperometric detection is generally used for the analysis of solutes with pK values above 7, which, owing to their

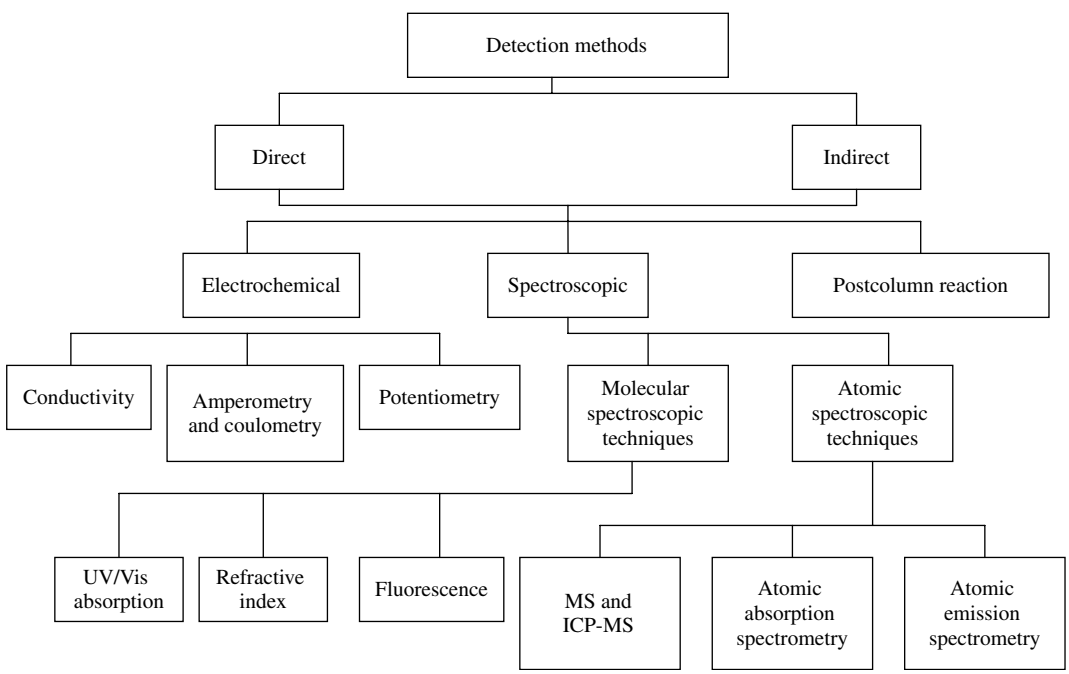

Fig. 1 Classification of detection methods for ion chromatography.

low dissociation, can hardly be detected by means of suppressed conductivity.

Conventional amperometric detectors employ a three-electrode detector cell consisting of a working electrode, a reference electrode, and a counter electrode. The electrochemical reaction at the working electrode is either oxidation or reduction. The required potential is applied to the working electrode. The electric current resulting from this electrochemical reaction serves as the analytical signal and is directly proportional to the concentration of the electrochemically active analyte. Generally, amperometric detection is carried out in a direct mode that requires electrochemically non-active coions in the mobile phase.

The potential applied to the working electrode may be constant during the period of separation or it may be applied in pulse mode. Application of this method includes determining ions like nitrite, bromide,[7] iodide, sulfite, thiosulfate, thiocyanate, cyanide, or heavy and transition metals.[8]

POTENTIOMETRIC DETECTION HAS ONLY FOUND LIMITED USE IN ROUTINE IC

The main disadvantages of potentiometric detectors in IC are: slow response of many electrodes and the fact that they respond well to only a few different species.[9]

UV/VIS DETECTION

UV/Vis detection is a very popular detection mode for high-performance liquid chromatography (HPLC) and although its significance in IC is smaller, it is considered a useful supplementary means of detection. A disadvantage of UV/Vis detection is that most inorganic anions do not have an appropriate chromophore. UV/Vis detection methods can be divided into direct and indirect methods. In UV/Vis detection, the change of absorbance during elution of an analyte ion is governed by the differences of molar absorbance of analyzed ions and coions in the mobile phase.

For direct UV/Vis detection, molar absorption of coions should be zero. UV/Vis transparent mobile phase includes alkane sulfonic acids and their salts, phosphate buffers, sodium perchlorate, and similar electrolytes that allow the direct UV detection of selected ions.[10]

Direct detection has gained great significance in determination of nitrite and nitrate,[11] as well as bromide and iodide in the presence of high chloride concentrations. Moreover, chromate, sulfide, thiocyanate, thiosulfate, and selected metal chloro- and cyano-complexes[12] can be determined by means of this method.

UV/Vis detection may also be performed indirectly. This method is called indirect photometric method. It is a more universally employed detection mode, for which a wavelength should be chosen where molar absorption of analyte is zero and high for eluate coions.[13] UV/Vis detection in combination with postcolumn reactions proves to be a versatile technique that provides enhanced sensitivity and selectivity for specific application.[14]

The instrumentation for postcolumn derivatization detection in IC is relatively simple. The effluent from the column is mixed with the reagent by means of a T-piece. The reagent is delivered by a pump or by pressure applied to the reagent bottle.

Next, a knitted polytetrafluoroethylene (PTFE) capillary can serve as the flow-through reactor, its length depending on the necessary reaction time.

OTHER SPECTROSCOPIC DETECTION METHODS

Chemiluminescence detection is another technique based on light emission. It is generally performed in a postcolumn reaction mode. The majority of chemiluminescence detection methods in IC is based on luminal reaction that involves aqueous alkaline oxidation of the luminal in the presence of a catalyst.[15]

In IC, fluorescence detection is rarely used as a detection method since very few ions fluoresce.[16] Refractive index detection is a non-selective detection. Only because of its moderate sensitivity, very poor selectivity, and sensitivity to baseline fluctuations, it is very rarely used in IC. The only advantage of refractive index detection is the ability to use comparatively concentrated eluants that allow the use of high-capacity ion exchangers.[17]

Atomic spectroscopic techniques in use for IC detection include both AAS and AES. The majority of AES detection techniques in IC is based on the ICP source.

In recent years, the coupling of IC with element-specific detection methods including AAS, ICP-AES, ICP-MS, and MS has gained significant importance.

ICP-MS offers unique advantages including element specificity, wide linear dynamic range, low detection limits and, ability to perform isotope dilution analysis.[18,19]

The most useful detection mode in IC seems to be MS. Because of its flexibility, this coupling method has numerous possible applications in ion analysis.[20,21] IC coupled with spectrometric detector (IC–MS) is a modern determination method for quantitative and qualitative analysis. Similar analytes are separated by IC and subsequently detected by a mass spectrometer. Both ionic substances (anionic and cationic) and polar substances (e.g., organic acids or sugars) can be determined with this very sensitive detection system.

Analyses using an MS detector are also characterized by a very low matrix influence and are therefore ideally suitable for cases involving coelution, eluate interference, or sample matrix influence. This means that MS represents a real alternative to conventional IC detectors such as conductivity, electrochemical or UV/Vis detectors. Because of IC–MS coupling, direct qualitative analysis of different species is possible. The mass-charge ratio is used for peak identification and resolving the molecular structure of the analyte. MS detection can be carried out in selected ion monitoring (SIM) or scan (*m/z*) mode.

In liquid chromatography with MS detection various ion sources can be used:

– electrospray ionization (ESI)
– atmospheric pressure chemical ionization (APCI)
– atmospheric pressure photochemical ionization (APPI)

ESI is a very soft ionization method. It shows the best sensitivity in IC for the polar and ionic analytes. By using ESI, in contrast to other ionization methods, multivalent ions also can be transferred to the gas phase. Further advantages of ESI are its dependability, simple handling and maintenance, and a wide range of use for polar and ionic substances in any molecular mass range.

In contrast to the conductivity detector, the MS detector is a mass-flow-dependent detector. This means that the flow rate influences the sensitivity of the signal. Flow rates below 1.0 ml/min should be used with ESI. In order to maximize the sensitivity of the detector the flow rate should be as low as possible. Various types of mass filters are used in IC–MS. Quadrupole is the most widespread one.

The advantages of IC–MS such as sensitivity and selectivity are noticeable in the analysis of drinking water (e.g., for the determination of perchlorate, the analysis of haloacetic acids or of disinfection by-products).[22] Other fields of application are: clinical and biochemical research (determination of organic acids, amines, or sugars),[23] pharmaceutical industry (peak identification and purity tests), petrochemical industry (determination of indicator substances), food industry, electroplating industry, analysis of hazardous substances, and environmental analysis.[24,25]

CONCLUSION

Of the many forms of detection used in IC, conductometric detection is still the most popular. However, all other methods such as electrochemical and spectroscopic methods are more often applied especially for the analysis of trace ions in samples with complex matrices.

The most powerful detection technique for the trace analysis in complex matrices seems to be MS, separately or with inductively coupled plasma source or an electrospray source.

REFERENCES

1. Buchberger, W.W. Detection techniques in ion analysis, what are our choices? J. Chromatogr. A, **2000**, *884*, 3–22.
2. Bucherberger, W.W.; Haddad, P.R. Advances in detection techniques for ion chromatography. J. Chromatogr. A, **1997**, *789*, 67–83.
3. Weiss, J. *Handbook of Ion Chromatography*; Wiley-VCH: Weinheim, Germany, 2004.
4. Haddad, P.R. *Ion Chromatography: Principles and Applications*; Elsevier: Amsterdam, 1990.
5. Haddad, P.R.; Jackson, P.E.; Shaw, M.J. Developments in suppressor technology for inorganic ion analysis by ion chromatography using conductivity detection. J. Chromatogr. A, **2003**, *1000*, 725–742.
6. Buchberger, W.W. Detection techniques in ion chromatography of inorganic ions. Trend. Anal. Chem. **2001**, *20*, 296–303.
7. Tirumalesh, K. Simultaneous determination of bromide and nitrate in contaminated waters by ion chromatography using amperometry and absorbance detectors. Talanta **2008**, *74*, 1428–1434.
8. Buldini, P.L.; Cavalli, S.; Mevoli, A.; Sharma, J.L. Ion chromatographic and voltamperometric determination of heavy and transition metals in honey. Food Chem. **2001**, *73*, 487–495.
9. Sahin, M.; Sahin, Y.; Ozcan, A. Ion chromatography–potentiometric detection of inorganic anions and cations using polypyrrole and overoxidized polypyrrole electrode. Sens. Actuat. B-Chem. **2008**, *133*, 5–14.
10. Connolly, D.; Paull, B. Fast separation of UV absorbing anions using ion-interaction chromatography. J. Chromatogr. A, **2001**, *917*, 353–359.
11. Moorcroft, M.J.; Davis, J.; Compton, R.G. Detection and determination of nitrate and nitrite: A review. Talanta **2001**, *54*, 785–803.
12. Karmarkar, S.V. Anion-exchange chromatography of metal cyanide complexes with gradient separation and direct UV detection. J. Chromatogr. A, **2002**, *956*, 229–235.
13. Breadmore, M.C.; Haddad, P.R.; Fritz, J.S. Optimisation of the separation of anions by ion chromatography–capillary electrophoresis using indirect UV detection. J. Chromatogr. A, **2001**, *920*, 31–40.
14. Dasgupta, P.K. Postcolumn techniques: A critical perspective for ion chromatography. J. Chromatogr. Sci. **1989**, *27*, 422–444.
15. Derbyshire, M.; Lamberty, A.; Gardiner, P.H. Optimization of the simultaneous determination of Cr(VI) and Cr(VI) by ion chromatography with chemiluminescence detection. Anal. Chem. **1999**, *19*, 4203–4207.
16. Miura, Y.; Hatakeyama, M.; Hosino, T.; Haddad, P.R. Rapid ion chromatography of L-ascorbic acid, nitrite, sulfite, oxalate, iodide and thiosulfate by isocratic elution utilizing a postcolumn reaction with cerium(IV) and fluorescence detection. J. Chromatogr. A, **2002**, *956*, 77–84.
17. Wong, D.; Jandik, P.; Jones, W.R.; Haganaars, A. Ion chromatography of polyphosphates with direct refractive index detection. J. Chromatogr. A, **1987**, *389*, 279–285.
18. Montes-Bayon, M.; De Nicola, K.; Caruso, J.A. Liquid chromatography–inductively coupled plasma mass spectrometry (Review). J. Chromatogr. A, **2003**, *1000*, 457–476.

19. Fernandez, R.G.; Alonso, J.I.G.; Sanz-Medel, A. Coupling of ICP–MS with ion chromatography after conductivity suppression for the determination of anions in natural and waste waters. J. Anal. Atom. Spectrom. **2001**, *16*, 1035–1039.
20. Jin, M.C.; Yang, Y.W. Simultaneous determination of nine trace mono- and di-chlorophenols in water by ion chromatography atmospheric pressure chemical ionization mass spectrometry. Anal. Chim. Acta **2006**, *566*, 193–199.
21. Haddad, P.R.; Nesterenko, P.N.; Buchberger, W. Recent developments and emerging directions in ion chromatography. J. Chromatogr. A, **2008**, *1184*, 456–473.
22. Charles, L.; Pepin, D. Electrospray ion chromatography tandem mass spectrometry of oxyhalides at sub-ppb levels. Anal. Chem. **1998**, *70*, 353–359.
23. Saccani, G.; Tanzi, E.; Pastore, P.; Cavalli, S.; Rey, A. Determination of biogenic amines in fresh and processed meat by suppressed ion chromatography–mass spectrometry using a cation-exchange column. J. Chromatogr. A, **2005**, *1082*, 43–50.
24. Mathew, J.; Gandhi, J.; Hedrick, J. Trace level perchlorate analysis by ion chromatography–mass spectrometry. J. Chromatogr. A, **2005**, *1085*, 54–59.
25. Soukup-Hein, R.J.; Remsburg, J.W.; Breitbach, Z.S. Evaluating the use of tricationic reagents for the detection of doubly charged anions in the positive mode by ESI–MS. Anal. Chem. **2008**, *80*, 2612–2616.

Detection of TLC Zones

Joseph Sherma
Department of Chemistry, Lafayette College, Easton, Pennsylvania, U.S.A.

INTRODUCTION

After development with the mobile phase, the thin-layer chromatography (TLC) plate is dried in a fume hood and heated, if necessary, to completely evaporate the mobile phase. Separated compounds are detected on the layer by viewing their natural color, natural fluorescence, or quenching of fluorescence. These are physical methods of detection and are non-destructive. Substances that cannot be seen in visible or ultraviolet (UV) light can be visualized with suitable detection reagents to form colored, fluorescent, or UV absorbing compounds by means of derivatization reactions carried out pre- or postchromatography. Although dependent upon the particular analyte, layer, and detection method chosen, sensitivity values are generally in the nanogram range for absorbance and picogram range for fluorescence.

Other detection methods include radioactivity for labeled compounds (a non-destructive physical method) and biological methods (e.g., immunochemical or enzymatic reactions). Coupled detection methods such as TLC/infrared spectrometry (TLC/IR) or TLC/mass spectrometry (TLC/MS) can be used for confirmation of zone identity as well as quantification in some cases.

DIRECT DETECTION

Compounds that are naturally colored (e.g., plant pigments, food colors, dyestuffs) are viewed directly on the layer in daylight, while compounds with native fluorescence (aflatoxins, polycyclic aromatic hydrocarbons, riboflavin, quinine) are viewed as bright zones on a dark background under longwave (366 nm) UV light. Compounds that absorb around 254 nm (shortwave), including most compounds with aromatic rings and conjugated double bonds and some unsaturated compounds, can be detected on an "F-layer" containing a phosphor or fluorescent indicator (often zinc silicate). When excited with 254 nm UV light, absorbing compounds diminish (quench) the uniform layer fluorescence and are detected as dark violet spots on a bright green background. Viewing cabinets or boxes (Fig. 1) incorporating 254 and 366 nm UV-emitting mercury lamps are available commercially for inspecting chromatograms in an undarkened room. Detection by natural color, fluorescence, or fluorescence quenching does not modify or destroy the compounds, and the methods are, therefore, suitable for preparative layer chromatography. Derivatization reactions modify or destroy the structure of the compounds detected, but they are often more sensitive than detection with UV radiation.

UNIVERSAL DETECTION REAGENTS

Postchromatographic universal reactions such as iodine absorption or spraying with sulfuric acid and heat treatment are quite unspecific and are valuable for completely characterizing an unknown sample. Absorption of iodine vapor from crystals in a closed chamber produces brown spots on a yellow background with almost all organic compounds except for some saturated alkanes. Iodine staining is non-destructive and reversible upon evaporation, while sulfuric acid charring is destructive. Besides sulfuric acid, 3% copper acetate in 8% phosphoric acid is a widely used charring reagent. The plate, which must contain a sorbent and binder that do not char, is typically heated at 120–130°C for 20–30 min to transform zones containing organic compounds into black to brown zones of carbon on a white background. Some charring reagents initially produce fluorescent zones at a lower temperature before the charring occurs at a higher temperature.

SELECTIVE DERIVATIZATION DETECTION

Selective derivatization reagents form colored or fluorescent compounds on a group- or substance-specific basis and aid in compound identification. They also allow the use of a TLC system with lower resolution, because interfering zones may not be detected. If the detection is to be the basis of a quantitative (densitometric) analysis, the reagent used should react with the analyte to produce the primary product in proportion to the quantity present in the zones and not produce any interfering secondary compounds.

Derivatization can be performed before or after development of the layer with the mobile phase. Prechromatographic derivatization is carried out either in solution prior to sample application or directly on the plate by applying the sample and reagents at the origin or in the preadsorbent (or concentration) area. Prechromatographic derivatization may enhance compound stability or chromatographic selectivity as well as serving for detection. Types of prechromatographic derivatization reactions that have been used include acid and

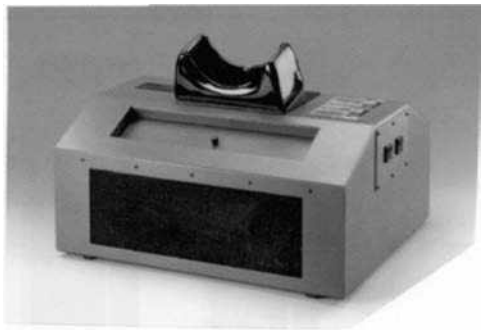

Fig. 1 Darkroom viewing cabinet with two overhead ports that accept one or two 8 W combination shortwave/longwave portable UV lamps.
Source: Photograph supplied by Analtech, Inc., Newark, Delaware.

alkaline hydrolysis, oxidation and reduction, halogenation, nitration and diazotization, hydrazone formation, esterification, and dansylation.

Derivatization reactions for detection are usually carried out postchromatography, and many hundreds of reagents have been reported in the literature. Selected examples are listed in Table 1.

APPLICATION OF DETECTION REAGENTS

Liquid chromogenic and fluorogenic detection reagents such as those in Table 1 can be applied by spraying or dipping the developed and dried layer. When a sequence of reagents is necessary, the layer is usually dried between each application.

Various types of aerosol sprayers that connect to air or nitrogen lines are available commercially for manual operation (Fig. 2), and this method is most widely used for reagent application. For safety purposes, spraying is carried out inside a laboratory fume hood or commercial TLC spray cabinet with a blower (fan) and exhaust hose, and protective eyeware and laboratory gloves are worn. The plate is placed on a sheet of paper or supported upright inside a cardboard spray box. The spray is applied from a distance of about 15 cm with a uniform up-and-down and side-to-side motion until the layer is completely covered. It is usually better to spray a layer two or three times lightly and evenly with intermediate drying rather than give a single, saturating application that might cause zones to become diffuse. Studies are required with each reagent to determine the optimum total amount of reagent that should be sprayed, but generally the layer is sprayed until it begins to become translucent. After visualization, zones should be marked with a soft lead pencil because zones formed with some reagents may fade or change color with time. A cordless electropneumatic sprayer with separate spray heads for low and high viscosity reagents is manufactured by Camag (Fig. 3). The ChromaJet DS 20 (Fig. 4) is a PC-controlled automatic apparatus that reproducibly sprays derivatization reagents on selected tracks of the layer; minimal reagent volumes are used, and operation can be documented in conformity with good laboratory practice (GLP) standards.

As with proper application using a fine-mist manual sprayer or an automated sprayer, dipping can provide uniform reagent application that leads to sensitive, reliable detection and reproducible results in quantitative densitometric analysis. The simplest method is to manually dip for a short time (5–10 sec) in a glass or metal dip tank. More uniform dip application of reagents can be achieved by use of a battery operated automatic, mechanical chromatogram immersion instrument (Fig. 5), which provides selectable, consistent vertical immersion and withdrawal speeds between 30 and 50 mm/sec and immersion times between 1 and 8 sec for plates with 10 or 20 cm heights. The immersion device can also be used for impregnation of layers with detection reagents prior to initial zone application and development, and for postdevelopment impregnation of chromatograms containing fluorescent zones with a fluorescence enhancement and stabilization reagent such as paraffin. Dip application to the layer cannot be used when two or more aqueous reagents must be used in sequence without intermediate drying. Dip reagents must be prepared in a solvent that does not cause the layer to be removed from the plate or the zones to be dissolved from the layer or to become diffuse; dip reagents are usually the same concentration or less concentrated than corresponding spray reagents.

Detection reagents can also be applied to the layer as a vapor, as mentioned above for iodine. Other reagents delivered to the layer by vapor exposure include *t*-butyl hypochlorite and HCl, both of which form fluorescent derivatives with a variety of compounds. The Analtech vapor-phase fluorescence (VPF) visualization chamber provides detection of compounds such as sugars, lipids, steroids, flavonoids, and antibiotics by induced fluorescence after heating the sealed chamber, containing the plate and ammonium bicarbonate crystals, on a hotplate to a temperature that decomposes the salt to ammonia.

HEATING THE LAYER

Layers often require heating to eliminate residual mobile phase after development, and again after spray or dip application of the detection reagent in order to complete the reaction upon which detection is based and ensure optimum derivative formation. Typical conditions are 5–15 min at 100–110°C. If a laboratory oven is used, the plate should be supported on a solid metal tray to help ensure uniform heat distribution. The plate heater shown in Fig. 6 usually provides more consistent heating conditions than an oven; it features a 20 × 20 cm flat, evenly

Table 1 Reagents used for postchromatographic derivatization of different classes of compounds.

Analyte(s)	Reagents and treatment	Result
Acidic or basic compounds	Solutions of pH indicators (e.g., bromocresol green, bromophenol blue)	Colored zones on pale background
Aldehydes	0.1 g 2,4-Dinitrophenylhydrazine in 100 ml methanol plus 1 ml conc. HCl	Orange-yellow or more colored zones on light-colored background
Alkaloids	0.85 g Basic bismuth nitrate, 40 ml water, and 10 ml glacial acetic acid mixed with 8 g potassium iodide in 20 ml water (Dragendorff reagent)	Yellow-brown zones
	0.3 g Hexachloroplatinic(IV) acid in 100 ml water mixed with 100 ml 6% potassium permanganate solution	Various colored and fluorescent zones; contrast of layer can be improved by heating
Amino acids	0.5% Ninhydrin in ethanol–glacial acetic acid (98 : 2); heat at 90–100°C for 5–10 min	Blue to purple zones
Amino acid derivatives	0.1% *p*-Dimethylaminobenzaldehyde in ethanol mixed (1 : 1) with conc. HCl (Ehrlich's reagent); heat at 60°C for 5 min	Different colored zones
Amphetamines	Spray with 0.5% aqueous Fast Black K salt, dry, spray with 0.5 *M* NaOH, spray again with Fast Black K solution	Orange-red and different violet colors
Antioxidants	Diazotized *p*-nitroaniline (800 mg *p*-nitroaniline in a mixture of 250 ml water and 20 ml HCl; 5 ml $NaNO_2$ added dropwise until solution is colorless)	Aromatic compounds give yellow to brown zones
Aromatic compounds	0.2 ml Formaldehyde (37%) in 10 ml conc. sulfuric acid (Marquis reagent); heat at 110°C for 20 min	Colored zones on light pink background; some may be fluorescent
Ascorbic acid	1–50 mg Cacotheline in 50 ml water, heat at 110°C for 20 min	Red-brown to violet zone on a yellow background
Carbohydrates	3% *p*-Anisidine hydrochloride in water-saturated butanol; heat at 110°C for 10 min	Red to brown zones
	1.2 g Ammonium vanadate in 95 ml water and 5 ml conc. sulfuric acid (Mandelin reagent)	Blue zones on yellow background
Flavonoids	1% Aluminum chloride solution in ethanol	Fluorescent zones
Lipids	5 g Phosphomolybdic acid in 100 ml absolute ethanol; heat at 100–150°C for 2–5 min	Blue zones on yellow layer background
Lipids and quinones	0.5–1.0 mg/ml Rhodamine 6G in ethanol	Fluorescent zones

(Continued)

Table 1 Reagents used for postchromatographic derivatization of different classes of compounds. *(Continued)*

Analyte(s)	Reagents and treatment	Result
Metal cations	0.25% Ethanol solution of alizarin, then ammonia vapor	Red-violet zones on violet background
Organic acids	100 mg 2,6-Dichloroindophenol sodium salt in 100 ml ethanol (Tillman reagent); heat at 100°C for 5 min	Red-orange zones on violet background
Pesticides (carbamates), sulfonamides, and primary amino compounds	1 g Sodium nitrite in 20 ml water diluted to 100 ml with conc. HCl–ethanol (17 : 83); dry plate; then 1% *N*-(1-naphthyl)ethylenediamine dihydrochloride in 10 ml water and 90 ml ethanol (Bratton–Marshall reagent)	Pink to violet zones
Pesticides (organophosphate)	2% 2,6-Dibromoquinone-4-chlorimide in glacial acetic acid; heat at 110°C for 10 min	Pink, orange, and brown zones on pale yellow background
Phenols	2% 4-Aminoantipyrene in 80% ethanol, then 4% potassium hexacyanoferrate(III) in ethanol–water (1 : 1) (Emerson reagent)	Red zones on light yellow background
Phenols, amino compounds, aromatic hydrocarbons, and coumarins	1% 2,6-Dibromoquinone-4-chloroimide in methanol (Gibbs reagent); heat at 110°C for 2–5 min	Different colored zones
Steroids	0.5 ml Anisaldehyde dissolved in 8 ml conc. sulfuric acid and diluted with 85 ml methanol plus 10 ml glacial acetic acid; heat at 100°C for 5–10 min	Violet-blue zones on light pink or colorless background; sometimes fluorescent zones
Sugars	5 g α-Naphthol in 160 ml ethanol, 20 ml sulfuric acid, and 13 ml water; heat at 110°C for 5 min	Blue-purple zones
Sulfonamides	15% Fluorescamine in acetone	Fluorescent zones
Terpenoids	0.5 ml Anisaldehyde mixed with 8 ml conc. sulfuric acid and diluted with 85 ml methanol and 10 ml glacial acetic acid; heat at 100°C for 5–10 min	Violet-blue zones on light pink or colorless background
	10% Antimony(III) chloride in chloroform; heat at 120°C for 5–10 min	Variously colored zones
Vitamin B_1	10 mg Potassium hexacyanoferrate and 1 g NaOH in 7 ml water and 13 ml ethanol	Bluish fluorescent zones
Vitamin E	Mixture (1 : 1) of 0.1 g iron(III) chloride hexahydrate in 50 ml ethanol with 0.25 g 2,2′-bipyridine (α,α′-dipyridyl) in 50 ml ethanol (Emmerie–Engle reagent)	Red zone

Fig. 2 Glass TLC reagent sprayer for use with an air line or the rubber bulb shown.
Source: Photograph supplied by Analtech.

heated ceramic surface; a grid to facilitate proper positioning of TLC or high-performance TLC (HPTLC) plates; programmable temperature between 25 and 200°C; and digital display of the programmed and actual temperatures. Prolonged heating time or excessive temperature can cause decomposition of the analytes and darkening of the layer background and should be avoided.

Some reagents can be impregnated into the layer before spotting of samples if the selectivity of the separation is not affected and the mobile phase does not strip the reagent during development. Detection takes place only upon heating after development. This method has been used for detection of lipids as blue spots on a yellow background on silica gel layers preimpregnated with phosphomolybdic acid by dipping, spraying, or development. Analtech sells precoated silica gel plates impregnated with 5% ammonium sulfate; heating at 150–200°C for 30–60 min in a closed container (the VPF Chamber, described above, can be used) generates sulfuric acid for charring detection of zones.

Fig. 3 TLC sprayer consisting of a charger and pump unit; homogeneous reagent aerosol particles in the 0.3–10 μm range are formed.
Source: Photograph supplied by Camag, Wilmington, North Carolina.

Fig. 4 ChromaJet DS 20 automated spray apparatus.
Source: Photograph supplied by Desaga Sarstedt-Gruppe GmbH, Wiesloch, Germany.

THERMAL DETECTION WITHOUT REAGENTS

Thermal derivatization (or thermochemical reaction) allows detection of zones without the use of reagents. For example, simple heating of amino-modified silica layers causes conversion of sugars, oligosaccharides, creatine, catecholamines, steroid hormones, and other compound types to stable fluorescent compounds. Heating times of 3–45 min and temperatures of 140–200°C have been used for different substances.

Fig. 5 Chromatogram immersion device set for 10 cm dipping depth with HPTLC plates. Vertical dipping and removal rates and the residence time in the reagent can be preselected.
Source: Photograph supplied by Camag, Wilmington, North Carolina.

Fig. 6 TLC plate heater.
Source: Photograph supplied by Camag.

BIOLOGICAL DETECTION

Several detection methods are based on the biological activities of certain compounds. Cholinesterase inhibiting pesticides (e.g., organophosphates, carbamates) are detected sensitively by treating the layer with the enzyme and a suitable substrate, which react to produce a colored product over the entire layer except where colorless pesticide zones are located due to their inhibition of the enzyme–substrate reaction.

TLC/immunostaining has been used to detect solasodine glycosides by separation of the compounds on a silica gel layer, transfer to a polyvinylidene difluoride membrane, and treatment of the membrane with sodium periodate solution followed by bovine serum albumin (BSA), resulting in a solasodine–BSA conjugate. Individual zones were stained by monoclonal antibody against solamargine.

Bioluminescence has been used for specific detection of separated bioactive compounds on thin layers (BioTLC). After development and drying of the mobile phase by evaporation, the layer is coated with micro-organisms by immersion of the plate. Single bioactive substances in multicomponent samples are located as zones of differing luminescence. The choice of the luminescent cells determines the specificity of the detection. A specific example is the use of the marine bacterium *Vibrio fischeri* with the BioTLC format. The bioluminescence of the bacterial cells is reduced by toxic substances, which are detected as dark zones on a fluorescent background with picogram level sensitivity.

BioTLC kits are commercially available from ChromaDex, Inc., (Santa Ana, California, U.S.A.).

RADIOACTIVITY DETECTION

Radioactive zones can be detected on thin layers by film autoradiography, digital autoradiography with a multiwire proportional chamber, use of charged–coupled devices, or bioimaging/phosphor imaging techniques. These methods differ in terms of factors such as simplicity, speed, sensitivity, resolution, linear range, and accuracy and precision of quantification, and the method of choice depends on the available instrumentation, the type of experiment, and the information needed.

ZONE IDENTIFICATION AND CONFIRMATION

The identity of the detected TLC zones is obtained initially by comparison of characteristic R_f values between samples and reference standards chromatographed on the same plate, where R_f equals the migration distance of the center of the zone divided by the migration distance of the mobile phase front, both measured from the start (origin). Identity is more certain if a selective chromogenic detection reagent yields the same characteristic color for sample and standard zones. Because the chromatogram is stored on the layer, multiple compatible detection reagents can be applied in sequence to confirm the identity of unknown zones. As an example, almost all lipids are detected as light green fluorescent zones by use of 2,7-dichlorofluorescein reagent, while absorption of iodine vapor differentiates between saturated and unsaturated lipids or lipids containing nitrogen. The identity of zones is confirmed further by recording UV or visible absorption spectra directly on the layer using a densitometer (in situ spectra), or by direct or indirect (after scraping and elution) measurement of fourier transform infrared (FT-IR), Raman, or mass spectra.

CONCLUSIONS

Details of reagent preparation, application and heating procedures, results, and selectivity of many hundreds of reagents for detection of all classes of compounds and ions, including those in Table 1, are available in the literature references listed.

BIBLIOGRAPHY

1. Bauer, K.; Gros, L.; Sauer, W. *Thin Layer Chromatography—An Introduction*; EM Science: Darmstadt, Germany, 1991; 41–46.
2. Cimpan, G. Pre- and postchromatographic derivatization. In *Planar Chromatography*; Nyiredy, Sz., Ed.; Springer Scientific Publisher: Budapest, Hungary, 2001; 410–445.

3. *Dyeing Reagents for Thin Layer Chromatography and Paper Chromatography*; E. Merck: Darmstadt, Germany.
4. Fried, B.; Sherma, J. *Thin Layer Chromatography—Techniques and Applications,* 4th Ed.; Marcel Dekker, Inc.: New York, NY, 1999; 145–175 (detection and visualization), 249–267 (radiochemical techniques).
5. Hazai, I.; Klebovich, I. Thin-layer radiochromatography. In *Handbook of Thin Layer Chromatography,* 3rd Ed; Sherma, J., Fried, B., Eds.; Marcel Dekker, Inc.: New York, NY, 2003; 339–360.
6. Jork, H.; Funk, W.; Fischer, W.; Wimmer, H. *Thin Layer Chromatography, Reagents and Detection Methods*; VCH Verlagsgesellschaft mbH: Weinheim, Germany, 1994; Vol. 1b.
7. Jork, H.; Funk, W.; Fischer, W.; Wimmer, H. *Thin Layer Chromatography, Physical and Chemical Detection Methods*; VCH Verlagsgesellschaft mbH: Weinheim, Germany, 1990; Vol. 1a.
8. Klebovich, I. Application of planar chromatography and digital autoradiography in metabolism research. In *Planar Chromatography*; Nyiredy, Sz., Ed.; Springer Scientific Publisher: Budapest, Hungary, 2001; 293–311.
9. Kreiss, W.; Eberz, G.; Weisemann, C. Bioluminescence detection for planar chromatography. Camag Bibliogr. Service (CBS) **2002**, *88*, 12–13.
10. Macherey-Nagel GmbH & Co. KG. TLC Catalog e2/5/0/1.98 PD; Dueren, Germany; A2–A81.
11. Maxwell, R.J. An efficient heating-detection chamber for vapor phase fluorescence TLC. J. Planar Chromatogr. Mod. TLC **1988**, *1*, 345–346.
12. Morlock, G.; Kovar, K.-A. Detection, identification, and documentation. In *Handbook of Thin Layer Chromatography,* 3rd Ed.; Sherma, J., Fried, B., Eds.; Marcel Dekker, Inc.: New York, NY, 2003; 207–238.
13. Stahl, E. *Thin Layer Chromatography—A Laboratory Handbook*; Academic Press: San Diego, CA, 1965; 485–502.
14. Tanaka, H.; Putalun, W.; Tsuzaki, C.; Shoyama, Y. A simple determination of steroidal alkaloid glycosides by thin layer chromatography immunostaining using monoclonal antibody against solamargine. FEBS Lett. **1997**, *404*, 279–282.
15. Touchstone, J.C. *Practice of Thin Layer Chromatography,* 3rd Ed.; Wiley-Interscience: New York, NY, 1992; 139–183.
16. Zweig, G.; Sherma, J. *Handbook of Chromatography*; CRC Press: Boca Raton, FL, 1972; Vol. 1, 103–189.

Detection Principles

Kiyokatsu Jinno
Department of Materials Science, Toyohashi University, Toyohashi, Japan

INTRODUCTION

Various methods of detection are employed in chromatography. Each approach for the detection of solutes is based on their physical or chemical properties. Some of the more commonly used detectors are discussed here for liquid chromatography (LC), gas chromatography (GC), and supercritical fluid chromatography (SFC).

LIQUID CHROMATOGRAPHY

The most commonly used detectors in LC are concentration-sensitive. The detector output signal is a function of the concentrations of the analytes passing through the detector cell. In order to use the information for quantitation, the detector must respond linearly to changes in concentration over a wide concentration range, which is called the linear dynamic range of the detector. Criteria for the evaluation of the quality or the suitability of the detector are as follows: the magnitude of the linear dynamic range, the noise level, the sensitivity, and the selectivity. The sensitivity is determined by the specific characteristics of the analytes and by the extent to which these differ from the characteristics of the sample matrix. The most important parameters are noise, drift, detection limit (sensitivity), selectivity, stability, and compatibility with various elution modes.

Noise is the high-frequency variation of the detector signal, which becomes visible when the baseline is recorded at the higher-sensitivity settings. To determine the noise level, parallel lines are drawn around the noise envelope and the distance between these lines; the actual noise level is expressed in detector signal units (for instance, AU, mV, or μA). This parameter is dependent upon the lamp, the amplifier, and the cell geometry, and is specified differently by many manufacturers. Static measurements usually provide better values for the noise level than those obtained under flow conditions. Noise levels are calculated using the mean of the baseline envelope. A measure for the sensitivity of a detector is the minimum detectable amount of a given compound (detection limit). Most LC detectors measure optical or spectroscopic characteristics of the analytes. Other detectors use electrical (conductivity) or electrochemical characteristics, such as oxidation or reduction electrochemical detector (EcD) of the analytes. A detector is said to be more selective when it measures a more unique characteristic of an analyte.

Ultraviolet (UV) Detector

UV detection is the most popular, i.e., most commonly utilized, in the LC detection mode. Depending on instrumental design, three types of UV detectors are used today: single wavelength detectors, where a fixed wavelength is used for the absorbance monitoring of the analytes; variable wavelength detectors, with which one can choose the most appropriate wavelength for the analyte detection; and UV detectors which provide spectral information, such as fast-scanning UV detectors and diode array detectors.

UV detectors make use of the spectral absorption properties of the analytes in the UV and visible (Vis) wavelength range. The absorption measured at a given wavelength generally follows Beer's law and is transformed to a concentration-dependent signal. The change in absorption is proportional to the concentration when all parameters are kept constant. The detector cell volumes range from 5 and 10 μl; the light path typically ranges from 6 to 10 mm.

The fixed wavelength detector is the most widely used in LC. It is simple in design and, consequently, the least expensive although it is still the most sensitive. Its widespread use is historic in origin and is due to the fact that the strong emission line of the mercury lamp at 254 nm is well suited for absorption measurements of many organic compounds, provided that they possess an aromatic system. Some advantages of the fixed wavelength detector are as follows:

1. The simple design; the detector is relatively inexpensive.
2. The mercury spectral line is very strong and narrow.
3. The intensity of the light beam entering the system allows for a wide linear response range and high sensitivity.

Variable wavelength detectors use a continuous light source in combination with monochromators to select the desired detection wavelength. The monochromator, in general, is a rotating diffraction grating which is positioned in the light path of the detector cell. Some instruments possess an additional variable bandwidth. In microprocessor-driven instruments, the desired wavelength and slit width can be selected and read on a display. Almost all instruments contain "classical" optics with spectral dispersion of the light occurring prior to passage through the flow cell. "Reversed optics" UV detectors have recently become

popular. A holographic grating is placed between the flow cell and the photodiodes; it disperses the light beam through the detector cell. This design makes it possible to obtain spectral information at any point in time, which can then be further processed depending on the requirements of the analysis. Spectral information can be obtained from the diode array within 40–200 msec. Even for very narrow peaks, it is possible to scan spectra without stopping the flow. The diode array detector contains no moving parts; consequently, the spectra are of high quality in terms of resolution and reproducibility. Data can be acquired and evaluated, and relevant spectra can be stored and compared with spectral libraries via a computer. Of course, this type detector can be useful as a variable wavelength detector and, also, this provides information on peak identity and peak purity; it is routinely used in method development for separation of UV-active compounds.

Refractive Index (RI) Detectors

RI detection is the oldest in various LC detection modes and is commonly used in carbohydrate and polymer analysis. The RI (n) is a bulk property of the eluate. The RI detector is therefore a universal and rather non-specific detector but offers relatively low sensitivity. In RI detection, the specific physical parameter is the RI increment, dn/dc, which detects the differential change in the RI (n) that is a dimensionless parameter, and dn/dc is therefore expressed in ml/g. For most compounds in common solvents, dn/dc lies between 0.8–0.15 ml/g. The actual parameter used in RI detection is the RI itself, whose minute changes are transformed into a detector signal. Three types of RI detectors are commercially available: Fresnel (reflection), deflection, and interference. Fresnel RI detectors measure the difference between the RI of a glass prism with reference to the eluate. At the glass/liquid phase boundary, part of the incident beam is completely reflected. The intensity of the transmitted light is then measured at a given angle. When the RI changes, the angle and the intensity of the beam hitting the photodiode changes accordingly.

In the deflection-type RI detector, the optical system is designed differently. The light beam actually passes through the detector cell twice. After passage through the detector and the reference cell, the light beam is reflected back through the detector cell. The beam is balanced by an optical zero control, divided into two beams of equal intensity by a prism, and focuses onto two photodiodes. One half of the detector cell is filled with pure mobile phase (reference cell), while the column eluate flows through the other half. The RI (n) is the same in each cell when only mobile phase passes through the cell. When an analyte passes through the flow cell, the RI (n) in the flow cell will change with respect to the reference cell. The light beam is deflected during forward and return passage through the cells. The resulting difference in light intensity is sensed by the photodiodes and the differential signal of the diodes is amplified and passed on to signal output devices.

In the interference-type RI detector, a monochromatic coherent light beam is split and the resulting two beams are directed through a reference and a sample cell, respectively. After passage through the cells, the difference in RI between the cells causes interference of two beams, which is measured by a photodiode.

Fluorescence (FL) Detector

Absorption of UV light by certain compounds triggers the emission of light with a longer wavelength. The spectral range of the emitted light depends on the excitation wavelength. Fluorescence emission can only be triggered at wavelengths at which the analytes absorb in the UV. Not all UV-absorbing compounds are also fluorescence emitters although some compounds possess native fluorescence. Non-fluorescent compounds can be converted into fluorescent compounds by derivatization with a suitable fluoresophore before (so-called pre-column derivatization) or after (post-column derivatization) LC separation. The most selective and most flexible design contains two diffraction gratings with variable wavelength monochromators at the excitation side and at the emission side of the system. These types of detectors contain an additional cut-off filter to control stray light/light-scattering and noise. In the stopped-flow mode, excitation, as well as emission spectra, of labile compounds can be scanned, and the optimum wavelengths for routine measurements can be determined. Of course, photodiode array detection is also available for this detector type.

Electrochemical Detectors

EcDs are used for quantitation of compounds which can be easily oxidized or reduced by an applied potential. The standard reduction potential at the electrode is measured and transformed into a detector signal. The number of compounds which can be electrochemically detected is, however, considerably smaller than the number of optically detectable compounds by UV, RI, and FL. To become oxidized or reduced, a compound must possess electrochemically active groups. EcDs are mainly used in clinical, food, and environmental analysis.

Gas Chromatography

In contrast to LC detectors, GC detectors often require a specific gas, either as a reactant gas or as fuel (such as hydrogen gas as fuel for flame ionization). Most GC detectors work best when the total gas flow rate through the detector is 20–40 ml/min. Because packed columns deliver 20–40 ml/min of carrier gas, this requirement is easily met. Capillary columns deliver 0.5–10 ml/min;

thus, the total flow rate of gas is too low for optimum detector performance. In order to overcome the problem when using capillary columns, an appropriate makeup gas should be supplied at the detector. Some detectors use the reactant gas as the makeup gas, thus eliminating the need for two gases. The type and flow rate of the detector gases are dependent on the detector and can be different even for the same type of detector from different manufacturers. It is often necessary to refer the specific instrument manuals for details to obtain the information on the proper selection of gases and flow rates. All detectors are heated, primarily to keep the analytes from condensing on the detector surfaces. Some detectors require high temperatures to function properly; some detectors are very sensitive to changes in temperature although others are only affected by very large changes in temperature. Some detectors are flow-sensitive; thus, their response changes or the baseline shifts according to the total gas flow rate through the detector.

Flame Ionization Detector (FID)

The FID is the most powerful and popular detector in GC, for which a basic structure is demonstrated in Fig. 1. Hydrogen and air are used to maintain a flame at the tip of the jet and into the flame where the organic components are burned. Ions are created in this combustion process; they are attracted to the charged collector electrode. This induced ion flow generates a current that can be measured and transformed to an output voltage by an electrometer. The amount of current generated should be dependent on the concentrations of the compounds introduced into the flame. The FID responds best to compounds containing a carbon–hydrogen bond. The lack of a carbon–hydrogen bond does not completely eliminate any response; however, the response is significantly depressed. Some notable compounds such as water, carbon monoxide, and carbon dioxide are non-responding. Typical sensitivities for most organic compounds are 0.1–1 ng. The linear range is 5–6 orders magnitudes. Helium and nitrogen are typical as the makeup gases for capillary columns. Nitrogen is less costly and provides slightly better sensitivity. Near universal response, ease of use, wide linear range, and good sensitivity make the FID suitable for a wide variety of samples. Since FID is a simple detector, there is little routine maintenance required. The response of an FID is dependent on the hydrogen and gas flow rates; therefore, periodic measurement of these gas flow rates is necessary to maintain a stable performance. FIDs are not very temperature-sensitive and temperature changes of 50°C or greater are needed before any performance alterations are observed. FIDs are not sensitive to changes in the carrier gas flow rates; thus, baseline shifts or drifting is rarely found by changing the experimental conditions.

Nitrogen–Phosphorus Detector (NPD)

An alkali metal bead, usually rubidium sulfate, is positioned above the jet in NPD, as seen in Fig. 2, and the current is applied to this bead, which causes it to achieve temperatures up to 800°C. The addition of hydrogen and air generates plasma around the bead, and carrier gas containing the solutes is delivered to the tip of the jet and the plasma. Specific ions are produced in the plasma from nitrogen- or phosphorus-containing compounds. These ions move to the charged collector. This movement of ions generates a current that is measured and transformed to an output voltage by an electrometer. The amount of the current is dependent on the amount of the compound introduced into the plasma. The NPD exhibits excellent selectivity and sensitivity for nitrogen- and phosphorus-containing compounds. The sensitivity is approximately 10,000 times

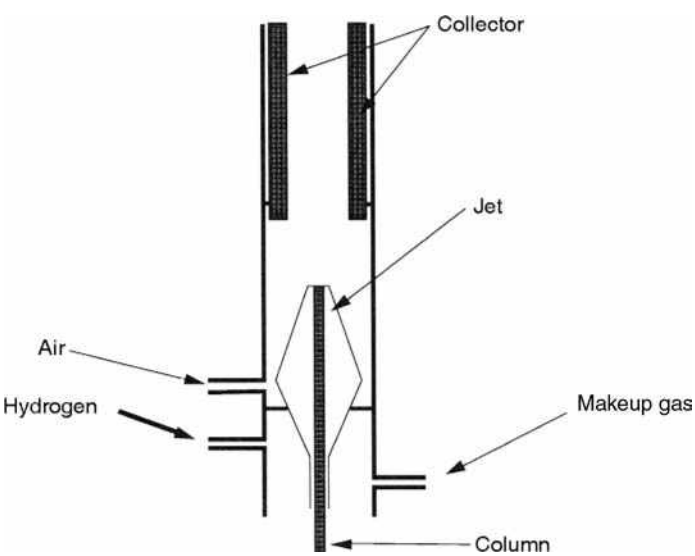

Fig. 1 Basic structure of FID for capillary GC.

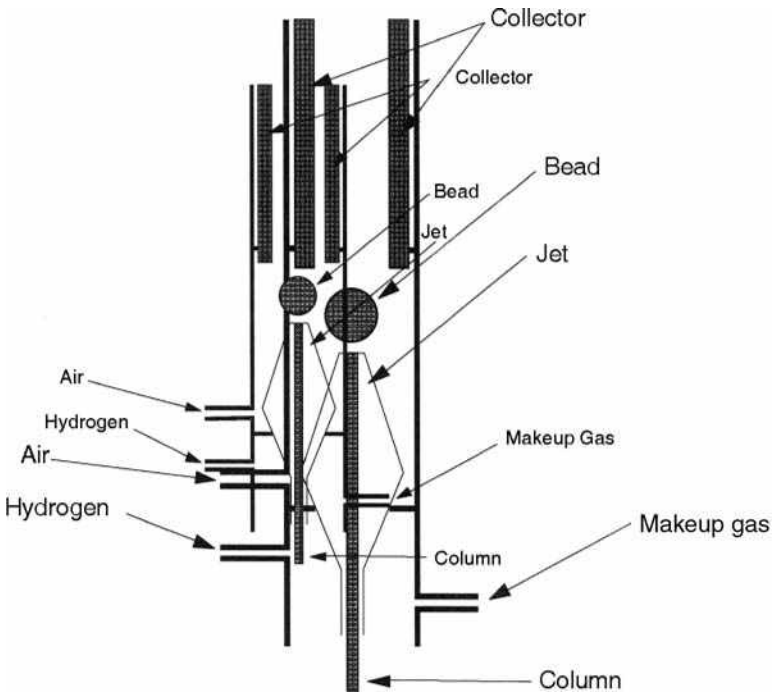

Fig. 2 Basic structure of NPD for capillary GC.

greater for nitrogen and phosphorus compounds than for hydrocarbons. Typical NPD sensitivities are in the range of 0.5–1 pg with a linear range of 5–6 orders. Helium is the preferred makeup gas. Many compounds in the sample may not contain nitrogen or phosphorus, so a response is not observed for these compounds and, therefore, specific detection for nitrogen and phosphorus can be attained. Peak separation, identification, and measurement are made much easier because there are fewer peaks in the chromatogram. Also, less preparation of the sample prior to final determination is required because fewer of the potential interferences yield a response in the detector signal. Pesticides and pharmaceuticals analysis are generally the fields of application of the NPD.

Flame Photometric Detector (FPD)

Hydrogen and air are used to maintain a flame at the tip of the jet in the FPD. The carrier gas containing the analytes is delivered to the tip of the jet and into the flame. Some FPDs use a dual jet or burner design, but the overall process is not significantly different. The solutes are burned in the flame, forming S2 and HPO. Due to excitation in the flame, light at 392 nm for S2 and at 526 nm for HPO are emitted. A photomultiplier tube is used to measure the light intensity after the optical filter. A current is generated, which can be measured and transformed to an output voltage by an electrometer. The amount of light created at each wavelength is dependent on the amount of compound introduced into the flame. The selectivity of the FPD for sulfur and phosphorus compounds is 3–4 orders of magnitude. Typical sensitivities are 10–100 pg for sulfur and 1–10 pg for phosphorus compounds. FPD responses are usually nonlinear for sulfur compounds. Nitrogen is the best makeup gas because its use results in the best sensitivity especially in the sulfur detection mode. FPDs are temperature- and flow-sensitive and, therefore, sensitivity changes are common when the temperature or carrier gas flow rates are changed. Increasing the detector temperature results in a decrease in sensitivity. FPD sensitivity for phosphorus compounds is comparable to NPD sensitivity. Due to some of the difficulties with NPDs, FPDs are frequently preferred for phosphorus-specific detection purposes. The increase of 500–1000 times in sensitivity of the FPD over the thermal conductivity detector (TCD) and FID often makes its nonlinear response behavior tolerable.

Electron-Capture Detector (ECD)

Carrier gas containing the solutes is delivered into the heated cell in the ECD. A ^{63}Ni source lining the cell acts as a source of electrons, and a moderating or auxiliary gas of nitrogen or argon/methane (95/5) is introduced into the cell to create thermal electrons which are attracted to the anode, creating a current. When an electronegative compound enters the cell, it captures thermal electrons and reduces the cell current. The amount of current reduction is measured and transformed to an output voltage by an electrometer. The size of the current loss is dependent on the amount of the compound entering the cell. The ECD primarily responds to compounds that contain a halogen, carbonyl, or nitrate group. Halogens have 100–100,000 times, nitrates have 100–1000 times, and carbonyls have 20–100 times better response than hydrocarbons.

Polyhalogenated compounds, or compounds containing multiple nitrate or carbonyl groups, yield significantly increased detector responses. Also, the response for different halogens and types of carbonyls are varied, depending upon the structures of the analytes. Sensitivities approaching 1 pg for halogens, 10 pg for nitrates, and 50 pg for carbonyls are typical. The linear range is 2–3 orders and poor; therefore, multiple-point calibration curves are required for accurate quantitation. The auxiliary gas is often used as the makeup gas in situations where makeup gas is necessary. Nitrogen is less costly and provides slightly better sensitivity than others. Argon/methane provides a slightly better linear dynamic range than nitrogen. The primary application of ECDs is for the detection of halogenated compounds. The flow rates of the carrier gas and auxiliary gas have a pronounced effect on the sensitivity and linear range of an ECD. The ECD temperature also affects the sensitivity.

Thermal Conductivity Detector (TCD)

The TCD consists of two heated cells, one of which is a sample cell and the other is a reference cell. The carrier gas containing the separated compounds enters the sample cell, while the reference cell is supplied with the same type and flow rate of carrier gas that flows into the sample cell. There is a TCD design that utilizes a single cell and a switching valve to accomplish the same task. Current is applied to the filaments, which causes them to reach an elevated equilibrium temperature when the current and gas flows are constant. When a compound that has a thermal conductivity different from that of the carrier gas is eluted from the column, it induces a change in the filament temperature. Because the reference cell filament remains at a constant temperature, the temperature difference between the two filaments is compared. The difference is measured via a Wheatstone bridge, which produces an output voltage. It is dependent on the amount of compound entering the sample cell. The best TCD sensitivity is established when the difference in thermal conductivities between the carrier gas and the component is maximized. Helium or hydrogen is usually the carrier gas of choice because these gases have thermal conductivities 10–15 times greater than that of most organic molecules, whereas nitrogen is only seven times higher than most organic molecules. This means that the TCD is a universal detector in GC although the sensitivity is relatively low, 5–50 ng per component or 10–100 times less than that of the FID. The linear range is five orders magnitude. TCDs are flow- and temperature-dependent.

Other detectors

There are a number of other GC detectors commercially available. Photoionization detectors (PIDs) are primarily used for the selective, low-level detection of the compounds which have double or triple bonds or an aromatic moiety in their structures. Electrolytic conductivity detectors (ELCDs) are used for the selective detection of chlorine-, nitrogen-, or sulfur-containing compounds at low levels. Chemiluminescence detectors are usually employed for the detection of sulfur compounds. The atomic emission detectors (AEDs) can be set up to respond only to selected atoms, or group of atoms, and they are very useful for element-specific detection and element-speciation work.

SFC

All detectors in GC and LC can be easily made useful for SFC. Basically, however, we can say that GC detectors are useful for capillary SFC, and LC detectors are useful for packed-column SFC. The most important and convenient features of SFC are that any detection systems available in chromatography can be useful and all work well.

BIBLIOGRAPHY

1. Gilbert, M.T. *High Performance Liquid Chromatography*; Wright Co.: Bristol, 1987.
2. Huber, L., George, S.A., Eds.; *Diode Array Detection in HPLC*; Marcel Dekker, Inc.: New York, 1993.
3. Jinno, K., Ed.; *Hyphenated Techniques in Supercritical Fluid Chromatography and Extraction*; Elsevier: Amsterdam, 1992.
4. Smith, R.M. *Gas and Liquid Chromatography in Analytical Chemistry*; John Wiley & Sons: Chichester, 1988.
5. Walker, J.Q., Ed.; *Chromatography Fundamentals, Applications, and Troubleshooting*; Preston Publications: Niles, IL, 1996.
6. Yeung, E.S., Ed.; *Detectors for Liquid Chromatography*; Wiley-Interscience: New York, 1986.

Detector Linear Dynamic Range

Raymond P.W. Scott
Scientific Detectors Ltd., Banbury, Oxfordshire, U.K.

INTRODUCTION

The linearity of most detectors deteriorates at high concentrations and, thus, the *linear dynamic range* of a detector will always be less than its dynamic range.

DISCUSSION

The symbol for the linear dynamic range is usually taken as (D_{LR}). As an example, the linear dynamic range of a flame ionization detector might be specified as

$$D_{LR} = 2 \times 10^5 \quad \text{for } 0.98 < r < 1.02$$

where r is the response index of the detector.

Alternatively, according to the ASTM E19 committee report on detector linearity, the linear range may also be defined as that concentration range over which the response of the detector is constant to within 5%, as determined from a linearity plot. This definition is significantly looser than that using the response index.

The lowest concentration in the linear dynamic range is usually taken as equal to the *minimum detectable concentration* or the *sensitivity* of the detector. The largest concentration in the linear dynamic range would be that where the response factor (r) falls outside the range specified, or the deviation from linearity exceeds 5% depending on how the linearity is defined. Unfortunately, many manufacturers do not differentiate between the dynamic range of the detector (D_R) and the linear dynamic range (D_{LR}) and do not quote a range for the response index (r). Some manufacturers do mark the least sensitive setting on a detector as N/L (non-linear), which, in effect, accepts that there is a difference between the linear dynamic range and the dynamic range.

BIBLIOGRAPHY

1. Fowlis, I.A.; Scott, R.P.W. A vapour dilution system for detector calibration. J. Chromatogr. **1963**, *11*, 1.
2. Scott, R.P.W. *Chromatographic Detectors*; Marcel Dekker, Inc.: New York, 1996.

Detector Linearity and Response Index

Raymond P.W. Scott
Scientific Detectors Ltd., Banbury, Oxfordshire, U.K.

INTRODUCTION

It is essential that any detector that is to be used directly for quantitative analysis has a linear response. A detector is said to be truly linear if the detector output (V) can be described by the simple linear function

$$V = Ac$$

where A is a constant and c is the concentration of the solute in the mobile phase (carrier gas) passing through it.

DISCUSSION

As a result of the imperfections inherent in all electromechanical and electrical devices, true linearity is a hypothetical concept, and practical detectors can only approach this ideal response. Consequently, it is essential for the analyst to have some measure of detector linearity that can be given in numerical terms. Such a specification would allow quantitative comparison between detectors and indicate how close the response of the detector was to true linearity. Fowlis and Scott[1] proposed a simple method for measuring detector linearity. They assumed that for an approximately linear detector, the response can be described by the power function

$$V = Ac^r$$

where r is defined as the response index of the detector.

For a truly linear detector, $r = 1$, and the proximity of r to unity will indicate the extent to which the response of the detector deviates from true linearity. The response of some detectors having different values for r are shown as curves relating the detector output (V) to solute concentration (c) in Fig. 1. It is seen that the individual curves appear as straight lines but the errors that occur in assuming true linearity can be quite large. The errors actually involved are shown in the following, which is an analysis of a binary mixture employing detectors with different response indices:

Solute	$r = 0.94$	$r = 0.97$	$r = 1.00$	$r = 1.03$	$r = 1.05$
1	11.25%	10.60%	10.00%	09.42%	09.05%
2	88.75%	89.40%	90.00%	90.58%	90.95%

It is clear that the magnitude of the error for the lower-level components can be as great as 12.5% (1.25% absolute) for $r = 0.94$ and 9.5% (0.95% absolute) for $r = 1.05$. In general analytical work, if reasonable linearity is assumed, then $0.98 < r < 1.03$. The basic advantage of defining linearity in this way is that if the detector is not perfectly linear, but the value for r is known, then a correction can be applied to accommodate the non-linearity.

There are alternative methods for defining linearity which, in the author's opinion, are somewhat less precise and less useful. The recommendations of the ASTM E19 committee on linearity measurement are as follows:

> The linear range of a detector is that concentration range of the test substance over which the response of the detector is constant to within 5% as determined from a linearity plot,—the linear range should be expressed as the ratio of the highest concentration on the linearity scale to the minimum detectable concentration.

This method for defining detector linearity is satisfactory up to a point and ensures a minimum linearity from the detector and, consequently, an acceptable quantitative accuracy. However, the specification is significantly "looser" than that given above, and it is not possible to correct for any non-linearity that may exist, as there is no correction factor provided that is equivalent to the response index. It is strongly advised that the response index should be determined for any detector that is to be used for quantitative analysis. In most cases, r need only be measured once, unless the detector undergoes some catastrophic event that is liable to distort its response, in which case, r may need to be checked again.

There are two methods that can be used to measure the response index of a detector: the *incremental method* of measurement and the *logarithmic dilution method* of measurement.[2] The former requires no special apparatus, but the latter requires a log-dilution vessel, which, fortunately, is relatively easy to fabricate. The incremental method of measurement is the one recommended for general use.

The apparatus necessary is the detector itself with its associated electronics and recorder or computer system, a mobile-phase supply, pump, sample valve, and virtually any kind of column. In practice, the chromatograph to be used for the subsequent analyses is normally employed. The solute is chosen as typical of the type of substances that will be analyzed and a mobile phase is chosen that will

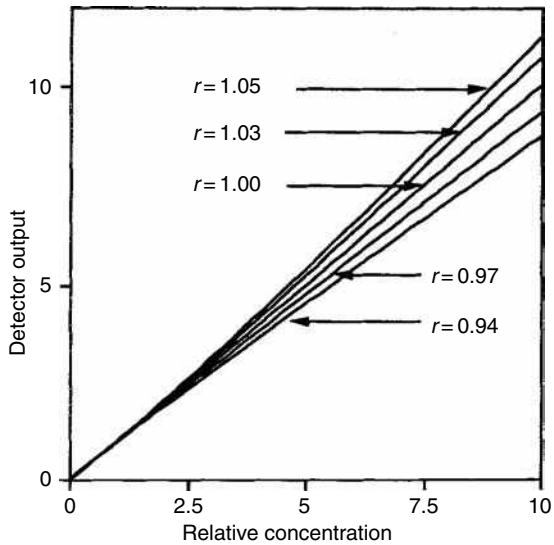

Fig. 1 Graph of detector output against solute concentration for detectors having different response indices.

elute the solute from the column in a reasonable time. Initial sample concentrations are chosen to be appropriate for the detector under examination.

Duplicate samples are placed on the column, the sample solution is diluted by a factor of 3 and duplicate samples are again placed on the column. This procedure is repeated, increasing the detector sensitivity setting where necessary until the height of the eluted peak is commensurate with the noise level. If the detector has no data acquisition and processing facilities, then the peaks from the chart recorder can be used. The width of each peak at 0.607 of the peak height is measured and the peak volume can be calculated from the chart speed and the mobile-phase flow rate. Now, the concentration at the peak maximum will be twice the average peak concentration, which can be calculated from

$$c_p = \frac{ms}{wQ}$$

where c_p is the concentration of solute in the mobile phase at the peak height (g/ml), m is the mass of solute injected, w is the peak width at 0.6067 of the peak height, s is the chart speed of the recorder or printer, and Q is the flow rate (ml/min).

The logarithm of the peak height y (where y is the peak height in millivolts) is then plotted against the log of the solute concentration at the peak maximum (c_p). Now,

$$\log(V) = \log(A) + (r)\log(c_p)$$

Thus, the slope of the $\log(V)/\log(c_p)$ curve will give the value of the response index (r). If the detector is truly linear, $r = 1$ (i.e., the slope of the curve will be sin $\pi/4 = 1$). Alternatively, if suitable software is available, the data can be curved fitted to a power function and the value of r extracted directly from the curve-fitting analysis. The same data can be employed to determine the linear range as defined by the ASTM E19 committee. In this case, however, a linear plot of detector output against solute concentration at the peak maximum should be used and the point where the line deviates from 45° by 5% determines the limit of the linear dynamic range.

REFERENCES

1. Fowlis, I.A.; Scott, R.P.W. A vapour dilution system for detector calibration. J. Chromatogr. **1963**, *11*, 1.
2. Scott, R.P.W. *Chromatographic Detectors*; Marcel Dekker, Inc.: New York, 1996.

Detector Noise

Raymond P.W. Scott
Scientific Detectors Ltd., Banbury, Oxfordshire, U.K.

INTRODUCTION

Detector noise is the term given to any perturbation on the detector output that is not related to the presence of an eluted solute. As the minimum detectable concentration, or detector sensitivity, is defined as that concentration of solute that provides a signal equivalent to twice the noise, the detector noise determines the ultimate performance of the detector. Detector noise has been arbitrarily divided into three types, *short-term noise*, *long-term noise*, and *drift*, all three of which are depicted in Fig. 1.

SHORT-TERM NOISE

Short-term noise consists of baseline perturbations that have a frequency that is significantly higher than that of the eluted peak. Short-term detector noise is usually not a serious problem in practice, as it can be easily removed by appropriate electronic noise filters that do not significantly affect the profiles of the peaks. The source of this noise is usually electronic, originating from either the detector sensor system or the amplifier electronics.

LONG-TERM NOISE

Baseline perturbations that have a frequency that is similar to that of the eluted peak are termed long-term noise. This type of detector noise is the most significant and damaging, as it is often indiscernible from very small peaks in the chromatogram. Long-term noise cannot be removed by electronic filtering without affecting the profiles of the eluted peaks and, thus, destroying the integrity of the chromatogram. It is clear in Fig. 1 that the peak profile can easily be discerned above the high-frequency noise, but it is lost in the long-term noise. Long-term noise usually arises from temperature, pressure, or flow-rate changes in the sensing cell. Long-term noise can be controlled by careful detector cell design, the rigorous stabilization of operating variables such as sensor temperature, flow rate, and sensor pressure. Long-term noise is the primary factor that ultimately limits the detector *sensitivity* or the *minimum detectable concentration*.

DRIFT

Baseline perturbations that have a frequency significantly larger than that of the eluted peak are called drift. In gas chromatography (GC), drift is almost always due to either changes in detector temperature, changes in carrier gas flow rate, or column bleed. As a consequence, with certain detectors, baseline drift can become very significant at high column temperatures. Drift is easily constrained by choosing operating parameters that are within detector and column specifications.

A combination of all three sources of noise is shown by the trace at the bottom of Fig. 1. In general, the sensitivity of the detector (i.e., in most cases, the amplifier setting) should never be set above the level where the combined noise exceeds 2% of the full scale deflection (FSD) of the recorder (if one is used), or appears as more than 2% FSD of the computer simulation of the chromatogram.

MEASUREMENT OF DETECTOR NOISE

The detector noise is defined as the maximum amplitude of the combined short- and long-term noise measured over a period of 10 min (the ASTM E19 committee recommends a period of 15 min). The detector must be connected to a column and carrier gas passed through it during measurement. The detector noise is obtained by constructing parallel lines embracing the maximum excursions of the recorder trace over the defined time period. The distance between the parallel lines, measured in millivolts, is taken as the measured noise (v_n), and the noise level (N_D) is calculated in the following manner:

$$N_D = v_n A = \frac{v_n}{B}$$

where v_n is the noise measured in volts from the recorder trace, A is the attenuation factor, and B is the alternative amplification factor.

Note: Attenuation is the reciprocal of amplification; manufacturers may use either function as a control of detector sensitivity.

The noise levels of detectors that are particularly susceptible to variations in column pressure or flow rate (e.g., the katharometer) are sometimes measured under static conditions (i.e., no flow of carrier gas). Such specifications

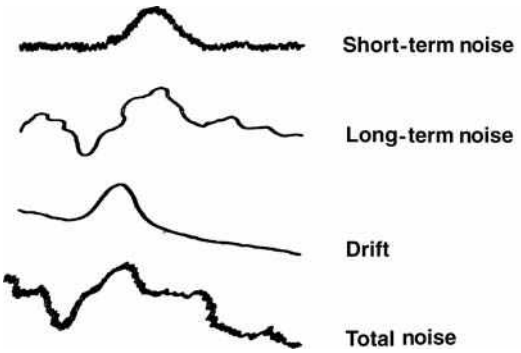

Fig. 1 Different types of detector noise.

are not really useful, as the analyst can never use the detector without a column flow. It could be argued that the manufacturer of the detector should not be held responsible for the precise control of the mobile phase, whether it may be a gas flow controller or pressure controller. However, all carrier supply systems show some variation in flow rates (and, consequently, pressure) and it is the responsibility of the detector manufacturer to design devices that are as insensitive to pressure and flow changes as possible.

At the high-sensitivity-range settings of some detectors, electronic filter circuits are automatically introduced to reduce the noise. Under such circumstances, the noise level should be determined at the lowest attenuation (or highest amplification) that does not include noise-filtering devices (or, at best, the lowest attenuation with the fastest response time) and then corrected to an attenuation of unity.

BIBLIOGRAPHY

1. Scott, R.P.W. *Chromatographic Detectors*; Marcel Dekker, Inc.: New York, 1996.
2. Scott, R.P.W. *Introduction to Gas Chromatography*; Marcel Dekker, Inc.: New York, 1998.

Diffusion Coefficients from GC

George Karaiskakis
Physical Chemistry Laboratory, Department of Chemistry, University of Patras, Patras, Greece

INTRODUCTION

One of the most important physicochemical applications of gas chromatography (GC) is for the measurement of diffusion coefficients of gases into gases, liquids, and on solids. The gas chromatographic subtechniques used for the measurement of diffusivities are briefly reviewed, focusing on their accuracy and precision, as well as on the corresponding sources of errors responsible for the deviation of the experimental diffusion coefficients measured by GC from those determined by other techniques or calculated from known empirical equations.

The diffusion coefficients can be determined by various gas chromatographic techniques based either on the broadening of the elution peaks, or on the perturbation imposed on the carrier gas flow rate.

DIFFUSION IN GASES

The diffusion coefficient of a gas A into another gas B, D_{AB}, is a function of temperature, T, pressure, p, and composition, x, even for binary mixtures at low pressure D_{AB} is almost independent of the gas composition. Several empirical equations describing the dependence of D_{AB} on T and p are available, among which the most important are the following:[1,2]

1. The Stefan–Maxwell equation:

$$D_{AB} = \frac{a}{n{\sigma_{AB}}^2}\left[\frac{8RT}{\pi}\left(\frac{1}{M_A}+\frac{1}{M_B}\right)\right]^{1/2} \quad (1)$$

where a is a constant taking various values ($1/3\pi$, 1/8, $1/2\pi$, and 3/32), depending on the researcher, n is the number of gas phase molecules per cubic centimeter, σ_{AB} is the collision diameter between the gas molecules A and B, R is the gas constant, T is the absolute temperature, and M_A, M_B are the molecular masses of solute A and carrier gas B, respectively.

2. The Chapman–Enskog equation:

$$D_{AB} = \frac{0.00263T^{3/2}}{p{\sigma_{AB}}^2}\left(\frac{1/M_A+1/M_B}{2}\right)^{1/2} \quad (2)$$

3. The Arnold equation:

$$D_{AB} = \frac{0.0083T^{3/2}(1/M_A+1/M_B)^{1/2}}{p({V_A}^{1/3}+{V_B}^{1/3})(1+c_{AB}/T)} \quad (3)$$

where V_A and V_B are molar volumes in cubic centimeters, at the boiling points, while c_{AB} is Sutherland's constant, which can be estimated in various ways.[1,2] The above equation, which introduces a second temperature dependent term in the denominator to account for molecular "softness," shows a dependence varying from $T^{3/2}$ to $T^{5/2}$.

4. The Gilliland equation:

$$D_{AB} = \frac{0.0043T^{3/2}(1/M_A+1/M_B)^{1/2}}{p({V_A}^{1/3}+{V_B}^{1/3})} \quad (4)$$

5. The Hirschfelder–Bird–Spotz (HBS) equation:

$$D_{AB} = \frac{0.00186T^{3/2}(1/M_A+1/M_B)^{1/2}}{p{\sigma_{AB}}^2\Omega_{AB}} \quad (5)$$

The term Ω_{AB} is the collision integral, depending in a complicated way on temperature and the interaction energy of the colliding molecules, ε_{AB}. Ω_{AB} values as a function of the reduced temperature $T^* = kT/\varepsilon_{AB}$, where k is the Boltzmann constant, have been tabulated.[3,4] The main disadvantage of the HBS equation is the difficulty encountered in evaluating σ_{AB} and Ω_{AB}.

6. Chen and Othmer provided the most explicit approximation of the HBS equation using the critical values of temperature, T_C, and volume, V_C:

$$D_{AB} = \frac{0.43(\frac{T}{100})^{1.81}(\frac{1}{M_A}+\frac{1}{M_B})^{1/2}}{p\left(\frac{T_{CA}T_{CB}}{10^4}\right)^{0.1405}\left[\left(V_{\frac{CA}{100}}\right)^{0.4}+\left(V_{\frac{CB}{100}}\right)^{0.4}\right]^2} \quad (6)$$

7. Fuller, Schettler, and Giddings[5] developed a successful equation in which atomic and structural volume increments and other parameters were obtained by a least-squares fit to over 340 measurements. In the Fuller et al. (FSG) method, which provides the best practical combination of simplicity and accuracy,

$$D_{AB} = \frac{0.00143T^{1.75}(1/M_A+1/M_B)^{1/2}}{p\left[(\sum v)_A{}^{1/3}+(\sum v)_B{}^{1/3}\right]^2} \quad (7)$$

$\sum v$ is determined by summing the relative atomic contributions given in literature.[1]

The Broadening Techniques

The GC broadening techniques for the measurement of gaseous diffusivities are the *continuous elution method*, introduced by Giddings,[2,6,7] and its *arrested elution* modification invented by Knox and McLaren.[2,6,7]

The continuous elution method is conducted in an open tube with circular cross section. The carrier gas flow rate is chosen such that the plate height, H, depends mainly on only one of the van Deemter terms, namely the longitudinal diffusion term. For correction reasons, the use of two different length columns is necessary, and the equation for H is:[2]

$$H = (L_1 - L_2)\left[\frac{t_1^2 - t_2^2}{(t_1 - t_2)^2}\right] \tag{8}$$

where L_1 and L_2 are the lengths of the two columns, respectively, while $(t_1 - t_2)$ and $(t_1^2 - t_2^2)$ are the corresponding differences for the first and second moments of the time base. Replacement of Eq. 8 by the Golay equation, describing band broadening in open tube, gives the final equation from which the diffusion coefficient D_{AB} is obtained:[2]

$$D_{AB} = \frac{v}{4}\left[H \pm \left(H^2 - \frac{r^2}{3}\right)^{1/2}\right] \tag{9}$$

where v is the average carrier gas velocity and r is the radius of the tube. When the flow velocity is slow, the determination of D_{AB} is done from the positive root, while the negative root is used at higher flow velocities. One of the main advantages of the method is the high speed of collecting data with high precision.

In a typical experiment of the arrested elution method,[2,6,7] a solute sample is injected into the column and eluted in the normal way without arresting the gas, so that its outlet velocity, v, can be obtained. Then, during the elution of the solute band, about halfway along the particular column, the flow is switched to a dummy column of equal resistance. After a delay time, t, of 1–20 min, the flow is reconnected to the column and the peak is eluted. The spreading of the band, during the delay time, can occur only by diffusion, and from the standard deviation δ (or the variance, σ^2) of the concentration profile, determined by the detector, the diffusion coefficient D_{AB} can be found from the following equation:[2]

$$\frac{d\sigma^2}{dt} = \frac{2D_{AB}}{v^2} \tag{10}$$

Eq. 10 shows that a plot of σ^2 against the delay time, t, should be a straight line with slope $2D_{AB}/v^2$, from which the D_{AB} value can be determined. The average reproducibility of the method, which is approximately $\pm 2\%$, depends mainly on the accurate measurement of v, since v is to the second power in Eq. 10.

Although the arrested elution method has two drawbacks (the need of several runs to get a D_{AB} value with a precision of 2%, and of constant flow rates over long periods for runs at various arrested times), in comparison with the continuous elution method, the former has also the following advantages: 1) Effects of zone broadening other than axial molecular diffusion and non-uniform flow profile do not affect the measurement; 2) no assumptions are made about the precise form of the flow profile, the smoothness of the column wall, or the accuracy in the knowledge of the column diameter.

Diffusion coefficients, for various binary gas mixtures, at various temperatures and pressures with their accuracy and precision, measured by gas chromatographic broadening techniques (GC-BTs; continuous, as well as arrested elution methods), are given in Table 3 of Ref.[2] and in Table 1 of Ref.[6] Representative data are collected here in Table 1.

The Flow Perturbation Techniques

The flow perturbation gas chromatographic methods used for the measurement of diffusion coefficients in gases are the *stopped-flow* and the *reversed-flow* techniques.

The stopped-flow technique[2,8] consists in stopping the carrier gas flow for short time intervals by using shut-off valves. Following each restoration of gas flow, a narrow peak (stop-peak) is recorded in the chromatographic trace, having the form of those of Fig. 2 in Ref.[2] The problem to be solved here is to determine the area under the curve of each stop-peak as a function of the time of the corresponding stop in the flow of the carrier gas. Since the stop-peaks are fairly symmetrical and have a constant half-width, their height from the baseline, H, rather than their area, is used to plot $\ln(Ht^{3/2})$ vs. the inverse time, $1/t$, according to the following equation:[8]

$$\ln(Ht^{3/2}) = \ln\left(\frac{mt_sL}{\pi^{1/2}D_{AB}^{1/2}}\right) - \frac{L^2}{4D_{AB}}\frac{1}{t} \tag{11}$$

where m is the injected amount of solute in moles, t_s the stopped-flow interval in seconds, and L the length of the diffusion column (cf. Fig. 1 of Ref.[2]) in centimeters, which permits calculation of the diffusion coefficient D_{AB} from the slope $-L^2/4D_{AB}$.

Table 1 Diffusion coefficients, D_{AB}, from GC-BTs.

Binary system A–B	T (K)	p (atm)	D_{AB} (cm^2/sec)	Precision[a] (%)	Accuracy[b] (%)
CH_4–H_2	298.0	1	0.73	2.7	0
C_2H_6–H_2	298.0	1	0.54	1.9	1.9
C_3H_8–H_2	298.0	1	0.44	6.8	2.2
C_4H_{10}–H_2	298.0	1	0.40	3.8	—
n-C_5H_{12}–H_2	353.0	1	0.4895	1.5	—
	373.0	1	0.5324	3.9	—
	393.0	1	0.5830	4.3	—
	423.0	1	0.6300	0.06	—
	453.0	1	0.7425	0.47	—
n-C_6H_{14}–H_2	353.0	1	0.4990	0.94	—
	373.0	1	0.4740	1.5	10
	393.0	1	0.5310	0.38	—
	423.0	1	0.5923	0.30	—
	453.0	1	0.6520	0.00	—
CH_4–He	298.0	1	0.6776	0.22	—
	298.0	1	0.6735	0.12	—
	373.0	1	1.005	—	—
	373.0	1	1.007	—	—
	248.0	9.97	0.0501	—	—
	248.0	29.9	0.0169	—	—
	248.0	49.8	0.0103	—	—
	248.0	59.8	0.00872	—	—
	273.0	9.97	0.0588	—	—
	273.0	29.9	0.0198	—	—
	273.0	49.8	0.0119	—	—
	273.0	59.8	0.0101	—	—
	298.0	9.97	0.0681	—	—
	298.0	29.9	0.0229	—	—
	298.0	49.8	0.0139	—	—
	298.0	59.8	0.0117	—	—
	323.0	9.97	0.0781	—	—
	323.0	29.9	0.0265	—	—
	323.0	49.8	0.0159	—	—
	323.0	59.8	0.0134	—	—
n-C_4H_{10}–He	298.0	1	0.364	0.27	—
	372.6	1	0.477	2.1	—
	423.0	1	0.634	0.95	—
	473.0	1	0.797	0.75	—
n-C_5H_{12}–He	298.0	1	0.288	0.35	—
	372.6	1	0.422	0.71	—
	423.0	1	0.565	1.2	—
	473.0	1	0.695	17	—
n-C_6H_{14}–He	298.0	1	0.27	1.8	—
	372.6	1	0.390	1.5	—
	417.0	1	0.574	—	
	423.0	1	0.513	2.5	
	473.0	1	0.629	1.9	
C_2H_6–N_2	298.0	1	0.14	18	—
C_3H_8–N_2	298.0	1	0.11	—	—
n-C_4H_{10}–N_2	298.0	1	<0.07	—	—
	298.0	1	0.0954	—	0.63
	302.4	1	0.100	—	1.5
n-C_5H_{12}–N_2	353.0	1	0.136	—	—

[a]Precision has been defined as: $100 \times$ Deviation/D_{AB}, where for two values, the high (D_{AB}^{high}) and the low (D_{AB}^{low}), the deviation is ($D_{AB}^{high} - D_{AB}^{low}$)/2.
[b]Accuracy has been defined as: $100 \times |D_{AB} - D_{lit}|/D_{AB}$, where D_{lit} are literature[2,6] values.

Diffusion coefficients from the stopped-flow technique, which are very sensitive to the precision with which L is measured, since D_{AB} is proportional to L^2, are given in literature[2,8] for some binary gas mixtures.

The *reversed-flow GC (RF-GC) technique*, introduced in 1980,[9] is based on reversing the direction of flow of the carrier gas from time to time. Its experimental setup is very simple and consists of the following parts:[2,10,11]

1. A conventional gas chromatograph with any kind of detector capable of detecting the solute(s) contained in the carrier gas.
2. A so-called sampling column constructed from a glass or stainless steel chromatographic tube of any diameter, and having a total length 0.6–2.0 m, depending on the particular application. The sampling column, which is coiled and accommodated inside the chromatographic oven, should be completely empty of any solid material for the determination of the diffusion coefficient of gases into pure gases or mixtures of gases, or it can be filled with a common chromatographic material for the measurement of the diffusion coefficient of ternary gas mixtures into pure gases.
3. A diffusion column, which is constructed from the same material as the sampling column, is connected perpendicularly to it, usually at its midpoint. The other end of the diffusion column is closed with an injector septum and is used as the injection point of the solute under study. The diffusion column, which is empty of any solid material, is a straight or coiled, relatively short (30–80 cm) piece of empty tubing placed inside the chromatographic oven.
4. The sampling and the diffusion column form the sampling cell, and this cell must now be connected to the detector and to the carrier gas inlet in such a way that the carrier gas flow through the sampling column can be reversed in direction by a four- or six-port valve that is connected with the two ends D_1 and D_2 of the chromatographic column, as well as with the inlet of the carrier gas and the detector, as shown in Fig. 1.

If pure carrier gas passes through the sampling column, nothing happens on reversing the flow. But if a solute comes out of the diffusion column as a result of its diffusion into the carrier gas, filling the diffusion column and also running along the sampling column, the flow reversal records the concentration of the solute at the junction $x = l'$ (cf. Fig. 1) at the moment of the reversal. This concentration recording has the form of extra chromatographic peaks, called *sample peaks*, superimposed on the otherwise continuous detector signal. The loading of the carrier gas with other substance(s) is due to its (their) slow diffusion into the carrier gas passing through the sampling column. The enrichment of carrier gas in the gas(es) contained in the diffusion column depends on the rate with which gas(es) enters (enter) the sampling column at the junction

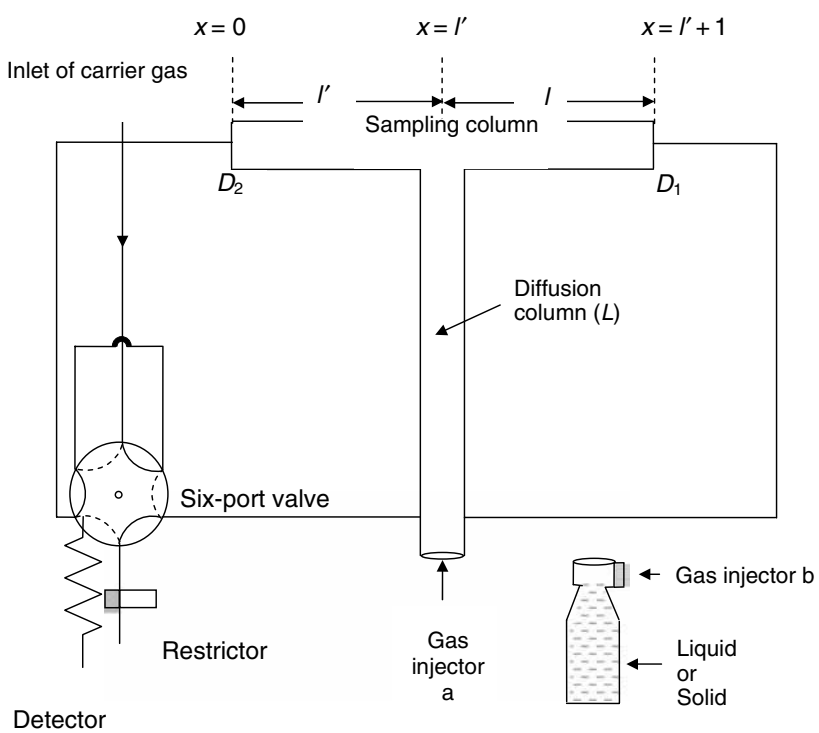

Fig. 1 Schematic representation of the reversed-flow GC technique for measuring diffusion coefficients. (a) Injection point for gaseous diffusivities; (b) injection point for liquid and solid diffusivities.

$x = l'$ of the two columns. By reversing the flow now, one can perform a sampling of the concentration of the analyte gas at this junction, each sample peak measuring (by its height H) this concentration at the time of the flow reversal. Repeating this sampling procedure at various times, t, and using suitable mathematical analysis, the following equations describing the variation of H with t, when the slow process under study is the gaseous diffusion, were derived:[10–13]

$$\ln(H^{1/M}t^{3/2}) = \ln(gN_1) - \frac{L^2}{4D_{AB}}\frac{1}{t} \tag{12}$$

$$\ln(H^{1/M}) = \ln(gN_2) - \frac{3D_{AB}}{L^2}t \tag{13}$$

where

$$N_1 = \frac{mL}{\dot{V}(\pi D_{AB})^{1/2}} \tag{14}$$

$$N_2 = \frac{\pi m D_{AB}}{\dot{V}L^2} \tag{15}$$

M is the response factor of the detector [$M = 1$ for flame ionization detector (FID)], g a proportionality constant pertaining to the detector calibration, m the injected amount of solute in moles, and V the volumetric flow-rate in cubic centimeters per second.

Plotting the left-hand side of Eq. 12, $\ln(H^{1/M}t^{3/2})$ vs. $1/t$, one can obtain the diffusion coefficient value of D_{AB} from the slope $-L^2/4D_{AB}$ of the straight line and the known value of the diffusion column length (L).

Eq. 13 shows that a plot of $\ln H$ vs. t (after the maximum of the diffusion band) is linear with the slope $-3D_{AB}/L^2$, from which the diffusion coefficient D_{AB} can be also determined.

The question that now naturally arises is: Which one of the two equations, namely Eqs. 12 and 13, is more accurate in the determination of the gaseous diffusion coefficients? The answer is not so simple and depends on both the gaseous system under study and the experimental conditions applied. Generally, Eq. 12 is used for short duration experiments and for long diffusion columns, while Eq. 13 is used for short column lengths (say 30–50 cm) and for experiments of long duration. The selection of the proper mathematical analysis to estimate the more accurate gaseous diffusion coefficient by RF-GC can also be based on the comparison of the two experimental values found from Eqs. 12 and 13 with those given in the literature or calculated from known empirical equations.

The diffusion coefficients of various gaseous hydrocarbons in carrier gases N_2, H_2, and He determined by the reversed-flow technique with the aid of Eq. 12 at various temperatures are compiled in Table 2. The values and their standard errors found by regression analysis using standard least-squares procedures are reduced to 1 atm after multiplication by the pressure of the experiment. This pressure is given in Table 2, so that one can find the actual values determined from the ratio D_{AB}/p. The precision of the method, defined as the relative standard deviation (%), can be judged from the data given for methane–helium. From the five values quoted, a precision of 0.9% is calculated. The experimental values of diffusion coefficient given in Table 2 are compared with those calculated theoretically with the equation of HBS (Eq. 5). The accuracy given in the last column of Table 2 is a measure of the deviation of the values found by the RF-GC method from the calculated ones, defined as:

$$\text{Accuracy } (\%) = \frac{\left|D_{AB}{}^{\text{found}} - D_{AB}{}^{\text{calcd}}\right|}{D_{AB}{}^{\text{found}}} \times 100 \tag{16}$$

All of the theoretical or semiempirical equations describing the dependence of the diffusion coefficient on temperature lead to the relationship[1,2,14]

$$D_{AB} = AT^n \tag{17}$$

where A is a complex function including molar masses or volumes, critical volumes or temperatures, volume increments, pressures, etc. depending on the special equation used. Eq. 17 shows that the exponent n can be found from the slope of the linear plot of $\ln D_{AB}$ against $\ln T$. The various values of n calculated from these plots, which vary between 1.59 and 1.77,[13,14] are very close to the value 1.50 suggested by the Stefan–Maxwell and the Gilliland and Arnold equations,[1] to the value 1.81 predicted by the Chen–Othmer equation,[1] and to the value 1.75 predicted by the FSG equation.[1,5]

The reversed-flow method for measurement of gas diffusion coefficients in binary mixtures can also be extended to simultaneous determination of effective diffusion coefficients for each substance in a multicomponent gas mixture.[15] This extension of the method is achieved by filling the column section l (Fig. 1) with a chromatographic material, which can affect the separation of all components of the gas mixture. Effective diffusion coefficients of various mixtures of gaseous hydrocarbons into the carrier gases N_2, H_2, and He, determined by RF-GC, with the aid of Eq. 12, can be found in the literature.[15]

Comparison of the Broadening with the Flow Perturbation Techniques

1. The accuracy of the RF-GC method, in comparison with the GC-BTs, is higher.[2] The mean percentage deviation of D_{AB} (for the binary mixtures C_2H_4–N_2 and C_2H_6–N_2 at various temperatures) determined by RF-GC[2] from the respective predicted values by means of the FSG equation is estimated at 3.4, while that of the GC-BTs is 5.7.[6]

Table 2 Diffusion coefficients of various solutes into three carrier gases at ambient temperatures and reduced to 1 atm pressure, determined by reversed-flow GC.

Carrier gas	Solute gas	T (K)	$\dot{V}$ (cm^3/sec)	p (atm)	D_{AB} ($\times 10^3$ cm^2/sec)		Accuracy[b] (%)
					D_{AB}^{found}	(D_{AB}^{calcd})[a]	
N_2	CH_4	296.0	0.260	1.96	272 ± 4	214	21.3
	C_2H_6	293.0	0.267	1.99	142 ± 0.03	144	1.4
	n-C_4H_{10}	295.5	0.300	2.15	98 ± 0.2	98.6	0.3
	C_2H_4	296.0	0.120	1.49	168 ± 2	156	7.1
		292.0	0.268	2.00	156 ± 0.4		0
		292.0	0.538	2.71	161 ± 0.4		3.1
	C_3H_6	298.0	0.260	1.96	124 ± 0.4	120	3.2
H_2	CH_4	293.0	0.287	1.70	699 ± 3	705	0.9
	C_2H_6	297.0	0.267	1.56	548 ± 5	556	1.5
	n-C_4H_{10}	296.0	0.273	1.60	386 ± 3	373	3.4
	C_2H_4	293.0	0.300	1.75	525 ± 5	559	6.5
	C_3H_6	296.0	0.273	1.60	485 ± 3	486	0.2
He	CH_4	295.7	0.250	1.78	527 ± 3	669	26.9
		295.0	0.283	2.03	520 ± 1		28.7
		296.0	0.283	2.03	522 ± 1		28.2
		296.0	0.283	2.03	514 ± 0.2		30.2
		296.7	0.283	2.03	522 ± 3		28.2
	C_2H_6	295.6	0.300	2.15	518 ± 3	507	2.1
	n-C_4H_{10}	290.0	0.283	2.03	333 ± 3	330	0.9
	C_2H_4	296.0	0.283	2.03	558 ± 4	544	2.5
	C_3H_6	291.0	0.283	2.03	412 ± 4	440	6.8

The actual values found at the pressure of the experiment, p, are simply D_{AB}/p. All errors given in this table are "standard errors" calculated by regressions analysis.
[a]This is defined by Eq. 16.
[b]Calculated by the HBS equation.

2. The precision of the RF-GC method was calculated to be 0.9%. The precision of the continuous elution technique was about 1%, while that of the arrested elution method was about 2%.[2]
3. The time needed for the determination of D_{AB} values by the continuous elution method is very short (≈5 min), while that by the arrested elution method is longer (≈3 hr), due to the requirement of repeating the experiments at a number of delay times. The corresponding time for the RF-GC method is about 30–60 min, depending on the binary gas mixture and the length of the diffusion column used.
4. The length of the empty diffusion column in RF-GC is relatively short (30–80 cm), compared to that used in the continuous elution method, where much longer (~15 m) columns are used.
5. In the continuous elution method, in order to eliminate the effect of extra zone broadening factors, the use of two columns is necessary. Such a correction procedure is not necessary in the arrested elution technique, resulting in more reliable D_{AB} values through a more time consuming procedure. RF-GC, being a dynamic technique under steady-state conditions, has also the advantage that extra zone broadening factors are not implied in D_{AB} determinations.

DIFFUSION OF GASES IN LIQUIDS

Diffusion coefficients in liquids are of great significance in many theoretical and engineering calculations involving mass transfer, such as absorption, extraction, distillation, and chemical reactions. The measurement of accurate diffusion coefficients of gases in liquids is not an easy task. Different values are often obtained from different workers in different laboratories, even by using similar measuring techniques.

GC, being a dynamic technique, has been successfully used during the last three decades for the measurement of diffusion coefficients in a large number of gas–liquid systems, especially polymer–solvent systems.

From the 1980s, the *chromatographic broadening technique* has been "substituted" in the literature by *inverse gas chromatography* (IGC). The two main IGC methods for the measurement of diffusion coefficients in liquids are *packed column IGC*[7] and *capillary column IGC*.[7]

In packed column IGC, the preparation of the column is usually done by packing the column with a chromatographic material, running a solution of the solvent through it, and removing the solvent by evaporating with a stream of an inert gas. The presence of film irregularities due to the porous character of most chromatographic supports in

packed columns is a problem that affects the accuracy of the measured diffusion coefficients.

An innovation in the use of IGC for the measurement of diffusion coefficients in liquids is the introduction of capillary columns, which solved the problem of the non-uniformity of the coating on the solid particles. A known concentration of a degassed solution is used to fill a capillary column, which is sealed at one end, and vacuum is applied to the other end. The evaporation of the solvent results in the deposition of a uniformly thin liquid layer on the capillary walls.

Data concerning diffusion coefficients of gases in liquids, determined by various IGC techniques, can be found in the literature.[2,6]

The Reversed-Flow Technique

The experimental setup of the RF-GC method for measuring diffusion coefficients of gases in liquids is similar to that of Fig. 1, the only difference being the end of the diffusion column, at which a vessel containing the liquid or the solid (when surface diffusion is studied) is placed.[16,17] Using suitable mathematical analysis, equations were derived by means of which diffusion coefficients of various gases into liquids, D_L, were determined.[16,17]

All calculations of D_L can be carried out simultaneously by a GW-BASIC personal computer program, written for non-linear least-squares regression analysis[18] and based on the experimental pair values H and t in centimeters and seconds, respectively. The experimental D_L values are of the same order of magnitude and, in some cases, very close to those obtained by other techniques or calculated theoretically from empirical equations. The precision (~13%) and the accuracy (8–47%) of the RF-GC method, as determined from the D_L values of Refs.[16,17], compared to those computed from the more accurate empirical equation of Wilke–Chang,[1] are relatively satisfactory, considering the difficulties in obtaining experimental D_L values, and the large dispersion of the predicted diffusion coefficients.[2]

SURFACE DIFFUSION

The only gas chromatographic method used for the measurement of diffusion coefficients of gases on solid surfaces is the RF-GC technique validating a recent mathematical analysis, also permitting the estimation of adsorption and desorption rate constants, local adsorbed concentrations, local isotherms, local monolayer capacities, and energy distribution functions.[19] The RF-GC technique has been successfully applied for the time-resolved determination of surface diffusion coefficients for physically adsorbed or chemisorbed species of O_2, CO, and CO_2 on heterogeneous surfaces of Pt/Rh catalysts supported on SiO_2.[19] All calculations for the surface diffusion coefficient, D_s, can be carried out simultaneously by the GW-BASIC personal computer program listed in Appendix A of Ref.[19] The D_s values clearly show their dependence on time, and are in relative agreement with those found by non-chromatographic techniques.[19]

CONCLUSIONS

The gas chromatographic broadening and flow perturbation techniques have been proven to be useful tools for the accurate measurement of diffusion coefficients of gases in gases and liquids, and on solids.

ACKNOWLEDGMENTS

The author thanks Ms. Margarita Barkoula for her kind assistance.

REFERENCES

1. Giddings, J.C. In *Dynamics of Chromatography*; Marcel Dekker, Inc.: New York, 1965; 237–241.
2. Karaiskakis, G.; Gavril, D. Determination of diffusion coefficients by gas chromatography. J. Chromatogr. A, **2004**, *1037*, 147–189.
3. Hirschfelder, J.O.; Curtis, C.F.; Bird, R.B. *Molecular Theory of Gases and Liquids*; John Wiley: New York, 1954; 1126–1127.
4. Bird, R.B.; Stewart, W.E.; Lightfoot, E.N. *Transport Phenomena*; John Wiley: New York, 1960; 744–746.
5. Fuller, E.N.; Schettler, P.D.; Giddings, J.C. A new method for prediction of binary gas-phase diffusion coefficients. Ind. Eng. Chem. **1966**, *58*, 19–27.
6. Maynard, V.R.; Grushka, E. Measurement of diffusion coefficients by gas-chromatography broadening techniques: A review. Adv. Chromatogr. **1975**, *12*, 99–140.
7. Yang, F.; Hawkes, S.; Lindstrom, F.T. Determination of precise and reliable gas diffusion coefficients by gas chromatography. J. Am. Chem. Soc. **1976**, *98*, 5101–5107.
8. Katsanos, N.A.; Karaiskakis, G.; Vattis, D. Diffusion coefficients from stopped-flow gas chromatography. Chromatographia **1981**, *14*, 695–698.
9. Katsanos, N.A.; Georgiadou, I. Reversed-flow gas chromatography for studying heterogeneous catalysis. J. Chem. Soc. Chem. Commun. **1980**, *5*, 242–243.
10. Katsanos, N.A.; Karaiskakis, G. Reversed-flow gas chromatography applied to physicochemical measurements. Adv. Chromatogr. **1984**, *24*, 125–180.
11. Katsanos, N.A. *Flow Perturbation Gas Chromatography*; Marcel Dekker, Inc.: New York, 1988; 113–161.
12. Katsanos, N.A.; Karaiskakis, G. Measurement of diffusion coefficients by reversed-flow gas chromatography instrumentation. J. Chromatogr. **1982**, *237*, 1–14.

13. Atta, K.A.; Gavril, D.; Karaiskakis, G. A new gas chromatographic methodology for the estimation of the composition of binary gas mixtures. J. Chromatogr. Sci. **2003**, *41*, 123–132.
14. Katsanos, N.A.; Karaiskakis, G. Temperature variation of gas diffusion coefficients measured by the reversed-flow sampling technique. J. Chromatogr. **1983**, *254*, 15–25.
15. Karaiskakis, G.; Katsanos, N.A.; Niotis, A. Measurement of diffusion coefficients in multicomponent gas mixtures by the reversed-flow technique. Chromatographia **1983**, *17*, 310–312.
16. Katsanos, N.A.; Kapolos, J. Diffusion coefficients of gases in liquids and partition coefficients in gas–liquid interphases by reversed-flow gas chromatography. Anal. Chem. **1989**, *61*, 2231–2237.
17. Atta, K.A.; Gavril, D.; Katsanos, N.A.; Karaiskakis, G. Flux of gases across the air–water interface studied by reversed-flow gas chromatography. J. Chromatogr. A, **2001**, *934*, 31–49.
18. Katsanos, N.A.; Arvanitopoulou, E.; Roubani-Kalantzopoulou, E.; Kalantzopoulos, A. Time distribution of adsorption energies, local monolayer capacities, and local isotherms on heterogeneous surfaces by inverse gas chrom atography. J. Phys. Chem. B. **1999**, *103*, 1152–1157.
19. Katsanos, N.A.; Gavril, D.; Karaiskakis, G. Time-resolved determination of surface diffusion coefficients for physically adsorbed or chemisorbed species on heterogeneous surfaces by inverse gas chromatography. J. Chromatogr. A, **2003**, *983*, 177–193.

Diode Array Detectors: Peak Identification

Ioannis N. Papadoyannis
H.G. Gika
Laboratory of Analytical Chemistry, Chemistry Department, Aristotle University of Thessaloniki, Thessaloniki, Greece

INTRODUCTION

The diode array detector (DAD), which arose from the analyst's needs to reduce data observations times in chromatography, has become a powerful tool in a research environment and in the quality assurance laboratory. Diode array adds a new dimension of analytical capability to liquid chromatography (LC) because it allows qualitative information to be obtained beyond simple identification by retention time.

Among the three advantages that DAD provides to the high-performance liquid chromatography (HPLC) analyst, peak identification is the one that allows the identification of unknown constituents in a sample whose matrix is complex.

PEAK IDENTIFICATION

The method-development laboratory is often set with a task of identifying unknown constituents in a complex sample. The identity or quantity of analytes is not well defined at this stage. Complicated sample-preparation steps and multiple HPLC analyses may be required to ascertain the nature of a sample. The diode array detector simplifies this process. In the case that more than 15 different peaks have been separated in a analysis of a multicomponent sample of known origin; more than a full day's work might be required just to establish the retention times of the unknowns with the use of a standard absorbance detector. A number of long-run HPLC analyses would have to be made with pure standards so that retention time correlations could be determined. This necessity is accomplished by the DAD's advantage of acquiring data in both the time and spectral domain.

The DAD has brought compound identification to HPLC. Previously, mass spectrometry (MS) was the sole domain in peak identification for gas or liquid chromatography (GC/MS or LC/MS). This can now be achieved as part of the HPLC analysis, and at a lower cost, because there is the ability to use an HPLC/DAD system as a scouting technique to check the possible identity of an unknown sample.

HPLC techniques often use absolute or relative retention times to identify compounds. Under well-defined conditions, UV/Visible spectra are useful data for the confirmation of peak identity. Thus, it is possible to qualify the compounds present through the use of spectra. This mode of identification by spectral similarity is also useful when retention times shift because of changing chromatography for similar sample runs.

However, spectral identity is a necessary but not a sufficient condition for compound identification. If the instrument parameters that determine how spectra are acquired are matched suitably, the spectral match of an unknown to a known spectrum can be used as strong indication of compound similarity or confirmation of identity. In a chromatogram, the retention time of a given peak offers an obvious means of preselection of candidate spectra through the application of a retention time window. All spectra from the set of possible candidates that fall in the window are compared to the unknown spectrum. The candidate with the best match factor above a certain threshold level is then used to identify the compound for the peak. Another possibility is to weigh both the match factor and the similarity in retention times and use the combined information for identification.

Peak identification is done by comparing a spectrum from an unknown peak to a spectrum from a user-created library. The best match of spectra is the closest to the correct identification. The comparison between the reference spectrum and the unknown spectrum is realized by the appropriate software.

With the DAD, spectra can be acquired automatically for each peak during the analysis. The spectra can be compared with those stored in a library, either interactively on the computer display or mathematically with the help of microprocessors. In Fig. 1, the spectral library matching is illustrated. The standard sample is analyzed and the spectrum of the target compound is registered in the library. The spectrum of the unknown sample is compared to standard spectra in the library.

SPECTRAL LIBRARIES

The UV spectra employed in HPLC can change for the same compound, depending on the mobile-phase environment at the time of elution. To have any success in applying similar approaches to compound identification, the separation system used to acquire spectra for standards and unknown analytes needs to be the same and well

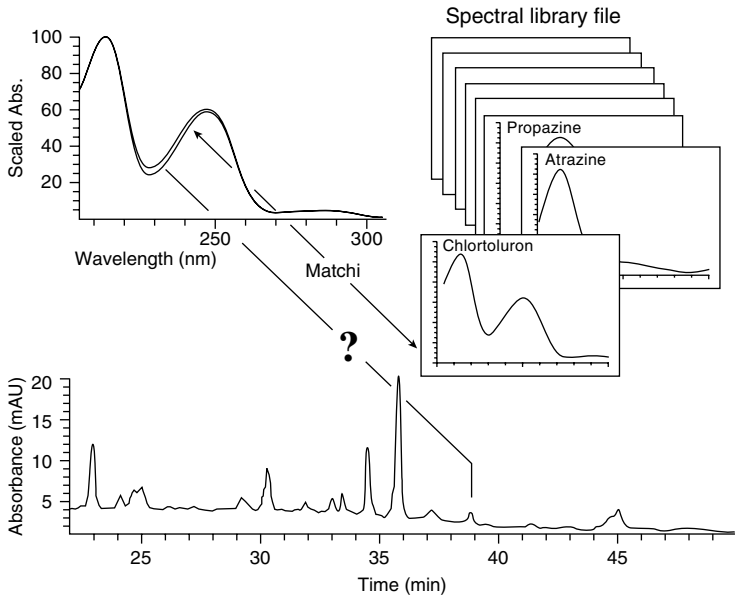

Fig. 1 Peak identification by spectral matching.

defined. Several examples taken from the recent literature make a strong case for the necessity of clearly defining the column and the mobile phase used.

Two primary approaches to the use of spectral libraries in HPLC can be described:

1. In the forward library search, an attempt is made to identify each compound in an unknown sample from a large library of standard compounds, previously recorded under defined chromatographic conditions. Each compound spectrum from the sample, analyzed under the same conditions, is searched against the library for identification. In case this is not possible, it may be classified by comparison with similar compounds from the library. Because the unknown sample may contain compounds that are not present in the library, it is desirable to obtain, at least, a list of likely matches for each unknown. In some instances, preselection of spectra is employed, based on the retention time indexing or on rough comparison of spectral features such as number and position of the primary absorbance maxima. This is done primarily to reduce the time needed to search the full compound library. In HPLC, it is found mainly in toxicological screening and drug-testing applications.
2. For reverse library searching, a limited library of standard compounds, all of which are expected to be present in the sample, is searched against the unknown spectrum in the current analysis. This search mode is an expansion of normal calibration procedures used currently in HPLC. Each peak of interest in a sample should be characterized through analysis of a standard. The spectral library, consequently, contains spectra for a limited number of compounds. In this case, we try to find the best match for each standard spectrum in the library by searching against all compound spectra identified in the current analysis. The question is to find all or some of the standard compounds in the unknown sample in a one-to-one assignment.

SPECTRAL MATCHING

Spectral matching can be defined as the process of comparing two spectra with the intention of determining their similarity. Once spectra could be digitized and the digital information manipulated mathematically, it became possible to base the comparison on a numeric evaluation of the digital data. Thus, in the modern definition, spectral matching is a procedure whereby the digital information available for a pair of spectra, each typically consisting of numerous discrete data points, is reduced to a single number indicative of the similarity between the two spectra. Ideally, this reduction in the number of data points does not involve any reduction in the information contained in the relationship of two spectra to each other. More specifically, most matching procedures presently employed are based on a point-by-point comparison of the two spectra in question to establish the presence or absence of significant differences.

Generally, there are three ways of performing spectral comparison: 1) overlay of spectra and visual determination, which is a subjective test; 2) evaluation of spectral differences between the reference spectrum and the unknown spectrum using the appropriate software. Larger differences suggest that the unknown is a different compound than the reference or that it is a mixture;

3) use of sophisticated software to calculate a numerical value that mathematically defines the closeness of the match.

Following are descriptions of the most common mathematical approaches used through spectral matching software.

Vectorial Approach to Spectral Matching

One approach that facilitates the definition and comparison of various matching procedures and eliminates the confusion associated with normalization is to view each spectrum as a vector in *N*-dimensional space. A spectrum data is considered as the group of the absorbance at each wavelength and it is represented with the vector.

$$(a(\lambda_1), (a(\lambda_2), a(\lambda_3), \ldots, a(\lambda_n))$$

where $a(\lambda_i)$ is the absorbance at the wavelength λ_i.

One spectrum corresponds to one vector:

$$\vec{S} = (a(\lambda_1), (a(\lambda_2), a(\lambda_3), \ldots, a(\lambda_n))$$

If there are two spectra, spectrum S_1 corresponds to S_1 and spectrum S_2 corresponds to S_2.

$$\vec{S}_1 = (a_1(\lambda_1), (a_1(\lambda_2), a_1(\lambda_3), \ldots, a_1(\lambda_n))$$
$$\vec{S}_2 = (a_2(\lambda_1), (a_2(\lambda_2), a_2(\lambda_3), \ldots, a_2(\lambda_n))$$

These vectors are simplified to a two-dimensional vector as shown in Fig. 2. The matching procedure can then be based either on determining the angle between the two vectors or on finding the distance between their tops. The first approach would seem to be independent of the relative magnitude of S_1 and S_2; the later definition implies normalization of S_1 and S_2 prior to the calculation of the distance.

If these spectra come from the same compound, the ratio between corresponding elements in S_1 and S_2 is constant and these vectors have the same direction. In that case, the angle θ in Fig. 2 becomes zero. As general rule, the more the angle approaches zero, the greater the similarity between the two spectra. The following equation describes the degree to which the two spectra correspond [similarity index (SI)] based on the cosine of the angle of their component vectors formed at each point of measurement:

$$\mathrm{SI} = \frac{\vec{S}_1 \cdot \vec{S}_2}{|\vec{S}_1| \cdot |\vec{S}_2|} = \cos\ \theta \tag{1}$$

or

$$\mathrm{SI} = \frac{\sum_{\lambda_i} a_1(\lambda_i) \cdot a_2(\lambda_i)}{\sqrt{\sum_{\lambda_i} a_1(\lambda_i)^2} \cdot \sqrt{\sum_{\lambda i} a_2(\lambda_i)^2}} \tag{2}$$

As the SI approaches zero, the pattern matching becomes poor (the angle θ between the vectors approaches 90°) and, conversely, as SI approaches unity, the pattern approaches a perfect match.

For easier manipulation, especially in the case of very similar spectra where differences may exist only in the third or fourth decimal place, the spectral match factor is often multiplied by 1000.

Another common measure of spectral similarity is the correlation coefficient *r* that is defined as:

$$r = \frac{\sum[(S_{1i} - \bar{S}_1)(S_{2i} - \bar{S}_2)]}{\sqrt{\sum(S_{1i} - \bar{S}_1)^2 \sum(S_{2i} - \bar{S}_2)^2}} \tag{3}$$

It expresses the correlation between paired absorbance values for the two spectra at each discrete wavelength interval. If we shift out two spectra S_1 and S_2 along the absorbance axis in a way that the mean absorbance for both spectra is zero, a process that is referred to as "mean centering," then $\bar{S}_1$ and $\bar{S}_2$ will both be zero.

Mean centering eliminates any spectral difference because of a fixed baseline offset that might be present in an individual spectrum. Eq. 3 further shows that the normalization of the spectral vectors to unit length is equivalent, in statistical terms, to the scaling of each spectrum by its standard deviation.

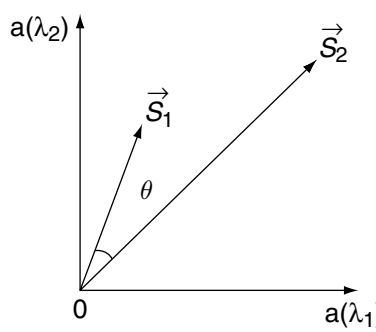

Fig. 2 Vectorial definitions of spectral matching.

Measures of Dissimilarity

Reliant on the ultimate relationship of geometry:

$$\cos^2 + \sin^2 = 1 \tag{4}$$

we can define a factor of dissimilarity of spectra. Thus, the sine square multiplied by 1000 could serve as an indicator of spectral dissimilarity.

Another possible measure of spectral dissimilarity, the Euclidean distance *e* between the tips of the two

vectors, as shown in Fig. 2, can also be related to sine and cosine:

$$e = S_1 - S_2 = \sqrt{\sin^2(S_1 - S_2) + [1 - \cos(S_1, S_2)]^2} \quad (5)$$

$$e = \sqrt{\sin^2(S_1 - S_2) + 1 - 2\cos(S_1 - S_2) + \cos^2(S_1 - S_2)} \quad (6)$$

and upon the Eq. 4

$$e = \sqrt{2 - 2\ \cos(S_1, S_2)} \quad (7)$$

$$e = \sqrt{1 - |\cos(S_1, S_2)|} \quad (8)$$

All the mathematical approaches mentioned above differ in the degree of change observed for spectral differences, most noticeably for angles below 15°. Between 0° and 10°, $\sin^2$, $\cos^2$, and cosine do not change very much, making it more difficult to differentiate among spectra with strong similarities. The rate of change varies, complicating the task of assessing the variability of the match score for different degrees of dissimilarity.

Normalization of Spectra

There are numerous procedures for the normalization of spectra, other than the one based on unit vector length. They all lead to the same result, if S_1 and S_2 differ only in concentration but there are essential differences in the case where S_1 and S_2 differ significantly.

The general normalization procedure for a given spectrum S follows the rule: $\langle S \rangle = NS$, where $\langle S \rangle$ corresponds to the normalized spectrum S and N is the appropriate normalization factor. Some of the more commonly used normalization procedures are presented below.

For vector normalization, N is defined as $N = 1/\sqrt{\sum S_i^2}$. Further, normalization to unit area can be achieved as $N = 1/\sum \mid S_i \mid$.

Vector normalization and area normalization are fairly resistant to noise because all data points are included and small random fluctuations, due to noise, tend to cancel each other.

There are also two normalization procedures that are based on the forcing of the absorbance at a specific wavelength to a specific value V. The wavelength used can be either the same for both spectra, $N = S_\lambda/V$ or the wavelength of maximum absorbance can be found over a specific wavelength range for each spectrum, $N = S_{max}/V$. In both cases, normalization is much more dependent on noise because a single absorbance value controls the normalization factor N.

FACTORS AFFECTING SPECTRAL COMPARISON

How to set a threshold level for the match factor to positively identify a compound spectrum is strongly dependent on a variety of factors. Below are mentioned those that play a major role in the success of the spectral matching procedure and are important tools in optimizing spectral comparison and threshold setting.

Wavelength Accuracy and Precision

Depending on the shape of the spectrum, small errors on the wavelength axis could translate into substantial errors on the absorbance axis and thus lead to false scores.

Detector Response Function

Initially, the optical resolution achieved by the spectrometer is governed by the size and shape of the entrance slit and determines the overall preservation of spectral fine structure. Secondly, the diode resolution obtained from the diode array is based on the geometry of the individual diodes, their spacing, and any grouping of diodes applied during processing of spectral data. Finally, stray light in the detector can cause deviations from Beer's law such that at low-light throughput absorbance no longer changes linearly with concentration. Thus, depending on the analyte's concentration, spectra will be distorted at higher absorbance values, resulting in an overall different shape when compared to a spectrum at lower concentrations.

Instrument Noise

The dissimilarity score for two identical spectra will never reach zero because of the presence of noise in the detector that cannot be compensated. There will always be some residual dissimilarity, which imposes a practical limit on the definition of a match threshold. The noise level of a given spectrum at a specific analyte concentration depends on the spectrometer, the characteristics of the diode array, and the scan speed of the detector, the lamp, and detector electronics.

Interference from Spectral Background

In most LC analyses, the spectra recorded contain some background absorption caused by either a change in the elution solvent, if a gradient system is employed, or by instabilities inherent in the instrumentation, or both. Therefore, some kind of background correction is typically indicated whenever spectra are compared, either for the purpose of determining whether a chromatographic peak contains an impurity or for the process of compound identification.

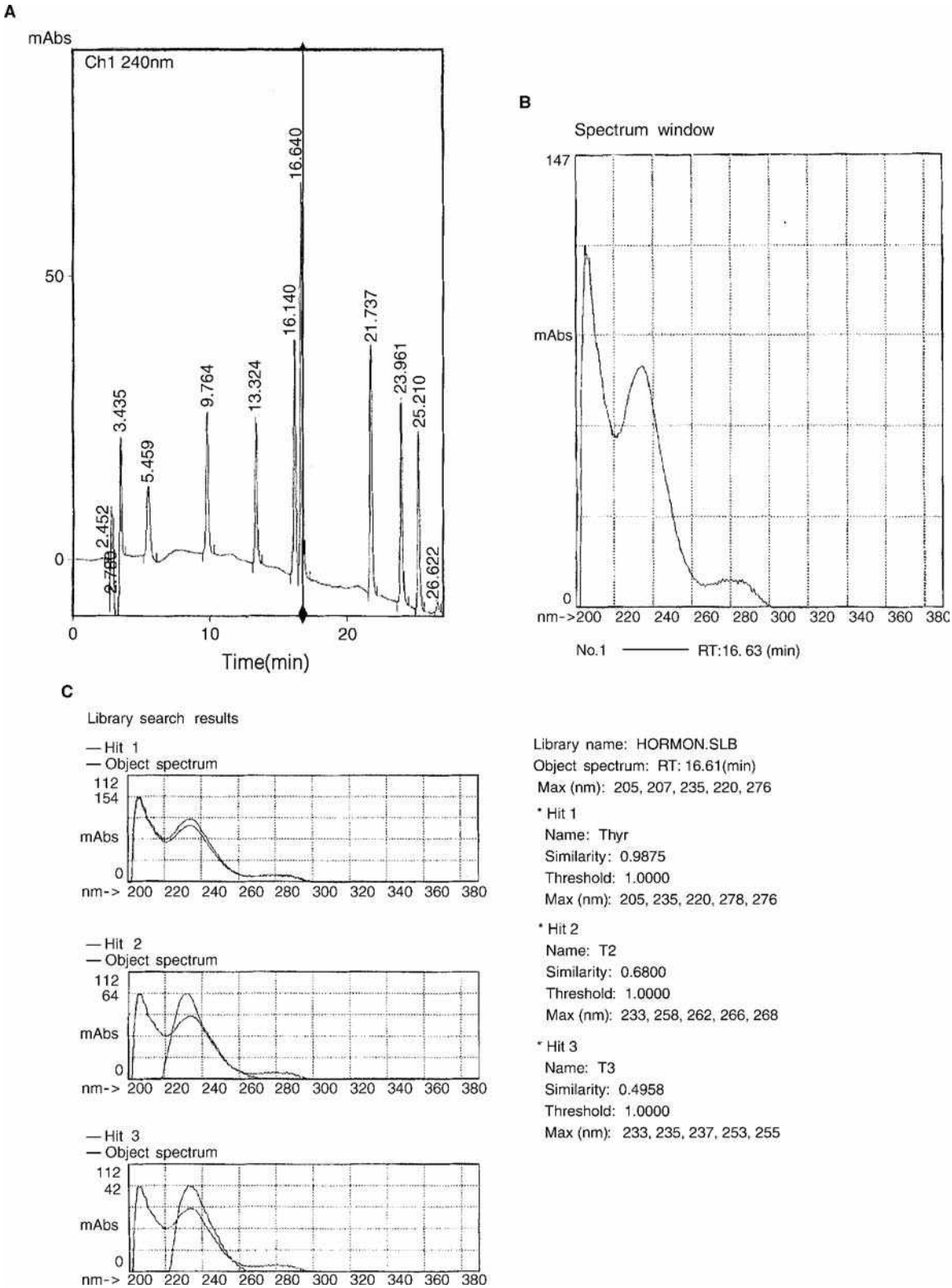

Fig. 3 A, HPLC chromatogram of standard solution containing tyrosine, thyronine, and some of their iodo derivatives. Detection was performed with a Shimadzu SPD-M6A photodiode array detector at 240 nm. The spectrum B, of the selected peak (thyronine) is acquired automatically and stored in the UV spectral library for comparison in further identification procedures. C, Normalized spectral comparison and report results of chromatogram's thyronine peak with the best matching library spectrum. The similarity index indicates the closest match.

Selection of Wavelength Range Employed for Matching

The selection of the appropriate wavelength determines the selectivity of spectral comparisons because instrument noise, which is the sum of all electronic and optical imperfections, will certainly favor some wavelength regions over others.

Processing of Spectral Data Prior to Matching

Prior to calculation of a dissimilarity score, spectra can be treated mathematically, either to improve their noise characteristics or to enhance differences for very similar spectra. One mode of pretreatment, from classical spectroscopy, involves the use of derivatives, especially of the second and higher derivatives, to enhance the fine structure of absorbance bands. Smoothing of spectral data to reduce noise is another pretreatment mode that could potentially improve the selectivity of spectral matching.

Impurities

The spectrum of the unknown compound to be identified should not contain any spectral impurities as caused by coeluting components. If a spectrum is known to contain a spectral impurity, it should be corrected for this impurity before the comparison with the standard spectra. Corrections for coeluting impurities are very difficult. If the impurity does not coelute completely, identification may still be possible, depending on the concentration and elution time of the impurity, relative to the main peak.

EXAMPLE OF APPLICATION

The identification of an unknown peak in a chromatographic analysis, performed by the Shimadzu SPD-M6A UV/Vis photodiode array detector, combined with data acquisition software Class M10A, is presented in Fig. 3A–C. The spectrum file of the selected peak is compared against reference spectra in a user-built library. Data processing through the mathematical approach mentioned above defines the best match. The numerical value of the SI indicates the spectrum of thyronine as the better match because, in this case, it is close to unity. The comparison is also made by visual evaluation through the overlaid spectra. The created spectral sublibrary consists of several iodothyronine and iodotyrosine spectra, which are those of interest in this application. Thus, the chromatographic peak, assuming it belongs to thyronine, can be identified among other related compounds by its UV spectrum, allowing qualitative analyses that are more accurate.

CONCLUSIONS

The mode of peak identification that the diode array detector provides allows identification of unknown peaks, not only by retention time but also by their UV spectra. The UV spectrum is very reproducible and its full shape is much more compound-specific than is generally assumed. It is a powerful tool that, beyond other applications, it can also be used as a scouting technique to find out the possible identity of an unknown sample. However, spectral identity is a necessary but not a sufficient precondition for compound identification. The information that is acquired by the comparison of an unknown and a known spectrum can be used as strong indication of compound similarity or confirmation of identity. Combinatorial estimation of retention time and spectral comparison results will give us a more definite idea.

BIBLIOGRAPHY

1. http://hplc.chem.shu.edu/new/HPLC_book/detectors/det_uvda.htm.
2. http://www.chem.agilent.com/cag/peak/peak3-99/article01.html.
3. http://www. Waters.com/waters_website/pittcon98/p996.htm.
4. Huber, L.; George, S.A. *Diode Array Detection in HPLC*; Chromatographic Science Series; Marcel Dekker, Inc.: New York, 1993; Vol. 62.
5. Kohn, A. LC/GC Int. Nov. **1994**, *7* (11), 652–660.
6. *SPDM6A Photodiode Array Detector, Instruction Manual*; Shimadzu: Columbia, MD, 1989.

Diode Array Detectors: Peak Purity Determination

Ioannis N. Papadoyannis
H. G. Gika
Laboratory of Analytical Chemistry, Chemistry Department, Aristotle University of Thessaloniki, Thessaloniki, Greece

INTRODUCTION

Peak purity analysis is an evaluation technique for detecting the presence of coeluting impurities in high-performance liquid chromatography (HPLC) data. Running a peak purity check prior to analytical quantitation helps to ensure accuracy. In the development of analytical methods, peak purity analysis can reveal the presence of contamination during standardization and, by doing so, can prevent the subsequent generation of false analytical data.

Peak purity analysis is also a useful addition to routine quality control procedures, especially in the analysis of pharmaceuticals and food products, for which contamination and quality of results are critical.

PEAK PURITY ANALYSIS WITH DIODE ARRAY DETECTOR

Peak purity analysis is designed to detect the presence of an impurity that is coeluting with the analyte peak. For impurity detection with a single-wavelength UV/Vis detector, one must see a shoulder, valley, or excessive tailing to suspect the presence of an impurity. The absence of these features on the chromatographic peak is not a foolproof assurance of peak purity. The impurity may not be seen simply because the chromatographic resolution is low (Fig. 1). A photodiode array detector can provide additional information by using the acquisition of UV/Vis spectra to determine peak purity.

A proper peak purity determination requires access to a significant portion of the eluting compound's spectrum without interrupting the separation. For this reason, peak purity analysis is performed using a multisignal UV/Vis diode array spectrophotometer as the HPLC detector. Unlike the diode array detector (DAD), the traditional variable-wavelength detector examines only a single wavelength of the sample spectrum, providing insufficient information for peak purity determination. The diode array spectrometer illuminates the sample with the entire spectrum of wavelengths emitted by the light source. Light transmitted by the sample is then broken into its component wavelengths by a diffraction grating and directed to a bank of photodiodes, each of which is dedicated to measure a narrow band of the spectrum. As no mechanical scanning is required, spectral acquisition can be accomplished in as little as 12 msec, well within the precision limits for HPLC peak elution. The rapid spectral acquisition makes it possible to perform peak purity determinations using selected multiple spectra as inputs. Therefore, the absence of any mechanical action in the acquisition of spectra enhances the reproducibility and the accuracy of the peak purity analysis. For coeluting peaks, a DAD makes it possible to differentiate both compounds, even when their spectral absorption overlaps the entire range of captured wavelength data.[1,2]

DIFFICULTIES OF PEAK PURITY CONFIRMATION

Before the quantitative information contained in a chromatographic peak can be used, the purity of the peak should be confirmed. Only after we are sure that no coeluting impurity was present, which could have contributed to the peak response, can we convert the peak's area or height into quantitative information based on the equivalent response of a pure standard. This peak purity analysis can be based on the comparison of the various spectra recorded during the elution of the peak. If the peak is pure, then, apart from concentration differences, the spectra taken at several points during a peak's elution should all be identical and the match scores obtained should be very close to the perfect match scores. If significant deviations are encountered, this can be seen as an indication of impurity.

Unfortunately, the inverse is not necessarily true. If the spectra are identical, based on the algorithm used for comparison, the peak can still be impure for one or several of three possible reasons:

1. The impurity is present at a much lower concentration than the main compound and is not detectable.
2. The impurity has the same or a very similar spectrum, compared to the main compound.
3. The impurity exhibits the same peak profile as does the main compound; that is, it completely coelutes with the main peak, across the entire peak.

One of the most important aspects of peak purity analysis that is often overlooked is the fact that any

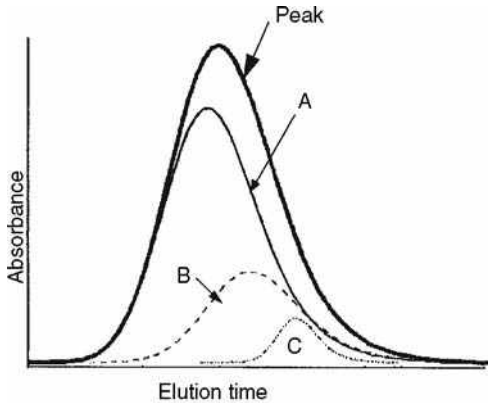

Fig. 1 Coelution of three compounds A, B, and C in the chromatographic peak. No shoulders, valleys, or excessive tailing are seen.

peak purity algorithm can only confirm the presence of impurities, but can never unambiguously prove that a peak is pure.

HPLC SIGNAL OVERLAY FOR PURITY ANALYSIS

One way of uncovering contributions because of impurities in an HPLC peak is to overlay peak profiles acquired at several wavelengths. As two different compounds are unlikely to exhibit identical absorption over multiple wavelengths, the presence of an impurity is revealed by the deviation of the profiles. To compensate for the differences in spectral intensity at different wavelengths, the signals to be compared are first normalized to the maximum absorbance value or to equal areas. Peaks free of impurities exhibit good overlap, but the presence of an impurity is indicated by a shift in the retention time maximum at different wavelengths (Fig. 2).

The signal overlay method is not considered to be very sensitive, and is highly dependent on the resolution of analyte and impurity peaks. If care is taken to correct for solvent background and if the signals are normalized to the highest absorbance value in the time range plotted, the resulting ratiogram can provide conclusive information. It is usually recommended as an additional qualifier in conjunction with other peak purity analysis methods.

In addition to signal overlap, the ratios of signals acquired at different wavelengths can be calculated and plotted. The resulting ratiograms are good *indicators* of peak purity. Any significant distortion of the ratiogram's ideally rectangular form is an indication of differential absorption and the presence of an impurity (Fig. 3). Peak purity analysis based on signals is generally limited to instances for which the spectra of both analytes and impurities are well known, a requirement for selecting the wavelengths best suited for comparison. Typical applications for this information would be routine evaluations such as quality control checks.

PEAK PURITY USING SPECTRAL DATA

Comparison of spectra is the most popular method of peak purity determination. The primary advantage of this approach is that prior knowledge of component spectra is not required. However, information derived using these techniques is not sufficient for determining the kind, number, and level of impurities present.

A number of selection criteria and data manipulation techniques can be applied prior to analysis to improve the quality of the analytical result. These include setting different spectrum acquisition modes, background corrections, normalization, and threshold settings.

Selection of Spectra for Comparison

Peak purity analysis software allows users to sample spectra at equidistant points across an HPLC peak. In

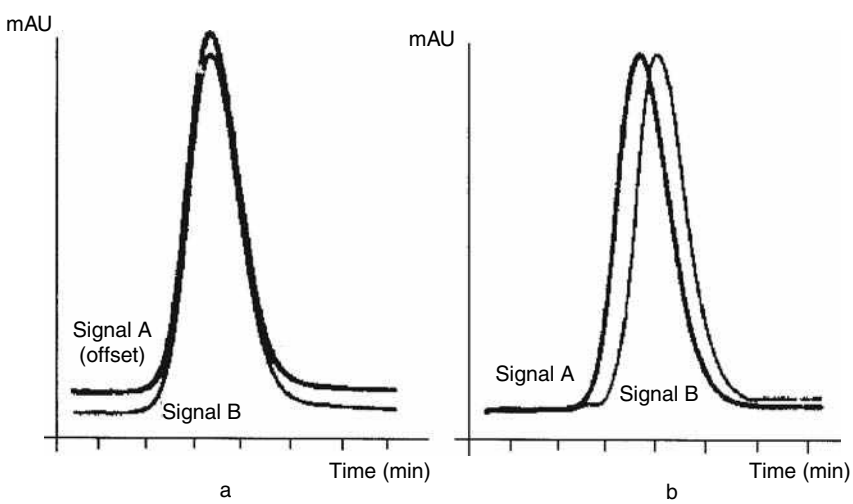

Fig. 2 Normalized signals for (a) pure and (b) impure peaks.

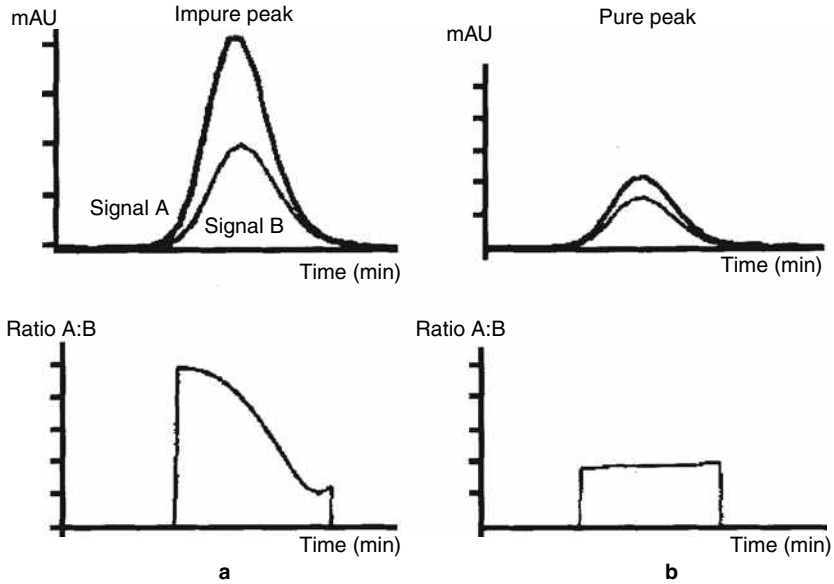

Fig. 3 Ratiograms taken from (a) an impure and (b) a pure peak.

general, the poorer the resolution between potentially coeluting peaks is, the more desirable it is to use greater numbers of data points to detect the impurity. Traditionally, spectra have been sampled upslope, at the apex, and downslope of the eluted peak. This selection pattern may overlook the presence of impurities near the peak extremities. However, acquisition of many spectra may increase calculation and display time without adding significant information.

Background Correction

A peak should not be labeled as impure because of spectral background, or because of tailing interference from a neighboring peak. Both effects can be corrected for by suitable background correction, with the understanding that spectral subtraction increases the noise of a spectrum and, thereby, lowers the ideal match factor.

Whether background correction needs to be applied depends on the separation system employed. If the instrument is balanced properly, then, for isocratic separations, the solvent background will be eliminated by the built-in automatic subtraction of the solvent spectrum, as present at the beginning of the analysis, from all recorded spectra. For gradient separations, background corrections will have to be applied after the analysis.

Different methods for correction are possible; the choice of method depends on the availability of spectra resulting from specific modes of spectral storage for different instruments. Ideally, all spectra are retained for an analysis, but because of processing and storage constraints, many instruments offer a mode of acquisition where spectra are stored only during the elution of a peak. Peak spectra can be limited to just the apex spectrum, or to a number of additional spectra across the peak, most commonly acquired at the baseline and the inflection points. If only apex spectra are available, no background correction is possible. For all other cases, the quality of background correction will depend on the availability of suitable baseline spectra.

In the simplest case, a single baseline spectrum is subtracted from all analyte spectra. This will work only for the elimination of constant spectral impurities. If several baseline spectra are available, linear combinations of those spectra can be used to generate a synthetic background spectrum at any point in the chromatogram. Ideally, the two spectra should be close to the beginning and the end of the peak being analyzed. If this is not possible because of incomplete separation of the peak from its neighbors, baseline spectra could be taken from the beginning and the end of a peak group.

If only slope and apex spectra are available, background correction is still possible, in a limited fashion, by subtracting the apex spectrum from the two slope spectra. For isocratic separations or gradient with slow changes in solvent background, this approach will produce two baseline-corrected slope spectra with a loss in signal that is equal to the difference in amplitude between slope and apex spectrum.

Spectrum Normalization

Spectra used for comparison during peak purity determination should be normalized to compensate for differences in concentration. Normalization can be based on setting equal absorbance maxima or maximum wavelength ranges, on setting equal area of spectra or spectral region of interest, or on using a matching algorithm that minimizes area differences by shifting and scaling spectra.

Absorbance Threshold

Setting an absorbance threshold improves the accuracy of spectral comparison by screening out spectra near the signal baseline. These spectra tend to have a relatively high degree of noise, which adversely affects the accuracy of both normalization and subsequent spectrum matching.

Spectrum Overlay

After spectra are acquired and processed, they are overlaid for visual evaluation (Fig. 4). Although significant deviations between the profiles can indicate the presence of an impurity, the converse is not necessarily true, and spectral profiles that match quite well may still mask the presence of an impurity. Factors that may contribute to nondetection of impurity include large concentration differences between analyte and impurity and either highly similar spectral profiles or identical chromatographic peak profiles and retention times for both analyte and impurity. As a rule of thumb, impurity concentrations in the 0.1–1% range may be detected when the spectra are dissimilar. However, if the spectra of the different components are highly similar and the HPLC peaks are not well resolved, the impurity detection limit is on the order of 5%.

ADVANCED TECHNIQUES

Simple peak purity analysis is relatively accurate when the impurity is present at significant concentration levels but, as the level of impurity diminishes, its impact on the target analyte spectrum becomes subtler and may require more sophisticated techniques. For this, statistical software routines are available for automated spectral comparisons. In these cases, peak purity determination and analysis of spectral differences are achieved using vector analysis algorithms. The more similar the spectra are, the closer the value is to 0.0°; the more spectrally different they are, the larger the value. All the spectral data points across the peak are analyzed; the data are converted into vectors, compared, and graphically plotted so that the results can be visualized. These software routines provide both numerical results and graphical representations such as similarity and threshold curves.

Similarity curves are plots of retention times versus similarity factors computed by comparing spectra across an eluted peak with one or more selected spectra. Similarity curves improve the sensitivity of detecting impurities because they extract and highlight subtle impurity-generated anomalies in an analyte spectrum that might otherwise go unnoticed.

The threshold curve is a plot of retention time versus a similarity factor threshold, below which the presence of an impurity cannot be distinguished from spectral noise. The threshold trace may be computed automatically from the standard deviation of a number of user-selected pure noise spectra. Alternatively, the threshold may be set at a fixed value. Similarity and threshold curves tend to rise at the extremities of the eluted peak, even when no impurity is present. As signal strength decreases, a larger proportion of the spectral response is caused by noise. If an impurity is present at a detectable concentration, the similarity curve will intersect the threshold (Fig. 5).

Peak purity software incorporating routines for data acquisition and reduction, extraction and comparison of spectra, and display of analytical results can be utilized in either an interactive or automated fashion. A desired sequence of operations can be recorded in a peak purity analysis method file and can run unattended after input parameters are selected. As the quality of the determination is highly dependent on the preanalysis data treatment,

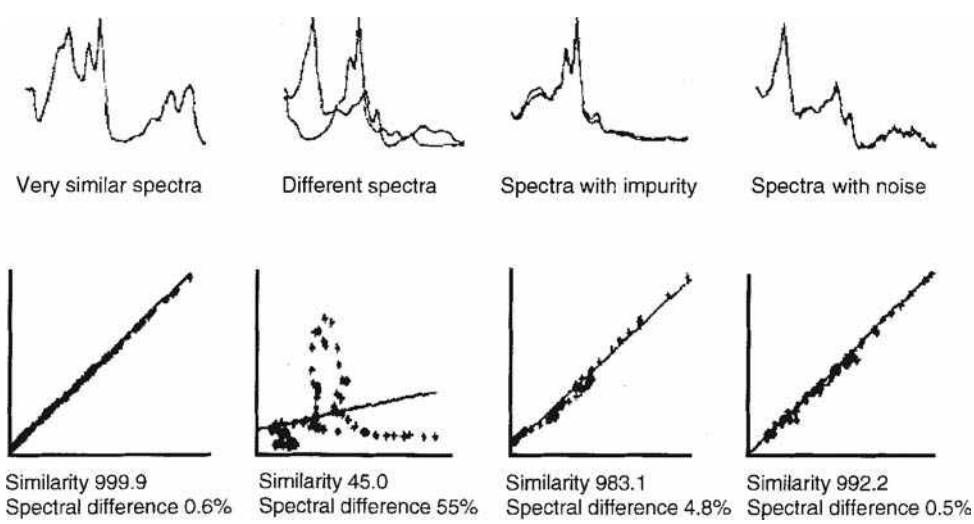

Fig. 4 Graphical display of similarity factors for different pairs of normalized spectra.

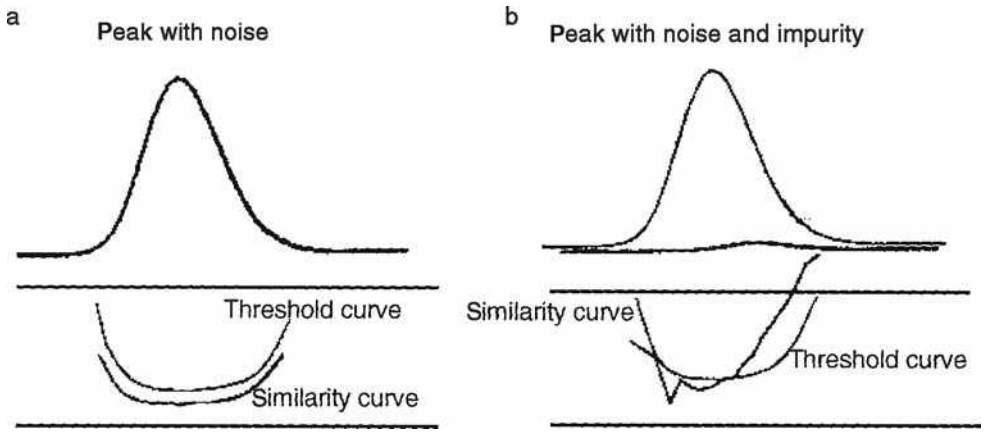

Fig. 5 Effect of impurity and noise on similarity and threshold curves of (a) a peak without impurity but with noise, and (b) a peak with impurity and noise.

results should be inspected visually to verify that peaks are properly baseline-separated and correctly integrated.

The evaluation of a peak purity analysis is assisted by a well-organized visual display of the output of various peak purity analysis techniques.[3–5]

CONCLUSIONS

Peak purity analysis is designed to detect the presence of an impurity that is coeluting with the analyte peak. A DAD, using the almost instantaneous acquisition of a considerable portion of the UV/Vis spectrum of eluted peak components, can give accurate information to determine peak purity. The spectral uniqueness of each compound is used to indicate when there are two or more components present in the peak, to identify peaks, and to assess purity.

Peak purity analysis is very useful in chromatographic method development, to confirm that all components have been chromatographically separated, and in quality control, to warn the analyst that an unexpected coeluting impurity has appeared.

REFERENCES

1. Huber, L.; George, S.A. *Diode Array Detection in HPLC*; Marcel Dekker, Inc.: New York, 1993.
2. Kohn, A. The application of peak purity analysis in liquid chromatography and capillary electrophoresis. LC-GC November **1994**, *7* (11) .
3. Shimadzu SPDM6A Photodiode Array Detector, Instruction Manual.
4. http://www.gentechscientific.com/879.htm
5. http://www.forumsci.co.il/HPLC/PEAK_PUR_web.pdf

Displacement Chromatography

John C. Ford
Department of Chemistry, Indiana University of Pennsylvania, Indiana, Pennsylvania, U.S.A.

INTRODUCTION

One of the three basic modes of chromatographic operation, displacement chromatography is useful for preparative separations and trace enrichment. Most liquid chromatographic methods have been performed in displacement mode. Solutes purified by displacement chromatography include metal cations, small organic molecules, antibiotics, sugars, peptides, proteins, and nucleic acids.

Displacement operation involves the introduction of a volume of sample onto the column, which has been previously equilibrated with a weak mobile phase. Since this is a weak mobile phase, the individual sample components are significantly retained by the stationary phase. Displacement occurs with the introduction of a new mobile phase containing a species with a higher affinity for the stationary phase than that of any of the solutes. The solutes are displaced from the stationary phase by this higher-affinity displacer and move further down the column, readsorbing. The solute with the highest affinity for the stationary phase moves the least before readsorbing and that solute with the lowest affinity for the stationary phase moves the most. This process repeats until a series of separated, but adjacent, bands is formed. Each band moves at the same velocity as that of the displacer front. Following elution, the column must be regenerated and re-equilibrated with the initial mobile phase before any subsequent displacement separation. This re-equilibration step can be lengthy and is frequently considered a major limitation to efficient displacement operation.

DEFINITION

Displacement chromatography is one of the three basic modes of chromatographic operation, the other two being frontal analysis and elution chromatography. Displacement chromatography is rarely, if ever, used for analytical separations, but is useful for preparative separations. It has also been used for trace enrichment.

Many, if not most, retentive chromatographic methods have been performed in the displacement mode, including normal-phase, reversed-phase, ion exchange, and metal affinity chromatographies. Much of the recent work has focused on the use of ion exchange displacement chromatography for the preparative purification of biotechnological products.[1,2] Solutes purified by displacement chromatography include metal cations, small organic molecules, antibiotics, sugars, peptides, proteins, and nucleic acids.

Tswett recognized the difference between elution and displacement development, although Tiselius was the first to clearly define these differences. While displacement was popular in the 1940s, that popularity waned in the 1950s. In the 1980s, there was a resurgence of interest in displacement operation due to the efficient utilization of the stationary phase possible in that mode. Frenz and Horvath[3] have published a comprehensive review of the history and applications of displacement chromatography.

Displacement chromatography is characterized by the introduction of a discrete volume of sample into the chromatographic column that has been previously equilibrated with a weak mobile phase, termed the carrier. This carrier is chosen so that the individual components of the sample (the solutes) are significantly retained by the stationary phase. The displacement is accomplished by following the sample with a new mobile phase containing some concentration of the displacer, a molecule with a higher affinity for the stationary phase than that of any of the solutes. The solutes are displaced from the stationary phase by the higher-affinity displacer and move further down the column, readsorbing. That solute with the highest affinity for the stationary phase moves the least before readsorbing, and that solute with the lowest affinity for the stationary phase moves the most. This process is repeated as the displacer solution moves further down the column until a series of separated, but adjacent, bands is formed, termed the isotachic train. Each component of the train moves at the same velocity as the velocity of the displacer front. Following elution of the isotachic train and the displacer solution from the column, the column must be regenerated and re-equilibrated with the carrier before any subsequent displacement separation. This re-equilibration step can be lengthy and is frequently considered a major limitation to efficient displacement operation.

Displacement chromatography requires the competitive isotherms of the solutes and the displacer to be convex upward and to not intersect each other. The isotherm of the displacer must have a higher saturation capacity than any of the solutes. The width, not the height, of the solute band within the isotachic train varies as the amount of solute in the sample varies. The height of the solute band is determined by its isotherm. The concentration of the eluted solutes can be greater than their concentrations in the

sample in displacement chromatography, unlike in isocratic elution chromatography, wherein dilution necessarily occurs.

The choice of displacer concentration is critical for successful displacement. If the displacer concentration is increased, then the solute concentrations in the isotachic train also increase. If the displacer concentration is decreased, then displacement does not occur and the solutes elute as overloaded peaks in the elution mode. Rhee and Amundson[5] have shown that there is a critical displacer concentration below which displacement cannot occur. This concentration depends primarily on the saturation capacities of the solutes and displacer.

When the solute isotherms cross one another, the situation becomes more complex. It then becomes possible to experience selectivity reversal, i.e., at one displacer concentration, the solutes elute in the order A first, then B, while at another displacer concentration, the order is B first, then A. In a study of this problem, Antia and Horvath[6] showed the existence of the separation gap. This is a region in the isotherm plane, the position of which depends on the ratio of the saturation capacities of the solutes in question. Outside the separation gap, displacement occurs in the normal fashion. However, within the separation gap, the displacement operation does not separate the displaced solutes, but results in the elution of a mixture of the solutes.

In addition to appropriate isotherm behavior and displacer concentration, other factors are important in determining the effectiveness of a displacement chromatographic method. Highly efficient columns and fast mass transfer kinetics are necessary to achieve sharp boundaries between the adjacent solute bands in the isotachic train. Diffuse boundaries mean significant regions of overlap between adjacent solute bands and thus low recovery of purified material.

Successful displacement requires the establishment of the isotachic train before elution of the solutes from the column. As might be expected, the column length is thus an important parameter in displacement chromatography. The column should be sufficiently long (or sufficiently efficient) to allow complete formation of the isotachic train, while lengths beyond that minimum do not improve the separation but increase the separation time. An inadequate length results in the elution of an incompletely formed isotachic train with inadequately resolved solute bands, again reducing the recovery yield.

Similarly, the sample size, column length, and displacer concentration jointly influence the establishment of the isotachic train and, thus, the effectiveness of the displacement separation. For a given displacer concentration and column length, increasing amounts of sample result in increasingly diffuse boundaries and, in sufficiently large samples, significant deterioration of the isotachic train. Likewise, for a given sample size and column length, increasingly high concentrations of displacer cause increasingly diffuse boundaries—termed overdisplacement.

Displacement chromatography has the attractive benefit of concentrating the solute. If the conditions are selected appropriately, large injection volumes of low concentration samples can result in isotachic trains having high solute concentrations, essentially identical to those obtained for narrow pulses of high concentration samples. This is one of the features that have caused the increased interest in displacement as a preparative mode. However, detailed comparisons of the production rates of displacement vs. overloaded elution operation are limited.[4] The limited experimental studies suggest that the displacement operation is superior, although regeneration time was not included in the production rate calculation. Alternately, extensive theoretical studies indicate that, for solutes having Langmuirian behavior, optimized overloaded elution chromatography is superior. Resolution of this issue currently awaits further studies.

REFERENCES

1. Antia, F.D.; Horvath, Cs. Displacement chromatography of peptides and proteins. In *HPLC of Peptides and Proteins: Separation, Analysis, and Conformation*; Mant, C., Hodges, R., Eds.; CRC Press: Boca Raton, 1990; 809–821.
2. Freitag, R. Displacement chromatography: Application to downstream processing in biotechnology. In *Bioseparation and Bioprocessing*; Subramanian, G., Ed.; Wiley-VCH Verlag GmbH: Weinheim, Germany, 1998; Vol. 1, 89–112.
3. Frenz, J.; Horvath, Cs. High-performance displacement chromatography. In *High-Performance Liquid Chromatography–Advances and Perspectives*; Horvath, Cs., Ed.; Academic Press: San Diego, 1988; Vol. 5, 211–314.
4. Guiochon, G.; Shirazi, S.G.; Katti, A.M. *Fundamentals of Preparative and Nonlinear Chromatography*; Academic Press: Boston, 1994; .
5. Rhee, H.-K.; Amundson, N.R. Analysis of multicomponent separation by displacement development. AIChE J. **1982**, *28* (3), 423–433.
6. Antia, F.D.; Horvath, Cs. Analysis of isotachic patterns in displacement chromatography. J. Chromatogr. **1991**, *556* (1–2), 119–143.

Displacement TLC

Maria Bathori
Department of Pharmacognosy, University of Szeged, Szeged, Hungary

INTRODUCTION

Displacement takes place in a broad scale when a stronger species replaces a weaker one. Displacement of ligands on the receptor is a typical phenomenon in pharmacology which explains drug–drug interactions.

Displacement equilibrium is also known in chromatography, by which ligands compete for binding sites. This competition can be preferentially utilized for either analytical or preparative scale separations.

DISPLACEMENT CHROMATOGRAPHY WITH COLUMN HPLC

Chromatography may be performed as elution, frontal, or displacement. When the mode of development is not specified, a chromatographic separation is considered to be an elution.

The displacement phenomenon in chromatography was recognized from the beginning of separation processes in the present-day sense.[1] Classical displacement chromatography (DC) was used to separate biologically active compounds, such as amino acids, peptides, and fatty acids.[2] High-performance displacement chromatography (HPDC) was developed in Horváth's laboratory at Yale University. They realized displacement type of development on a microparticulate stationary phase; various applications were accomplished to demonstrate the power of HPDC in preparative scale separation of compounds of biological and medical interest.[3–6]

Experimental work of Kalász et al.[6] resulted in the statement of the characteristics and basic rules of DC. They conceived properties of the fully developed displacement train, factors affecting displacement development, efficacy of separation, analysis of displaced fractions, determination of displacement diagrams from Langmuirian isotherms, as well as selection of the column, carrier, and displacer for DC. Concentration of the sample is a particular feature of DC. However, the displacer in the carrier is also definitely concentrated through the development of the displacement train.

Furthermore, certain prerequisites of HPDC were stated, such as the limit of the mobile phase flow velocity, slight overlapping of peaks during fractionation, etc.

Displacement thin-layer chromatography (D-TLC) also stemmed from the activity of Horváth's group at Yale University. Experimental work with D-TLC has proven the validity of the rules of DC, found by using HPLC.[5,6] Kalász et al.[6–8] continued the research on D-TLC, mainly with the separation of steroids.

There are basic unique characteristics solely for DC. DC works with a mobile phase containing both the carrier and the displacer. A special front moves forward during the development; it is the front of the displacer. Of course, certain compounds are moving forward ahead of the displacer front; that is, the displacer (front) displaces the components from the binding sites of the stationary phase. This complex of the components is terminated by the displacer and the components, and also the displacer is moving forward in the form of clearly defined zone(s) instead of as the Gaussian peaks seen with elution chromatography. The concentration (zone height or peak height) of individual displaced zones is determined by the crossing point of the Langmuirian isotherm and the operating line, instead of the amount of sample components (Table 1).

DISPLACEMENT THIN-LAYER CHROMATOGRAPHY

D-TLC started with the experiments of Kalász and Horváth,[5–7] who stated the basic rules of D-TLC. A direct connection was found between the volumetric load of HPLC and the size (length) of sample in TLC. The size of displaced zones depends on the weight size of the load, but never on the volume of the injected sample with D-HPLC. Similarly, the dimensions of the displaced band are independent from that of the spotted sample. A surprisingly short distance of advancement totally developed the displacement train, e.g., a 20 mm development. It is even more surprising that 75 μg of the sample load could become part of a displacement train after having utilized about 250 mg of stationary phase.[6,7]

D-TLC has several analogs to column displacement HPLC, such as:

- A displacer is supplied after the samples have been loaded onto the stationary phase.
- A displacer front is generated in situ on the stationary phase.
- The sample components start to move because of the effect of displacer, and the displacer front forms a displacement train of adjacent spots.

Table 1 Comparison of elution and displacement modes of development.

Elution development	Displacement development
Linear and non-linear (overloaded) elution.	
The components are diluted (relative to their concentrations in the sample).	The components are concentrated (relative to their concentrations in the sample).
There is one mobile phase, consisting of the elements of the eluent. Gradient elution can also be performed by the use of several mobile phases. Either stepwise gradient or continuous gradient elution is possible.	There are two consecutively supplied mobile phases, the carrier and the displacer. This latter consists of an adequate amount of displacer in the carrier.
The components travel with different migration speeds.	Isotachic migration of the component zones in the fully developed displacement train.
Gaussian (or quasi-Gaussian) peaks.	Adjacent square-wave-shaped zones.
The peak area is proportional to the amount of the component. In some approximations, the peak height is considered instead of peak area.	The zone height is determined by the crossing of the Langmuirian isotherm of the component with the operating line. The zone width is proportional to the amount of the component.
Separation means physical removal of the peaks from each other, the maximum of peaks have to be far away from each other, the distance should be at least one peak width measured at the baseline.	The adjacent zones of a totally developed displacement train touch each other, even in the optimal separation.

- After having reached the state of a fully developed displacement train, all bands move with the same velocity, which is the velocity of the displacer front.

There are two conditions required for any component in the displacement train:

- The component has to show very moderate movement on the stationary phase from the effect of carrier.
- The displacer has to have stronger absorption to the displacement train than the component to be displaced.

There are four different migration types of any solute in the displacing system; for example,

1. The solute is displaced in the front of the displacer.
2. The solute migrates faster than the displacer front.
3. The solute migrates slower than the displacer front.
4. The solute remains at the start.

Cases 1–3 are given in Fig. 1. Case no. 1 generally represents the real displacement (bonafide displacement).[9] Further proof of the bonafide displacing process can be given by the use of spacers, varying the front distance (and, thereby, the displacement front distance), and control of the load vs. spot length principle. This latter rule means that the higher the load, the longer will be the spot length. Bonafide displacement and quasi-displacement can also be differentiated on the basis of the chromatogram. Bonafide displacement gives a homogenous peak, which consists of both the displacer front and the displaced component. In the case of quasi-displacement, the two peaks are partially separated, and the peak of the displaced component is a little bit wider. A change of carrier generally solves this problem. Participation in the displacement train is the principal assignment.

Kalász et al.[10] showed that even a very short distance (e.g., 2 cm in the case of 5% displacer) may be sufficient for the formation of a fully developed displacement train. HPDC is devoted to preparative scale separation.[3] Fractions result in HPDC; the fractions are collected and analyzed "off-line." The appropriate fractions can be combined to yield the pure compounds. D-TLC was grown into an approach for scouting the optimum conditions for HPDC. Its goals are to find the proper carrier, the proper displacer, and the appropriate displacer concentration in the carrier. A series of experiments proved that the results of D-TLC can be transferred to HPDC.[5]

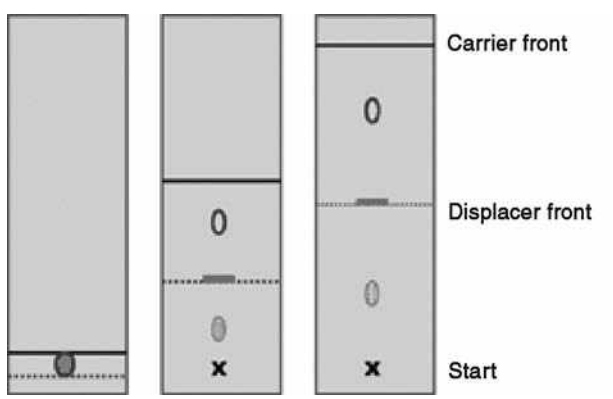

Fig. 1 Development of displacement chromatogram can take place on a plane. The faster-running front represents the carrier, and the slower-running front is the displacer in the carrier. Certain components can be eluted by the carrier (blue open circle), and another one is eluted with the displacer (green circle, shaded). If there is any component displaced, it is located just before the displacer front (red square, filled).

Even the zone-concentrating effect of the increase of displacer concentration was directly proven using off-line quantitative determination of the fractions obtained by HPDC.[5] However, the major field of application of D-TLC remains qualitative analysis, such as identification of compounds such as metabolites. D-TLC is mainly performed for such analytical purposes. On plain silica stationary phase, the 20:1:4:2 mixture of *n*-butanol–hydrochloric acid–water–methanol properly displaced several morphine derivatives, including morphine, azido-dihydroisomorphine, 14-hydroxy-dihydromorphine, dihydromorphine, 14-hydroxy-azido-dihydroisocodeine, 14-hydroxy-azido-dihydroisomorphine, codeine, azido-dihydroisocodeine, and 14-hydroxy-dihydrocodeine. Nonetheless, the adequate choice of the displacement system can alter the order of components and even the participation of the components in the displacement train. Using the same stationary phase (plain silica), the chlorinated hydrocarbon carriers (chloroform, dichloromethane, and dichloroethane) make less migration possible, as compared with the *n*-butanol–methanol–water–hydrochloric acid system. When triethanolamine displacer in chloroform carrier was used, certain otherwise eluted components became part of the displacement train. The ECAM (*O*-ethyl-*N*-cyclopropyl-norazido-dihydroisomorphine), CAM (*N*-cyclopropyl-norazido-dihydroisomorphine), norazido-dihydroisomorphine, normorphine, and nalorphine changed their situation from eluted positions to displaced ones. The most surprising change happened in the case of 6-amino-dihydromorphine, which was eluted with the carrier well before the displacer front, but it was left behind the displacer front in chlorinated hydrocarbon carrier and triethanolamine displacer. This phenomenon can be explained by the reaction of amino group to the change of acidic to basic conditions caused by substituting triethylamine for the hydrochloric acid. The change of the stationary phase from silica to alumina also altered the components, in the displacement train, and the lengths of the displaced zones were changed as well. Remarkably, certain components show faster mobility on alumina when chloroform carrier is used. In addition, the displacement zones are also generally longer.[11] The change of the stationary phase from plain silica to reversed-phase silica (TLC plate RP-18 F_{254}s, precoated, layer thickness 0.25 mm) turned the order of components upside-down (Fig. 2). Some of the components, however, remained in the displacement train, e.g., azido-dihydroisomorphine, ethylmorphine, and norazido-dihydroisomorphine. Preparative work can also be performed by scraping the spots from the plate. D-TLC separation of morphine analogs was performed using volatile mobile phases including the carrier and the displacer. The mixture of *n*-butanol–hydrochloric acid–water–methanol (20:1:4:2) can be preferentially used for preparative separation of semisynthetic

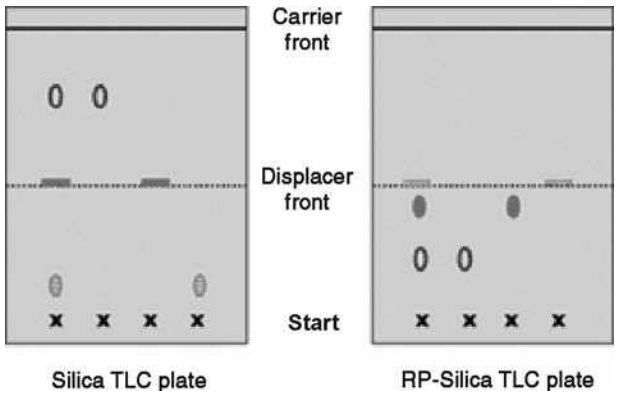

Fig. 2 The order of the spots is generally reversed when the stationary phase is changed from plain silica to reversed-phase silica.

morphine derivatives. The separation includes the removal of the intermediates of the synthesis as well as the purification of the member of metabolic pathway. Another important factor to be considered was the concentration of displacer in the carrier. The higher the displacer concentration, the larger will be the R_F of its front (i.e., R_D). The displacer front could reach the migration position of certain eluted components, which may be part of the displacement train.[9]

DC of substituted phenylisopropylamines can be easily accomplished. Both normal phase and octadecyl-substituted silica (reversed-phase) plates were used with the chloroform/triethanolamine and water–acetonitrile/tetrabutylammonium chloride carrier/displacer pairs, respectively. Only a few exceptionally behaving compounds moved faster or slower than the displacer front in the normal-phase and reversed-phase systems, respectively. The displacement chromatogram of HPDC can be characterized as series of sequentially increasing steps of the weight distribution or that of ultraviolet absorbance. This is the reason why off-line detection is used to characterize HPDC. D-TLC would have a similar profile, but specific detection may improve differentiation of the individual components. Further possibility is given by the application of spacers.

Kalász et al.[12] used spacer to improve separation of radiolabeled metabolites, and the method was called spacer D-TLC. They also constructed specific parameters of DC, especially for calculation of the resolution (R_D), yield (Y), loss (L), and efficiency (E). Displacement of radiolabeled compounds was readily visualized using X-ray film with contact autoradiography.[6,12,13] Two-dimensional chromatography can be simply arranged when a planar stationary phase is used. The stationary phase must be rotated 90° after the 1st dimensional development; then, the system is ready for the 2nd dimensional run. Elution type of development followed by displacement is an easy and useful means of two-dimensional thin-layer chromatography

(2D-TLC). The 2D-TLC method has several increments to the elution–elution developments, such as the discrimination factors are different in the 1st and in the 2nd dimensional separations. The spots are concentrated through the 2nd dimensional development. Use of a spacer may further increase the separation of the spots that are located close to each other. Extensive work was devoted to the D-TLC using forced flow of the mobile phase (FFMP)[6,14] and to the comparison of the effect of forced flow of the mobile phase to that of the classical (capillary flow) TLC.[8]

The decrease of the mobile phase flow rate from 0.6 to 0.5 and then to 0.3 caused the appearance of the doubled fronts, such as alpha and beta fronts of the carrier and also α and β fronts of the displacer. This phenomenon can be explained by a particular characteristic of planar chromatography, as the mobile phase runs on a dry stationary phase. In addition to the chromatographic occurrences, there is an additional process; it is the wetting of the stationary phase with the components of the mobile phase. If the mobile phase supply is not adequate (this is the case of slow-traveling mobile phase), the wetting of the dry stationary phase is the rate-limiting step. Such cases are unknown in either HPDC or HPLC, when the stationary phase is presaturated and extensively washed by the mobile phase prior to loading a sample. Therefore development of HPDC is restrained by the high flow velocity of the mobile phase, and that of D-TLC is limited by using a slow velocity. 2D-TLC is the proper choice for separation of a single compound from a multicomponent mixture. When the 2nd dimensional run is carried out using D-TLC, one or several components can be well separated from all others. In addition, the displaced components are extensively concentrated.[14]

When varying the conditions of D-TLC, various components can be a part of the displacement train. An interesting application of DC is given by the identification of metabolically generated radi olabeled formaldehyde from the radiolabeled (–)-deprenyl [(–)-C^{14}-*N*-methyl-*N*-propynyl-phenyl-isopropylamine]. The analysis was carried out after reacting the metabolites in a urine sample with 2,4-dinitrophenylhydrazine. The essence of the identification included the use of a standard (2,4-dinitrophenylhydrazone of formaldehyde) and comparing the urine samples with, and without, reaction of 2,4-dinitrophenylhydrazine.[15,16] This method has been called reaction-displacement thin-layer chromatography.[16] Kalász et al.[9,17] reported front deformation when the stationary phase per load mass ratio was under 10, e.g., when 0.5 or 1 mg of solute was loaded onto 2.5 mg of the stationary phase.

The list of substances subjected to planar displacement chromatography includes a broad range of organic compounds. For instance, Kalász and Horváth[5] separated three corticosteroids, Reichstein's Q, Reichstein's S, and Reichstein's H compounds. Kalász[13] also separated phenylalkylamines, e.g., deprenyl, deprenyl metabolites, and related compounds. Báthori et al.[18–21] separated ecdysteroids; Kamano et al.[22] separated toad-poison bufadienolides, such as resibufogenin, cinobufagin, bufalin, bufotalin, cinobufotalin, telocinobufagin, and gamabufotalin. Kalász et al.[10] separated morphine and semisynthetic morphine derivatives from each other. Kalász et al.[15,16] also identified formaldehyde as an efferent metabolite of *N*-demethylation.

CONCLUSIONS

There are advantages which are offered by D-TLC. The planar stationary phase offers numerous advantages which cannot easily be realized using column (or capillary) arrangements. The entire displacement process can be readily visually followed. The separation can be directly evaluated. Sensitivity of the UV/visible scanners is well suited for the concentrations of substances in the displacement train. Radioactive spots on the planar stationary phase may be easily monitored by the use of X-ray film or digital autoradiography (DAR). Spacers can be inserted between the displaced bands. The plates are disposable; therefore the regeneration process is generally ignored. Two-dimensional developments (elution displacement) can be easily performed. The actual concentration of displacer in the carrier can be calculated on the basis of its retardation. A detailed general summary of D-TLC is also given in a recently published book on TLC.[23]

ACKNOWLEDGMENTS

This project was sponsored by the grant of OTKA T032185. The advice of Ms. Bogi Kalász is appreciated.

REFERENCES

1. Ettre, L.S. Evolution of Liquid Chromatography. In *High-Performance Liquid Chromatography. Advances and Perspectives*; Horváth, Cs., Ed.; Academic Press: New York, 1980; Vol. 1, 25.
2. Tiselius, A. Displacement development in adsorption analysis. Ark. Kemi, Mineral. Geol. **1943**, *16A*, 1–18.
3. Horváth, Cs.; Nahum, A.; Frenz, J. High-performance displacement chromatography. J. Chromatogr. **1981**, *218*, 365–393.
4. Kalász, H.; Horváth, Cs. Preparative scale separation of polymyxin B's by high performance displacement chromatography. J. Chromatogr. **1981**, *215*, 295–302.
5. Kalász, H.; Horváth, Cs. High-performance displacement chromatography of corticosteroids. Scouting for displacer and analysis of the effluent by thin-layer chromatography. J. Chromatogr. **1982**, *239*, 423–438.
6. Kalász, H.; Kerecsen, L.; Knoll, J.; Báthori, M. Displacement Chromatography of Steroids. In *Steroid Analysis,* Proceedings of the Symposium on the Analysis

of Steroids, Sopron, Hungary, 1987, Görög, S., Ed.; Akadémiai Kiadó: Budapest, 1988, pp. 405–410.
7. Kalász, H.; Horváth, Cs. Effects of Operating Conditions in Displacement Thin-Layer Chromatography. In *New Approaches in Liquid Chromatography*; Kalász, H., Ed.; Elsevier: Amsterdam, 1984; 57–67.
8. Kalász, H.; Báthori, M.; Kerecsen, L.; Tóth, L. Displacement thin-layer chromatography of some plant ecdysteroids. J. Planar Chromatogr. **1993**, *6*, 38–42.
9. Bariska, J.; Csermely, T.; Fürst, S.; Kalász, H.; Báthori, M. Displacement thin-layer chromatography. J. Liq. Chromatogr. Relat. Technol. **2000**, *23*, 531–549.
10. Kalász, H.; Kerecsen, L.; Csermely, T.; Götz, H.; Friedmann, T.; Hosztafi, S. Displacement thin-layer chromatographic investigation of morphine and its semisynthetic derivatives. J. Liq. Chromatogr. **1996**, *19*, 23–35.
11. Kalász, H.; Báthori, M.; Csermely, T. Planar versus microcolumn chromatography. Am. Lab. **2000**, *32* (9), 28–32.
12. Kalász, H.; Báthori, M.; Matkovics, B. Spacer and carrier spacer-displacement thin-layer chromatography. J. Chromatogr. **1990**, *520*, 287–293.
13. Kalász, H. Carrier displacement chromatography for identification of deprenyl and its metabolites. J. High Resol. Chromatogr. Chromatogr. Commun. **1983**, *6*, 49–50.
14. Kalász, H.; Báthori, M.; Ettre, L.S.; Polyák, B. Displacement thin-layer chromatography of some plant ecdysteroids with forced-flow development. J. Planar Chromatogr. **1993**, *6*, 481–486.
15. Kalász, H.; Szarvas, T.; Szarkáné-Bolehovszky, A.; Lengyel, J. TLC analysis of formaldehyde produced by metabolic *N*-demethylation. J. Liq. Chromatogr. Relat. Technol. **2002**, *25*, 1589–1598.
16. Kalász, H.; Lengyel, J.; Szarvas, T.; Morovjan, Gy.; Klebovich, I. J. Planar Chromatogr. Submitted.
17. Kalász, H.; Báthori, M. Spacer displacement chromatography of steroids. Experiments, considerations and calculations. Invertebr. Reprod. Dev. **1990**, *18*, 119–120.
18. Kalász, H.; Kerecsen, L.; Nagy, J. Conditions dominating displacement thin-layer chromatography. J. Chromatogr. **1984**, *316*, 95–104.
19. Csermely, T.; Kalász, H.; Rischák, K.; Báthori, M.; Tarjányi, Zs.; Fürst, S. Planar chromatography of (−)-deprenyl and some structurally related compounds. J. Planar Chromatogr. **1998**, *11*, 247–253.
20. Lengyel, J.; Magyar, K.; Hollósi, I.; Bartók, T.; Báthori, M.; Kalász, H.; Fürst, S. Urinary excretion of deprenyl metabolites. J. Chromatogr. **1997**, *762*, 321–326.
21. Kalász, H.; Kerecsen, L.; Csermely, T.; Götz, H.; Friedmann, T.; Hosztafi, S. Thin-layer chromatographic investigation of some morphine derivatives. J. Planar Chromatogr. **1995**, *8*, 17–22.
22. Kamano, Y.; Kotake, A.; Nogawa, T.; Tozawa, M.; Pettit, G. Application of displacement thin-layer chromatography to toad-poison bufadienolides. J. Planar Chromatogr. **1999**, *12*, 120–123.
23. Kalász, H.; Báthori, M. Displacement Chromatography and Its Application Using a Planar Stationary Phase. In *Planar Chromatography, a Retrospective View for the Third Millenium*; Nyiredy, Sz., Ed.; Springer: Budapest, 2001; 220–233.

Distribution Coefficient

M. Caude
A. Jardy
Analytical Chemistry Department, City of Paris Industrial Physics and Chemistry Higher Educational Institution (ESPCI), Paris, France

INTRODUCTION

In high-performance liquid chromatography (HPLC), as in many chromatographic techniques, separations result from the great number of repetitions of the analyte distribution between the mobile and stationary phases that are linked. At each elementary step, the distribution is governed by the distribution equilibrium

$$X_M \rightleftharpoons X_S$$

where X stands for the solute and the subscripts M and S for the mobile phase and the stationary phase, respectively. Conventionally, this equilibrium is characterized by the distribution coefficient

$$K = \frac{C_S}{C_M} \tag{1}$$

where C_S and C_M are the molar concentrations of the solute X in the two phases. The distribution coefficient is also sometimes defined in terms of mole fractions of the solute in both phases. In elution analytical chromatography, concentrations are low enough to be comparable to the activities as an approximation. Although K should be dimensionless, as any thermodynamic constant, some authors use different units for the concentrations in both phases. For example, in LSC chromatography, concentrations are given in moles per square meter for the adsorbent. In such a case, K should be considered as an "apparent" constant, the dimension of which is m. However, in practice, the product in Eq. 2 must have the dimension of a volume.

K is interrelated with the retention factor k' by

$$k' = Kq$$

where q is the phase ratio, defined as the ratio of stationary phase volume V_S to the mobile phase volume V_M. Under linear conditions, K is linked to the solute retention volume (first-order moment of the elution peak) through

$$V_R = V_M + KV_S \tag{2}$$

The distribution coefficient is the reflection of the ternary interactions schematically represented by

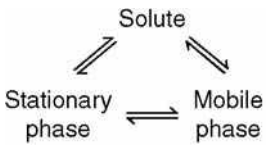

These interactions are as follows:

Solute ↔ stationary phase for the retention
Solute ↔ mobile phase for the solubilization
Mobile phase ↔ stationary phase because of the competition between at least one constituent of the mobile phase (the strongest, also called the modifier) and the solute toward the active sites.

For an isobaric and isothermal process, the equilibrium constant K is given by

$$\ln K = -\frac{\Delta G}{RT} \tag{3}$$

where ΔG° is the difference in standard Gibbs free energy linked with the solute transfer from the mobile phase to the stationary phase:

$$\Delta G = -\frac{\Delta G}{RT} \tag{4}$$

where H° and S° are the enthalpy and entropy, respectively.

In many cases, the value of H° is independent of temperature so that linear van't Hoff plots ($\ln K$ vs. $1/T$) are observed. However, irregular retention behaviors are often observed, in practice, due to the dependence of H° on the temperature.

Relationship (3) shows, clearly, the obtaining of reproducible results needed to thermoregulate the chromatographic apparatus, especially the column and mobile phase. Similarly, Eq. 3 explains why temperature changes implemented in order to increase efficiency can affect, drastically, the selectivity.

From Eq. 1, K can be related to the sorption isotherm, as it corresponds to the chord slope at each point. Therefore, Eq. 2 is valid only if K is constant; that is, the sorption

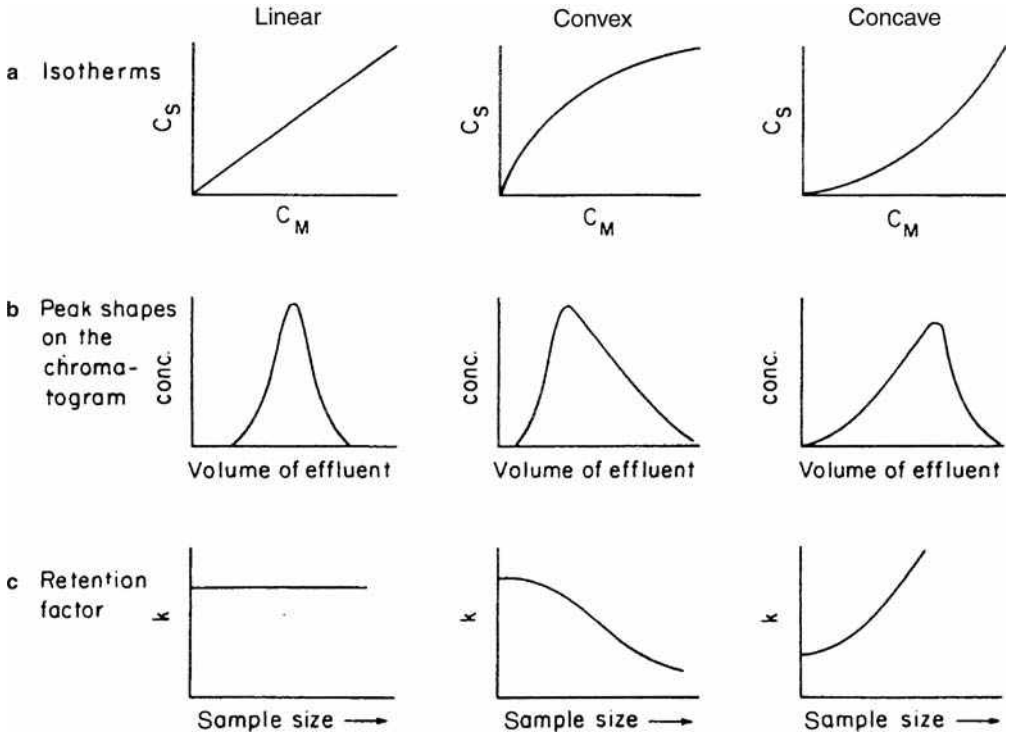

Fig. 1 Effect of isotherm shape on certain chromatographic properties. a, Three different shapes of sorption isotherms encountered in chromatography; b, peak shapes resulting from these isotherms; c, dependence of the retention factor on the amount of solute injected. **Source:** From *An Introduction to Separation Science*.[1]

isotherm is linear or, at least, is in a region where it becomes linear (i.e., if the dilution is great enough). The effect of the isotherm shape is shown in Fig. 1.

For the low concentrations used in LC, the elution peak is Gaussian in shape and its retention factor is independent of the sample size. When isotherms are non-linear (convex or concave, as illustrated in Fig. 1), an asymmetric elution peak is obtained and the retention factor measured at the peak apex is dependant on the sample size. This peak asymmetry is due to the dependence of the solute migration velocity vs. the slope of the isotherm, which varies the solution concentration in the mobile phase.

REFERENCE

1. Karger, B.L.; Snyder, L.R.; Horvath, C. *An Introduction to Separation Science*; John Wiley & Sons: New York, 1973; 12–33.

BIBLIOGRAPHY

1. Katz, E.; Eksteen, R.; Schoenmakers, P.; Miller, N. *Handbook of HPLC*; Marcel Dekker, Inc.: New York, 1998; Chap. 1.
2. Rosset, R.; Caude, M.; Jardy, A. *Chromatographies en Phases Liquide et Supercritique*; Masson: Paris, 1991; 729–730.

DNA Sequencing: CE

Feng Xu
Yoshinobu Baba
Department of Medicinal Chemistry, University of Tokushima, Tokushima, Japan

INTRODUCTION

Cells store their hereditary information in the form of double-stranded DNA, formed of the same four monomers—adenine (A), thymine (T), cytosine (C), and guanine (G). Using capillary electrophoresis (CE), scientists can read out the complete sequence of monomers in DNA molecules and thereby decipher the hereditary information that each organism contains. Large-scale DNA sequencing projects need instruments that generate high throughput at low cost. One approach to increase the CE throughput is to run a large number of capillaries in parallel, so-called capillary array electrophoresis (CAE). The Human Genome Project was initiated in 1990 with the goal of sequencing the 3 billion nucleotides present within human chromosomes. In 2001, the "first draft" of the entire human genome was published,[1,2] which made it possible to see for the first time exactly how genes are arranged along human chromosomes. With the appearance of the first multicapillary instrument in 1990, traditional slab gel electrophoresis was gradually replaced by CAE due to higher DNA sequencing performance. The early experimental result of sequencing of 29–512 bases with >97% accuracy was obtained in 9.5 hr at a field strength of 50 V/cm by using a laser beam scanning across a capillary array.[3] Later, the appearance of 96-capillary array electrophoresis greatly speeded the DNA sequencing in the Human Genome Project. In the meantime, the new technique of microfabricated CAE (μCAE, or microchip electrophoresis) combines the advantages of CE (system automation, reproducibility, and accurate quantification) with those of microfabrication (high speed and multiplex analysis), and will find its position in DNA sequencing.

This entry gives an overview of the fundamentals of DNA sequencing by CAE, μCAE, and four-color laser-induced fluorescence (LIF) detection, as well as some major factors (sieving matrix, sample preparation, electric field strength, etc.) influencing the sequencing accuracy and efficiency.

FOUR-COLOR LASER-INDUCED FLUORESCENCE DETECTION AND CAPILLARY ARRAY ELECTROPHORESIS

Laser-induced fluorescence is the standard CE detection method in DNA sequencing, due to its high sensitivity and the fact that the identity of the terminal base of each DNA can be encoded in the wavelength and intensity of the fluorescent emission. The DNA sequencing fragments are fluorescently labeled with four different dyes on each base, and are then detected by a four-color LIF detector.

Instrumentation design of detector systems for CAE and microfabricated devices has reached a mature stage. The two most successful LIF detector designs are the scanning confocal detector[4] and the multisheath flow detector.[5] A schematic of the scanning confocal detector (four-color planar fluorescence scanner) is shown in Fig. 1. The design adopts a scanning technology through capillaries that are illuminated by a single laser beam. The capillary bundle is placed on a planar translation stage, which moves at 1 cm/sec perpendicular to the direction of electrophoresis. The fluorescence, collected at right angles from the capillaries, is divided into four detection channels by dichroic beam splitters and band-pass filters, and then focused through a pinhole on four photomultiplier tubes and simultaneously recorded in four spectral channels. Using automated sample and gel-matrix loading, the total run time for sequencing more than 500 bases is <2 hr. The scanning confocal detector is adopted in the first commercial 96-capillary array MegaBACE 1000 system from Molecular Dynamics (Amersham-Pharmacia Biotech)[6] for DNA sequencing by CAE. The system uses linear polyacrylamide (LPA) as the separation matrix, and has a turnaround time of 2 hr per run. The capillaries have a life of ~130 runs and can be run with both dye primer and dye terminator reactions. An average read length of >550 bases at 98.5% accuracy is feasible with the M13 standard template. Another high-throughput rotary-scanner detection device was designed (as shown in Fig. 2), in order to analyze over 1000 capillaries in parallel. Currently, the device accommodates 128 capillaries. A microscope objective and a mirror assembly revolve inside a ring of capillaries, exciting fluorophores and collecting fluorescence from each capillary.

In the second detector design, multisheath flow detector, the capillaries are illuminated with a line-focused laser beam. Fluorescence is collected at right angles and imaged onto a CCD camera. The use of the CCD camera ensures that all capillaries are monitored simultaneously. To eliminate light scattering, the capillary array is inserted into a

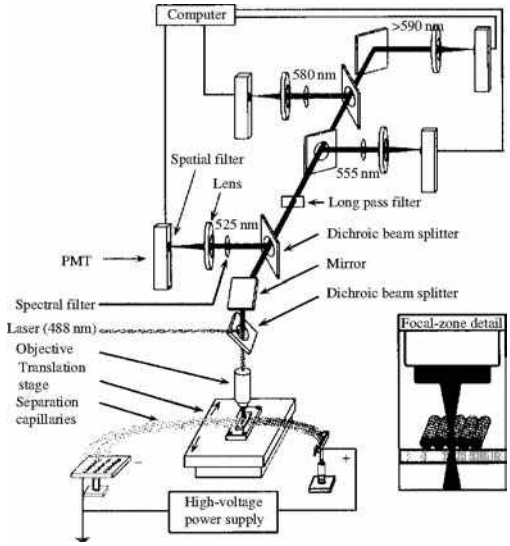

Fig. 1 Four-color planar confocal fluorescence CAE scanner using an excitation of 488 nm from argon ion laser.
Source: From DNA-sequencing using a four-color confocal fluorescence capillary array scanner, in Electrophoresis.[33]

rectangular quartz cuvette that holds the capillaries like the teeth of a comb (Fig. 3). A simple siphon pumps the sheath fluid through the interstitial spaces between the capillaries, and draws a sample from each capillary as a thin stream in the open region below the capillaries. A single laser beam

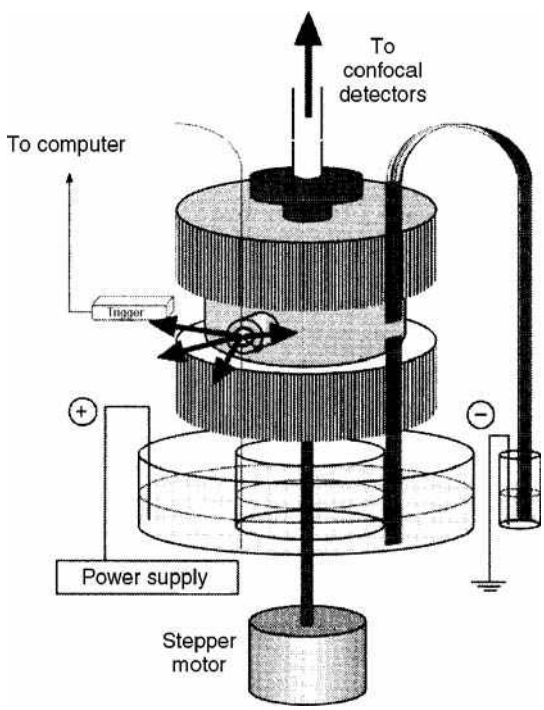

Fig. 2 Rotary confocal scanning detector.
Source: From Ultra-high throughput rotary capillary array electrophoresis scanner for fluorescent DNA sequencing and analysis, in Electrophoresis.[34]

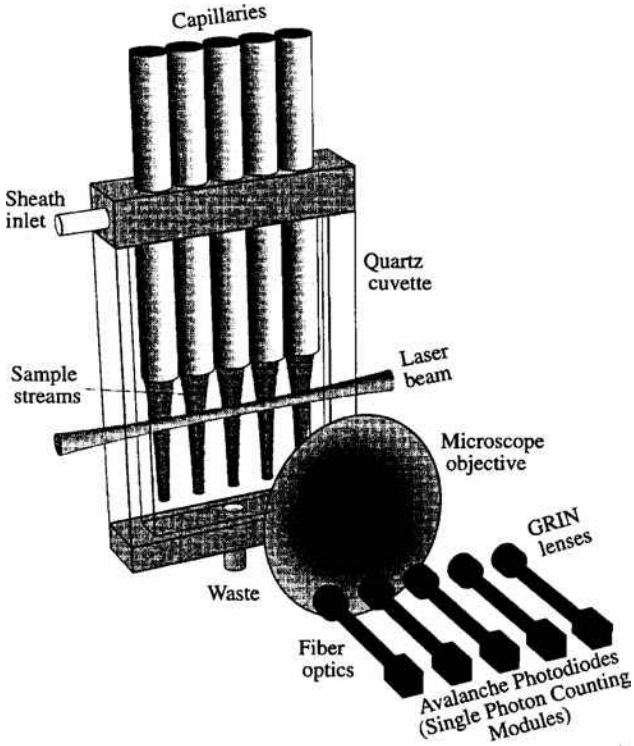

Fig. 3 The sheath-flow cuvette fluorescence detection chamber for an array of five capillaries. The chamber is tapered. A single laser beam is used to illuminate fluorescence from the five sample streams isolated by the sheath flow fluid.
Source: From A multiple-capillary electrophoresis system for small-scale DNA sequencing and analysis, in Nucleic Acids Res.[35]

skims all flow streams. Since the laser beam only traverses the sheath fluid and DNA streams, the low-power beam can excite fluorescence from all samples simultaneously. The detector has no moving parts. This design has been incorporated in a second commercial system, ABI PRISM 3700 from PE Biosystems (Applied Biosystems).[7] The system uses four dyes, and simultaneously detects 96 capillaries with a turnaround time of 2 hr to obtain 550 bases with 98.5% accuracy using POP-6 (6% poly-*N*,*N*-dimethylacrylamide; pDMA) as the sieving matrix.

RIKEN Japan has produced an extra-high-throughput autosequencer (RISA sequencer) that consists of a 384-capillary array. Cross-linked acrylamide is used as the sieving matrix and a scanning laser fluorescence as the detector.[8] The read length, with more than 99% accuracy, is 650 bases.

MICROCHIP ELECTROPHORESIS

Microchip electrophoresis is superior to CE in that it allows facile monolithic array construction, precise controlling of picoliter sample injection amount, quick electrophoretic

separation speed, and potential for integration with sample pretreatment.

The first instance of DNA separation by microchip electrophoresis was in 1994.[9] A mixture of DNA oligomers from 10 to 15 bases was efficiently separated. Since then, microchip electrophoresis for DNA separation has developed very quickly. DNA sequencing of 200 bases by microchip takes only 10 min in cross-linked polyacrylamide gels.[10] By using 4% LPA in 7 cm-long coated microchannels, 600 bases were separated in 20 min at 160 V/cm.[11] Four-color LIF detection is feasible in micrototal analysis system (μTAS) use.

Long read lengths need long separation channels, because separation resolution scales with the square root of channel length. In order to adapt the radial chip design to modern wafer-scale fabrication for increasing the effective separation lengths, Mathies's group developed pinched turn geometries (hyperturns) in folding channels (Fig. 4).[12] A unique rotary design and a rotary confocal scanning system run 96 samples in a radial configuration at a time. DNA sequencing with an average read length of 430 bases at a rate of 1.7 kb/min was achieved in 96-lane microchip CAE. Ehrlich and coworkers[36] fabricated very long microchannels of 40 cm in large glass plates and obtained an average read length of 800 bases in 80 min with 98% accuracy (Fig. 5). Capillary array electrophoresis on a chip brings new potentials to high-throughput DNA sequencing on miniaturized CE platforms.

FACTORS INFLUENCING SEQUENCING

A key parameter of an electrophoresis system is the read length per unit time. Since the read length for the present commercial instrument is limited to 500–600 bases with >99% accuracy in 2 hr, sequencing of long read lengths, for example, >1000 bases, is very much required. Long read lengths in a short time reduce the number of sequencing reactions needed, because the number of primers required for directed sequencing strategy and the number of templates generated and sequenced in shotgun sequencing are inversely proportional to the read length. In addition, long read lengths minimize the computational effort required to assemble shotgun-generated data into finished sequences. The read length is influenced by a number of factors, e.g., polymer matrix, capillary temperature, field strength, effective channel length, base-calling algorithms, etc. but the most important is resolution. Heller[13] summarized in detail how various factors affect resolution (Fig. 6). Diffusion is thought to be an ultimate limitation to the resolution of polymer matrix-based separation. Long separation channels, modest electric fields, high temperature, and medium concentrations of polymer matrices are feasible for obtaining higher resolution and longer read length.

According to polymer theory, with a semidilute polymer solution above an overlap threshold concentration, c^*, fully entangled networks are formed by the interaction of polymer tangles, thereby forming dynamic pores in the polymer network for DNA separation. Depending on DNA size, the DNA molecules can either be sieved through the polymer network (Ogston model) or reptate in a virtual tube (reptation model).[14] The Ogston model

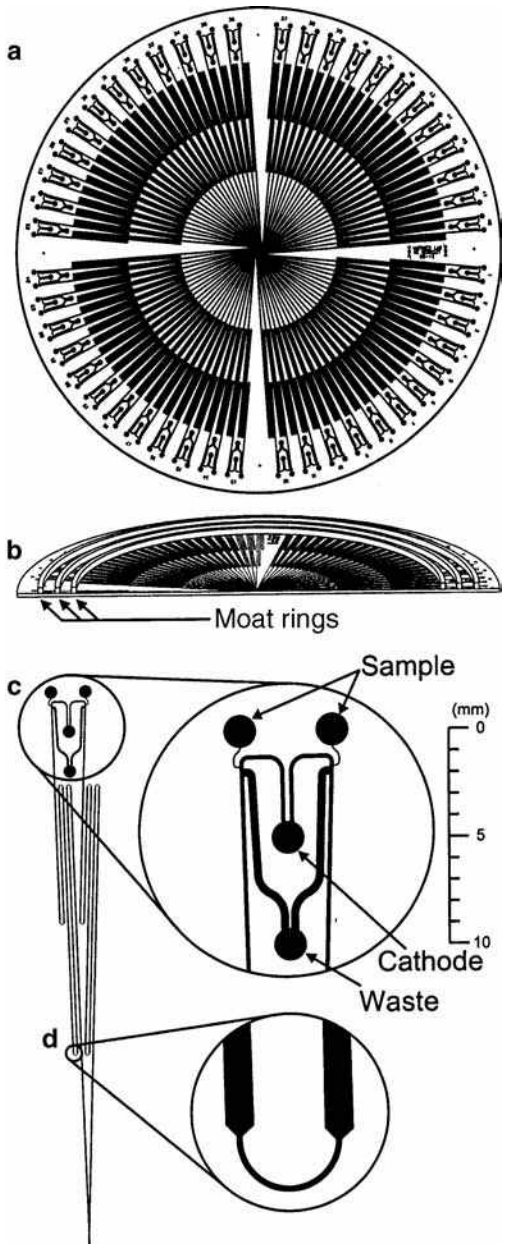

Fig. 4 Capillary array electrophoresis on a microchip with 96 channels. a, Overall layout of the 96-lane DNA sequencing microchannel plate (μCP). b, Vertical cut-away of the MCP. c, Expanded view of the injector. Each doublet features two sample reservoirs and common cathode and waste reservoirs. d, Expanded view of the hyperturn region.
Source: From High throughput DNA sequencing with a microfabricated 96-lane capillary array electrophoresis bioprocessor, in Proc. Natl. Acad. Sci. U.S.A.[12]

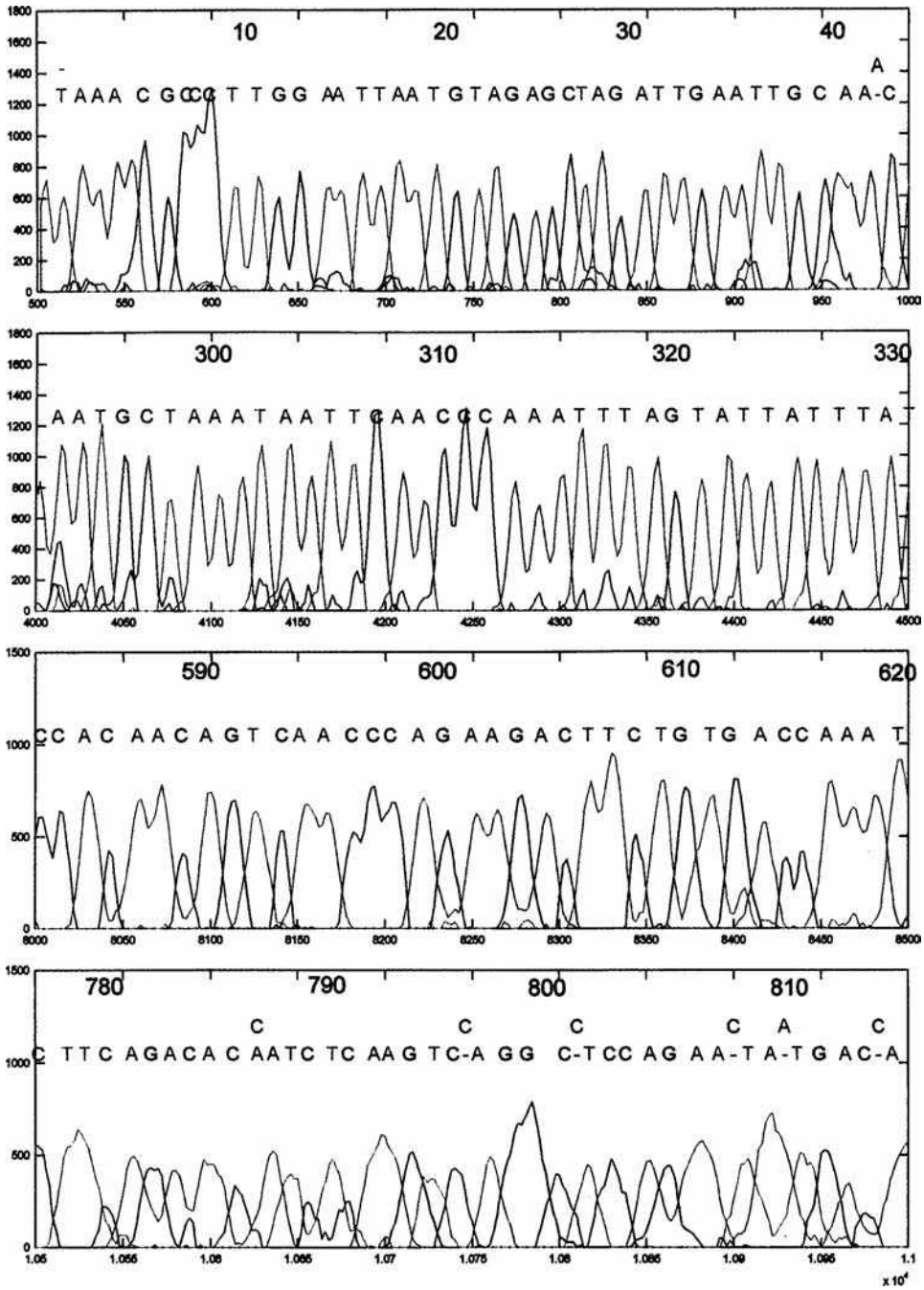

Fig. 5 Eight hundred base reads of a four-color DNA sequencing sample in a 40 cm-long microchannel. The four panels show the processed sequencing profiles and base calls at the beginning, the middle, and the end of the run. Conditions: 150 V/cm, 50°C, and 2% (w/v) LPA in 1 × TTE/7 *M* urea.
Source: From Eight hundred-base sequencing in a microfabricated electrophoretic device, in Anal. Chem.[36]

describes the separation of DNA molecules smaller than the polymer pore size. The reptation model can depict the electrophoresis behavior of DNA molecules larger than the polymer pore size. Larger DNA fluctuates in effective length during migration. The mobility of a DNA fragment is inversely proportional to its size (reptation without orientation). If the DNA molecule is very large, its mobility is size independent (reptation with orientation), in which case the resolution approaches zero. In DNA sequencing by electrophoresis, one can extend the

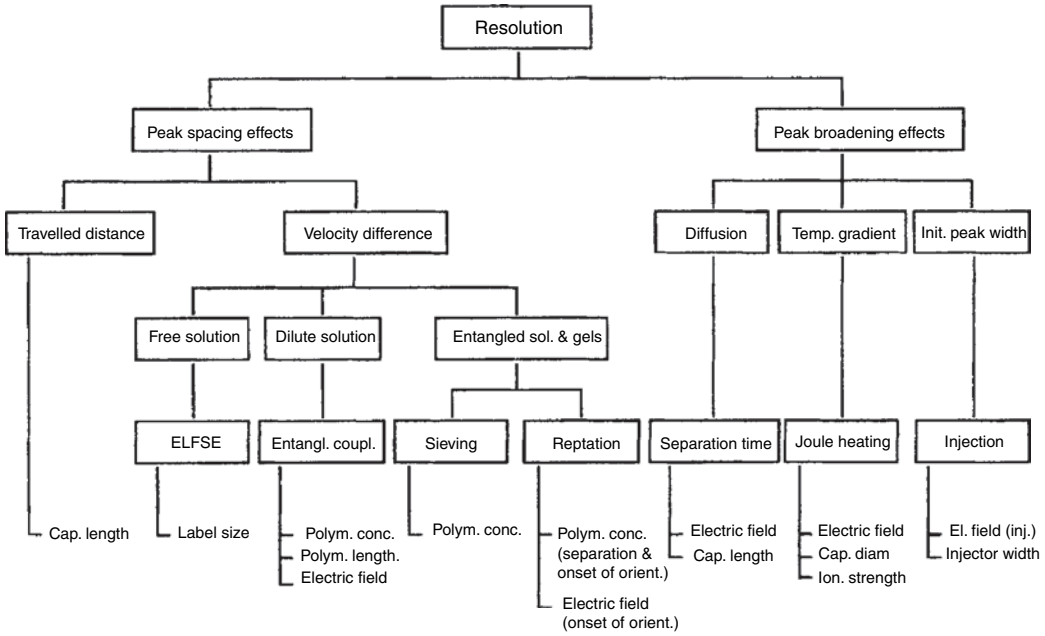

Fig. 6 Overview of the influence of different parameters on resolution during separation of DNA by CE. Only tunable parameters with strong influence are shown.
Source: From Principle of DNA separation with capillary electrophoresis, in Electrophoresis.[13]

reptation-without-orientation range by optimizing various parameters that influence resolution. Then the position of zero resolution is shifted to a higher base number.

Separation Matrix

Earlier DNA sequencing by CE used cross-linked polyacrylamide gels. The polyacrylamide capillary has a rather limited life. When the separation medium has degraded, the entire capillary must be replaced. The replacement is quite tedious because of alignment constraints of the optical system with the narrow-diameter capillaries. In contrast, low-viscosity polymers are attractive for DNA sequencing by CE. They can be pumped from the capillary and replaced with fresh matrix after each run without replacement of the capillary or realignment of the optical system. A range of polymeric solutions have been tested. LPA, pDMA, and polyethylene oxide (PEO) are the most widely used ones. Nowadays, gel-filled capillaries have almost fully been substituted by polymer solution-filled capillaries.

Linear polyacrylamide represents the best replaceable sieving polymer in terms of read length and speed. It can generate DNA sequencing read lengths beyond 1000 bases within 1 hr with a run-to-run base calling accuracy of 99.2% for the first 800 bases and 98.1% for the first 900 bases.[15] At a high polymer concentration, both long and short chains give equally good resolution for single-stranded DNA. For separating a larger size range, it is better to use long polymer chains and lower polymer concentrations. This leads to a more uniform resolution in function of DNA size. Mixing two populations of polymers, each with a narrow but different range of molar mass, has become popular. It facilitates fine-tuning of the separation performance over a broad range of DNA sizes. With a novel LPA formulation comprising 0.5% w/w 270 kDa/2% w/w 17 MDa LPAs operated at 70°C and 125 V/cm, an ultralong read length of 1300 bases was reached in 2 hr with 98.5% accuracy.[16] The high performance is attributed to better thermostability of the LPA formulation, optimized temperature and electric field, adjustment of the sequencing reaction, and refinement of the base-calling software.

PEO, pDMA, and polyvinylpyrrolidone (PVP) have self-coating abilities, which allows DNA sequencing in bare fused-silica capillaries. A mixture of two molecular mass populations of PEO is possible to separate DNA sequencing fragments over 1000 bases, too, but the separation time exceeds 7 hr.[17] pDMA[18] and PVP[19] are low-viscosity sieving matrices (<100 cP). They have moderate separation efficiencies and can provide maximum read lengths of about 500–600 bases.

Copolymers of LPA and pDMA combine the excellent sieving performance of LPA with the good self-coating property of pDMA. On uncoated capillaries at room temperature, 700 bases can be obtained with resolution $R > 0.55$.[20]

Sieving matrices with "built-in thermal viscosity switches" are alternatives in DNA sieving. The 3–5% grafted copolymer solution, which has a hydrophilic LPA backbone and comblike poly(*N*-isopropylacrylamide) (pNIPA; M_w 650–1800 kDa) side chains, exhibits a viscosity lower than

300 cP at room temperature, and a high viscosity (10,000 cP) at 66°C, suitable for DNA sequencing with a read length of 800 bases ($R > 0.5$) in less than 1 hr.[21]

In order to avoid intramolecular base pairing of DNAs, sequencing has to be run under denaturing conditions. A denaturing agent, such as urea or formamide, is added during gel polymerization or to the buffer in the case of polymer solutions. Most researchers use urea at a concentration of 7–8 *M*. The addition of formamide up to 40% increases the denaturing capacity of the matrix. The denaturing power of these agents alone is not sufficient, and the separation has to be performed at an elevated temperature. Generally, a temperature of 50–60°C is used to keep the DNA fragments completely denatured. Furthermore, higher temperature operation increases sequencing rate and read length as well as resolutions.[22] For 600-base separation, the maximum separation efficiency was also found at 60°C.[23] Temperature stability is important for DNA sequencing by CE. Even millidegree temperature oscillations have a detrimental effect on DNA read lengths.[24] Beyond a point, the efficiency diminishes seriously.

Sample Preparation

Sample preparation is an important step in the sequencing protocol. The presence of impurities [salt, proteins, unincorporated deoxynucleotides (dNTPs), dideoxynucleotides (ddNTPs), etc.] in DNA samples has deleterious effects both on the sequencing run and on capillary lifespan. DNA sequencing samples are typically synthesized following the Sanger enzymatic method.[25] Four reactions are set up, each with a different A, T, C, or G modified by replacing an H atom from the OH group in the C3 position of the sugar. This ddNTP is incapable of forming the next bond in the DNA chain; therefore, synthesis of that chain is terminated when a ddNTP is incorporated. The four reactions (with either labeled ddATP, ddTTP, ddCTP, or ddGTP) are performed, followed by ethanol precipitation to remove excess reagents and salts. The precipitated DNA is dissolved in formamide for electrophoretic injection and sequencing.

Since the beginning of DNA sequencing by CE, DNA labeled with four dyes (FAM, JOE, ROX, and TAMRA) has been standardized.[26] The four-color confocal fluorescence scanner utilizes excitation at either two laser wavelengths (e.g., 488 and 543 nm) or a single laser beam (e.g., 488 nm). New energy-transfer (ET) primers have higher molar absorbances. They contain a common donor dye at the 5′ end and an acceptor dye about 8–10 nucleotides away. Using a single laser at 488 nm, the excitation is transferred by resonance ET to the acceptor dye; then higher fluorescence intensities are observed,[27] which results in longer read lengths, higher base-calling accuracies, and reduced template amount. Now the ET primers have gained wide acceptance and are widely used for DNA sequencing in CAE.[28]

Effect of Electric Field Strength

With decreasing electric field, the onset of reptation-with-orientation is shifted to larger DNA sizes, which extends the size range to be separated. This effect is confirmed by many experiments. An electric field strength of 600 V/cm produces an ultrafast analysis time of 3–4 min, but the read length degrades to 300 bases.[29] At the expense of an analytical time of 7 hr, a low-field strength of 75 V/cm can extend the read length up to 1000 bases in PEO matrices.[17] Baba's group[30] proposed electric field step gradients, with an initial voltage ramp (up to 220 V/cm) for accelerating short fragments, followed by a voltage plateau, a voltage decrement, and a lower voltage constant of 90–130 V/cm for longer DNA fragments. A 20% extension of the read length was obtained, up to 800 bases at 60°C with high accuracy.

WALL COATING

Single-stranded DNA has a more hydrophobic character than double-stranded DNA and presents stronger interaction with the silica wall. Thus, capillary wall coating is greatly preferred. A few of polymers, such as pDMA, PEO, and PVP, as mentioned, have self-coating abilities. They can be used for DNA sequencing in bare capillaries or bare microchips. However, the life of the bare walls is limited because their performance deteriorates with repeated runs. Therefore, extensive and, sometimes, harsh rinsing is indispensable between runs.

Most polymeric matrices require an inner coating of separation channels to prevent both electro-osmotic flow (EOF) and DNA–channel wall interactions. The acrylamide coating procedure developed by Hjertén[31] is the most commonly used permanent covalent coating method. The disadvantage is that the coating cannot endure for long due to easy hydrolysis of the –Si–O–Si– bond. Hence, some more stable covalent coating procedures[32] have been developed to extend the wall-coating life.

CONCLUSIONS

Capillary array electrophoresis has become a standard method to decipher genomes within a short time, and has played an important role in large-scale DNA sequencing. With further increase of the capillary number in the array, it will become difficult to manufacture and work with. The problem is being solved by a transition to μCAE systems. The quality of sequencing separations on microchips is rapidly approaching that obtained using conventional

CAE. Hyphenation of sample automatic processing steps to μCAE will further lead to increase in efficiency and quality of DNA sequencing, reduction of overall cost, and automation of the whole process. It is plausible that high-throughput DNA sequencing by CAE and μCAE will afford a rapid means for human genetic counseling, disease diagnosis, and clinical therapy.

ACKNOWLEDGMENTS

The work was partially supported by the CREST program of the Japan Science and Technology Agency (JST); a grant from the New Energy and Industrial Technology Development Organization (NEDO) of the Ministry of Economy, Trade, and Industry, Japan; a Grant-in-Aid for Scientific Research from the Ministry of Health and Welfare, Japan; a Grant-in-Aid for Scientific Research from the Ministry of Education, Science, and Technology, Japan; a Grant-in-Aid of the 21st Century COE program, Human Nutritional Science on Stress Control, from the Ministry of Education, Science, and Technology, Japan; and a Grant-in-Aid from Shimadzu Corp., Japan.

REFERENCES

1. Lander, E.S.; Linton, L.M.; Birren, B.; Nusbaum, C.; Zody, M.C.; Baldwin, J.; et al. Initial sequencing and analysis of the human genome. Nature **2001**, *409* (6822), 860–921.
2. Venter, J.C.; Adams, M.D.; Myers, E.W.; Li, P.W.; Mural, R.J.; Sutton, G.G.; et al. The sequence of the human genome. Science **2001**, *291* (5507), 1304–1351.
3. Zagursky, R.J.; McCormick, R.M. DNA sequencing separations in capillary gels on a modified commercial DNA sequencing instrument. Biotechniques **1990**, *9* (1), 74–79.
4. Mathies, R.A.; Huang, X.C. Capillary array electrophoresis: An approach to high-speed, high-throughput DNA sequencing. Nature **1992**, *359* (6391), 167–169.
5. Kambara, H.; Takahashi, S. Multiple-sheathflow capillary array DNA analyzer. Nature **1993**, *361* (6412), 565–566.
6. Bashkin, J.S.; Bartosievicz, M.; Roach, D.; Leong, J.; Barker, D.; Johnston, R. Implementation of a capillary array electrophoresis instrument. J. Capillary Electrophor. **1996**, *3* (2), 61–68.
7. Swerdlow, H.; Zhang, J.Z.; Chen, D.Y.; Harke, H.R.; Grey, R.; Wu, S.L.; Dovichi, N.J.; Fuller, C. Three DNA sequencing methods using capillary gel electrophoresis and laser-induced fluorescence. Anal. Chem. **1991**, *63* (24), 2835–2841.
8. Shibata, K.; Itoh, M.; Aizawa, K.; Nagaoka, S.; Sasaki, N.; Carninci, P.; et al. RIKEN integrated sequence analysis (RISA) system—384-format sequencing pipeline with 384 multicapillary sequencer. Genome Res. **2000**, *10* (11), 1757–1771.
9. Effenhauser, C.S.; Paulus, A.; Manz, A.; Widmer, H.M. High-speed separation of antisense oligonucleotides on a micromachined capillary electrophoresis device. Anal. Chem. **1994**, *66* (18), 2949–2953.
10. Woolley, A.T.; Mathies, R.A. Ultra-high-speed DNA sequencing using capillary electrophoresis chips. Anal. Chem. **1995**, *67* (20), 3676–3680.
11. Liu, S.; Shi, Y.; Ja, W.W.; Mathies, R.A. Optimization of high-speed DNA sequencing on microfabricated capillary electrophoresis channels. Anal. Chem. **1999**, *71* (3), 566–573.
12. Paegel, B.M.; Emrich, C.A.; Wedemayer, G.J.; Scherer, J.R.; Mathies, R.A. High throughput DNA sequencing with a microfabricated 96-lane capillary array electrophoresis bioprocessor. Proc. Natl. Acad. Sci. U.S.A. **2002**, *99* (2), 574–579.
13. Heller, C. Principle of DNA separation with capillary electrophoresis. Electrophoresis **2001**, *22* (4), 629–643.
14. Xu, F.; Baba, Y. Polymer solutions and entropic-based systems for double-stranded DNA capillary electrophoresis and microchip electrophoresis. Electrophoresis **2004**, *25* (14), 2332–2345 (and references therein).
15. Salas-Solano, O.; Carrilho, E.; Kotler, L.; Miller, A.W.; Goetzinger, W.; Sosic, Z.; Karger, B.L. Routine DNA sequencing of 1000 bases in less than one hour by capillary electrophoresis with replaceable linear polyacrylamide solutions. Anal. Chem. **1998**, *70* (19), 3996–4003.
16. Zhou, H.; Miller, A.W.; Sosic, Z.; Buchholz, B.; Barron, A.E.; Kotler, L.; Karger, B.L. DNA sequencing up to 1300 bases in two hours by capillary electrophoresis with mixed replaceable linear polyacrylamide solutions. Anal. Chem. **2000**, *72* (5), 1045–1052.
17. Kim, Y.; Yeung, E.S. Separation of DNA sequencing fragments up to 1000 bases by using poly(ethylene oxide)-filled capillary electrophoresis. J. Chromatogr. A, **1997**, *781* (1–2), 315–325.
18. Madabhushi, R.S. Separation of 4-color DNA sequencing extension products in noncovalently coated capillaries using low viscosity polymer solutions. Electrophoresis **1998**, *19* (2), 224–230.
19. Gao, Q.F.; Yeung, E.S. A matrix for DNA separation: Genotyping and sequencing using poly(vinylpyrrolidone) solution in uncoated capillaries. Anal. Chem. **1998**, *70* (7), 1382–1388.
20. Song, L.; Liang, D.; Kielscawa, J.; Liang, J.; Tjoe, E.; Fang, D.; Chu, B. DNA sequencing by capillary electrophoresis using copolymers of acrylamide and *N*,*N*-dimethylacrylamide. Electrophoresis **2001**, *22* (4), 729–736.
21. Sudor, J.; Barbier, V.; Thirot, S.; Godfrin, D.; Hourdet, D.; Millequant, M.; Blanchard, J.; Viovy, J.-L. New block–copolymer thermoassociating matrices for DNA sequencing: Effect of molecular structure on rheology and resolution. Electrophoresis **2001**, *22* (4), 720–728.
22. Kleparnik, K.; Foret, F.; Berka, J.; Goetzinger, W.; Miller, A.W.; Karger, B.L. The use of elevated column temperature to extend DNA-sequencing read lengths in capillary electrophoresis with replaceable polymer matrices. Electrophoresis **1996**, *17* (12), 1860–1866.
23. Salas-Solano, O.; Ruiz-Martinez, M.C.; Carrilho, E.; Kotler, L.; Karger, B.L. A sample purification method for rugged and high-performance DNA sequencing by capillary

electrophoresis using replaceable polymer solutions. B. Quantitative determination of the role of sample matrix components on sequencing analysis. Anal. Chem. **1998**, *70* (8), 1528–1535.
24. Voss, K.O.; Roos, H.P.; Dovichi, N.J. The effect of temperature oscillations on DNA sequencing by capillary electrophoresis. Anal. Chem. **2001**, *73* (6), 1345–1349.
25. Sanger, F.; Nicklen, S.; Coulson, A.R. DNA sequencing with chain-terminating inhibitors. Proc. Natl. Acad. Sci. U.S.A. **1977**, *74* (12), 5463–5467.
26. Carson, S.; Cohen, A.S.; Belenkii, A.; Ruiz-Martinez, M.C.; Berka, J.; Karger, B.L. DNA sequencing by capillary electrophoresis: Use of a two-laser-two-window intensified diode array detection system. Anal. Chem. **1993**, *65* (22), 3219–3226.
27. Ju, J.; Glazer, A.N.; Mathies, R.A. Energy transfer primers: A new fluorescence labeling paradigm for DNA sequencing and analysis. Nat. Med. **1996**, *2* (2), 246–249.
28. Soper, S.A.; Legendre, B.L., Jr.; Willams, D.C. On-line fluorescence lifetime determinations in capillary electrophoresis. Anal. Chem. **1995**, *67* (23), 4358–4365.
29. Muller, O.; Minarik, M.; Foret, F. Ultrafast DNA analysis by capillary electrophoresis/laser-induced fluorescence detection. Electrophoresis **1998**, *19* (8–9), 1436–1444.
30. Endo, Y.; Yoshida, C.; Baba, Y. DNA sequencing by capillary array electrophoresis with an electric field strength gradient. J. Biochem. Biophys. Meth. **1999**, *41* (2–3), 133–141.
31. Hjertén, S. High-performance electrophoresis: Elimination of electroendosmosis and solute adsorption. J. Chromatogr. **1985**, *347*, 191–198.
32. Dolnik, V.; Xu, D.; Yadav, A.; Bashkin, J.; Marsh, M.; Tu, O.; Mansfield, E.; Vainer, M.; Madabhushi, R.; Barker, D.; Harris, D. Wall coating for DNA sequencing and fragment analysis by capillary electrophoresis. J. Microcol. Sep. **1998**, *10* (2), 175–184.
33. Kheterpal, I.; Scherer, J.R.; Clark, S.M.; Radhakrishnan, A.; Ju, J.; Ginther, C.L.; Sensabaugh, G.F.; Mathies, R.A. DNA-sequencing using a four-color confocal fluorescence capillary array scanner. Electrophoresis **1996**, *17* (12), 1852–1859.
34. Scherer, J.R.; Kheterpal, I.; Radhakrishnan, A.; Ja, W.W.; Mathies, R.A. Ultra-high throughput rotary capillary array electrophoresis scanner for fluorescent DNA sequencing and analysis. Electrophoresis **1999**, *20* (7), 1508–1517.
35. Zhang, J.; Voss, K.O.; Shaw, D.F.; Roos, K.P.; Lewis, D.F.; Yan, J.; Jiang, R.; Ren, H.; Hou, J.Y.; Fang, Y.; Puyang, X.; Ahmadzadeh, H.; Dovichi, N.J. A multiple-capillary electrophoresis system for small-scale DNA sequencing and analysis. Nucleic Acids Res. **1999**, *27* (24), e36.
36. Koutny, L.; Schmalzing, D.; Salas-Solano, O.; El-Difrawy, S.; Adourian, A.; Buonocore, S.; Abbey, K.; McEwan, P.; Matsudaira, P.; Ehrlich, D. Eight hundred-base sequencing in a microfabricated electrophoretic device. Anal. Chem. **2000**, *72* (14), 3388–3391.

Drug Development: LC/MS in

Mohamed Abdel-Rehim
Research and Development, AstraZeneca, Södertälje, and Department of Chemistry, Karlstad University, Karlstad, Sweden

Eshwar Jagerdeo
Federal Bureau of Investigation Laboratory, Quantico, Virginia, U.S.A.

Abstract
Impressive progress has been made in the instrumentation and application of liquid chromatography–mass spectrometry (LC–MS) in the past few decades. In recent years, the use of LC–MS has become more important in drug discovery and development. In quantitative bioanalysis, LC–MS has become the method of choice for drug analysis in biological samples. The use of liquid chromatography in combination with mass spectrometry in routine therapeutic drug-monitoring activity is becoming more and more important. This entry will attempt to provide an overview as well as an understanding of the importance of liquid chromatography–mass spectrometry/tandem mass spectrometry (LC–MS, LC–MS/MS) in drug development. The role of LC–MS/MS in drug discovery and development will be discussed. Different sample preparation methods for plasma handling will be presented. High-throughput LC–MS/MS is summarized. Applications of LC–MS in metabolism studies and clinical studies will be presented.

INTRODUCTION

Even though the first mass spectrometer (MS) that was constructed by Sir J.J. Thomson[1] more than 110 years ago (1897) for the determination of mass-to-charge ratios (*m/z*) of ions, today it is almost a ubiquitous research instrument. A clear demonstration of MS took place in 1918–1919 by Francis W. Aston (University of Cambridge) and Arthur J. Dempster (University of Chicago). The first commercial MS instrument was introduced in the 1940s in the United States by Consolidated Engineering Corporation (Pasadena, California). In 1946, the concept of time-of-flight mass spectrometry (TOF-MS) was suggested by William E. Stephens.[1] The direct coupling of gas chromatography (GC) and TOF-MS was achieved in 1950s by Roland S. Gohlke and McLafferty.[1] The most popular type of tandem MS instrument (triple quadrupole) was invented by Richard A. Yost in 1987.[1] Two recently developed MS techniques (1980s) have had a major impact on the ability to use MS for the study of biomolecules: electrospray ionization–MS (ESI–MS)[1] and matrix-assisted laser desorption/ionization–MS (MALDI–MS).[1]

In the 1990s and 2000s, new products were designed and developed exclusively for LC–MS performance. A broader scale of application occurred with the development of LC–MS-based methods for the analysis of novel pharmaceuticals.

Today, MS is one of the most powerful analytical techniques particularly in pharmaceutical analysis where good selectivity and high sensitivity are often needed. Liquid chromatography–mass spectrometry (LC–MS) has become a highly developed tool for the determination of drugs in plasma samples. The more recent developments in ionization technologies make MS an important tool for biological research. In the pharmaceutical industry the measurement of drug level in plasma answers key questions that are asked during drug discovery and development. The more rapid these measurements the more quickly drugs progress toward regulatory approval. It is important to minimize the analysis times where possible. The enhancement of the LC–MS technique during the past few years has led to decreased analysis times and increased throughput in the bioanalytical field. Due to its selectivity the use of MS has strongly increased for applications in biological samples. The advent of modern, user-friendly MS has led to a reconsideration of the application of MS in the analytical process. In many instances this re-evaluation has resulted in an explosive increase in the use of the technique in industry, particularly for drug discovery/pharmacological and genomic/proteomic applications. MS technologies such as matrix-assisted laser desorption/ionization (MALDI) and ESI have simplified the analysis of proteins, peptides, and drug metabolites. In general, low detection limits ranging from the picomole to the femtomole level are achieved.

DISCUSSION

In recent years, there has been an explosion in the use of LC–MS/MS as a fundamental analytical tool for drug metabolism and pharmacokinetics (DMPK) applications, e.g., metabolite identification, pharmacokinetic (PK) analysis,

cytochrome P450 (CYP) inhibition/induction, parallel artificial membrane permeation assay (PAMPA), and Caco-2 permeability. The choice of ESI vs. atmospheric pressure chemical ionization (APCI) should be addressed seriously, given the well-recognized fact that ESI is not a uniform ionization method. The greater the polarity of a compound, the more likely it is to occur as an ion in solution and it can be observed using ESI. Thus, in a complex mixture only a limited number of the components of the mixture are likely to be observed. Another way to look at it is to say that there is only a certain amount of ionization available and that it will be distributed in favor of the most polar species present. For instance, it is not uncommon that the purpose of a chemical reaction is to convert a polar precursor into a less polar product, for example, the addition of a protecting group onto an amine. Here the user may have a difficult time determining the level of completion of such a reaction if trying to monitor it by ESI. On the other hand, APCI is more even in its ability to ionize a range of compounds and would therefore be suited to answering such questions. However, APCI also has disadvantages in that the ionization process is more energetic and therefore more likely to generate fragments. Also, it is limited in its molecular mass range to about 1000 Da. This mass range limitation would be highly detrimental in cases where many analytes exceed 1000 Da. Arguments can be put forward for either method, but we would recommend ESI based on the simplicity of the spectra and the very wide range of structures for which data can be obtained. Today, most applications utilize the ESI interface (about 80% of published papers) vs. atmospheric pressure chemical ionization. ESI is an interface that is relatively easy to use.

The Role of LC–MS, LC–MS/MS in Drug Discovery and Development

The main purpose of drug discovery is to generate lead compounds with suitable pharmaceutical properties for preclinical evaluation and ensure high speed and high quality. High-capacity screening and high throughput are required. It was estimated that screening of 100,000 compounds are required for the discovery of only one quality lead compound.[2] The identification and optimization of a lead compound can take up to 3–6 years.[2] Therefore, drug discovery advances need fast, selective, and high-throughput screening methods. In addition, the drug development consists of four discrete stages: 1) drug discovery; 2) preclinical development; 3) clinical development; and 4) manufacturing. Due to its sensitivity, selectivity, speed, and simplicity, the LC–MS technology is applied nearly in every stage of drug development (Table 1). Additionally, the ease of method development and operation and the achieved level of automation make LC–MS an attractive tool in drug analysis. The role of LC–MS already starts in the drug discovery stage and continues until or after the manufacturing stage (Table 1). In spite of several chromatographic techniques such as GC, supercritical fluid chromatograph (SFC), and capillary electrophoresis (CE) have been interfaced to MS, LC–MS remains dominated in bioanalysis. The use of ionization technique depends on the structure and the acidity or basicity of the analyte studied. Normally, positive and negative ion ESI is preferred for basic and acidic drugs, respectively, while APCI is more suited for the less basic/acidic or neutral molecules.

LC–MS Instrumentation

Atmospheric pressure ionization (ESI and APCI) has become the dominant technique. The development of ESI led to a huge increase in the use of LC–MS, which was established to be a capable ionization technique, especially for polar compounds, and was found to be very compatible with solvents used for reversed-phase LC. Today, numerous manufacturers offer well-integrated LC–MS systems with the best performance. The ESI sources are usually orthogonal to the analyzer, which results in the maintenance of high

Table 1 LC/MS analysis activities at every stage of drug development.

Stage	Milestone	Highlight	LC/MS analysis behavior
Drug discovery	Lead candidate	Screening	1-Protein identification
			2-Metabolic stability profiles
			3-Molecular weight determination for medicinal chemistry support
Preclinical development	IND/CTA	Evaluation	1-Impurity
			2-Degradent
			3-Metabolicidentification
			4-Quantitative bioanalysis
Clinical development	NDA/MAA	Registration	1-Quantitative bioanalysis
			2-Structure identification
Manufacturing	Marketing sales	Compliance	1-Impurity
			2-Degrading identification

IND: Investigational New Drug; CTA: Clinical Trial Application; NDA: New Drug Application; MAA: Marketing Authorization Application.

performance by reducing source contamination, for example, the "Z-spray" ESI. In the past 10 years there has been an increasing demand from the pharmaceutical industry for faster analytical methods, to accelerate the drug development process. LC–MS is the most well-known technique, with its high sensitivity and selectivity. Ultra-performance liquid chromatography (UPLC) with fast gradients of only a few minutes are now used on short columns (typically 5 cm long, 1.7–1.9 μm particle size), compared to separations formerly on 10–25 cm long columns (3–5 μm particle size) with 10–30 min gradients.[3] However, suppression effects can be a significant problem and therefore a sample preparation is needed. Fraction collection system connected with LC–MS has also been introduced by several manufacturers. Moreover, coupling of LC with UV detection in parallel with MS provides further structural information and indication of purity and may display analytes not observed on the MS because of inability to ionize or ion suppression. The fast acquisition TOF-MS gives the possibility to maximize sample throughput with multiple inlet systems into one MS. Further developments include high capacity of vacuum pumps, resulting in lower MS background and in higher sensitivity. In addition, combinatorial chemistry has led to the use of 96-well microtiter plates and their coupling with analytical systems. The applications of MS/MS stages, as available on ion-trap MS systems, can be of enormous help in structure elucidation in drug metabolism studies. The result of this improved ability to analyze many more samples in a given time and faster acquisition MS instruments is the production of large amounts of data. This is becoming a major issue, and improvements in data management using automated processing are needed. Today there are powerful software tools that have been developed and are available from all major instrument manufacturers.

High-Throughput LC–MS

The development of faster and higher-throughput analytical methods is required for speed and capable use of time in the pharmaceutical industry. The development of combinatorial chemistry techniques and other new strategies has led to an increase in the number of possible drug candidates. This has produced a need for high throughput in bioanalyses for toxicological and pharmacokinetic studies. The trace level of drugs and metabolites in plasma remains a challenge in quantitative bioanalysis. Also, the need for same-day rotate of results from large numbers of biological samples makes high-throughput bioanalysis more essential.

Due to its sensitivity, selectivity, and potential for the development of high-throughput methods of analysis, LC–MS/MS has revolutionized the strategies and achievement of modern drug discovery and development in the pharmaceutical industry. Furthermore, UPLC–MS has the advantage of increased chromatographic performance generated by sub-2 μm particle stationary phases run at high mobile phase linear velocities. This results in increased resolution, peak capacity, and more sensitive high-throughput assays. However, efforts to further improve the sample throughput capabilities of modern techniques and strategies are ongoing.[4]

The higher selectivity attainable due to the use of LC–MS/MS is frequently reduced by decreasing the quality of the sample pretreatment and/or the chromatography. The motivation of this is an increase in the sample throughput. However, this often puts serious demands on the sample pretreatment methods. Also, the off-line sample pretreatment appeared to be the rate-limiting step. Speeding up the sample preparation is one of the most important factors in bioanalysis. One of the most applied approaches is the use of SPE or LLE in a 96-well plate format. Online sample preparation in a 96-well plate format was described by different authors.[4] Off-line sample preparation seems to be preferred by many researchers.

Severe matrix problems may be experienced in quantitative bioanalysis, especially in ESI. Signal suppression due to unknown matrix interferences is often observed. Changes in the sample preparation procedures may solve the problem, but in some cases changing over to APCI, when appropriate, appears to be the only likely solution. Signal suppression is described in the next section.

ION SUPPRESSION IN MS

Although the MS technique is particularly sensitive and robust, there is potential for ion suppression,[5] particularly with ESI interface. The matrix problems may be practiced in quantitative bioanalysis, particularly in ESI. Ion suppression was also observed with APCI interface during studies on a drug compound and metabolites.[6] Ion suppression is a well-known phenomenon in LC–MS bioanalysis, and in recent years the occurrence of ion suppression has become the most important concern in quantitative bioanalysis using LC–MS. A well-defined example of signal suppression was described by Annesley[7] and Matuszewski, Constanzer, and Chavez-eng.[8] Ion suppression can give rise to incorrect data interpretation, that is, poor accuracy and precision. Weaver and Riley[5] described how the effect of ion suppression of polyethylene glycol (PEG 400) could lead to incorrectly determined PK parameters and decreased sensitivity of the analytical method. Ion suppression is not only a result of endogenous material present in biological samples but it can also be caused by LC mobile-phase additives.[9] Even typically used mobile-phase components such as triflouroacetic acid (TFA) or methanol cause ion suppression. For example, TFA has been used in HPLC–UV analyses to improve the peak shape and to reduce the retention times but for MS analyses, TFA causes signal suppression. Annesley reported that the methanol used in the mobile phase could be a source of differential ionization or ion suppression.[10] van Hout et al.[11] showed that the percentage of ion

suppression relates to the matrix/analyte ratio, in another words it depends on the analyte concentration [ion suppression degree is proportional to 1/(analyte concentration)]. Two important points can be concluded from the van Hout et al. paper, the first is decreasing the matrix/analyte ratio through more extensive sample cleanup or through better chromatographic separation and the second is the importance of performing ion suppression validations.

The frequency of ion suppression or other deleterious effects can be evaluated by different experimental methods. The most common method is the comparison of the instrument response for an injected sample prepared in the mobile phase to the same concentration added to a preextracted blank sample matrix. The second method involves postcolumn continuous infusion of the compound into the MS instrument. In the third method, standard line slope comparison is also used to evaluate ion suppression.[12–16] Full-scan mass spectra can also be a useful method to study what impurities (in the blank of extracted sample matrix or in the LC mobile phase) are responsible for ion suppression and to try to remove these compounds.

Elimination of ion suppression requires changes in: 1) the sample pretreatment procedures; 2) the LC mobile-phase composition; 3) the LC mobile phase pH; and 4) the LC column polarity. In some cases changing the ionization source (e.g., ESI over to APCI) appears to be the feasible solution. At last the studies about ion suppression may further our understanding of the fundamental chemistry and physics of the ESI process.

ROLE OF SAMPLE PREPARATION PRIOR TO INJECTION

When the analytes are present in a complex matrix, e.g., plasma, the sample preparation is of crucial importance for the analysis. Biological fluids such as plasma and urine are much more complex than many others due to the presence of proteins, salts, acids, bases, and various organic compounds with chemistry similar to that of the analytes of interest. Thus, the extraction methods for biological samples are difficult. If an unsuitable sample preparation method has been employed before the injection, the whole analytical process can be wasted. The purpose of the sample preparation is: 1) the removal of interfering substances to eliminate ion suppression; 2) the conversion of analytes into a more suitable form for injection, separation, and detection; and 3) the preconcentration of the analytes to improve sensitivity. The procedure must be highly reproducible, with a high recovery of the target analytes. Further, an ideal sample preparation method should involve a minimum number of working steps and it should be fully automated. Because of the low concentration levels of drug in plasma and the variety of metabolites, the selected extraction technique should be virtually exhaustive. In this section, we will discuss about a well-applied sample preparation for drug analysis that is used with real samples from clinical institutions or pharmaceutical industry. Commonly used sample preparation methods[4,17] in the pharmaceutical industry are solid-phase extraction (SPE), liquid–liquid extraction (LLE), and protein precipitation (PP). SPE gives both high recovery and good chromatography. LLE and SPE are the most important sample preparation methods in LC–MS. The growing number of samples to be analyzed requires high-throughput and fully automated analytical techniques. Recent developments of sample handling techniques are directed, from one side, toward automation and online coupling of sample preparation units and detection systems and, from another, toward development of more selective sorbents such as immunosorbents, molecular imprinted polymers, and restricted access materials (RAM).

The limiting step in achieving fast bioanalysis is off-line sample preparation. This indicates the clear need of online sample pretreatment for speeding up sample preparation. One of most widely applied approaches is the 96-well plate format. While off-line sample pretreatment seems to be preferred by many researchers, online strategies are described as well.[4]

Liquid–Liquid Extraction

LLE is a simple sample preparation method. It has been widely used for the preparation of aqueous samples for many decades. It is a useful and easy method to extract the analytes from plasma to an organic solvent after shaking. LLE involves mixing an immiscible organic solvent with an aqueous solvent (e.g., plasma, urine, serum) to extract the analyte into the organic phase. The organic phase may be transferred, evaporated to dryness, and reconstituted prior to analysis. This method can give good recovery and a very clean sample. Initially volume of milliliters of solvent was needed but today 100–500 μl can be used for 96-well plates.[4] The analytes are extracted in an uncharged form by adjusting the plasma pH. Using LLE the analytes can also be extracted into the organic phase as an ion pair using an ion-pair reagent. Also, the analyte can be concentrated by the evaporation of the solvent and by redissolving the analyte in less volume prior to injection. The disadvantage of the LLE method is that it is difficult to obtain high recovery for polar analytes such as metabolites and it is not easy to automate it. Also, analytes with low K_D (distribution constant, K_D = concentration in organic phase/concentration in aqua phase) give bad recovery.

New progresses to establish LLE have been done in the past 10 years and is still under development. Examples of these include single-drop-liquid-phase microextraction (SD-LPME), LPME, and supported membrane extraction (SME). Single drop-LPME is based on a drop of organic solvent hanging at the end of a syringe needle.

Solid-Phase Extraction

SPE is a simple method that uses a small volume of a solid phase (10–100 mg) to isolate desired analytes from a sample. SPE has been in use for more than 50 years. Today SPE is the most popular sample preparation method. SPE can be performed off-line or online by direct connection to the chromatographic system. However, a key SPE problem is- method development. In the development of SPE the most important goal was to obtain extracts free from matrix interferences in a few steps (conditioning of the sorbent, applying of the sample, washing and elution). The most important parameters in SPE are the selection of the type and amount of the sorbent, the determination of the sample volume that can be applied without loss in recovery, the composition and volume of the washing solution that can be applied without loss of the analytes, and finally the composition and volume of the elution solution.[18] The availability of cleaner and more reproducible sorbents, and the large choice of sorbents over past few years, has led to an increasing acceptance and growing interest in this method. Compared to LLE, SPE has a number of potential advantages: SPE can easily be automated, gives more efficient separation of interferences from analytes, reduces organic solvent consumption, and is more efficient in analyte recovery. In SPE, higher recovery takes one step, while in LLE it takes many more steps. One major disadvantage of SPE is that the cartridges tend to vary from lot to lot.

Protein Precipitation

Precipitation is a widely used sample preparation method in bioanalysis. The most common type of precipitation for proteins is salt induced or by addition of an organic solvent (methanol, acetonitrile) or by changing the sample pH by adding acids such as sulfuric acid or hydrochloric acid. Today there is a PP microplate in the 96-well format (Biotage AB and Whatman). Many applications on this technique have been published.

Microextraction-Related Techniques in Bioanalysis

Solid-Phase Microextraction

Solid-phase microextraction (SPME) was introduced in the early 1990s by Arthur and Pawliszyn.[19] SPME is a simple solvent-free sample preparation method for GC and LC. The extraction is based on the partitioning of the analyte between the organic phase on the fused silica fiber and the matrix. Many factors such as pH, temperature, salt concentration, and stirring affect the equilibrium constant and the equilibration time.[19] Fiber lifetime is a significant issue. SPME fiber is quite sensitive to complex matrix such as plasma. In addition, type of polymer, temperature, duration, and additives coming from the sample solution influence the stability of the coating. It should be noted that additives such as sodium hydroxide and salt could catalyze polymer thermal degradation. In some bioanalytical studies, fiber lifetime decreased to about 20 samplings instead of 80.[20]

Microextraction by Packed Sorbent

Microextraction by packed sorbent (MEPS) is a new development in the field of sample preparation and sample handling.[21] It entails the miniaturization of conventional SPE packed-bed devices from milliliter bed volumes to microliter volumes. MEPS can be connected online to GC or LC without any modifications. This approach to sample preparation is very promising for many reasons: 1) it is easy to use; 2) it is a fully automated online procedure; 3) it is rapid; and 4) the cost of analysis is minimal compared to conventional solid-phase extraction. In MEPS about 1 mg of the solid packing material is packed inside a syringe (100–250 μl) as a plug or between the barrel and the needle as a cartridge. Sample preparation takes place on the packed bed. The bed can be coated to provide the selective and suitable sampling conditions. MEPS differs from commercial SPE in that the packing is integrated directly into the syringe and not into a separate column. Moreover, the packed syringe can be used several times, more than 100 times using plasma or urine samples, whereas a conventional SPE column is used only once. MEPS can handle small sample volumes (10 μl plasma, urine, or water) as well as large volumes (1000 μl). The superior performance of MEPS was recently illustrated by online LC–MS and GC–MS assays of drugs and metabolites in water, urine, plasma, and blood samples.

The MEPS technique has been used to extract a wide range of analytes in different matrices (urine, plasma, blood). Several drugs such as local anesthetics and their metabolites, the anticancer drugs roscovitine, olomoucine, busulfan, cyclophosphamide, β-blockers acebutolol and metoprolol, the neurotransmitters dopamine and serotonin, methadone, and cocaine and cocaine metabolites have been extracted from biological samples such as blood, plasma, and urine using MEPS.[21–26]

APPLICATION OF LC–MS IN DRUG AND METABOLITES ANALYSIS

The most important application of LC–MS in drug development has been in drug metabolism studies. Furthermore, LC–MS has an important role in the analysis and identification of impurities, in degradation products in pharmaceuticals, and in the isolation and characterization of potential drug substances from natural or synthetic sources. Additionally, quantitative bioanalysis of drugs and

metabolites in biological samples is the most important application area of LC–MS in drug development. Quantitative bioanalysis is necessary for preclinical and clinical drug testing to make available pharmacokinetic and pharmacodynamic data. The use of LC–MS in quantitative bioanalysis is favored due to low detection limits in picograms, high selectivity against possibly interfering solutes in the biological matrix, and the capability to use isotopically labeled compounds as internal standards. As a result, LC–MS/MS has become the method of choice for quantitative bioanalysis in the pharmaceutical industry.

The metabolism of a potential new drug must be investigated before it can be considered for further development into a therapeutic agent.[27] A good drug candidate should preferably be metabolically stable and should have a good pharmacokinetic profile with high bioavailability and long half-life. Some metabolites may also be more pharmacologically active or more toxic than the parent drug. The characterization of the metabolites, major and active, helps in the discovery of new drug candidates with enhanced pharmacological activity, metabolic stability, and toxicology profile. The LC–MS technique is the preferred tool for the study of drug metabolism because of its sensitivity and selectivity. The use of LC–MS provides information about molecular weight and fragmentation patterns for structure elucidation.

In Vitro and In Vivo Drug Metabolism

Today, in vitro systems are a basic part of drug metabolism during drug discovery.[27] This has several advantages such as high speed, reduction in the use of animals, and the ability to investigate specific aspects of the metabolic disposition of a compound. Metabolic stability influences both oral bioavailability and plasma half-life of a compound, which in turn, affect its efficacy. Commonly, the initial studies of drug metabolism have been carried out in vitro with liver microsomal preparations or hepatocytes. These provide good indication of the metabolic fate of a drug.

In vivo metabolism studies entail analysis and determination of drugs and metabolites in blood, urine, and feces. These matrices contain a larger amount of endogenous compounds that could coelute and interfere with LC–MS analysis. A good sample preparation technique and capable chromatographic separation (LC, UPLC) and a selective detection technique (MS/MS) are therefore important for successful in vivo metabolism studies.

An example of the application of LC–MS and UPLC–MS in vitro and in vivo metabolism studies is the study of the metabolism of prazosin (antihypertensive agent being investigated for the treatment of posttraumatic stress disorder). The in vivo metabolism of prazosin in rat was first reported in 1977,[28] and six metabolites were characterized, though at that time analytical techniques were not as advanced, nor were the MS as sensitive as today. Studies have shown that prazosin can improve sleep and reduce severe nightmares in both civilians and military war veterans experiencing posttraumatic stress disorder (PTSD), as well as those from Operation Iraqi War, 2003.[29] The new interest in the use of prazosin in the clinic led to its metabolism being investigated in vitro using liver microsomes from rats, dogs, and humans; rat and human cryopreserved hepatocytes and more metabolites were characterized. Erve et al.[30] reinvestigated the in vivo metabolism study of prazosin in rat using a quadrupole TOF-MS coupled with UPLC, to identify metabolites revealed by in vitro studies; consequently, six new metabolites were identified (Fig. 1). The structures of the metabolites M1–M8, M10, M11, and M13 were confirmed by comparison of MS/MS spectra with those obtained from metabolites formed in vitro and reported elsewhere. For M7, nuclear magnetic resonance (NMR) spectroscopy was also performed to provide additional support for the proposed structure. For M16–M21, tentative structures were proposed based on interpretation of MS/MS spectra, H–D exchange, and accurate mass as discussed in detail.[30]

LC–MS in Clinical Applications

LC–MS determination of drugs and metabolites in clinical studies is a key function in the success and effectiveness of clinical development of drugs. LC–MS has established an obvious advantage for quantitative pharmacokinetic studies in terms of analysis time, cost, and sample throughput. LC–MS/MS has powerful capacity in quantity bioanalysis. LC–MS in clinical applications such as in the diagnosis of inherited and acquired metabolic disorders, gastrointestinal disorders, cancer and diabetes, and therapeutic drug monitoring is still frequently required.

Today LC–MS is a useful alternative to GC–MS for the analysis of biological carboxilic acids.[31] Simultaneous determination of anticancer drugs such as busulfan, cyclophosphamide, and rescovitine in patients' samples are reported using LC–MS/MS after online sample pretreatment.[22–24] Quantitation of antibiotics such as penicillins, nitrofurans, tetracyclines, cephalosporins, and sulfonamides at low concentration levels in biological samples was performed using LC–MS/MS. Salvador et al.[32] have developed an LC–MS/MS assay for the determination of a new antibacterial agent (AVE6971) and validated the assay in human white blood cells (WBC). The assay involved a lysing procedure of WBC and ultracentrifugation of the extracts. Determination of drugs with a nitrogen-containing-saturated ring such as morphine, codeine, cocaine, and 6-monoacetylmorphine in body fluids utilizing LC–MS/MS has been reported. A number of publications have also covered the application of LC–MS/MS for determination of neurosteroids and steroids such as 3-ketosteroids metandienone, nandrolone, and testosterone with limit of detection (LODs) between 2.5 and 250 fmol (in different matrices), depending on the analyte by using atmospheric pressure photoionization (APPI–MS).[33] Type-amide local anesthetics such as ropivacaine in human plasma were analyzed using LC–MS/MS. Table 2 summarizes the

Fig. 1 Proposed in vivo metabolism of prazosin. Bold indicates metabolites not previously reported in vivo.
Source: From Metabolism of prazosin in rat and characterization of metabolites in plasma, urine, faeces, brain and bile using liquid chromatography/mass spectrometry (LC/MS), in Xenobiotica.[30]

Table 2 Operating and conditions of LC/MS/MS of different drugs.

Drug	Column	Mobile phase	Sample preparation	LOD/ LOQ	Refs.
Local anaesthetics	Hypersil Gold (100 × 2.1 mm)	Methanol and water (1:1) 0.1% HCOOH	MEPS	2 n*M*	[22]
Busulfan	Hypersil Gold (100 × 2.1 mm)	Acetonitrile and water 0.1% HCOOH	MEPS	5 μg/ml	[23]
Cyclophosphamide	Zorbax SB-C8 (50 × 2.1 mm)	Acetonitrile and water 0.1% HCOOH	MEPS	0.5 μg/ml	[24]
Roscovitine and Olomoucine	Zorbax SB-C8 (50 × 2.1 mm)	Acetonitrile/methanol/water 0.1% HCOOH	MEPS	0.5, 1.0 μg/L	[25]
Acebutolol and metoprolol	Zorbax SB-C18 (50 × 2.1 mm)	Acetonitrile and water 0.1% HCOOH	MEPS	1.0 μg/L	[26]
Immunosuppressive	CP ChromSphere (20 × 3 mm)	Methanol and 10 m*M* ammonium formate	Protein precipitation	2 n*M*	[34]
Antibiotics	Caltrex Resorcinearene (125 × 2 mm)	Formate buffer-acetonitrile (40:60, v/v)	SPE	3–18 ng/ L	[35]
Cefdinir	RP18 Waters (50 × 2.1 mm)	Methanol–water (25:75, v/v) 0.075% HCOOH	Protein precipitation	5 μg/L	[36]
Anabolic and corticosteroids	C-18 RP (50 × 2.1 mm)	Acetic acid, ammonium acetate, and methanol	LLE	0.1–2 μg/L	[37]
Amphetamines	C18 (40 × 2.1 mm)	Trifluoroacetic acid (ion paring)	SPE	1 μg/L	[38]
Amisulpride	Polar-RP (75 × 4.6 mm)	5 m*M* ammonium formate and acetonitrile (30:70, v/v)	LLE	0.5 μg/L	[39]
Ziprasidone	C8 (150 × 2.1 mm)	2 mmol L−1 Ammonium acetate in acetonitrile–water (9:1, v/v)	LLE	0.1 μg/L	[40]

conditions of LC–MS/MS for some classes of drugs in biological samples. In addition, in a clinical study Abdel-Rehim, Bielenstein, and Askemark[41] showed how the use of LC–MS/MS leads to more reliable results than the use of LC–UV/ LC–MS for the quantification of ropivacaine and its metabolites. In their investigation analysis of urine samples from a clinical study of ropivacaine and its metabolites, 3-hydroxyropivacaine (3-OH-ropivacaine) and PPX, by an LC–UV method showed high concentrations of 3-hydroxyropivacaine, 2–50 times higher than expected. In the study, the patients were treated with a number of drugs in combination with ropivacaine. These drugs were paracetamol, lidocaine, fentanyl, morphine, and trimethoprim. When the fraction of 3-hydroxyropivacaine was collected from LC–UV and analyzed by LC–MS, only a high signal with mass number 291 [3-hydroxyropivacaine (MH+)] was observed. This observation indicates that it may be a drug or a metabolite having the same mass number as 3-hydroxyropivacaine and eluting at the same retention time on the LC system that gives a high signal in UV and MS detection. The examination of the drugs given showed that trimethoprim has the same molecular weight as 3-hydroxyropivacaine. The analysis of trimethoprim by LC–UV and LC–MS showed that under the given conditions it has the same retention time as 3-hydroxyropivacaine. The tuning of 3-hydroxyropivacaine and trimethoprim by tandem MS/MS showed that both substances have the same precursor ions (*m/z*: 291) but different product ions (*m/z*: 126 and 123 for 3-hydroxyropivacaine and trimethoprim, respectively) (Fig. 2A and B).

Analysis and Identification of Impurities and Degradation Products

The impurities in pharmaceuticals are mainly produced during the synthetic process from raw chemicals, intermediates, solvents, and by-products. Raw chemicals and intermediates for drug manufacturing do not always have the same purity requirements as the final pharmaceuticals. By-products are generated during synthesis and are another source of pharmaceutical impurities. Impurities may also occur from the components used in dosage formulation and/or in the process of formulation where temperature, humidity, and light may all participate. The most common degradation processes are oxidation, hydrolysis, and dehydration; other processes include adduct formation with excipients, dimerization, and rearrangement. Thus the investigation and the evaluation of drug impurities is a demand from drug regulation authorities. It is important to ensure that the observed impurities do not have any pharmacological and toxicological effects. Study and screening of impurities and degradation products in formulated

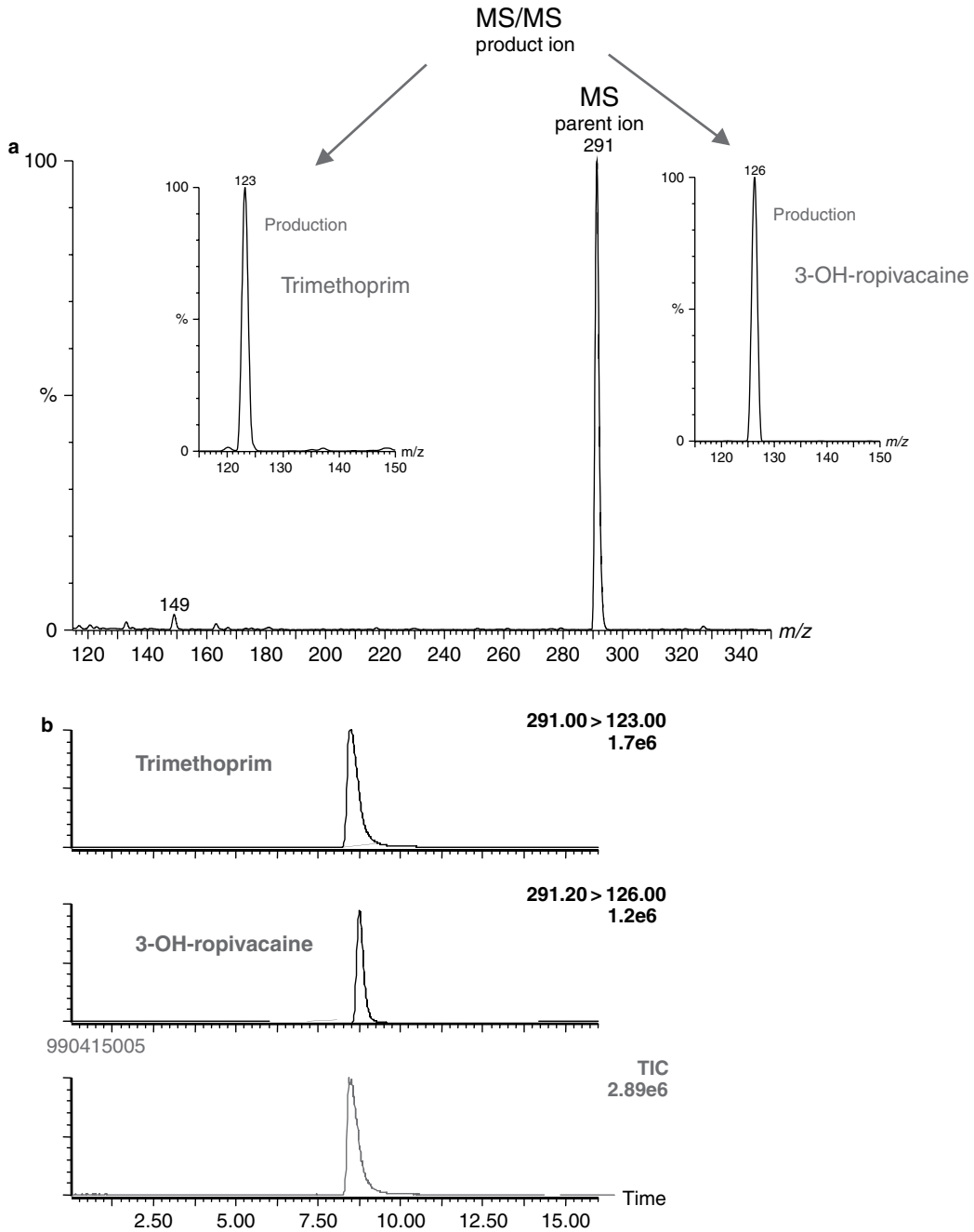

Fig. 2 a, Mass chromatogram (LC–MS and product ions from MS/MS) for the fraction of 3-OH-ropivacaine including trimethoprim collected from LC–UV. b, Mass chromatogram of patient's urine sample shows 3-OH-ropivacaine and trimethoprim by LC–MS–MS.

pharmaceuticals are necessary for ensuring that no compounds with deleterious effects are produced during their shelf life. The identification of degradation products will help in the understanding of potential side effects associated with degradation. This will also aid in the design of a more constructive formulation and for synthesis of new drugs with better stability. According to ICH (International Conference on Harmonization) guidelines on impurities in new drug products, identification of impurities below the 0.1% level is not considered to be necessary except for the potential impurities that are expected to be unusually potent or toxic.[42]

Since impurities and degradents are usually present in quite small quantities as compared to the drug, LC–MS is widely used for analysis of impurities.[43] However, it is useful to use a UV in combination with MS for the estimation and identification of impurities especially for the

unknowns. In addition, NMR and Fourier transform ion cyclotron resonance mass spectrometry (FTICR-MS) are also used for studying impurities.[42]

Additionally, LC–MS is the method of choice for the separation and detection of chiral impurities in pharmaceuticals. The analysis of chiral impurities in pharmaceuticals is of importance because the D-isomer of a drug can have a different pharmacological, metabolic, and toxicological activity from the L-isomer. Chiral impurities of amino acids, present in peptide drugs, have been separated and determined by LC–MS.[43] The selectivity of MS detection eliminated interference from other peaks that appeared when a UV detector was used for detection.

FUTURE TRENDS AND PERSPECTIVES

The combination of LC with MS has created a powerful tool for the analysis and quantitation of a variety of drugs and metabolites in complex matrices. LC–MS has turned out to be a particularly sensitive and selective technique for the analysis and quantitation of pharmaceuticals. It is a fundamental analytical tool for the studies of drug metabolism of new drug candidates and the identification and characterization of impurities and degradents in pharmaceuticals. Further transfer of the routine activity of immunosuppressants from immunoassays to LC–MS, which allows the automation of sample preparation, shortens analytical run times and is probably cost-effective despite heavy investment costs.

Technical progress in MS continues, with improvements in sensitivity and resolution. The trend is toward the further development of hybrid instruments such as Q-TOF/FTICR. Application of accurate mass measurement is a convenient tool to enable offering information about molecular weight and fragmentation patterns for structure elucidation. Further requirements for high-resolution sequencing of proteomics in pharmaceutical development will have implication for MS. The combination of online high-throughput sample preparation techniques with LC–MS/MS will lead to even faster analysis and cost-effective.

Because of the use of microfluidic systems, it might be possible in the future to use online miniaturized chip separation with miniaturized MS for rapid on-site analysis. Additionally, coupling of LC–NMR/MS will be a invaluable system that will allow the obvious identification of metabolites.

REFERENCES

1. Siuzdak, G. *The expanding role of Mass Spectrometry in Biotechnology*; MCC Press: San Diego, California, 2006.
2. Lee, M. *LC/MS Applications in Drug Development*; John Wiley & Sons, Inc.: Canada, 2002.
3. http://www.waters.com/waters/nav.htm?locale=en_SE&cid=514514
4. Wells, D.A. *High Throughput Bioanalytical Sample Preparation Method and Automation Strategies*; Elsevier Science B.V.: Amsterdam, The Netherland, 2003.
5. Weaver, R.; Riley, R.J. Identification and reduction of ion suppression effects on pharmacokinetic parameters by polyethylene glycol 400. Rapid Commun. Mass Spectrom. **2006**, *20*, 2559–2564.
6. Sangster, T.; Spence, M.; Sinclair, P.; Payne, R.; Smith, C. Unexpected observation of ion suppression in a liquid chromatography/atmospheric pressure chemical ionization mass spectrometric bioanalytical method. Rapid Commun. Mass Spectrom. **2004**, *18*, 2559–2564.
7. Annesley, T.M. Ion suppression in mass spectrometry. Clin. Chem. **2003**, *49* (7), 1041–1044.
8. Matuszewski, B.K.; Constanzer, M.L.; Chavez-eng, C.M. Strategies for the assessment of matrix effect in quantitative bioanalytical methods based on HPLC–MS/MS. Anal. Chem. **2003**, *75* (13), 3019–3030.
9. Mallet, C.R.; Lu, Z.; Mazzeo, J.R. A study of ion suppression effects in electrospray ionization from mobile phase additives and solid-phase extracts. Rapid Commun. Mass Spectrom. **2004**, *18*, 49–58.
10. Annesley, T.M. Methanol-associated matrix effects in electrospray ionization tandem mass spectrometry. Clin. Chem. **2007**, *53* (10), 1827–1834.
11. van Hout, M.W.J.; Hoffland, C.M.; Niederlander, H.A.G.; de Jong, G.J. On-line coupling of solid-phase extraction with mass spectrometry for the analysis of biological samples. II. Determination of clenbuterol in urine using multiple-stage mass spectrometry in an ion-trap mass spectrometer. Rapid Commun. Mass Spectrom **2000**, *14*, 2103–2111.
12. Matuszewski, B.K.; Constanzer, M.L.; Chavez-Eng, C.M. Matrix effect in quantitative LC/MS/MS analyses of biological fluids: A method for determination of finasteride in human plasma at picogram per milliliter concentrations. Anal. Chem. **1998**, *70*, 882–889.
13. Bonfiglio, R.; King, R.C.; Olah, T.V.; Merkle, K. The effects of sample preparation methods on the variability of the electrospray ionization response for model drug compounds. Rapid Commun. Mass Spectrom. **1999**, *13* (12), 1175–1185.
14. Muller, C.; Schafer, P.; Stortzel, M.; Vogt, S.; Weinmann, W. Ion suppression effects in liquid chromatography–electrospray ionisation transport-region collision induced dissociation mass spectrometry with different serum extraction methods for systematic toxicological analysis with mass spectra libraries. J. Chromatogr. B, **2002**, *773*, 47–52.
15. Hsieh, Y.; Chintala, M.; Mei, H.; Agans, J.; Brisson, J.-M.; Ng, K.; Korfmacher, W.A. Quantitative screening and matrix effect studies of drug discovery compounds in monkey plasma using fast-gradient liquid chromatography/tandem mass spectrometry. Rapid Commun. Mass Spectrom. **2001**, *15* (24), 2481–2487.
16. Matuszewski, B.K. Standard line slopes as a measure of a relative matrix effect in quantitative HPLC–MS bioanalysis. J. Chromatogr. B, **2006**, *830*, 293–300.
17. van Hout, M.W.J.; Niederlandär, H.A.G.; de Zeeuw, R.A.; de Jong, G.J. New developments in integrated sample

preparation for bioanalysis. In *Handbook of Analytical Separations*, Ian D. Wilson, Ed.; series editor: Roger M. Smyth; Elsevier: Amsterdam, The Netherlands, 2003; Vol. 4.
18. Poole, C.F. New trends in solid-phase extraction. Trends Anal. Chem. **2003**, *22* (6), 362–373.
19. Pawliszyn, J. Solid phase microextraction theory and practice. Wiley-VCH: New York, USA, 1997.
20. Abdel-rehim, M.; Hassan, Z.; Blomberg, L; Hassan, M. Determination of busulphan in plasma samples by gas chromatography–mass spectrometry (GC–MS) using on-line derivatization utilizing solid-phase microextraction (SPME). Ther. Drug Monit. **2003**, *25*, 400–406.
21. Abdel-Rehim, M. New trend in sample-preparation: On-line microextraction in packed syringe (MEPS) for LC and GC applications Part I: Determination of local anaesthetics in human plasma samples using MEPS on-line with GC–MS-MS. J. Chromatogr. B, **2004**, *801* (2), 317–321.
22. Abdel-Rehim, M.; Altun, Z.; Blomberg, L. New trend in sample-preparation: On-line microextraction in packed syringe (MEPS) for LC and GC applications. Part II: Determination of ropivacaine and its metabolites in human plasma samples using MEPS on-line with LC–MS-MS, J. Mass Spectrom. **2004**, *39*, 1488–1493.
23. Abdel-Rehim, M.; Hassan, Z.; Skansen, P.; Hassan, M. Simultaneous determination of busulphan in plasma samples by liquid chromatography–electrospray ionization mass spectrometry utilizing microextraction in packed syringe (MEPS) as on-line sample preparation method. J. Liq. Chromatogr. Relat. Technol. **2007**, 30, 3029–3041.
24. Said, R.; Hassan, Z.; Hassan, M.; Abdel-Rehim, M. Rapid quantification of cyclophosphamide in patients plasma samples using microextraction in packed syringe (MEPS) on-line with liquid chromatography–tandem mass spectrometry. J. Liq. Chromatogr. Relat. Technol. **2008**, *31*, 683–694.
25. Vita, M.; Skansen, P.; Hassan M.; Abdel-Rehim, M. Development and validation of a liquid chromatography and tandem mass spectrometry method for determination of roscovitine in plasma and urine samples utilizing on-line sample preparation. J. Chromatogr. B, **2005**, *817*, 303–307.
26. El-Beqqali, A.; Kussak, A.; Abdel-Rehim, M. Microextraction in packed syringe/liquid chromatography/electrospray tandem mass spectrometry for quantification of acebutolol and metoprolol in human plasma and urine samples. J. Liq. Chromatogr. Relat. Technol. **2007**, *30* (4), 575–586.
27. *Drug Metabolism in Drug Design and Development*; Donglu Zhang, Mingshe Zhu, Humphreys, W.G., Eds.; John Wiley & Sons, Inc: Hoboken, New Jersey, USA, 2008.
28. Taylor, J.A.; Twomey; T.M.; Schach Von Wittenau, M. The metabolic fate of prazosin. Xenobiotica **1977**, *7* (6), 357–364.
29. Daly Christine, M.; Doyle Michael, E.; Radkind, M.; Raskind, E.; Daniels, C. Clinical case series: The use of prazosin for combat-related recurrent nightmares among Operation Iraqi freedom combat veterans. Military Med. **2005**, *170*, 513–515.
30. Erve, J.C.L.; Vashishtha, S.C.; Ojewoye b, O.; Adedoyin, A.; Espina, R.; DeMaio, W.; Talaat, R.E. Metabolism of prazosin in rat and characterization of metabolites in plasma, urine, faeces, brain and bile using liquid chromatography/mass spectrometry (LC/MS). Xenobiotica, May **2008**, *38* (5), 540–558.
31. Johnson, D.W. Contemporary clinical usage of LC/MS: Analysis of biologically important carboxylic acids. Clin. Biochem. **2005**, *38*, 351–361.
32. Salvador, A.; Gautier, J.-Y.; Pasquier, O.; Merdjan, H. Liquid chromatography–tandem mass spectrometric determination of a new antibacterial agent (AVE6971) in human white blood cells. J. Chromatogr. B, **2007**, *855*, 173–179.
33. Smyth, W.F.; Rodriguez, V. Recent studies of the electrospray ionisation behaviour of selected drugs and their application in capillary electrophoresis–mass spectrometry and liquid chromatography–mass spectrometry. J. Chromatogr. A, **2007**, *1159*, 159–174.
34. Abdel-Rehim, M.; Bielenstein, M.; Askemark, Y. Determination of ropivacaine and its metabolites in urine: The advantage of LC–MS-MS over LC–UV and LC–MS. Analytica Chimica Acta **2003**, *492*, 253–260.
35. Roy, J. Pharmaceutical impurities—A mini-review. AAPS PharmSciTech **2002**, *3* (2), article 6.
36. Lim, C.-K; Lord, G. Current developments in LC–MS for pharmaceutical analysis. Biol. Pharm. Bull. **2002**, *25* (5), 547–557.
37. Bogusz, M.J.; Al Enazi, E.; Hassan, H.; Abdel-Jawaad, J.; Al Ruwaily, J.; Al Tufail, M. Simultaneous LC–MS–MS determination of cyclosporine A, tacrolimus, and sirolimus in whole blood as well as mycophenolic acid in plasma using common pretreatment procedure. J. Chromatogr. B, **2007**, *1159*, 159–174.
38. Scheuch, E.; GieÔmann, T.; Siegmund, W. Quantitative determination of nystatin in human plasma using LC–MS after inhalative administration in healthy subjects. J. Chromatogr. B, **2006**, *844*, 84–88.
39. Chen, Z.-J.; Zhang, J.; Yu, J.-C.; Cao, G.-Y.; Wu, X.-J.; Shi, Y.-G. Selective method for the determination of cefdinir in human plasma using liquid chromatography electrospray ionization tandem mass spectrometry. J. Chromatogr. B, **2006**, *834*, 163.
40. Thevis, M.; Schänzer, W. Current role of LC–MS(/MS) in doping control. Anal. Bioanal. Chem. **2007**, *388*, 1351–1358.
41. Fuh, M.R.; Wu, T.Y.; Lin, T.Y. Determination of amphetamine and methamphetamine in urine by solid phase extraction and ion-pair liquid chromatography–electrospray–tandem mass spectrometry. Talanta **2006**, *68*, 987–991.
42. Gschwend, M.H.; Arnold, P.; Ring, J.; Martin, W. Selective and sensitive determination of amisulpride in human plasma by liquid chromatography–tandem mass spectrometry with positive electrospray ionisation and multiple reaction monitoring J. Chromatogr. B, **2006**, *831*, 132.
43. Al-Dirbashi, O.Y.; Aboul-Enein, H.Y.; Al-Odaib, A.; Jacob, M.; Rashed, M.S. Rapid liquid chromatography—tandam mass sepectrometry method for quantification of ziprasidone in human plasma. Biomed. Chromatogr. **2006**, *20* (4), 365.

Drugs: HPLC Analysis of NSAIDs

Adrian Florin I. Spac
Department of Chemistry, Grigore T. Popa University of Medicine and Pharmacy, Iasi, Romania

Vasile I. Dorneanu
Analytical Chemistry Department, Grigore T. Popa University of Medicine and Pharmacy, Iasi, Romania

INTRODUCTION

Non-steroidal anti-inflammatory agents are of prime clinical interest in the control of pain and inflammation associated with a wide variety of rheumatoid- and non-rheumatoid-related disorders. In a continuous search for well-tolerated and effective agents for the treatment of human diseases, over 100 groups of new chemical entities have been synthesized and disclosed in the literature as potential anti-inflammatory drugs.

As their name implies, non-steroidal anti-inflammatory drugs (NSAIDs) are drugs that block or inhibit the inflammation processes without the use of steroid drugs. The most commonly used NSAIDs are aspirin, ibuprofen, and naproxen.

NSAIDs remain the mainstay of therapy for patients with chronic pain. NSAIDs are essential analgesics, especially for pain associated with inflammation. Inflammation results in increased local prostaglandin (PG) production, which also occurs in the central nervous system (CNS). Increased PGs in the CNS result in central sensitization and increased pain. The NSAIDs main mode of action is blocking the PG production by binding and inhibiting cyclooxygenase (COX), the main enzyme in the synthesis of PGs from arachidonic acid. NSAIDs inhibit PG production both at the site of injury and in the CNS, i.e., they have both a peripheral and a central action. While the result of this effect is mainly a reduction in inflammation and peripheral nociceptor sensitization, there is some evidence that NSAIDs have a central analgesic action as well, although the exact mechanism remains unclear. However, inhibition of PG synthesis does not account for the total analgesic effect of NSAIDs.

NSAID CLASSIFICATION

NSAIDs are, as a group, the most frequently consumed drugs worldwide. They also cause the most, and often dangerous, side effects reported to the US Food and Drug Administration, the majority of which are because of damage of the gastrointestinal (GI) tract and kidneys. This explains the continuous interest of pharmacologists, clinical pharmacologists, and pharmacoepidemiologists in this group of drugs.

Although NSAIDs are effective in the treatment of pain and inflammation, their routine and long-term administration is limited, because of their GI and renal side effects. COX isozymes are the main targets of NSAIDs. While the inhibition of COX-2 is related to anti-inflammatory effects, that of COX-1 is associated with the adverse effects. The idea behind developing COX-2 inhibitors was to have a NSAID devoid of GI toxicity. However, GI toxicity depends on multiple factors, not just COX-2 selectivity.

Based on an increasing body of data, Frolich[1] proposes a simple alternative to the usual chemical classification of NSAIDs, allowing one to predict a drug's major effects according to its relative inhibition of the constitutive and inducible COX isoenzymes.

According to COX enzyme selectivity,[2] NSAIDs are classified into the following:

1. COX-1 selective group-1, which include low- dose aspirin.
2. Non-selective group-2 with similar inhibition activity for COX-1 and COX-2, which includes high-dose aspirin, diclofenac, ibuprofen, indomethacin, mefenamic acid, naproxen, paracetamol, piroxicam, and others.
3. COX-2 selective group-3, which includes ketorolac, meloxicam, nabumetone, nimuselide, and others.
4. COX-2 highly selective group-4, which includes celecoxib, rofecoxib, etc.

Based on their chemical structures, NSAIDs areas follows:

1. Carboxylic acids
   a. Salicylic acids and esters (e.g., ASA, diflunisal, and benorylate)

   b. Acetic acids
      i. Phenylacetic acids (e.g., diclofenac)
      ii. Carbo- and heterocyclic acetic acids (e.g., indomethacin, ketorolac, sulindac, and tolmetin)
   c. Propionic acids (e.g., flurbiprofen, ketoprofen, tiaprofenic acid, ibuprofen, naproxen, and fenoprofen)
   d. Fenamic acids (e.g., mefenamic Acid)
2. Enolic acids
   a. Pyrazolones (e.g., phenylbutazone)
   b. Oxicams (e.g., piroxicam and meloxicam)
3. Cox-II Inhibitors (e.g., celecoxib, valdecoxib, and rofecoxib)

ANALYSIS OF NSAIDS

High-performance liquid chromatography (HPLC) possesses many of the attributes of gas chromatography, plus some of the advantages of liquid-phase separation. Without derivatization, the high polarity and low volatility of many non-steroidal anti-inflammatory agents restrict the use of gas chromatographic methods. The thermally labile compounds and their derivatives may also limit the applicability of gas chromatography for the analysis of these classes of drugs.

A great number of HPLC techniques have been developed and successfully applied for the analysis of NSAIDs from pharmaceutical forms or from biological media (urine, plasma, whole blood, etc.).

Selection of a procedure, which is most suitable for solving a specific problem, depends on the analyst's need for measuring the drugs only or the drugs and their respective metabolites.

SAMPLE PREPARATION

The most critical step in generating accurate, reliable results is good sample preparation. Only in rare instances, is cleanup not required, and the drug concentration is simply adjusted before the drug is injected directly into the chromatograph.

Most samples are not ready for direct introduction into instruments. For example, the substances have to be extracted into a solution, which can be analyzed. There might be several processes within sample preparation itself. Some steps commonly encountered are homogenization, size reduction, extraction, concentration, derivatization, the cleanup, and the analysis. These processes depend on the sample, the matrix, and the concentration level at which the analysis needs to be carried out. For instance, trace analysis requires more stringent sample preparation than major component analysis.

Considering the solubilities of the NSAIDs in solvents such as methanol or acetonitrile, for the analysis from pharmaceutical formulations (tablets, syrups, supositories, etc.), the easy way to prepare the sample is to dissolve it in the following:

1. Pure solvents
   a. Methanol[3–10] for aspirin, diclofenac, mefenamic acid, tolfenamic acid, ibuprofen, tenoxicam, nabumetone, etc.
   b. Acetonitrile[11,12] for diflunisal, indomethacin, fenoprofen, ibuprofen, ketoprofen, naproxen, mefenamic acid, diclofenac, piroxicam, etc.
2. Aqueous methanol or acetonitrile[10,13–15] for tolmetin, bufexamac, nabumetone, benzydamine, etc.
3. The mobile phase used in HPLC[16,17] for diclofenac, oxyphenbutazone, etc.
4. THF/propan-2-ol[15] (for benzydamine hydrochloride from creams).

The obtained solution can be analyzed after centrifugation and filtration.

In other cases, e.g., for pharmacokinetic studies, the NSAIDs must first be extracted from biological media (urine, plasma, serum, whole blood, tissues, etc.).

The main challenge, when dealing with the preparation of biological samples, is that they are exceedingly complex. These substances might interfere by interaction with the drug itself, or possibly with the column packing or detector of the chromatographic system. Thus, additional procedures are almost always required, prior to the chromatography, to reduce the number of interfering substances, so that HPLC can resolve the remaining components efficiently, with a lower noise level and detection limit.

The purification of the drug, once it is freed from its environment, depends upon the chemical nature of the drug and its contaminants. Those purification conditions that selectively extract the drug should be chosen leaving, as much as possible, the endogenous material unextracted, while providing quantitative recovery of the drug.

The sample preparation for the analysis of drugs in biological fluids consists of a number of operations that are used for the release of the drug from a conjugate or biological matrix; removal of endogenous compounds that could interfere with the assay; and techniques for liquid handling.

In the case of NSAIDs, the most encountered techniques are liquid–liquid extraction or solid-phase extraction (SPE).

Table 1 Salicylic acids and esters.

Stationary phase	Mobile phase	Detection	Comments	Refs.
3 μm ODS column 10 cm × 4.6 mm I.D.	0.01 *M* phosphate buffer(pH = 3) : CH_3OH (19 : 1) (0.6 ml/min)	Ultraviolet (UV), 216 nm	Linear from 40–42.5 μg aspirin/ml Detection limit: 157 ng/ml Precision ranged from 0.12 to 1.95%	[72]
Bondapak ODS C18 (30 cm × 4 mm I.D.) 10 μm	0.03 *M* sodium acetate (pH = 3.5 with glacial acetic acid) : methanol (5 : 2) (1 ml/min)	UV, 280 nm	Separation from methanolic solution Linear from 0.85–12 mg aspirin/ml Detection limit: 2.7 ng Recovery: 100.4% with RSD (n = 6) of 0.98%	[3]
Nucleosil C8 (25 cm × 4.6 mm, 5 μm	H_2O : acetonitrile : H_3PO_4 (325 : 175 : 1); 1 ml/min	UV, 225 nm	Linear for 0.2–5 μg/ml Detection limit: 0.05 μg aspirin/ml	[73]
LiChrospher 100 RP-18 (5 μm)	KH_2PO_4 (pH 2.5)/acetonitrile	UV, 234 nm	Linear from 0.1–2 μg aspirin/ml Accuracy: 99.7–101.3%; RSD: 3.3–4.3% Detection limit: 0.05 μg/ml	[74]
Nucleosil C8 (25 cm × 4.6 mm I.D.) 5 μm	H_2O : methanol : acetonitrile : OPA (650 : 200 : 150 : 1) at 1 ml/min	UV, 225 nm	SPE from plasma in acid medium (SPE PEEK column, 10 mm × 4.3 mm I.D., packed with 30 μm Hypersil C18; washed with water : OPA (1000 : 1) at pH 2.5 for 2 min at 1 ml/min) Linear from 0.1–5.00 μg aspirin/ml Detection limit 0.04 μg/ml	[75]
Develosil ODS (10 μm)	Water : methanol (4 : 6)	FTIR		[76]
Spherisorb ODS-5 (25 cm × 4.6 mm)	H_2O : methanol : acetic acid (71 : 25 : 4; pH 2.5) 1.2 ml/min	UV, 254 nm	Linear from 2.5–10 mg/L	[63]

(Continued)

Table 1 Salicylic acids and esters. *(Continued)*

Stationary phase	Mobile phase	Detection	Comments	Refs.
C-18 (30 cm × 3.9 mm I.D., 10 μm) fitted with a C18 guard column (1 cm × 4.6 mm I.D., 30 μm)	0.01 *M* phosphate buffer (pH 7) : acetonitrile : methanol (58 : 26.3 : 15.7) 1 ml/min	UV, 262 nm	Linear from 5–50 μg diflunisal/ml	[77]
Spherisorb S5 ODS2 (15 cm × 3.8 mm, 5 μm) and a Novapak C18 guard column	Gradient elution (1 ml/min) 10% CH_3CN in 10 m*M* potassium phosphate buffer of pH 3.1 : 60% CH_3CN in 10 m*M* potassium phosphate buffer of pH 3.1 [100 : 0 (held for 1 min) to 1 : 1 (held for 20 min) over 5 min then to 0 : 100 (held for 10 min) over 10 min]	UV, 195–650 nm	250 μl blood mixed with 250 μl acetonitrile containing p-methylphenylphenylhydantoin (IS; 80 mg/L), set aside for 10 min then centrifuged at 10,000 g for 10 min Recovery: 100% for diflunisal	[78]
Brownlee RP-18 (10 cm × 4.6 mm) 5 μm	25 μ*M* ammonium phosphate buffer (pH 3.0) in 75% methanol	Amperometric at +0.9 V; UV, 254 nm	Plasma mixed with buffer solution (pH = 3.0), methanol, H_2O, and IS and centrifuged; the supernatant applied to a Sep-Pak C18 cartridge, washed with H_2O and the drugs eluted with methanol; after evaporating to dryness, the residue is dissolved in mobile phase	[79]
Hypersil ODS (25 cm × 4 mm) 5 μm	Acetonitrile—acetate buffer (pH 4.8 or 4.2)	UV, 254, 240, 280, 220, 260, 240, 280, and 360 nm	The drugs were extracted with acetonitrile Detection limits ranged from 1 mg/L to 5 mg/L The mentioned detection wavelengths are for diflunisal, indomethacin, fenoprofen, ibuprofen, ketoprofen, naproxen, mefenamic acid, and piroxicam, respectively;	[11]
4 μm Novapak C18 and Bondapak C18 Corasil guard column	Methanol–0.01 *M* Na_2HPO_4 (adjusted to pH 2.7 with H_3PO_4 and containing 4% of Na_2SO_4) (27 : 23), 2 ml/min	UV, 226 nm	Diflunisal recovery: 95% Linearity: 0.3–500 μg/ml	[60]

Table 2 Phenylacetic acids.

Stationary phase	Mobile phase	Detection	Comments	Refs.
Novapak C18 (15 cm × 3.9 mm I.D., 4 μm), Novapak C18 guard column (2 cm × 3.9 mm)	CH_3CN : 10 m*M* acetate buffer of pH 4 (21 : 29); 1 ml/min	UV, 210 nm	SPE (C18) from urine, washed with 1 ml CH_3CN : 0.1 *M* acetate buffer of pH 5 (3 : 7), an air segment of 1.5 ml for partial drying and eluted with 1 ml acetonitrile : buffer (1 : 1); the eluate is evaporated at 45°C under N_2, the residue dissolved in 0.2 ml mobile phase SPE (C18) from urine, washed with 1 ml CH_3CN : 0.1 *M* acetate buffer of pH 5 (3 : 7), an air segment of 1.5 ml for partial drying and eluted with 1 ml acetonitrile : buffer (1 : 1); the eluate is evaporated at 45°C under N_2, the residue dissolved in 0.2 ml mobile phase Linearity: 0.02–1 μg diclofenac sodium/ml	[80]
LiChroCART RP-18 (12.5 cm × 4 mm, 5 μm); Pelliguard LC-18 guard column (5.0 cm × 4.6 mm I.D., 40 μm)	CH_3CN : H_2O adjusted to pH 3.45 with acetic acid (2 : 3) (0.8 ml/min for 6.5 min and then 1.9 ml/min)	UV, 240 nm	Tablets dissolved in mobile phase Linearity: 90–300 μg diclofenac sodium/ml Average recovery: 100.7%	[16]
Regis SPS 100 RP-8 (15 cm × 4.6 mm I.D.); 5 μm	30 m*M* sodium acetate : CH_3CN (3 : 2), adjusted to pH 3 with 85% H_3PO_4, or CH_3CN : sodium acetate (1 : 1) 1.3 ml/min	Electrochemical detection at +0.95 V	Diclofenac sodium from human aqueous humor Linearity: 1–1,000 ng/ml diclofenac sodium Detection limit: 0.5 ng/ml	[66]
Shendon-Phenyl or Shendon-ODS (25 cm × 4.6 mm I.D.), 5 μm	11.1% CH_3OH in CO_2 at 45°C, or 80% CH_3OH containing 0.1% CH_3COOH; 1 ml/min)	UV, 225 or 254 nm	Tablets dissolved in CH_3OH Linearity: 0.3–20 μg/ml diclofenac sodium Detection limit: 0.1–0.2 μg/ml	[81]
Purospher RP-18 (12.5 cm × 4 mm I.D.), 40°C	CH_3OH : 20 m*M* H_3PO_4 (1 : 3) 0.8 ml/min	UV, 220 nm	Diclofenac from pharmaceuticals	[82]
Spherisorb C18 (25 cm × 4.6 mm, 5 μm)	CH_3CN : 0.1 *M* sodium acetate (7 : 13) at pH 6.3; 1 ml/min	UV, 278 nm	Linearity: 0.02 (detection limit)–5 μg/ml diclofenac Recovery of 0.02–4 μg/ml from plasma is 97.2–100.3%	[83]

(Continued)

Table 2 Phenylacetic acids. *(Continued)*

Stationary phase	Mobile phase	Detection	Comments	Refs.
Supercritical fluid chromatography: JASCO C18 (25 cm × 4 mm, 10 μm), 45°C	CO_2 containing 16.67% CH_3OH (3 ml/min), 9.81 MPa	UV, 220 nm	Ibuprofen from tablets	[84]
Zorbax C8 column (25 cm × 4.5 mm I.D.)	CH_3CN : 50 m*M* disodium hydrogen phosphate buffer of pH 3.3 (buffer A) (1 : 1); 1.5 ml/min	UV, 220 nm	Paracetamol, chlorzoxazone, and diclofenac sodium in drug formulations were shaken with CH_3CN; the solution is filtered and diluted with buffer A Linearity: 4–20 μg/ml diclofenac sodium; Average recovery of 50 mg is 99.24%.	[12]
Machery-Nagel-Nitrile (25 cm × 4 mm I.D.), 10 μm	H_2O : CH_3OH (17 : 3, containing 0.01 *M* sodium acetate and anhydrous acetic acid with the pH adjusted to 4.6) 2.5 ml/min	UV, 220 nm	Paracetamol, chlormezanone, and diclofenac sodium from tablets, methanolic solution Linearity: 2–200 μg/ml diclofenac sodium Recovery: 98–101.98%	[4]
Nucleosil 5C18 (10 cm × 3 mm I.D.) 5 μm	For urine: CH_3CN : 1% acetic acid (9 : 11), 0.5 ml/min For plasma: the same solvents from 48% CH_3CN (held for 8 min) to 90% CH_3CN from 8.1 to 9.9 min	UV, 220 nm	Alclofenac in plasma, extracted with ethyl ether, evaporated to dryness, and the residue dissolved in the mobile phase Alclofenac in urine, SPE on an Adsorbex C18 column with elution with CH_3OH : H_2O (4 : 1) Linearity: to 10 and 20 μg/ml with limits of quantitation of 0.1 and 1 μg/ml in plasma and urine, respectively	[19]
Hypersil C18 (10 cm × 4.6 mm I.D.), 5 μm	CH_3OH : 0.1 *M* acetic acid containing 0.01% heptanesulfonic acid (3 : 2) 1.5 ml/min	UV, 240 nm	Fenclofenac from plasma: adding 0.1 *M* phosphate buffer of pH 7.2 and H_2O; SPE on Isolute C18 preconditioned with CH_3OH and H_2O, washed with phosphate buffer and hexane and dried under reduced pressure (68 kPa) for 2 min, eluted with ethyl acetate : hexane (1 : 1), evaporated to dryness at 40°C under N_2; the residue dissolved in 0.1 ml of methanol plus 0.15 ml of phosphate buffer	[85]

Table 3 Carbo- and heterocyclic acetic acids.

Stationary phase	Mobile phase	Detection	Comments	Refs.
Alltima C8 (10 cm × 2.1 mm I.D.), 5 μm	CH_3OH : 40 m*M* ammonium acetate buffer of pH 5.1 (4 : 1) 0.3 ml/min	Electrospray MS; m/z = 357.9/139.0	Plasma is mixed with 50 m*M* ammonium formate buffer of pH 3.5 and IS (mefanamic acid; 100 mg/L in aqueous 50% methanol); the mixture is applied to C18 SPE cartridges preconditioned with methanol and 50 m*M* ammonium formate buffer of pH 3.5; after washing with 50 m*M* ammonium formate buffer of pH 3.5, the analytes were eluted with methanol and evaporated to dryness under air flow at 40°C; the sample is reconstituted with mobile phase Linearity: 5–2,000 μg/L indomethacin	[36]
Spherisorb column (20 cm × 3.9 mm I.D.), 5 μm	CH_3CN : 0.5% acetic acid (1 : 1) 1.5 ml/min	UV, 254 nm	Tissue homogenized with 0.25 *M* Na_2HPO_4 of pH 3.5; a portion is mixed with IS then extracted with CH_2Cl_2 and centrifugated at 2,000 g for 20 min; the extract is evaporated to dryness and the residue (from liver or muscle) is redissolved in methanol. For the residue resulting from fat, it is mixed with methanol, and the unstable emulsion obtained is allowed to stand for 10 min until total phase separation occurred Linearity: 20 ng/g (detection limit) to 500 ng/g indomethacin	[67]
μ-Bondapak C18 (25 cm × 4.6 mm I.D.) 10 μm; 30°C	CH_3OH : 0.035 *M* H_3PO_4 of pH 5.5 (19 : 6), 1 ml/min	UV, 260 nm	Plasma is mixed with IS solution, phosphate buffer of pH 7, and NaCl; the mixture is extracted with ethyl acetate; the organic phase is heated at 50°C to dryness, the residue is dissolved in methanol and centrifuged at 3,000 rpm Linearity: 0.125–50 μg/ml indomethacin Detection limit: 62.5 ng/ml	[68]
Chiralpak AD (25 cm × 4.6 mm), 10 μm and Chiralpak AD guard column (5 cm × 4.6 mm)	0.05% trifluoro acetic acid (TFA) in hexane : ethanol (17 : 3) 1 ml/min	UV, 340 nm	Enantiomers of sulindac	[56]
Spherisorb S5 ODS-2 (25 cm × 4.6 mm I.D.) 5 μm	2% acetic acid of pH 3.5 : CH_3CN : THF (25 : 24 : 1) 1 ml/min	UV, 340 nm	For sulindac from urine, the sample is injected directly or after dilution, acidification to 0.2 *M* with 1 *M* HCl and addition of 10 μg indomethacin (IS)	[56]

(Continued)

Table 3 Carbo- and heterocyclic acetic acids. *(Continued)*

Stationary phase	Mobile phase	Detection	Comments	Refs.
Inertsil ODS-2 (15 cm × 4.6 mm), 5 μm	50 m*M* phosphate buffer(pH = 5) : CH_3CN (29 : 21), 0.9 ml/min	UV, 230 or 320 nm	Urine samples acidified to pH 5 with acetate buffer and purified by SPE on a Sep-Pak silica cartridge; the NSAIDs were eluted from the cartridge with ethyl acetate Detection limits: 0.005 μg/ml for naproxen and 0.05 μg/ml for sulindac, piroxicam, loxoprofen, ketoprofen, felbinac, fenbufen, flurbiprofen, diclofenac, ibuprofen, and mefenamic acid in human urine	[47]
Octyl column (15 cm × 4.6 mm), 5 μm	CH_3CN : CH_3COOH : H_2O (75 : 2 : 123) 2 ml/min or 1 ml/min for feces	UV, 329 nm	Plasma is mixed with 50% H_3PO_4, indomethacin solution (IS), and extracted with CH_2Cl_2; the organic phase is evaporated to dryness under N_2 at 37°C and reconstituted in mobile phase Urine is treated at 37°C for 2 hr with betaglucuronidase and extracted as for plasma Fecal supernatants were mixed with IS, evaporated to dryness and reconstituted in mobile phase; Linearity: 0.025–10, 0.02–2, and 250–100 μg/ml for active metabolite of sulindac in plasma, urine, and feces, respectively	[58]
Hypersil ODS (15 cm × 4.5 mm), 5 μm; 17°C	CH_3OH : 0.02 *M* KH_2PO_4 (pH 4.5) (57 : 43) 1.25 ml/min	UV, 245 nm	Plasma is mixed with 0.15 *M* KH_2PO_4 buffer (pH = 3), IS, and ethyl ether; after centrifugation, the organic phase is evaporated to dryness and the residue is dissolved in the mobile phase Linearity: 10–1000 ng/ml acemetacin	[37]
Nucleosil 5 C18 (12.5 cm × 4.6 mm)	0.02 *M* phosphate buffer of pH 4.5 : CH_3OH (9 : 11) 1.4 ml/min	UV, 254 nm	Acemetacin is extracted from plasma (adjusted to pH = 3) with ethyl ether, the solvent is evaporated and the residue is dissolved in the mobile phase	[30]
LiChrosorb RP-18 (25 cm × 4 mm), 7 μm	1% aqueous acetic acid : acetonitrile (1 : 1) 1.3 ml/min	UV, 227 nm	Serum or urine is mixed with IS, diluted with H_2O, adjusted to pH = 1 with 1 *M* HCl, extracted twice with isooctane/isopropanol (19 : 1); the combined organic layers were evaporated to dryness with N_2 and reconstituted in mobile phase	[35]

μ-Bondapak C18 (25 cm × 5 mm)	Methanol-aq. 1% formic acid (77 : 23)	UV, 310 nm	Fentiazac is extracted from plasma at pH = 2 into CH_2Cl_2	[31]
LiChrosorb RP-8 (25 cm × 4 mm) 7 μm	Methanol : 5 m*M* phosphate buffer of pH 3 (4 : 1) 1 ml/min	UV, 254 nm	Fentiazac from tablets and suppositories is extracted with methanol Linearity: 8–18 μg/ml fentiazac	[86]
Brownlee silica (22 cm × 4.6 mm) 5 μm (23°C) in series with a 7 μm silica precolumn (1.5 cm × 4.6 mm)	5 m*M* sodium phosphate : H_3PO_4 buffer of pH 2.6 (19 : 1) containing 0 to 10% CH_3CN 1 ml/min	UV	Indomethacin, sulindac and tolmetin were extracted from capsules or table ts using aq. 0 to 10% acetonitrile	[87]
Zorbax ODS or ultrasphere ODS (25 cm × 4.6 mm) 5 μm or μ Bondapak C18 (30 cm × 3.9 mm) 10 μm	1.36 g/L KH_2PO_4 and 3.39 g/L of PIC A in H_2O : methanol : acetic acid (350 : 650 : 1) 1 ml/min	UV, 317 nm	Tolmetin from tablets or capsule powder is dissolved in and diluted with sodium zomepirac dihydrate solution (IS) and aq. 50% methanol Linearity: 10–30 μg/ml tolmetin; Detection limit: 1 μg/ml	[13]
Spherisorb ODS (12.5 cm × 4.9 mm) 5 μm	CH_3CN : aq. 1% H_3PO_4 (1 : 1) 2 ml/min	UV, 313 nm	Urine and plasma samples were centrifuged and an aliquot of the supernatant so lution is subjected to HPLC o n a cleanup column of Spherisorb ODS (4 cm × 4.6 mm), 10 μm) with a mobile phase (1.5 ml/min) of aq. 0.5% H_3PO_4 Linearity: 0.5–100 μg/ml zomepirac sodium	[88]

Table 4 Fenamic acids.

Stationary phase	Mobile phase	Detection	Comments	Refs.
Nucleosil C18 5 μm	H_2O : methanol (23 : 73) 0.8 ml/min	UV, 280 nm	Plasma containing flufenamic acid, mefenamic acid (IS), and 1 *M* HCl were mixed, then extracted with CH_2Cl_2 by shaking for 20 min; the organic phase is evaporated to dryness and the residue reconstituted in methanol Linearity: 0.5–15 μg/ml flufenamic acid Detection limit: 0.1 μg/ml	[41]
Supelcosil LC-8 (25 cm × 4.6 mm I.D.) 5 μm	50% acetonitrile adjusted to pH = 3.3 with CH_3COOH; 2 ml/min for 13 min then to 2.7 ml/min (held for 11 min) in 17 min	UV, 280 nm	Plasma-containing flufenamic acid is mixed with acetonitrile; after centrifugation, the supernatant is evaporated to dryness at 45°C under N2 and the residue is reconstituted in the mobile phase	[20]
LiChrosorb RP-18 (25 cm × 4 mm) 10 μm	65 m*M* ammonium acetate–methanol (1 : 3–3 : 7 in 6 min) 0.8 ml/min	UV, 282 nm	Flufenamic acid, mefenamic acid and tolfemanic acid were determined in serum, urine, and pharmaceuticals Detection limits (ng injected) were 0.5 for flufenamic acid, 0.7 for mefenamic acid, and 1.0 for tolfenamic acid	[89]
Shimpack CLC-ODS (15 cm × 6 mm)	Aq. 85% methanol containing 0.05 *M* $NaClO_4$ and 0.57% of acetic acid 0.6 ml/min	Electrochemical detection with a vitreous-carbon electrode at +1.0 V vs. Ag/AgCl	Serum is mixed with 10 m*M* phosphate buffer (pH 5.6) and *N*-phenylanthranilic acid as IS; proteins were removed by precipitation with acetonitrile, and, after centrifugation, the supernatant solution is concentrated to dryness and the residue is dissolved in methanol Serum recoveries of mefenamic acid (4–21 ng) and flufenamic acid (8–25 ng) were 96–119% and 98–103%, respectively; The corresponding detection limits were 0.4 and 6.3 pg	[21]
Nucleosil C18 (25 cm × 4.6 mm I.D.) 5 μm	H_2O adjusted to pH 3 with H_3PO_4/CH_3CN (45 : 55) 1.5 ml/mm	UV, 210 nm	Mefenamic acid sample is dissolved in methanol The method is applied in analysis of related substances in mefenamic acid	[90]
		UV, 210 nm		[5]

Hypersil ODS (20 cm × 2.1 mm I.D.) 5 μm	2 m*M* phosphate buffer of pH 3.2 : CH_3CN 19 : 1 to 1 : 1 (held for 10 min) in 20 min and then to 19 : 1 in 1 min; 0.4 ml/min		Blood containing mefenamic acid is vortex mixed with saturated NH_4Cl for 10 sec, and the mixture is extracted with ethyl acetate containing heptabarbitone (IS); the mixture is centrifuged at 2,500 rpm for 10 min, a portion of the upper organic layer is removed and evaporated to dryness; the residue is dissolved in CH_3CN and vortex mixed with CH_3CN-saturated hexane for 10 sec	
Vydac stainless steel C18 bonded-phase silica (25 cm × 4.6 mm I.D.) 5 μm	CH_3CN : 10 m*M* H_3PO_4 (3 : 2) of pH 2.6, 0.9 ml/min	UV, 280 nm	Plasma is vortex mixed with the IS (indomethacin for the determination of mefenamic acid or mefenamic acid for indomethacin in acetonitrile) and acetonitrile; the mixture is centrifuged at 9,000 g for 3 min, and a portion of the supernatant liquid is evaporated to dryness; the residue is dissolved in mobile phase Linearity: 0.1–10 μg/ml Detection limits: 0.06 and 0.08 μg/ml for indomethacin and mefenamic acid, respectively;	[22]
Spherisorb ODS (10 cm × 3 mm) 10 μm	CH_3OH : phosphate buffer (9 : 11) 0.85 ml/min	UV, 280 nm	Urine samples containing meclofenamic acid were hydrolyzed with 10 *M* NaOH, the pH is adjusted to 3 with H_3PO_4, and the analytes were extracted into CH_2Cl_2; the organic extracts were washed with citrate buffer of pH 5.2 and extracted with 0.1 *M* NaOH, the alkaline aq. phase is adjusted to pH 5.2 with H_3PO_4, and the analytes were extracted into heptane; the heptane is evaporated and the residue is dissolved in methanol	[32]
Stainless steel column (10 cm × 3.0 mm) packed with Spherisorb ODS (10 μm)	40% of methanol in phosphate buffer solution of pH 6.1, 0.8 ml/min	UV, 280 nm	Meclofenamic acid from plasma and citrate buffer solution (pH 4.6) containing diclofenac sodium (IS) were mixed with CH_2Cl_2; the mixture is centrifuged, the organic phase is evaporated to dryness, and the residue is dissolved in the mobile phase Linearity: 0.20–4.8 μg/ml meclofenamic acid	[42]
LiChrospher C18 (15 cm × 4.6 mm I.D.) 5 μm; 30°C	Methanol : 0.07 *M* phosphate buffer of pH 3 (9 : 1) 2 ml/min	UV, 286 nm	Linearity: 50–500% of the expected working assay of tolfenamic acid and RSD were <1%; Mean recoveries were 99.7%	[91]

(Continued)

Table 4 Fenamic acids. *(Continued)*

Stationary phase	Mobile phase	Detection	Comments	Refs.
LiChrospher 100 RP-18 (25 cm × 4 mm I.D.) 5 μm	CH_3CN : 10 m*M* H_3PO_4 (3 : 2) 1.1 ml/min	UV, 280 nm	Plasma containing tolfenamic acid is diluted with acetonitrile containing phenylbutazone (IS), vortex mixed for 1 min and centrifuged at 9,000 g for 3 min; the supernatant is separated and evaporated to dryness, and the residue is redissolved in mobile phase Linearity: 0.2–5 μg/ml telfenamic acid Detection limit: 50 ng/ml	[23]
LiChrosorb RP-18 (25 cm × 4 mm) 10 μm	Acetate buffer (pH 4.6) : CH_3OH (9 : 41) 1.9 ml : min	UV, 282 nm	Powdered capsule contents or suspension were dissolved in methanol; the diluted suspensions were sonicated for 10 min, centrifuged at 3,500 rpm for 10 min, and a portion of the supernatant solution is diluted with methanol. Portions of the solution. (1–3 ml for capsule contents or 10–30 ml for suspensions) were mixed with 6 ml of caffeine solution (IS) and diluted with methanol Linearity: 0.1–10.0 ng/μl tolfenamic acid	[6]
GSK ODS-2 C18 Microbore, 5 μm (15 cm × 1 mm I.D.)		UV or electrospray ionization MS	Samples containing niflumic acid is extracted with ethanol	[92]
Hypersil ODS (10 cm × 2.1 mm I.D.) 5 μm	Gradient elution with hexane : 95% propan-2-ol; 0.4 ml/min	Atmospherc pressure-ionization (API)-MS detection or PBMS detection	Urine containing flunixin is adjusted to pH 7 with 1 *M* NaOH (or 1 *M* HCl) and centrifuged at 500 g for 15 min supernatant is applied to a Bond Elut Certify II SPE ml cartridge and washed with H_2O, CH_3OH, and hexane. Flunixin is eluted with 10% acetic acid in hexane and naproxen (IS) for API-MS or ketoprofen (IS) for particle-beam (PB)-MS; the eluates were evaporated to dryness under N_2 and the residues were dissolved in methanol for API-MS or hexane : propan-2-ol (1 : 1; solvent B) for PB-MS.	[64]

Table 5 Propionic acids.

Stationary phase	Mobile phase	Detection	Comments	Refs.
Tris-(4-methyl benzoate) cellulose covalently bound to silica gel (15 cm × 4.6 mm I.D.) (10 μm)	Methanol/0.1*M* perchlorate buffer of pH 2 1 ml/min	UV, 230; 254 nm	Benoxaprofen, carprofen, fenoprofen, flurbiprofen, ibuprofen, ketoprofen, pirprofen, and tiaprofenic acid derivatized to their amides using 1-naphthylmethylamine or benzylamine in the presence of 1-hydroxybenzotriazole as catalyst and 1-ethyl-3-dimethylaminopropyl-carbodiimide as coupling agent	[93]
Ultron ES-OVM chiral column (15 cm × 4.6 mm) packed with ovomucoid protein chemically bonded to silica	Phosphate buffer (pH 5.8)/an organic modifier (e.g., methanol, ethanol, propanol, propan-2-ol, butanol, butan-2-ol, and 2-methylpropan-2-ol) 1 ml/min	fluorimetric (λ_{ex} = 227 nm) or UV at 214 nm	Racemic mixtures of flurbiprofen, benoxaprofen, benzoin, and verapamil	[94]
CHIRAL-AGP (50 and 10.0 cm × 4 mm I.D.) of (5 μm), CHIRAL-AGP precolumn (1 cm × 3 mm I.D.)	Buffers/uncharged modifiers such as methanol, ethanol, propan-1-ol, propan-2-ol, or acetonitrile; 0.9 ml/min	UV, 225 nm	Naproxen, tiaprofen, flurbiprofen, carprofen, ketoprofen, ibuprofen, fenoprofen, and indoprofen	[95]
Ultrasphere ODS (15 cm × 4.6 mm, 5 μm)	Gradient of 35% of acetonitrile 9 m*M* and 45 or 50% of acetonitrile 5 m*M*; 2 ml/min	λ_{em} = 365 nm, λ_{ex} = 235 or 290 nm for urine or plasma, respectively	Carprofen Plasma is acidified with H_3PO_4 and extracted with ethyl acetate, the organic phase is evaporated; residue dissolved in 28% of acetonitrile in aqueous 10 m*M* tetrabutylammonium hydrogen sulfate pH = 2.5 (solution A); Urine is mixed with solution A and centrifuged	[48]
LiChrosorb Si 60 (25 cm × 4 mm); similar precolumn (3 cm × 4 mm)	CH_2Cl_2 : methanol : acetic acid (98 : 1 : 1); 1.5 ml/min	λ_{ex} = 305 nm λ_{em} = 375 nm	Carprofen Plasma is extracted with butyl acetate in the presence of acetate buffer (pH 2.8)	[52]
C-18 Spherisorb (25 cm × 4.6 mm × 5 μm)	CH_3CN : 0.1 *M* sodium acetate (7 : 13), pH = 6.3, 1 ml/min	UV, 278 nm	Flurbiprofen and diclofenac. Plasma is spiked with IS solution, 2.5 *M O*-phosphoric acid is added, and the mixture is vortex mixed, and 1.5 ml hexane/propan-2-ol (4 : 1) is added; The mixture is vortexed and centrifuged The organic layer is separated and evaporated to dryness at 37°C under N_2 The residue is reconstituted in mobile phase	[53]

(Continued)

Table 5 Propionic acids. *(Continued)*

Stationary phase	Mobile phase	Detection	Comments	Refs.
C18 (25 cm × 4.6 mm × 5 μm)	Acetonitrile : H_2O_2 : H_3PO_4 (1200 : 800 : 1) 1.5 ml/min	$\lambda_{ex} = 250$ nm $\lambda_{em} = 285$ nm	Flurbiprofen from plasma: deproteinized by vortexing and centrifuging with acetonitrile	[24]
Spherisorb ODS2 (15 cm × 4 mm I.D.), 5 μm	Linear gradient elution with 0.1 *M* formate buffer of pH 3% methanol, (9 : 1–9 : 11 over 10 min, and to 0 : 100 over 20 min); 1.5 ml/min	UV, 254 nm	Ketoprofen, caffeine, indoprofen, fenbufen, naproxen, and ibuprofen in pharmaceutical formulations and blood plasma	[96]
YWG-C18 (25 cm × 4.6 mm I.D.)	380 mg NaH_2PO_4 and 50 mg Na_2HPO_4 in 1 L H_2O adjusted to pH 3 : methanol (1 : 3) 1 ml/min	UV, 220 nm	Ibuprofen Syrup is dissolved in and diluted with methanol. A portion of the solution is mixed with diphenylamine (IS) and the mixture is diluted with methanol	[7]
Column packed with an amide derivative made from (*R*)-1-naphthylglycine and 3,5-dinitrobenzoic acid; (25 cm × 4.6 mm I.D.)	Aqueous 70% methanol containing 0.01 *M* ammonium acetate with pH adjusted to 5.9 with acetic acid; 1 ml/min	UV, 254 nm	Ibuprofen enantiomers	[97]
Chiralcel OD column (15 cm × 4.6 mm I.D.) 25°C	Hexane : propan-2-ol, 100 : 1 containing 0.1% TFA; 1 ml/min	UV, 230 or 254 nm	Ibuprofen or flurbiprofen Plasma is applied to a Sep-pak C18 cartridge for SPE, with 10 ml H_2O for percolation and 5 ml acetonitrile for elution The eluate is evaporated then dissolved in mobile phase	[61]
LiChroCART RP-18	Acetonitrile : 10 m*M* phosphate buffer of pH 6.5 (19 : 31)	UV, 275 nm or fluorimetric $\lambda_{ex} = 275$ nm $\lambda_{em} = 433$ nm	Enantiomers of indoprofen in plasma Plasma is mixed with racemic indobufen (IS), acidified, and extracted with ethyl ether The drug is coupled with leucinamide via reaction with ethyl chloroformate; The enantiomers are then extracted into ethyl acetate and transferred into methanol	[38]

Hypersil HAS (15 cm × 4.6 mm I.D.), 7 μm; operated at 28°C	50 m*M* phosphate buffer of pH = 7.4 : acetonitrile (17 : 3); addition of 3.5% propan-2-ol and 15% acetonitrile if the phosphate concentration decreased from 50 to 25 m*M*; 0.6 ml/min	UV, 232 nm	Ketoprofen from human serum albumin. The unbound enantiomers in the mixed buffer (0.067 *M* phosphate and pH 7.4) solution of the drug racemate with human serum albumin were sampled with a microdialysis probe after 10 min incubation at 37°C After 12 min, the dialysate is collected for 30 min	[98]
Bioptic AV-1 (15 cm × 4.6 mm)	Acetonitrile : buffer pH 7, 0.1 *M* (5 : 95); 0.6 ml/min	UV, 254 nm	Ketoprofen, ibuprofen, and fenprofen enantiomers Samples were prepared in methanol	[99]
α 1 acid glycoprotein-immobilized silica	4 m*M* potassium dihydrogen phosphate buffer/propan-2-ol (199 : 1) 0.8 ml/min	UV, 263 nm	Inactive (*R*)-enantiomer in the pharmacologically active (*S*)-enantiomer of naproxen	[100]
Zorbax Sil (25 cm × 4.6 mm)	Cyclohexane : ethyl acetate (7 : 3), 0.8 ml/min	UV, 272 nm	Naproxen enantiomers	[101]
Tris-(4-methyl benzoate) cellulose covalently bound to silica gel (15 cm × 4.6 mm I.D.); 10 μm	Methanol : 0.1 *M* perchlorate buffer of pH 2; 1 ml/min	UV, 230 and 254 nm	Benoxaprofen, carprofen, fenoprofen, flurbiprofen, ibuprofen, ketoprofen, pirprofen, and tiaprofenic acid after derivatization to their amides using 1-naphthyl methylamine or benzylamine in the presence of 1-hydroxy benzotriazole as catalyst and 1–ethyl–3–dimethyl aminopropyl-carbodiimide as coupling agent	[102]

Table 6 Other acids.

Stationary phase	Mobile phase	Detection	Comments	Refs.
Chiralpak AD	Propan-2-ol : 90 m*M*	UV, 313 nm	Ketorolac and its enantiomers from blood	[103]
Chiral-AGP (10 cm × 4 mm, 5 μm) packed with α 1-acid glycoprotein immobilized on silica	NaH_2PO_4 : 10 m*M* Na_2HPO_4 : 2 m*M* dimethyloctylamine (pH 5.5; 17 : 183) 0.5 ml/min	UV, 320 nm	Ketorolac from plasma Plasma is spiked with S-(+)-naproxen in methanol-IS, extracted with tertbutyl methyl ether The aqueous phase is acidified to pH 1 with HCl, and backextracted into tertbutyl methyl ether The organic phase is removed, evaporated to dryness, and the residue redissolved in mobile phase Linearity : 20–20,000 ng/ml Quantitation limit: 5 ng/ml	[54]
C8 (25 cm × 4.6 mm); 10 μm	Acetonitrile : methanol : 0.01 *M* KH_2PO_4 of pH 4.2 (1 : 1 : 2)	UV, 319 nm	Ketorolac tromethamine in ophthalmic formulations after dilution with water Linearity: 20–70 μg/ml	[104]
Bondapak/μ Porasil C18 (15 cm × 3.9 mm)	Acetonitrile : 0.05 *M* H_3PO_4 (1 : 1) of pH 2, 1 ml/min	Vitreous C electrode in the pulsed mode at 0, 1000, and 12000 mV vs. Ag/AgCl	Ketorolac from tablets Linearity: 1–50 μ*M* ketorolac Detection limit: 0.359 μ*M*	[105]
Microsorb silica (15 cm × 4.6 mm), 5 μm	Ethyl acetate : hexane (2 : 3)	UV, 317 nm	Ketorolac from plasma Plasma is mixed with IS, acidified, extracted with ethyl acetate/hexane and the extract is derivatized with (+)-R-1-(1-naphthyl)ethylamine Linearity: 0.02–2 μg/ml	[50]

Chiral AGP (10 cm × 4 mm); 5 μm	Propan-2-ol : 0.05 *M* phosphate buffer of pH 5.5 (1 : 19), 0.4 ml/min	UV, 317 nm	Plasma (containing ketorolac) is mixed with IS and subjected to SPE on C18 columns using H_2O, aqueous 20% methanol, and hexane for washing and ethyl acetate : hexane (3 : 7) for elution The eluate is dried and reconstituted in mobile phase Linearity: 0.02–2 μg/ml	[44]
Waters Novapak C18 (15 cm × 3.9 mm) 4 μm	H_2O : acetonitrile : triethylamine : 85% H_3PO_4 : cyclam (800 : 200 : 10 : 3 : variable), 2 ml/min	UV, 255 nm	Analysis of tenidap	[106]
Novapak C18	Aqueous 35% methanol containing 2 m*M* triethylamine, 1 ml/min	MS	Tenidap and its stable isotope analog in serum IS solution in aqueous 75% methanol is vortex mixed with 0.05 *M* Na_2CO_3 Serum is added and the resulting mixture is again vortex mixed and extracted with ethyl acetate Following centrifugation, the organic layer is evaporated to dryness, the residue is dissolved in 2 m*M* triethylamine in methanol, sonicated and vortex mixed. Triethylamine–H_2O is added, and the solution is vortex mixed Linearity: 0.1–25 μg/ml tenidap	[55]

Table 7 Oxicams.

Stationary phase	Mobile phase	Detection	Comments	Refs.
Haisil 120 BD C18 (12 cm × 3 mm I.D.), 5 μm; at 30°C	THF : methanol : 30 m*M* H_3PO_4 buffer containing 0.015% KCl adjusted to pH 2.7 with 4 *M* NaOH (2 : 8 : 15); 0.5 ml/min	Amperometric at +0.65 V	Extraction of piroxicam from plasma, subcutaneous tissue or synovial capsule homogenate, synovial fluid from alkaline medium with CH_2Cl_2/hexane (1 : 4) and evaporation of the extract, with the residues dissolved in mobile phase Linearity: 0.72–600 ng/ml	[44]
LiChrospher 100 RP-18 (11.9 cm × 3 mm I.D.), 5 μm	Methanol : acetate buffer of pH = 4.3 (9 : 11)	UV, 280 nm and 254 nm	Piroxicam in 2.5% NH_4OH	[107]
Kromasil C18 (15 cm × 4 mm I.D.), 5 μm	Acetonitrile : 20 m*M* phosphate buffer of pH 3.1; 1 ml/min	UV, 360 nm	Piroxicam from plasma (A) plasma is applied to a Bond-Elut C8 SPE cartridges, washed with 2 ml 0.15 m*M* phosphate buffer of pH 3.5, dried under vacuum and eluted with 0.4 ml mobile phase; (B) plasma applied to the SPE cartridges packed with 40 μm C8-bonded phase, washed with 1 ml 75 m*M* phosphate buffer of pH 3.5 and eluted with mobile phase; Linearity: 0.05–2.5 μg/ml Detection limit: 25 ng/ml (A) and 7.5 ng/ml (B)	[71]
LiChrosorb RP-C8 (25 cm × 4.6 mm I.D.); 10 μm	0.02 *M* sodium acetate (containing 5 m*M* heptane sulfonic acid sodium salt; pH = 3.5) : methanol : acetonitrile (11 : 8 : 1); 1.5 ml/min	UV, 300 nm and 375 nm	Tenoxicam from tablets Powdered tablets equivalent to one tablet dissolved in methanol	[8]
Nucleosil C18 (25 cm × 4.6 mm I.D.), 5 μm	10 m*M* NaH_2PO_4, 1 m*M* sodium lauryl sulfate and acetonitrile : H_2O (7 : 13) adjusted to pH 2.8 with H_3PO_4; 1.5 ml/min	UV, 355 nm	Tenoxicam from plasma; to 1 ml plasma is added ketorolac (IS) and 100 μl 1.5% $ZnSO_4$; the sample is vortex mixed for 2 min; 3 ml methanol is added followed by further mixing for 2 min; buffer (0.44 ml; 100 m*M* NaH_2PO_4 and 10 m*M* sodium lauryl sulfate, adjusted to pH 2.8 with H_3PO_4) is added and after mixing the solution, it is centrifuged at 2000 g for 10 min at 27°C	[26]
LiChrospher 100 RP-18 (12.5 cm × 4 mm); 5 μm	0.1 *M* phosphate buffer of pH 7.4 : methanol (3 : 2); 1.1 ml/min	UV, 355 nm	Tenoxicam from plasma; plasma is mixed with 1 ml of 1 *M* HCl, 1 ml H_2O and 100 μl of piroxicam solution (IS) The mixture is extracted with 5 ml of CH_2Cl_2, mixed 5 min and centrifugated at 1800 g for 10 min The extract is evaporated to dryness under N at 30°C and the residue is dissolved in 100 μl mobile phase Linearity: 5–2000 ng/ml Detection limit: 5 ng/ml	[43]

Viosfer LC-18 (25 cm × 4.6 mm); 10 μm	Methanol : Na_2HPO_4 buffer of pH 3 (9 : 11); 1.2 ml/min	UV, 361 nm	Tenoxicam from plasma Plasma is mixed with 1-(2-hydroxyethyl)-3-hydroxy-7-chloro-1, 3-dihydro-(*O*-fluorophenyl)-2H-1, 4–benzodiazepin-2-one solution (3 μg/ml; IS) and the mixture is applied to a Bakerbond SPE extraction column Elution with acetonitrile, evaporation to dryness, and the residue dissolved in mobile phase Linearity: 0.1–10 μg/ml Detection limit: 0.05 μg/ml;	[108]
Hypersil ODS2 (250 mm × 4.6 mm) 5 μm	Methanol : H_2O : triethylamine : acetic acid (2,5 : 1,5 : 15 : 7)	UV, 355 nm	Meloxicam from plasma Plasma is acidified with HCl and extracted with ethyl ether Linearity: 0.03–8.0 mg/L Detection limit: 2.5 ng/ml Recovery: 93.6–97.7%	[39]
LiChrosphere RP-18	*Tris*-acetic acid buffer : tetrabutylammonium reagent : THF : acetonitrile	UV, 360 nm	Analysis of tenoxicam, piroxicam, isoxicam, cinnoxicam, meloxicam, and lornoxicam from pharmaceutical preparations	[109]
LiChrospher C18 (125 mm × 4.0 mm) 5 μm	Sodium acetate buffer (pH = 3.3; 170 m*M*) : acetonitrile (62 : 38)	UV, 355 nm	Meloxicam from plasma Plasma proteins were precipitated with $HClO_4$ (70%) and acetonitrile mixture (1 : 1 v/v) Linearity: 50–1500 ng/ml	[27]
LiChroCART 125-4 LiChrospher RP-8	0.05 *M* phosphate buffer : 30% acetonitrile : 25 m*M* *t*-butylamine (pH = 7.0)	UV, 364 nm	Meloxicam from plasma Plasma is introduced on the LiChrospher alkyl-diol silica precolumn using a 0.05 *M* phosphate buffer (pH = 6.0); The precolum is washed with the buffer and is backflushed with the mobile-phase transferring the analyte to the HPLC system	[69]
YMC Cyano (50 mm × 4.6 mm)	H_2O : acetonitrile : formic acid (50 : 50 : 0.1); 1.0 ml/min	MS in positive ion ESI mode	Meloxicam from plasma Plasma is treated with potassium phosphate (1.0 *M*, pH = 7.0) and extracted with ethyl acetate : cyclohexane (9 : 1) The organic layer is evaporated and reconstituted Linearity: 50.0–3000 ng/ml	[51]

Table 8 Pyrazolidindiones.

Stationary phase	Mobile phase	Detection	Comments	Refs.
Ultracarb 5 C18 ODS (15 cm × 4.6 mm I.D.) equipped with Supelcosil LC-18DB guard column (2 cm × 4.6 mm I.D.) at 35°C	0.02 *M* sodium phosphate buffer (pH = 7) : methanol (1 : 1); 1 ml/min	UV, 264 nm	Phenylbutazone from plasma; Plasma is ultrafiltered into a 2 ml centrifugal concentrator with molecular-mass cut-off membrane The ultrafiltrates is centrifuged at 4500 g for 2 hr at 4°C Linearity: 20–2000 ng/ml Detection limit: 3.4 ng/m Recovery: 89.9–93.7%	[18]
SPS-5PM-55-100-C18 (15 cm × 4.6 mm I.D.) and similar guard column	Acetonitrile : 0.05 *M* phosphate buffer (pH = 7.5) (3 : 17) 1 ml/min	UV, 265 nm	Phenylbutazone and oxyphenbutazone in serum Direct injection after filtering; Linearity: 0.5–20 μg/ml Detection limit: 0.25 μg/ml	[110]
LiChrospher 100 RP-18 (12.5 cm × 4 mm I.D.), 5 μm; similar guard column (40 × 4 mm) at 35°C	0.1 *M* acetic acid : methanol (9 : 11); 1 ml/min	UV, 254 nm	Phenylbutazone and oxyphenbutazone from plasma and urine Plasma is deproteinized by adding acetonitrile and centrifuging Urine is acidified with 2 *M* acetate buffer (pH = 3.5) and extracted with CH_2Cl_2 : methanol (19 : 1); the organic layer is washed with saturated $NaHCO_3$, filtered, and evaporated at 40°C to dryness under N_2; the residue is dissolved in methanol Detection limit: 0.5 μg/ml Quantitation limit: 1 μg/ml	[33]
LiChrosorb RP-18 (25 cm × 4.5 mm)	80% methanol (adjusted to pH 3 with H_3PO_4); 1 ml/min	UV, 250 nm	Azapropazone and its principal 8-hydroxy-metabolite in plasma, urine, and GI mucosa Mucosa homogenate is extracted with HCl_3 : methanol (4 : 1), the extract is evaporated to dryness and the residue is dissolved in methanol This solution or acidified urine or plasma, is cleaned on Sep-Pak C18 and eluated with methanol	[57]

Ultrasphere ODS (15 cm × 4.6 mm); 5 μm and Nova-Pak precolumn	Acetonitrile : 0.02 *M* $(NH_4)_2SO_4$ (11 : 9); 1.5 ml/min	UV, 340 nm	Indomethacin, suxibuzone, phenylbutazone, and oxyphenbutazone in plasma Plasma is mixed with indomethacin solution (IS); adjusted to pH = 3.4 with 0.345 *M* citrate buffer The solution is passed through a Bond Elut cartridge of phenyl sorbent, washed with H_2O, dried and eluted with hexane : ethyl ether (1 : 1); the organic phase is evaporated to dryness under N_2 at 40°C and the residue is dissolved in methanol Linearity: up to 50 μg/ml Detection limit: 0.05 μg/ml Recovery: 90.8–101.5%	[62]
LiChrosorb RP-8 (25 cm × 4 mm, 10 μm), LiChrosorb RP-8 (3 cm × 4 mm, 7 μm) as precolumn	Acetonitrile : methanol : H_2O (5 : 1 : 4) adjusted to pH 3.5 with acetic acid; 1 ml/min	UV, 254 nm	Oxyphenbutazone from tablets Powdered tablets equivalent to ~25 mg of oxyphenbutazone were dissolved in mobile phase Linearity: 10–100 μg/ml	[17]
Nucleosil 5C18 (10 cm × 3 mm)	[H_2O : acetic acid (30 : 1)] : methanol (2 : 3); 0.4 ml/min	UV, 240 nm	Mofebutazone and its 4-hydroxy-metabolite in plasma and urine To 1 ml of plasma were added 1 ml of 1 *M* acetate buffer (pH = 5.3) and 0.1 ml of phenylbutazone in methanol : ascorbic acid (100 : 1) as IS An ethyl ether extract of the mixture is evaporated to dryness at 40°C under N_2 and the residue is dissolved in methanol Linearity: 1–25 μg/ml	[40]
LiChrosorb RP-8 or -18 (15 cm × 4.6 mm, 5 μm)	Ethanol : citrate buffer of pH = 2.5 (12 : 13); 1 ml/min	UV, 254 nm	Acidified plasma or urine is extracted with 1-chloro butane : $CHCl_3$ (1 : 1) Detection limit: 10 ng/ml	[34]
Radial-Pak C18	Acetonitrile : 0.02 *M* phosphate buffer (pH = 7) (13 : 37)	UV, 254 nm	Sulphinpyrazine and four of its metabolites in plasma Deproteinization with acetonitrile Linearity: 0.2–100 μg/ml	[25]

Table 9 Non-acids compounds.

Stationary phase	Mobile phase	Detection	Comments	Refs.
μ Bondapak C18 (30 cm × 4 mm) 8–10 μm	H_2O : methanol (40 : 60) pH = 3.0 with H_3PO_4 1 ml/min	UV, 280 nm	Bufexamac in cream and ointment About 1 g of sample, containing ~50 mg of bufexamac, is mixed with hexane and aqueous 80% methanol; the layers were separated after shaking and the extraction is repeated with aqueous methanol Recovery 91.2–103.2%	[111]
Shim-pack CLC-ODS (15 cm × 4.6 mm I.D.)	Methanol : 50 m*M* acetate buffer at pH = 3.5 (13 : 7); 1 ml/min	UV, 254 nm	Determination of nabumetone in pharmaceutical products after the sample is dissolved in methanol Linearity: 86.4–345.6 μg/ml	[9]
Supelcosil LC-8 (15 cm × 4.6 mm, 5 μm)	H_2O : acetonitrile (50 : 50) containing 1.5 ml/L triethyl amine and 8 ml/L acetic acid; pH = 4.5; 2 ml/min	UV, 270 nm	Analysis of nabumetone and its major metabolite from plasma and tablets Powdered tablets (~one tablet) were sonicated in 30 ml aqueous 50% acetonitrile containing methoxy acetophenone (IS); the resulting solution is diluted with IS solution Plasma is shaken with 10 ml *n*-hexane : ethyl acetate (1 : 1) and 0.5 ml 1 *M* HCl; the mixture is centrifuged and the organic layer is evaporated to dryness; the residue is dissolved in aqueous 50% acetonitrile	[14]

			Recovery: 99.8–100.9%	
Spherisorb C18 (15 cm × 4.6 mm, 5 μm)	H_2O : acetonitrile (45 : 55) 1 ml/min	UV, 331 nm	Determination of nabumetone from pharmaceutical products Powdered tablets were dissolved in methanol with sonication then filtered The filtrate is diluted with the mobile phase and mixed with methanolic naproxen solution (IS) Linearity: 20–90 μg/ml	[10]
Wakosil ODS 5C18 (150 × 4.6 mm, 5 μm)	0.5 g of 1-heptanesulfonic acid sodium salt in 1 Lacetonitrile : water : triethyl amine (500 : 500 : 1); pH = 3 with H_3PO_4	UV, 270 nm or fluorimetric (λ_{ex} = 280 nm, λ_{em} = 350 nm)	Determination of naproxen and nabumetone in urine and pharmaceutical products Urine is purified by SPE (Bond-Elut Certify II)	[112]
μ Bondapak C18 (30 cm × 4 mm, 10 μm)	H_2O : acetonitrile (1 : 1) pH = 3; 2.0 ml/min	UV	Determination of proquazone from serum or urine Serum or urine is mixed with 0.2 *M* Na acetate buffer (pH = 5); the proteins were precipitated with H_2SO_4/Na_2WO_4; The obtained solution is extracted with $CHCl_3$, the organic layer is evaporated to dryness and the residue is dissolved in methanol Linearity: up to 2 μ*M* Detection limit: 0.02 μ*M*	[28]

Table 10 Compounds with alkaline character.

Stationary phase	Mobile phase	Detection	Comments	Refs.
LiChrospher 60 RP Select B (10 cm × 4.6 mm, 5 μm)	Acetonitrile : 0.05 *M* ammonium acetate (pH 7) (11 : 9); 0.9 ml/min	UV, 230 nm	Benzydamine hydrochloride is dissolved in H_2O Gels were dissolved in aqueous acetonitrile Creams were dissolved in propan-2-ol/THF	[113]
μ Bondapak C18 (30 cm × 3.9 mm), 10 μm	Methanol : acetonitrile : H_2O (9 : 10 : 1) containing 0.05% of aqueous 25% NH_3; 2 ml/min	Fluorimetric $\lambda_{ex} = 303$ nm; $\lambda_{em} = 377$ nm	Benzydamine from biological fluids Extracted from plasma or urine with ethyl ether Detection limit: 0.5 ng/ml in plasma, 1 ng/ml in urine	[29]
Novapak C18 (15 cm × 3.9 mm), 5 μm at 30°C	Acetonitrile : H_2O : anhydrous acetic acid (124 : 75 : 1), containing 5 m*M* Na-dodecyl sulfate at pH = 4; 0.9 ml/min	UV, 305 nm	Benzydamine hydrochloride in pharmaceutical products Gels were dissolved in H_2O : acetonitrile (1 : 1) Creams were dissolved in THF : propan-2-ol (1 : 2) Linearity: 18.75–600 μg/ml Detection limit: 3 μg/ml (gel); 7.8 μg/ml (cream)	[15]
ODP-50 (15 cm × 4.6 mm, 5 μm) at 55°C	5 m*M* tetrabutylammonium bromide in 0.02 *M* phosphate buffer of pH = 6.5 : acetonitrile : THF (30 : 5 : 1)	UV, 295 nm	Tiaramide metabolites in urine and plasma To 5 ml urine were added 100 μl IS, and 5 ml 0.5 *M* phosphate buffer (pH = 7); the mixture is vortexed, centrifugated 5 min at 3000 rpm, and purified with a Bond-Elut PH cartridge, washing with 4 × 10 ml ice-cold 50 m*M* phosphate buffer (pH = 7); the elution is made with 5 ml ice-cold 30% aqueous methanol To 3 ml plasma were added 60 μl IS and 5 ml 0.5 *M* phosphate buffer were added and prepared as above Linearity: up to 10 μg/ml; detection limit: 20 ng/ml	[70]
ODS-bonded material	Methanol : 15 m*M* phosphate buffer of pH 8 (11 : 9)	UV, 225 nm	Tiaramide and its metabolites were extracted with $CHCl_3$ from plasma at pH = 6; the organic phase is evaporated to dryness; the residue is dissolved in the mobile phase	[46]

Table 11 Sulphoanilide analog (nimesulide).

Stationary phase	Mobile phase	Detection	Comments	Refs.
RP C18	Linear gradient	UV, 240 and 280 nm	Nimesulide from plasma Recovery: 96.0%;	[114]
Supelcosil LC-18 DB	50 m*M* sodium phosphate buffer (pH = 3.0) : acetonitrile (gradient elution); 1 ml/min;	UV, 230 nm	Analysis of main urinary metabolites Urine is purified by solvent extraction before and after enzymatic hydrolysis	[115]
Spherisorb ODS 2 (12.5 cm × 4.6 mm)	50 m*M* phosphate buffer (pH = 5.5) containing 10% methanol; 1 ml/min	UV, 280 nm	Determination of nimesulide from biological media	[116]

Table 12 COX-2 inhibitors.

Stationary phase	Mobile phase	Detection	Comments	Refs.
BDS-Hypersil C18 (10 cm × 4.6 mm, 5 μm)	H_2O : acetonitrile (65 : 35); 1.2 ml/min	Postcolumn photolysis at 254 nm; fluorimetric $\lambda_{ex} = 250$ nm; $\lambda_{em} = 375$ nm	Determination of rofecoxib from plasma 1 ml plasma is vortex mixed 50 μl acetonitrile, 25 μl of 4-(4-methanesulponylphenyl)-3-(4-methyl phenyl)-5H-furan-2-one (IS; 0.4 μg/ml in acetonitrile) and 1 ml 0.1 *M* acetate buffer The mixture is extracted with 8 ml hexane : CH_2Cl_2 (1 : 1) and centrifuged at 1500 g for 5 min The organic layer is evaporated to dryness at 50°C under N_2 and the residue is reconstituted in 1 ml mobile phase Linearity: up to 100 ng/ml; detection limit: 0.5 ng/ml	[45]
Thermohypersil-Keystone C18 (250 mm × 4.6 mm) 5 m	H_2O : acetonitrile (60 : 40), 1 ml/min	UV, 272 nm	Determination of rofecoxib from plasma 1 ml of plasma is mixed with 0.3 ml of saturated borate solution, extracted with 3 ml of ethyl acetate and centrifuged at 3000 rpm for 10 min The organic layer is evaporated to dryness under N_2, the residue is dissolved in the mobile phase Linearity: 50–450 ng/ml; quantitation limit: 50 ng/ml	[49]
C18 (100 mm × 3.0 mm)	Acetonitrile : water (1 : 1) 0.4 ml/min	MS with chemical ionization	Determination of rofecoxib after extraction from basified plasma by solvent extraction; organic extract is dried and reconstituted in mobile phase	[59]
Novapak C 8 (150 mm × 3.8 mm)	Acetonitrile : tetrahydrofuran : sodium acetate buffer (pH = 5.0) (30 : 8 : 62)	UV, 215 nm	Determination of celecoxib plasma after SPE using C18 extraction cartridges Linearity: 40–4000 ng/ml; recovery: >88%	[117]

Octadecyl-bonded phase	Mobile phase containing acetonitrile and a phosphate buffer	UV	Determination of celecoxib from acidified plasma after SPE on a poly (divinyl benzene-co-*N*-vinyl pyrrolidone) and elution with a mixture of acetonitrile : methanol (1 : 1); the eluate is evaporated to dryness and the residue is dissolved in methanol Linearity: 0.01–2 mg/L Detection limit: 0.005 mg/L Quantitation limit: 0.002 mg/L	[65]
Zorbax XDB	Acetonitrile : water (50 : 50) containing 10 m*M* 4-methyl morpholine (pH = 6.0)	MS–MS	Determination of valdecoxib, its hydroxylated metabolite and carboxylic acid metabolite in human urine after SPE (Zymark RapidTrace automation system) Linearity: 1–200 ng/ml Quantitation limit: 1 ng/ml	[118]
Zorbax XDB-C8	Acetonitrile : water (50 : 50) containing 10 m*M* ammonium acetate	MS	Determination of valdecoxib and its hydroxylated metabolite in human plasma after SPE (Zymark RapidTrace automation system); Linearity: 0.5–200 ng/ml Quantitation limit: 0.5 ng/ml	[119]

For instance, the NSAIDs are extracted from biological media with different procedures.

1. Plasma is ultrafiltered into a centrifugal concentrator with a molecular-mass cut-off membrane, and the ultrafiltrate is centrifuged.[18]
2. The proteins from biological fluids are removed with acetonitrile,[11,17,19–25] methanol,[26] $HClO_4$/acetonitrile,[27] or H_2SO_4/Na_2WO_4,[28] and, after centrifugation, the supernatant solution is evaporated to dryness and the residue is dissolved in the mobile phase [20,22,23] or in methanol.[21]
3. By liquid–liquid extraction from the following:
   a. Urine with ethyl ether,[29] CH_2Cl_2,[30–32] CH_2Cl_2/methanol,[33] $CHCl_3$/1-chlorobutane,[34] or isooctane/isopropanol[35]
   b. Plasma with ethyl ether,[29,30,36–40] CH_2Cl_2,[30,41–43] CH_2Cl_2/hexane,[44,45] $CHCl_3$,[46] $CHCl_3$/1-chlorobutane,[34] ethyl acetate,[47–49] ethyl acetate/hexane,[14,50] ethyl acetate/cyclohexane,[51] butyl acetate,[52] hexane/propan-2-ol,[53] and tert butyl methyl ether[54]
   c. Serum with isooctane/isopropanol[35,55]
   d. Blood with ethyl acetate[45]
   e. Tissue with CH_2Cl_2,[56] CH_2Cl_2/hexane,[44] and $CHCl_3$/methanol[57]

The obtained solution is evaporated and the residue is reconstituted in mobile phase,[30,35–37,42–46,53,54,58,59] acetonitrile,[5] acetonitrile/water,[14] methanol,[21,33,40,47,56,57] triethylamine in methanol,[55] 28% CH_3CN in aqueous 10 m*M* tetrabutylammonium hydrogen sulfate, pH = 2.5.[48]

4. Separation by SPE is done at a controlled pH value for absorption and for elution.

For instance, the sample, more often in an acid medium, is applied to a C_{18} cartridge, this is washed with water,[60–62] water/*O*-phthaldehyde,[63] water/methanol/hexane,[50,64] methanol/CH_3CN,[65] CH_3CN/acetate buffer,[66] phosphate buffer/hexane,[67] ammonium formate buffer,[68] or phosphate buffer.[69,70]

For elution, solutions of methanol,[57,60] methanol/water,[36,70] acetonitrile,[43,61] acetonitrile/buffer,[66] 10% acetic acid in hexane,[64] ethyl acetate,[37] ethyl acetate/hexane,[50,67] ethyl ether/hexane,[62] or mobile phase are used.[69] The obtained solution is injected directly[63] or after evaporating to dryness in the normal condition or under nitrogen, the residue being dissolved in mobile phase,[43,50,60,61,66,68] methanol/buffer,[67] methanol,[62,64,65] or hexane/propan-2-ol.[64]

If the SPE is done on a C_8-bonded phase, then the cartridge is washed with a buffer with pH value lower than 4 and eluted with mobile phase.[71]

HPLC

Reverse-phase HPLC systems most often employ aqueous buffers, methanol, or acetonitrile as part of the mobile phase. The biological samples are injected, after purification, using one of the previously methods (e.g., liquid–liquid extraction or SPE), as well as aqueous or alcoholic extracts of pharmaceutical preparations. In addition, increased specificity of spectrophotometric detectors in HPLC often obviates the need for extraction cleanup prior the injection.

Because of the large number of individual nonsteroidal anti-inflammatory agents, the analytical conditions for HPLC will be presented for a few selected compounds.

In the context of this review, the procedures for some NSAIDs are briefly presented; for adapting a particular analytical procedure to the instrumentation available in a specific laboratory, we strongly recommend using the original literature for the most complete descriptions of the methods.

For convenience of the reader and analyst, the liquid chromatographic conditions included in this entry are summarized in tabular form (Tables 1–12). All entries are listed according to their chemical structures.

REFERENCES

1. Frolich, J.K. A classification of NSAIDs according to the relative inhibition of cyclooxygenase isoenzymes—Trends. Pharmacol. Sci. **1997**, *18* (1), 30–34.
2. Thomas, A.T.; Sibin, A.K.; Vinu, M.J. A drug utilization study to evaluate the rationality in the use of NSAID and anti Ulcer Agents. Calicut Med. J. **2003**, *1* (1), e9.
3. Nan, N.; Zhu, J.H. Reversed-phase HPLC determination for pain release compound preparation containing codeine phosphate and aspirin. Yaowu. Fenxi. Zazhi. **1999**, *19* (1), 7–9.
4. Argekar, A.P.; Shah, S.J. A fast and accurate HPLC method for the simultaneous determination of paracetamol, chlormezanone and diclofenac sodium in tablets. Indian Drugs **1997**, *34* (8), 437–442.
5. Lo, D.S.T; Chao, T.C.; Ng-Ong, S.E.; Yao, Y.J.; Koh, T.H. Acidic and neutral drugs screen in blood with quantitation using microbore high-performance liquid chromatography-diode array detection and capillary gas chromatography-flame ionization detection. Forensic Sci. Int. **1997**, *90* (3), 205–214.
6. Papadoyannis, I.; Georgarakis, M.; Samanidou, V.; Zotou, A. Rapid assay for the determination of tolfenamic acid in pharmaceutical preparations and biological fluids by high-performance liquid chromatography. J. Liq. Chromatogr. **1991**, *14* (15), 2951–2967.
7. Wang, R.L.; Zhang, Q.W.; Niu, L.H.; Dong, W.L. HPLC determination of ibuprofen in syrups. Yaowu Fenxi Zazhi **1999**, *19* (2), 136–137.

8. El-Walily, A.F.M; Blaih, S.M.; Barary, M.H.; El-Sayed, M.A.; Abdine, H.H.; El-Kersh, A.M. Simultaneous determination of tenoxicam and 2-aminopyridine using derivative spectrophotometry and high-performance liquid chromatography. J. Pharm. Biomed. Anal. **1997**, *15* (12), 1923–1928.
9. Zhao, Y.; Zhe, X.J.; Wang, N. Determination of nabumetone in its preparations by high-performance liquid chromatography. Yaowu Fenxi Zazhi **1999**, *19* (2), 139–140.
10. Sane, R.T.; Patel, M.K.; Kulkarni, U.D.; Tirodkar, V.B. Application of different analytical techniques for the quantitation of nabumetone from its dosage form. Indian Drugs **1993**, *30* (9), 468–472.
11. Streete, P.J. Rapid high-performance liquid-chromatographic methods for the determination of overdose concentrations of some non-steroidal anti-inflammatory drugs in plasma or serum. J. Chromatogr. Biomed. Appl. **1989**, *87*, 179–193, 495.
12. Ravisankar, S.; Vasudevan, M.; Nanjan, M.J.; Suresh, B. Reversed phase HPLC method for the estimation of paracetamol, chlorzoxazone and diclofenac sodium in formulations. Indian Drugs **1997**, *34* (11), 663–665.
13. Stromberg, R. Statistical optimization of a reversed-phase ion-pair liquid-chromatographic method for the analysis of tolmetin sodium in dosage forms. J. Chromatogr. **1988**, *448* (1), 1–9.
14. Al-Momani, I.F. Determination of nabumetone and its major metabolite in plasma and tablet formulations by reverse-phase HPLC. Anal. Lett. **1997**, *30* (14), 2485–2492.
15. Benson, H.A.E.; McElnay, J.C. High-performance liquid chromatography assay for the measurement of benzydamine hydrochloride in topical pharmaceutical preparations. J. Chromatogr. **1987**, *394* (2), 395–399.
16. Gonzalez, L.; Yuln, G.; Volonte, M.G. Determination of cyanocobalamin, betamethasone and diclofenac sodium in pharmaceutical formulations, by high-performance liquid chromatography. J. Pharm. Biomed. Anal. **1999**, *20* (3), 487–492.
17. Shakya, A.K.; Talwar, N.; Singhai, A. High-performance liquid-chromatographic determination of oxyphenbutazone in tablets. Indian Drugs **1991**, *28* (4), 192–193.
18. de-Veau, E.J.I. Determination of non-protein bound phenylbutazone in bovine plasma using ultrafiltration and liquid chromatography with ultraviolet detection. J. Chromatogr. B, Biomed. Appl. **1999**, *721* (1), 141–145.
19. Delbeke, F.T.; Landuyt, J.; Debackere, M. Determination of alclofenac in equine plasma and urine by high-performance liquid chromatography. J. Chromatogr. Biomed. Appl. **1993**, *132* (2), 209–214, 621.
20. Benoni, G.; Terzi, M.; Adami, A.; Grigolini, L.; Del-Soldato, P.; Cuzzolin, L. Plasma concentrations and pharmacokinetic parameters of nitrofenac using a simple and sensitive HPLC method. J. Pharm. Sci. **1995**, *84* (1), 93–95.
21. Shimada, K.; Nakajima, M.; Wakabayashi, H.; Yamato, S. Determination of mefenamic and flufenamic acids in serum by HPLC with electrochemical detection. Bunseki Kagaku **1989**, *38* (11), 632–635.
22. Niopas, I.; Mamzoridi, K. Determination of indomethacin and mefenamic acid in plasma by high-performance liquid chromatography. J. Chromatogr. B, Biomed. Appl. **1994**, *656* (2), 447–450.
23. Niopas, I.; Georgarakis, M. Determination of tolfenamic acid in human plasma by HPLC. J. Liq. Chromatogr. **1995**, *18* (13), 2675–2682.
24. Park, K.M.; Gao, Z.G.; Kim, C.K. Assay of flurbiprofen in rat plasma using HPLC with fluorescence detection. J. Liq. Chromatogr. Relat. Technol. **1997**, *20* (12), 1849–1855.
25. Tam, Y.K.; Ferguson, S.M.; Yau, M.L.; Wyse, D.G. Simple and rapid high-performance liquid-chromatographic method for analysis of sulphinpyrazine and four of its metabolites in human plasma. J. Chromatogr. Biomed. Appl. **1984**, *35* (2), 310, 438–444.
26. Mason, J.L.; Hobbs, G.J. Simple method for the analysis of tenoxicam in human plasma using high-performance liquid chromatography. J. Chromatogr. B, Biomed. Appl. **1995**, *665* (2), 410–415.
27. Dasandi, B.; Shivaprakash, S.H.; Bhat, K.M. LC determination and pharmacokinetics of meloxicam. J. Pharm. Biomed. Anal. **2002**, *28* (5), 999–1004.
28. Lempiainen, M.; Makela, A.L. Determination of proquazone and its *m*-hydroxy-metabolite by high-performance liquid chromatography. Clinical application: pharmacokinetics of proquazone in children with juvenile rheumatoid arthritis. J. Chromatogr. Biomed. Appl. **1985**, *42* (1), 105–113, 341.
29. Baldock, G.A.; Brodie, R.R.; Chasseaud, L.F.; Taylor, T. Determination of benzydamine and its N-oxide in biological fluids by high-performance liquid chromatography. J. Chromatogr. Biomed. Appl. **1990**, *94* (1), 113–123, 529.
30. Schoellnhammer, G.; Dell, H.D.; Doersing, K.; Kamp, R. Quantitative determination of acemetacin and its metabolite indomethacin in blood and plasma by column liquid chromatography. J. Chromatogr. Biomed. Appl. **1986**, *48* (2), 331–338, 375.
31. Dowell, P.S. Simultaneous determination of fentiazac and *p*-hydroxyfentiazac in plasma by high-performance liquid chromatography with ultra-violet detection. Analyst (London) **1983**, *108* (1293), 1535–1537.
32. Johansson, I.M.; Anler, E.L.; Bondesson, U.; Schubert, B. Isolation of meclofenamic acid and two metabolites from equine urine: a comparison between horse and man. J. Pharm. Biomed. Anal. **1986**, *4* (2), 171–179.
33. Neto, L.M.R; Andraus, M.H.; Salvadori, M.C. Determination of phenylbutazone and oxyphenbutazone in plasma and urine samples of horses by high-performance liquid chromatography and gas chromatography-mass spectrometry. J. Chromatogr. B, Biomed. Appl. **1996**, *678* (2), 211–218.
34. Lentjes, E.G.W.M.; Tan, Y.; Van-Ginneken, C.A.M Determination of sulphinpyrazone and four metabolites in plasma and urine by high-pressure liquid chromatography. Pharm. Weekbl Sci. Ed. **1985**, *7* (6), 252–259.
35. Koupai-Abyazani, M.R.; Esaw, B.; Laviolette, B. Etodolac in equine urine and serum: determination by high-performance liquid chromatography with ultraviolet detection, confirmation and metabolite identification by atmospheric pressure ionization mass spectrometry. J. Anal. Toxicol. **1999**, *23* (3), 200–209.
36. Taylor, P.J.; Jones, C.E.; Dodds, H.M.; Hogan, N.S.; Johnson, A.G. Plasma indomethacin assay using high-

performance liquid chromatography-electrospray tandem mass spectrometry: application to therapeutic drug monitoring and pharmacokinetic studies. Ther. Drug. Monit. **1998**, *20* (6), 691–696.
37. Notarianni, L.J.; Collins, A.J. Method for the determination of acemetacin, a non-steroidal anti-inflammatory drug, in plasma by high-performance liquid chromatography. J. Chromatogr. Biomed. Appl. **1987**, *57*, 305–308, 413.
38. Bjorkman, S. Determination of the enantiomers of indoprofen in blood plasma by high-performance liquid chromatography after rapid derivatization by means of ethyl chloroformate. J. Chromatogr. Biomed. Appl. **1985**, *40* (2), 339–346.
39. Ding, Li; Chen, H.; Jiang, H.; Hou, Y.; Zhang, Z. Determination of meloxicam in human plasma by HPLC and relative bioavailability of meloxicam dispersible tablets. Zhongguo Yiyao Gongye Zazhi **2002**, *33* (3), 131–133.
40. Delbeke, F.T.; Debackere, M. Determination of mofebutazone and its 4-hydroxy-metabolite in plasma and urine by high-performance liquid chromatography. J. Chromatogr. **1986**, *369* (2), 440–444.
41. Cerretani, D.; Micheli, L.; Fiaschi, A.I.; Giorgi, G. High-performance liquid chromatography of flufenamic acid in rat plasma. J. Chromatogr. B, Biomed. Appl. **1996**, *678* (2), 365–368.
42. Johansson, I.M.; Eklund, M.L. Liquid-chromatographic determination of meclofenamic acid in equine plasma. J. Liq. Chromatogr. **1984**, *7* (8), 1609–1626.
43. Munera-Jaramillo, M.I.; Botero-Garces, S. Determination of tenoxicam in plasma by high-performance liquid chromatography. J. Chromatogr. Biomed. Appl. **1993**, *127* (2), 349–352, 616.
44. De-Jager, A.D.; Ellis, H.; Hundt, H.K.L; Swart, K.J.; Hundt, A.F. High-performance liquid chromatographic determination with amperometric detection of piroxicam in human plasma and tissues. J. Chromatogr. B, Biomed. Appl. **1999**, *729* (1–2), 183–189.
45. Woolf, E.; Fu, I.; Matuszewski, B. Determination of rofecoxib, a cyclooxygenase-2 specific inhibitor, in human plasma using high-performance liquid chromatography with post-column photochemical derivatization and fluorescence detection. J. Chromatogr. B, Biomed. Appl. **1999**, *730* (2), 221–227.
46. Naito, S.; Tanase, A.; Yoshihara, H.; Tominaga, H. Simultaneous determination of tiaramide and its metabolites by high-performance liquid chromatography. Pharm. Res. **1985**, *2* (3), 140–142.
47. Hirai, T.; Matsumoto, S.; Kishi, I. Simultaneous analysis of several non-steroidal anti-inflammatory drugs in human urine by high-performance liquid chromatography with normal solid-phase extraction. J. Chromatogr. B, Biomed. Appl. **1997**, *692* (2), 375–388.
48. Iwakawa, S.; Suganuma, T.; Lee, S.F.; Spahn, H.; Benet, L.Z.; Lin, E.T. Direct determination of diastereomeric carprofen glucuronides in human plasma and urine and preliminary measurements of stereoselective metabolic and renal elimination after oral administration of carprofen in man. Drug Metab. Dispos. **1989**, *17* (4), 414–419.
49. Mandal, U.; Ganesan, M.; Jayakumar, M.; Pal, T.K.; Chattaraj, T.K.; Ray, K.; Banerjee, S.N. High performance liquid chromatographic determination of Cox-2 inhibitor rofecoxib in human plasma. JIMA **2003**, *10* (08),
50. Tsina, I.; Tam, Y.L.; Boyd, A.; Rocha, C.; Massey, I.; Tarnowski, T. An indirect (derivatization) and a direct HPLC method for the determination of the enantiomers of ketorolac in plasma. J. Pharm. Biomed. Anal. **1996**, *15* (3), 403–417.
51. http://www.cedracorp.com/CEDRA_meloxicam_abstract.htm (accessed August 2005).
52. Ascalone, V.; Dal-Bo, L. Rapid and simple determination of carprofen in plasma by high-performance liquid chromatography with fluorescence detection. J. Chromatogr. Biomed. Appl. **1983**, *27* (1), 230–236, 276.
53. Giagoudakis, G.; Markantonis, S.L. An alternative high-performance liquid-chromatographic method for the determination of diclofenac and flurbiprofen in plasma. J.Pharm. Biomed. Anal. **1998**, *17* (4–5), 897–901.
54. Campanero, M.A.; Lopez Ocariz, A.; Garcia Quetglas, E.; Sadaba, B.; Azanza, J.R. Determination of ketorolac enantiomers in plasma using enantioselective liquid chromatography. Application to pharmacokinetic studies. Chromatographia **1998**, *48* (3–4), 203–208.
55. Avery, M.J.; Mitchell, D.Y.; Falkner, F.C.; Fouda, H.G. Simultaneous determination of tenidap and its stable isotope analog in serum by high-performance liquid chromatography—atmospheric pressure chemical-ionization tandem mass spectrometry. Biol. Mass. Spectrom. **1992**, *21* (7), 353–357.
56. Slovakova, A.; Freiin-von-Maltzan, X.; Patel, B.K.; Drake, A.F.; Hutt, A.J. Chromatographic resolution, chiroptical characterization and urinary excretion of the enantiomers of sulindac. Chromatographia **1998**, *48* (5–6), 369–376.
57. Rainsford, K.D. Distribution of azapropazone and its principal 8-hydroxy-metabolite in plasma, urine and gastrointestinal mucosa determined by H.P.L.C. J. Pharm. Pharmacol. **1985**, *37* (5), 341–345.
58. Ray, G.F.; Lanman, R.C.; Fu, C.J.; Paranka, N.S.; Pamukcu, R.; Wheeler, S.C. Determination of FGN-1 (an active metabolite of sulindac) in human plasma, urine, and faeces by HPLC. J. Pharm. Biomed. Anal. **1995**, *14* (1–2), 213–220.
59. Chavez-Eng, C.M.; Constanzer, M.L.; Matuszewski, B.K. Determination of rofecoxib (MK-0966), a cyclooxygenase-2 inhibitor, in human plasma by high-performance liquid chromatography with tandem mass spectrometric detection. J. Chromatogr. B Biomed. Sci. Appl. **2000**, *748* (1), 31–39.
60. Dickinson, R.G.; King, A.R. Reactivity considerations in the analysis of glucuronide and sulphate conjugates of diflunisal. Ther. Drug. Monit. **1989**, *11* (6), 712–720.
61. Kanazawa, H.; Kunito, Y.; Matsushima, Y.; Okubo, S.; Mashige, F. Stereospecific analysis of chiral drugs in plasma by chromatography-chiroptical detector. Chromatography **1999**, *20* (1), 81–87.
62. Caturla, M.C.; Cusido, E. Solid-phase extraction for the high-performance liquid-chromatographic determination of indomethacin, suxibuzone, phenylbutazone and oxyphenbutazone in plasma, avoiding degradation of compounds. J. Chromatogr. Biomed. Appl. **1992**, *119* (1), 101–107, 581.

63. Ogunbona, F.A. Simultaneous liquid-chromatographic determination of aspirin and the metabolites in human urine. J. Chromatogr. Biomed. Appl. **1986**, *50*, 377, 471–474.
64. Stanley, S.M.R; Owens, N.A.; Rodgers, J.P. Detection of flunixin in equine urine using high-performance liquid chromatography with particle-beam and atmospheric-pressure-ionization mass spectrometry after solid-phase extraction. J. Chromatogr. B, Biomed. Appl. **1995**, *667* (1), 95–103.
65. Guermouche, M.H.; Gharbi, A. Simplified solid-phase extraction procedure and liquid chromatographic determination of celecoxib in rat serum. Chromatographia **2004**, *60* (5–6), 341.
66. Kuhlmann, O.; Stoldt, G.; Struck, H.G.; Krauss, G.J. Simultaneous determination of diclofenac and oxybuprocaine in human aqueous humor with HPLC and electrochemical detection. J. Pharm. Biomed. Anal. **1998**, *17* (8), 1351–1356.
67. Cristofol, C.; Perez, B.; Pons, M.; Valladares, J.E.; Marti, G.; Arboix, M. Determination of indomethacin residues in poultry by high-performance liquid chromatography. J. Chromatogr. B, Biomed. Appl. **1998**, *709* (2), 310–314.
68. Zhang, D.; Zeng, J.Z.; Bianba, C.; Jiang, X.H. Determination of plasma drug concentration and bioavailability of indomethacin controlled release capsule by high-performance liquid chromatography. Sepu. **1997**, *15* (6), 515–517.
69. Baeyens, W.R.G.; Van der Weken, G.; D'haeninck, E.; Garcia Campana, A.M.; Vankeirsbilck, T.; Vercauteren, A.; Deprez, P. Application of an alkyl–diol silica precolumn in a column-switching system for the determination of meloxicam in plasma. J. Pharm. Biomed. Anal. **2003**, *32* (4), 839–846.
70. Takeda, A.; Shinohara, T. Simultaneous analysis of tiaramide metabolites in horse urine and plasma by solid-phase extraction and reversed-phase ion-pair liquid chromatography. J. Anal. Toxicol. **1995**, *19* (6), 435–442.
71. Yritia, M.; Parra, P.; Fernandez, J.M.; Barbanoj, J.M. Piroxicam quantitation in human plasma by high-performance liquid chromatography, with online and off-line solid-phase extraction. J. Chromatogr. A, **1999**, *846* (1–2), 199–205.
72. Spell, J.C.; Stewart, J.T. Analysis of an analgesic mixture utilizing a non-porous octadecylsilane stationary phase for reversed-phase fast HPLC. J. Liq. Chromatogr. Relat. Technol. **1999**, *22* (2), 297–305.
73. McMahon, G.P.; O′Connor, S.J.; Fitzgerald, D.J.; le-Roy, S.; Kelly, M.T. Determination of aspirin and salicylic acid in transdermal perfusates. J. Chromatogr. B, Biomed. Appl. **1998**, *707* (1–2), 322–327.
74. Pirola, R.; Bareggi, S.R.; De-Benedittis, G. Determination of acetylsalicylic acid and salicylic acid in skin and plasma by high-performance liquid chromatography. J. Chromatogr. B, Biomed. Appl. **1998**, *705* (2), 309–315.
75. McMahon, G.P.; Kelly, M.T. Determination of aspirin and salicylic acid in human plasma by column-switching liquid chromatography using online solid-phase extraction. Anal. Chem. **1998**, *70* (2), 409–414.
76. Fujimoto, C.; Oosuka, T.; Jinno, K. New sampling technique for reversed-phase liquid chromatography–Fourier-transform infra-red spectrometry. Anal. Chim. Acta **1985**, *178* (2), 159–167.
77. Ugwu, S.O.; Alcala, M.J.; Bhardwaj, R.; Blanchard, J. Characterization of the complexation of diflunisal with hydroxypropyl-β-cyclodextrin. J. Pharm. Biomed. Anal. **1999**, *19* (3–4), 391–397.
78. Drummer, O.H.; Kotsos, A.; McIntyre, I.M. Class-independent drug screen in forensic toxicology using a photodiode array detector. J. Anal. Toxicol. **1993**, *17* (4), 225–229.
79. Kazemifard, A.G.; Moore, D.E. Liquid chromatography with amperometric detection for the determination of non-sterodial anti-inflammatory drugs in plasma. J. Chromatogr. Biomed. Appl. **1990**, *98*, 125–132, 533.
80. Bakkali, A.; Corta, E.; Berrueta, L.A.; Gallo, B.; Vicente, F. Study of the solid-phase extraction of diclofenac sodium, indomethacin and phenylbutazone for their analysis in human urine by liquid chromatography. J. Chromatogr. B, Biomed. Appl. **1999**, *729* (1–2), 139–145.
81. Patil, S.T.; Sundaresan, M.; Bhoir, I.C.; Bhagwat, A.M. Packed column supercritical-fluid-chromatographic separation and estimation of acetaminophen, diclofenac sodium and methocarbamol in pharmaceutical dosage forms. Talanta **1998**, *47* (1), 3–10.
82. Battermann, G.; Cabrera, K.; Heizenroeder, S.; Lubda, D. HPLC analysis of active ingredients of pharmaceuticals. LaborPraxis **1998**, *22* (9), 30.32–34.
83. Giagoudakis, G.; Markantonis, S.L. An alternative high-performance liquid-chromatographic method for the determination of diclofenac and flurbiprofen in plasma. J. Pharm. Biomed. Anal. **1998**, *17* (4–5), 897–901.
84. Bhoir, I.C.; Raman, B.; Sundaresan, M.; Bhagwat, A.M. Isocratic simultaneous supercritical fluid chromatography—separation and estimation of ibuprofen and methocarbamol in solid dosage form. Indian Drugs **1998**, *35* (3), 134–139.
85. Taylor, M.R.; Westwood, S.A. Quantitation of phenylbutazone and oxyphenbutazone in equine plasma by high-performance liquid chromatography with solid-phase extraction. J. Chromatogr. A, **1995**, *697* (1–2), 389–396.
86. Cavrini, V.; Di-Pietra, A.M.; Raggi, M.A. Analysis of fentiazac in pharmaceutical dosage forms by reversed-phase high-performance liquid chromatography. J. Pharm. Biomed. Anal. **1983**, *1* (2), 235–240.
87. Lampert, B.M.; Stewart, J.T. Determination of non-steroidal anti-inflammatory analgesics in solid dosage forms by high-performance liquid chromatography on underivatized silica with aqueous mobile phase. J. Chromatogr. **1990**, *504* (2), 381–389.
88. Mueller, H.; Zulliger, H.W. Continuous body-fluid monitoring for zomepirac by fully automated high-performance liquid chromatography. Arzneim. Forsch. **1985**, *35* (I)(1), 152–154.
89. Papadoyannis, I.N.; Zotou, A.C.; Samanidou, V.F. Simultaneous reversed-phase gradient-HPLC analysis of anthranilic acid derivatives in anti-inflammatory drugs and samples of biological interest. J. Liq. Chromatogr. **1992**, *15* (11), 1923–1945.
90. Miller, J.H.Mc.B.; Ceva, P.; Dujardin, V.; Skellern, G.G.; Herne, S. The development of a liquid-chromatographic method to limit related substances in mefenamic acid and a survey of the purity of samples of diverse origin. Pharmeuropa **1998**, *10* (4), 502–509.
91. Rozou, S.; Antoniadou Vyza, E. An improved HPLC method overcoming Beer's law deviations arising from

supramolecular interactions in tolfenamic acid and cyclodextrins complexes. J. Pharm. Biomed. Anal. **1998**, *18* (4–5), 899–905.
92. Song, Y.; Her, G.R.; Wen, K.C. Analysis of synthetic drugs in adulterated Chinese medicine by high-performance liquid chromatography-electrospray mass spectrometry. Yaowu Shipin. Fenxi. **1997**, *5* (4), 295–301.
93. van-Overbeke, A.; Baeyens, W.; van-den-Bossche, W.; Dewaele, C. Separation of 2-arylpropionic acids on a cellulose-based chiral stationary phase by RP [reversed-phase]-HPLC. J. Pharm. Biomed. Anal. **1994**, *12* (7), 901–909.
94. Iredale, J.; Aubry, A.F.; Wainer, I. Effects of pH and alcoholic organic modifiers on the direct separation of some acidic, basic and neutral compounds on a commercially available ovomucoid column. Chromatographia **1991**, *31* (7–8), 329–334.
95. Hermansson, J.; Hermansson, I. Dynamic modification of the chiral bonding properties of a CHIRAL-AGP column by organic and inorganic additives. Separation of enantiomers of anti-inflammatory drugs. J. Chromatogr. A, **1994**, *666* (1–2), 181–191.
96. Martin, M.J.; Pablos, F.; Gonzalez, A.G. Simultaneous determination of caffeine and non-steroidal anti-inflammatory drugs in pharmaceutical formulations and blood plasma by reversed-phase HPLC from linear gradient elution. Talanta **1999**, *49* (2), 453–459.
97. Zhang, Y.H.; Yun, Z.H. Direct resolution of ibuprofen enantiomers by reversed-phase high-performance liquid chromatography with an amide derivative as chiral stationary phase. Fenxi Huaxue **1999**, *27* (3), 309–311.
98. Zou, H.F.; Wang, H.L.; Zhang, Y.K. Stereoselective binding of warfarin and ketoprofen to human serum albumin determined by microdialysis combined with HPLC. J. Liq. Chromatogr. Relat. Technol. **1998**, *21* (17), 2663–2674.
99. Haque, A.; Stewart, J.T. Chiral separations of selected pharmaceuticals on avidin column. J. Liq. Chromatogr. Relat. Technol. **1998**, *21* (17), 2675–2687.
100. Rose, U.; Kaltenbach, T. Control of the enantiomeric purity of S-naproxen by chiral chromatography. Pharmeuropa **1999**, *11* (1), 16–20.
101. Xu, X.Z.; Xu, G.L.; Xia, X.J. Separation of naproxen enantiomers by high-performance liquid chromatography. Fenxi Huaxue **1998**, *26* (4), 435–438.
102. van-Overbeke, A.; Baeyens, W.; van-den-Bossche, W.; Dewaele, C. Separation of 2-arylpropionic acids on a cellulose-based chiral stationary phase by RP [reversed-phase]-HPLC. J. Pharm. Biomed. Anal. **1994**, *12* (7), 901–909.
103. Jamali, F.; Lovlin, R.; Corrigan, B.W.; Davies, N.M.; Aberg, G. Stereospecific pharmacokinetics and toxicodynamics of ketorolac after oral administration of the racemate and optically pure enantiomers to the rat. Chirality **1999**, *11* (3), 201–205.
104. Kumar, T.R.S; Shedbalkar, V.P.; Bhalla, H.L. High-performance liquid-chromatographic determination of ketorolac tromethamine in ophthalmic formulations. Indian Drugs **1997**, *34* (9), 532–535.
105. Squella, J.A.; Lemus, I.; Sturm, J.C.; Nunez-Vergara, L.J. Voltammetric behaviour of ketorolac and its HPLC-EC determination in tablets. Anal. Lett. **1997**, *30* (3), 553–564.
106. Colgan, S.T.; Hammen, P.D.; Knutson, K.L.; Bordner, J. Investigation of cyclam-containing mobile phases for the liquid-chromatographic analysis of tenidap. J. Chromatogr. Sci. **1996**, *34* (3), 111–114.
107. Bartsch, H.; Eiper, A.; Kopelent-Frank, H. Stability indication assays for the determination of piroxicam: Comparison of methods. J. Pharm. Biomed. Anal. **1999**, *20* (3), 531–541.
108. Carlucci, G.; Mazzeo, P.; Palumbo, G. Determination of tenoxicam in human plasma using solid-phase extraction and high-performance liquid chromatography with ultraviolet detection. J. Liq. Chromatogr. **1992**, *15* (4), 683–695.
109. Joseph-Charles, J.; Bertucat, M. Simultaneous high performance liquid chromatographic analysis of nonsteroidal anti- inflammatory oxicams in pharmaceutical preparations. J. Liq. Chromatogr. Relat. Technol. **1999**, *22* (13), 2009–2021.
110. Haque, A.; Stewart, J.T. Direct injection HPLC method for the determination of phenylbutazone and oxyphenbutazone in serum using a semipermeable surface column. J. Pharm. Biomed. Anal. **1997**, *16* (2), 287–293.
111. Kamata, K.; Akiyama, K. Determination of bufexamac in cream and ointment by high-performance liquid chromatography. J. Chromatogr. **1986**, *370* (2), 344–347.
112. Mikami, E.; Goto, T.; Ohno, T.; Matsumoto, H.; Nishida, M. Simultaneous analysis of naproxen, nabumetone and its major metabolite 6-methoxy-2-naphthylacetic acid in pharmaceuticals and human urine by high-performance liquid chromatography. J. Pharm. Biomed. Anal. **2000**, *23* (5), 917–925.
113. Wang, J.; Moore, D.E. Study of the photodegradation of benzydamine in pharmaceutical formulations using HPLC with diode array detection. J. Pharm. Biomed. Anal. **1992**, *10* (7), 535–540.
114. Fiori, M.; Farnè, M.; Civitareale, C.; Nasi, A.; Serpe, L.; Gallo, P. The use of bovine serum albumin as a ligand in affinity chromatographic clean-up of non-steroidal anti-inflammatory drugs from bovine plasma. Chromatographia **2004**, *60* (5, 6), 253.
115. Carini, M.; Aldini, G.; Stefani, R.; Marinello, C.; Facino, R.M. Mass spectrometric characterization and HPLC determination of the main urinary metabolites of nimesulide in man. J. Pharm. Biomed. Anal. **1998**, *18* (1–2), 201–211.
116. Tardieu, D.; Jaeg, J.P.; Deloly, A.; Corpet, E.D.; Cadet, J.; Petit, C.R. The COX-2 inhibitor nimesulide suppresses superoxide and 8-hydroxy-deoxyguanosine formation, and stimulates apoptosis in mucosa during early colonic inflammation in rats. Carcinogenesis **2000**, *21* (5), 973–976.
117. Chow, H.H.S; Anavy, N.; Salazar, D.; Frank, D.H.; Alberts, D.S. Determination of celecoxib in human plasma using solid-phase extraction and high-performance liquid chromatography. J. Pharm. Biomed. Anal. **2004**, *34* (1), 167–174.
118. Zhang, J.Y.; Fast, D.M.; Breau, A.P. Determination of valdecoxib and its metabolites in human urine by automated solid-phase extraction-liquid chromatography-tandem mass spectrometry. J. Chromatogr. B Analyt. Technol. Biomed. Life Sci. **2003**, *785* (1), 123–134.
119. Zhang, J.Y.; Fast, D.M.; Breau, A.P. Development and validation of an automated SPE-LC-MS/MS assay for valdecoxib and its hydroxylated metabolite in human plasma. J. Pharm. Biomed. Anal. **2003**, *33* (1), 61–72.

Dry-Column Chromatography

Mark Moskovitz
Dynamic Adsorbents, Inc., Atlanta, Georgia, U.S.A.

INTRODUCTION

Dry-column chromatography (DCC) is a modern chromatographic technique that allows easy and rapid transfer of the operating parameters of analytical thin-layer chromatography (TLC) to preparative column chromatography (CC). The dry-column technique bridges the gap between preparative CC and analytical TLC.

DISCUSSION

TLC has become an important technique in laboratory work, because it permits the rapid determination of the composition of complex mixtures. TLC allows the isolation of substances in micro amounts. If, however, milligrams or even grams of substance are required, CC has to be applied, as TLC would involve a high cost and excessive time. In many cases, even the so-called thick layer or prep layer is but a poor choice because of time, cost, and sometimes inadequate transferability of the parameters of the analytical technique. In addition, the transfer from TLC to CC, however, often proves to be difficult because the CC adsorbent is not usually analogous to the TLC adsorbent.

It is imperative that when transferring conditions of TLC separations to preparative columns, the conditions responsible for the TLC separation be meticulously transferred. Both CC and TLC use the same principle of separation. For normal operating conditions, a TLC layer has a chromatographic activity of II–III of the Brockmann and Schodder scale. Therefore, the sorbent used for DCC has to be brought to the same grade of activity. TLC layers often contain a fluorescent indicator in which case the DCC sorbent has to contain the same phosphor.

In TLC, the silica or alumina layer is "dry" before it is used and contacts the solvent only after it has been placed into the developing chamber. This is why, in DCC, the dry column is charged with the sample. Contrary to the normal CC, DCC is a non-elution technique. Therefore, only a limited amount of eluent is used in DCC to merely fill the interstitial volume between the adsorbent particles.

Scientific Adsorbents, Inc. DCC adsorbents, which are commercially available from Scientific Adsorbents, Inc. (Atlanta, Georgia, U.S.A.) are adjusted to meet the physical-chemical properties of TLC as closely as possible. These adjustments are made during the manufacturing cycle, and the material is packaged ready to use. With similar physical-chemical properties, the values obtained for the substances under investigation from TLC are practically identical to those obtained with DCC.

Using these especially adjusted adsorbents for DCC, one can use the same sorbent and the same solvent for the column work and can transfer the TLC results to a preparative scale column operation rapidly, saving time and money. DCC materials are available corresponding with the most common thin layers: silica DCC and alumina DCC.

These DCC sorbents have found wide use when it is necessary to scale up TLC separations in order to prepare sufficient quantities of compounds for further chemical reactions and/or analytical processes. DCC can be practically used for every separation achievable by TLC (Fig. 1).

SIMPLIFIED PROCEDURE

Preparation

1. Use the same solvent system that was developed on a TLC plate.
2. Cut a Nylon tube to the desired length. To isolate 1 g of material, use approximately 300 g of sorbent in a 1 m × 740 mm tube (Fig. 2).
3. Close the tube by rolling one end and securing it by a seal or a clip/staple.
4. Insert a small pad or wad of glass wool at the bottom of the column; pierce holes at the bottom with a needle.

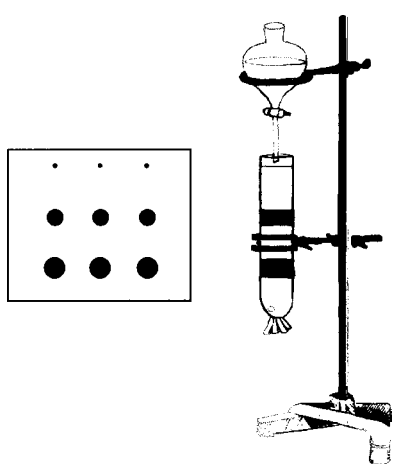

Fig. 1 Dry column chromatography (DCC).

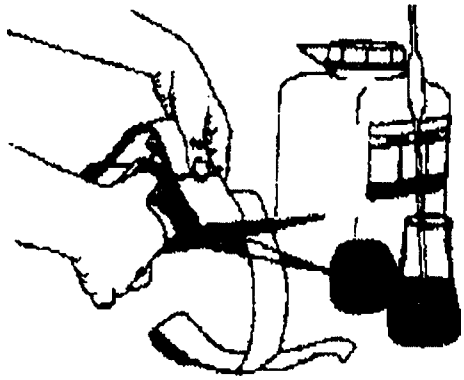

Fig. 2 Cut a nylon tube to the desired length.

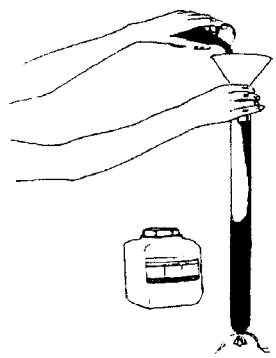

Fig. 3 Dry fill the column to three-fourths of its length.

5. Dry fill the column to three-fourths of its length (Fig. 3).
6. The sample to be separated should be combined with at least 10 times its weight of the same sorbent in a conical test tube.
7. Add an additional centimeter of sorbent on top of the sample, followed by a small pad of glass wool (Fig. 4).
8. Fasten the tube to a clamp on a stand.

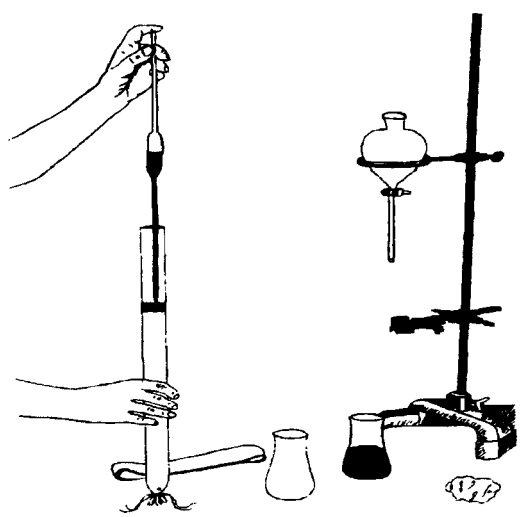

Fig. 4 Add sorbent and a small pad of glass wool.

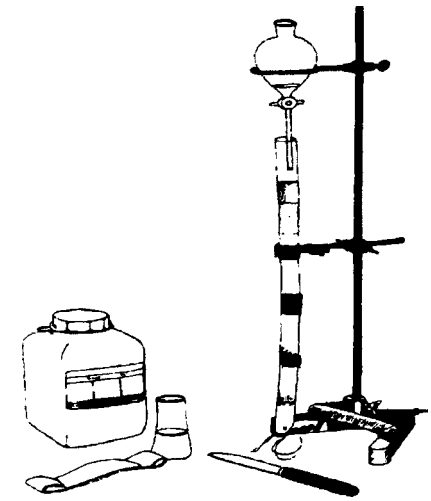

Fig. 5 Add solvent.

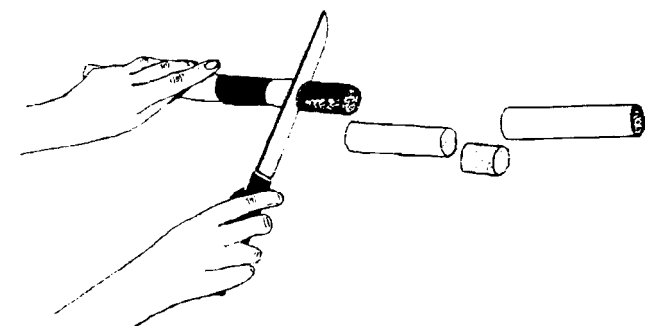

Fig. 6 Slicing the column.

9. Open the stopcock of the solvent reservoir and add solvent until it reaches the bottom of the column. Stop. Elapsed time: approximately 30 min. (Fig. 5).
10. Find the locations of the separated bands by visible, ultraviolet (UV), or UV quenching. Alternatively, cut a 1/16 in. vertical slice off the tube. Spray the exposed area with an appropriate visualization reagent and align with the untreated column to identify (mark) the separated bands.
11. Mark the location of the bands on the Nylon tube.
12. Remove the column from the clamp.
13. Slice the column into the desired sections (Fig. 6).
14. Elute the pure compounds from the sliced sections with polar solvents.

BIBLIOGRAPHY

1. Love, B.; Goodman, M.M. Chem. Ind. (London) **1967**, 2026.
2. Love, B.; Snyder, K.M. Chem. Ind. (London) **1965**, 15.

Dual CCC

David Y.W. Lee
McLean Hospital, Harvard Medical School, Belmont, Massachusetts, U.S.A.

INTRODUCTION

Dual countercurrent chromatography (DuCCC) is a powerful separation method, which allows the performance of classic countercurrent distribution in a highly efficient manner. The system consists of a multilayer coiled column integrated with two inlet and two outlet flow tubes for a non-miscible two-phase solvent system and a sample feed line, which is connected to the middle of the coiled column. Subjecting the system to a particular combination of centrifugal and planetary motions produces a unique hydrodynamic effect, which allows two immiscible liquids to flow countercurrently through the coiled column. The sample solution is fed at the middle portion of the column and eluted simultaneously through the column in opposite directions by the two solvents. This distinct feature of maintaining constant fresh two mobile phases within the coiled column permits a rich domain of applications. The principles of DuCCC and its applications in the purification of natural products and synthetic peptides are reviewed.

DISCUSSION

The development, in the 1980s, of modem high-speed countercurrent chromatography (HSCCC) based on the fundamental principles of liquid–liquid partition has caused a resurgence of interest in the separation sciences. The advantages of applying continuous liquid–liquid extraction, a process for separating of a multi-component mixture according to the differential solubility of each component in two immiscible solvents, have long been recognized. For instance, the countercurrent distribution method, which prevailed in the 1950s and 1960s, was applied successfully to fractionate commercial insulin into two subfractions, which differed only by one amide group in a molecular weight of 6000.[1] In recent years, significant improvements have been made to enhance the performance and efficiency of liquid–liquid partitioning.[2–8] The high-speed centrifugal partition chromatographic (CPC) technique utilizes a particular combination of coil orientation and planetary motion to produce a unique hydrodynamic, unilateral phase distribution of two immiscible solvents in a coiled column. The hydrodynamic properties can effectively be applied to perform a variety of liquid–liquid partition chromatographies including HSCCC,[2] foam countercurrent chromatography.[8–9] and DuCCC [10–11] In most cases, for the two-phase solvent system selected for HSCCC, one liquid phase serves as a stationary phase and the second phase is used as a mobile phase. An efficient separation can be achieved by continuous partitioning of a mixture between the stationary phase and the mobile phase.

By definition, this mode of separation should be called high-speed liquid–liquid partition chromatography or centrifugal partition chromatography, because only one solvent phase is mobile. In the case of DuCCC, for the two-phase solvents countercrossing each other inside the coiled column from opposite directions, both phases are mobile and there is no stationary phase involved.

The name "dual" countercurrent chromatography is redundant; however, it is useful to distinguish it from ordinary HSCCC. DuCCC shares several common advantages with other types of liquid–liquid partition chromatography. For instance, there are an unlimited number of two-phase solvent systems which can be employed, and there are no sample losses from irreversible adsorption or decomposition on the solid support. In addition, DuCCC is extremely powerful in separating crude natural products, which usually consist of multicomponents with an extremely wide range of polarities. In a standard operation, the crude sample is fed through the middle portion of the column. The extreme polar and non-polar components are readily eluted from the opposite ends of the column followed by components with decreasing orders of polarity in one phase and increasing order of polarity in the other phase. A component with a partition coefficient equal to 1.0 will remain inside the coiled column. Essentially, the DuCCC resembles a highly efficient performance of classic countercurrent distribution. They differ in that CCC is a dynamic process, whereas CCD is an equilibrium process. The principles, instrumentation of DuCCC, and its capabilities in natural products isolation are illustrated in the remainder of the entry.

PRINCIPLES AND MECHANISM

The fundamental principle of separation for modem DuCCC is identical to classic countercurrent distribution. It is based on the differential partitions of a multicomponent mixture between two countercrossing and immiscible solvents.The separation of a particular component within a complex mixture is based on the selection of a two-phase

solvent system, which provides an optimized partition coefficient difference between the desired component and the impurities. In other words, DuCCC and HSCCC cannot be expected to resolve all the components with one particular two-phase solvent system. Nevertheless, it is always possible to select a two-phase solvent system, which will separate the desired component. In general, the crude sample is applied to the middle of the coiled column through the sample inlet, and the extreme polar and nonpolar components are readily eluted by two immiscible solvents to opposite outlets of the column.

Contrary to the classic countercurrent distribution method, modern DuCCC allows the entire operation to be carried out in a continuous and highly efficient manner. DuCCC is based on the ingenious design of Ito.[8] A cylindrical coil holder is equipped with a planetary gear, which is coupled to an identical stationary sun gear (shaded) placed around the central axis of the centrifuge. This gear arrangement produces an epicyclic motion; the holder rotates about its own axis relative to the rotating frame and simultaneously revolves around the central axis of the centrifuge at the same angular velocity as indicated by the pair of arrows. The epicyclic rotation of the holder is necessary to unwind the twist of the five flow tubes caused by the revolution, eliminating the use of rotary seals to connect each flow tube.

As shown in Fig. 1, this unique design enables the performance of DuCCC using five flow channels connected directly to the column without using a rotational seal. When a column with a particular coil orientation is subjected to an epicyclic rotation, it produces a unique hydrodynamic phenomenon in the coiled column in which one phase entirely occupies the head side and the other phase occupies the tail side of the coil column. This unilateral phase distribution enables the performance of DuCCC in an efficient manner. A theoretical calculation of the hydrodynamic forces resulting from such an epicyclic rotation is very complicated and has not been elucidated.

METHODS AND APPARATUS

The DuCCC experiments are performed with a tabletop (type J) high-speed plant centrifuge equipped with a multilayer coiled column connected to five flow channels. The multilayer coiled column is prepared from 2.6 mm inner diameter PTFE tubing by winding it coaxilially onto the holder to a total volume capacity of 400 ml. The multilayer coiled column is subjected to an epicyclic rotation at 500–800 rpm. The fractions are collected simultaneously from both ends of the column and analyzed by thin-layer chromatography (TLC) or high-performance liquid chromatography (HPLC).[8,12]

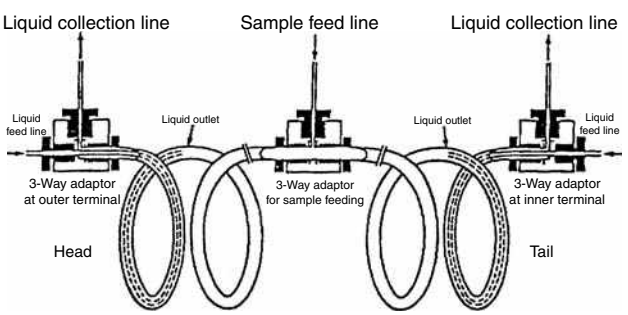

Fig. 1 Column design for DuCCC.

APPLICATIONS

In the past decade, the rapid development of sophisticated spectroscopic techniques, including various two-dimensional nuclear magnetic resonance (2D NMR) methods, automated instrumentation and routine availability of x-ray crystallography has greatly simplified structural elucidation in natural product investigations. Consequently, the challenge to today's chemists has shifted to one's capability of isolating the bioactive components from crude extracts of either plants or animals. The extract of crude natural products usually is comprised of hundreds of components over a wide range of polarities. In isolating these natural products, it is essential to preserve the biological activity while performing chromatographic purifications. DuCCC represents one of the most efficient methods for isolation of the desired compound from a complex mixture.

Dual CCC has several advantages over HSCCC or CPC[13] in dealing with crude natural products. One distinct feature of DuCCC is the capability of performing normal-phase and reversed-phase elusions simultaneously. This provides a highly efficient and unique method for separation of crude natural products. In many instances, fractions eluted from DuCCC are pure enough for recrystallization or structural study. For example, an HPLC trace of the crude ethanol extract of *Schisandra rubriflora* shows that the major bioactive lignan, schisanhenol, is closely eluted with its acetate, it has been a major problem to isolate the pure schisanhenol. The fractions collected from DuCCC after injection of a crude ethanol extract of *Schisandra rubriflora* (125 mg) were analyzed by TLC and reversed-phase HPLC. The solvent system employed for DuCCC was hexane:ethyl acetate:methanol:water (10:5:5:1).

The upper phase, being less polar than the lower phase, results in a sequence of elution similar to normal-phase chromatography, whereas the lower phase provides a sequence of elution resembling reversed-phase chromatography. The bioactive components, schisanhenol acetate and schisanhenol, were eluted in the lower phase. Reversed-phase HPLC analyses of fractions 36–40 accounted for 32 mg of almost pure schisanhenol.[6] A total of 4 mg of schisanhenol acetate was also obtained from fractions 50–57. As evidenced by this experiment, DuCCC offers an excellent method for semipreparative isolation of bioactive components from very crude natural products.[11] The

isolation of the topoisomerase inhibitor boswellic acid acetate from its triterpenoic acid mixture has also been accomplished by DuCCC.[12] As shown in Fig. 2, when an isomeric mixture of triterpenoic acids (400 mg) was subjected to DuCCC, using a hexane:ethanol:water (6:5:1) as the solvent system, 215 mg of the boswellic acid acetate and 135 mg of the corresponding boswellic acid were obtained. Some highly polar impurities were eluted immediately in the solvent front, from fraction 1 to 4. The isomeric boswellic acid was eluted in the lower-phase solvent and the less polar acetates were eluted simultaneously in the upper-phase solvent. Although the isomers were only partially resolved by DuCCC, this experiment demonstrates that DuCCC is a highly efficient system for preparative purification.

The conformationally restricted cyclic, disulfide containing, enkephalin analogue (D-Pen, D-Pen) enkephalin (DPDPE) was synthesized by solid-phase methods. Its purification was accomplished previously by partition on Sephadex G-25 block polymerizate using the solvent system (1-butanol:acetic acid:water: 4:1:5), followed by gel filtration on Sephadex G-15 with 30% acetic acid as the eluent.[14] DuCCC demonstrated a highly efficient and one step method for the purification of DPDPE. The crude DPDPE (500 mg), which contained impurities and salts, was purified by DuCCC with a two-phase solvent system consisting of 1-butanol containing 0.1% TFA and water also containing 0.1% TFA in a 1:1 (v/v) ratio. The desired DPDPE was eluted from the upper phase in fractions 15–19. The purity of each fraction collected was monitored by HPLC. A total of 24 mg pure DPDPE was obtained within 2 hr. As evidenced, DuCCC can be a highly costeffective procedure for the purification of polypeptides.

CONCLUSION

The capability and efficiency of DuCCC in performing classic countercurrent distribution has been demonstrated in the isolation of bioactive lignans and triterpenoic acids from crude natural products and in the purification of synthetic polypeptides. DuCCC provides excellent resolution and sample loading capacity. It offers a unique feature of elution of the non-polar components in the upper-phase solvent (assuming the upper phase is less polar than the lower phase) and concomitant elution of the polar components in the lower phase. This capability results in an efficient and convenient preparative method for purification of the crude complex mixture. The capability of DuCCC has not yet been fully explored. For instance, a particular solvent system can be selected to give the

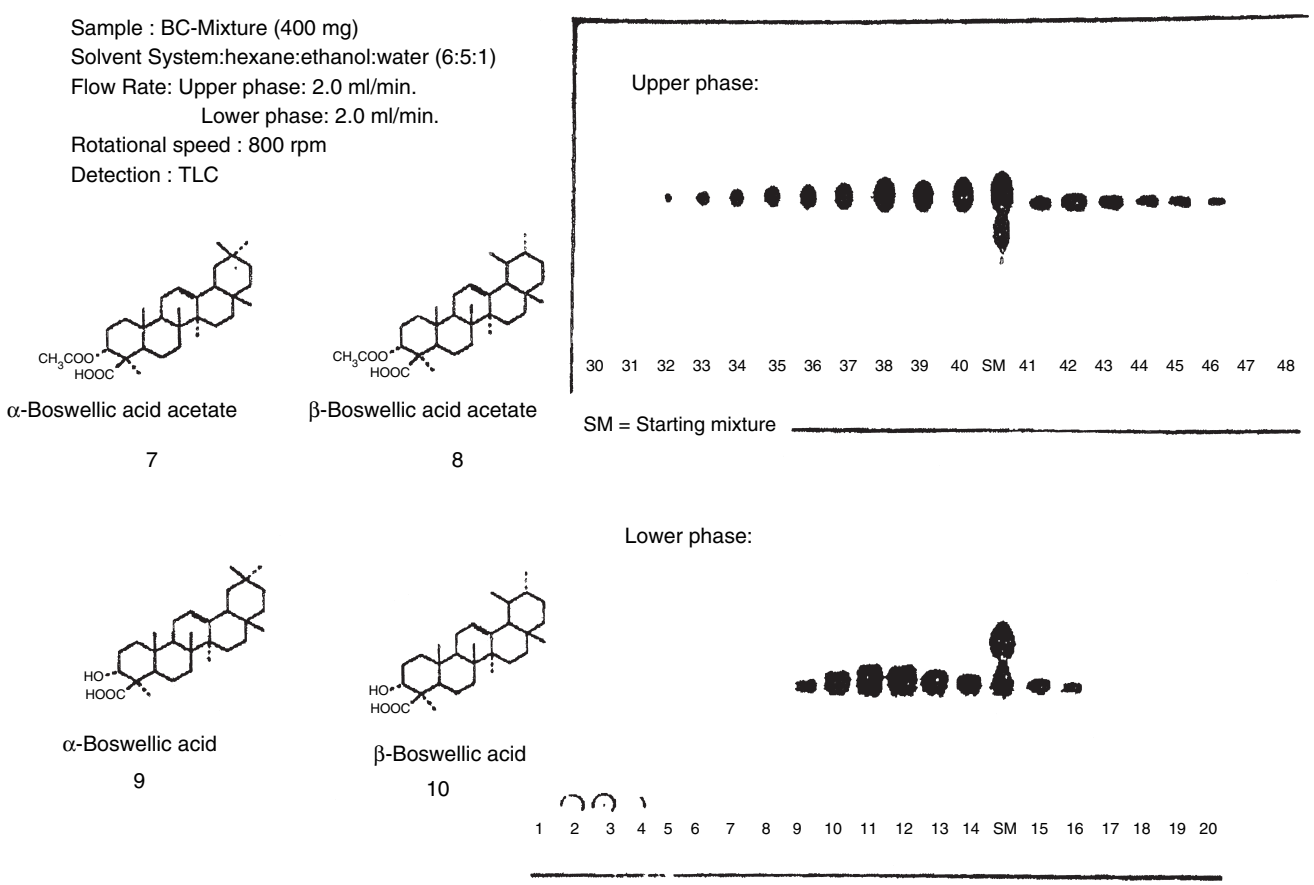

Fig. 2 DuCCC of triterpenoic acids.

desired bioactive component a partition coefficient of 1. This will allow the "stripping" of the crude extract with DuCCC to remove the impurities or inactive components. Consequently, the bioactive component will be concentrated inside the column for subsequent collection. This strategy can also be applied to extract and concentrate certain metabolites in biological fluids such as urine or plasma. Because there is no saturation of the stationary phase, a large amount of sample can also be processed by DuCCC. In addition, the system can be easily automated with computer-assisted sample injection and fractionation.

REFERENCES

1. Craig, L.C.; Hausmann, W.; Ahrens, P.; Harfenist, E. Determination of weight curves in column processes. J. Anal. Chem. **1951**, *23* (9), 1326.
2. Ito, Y. High-speed countercurrent chromatography. CRC Crit. Rev. Anal. Chem. **1986**, *17*, 65–143.
3. Lee, Y.W.; Ito, Y.; Fang, Q.C.; Cook, C.E. Dual countercurrent chromatography. J. Liquid Chromatogr. & Relat. Technol. **1988**, *11* (1), 75–89.
4. Zhang, T.Y.; Hua, X.; Xiao, R.; Kong, S. Separation of flavonoids in crude extract from sea buckthorn by countercurrent chromatography with two types of coil planet centrifuge. J. Liquid Chromatogr. & Relat. Technol. **1988**, *11* (1), 233–244.
5. Lee, Y.W.; Cook, C.E.; Fang, Q.C.; Ito, Y. Application of analytical high-speed counter-current chromatography to the isolation of bioactive natural products. J. Chromatogr. & Relat. Technol. **1989**, *477*, 434–438.
6. Brill, G.M.; McAlpine, J.B.; Hochlowski, E.J. Use of coil planet centrifuge in the isolation of antibiotics. J. Liquid Chromatogr. & Relat. Technol. **1985**, *8* (12), 2259.
7. Martin, D.G.; Peltonen, R.E.; Nielsen, J.W. Preparative resolution of an actinomycin complex by countercurrent chromatography in the ito coil planet centrifuge. J. Antibiot. **1986**, *39*, 721.
8. Ito, Y. Foam countercurrent chromatography based on dual counter-current system. J. Liquid Chromatogr. & Relat. Technol. **1985**, *8* (12), 2131.
9. Oka, H.; Harada, K.-L.; Suzuki, M.; Nakazawa, H.; Ito, Y. Foam counter-current chromatography of bacitracin: I. Batch separation with nitrogen and water free of additives. J. Chromatogr. & Relat. Technol. **1989**, *482* (1), 197.
10. Lee, Y.W.; Cook, C.E.; Ito, Y. Dual countercurrent chromatography. J. Liquid Chromatogr. & Relat. Technol. **1988**, *11* (1), 37–53.
11. Lee, Y.W.; Fang, Q.C.; Ito, Y.; Cook, C.E. The application of true countercurrent chromatography in the isolation of bioactive natural products. J. Nat. Products **1989**, *52* (4), 706–710.
12. Lee, W., unpublished data.
13. Murayarna, W.; Kosuge, Y.; Nakaya, N.; Nunogaki, Y.; Nunogaki, N.; Cazes, J.; Nunogaki, H. Preparative separation of unsaturated fatty acids esters by centrifugal partition chromatography (CPC). J. Liquid Chromatogr. & Relat. Technol. **1988**, *11* (1), 283–300.
14. Mosberg, H.J.; Hurst, R.; Hruby, V.J.; Gee, K.; Yamamura, H.I.; Galligan, J.J.; Burks, T.F. Bis-penicillamine enkephalins possess highly improved specificity toward delta opioid receptors. Proc. Natl. Acad. Sci. USA **1983**, *80*, 5871–5874.

Eddy Diffusion in LC

J.E. Haky
Department of Chemistry and Biochemistry, Florida Atlantic University, Boca Raton, Florida, U.S.A.

INTRODUCTION

Among the causes of widening of peaks corresponding to components of a mixture undergoing separation by liquid chromatography (LC) is the phenomenon known as eddy diffusion. This results from molecules of a solute traversing a packed bed of a column through different pathways, in and around the stationary phase. Some molecules travel more rapidly through the column through more open, shorter pathways, whereas others will encounter longer, restricted areas and lag behind. The result is a solute band that passes through the column with a Gaussian distribution around its center.[1]

DISCUSSION

The degree of band broadening of any chromatographic peak may be described in terms of the height equivalent to a theoretical plate, H, given by

$$H = \frac{L}{N} \tag{1}$$

where L is the length of the column (usually measured in cm) and N is the number of theoretical plates, which can be calculated from Eq. 2, where t_R and W are the retention time and width of the peak of interest, respectively:

$$N = 16\left(\frac{t_R}{W}\right)^2 \tag{2}$$

Because higher values of N correspond to lower degrees of band broadening and narrower peaks, the opposite is true for H. Therefore, the goal of any chromatographic separation is to obtain the lowest possible values for H.

The contribution of eddy diffusion and other factors to band broadening in LC can be quantitatively described by the following equation, which relates the column plate height H to the linear velocity of the solute, μ:

$$H = A\mu^{0.33} + \frac{B}{\mu} + C\mu + D\mu \tag{3}$$

where A, B, C, and D are constants for a given column.[2] The linear velocity μ is related to the mobile-phase flow rate and is determined by

$$\mu = \frac{L}{t_0} \tag{4}$$

where t_0 (the so-called "dead time") is determined from the retention time of a solute which is known not to interact with the stationary phase of the column. The first term in Eq. 4, $A\mu^{0.33}$, includes the contribution of eddy diffusion to chromatographic band broadening. This term, which is dependent on the cube root of the linear velocity, is less dependent on mobilephase flow rate than the other terms in the equation, which are either directly or inversely proportional to linear velocity.

Minimizing eddy diffusion in an LC column results in a lower $A\mu^{0.33}$ term in Eq. 3, which minimizes band spreading and gives narrower chromatographic peaks. The most common methods used for this purpose, in LC, are the following: a) Using a column of the smallest practical diameter. This obviously reduces the number of alternate pathways which a solute can take through the column; b) Using a stationary phase of smallest practical particle size. Giddings[3] and others have shown that the effects of eddy diffusion are directly proportional to the average diameter of stationary-phase particles. Thus, smaller stationary-phase particles give narrower peaks; c) Making sure the column is uniformly packed. Again, this limits open space in the column, thus minimizing the number of pathways.

Those who prepare and/or manufacture LC columns must use the above methods to limit the effects of eddy diffusion on the chromatographic separations. However, there are practical limitations. Column and stationary-phase particle diameters can only be reduced to points that are compatible with the pressure limitations of the pumps used in chromatographic instruments and the required sample capacities of the columns. The degree of training and experience of those who pack the columns

may also limit the quality of the procedure used in packing the column. Nevertheless, most commercial manufacturers of LC columns have adopted column designs and packing procedures which generally reduce the effects of eddy diffusion on modern LC separations to an inconsequential level. Still, these effects may increase as a column ages, and practicing chromatographers should be on the watch for them.

REFERENCES

1. Poole, C.F.; Poole, S.K. *Chromatography Today*; Elsevier: New York, 1991; .Chap. 1.
2. Snyder, L.R.; Kirkland, J.J. *Introduction to Modern Liquid Chromatography,* 2nd Ed.; John Wiley & Sons: New York, 1979; 15–37.
3. Giddings, J.C. *Dynamics of Chromatography*; Marcel Dekker, Inc.: New York, 1965; 35–36.

Efficiency in Chromatography

Nelu Grinberg
Analytical Research Department, Merck Research Laboratories, Rahway, New Jersey, U.S.A.

Rosario LoBrutto
Merck Research Laboratories, Rahway, New Jersey, U.S.A.

INTRODUCTION

One of the most important characteristics of a chromatographic system is the efficiency or the number of theoretical plates, *N*.

DISCUSSION

The number of theoretical plates can be defined from a chromatogram of a single band as

$$N = \left(\frac{t_R}{\sigma_t}\right)^2 = \frac{L^2}{{\sigma_t}^2} \tag{1}$$

where, for a Gaussian shaped peak, t_R is the time for elution of the band center, σ_t is the band variance in time units, and L is the column length.[1] N is a dimensionless quantity; it can also be expressed as a function of the band elution volume and variance in volume units:

$$N = \left(\frac{V_R}{\sigma_v}\right)^2 = 5.56\left(\frac{t_R}{W_{1/2}}\right)^2 \tag{2}$$

In a chromatographic system, it is desirable to have a high column plate number. The column plate number increases with several factors:[2]

- Well-packed column
- Longer columns
- Smaller column packing particles
- Lower mobile-phase viscosity and higher temperature
- Smaller sample molecules
- Minimum extracolumn effects.

In an open-bed system, N can be measured from the distance passed by a zone along the bed:

$$N = \left(\frac{d_R}{\sigma_d}\right)^2 \tag{3}$$

where d_R is the distance from the point of sample application to the point of the band center and σ_d is the variance of the band in distance units.[1]

In fact, the plate theory describes the movement of a particular zone through the chromatographic bed. As the zone is washed through the first several plates, a highly discontinuous concentration profile is obtained, with the solute being distributed in plates following the Poisson distribution.[3] At an intermediate stage (approximately 30–50 plates), much of the abrupt discontinuity disappears due to a similar concentration of the analyte in the neighboring plates. As the process continues (after 100 plates), the concentration profile is smooth and, even though the distribution is still Poisson, it can be approximated by a Gaussian curve. The standard deviation, of the Gaussian curve, which is a direct measure of the zone spreading, is found to be

$$\sigma = \sqrt{HL} \tag{4}$$

where H is the plate height and L is the distance migrated by the center of the zone. In practice, the plate height is used to describe the zone spreading, including both nonequilibrium and longitudinal effects. In a uniform column, free from concentration and velocity gradients, the plate height is defined as

$$H = \frac{\sigma^2}{L} \tag{5}$$

In a non-uniform column, the zone spreading varies from point to point and its local value is

$$H = \frac{d\sigma^2}{dL} \tag{6}$$

which represents the increment of plate height in the variance σ^2 per unit length of migration. In practice, the smaller the value of H, the smaller the magnitude of band spreading per unit length of the column. The determination of H does not require the measurement of, as long as N is known. Thus, combining Eqs. 1 and 6 yields[4]

$$H = L\left(\frac{\sigma}{L}\right)^2 = \frac{L}{N} \tag{7}$$

In practice, because the separation in a particular chromatographic column is linked to the time spent by the analyte in the stationary phase and the time spent by the analyte in the mobile phase is irrelevant for the separation, a new parameter is defined (i.e., *effective plate number*, N_{eff}). The effective plate number is related to the separation factor k' and N by

$$N_{\text{eff}} = N\left(\frac{k'}{1+k'}\right)^2 \tag{8}$$

Similarly, an expression for H_{eff} can be written

$$H_{\text{eff}} = H\left(\frac{1+k'}{k'}\right)^2 \tag{9}$$

The effective parameters are more meaningful when comparing different columns.[4]

There are several major contributions that will influence the band broadening and, consequently, H:[5] eddy diffusion, mobile-phase mass transfer, longitudinal diffusion, stagnant mobile-phase mass transfer, and stationary-phase mass transfer. The effect of each process on the band broadening and, consequently, on the plate height is related to all the experimental variables: mobile-phase velocity, u; particle diameter, d_p; sample diffusion coefficient in the mobile phase, D_m; the thickness of the stationary-phase layer, d_f; and the sample diffusion coefficient in the stationary phase, D_s. In general, H will vary with the velocity of the mobile phase, u, as it travels through the column. In a gas chromatography (GC) system, a plot of u vs. H will lead to a curve which has a hyperbolic shape,[6] characterized by the equation

$$H = A + \frac{B}{u} + Cu \tag{10}$$

Eq. 10 is known as the van Deemter equation, and no correction was made for gas compressibility. Using the reduced parameters $h = Hd_p$ and $v = ud_pD_m$, Eq. 10 becomes

$$h = a + \frac{b}{v} + cv \tag{11}$$

where A, B, C, a, b, and c are constants for a particular sample compound and set of experimental conditions as the flow rate varies. The B term in Eq. 10 relates to band broadening occurring by diffusion in the gas phase in the longitudinal direction of the column. According to Einstein's equation for diffusion,

$$\sigma^2 = 2D_m t_0 = \frac{2D_m L}{u} \tag{12}$$

Because $H = \sigma^2 L$, the B term becomes

$$B = 2\frac{D_m}{u} \tag{13}$$

The inverse velocity term in Eq. 13 becomes important at low velocities. Because the D_m in liquids is 10^5 times smaller than in gases, the longitudinal term plays no practical role in band broadening in LC. The A term in Eq. 10 describes the non-homogeneous flow, also called eddy diffusion. In this case,

$$\frac{\sigma^2}{L} = 2\lambda d_p = A \tag{14}$$

where λ is a packing correction factor of $\sim$0.5. In classical GC, the A term is a constant, representing a lower limit on column efficiency, equivalent to $H = d_p$ or $h = 1$.

At velocities above $H_{\min}$, the C term controls H and relates to non-equilibrium resulting from resistance to mass transfer in the stationary and mobile phases.[6]

In HPLC, the van Deemter equation still holds. However, Giddings[3] argued that the equation is too simplistic because it ignores the coupling that exists between the flow velocity and the radial diffusion in the void space of the packing around the particles. He suggested replacing the term A by a term $a(1 + bu^{-1})$ to account for the flow velocity, because both the eddy diffusion and the radial diffusion are responsible for the transfer of the molecules between the different flow paths of unequal velocity. To include the coupling between the laminar flow and the molecular diffusion in porous media, Horvath and Lin[7] introduced a new parameter, δ, which is the thickness of the stagnant film surrounding each stationary-phase particle. However, at high velocities required in high-performance liquid chromatography (HPLC), Horvath and Lin's model reduces to the Knox equation, which is a variation of the van Deemter equation:[8]

$$h = av^{0.33} + \frac{b}{v} + cv \tag{15}$$

where a, b, and c are empirical parameters related to the analyte and the experimental flow rate conditions.

REFERENCES

1. Karger, B.L.; Snyder, L.R.; Horvath, Cs. *An Introduction to Separation Science*; John Wiley & Sons: New York, 1973; 136.
2. Snyder, L.R.; Kirkland, J.J.; Glajch, J.L. *Practical HPLC Method Development*; John Wiley & Sons: New York, 1997; 42.
3. Giddings, J.C. *Dynamic of Chromatography, Part I, Principles and Theory*; Marcel Dekker, Inc.: New York, 1965; 23, 61.
4. Horvath, Cs.; Melander, W.R. *Chromatography, Fundamentals and Applications of Chromatographic and Electrophoretic Methods, Part A: Fundamentals and Techniques*; Heftmann, E., Ed.; Elsevier Scientific: Amsterdam, 1983; A45.
5. Snyder, L.R.; Kirkland, J.J. *Introduction to Modern Liquid Chromatography,* 2nd Ed.; John Wiley & Sons: New York; 168.
6. Karger, B.L. *Modern Practice of Liquid Chromatography*; Kirkland, J.J., Ed.; Wiley–Interscience: New York, 1971; 23.
7. Horvath, Cs.; Lin, H.J. Band spreading in liquid chromatography: General plate height equation and a method for the evaluation of the individual plate height contributions. J. Chromatogr. **1978**, *149*, 43.
8. Guiochon, G.; Shirazi, S.G.; Katti, A.M. *Fundamentals of Preparative and Nonlinear Chromatography*; Academic Press: Boston, 1994; 201.

Efficiency of a TLC Plate

Wojciech Markowski
Department of Inorganic and Analytical Chemistry, Medical University of Lublin, Lublin, Poland

INTRODUCTION

Chromatography, by definition, is a separation methodology for a multicomponent sample mixture, which is based on differentiating movement zones of the sample. An essential feature of chromatographic separation is that the components of the sample are transported through the separation medium—in the case of thin-layer chromatography (TLC), through an open bed. Differences in interaction with the medium lead to a selective redistribution of the component zones, from overlapping zones at the start following injection, toward largely individual regions inside the separation medium. The appearance of individual component zones, after the development process, can be recorded with the aid of scanning densitometry, to convert the plate chromatogram into realistic two-dimensional representation of the chromatographic process in a form suitable for evaluation of kinetic parameters. The underlying fundamental processes responsible for chromatographic separations can be explained by thermodynamic and kinetic considerations. Thermodynamic relationships are responsible for retention and selectivity, and kinetic properties are responsible for band broadening. Thus, the position and separation of peaks in a chromatogram are thermodynamic properties, whereas the axial dimensions of the peaks are governed by kinetic considerations, and both phenomena must be considered to optimize resolution. As Giddings[1] emphases in his book, "separation is the art and science of maximizing separative transport relative to the dispersive transport."

RESOLUTION

The most useful criterion for the estimation of the quality of a separation is the resolution. The resolution is given by:[2]

$$R_s = \frac{(z_f - z_o)(R_{f(2)} - R_{f(1)})}{0.5(w_1 + w_2)} \quad (1)$$

where $R_{f(1)}$ and $R_{f(2)}$ are the R_f values of chromatographic spots 1 and 2, respectively; and w_1 and w_2 are widths of spots at the base. Eq. 1 clearly shows the two competing aspects of a chromatographic separation: the separation distance achieved by the primary separation process (numerator) is opposed by the "blurring" action of the zone broadening (denominator). Eq. 1 allows for direct calculation of R_s based on the parameters measured on the chromatogram. Eq. 1 can be transformed to the form:[3]

$$R_s = (1 - R_{f(1)})\left[1 - \frac{R_{f(1)}}{R_{f(2)}}\right]N^{0.5} \quad (2)$$

Eq. 2 demonstrates that the plate resolution, as in other forms of chromatography, depends on the number of theoretical plates N, the selectivity, and the retention coefficient of the solute for the particular layer concerned.

CONCEPT OF THEORETICAL PLATES AND THEIR MEASUREMENT

The measurement of plate efficiency is depicted in Fig. 1a and b.[4] The number of "theoretical plates" is a measure of the quality or "efficiency" of a chromatographic layer. By analogy with the theoretical plates of a distillation column, the chromatographic separations distance and the layer are divided into theoretical separation plates. For a given problem, sorbent, and solvent, a specific minimum number of theoretical plates is necessary to achieve the desired separation. For a capillary flow-controlled system, the mobile-phase velocity is not constant throughout the chromatogram and, at any position within the chromatogram, its value depends on the system variables. The mobile-phase velocity is not under external control and its range cannot be varied independently to study the relationship between the layer plate height and the mobile-phase velocity. Because all zones do not migrate the same distance in TLC, individual zones experience only those theoretical plates through which they travel and the plate height is directly dependent on the migration distance. A further complicating factor is that the size of the starting zone applied to the layer is always a finite value with respect to the size of a developed zone. Therefore, it is not adequate to use the measured zone width as the starting point from which to determine the extent of zone broadening for the layer. The plate number N can be experimentally determined via the "H value" (i.e., "height equivalent to a theoretical plate," or HETP).[5] The measured H value is an average over the separation length and the symbol H_{obs} or $\bar{H}$ is given and is obtained from the integration of the expression for the local plate height H_{loc} (quantity introduced by Giddings[1,4]):

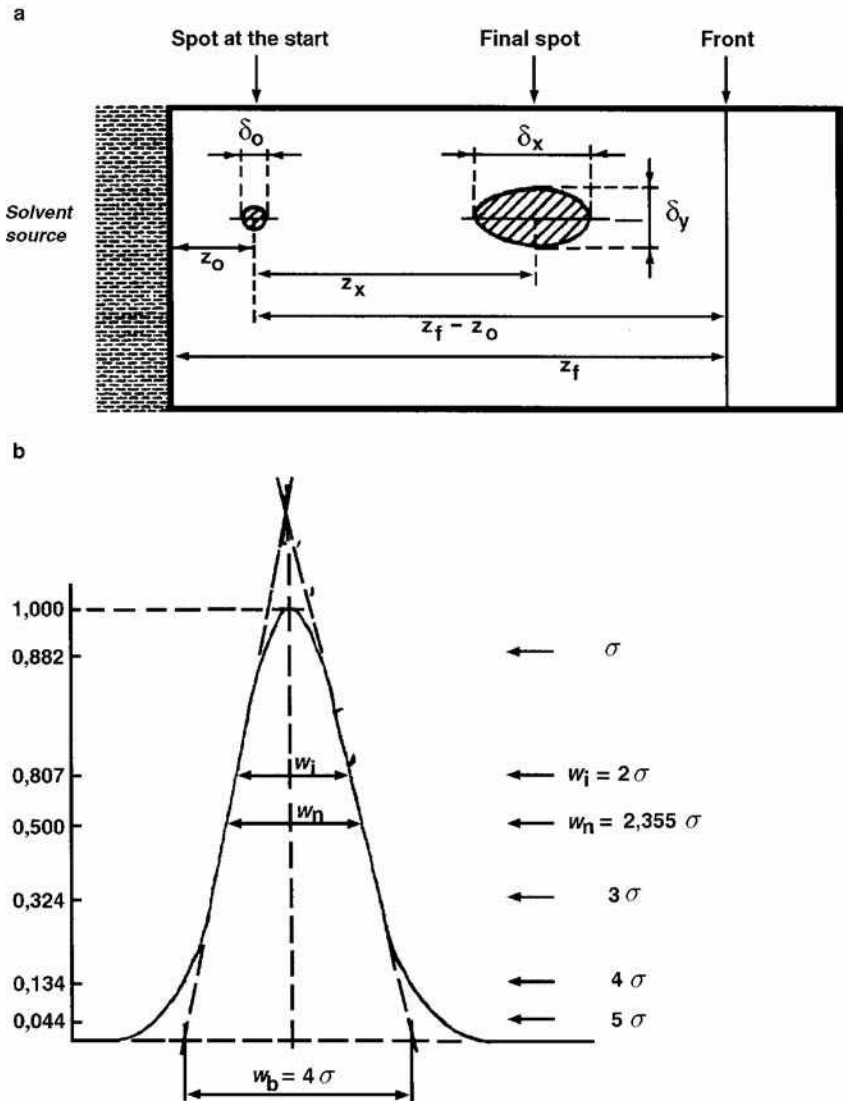

Fig. 1 a, Basic symbols for TLC spot migration. z_x is the migration length of the spot, $z_f - z_o$ is the separation length, and z_f is the front migration length; and b, Width of a Gaussian band at different percentages of maximum height.

$$N = \frac{z_f - z_o}{H} \tag{3}$$

$$H_{loc} = \frac{d\sigma_x^2}{dz} \tag{4}$$

and, in practical terms,

$$\overline{H} = H_{obs} = \frac{\int_{z_o}^{z_x} H_{loc} dz}{\int_{z_o}^{z_x} dz} = \frac{\sigma_x^2}{z_x} = \frac{b_{0.5}^2}{5.54 z_x} \tag{5}$$

The average plate number N of the whole separation length is:

$$N \approx \overline{N} = \frac{z_f - z_o}{H_{obs}} = \frac{z_x}{H_{obs} R_f} \tag{6}$$

Hence, the average theoretical plate number can be calculated from the experimental data for $b_{0.5}$ and the lengths z_f and z_x in the chromatogram. To obtain reliable H values, it is recommended that the experiment comply with the following rules:[4]

1. The band maximum should be at least 10 times greater than the detection limit.
2. Asymmetrical or poorly resolved spots should not be used for determining H.
3. Only σ_{chrom}^2 should be used.

Failure to do this results in excessively high H values. The measured zone variance σ_x^2 in the direction of flow is composed of:

$$\sigma_x^2 = \sigma_{spotting}^2 + \sigma_{chrom}^2 + \sigma_{inst}^2 + \sigma_{other}^2 \tag{7}$$

The contribution of the length of the starting zone to the length of the separated zone could be removed by considering their variances, such that:

$$\sigma_{\text{chrom}}{}^2 = \sigma_{\text{x}}{}^2 - \sigma_{\text{spotting}}{}^2 \quad (8)$$

where $\sigma_{\text{x}}{}^2$ is the variance of the developed zone, $\sigma_{\text{chrom}}{}^2$ is the variance due to the zone expansion during the migration through the layer, and $\sigma_{\text{spotting}}{}^2$ is the variance associated with sample application; here, we are assuming that the contributions to zone broadening associated with the properties of the detection and recording devices $\sigma_{\text{inst}}{}^2$ are negligible. The form of the starting zone is immaterial—only its dimension and sample distribution along its axis parallel to the direction of development (first-order approximation) are significant. It is obvious that the characteristic dimension of the starting zone in the direction of migration is never infinitely small compared with the same characteristic dimension of the zone after normal development. The determination of peak variance is straightforward for developed zones, but presents some difficulty for the undeveloped starting zone. The starting zone is applied to the dry layer. At the start of the migration process, it is contacted by the advancing mobile phase, which is moving at its highest velocity and is probably not fully saturated at its leading edge. Several processes take place quickly, which can lead to changes in the dimensions of the starting zone at the moment the chromatogram begins. The solvent front contacts the bottom portion of the starting zone first, pushing it forward with a characteristic migration velocity (which depends on the solute R_{f} value) into the upper portion of the starting zone, which is fixed in position until it is contacted by the advancing mobile phase. This causes a reconcentration of the starting zone and a reduction of its characteristic dimension in the direction of development. In addition, because the flow of mobile phase is unsaturated, all the pores holding sample will not be filled simultaneously; adsorbed samples may not be displaced from the sorbent surface instantaneously, and localized solvent saturation may limit the rate of solute dissolution in the mobile phase. The dimensions of the starting zone in the direction of migration are too large to ignore.

It can be assumed that the variance of the starting zone is equivalent to the properties of the sample zone, after it has been transported a few millimeters from its point of application by the mobile phase. In this way, some account is taken of the capacity of the mobile phase to reshape the deposited sample zone at the beginning of the chromatogram.[6]

CAPILLARY FLOW

As normally practiced in TLC, capillary forces control the migration of the mobile phase through the layer. Under these conditions, the velocity at which the solvent front moves is a function of the distance of the front from the solvent entry position and declines as this distance increases.[4] There are two consequences of this effect:

1. The mobile-phase velocity is not constant throughout the chromatogram.
2. The mobile-phase velocity is set by the system variables and cannot be independently optimized unless forced flow development conditions are used.

If the migration distance is not excessively long, then the solvent front position as a function of time is adequately described by:

$$z_{\text{f}}{}^2 = \chi t \quad (9)$$

where z_{f} is the distance of the solvent front position above the solvent entry position, χ is the mobile-phase velocity constant, and t is the elapsed time since the solvent commenced migration through the layer. At any position on the layer, the solvent front will be moving with a velocity given by:

$$u_{\text{f}} = \frac{\chi}{2z_{\text{f}}} \quad (10)$$

There are two features of importance when using Eqs. 9 and 10. The velocity constant χ depends on the identity of the solvent; layer characteristics such as average particle size, layer permeability, layer thickness, etc.; and the state of equilibrium between solvent vapors in contact with the layer and the bulk solvent moving through the layer. As the solvent permeates the layer, the channels of narrower diameter are filled first, leading to more rapid advancement of the mobile phase. Large pores below the solvent front fill more slowly, resulting in an increase in the thickness of the layer of mobile phase. The bulk mobile-phase velocity, representing saturated flow through the region occupied by the sample zones, is moving at a lower velocity than the solvent u_{f} front velocity. As a reasonable approximation, the bulk solvent velocity is usually taken to be 0.8 u_{f}.[6] The velocity constant χ is related to the experimental condition by Eq. 11:

$$\chi = 2\kappa_{\text{o}} d_{\text{p}} \frac{\gamma}{\eta} \cos\theta \quad (11)$$

where κ_{o} is the layer permeability constant, d_{p} is the average particle diameter, γ is the surface tension, η is the viscosity of the mobile phase, and θ is the contact angle. The layer permeability constant is dimensionless and takes into account the effect of porosity on the permeability of the layer and the difference between the bulk liquid velocity and the solvent front velocity. A typical value of permeability is $1 - 2 \times 10^{-3}$,[6] virtually identical

with typical column values. Assuming a narrow particle size distribution, Eq. 11 indicates that the velocity constant should increase linearly with average particle size. The solvent front velocity should be larger for coarse particle layers than for fine particle layers, in good agreement with experimental observations. In addition, from Eq. 11, we see that the velocity constant depends linearly on the ratio of the surface tension of the solvent to its viscosity, and the solvents that maximize this ratio are most useful for TLC. The contact angle for most mobile phases on polar adsorbent layers is generally close to zero and there does not exist the problem of wetting. In the case of reversed-phase layers containing bonded, long-chain, alkyl groups, it is not possible to apply the mobile phase with a content of water below 40%. The optimum mobile-phase velocity for a separation can be established by forced flow development[6] and it is considerably higher than the mobile-phase velocity obtained by the use of capillary flow under different experimental conditions. This is illustrated in Fig. 2(a) and (b).

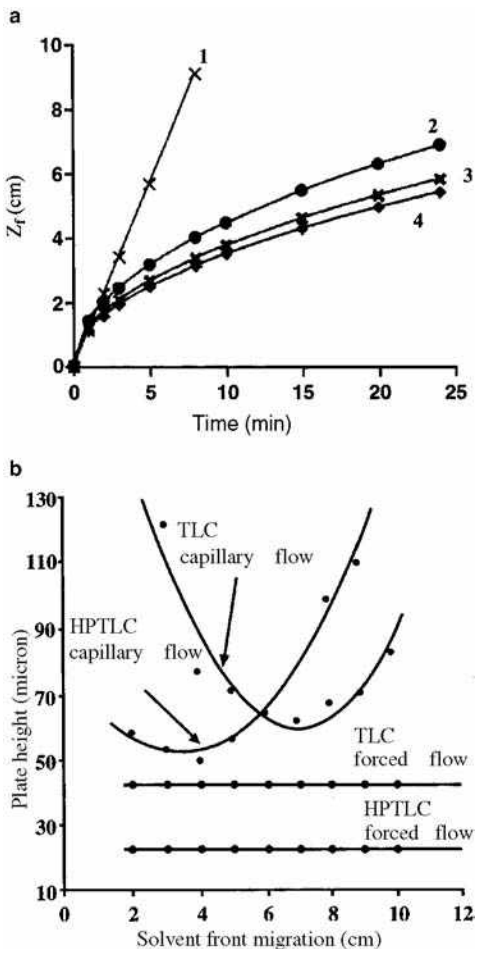

Fig. 2 a, Plot of solvent front migration distance z_f for dichloromethane on a high-performance silica gel layer as a function of time under different experimental conditions. Identification: 1 = forced flow development at u_{opt}; 2 = capillary flow in a saturated developing chamber; 3 = capillary flow in a sandwich chamber; and 4 = capillary flow in an unsaturated developing chamber; and b, Variation of the observed plate height as a function of the solvent front migration distance for conventional TLC and high-performance thin-layer chromatography (HPTLC) silica layers under capillary flow and forced flow (u_{opt}) conditions.

BAND-BROADENING INTERPRETATION

The kinetic contributions to zone broadening are evaluated by fitting data for the column plate height, as a function of the mobile-phase velocity, to a mathematical model describing the relationship between the two parameters. Several models have been used in the above experiment, but those by de Ligny and Remijnsee[7] and Knox and Pryde,[12] and developed by Guiochon and Siouffi,[9] are most widely used and, at least for a first approximation, allow for comparison and determination of the differences between TLC and column chromatography:[7–11]

$$\bar{H} = \frac{3A_k d^{5/3}\theta^{1/3}}{2(2D_m)^{1/3} z_f^{1/3}} \frac{(z_f^{2/3} - z_0^{2/3})}{z_f - z_o} + \frac{B_k D_m}{\theta d_p}(z_f - z_o) + \frac{C_k \theta d_p^{3}}{2D_m(z_f - z_o)} \lg \frac{z_f}{z_o} \quad (12)$$

where d_p is the average particle size, χ is the mobile-phase velocity constant, and D_m is the solute diffusion coefficient in the mobile phase. A_k, B_k, and C_k are dimensionless coefficients characterizing the packing quality (A_k), the diffusion in the mobile phase (B_k), and the resistance to mass transfer (C_k). Eq. 12 can be helpful in the interpretation of the influence of layer structure on plate height. Results of simulations of the relationship between plate height and different parameters are presented in Fig. 3 and parameters used in simulation are presented in Table 1.

UNIDIMENSIONAL MULTIPLE DEVELOPMENT

Unidimensional multiple development provides a complementary approach to forced flow for minimizing zone broadening.[13] All unidimensional multiple development techniques employ successive repeated development of the layer in the same direction, with removal of the mobile phase between developments. Approaches differ in the changes made (e.g., mobile-phase composition and solvent front migration distance) between consecutive development steps; the total number of successive development steps employed can also be varied. Capillary forces are responsible for migration

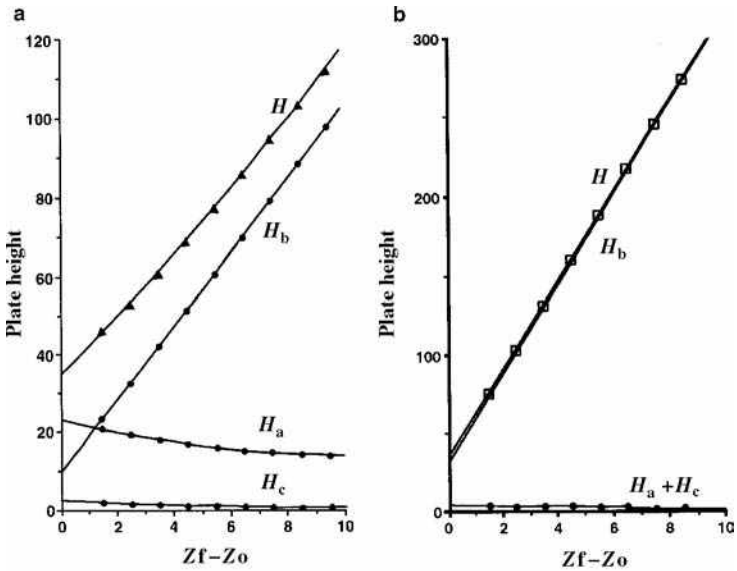

Fig. 3 a, Simulation of the average plate height for a TLC layer by use (Eq. 12) and properties listed in Table 1. The contribution from flow anisotropy is represented by H_a, that from longitudinal diffusion by H_b, and that from resistance to mass transfer by H_c; and b, Simulation of the average plate height for an HPTLC layer by use (Eq. 12) and properties listed in Table 1. The contribution from flow anisotropy is represented by H_a, that from longitudinal diffusion by H_b, and that from resistance to mass transfer by H_c.

of the mobile phase, but a zone-focusing mechanism is used to counteract the normal zone broadening that occurs in each successive development. Each time the solvent front traverses the stationary sample zone, the zone is compressed in the direction of development. The compression occurs because the mobile phase contacts the bottom edge of the zone first; here, the sample molecules start to move forward before those molecules are still ahead of the solvent front. When the solvent front has moved beyond the zone, the focused zone migrates and is subject to the normal zone-broadening mechanisms. Experiment indicates that, beyond a minimum number of development steps, zone widths converge to a constant value that is roughly independent of migration distance.

SOLVENT GRADIENTS

A similar phenomenon, compression of chromatographic zones, occurs in gradient TLC when the concentration of mobile phase delivered to the layer is varied in a stepwise manner. In the case where the concentration front traverses the sample zone, the zone is compressed in the direction of development. The compression takes place on the length equal to the diameter of the spot. Application of multicomponent eluent for the development of the layer, when the components differ in polarity, causes the creation of a natural gradient in the mobile phase. The gradient appears as multiconcentration fronts.[14] As in step gradients, the compression takes place and the widths of the spots are much smaller. This should improve resolution.

Table 1 Characteristic properties of precoated layers and HPLC columns.

Property	HPTLC	TLC	HPLC
Porosity total	0.65–0.70	0.65–0.75	0.8–0.9
Interparticle	0.35–0.45	0.35–0.45	0.4–0.5
Intraparticle	0.28	0.28	0.4–0.5
Flow resistance parameter	875–1500	600–1200	500–1000
Apparent particle size (μm)	5–7	8–10	d_p
Minimum plate height (μm)	22–25	35–45	2–3 d_p
Optimum velocity (cm/sec)	0.03–0.05	0.02–0.05	0.2
Minimum reduced plate height	3.5–4.5	3.5–4.5	1.5–3
Optimum reduced velocity	0.7–1.0	0.6–1.2	3–5
Separation impedance 9,000–70,000	10,500–19,800	11,100–60,200	2,000–9,000
Mean pore diameter (Si 60) (nm)	5.9–7.0	6.1–7.0	
Knox coefficients			
A_k	0.75	2.83	0.5–1
B_k	1.56	1.18	1–4
C_k	1.42	0.84	0.05

Adapted from Poole[6] and Knox & Pryde.[12]

Table 2 Zone capacity calculated or predicted for different separation conditions in TLC.[6]

Method	Dimensions	Zone capacity
(A) *Predictions from theory*		
Capillary flow	1	<25
Forced flow	1	<80 (up to 150, depending on pressure limit)
Capillary flow	2	<400
Forced flow	2	Several thousands
(B) *Based on experimental observations*		
Capillary flow	1	12–14
Forced flow	1	30–40
Capillary flow (AMD)	1	30–40
Capillary flow	2	~100
2		
(C) *Predictions based on results in (B)*		
Forced flow	2	~1500
Capillary flow (AMD)	2	~1500

MOVING PLATE

Changing the solvent entry position for each, or some, of the development steps enables the separation in each segment to be achieved in the shortest possible time under favorable capillary flow conditions. With as few as 10 developments, it is relatively easy to achieve 15,000–25,000 apparent theoretical plates for a zone migration distance of 6–11 cm.[6,15,16]

ZONE CAPACITY

The potential of a chromatographic system to achieve a particular separation can be estimated from its zone capacity, also referred to as the separation number (SN). It provides a method of comparison of different TLC systems and an indication of the possibility of separating a given mixture:[8]

$$\mathrm{SN} = \frac{z_\mathrm{f}}{b_0 + b_1} - 1 \qquad (13)$$

where b_0 is the extrapolated width of the starting spot at half-height of the concentration curve, and b_1 is the extrapolated width of the spot with $R_\mathrm{f} = 1$. Some typical results for the zone capacity, either predicted from theory or by experiment, are summarized in Table 2.[6] Experimental observations are indicated for zone capacity of approximately 12–14 for a single development in a capillary flow, increasing to 30–40 if forced flow is used. Use of capillary flow and the zone-focusing mechanism of multiple development leads to a zone capacity similar to that for forced flow.

CONCLUSIONS

In capillary flow conditions, there is an inadequate range of mobile-phase velocities, which does not allow working at u_opt values; the role of the binder remains not completely clear. The zone-focusing mechanism causes an increase of separation performance of the system in the most simple way. Forced flow offers a modest increase in performance with a reduction in separation time.

REFERENCES

1. Giddings, J.C. *Unified Separation Science*; John Wiley & Sons, Inc.: New York, 1991; 10.
2. Kowalska, T. Theory and mechanism of thinlayer chromatography. In *Handbook of Thin Layer Chromatography,* 2nd Ed.; Sherma, J., Fried, B., Eds.; Marcel Dekker, Inc.: New York, 1996; Vol. 71, 49–80.
3. Cazes, J.; Scott, R.P.W. Thin layer chromatography. In *Chromatography Theory*; Marcel Dekker, Inc.: New York, 2002; 443–454.
4. Geiss, F. *Fundamentals of Thin Layer Chromatography*; Hüthig: Heidelberg, 1987; 9–82.
5. Van Deemter, J.J.; Zuiderweg, F.; Klinkenberg, A. Longitudinal diffusion and resistance to mass transfer as causes of nonideality in chromatography. Chem. Eng. Sci. **1956**, *5*, 271.
6. Poole, C.F. Kinetic theory of planar chromatography. In *Planar Chromatography. A Retrospective View for the Third Millenium*; Nyiredy, Sz., Ed.; Springer: Budapest, 2001; 13–32.
7. de Ligny, C.L.; Remijnsee, A.G. Peak broadening in paper chromatography and related techniques: III. Peak broadening in thin-layer chromatography on cellulose powder. J. Chromatogr. **1968**, *33*, 242–254; 257–268.
8. Zlatkis, A.; Kaiser, R.E. *HPTLC High Performance Thin Layer Chromatography*; Elsevier: Amsterdam, 1977; 15–38.
9. Guiochon, G.; Siouffi, A. Band broadening and plate height equation. III. Flow velocity. J. Chromatogr. Sci. **1978**, *16*, 470–481; 598–609.
10. Belenkii, B.B.; Nesterov, V.V.; Smirnov, V.V. Differential equation for thin layer chromatography

and its solution. Russ. J. Phys. Chem. **1968**, *42*, 773–775; 1527–1530.
11. Belenkii, B.B.; Nesterov, V.V.; Smirnov, V.V. Comparison of theory with experimental results. Russ. J. Phys. Chem. **1968**, *42*, 773–775; 1527–1530.
12. Knox, J.H.; Pryde, A. Performance and selected applications of a new range of chemically bonded packing materials in high-performance liquid chromatography. J. Chromatogr. **1975**, *112*, 171–188.
13. Poole, C.K.; Poole, S.K. Instrumental thin-layer chromatography. Anal. Chem. **1994**, *66*, 27A–37A.
14. Poole, C.K.; Poole, S.K. *Chromatography Today*; Elsevier: Amsterdam, 1991.
15. Niederwieser, A.; Honegger, C.C. Gradient techniques in thin-layer chromatography. In *Advances in Chromatography*; Giddings, J.J.; Keller, R.A., Eds.; Marcel Dekker, Inc.: New York, 1966; Vol. 2, 123.
16. Fernando, W.P.N.; Poole, C.F. Determination of kinetic parameters for precoated silica gel thin-layer chromatography plates by forced flow development. J. Planar Chromatogr. **1991**, *4*, 278–287.

BIBLIOGRAPHY

1. Grinberg, N.; LoBrutto, R. Efficiency in chromatography. In *Encyclopedia of Chromatography*, 3rd Ed.; Cazes, J., Ed.; Taylor & Francis: New York, 2010; 685–687.
2. Grinberg, N., Ed.; *Modern Thin Layer Chromatography*; Marcel Dekker, Inc.: New York, 1990.
3. Tijssen, R. The mechanisms and importance of zone-spreading. In *Handbook of HPLC*; Katz, E. Eksteen, R. Schoenmakers, P., Miller, N., Eds.; Marcel Dekker, Inc.: New York, 1998; 55–142.
4. Fernando, W.P.N.; Poole, C.F. Comparison of the kinetic properties of commercially available precoated silica gel plates. J. Planar Chromatogr. 1993; *6*, 357–361.

Electrochemical Detection

Peter T. Kissinger
Chairman and CEO, Bioanalytical Systems, Inc., West Lafayette, Indiana, U.S.A.

INTRODUCTION

With respect to chromatography, "electrochemical detection" means amperometric detection. Amperometry is the measurement of electrolysis current vs. time at a controlled electrode potential. It has a relationship to voltammetry similar to the relationship of a UV detector to spectroscopy. While conductometric detection is used in ion chromatography, potentiometric detection is never used in routine practice. Electrochemical detection has even been used in gas chromatography (GC) in a few unusual circumstances. It has even been attempted with thin-layer chromatography (TLC). Its practical success has only been with liquid chromatography (LC), and that will be the focus here.

Most chemists remember electrochemistry as a difficult subject they heard about in physical chemistry courses, and they regard it as having something to do with batteries. Both of these impressions are true! What is important here is to understand that: 1) redox reactions can be made to occur at surfaces (electrodes); and 2) amazingly enough, such reactions are not just the fate of metals ($Fe^{+++} \rightarrow Fe^{++}$) but actually occur quite widely among organic compounds of interest, such as drugs, pesticides, explosives, food additives, neurotransmitters, DNA, etc. There are good references for the novice wishing to understand the analytical electrochemistry of organic substances.[1] I present a few common examples below for both oxidations (electrons are lost; the process is anodic) and reductions (electrons are gained by the analyte; the process is cathodic).

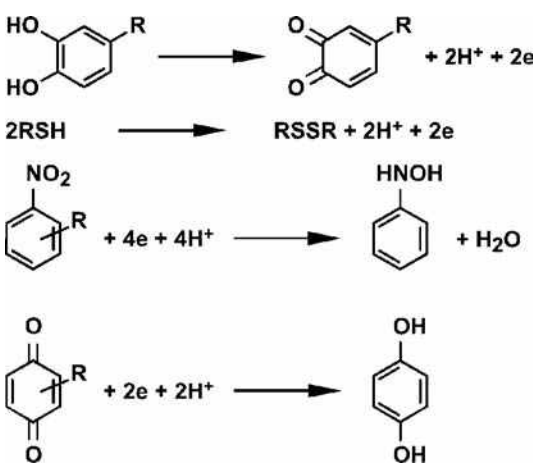

While we all remember (or try not to) the confusing math associated with electrochemistry and thermodynamics, all we need here is an appreciation of the fact that current, i, is proportional to the moles, N, of analyte reacted per unit time. The latter is proportional to concentration at a constant flow rate through a detector cell. The key equation is

$$i = \frac{dQ}{dt} = nF\frac{dN}{dt}$$

where Q is the amount of electricity (charge in coulombs), n is the number of electrons, and F is the Faraday constant. As one can see from the above examples, most organic analytes are involved in reactions where $n = 1$, 2, or 4. To use an electrochemical detector, it is very important to know that i is proportional to concentration and the amount injected, just as UV absorbance is proportional to concentration or the amount injected.

LC/electrochemistry (LCEC) is now over 30 years old.[1] In recent years, an emphasis has been placed on miniaturizing the technology to accommodate the study of smaller biological samples, often with a total available volume of only a few microliters. Both LC and electrochemistry are largely controlled by surface science. Considering this fact, both technologies benefit from reducing the distance from the bulk of the solution phase to the surface. In LC, this is accomplished by using smaller diameter stationary phase particles. In electrochemistry, it is accomplished by using packed bed or porous electrodes and/or thin-layer cells with greatly restricted diffusion pathways.

For analytical purposes, there is no loss in concentration detection limit by reducing the total surface area available in both methodologies. In LC, this reduction is accomplished by using smaller diameter columns and in EC, by using smaller electrodes. With LC column diameters of 0.1–1.0 mm and radial flow thin-layer cells with dead volumes of a few tens of nanoliters, it is possible to build analytical instruments suitable for routine use by neuroscientists, drug metabolism groups, and pharmacokinetics experts. LC/electrochemistry has been used for foods, industrial chemicals, and environmental work. Nevertheless, biomedical applications have dominated. It shows no potential for preparative chromatography and is generally used when nanograms or picograms hold some appeal.

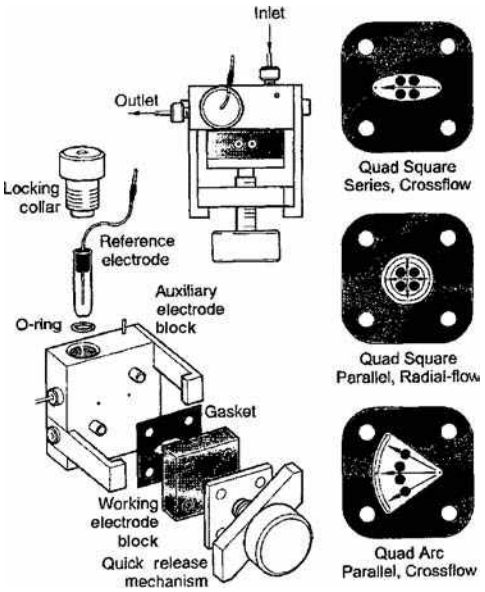

Fig. 1 One example of a sandwich type thin-layer LCEC detector with adjustable dead volume, flow pattern, and up to four channels. **Source:** From Four channel liquid chromatography/electrochemistry, in Curr. Sep.[2]

DETECTOR CELLS

A wide variety of detector cells have been used for LCEC.[1] The choice can be baffling to a non-expert. These all "work" to some degree. The key issues:

1. An electrode (the "working electrode") exposed to the mobile phase in a dead volume (small) appropriate to the column diameter chosen.
2. A place to locate at least one other electrode (a "counterelectrode") or preferentially two (an auxiliary electrode and a reference electrode).
3. The possibility for a choice of different working electrode materials (see following section).
4. The possibility of multiple channels in series or parallel.

Fig. 1 is representative of one choice that meets these criteria.[2] Such a cell is normally described as a "thin-layer sandwich configuration." The working electrode(s) is (are) in the form of an interchangeable block. Electrodes of different sizes, shapes, or materials can be accommodated with a flow pattern established by a gasket shape and thickness. Such cells can easily be adapted for LC flow rates of 5–5000 μl/min. Different designs are used for capillary separation tools such as capillary electrophoresis (CE).

ELECTRODE MATERIALS

The most common electrode material used in LCEC is carbon, either as solid "glassy carbon" disks in thin-layer cells, or as a high surface area porous matrix through which the mobile phase can flow. Gold electrodes are useful to support a mercury film, and these are primarily used to determine thiols and disulfides, and also for carbohydrates using pulsed electrochemical detection (PED) with high pH mobile phases. Platinum electrodes are occasionally useful for specific analytes, but are most frequently employed to determine hydrogen peroxide following an oxidase immobilized enzyme reactor (IMER). More recently, copper electrodes have begun to attract serious interest for determination of carbohydrates in basic mobile phases. Glassy carbon is the overwhelming favorite choice due to its wide range of applicable potentials and its rugged convenience. Bulk glassy carbon is difficult to use in geometries other than disks and plates. There are a number of other geometries that have practical interest for multiple electrode detectors. One of the more valuable recent contributions to LCEC derives from the ability to deposit conducting vitreous carbon films on silicon or quartz substrates using lithography techniques. The lithography technology makes it possible to lay down a variety of electrode geometries, which could not possibly be manufactured in small sizes by traditional machining. While such electrodes are still at the research stage, they show considerable promise. Detector cells with 2, 4, or even 16 electrodes are commercially available. There are obvious parallels with diode array detection (DAD). When two electrodes are used in series, there are similarities to fluorescence or MS/MS in the way that selectivity is often enhanced.

PULSED ELECTROCHEMICAL DETECTION

There are many substances that would appear to be good candidates for LCEC from a thermodynamic point of view, but that do not behave well due to kinetic limitations. Johnson and coworkers at Iowa State University used some fundamental ideas about electrocatalysis to revolutionize the determination of carbohydrates, nearly intractable substances that do not readily lend themselves to ultraviolet absorption (LCUV), fluorescence (LCF), or traditional d.c. amperometry (LCEC).[3] At the time this work began, the LC of carbohydrates was more or less relegated to refractive index detection (LCRI) of microgram amounts. The importance of polysaccharides and glycoproteins, as well as traditional sugars, has focused a lot of attention on PED methodology. The detection limits are not competitive with d.c. amperometry of more easily oxidized substances such as phenols and aromatic amines; however, they are far superior to optical detection approaches.

POSTCOLUMN REACTIONS

Electrochemical detection is inherently a "chemical" rather than a "physical" technique (such as ultraviolet, infrared,

fluorescence, or refractive index). It is therefore not surprising to find that many imaginative postcolumn reactions have been coupled to LCEC. These include photochemical reactions, enzymatic reactions, halogenation reactions, and Biuret reactions. In each case, the purpose is to enhance selectivity and therefore improve limits of detection. While simplicity is sacrificed with such schemes, there are many published methods that have been quite successful.

CAPILLARY ELECTROPHORESIS AND CAPILLARY ELECTROCHROMATOGRAPHY (CEC)

Since there is LCEC, it is only logical that there should be CEEC and CEC/EC. This area was pioneered by Andrew Ewing at the Pennsylvania State University. Richard Zare (Stanford University) and Susan Lunte (Kansas University) have explored this idea in a number of unique ways. The basic technology has been recently reviewed.[4] There are several fundamental problems that do not occur with LCEC. First, the capillaries must be of small diameter to properly dissipate resistive heating. Thus, the electrodes used in CEEC are normally carbon fibers or metallic wires placed in or at the capillary end. Second, the electrical current through the capillary that establishes the electroosmotic pumping is much larger than the electrolysis current measured in determining analytes of interest. The ionic and electrolytic currents need to be "decoupled" in some way. A third concern is that the flow rate in CE or CEC is not independent of the choice of "mobile phase" or even the sample, whereas in LC it is easily predetermined and maintained by a volume displacement pump. In spite of these concerns, CE is very attractive because of its high resolution per unit time and the small sample volumes required. In the case of CEEC, the concentration detection limits are frequently superior to those of optical detectors for suitable analytes. This is because electrochemical detection is a surface (not volume) dependent technique. In the grand scheme of things, at this writing, CE and CEC are very rarely used vs. LC, and therefore CEEC and CEC/EC must be considered academic curiosities until this situation changes.

CONCLUSIONS

Electrochemical detection has matured considerably in recent years and is routinely used by many laboratories, often for a very specific biomedical application. The most popular applications include acetylcholine, serotonin, catecholamines, thiols and disulfides, phenols, aromatic amines, macrocyclic antibiotics, ascorbic acid, nitro compounds, hydroxylamines, and carbohydrates. As the last century concluded, it is fair to say that many applications for which LCEC would be an obvious choice are now pursued with LC/MS/MS. This only became practical in the 1990s and is clearly a more general method applicable to a wider variety of substances. In a similar fashion, LC/MS/MS has also largely supplanted LCF for new bioanalytical methods. Nevertheless, there remain a number of key applications for these more traditional detectors, known for their selectivity (and therefore excellent detection limits). Likewise, it will be quite a few years before LC/MS/MS is affordable worldwide. An interesting recent development is the combination of electrochemical detector flow cells with MS in various configurations including EC/LC/MS/MS and LC/EC/MS/MS.[5] This enables information-rich solution phase redox chemistry to be combined with gas phase ion chemistry, adding a new dimension for complex samples. It also provides new mechanistic information on the electrochemical detection process.[6]

REFERENCES

1. Kissinger, P.T., Heineman, W.R., Eds.; *Laboratory Techniques in Electroanalytical Chemistry,* 2nd Ed.; Marcel Dekker Inc.: New York, 1996.
2. Solomon, B.P.; Long, H.; Zhu, Y.; Gunaratna, C.; Coury, L. Four channel liquid chromatography/electrochemistry. Curr. Sep. **2000**, *18* (4), 114.
3. LaCourse, W.R. *Pulsed Electrochemical Detection in High-Performance Liquid Chromatography*; John Wiley & Sons: New York, 1997.
4. Holland, L.A.; Lunte, S.M. Capillary electrophoresis coupled to electrochemical detection: A review of recent advances. Anal. Commun. **1998**, *35*, 1H–4H.
5. Bŏkman, C.F.; Zettersten, C.; Sjŏberg, P.J.R.; Nyholm, L. A setup for the coupling of a thin-layer electrochemical flow cell to electrospray mass spectrometry. Anal. Chem. **2004**, *76* (7), 2017–2024.
6. Arakawa, R.; Yamaguchi, M.; Hotta, H.; Osakai, T.; Kimoto, T. Product analysis of caffeic acid oxidation by on-line electrochemistry/electrospray ionization mass spectrometry. J. Am. Soc. Mass. Spectrom. **2004**, *15*, 1228–1236.

Electrochemical Detection in CE

Oliver Klett
Institute of Chemistry, Uppsala University, Uppsala, Sweden

INTRODUCTION

Capillary electrophoresis (CE) is a powerful separation tool which has its primary strength in the high separation efficiency and short analysis times.

DISCUSSION

By decreasing the internal diameter (I.D.) of the capillaries used, the situation can be further improved due to the possibility of using higher separation voltages. Such a miniaturization, however, often involves a challenge regarding how the detection is to be made in the narrow capillaries for sample volumes in the nanoliter to subpicoliter range. Electrochemical (EC) methods, usually based on the use of microelectrodes, are relatively inexpensive and are readily miniaturized and adapted to such low volumes and capillary sizes without loss of performance. Electrochemical detection is based on the monitoring of changes in an electrical signal due to a chemical system at an electrode surface, usually as a result of an imposed potential or current. The principles, advantages, and drawbacks of currently used EC methods will be discussed briefly below.

In a solution, the equilibrium concentrations of the reduced and oxidized forms of a redox couple are linked to the potential (E) via the Nernst equation

$$E = E^{0\prime} + \frac{RT}{nF}\ln\left(\frac{c(\text{ox})}{c(\text{red})}\right) \quad (1)$$

with $E^{0\prime}$ the standard potential and c(ox) and c(red) the concentration of the oxidized and reduced forms, respectively; the other symbols have their usual meaning.

In electrochemical detection, the potential of a working electrode can be measured versus a reference electrode, usually while no net current is flowing between the electrodes. This type of detection is referred to as "potentiometry." Alternatively, a potential is applied to the working electrode with respect to the reference electrode while the generated oxidation or reduction current is measured. This technique is referred to as "amperometry." When applying a negative potential to the working electrode, the energy of the electrons in the electrode is increased and, eventually, an electron can be transferred to the lowest unoccupied level of a species in the nearby solution. This species is thus reduced; vice versa, species can be oxidized by applying a sufficiently high positive potential. In both cases, the generated current (i) can be expressed by

$$i = -aFDnc\delta_N^{-1} \quad (2)$$

with a being the electrode area, D the diffusion coefficient, δ_N the thickness of diffusion layer; the other symbols have their usual meaning. For each redox couple, there exists a potential, the standard potential E^0, for which the reduced and oxidized forms are present in equal concentrations. By applying a potential more positive than E^0, the concentration of the reduced form is forced to decrease at the electrode surface while the concentration of the oxidized form increases. This process is the cause of the current measured in amperometric techniques. By choosing the applied potential, it is also possible to discriminate between different analytes. The range of potentials that can be applied in amperometric detection is, however, generally limited by redox processes involving the solvent [e.g., the oxidative and reductive evolution of oxygen ($2H_2O \rightarrow O_2 + 4H^+ + 4e^-$) and hydrogen ($H_2O + e^- \rightarrow 0.5\ H_2 + OH^-$), respectively, in water]. A wide range of physiologically and pharmacologically important substances, as well as many heavy metals, transition metals, and their complexes, exhibit standard potentials within this accessible potential range. In fact, many metabolic pathways involve redox processes taking place in aqueous systems. Neurotransmitters of the catechol type (*O*-dihydroxy benzene derivatives) were consequently among the first reported analytes for electrochemical detection in CE (CE/EC). Detection limits down to can be achieved in this way.

The choice of working electrode material is an important factor in amperometric detection. For catechols and similar substances, such as phenolic acids, electrodes made of glassy carbon have shown good performances. Other good detectable and biological important substances include thiols and disulfides (e.g., cysteine, glutathione, and their disulfides which are best detected on an Au/Hg amalgam electrode); amino acids and peptides, which can be detected using Cu electrodes, and carbohydrates, glycopeptides, and nucleotides, detected on Au, Cu, or Ni electrodes.

Commonly in amperometric detection, a fiber or disk microelectrode is used where the electrode is positioned in or close to the outlet of the capillary (see Fig. 1). A complication when working with EC in CE is the need for careful alignment of the electrode(s) and capillary

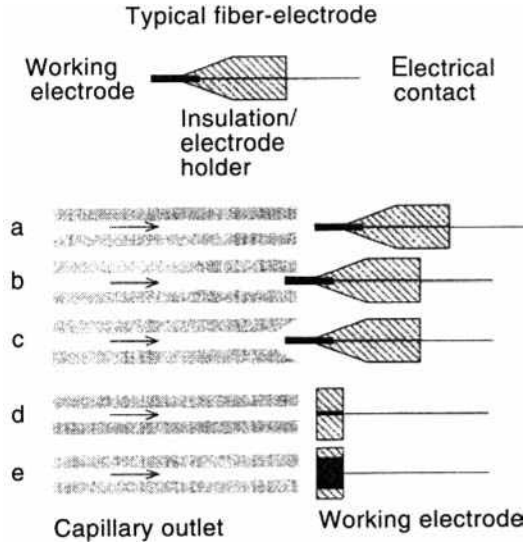

Fig. 1 Electrode setups for CE/EC with fiber microelectrodes: (a) end column, (b) on-column, (c) improved on-column, (d) wall tube, and (e) wall-jet detection.

outlet. This alignment, which mostly is carried out with micromanipulators under a microscope, is essential to ensure both a good sensitivity and reproducibility and, hence, constitutes the main challenge while adapting EC for routine CE. Another complication in CE/EC involves the interference of the high-voltage (HV) separation field on the EC detection. In the first combination of EC and CE, it was assumed that the HV field had to be totally removed from the detection area. This was done by various kinds of decouplers, which unfortunately also introduced additional band broadening and decreased sensitivities. Furthermore, the manufacturing of the decouplers requires considerable labor-intensive experience and skill.

A later approach is based on the utilization of small-inner-diameter (<25 μm) capillaries to reduce the influence of the HV field.

In potentiometry, all ions present in the solution principally contribute to the potential of the working electrode. As the ratio between the analyte concentration and that of other species in the solution generally is rather low, the analyte contribution to the detector signal is often low, which results in relatively poor detection limits. To circumvent this problem, ion-selective membranes (ISM), which permit only some ions to pass through the membranes, are commonly employed. In this way, detection limits down to 10^{-7} mol/L can be achieved. The ISM also reduces the influence from matrix components, which allows measurements in complex matrices such as blood or serum without interferences. The long-term stability of these electrode may, however, be a problem, as the electrodes might have to be replaced after a few hours or days. Common analytes are inorganic anions and cations, especially alkali and alkaline earth metals ions. A further application is the indirect detection of amino acids, where the complexing of amino acids with Cu^+ ions selectively alters the potential of a copper electrode.

In conductometry, two working electrodes placed either in or at the end of the capillary, along the capillary axis, are commonly employed. A high-frequency AC potential is applied between the working electrodes and the conductance (L) of the solution is continually monitored. In this way, the passing of any zone deviating in its ion composition from the background is detected. As the ion mobilities contribute to the magnitude of the signal as seen in Eq. 3, slowly moving large molecules and low charged biomolecules are less straightforwardly detected, whereas detection limits down to some hundred parts per thousand have been reported for small inorganic and organic ions:

$$L = \frac{FA\Sigma i|z_i|u_i c_i}{l} \tag{3}$$

with A as the cross-sectional area perpendicular to the AC field, l the electrode distance, and u the mobility. Applications have been described for ions up to a size of sulfate or Cd^+ and MES or benzylamine, respectively.

BIBLIOGRAPHY

The field of electrochemical detection in CE have been extensively reviewed in Refs.[1–3] Instructive applications can be found for amperometry in Ref.,[4] for potentiometry in Ref.,[5] and for conductometry in Ref.[6] An example of miniaturized on-chip EC/CE is given in Ref.[7] The theoretical aspects of electrochemical detection have been discussed in detail in Ref.[8]

REFERENCES

1. Voegel, P.D.; Baldwin, R.P. Electrophoresis **1997**, *18* (12–13), 2267–2278.
2. Holland, L.A.; Chetwyn, N.P.; Perkins, M.D.; Lunte, S.M. Capillary electrophoresis in pharmaceutical analysis. Pharmaceut. Res. **1997**, *14* (4), 372–387.
3. Kappes, T.; Hauser, P.C. Electrochemical detection methods in capillary electrophoresis and applications to inorganic species. J. Chromatogr. A, **1999**, *834* (1–2), 89–101.
4. Holland, L.A.; Lunte, S.M. Postcolumn reaction detection with dual-electrode capillary electrophoresis-electrochemistry and electrogenerated bromine. Anal. Chem. **1999**, *71* (2), 407.
5. Kappes, T.; Hauser, P.C. Potentiometric detection in capillary electrophoresis with a metallic copper electrode. Anal. Chim. Acta **1997**, *354*, 129–134.
6. Haber, C.; et al., Conductivity detection in capillary electrophoresis—a powerful tool in ion analysis. J. Capillary Electrophoresis **1996**, *3* (1), 1–11.
7. Woolley, A.T.; Lao, K.; Glazer, A.N.; Mathies, R.A. Capillary electrophoresis chips with integrated electrochemical detection. Anal. Chem. **1998**, *70* (4), 684.
8. Brett, C.M.A.; Oliveira Brett, A.M. *Electrochemistry*; Oxford University Press: Oxford, 1993.

Electrokinetic Chromatography Including MEKC

Hassan Y. Aboul-Enein
Pharmaceutical and Medicinal Chemistry Department, Pharmaceutical and Drug Industries Research Division, National Research Center, Dokki, Cairo, Egypt

Vince Serignese
Pharmaceutical Analysis Laboratory, King Faisal Specialist Hospital and Research Center, Riyadh, Saudi Arabia

INTRODUCTION

Separation science technology has provided the analyst with numerous methods for quantitative determinations, the more established being high-performance liquid chromatography (HPLC) and gas chromatography (GC). With huge advancements in computer technology, extremely sensitive methods have been made available to the user such as tandem mass spectrometry (MS–MS), liquid chromatography/mass spectroscopy (LC/MS), and GC/MS. However, an electrophoretic technique which has been developed through joint efforts from a number of scientific disciplines is rapidly generating interest for its wide applicability and highly sensitive assays. The field of capillary electrophoresis (CE) borrows principles from conventional electrophoresis, LC, and GC. High-performance capillary electrophoresis (HPCE) refers to all techniques that have been developed on the subject. In this entry, the electrokinetic chromatographic (EKC) analysis method will be discussed, with emphasis on micellar electrokinetic chromatographic (MEKC). Before doing so, some fundamental principles of CE will be discussed.

ELECTROPHORETIC AND ELECTRO-OSMOTIC MIGRATION

Capillary zone electrophoresis (CZE)[1] is a basic mode of HPCE and serves as a good starting point for laying the background information on EKC and MEKC. Only ionic or charged compounds are separated, based on their differential eletrophoretic mobilities. Fig. 1 illustrates the setup for a CE system. In summary, electrolyte buffer solutions and electrodes are present at both ends of the open-tube fused-silica capillary. A positive high-voltage power supply is the source of current. A sample is injected hydrostatically or electrokinetically at the positive end of the capillary (capillary head) and, in the presence of an applied voltage potential, moves toward the negative electrode, where it is detected by an ultraviolet (UV) absorbance instrument. The signal produced is recorded as a chromatogram where sample components are identified as chromatographic peaks according to their retention times, and peak areas or heights are calculated for quantitative purposes.

During analyte migration, electrophoresis and electro-osmosis are taking place. The velocity (v_s, cm/sec) and mobility (μ_s, cm^2/V sec) of the solute are defined by the following equations:

$$v_s = v_{co} + v_{cp} \tag{1}$$

$$\mu_s = \mu_{co} + \mu_{cp} \tag{2}$$

where v_{co} and μ_{co} are electro-osmotic velocity and mobility, respectively, v_{cp} and μ_{cp} and are electrophoretic velocity and mobility, respectively. The relationship between velocity and mobility is given by

$$v = \mu E \tag{3}$$

where E (V/cm) is the electric field strength. Because E is constant for all solutes in a separation analysis, the solute velocities are differentiated by their mobilities.

Electrophoresis is an electrokinetic phenomenon whereby charged compounds in an electric field move through a continuous medium and separate by preferentially obtaining different electrophoretic mobilities according to their charges and sizes. Cations move toward the negative electrode (cathode) and anions move toward the positive electrode (anode).

Electro-osmosis is created by the electric doublelayer effect.[2] A fused-silica capillary at neutral pH attains fixed negative charges at the inner wall surface as its silanol groups undergo ionization. A layer of hydrated cations will form adjacent to the inner wall to counter the fixed negative charges. An applied voltage potential will cause the positively charged layer to migrate toward the cathode with a flat velocity profile, simultaneously dragging the bulk solution inside the capillary and transporting charged compounds at the electro-osmotic flow velocity. It is assumed that v_{co} is faster than v_{cp} and determines the direction of solute migration. Hence, a cation will have its sum total (Eq. 1) greater than the individual component velocities ($v_s > v_{co}$) and the anion will migrate slower than the electro-osmotic flow ($v_s < v_{co}$).

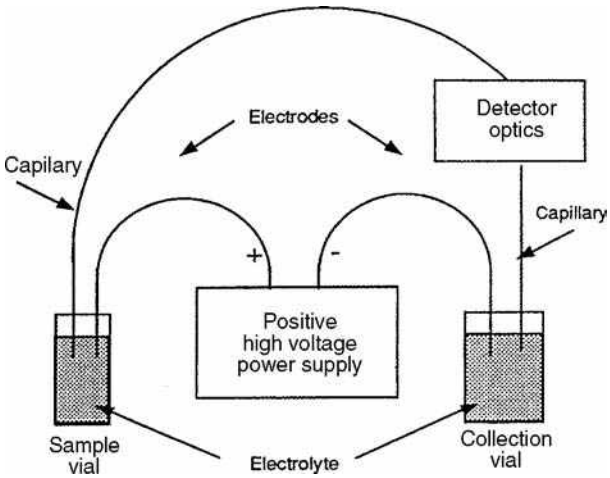

Fig. 1 Diagram of a CE system.
Source: Reprinted from Waters Quanta 4000E CE System Operator's Manual, Waters Corp., 1993.

Electro-osmosis need not be present in open-tube CE. Coatings exist that can be applied to the capillary surface to eliminate the electrical double layer. However, electro-osmotic flow can be used to reduce solute retention times, which can be advantageous for certain analyses.

As previously mentioned, electrophoretic separations using open-tube capillaries are based on solute differential mobility, which is a function of charge and molecular size. A different approach is required for separating neutral or uncharged compounds. Because charge is absent, electrophoretic mobility is zero. Electro-osmotic flow would allow them to migrate, but their velocities would be equal. Separation would not be possible with the above method.

ELECTROKINETIC CHROMATOGRAPHY

Terabe[3] developed a method that separates neutral or uncharged compounds; he named it electrokinetic chromatography. The experimental design is that of CZE (Fig. 1). The difference lies in the separation principle. In LC, a solute freely distributes itself between two phases [i.e., a mobile phase usually made of a mixture of aqueous and organic solvents and a stationary phase (a solid material packed in a steel housing known as a chromatographic column)]. Under high pressure, the mobile phase is delivered by a liquid chromatographic pump and continuously solvates the stationary phase, thereby transporting nonvolatile compounds of interest that are introduced into the system via chromatographic injection. Separation is based on their phase-distribution profiles. EKC follows the above principle but uses electro-osmosis and electrophoresis to displace analytes and "chromatographic phases" in capillaries.

The electrolyte buffer solution is analogous to the mobile phase. A charged substance, referred to as the carrier, is dissolved in the electrolyte buffer. The neutral solute present in the separation medium will partition itself between the carrier (incorporated form) and the surrounding solution (free form). The carrier ("chromatographic phase") corresponds to the stationary phase in conventional chromatography with modifications, in that it is not a fixed support and exists homogeneously in solution. For this reason, the carrier is called the "pseudo-stationary phase." As discussed in the previous section, the charged carrier will transport the incorporated solute electrophoretically (here, is the carrier velocity) at a slower velocity than the free solute migrating with the electro-osmotic flow velocity in the opposite direction. The point to keep in mind is that the carrier migrates with a different velocity than the bulk solution. The variation of the ratio of the amount of incorporated solute to the amount of total solute between separands in a sample mixture will lead to sample component separation.

MICELLES IN ELECTROKINETIC CHROMATOGRAPHY

Different types of EKC have been developed. Cyclodextrins (CDEKC) have been used to form inclusion complexes with solutes to effect their separation. Other examples of EKC include microemulsion electrokinetic chromatography (MEEKC). The MEKC technique (for a detailed treatise, the reader is referred to Ref.[4]) utilizes the presence of micelles in the electrolyte buffer solution to influence the migration time of solutes. In this case, the separation carrier is the micelle.[5]

Surfactants produce micelles. Their amphophilic nature classifies them as detergents, surface-active agents that are composed of a hydrophilic group and a hydrophobic hydrocarbon chain. In addition to what is known as the critical micelle concentration (CMC), individual surfactant molecules (monomers) interact with each other to form aggregates or micelles, establishing a state of equilibrium between a constant monomer concentration and a rapidly increasing micelle concentration.

As shown in Fig. 2, micelles are depicted as "round-like" structures with their polar moieties exteriorly located in the vicinity of the aqueous medium and their hydrophobic tails oriented inward forming a cavity. The sizes and shapes of the structures formed when monomer units aggregate is affected by electrolyte concentration, pH, temperature, and hydrocarbon chain length. During aggregation, interactions occur not only between the aggregates but also among the monomer units within the aggregate structure. Monomer unit distribution (the number of surfactant molecules in an aggregate) is characteristic of the surfactant used. Fig. 2 displays several forms of aggregates that exist in solution and Table 1 gives examples of surfactants.

Basically, MEKC is an EKC application with the micelle as the designated carrier. A surfactant at a concentration above the CMC is added to the running buffer and

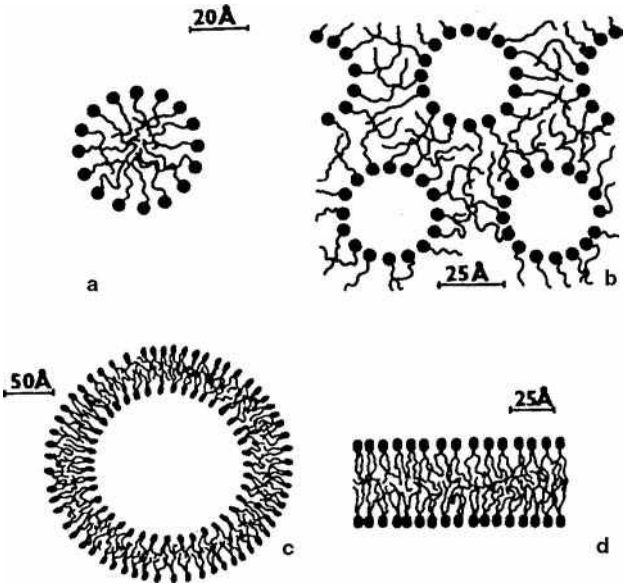

Fig. 2 Examples of aggregate structures of surfactants in solution: (a) micelle; (b) inverted micelles; (c) bilayer vesicle; (d) bilayer.
Source: From Physics of amphiphiles: micelles, vesicles and microemulsions, in Proceedings of the International School of Physics "Enrico Fermi," CourseXC.[6]

initiates micelle formation. Because the separation principle has already been dealt with and the flow scheme in Fig. 3 is an illustrative summary notated for MEKC, it is clear that a neutral analyte residing in the hydrophobic interior of a micelle (depicted as a sphere in Fig. 3) will be transported with the micelle's velocity (v_{mc}). The free analyte will migrate with the electro-osmotic flow velocity (v_{co}).

The chromatographic aspect (solute partitioning) of the separation[8] can be explained in terms of a commonly used parameter in chromatography, the retention or capacity factor. We begin with the following equation:

$$k' = \frac{n_{mc}}{n_{aq}} \tag{4}$$

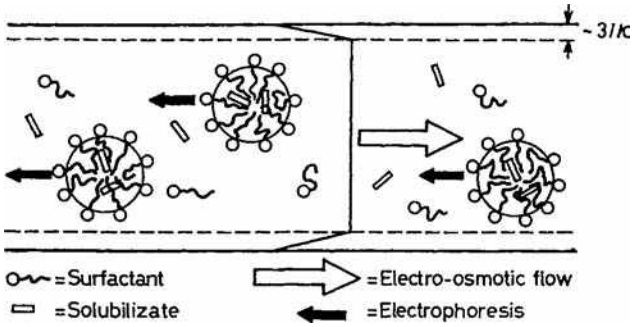

Fig. 3 Schematics of the separation principle of MEKC.
Source: From Micellar electrokinetic chromatography, in *Capillary Electrophoresis Technology*.[8]

where n_{mc} and n_{aq} are the mole amounts of the analyte in the micellar and aqueous phases, respectively. The corresponding mole fractions are given by

$$\frac{n_{mc}}{n_{mc} + n_{aq}} \text{ and } \frac{n_{aq}}{n_{mc} + n_{aq}}$$

where $n_{mc} + n_{aq}$ is the total amount of analyte present in the electrolyte buffer. The relationship in Eq. 4 and appropriate substitutions transform the above ratios into $k'/(1 + k')$ for the micelle analyte mole fraction and $1/(1 + k')$ for the aqueous analyte mole fraction. The total analyte velocity (v_s) takes the form

$$v_s = \frac{1}{1 + k'} v_{co} + \frac{k'}{1 + k'} v_{mc} \tag{5}$$

where $[1/(1 + k')]$ represents the velocity of the analyte mole fraction in the aqueous phase and $[k'/(1 + k')]v_{mc}$ is the velocity of the analyte mole fraction in the micellar phase.

Because velocity is a function of length (the capillary length from the point of injection to the detector cell) over time ($v = l/t$), we can substitute and rearrange the terms in Eq. 5 to obtain a relationship between the migration time (t_R) of the analyte and k':

Table 1 Some common surface-active agents.

Anionic	
Sodium stearate	$CH_3(CH_2)_{16}COO^-Na^+$
Sodium oleate	$CH_3(CH_2)_7CH{=}CH(CH_2)_7COO^-Na^+$
Sodium dodecyl sulfate	$CH_3(CH_2)_{11}SO_4^-Na^+$
Sodium dodecyl benzene sulfonate	$CH_3(CH_2)_{11} \cdot C_6H_4 \cdot SO_3^-Na^+$
Cationic	
Laurylamine hydrochloride	$CH_3(CH_2)_{11}NH_3^+Cl^-$
Cetyltrimethylammonium bromide	$CH_3(CH_2)_{15}N(CH_3)_3^+Br^-$
Nonionic	
Polyethylene oxides	$CH_3(CH_2)_7 \cdot C_6H_4 \cdot (O \cdot CH_2 \cdot CH_2)_8OH$

Source: From *Introduction to Colloid and SurfaceChemistry*.[7]

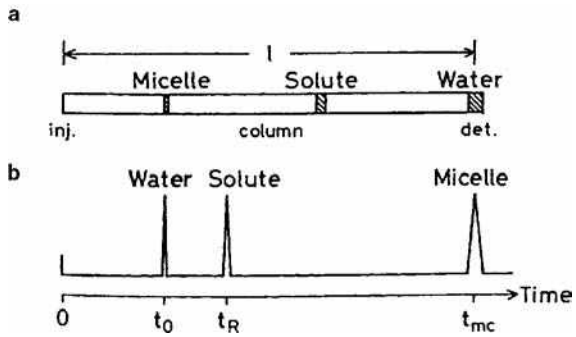

Fig. 4 (a) Representation of zone migration inside the capillary tube and (b) the corresponding chromatogram.
Source: From Electrokinetic chromatography with micellar solution and opentubular capillary, in Anal. Chem.[9]

$$T_R = \frac{1 + k'}{1 + (t_0/t_{mc})k'} t_0 \tag{6}$$

$$k' = \frac{t_R - t_0}{(1 - t_R/t_{mc})t_0} \left[\left(\frac{1 - t_R}{t_{mc}} \right) t_0 \right]^{-1} \tag{7}$$

Fig. 4a is a snapshot of the capillary tube following a sample injection at its positive end (inj.). The micelle, neutral solute, and aqueous solution (water) migrate toward the negative electrode (det.), establishing zones depicted by vertical bands, as they separate inside the capillary. The corresponding chromatogram in Fig. 4b shows the migration order where the t_R value for a neutral analyte is range bound between the migration times of the micelle (t_{mc}) and water (t_0). This limitation is reflected in the denominator of Eq. 6. When t_{mc} approaches infinity, the micelle is assumed to be stationary. The ratio t_0/t_{mc} will become zero and Eq. 6 turns into

$$t_R = 1 + k' \tag{8}$$

In this case, a neutral solute completely solubilized within the micelle will have a t_R value approaching infinity as its k' value does the same. Solute elution is assumed not to occur. Similarly, the free neutral analyte is unretained and its k' is equal to zero. Therefore, the t_R value will be equal to t_0 (Eq. 8). This explains why the neutral solute can migrate no slower than the micelle (t_{mc}) and no faster than the aqueous solution (t_0).

Although the above discussion focuses on neutral analyte separation, MEKC can be applied to ionic species which have their own electrophoretic mobilities and a broader migration time range.

CONCLUSIONS

The purpose of this entry was to provide the reader with a basic understanding of CE and to describe how a technique such as MEKC uses basic principles of chromatography to perform separations which are not possible electrophoretically. As the applications for electrokinetic chromatography rapidly expand, the future direction will develop on two fronts:

1. The development of novel separation carriers that will broaden the species range of separable analytes. EKC is suitable for separating small molecules, considering the size of the cavities of the established carriers.
2. The scope for further partition mechanisms, as new separation carriers are discovered, is promising. The separation principle is basic chromatography and with research efforts introducing new carriers in the pipeline, modified versions of the separation mechanism are possible.

Its rapid analysis time, low sample and solvent volume requirements, high resolution, and selectivity will continue to attract researchers who are involved in separation analysis.

REFERENCES

1. Radola, B.J., Ed.; *Capillary Zone Electrophoresis*; VCH: Weinheim, 1993.
2. Karger, B.L.; Foret, F. Capillary electrophoresis: Introduction and assessment. In *Capillary Electrophoresis Technology*; Guzman, N.A., Ed.; Marcel Dekker, Inc.: New York, 1993; 3–64.
3. Terabe, S. Electrokinetic chromatography: An interface between electrophoresis and chromatography. Trends Anal. Chem. **1989**, *8*, 129.
4. Muijselaar, P. Micellar electrokinetic chromatography: Fundamentals and applications. In *Ph.D. thesis*; Eindhoven University of Technology: Eindhoven, The Netherlands, 1996.
5. Foret, F.; Kivánková, L.; Boek, P. Principles of capillary electrophoretic techniques: Micellar electrokinetic chromatography. In *Capillary Zone Electrophoresis*; Radola, B.J., Ed.; VCH: Weinheim, 1993; 67–74.
6. Israelchvilli, J.N. Physics of amphiphiles: Micelles, vesicles and microemulsions. Proceedings of the International School of Physics "Enrico Fermi," CourseXC, North-Holland, Amsterdam, 1985; Degiorgio, V. Corti, M., Ed.; North-Hollsnd, 24–37.
7. Shaw, D.J. *Introduction to Colloid and Surface Chemistry*; Butterworths: London, 1966; 57–72.
8. Terabe, S. Micellar electrokinetic chromatography. In *Capillary Electrophoresis Technology*; Guzman, N.A., Ed.; Marcel Dekker, Inc.: New York, 1993; 65–87.
9. Terabe, S.; Otsuka, K.; Ando, T. Electrokinetic chromatography with micellar solution and open-tubular capillary. Anal. Chem. **1985**, *57*, 834.

Electron-Capture Detector

Raymond P.W. Scott
Scientific Detectors Ltd., Banbury, Oxfordshire, U.K.

INTRODUCTION

The electron-capture detector (ECD) is probably the most sensitive gas chromatography (GC) detector presently available. However, like most high-sensitivity detectors, it is also very specific and will only sense those substances that are electron capturing (e.g., *halogenated* substances, particularly fluorinated materials).

DISCUSSION

The ECD detector was invented by Lovelock[1] and functions on an entirely different principle from that of the argon detector. A low-energy β-ray source is used in the sensor to produce electrons and ions. The first source to be used was tritium absorbed onto a silver foil, but, due to its relative instability at high temperatures, this was replaced by the far more thermally stable ^{63}Ni source. The detector can be made to function in two ways: either a constant potential is applied across the sensor electrodes (the DC mode) or a pulsed potential is used (the pulsed mode).

A diagram of the ECD is shown in Fig. 1. In the DC mode, a constant electrode potential (a few volts) is employed that is just sufficient to collect all the electrons that are produced and provide a small standing current. If an electron-capturing molecule (e.g., a molecule containing a halogen atom which has only seven electrons in its outer shell) enters the sensor, the electrons are captured by the molecules and the molecules become charged. The mobility of the captured electrons are much reduced compared with the free electrons and, furthermore, are more likely to be neutralized by collision with any positive ions that are also generated. As a consequence, the electrode current falls dramatically. In the pulsed mode of operation, which is usually the preferred mode, a mixture of methane in argon is usually employed as the carrier gas. Pure argon cannot be used very effectively as the carrier gas, as the diffusion rate of electrons in argon is 10 times less than that in a 10% methane–90% argon mixture. The period of the pulsed potential is adjusted such that relatively few of the slow negatively charged molecules reach the anode, but the faster moving electrons are all collected. During the "off-period," the electrons reestablish equilibrium with the gas. In general use, the pulse width is set at about 1 μs and the frequency of the pulses at about 1 kHz. This allows about 1 ms for the sensor to reestablish equilibrium in the cell before the next electron collection occurs. The peak potential of each pulse is usually about 30 V but will depend on the geometry of the sensor and the strength of the radioactive source. The average current resulting from the electrons collected at each pulse is about 1×10^{-8} A and usually has an associated noise level of about 5×10^{-12} A. Both the standing current and the noise will also vary with the strength of the radioactive source that is used.

The sensor consists of a small chamber, 1 or 2 ml in volume, with metal ends separated by a suitable insulator. The metal ends act both as electrodes and as fluid conduits for the carrier gas to enter and leave the cell. The cell contains the radioactive source, electrically connected to the conduit through which the carrier gas enters and to the negative side of the power supply. A gauze "diffuser" is connected to the exit of the cell and to the positive side of the power supply. In the pulsed mode, the sensor operates with oxygen-free nitrogen or argon–methane mixtures. The active source is ^{63}Ni, which is stable up to 450°C. The sensor is thermostatted in a separate oven which can be operated at temperatures ranging from 100°C to 350°C. The column is connected to the sensor at the base and makeup gas can be introduced into the base of the detector. If open tubular columns are employed, the columns are operated with hydrogen or helium as the carrier gas. The ECD is extremely sensitive (i.e., minimum detectable concentration $\sim 1 \times 10^{-13}$ g/ml) and is widely used in trace analysis of halogenated compounds—in particular, pesticides.

In the DC mode, the linear dynamic range is relatively small, perhaps two orders of magnitude, with the response index lying between 0.97 and 1.03. The pulsed mode has a much wider linear dynamic range and values up to five orders of magnitude have been reported. The linear dynamic range will also depend on the strength of the radioactive source and the detector geometry. The values reported will also rest on how the linearity is measured and defined. If a response index lying between 0.98 and 1.02 is assumed, then a linear dynamic range of at least three orders of magnitude should be obtainable from most pulsed-mode ECD.

PULSED-DISCHARGE ELECTRON-CAPTURE DETECTOR

The pulsed-discharge ECD is a variant of the pulsed ECD detector, a diagram of which is shown in the lower part of

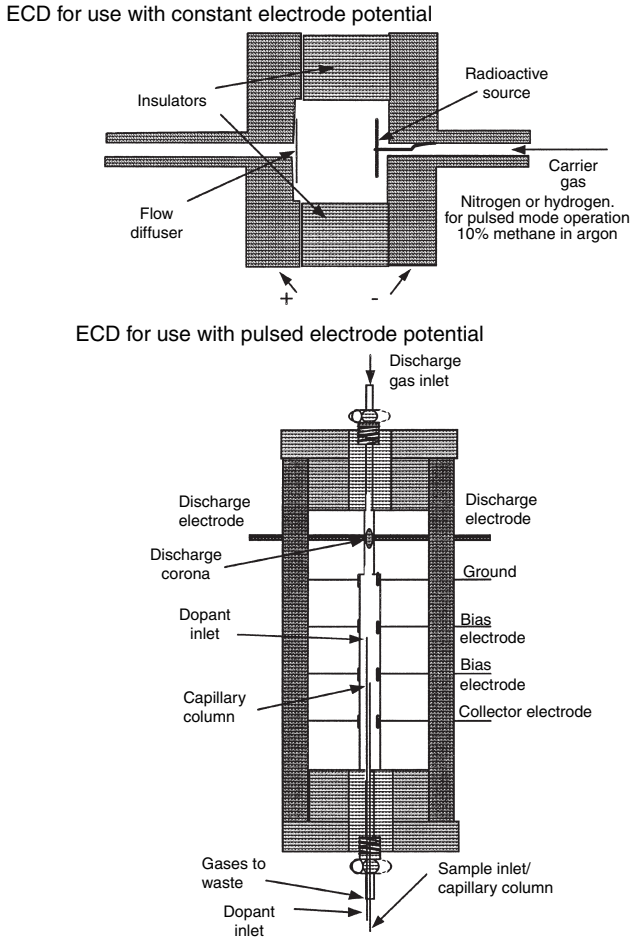

Fig. 1 The two types of electron capture detector.
Source: Courtesy of Valco Instruments Company, Inc.

Fig. 1. The detector functions in exactly the same way as that of the traditional ECD but differs in the method of electron production. The sensor consists of two sections: the upper section, where the discharge takes place, has a small diameter and the lower section where the column eluent is sensed and the electron capturing occurs, has a wider diameter. The potential across the discharge electrodes is pulsed at about 3 kHz with a discharge pulse width of about 45 μs for optimum performance. The discharge produces electrons and high-energy photons (which can also produce electrons) and some metastable helium atoms. The helium doped with propane enters just below the second electrode, metastable atoms are removed, and electrons are generated both by the decay of the metastable atoms and by the photons. The electrons are collected by appropriate potentials applied to each electrode in the section between the third and fourth electrode and, finally, collected at the fourth electrode. The collector electrode potential (the potential between the third and fourth electrodes) is pulsed at about 3 kHz with a pulse width of about 23 μs and a pulse height of 30 V.

The device functions in the same way as the conventional ECD with a radioactive source. The column eluent enters just below the third electrode, any electron-capturing substance present removes some of the free electrons, and the current collected by the fourth electrode falls. The sensitivity claimed for the detector is 0.2–1.0 ng, but this is not very informative as its significance depends on the characteristics of the column used and on the k' of the solute peak on which the measurements were made. The sensitivity should be given as that solute *concentration* that produces a signal equivalent to twice the noise. Such data allow a rational comparison between detectors. The sensitivity or minimum detectable concentration of this detector is probably similar to the conventional pulsed an estimate from the published data. The modified form of the ECD, devoid of a radioactive source, is obviously an attractive alternative to the conventional device and appears to have similar, if not better, performance characteristics.

The high sensitivity of the ECD makes it very popular for use in forensic and environmental chemistry. It is very simple to use and is one of the less expensive, high-sensitivity selective detectors available.

REFERENCE

1. Lovelock, J.E.; Lipsky, S.R. Electron affinity spectroscopy—A new method for the identification of functional groups in chemical compounds separated by gas chromatography. J. Am. Chem. Soc. **1960**, *82* (2), 431.

BIBLIOGRAPHY

1. Scott, R.P.W. *Introduction to Gas Chromatography*; Marcel Dekker, Inc.: New York, 1998.
2. Scott, R.P.W. *Chromatographic Detectors*; Marcel Dekker, Inc.: New York, 1996.

Electro-Osmotic Flow

Danilo Corradini
Institute of Chromatography, Rome, Italy

INTRODUCTION

Electro-osmosis refers to the movement of the liquid adjacent to a charged surface, in contact with a polar liquid, under the influence of an electric field applied parallel to the solid–liquid interface. The bulk fluid of liquid originated by this electrokinetic process is termed electro-osmotic flow (EOF). It may be produced both in open and in packed capillary tubes, as well as in planar electrophoretic systems employing a variety of supports, such as paper or hydrophilic polymers.

DISCUSSION

The formation of an electric double layer at the interfacial region between the charged surface and the surrounding liquid is of key importance in the generation of the EOF.[1–3] Most solid surfaces acquire a superficial charge when are brought into contact with a polar liquid. The acquired charge may result from dissociation of ionizable groups on the surface, adsorption of ions from solution, or by virtue of unequal dissolution of oppositely charged ions of which the surface is composed. This superficial charge causes a variation in the distribution of ions near the solid–liquid interface. Ions of opposite charge (counterions) are attracted toward the surface, whereas ions of the same charge (co-ions) are repulsed away from the surface. This, in combination with the mixing tendency of thermal motion, leads to the generation of an electric double layer formed by the charged surface and a neutralizing excess of counterion over co-ions distributed in a diffuse manner in the polar liquid. Part of the counterions are firmly held in the region of the double layer closer to the surface (the compact or Stern layer) and are believed to be less hydrated than those in the diffuse region of the double layer where ions are distributed according to the influence of electrical forces and random thermal motion. A plane (the Stern plane) located at about one ion radius from the surface separates these two regions of the electric double layer.

Certain counterions may be held in the compact region of the double layer by forces additional to those of purely electrostatic origin, resulting in their adsorption in the Stern layer. Specifically, adsorbed ions are attracted to the surface by electrostatic and/or van der Waals forces strongly enough to overcome the thermal agitation. Usually, the specific adsorption of counterions predominates over co-ion adsorption.

The variation of the electric potential in the electric double layer with the distance from the charged surface is depicted in Fig. 1. The potential at the surface (ψ_0) linearly decreases in the Stern layer with respect to the value of the zeta potential (ζ). This is the electric potential at the plane of shear between the Stern layer (plus that part of the double layer occupied by the molecules of solvent associated with the adsorbed ions) and the diffuse part of the double layer. The zeta potential decays exponentially from ζ to zero with the distance from the plane of shear between the Stern layer and the diffuse part of the double layer. The location of the plane of shear, a small distance further out from the surface than the Stern plane, renders the zeta potential marginally smaller in magnitude than the potential at the Stern plane (ψ_δ). However, in order to simplify the mathematical models describing the electric double layer, it is customary to assume identity of ψ_δ and ζ, and the bulk experimental evidence indicates that errors introduced through this approximation are usually small.

According to the Gouy–Chapman–Stern–Grahame (GCSG) model of the electric double layer,[4] the surface density of the charge in the Stern layer is related to the adsorption of the counterions, which is described by a Langmuir-type adsorption model, modified by the incorporation of a Boltzman factor. Considering only the adsorption of counterions, the surface change density σ_S of the Stern layer is related to the ion concentration C in the bulk solution by the following equation:

$$\sigma_S = zen_0 \frac{C}{V_m} \exp\left(\frac{ze\xi + \Phi}{kT}\right) \times \left[1 + \frac{C}{V_m} \exp\left(\frac{ze\xi + \Phi}{kT}\right)\right]^{-1} \quad (1)$$

where e is the elementary charge, z is the valence of the ion, k is the Boltzman constant, T is the temperature, n_0 is the number of accessible sites, V_m is the molar volume of the solvent, and Φ is the specific adsorption potential of counterions.

The surface charge density of the diffuse part of the double layer is given by the Gouy–Chapman equation

$$\sigma_G = (8\varepsilon kTc_0) \sinh\left(\frac{ze\xi}{2kT} f\right) \quad (2)$$

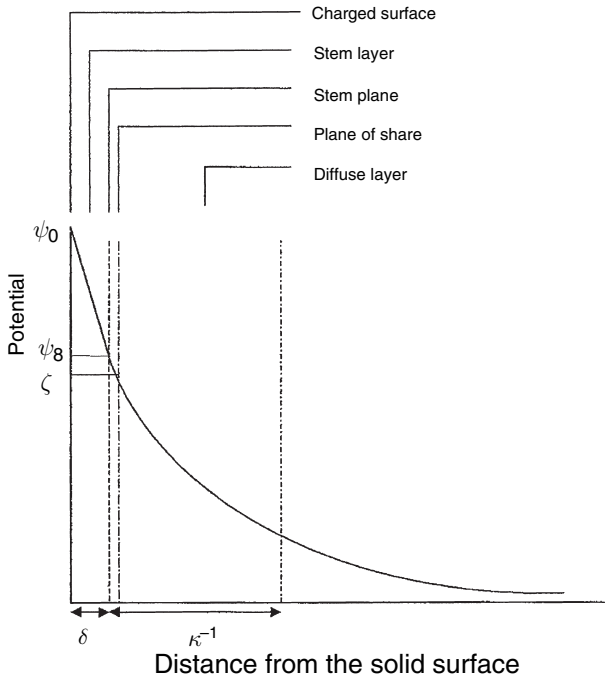

Fig. 1 Schematic representation of the electric double layer at a solid–liquid interface and variation of potential with the distance from the solid surface: ψ_0, surface potential; ψ_δ, potential at the Stern plane; ζ, potential at the plane of share (zeta potential); δ, distance of the Stern plane from the surface (thickness of the Stern layer); κ^{-1}, thickness of the diffuse region of the double layer.

where ε is the permittivity of the electrolyte solution and c_0 is the bulk concentration of each ionic species in the electrolyte solution.

At low potentials, Eq. 2 reduces to

$$\sigma_G = \frac{\varepsilon\xi}{\kappa^{-1}} \tag{3}$$

where κ^{-1} is the reciprocal Debye–Hückel parameter, which is defined as the "thickness" of the electric double layer. This quantity has the dimension of length and is given by

$$\kappa^{-1} = \left(\frac{\varepsilon kT}{2e^2 I}\right)^{1/2} \tag{4}$$

in which I is the ionic strength of the electrolyte solution.

Eq. 3 is identical to the equation that relates the charge density, voltage difference, and distance of separation of a parallel-plate capacitor. This result indicates that a diffuse double layer at low potentials behaves like a parallel capacitor, in which the separation distance between the plates is given by κ^{-1}. This explains why κ^{-1} is called the double-layer thickness.

Eq. 2 can be written in the form

$$\xi = \frac{\sigma_G \kappa^{-1}}{\varepsilon} \tag{5}$$

which indicates that the zeta potential can change due to variations in the density of the electric charge, in the permittivity of the electrolyte solution, and in the thickness of the electric double layer, which depends, throughout the ionic strength (see Eq. 4), on the concentration and valence of the ions in solution.

The dependence of the velocity of the electro-osmotic flow (v_{eo}) on the zeta potential is expressed by the Helmholtz–von Smoluchowski equation

$$v_{eo} = \frac{\varepsilon_0 \varepsilon \zeta}{\eta} E \tag{6}$$

where E is the applied electric field, ε_0 is the permittivity of vacuum, and ε and η are the dielectric constant and the viscosity of the electrolyte solution, respectively. This expression assumes that the dielectric constant and viscosity of the electrolyte solution are the same in the electric double layer as in the bulk solution.

The Helmholtz–von Smoluchowski equation indicates that under constant composition of the electrolyte solution, the EOF depends on the magnitude of the zeta potential, which is determined by the different factors influencing the formation of the electric double layer, as discussed earlier. Each of these factors depends on several variables, such as pH, specific adsorption of ionic species in the compact region of the double layer, ionic strength, and temperature.

The specific adsorption of counterions at the interface between the surface and the electrolyte solution results in a drastic variation of the charge density in the Stern layer, which reduces the zeta potential and, hence, the EOF. If the charge density of the adsorbed counterions exceeds the charge density on the surface, the zeta potential changes sign and the direction of the EOF is reversed.

The ratio of the velocity of the EOF to the applied electric field, which expresses the velocity per unit field, is defined as electro-osmotic coefficient or, more properly, electro-osmotic mobility (μ_{eo}).

$$\frac{v_{eo}}{E} = \mu_{eo} = \frac{\varepsilon_0 \varepsilon \xi}{\eta} \tag{7}$$

Using SI units, the velocity of the electro-osmotic flow is expressed in meters per second (m/sec) and the electric field in volts per meter (V/m). Consequently, in analogy to the electrophoretic mobility, the electro-osmotic mobility has the dimension square meters per volt per second. Because electro-osmotic and electrophoretic mobilities are converse manifestations of the same underlying phenomenon, the Helmholtz–von Smoluchowski equation applies to electro-osmosis as well as to electrophoresis. In fact, when an electric field is applied to an ion, this moves relative to the electrolyte solution, whereas in the case of electro-osmosis, it is the mobile diffuse layer that moves under an applied electric field, carrying the electrolyte solution with it.

According to Eq. 6, the velocity of the EOF is directly proportional to the intensity of the applied electric field. However, in practice, the non-linear dependence of the EOF on the applied electric field is obtained as a result of Joule heat production, which causes an increase of the electrolyte temperature with a consequent decrease of viscosity and variation of all other temperature-dependent parameters (protonic equilibrium, ion distribution in the double layer, etc.). The EOF can also be altered during a run by variations of the protonic and hydroxylic concentration in the anodic and cathodic electrolyte solutions as a result of electrolysis. This effect can be minimized by using electrolyte solutions with a high buffering capacity and electrolyte reservoirs of relatively large volume and by frequent replacement of the electrolyte in the electrode compartments with fresh solution.

The magnitude and direction of the EOF depend also on the composition, pH, and ionic strength of the electrolyte solution.[5–7] Both the pH and ionic strength influence the protonic equilibrium of fixed-charged groups on the surface and of ionogenic substances in the electrolyte solution which affect the charge density in the electric double layer and, consequently, the zeta potential. In addition, the ionic strength influences the thickness of the double layer (κ^{-1}). According to Eq. 4, increasing the ionic strength causes a decrease in κ^{-1}, which is currently referred to as the compression of the double layer that results in lowering the zeta potential. Consequently, increasing the ionic strength results in decreasing the EOF.

The charge density in the electric double layer and, hence, the EOF are also influenced by the adsorption of potential-determining ions in the Stern region of the electric double layer. A variety of additives can be incorporated into the electrolyte solution with the purpose of controlling the EOF by modifying the solid surface dynamically. These include simple and complex ionic compounds, ionic and zwitterionic surfactants, and neutral and charged polymers. The incorporation of these additives into the electrolyte solution may result either in increasing or in reducing the EOF, or even in reversing its direction. The impact of these additives on the EOF is generally concentration dependent. Such behavior is in accordance to the Langmuir-like adsorption model describing the variation of the charge density in the Stern layer on the concentration of adsorbing ions in the electrolyte solution (see Eq. 1).

The proper control of the EOF can be also obtained by adding organic solvents to the electrolyte solution. The influence of organic solvents on the EOF may result from a multiplicity of mechanisms. Organic solvents are expected to influence both the dielectric constant and viscosity of the bulk electrolyte solution. Generally, this leads to the variation of the ratio of the dielectric constant to the viscosity of the electrolyte solution, to which the EOF depends according to Eq. 6. In addition, the local viscosity within the electric double layer[8] can be varied by the adsorption of the organic–solvent molecules in the Stern layer, which may also influence the adsorption of counterions, depending on the different solvation properties of the organic solvent. Organic solvents may also influence the zeta potential by affecting the ionization of potential-determining ions on the surface.

Different methods can be employed to measure the magnitude of the EOF.[9] One possibility involves measuring the velocity of the EOF by measuring the change in weight or in volume in one of the electrolyte solution reservoirs. The addition of an electrically neutral dye to one electrode reservoir and its detection in the other where the EOF is directed is another possible method. Other methods based on monitoring electric current while an electrolyte solution of different conductivity is drawn into the system by electro-osmosis or determining the zeta potential from streaming potential measurements are less popular and accurate. More common is the method of calculating the electro-osmotic velocity from the migration time of an electrically neutral marker substance incorporated into the sample solution. The selected compound must be soluble in the electrolyte solution, neutral in a wide pH range, and easily detectable. In addition, it should neither become partially charged by compellation with the components of the electrolyte solution nor interact with the capillary tube, the chromatographic stationary phase, or the slab gel employed in capillary electrophoresis (CE), capillary electrochromatography, and planar electrophoresis, respectively. This method has the advantage of simplicity and can be used to monitor the EOF during analysis in any of the above techniques, provided that the analytes and the EOF are directed toward the same electrode.

REFERENCES

1. Hiemenz, P.C. *Principles of Colloid and Surface Chemistry,* 2nd Ed.; Marcel Dekker, Inc.: New York, 1986; 677–735.
2. Adamson, A.W. *Physical Chemistry of Surfaces,* 5th Ed.; John Wiley & Sons: New York, 1990; 203–257.
3. Shaw, D.J. *Introduction to Colloid and Surface Chemistry,* 3th Ed.; Butterworths: London, 1980; 148–182.
4. Grahame, D.C. The electrical double layer and the theory of electro-capillarity. Chem. Rev. **1947**, *41*, 441–501.
5. Lukacs, K.D.; Jorgenson, J.W. J. High Resolut. Chromatogr. Chromatogr. Commun. **1985**, *8*, 407–411.
6. Altria, K.D.; Simpson, C.F. High voltage capillary zone electrophoresis: Operating parameter effects upon electro-endosmotic flows and electrophoretic mobilities. Chromatographia **1987**, *24*, 527–532.
7. Cikalo, M.G.; Bartle, K.D.; Myers, P. Attempt to define the role of the length of the packed section in capillary electrochromatography. J. Chromatogr. A, **1999**, *836*, 35–51.
8. Hjerten, S. Free zone electrophoresis. Chromatogr. Rev. **1967**, *9*, 122–219.
9. Van de Goor, A.A.A.M.; Wanders, B.J.; Everaerts, F.M. Modified methods for off- and on-line determination of electroosmosis in capillary electrophoretic separations. J. Chromatogr. **1989**, *470*, 95–104.

Electro-Osmotic Flow in Capillary Tubes

Danilo Corradini
Institute of Chromatography, Rome, Italy

INTRODUCTION

The electro-osmotic flow in open capillary tubes is generated by the effect of the applied electric field across the tube on the uneven distribution of ions in the electric double layer at the interface between the capillary wall and the electrolyte solution. In bare fused-silica capillaries, ionizable silanol groups are present at the surface of the capillary wall, which is exposed to the electrolyte solution. In this case, the electric double layer is the result of the excess of cations in the solution in contact with the capillary tube to balance the negative charges on the wall arising from the ionization of the silanol groups. Part of the excess cations are firmly held in the region of the double layer closer to the capillary wall (the compact or Stern layer) and are believed to be less hydrated than those in the diffuse region of the double layer.[1] When an electric field is applied across the capillary, the remaining excess cations in the diffuse part of the electric double layer move toward the cathode, dragging their hydration spheres with them. Because the molecules of water associated with the cations are in direct contact with the bulk solvent, all the electrolyte solution moves toward the cathode, producing a pluglike flow having a flat velocity distribution across the capillary diameter.[2]

DISCUSSION

The flow of liquid caused by electro-osmosis displays a pluglike profile because the driving force is uniformly distributed along the capillary tube. Consequently, a uniform flow velocity vector occurs across the capillary. The flow velocity approaches zero only in the region of the double layer very close to the capillary surface. Therefore, no peak broadening is caused by sample transport carried out by the electro-osmotic flow. This is in contrast to the laminar or parabolic flow profile generated in a pressure-driven system, where there is a strong pressure drop across the capillary caused by frictional forces at the liquid–solid boundary. A schematic representation of the flow profile due to electro-osmosis in comparison to that obtained in the same capillary column in a pressure-driven system, such as a capillary high-performance liquid chromatography (HPLC), is displayed in Fig. 1.

The dependence of the velocity of the electro-osmotic flow (v_{co}) on the applied electric field (E) is expressed by the Helmholtz–von Smoluchowski equation

$$v_{co} = -\frac{\varepsilon_0 \varepsilon_r \zeta}{\eta} E \tag{1}$$

where ζ is the zeta potential, ε_0 is the permittivity of vacuum, ε_r is the dielectric constant, and η is the viscosity of the electrolyte solution. This expression assumes that the dielectric constant and viscosity of the electrolyte solution are the same in the electric double layer as in the bulk solution. The term $-\varepsilon_0 \varepsilon_r \zeta/\eta$ is the defined electro-osmotic coefficient or, more properly, electro-osmotic mobility (μ_{co}) and expresses the velocity of the electro-osmotic flow per unit field. Accordingly, the Helmholtz–von Smoluchowski equation can be written

$$\mu_{co} = \frac{v_{co}}{E} \tag{2}$$

In a capillary tube, the applied electric field E is expressed by the ratio where V is the potential difference in volts across the capillary tube of length L_T (in meters). The velocity of the electro-osmotic flow, v_{co} (in meters per second), can be evaluated from the migration time t_{cot} (in seconds) of an electrically neutral marker substance and the distance L_D (in meters) from the end of the capillary where the samples are introduced to the detection windows (effective length of the capillary). This indicates that, experimentally, the electro-osmotic mobility can be easily calculated using the Helmholtz–von Smoluchowski equation in the following form:

$$\mu_{co} = \frac{L_T L_D}{V t_{co}} \, (\mathrm{m^2/V/s}) \tag{3}$$

which demonstrates that, by analogy to the electrophoretic mobility, the electro-osmotic mobility has the dimension of square meters per volt per second.

The electrically neutral marker substance employed to measure the velocity of the electro-osmotic flow has to fulfill the following requirements. The compound must be soluble in the electrolyte solution and neutral in a wide pH range and no interaction with the capillary wall must occur. In addition, the electrically neutral marker substance should be easily detectable in order to allow a small amount to be injected. If the electrically neutral marker interacts with the capillary wall or becomes partially charged by complexation with the components of the electrolyte solution, the measured electro-osmotic velocity

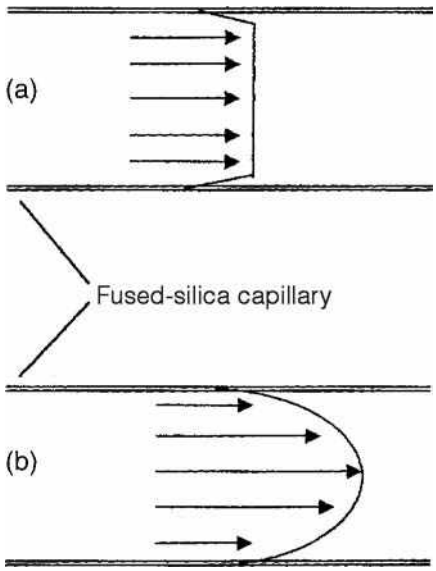

Fig. 1 Schematic representation of the flow profiles obtained with the same capillary column connected to an electric-driven system (a) and to a pressure-driven system (b). Arrows indicate flow velocity vectors.

may appear slower or faster than the real flow. Some compounds that adequately serve as electrically neutral markers include benzyl alcohol, riboflavin, acetone, dimethyl-formamide, dimethyl sulfoxide, and mesityl oxide.

Alternatively, the velocity of the electro-osmotic flow can be measured by weighing the volume of the electrolyte solution displayed by electro-osmosis from the anodic to the cathodic reservoir. When detection is performed by ultraviolet (UV) absorbance, a "solvent dip" equal to the electro-osmotic flow appears in the electropherogram after any sample injection. In most cases, the sample solvent has a lower UV absorbance than the electrolyte solution, resulting in a negative UV signal. On the other hand, if the UV absorbance of the sample solvent is higher than that of the electrolyte solution, a positive system peak can be observed at the time corresponding to the velocity of the electro-osmotic flow. The time at which the "solvent dip" appears in the electropherogram can be used to measure the velocity of the electro-osmotic flow in a very simple but less accurate way than those using an electrically neutral marker substance or the weight of the displaced liquid.

The Helmholtz–von Smoluchowski equation indicates that under constant composition of the electrolyte solution, the electro-osmotic flow depends on the magnitude of the zeta potential which is determined by many different factors, the most important being the dissociation of the silanol groups on the capillary wall, the charge density in the Stern layer, and the thickness of the diffuse layer. Each of these factors depends on several variables, such as pH, specific adsorption of ionic species in the compact region of the electric double layer, ionic strength, viscosity, and temperature.

Secondary equilibrium in solution, generation of Joule heat, and variation of protonic and hydroxylic concentration due to electrolysis may alter the hydrogen ion concentration in the capillary tube when electrolyte solutions having low buffering capacities are employed. A change in the protonic equilibrium directly influences the zeta potential through the variation of the charge density on the capillary wall resulting from the deprotonation of the surface silanol groups, which increases with increasing pH. The shape of a curve describing the dependence of the zeta potential on the electrolyte pH resembles a titration curve, the inflection point of which may be interpreted as the pK_a value of the surface silanol groups. At acidic pH, the ionization of the surface silanol groups is suppressed and the zeta potential approaches zero, determining the virtual annihilation of the electro-osmotic flow. Under alkaline conditions, the silanol groups are fully charged and the zeta potential reaches its maximum value, which corresponds to a plateau value of the electro-osmotic flow. Between these extreme conditions, the zeta potential rapidly increases with increasing pH up to the complete dissociation of the silanol groups, determining the well-known sigmoidal pH dependence of the electro-osmotic flow. The concentration and ionic strength of the electrolyte solution also have a strong impact on the electro-osmotic flow. The ionic strength influences the thickness of the diffuse part of the electric double layer to which the zeta potential is directly proportional. Because the thickness of the diffuse part of the electric double layer is inversely proportional to the square root of the ionic strength, the electro-osmotic flow decreases with the concentration of the electrolyte solution according to the following relationship:[3]

$$\mu_{co} \approx \frac{e}{3 \times 10^7 \mid z \mid \eta\sqrt{C}} \tag{4}$$

where, e, z, η, and C are the total charge per unit surface area, the electron valence of the electrolyte, the viscosity, and the concentration of the electrolyte in the bulk solution, respectively.

Another model that accounts for the decrease of the electro-osmotic flow with increasing the electrolyte concentration relates the electro-osmotic mobility to the concentration of a monovalent counterion, introduced with the buffer, according to the following relationship:[4]

$$\mu_{co} = \frac{Q_0}{\eta(1 + K_{wall}[M^+])}\left(d_0 + \frac{1}{K'\sqrt{[M^+]}}\right) \tag{5}$$

where η is the viscosity of the electrolyte solution and K' is a constant that, for a dilute aqueous solution at 25°C, is equal to 3×10^9/m $(\text{mol/L})^{-1/2}$. The first term on the right side of Eq. 5 is related to the dependence of the surface charge on the concentration of the monovalent cation in the

electrolyte solution. The model postulates that the initial charge per unit area at the surface of the silica capillary wall (Q_0) is reduced by the factor $1/1 + K_{wall}[M^+]$ upon incorporating a monovalent buffer of concentration $[M^+]$ into the electrolyte solution. This is a result of the neutralization of the free silanol groups on the capillary surface caused by the adsorption of the monovalent cations. The constant K_{wall} is defined as the equilibrium constant between the cations in the buffer solution and adsorption sites on the capillary wall. The second term describes the influence of the concentration of the monovalent cation on the thickness of the mobile region of the electric double layer. This is postulated to be composed of a fixed thickness (d_0) and the Debye–Hückel thickness $\delta = 1/K'[M^+]^{1/2}$, which is inversely proportional to the square root of the concentration of the monovalent ion. According to this model, increasing the concentration of the monovalent buffer cation in the bulk solution influences the electro-osmotic mobility by reducing the Debye–Hückel thickness of the diffuse double layer and by neutralizing the negative charges on the capillary wall resulting from the ionization of the silanol groups.

Certain counterions, such as polycationic species, cationic surfactants, and several amino compounds can be firmly held in the compact region of the electric double layer by forces additional to those of simple Coulombic origin. The specific adsorption of counterions at the interface between the capillary wall and the electrolyte solution results in a drastic variation of the positive charge density in the Stern layer, which reduces the zeta potential and, hence, the electro-osmotic flow. If the positive charge density of the adsorbed counterions exceeds the negative charge density on the capillary wall resulting from the ionization of silanol groups, the zeta potential becomes positive and the concomitant electro-osmotic flow is reversed from cathodic to anodic.

The dependence of the electro-osmotic flow on the specific adsorption of counterions in the electric double layer can be described by a model which correlates the electro-osmotic mobility to the charge density in the Stern part of the electric double layer (arising from the adsorption of counterions) and the charge density at the capillary wall (resulting from the ionization of silanol groups).[5] According to this model, the dependence of the electro-osmotic mobility on the concentration of the adsorbing ions (C) in the electrolyte solution is expressed as

$$\mu_{co} = \frac{\kappa^{-1}}{\eta}\left\{ze n_0 \frac{C}{V_m}\exp\left(\frac{ze\psi_d + \Phi}{kT}\right) \times\left[1 + \frac{C}{V_m}\exp\left(\frac{ze\psi_\delta + \Phi}{kT}\right)\right]^{-1} - \left(\frac{\gamma}{1 + [H^+]/K_a}\right)\right\} \quad (6)$$

where κ^{-1} is the Debye–Hückel thickness of the diffuse double layer, is the viscosity of the electrolyte solution, e is the elementary charge, z is the valence of the adsorbing ion, k is the Boltzman constant, T is the absolute temperature, is the number of accessible sites in the Stern layer, is the molar volume of the solvent, Φ is the specific adsorption potential of counterions, γ is the sum of the ionized and protonated surface silanol groups, $[H^+]$ is the bulk electrolyte hydrogen ion concentration, and is the silanol dissociation constant. According to this equation, at constant ionic strength, viscosity, and pH, the electro-osmotic mobility depends mainly on the surface density of the adsorbed counterions in the Stern region of the electric double layer, which follow a Langmuir-type adsorption model.

The reversal of the direction of the electro-osmotic flow by the adsorption onto the capillary wall of alkylammonium surfactants and polymeric ion-pair agents incorporated into the electrolyte solution is widely employedin capillary zone electrophoresis (CZE) of organic acids, amino acids, and metal ions. The dependence of the electro-osmotic mobility on the concentration of these additives has been interpreted on the basis of the model proposed by Fuerstenau[6] to explain the adsorption of alkylammonium salts on quartz. According to this model, the adsorption in the Stern layer as individual ions of surfactant molecules in dilute solution results from the electrostatic attraction between the head groups of the surfactant and the ionized silanol groups at the surface of the capillary wall. As the concentration of the surfactant in the solution is increased, the concentration of the adsorbed alkylammonium ions increases too and reaches a critical concentration at which the van der Waals attraction forces between the hydrocarbon chains of adsorbed and freesurfactant molecules in solution cause their association into hemimicelles (i.e., pairs of surfactant molecules with one cationic group directed toward the capillary wall and the other directed out into the solution).

Lowering the velocity or reversing the direction of the electro-osmotic flow may have a beneficial effect of on the resolution of two adjacent peaks, as evidenced by the following expression for resolution in electrophoresis elaborated by Giddings:[7]

$$R_s = \frac{\sqrt{N}}{4}\left(\frac{\Delta\mu}{\mu_{av} + \mu_{co}}\right) \quad (7)$$

where N is the number of theoretical plates, $\Delta\mu$ and μ_{av} are the difference and the average value of the electrophoretic mobilities of two adjacent peaks, respectively, and μ_{co} is the electro-osmotic mobility. According to this equation, the highest resolution is obtained when the electro-osmotic mobility has the same value but opposite direction of the average electrophoretic mobility of the two adjacent peaks.

Neutral polymeric molecules, such as polysaccharides and synthetic polymers, may also adsorb onto the Stern

layer, causing a variation of viscosity in the double layer with distance from the capillary wall, which affects the electro-osmotic mobility according to the following relationship:[2]

$$\mu_{co} = \frac{\varepsilon_r}{4\pi} \int_0^{\zeta} \frac{1}{\eta} d\psi \tag{8}$$

where ε_r is the dielectric constant, ζ is the zeta potential, η is the viscosity, and ψ is the electric potential. The value of the integral in this expression will approach zero when the viscosity in the double layer approaches infinity. Accordingly, the electro-osmotic flow is drastically reduced when the local viscosity of the double layer is increased as a result of the adsorption of a neutral polymer onto the Stern layer. It is worth noting that at constant value of the viscosity in the electric double layer, Eq. 8 is equivalent to the Helmholtz–von Smoluchowski expression for the electro-osmotic flow.

The incorporation of an organic solvent into the aqueous electrolyte solution also leads to a variation of the electro-osmotic flow.[8] The general trend is that the electro-osmotic flow decreases steadily with increasing concentration of the organic solvent in the hydro-organic electrolyte solution. This effect can be attributed, to some extent, to the increasing viscosity and decreasing dielectric constant of most hydro-organic electrolyte solutions with increasing concentration of organic solvent. However, in most cases, the decrease of the electro-osmotic flow is also observed at organic solvent concentrations greater than 50–60% (v/v), at which the ratio of the dielectric constant and the viscosity, ε_r/η is generally increasing. This indicates that the variation of the electro-osmotic flow caused by the incorporation of an organic solvent into the electrolyte solution cannot be solely related to the changes of the ratio ε_r/η.

Similar to the neutral polymers, organic solvents can adsorb at the interface between the capillary wall and the electrolyte solution, through hydrogen-bonding or dipole interaction, thus increasing the local viscosity within the electric double layer. Organic solvents may also influence the zeta potential by affecting the ionization of the silanol groups at the capillary surface, whose has been found to be shifted toward higher values with increasing the content of organic solvents in the electrolyte solution. The dependence of the zeta potential on the fraction of an organic solvent incorporated into the electrolyte solution may be also related to the variation of both the dielectric constant and the adsorption of counterions in the Stern layer. In practice, introducing a neutral polymer or an organic solvent into the electrolyte solution results in multiple changes, generally involving the viscosity and the dielectric constant of the bulk solution, the ionization of the silanol groups on the capillary wall, and the charge density in the Stern layer, as well as the local viscosity and the dielectric constant of the electric double layer.

REFERENCES

1. Hiemenz, P.C. *Principles of Colloid and Surface Chemistry,* 2nd Ed.; Marcel Dekker, Inc.: New York, 1986; 677–735.
2. Hjertén, S. Free zone electrophoresis. Chromatogr. Rev. **1967**, *9*, 122–219.
3. Tsuda, T.; Nomura, K.; Nakagawa, G. Open-tubular microcapillary liquid chromatography with electro-osmosis flow using a UV detector. J. Chromatogr. **1982**, *248*, 241–247.
4. Salomon, K.; Burgi, D.S.; Helmer, J.C. Valuation of fundamental properties of a silica capillary used for capillary electrophoresis. J. Chromatogr. **1991**, *559*, 69–80.
5. Corradini, D.; Rhomberg, A.; Corradini, C. Electrophoresis of proteins in uncoated capillaries with amines and amino sugars as electrolyte additives. J. Chromatogr. A, **1994**, *661*, 305–313.
6. Fuerstenau, D.W. Streaming potential studies on Quartz in solutions of aluminum acetates in relation to the formation of Hemi-Micelles at the Quartz-solution interface. J. Phys. Chem. **1956**, *60(7)*, 981–985.
7. Giddings, J.C. Generation of variance, theoretical plates resolution and peak capacity in electrophoresis and sedimentation. Separ. Sci. **1969**, *4*, 181–189.
8. Schwer, C.; Kenndler, E. Electrophoresis in fused-silica capillaries: the influence of organic solvents on the electro-osmotic velocity and the zeta potential. Anal. Chem. **1991**, *63*, 1801–1807.

Electro-Osmotic Flow Nonuniformity: Influence on Efficiency of CE

Victor P. Andreev
Institute for Analytical Instrumentation, Russian Academy of Sciences, St. Petersburg, Russia

INTRODUCTION

There are two types of nonuniformities of electro-osmotic flow (EOF) that can contribute significantly to the solute peak broadening and are important for capillary electrophoresis (CE). The first is the transversal nonuniformity of the usual EOF in the capillary with the zeta potential of the walls and longitudinal electric field strength constant and independent of coordinates. The second one is the nonuniformity of EOF caused by the dependence of the zeta potential of the walls or electric field strength on coordinates.

DISCUSSION

The first type of EOF nonuniformity was described in the classical article by Rice and Whitehead[1] written much earlier than the first works on CE. The equation for the EOF velocity profile in the infinitely long tube with radius a was given by

$$V(r) = \frac{\zeta \varepsilon \varepsilon_0 E}{\eta}\left(1 - \frac{I_0(\kappa r)}{I_0(\kappa a)}\right) \quad (1)$$

where ζ is the zeta potential of the wall, ε and η are the dielectric constant and viscosity of the buffer, respectively, ε_0 is the permitivity of the free space, $\kappa^{-1} = (\varepsilon\varepsilon_0\kappa_B T2ne^2)^{1/2}$ is the Debye layer thickness, κ_B is the Boltzmann constant, T is the temperature, n is the number of ions per unit volume (proportional to the concentration of buffer C_0), e is the proton charge, and $I_0(x)$ is the modified Bessel function. It is evident from Eq. 1 that the nonuniformity of the EOF profile can be substantial only if the capillary radius and Debye length are commensurate. In fact, for the case of $\kappa a \approx 1$, the profile of EOF according to Eq. 1 is very close to parabolic. Luckily, it is not the case of usual capillaries for CE with $a \geq 25$ μm because, even for distilled water, $\kappa^{-1} \approx 0.1$ μm. Another important result of Ref.,[1] is the prediction of the EOF profile in the long capillary with closed ends. In such a capillary, liquid moves in one direction in the vicinity of the walls and in the opposite direction near the axis of the capillary, thus making the total flow through the cross section equal to zero. With this result, it is quite evident that CE must be realized in a capillary with open ends; otherwise, nonuniformity of EOF would ruin the separation.

Results of Ref.,[1] were produced by employing a linear approximation of the exponential terms in the Poisson–Boltzmann equation for electrical potential and charge distribution. Strictly speaking, this linearization is valid only for $|\zeta| \ll kT/e \approx 0.03$ V, whereas the range of the values of the zeta potential is $|\zeta| \leq 0.1$ V. In Ref.,[2] the Poisson–Boltzmann equation and the Navier–Stokes equations for EOF velocity profile were solved numerically without linearization. The dependence of buffer viscosity on temperature and the existence of temperature gradients due to Joule heating were also taken into consideration. Calculated EOF profiles were compared with and predicted by Eq. 1, showing that the difference in flow profiles for $|\zeta| = 0.1$ V could be significant, especially for thin capillaries and low buffer concentrations ($ka \approx 10$). Calculated flow profiles were used to predict the stationary value of height equivalent to the theoretical plate (HETP) by using the results of generalized dispersion theory. It was shown that for low buffer concentrations ($C_0 \leq 10^{-4}$ M), the contribution of electro-osmotic flow nonuniformity to the HETP value could be larger than the contribution of the thermal effects and molecular diffusion.

A similar approach was used in Ref.,[3] where the contributions of EOF nonuniformity (H_{co}) and molecular diffusion (H_{diff}) to HETP were compared for different values of solute diffusion coefficients. It was shown[3] that for the typical CE velocities of EOF (1–2 mm/sec) and rather high buffer concentration ($C_0 = 10^{-2}$ M), $H_{co}H_{diff} \geq 1$ for $D \leq 2 \times 10^{-12}$/m^2/sec. For lower buffer concentrations, the influence of EOF nonuniformity is substantial for smaller molecules also ($H_{co} = 1.3 \times 10^{-8}$ m, $H_{diff} = 1.6 \times 10^{-8}$ m for $D = 2.4 \times 10^{-11}$ m^{2}sec, corresponding to α_2-macroglobulin).

The joint effect of EOF nonuniformity and particle–wall electrostatic interactions was studied in Ref.[4] Two types of solute particles were examined: one with the charge of the same sign as the zeta potential of the wall, and the other of the opposite sign. The particles of the first type are moving electrophoretically in the direction opposite to the direction of EOF and are electrostaticaly subtracted by the wall, whereas the particles of the second type are attracted by the wall and are moving

electrophoretically in the same direction as EOF. Particles of the second type spend a large portion of time in the vicinity of the capillary wall and, so, EOF nonuniformity contributes significantly to peak broadening, whereas for the particles subtracted by the wall, the influence of EOF nonuniformity is negligible because their residence time in the vicinity of the wall is close to zero. For example, for the particles with $D = 5 \times 10^{-11}$ m^{2}sec, in the capillary with $a = 10$ μm, $\zeta = -0.1$ V, and $E = 40$ kV/m, filled with diluted buffer ($C_0 = 10^{-5}$ M), one has HETP ≈ 10 μm for particles attracted by the wall, whereas for particles subtracted by the wall, HETP ≈ 0.1 μm. For neutral particles not interacting with the walls, HETP ≈ 0.2 μm was predicted. The difference was much less dramatic for the case of the higher buffer concentrations and the lower zeta potential. For example, for $\zeta = -0.02$ V, $C_0 = 10^{-3}$ M and the rest of parameters being the same as described earlier, HETP is determined mainly by molecular diffusion and is close to 0.1 μm.

The influence of EOF nonuniformity on efficiency of CE in the capillary with the zeta potential of the wall being the function $\zeta(x)$ of the longitudinal coordinate x was studied in Ref.[5] To calculate the EOF velocity profile, an important approximation was justified by the fact that usually $\kappa a \gg$ in CE. Thus, the doublelayer region was neglected and the following boundary condition was formulated:

$$V_x(x, a, t) = \frac{\varepsilon\varepsilon_0 E}{\eta}\zeta(x) \tag{2}$$

With this boundary condition, the Navier–Stokes equations for longitudinal V_x and radial V_r components of EOF velocity were solved numerically, and the calculated EOF profiles were used to simulate the solute peak shapes. The situation where the part of the capillary length was modified to the zero value of the zeta potential and the part of capillary was not modified ($\zeta \neq 0$) was studied. It was shown that the radial component of the velocity is non-zero only in the rather short transition region between the uncovered and covered parts of the capillary. At a distance of a few capillary diameters from the transient region, the radial flows are negligible and the axial component of the velocity in the covered section of the capillary has an almost parabolic profile. Peak shapes and peak variances were studied, and the general conclusion of Ref.,[5] was that the main contribution to the peak width was from the parabolic velocity profiles, the contribution of the radial flow in the transient regions being less significant. Based on this result, the mathematical model of CE in the capillary made of several sections with various non-equal values of the zeta potentials and radii was developed.[6] For each of the sections, the total flow was considered to be the sum of EOF caused by electrical potential differences along the section and the Poiseuille flow, caused by the pressure drop along the section. The values of the pressure drops and potentials differences were determined by the solution of the set of $2N$ algebraic equations, where N is the number of sections in the capillary. These equations reflect the fact that the total flow of liquid and total current are constant along the capillary, and the sums of pressure drops and potential differences at the sections are equal to the total pressure drop and total potential difference at the whole capillary, respectively. The lengths of the sections were considered to be much larger than the capillary radius, so the results of the model are valid everywhere except the immediate vicinity of the points where the radius of capillary or the zeta potential of the wall change their values. When calculating the values of HETP in such a capillary, particle–wall electrostatic interactions were taken into consideration, and it was shown that HETP values are considerably larger for particles attracted by the wall. It was also shown that differences in the values of the zeta potential contributes to HETP much more significantly than the differences in radii values. The situation that might happen in the case of a bubble-cell detector was modeled and considerable growth of HETP was predicted.

In Ref.,[7] the case was studied in which the zeta potential of the wall was the linear function of the longitudinal coordinate. This situation may happen when the value of the zeta potential is controlled by the external electrical potential applied to the wall. Electrical potential value inside the capillary is naturally a linear function of the longitudinal coordinate x; therefore, if the electrical potential applied to the outer boundary of the capillary wall is constant, then the potential difference across the wall is a linear function of x. The theoretical approach used in Ref.,[7] is similar to the one in Ref.[5] Secondary parabolic flow was shown to be generated, leading to the increase of HETP. It was predicted theoretically, and verified experimentally, that a pressure profile superimposed on the capillary can, in some cases, compensate for the disturbed profile and reduce the HETP value.

In Ref.,[8] the mathematical model of CE in rectangular channels with non-equal values of the zeta potentials of the walls was developed. This model may be of interest for the case of CE on a microchip, where the microgroves are produced by wet chemical etching and, so, the walls of the groove can have different values of zeta potential than the cover plate that is not etched. Flow profiles for the channels with different aspect ratios and different combinations of the zeta potential values were examined. It was shown, for example, that a 10% difference in the values of the zeta potentials of upper and lower walls can cause a sixfold growth of the HETP value.

The above-mentioned examples show that EOF nonuniformities may occur in different situations and must be given considerable attention, as they can reduce the CE efficiency dramatically.

REFERENCES

1. Rice, C.L.; Whitehead, R. Electrokinetic flow in a narrow cylindrical capillary. J. Phys. Chem. **1965**, *69*, 4017.
2. Andreev, V.P.; Lisin, E.E. Investigation of the electroosmotic flow effect on the efficiency of capillary electrophoresis. Electrophoresis **1992**, *13*, 832.
3. Gas, B.; Stedry, M.; Kenndler, E. Contribution of the electroosmotic flow to peak broadening in capillary zone electrophoresis with uniform zeta potential. J. Chromatogr. A, **1995**, *709*, 63.
4. Andreev, V.P.; Lisin, E.E. On the mathematical model of capillary electrophoresis. Chromatographia **1993**, *37*, 202.
5. Potocek, B.; Gas, B.; Kenndler, E.; Stedry, M. Electroosmosis in capillary zone electrophoresis with nonuniform zeta potential. J. Chromatogr. A, **1995**, *709*, 51.
6. Andreev, V.P.; Shirokih, N.V. Electroosmotic flow profile in the capillary made of several sections, 20th Int. Symp. on Capillary Chromatography, Proceedings on CD, 1998 paper H 11.
7. Keely, C.A.; van de Goor, T.A.A.M.; McManigill, D. Modeling flow profiles and dispersion in capillary electrophoresis with nonuniform zeta potential. Anal. Chem. **1994**, *66*, 4236.
8. Andreev, V.P.; Dubrovsky, S.G.; Stepanov, Y.V. Mathematical modeling of capillary electrophoresis in rectangular channels. J. Microcol. Separ. **1997**, *9*, 443.

Electrophoresis in Microfabricated Devices

Xiuli Lin
Christa L. Colyer
Department of Chemistry, Wake Forest University, Winston-Salem, North Carolina, U.S.A.

James P. Landers
Department of Chemistry, University of Virginia, Charlottesville, Virginia, U.S.A.

Abstract
Almost 20 years after the first demonstration of electrophoresis on a microchip (μ-chip) substrate, advances in microfabrication techniques and electrophoretic separation methodologies have resulted in the development of integrated systems offering high-efficiency separations coupled to sophisticated sample handling and detection schemes. The miniaturization of chemical analysis systems employing electrokinetic phenomena is explored in this entry, with particular reference to applications involving three major classes of analytes: DNA, proteins, and cells.

INTRODUCTION

The transposition of capillary electrophoresis (CE) methods from conventional capillaries to channels on planar chip substrates is an emergent separation science that has attracted widespread attention from analysts in many fields. Owing to the miniaturization of the separation format, CE-like separations on a chip typically offer shorter analysis times and lower reagent consumption augmented by the potential for portability of analytical instrumentation. Microchip (μ-chip) electrophoresis substrates boast optically flat surfaces, short diffusion distances, low Reynolds numbers, and high surface (or interface)-to-volume ratios. By exploiting these physical advantages of the chip over conventional capillaries, efficient μ-chip electrophoresis systems can accomplish multiple complicated tasks that may not be realized by a conventional CE system alone.

The first published demonstration of electrophoresis on a chip appeared almost 20 years ago and, although the separation efficiencies and analysis times in this pioneering work did not represent significant improvements over those achievable by way of conventional CE, this work demonstrated the feasibility of miniaturizing a chemical analysis system involving electrokinetic phenomena for sample injection, separation, and solvent pumping. Within 2 years of the first publication in this field, analysis times on the order of seconds and even milliseconds had been demonstrated with similar μ-chip systems, and efficiencies in excess of 100,000 theoretical plates were routinely obtained. Subsequently, the integration of other functionalities such as sample manipulations and chemical reactions, alongside electrophoretic separation, has vaulted μ-chip electrophoresis to new heights. In order to provide a rudimentary introduction to this important analytical technique, this entry will present the fundamentals of μ-chip fabrication methods and materials, sample introduction and detection methods, as well as selected recent *case studies* or notable applications of electrophoresis in microfabricated devices for various classes of analytes and various fields of study.

ADVANCES IN μ-CHIP FABRICATION AND DESIGN

The name "μ-chip" refers to the scale of the dimensions of the separation channels or other fluidic features as opposed to the dimensions of the substrate itself, which tend to be on the order of 1–2 mm in thickness and anywhere from 1 to 10 cm in length (or diameter for circular substrates). The evolution of μ-chip-based electrophoretic systems benefited initially from the tremendous advances in semiconductor microfabrication technologies witnessed over the past two decades. Although semiconducting substrates are not ideally suited to electrophoretic applications due to the high voltages applied for separation and fluid manipulation, many of the established semiconductor microfabrication techniques were modified for the insulating glass or quartz substrates that were most commonly encountered in early developments in the field of μ-chip electrophoresis. Micromachining of silicon and glass can involve wet and dry etching, photolithography, electron beam lithography, or a variety of other techniques, all of which require the use of clean-room facilities and equipment. Limitations posed by these high-cost and complicated (and potentially harmful) fabrication procedures have, in part, led to greater interest in polymer-based μ-chips. The trend toward the use of polymeric substrate materials, such as

polycarbonate, poly(dimethylsiloxane) PDMS, and poly(-methyl methacrylate) PMMA, has also been driven by the need for disposable μ-chips that are compatible with a wide variety of cellular, biological, and clinical samples (akin to the disposable plastic pipette tips, tubes, beads, plates, etc. commonly encountered in modern laboratories). Polymer μ-chip substrates are typically fabricated by a number of technologies, including in situ polymerization, replica molding, hot embossing, laser ablation, imprinting, and injection molding, the last of which is perhaps the best-known and the most frequently used technique in industrial settings. A thorough review of polymer microfabrication technologies is presented by Becker and Gärtner.[1] Even more recently, improvements in polymer μ-chip fabrication methods have been described, which involve a two-stage embossing technique and solvent welding on PMMA with water as a sacrificial layer.[2] With this technique, the tedious procedure of fabricating the primary mold can be avoided, and thus the overall time needed for fabrication is decreased considerably.

The concept of a *lab-on-a-chip* or a *micro-total-analysis-system* (μ-TAS) has pushed the development of even more advanced design features on chips. Sophisticated channel features such as weirs, pressure valves, and posts (columns) can be found with increasing frequency on chips. Weirs can be used to outline a specific area in the channel where beads or solgels with immobilized enzymes can be packed. Liquid can flow through these physical obstacles but the beads are held in place because of their larger size. Elastomeric materials that function as diaphragm pumps or valves can be manufactured from PDMS sandwiched between the channel and cover plate of the chip. This way, fluid movement in the chip can be manipulated by pressure as well as by electrokinetic means. Many other novel chip designs and features have been reported in the literature. For example, Inoue et al.[3] recently fabricated an I-shaped microchannel array (IMA) chip by integrating 12 independent microchannels, 2 electrodes, and 24 reservoirs onto a 3 × 2 cm area in a PDMS–glass hybrid μ-chip, complete with an integrated electrical wiring system to facilitate the autonomous regulation of sample plugs and high-throughput electrophoretic assays, as illustrated in Fig. 1. Also, Liu et al.[4] have developed 3-D microfluidic networks with an integrated combinatorial mixer for high-throughput combinatorial cell-based assays.

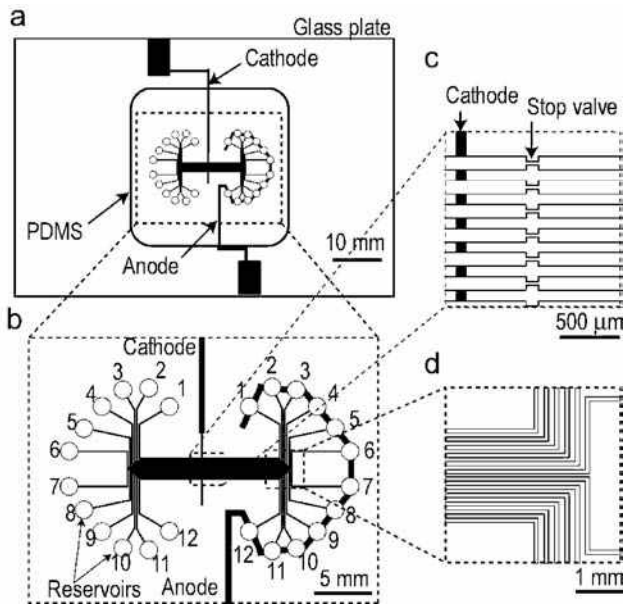

Fig. 1 Design of the IMA chip. a, Top view. The device consists of a 2 mm thick PDMS part with microchannels and a 1 mm thick glass plate with Au thin-film electrodes. b, Magnified view of the channel layout. The 12 I-shaped microchannels are arranged symmetrically with respect to both the horizontal and vertical axes. Each channel is 80 μm wide, 25 μm deep, and 28 mm long. The reservoirs with a diameter of 2 mm are punched in the PDMS part. The cathode is 80 μm wide and 200 nm thick. The anode is 400 μm wide and 200 nm thick. The distance between the cathode and the anode along the microchannels is 14.4 mm. c, Magnified view around the cathode. Each channel has a passive stop valve (8 μm wide and 80 μm long). The distance between adjacent channels (center to center) is 160 μm. The distance between the cathode and the passive stop valves is 0.4 mm. d, Magnified view around the corners of the microchannels.
Source: From I-shaped microchannel array chip for parallel electrophoretic analyses, in Anal. Chem. Copyright 2007, American Chemical Society.[3]

SAMPLE INJECTION ON μ-CHIPS

Reproducible sample introduction is a crucial factor in μ-chip-based electrophoretic separations. Various μ-chip sample introduction schemes are illustrated in Fig. 2. Of the many proposed injection methods, electrokinetic injection based on electro-osmotic flow (EOF) is most commonly encountered on chips, because electrically driven fluid flow is easier to generate and control than pressure-driven flow. Electrokinetic sample injection is generally achieved through a simple cross, "T," or "double-T" arrangement of etched channels to form the injection structure. Each injector design has different injection modes depending on the applied electric field sequences. For example, the original T-geometry (which can suffer from sample leakage problems) can be operated in floating, pinched, reversed pinched, dynamic, gated, gated with diffusion, and double-L injection modes.

Research still continues into the development of enhanced electrokinetic injection techniques for μ-chips. Modifications made to the outlet end of the separation channel, such as its connection to a length of fused silica capillary to facilitate chip interfacing with off-chip detection systems for example, can be adopted equally well for chip inlets and sample introduction. The use of conventional capillary to interface between macroscale sample reservoirs and μ-chip platforms has been successfully

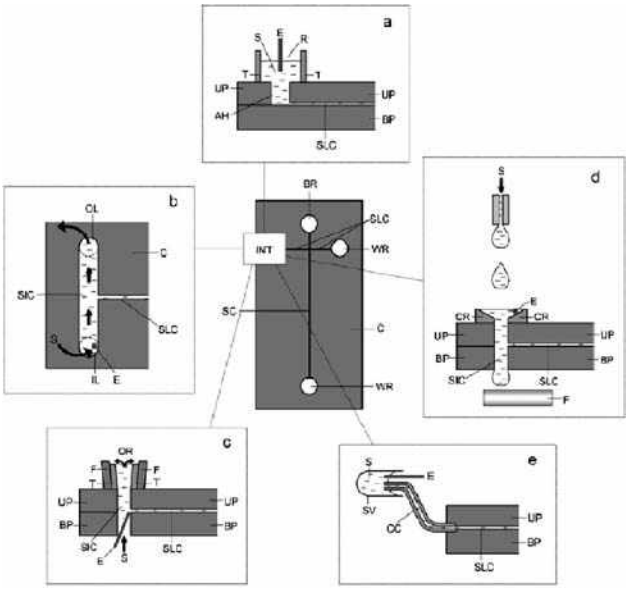

Fig. 2 Schematic diagrams of a typical capillary electrophoresis microchip employing different sample introduction systems. Abbreviations: C, chip; BR, buffer reservoir; INT, interfacing; SLC, sample loading channel; WR, waste reservoir; SC, separation channel; UP, upper plate of the chip; BP, base plate; S, sample; AH, access hole; E, electrode; T, tube; R, reservoir, SIC, sample introduction channel; IL, inlet; OL, outlet; F, filter paper; OR, overflow reservoir; CR, conical reservoir; CC, connecting capillary sample probe; SV, sample vial. a, Simple on-chip sample reservoir for electrokinetic cross or double-T type injector; b, large flow channel for on-chip continuous sample introduction; c, flow-through sampling reservoir with guided overflow design; d, flow-through sampling reservoir with falling-drop modification; e, fused-silica capillary "sampling probe" from sample vial to CE chip.

Source: Reprinted with permission from Springer Science+Business Media, from Sample introduction for microfluidic systems, in Anal. Bioanal. Chem.[5]

demonstrated[5] and has even been commercialized in the form of *sipper chips*, which are capable of sampling from up to 12 microtiter wells simultaneously via short lengths of conventional capillary interfaced to the bottom of the chip. In more recent work, Chang et al.[6] developed microfluidic electrophoresis devices with an enhanced injection scheme whereby a single- or a double-circular barrier is introduced in the intersection region of the microchannels in order to prevent sample leakage into the separation channel and to improve the sample plug definition.

Two of the main limitations of electrokinetic injection are its strong dependency on the surface properties of the channel walls and a bias toward different species depending upon their size and charge. Pressure-based injection techniques (such as pneumatic or hydrodynamic injection, based upon the hydrophobicity and wettability of channel surfaces) can solve the sampling bias problem, and so considerable effort has been devoted to the optimization of pressure injection. Karlinsey et al.[7] proposed a valved chip design that can perform both pressure and electrokinetic injections; Chen et al.[8] proposed a semihydrodynamic (SHD) injection coupled with a high-salt stacking method, which proved to be superior to regular hydrodynamic injection; Wang et al.[9] proposed an improved hydrostatic pressure sample injection method entailing nothing more than a simple tilt of the microchip, requiring no additional hardware and thus enabling this technology for disposable devices.

DETECTION ON μ-CHIPS

From the beginning, detection has been one of the main challenges for analytical microsystems, as very sensitive techniques are needed as a consequence of the ultrasmall sample volumes used in micrometer-sized environments. As μ-chip electrophoresis devices continue to advance, greater emphasis is being placed on detector design and configuration in order to achieve maximum sensitivity with low cost and ease of manufacture. The most common detection schemes employed in conjunction with μ-chip separations include optical [especially, laser-induced fluorescence (LIF) detection, chemiluminescence detection, and ultraviolet–visible (UV–Vis) absorbance], electrochemical, and mass spectrometric methods, although less commonly encountered chip detection methods such as refractive index, Raman, surface plasmon resonance, thermal lens, infrared, and nuclear magnetic resonance (NMR) have been used with success too.

LIF is the most widespread of all chip detection methods because of its high sensitivity despite small separation channel dimensions and the convenience of optically flat chip surfaces for detection purposes. However, since relatively few analytes are natively fluorescent, LIF detection often necessitates the development of selective and sensitive labeling strategies for each assay. Specialized on-chip LIF detection schemes such as the utilization of Hadamard transform CE with caged fluorescent labels have rendered detection limits down to as few as 18 molecules per injection event.[10]

Electrochemical detection (ECD) modes include amperometry, conductimetry, and potentiometry, with the first of these being employed most frequently. ECD is ideal for use with μ-chip electrophoresis systems because of the ease of miniaturization with no diminution in analytical performance and the ease of incorporating detection electrodes directly onto the chip by standard microfabrication procedures. Electroactive analytes can be easily detected using ECD methods, although non-electroactive compounds can also be detected by using derivatization agents, analogous to the use of derivatization in LIF detection schemes. Decoupling the electric field used to drive the electrophoretic separation from the ECD signal poses a

challenge on μ-chip electrophoresis substrates, just as it does with conventional CE capillaries. Recent fabrication developments involving gold nanoelectrode assemblies as working and decoupler electrodes in PMMA chips have enabled higher signal response (relative to a bulk gold working electrode) and reduced charging current and baseline drift (relative to a conventional palladium decoupler).[11] The development of a sheath flow ECD design,[12] which relies on gravity-driven flow of a sheath buffer to carry the electroactive analytes to the detection electrodes, is able to reduce the dependence of the ECD signal on electrode position, further improving the potential of ECD schemes for μ-chip-based electrophoretic analyses.

Mass spectrometry (MS) is a powerful alternative to ECD and optical detection schemes, especially for large biological molecules. The typical flow rates encountered in microfluidics (nanoliter to microliter per minute) are well suited to electrospray ionization mass spectrometry (ESI–MS). The integration of the ionization process onto microfluidic devices is challenging owing to the planar nature of microfabricated systems. Much work in this field deals with ways to create suitable tips for the generation of electrospray from the chip. One method for interfacing electrospray ionization with microfluidic devices involves gluing or bonding electrospray emitters, such as fused-silica capillaries or nanospray needles, to the end of the chip at the outlet of the microchannel. Another method is to integrate electrospray tips during the chip fabrication process. Advances in sheathless CE/ESI–MS interfaces have been reviewed by Zamfir.[13] Recognizing the potential for complementarity of microfabricated separation substrates and microfabricated detectors, Whitten, Reilly, and Ramsey have advanced a miniaturized ion-trap mass analyzer,[14] which shows spectral resolution comparable to conventional mass analyzers with slight compromises in sensitivity.

APPLICATIONS OF μ-CHIP ELECTROPHORESIS

One of the most impressive aspects of μ-chip electrophoresis is the diversity of analytes and the breadth of research fields that have been served by this technology. A comprehensive review of applications is not possible here, but instead, we will present a brief summary of interesting examples employing μ-chip electrophoresis for three major classes of analytes: DNA, proteins, and cells.

ELECTROPHORESIS OF DNA ON CHIPS

Since the first DNA separations on a single-lane μ-chip in the mid 1990s, improved fabrication and detection methods have allowed for a remarkable increase in the throughput and performance capabilities of these devices. Now, DNA analysis is one of the leading applications of μ-chip electrophoresis. Early DNA applications included the separation of oligonucleotides (10–25 bases) and sizing of longer DNA fragments. Sieving matrices such as linear poly(acrylamide) (LPA), hydroxyethyl cellulose (HEC), hydroxypropyl cellulose (HPC), and hydroxypropylmethyl cellulose (HPMC) are often used for DNA fragment sizing. The formation of hydrogen bonds between polyhydroxy buffer additives and DNA analytes enhances the separation, as demonstrated by Xu, Jabasini, and Baba,[15] who separated DNA restriction fragments ranging in size from 72 to 1353 bp in a 3 cm long channel in 170 sec with HPMC. The application of μ-chip electrophoresis methods to more sophisticated DNA assays, including DNA sequencing, genotyping, and polymerase chain reaction (PCR) amplification, logically followed, and will be considered here.

Among the technologies being developed to reduce sequencing costs, μ-chip CE is most suitable for the de novo sequencing and assembly of large and complex genomes. DNA sequencing relies upon the Nobel Prize–winning Sanger dideoxy chain termination reaction, which is based on the controlled interruption of the enzymatic replication of an ssDNA template by a DNA polymerase. The Sanger reaction was used to produce a "ladder" of template-complementary DNA fragments that differ in length by one base and that bear unique fluorescent labels according to their terminal nitrogenous base, and so after separating these fragments (e.g., by μ-chip electrophoresis) and detecting the base-specific labels, the original sequence order of the fragments can be obtained by computational reassembly. Fredlake et al.[16] recently reported a microfluidic chip-based system that provides ultrafast DNA Sanger sequencing with read lengths up to 600 bases in 6.5 min.

Functional genomic studies focus on the analysis of gene variants in human populations for the purpose of disease diagnosis, prognosis, and management. Techniques such as single-nucleotide polymorphism (SNP) detection, single-stranded conformation polymorphism (SSCP) detection, heteroduplex analysis (HA), allele-specific PCR (ASPCR), and short tandem repeat (STR) analysis are commonly used for DNA mutation analysis. Single-nucleotide polymorphisms are single-base-pair changes or deletions in a natural DNA sequence, and there is an estimated number of 2–3 million SNPs that can differ between any two individuals' genomes. STRs are short stretches of repetitive DNA sequences that are distributed throughout the genome of every individual. Each genetic locus consists of 7–20 repeats of a specific 2- to 7-base sequence. By electrophoretic separation of these repeats, the DNA can be sequenced and genotyped. Because of the effectiveness of STR analysis, the Federal Bureau of Investigation (FBI) created a national criminal database—the Combined DNA Index System (CODIS)—in 1998. Owing to the rigorous demands of the database, analysis techniques need to possess high

reproducibility and throughput capability, and they should be fast, automated, and easily adaptable by instrument operators. To address these requirements, Goedecke et al. developed "GeneTrack," a multiplexed DNA analysis instrument.[17] It consisted of two units, the support and the top unit, with the former containing the necessary power supplies and the data acquisition system, and the latter containing the laser, optics, and the electrode board. The heart of the instrument, a microfabricated device, consisted of two glass plates thermally bonded together. Sixteen separation channels were wet-etched on one of the plates; sample injection was achieved using a classic double-T injector. The inner channel surfaces were silanized by following a modified Hjerten method and finally filled with LPA as the sieving media. Fluorescence detection was arranged with a multiline argon ion laser and four photomultiplier tubes (PMTs) that allowed for four-color detection when coupled with a system of dichroic mirrors. The developed system was validated by analyzing the DNA template 9947a with the PowerPlex® 16 PCR kit from Promega. All the 16 lanes on the microchip were used for the analysis, which was repeated 6 times over 4 days. It was reported that 92 out of the 96 total lanes performed successfully. Also, after statistical testing, the instrument was shown to have 0.4–0.9 bp absolute signal accuracy for the full 13-locus STR DNA determination as required by the CODIS. For the specific TH01 DNA locus it was shown that the required single-base-pair resolution was reliably achieved. The authors concluded by stating that "the system is optimized for the forensics 'casework' application and is expected to exceed current capillary systems in sample economy, critical temperature/environmental stability, and software features."

Improved throughput and reduced cost have governed genotyping assay development. A capillary array electrophoresis (CAE) bioanalyzer with 384 lanes etched radially around the center of a round, 200 mm diameter borosilicate glass wafer with a common central anode was developed.[18] The utility of this system was demonstrated for the simultaneous genotyping of the DNA from 384 individuals for a hereditary hemochromatosis (HHC)-related mutation in the human HFE gene. HHC is not only one of the most common autosomal recessive diseases in the United States, but its diagnosis also remains troublesome. The genotyping success rate for the 384-lane chip was found to be 98.7% with a relative mobility deviation of less than 2.2%. Electrophoresis of the samples was completed in 325 sec. It was concluded that the μ-chip device outperformed the best commercially available 96-capillary instruments by a factor of 20 and that it could be ideal for gene mapping, pharmacogenomic screening, forensics, and proteomics.

PCR is an enzyme-mediated process whereby, in response to temperature cycling, a single DNA molecule can be rapidly amplified into many billions of molecules. Scaling down PCR technology to allow its integration with microfluidic systems is essential to the analysis of DNA in this realm. For example, Prakash et al.[19] have used off-chip, real-time PCR to validate a recently developed chip technology that integrates PCR with CE to detect the respiratory pathogen *Bordetella pertussis*. This chip technology used less than 3 μl for PCR and only 0.3 μl for subsequent CE analysis to identify *B. pertussis* from the equivalent genetic content of two or fewer cells, as illustrated in Fig. 3. Another recent technology developed by Easley, Humphrey, and Landers[20] provides a non-contact, infrared-mediated system for μ-chip DNA amplification via PCR, which focuses on heat transfer modeling and subsequent fabrication of thermally isolated reaction chambers in glass devices. These devices are compatible with standard photolithography and wet-etching techniques and can realize rapid temperature control. Notably, this is the fastest static PCR in glass devices reported to date: 25 thermal cycles are completed in only 5 min in thermally isolated PCR chambers of 270 nl volume for DNA amplification. The recurring goals of low cost, low sample requirement, and high throughput for DNA analysis are clearly met by integrated μ-chip electrophoresis devices.[21]

ELECTROPHORESIS OF PROTEINS ON CHIPS

On-chip protein analysis encompasses a wide range of applications and technical developments. On-chip protein assays began with simple demonstrations of 1-D separations: sodium dodecyl sulfate (SDS) gel-based molecular sizing, isoelectric focusing (IEF), capillary electrochromatography (CEC), and micellar electrokinetic chromatography (MEKC). However, the sequential coupling of these methods in two orthogonal dimensions was subsequently demonstrated on a chip, to reproduce the more traditional 2-D separations fundamental to proteomic studies. A simultaneous 2-D microchip design consisting of an IEF microchannel orthogonal to an array of SDS-PEO [poly(ethylene oxide)] gel microchannels on a plastic substrate as small as 2 × 3 cm, as reported by Li et al.,[22] offered an alternative to the inherently serial nature of most 2-D microchip designs. This design permitted the focused and concentrated protein fractions from the IEF channel to be simultaneously injected and separated (on the basis of protein size) in the multiple, parallel SDS-gel channels in the orthogonal array, yielding a comprehensive protein separation in less than 10 min with a peak capacity of about 1700. Furthermore, it was proposed that the peak capacity could be increased by simply raising the density of microchannels in the second-dimension array, which would have the effect of increasing the number of fractions from the IEF dimension that could be simultaneously analyzed in the size-based SDS–PEO separation dimension.

However, fluorescent derivatization of proteins is not compatible with IEF (as the derivatization may alter the

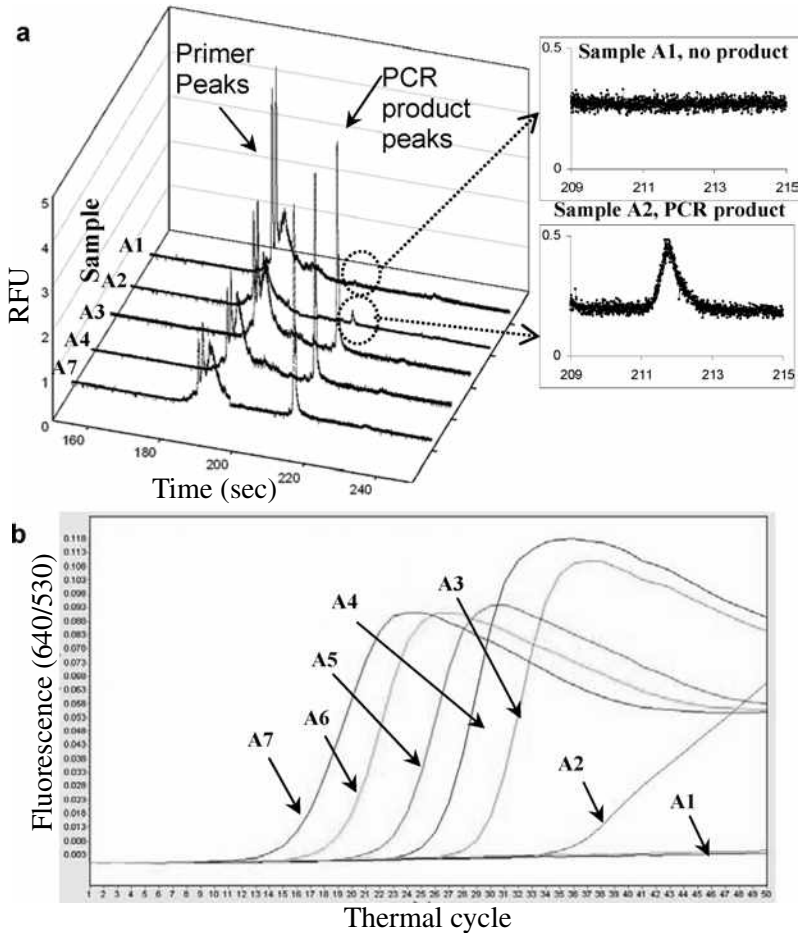

Fig. 3 Integration of PCR with CE to detect the respiratory pathogen *Bordetella pertussis*. a, The 3-D plot shows the CE analysis of different concentrations of *B. pertussis* samples run on the integrated chip. For clarity, the PCR product ''Time vs. RFU'' for samples A2 and A1 are shown in magnified inserts. b, Real-time PCR LightCycler® amplification profile of the IS481 hybridization probe assay with a dilution series of *B. pertussis*, for samples A7–A1. In CE the PCR amplification is analyzed based on the fluorescence intensity of the amplified DNA and time, while in real-time PCR it is analyzed at the amplification stage itself by the fluorescence of the hybridization probe at each thermal cycle.
Source: Reprinted with permission from Springer Science+Business Media, from Identification of respiratory pathogen *Bordetella pertussis* using integrated microfluidic chip technology, in Microfluid. Nanofluid.[19]

isoelectric point of the labeled protein), and so Shadpour and Soper[23] recently described an alternative 2-D electrophoretic separation of derivatized proteins ranging in size from 38 to 110 kDa using an embossed PMMA microchip. In this work, separation in the first dimension (30 mm length) was based on size using SDS-microcapillary gel electrophoresis while separation in the second dimension (10 mm length) was based on pseudostationary phase partitioning using MEKC. LIF detection followed the MEKC dimension to provide for the sensitive determination of proteins conjugated with the Alexa Fluor® 633 label. Average plate numbers of 4.8×10^4 and 1.2×10^4 were obtained for the first and second dimensions, respectively, while the full 2-D separation was performed in about 12 min with a peak capacity of about 1000.

Covalent derivatization of proteins in this instance dictated the modes of separation and enhanced detection sensitivity. Non-covalent dye–protein interactions can alternatively be exploited to facilitate protein determination by μ-chip electrophoresis with LIF detection, thus offering greater selectivity and sensitivity than is possible with absorbance detection while entailing a simpler and faster labeling protocol than required by conventional covalent labels. Sloat et al.[24] recently employed the asymmetric squarylium dye Red-1c as a non-covalent label in both on-column and pre-column derivatization methods for protein determination by μ-chip electrophoresis with LIF detection. This was the first demonstration of Krylov's non-equilibrium CE of equilibrium mixtures (NECEEM) theory[25] to calculate binding constants for dye–protein complexes in microchip substrates based on areas beneath bound and free dye peaks in the resulting electropherograms (Fig. 4), with the aim of developing more selective and sensitive non-covalent chip-based labeling strategies for CE–LIF protein assays.

Beyond their rapidly developing role in 1-D and 2-D protein separations and protein-binding studies, μ-chip platforms also offer advantages in other aspects of protein assays, such as sample "prep" and direct transfer to MS detection systems. Whereas traditional protein assays may require spot excision and proteolytic digestion following 1-D or 2-D gel-based separations, concluding with

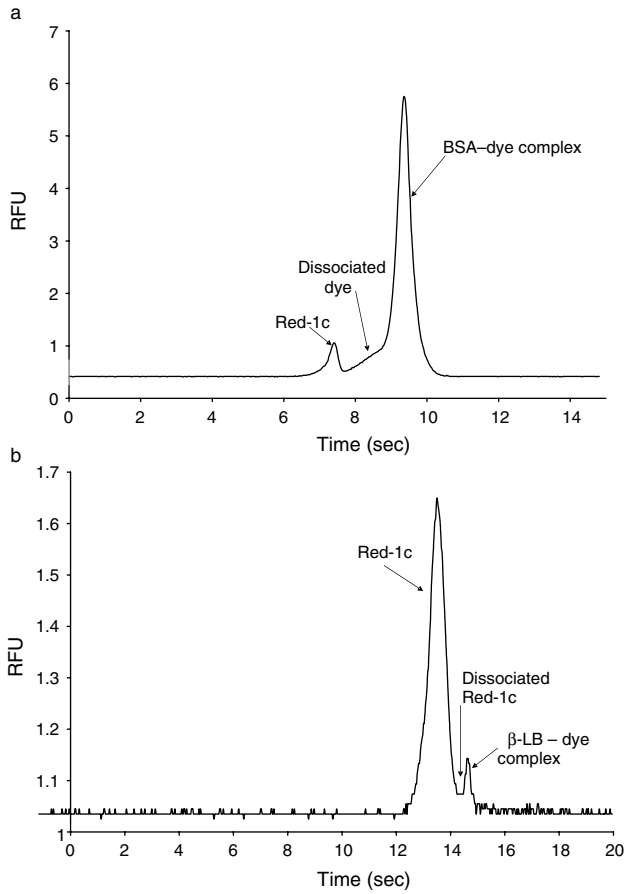

Fig. 4 The separation of free dye and protein–dye complex by micro-chip NECEEM. a, BSA–Red-1c complex. Sample and experimental details: Precolumn labeling of 0.50 μmol BSA with 5.0 μmol Red-1c; 60 sec injection; 2500 V separation voltage; 6 mm effective separation channel length; 800 V PMT voltage; b, β-lactoglobulin B–Red-1c complex. Sample and experimental details: Precolumn labeling of 75 μmol β-lactoglobulin B with 5.0 μmol Red-1c; 10 mm effective separation channel length; 100 mmol boric acid buffer (pH 9.5) with 100 mmol KCl.

Source: Reproduced with permission from Protein determination by microchip capillary electrophoresis using an asymmetric squarylium dye: Non-covalent labeling and non-equilibrium measurement of association constants, in Electrophoresis. Copyright Wiley-VCH Verlag GmbH & Co. KGaA.[24]

detection of the resulting digestion fragments by mass spectrometry, μ-chip electrophoresis systems can integrate these many functionalities or can provide suitable alternatives to them. A microfabricated CE–MS device recently developed by Mellors et al.[26] performs electrospray ionization directly from the corner of the chip to a mass spectrometer to detect peptides and proteins with efficiencies in excess of 1 million plates per meter. A positively charged surface coating reversed the direction of EOF in the chip channels and prevented interactions between the analytes and channel surfaces. This work, which also identified 37 peptide fragments from the tryptic digest of bovine serum albumin (BSA), accounting for 58% coverage of the total sequence of BSA, offers much promise for future proteomic studies employing similar μ-chip technologies.

ELECTROPHORESIS OF CELLS ON CHIPS

Understanding biological chemistry from both structural and functional perspectives necessitates tools capable of analysis not only on the molecular level (e.g., of proteins and DNA) but also on the cellular level. Extending the realm of the so-called lab-on-a-chip to the lab-in-a-cell concept requires three particular areas to be addressed, including cell sorting or trapping, cell treatment, and cell analysis. Most cells have a net negative charge near physiological pH, and so an electric field can be used to transport them. Li and Harrison[27] first took advantage of this fact in their demonstration of electrophoretic and electro-osmotic pumping of three cell types—baker's yeast, *Escherichia coli*, and canine erythrocytes (red blood cells)—within a network of microfabricated capillary channels. EOF in their uncoated glass chips exceeded the electrophoretic mobility of the cells, and so the net transport of cells toward the cathode was observed at near physiological pH values. Cell velocities of up to 0.5 mm/sec in channels with 15 × 50 μm cross-sections were observed. Care was taken to avoid cell lysis caused by the application of the separation voltage (less than 600 V/cm and typically about 100 V/cm), although high electric fields (1–10 kV/cm) have been shown to cause cell membrane permeation. Cell adhesion to the channel walls was observed in the case of yeast and *E. coli*; however, reduction of cell counts significantly relieved this problem, as did wall treatment with a commercial trichlorohexadecylsilane agent, rendering the walls hydrophobic. This wall treatment, however, also substantially reduced the EOF, so that the electrophoretic mobility of the negatively charged canine erythrocytes in isotonic solution (toward the anode) exceeded the EOF toward the cathode. Furthermore, Li and Harrison were able to demonstrate the second component of cell analysis—namely, cell treatment—by successfully using electrokinetic effects to mix streams of canine erythrocytes and SDS directly on the chip and subsequently observing the resulting cell lysis. Thus, this successful demonstration of cell sorting or directed cell transport and cell lysing by an electrokinetic, valveless control scheme within a system of four intersecting channels clearly established the utility of electrophoresis on microfabricated devices for cellular analysis.

Single-cell analysis is essential to the growing pursuits of proteomics and systems biology. Thus, more and more sophisticated chip-based cellular assays have followed this pioneering work. For example, Huang et al.[28] recently developed a microfluidic device with a three-state valve to

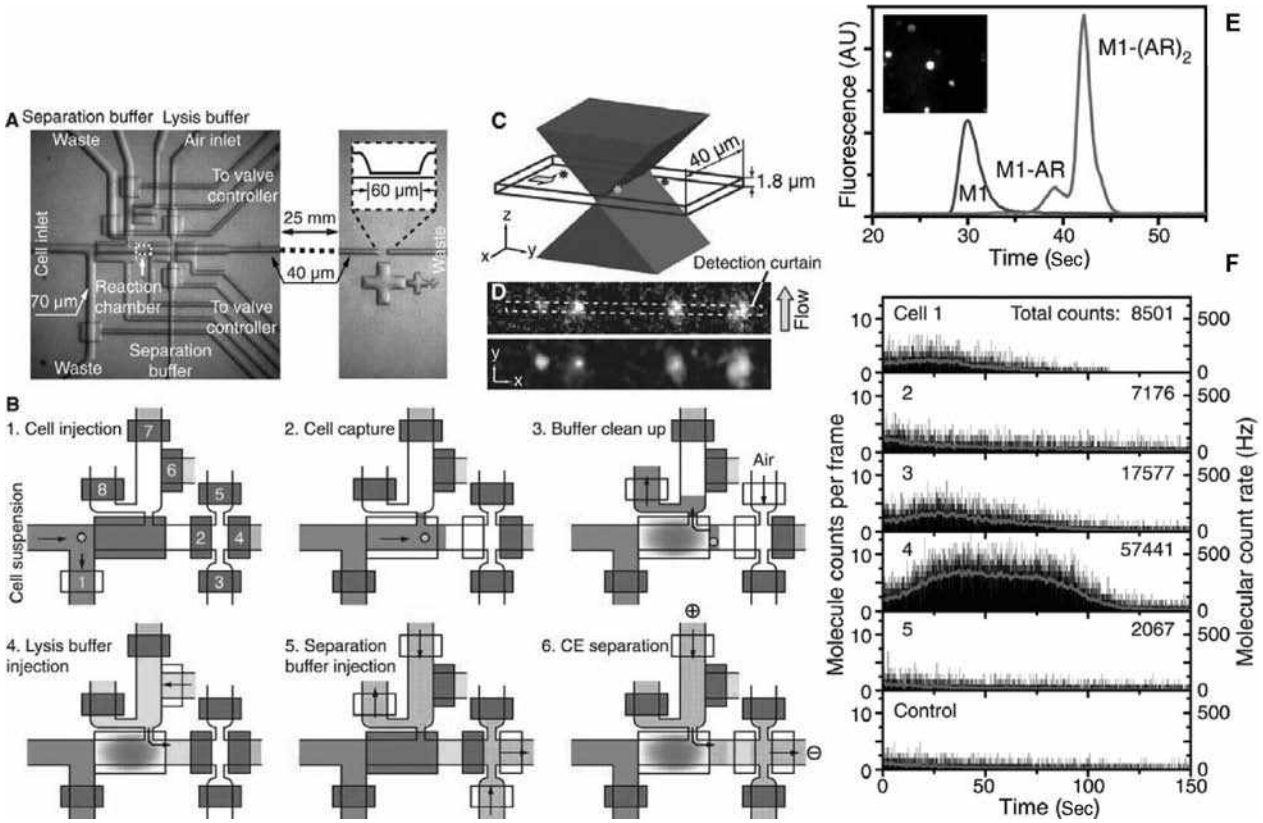

Fig. 5 The single-cell analysis chip and the analysis of β_2AR in Sf9 cells. A, Layout of the single-cell chip, showing the cell-manipulation section on the left and the molecule-counting section on the right; B, Analysis procedure for a mammalian or insect cell; C, Schematic illustration of the excitation laser focused by the microscope objective and the dimensions of the molecule-counting channel; D, One frame from the CCD images of fluorescent molecules flowing across the molecule-counting section (upper panel) and the identification results (lower panel); E, Electropherogram of Cy5-labeled M1 antibody against FLAG (M1); measurements are shown before and after adding an excess amount of purified β_2AR (AR) in a double-T chip; F, Molecule-counting results of Sf9 cells expressing β_2AR, showing the electropherogram of the M1–AR complexes. The red (solid) line represents the average count rate.
Source: Reprinted with the permission of AAAS, modified from Counting low-copy number proteins in a single cell, in Science.[28]

integrate the isolation of an individual cell from a bulk suspension; the accurate metering and delivery of chemical reagents; the performance of cell lysis and chemical derivatization reactions; and the separation of derivatized cell contents by CE–LIF. Between the three-state valve and a conventional two-state valve in this system is the reaction chamber in which both cell capture and the labeling of proteins were achieved (see Fig. 5). The latter function involved fluorescent–antibody binding by injecting a lysing/labeling buffer into the reaction chamber to release the cell contents. In order to achieve high-efficiency counting of molecules in micrometer-sized channels, cylindrical optics were used to form a rectangular, curtain-shaped detection region across the channel. By combining this microfluidic device with single-molecule fluorescence counting, β_2 adrenergic receptors expressed in Sf9 cells were quantified and phycobiliprotein content in individual cyanobacterial cells (*Synechococcus* sp. PCC 7942) was also determined.

Greif et al.[29] reported on novel chip architectures for single-cell analysis based on full-body quartz glass (QG) μ-chips. The enhanced sensitivity of QG chips as compared to PDMS chips and PDMS quartz window (PQW) chips employing native UV laser-induced fluorescence (UV-LIF) detection was shown. The combination of a higher pH for the separation buffer and the use of dodecyl-β-D-maltoside (DDM) and methylcellulose (MC) as dynamic wall coatings resulted in higher detection sensitivities and separation efficiencies for single-cell electropherograms of *Spodoptera frugiperda* (Sf9) insect cells. This method offers promise for label-free protein fingerprinting of single cells.

CONCLUSIONS AND FUTURE PERSPECTIVES

The advantages typically associated with CE, such as reduced sample and reagent consumption, reduced analysis time, and increased separation efficiency, are augmented when the CE system is transposed to a μ-chip substrate. Beyond electrophoresis, however, μ-chip substrates offer the distinct advantage of functional process integration.

Analytical processes such as sample preparation, injection, reaction, and detection can be seamlessly tied to electrophoretically driven separations on microfabricated chips en route to the realization of a true lab-on-a-chip.

The very nature of μ-chip electrophoresis systems, characterized by their capacity for high-throughput, high-speed, high-sensitivity, and low-sample-consumption assays, makes them inherently well suited to the clinical setting, as documented in a recent review article by Dewald, Poe, and Landers.[30] Likewise, these same characteristics render μ-chip electrophoresis systems invaluable to numerous other realms, such as forensics, environmental analysis, oceanography, and homeland security. However, the full realization of portable, field-based, or point-of-care analysis systems still lags behind the promise of research-based systems, and this deficiency needs to be remedied through continued advances in interfacing, engineering, and commercialization. As the complexity of chip designs increases, and as we strive to fully realize the advantages offered by the microfluidics regime of the chip, we must continue to carefully manage methods of physically addressing their small structures and volumes, and of interfacing to the macroscale world beyond the chip. In this regard, passive approaches to controlling fluid flow through complex chip architectures without active valves will become key.[31]

Although chip fabrication techniques are quite well established and varied, they are still not accessible to the majority of analysts. Fabrication processes must continue to be refined to allow routine chip construction at the hands of analysts in regular research labs, or ideally, the chips themselves must be made more readily available at low cost and in a variety of application designs for all potential users. Miniaturization, or careful arrangement of the apparatus accompanying the electrophoresis chip, including power supplies, detection systems, computer controllers, and other components, into compact and robust systems, must be considered in order to take full advantage of the chip's small size. It is in this respect that novel, cost-effective approaches for rapid chip prototyping will be critical not only to application development, but possibly to mass fabrication of single-use, disposable microdevices.[32]

Despite these remaining challenges, which offer exciting opportunities for discovery in numerous fields of study, it should be noted that electrophoretic separations remain the cornerstone of μ-chip-based analysis systems, and so the fields of analytical chemistry and separation science must continue to take the lead in the development of these promising and important tools, techniques, and technologies.

ACKNOWLEDGMENTS

C.L. Colyer gratefully acknowledges support of this work by the National Science Foundation under Grant No. CHE-0809756.

REFERENCES

1. Becker, H.; Gärtner, C. Polymer microfabrication methods for microfluidic analytical applications. Electrophoresis **2000**, *21* (1), 12–26.
2. Koesdjojo, M.T.; Tennico, Y.H.; Reincho, V.T. Fabrication of a microfluidic system for capillary electrophoresis using a two-stage embossing technique and solvent welding on poly(methyl methacrylate) with water as a sacrificial layer. Anal. Chem. **2008**, *80* (7), 2311–2318.
3. Inoue, A.; Ito, T.; Makino, K.; Hosokawa, K.; Maeda, M. I-shaped microchannel array chip for parallel electrophoretic analyses. Anal. Chem. **2007**, *79* (5), 2168–2173.
4. Liu, M.C.; Ho, D.; Tai, Y.C. Monolithic fabrication of three-dimensional microfluidic networks for constructing cell culture array with an integrated combinatorial mixer. Sens. Actuators B, **2008**, *129* (2), 826–833.
5. Fang, Q. Sample introduction for microfluidic systems. Anal. Bioanal. Chem. **2004**, *378* (1), 49–51.
6. Chang, C.L.; Hou, H.H.; Fu, L.M.; Tsai, C.H. A low-leakage sample plug injection scheme for crossform microfluidic capillary electrophoresis devices incorporating a restricted cross-channel intersection. Electrophoresis **2008**, *29* (15), 3135–3144.
7. Karlinsey, J.M.; Monahan, J.; Marchiarullo, D.J.; Ferrance, J.P.; Landers, J.P. Pressure injection on a valved microdevice for electrophoretic analysis of submicroliter samples. Anal. Chem. **2005**, *77* (11), 3637–3643.
8. Chen, C.C.; Yen, S.F.; Makamba, H.; Li, C.W.; Tsai, M.L.; Chen, S.H. Semihydrodynamic injection for high salt stacking and sweeping on microchip electrophoresis and its application for the analysis of estrogen and estrogen binding. Anal. Chem. **2007**, *79* (1), 195–201.
9. Wang, W.; Zhou, F.; Zhao, L.; Zhang, J.R.; Zhu, J.J. Improved hydrostatic pressure sample injection by tilting the microchip towards the disposable miniaturized CE device. Electrophoresis **2008**, *29* (3), 561–566.
10. Braun, K.L.; Hapuarachchi, S.; Fernandez, F.M.; Aspinwall, C.A. High-sensitivity detection of biological amines using fast Hadamard transform CE coupled with photolytic optical gating. Electrophoresis **2007**, *28* (17), 3115–3121.
11. Chen, C.M.; Chang, G.L.; Lin, C.H. Performance evaluation of a capillary electrophoresis electrochemical chip integrated with gold nanoelectrode ensemble working and decoupler electrodes. J. Chromatogr. A, **2008**, *1194* (2), 231–236.
12. Ertl, P.; Emrich, C.A.; Singhal, P.; Mathies, R.A. Capillary electrophoresis chips with a sheath-flow supported electrochemical detection system. Anal. Chem. **2004**, *76* (13), 3749–3755.
13. Zamfir, A.D. Recent advances in sheathless interfacing of capillary electrophoresis and electrospray ionization mass spectrometry. J. Chromatogr. A, **2007**, *1159* (1–2), 2–13.
14. Whitten, W.B.; Reilly, P.T.A.; Ramsey, J.M. High-pressure ion trap mass spectrometry. Rapid Commun. Mass Spectrom. **2004**, *18* (15), 1749–1752.
15. Xu, F.; Jabasini, M.; Baba, Y. DNA separation by microchip electrophoresis using low-viscosity hydroxypropylmethylcellulose-50 solutions enhanced by polyhydroxy compounds. Electrophoresis **2002**, *23* (20), 3608–3614.

16. Fredlake, C.P.; Hert, D.G.; Kan, C.W.; Chiesl, T.N.; Root, B.E.; Forster, R.E.; Barron, A.E. Ultrafast DNA sequencing on a microchip by a hybrid separation mechanism that gives 600 bases in 6.5 minutes. Proc. Natl. Acad. Sci. U.S.A. **2008**, *105* (2), 476–481.
17. Goedecke, N.; McKenna, B.; El-Difrawy, S.; Carey, L.; Matsudaira, P.; Ehrlich, D. A high-performance multilane microdevice system designed for the DNA forensics laboratory. Electrophoresis **2004**, *25* (10–11), 1678–1686.
18. Emrich, C.A.; Tian, H.; Medintz, I.L.; Mathies, R.A. Microfabricated 384-lane capillary array electrophoresis bioanalyzer for ultrahigh-throughput genetic analysis. Anal. Chem. **2002**, *74* (19), 5076–5083.
19. Prakash, A.R.; De La Rosa, C.; Fox, J.D.; Kaler, K.V.I.S. Identification of respiratory pathogen *Bordetella pertussis* using integrated microfluidic chip technology. Microfluid. Nanofluid. **2008**, *4* (5), 451–456.
20. Easley, C.J.; Humphrey, J.A.C.; Landers, J.P. Thermal isolation of microchip reaction chambers for rapid non-contact DNA amplification. J. Micromech. Microeng. **2007**, *17* (9), 1758–1766.
21. Easley, C.J.; Karlinsey, J.M.; Bienvenue, J.M.; Legendre, L.A.; Roper, M.G.; Feldman, S.H.; Hughes, M.A.; Hewlett, E.L.; Merkel, T.J.; Ferrance, J.P.; Landers, J.P. A fully-integrated microfluidic genetic analysis system with sample-in-answer-out capability. Proc. Natl. Acad. Sci. USA **2006**, *103* (51), 19272–19277.
22. Li, Y.; Buch, J.S.; Rosenberger, F.; DeVoe, D.L.; Lee, C.S. Integration of isoelectric focusing with parallel sodium dodecyl sulfate gel electrophoresis for multidimensional protein separations in a plastic microfluidic network. Anal. Chem. **2004**, *76* (3), 742–748.
23. Shadpour, H.; Soper, S.A. Two-dimensional electrophoretic separation of proteins using poly(methyl methacrylate) microchips. Anal. Chem. **2006**, *78* (11), 3519–3527.
24. Sloat, A.L.; Roper, M.G.; Lin, X.; Ferrance, J.P.; Landers, J.P.; Colyer, C.L. Protein determination by microchip capillary electrophoresis using an asymmetric squarylium dye: Noncovalent labeling and nonequilibrium measurement of association constants. Electrophoresis **2008**, *29* (16), 3446–3455.
25. Okhonin, V.; Krylova, S.M.; Krylov, S.N. Nonequilibrium capillary electrophoresis of equilibrium mixtures, mathematical model. Anal. Chem. **2004**, *76* (5), 1507–1512.
26. Mellors, J.S.; Gorbounov, V.; Ramsey, R.S.; Ramsey, J.M. Fully integrated glass microfluidic device for performing high-efficiency capillary electrophoresis and electrospray ionization mass spectrometry. Anal. Chem. **2008**, *80* (18), 6881–6887.
27. Li, P.C.H.; Harrison, D.J. Transport, manipulation, and reaction of biological cells on-chip using electrokinetic effects. Anal. Chem. **1997**, *69* (8), 1564–1568.
28. Huang, B.; Wu, H.K.; Bhaya, D.; Grossman, A.; Granier, S.; Kobilka, B.K.; Zare, R.N. Counting low-copy number proteins in a single cell. Science **2007**, *315* (5808), 81–84.
29. Greif, D.; Galla, L.; Ros, A.; Anselmetti, D. Single cell analysis in full body quartz glass chips with native UV laser-induced fluorescence detection. J. Chromatogr. A, **2008**, *1206* (1), 83–88.
30. Dewald, A.H.; Poe, B.L.; Landers, J.P. Electrophoretic microfluidic devices for mutation detection in clinical diagnostics. Exp. Opin. Mol. Diag. **2008**, *2* (8), 963–977.
31. Leslie, D.J.; Easley C.J.; Seker, E.; Karlinsey, J.; Utz, M.; Begley, M.R.; Landers, J.P. Frequency-specific flow control in microfluidic circuits with passive elastomer features. Nature Phys. **2009**, *5* (3), 231–235.
32. Lago, C.L.; Neves, C.A.; Pereira de Jesus, D.; da Silva, H.D.; Brito-Neto, J.G.; Fracassi da Silva, J.A. Microfluidic devices obtained by thermal toner transferring on glass substrate. Electrophoresis **2004**, *25* (21–22), 3825–3831.

Electrospray Ionization Interface for CE/MS

Joanne Severs
Bayer Pharmaceuticals, Berkeley, California, U.S.A.

INTRODUCTION

The development of the electrospray ionization (ESI) source for mass spectrometry (MS) provided an ideal means of detection for capillary electrophoretic (CE) separations. The ESI source is currently the preferred interface for CE/MS, due to the fact that it can produce ions directly from liquids at atmospheric pressure and with high sensitivity and selectivity for a wide range of analytes.

DISCUSSION

ESI is initiated by generating a high potential difference between the spray capillary tip and a counterelectrode.[1] This electric field leads to the production of micron-sized droplets with an uneven charge distribution, generally accepted to be due to an electrophoretic mechanism acting on electrolytes in the solvent.[2] This mechanism, combined with a shrinkage of the droplets due to solvent evaporation (aided by heat and an applied gas flow into the source), leads to electrostatic repulsion overcoming surface tension in the droplet. The "Rayleigh" limit is reached, a "Taylor cone" is formed, and smaller highly charged droplets are emitted, eventually leading to the production of gas-phase ions.[1–3] These ions are accelerated through a skimmer into successive vacuum stages of the mass analyzer. The ESI source has been demonstrated to act as an electrolytic cell, generating electrochemical oxidation and reduction.[2] The exact ionization mechanism will vary with experimental conditions and is still an area of continuing in-depth research and discussion.[3]

ESI is classified as a "soft" ionization technique. It produces molecular-weight information and very little, if any, fragmentation of the analyte ion, unless induced in the vacuum region of the mass analyzer. The number of charges accumulated by an analyte ion is proportional to its number of basic or acidic sites. The spray polarity and conditions, solution pH and nature, as well as solute concentration will all effect the charge state distribution observed in the mass spectrum. Multiple charging of an analyte ion encourages the release of very high-molecular-weight ions. It is mainly due to this fact that ESI has gained such enormous interest, especially among biochemists. Employing only small, relatively inexpensive mass analyzers, spectrometrists are able to obtain high-sensitivity information on analytes with molecular weights of up to 200 kDa. The multiple-charging phenomenon means that the mass-to-charge (m/z) range of the analyzer does not generally need to exceed 3000. A deconvolution algorithm,[4] generally built nowadays into the instrument software, can be applied to the series of multiple-charged, molecular-ion peaks, and a single peak, representing the molecular weight, is then displayed on a "true mass" scale. The m/z scale is calibrated with standards of known exact mass. Whereas ESI/MS has made the largest impact on large biomolecule analysis, CE/ESI/MS has also been applied with great success to the analysis of many small-molecule applications.

The development of the first CE/MS was prompted by the early reports on ESI/MS by Fenn and coworkers in the mid-1980s,[1] when it was recognized that CE would provide an optimal flow rate of polar and ionic species to the ESI source. In this initial CE/MS report, a metal coating on the tip of the CE capillary made contact with a metal sheath capillary to which the ESI voltage was applied.[5] In this way, the sheath capillary acted as both the CE cathode, closing the CE electrical circuit, and the ESI source (emitter). Ideally, the interface between CE and MS should maintain separation efficiency and resolution, be sensitive, precise, linear in response, maintain electrical continuity across the separation capillary so as to define the CE field gradient, be able to cope with all eluents presented by the CE separation step, and be able to provide efficient ionization from low flow rates for mass analysis.

Several research groups have presented work on the development of CE/ESI/MS interfaces. The interfaces developed can be categorized into three main groups: coaxial sheath flow, liquid junction, and sheathless interfaces. A schematic of the sheath-flow interface first developed for CE/ESI/MS by Smith et al.[6] is illustrated in Fig. 1a. A sheath liquid, with an electrolytic content, is infused into the ESI source at a constant rate, through the coaxial sheath capillary which surrounds the end of the separation capillary and terminates near the end of the separation capillary. This sheath liquid mixes with the separation buffer as it elutes from the tip of the CE, thus providing the necessary electrical contact between the ESI needle and the CE buffer, and closing the CE circuit. Because the CE terminus and ESI source are at the same voltage, if the ESI source requires a high voltage (2–5 kV) (rather than ground potential), then the ESI voltage chosen

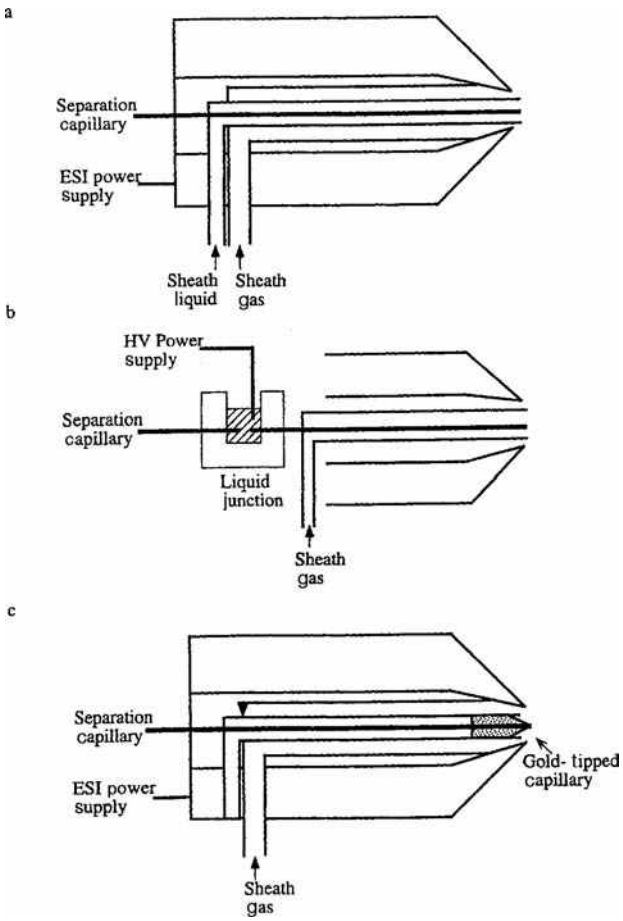

Fig. 1 Schematic illustration of CE/MS interfaces to an ESI. **Source:** a, a coaxial sheath-flow interface; b, a liquid-junction interface; c, a sheathless interface.

also directly affects the potential difference across the separation capillary. To date, the sheath–liquid interface has been the most widely used and accepted system, being the simplest to construct, with numerous results published employing sheath liquids typically containing 60–80% organic solvent, modified with 1–3% acid in water and typically introduced at flow rates of 1–4 μl/min. The composition of the sheath liquid should be optimized for the specific systems under investigation. Recent reports have confirmed that the relative dimensions and positioning of the separation and sheath capillaries also influence sensitivity and stability.

Although the additional flow of an organic-containing electrolyte into the ESI source moderately extends the range of CE buffer systems that can be used, the CE buffer composition still has a dramatic effect on the ESI signal, minimizing the buffer choice for best sensitivity to volatile solutions. Reports have also highlighted the need for a considered selection of sheath-liquid composition due to the possibility of formation of moving ionic boundaries inside the capillary.[7] The possibility of these effects occurring should be considered and minimized when transferring a CE method from an alternative detection system to MS. It should be noted, however, that these effects are minimized or eliminated when there is a sufficiently strong flow toward the CE terminus.

A "liquid-junction interface" has also been suggested and applied for CE/ESI/MS.[8] Electrical contact with this interface is established through the liquid reservoir which surrounds the junction of the separation capillary and a transfer capillary, as shown in Fig. 1b. The gap between the two capillaries is approximately 10–20 μm, allowing sufficient makeup liquid from the reservoir to be drawn into the transfer capillary while avoiding analyte loss. The flow of makeup liquid into the transfer capillary is induced by a combination of gravity and the Venturi effect of the nebulizing gas at the capillary tip.[8]

In comparisons of coaxial sheath-flow and liquid-junction interfaces, it has been noted that although both provide efficient coupling, the former is generally easier to operate. One of the major disadvantages in employing the liquid-junction interface is in establishing a reproducible connection inside the tee piece. Also, the use of a transfer capillary, which has no potential difference applied across it, can lead to peak broadening. Advantages of this interface, however, include the possibility of combining different outer-diameter capillaries through the junction and the extra mixing time provided for the makeup liquid and CE eluant.

The problem with both interfaces described so far is that they depend on the addition of excess electrolyte to the ESI source to maintain the circuit, generally leading to a decrease in analyte sensitivity. As previously mentioned, the first CE/MS interface reported made electrical connection between the separation buffer and the ESI needle via a metal coating on the tip of the CE capillary,[5] as represented in Fig. 1c. Although femtomole detection limits and separation efficiencies of up to half a million theoretical plates were achieved, problems included a high dependence on the buffer system used and the need to regularly replace the metal coating on the capillary tip.

The further development of interfaces which do not rely on an additional liquid flow are currently underway. Generally, they have employed metal deposition on the CE terminus that is tapered (by chemical etching or mechanical pulling) to provide an increased electric field at the capillary tip. These so-called "microspray" and "nanospray" approaches, with more effective ionization mechanisms, have been adopted recently by several groups for interfacing infusion systems, LC and CE to ESI/MS, and in all cases, significant gains in sensitivity and sample usage have been observed.[9,10] Attomole level detection limits from nanoliter sample volumes can now be attained, and the ability to form an electrospray from a purely aqueous solution is now possible. Alternative

sheathless interfaces have also been briefly investigated.[11] Stability problems still need consideration in most cases. An interface which does not use an additional makeup flow can, as well as aiding sensitivity, also avoid such problems as charge state distribution shifts in the mass spectrum. In addition, the ability to electrospray purely aqueous systems is often advantageous for looking at fragile biological and non-covalently bound analytes. In some cases, however, a makeup liquid may be found necessary. For example, for certain separations, the EOF may need to be minimized or eliminated in the CE capillary, and thus flow rates into the source will not be sufficiently high as to maintain a stable electrospray. If a capillary needs to be coated to avoid analyte interaction with the capillary wall, then a cationic coating, which reverses the electro-osmotic flow (EOF) rather than eliminating it, should preferably be chosen if a sheathless system is to be employed. Also, it may be found that a makeup liquid is necessary to increase the volatility of a specific CE electrolyte system.

Another disadvantage at present in using the sheathless interface is the time dispensed in preparing the tapered, coated tips. Although the coatings now employed are more stable than those initially used, the tips do not regularly survive more than a day or two of use. This can, however, be due to the tip "plugging" rather than the metal coating deteriorating. Filtering of electrolyte and analytes and rinsing of the capillary can, therefore, often prolong the capillary lifetime.

An instrumental attribute which aids the development and interfacing of CE to ESI/MS is the ability to pressurize the CE, at low pressure for sample injection and higher pressures for capillary content elution. Balancing of the heights of the capillary termini is also an important consideration in order to avoid syphoning effects. In all cases of CE/ESI/MS application, safety, with respect to the electrical circuits, should be considered. It should be verified that all circuits have a common ground, and the addition of a resistor in the ESI power supply line when interfaced to CE is a wise precaution.

An incompatability that does need to be considered in CE/MS method development is the use of certain CE buffer systems and additives which are detrimental to the ESI process. For example, although sample concentration can be increased by the use of more conductive buffers, this approach is not advantageous for ESI/MS detection. These characteristics result in a significant demand upon ESI interface efficiency.[12] Ideally, the chosen CE buffer should be volatile, such as ammonium acetate or formate. The use of pure acids or bases rather than a true buffer has also been shown to be advantageous for certain molecules. Non-aqueous buffer systems are also being employed more widely.

Capillary electrokinetic chromatography (CEKC) with ESI/MS requires either the use of additives that do not significantly impact the ESI process or a method for their removal prior to the electrospray. Although this problem has not yet been completely solved, recent reports have suggested that considered choices of surfactant type and reduction of EOF and surfactant in the capillary can decrease problems. Because most analytes that benefit from the CEKC mode of operation can be effectively addressed by the interface of other separations methods with MS, more emphasis has until now been placed upon interfacing with other CE modes. For "small-molecule" CE analysis, in which micellar and inclusion complex systems are commonly used, atmospheric pressure chemical ionization (APCI) may provide a useful alternative to ESI, as it is not as greatly affected by involatile salts and additives.

The efficiency of the ESI detection process for CE/MS can be considered in terms of the simple model of Kebarle and Tang[2] and has been discussed in great detail by Smith and coworkers.[12] These considerations indicate that analyte sensitivity in CE/ESI/MS may be increased by reducing the mass flow rate of the background components. This decrease in background flow rates can be experimentally accomplished by decreasing the electric field or employing smaller-diameter capillaries, and this predicted increase in analyte sensitivity is now well supported by experimental studies.[12]

To reduce the elution speed of the analyte ions into the source, the electrophoretic voltage can be decreased just prior to elution of the first analyte of interest, minimizing the experimental analysis time while allowing more scans to be recorded without a significant loss in ion intensity.[12] Alternatively, the use of smaller-diameter capillaries than conventionally used for CE also increases sensitivity.[12] A capillary diameter should, ideally, be commercially available, amenable to alternative detection methods, provide the necessary detector sensitivity, and be free from clogging. Capillary internal diameters of between 20 and 40 μm have been shown to be optimal and are compatible with "microspray" techniques.

The further development of microscale preconcentration and cleanup techniques and the resulting improvements in CE/MS concentration detection limits are likely to expand the use of this analytical technique. The more common use of small-diameter capillaries and even tiny etched microplate devices,[11] along with the improvements in ESI spray techniques are pushing research along. Further investigations into improving interface design, durability, reproducibility, and sensitivity are still necessary. The availability of improved, less expensive, and smaller mass spectrometers will almost certainly lead to increased use of CE/MS. However, the sensitivity and selectivity already demonstrated by CE/MS systems, in combination with the minute analyte volumes sampled, already make this a highly powerful technique.

REFERENCES

1. Whitehouse, C.M.; Dreyer, R.N.; Yamashita, M.; Fenn, J.B. Electrospray interface for liquid chromatographs and mass spectrometers. Anal. Chem. **1985**, *57*, 675–679.
2. Kebarle, P.; Tang, L. From ions in solution to ions in the gas phase. Anal. Chem. **1993**, *65*, 972A.
3. Ikonomou, M.G.; Blades, A.T.; Kebarle, P. Electrospray-ion spray: A comparison of mechanisms and performance. Anal. Chem. **1991**, *63*, 1989–1998.
4. Mann, M.; Meng, C.K.; Fenn, J.B. Interpreting mass spectra of multiply charged ions. Anal. Chem. **1989**, *61*, 1702–1708.
5. Olivares, J.A.; Nguyen, N.T.; Yonker, C.R.; Smith, R.D. On-line mass spectrometric detection for capillary zone electrophoresis. Anal. Chem. **1987**, *59*, 1230–1232.
6. Smith, R.D.; Olivares, J.A.; Nguyen, N.T.; Udseth, H.R. Capillary zone electrophoresis–mass spectrometry using an electrospray ionization interface. Anal. Chem. **1988**, *60*, 436–441.
7. Foret, F.; Thompson, T.J.; Vouros, P.; Karger, B.L.; Gebauer, P.; Bocek, P. Liquid sheath effects on the separation of proteins in capillary electrophoresis/electrospray mass spectrometry. Anal. Chem. **1994**, *66*, 4450–4458.
8. Lee, E.D.; Mück, W.; Henion, J.D.; Covey, T.R. Liquid junction coupling for capillary zone electrophoresis/ion spray mass spectrometry. Biomed. Environ. Mass Spectrom. **1989**, *18*, 844–850.
9. Chowdhury, S.K.; Chait, B.T. Method for the electrospray ionization of highly conductive aqueous solutions. Anal. Chem. **1991**, *63*, 1660–1664.
10. Wilm, M.; Mann, M. Analytical Properties of the nanoelectrospray ion source. Anal. Chem. **1996**, *68*, 1–8.
11. Figeys, D.; Aebersold, R. Electrophoresis **1998**, *19*, 885–892.
12. Wahl, J.H.; Goodlett, D.R.; Udseth, H.R.; Smith, R.D. Electrophoresis **1993**, *14*, 448–457, J.P. Landers, Capillary electrophoresis–mass spectrometry, in *Handbook of Capillary Electrophoresis*, CRC Press, Boca Raton, FL, 1997, and references therein.

Eluotropic Series of Solvents for TLC

Simion Gocan
Department of Analytical Chemistry, Babes-Bolyai University, Cluj-Napoca, Romania

INTRODUCTION

The easiest way to vary the relative adsorption of the sample (and its R_f value, migration rate, respectively) is to change the solvent: strong (polar) eluents decrease adsorption, and weak (no polar) eluents increase it. When benzene, for instance, is used as solvent on silica gels or alumina layers, the ethers and esters are found on top of the chromatogram (with high R_f values), ketones and aldehydes are approximately in the center (medium R_f values), and the alcohols are below them (low R_f values), whereas the acids remain at the starting point ($R_f = 0$). Thus the separation sequence follows the polarities of the compounds.

The dielectric constant may be taken as an indication of solvent polarity, but the interfacial tension between solvents and polar adsorbents, approximated by the interfacial tension between the solvent and water, has been suggested as a fundamental basis for correlating solvent strength.

The physical factors that determine solvent strength in a given adsorption system have long been understood in general terms. Solvent strength can be interpreted in terms of the following basic contributions: 1) interactions between solvent molecules and a sample molecule in solution; 2) interactions between solvent molecules and a sample molecule in the adsorbed phase; and 3) interactions between an adsorbed solvent molecule and the adsorbent.

ELUOTROPIC SERIES

Normal-Phase Thin-Layer Chromatography (NPTLC)

A series of authors has defined the solvent relative strength for polar adsorbents in the form of eluotropic series, grouping them in order of their chromatographic elution strength, with both pure solvents and mixtures of solvents included. The most familiar of these is, of course, the one set up by Trappe,[1] and variations of this have been published from time to time. Trappe gave the following series (listed in order of increasing elution power): light petroleum, cyclohexane, carbon tetrachloride, trichloroethylene, toluene, benzene, dichloromethane, chloroform, ether, ethyl acetate, acetone, *n*-propanol, ethanol, and methanol.

The eluotropic series of pure solvents is generally referred to a particular adsorbent. The magnitude of ε^o, the solvent strength parameter, can be defined as the adsorption energy of the solvent per unit of the standard activity surface. All these ε^o values are relative to the solvent pentane, for which ε^o is defined equal to zero. This parameter is defined as a measure of the degree of the adsorption interaction of the solvent with the stationary phase. As a function of this magnitude, the eluotropic series for various polar adsorbents is presented in Table 1.

It is well recognized that the eluotropic series of solvents, according to Snyder, is suited for monoactive site-type adsorbents, but in the case of multiactive site-type adsorbents (e.g., alumina), their imperfection becomes acute. Thus for multiactive-site-type adsorbents, the eluotropic series sequence and eluent strength values are highly dependent on the class of test solutes employed.[7]

A practical eluotropic series of solvents, based on the expended solubility parameter concept, was reported.[8] This series was defined based on partial specific solubility parameter (δ_s) that is equal to the sum of Keeson (δ_o) and acid–base ($2\delta_a\delta_b$), which represents the contribution to interaction forces introduced to characterize the solute, the mobile, and the stationary phase in liquid–solid chromatography. Exactly the same two interaction forces define ε^o and, consequently, there should exist a direct relation between ε^o and $\delta_s{}^2 = \delta_o{}^2 + 2\delta_a\delta_b$. Unfortunately, the general correlation for all the solvents on alumina is poor ($r^2 = 0.75$).

Snyder[2] has shown that there is a correlation between the ε^o values for a certain polar adsorbent (i.e., silica gel, Florisil, magnesia, and alumina). These values can be estimated from values for alumina using the following equations:

$$\varepsilon^o_{\text{silica gel}} = 0.77\varepsilon^o_{\text{alumina}}$$

$$\varepsilon^o_{\text{Florisil}} = 0.52\varepsilon^o_{\text{alumina}}$$

and

$$\varepsilon^o_{\text{magnesia}} = 0.58\varepsilon^o_{\text{alumina}}$$

Table 1 Relative strengths of different solvents on various adsorbents: eluotropic series.

	ε^o					
Solvent	**Al_2O_3[2]**	**Silica gel[2]**	**Florisil[2]**	**MgO[2]**	**P_i'[3,4]**	**S_i[5]**
n-Pentane	0.00	0.00	0.00	0.00		
n-Hexane	0.01				0.1 (–)[a]	
					–0.14	
Cyclohexane	0.04				0.2 (VIa)	
Carbon tetrachloride	0.18	0.11	0.04	0.10	1.6 (–)[a]	
					1.56	
m,*p*-Xylene	0.25				2.7 (VII)	
Amyl chloride	0.26					
o-Xylene	0.27					
Isopropyl ether	0.28				2.4 (I)	
Isopropyl chloride	0.29					
Toluene	0.29				2.4 (VII)	
Benzene	0.32	0.25	0.17	0.22	2.7 (VII)	
					3.19	
Ethyl ether	0.38	0.38	0.30	0.21	2.8 (I)	
					3.15	
Chloroform	0.40	0.26	0.19	0.26	4.1 (VIII)[b]	
					4.31	
Methylene chloride	0.42	0.32	0.23	0.26	3.1 (V)	
Methyl isobutyl ketone	0.43					
1,2-Dichloroethane	0.43				3.1 (V)	
					4.29	
Acetone	0.56	0.47			5.1 (VIa)	3.4
					5.10	
Ethyl acetate	0.58	0.38			4.4 (VIa)	
					4.24	
Methyl acetate	0.60			0.28		
Amyl alcohol	0.61					
Dioxane	0.63	0.49			4.8 (VIa)	3.5
					5.27	
Pyridine	0.71				5.3 (III)	
Butyl-cellosolve (C_4H_9-O-C_2H_4OH)	0.74					
Acetonitrile	0.79	0.50			5.8 (VIb)	3.4
					5.64	
Tetrahydrofuran					4.0 (III)	4.4
					4.28	
Isopropanol	0.82				3.9 (II)	4.2
					3.92	
Methanol	0.95				5.1 (II)	2.9
					5.10	
Ethanol					4.3 (II)	3.6
Acetic acid					6.0 (IV)	
					6.13	
Water					10.2 (VIII)	0.0
					10.2	

I–VIII represent groups from Snyder's classification.
[a]Selectivity group irrelevant because of low P' values.
[b]Close to group and VIII.

The values calculated by means of these equations show the standard deviation of ε^o values $\pm$ 0.004 units with respect to the experimental values.

The relationships between eluent strength and composition for binary (one to two) and ternary (one to three) solvents have been derived:[2]

$$\varepsilon_1 - \varepsilon_2 = \varepsilon_1 + \frac{\log[X_2 10^{\alpha n_2(\varepsilon_2 - \varepsilon_1)} + 1 - X_2]}{\alpha n_2} \quad (1)$$

$$\varepsilon_1 \rightarrow \varepsilon_3 = \varepsilon_2 - \frac{\log[X_3 10^{\alpha n_3(\varepsilon_3 - \varepsilon_2)} + X_2]}{\alpha n_3} \quad (2)$$

Eluent strength is assumed to increase in the order $\varepsilon_1 < \varepsilon_2 < \varepsilon_3$ for solvents A, B, and C; n_2 and n_3 are the effective molecular areas of adsorbed solvent molecules B and C, respectively (with the exception of certain very strong solvents); X_2 and X_3 are the mole fractions of B and C in the solvent mixtures; and α represents the adsorbent's surface activity. To use Eqs. 1 and 2, we must know the activity degree of the adsorbent. Consequently, the α (adsorbent surface activity function) values for a few adsorbents with respect to water content are presented in Table 2. Based on the data in Tables 1 and 2, and by using Eq. 1, an infinite number of such series can be established.

The principle of the variation of solvent composition while holding solvent strength constant was first developed by Neher[9] for separation of steroids. Fig. 1 is a representation of the eluotropic series of Neher for application in this fashion. Six solvents, which will act as solvent S_1 (100% concentration, on the left), are arranged vertically, whereas the same solvents, acting as solvent S_2 (100% concentration, on the right of the horizontal lines) in a binary solvent eluotropic series, are arranged horizontally. We can obtain a very large number of binary systems, of the same or different strength, by means of this nomogram. The dashed line X determines 12 compositions of binary systems of the same average eluotropic properties. These

Table 2 α Values for some common chromatographic adsorbents.

H_2O[a] (%)	Alumina	Silica gel (wide pore) TLC	Florisil	Magnesia
0	1.00	0.83	1.61	1.00
0.5	0.90	0.79	1.18	1.00
1.0	0.84	0.75	1.00	1.00
2.0	0.75	0.71	0.90	0.98
4.0	0.63	0.70	0.81	0.93
7.0	0.59	0.69	0.79	0.86
10.0	0.59	0.69		
15.0	0.59			

[a]Water added to activated adsorbent.

Source: From The mobile phase in thin-layer chromatography, in *Modern Thin-Layer Chromatography*.[6]

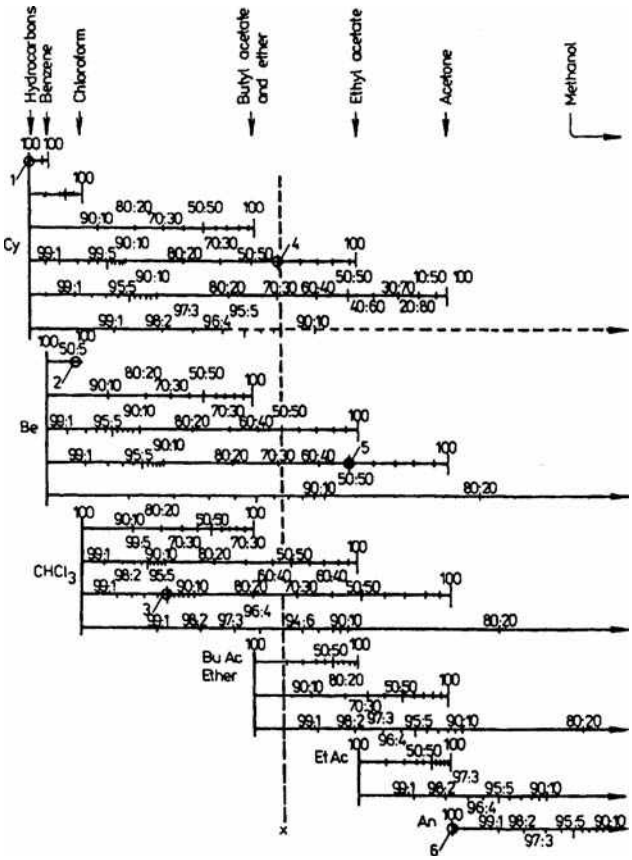

Fig. 1 Eluotropic series of Neher. Cy = cyclohexane; Be = benzene; BuAc = butyl acetate; EtAc = ethyl acetate; An = acetone.

systems are called equieluotropic systems. The nomogram in Fig. 1 corresponds to adsorption on silica gel.

Saunders[10] obtained another nomogram by using six very common solvents. With the help of the nomogram presented in Fig. 2, we can achieve binary solvent mixtures of certain strength in the interval 0.0–0.75. In this graph, ε^o is plotted across the top and in various binary solvent compositions in each of the horizontal lines below it. Each line corresponds to the range 0–100% by volume of binary solvent composition. Its manner of use is similar to that described for Neher's nomogram.

For NPTLC, the solvent strength weighting factor S_i is the same as the polarity index P' given in Table 1. The polarity index P' is given by the sum of the logarithms of the polar distribution constants for ethanol, dioxane, and nitromethane, and the selectivity parameters x_i is given as the ratio of polar distribution constant for solute I to the total solvent polarity (P'). The sum of the three values for x_i will be normalized up to 1.0. Snyder was able to show that the many solvents available could be grouped into eight classes with distinctly different selectivities. Solvents within the same selectivity group exhibit similar separation properties (Table 1).[3] The polarity index P' of a mixed

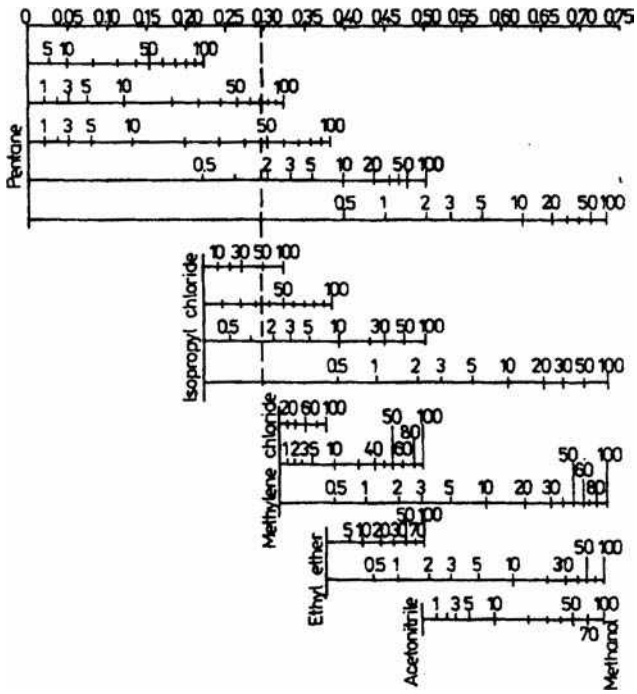

Fig. 2 Mixed solvent strengths on silica gel after Saunders.
Source: From Solvent selection in adsorption liquid chromatography, in Anal. Chem.[10]

mobile phase is the arithmetic average of the solvent polarity index weighting factor adjusted according to the volume fraction of each solvent as is given by:[11]

$$P' = \Sigma_i P_i' \phi_i \tag{3}$$

where P_i' is the polarity index weighting factor of solvent i (Table 1) and ϕ_i is the volume fraction of solvent i. For a binary solvent mixture containing 95% dichloromethane and 5% methanol, the polarity index of the mixed solvent is calculated as follows:

$$P' = (4.29)(0.95) + (5.10)(0.05) = 4.33$$

Reversed-Phase Thin-Layer Chromatography (RPTLC)

A general characteristic of RTLPC systems is that the stationary phase is non-polar vs. the mobile phase that is polar. Thus a decrease in polarity of the mobile phase leads to a decrease in retention. This situation is the reverse of the general trends observed in NPTLC. A decrease in polarity of the mobile phase can be realized by increasing the volume fraction of organic solvent in an aqueous organic mobile phase. The most common method for varying the chromatographic selectivity for neutral molecules is to change the type of organic modifier in the mobile phase. Eq. 4 can often be used as an acceptable approximation for the variation of the retention with the volume fraction of organic solvent in the mobile phase:[11]

$$\log k = \log k_w - S\phi \tag{4}$$

where k is the solute capacity factor, k_w is the solute capacity factor with pure water as the mobile phase, ϕ is the volume fraction of organic solvent, and S is a solute-dependent factor related to the solvent strength of the organic solvent.

The literature data suggest that RPTLC solvent strength varies as water (weakest) < methanol < acetonitrile < ethanol < tetrahydrofuran < propanol < (methylene chloride) (strongest). Thus solvent strength increases as solvent polarity decreases.

The eluotropic scale is a relative one; it is necessary to choose a reference. To obtain a positive value for solvent eluotropic strength, the reference solvent has to be water. The S values determined from the slope of Eq. 4 can be used as descriptor, in a semiquantitative way, of the solvent strength (S_i) of the organic solvent.[11] Some typical S_i values for common solvents are presented in Table 1. The solvent strength of a mixed mobile phase (S_T) is the arithmetic average of the solvent strength weighting factors adjusted according to the volume fraction ϕ of each solvent Eq. 5:

$$S_T = \Sigma_i S_i \phi_i \tag{5}$$

where S_i is the solvent strength weighting factor of solvent i and ϕ_i is the volume fraction of solvent i. If we want to change solvent selectivity to adjust resolution, then the volume fraction of the new solvent required to obtain an isoeluotropic mixture could be calculated from Eq. 5. For example, for methanol–water (60:40), $S_T = 1.56$; using acetonitrile as an example and the same value of $S_T = 1.56$, we obtain $1.56 = 3.2\phi_a + 0\phi_w = 0.49$. Thus a mixture of acetonitrile–water (49 : 51) is similar in solvent strength to a mixture of methanol–water (60:40). In a similar manner, it is possible to calculate several eluotropic eluents.

TLC APPLICATIONS

In adsorption TLC, there exists a competition between the sample and eluent molecules for a place on the adsorbent surface. If we assume that one molecule of sample (X) replaces m solvent molecules (S) on adsorption, we may represent the adsorption process as:

$$X_1 + mS_a \Leftrightarrow X_a + mS_1 \tag{6}$$

In this case, Snyder[2] found an important relationship for adsorption chromatography:

$$\log K^{o} = \log V_a + \alpha(S^{o} - A_s\varepsilon^{o}) \quad (7)$$

where the sample adsorption distribution coefficient K^{o} [ml/g] is defined as being equal to the ratio of sample concentrations in adsorbent and unadsorbed phases; V_a is adsorbent surface volume [ml]; S^{o} is dimensionless free energy of adsorption of a sample compound on adsorbent of standard activity ($\alpha = 0$) from pentane as solvent; and A_s is molecular area of adsorbed sample. For adsorbents of the same type, Eq. 7 expresses K^{o} as a function of some fundamental properties of the sample (S^{o}, A_s), adsorbent (V_a, α), and solvent (ε^{o}). The parameter ε^{o} defines the effect of the solvent on the adsorption of a given sample; therefore it may be equated with solvent strength. The larger is the solvent strength parameter ε^{o}, the smaller is the value of K^{o} for a given sample and adsorbent. Eq. 7 predicts that sample separation order can vary with solvent for sample components of different sizes (A_s). Let K^{o} and ε^{o} for solvent 1 be K_1 and ε_1, and K_2 and ε_2 for solvent 2. Thus from Eq. 4, the ratio of K values for a sample component adsorbent from two solvents is given as:

$$\log(K_1/K_2) = \alpha A_s(\varepsilon_2 - \varepsilon_1) \quad (8)$$

According to Eq. 8, the change in K on changing the solvent is predicted to be proportional to the difference in eluent strengths ($\varepsilon_2 - \varepsilon_1$) and to the sample molecule size A_s.

For the TLC or other bed, there were analogous relationships derived:[2]

$$R_{M'} = \log(V_a W/V^{o}) + \alpha(S^{o} - A_s\varepsilon^{o}) \quad (9)$$

where $R_{M'} = \log[(1/\xi R_f) - 1]$, W is total weight of adsorbent in the bed, V^{o} is bed void volume equal to the volume of solvent in a solvent wet bed, and $(R_f)_{true} = \xi(R_f)_{exp}$. Eq. 9 can be written for a given sample and adsorbent, for solvents 1 and 2, respectively. Then, subtracting the second equation from the first gives:

$$(R_{M'})_1 - (R_{M'})_2 = \alpha A_s(\varepsilon_2 - \varepsilon_1) \quad (10)$$

Eq. 10 can be useful in estimating the effect on sample R_f values of a change in solvent strength.

Eqs. 7 and 9 are a generally reliable relationship for adsorption systems with weak or moderately strong solvents. But, in their derivation, two major approximations were made:[2] 1) interactions between solvent and sample molecules are assumed unimportant; and 2) interactions between the adsorbent and various adsorbed molecules are assumed to be fundamentally similar in type. Both of these assumptions can be defended in the case of weak solvent systems, but they are poor approximations for strong solvents. These equations are concerned only with the primary effect of the solvent on sample adsorption. However, in the case of the majority of adsorption systems based on weak or moderately strong solvents, these approximate relationships are adequate for most purposes. For the strongest solvent systems (e.g., alcohols, acids, water, and their solutions), these equations can be corrected for secondary solvent effect by addition of a correction term Δ_{eas}:

$$R_{M'} = \log(V_a W/V^{o}) + \alpha(S^{o} - A_s\varepsilon^{o}) + \Delta_{eas} \quad (11)$$

where Δ_{eas} represents the secondary adsorption effect and is a complex function of solvent elution strength, adsorbent activity, solute structure, and various possible interactions between the solute adsorbent, and solvent and adsorbent. These aspects are largely discussed in Ref.[2] If $(\Delta_{eas})_1$ and $(\Delta_{eas})_2$ refer to the secondary solvent effects for a particular sample and solvents 1 and 2, respectively, then we can write:

$$(R_{M'})_1 - (R_{M'})_2 = \alpha A_s(\varepsilon_2 - \varepsilon_1) + (\Delta_{eas})_1 - (\Delta_{eas})_2 \quad (12)$$

Eq. 12 gives the difference in $\Delta R_{M'}$ values for a particular sample (A_s) in two solvents 1 and 2, with ε_1 and ε_2, respectively, as a function of adsorbent activity α, and the secondary solvent terms for the particular solvent contribution. The largest Δ_{eas} values were found for samples with free hydroxyl groups, and between these samples, two free hydroxyl groups in the sample molecule give a larger value of Δ_{eas} than does a single free hydroxyl. Sample molecules with intramolecularly bonded hydroxyl groups give much smaller values of Δ_{eas}, but limited hydrogen bonding of these groups with basic solvents is still possible. For the same sample molecule, the Δ_{eas} value will be a function of the eluent composition.

Now let us write Eq. 11 for a particular eluent and sample molecules 1 and 2, respectively:

$$(R_{M'})_1 - (R_{M'})_2 = \alpha(S_1^{o} - S_2^{o}) + \alpha\varepsilon(A_{s2} - A_{s1}) + (_{eas})_1 - (_{eas})_2 \quad (13)$$

In this equation, we find the different source and the selectivity between the two solutes, which can differ by the difference in energy of adsorption ($S_1{}^{o} - S_2{}^{o}$), molecular size ($A_{s2} - A_{s1}$), and secondary adsorption effect $(\Delta_{eas})_1 - (\Delta_{eas})_2$. These considerations are valuable for a large number of compounds, but in the case of some isomers, the second terms of Eq. 13 can be considered practically equal to zero and only difference sources for selectivity remain in the difference in energy of adsorption and the secondary adsorption effect. The secondary adsorption effect plays a major role in the separation of the isomers. For instance, in adsorption on silica gel with benzene–pyridine (90:10, vol/vol) as eluent, the following Δ_{eas} values: -0.90 ± 0.17 and $+0.05 \pm 0.11$ for *m*-hydroxybenzaldehyde and *O*-hydroxybenzaldehyde, respectively,

were obtained. These sample molecules can be very easily separated.

Adsorption TLC selection of the mobile phase is conditioned by sample and stationary-phase polarities. The following polarity scale is valid for various compound classes in NPTLC in decreasing order of K values: carboxylic acids > amides > amines > alcohols > aldehydes > ketones > esthers > nitro compounds > ethers > halogenated compounds > aromatics > olefins > saturated hydrocarbons > fluorocarbons. For example, retention on silica gel is controlled by the number and functional groups present in the sample and their spatial locations. Proton donor/acceptor functional groups show the greatest retention, followed by dipolar molecules, and, finally, non-polar groups.

The activity degree is another important characteristic for adsorbents. As is well known, the adsorbent is in contact with large amounts of water in the thin-layer preparation process water that has to be removed by drying at 100–120°C for approximately 30–60 min. This process is known as activation. The activity of the layer is directly correlated with the water content of the adsorbent. The silanol groups show a great affinity for water, which is bound by hydrogen bonds. Thus the activity degree can be controlled by the content of physisorbed water onto the adsorbent. Lower R_f values will be obtained on the adsorbent with a high degree of activity.

Generally speaking, the first problem with which the analyst is confronted concerns gathering information regarding the mixture to be separated, in terms of mixture polarity and the range of molecular masses. For example, if the mixtures that have to be separated are non-polar, then we can select an active stationary phase and non-polar mobile phase from the following scheme:

Sample to be separated:	non-polar → medium polar → polar
Stationary phase:	active → medium active → inactive
Mobile phase:	non-polar → medium polar → polar

Several mobile-phase optimization strategies in TLC are based on the use of isoeluotropic solvents (i.e., solvent mixtures of identical strengths but different selectivities). Selecting mobile phase will be achieved based on the eluotropic series (Figs. 1 and 2). These considerations are very general. The selection and optimization of one system of eluent is a more complex problem and must be discussed for each particular system. For example, the separation of 13 phenylurea and *s*-triazine herbicides was performed by overpressured layer chromatography (OPLC) with a binary mobile phase.[12] The optimization of the mobile-phase composition for the separation of these herbicides on silica gel was achieved by means of the "ELUO" method in which solvents are selected from an eluotropic series based on solvent power. The method is complementary to the "PRISMA" method for optimizing the compositions of binary, ternary, and quaternary mobile phase for OPLC and TLC.[13] The phenylurea herbicides could be separated with hexane–ethyl acetate (1:1, vol/vol), ethyl ether–benzene (9:1, vol/vol), or chloroform–ethyl acetate, and triazine herbicides could be separated with hexane–ethyl acetate (13:7, vol/vol), ethyl ether–benzene (9:1, vol/vol), or chloroform–ethyl acetate (3:1, vol/vol). The simultaneous separation of the herbicide classes could not be achieved and compounds that were chemically closely related were not well separated.

To maximize the differences in selectivity, solvents must be selected from different selectivity groups that are situated close to the Snyder's triangle apexes. For example, for NPTLC, a suitable selection could be solvents from several groups of Snyder's classifications (I, VII, and VIII), mixed with hexane to control solvent strength.[3]

REFERENCES

1. Trappe, W. Eluotropic series of solvents. Biochem. Z. **1940**, *305*, 150.
2. Snyder, L.R. *Principles of Adsorption Chromatography*; Marcel Dekker: New York, 1968.
3. Snyder, L.R. Classification of the solvent properties of common liquids. J. Chromatogr. Sci. **1978**, *16*, 223–234.
4. Poole, C.V.; Poole, S.K. *Chromatography Today*; Elsevier: Amsterdam,1991.
5. Snyder, L.R.; Dolan, J.W.; Gant, J.R. Gradient elution in high-performance liquid chromatography: I. Theoretical basis for reversed-phase systems. J. Chromatogr. **1979**, *165*, 3–9.
6. Gocan, S. The mobile phase in thin-layer chromatography. In *Modern Thin-Layer Chromatography*; Grinberg, N., Ed.; Marcel Dekker: New York, 1990; 139, Chap. 3.
7. Kovalsca, T.; Klama, B. JPC, J. Planar Chromatogr. Mod. TLC **1997**, *10*, 353–357.
8. Buchmann, M.L.; Kesselring, U.K. Pharm. Acta Helv. **1981**, *56*, 166–273.
9. Neher, R. *Thin Layer Chromatography*; Marini-Bettolo, G.B., Ed.; Elsevier: Amsterdam,1964; 75–86.
10. Saunders, D.L. Solvent selection in adsorption liquid chromatography. Anal. Chem. **1974**, *46*, 470–473.
11. Poole, C.F.; Poole, S.K. *Chromatography Today*; Elsevier: Amsterdam,1991.
12. Tekei, J. JPC, J. Planar Chromatogr. -Mod. TLC **1990**, *3*, 326–330.
13. Nyiredy, S.Z.; Meier, B.; Erdelmeier, C.A.J.; Sticher, O. PRISMA: Ageometrical design for solvent optimization in HPLC. HRC CC **1985**, *8*, 186–188.

Elution Chromatography

John C. Ford
Department of Chemistry, Indiana University of Pennsylvania, Indiana, Pennsylvania, U.S.A.

INTRODUCTION

By far the most common chromatographic mode of operation, elution chromatography is virtually the only mode used for analytical separations. Separation in elution chromatography occurs due to differences in migration velocities among the sample components. These differences are related to the affinities of the solutes for the mobile phase, of the solutes for the stationary phase, and of the mobile phase for the stationary phase, and to the properties of the stationary phase itself. Band broadening is typically caused by axial diffusion and mass transfer considerations. The plate number is a measure of the column efficiency, i.e., the ratio of separative to dispersive transport. The resolution is a measure of the overall quality of the separation of two solutes; resolution is a combination of the thermodynamic factors causing separative transport and the kinetic factors causing dispersive transport. Developing a useful elution separation requires more than obtaining the minimal resolution of the solutes of interest. A successful method should not only achieve the desired separation but should also do so in a cost-effective and robust manner. High-performance liquid chromatography (HPLC) method development has its own, extensive literature, reflecting the importance of HPLC as an analytical technique. Some considerations for practical separations are also discussed.

DEFINITION

Elution chromatography is one of the three basic modes of chromatographic operation, the other two being frontal analysis and displacement chromatography. All three modes were known to Tswett in the early 1900s, although a systematic definition was not made until 1943. Elution chromatography is by far the most common chromatographic mode and is virtually the only mode used for analytical separations. Most theoretical work has been directed at the elution mode, although frequently the results are applicable to other modes as well.

The current IUPAC nomenclature for chromatography defines elution chromatography as "a procedure in which the mobile phase is continuously passed through or along the chromatographic bed and the sample is introduced into the system as a finite slug."[1] Typically, the volume of the sample is small compared to the volume of the column. The individual components of the sample (the solutes) move through the column at different average velocities, each less than the velocity of the mobile phase. The differences in velocities are caused by differences in the interactions of the solutes with the stationary and mobile phases. Assuming essentially equivalent interactions with the mobile phase, solutes that interact strongly with the stationary phase spend less time on average in the mobile phase and consequently have a lower average velocity than components that interact weakly with the stationary phase. If the difference between the average velocities of two solutes is sufficiently large, if the dispersive transport within the column is sufficiently small, and if the column is sufficiently long, the solute bands are resolved from one another by the time they exit the column.

Elution chromatography can be performed with a constant mobile phase composition (isocratic elution) or with a mobile phase composition that changes during the elution process (gradient elution). The following discussion focuses on isocratic operation. Further, each of the mechanistic categories of chromatography (ion exchange, reversed-phase, normal phase, etc.) can be performed in the elution mode and additional information on elution chromatography can be obtained by reference to the appropriate sections of this encyclopedia.

Elution chromatography is categorized as being linear or non-linear, depending on the distribution isotherm, and as being ideal or non-ideal, with ideal behavior requiring both infinite mass transfer kinetics and negligible axial dispersion. Although truly linear distribution isotherms are rare, at low solute concentrations or over small ranges of solute concentration, sufficient linearity may exist to approximate linear elution. Linear, ideal elution would result in band profiles that are identical to the injection profiles—an unrealistic situation. Under linear, non-ideal elution conditions, thermodynamic factors control band retention and kinetic factors such as mass transfer resistances control the band shape. Guiochon, Shirazi, and Katti[2] have discussed the relationship between the isotherm and chromatographic behavior extensively.

The retention of a solute in elution chromatography is usually expressed as the retention factor, k (capacity factor or k'), given by $k = (t_R - t_M)/t_M$, where t_R is the retention time of the solute, and t_M is the hold up time (void time, dead time, or t_0). The hold up time is the time required to elute a component that is not retained at all by the stationary phase. One can relate k to the distribution coefficient, K, by $k = K\beta$, where φ is the phase ratio, the ratio of the stationary phase volume to the mobile phase volume. Rearranging

the definition of retention factor, we find that $t_R = t_M(1 + k) = t_M(1 + K\beta)$. Since it is usually reasonable to assume that t_M and β are the same for different solutes, the retention time differences are due to distribution coefficient differences. Under appropriate conditions, the distribution coefficient can be related to the thermodynamic distribution constant and elution chromatographic measurements can be used for physicochemical determinations of thermodynamic parameters.

Differences in solute retention are usually expressed as the separation factor (selectivity coefficient or α), given by $\alpha = k_b/k_a$, where k_a and k_b are the retention factors of the two solutes in question. By convention, k_b is the more retained solute and $\alpha > 1$, although this is not always followed. Since again it is reasonable to assume that φ is the same for different solutes, $\alpha = K_b/K_a$, where K_a and K_b are the distribution coefficients of the two solutes, and again, retention time differences are due to distribution coefficient differences. If two solutes have the same distribution coefficient (i.e., $\alpha = 1$) in a particular combination of mobile and stationary phases, they cannot be separated by elution chromatography in that system. However, $\alpha \neq 1$ is a necessary, but not sufficient, condition for a successful separation.

As a solute moves through the column, it undergoes dispersive transport as well as separative transport. Under typical elution chromatographic conditions, the dispersive transport is caused by axial diffusion and mass transfer considerations, such as slow adsorption–desorption kinetics. This dispersive transport results in band spreading lowering column efficiency, which can prevent adequate separation of different solutes. The plate number (plate count, number of theoretical plates, theoretical plate number, or N), defined as $N = t_R^2/\sigma_t^2$, where σ_t^2 is the variance of the band in time units, is a measure of the column efficiency, i.e., the ratio of separative to dispersive transport. Several alternate forms of this equation are commonly used, usually based on the assumption of Gaussian peak shape. The effective plate number, N_{eff}, is a combination of the plate number and the capacity factor, i.e., $N_{eff} = N[k/(1 + k)]^2$, and is generally more useful than N for comparing the resolving power of different columns.

Another common measure of column efficiency is the plate height [height equivalent to a theoretical plate (HETP), H], defined by $H = L/N$, where L is the length of the column, usually in centimeters. This is frequently presented as the reduced plate height, h, the ratio of the plate height to the diameter of the packing material. A "good" column has a high plate count (a low plate height; $2 < h < 5$).

The overall quality of the separation of two solutes is measured by their resolution (R_s), a combination of the thermodynamic factors causing separative transport and the kinetic factors causing dispersive transport, and is an index of the effectiveness of the separation. Defined by $R_s = (t_{r,b} - t_{r,a})/\frac{1}{2}[(w_{t,b} + w_{t,a})]$, where a and b refer to the two solutes, $t_{r,x}$ is the retention time of solute x, and $w_{t,x}$ is the peak width at the base of solute x in units of time, it is frequently estimated by use of the fundamental resolution equation

$$R_s = \left(\frac{\sqrt{N}}{4}\right)\left(\frac{\alpha - 1}{\alpha}\right)\left(\frac{k_b}{1 + k_b}\right)$$

where k_b is the retention factor of the more retained solute, α is the separation factor of the solute pair under consideration, and N is the plate count. This equation assumes that the peak shapes are Gaussian and that the peak widths are equivalent.

Easy recognition of the two peaks over a wide range of relative concentrations is possible for $R_s = 1$, and this is essentially the practical minimum resolution desirable. It is usually stated that $R_s = 1$ corresponds to a peak purity of about 98%; however, this is correct only for equal concentrations of the two solutes. As the ratio of relative concentrations of the two solutes deviates from 1, the recovery of the lower concentration solute at a given level of purity becomes poorer.

Examination of the fundamental resolution equation shows that improvements in resolution can be obtained by: 1) increasing the column efficiency. The dependence of R_s on $\sqrt{N}$, rather than N, means that this method is most effective when the column efficiency is initially low. In other words, when using efficient columns to develop a separation, major improvements in R_s are not generally obtained by increasing N; 2) increasing α. If α is close to 1.0, the greatest increase in R_s can be obtained by changing those parameters that influence α, i.e., the mobile phase composition, the choice of stationary phase, the temperature, or, less frequently, the pressure. Increasing α from 1.1 to 1.2 increases R_s by more than 80%. However, as α increases, the amount of increase in R_s decreases, so that increasing α from 2.1 to 2.2 increases R_s by only about 4%; 3) increasing k. If k_b (and thus k_a) < 1, R_s can be significantly increased by changing the mobile phase composition to increase k_b. As for α, the amount of increase decreases as k_b increases, so that while changing k_b from 0.5 to 1.5 improves R_s by about 80%, increasing k_b from 1.5 to 2.5 increases R_s by about 20%. Moreover, increasing k_b increases the analysis time, so that this approach is also of limited practicality.

To summarize, the most successful approach to obtaining adequate R_s is usually to increase α by varying the mobile phase composition—e.g., choice of solvent(s), pH, or temperature—or by varying the stationary phase. Increasing R_s by increasing N or k_b works in selected instances, but is not as generally applicable.

Developing an elution separation method to be used for the analysis of numerous samples requires more than obtaining the minimal resolution of the solutes of interest.

A successful method should not only achieve the desired separation but should also do so in a cost-effective and robust manner. HPLC method development has its own, extensive literature, reflecting the importance of HPLC as an analytical technique.

Snyder, Kirkland, and Glajch state the goals of HPLC method development as: 1) precise and rugged quantitative analysis requires that R_s be greater than 1.5; 2) a separation time of <5–10 min; 3) ≤2% relative standard deviation (RSD) for quantitation in assays (≤5% for less-demanding analyses and ≤15% for trace analysis); 4) a pressure drop of <150 bar; 5) narrow peaks to give large signal/noise ratios; and 6) minimal mobile-phase consumption per run. Additionally, thorough testing of the robustness of proposed methods is recommended.

REFERENCES

1. Section 9.2.1.2 of International Union of Pure and Applied Chemistry Compendium of Analytical Nomenclature; http://www.iupac.org/publications/analytical_compendium (accessed November 2004).
2. Guiochon, G.; Shirazi, S.G.; Katti, A.M. *Fundamentals of Preparative and Nonlinear Chromatography*; Academic Press: Boston, 1994.

BIBLIOGRAPHY

1. Bidlingmeyer, B.A. *Practical HPLC Methodology and Applications*; John Wiley & Sons: New York, 1992.
2. Giddings, J.C. *Unified Separation Science*; John Wiley & Sons: New York, 1991.
3. Karger, B.L.; Snyder, L.R.; Horvath, Cs. *An Introduction to Separation Science*; John Wiley & Sons: New York, 1973; 11–167.
4. Meyer, V.R. *Practical High-Performance Liquid Chromatography,* 3rd Ed.; John Wiley & Sons: New York, 1998.
5. Rizzi, A. Retention and selectivity. In *Handbook of HPLC*; Katz, E. Eksteen, R. Schoenmakers, P., Miller, N., Eds.; Marcel Dekker: New York, 1998; 1–54.
6. Snyder, L.R.; Kirkland, J.J.; Glajch, J.L. *Practical HPLC Method Development,* 2nd Ed.; John Wiley & Sons: New York, 1997.
7. Snyder, L.R.; Kirkland, J.J.; Glajch, J.L. *Introduction to Modern Liquid Chromatography,* 2nd Ed.; John Wiley & Sons: New York, 1979.

Elution Modes in FFF

Josef Chmelík
Institute of Analytical Chemistry, Academy of Sciences of the Czech Republic, Prague, Czech Republic

INTRODUCTION

Field-flow fractionation (FFF) is, in principle, based on the coupled action of a non-uniform flow velocity profile of a carrier liquid with a non-uniform transverse concentration profile of the analyte caused by an external field applied perpendicularly to the direction of the flow. Based on the magnitude of the acting field, on the properties of the analyte, and, in some cases, on the flow rate of the carrier liquid, different elution modes are observed. They basically differ in the type of the concentration profiles of the analyte. Three types of the concentration profile can be derived by the same procedure from the general transport equation. The differences among them arise from the course and magnitude of the resulting force acting on the analyte (in comparison to the effect of diffusion of the analyte). Based on these concentration profiles, three elution modes are described.

BACKGROUND INFORMATION

FFF represents a family of versatile elution techniques suited for the separation and characterization of macromolecules and particles. Separation results from the combination of a non-uniform flow velocity profile of a carrier liquid and a non-uniform transverse concentration profile of an analyte caused by the action of a force field. The field, oriented perpendicularly to the direction of the flow, forms a specific concentration distribution of the analyte inside the channel. Because of the flow velocity profile, different analytes are displaced along the channel with different mean velocities, and, thus, their separation is achieved.

According to the original concept,[1] the field drives the analytes to the accumulation wall of the channel. This concentrating effect is opposed by diffusion, driven by Brownian motion of the analytes, which causes a steady state when the convective flux is exactly balanced by the diffusive flux. The concentration profile is exponential and the corresponding elution mode is referred to as the normal mode. Recently, it has been called the Brownian elution mode.[2]

During last two decades, new elution modes were described[3–5] that were not suggested in the original concept.[1] Basically, they differ in the type of the analyte concentration profile.

In 1978, Giddings and Myers described another elution mode for large particles under conditions when diffusion effects can be neglected.[3] The particles form a layer on the channel wall and, under the influence of the carrier liquid flow, they roll on the channel bottom to the channel outlet. This elution mode is referred as the steric mode.[3]

The above-mentioned elution modes apply to the situation when the resulting force acting on the analytes does not change its orientation inside the channel. However, there exist conditions when the resulting force acting on analytes may change its orientation inside the channel [e.g., two counteracting forces, a gradient of a property (pH, density) of the carrier liquid, influence of hydrodynamic lift forces]. Under such conditions, the analytes form narrow zones at the positions where the resulting forces acting on them equal zero. The resulting force is changing its sign below and above this position in such a way that the analyte is focused into this equilibrium position. The concept of formation of narrow zones of analytes inside the FFF channel was first described in 1977 by Giddings.[6] In 1982, a technique utilizing sedimentation–flotation equilibrium and centrifugal field was suggested.[7] However, this technique has not been yet verified experimentally. Later, the general features of this elution mode were described and several techniques were implemented; for a review, see Ref.[8] The mode was called either the hyperlayer[4] or focusing[5] elution mode.

Some other elution modes have been described. They are induced by various factors—cyclical field, secondary chemical equilibria, adhesion chromatography, asymmetrical electro-osmotic flow; for a review, see Ref.[2] However, the number of their implementations is rather limited, and for this reason, these modes are not discussed here.

THEORY

FFF experiments are mainly performed in a thin ribbonlike channel with tapered inlet and outlet ends (Fig. 1). This simple geometry is advantageous for the exact and simple calculation of separation characteristics in FFF. Theories of infinite parallel plates are often used to describe the behavior of analytes because the cross-sectional aspect ratio of the channel is usually large and, thus, the end effects can be neglected. This means that the flow velocity

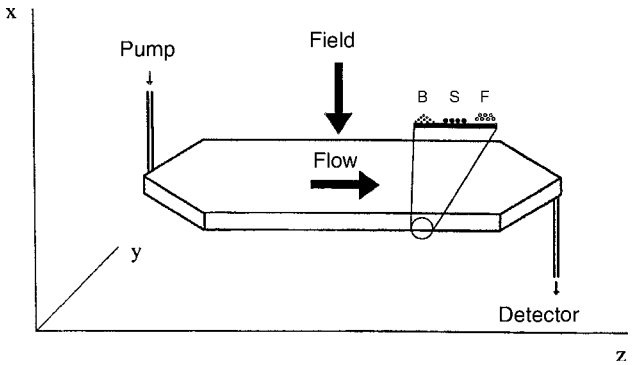

Fig. 1 The orientation of the field and flow in the given coordinate system. The zoomed inset shows the schematic representation of the zone shapes in particular elution modes (B for Brownian, S for steric, and F for focusing).

and concentration profiles are not dependent on the coordinate y. It has been shown that, under suitable conditions, the analytes move along the channel as steady-state zones. Then, equilibrium concentration profiles of analytes can be easily calculated.

Generally, the concentration profile of analytes in FFF can be obtained from the solution of the general transport equation. For the sake of simplicity, the concentration profile of the steady-state zone of the analyte along the axis of the applied field is calculated from the one-dimensional transport equation:

$$J_x = W_x c(x) - D\frac{\partial c}{\partial x} \tag{1}$$

where J_x and W_x are the components of the flux density of the analyte and of the transport velocity of the analyte along the axis of the applied field, $c(x)$ is the analyte concentration distribution along the direction of the applied field, and D is the total effective diffusion coefficient. The term $W_x c(x)$ corresponds to the x component of the convective flux of the analyte and the term $D(\partial c/\partial x)$ corresponds to the x component of the diffusive flux of the analyte. W_x equals the sum of the x components of the transport velocity of the analyte induced by the external field applied U_x and the transport velocity of the analyte induced by the carrier liquid flow $v_x (W_x = U_x + v_x)$. Because of the direction of the carrier liquid flow inside the FFF channel, the component v_x equals zero (the x axis is perpendicular to the direction of the flow) and, thus, W_x equals U_x.

Following the treatment given by Giddings,[9] imposing for the condition of the steady-state zone of the analyte, which is characterized by the null flux density, and applying the equation of continuity, the general solution of the analyte concentration profile can be expressed in the form

$$c(x) = c_0 \exp\left[\int_0^x \left(\frac{U_x}{D}\right) dx\right] \tag{2}$$

The integration limit $x = 0$ corresponds to the accumulation wall boundary. The particular solutions for the concentration profile are dependent on the course of the force field inducing the transport of the analyte, and the ratio of U_x and D.

The equation of the field-induced transport velocity was derived by Giddings:[10]

$$U_x = -ax^n \tag{3}$$

where a is constant and n equals 0 or 1. If $n = 0$, then U_x is constant; if $n = 1$, then U_x is dependent on the position inside the channel.

DISCUSSION

Brownian Elution Mode

The field-induced velocity of the analyte in the separation channel is constant and comparable with its diffusive motion (U_x = constant, $U_x t \approx \sqrt{2Dt}$, where t is time). The resulting concentration profile of the analyte is given by the exponential relationship[9]

$$c(x) = c_0 \exp\left(-\frac{|U_x|}{D}x\right) \tag{4}$$

where c_0 is the maximum concentration at the accumulation channel wall. The elution mode with the exponential concentration profile is called Brownian.[2]

It is known that there are two main factors influencing the behavior of analytes in this elution mode: the properties of the analytes (characterized by the so-called analyte–field interaction parameter[11] and the diffusion coefficient) and the strength of the field applied.

In Brownian elution mode, the retention ratio R is indirectly dependent on both the applied force F and the thickness of the channel w, and independent on the flow rate.[9] It can be expressed in an approximate form:

$$R = \frac{6kT}{Fw} \tag{5}$$

where k is the Boltzmann constant and T is the absolute temperature.

Steric Elution Mode

The velocity of transport induced by the force field in the separation channel is constant and much higher than the velocity caused by the diffusive motion of the analyte (U_x = constant, $U_x t \gg \sqrt{2Dt}$). In this case, the analyte forms a layer on the accumulation channel wall and its concentration in any other position inside the channel

equals zero. The particle radius r_p describes the distance of the particle center from the accumulation wall:

$$c(r_p) = c_0 \quad \text{and} \quad c(x \neq r_p) = 0 \tag{6}$$

The elution mode is called steric.[3] The retention ratio can be expressed in the form

$$R = \frac{6r_p}{w} \tag{7}$$

This shows that R is independent of both the field applied and the flow rate, and it is dependent only on the particle radius and the channel thickness. In fact, the retention ratio values corresponding to the pure steric elution mode have been seldom observed experimentally.[12] The observed values often correspond to the focusing elution mode as a result of the action of some additional forces influencing retention behavior of analytes.

Focusing Elution Mode

In this elution mode, the velocity of analyte transport induced by a force field in the separation channel is dependent on the position across the channel ($U_x \neq$ constant). Based on Eq. 3, the non-constant transport velocity can be, in the simplest case, described as

$$U_x = -a(x - s) \tag{8}$$

where s is the distance of the center of the focused zone from the channel wall (i.e., the position where the resulting force acting on the analyte equals zero). Combining this equation with Eq. 2, we obtain a relation for the resulting concentration profile of the analyte:

$$c(x) = c_0 \exp\left(-\frac{a}{2D}(x - s)^2\right) \tag{9}$$

where c_0 is the maximum concentration at the center of the focused zone at the position s. The concentration profile of the analyte across the channel thickness, in this simplest case, is Gaussian. In other cases, where other secondary effects act on the retention in the focusing elution mode, the observed concentration profile is more complex. However, even in these cases, the main feature remains the same; that is, the maximum concentration of the analyte is at the equilibrium position, where the resulting force acting on the analyte is zero, and not on the channel wall as in the case of the Brownian and steric elution modes. The elution mode is called focusing[5] or hyperlayer.[4] In the focusing elution mode, the retention ratio can be expressed in a form formally similar to the expression given for the steric elution mode (see Eq. 7):

$$R = \frac{6s}{w} \tag{10}$$

At least two counteracting forces are necessary for the formation of the focused zone of the analyte. The center of the zone is located at the position s where the resulting force is zero. Changing of both forces can control the resulting position of the particle zone.

CONCLUSIONS

In the majority of FFF techniques, the retention ratio is dependent on the analyte size. This dependence for Brownian and steric mode is described by Eq. 11, derived by Giddings:[13]

$$R = 6(\alpha - \alpha^2) + 6\lambda(1 - 2\alpha)\left[\coth\left(\frac{1 - 2\alpha}{2\lambda}\right) - \frac{2\lambda}{1 - 2\alpha}\right] \tag{11}$$

where $\alpha = d/2w$, $\lambda = kT/Fw$ and d is the analyte diameter. The curve describing this dependence is shown in Fig. 2. The values of R for the focusing mode lie above the curve. This complex situation shows that determination of the elution mode is very important for evaluation of the measured retention data because different elution modes can act on particular analytes in the same experiment.

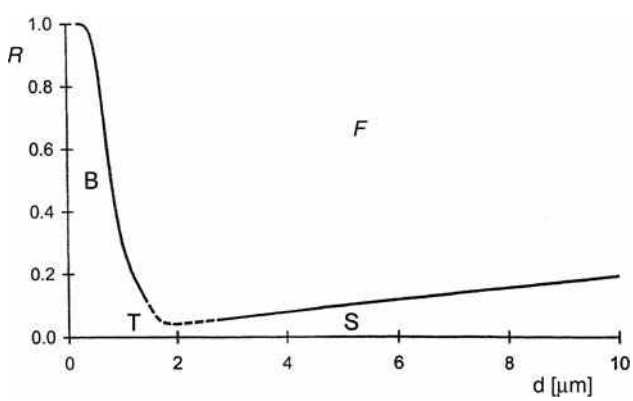

Fig. 2 Schematic representation of the dependence of the retention ratio R on the analyte size. Curve B corresponds to Brownian mode and the line S to the steric mode. The dashed part T denotes the transition between these two modes. The area F shows the range of applicability of the focusing mode.

ACKNOWLEDGMENT

This work was supported by Grant No. A4031805 from the Grant Agency of Academy of Sciences of the Czech Republic.

REFERENCES

1. Giddings, J.C. A new separation concept based on a coupling of concentration and flow non-uniformities. Separ. Sci. **1966**, *1*, 123.
2. Martin, M. *Advances in Chromatography*; Brown, P.R., Grushka, E., Eds.; Marcel Dekker, Inc.: New York, 1998; Vol. 39, 1–138.
3. Giddings, J.C.; Myers, M.N. Steric field-flow fractionation: A new method for separating 1 to 100 μm particles. Separ. Sci. Technol. **1978**, *13* (8), 637.
4. Giddings, J.C. Hyperlayer field-flow fractionation. Separ. Sci. Technol. **1983**, *18* (8), 765.
5. Janća, J.; Chmelík, J. Focusing in field-flow fractionation. Anal. Chem. **1984**, *56*, 2481.
6. Giddings, J.C. Hyperlayer field-flow fractionation: State of development. Am. Lab. **1992**, *24*, 20D.
7. Janća, J. Sedimentation-flotation focusing field-flow fractionation. Makromol. Chem. Rapid Commun. **1982**, *3*, 887.
8. Janća, J.; Chmelík, J.; Jahnová, V.; Nováková, N.; Urbánková, E. Principle, theory and applications of focusing field-flow fractionation. Chem. Anal. **1991**, *36*, 657.
9. Giddings, J.C. *Unified Separation Science*; John Wiley & Sons: New York, 1991.
10. Giddings, J.C. Nonequilibrium theory of field-flow fractionation. J. Chem. Phys. **1968**, *49*, 81.
11. Giddings, J.C.; Caldwell, K.D. *Physical Methods of Chemistry*; Rossiter, B.W., Hamilton, J.F., Eds.; John Wiley & Sons: New York, 1989; Vol. 3B, 867.
12. Pazourek, J.; Wahlund, K.-G.; Chmelík, J. Effect of flowrate and ionic strength on retention of nonporous micron-sized silica gel particles in gravitational field-flow fractionation. J. Microcol. Separ. **1996**, *8* (5), 331.
13. Giddings, J.C. Separ. Sci. Technol. **1978**, *13*, 241; **1979**, *14*, 869.

Elution Volumes: Concentration Effects on SEC

Rosa Garcia-Lopera
Iolanda Porcar
Institute of Materials Science, University of Valencia, Valencia, Spain

Concepción Abad
Department of Biochemistry and Molecular Biology, University of Valencia, Valencia, Spain

Agustín Campos
Institute of Materials Science, University of Valencia, Valencia, Spain

INTRODUCTION

Size exclusion chromatography (SEC) elution behavior of different solvent/polymer/gel systems has been analyzed from chromatographic, thermodynamic, and hydrodynamic points of view, in two organic column packings, based on polystyrene/divinylbenzene (PS/DVB) copolymer, named: μ-Styragel and TSK Gel H_{HR}. Although both packings present similar chromatographic properties, some differences arise when eluting the same systems. The values of the adsorption distribution coefficients, K_p, have been correlated with the preferential solvation coefficient, λ, for both packings, showing that those systems with lower and negative λ values (denoting higher preferential solvation of the polymer by the gel packing) are those with $K_p > 1$. In addition, the main goal has been to make use of the λ values to adequately interpret the concentration effects (injected polymer concentration) on the elution volumes. In this regard, the experimental concentration effects have been completely explained taking into account not only the conventional hydrodynamic factors, but also thermodynamic aspects such as the preferential solvation phenomenon.

CONCENTRATION EFFECTS

SEC columns separate molecules according to their hydrodynamic volumes in solution. In an ideal experiment, only entropic effects play a role, and molecules are solely separated by size. However, in most cases, enthalpic processes owing to polymer gel–polymer solute interactions, in addition to solvent–polymer and solvent–gel matrix interactions, have to be taken into account, because they affect the values of the sample elution volumes.[1–7] When these non-exclusion secondary mechanisms are present, mainly as adsorption, the polymer–polymer interactions increase and shift the retention volumes of solute macromolecules to higher values. Both the exclusion of macromolecules and the interaction with the column packing are affected by the sample concentration or by the eluent applied, which is evidenced even for the inactive gel packing based on PS/DVB cross-linked materials.[2,8]

The concentration effect, i.e., the dependence of the elution volume on the injected polymer concentration, especially for good solvents, can be considered as a factor affecting the quantitative evaluation of polymer-packing interactions in SEC. This effect has been mainly interpreted on the basis of hydrodynamic factors.[9–19] Other authors have attempted to formulate theoretical models to account for concentration effects in SEC. Among them, the work carried out by Song and coworkers[15,19–22] deserves to be mentioned, on both narrow and polydisperse polymers. They successfully predicted the shifts of retention volumes, the axial spreading, and the skewing of chromatograms caused by the concentration effects. More recently, Lou et al.,[23] have performed simulations of SEC retention behavior of supramolecular complexes by including the concentration effects as a factor affecting the sample retention time. Skrinarova, Bleha, and Cifra[24] have studied the influence of the concentration effects on the partitioning of flexible polymers into pores with attractive walls by regarding the effect as a confined adsorption. Lastly, a simple analytical equation that is able to evaluate the distribution coefficients in SEC of polymers as a function of molar mass, injected sample concentration, and solvent quality has been presented.[25] The equation has been proven to be accurate, both in wide- and narrow-pore regimes, for a wide range of polymer concentrations, opening the possibility to analyze experimental data in concentrated solutions.

In the present work, the concentration effect has been correlated with the preferential solvation phenomenon. First, the observed non-exclusion mechanism has been quantified by means of the distribution coefficient, K_p, representing the concentration ratio of macromolecules inside the pores (i.e., in the quasistationary phase) to those in the mobile phase. Second, the shifts in the elution volume owing to either adsorption or, on the contrary, incompatibility of the solute with the gel packing, have been related to the preferential or selective sorption phenomenon. From a thermodynamic viewpoint, the

preferential adsorption coefficient, λ, is an equilibrium property that reflects the solvent–polymer–solute composition, both close to and far from the polymer gel. This magnitude is related to the chromatographic parameter K_p, to study the adsorption phenomena in the chromatographic systems, given that negative λ values will indicate preferential sorption of the solute polymer onto the gel packing, which occurs when $K_p > 1$. Conversely, positive λ values will denote incompatibility between both components, which accounts for $0 < K_p < 1$ values. The chromatographic data from previous work,[26–28] together with λ values, have successfully served to explain the observed concentration effect on the elution behavior of different solvent(1)/polymer(2)/gel(3) ternary systems in two commercial SEC packings, namely, μ-Styragel and TSK Gel H_{HR}.

EXPERIMENTAL TECHNIQUE

Chemicals

Polybutadiene (PBD) standards with a weight-average molar mass, in daltons, $\overline{M_w}$ = 5,900, 13,400, 18,100, 67,300, 90,000, 268,000, and 1,120,000 (polydispersity, I = 1.03–1.05) were purchased from Polymer Source, Inc. (Dorval, Canada); poly(dimethylsiloxane) (PDMS) standards with $\overline{M_w}$ = 8,100, 41,500, 76,035, 188,400, and 681,600 Da (I = 1.10–1.40) were supplied by Polymer Laboratories (Shropshire, U.K.).

Tetrahydrofuran (THF), benzene (Bz), toluene (Tol), 1–4 dioxane (Diox), and cyclohexane (CHX), of chromatographic grade, from Scharlau (Barcelona, Spain) were used as solvents or eluents.

Chromatography

Waters liquid chromatography equipment with a refractive index detector was used for SEC experiments and has been recently described.[26,27] Two sets of columns (7.8 mm I.D. × 300 mm length) based on a PS/DVB copolymer and with the following characteristics were compared: (i) three μ-Styragel columns from Waters (Milford, Massachusetts, U.S.A.) with nominal pore size of 10^3, 10^4, and 10^5 Å; 15 μm particle size; pore exclusion volume, V_p = 18.1 ml; total exclusion volume, V_0 = 17.7 ml; and (ii) three TSK Gel H_{HR} from Tosohaas, Tosoh Corp. (Tokyo, Japan) with pore sizes G2500, G4000, and G6000; 5 μm particle size; and V_p = 21.0 ml and V_0 = 16.4 ml. The volumes V_0 and V_p were determined with a PS standard of high-molar mass ($\overline{M_w}$ = 3,800,000) and with small molecules such as Tol or Bz in THF, respectively. All chromatographic experiments were performed at room temperature and the columns were equilibrated overnight prior to starting any experiment.

Chromatograms were obtained at a flow rate of 1.0 ml/min by injection of 100 μl of sample solution. The injected polymer concentration, c_2, ranged between 0.1 and 0.8 g/100 ml.

RESULTS AND DISCUSSION

Partitioning in SEC

Chromatographic separation of macromolecules by size depends on the strength and type of interactions in the chromatographic system and is characterized by being the retention or elution volume, V_e. For non-ideal SEC (when secondary mechanisms such as adsorption appear), V_e is given by:

$$V_e = V_0 + K_{SEC} K_p V_p \quad (1)$$

where V_0 is the interstitial or total exclusion volume of the column; V_p, the pore or packing volume; K_{SEC}, the distribution coefficient for ideal SEC based only on entropic effects; and K_p, the distribution coefficient accounting for interactions between the components of the system, such as solute–solvent, solvent–gel, or solute–gel (enthalpically driven) interactions. In the case of "ideal" SEC, separation is exclusively directed by conformational size changes of macromolecules; thus, the global distribution coefficient of the solute between the stationary and the mobile phases is $K_D = K_{SEC}$ and $K_p = 1$. However, if enthalpic effects, mainly owing to interactions between the polymeric solutes and the pore walls, take place, the retention volume is given by Eq. 1 with $K_p < 1$ when solute–gel interactions are repulsive or with $K_p > 1$ when attractive, such as the reversible adsorption of the polymer onto the matrix packing.

The primary elution data, in terms of the Universal Calibration plot, $\log(M[\eta])$ vs. elution volume for the systems: THF/PBD, Bz/PBD, Diox/PBD, Tol/PDMS, Bz/PDMS, and CHX/PDMS in both packings have been taken from the literature.[26,27] To better explain the elution trend, here, we have selected three values of the hydrodynamic volumes, ($M[\eta] = V_h = 10^6$, 10^7, and 10^8 ml/mol), which are representative of the most effective mass-separation range. According to Eq. 1, the obtained K_p values for the different assayed chromatographic systems are compiled in Table 1. In general, $K_p > 1$ and increases its value as V_h increases, leading to secondary mechanisms owing to the increasing polymer–gel matrix interactions. It is also observed that the lowest K_p values, and, therefore, the lowest adsorption effects occur in the TSK Gel H_{HR} columns, which could be attributed to their lower cross-linking degree with respect to μ-Styragel.[27]

Table 1 Experimental K_p values for different chromatographic systems eluted in two types of column packings at three hydrodynamic volumes (in ml/mol).

Packing	System	K_p[a]	K_p[b]	K_p[c]
μ-Styragel	THF/PBD	1.006	0.992	0.958
	Bz/PBD	1.293	1.298	1.325
	Diox/PBD	1.636	1.853	2.490
	Tol/PDMS	1.061	1.089	1.181
	Bz/PDMS	1.077	1.043	0.962
	CHX/PDMS	1.159	1.171	1.217
TSK Gel H_{HR}	THF/PBD	0.981	0.966	0.935
	Bz/PBD	1.205	1.160	1.038
	Diox/PBD	1.265	1.364	1.659
	Tol/PDMS	1.097	1.095	1.103
	Bz/PDMS	1.246	1.244	1.243
	CHX/PDMS	1.408	1.462	1.638

[a] $V_h = 10^6$.
[b] $V_h = 10^7$.
[c] $V_h = 10^8$.

Quantitative Evaluation of the Enthalpic Polymer–Gel Interactions

The attractive interactions given by K_p have allowed quantification of the composition of each component of the ternary solvent (1)/polymer (2)/gel matrix (3) system in terms of volume fractions, ϕ_i ($i = 1$, 2, or 3), by means of a thermodynamic approach, and equations were recently derived.[26,27] Altogether, an increase of K_p as ϕ_3 increases was observed in most of the systems, evidencing more interactions between segments of the polymeric solute (2) and the gel matrix (3) (data not shown). The highest polymer–gel interaction was observed for the system Diox/PBD in both packings studied here, and is even more pronounced in the case of μ-Styragel in accordance with its higher cross-linking degree or chain density per volume unit.

Preferential Solvation

The preferential solvation phenomenon in a ternary polymer system indicates which component, (1) or (2), is preferentially adsorbed by component (3); it is quantified by means of the preferential solvation coefficient, λ. From a chromatographic point of view, adsorption or, conversely, incompatibility between solute (2) and gel matrix (3) can be detected through the coefficient K_p, as seen before. Therefore, both parameters, λ and K_p, have a similar physical meaning in the sense that an equilibrium between a binary and a ternary phase is established and, consequently, one could try to relate them. Accordingly, it is expected that when $K_p > 1$ [meaning compatibility between polymer (2) and gel matrix (3)], values of $\lambda < 0$ will be obtained, denoting a preferential solvation of component (2) toward the gel (3). On the contrary, because $\lambda > 0$ means preferential solvation of solvent (1) by the gel matrix (3), the polymer (2) would be eluted earlier, giving $K_p < 1$.

In fact, the preferential solvation coefficient, λ, represents the volume of solvent (1) or polymer (2) (in ml) adsorbed by the mass (in grams) of polymer (3), and can be calculated at finite polymer composition, ϕ_3, by

$$\lambda(u_1, \phi_3) = B_1(u_1)\bar{v}_3 + B_2(u_1)\bar{v}_3\phi_3 \tag{2}$$

where $\bar{v}_3$ is the partial specific volume of component (3), the polymer constitutive of the gel matrix, and B_1 and B_2 are obtained as follows.[26]

$$B_1 = -\frac{M_{13}}{M_{11}} \tag{3}$$

$$B_2 = -\frac{\left(\frac{M_{13}}{M_{11}}\right)^2 M_{111} - 2\frac{M_{13}}{M_{11}}M_{113} + M_{133}}{2M_{11}} \tag{4}$$

B_1 and B_2 are the corresponding M_{ij} and M_{ijk} functions dependent on the system composition and on the interaction functions, and have been recently given (see Eqs. 6–10) in Ref.[28] The calculation of the preferential solvation parameter has mainly served to be compared and related to the non-ideal chromatographic behavior expressed through K_p. In this regard, Figs. 1–3 show the theoretical variation of λ with ϕ_2 at different V_h (solid lines) together with single λ values, calculated with the real (ϕ_2, ϕ_3) composition data[28] for both packings (empty symbols for μ-Styragel and filled ones for TSK Gel H_{HR}). Concretely, Fig. 1 plots the above-mentioned dependence for PBD as polymeric solute in THF (part a) and in Bz (part b). As can be seen, in THF, the λ values are close to zero, in good accord with the K_p values close to unity obtained in this eluent, which is usually considered as non-interactive for "ideal" SEC. However, in Bz, the λ values are always negative, which means that the PS gel matrix is preferentially solvated by the PBD; in consequence, the solute will be eluted later, being in agreement with the $K_p > 1$ obtained in both packings.

In Fig. 2, the data for the Diox/PBD system have been plotted for μ-Styragel (part a) and for TSK Gel H_{HR} (part b) columns. Again, in this eluent, λ values are also negative, denoting values of $K_p > 1$, as experimentally observed in both packings.

In summary, the comparison of the PBD behavior, in the three eluents assayed, reveals that $\lambda^{\mu-\text{Styragel}}$ is always lower than $\lambda^{\text{TSK Gel H}_{HR}}$, i.e., the preferential solvation of PBD solute onto the PS gel is higher in the μ-Styragel columns, in accordance with the general trend $K_p^{\mu-\text{Styragel}} > K_p^{\text{TSK Gel H}_{HR}}$ pointed out in Table 1.

On the other hand, Fig. 3 compares the preferential solvation behavior of PDMS by PS gels in three solvents: Tol (part a), Bz (part b), and CHX (part c). As seen, in Tol,

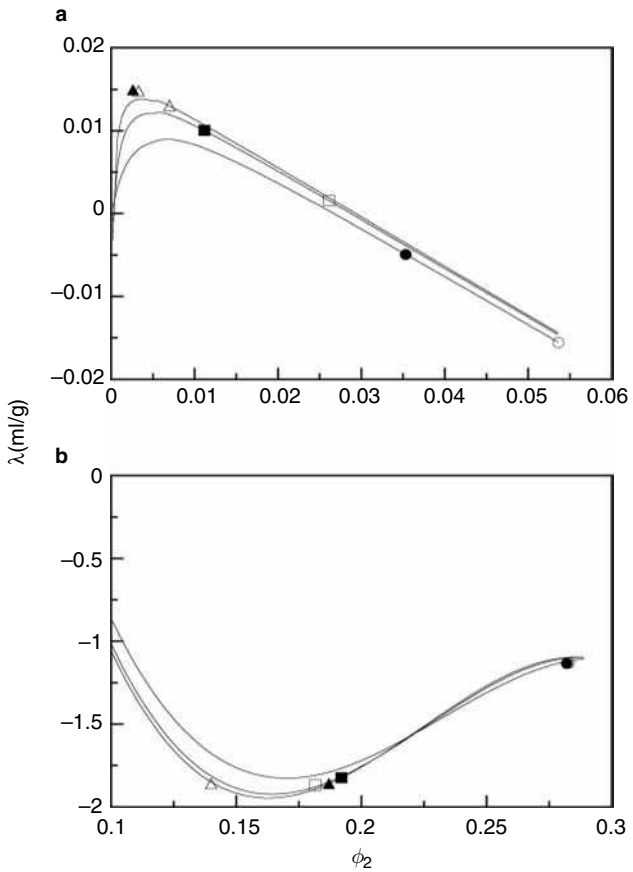

Fig. 1 Plot of the preferential solvation coefficient, λ, as a function of the volume fraction of polymer(2), ϕ_2, at three hydrodynamic volumes, $V_h = 10^6$ (○●); 10^7 (□■), and 10^8 (△▲) ml/mol for different systems: (a) THF/PBD/PS and (b) Bz/PBD/PS eluted in μ-Styragel (empty symbols) and TSK Gel H_{HR} (solid symbols) columns. Solid line has been calculated with equations and ϕ_3 values given in Ref. 28.
Source: From An analysis of the concentration effects on elution volumes through the preferential solvation parameter in two SEC packings, in Macromol. Chem. Phys.[28]

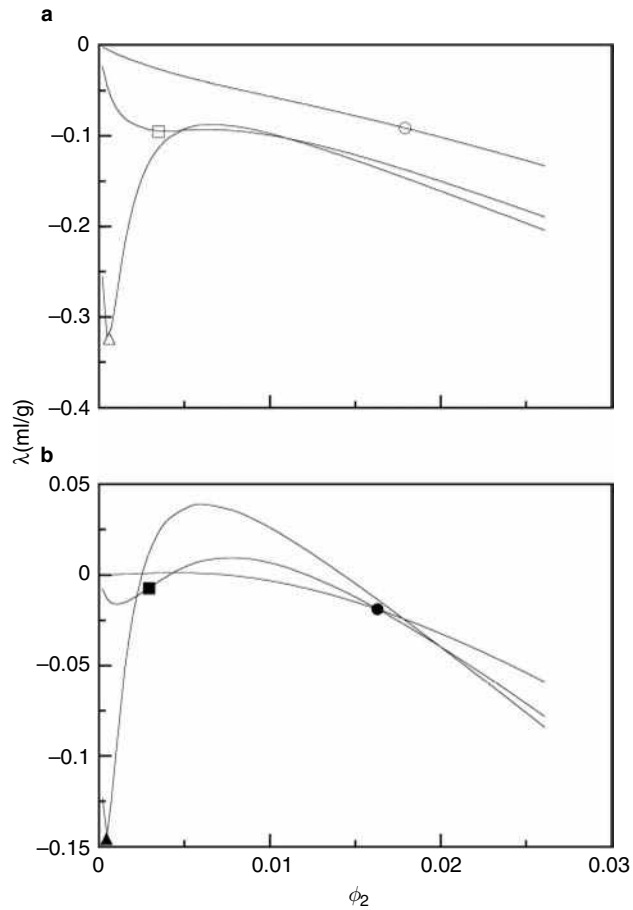

Fig. 2 Plot of the preferential solvation coefficient, λ, as a function of the volume fraction of polymer(2), ϕ_2, at three hydrodynamic volumes, $V_h = 10^6$ (○●); 10^7 (□■), and 10^8 (△▲) ml/mol for the system Diox/PBD/PS eluted in: (a) μ-Styragel (empty symbols) and (b) TSK Gel H_{HR} (solid symbols). Solid line has been calculated with equations and ϕ_3 values given in Ref. 28.
Source: From An analysis of the concentration effects on elution volumes through the preferential solvation parameter in two SEC packings, in Macromol. Chem. Phys.[28]

as ϕ_2 increases, λ also does in positive value and reaches the highest values, denoting the poorest preferential solvation of the PDMS polymer on the matrix or, in other words, the best solvation of the solvent. Consequently, this tendency will be reflected by early solute elution and the lowest K_p values, in agreement with data compiled in Table 1. Also, the λ punctual values, in TSK Gel H_{HR}, are slightly higher than in μ-Styragel, as reflected in their respective K_p data. In Bz, λ values are close to zero, especially for the μ-Styragel columns, in which the K_p values approach unity, denoting no solute–gel attractive interactions, in accordance with the fact that $\lambda \approx 0$ means no preferential salvation, neither for the solute (2) nor for the solvent (1) by the gel (3). Finally, in CHX as eluent, no differences in both packings, among the punctual λ values, are noticed. However, only in CHX, λ tends to diminish as ϕ_2 increases indicating an increase in their K_p values, compared with those observed in Tol and in Bz, which is, again, in good agreement with the experimental chromatographic behavior noticed in both types of SEC columns.

Finally, further evidence on the correlation between the λ and K_p magnitudes is noticed independently of the column packing used. As a general trend, as the hydrodynamic volume increases (from 10^6 to 10^8 ml/mol), λ decreases and K_p data increase, which was also observed in previous studies.[26,27]

Concentration Effects on Elution Volumes

Another complicating factor in the quantitative evaluation of polymer-packing interactions by SEC is the concentration effect, i.e., the dependence of elution volumes, V_e, on the

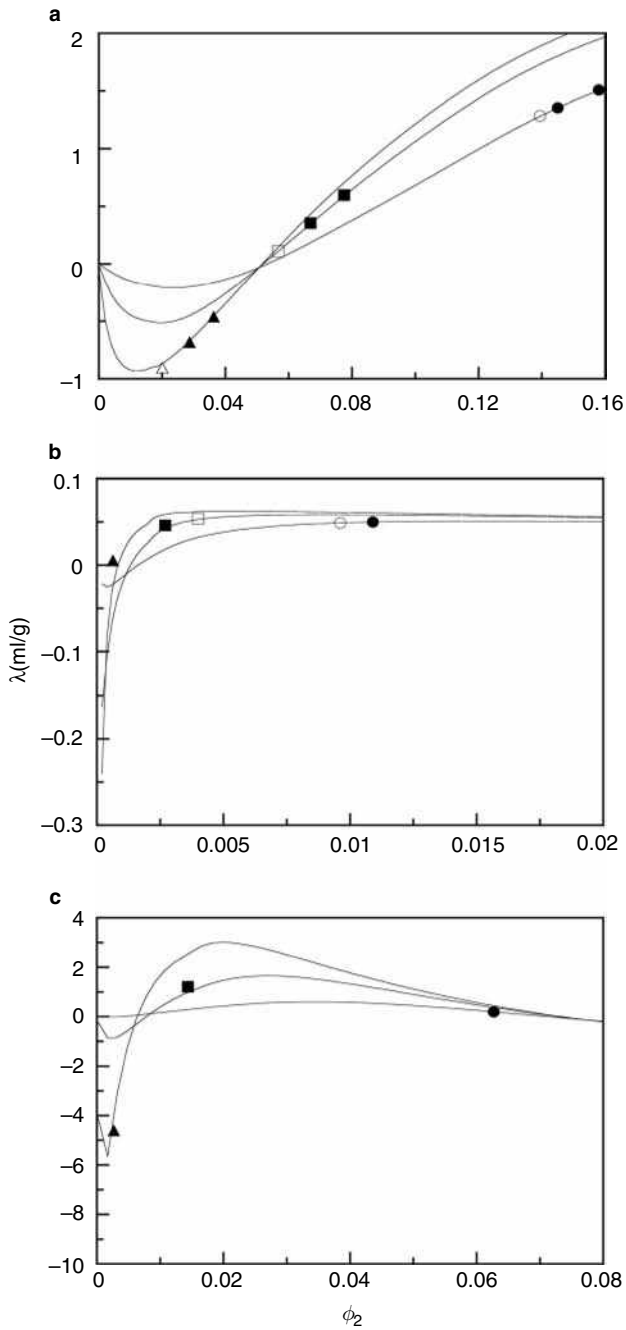

Fig. 3 Plot of the preferential solvation coefficient, λ, as a function of the volume fraction of polymer(2), ϕ_2, at three hydrodynamic volumes, $V_h = 10^6$ (○●); 10^7 (□■), and 10^8 (△▲) ml/mol for different systems: (a) Tol/PDMS/PS; (b) Bz/PDMS/PS; and (c) CHX/PDMS/PS eluted in μ-Styragel (empty symbols) and TSK Gel H_{HR} (solid symbols) columns. Solid line has been calculated with equations and ϕ_3 values given in Ref. 28. **Source:** From An analysis of the concentration effects on elution volumes through the preferential solvation parameter in two SEC packings, in Macromol. Chem. Phys.[28]

injected polymer concentration, c_2. As reported,[9] the slopes of linear plots, V_e vs. c_2, strongly depend on the thermodynamic quality of the eluent for the polymer, and become higher as the molar mass of the polymer increases, especially for good solvents. As usually found in the literature,[9–14,17,18] the hydrodynamic volume of the polymer decreases as the injected polymer concentration increases, making its V_e to be higher than the one obtained at zero concentration, especially for high-molar masses. Therefore, to avoid concentration effects on the elution volumes, all polymeric solute samples should be injected at different concentrations and then extrapolated to zero concentration.

Next, we need to clarify whether this hydrodynamic effect can be also influenced by the thermodynamic effect owing to the preferential solvation of the polymer (2) onto the gel (3) as the volume fraction of the polymer injected, ϕ_2, increases. For this purpose, Fig. 4 shows the dependence of the elution volumes on the solute concentration for different solvent/PBD systems in μ-Styragel (Fig. 4a) and in TSK Gel H_{HR} (Fig. 4b) columns; and Fig. 5 plots the same dependence for several solvent/PDMS systems in the

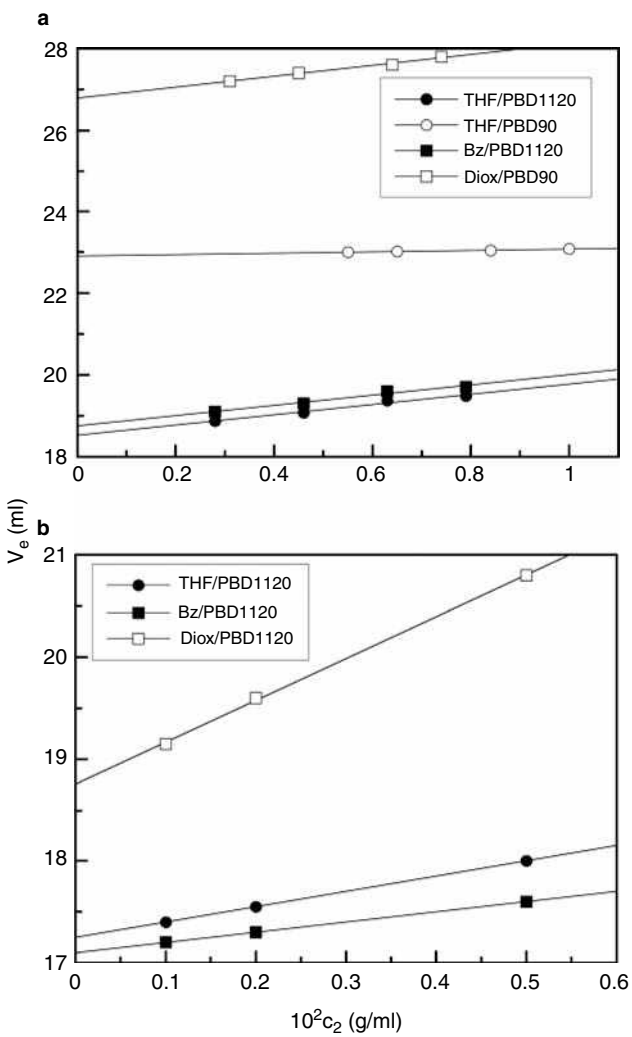

Fig. 4 Dependence of elution volumes, V_e, on the injected polymer concentration, c_2, for different solvent/PBD systems eluted in: (a) μ-Styragel and (b) TSK Gel H_{HR} column packings.

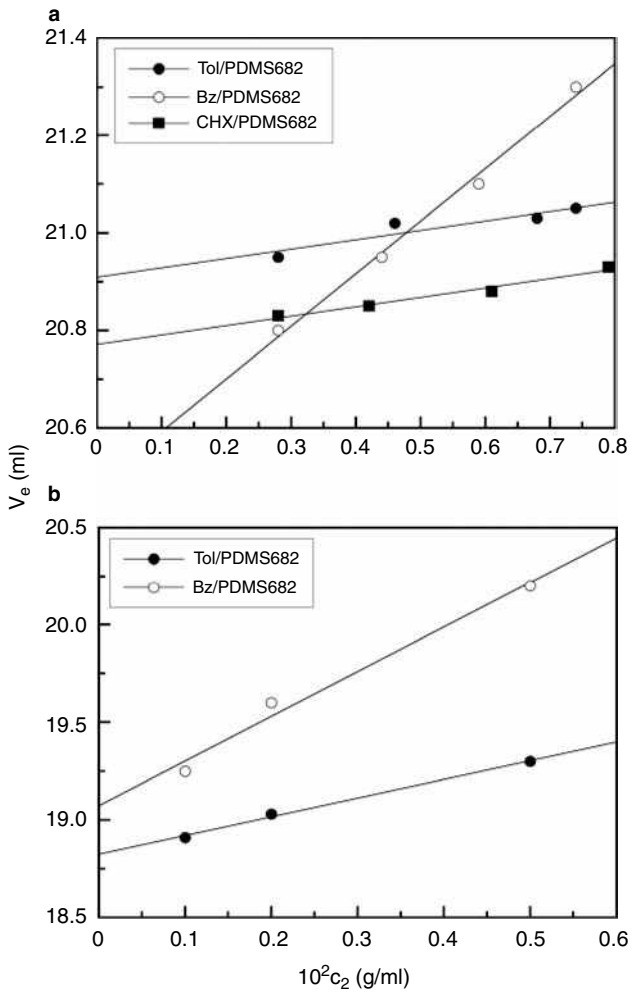

Fig. 5 Dependence of elution volumes, V_e, on the injected polymer concentration, c_2, for different solvent/PDMS systems eluted in: a, μ-Styragel and b, TSK Gel H_{HR} column packings.

same packings (parts a and b, respectively). As seen, the elution volumes always increase with increasing polymer concentration (positive slopes) owing to the decrease in the respective hydrodynamic volumes, as expected. A detailed analysis of this trend can be made, based not only on hydrodynamic, but also on thermodynamic considerations, because these slopes could also be a sensitive function of the polymer–gel and solvent–gel interactions.

Firstly, to discuss the thermodynamic quality of the solvents used, in Table 2, the values of the MHS exponent, a, for all the systems here studied, have been compiled. As known, a represents the thermodynamic affinity of the solvent by the polymer or, in other words, the magnitude representative of the solvent–polymer interactions. Hence, a value of $a = 0.50$ means a poor or "theta" solvent, i.e., a solvent in which the polymer has unperturbed dimensions; and, as a increases, the polymer coil becomes more expanded. Therefore, in the light of values in Table 2, at a given molar mass, for PBD, the solvent affinity will be

Table 2 Mark–Houwink–Sakurada (MHS) exponents for different solvent/polymer systems at 25°C.

System	a
THF/PBD	0.76
Bz/PBD	0.60
Diox/PBD	0.54
Tol/PDMS	0.60
Bz/PDMS	0.57
CHX/PDMS	0.53

THF > Bz > Diox, and for PDMS, the order is Tol > Bz > CHX. In this sense, the effect of the injected polymer concentration on the magnitude of the hydrodynamic volume should also follow the mentioned order, and it should be expected for the respective slopes of the V_e vs. c_2 plots. Consequently, and independently of the columns used, for PBD, it was expected that the concentration effect would be the most accentuated in THF and for PDMS in Tol. However, as can be seen in Figs. 4 and 5, this expected tendency is not accomplished in most systems.

For the sake of discussion, Table 3 contains the values of the slopes of Figs. 4 and 5. First, in the case of TSK Gel H_{HR}, when eluting PBD1120 (M = 1,120,000 g/mol), the slope values reveal that the concentration effect is more pronounced in Diox, contrary to the expected behavior based only in its a value (the lowest). Therefore, in addition to the hydrodynamic size of the macromolecules, other factors may be responsible for these deviations. In this sense, the reversible sorption of the polymeric solute onto the gel surface is likely playing a major role on increasing the elution volumes and, consequently, on enhancing the concentration effects. For this reason, it seems reliable to try to understand the observed concentration effects with the aid of the preferential solvation coefficient evaluated in the preceding section. In this regard, the comparison of λ values given in Figs. 1 and 2 show that the increase in negative value (meaning increasing polymer–gel adsorption) is more acute as PBD concentration (ϕ_2) increases, and in Diox as eluent. Both facts corroborate the major

Table 3 Slopes of the dependence of SEC elution volumes on the injected polymer concentration in the two gel packings.

System	$\Delta V_e/\Delta c_2$ (ml²/g) μ-Styragel	TSK Gel H_{HR}
THF/PBD (90)[a]	16.52	
THF/PBD (1120)	125.5	150.0
Bz/PBD (1120)	125.5	100.0
Diox/PBD (90)	133.0	
Diox/PBD (1120)		409.3
Tol/PDMS (682)	19.05	97.86
Bz/PDMS (682)	107.2	230.7
CHX/PDMS (682)	19.43	

[a]Figures in parenthesis refer to polymer molar mass in kD.

influence of λ on the concentration effect than the influence of the solvent affinity, because the elution volumes increase much more than if the preferential solvation phenomenon was not present.

Secondly, Fig. 4a shows the concentration effect obtained in the μ-Styragel packing for PBD1120 in THF and Bz as eluents. Taking into account only hydrodynamic considerations (see the a values), in THF, the slope should be a little higher than in Bz, but, as seen in Table 3, the same slopes are obtained. Again, this fact can be explained if the solvent hydrodynamic effect is compensated by the preferential solvation. Because λ values are more negative in Bz than in THF as ϕ_2 increases, this causes the PBD solute to be eluted similarly in both eluents, i.e., with an equal concentration effect, even though their solvation qualities were different. In addition, a similar behavior is observed for a polymer with low molar mass, such as PBD90 (M = 90,000 g/mol) in μ-Styragel columns eluted in THF and Diox (also plotted in Fig. 4a). From the respective a values, THF is a better solvent for PBD than Diox; thus, if only considering hydrodynamic factors, the concentration effect should be more important in THF as eluent. However, we find the opposite from their slope values (Table 3), which implies that the sorption of the PBD onto the gel matrix, when eluted in THF, is less significant than in Diox. This experimental trend is, again, clearly supported by the λ values depicted in Figs. 1a and 2a, which are much more negative in Diox than in THF, denoting a major solute–gel interaction in the former eluent, and, consequently, a higher influence of the preferential sorption.

Finally, Fig. 5 shows the behavior followed by the other polymer, PDMS682 (M = 6,82,000 g/mol), in both packings. In the case of μ-Styragel, Fig. 5a shows the behavior of PDMS682 in three solvents: Tol, Bz, and CHX. From the a data in Table 2, it is clearly seen that they are very similar; so it is expected that the hydrodynamic influence on the elution volumes should be nearly the same. Nevertheless, from the slope values in Table 3, the concentration effect is more acute in Bz than in Tol or in CHX. This behavior could again be understood through their respective thermodynamic λ data, which tend to give negative values when ϕ_2 increases (Fig. 3c), denoting more PDMS–gel attractive interactions in Bz than in the other two solvents assayed. With respect to the TSK Gel H_{HR} (part b), the concentration effect has been studied in two solvents with quite similar thermodynamic qualities: Tol and Bz. Therefore, a similar influence of the hydrodynamic factor on the concentration effect should be expected. However, the slope of the V_e vs. c_2 dependence in Bz is more than twice that in Tol. Again, this discrepancy can be properly attributed to the preferential sorption effect. In this sense, from the comparison of Figs. 3a and b, the Tol/PDMS system shows positive λ values as increasing ϕ_2 denote a lesser adsorption of the polymer onto the gel matrix, and lower elution volumes; the contrary is observed for Bz/PDMS system, supporting the experimental concentration effect depicted in Fig. 5a.

A final comparison of the concentration effects in both gel packings, for a given solvent/polymer system and a given molar mass, through their respective slope values reveals that, in general, the slopes in TSK gel H_{HR} are higher than those in μ-Styragel. In other words, the solute concentration influence is more accentuated in the gel that presents lower polymer–gel interactions and lower degree of cross-linking (or higher pore volume).[27] In consequence, for the same Δc_2, the hydrodynamic size of the polymer coil can decrease more in these columns, exhibiting, then, a higher change in the elution volumes.

In summary, as a main conclusion, there is a clear and quantitative influence of the preferential solvation effect on the polymer elution behavior in SEC. In the past,[10–12] the dependence of elution volumes on the sample concentration injected had been only attributed to conventional hydrodynamic aspects (solvent quality affecting the coil size), although never before the thermodynamic effects had been taken into account.

CONCLUSIONS

The comparison of the K_p data of different solvent–polymer systems in two column packings based on PS gels shows that adsorption of solutes onto the gel as secondary mechanism is more pronounced in μ-Styragel than in TSK Gel H_{HR}.

The observed solute–gel attractive interactions have been quantitatively analyzed through the values of the preferential solvation coefficient for all systems in both gels. The correlation between the thermodynamic parameter λ with the chromatographic distribution coefficient, K_p, has revealed that the lower the λ values, the higher the preferential solvation of the polymer by the gel and, consequently, the higher the K_p values. In general, the comparison in both packings yields that $\lambda^{\mu-\text{Styragel}} < \lambda^{\text{TSK Gel H}_{HR}}$, in agreement with the experimental chromatographic tendency $K_p^{\mu-\text{Styragel}} > K_p^{\text{TSK Gel H}_{HR}}$.

Finally, the most noticeable result has been the understanding of the usually observed concentration effects on the elution volumes based not only on hydrodynamic aspects, but also on the important influence of thermodynamic factors such as the preferential solvation. In this sense, it has been quantitatively shown that, for a given solvent/polymer system and a given molar mass, the concentration effect is more acute in the packing that presents lower polymer–gel sorption and lower degree of cross-linking.

ACKNOWLEDGMENT

Financial support from Ministerio de Ciencia y Tecnología (Spain) under Grant No. MAT2003-00668 is gratefully acknowledged.

REFERENCES

1. Mori, S.; Barth, H.G. Fundamental concepts. In *Size Exclusion Chromatography*; Springer: Berlin, 1999; 11–21.
2. Berek, D. Interactive properties of polystyrene/divinylbenzene based commercial SEC columns. In *Column Handbook for Size Exclusion Chromatography*; Wu, C., Ed.; Academic Press: San Diego, CA, , 1999; 445–457.
3. Nagata, M.; Kato, T.; Furutani, H. Comparison of a multipore column with a mixed-bed column for size exclusion chromatography. J. Liq. Chromatogr. Relat. Technol. **1998**, *21* (10), 1471–1484.
4. Berek, D.; Janco, M.; Meira, G.R. Liquid chromatography of macromolecules at the critical adsorption point. II. Role of column packing: Bare silica gel. J. Polym. Sci. Part A: Polym. Chem. **1998**, *36* (9), 1363–1371.
5. Nguyen, S.H.; Berek, D.; Chiantore, O. Reconcentration of diluted polymer solutions by full adsorption/desorption procedure-1. Eluent switching approach studied by size exclusion chromatography. Polymer **1998**, *39* (21), 5127–5132.
6. Berek, D. Evaluation of high-performance liquid chromatography column retentivity using macromolecular probes I. J. Chromatogr. A, **2002**, *950* (1–2), 75–80.
7. García-Lopera, R.; Gómez, C.M.; Falo, M.; Abad, C.; Campos, A. Chromatographic evaluation of resolution and secondary mechanisms of pure and mixed sets of SEC columns: TSK-Gel H_{HR} and TSK-Gel H_{XL}. Chromatographia **2004**, *59* (5/6), 355–360.
8. Dickie, R.A., Labana, S.S., Bauer, R.S., Eds.; *Cross-linked Polymers: Chemistry, Properties and Applications*; ACS Symp. Ser. ACS: Washington, 1998; 367.
9. Berek, D.; Bakos, D.; Bleha, T.; Soltes, L. Gel-permeation chromatography in mixed eluents effects of sorption on porasil gels. Makromol. Chem. **1975**, *176* (2), 391–398.
10. Mahabadi, H.K.; Rudin, A. Effect of solvent on concentration-dependence of hydrodynamic volumes and GPC elution volumes. Polym. J. **1979**, *11* (2), 123–131.
11. Bleha, T.; Mlynek, J.; Berek, D. Concentration-dependence of chain dimensions and its role in gel chromatography. Polymer **1980**, *21* (7), 798–804.
12. Janca, J.; Pokorny, S.; Zabransky, J.; Bleha, T. On the concentration effects in steric exclusion chromatography under stationary equilibrium conditions. J. Liq. Chromatogr. **1984**, *7* (9), 1887–1901.
13. Mori, S. *Steric Exclusion Liquid Chromatography of Polymers*; Janca, J., Ed.; Chromatogr. Sci. Ser.; Marcel Dekker: New York, 1984; Vol. 25, 192.
14. Figueruelo, J.E.; Campos, A.; Soria, V.; Tejero, R. A model accounting for concentration effects in exclusion chromatography. J. Liq. Chromatogr. **1984**, *7* (6), 1061–1078.
15. Song, M.S.; Hu, G.X. Study on the concentration effect in gel-permeation chromatography. 1. A new model-theory for concentration-dependence of hydrodynamic volumes and GPC elution volumes. J. Liq. Chromatogr. **1985**, *8* (14), 2543–2556.
16. Chiantore, O.; Guaita, M. Concentration effects in size-exclusion chromatography of polymers. Separation of the contributions from viscosity and hydrodynamic volume contraction. J. Chromatogr. **1986**, *353*, 285–293.
17. Tejero, R.; Soria, V.; Campos, A.; Figueruelo, J.E.; Abad, C. Quantitative prediction of concentration effects in steric exclusion chromatography. J. Liq. Chromatogr. **1986**, *9* (4), 711–726.
18. Soria, V.; Campos, A.; Tejero, R.; Figueruelo, J.E.; Abad, C. Concentration effects in SEC for polymer polymer solvent systems. J. Liq. Chromatogr. **1986**, *9* (6), 1105–1121.
19. Song, M.S.; Hu, G.X. Study on the concentration effects in gel-permeation chromatography. 2. A model-theory of concentration effects for polydispersed polymers. J. Liq. Chromatogr. **1988**, *11* (2), 363–381.
20. Hu, G.X.; Song, M.S. Study on the concentration effects in GPC: 5. A new method for calibration on universal calibration curves with polydispersed polymers. Polym. Test. **1991**, *10* (1), 59–67.
21. Hu, G.X.; Song, L.X.; Song, M.S. Study on the concentration effects in GPC: 6. A new method for determination of the radius of gyration for macromolecules. Polym. Test. **1991**, *10* (2), 91–99.
22. Song, M.S.; Hu, G.X.; Li, X.Y.; Zhao, B. Study on the concentration effects in size exclusion chromatography. VII. A quantitative verification for the model theory of concentration and molecular mass dependences of hydrodynamic volumes for polydisperse polymers. J. Chromatogr. A, **2002**, *961* (2), 155–170.
23. Lou, X.; Zhu, Q.; Lei, Z.; van Dongen, J.L.J.; Meijer, E.W. Simulation of size exclusion chromatography for characterization of supramolecular complex: A theoretical study. J. Chromatogr. A, **2004**, *1029* (1,2), 67–75.
24. Skrinarova, Z.; Bleha, T.; Cifra, P. Concentration effects in partitioning of macromolecules into pores with attractive walls. Macromolecules **2002**, *35* (23), 8896–8905.
25. Fleer, G.J.; Skvortsov, A.M. Theory for concentration and solvency effects in size-exclusion chromatography of polymers. Macromolecules **2005**, *38* (6), 2492–2505.
26. García, R.; Gómez, C.M.; Figueruelo, J.E.; Campos, A. Thermodynamic interpretation of the SEC behavior of polymers in a polystyrene gel matrix. Macromol. Chem. Phys. **2001**, *202* (9), 1889–1901.
27. García, R.; Recalde, I.B.; Figueruelo, J.E.; Campos, A. Quantitative evaluation of the swelling and crosslinking degrees in two organic gel packings for SEC. Macromol. Chem. Phys. **2001**, *202* (17), 3352–3362.
28. García-Lopera, R.; Gómez, C.M.; Abad, C.; Campos, A. An analysis of the concentration effects on elution volumes through the preferential solvation parameter in two SEC packings. Macromol. Chem. Phys. **2002**, *203* (18), 2551–2559.

Enantiomers: TLC Separation

Luciano Lepri
Alessandra Cincinelli
Department of Chemistry, University of Florence (UNIFI), Florence, Italy

Abstract
The most popular thin layer chromatography (TLC) techniques for separation of enantiomers are described here: 1) use of non-chiral phases for indirect resolution of optical isomers after derivatization to obtain the corresponding diastereoisomers; and 2) direct resolution of enantiomers using chiral stationary phases or chiral mobile phases. Advantages and limits of all reported techniques are discussed.

INTRODUCTION

Enantiomers are compounds that have the same chemical structure but different conformations, whose molecular structures are not superimposable on their mirror images, and, because of their molecular asymmetry, these compounds are optically active. The most common cause of optical activity is the presence of one or more chiral centers, which are usually related to tetrahedral structures formed by four different groups around carbon, silicon, tin, nitrogen, phosphorous, or sulfur.

Many molecules are chiral, even in the absence of stereogenic centers; that is, molecules containing adjacent π systems, which cannot adopt a coplanar conformation because of rotational restrictions due to steric hindrance, can exist in two mirror forms (atropisomers). This is the case for some dienes or olefins, for some non-planar amides, and for the biphenyl or binaphthyl types of compounds.

Optical isomers can be designated by the symbols D and L, which are used to indicate the relationship between configurations based on D(+)-glyceraldehyde as an arbitrary standard. If this relationship is unknown, the symbols (+) and (−) are used to indicate the direction of rotation of plane polarized light (i.e., dextrorotatory and levorotatory). In 1956, Cahn, Ingold, and Prelog[1] presented a new system, the *R* and *S* absolute configurations of compounds.

Many enantiomers show different physiological behaviors, and it is therefore desirable to have reliable methods for the resolution of racemates and the determination of enantiomeric purity. To this end, thin layer chromatography (TLC) is a simple, sensitive, economic, and fast method, which allows easy control of a synthetic process and can be used for preparative separations.

TLC SEPARATION OF ENANTIOMERS BY USE OF DIASTEREOMERIC DERIVATIVES

Because the stationary phases originally used in LC were achiral, much research was devoted to the separation of enantiomers as diastereomeric derivatives produced by reaction with an optically pure reagent (A_R). The resultant diastereomers could, because of their different physicochemical properties, then be separated on conventional stationary phases.

In addition, a significant increase in the sensitivity of detection and the location, on the layers, of some compounds that are not otherwise identifiable can be achieved by this method. There are, however, some disadvantages: 1) it is necessary to use derivatization reagents with 100% optical purity; 2) quantitation is founded on the assumption that the reaction is complete and not associated with racemization; and 3) the two chiral centers should be as close as possible to each other in order to maximize the difference in chromatographic properties.

Many chiral derivatization reactions have been used, and the compounds examined are mostly amphetamines, β-blocking agents, amino acids, and anti-inflammatory drugs. Silica gel and, to a lesser extent, silanized silica have been used as stationary phases. The ΔR_f values obtained for the diastereomeric pairs were usually not very high (0.04–0.07), with the exception of amino alcohol and amino acid diastereomers obtained with Marfey's reagent (0.06–0.22). Recently,[2] Marfey's reagent (1-fluoro-2,4-di-nitrophenyl-5-L-alaninnamide, FDNP-L-Ala-NH_2) and the two variants with phenylalaninamide (FDNP-L-Phe-NH_2) and valinamide (FDNP-L-Val-NH_2) were used to separate 17 DL-amino acids by normal- and reversed-phase TLC on SILG/UV_{254} and RP-18W/UV_{254} plates, respectively. In normal-phase chromatography ΔR_f values of diastereomeric pairs were included between 0.13

and 0.39 (FDNP-L-Ala-NH_2), 0.12 and 0.50 (FDNP-L-PHe-NH_2), and 0.21 and 0.55 (FDNP-L-Val-NH_2) by eluting with phenol–water 3 + 1 (v/v).

In reversed-phase chromatography ΔR_f for the three different derivatives were 0.02–0.09, 0.03–0.10, and 0.14–0.55, respectively, with acetonitrile (30–50%) in triethylamine phosphate buffer, pH = 5.5, as eluent. Resolution was always better for diastereosomers obtained with FDNP-L-Val-NH_2 under normal- and reversed-phase conditions. Derivatives appeared as bright yellow spots.

This procedure has become more and more important owing to the occurrence of D-enantiomers of amino acids in tissues of various organisms. In addition, amino acid residues in dietary proteins have been reported to have been significantly racemized.

TLC SEPARATIONS OF ENANTIOMERS BY CHIRAL CHROMATOGRAPHY

In chiral chromatography, the two diastereomeric adducts A_RE_R and A_RE_S are formed during elution, rather than synthetically, prior to chromatography. The adducts differ with respect to their stability in the use of chiral stationary phases (CSPs) or chiral-coated stationary phases (CCSPs) and/or in their interphase distribution ratio with the addition of a chiral selector to the mobile phase (CMP). The difference between the interactions of the chiral environment with the two enantiomers is called enantioselectivity.

According to Dalgliesh,[3] three active positions on the selector must interact simultaneously with the active positions of the enantiomer to reveal the differences between optical antipodes. This is a sufficient condition for resolution to occur, but it is not necessary. Chiral discrimination may happen as a result of hydrogen bonding and steric interactions, making only one attractive force necessary in this type of chromatography. Moreover, the formation of specific chiral cavities in a polymer network (as in the "Molecular Imprinting Techniques" section) could make it possible to base enantiomeric separations mainly on steric fit.

CHIRAL STATIONARY PHASES AND CHIRAL-COATED STATIONARY PHASES

Few chiral phases are used in TLC; one of the main reasons for this is that stationary phases with very high ultraviolet (UV) background can be used only with fluorescent or colored solutes. For example, amino-modified ready-to-use layers bonded or coated with Pirkle-type selectors, such as *N*-(3,5-dinitrobenzoyl)-L-leucine or *R*(–)-α-phenylglycine, are pale yellow and strongly absorb UV radiation.

Another reason is the high price of most CSPs. In spite of this, Pirkle-type CSPs, based on a combination of aromatic π–π bonding interactions, hydrogen bonding, and dipole interactions, allow the resolution of racemic mixtures of 2,2,2-trifluoro-1-(9-anthryl) ethanol, 1,1′-bi-2-naphthol, benzodiazepines, hexobarbital, and β-blocking agents derivatized with achiral 1-isocyanatonaphthalene. However, the most widely used CSPs or CCPs are polysaccharides and their derivatives (cellulose, cellulose triacetate, tribenzoate, and tricarbamate) and silanized silica gel impregnated with an optically active copper (II) complex of (2*S*,4*R*,2′*RS*)-*N*-(2′-hydroxydodecyl)-4-hydroxyproline (ChiralPlate, Macherey-Nagel, and high-performance thin layer chromatography [HPTLC] Chir, Merck, Germany) for chiral ligand exchange chromatography (CLEC). The chiral layer on the latter plates is combined with a so-called concentrating zone. β-Cyclodextrin bonded to silica gel H has also been used for the resolution of some racemic drugs and binaphthalenes.

CLEC is based on the copper (II) complex formation of a chiral selector and the respective optical antipodes. Differences in retention of the enantiomers are caused by dissimilar stabilities of their diastereomeric metal complexes. The requirement of sufficient stability of the ternary complex involves five-membered ring formation, and compounds such as α-amino and α-hydroxy acids are the most suitable.

The D-enantiomer of such bidentate compounds was generally retained more than L-enantiomer. Mixtures of methanol/acetonitrile/water or dichloromethane/methanol were often used as eluents. Chiral recognition based on CLEC was also involved in the enantiomer separation of amino acids and β-adrenergic blocking agents on silica gel plates coated with the copper(II) complex of enantiomeric amino acids (L-proline, L-arginine, and 1R,3R,5R-2-azobicyclo[3.3.0]octan-3-carboxylic acid).[4]

The resolution of optical antipodes on polysaccharides is mainly governed by the shape and size of the solutes (inclusion phenomena) and only to a minor extent by other interactions involving the functional groups of the molecules. The type and composition of the aqueous–organic eluents affect the separation because these result in different swelling of polysaccharides.

Commercially available silica gel plates coated with acid or basic chiral selectors [D-galacturonic acid, L-(+)-tartaric acid, L-lactic acid, (–)-brucine] were used for the separation of racemic ephedrine, atropine, neutral amino acids, and their 3-phenyl-2-thiohydantoins (PTH) derivatives. The use of amino acids as chiral selectors involved further possibilities of enantiomer separation owing to the simultaneous presence of basic and acidic groups. In fact, L-aspartic acid, L-lysine, L-histidine, L-arginine, and L-serine resolved racemic alkaloids, β-blockers, profens, some amino acids, and their Dns derivatives. Macrocyclic antibiotics [i.e., (–)-erythromycin and (–)-vancomycin] were also used as chiral agents for the separation of enantiomeric DNs amino acids. The mechanisms of chiral recognition was investigated by Aboul-Enein, El-Awady, and Heard;[5] they hypothesized that the formation of

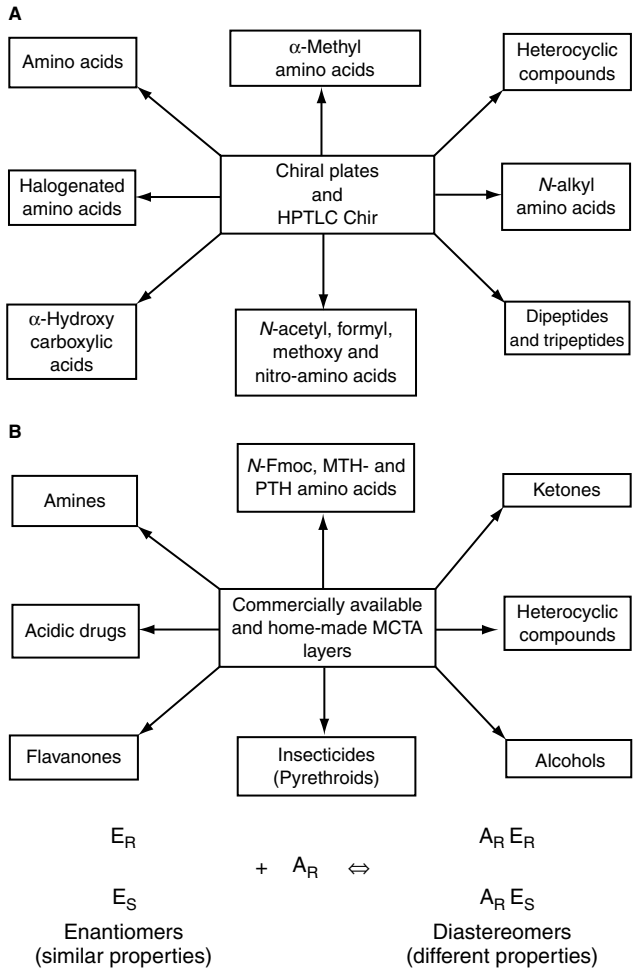

Fig. 1 Classes of chiral organic compounds resolved (A) by ligand exchange chromatography on Chiral plate and HPTLC Chir plates and (B) on MCTA layers.

diastereoisomers should occur within the pores of silica gel to obtain chiral discrimination.

A peculiar behavior of enantiomeric non-steroidal anti-inflammatory drugs (i.e., ibuprofen, naproxen, 2-phenylpropionic acid) was found by Sajewicz et al.[6] on 20 × 20 cm silica gel 60 F_{254} plates impregnated with L-arginine by using acetonitrile/methanol/water mixtures (5+1+0.75, 5+1+1, or 5+1+1.5 v/v/v) as eluents. The migration of the enantiomers of 2-arylpropionic acids deviates markedly from the strict vertical in the mutually opposite direction; the maximum sum of the left- and right-handed deviation was 4 ± 2 mm for ibuprofen, 6 ± 2 mm for nanoproxen, and 7 ± 2 for 2-phenylpropionic acid. Such deviations can improve resolution of racemic ibuprofen whose enantiomers are insufficiently separated by one-dimensional chromatography ($\Delta R_f = 0.03$). Better resolution is possible using a two-dimensional technique. As a consequence of these results, the application of densitometry to chiral separation of 2-arylpropionic acids must be used very cautiously.

In CSPs, owing to the nature of the polymer structure, the simultaneous participation of several chiral sites or several polymer chains is conceivable. In CCSPs, the chiral sites are distributed on the surface or in the network of the achiral matrix relatively far away from each other, and only bimolecular interaction is generally possible with the optical antipodes. A survey of the optically active substance classes separated with Chiral plate and HPTLC Chir layers and with microcrystalline cellulose triacetate (MCTA) plates is shown in Fig. 1. Cellulose tribenzoate and tricarbamate have recently been used for the separation of enantiomeric aromatic alcohols, Troger's base, and benzoin ethyl ether.

MOLECULAR IMPRINTING TECHNIQUES

This technique is based on the preparation of synthetic polymers with specific selectivity by using chiral imprinting molecules mixed with functional and cross-linking monomers (usually methacrylic acid and ethylene glycol dimethacrylate, respectively), capable of interacting with such molecules.

After polymerization, imprinting molecules (templates) are removed by extraction, leaving cavities that correspond to those of the template. The resulting product is called a molecular imprinting polymer (MIP).

MIPs containing L- or D-phenylalanine anilide, quinine, (+)-ephedrine, (+)-pseudoephedrine, (+)-norephedrine, R-(+)-propranolol, S-(+)-naproxen, and S-(–)-timolol were prepared and non-commercial microlayers (2.5 × 7 cm) were obtained by mixing the polymer (8100 mg) and gypsum (100 mg) as binders, with 1.9 ml water and 10 μl ethanol as wetting agent. Such polymers are easy to recognize and they usually separate enantiomers of molecules having structures similar to that of original template.[7]

CHIRAL MOBILE PHASES

Chiral mobile phases enable the use of conventional stationary phases and show only minor detection problems compared to CSPs or CCSPs. However, high-cost chiral selectors (e.g., γ-cyclodextrin) are certainly not advisable for TLC. Enantiomer separations can be achieved using chiral mobile phases in both normal- and reversed-phase chromatography. The first technique uses silica gel and, mostly, diol F_{254} HPTLC plates (Merck) and, as chiral selectors, D-galacturonic acid for ephedrine, *N*-carbobenzoxy (CBZ)-L-amino acids or peptides and 1*R*(–)-ammonium-10-camphorsulfonate for several drugs, and 2-*O*-[(*R*)-2-hydroxypropyl)]-β-cyclodextrin for underivatized amino acids. Extremely high ΔR_f values (0.05–0.25) were observed for the various pairs of enantiomers, proving the strong enantioselectivity of this system.

Most separations were effected by reversed-phase chromatography on hydrophobic silica gel (RP-18W/UV_{254} and

Sil C_{18}-50/UV_{254} from Macherey-Nagel, Germany; KC2F, KC18F, and chemically bonded diphenyl-F from Whatman, U.S.A.; and RP-18W/F_{254} from Merck, Germany) as stationary phase and β-cyclodextrin and its derivatives, bovine serum albumin (BSA), and the macrocyclic antibiotic vancomycin as chiral agents. Enantiomers that selectively interact with β-cyclodextrin cavities are generally *N*-derivatized amino acids, whereas the use of BSA as chiral selector is able to resolve many *N*-derivatized amino acids, tryptophan and its derivatives, derivatized lactic acid, and unusual optical antipodes such as binaphthols.

In particular, the resolution of dansyl-D- and L-amino acids by reversed-phase TLC using aqueous mobile phases containing methanol or acetonitrile and β-cyclodextrin as chiral selector is very useful for stereochemical analysis of amino acids from small peptides, since a significant number of naturally occurring peptides and peptide antibiotics isolated from plants and microorganisms contain at least one amino acid in D-configuration.[8]

QUANTITATIVE ANALYSIS OF TLC-SEPARATED ENANTIOMERS

Although TLC/mass spectrometry (MS) has been shown to be technically feasible and applicable to a variety of problems, TLC is generally coupled with spectrophotometric methods for quantitative analysis of enantiomers. Optical quantitation can be achieved by in situ densitometry by the measurement of UV/VIS absorption, fluorescence, or fluorescence quenching, or after extraction of solutes from the scraped layer. The evaluation of detection limits for separated enantiomers is essential because precise determination of trace levels of a D- or L-enantiomer in an excess of the other becomes more and more important. Detection limits as low as 0.1% of an enantiomer in the other were obtained.

REFERENCES

1. Cahn, R.S.; Ingold, C.K.; Prelog, V. Specification of asymmetric configuration in organic chemistry. Experientia **1956**, *12*, 81–94.
2. Bushan, R.; Bruckner, H.; Kumar, V.; Gupta, D. Indirect TLC resolution of amino acid enantiomers after derivatization with Marfey's reagent and its chiral variants. J. Planar Chromatogr. Mod. TLC **2007**, *20*, 165–171.
3. Dalgliesh, C.E. The optical resolution of aromatic amino acids on paper chromatograms. J. Chem. Soc. III **1952**, 3940–3943.
4. Bhushan, R.; Gupta, D. Ligand exchange TLC resolution of some racemic β-adrenergic blocking agents. J. Planar Chromatogr. Mod. TLC **2006**, *19*, 241–245.
5. Aboul-Enein, H.Y.; El-Awady, M.I.; Heard, C.H. Enantiomeric resolution of some 2-arylpropionic acids using L-(–)serine impregnated silica as stationary phase by thin layer chromatography. J. Pharm. Biomed. Anal. **2003**, *32*, 1055–1059.
6. Sajewicz, M.; Pietra, R.; Drabik, G.; Namyolo, E.; Kowalska, T. On the stereochemistry peculiar two-dimensional separation of 2-arylpropionic acids by chiral TLC. J. Planar Chromatogr. Mod. TLC **2006**, *19*, 273–277
7. Suedee, R.; Srichana, T.; Saelim, J.; Thavonpibulbut, T. Thin layer chromatographic separation of chiral drugs on molecularly imprinted chiral stationary phases. J. Planar Chromatogr. Mod. TLC **2001**, *14*, 194–198.
8. Le Fevre, J.W.; Gublo, E.J.; Botting, C.; Wall, R.; Nigro, A.; Pham, M.L.T.; Ganci, G. Qualitative reversed-phase thin-layer chromatographic analysis of the stereochemistry of D- and L-α-amino acids in small peptides. J. Planar Chromatogr. Mod. TLC **2000**, *13*, 160–165.

BIBLIOGRAPHY

1. Lepri, L.; Del Bubba, M.; Cincinelli, A. Chiral separations by TLC. In *Planar Chromatography, A Retrospective View for the Third Millennium*; Nyiredy, Sz., Ed.; Springer Scientific Publisher: Hungary, 2001; 517–549.
2. Prosek, M.; Puki, M. Basic principles of optical quantitation in TLC. In *Handbook of Thin Layer Chromatography*; Sherma, J.; Fried, B., Eds.; Marcel Dekker, Inc.: New York, 1996; 273–306.
3. Kowalska, T.; Sherma, J. Thin layer chromatography in chiral separations and analysis. In *Chromatographic Science Series*; CRC Press: Taylor & Francis Group, Boca Raton, FL, 2007.

Enantioseparation by CEC

Yulin Deng
Neuropsychiatry Research Unit, University of Saskatchewan, Saskatoon, Saskatchewan, Canada

INTRODUCTION

Capillary electrochromatography (CEC) is considered to be a hybrid technique that combines the features of both capillary high-performance liquid chromatography (HPLC) and capillary electrophoresis (CE). In CEC, a mobile phase is driven through a packed or an open tubular coating capillary column by electro-osmotic flow (EOF)[1,2] and/or pressurized flow.[3] The first electrochromatographic experiments were done in early 1974 by Pretorius et al.,[4] who applied an electric field across a packed column. This allows the analyte to partition between the mobile and stationary phases. As a high voltage is applied, electrophoretic mobility should also contribute to the chromatographic separation for charged analyses. The ability of CEC to combine electrophoretic mobility with partitioning mechanisms is one of its strongest advantages. For electro-osmotically driven-capillary electrochromatography (ED-CEC), the resulting flow profile is almost pluglike; thus, a high column efficiency, comparable to that in CE, can be obtained. For pressure-driven capillary electrochromatography (PD-CEC), although dispersion caused by flow velocity differences causes zone broadening, plate numbers are higher than in capillary HPLC due to the contribution of the electric field to total flow rate. Unlike ED-CEC, the use of an HPLC pump provides stable flow conditions and, thus, offers improvements in retention reproducibility, in sample introduction (e.g., split injection), in suppression of bubble formation, and in gradient elution. More importantly, because the solvent can be mainly driven by pressurized flow, the change of the direction of electric field is no longer limited, and the separation of mixtures of cationic, anionic and neutral compounds becomes possible in a single run. Additionally, neutral molecules can be separated without micelles or other organic additives; this makes CEC more amenable to coupling with mass spectrometry.

Chiral separation in CE is usually achieved by the addition of chiral complexing agents to form *in situ* diastereometric complexes between the enantiomers and the chiral complexing agent. Many of the chiral selectors successfully used in HPLC[5] can also be applied in CE, and thus the experience from both HPLC and CE can be transferred to CEC. During the last few years, interest in CEC has increased due to the improvement in the preparation of capillary columns[6,7] and in the stability and efficiency of separations.[6–9] A limited but dramatically increasing number of chiral separations in CEC have been reported so far. This review will be mainly devoted to recent developments and applications. We are also interested in exploring the potential advantages offered by CEC and, in particular, its practical utility for enantioseparation.

ENANTIOSELECTIVITY IN CEC

CEC is a more complicated system than CE and HPLC due to the combination of both electrophoretic and chromatographic transport mechanisms. It is difficult to define an effective selectivity (separation factor) as in the case of general chromatography or general electrophoresis. To better illustrate the interactions that control selectivity, we defined a relative selectivity and postulated a model that illustrates the effect of separation parameters on the enantioselectivity.[10]

For enantioseparation chiral stationary phases (CSPs), an expression of the relative selectivity is obtained:

$$\alpha_{\mathrm{r}} = \frac{\phi(K_{\mathrm{f2}} - K_{\mathrm{f1}})}{1 + \phi K_2 + \phi K_{\mathrm{f2}}} \tag{1}$$

Interestingly, this equation indicates that the electrophoresis mechanism does not influence the enantioselectivity and the electric field only plays a role in driving the mobile phase.

For enantioseparation with chiral additives in CEC, we derived another expression:

$$\alpha_r = \frac{(K_{\mathrm{f1}} - K_{\mathrm{f2}})[\phi K v_{\mathrm{c}} + (\mu_{\mathrm{c}} - \mu_{\mathrm{f}})E][\mathrm{C}]_{\mathrm{m}}}{(1 + \phi K + K_{\mathrm{f2}}[\mathrm{C}]_{\mathrm{m}})(v_{\mathrm{f}} + v_{\mathrm{c}} K_{\mathrm{f1}}[\mathrm{C}]_{\mathrm{m}})} \tag{2}$$

where v_f and v_c are the apparent flow velocity of the free analyte and the complexed analyte, respectively. Both Eqs. 1 and 2 show that the enantioselectivity is not only dependent on the difference in formation constants (K_{f}) between a pair of enantiomers with the chiral agents but also is influenced by some experimental factors. Substantially, chiral recognition of enantiomers is the direct result of the transient formation of diastereomeric complex between enantiomeric analytes and the chiral complexing agent (i.e., the difference in formation constants). However, the importance of experimental factors lies in the fact that they can convert the intrinsic difference into the apparent difference in migration velocity along the column. Therefore, the overall selectivity in chiral separation

can be considered to be made up of two contributing factors: the intrinsic difference (intrinsic selectivity) in formation constants of a pair of enantiomers, and the conversion efficiency (exogenous selectivity) of the intrinsic difference into the apparent difference in the migration velocity. According to Eq. 2, these experimental factors may include the equilibrium concentration of a chiral selector, the electric field strength, and the properties of the stationary phase.

In CEC with chiral additives, Eq. 2 shows that there exists a maximum selectivity at the optimal concentration of chiral selector. The optimal concentration is not nly dependent on the formation constants (K_{f1}, K_{f2}) butalso on properties of the column (ϕ and K) {i.e., $[C]_{opt} = \sqrt{(1+\phi K)/K_{f1}K_{f2}}$}.

Unlike in the case of a chiral column, the selectivity in CEC with chiral additives is determined by both partition and electrophoresis, and the electric field either increases or decreases the selectivity. Table 1 summarizes the relationship between the direction of field strength and the electrophoretic mobility of the free and complexed analytes. For PD-CEC, the solvent is mainly driven by pressurized flow; thus, there is no limitation to change the direction of electric field.

For enantioseparation on CSPs in CEC, non-stereospecific interactions, expressed as ϕK, contribute only to the denominator as shown in Eq. 1, indicating that any non-stereospecific interaction with the stationary phase is detrimental to the chiral separation. This conclusion is identical to that obtained from most theoretical models in HPLC. However, for separation with a chiral mobile phase, ϕK appears in both the numerator and denominator Eq. 2. A suitable ϕK is advantageous to the improvement of enantioselectivity in this separation mode. It is interesting to compare the enantioselectivity in conventional CE with that in CEC. For the chiral separation of salsolinols using β-CyD as a chiral selector in conventional CE, a plate number of 178,464 is required for a resolution of 1.5. With CEC (i.e., $\phi K = 10$), the required plate number is only 5976 for the same resolution.[10] For PD-CEC, the column plate number is sacrificed due to the introduction of hydrodynamic flow, but the increased selectivity markedly reduces the requirement for the column efficiency.

Table 1 Relationship between the field strength and the electrophoretic mobility for getting high enantioselectivity in CEC.

Direction of μ_{ep}		Size relationship	
μ_f	μ_c	(absolute value)	Direction of E
+	+	$\mu_f < \mu_c$	+
+	+	$\mu_f > \mu_c$	−
+	−	[a]	−
−	−	$\mu_f < \mu_c$	−
−	−	$\mu_f > \mu_c$	+
−	+	[a]	+

[a]The selection of direction of electric field is not influenced by size relationship in absolute values between the electrophoretic mobility of the free and complexed analytes.

CHIRAL SEPARATION IN CEC

There are different ways of performing chiral separation by CEC. Mayer and Schurig immobilized the chiral selectors by coating or chemically binding them to the wall of the capillary.[11,12] Permethylated β- or γ-CyD was attached via an octamethylene spacer to dimethylpolysiloxane (Chirasil-Dex) as the stationary phase. A high efficiency (~250,000/M) was obtained for the separation of 1,1′-dinaphthyl-2,2′-diyl hydrogenphosphate. An alternative coating approach was developed by Sezeman and Ganzler. Linear acrylamide was coated on the capillary wall, and after polymerization, CyD derivatives were bound to the polymer.[13]

Chiral separation can also be performed with packed capillaries. β-CyD-bonded CSPs that are most frequently used in HPLC and CE were successfully applied in CEC. The separation of a variety of chiral compounds, such as some amino acid derivatives benzoin and hexobarbital was achieved by using CSPs bonded with different CyD derivatives.[14,15] Proteins are not ideal for use as buffer additives in CE because of their large detector response; however, CEC may be a good way to use this type of chiral selectors. Lloyd et al. have performed CEC enantioseparation by using commercially available protein CSPs, such as AGP and HAS.[16,17] The resolution obtained on protein CSPs was good; the efficiency, however, was rather poor. Another HPLC–CSP based on cellulose derivatives has been also reported for enantioseparation by CEC.[18] CSPs modified by covalent attachment of poly-*N*-acryloyl-L-phenylalanineethylester or by coating with cellulose tris(3,5-dimethylphenylcarbamate) can be performed in the reversed-phase mode. Acetonitrile as organic modifier was found to be advantageous for this type of CSP. An anion-exchange-type CSP was recently developed for the separation of N-derivatized amino acids.[19] The new chiral sorbent was modified with a basic *tert*-butyl carbamoyl quinine. Enantioselectivity obtained in CEC was as high as in HPLC and efficiency was typically a factor of 2–3 higher than in HPLC. A recent innovative approach is the use of imprinted polymers as CSPs in CEC.[20,21] Imprinted polymers possess a permanent memory for the imprinted species, and, thus, their enantioselectivity is predetermined by the enantiomeric form of the templating ligand. The use of imprint-based CSPs in HPLC is hampered by their poor chromatographic performance. CEC, however, was found to greatly improve the efficiency of the imprint-based separation. The most successful approach is the use of capillary columns filled with a monolithic, superporous imprinted polymer obtained by

an *in situ* photo-initiated polymerization process. This technique enables imprint-based column to be operational within 3 hr from the start of preparation. Generally, the imprint-based CSPs show high enantioselectivity but somewhat low efficiency and are limited to the separation of very closely related compounds.

Enantioseparation can be achieved on a conventional achiral stationary phase by the inclusion of an appropriate chiral additive into the mobile phase. It is theoretically predicted that the enantioselectivity in CEC with a chiral additive may be higher than that using a chiral column with the same chiral selector.[10] Lelievre et al. compared an HP-β-CyD column and HP-β-CyD as an additive in the mobile phase with an achiral phase (ODS) to resolve chlortalidone by CEC.[22] It was demonstrated that resolution on ODS with the chiral additive was superior on the CSP; however, efficiency was low. With an increasing amount of acetonitrile, the peak shape was improved and the migration time was decreased. We achieved the separation of salsolinol by the use of CEC with β-CyD as a chiral additive in the mobile phase containing sodium 1-heptanesulfonate, as shown in Fig. 1. Salsolinol is a hydrophilic amine and is difficult to enantioseparate due to the small k' values on the reversed stationary phases. Sodium 1-heptanesulfonate was used as a counterion to improve the retention.

In conclusion, CEC has great potential in separation technology. Our theoretical model as well as many published practices in CEC show clearly that the benefit of combining electrophoresis and partitioning mechanisms in CEC is the increase in selectivity for the separation. The intrinsic difference in formation constants is critical, but the experimental factors, such as electric field or the stationary and mobile phases, can also contribute to the improvement of the overall enantioselectivity via increasing the conversion efficiency. However, only when both electrophoretic and partitioning mechanisms act in the positive effects, can high overall enantioselectivity in CEC be obtained.

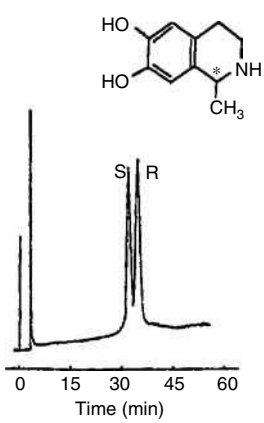

Fig. 1 Electrochromatogram of salsolinol enantiomers on a packed capillary column. Column: ODS-C18, 29 cm (23 cm effective length) × 75 μm I.D.; applied electric field strength: ~250 V/cm; mobile phase: 20 m*M* sodium phosphate buffer (pH 3.0) containing 12 m*M* β-cyclodextrin and 5 m*M* sodium 1-heptanesulfonate. The pump was set at the constant pressure of 100 kg/cm^2.

REFERENCES

1. Tsuda, T.; Nomura, K.; Nagakawa, G. Open-tubular microcapillary liquid chromatography with electro-osmosis flow using a UV detector. J. Chromatogr. **1982**, *248*, 241.
2. Jorgenson, J.W.; Lukacs, K.D. High-resolution separations based on electrophoresis and electroosmosis. J. Chromatogr. **1981**, *218*, 209.
3. Tsuda, T. Direct chiral separations by capillary electrophoresis using capillaries packed with an .alpha.1-acid glycoprotein chiral stationary phase. LC–GC Int. **1992**, *5*, 26.
4. Pretorius, V.; Hopkins, B.J.; Schieke, J.D. J. Chromatogr. **1974**, *99*, 23.
5. Deng, Y.; Maruyama, W.; Kawai, M.; Dostert, P.; Naoi, M. *Progress in HPLC and HPCE*; VSP: Utrecht, 1997; Vol. 6, 301.
6. Boughtflower, R.J.; Underwood, T.; Paterson, C.J. Capillary electrochromatography: some important considerations in the preparation of packed capillaries and the choice of the mobile phase buffers. Chromatographia **1995**, *40*, 329.
7. Yan, C . U.S. Patent 5453163 1995.
8. Taloy, M.R.; Teale, P.; Westwood, S.A.; Perrett, D. Analysis of corticosteroids in biofluids by capillary electrochromatography with gradient elution. Anal. Chem. **1997**, *69*, 2554.
9. Eimer, T.; Unger, K.K.; Tsuda, T. Pressurized flow electrochromatography with reversed phase capillary columns. Fresenius J. Anal. Chem. **1995**, *352*, 649.
10. Deng, Y.; Zhang, J.; Tsuda, T.; Yu, P.H.; Boulton, A.A.; Cassidy, R.M. Modeling and optimization of enantioseparation by capillary electrochromatography. Anal. Chem. **1998**, *70*, 4586.
11. Mayer, S.; Schurig, V. Enantiomer separation by electrochromatography on capillaries coated with chirasil-dex. J. High Resolut. Chromatogr. **1992**, *15*, 129.
12. Mayer, S.; Schurig, V. Enantiomer separation by electrochromatography in open tubular columns coated with chirasil-dex. J. Liquid Chromatogr. **1993**, *16*, 915.
13. Sezemam, J.; Ganzler, K. Use of cyclodextrins and cyclodextrin derivatives in high-performance liquid chromatography and capillary electrophoresis. J. Chromatogr. A, **1994**, *668*, 509.
14. Li, S.; Lloyd, D.K. Packed-capillary electrochromatographic separation of the enantiomers of neutral and anionic compounds using β-cyclodextrin as a chiral selector: effect of operating parameters and comparison with free-solution capillary electrophoresis. J. Chromatogr. A, **1994**, *666*, 321.
15. Wistuba, D.; Czesla, H.; Roeder, M.; Schurig, V. Enantiomer separation by pressure-supported electrochromatography

using capillaries packed with a permethyl-β-cyclodextrin stationary phase. J. Chromatogr. A, **1998**, *815*, 183.
16. Li, S.; Lloyd, D.K. Direct chiral separations by capillary electrophoresis using capillaries packed with an .alpha.1-acid glycoprotein chiral stationary phase. Anal. Chem. **1993**, *65*, 3684.
17. Lloyd, D.K.; Li, S.; Ryan, P. Protein chiral selectors in free-solution capillary electrophoresis and packed-capillary electrochromatography. J. Chromatogr. A, **1995**, *694*, 285.
18. Krause, K.; Girod, M.; Chankvetadze, B.; Blasehk, G. Enantioseparations in normal- and reversed-phase nano-high-performance liquid chromatography and capillary electrochromatography using polyacrylamide and polysaccharide derivatives as chiral stationary phases. J. Chromatogr. A, **1999**, *837*, 51.
19. Lammerhofer, M.; Lindner, W. High-efficiency chiral separations of N-derivatized amino acids by packed-capillary electrochromatography with a quinine based chiral anion exchange type stationary phase. J. Chromatogr. A, **1998**, *829*, 115.
20. Schweitz, L.; Andersson, L.I.; Nilsson, S. Capillary electrochromatography with predetermined selectivity obtained through molecular imprinting. Anal. Chem. **1997**, *69*, 1179.
21. Schweitz, L.; Andersson, L.I.; Nilsson, S. Molecular imprint-based stationary phases for capillary electrochromatography. J. Chromatogr. A, **1998**, *817*, 5.
22. Lelievre, F.; Yan, C.; Zare, R.N.; Gareil, P. Capillary electrochromatography: operation characteristics and enantiomeric separations. J. Chromatogr. A, **1996**, *723*, 145.

Enantioseparation in HPLC: Thermodynamic Studies

Damián Mericko
Jozef Lehotay
Institute of Analytical Chemistry, Slovak University of Technology, Bratislava, Slovakia

INTRODUCTION

Systematic thermodynamic studies with a large set of structurally related compounds can be useful to acquire insight into the separation and retention mechanism using a chiral stationary phase (CSP), or stationary phases in general. In addition, such studies can serve as predictors of expected separation for the enantiomers of analytes based on their structures.

The effect of temperature on the distribution of analytes at infinite dilution between the stationary and the liquid phases is well known. With the respect to all knowledge, it is still interesting to observe how the temperature of a chromatographic column influences the separation. In chromatographic separations, the temperature of the column plays an important role. Hence, the temperature is a critical parameter in chromatography; studying its effect on a separation and retention is the key to understanding the mechanism governing the chromatographic process.

The understanding of mechanistic aspects of chiral recognition in chromatography is important because it allows one to design improved chromatographic systems and it addresses fundamental concepts in chiral recognition also for disciplines outside of separation science.[1]

Temperature has a major impact on retention selectivity (enantioselectivity), resolution, and column efficiency for chromatographic enantiomer separations and can provide valuable information about solute conformational changes, the stationary phase transitions, as well as the chromatographic retention.[2,3]

Earlier results suggest that there are at least two completely different effects of temperature in reversed-phase high-performance liquid chromatography (RP-HPLC) which can affect resolution. One effect changes the separation factor (α), the peak-to-peak separation distance. A decrease in analysis temperature usually results in larger α-values for enantiomeric pairs. This fact is also well known from the general practice of chromatography. This occurs because the partition coefficients and, therefore, the free energy change ΔG of transfer of the analyte between the stationary phase and the mobile phase vary with temperature. This is the *thermodynamic effect*.[4]

In the case of multicomponent or ionisable mobile phases or an ionisable solute, both the distribution of the solvent components and the pK_a of the ionisable compound can also vary with temperature.

Another completely different effect of temperature is the influence on viscosity and on diffusion coefficients. This is largely a kinetic effect, which improves efficiency (i.e., peak width). There are two different mass transfer effects here. One is mobile mass transfer. An increase of temperature reduces the viscosity of the mobile phase. However, an increase of the temperature also increases the diffusion coefficients of the solute in both the mobile phase and the stationary phase (enhancing stationary phase mass transfer).[4]

In many cases, a temperature increase often produces a trade-off for resolution. The increased efficiency is good for resolution, while the lessening of the peak-to-peak separation is bad for resolution.

The temperature can also have the following additional effects that can influence separations:[5]

- Changes in the population of vibrational and rotational energy levels of the chiral solute
- Displacement of solute–solvent equlibria
- Displacement of conformational equlibria, and
- Aggregation and microcrystallization of the chiral solute.

In the case of chiral compounds, especially racemic mixtures, there are also some well-known effects of temperature, such as changing of elution order or coelution of enantiomers due to change of the temperature during the separation.

Moreover, there are many examples of enantiomerization processes which are accelerated by changing the temperature, which are not discussed in this text.

THEORETICAL ASPECTS OF THERMODYNAMIC STUDY

The retention of a solute in a chromatographic system is determined, first, by the magnitude of the distribution coefficient of the solute between the two phases and, second, by the amount of stationary phase available to the solute for interaction. The distribution coefficient in

chromatography is the equilibrium constant and, consequently, it can be treated rationally by conventional thermodynamics.

It follows that the distribution coefficient can be expressed in terms of the *standard energy* of solute exchange between the phases employing the traditional and well-established Arrhenious relationship (Eq. 1).

$$RT \ln K = -\Delta G \quad (1)$$

Now, classical thermodynamics gives another expression for the *free change of energy* (Eq. 2), which separates it into two parts, the *free change of enthalpy* and the *free change of entropy*.

$$\Delta G = \Delta H - T\Delta S \quad (2)$$

The change of enthalpy and change of entropy represent two distinctly different portions of the energy associated with distribution and are related to quite different parts of the distribution processes. The enthalpy term represents the energy involved when the solute molecules break their interactions with the mobile phase and interact with, and enter, the stationary phase. These interactions result from intermolecular forces that are electrical in nature and are accompanied by the absorption or evolution of heat. However, when the solute interacts with the stationary phase, because the interactive forces between the solute and the stationary phase molecules are stronger than those between the solute molecules and the mobile phase, the solute molecules are held more tightly and, consequently, are more restricted. This motion restriction, reduced freedom of movement or loss of randomness is measured as the entropy change. Thus, the free energy change is made up of an actual energy or free enthalpy change resulting from the intermolecular forces between solute and stationary phase and free entropy change that reflects the resulting restricted movement, or loss of randomness, of the solute while preferentially interacting with the stationary phase.

Direct enantiomeric separations are based on the formation of reversible diastereomeric associates or complexes that are created by intermolecular interactions of individual enantiomers with a chiral selector.[6] Diastereomeric association complexes can be depicted as follows (Fig. 1):

A_R and A_S are analytes in R and S configurations. If enantiomeric resolution is observed, the equilibrium

$$CSP + A_R \overset{K_R}{\Leftrightarrow} CSP\text{-}A_R$$

$$CSP + A_S \overset{K_S}{\Leftrightarrow} CSP\text{-}A_S$$

Fig. 1 Formation of diastereomeric association complexes.

(association) constants K_R and K_S have different values. Chromatographic retention depends upon the free energy of the partitioning process of the analyte between the mobile phase and the stationary phase. If the equilibrium constants are denoted by K_R and K_S, respectively, the expression for the change in free energy is as follows:

$\Delta G = -RT \ln K$, Will give the free energy difference :
$\Delta(\Delta G) = \Delta G_R - \Delta G_S$.

The free energy difference, $\Delta(\Delta G)$, can be calculated according Eq. 3 follows (if A_S is less retained analyte, $K_R > K_S$):

$$-\Delta(\Delta G) = RT \ln \frac{K_R}{K_S} \quad (3)$$

where R represents gas constant and T is temperature in Kelvin. Unfortunately, measuring K_R and K_S is not feasible in most cases. To a first approximation, $\Delta(\Delta G)$ can be calculated from the separation factor (α) as follows in Eq. 4:

$$-\Delta(\Delta G) = RT \ln \alpha \quad (4)$$

In the separations of the enantiomers by chromatography, the separation factor (α) is determined by the difference between the free energy of sorption (association) of each enantiomer. From the definition of k' (capacity factor) is clear that $k' = KV_s/V_m$ ($V_s/V_m = \phi$, ϕ is phase ratio of the chromatographic column) and the α value can be given as $\alpha = k'_R/k'_S$, thus, the free energy difference associated with a given α value can be easily computed from chromatographic data.

In certain cases, α values of 30 or more have been found, which then correspond to $\Delta(\Delta G)$ values in the range of 2 kcal/mol (8.4 kJ/mol). Generally, such values are obtained owing to very low retention of the first enantiomer eluted. This means that a very enantioselective sorption process is operating in the column, i.e., one of the enantiomers is virtually unbound by the CSP for steric reasons. Such phenomena are not easily explained by the three-point interaction model, but rather indicate the operation of a sort of "chiral steric exclusion" mechanism, more in line with a "steric fit" concept involving only one binding interaction.[7]

To calculate the thermodynamic parameters and acquire some information for an understanding of enantiomeric retention, selectivity and/or mechanism for the CSP, we need to involve the enthalpy and entropy terms (by an application of the Gibbs–Helmholtz equation: $G = H–TS$) as it is in Eq. 5:

$$\ln \alpha = -\frac{\Delta(\Delta H)}{RT} + \frac{\Delta(\Delta S)}{R} \quad (5)$$

Thus, from a study of the dependence of α on temperature, $\ln \alpha$ may be plotted as a function of $1/T$. This expression of

ln α as a function of $1/T$ is one form of the van't Hoff equation. Using a linear regression model on this kind of dependence, $\Delta(\Delta H)$, from the slope of the line, and $\Delta(\Delta S)$, from the intercept, can be determined. The value of $\Delta(\Delta H)$ represents the difference in change of enthalpy between the couple of enantiomers and $\Delta(\Delta S)$, in turn, difference in change of entropy for a couple of enantiomers, for more and less retained one.

In general, the corresponding $\Delta(\Delta H)$ and $\Delta(\Delta S)$ values can be obtained as the differences $\Delta H_R - \Delta H_S$ and $\Delta S_R - \Delta S_S$, or can be estimated from the selectivity factor (α), which is related to the difference in Gibbs energy of association $\Delta(\Delta G)$ for an enantiomeric pair as was already mentioned. The values of $\Delta(\Delta H)$ and $\Delta(\Delta S)$ obtained by the two methods should be identical within experimental error.[4]

According to this, the van't Hoff plot is usually a plot of either the logarithm of the retention factors (ln k_i') of an analyte or the selectivity factors (ln α) for two analytes vs. the inverse of absolute temperature ($1/T$).

Chromatographic retention is often used to calculate the partial molar enthalpy (ΔH_i) of transfer of solute from the mobile phase to the stationary phase. The transfer enthalpy can be used to characterize or compare various stationary phases using a particular mobile phase. Typically, the transfer enthalpy (ΔS_i) is obtained by invoking a form of the van't Hoff Eq. 6:

$$\ln\ k_i\ =\ \frac{-\Delta H_i}{RT} + \frac{\Delta S_i}{R} + \ln\ \phi \tag{6}$$

where k, ΔH_i, ΔS_i, R, T, and ϕ are the retention factor for the solute, partial molar enthalpy of transfer, partial molar entropy of transfer, the gas constant, the absolute temperature, and the phase ratio (that, is the volume of the stationary phase) (V_s), divided by the volume of the mobile phase (V_m), respectively. The procedure involves plotting ln k' against $1/T$, then setting the slope equal to $-\Delta H_i/R$ and solving for ΔH_i, and enable to determine ΔS_i, from the intercept ($\Delta S_i + \ln \phi$) of the plot. The limitation of this determination relates to the calculation of ΔS_i from the intercept, because it requires the knowledge of the phase ratio ϕ. When the dead volume of the column and the technical data are known, the phase ratio (ϕ) can be calculated.

The problem may often occur in the case of a commercial stationary phase. For example, in the case of RP-HPLC, if the information about bonding chemistry, starting silica, and surface coverage for commercial stationary phases is not available, it is typically not possible to calculate the phase ratio. In addition, since the bonding density of commercial columns is usually not accurately known, it is virtually impossible to assess the role of surface coverage, and more broadly, the stationary phase, on the retention mechanism.[8,9]

Dorsey and Cole[10] have published the way of calculation of phase ratio in RP-HPLC. They used monomeric (self prepared and packed) C_{18}, stationary phases. The volume of the stationary phase (V_s) was determined using the following Eq. 7:

$$V_s = \frac{(\%C)(M)(W_p)}{(100)(12.011)(n_C)(\rho)} \tag{7}$$

where %C is the carbon loading as determined from elemental analysis, M is the molecular weight of the bonded alkyl ligand (g/mol), W_p is the weight of the bonded packing contained in the chromatographic column, n_C is the number of the carbons in the alkyl ligand, and ρ is the density (g/cm^3). V_m was determined by using the gravimetric method with methylene chloride and methanol as the two pure liquids. They assumed that V_m for these columns would be essentially constant (within experimental error), since they were all prepared using the same starting silica.

The advantage of using van't Hoff plot of the logarithm of the enantioselectivity factor (ln α) vs. reciprocal absolute temperature ($1/T$) is that it does not require the knowledge of phase ratio for determination $\Delta(\Delta H)$ and $\Delta(\Delta S)$ values. In turn, it does not bring a solution of determination of the entropy of the solute transfer from the mobile phase to stationary phase (ΔS_i).

LINEAR VAN'T HOFF BEHAVIOR

In general, van't Hoff equation assumes that there is a single adsorption mechanism (hence, that the surface is homogeneous). The plot of ln k vs. $1/T$ is linear only if the associated thermodynamic parameters, ΔH and ΔS, are invariant with temperature changes. According to Gritti and Guiochon,[11] these assumptions are not likely to be fulfilled in reversed phase liquid chromatography (RPLC). First, they showed that RP-HPLC stationary phases are heterogeneous. Secondly, it is known that the structure of the alkyl bonded chains changes somewhat with temperature. Despite this, a majority of the plots of ln k' vs. $1/T$ found in the literature are mainly linear, or nearly so. Finally, the issue of linearity or non-linearity of van't Hoff plots is often matter of temperature range of thermodynamic study. According to previous considerations, there are two basic forms (of decrease of analyte retention with increasing temperature) that the linear van't Hoff curve can take. These two types of curves relate to the two basic types of chromatography.

The first is *interactive* (system A) chromatography where the major retentive mechanism results from solute phase interactions and the second *exclusion* (system B) chromatography, where the major retention mechanism depends on the amount of stationary phase available to each solute.[12]

For system A, it is characteristic to have a relatively very large enthalpy contribution (the slope of the van't Hoff curve is steep) with, conversely, a very low entropy contribution (the intercept is relatively small). The large value of the slope means that molecular forces dominate the distribution in favor of the stationary phase. It can be said that molecules are retained in the stationary phase as a result of molecular interactions. Thus, the change in enthalpy is the major contribution to the change in free energy and it can be said, *in thermodynamic terms*, *the distribution is energy driven*.

System B, in turn, seems to be a completely different type in comparison with system A. In this distribution system, there is a very high entropy contribution in comparison with the entropy contribution in system A. On the other hand, this distribution system shows a relatively small enthalpy contribution; in comparison with system A. Molecular forces do not dominate this distribution system. The elatively large entropy change is a measure of the loss of randomness or freedom that happens when the solute molecule transfers from one phase to the other. The more random and "more free" the solute molecule is in a particular environment, the greater will be its entropy in that environment. The large entropy change shown in system B indicates that the solute molecules are more constrained in the stationary phase (i.e., confined in the pores of the exclusion medium) than they were in the mobile phase. This restriction is responsible for the greater distribution of the solute in the stationary phase and its greater retention. Because the change in entropy is the major contribution to the change in standard energy, *in thermodynamic terms*, *the distribution is entropically driven.*

It is important to understand that chromatographic separations cannot be exclusively *energetically driven* or *entropically driven*; both components will always be present to a greater or lesser extent. It is by the careful adjustment of both the *energetic* and *entropic* components of a distribution that very difficult and subtle separations can be accomplished.[12] For both systems, there is characteristic plus value of the slope, which means that the process of molecule transfer between the stationary and mobile phase has negative value of change of enthalpy and the heat energy is released. Then it is clear that, in this case, the increase of the temperature is responsible for a decrease in retention and usually in enantioselectivity as well.

However, if the van't Hoff plots are linear, it indicates that the retention and/or selective processes governing the separation are unchanged over the temperature range studied. Furthermore, it can be assumed that a separation is a) thermodynamically reversible, b) (ΔH) and (ΔS) values are temperature independent, c) the enantiomers are retained in single associative mechanism, and d) a solvation–desolvation equilibrium does not obscure the association process of the enantiomers with the CSP.[13]

Enantioselective retention mechanisms are sometimes influenced by temperature to a greater extent than ordinary reversed-phase separations. Péter et al.[4] show some examples of how strongly can chiral recognition be dependent upon the temperature. It is must not be just in the case of separation of amino acid enantiomers by a chiral ether stationary phase, but it can be observed also on other CSPs, such as cyclodextrins, α_1-glycoprotein, and chiral macrocyclic antibiotics. Peter et al. explored the effect of the temperature on retention of β-methyl amino acids using teicoplanin CSP. They observed linear van't Hoff plots in the studied temperature range, 1.5–50°C. They suggested that the values of the thermodynamic parameters depend upon the structures of the compounds. They found that chiral recognition and enantioselective retention results from the distinct hydrogen-bonding, steric, and hydrophobic interactions that occur when two amino acid enantiomers are retained at the same CSP site. From the structure of the teicoplanin CSP, it is clear that the main contributor leading to the retention of both enantiomers on this CSP is the charge–charge interaction between the carboxylate group of the amino acid and the ammonium group of the teicoplanin molecule. Sun et al.[14] showed how chiral selectivity can be improved when simultaneously vancomycin as CSP and vancomycin as chiral mobile phase additive are used. They summarized that, with increasing concentration (up to 2 mmol/L) of vancomycin, a favorable effect on selectivity and an increase in enantiomeric resolution of warfarin, fluorbiprofen, and ketoprofen is observed. They observed a significant increase in the enthalpy and entropy differences between the two enantiomers for some very polar compounds, which indicates a change of the retention mechanism for the CSP-analyte.

In general, it is widely known that decreasing the temperature improves the separation, except for some anomalous behaviors. Takagi et al.[15] explored the effect of the temperature on chiral and achiral separations of diacylglycerol derivatives by HPLC using a commercial sumichiral OA-4100 chiral column. They observed a linear relationship between the logarithm of the enantioselectivity factor and the reciprocal of the absolute temperature. They assumed that, in a case of the use of hexane-1,2-dichloroethane as a mobile phase, the separation by carbon number is controlled by entropy differences, whereas separation by double bond number is based on the enthalpy contributions. In addition, they assumed that separation according to carbon number is nearly independent of the temperature, whereas that according to the number of the double bonds is dependent upon the temperature.

The isocratic retention of enantiomers of chiral analytes, e.g., tryptophan, 1,2,3,4-tetrahydroisoquinoline and γ-butyrolactone analogs, was studied on ristocetin A CSP at different temperatures and with various mobile phases. A linear dependence of van't Hoff plots was

observed. According to negative ΔH_i values for all enantiomers, Peter et al.[16] assumed that the transfer of the enantiomers from the mobile to the stationary phase is enthalpically favored. For all studied compounds in reversed phase mode (four different RP mobile phase of 0.1% TEAA–MeOH were used; 80:20, 60:40, 40:60, and 20:80), the change of enthalpy for the second-eluted isomer was always greater (i.e., more negative) than that for the first-eluted isomer. Probably, this means that the association between the second-eluted enantiomer and the CSP is more favorable than for the first enantiomer. In the case of $\Delta(\Delta H_i)$, the more negative value means that the interactions for these analytes are enthalpically favored. On the other hand, the more negative difference in entropy change can be explained by the fact that the difference in degrees of freedom of these enantiomers on the CSP is larger.

The influence of temperature on the performance of an enantioselective anion-exchange type chiral selector was investigated.[2] The resolution of 23 *N*-acylated amino acid Selectands (SAs) enantiomers was studied under linear chromatographic conditions over temperature range of 0–85°C with hydro-organic buffers (pH 6) as mobile phases on a covalently immobilized quinine *tert*-butylcarbamate chiral stationary phase. Using the quinine *tert*-butylcarbamate derived chiral stationary phase, the enantioselective interaction of *N*-acylated amino acids is strongly enthalpy-driven. The thermodynamics of enantioselective adsorption is correlated to structural and electronic properties of the *N*-acyl group and the side chain of the SAs.

Armstrong et al.[17] have studied the effect of temperature (carried out from 0°C to 45°C) on resolution behavior of proglumide, 5-methyl-5-phenylhydantoin, and *N*-carbamyl-D-phenyl-alanine on a vancomycin column. It has been observed that values of k, α, and resolution factor for all the three studied molecules have decreased with the increase in temperature, indicating the enhancement of chiral resolution at low temperature.

By varying the column temperature, linear van't Hoff for D,L-dansyl amino acids retention and enantioselectivity using immobilized human serum albumin as CSP were acquired and thermodynamic parameters were calculated. These linear behaviors were thermodynamically what was expected when there was no change in retention and enantioselective interactions over the temperature range (20–40°C) studied.[18]

Ding et al.[19] described the chiral separation of enantiomers of several dansyl-amino acids by HPLC in the reversed-phase mode. The natural logarithms of selectivity factors ($\ln \alpha$) of all the investigated compounds depended linearly upon the reciprocal of temperature ($1/T$). For most processes of enantioseparation, enantioselectivity, α, decreased with increasing of temperature, and the processes of chiral recognition were enthalpy-controlled. It is very interesting that enantioselectivity, α, increased with increasing temperature for dansyl-threonine (Dns-Thr) at a pH of 7.0; the enthalpy and entropy differences were all positive, indicating that the process of chiral recognition was controlled entropically. It can be concluded that the chiral recognition mechanisms are different for Dns-Thr at different pH's.

Usually, as most HPLC separations are enthalpy controlled, with prominal, a special case was found where the temperature dependence of the separation is entropy controlled. Thermodynamic data for chiral separation of prominal showed a straight line with a negative slope of $\ln \alpha$ vs. $1/T$.[20]

There have also been published other cases of inverse dependencies, with negative slope and with positive value of ΔH_i (so called anomalous behavior). They may occur, for example, in a case of separation of some bases in RP-HPLC. Their retentions increase with increasing the temperature. This may be due to a decrease in the pK_a's of the bases with temperature and, so, the change in protonization with the temperature may contribute to anomalous retention effects.[21]

Yan Lu et al.[22] observed another dramatic example. They used molecularly imprinted polymers (MIPs) as stationary phases for the study of chiral recognition in an aqueous environment. Thermodynamic studies at different pH (pH_{app} 6.4 and pH_{app} 4) revealed that the interaction between the pyridyl group of 4-L-phenylalanylamino-pyridine (4-L-PheNHPy) and the carboxylic acid group on the MIPs is also strong, implying that it also plays a profound role in determining the highly chiral selectivity of MIPs. In addition, it confirmed a different retention mechanism of 4-L-PheNHPy at different pH's of the mobile phases. Whereas, at pH_{app} 6.4, a linear van't Hoff plot showed an increase of $\ln k'$ with increasing temperature, in the case of pH_{app} 4, there was observed a completely inverse dependence. The decrease of $\ln k'$ with increasing temperature at pH_{app} 4 is attributed to enthalpy gained from the binding that is less than the enthalpy lost during the desolvation, which resulted in an endothermic process.

CHANGES IN ELUTION ORDER

In the case of enantioseparation, the slope of the straight van't Hoff line will then be proportional to the enthalpy difference, and $\ln \alpha = 0$ (the individual enantiomers will coelute) will give the temperature at which the enthalpy and entropy contributions cancel each other.[23] This temperature is known as the enantioselective temperature (T_{iso}) and can be defined as in Eq. 8. At this temperature, $\Delta(\Delta G) = 0$ and the enantiomers are not separated. Above T_{iso}, an inversion in the elution order of the enantiomers is expected. Knowing the T_{iso} of certain analytes under given experimental conditions might be helpful for

the determination of optical purities, as the elution order will be reversed.[13]

$$T_{iso} = \frac{\Delta(\Delta H)}{\Delta(\Delta S)} \quad (8)$$

This phenomenon has been mostly observed in gas chromatography (GC) at relatively high temperature (in comparison with HPLC, which is usually performed at relatively low temperatures), because solvation effects are essentially absent. Despite this, also in HPLC, some cases of change in elution order of the enantiomers have been achieved.[24]

Hermansson and Schill,[25] in 1988, first reported the inversion of the enantiomeric elution order for pseudoephedrine occurring on an α_1-acid glycoprotein-based (AGP) column with the addition of octanoic acid to the eluent. These effects might be due to a blocking of one or more of several chiral binding sites and conformational change of the protein as a consequence of variation of the properties of the mobile phase.

Later, in 1990, Haginaka[26] observed the inversion of the elution order of propanolol (PP) and its ester derivates (*O*-acetyl, -propyl, -butyl, and valeryl PP) on an ovomucoid-bonded column.

Pirkle and Murray[27] first reported the temperature-dependent elution order reversal in PI-basic proline-derivatized CSPs in 1993. They used (*RS*)-*N*-(3,5-dinitrobenzoyl)-α-phenylethylamine as the solute to investigate the response of the chromatographic behavior by changing the temperature on the CSP.

The reversal of enantiomeric elution order for the polysaccharide CSP was first reported by Okamoto et al. in 1991.[28] They found that the reversal of the elution order of the enantiomers on a modified cellulose column was associated with changes in the mobile phase modifiers during the investigation of the direct chromatographic enantioseparation of pyriproxyfen, an insect growth regulator. If one can find such phenomena, although very rare in HPLC, it will be important to understand the reasons for this behavior and to anticipate when such inversions of elution order are likely to occur.

The temperature is the determining factor for the discrimination process of (*R*)-(−) and (*S*)-(+)-sotalol by immobilized cellobiohydrolase 1 (CBH 1), as it influences, not only the extent, but also the sign of enantioselectivity. An inversion of the enantiomeric elution order was also induced by changes in the organic modifier added to the buffer solution.[29]

The presented examples emphasize the importance of careful temperature control in order to achieve reproducible separations in chiral chromatography. Although reversals in enantioselectivity are rare in HPLC, general predictions of the enantiomeric elution order on CSPs should be critically considered, especially if the extent of chiral recognition is marginal.

NON-LINEAR VAN'T HOFF BEHAVIOR

Since many of the studies showing linear van't Hoff behavior were conducted over a narrow temperature range (typically 20–50°C), it is possible that the deviation from linearity usually observed at about 20–25°C might have been missed.[8,9] On the other hand, if the stationary phase in HPLC undergoes a change in conformation at a certain temperature (transition temperature), the enthalpy and entropy of retention process will change, and non-linear van't Hoff plots will be obtained. Since both enthalpy and entropy of adsorption are influenced by any changes in solvation, which accompany analyte adsorption, it is conceivable that mobile phase composition might influence not only the magnitude, but also the sign of $\Delta(\Delta G)$. This implies that the elution order of a particular pair of enantiomers from a given CSP in HPLC could be mobile phase dependent.[13]

Despite the fact that van't Hoff plots are usually linear, Pirkle[30] showed that van't Hoff plots data obtained by temperature study of conformationally rigid spirolactam 1 are non-linear. The combination of using mobile phases of hexane containing 20, 10, or 5% (v/v) 2-propanol and use of CSP derived from (*R*)-*N*-(3,5-dinitrobenzoyl)phenylglycine for separation of spirolactam is responsible for the curvature of van't Hoff lines. At low temperatures, residual silanol groups and strands of bonded phase adsorb the 2-propanol. The lack of strong dependence of ΔH on 2-propanol concentration suggests that the stationary phase and analytes are saturated with 2-propanol below 25°C, even when 2.5% 2-propanol is present. As the temperature increases, thermal desorption of 2-propanol leads to the formation of sites at which analyte adsorption is more exergonic, owing to the reduced need to displace 2-propanol. This can increase retention of the analyte provided the magnitude of the effect is sufficiently great.

In general, non-linear van't Hoff behavior may be indicative of a change in the mechanism of retention. Basically, any reversible process which alters the enthalpy and entropy of adsorption can, in principle, give rise to non-linear van't Hoff plots. Dissociative processes, such as ionisation, change in conformation, or changes in the extent to which the mobile phase interacts with either the analyte or stationary phase are examples of such reversible processes. In addition, the presence of multiple types of retention mechanisms or multiple types of binding sites may also lead to non-linear van't Hoff plots.[30]

Another example of curvature of van't Hoff plots relates to irreversible changes in the conformation of carbamate-derivatized amylose and cellulose CSP, which was observed for the normal-phase separation of the enantiomers of a dihydropyrimidinone acid and methyl ester. The apparent conformational change was thermally induced and depended upon the polar component of the mobile phase. The irreversible change in the conformation of

these CSPs, caused by modifiers and temperature, can also play an important role in projecting large-scale enantioseparation, such as simulated moving bed (SMB) chromatography.[31]

If the van't Hoff plot ($\ln k_i'$ vs. $1/T$) is not a straight line, it is often presumed that ΔH_i varies with temperature; ΔH_i is then evaluated from the slope at any particular $1/T$ value. This is valid if the phase ratio (ϕ) is constant with respect to temperature. Chester and Coym[32] have considered two questions regarding the interpretation of van't Hoff plots: if linearity is observed, does it imply that ΔH_i is constant with temperature (or does curvature imply that ΔH_i changes with temperature)? Is the phase ratio constant and does it have any influence on the curvature or slope of a van't Hoff plot?

They showed that, when the possibility of change in the phase ratio is considered, it becomes apparent that, nonlinear van't Hoff behavior may, or may not, be due to changes in enthalpy or entropy. Considering the molecular difference between two solutes instead of the solutes themselves can eliminate the phase ratio influence. Some cases show that in the resulting selectivity, van't Hoff plots may be linear, even when the van't Hoff plots of solutes are nonlinear. In such cases, temperature-dependent phase ratio changes, and not necessarily changes in the transfer enthalpy, may be responsible for the curved van't Hoff plots of individual solutes. In addition, the different solutes in RP-HPLC may also be responsible for different thermodynamic phase ratios.

ENTHALPY–ENTROPY COMPENSATION

Despite the fact that, in some cases, small differences in ΔH and ΔS can be observed (for various solutes, but on the same column with the same mobile phase), these differences could be found to be essentially insignificant when compared to a change in stationary-phase bonding density using enthalpy–entropy compensation. Enthalpy–entropy compensation is a term used to describe a compensation temperature, which is system independent for a class of similar experimental systems.[10,33] Melander et al.[34] have used the enthalpy–entropy compensation method in studies of hydrophobic interactions and separation mechanisms in reversed phase HPLC. Mathematically, enthalpy–entropy compensation can be expressed by the formula 9:

$$\Delta H_i = \beta \Delta S_i + \Delta G_\beta \tag{9}$$

where ΔG_β is the Gibbs free energy of the enantiomeric interactions (physicochemical interaction) in the chromatographic system at the compensation temperature (β), (β and ΔG_β are constants). The values of ΔH and ΔS are the corresponding changes in enthalpy and entropy, respectively. According to Eq. 7, when enthalpy–entropy compensation is observed with a group of compounds in a particular chemical transformation (or interaction in the case of chromatographic retention), all of the compounds have the same ΔG_β at the compensation temperature β. For example, if enthalpy–entropy compensation is observed in liquid chromatography (LC) or GC for a group of compounds, all the compounds will have the same net retention at the compensation temperature β, although their temperature dependencies may differ.[17] In order to express the free energy change ΔG_T measured at a given temperature T, the Gibbs–Helmholtz relationship can be rewritten using Eq. 10.

$$\Delta G_T = \Delta H\left(1 - \frac{T}{\beta}\right) + \frac{(T\Delta G_\beta)}{\beta} \tag{10}$$

Eq. 8 shows that a plot of ΔG_T for different compounds at a constant temperature T vs. the corresponding ΔH_i produces a straight line, and the compensation temperature β can be evaluated from the slope. Combination of Eqs. 6 and 9 leads to Eq. 11, which shows that plots of $\ln k_i'$ on $-\Delta H_i$ can be used to determine the compensation temperature β.

$$\ln k_i = \frac{-\Delta H_i}{R}\left(\frac{1}{T} - \frac{1}{\beta}\right) - \frac{\Delta G_\beta}{R_\beta} + \ln \phi \tag{11}$$

A similarity in values for the compensation temperature suggests that the solutes are retained by essentially identical interaction mechanisms and, thus, the compensation study is a useful tool for comparing retention mechanisms in different chromatographic systems.[35,36]

In addition, calculation of compensation temperature can be also used in order to compare GC and LC retention processes and, therefore, enthalpy–entropy compensation theory is often applied.[37]

CONCLUSION

There are many parameters which control the enantiomeric resolution by HPLC. The most important of them include parameters of the stationary phase, such as particle size of CSP, pore size of column, and kind of chiral selector, composition, and pH of the mobile phase, flow rate of mobile phase, and temperature. Systematic variation of column temperature should be considered as one way to improve chiral separations in HPLC. From the practical point of view, it is easier to vary column temperatures than mobile phase composition. In addition, variable temperature runs can provide useful information concerning the thermodynamic parameters for the CSP–analyte interactions. The effect of temperature on the resolution

and selectivity factors for a set of structurally related chiral compounds is often interpreted using van't Hoff plots generated from the chromatographic data. The study of temperature effects helps to estimate the interaction/separation behavior on the CSP and is the key to understanding the mechanism governing the chromatographic process.

REFERENCES

1. Špánik, I.; Krupčík, J.; Schurig, V. Comparison of two methods for the gas chromatographic determination of thermodynamic parameters of enantioselectivity. J. Chromatogr. A, **1999**, *843*, 123.
2. Oberleitner, W.R.; Maier, N.M.; Lindner, W. Enantioseparation of various amino acid derivatives on a quinine based chiral anion-exchange selector at variable temperature conditions. Influence of structural parameters of the analytes on the apparent retention and enantioseparation characteristics. J. Chromatogr. A, **2002**, *960*, 97–108.
3. Zarzycki, P.K. Simple chamber for temperature-controlled planar chromatography. J. Chromatogr. A, **2002**, *971*, 193–197.
4. Péter, A.; Török, G.; Armstrong, D.W.; Tóth, G.; Tourwé, D. Effect of temperature on retention of enantiomers of β-methyl amino acids on a teicoplanin chiral stationary phase. J. Chromatogr. A, **1998**, *828*, 177.
5. Ahuja, S. *Chiral Separation by Chromatography*; ACS: Washington, DC, 2000; 112.
6. Feibush, B.; Gil-Av, E. Interaction between asymmetric solutes and solvents: peptide derivatives as stationary phases in gas liquid partition chromatography. Tetrahedron **1970**, *26*, 1361.
7. Allenmark, S. *Chromatographic Enantioseparation, Methods and Applications*; 2nd Ed.; Ellis Horwood: New York, 1991.
8. Tchapla, A.; Heron, S.; Colin, H.; Guiochon, G. Role of temperature in the behavior of a homologous series in reversed phase liquid chromatography. Anal. Chem. **1988**, *60*, 1443–1448.
9. Yamamoto, F.M.; Rokushika, S.; Hatano, H. Comparison of thermo-dynamic retention behavior on various C 18 columns different in their hydrophobicity. J. Chromatogr. Sci. **1989**, *27*, 704–709.
10. Cole, L.A.; Dorsey, J.G. Temperature dependence of retention in reversed-phase liquid chromatography. 1. Stationary-phase considerations. Anal. Chem. **1992**, *64*, 1317–1323.
11. Gritti, F.; Guiochon, G. Critical contribution of non-linear chromatography to the understanding of retention mechanism in reversed-phase liquid chromatography. J. Chromatogr. A, **2005**, *1099*, 31.
12. Beesley, T.E.; Scott, R.P.W. *Chiral Chromatography*; Wiley: New York, 1998.
13. Okamoto, M. Reversal of elution order during the chiral separation in high performance liquid chromatography. J. Pharm. Biomed. Anal. **2002**, *27*, 401–407.
14. Sun, Q.; Olesik, S.V. Chiral separation by simultaneous use of vancomycin as stationary phase chiral selector and chiral mobile phase additive. J. Chromatogr. B, **2000**, *745*, 159–166.
15. Takagi, T.; Suzuki, T. Effect of temperature on chiral and achiral separations of diacylglycerol derivatives by high-performance liquid chromatography on a chiral stationary phase. J. Chromatogr. A, **1992**, *625*, 163–168.
16. Péter, A.; Vékes, E.; Armstrong, D.W. Effects of temperature on retention of chiral compounds on a ristocetin A chiral stationary phase. J. Chromatogr. A, **2002**, *958*, 98–107.
17. Armstrong, D.W.; Tang, Y.; Chen, S.; Zhou, Y.; Bagwill, C.; Chen, J.R. Macrocyclic antibiotics as a new class of chiral selectors for liquid chromatography. Anal. Chem. **1994**, *66*, 1473–1484.
18. Peyrin, E.; Guillaume, Y.C. Effect of tetrabutylammonium chloride as eluent modifier on the retention and enantioselectivity of D,L-dansyl amino acids using immobilized human serum albumin. Talanta **1999**, *49*, 415–423.
19. Ding, G.S.; Liu, Y.; Cong, R.Z.; Wang, J.D. Chiral separation of enantiomers of amino acid derivatives by high-performance liquid chromatography on a norvancomycin-bonded chiral stationary phase. Talanta **2004**, *62*, 997–1003.
20. Cabrera, K.; Lubda, D. Influence of temperature on chiral high-performance liquid chromatographic separations of oxazepam and prominal on chemically bonded β-cyclodextrin as stationary phase. J. Chromatogr. A, **1994**, *666*, 433–438.
21. McCalley, D. Effect of temperature and flow-rate on analysis of basic compounds in high-performance liquid chromatography using a reversed-phase column. J. Chromatogr. A, **2000**, *902*, 311–321.
22. Lu, Y.; Li, Ch.; Zhang, H.; Liu, X. Study on the mechanism of chiral recognition with molecularly imprinted polymers. Anal. Chem. Acta **2003**, *489*, 33–43.
23. Stringham, R.W.; Blackwell, J.A. Factors that control successful entropically driven chiral separations in SFC and HPLC. Anal. Chem. **1997**, *69*, 1414–1420.
24. Pirkle, W.H.; Pochapsky, T.C. Considerations of chiral recognition relevant to the liquid chromatography separation of enantiomers. Chem. Rev. **1989**, *89*, 347–362.
25. Hermansson, J.; Schill, G. Resolution of enantiomeric compounds by slica-bonded α_1-acid glycoprotein. In *Chromatographic Chiral Separation*; Zief, M., Crane, L.J., Eds.: Marcel Dekker: New York, 1988; 245.
26. Haginaka, J.; Wakai, J.; Takahashi, K.; Yasuda, H.; Katagi, T. Chiral separation of propranolol and its ester derivatives on an ovomucoid-bonded silica: influence of pH, ionic strength and organic modifier on retention, enantioselectivity and enantiomeric elution order. Chromatographia **1990**, *29*, 587–592.
27. Pirkle, W.H.; Murray, P.G. An instance of temperature-dependent elution order of enantiomers from a chiral brush-type HPLC column. J. High Resol. Chromatogr. **1993**, *16*, 285–288.

28. Okamoto, M.; Nakazawa, H. Reversal of elution order during direct enantiomeric separation of pyriproxyfen on a cellulose-based chiral stationary phase. J. Chromatogr. A, **1991**, *588*, 177–180.
29. Fulde, K.; Frahm, A.W. Temperature-induced inversion of elution order in the enantioseparation of sotalol on a cellobiohydrolase I-based stationary phase. J. Chromatogr. A, **1999**, *858*, 33–43.
30. Pirkle, W.H. Unusual effect of temperature on the retention of enantiomers on a chiral column. J. Chromatogr. A, **1991**, *558*, 1–6.
31. Wang, F.; O'Brien, T.; Dowling, T.; Bicker, G.; Wyvratt, J. Unusual effect of column temperature on chromatographic enantioseparation of dihydropyrimidinone acid and methyl ester on amylose chiral stationary phase. J. Chromatogr. A, **2002**, *958*, 69–77.
32. Chester, T.L.; Coym, J.W. Effect of phase ratio on van't Hoff analysis in reversed-phase liquid chromatography, and phase-ratio-independent estimation of transfer enthalpy. J. Chromatogr. A, **2003**, *1003*, 101–111.
33. Boots, H.M.J.; de Bokx, P.K.J. Theory of enthalpy–entropy compensation. Phys. Chem. **1989**, *93*, 8240–8243.
34. Melander, W.; Campbell, D.E.; Horvath, Cs. Enthalpy–entropy compensation in reversed-phase chromatography. J. Chromatogr. A, **1978**, *158*, 215.
35. Berthod, A.; Li, W.; Armstrong, D.W. Multiple enantioselective retention mechanisms on derivatized cyclodextrin gas chromatographic chiral stationary phases. Anal. Chem. **1992**, *64*, 873–879.
36. Krug, R.R.; Hunter, W.G.; Grieger, R.A. Enthalpy–entropy compensation. 1. Some fundamental statistical problems associated with the analysis of van't Hoff and Arrhenius data. J. Phys. Chem. **1976**, *80*, 2335.
37. Limsavarn, L.; Dorsey, J.G. Influence of stationary phase solvation on shape selectivity and retention in reversed-phase liquid chromatography. J. Chromatogr. A, **2006**, *1102*, 143–153.

End Capping

Kiyokatsu Jinno
Department of Materials Science, Toyohashi University, Toyohashi, Japan

INTRODUCTION

A typical stationary phase for chromatography, especially liquid chromatography (LC), is a chemically alkyl (C_{18})-bonded phase on silica gel particles. For the preparation of this type of bonded phase, alkylsilane is used to react with the silica gel surface by a silane-coupling reaction. In order to perform this synthesis, the silica gel to be bonded is treated to remove heavy metals and to prepare the surface for better bonding. Generally, only one of the functional groups bonds to form a Si–O–Si bond. Less often, two of the functional groups react to form adjacent Si–O–Si bonds. The remaining functional groups on each reagent molecule hydrolyze to form Si–O–H groups during workup, following the initial reaction. These groups, however, which form with the di- and tri- functional reagents, can cross-link with one another near the surface of the silica gel support. Thus, bonded phases made with any di- or tri- functional reagents are termed "polymeric" phases. A monofunctional silane reagent can only bond to the silanols and any excess is washed free as the ether resulting from hydrolysis of the reagent. Any packing made with a monofunctional silane reagent is referred to as a "monomeric" bonded phase. These schemes are summarized in Fig. 1a(i) and (ii). Other chemically bonded phases, such as cyano-, amino-, and shorter or longer alkyl phases are synthesized by similar bonding chemistries.

DISCUSSION

The products made by the above synthetic processes still have large numbers of residual silanols, which lead to poor peak shapes or irreversible adsorption, because chemically bonded groups on the silica gel surface have large, bulky molecular sizes and, after the bonding, the functionalized silane cannot react with the silanols around the bonded ligands. Because such alkyl-bonded phases are used for reversed-phase (RP) separations, especially for chromatography of polar molecules, any silanol groups that remain accessible to solutes after the bonding are likely to make an important contribution to the chromatography of such solutes; this is generally detrimental to the typical RP LC separations. It is a common fact that the residual silanols produce peak tailing for highly polar compounds which will interact with these silanol groups with deleterious effects. Therefore, the attempt to reduce the number of residual silanols on the silica gel is a common procedure in the preparation of chemically bonded stationary phases, where the surface of a RP material is ensured to be uniformly hydrophobic, for example, by blocking residual silanol groups with some functional groups. This process is the so-called "end capping." The end-capping process is possible with a smaller molecule than alkylchlorosilanes, such as a trimethyl-substituted silane (from trimethylchlorosilane or hexamethyldisilazane) as seen in Fig. 1a(iii). Because the molecular weights of these reagents are small, they do not add much to the total percent carbon, compared with the initial-bonded phase. It must be known that all chemically bonded phases on silica gel cannot be end-capped by this process, because the above reagents can react with diol and amino phases, and not only with silanol groups on the surface. To block, end cap, and then unblock these phases would be very time-consuming and too expensive to be practical. If the final-bonded phase is, in fact, a diol, this silane-bonding reagent is made from glycerol and has the structure Si–O–CHOH–CH_2OH. The cyano or amino phases are most often attached with a propyl group between the silicon atom and the CN or NH_2 group.

Often, when various bonded phases are studied for suitability for a particular separation, the question arises as to which is bonded most completely. This is a common question, because all phases, no matter how they are bonded, will have some residual silanols, even after an end-capping process. It is impossible for the bulkier bonding reagents to reach any but the most sterically accessible silanols. It is much easier for the smaller solutes to reach the silanols, however, and be affected by them. The final surface of the silica gel has three different structures, as demonstrated in Fig. 1b(i), (ii), and (iii), for a monomeric C_{18}, end capped by trimethylchlorosilane and residual silanols, respectively.

The presence of residual silanol groups can be detected most readily by using Methyl Red indicator,[1] which turns red in the presence of acidic silanol groups, but a more sensitive test is to chromatograph a polar solute on the RP material.

To test, chromatographically, any phase for residual silanols, the column has to be conditioned with heptane or hexane (which has been dried overnight with spherical 4A molecular sieves). The series of solvents to use if the column has been used with water or a water-organic-mobile phase, such as water → ethanol → acetone → ethyl acetate → chloroform

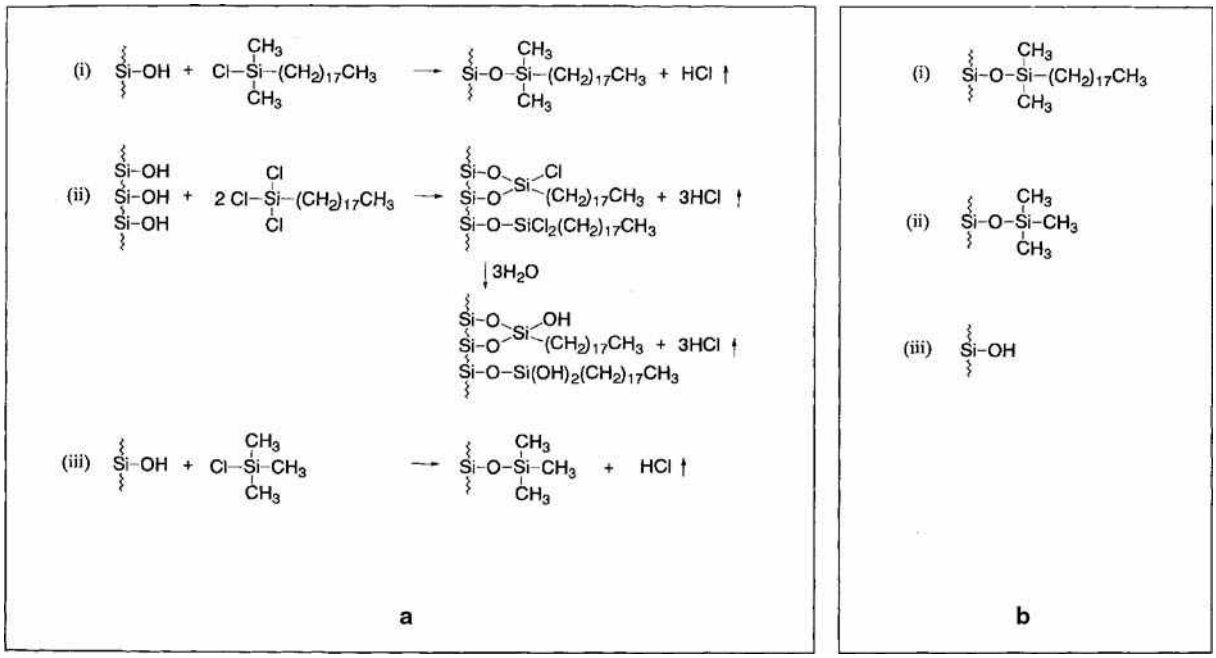

Fig. 1 a, Scheme of bonding chemistry for chemically bonded C_{18} silica phase: (i) synthesis of monomeric C_{18}; (ii) synthesis of polymeric C_{18}; (iii) end-capping process. b, Surface structure of a monomeric C_{18} phase: (i) monomeric C_{18} ligand; (ii) end-capped trimethyl ligand; (iii) residual silanol.

→ heptane. Once activated, a sample of nitrobenzene or nitrotoluene is injected, eluted with heptane or hexane, and detected at 254 nm. The degree of retention is then a sensitive guide to the presence or absence of residual silanols; if the solute is essentially unretained, the absence of silanols may be assumed. The better the bonding, the faster the polar compound will be eluted from the column. A well-bonded and end-capped phase will have a retention factor of between 0 and 1. Less well-covered silicas can have retention factors greater than 10. This is a comparative test, but it can also be useful for examining a phase to see if the end-capping reagent or primary phase has been cleaved by the mobile phase used over a period of time. Other methods to measure the silanol content of silica and bonded silica have been discussed by Unger.[2] Solid-state nuclear magnetic resonance spectrometry is the most powerful method to identify the species of residual silanol groups on the silica gel surface.[3]

In order to avoid the contribution of the residual silanols to solute retention, many packing materials that should not have silanols have been developed.[4] They are polymer-based materials and also polymer-coated silica phases. These polymer-based or polymer-coated phases can be recommended as very useful and stable stationary phases in LC separations of polar compounds; they also offer much better stability for use at higher pH alkaline conditions.

REFERENCES

1. Karch, K.; Sebestian, I.; Halasz, I. Preparation and properties of reversed phases. J. Chromatogr. **1976**, *122*, 3.
2. Unger, K.K., Ed.; *Packings and Stationary Phases in Chromatographic Techniques*; Marcel Dekker, Inc.: New York, 1990.
3. Pursch, M.; Sander, L.C.; Albert, K. Understanding reversed-phase LC with solid-state NMR. Anal. Chem. **1999**, *71*, 733A.
4. Unger, K.K. *A Guide to Practical HPLC*; GIT Verlag: Darmstadt, 1999.

Enoxacin: CE and HPLC Analysis

Hassan Y. Aboul-Enein
Pharmaceutical and Medicinal Chemistry Department, Pharmaceutical and Drug Industries Research Division, National Research Center, Dokki, Cairo, Egypt

Imran Ali
Department of Chemistry, Jamia Millia Islamia (A Central University), New Delhi, India

INTRODUCTION

Enoxacin, 1-ethyl-6-fluoro-1,4-dihydro-4-oxo-7-(1-piperazinyl)-1,8-naphthyridine-3-carboxylic acid (ENX; Fig. 1), is a new broad spectrum fluorinated 4-quinolone antibacterial agent.[1] It has a broad spectrum of antibacterial activity and is particularly potent against Gram-negative organisms and staphylococci.[2] The 4-quinolone antibiotics have been used in the treatment of many soft tissue infections including bacterial prostatitis.[3] ENX is excreted, mainly, in urine as the unchanged drug. It is metabolized by oxidation (to oxo-enoxacin), by conjugation with formic and acetic acid (ring opening), and by deamination of the piperazinyl ring. Its major metabolite, oxo-enoxacin, accounts for 10–15% of the administered dose and each of the other metabolites constitutes less than 1% of the dose.[2] It has also been reported that ENX has potent competitive inhibitory effects on theophylline metabolism, causing elevated plasma theophylline concentration and potential toxicity.[4] Because of these properties of ENX, it is very important to develop suitable analytical methods for this substance. High-performance liquid chromatography (HPLC) is the most commonly employed method for the determination of ENX and its metabolites in plasma, urine, and tissues.[5–12] Capillary electrophoresis (CE) is becoming a reliable, preferable, and alternative method, especially for the analysis of drugs in biological matrices.[13,14] CE offers some advantages such as rapidity, short analysis time, and low cost.[15–17] Only one report on the analysis of ENX by CE is presented by Tuncel et al.[18] Further, the authors have also carried out the analysis of ENX by HPLC and compared this method with the CE method in pharmaceutical dosage forms and in biological fluids.

DETERMINATION OF ENX BY CE

Instruments

The experiments were conducted using a Spectrophoresis 100 system equipped with a modular injector and high-voltage power supply, and a model Spectra FOCUS scanning CE detector (Thermo Separation Products, California, U.S.A.) connected to a Model Etacomp 486 DX 4-100 computer which processed the data using PC 1000 (Version 2.6) running under the OS/2 Warp program (Version 3.0). The analysis was performed in a fused silica capillary which has a total length of 88 cm, an effective length of 58 cm, and an I.D. of 75 μm (Phenomenex, California, U.S.A.). The pHs of the solutions were measured with a Multiline P4 pH meter with SenTix glass electrode (WTW, Weilheim, Germany). All the solutions were filtered using a Phenex microfilter (25 mm, 0.45 μm) (Phenomenex) and were degassed using a model B-220 ultrasonic bath (Branson, Connecticut, U.S.A.).

Chemicals

Acetonitrile, methanol (HPLC grade), ethanol, propanol, hydrochloric acid, sodium hydroxide, borax, acetylpipemidic acid (internal standard (IS) for CE), and 3,4-dihydroxybenzylamine HBr (IS for HPLC) were from Merck (Darmstadt, Germany). Enoxacin was generously provided by Eczacibasi Ilac Sanayi ve Ticaret A.S. (Istanbul, Turkey). Blood samples were withdrawn from healthy volunteers after obtaining their consent. The serum samples were separated by centrifuging for 10 min at 5000 × *g*. Double-distilled water was used to prepare all the solutions. A stock solution of ENX (10 mg/25 ml of methanol) was prepared. Dilutions were made in the range of 2.5×10^{-5} to 1.2×10^{-4} *M*, each containing 0.25 μmol IS (acetylpipemidic acid) for CE and 0.11 μmol IS (3,4-dihydroxybenzylamine HBr) for HPLC. All the dilutions for CE were prepared in a background electrolyte. The background electrolyte was a 20 m*M* borate buffer at pH 8.6 for the CE experiments. The dilutions were analyzed by applying a +30 kV potential, injecting the sample 1sec and detecting at 265 nm where ENX and acetylpipemidic acid (IS) absorb the monochromatic light equivalently.

Procedure for CE Analysis

The fused silica capillary tubing was filled with the background electrolyte (pH 8.6; 20 m*M* borate). Both ends of the tube were dipped into a reservoir (8 ml) and a vial (1.1 ml) filled with the background buffer. The end part

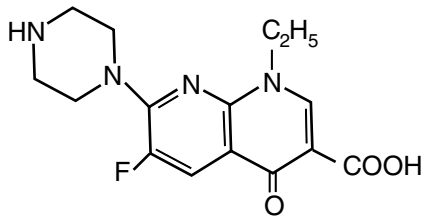

Fig. 1 The chemical structure of ENX.

where the sample (side of vial) was introduced was connected with a platinum electrode to the positive high-voltage side of the power supply. The reservoir side at the detector end was connected with a platinum electrode to the ground. Samples at a concentration of 7.7×10^{-5} *M* for the optimization of CE parameters were introduced by 1sec of vacuum injection corresponding to almost 65 nl. Before each run, the capillary was purged for 2 min with 0.1 *M* sodium hydroxide solution, then for another 2 min with double-distilled water. It was then equilibrated by passing the background electrolyte for 5 min prior to operation.

A background electrolyte consisting of borax was preferred for conducting the initial CE experiments because ENX has a carboxylic group on its structure. Several pH values were tested in the range from 8.45 to 9.95 using the concentration of 20 m*M* borax buffer. It was observed that the ENX (1.26×10^{-4} *M*) peak appeared in all the studied pH values, but the migration time of ENX, as expected, increased with increasing pH. Phosphate and citrate buffers of the same pH and concentration (8.6, 20 m*M*) were used to compare the effect of the nature of the buffer components. The migration time (t_M) of ENX was not affected by the buffer components, but the repeatability of the peak areas decreased with the use of citrate and phosphate buffers. It is concluded that some optimization studies are required if these buffer systems are to be used.

The influence of borax buffer concentration was investigated in the range from 10 to 100 m*M*. The sharpest peaks were obtained in the use of 10–30 m*M* concentrations and the t_M of ENX was almost constant, and an increase was observed in the use of borax concentration above 30 m*M*, but peak deformation also occurred due to the heat production by the Joule effect. In order to achieve optimization of the proposed analytical procedure, low buffer concentration was considered to decrease the electrophoretic mobility that corresponds to short analysis time. Based on the above results, the most convenient buffer system was 20 m*M* borate buffer at pH 8.6. Since the separation depends on the conditioning of the capillary inner surface in the CE analysis, the t_M and peak integration values might be very similar to the HPLC techniques.

The electropherogram of ENX and acetylpipemidic acid (IS) in the background electrolyte is shown in Fig. 2. The signal of electroosmosis and the migration time of the peaks of ENX and IS appeared at 3.8, 4.8, and 5.5 min, respectively. From the integration data, the net mobility toward the cathode (electroosmosis) and the ENX and IS toward the anode (electrophoretic) were 7.56×10^{-4}, 5.96×10^{-4}, and 4.6×10^{-4} $cm^2/V/sec$, respectively. The capacity factors were 3.82 (ENX) and 4.53 (IS).

Certain evaluation methods were examined based on the quantification processes. These can be divided into three

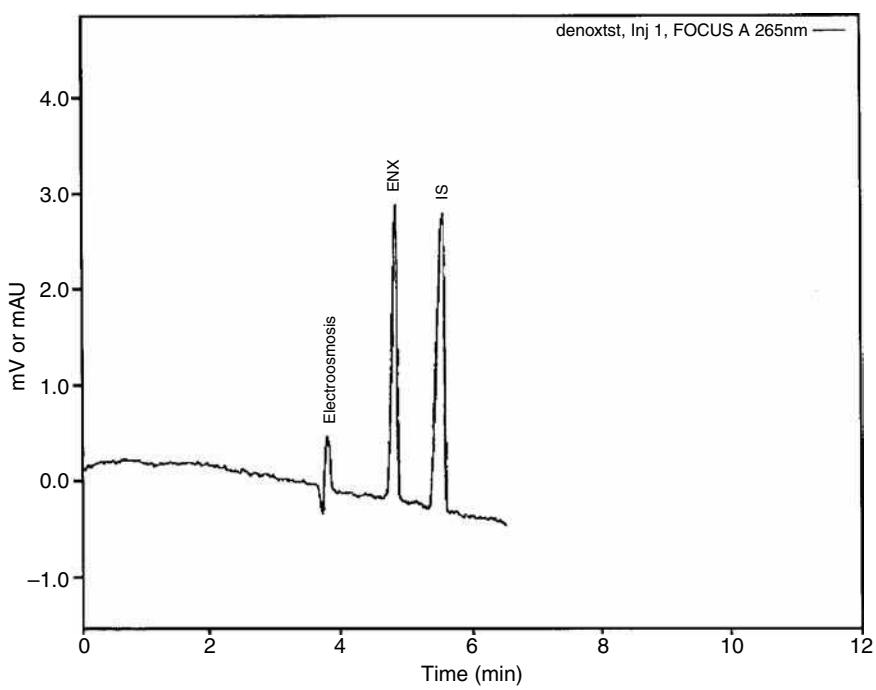

Fig. 2 Typical electropherogram of standard ENX (7.7×10^{-5} *M*) and IS (acetylpipemidic acid, 5.18×10^{-5} *M*). Conditions: 20 n*M* boratem pH 8.6; injection, hydrodynamically 1 sec; applied voltage, +30 kV; capillary, uncoated fused silica, 75 μm I.D., 88 cm total, and 58 cm effective length; detection at 265 nm.

Table 1 Precision of peak areas (days = 3; $n = 6$).

Precision of peak areas (RSD%)	PN no. IS	IS no. PN	IS and PN
Repeatability	2.80	0.99	0.99
Intermediate precision	3.24	2.86	1.36

groups, employing only the values of peak normalization (PN). The effect of the use of IS and certain evaluation methods, such as correction of peak area (normalization), was calculated by dividing the related peak area into t_M on which the precision was examined. These can be divided into three groups: a) employing only the area values of PN (PN no IS); b) computing the ratio values (IS no PN); and c) using the area values of peak normalized IS and ENX (IS and PN). The precision of the peak areas was calculated as shown in Table 1.

The success of the CE experiments from an analytical point of view depends on the conditioning of the capillary surface. Therefore, cleaning and conditioning processes, as explained in the experimental part, must be repeated after each injection to provide optimum resolution and reproducibility. The precision of the peak area was also assessed by considering certain evaluations, such as the effects of correction of peak area (normalization), which were found by the division of the related peaks into the corresponding migration times; the use of an internal standard was studied.

As seen from Table 1, the lowest RSD% values were obtained from those of IS and PN. Thus, such evaluation was considered throughout the rest of the study. A series of standard ENX solutions in the concentration range of 2.5×10^{-5} through 1.2×10^{-4} M, with each solution containing 0.25 μmol at a fix concentration of IS, were prepared and injected ($n = 3$). Linear regression lines were obtained by plotting the ratios of normalized peak areas to those of the internal standard vs. the analyte concentration. The calibration equation was computed using a regression analysis program, considering the ratio values vs. the related concentrations. The results are presented in Table 2.

Method Validation and Accuracy

From the electropherogram in Fig. 2, no interference from the formulation excipients could be observed at the migration times of ENX and IS. The limit of the detection (LOD) was 3.85×10^{-7} M, while the limit of quantification (LOQ) was 1.16×10^{-6} M. The results indicate good precision. Method accuracy was determined by analyzing a placebo (mixture of excipients) spiked with ENX at three concentration levels ($n = 6$) covering the same range as that used for linearity. Mean recoveries with 95% confidence intervals are given in Table 3.

Table 3 Precision of the method (spiked placebos).

Concentration levels (%)	50	100	150
Repeatability (days = 3; $n = 6$, RSD%)	2.0	2.5	2.1
Intermediate precision (days = 3; $n = 6$, RSD%)	3.3	3.0	3.1

Determination of ENX by HPLC

HPLC experiments were carried out using a Model 510 Liquid Chromatograph equipped with a Model 481 UV detector (Waters Associates, Milford, Massachusetts, U.S.A.). The chromatograms were processed by means of a chromatographic workstation (Baseline 810). Separation was performed on a reversed-phase Supelcosil LC-18 column (250 × 4.6 mm I.D., 5 μm particle size) (Supelco, St. Louis, Missouri, U.S.A.). The samples were injected into a 50 μl loop using a Rheodyne 7125 valve (Rheodyne, Cotati, California, U.S.A.).

Procedure for HPLC Analysis

The HPLC conditions were optimized by using different mobile and stationary phases. During HPLC experiments, a 10 mM phosphate buffer (pH 4.0)/acetonitrile (85:15, v/v) was used as a mobile phase. 3,4-Dihydroxybenzylamine-HBr (IS) was found to be a suitable internal standard for the HPLC experiments. The flow rate was 1.5 ml/min and detection was carried out at 260 nm. The ENX in tablet and the serum were identified by comparing the retention times of the pure ENX under the identical chromatographic conditions.

RESULTS AND DISCUSSION

Under the described chromatographic conditions, ENX has a retention time of 10.03 min, whereas IS eluted at 2 min.

Table 2 Linearity and accuracy of the method (spiked placebos).

Regression parameters			
Linearity	$r^2 = 0.9998$	intercept (mean ± SD) = $-0.02342 \pm 7.32 \times 10^{-3}$	slope (mean ± SD) = 9813.18 ± 102.31
Accuracy	50%	100%	150%
Mean recovery ±CI%	101.4 ± 2.12	101.1 ± 2.63	100.4 ± 2.25

Peak area ratios were linearly proportional to ENX concentrations in the range 3.12×10^{-6} through 3.12×10^{-4} *M*, with a detection limit of 1.56×10^{-6} *M*. The calibration equation was found to be [$R = -0.51 + 2.1 \times 10^5$ *C* (M); $r = 0.9992$], where *C* (M) is the molar concentration of ENX. The results of the HPLC experiments were compared with those obtained by the CE experiments. As described earlier, various reports on enoxacin analysis by HPLC are available. The different stationary phases used are μ-Bondapak C_{18}, Spherisorb S5 ODS2, Nucleosil C_{18}, Hypersil ODS, etc. The mobile phases used for the analysis of ENX are different ratios of water–acetonitrile, buffers–acetonitrile, acetonitrile–salt solutions, methanol–salt solutions, etc.[5–12]

Analysis of ENX in Tablets by CE and HPLC Methods

Enoxacin tablets (containing 400 mg active material) were obtained from the local market. Ten ENX tablets were accurately weighed. The average weight of one tablet was calculated, and then the tablets were finely powdered in a mortar. A sufficient amount of tablet powder, equivalent to 10 mg of ENX, was accurately weighed, then transferred to a 25 ml volumetric flask, and methanol was added to dissolve the active material. It was magnetically stirred for 10 min and made up to the final volume with the related solvent. The solution was then centrifuged at 5000 × *g* for 10 min. The supernatant and a fixed amount of IS solution were diluted with a background electrolyte or mobile phase to carry out either the CE or the HPLC assay. The electropherograms of ENX in tablets with IS are shown in Fig. 3.

Analysis of ENX in Serum by CE and HPLC Methods

For the CE analysis, 0.25 μmol of ENX (in 1 ml) was added to 1 ml of serum and was vigorously shaken. Then 3 ml of ethanol was added and mixed well using a shaker. The precipitated proteins were separated by centrifuging for 10 min at 5000 × *g*. A specific amount of clear supernatant was transferred to a tube, IS solution was added, and the final solution was directly injected to the CE instrument under the same conditions. It was reported that some determinations have been carried out by directly injecting the supernatant of the homogenates and urine into the CE.[16] This kind of application shortens the total analysis time. For HPLC, the precipitation of proteins of 1 ml serum was achieved according to the methods described by Nangia et al.,[7] i.e., by adding 50 μl $HClO_4$ (60% w/v), centrifuging for 10 min at 5000 × *g*, and directly injecting the supernatant into the column of the HPLC system under the conditions

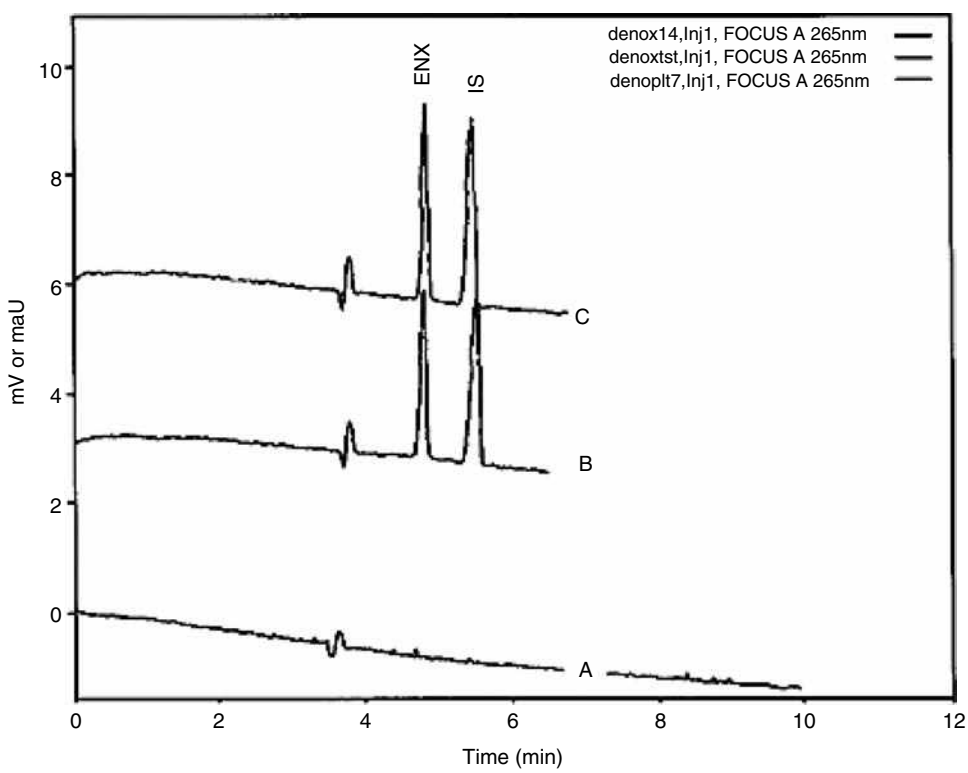

Fig. 3 Electropherograms of (a) inactive ingredients of a tablet solution of ENX; (b) standard ENX (7.7×10^{-5} *M*) and IS (acetylpipemidic acid, 5.18×10^{-5} *M*); and (c) enoxacin tablet solution containing IS. Conditions are the same as in Fig. 2.

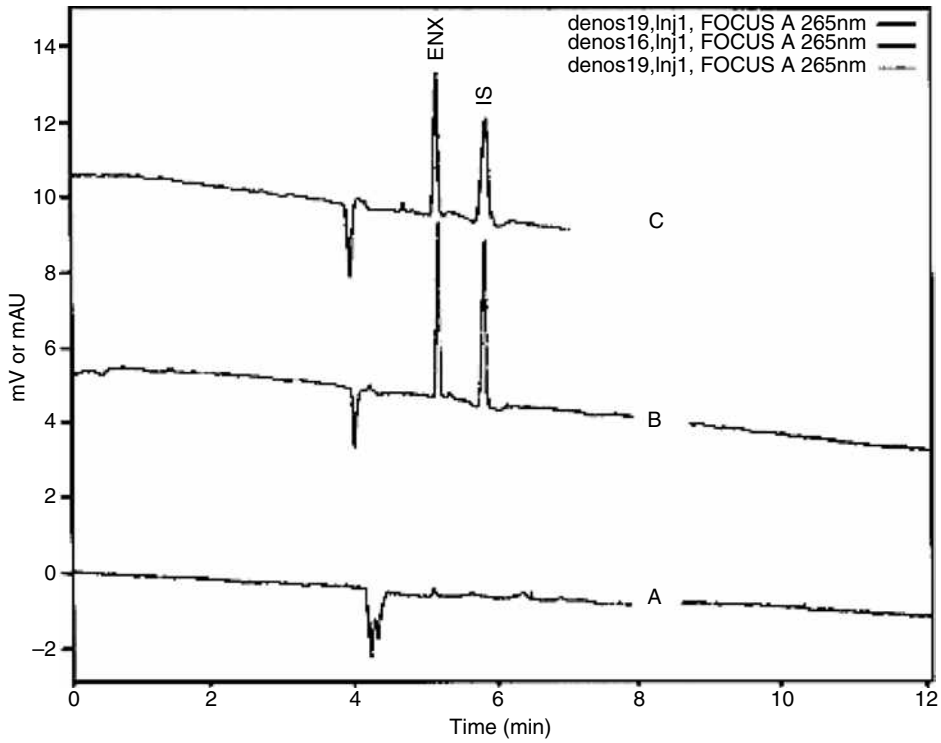

Fig. 4 Electropherogram of (a) blank serum deproteinized with ethanol; (b) serum spiked with the standard ENX solution (0.25 μmol) and IS (0.15 μmol); and (c) water spiked with the standard ENX solution (0.25 μmol). Conditions are the same as in Fig. 2.

mentioned above. The electropherograms of ENX with IS in the serum are given in Fig. 4.

CONCLUSIONS

A typical electropherogram is shown in Fig. 2, which indicates no interferences from the tablet excipients. In order to examine the applicability and validity of the CE method, ENX pharmaceutical tablets were analyzed by CE and HPLC methods. Results of the comparative studies are shown in Table 4. The results indicate that both methods, i.e., by CE and HPLC, show insignificant differences at the 95% probability level and the ENX tablet formulations satisfy the official requirements.[19] Certain experiments were conducted to elucidate the recovery of ENX and to validate the CE studies. Three sets of experiments with definite amounts of ENX were added to the serum and to the double-distilled water, and were analyzed. The same experiment was also performed without any ENX. The recovery was found to be 89.7 ± 0.63 (RSD%). The recovery experiments were also tested by HPLC and were found to be 78.8 ± 4.94 (RSD%). The difference between the methods could be due to the different precipitation procedures applied.

These results show that the proposed CE method is simple, rapid, and low cost, as compared to HPLC, especially for the quality-control analysis of ENX. It has also been observed that the amount of ENX found (Table 4) was always greater with CE than with HPLC. The presented CE method can be used for the analysis of ENX at trace levels in unknown matrices and also for routine quality control of ENX.

Table 4 Comparative studies for the determination of ENX tablet.

No. of experiment	Amount found (mg) using CE	Amount found (mg) using HPLC
1	419.7	410.1
2	428.5	417.4
3	422.3	414.9
4	417.1	419.9
5	419.4	417.4
Mean	421.4	415.9
RSD%	1.04	0.89
$t_{calculated}$	2.13	
t_{table}		2.78 ($p = 0.05$)

Declared amount, 400 mg per tablet.

REFERENCES

1. Wolfson, J.S.; Hooper, C. Quinolone Antimicrobial Agents; American Society for Microbiology: Washington, DC, 1989.
2. Henwood, J.M.; Monk, J.P. Enoxacin: A review of its antibacterial activity, pharmacokinetic properties and therapeutic use. Drugs **1988**, *36*, 32–66.
3. Guimaraes, M.A.; Noone, P. The comparative in-vitro activity of norfloxacin, ciprofloxacin, enoxacin and

nalidixic acid against 423 strains of gram-negative rods and staphylococci isolated from infected hospitalised patients. J. Antimicrob. Chemother. **1986**, *17*, 63–68.
4. Wijnands, W.J.; Vree, T.B.; Van Herwaarden, C.L. The influence of quinolone derivatives on theophylline clearance. Br. J. Clin. Pharmacol. **1986**, *22*, 677–683.
5. Vree, T.B.; Baars, A.M.; Wijnands, W.J.A. High performance liquid chromatography and preliminary pharmacokinetics of enoxacin and its 4-oxo metabolite in human plasma, urine and saliva. J. Chromatogr. Biomed. Appl. **1985**, *343*, 449–454.
6. Griggs, D.J.; Wise, R. A simple isocratic high pressure liquid chromatographic assay of quinolones in serum. J. Antimicrob. Chemother. **1989**, *24*, 437–445.
7. Nangia, A.; Lam, F.; Hung, C.T. Reversed phase ion-pair high performance liquid chromatographic determination of fluoroquinolones in human plasma. J. Pharm. Sci. **1990**, *79*, 988–991.
8. Goebel, K.J.; Stolz, H.; Ehret, I.; Nussbaum, W. A validated ion-pairing high performance liquid chromatographic method for the determination of enoxacin and its metabolite oxo-enoxacin in plasma and urine. J. Liq. Chromatogr. **1991**, *14*, 733–751.
9. Zhai, S.; Korrapati, M.R.; Wei, X.; Muppalla, S.; Vestal, R.E. Simultaneous determination of theophylline, enoxacin and ciprofloxacin in human plasma and saliva by high performance liquid chromatography. J. Chromatogr. Biomed. Appl. **1995**, *669*, 372–376.
10. Davis, J.D.; Aarons, L.; Houston, J.B. Simultaneous assay of fluoroquinolones and theophylline in plasma by high performance liquid chromatography. J. Chromatogr. Biomed. Appl. **1993**, *621*, 105–109.
11. Hamel, B.; Audran, M.; Costa, P.; Bressolle, F. Reversed phase high performance liquid chromatographic determination of enoxacin and 4-oxo-enoxacin in human plasma and prostatic tissue: Application to a pharmacokinetic study. J. Chromatogr. A, **1998**, *812*, 369–379.
12. Barbosa, J.; Berges, R.; Sanz-Nebot, V. Retention behaviour of quinolone derivatives in high performance liquid chromatography: Effect of pH and evaluation of ionization constants. J. Chromatogr. A, **1998**, *823*, 411–422.
13. Boone, C.M.; Douma, J.W.; Franke, J.P.; de Zeeuw, R.A.; Ensing, K. Screening for the presence of drugs in serum and urine using different separation modes of capillary electrophoresis. Forensic Sci. Int. **2001**, *121*, 89–96.
14. Lemos, N.P.; Bortolotti, F.; Manetto, G.; Anderson, R.A.; Cittadini, F.; Tagliaro, F. Capillary electrophoresis: A new tool in forensic medicine and science. Sci. Justice **2001**, *41*, 203–210.
15. Baker, D.R. *Capillary Electrophoresis*; J. Wiley & Sons, Inc.: New York, 1995.
16. Xu, Y. Capillary electrophoresis. Anal. Chem. **1995**, *67*, 463R–473R.
17. Altria, K.D. Overview of capillary electrophoresis and capillary electrochromatography. J. Chromatogr. **1999**, *856*, 443–463.
18. Tuncel, M.; Dogrukol-Ak, D.; Senturk, Z.; Ozkan, S.A.; Aboul-Enein, H.Y. Capillary electrophoretic behaviour and determination of enoxacin in pharmaceutical preparations and human serum. J. Liq. Chromatogr. Relat. Technol. **2001**, *24*, 2455–2467.
19. United States Pharmacopoeia (USP) 22, NF-17; U.S. Pharmacopeial Convention: Rockville, Maryland, 1990.

Environmental Applications of Reversed-Flow GC

John Kapolos
Department of Agricultural Products Technology, Technological Educational Institute of Kalamata, Kalamata, Greece

INTRODUCTION

The reversed-flow gas chromatography (RFGC) technique, a subtechnique of the inverse gas chromatography (IGC), can be used for the determination of physicochemical quantities pertaining to environment and pollutants. Experimental setup and appropriate mathematical analysis for the calculation of physicochemical parameters are reviewed, taking into account: i) the interaction between air pollutant(s) and a solid surface in the absence, or in the presence, of a chemical reaction between two pollutants in the gas phase over the solid material (synergistic effects) and ii) exchange of gas pollutant(s) between atmospheric and water environment.

REVERSED-FLOW GAS CHROMATOGRAPHY

Interaction Between Air Pollutant(s) and a Solid Surface

One of the most important effects of atmospheric pollution is the damage to historic monuments and buildings and, generally, to cultural heritage. Volatile hydrocarbons, nitric oxide, nitrogen dioxide, sulfur dioxide, aromatic hydrocarbons, and suspended particulate matter are emitted by a number of processes, either anthropogenic or not. In addition, ozone plays a significant role in atmospheric pollution because of its relationship with chemical and photochemical changes. All these effects start with the deposition of air pollutants onto solid surfaces and lead to permanent corrosion and damage. The exterior surfaces of monuments have been attacked by more than one pollutant and, in addition, by secondary pollutants that are produced by chemical reactions in the gas phase, and have led to deterioration of the buildings and monuments.

The RFGC technique, a flow perturbation method developed in 1980,[1] is used to measure the following directly from experimental data: rate constants for adsorption, desorption, and chemical reaction of gaseous pollutants with the solid surface of the objects, diffusion coefficients of the pollutants which are diffused into the pores of the solid, deposition velocities and reaction probabilities for the action of air pollutants on the same surfaces, adsorption energies, local monolayer capacities, local adsorption isotherms, and probability density functions for the deposition of the pollutants onto the surface of the cultural heritage objects.[2,3] All the above quantities can be calculated, including, or not, apparent first-order rate constants for the chemical reaction of two pollutants in the gaseous phase above the solid surface (synergistic effects).[2,4]

A commercial gas chromatograph, equipped with an appropriate detector (depending on the kind of pollutant under study), is required to apply the RFGC technique.[5,6] The experimental arrangement is very simple and the traditional gas chromatograph is slightly modified to include a T-shape cell constructed from glass or stainless steel chromatographic tube inside the chromatographic oven, and a four- or six-port gas valve inside or outside the oven. The diffusion column (20–80 cm × 3–5 mm I.D.), connected perpendicularly to the sampling column (0.6–2.0 m × 3–5 mm I.D.) at its midpoint, contains only stagnant carrier gas (nitrogen or air), which also flows through the empty sampling column, either from D_1 to D_2 or vice versa. Near the closed end of the diffusion column, a small length (4–9 cm) is filled with particles of the solid under study. The sampling column is devoid of any solid or liquid material, and, for separation purposes, an additional separation column is placed before the detector.

After the solid bed is conditioned by heating it in situ, under a continuous carrier gas flow, the bed is cooled to the working temperature and a small volume of gas (0.5–1.0 cm^3 at atmospheric pressure) or liquid (1–5 μl) pollutant is introduced through the injector into the solid bed. When studying synergistic effects, two pollutants are introduced simultaneously or within a short interval of no more than a few seconds to the system.

After the appearance of the continuously rising concentration–time curve, the reversing procedure for the carrier gas flow by means of the four- or six-port valve is initiated. This reversal procedure, for a period shorter than the gas hold-up time in the sampling column, creates narrow and fairly symmetrical chromatographic peaks over the continuous elution curve.[7,8,9] These extra chromatographic peaks, called "sample peaks," and their heights H are measured as a function of the time t during the reversal procedure. The height is proportional to the concentration c, of the injected pollutant, at the junction point $z = 0$ and $x = l'$ of the sampling column (Fig. 1), at time t. The

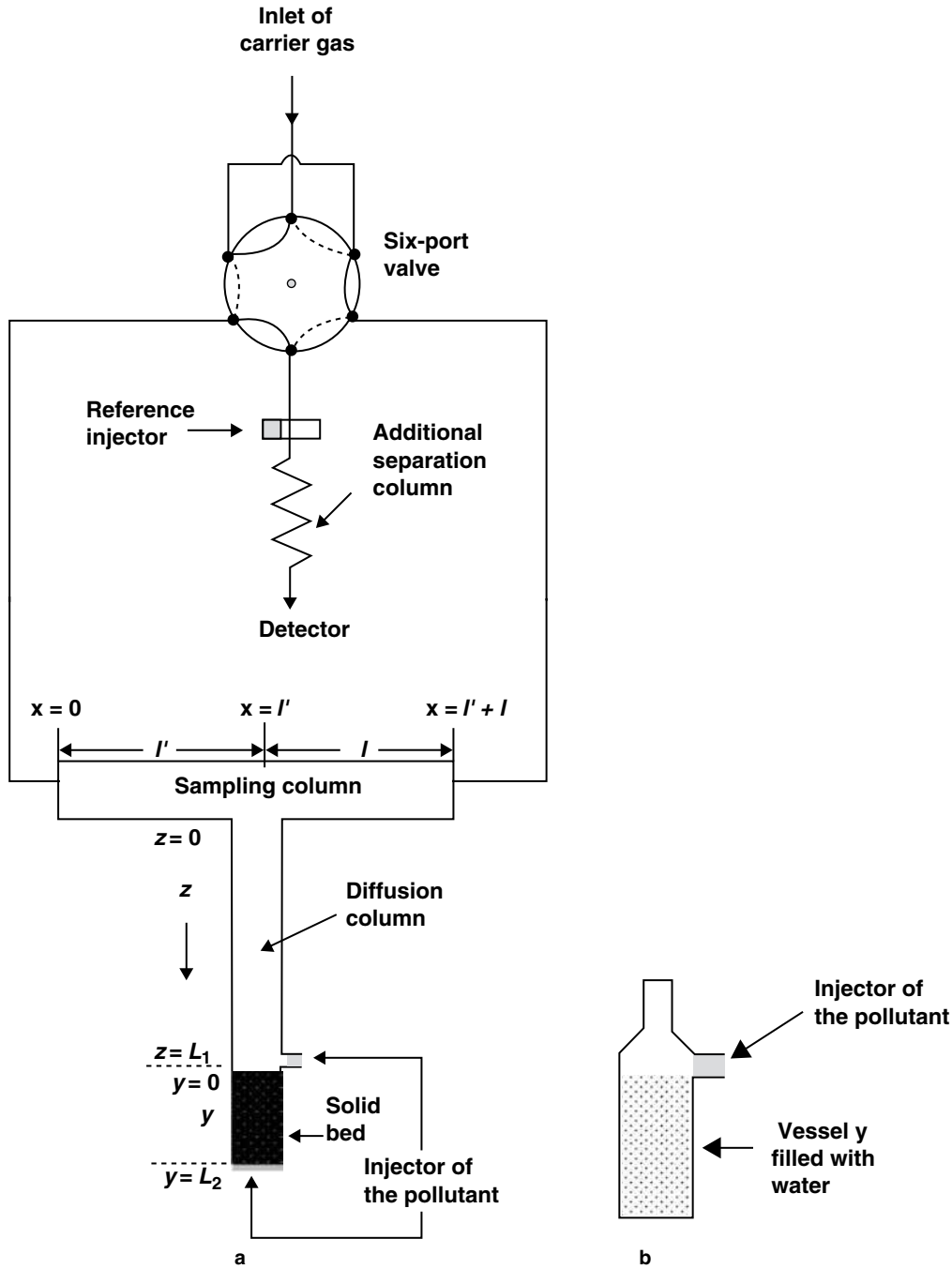

Fig. 1 Schematic representation of columns and gas connections for studying (a) the interaction between air pollutant(s) and a solid surface and (b) exchange of gas pollutant(s) between atmospheric and water environments.

mathematical expression of the above has been derived theoretically:[7,10]

$$H^{\frac{1}{M}} = gc(l', t) \tag{1}$$

where M (dimensionless) is the response factor for the detector ($M = 1$ for the linear FID and g is the proportionality constant (cm per mol/cm^3).

Now a question arises; is there any relationship between the measured concentration $c(l', t)$ and the physicochemical quantities pertaining to the various phenomena occurring in the solid bed region? For an answer, one must solve the mathematical equations describing all the physicochemical actions taking place in such systems.

First, the local (with respect to time) adsorption isotherm of the pollutant

$$c_s^* = \frac{a_y}{a_s} k_1 \int_0^t c_y(\tau) d\tau \tag{2}$$

Second, the mass balance equation for the pollutant in the region z (diffusion column)

$$\frac{\partial c_z}{\partial t} = D_z \frac{\partial^2 c_z}{\partial z^2} \tag{3}$$

Next, the mass balance equation for the same pollutant in region y, filled with the solid material under study

$$\frac{\partial c_y}{\partial t} = D_y \frac{\partial^2 c_y}{\partial y^2} - k_R \frac{a_s}{a_y} (c_s^* - c_s) \tag{4}$$

Finally, the rate of change of the adsorbed concentration:

$$\frac{\partial c_s}{\partial t} = k_R (c_s^* - c_s) - k_2\ c_s \tag{5}$$

where c_s^* is the local adsorbed concentration of the pollutant in equilibrium with that in the gaseous state (mol/g), n_s the initially adsorbed equilibrium amount of the pollutant (mol), a_s the amount of the solid material per unit length of column bed (g/cm), y the length coordinate along section L_2 (cm), a_y the cross-sectional area of the void space in region y (cm^2), k_1 the local adsorption parameter describing the local experimental isotherm of the pollutant on the solid surface, which varies with time (1/sec), c_y the gaseous concentration of the pollutant in the gas phase above the solid (mol/cm^3), τ the dummy variable for time (sec), c_z the gaseous concentration of the pollutant as a function of time t and length coordinate z along the column (mol/cm^3), D_z the diffusion coefficient of the pollutant in the carrier gas (cm^2/sec), D_y the effective diffusion coefficient of the pollutant in the region of the solid bed (cm^2/sec), k_R the rate constant for adsorption/desorption of the pollutant on the bulk solid (1/sec), c_s the concentration of the pollutant adsorbed on the solid (mol/g), and k_2 the rate constant of a possible first-order or pseudo-first-order surface reaction of the adsorbed pollutant (1/sec).

By taking the following initial conditions into consideration, $c_z(0,\ z) = 0$, $c_y(0,\ y) = (n_A/a_y)\ \delta(y - L_2)$, and $c_s(0,y) = 0$, where n_A is the amount (mol) of the pollutant introduced as a pulse at $y = L_2$, the system of the above partial differential (Eqs. 2–5) is solved by using double Laplace transformation of all terms with respect to time and length coordinates. By means of certain approximations and algebraic manipulations,[3] the t Laplace transform of the measurable concentration $c(l',\ t)$ of the pollutant in the sampling column at time t is given by the equation:

$$C(l',\ p) = G \frac{p^2 + kp}{(p - B_1)(p - B_2)(p - B_3)} \tag{6}$$

where

$$G = \frac{n_A a_1 a_2}{\dot{V}(a_1 + a_2 + a_2 Q)} \tag{7}$$

$$a_1 = \frac{2D_z}{L_1^2};\quad a_2 = \frac{2D_y}{L_2^2};\quad Q = \frac{2a_y L_2}{a_z L_1} \tag{8}$$

$$k = k_2 + k_R \tag{9}$$

L_1 and L_2 are the lengths of the sections z and y, respectively, α_z is the cross-sectional area of the region z (cm^2), $\dot{V}$ is the volumetric flow rate of the carrier gas, and B_1, B_2, and B_3 are the roots of the third degree polynomial of the denominator in Eq. 6.

The inverse Laplace transformation with respect to p of Eq. 6 leads to the equation:

$$c(l', t) = G\Big[A_1^0 \exp(B_1 t) + A_2^0 \exp(B_2 t) + A_3^0 \exp(B_3 t)\Big] \tag{10}$$

where

$$A_1^0 = \frac{B_1^2 + kB_1}{(B_1 - B_2)(B_1 - B_3)} \tag{11}$$

$$A_2^0 = \frac{B_2^2 + kB_2}{(B_2 - B_1)(B_2 - B_3)} \tag{12}$$

$$A_3^0 = \frac{B_3^2 + kB_3}{(B_3 - B_1)(B_3 - B_2)} \tag{13}$$

and the relationships between the physicochemical parameters previously defined, k_1, k_R, k_2, and D_y, and the exponential coefficients of time are as follows:

$$X = \frac{a_1 a_2}{a_1 + a_2 + a_2 Q} + k = -(B_1 + B_2 + B_3) \tag{14}$$

$$Y = \frac{a_1 a_2 k + (a_1 + a_2 Q) k_1 k_R}{a_1 + a_2 + a_2 Q} = B_1 B_2 + B_1 B_3 + B_2 B_3 \tag{15}$$

$$Z = \frac{a_1 + a_2 Q}{a_1 + a_2 + a_2 Q} k_1 k_2 k_R = -B_1 B_2 B_3 \tag{16}$$

where X, Y, and Z are auxiliary parameters.

As the height H of the extra chromatographic peaks, obtained by the repeated flow reversals, is proportional to

the gaseous concentration (Eq. 1) with a proportionality constant g (cm per mol/cm^3), we can write Eq. 10 as:

$$H^{\frac{1}{M}} = gG\sum_{i=1}^{3} A_i^0 \exp(B_i t) = \sum_{i=1}^{3} A_i \exp(B_i t) \tag{17}$$

where $A_i = gGA_i^0$ in cm.

Using a non-linear regression analysis PC program in GW-BASIC,[10] one can calculate the exponential and preexponential coefficients from the measured pairs H, t. From these, in turn, the calculation of the physicochemical quantities mentioned above is carried out as follows:

First, the value of k of Eq. 9 is calculated by dividing Eqs. 11 and 12 by Eq. 13. The results are

$$\frac{A_2^0(B_2 - B_1)(B_2 - B_3)}{A_1^0(B_1 - B_2)(B_1 - B_3)} = \frac{B_2^2 + kB_2}{B_1^2 + kB_1} = A_{21};$$

$$\frac{A_3^0(B_3 - B_1)(B_3 - B_2)}{A_1^0(B_1 - B_2)(B_1 - B_3)} = \frac{B_3^2 + kB_3}{B_1^2 + kB_1} = A_{31} \tag{18}$$

The mean value of k's, found from the above two relationships, is further used. The a_2 by Eq. 14 and then D_y by Eq. 8 are easily calculated, while the value of D_z is obtained from the literature or calculated by well-known equations.[11,12]

The values of k_1, k_R, and k_2 are computed by using, after rearrangement, Eqs. 15, 16, and 9. First, by dividing Eq. 16 by Eq. 15, one obtains the value of k_2; then, subtracting that from k yields k_R and, finally, by dividing Eq. 15 by k_R, we find k_1.

From the above-calculated parameters, through the following Eqs. 19 and 20, the overall deposition velocity (V_d), which is equivalent to an overall mass transfer coefficient of the gaseous pollutant to the solid surface, corrected for the activated adsorption/desorption and surface reaction, and the reaction probability γ of the pollutant with the surface under study are found:

$$V_d = \frac{k_1 V'_G(\text{empty})\varepsilon}{A_S} \cdot \frac{k_2}{k_R + k_2} \tag{19}$$

$$\frac{1}{\gamma} = \left(\frac{R_g T}{2\pi M_B}\right)^{\frac{1}{2}} \cdot \frac{1}{V_d} + \frac{1}{2} \tag{20}$$

where A_S is the total surface area of solid (cm^2) V'_G the gaseous volume of the section y of the experimental cell (Fig. 1a) (cm^3), R_g the ideal gas constant (J/K/mol), M_B the molar mass of pollutant, (kg/mol), and T the absolute temperature (K).

For calculating adsorption energies, local monolayer capacities, local adsorption isotherms, and probability density functions for the deposition of the pollutants onto the surface of the objects, the height H of the reversed-flow peaks and the physicochemical parameters B_i and A_i are used. The necessary relationships are as follows:

First, Eq. 10 of Ref.[13], which describes the local adsorption isotherm θ_t on the solid surface

$$\theta_t = \frac{c_s^*}{c_{\max}^*} = 1 - \exp(-KR_g T c_y) \tag{21}$$

where c_s^* and c_y have been defined after Eq. 5, $c_{\max}^*$ is the local monolayer capacity, with respect to time, ε is the adsorption energy, and K is the Langmuir constant[14] given by the relationship:

$$K = K^0(T)\exp\left(\frac{\varepsilon}{RT}\right) \tag{22}$$

where $K^0(T)$ is described by statistical mechanics[15] as

$$K^0 = \frac{h^3}{(2\pi m)^{\frac{3}{2}}(kT)} \cdot \frac{v_s(T)}{b_g(T)} \tag{23}$$

where k is the Boltzmann constant, m the molecular mass of the pollutant, h the Plank constant, and the ratio $v_s(T)/b_g(T)$ of two partition functions, namely that of the adsorbed molecule, $v_s(T)$, and that for rotations–vibrations in the gas phase $b_g(T)$. This ratio is taken approximately as unity.[14]

Second the gaseous concentration c_y (mol/cm^3) in the solid bed space is given by the equation:

$$c_y = \frac{uL_1}{gD_z}\sum_{i=1}^{3} A_i \exp(B_i t) \tag{24}$$

while the equilibrium adsorbed concentration c_s^* (mol/g) is obtained as

$$c_s^* = \frac{a_y}{a_s} k_1 \frac{uL_1}{gD_z}\sum_{i=1}^{3} \frac{A_i}{B_i}[\exp(B_i t) - 1] \tag{25}$$

where g, D_z, and L_1 have been defined above, u (cm/sec) is the corrected linear velocity of the carrier gas, and A_i and B_i are the parameters of Eq. 17.

Finally, the probability density function for the adsorption energy ε as the random variable and the time t as a structural parameter, $f(\varepsilon,t)$ can be based on the relationship:[16]

$$f(\varepsilon, t) = \frac{\partial c_{\max}^*}{\partial \varepsilon} = \frac{\partial c_{\max}^*/\partial t}{\partial \varepsilon/\partial t} \tag{26}$$

From the above Eqs. 21–26, the time distribution physicochemical parameters for the adsorption of the pollutants on the surface of the monuments can be calculated.

The adsorption energy ε is expressed by the next relationship, which is derived from Eq. 22:

$$\varepsilon = RT \ln\left(\frac{K}{K^0}\right) \tag{27}$$

The local isotherm θ_t is calculated with Eq. 21, where c_y is given by Eq. 24 and KR_gT by Eq. 12 of Ref.[17]

The local monolayer capacity $c^*_{\max}$ is obtained as a combination of Eqs. 21 and 25, and the calculated value of θ_t according to the relationship:

$$c^*_{\max} = \frac{c^*_s}{\theta_t} \tag{28}$$

Finally, the probability density function over time for the adsorption energy is given as follows:

$$f(\varepsilon, t) = \frac{1}{RT}\left[\frac{KRT(\partial c^*_s/\partial t) + (\partial^2 c^*_s/\partial c_y \partial t)}{\partial(KR_gT)/\partial t} - \frac{\partial c^*_s/\partial c_y}{KR_gT}\right] \tag{29}$$

The expressions for all derivatives with respect to time in the above relationship have been given in detail elsewhere.[16,18]

From the above mathematical analysis, the answer to the question (Is there any relationship between the measured concentration $c(l', t)$ and the physicochemical quantities pertaining to the various phenomena occurring in the solid bed region?) is obtained. Using only measurable experimental quantities, such as the height H of the extra chromatographic peaks and the time t when those peaks occur, RFGC was used to study the action of air pollutants, such as SO_2, NO_2, $(CH_3)_2S$, O_3, and volatile hydrocarbons on pure $CaCO_3$, Penteli marbles, inorganic pigments as well as surfaces of cultural and artistic value inside museums.[2–6,8,9] Synergistic effects of two gaseous substances,[4] effects of airborne particles deposited on solid surfaces, and characterization and comparison of the behavior of coverage which protects materials against air pollutants can also be carried out.

Finally, from the above-calculated physicochemical quantities, a mechanism for the interaction of air pollutant and a solid surface can be proposed.[8]

Exchange of Gaseous Pollutant(s) Between Atmospheric and Water Environments

Aside from the above interactions between air pollutants and solid surfaces, the RFGC was recently applied to describe and quantify the physical and chemical phenomena controlling the exchange of gas pollutants between the atmospheric and water environments and vice versa. These phenomena are of great significance in environmental chemistry,[19] either owing to the solubilities of air pollutants in water or owing to their ability to migrate from water to the atmosphere. A good example is dimethyl sulfide, which is emitted by oceanic phytoplankton and constitutes the major natural source of sulfur in the troposphere.

For a description of the mechanism involving the above phenomena, the following physicochemical quantities should be calculated:

i. Diffusion coefficient of the pollutant in the carrier gas (D_z, cm^2/sec).
ii. Diffusion coefficient of the pollutant in the water (D_L, cm^2/sec).
iii. Partition coefficient of the pollutant between the water at the interface and the carrier gas (K, dimensionless).
iv. Partition coefficient of the pollutant between the bulk water and the carrier gas (K', dimensionless).
v. Partition coefficient of the pollutant between the water at the interface and the bulk (K'', dimensionless).
vi. Henry's law constant for the dissolution of the pollutant in the water (H^+, atm).
vii. Overall mass transfer coefficients of the gas in the carrier gas (K_G, cm/sec) and in the liquid water (K_L, cm/sec).
viii. Gas (k_G, cm/sec) and liquid (k_L, cm/sec) film transfer coefficients.
ix. Gas (r_G, sec/cm) and liquid (r_L, sec/cm) phase resistances for the transfer of the pollutant to the water.
x. Thickness of the stagnant film in the liquid phase (z_L, cm).

The experimental setup which is used for the calculation of the above-mentioned parameters is described above. The only difference is an additional vessel at the end of the diffusion column where liquid water is placed instead of the solid bed (Fig. 1b). The experimental procedure is identical to the previously described one (except, of course, for the condition of the solid bed).

The height of the extra chromatographic peaks is again proportional to the measurable concentration $c(l', t)$ of the pollutant and is given by an equation analogous to Eq. 17, which is reproduced in detail elsewhere.[20]

$$\frac{H}{2} = c(l', t) = A_1 \exp(B_1 t) + A_2 \exp(B_2 t) + A_3 \exp(B_3 t) \tag{30}$$

where the pre-exponential coefficients A_1, A_2, and A_3 can be written as explicit functions of B_1, B_2, and B_3, the geometrical characteristics of the cell and other experimental quantities, but this is not needed for the calculation

of the above-mentioned physicochemical quantities. The exponential coefficients of time B_1, B_2, and B_3 are used first for the calculation of D_L, K, and H^+ according to the following equations:[20]

$$X = \frac{9AD_z}{KL_1L_2} + \frac{6D_z}{L_1^2} + \frac{6D_L}{L_2^2} = -(B_1 + B_2 + B_3) \quad (31)$$

$$Y = \frac{18AD_z^2}{KL_1^3L_2} + \frac{18AD_zD_L}{KL_1L_2^3} + \frac{36D_zD_L}{L_1^2L_2^2} = B_1B_2 + B_1B_3 + B_2B_3 \quad (32)$$

$$Z = \frac{36AD_z^2D_L}{KL_1^2L_2^3} = -B_1B_2B_3 \quad (33)$$

$$H^+ = \frac{R_gTd}{KM_L} \quad (34)$$

where X, Y, and Z are auxiliary parameters, A is the ratio of cross-sectional areas in z and y regions, α_z and α_L, respectively (cm^2), L_1 and L_2 are lengths in z and y regions, respectively (cm), d is the density of the liquid, M_L is the molar mass of the liquid, and D_z is the diffusion coefficient of the pollutant in carrier gas, which can be determined when the vessel y is empty.

For the calculation of the other parameters K_G and K_L, and, from them, k_G, k_L, r_G, r_L, z_L, K, K' and K'', the following equations are adopted:[20]

$$X_1 = \frac{12D_z/L^2 + 4k/L + k'}{1 + kL/5D_z} = (-B_1 + B_2 + B_3) \quad (35)$$

$$Y_1 = \frac{24D_z^2/L^4 + 24kD_z/L^3 + 12k'D_z/L^2}{1 + kL/5D_z} = B_1B_2 + B_1B_3 + B_2B_3 \quad (36)$$

$$Z_1 = \frac{24k'D_z^2/L^4}{1 + k_L/5D_z} = -B_1B_2B_3 \quad (37)$$

$$K_L = \frac{k'V_L}{a_L}; \quad K_G = \frac{ka_z}{a_L}; \quad \frac{1}{K_L} = \frac{1}{k_L} + \frac{K'}{k_G}; \quad z_L = \frac{D_L}{k_L}; \quad K'' = \frac{K}{K'} \quad (38)$$

where X_1, Y_1, and Z_1 have different physicochemical meaning than the above X, Y, and Z, $L = L_1$ (gas phase), $k = K_Ga_L/a_z$, and $k' = K_La_L/V_L$ (liquid volume).

From the above equations, it is clearly defined that only the measurable height H of the extra chromatographic peaks and the time t when these peaks are produced are needed for the calculation of all the physicochemical quantities which are necessary for the description of the flux of gaseous pollutants across the air–water interface.

Until now, RFGC was used for studying the system vinyl chloride/water,[20] SO_2/water, and the effects of surfactants in reducing air–water exchange rates.[21]

CONCLUSIONS

Reversed-flow gas chromatography, which is a subtechnique of inverse gas chromatography, can be applied to determination of necessary physicochemical quantities for the interaction between air pollutants and cultural objects and exchange of air pollutants between atmospheric and water environments.

REFERENCES

1. Katsanos, N.A.; Georgiadou, I. Reversed-flow gas chromatography for studying heterogeneous catalysis. J. Chem. Soc. Chem. Commun. **1980**, *5*, 242–243.
2. Abatzoglou, C.; Iliopoulou, E.; Katsanos, N.A.; Roubani-Kalantzopoulou, F.; Kalantzopoulos, A. Deposition parameters of air pollutants on solid surfaces, measured in the presence of surface and gaseous reactions, with a simultaneous determination of the experimental isotherm. J. Chromatogr. A, **1997**, *775*, 211–224.
3. Bakaoukas, N.; Koliadima, A.; Farmakis, L.; Karaiskakis, G.; Katsanos, N.A. Dependence of adsorption rates with lateral interactions on local surface coverage of heterogeneous surfaces. Chromatographia **2003**, *57*, 783–791.
4. Siokos, V.; Kapolos, J.; Roubani-Kalantzopoulou, F. Physicochemical characterization of inorganic pigments in the presence of gaseous pollutants. The role of ozone. Z. Phys. Chem. **2002**, *216*, 1311–1321.
5. Vassilakos, C.; Katsanos, N.A.; Niotis, A. Physicochemical damage parameters for the action of SO_2 and NO_2 on single pieces of marble. Atm. Environ. **1992**, *26A*, 219–223.
6. Kalantzopoulos, A.; Abatzoglou, C.; Roubani-Kalantzopoulou, F. Environmental catalysis studied by the reversed-flow gas chromatography. Measurements, mechanism and models. Colloids Surf. **1999**, *151*, 377–387.
7. Katsanos, N.A. *Flow Perturbation Gas Chromatography*; Marcel Dekker, Inc.: New York, 1988; 93, 108.
8. Zachariou-Rakanta, H.; Kalantzopoulos, A.; Roubani-Kalantzopoulou, F. Chromatographic study of the influence of nitrogen dioxide on the reaction between volatile hydrocarbons and inorganic pigments. J. Chromatogr. A, **1997**, *776*, 275–282.
9. Kalantzopoulos, A.; Birbatakou, S.; Roubani-Kalantzopoulou, F. Benzene and toluene influence with or without nitrogen dioxide on inorganic pigments of works of art. Atm. Environ. **1998**, *32*, 1811–1816.
10. Sotiropoulou, V.; Vassilev, G.P.; Katsanos, N.A.; Metaxa, H.; Roubani-Kalantzopoulou, F. Simple determinations of experimental isotherms using diffusion denuder tubes. J. Chem. Soc. Faraday Trans. **1995**, *91* (3), 485–492.
11. Bird, R.B.; Stewart, W.E.; Lightfoot, E.N. *Transport Phenomena*; Wiley: New York, 1960; 744–746.

12. Fuller, E.N.; Schettler, P.D.; Giddings, J.C. A new method for prediction of binary gas-phase diffusion coefficients. Ind. Eng. Chem. **1966**, *58*, 19–27.
13. Katsanos, N.A.; Arvanitopoulou, E.; Roubani-Kalantzopoulou, F.; Kalantzopoulos, A. Time distribution of adsorption energies, local monolayer capacities, and local isotherms on heterogeneous surfaces by inverse gas chromatography. J. Phys. Chem. B, **1999**, *103*, 1152–1157.
14. Heuchel, M.; Jaroniec, M.; Gilpin, R.K. Application of a new numerical method for characterizing heterogeneous solids by using gas solid chromatographic data. J. Chromatogr. **1993**, *628*, 59–67.
15. Fowler, R.H. *Statistical Mechanics,* 2nd Ed.; Cambridge University Press: Cambridge, 1936; 829.
16. Katsanos, N.A.; Iliopoulou, E.; Roubani-Kalantzopoulou, F.; Kalogirou, E. Probability density functions for adsorption energies over time on heterogeneous surfaces by inverse gas chromatography. J. Phys. Chem. B, **1999**, *103*, 10228–10233.
17. Katsanos, N.A.; Iliopoulou, E.; Plagianakos, V.; Mangou, H. Interrelations between adsorption energies and local isotherms, local monolayer capacities, and energy distribution functions, as determined for heterogeneous surfaces by inverse gas chromatography. J. Colloids Interf. Sci. **2001**, *239*, 10–19.
18. Roubani-Kalantzopoulou, F.; Artemiadi, T.; Bassiotis, I.; Katsanos, N.A.; Plagianakos, V. Time separation of adsorption sites on heterogeneous surfaces by inverse gas chromatography. Chromatographia **2001**, *53*, 315–320.
19. Lis, P.S.; Slater, P.G. Flux of gases across air–sea interface. Nature **1974**, *247*, 181–184.
20. Rashid, K.A.; Gavril, D.; Katsanos, N.A.; Karaiskakis, G. Flux of gases across the air–water interface studied by reversed-flow gas chromatography. J. Chromatogr. A, **2001**, *934*, 31–49.
21. Atta, K.R.; Gavril, D.; Loukopoulos, V.; Karaiskakis, G. Study of the influence of surfactants on the transfer of gases into liquid by inverse gas chromatography. J. Chromatogr. A, **2004**, *1023*, 287–296.

Environmental Applications of SFC

Yu Yang
Department of Chemistry, East Carolina University, Greenville, North Carolina, U.S.A.

INTRODUCTION

Because supercritical fluids have liquid like solvating power and gaslike mass-transfer properties, supercritical fluid chromatography (SFC) is considered to be the bridge between gas chromatography (GC) and liquid chromatography (LC) and possesses several advantages over GC and LC, as summarized in Table 1. For example, SFC can separate non-volatile, thermally labile, and high-molecular-weight compounds in short analysis times. Another advantage of SFC is its compatibility with both GC and high-performance liquid chromatography (HPLC) detectors. Because of these advantages of SFC, there is a large number of SFC applications in environmental analysis. However, only selected recent works are reviewed here. Although sample preparation is often required before SFC analysis to remove the analytes from environmental matrices and to enrich them, sample preparation is not intensively discussed in this review. To facilitate the discussion, the environmental pollutants are classified and reviewed separately in this entry.

PESTICIDES AND HERBICIDES

The analysis of pesticides and herbicides has mainly been done either by GC with selective detectors or by HPLC with ultraviolet (UV) detection. As summarized in Table 1, GC is limited to thermally stable volatile compounds, whereas the HPLC with UV can only detect compounds with chromophores. These limitations of GC and HPLC led to the use of SFC in the analysis of pesticides and herbicides. Among the SFC works in environmental analysis, one-third of the works concerns the analysis of pesticides and herbicides.

Many detectors have been used to detect pesticides and herbicides in SFC. Among these detectors, the flame ionization detector (FID) is most commonly used for detection of a wide range of pesticides and herbicides, with a detection limit ranging from 1 ppm (for carbonfuran) to 80 ppm (for Karmex, Harmony, Glean, and Oust herbicides). The UV detector has frequently been used for the detection of compounds with chromophores. The detection limit was as low as 10 ppt when solid-phase extraction (SPE) was online coupled to SFC. The mass spectrometric detector (MSD) has also been used in many applications as a universal detector. The MSD detection limit reached 10 ppb with online SFE (supercritical fluid extraction)–SFC. Selective detection of chlorinated pesticides and herbicides has been achieved by an electron-capture detector (ECD). The limit of detection for triazole fungicide metabolite was reported to be 35 ppb. Other detectors used for detection of pesticides and herbicides include thermoionic, infrared, photometric, and atomic emission detectors.

A variety of both packed and open tubular columns have been used for separation of pesticides and herbicides. The columns were either used separately or coupled in series to achieve better separations. Although environmental water samples were mostly analyzed by SFC, analyses of pesticides and herbicides from soil, foods, and other samples were also reported.

POLYCHLORINATED BIPHENYLS

Since 1929, polychlorinated biphenyls (PCBs) have been produced and used as heat-transfer, hydraulic, and dielectric fluids. Because of their chemical and physical stability, PCBs have been found in many environmental samples. Generally, PCBs have been analyzed by GC with electron-capture detection. There are many reports on subcritical and supercritical fluid extraction of PCBs, but only a few on supercritical fluid separation of PCBs.

Among the works of supercritical fluid separations of PCBs, UV has been the most popular detector. A Microbore C_{18} column was used to separate individual PCB congeners in Aroclor mixtures. Density and temperature programming was also utilized for separation of PCBs. Both packed (with phenyl and C_{18}) and capillary (Sphery-5 cyanopropyl) columns were used in this work. Carbon dioxide, nitrous oxide, and sulfur hexafluoride were tested as mobile phases for the separation of PCBs.

A HD and MSD were also used for detection of PCBs in SFC. Capillary columns packed with aminosilane-bonded silica and open-tubular columns coated with polysiloxane were employed for PCB separation in these works.

POLYCYCLIC AROMATIC HYDROCARBONS

Polycyclic aromatic hydrocarbons (PAHs) have routinely been analyzed by GC and LC. However, both techniques have limitations in terms of analyte molecular weight and analysis time. The greater molecular weight range of SFC

Table 1 Comparison of characteristics of GC, SFC, and LC.

	GCX[a]	SFC	LC[b]
Suitability for polar and thermolabile compounds	Low	High	High
Size of analyte molecule	Small-Medium	Small-Large	Small-Large
Sample capacity	Low	High (packed column)	High
Possibility of introducing selectivity in the mobile phase	Low	High	Medium
Toxicity and disposal cost of the mobile phase	No	No (with pure CO_2) Low (with modifier)	High
Efficiency	High	Medium-High	Low
Use of gas-phase detectors	Yes	Yes	No
Analysis time	Medium	Medium	Long

[a]Only capillary GC is used for these evaluations. Fast GC and packed column GC are not included here.
[b]Capillary HPLC is not included.

with respect to GC makes it better suited for determining a wide range of PAHs. SFC also has advantages over HPLC for the analysis of PAHs when the same kind of columns is used. Supercritical fluid has similar solvating power as a liquid does, and the solute diffusion coefficients are much greater than those found in liquids. Therefore, comparable efficiencies to HPLC can be obtained by SFC in shorter analysis time. Because of these characteristics of SFC, the separation of PAHs by SFC with different kinds of packed and capillary columns is a well-investigated and established method.

The most popular detector for PAHs is the UV detector. The detection limit was 0.2–2.5 ppb for 16 PAHs. A diode-array detector was also used for PAHs in SFC, and the detection limit was reported to be as low as 0.4 ppb. Other detections used for PAHs include mass spetrometric, thermoionic, infrared, photoionization, sulfur chemiluminescence, and fluorescence detectors.

Although has mainly been used as the mobile phase in SFC, modifiers have often been added to to increase the solvating power of the mobile phase. Although the most frequently used modifier has been methanol, many other modifiers were also tested. The modifier effect on retention is discussed separately in this encyclopedia. Because organic modifiers are incompatible with FID, FID was rarely used for PAHs in SFC.

Fast separations of 16 PAHs were achieved within 6–7 min using packed columns. A comparison study of the PAH molecular shape recognition properties of liquid-crystal-bonded phases in packed-column SFC and HPLC found that the selectivity was enhanced in SFC. The result of an interlaborotory round-robin evaluation of SFC for the determination of PAHs also shows that SFC possesses distinct advantages over GC/MS and nuclear magnetic resonance (NMR) including speed, cost, and applicability.

POLAR POLLUTANTS

Because carbon dioxide is non-polar, the separation of polar compounds by supercritical carbon dioxide is difficult. Thus, polar modifiers are often used for the separation of phenols and amines. Derivatization has also been employed to obtain non-polar analytes in some applications. The UV detector has mainly been used for the detection of polar compounds. Oxidative and reductive amperometric detection was also utilized with a detection limit of 250 pg for oxidative detection of 2,6-dimethylphenol. The detection of amines has generally been achieved by FID. Other detectors used for the detection of polar analytes include Fourier transform infrared (FTIR), photodiode array, and flame photometry.

It should be pointed out that separation of more than one class of organic compounds can be achieved by SFC. For example, Fig. 1 shows the chromatogram of 35 PAHs, herbicides, and phenols from a contaminated water sample. Solid-phase extraction was used for sample preparation. Five Hypersil silica columns were coupled in series for separation of these contaminants. The percentage of methanol (as modifier) was varied from 2% (5 min) to 10% (29 min) at 0.5%/min. A pressure program was also applied. A diode-array detector was used in this work.

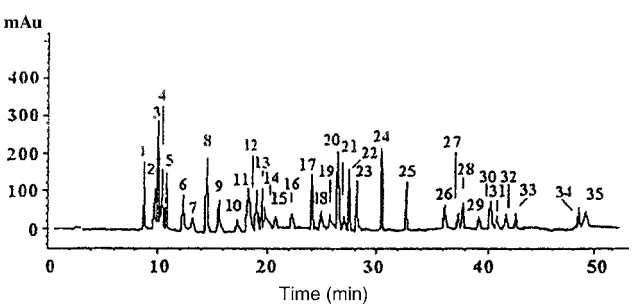

Fig. 1 Chromatogram of PAHs, herbicides, and phenols obtained by supercritical carbon dioxide modified with methanol. **Source:** From Packed-column supercritical fluid chromatography coupled with solid-phase extraction for the determination of organic microcontaminants in water, in J. Chromatogr. A.[1] Copyright 1998, with permission from Elsevier.[1] Packed-column supercritical fluid chromatography coupled with solid-phase extraction for the determination of organic microcontaminants in water, *J. Chromatogr. A 823*: 164, 1998. Copyright 1998, with permission from Elsevier Science.

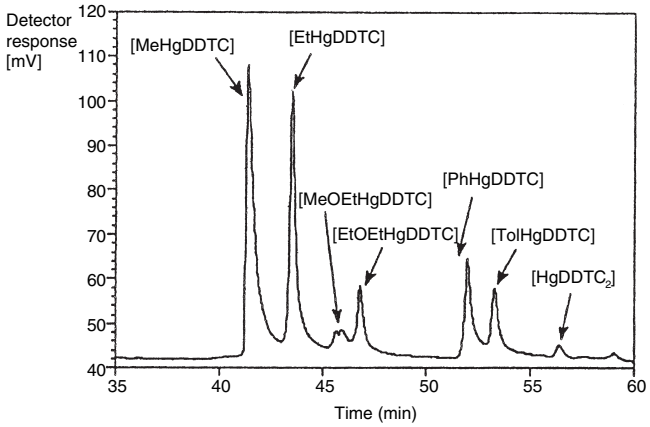

Fig. 2 Chromatogram of a standard mixture after complexation with sodium diethyldithiocarbamate. Composition of the standard: mercury dichloride, methylmercury chloride, ethylmercury chloride, methoxyethylmercury chloride, ethoxyethylmercury chloride, phenylmercury chloride, and tolymercury chloride.
Source: From Interfacing supercritical fluid chromatography with atomic fluorescence spectrometry for the determination of organomercury compounds, in J. Chromatogr. A.[2] Copyright 1997, with permission from Elsevier Science.[2]

ORGANOTIN, MERCURY, AND OTHER INORGANIC POLLUTANTS

Organotin compounds are used extensively as biocides and in marine antifouling paints. These compounds accumulate in sediments, marine organisms, and water, as they are continuously released into the marine environment. Many of these organotin compounds are toxic to aquatic life. Most organotin separation techniques have been based on the GC resolution of volatile derivatives and coupled to elemental detection techniques that are often not sensitive enough to detect trace organotin compounds. However, the separation of organotin compounds was achieved by capillary columns (SB-Biphenyl-30 or SE-52) with pure CO_2 as the mobile phase. Inductively coupled plasma–mass spectrometry (ICP–MS) was used in most of the applications to improve the sensitivity for detecting trace organotin species. The reported detection limits range from 0.2 to 0.8 pg for tetrabultin chloride, tributyltin chloride, triphenyltin chloride, and tetraphenyltin. However, the detection limits obtained by FID are 15- to 45-fold higher than those obtained by ICP–MS for the above-mentioned organotin compounds. Flame photometric detector was also used to detect organotin species with a detection limit of 40 pg for tribultin chloride.

The separation of organomercury was conducted by using a SB-methyl-100 capillary column and pure CO_2 as the mobile phase. FID and atomic fluorescence were used for detection. The same column was also used for separation of mercury, arsenic, and antimony species using carbon dioxide as the mobile phase. A chelating reagent, bis(trifluoroethyl)dithiocarbamate, was used in this case to convert the metal ions to organometallic compounds before the separation. The detection limit of FID was 7 and 11 pg for arsenic and antimony, respectively.

Fig. 2 shows an example of separating organomercury using supercritical A 10 m 50 mm-inner CO_2. A 10 m × 50 μm inner diameter SB-Methyl 100 column was used for the separation. Due to their poor solubility in supercritical carbon dioxide, monoorganomercury compounds were derivatized by diethyldithiocarbamate. An interface for a system consisting of SFC and atomic fluorescence spectrometry was developed for the detection of organomercurials.

In closing, supercritical fluid chromatography is a promising technique for the analysis of environmental pollutants. The analytes range from inorganic species to polar and non-polar organic compounds. The sample matrices cover water, soil, sediments, sludge, and air particulate matters. The sample preparation has been done by solid-phase extraction, supercritical fluid extraction, or traditional solvent extraction. Modifiers are often used to enhance the solubility of analytes and to yield a better separation for polar and high-molecular-weight analytes. Packed columns are preferred for trace analysis because of their high sample capacity. Both gas-phase and liquid-phase detectors have been used in SFC to detect a wide range of environmental pollutants.

REFERENCES

1. Toribio, L.; del Nozal, M.J.; Bernal, J.L.; Jimenez, J.J.; Serna, M.L. Packed-column supercritical fluid chromatography coupled with solid-phase extraction for the determination of organic microcontaminants in water. J. Chromatogr. A, **1998**, *823*, 164.
2. Knochel, A.; Potgeter, H. Interfacing supercritical fluid chromatography with atomic fluorescence spectrometry for the determination of organomercury compounds. J. Chromatogr. A, **1997**, *786*, 192.

BIBLIOGRAPHY

1. Bayona, J.M.; Cai, Y. The role of supercritical fluid extraction and chromatography in organotin speciation studies. Trends Anal. Chem. **1994**, *13*, 327–332.
2. Berger, T.A. Separation of polar solutes by packed column supercritical fluid chromatography. J. Chromatogr. A, **1997**, *785*, 3–33.

3. Chester, T.L.; Pinkston, J.D.; Raynie, D.E. Supercritical fluid chromatography and extraction. Anal. Chem. **1998**, *70*, 301R–319R.
4. Dressman, S.F.; Simeone, A.M.; Michael, A.C. Supercritical fluid chromatography with electrochemical detection of phenols and polyaromatic hydrocarbons. Anal. Chem. **1996**, *68*, 3121–3127.
5. Juvancz, Z.; Payne, K.M.; Markides, K.E.; Lee, M.L. Multidimensional packed capillary coupled to open tubular column supercritical fluid chromatography using a valve-switching interface. Anal. Chem. **1990**, *62*, 1384–1388.
6. Knochel, A.; Potgeter, H. Optimisation of expression and purification of the recombinant Yol066 (Rib2) protein from Saccharomyces cerevisiae. J. Chromatogr. A, **1997**, *786*, 188–193.
7. Laintz, K.E.; Shieh, G.M.; Wai, C.M. Simultaneous determination of arsenic and antimony species in environmental samples using bis(trifluoroethyl)dithiocarbamate chelation and supercritical fluid chromatography. J. Chromatogr. Sci. **1992**, *30*, 120–123.
8. Luffer, D.R.; Novotny, M. Element-selective detection after supercritical fluid chromatography by means of a Surfatron plasma in the near-infrared spectral region. J. Chromatogr. **1990**, *517*, 477–489.
9. Medvedovici, A.; David, F.; Desmet, G.; Sandra, P. Fractionation of nitro and hydroxy polynuclear aromatic hydrocarbons from extracts of air particulates by supercritical fluid chromatography. J. Microcol. Separ. **1998**, *10* (1), 89–97.
10. Medvedovici, A.; Kot, A.; David, F.; Sandra, P. The use of supercritical fluids in environmental analysis. In *Supercritical Fluid Chromatography with Packed Columns*; Anton, K., Berger, C., Eds.; Marcel Dekker, Inc.: New York, 1998; 369–401.
11. Moyano, E.; McCullagh, M.; Galceran, M.T.; Games, D.E. Supercritical fluid chromatography-atmospheric pressure chemical ionisation mass spectrometry for the analysis of hydroxy polycyclic aromatic hydrocarbons. J. Chromatogr. A, **1997**, *777*, 167–176.
12. Mulcahey, L.J.; Rankin, C.L.; McNally, M.E.P. Environmental applications of supercritical fluid chromatography. In *Advances in Chromatography*; 1994; *Vol. 34*, 251–308.
13. Shan, S.; Ashraf-Khorassani, M.; Taylor, L.T. Analysis of triazine and triazole herbicides by gradient-elution supercritical fluid chromatography. J. Chromatogr. **1990**, *505*, 293–298.
14. Smith, R.M.; Briggs, D.A. Separation of homologous aromatic alcohols and carboxylic acids by packed column supercritical fluid chromatography. J. Chromatogr. A, **1994**, *688*, 261–271.

Environmental Materials: Supercritical Fluid Extraction of Polynuclear Aromatic Hydrocarbons

Maria de Fatima Alpendurada
Faculty of Pharmacy, University of Porto, Porto, Portugal

INTRODUCTION

Supercritical fluid extraction (SFE), usually with carbon dioxide and, often, with a modifier, has become of increasing interest in the last few years because of its selectivity, preconcentration effect, efficiency, simplicity, rapidity, cleanness, and safety, mainly concerning the extraction of organic compounds prior to separation and detection by chromatographic techniques. It has several advantages over classical solvent extractions, in comparison with recent extraction techniques. Approaches to obtain quantitative extractions, including fluid choice, extraction flow rate, modifiers, pressure, and temperature, are presented, as well as the potential for SFE to extract polynuclear aromatic hydrocarbons (PAHs) from soils, sediments, and biota. Improvements and new environmental applications are also reported.

PARAMETERS INFLUENCING THE SUPERCRITICAL FLUID EXTRACTION PROCESS AND APPLICATIONS

Since the first applications of SFE were published by Zosel in 1978, this extraction technique has developed into a key method for the separation of the contaminants from both sediment and biological matrices. SFE has a number of advantages over classical solvent extraction methods: It is faster, more selective, and less toxic, particularly when compared with techniques using solvents such as dichloromethane, thus reducing safety hazards. It has received the attention of some researchers who have reviewed and developed this technique and its suitability to the analysis of environmental matrices.[1–3] The application of SFE to PAHs was reviewed, and new analytical strategies involving the need for modified supercritical fluids to improve extraction efficiency, restrictor prevention from blocking, collection form of the eluant, and general operation conditions, has been demonstrated. This technique is radically different from liquid–solid extraction (LSE), subcritical water extraction, microwave-assisted extraction (MAE), and accelerated solvent extraction (ASE)—also known as pressurized liquid extraction or pressurized fluid extraction—because the main constituent of the solvent system, CO_2, separates from the extracts upon venting to the atmosphere, leaving the analytes that are trapped either on a solid phase, such as C_{18}, or in an organic solvent. The influence in the extraction process of various parameters will depend on a number of steps controlling the transport of analytes from the matrix to the bulk fluid, e.g., temperature, pressure, solvent type, and extraction time. Interested readers should consult an excellent review regarding the mechanisms controlling the binding, release, and transport in environmental materials.[4] Supercritical fluid extraction, at low (50°C) and high (200°C) temperatures, and an 18 hr Soxhlet extraction with dichloromethane for railway soil and diesel soot samples were compared for the PAHs extraction.[5] The samples were mixed with anhydrous Na_2SO_4. The mean recoveries for the 17 PAHs examined in the railway soil was 50% at 50°C, 81% at 200°C, and 90% at 350°C. For the diesel soot, the recovery for 13 PAHs was 51% at 50°C, 71% at 200°C, and 118% at 350°C. Although higher temperatures favored better recoveries for the higher-molecular-weight PAHs, it was also suspected that the two- to three-ring PAHs were actually generated at these elevated temperatures. So a 30 min extraction at 200°C was selected as the optimum. Temperature and organic modifiers—10% MeOH, diethylamine, and/or toluene—using a marine sediment (SRM 1941) diesel soot and air particulate matter (SRM 1649) were also examined. The best recoveries were obtained with CO_2–diethylamine at 200°C with a 15 min-static and 15 min-dynamic extraction time. Also, supercritical water at 250°C, CO_2 at 200°C, and CO_2 with 19% toluene at 80°C were compared for the extraction of PAHs from urban air. Surprisingly, the water was generally as effective as the other solvents under these conditions.[2] However, unlike CO_2, the water had to be subsequently removed from the extract. After optimization of the SFE-CO_2 extraction method for PAHs, similar results were obtained by using the acetone with MAE, ASE with acetone/dichloromethane, or Soxhlet with dichloromethane.

The use of a binary modifier, which is added to the extraction cell at the time of the extraction, rather than continuously, in the CO_2 stream showed an almost matrix-independent SFE method for the PAHs.[6] The modifiers, diethylamine, trifluoroacetic acid, citric acid, isopropylamine, and tetrabuthyl ammonium hydroxide, all individually at a 1% level in toluene, were tested for the extraction of CRM 392, sewage sludge, and marine sediment. The extractions were reproducible and

comparatively complete and, with the correct binary modifier, did not require any prior matrix treatment, e.g., with HCl. Diethylamine at 200°C gave the highest recoveries to examine the effect on the SFE of PAHs from marine sediment, diesel soot, and air particulates. Online coupling of an SFE system with a GC/MS instrument was performed by a homemade, suitably shaped accumulation cell,[7] eliminating the effect of CO_2 flow on the MS detector. Moreover, it enables multistep extraction based on the direct addition of a modifier into the extraction cell. The quantitative determination of PAHs and other organic pollutants in sewage sludge was performed by using SFE as a fast extraction method, followed by a short cleanup step. The extraction step was validated with CRMs.[8] Improving the extraction capacity of the supercritical fluid—higher temperature, higher pressure, stronger modifier effect—by using a ternary mixture of CO_2 modified with methanol/dichloromethane, 5:1, a more robust and applicable method to a larger range of matrices was obtained.[9] Fernández[10] used an experimental design to optimize the SFE of PAHs from sediment. Under the optimum conditions, the recovery of total PAHs was ~15% higher with SFE than with the comparative Soxhlet extraction. A five-level factorial experimental design was used to examine the optimum conditions for the extraction of two- to six-ring PAHs from sediment with pressure, temperature, and organic modifier. Depending on the nature of the matrix and the concentration of the compounds to be determined, the SFE system can be directly connected to the detector. All of the different extraction techniques mentioned above can be used for the extraction of PAHs in very complex environmental materials. A very recently developed work reported an extraction/cleanup procedure by SFE for biological samples (liver) and subsequent high-performance liquid chromatography HPLC-FL determination of those compounds in the enriched extract.[11]

COMMENTS ON THE EXTRACTION TECHNIQUES

Most recent studies on the previously discussed extraction techniques have made a direct comparison with the efficiency of Soxhlet extraction to validate the system used, effectively resulting in a benchmark method. Regarding these studies of extraction of PAHs from solid environmental samples, some overall observations can be made. With the exception of a few reports, the modern methods of extraction offer no greater efficiency than the centenary Soxhlet extraction method. Also, in terms of extraction, the extent of good agreement between data obtained by a wide range of extraction methods should suggest that there may not be any significant advantage with any particular method. Because one of the advantages of using MAE, ASE, and SFE is the use of small volumes of toxic organic solvents, in a number of cases the use of multiple extractions with a fresh change of solvent will approach the volume to the classical extraction method. Another apparent advantage of MAE, ASE, subcritical water extraction, and SFE is that the extractions are faster and, therefore, labor saving. The actual extraction cycle is short for MAE and ASE, ~5–10 min. However, for multiple extractions, there is little time between cycles for the analyst to undertake other tasks and also to attend the system while it is in use. The main advantage of Soxhlet extraction is that, once it has been set up, it can be left unattended for the full duration of the extraction, ~8–24 r. In many cases, the extent of the labor saved associated with MAE, ASE, and SFE is considerably exaggerated. Table 1 shows the conditions used to compare Soxhlet, ASE, SFE, and subcritical water extractions of PAHs. Also, the extraction quality greatly differed. In the case of Soxhlet and ASE, they were much darker, while extracts from subcritical water were orange, and the extracts from SFE (with CH_2Cl_2) were light yellow.[12] The organic solvent extracts also yielded more artifact peaks in the GC/MS and GC-flame ionization detection chromatograms, especially when compared to supercritical CO_2 (Figs. 1 and 2). Based on elemental analysis (carbon and nitrogen) of the solid residues after each extraction, subcritical water, ASE, and Soxhlet extraction had poor selectivity for PAHs vs. soil organic matter (~25–33% of the bulk solid organic matter was extracted along with PAHs), while SFE with pure CO_2 removed only 8% of the bulk organic matrix.

Table 1 Conditions used to compare soxhlet, ASE, SFE, and subcritical water extractions of PAHs.

Conditions	Soxhlet	ASE	SFE	Subcritical water
Sample size (g)	2	2	2	2
Extraction solvent	DCM–acetone	DCM–acetone	pure CO_2	water
Collection solvent	—	—	DCM	toluene
Pressure (bar)	ambient	70	400	50
Temperature (°C)	b.p. of solvent	100	150	300, 250
Flow rate	15 min/cycle	1 ml/min	1 ml/min	1 ml/min
Time	18 hr	50 min	60 min	30, 60 min
Solvent volume (ml)	150	15	15	10, 20

These conditions were used for determination of PAHs in soil samples collected from an abandoned gas-manufacturing plant.
Source: From Comparison of Soxhlet extraction, pressurized liquid extraction, supercritical fluid extraction and subdritical water extraction for environmental solids: Recovery, selectivity and effects on sample matrix, in J. Chromatogr. A.[12]

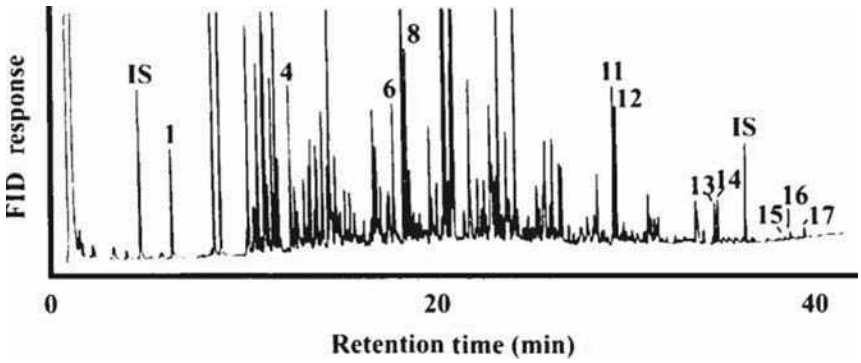

Fig. 1 GC-flame ionization detection chromatogram of a complex mixture of PAHs extracted by SFE from a contaminated soil. (1) naphthalene, (2) 2-methylnaphthalene, (3) 1-methylnaphthalene, (4) acenaphthene, (5) fluorene, (6) dibenzothiophene, (7) phenanthrene, (8) anthracene, (9) fluoranthene, (10) pyrene, (11) benzo(a)anthracene, (12) chrysene, (13) benzo(e)pyrene, (14) benzo(a)pyrene, (15) indeno(1,2,3-cd)pyrene, (16) dibenzo(a,h)anthracene, (17) benzo(g,h,i)perylene.
Source: From Comparison of Soxhlet extraction, pressurized liquid extraction, supercritical fluid extraction and subdritical water extraction for environmental solids: Recovery, selectivity and effects on sample matrix, in J. Chromatogr. A.[12]

Neither MAE nor ASE is currently in a configuration that would readily lead to the automation of sample preparation. Supercritical fluid extraction can be used as online system that can then be connected to the chromatographic and detection systems. Connected online with the GC/MS, SFE was successfully used for the determination of PAHs in marine sediments. Using either CO_2 alone or modified with toluene or MeOH in the extraction, the PAHs were cryofocused in the accumulation cell of the GC and then directly chromatographed.[7] For the study of PAHs in marine sediments, a new extraction technique, which consists of the combination of ASE (dynamic and static mode) and SFE (dynamic mode), was developed, with an extraction time longer than in ASE but shorter than in SFE, and better recoveries for five- to six-ring PAHs than in the conventional ASE and SFE.[13] Polynuclear aromatic hydrocarbons in tap and river water were extracted by SFE, online, with solid-phase extraction disks.[14] Table 2 presents the extraction conditions for SFE of PAHs from different environmental materials, as reported in the literature.

FUTURE TRENDS IN SFE

SFE with CO_2, whose most important benefits have already been mentioned, also shows significant limitations that are worth studying to understand the field of

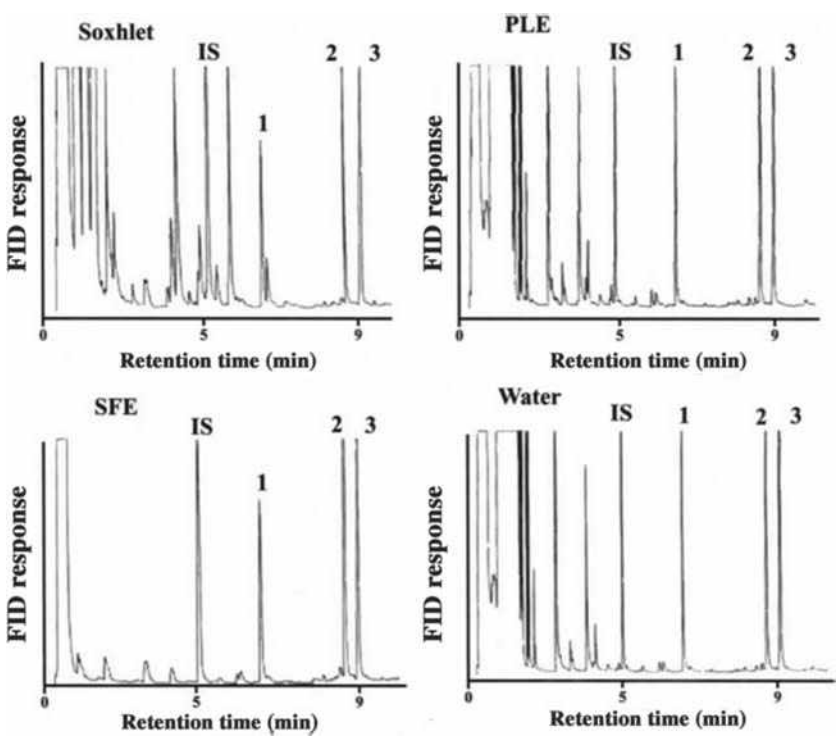

Fig. 2 GC-flame ionization detection chromatograms containing early artifact peaks from different solvent extraction methods: Soxhlet, ASE (PLE), SFE, and subcritical water extraction of a soil sample collected from a manufacturing gas plant site. The numbers refer to PAHs identified in the legend of Fig. 1.
Source: From Comparison of Soxhlet extraction, pressurized liquid extraction, supercritical fluid extraction and subdritical water extraction for environmental solids: Recovery, selectivity and effects on sample matrix, in J. Chromatogr. A.[12]

Table 2 Extraction conditions for SFE of PAHs from different environmental materials.

Matrix	Reference material	Extractant	Temp. (°C)	Pressure (bar)	Extraction time (min)	Mode	Solvent collection	Recovery (%)	Refs.
Marine sediment	NIST 1649	CO_2 100%	200	450	15 + 30	static + dynamic	DCM	—	[5]
Sediment	NRCC HS-6	CO_2 100% or + 3 × 20 ul MeOH	70	200	15	dynamic	MeOH	80–100	[7]
Sewage sludge	CRM 088	CO_2 100% (step 1)	80	121	10 + 10	static + dynamic	toluene		[8]
		CO_2 + 1% MeOH and 4% DCM (step 2)	120	335	10 + 30	static + dynamic	toluene		[8]
		CO_2 100% (step 3)	120	335	5 + 10	static + dynamic	toluene	104–122	[8]
Soil	—	CO_2 + MeOH + DCM 5 : 1	95	450	15	dynamic	MeOH	90	[9]
Sediment	—	CO_2 100% or CO_2 + 2 to 10% methanol	140	340	15	dynamic	hexane	—	[10]
Soil	—	CO_2 100%	150	400	60	dynamic	DCM	>90%	[12]

The following abbreviations are used for organic solvents used: MeOH = methanol; DCM = dichloromethane.

application of the technique and to help in seeking alternatives in this context. The main drawbacks that SFE has to cope with are the difficulties in extracting polar analytes, the different efficiencies obtained from spiked and natural samples, and sometimes the need for a cleanup step before the analysis.[12] To point out the future trends in this extraction technique, it is mandatory to consider the latest contributions in this area. The coupling of supercritical CO_2 with subcritical water is a very recent and promising alternative that has proven to successfully extract nonpolar analytes.[14] The development of new analyte collection methods, with reduced solvent consumption resulting in more concentrated extracts, is also a target of current research. Another important future trend in SFE is the possibility of performing fieldwork.[15] In this context, a single SFE method for field extraction of PAHs in soil has been developed for the U.S. Department of Defense and it is currently being tested. The approach uses dry ice (thus avoiding compressed CO_2 tanks), and works well for nonpolar analytes, but requires the use of modifiers for the extraction of polar analytes. Increased energy costs and regulatory requirements for waste reduction and site remediation have created increased interest in the benefits and application of SFE. Current research is being conducted to develop methods for application to large-scale soil remediation. Such applications will occur as the SFE knowledge base expands.[16] Taking into account the breakthroughs in other alternatives, such as ASE, MAE, and Soxhlet, before selecting SFE as a primary extraction method, its main benefits and limitations should be weighted. Thus considering the characteristics of the matrix and the analytes involved, the analyst must select the most appropriate alternative.

CONCLUSIONS

It has become clear that the environmental chemist should be more diligent in developing methods that are more environmentally friendly and provide a safer work environment. Following the Montreal Protocol, there is a gradual phasing out of the use of chlorinated solvents. While it has the major environmental impact in the dry cleaning and bulk chemical industry, it seems inappropriate to continue developing methods that require chlorinated solvents when, with a review of literature and some practice, suitable alternatives can be found. The accreditation bodies could play an important role to clearly move the existence of methodologies that use organic solvents.

In this context, SFE has a great potential for replacing older extraction methods, e.g., Soxhlet extraction. Despite important limitations described elsewhere, with the help of special strategies for the extraction of moderately polar and highly polar analytes, the SFE range of applications will dramatically increase in the near future.

REFERENCES

1. Camel, D.; Tambuté, B.; Caude, M. Analytical-scale supercritical fluid extraction: A promising technique for the determination of pollutants in environmental matrices. J. Chromatogr. A, **1993**, *642* (1–2), 263–281.
2. Hawthorne, S.B.; Miller, D.J.; Burford, M.D.; Langenfeld, J.J.; Eckert-Tilotta, S.; Louie, P.K. Factors controlling quantitative supercritical fluid extraction of analytical samples. J. Chromatogr. A, **1993**, *642* (1–2), 301–317.
3. Janda, V.; Bartle, D.K.; Clifford, A.A. Supercritical fluid extraction in environmental analysis. J. Chromatogr. A, **1993**, *642* (1–2), 283–299.

4. Dean, J.R. Extraction of polycyclic aromatic hydrocarbons from environmental matrices: Practical considerations for supercritical fluid extraction. Analyst **1996**, *121*, 85R–89R.
5. Yang, Y.; Gharaibeh, A.; Hawthorne, B.; Miller, J.D. Combined temperature/modifier effects on supercritical CO_2 extractions efficiencies of polycyclic aromatic hydrocarbons from environmental samples. Anal. Chem. **1995**, *67*, 641–646.
6. Hawthorne, S.B.; Yang, Y.; Miller, J.D. Extraction of organic pollutants from environmental solids with sub- and supercritical water. Anal. Chem. **1994**, *66*, 2912–2920.
7. Fuoco, R.; Ceccarini, A.; Onor, M.; Lottici, S. Supercritical fluid extraction combined on-line with cold-trap gas chromatography/mass spectrometry. Anal. Chim. Acta **1997**, *346* (1), 81–86.
8. Berset, J.D.; Holzer, R. Quantitative determination of polycyclic aromatic hydrocarbons, polychlorinated biphenyls and organochlorine pesticides in sewage sludges using supercritical fluid extraction and mass spectrometric detection. J. Chromatogr. A, **1999**, *852*, 545–558.
9. Gonçalves, C.; De-Rezende Pinto, M.; Alpendurada, M.F. Benefits of a binary modifier with balanced polarity for an efficient supercritical fluid extraction of PAHs from solid samples followed by HPLC. J. Liq. Chromatogr. Relat. Technol. **2001**, *24* (19), 2943–2959.
10. Fernández, I.; Dachs, J.; Bayona, M.J. Application of experimental design approach to the optimization of supercritical fluid extraction of polychlorinated biphenyls and polycyclic aromatic hydrocarbons. J. Chromatogr. A, **1996**, *719* (1), 77–85.
11. Amigo, S.G.; Falcon, M.S.G.; Yusty, M.A.L.; Lozano, J.S. Supercritical liqud extraction of polycyclic aromatic hydrocarbons from liver samples and determination by HPLC-FL. Fresenius' J. Anal. Chem. **2000**, *367* (6), 572–578.
12. Hawthorne, S.B.; Grabanski, C.B.; Martin, E.; Miller, D.J. Comparison of Soxhlet extraction, pressurized liquid extraction, supercritical fluid extraction and subdritical water extraction for environmental solids: Recovery, selectivity and effects on sample matrix. J. Chromatogr. A, **2000**, *892*, 421–433.
13. Notar, M.; Leskovsek, H. Determination of polycyclic aromatic hydrocarbons in marine sediments using a new ASE–SFE extraction technique. Fresenius' J. Anal. Chem. **2000**, *366* (8), 500–846.
14. Luque de Castro, D.C.; Jiménez-Carmona, M.M. Where is supercritical fluid extraction going? Trends Anal. Chem. **2000**, *19* (4), 223–228.
15. Bowadt, S.; Mazeas, L.; Millert, D.J.; Hawthorne, S.B. Field portable determination of polychlorinated biphenyls and polynuclear aromatic hydrocarbons in soil using supercritical fluid extraction. J. Chromatogr. A, **1997**, *785*, 205–217.
16. Green, T.; Bonner, J.S. Environmental application of supercritical fluid extraction. Danger. Prop. Ind. Mater. Rep. **1991**, *11* (4), 304–310.

Environmental Pollutants: CE Analysis

Imran Ali
Department of Chemistry, Jamia Millia Islamia (A Central University), New Delhi, India

Hassan Y. Aboul-Enein
Pharmaceutical and Medicinal Chemistry Department, Pharmaceutical and Drug Industries Research Division, National Research Center, Dokki, Cairo, Egypt

INTRODUCTION

The quality of the environment is degrading continuously, due to the accumulation of various undesirable constituents. Water resources, the most important and useful components of the environment, are most affected by pollution. The ground and surface water at many places in the world are not suitable for drinking purposes, due to the presence of esthetic and toxic pollutants. Therefore, the importance of water quality preservation and improvement is essential and continuously increasing.[1,2] The most important toxic pollutants are inorganic and organic chemicals. Therefore, determination of these water pollutants at trace levels is essential in environmental hydrology.

PRINCIPLE OF CAPILLARY ELECTROPHORESIS (CE)

The schematic representation of a CE apparatus is shown in Fig. 1. The mechanism of separation of water pollutants in CE is based on the electro-osmotic flow (EOF) and electrophoretic mobilities of the pollutants. The EOF propels all pollutants (cationic, neutral, and anionic) toward the detector and, ultimately, separation occurs due to the differences in the electrophoretic migration of the individual pollutants. Under the CE conditions, the migration of the pollutant is controlled by the sum of the intrinsic electrophoretic mobility (μ_{ep}) and the electro-osmotic mobility (μ_{eo}), due to the action of EOF. The observed mobility (μ_{obs})of the pollutants is related to μ_{eo} and μ_{ep} by the following equation:

$$\mu_{obs} = \mu_{eo} + \mu_{ep} \tag{1}$$

The electrophoretic mobilities of cations (μ_{obs}) can be related to the limiting ionic equivalent conductivity, λ_{ekv}, by the following equation:

$$\mu_{obs} = \lambda_{ekv}/F = q_i/6\pi\eta r_i \tag{2}$$

where, F is the Faraday constant ($F = 9.6487 \times 10^4$ A sec/mol), λ_{ekv} (cm^2/mol/ohm) is related, by the Stokes law, to the charge of the hydrated cation q_i, to the dynamic viscosity of the electrolyte, η (g cm^2/sec), and to the radius of the hydrated cation r_i (cm). The μ_{ep} values can be calculated from the experimental data, the mobility of the cation (μ_{obs}), and the mobility of the EOF μ_{eo}, according to the following equation:

$$\begin{aligned}\mu_{ep} &= \mu_{obsp} - \mu_{eo} \\ &= [1/t_{m(ion)} - 1/t_{m(eo)}][l_T \cdot L_d/V]\end{aligned} \tag{3}$$

where, $t_{m(ion)}$, $t_{m(eo)}$, l_T and L_d are the migration time of the cation (sec), migration time of the EOF (sec), the overall capillary length, and the length of the capillary to the detector (cm), respectively. Thus, EOF plays an important role in the determination of metal ions by CE. The determination of water pollutants can be carried out by several modes of CE. The various modes of CE include capillary zone electrophoresis (CZE), micellar capillary electrokinetic chromatography (MECC), capillary isotachophoresis (CIEF), capillary gel electrophoresis (CGE), ion-exchange electrokinetic chromatography (IEEC), capillary isoelectric focusing (CIEF), affinity capillary electrophoresis (ACE), capillary electrochromatography (CEC), separation on microchips (MC), and non-aqueous capillary electrophoresis (NACE).[6] However, most of the water pollutant analyses have been carried out in the CZE mode.

SAMPLE PRETREATMENT

The treatment of the samples from environmental matrices is an important issue in CE. Little attention has been given for the water sample treatment in CE analysis of environmental pollutants. Soil samples have been extracted by the usual methods. Besides, the sediment samples were digested using strong acids. The samples containing a highly ionic matrix may cause problems in CE. EOF in the capillary can be altered by the influence of the sample matrix, resulting in poor resolution. Additionally, the

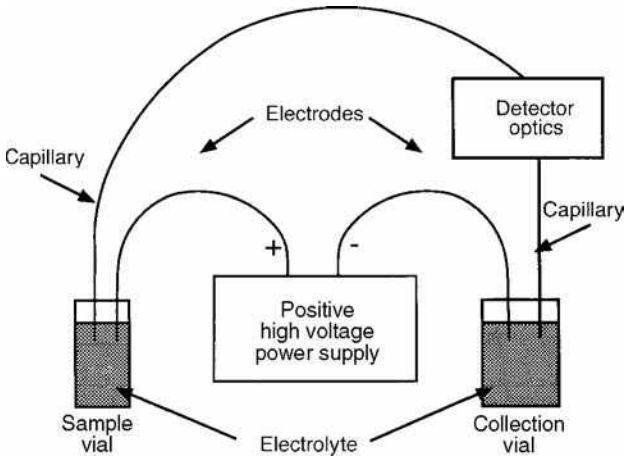

Fig. 1 Diagram of the CE system.
Source: Reprinted from Waters Quanta 4000E Capillary Electrophoresis System Operator's Manual, Waters Corp., Milford, Massachusetts, U.S.A., 1993.

detector baseline is usually perturbed when the pH of the sample differs greatly from the pH of the background electrolyte (BGE). The samples containing UV absorbing materials are also problematic in the detection of the environmental pollutants. Due to all of these factors, some authors have suggested sample cleanup processes, solid/liquid phase extractions, and sample preparations prior to loading onto CE.[8–11] Real samples often require the application of simple procedures, such as filtration, extraction, dilution, etc. Electromigration of sample cleanup suffers severely from matrix dependence effects; even then, it has been used for preconcentration in inorganic analysis. The sample treatment methods have been discussed in several reviews.[5–7,10] The use of ion-exchange and chelating resins to preconcentrate the metal ion samples prior to CE application has been reported.[7,10] An online dialysis sample cleanup method for CE analysis has also been presented. Besides, several reports have been published on dialysis and electrodialysis for sample cleanup prior to CE injection.[5–7,10]

DETECTION

Generally, UV detection is used for the determination of most environmental pollutants. However, the use of UV detectors in CE for metal ion and anion analysis is not suitable due to the poor absorbance of UV radiation by metal ions and anions. The most common method to solve this problem is indirect UV detection. The main advantage of the indirect UV detection method is its universal applicability. The complexation of metal ions with ligands also increases the sensitivity of their detection. The complexing agent is either added to the electrolyte (in situ, online complexation) or to the sample before the introduction into the capillary column (off-line complexation). The most commonly used ligands are azo dyes, quinoline dyes, porphyrin, dithiocarbamate, aminopolycarboxylic acids, 4-(2-pyridylazo) resorcinol, 8-hydroxyquinoline-5-sulfonic acid, ethylenediaminetetraacetic acid, cyanides, various hydroxy carboxylic acids, crown ethers, and other organic chelating agents. Besides, UV visualizing agents (probe) have also been used to increase the sensitivity of detection in the UV mode. The important probes include, e.g., Cu(II) salts, chromate, aromatic amines, and cyclic compounds, e.g., benzylamine, 4-methylbenzylamine, dimethylbenzylamine, imidazole, *p*-toludine, pyridine, creatinine, ephedrine, and anionic chromophores (benzoate and anisates).[5–7,10,12] Care must be taken to avoid the interaction of the cations and visualizing agent with the capillary wall. Besides, the visualizing agents should exhibit a mobility close to that of the cations, its UV absorbance should be as high as possible, and the detector noise as low as possible. Furthermore, sensitivity of the UV detection has been increased by using a double beam laser as the light source.

To overcome the problem of detection in CE, many workers have used inductively coupled plasma-mass spectrometry (ICP-MS) as the method of detection.[5–7,10–12] Electrochemical detection in CE includes conductivity, amperometry, and potentiometry detection. The detection limit of amperometric detectors has been reported to be up to 10^{-7} *M*. A special design of the conductivity cell has been described by many workers. The pulsed-amperometric and cyclic voltametry waveforms, as well as multi step wave forms, have been used as detection systems for various pollutants. Potentiometric detection in CE was first introduced in 1991 and was further developed by various workers.[5–7,10,12] 8-Hydroxyquinoline-5-sulfonic acid and lumogallion exhibit fluorescent properties and, hence, have been used for metal ion detection in CE by fluorescence detectors.[5–7,10,12] Overall, fluorescence detectors have not yet received wide acceptance in CE for metal ions analysis, although their gains in sensitivity and selectivity over photometric detectors are significant. Moreover, these detectors are also commercially available. Some other devices, such as chemiluminescence, atomic emission spectrometry (AES), refractive index, radioactivity, and X-ray diffraction, have also been used as detectors in CE for metal ions analysis,[12] but their use is still limited.

SEPARATION EFFICIENCY IN CAPILLARY ELECTROHPORESIS

From the literature available and discussed herein, it may be assumed that the selectivity of various environmental pollutants by CE is quite good. However, the detection sensitivity for metal ions and anions is poor. Therefore,

Table 1 The applications of capillary electrophoresis for the determination of environmental pollutants.

Pollutants	Sample matrix	Electrolytes	Detection	Detection limit
Metal Ions in Water, Sediment, and Soil[5–7]				
Arsenic and selenium	Drinking water	20 m*M* KHP, 20 m*M* Boric acid (pH 9.03) hydrodynamically modified EOF	Hydride generation ICP-MS	6–58 ng/L
		75 m*M* Dihydrogen phosphate, 25 m*M* tetraborate (pH 7.65)	Direct UV 195	12 μg/L
		Chromate, 0.5 m*M* TTAOH (pH 10.5)	Indirect UV 254 nm	10 μg/L
Mg, Ca, Na, and K	Well water	5 m*M* Imidazole, 6.5 m*M* HIBA 2 m*M* 18-crown-6 (pH 4.1)	Indirect UV 214 nm	—
Alkali and alkaline Earth metals	Tap and mineral waters	10 m*M* Imidazole (pH 4.5)	Indirect UV 214 nm	0.05 mg/L
Uranyl cation (UrO_2^{2+})	River water	10 m*M* Perchloric acid, 1 m*M* phosphate, 0.6 m*M* borate, 0.01–0.1 m*M* arsenazo III 650 nm, 50–150 m*M* NaCl, 10% MeOH	Direct UV–VIS	10 μg/L
Zn and other transition metals	Tap water	10 m*M* Borate buffer, 0.1 m*M* HQS (pH 9.2)	Direct UV 254 nm	3–225 μg/L
Al	River, reservoir, and spring waters	40 m*M* AcOH, 10 m*M* NH_4Ac (pH 4.0)	Fluorescence 419 and 576 nm	19 μg/L
Ca, Mg, Ba, Na, K, and Li	Mineral water	3–5 m*M* Imidazole, pH 4.5	Indirect 214 nm	0.05 ppb
Cu, Ni, Co, Hg, Mn, Fe, Pb, Pd, Zn, Cd, Mg, Sr, Ca, and Ba	River water	2 m*M* $Na_2B_4O_7$, 2 m*M* EDTA pH 4.4	Direct UV 200 and 214 nm	10 μ*M*
Ca, Sr, Ba, Li, Na, K, Rb, Sc, and Mg	Tap, rain, and mineral waters	5 m*M* Benzimidazole, tartarate, pH 5.2, + 0.1% HEC or methy-HEC, + 40 m*M* 18C6	Indirect UV 254 nm	—

Chromate	Wastewater	0.02 m*M* Phosphate buffer (pH 7)	Direct UV	—
Fe, Ni, Pd, Pt, and Cu(I) cyano complexes	Leaching solutions of automobile catalytic converters	20 m*M* Phosphate buffer, 100 *M*m NaCl, 1.2 m*M* TBABr, 40 μ*M* TTABr (pH 11)	Direct UV 208 nm	20 μg/L
Speciation of Metal Ions[5–7]				
Arsenic species	Drinking water	0.025 m*M* Phosphate buffer, pH 6.8	Direct UV 190 nm	<2 mg/L
	Water	50 m*M* CHES, 20 m*M* LiOH	Conductivity	0.4 mg/L
	Tin mining	15 m*M* Phosphate buffer, 1 m*M* CTAB 50 m*M* CHES, 0.03% Triton X-100 20 m*M* LiOH, pH 9.4	Conductivity	0.4 mg/L
As(III), As(V), and dimethyl arsenic acid	Process water		ICP-MS	1 ppb
—	60 m*M* Calcium chloride (pH 6.7) cetyltrimethyl ammonium bromide, pH 10.0			
Arsenic and selenium species	Drinking water	20 m*M* KHP, 20 m*M* Boric acid (pH 9.03) hydrodynamiccally modified EOF	Hydride generation ICP-MS	6 ng/L
	Tap and drinking waters	75 m*M* Dihydrogen phosphate 25 m*M*, tetraborate (pH 7.65)	Direct UV 12 μg/L 195 nm	—
	—	20 m*M* Na_2HPO_4, 5 m*M* DTPA, pH 8.0 or 8.5	Indirect UV 214 nm	10^{-6} *M*
Cr(IV) and Cr(VI)	Rinse water from chromium platings	1 m*M* CDTA, 10 m*M* Formate buffer (pH 3.8)	Direct UV 214 and 254 nm	10 μg/L
	Chromium plating water	10 m*M* Formate buffer, 1 m*M* CDTA (pH 3.0)	Direct UV 214 nm	10 ppb
	Electroplating water	10 m*M* Formate buffer (pH 3.0)	Indirect UV 214 nm	50 ppb
	Wastewater	20 m*M* Na_2HPO_4, 0.05 m*M* TTAOH	Direct UV 214 and 254 nm	—
Fe(II) and Fe(III)	Electroplating waters	20 m*M* Phosphate buffer (pH 7.0)	Direct UV 214 nm	10^{-5} *M*

(Continued)

Table 1 The applications of capillary electrophoresis for the determination of environmental pollutants. *(Continued)*

Pollutants	Sample matrix	Electrolytes	Detection	Detection limit
Hg(II), CH_3Hg^+, and $CH_3CH_2Hg^+$	—	25 m*M* $Na_2B_4O_7 \cdot 10\,H_2O$, pH 9.3	ICP-MS	81–275 ppb
Ir(II) and Ir(III)	4 m*M* H^+, 23 m*M* Cl^-, pH 2.4			Indirect UV 214 nm
—				
Pb(II), triethyl lead (IV), trimethyl lead (IV), and diphenyl lead (IV)	Na_2HPO_4–$Na_2B_4O_7$, 2.5 m*M* TTHA, 2.0 m*M* SDS, pH 7.5			Indirect UV 220 nm
ppb level				
Pt(II) and Pt(IV)	4 m*M* H^+, 23 m*M* Cl^-, pH 2.4		Indirect UV 214 nm	—
V(IV) and V(V)	Electroplating bath	20 m*M* Na_2HPO_4, 5 m*M* DTPA, pH 8.0 or 8.5	Indirect UV 214 nm	10^{-6} *M*
Anions Analysis[7,10]				
F^-	Rain water	1.13 m*M* PMA, 0.8 m*M* TEA, 2.13 m*M* HMOH, pH 7.7	Indirect UV 254 nm	0.6 μ*M*
F^-, Cl^-, Br^-, SO_4^{-2}, NO_3^-, NO_2^-, PO_4^{-3}, and thiosulphate	Tap water	2.25 m*M* PMA, 6.5 m*M* NaOH, 0.75 m*M* HMOH, 1.6 m*M* TEA, pH 7.7	Indirect UV 250 nm	1–3 mg/L
$HClO_4^-$, Br^-, F^-, NO_3^-, and NO_2^-	Tap water	20 m*M* Sodium sulfate, pH 2.5	Ionselective microelectrode	5 μg/L
Br^-, BrO_4^-, I^-, IO_4^-, NO_3^-, NO_2^-, and selenite organic and inorganic anions	River water Water from dumping area	Phosphate buffer, pH 2.9 9 m*M* PDCA, 0.05 m*M* TTABr, pH 7.8	Direct UV 200 nm Indirect UV 254 nm	— —
Br^-, NO_2^-, $S_2O_3^-$, NO_3^-, N_3^-, $Fe(CN)_6^{-4}$, MoO_4^{-2}, WO_4^{-2}, CrO_x^{-3}, and ReO_4^-	—	10 m*M* Borate, 220 m*M* NaCl, pH adjusted to 8.5 by sodium hydroxide	UV 214 nm	—
Phenols and its Derivatives[3,8]				
Alkyl phenols	1.25 m*M* $Na_2B_4O_7$, 15 m*M* NaH_2PO_4 pH 11.0 with 0.001% HDB		UV 254 nm	—
Chlorophenols	50 m*M* Na_2HPO_4/NaH_2PO_4, pH 6.9		UV 214 nm	0.06 mg/L

Miscellaneous derivatives of phenols	10 m*M* $Na_2B_4O_7/Na_3PO_4$, pH 9.8 20 m*M* CHES, pH 10.1 15 m*M* Na_3BO_3, pH 9.9	 Amperometric Indirect fluorimetry	UV 210 nm 0.03 mg/L 0.01 mg/L	0.3 mg/L
Pentachlorophenols	Drinking water	40 m*M* Sodium borate, pH 10	—	ng level
Chloro- and nitrophenols	Tap water	20 m*M* Sodium borate	—	μg level
Pesticides[9]				
Hexazinone and its metabolite	Ground water	50 m*M* SDS, 12 m*M* Sodium phosphate, 10 m*M* Sodium borate, and 15% MeOH, pH 9.0	UV 220–247 nm	—
Primisulfuron and triasulfuron	Water and soil	25 m*M* NaH_2PO_4 + 50 m*M* LiDS buffer	UV at 214 nm	—
Triazines and chlorotriazines	Tap and river Water	30 m*M* Sodium borate, 30 m*M* SDS, pH 9.3	UV at 210 nm	—
Chlorinated acid herbicides and related compounds	Water	5 m*M* Ammonium acetate in isopropanol-water (40 : 60, v/v), pH 10	MS	—
Chlorphyrifos	Air and soil	—	—	—
Triazine pesticides	50 m*M* Ammonium acetate, 0.7 m*M* CTAB, pH 4.5	MS and UV (230 nm)	—	
Polyaromatic Hydrocarbons[4]				
PAHs	Standard	8 m*M* $Na_2B_4O_7$, pH 9.0, 50 m*M* DOSS, 40% acetonitrile	UV 254 nm	—
	Standard	5 m*M* Resorcarene, pH 13.25, 6 *M* Urea, 50% acetonitrile	UV 260 nm	
Amines[4]				
Methyl, dimethyl trimethyl, and ethyl amines	Atmospheric aerosols	5 m*M* DHBP, 6 m*M* glycine, 2 m*M* 18-crown-6 ether, pH 6.5	Indirect UV 280 nm	—

(Continued)

Table 1 The applications of capillary electrophoresis for the determination of environmental pollutants. *(Continued)*

Pollutants	Sample matrix	Electrolytes	Detection	Detection limit
Substituted anilines	Tap and ground water, soil, and sediment	50 m*M* NaH_2PO_4, pH 2.35, 7 m*M* 1,3-diaminopropane	UV 280 nm	0.06 mg/L
Heterocyclic aromatic amines	Rain water	50 m*M* NaH_2PO_4–20 m*M* citric acid, 30 m*M* NaCl, 26% methanol	UV 190, 240, and 263 nm	0.05 mg/L
Carbonyls[4]				
Acetaldehyde, benzaldehyde, formaldehyde, and glyoxal	Rain water	5 m*M* Na_3PO_4–10 m*M* $Na_2B_4O_7$, pH 8.0, 20% acetonitrile	Laser-induced fluorescence 325 and 442 nm	—
Dyes[4,8]				
Synthetic cationic dyes	Standard	10 m*M* Citric acid, pH 3.0, 0.1% PVP	UV 214 nm	—
Anionic synthetic azo dyes	Standard	10 m*M* BTP-HCl, pH 6.5, 0.5% PEG, 0.05% PVP	UV 214 nm	—
Photoactive dyes	Coffee and beans	50 m*M* Boric acid/10 m*M* sodium borate, pH 8.5	—	0.08 μg/L
Chiral Separations[9,16]				
Fenoprop, mecoprop, and dichlorprop	20 m*M* Tributyl-β-CD in 50 m*M*, ammonium acetate, pH 4.6	MS	—	
2-Phenoxypropionic acid, dichloroprop, fenoprop, fluaziprop, haloxyfop, and diclofop enantiomers	—	10 – 4 *M* 75 m*M* Britton-Robinson buffer with 6 m*M* Vancomycin	—	—
Imazaquin isomer	—	50 m*M* Sodium acetate, 10 m*M* dimethyl-β-CD, pH 4.6	—	—
Phenoxy acid herbicides	—	200 m*M* Sodium phosphate, pH 6.5 with various concentrations of OG and NG	—	—
Diclofop		—	—	

	50 m*M* Sodium acetate, 10 m*M* trimethyl-β-CD, pH 3.6			
Imazamethabenz isomers	50 m*M* Sodium acetate, 10 m*M* dimethyl-β-CD, pH 4.6	—	—	
2-(2-methyl-4-chlorophenoxy) propionic acid,	—	0.05 *M* Lithium acetate containing α-cyclodextrins	UV 200 nm	—
2-(2-methyl-4,6-dichlorophenoxy) propionic acid	0.05 *M* Lithium acetate containing β-cyclodextrin		UV 200 nm	—
2-(2,4-dichlorophenoxy) propionic acid propionic acid, and	0.05 *M* Lithium acetate containing heptakis-(2,6-di-*O*-methyl)- β-cyclodextrin	UV 200 nm	—	
2-(2-methyl-4-chlorophenoxy) propionic acid	0.03 *M* Lithium acetate containing heptakis-(2,6-di-*O*-methyl)-β-cyclodextrin		UV 200 nm	—
1,1′-Binaphthyl-2-2′-dicarboxylic acid, 1,1′-binaphthyl-2,2′-dihydrogen phosphate, and 2,2′-dihydroxy-1-1′-binaphthyl-3,3′-dicarboxylic acid	—	0.04 *M* Carbonate, pH 9.0, with non-cyclooligosaccharides	UV 215–235 nm	—

AcOH, Acetic acid; BTP, Bis-trispropane; CD, Cyclodextrin; CDTA, Cyclohexane-1,2-diaminetetraacetic acid; CHES, 2-(*N*-Cyclohexylamino)-ethanesulphonic acid; CTAB, Cetyltrimethylammonium bromide; DHBP, 1,1′-Di-*n*-heptyl-4,4′-bipyridinium hydroxide; DOSS, Sodium dioctyl sulfosuccinate; DTPA, Diethylenetriaminepenta acetic acid; EDTA, Ethylenediaminetetraacetic acid; EOF, Electroosmotic flow; HDB, Hexadimethrine bromide; HEC, Hydroxyethyl cellulose; HIBA, α-Hydroxyisobutyric acid; HMOH, Hexamethonium hydroxide; HQS, 8-Hydroxyquinoline-5-sulfonic acid; ICP-MS, Inductively coupled plasma-mass spectrometer; KHP, Potassium hydrogenphthalate; LiOH, Lithium hydroxide; MeOH, Methanol; MES, Morpholinoethanesulfonic acid; NaAc, Sodium acetate; NaCl, Sodium chloride; NH_4Ac, Ammonium acetate; NaOH, Sodium hydroxide; NG, Nonyl-β-D-glucopyranoside; OG, Octyl-β-D-glucopyranoside; PAHs, Polyaromatic hydrocarbons; PDCA, Pyridine-2,6-dicarboxylic acid; PEG, Polyethylene glycol; PMA, Pyromellitic acid; PVP, Polyvinylpyrrolidine; RSD, Lower standard deviation; SDS, Sodium dodecyl sulfate; TBABr, Tetrabutylammonium bromide; TEA, Triethanolamine; TTABr, Tetradecyl-trimethylammonium bromide; TTAOH, Tetradecyl-trimethylammonium hydroxide; TTHA, Triethylenetetraminehexa acetic acid; and UV, Ultraviolet.

many attempts have been made to solve this problem. Organic solvents have been added to the BGE to improve the selectivities of many of the pollutants. It has also been reported that the organic solvents ameliorate the solubility of hydrophobic complexes, reduce the adsorption onto the capillary wall, regulate the distribution of complexes between aqueous phase and micellar phase, adjust the viscosity of the separation medium and, accordingly, accomplish an improvement in detection. The pH of the electrolyte solution is very important from the selectivity point of view. The pH controls the behavior of EOF, acid/base dissociation equilibria of complexes, and the state of existing complexes. Therefore, the selectivity can be improved by adjusting the pH of the BGE. Besides, ion pairing can be used to improve the separation in CE. Six types of ion pairing agents have been developed and used. Ion pairing has also been used in MECC for the improvement of the separation of hydrophobic or weakly hydrophobic metal complexes. In addition, the selectivity of the separation of environmental pollutants has also been increased by varying the partition and ion-association (micellar interactions) mechanisms.

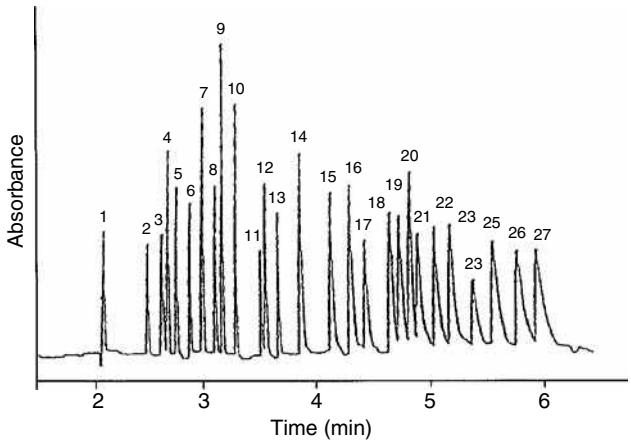

Fig. 2 The electropherogram of the separation of alkali, alkaline earth, transition metals, and lanthanoids on a fused silica capillary (60 cm × 75 μm) using 15 n*M* lactic acid, 8 m*M* 4-methylbenzylamine and 5% MeOH, pH 4.25, as running electrolyte with 30 kV as the separation voltage, 20°C temperature, and UV detection (214 nm).[5] Peaks: 1 = K; 2 = Ba; 3 = Sr; 4 = Na; 5 = Ca; 6 = Mg; 7 = Mn; 8 = Cd; 9 = Li; 10 = Co; 11 = Pb; 12 = Ni; 13 = Zn; 14 = La; 15 = Ce; 16 = Pr; 17 = Nd; 18 = Sm; 19 = Gd; 20 = Cu; 21 = Tb; 22 = Dy; 23 = Ho; 24 = Er; 25 = Tm; 26 = Yb; and 27 = Lu.

APPLICATIONS

During the last decade, CE has been increasingly used for the determination of environmental pollutants. Some of the methods of pre-treatment of waste environmental samples have been carried out prior to the injection into the CE system, as discussed above. CE has been applied for the determination of inorganic and organic pollutants. The major inorganic pollutants include metal ions and anions. On the other hand, the most common toxic organic environmental pollutants analyzed by CE are phenols, pesticides, polynuclear aromatic hydrocarbons, amines, carbonyl compounds, surfactants, dyes, and others. Recently, chiral separation of pollutants and xenobiotics has emerged as the most important issue for the environmental chemist. Therefore, CE has also been used for the analysis of the chiral pollutants. The application of CE for the determination of environmental pollutants is summarized in Table 1, which contains the type of pollutants, their sources, BGE used, detection method, and detection limit. As a specimen sample, a typical electropherogram of separated metal ions in a water sample by CE is shown in Fig. 2.[5]

Validation of Methods

There are only a few studies dealing with method validation of the determination of environmental pollutants by CE. However, some authors have demonstrated the application of their developed separation methods. The accuracy determination for Na, K, Ca, and Mg metal ions has been presented.[5–7] Similarly, the precision of migration times and peak areas for seven alkali and alkaline earth metals has been measured; RSD values were less than 0.4% for migration times and from 0.8% to 1.8% for peak areas.[5–7] In one of the experiments, the reported %RSD varied from 2.79 to 3.38 for Zn, Cu, and Fe metal ions.[13] Several other studies have shown reliable results with recoveries close to 100%, or good agreement with the results obtained by other methods.[13] In spite of this, the precision of linearity, sensitivity, and reproducibility of CE methods for metal ions and anions analysis are not better than ion chromatography.

CONCLUSIONS

The determination of environmental pollutants at trace level is currently a very important and challenging issue. Gas chromatography (GC) and high-performance liquid chromatography (HPLC) have been used for the analysis of environmental pollutants but, in recent years, CE has also been used for the determination of environmental pollutants. A search of the literature indicates several reports of the analysis of environmental pollutants by CE, but CE could not have yet achieved a place in the routine analysis of these pollutants. The reason for this is the poor detection of metal ions and anions and the poor reproducibility of CE methods. Therefore, many workers have suggested various modifications and alternatives to make CE a

method of choice. To obtain good sensitivity and reproducibility, the selection of the capillary wall chemistry, pH and ionic strength of the BGE, complexing and visualizing agents, detectors, and optimization of BGE have been described and suggested.[5–7,12–15]

Apart from the points discussed for improvement of CE applications for the determination of environmental pollutants, some other aspects should also be addressed so that CE can be used as the routine method of choice in this field. The important points relating to this include the development and wide use of fluorescent and radioactive complexing agents, since detection by fluorescent and radioactive detectors is more sensitive and reproducible with low limits of detection. To make CE application more reproducible, the BGE should be developed in such a way to ensure its physical and chemical properties remain unchanged during the experimental run. The non-reproducibility of the methods may be due to the heating of BGE during a long analysis. Therefore, to keep the temperature constant throughout the experiments, a cooling device should be included in the instrument. Besides, especially for the determination of anions, the CE instrument should be designed with the facility to reverse the electrodes. There are only a few reports dealing with method validation. To make the developed method more applicable, the validation of the methodology should be performed. All the capabilities and possibilities of CE have not yet been explored but they are underway. However, eventually CE will be realized as a widely recognized method of choice for the determination of environmental pollutants.

In summary, there is much to be developed for the advancement of CE for the analysis of environmental pollutants. Definitely, CE will prove itself as the best technique for the determination of environmental pollutants within the next few years; it will achieve the status of the technique of routine analysis in most of the environmental laboratories.

REFERENCES

1. Franklin, L.B. *Wastewater Engineering: Treatment, Disposal and Reuse*; McGraw-Hill, Inc.: New York, 1991.
2. Droste, R.L. *Theory and Practice of Water and Wastewater Treatment*; John Wiley & Sons, Inc.: New York, 1997.
3. Crego, A.L.; Marina, M.L. Capillary zone electrophoresis versus micellar electrokinetic chromatography in the separation of phenols of environmental interest. J. Liq. Chromatogr. & Relat. Technol. **1997**, *20*, 1–20.
4. Dabek-Zlotorzynska, E. Capillary electrophoresis in the determination of pollutants. Electrophoresis **1997**, *18*, 2453–2464.
5. Pacakova, V.; Coufal, P.; Stulik, K. Capillary electrophoresis of inorganic cations. J. Chromatogr. A, **1999**, *834*, 257–275.
6. Liu, B.F.; Liu, B.L.; Cheng, J.K. Analysis of inorganic cations as their complexes by capillary electrophoresis. J. Chromatogr. A, **1999**, *834*, 277–308.
7. Valsecchi, S.M.; Polesello, S. Analysis of inorganic species in the environmental samples by capillary electrophoresis. J. Chromatogr. A, **1999**, *834*, 363–385.
8. Martinez, D.; Cugat, M.J.; Borrull, F.; Calull, M. Solid phase extraction coupling to capillary electrophoresis with emphasis on environmental analysis. J. Chromatogr. A, **2000**, *902*, 65–89.
9. Malik, A.K.; Faubel, W. A review of analysis of pesticides using capillary electrophoresis. Crit. Rev. Anal. Chem. **2001**, *31*, 223–279.
10. Haddad, P.R.; Doble, P.; Macka, M. Development in sample preparation and separation techniques for the determination of inorganic ions by ion chromatography and capillary electrophoresis. J. Chromatogr. A, **1999**, *856*, 145–177.
11. Dabek-Zlotorzynska, E.; Aranda-Rodriguez, R.; Keppel-Jones, K. Recent advances in capillary electrophoresis and capillary electro-chromatography of pollutants. Electrophoresis **2001**, *22*, 4262–4280.
12. Timerbaev, A.R.; Buchberger, W. Prospects for the detection and sensitivity enhancement of inorganic ions in capillary electrophoresis. J. Chromatogr. A, **1999**, *834*, 117–132.
13. Macka, M.; Haddad, P.R. Determination of metal ions by capillary electrophoresis. Electrophoresis **1997**, *18*, 2482–2501.
14. Horvath, J.; Dolnike, V. Polymer wall coating for capillary electrophoresis. Electrophoresis **2001**, *22*, 644–655.
15. Mayer, B.X. How to increase precision in capillary electrophoresis. J. Chromatogr. A, **2001**, *907*, 21–37.
16. Marina, M.L.; Crego, A.L. Capillary electrophoresis: A good alternative for the separation of chiral compounds of environmental interest. J. Liq. Chromatogr. & Relat. Technol. **1997**, *20*, 1337–1365.

BIBLIOGRAPHY

1. Kallenborn, R.; Huhnerfuss, H. *Chiral Environmental Pollutants: Trace Analysis and Ecotoxicology*; Springer-Verlag: Berlin, 2000.
2. Sovocool, G.W.; Brumley, W.C.; Donnelly, J.R. Capillary electrophoresis and capillary electrochromatography of organic pollutants. Electrophoresis **1999**, *20*, 3297–3310.

Environmental Research: Ion Chromatography

Rajmund Michalski
Institute of Environmental Engineering, Polish Academy of Science, Zabrze, Poland

Abstract
Water, wastewater, and soil and air pollution analyses are the most important part of environmental analysis. Determination of common inorganic anions and cations is mandatory. Ion chromatography has almost replaced most of the wet chemical methods used in water analysis. This entry is a review of application of ion chromatography to environmental research.

INTRODUCTION

Environmental analysis is one of the most important fields of application for ion chromatography; it can be divided into water, soil, and air analysis. Ion chromatography has become an essential tool for the analytical chemist, especially in the area of anion analysis. In many cases, this method has replaced the conventional wet chemical methods, which are labor-intensive, time-consuming, and occasionally susceptible to interferences.

In addition to environmental applications, ion chromatography is now routinely being used for the analysis of ionic compounds in diverse areas such as power plant chemistry, semiconductor industry, food and beverages, household products and detergents, pharmaceuticals, biotechnology, and agriculture. In this entry, the application of ion chromatography in environmental research is described.

APPLICATION OF ION CHROMATOGRAPHY IN ENVIRONMENTAL ANALYTICAL CHEMISTRY

Environmental analytical chemistry can be regarded as the study of a series of factors that affect the distribution and interaction of elements and substances present in the environment, the ways they are transported and transferred, as well as their effects on biological systems.[1] An important job for analytical chemistry today is environmental analysis. This task can be performed using modern analytical techniques and methods. In the range of ionic compounds, the most important one is ion chromatography.

Modern ion chromatography was first reported in 1975 in a landmark paper by Small, Stevens, and Bauman.[2] At present, there are two main types of ion chromatography: suppressed ion chromatography and non-suppressed ion chromatography. Ion exchange remains the primary separation mode used in ion chromatography today, although the apparatus used for the separation of the ionic species includes ion pairing, ion exclusion, and chelation chromatography.

In recent years, the importance of monitoring and controlling environmental pollutants has become apparent in all parts of the world. As a result, analysts have increased their efforts to identify and determine toxic substances in air, water, wastewaters, food, and other sectors of our environment. Ion chromatography has been demonstrated to be a valuable tool for these analyses.

The primary concern when collecting environmental samples for analysis using any analytical technique (including ion chromatography) is that the sample must be a representative of the total sample matrix and that no contamination occurs during the sampling process. Moreover, appropriate methods for storage and preservation of the sample are definitely required.

In the range of environmental applications of ion chromatography, inorganic anions are, by far, the most important. The primary reason for this is the lack of alternative methods for anion analysis, which is not the case for cation analysis where many other instrumental techniques are readily available [e.g., atomic absorption spectrometry (AAS); inductively coupled plasma-atomic emission spectrometry (ICP-AES); and ICP-mass spectrometry (ICP-MS)].

However, ion chromatography has an advantage over spectroscopic techniques for cation analysis in the area of metal speciation. Moreover, ion chromatography is particularly beneficial for the simultaneous determination of cations and ammonia in wastewater containing amines. Examples of anion and cation chromatograms are given in Figs. 1 and 2, respectively.

During the development of ion chromatography, many comparisons between wet chemistry methods and ion chromatography were performed to validate the latter technique.[3] Recently, ion chromatography has become a well-established mature technique for the analysis of ionic species, and many standard organizations have regulatory methods of analysis based upon ion chromatography.[4]

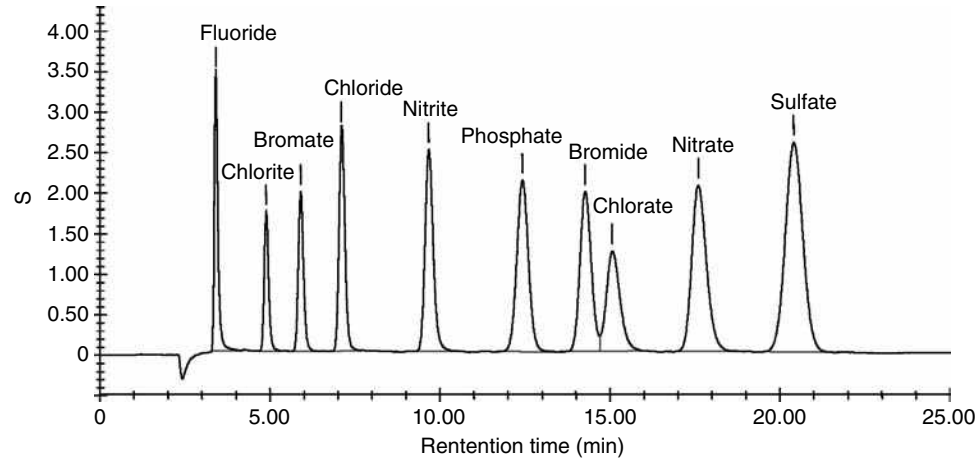

Fig. 1 Separation of inorganic anions standard.

Regulatory standards for water analysis require an analytical method with a detection limit of at least 25% of the parametric value. This method must be relatively simple, accurate, cheap, and adequate for routine laboratories. Ion chromatography meets these requirements. The separation and detection methods employed in ion chromatography as well as the selection of ionic species that may be analyzed with the ion chromatography method are summarized in Table 1 (inorganic anions), Table 2 (organic anions), and Table 3 (inorganic and organic cations). A survey of the detection methods used is given in Table 4.

WATER AND WASTEWATER ANALYSIS

Water in the environment occurs under various categories; it supports an incredible diversity of plant and animal life. It also plays an especially important role in human life and existence. It is also used by the industry and for agricultural purposes. For these and many more reasons, the knowledge of water quality is very meaningful and essential. Natural waters are dynamic systems that contain inert and living matter, organic and inorganic species, dissolved compounds, and insoluble substances. Moreover, the composition of water samples can change drastically during or after sampling.

One of the main environmental problems is the pollution of water by inorganic and organic compounds; they influence the quality of upgraded water and can cause health risks. Therefore, analysis of water is highly necessary, and it is critical to apply a method that enables the determination of more than one compound simultaneously.

Water-soluble inorganic ions can be determined by flow injection analysis, spectroscopic techniques, titration, and, most important of all, ion chromatography. The main focus of the application of ion chromatography in environmental

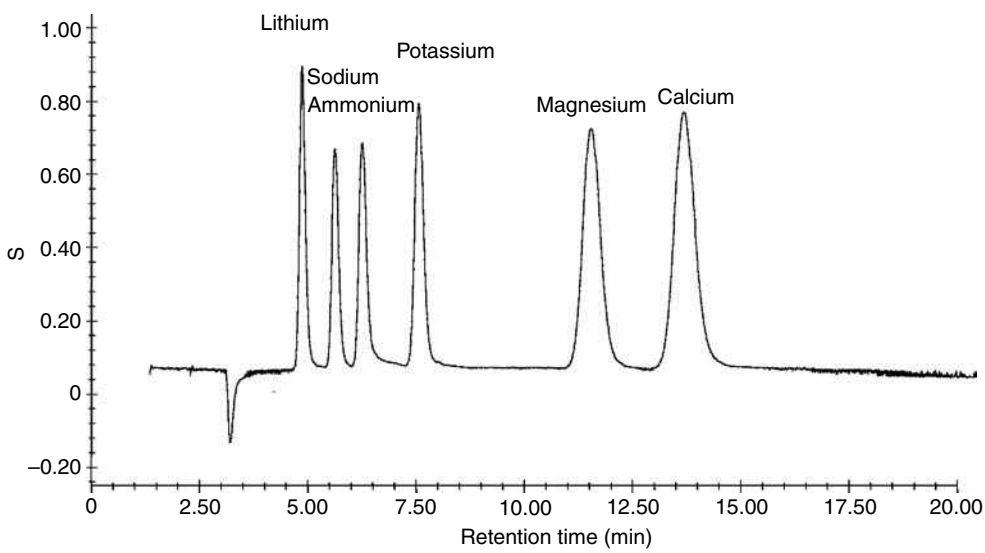

Fig. 2 Separation of alkali and alkaline earth metals.

Table 1 Inorganic anions determined by ion chromatography method.

Analyte groups		Analytes	Separation mechanism	Detection mode
Hydrophilic	Strong acids	F^-, Cl^-, Br^-, NO_2^-, NO_3^- PO_4^{3-}, SO_3^{2-}, SO_4^{2-}, ClO_2^-, ClO_3^-	Anion exchange	Conductivity, UV
		Arsenate, selenate, selenite	Anion exchange, ion exclusion	Conductivity
	Weak acids	$H_2BO_3^-$, CO_3^{2-}, SiO_3^{2-}	Ion exclusion, anion exchange	Conductivity, UV/Vis
Hydrophobic		CN^-, HS^-, I^-, BF_4^-, $S_2O_3^{2-}$, SCN^-, ClO_4^-	Ion exclusion, anion exchange	Amperometry, conductivity
Polyvalent chelating agents		EDTA, NTA	Anion exchange	UV/Vis
Polyvalent phosphates		$H_2PO_4^-$, HPO_3^-, HPO_4^{2-}, $P_2O_7^{4-}$, $P_3O_{10}^{5-}$	Anion exchange	Conductivity
Metal complexes		$Au(CN)_2^-$, $Au(CN)_4^-$, $Fe(CN)_6^{4-}$ $Fe(CN)_6^{3-}$, $Cu(EDTA)_2^-$, $Ni(EDTA)_2^-$	Ion pair, anion exchange	Conductivity

analytical chemistry is the qualitative and quantitative analysis of anions and cations in all kinds of waters.[5] These applications include the following:

- Determination of inorganic and organic anions and cations in all kinds of surface and groundwater (drinking water as well as sea, river, lake, streams, ground, and swimming pool water) and wastewater.[6–8]
- Determination of common anions and cations in rainwater.[9]
- Analysis of snow and ice samples.[10]

Natural waters encompass a wide variety of sample matrices including rainwater; mineral spring waters; groundwaters; surface waters (river, stream, lake, and pond waters); soil pore waters; runoff waters; snow, hail, and sleet; ice and ice cores; and well and bore waters.

In the past, drinking water disinfection was done through chlorination, until the 1970s when it was discovered that carcinogenic compounds such as trihalomethanes can be produced during this process.

In this connection, many drinking water utilities are changing their primary disinfectants from chlorine to alternative disinfectants, such as ozone, chlorine dioxide, and chloroamines, which reduce regulated trihalomethanes and some organochlorine compound levels but, at the same time, often increase levels of other potentially toxicologically important compounds, such as inorganic oxyhalide by-products (bromate, chlorite, and chlorate). Some of them have been classified as probable human carcinogens.

Bromate is a disinfection by-product that is produced from the ozonation of source water that contains naturally occurring bromide, whereas chlorite and chlorate are produced as a result of using chlorine dioxide as a disinfectant. Recently, bromate has become the most important inorganic oxyhalide by-product, and its concentration in drinking water has to be controlled. Another challenge is seawater, which represents a very difficult matrix for the analysis of trace ionic constituents, because chloride, sulfate, and sodium are the primary ions and they are present at extremely high concentrations.[11]

Determination of trace anions in water matrices containing high concentrations of salt can also be made by

Table 2 Organic anions determined by ion chromatography methods.

Analyte groups		Analytes	Separation mechanism	Detection mode
Carboxylic acids	Monovalent	Aliphatic, $C < 5$	Ion exclusion, anion exchange	Conductivity
		Aliphatic, $C > 5$, aromatic	Ion pair, anion exchange	Conductivity, UV
	Mono-, di-, and trivalent	Hydroxy carboxylic acids, di- and trivalent carboxylic acids	Ion exclusion	Conductivity
Sulfonic acids		Alkylsulfonates, $C < 8$, toluene, xylene, benzene sulfonates	Ion exclusion, anion exchange	Amperometry, conductivity
		Alkylsulfonates, $C > 8$, aromatic sulfonates	Ion pair, anion exchange + reversed phase	Conductivity
Alcohols and phenols		Phenols	Anion exchange	UV, amperometry
		Aliphatic alcohols	Ion exclusion, reversed phase, anion or cation exchange	Amperometry

Table 3 Cations determined by ion chromatography methods.

Analyte groups		Analytes	Separation mechanism	Detection mode
Inorganic	Group I and II metals	Li^+, Na^+, K^+,, Rb^+, Cs^+, g^{2+}, Ca^{2+}, Sr^{2+}, Ba^{2+}, amines, alkanolamines	Cation exchange	Conductivity
	Transition metals	Cu^{2+}, Ni^{2+}, Zn^{2+}, Co^{2+}, Cd^{2+}, Pb^{2+}, Mn^{2+}, Fe^{2+}, Fe^{3+}, Sn^{2+}, Sn^{4+}, Cr^{3+}, V^{4+}, V^{5+}	Ion exclusion, anion exchange	Conductivity, UV/Vis
	Lanthanide metals	La^{3+}, Ce^{3+}, Pr^{3+}, Nd^{3+}, Sm^{3+}, Eu^{3+}, Gd^{3+}, Tb^{3+}, Dy^{3+}, Ho^{3+}, Er^{3+}, Tm^{3+}, Yb^{3+}, Lu^{3+}	Anion exchange, cation exchange	UV/Vis
Organic	Low-molecular-weight amines, alkylamines, mono-, di-, tri-, tetramethylamine, alkanolamines, monoethanolamine, diethanolamine	CH_3NH_2, $C_2H_5NH_2$, $(CH_3)_2NH$, $(CH_3)_3N$, $C_6H_5NH_2$, $C_6H_{11}NH_2$, $C_{10}H_{21}NH_2$, $[R_1R_2R_3R_4]N^+$	Cation exchange, ion pair	Conductivity
	High-molecular-weight amines, alkylamines, aromatic amine, cyclohexamines, quaternary ammonium ions, polyamines		Cation exchange, ion pair	Conductivity, UV

multidimensional suppressed ion chromatography. In this method, trace concentrations of anions can be separated from the matrix anions (e.g., chloride, nitrate, and sulfate) by collecting a selected portion of the ion chromatogram on a concentrator column after suppression and reinjecting the concentrated amount of trace anions under the original chromatographic conditions.

The analysis of brines by ion chromatography is complicated by the high ionic strength and excess of NaCl in the sample. Ion chromatography can be used for

Table 4 Survey of the detection methods used in ion chromatography.

Detection mode	Principle	Applications
Conductivity	Electrical conductivity	Anions and cations with pK_a or $pK_b < 7$
Amperometry	Oxidation or reduction on Ag/Pt/Au/ glassy carbon and carbon paste electrodes	Anions and cations with pK_a or $pK_b > 7$
UV/Vis detection with or without postcolumn derivatization	UV/Vis light absorption	UV-active anions and cations, transition metals after reaction with 4-(2-pirydyloazo) rezorcinol (PAR), aluminum after reaction with tiron, lanthanides after reaction with arsenazo I, polyvalent anions after reaction with iron(III), silicate and orthophosphate after reaction with molybdate
Fluorescence in combination with postcolumn derivatization	Excitation and emission	Ammonium, amino acids, and primary amines after reaction with *O*-phenylamine (OPA)
Refractive index	Change in refractive index	Anions and cations at higher concentrations
Inductively coupled plasma-optical emission spectrometry (ICP-OES), inductively coupled plasma-mass spectrometry (ICP-MS)	Atomic emission	Hyphenation techniques for selective and sensitive transition metal analysis
MS	Electrospray ionization	Hyphenation technique for structural elucidation of organic anions and cations

the analysis of inorganic ions in natural waters brines, which include seawaters, subsurface brines, geothermal brines, and high-salinity groundwaters. A review of the application of ion chromatography for the analysis of high ionic strength waters and aqueous matrices has been described by Singh, Abbas, and Smesko.[12] The determination of cyanide in various samples is very important environmentally because of its large-scale industrial uses and its extreme toxicity. In all of the analytical methods developed so far, for cyanide and sulfide, removal of interferences is a necessary first step when analyzing most environmental samples. With the ion chromatography method cyanide and sulfide are separated and are thus determined simultaneously.[13]

Polyphosphates are widely used in industrial water treatment applications on account of their sequestering and dispersing properties.[14] Chelating agents such as nitriltriacetate acid (NTA) and ethylenediaminetetraacetic acid (EDTA) can also be determined rapidly by the same approach used for polyphosphonates.

The determination of various oxidation states of elements is of great interest as well. Until recently, analytical methods allowed analysts to determine only the total content of analytes, but it was soon realized that this analytical information was insufficient. Biochemical and toxicological investigation has shown that, for living organisms, the chemical form of a specific element or the oxidation state in which that element is introduced into the environment is as important as its quantity.[15] Ion chromatography plays an important role in hyphenated techniques used for species analysis, as an effective and reliable separation method.[16]

Besides the common inorganic anions (F^-, Cl^-, Br^-, NO_3^-, PO_4^{3-}, and SO_4^{2-}) and cations (Na^+, K^+, NH_4^+, Mg^{2+}, and Ca^{2+}), chromate and arsenite are of primary concern because of their greater toxicities as compared to chromium(III) and arsenate, respectively. Hexavalent chromium is a toxic form of chromium that must be monitored in manufacturing wastes. Ion chromatography with postcolumn addition of diphenylcarbazide is probably the most specific and sensitive method available for the determination of hexavalent chromium.

The simultaneous analysis of alkali and alkaline earth metals is another important ion chromatographic application in the field of drinking water and surface water analysis. Environmental samples with low levels of ammonium, in matrices with high concentration of sodium, are a typical case. Unfortunately, ammonium and sodium ions have similar selectivities for the common stationary phases. This problem can be solved by a column-switching technique[17] or by applying appropriate columns and eluents. Owing to the strong environmental impact, trace heavy metal ion determination and speciation have received particular attention in recent years.

There is a significant number of ion chromatography methods developed for the determination of metal pollutants in a wide variety of environmental samples. The review of the current state and progress of ion chromatography as an analytical tool for trace metal analysis in environmental samples is described by Shaw and Haddad.[18] Ion chromatographic separation by anion exchange of metal ions involves their presence as negatively charged complexes, which can be achieved off-line or online. In the off-line method, metal complexes are formed before the chromatographic separation, because complexes must be stable enough to avoid decomposition during separation or a ligand must be added to the eluent. In the online method, complexation is performed in the chromatographic column by adding the proper ligand to the eluent. Among the many ligands (mainly organic acids) used for simultaneous ion chromatography of metals, the most common additives are oxalic acid, pyridine-2,6-dicarboxylic acid (PDCA), and EDTA.

At an appropriate pH, EDTA forms negatively charged complexes with divalent or trivalent metal ions, and simultaneous separation of anions from metal ions is also feasible with this ligand.[19] Ion chromatography is increasingly being used for the separation of lanthanides. The separation of each rare earth element can be performed with either a cation- or an anion-exchange mechanism, depending on the eluent composition and the properties of the stationary phase.

SOIL ANALYSIS

Soil is one of the most complex environmental components; it is the vehicle by which pollutants generated by human action—particularly, agricultural and industrial activities—are driven from the ground surface to the underground waters.

Extension of ion chromatography to the analysis of soil has been hindered by the sample preparation problems associated with soil samples. Sample preparation includes crushing, homogenization, digestion, dissolution, stabilization, and filtration. Ion chromatographic procedures require that any sample that is to be analyzed be in a solution, most preferably in aqueous form. Dissolution of the sample in acids should be avoided when determining anions, unless a subsequent high dilution with water is possible, because the acid anions that are added could result in overloading of the analytical column. Analysis of the total nitrogen, phosphorous, and sulfur, and their corresponding oxidized anions, e.g., nitrite, nitrate, phosphate, and sulfate, is of importance when assessing soil conditions and fertility. Most, if not all, of the inorganic species important in agriculture exist as ions.[20]

The control of landfills, especially of hazardous waste landfills, is becoming increasingly important. For environmental control purposes, the leachates from hazardous waste landfills and leachability test samples have to be analyzed regularly.[21]

The quantitation of inorganic ions in sludge, leachates, and similar solid wastes by ion chromatography is similar, in practice, to the analysis of soil samples. Such samples are typically leached under aqueous conditions, then filtered and pretreated using solid-phase extraction (SPE), if necessary, before injection. Sludges and solid-waste samples can be prepared for analysis by ion chromatography using combustion methods.[22]

AIR POLLUTION

Atmospheric pollutants can occur in a variety of forms, namely, fumes, dust, gases and vapors, and mists and aerosols. The knowledge of the distribution of atmospheric pollutants between the gaseous and the particulate phase is very important for the environmental analytical chemist. Gases and particles, in fact, are very different in terms of their adverse effects on human health and on the ecosystem; they generally involve different formation pathways and removal processes.

The major areas where ion chromatography is used are for the analysis of atmospheric particulates, aerosols, acid rain, sulfur dioxide flue gas, and automobile exhaust.[23] Ion chromatographic applications in the area of air hygiene include the determination of:

- NO_2^-, NO_3^-, SO_3^{2-}, SO_4^{2-}, and NH_4^+ in ambient aerosols and in motor vehicle exhaust.
- Trace anions (F^-, Cl^-, NO_3^-, and SO_4^{2-}) and cations (Na^+, NH_4^+, and K^+) in precipitation samples.
- SO_2 and NO_x in the atmosphere and in combustion products.
- Heavy metals in flue dust.
- Common toxic substances, such as formaldehyde, in industrial environment.
- Specific toxic substances in industrial environments.

Measurements may be made directly with the extracts from filters, bulk collectors, particle collectors, solution bubblers, or diffusion tubes, or following concentration on solid cartridges or guard columns. Usually, air is first passed through the collected material and is then extracted into solutions for analysis.

Ammonia can be converted to the ammonium cation, sulfur dioxide to the more stable sulfate anion, and nitrogen dioxide to nitrite and nitrate ions. In addition, organic anions, which include carboxylic acids and amines, can be determined. Sulfur dioxide, which results primarily from the combustion of coal and petroleum, is one of the six major air pollutants; therefore, it is necessary to have a reliable analytical method for its determination. The United States Environmental Protection Agency (U.S. EPA) has been evaluating ion chromatography method for ambient SO_2 monitoring. It was noted that this method has no temperature stability problems and eliminates the use of the toxic chemical potassium tetrachloromercurate used in the previously recommended methods. The hydrogen peroxide-absorbing reagent is a very efficient collector of sulfur dioxide.

Coupling of the annular denuder sampling techniques with ion chromatography provides a valuable solution to the problem of precise and accurate measurement of atmospheric inorganic pollutants, with discrimination of the gaseous and the particulate phase.[24]

Heavy and transition metals, normally present in atmospheric particulates, can be separated and detected by isocratic ion chromatography with a postcolumn reaction and spectrophotometric detection.[25]

CONCLUSION

Since its introduction in 1975 ion chromatography has been used in most areas of analytical chemistry and has become a versatile and powerful technique for the analysis of a vast number of ions present in the environment. The most important aims in ion chromatography development are new stationary phases, miniaturized inductively coupled (IC) systems, enhanced peak capacity through the use of complex eluent profiles and the associated computer tools for simulation and prediction of retention, and hyphenated IC systems.

The development of ion chromatography allows the determination of ionic contaminants in environmental samples with very low detection limits and expands the range of determined analytes. Ion chromatography will continue to develop as more and more ionic contaminants become regulated at increasingly lower limits in the future.

REFERENCES

1. Pérez-Bendito D.; Rubio S.; Weber S.G. *Environmental Analytical Chemistry*; Wilson & Wilson's, Comprehensive Analytical Chemistry, Elsevier: Amsterdam, **1999**.
2. Small H. Stevens T.S.; Bauman, W.C. Novel ion exchange chromatographic method using conductometric detection Anal. Chem. **1975**, *47*, 1801–1886.
3. Marchetto, A.; Mosello, R.; Tartari G.A.; Muntau H.; Bianchi M.; Geiss H.; Serrini G; Lanza G.S. Precision of ion chromatographic analyses compared with that of

other analytical techniques through intercomparison exercises. J. Chromatogr. A, **1995**, *706*, 13–19.
4. Michalski, R. Ion chromatography as a reference method for the determination of inorganic ions in water and wastewater. Crit. Rev. Anal. Chem. **2006**, *36* (2), 107–127.
5. Jackson, P.E. Ion chromatography in environmental analysis. In *Encyclopedia of Analytical Chemistry,* Meyers, R.A., Ed.; Wiley: Chichester, U.K., **2000**; 2779–2801.
6. Weiss J. *Handbook of Ion Chromatography*; Wiley-VCH: Weinheim Germany.
7. Jackson P.E. Determination of inorganic ions in drinking water by ion chromatography. Trends Anal. Chem. **2001,** *20*, 320–329.
8. Haddad P.R. In *Ion Chromatography. Principles and Applications*; J. Chromatogr. Library Series. Elsevier: Amsterdam, **1990**, *46*.
9. Oikawa, K.; Murano, K.; Enomoto, Y.; Wada, K.; Inomata, T. Automatic monitoring system for acid rain and snow based on ion chromatography. J. Chromatogr. **1994**, *671*, 211–215.
10. Buck, C.F.; Mayewski, P.A.; Spencer, M.J.; Whitlow, M.S.; Twickler, M.S.; Barrett, D. Determination of majors ions in snow and ice cores by ion chromatography. J. Chromatogr. **1992,** *594*, 225–228.
11. Carrozzino, S.; Righini, F.; Ion chromatographic determination of nutrients in sea water. J. Chromatogr. **1995**, *706*, 277–280.
12. Singh, R.P.; Abbas, N.M.; Smesko, S.A. Suppressed ion chromatography analysis of anions in environmental waters containing high salt concentration. J. Chromatogr. **1996**, *733*, 73–91.
13. Otu, E.O.; Byerley, J.J.; Robinson, C.W. Ion chromatography of cyanide and metal cyanide complexes: A review Int. J. Environ. Anal. Chem. **1996**, *63* (1), 81–90.
14. Ruiz-Calero, V.; Galceran, M.T. Ion chromatographic separations of phosphorus species: A review. Talanta **2005**, *66* (2), 376–410.
15. Kot, A.; Namiesnik, J. The role of speciation in analytical chemistry. Trend. Anal. Chem. **2000**, *19*, 69–79.
16. Ellis, L.A.; Roberts, D.J. Chromatographic and hyphenated methods for elemental speciation analysis in environmental media. J. Chromatogr. **1997**, *774*, 3–19.
17. Umile, C.; Huber, J.F.K. Determination of inorganic and organic anions in one run by ion chromatography with column switching. J. Chromatogr. **1993**, *640*, 27–31.
18. Shaw, M.J.; Haddad, P.R. The determination of trace metal pollutants in environmental matrices using ion chromatography. Environ. Int. **2004**, *30*, 403–431.
19. Sarzanini, C.; Bruzzoniti, M.C. Metal species determination by ion chromatography Trends. Anal. Chem. **2001**, *20* (6–7), 304–310.
20. Goyal S.S. Applications of column liquid chromatography in inorganic analysis in agricultural research. J. Chromatogr. **1997**, *789*, 519–527.
21. Gade, B. Ion chromatographic investigations of leachates from a hazardous-waste landfill. J. Chromatogr. **1993**, *640*, 227–230.
22. Miyake, Y.; Kato, M.; Urano, K. A method for measuring semi- and non-volatile organic halogens by combustion ion chromatography. J. Chromatogr. A, **2007**, *1139*, 63–69.
23. Sawicki, E.; Mulik, J.D.; Wittgenstein, E., Eds., *Ion Chromatographic Analysis of Environmental Pollutants*; Ann Arbor Science Publishers: Ann Arbor, MI, 1978.
24. Perrino, C.; Concetta, M.; Scianò, T.; Allegrini, I. Use of ion chromatography for monitoring atmospheric pollution in background networks. J. Chromatogr. **1999**, *846* (1–2), 269–275.
25. Caselli, B.M.; Gennaro, G.; Ielpo, P.; Traini, A. Analysis of heavy metals in atmospheric particulate by ion chromatography. J. Chromatogr. **2000**, *888* (1–2), 145–150.

Essential Oils: GC Analysis

M. Soledad Prats Moya
Alfonso Jiménez
Department of Analytical Chemistry, Nutrition and Food Sciences, University of Alicante, Alicante, Spain

Abstract
The use of essential oils is increasing because of the increase in the number of their applications and in the framework of natural and environmentally friendly materials. Many times the analysis of their components is quite complex due to the high number and the diversity of compounds in their composition. In this entry a general overview of the extraction methods is given by comparing conventional liquid–liquid and solid–liquid methods with new alternative ones, such as supercritical fluid extraction and microwave-assisted extraction. Gas chromatography methods and examples are treated and important issues such as detection systems, modern libraries for compounds identification, as well as multidimensional or hyphenated techniques are discussed. The use of these modern techniques and methods has improved resolution and sensitivity in essential oils determination and could open the possibility of future work in this area of chromatography.

INTRODUCTION

Natural products have served as an important source of drugs since ancient times. In recent years, a renewed interest in obtaining biologically active compounds from natural sources has been observed. Essential oils are highly concentrated substances present in aromatic plants that can be extracted from flowers, leaves, stems, roots, seeds, barks, resins, or fruit rinds. The levels of essential oils found in plants can be anywhere from 0.01 to 10 wt% of the total. This is why tons of plant materials are required for just a few hundred grams of oil. These oils are often used for their flavor and their therapeutic or odoriferous properties. They are used in a wide selection of products such as foods, medicines, and cosmetics.

Pure essential oils are complex mixtures of more than 200 components. They can be essentially classified into two groups: a volatile fraction constituting 90–95% of the oil in weight, containing the monoterpene and sesquiterpene hydrocarbons, as well as their oxygenated derivatives along with aliphatic aldehydes, alcohols, and esters; and a non-volatile residue that comprises 1 to 10 wt% of the oil, containing hydrocarbons, fatty acids, sterols, carotenoids, waxes, and flavonoids. Essential oils are characterized by two or three major components at fairly high concentrations (20–80%) while the rest of the components are present in trace amounts. Essential oils and their constituents are categorized as Generally Recognized As Safe (GRAS) by the U.S. Food and Drug Administration.[1]

OVERVIEW

Because of the enormous amount of raw material necessary to obtain a small amount of essential oil, many products on the market have been polluted with low-quality commercial oils to reduce their cost, a fact not always indicated on the label. Therefore it is important to study the chemical composition of the volatile fraction once the essential oil is extracted. This fraction is characterized by the complexity in the separation of its components, which belong to various classes of compounds and which are present in a wide range of concentrations. Therefore it is complicated to establish a composition profile of essential oils and to identify possible adulterations.

The gas chromatographic (GC) technique is almost exclusively used for the qualitative analysis of volatiles. The analysis of essential oils was developed in parallel with the technological developments in GC. Some of these developments were the application of more selective new column stationary phases and mass spectrometry (MS) detection devices which allow to identify the compounds. However, advances in instrumentation were not the only important factor in the development of analytical methods for essential oils in plants. Sample extraction and concentration techniques were also improved recently, in order to reduce the extraction time, to improve the extraction yield, and to enhance the quality of the extracts. The most outstanding improvements in the determination of the composition of essential oils came from the development of total analysis systems, i.e., systems where sample

preparation and analysis are integrated into a single online step. The great amount of information on the application of GC and hyphenated techniques to essential oils has led to much research in this field, and to the publication of recent reviews.[2–5]

EXTRACTION METHODS

Extraction of essential oils is one of the most time- and effort-consuming processes in the analysis of the constituents of plants. The extraction products can vary in quality, composition and quantity depending on the type of soil, weather, plant organs, and other factors.[6] Various extraction methods were traditionally employed, depending on the material or the available devices. The most common methods for essential oil isolation are steam distillation (SD) and hydro-distillation (HD). In the first method, water steam is passed through the raw material, which drives out most of its volatile fragrant compounds. SD is commonly used for fresh plant materials, such as flowers, leaves, and stems. In the HD method the plant is inserted into water in a Clevenger-type apparatus and subjected to heating; the vapor, which contains the volatile compounds, is passed through a cooler for condensation, with subsequent collection of the extract.[7]

An alternative method, useful for much smaller samples, involves extraction with organic solvents, such as dichloromethane or hexane, followed by evaporation of solvents from the extract.[8] However, this approach is not very popular when the extracts obtained are to be used in the cosmetic or food industry, because of the possible toxic organic solvent residue.

These conventional methods used to isolate valuable compounds from aromatic plants have important drawbacks, such as low yields, formation of by-products due to the degradation of thermally unstable and unsaturated compounds by temperature or hydrolytic effects, as well as large extraction times.[9] Therefore, some alternative extraction methods were proposed to overcome these drawbacks.

Supercritical fluid extraction (SFE) using CO_2 as extractant has shown good potential for the isolation of organic compounds from various samples, by minimizing sample handling, eliminating the use of residual solvents, and allowing the use of lower temperatures, which reduces the deterioration of heat-labile compounds.[10] As a consequence, a great number of applications using SFE were successfully developed in the last decade for different sorts of herbs.[11–13] By varying the temperature and pressure of the CO_2 during extraction, the flavor or odor components can be selectively extracted.[14] Nevertheless, there are two main limitations in the use of supercritical CO_2 extraction: the high costs and the lack of quantitative extraction of polar analytes from solid matrices, caused by the poor solvating power of this fluid.[15]

The use of superheated water extraction (SWE) is a good alternative to SFE since the pressure is not a critical factor due to the low compressibility of water over the typical temperature ranges.[16] The extract obtained using SWE is a relatively dilute aqueous solution, but some care must be taken with the solubility changes of the analytes on cooling the extract as precipitation problems can occur.

The use of high temperatures for rapid extraction has been extended to pressurized liquid extraction (PLE). This technique uses organic solvents at elevated temperature and pressure, improving the speed of the extraction process.[17] The extractor design, capable of withstanding high pressures, allows the extraction temperature to be raised above the boiling point of the solvent while the high pressure allows maintaining the solvent in a liquid state at a high temperature. Under these conditions, the extraction process is favored by the high solvent strength. Some authors have claimed that PLE is the most efficient sample preparation method in determining essential oils in some herbs.[18] However, coextraction of non-volatile ingredients is recognized as the main drawback of this method.

Another possibility for essential oils extraction is the use of microwave-assisted extraction (MAE). This methodology appeared to be quite attractive for the isolation of essential oils. The main advantage of using MAE for essential oils extraction is the effective heat transfer that allows quicker times of extraction as compared to classical methods. In the last few years, different applications using microwave energy have been developed.[19] A recent modification of this technique is solvent-free microwave extraction (SFME), where the sample is placed in the reactor inside the microwave oven without any solvent.[20–21] A cooling system outside the microwave oven cool the extract continuously. Finally, the mixture of water and essential oil is collected and separated in a vessel.

Even though SFE, SWE, PLE, and MAE give better yields for essential oils extraction, high sample temperatures with possible formation of undesirable by-compounds is a shortcoming. Therefore, extraction techniques with no sample heating have been recently applied to essential oils. Ultrasound-assisted extraction (USAE) is a low-cost technique that is carried out at ambient temperature. Moreover, USAE uses quite simple equipment.[18] The main shortcoming of USAE is the potential formation of free radicals during sonication of the solvent, which can lead to degradation of some labile compounds by oxidation.[22–23]

The use of these alternative extraction techniques has been generalized to many essential oils and different samples as previously mentioned. These techniques have improved recoveries in the determination of most organic additives, as well as permitted considerable reductions in solvent volume and extraction time. However, the comparison of extraction methods was usually reduced to relative

recoveries of target analytes, ignoring important analytical parameters of the method. Selectivity is one of these, as the coextraction of other organics from the matrix usually requires a postextraction cleanup step before chromatographic analysis. Therefore, there is still much effort to be carried out in this field in order to optimize the extraction of essential oils from different natural matrices. The selection of the best extraction method and the best conditions depends on the components to be extracted, and this is something to be carefully considered. The application of chemometrics based, for example, on the use of central composite designs (CCD) and multilinear regression analysis has recently been shown to be a good alternative for the optimization of extraction parameters, such as temperature, pressure, and static time.[24,25] In addition, several mathematical models have been presented in literature for essential oils extraction.[12,13,26]

CONCENTRATION OF ANALYTES

Another important aspect to be taken into account for a reproducible and accurate separation and determination of essential oils is the concentration of each component after extraction. In many cases, a preconcentration of the sample, prior to any other step in the analytical process, is necessary to assure a concentration range for an accurate determination. This is the way small amounts of each constituent in plants or complex matrices, such as pharmaceuticals, can be collected and concentrated using the headspace technique (HS-GC), which involves volatilization of the terpenoids and other substances in a closely confined space, followed with analysis of constituents in the gaseous phase.[27,28] HS sampling can be used when essential oils must be selectively introduced to a GC to avoid transfer of non-volatile constituents, which may increase running times or complicate separation. This process can be carried out as an equilibrium process (static headspace) or as a continuous one (dynamic headspace). In the last few years, different publications have appeared using HS associated to a concentration technique like solid-phase microextraction (SPME), sorptive extraction (SE), and single-drop microextraction (SDME). In particular, the coupling of HS to SPME has been reported as a powerful separation tool for essential oils analysis due to its simplicity.[29–32] Results were compared to those from steam-distilled samples and, in general, most of the monoterpene compounds were detected at higher levels by using HS-SPME with 30 sec extraction time. In addition, detailed information about terpenic compounds was obtained by using HS-SPME.[29]

Some authors have proposed the use of HS-sorptive extraction (HSSE) where the analytes are adsorbed onto a thick film of polydimethylsiloxane (PDMS) coating a glass-coated iron stir bar. This stir bar is suspended in the headspace volume from where the analytes are adsorbed by the PDMS coating. After sampling, the stir bar is placed in a glass tube and transferred to a thermodesorber from where the analytes are thermally recovered and further analyzed by GC. This concentration technique is very effective for trace analysis.[33]

GC ANALYSIS

The separation of essential oil components is usually carried out by GC with fused-silica capillary columns. The information obtained from high-resolution GC analysis of the volatile fraction of essential oils must be enough to determine any adulteration or loss of quality. Therefore a selective and accurate separation is absolutely necessary in the case of industrial analysis.

The properties and conditions of columns are variable, depending on the polarity of the components to be separated. The most commonly used columns include stationary phases, such as DB-1, Carbowax, OV-1, OV-101, PEG 20M, BP5, and DB-5, which cover a wide range of polarities. Column lengths normally range from 25 to 100 m, and stationary-phase film thickness ranges from 0.2 to 0.7 μm. Elution of components is usually performed with a temperature gradient ranging from 50°C to 280°C.

The developments in new stationary phases have led to the production of thermally and chemically stable phases, with greater selectivity and efficiency. It is advantageous to use a more selective phase for a given separation as the overlapping of peaks in the final chromatogram is often a significant drawback of chromatographic techniques in natural samples.[34] The discovery of chiral phases (mostly based on cyclodextrin derivatives) allows the resolution of enantiomers of volatile components. These phases can give different elution sequences for a range of polarities and provide a distinct advantage in identification because of large changes in solute relative retention times.[35]

An important drawback in the separation of essential oils is the time required for complete GC resolution of the components of interest, which can sometimes take hours. In fact, the analysis of essential oils is usually carried out with slow temperature programs, which take long times for the development of the whole chromatogram. There are several ways to reduce analysis time in GC. The most common approach is to use shorter capillary columns with reduced internal diameter (I.D.) and film thickness, i.e., narrow bore columns. When using these columns, the optimum carrier gas velocity is higher, and it is possible to work with higher average linear velocity without loss of efficiency. However, this increase in linear velocity must be linked with some specific conditions of measurement, such as fast oven heating, fast acquisition rate, high inlet pressures, and higher split ratios. In the last few years, several studies have been carried out in this area, using columns of 1, 2, 5 or 10 m length, 0.10 mm I.D., and

0.10 μm stationary-phase film thickness. These columns offer the most effective compromise between separation efficiency and analysis time. Time can decrease from tens of minutes to minutes or even seconds while keeping a resolution suitable for normal determinations.[35–38]

DETECTION AND CHARACTERIZATION OF CONSTITUENTS

The flame ionization detector (FID) is still widely applied for the detection and quantification of some of the essential oil components, such as terpenoids. As usual in GC–FID, the primary criterion for the identification of peaks is the comparison of the standard retention times with the retention times of peaks in the sample's chromatogram. However, this procedure is sometimes not useful as the identification is quite difficult and overlapping of peaks makes determination not possible.

The easiest and most frequently used way to identify essential oil components when using GC–FID is comparison with Kovats retention indices (RI). The use of this type of retention data, derived from two GC columns of different polarities, allows highly reliable identification of a large number of components in a particular sample.

By far, MS is the most popular detection technique for performing chromatographic studies of essential oils. The use of retention indices, in conjunction with GC–MS studies, is well established. Many laboratories use such procedures in their routine analyses to confirm the identities of unknown components. However, a feature of MS for essential oils is that mass spectra are not particularly unique in many cases because of the large number of isomers of the same molecular formula, but with different structures, that could exist. Therefore their mass spectra are similar and their identification is sometimes not easy. The most common approach to solve this problem, as well as the presence of unknowns on which very little other structural information is available, is the use of algorithms and powerful MS databases, as has been recently proposed.[37] Two different MS databases are commonly used as references: National Institute of Standards and Technology (NIST)/Environment Protection Agency (EPA)/National Institutes of Health (NIH)[38] and the Registry of Mass Spectral Data.[39] The first one contains more than 191,000 mass spectra of different chemicals. The largest database is the Registry of Mass Spectral Data, called the Wiley database, containing more than 400,000 different spectra, resulting from the work of many researchers in the field of MS. One of the commonly used algorithms was proposed by Oprean et al.[40] who consider two parameters as identification criteria for an unknown peak, i.e., the match index of the unknown mass spectrum with spectral libraries, and the relative retention indices computed from the retention times of the unknowns relative to a mixture of *n*-alkanes.

One of the most recently proposed methods to improve the analysis of complex mixtures, especially for deconvolution of overlapping mass spectra, is time-of-flight mass spectrometry (TOF-MS). This technique allows assignment of a spectrum to each individual solute in significantly overlapping elution profiles. This is an important advantage that can be exploited when fast GC methods are applied for complex samples because each overlapping peak may be deconvoluted and the individual spectrum of each overlapping solute may be obtained. Although great efforts have recently been carried out in this field, it remains to be determined if TOF-MS can be used on a routine basis even though a lot of works have been published using this detector in the last few years.[41–42]

The identification of compounds comprising more than 1 wt% in the oils can be also carried out by ^{13}C-NMR and computer-aided analysis.[43] The chemical shift of each carbon in the experimental spectrum can be compared with those of the spectra of pure compounds. These spectra are listed in the laboratory spectral database, which contains approximately 350 spectra of mono-, sesqui-, and diterpenes, as well as in the literature data. Each compound can be unambiguously identified, taking into account the number of identified carbons, the number of overlapped signals, as well as the difference between the chemical shift of each resonance in the mixture and in the reference.

The combination of GC with olfactometry is another possibility for detection that has been used in essential oils analysis.[41,44] Olfactometry adapters are commercially available and should include humidity of the GC effluent at the nose adapter and provide auxiliary gas flow. The correlation among eluted peaks with specific odors allows accurate retention indices or retention times to be established for the essential oil components. Some of them can be detected in this way after applying chemometric techniques, such as cluster analysis and principal component analysis, to the data from the sensors. A limitation of GC with olfactometry is that peak coelution in complex samples makes identification of the compound(s) responsible for an odor difficult, particularly where trace odorants coelute with larger odor-inactive peaks. One possible solution for identifying character-impact odorants where coelution occurs is to use comprehensive two-dimensional GC (GC × GC).[44]

HYPHENATED OR MULTIDIMENSIONAL ANALYSIS OF ESSENTIAL OILS

Hyphenated or multidimensional techniques have recently been introduced for the analysis of essential oils. Various approaches were recently proposed to obtain better results in the identification and quantification of essential oil components. Thus it is possible to use systems that incorporate separations prior to GC, multicolumn separations, and specific identification methods.

With respect to separations preceding GC analysis, some hyphenated techniques have been successfully used when there is a lack of resolution of the single-capillary GC method. One of these is the combination of high-performance liquid chromatography (HPLC) with GC. The prior HPLC step achieves the isolation of components of similar chemical composition, primarily based on polarity. Hence, this will separate saturated hydrocarbons from unsaturated or aromatic hydrocarbons, for example.[45] These systems are fully automated, but there is a problem with off-line sampling of HPLC fractions. The selection of the HPLC injection port will determine the particular method of separation. Therefore in this instrumental arrangement, each transferred fraction must be separately analyzed before the introduction of a subsequent fraction into the GC system. In general, the prior separation will be introduced to simplify the subsequent GC analysis, leading to improved resolution.

MULTIDIMENSIONAL GC

If highly complex samples, such as natural tissues, have to be studied, one way to improve the separation power is to couple, through an interface, two independent columns. The application of multidimensional GC (MDGC) to essential oils analysis was a great development in the determination of such complex samples.[46] This is an adequate approach when there are some zones on the chromatogram where peaks are not well resolved. The fractions corresponding to the zones with unresolved peaks are transferred to a second column containing a different stationary phase, where they are separated and completely resolved.

However, this evident improvement in instrumentation is only available to relatively few regions of the chromatographic analysis, as overlapping of peaks can be too complex for a complete resolution of each component, even after applying multiple-column couplings. The use of conventional MDGC technology is not possible for the entire analysis because this would involve transferring all the components to the second column, with the inherent technical problems of selectivity and sensitivity losses. This is why the MDGC analysis of essential oils is not focused on the increase of resolution for the whole sample, but only for specific components of interest in the quality control of the natural product.

Alternatively, when, across-the-board screening of an entire sample is required, MDGC is too time-consuming and complicated, and a comprehensive, i.e., a GC × GC, approach has to be used.[47] In this case, the entire first-column (first-dimension) eluate, cut into small adjacent fractions to maintain the first-dimension resolution, is subjected to further analysis on the second (second-dimension) column. GC × GC provide superior analyses compared to MDGC and single-column GC analysis, as can be seen in a recently published review.[48]

Finally, the most powerful option available for volatiles analysis is the introduction of a third mass spectrometric dimension in a comprehensive GC system.[49] MS techniques improve component identification and sensitivity, especially for the limited spectral fragmentation produced by soft ionization methods, such as chemical ionization (CI) and field ionization (FI). The use of MS to provide a unique identity for overlapping components in the chromatogram makes identification much easier. However, quadrupole conventional MS is unable to reach the resolution levels required for such separations. Only TOF-MS possesses the necessary speed of spectral acquisition to give more than 50 spectra per second.

CONCLUSIONS

The identification and determination of essential oils in many natural samples have improved greatly with the use of more powerful analytical techniques, such as fast extraction methods, better chromatographic detectors, and comprehensive GC. This improvement in analytical parameters opens a great future for the development of analytical methods for essential oils determinations, even at low limits of detection.

REFERENCES

1. http://www.cfsan.fda.gov/~lrd/FCF170.html (accessed December 2008).
2. Marriot, P.J.; Shellie, R.; Cornwell, C. Gas chromatographic techniques for the analysis of essential oils. J. Chromatogr. A, **2001**, *936*, 1–22.
3. Bicchi, C.; Rubiolo, P.; Cordero, C. Separation science in perfume analysis. Anal. Bioanal. Chem. **2006**, *384*, 53–56.
4. Adams, R.P. *Identification of Essential Oil Components by Gas Chromatography–Mass Spectrometry*, 4th Ed., Allured Publishing Co. Carol Stream: IL, USA, 2007.
5. Bakkali, F.; Averbeck, S.; Averbeck, D.; Idaomar, M. Biological effects of essential oils—A review. Food Chem. Toxic. **2008**, *46*, 446–475.
6. Angioni, A.; Barra, A.; Coroneo, V.; Dessi, S.; Cabras, P. Chemical composition, seasonal variability, and antifungal activity of Lavandula stoechas L. ssp. stoechas essential oils from stem/leaves and flowers. J. Agric. Food Chem. **2006**, *54*, 4364–4370.
7. Griffiths, D.W.; Robertson, G.W.; Birch, A.N.E.; Brennan, R.M. Evaluation of thermal desorption and solvent elution combined with polymer entrainment for the analysis of volatiles released by leaves from midge (*Dasineura tetensi*) resistant and susceptible blackcurrant

(*Ribesnigrum* L.) cultivars. Phytochem. Anal. **1999**, *10*, 328–334.
8. Zhu, W.; Lockwood, G.B. Enhanced biotransformation of terpenes in plant cell suspensions using controlled release polymer. Biotechnol. Lett. **2000**, *22*, 659–662.
9. Laguerre, M.; Lecomte, J.; Villeneuve, P. Evaluation of the ability of antioxidants to counteract lipid oxidation: Existing methods, new trends and challenges. Prog. Lipid Res. **2007**, *46*, 244–282.
10. Hyötyläinen, T. On-line coupling of extraction with gas chromatography. J. Chromatogr. A, **2008**, *1186*, 39–50.
11. Tezel, A.; Hortaçsu, A.; Hortaçsu, O. Multi-component models for seed and essential oil extraction. J. Supercritical Fluids **2000**, *19*, 3–17.
12. Pourmortazavi, S.M.; Hajimirasdeghi, S.S. Supercritical Fluid Extraction in plant essential and volatile oil analysis. J. Chromatogr. A, **2007**, *1163*, 2–24.
13. Stamenić, M.; Zizovic, I.; Orlović A.; Skala D. Mathematical modeling of essential oil SFE on the micro-scale—Classification of plant material. J. Supercritical Fluids **2008**, *46*, 285–292.
14. Khajeh, M.; Yamini, Y.; Bahramifar, N.; Sefidkon, F.; Pirmoradei, M.R. Comparison of essential oils composition of *Ferula assa-foetida* obtained by supercritical carbon dioxide extraction and hydrodistillation methods. Food Chem. **2005**, *91*, 639–644.
15. Rostagno, M.A.; Araujo, J.M.A.; Sandi, D. Supercritical fluid extraction of isoflavones from soybean flour. Food Chem. **2002**, *78*, 111–117.
16. Smith, R.M. Review. Extractions with superheated water. J. Chromatogr. A, **2002**, *975*, 31–46.
17. Ong, E.S. Extraction methods and chemical standardization of botanicals and herbal preparations. J. Chromatogr. B, **2004**, *812*, 23–33.
18. Dawidowicz, A.L.; Rado, E.; Wianowska, D.; Mardarowicz, M.; Gawdzik, J. Application of PLE for the determination of essential oil components from *Thymus vulgaris L.* Talanta **2008**, *76*, 878–884.
19. Bendahou M.; Muselli, A.; Grignon-Dubois, M.; Benyoucef, M.; Desjobert, J.M.; Bernardini, A.F.; Costa, J. Antimicrobial activity and chemical composition of *Origanum glandulosum* Desf. essential oil and extract obtained by microwave extraction: Comparison with hydrodistillation. Food Chem. **2008**, *106*, 132–139.
20. Lucchesi, M.E.; Smadja, J.; Bradshaw, S.; Louw, W.; Chemat, F. Solvent free microwave extraction of *Elletaria cardamomum* L. A multivariate study of a new technique for the extraction of essential oil. J. Food Eng. **2007**, *79*, 1079–1086.
21. Abert-Vian, M.; Fernandez, X.; Visinoni F.B.Y.; Chemat, F. Microwave hydrodiffusion and gravity, a new technique for extraction of essential oils. J. Chromatogr. A, **2008**, *1190*, 14–17.
22. Luque de Castro, M.D.; Priego-Capote, F. *Analytical Applications of Ultrasound*; Elsevier: Amsterdam, 2007.
23. Roldán-Gutierrez, J.M.; Ruiz-Jiménez, J.; Luque de Castro, M.D. Ultrasound-assisted dynamic extraction of valuable compounds from aromatic plants and flowers as compared with steam distillation and superheated liquid extraction. Talanta **2008**, *75*, 1369–1375.
24. Zhao, C.X.; Li, X.N.; Liang, Y.Z.; Fang, H.Z.; Huang, L.F.; Guo, F.Q. Comparative analysis of chemical components of essential oils from different samples of Rhododendron with the help of chemometrics methods. Chemometries and Intelligent Laboratory Systems. **2006**, *82*, 218–228
25. Zaibunnisa, A.H.; Norashikin, S.; Mamot, S.; Osman, H. An experimental design approach for the extraction of volatile compounds from turmeric leaves (*Curcuma domestica*) using pressurised liquid extraction (PLE). Food Sci. Tech. **2009**, *42*, 233–238.
26. Dehghani, M.; Mastali, M.; Esmaeilzadeh, F.; Safavi, A.A. Dynamic Modeling of the Essential Oil Extraction Based on Artificial Neural Networks, 12th International Conference on Intelligent Engineering Systems, Miami, Florida, February 25–29, 2008.
27. Krizman, M.; Baricevic, D.; Prosek, M. Fast quantitative determination of volatile constituents in fennel by headspace-gas chromatography. Anal. Chim. Acta **2006**, *557*, 267–271.
28. Tranchida, P.Q.; Lo Presti, M.; Costa, R.; Dugo, P.; Dugo, G.; Mondello, L. High-throughput analysis of bergamot essential oil by fast solid-phase microextraction–capillary gas chromatography–flame ionization detection. J. Chromatogr. A, **2006**, *1103*, 162–165.
29. Rohloff, J. Essential oil composition of sachalinmint from Norway detected by solid phase microextraction and gas chromatography–mass spectrometry analysis. J. Agric. Food Chem. **2002**, *50*, 1543–1547.
30. Deng, C.; Wang, A.; Shen, S.; Fu, D.; Chen, J.; Zhang, X. Rapid analysis of essential oil from *Fructus Amomi* by pressurized hot water extraction followed by solid-phase microextraction and gas chromatography–mass spectrometry. J. Pharm. Biomed. **2005**, *38*, 326–331.
31. López, P.; Huerga, M.A.; Batlle, R.; Nerín, C. Use of solid phase microextraction in diffusive sampling of the atmosphere generated by different essential oils. Anal. Chim. Acta **2006**, *559*, 97–104.
32. Jalali Heravi, M.; Sereshti, H. Determination of essential oil components of *Artemisia haussknechtii* Boiss using simultaneous hydrodistillation-static headspace liquid phase microextraction-gas chromatography–mass spectrometry. J. Chromatogr. A, **2007**, *1160*, 81–89.
33. Bicchi, C.; Cordero, C.; Liberto, E.; Rubiolo, P.; Sgorbini, B.; Sandra, P. Impact of phase ratio, polydimethylsiloxane volume and size, and sampling temperature and time on headspace sorptive extraction recovery of some volatile compounds in the essential oil field. J. Chromatogr. A, **2005**, *1071*, 111–118.
34. Cordero, C.; Rubiolo, P.; Sgorbini, B.; Galli, M.; Bicchi, C. Comprehensive two-dimensional gas chromatography in the analysis of volatile samples of natural origin: A multidisciplinary approach to evaluate the influence of second dimension column coated with mixed stationary phases on system orthogonality, J. Chromatogr. A, **2006**, *1132*, 268–279.
35. Bicchi, C.; Liberto, E.; Cagliero, C.; Cordero, C.; Sgorbini, B.; Rubiolo, P. Conventional and narrow bore short capillary columns with cyclodextrin derivatives as chiral selectors to speed-up enantioselective gas chromatography and enantioselective gas chromatography–mass spectrometry analyses. J. Chromatogr. A, **2008**, *1212*, 114–123.

36. Poynter, S.D.H.; Shellie, R.A. High-speed, low-pressure gas chromatography–mass spectrometry for essential oil analysis. J. Chromatogr. A, **2008**, *1200*, 28–33.
37. http://www.nist.gov/srd/nist1a.htm (accessed December 2008).
38. http://webbook.nist.gov/chemistry/ (accessed December 2008).
39. http://eu.wiley.com/WileyCDA/Section/id-301546.html (accessed December 2008).
40. Oprean, R.; Oprean, L.; Tamas, M.; Sandulescu, R.; Roman, L. Essential oils analysis. II. Mass spectra identification of terpene and phenylpropane derivatives. J. Pharm. Biomed. **2001**, *24*, 1163–1168.
41. Eyres, G.T.; Marriott, P.J.; Dufour, J.P. Comparison of odor-active compounds in the spicy fraction of hop (*Humulus lupulus* L.) essential oil from four different varieties. J. Agric. Food Chem. **2007**, *55* (15), 6252–6261.
42. Tran, T.C.; Marriott, P.J. Comprehensive two-dimensional gas chromatography–time-of-flight mass spectrometry and simultaneous electron capture detection/nitrogen phosphorous detection for incense analysis. Atmos. Environ. **2008**, *42*, 7360–7372.
43. Khadri, A.; Serralherio, M.L.M.; Nogueira, J.M.F.; Neffati, M.; Smiti, S.; Araujo, M.E.M. Antioxidant and antiacetylcholinesterase activities of essential oils from *Cymbopogon schoenanthus* L. *Spreng*. Determination of chemical composition by GC–mass spectrometry and ^{13}C NMR. Food Chem. **2008** *109*, 630–637.
44. Eyres, G.T.; Marriott, P.J.; Dufour, J.P. The combination of gas chromatography–olfactometry and multidimensional gas chromatography for the characterisation of essential oils. J. Chromatogr. A, **2007**, *1150*, 70–77.
45. Mondello, L; Dugo, G.; Bartle, K.D. On-line microbore high performance liquid chromatography capillary gas chromatography for food and water analysis—A review. J. Microcolumn. **1996**, *8*, 275–310.
46. Bertsch, W. Two-dimensional gas chromatography. Concepts, instrumentation, and applications-part 1. Fundamentals, conventional two-dimensional gas chromatography, selected applications. J. High Resol. Chromatogr. **1999**, *22*, 647–665.
47. Dallüge, J.; Beens, J.; Brinkman, U.A.T. Comprehensive two dimensional gas chromatography: A powerful and versatile analytical tool. J. Chromatogr. A, **2003**, *1000*, 69–108.
48. Adahchour, M.; Beens, J.; Brinkman, U.A.Th. Recent developments in the application of comprehensive two-dimensional gas chromatography. J. Chromatogr. A, **2008**, *1186*, 67–108.
49. Shellie, R.; Marriot, P.; Morrison, P. Concepts and preliminary observations on the triple-dimensional analysis of complex volatile samples by using GC×GC-TOFMS. Anal. Chem. **2001**, *73*, 1336–1344.

Evaporative Light Scattering Detection

Juan G. Alvarez
Department of Obstetrics and Gynecology, Beth Israel Deaconess Medical Center, Boston, Massachusetts, U.S.A.

INTRODUCTION

High-performance liquid chromatography (HPLC) is mainly carried out using light absorption detectors as ultraviolet (UV) photometers and spectrophotometers (UVD) and, to a lesser extent, refractive index detectors (RIDs). These detectors constitute the main workhorses in the field.[1] The sensitive detection of compounds having weak absorption bands in the range 200–400 nm, such as sugars and lipids is, however, very difficult with absorption detectors. The use of the more universal RID is also restricted in practice because of its poor detection limit and its high sensitivity to small fluctuations of chromatographic experimental conditions, such as flow rate, solvent composition, and temperature.[2] Moreover, if the separation of complex samples requires the use of gradient elution, the application of RID becomes almost impossible. Although for some solutes the use of either a reaction detector (RD) or a fluorescence detector (FD) is possible, this is not a general solution. In this regard, the analysis of complex mixtures of lipids or sugars by HPLC remains difficult owing to the lack of a suitable detector.

The miniaturization of detector cells is also extremely difficult and the technological problems have not yet been solved because the detection limit should also be decreased or, at least, kept constant.[2–6] Some progress in the design of very small cells for UVD and FD has been reported,[3–7] but the miniaturization of RD and RID seems much more difficult in spite of some suggestions.[8] Similarly, the development of open tubular columns is plagued by the lack of a suitable detector with a small contribution to band broadening. A non-selective detector more sensitive than the RID and easier to use with a small contribution to band broadening is thus desirable in HPLC. The mass spectrometer would be a good solution if it were not so complex[10] and expensive. The electron-capture detector (ECD)[11] and flame-based detectors have been suggested.[12] Both are very sensitive and could be made with very small volumes. Unfortunately, the ECD can be used only with volatile analytes and it is very selective. Both ECD and flame-based detectors are very sensitive to the solvent flow rate, and noisy signals are often produced. The adaptability of these detectors to packed columns is thus difficult. This probably explains why the ECD has been all but abandoned.

The evaporative light-scattering analyzer,[13,14] on the other hand, is an alternative solution which seems very attractive for a number of reasons. As most analytes in HPLC have a very low vapor pressure at room temperature and the solvents used as the mobile phase have a significant vapor pressure, some kind of phase separation is conceivable.

EVAPORATIVE LIGHT-SCATTERING DETECTOR

Principle of Operation

The unique detection principle of evaporative light-scattering detectors involves nebulization of the column effluent to form an aerosol, followed by solvent vaporization in the drift tube to produce a cloud of solute droplets (or particles), and then detection of the solute droplets (or particles) in the light-scattering cell.

Detector Components

Nebulizer: The nebulizer is connected directly to the analytical column outlet. In the nebulizer, the column effluent is mixed with a steady stream of nebulizing gas, usually nitrogen, to form an aerosol. The aerosol consists of a uniform dispersion of droplets. Two nebulization properties can be adjusted to regulate the droplet size of the analysis. These properties are gas and mobile-phase flow rates. The lower the mobile-phase flow rate, the less gas and heat are needed to nebulize and evaporate it. Reduction of flow rate by using a 2.1 mm I.D. column should be considered when sensitivity is important. The gas flow rate will also regulate the size of the droplets in the aerosol. Larger droplets will scatter more light and increase the sensitivity of the analysis. The lower the gas flow rate, the larger the droplets. It is also important to remember that the larger the droplet, the more difficult it will be to vaporize in the drift tube. An unvaporized mobile phase will increase the baseline noise. There will be an optimum gas flow rate for each method which will produce the highest signal-to-noise ratio.

Drift tube: In the drift tube, volatile components of the aerosol are evaporated. The non-volatile particles in the mobile phase are not evaporated and continue down the drift tube to the light-scattering cell to be detected. Non-volatile impurities in the mobile phase or nebulizing gas will produce noise. Using the highest-quality gas,

solvents, and volatile buffers, preferably a filter, will greatly reduce the baseline noise. Detector noise will also increase if the mobile phase is not completely evaporated. The sample may also be volatilized if the drift-tube temperature is too high or the sample is too volatile. The optimal temperature in the drift tube should be determined by observing the signal-to-noise ratio with respect to temperature.

Light-scattering cell: The nebulized column effluent enters the light-scattering cell. In the cell, the sample particles scatter the laser light, but the evaporated mobile phase does not. The scattered light is detected by a silicone photodiode located at a 90° from the laser. The photodiode produces a signal which is sent to the analog outputs for collection. A light trap is located 180° from the laser to collect any light not scattered by particles in the aerosol stream.

The signal is related to the solute concentration by the function $\Lambda = am^x$, where x is the slope of the response line, m is the mass of the solute injected in the column, and a is the response factor.

APPLICATIONS

Evaporative light-scattering detection finds wide applicability in the analysis of lipids and sugars. The analysis of lipids and sugars by HPLC has classicaly been hampered due to the lack of absorbing chromophores in these molecules. Accordingly, most analyses are carried out by GC, requiring derivatization in the case of the sugars or being especially difficult like the separation of the high-molecular-weight triglycerides, or even impossible for the important class of phospholipids, which cannot withstand high temperatures. Specific applications are as follows:

1. Use of evaporative light scattering detector in reversed-phase chromatography of oligomeric surfactants. Y. Mengerink, H. C. De Man, and S. J. Van Der Wal, J. Chromatogr. 552: 593 (1991).
2. A rapid method for phospholipid separation by HPLC using a light-scattering detector: W. S. Letter, J. Liq. Chromatogr. 15: 253 (1992).
3. Detection of HPLC separation of glycophospholipids: J. V. Amari, P. R. Brown, and J. G. Turcotte, Am. Lab. 23 (Feb. 1992).
4. Analysis of fatty acid methyl esters by using supercritical fluid chromatography with mass evaporative light-scattering detection: S. Cooks and R. Smith, Anal. Proc. 28, 11 (1991).
5. HPLC analysis of phospholipids by evaporative light-scattering detection: T. L. Mounts, S. L. Abidi, and K. A. Rennick, J. AOCS 69: 438 (1992).
6. Determination of cholesterol in milk fat by reversed-phase high-performance liquid chromatography and evaporative light-scattering detection: G. A. Spanos and S. J. Schwartz, LC–GC 10(10): 774 (1992).
7. A qualitative method for triglyceride analysis by HPLC using ELSD: W. S. Letter, J. Liq. Chromatogr. 16: 225 (1993).
8. Detect anything your LC separates, P. A. As-mus, Res. Dev. 2: 96 (1986).
9. Rapid separation and quantification of lipid classes by HPLC and mass (light scattering) detection: W. H. Christie, J. Lipid Res. 26: 507 (1985).

REFERENCES

1. Scott, R.P.W. *Liquid Chromatography Detectors*; Elsevier: Amsterdam, 1977.
2. Colin, H.; Krstulovic, A.; Guiochon, G. Analysis **1983**, *11*, 155.
3. Scott, R.P.W.; Kucera, P. Mode of operation and performance characteristics of microbore columns for use in liquid chromatography. J. Chromatogr. **1979**, *169*, 51–72.
4. Knox, J.H.; Gilbert, M.T. Kinetic optimization of straight open-tubular liquid chromatography. J. Chromatogr. **1979**, *186*, 405–418.
5. Guiochon, G. Conventional packed columns vs. packed or open tubular microcolumns in liquid chromatography. Anal. Chem. **1981**, *53*, 1318–1325.
6. Guiochon, G. *Miniaturization of LC Equipment*; Kucera, P., Ed.; Elsevier: Amsterdam, 1983.
7. Kucera, P.; Umagat, H. Design of a post-column fluorescence derivatization system for use with microbore columns. J. Chromatogr. **1983**, *255*, 563–579.
8. Jorgenson, J.W.; Guthrie, E.J. Liquid chromatography in open-tubular columns: Theory of column optimization with limited pressure and analysis time, and fabrication of chemically bonded reversed-phase columns on etched borosilicate glass capillaries. J. Chromatogr. **1983**, *255*, 335–348.
9. Arpino, P.J.; Guiochon, G. LC/MS coupling. Anal. Chem. **1979**, *51* (7), 682A.
10. Willmont, F.W.; Dolphin, R.J. A novel combination of liquid chromatography and electron capture detection in the analysis of pesticides. J. Chromatogr. Sci. **1974**, *12*, 695.
11. McGuffin, V.L.; Novotný, M. Micro-column high-performance liquid chromatography and flame-based detection principles. J. Chromatogr. **1981**, *218*, 179–187.
12. Charlesworth, J.M. Evaporative analyzer as a mass detector for liquid chromatography. Anal. Chem. **1978**, *50*, 1414–1420.
13. Macrae, R.; Dick, J.J. Analysis of carbohydrates using the mass detector. J. Chromatogr. **1981**, *210*, 138–145.

BIBLIOGRAPHY

1. Jorgenson, J.W.; Smith, S.L.; Novotný, M. Light-scattering detection in liquid chromatography. J. Chromatogr. **1977**, *142*, 233–240.

Evaporative Light Scattering Detection for LC

Sarah S. Chen
Analytical Science, GlaxoSmithKline, King of Prussia, Pennsylvania, U.S.A.

INTRODUCTION

Evaporative light scattering detection (ELSD) is a powerful technique that can be applied in liquid chromatography (LC) to all solutes having lower volatility than the mobile phase. It consists of a nebulizer that transforms the eluent from the high-performance liquid chromatography (HPLC) into an aerosol, a drift tube to vaporize the solvent, and a light scattering cell (Fig. 1). When using ELSD in conjunction with LC, the eluent is nebulized immediately into a stream of warm gas. The solvent then vaporizes leaving a cloud of solute particles. The particles are subjected to a light source and scattering occurs in the scattering chamber. The amount of light scattered by the particles is proportional to the analyte concentration. These principles make ELSD a universal detector that can be used for analytes with low UV chromophores. Evaporative light scattering detection has been used for the detection of polymers in size-exclusion chromatography (SEC).[1] It has also been used in the detection of small molecules in reversed phase and normal phase LC.[2–4]

THEORY AND INSTRUMENTATION

Light scattering detection cannot be used if the analyte particles or solvent vapors absorb at the wavelength range of the light source. When particles are hit with a beam of light, the light may be absorbed, refracted, reflected, or scattered. Reflection and refraction always occur together and they prevail when the wavelength of light approaches the particle's size.[5] The sum of the reflection and refraction intensities equals the intensity of the incident light when there is no absorbance. Scattering occurs when the particle diameter is close to one-tenth of the wavelength. There are two types of scattering: Mie scattering and Rayleigh scattering. Mie scattering occurs when the ratio of particle diameter to the wavelength of light is greater than 0.1.[6] Rayleigh scattering occurs when the ratio is less than 0.1.[7] These numbers are approximate and a transition region does exist. The property of scattering has been used in the ELSD for LC. In ELSD, the eluent for LC is nebulized, and the amount of light scattered by the nebulized eluent particles is proportional to the analyte concentration.

Evaporative light scattering detection involves three successive and interrelated processes: nebulization of the chromatographic eluent, evaporation of the volatile solvent (mobile phase), and scattering of light by residual analyte particles. The three major parts of the system are the nebulizer, drift tube, and light-scattering cell.

Nebulizer

The nebulizer is normally interfaced directly to the LC column. It combines the eluent with a stream of gas to produce an aerosol. Much of the theoretical and practical basis of nebulization comes from atomic spectroscopy. The average droplet diameter and uniformity of the aerosol are the most important factors for ELSD sensitivity and reproducibility. As larger solute particles scatter light more intensely, an aerosol with large droplets and a narrow droplet size distribution leads to the most precise and sensitive detection. A good nebulizer should produce a uniform aerosol of large droplets with narrow droplet size distribution. The droplets cannot be too large, however; otherwise, the solvent in a droplet will not be completely vaporized and errors in detection will occur. The nebulizer properties that can be adjusted to obtain the desired droplet properties are, primarily, the gas flow rate and the LC mobile phase flow rate.[8]

Drift Tube

Volatile components of the aerosol produced by the nebulizer are evaporated in the drift tube to produce non-volatile particles in a dispersed mixture of carrier gas and solvent vapors. Ideally, the temperature in the drift tube should be high enough to ensure the complete evaporation of solvents, yet not so high as to be able to volatilize the analytes. If solvent removal is incomplete, detector noise will increase. When extremely large droplets reach the light scattering cell, they will be seen as spikes. If the drift tube temperature is too high, solute may be vaporized or partially vaporized, resulting in decreased sensitivity and accuracy. Droplet aggregation is another phenomenon that can occur in the drift tube. It can cause incomplete solvent removal and detector signal spiking. Overall, the drift tube should be wide enough, long enough, and hot enough to ensure complete and rapid solvent removal. Its outlet into the light-scattering cell should be shaped to send all of the particles past the detector window. There has been an increased need for a low temperature ELSD to address the detection of thermally labile compounds and volatile compounds. A low-temperature ELSD that can evaporate solvent at near-ambient temperature, 26–40°C, is now available from several vendors. These instruments are designed in a way that extremely large

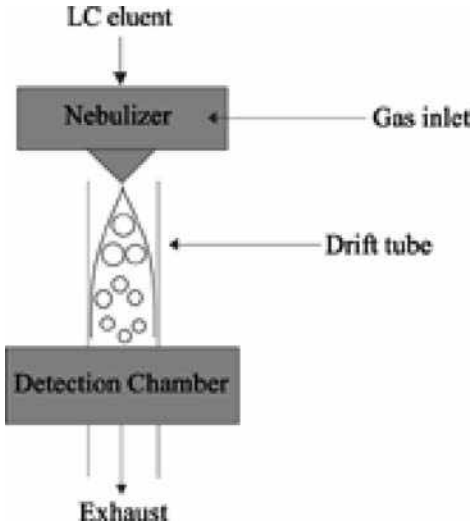

Fig. 1 Schematic diagram of evaporative light scattering detector.

droplets are expelled to waste. Only droplets of optimum size can survive and the surface area of these droplets will allow maximum vaporization of solvents at moderate drift tube temperatures.

Light Scattering Cell

The particle cloud leaves the drift tube and enters into a light scattering cell. Laser light is passed into the cell through a window, scattered by the analyte, and detected at an angle to the incident light. Single wavelength light at 632, 650, or 670 nm has been generally used in various instrument designs. Other instruments use a polychromatic light source. It is believed that a polychromatic light source emits a distribution of wavelengths where specific absorbance effects are minimized and mass sensitivity predominates over structural sensitivity. The response increases monotonically with analyte mass because of the averaging effects that occur when polychromatic scattered light is collected. Thus a polychromatic light source can be found more often than a single wavelength source in instruments. The detector is usually constructed in a way that material in the particle cloud will not stick to the window and fumes are properly vented. In addition, light traps are used to dissipate non-scattered light.

EXPERIMENTAL CONSIDERATIONS

The response factor of an ELSD largely depends on the size of analyte particles entering the detection chamber. After exiting from the HPLC column, the eluent stream is nebulized, and a scavenger gas stream carries the effluent cloud through a hot drift tube where the solvent vaporizes. The droplet shrinks to the volume of the non-volatile material contained in the eluent. The average particle size in the cloud at a given time and the particle size distribution can be derived from the elution profile of the analyte and the droplet size distribution given by the nebulizer. The average diameter, D_o, of the particles formed in a concentric nebulizer is given by the Atkinson equation:[9]

$$D_o = \frac{A\sigma_1^{1/2}}{u\rho_1^{1/2}} + B\left(\frac{\eta_1}{(\sigma_1\rho_1)^{1/2}}\right)^{0.45}\left(\frac{1000Q_1}{Q_g}\right)^{1.5} \quad (1)$$

where A and B are constants, σ_1 is the surface tension of the mobile phase, ρ_1 is the density of the mobile phase, η_1 is the viscosity of the mobile phase, u is the relative velocity of the gas and liquid streams in the nebulizer (i.e., the cross-section average velocity of the gas stream between the gas and the liquid nozzles, minus the cross-sectional average velocity of the solvent in the liquid tube), Q_1 is the volume flow rate of the mobile phase, and Q_g is the volume flow rate of the scavenger gas.

Eq. 1 predicts that the average droplet size depends on the gas and solvent flow rate. It also predicts that the average droplet size will depend on the nature of the solvent, because of the dependency on the density, surface tension, and viscosity of the nebulized liquid. The initial droplet size formed in the nebulizer has little to do with the property of the analyte as it predominantly contains mobile phase. The final droplet size in the scattering chamber is dependent on the analyte concentration. When optimizing detector conditions, the experimental parameters that can be adjusted are nebulizer gas flow rate, mobile phase flow rate, and drift tube temperature.

Effect of Scavenger Gas Flow Rate

While keeping mobile phase constant, a plot of the response for a constant sample amount vs. the scavenger gas flow rate exhibits a maximum at an intermediate flow rate, and so does the plot of the signal-to-noise ratio vs. flow rate. At large flow rates, the decrease in response is due to the fact that the average particle size of the solute cloud decreases with increasing gas flow rate according to Eq. 1. The response decreases accordingly with the particle size. At low flow rate, the response factor decreases rapidly with decreasing flow rate, while the noise increases and spikes appear. This is related to the fact that the flow velocity of the scavenger gas in the concentric nebulizer should be in the sonic range in order for the nebulizer to function properly. A low gas flow rate results in very large droplets that vaporize too slowly; hence a spike appears. Precipitation or aggregation can occur if the nebulizer gas pressure is too low. Precipitation in the drift tube can also cause a decrease in sensitivity.

Effect of Mobile Phase Flow Rate

An increase in eluent flow rate will result in increased droplet size and high response factor. However, a flow rate that is too high will result in the incomplete vaporization of the mobile phase and high background noise. When

ELSD is used in conjunction with LC, the effect of flow rate on the separation should also be considered.

Effect of Drift Tube Temperature

The solvent contained in the droplets formed in the nebulizer must be completely vaporized during the migration of these droplets down through the drift tube. Thus a compromise between the scavenger gas pressure, the mobile phase flow velocity, and drift tube temperature has to be chosen. The residence time of the droplets of solution in the drift tube should be large enough and the drift tube temperature should be high enough to ensure the complete vaporization of solvents. Meanwhile, the temperature must be low enough so that the analytes are not vaporized, as this would result either in a systematic error (small extent of analyte vaporization) or in a total loss of signal (total vaporization of analyte). Low temperatures avoid evaporation of semivolatile analytes and destruction of thermally labile compounds. Vaporization of the solvent is facile with organic mobile phases such as acetonitrile, hexane, or chloroform, but relatively difficult with aqueous mobile phases.

Other Considerations

The response of the evaporative light scattering detector is not linear. This is because the droplets scatter light with an intensity that increases much faster than the third power of their diameter.[10] The response of the detector is not linear but is given by

$$A = aC^b \tag{2}$$

where A is the response of the detector, a and b are numerical coefficients, C is the concentration of solute. The data can be plotted as log A vs. log C to obtain a graph that has a large linear region with a slope b and an ordinate a. This region can be used for quantitation. Slope b tends to be similar for similar compounds and falls between 1 and 2. A slope of 2 is the limiting value for Rayleigh scattering.[11]

One advantage of ELSD is that a wide range of solvents can be used, including acetone and chloroform which are not useful with UV detection. One drawback is that the solvent must be significantly more volatile than the analytes; thus the use of non-volatile buffers should be strictly avoided. Only high-quality HPLC solvents with minimum particulates should be used.

If the solvents remain clean and totally volatilized, baseline drift should not be observed during gradient elution. However, sensitivity may change in solvent gradients, mainly due to the change in droplet size as a result of the change in eluent properties such as surface tension, viscosity, and density. In general, shallow gradients are preferable.

Outlet waste gas stream from the ELSD may contain organic solvent vapors. For safety reasons, it is essential to ensure that the outlet of ELSD is properly directed to a safe vented outlet (e.g., a fume hood). Waste ventilation should occur at atmospheric pressure. A vacuum or restriction may result in pressure changes within the optical detection chamber and cause detector baseline instability.

CONCLUSIONS

Evaporative light scattering detection can be used as a universal detector for LC. Its operation includes the nebulization of the eluent in the nebulizer, solvent evaporation in the drift tube, and scattered light detection at the light scattering chamber. Experimental conditions which can be adjusted in most ELSD systems to optimize the detector sensitivity are the nebulizer gas flow rate, mobile phase flow rate, and drift tube temperature. The detector response is non-linear, but can be used in quantitative work if a calibration curve is obtained.

REFERENCES

1. Nagy, D.J. Characterization of nonionic and cationic amine-functional polymers by aqueous SEC-MALLS. J. Appl. Polym. Sci. **1996**, *62* (5), 845.
2. Toussaint, B.; Duchateau, A.L.L.; van der Wal, Sj.; Albert, A.; Hubert, Ph.; Crommen, J. Determination of the enantiomers of 3-tert.-butylamino-1,2-propanediol by high-performance liquid chromatography coupled to evaporative light scattering detection. J. Chromatogr. A, **2000**, *890(2)*, 239–249.
3. Risley, D.S.; Strege, M.A. Chiral separations of polar compounds by hydrophilic interaction chromatography with evaporative light scattering detection. Anal. Chem. **2000**, *72*, 1736–1739.
4. Chen, S.; Yuan, H.; Grinberg, N.; Dovletoglou, A.; Bicker, G. Enantiomeric separation of trans-2-aminocyclohexanol on a crown ether stationary phase using evaporative light scattering detection. J. Liq. Chromatogr. & Relat. Technol. **2003**, *26* (3), 425–442.
5. Charlesworth, J. Enantiomeric separation of trans-2-aminocyclohexanol on a crown ether stationary phase using evaporative light scattering detection. Anal. Chem. **1978**, *50* (11), 1402–1414.
6. Righezza, M.; Guiochon, G. Effects on the nature of the solvent and solutes on the response of a light-scattering detector. J. Liq. Chrom. Relat. Techol. **1988**, *11* (9,10), 1967–2004.
7. Mourey, T.; Oppenheimer, L. Principles of operation of an evaporative light-scattering detector for liquid chromatography. Anal. Chem. **1984**, *56*, 2427–2434.
8. Stolyhwo, A.; Colin, H.; Martin, M.; Guiochon, G. Study of the qualitative and quantitative properties of the light scattering detector. J. Chromatogr. **1984**, *288*, 253–275.
9. Nukiyama, S.; Tanasawa, Y. Trans. Soc. Mech. Eng. Tokyo **1938**, *4*, 86.
10. Guiochon, G.; Moysan, A.; Holley, C. Influence of various parameters on the response factors of the evaporative light scattering detector for a number of non-volatile compounds. J. Liq. Chromatogr. **1988**, *11* (12), 2547–2570.
11. Oppenheimer, L.; Mourey, T. Examination of the concentration response of evaporative light-scattering mass detectors. J. Chromatogr. **1985**, *323*, 297–304.

Evaporative Light Scattering Detection for SFC

Christine M. Aurigemma
William P. Farrell
Pfizer Global Research and Development, Pfizer Inc., La Jolla, California, U.S.A.

INTRODUCTION

The evaporative light-scattering detector (ELSD) was originally developed for use with high-performance liquid chromatography (HPLC) to detect nonvolatile compounds by mass rather than ultraviolet (UV) absorbance detection.[1] The response is dependent on the light scattered from particles of the solute remaining after the mobile phase has evaporated and is proportional to the total amount of the solute. Because no chromophore is necessary, a response can be measured for any solute less volatile than the mobile phase.

DISCUSSION

Although ELSD is considered a universal detector for HPLC,[2] there are additional advantages obtained from coupling ELSD to packed column supercritical fluid chromatography (SFC). SFC provides better selectivity and faster analysis times over HPLC as a result of the low-viscosity and high solute diffusion coefficients characteristic of supercritical fluids.[3] Detection limits for some solutes are improved using ELSD with SFC relative to HPLC.[4] In order to increase solvating power and improve peak shape, CO_2 is often modified with a polar organic solvent such as methanol.[5,6] Using this binary fluid allows for improved separation efficiency of compounds having a wide range of polarities that may otherwise require a buffer.

When compared to other mass-sensitive detectors such as flame ionization (FID), refractive index (RI), and mass spectrometry (MS), the ELSD can detect analytes without interference from organic modifiers and additives. The use of organic solvents in FID limits usefulness due to an increase in baseline noise, and FID cannot be used with HPLC. RI detectors, in general, are less sensitive than other detectors and are incompatible with gradient elution. Although the MS can be used with modifier gradients, ionization efficiencies can vary over orders of magnitude depending on the solute and mode of ionization. The ELSD is more practical than conventional UV detectors because solutes lacking in UV-absorbing chromophores can be directly detected without any sample derivatization or pretreatment. Baseline disturbances due to absorption of the mobile-phase solvents are not observed with ELSD. However, solvents containing trace levels of impurities and columns with low bleed characteristics must be employed for high-sensitivity work. The ELSD can be optimized to generate a narrow range of response factors to components within a structural class, and the use of appropriate standards would allow for quantitative analysis of these compounds.

Because organic solvent gradients do not interfere with ELSD, the detector is an ideal choice for coupling with SFC. A wide range of SFC–ELSD biomedical and pharmaceutical applications have demonstrated higher sensitivity, shorter analysis times, and better separation efficiencies with SFC than HPLC. Compounds without UV chromophores, such as carbohydrates and ginkgolide extracts, have been reported by Lafosse et al.,[3] Carraud et al.,[4] and Strode et al.,[7] using SFC modifier gradients. More efficient baseline separations of these compounds were achieved by SFC–ELSD than with HPLC, and no time-consuming derivatization steps were necessary. The analysis of triglycerides using SFC–ELSD, which required a polar organic modifier to elute, yielded a significant increase in sensitivity over HPLC–ELSD.[4] Underivatized amino acids were also effectively separated by SFC– ELSD.[3] A more complete review of the various SFC–ELSD interfaces and applications was recently published by Lafosse.[2]

Evaporative light-scattering detection response was found to have an exponential relationship to the mass of the solute by the equation:

$$A = am^b \tag{1}$$

where A is the peak area of the ELSD signal, m is the solute mass, and a and b are constants which depend on the nature of the mobile phase and of the solutes.[8] Because the peak area response is proportional to the amount of solute, a linear response would be more desirable if quantitation of sample components is required. Linearity can be achieved by plotting calibration curves on a log–log scale as in Eq. 2:

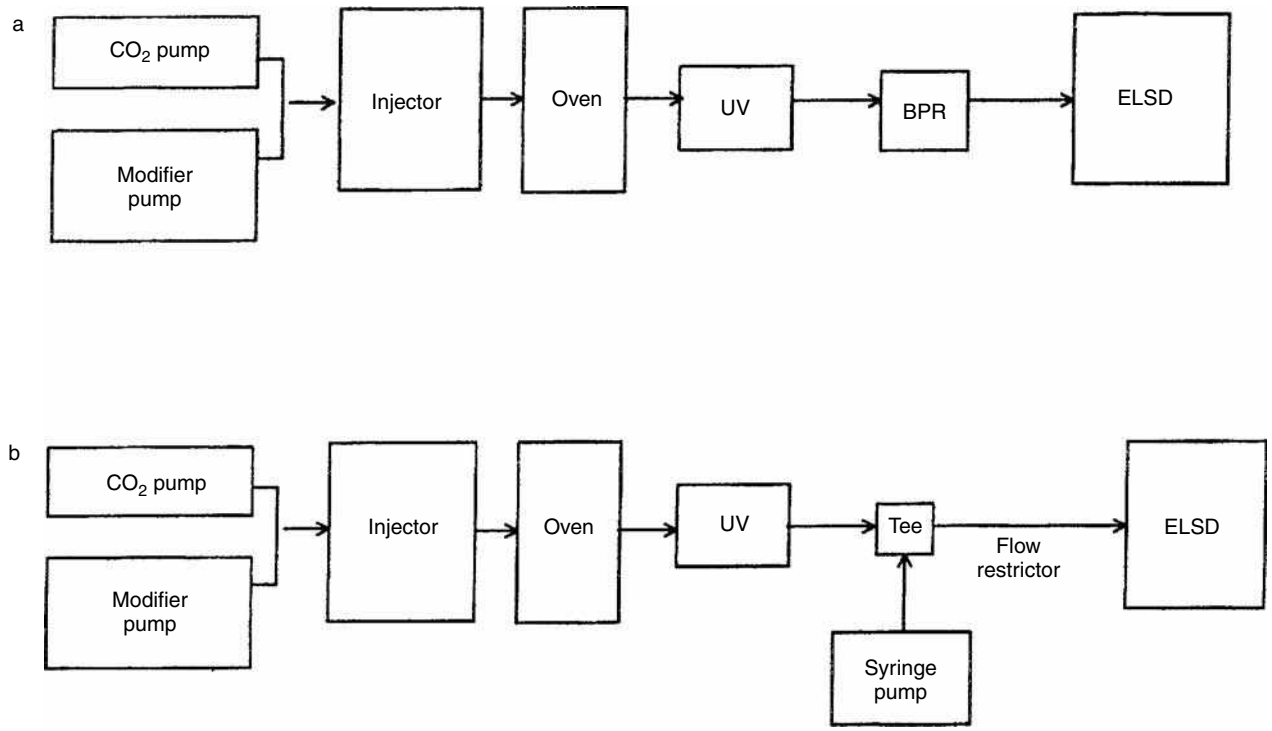

Fig. 1 Two common arrangements for SFC–ELSD coupling: (a) shows pressure control by a back-pressure regulator (BPR), and in (b), the pressure is regulated by a makeup fluid delivered by a pressure-controlled syringe pump.
Source: From Pressure-regulating fluid interface and phase behavior considerations in the coupling of packed-column supercritical fluid chromatography with low-pressure detectors, in J. Chromatogr. A.[12]

$$\log A = b \log m + \log a \quad (2)$$

The ELSD detector response is influenced by the functions of its three main units: the nebulizer, drift tube, and light-scattering cell. As the mobile phase passes through the nebulizer, it becomes dispersed by a flow of carrier gas such as nitrogen and forms an aerosol. The resultant droplets vary in size depending on factors including the flow rate of the nebulizer gas and the geometry of the nebulizer.[6] The droplets then travel through a heated drift tube where the mobile phase is evaporated, leaving behind only unsolvated particles. Upon exiting the drift tube, the solute particles enter a detection chamber and pass through a beam of light from either a polychromatic (tungsten lamp) or a monochromatic (laser) source. The light is scattered and a photomultiplier or photodiode detector, which measures the light intensity, produces a chromatographic signal. Refer to Ref.[1] for a more detailed discussion of the principles of light scattering.

When coupling a low-pressure detector such as the ELSD with SFC, detection takes place at atmospheric pressure, usually downstream of the back-pressure regulator.[2] Fig. 1a shows a common SFC–ELSD interface with downstream pressure control. Factors affecting ELSD response in this configuration include nebulizer design, evaporation conditions, carrier gas flow rate, and the use of makeup fluid.

Most commercial ELSDs employ a standard or modified HPLC nebulizer (Venturi flow type). It was believed that this nebulizer was not necessary for SFC because nebulization of the SFC mobile phase is accomplished by gas expansion in a restrictor which controls pressure and mobile-phase flow rates. To counter the cooling effects of CO_2 decompression in the linear fused-silica restrictor and improve heat transfer, Nizery et al., using a Cunow Clichy Model DDL 10 detector, placed the restrictor tip into a heated brass ring and applied heat to a small section of tubing between the restrictor and the drift tube.[9] They found that baseline noise resulting from the formation of ice crystals decreased and the performance of the ELSD was unaffected.

The droplet sizes formed and the flow rate of the particles in the drift tube are influenced by the design of the nebulizer. In order to maintain a constant nebulization, droplet sizes should not be too large making them difficult to evaporate or too small where solute vaporization could occur. This requires sufficient liquid and a carrier gas (usually nitrogen). Carraud et al., replaced a conventional ELSD nebulizer (Cunow Clichy Model DDL 10) with a short fused-silica restrictor and determined that the ELSD signal response was dependent on the CO_2 flow rate, although this was later disproved.[4]

Larger particle sizes produce higher intensities of scattered light. In order to obtain maximal ELSD sensitivity,

evaporator temperatures must be sufficient to allow for the formation of appropriately sized particles. A loss in sensitivity is observed if temperatures are too high because smaller particles may result from sublimation of some compounds. Upnmoor and Bruner[10] studied the effects of varying evaporator temperature on ELSD sensitivity and found that the optimal range of temperatures was between 40°C and 70°C. At lower temperatures, longer residence times required in the drift tube produced peak broadening as well as an increase in baseline noise.

The flow rate of the carrier gas (usually N_2) influences the residence time of the sample in the light-scattering chamber. Low gas flows may allow solute bands to broaden as they travel in the drift tube to the detector. Strode and Taylor[11] observed a decrease in ELSD signal with an increase in the carrier gas flow rate. However, the increase in gas flow improved peak width compared to that observed with the UV detector. It was later found that the total flow of gas (carrier gas plus the decompressed CO_2) through the detector influenced the signal response and the peak width.[11]

Most SFC–ELSD instruments employ a direct connection of the outlet of a back-pressure regulator to the detector inlet, as outlined in Fig. 1a. By operating in this manner, peak broadening in the transfer line between the back-pressure regulator and the detector may occur. Additionally, the pressure decrease in the transfer line may affect the strength of the mobile phase and, thus, the ability of the solutes to become completely solubilized. Pinkston bypassed the back-pressure regulator with a post-column tee that introduced a makeup fluid such as methanol from a high-pressure syringe pump under pressure control.[12] A fused-silica linear restrictor at the ELSD inlet maintained the pressure and was regulated by the flow of the makeup fluid, as shown in Fig. 1b. Pinkston theorized that this method of pressure control would prevent mass-transfer problems that diminish detector sensitivity and decrease the dependence of the ELSD response on mobile-phase composition.[12] The flow of makeup solvent enhanced the solubility of the analytes in the mobile phase. Additionally, the efficiency of forming appropriately sized particles in the ELSD was improved, generating better peak shapes and higher signal-to-noise ratios.

In conclusion, an ELSD with SFC provides a sensitive analytical tool for qualitative and quantitative analysis of solutes. Detection depends only on the solute being less volatile than the least volatile mobile-phase component. Detection is independent of the basicity or presence of a chromophore for a given solute. The detector response is a logarithmic function of the mass of the solute. The SFC–ELSD combination should be considered whenever a universal high-throughput analysis is needed.

REFERENCES

1. Strode, J.T.B.; Taylor, L.T.; Anton, K.; Bach, M.; Pericles, N. *Supercritical Fluid Chromatography with Packed Columns: Techniques and Applications*; Marcel Dekker, Inc.: New York, 1997; 97–123.
2. Lafosse, M. Evaporative light scattering detection in SFC. Chromatogr. Princ. Pract. **1999**, 201–218.
3. Lafosse, M.; Elfakir, C.; Morin-Allory, L.; Dreux, M. The advantages of evaporative light scattering detection in pharmaceutical analysis by high performance liquid chromatography and supercritical fluid chromatography. J. High Resolut. Chromatogr. **1992**, *15*, 312–318.
4. Carraud, P.; Thiebaut, D.; Caude, M.; Rosset, R.; Lafosse, M.; Dreux, M. Supercritical fluid chromatography/light-scattering detector: A promising coupling for polar compounds analysis with packed columns. J. Chromatogr. Sci. **1987**, *25*, 395–398.
5. Berger, T.A. *Packed Column SFC*; The Royal Society of Chemistry: Cambridge, 1995.
6. Dreux, M.; Lafosse, M. LC-GC Int. **1997**, *10*, 382–390.
7. Strode, J.T.B.; Taylor, L.T.; van Beek, T.A. Supercritical fluid chromatography of ginkgolides A, B, C and J and bilobalide. J. Chromatogr. A, **1996**, *738*, 115–122.
8. Dreux, M.; Lafosse, M.; Morin-Allory, L. The evaporative light scattering detector—A universal instrument for nonvolatile solutes on LC and SFC. LC-GC Int. **1996**, *9*, 148–153.
9. Nizery, D.; Thiebaut, D.; Caude, M.; Rosset, R.; Lafosse, M.; Dreux, M. Improved evaporative light-scattering detection for supercritical fluid chromatography with carbon dioxide-methanol mobile phases. J. Chromatogr. **1989**, *467*, 49–60.
10. Upnmoor, D.; Brunner, G. Packed column supercritical fluid chromatography with light-scattering detection. I. Optimization of parameters with a carbon dioxide/methanol mobile pase. Chromatographia **1992**, *33*, 255–260.
11. Strode, J.T.B., III; Taylor, L.T. Evaporative light scattering detection for supercritical fluid chromatography. J. Chromatogr. Sci. **1996**, *54*, 261–270.
12. Chester, T.L.; Pinkston, J.D. Pressure-regulating fluid interface and phase behavior considerations in the coupling of packed-column supercritical fluid chromatography with low-pressure detectors. J. Chromatogr. A, **1998**, *807*, 265–273.

Exclusion Limit in GPC/SEC

Iwao Teraoka
Department of Chemistry, Polytechnic University, Brooklyn, New York, U.S.A.

INTRODUCTION

A given gel permeation chromatography–size-exclusion chromatography (GPC–SEC) column can analyze the molecular weight (MW) of a polymer only over a limited range of MWs. Figure 1 illustrates a typical calibration curve for the column. The logarithm of the MW is plotted as a function of the retention time t_R. At low and high ends of MW, t_R barely depends on MW, effectively limiting the range of analysis to $M_1 < \text{MW} < M_2$. The exclusion limit refers to M_2.

DISCUSSION

The sharp slope of the calibration curve at the high-MW end of the calibration curve is caused by a drastic decline of the partition coefficient as the chain dimension increases beyond the accessible pore size of the column packing material. Polymer chains of MW $> M_2$ have a molecular size dimension which is much greater than the pore size. It is virtually impossible for these chains to enter the stationary-phase pores. Thus, at almost every plate in the column, they are partitioned to the mobile phase, thus eluting with little separation at around the dead time (volume) of the column. By contrast, polymer chains smaller or comparable to the available pore sizes can pentrate the pores to be partitioned to the stationary phase with a partition coefficient which depends on their chain dimensions. The dependence of the partition coefficient on the chain dimension allows polymer chains of different MWs to be separated and elute at different times. Columns packed with porous materials of a larger pore size have greater M_1 and M_2.

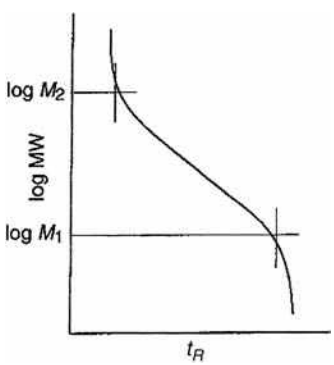

Fig. 1 Calibration curve of GPC–SEC column. Logarithm of the molecular weight, M, is plotted as a function of the retention time (volume) t_R (V_R).

For the high-MW chains that are excluded by the pores, there is a small dependence of t_R (V_R) on MW. The latter is mostly caused by the velocity gradient of the mobile phase and the population gradient of the polymer near the stationary-phase particles' surface. The mobile phase flows more slowly near the particles' surface because of the no-slip boundary condition of the fluid at the particles' surface. Among sufficiently long polymer chains to be excluded by the pore, those with a smaller dimension can more easily approach the particles' surface, compared with those of a greater dimension. Therefore, shorter chains flow more slowly. Longer chains stay away from the particles and flow along the fastest-flowing mobile phase, eluting earlier than other components. This mode of separation is called "hydrodynamic chromatography."

Extra-Column Dispersion

Raymond P.W. Scott
Scientific Detectors Ltd., Banbury, Oxfordshire, U.K.

INTRODUCTION

In addition to the dispersion that takes place during the normal function of the column, dispersion can also occur in connecting tubes, injection system, and detector sensing volume, and as a result of injecting a finite sample mass and sample volume onto the column.

DISCUSSION

The major sources of extra column dispersion are as follows:

1. Dispersion due to the sample volume (σ_S^2).
2. Dispersion occurring in valve-column and column-detector connecting tubes (σ_T^2).
3. Dispersion in the sensor volume from Newtonian flow (σ_{CF}^2).
4. Dispersion in the sensor volume from peak merging (σ_{CM}^2).
5. Dispersion from the sensor and electronics time constant (σ_t^2).

The sum of the variances will give the overall variance for the extra-column dispersion (σ_E^2). Thus,

$$\sigma_E^2 = \sigma_S^2 + \sigma_T^2 + \sigma_{CF}^2 + \sigma_{CM}^2 + \sigma_t^2 \quad (1)$$

Eq. 1 shows how the various contributions to extra-column dispersion can be combined. According to Klinkenberg,[1] the total extra-column dispersion must not exceed 10% of the column variance if the resolution of the column is not to be seriously denigrated; that is,

$$\sigma_E^2 = \sigma_S^2 + \sigma_T^2 + \sigma_{CF}^2 + \sigma_{CM}^2 + \sigma_t^2 = 0.1\sigma_c^2$$

In practice, σ_T^2, σ_{CF}^2, σ_{CM}^2, and σ_t^2 are all kept to a minimum to allow the largest contribution to extra-column dispersion to come from σ_S^2. This will allow the largest possible sample to be placed on the column, if so desired, to aid in trace analysis. Each extra-column dispersion process can be examined theoretically and two examples will be the evaluation of σ_S^2 and σ_T^2.

MAXIMUM SAMPLE VOLUME

Consider the injection of a sample volume (V_i) that forms a rectangular distribution of solute at the front of the column. The variance of the final peak will be the sum of the variance of the sample volume plus the normal variance from a peak for a small sample. Now, the variance of a rectangular distribution of sample volume (V_1) is $V_i^2/12$, and assuming the peak width is increased by 5% due to the dispersing effect of the sample volume (a 5% increase in standard deviation is approximately equivalent to a 10% increase in peak variance), then by summing the variances,

$$\frac{V_i^2}{12} + [\sqrt{n}(\nu_m + K\nu_s)]^2 = [1.05\sqrt{n}(\nu_m + K\nu_s)]^2$$

where the dispersion due to the column alone is $[\sqrt{n}(\nu_m + K\nu_s)]^2$ (see *Plate Theory*, p. 1829). Simplifying and rearranging,

$$V_i^2 = n(\nu_m + K\nu_s)^2(1.22)$$

Bearing in mind that

$$V_r = n(\nu_m + K\nu_s)$$

then

$$V_i = \frac{1.1V_r}{\sqrt{n}}$$

Thus, the maximum sample volume that can be tolerated can be calculated from the retention volume of the solute concerned and the efficiency of the column. A knowledge of the maximum sample volume can be important when the column efficiency available is only just adequate, and the compounds of interest are minor components that are only partly resolved.

DISPERSION IN CONNECTING TUBES

The column variance is given by V_r^2/n, and for a peak eluted at the dead volume, the variance will be V_0^2/n (see *Plate Theory*, p. 1829). Thus, for a connecting tube of radius r_t and length l_t, the dead volume (V_0) (i.e., the volume of the tube) is

$$V_0 = \pi r_t^2 l_t$$

Thus,

$$\sigma_E^2 = \frac{0.1(\pi r_t^2 l_t)^2}{n}$$

Now, for the dead volume peak from an open tube, $n = 1/0.6r_t$ (see *Open-Tubular Columns: Golay Dispersion Equation*, p. 1635). Thus,

$$\sigma_E^2 = 0.06\pi^2 r_t^5 l_t$$

However, when assessing the length of tube that can be tolerated, it must be remembered that the 10% increase in variance that can be tolerated before resolution is seriously denigrated involves *all* sources of extra-column dispersion, not just for a connecting tube. In practice, the connecting tube should be made as short as possible and the radius as small as possible commensurate with reasonable pressures and the possibility that if the radius is too small, the tube may become blocked. The different sources of extra-column dispersion have been examined in Refs.[2,3]

REFERENCES

1. Klinkenberg, A. *Gas Chromatography 1960*; Scott, R.P.W., Ed.; Butterworths: London, 1960; 194.
2. Scott, R.P.W. *Liquid Chromatography Column Theory*; John Wiley & Sons: New York, 1992; 19.
3. Scott, R.P.W. *Introduction to Gas Chromatography*; Marcel Dekker, Inc.: New York, 1998.

BIBLIOGRAPHY

1. Scott, R.P.W. *Chromatographic Detectors*; Marcel Dekker, Inc.: New York, 1998.

Extra-Column Volume

Kiyokatsu Jinno
Department of Materials Science, Toyohashi University, Toyohashi, Japan

INTRODUCTION

Three mechanisms produce dispersion of a band of solute in a chromatographic system as it passes through the separation column: 1) eddy diffusion; 2) longitudinal diffusion; and 3) mass transfer effects. These effects are discussed, in some detail, in this entry.

EXTRA-COLUMN BAND BROADENING

Three mechanisms produce dispersion of a band of solute in a chromatographic system as it passes through the separation column.

a. Eddy diffusion and flow dispersion, which is the term for the dispersion produced because of the existence of different flow paths through which solutes can progress through the column. These differences of traveling distance arise because the stationary phase particles have different sizes and shapes, and because the packing of the column is imperfect, causing gaps or voids in the column bed. To reduce dispersion due to the multiple path effect, we need to pack the column with small particles, with as narrow a size distribution as possible.
b. Longitudinal diffusion, which also arises because of diffusion of solute in the longitudinal (axial) direction in the column. This is an important source of dispersion in gas chromatography (GC), but less so in liquid chromatography (LC), because rates of diffusion are very much slower in liquids than they are in gases. This effect becomes more serious the longer the solute species spend in the column; so, unlike flow dispersion, using a rapid flow rate of mobile phase reduces this effect.
c. Mass transfer effects, which arise because the rate of the distribution process (sorption and desorption) of the solute species between mobile and stationary phases may be slow, compared to the rate at which the solute is moving in the mobile phase.

Except for the above general dispersions produced in the separation mechanisms, an unexpected, but important, dispersion can be produced outside the separation column by dead volumes in other parts of the chromatographic system, such as in the injector, the detector, the connecting tubing, and connectors. The combined effect of all of these parts is called "extra-column volume" and the dispersion produced by this volume is called "extra-column dispersion."[1–4] Fig. 1 demonstrates an example of this extra-column dispersion, in which different dead volumes are inserted between the column and the detector. One can see, from this figure, that the effect of extra-column volume can cause a serious loss in separation performance of the chromatographic system.

The variance (the square of the standard deviation) of the observed peak (σ^2) can be expressed as the sum of the peak variances caused only by the contribution of the column ($\sigma_p{}^2$) and all the contributions to the peak broadening due to the extra-column volume ($\sigma_{ex}{}^2$). This is expressed as

$$\sigma^2 = \sigma_p{}^2 + \sigma_{ex}{}^2 \tag{1}$$

Since the peak volume is four times the standard deviation (σ_s), Eq. 1 can be rewritten as

$$V_t{}^2 = V_p{}^2 + V_{ex}{}^2 \tag{2}$$

where V_p is the peak volume obtained only from column contribution and V_{ex} is the extra-column peak volume corresponding to the contributions of the injector, detector

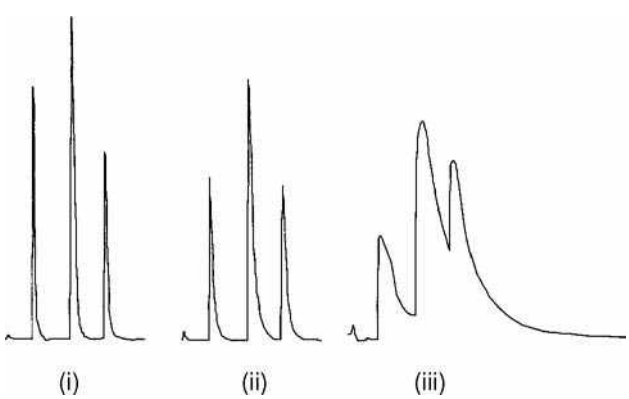

Fig. 1 Extra-column effects on the chromatogram. (i) Normal chromatogram for a test separation; (ii) chromatogram obtained by inserting 75 μl of extra volume between the column and the detector inlet tube; (iii) chromatogram obtained by inserting 2 ml of extra volume between the column and the detector inlet tube.

Table 1 Maximum extra-column peak volumes for peaks eluted by various columns.[a]

	Column type (length, mm; I.D., mm)		
	Conventional (250; 4.6)	**Semi-microcolumn (250; 1.5)**	**Microcolumn (250; 0.5)**
Maximum extra column			
Peak volume (V_{ex}, μl)	53	5.5	0.6
Peak volume (V_p, μl)	116	12	1.4

[a]The above numbers have been estimated by assuming as follows: Column porosity = 0.7; retention factor = 0; and theoretical plate number = 10,000.

cell, and connecting tubing. Dividing Eq. 2 by V_p^2 produces

$$(V_t/V_p)^2 = 1 + (V_{ex}/V_p)^2 \quad (3)$$

Therefore, if the observed peak is allowed to have a volume 10% greater than the column peak volume, the extra-column peak volume should be one-half (~46%) of the column peak volume. Table 1 lists column peak volumes and maximum extra-column peak volumes for various types of columns for LC; because the largest contribution from this extra-column volume should be considered in liquid phase separations, the diffusion coefficients in liquids are very small.

From Table 1, it is very clear that, as the absolute volume of a microcolumn is relatively small, the extra-column volume will contribute significantly to disturb the separation performance of the chromatography system. Because the small extra-column volume is still a large portion of the total system volume which, in turn, is much smaller than the conventional column system, and it is hard to eliminate such small extra-column volume, even if attempts to reduce are applied, a serious problem would be produced. Most typical discussions on the applicability of microcolumn separations in LC are concerned with how to reduce the extra-column volume; this makes microcolumn LC techniques still unpopular, although many advantages are proven and acknowledged. In conclusion, the minimum column volume one can use will depend on the amount of extra-column dispersion and on what we consider to be an acceptable increase in peak width that is produced by the extra-column effects. In practice, this acceptable increase is assumed to be 10%, based on an unretained solute and, if we take 50 μl as a typical value for extra-column dispersion, then the minimum column diameter in LC works out to about 4.6 mm for a column 25 cm long, which is the most popular conventional LC separation column configuration that is commercially available.

REFERENCES

1. Knox, J.H. Practical aspects of LC theory. J. Chromatogr. Sci. **1977**, *15* (9), 352–364.
2. Golay, M.J.E.; Atwood, J.G. Early phases of the dispersion of a sample injected in poiseuille flow. J. Chromatogr. **1979**, *186*, 353.
3. Katz, E.D.; Scott, R.P.W. Low-dispersion connecting tubes for liquid chromatography systems. J. Chromatogr. **1983**, *268*, 169.
4. Hupe, K.P.; Jonker, R.J.; Rozing, G. Determination of band-spreading effects in high-performance liquid chromatographic instruments 1. J. Chromatogr. **1984**, *285*, 253.

Fast GC

Richard C. Striebich
University of Dayton Research Institute, Dayton, Ohio, U.S.A.

INTRODUCTION

The examination of ways to conduct fast gas chromatography (GC) has been a popular research topic since the 1960s, and even more so in the past 10 years. The need to analyze complex mixtures by GC is often a balance between the ability to separate adjacent peaks in a chromatogram (resolution) and analysis time. Especially with complex mixtures, analysts can use longer columns and much slower programing rates to increase resolution; however, there is a penalty to be paid in analysis time. Because petroleum samples are arguably the most complex samples known, a good deal of work has been performed to provide the greatest possible resolution without regard for the consideration of time. Some GC petroleum analyses have been reported, which take 2–4 hr and longer.[1] However, there is a definite application for faster analyses with less resolution.

The history, methods, and applications for conducting fast analyses by GC are delineated in several excellent reviews.[2–6] In these works, the authors discuss several ways to shorten analysis time, such as the following:

1. Decrease the column length.
2. Increase the carrier gas flow rate.
3. Use multichannel columns.[6]
4. Provide rapid heating of the column with heating rates up to 1200°C/min and sometimes higher.[2]

Fast GC in these instances is best described as conducting analyses as fast as is possible to provide just enough separation of the compounds of interest. Oftentimes, in the search for maximum resolution, compounds can be overseparated, which usually lengthens the time of analysis.

OVERVIEW

In petroleum analyses, and specifically for aviation fuels, there are a good many separations where complete resolution is not needed. GC fingerprinting of different types of fuels (diesel, gasoline, aviation fuels, kerosene, etc.) can be performed quickly to characterize the mixtures in useful ways. Simulated distillation[1] is one good example of a chromatographic analysis that has low resolution, but can be conducted very quickly, (i.e., $\ll$ 5 min). Fortunately, excellent resolution is not usually necessary to obtain the critical information about distillation range,[7] and so this application is a good example of fast GC where limited resolution is acceptable. In this entry, we introduce simple fast GC concepts that can speed up the low-resolution analysis of petroleum products.

EXPERIMENTAL

Short (3–7 m) microbore gas chromatographic columns (0.10 mm internal diameter, 0.17 μm film thickness) can be used to provide much faster analyses with acceptable resolution for at least two different types of useful analyses: *fuel GC fingerprinting* and *simulated distillation analysis*. The detector for the instrument used for these analyses is a hydrogen flame ionization detector (FID) capable of very fast sampling rates (adjustable up to 200 Hz), which is necessary because of the narrow peaks that are generated. Carrier gas is one of the parameters investigated; both helium and hydrogen carrier gases were used, with high-pressure hydrogen routinely providing the best and fastest separations (in agreement with previous work and theory). In this work, the programing rates were limited to that which was available using an Agilent 6890 instrument with a fast heating option (i.e., input rates to 120°C/min with trackable rates to approximately 75°C/min). No attempts were made to increase programing rate by resistively heating the column.

RESULTS AND DISCUSSION

Analysis of aviation fuels by capillary GC can be performed using a variable level of resolution (peak separation) by changing the conditions of the GC. For the purposes of this work, the approximate resolution required was that obtained with conventional methods. That is, an experiment that is completed in 20–30 min is typical because it is fast enough to be productive with regard to research and testing, and provides enough resolution to obtain the needed useful information. In addition to this level of resolution, we briefly examined the output of a GC analysis conducted using a column of 50 μm internal diameter, half the diameter of typical fast GC columns. These conditions represent our laboratory's (present-day) limit of speed and resolving power (Fig. 1).

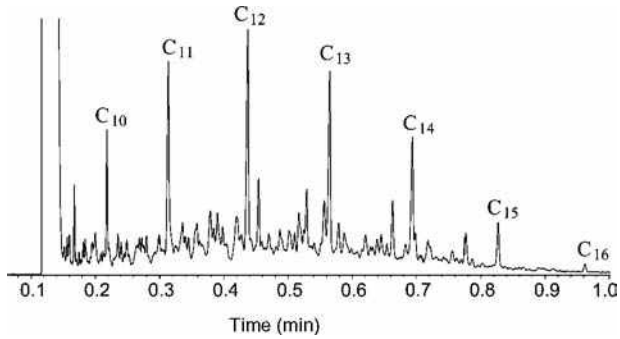

Fig. 1 Fast GC analysis of aviation turbine engine fuel using a typical laboratory GC instrument. Conditions: hydrogen carrier gas; temperature programming rate, 70–170°C at 120°C/min (actual 75°C/min); microbore column: 3 m × 0.10 mm I.D.

Effect of Column Dimensions

Table 1 shows a comparison of the general relationship that exists between GC efficiency as measured by the number of theoretical plates per meter and a particular column dimension. Because microbore columns (0.10 mm internal diameter) have more resolving power per meter, the length of these columns can be typically one third the length of standard bore columns (0.25 mm internal diameter) and still provide approximately the same resolution. Thus fast GC is really faster because of the use of shorter columns, which are more efficient because of their smaller inner diameter. Fig. 2a shows a typical high-resolution analysis using a conventional 30-m column (0.25 mm internal diameter) and a fast chromatogram with similar resolution, but with greatly reduced time. Changing column diameter and length is one of the easiest ways to decrease analysis times, but it is not without a price. Usually, this cost is in decreased column capacity (mass of solute chromatographed without overloading), or in the need to increase carrier head pressure.[4,6]

Effect of Carrier Gas

The widely accepted carrier gas for fast GC analyses is hydrogen, whereas in the United States, helium is the usual choice for conventional analyses. The use of hydrogen is typically better because faster optimal linear velocities are possible at the same generated resolution. Column efficiency is usually expressed in terms of *H* (i.e., the height equivalent of a theoretical plate, which, when minimized, expresses an optimal efficiency of separation between two components). By plotting the average velocity of the carrier gas vs. the *H* value, a van Deemter plot is generated. The optimal velocity of the carrier gas for the most efficient separation is higher for hydrogen carrier gas. Thus hydrogen can operate at higher carrier gas velocities without loss of resolution. Although helium carrier gas can be used above its optimal velocity, significant resolution decreases will occur at high flow rates.

Table 1 Chromatographic column diameter vs. efficiency.

Column internal diameter (I.D.) [mm]	Theoretical plates per meter
0.10	12,500
0.18	6,600
0.20	5,940
0.25[a]	4,750
0.32	3,710
0.45	2,640
0.53	2,240

[a]Most typically used in our laboratory.
Source: From *GC Reference Guide*.[8]

Because the van Deemter plot for hydrogen is flatter for higher velocities than it is for helium, less resolution is lost with higher velocities of hydrogen, compared to helium.

Effect of Temperature Programing

The ability to quickly ramp column temperature is an excellent way to increase analysis speed, given appropriate carrier gas flow rates and fast detector sampling rates. Along with column dimensions and operation above optimal velocities of hydrogen carrier gas, analyses can be performed extremely fast and with high resolution. Temperature programing for all of the experiments shown was at 70°C/min, which was approximately the fastest rate that the GC oven could reasonably track. Temperature programing rates of up to 120°C/min are possible to input into the GC, but the heaters cannot reliably heat the large oven at this rate. Clearly, faster temperature programs, using resistively heated columns and sheaths,[2] would lead to faster analyses. However,

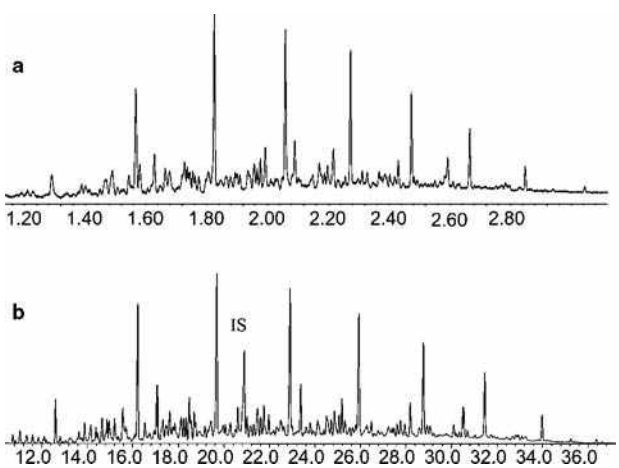

Fig. 2 Comparison of conventional 3 m × 0.25 mm I.D. (standard bore) column (b) with a 10 m × 0.10 mm I.D. column (a) with similar resolution.

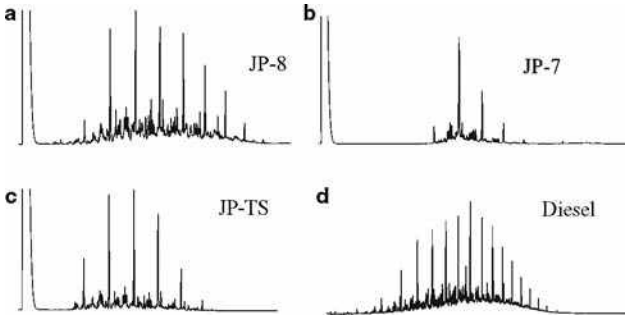

Fig. 3 Fast GC analysis of four fuels including (a) JP-8, (b) JP-7, (c) JP-TS, and (d) diesel fuel.

resolution is sacrificed if the column is heated so fast that large portions of the column act as a transfer line for GC solutes, whose boiling points have been exceeded too quickly. It is difficult to balance speed and accuracy with mixtures with wide boiling range.

APPLICATIONS

Fuel samples were examined using conditions similar to those used in this study, with 100 μm capillary columns and conventional GC instrumentation (Agilent 6890). Jet fuels are more of an analytical challenge because of their multicomponent nature; indeed, any analysis of jet fuel probably contains many unresolved solute zones. Enough chromatographic separation must be generated to conduct the particular task of the analysis, but must also be balanced with acceptable speed. The following applications show separations of various mixtures conducted with speed as the primary consideration.

Fuel GC Fingerprinting

Fig. 3 shows four examples of fuel "fingerprinting"; the normal alkane distribution helps to indicate the fuel type.

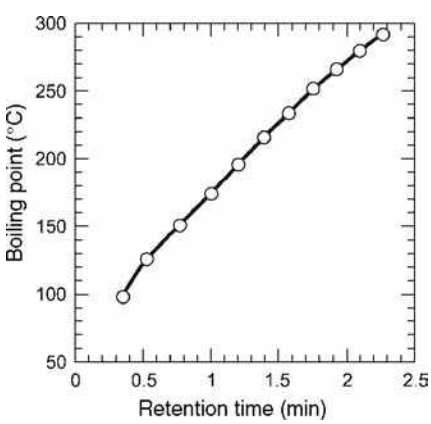

Fig. 4 Calibration curve for simulated distillation of JP-8, JP-TS, and JP-7.

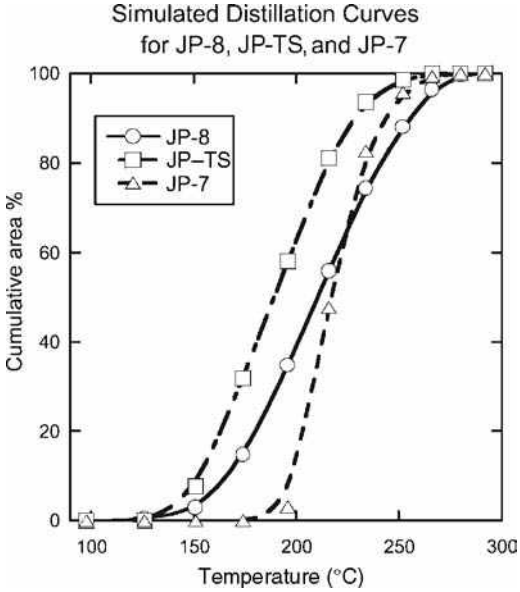

Fig. 5 Simulated distillation analysis of JP-8, JP-TS, and JP-7.

Because of the high resolution in this example, it is possible to obtain useful information from the chromatogram and to be able to compare this output tracing to those generated by other fuels. In many cases of fuel contamination, mixing of fuels, mislabeling of containers, and other commonly encountered problems, it is necessary to perform a "general pattern recognition" to identify or characterize the fuel.

Simulated Distillation

By conducting a calibration curve based on the boiling points of *n*-alkanes, it is possible to estimate the distillation temperatures according to the ASTM D2887 method.[9] Figs. 4 and 5 show the calibration and the simulated distillation curves, respectively, for JP-8, JP-TS, and JP-7, which were obtained from the fast GC analyses. These analyses are directly comparable to fuel specification tests for distillation range. Even analyses faster than these are possible because simulated distillation is a technique where very low resolution is required and generated. Relatively high resolution was maintained for these runs because the chromatographic data were correlated to other specification properties, such as freeze point and flash point.[7]

CONCLUSIONS

Fast GC has great potential as a highly productive investigative tool in today's analytical laboratory. It is becoming more widely used as more advanced GC systems are introduced. We have shown applications of GC analyses with acceptable resolution for aviation fuels, analyzed in fewer than 5 min. The speed of analysis may eventually improve

to the point where the GC could produce jet fuel analyses in much less than 1 min.

ACKNOWLEDGMENTS

This work was partially supported by the Fuels Branch of the Air Force Research Laboratory, Propulsion Sciences and Advanced Concepts Division, AFRL/PRSF under the program entitled "Advanced Integrated Fuel/Combustion System" (contract no. F33615-97-C-2719). Mr. Robert Morris was the technical monitor.

REFERENCES

1. Altgelt, K.H., Gouw, T.H., Eds.; *Chromatography in Petroleum Analysis*; Marcel Dekker, Inc.: New York, NY, 1979; 75–89.
2. McNair, H.M.; Reed, G.L. Fast gas chromatography: The effect of fast temperature programming. J. Microcolumn Sep. **2000**, *12* (6), 351–355.
3. Cramers, C.A.; Janssen, H.-G.; van Deursen, M.M.; Leclercq, P.A. High-speed gas chromatography: An overview of various concepts. J. Chromatogr. A, **1999**, *856*, 315–329.
4. Cramers, C.A.; Leclercq, P.A. Strategies for speed optimization in gas chromatography: An overview. J. Chromatogr. A, **1999**, *842*, 3–13.
5. David, F.; Gere, D.R.; Scanlan, F.; Sandra, P. Instrumentation and applications of fast high-resolution capillary gas chromatography. J. Chromatogr. A, **1999**, *842*, 309–319.
6. van Lieshout, M.; van Deursen, M.; Derks, R.; Janssen, H.-G.; Cramers, C. A practical comparison of two recent strategies for fast gas chromatography: Packed capillary columns and multicapillary columns. J. Microcolumn Sep. **1999**, *11* (2), 155–162.
7. Striebich, R.C. Fast gas chromatography for middle-distillate aviation turbine fuels. Assoc. Can. Stud. Pet. Chem. Prepr. **2002**, *47* (3), 219–222.
8. J&W Inc., *GC Reference Guide*; Folsom, CA, 1998; 13.
9. ASTM D2887-93, Boiling Range Distribution of Petroleum Fractions by Gas Chromatography. In *Section 5 Annual Book of ASTM Standards*; Conshohocken, PA, 1996; 192–201.

Fatty Acids: GC Analysis

Susana Casal
Beatriz Oliveira
Requimte, Bromatology Service, Faculty of Pharmacy, University of Porto, Porto, Portugal

Abstract
Fatty acids (FAs) are key molecules in living organisms. Gas chromatography (GC) is the most common analytical tool in fatty acid analysis, with broad applications in nutritional, biochemical, biomedical, microbiological, and agricultural fields. While the volatile short-chain FAs can be analyzed directly, for most samples the use of derivatives, mainly methyl esters (FAMEs), is mandatory. Several reagents can be used directly on the sample or, more commonly, on their lipid extracts. Depending on the type of the chromatographic column, different information can be retrieved. In medium polar columns (carbowax type) the FAs elute in a predictable order determined by their carbon chain length and the number of double bonds. The highly polar cyanosilicone phases allow the separation of polar compounds with close boiling points, like geometrical or positional isomers. Although flame ionization detection (FID) has proven to be a robust tool, it lacks selectivity, of special concern in misidentifications. Mass spectrometry (MS) is becoming increasingly popular, being essential in the recent two-dimensional gas chromatographic methods.

INTRODUCTION

Analysis of fatty acids (FAs) may be required for a variety of reasons. It may be important in food process control, quality assurance, detection of adulteration, or for regulatory reasons such as labeling. In the biological field, information on the FA composition in blood and tissues may be important for nutritional and health reasons—especially for FAs of functional significance (e.g., long-chain omega-3 acids)—or for the diagnosis of some metabolic diseases.

Depending on the situation, FA analysis might be used to generate a profile where all FAs are expressed as a weight percentage of the total FAs, as is usual in food characterization, or for the quantification of each FA in units of milligrams per gram. Food labeling requirements, for instance, can be limited to the saturated and *trans* FAs or can also include monounsaturated and polyunsaturated groups. This last fraction may be broken down further into total omega-6 and omega-3 with the latter detailed into individual FAs: docosahexaenoic acid (DHA), eicosapentaenoic acid (EPA), and α-linolenic acid (ALA). Irrespective of the details, all these labels would require a FA profile to be obtained by a suitable chromatographic technique.

Capillary chromatography is by far the most common analytical tool in the analysis of FAs in food and other matrices, mainly as their methyl esters (FAMEs). The purpose of this entry is to provide some insights into this methodology, mainly for those initiating their work in this area. The reasons behind its popularity and the details involved in the process, as well as its main applications, will be discussed here. There is insufficient room in this entry to address all related details, but important reviews will be identified for those who might be interested.

FA CHEMISTRY

FAs constitute a wide range of molecules, ubiquitous in biological systems, occurring as components of virtually all lipids. They are found as esters of glycerol in triacylglycerides (>90%), diacylglycerides, and monoacylglycerides; as esters of other polar lipids such as lecithin; as sterol esters, esterified with natural aliphatic alcohols in waxes; and as free FAs (up to 1%). They are important sources of energy, as well as structural components of cell membranes, signaling molecules, and precursors of eicosanoids (EPA and arachidonic acid). Special attention is usually devoted to the essential FAs, linoleic and ALA, whose presence in food is of great importance.[1]

Chemically, FAs are aliphatic carboxylic acids, comprising an alkyl (hydrocarbon) chain with a methyl group at one end and a carboxylic group at the other. They can be grouped according to chain length, the number of double bonds (i.e., degree of unsaturation), its position and configuration, and the occurrence of additional functional groups along the chain. More than 400 FAs are known, occurring naturally or synthesized in the laboratory, but only a few of them are quantitatively important; they represent about 95% of the total FAs present in food lipids for human or animal consumption.[1] Indeed, most papers usually report only a dozen FAs, and less than 30 are present in most analytical standards. Recent gas chromatographic techniques, however, are able to identify more than 100 FAs in a single drop of blood.[2]

The major FAs comprise saturated, monounsaturated, and polyunsaturated ones, according to their chemical structures and properties. Most of them are unbranched and contain an even number of carbon atoms. Odd carbon number FAs are less common and are almost restricted to animal food of ruminant origin, namely milk, cheese, and meat, usually in trace amounts. Although rare in plant lipids, branched-chain acids are the major components of Gram-positive bacteria lipids. Small amounts of branched *iso* and *anteiso* FAs also occur in animal fats, waxes, and marine oils.

FA nomenclature is a complex issue. Their systematic names are rather extensive, and the trivial names, when existent, are often difficult to associate with the correspondent FA. In shorthand notations, the chain length (*c*) and the number of double bonds (*d*) is usually simplified to *c*:*d* but it does not specify the double-bond positions. The Greek letters Δ (delta) and ω (omega) are frequently used for this complementary purpose. Delta, followed by a numeral or numerals (Δ*x*,*y*), is used to allocate the position of one or more double bonds in the hydrocarbon chain, counting from the carboxyl group. Omega (ω) is used to indicate how far a double bond is from the terminal methyl group, irrespective of the chain length. The "*n*-*x*" system (*n*-minus) is analogous to the "ω" naming system. The omega terminology is usually used by biochemists/nutritionists, because it enhances the structural relationship between the different biosynthetic families and also because of the attention currently paid to the omega-3 fatty acids. This system is now superseding the classical one traditionally used by food chemists.

In nature, the monounsaturated (MUFA) and polyunsaturated FA (PUFA) double bonds are commonly in the *cis* (*c*-) or *E*-configuration, each being separated from the next by a methylene group (non-conjugated FAs). Therefore, unless otherwise indicated, the double bond is in the *cis* configuration. Whenever a *trans*-bond is present, it is indicated by an additional *trans*, "*t*-," or "*Z*-."

Detailed information regarding the formulas and molecular structures of different FAs is likely to be found in recent specialized chemical or biochemical books. Some of the more important FAs, their structures, systematic and trivial names, as well as their main sources, are summarized in Table 1.

GAS–LIQUID CHROMATOGRAPHY

Gas–liquid chromatography (GLC), or gas chromatography (GC), was first developed by lipid analysts. From its beginning more than 60 years ago, the instrumentation has become more sophisticated and accurate with the development of new detectors, capillary columns, temperature and pressure programming, etc. Many reviews and books detail these developments. Among the more comprehensive ones are the several books published by Dr. William W. Christie and his regularly updated website Lipid Library,[3] whose reading is recommended to all beginners in this field, as well as to those seeking answers to analysis problems.

Nowadays most gas chromatographs have similar configuration. In the injector category, the split–splitless is the most frequently used one with reproducible results, but particular attention should be paid when analyzing volatile FAs, because there is some discrimination in the usual split injectors. Hydrogen and helium are both efficient for FA separation but, while the former gives the best separation results and is less expensive, the latter is much safer and will resolve most situations. Detection in routine analysis is usually performed with a flame ionization detector (FID) that responds to non-oxidized carbon in a linear relationship. However, the carboxyl carbon is not appreciably ionized during combustion and, for maximum precision, the response factor must be known or calculated to correct the experimental data. These corrections are of particular importance for quantitative analysis. The correction factors are easily estimated from the ratio of known proportions of standards to the detected peak areas.

The analysis of FAs by GC in their free form is practically restricted to the volatile short chains (less than 10 carbons) present in lipid extracts, such as in milk fat, and cheese samples. For most FA mixtures, the use of ester derivatives, mainly methyl esters, is recommended. These esters are more volatile than the corresponding free FAs and, therefore, more suitable for analysis by GC in the gaseous form. They are also less polar, thereby reducing their adsorption onto the support and dimerization in the vapor phase with subsequent reduction in peak tailing and/or ghosting, improved peak shape, and resolution.

DERIVATIZATION OF FAs

Fatty acid methyl esters (FAMEs), esterified in the carboxylic group, are by far the most widely used derivatives. The boiling points of the methyl esters are markedly lower than those of the free FAs, being also more soluble in organic solvents. Several methods have been proposed for their preparation, based on the presence of free FAs, short-chain FAs, or highly PUFA.

During the transesterification process, the esterified FAs react with methanol, in the presence of a strong acidic or basic catalyst, producing a mixture of FAMEs and glycerol (Fig. 1). The reaction is reversible, but an excess of the alcohol is used to increase the yields of the methyl esters and to allow their phase separation from the released glycerol. Most FAs, including long-chain PUFA, can be treated with acidic or alkaline reagents with no adverse effects. However, some FAs, including conjugated linoleic acids (CLAs), form artifacts with acidic reagents. Also, for the derivatization of FAs containing epoxy, hydroperoxy, cycloprophenyl, and cyclopropyl groups, specific procedures have been developed.

Methylation is usually performed on lipids isolated from the matrix by several classical methodologies, but it

Table 1 Nomenclature of the most common fatty acids and their major sources.

Systematic name[a]	Shorthand notation[b] *c:d (n–x)*	Common name	Simplified formula	Major sources
Saturated fatty acids				
Butanoic	4:0	Butyric	$CH_3(CH_2)_2COOH$	Ruminant milk fats
Hexanoic	6:0	Caproic	$CH_3(CH_2)_4COOH$	Ruminant milk fats
Octanoic	8:0	Caprylic	$CH_3(CH_2)_6COOH$	Milk fats, palm kernel oil
Decanoic	10:0	Capric	$CH_3(CH_2)_8COOH$	Milk fats, coconut oil
Dodecanoic	12:0	Lauric	$CH_3(CH_2)_{10}COOH$	Coconut oil, palm kernel oil
Tetradecanoic	14:0	Myristic	$CH_3(CH_2)_{12}COOH$	Dairy products, plant seed fats
Hexadecanoic	16:0	Palmitic	$CH_3(CH_2)_{14}COOH$	Almost ubiquitous
Octadecanoic	18:0	Stearic	$CH_3(CH_2)_{16}COOH$	Almost ubiquitous
Eicosanoic	20:0	Arachidic	$CH_3(CH_2)_{18}COOH$	Peanut oil
Docosanoic	22:0	Behenic	$CH_3(CH_2)_{20}COOH$	Peanut oil, waxes
Tetracosanoic	24:0	Lignoceric	$CH_3(CH_2)_{22}COOH$	Peanut oil, waxes
Monounsaturated fatty acids				
9-Dodecenoic	12:1 *n*–3	Lauroleic	$CH_3–CH_2–CH{=}(CH_2)_7–COOH$	Cow milk fats
9-Tetradecenoic	14:1 *n*–5	Myristoleic	$CH_3–(CH_2)_3–CH{=}CH–(CH_2)_7–COOH$	Milk fats, liver fat
9-Hexadecenoic	16:1 *n*–7	Palmitoleic	$CH_3–(CH_2)_5–CH{=}CH–(CH_2)_7–COOH$	Fish oils, animal fats
6-Octadecenoic	18:1 *n*–12	Petroselinic	$CH_3–(CH_2)_{10}–CH{=}CH–(CH_2)_4–COOH$	Umbelliferae seed oils
9-Octadecenoic	18:1 *n*–9	Oleic	$CH_3–(CH_2)_7–CH{=}CH–(CH_2)_7–COOH$	Almost ubiquitous
*t*9-Octadecenoic	*t*18:1 *n*–9	Elaidic	$CH_3–(CH_2)_7–CH{=}CH–(CH_2)_7–COOH$	Hydrogenated fats
11-Octadecenoic	18:1 *n*–7	*cis*-Vaccenic	$CH_3–(CH_2)_5–CH{=}CH–(CH_2)_9–COOH$	
*t*11-Octadecenoic	*t*18:1 *n*–6	Vaccenic	$CH_3–(CH_2)_5–CH{=}CH–(CH_2)_9–COOH$	Ruminant fats and milk fats
11-Eicosenoic	20:1 *n*–9	Gondoic	$CH_3–(CH_2)_7–CH{=}CH–(CH_2)_9–COOH$	Rapeseed and mustard seed oils
9-Eicosenoic	20:1 *n*–11	Gadoleic	$CH_3–(CH_2)_9–CH{=}CH–(CH_2)_7–COOH$	Marine oils
11-Docosenoic	22:1 *n*–11	Cetoleic	$CH_3–(CH_2)_9–CH{=}CH–(CH_2)_9–COOH$	Marine oils
13-Docosenoic	22:1 *n*–9	Erucic	$CH_3–(CH_2)_7–CH{=}CH–(CH_2)_{11}–COOH$	Rapeseed and mustard seed oils
15-Tetracosenoic	24:1 *n*–9	Nervonic	$CH_3–(CH_2)_7–CH{=}CH–(CH_2)_{13}–COOH$	Marine oils, brain lipids

(Continued)

Table 1 Nomenclature of the most common fatty acids and their major sources. *(Continued)*

Systematic name[a]	Shorthand notation[b] *c:d (n–x)*	Common name	Simplified formula	Major sources
Polyunsaturated fatty acids				
4,7,10-Hexadecatrienoic	16:3 *n*–6	Hiragonic	$CH_3–(CH_2)_2–(CH{=}CH–CH_2)_2–CH–(CH_2)_2–COOH$	Marine oils
9,12-Octadecadienoic	18:2 *n*–6	Linoleic	$CH_3–(CH_2)_4–(CH{=}CH–CH_2)_2–(CH_2)_6–COOH$	Vegetable oils
*cis*9, *trans*11-Octadecadienoic	CLA	Rumenic	$CH_3–(CH_2)_5–(CH{=}CH–)_2–(CH_2)_7–COOH$	Ruminant milk fats
6,9,12-Octadecatrienoic	18:3 *n*–6	γ-Linolenic	$CH_3–(CH_2)_4–(CH{=}CH–CH_2)_3–(CH_2)_3$-COOH	Evening primrose, borage
9,12,15-Octadecatrienoic	18:3 *n*–3	α-Linolenic	$CH_3–CH_2–(CH{=}CH\text{-}CH_2)_3–(CH_2)_6–COOH$	Soya, walnut, and linseed oils
6,9,12,15-Octadecatetraenoic	18:4 *n*–3	Stearidonic	$CH_3–CH_2–(CH{=}CH–CH_2)_4–(CH_2)_3–COOH$	Black currant seed oil, fish oils
11,14-Eicosadienoic	20:2 *n*–6		$CH_3–(CH_2)_4–(CH{=}CH–CH_2)_2–CH–(CH_2)_7–COOH$	
5,8,11-Eicosatrienoic	20:3 *n*–9	Mead	$CH_3–(CH_2)_7–(CH{=}CH–CH_2)_2–CH–(CH_2)_3–COOH$	
5,8,11,14-Eicosatetraenoic	20:4 *n*–6	Arachidonic	$CH_3–(CH_2)_4–(CH{=}CH–CH_2)_4–(CH_2)_2–COOH$	Animal fats (egg yolk, liver)
5,8,11,14,17-Eicosapentaenoic	20:5 *n*–3	EPA	$CH_3–CH_2–(CH{=}CH–CH_2)_5–(CH_2)_2–COOH$	Fish oils
13,16-Docosadienoic	22:2 *n*–6		$CH_3–(CH_2)_4–(CH{=}CH–CH_2)_2–(CH_2)_{10}–COOH$	
7,10,13,16-Docosatetraenoic	22:4 *n*–6	Adrenic	$CH_3–(CH_2)_4–(CH{=}CH–CH_2)_4–(CH_2)_4–COOH$	Adrenal and liver lipids
7,10,13,16,19-Docosapentaenoic	22:5 *n*–3	DPA	$CH_3–CH_2–(CH{=}CH–CH_2)_5–(CH_2)_4–COOH$	Fish oils, brain tissues
4,7,10,13,16,19-Docosahexaenoic	22:6 *n*–3	DHA	$CH_3–CH_2–(CH{=}CH–CH_2)_6–CH_2–COOH$	Fish oils, brain tissues

[a]*cis* unless specified;
[b]*c* = number of carbon atoms; *d* = number of double bonds; (*n*–*x*) = double-bond position when counting from the methyl end.

can also be performed by a one-step procedure combining lipid extraction and transesterification directly on small amounts of dried sample.

Acid-Catalyzed Transesterification

Acidic reagents, including hydrochloric acid, sulfuric acid, boron trifluoride (Lewis acid), and acetyl chloride in methanol, catalyze the formation of methyl esters from both esterified FAs (the form in which FAs are normally found) and free FAs (normally present only in small amounts, but formed when samples are subjected to hydrolytic treatments) when heated with a large excess of anhydrous methanol.

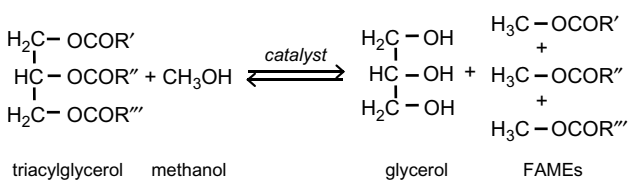

Fig. 1 Transesterification of triacylglycerols.

Acetyl chloride (5% in methanol) is often the preferred choice for samples containing sensitive FAs or when unknown substances are present in the samples. Usually, the lipids are dissolved in the reagent and heated overnight at 50°C, or for 2 hr at 80°C. Methyl esters are then extracted twice with an appropriate solvent, and the extract is further washed for removing acidity.

Boron trifluoride (12–14% in methanol) is probably the more frequently described derivatization agent in the literature for FAs methylation; it is recommended by several official institutions such as American Organization of

Analytical Chemists (AOAC) and by the ISO standards.[4,5] Special attention should be given to its toxicity. In the initial procedure, as described by Morrison and Smith,[6] the reagent is added directly to the lipid extract (about 10 mg) and heated for different periods depending on the FA's form (free or conjugated). Currently, this reagent is more frequently used after the saponification of glycerides and phospholipids with methanolic NaOH or KOH, as described in the official standards. Nevertheless, several authors have claimed the formation of artifacts and loss of PUFA with this reagent. It should be noted, for instance, that the use of old reagents or solutions that are too concentrated must be avoided.[3]

Base-Catalyzed Transesterification

Base-catalyzed transesterification proceeds faster than the acid-catalyzed reaction and requires lower temperatures. For this reason, combined with the fact that the alkaline catalysts are less corrosive than acidic compounds and lead to the formation of fewer artifacts, they are more frequently used. This type of catalysis is also recommended for samples containing short-chain FAs or labile FAs (polyunsaturated, conjugated unsaturations).

The first step is the reaction of the base with methanol, producing a methoxide and the protonated catalyst. The nucleophilic attack of the methoxide at the carbonyl group of the triglyceride liberates the methyl ester and the diglyceride, starting another cycle until all methyl esters are formed and glycerol released. Free FAs are not susceptible to nucleophilic attack by alcohols or bases and, thus, are not esterified under these conditions. Therefore, samples containing free FAs should be methylated by other methods. Absence of water must be guaranteed; otherwise, free FAs will be formed by hydrolysis.

Sodium methoxide (1–2 *M* in anhydrous methanol) is probably the most useful basic transesterifying agent. It can be prepared in the laboratory, with adequate precautions, simply by dissolving clean sodium in dry methanol, and it is stable for several months at 4°C. Glycerolipids are rapidly transesterified (2–5 min) at room temperature.

The simplest methylation method uses KOH (2 *M* in methanol). It is recommended, for instance, in the analysis of vegetable oils or virgin olive oil with reduced acidity (small amounts of free acids) by several European standards. The reaction is rapid and occurs at room temperature. It must be pointed out that sterol esters and waxes, as well as free FAs, do not react under these conditions, as mentioned earlier.

Other FA Derivatives

The *tert*-butyldimethylsilyl (tBDMSi) derivatives have high thermal and hydrolytic stability and improved sensitivity (two- to sixfold) when compared to the methyl esters, being adequate for samples with very small lipid amounts. Their stability, however, is limited to about three days.[7]

In cyanomethyl derivatization, particularly suited for use with the nitrogen–phosphorus detector, cyanomethyl esters are formed by alkylation of the carboxyl group ($R–COO–CH_2–CN$). The method is rapid, inexpensive, and is resistant to contaminants frequently found during the chromatographic separation of very-long-chain FAs.[8]

GC COLUMNS

The flexible fused silica columns have been commercially available for over three decades and allow substantial improvements in the separation of FAMEs, especially from oil samples rich in PUFAs, such as fish oil. Nevertheless, for some simple work, packed columns are still quite effective. The stationary phases for GC FAME analysis are almost exclusively polar polyesters. These are usually classified according to their degree of polarity, and usually only two main types are used: those with medium polarity such as the carbowax type [polyethylene glycol (PEG) under various trade names] and those with high polarity, with cyanopropil polysiloxane stationary phases, such as HP-88, CP-Sil88, BPX70, SP-2340, or SP-2560.[9]

To prevent misidentification of FAMEs, the GC column used should elute the compounds primarily by carbon chain length and next by the number of double bonds. There should be minimal overlap in the elution order among FAMEs having different chain lengths. This situation is fully accomplished by the PEG-phase capillary columns that are able to resolve these compounds with little or no overlap in the elution order of FAMEs of different carbon chain lengths. Complex FAME mixtures, with chain lengths up to 24 carbons and up to 6 double bonds, including all omega-3 and omega-6 fatty acids, can be separated on capillary columns of medium polarity and length.

Fig. 2 represents the chromatogram of a standard mixture of FAMEs eluted on a Carbowax-type column. For many samples, this type of column may be all that is required and should be the first column to buy for general FA analysis. Carbowax-type columns (Carbowax-20M, CP-Wax 52CB, DB-Wax, etc.) with dimensions of 25–30 m length and 0.25 mm I.D., and a film thickness of 0.2 μm, are preferred because of their stability and the predictable order in which all compounds elute. In fact, all FAMEs of a given chain length elute before those that are two carbons longer, the only exception being that 22:6 elutes between 24:0 and 24:1. Double-bond positional isomers are also separated, with the isomer with double bonds nearer to the ester group eluting first.

The high polarity of the cyanosilicone phases allows separation of polar compounds with close boiling points, like geometrical groups (*cis*, *trans*) or positional isomers, and complex samples such as polyunsaturated marine oils, being essential for the analysis of *trans* FAs and conjugated linoleic acid (CLA) isomers. As the separation on these phases is dependent on both polar interactions and boiling

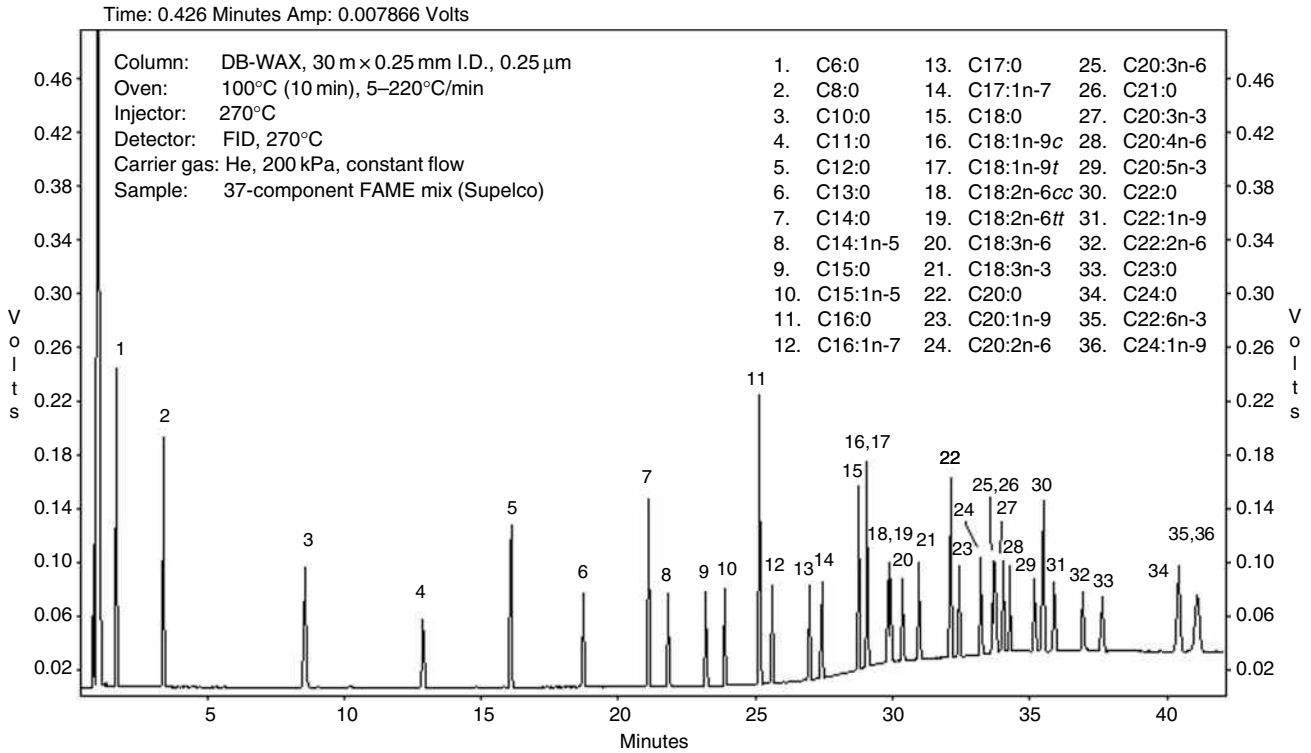

Fig. 2 Chromatogram of a standard mixture of fatty acid methyl esters (FAMEs) eluted on a 30 m DB-Wax column.

point, there is crossover in the elution sequence among FAMEs of different chain lengths and degrees of unsaturation. Also, a small alteration in the temperature program might induce alterations in the elution order, requiring special attention to avoid misidentifications. Fig. 3 represents the chromatogram of a standard mixture of 41 FAMEs

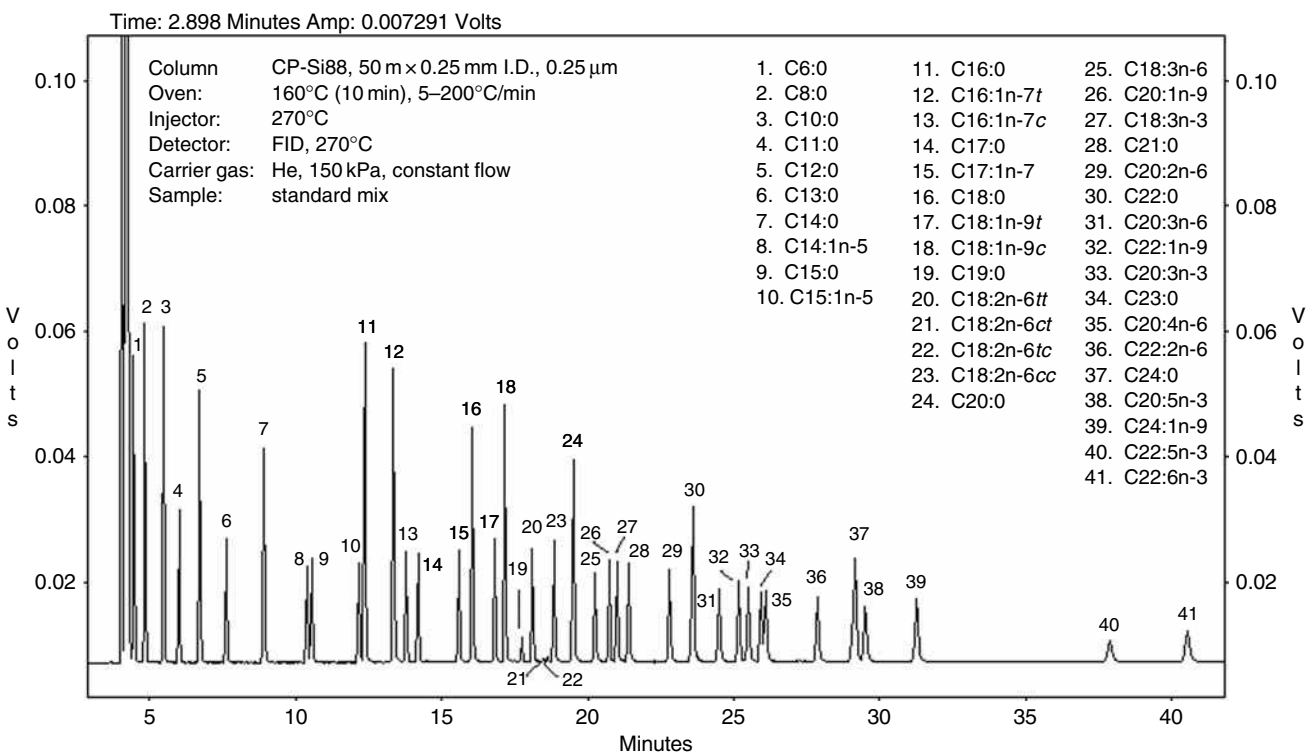

Fig. 3 Chromatogram of a standard mixture of fatty acid methyl esters (FAMEs) eluted on a 50 m CP-Sil88 column.

eluted on a 50 m CP-Sil88 column, where the separation of the *cis–trans* isomers is evident (see peaks 17 and 18, and 20–23). Nowadays, for most food FAs analyses, these polar columns are increasingly being selected because they provide simultaneous information on all the FA classes required for nutritional label, i.e., saturated, monounsaturated, polyunsaturated, together with *trans* fatty acids.

The non-polar phases, usually silicone liquid phases, are seldom used for FA analysis. Despite their high stability at high temperatures and low bleeding, separation occurs primarily on the basis of the boiling points of the FAMEs. For acids of each chain length, the unsaturated compounds elute before the saturated ones, but there is considerable overlap among unsaturated acids of the same chains length, with 18:1, 18:2, and 18:3 practically coeluting.

Irrespective of the column choice, bounded phases are recommended because they allow rinsing to remove contaminant material, besides presenting higher thermal stability and lower bleeding.

QUALITATIVE AND QUANTITATIVE ANALYSIS OF FAs

Qualitative Analysis

The number of individual FAs will vary greatly depending on sample complexity. Although less than 20 FAs are of importance in vegetable oils, the FA profile of a fish oil, for instance, is reasonably complex because of the range of chain lengths, degrees of unsaturation, and the presence of positional isomers. The additional presence of a partially hydrogenated vegetable oil (containing *trans* fatty acids), coconut or palm kernel oil (containing short-chain acids), or butterfat (containing *trans* fatty acids, short-chain acids, branched-chain FAs, and CLA), for instance, would complicate the mixture further. Indeed, in some cases, two different columns (varying in the type of chemical phase, length, internal diameter, and phase thickness) may be necessary to separate all the components in the sample.

Identification of the FAs can be achieved, more or less accurately, with conventional methods or, more acceptably, with mass spectrometry (MS). The conventional methods are based on comparison between the retention times of the components to be identified with those of known FAs in a synthetic or natural mixture. It is convenient to use commercially available standard mixtures of saturated, and mono- and polyunsaturated FAMEs (from Sigma, Matreya, Nu-Chek-Prep, Larodan, etc.). In their absence, natural lipid extracts are also useful. A good start can be made with the methylation of peanut oil, because it contains the most common FAs (16:0, 18:0, 18:1, 18:2) together with several long-chain saturated FAs (20:0, 22:0, 24:0) (Fig. 4). For the analysis of complex marine oils, the use of FAMEs, prepared from cod liver oil or salmon oil containing very different highly polyunsaturated *n*-3 fatty acids, is

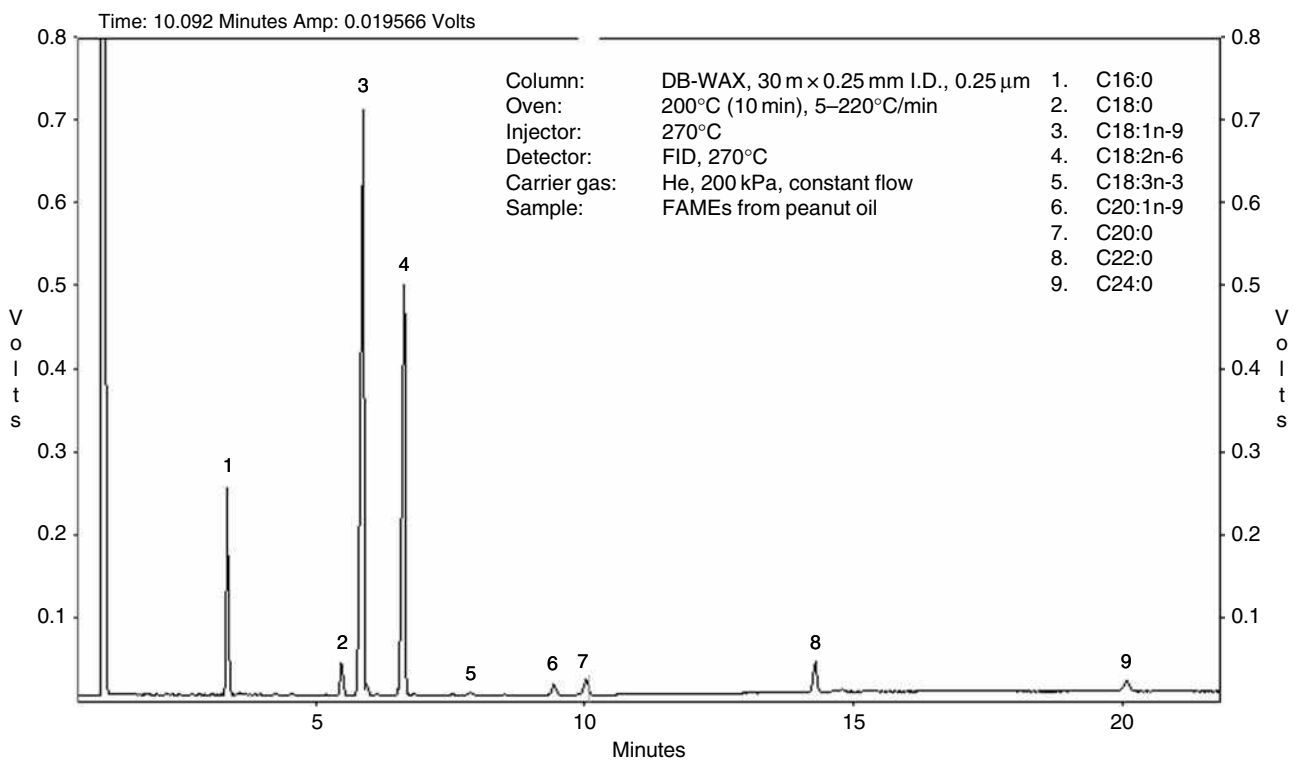

Fig. 4 Chromatogram of refined peanut oil fatty acid methyl esters (FAMEs) eluted on a 30 m DB-Wax column.

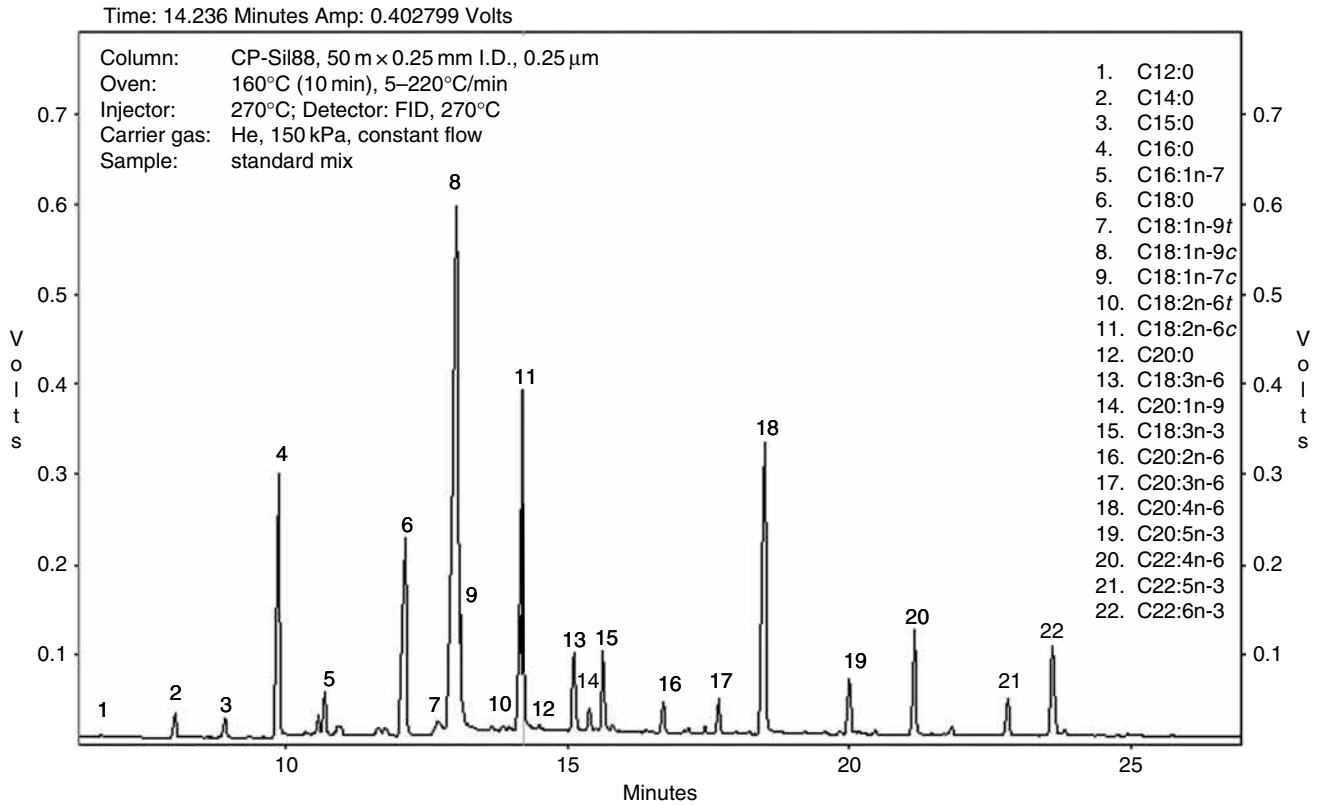

Fig. 5 Chromatogram of a commercial sample of animal origin (PUFA-2, from Supelco) eluted on a 50 m CP-Sil88 column.

recommended. Several natural mixtures from animal sources are also commercialized (Fig. 5). The qualitative composition of these samples has been well established, and they generally contain a wider range of FAs than do synthetic mixtures. Reference lipid samples of animal and vegetable origin may be procured from several official institutions.

In practice, it is convenient to base the identification not exclusively on retention time, which is temperature and gas flow rate dependent, but on relative retention times of FAs commonly occurring in nature, namely, palmitic acid (16:0) or stearic acid (18:0). The relative values can also be used to tentatively identify unknown acids if analysis is carried out under the same isothermal conditions.

Another means of identifying FAs of a homologous series is to use a well-known property of their elution under isothermal conditions: the linear relationship between the number of carbons in the aliphatic chain and the logarithms of the corrected retention times. The same linear relationship exists between a homologous series of *cis*-monoenes, dienes, trienes, etc. but attention must be paid to the fact that the retention times depends on the positions of the double bonds. This may be of some help in tentatively identifying unknown components. However, it does not offer any certainty and cannot be utilized in temperature-programmed analyses of mixtures comprising a wide range of FAs, differing both in chain length and in the degree of unsaturation.

Alternatively, the identification of FAMEs is possible using the concept of equivalent chain length (ECL), by expressing their elution positions relative to those of known straight-chain saturated FAMEs, under isothermal conditions. Details for the calculation of ECL and tables for a large number of FAMEs are available in specialized reports.[10] Recently a method was developed that allows this identification with temperature and pressure programming on a single capillary column.[11]

Quantitative Analysis

The quantification of FAs can be expressed in different forms, depending on the accuracy of the analysis in question.

Normalization

In most analyses, each FAME can be expressed as a weight percentage of the total FAMEs represented in the chromatogram. The areas under the GC peaks are approximately equivalent to the masses of the FAMEs they represent. Therefore, the area percentage of each peak (as a

percentage of the total areas of all FAME peaks) is approximately equal to the weight percentage of each FAME. This response represents a close approximation of weight percentage for simple vegetable oils, but is only an approximation.

In the simplest case, the percentage by weight of each component, expressed as methyl ester, is calculated by:

$$\%A = 100 \times \frac{\text{Area A}}{\text{Sum of all peaks' areas}} \quad (1)$$

However, with this approach, the longer- and the shorter-chain FAMEs are, respectively, overestimated and underestimated, because there is no exact linearity of the detector response to the FA mass. The response of the detector should be checked with a calibrated standard mixture. This correction is more important in studies concerning highly unsaturated FAs, high amounts of short-chain FAs, FAs with large differences in molecular weights, or even the presence of FAs with secondary groups. In these cases, correction factors must be used to convert peak areas into weight percentages. The area percentages are multiplied by a theoretical response correction factor (tables are published, e.g., Christie[9]), and are renormalized to give the true weight percentages. The corrections will only make small differences for chain lengths C_{14}–C_{24}, but will make significant differences for shorter chain lengths. These factors can easily be determined by analyzing known reference standard mixtures of methyl esters under chromatographic conditions identical to those of the sample.

One must also intend to express the results in FA percentages instead of FAME percentages. In such situations, the response factors should also consider the conversion of the methyl esters to the free acids based on their molecular weights. Furthermore, total fat is the sum of FAs from all sources, expressed as triglycerides. Thus, expressing the measured FAs as triglycerides requires the mathematical equivalent of condensing each of the three FAs with one glycerol.

It should also be noted that even these normalized peaks may still not be representative of the weight content of FAs in the sample. Some lipid samples can contain other forms of FAs that will not appear in the chromatographic run, such as polymerized FAs, making the FA proportions incorrect. Therefore, an internal standard should be used in critical cases, to give the sample content of a particular FA in absolute amounts (milligrams per gram of the sample). The use of suitable internal standards will also prevent one disadvantage of area normalization: error propagation (i.e., if one FA is wrongly estimated, or omitted when unknown, the results for the others are also affected).

In biochemical studies, however, the results should be expressed as a molar percentage, because it expresses the relative number of molecules of each type of acid, or glyceride component, present in a fat. The difference between the two modes of expression becomes especially

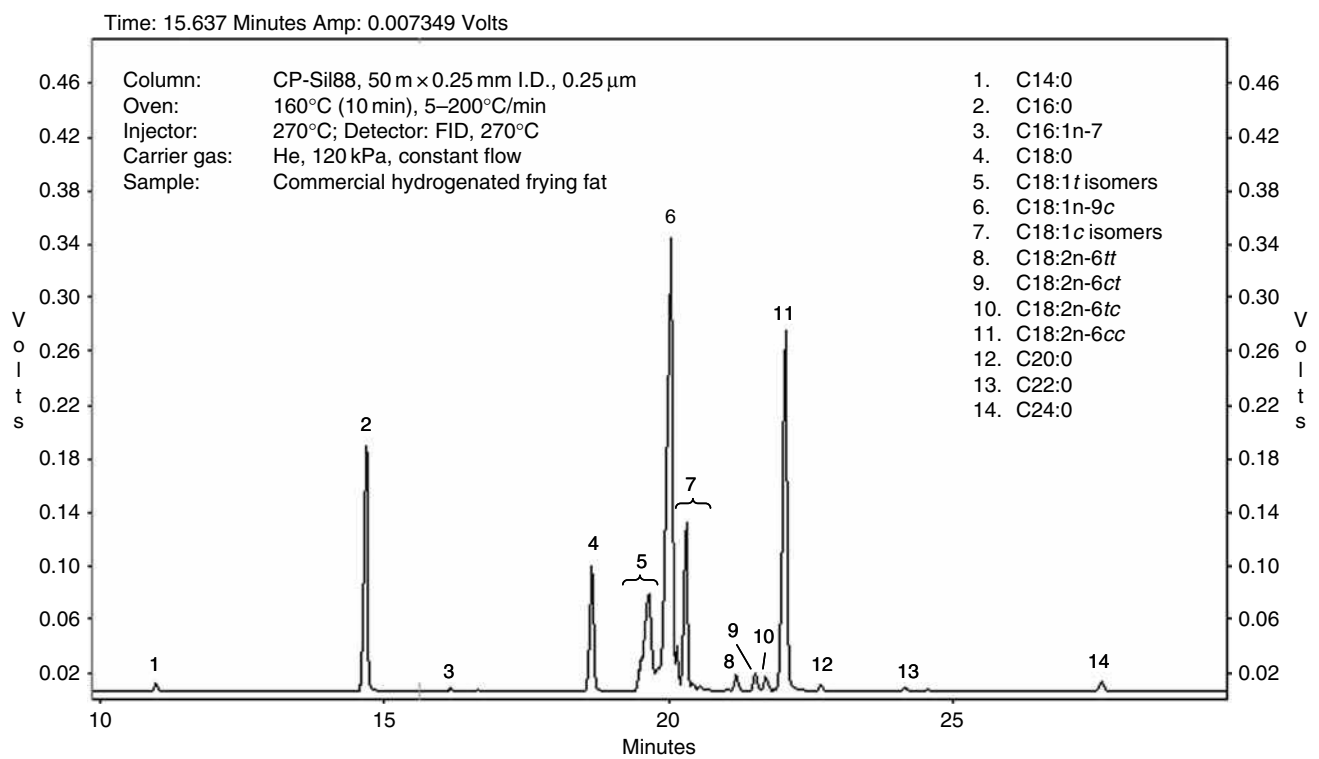

Fig. 6 Separation of *trans* isomers of a partially hydrogenated fat on a 50 m CP-Sil88 column.

significant when FAs of widely differing molecular weights are present in the same fat.

Absolute Amounts

In some cases, one has to measure the absolute amount of each FA, requiring the use of appropriate internal standards. This is best accomplished by adding a precise quantity of a FAME that is not present in the mixture—generally an odd-chain FA (11:0, 13:0, 15:0, 17:0, 23:0, or 29:0)—as an internal standard, but the analyst should be aware of the fact that odd-chain FAs are not always absent, and some can be significant components of dairy products. For a more complete and precise standardization, the internal standard should be added to the sample from which the lipids are to be extracted, in order to take the extraction yield into account.

The internal standard should, preferably, be in a form similar to that in which the bulk of FAs occur in the sample (often as triglycerides, although sometimes as phospholipids or cholesterol esters). Triundecanoin ($3 \times$ C11:0), for instance, is frequently used for milk fat; 23:0 is more suitable for determining EPA and DHA.

The response factor (F) for each FA in a calibrated standard is calculated as shown below:

$$F_{FA} = \frac{(\text{Area}_{FA} \times \text{Weight}_{IS})}{(\text{Area}_{IS} \times \text{Weight}_{FA})} \quad (2)$$

The FAME amount in a sample can be calculated from the following equation:

$$\text{FAME (mg/g)} = 1000 \times \frac{(\text{Area}_{FA} \times \text{Weight}_{IS} \times F_{FA})}{(\text{Area}_{IS} \times \text{Weight}_{sample})} \quad (3)$$

If the internal standard was added as a triacylglyceride, the concentrations obtained using the equation would also be of triacylglycerides.

SPECIAL APPLICATIONS

GC–MS Analysis

Mass spectrometry, coupled to GC (GC–MS), is probably the most powerful tool available for the identification of FAs separated by GC. Although generally used for structural analysis, the mass spectrometer also has a quantitative performance comparable to that of FID.[12]

Electron impact MS can be easily used for the identification of saturated FAs because their spectra are characterized by one prominent molecular ion and several ions with reduced mass (in steps of 14 amu, owing to the loss of successive methylene groups). Methyl esters, picolinylesters, pyrrolidines, and oxazolines are the derivatives used for this purpose.[3,13]

Mass spectrometry is particularly suitable for locating double bonds in PUFA, but this requires derivatives that fix the double-bond position. Good examples are those containing a nitrogen atom because these bonds have a pronounced tendency to ionize and migrate along the aliphatic chain, as in methyl esters or trimethylsilyl ethers. Picolinyl esters are the most widely used derivatives because they offer a specific mass fragmentation pattern with a particular value at the double-bond location. 4,4-Dimethyloxazoline (DMOX) derivatives are also becoming increasingly popular for this purpose. They have chromatographic properties similar to those of methyl esters, elute slightly later, and the peak resolution is usually retained. In the mass spectra, simple radical-induced cleavages occur at every carbon in the chain, resulting in gaps of 14 amu between adjacent methylene groups in a saturated chain and a gap of 12 amu when a double bond is present.[3,13]

GC–MS does not distinguish between geometrical isomers, but this can be achieved using the IR spectra obtained by GC-Fourier transform infrared (FTIR) spectrometry of the methyl esters.

Short-Chain FAs

When short-chain FAs are present in the lipid sample, the quantitative recovery of their methyl esters is questionable because of their volatility and partial solubility in water.

If short-chain acids are present (indicated by a series of peaks eluting just after the solvent front), then GC conditions should be adjusted to include a low-temperature step (often at 70°C) before the normal starting temperature. It is also extremely important to prevent the loss of the most volatile compounds during the injection procedure. Despite their suitability for most FAs, split injectors' tendency to lose short-chain FAs, especially those with lower molecular weights, is a reality.

The problem can be resolved partially by preparing derivatives with higher molecular weights, usually isopropyl or butyl esters in dairy products, where methanol is replaced by isopropanol or butanol with appropriate catalysts.[14]

trans Fatty Acids

There is a confirmed relationship between the consumption of foods containing *trans* fatty acids and high-low-density lipoprotein (LDL)-cholesterol levels associated with increased risk of coronary heart disease, a leading cause of death in the United States and a growing concern in Europe.

trans Fatty acids, also known as *trans* fat, are naturally present in dairy products, meats, and refined oils at levels of no concern. However, the actual main sources are the man-made partially hydrogenated fats, designed to

increase the shelf life and applicability of polyunsaturated oils. During the hydrogenation process, *cis*-fatty acids are partially converted to their *trans* isomers, which will be present in the final product if the hydrogenation process is incomplete. These edible fats are frequently used in fried or baked foods, cookies, snacks, salad dressings, and other processed foods.[15]

trans Fatty acids from dairy foods, mostly monoethylenic, have been known for decades and were traditionally determined by IR spectroscopy. Indeed, there was no exact knowledge of the man-made *trans* ethylenic bonds in hydrogenated PUFA until their discovery by capillary GLC, in the 1970s. Although in the beginning no special attention was devoted to their high levels, the *trans* fatty acids by virtue of their impact on blood lipid composition created a very strong demand for comprehensive analyses of edible fats. In fact, the U.S. Food and Drug Administration (FDA) has amended its regulation on nutritional labeling, requiring the inclusion of *trans* fatty acids in food nutritional information, with effect from January 2006. This necessitated reliable analytical methods for the determination of *trans* fatty acid levels.

The chromatographic technique of choice for this purpose is GC, but some adjustments have to be made to achieve an accurate separation of the *trans* isomers from the naturally present *cis*-isomers. Although for most analyses, namely for food labeling, only the total *trans* content is of interest, cases exist, in biological studies for instance, where a specific isomer needs to be quantified. Another factor to consider is the complexity of the *trans* fatty acids present in samples: it can be low, as in dairy products, or high, as in partially hydrogenated fats where the octadecenoic isomer group can constitute up to 26 *cis* and *trans* isomers with double-bond positions ranging from 4 to 16.

The chromatographic separation of *cis–trans* FAMEs requires specific columns. Preferably, a single capillary GLC method should yield detailed information on all types of FAs, allowing labeling of saturated, monounsaturated, polyunsaturated, and total *trans* levels, in a rapid analysis because more samples are continually analyzed on a day-to-day basis.

Long (50–100 m), highly polar (cyanopropyl) columns are used for separating *trans* polyenes[16] that elute earlier than the corresponding *cis*-isomers. The columns most suitable for isomer separation include the SP-2340, SP-2560, CP-Sil88; the last two, both 100 m long, are currently considered the most progressive for *cis–trans* isomer separation. Fig. 6 represents a chromatogram from a commercial hydrogenated frying fat, in which a huge amount of *trans* was detected (21%).

It should be noted that, with cyanopropyl columns (in contrast to the carbowax columns), even though retention time increases with chain length and degree of unsaturation, there is considerable chain length overlap. Furthermore, the resolution of isomeric FAs depends greatly on the column operating temperature. Varying the column temperature by 5–10°C affects the relative elution order of some 18:1 isomers, as well as of 11*c*-20:1 and geometric isomers of ALA. If the analyst is not aware of these variations, misidentification of FAs is possible, leading to inaccurate compositional reports.

When the *trans* fatty acids are difficult to separate by GC, silver-ion chromatography is a useful tool for simplifying any complex FAME sample into fractions according to the number, geometry (*cis* double bonds are held stronger than *trans* double bonds), and even positions of the double bonds. This separation principle can also be applied during sample preparation; special Ag-SPE phases are used for the separation of *trans* and *cis* isomers, the two fractions analyzed separately by GC.

Conjugated Linoleic Acids

These FAs, although chemically "*trans*," are regarded as a distinct class because of the claims on their beneficial health effects, intensively discussed nowadays.

Initial separation of commercial CLA can be achieved by GC but, depending on the sample's complexity, other chromatographic methodologies such as selected-ion recording (SIR) GC–MS with DMOX derivatives or silver-ion HPLC might be necessary to achieve full identification and quantification of the isomers.

It is recognized that long, polar cyanopropyl columns, such as CP-Sil88 or SP-2560, similar to those used for the separation of normal *trans* isomers, are required to achieve optimum separation of CLA isomers. If one is interested only in the two usually encountered major isomers—9*c*, 11*t* and 10*t*, 12*c*—most of the 50 m columns will be sufficient. For a better separation of minor or coeluting isomers a 100-m column is mandatory. Typical conditions might involve complex temperature programming and long running times, usually more than 80 min, and the elution of CLA isomers occur just after 18:3 *n*–3 and before 20:2 *n*–6. Quantification, in milligram of CLA per gram of the sample, would be carried out by adding an appropriate internal standard during extraction. Nevertheless, some isomers are accurately quantifiable by Ag-HPLC only.[17]

Special attention must also be devoted to the derivatization method, as isomerization and oxidation can occur under acidic conditions, thereby altering the original CLA content. Methylation procedures suitable for CLA have been the subject of extensive investigation. CLAs, if present entirely in an esterified form, can be converted to methyl esters with alkaline reagents such as sodium methoxide without causing any changes. However, commercial CLA mainly occur in free-acid form, which cannot be methylated under alkaline conditions. The usual approach is to use an alkaline method for esterified CLA, such as sodium methoxide, followed by

a mild acid method (hydrochloric acid, 80°C for 10 min) or trimethylsilyldiazomethane.

Fast GC in FAME Analysis

The traditional GC separation with a reduced run time, i.e., fast GC, is now the cutting edge and can be achieved by the use of shorter capillary columns, columns with reduced internal diameter, thinner stationary-phase films, H_2 as the carrier gas, higher carrier gas velocities, faster oven temperature programming rates, and combinations of these parameters. However, one must be careful to understand the impact of these changes on the chromatographic resolution. Despite the unavoidable decrease in efficiency, the overall analytical results are obtained with 95% reduction in analytical time, typically less than 2 min.[18]

Comprehensive Two-Dimensional Gas Chromatography

This chromatographic technique, known as GC × GC or 2-D-GC, has emerged in the past decade as a powerful separation technique, able to resolve coeluting peaks in complex samples. The separation can be performed, for instance, by boiling point in the first column and by polarity in the second, with columns usually coupled with a cryogenic modulator. The modulator repeatedly focuses a small portion of the first column eluate and injects it onto the second column. The second column, being very short and narrow, performs a flash (several seconds) separation for each modulation portion injected. Overall separation capacity of the system is greatly enhanced compared to the 1-D separation systems. Scan rate is a key to higher analytical resolution, and hence time-of-flight mass spectrometers (TOF-MS) are increasingly used.[19]

SOME RECOMMENDATIONS

- Lipid extraction, preceding FA analysis, is an important process and it should be performed correctly to achieve plausible results. Sometimes, incomplete lipid recovery may not be a problem if the material recovered is a representative sample; however, it can be misleading if FA compositional data are needed. If hydrolytic methods are used during extraction, or if the presence of free FAs is in order, an adequate derivatization method must be chosen to guarantee the methylation of both triacylglycerols and free FAs.
- Often for sample preservation before analysis, samples are freeze-dried. The possibility of oxidative damage is high in this situation, which can be reduced by following some guidelines. First, the lipids must be kept in the original matrix as long as possible and frozen at the lowest possible temperature, preferably −30°C or lower, to avoid enzymatic lipolysis. Autoxidation during storage can be reduced by flushing with nitrogen and adding a small amount of butylated hydroxyanisole (BHA) or butylated hydroxytoluene (BHT). Second, if extraction is mandatory, then total lipid extraction is done immediately, and the lipids are stored in solution or partially dried by solvent removal with nitrogen, at −30°C or lower, always in the presence of an appropriate antioxidant.
- Finally, it must be pointed out that, when interpreting the results of FA analyses, one should take into account the fact that FA composition is subject to considerable variations—depending on the breed and feed, in the case of animal fats, and on the plant variety, geographic location of the area of cultivation, and climate in the case of plant fat. Therefore, guideline values for individual oils and fats can differ from country to country.

REFERENCES

1. Belitz, H.D.; Grosch, W.; Schieberle, P. *Food Chemistry*; Springer: Berlin, 2004; 157–169.
2. Bicalho, B.; David, F.; Rumplel, K.; Kindt, E.; Sandra, P. Creating a fatty acid methyl ester database for lipid profiling in a single group of human blood using high resolution capillary gas chromatography and mass spectrometry. J. Chromatogr. A, **2008**, *1211*, 120–128.
3. http://www.lipidlibrary.co.uk (accessed December 2008).
4. Horwitz, W., Ed. AOAC official method 969.33—fatty acids in oils and fats—preparation of methyl esters, boron trifluoride method. *Official Methods of Analysis of AOAC International*, 17th Ed.; AOAC International: Gaithersburg, MD, 2000.
5. International Standard Organization. ISO 5509:2000-International Standard-Animal and vegetable fat and oil-preparation of methyl esters of fatty acids. International Standards Organization: Switzerland, 2000.
6. Morrison, W.R.; Smith, L.M. Preparation of fatty acid methyl esters and dimethylacetals from lipids with boron fluoride-methanol. J. Lipid Res. **1964**, *5*, 600–608.
7. Woo, K.L.; Kim, J.-I. New hydrolysis method for extremely small amount of lipids and capillary gas chromatographic analysis as *N*(*O*)-*tert*-butyldimethylsilyl fatty acid derivatives compared with methyl esters derivatives. J. Chromatogr. A, **1999**, *862*, 199–208.
8. Paik, M.-J.; Lee, K.O.; Shin, H.-S. Determination of very-long-chain fatty acids in serum by gas chromatography–nitrogen-phosphorous detection following cyanomethylation. J. Chromatogr. B, **1999**, *721*, 3–11.
9. Christie, W.W. *Gas Chromatography and Lipids*; The Oily Press Ltd.: Ayr, Scotland, 1989.

10. Christie, W.W. *Lipid Analysis*; Pergamon Press: New York, 1982.
11. Mjøs, S.A. Identification of fatty acids in gas chromatography by application of different temperature and pressure programs on a single capillary column. J. Chromatogr. A, **2003**, *1015*, 151–161.
12. Dodds, E.D.; McCoy, M.R.; Rea, L.D.; Kennish, J.M. Gas chromatographic quantification of fatty acid methyl esters: Flame ionization detection vs. electron impact mass spectrometry. Lipids **2005**, *40*, 419–428.
13. Dobson, G.; Christie, W.W. Structural analysis of fatty acids by mass spectrometry of picolinyl esters and dimethyloxazoline derivatives. Trends Anal. Chem. **1996**, *15*, 130–136.
14. Wolff, R.L.; Bayard, C.C.; Fabien, R.J. Evaluation of sequential methods for the determination of butterfat fatty acid composition with emphasis on *trans*-18:1 acids. Application to the study of seasonal variations in French butters. J. Am. Oil Chem. Soc. **1995**, *72*, 1471–1483.
15. Hunter, J.E. Safety and health effects of *trans* fatty acids. In *Fatty Acids in Foods and Their Health Implications*, 3rd Ed., Chow, C.K., Ed.; Marcel Dekker: New York, 2008; 757–790.
16. Ratnayake, W.M.I.; Plouffe, L.J.; Pasquier, E.; Gagnon C. Temperature-sensitive resolution of *cis*- and *trans*-fatty acid isomers of partially hydrogenated vegetable oils on SP-2560 and CP-Sil 88 capillary columns. J. AOAC Int. **2002**, *85* (5), 1112–1118.
17. Kramer, J.K.G.; Cruz-Hernandez, C.; Zhou, J. Conjugated linoleic acids and octadecenoic acids: Analysis by GC. Eur. J. Lipid Technol. **2001**, *103*, 600–608.
18. Mondello, L.; Casilli, A.; Tranchida, P.Q.; Costa, R.; Chiofalo, B.; Dugo, P.; Dugo, G. Evaluation of fast gas chromatography and gas-chromatography-mass spectrometry in the analysis of lipids. J. Chromatogr. A, **2004**, *105*, 237–247.
19. Akoto, L.; Stellaard, F.; Irth, H.; Vreuls, R.J.J.; Pel, R. Improved fatty acid detection in micro-algae and aquatic meiofauna species using a direct thermal desorption interface combined with comprehensive gas chromatography–time-of-flight mass spectrometry. J. Chromatogr. A, **2008**, *1186*, 254–261.

Fatty Acids: Silver Ion TLC

Boryana Nikolova-Damyanova
Institute of Organic Chemistry, Bulgarian Academy of Sciences, Sofia, Bulgaria

INTRODUCTION

Fatty acids (FA) are basic structural elements of lipid molecules, determining many of their chemical and physical properties. Therefore determination of FA composition is mandatory for lipid analysis. For many years, silver ion thin-layer chromatography (Ag-TLC) has been one of the basic separation techniques employed in lipid analysis, the resolution of FA mixtures being one of the main tasks. FAs are separated according to the number, the configuration and, to some extent, the positions of the double bonds. While gas chromatography (GC) has always been the basic method in FA analysis, the specific separation features of Ag-TLC make this technique indispensable in performing certain analytical tasks. The complementary employment of GC or/and GC/MS together with Ag-TLC is probably the most powerful tool for elucidation of fatty acid composition in complex lipid samples.

SILVER ION COMPLEXATION WITH DOUBLE BONDS

The use of Ag-TLC in fatty acid analysis is based on the ability of Ag(I) to form weak, reversible charge-transfer complexes with olefinic double bonds. It is now considered that a σ-type bond is formed between the occupied $2p\pi$ orbitals of the olefinic bond, and the free 5s and 5p orbitals of Ag(I) and a weaker π-acceptor backbond is formed between the occupied 4d orbitals of Ag(I) and the free antibonding $2p\pi^*$ orbitals of the olefinic bond. Quantitative data on equilibrium constants exists for some short-chain mono- and diolefins only. The retention of longer-chain unsaturated compounds, such as FAs, is described on the basis of data collected by different silver ion separation techniques (mostly GC and Ag-TLC) and is supposed to depend on the strength of complexation with Ag(I). The latter, in turn, depends on the number, configuration, and the distance between double bonds. Thus the migration rules in Ag-TLC can be summarized as follows:

- The stronger FAs are held, the higher is the number of double bonds in the chain.
- FAs with *trans* double bonds are held less strongly than FA with *cis* double bonds.
- The retention of FAs with more than one double bond depends on the distance between the bonds, the order of decreasing retention being separated double bonds > methylene interrupted double bonds > conjugated double bonds.
- Longer-chain FAs are less strongly held than shorter-chain FA of the same unsaturation.
- FAs with an olefinic double bond are more strongly held than FAs with an acetylenic bond.
- Deuterated FAs are more strongly held than hydrogen analogs.

Although there is evidence that complexation with silver ions is the governing interaction in Ag-TLC, other factors should also be considered. Thus silica gel, which is the most widely used supporting material, possesses appreciable polarity and adsorption activity. Therefore, in many cases, an impact of mixed retention mechanism on migration, geometry of spots, and selectivity of resolution is to be expected. Also, the mobile-phase solvents are active elements of the chromatographic system and interactions both with the supporting material and FA is possible; this may also have a serious effect on the whole separation process.

SOME PRACTICAL CONSIDERATIONS

Both homemade and precoated glass plates are used in Ag-TLC. Silica gel G (with calcium sulfate as binder) is usually the supporting material. Layer thickness varied between 0.2–0.3 mm for analytical plates and 0.5–1.0 mm for preparative plates. Fully automated spreaders are now available, but simple spreaders are also effective. Some practice is needed to prepare the layer in the laboratory; thus precoated plates are often preferred.

The impregnation of the layer with silver ions is performed by either incorporating the silver salt into the silica gel slurry or by immersing or spraying the plate with water, ethanol, methanol, ammonia, or acetonitrile solutions of the salt. Silver nitrate is normally used. The only method that affords proper control of the Ag(I) content in the layer is to add silver nitrate to the slurry. However, this is inconvenient and messy and is less used now. Because it is evident from analytical practice that the content of silver ions in the layer is not critical over rather broad limits, immersion and spraying are considered equally good. Immersion procedures can be sufficiently well standardized to provide satisfactory results, and can be applied both to homemade and precoated plates. Spraying procedures are also often used in FA analysis, although they are less easily

standardized and are messier. Spraying may have to be repeated from two to six times until the layer is properly wetted. This is especially important for precoated plates.

The concentrations of impregnating solutions vary depending on the purpose. Immersion or dipping is carried out most often with 0.5–20% solutions of silver nitrate, while 10–40% solutions of silver nitrate are recommended for the spraying procedure.

After impregnation, the plates are air-dried, preserved in a dark place, and activated (between 5 and 30 min at 110–120°C in an oven) before sample application.

In spite of all precautions, humidity is not easy to control and is one of the main reasons for the relatively poor overall reproducibility of separations in Ag-TLC.

FAs are subjected to Ag-TLC usually in the form of methyl esters. The methods for methylation and transmethylation are simple, easy to perform, and with practically 100% yield. Methyl esters are particularly suitable when Ag-TLC is used as a complementary method with GC. Butyl and isopropyl esters were employed for the fractionation of butterfat FAs by Ag-TLC because these derivatives provided better resolution in GC. Conversion of positionally isomeric 18 : 1 and 20 : 1 FAs into phenacyl esters ensured complete resolution of the components by Ag-TLC; however, this is not possible when using methyl esters.

Mobile phases generally consist of two- and, rarely, three-component mixtures. Hexane or petroleum ether (BP 40–60°C), chloroform, benzene, and toluene are most often the major components, while smaller proportions of diethyl ether, acetone, methanol, ethanol, or acetic acid may be added.

The conventional approach is to perform the development in closed standard rectangular tanks lined with filter paper to saturate the atmosphere with the mobile-phase

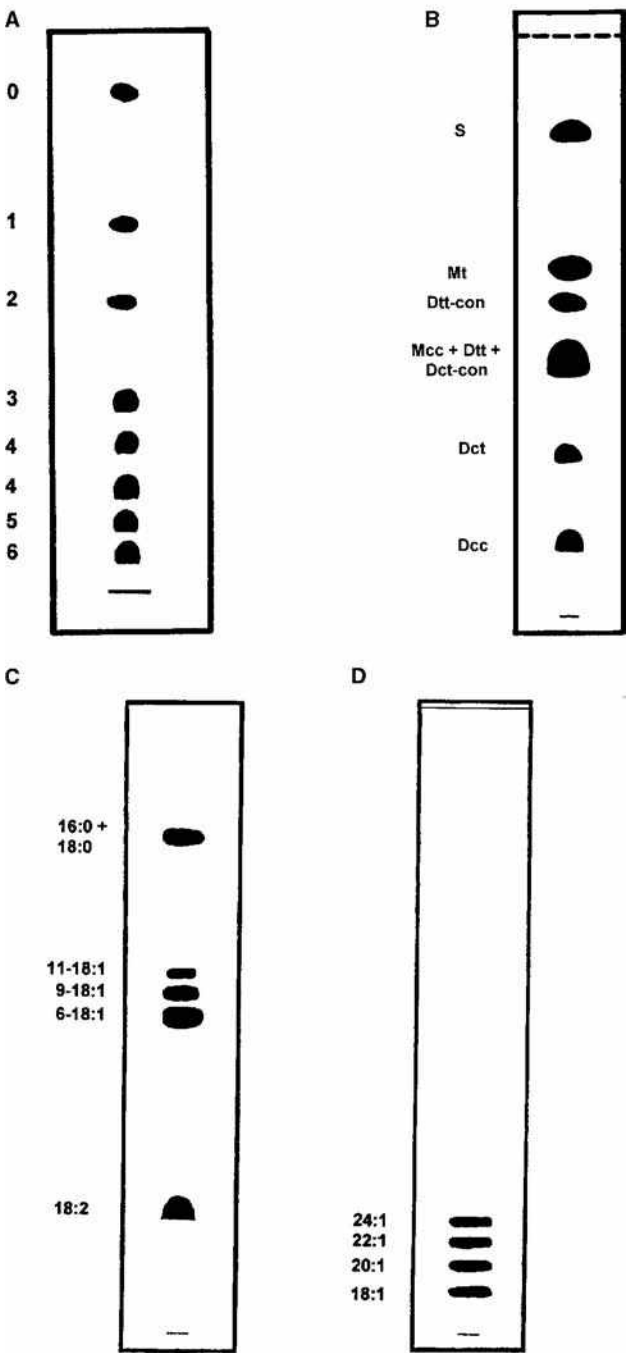

Fig. 1 A, Separation of a reference mixture of fatty acid methyl esters by Ag-TLC according to the number of double bonds. The plate was impregnated by dipping with 0.5% methanolic silver nitrate (w/v) and developed with 5 ml of light petroleum ether–acetone–formic acid, 97 : 2 : 1 (v/v/v); spots were detected by treating the plate in sequence with bromine and sulfuryl chloride vapors, followed by heating at 180–200°C. Numbers alongside denote the number of double bonds. B, Separation of reference mixture of fatty acid methyl esters by Ag-TLC according to the configuration of the double bond. The plate was impregnated with silver nitrate as in A, and developed with 2 ml of light petroleum–acetone, 100 : 2 (v/v) followed by 3 ml light petroleum–acetone, 100 : 7 (v/v). The spots are detected as in A. S, saturated; M, monoenoic; D, dienoic fatty acid methyl esters; c, *cis*; t, *trans*; con, conjugated double bonds. C, Separation of fatty acid phenacyl esters in *Pimpinella anisum* seed oil by Ag-TLC according to the position of the double bond in the chain. Plate was impregnated by dipping with 1% methanolic silver nitrate and was developed twice with mobile phase chloroform–acetone, 100 : 0.25 (v/v); *a* − *c*:*n* denotes the position of the double bond − the number of carbon atoms in the chain: the number of double bonds. (D) Separation of reference mixture of fatty acid methyl esters by Ag-TLC according to the chain length. The plate was sprayed with 20 ml acetonitrile containing 2 g silver nitrate until the layer was saturated. It was then activated for 30 min at 110°C and developed with toluene–hexane, 40 : 60 (v/v) in saturated closed standard tank. Spots were visualized by charring (the procedure was not specified).

vapors. Equal, and in many cases better, results are achieved by development in "open" cylindrical containers where a fixed volume of the mobile phase is added, passed through the plate, and permitted to evaporate from the upper edge of the plate.

Detection of separated zones depends on the analytical task. Destructive procedures are used for qualitative analysis and for quantification by photodensitometry. They consist in carbonization of the FAs by heating at 180–200°C after treating the plate with charring reagents. These can be introduced by spraying, by treatment with the respective vapors, or by incorporation of the reagent into the layer. Up to 50% ethanolic sulfuric or phosphomolybdic acids and copper acetate–phosphoric acid have been used as spraying reagents. Reliable results have been obtained by saturating the silica-gel layer with vapors of sulfuryl chloride. Non-destructive procedures are used in preparative Ag-TLC. It is performed by spraying the plate with a fluorescent indicator, mostly 2,7-dichlorofluorescein in ethanol, and viewing under UV light. The bands are then scraped from the plate and extracted with diethyl ether or hexane–methanol (in appropriate proportions). The excess silver ions and indicator are removed by passing the extract through a small silica column, or by washing with bicarbonate, ammonia, or sodium chloride solutions.

Examples of the separation of fatty acid derivatives by Ag-TLC are given in Fig. 1.

CONCLUSIONS

Silver ion TLC is a simple but reliable approach for separation, identification, quantification, and preparative isolation of fatty acids in lipid samples, depending on the number, configuration, position, and chain length (see Refs.[1–9] for additional information).

ACKNOWLEDGMENT

The partial financial support of the Bulgarian National Science Fund, Contract No. X1009, is gratefully acknowledged.

REFERENCES

1. Morris, L.J. Separation of lipids by silver ion chromatography. J. Lipid Res. **1967**, *7*, 717–732.
2. de Ligny, C.L. The investigation of complex association by gas chromatography and related chromatographic and electrophoretic methods. In *Advances in Chromatography*; Grushka, E., Cazes, J., Brown, P.R., Eds.; Marcel Dekker: New York; Vol. 14, 265–304.
3. Christie, W.W. *Lipid Analysis*; Pergamon Press: Oxford, 1982.
4. Christie, W.W. *Gas Chromatography and Lipids*; The Oily Press: Ayr, 1989.
5. Nikolova-Damyanova, B. Silver ion chromatography and lipids. In *Advances in Lipid Methodology—One*; Christie, W.W., Ed.; The Oily Press: Ayr, 1992; 181–237.
6. Firestone, D.; Shepperd, A. Determination of *trans* fatty acids. In *Advances in Lipid Methodology—One*; The Oily Press: Ayr, 1992; 273–322.
7. Nikolova-Damyanova, B. Quantitative thin-layer chromatography of triacylglycerols: Principles and application. J. Liq. Chromatogr. Relat. Technol. **1999**, *22*, 1513–1537.
8. Fried, B.; Sherma, B. *Thin-Layer Chromatography*; Marcel Dekker: New York, 1999; 197–222.
9. Nikoliova-Damyanova, B.; Momchilova, Sv. Silver ion TLC of fatty acids—a survey. J. Liq. Chromatogr. Relat. Technol. **2001**, *24*, 1447–1466.

FFF Fundamentals

Josef Janca
Department of Chemistry, University of La Rochelle, La Rochelle, France

INTRODUCTION

Field-flow fractionation (FFF) is a separation method suitable for the analysis and characterization of macromolecules and particles. The separation is based on the interaction of the effective physical or chemical forces (e.g., temperature gradient; electric, magnetic, gravitational, or centrifugal forces; chemical potential gradient; etc.) with the separated species. The field, acting across a separation channel, concentrates them at a given position inside the channel. The formed concentration gradient induces an opposite diffusion flux. This leads to a steady-state distribution of the sample components across the channel. The velocity of the longitudinal flow of the carrier liquid also varies across the channel. A flow velocity profile is established inside the channel. As a result, the components of the separated sample are transported in the longitudinal direction at different velocities depending on their transversal positions within the flow of the carrier liquid. This general principle of FFF is demonstrated in Fig. 1.

DISCUSSION

One of three mechanisms, *polarization*,[1] *steric*,[2] and *focusing*,[3] can lead to the formation of different concentration distributions across the fractionation channel. The components of the fractionated sample are either concentrated in the direction of the accumulation wall (polarization FFF), totally compressed at the accumulation wall of the channel (steric FFF), or focused at different positions (focusing FFF), as shown in Fig. 1. Steady state inside the channel is reached in a short time due to the small channel thickness. The strength of the field can be controlled within a wide range in order to manipulate the retention conveniently. Many operational variables in FFF can be manipulated during the experiment by suitable programming.

The *polarization* and *steric* FFF methods are classified according to the nature of the applied field, whereas the *focusing* FFF methods are classified by considering the combination of various gradients and fields emphasizing the focusing processes. Polarization FFF methods make use of the formation of an exponential concentration distribution of each sample component across the channel with the maximum concentration at the accumulation wall, which is a consequence of the constant and position-independent velocity of transversal migration of the affected species due to the field forces. This concentration distribution is combined with the velocity profile formed in the flowing liquid. In steric FFF, the field strength is so high that all species interacting with the field are in contact with the accumulation wall. As a result, the proper size of the retained species determines their position in the flow velocity profile and, consequently, their elution velocity along the channel. Focusing FFF methods make use of transversal migration of each sample component under the effect of driving forces whose intensity varies across the channel. As a result, the sample components are focused at the positions where the intensity of the effective forces is zero and are transported longitudinally with different velocities according to the established flow velocity profile. The concentration distribution within a zone of a focused sample component can be described by Gaussian or similar distribution function.

PRINCIPLE AND THEORY

The carrier liquid flows in the direction of the channel's longitudinal axis, whereas the field forces act perpendicularly across the channel. The driving forces can be generated by a single field or by the coupled action of two or more different fields. Polarizing and focusing forces can operate simultaneously, resulting in a complex mechanism of separation. The field force F and, consequently, the velocity U are independent of position in the direction of the x-axis in polarization and steric FFF:

$$F \neq 0 \quad \text{and} \quad U \neq 0 \quad \text{for} \quad 0 < x < w \tag{1}$$

where w is the distance between the main channel walls in the direction of the x-axis, with $x = 0$ at the accumulation wall. On the other hand, the following hold for the x-axis-dependent direction of the field force in focusing FFF:

$$F = F(x) \quad \text{and} \quad U = U(x) \quad \text{within} \quad 0 < x < w \tag{2}$$

$$F(x) = 0 \quad \text{and} \quad U(x) = 0 \quad \text{for } x = x_{\max} \text{ with } 0 < x_{\max} < w \tag{3}$$

$$F(x) > 0 \quad \text{and} \quad U(x) > 0 \quad \text{for } x < x_{\max} \tag{4}$$

$$F(x) < 0 \quad \text{and} \quad U(x) < 0 \quad \text{for } x > x_{\max} \tag{5}$$

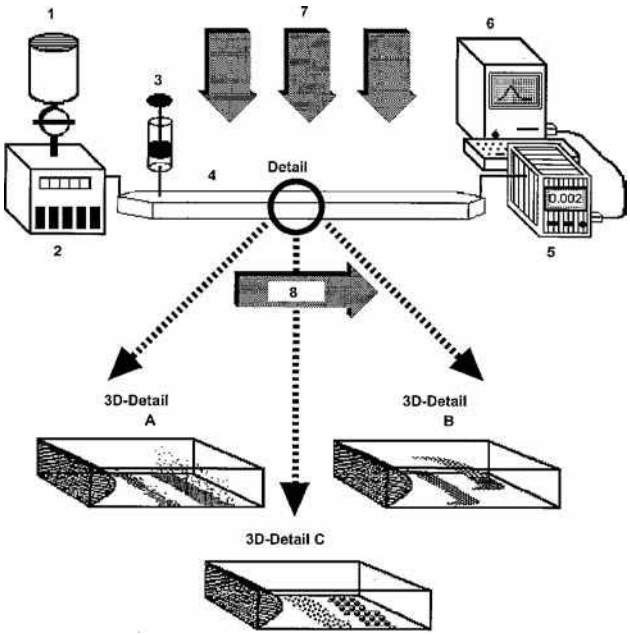

Fig. 1 Principle of field-flow fractionation. 1—Solvent reservoir, 2–carrier liquid pump, 3—injection of the sample, 4—separation channel, 5—detector, 6—computer for data acquisition, 7—transversal effective field forces, 8—longitudinal flow of the carrier liquid. A—Section of the channel demonstrating the principle of polarization FFF with two distinct zones compressed differently at the accumulation wall and the parabolic flow velocity profile. B—Section of the channel demonstrating the principle of focusing FFF with two distinct zones focused at different positions and the parabolic flow velocity profile. C—Section of the channel demonstrating the principle of steric FFF with two zones eluting at different velocities according to the distance of their centers from the accumulation wall.

where the coordinate x_{max} corresponds to the position at which the concentration distribution of a sample component across the channel attains its maximal value.

POLARIZATION FFF

The equilibrium concentration distribution in the direction of the x-axis across the channel of a given component of the sample can be calculated from the continuity equation:

$$-D\frac{\partial c}{\partial x} - Uc = 0 \tag{6}$$

where D is the diffusion coefficient and c is the concentration. The solution of Eq. 6 gives the exponential concentration distribution of the sample component across the channel:[4]

$$c(x) = c(0)\exp(-xU/D) \tag{7}$$

By defining the mean layer thickness, $\ell = D/U$, Eq. 7 can be rewritten:

$$c(x) = c(0)\exp(-x/\ell) \tag{8}$$

The mean layer thickness is practically equal to the center of gravity of the concentration distribution.

STERIC FFF

The radius (or hydrodynamic equivalent of the radius) of the retained species determines the distance of the center of such a species from the accumulation wall. There is no distribution of concentration of the retained component across the channel. Consequently, the ratio α is a decisive parameter determining the retention in steric FFF:[2]

$$R = 6(\alpha - \alpha^2) \tag{9}$$

where $\alpha = r/w$, and r is the radius of the retained species.

FOCUSING FFF

It holds for a focused species at equilibrium that:

$$D\frac{\partial c}{\partial x} - U(x)c = 0 \tag{10}$$

The force $F(x)$, acting on one particle undergoing the focusing, can be written as:

$$F(x) = U(x)f \tag{11}$$

with the friction coefficient defined by:

$$f = kT/D \tag{12}$$

where k is the Boltzmann constant and T is the absolute temperature. Then the following holds:

$$\frac{\mathrm{d}c}{\mathrm{d}x} = \frac{F(x)c}{kT} \tag{13}$$

The focusing force can be approximated by:[5]

$$F(x) = -\left|\left(\frac{\mathrm{d}F(x)}{\mathrm{d}x}\right)_{x\approx x_{max}}\right|(x - x_{max}) \tag{14}$$

where $[\mathrm{d}F(x)/\mathrm{d}x]_{x\approx x_{max}}$ is the gradient of the driving force. The solution is:

$$c(x) = c_{\max} \exp\left[-\frac{1}{2kT}\left|\left(\frac{\mathrm{d}F(x)}{\mathrm{d}x}\right)_{x\approx x_{\max}}\right|(x - x_{\max})^2\right] \tag{15}$$

which is the Gaussian concentration profile of a single focused component. A more accurate approach[5] is based on the real gradient of the focusing forces and results in a concentration distribution of the focused species that is not Gaussian.

FLOW VELOCITY PROFILES

The separation is usually carried out in a belt-shaped narrow channel of constant thickness. The cross-section of the channel is rectangular. The 2D velocity distribution in a plane parallel to the sidewalls in such a channel (provided that the flow is isoviscous) is parabolic:

$$v(x) = \frac{Px(w - x)}{2L\mu} \tag{16}$$

where $v(x)$ is the longitudinal velocity at the x-co-ordinate, ΔP is the pressure drop along a channel of length L, and μ is the viscosity of the carrier liquid. The average velocity is:

$$\langle v(x)\rangle = \frac{\Delta P w^2}{12L\mu} \tag{17}$$

Other shapes of flow velocity profiles can be formed in channels whose cross-section is not rectangular but, for example, trapezoidal. The use of such non-parabolic flow velocity profiles can be advantageous, especially in focusing FFF.

SEPARATION

Separation is due to the coupled action of the concentration and flow velocity distributions. The concentration distribution across the channel of each sample component is established and the sample components are eluted along the channel with different velocities depending on the distance of their centers of gravity from the accumulation wall. The average velocity of the zone of a retained sample component is:

$$\langle v\rangle = \langle c(x)v(x)\rangle / \langle c(x)\rangle \tag{18}$$

The retention ratio R is defined as the average velocity of a retained sample component to the average velocity of the carrier liquid:

$$R = \frac{\int_0^w c(x)v(x)\mathrm{d}x \int_0^w \mathrm{d}x}{\int_0^w c(x)\mathrm{d}x \int_0^w v(x)\mathrm{d}x} \tag{19}$$

where $v(x)$ and $c(x)$ are the local velocity and concentration, respectively, of the retained species. From the practical point of view, the retention ratio R can be expressed as the ratio of the experimental retention time t_0 or the retention volume V_0 of an unretained sample component to the retention time t_r or the retention volume V_r of the retained sample component. Provided that a relationship exists between the position of the center of gravity of the zone and the molecular parameters of the sample component, these parameters can be calculated from the retention data without calibration.

The retention ratio in polarization FFF is thus given by:[6]

$$R = 6\lambda\left[\coth\left(\frac{1}{2\lambda}\right) - 2\lambda\right] \tag{20}$$

where $\lambda = l/w$. If λ is small, the following approximations hold:

$$\lim_{\lambda\to 0} R = 6(\lambda - 2\lambda^2) \quad \text{or} \quad \lim_{\lambda\to 0} R = 6\lambda \tag{21}$$

The retention parameter λ relates the dispersive effect of thermal energy to the structuring effect of the field on the retained species:

$$\lambda = \frac{kT}{Fw} \tag{22}$$

When the size of the separated species is commensurable with the thickness of the channel, the limit retention ratio in this mode of steric FFF is:[3]

$$\lim_{\alpha\to 0} R = 6\alpha \tag{23}$$

where $\alpha = r/w$; r is the particle radius.

The retention ratio in focusing FFF carried out in a channel of rectangular cross-section is given by the approximate relationship:[7]

$$R = 6\left(\Gamma_{\max} - {\Gamma_{\max}}^2\right) \tag{24}$$

where $\Gamma_{\max} = x_{\max}/w$ is the dimensionless co-ordinate of the maximal concentration of the focused zone.

METHODS AND APPLICATIONS

The retention is related to the size, charge, diffusion coefficient, thermal diffusion factor, and so forth of the separated species in polarization FFF, whereas it is exclusively

the size that determines the retention in steric FFF. As concerns focusing FFF, the retention is usually related to the intensive properties of the fractionated species. Consequently, FFF can be used to characterize the properties related to retention. Only the polarization and steric FFF methods are described here.

The particular methods of polarization and steric FFF are denominated by the nature of the applied field. The most important of them are described in the following subsections.

Sedimentation FFF

Sedimentation FFF is shown schematically in Fig. 2a. The separation channel is situated inside a centrifuge rotor and the centrifugal forces are applied radially.[8] The method can be used for the analysis and characterization of various latexes, inorganic particles, emulsions, biological cells, etc. The retention parameter λ depends on the effective mass of the particles:

$$\lambda = 6kT/(\pi d^3 g w \Delta\rho) \tag{25}$$

where g is the gravitational or centrifugal acceleration and $\Delta\rho$ is the density difference between the particles and the carrier liquid. The calculation of the particle size distribution is possible directly from the retention data.

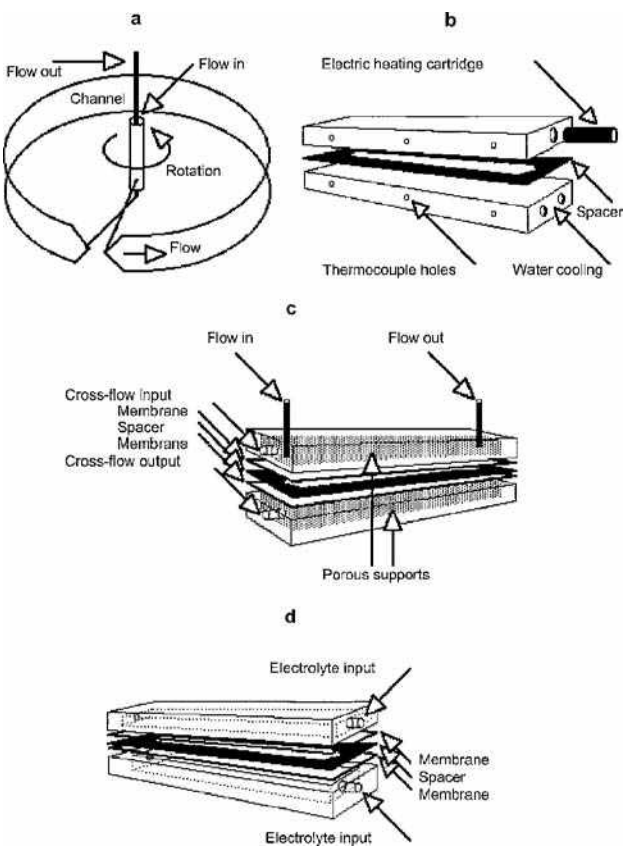

Fig. 2 Methods of polarization FFF. a, Sedimentation FFF; b, thermal FFF; c, flow FFF; and d, electric FFF.

Thermal FFF

Thermal FFF was the first experimentally implemented method.[9] It is used mostly for the fractionation of macromolecules. The temperature difference between two metallic bars, forming the channel walls with highly polished surfaces and separated by a spacer in which the channel proper is cut, produces the flux of the sample components, usually toward the cold wall. The channel for thermal FFF is shown in Fig. 2b. The relation between λ and the operational variables is given by:

$$\lambda = \frac{D}{wD_T(\mathrm{d}T/\mathrm{d}x)} \tag{26}$$

where D_T is the coefficient of the thermal diffusion, which depends on the chemical composition and structure of the fractionated species but not on their size. On the other hand, the diffusion coefficient D depends on the size. As a result, the differences in thermal diffusion coefficients allow fractionation according to differences in chemical composition and structure, whereas different diffusion coefficients allow fractionation based on the size differences. The performances favor thermal FFF over its competing methods.

Flow FFF

Flow FFF is a universal method because the cross-flow field acts on all fractionated species in the same manner and the separation is due to the differences in diffusion coefficients.[10] The channel, schematically demonstrated in Fig. 2c, is formed between two parallel semipermeable membranes. The carrier liquid can permeate through the membranes but not the separated species. The retention parameter λ is related to the diameter d_p of the separated species:

$$\lambda = kTV_0/\left(3\pi\mu V_c w^2 d_p\right) \tag{27}$$

where V_0 is the void volume of the channel, μ is the viscosity of the carrier liquid, and V_c is the volumetric velocity of the cross-flow. The separations of various kinds of particles such as proteins, biological cells, colloidal silica, polymer latexes, etc. as well as of soluble macromolecules have been described.

Electric FFF

Electric FFF uses the electric potential across the channel to generate the transversal flux of the charged species.[11] The walls of the channel can be formed by semipermeable

membranes that allow the passage of small ions but not of the separated species. The channel is shown in Fig. 2d. The dependence of the retention parameter λ on the electrophoretic mobility μ_e, and on the diffusion coefficient of the charged particles, is given by:

$$\lambda = D/(\mu_e E w) \tag{28}$$

where E is the electric field strength. As a result, the ratio of the diffusion coefficient to the electrophoretic mobility determines the retention. Species exhibiting only small differences in electrophoretic mobilities but significant differences in diffusion coefficients can be separated. Electric FFF is especially suited for the separations of biological cells as well as for charged polymer latexes and other colloidal particles and charged macromolecules.

Other Polarization FFF Methods

Other polarization FFF methods have recently been proposed theoretically and some of them implemented experimentally. Their use in current laboratory practice needs further development in methodology and instrumentation. One of the most recent review papers summarizes the state of the art of the polarization FFF methods.[12]

Steric FFF Methods

Any field force can be exploited to create conditions for effective action of the steric exclusion mechanism. The only condition is, as mentioned above, that the field strength be high enough to compress all retained species to the accumulation wall. In experimental practice, sedimentation FFF, flow FFF, and thermal FFF are the techniques actually applied in steric mode to separate effectively some particulate species.

REFERENCES

1. Giddings, J.C. A new separation concept based on a coupling of concentration and flow nonuniformities. Sep. Sci. **1966**, *1*, 123.
2. Giddings, J.C.; Myers, M.N. Steric field-flow fractionation: A new method for separating 1–100 μm particles. Sep. Sci. Technol. **1978**, *13*, 637.
3. Janča, J. Sedimentation–flotation focusing field-flow fractionation. Makromol. Chem. Rapid Commun. **1982**, *3*, 887.
4. Janča, J. *Field-Flow Fractionation: Analysis of Macromolecules and Particles*; Marcel Dekker, Inc.: New York, 1988.
5. Janča, J. *Chromatographic Characterization of Polymers, Hyphenated and Multidimensional Techniques*; Provder, T., Barth, H.G., Urban, M.W., Eds.;Advances in Chemistry Series 247; ACS: Washington, D.C., 1995.
6. Hovingh, M.E.; Thompson, G.H.; Giddings, J.C. Column parameters in thermal field-flow fractionation. Anal. Chem. **1970**, *42*, 195.
7. Janča, J.; Chmelik, J. Focusing in field-flow fractionation. Anal. Chem. **1984**, *56*, 2481.
8. Giddings, J.C.; Myers, M.N.; Moon, M.H.; Barman, B.N. In *Particle Size Distribution*; Provder, T., Ed.; ACS Symposium Series No. 472; ACS: Washington, D.C., 1991.
9. Jeon, S.J.; Schimpf, M.E. *Particle Size Distribution III: Assessment and Characterization*; Provder, T., Ed.; ACS: Washington, D.C., 1998.
10. Ratanathanawongs, S.K.; Giddings, J.C. *Chromatography of Polymers: Characterization by SEC and FFF*; Provder, T., Ed.; ACS Symposium Series 521; ACS: Washington, D.C., 1993.
11. Schimpf, M.E.; Caldwell, K.D. Electrical field-flow fractionation for colloid and particle analysis. Am. Lab. **1995**, *27*, 64.
12. Cölfen, H.; Antonietti, M. Field-flow fractionation techniques for polymer and colloid analysis. In new developments in polymer analytics I. Adv. Polym. Sci. **2000**, *150*, 67.

FFF with Electro-Osmotic Flow

Victor P. Andreev
Institute for Analytical Instrumentation, Russian Academy of Sciences, St. Petersburg, Russia

INTRODUCTION

It is well known that the essence of field-flow fractionation (FFF) is in the interaction between the distribution of the sample particles in the transversal field and the non-uniformity of the longitudinal flow profile. The classical FFF is realized in the channel with the flow driven by the pressure drop. The flow, in this case, is called Poiseuille flow and its profile is parabolic.

DISCUSSION

Electro-osmotic flow (EOF) is widely used for the propulsion of liquid in modern chromatographic methods, so it was natural to study the possibility of FFF with EOF, generated by applying an electric field, E, along a channel or a tube with charged (having the non-zero zeta-potentials) walls. The usual EOF is very close to uniform. For the cylindrical tube of radius a, the EOF velocity profile is described by

$$V(r) = \frac{\zeta\varepsilon\varepsilon_0 E}{\eta}\left(1 - \frac{I_0(\kappa r)}{I_0(\kappa a)}\right) \tag{1}$$

where ζ is the zeta-potential of the wall, ε and η are the dielectric constant and viscosity of the buffer, respectively, ε_0 is the permitivity of the free space, $\kappa^{-1} = (\varepsilon\varepsilon_0 k_B T/2ne^2)^{1/2}$ is the Debye layer thickness [k_B is the Boltzman constant, T is the temperature, n is the number of ions per unit volume (proportional to the concentration of buffer C_0), e is the proton charge], and $I_0(x)$ is the modified Bessel function. As can be seen from Eq. 1, the velocity profile of the EOF in the tube is very close to uniform everywhere except the Debye layer vicinity of the wall. Thus, it is hard to exploit such a profile for FFF unless the concentration of buffer is very low.

That is why it was proposed[1,2] to realize the asymmetrical FFF in the flat channel by making its walls of different materials or chemically modifying them. If the channel walls have non-equal values of the zeta-potentials, then the shape of the EOF profile can be quite different from uniform. The flow profiles that can be generated in the FFF channel with the applied electric field E and pressure drop Δp are presented in Fig. 1. These profiles can be described by

$$V(r) = \frac{\zeta_2\varepsilon\varepsilon_0 E}{\eta}\cdot\left[(\zeta_R - 1)\frac{\sinh kY}{\sinh k} + (\zeta_R + 1)\right.$$
$$\left.\frac{\cosh kY}{\cosh k} + (1 - \zeta_R)Y - (1 + \zeta_R)\right] + V_0(1 - Y^2) \tag{2}$$

where $\zeta_R = \zeta_1/\zeta_2$ is the ratio of the zeta-potential of the accumulation wall to the zeta-potential of the depletion wall, $k = \kappa w/2$, w is the channel depth, $Y = 1 - 2y/w$, and $V_0 = \Delta p/2\eta L$.

For large values of k, the first two terms in the square brackets are substantially non-zero only in the Debye layer vicinity of the walls, whereas everywhere else the EOF profile is dominated by the last two linear terms in the square brackets. Therefore, the asymmetric EOF profile can be close to trapezoidal or close to triangular depending on the exact values of the zeta-potentials of the walls. If the signs of the zeta-potentials of the walls are different, then the liquid moves in one direction near one wall and in the opposite direction near another wall (this case can be interesting for the preseparation of the particles having different densities). The last term in Eq. 2 corresponds to the pressure-driven Poiseuille flow.

Having Eq. 2 for flow profile enables one to calculate the retention ratio R and χ coefficient describing the Taylor dispersion part of the theoretical plate height H for arbitrary flow profile, according to[3]

$$H = \frac{2D}{R\langle V\rangle} + \chi\frac{w^2\langle V\rangle}{D} \tag{3}$$

where $\langle V\rangle$ is the average velocity of the flow and D is the diffusion coefficient of sample molecules. Usually, in FFF, the second term of Eq. 3 is much larger than the first one.

Comparison of R and χ values for the flow profiles presented in Fig. 1 for the case of the FFF parameter $\lambda \ll 1$ gives $R = 6\lambda$ and $\chi = 24\lambda^3$ for classical FFF with Poiseuille flow and $R = 2\lambda$ and $\chi = 8\lambda^3$ for FFF with a triangular EOF ($\zeta_1 = 0$). The most interesting result corresponds to the case of FFF with a combined triangular EOF and counterdirected Poiseuille flow (with $V_0 = \zeta_2\varepsilon\varepsilon_0 E/4\eta$ leading to $dV/dY = 0$ for $Y = 0$). In this case, $R = 6\lambda^2$ and $\chi = 24\lambda^4$. Thus, the selectivity $S = d\ln R/d\ln\lambda = 2$ and is twice as large as in the case of classical FFF and FFF with a triangular EOF. The χ coefficient is very small for $\lambda \ll 1$, so that the Taylor dispersion is very low and efficiency is high. The function $F = S/\sqrt{\chi}$

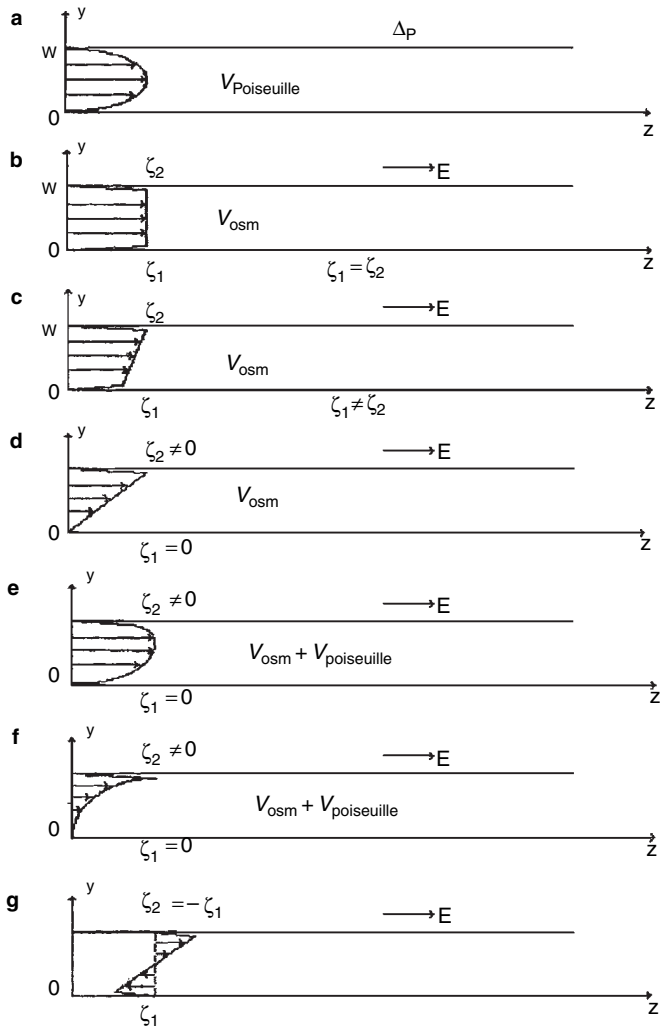

Fig. 1 Outline of the flow profiles in the FFF channels: a, Poiseuille flow; b, EOF (the equal zeta-potentials of the walls; c, trapezoidal EOF (the non-equal zeta-potentials of the walls); d, triangular EOF (the zero zeta-potential of the accumulating wall); e, codirected triangular EOF and Poiseuille flow; f, counterdirected triangular EOF and Poiseuille flow; and g, antisymmetric EOF (different signs of the zeta-potentials of the walls).

(fractionating power), characterizing the resolution for the given value of $\langle V \rangle$, is proportional to λ^{-2} in this case; in the rest of the cases, it is proportional to $\lambda^{-3/2}$. The situation with this kind of combined flow is very similar to the one described in Ref.[4] for the case of Poiseuille flow combined with the natural convection flow in the thermogravitational FFF channel.

High selectivity, efficiency, and fractionating power makes FFF with combined EOF and Poiseuille flows very interesting, as it can, at least theoretically, lead to finer separations for given values of λ. Experimental realization of FFF with asymmetrical EOF have not yet been reported due to some technical problems. However, considerable progress in this field is accomplished by a Finnish group (Riekkola, Vastamaki, and Jussila) working on the experimental realization of thermal FFF with asymmetrical EOF[5] and a Russian group (Andreev, Stepanov, and Tihomolov) working on gravitational FFF with asymmetrical EOF.[6]

The situation is more complicated, even theoretically, when the sample particles are charged. In this case, they are not only moving with the longitudinal flow (here, asymmetrical EOF) but are also forced by the longitudinal electric field to move along the channel electrophoretically. If the electrophoretic mobilities of the particles are different, then there are two types of separations combined: The FFF type due to the difference in λ values and the capillary zone electrophoresis (CZE) type due to the difference in electrophoretic mobilities. A great variety of variants of FFF and CZE combinations in the FFF channel with asymmetrical EOF could be imagined, depending on various factors such as the ratio of the zetapotentials of the channel walls, the sign and the value of the ratio of eletrophoretic and electro-osmotic velocities, and the type of the transversal field. Some of these combinations are examined in Ref.[6] They could lead both to the new possibilities of the method and to some new complications in the interpretation of the experimental results.

Another possibility for realizing FFF with EOF is to reduce the concentration of the buffer, thus making the Debye length commensurate, if not with the depth of the channel, then with the thickness $l = \lambda w$ of the layer of sample particles compressed to the accumulating wall of

FFF channel (for $C_0 = 10^{-5}M$ Debye length, $\kappa^{-1} = 0.1$ μm). In this case, EOF will be non-uniform enough to realize FFF in a channel with equal zeta-potentials of the walls.

In Ref.[7] the mathematical model of CZE, taking into consideration EOF non-uniformity and particle–wall electrostatic interactions, was developed. It was shown that for the particles electrostatically attracted by the wall of the capillary, two mechanisms of separation exist. The first is the usual CZE mechanism and it dominates for the case of high buffer concentrations; the second is the FFF accompanying the CZE mechanism and it dominates for low buffer concentrations. As is usual in CZE, the total velocity of the particle is the sum of its electrophoretic velocity and electro-osmotic velocity of the flow. The larger the electrical charge of sample particles, the stronger they are attracted to the wall and the higher is their concentration in the Debye layer vicinity of the wall, where the EOF is substantially non-uniform. Thus, for the particles with a higher charge, the mean velocity of movement with EOF will be lower than for the particles with the lower charge. Especially interesting with this type of FFF is for the particles with equal electrophoretic mobilities but different charges. Such types of particles (e.g., DNA fragments) cannot be fractionated by usual CZE, but can be fractionated by FFF accompanying CZE, where the separation is due to the difference of electrical charges, not the difference of mobilities. Note that for this type of FFF, there is no need for any external transversal field, because the particles are attracted to the walls by the field of the electrical double layer. As is usual in FFF, there is the transition point from normal diffusional FFF to steric FFF mode, taking place when the size of the particle is commensurable with λw. In Ref.,[8] it was theoretically predicted that steric FFF accompanying the CZE mode can be realized for the separation of DNA fragments in the range of 20–3000 bases with high resolution and speed. To realize this type of separation, one needs to develop a modified capillary with the positive value of the zeta-potential of the wall and without the irreversible sorption of DNA fragments on the walls. Such an attempt seems to be worthy because, unlike DNA separation by CZE in gel or polymer solution, in the case of FFF/CZE there is the possibility of online coupling with a mass spectrometer without the risk of gel particles going inside the spectrometer.

REFERENCES

1. Andreev, V.P.; Miller, M.E.; Giddings, J.C. Field-flow fractionation with asymmetrical electroosmotic flow. 5th Int. Symp on FFF, 1995.
2. Andreev, V.P.; Stepanov, Y.V.; Giddings, J.C. Field-flow fractionation with asymmetrical electroosmotic flow. I. Uncharged particles. J. Microcol. Separ. **1997**, *9*, 163.
3. Martin, M.; Giddings, J.C. Retention and non-equilibrium peak broadening for generalized flow profile in FFF. J. Phys. Chem. **1981**, *85*, 727.
4. Giddings, J.C.; Martin, M.; Myers, M.N. Thermogravitational FFF: an elution thermogravitational column. Separ. Sci. Technol. **1979**, *14*, 611.
5. Vastamaki, P.; Jussila, M.; Riekkola, M.-L. The effect of electrically-conductive wall coating on retention in ThFFF. 7th Int. Symp. on FFF, 1998.
6. Andreev, V.P.; Stepanov, Y.V. Field-flow fractionation with asymmetrical electroosmotic flow. II. Charged particles. J. Liquid Chromatogr. Relat. Technol. **1997**, *20*, 2873.
7. Andreev, V.P.; Lisin, E.E. On the mathematical model of capillary electrophoresis. Chromatographia **1993**, *37*, 202.
8. Andreev, V.P.; Stepanov, Y.V. Steric FFF accompanying capillary electrophoresis. 5th Int. Symp on FFF, 1995.

FFF: Data Treatment

Josef Janca
Department of Chemistry, University of La Rochelle, La Rochelle, France

INTRODUCTION

Field-flow fractionation (FFF) methods are classified into two main categories:[1–3] *polarization* FFF and *focusing* FFF. Their basic characterization is given in the entry *FFF Fundamentals*, p. 849. Whereas the polarization FFF methods allow to fractionate the samples on the basis of the differences in the extensive properties (such as the molar mass or particle size, etc.) of the individual species, the focusing FFF methods discriminate among the species, according to their intensive property differences (such as the charge or density, etc.). This entry deals with the data treatment of the experimental results from polarization FFF, thus with the quantitative characterization of the extensive properties. However, a principally identical approach can be applied to the intensive properties data treatment of the results obtained from the focusing FFF experiments.

In general, the methodology of the data treatment, concerning the separations of the macromolecular or particulate samples, does not depend on the particular separation method or technique. The basics of this methodology were elaborated in parallel with the development of size-exclusion chromatography (SEC)[4] and of the techniques of particle size analysis,[5] but they originate at the very beginning[6,7] of liquid chromatography (LC) of macromolecules and remain substantially unchanged until today.

Macromolecular or particulate samples fractionated by the FFF are usually not uniform but exhibit a distribution of the concerned extensive or intensive parameter[8] or, in other words, a polydispersity. Molar mass distribution (MMD), sometimes called molecular weight distribution (MWD), or particle size distribution (PSD) describes the relative proportion of each molar mass (molecular weight), M, or particle size (diameter), d_p, species composing the sample. This proportion can be expressed as a number of the macromolecules or particles of a given molar mass or diameter, respectively, relative to the number of all macro molecules or particles in the sample:

$$N(M) = \frac{n_i(M)}{\sum_{i=1}^{\infty} n_i} \qquad N(d_p) = \frac{n_i(d_p)}{\sum_{i=1}^{\infty} n_i} \tag{1}$$

or as a mass (weight) of the macromolecules or particles of a given molar mass or diameter relative to the total mass of the sample:

$$W(M) = \frac{m_i(M)}{\sum_{i=1}^{\infty} m_i} \qquad W(d_p) = \frac{m_i(d_p)}{\sum_{i=1}^{\infty} m_i} \tag{2}$$

Accordingly, the MMD (MWD) and PSD are called number or mass (weight) MMD or PSD, respectively. FFF provides a fractogram which has to be treated to obtain the required MMD or PSD. These distributions can be used to calculate various average molar masses or particle sizes and polydispersity indices.

AVERAGE MOLAR MASSES, PARTICLE SIZES, AND POLYDISPERSITIES

As mentioned, in addition to the MMD and PSD, various average molar masses, particle sizes, and polydispersity indexes can be calculated from the FFF fractograms. If the detector response, h, is proportional to the mass of the macromolecules or particles, the mass-average molar mass or mass average particle diameter can be calculated from

$$\overline{M_m} = \overline{M_w} = \frac{\sum_{i=1}^{\infty} M_i h_i}{\sum_{i=1}^{\infty} h_i} \qquad \overline{d_m} = \overline{d_w} = \frac{\sum_{i=1}^{\infty} d_i h_i}{\sum_{i=1}^{\infty} h_i} \tag{3}$$

and the corresponding number average values are calculated from

$$\overline{M_n} = \frac{\sum_{i=1}^{\infty} M_i n_i}{\sum_{i=1}^{\infty} n_i} = \frac{\sum_{i=1}^{\infty} h_i}{\sum_{i=1}^{\infty} (h_i/M_i)} \qquad \overline{d_n} = \frac{\sum_{i=1}^{\infty} d_i n_i}{\sum_{i=1}^{\infty} n_i} = \frac{\sum_{i=1}^{\infty} h_i}{\sum_{i=1}^{\infty} (h_i/d_i)} \tag{4}$$

The width of the MMD or PSD (polydispersity) can be characterized by the index of polydispersity:

$$I_{\mathrm{MMD}} = \frac{\overline{M_m}}{\overline{M_n}} \qquad I_{\mathrm{PSD}} = \frac{\overline{d_m}}{\overline{d_n}} \tag{5}$$

PRACTICAL DATA TREATMENT

Provided that the correction for the zone broadening should not be applied, the first step in the data treatment is to convert the retention volumes (or the retention ratios R) into the corresponding molecular or particulate parameter, characterizing the fractionated species. Whenever the zone broadening correction procedure has to be applied, the data treatment protocol is modified, as described in the entry *Zone Dispersion in FFF*, p. 2455.

The dependences of the retention ratio R on the size of the fractionated species (molar mass for the macromolecules or particle diameter for the particulate matter) are presented for various polarization FFF methods in the entry *FFF Fundamentals*, p. 849. The raw, digitized fractogram, which is a record of the detector response as a function of the retention volume, is represented by a differential distribution function $h(V)$. It can be processed to obtain a series of the height values h_i corresponding to the retention volumes V_i, as shown in Fig. 1. Subsequently, the retention volumes are converted into the retention ratios R_i:

$$R_i = \frac{V_0}{V_i} \tag{6}$$

The retention ratio R in polarization FFF is related to the retention parameter λ (see *FFF Fundamentals*, p. 849) by

$$R = 6\lambda\left[\coth\left(\frac{1}{2\lambda}\right) - 2\lambda\right] \tag{7}$$

or by an approximate relationship

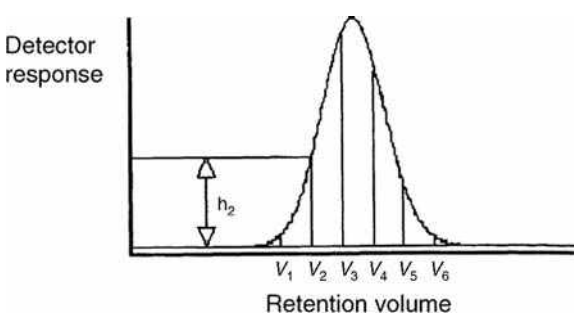

Fig. 1 Treatment of an experimental FFF fractogram of a polydisperse sample.

$$(\lim R)_{\lambda\to 0} = 6\lambda \tag{8}$$

and the parameter λ is directly related to the molecular or particulate parameters by the general relationships

$$\lambda = f(M^{-n}) \quad \text{or} \quad \lambda = f(d_p^{-n}) \tag{9}$$

where the exponent $n = 1$, 2, or 3. As concerns the focusing FFF methods, similar relationships exist between the retention ratio R and the intensive properties of the fractionated species.

Having the V_i values converted into the R_i values by using Eq. 6, the corresponding molar mass M_i or the particle diameter d_i values are calculated by applying Eqs. 7–9. The difficulty is that Eq. 7 is a transcendental function $R = f(\lambda)$ for which the inversion function $\lambda = f'(R)$ does not exist. As a result, Eq. 8 can be used as a first approximation to estimate the λ_i values from the experimental R_i data, and by applying a rapidly converging iteration procedure, the accurate λ_i values can be calculated. The subsequent attribution of the corresponding M_i or d_i values to the calculated λ_i values, by using the appropriate relationship, Eq. 9, is not mathematically complicated.

In order to obtain an accurate result, the regular segmentation ΔV_i of the raw fractogram must be converted into the ΔR_i and, thereafter, into the appropriate increment of the molar mass ΔM_i or of the particle diameter Δd_i. The corresponding conversions of the raw experimental fractograms into the MMD or PSD can be carried out according to the following protocol. Eqs. 3 and 4 can be rewritten in integral form:

$$\overline{M_m} = \frac{\int_0^\infty W(M)M\,dM}{\int_0^\infty W(M)\,dM} \qquad \overline{d_m} = \frac{\int_0^\infty d_p W(d_p)\,dd_p}{\int_0^\infty W(d_p)\,dd_p} \tag{10}$$

and

$$\overline{M_n} = \frac{\int_0^\infty N(M)M\,dM}{\int_0^\infty N(M)\,dM} \qquad \overline{d_n} = \frac{\int_0^\infty d_p N(d_p)\,dd_p}{\int_0^\infty N(d_p)\,dd_p} \tag{11}$$

where it holds for the normalized MMD or PSD:

$$\int_0^\infty W(M)\,dM = \int_0^\infty W(d_p)\,dd_p = \int_0^\infty N(M)\,dM = \int_0^\infty N(d_p)\,dd_p = 1 \tag{12}$$

By considering all of the above-mentioned transformations, Eqs. 10–12 give

$$\overline{M_m} = \int_0^\infty W(M)M\left(\frac{\partial M}{\partial \lambda}\right)\left(\frac{\partial \lambda}{\partial R}\right)\left(\frac{\partial R}{\partial V}\right)dV \left(\int_0^\infty W(M)dV\right)^{-1}$$

$$\overline{d_m} = \int_0^\infty W(d_p)d_p\left(\frac{\partial d_p}{\partial \lambda}\right)\left(\frac{\partial \lambda}{\partial R}\right)\left(\frac{\partial R}{\partial V}\right)dV \left(\int_0^\infty W(d_p)dV\right)^{-1}$$

$$\overline{M_n} = \int_0^\infty N(M)M\left(\frac{\partial M}{\partial \lambda}\right)\left(\frac{\partial \lambda}{\partial R}\right)\left(\frac{\partial R}{\partial V}\right)dV \left(\int_0^\infty N(M)dV\right)^{-1}$$

$$\overline{d_n} = \int_0^\infty N(d_p)d_p\left(\frac{\partial d_p}{\partial \lambda}\right)\left(\frac{\partial \lambda}{\partial R}\right)\left(\frac{\partial R}{\partial V}\right)dV \left(\int_0^\infty N(d_p)dV\right)^{-1} \quad (13)$$

Any of Eq. 13 can further be rewritten in a numerical form of Eqs. 3 and 4, which are convenient for the data treatment and calculations using the discrete M_i or d_i and h_i values. The acquisition of the experimental data and the treatment of the fractogram is easily performed by a computer connected online to the separation system.

REFERENCES

1. Janča, J. *Field-Flow Fractionation: Analysis of Macromolecules and Particles*; Marcel Dekker, Inc.: New York, 1988.
2. Janča, J. Isoperichoric focusing field-flow fractionation for characterization of particles and molecules. J. Liq. Chromatogr. Relat. Technol. **1997**, *20*, 2555.
3. Cölfen, H.; Antonietti, M. "Field-flow fractionation techniques for polymer and colloid analysis" in "new developments in polymer analytics I.". Adv. Polym. Sci. **2000**, *150*, 67.
4. Quivoron, C. *Steric Exclusion Chromatography of Polymers*; Janča, J., Ed.; Marcel Dekker, Inc.: New York, 1984.
5. Barth, H.G., Ed.; *Modern Methods of Particle Size Analysis*; John Wiley & Sons: New York, 1984.
6. Cazes, J. Gel permeation chromatography. Part I. J. Chem. Educ. **1966**, *43*, A567.
7. Cazes, J. Gel permeation chromatography. Part II. J. Chem. Educ. **1966**, *43*, A625.
8. Dawkins, J.V. *Comprehensive Polymer Science*; Booth, C., Price, C., Eds.; Pergamon Press: Oxford, 1989; Vol. 1.

FFF: Frit-Inlet Asymmetrical Flow

Myeong Hee Moon
Department of Chemistry, Kangnung National University, Kangnung, South Korea

INTRODUCTION

Frit-inlet asymmetrical flow field-flow fractionation (FIA-FlFFF)[1–3] utilizes the frit-inlet injection technique, with an asymmetrical flow FFF channel which has one porous wall at the bottom and an upper wall that is replaced by a glass plate. In an asymmetrical flow FFF channel, channel flow is divided into two parts: axial flow for driving sample components toward a detector, and the cross-flow, which penetrates through the bottom of the channel wall.[4,5] Thus, the field (driving force of separation) is created by the movement of cross-flow, which is constantly lost through the porous wall of the channel bottom. FIA-FlFFF has been developed to utilize the stopless sample injection technique with the conventional asymmetrical channel by implementing an inlet frit nearby the channel inlet end and to reduce possible flow imperfections caused by the porous walls.

DISCUSSION

The asymmetrical channel design in flow FFF has been shown to offer high-speed and more efficient separation for proteins and macromolecues than the conventional symmetrical channel. However, an asymmetrical channel requires a focusing-relaxation procedure for sample components to reach their equilibrium states before the separation begins. The focusing-relaxation procedure is achieved by two counterdirecting flow streams from both the channel inlet and outlet to a certain point slightly apart from the channel inlet end for a period of time. This is a necessary step equivalent to the stop-flow procedure as is normally used in a conventional symmetrical channel system. Although the stop-flow and the focusing-relaxation procedures are essential in each technique (symmetrical and asymmetrical channels, respectively), they are basically cumbersome in system operation due to the stoppage of flow with valve operations. In addition, they often cause baseline shifts during the conversion of flow. For these reasons, the frit-inlet injection technique, which can be an alternative to bypass those flow-halting processes, is adapted to an asymmetrical flow FFF channel in order to take advantage of hydrodynamic relaxation of sample components.

The frit-inlet injection device was originally applied to the conventional symmetrical channel in order to bypass the stop-flow procedure.[6] However, the lowest axial flow rate that can be manipulated in a frit-inlet symmetrical system is limited, because the total axial flow rate becomes the sum of the injection flow rate and frit flow rate, and the incoming cross-flow penetrates through the bottom wall at the same rate. The relatively high axial flow rate in a symmetrical system needs a very high cross-flow rate in order to separate relatively low-retaining materials, such as proteins or low-molecular-weight components.

Compared to the limited choice in the selection of flow rate conditions, application of the frit-inlet injection technique to an asymmetrical flow FFF channel can be more flexible in allowing the selection of a low axial flow rate condition which is suitable for low-retaining materials without the need of using a very high cross-flow rates and for the reduction of injection amount resulting from the concentration effect.

In FIA-FlFFF, sample materials entering the channel are quickly driven toward the accumulation wall and are transported to their equilibrium positions by the compressing action of a rapidly flowing frit flow entering through the inlet frit. The schematic view of an FIA-FlFFF channel is shown in Fig. 1. In the relaxation segment of a FIA-FlFFF channel, the frit flow stream and the sample stream of relatively low speed will merge smoothly. During this process, sample materials are expected to be pushed below the inlet splitting plane formed by the compressing effect of frit flow, as illustrated in Fig. 1b. Thus, sample relaxation is achieved hydrodynamically in the relaxation segment (under the inlet frit region), and the sample components are continuously carried to the separation segment where the separation of sample components takes place. System operation requires only a simple one-step injection procedure, with no need for valve switching or interruption of flow. This is far simpler and more convenient than the operation of the conventional relaxation techniques, such as stop-flow and focusing-relaxation procedures.

In the first experimental work on FIA-FlFF,[1] the system efficiency was studied by examining the effect of the ratio of injection flow rate to frit flow rate on hydrodynamic relaxation; the initial tests showed a possibility f using hydrodynamic relaxation in asymmetrical flow FFF with a number of polystyrene latex standards, in both normal and steric/hyperlayer modes of FFF. Normally, relaxational band broadening under hydrodynamic relaxation arises from a broadened starting band. The length of an

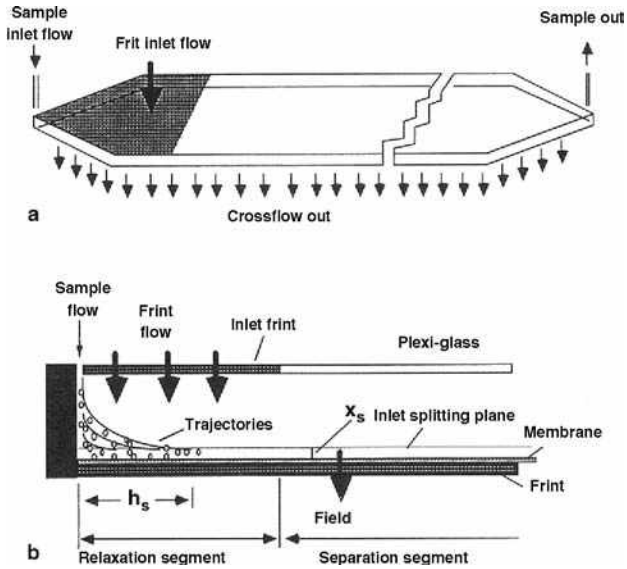

Fig. 1 Schematic view of an FIA-FIFFF channel.

initial sample band during hydrodynamic relaxation is dependent on flow rates as

$$h_s = \frac{\dot{V}_s}{\dot{V}_f}\frac{\dot{V}}{\dot{V}_c}L \tag{1}$$

where L is the channel length; $\dot{V}_s$, $\dot{V}_f$, $\dot{V}$, and $\dot{V}_c$ represent the flow rates of the sample stream, frit stream, effective channel flow, and cross-flow, respectively. Eq. 1 suggests that a small ratio of sample flow rate to frit flow rate, with a combined high cross-flow rate, is preferable in reducing h_s, leading to minimized relaxational band broadening.

Experimentally, the optimum ratio of V_s/V_f has been found to be about 0.03–0.05 for the separation of latex beads and for proteins.

Retention in the separation segment of the FIA-FlFFF channel is expected to be equivalent to that observed in a conventional asymmetrical channel system, if complete hydrodynamic relaxation can be obtained. It will follow basic principles, as shown by the retention ratio, R, given by

$$R = \frac{t^0}{t_r} = 6\lambda\left[\coth\left(\frac{1}{2\lambda} - 2\lambda\right)\right]\left(\text{where } \lambda = \frac{D}{w^2}\frac{V^0}{\dot{V}_c}\right) \tag{2}$$

where t^0 is the void time, t_r is the retention time, λ is the retention parameter, D is the diffusion coefficient, w is the channel thickness, and V^0 is the channel void volume. The void time in an FIA-FlFFF channel system is complicated to calculate, because sample flow and frit flow enter the channel simultaneously, and part of the merged flow exits through the accumulation wall. For this reason, channel flow velocity varies along the axial direction of channel. By considering these, the determination of void time can be represented as

$$t^0 = \frac{V^0 A_f/A_c}{\dot{V}_f - \dot{V}_c A_f/A_c}\ln\left(\frac{\dot{V}_s + \dot{V}_f - \dot{V}_c A_f/A_c}{\dot{V}_s}\right) + \frac{\dot{V}^0}{\dot{V}_c}\ln\left(\frac{\dot{V}_s + \dot{V}_f - \dot{V}_c A_f/A_c}{\dot{V}_{\text{out}}}\right) \tag{3}$$

where $\dot{V}_{\text{out}}$ is the channel outflow rate and A_f and A_c are the area of the inlet frit and the accumulation wall, respectively. Eq. 3 represents the void time calculation in terms of volumetric flow rate and channel dimensions only; it is valid for any channel geometry, such as rectangular, trapezoidal, and even exponential design. Retention in FIA-FlFFF has been shown to follow the general principles of FFF with the confirmation of experimental work. It has also been found that the trapezoidal channel design provides a better resolving power for the separation of protein mixtures than a rectangular channel in FIA-FlFFF.

REFERENCES

1. Moon, M.H.; Kwon, H.S.; Park, I. Stopless flow injection in asymmetrical flow field-flow fractionation using a frit inlet. Anal. Chem. **1997**, *69*, 1436.
2. Moon, M.H.; Kwon, H.S.; Park, I. Stopless separation of proteins by frit-inlet asymmetrical flow field-flow fractionation. J. Liquid Chromatogr. Relat. Technol. **1997**, *20* (16–17), 2803.
3. Moon, M.H.; Stephen Williams, P.; Kwon, H.S. Retention and efficiency in frit-inlet asymmetrical flow field-flow fractionation. Anal. Chem. **1999**, *71*, 2657.
4. Litzén, A.; Wahlund, K.-G. Zone broadening and dilution in rectangular and trapezoidal asymmetrical flow field-flow fractionation channels. Anal. Chem. **1991**, *63*, 1001.
5. Litzén, A. Separation speed, retention, and dispersion in asymmetrical flow field-flow fractionation as functions of channel dimensions and flow rates. Anal. Chem. **1993**, *65*, 461.
6. Giddings, J.C. Optimized field-flow fractionation system based on dual stream splitters. Anal. Chem. **1985**, *57*, 945.

Fipronil Residue in Water

Silvia H.G. Brondi
Embrapa Livestock Southeast, São Carlos, Brazil

Fernanda C. Spoljaric
Chemical Institute of São Carlos, University of São Paulo, São Carlos, Brazil

Fernando M. Lanças
Institute of Chemistry of São Carlos (USP), University of São Paulo, São Carlos, Brazil

INTRODUCTION

The present work consists of a comparative study of three different extraction techniques—specifically, liquid–liquid extraction (LLE), solid-phase extraction (SPE), and supercritical fluid extraction (SFE)—for the trace analysis of fipronil insecticide in water samples. The extracted fipronil was analyzed via high-resolution gas chromatography using electron capture detection (HRGC–ECD). The extraction methods presented linear calibration all over the investigated concentration range (0.1–1.0 μg/L). The limit of detection (LOD) was determined at 0.1 μg/L concentration level, and precision, measured by the relative standard deviations (RSD), was 7.7% for LLE, 7.8% for SPE, and 0.5% for SFE.

FIPRONIL RESIDUES IN WATER

The principal application of pesticides is related to food crops, but even given the extensive use of pesticides, about one-third of the world's total crops yield is destroyed by pests and weeds during growth, harvesting, and storage.[1] Although these pesticides are considered essential for agricultural development, some of them can cause serious ambient contamination.[2–4]

Fipronil is a highly effective, broad-spectrum insecticide with potential value for the control of a wide range of crop, public hygiene, amenity, and veterinary pests.[5] It belongs to a relatively new insecticide class, the phenylpirazoles. It was discovered in 1987 by Rhône-Poulenc researchers in Ongar, England,[6] and exhibits a mode of action that differs from traditional organophosphate, carbamate, and pyrethroid insecticides. Fipronil acts by blocking the GABA-gated chlorine channels of neurons in the central nervous system.

In recent years, there has been much discussion about the toxicity of fipronil. It is classified as a World Health Organization (WHO) class II moderately hazardous pesticide.[7] Fipronil is a relatively new insecticide that has not been used long enough to evaluate the risk; it may be dangerous to human health.[5]

Because of the rigorous limits for water purity, methods for extraction and preconcentration of pesticides present in water have become necessary. For these purposes, LLE, SPE, and SFE were used in this work.

Liquid–liquid extraction is a simple and convenient technique used to separate organic compounds from solutions or aqueous suspensions where they are present. Although LLE is often considered the conventional extraction method, it presents disadvantages because it consumes large volumes of organic solvents, which are expensive and represent a danger to health and the environment.[4]

Solid phase extraction is used in the analysis of both polar and non-polar analytes, where the matrix and the analyte of interest are usually dissolved in a liquid. It is applied to pesticide analysis in water samples because this is an easy and fast process.[8] According to Font et al.[9] the recovery of pesticides from water samples through SPE depends on the type of water, pH, and treatment of the sorbent.

Comparing LLE with SPE, Majors[10] concluded that SPE presents advantages because it reduces the consumption of solvents, has fewer steps, is less laborious and more efficient, and prevents emulsions.

Supercritical fluid extraction is a newer technique that is also used in the extraction of pesticide residues, presenting advantages in relation to other techniques, including economy of samples, solvents, reagents, and time. It also usually presents a larger recovery in the analysis of real samples.[11] Levy[12] claims that not much literature is available regarding organic pollutant supercritical fluid extraction in the aqueous matrix due to the mechanical difficulty of retaining the liquid and polar matrix in the extraction cell. Carbon dioxide has been the most widely used solvent due to its mild critical conditions, high volatility, low viscosity, high diffusivity, low cost,[13] and other favorable properties.

This entry describes the development and validation of analytical methodologies using LLE, SPE, and SFE,

followed by gas chromatography with electron capture detection analysis for the determination of fipronil residue in water.

EXPERIMENTAL

Chemicals

The fipronil standard, more than 99% pure, was obtained from Chem Service (West Chester, Pennsylvania, U.S.A.). The fipronil standard solution was prepared in ethyl acetate. Mallinckrodt (Phillipsburg, New Jersey, U.S.A.) supplied all the nanograde solvents for pesticide-residue analyses. Several adsorbents—such as octadecyl silane (35–75 mesh, Supelco), chromossorb (100–120 mesh, Johns Manville), florisil (100–200 mesh, Riedel), silica gel 60 (70–230 mesh, Merck), and XAD-7 (20–60 mesh, Rohm and Haas)—were tested as sorbents in the SPE cartridges. Different modifiers (hexane, acetone, methanol), various temperature (50, 60°C), and pressure conditions (120, 250, and 300 atm) were tested for supercritical fluid extraction. The water was purified with a Millipore Milli Q Plus System (Bedford, Massachusetts, U.S.A.).

Extraction

For all three extraction methods investigated—specifically, LLE, SPE, and SFE—100 ml of water purified in a Milli-Q system (Millipore, Eschborn, Germany) was enriched with the analytical standards mixture at 0.1 mg/L concentration level.

The best results obtained through each extraction method are described below. In LLE, 60 ml of dichlomethane was used to remove analytes from the aqueous matrix. In SPE, 1.0 g of C_{18} (octadecyl silane) sorbent was used as solid support, and ethyl acetate was used for both phase condition and compound elution. In SFE, the C_{18} phase was used as support for the sample and CO_2 in a supercritical state modified with acetone in the compound extraction at 60°C, while a pressure of 300 atm was used as the mobile phase.

GC–ECD ANALYSIS

The extracts analyses were performed using a HP 5890 series II gas chromatograph equipped with a Ni^{63} electron capture detector (Palo Alto, California, U.S.A.) and a Croma-5 coated with 0.25 mm film of cross-linked 5% phenyl methyl polysiloxane stationary phase, 30 m × 0.25 mm I.D. (Croma, São Carlos, São Paulo State, Brazil). A volume of 1 μl was injected under the following temperature conditions: injector at 250°C and detector 300°C. The initial oven temperature was settled at 140°C, programmed at 4°C/min to 270°C for 1 min. The split ratio was 1:20.

RESULTS AND DISCUSSION

Few analytical methods have been reported for the determination of fipronil residues.[6] Fig. 1 presents the fipronil insecticide chromatogram obtained by gas chromatography with electron capture detection, prepared in ethyl acetate at 0.1 mg/L concentration.

The three extraction techniques evaluated—LLE, SPE, and SFE—are appropriate for fipronil analysis in water samples. The recovery results obtained using LLE, SPE, and SFE were in the 98.0–102.8% range. Table 1 presents the recovery and RSD values obtained when LLE, SPE, and SFE were applied. These results are consistent with the acceptable range.[14,15] The extraction methods presented linear calibration at the investigated concentration range (0.1–1.0 μg/L) with correlation coefficient (r) higher than 0.99.

Due to the high amount of solvents used, LLE presents some drawbacks: costly solvent fees, environmental contamination, and work safety conditions due to

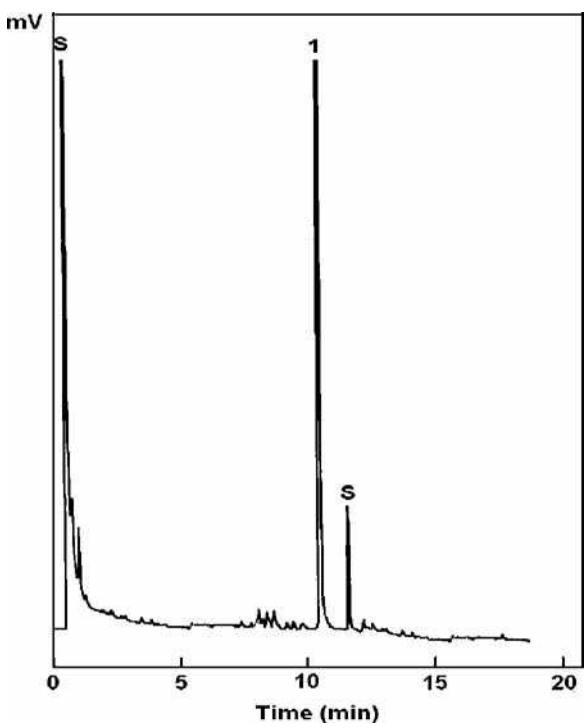

Fig. 1 Chromatogram of fipronil pesticide obtained by gas chromatography/electron capture detector at 0.1 mg/L concentration. S = ethyl acetate solvent; 1 = fipronil.

Table 1 Extraction recovery (%) and corresponding relative standard deviation (RSD) obtained through liquid–liquid extraction (LLE), solid phase extraction (SPE), and supercritical fluid extraction (SFE) in water samples enriched with 0.1 mg/L of fipronil pesticide.

	Recovery (%)±RSD (%)		
Pesticide	**LLE**	**SPE**	**SFE**
Fipronil	102.8 ± 7.7	102.1 ± 7.8	98.0 ± 0.5

the manipulation of organic solvents.[16,17] Solid phase extraction has some advantages over the conventional extraction techniques, such as LLE: simplicity, quick extraction, purer extracts, freedom from interference, lower operational cost, selective extraction, and small volume consumption of high-purity solvents. It also allows extraction and sampling in the field for later transport and storage.[10] The results obtained in our research group, which substituted SFE for other pesticide extractions in different matrices, presented excellent recovery results, besides sample, solvent, reagent, and time-saving advantages.[1,18]

Although the data showed that the three extraction methods were able to isolate the fipronil residue from water samples, the best results were obtained by using SPE and SFE, which are faster and cheaper, making them more useful techniques for the analysis of fipronil in drinking water.

The LOD was calculated by multiplying the average value of the noise sampled at the retention time of each analyte by 3,[19] and the limit of quantification was ten times the average value of the noise in this same region.[20] The detection limit found was 0.1 μg/L, and the quantification limit was 0.3 μg/L. It is possible to determine fipronil residues in water at a concentration similar to the European Union maximum admissible, 0.1 μg/L.[21]

CONCLUSION

The three extraction techniques evaluated—LLE, SPE, and SFE—are adequate for fipronil residue analysis in water samples, with good recovery results. Solid-phase extraction and SFE are the preferred techniques, as they are more sensitive and faster. Another advantage of these techniques is that they reduce the consumption of organic solvents associated with risks to health and the environment, as well as the high costs of their use and discard. However, as fipronil is a relatively new insecticide, it has not been in use long enough for researchers to evaluate the risk it may pose to human health.

ACKNOWLEDGMENT

The authors are grateful to FAPESP (São Paulo State Research Foundation) for the financial support given to this research.

REFERENCES

1. Lanças, F.M.; Barbirato, M.A.; Galhiane, M.S.; Rissato, S.R. Off-line SFE–CZE analysis of carbamate residues. Chromatographia **1996**, *42*, 547–550.
2. Knutsson, M.; Nilvé, G.; Mathiasson, L.; Jonson, J.A. Supported liquid membranes for sampling and sample preparation of pesticides in water. J. Chromatogr. A, **1996**, *754*, 197–205.
3. Hogendoorn, E.A.; Hoogerbrugge, R.; Baumann, R.A.; Meiring, H.D.; de Jong, M.P.I.M.; van Zoonen, P. Screening and analysis of polar pesticides in environmental monitoring programmes by coupled-column liquid chromatography and gas chromatography–mass spectrometry. J. Chromatogr. A, **1996**, *754*, 49–60.
4. Hatrík, S.; Tekel, J. Extraction methodology and chromatography for the determination of residual pesticides in water. J. Chromatogr. A, **1996**, *733*, 217–233.
5. Tingle, C.C.; Rother, J.A.; Dewhurst, C.F.; Lauer, S.; King, W.J. Fipronil: environmental fate, ecotoxicology, and human health concerns. Rev. Environ. Contam. Toxicol. **2003**, *176*, 1–66.
6. Madsen, J.E.; Sandstrom, M.W.; Zaugg, S.D. Methods of analysis by the U.S. Geological Survey National Water Quality Laboratory—a method supplement for the determination of fipronil and degradates in water by gas chromatography/mass spectrometry. U.S. Geological Survey Open-File Report 02-462, Method ID: O-1126-02; 2003.
7. AccuStandard. *Pesticides and Their Metabolites*. Available at: www.accustandard.com (accesed January 2006).
8. Albanis, T.A.; Hela, D.G. Multi-residue pesticide analysis in environmental water samples using solid-phase extraction discs and gas chromatography with flame thermionic and mass-selective detection. J. Chromatogr. A, **1995**, *707*, 283–292.
9. Font, G.; Manes, J.; Moltó, J.C.; Picó, Y. Solid-phase extraction in multiresidue pesticide analysis of water. J. Chromatogr. **1995**, *642*, 135–161.
10. Majors, R.E. A review of modern solid-phase extraction. LC–GC. **1998**, *8*, 15–22.
11. Lanças, F.M.; Galhiane, M.S.; Barbirato, M.A. Supercritical fluid extraction of oxadixyl from food crops. Chromatographia **1994**, *39*, 11–14.
12. Levy, J.M. Supercritical fluid extraction of phenoxy acids from water. J. High Resolut. Chromatogr. **1995**, *18*, 446–448.
13. O'Keeffe, M.J.; O'Keeffe, M.; Glennon, J.D.; Lightfield, A.; Maxwell, R.J. Supercritical fluid extraction of clenbuterol from bovine liver tissue. Analyst **1998**, *12*, 2711–2714.

14. Garp, A. *Validation of Analytical Methodologies for Determination of Pesticides Residues (Roteiro para Validação de Metodologia Analítica Visando a Determinação de Resíduos de Pesticidas)*; Ministry of Agriculture: Brasília, Brazil, 1997.
15. Gou, J.; Tragas, C.; Lord, H.; Pawliszyn, J. On-line coupling of in-tube solid phase microextraction (SPME) to HPLC for analysis of carbamates in water samples: Comparison of two commercially available autosamplers. J. Microcolumn Sep. **2000**, *12*, 125–134.
16. Barrionuevo, W.R.; Lanças, F.M. Comparison of liquid–liquid extraction (LLE), solid-phase extraction (SPE), and solid-phase microextraction (SPME) for pyrethroid pesticides analysis from enriched river water. Bull. Environ. Contam. Toxicol. **2002**, *69*, 123–128.
17. Moret, S.; Conte, L.S. Polycyclic aromatic hydrocarbons in edible fats and oils: Occurrence and analytical methods. J. Chromatogr. A, **2000**, *882*, 245–252.
18. Lanças, F.M.; Galhiane, M.S.; Rissato, S.R.; Barbirato, M.A. Effect of temperature, collection mode and modifier on the supercritical CO_2 extraction of dicofol residues from fish samples. J. High Resol. Chromatogr. **1997**, *20*, 369–374.
19. Leite, F. *Validation Procedures in Chemical Analysis (Validação em Análise Química)*; Editora Átomo Ltda: Campinas, Brazil, 1996; 64.
20. Chasin, A.A.M.; Nascimento, E.S.; Ribeiro-Neto, L.M.; et al. Validation of analytical methodologies for toxicological analysis (validação de métodos em análises toxicológicas: uma abordagem geral). Rev. Bras. Toxicol. **1998**, *11*, 1–6.
21. Mol, H.G.J.; Janssen, H.G.M.; Cramers, C.A.; Vreuls, J.J.; Brinkman, U.A.T. Trace-level analysis of micropollutants in aqueous samples using gas-chromatography with online sample enrichment and large-volume injection. J. Chromatogr. A, **1995**, *703*, 277–307.

Flame Ionization Detector for GC

Raymond P.W. Scott
Scientific Detectors Ltd., Banbury, Oxfordshire, U.K.

INTRODUCTION

The flame ionization detector (FID) is, by far, the most commonly used detector in GC and is probably the most important. It is a little uncertain as to who was the first to invent the FID; some gave the credit to Harley, Nel, and Pretorius,[1] others to McWilliams and Dewer.[2] In any event, it would appear that both contenders developed the device at about the same time, and independently of one another; the controversy had more patent significance than historical interest. The FID is an extension of the flame thermocouple detector and is physically very similar, the fundamentally important difference being that the ions produced in the flame are measured, as opposed to the heat generated.

DISCUSSION

The principle of detection is as follows. Hydrogen is mixed with the column eluent and burned at a small jet. Surrounding the flame is a cylindrical electrode and a relatively high voltage is applied between the jet and the electrode to collect the ions that are formed in the flame. The resulting current is amplified by a high-impedance amplifier and the output fed to a data acquisition system or a potentiometric recorder.

A detailed diagram of the FID sensor is shown in Fig. 1. The body and the cylindrical electrode is usually made of stainless steel and stainless-steel fittings connect the detector to the appropriate gas supplies. The jet and the electrodes are insulated from the main body of the sensor with appropriate high-temperature insulators. Some care must be taken in selecting appropriate insulators as many glasses (with the exception of fused quartz) and some ceramic materials become conducting at high temperatures (200–300°C).[3]

As a result of the relatively high voltages used in conjunction with the very small ionic currents being measured, all connections to the jet or electrode must be well insulated and electrically screened. In addition, the screening and insulating materials must be stable at the elevated temperature of the detector oven. In order to accommodate the high temperatures that exist at the jet tip, the jet is usually constructed of a metal that is not easily oxidized, such as stainless steel, platinum, or platinum–rhodium. The detector electronics consist of a high-voltage power supply and a high-impedance amplifier. The jet and electrode can be connected to the power supply and amplifier in basically two configurations. The floating jet configuration is the most commonly used and in this arrangement, + 250 to + 400 V is applied to the cylindrical electrodes and the jet is connected to a ground by a very high resistance. The signal developed across the resistance is amplified, modified, and passed to a recorder of the data acquisition system. In the second alternative, the jet is grounded and the high-voltage power supply is electrically floated. Then, + 250 to + 400 V is applied to the cylindrical electrodes and the negative terminal of the power supply is connected to a ground by a very high resistance. The signal that is developed across the resistance is again amplified, modified, and passed to a recorder of the data acquisition system.

RESPONSE MECHANISM OF THE FID

The FID has a very wide dynamic range, has a high sensitivity, and, with the exception of about half a dozen low-molecular-weight compounds, will detect all substances that contain carbon. The response mechanism of the FID has been carefully investigated by a number workers. It was originally thought that the ionization mechanism in the FID flame is similar to the ionization process in a hydrocarbon flame, but it quickly became apparent that ionization in the hydrogen flame is many times higher than could be accounted for by thermal ionization alone. It would appear that the ionization potentials of organic materials become much lower when they enter the flame.

The generally accepted explanation of this effect is that the ions are not formed by thermal ionization but by thermal emission from small carbon particles that are formed during the combustion process. Consequently, the dominating factor in the ionization of organic material is not their ionization potential but the work function of the carbon that is transiently formed during their combustion. The flame plasma contains both positive ions and electrons which are collected on either the jet or the plate, depending on the polarity of the applied voltage. Initially, the current increases with applied voltage, the magnitude of which depend on the electrode spacing. The current continues to increase with the applied voltage and eventually reaches a plateau at which the current remains sensibly constant. The voltage at which this plateau is reached also depends on the electrode distances.

As soon as the electron–ion pair is produced, recombination starts to take place. The longer the ions take to reach the electrode and be collected, the more the recombination

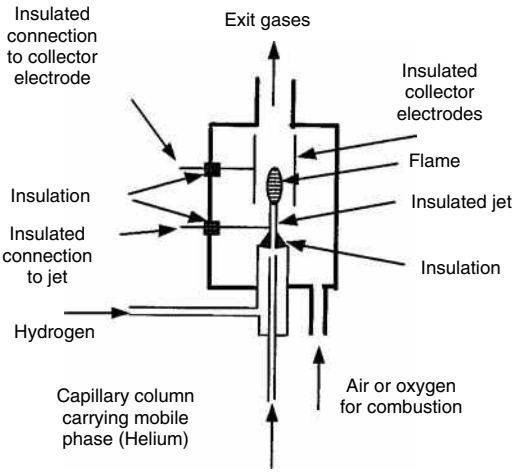

Fig. 1 The FID sensor.

takes place. Thus, the greater the distance between the electrodes and the lower the voltage, the greater the recombination. As a result, initially the current increases with the applied voltage and then eventually flattens out, and at this point, it would appear that all the ion–electron pairs were being collected. In practice, the applied voltage would be adjusted to suit the electrode geometry and ensure that the detector operates under conditions where all electrons and ions are collected.

It was also shown that the airflow should be at least six times that of the hydrogen flow for stable conditions and complete combustion. The base current from the hydrogen flow depends strongly on the purity of the hydrogen. Traces of hydrocarbons significantly increase the base current, as would be expected. Consequently, very pure hydrogen should be employed with the FID if maximum sensitivity is required. Employing purified hydrogen, Desty et al., reported a base current of 1.45×10^{-12} A for a hydrogen flow of 20 ml/min. This was equivalent to 1×10^{-7} C/mol. The sensitivity reported for *n*-heptane, assuming a noise level equivalent to the base current from hydrogen of $\sim 2 \times 10^{-14}$ A (a fairly generous assumption), was 5×10^{-12} g/ml at a flow rate of 20 ml/min. It follows that although the sensitivity is amazingly high, the ionization efficiency is still very small ($\sim$0.0015%). The general response of the FID to substances of different type varies very significantly from one to another. For a given homologous series, the response appears to increase linearly with carbon number, but there is a large difference in response between different homologous series (e.g., hydrocarbons and alcohols).

The linear dynamic range of the FID covers at least four to five orders of magnitude for $0.98 < r < 1.02$. This is a remarkably wide range that also helps explain the popularity of the detector. Examination of the different commercially available detectors shows considerable difference in electrode geometry and operating electrode voltages, yet they all have very similar performance specifications.

OPERATION OF THE FID

The FID is one of the simplest and most reliable detectors to operate. Generally, the appropriate flow rates for the different gases are given in the detector manual. The hydrogen flow usually ranges between 20 and 30 ml/min and the airflow is about six times that of the hydrogen flow (e.g., 120–200 ml/min. The column flow that can be tolerated is usually about 20–25 ml/min, depending on the chosen hydrogen flow. However, if a capillary column is used, the flow rate may be less than 1 ml/min for very small-diameter columns. The mobile phase can be any inert gas—helium, nitrogen, argon, and so forth. To some extent, the detector is self-cleaning and rarely becomes fouled. However, this depends a little on the substances being analyzed. If silane derivatives are continuously injected on the column, then silica is deposited both on the jet and on the electrodes and may need to be regularly cleaned. In a similar way, the regular analysis of phosphate-containing compounds may eventually contaminate the electrode system. Electrode cleaning is best carried out by the qualified instrument service engineer.

Apparently, the sole disadvantage of the FID as a general detector is that it normally requires three separate gas supplies, together with their precision flow regulators. The need for three gas supplies is a decided inconvenience but is readily tolerated in order to take advantage of the many other attributes of the FID. The detector is normally thermostatted in a separate oven; this is not because the response of the FID is particularly temperature sensitive but to ensure that no solutes condense in the connecting tubes.

The FID has an extremely wide field of application and is used in the analysis of hydrocarbons, solvents, essential oils, flavors, drugs, and their metabolites—in fact, any mixture of volatile substances that contain carbon.

REFERENCES

1. Harley, J.; Nel, W.; Pretorius, V. Flame ionization detector for gas chromatography. Nature **1958**, *181*, 177.
2. McWilliams, I.G.; Dewer, R.A. In *Gas Chromatography 1958*; Desty, D.H., Ed.; Butterworths: London, 1957; 142.
3. Beres, S.A.; Halfmann, C.D.; Katz, E.D.; Scott, R.P.W. A new type of argon ionisation detector. Analyst **1987**, *112*, 91.

BIBLIOGRAPHY

1. Scott, R.P.W. *Chromatographic Detectors*; Marcel Dekker, Inc.: New York, 1996.
2. Scott, R.P.W. *Introduction to Analytical Gas Chromatography*; Marcel Dekker, Inc.: New York, 1998.

Flash Chromatography

Mark Moskovitz
Gary Witman
Dynamic Adsorbents, Inc., Atlanta, Georgia, U.S.A.

Abstract
Flash chromatography offers an affordable, simple, fast, and convenient solution for the purification of synthetic and natural organic compounds from crude mixtures. It plays a critical role in the purification of natural plant alkaloids. Due to modularity of design and ease of use flash has become the scale-up process in the purification of products initially isolated using thin-layer chromatography (TLC) chemistry. Prepackaged flash columns are offered with more than 30 different phase chemistries having corresponding TLC plates. Using either isocratic or gradient elution techniques with flash chromatography it is possible to separate out a desired compound(s) on a single run.

INTRODUCTION

It has been 30 years since Still, Kahn, and Mitra published their seminal article.[1] This short, elegant paper established the separation technique that has eventually evolved into flash chromatography. In the subsequent three decades, dramatic advances in the life sciences have placed increasing demands on the separation sciences. These have been especially prominent in producing enhanced methods for the purification of synthetic and natural organic compounds. For many separation demands, there has been no advancement since this original paper.

Initially developed at Columbia University, flash chromatography is "an air pressure driven hybrid of medium pressure and short column chromatography which has been optimized for particularly rapid separations."[1] The resolution is measured in terms of the ratio of retention time (r) to peak width (w, $w/2$). It is measured by baseline resolution in the valley between the peaks and the distance from peak to peak. Sample size can be increased dramatically if less resolution is required. This innovative work by the Columbia University team demonstrated that column performance was quite sensitive to the rate of elution, and the best performance was accomplished with relatively high eluent flow rates.

Initially, flash chromatography was performed as a manual operation using self-packed glass columns. As the technology evolved, this chromatographic process became increasingly automated and simple in design. Self-packed glass columns have been replaced with disposable prepackaged cartridge columns that are modular in design and capable of withstanding high pressures and corrosive eluent agents. Furthermore, these prepackaged flash columns have translucent casings. The casings allow organic synthesis chemists to determine when the column is equilibrated, and when it has dried at the conclusion of the run.

Fig. 1 shows an example of commercially prepacked flash cartridges.

In addition, cartridge columns provide high-purity fractions, consistent flow rates from column to column, and reproducible results. They are simple to use and can be replaced in as little time as 20 min. Solvent waste is minimized as chemists are able to visually confirm when the equilibration occurs. Vendors now provide columns packed with 10–60 μm diameter irregular or spherical packings with more than 30 different phase chemistries that have corresponding thin-layer chromatographic (TLC) plates. This allows for method development and purity checks to be performed during flash chromatography experiments. Compressed air-driven pumps can now deliver solvent at flow rates of liters per minute with high-pressure capability. Furthermore, stationary-phase silica packing is now complemented and is increasingly being replaced by superior adsorbent materials such as alumina.

Flash chromatography can be employed to separate many crude mixtures, such as peptides and natural plant compounds, to high-purity levels. Subsequently, costly analytical high-performance liquid chromatography (HPLC) separation methods can easily be converted to flash purification methods. The selection of the proper flash system and cartridges can simplify the process, saving the chromatographer valuable time and significant amounts of money.

Fig. 2 shows an example of a flash chromatography system.

Eluents can be sampled using isocratic, step gradient, or linear gradient elution methods for up to dozens of segments. For complex mixtures of components that exhibit a broad range of retentivity, as in the isolation of natural product extracts, the use of gradient elution allows the separation of the whole sample in a single run.[2] When compounds are well resolved by TLC, isocratic separation

Fig. 1 Examples of typical flash chromatography cartridges.

is usually sufficient to achieve separation. More complex or poorly resolved samples may require gradient elution. In this situation, the stronger solvent concentration is increased during the sample purification. Elution mode can also effect separation.

THEORY/METHODOLOGY

In preparative chromatography, it is essential to remove the mobile phase from the collected fraction. Therefore, to simplify separations, all eluent components, including buffers, should be volatile. Best separations are achievable if one can inject a large amount of sample dissolved in a relatively small volume of mobile phase. The critical properties of the solvents are the viscosity of the concentration sample solution in the mobile phase and the elution strength of the sample solvent compared to the mobile phase.[3] Ultimately, the goal is to select a phase system having sufficient sample solubility. This will determine the possible column loading, the performance, the throughput of the system, and the concentration of the collected fractions.

Properties of the flash system that need to be addressed include selecting eluents allowing for high loading capacity, using air-driven pumps with enhanced performance, and selecting the right sorbent media to get the highest concentration of the selected fractions.

One fundamental principle in dealing with flash chromatography is to assure that separation purification is first achieved using TLC. By doing so, the mobile and separation media, as well as elution techniques desired for scale-up, are tested first on a smaller scale. Using similar materials, it is possible to then scale up from TLC to preparative or industrial scale purification. The same stationary-phase (sorbent) packing material, such as silica gel or alumina, can be provided by vendors, such as Dynamic Adsorbents, Inc., Georgia, United States, and is used for both TLC and flash chromatography. This consistency in sorbent packing media assures identical chromatographic selectivity. The scaling-up process is easier if the packing material is the same, or at least from the same batch or manufacturing process, as that used in the TLC analytical and preparative scales.[4] TLC retention factor (R_f) values correlate directly with the separation on a column. TLC R_f is inversely proportional to flash cartridge retention, which is also measured in column volumes.

Preparative flash chromatography methods can be achieved in as little time as 2–3 days. To optimize separation conditions, dozens of TLC evaluations can be simultaneously run in small beakers. This is achieved by having a different solvent system in each beaker. Each TLC

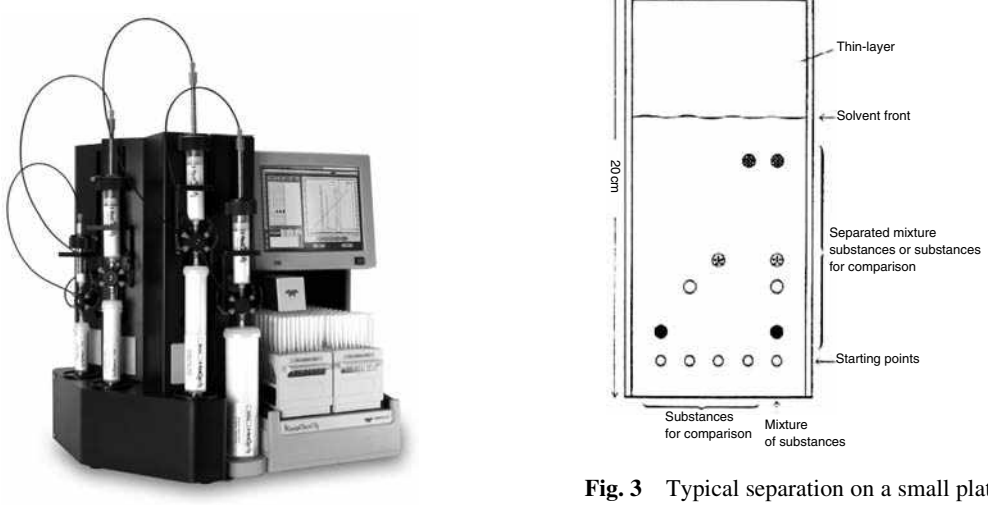

Fig. 2 Example of a flash chromatography system.

Fig. 3 Typical separation on a small plate.
Source: From Column Chromatography with Dynamic Adsorbents, Inc. 2nd Ed.[5]

system requires 10 min or less to run. Through this technique it is possible to optimize the developing solvent system. This can be accomplished by using a Vario chamber enabling simultaneous, side-by-side development, with six different solvents on the same TLC plate. Developing a pilot scale purification process requires 2–5 hr of TLC, and 2–4 hr of laboratory work to confirm a small-scale cartridge (Fig. 3).

Without TLC plates, method development for the separation and purification of compounds consists of running small-scale analytical or small-scale flash chromatography. Once mobile and stationary phases for optimal sample purification are identified, the full sample batch is purified by using preparative flash techniques. Prerequisites for a successful method transfer include the need for similar sorbents, identical composition of the mobile phase, and adherence to reproducible chromatographic conditions in TLC and preparative chromatography.[6] Manufacturers of media have addressed the demands of end users and have provided products with defined pore structure, chemical purity, as well as specific pore volume and surface characteristics. The contemporary selectivity of TLC media as flash grade alumina or silica gel media is basically identical. As resolution decreases with increasing particle size, there is a trend in flash chromatography toward using smaller particle size material and increasing pump pressure to quickly drive the eluent through the stationary phase.

Pilot scale manufacturing may require hundreds of grams of material. Flash chromatography provides the means to purify large volumes of material. Columns typically use 40–60 μm diameter silica or alumina particles. They permit high flow rates and effective separations with modest system pressures in the range of 40–100 psi. Through the use of these larger particles and radial compression technology, it is possible to achieve excellent separation at a fraction of the cost of HPLC systems.

The goals of preparative flash chromatography are to produce a highly concentrated fraction, to collect and transfer the fraction without contamination, and to perform the separation as quickly and cheaply as possible (Fig. 4).[7]

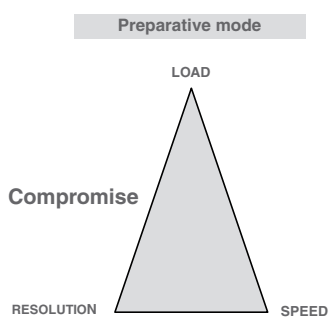

Fig. 4 Preparative mode compromise.

When the column dimensions are changed to optimize a separation, or to scale a separation to be preparative or narrow bore, the mobile-phase flow rate is adjusted in proportion to the cross sectional area of the column. This then maintains consistent linear velocity and retention times.

$$\text{Flow rate}_{\text{final}} = \frac{(D_{final})^2}{(D_{initial})^2} \quad (1)$$

When scaling up run times on a preparative column from small-scale analytic testing, a simple procedure is followed:

$$\text{Run time (prep)} = \text{Run time (analytical)} \times \frac{\text{Column length (analytical)}}{\text{Column length (preparative)}} \quad (2)$$

To retain the same end product resolution while increasing the column diameter, the gradient shape must be maintained by keeping constant the ratio of the gradient volume to the column volume.

SCALE-UP UTILITY OF FLASH CHROMATOGRAPHY

Among the factors affecting the purification efficiency of flash chromatography are sample homogeneity and sample concentration. When the compound and reaction by-products are highly diluted or dissolved in an overly polar solvent, the compound peak broadens, leading to loss of resolution. Simply put, volume overloading causes significant band broadening that degrades sample resolution.

Because small-diameter narrow particle range adsorbents are more expensive to manufacture, there is a cost advantage for using larger-diameter materials in preparative columns. There are also other advantages to using larger particle sizes. For example, when the column overload increases, the sample band widths start to increase and the column plate number becomes more a function of sample size than of the column conditions. As a result, it is often advantageous to use larger particles. Larger particles have higher loadability, cause lower back pressure, and therefore increase flow rate while decreasing elution time.[8]

Oftentimes, the objective of preparative flash separations may be different from the objective of analytical separations. Speed and sensitivity may be less important than product purity in preparative chromatography. Preparative columns may operate at flow rates lower than in analytic columns with gradient profiles altered in order to compensate for the less efficient mass transfer of larger adsorbent particles.

There is a major advantage in the use of alumina oxide (alumina) over silica gel ($SiO_2 \times H_2O$) for flash

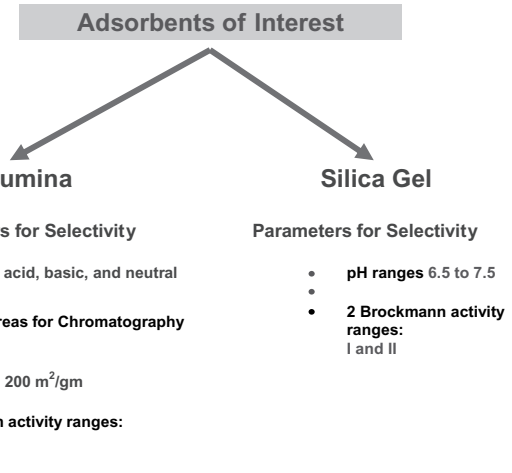

Fig. 5 Graph shows advantages of alumina over silica.

chromatography purification applications (Fig. 5). Owing to its amphoteric character, alumina oxides can be used in specifically defined pH ranges.

Using flash grade silica, or alumina with a high-purity clean particle size distribution, is essential. The particle size distribution of the silica or alumina flash product of 32–63 μm or 230–400 mesh is the favored industry average. This ensures a more uniform adsorbent-packed column or cartridge, providing superior resolution and separation.

The importance of the clean particle size distribution varies depending on the type of chromatography being performed. In medium pressure liquid chromatography (MPLC), it is very important that silica or alumina particles of a very clean particle distribution be used (no fines and no large particles). Separation chemists need to remember that not all 40–63 μm silica gels are the same. Additionally, it is also very important to use an alumina or silica gel containing as little metal contamination as possible as demonstrated by Dynamic Adsorbents, Inc., media.

In flash chromatography, one requires an adsorbent with a much higher percentage of particles between 32

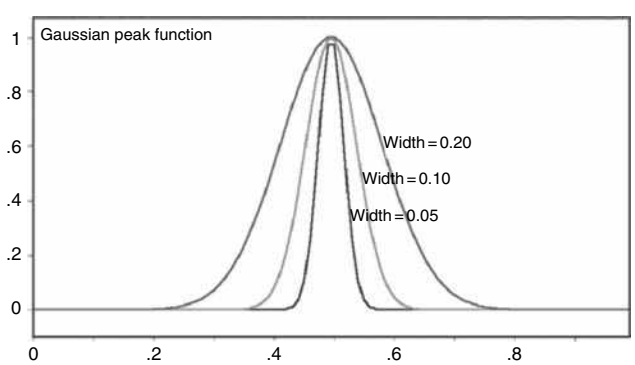

Fig. 6 An example of ideal Gaussian curves.

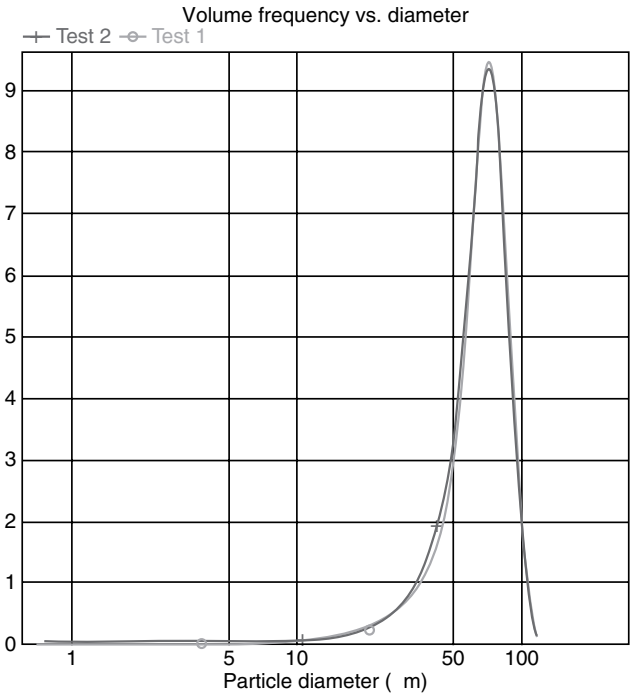

Fig. 7 Typical Micromeritics saturn instrument scan for illustrating and determining particle size distribution.

and 63 μm and a very low level of small particles, or fines, below 32 μm. Fines increase backpressure, which may result in clogging—a complication of the separation process that is particularly dangerous when using glass columns. Fines can also pass through filters and contaminate the final product, therefore rendering the final product useless. Using a sorbent containing fewer fines provides a more regular, stable, and reproducible chromatography bed. This achieves a faster, more even flow rate that yields superior separations.

An adsorbent having 90% particles on average would be the ideal range. The connection between particle size distribution and column performance is important. When the range in particle size is broad, column packing becomes uneven. Furthermore, some regions may be mainly composed of large particles where the solvent will flow quickly, meeting very little resistance. In a similar situation, there are other regions composed primarily of smaller particles causing uneven flow characteristics secondary to more solvent resistance. The solvent will take the path of least resistance through the column and flow around the pockets of small particles and not straight through the column. This uneven flow greatly affects the separation as the peaks will have different retention times depending on the flow path when the solvent emerges from the column. When the sample exits the column, compounds will give peaks that are broad and poorly separated (Fig. 6).

Table 1 Functionalized silica gel.

Functionalization	Suitable solvent
Amine (most organic compounds)	Hexane, ethyl acetate, methylene chloride, chloroform, methanol, ethanol, isopropranol, water, acetonitrile
Cyano (most organic compounds)	Hexanes, ethyl acetate, methylene chloride, chloroform, methanol, ethanol, isopropanol, water, acetonitrile
C-2, C-8, C-18	Methanol, ethanol, isopropanol, water, acetonitrile, etc.
Fluoro-tagged (separate organic compounds from fluorinated compounds and separation of fluorinated compounds by degrees). Fluorous silica gel may be used in the purification of peptides, oligonucleotides, and oligosaccharides. The orthogonal nature of this purification enables desired oligomers to separate from truncations and deletion sequences.	Methanol, water. This is a two-step separation. Fluorous molecules are selectively retained on the stationary phase while non-fluorous molecules are not. The fluorous component is eluted with a fluorophilic solvent, without the need for buffers or fluorinated solvents.

Uneven solvent flow will give broad peaks that are poorly separated from other components.

A more even particle distribution provides a narrower Gaussian peak and purer compounds (Fig. 7).

APPLICATION

Flash chromatography is playing a leading role in the purification of natural plant alkaloids. These are increasingly being looked upon as the major source for pharmaceutical agents. In areas such as antineoplastic and anti-infective agents, natural products are the dominant source of successful new bioactive compounds.[9,10] Among the estimated 420,000 plant species on Earth, less than 10% have been phytochemically investigated. Within each plant species lay multiple metabolites that still need to be screened as pharmaceutical agents.[11] The following are purified using alumina oxide as an adsorbent in flash chromatography processes:

Alkaloids—basic, medium activity isolation of ergo, opium, rauwolfia, and other alkaloids
Antibiotics—neutral isolation, purification
Essential oils—basic, neutral removal of terpenes
Plant extraction—basic, neutral, acid isolation of active substances
Degradation of organic solvents—basic, highly active
Enzymes—neutral purification
Glycosides—neutral isolation of digitalis, strophanthus glycosides
Lipids—non-polar lipids, glycolipids, and phospholipids
Removal of peroxides—basic, highly active from organic solvents
Hormones—neutral isolation and purification of ketosteroids from neutral materials
Purification of organic solvents—basic, highly active for technical purposes
Oils—basic clarification of fatty oils, separation of fatty acids

A cardinal reason for using alumina, rather than silica gel as the sorbent for purifying organic compounds, is that natural compounds contain amines or nitrogen-containing heterocyclic structures. The amphoteric property of alumina is the chemical mechanism for superior separation of natural products containing alkaloids. These are cyclic organic compounds in a negative oxidation state.

Silica gel can be used in either normal- or reversed-phase conditions. Normal-phase silica is slightly acidic and has some acid-sensitive compounds that will break down when using silica for separation/purification. Compounds that have an acidic or basic moiety may streak or tail with normal or reversed-phase silica. This may occur when interacting with residual surface silanol groups on normal-phase chromatographic support. This interaction between functional groups and the silanol groups causes peak streaking and tailing, which then leads to a deterioration in chromatographic purification. For acidic and basic organic compounds, it is recommended that alumina oxide be used as the adsorbent agent.

An option for using silica gel as the sorbent for purifying acidic or basic compounds would be to add a mobile-phase modifier. This process reduces peak tailing and sharpens peaks. However, when using modifiers (such as triethylamine or ammonium hydroxide for basic compound separations), the added modifier remains after evaporation of the volatile solvents such as dichloromethane and methanol. Removal of the modifier then requires the additional steps of extraction, or washing, with a suitable solvent. Additionally, this may also be achieved by concentrating the mixture down to an oil. In practice, using alumina as the sorbent provides a far simpler solution and a much cleaner product. Silica gel is commercially functionalized in C-2, C-8, C-18, amine, cyano, diol, fluoro-tagged products, and many others (Table 1).

When reusing a functionalized silica column, it is recommended to always flush the column with the highest polarity solvent that was used in the previous separation or purification. Subsequently, purge the column with air following flushing. Purging with air, and keeping the column in a desiccator when not in usage, increases the life expectancy of the column.

CONCLUSION

Advances in media, eluent materials, and air-driven pumps allow today's chromatographer to achieve the defined goals of preparative flash chromatography. Highly concentrated fractions are collected and transferred without contamination. Flash separations are performed quickly and as cheaply as possible. The need for more costly preparative HPLC has now been eliminated in many settings.

REFERENCES

1. Still, W.C.; Kahn, M.; Mitra, A. Rapid chromatographic technique for preparative separations with moderate resolution. J. Org. Chem. **1978**, *43*, 2923–2925.
2. Crietier, G.; Rocca, J.L. Gradient Elution in preparative reversed phase liquid chromatography. J. Chromatogr. A, **1994**, *658*, 195–205.
3. Porsch, B. Some specific problems in the practice of preparative high performance liquid chromatography. J. Chromatogr. A, **1994**, *658*, 179–194.
4. Majors, R.E. Developments in preparative scale chromatography. LC–GC Europe **2004**, *17* (12), 630–638.
5. Moskovitz, M. Column Chromatography with Dynamic Adsorbents, Inc., 2nd Ed., 2007.
6. Reuke, S.; Hauck, H.E. Thin layer chromatography as a pilot technique for HPLC demonstrated for pesticide samples. Fresenius J. Anal. Chem. **1995**, *351*, 739–744.
7. Guiochon, G.; Katti, A. Preparative liquid chromatography. Chromatographia **1987**, *24*, 165–189.
8. Snyder, L.R.; Kirkaland, J.J.; Glajch, J.L. *Practical HPLC Method Development*, 2nd Ed.; John Wiley & Sons: New York, 1997.
9. Baker, D.D.; Alvi, K.A. Small-molecule natural products: New structures, new activities. Curr. Opin. Biotechnol. **2004**, *15* (6), 576–583.
10. Newman, D.J.; Cragg, G.M.; Snader, K.M. Natural products as sources of new drugs over the period 1981–2002. J. Nat. Prod. **2003**, *66*, 1022–1037.
11. Hostettmann, K.; Potterat, O.; Wolfender, J.L. The potential of higher plants as a source of new drugs. Chemia **1998**, *4*, 10–17.

Flash Chromatography: TLC for Method Development and Purity Testing of Fractions

Joseph Sherma
Department of Chemistry, Lafayette College, Easton, Pennsylvania, U.S.A.

INTRODUCTION

Flash chromatography (FC) is a type of preparative column liquid chromatography (LC) that was first described in 1978. As traditionally performed in most laboratories today, and taught in college organic chemistry laboratory courses, sorbent (usually ~40–60 micron diameter silica gel, 60 Å pore size) is manually dry packed into a glass tube (e.g., 10–20 cm length and 10–50 mm I.D.) fitted with a stopcock at the bottom. Sample is applied (after filtration if necessary) on to the top of the column, a relatively non-polar eluent (mobile phase) is forced through using a vacuum manifold, air pressure, or a low-pressure (<100 psi) pump, and fractions of effluent are collected (~ every 0.5 column volume) and analyzed. The volume of eluent, flow rate, sample load, and fraction size are determined by the size of the column; in general, longer columns give better resolution and wider columns higher sample loading. Sample sizes separated by FC are typically at milligram to gram levels, but scale up to 10s or even 100s of grams is possible. FC is faster than traditional column purification using gravity flow and larger silica gel particles; it is less efficient and has lower separation power when compared with analytical column high-performance liquid chromatography (HPLC), but higher sample amounts can be purified.

Modern online FC systems have made the method faster, safer, and more flexible and reproducible by incorporating reusable plastic cartridges prepacked with the sorbent and other features such as eluent (isocratic or gradient) pumped at a high rate by a medium pressure pump, ultraviolet (UV) detection, computer software control, and automated fraction collection (Figs. 1 and 2 show typical modern FC systems). These systems are applied in sample cleanup, natural products purification, organic synthesis, combinatorial chemistry, drug discovery, pharmaceutical intermediate purification, and many other areas. Normal phase (NP) FC of polar compounds on silica gel columns is still the most widely used mode, but reversed phase (RP; e.g., C_{18} octadecyl silane), celite, ion exchange, and other types of sorbents are becoming used more frequently. This entry will focus only on NP-FC.

THIN-LAYER CHROMATOGRAPHY AS A PILOT METHOD FOR FC

Isocratic Elution FC

Thin-layer chromatography (TLC) of the sample mixture is most often used to predict the optimum isocratic eluent composition in traditional and modern FC. For rapid elution and separation, the TLC mobile phase should provide an R_f value of 0.15–0.35 for the component of interest, and the difference in R_f values (delta-R_f) should be 0.15 or greater between components to be separated. R_f is defined as the distance traveled by the compound zone divided by the distance traveled by the mobile phase front.

In terms of column volumes (CVs), the ideal FC mobile phase elutes the desired component in 3–6 CVs and will separate two components if their CVs differ by 1 or more. A CV is defined as the volume of solvent filling the sorbent pores and spaces between particles in a column of any dimensions, and it is related to R_f by the equation $CV = 1/R_f$. As examples, an R_f of 0.90 indicates that 1.1 CV will be required to elute the compound from the column, R_f 0.50 requires 2.0 CV, and R_f 0.10 requires 10 CV.

When adjusting mobile phases to meet the R_f and delta-R_f or CV and delta-CV requirements, it should be remembered that when using NP silica gel, mobile-phase strength and component mobility increase when the solvent composition becomes stronger (more polar) [e.g., hexane–ethyl acetate (9:1, v/v) replaced by (8:2, v/v)], and selectivity is changed by using a different solvent combination that maintains a similar, favorable retention [e.g., hexane–dichloromethane (1:2) instead of hexane–ethyl acetate (1:1)]. Table 1 gives solvent strength values that allow calculation of mobile phases with similar strengths but different selectivities that may improve resolution using the equation:

$$\begin{aligned}\text{Solvent strength} = {} & (\text{solvent A}\% \\ & \times \text{solvent A strength})/100 \\ & + (\text{solvent B}\% \\ & \times \text{solvent B strength})/100.\end{aligned}$$

Fig. 1 VersaFlash high throughput flash purification (HTFP) system shown with two stacked prepacked 40 × 75 mm (51 g) cartridges inserted in the support stand and 110 × 300 mm (1.35 kg), 80 × 150 mm (410 g), and 23 × 110 mm (23 g) cartridges on the right side of the eluent pump. The 3-way valve injector at the upper right allows direct application of sample onto cartridges using a syringe. The outlet tubing can be used for manual sample collection or connection to an automated fraction collector or UV detector.
Source: Photograph supplied by Supelco, Bellefonte, Pennsylvania.

Table 1 Solvent strength values of different solvents used to prepare TLC mobile phases and FC eluents.

Solvent	Strength
Methanol	0.95
Ethanol	0.88
2-Propanol	0.82
Acetonitrile	0.65
Ethyl acetate	0.58
Tetrahydrofuran	0.57
Acetone	0.56
Dichloromethane	0.42
Chloroform	0.40
Diethyl ether	0.38
Toluene	0.29
Hexane	0.01
Heptane	0.01
Iso-octane	0.01

With this equation, it is found that hexane–ethyl acetate (50:50) has a solvent strength of 0.30, hexane–ethyl acetate (60:40) is 0.24, and hexane–dichloromethane (30:70) is 0.30. A greater TLC separation will lead to a greater difference in CV values and allow more samples to be applied to the column. For example, if impurity A is separated from the compound of interest (target compound) B with respective R_f values of 0.55 (1.8 CV) and 0.40

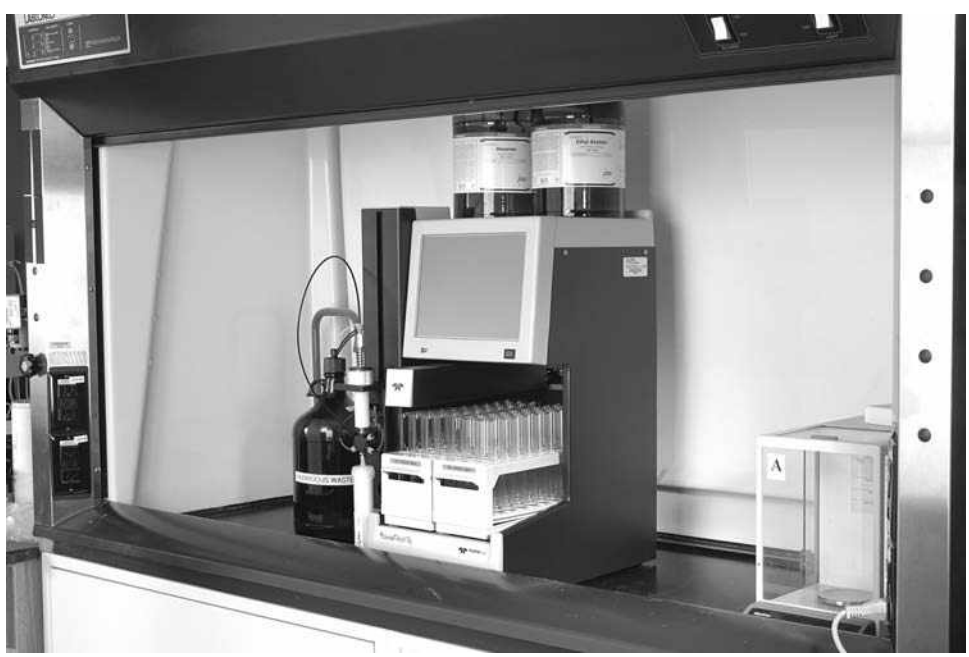

Fig. 2 CombiFlash R_f automated FC instrument, which features a PC touchscreen controller with PeakTrack software, linear and/or step gradients, 4–330 g column sizes, two fraction collection racks each holding seventy 18 × 150 mm tubes, six-position motor powered sample loading valve, and UV variable dual-wavelength detector.
Source: Photograph supplied by Teledyne Isco, Inc., Lincoln, Nebraska.

(2.5 CV), delta-CV is 0.7 and only a small amount of sample can be purified before overload and loss of resolution occurs. Both R_f values are outside the optimal 0.15–0.35 range. If a weaker mobile phase can be used giving separation within the optimal range with respective R_f values of 0.35 (2.9 CV) and 0.20 (5.0 CV), the delta-CV is 2.1 and a greater than five-fold sample load increase is potentially possible.

For the best transfer of TLC results to FC, the sorbents used in both methods should match as closely as possible (same manufacturer). Differences in the sorbents (e.g., moisture content, particle size, pore size, shape, TLC binding agents), as well as in the basic chromatographic processes (closed column compared with an open layer, mobile phase velocity, relative humidity) may cause the TLC conditions not to be directly transferable to FC and require application of a predetermined correction factor to the TLC results.

Traditional large volume glass TLC chambers (N-tanks) are usually used for development of 20×20 cm commercially precoated silica gel TLC plates with the mobile phase when scouting FC eluents. However, microscope slide size TLC plates (2.5×7.5 cm) developed in small-capped jars can be used if available with silica gel matching the FC column. For faster method development, the Uniflash (Hologent Technologies, Inc., Baldwin Park, California, U.S.A.) Planar Station horizontal chamber allows four different mobile phases to be evaluated simultaneously on two microscope slide plates precoated with Merck silica gel 60 or their own UniFlash silica; other manufacturers offer different microscope slide plates that may transfer more directly to the FC column to be used. The Planar Station has a base with four separate wells each holding up to 1 ml of mobile phase, Teflon plate holder supporting two microscope slide TLC plates, and 0.5 in. thick glass cover that achieves vapor saturation of the individual mobile phases with the plate surface. Mobile phase is added to each well, the plate holder is placed in the plate loading position over the base, the plates are spotted with sample at both ends, and they are placed face down on the plate holder such that they contact the top edges of the mobile phase wicks. The cover plate is placed on the plate holder over the TLC plates, creating four separate sealed chambers. The plate holder/cover assembly is shifted to the development position over the base, causing the bottom edge of each wick to contact the respective mobile phase in the wells of the base. Mobile phase is drawn up to the plates to produce a total of four unique chromatograms. In examples of possible patterns of usage, the wells can be filled with mobile phases consisting of four different solvent combinations, or a single solvent pair with four different percentage compositions.

Sample solutions are generally applied to the origin line of the TLC plate using a micropipette. Separated zones that are naturally colored are detected by viewing in daylight, naturally fluorescent zones are detected in a viewing box under 254 or 366 nm UV light, and compounds that absorb 254 nm UV light are detected as dark zones on a bright green background on plates containing a fluorescent phosphor by viewing under 254 nm UV light (fluorescence quenching detection).

Gradient Elution FC

Step or continuous (linear) gradients may be required for FC separation of complex mixtures. For predicting step gradients, TLC is used to choose different solvent mixtures that elute each component with R_f 0.15–0.35, and the calculated number of CVs of each required for component elution is used for FC starting with the weakest (least polar). For linear gradients, TLC is used to find weak (all R_f values are low) and strong (all high R_f values) solvents, and an FC gradient is run from pure weak solvent to pure strong solvent.

Teledyne Isco, Inc., offers PeakTrak 2.0 software featuring an R_f to gradient calculator for use with their CombiFlash automated FC purification systems (Fig. 2). Only two thin layer developments of the crude reaction mixture with different mobile phases providing R_f values within the range of 0.2–0.8 are needed. The mobile-phase composition and corresponding R_f values are entered into the calculator, and the software gives a gradient profile specific to the sample for separation between the target compound and the nearest impurity. The linear gradient suggested may include an isocratic hold to provide greater sharpening and separation of the FC peaks of the two compounds, compared with fully isocratic or linear gradient separation. An auto scale-up feature is also included in the software.

ANALYSIS OF FC FRACTIONS

Collected FC fractions are analyzed by TLC to determine if the compound of interest is present and to determine its purity. The mobile phase should be reoptimized, if necessary, for separation of the compounds most likely to be present in each fraction. R_f values and detection characteristics of the compound zones separated from fractions are compared with those of standards (if available) developed on the same plate to aid identification of the zones. The ability to apply multiple standards and samples onto

one plate is an advantage in terms of speed and cost of analysis.

CONCLUSION

TLC is the most widely used technique for method development and determining the purity of fractions in FC. In this entry, it is shown how both isocratic and gradient eluents can be easily and rapidly optimized by TLC on layers corresponding to FC columns.

BIBLIOGRAPHY

1. Armarego, W.L.F.; Chai, C.L.L. *Purification of Laboratory Chemicals*; Elsevier: Amsterdam, The Netherlands, 2003; 21 pp.
2. Flash Chromatography-Method Development, at: www.merck.de/servlet/PB/show/1452390/Merck%20Flash%20Chromatography%20-%20Method%20Development.ppt (accessed August 2007)
3. Fried, B.; Sherma, J. *Thin Layer Chromatography,* 4th Ed.; Marcel Dekker, Inc.: New York, NY, 1999.
4. Introduction to Flash Chromatography, at: http://www.-labhut.com/education/flash/index.php (accessed August 2007)
5. Keese, R. *Practical Organic Synthesis—A Student's Guide*; John Wiley & Sons, Inc.: New York, NY, 2006; Chapter 5.
6. Purifying the First Hundred Grams, at: http://www.-biotage.com/Print.aspx?id=21990 (accessed August 2007)
7. Sherma, J. Flash chromatography. J. AOAC Intl. **2005,** *88*, 16A–22A.
8. Sherma, J., Fried, B., Eds.; *Handbook of Thin Layer Chromatography,* 3rd; Marcel Dekker, Inc.: New York, NY, 2003.
9. Solvent Strength Optimization, at: http://www.biotage.com/Print.aspx?id=21978 (accessed August 2007)
10. Talamona, A. *Laboratory Chromatography Guide*; Buchi Labortechnik AG: Flawil, Switzerland, 2007; 12–26.
11. Thomason, V. Optimized flash chromatography purification: From TLC to large scale in three steps. 2006, Teledyne Isco, Inc., P.O. Box 82531, Lincoln, NE 68501.

Flavonoids: CCC Separation

L.M. Yuan
Department of Chemistry, Yunnan Normal University, Kunming, China

INTRODUCTION

Various countercurrent chromatography (CCC) methods employ two-phase solvent systems for separation of flavonoids. $CHCl_3$: CH_3OH : H_2O (4 : x : 2, for which x is between 2.5 and 4 for different samples) may be used for their prefractionation. Two-phase solvent systems can be divided into four types: $CHCl_3$: CH_3OH : H_2O, $CHCl_3$: CH_3OH : *n*-BuOH :H_2O, EtOAc : PrOH : H_2O or BuOH : HOAc : H_2O, and *n*-C_6H_{14} : EtOAc : CH_3OH : H_2O, respectively. CCC fractionation permits the use of either stepwise elution or gradient elution, and analytical-scale CCC can also be carried out for separation of flavonoids.

FLAVONOIDS

Flavonoids are polyphenolic compounds and have a wide polarity range. Successful CCC depends on the appropriate choice of a solvent system. The partition of solutes between two immiscible solvent phases is an ideal method for the separation of flavonoids because the phenomenon of irreversible adsorption, tailing, sample loss, and denaturation, which plague analysts using other forms of liquid chromatography (LC), are avoided.

SEPARATION OF FLAVONOIDS BY CCC

Flavonoids are a specific class of polyphenols. It is generally believed that flavonoids include a wide variety of phenolic compounds, such as flavones, flavonols, flavanones, flavanonols, anthocyanidins, flavan-3,4-diols, xanthones, flavan-3-ols, isoflavones, isoflavanones, chalcones, dihydrochalcones, aurones, and homoisoflavones. Their separation poses special problems because there is often irreversible adsorption and even hydrolysis on solid supports.

The development of CCC began in the mid-1960s. Among various types of CCC modes for the separation of flavonoids, the main techniques are droplet countercurrent chromatography (DCCC), rotary locular countercurrent chromatography (RLCCC), and centrifuge partition chromatography (CPC). Today, the cartridge and multilayer coil CPC methods are the leading techniques.

The selection of a solvent system is the most important step in performing CCC. Selecting a solvent system for CCC means *simultaneously* choosing the column and the eluent. The chromatographic literature contains numerous examples of solvent systems used in various CCC systems for separation of flavonoids,[1–6] and consultation of these references may give some leads as to possible systems that would be useful for a particular separation. The selection of appropriate biphasic solvent systems also may be aided by thin-layer chromatography (TLC) or high-performance liquid chromatography (HPLC) experiments.

One quite remarkable comparative separation of flavonoids by DCCC, RLCC, and cartridge and multilayer coil CPC methods, with the same solvent system (chloroform–methanol–water, 33 : 40 : 27), is shown in Fig. 1.[7,8]

Elutions of the three peaks were similar and according to the order of increasing polarity: hesperetin, kaempferol, quercetin. The above peak effect can be seen in the various CCC methods, which have similar two-phase solvent systems, for the separation of flavonoids, but DCCC and RLCC require much more time than CPC.

A versatile two-phase solvent system for flavonoid prefractionation by high-speed CCC was introduced.[9] The

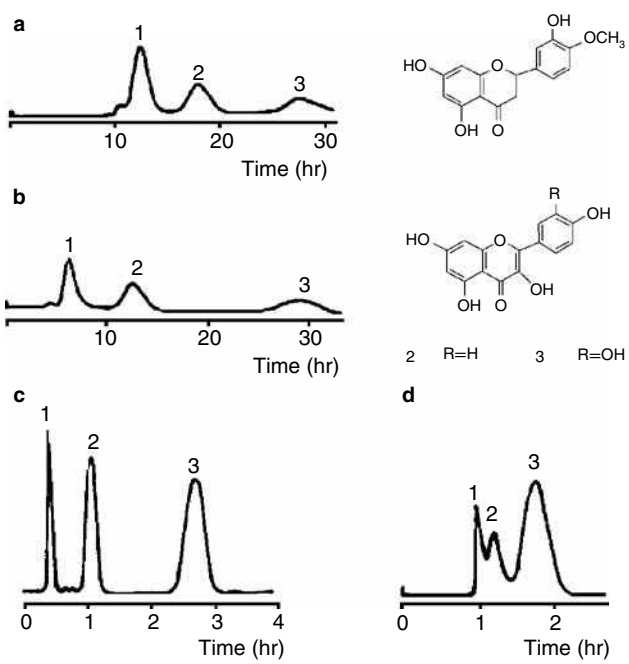

Fig. 1 Chromatograms of hesperetin (1), kaempferol (2), and quercetin (3) by different countercurrent chromatographic methods. Solvent system: chloroform–methanol–water (33 : 40 : 27). a, DCCC; b, RLCC; c, multilayer coil CPC system; and d, cartridge CPC system.
Source: Reprinted with permission from Elsevier Science.

Table 1 Separations of flavonoids by CCC.

Sample	Solvent system
Flavonoids	$CHCl_3$: CH_3OH : H_2O, 4 : 3 : 2
	$CHCl_3$: CH_3OH : H_2O, 7 : 13 : 8
	$CHCl_3$: CH_3OH : H_2O, 33 : 40 : 27
	$CHCl_3$: CH_3OH : H_2O, 5 : 6 : 4
Flavonol glycosides	$CHCl_3$: CH_3OH : H_2O, 7 : 13 : 8
Isoflavonol glycosides	$CHCl_3$: CH_3OH : H_2O, 7 : 13 : 8
Baccharis trimera	$CHCl_3$: CH_3OH : H_2O, 13 : 7 : 4
Orthosiphon spicatus	$CHCl_3$: CH_3OH : H_2O, 13 : 7 : 4
Epilobium parviflorum	$CHCl_3$: CH_3OH : H_2O, 7 : 13 : 8
Licorice	$CHCl_3$: CH_3OH : H_2O, 7 : 13 : 8
Sea buckthorn	$CHCl_3$: CH_3OH : H_2O, 4 : 3 : 2
Daphne genkwa sieb et zucc	$CHCl_3$: CH_3OH : H_2O, 4 : 3 : 2
Strychnos variabilis	$CHCl_3$: CH_3OH : H_2O, 5 : 6 : 4
Pericarpium citri reticulata	$CHCl_3$: CH_3OH : H_2O, 4 : 4 : 2
Radix puerariae	$CHCl_3$: CH_3OH : H_2O, 4 : 2.9 : 2
Radix glycyrrhizae	$CHCl_3$: CH_3OH : H_2O, 4 : 4 : 2
Radix scutellariae	$CHCl_3$: CH_3OH : H_2O, 4 : 3.8 : 2
Flos genkwa	$CHCl_3$: CH_3OH : H_2O, 4 : 3.6 : 2
Flavonoids	$CHCl_3$: CH_3OH : 5% HCl, 5 : 5 : 3
Flavonoid glycosides	$CHCl_3$: CH_3OH : *n*-BuOH : H_2O, 10 : 10 : 1 : 6
Flavonol glycosides	$CHCl_3$: CH_3OH : *n*-BuOH : H_2O, 7 : 6 : 3 : 4
	$CHCl_3$: CH_3OH : *n*-BuOH : H_2O, 10 : 10 : 1 : 6
Galipea trifoliata	$CHCl_3$: CH_3OH : *n*-BuOH : H_2O, 10 : 10 : 2 : 6
Arnica species	$CHCl_3$: CH_3OH : *n*-BuOH : H_2O, 10 : 10 : 1 : 6
Flavonol glycosides	$CHCl_3$: CH_3OH : *i*-PrOH : H_2O, 5 : 6 : 1 : 4
Bidens pilosa	$CHCl_3$: CH_3OH : *i*-PrOH : H_2O, 5 : 6 : 1 : 4
Picea abies	$CHCl_3$: CH_3OH : *i*-PrOH : H_2O, 5 : 6 : 1 : 4
Alangium premnifolium	$CHCl_3$: CH_3OH : *i*-PrOH : H_2O, 9 : 12 : 2 : 8
G. biloba	$CHCl_3$: CH_3OH : PrOH : H_2O, 5 : 6 : 1 : 4
Vaccinium uliginosum	$CHCl_3$: CH_3OH : PrOH : 5% HOAc, 31.2 : 37.5 : 6.25 : 25
Oxytropis ochrocephala	$CHCl_3$: CH_3OH : EtOH : H_2O, 2 : 5 : 8 : 5
Tephrosia vogelii	$CHCl_3$: CH_3OH : EtOH : H_2O, 7 : 3 : 3 : 4
Flavonoid glycosides	EtOA : PrOH : H_2O, 4 : 2 : 7
Arnica montana	EtOA : PrOH : H_2O, 4 : 2 : 7
Stryphnodendron adstringens	EtOA : PrOH : H_2O, 35 : 2 : 2
Anthocyanidins	EtOA : PrOH : H_2O, 140 : 8 : 80
Flavonoid glycosides	EtOA : BuOH : H_2O, 2 : 1 : 2
Crossopteryx febrifuga	EtOA : BuOH : H_2O, 2 : 1 : 2
	EtOA : EtOH : H_2O, 2 : 1 : 2
Tephrosia vogelii	EtOA : 94% EtOH : H_2O, 2 : 1 : 2
Flavonoid glycosides	BuOH : HOAc : H_2O, 4 : 1 : 5
Anthocyanidins glycosides	BuOH : HOAc : H_2O, 4 : 1 : 5
Sambucus nigra	BuOH : HOAc : H_2O, 4 : 1 : 5

(Continued)

Table 1 Separations of flavonoids by CCC. *(Continued)*

Sample	Solvent system
Pavetta owariensis	BuOH : PrOH : H_2O, 4 : 1 : 5
Arnica species	CH_2Cl_2 : PrOH : H_2O, 7 : 13 : 8
Biflavonoids	*n*-C_6H_{14} : EtOAc : CH_3OH : H_2O, 2 : 8 : 5 : 5
Brackenridgea zanguebarica anthocyanidins	*n*-C_6H_{14} : EtOAc : CH_3OH : H_2O, 8 : 8 : 6 : 6 *n*-C_6H_{14} : EtOAc : CH_3OH : H_2O, 8 : 6 : 7 : 10 *n*-C_6H_{14} : EtOAc : BuOH : HAc : 1% HCl, 2 : 1 : 3 : 1 : 5
Gradient elution	
G. biloba	EtOAc → EtOAc-*i*-BuOH, 6 : 4
Esenbeckia pumila	Et_2O → EtOAc-PrOH-H_2O (10 : 1 : 2) → EtOAc-PrOH-H_2O (4 : 1 : 2)

flavonoid compounds encompass a wide polarity range and exhibit good solubility in methanol. The two-phase solvent system composed of $CHCl_3$:CH_3OH : H_2O = 4 : *x* : 2, in which *x* was between 2.5 and 4 for different samples, was selected for the separation of crude flavonoid extracts because this solvent system contains methanol and provides nearly equal volumes of the upper and lower phases with reasonably short settling times. Changing the ratio of methanol in the solvent system permitted changing, simultaneously, the selectivity of the upper and lower phases, as methanol can dissolve in chloroform and water and may change the polarity of the two phases.

The previous applications of CCC are summarized in Table 1. One may use this table to search for suitable solvent systems that have been previously used for similar compounds.

In Table 1, the various two-phase solvent systems are divided into four types. It has been shown that the solvent system chloroform–methanol–water has been used for the greatest number of applications. $CHCl_3$: CH_3OH : H_2O is a versatile CCC solvent system for flavonoid separations as well.

The second most used two-phase solvent system is $CHCl_3$: CH_3OH : *n*-BuOH (*i*-PrOH or PrOH) : H_2O. It is similar to $CHCl_3$: CH_3OH : H_2O, but CH_3OH is partially replaced by BuOH, *i*-PrOH, or PrOH. The desirable *K* value may be obtained by varying the ratios.

The third most used type of two-phase solvent system is EtOAc : PrOH (BuOH or EtOH) : H_2O or BuOH : HOAc (or PrOH) : H_2O. It is a more polar solvent system and is useful for the separation of flavonoid glycosides.

The final type of solvent system is *n*-C_6H_{14} : EtOAc : CH_3OH : H_2O. Sometimes CH_3OH also may be substituted by other solvents such as BuOH. It is a slightly more hydrophobic solvent system than $CHCl_3$: CH_3OH : H_2O.

Analogous to HPLC, CCC fractionation permits the use of either stepwise elution or gradient elution, provided that some precautions are taken. For example, in the isolation of extracts of *Ginkgo biloba*, one starts with water as a stationary phase, eluting with ethyl acetate with increasing amounts of *i*-butanol and finally reaching the 6 : 4 proportion of ethyl acetate : *i*-butanol at the end of the elution.[10]

Samples ranging in size from microgram to gram quantities can be separated with the range of available instruments. Analytical-scale CCC also was carried out for the separation of flavonoids.[11]

CONCLUSIONS

The application of CCC to the separation of flavonoids has been proven to be very successful. Chloroform–methanol–water can be chosen as starting point and, by modifying the relative proportions of methanol or by replacing methanol with other solvents, it is possible finally to obtain the required distribution of sample components between the two phases. EtOA : PrOH : H_2O and *n*-C_6H_{14} : EtOAc : CH_3OH : H_2O also are very useful solvent systems. The technique is versatile and can be employed for the initial fractionation of crude extracts for the separation of closely related flavonoids and/or the isolation of pure products.

ACKNOWLEDGMENT

This work is supported by the National Natural Science Foundation, Yunnan Province Natural Science Foundation, and TRAPOYT of China.

REFERENCES

1. Ito, Y. High-speed countercurrent chromatography. Crit. Rev. Anal. Chem. **1986**, *17*, 65–143.
2. Marston, A.; Slacanin, I.; Hostettmann, K. Centrifugal partition chromatography in the separation of natural products. Phytochem. Anal. **1990**, *1*, 3–17.
3. Marston, A.; Hostettmann, K. Counter-current chromatography as a preparative tool—applications and perspectives. J. Chromatogr. A, **1994**, *658*, 315–341.

4. Yuan, L.M.; Fu, R.N.; Zhang, T.Y. Separation of bioactive components from medicinal plants by high-speed countercurrent chromatography. Chin. J. Med. Anal. **1998**, *18* (1), 60–64.
5. Hostettmann, K.; Hostettmann, M.; Marston, A. Countercurrent chromatography. In *Preparative Chromatography Techniques*; Springer-Verlag: Berlin, 1986; 80–126.
6. Ito, Y.; Conway, W.D. High-speed countercurrent chromatography of natural products. In *High-Speed Countercurrent Chromatography*; Wiley-Interscience: New York, 1996; 189–251.
7. Slacanin, I.; Marston, A.; Hostettmann, K. Modifications to a high-speed counter-current chromatograph for improved separation capability. J. Chromatogr. **1989**, *482*, 234–239.
8. Marston, A.; Borel, C.; Hostettmann, K. Separation of natural products by centrifugal partition chromatography. J. Chromatogr. **1988**, *450*, 91–99.
9. Yuan, L.M.; Ai, P.; Chen, X.X.; Zi, M.; Wu, P.; Li, Z.Y.; Chen, Y.G. Versatile two-phase solvent system for flavonoid prefractionation by high-speed countercurrent chromatography. J. Liq. Chromatogr. Relat. Technol. **2002**, *25* (5), 10.
10. Vonhaelen, M.; Vanhaelen-Fastre, R. Counter-current chromatography for isolation of flavonol glycosides from *Ginkgo biloba* leaves. J. Liq. Chromatogr. **1988**, *11*, 2969–2975.
11. Zhang, T.Y.; Xiao, R.; Xiao, Z.Y.; Pannell, L.K.; Ito, Y. Rapid separation of flavonoids by analytical high-speed countercurrent chromatography. J. Chromatogr. **1988**, *445*, 199–206.

Flavonoids: HPLC Analysis

Marina Stefova
Trajce Stafilov
Institute of Chemistry, Faculty of Science, Sts. Cyril and Methodius University, Skopje, Republic of Macedonia

Svetlana Kulevanova
Institute of Pharmacognosy, Faculty of Pharmacy, Sts. Cyril and Methodius University, Skopje, Republic of Macedonia

INTRODUCTION

Flavonoids are widely spread plant secondary metabolites called C_6–C_3–C_6 phenolics, which are classified in three groups, depending on the nature of the C_3 fragment and the type of the heterocyclic ring, as follows: 1) chromone derivatives (flavones, flavonols, flavanones, and flavanonols); 2) chromane derivatives (catechines and antocyanidines); and 3) flavonoids with open propane chain (chalcones) and with a furane ring (aurones). From all of these, flavones, flavonols, and flavanones are the most abundant in the plant kingdom and their skeleton is given in Fig. 1. Substitution in the positions 3, 5, 6, 7, 8, 2′, 3′, 4′, 5′, and 6′ gives all the compounds from these groups, with hydroxylation, methoxylation, and glycosylation being the most common substitution. Thousands of various flavonoids with various substitution patterns are recognized today as *free* flavones, flavonols, and flavanones, i.e., *aglycones*, and as *flavonoid glycosides*, which consist of flavonoid, non-sugar component *aglycone*, connected to the *sugar moiety* (mostly monosaccharides and disaccharides). Bonding to sugars makes flavonoids soluble in water and enables their easy transport within plants.

Flavonoids are a well-defined group of compounds with established physical and chemical characteristics. This especially counts for their absorption of ultraviolet (UV) radiation, which makes their UV spectra very characteristic and UV spectroscopy a method of choice for their characterization.[1] Two main absorption bands are observed: 1) band I (300–380 nm) due to absorption of ring B; and 2) band II (240–280 nm) due to absorption of ring A. The position of these bands gives information about the kind of the flavonoid and its substitution pattern; thus UV spectroscopy is used as a main method for the identification and the quantification of flavonoids for decades.

There are several published information regarding the isolation and the identification of flavonoids in plant material using different methods, mainly chromatographic and spectroscopic. Today, high-performance liquid chromatography (HPLC) is established as the most convenient method which enables separation and identification of flavonoids using various detection systems.[2–4] As for the quantitative analysis, much data have been published in the last few years confirming the suitability of this technique for simultaneous determination of flavonoid compounds in various samples, which gives an insight into the distribution of flavonoids in the studied material. HPLC methods are developed for qualitative and quantitative analyses of flavonoids in fruits and beverages, wine, honey, propolis, and, especially, in various plant materials[5–14] using different detection systems, from which UV diode array detectors are settled as the most suitable for these compounds and the most accessible as well.

EXPERIMENTATION

Stationary Phases

HPLC is the method of choice for the separation of complex mixtures containing non-volatile compounds such as various flavonoids in extracts prepared from different samples. A survey of literatures revealed that most researchers have used C_{18}-reversed stationary phases, which proved to be superior to the normal phase technique. The reversed phases are suitable for separating flavonoids in a wide range of polarities, as Vande Casteele et al.[15] have demonstrated the separation of 141 flavonoids from polar triglycosides to relatively non-polar polymetoxylated aglycones belonging to the classes of flavones, flavonols, flavanones, dihydroflavonols, chalcones, and dihydrochalcones.

The use of normal phase silica columns was also described but after acetylation of the flavonoids and then isocratic elution on silica gel.[16] Polystyrene divinylbenzene as a stationary phase was also found to give satisfactory separation and good peak shapes without using acidic

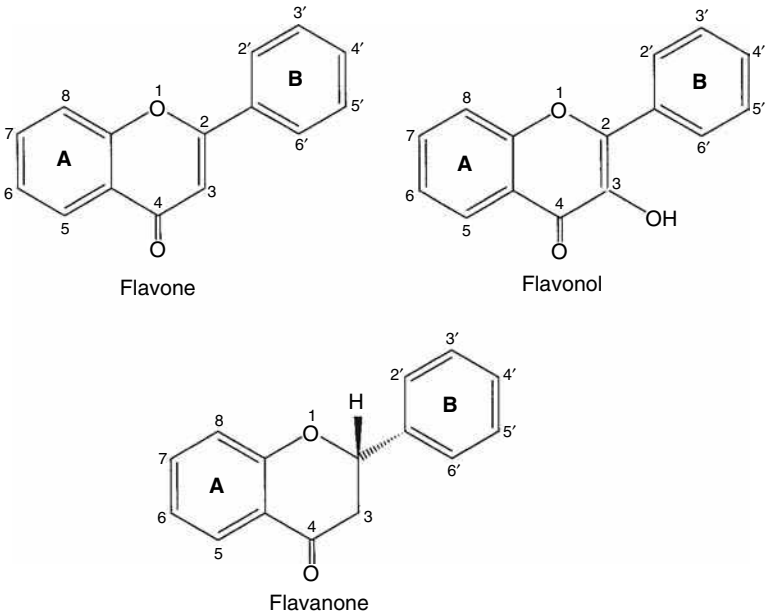

Fig. 1 Structure of flavone, flavonol, and flavanone.

mobile phases,[17] which are not so favorable for use with reversed phases.

The choice of a column involves matching the class of flavonoids to be separated to the characteristics of the stationary phase capable of providing satisfactory retention, selectivity, and peak shapes. As for the dimensions, the most popular are 150 and 250 mm long, with 5 μm particle size, although phases with 3 μm particles are becoming more popular because of better efficiency and less solvent consumption. The use of guard columns is recommended in order to extend their lifetime by protecting the analytical column from impurities in the samples prepared from various natural products.

Mobile Phases

The preferred solvent system used for the separation of flavonoids on reversed-phase stationary phases is methanol–water, followed closely by acetonitrile–water. Usually, acetic or formic acid is added (sometimes phosphoric acid, potassium dihydrogen phosphate, ammonium dihydrogen phosphate, and perchloric acid), which enables improved separation and prevention of peak tailing with respect to the phenolic character of the flavonoids. Ion pairing has also been used for improving the separation of neutral glycosides from flavonol sulfates.[4]

Often, gradient elution with a linear gradient, combined with isocratic steps, usually gives the best separation of flavonoids, differing in the degree of saturation, hydroxylation, methylation, and/or glycosylation. Optimization of the elution program is usually performed by changing the elution program until a satisfactory resolution and analysis time is achieved, depending on the analysis purpose, i.e., qualitative or quantitative analysis.

Detection Systems

Identification of flavonoids separated by HPLC is commonly performed by comparing the obtained retention times with the ones of authentic samples as well as by analysis of their characteristics collected by the detector.

Detection of flavonoids separated by HPLC can be performed using several detection systems. Photodiode array detectors (DADs) are the most convenient for use because of their availability and easy maintenance, and mainly because of the valuable information for the identification of flavonoids contained in their UV [or ultraviolet–visible (UV–Vis)] spectra. The sophisticated software packages enable storage of all the spectra obtained during the elution process, which can later be analyzed and compared to the spectra from a library previously prepared from authentic samples of flavonoids. An experienced analyst working on flavonoids can recognize the peaks from flavonoids in the chromatogram from the spectra, which are, as previously mentioned, very characteristic, although they are not enough for identification. As for the quantitative analysis, scanning over a wide wavelength range enables measuring all the components at wavelengths of their absorption maxima, which provides maximum sensitivity.

Fluorescence detectors have also been employed for flavonoid determination, offering higher sensitivity and selectivity, as suggested by the results in the analysis of

3′,4′,5′-trimethoxyflavone, which has been determined by excitation at 330 nm and by detection at 440 nm.[18]

Overcoming the difficulty in introducing the liquid sample into the mass spectrometer in the last decade enabled their use for HPLC detection, even in routine practical applications. The atmospheric pressure chemical ionization, thermospray, and electrospray ionization systems have proved to be most convenient for flavonoid analysis by HPLC/MS.[18,19] Mass spectrometry is a more specific and extremely selective detection technique, although it is not enough for structure elucidation (it reveals the structural fragments that are present, but not the exact substitution pattern). It offers the molecular weight of the molecular ion, which helps the tentative identification of the flavonoid. The use of HPLC/MS/MS gives additional information about the characteristic fragmentation pattern—"fingerprint" of the substance, which is very useful for qualitative and quantitative analyses in complex matrices. An excellent illustration of the use of HPLC/MS for the identification of flavonoids is presented in the work of Huck et al.,[19] who have isolated and characterized polymethoxylated flavones from *Primulae veris flos* using HPLC/ESI/MS. The six detected flavonoid compounds were found to be mono-, di-, tri-, and pentametoxyflavones, but their exact substitution pattern could not be revealed, except for 3′,4′,5′-trimetoxyflavone, for which ^{13}C NMR spectral data were available.

As regards the sensitivity of the MS detection in HPLC analysis of flavonoids, this technique has proved to be the most sensitive as compared to UV and fluorescence detection. A very comprehensive comparison of the four detection systems—UV, fluorescence, and two MS systems [atmospheric pressure chemical ionization (APCI) and electrospray ionization (ESI)]—for the determination of the previously identified 3′,4′,5′-trimethoxyflavone[18] is presented in Table 1. Fluorescence detection is 10 times more sensitive than UV detection, whereas MS detection is 50 times more sensitive than UV detection and 5 times more sensitive than fluorescence detection.

Similar assay of the detection systems is performed by Stecher et al.,[9] who analyzed flavonols and stilbenes in wine and biological products and found that ESI/MS detection gave two, three, and nine times lower limit of detection (LOD) for myricetin, quercetin, and kaempferol, respectively, as compared to UV absorbance detection at 377 nm (absorption maximum of flavonols).

A significant amount of literature regarding the antioxidant properties of flavonoids and other plant polyphenols is available. As the essence of redox chemistry involves electron transfer, it seems natural that electrochemical detection rivals spectrophotometric detection techniques for the compounds that are supposed to be antioxidants. With the improvements in electrochemical detector geometries and electronics over the last decade, coupled with a requirement for increased sensitivity, the use of electrochemical detectors offers significant additional advantages when combined with the traditional UV–VIS detection in the analysis of flavonoids and other plant polyphenols.[20]

APPLICATIONS

Several information regarding HPLC analysis of flavonoids, often together with other phenolic constituents, in various samples, such as fruits, vegetables, juices, wines, honey, propolis, and, especially, plant material, are published. The enormous interest in studying these compounds is a result of their potential importance to health and antioxidant defense mechanisms, which has imposed the need for developing methods for their identification and quantification in various natural products. Reversed-phase HPLC (RP HPLC) with combined isocratic and gradient elution with acidic mobile phases and UV diode array or mass spectrometer detector is the most often used system for flavonoid analysis. Depending on the nature of the sample, a variety of sample preparation techniques has been developed in order to achieve good recovery of the analyzed compounds in a simple sample preparation procedure. The procedure includes extraction of the flavonoids in a polar solvent; this extract is then used either for injection onto the column (after filtration) or for further fractionation and purification of the flavonoids to obtain a relatively "clean" sample for injection. The latter step can be carried out in

Table 1 Regression equations for the calibration curves (logarithmic), regression coefficients, and detection limits for the determination of 3′,4′,5′-trimethoxyflavone.

Detection method	Regression equation	Regression coefficient (R^2)	Detection limit
UV at 213 nm	$y = 0.990x + 13.158$	0.9986	0.244 ng
Fluorescence at 330/440 nm	$y = 0.879x + 12.926$	0.9946	24.4 pg
ESI–MS	$y = 0.692x + 17.349$	0.9956	5.00 pg
APCI–MS	$y = 0.899x + 15.798$	0.9997	5.00 pg

Source: From Evaluation of detection methods for the reversed-phase HPLC determination of 3′,4′,5′-trimethoxyflavone in different phytopharmaceutical products and in human serum, in Phytochem. Anal.[18]

several ways: by liquid–liquid extraction in suitable solvents; by chromatographic techniques (thin layer or column chromatography) on various stationary phases (silica, reversed phases, Amberlite, and Sephadex); or by solid-phase extraction techniques using different adsorbents, which in the last decade has been found very convenient for the isolation of flavonoids from complex matrices.

Flavonoids in Fruits, Juices, and Wine

During the past decades, extensive analytical research has been performed on the separation of phenolic constituents in various fresh fruits and fruit products. A very thorough examination was performed by Barberán et al.,[11] on samples of several types of fresh nectarines, peaches, and plums using RP HPLC/DAD/ESI/MS and combined isocratic and gradient elution with a mobile phase of water–methanol with 5% formic acid. The samples were prepared by extraction of a homogenized frozen fruit material with water–methanol (2:8), by centrifugation, by filtration, and by injection into the column. This procedure recovers 85–92% of all phenolic compounds including hydroxycinnamates, procyanidins, flavonols, and anthocyanins. In the chromatograms obtained for nectarin and peach samples, three peaks from flavonols (quercetin 3-glucoside, quercetin 3-rutinoside, and, probably, quercetin 3-galactoside), several peaks from flavan-3-ols (catechin, epicatechin, and dimer procyanindines), and two anthocyanin pigments (cyanidine 3-glucoside and cyanidine 3-rutinoside) have been identified by comparing the retention data, the UV, and the mass spectra of the detected flavonoids with the ones obtained for authentic markers. Quantification was done using external standards: quercetin 3-rutinoside for flavonols at 340 nm, cyanidine 3-rutinoside for anthocyanins at 510 nm, and catechin for flavan-3-ols at 280 nm.

An HPLC/DAD method was developed for the separation and the determination of flavonoid and phenolic antioxidants in commercial and freshly prepared cranberry juice.[6] Two sample preparation procedures were used: with and without hydrolysis of the glycoside forms of flavonoids carried out by the addition of HCl in the step prior to solid-phase extraction (SPE). The flavonoid and phenolic compounds were then fractionated into neutral and acidic groups via a SPE method (Sep-Pak C_{18}), followed by a RP HPLC separation with gradient elution with water–methanol–acetic acid and a detection at 280 and 360 nm. A comparison of the chromatograms obtained for extracts prepared with and without hydrolysis showed that flavonoids and phenolic acids exist predominantly in combined forms such as glycosides and esters. In a freshly squeezed cranberry juice, for instance, 400 mg of total flavonoids and phenolics per liter of sample was found, 56% of which were flavonoids. Quercetin was the main flavonoid in the hydrolyzed products, where it accounted for about 75% of the total flavonoids, while it was absent in the unhydrolyzed products.

The flavonoid constituents of *Citrus* have attracted attention in the last decade because of their biological activities (anticarcinogenic, anti-inflammatory effects, etc.) together with the chemotaxonomic importance of the specific flavanone glycosides found in this species. The presence of 12 flavonoids (9 flavanone glycosides, 2 flavanone aglycones, and 1 flavone glycoside) was detected in samples from leaves and fruits of *Citrus aurantium*.[7] The use of different extraction solvents was studied (methanol, dioxane–methanol 1:1, 0.1% NaOH aq., 0.01% KOH methanolic, pyridin, dimethylformamide, and dimethylsulfoxide), with dimethylsulfoxide representing the best results. Also, an exhaustive description of the optimization process by studying the quantitative chromatographic parameters—k', w, α, N, height equivalent to a theoretical plate (HETP), and R—is given with the discussion of the effects of the variation of the methanol (acetonitrile) content in the mobile phase, the degree of mobile phase acidity, together with the influence of the structural

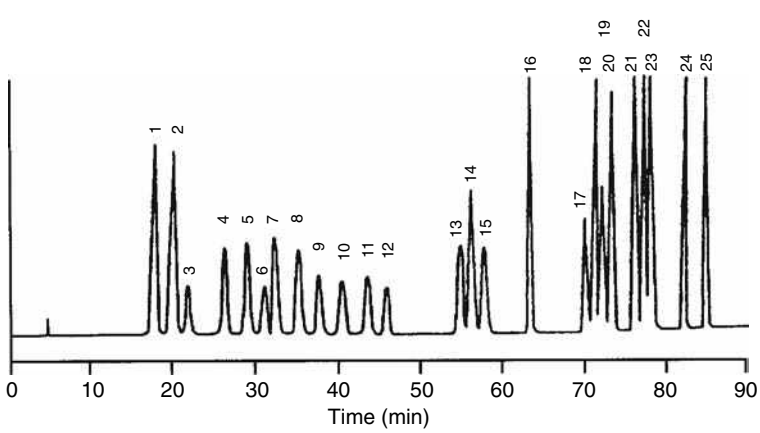

Fig. 2 Separation of 25 flavonoid standards (1—eriocitrin; 2—neoeriocitrin; 3—robinetin; 4—narirutin; 5—naringin; 6—rutin; 7—hesperidin; 8—neohesperidin; 9—isorhoifolin; 10—rhoifolin; 11—diosmin; 12—neodiosmin; 13—neoponcirin; 14—quercetin; 15—poncirin; 16—luteolin; 17—kaempferol; 18—apigenin; 19—isorhamnetin; 20—diosmetin; 21—rhamnetin; 22—isosakuranetin; 23—sinensetin; 24—acacetin; 25—tangeretin) using C_{18} Lichrospher 100, 250 × 4.0 mm, 5 μm, Merck; gradient elution with 0.01 *M* phosphoric acid–methanol with flow rate of 0.6 ml/min at 40°C and detection at 285 nm.

Source: From High—performance liquid chromatographic determination of naturally occurring flavonoids in *citrus* with a photodiode-array detector, in J. Chromatogr. A.[8]

characteristics of the studied flavonoids on their behavior in the reversed-phase chromatographic system.

Another thorough procedure for flavonoid analysis in *Citrus* samples is presented in the work of Nogata et al.[8] They developed a method for separation of 9 flavanones, 10 flavones, and 6 flavonols using a RP HPLC system with gradient elution with 0.01 *M* phosphoric acid–methanol and for detection at 285 nm, which is presented in Fig. 2. Identification was carried out by comparing the retention data and the spectra of the sample components with the ones of the standards. For quantitative analysis, all flavonoids exhibited good linearity ($r = 0.988$–1.00) between concentration and peak area in the investigated concentration range (10–200 ppm) with detection limits from 0.5 to 2.5 ppm.

To investigate the probable health benefits of flavonoids and stilbenes in red wine, a RP HPLC method with enhanced separation efficiency, selectivity, sensitivity, and speed has been established for the determination of the flavonols quercetin, myricetin, and kaempferol and the stilbenes *cis*- and *trans*-resveratrol in a single run.[9] The sample preparation step for wines and grape juices included only filtration prior to injection. Identification was carried out by the comparison of the retention data, the UV, and the mass spectra of the flavonoids and the stilbenes with the ones obtained for standards. Quantitative analysis using external standards showed good linearity ($R^2 > 0.999$ for UV and $R^2 > 0.9878$ for MS detection), recoveries between 95% and 105%, and limits of detection in the nanogram range, with MS being more sensitive.

An interesting improvement in the sample preparation step has been suggested[10] using only filtering of the sample prior to injection into the system composed of two columns: clean-up column (50×2.1 mm packed with C_{18} stationary phase, 5 μm) and analytical column (250×2.1 mm, C_{18}, 5 μm). A column-switching procedure enables the sample introduced in the first column to be cleaned from the disturbing matrix compounds for 2 min (elution phosphate buffer, pH = 7, with 10% acetonitrile), and then by a gradient of the mobile phase (phosphate buffer, pH = 2.5, with acetonitrile); the retained analytes—flavonoids—are eluted to the analytical column, where they are separated and detected at 365 nm. The method was used for the determination of flavonoid profiles of berry wines containing the flavonols quercetin, myricetin, kaempferol, rutin, and isoquercitrin.

Flavonoids of Honey and Propolis

A very interesting application of flavonoid analysis by HPLC has been carried out by Barberán et al.[11] on honey samples. They used RP HPLC/DAD for the analysis of 20 flavonoid aglycones, which could be considered as markers for the floral origin of honey. Different solvent systems were applied to the analysis of flavonoids from citrus and rosemary honeys. The sample preparation included dilution with water and HCl (pH = 2–3) for hydrolysis of glycosides, followed by purification using chromatography on Amberlite XAD-2 and Sephadex LH-20. The flavonoid markers of the botanical origin, hesperetin and apigenin, were detected using methanol–water and acetonitrile–water mixtures with formic acid. Quercetin and kaempferol were separated using Prizma-optimized conditions, whereas tectochrysin was eluted with methanol–water and acetonitrile–water mixtures by increasing the content of the organic solvent at the end of the elution programs. The use of diode array detection was found essential in studies of the floral origin of honey by flavonoid analysis.

Flavonoid analysis has also been carried out in propolis, another beehive product rich in flavonoids, which are partly responsible for its pharmacological activity.[12] Qualitative and quantitative analyses were performed by using a reversed-phase column and isocratic elution with water–methanol–acetic acid (60:75:5) and by monitoring at 275 and 320 nm. The propolis sample was cut into small pieces, extracted with boiling methanol, and the methanolic extract was then diluted with water and, subsequently, extracted with light petroleum and diethyl ether. The last extract contained the propolis flavonoids pinocembrin (21.4%), galangin (5%), chrysin (4.8%), quercetin (2.2%), and tectochrysin (1.1%).

Plant Material

Flavonoids play important roles in plant biochemistry and physiology; they are responsible for the biological effects of plants and their extracts as well as preparations on humans. HPLC is found very suitable for the detection and the determination of flavonoids present in various plants and plant products; the so-called HPLC fingerprint analysis is suggested for quality control and standardization because of the ability of good separation and resolution of complex mixtures as well as peak purity control. One of the limitations of the assays of flavonoids in plant material is the fact that many compounds, especially glycosides, are not commercially available. One of the possible solutions to this problem is the hydrolysis of flavonoid glycosides during the extraction procedure, which aids the identification on flavonoid aglycones. Such a procedure (the extraction in acetone with the addition of HCl for hydrolysis of glycosides) is proposed for the screening of flavonols and the determination of quercetin in medicinal plants using RP HPLC with gradient elution with water–acetonitrile–acetic acid and UV

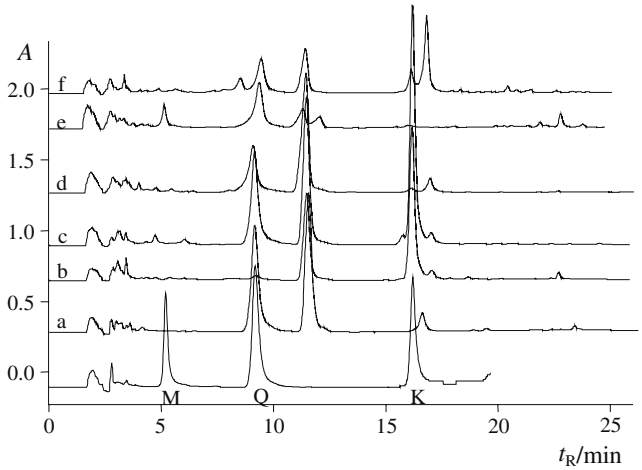

Fig. 3 Chromatograms obtained for extracts of the following: a) *H. herba*; b) *R. pseudoacaciae flos*; c) *P. spinosae flos*; d) *Sambuci flos*; e) *B. folium*; and f) *Primula flos*, and for mixture of authentic samples of myricetin (M), quercetin (Q), and kaempferol (K) using: C18 (250 × 4.6 mm, 5 μm, Varian); gradient elution with 5% acetic acid–acetonitrile with flow rate of 1.0 ml/min at 30°C and detection at 367 nm.
Source: From Assay of flavonols and quantification of quercetin in medicinal plants by HPLC with UV-diode array detection, in J. Liq. Chromatogr. Relat. Technol.[13]

diode array detection.[13] Quercetin was found to be the most abundant, especially in *Hyperici herba* and *Pruni spinosae flos*, kaempferol in *Robiniae pseudoacaciae flos* and *P. spinosae flos*, whereas myricetin was detected only in *Betulae folium*, as can be seen in the chromatograms presented in Fig. 3. The content of quercetin ranged from 0.026% in *Bursae pastoris herba* to 0.552% in *Hyperici herba*.

Another quantitative RP HPLC method, based on the reduction of the complex flavonoid glycoside pattern by acid hydrolysis to one major aglycone (quercetin) and one C-glycoside (vitexin), was developed and employed for the characterization of Crataegus leaves and flowers.[14] A qualitative fingerprint method was also developed for the separation and the identification of all characteristic flavonoids (glycosides and aglycones). Samples for fingerprint analysis were prepared by extraction with 80% methanol and then filtered through Bond Elut C_{18} cartridge prior to injection. Elution was performed by a mobile phase composed of tetrahydrofuran–acetonitrile–methanol and 0.5% orthophosphoric acid and was monitored at 370, 336, and 260 nm. For quantitative analysis, extraction was carried out with methanol in a Soxhlet apparatus, HCl was added to the methanolic extracts for the hydrolysis of glycosides, and, finally, they were filtered through Bond Elut C_{18} before injection. Separation and quantification of vitexin and quercetin were performed for characterization and standardization of the plant material as well as its extracts and preparations.

Structure–RP HPLC Retention Relationships of Flavonoids

The ability to predict the chromatographic mobility of a compound under given conditions, based on its structure, offers many advantages in analysis. The elution sequence of individual flavonoids can be interpreted by assuming that the compounds are first adsorbed on the reversed stationary phase by "hydrophobic interaction," and then subsequently eluted with the mobile phase according to the extent of hydrogen bond formation. Therefore the hydrogen bond donating and/or accepting ability of a given substituent as well as its contribution to the hydrophobic interaction have to be considered. The retention data of 141 flavonoids[15] imply the balance between these two effects, resulting in almost identical retention of tricetin pentamethylether (pentamethoxy flavone) and unsubstituted flavone.

Hydroxylation in positions other than 3 and 5 decreases retention owing to increasing polarity (hydrogen bond formation ability). The presence of an OH group in positions 3 and 5 is specific because of the formation of an intramolecular hydrogen bond with the carbonyl group on C-4, which is the strongest hydrogen bond acceptor in flavones and isoflavones. This is the reason for the increase in retention, especially when OH is substituted in position 5, whereas another OH group in position C-3 only slightly lowers the retention. This produces poor separation of the so-called critical pairs

flavone–flavonol differing only in the OH group in position 3.

Methylation of the OH groups more or less prevents their effect, which means that flavonoids and their partial methyl ethers are easily separated. On the other hand, the introduction of additional methoxy groups has little or no effect on retention—introducing another type of critical pair differing only in one methoxy group.

Glycosylation of an OH group means introducing a hydrophilic moiety together with shielding (by hydrogen bonding or just by steric hindrance) some hydrophilic substituents already present in the vicinity. The shielding effect plays a role when an OH group located *ortho* to another OH group is glycosylated (e.g., glycosylation of 7- or 4′-OH without an adjacent *ortho*-OH decreases the t_R values by 4.26–3.83 min, whereas, in the presence of an *ortho*-OH, the decrease is only 2.28–1.55 min[15]). The fact that the t_R value of luteolin-5-β-D-glucopyranoside is only 0.37 min smaller than that of the corresponding 7-β-D-glucopyranoside can also be explained by the shielding effect of sugar on the carbonyl group. The contributions of various types of sugars to the hydrophilic interaction decrease from hexoses through pentoses to methylpentoses.

Saturation of the C_3 ring, which means transformation of flavones to flavanones and of flavonols to dihydroflavonols, affects the retention in a very complex way. The saturation itself has a small effect; however, in the presence of OH groups, the retention is always decreased. This is explained by the interruption of the conjugation in the system, affecting the acidity and therefore the hydrogen bond accepting and donating abilities of the OH groups, especially the 3-OH groups which are phenolic in flavones and alcoholic in flavanones.

CONCLUSIONS

RP HPLC has proved to be the method of choice for the separation of a variety of flavonoids in different samples. The phenolic nature of these compounds requires the use of acidic mobile phases for satisfactory separation and peak shapes, whereas the detection is usually carried out with photodiode array detectors which are also very helpful for their identification of the characteristic absorption spectra of the flavonoids. In the last decade, mass spectrometers connected to HPLC systems introduced a greater selectivity and sensitivity in flavonoid analysis. Improving the characteristics of the stationary phases and developing more sophisticated instruments as well as devices for more efficient and faster sample preparation are the challenges for all modern analysts. Discovering the beneficial health effects of flavonoids and the "going-back-to-nature" trend motivates the development of more efficient and fast procedures for their identification and quantification, with HPLC remaining the most powerful technique for their separation from the complex mixtures.

REFERENCES

1. Mabry, T.J.; Markham, K.R.; Thomas, M.B. *The Systematic Identification of Flavonoids*; Springer-Verlag: New York, 1970.
2. Harborne, J.B. *Phytochemical Methods (A Guide to Modern Techniques of Plant Analysis)*; Chapman and Hall: London, 1984.
3. Wollenweber, E.; Jay, M. Flavones and flavonols. In *The Flavonoids*; Harborn, J.B., Ed.; Chapman and Hall: London, 1988.
4. Daigle, D.J.; Conkerton, E.J. Analysis of flavonoids by HPLC: An update. J. Liq. Chromatogr. **1988**, *11* (2), 309–325.
5. Barberán, F.A.T.; Gil, M.I.; Cremin, P.; Waterhouse, A.L.; Hess-Pierce, B.; Kader, A.A. HPLC–DAD–ESIMS analysis of phenolic compounds in nectarines, peaches, and plums. J. Agric. Food Chem. **2001**, *49*, 4748–4760.
6. Chen, H.; Zuo, Y.; Deng, Y. Separation and determination of flavonoids and other phenolic compounds in cranberry juice by high-performance liquid chromatography. J. Chromatogr. A, **2001**, *913*, 387–395.
7. Castillo, J.; Benavente-García, O.; Del Rio, J.A. Study and optimization of *citrus* flavanone and flavones elucidation by reverse phase HPLC with several mobile phases: Influence of the structural characteristics. J. Liq. Chromatogr. **1994**, *17* (7), 1497–1523.
8. Nogata, Y.; Ohta, H.; Yoza, K.I.; Berhow, M.; Hasegawa, S. High-performance liquid chromatographic determination of naturally occurring flavonoids in *citrus* with a photodiode-array detector. J. Chromatogr. A, **1994**, *667*, 59–66.
9. Stecher, G.; Huch, C.W.; Popp, M.; Bonn, G.K. Determination of flavonoids and stilbenes in red wine and related biological product by HPLC and HPLC–ESI–MS–MS. Fresenius' J. Anal. Chem. **2001**, *371*, 73–80.
10. Ollanketo, M.; Riekkola, M.L. Column-switching technique for selective determination of flavonoids in finnish berry wines by high-performance liquid chromatography with diode array detection. J. Liq. Chromatogr. Relat. Technol. **2000**, *23* (9), 1339–1351.
11. Barberán, F.A.T.; Ferreres, F.; Blázquez, M.A.; García-Viguera, C.; Tomás-Lorente, F. High-performance liquid chromatography of honey flavonoids. J. Chromatogr. **1993**, *634*, 41–46.
12. Bankova, V.S.; Popov, S.S.; Marekov, N.L. High-performance liquid chromatographic analysis of flavonoids from propolis. J. Chromatogr. **1982**, *242*, 135–143.
13. Stefova, M.; Kulevanova, S.; Stafilov, T. Assay of flavonols and quantification of quercetin in medicinal

plants by HPLC with UV-diode array detection. J. Liq. Chromatogr. Relat. Technol. **2001**, *24* (15), 2283–2292.
14. Rehwald, A.; Meier, B.; Sticher, O. Qualitative and quantitative reversed-phase high-performance liquid chromatography of Crataegus leaves and flowers. J. Chromatogr. A, **1994**, *677*, 25–33.
15. Vande Casteele, K.; Geiger, H.; Van Sumere, C.F. Separation of flavonoids by reversed-phase high-performance liquid chromatography. J. Chromatogr. **1982**, *240*, 81–94.
16. Galensa, R.; Herrmann, K. Analysis of flavonoids by high-performance liquid chromatography. J. Chromatogr. **1980**, *189*, 217–224.
17. Jagota, N.K.; Cheathan, S.F. HPLC separation of flavonoids and flavonoid glycosides using a polystyrene/divinylbenzene column. J. Liq. Chromatogr. **1992**, *15* (4), 603–615.
18. Huck, C.W.; Bonn, G.K. Evaluation of detection methods for the reversed-phase HPLC determination of 3′,4′,5′-trimethoxyflavone in different phytopharmaceutical products and in human serum. Phytochem. Anal. **2001**, *12*, 104–109.
19. Huck, C.W.; Huber, C.G.; Ongania, K.H.; Bonn, G.K. Isolation and characterization of methoxylated flavones in the flowers of *Primula veris* by liquid chromatography and mass spectrometry. J. Chromatogr. A, **2000**, *870*, 453–462.
20. Milbury, P.E. Analysis of complex mixtures of flavonoids and polyphenols by high-performance liquid chromatography electrochemical detection methods. Methods Enzymol. **2001**, *335*, 15–26.

Flavonoids: SFC Analysis

Xia Yang
Huwei Liu
Institute of Analytical Chemistry, Peking University, Beijing, China

INTRODUCTION

Several kinds of flavonoids are efficiently separated and analyzed using packed or capillary column supercritical fluid chromatography (SFC). The composition of mobile phase, stationary phase, temperature, and pressure all affect the resolution. This entry mainly focuses on the separation of polymethoxylated flavones, polyhydroxyl flavonoids, and flavonol isomers.

FLAVONOIDS

As a result of the development of chromatography technology, supercritical fluid chromatography (SFC) has been used to separate more and more compounds, owing to the low viscosity and high diffusivity of its mobile phase compared to the liquid mobile phase in HPLC. Supercritical carbon dioxide is the most popular SFC mobile phase because it is non-toxic, non-flammable, and easy to obtain, and it has a near-ambient critical temperature (approximately 31°C at 74 bar). However, CO_2 has weak solvating power for polar compounds. Supercritical fluids that are substantially more polar than carbon dioxide generally tend to have extreme critical temperatures and pressures (e.g., water with a critical temperature near 400°C), which makes them difficult or dangerous to work with and raises questions about the effect of such conditions on labile solutes themselves.[1] So CO_2 is the best choice, but it is often modified by such polar organic solvents as methanol, ethanol, etc. However, this binary mobile phase cannot elute very polar compounds efficiently. To widen the applicability of SFC, a small amount ($< 1\%$) of additive is added to a modifier to form a ternary mixture with CO_2. Organic acids, such as trifluoroacetic acid and citric acid, were used as additives to cause polar solutes (e.g., hydroxybenzoic and polycarboxylic acids) to be eluted rapidly and efficiently from packed SFC columns.[2–4]

Flavonoids are a group of naturally occurring substances derived from flavone (phenyl-γ-benzopyrone) that are widely distributed in the plant kingdom and used in herbal medicines throughout the world. They are 15-carbon compounds consisting of two aromatic rings and, based on the oxidation level of another ring, are classified into several groups, i.e., chalcones, flavanones, flavones, isoflavones, and flavonols, which are collectively known as the "yellow pigments," and the colored "anthocyanin pigments." Flavonoid compounds may undergo further enzymatic hydroxylation, methylation, glycosylation, sulfonation, acylation, and/or prenylation reactions, resulting in the immense diversity of flavonoid structures. There are more than 5000 identified flavonoid compounds found in nature.

Traditionally, flavonoids have been separated and analyzed by high-performance liquid chromatography (HPLC)[5,6] and gas chromatography (GC).[7] However, recent developments of SFC may permit a more accurate and complete analysis of plant phenolic compounds. Supercritical fluid chromatography brings together the advantages of both HPLC and GC techniques because it may be readily employed in the analysis of non-volatile and thermolabile compounds and provides facile coupling to detector technologies such as mass spectrometry and Fourier transform infrared (FTIR) spectroscopy. In recent years, SFC has been used to separate flavonoid compounds, most of which are polymethoxylated flavones and polyhydroxylflavonoids.

SEPARATION OF FLAVONOIDS

Separation of Polyhydroxylflavonoids by Packed-Column SFC

Liu et al.[8] separated polyhydroxylflavonoids, quercetin, and risetin by packed-column SFC with a ternary mobile phase. They designed an SFC apparatus with two syringe pumps and a variable-wavelength UV detector. A manual back-pressure regulator was also used to control the flow rate. This experiment showed that there are several factors affecting the result.

Mobile Phase

Neither pure supercritical CO_2 nor ethanol-modified CO_2 eluted all the flavonoids tested in this experiment. But when phosphoric acid and ethanol modifiers were added to the mobile phase together, the separation on a silica-based column was significantly improved, and quercetin and risetin were eluted rapidly and efficiently. With an increase of phosphoric acid concentration, the peak shapes were also improved. Because the phosphoric acid molecules could be adsorbed onto the active sites of the

stationary phase, which could prevent solute molecules from being strongly adsorbed, the interaction between solutes and stationary phase was eliminated, making the solutes easily elute from the chromatographic system.

Stationary Phase

The polarity of the column packing is in the following order: cyanopropyl > phenyl > ODS C_{18}. It is understandable that the ODS column is not suitable for the separation because of its low polarity. Both the cyanoprophyl and phenyl columns could separate these solutes efficiently, but the latter exhibited shorter separation times.

Pressure and Temperature

The capacity factor for the separation of flavonoids is decreased with the increase of operating pressure, in addition to the effect of the decrease in modifier concentration, thus indicating that the pressure effect is a very important one.

The retention times of solutes slightly increased with increasing temperature in the range of 40.0–65.0°C. As the volatilities of the solutes were increased with an increase in the temperature (which is favorable to shorten the retention time), the density of the mobile phase decreases with the temperature, which is not favorable for eluting the solute. In the range of temperatures mentioned above, the second factor is dominant; thus a lower temperature is desirable for the separation of quercetin and risetin.

Separation of Polymethoxylated Flavones by Packed-Column SFC

Morin et al.[9] successfully separated polymethoxylated flavones (PMFs) by packed-column SFC, illustrating that the SFC procedure is considerably faster than HPLC, with good resolution and adequate accuracy for the quantitative analysis of the PMFs. The chromatographic system consisted of a bare silica column (250 × 4.6 mm I.D.) with a carbon dioxide–methanol mobile phase and UV detection (313 nm). The pressure was controlled by a manual back-pressure regulator connected in series after the detector and maintained at 40°C with a water bath. Six compounds, including tangeretin, heptamethoxyflavone, nobiletin, sinensetin, tetramethylisoscutellarein, and isosinensetin (Table 1), were separated in less than 12 min as shown in Fig. 1. The resolution between nobiletin and heptamethoxyflavone is greater than 1.5, whereas reversed-phase HPLC required the use of water–tetrahydrofuran solvent to resolve these two compounds satisfactorily. If the carbon dioxide and methanol flow rates are increased from 3 and 0.3 ml/min to 9 and 0.9 ml/min, respectively, the polymethoxylated flavones (tangeretin, nobiletin, sinensetin, and tetramethylisoscutellatrein) are separated in 2 min

Table 1 Structures of polymethoxylated flavones.

PMF	Systematic name
Heptamethoxyflavone	3,5,6,7,8,3′,4′-Heptamethoxyflavone
Hexamethoxyflaxone	3,5,6,7,3′,4′-Hexamethoxyflavone
Nobiletin	5,6,7,8,3′,4′-Hexamethoxyflavone
Sinensetin	5,6,7,3′,4′-Pentamethoxyflavone
Tangeretin	5,6,7,8,4′-Pentamethoxyflaxone
Isosinensetin	5,7,8,3′,4′-Pentamethoxyflavone
Tetramethylisoscutellarein	5,8,7,4′-Tetramethoxyflavone
Tetramethylscutellarein	5,6,7,4′-Tetramethoxyflavone

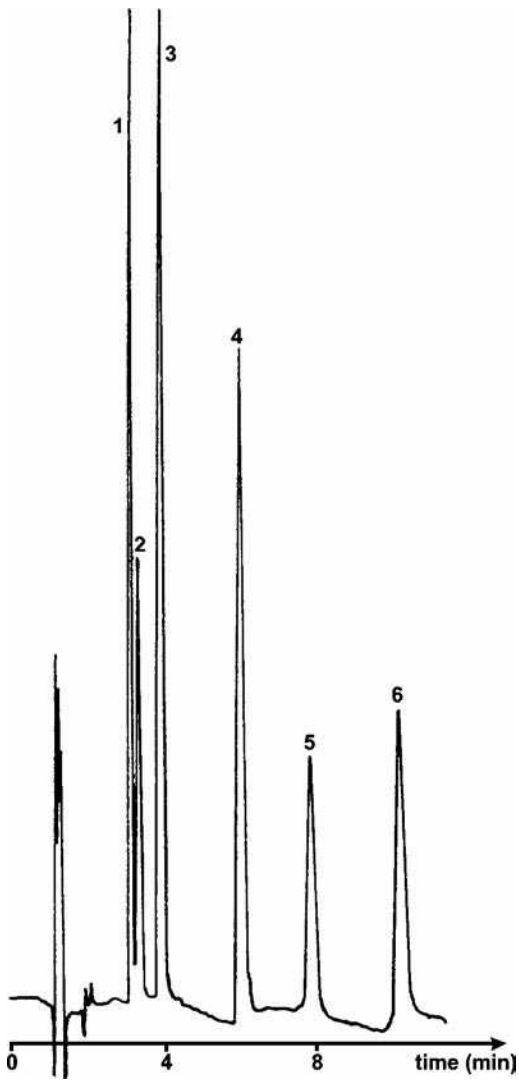

Fig. 1 SFC separation of synthetic mixture of polymethoxylated flavones. Column, 250 × 4.6 mm I.D.; stationary phase, Zorbax (5 μm) silica; mobile phase, carbon dioxide modified with 10% methanol; inlet pressure, 220 atm; outlet pressure, 200 atm; column temperature, 40°C; carbon dioxide flow-rate, 3 ml/min; methanol flow-rate, 0.3 ml/min; UV detection at 313 nm. Peaks: 1 = tangeretin; 2 = heptamethoxyflavone; 3 = nobiletin; 4 = sinensetin; 5 = tetramethylisoscutellarein; 6 = isosinensetin.

without any significant loss of efficiency and resolution. Thus packed-column SFC appears to be useful for rapid analyses of the main polymethoxylated flavonones.

Separation of Flavonol Isomers by Packed-Column SFC

Flavonol isomers, which differ only in the position of hydroxyl group on their chemical structures, showed different chromatographic behaviors. Liu et al.[10] separated three flavonol isomers (3-hydroxyflavone, 6-hydroxyflavone, and 7-hydroxyflavone) by a lab-constructed packed column SFC system with carbon dioxide modified with ethanol containing 0.5% (V/V) phosphoric acid as the mobile phase. The effects of temperature, pressure, composition of mobile phase, and packed-column type on the separation were studied. It was indicated that the addition of phosphoric acid to the mobile phase enabled flavonol isomers to be eluted from the column. It was also shown that a phenyl-bonded silica column was better and the ODS column was not as effective for the isomer separation. Increasing pressure shortened the retention time of each compound, with good resolution, and higher temperature led to longer retention times, and even the loss of the bioactivities of these components. Under selected conditions, the separation of these isomers was very satisfactory, as illustrated in Fig. 2.

Separation of Polymethoxylated and Polyhydroxylated Flavones by Open-Tubular Capillary SFC

Solvent modifiers and additives can be used to adjust the retention and selectivity of separation in packed-column SFC. Similar effects have been reported with open-tubular capillary SFC.[11] The advantage of capillary column over packed column arises from the differences in permeability. Pressure ramps are much easier to use in capillary columns to modify the solvent strength (via density modification) as compared to packed columns. Therefore it should be entirely feasible, with capillary SFC, to combine the benefit of solvent density (pressure) programming with simultaneous modification of the solvent strength.[12,13]

Hadj-Mahammed et al.[11] analyzed a mixture of flavone, 5-methoxyflavone, and tangeretin by supercritical CO_2 SFC on capillary columns with two types of detectors: flame ionization (FID) and FTIR. Peak identification was achieved with the help of the FTIR fingerprint of each compound. However, the separation was satisfactory only by the use of supercritical CO_2 density programs, without the use of a phase modifier. The separations were accomplished using a Carlo Erba SFC system equipped with a Model SFC 300 pump and a Model SFC 3000 oven. The fused silica capillary columns were BP1 (12 m × 0.1 mm I.D.; 0.1 μm film of dimethylpolysiloxane) and DB5 (15 m × 0.1 mm I.D.; 0.4 μm film of 94% dimethyl-, 5% diphenyl-, and 1% vinylpolysiloxane). The two supercritical CO_2 density programs used in this work were P1 [from 0.127 g/ml (at a pressure of 73.3 bars) to 0.689 g/ml (324.2 bars) isothermally at 100°C] and P2 [from 0.111 g/ml (at a pressure of 79.0 bars) to 0.511 g/ml (318.5 bars) isothermally at 150°C].

On the DB5 capillary column, satisfactory separation of hydroxyl- and methoxyflavones could be obtained using either of the two gradient systems, but the retention times of the analytes for P2 were shorter than those for P1. This is due to the variation in the solubilities of flavones in the supercritical mobile phase when the density gradient was employed. The polarity effect of the stationary phase (BP1 phase is less polar than the DB5) is illustrated in Table 2. It can be seen that, on BP1, the flavones are less retained and the analysis time is decreased by nearly half, while conserving a satisfactory separation.

In summary, the use of a polar capillary column and an appropriate gradient of supercritical CO_2 density at a temperature of about 150°C permits the flavonoids to be separated rapidly and effectively.

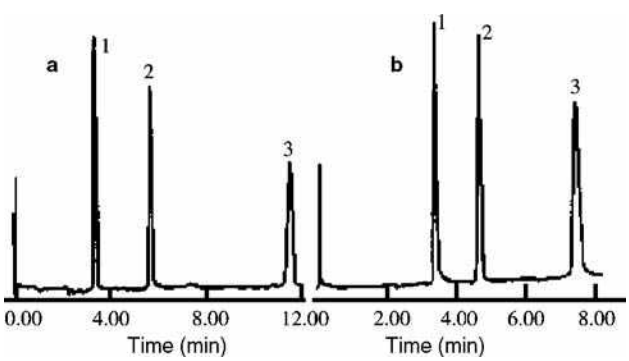

Fig. 2 Effect of stationary phase Pressure: 25 MPa, temperature: 50°C, mobile phase: carbon dioxide-ethanol with 0.5% phosphoric acid: 90 : 10, flowrate: 1.05 ml/min, stationary phase: a) cyano column, b) phenyl column.

Table 2 Comparison of retention times and capacity factors of flavones analyzed using capillary columns DB5 and BP1 with supercritical CO_2 density program P2.

	DB5		BP1	
Flavones	t_R (min)	k'	t_R (min)	k'
Flavone	17.93	2.40	9.52	1.36
5-Methoxyflavone	20.83	2.93	11.82	1.93
Tangeretin	25.84	3.90	16.53	3.10

CONCLUSIONS

Both packed-column and open-tubular capillary SFC can be used to separate flavonoids, and, in most cases, the separation is improved by changing the composition of mobile phase, stationary phase, temperature, and pressure.

Although HPLC has been used more often than SFC for the separation of flavonoids until now, SFC still has its particular merits and can be listed as the promising approach.

ACKNOWLEDGMENTS

This study is financially supported by the National Nature Science Foundation of China (NSFC), Grant Nos. 20275001 and 90209056.

REFERENCES

1. Berger, T.A.; Deye, J.F. Separation of benzene polycarboxylic acids by packed column supercritical fluid chromatography using methanol–carbon dioxide mixtures with very polar additives. J. Chromatogr. Sci. **1991**, *29*, 141.
2. Berger, T.A.; Deye, J.F. Separation of phenols by packed column supercritical fluid chromatography. J. Chromatogr. Sci. **1991**, *29*, 54–59.
3. Berger, T.A.; Deye, J.F. Separation of hydroxybenzoic acids by packed column supercritical fluid chromatography using modified fluids with very polar additives. J. Chromatogr. Sci. **1991**, *29*, 26–30.
4. Berger, T.A.; Deye, J.F. Separation of benzene polycarboxylic acids by packed column supercritical fluid chromatography using methane–carbon dioxide mixtures with very polar additives. J. Chromatogr. Sci. **1991**, *29*, 141–146.
5. Sendra, J.M.; Swift, J.L.; Izquierdo, L. C_{18} solid-phase isolation and high-performance liquid chromatography/ultraviolet diode array determination of fully methoxylated flavones in citrus juices. J. Chromatogr. Sci. **1988**, *26*, 443.
6. Hermburger, B.; Galensa, R.; Herrmann, K. High-performance liquid chromatography determination of polymethoxylated flavones in orange juice after solid-phase extraction. J. Chromatogr. **1988**, *439*, 481.
7. Drawert, F.; Leupold, G.; Pivernetz, H. Quantitative gaschromatographische bestimmung von Rutin, Hesperidin and Naringin in Orangensaft. Chem. Mikrobiol. Technol. Lebensm. **1980**, *20*, 111–114.
8. Liu, Z.; Zhao, S.; Wang, R.; Yang, G. Separation of polyhydroxylflavonoids by packed-column supercritical fluid chromatography. J. Chromatogr. Sci. **1999**, *37*, 155–158.
9. Morin, P.; Gallois, A.; Richard, H.; Gaydou, E. Fast separation of polymethoxylated flavones by carbon dioxide supercritical fluid chromatography. J. Chromatogr. **1991**, *586*, 171–176.
10. Liu, Z.; Zhao, S.; Wang, R.; Yang, G. Separation of flavonol isomers by packed column supercritical fluids chromatography. Chin. J. Chromatogr. **1997**, *15* (4), 288–291.
11. Hadj-Mahammed, M.; Badjah-Hadj-Ahmed, Y.; Meklati, B.Y. Behaviour of polymethoxylated and polyhydroxylated flavones by carbon dioxide supercritical fluid chromatography with flame ionization and fourier transform infrared detectors. Phytochem. Anal. **1993**, *4*, 275–278.
12. Schmitz, F.P.; Hilger, H.; Lorenschat, B.; Klesper, E. Separation of oligomers with UV-absorbing side groups by supercritical fluid chromatography using eluent gradients. J. Chromatogr. **1985**, *346*, 69.
13. Blilie, A.L.; Greibrokk, T. Gradient programming and combined gradient-pressure programming in supercritical fluid chromatography. J. Chromatogr. **1985**, *349*, 317–322.

Flow FFF

Myeong Hee Moon
Department of Chemistry, Kangnung National University, Kangnung, South Korea

INTRODUCTION

Flow field-flow fractionation (flow FFF or FlFFF) is one of the FFF subtechniques in which particles and macromolecules are separated in a thin channel by aqueous flow under a field force generated by a secondary flow. As with other FFF techniques, separation in FlFFF is based on the applied force directed across the axis of separation flow. In FlFFF, this force is generated by cross-flow of liquid delivered across the channel walls. In order to maintain the uniformity of cross-flow moving in a typical rectangular channel, two ceramic permeable frits are used as channel walls and the flow stream enters and exits through these walls. The force applied in FlFFF is a Stokes force that depends only on the sizes of sample components.

PRINCIPLES

In FlFFF, particles or macromolecules entering the channel are driven toward an accumulation wall by the cross-flow. Normally, a sheet of semipermeable membrane is placed at the accumulation wall in order to keep sample materials from being lost by the wall. While sample components are being transported close to the accumulation wall, they are projected against the wall by Brownian diffusion. The diffusive transport against the wall leads the sample components to be differentially distributed against the wall, according to their sizes: The larger particles, having a small diffusion coefficient, are placed at an equilibrium position closer to the vicinity of accumulation wall than the smaller ones. Thus, small particles, which are located further from the wall, will be exposed to the fast streamline of a parabolic flow profile, and they will be eluted earlier than the larger ones. This is the typical elution profile that can be observed in the normal operating mode of FFF (denoted as Fl/Nl FFF). Retention time in Fl/Nl FFF is inversely proportional to the diffusion coefficient of the sample; it is represented as

$$t_r = \frac{w^2}{6D}\frac{\dot{V}_c}{\dot{V}}\left(\text{where } D = \frac{kT}{3\pi\eta d_s}\right) \tag{1}$$

where w is the channel thickness, D is the diffusion coefficient, $\dot{V}_c$ is the cross-flow rate, and $\dot{V}$ is the channel flow rate. Because the diffusion coefficient D is inversely proportional to the viscosity of carrier solution η and hydrodynamic radius d_s, the retention time can be simply predicted provided the particle diameter or the diffusion coefficient is known. Conversely, the particle diameter of an unknown sample can be calculated from experimental retention time by rearranging Eq. 1.

As the particle size becomes large at or above 1 μm, the diffusional process of particles becomes less dominant in FFF. In this regime, a particle's retention is largely governed by the particle size itself, in which the center of large particles is located at a higher position than small ones. Thus, large particles meet the faster streamlines and they elute earlier than the small ones; the elution order is reversed. However, it is known, from experimental results, that particles migrate at certain positions elevated from the wall due to the existence of hydrodynamic lift forces that act in the opposite direction to the field. This is described as the steric/hyperlayer operating mode of separation in flow FFF and is denoted by Fl/Hy FFF. Whereas the theoretical expectation of particle retention in Fl/Nl FFF is clearly understood, retention in Fl/Hy FFF is not predictable because the hydrodynamic lift forces are not yet completely understood. Therefore, the particle size calculation in Fl/Hy FFF relies on the calibration process in which a set of standard latex particles of known diameter is run beforehand as

$$\log t_r = -S_d \log d_s + \log t_{r1} \tag{2}$$

where S_d is the diameter-based selectivity and t_{r1} is the interpolated intercept representing the retention time of a unit diameter. The S_d values found experimentally are about 1.5 in Fl/Hy FFF. By using Eq. 2, the particle diameters of unknown samples can be calculated once the calibration parameters S_d and t_{r1} are provided.

TYPES OF CHANNEL IN FIFFF

There are two main categories of flow FFF channel systems, depending on the use of frit wall. The above-described flow FFF system has a frit on both walls; this is classified as a symmetrical channel, as shown in Fig. 1a. An asymmetrical channel system is being widely studied in which only one permeable frit wall is used, at the accumulation wall, and the depletion wall is replaced with a glass plate (Fig. 1b). In an asymmetrical channel, part of the flow entering the channel is lost by the accumulation wall and this acts as a field force to retain the sample components in the channel, as does the cross-flow in a symmetrical channel.

The separation efficiency of an asymmetrical flow FFF system has been known to be higher than that of a conventional symmetrical channel. Because an asymmetrical channel utilizes only one frit, non-uniformity of flow that could arise from the imperfection of frits can be reduced. In addition, the initial sample band can be kept narrower in an asymmetrical channel, due to the focusing–relaxation procedure, which is an essential process in an asymmetrical channel. The relaxation processes, which provide an equilibrium status for sample components, are necessary in both symmetrical and asymmetrical channels for a period of time prior to the separation. For a symmetrical channel, this is normally achieved by stopping channel flow immediately after sample injection, while the cross-flow is applied.

During the relaxation process, sample components seek their equilibrium positions where the drag of the cross-flow is counterbalanced with diffusive transports (or lift forces) against the walls. After relaxation, flow is resumed and separation begins. However, in an asymmetrical channel, the relaxation process is achieved by two convergent focusing flow streams originating at the channel inlet and outlet (focusing–relaxation). Thus, injected sample can be focused at a certain position near the inlet end and the broadening of the initial sample band can be better minimized. This will lead to a decrease in band broadening of an eluted peak in an asymmetrical channel.

In asymmetrical flow FFF, two channel designs are utilized: rectangular and trapezoidal. Because flow velocity decreases along the axis of migration, a trapezoidal channel in which the channel breadth decreases toward the outlet is known to be more efficient in eluting low-retaining materials such as high-molecular-weight proteins. Retention in an asymmetrical flow FFF system follows the basic FFF principle and the retention time is calculated as

$$t_r = \frac{w^2}{6D}\ln\left(1 + \frac{\dot{V}_c}{\dot{V}_{\text{out}}}\right) \tag{3}$$

where $\dot{V}_c$ is the cross-flow rate and $\dot{V}_{\text{out}}$ is the outlet flow rate.

In addition to the rectangular channels in FlFFF described thus far, a cylindrical channel system has been developed with the use of hollow fibers in which the fiber wall is made of a porous membrane, as shown in Fig. 1c. It also requires a focusing–relaxation process, as does an asymmetrical channel. Retention in hollow-fiber flow FFF (HF-FlFFF) is controlled by the radial flow, which effectively acts as the cross-flow of a conventional flow FFF system, and the retention in a hollow fiber resembles that of an asymmetrical channel system.

However, the retention ratio in HF-FlFFF is approximately 4λ for a sufficiently retained component, which is somewhat different from that of a conventional channel system ($R \cong 6\lambda$). The retention time in a hollow fiber is calculated as

$$t_r = \frac{r_f^2}{8D}\ln\left(1 + \frac{\dot{V}_{\text{rad}}}{\dot{V}_{\text{out}}}\right) \tag{4}$$

where r_f^2 is the radius of the fiber and $\dot{V}_{\text{rad}}$ is the radial flow rate. Although a number of experiments have indicated a

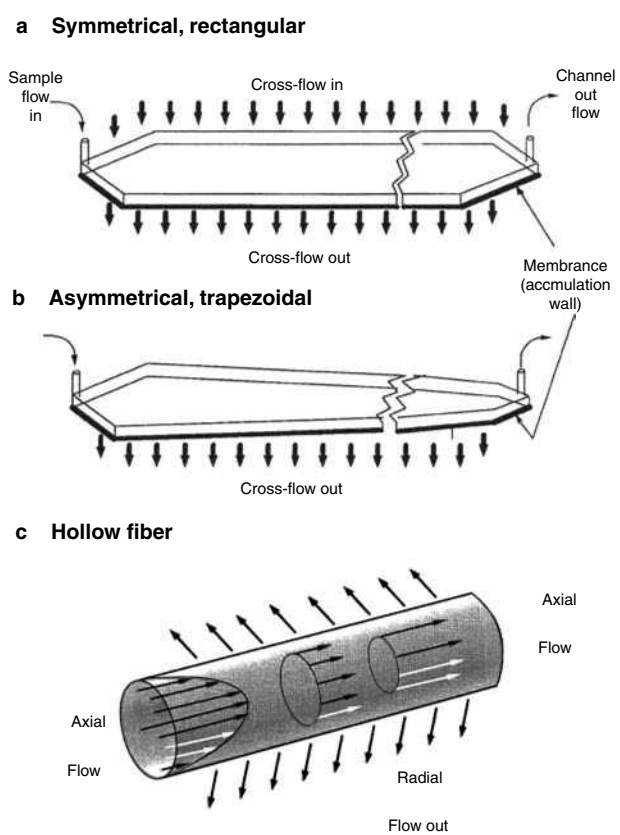

Fig. 1 Types of channel in FFF.

great potential of hollow fibers as an alternative for a flow FFF channel, a great deal of study related to their performance and optimization is needed.

BIBLIOGRAPHY

1. Giddings, J.C. Field flow fractionation: Separation and characterization of macro molecular, colloidal, and particulate materials. Science **1993**, *260*, 1456.
2. Giddings, J.C.; Yang, F.J.; Myers, M.N. Theoretical and experimental characterization of flow field-flow fractionation. Anal. Chem. **1976**, *48*, 1126.
3. Jönsson, J.A.; Carlshaf, A. Flow field flow fractionation in hollow cylindrical fibers. Anal. Chem. **1989**, *61*, 11.
4. Litzén, A.; Wahlund, K.-G. Improved separation speed and efficiency for proteins, nucleic acids and viruses in asymmetrical flow field flow fractionation. J. Chromatogr. **1989**, *476*, 413.
5. Litzén, A.; Wahlund, K.-G. Zone broadening and dilution in rectangular and trapezoidal asymmetrical flow field-flow fractionation channels. Anal. Chem. **1991**, *63*, 1001.
6. Moon, M.H.; Kim, Y.H.; Park, I. Size characterization of liposomes by flow field-flow fractionation and photon correlation spectroscopy: Effect of ionic strength and pH of carrier solutions. J. Chromatogr. **1998**, *813*, 91.
7. Ratanathanawongs, S.K.; Giddings, J.C. *Chromatography of Polymers: Characterization by SEC and FFF*; ACS Symposium Series; Provder, T., Ed.; American Chemical Society: Washington, D.C., 1993; Vol. 521, 13–29.

Fluorescence Detection in CE

Robert Weinberger
CE Technologies, Inc., Chappaqua, New York, U.S.A.

INTRODUCTION

One cannot overestimate the importance of fluorescence detection in high-performance-capillary electrophoresis (HPCE).[1] The success of the human genome project along with the forthcoming revolutions in forensic testing and genetic analysis might not have occurred without the sensitivity and selectivity of laser induced fluorescence (LIF) detection.

BASIC CONCEPTS

The stunning sensitivity of fluorescence detection arises from two areas: (a) detection is performed against a very dark background and (b) the use of the laser as an excitation source provides a high photon flux. The combination of the two can yield single-molecule detection in exceptional circumstances, although picomolar ($10^{-12}M$) is typically obtained. Under conditions that are easy to replicate, LIF detection is often times more sensitive compared to ultraviolet (UV) absorption detection.

Most molecules absorb light in the ultraviolet or visible portion of the spectrum, but only few produce significant fluorescence. This provides for the extreme selectivity of the technique. Molecular fluorescence is usually quenched through vibronic or collosional events resulting in a radiationless decay of excited singlet-state energy to the ground state. In aromatic structurally rigid molecules, quenching is less significant and the quantum yield increases.

The selectivity of fluorescence is to itself a problem because the technique is applicable to fewer separations. Sophisticated derivatization schemes have been developed for these applications to take advantage of the attributes contributed by fluorescence detection. Because there are two instrumental parameters to adjust, the excitation and emission wavelengths, the inherent selectivity of the method is further enhanced.

The fundamental equation governing fluorescence is

$$I_f = \Phi_f I_0 abc E_x E_c E_m E_{\text{pmt}}$$

where I_f is the measured fluorescence intensity, Φ_f is the quantum yield (photons emitted/photons absorbed), I_0 is the excitation power of the light source, a, b, and c are the Beer's Law terms, and the E terms are the efficiencies of the excitation monochromator or filter, the optical portion of the capillary, the emission monochromator or filter, and the detector (photomultiplier or charge-coupled device), respectively. It is no wonder why optimization of fluorescence detection is difficult for the uninitiated.

EXCITATION SOURCES

The optimal excitation wavelength is usually a combination of the power of the light source and the molar absorptivity of the solute at the selected wavelength. The argon-ion laser is used for most DNA applications since the primers, intercalators, and dye terminators have been optimized for 488 nm excitation. For other applications, particularly for small molecules, where native fluorescence is measured, a tunable light source is desirable. The deuterium lamp is useful for low-UV excitation and the xenon arc is superior in the near-UV to visible region. With a 75-W xenon arc, the limit of detection (LOD) is 2 ng/ml ($6 \times 10^{-9}M$) for fluorescein using fiber-optic collection of the fluorescence emission.[2] This is a 100-fold improvement compared to absorption detection. By using a microscope objective to focus the light along with a sheath-flow cuvette (to reduce scattering, see below) and lens to collect the light, the LOD is reduced to 8×10^{-11}.[3] Nevertheless, the LOD using conventional tunable sources will never be superior to that found with the laser.

It is possible to select lasers other than the argonion laser for LIF detection. A 625 nm diode laser is available on a commercial unit (Beckman P/ACE and MDQ). Tunable dye lasers would be desirable but cost and reliability has precluded widespread use. The KrF laser is particularly useful because it emits in the UV at 248 nm. If fiber optics are employed to direct the laser light, then a UV transparent fiber optic must be used. A table of lasers and their wavelengths of emission is given in Table 1.

Lower-power lasers are often used in HPCE. Because scattered light is the factor that often limits detectibility, raising the power levels is ineffective. At high laser power, photobleaching becomes more likely to occur as well.

Table 1 Laser light sources for LIF detection.

Laser	Available wavelengths
Ar ion (air-cooled)	457, 472, 476, 488, 496, 501, 514
Ar ion (full frame)	275, 300, 305, 333, 351, 364, 385, 457, 472, 476, 488, 496, 501, 514
Ar ion (full frame, frequency doubled)	229, 238, 244, 248, 257
ArKr	350–360, 457, 472, 476, 488, 496, 501, 514, 521, 514, 521, 531, 568, 647, 752
HeNe	543, 594, 604, 612, 633
Excimer	
XeCl (pulsed)	308
KrF (pulsed)	248
Nitrogen (pulsed)	337
Nitrogen-pumped dye (tunable)	360–950
Solid state	
YAG (frequency doubled)	532
YAG (frequency quadrupled)	266
Diode lasers	
Frequency doubled ($LiNbo_3$)	415
Frequency doubled (KTP)	424
Frequency tripled (Nd-doped YLiF)	349

Source: From Capillary Electrophoresis.[13]

METHODS FOR COLLECTING FLUORESCENT EMISSION

The goal here is to minimize the collection of scattered radiation and optimize the collection of emitted fluorescence. Scattered radiation comes from two sources: Rayleigh scattering and Raman scattering. Rayleigh scattering occurs at the wavelength of excitation. To optimize the LOD, virtually all of this radiation must be excluded from detection. Raman scattering is observed at longer wavelengths than Rayleigh scattering and it is times less intense. Despite the weakness of Raman scattering, this effect can significantly elevate the background if left unchecked. Bandpass and/or cutoff filters are often used to reduce the impact of scattering. It is important to ascertain that the selected filter does not fluoresce as well.

Fiber optics held at right angles to the capillary can be employed to route emitted light toward the photomultiplier tube (PMT).[2] The Beckman LIF detector employs a collecting mirror to increase the amount of collected emission. One problem with both of these approaches is the failure to prevent small amounts of scattered light from reaching the PMT. Cutoff and/or bandpass filters are not 100% efficient in this regard. This is particularly important when lasers are used because of the intense scattering of light.

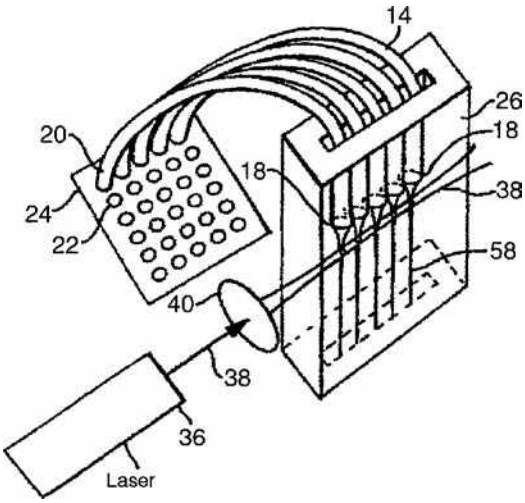

Fig. 1 Multiple-capillary instrument employing the sheath-flow technique. Key: 14, capillary; 18, capillary outlet; 20, capillary inlet; 22, buffer well; 24, microtiter plate; 26, quartz chamber; 36, laser; 38, laser beam; 40, lens; 58, fluidic stream. The electrodes are not shown nor is the device for delivering the sheath fluid.
Source: Reprinted in part from U.S. Patent No. 5,741,412.

The sheath-flow design is an important advance in reducing scattering because detection occurs after the solutes have exited the capillary.[4] Scattering occurs whenever a refractive index (RI) change occurs in the optical path.These RI changes include the air–capillary interface and the buffer–capillary interface. Eliminating the capillary from the optical path effectively removes four scattering surfaces. This becomes most important in multiple-capillary systems such as the DNA sequencer because many surfaces are now involved. The sheath-flow device patented in 1998[5] is illustrated in Fig. 1 for a five-capillary system. In actual practice, 96 capillaries are employed. The laser beam is sufficiently strong that attenuation is not significant or at least can be compensated for in the software. Fluorescence from each capillary is then imaged onto a charge-coupled device (CCD) camera.

For single-capillary systems, a conventional PMT is used for detection. Light is routed to that PMT either with fiber optics, a collecting mirror, epiillumination microscopy, or a microscope objective. For multiple-capillary systems, the system must be scanned[6] or the light imaged onto a CCD camera.

DERIVATIZATION

Derivatization is important in capillary electrophoresis to enhance the detectibility of solutes that are non-fluorescent.[7] The chemistry can occur precapillary, on capillary, postcapillary. Typically, the solutes are amino acids,

catecholamines, peptides, or proteins, all of which contain primary or secondary amine groups.

Reagents such as *ortho*-phthaldehyde (OPA), naphthalenedialdehyde (NDA), 3-(4-carboxy-benzoyl)-2-quinoline carboxaldehyde (CBQCA), fluorescein, and fluorenylmethyl chloroformate (FMOC) are all useful for precapillary derivatization, the most common of the three techniques. For carbohydrates, reagents such as aminopyrene naphthalene sulfonate (APTS) are used for precapillary derivatization. For chiral recognition, prederivatization with optically pure fluorenylethyl chloroformate (FLEC) provides for both enantioseparation by micellar electrokinetic capillary chromatography (MECC or MEKC) and a tag that absorbs at 260 nm and emits above 305 nm. Reagents for derivatizing carbonyl, hydroxyl, and other functional groups are also available.

For on-capillary and postcapillary derivatization, the reagent must not fluoresce until reacted with the solute. For these purposes, NDA and OPA are the best choices. With on-capillary derivatization, it is possible to use a reagent that fluoresces, but its removal prior to solute detection can be difficult.

The advantage of precapillary and on-capillary derivatization is the lack of the need for additional instrumentation beyond the basic HPCE instrumentation. The disadvantage of precapillary derivatization is the need for extra sample-handling steps. For postcapillary derivatization, the need for additional miniaturized instrumentation is the principle disadvantage. This problem may be overcome when dedicated microfabricated systems become available.

Important non-DNA application areas for precapillary derivatiation with LIF detection include the determination of amino acids and amines in cerebrospinal fluid to distinguish disease states such as Alzheimer's disease and leukemia from the normal population. In vivo monitoring of microdialysates from the brain of living animals has been employed for the determination neuropeptides, amphetamine, neurotransmitters, and amino acids. The contents of single neurons and red blood cells have been studied as well.

A variant of postcapillary derivatization is chemiluminescence (CL) detection.[8] In this case, the chemical reaction replaces the light source for excitation. The detector is a PMT run at high voltage. Solutes can be tagged with CL reagents such as luminol or directly excited via the peroxyoxalate reaction. The latter works best for aminoaromatic hydrocarbons such as dansylated amines. The LODs using CL detection approach laser levels because of the low background. However, the need for specialized apparatus has limited the applicability of CL detection.

FLUORESCENCE DETECTION FOR MICROFABRICATED SYSTEMS

The so-called micro-total analytical systems (mTAS) can integrate sample handling, separation, and detection on a single chip.[9] Postcapillary reaction detectors can be incorporated as well.[10] Fluorescence detection is the most common method employed for these chip-based systems. A commercial instrument (Agilent 2100 Bioanalyzer) is available for DNA and RNA separations on disposable chips using a diode laser for LIF detection. In research laboratories, polymerase chain reaction (PCR) has been integrated into a chip that provides size separation and LIF detection.[11]

INDIRECT FLUORESCENCE DETECTION

When detecting solutes that neither absorb nor fluoresce, indirect detection can be employed. With this technique, a reagent is added to the background electrolyte that absorbs or fluoresces and is of the same charge for the solute being separated. This reagent elevates the baseline. When solute ions are present, they displace the additive as required by the principle of electroneutrality. As the separated ions migrate past the detector window, they are measured as negative peaks relative to the high baseline. The advantage of indirect fluorescence compared to indirect absorption is an improved LOD.

The sensitivity of indirect detection is given by the following equation:[12]

$$C_{\mathrm{LOD}} = \frac{C_R}{(\mathrm{DR})(\mathrm{TR})}$$

where the CLOD is the concentration limit of detection, is the concentration of the reagent, D_R is the dynamic reserve, and TR is the transfer ratio. Thus, the lowest CLOD occurs when the reagent concentration is minimized.

With 100 μm fluorescein, a mass limit of detection of 20 μ*M* was measured for lactate and pyruvate in single red blood cells. Fluorescein is a good reagent because it absorbs at 488 nm and thus matches the argon-ion laser emission wavelength. In indirect absorption detection, the additive concentration is usually 5–10 m*M*. Band broadening due to electrodispersion is less unimportant in indirect fluorescence detection because the solute concentration is so low. At higher solute concentrations, the system will be less useful because of electrodispersion. The concentration of the indirect reagent could be increased, but then indirect absorption detection becomes applicable.

With the advent of microfabricated systems that employ LIF detection, it is expected that indirect fluorescence will gain importance as a general-purpose detection scheme.

REFERENCES

1. MacTaylor, C.E.; Ewing, A.G. Critical review of recent developments in fluorescence detection for CE. Electrophoresis **1997**, *18*, 2279.
2. Albin, M.; Weinberger, R.; Sapp, E.; Moring, S. Fluorescence detection in capillary electrophoresis: Evaluation of derivatizing reagents and techniques. Anal. Chem. **1991**, *63*, 417.
3. Arriaga, E.; Chen, D.Y.; Cheng, X.L.; Dovichi, N.J. High-efficiency filter fluorometer for capillary electrophoresis and its application to fluorescein thiocarbamyl amino acids. J. Chromatogr. **1993**, *652*, 347.
4. Cheng, Y.F.; Dovichi, N.J. Subattomole amino acid analysis by capillary zone electrophoresis and laser induced fluorescence. Science **1988**, *242*, 562.
5. Dovichi, N.J.; Zhang, J.Z . U.S. Patent 5,741,412 (April 21, 1998).
6. Huang, X.C.; Quesada, M.A.; Mathies, R.A. Capillary array electrophoresis using laser-excited confocal fluorescence detection. Anal. Chem. **1992**, *64*, 967.
7. Bardelmeijer, H.A.; et al., Pre-on, and post-column derivatization in capillary electrophoresis. Electrophoresis **1997**, *18*, 2214.
8. Staller, T.D.; Sepaniak, M.J. Chemiluminescence detection in capillary electrophoresis. Electrophoresis **1997**, *18*, 2291.
9. Manz, A.; et al., Capillary electrophoresis integrated onto a planar microstructure (review). Analusis **1994**, *22*, M25.
10. Jacobson, S.C.; Koutny, L.B.; Hergenroeder, R.; Moore, A.W., Jr. Microchip capillary electrophoresis with an integrated postcolumn reactor. Anal. Chem. **1994**, *66* (20), 3472–3476.
11. Waters, L.C.; et al., Microchip device for cell lysis, multiplex PCR amplification, and electrophoretic sizing. Anal. Chem. **1998**, *70*, 158.
12. Yeung, E.S.; Kuhr, W.G. Indirect detection methods for capillary separations. Anal. Chem. **1991**, *63* (5), A275.
13. Schwartz, H.E.; Ulfelder, K.J.; Chen, F.-T.A.; Pentoney, J. J. Capillary Electrophoresis **1994**, *1*, 36.

Fluorescence Detection in HPLC

Ioannis N. Papadoyannis
Anastasia Zotou
Laboratory of Analytical Chemistry, Chemistry Department, Aristotle University of Thessaloniki, Thessaloniki, Greece

INTRODUCTION

Detection based on analyte fluorescence can be extremely sensitive and selective, making it ideal for trace analysis and complex matrices. Fluorescence has allowed liquid chromatography (LC) to expand into a high-performance technique. High-performance liquid chromatography (HPLC) procedures with fluorescence detection are used in routine analysis for assays in the low nanogram per milliliter range and concentrations as low as picogram per milliliter often can be measured. The linearity range for these detectors is similar to that of ultraviolet (UV) detectors (i.e., 10^3–10^4).

DISCUSSION

One major advantage of fluorescence detection is the possibility of obtaining three orders of magnitude increased sensitivity over absorbance detection and its ability to discriminate analyte from interference or background peaks. Contrary to absorbance, fluorescence is a "low-background" technique. In an absorbance detector, the signal measured is related to the difference in light intensity in the presence of the sample vs. the signal in the absence of the sample. For traces of analyte, this difference becomes extremely small and the noise level of the detector increases significantly. In a fluorescence detector, however, the light emitted from the analyte is measured against a very low-light (dark) background and, thus, against a very low noise level. The result is a much lower detection limit, which is limited by the electronic noise of the instrument and the dark current of the photomultiplier tube.

Another major advantage of fluorescence detection is selectivity. The increased selectivity of fluorescence vs. absorbance is mainly due to the following reasons: (a) Most organic molecules will absorb UV/visible light but not all will fluoresce. (b) Fluorescence makes use of two different wavelengths (excitation and emission) as opposed to one in absorbance, thus decreasing the chance of detecting interfering chromatographic peaks.

Quantitative analysis can be performed with fluorescence detection even when poor column resolution occurs, provided there is enough detection selectivity to resolve the peaks.

One of the weak points of fluorescence is that relatively few compounds fluoresce in a practical range of wavelengths. However, chemical derivatization allows many non-fluorescent molecules containing derivatizable functional groups to be detected, thus expanding the number of applications. Fluorescence derivatization can be accomplished either via precolumn or postcolumn methods.

THEORETICAL BACKGROUND OF FLUORESCENCE DETECTION

Fluorescence is a specific type of luminescence. When a molecule is excited by absorbing electromagnetic radiation (a photon) supplied by an external source (i.e., an incandescent lamp or a laser), an excited electronic singlet state is created. Eventually, the molecule will attempt to lower its energy state, either by reemitting energy (heat or light) by internal rearrangement or by transferring the energy to another molecule through a molecular collision. This process distinguishes fluorescence from chemiluminescence, in which the excited state is created by a chemical reaction. If the release of electromagnetic energy is immediate or stops upon the removal of the excitation source, the substance is said to be fluorescent.

In fluorescence, the excited state exists for a finite time (1–10 ns). If, however, the release of energy is delayed or persists after the removal of the exciting radiation, then the substance is said to be phosphorescent.

Once a photon of energy $h\nu_{ecx}$ excites an electron to a higher singlet (absorbance) state (1 fs), emission of the photon $h\nu_{em}$ occurs at longer wavelengths. This is due to the competing non-radiative processes (such as heat or bond breakage) occurring during energy deactivation. The difference in energy or wavelength represented by $h\nu_{em} - h\nu_{exc}$ is called the *Stokes shift*.

The fluorescence signal, I_f, is given by

$$I_f = \varphi I_0\left(1 - e^{-kcl}\right)$$

where φ is the quantum yield (the ratio of the number of photons emitted to the number of photons absorbed), I_0 is the intensity of the incident light, c is the concentration of the analyte, k is the molar absorbance, and l is the path length of the cell.

With few exceptions, the *fluorescence excitation spectrum* of a single fluorophore in dilute solution *is identical to its absorption spectrum*. Under the same conditions, the *fluorescence emission spectrum is independent of the excitation wavelength*, due to the partial dissipation of the excitation energy during the excited lifetime. The emission intensity is proportional to the amplitude of the fluorescence excitation spectrum at the excitation wavelength.

DEACTIVATION PATHWAYS IN FLUORESCENCE

The excited state exists for a finite time (1–10 ns) during which the fluorophore undergoes conformational changes and is also subject to several interactions with its molecular environment. The processes which deactivate the excited state may be radiational or non-radiational (see Fig. 1) and are the following.

Internal Conversion

A transition from a higher (S_3, S_2) to the first singlet excited energy state occurs (S_1) through an internal conversion (in 1 ps). Internal conversion is increased with increasing solvent polarity.

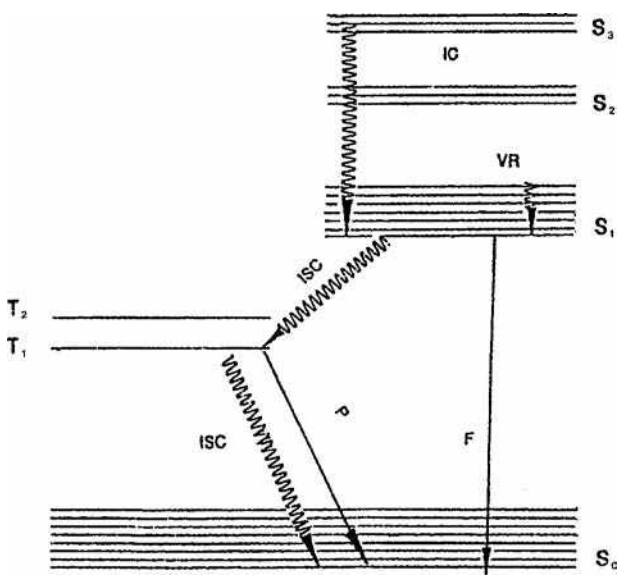

Fig. 1 Deactivation pathways in fluorescence; S_1, S_2, and S_3 are singlet excited states; S_0 is the ground state; T_1 and T_2 are triplet excited states; VR is vibrational relaxation, IC is internal conversion, ISC is intersystem crossing, P is phosphorescence, and F is fluorescence.

External Conversion (Quenching)

This is a chemical or matrix effect and can be defined as a bimolecular process that reduce the fluorescence quantum yield without changing the emission spectrum. Fluorescence radiation is transferred to foreign molecules after collisions.

Vibrational Relaxation

The energy of the first excited singlet state is partially dissipated through vibrations, yielding a relaxed singlet excited state. *Increased vibrations lower the fluorescence intensity*, due to the fact that they occur much faster (1 ps) than the fluorescence event. The molecular structure itself will determine the amount of vibrations. Rigid and planar molecules usually do not favor vibrations and they are prone to fluoresce.

Intersystem Crossing (Photobleaching)

This is a non-radiational process under high-intensity illumination conditions and in the same timescale as fluorescence (1–10 ns). It is defined as a transition from the first excited singlet (S_1) to the excited triplet (T_1) state. This is a "forbidden" transfer and necessitates the change of electron spin. *The quantum yield of fluorescence is reduced and phosphorescence also occurs*.

Phosphorescence

This event occurs due to a radiational relaxation to the ground singlet (S_1) state and in the 0.1 ms to 10 sec time frame. Therefore, the emission is at even longer wavelengths than in fluorescence. Energy addition to the molecule in the form of heat or collisions of two triplet-state molecules can cause delayed fluorescence.

FACTORS AFFECTING FLUORESCENCE

Molecular structure and environmental factors such as acidity, solvent polarity, and temperature variations exert significant influence on fluorescence intensity. Also, variations in mobile-phase composition will cause excitation and emission-wavelength changes in the fluorophore.

Molecular Structure

Common fluorophores possess aromaticity and electron-donating substituents on the ring. Only compounds with a high degree of conjugation will fluoresce. The possible molecular transitions resulting in fluorescence are $\sigma \rightarrow \sigma^*$, occurring only on alkanes in the vacuum UV region, and $\pi \rightarrow \pi^*$ with very high extinction coefficients, occurring in alkenes, carbonyls, alkynes, and azo

compounds. The majority of strong fluorophores undergo this transition and the excited state is more polar than the ground state.

Solvent Polarity

Polar solvents affect the excited state differently in $\pi \rightarrow \pi^*$ and $n \rightarrow \pi^*$ transitions. The excited state in $\pi \rightarrow \pi^*$ transition is stabilized. A reduction in the energy gap will occur and the emission will be shifted to a longer wavelength (red shift). Therefore, the difference between excitation and emission wavelengths will be greater in polar solvents.

Temperature

A rise in temperature increases the rate of vibrations and collisions, resulting in increased intersystem crossing, internal and external conversion. Consequently, the fluorescence intensity is inversely proportional to the temperature increase. Additionally, an increased temperature causes a red shift of the emission wavelength.

Acidity

Acidity can drastically affect the fluorescence intensity. The pK_a of concern is the pK_a of the excited state. Because protonation is faster than fluorescence, the pK_a can be quite different than it is for the molecule in the ground state. Therefore, a pH optimization vs. fluorescence intensity is needed for molecules that are particularly prone to pH changes.

FLUORESCENCE DETECTOR INSTRUMENTATION

Fluorescence detectors for HPLC use come in many designs from the manufacturer. Differences in detector design can lead to markedly different results during interlaboratory comparisons.

Fluorescence detectors are based either on the straight-path design (similar to UV photometers) or on the more often encountered right-angle design. The common excitation source lamps used are continuous deuterium, xenon, xenon–mercury, and pulsed xenon. Recently, the use of high-power light sources for excitation, such as laser sources, allows the development of much smaller volume flow cells with less scatter (noise), resulting in improved efficiency. Photomultiplier tubes are commonly used as the photodetectors (photocells) vs. photodiodes in UV detectors. They convert a light signal to an electronic signal.

Detector flow cells are the link between the chromatographic system and the detector system. The cell cuvettes are made of quartz, with either cylindrical or square shapes and volumes between 5 and 20 μl. The sensitivity is directly proportional to the volume. However, resolution decreases with increasing volume. Fluorescence is normally measured at an angle perpendicular to the incident light. An angle of 90° has the lowest scatter of incident light. However, fluorescence from the flow cell is isotropic and can be collected from the entire 360°.

With the straight-path design, a standard UV cell can be used, but the filters must be selected so as to prevent stray light from reaching the photodetector. The right-angle design often uses a cylindrical cell. This design is less efficient than the straight-path cell because light-scattering problems result in a lower light intensity reaching the photodetector. However, this design is less susceptible to interference from stray light from the lamp, because the photodetector is not in line with the lamp.

With respect to monochromator type, three general detector designs are available: filter–filter, grating–filter, and grating–grating, where either a filter or monochromator grating is used to select the correct excitation and emission wavelengths. Gratings allow a choice of any desired wavelength, whereas filters are limited to a single wavelength.

Fluorescence detectors that use *filters* to select excitation and emission wavelengths are called *filter fluorometers*. This type of detector is the most sensitive, yet the simplest and least expensive. A diagram of this simple form of fluorescence detector is shown in Fig. 2. Usually, in order to enhance the fluorescence collected from the flow cell, lenses are employed along with filters. The lenses are positioned before the excitation filter and after the flow cell to focus and collect the light.

The ultimate in fluorescence detection is a detector that uses a diffraction grating to select the excitation wavelength

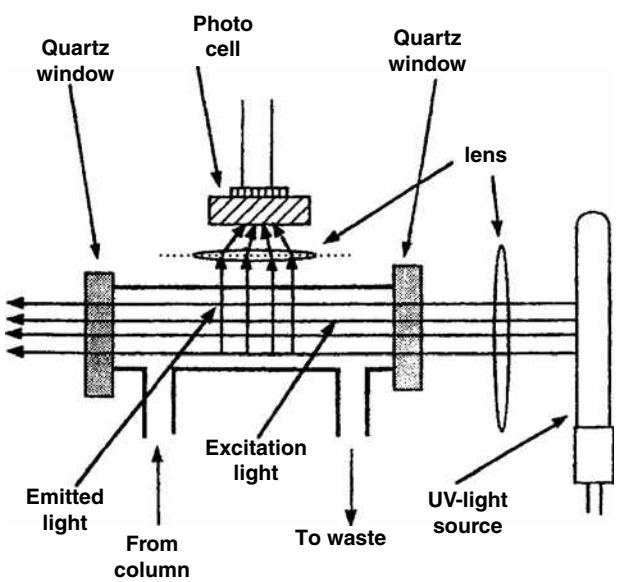

Fig. 2 Schematic of a single-wavelength fluorescence detector.

and a second grating to select the wavelength of the fluorescent light. These dual monochromatic *grating–grating* fluorescence detectors are called *spectrofluorometers*. If the gratings are used in the scanning mode, the detector is a *scanning spectrofluorometer*. A fluorescence or excitation spectrum can be provided by arresting the flow (stop-flow technique) of the mobile phase when the solute resides in the detecting cell or by scanning the excitation or fluorescent light, respectively. In this way, it is possible to obtain excitation spectra at any chosen fluorescent wavelength or fluorescence spectra at any chosen excitation wavelength.

The *grating–filter* detector is a hybrid between the filter–filter and the grating–grating types. Both high sensitivity and intermediate selectivity are achieved. The use of a filter in combination with gratings is ideal for lowering the background.

Grating–grating fluorometers are convenient for method development, because they permit selection of any excitation or emission wavelength. Filter–filter instruments, on the other hand, are simpler, easier in use, less expensive, more sensitive, and better suited for transferring an HPLC method between laboratories.

With the vast development of technology, fluorescence detectors have become programable. Optimization of wavelength-pair maxima for each analyte can be time programmed during the chromatographic run.

The proper use of fluorescence detectors necessitates knowledge and understanding of noise sources. Dual monochromatic detectors have stray light leakage. When the wavelength pair is close, the background noise can significantly limit the detection limit. The *stray light*, along with *reflection* and *scattering*, increases the blank signal, resulting in reduced signal-to-noise ratio. Reflection occurs at interfaces that have a difference in the refractive index. Scattering can be of *Rayleigh* or *Raman* type.

In Rayleigh scatter, the wavelength of the absorbed and emitted photons are the same. Ultraviolet wavelengths scatter more than visible. Rayleigh scatter can be a significant problem when the wavelength pair overlaps (less than 50 nm) and instruments do not have filter accommodations and adjustable slits.

Raman scatter can also be troublesome. Depending on the wavelength pair of the sample, Raman scatter from the mobile phase can overlap the fluorescence signal and, thus, can be misdiagnosed as the fluorescence signal itself. This problem arises during increasing instrument sensitivity. However, satisfactory separation can be achieved by changing the excitation wavelength because emission is independent of the excitation wavelength.

To summarize, in terms of instrumental operation, the following practices should be followed: proper zeroing of the blank and non-tampering with the gain during serial dilutions. Increased sensitivity should be accomplished by varying the full-scale range.

The basic sequence in instrumental adjustments is to select the minimum gain necessary to allow a full-scale deflection, at the least sensitive scale. When linear curves are prepared, the gain need not be adjusted. Amplification should always be done using the range control. Any small changes in the gain during calibration will cause non-linearity. Once the gain has been set, the zero can be set. To ensure reproducibility, zeroing the detector from time to time during the day is recommended, because the dark current can change during the day.

BIBLIOGRAPHY

1. Dolan, J.W.; Snyder, L.R. *Troubleshooting LC Systems*; Humana Press: Clifton, NJ, 1989; 337–339.
2. Gilbert, M.T. *High Performance Liquid Chromatography*; IOP Publishing: Bristol, U.K., 1987; 34–35.
3. Hancock, W.S.; Sparrow, J.T. *HPLC Analysis of Biological Compounds, A Laboratory Guide*; Marcel Dekker, Inc.: New York, 1984; 166–169.
4. Haugland, R.P. *Handbook of Fluorescent Probes and Research Chemicals,* 6th Ed.; Molecular Probes, Inc.: Eugene, OR, 1996; 1–4.
5. O'Flaherty, B. Fluorescence detection. In *A Practical Guide to HPLC Detection*; Parriott, D., Ed.; Academic Press: San Diego, CA, 1993; 111–139.
6. Papadoyannis, I.N. *HPLC in Clinical Chemistry*; Marcel Dekker, Inc.: New York, 1990; 74–75.
7. Scott, R.P.W. *Techniques and Practice of Chromatography*; Marcel Dekker, Inc.: New York, 1995; 288–292.
8. Scott, R.P.W. *Chromatographic Detectors, Design, Function and Operation*; Marcel Dekker, Inc.: New York, 1996; 199–211.
9. Snyder, L.R.; Kirkland, J.J. *Introduction to Modern Liquid Chromatography,* 2nd Ed.; John Wiley & Sons: New York, 1979; 145–147.
10. Snyder, R.L.; Kirkland, J.J.; Glajch, J.L. *Practical HPLC Method Development*; John Wiley & Sons: New York, 1997; 81–84.

Foam CCC

Hisao Oka
Food-Related Chemistry, Laboratory of Chemistry, Aichi Prefectural Institute of Public Health, Nagoya, Japan

Yoichiro Ito
National Heart, Lung, and Blood Institute (NHLBI), National Institutes of Health (NIH), Bethesda, Maryland, U.S.A.

INTRODUCTION

When a foam moves through a liquid, it carries particles caught at its interface, resulting in accumulation of these particles at the surface. For many years, this phenomenon has been utilized for the separation of minerals and metal ions. Since the method only employs inert gas and aqueous solution, it should have great potential for the separation of biological samples. This idea has been materialized using the high-speed countercurrent chromatographic (HSCCC) system. In this foam CCC method, foam and liquid undergo rapid countercurrent movement through a long, fine Teflon tube (2.6 mm I.D. × 10 m) under a centrifugal force field. This foam CCC technology has been applied to the separation of a variety of samples.

APPARATUS OF FOAM CCC

Fig. 1a illustrates a cross-sectional view of the foam CCC apparatus. The rotary frame holds a coiled separation column and a counterweight symmetrically at a distance of 20 cm from the central axis of the centrifuge. When the motor drives the rotary frame, a set of gears and pulleys produces synchronous planetary motion of the coiled column in such a manner that the column revolves around the central axis of the centrifuge while it rotates about its own axis at the same angular velocity in the same direction. The rotating force field resulted from this planetary motion induces countercurrent movement between the foam and its mother liquid through a long, narrow, coiled tube. Introduction of a sample mixture into the coil results in the separation of sample components. The foam active components are quickly carried with the foaming stream and are collected from one end of the coil, while the rest moves with the liquid stream in the opposite direction and is collected from the other end of the coil.

Fig. 1b illustrates the column design for foam CCC. The coiled column consists of a 10 m long, 2.6 mm I.D. Teflon tube of 50 ml capacity. The column is equipped with five flow channels. The liquid is fed from the liquid feed line at the tail and collected from the liquid collection line at the head. Nitrogen gas is fed from the gas feed line at the head and discharged through the foam collection line at the tail, while the sample solution is introduced through the sample feed line in the middle portion of the coil. The head–tail relationship of the rotating coil is conventionally defined by an Archimedean screw force, where all objects of different density are driven toward the head. Liquid feed rate and sample injection rate are each separately regulated with a needle valve, while the foam collection line is left open to the air.

APPLICATION

Foam CCC can be applied to two types of samples with: 1) affinity to the foam producing carrier; and 2) direct affinity to the gas–liquid interface.

Foam Separation Using Surfactants

This technique was demonstrated for the separation of methylene blue and dinitrophenyl (DNP)-leucine having affinity to the foam producing carrier. Sodium dodecyl sulfate (SDS) and cetyl pyridinium chloride (CPC) were used as carriers to study the effects of their electric charges on the foam affinity of various compounds. When the sample mixture was introduced with the anionic SDS surfactant, the positively charged methylene blue was adsorbed onto the foam and quickly eluted through the foam collection line while the negatively charged DNP-leucine was carried with the liquid stream in the opposite direction and eluted through the liquid collection line. Similarly, when the same sample mixture was introduced with the cationic CPC surfactant, the negatively charged DNP-leucine was totally eluted through the foam collection line and the positively charged methylene blue through the liquid collection line.

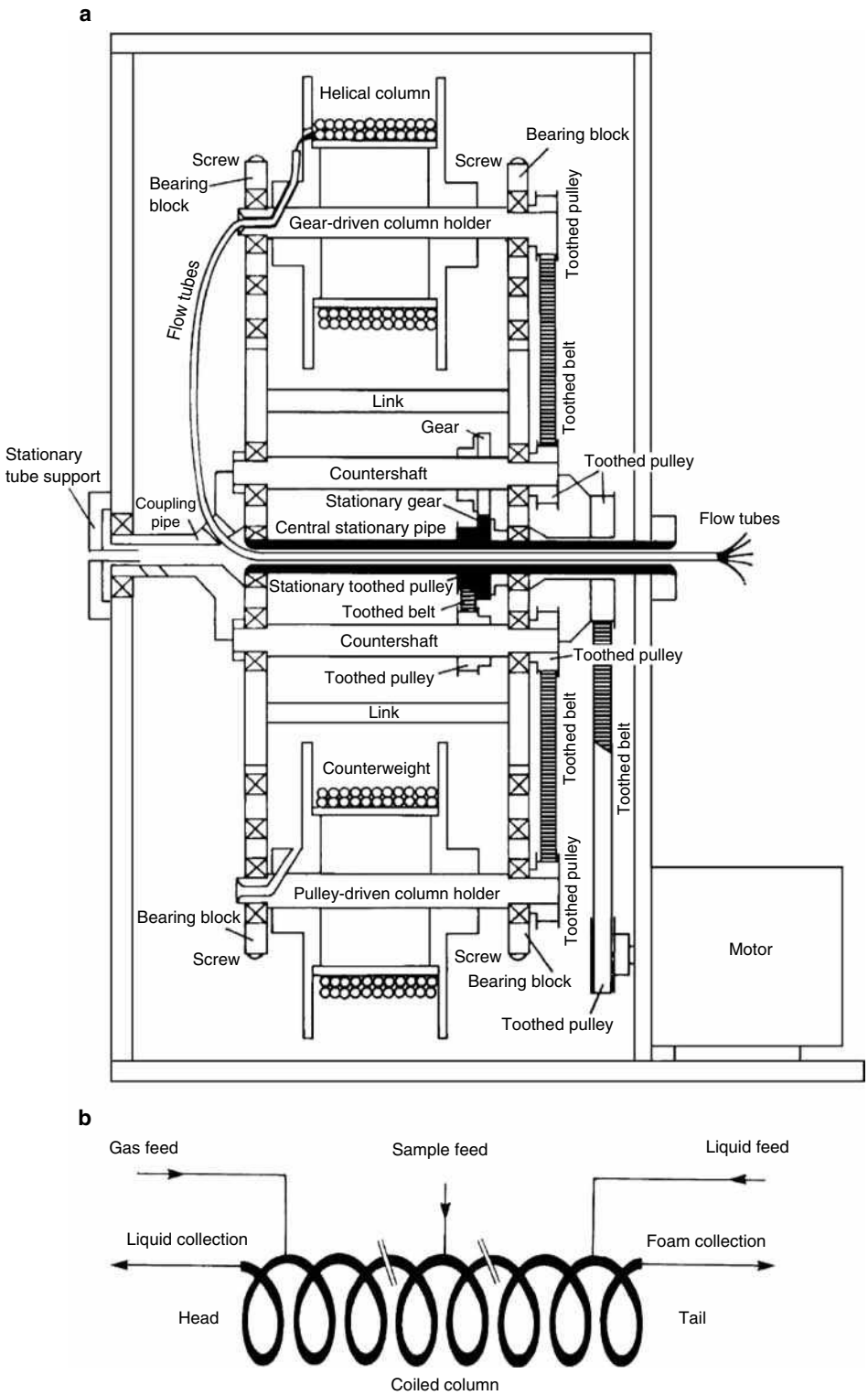

Fig. 1 a) Foam CCC apparatus; and b) column design for foam CCC.

Foam Separation Without Surfactant

Many natural products have foaming capacity so that foam CCC may be performed without surfactant. This possibility was demonstrated using bacitracin complex (BC) as a test sample because of its strong foaming capacity. Bacitracin complex is a basic cyclic peptide antibiotic consisting of more than 20 components, but except for the major components BCs-A and -F, the chemical structures of the other components are still unknown.

The foam CCC experiment for the separation and enrichment of BC components was conducted using nitrogen gas and distilled water entirely free of surfactant or other additives.

Batch sample loading

Foam CCC of BC components was initiated by simultaneously introducing distilled water through the liquid feed line at the tail and nitrogen gas through the gas feed line at the head into the rotating column, while the needle valve in the liquid collection line was fully open. After steady state hydrodynamic equilibrium was reached, the pump was stopped and the sample solution was injected into the sample feed line at the middle of the column. After the lapse of a predetermined standing time, the needle valve opening was adjusted to the desired level and pumping was resumed. Effluents were collected at 15 sec intervals. The bacitracin components were separated in the order of hydrophobicity of the molecule in the foam fractions, with the most hydrophobic compounds being eluted first. This method can also be applied to continuous sample feeding as described below.

Continuous sample feeding

The experiment was initiated by introducing nitrogen gas into the gas feed line at the head of the rotating column. Then, a 2.5 L volume of the BC solution was continuously introduced into the coil through the sample feed line at 1.5 ml/min. The hydrophobic components produced a thick foam that was carried with the gas stream and collected from the foam collection line at the tail, while the other components stayed in the liquid stream and eluted from the liquid collection line at the head. High-performance liquid chromatography (HPLC) analysis of the foam fraction revealed that the degree of enrichment increased with the hydrophobicity of the components. These results clearly indicate that the present method is quite effective for the detection and isolation of small amounts of natural products present in a large volume of aqueous solution.

Recycling sample injection

In this system, the effluent from the liquid outlet is directly returned into the column through the sample feed line so that the sample solution is continuously recycled for repetitive foam fractionation (Fig. 2). The utility of this system was demonstrated in the separations of microcystin extract and bacitracin complex from large volumes of sample solution. Microcystins were separated and enriched in decreasing order of hydrophobicity. Bacitracin A, a hydrophobic major component, in the bacitracin complex was highly enriched in the foam fraction and almost completely isolated from other components. This recycling foam CCC method may be effectively applied for the separation and enrichment of various foam-active components from crude natural products.

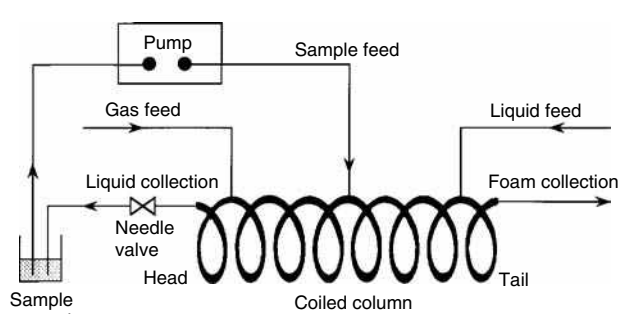

Fig. 2 Foam CCC system with recycle sample injection.

The general procedure for foam CCC using this recycling sample injection is as follows: 1) Clamp the liquid feed inlet (no liquid feed is employed); 2) rotate the column at 500 rpm; 3) fully open the needle valve; 4) introduce nitrogen gas at 80 psi through the gas feed line; 5) introduce the sample at a flow rate of 9.0 ml/min through the sample feed line for 20 min; 6) stop the pumping; 7) close the needle valve; 8) resume the pumping at a flow rate of 1.0 ml/min; 9a) when foam emerges, fractionate effluents from foam outlet at 2.5 min intervals; 10) increase the flow rate to 1.5 ml/min; 9b) when failing to elute at step 8, increase the flow rate to 1.5 ml/min or until the foam is eluted.

Foaming parameters

For application of foam CCC to various natural products, it is desirable to establish a set of physicochemical parameters that reliably indicate their applicability to foam CCC. Two parameters were selected for this purpose, i.e., "foaming power" and "foam stability," which can be simultaneously determined by the following simple procedure. In each test, the sample solution (20 ml) is delivered into a 100 ml graduated cylinder with a ground stopper and the cylinder vigorously shaken for 10 sec. The foaming power is expressed as the volume ratio of the resulting foam to the remaining solution, and the foam stability by the duration of the foam.

In order to correlate the foaming parameters to the foam productivity in foam CCC, the following five samples were selected because of their strong foaming capacities: bacitracin, gardenia yellow, rose bengal, phloxine B, and senega methanol extract. The results of our studies indicated that a sample having foaming power greater than 1.0 and foam stability of over 250 min could be effectively enriched by foam CCC. These minimum requirements of foaming parameters derived from the bacitracin experiment were found to be well applicable to four other samples.

CONCLUSIONS

Foam CCC can be successfully applied to a variety of samples having foam affinity with or without surfactants.

The method offers significant advantages over conventional foam separation methods by allowing the efficient chromatographic separation of sample in both batch loading and continuous feeding. We believe that the foam CCC technique has great potential in the enrichment, stripping, and isolation of foam active components from various natural and synthetic products in both research laboratories and industrial plants.

BIBLIOGRAPHY

1. Bhatnagar, M.; Ito, Y. Foam countercurrent chromatography on various test samples and the effects of additives on foam affinity. J. Liq. Chromatogr. **1988**, *11*, 21.
2. Ito, Y. Foam countercurrent chromatography: New foam separation technique with flow-through coil planet centrifuge. Sep. Sci. **1976**, *11*, 201.
3. Ito, Y. Foam countercurrent chromatography based on dual countercurrent system. J. Liq. Chromatogr. **1985**, *8*, 2131.
4. Ito, Y. Foam countercurrent chromatography with the cross-axis synchronous flow-through coil planet centrifuge. J. Chromatogr. **1987**, *403*, 77.
5. Oka, H.; Harada, K.-I.; Suzuki, M.; Nakazawa, H.; Ito, Y. Foam countercurrent chromatography of bacitracin with nitrogen and additive-free water. Anal. Chem. **1989**, *61*, 1998.
6. Oka, H.; Harada, K.-I.; Suzuki, M.; Nakazawa, H.; Ito, Y. Foam countercurrent chromatography of bacitracin I. Batch separation with nitrogen and water free of additives. J. Chromatogr. **1989**, *482*, 197.
7. Oka, H.; Harada, K.-I.; Suzuki, M.; Nakazawa, H.; Ito, Y. Foam countercurrent chromatography of bacitracin II. Continuous removal and concentration of hydrophobic components with nitrogen gas and distilled water free of surfactants or other additives. J. Chromatogr. **1991**, *538*, 213.
8. Oka, H. Foam countercurrent chromatography of bacitracin complex. In *High-Speed Countercurrent Chromatography*; Ito, Y., Conway, W.D., Eds.; John Wiley & Sons, Inc.: New York, 1996; 107–120 (Chapter 5).
9. Oka, H.; Iwaya, M.; Harada, K.-I.; Muarata, H.; Suzuki, M.; Ikai, Y.; Hayakawa, J.; Ito, Y. Effect of foaming power and foam stability on continuous concentration with foam countercurrentchromatography. J. Chromatogr. A, **1997**, *791*, 53.
10. Oka, H.; Iwaya, M.; Harada, K.-I.; Suzuki, M.; Ito, Y. Recycling foam countercurrent chromatography. Anal. Chem. **2000**, *72*, 1490.

Food Analysis: Ion Chromatography

Rajmund Michalski
Institute of Environmental Engineering, Polish Academy of Science, Zabrze, Poland

Abstract
Ion chromatography (IC) plays an important role not only in the determination of anions and cations in water and wastewater but also in analysis of different kinds of samples such as food and beverages. The entry is a short review of food sample pretreatment and application of IC for the analysis of inorganic and organic ions.

INTRODUCTION

Ion chromatography (IC) has become a useful tool for the analytical chemist especially in the area of inorganic and organic anions and cations analysis.

Originally, IC was developed as a chromatographic method for inorganic anions, using ion-exchange stationary phases and conductivity detection. Recently, the definition of IC has been broadened to include other separation modes such as ion pair chromatography and ion exclusion chromatography, which are based on different separation mechanisms than simply ion exchange.

Ions that are most commonly determined in food samples are: inorganic anions, carboxylic acids, metal ions, and organic cations. Some anion-exchange stationary phases do not always allow a baseline-resolved separation of all inorganic and organic ions under isocratic conditions.

The introduction of gradient elution greatly improved these analyses. The reason IC easily deals with complex matrices lies not only in the stability and resistance to contamination of the stationary phases used, but also in the sensitivity and specificity of the detection methods employed.

IC is increasingly being adopted by many test and research laboratories in food and beverage industry.[1,2] A survey of the application of IC in food and beverage industry is given in Table 1.[3]

SAMPLE PREPARATION FOR FOOD ANALYSIS

Regarding the application of IC for foodstuff analysis, the crucial step is sample preparation. Adequate sample preparation has growing importance because it allows full exploitation of the potential of IC. Thus, it is essential to modernize traditional sample preparation techniques in food analysis, which very often result in solutions that are easily contaminated by high quality of reagents involved or prone to causing IC column contamination.

Sometimes, sample extraction with deionized water and membrane filtration is completely sufficient. In case of a complex sample matrix, more sophisticated sample preparation procedures are required.

The most often used and promising techniques for obtaining solutions for direct IC injection of food samples are: accelerated solvent extraction (ASE), supercritical fluid extraction (SFE), solid-phase extraction (SPE), and UV photolysis and pyrolysis.[4] The ASE technique basically employs the principles of traditional solvent extraction but at higher temperature and pressure, in which conditions solvents show better extraction properties.

SFE uses the principles of traditional liquid–solid extraction. It is extensively used for the separation of organic compounds from food as well as for the separation of inorganic compounds.

SPE offers many advantages over liquid–liquid extraction and permits removal of interferents and analyte concentration at the same time. The extraction conditions are mainly affected by pH, matrix ionic strength of the elution solvent, flow rate, and physicochemical characteristic of the sorbent bed.

The UV digestion of any sample is directly proportional to the UV intensity and irradiation time, and is inversely proportional to the concentration of organic substance.

Microwave-oven digestion involves heating the samples with acids in a polytetrafluoroethylene (PTFE) vessel using microwave radiation. The PTFE vessels are transparent to microwaves and the sample directly absorbs electromagnetic energy that is transmitted to the polar molecules present in the sample, forcing them to vibrate at high frequency. This results in high sample temperatures without the vessel being heated.

Pyrohydrolysis is a technique that uses decomposition of the matrix by superheated water vapors. This technique can be used for the determination of halogens, borates, nitrates, sulfates, etc. in various food matrices.

Table 1 Areas and typical examples of ion chromatography application in the food and beverage analysis.

Application area	Analytical examples
Baby food	Determination of iodide, amines, and transition metals
Beverages	Determination of inorganic anions and cations in the water being used; in sweeteners and flavors and in the finished products; organic acids and carbohydrates in beer, wine, and juice
Canned food	Determination of chloride, nitrite, nitrate, sodium, potassium, organic acids, and transition metals in canned fruit and canned vegetables, species, vinegar, and fish
Cereal products	Determination of bromate and propionate in bakery products
Fats, oils, carbohydrates, and flavors	Determination of fatty acids and carbohydrates in corn syrup
Meat processing	Determination of nitrite/nitrate ratio in meat products; nitrate in the water being used
Milk production	Determination of iodide in whole milk; chloride and/or sodium in butter; lactate, pyruvate, and citrate in cheese

APPLICATION OF IC IN BEVERAGE AND FOOD ANALYSIS

The methods used to evaluate foodstuff quality are commonly required to be reliable, rapid, and convenient. IC meets these requirements, although simply suppressed conductivity detection is sufficient only for the detection of selected ions such as chloride, sulfate, sodium, potassium, magnesium, and calcium. Its application strongly depends on sample matrix. Sometimes an alternative detection mode should be used.

Generally speaking, most inorganic anions and cations have weak absorption in UV–Visible spectral region. Thus, only selected ions can be determined by UV detection.[5] Therefore other detection techniques such as amperometry, spectrometry, and refractive index are used for food analysis. The best detection limit is offered by mass spectrometry because of the reduction of chemical noise especially in complex matrices.[6]

The determination of anions and cations in alcoholic and non-alcoholic beverages is of importance from both health-related and manufacturing perspectives. It concerns the determination of inorganic and organic anions and cations,[7,8] and carbohydrates[9,10] in beverages of all kinds (e.g., beer, wine, fruit juices, refreshers, coffee, and tea).

The analysis of organic acids, carbohydrates, sulfites, ascorbic acid, and ethanol is of primary interest for characterizing beer and monitoring of brewing process. For monitoring the brewing process in terms of carbohydrates, anion-exchange chromatography with pulsed amperometric detection is the method of choice.

The spectrum of organic acids in wine is extremely complex and represents a challenge for IC analysis due, in part, to large concentration differences.[11] In many cases, a number of organic additives are added to refreshing drinks. These additives include sweeteners such as saccharin or aspartame, preservatives such as benzoic acid, and flavors such as citric acid and caffeine. They can be simultaneously analyzed using a multimode phase with anion-exchange and reversed-phase, and simultaneous conductive and UV detection.

Sweeteners such as saccharine, sodium cyclamate, and acesulfam-K are more and more frequently used in food industry instead of sugar or glucose syrup. These compounds in alkaline medium exist as anions, thus anion-exchange chromatography with conductivity detection provides an alternative to reversed-phase liquid chromatography (RPLC) with UV/Vis detection.[12]

A serious analytical problem is the analysis of preservatives used in food preparation. Usually, separation is carried out on chemically modified silica, utilizing suppressed conductivity detection and UV/Vis detection for preservatives containing chromophores.[13]

As in the case of inorganic anions (Cl^-, NO_2^-, NO_3^-, PO_4^{3-}, SO_4^{2-}), many inorganic cations (e.g., Na^+, K^+, NH_4^+, Mg^{2+}, and Ca^{2+}) are introduced into beverages with water. Others are introduced as counterions to added ingredients. These ions are monitored due to restrictions imposed by different countries and for purposes of mass balance. Thus, the content of these ions needs to be monitored by the manufacturer to maintain high quality of the product. The quality of beverages, in a sense, is based on ion controlling, because some ions such as K^+ and Na^+ are beneficial to human health; some of them are not.

Some organic acids such as citrate and malate, and inorganic anions such as phosphate are monitored due to their function as acidifiers or flavor enhancers. In addition, the presence of some organic acids can be used to reveal potential food adulteration.[14] As an alternative to ion-exchange chromatography, ion-exclusion chromatography is also used for determining organic acids especially in milk products and fruit juices.[15]

Ions determined in food samples can be divided into: nitrogen, sulfur and phosphorus compounds, halides, and inorganic and organic cations. For health purposes, the determination of nitrogen compounds such as nitrite, nitrate, ammonium, and biogenic amines is of great importance. Nitrates are naturally present in many foodstuffs, noticeably

vegetables, where their content varies to a great extent because of the widespread nitrogenous fertilizers in use.

Vegetables are not the only source of nitrate intake. Potassium and sodium salts of both nitrate and nitrite are commonly used in food industry, in curing meat, for fixing the color, for inhibiting the microbial growth, and for obtaining the characteristic flavor.[16]

The determination of nitrite and nitrate in meat and sausage products is an important problem, because their tolerated concentrations are strictly limited. Sample preparation includes homogenization of the sample, its extraction with a 5% borax buffer in a hot water bath, and subsequent Carrez precipitation with 15% potassium hexacyanoferrate(II) and 30% zinc sulfate solution.

The nitrate content is also important for monitoring the food adulteration in dairy industry.

The determination of nitrite and nitrate is usually performed simultaneously by using a bicarbonate/carbonate or hydroxide eluent and suppressed conductivity detection, alone or coupled with UV/Vis detection in the case of complex matrices.

Sulfur species commonly used in the food industry as preventing agents are sulfites. Moreover, sulfate concentration can be affected by technological use of sulfites.

Sulfate can be determined simultaneously with other inorganic species of sulfur such as thiosulfate and dithionate, using conductivity, UV/Vis or amperometric detectors.

Total phosphorus content is one of the parameters used to define product quality and originality. Phosphorus compounds are present in most vegetables and foods. Some of them such as proteins and phospholipids are important indicators of metabolic activity. Inorganic phosphates are extensively used as fertilizers, so the same considerations that apply for nitrogen species are also valid for phosphorus content in food samples.

Phosphorus concentration in milk affects almost all aspects of cheese manufacturing, and in soft drinks production, where it acts as acidifier and flavor.[17] Polyphosphates are widely used as additives: in meat-based products for reducing water loss, to increase the uptake of water for economic purposes, in fruit juices as flavor and color preservatives, in diary industry as additive for cheese, etc.

The most common way of phosphate determination is its separation with bicarbonate/carbonate or hydroxide eluent followed by suppressed conductivity detection. Yet this does not suffice for polyphosphates determination in food samples that have to be determined by means of gradient IC. When determining orthophosphate content, it should be noted that only free PO_4^{3-} ions, and not the total phosphate, are detected by IC. The reason is that some phosphate is bound by calcium especially in fruit juices.[18]

Next group of anions determined in food samples are halides. The principal source of fluoride intake is water, however, other foods such as tea[19] and fish can be a source of fluoride as well. In dairy products such as cream and cheese, fluoride content is very high and can exceed by threefold the original fluoride concentration in milk.

Chloride is one of the most common inorganic anions in food. Its content is usually related to presence of sodium. In food industry, it is commonly added in the form of NaCl as a preservative or to enhance sapidity of the final products.

The bromide content in food is mainly related to disinfecting with methyl bromide. Some plants such as carrot, celery, and tomato accumulate bromide and its determination can be used as a marker of methyl bromide treatment. High bromide concentration in soft drinks can derive from the addition of brominated vegetable oils.

Bromate is a potential carcinogenic agent; thus its determination even at trace levels is important in drinking water. There is some health risks concerning with residual bromate in bakery products, because bromate salts are used as dough conditioners in baking industry. The majority of bromate is reduced to bromide during baking processes, however residual bromate has still been found in some baked goods.[20]

Common sources of iodide include not only iodized table salt and seafood, but also other foods such as eggs and milk. In standard analytical conditions, IC allows simultaneous determination of fluoride, chloride, and bromide with suppressed conductivity detection, while iodide is usually determined separately with amperometric detection.

Among many other anionic species determined in foodstuff, the most important are: cyanide, carbonate, and certain anionic metal complexes. Cyanides are very toxic compounds; concentrations as low as a few ppm are dangerous for human health. Cyanide is naturally present in some vegetables, such as cassava, sorghum, and fruit seeds. Amperometric detection provides high sensitivity for cyanide.

Carbonate is naturally present in fermented beverages or added to soft drinks. Taking into consideration of its weak acidity, the separation technique of choice is ion exclusion chromatography coupled with conductivity detection.

Selected metal anionic forms such as arsenic species are toxic compounds and their presence must be detected at very low levels. Similar to inorganic arsenic species, simultaneous determination of selenite and selenate, as well as Cr(III)/Cr(VI), provides important information about oxidation states and their influence on food quality and human health.

These species can be determined by UV/Vis or amperometric detection, coupled with suppressed conductivity, or by hyphenated techniques such as ion chromatography–mass spectrometry (IC–MS) or ion chromatography-inductively coupled plasma–mass spectrometry (IC-ICP–MS).[21]

Inorganic cations such as sodium, potassium, ammonium, calcium, magnesium, heavy and transition metals, and organic amines are present in foods and their concentrations can significantly vary.

IC allows simultaneous determination of alkaline and alkaline earth metals, as well as ammonium and biogenic

amines with conductivity detection, while heavy and transition metals are more commonly determined by post-column derivatization technique by absorbance detection.[22] The main advantage of post-column derivatization technique by UV detection is the simultaneity of the procedure and the ability to distinguish between different oxidation states.[23]

Another important application of IC in food industry is determination of biogenic amines. Usually, they are separated by ion-pair chromatography on a chemically bonded reversed phase, using UV detection, amperometry[24], or MS detection.[25]

CONCLUSION

IC has been applied successfully to analysis of inorganic and organic ions in foodstuffs. Its reliability and versatility in analyzing complex matrices typical of food samples with high selectivity, sensitivity, and reproducibility provides a rapid and convenient means to obtain complex profiles of ionic components.

New developments in sample preparation, higher capacity of ion-exchange stationary phases coupled with high efficiency, different selectivity, solvent compatibility, and major diffusion of IC detection techniques other than conductivity cause more widespread usability of IC in food industry.

REFERENCES

1. Buldini, P.L.; Cavalli, S.; Trifirò, A. State-of-the-art ion chromatographic determination of inorganic ions in food. J. Chromatogr. A, **1997**, *789*, 529–548.
2. Pereira, C.F. Application of ion chromatography to the determination of inorganic anions in foodstuffs. J. Chromatogr. A, **1992**, *624*, 457–470.
3. Weiss, J. *Handbook of Ion Chromatography*. Wiley-VCH: Weinheim, Germany, 2004; 711–756.
4. Smith, R. Before the injection–modern methods of sample preparation for separation techniques. J. Chromatogr. A, **2003**, *1000*, 3–27.
5. Fernandes, C.; Leite, R.S.; Lancas, F.M. Rapid determination of bisphosphonates by ion chromatography with indirect UV detection. J. Chromatogr. Sci. **2007**, *45*, 236–241.
6. Saccani, G.; Tanzi, E.; Cavalli, S. Determination of nitrite, nitrate, and glucose-6-phosphate in muscle tissues and cured meat by IC/MS. J. AOAC Inter. **2006**, *89*, 712–719.
7. Horie, H.; Kohata, K. Analysis of tea components by high performance liquid chromatography and high performance capillary electrophoresis (Review). J. Chromatogr. A, **2000**, *881*, 425–438.
8. Alcazar, A.; Fernandez-Caceres, M.J.; Martin, M.J.; Pablos, F.; Gonzalez, A.G. Ion chromatography determination of some organic acids, chloride and phosphate in coffee and tea. Talanta **2003**, *61*, 95–101.
9. Mato, I.; Suarez-Luque, S.; Huidobro, J.F. A review of the analytical methods to determine organic acids in grape juices and wines. Food Res. Intl. **2005**, *38*, 1175–1188.
10. Yan, Z.; Zhang, X.D.; Niu, W.J. Simultaneous determination of carbohydrates and organic acids in beer and wine by ion chromatography. Microchim. Acta. **1997**, *127*, 189–194.
11. Prusisz, B.; Mulica, K.; Pohl, P. Ion exchange and ion exclusion chromatographic characterization of wines using conductivity detection. J. Food Drug Anal. **2008**, *16*, 95–103.
12. Zhu, Y.; Guo, Y.Y.; Ye, M.L. Separation and simultaneous determination of four artificial sweeteners in food and beverages by ion chromatography. J. Chromatogr. A, **2005**, *1085*, 143–146.
13. Chen, Q.C.; Wang, J. Simultaneous determination of artificial sweeteners, preservatives, caffeine, theobromine and theophylline in food and pharmaceutical preparations by ion chromatography. J. Chromatogr. A, **2001**, *937*, 57–64.
14. Yoshikawa, K.; Okamura, M.; Inokuchi M. Ion chromatographic determination of organic acids in food samples using a permanent coating graphite carbon column. Talanta **2007**, *72*, 305–309.
15. Chinnici, F.; Spinabelli, U.; Riponi, C. Optimization of the determination of organic acids and sugars in fruit juices by ion-exclusion liquid chromatography. J. Food Comp. Anal. **2005**, *18*, 121–130.
16. Siu, D.C.; Henshall, A. Ion chromatographic determination of nitrate and nitrite in meat products. J. Chromatogr. A, **1998**, *804*, 157–160.
17. Cataldi, T.R.I.; Angelotti, M.; D'Ericha, L.; Alteri, G.; Di Renzo, G.C. Ion-exchange chromatographic analysis of soluble cations, anions and sugars in milk whey. Eur. Food Res. Technol. **2003**, *216*, 75–82.
18. Sekiguchi, Y.; Matsunaga, A.; Yamamoto, A. Analysis of condensed phosphates in food products by ion chromatography with an on-line hydroxide eluent generator. J. Chromatogr. A, **2000**, *881*, 639–644.
19. Michalski, R. Simultaneous determination of common inorganic anions in black and herbal tea by suppressed ion chromatography. J. Food Qual. **2006**, *29*, 607–616.
20. Wang, K.; Liu, H.; Huang, J.; Chen, X.; Hu, Z. Determination of bromate in bread additives and flours by flow injection analysis. Food Chem. **2000**, *70*, 509–514.
21. Vela, N.P.; Heitkemper, D.T. Total arsenic determination and speciation in infant food products by ion chromatography-inductively coupled plasma–mass spectrometry. J. AOAC Int. **2004**, *87*, 244–252.
22. Buldini, P.L.; Cavalli, S.; Mevoli, A. Ion chromatographic and voltammetric determination of heavy and transition metals in honey. Food Chem. **2001**, *73*, 487–495.
23. Benramdane, L.; Bressolle, F.; Vallon, J.J. Arsenic speciation in humans and food products: A review. J. Chromatogr. Sci. **1999**, *37*, 330–344.
24. De Borba, B.M.; Rohrer, J.S. Determination of biogenic amines in alcoholic beverages by ion chromatography with suppressed conductivity detection and integrated pulsed amperometric detection. J. Chromatogr. A, **2007**, *1155*, 22–30.
25. Gianotti, V.; Chiurminatto, U.; Mazzucco, E. A new hydrophilic interaction liquid chromatography tandem mass spectrometry method for the simultaneous determination of seven biogenic amines in cheese. J. Chromatogr. A, **2008**, *1185*, 296–300.

Food Colors: TLC Analysis and Scanning Densitometry

Hisao Oka
Food-Related Chemistry, Laboratory of Chemistry, Aichi Prefectural Institute of Public Health, Nagoya, Japan

Yuko Ito
Tomomi Goto
Aichi Prefectural Institute of Public Health, Nagoya, Japan

INTRODUCTION

Many synthetic and natural colors are used in foods all over the world. In Japan, 12 synthetic and 66 natural colors are generally permitted for use in foods. The Japanese government requires labeling on the package concerning kinds of colors that have been used in the contained foods. However, non-permitted colors are also frequently detected in food, and also unlabeled foods are found in the market. Thus, the inspection of colors in foods has been performed by a public health agency.

The analyses of colors in foods have been mainly achieved by thin-layer chromatography (TLC), because TLC is a simple and effective technique for the separation of components in a mixture. However, the only useful information obtained from a TLC plate to identify a component is the R_f value; the identification of the separated components is difficult unless an appropriate spectrometric method, such as ultraviolet-visible absorption spectrometry, is used. A stepwise operation, including individual component separation by TLC and measurement of the spectrum, is laborious and time-consuming, because it requires extra steps such as extraction of the desired compound from the TLC plate and elimination of adsorbents.

TLC/scanning densitometry is a useful tool for the identification of the target compounds on a TLC plate, because the combined methods can separate and then directly measure ultraviolet-visible absorption spectra of the compounds without the laborious and time-consuming procedures described above. In this entry, we deal with the identification of synthetic and natural colors in foods using TLC/scanning densitometry.

SYNTHETIC COLORS

A simple and rapid identification method for synthetic colors in foods has been established, using TLC/scanning densitometry.[1] Forty-five synthetic colors were able to be completely separated on a C18 TLC plate by complementary use of the following four solvent systems: 1) acetonitrile–methanol–5% sodium sulfate (3:3:10); 2) methyl ethyl ketone–methanol–5% sodium sulfate (1:1:1); 3) acetonitrile–methanol–5% sodium sulfate (1:1:1); and 4) acetonitrile–dichloromethane–5% sodium sulfate (10:1:5). We measured the visible absorption spectra of the synthetic colors on the developed C18 TLC plates by scanning densitometry to identify them. The spectra of the colors purified from foods were in close agreement with those of the standard colors, and the reliability of identification was established.

Next, we successfully applied this technique to the identification of an unknown synthetic color in a pickled vegetable.[2] This color was suspected to be orange II (Or-II), which is not permitted for use in foods in Japan. It was difficult to identify Or-II by conventional analytical methods for food colors, including TLC and high-performance liquid chromatography (HPLC), because there are actually three isomers in total: orange I (Or-I), orange RN (Or-RN), and Or-II, due to differences in the positions of hydroxyl groups in the molecules. Under conventional TLC or HPLC conditions, it is hard to separate these isomers from each other. As shown in Fig. 1 (left), the unknown color showed the same R_f value as those of Or-II and Or-RN, although it showed a different R_f value from Or-I. In order to identify the unknown color, we measured the visible absorption spectrum of the color using TLC/scanning densitometry and compared it with those of Or-II and Or-RN. Both spectra of the unknown color and Or-II gave maximum absorption at only 485 nm; however, that of Or-RN showed maximum absorption at 485 and 400 nm. Therefore, we identified the unknown color in the pickled vegetable to be Or-II.

Thus, TLC/scanning densitometry is shown to be effective for the identification of an unknown synthetic color in foods.

NATURAL COLORS

Lac Color and Cochineal Color

Lac color is a natural food additive extracted from a stick lac, which is a secretion of the insect *Coccus laccae*

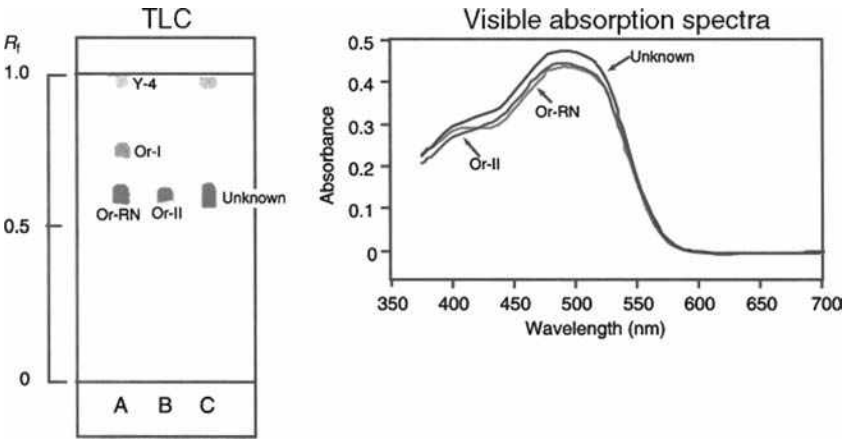

Fig. 1 TLC and visible absorption spectra of synthetic colors extracted from a pickled vegetable under TLC/scanning densitometry. (A) Standards of tartrazine (Y-4), orange I (Or-I), and orange RN (Or-RN). (B) Standard of orange II (Or-II). (C) Extract of the sample. TLC/scanning densitometric conditions. Plate: RP-18 (E. Merck). Solvent system: methyl ethyl ketone-methanol-5% sodium sulfate (1:1:1). Apparatus: Shimadzu CS-9000. Wavelength scanning range: 370–700 nm. Slit size: 0.4 × 0.4 mm. Measuring mode: reflecting absorption.

(*Laccifer lacca* Kerr), and is widely used for coloring food. It is known that the red color is derived from a water-soluble pigment including laccaic acids A, B, C, and E. Cochineal color extracted from the dried female bodies of the scale insect (*Coccus cacti* L.) is water-soluble and has a reddish color. The main coloring component is carmic acid.

Because these colors are frequently used in juice, jam, candy, jelly, etc. it is required to establish a simple and rapid analysis method using TLC. However, as described in the "Introduction," the only useful information obtained from a TLC plate to identify a component is the R_f value. Therefore, we applied TLC/scanning densitometry to the identification of lac and cochineal colors in foods.[3]

TLC conditions

After various experiments, the best results were obtained using methanol–0.5 mol/L oxalic acid (5:4.5) as the solvent system, with a C18 TLC plate. As shown in Fig. 2 (left), the lac color standard was separated into two spots at R_f values of 0.60 and 0.29, and cochineal color standard gave a spot at R_f value of 0.52. Anthraquinone compounds, such as lac and cochineal colors, showed extreme tailing on the C18 TLC plate using conventional TLC conditions. We have previously found that the use of a solvent system containing oxalic acid is effective for controlling the tailing of anthraquinone compounds. Therefore, we decided to use a solvent system containing oxalic acid and tried various TLC conditions. Finally, we found the best conditions described above.

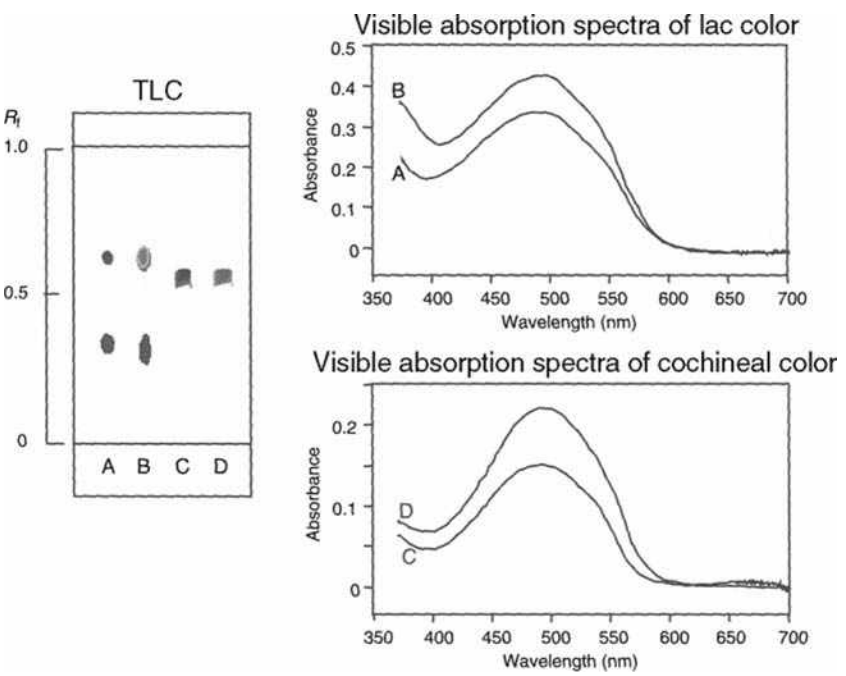

Fig. 2 TLC and visible absorption spectra of lac color and cochineal color extracted from commercial foods under TLC/scanning densitometric conditions. (A) Lac color standard. (B) Extract of jelly. (C) Cochineal color standard. (D) Extract of spagetti sauce. Plate: RP-18 (E. Merck). Solvent system: methanol-0.5 mol/L oxalic acid (5.5:4.5). Other conditions: see Fig. 1.

Measurement of visible absorption spectrum by scanning densitometry

Reflection spectra of the spots of lac color standard at R_f values of 0.60 and 0.29 and cochineal color standard at R_f value of 0.52 on the TLC plate were taken under the conditions described above. The obtained spectra showed good agreement with the spectra obtained from methanol solutions. Therefore, we considered that TLC/scanning densitometry is effective for the identification of these natural colors.

Application to commercial food

Reproducibility of the R_f value by reversed-phase TLC (RP-TLC). In order to examine the effects of the contaminants contained in the sample on the R_f value, 122 commercial foods (41 foods for lac color and 81 foods for cochineal color) were analyzed by C18 TLC as described above. The obtained R_f values of the spots were then compared. The difference between the R_f value of the standard color and the R_f value of the color in the sample was expressed as the ratio between the R_f value of the color in the sample (Ra) and the R_f value of the standard color (Rs); the reproducibility was evaluated according to the coefficient of variation of this ratio.[4] With respect to lac color, the average Ra/Rs values were 0.99 with a coefficient of variation of 8.1% and 1.00 with 4.6% for spots at R_f values of 0.29 and 0.60, respectively. Cochineal color gave an average Ra/Rs value of 0.99 with a coefficient of variation of 5.9%. These results suggest that the spots extracted from the samples appear nearly at the same positions as those of the lac color and the cochineal color standard without being affected by contaminants in the sample, and that the identification of the color is reliable and reproducible.

Identification by TLC/scanning densitometry. The visible absorption spectra of the spots of the lac and cochineal colors on the C18 TLC plates, for which the reproducibility of the R_f value had been evaluated, were measured using a scanning densitometer. Fig. 2 shows the typically obtained TLC chromatograms and spectra obtained from the spots. The spectra of the colors purified from foods were in good agreement with those of the standard colors; thus, the reliability of identification was then established.

Paprika Color

Paprika color is obtained by extraction from the fruit of red peppers (*Capsicum annuum*) and contains capsanthin and its esters, formed from acids, such as lauric acid, myristic acid, and palmitic acid, in large amounts as its color components. Commercially available paprika colors are known to have different compositions of these color components, depending on the material from which the paprika color is extracted; this makes the identification of paprika color, based on the analysis of the color components, impossible, causing difficulty in developing a simple, rapid, and reliable identification method for the paprika color in foods. Therefore, we investigated a TLC/scanning densitometric method for the identification of paprika color using capsanthin, which is a main product of saponification, as an indicator.[5]

TLC conditions

When a paprika color standard, before saponification, was subjected to C18 TLC, a number of overlapping spots were observed, and a satisfactory separation could not be obtained. This was probably due to the paprika color containing a large number of esters. Paprika color is known to be hydrolyzed into a carotenoid and a fatty acid when saponified under mild conditions. Thus, a paprika color standard, after saponification, was subjected to TLC using a solvent system of acetonitrile–acetone–*n*-hexane (11:7:2) on a C18 plate. It was found that the paprika color standard, after saponification, was satisfactorily separated into a main spot having an R_f value of 0.50 and two subspots having R_f values of 0.60 and 0.75 (Fig. 3A). The main

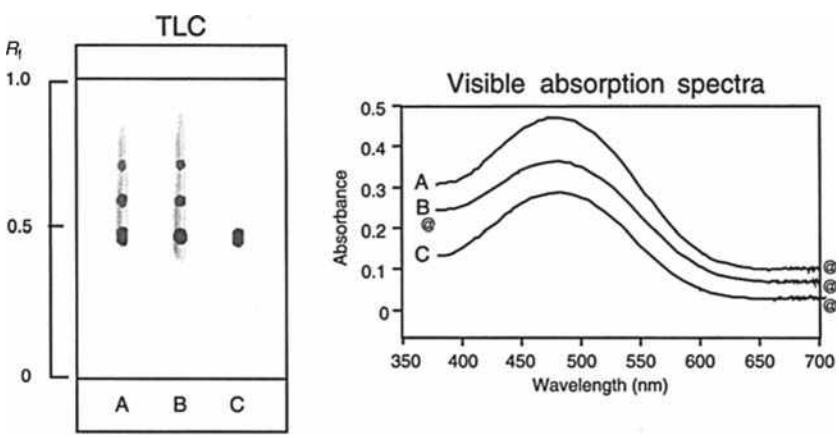

Fig. 3 TLC and visible absorption spectra of hydrolyzed paprika colors extracted from commercial foods under TLC/scanning densitometric conditions. (A) Hydrolyzed paprika color standard. (B) Hydrolyzed extract of rice-cracker. (C) Capsanthin. Plate: RP-18 (E. Merck). Solvent system: acetonitrile–acetone–*n*-hexane (11:7:2). Other conditions: see Fig. 1.

spot was identical with the spot of the capsanthin standard in terms of its R_f value, color, and shape (Fig. 3C).

As described above, it was suggested that the paprika color is hydrolyzed into a carotenoid and a fatty acid by saponification under mild conditions. Next, the saponification conditions were investigated; based on various experimental results, the following saponification conditions were selected: reaction time, 24 hr; amount of 5% sodium hydroxide–methanol solution, 2 ml.

Measurement of visible absorption spectrum by scanning densitometry

The separated spots, obtained by subjecting a paprika color standard, after saponification, to C18 TLC under the conditions described above, were then subjected to scanning densitometry. The visible absorption spectra were scanned in the wavelength range of 370–700 nm, and excellent visible absorption spectra were obtained (Fig. 3A). The spectrum of the main spot ($R_f = 0.50$) of the paprika color, after saponification, showed its maximum absorption wavelength at 480 nm, which identically matches the spectrum of the capsanthin standard (Fig. 3C).

Application to commercial foods

Reproducibility of the Rf value by RP-TLC. The paprika color in 42 samples from commercially available foods, that had a label stating the use of paprika color, were analyzed by C18 TLC to examine the influence of the coexisting substances from the sample on the R_f value. The obtained R_f values of the main spot ($R_f = 0.50$) of saponified paprika color were then compared, and Ra/Rs value was computed. The average Ra/Rs value was 1.01 with a coefficient of variation of 2.6%, suggesting that the spot extracted from the samples appear nearly at the same position as that of the paprika color standard without being affected by contaminants in the sample and that the identification of the color is reliable and reproducible.

Identification by RP-TLC/scanning densitometry. The visible absorption spectra of the main spot of the saponified paprika color on the C18 TLC plates, for which the reproducibility of the R_f value had been evaluated, were measured using a scanning densitometer. Fig. 3 shows the typically obtained TLC chromatograms and spectra obtained from the spots. The spectra of the colors purified from foods were in good agreement with those of the standard colors, and the identification reliability was then destablished.

Gardenia Yellow

Gardenia yellow is a yellow color obtained by extracting or hydrolyzing the fruit of the *Gardenia augusta* MERR. var. *gardiflora* HORT. with water or ethanol and is widely used for the coloring of noodles, candies, and candied chestnuts. The yellow color is derived from the carotinoids crocin and crocetin. Crocetin is the hydrolysis product of crocin. Gardenia yellow has been conventionally analyzed by a method based on reversed-phase chromatography/scanning densitometry using crocin as the indicator. However, when this method was applied to samples containing caramel or anthocyanins, their spots overlapped with that of crocin, which made it difficult to identify the gardenia yellow. Therefore, we evaluated an analytical method for gardenia yellow based on C18 TLC/scanning densitometry using crocetin as the indicator by hydrolyzing crocin, extracted from food samples, into crocetin.[6]

Hydrolysis and TLC conditions

In order to examine the optimal hydrolysis conditions of crocin, a standard crocin solution was hydrolyzed by varying the pH of the solution, temperature, and incubation time; the degree of hydrolysis was followed by C18 TLC as described below. Samples of crocin were completely hydrolyzed to crocetin by adjusting the pH to 11 or above with 0.1 mol/L sodium hydroxide and incubating them at 50°C for 30 min. Therefore, we applied these conditions to hydrolyze crocin to crocetin in the subsequent work.

Next, we investigated the optimal TLC conditions for the separation of crocin and crocetin and found that the combined use of a C18 TLC plate and solvent system of acetonitrile–tetrahydrofuran–0.1 mol/L oxalic acid (7:8:7) gave a satisfactory separation. Under these TLC conditions, crocin gives three spots at R_f values of 0.74, 0.79, and 0.83, and crocetin gives one spot at an R_f value of 0.51 (Fig. 4, left).

Measurement of visible absorption spectrum by scanning densitometry

Reflection spectra of the spots on the TLC plates separated under the conditions described above were measured at scanning wavelengths of 370–700 nm. Fig. 4 (right) shows the visible absorption spectra obtained; the maximum absorption wavelengths were 435 and 460 nm, being in complete agreement with the visible absorption spectrum for the standard preparation of crocetin.

Application to commercial foods

As described above, foods that contained caramel or anthocyanins, for which the identification of gardenia yellow was impossible by the analytical method using crocin as an indicator due to the appearance of interfering spots at the same positions as the spots of crocin on the C18 TLC plates, were analyzed by the present method. As shown in Fig. 4 (left), crocetin appeared as a clear spot on the plate, and the shape and R_f value of the spot were in close agreement with those of the standard preparation. Hence, gardenia yellow can be identified using crocetin as the indicator.

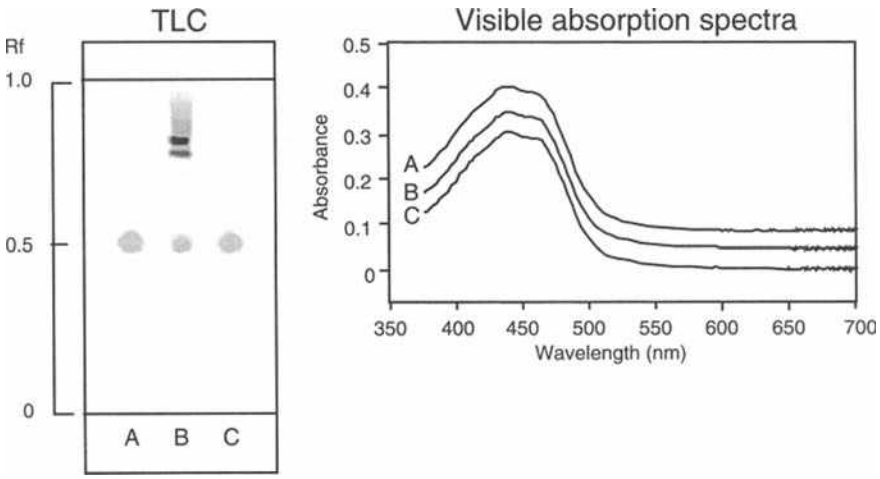

Fig. 4 TLC and visible absorption spectra of the hydrolyzed gardenia yellow extracted from commercial foods under TLC/scanning densitometry. (A) Hydrolyzed gardenia yellow standard. (B) Candy containing gardenia yellow and anthocyanin. (C) Crocetin. Plate: RP-18 (E. Merck). Solvent system: acetonitrile-tetrahydrofuran-0.1 mol/L oxalic acid (7:8:7). Other conditions: see Fig. 1.

Reproducibility of the R_f value by RP-TLC. To examine the influence of the contaminants contained in the sample on the R_f value, 37 commercial foods were analyzed by C18 TLC. The obtained R_f values of the spots were then compared. The mean value of Ra/Rs was 0.99, and the coefficient of variation was 2.5%. These results suggest that the spots of crocetin generated by hydrolysis appear nearly at the same positions as those of the standard color, without being affected by contaminants in the sample, and that the identification of the color is reliable and reproducible.

Identification by RP-TLC/scanning densitometry. The visible absorption spectra of the crocetin spots on the reversed-phase TLC plates, for which the reproducibility of the R_f value had been evaluated, were measured using a scanning densitometer. Fig. 4 shows the typically obtained TLC chromatograms and spectra obtained. The spectra of the colors purified from foods were in close agreement with that of the standard dye, and the identification reliability was then established.

CONCLUSIONS

We introduced the identification of food colors in foods using TLC/scanning densitometry and consider the method to be sufficiently applicable to routine analyses at facilities such as the Centers of Public Health and the Food Inspection Office. Also, we consider that TLC/scanning densitometry is applicable to the identification of various food additives, drugs, and pesticides in foods. However, TLC/scanning densitometry has a limitation: It can be applied only to samples which have chromophores in the molecules. Recently, applications of the TLC/matrix-assisted laser desorption ionization time-of-flight mass spectrometry (TOF-MS),[7] TLC/fast atom bombardment MS,[7] and TLC/multiphoton ionization TOF-MS[8] have been reported. Combined uses of these techniques and TLC/scanning densitometry can develop further applications of TLC.

REFERENCES

1. Ohno, T.; Ito, Y.; Mikami, E.; Ikai, Y.; Oka, H.; Hayakawa, J.; Nakagawa, T. Identification of coal tar dyes in cosmetics and foods using reversed phase TLC/scanning densitometry. Jpn. J. Toxicol. Environ. Health **1996**, *42*, 53–59.
2. Ueno, E.; Ohno, T.; Oshima, H.; Saito, I.; Ito, Y.; Oka, H.; Kagami, T.; Kijima, H.; Okazaki, K. Identification of small amount of coal tar dyes in foods by reversed phase TLC/scanning densitometry with sample concentration techniques. J. Food Hyg. Soc. Jpn. **1998**, *39*, 286–291.
3. Itakura, Y.; Ueno, E.I.; Ito, Y.; Oka, H.; Ozeki, N.; Hayashi, T.; Yamada, S.; Kagami, T.; Miyazaki, Y.; Otsuji, Y.; Hatano, R.; Yamada, E.; Suzuki, R. Analysis of lac and cochineal colors in foods using reversed phase TLC/scanning densitometry. J. Food Hyg. Soc. Jpn. **1999**, *40*, 183–188.
4. Ozeki, N.; Oka, H.; Ikai, Y.; Ohno, T.I.; Hayakawa, J.; Sato, T.; Ito, M.; Ito, Y.; Hayashi, T.; Yamada, S.; Kagami, T.; Miyazaki, Y.; Otsuji, Y.; Hatano, R.; Yamada, E.; Suzuki, R. Application of reversed phase TLC to the analysis of coal tar dyes in foods. J. Food Hyg. Soc. Jpn. **1993**, *34*, 542–545.
5. Hayashi, T.; Ueno, E.; Ito, Y.; Oka, H.; Ozeki, N.; Itakura, Y.; Yamada, S.; Kagami, T.; Miyazaki, Y. Analysis of β-carotene and paprika color in foods using reversed phase TLC/scanning densitometry. J. Food Hyg. Soc. Jpn. **1999**, *40*, 356–362.
6. Ozeki, N.; Oka, H.; Ito, Y.; Ueno, E.; Goto, T.; Hayashi, T.; Itakura, Y.; Ito, T.; Maruyama, T.; Tsuruta, M.; Miyazawa, T.; Matsumoto, H. A reversed-phase thin-layer chromatography/scanning densitometric method for the analysis of gardenia yellow in food using crocetin as an indicator. J. Liq. Chromatogr. **2001**, *24*, 2849–2860.
7. Wilson, I.D. The state-of-the-art in thin-layer chromatography–mass spectrometry: A critical appraisal. J. Chromatogr. A, **1999**, *856*, 429–442.
8. Krutchinsky, A.N.; Dolgin, A.I.; Utsal, O.G.; Khodorkovski, A.M. Thin-layer chromatography–laser desorption of peptides followed by multiphoton ionization time-of-flight mass spectrometry. J. Mass Spectrom. **1995**, *30*, 375–379.

Food: Drug Residue Analysis by LC/MS

Nikolas A. Botsoglou
Laboratories of Nutrition, Faculty of Veterinary Medicine, Aristotle University of Thessaloniki, Thessaloniki, Greece

Abstract
Analyzing drug residues in animal-derived food is complicated as it is not known whether residues exist, and if they exist, the type and quantity are not known. The possibility for unambiguous identification of illegal drug residues is offered by coupling liquid chromatography (LC) with mass spectrometry (MS). The major problems that frequently appear when LC is coupled with MS and their elimination are discussed in this entry.

INTRODUCTION

Numerous detection systems that are based on almost all kinds of known analytical techniques have been developed for screening, identifying, and quantifying drug residues in food. Each detection system has its own advantages and drawbacks, which must be carefully considered before selecting the most convenient system for a particular analyte in a particular matrix. Screening assays based on microbiological or immunochemical detection offer the advantage to screen rapidly and at low cost a large number of food samples for potential residues but cannot provide definitive information on the identity of violative residues found in suspected samples. Analyzing drug residues in food is complicated as it is not known whether residues exist, and if they exist, the type and quantity are not known. For samples found positive by the screening assays, residues can be tentatively identified and quantified by combining an efficient liquid chromatographic (LC) separation and a selective physicochemical detection system such as UV, fluorescence, or electrochemical. The potential of pre- or postcolumn derivatization can further enhance the selectivity and sensitivity of LC analysis. Nevertheless, unequivocal identification is not possible unless a more efficient detection system is employed. The possibility for unambiguous identification of the analytes is offered by coupling LC with mass spectrometers (LC–MS). MS detection systems use the difference in mass-to-charge ratio (m/z) of ionized atoms or molecules to separate them from each other. Molecules have distinctive fragmentation patterns that provide structural information to identify structural components.

LC–MS COUPLING

When LC is coupled with MS, three major problems generally appear. The first concerns the ionization of non-volatile and/or thermolabile analytes. Since MS operation is based on magnetic and electric fields that exert forces on charged ions in a vacuum, a compound must be charged or ionized in the source to be introduced in the gas phase into the vacuum system of the MS. This is easily attainable for heat-volatile samples, but thermally labile analytes may decompose upon heating. The second is due to the mobile-phase incompatibility as a result of the frequent use of non-volatile mobile-phase buffers and additives in LC. This is why routine or long-term use of non-volatile mobile-phase constituents such as phosphate buffers and ion-pairing agents is prohibited by all current LC–MS methods. As far as the third problem is concerned, this is related to the apparent flow rate incompatibility as expressed in the need to introduce a mobile phase eluting from the column at a flow rate of around 1 ml/min into the high vacuum of the MS. To eliminate these problems, several different interfaces that provide broad analytical coverage have been developed. The main limitation of the LC–MS interfaces is the lack of fragmentation data provided for structure determination because most interfaces operate in a basically chemical ionization (CI) mode, providing mild ionization and making identification of unknowns difficult or impossible. Hence, the choice of a suitable interface for a particular application has always to be related to the analytes considered, especially their polarity and molecular mass, and the specific analytical problem as well.[1]

Among the currently available interfaces for drug residue analysis, more interesting appear the particle-beam (PB) interface, the thermospray (TSP) interface that works well with substances of medium polarity, and the atmospheric pressure ionization (API) interfaces that have opened up powerful application areas to LC–MS for ionizable compounds. Among API interfaces, most versatile appear to be the electrospray (ESP) interface and its variants including the ion spray

(ISP), the turbo ISP and the Z-spray interfaces, which are suitable for substances ranging from polar to ionic and from low to high molecular mass. The ISP and turbo ISP, in particular, are compatible with flow rates commonly used with conventional LC columns, whereas both ESP and ISP appear to be valuable in terms of analyte detectability. Complementary to ESP and ISP interfaces with respect to the analyte polarity is the atmospheric pressure chemical ionization (APCI) interface that is equipped with a heated nebulizer. This is a powerful interface for both structural confirmation and quantitative analysis. API interfaces coupled to LC and tandem mass spectrometry (LC–MS–MS) have opened a new era in qualitative and quantitative analysis of veterinary drug residues. Depending on the quantitative or confirmatory nature of analysis, two types of mass spectrometers can be employed. The triple quadrupole instruments will produce ions with collision-induced fragmentation such as daughter ions for multiple reaction monitoring, while the ion trap spectrometers can produce MS^n fragment ions such as granddaughter ions. The advantages and disadvantages of these two types of instruments have been investigated in literature.[2]

PB INTERFACE

PB interface is an analyte enrichment interface in which the column effluent is pneumatically nebulized into a near atmospheric pressure desolvation chamber connected to a momentum separator, where the high-mass analytes are preferentially directed to the MS ion source, while the low-mass solvent molecules are efficiently pumped away. With this interface mobile phase, flow rates within the range 0.1–1.0 ml/min can be applied. PB–MS appears to have high potential as an identification method for residues of some antibiotics in foods as it generates library-searchable EI spectra and CI solvent-independent spectra. Limitations of the PB–MS interface, as compared with other LC–MS interfaces, include lower sensitivity, difficulty in quantification, and lower response with highly aqueous mobile phases. The low sensitivity can be attributed in part to chromatographic band broadening during the transmission of the sample through the interface and in part to non-linearity effects that appear at low analyte concentrations.[3]

LC–PB–MS has been investigated as a potential confirmatory method for the determination of malachite green in incurred catfish tissue,[4] and cephapirin, furosemide, and methylene blue in milk, kidney, and muscle tissue, respectively.[5] LC–PB–MS has also been investigated for the analysis of ivermectin residues in bovine liver and milk.[6] The specificity required for regulatory confirmation was obtained by monitoring the molecular ion and characteristic fragment ions of the drug under negative-ion chemical ionization (NCI) and selective ion monitoring (SIM) conditions. Quantification and confirmation of tetracycline, oxytetracycline, and chlortetracycline residues in milk[7] and chloramphenicol residues in calf muscle[8] have been also carried out using LC–PB–NCI–MS.

THERMOSPRAY INTERFACE

TSP interface is widely used for the determination of drug residues in foods.[1] TSP is typically used with reversed-phase columns and volatile buffers. Aqueous mobile phases containing an electrolyte such as ammonium acetate are passed through a heated capillary prior to entering a heated ion source. Since the end of the capillary lies opposite a vacuum line, nebulization takes place and a jet of vapor containing a mist of electrically charged droplets is formed. As the droplets move through the hot source area, they continue to vaporize, and ions present in the eluent are ejected from the droplet and sampled through a conical exit aperture in the mass analyzer. The ionization of the analytes takes place by means of direct ion evaporization of the sample ion or by solvent-mediated CI reactions. With ionic analytes, the mechanism of ion evaporation is supposed to be primarily operative as ions are produced spontaneously from the mobile phase. Drawbacks of LC–TSP–MS are the requirements for volatile modifiers and the control of temperature, particularly for thermolabile compounds.[9] Also, ion evaporation often yields mass spectra with little structural information. Lack of structural information from LC–TSP–MS applications can be overcome by the use of LC–TSP–MS–MS. Use of this tandem MS approach provides enhanced selectivity, generally at the cost of a loss of sensitivity as a consequence of decreased ion transmission.

LC–TSP–MS has been successfully applied for detection/confirmation of nicarbazin residues in chicken tissues using negative-ion detection in the SIM mode.[10] LC–TSP–MS in the SIM mode has also been used for quantification of residues of moxidectin in cattle tissues and fat,[11] and nitroxynil, rafoxanide, and levamisole in muscle.[12] Confirmatory methods based on LC–TSP–MS have further been reported for determination of penicillin G,[13] cephapirin,[14] and various penicillin derivatives[15] in milk. Comparative evaluation of the confirmatory efficiency of LC–TSP–MS and LC–TSP–MS–MS in the assay of maduramycin in chicken fat showed the former approach to be marginally appropriate whereas the latter highly efficient.[16] Tandem LC–MS–MS has also been successfully applied for analyzing residues of chloramphenicol in milk and fish.[17]

ESP AND ITS VARIANTS ION SPRAY, TURBO ION SPRAY, AND Z-SPRAY INTERFACES

The ESP interface, a widely applicable soft ionization technique, operates at the low microliter/minute flow rate, necessitating use of either capillary columns or post-column splitting of the mobile phase. For ESP ionization, the analytes must be ionic or have an ionizable functional group or be able to form an ionic adduct in solution. The analytes are commonly detected as deprotonated species or as cation adducts of a proton or an alkali metal ion. The first step in the ESP is the nebulization of the liquid into small droplets. This process is supported by the introduction of a drying gas as well as a nebulizer gas such as nitrogen, by different techniques. In the most commonly used approach, a coaxial nebulizing gas of nitrogen or air is used for evaporation of the aqueous eluents at higher LC flow rates.[18] The influence of the LC mobile phase on the ESP process has been studied by several workers.[19,20] When using positive-ion ESP ionization, use of ammonium acetate as a mobile-phase modifier is generally unsuitable. Instead, organic modifiers, such as heptafluorobutyric or trifluoroacetic acid, usually at a concentration of 0.1% are strongly recommended. For negative-ion applications, the choice of the modifier is even more limited, triethylamine being the only suitable compound.

ISP interface is a pneumatically assisted ESP. However, unlike the ESP interface, ISP allows higher flow rates (0.05–0.20 ml/min) by virtue of pneumatically assisted vaporization. A capillary is housed inside an external tube through which the nebulizing gas is coaxially directed. To avoid source contamination by non-volatile compounds such as salts, off-axis ESP nebulization instead of on-axis with the sampling orifice has been developed by several manufacturers. ISP and turbo ISP interfaces are generally used off-axis positioned at 30–45° relative to the axis or in the case of the Z-spray source the ESP nebulization is performed orthogonally to the sampling cone. Since both ESP and ISP produce quasi-molecular ions, more sophisticated techniques such as LC–MS–MS are required to obtain diagnostic fragment ions and, thus, analyte structure elucidation. Identification can often be achieved by using daughter ion MS–MS scans and collisionally induced dissociation (CID), most commonly on a triple quadrupole MS; in this way, dissociation of the quasi-molecular ion occurs and diagnostic structural information can be obtained.

The turbo ISP interface has been developed for conventional LC systems with high flow rates. Relatively high gas temperatures must be applied to achieve sufficient heat transfer to the evaporating droplets. The Z-spray interface is another variant where the ESP nebulization is performed with concurrent desolvation gas. Ions are extracted orthogonally from the spray into the sampling cone, while large droplets and non-volatile material are collected onto a baffle plate. From the expansion area behind the sampling cone the ions are again extracted orthogonally into the high-vacuum region of the spectrometer.[18]

LC–ESP–MS has been successfully used for multiresidue assay of penicillins in milk ultrafiltrate at the 100 ppb level after postcolumn splitting of the eluent and recording under SIM conditions in the positive-ion mode.[21] Significantly lower detection limits have been reported by other workers who described an LC–ESP–MS confirmatory procedure for the simultaneous determination of five penicillins in milk and meat under SIM conditions in the negative-ion mode.[22] Further, ESP has been shown to be useful in the analysis of several classes of veterinary drugs including sulfonamides and tetracyclines, which exhibit spectra with four common ions; however, this was not possible for the group of β-agonists because of their more diverse chemical structure.[23] Negative-ion ESP–MS has also been used for the detection/identification of a number of non-steroidal anti-inflammatory drugs, including phenylbutazone, flunixin, oxyphenbutazone, and diclofenac.[24] LC–ESP–MS has been found suitable for the determination of four coccidiostats in poultry products.[25] In addition, LC–ESP–MS–MS has been proposed for quantification/confirmation of 10 sulfonamides in liver and kidney tissues of bovine, swine, and chicken.[26] LC–ESP triple quadrupole MS–MS has also been applied for the assay of five macrolides in bovine, swine, and poultry tissues, bovine milk, and eggs,[27] 11 fluoroquinolones in porcine kidney,[28] mebendazole, and its metabolites in sheep liver and muscle,[29] and multiclass veterinary drugs in animal muscles,[30,31] eggs,[32] and shrimps.[33]

LC–ISP–MS has also been shown to be an attractive approach for the determination of semduramicin in chicken liver.[34] Tandem MS using CID of the molecular ions further enhanced the specificity, providing structure elucidation and selective detection down to 30 ppb. LC–ISP–MS has also been successfully applied for the assay of 21 sulfonamides in salmon flesh.[35] Coupling of LC with either ISP–MS or ISP–MS–MS has also been investigated as an attractive alternative for the determination of erythromycin A and its metabolites in salmon tissue.[36] The combination of these methods permitted identification of a number of degradation products and metabolites of erythromycin at the 10–50 ppb level. Tandem MS with CID has also been applied for the specific monitoring of danofloxacin and its metabolites in chicken and cattle tissues at levels down to 50 ppb.[37] LC–ISP triple quadrupole MS–MS has also been proposed for confirmation of aminoglycoside residues in bovine kidney.[38]

ATMOSPHERIC PRESSURE CHEMICAL IONIZATION INTERFACE

Complementary to ESP and its variants with respect to analyte polarity is the APCI interface. This is equipped with a heated nebulizer that can be used for LC flow rates

of 0.5–1.5 ml/min. The nebulized liquid effluent is swept through the heated tube by a coaxial nitrogen stream at high temperature. The heated mixture of solvent and vapor is then introduced in the ionization source where a corona discharge electrode initiates APCI. Ionization in APCI is primarily based on gas-phase chemical reactions and contains charge transfer from solvent-based reagent gas to the analyte molecules. The reagent gas is generated by a series of ion–molecule reactions initiated by the corona discharge electrode.[39] The spectra and chromatograms from APCI are somewhat similar to those from TSP, but the technique is more robust, especially with gradient LC and often more sensitive. APCI is particularly useful for heat-labile and low-mass or high-mass compounds. In contrast to TSP interface, no extensive temperature optimization is needed with APCI. The applicability of the APCI interface is restricted to the analysis of compounds with lower polarity and lower molecular mass compared with ESP and ISP.

Applications include the LC–APCI–MS multiresidue determination of quinolone antibiotics,[40] the determination of tetracyclines in muscle at the 100 ppb level,[41] and the determination of fenbendazole, oxfendazole, and the sulfone metabolite in muscle at the 10 ppb level.[42] In addition, LC–APCI–MS–MS has been proposed for the determination of the coccidiostats dimetridazole and ronidazole residues and their common metabolites in poultry muscle and eggs,[43] for the determination of residues of five coccidiostats in both positive and negative modes,[44] and for the quantification of tranquillizers and β-blockers in muscle and liver tissues of food-producing animals.[45]

Although the detection capability of LC–MS–MS is very powerful, the cleanup process of the sample prior to instrumental analysis must always be kept in mind because the better the cleanup the better the results of the hyphenated technique used. Investigation of sample matrix effects, ion suppression, and "cross talk" effects that can reduce the ion intensity of the analytes and lead to poor reproducibility and accuracy should always be part of the validation of LC–MS–MS assays in residue analysis.

CONCLUSION

The need to use veterinary drugs in animal husbandry will continue well into the future, and therefore monitoring of edible animal products for violative residues will remain an area of increasing concern and importance, due to the potential impact on human health. The successful hyphenation of LC with MS has led to development of highly flexible, computer-aided analytical methods that offer the required possibility for unambiguous identification of drug residues in food. LC–MS is now in a mature state, but it still cannot be considered routine in the field of drug residue analysis. Possible reasons are the high initial cost, which is 2–4 times higher than that of gas chromatography (GC)–MS, and the poor detection limits, which are approximately 100 times higher than in GC–MS. Coupling of LC with tandem MS is a solution for improving detection limits by reducing the background noise, but this combination is 2 or 3 times more expensive than its LC–MS analogue. However, there are also disadvantages to the LC–MS–MS technique as high background noise can be observed due to solvent/salt concentrations. In addition, screening by multiresidue analysis in the scan mode is normally not possible due to the low sensitivity. Moreover, the search and identification of unknowns is difficult since spectrum libraries are not available due to influence of the experimental conditions and variation of spectra and MS–MS data between instruments supplied by different manufacturers.

REFERENCES

1. Botsoglou, N.A.; Fletouris, D.J. *Drug Residues in Food. Pharmacology, Food Safety, and Analysis*; Marcel Dekker, Inc.: New York, 2001.
2. De Wash, K.; Alam, Z.; Benoot, J.; Van Hoof, N.; Poelmans, S.; De Brabander, H. In Poster presented at 4th International Symposium on Hormone and Veterinary Drug Residue Analysis, Antwerp, June 2002.
3. Tinke, A.P.; Van der Hoeven, R.A.M.; Niessen, W.M.A.; Tjaden, U.R.; Van der Greef, J. Some aspects of peak broadening in particle-beam liquid-chromatography mass-spectrometry. J. Chromatogr. **1991**, *554*, 119–124.
4. Turnipseed, S.B.; Roybal, J.E.; Rupp, H.S.; Hurlbut, J.A.; Long, A.R. Particle beam liquid chromatography—mass-spectrometry of triphenylmethane dyes: Application to confirmation of malachite green in incurred catfish tissue. J. Chromatogr. **1995**, *670*, 55–62.
5. Voyksner, R.D.; Smith, C.S.; Knox, P.C. Optimization and application of particle beam high-performance liquid-chromatography mass-spectrometry to compounds of pharmaceutical interest. Biomed. Environ. Mass Spectrom. **1990**, *19*, 523–534.
6. Heller, D.N.; Schenck, F.J. Particle beam liquid-chromatography mass-spectrometry with negative-ion chemical ionization for the confirmation of ivermectin residues in bovine milk and liver. Biol. Mass Spectrom. **1993**, *22*, 184–193.
7. Kijak, P.J.; Leadbetter, M.G.; Thomas, M.H.; Thompson, E.A. Confirmation of oxytetracycline, tetracycline and chlortetracycline residues in milk by particle beam liquid-chromatography mass-spectrometry. Biol. Mass Spectrom. **1991**, *20*, 789–795.
8. Delepine, B.; Sanders, P. Determination of chloramphenicol in muscle using a particle beam interface for combining liquid-chromatography with negative-ion chemical ionization mass-spectrometry. J. Chromatogr. **1992**, *582*, 113–121.
9. Niessen, W.M.A.; Van der Greef, J. *Liquid Chromatography–Mass Spectrometry, Principles and Application*; Marcel Dekker, Inc.: New York, 1992.

10. Lewis, J.L.; Macy, T.D.; Garteiz, D.A. Determination of nicarbazin in chicken tissues by liquid-chromatography and confirmation of identity by thermospray liquid-chromatography mass-spectrometry. J. Assoc. Off. Anal. Chem. **1989**, *72*, 577–581.
11. Khunachak, A.; Dakunha, A.R.; Stout, S.J. Liquid-chromatographic determination of moxidectin residues in cattle tissues and confirmation in cattle fat by liquid-chromatography mass-spectrometry. J. AOAC Int. **1993**, *76*, 1230–1235.
12. Cannavan, A.; Blanchflower, W.J.; Kennedy, D.G. Determination of levamisole in animal tissues using liquid-chromatography thermospray mass-spectrometry. Analyst **1995**, *120*, 331–333.
13. Boison, J.O.K.; Keng, L.J.-Y.; MacNeil, J.D. Analysis of penicillin-G in milk by liquid-chromatography. J. AOAC Int. **1994**, *77*, 565–570.
14. Tyczkowska, K.L.; Voyksner, R.D.; Aronson, A.L. Development of an analytical method for cephapirin and its metabolite in bovine milk and serum by liquid-chromatography with UV-Vis detection and confirmation by thermospray mass-spectrometry. J. Vet. Pharmacol. Therap. **1991**, *14*, 51–60.
15. Voyksner, R.D.; Tyczkowska K.L.; Aronson, A.L. Development of analytical methods for some penicillins in bovine milk by ion-paired chromatography and confirmation by thermospray mass-spectrometry. J. Chromatogr. **1991**, *567*, 389–404.
16. Stout, S.J.; Wilson, L.A.; Kleiner, A.I.; Dacunha, A.R.; Francl, T.J. Mass-spectrometric approaches to the confirmation of maduramicin-alpha in chicken fat. Biomed. Environ. Mass Spectrom. **1989**, *18*, 57–63.
17. Ramsey, E.D.; Games, D.E.; Startin, J.R.; Crews, C.; Gilbert, J. Detection of residues of chloramphenicol in crude extracts of fish and milk by tandem mass-spectrometry. Biomed. Environ. Mass Spectrom. **1989**, *18*, 5–11.
18. Balizs, G.; Hewitt, A. Determination of veterinary drug residues by liquid chromatography and tandem mass spectrometry. Anal. Chim. Acta **2003**, *492*, 105–131.
19. Zhou, S.; Hamburger, M. Effects of solvent composition on molecular ion response in electrospray mass spectrometry: Investigation of the ionization processes. Rapid Commun. Mass Spectrom. **1995**, *9*, 1516–1521.
20. Zhou, S.; Hamburger, M. Application of liquid chromatography-atmospheric pressure ionization mass spectrometry in natural product analysis evaluation and optimization of electrospray and heated nebulizer interfaces. J. Chromatogr. **1996**, *755*, 189–204.
21. Straub, R.F.; Voyksner, R.D. Determination of penicillin-G, ampicillin, amoxicillin, cloxacillin and cephapirin by high-performance liquid-chromatography electrospray mass-spectrometry. J. Chromatogr. **1993**, *647*, 167–181.
22. Tyczkowska, K.L.; Voyksner, R.D.; Straub, R.F.; Aronson, A.L. Simultaneous multiresidue analysis of beta-lactam antibiotics in bovine milk by liquid-chromatography with ultraviolet detection and confirmation by electrospray mass-spectrometry. J. AOAC Int. **1994**, *77*, 1122–1131.
23. Harris, J.; Wilkins, J. The application of HPLC–Cone voltage assisted fragmentation electrospray mass spectrometry to the determination of veterinary drug residues. In *Residues of Veterinary Drugs in Food*, Proceedings of the Euroresidue III Conference, Veldhoven, May 6–8, 1996; Haagsma, N., Ruiter, A., Eds.; Faculty of Veterinary Science, University of Utrecht, Utrecht: The Netherlands, 1996.
24. Gowik, P.; Julicher, B. Behaviour of some selected NSAID's under electrospray LC–MS conditions. In *Residues of Veterinary Drugs in Food*, Proceedings of the Euroresidue III Conference, Veldhoven, May 6–8, 1996; Haagsma, N., Ruiter, A., Eds.; Faculty of Veterinary Science, University of Utrecht, Utrecht: The Netherlands, 1996.
25. Blanchflower, W.J.; Kennedy, D.G. Determination of lasalocid in eggs using liquid chromatography–electrospray mass-spectrometry. Analyst **1995**, *120*, 1129–1132.
26. Ito, Y.; Oka, H.; Ikai, Y.; Matsumoto, H.; Miyazaki, Y.; Nagas, H. Application of ion-exchange cartridge clean-up in food analysis: V. Simultaneous determination of sulphonamide antibacterials in animal liver and kidney using high-performance liquid chromatography with ultraviolet and mass spectrometric detection. J. Chromatogr. **2000**, *898*, 95–102.
27. Dubois, M.; Fluchard, D.; Sior, E.; Delahaut, Ph. Identification and quantification of five macrolide antibiotics in several tissues, eggs and milk by liquid chromatography–electrospray tandem mass spectrometry. J. Chromatogr. **2001**, *753*, 189–202.
28. Van Vyncht, G.; Janosi, A.; Bordn, G.; Toussaint, B.; Maghuin-Rogister, G.; DE Pauw, E.; Rodriguez, A.R. Multiresidue determination of (fluoro)quinolone antibiotics in swine kidney using liquid chromatography–tandem mass spectrometry. J. Chromatogr. **2002**, *952*, 121–129.
29. De Ruyck, H.; Daeselerie, E.; De Ridder, H.; Van Renterghem, R. Liquid chromatographic-electrospray tandem mass spectrometric method for the determination of mebendazole and its hydrolysed and reduced metabolites in sheep muscle. Anal. Chim. Acta **2003**, *483*, 111–123.
30. Tang, H.P.; Ho, C.; Lai, S.S.-L. High-throughput screening for multiclass veterinary drug residues in animal muscle using liquid chromatography/tandem mass spectrometry with on-line solid-phase extraction. Rapid Commun. Mass Spectrom. **2006**, *20*, 2565–2572.
31. Yamada, R.; Kozono, M.; Ohmori, T.; Morimatsu, F.; KItayama, M. Simultaneous determination of residual veterinary drugs in bovine, porcine, and chicken muscle using liquid chromatography coupled with electrospray ionization tandem mass spectrometry. Biosci. Biotechnol. Biochem. **2006**, *70*, 54–65.
32. Heller, D.N.; Nochetto, C.B. Development of multiclass methods for drug residues in eggs: Silica SPE cleanup and LC–MS/MS analysis of ionophore and macrolide residues. J. Agric. Food Chem. **2004**, *52*, 6848–6856.
33. Li, H.; Kijak, P.J.; Turnipseed, S.B.; Cui, W.J. Analysis of veterinary drug residues in shrimp: A multiclass method by liquid chromatography–quadrupole ion trap mass spectrometry. J. Chromatogr. **2006**, *836*, 22–38.
34. Schneider, R.P.; Lynch, M.J.; Ericson, J.F.; Fouda, H.G. Electrospray ionization mass-spectrometry of semduramicin and other polyether ionophores. Anal. Chem. **1991**, *63*, 1789–1794.
35. Pleasance, S.; Blay, P.; Quilliam, M.A.; O'Hara, G. Determination of sulfonamides by liquid-chromatography,

ultraviolet diode-array detection and ion-spray tandem mass-spectrometry with application to cultured salmon flesh. J. Chromatogr. **1991**, *558*, 155–173.
36. Pleasance, S.; Kelly, J.; Leblanc, M.D.; Quilliam, M.A.; Boyd, R.K.; Kitts, D.D.; McErlane, K.; Bailey, M.R.; North, D.H. Determination of erythromycin: A in salmon tissue by liquid-chromatography with ionspray mass-spectrometry. Biol. Mass Spectrom. **1992**, *21*, 675–687.
37. Schneider, R.P.; Ericson, J.F.; Lynch, M.J.; Fouda, H.G. Confirmation of danofloxacin residues in chicken and cattle liver by microbore high-performance liquid-chromatography electrospray-ionization tandem mass-spectrometry. Biol. Mass Spectrom. **1993**, *22*, 595–599.
38. McLaughlin, L.G.; Henion, J.D.; Kijak, P.J. Multiresidue confirmation of aminoglycoside antibiotics in bovine kidney by ion spray high performance liquid chromatography/tandem mass spectrometry. Biol. Mass Spectrom. **1994**, *23*, 417.
39. Niessen, W.M.A. State-of-the-art in liquid chromatography–mass spectrometry. J. Chromatogr. **1999**, *12*, 179–197.
40. Doerge, D.R.; Bajic, S. Multiresidue determination of quinoloe antibiotics using liquid-chromatography coupled to atmospheric-pressure chemical-ionization mass-spectrometry and tandem mass-spectrometry. Rapid Commun. Mass Spectrom. **1993**, *9*, 1012–1016.
41. McCracken, R.J.; Blanchflower, W.J.; Haggan, S.A.; Kennedy, D.G. Simultaneous determination of oxytetracycline, tetracycline and chlortetracycline in animal tissues using liquid-chromatography, postcolumn derivatization with aluminum, and fluorescence detection. Analyst **1995**, *120*, 1761–1766.
42. Blanchflower, W.J.; Cannavan, A.; Kennedy, D.J. Determination of fenbendazole and oxfendazole in liver and muscle using liquid-chromatography mass-spectrometry. Analyst **1994**, *119*, 1325–1328.
43. Sams, M.J.; Strutt, P.R.; Barnes, K.A.; Damant, A.P.; Rose, M.D. Determination of dimetridazole, ronidazole and their common metabolite in poultry muscle and eggs by high performance liquid chromatography with UV detection and confirmatory analysis by atmospheric pressure chemical ionization mass spectrometry. Analyst **1998**, *123*, 2545–2549.
44. Mortier, L.; Daeselerie, E.; Delahaut, P. Simultaneous detection of five coccidiostats in eggs by liquid chromatography–tandem mass spectrometry. Anal. Chim. Acta **2003**, *483*, 27–37.
45. Delahaut, P.; Levaux, C.; Eloy, P.; Dubois, M. Validation of a method for detecting and quantifying tranquillizers and a β-blocker in pig tissues by liquid chromatography–tandem mass spectrometry. Anal. Chim. Acta **2003**, *483*, 335–340.

Food: Penicillin Antibiotics Analysis by LC

Yuko Ito
Tomomi Goto
Aichi Prefectural Institute of Public Health, Nagoya, Japan

Hisao Oka
Food-Related Chemistry, Laboratory of Chemistry, Aichi Prefectural Institute of Public Health, Nagoya, Japan

INTRODUCTION

Penicillin antibiotics are part of a wide variety of antimicrobial agents that are used as veterinary drugs to prevent and treat infectious diseases. Such use may lead to problems with residues in the livestock products. To provide safe products for consumers, the quantification of these residues in foods is required.

As most of the penicillins dissolve easily in water, high-performance liquid chromatography (HPLC) appears to be the best-suited approach for the analysis of residual penicillins in food. However, many HPLC methods require derivatization or special instrumentation because penicillins do not have any specific, strong ultraviolet (UV) absorption. Above all, the derivatization technique using mercury (II) chloride and 1,2,4-triazole or imidazole was applied to many analyses of penicillins. On the other hand, because it is not desirable to use toxic reagents such as mercury (II) chloride, there is a great need for a simpler, safer analytical method. To analyze the penicillins in food using a UV detector, a device is needed for sample preparation and chromatographic separation to remove interfering compounds which originate from the sample matrix. Because animal tissues (primarily muscle, kidney, and liver) include large amounts of sample matrix in comparison with milk, this causes difficulties for the development of simultaneous analysis of penicillins in these tissues. However, using an ion-exchange cartridge, in combination with ion-pair HPLC, has been reported to be very effective for simultaneous determination of the penicillins in the tissues. On the other hand, liquid chromatography/mass spectrometry (LC/MS) methods have also been published for the analysis of residual penicillins in food because mass spectrometric techniques can confirm and determine them, with high sensitivity and selectivity.

In this entry, we deal with the simultaneous determination of penicillins in animal muscle, liver, and kidney using ultraviolet (UV)–HPLC and LC/MS.

UV–HPLC METHOD

Benzylpenicillin (PCG), phenoxymethylpenicillin (PCV), oxacillin (MPIPC), cloxacillin (MCIPC), nafcillin (NFPC), and dicloxacillin (MDIPC), all of which are representative weakly acidic penicillins, are widely used as veterinary drugs for livestock. We have reported, in our previous studies,[1,2] the applicability of sample cleanup with an ion-exchange cartridge, in combination with ion-pair HPLC, for the analysis of ionizable compounds. We therefore applied the same technique to develop an analytical method for the quantitative determination of these residual penicillins in bovine muscle, kidney, and liver.[3,4]

HPLC Conditions

After examination of several ion-pair reagents for acidic compounds, 12 m*M* of cetyltrimethylammonium chloride was chosen because it gave the best result in the separation of penicillins. When the pH of the mobile phase was adjusted to 6.2, the six penicillins exhibited good separations from each other, with adequate capacity factors.

Thus a satisfactory separation of the penicillins was obtained using TSKgel ODS-80Ts (5 μm, 150 × 4.6, I.D.) column and acetonitrile-0.02 *M* phosphate buffer, pH 6.2, (4.3 : 5.7, v/v) containing 12 m*M* of cetyltrimethylammonium chloride, as the mobile phase (Fig. 1a).

Sample Extraction

Although the repeated (three times) extraction of the penicillins with 2% NaCl aqueous solution (60, 40, 40 ml) from bovine muscle was very simple and gave satisfactory extraction efficiency, the same extraction procedure could not be applied to bovine kidney and liver. Because the resultant extracts were foamy and viscous, it caused the serious problems in the sample cleanup procedure. To avoid these problems, the addition of aqueous solutions of sodium tungstate and sulfuric acid to the extraction solution (2% NaCl), as deproteinization reagents, yielded satisfactory results. After a series of preliminary experiments, we decided to use 55 or 50 ml of 2% NaCl aqueous solution and 5 or 10 ml of the deproteinization reagent (5% sodium tungstate aqueous solution-0.17 *M* sulfuric acid solution, 1 : 1) as the first extraction solution for bovine kidney and liver. For the remaining two extractions, for each, 40 ml of 2% NaCl

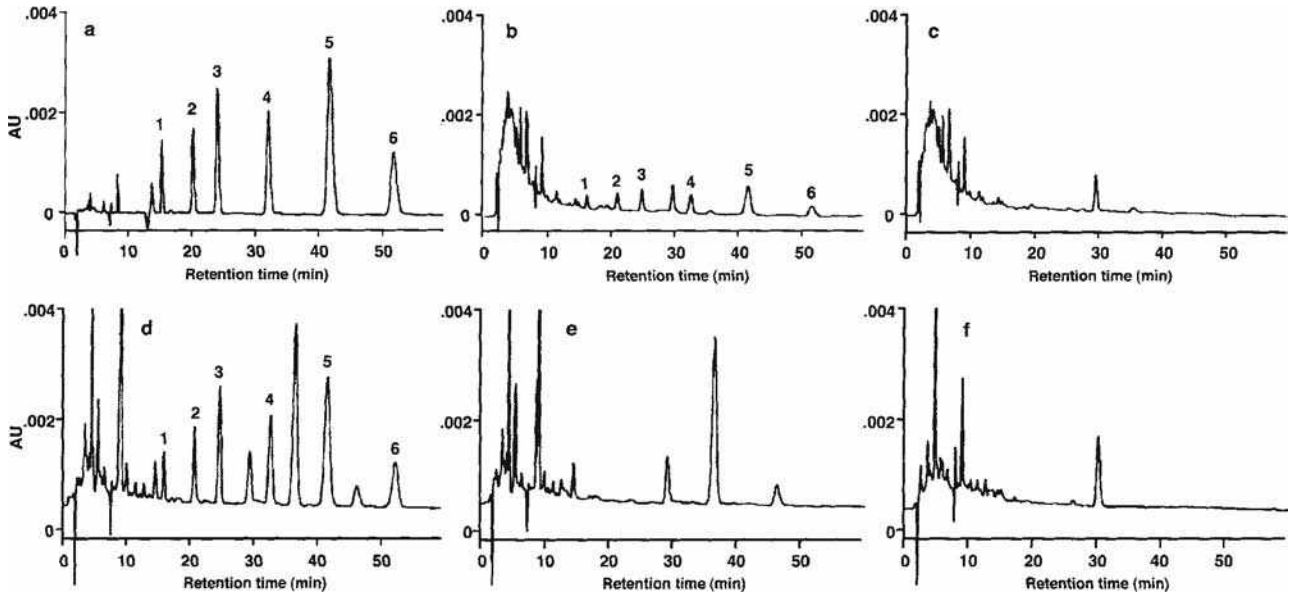

Fig. 1 Typical HPLC chromatograms of bovine tissue samples. a) Standard of six penicillins; b) muscle sample fortified at a concentration of 0.1 mg/kg each of penicillins; c) muscle sample; d) liver sample fortified at a concentration of 0.5 mg/kg each of penicillins; e) liver sample; f) kidney sample. 1) Benzylpenicillin; 2) phenoxymethylpenicillin; 3) oxacillin; 4) cloxacillin; 5) nafcillin; 6) dicloxacillin. Operating conditions—column: TSKgel ODS-80Ts (150 × 4.6 I.D.); mobile phase: acetonitrile-0.02 *M* phosphate buffer, pH 6.2, (4.3 : 5.7, v/v) containing 12 m*M* cetyltrimethylammonium chloride.; flow-rate: 0.8 ml/min; detector: UV 220 nm; column temp.: 30°C.

aqueous solution was used in the same manner as was used for muscle samples.

Purification of Crude Extracts

Pre-cleanup method

Because the tissue extract contains many substances which interfere with the ion-exchange capacity of the cartridge, it was necessary to develop a pre-cleanup method to retain the residual penicillins present in the tissue samples on the ion-exchange cartridge. It had been reported that washing a crude extract-loaded C18 cartridge with an aqueous methanolic solution containing NaCl was effective as a pre-cleanup of samples for the determination of PCG.[5] After several experiments, the following pre-cleanup method was developed: the crude extract-loaded Bond Elut C18 cartridge was washed with 15% methanol containing 2% NaCl, followed by water; finally, the elution was carried out with 5 ml of 55% methanol.

Ion-exchange cartridge cleanup method

It is desirable to use the same solution for HPLC mobile phase and for the elution solvent from the cleanup cartridges to assure good reproducibility of the HPLC determination of the penicillins. After the investigation of the selected ion-exchange cartridges using 2 ml of the above-described mobile phase as the elution solvent, Sep-Pak Accell Plus QMA (QMA) produced the best results with all of the penicillins being completely eluted.

Even after the QMA cartridge cleanup procedure with the C18 cartridge pre-cleanup describe above, there were nevertheless small amounts of the interfering substances overlapping the peaks of the penicillins. We therefore tried to wash the QMA cartridge to improve the cleanup. Judging from the results of several experiments, on the basis of the chemical properties of the QMA cartridge, we decided to use 3 ml each of 55% methanol and water for muscle samples and to use 3 ml each of 55% methanol, 10 m*M* acetic acid methanolic solution, and water for the kidney and liver samples.

Recoveries

Bovine tissue samples were fortified with the six penicillins (0.5 or 0.1, or 0.05 mg/kg of each) and performed the analyses according to the procedure described above. As shown in Table 1, satisfactory recoveries (over 71%) and corresponding coefficients of variation (C.V., less than 8.7%) were obtained for these low concentrations of the penicillins. The detection limit was 0.02 mg/kg for each penicillin in the meat, and those were 0.02 mg/kg for MPIPC, MCIPC, and NFPC, 0.03 mg/kg for PCV, 0.04 mg/kg for PCG, and 0.05 mg/kg for MDIPC in the bovine kidney and liver (S/N ratio = 3). Fig. 1 shows typical chromatograms of standard solution (a), fortified bovine muscle and liver samples (b and d), their

Table 1 Recoveries of penicillins from bovine tissues.

	Muscle			Liver			Kidney		
Penicillins	Fortified (mg/kg)	Recovery[a](%)	C.V. (%)	Fortified (mg/kg)	Recovery[a](%)	C.V. (%)	Fortified (mg/kg)	Recovery[a](%)	C.V. (%)
Benzylpenicillin	0.5	92	2.9	0.5	82	4.2	0.5	83	4.7
	0.1	83	7.0	0.1	86	7.4	0.1	82	5.8
	0.05	77	6.4						
Phenoxymethylpenicillin	0.5	90	2.4	0.5	88	1.4	0.5	82	1.8
	0.1	82	4.8	0.1	83	4.1	0.1	86	7.8
	0.05	84	5.4						
Oxacillin	0.5	86	1.9	0.5	91	1.4	0.5	92	3.2
	0.1	74	3.5	0.1	96	3.4	0.1	92	4.2
	0.05	80	3.9						
Cloxacillin	0.5	85	1.8	0.5	91	2.9	0.5	89	2.9
	0.1	86	3.1	0.1	92	8.7	0.1	90	2.7
	0.05	82	4.0						
Nafcillin	0.5	89	1.7	0.5	84	1.7	0.5	80	3.5
	0.1	85	2.6	0.1	84	3.8	0.1	89	3.8
	0.05	90	5.2						
Dicloxacillin	0.5	83	4.4	0.5	73	3.1	0.5	79	5.9
	0.1	71	2.6	0.1	89	6.4	0.1	89	4.3
	0.05	79	6.4						

C.V.: coefficient of variation.
[a]Average of five trials.

corresponding controls (c and e), and bovine kidney sample (f), respectively. As shown by these chromatograms, satisfactory separation of PCs and cleanup effects were achieved by using the ion-exchange cartridge cleanup in combination with the ion-pair HPLC described above.

LC/MS METHOD

Because mass spectrometric techniques can confirm and determine substances, with high sensitivity and selectivity, LC/MS methods have been published for the analysis of residual penicillins in food. However, only a few methods have been reported for the simultaneous analysis of penicillins in animal tissues; moreover, these methods are less sensitive than the UV–HPLC methods. It seemed that their insufficient sample cleanup and separation under their LC conditions led to the lack of sensitivity. Accordingly, based on our determination method using the UV–HPLC approach described above, we decided to develop an accurate and highly sensitive confirmation method for penicillins in bovine tissues using ESI LC/MS/MS with a product ion scan mode.[6] First, we reconstructed the LC conditions for ESI LC/MS analysis; hence 30% acetonitrile aqueous solution containing 2 m*M* of di-*n*-butylamine acetate (DBAA), which was a volatile ion-pair reagent, was selected as the mobile phase. Gradient elution was used to increase the sensitivity. Then, we investigated whether or not the mobile phase described above can be used as the elution solvent for the cartridges used for cleanup. Because the mobile phase for

Table 2 Diagnostic ions of penicillins.

	Product ions[a]			
Penicillins	$[M–H]^-$	$[M–H–CO_2]^-$	$[M–H–141]^-$	Precursor ion[a] $[M–H]^-$
Benzylpenicillin	333	289	192	333
Phenoxymethylpenicillin	349	305	208	349
Oxacillin	400	356	259	400
Cloxacillin	434	390	293	434
Nafcillin	413	369	272	413
Dicloxacillin	468	424	327	468

[a]*m/z*.

ESI LC/MS analysis did not show satisfactory results, we decided to use the 30% acetonitrile aqueous solution containing 50 m*M* DBAA as the elution solvent.

Next, the optimal MS/MS conditions were investigated. Electrospray ionization mass spectra recorded for the six penicillins gave $[M–H]^-$, $[M–H–CO_2]^-$, and $[M–H–141]^-$. When $[M–H]^-$ serves as a precursor ion for MS/MS, $[M–H–CO_2]^-$ and $[M–H–141]^-$ were generated as product ions (listed in Table 2), and they are very useful for the confirmation of penicillins. After a series of detailed examinations, the other MS/MS conditions including the compound-specific parameters were selected. To provide the applicability of the present method, the fortified bovine tissues, at a concentration of 0.05 mg/kg of each six penicillins, were analyzed. As shown in Fig. 2 left, all six penicillins from the liver sample appeared as separate peaks on the mass chromatograms monitored at $[M–H–141]^-$ under ESI LC/MS/MS conditions. Fig. 2 right shows the tandem mass spectra of the penicillins recorded at the top of each peak on the mass chromatograms shown in Fig. 2 left. All of these mass chromatograms and tandem mass spectra of fortified samples were almost the same as for the respective

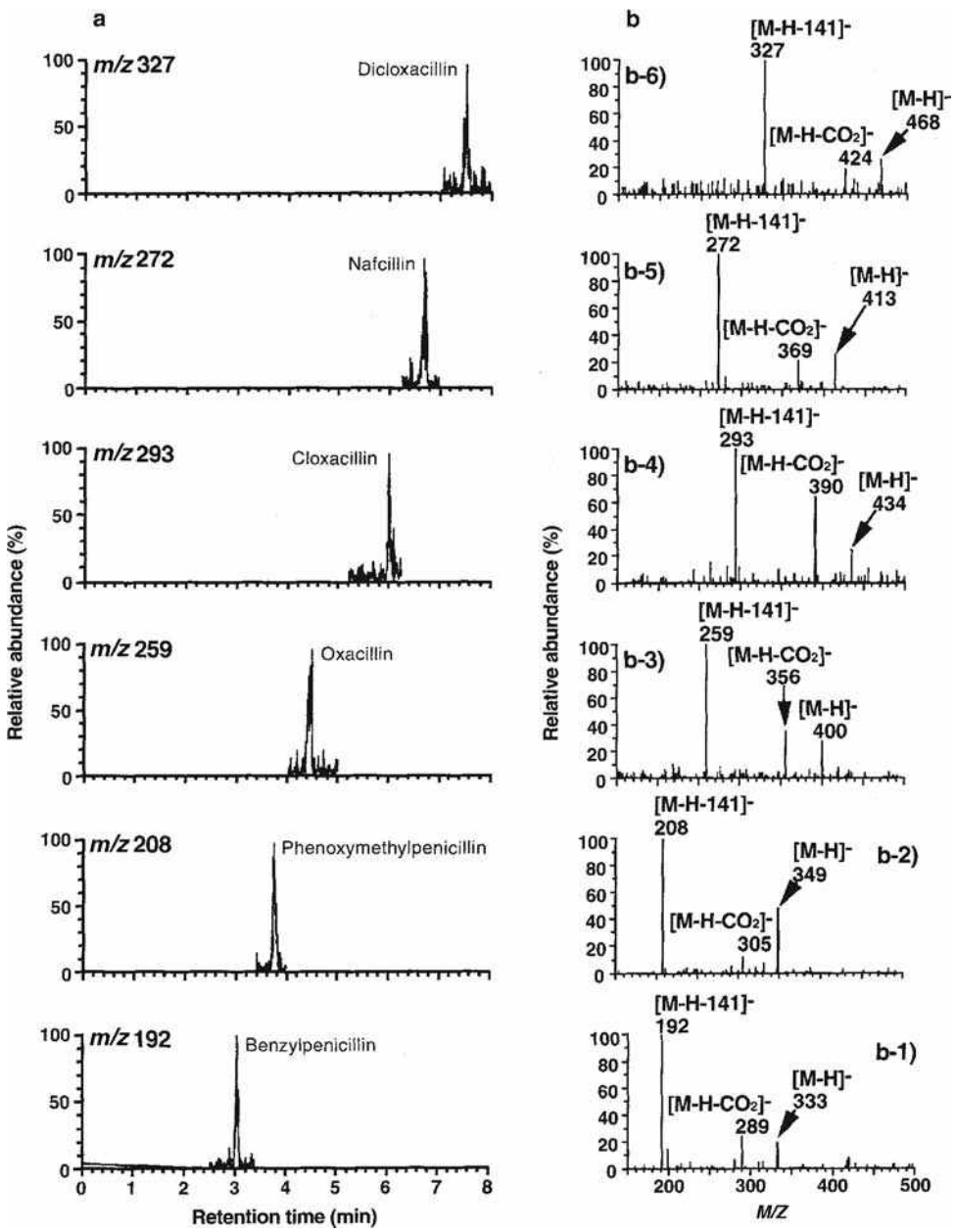

Fig. 2 ESI LC/MS/MS analysis of penicillins fortified at a concentration of 0.05 mg/kg in bovine liver. a, Mass chromatograms monitored at $[M–H–141]^-$; b, tandem mass spectra of penicillins recorded at the top of each peak on the mass chromatograms (a). (b-1) Benzylpenicillin; (b-2) phenoxymethylpenicillin; (b-3) oxacillin; (b-4) cloxacillin; (b-5) nafcillin; (b-6) dicloxacillin.

standards. Based on the results of the analyses of the fortified samples at 0.02 mg/kg, the lower limit of confirmation of the present method for muscle sample was estimated to be 0.02 mg/kg for all six penicillins, and those for kidney and liver were between 0.02 and 0.03 mg/kg.

As described above, we can hardly find the applicable LC/MS determination method of residual penicillins in animal tissue sample; however, those of penicillins in milk sample can be found. Recently, Riediker and Stadler[7] reported the quantitative method for residual amoxicillin, ampicillin, MCIPC, MDIPC, and PCG in milk using ESI LC/MS/MS with a multiple ion monitoring mode and a stable isotope-labeled internal standard. A stable isotopically labeled compound is reasonable and useful for an internal standard of determination method using mass spectrometric techniques. The mixture of acetonitrile and water, including formic acid, as the LC mobile phase and gradient elution were selected. The milk sample with added internal standard (deuterated PCG) was washed with *n*-hexane and condensed before applying C18 cartridge for cleanup. The provided sample solution was filtered through a cutoff filter device (nominal molecular weight limit 10,000). For quantitation, matrix-matched calibration curves were established using a blank milk sample fortified at different concentrations of each target analyte. The mean recoveries of all target penicillins ranged from 76% to 94% at a single analyte concentration of 0.004 mg/kg. The LOQs were in the range of 0.0004–0.0008 mg/kg (mean of blank intensity +10 SD).

CONCLUSIONS

We introduced the LC analysis for residual penicillin antibiotics in food, especially in bovine tissues. To avoid the use of special instruments and toxic reagents, the combination of ion-exchange cartridge cleanup and ion-pair HPLC was very effective and was able to provide sufficient sensitivity and quantitation for the measurement of penicillins. Moreover, it was also able to be used for the development of the confirmation method using ESI LC/MS. The detection limits of all of these methods are able to satisfy the MRLs established by the WHO, FDA, EU, and Japan; so we strongly recommend these methods for the analysis of residual penicillins in tissues to provide safe products for consumers.

REFERENCES

1. Oka, H.; Ikai, Y.; Kawamura, N.; Uno, K.; Yamada, M.; Harada, K.; Uchiyama, M.; Asukabe, H.; Mori, Y.; Suzuki, M. Improvement of chemical analysis of antibiotics. IX. A simple method for residual tetracyclines analysis in honey using a tandem cartridge clean-up system. J. Chromatogr. **1987**, *389*, 417–426.
2. Ito, Y.; Ikai, Y.; Oka, H.; Hayakawa, J.; Kagami, T. Application of ion-exchange cartridge clean-up in food analysis. I. Simultaneous determination of thiabendazole and imazalil in citrus fruit and banana using high-performance liquid chromatography with ultraviolet detection. J. Chromatogr. A, **1998**, *810*, 81–87.
3. Ito, Y.; Ikai, Y.; Oka, H.; Kagami, T.; Takeba, K. Application of ion-exchange cartridge clean-up in food analysis. II. Determination of benzylpenicillin, phenoxymethylpenicillin, oxacillin, cloxacillin, nafcillin and dicloxacillin in meat using liquid chromatography with ultraviolet detection. J. Chromatogr. A, **1999**, *855*, 247–253.
4. Ito, Y.; Ikai, Y.; Oka, H.; Matsumoto, H.; Kagami, T.; Takeba, K. Application of ion-exchange cartridge clean-up in food analysis. III. Determination of benzylpenicillin, phenoxymethylpenicillin, oxacillin, cloxacillin, nafcillin, and dicloxacillin in bovine liver and kidney by liquid chromatography with ultraviolet detection. J. Chromatogr. A, **2000**, *880*, 85–91.
5. Terada, H.; Asanoma, M.; Sakabe, Y. Studies on residual antibacterials in foods. III. High-performance liquid-chromatographic determination of penicillin G in animal tissues using an on-line pre-column concentration and purification system. J. Chromatogr. **1985**, *318*, 299–306.
6. Ito, Y.; Ikai, Y.; Oka, H.; Matsumoto, H.; Miyazaki, Y.; Takeba, K.; Nagase, H. Application of ion-exchange cartridge clean-up in food analysis. IV. Confirmatory assay of benzylpenicillin, phenoxymethylpenicillin, oxacillin, cloxacillin, nafcillin and dicloxacillin in bovine tissues by liquid chromatography–electrospray ionization tandem mass spectrometry. J. Chromatogr. A, **2001**, *911*, 217–223.
7. Riediker, S.; Stadler, R.H. Simultaneous determination of five β-lactam antibiotics in bovine milk using liquid chromatography coupled with electrospray ionization tandem mass spectrometry. Anal. Chem. **2001**, *73*, 1614–1621.

Food: Quinolone Antibiotics Analysis by LC

Nikolas A. Botsoglou
Laboratories of Nutrition, Faculty of Veterinary Medicine, Aristotle University of Thessaloniki, Thessaloniki, Greece

Elias Papapanagiotou
Laboratories of Food Hygiene, Faculty of Veterinary Medicine, Aristotle University of Thessaloniki, Thessaloniki, Greece

Abstract
Quinolone antibiotics, however valuable they may be for increasing food animal productivity, present a concern for public health, considering the potential presence of their residues in the edible products of treated animals. Residues of quinolones in animal-derived food are rather difficult to analyze by chromatographic methods due to their inherent physicochemical characteristics. An overview of the isolation, separation, quantification, and confirmation procedures that may be used to analyze for violative quinolone residues in foods is presented in this entry.

INTRODUCTION

With the extensive use of drugs in animal production, violative residues of the parent drugs and/or metabolites have a high potential to be present in meat, milk, eggs, and honey. The level of residues and the individual drugs they originate from determine the public health significance of such an adulteration of the food supply. The European Union (EU) and the Joint FAO/WHO Expert Committee on Food Additives (JECFA) have established maximum residue limits (MRLs) for several quinolones.

Quinolones constitute an expanding group of synthetic antibiotics that are widely used in combating various diseases in animal husbandry and aquaculture. It is estimated that during the last decade, oxolinic acid, one of the earliest members of this group of drugs, has been by far the most widely used drug in fish farming for prophylaxis and treatment of bacterial fish disease. Oxolinic acid along with nalidixic acid comprises the main members of the first-generation quinolones whose basic molecular structure includes a quinolone ring and a carboxylic acid group. Ciprofloxacin, danofloxacin, difloxacin, enrofloxacin, flumequine, marbofloxacin, norfloxacin, ofloxacin, and sarafloxacin make up the main members of the second-generation quinolones that contain a fluorine atom and a piperazine ring in their molecule, and are collectively called fluoroquinolones. Both first- and second-generation quinolones are analyzed in food of animal origin mainly by liquid chromatographic (LC) methods. An overview of the analytical methodology for the determination of quinolone residues in food is provided in this entry.

ANALYSIS OF QUINOLONES

Quinolones are amphoteric compounds soluble in polar organic solvents such as acetonitrile, methanol, ethanol, dimethylformamide, dichloromethane, and ethyl acetate.[1] They are slightly soluble in water and insoluble in nonpolar solvents such as hexane, petroleum ether, and isooctane. Most of these drugs are fluorescent and are quite stable in aqueous solution toward light except miloxacin, which is reported to be unstable. These inherent characteristics have made quinolones a difficult group of compounds to be analyzed by chromatographic methods.

Sample Extraction

Mincing and/or homogenization of muscle, kidney, and liver samples is usually required before some type of extraction is applied. Drying of tissue samples with anhydrous sodium sulfate prior to extraction is another procedure often employed to enhance the recovery of the analytes.[2–5] Sample extraction and precipitation of concurrent proteins can be accomplished with a great variety of organic solvents including ethyl acetate,[2–4] acetone,[6–8] methanol,[9] acetonitrile,[10,11] ethanol,[5] ethylenediaminetetraacetic acid (EDTA)–McIlvaine buffer solution,[12] EDTA and methanol/water,[13] and trichloroacetic acid and acetonitrile.[14,15]

Enhancement of the extraction efficiency can be achieved by properly acidifying the sample homogenate.[5,9] In acidic conditions, particularly at pH values lower than 3, quinolones, being zwitterions, are fully

protonated and, therefore, are becoming less bound by the matrix and more soluble in organic extraction solvents. Nevertheless, extraction of quinolones from food samples has also been accomplished by aqueous solutions such as water, alkaline buffers, and trichloroacetic acid.[16–18]

Supercritical fluid extraction (SFE) using supercritical CO_2 containing 30% (v/v) methanol has been applied for the extraction of four fluoroquinolones from chicken tissues,[19] while supercritical CO_2 containing 20% (v/v) methanol has also been used for the extraction of the same four fluoroquinolones from eggs.[20]

Another extraction procedure based on buffered QuEChERS methodology (quick, easy, cheap, effective, rugged, and safe) has recently been reported for the multiresidue determination of 18 drugs in milk. In this procedure, extraction of milk samples was carried out with acetonitrile while no extract cleanup was required.[21] Extract cleanup was also not applied in the multiresidue determination of 39 antibiotics, including tetracyclines, quinolones, penicillins, sulfonamides, and macrolides in chicken muscle after extraction with methanol/water containing EDTA and direct injection into an ultra-performance LC–mass spectrometery (MS)–MS system.[13]

Extract Cleanup

Various cleanup procedures including conventional liquid–liquid partitioning, solid-phase extraction, matrix solid-phase dispersion, and online dialysis/trace enrichment have all been employed to eliminate or reduce interfering compounds and also to concentrate the analyte(s). In many instances, more than one of these cleanup procedures have been used in combination to enhance cleanup efficiency.[1]

Liquid–liquid partitioning is employed either to extract the analytes from an organic sample extract into an aqueous solution or to wash out interfering substances from the organic or aqueous sample extracts. In general, quinolones are partitioned from chloroform or ethyl acetate sample extracts into alkaline aqueous buffers, to be then back-extracted into the organic solvent under acidic conditions.[7,8] To remove lipids, sample extracts are often also partitioned with *n*-hexane[2–4,6–8,11,12] or diethyl ether.[10]

Solid-phase extraction is also often used to remove interfering coextracted compounds. Solid-phase extraction columns contain either non-polar reversed-phase C_{18} sorbents or polar sorbents (such as alumina, aminopropyl acid, and propylsulfonic acid).[1,5,15,18,21–23] Matrix solid-phase dispersion cleanup using reversed-phase C_{18} material has been also employed for the determination of oxolinic acid in catfish muscle.[24] In-tube solid-phase microextraction (SPME) based on poly(methacrylic acid–ethylene glycol dimethacrylate) (MAA–EGDMA) monolith coupled to high-preformance liquid chromatography (HPLC) with ultraviolet (UV) and fluorescence detection (FLD) was developed for the determination of five fluoroquinolones in eggs.[25]

Online dialysis and subsequent trace enrichment has been further described for extraction/cleanup of flumequine residues from fish muscle[12] or oxolinic acid and flumequine from chicken liver[6] and salmon muscle.[12] This process involves online use of diphasic dialysis membrane, trapping of the analytes onto a preconcentration column filled with reversed-phase C_{18} or polymeric material, rinsing of the coextracted interfering compounds to waste, and finally, flushing of the concentrated analytes onto the analytical column.

Molecular imprinted polymer microspheres against enrofloxacin have been developed and off-line molecular imprinted solid-phase extraction (MISPE) has been applied for the extraction of enrofloxacin from bovine milk.[26]

LC Separation

Following their extraction and cleanup, residues of quinolones can be analyzed by either gas or liquid chromatography. Among these chromatographic techniques, liquid chromatography seems to be the method of choice since gas chromatography necessitates reduction of analytes such as oxolinic acid, nalidixic acid, and piromidic acid by sodium tetrahydroborate prior to their determination in fish muscle.[27] Since quinolones are polar compounds, LC is generally carried out with non-polar reversed-phase stationary phases that are based on octadecyl, octyl, phenyl, or polymeric sorbents. Recommended mobile phases are fairly polar, containing tetrahydrofuran, methanol, and/or acetonitrile as organic modifiers.[20–22,28] In most applications, phosphoric acid is added into the mobile phase prior to chromatography.[14,17] By acidifying the mobile phase pH at values lower than 3, the ionization of the carboxylate moiety of the analytes is suppressed, and thus, the retention is increased and the separation is improved. Nevertheless, the recorded chromatographic peaks generally tail, and elimination or significant reduction of peak tailing can be generally achieved by addition to the mobile phase of counterions[10,16] or oxalic acid and citric acid.[2–4,13,23]

Detection

Ultraviolet,[23,25] fluorimetric,[12,14,15,17,18,20,25] chemiluminescence,[28] and mass spectrometric[12,13,21–23] detections have been successfully used for the determination of residues of quinolones in food. Quinolones exhibit remarkable UV absorption and are, therefore, ideal for direct determination by UV detection anywhere in the wavelength range of 254–295 nm. However, fluorimetric detection is the most popular because of the inherent fluorescence of these drugs and the advantages in terms of selectivity and sensitivity that this detection offers.

Confirmation

Each detection system has its own advantages and disadvantages, which must be carefully considered in the selection of the most convenient system for a particular analyte in a particular matrix. Screening assays based on ultraviolet and fluorimetric detection offer the advantage to rapidly screen a large number of food samples for potential residues at a low cost, but cannot provide definitive information on the identity of violative residues found in suspected samples. The problem of analyzing drug residues in food is complicated by the fact that it is not known whether residues exist, and if they exist, their type and quantity are not known. In the past, confirmation of the identity of LC peaks in suspected samples was obtained by means of a derivatization process in which the analytes are converted to the corresponding decarboxylated derivatives, which are then analyzed by gas chromatography (GC)–MS.[7,8] Nowadays, the possibility for unambiguous identification of the analytes is offered by coupling LC–MS. MS detection systems use the difference in mass-to-charge ratio (m/z) of ionized atoms or molecules to separate them from each other. Molecules have distinctive fragmentation patterns that provide structural information to identify structural components. Thus, LC–MS–MS in the multiple reaction monitoring mode has been used to detect/confirm residues of eight quinolones in pig muscle.[23] Additionally, ultra-performance LC coupled with MS–MS has been used in confirmatory multiresidue, multiclass analysis of various quinolone residues in poultry, ovine, and porcine tissues,[13] milk,[21] and eggs.[12] The latest introduction of new MS techniques such as the combination of ultra-performance LC with time-of-flight (TOF)–MS has offered an additional powerful analytical tool for both screening and confirmatory analysis of drug residues in foods of animal origin. Applications include ultra-performance LC coupled with TOF–MS for the confirmatory multiresidue, multiclass analysis of 11 quinolones in milk.[22] However, one should always bear in mind that the confirmatory analysis of suspected samples has to be better carried out by MS–MS techniques, since criteria for confirmation of the identity of drug residues by TOF–MS are not yet included in the EU guidelines.[29]

CONCLUSION

An analyst has a wide range of efficient extraction, cleanup, separation, and detection procedures to choose from. The choice will depend on the nature of the sample matrix, whether it is solid or liquid, fatty or non-fatty, and the expected range and levels of quinolone residues in food.

REFERENCES

1. Botsoglou, N.A.; Fletouris, D.J. *Drug Residues in Food: Pharmacology, Food Safety, and Analysis*; Marcel Dekker: New York, 2001.
2. Larocque, L.; Schnurr, M.; Sved, S.; Weninger, A. Determination of oxolinic acid residues in salmon muscle-tissue by liquid chromatography with fluorescence detection. J. Assoc. Off. Anal. Chem. **1991**, *74*, 608–611.
3. Carignan, G.; Larocque, L.; Sved, S. Assay of oxolinic acid residues in salmon muscle by liquid chromatography with fluorescence detection-interlaboratory study. J. Assoc. Off. Anal. Chem. **1991**, *74*, 906–909.
4. Degroodt, J.M.; Wyhowski de Bukanski, B.; Srebrnik, S. Oxolinic acid and flumequine in fish tissues: Validation of an HPLC method; Analysis of medicated fish and commercial fish samples. J. Liq. Chromatogr. **1994**, *17*, 1785–1794.
5. Roybal, J.E.; Pfenning, A.P.; Turnipseed, S.B.; Walker, C.C.; Hurlbut, J.A. Determination of 4 fluoroquinolones in milk by liquid chromatography. J. AOAC Int. **1997**, *80*, 982–987.
6. Eng, G.Y.; Maxwell, R.J.; Cohen, E.; Piotrowski, E.G.; Fiddler, W. Determination of flumequine and oxolinic acid in fortified chicken tissue using online dialysis and high-performance liquid chromatography with fluorescence detection. J. Chromatogr. **1998**, *799*, 349–354.
7. Pfenning, A.P.; Munns, R.K.; Turnipseed, S.B.; Roybal, J.E.; Holland, D.C.; Long, A.R.; Plakas, S.M. Determination and confirmation of identities of flumequine and nalidixic, oxolinic, and piromidic acids in salmon and shrimp. J. AOAC Int. **1996**, *79*, 1227–1235.
8. Munns, R.K.; Turnipseed, S.B.; Pfenning, A.P.; Roybal, J.E.; Holland, D.C.; Long, A.R.; Plakas, S.M. Determination of residues of flumequine and nalidixic, oxolinic, and piromidic acids in catfish by liquid chromatography with fluorescence and UV detection. J. AOAC Int. **1995**, *78*, 343–352.
9. Pouliquen, H.; Gouelo, D.; Larhantec, M.; Pilet, N.; Pinault, L. Rapid and simple determination of oxolinic acid and oxytetracycline in the shell of the blue mussel (Mytilus-Edulis) by high-performance liquid chromatography. J. Chromatogr. **1997**, *702*, 157–162.
10. Hormazabal, V.; Yndestad, M. Rapid assay for monitoring residues of enrofloxacin in milk and meat tissues by HPLC. J. Liq. Chromatogr. **1994**, *17*, 3775–3782.
11. Meinertz, J.R.; Dawson, V.K.; Gingerich, W.H.; Cheng, B.; Tubergen, M.M. Liquid chromatographic determination of sarafloxacin residues in channel catfish muscle tissue. J. AOAC Int. **1994**, *77*, 871–875.
12. Jia, X.; Shao, B.; Wu, Y.; Yang, Y.; Zhang, J. Simultaneous determination of tetracyclines and quinolones antibiotics in egg by ultra-performance liquid chromatography–electrospray tandem mass spectrometry. J. AOAC Int. **2008**, *91*, 461–468.
13. Chico, J.; Rubies, A.; Centrich, F.; Companyo, R.; Prat, M.D.; Granados, M. High-throughput multiclass method for antibiotic residue analysis by liquid chromatography–tandem mass spectrometry. J. Chromatogr. A, **2008**, *1213*, 189–199.
14. Cho, H.-J.; Abd El-Aty, A.M.; Goudah, A.; Sung, G.-M.; Yi, H.; Seo, D.-C.; Kim, J.-S.; Shim, J.-H.; Jeong, J.-Y.;

Lee, S.-H.; Shin, H.-C. Monitoring of fluoroquinolone residual levels in chicken eggs by microbiological assay and confirmation by liquid chromatography. Biomed. Chromatogr. **2008**, *22*, 92–99.

15. Yang, G.; Lin, B.; Zeng, Z.; Chen, Z.; Huang, X. Multiresidue determination of eleven quinolones in milk by liquid chromatography with fluorescence detection. J. AOAC Int. **2005**, *88*, 1688–1694.
16. Thanh, H.H.; Andresen, A.T.; Agasoster, T.; Rasmussen, K.E. Automated column-switching high-performance liquid chromatographic determination of flumequine and oxolinic acid in extracts from fish. J. Chromatogr. **1990**, *532*, 363–373.
17. Anadon, A.; Martinez, M.A.; Martinez, M.; De La Cruz, C.; Diaz, M.J.; Martinez-Larranaga, M.R. Oral bioavailability, tissue distribution and depletion of flumequine in the food producing animal, chicken for fattening. Food Chem. Toxicol. **2008**, *46*, 662–670.
18. Verdon, E.; Couedor, P.; Roudaut, B.; Sanders, P. Multiresidue method for simultaneous determination of ten quinolone antibacterial residues in multimatrix/multispecies animal tissues by liquid chromatography with fluorescence detection: Single laboratory validation study. J. AOAC Int. **2005**, *88*, 1179–1192.
19. Choi, J.H.; Abd El-Aty, A.M.; Shen, J.Y.; Kim, M.R.; Shim, J.H. Analysis of fluoroquinolone residues in edible chicken tissues using supercritical fluid extraction. Berl Munch Tierarztl Wochenschr **2006**, *119*, 456–460.
20. Shim, J.H.; Lee, M.H.; Kim, M.R.; Lee, C.J.; Kim, I.S. Simultaneous measurement of fluoroquinolones in eggs by a combination of supercritical fluid extraction and high pressure liquid chromatography. Biosci. Biotechnol. Biochem. **2003**, *67*, 1342–1348.
21. Aguilera-Luiz, M.M.; Martinez Vidal, J.L.; Romero-Gonzalez, R.; Frenich, A.G. Multi-residue determination of veterinary drugs in milk by ultra-high-pressure liquid chromatography–tandem mass spectrometry. J. Chromatogr. A, **2008**, *1205*, 10–16.
22. Stolker, A.A.M.; Rutgers, P.; Oosterink, E.; Lasaroms, J.J.P.; Peters, R.J.B.; van Rhijn, J.A.; Nielen, M.W.F. Comprehensive screening and quantification of veterinary drugs in milk using UPLC–TOF–MS. Anal. Bioanal. Chem. **2008**, *391*, 2309–2322.
23. Hermo, M.P.; Barron, D.; Barbosa, J. Development of analytical methods for multiresidue determination of quinolones in pig muscle samples by liquid chromatography with ultraviolet detection, liquid chromatography–mass spectrometry and liquid chromatography–tandem mass spectrometry. J. Chromatogr. A, **2006**, *1104*, 132–139.
24. Jarboe, H.H.; Kleinow, K.M. Matrix solid-phase dispersion isolation and liquid chromatographic determination of oxolinic acid in channel catfish (Ictalurus-Punctatus) muscle tissue. J. AOAC Int. **1992**, *75*, 428–432.
25. Huang, J.-F.; Lin, B.; Yu, Q.-W.; Feng, Y.-Q. Determination of fluoroquinolones in eggs using in-tube solid-phase microextraction coupled to high-performance liquid chromatography. Anal. Bioanal. Chem. **2006**, *384*, 1228–1235.
26. Qu, G.; Wu, A.; Shi, X.; Niu, Z.; Xie, W.; Zhang, D. Improvement on analyte extraction by molecularly imprinted polymer microspheres toward enrofloxacin. Anal. Lett. **2008**, *41*, 1443–1458.
27. Takatsuki, K. Gas chromatographic mass spectrometric determination of oxolinic, nalidixic, and piromidic acid in fish. J. AOAC Int. **1992**, *75*, 982–987.
28. Wan, G.-H.; Cui, H.; Pan, Y.-L.; Zheng, P.; Liu, L.-J. Determination of quinolones residues in prawn using high performance liquid chromatography with Ce(IV)–$Ru(bpy)_3^{2+}$–HNO_3 chemiluminescence detection. J. Chromatogr. B, **2006**, *843*, 1–9.
29. European Union. Commission Decision 2002/657/EC of 12 August 2002. Off. J. Eur. Comm. **2002**, *L221*, 8–36.

Food: β-Agonist Residue Analysis by LC

Nikolas A. Botsoglou
Laboratories of Nutrition, Faculty of Veterinary Medicine, Aristotle University of Thessaloniki, Thessaloniki, Greece

Evropi Botsoglou
Laboratory of Hygiene of Foods of Animal Origin, Department of Veterinary Medicine, University of Thessaly, Karditsa, Greece

Abstract
β-Agonists are synthetic compounds that, in addition to their therapeutic use in veterinary medicine, are able to promote live weight gain in food-producing animals. Such a use, however, may result in the presence of residues in the edible products of treated animals that may cause a real health problem to consumers. An overview of the isolation, separation, quantification, and confirmation procedures that may be used to analyze for violative β-agonist residues in foods is presented in this entry.

INTRODUCTION

β-Agonists are synthetically produced compounds that, in addition to their regular therapeutic role in veterinary medicine as bronchodilatory and tocolytic agents, can promote live weight gain in food-producing animals. They are also referred to as repartitioning agents, because their effect on carcass composition is to increase the deposition of protein while reducing fat accretion. For use in lean-meat production, doses of 5–15 times greater than the recommended therapeutic dose would be required, together with a more prolonged period of in-feed administration, which is often quite near to slaughter to obviate the elimination problem. Such a use would result in significant residue levels in edible tissues of the treated animals which might, in turn, exert adverse effects on the cardiovascular and central nervous system of the consumers.[1]

There are a number of well-documented cases where consumption of liver and meat from animals illegally treated with these compounds, particularly clenbuterol, has resulted in massive human intoxification.[1] In Spain, a food-borne clenbuterol poisoning outbreak occurred in 1989–1990, affecting 135 persons. Consumption of liver containing clenbuterol in the range 160–291 ppb was identified as the common point in the 43 families affected, while symptoms were observed in 97% of all family members who consumed liver. In 1992, another outbreak occurred in Spain, this time affecting 232 persons. Clinical signs of poisoning in more than half of the patients included muscle tremors and tachycardia, frequently accompanied by nervousness, headaches, and myalgia. Clenbuterol levels in the urine of the patients were found to range from 11 to 486 ppb. An incident of food poisoning by residues of clenbuterol in veal liver occurred also in the fall of 1990 in the cities of Roanne and Clermont-Ferrand, France. A total of 22 persons from eight families were affected.[1] An outbreak of poisoning occurred also in Italy in May 1997 affecting 15 individuals who ingested about 200 g veal meat contaminated with clenbuterol residues at 1140–1480 ng/g.[2] In addition, four cases of acute food poisoning in 50 people who ingested lamb and bovine meat containing clenbuterol residues at 300–1400 ng/g levels were recorded in Portugal in 1998–2002.[3] Apart from the above-mentioned cases, two farmers in Ireland were also reported to have died while preparing clenbuterol as feed for livestock.

Although, without exception, these incidents have all been caused by the toxicity of clenbuterol, the entire group of β-agonists is now being treated with great suspicion by regulatory authorities, and the use of all β-agonists in farm animals for growth-promoting purposes has been prohibited by regulatory agencies in Europe, Asia, and the Americas. Clenbuterol, in particular, has been banned by the FDA for any animal application in the United States, whereas it is highly likely to be banned even for therapeutic use in the European Union in the near future. However, veterinary use of some β-agonists such as clenbuterol, cimaterol, and ractopamine is still licensed in several parts of the world for therapeutic purposes. As a result, a recent screening assay in Turkey showed a high incidence rate (68.3%) of clenbuterol residues in ultra-high temperature (UHT) milk, with 21.7% of the samples exceeding the level of 50 ng/L.[4]

Monitoring programs have shown that β-agonists have been used illegally in parts of Europe and United States by some livestock producers.[1] In addition, new analogues, often with deviating structural properties, are continuously introduced in the illegal practice of application of growth-promoting β-agonists in cattle rearing. As a result, specific

knowledge of the target residues appropriate for surveillance is very limited for many of the β-agonists that have potential black-market use.[5] Hence, continuous improvement of detection methods is necessary to keep pace with the rapid development of these new unknown β-agonists. Both gas and liquid chromatography (LC) methods can be employed for the determination of β-agonist residues in biological samples. However, LC methods are receiving wider acceptance, as gas chromatographic methods are generally complicated by the necessity for derivatization of the polar hydroxyl and amino functional groups of β-agonists. In this entry, an overview of the analytical methodology for the determination of β-agonists in food by LC is provided.

ANALYSIS OF β-AGONISTS BY LC

Included in this group of drugs are certain synthetically produced phenethanolamines such as bambuterol, bromobuterol, carbuterol, cimaterol, clenbuterol, dobutamine, fenoterol, isoproterenol, mabuterol, mapenterol, metaproterenol, pirbuterol, ractopamine, reproterol, rimiterol, ritodrine, salbutamol, salmeterol, terbutaline, tulobuterol, and zilpaterol. Except zilpaterol, these drugs fall into two major categories: substituted anilines, including clenbuterol, and substituted phenols, including salbutamol. This distinction is important because most methods for drugs in the former category depend on the pH adjustment to partition the analytes between organic and aqueous phases. The pH dependence is not valid, however, for drugs in the latter category, as phenolic compounds are charged under all pH conditions.

Extraction Procedures

β-Agonists are relatively polar compounds, which are soluble in methanol and ethanol, slightly soluble in chloroform, and almost insoluble in benzene. When analyzing liquid samples for residues of β-agonists, deconjugation of bound residues using β-glucuronidase/sulfatase enzyme hydrolysis before sample extraction is often recommended.[6,7] Semisolid samples, such as liver and muscle, require usually more intensive sample pretreatment for tissue breakup. Most popular approach is sample homogenization in dilute acids such as hydrochloric or perchloric acid or in an aqueous buffer.[6–9] In general, dilute acids allow high extraction yields for all categories of β-agonists because the aromatic moiety of these analytes is uncharged under acidic conditions while their aliphatic amino group is positively ionized. Following centrifugation of the extract, the supernatant may be further treated with β-glucuronidase/sulfatase or subtilisin A to allow hydrolysis of the conjugated residues.

Cleanup Procedures

The primary sample extract is subsequently subjected to cleanup using several different approaches including conventional liquid–liquid partitioning, diphasic dialysis, solid-phase extraction, and immunoaffinity chromatography cleanup. In some instances, more than one of these procedures is applied in combination to achieve better extract purification.

Liquid–liquid partitioning cleanup is generally carried out at alkaline conditions using ethyl acetate, ethyl acetate–*tert*-butanol mixture, diethyl ether, or *tert*-butyl methyl ether/*n*-butanol as extraction solvents.[8,10,11] The organic extracts are then either concentrated to dryness or repartitioned with dilute acid to facilitate back extraction of the analytes into the acidic solution. A literature survey shows that liquid–liquid partitioning cleanup resulted in good recoveries of substituted anilines such as clenbuterol,[10,11] but it was less effective for more polar compounds such as salbutamol.[8] Diphasic dialysis can be also used for purification of the primary sample extract. This procedure was only applied in the determination of clenbuterol residues in liver using *tert*-butyl methyl ether as the extraction solvent.[9]

Solid-phase extraction is, generally, better suited to the multiresidue analysis of β-agonists. This procedure has become the method of choice for the determination of β-agonists in biological matrices because it is not labor- and material intensive. It is particularly advantageous because it allows better extraction of the more hydrophilic β-agonists including salbutamol. β-Agonists are better suited to reversed-phase solid-phase extraction owing, in part, to their relatively non-polar aliphatic moiety, which can interact with the hydrophobic octadecyl- and octyl-based sorbents of the cartridge.[12–14] By adjusting the pH of the sample extracts at values above 10, optimum retention of the analytes can be achieved. Adsorption solid-phase extraction using a neutral alumina sorbent has also been recommended for improved cleanup of liver homogenates.[8] Ion-exchange solid-phase extraction is another cleanup procedure successfully used in the purification of liver and tissue homogenates.[15] As multiresidue solid-phase extraction procedures covering β-agonists of different types, in general, present analytical problems, mixed-phase solid-phase extraction sorbents, which contained a mixture of reversed-phase and ion-exchange material, were also employed to improve the retention of the more polar compounds.[12,16–20] Toward this direction, several different sorbents were designed and procedures that utilized different interaction mechanisms were described, such as those using matrix solid-phase dispersion in combination with molecularly imprinted polymers for the extraction of clenbuterol from liver.[21] Molecular imprints as sorbents for solid-phase extraction are very selective, but the production of a constant-quality material still causes reproducibility problems.[17,22]

Immunoaffinity chromatography, owing to its high specificity and sample cleanup efficiency, has also gained widespread acceptance for the determination of β-agonists in biological matrices.[6,7,15,23] The potential of online immunoaffinity extraction for the multiresidue determination of β-agonists in bovine urine has been demonstrated, using an automated column-switching system.[23]

Separation Procedures

Following extraction and cleanup, β-agonist residues can be analyzed by LC. Gas chromatographic separation of β-agonists is generally complicated by the necessity for derivatization of their polar hydroxyl and amino functional groups. LC reversed-phase chromatography is commonly used for the separation of the various β-agonist residues owing to their hydrophobic interaction with the C_{18} sorbent. Efficient reversed-phase ion-pair separation of β-agonists has also been reported using sodium dodecyl sulfate as the pairing ion.[24]

Detection Procedures

Following LC separation, detection is often performed in the ultraviolet region at wavelengths of 245 or 260 nm. However, poor sensitivity and interference from coextractives may occur at these low detection wavelengths unless sample extracts are extensively cleaned up and concentrated. This problem may be overcome by postcolumn derivatization of the aromatic amino group of the β-agonist molecules to the corresponding diazo dyes through a Bratton–Marshall reaction, and detection at 494 nm.[24] Although spectrophotometric detection is generally acceptable, electrochemical detection appears more appropriate for the analysis of β-agonists, owing to the presence of oxidizable hydroxyl and amino groups on the aromatic part of their molecules. This method of detection has been applied in the determination of clenbuterol residues in bovine retinal tissue with sufficient sensitivity for this tissue.[11] Potentiometric detection with poly(vinyl chloride)-based liquid membrane electrode coatings has also been applied for a series of 18 exogenic β-agonist residues in LC systems.[25] Recently, a novel detection method using chemiluminescence has been reported for multiresidue determination of β-agonists including terbutaline, salbutamol, and clenbuterol in pig liver.[26] The procedure is based on the enhancement effect of β-agonists on the chemiluminescent reaction between the luminal and the complex of trivalent copper and periodate, which was electrogenerated online by constant-current electrolysis. However, the highest sensitivity and selectivity is offered by mass spectrometry (MS). Currently, coupling LC with MS appears to be the method of choice for the determination of β-agonists in biological samples although some drawbacks have started to appear. Main source of these drawbacks is the existence of matrix effects in general, and the ion suppression phenomenon in particular.[27] This phenomenon affects many aspects of the performance of the method, such as detection capability, repeatability, and accuracy. The cause of ionization suppression is a change in the droplet solution properties of the spray arising from the presence of coeluting non-volatile or less volatile solutes. Polar compounds such as β-agonists seem to be particularly susceptible to ion suppression. A possible solution to overcome false compliant results is the use of a proper internal standard, preferably an isotope-labeled one, to incorporate corrections for the ion suppression effect in cases where the ion signal is not suppressed completely.[28]

Confirmation Procedures

The requirements for unambiguous identification of these drugs have led to the large utilization of MS as the confirmatory procedure. Ion spray LC–MS/MS has been used to monitor five β-agonists in bovine urine,[23] while atmospheric-pressure chemical ionization LC–MS/MS has been employed for the identification of ractopamine residues in bovine urine.[12]

CONCLUSION

This literature overview shows that a wide range of efficient extraction, cleanup, separation, and detection procedures is available for the determination of β-agonists in food. However, continuous improvement of detection methods is necessary to keep pace with the continuous introduction of new unknown β-agonists that have potential black-market use, in illegal practice.

REFERENCES

1. Botsoglou, N.A.; Fletouris, D.J. *Drug Residues in Food: Pharmacology, Food Safety, and Analysis*; Marcel Dekker, Inc.: New York, 2001.
2. Brambilla, G.; Cenci, T.; Franconi, F.; Galarini, R.; Macri, A.; Rondoni, F.; Strozzi, M.; Loizzo, A. Clinical and pharmacological profile in a clenbuterol epidemic poisoning of contaminated beef meat in Italy. Toxicol. Lett. **2000**, *114*, 47–53.
3. Barbosa, J.; Cruz, C.; Martins, J.; Silva, J.M.; Neves, C.; Alves, C.; Ramos, F.; Da Silveira, M.I.N. Food poisoning by clenbuterol in Portugal. Food Addit. Contam. **2005**, *22*, 563–566.
4. Unusan, N. Determination of clenbuterol in UHT milk in Turkey. Inter. J. Food Sci. Tech. **2008**, *43*, 617–619.
5. Kuiper, H.A.; Noordam, M.Y.; van Dooren-Flipsen, M.M.H.; Schilt, R.; Roos, A.H. Illegal use of beta-adrenergic agonists: European Community. J. Anim. Sci. **1998**, *76*, 195–207.

6. Van Ginkel, L.A.; Stephany, R.W.; Van Rossum, H.J. Development and validation of a multiresidue method for β-agonists in biological samples and animal feed. J. AOAC Int. **1992**, *75*, 554–560.
7. Visser, T.; Vredenbregt, M.J.; De Jong, A.P.J.M.; Van Ginkel, L.A.; Van Rossum, H.J.; Stephany, R.W. Cryotrapping gas chromatography Fourier-transform infrared spectrometry: A new technique to confirm the presence of β-agonists in animal material. Anal. Chim. Acta **1993**, *275*, 205–214.
8. Leyssens, L.; Driessen, C.; Jacobs, A.; Czech, J.; Raus, J. Determination of beta-2-receptor agonists in bovine urine and liver by gas-chromatography–tandem mass spectrometry. J. Chromatogr. **1991**, *564*, 515–527.
9. González, P.; Fente, C.A.; Franco, C.; Vázquez, B.; Quinto, E.; Cepeda, A. Determination of residues of the β-agonist clenbuterol in liver of medicated farm animals by gas chromatography–mass spectrometry using diphasic dialysis as an extraction procedure. J. Chromatogr. **1997**, *693*, 321–326.
10. Wilson, R.T.; Groneck, J.M.; Holland, K.P.; Henry, A.C. Determination of clenbuterol in cattle, sheep, and swine tissues by electron ionization gas chromatography–mass spectrometry. J. AOAC Int. **1994**, *77*, 917–924.
11. Lin, L.A.; Tomlinson, J.A.; Satzger, R.D. Detection of clenbuterol in bovine retinal tissue by high-performance liquid chromatography with electrochemical detection. J. Chromatogr. **1997**, *762*, 275–280.
12. Elliott, C.T.; Thompson, C.S.; Arts, C.J.M.; Crooks, S.R.H.; Van Baak, M.J.; Verheij, E.R.; Baxter, G.A. Screening and confirmatory determination of ractopamine residues in calves treated with growth-promoting doses of the β-agonist. Analyst **1998**, *123*, 1103–1107.
13. Van Rhijn, J.A.; Heskamp, H.H.; Essers, M.L.; Van de Wetering, H.J.; Kleijnen, H.C.H.; Roos, A.H. Possibilities for confirmatory analysis of some beta-agonists using two different derivatives simultaneously. J. Chromatogr. **1995**, *665*, 395–398.
14. Gaillard, Y.; Balland, A.; Doucet, F.; Pepin, G. Detection of illegal clenbuterol use in calves using hair analysis. J. Chromatogr. **1997**, *703*, 85–95.
15. Lawrence, J.F.; Menard, C. Determination of clenbuterol in beef-liver and muscle-tissue using immunoaffinity chromatographic cleanup and liquid-chromatography with ultraviolet absorbency detection. J. Chromatogr. **1997**, *696*, 291–297.
16. Ramos, F.; Santos, C.; Silva, A.; Da Silveira, M.I.N. Beta(2)-adrenergic agonist residues: Simultaneous methylboronic and butylboronic derivatization for confirmatory analysis by gas-chromatography–mass-spectrometry. J. Chromatogr. **1998**, *716*, 366–370.
17. Stolker, A.A.M.; Brinkman, U.A.Th. Analytical strategies for residue analysis of veterinary drugs and growth-promoting agents in food-producing animals: A review. J. Chromatogr. **2005**, *1067*, 15–53.
18. Williams, L.D.; Churchwell, M.I.; Doerge, D.R. Multiresidue confirmation of beta-agonists in bovine retina and liver using LC-ES/MS/MS. J. Chromatogr. **2004**, *813*, 35–45.
19. van Hoof, N.; Schilt, R.; van der Vlis, E.; Boshuis, P.; van Baak, M.; Draaijer, A.; de Brabander, H. Detection of zilpaterol (Zilmaxo) in calf urine and faeces with liquid chromatography–tandem mass spectrometry. Anal. Chim. Acta **2005**, *529*, 189–197.
20. Blanca, J.; Munoz, P.; Morgado, M.; Mendez, N.; Aranda, A.; Reuvers, T.; Hooghuis, H. Determination of clenbuterol, ractopamine and zilpaterol in liver and urine by liquid chromatography–tandem mass spectrometry. Anal. Chim. Acta **2005**, *529*, 199–205.
21. Crescenzi, C.; Bayoudth, S.; Cormack, P.A.G.; Klein, T.; Ensing, K. Determination of clenbuterol in bovine liver by combining matrix solid-phase dispersion and molecularly imprinted solid-phase extraction followed by liquid chromatography/electrospray ion trap multiple-stage mass spectrometry. Anal. Chem. **2001**, *73*, 2171–2177.
22. Widstrand, C.; Larsson, F.; Fiori, M.; Civitareale, C.; Mirante, S.; Brambilla, G. Evaluation of MISPE for the multi-residue extraction of β-agonists from calves urine. J. Chromatogr. **2004**, *804*, 85–91.
23. Cai, J; Henion, J. Quantitative multi-residue determination of β-agonists in bovine urine using on-line immunoaffinity extraction coupled-column packed capillary liquid chromatography–tandem mass spectrometry. J. Chromatogr. **1997**, *691*, 357–370.
24. Courtheyn, D.; Desaever, C.; Verhe, R. High-performance liquid chromatographic determination of clenbuterol and cimaterol using postcolumn derivatization. J. Chromatogr. **1991**, *564*, 537–549.
25. Bazylak, G.; Nagels, L.J. Potentiometric detection of exogenic beta-adrenergic substances in liquid chromatography. J. Chromatogr. **2002**, *973*, 85–96.
26. Zhang, Y.; Zhang, Z.; Sun, Y.; Wie, Y. Development of an analytical method for the determination of beta(2)-agonist residues in animal tissues by high-performance liquid chromatography with online electrogenerated [Cu(HIO(6)(2)](5)(-)-Luminol chemiluminescence detection. J. Agric. Food Chem. **2007**, *55*, 4949–4956.
27. Antignac, J.-P.; de Wasch, K.; Monteau, F.; de Brabander, H.F.; Andre, F.; le Bizec, B. The ion suppression phenomenon in liquid chromatography–mass spectrometry and its consequences in the field of residue analysis. Anal. Chim. Acta **2005**, *529*, 129–136.
28. de Brabander, H.F.; le Bizec, B.; Pinel, G.; Antignac, J.-P.; Verheyden, K.; Mortier, V.; Courtheyn, D.; Noppe, H. Past, Present, and future of mass spectrometry in the analysis of residues of banned substances in meat-producing animals. J. Mass Spectrom. **2007**, *42*, 983–998.

Food: Vitamin B_{12} and Related Compound Analysis by TLC

Fumio Watanabe
Emi Miyamoto
Department of Health Science, Kochi Women's University, Kochi, Japan

INTRODUCTION

Vitamin B_{12} (B_{12} or CN-B_{12}) is synthesized only in certain bacteria. Usual dietary sources of B_{12} are animal food products (meat, milk, eggs, and shellfish), but not generally plant food products. However, some plant foods (e.g., edible algae) contain large amounts of B_{12}. Various B_{12} compounds with different upper (L) and/or lower (R) ligands naturally occur (Fig. 1), especially MeB_{12} and $AdoB_{12}$, which function as coenzyme forms of B_{12}. Some food products contain unidentified or inactive B_{12}-related compounds, which may not be bioavailable in humans. Appreciable loss of B_{12} also occurs in foods during cooking and/or other food processing.

This entry summarizes the purification and characterization of B_{12} compounds found in various food products and of B_{12} degradation compounds formed by cooking and/or food processing, using thin-layer chromatography (TLC) as a powerful separation and analytical tool.

PURIFICATION AND CHARACTERIZATION OF VITAMIN B_{12} AND RELATED COMPOUNDS BY TLC

Commercially Available Reagents

Some commercially available B_{12} reagents, especially OH-B_{12} and dicyanocobinamide, contain small amounts of impurities (Fig. 2). Each B_{12} reagent should be purified with silica gel 60 TLC and then used for experiments as an authentic "standard" material. The authentic OH-B_{12}, purified by TLC on silica gel, has been used in the experiments conducted in the authors' laboratory.[1]

Vitamin B_{12} Degradation Products by Cooking and/or Food Processing

To determine whether the loss of B_{12} in microwave-treated foods is derived from the conversion of B_{12} to some inactive B_{12} degradation products, the OH-B_{12} that predominates in food is treated by microwave heating for 6 min and then analyzed by TLC on silica gel 60 with 1-butanol-2-propanol–water (10:7:10 vol/vol) as the solvent. The treated OH-B_{12} is separated into three red spots [major compound I with an R_f of 0.03, identical R_f of intact OH-B_{12}, and minor compound II (about 18.2%) with an R_f of 0.16 and compound III (4.2%) with an R_f of 0.27].[2] Although a novel OH-B_{12} degradation product with an R_f of 0.12 has not been separable from intact OH-B_{12} by the TLC system, it can be completely separated by silica gel 60 column chromatography.[1]

The OH-B_{12} degradation products with R_f values of 0.12 and 0.16 are further purified to homogeneity by the use of silica gel 60 TLC and reversed-phase (RP) high-performance liquid chromatography (HPLC).[1,2] The ^1H nuclear magnetic resonance (NMR) spectra of the OH-B_{12} degradation products show that the degradation product with an R_f of 0.12 is a B_{12} compound with the lower ligand structure changed slightly, but that with an R_f of 0.16 is a B_{12} compound without the base portion in the lower ligand.[1,2] Structural information on the degradation compound with an R_f of 0.27 is not available because a purified sample was not obtained for NMR study. Although the degradation product with an R_f of 0.12 has about 13% and 23% biological activity of authentic B_{12} in hog intrinsic factor (IF; the most specific mammalian B_{12}-binding protein) and *Lactobacillus delbrueckii* ATCC 7830 (a micro-organism for B_{12} bioassay), respectively, the product with an R_f of 0.16 does not show any biological activity.[1,2] Intravenous administration of both purified degradation products to rats indicates that the compounds are not toxic.[1,2] These results indicate that the conversion of B_{12} to these inactive B_{12} degradation products occurs in food during microwave heating.

Appreciable loss of B_{12} occurs in the multivitamin–mineral food supplements containing B_{12} because B_{12} is converted to inactive B_{12} compounds by the addition of substantial amounts of vitamin C in the presence of copper.[3] The destruction of B_{12} is probably concerned with radicals generated by vitamin C in the presence of copper. Although vitamin C alone or metal ion (Cu^{2+}) alone does not decompose B_{12}, B_{12} is destroyed significantly by mixing vitamin C and Cu^{2+} together (vitamin C–Cu^{2+} system).[4] Many B_{12} degradation compounds (ladderlike red-colored spots) are separated from the B_{12} treated with the vitamin C–Cu^{2+} system by TLC on silica gel 60.[4] Some of the B_{12} compounds formed appear to block B_{12} metabolism in mammalian cells.[3]

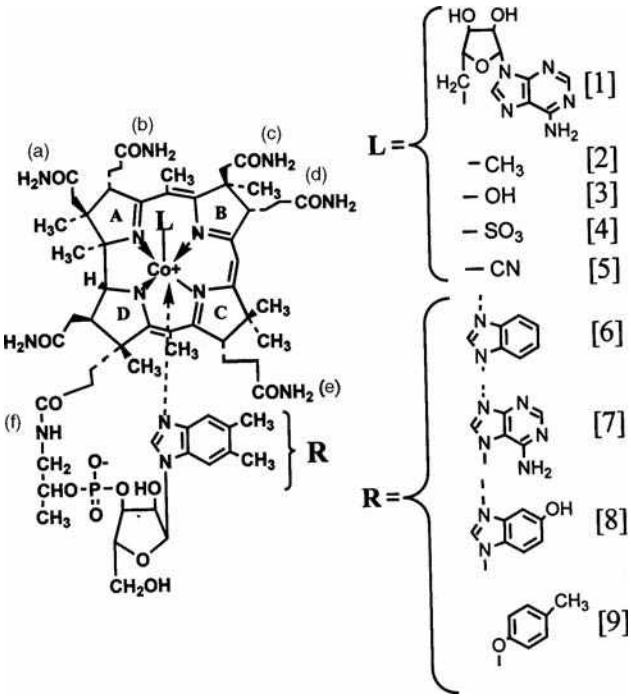

Fig. 1 Structural formulae of B_{12} compounds. The partial structures of B_{12} compounds show only those portions of the molecule that differ from B_{12}. 1, $AdoB_{12}$; 2, MeB_{12}; 3, OH-B_{12}; 4, SO_3^- B_{12}; 5, CN-B_{12} or B_{12}; 6, benzimidazolyl cyanocobamide; 7, pseudovitamin B_{12}; 8, 5-hydroxybenzimidazolyl cyanocobamide; and 9, *p*-cresolyl cyanocobamide.

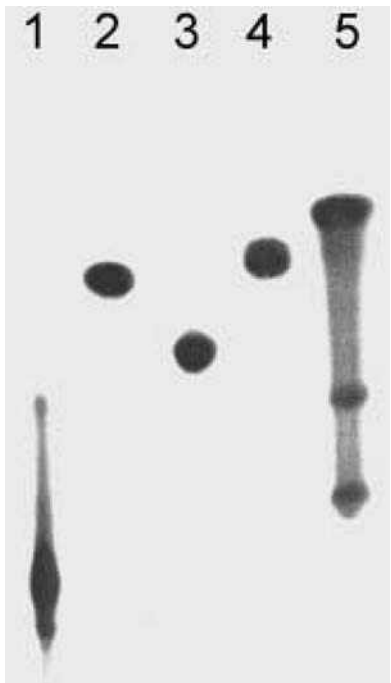

Fig. 2 Silica gel 60 TLC pattern of commercially available B_{12} reagents. The concentrated solution (4 μl) was spotted on the silica gel TLC sheet and developed with 2-propanol–NH_4OH (28%)–water (7:1:2 vol/vol) at room temperature in the dark. 1, OH-B_{12}; 2, CN-B_{12}; 3, $AdoB_{12}$; 4, MeB_{12}; and 5, dicyanocobinamide.

Vitamin B_{12} Compounds from Foods

Shellfish

The shellfish that siphon large quantities of B_{12}-synthesizing micro-organisms from the sea are known to be excellent sources of B_{12}. These micro-organisms can synthesize various B_{12} compounds (including inactive B_{12} compounds for humans). B_{12} contents of various edible shellfish were determined by both *L. delbrueckii* ATCC 7830 microbiological and IF chemiluminescence methods. The values determined by the microbiological method were 1.2-fold to 19.8-fold greater in the shellfish than the values determined by the IF chemiluminescence method.[5] To clarify why such differences in the B_{12} contents determined by the two methods occur, some B_{12} compounds have been purified from edible shellfish (oyster, mussel, and short-necked clam) using silica gel 60 TLC and a RP HPLC method, and subsequently characterized.[5]

The R_f values (0.18 and 0.59) of the red-colored B_{12} compounds purified from these shellfish are identical to those of authentic B_{12}, but not to those of benzimidazolyl cyanocobamide (R_f values: 0.15 and 0.55), 5-hydroxybenzimidazolyl cyanocobamide (R_f values: 0.16 and 0.47), pseudo-B_{12} (R_f values: 0.14 and 0.46), and *p*-cresolyl cyanocobamide (R_f values: 0.27 and 0.64) in two solvent systems [1-butanol-2-propanol–water (10:7:10) and 2-propanol–NH_4OH (28%)–water (7:1:2), respectively] by TLC on silica gel.[5] Although the higher values in the determination of B_{12} by the microbiological method may be because of the occurrence of B_{12} substitution compounds (probably deoxyribosides and/or deoxynucleotides), the edible shellfish would be excellent B_{12} sources, judging from the values (6 μg/100 g) determined by the IF chemiluminescence method.

Edible Algae

Edible algae are known to be rich in vitamins and minerals, as well as being good dietary fibers. Dried lavers (nori) appear to be the most widely eaten edible algae worldwide, and they have been reported to contain substantial amounts of B_{12}.[6] As the bioavailability of the laver B_{12} in mammals is not well understood, B_{12} compounds have been purified from the dried purple (*Porphyra yezoensis*) and green (*Enteromorpha prolifera*) lavers using silica gel 60 TLC and a RP-HPLC method and subsequently characterized.[7,8]

The silica gel 60 TLC and RP-HPLC patterns of the pink-colored compound purified from each laver are identical to those of authentic B_{12}, but not to those of B_{12} compounds inactive for humans.[7,8]

Algal Health Food

A health food fad involves tablets of *Spirulina* sp. (blue-green algae). When the B_{12} concentration of algal health food (*Spirulina* tablets) has been determined by both *L. delbrucekii* ATCC 7830 microbiological and IF chemiluminescence methods, the values determined by the microbiological method are about sixfold to ninefold greater in the *Spirulina* tablets than the values determined by the IF chemiluminescence method.[9] To evaluate whether the B_{12} found in the *Spirulina* tablets is true B_{12} or inactive B_{12}-related compound, B_{12} compounds have been purified from the *Spirulina* tablets using silica gel 60 TLC and a RP-HPLC, and then characterized.[9]

The major (83%) and minor (17%) B_{12} compounds purified from the *Spirulina* tablets are identified as pseudo-B_{12} and B_{12}, respectively, judging from TLC, HPLC, ^{1}H NMR spectroscopy, ultraviolet–visible spectroscopy, and biological activity data.[9] The *Spirulina* tablets are not suitable for use as a B_{12} source, especially for vegetarians, because pseudo-B_{12} appears to be inactive for humans.

In the case of other algal health foods (e.g., *Chlorella* tablets[10] and a coccolithophorid alga[11]), some B_{12} compounds have also been purified using TLC on silica gel 60 and then characterized. They contain substantial amounts of true active B_{12}.

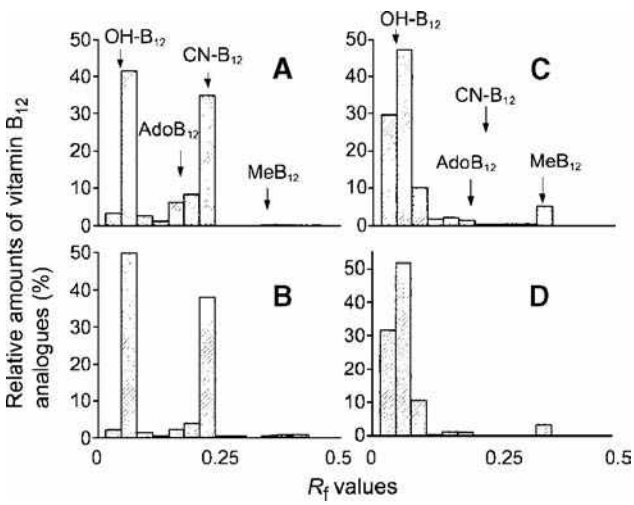

Fig. 3 Silica gel 60 TLC analysis of B_{12} compounds of dried green and purple lavers. The green laver B_{12} compounds were determined according to the chemiluminescence B_{12} assay (A) and microbiological B_{12} assay (B) methods. The purple laver B_{12} compounds were determined according to the chemiluminescence B_{12} assay (C) and microbiological B_{12} assay (D) methods. The R_f values of authentic OH-B_{12}, AdoB$_{12}$, CN-B_{12}, and MeB$_{12}$ on this TLC system [1-butanol-2-propanol–water (10:7:10 vol/vol) as a solvent] were 0.03, 0.20, 0.22, and 0.36, respectively. **Source:** From Vitamin B_{12}, in *Present Knowledge in Nutrition*.[3] © American Chemical Society, 1999.

VITAMIN B_{12} BIOASSAY AFTER TLC SEPARATION

To evaluate whether foods contain true B_{12} or not, B_{12} compounds can be separated by TLC and then assayed. Various kinds of fish sauces, traditional food supplements in the diet, are widely used in the world as condiments, and sometimes substituted for soybean sauces. Although a fish sauce (Nam-pla) appears to contribute a major source of B_{12} in Thailand, B_{12} compounds found in the nine selected fish sauces were separated by TLC on silica gel 60 and then determined with the *Lactobacillus* microbiological method, indicating that most B_{12} is derived from unidentified B_{12} compounds[12] and suggesting that fish sauce may not be suitable for use as a B_{12} source.

Coenzyme forms of B_{12} are also separated by TLC and then assayed. Occurrence of B_{12} coenzymes in the dried purple and green lavers is shown by the use of silica gel 60 TLC (Fig. 3).[13] The dried green laver contains four known types of biologically active B_{12} compounds (approximately OH-B_{12}, 45%; CN-B_{12}, 35%; AdoB$_{12}$, 6%; and MeB$_{12}$, 0.2%), and the non-coenzyme forms (OH and CN forms) of B_{12} predominated. Most B_{12} (about 80%) found in the dried purple laver are recovered in the OH-B_{12} fraction.

ONE-DIMENSIONAL AND TWO-DIMENSIONAL BIOAUTOGRAPHY

Because levels of B_{12} are very low in foods, tissues, and body fluids, bioautography is used before densitometry. A selected strain of *Escherichia coli* is used as the microorganism for the bioautography. Growth spots are enhanced by the addition of 2,3,5-triphenyltetrazolium chloride, which is converted to the red-colored formazan by *E. coli* growth.

The one-dimensional bioautography of authentic B_{12} compounds, cobinamide, and extracts of three edible algae, using TLC on mixture of silica gel and cellulose, is shown in Fig. 4.[14] The R_f value of a dominant red color spot found in the extract of Maruba-amanori is identical to that of authentic MeB$_{12}$. A single spot corresponding to CN-B_{12} is found in the extract of Wakame.

A sensitive two-dimensional bioautography has also been developed to investigate B_{12} metabolism in health and a wide range of diseases,[15] but it has hardly been used for food B_{12} analysis.

CONCLUSIONS

To evaluate whether food products contain true B_{12} or inactive (or unidentified) B_{12}-related compounds, B_{12} compounds were purified and analyzed by TLC on silica gel 60.

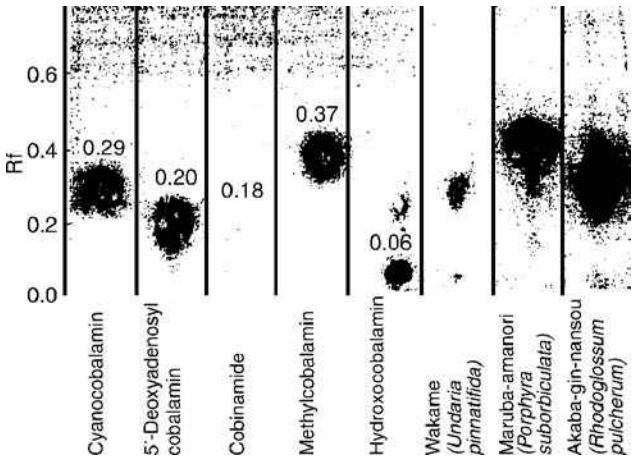

Fig. 4 Bioautogram of B_{12} and related compounds in the edible algae. A TLC plate was prepared from a slurry mixture of three weights of powdered cellulose (Whatman, Microgranular Cellulose, and CC41) and one weight of silica gel (Silica gel G, Type 60; Merck). Extracts of the edible algae, solutions of authentic B_{12} compounds, and cobinamide were applied at one of the plate, and developed with 2-butanol–NH_4OH (28%)–water (75:2:25 vol/vol). After drying the cellulose–silica gel plate, agar containing basal medium and *E. coli* 215 was overlayed and then incubated at 30°C for 20 hr. After spraying methanol solution of 2,3,5-triphenyltetrazolium salt on the gel plate, the position of B_{12} was visualized as red color by *E. coli* growth.
Source: From Effects of microwave heating on the loss of vitamin B_{12} in foods, in Agric. Food Chem.[2] © Center for Academic Publications Japan, 1996.

Sensitive one-dimensional or two-dimensional bioautography was also available in samples with lower levels of B_{12}.

The results presented here indicate that TLC offers great advantages (simplicity, flexibility, speed, and relatively low cost) for the separation and analysis of B_{12} compounds in foods.

REFERENCES

1. Watanabe, F.; Abe, K.; Katsura, H.; Takenaka, S.; Mazumder, S.A.M.Z.H.; Yamaji, R.; Ebara, S.; Fujita, T.; Tanimori, S.; Kirihata, M.; Nakano, Y. Biological activity of hydroxovitamin B_{12} degradation product formed during microwave heating. J. Agric. Food Chem. **1998**, *46* (12), 5177–5180.
2. Watanabe, F.; Abe, K.; Fujita, T.; Goto, T.; Hiemori, M.; Nakano, Y. Effects of microwave heating on the loss of vitamin B_{12} in foods. J. Agric. Food Chem. **1998**, *46* (1), 206–210.
3. Herbert, V. Vitamin B_{12}. In *Present Knowledge in Nutrition*; Brown, M.L., Ed.; International Life Science: Washington, DC, 1990; 170–179.
4. Takenaka, S.; Sugiyama, S.; Watanabe, F.; Abe, K.; Tamura, Y.; Nakano, Y. Effects of carnosine and anserine on the destruction of vitamin B_{12} with vitamin C in the presence of copper. Biosci. Biotechnol. Biochem. **1997**, *61* (12), 2137–2139.
5. Watanabe, F.; Katsura, H.; Takenaka, S.; Enomoto, T.; Miyamoto, E.; Nakatsuka, T.; Nakano, Y. Characterization of vitamin B_{12} compounds from edible shellfish, clam, oyster, and mussel. Int. J. Food Sci. Nutr. **2001**, *52*, 263–268.
6. Watanabe, F.; Takenaka, S.; Kittaka-Katsura, H.; Ebara, S.; Miyamoto, E. Characterization of bioavailability of vitamin B_{12}-compounds from edible algae. J. Nutr. Sci. Vitaminol. **2002**, *48* (5), 325–331.
7. Watanabe, F.; Takenaka, S.; Katsura, H.; Miyamoto, E.; Abe, K.; Tamura, Y.; Nakatsuka, T.; Nakano, Y. Characterization of a vitamin B_{12} compound in the edible purple laver, *Porphyra yezoensis*. Biosci. Biotechnol. Biochem. **2000**, *64* (12), 2712–2715.
8. Watanabe, F.; Katsura, H.; Miyamoto, E.; Takenaka, S.; Abe, K.; Yamazaki, Y.; Nakano, Y. Characterization of vitamin B_{12} in an edible green laver (*Entromopha prolifera*). Appl. Biol. Sci. **1999**, *5*, 99–107.
9. Watanabe, F.; Katsura, H.; Takenaka, S.; Fujita, T.; Abe, K.; Tamura, Y.; Nakatsuka, T.; Nakano, Y. Pseudovitamin B_{12} is the predominant cobamide of an algal health food, *Spirulina* tablets. J. Agric. Food Chem. **1999**, *47* (11), 4736–4741.
10. Kittaka-Katsura, H.; Fujita, T.; Watanabe, F.; Nakano, Y. Purification and characterization of a corrinoid compound from *Chlorella* tablets as an algal health food. J. Agric. Food Chem. **2002**, *50* (17), 4994–4997.
11. Miyamoto, E.; Watanabe, F.; Ebara, S.; Takenaka, S.; Takenaka, H.; Yamaguchi, Y.; Tanaka, N.; Inui, H.; Nakano, Y. Characterization of a vitamin B_{12} compound from unicellular coccolithophorid alga (*Pleurochrysis carterae*). J. Agric. Food Chem. **2001**, *49* (7), 3486–3489.
12. Takenaka, S.; Enomoto, T.; Tsuyama, S.; Watanabe, F. TLC analysis of corrinoid compounds in fish sauce. J. Liq. Chromatogr. Relat. Technol. **2003**, *26* (16), 2703–2707.
13. Watanabe, F.; Takenaka, S.; Katsura, H.; Mazumder, S.A.M.Z.H.; Abe, K.; Tamura, Y.; Nakano, Y. Dried green and purple lavers (nori) contain substantial amounts of biologically active vitamin B_{12} but less of dietary iodine relative to other edible seaweeds. J. Agric. Food Chem. **1999**, *47* (6), 2341–2343.
14. Yamada, S.; Shibata, Y.; Takayama, M.; Narita, Y.; Sugawara, K.; Fukuda, K. Content and characteristics of vitamin B_{12} in some seaweeds. J. Nutr. Sci. Vitaminol. **1996**, *42* (6), 497–505.
15. Linnell, J.C. Hydrophilic vitamins. In *Handbook of Thin-Layer Chromatography: Second Edition, Revised and Expanded*; Sherma, J., Fried, B., Eds.; Marcel Dekker, Inc.: New York, 1996; 1047–1054.

Forensic Applications of GC

John Kapolos
Department of Agricultural Products Technology, Technological Educational Institute of Kalamata, Kalamata, Greece

Christodoulos Christodoulis
Department of Chemical and Physical Examinations, Forensic Science Division, Hellenic Police Headquarter, Athens, Greece

INTRODUCTION

Forensic science, also referred to as "forensics," is the application of science to law. Forensic science uses various laboratory techniques to detect the presence of substances on a victim or a suspected criminal, or at a crime scene. In a forensic laboratory, quite a large variety of materials, such as explosives, tear gases, other toxic substances, biological fluids (blood, saliva, semen, etc.), bones, ignitable liquids, drugs, firearms and bullets, banknotes and other documents, paints and paint marks, glasses, plastic materials, hairs and fibers, other inorganic or organic materials, etc. as well as debris from explosions or arsons are examined as evidence. All of this evidence is known as "exhibits." The examinations have two purposes: to identify the exhibits (to clarify their chemical composition, their possible uses, etc.) or to compare them with reference materials to determine their common origin or lack thereof.

One of the most widely used forensic techniques for examining most of the above referring exhibits is the gas chromatography (GC) technique. In this entry, the experimental procedures for applying GC to exhibits examination are summarized.

FORENSIC APPLICATIONS OF GC

A court substantiates the imputation of guilt through three methods: a suspect's confession, the testimony of witnesses, and laboratory results from exhibit examinations. Taking into account all the necessary actions for collecting, packaging, and transferring of exhibits into a forensic laboratory to prevent contamination, as well as applying appropriate methodologies for their examination, the third way is the most reliable, because exhibits always tell the truth.

In a forensic laboratory, depending on the types of exhibits (paints, biological fluids, explosives, drugs, explosive devices, firearms, debris, etc.) and cases investigated, a variety of experimental procedures is applied, such as extraction, condensation, dilution, polymerase chain reaction (PCR), etc. as well as analytical techniques like GC, high-performance liquid chromatography (HPLC), thin-layer chromatography (TLC), X-ray diffraction (XRD) and X-ray fluorescence spectroscopy (XRF), Fourier transform-infra red spectroscopy (FTIR), UV/Vis spectroscopy, atomic absorption spectroscopy (AAS), scanning electron microscopy (SEM), electrophoresis, etc.

Of the above-mentioned techniques, GC is used for the:

1. Determination of alcohol concentration in biological specimens
2. Detection of ignitable liquid residues
3. Identification of explosive materials and examination of postexplosion exhibits
4. Drug analysis and profiling, as well as determination of drugs of abuse in biological specimens (forensic toxicology)
5. Examination of paints and paint marks from crime scenes
6. Analysis of tear gases.

Determination of Alcohol Concentration in Biological Specimens

Ethyl alcohol, ethanol, or alcohol is the active constituent of alcoholic drinks, in which it is contained in various concentrations (3–5% in beer; 9–12% in wines; and 20–60% in alcoholic distillations, such as brandy, whisky, etc.). Immediately after consumption, the reception of alcohol follows its absorption from the gastrointestinal tract and its rapid distribution into tissues, depending on their water content. Blood is an aqueous tissue; thus, a high percentage of alcohol will exist in blood after consumption of an alcoholic beverage.

After absorption, the metabolism of alcohol begins, mainly in the liver, where approximately 95% of the received quantity is metabolized. Also, because of respiration and eliminations, an amount of the received alcohol is excreted. The rate of alcohol reduction in the blood due to metabolism and excretion depends on many factors (e.g., age, physical fitness, the received quantity of ethanol, etc.) and differs among individuals.

The central nervous system is powerfully influenced by ethyl alcohol; the intensity of this influence is proportional to the content of ethyl alcohol in the blood. This influence is expressed by the weakness of an individual and ensuing difficulty in executing fine work, as well as in controlling a vehicle.[1] In all developed countries, operating any vehicle under the influence of alcohol is prohibited, with special rules established for its prohibition. Either through formal driver controls or at accident investigations by police authorities, but also in many other instances (falls from great heights, other work accidents, etc.), the determination of alcohol concentration is required.

Biological specimens (blood, urine, or other body fluids), as well as air breathed, can be used for measuring alcohol concentration. Blood is the most widely used biological specimen for this purpose in forensic laboratories. The officially recognized method for the determination of blood alcohol concentration is automated headspace GC. According to Henry's Law, at equilibrium in a sealed vessel, volatile compounds in the liquid state will be present in the vapor state at a concentration proportional to the concentration of the liquid. By sampling this vapor (i.e., the headspace) through a GC, volatile compounds may be qualitatively identified and quantitatively measured. The height or area under the chromatographic peaks generally can be used for quantitative determinations.

This is a precise, fast, and specialized method, with no pretreatment of the sample required, and it allows for the simultaneous determination of other volatile substances existing in the sample (methanol, isopropyl alcohol, etc.). The method is offered for continuous operation, does not require any modifications of commercial GCs, and is completely automated.

Experimental Procedure

A commercial GC equipped with a flame ionization detector is required. The GC is connected to an automatic headspace sampler, where sample vials are placed. Helium as carrier gas and *tert*-butanol as internal standard are used. Carbowax 1500 or 1540 (poly ethylene glycols) or other polar materials can be used as stationary phases.

The alcohol concentration in the sample is calculated with the assistance of standard samples containing ethanol in water at known concentrations and the amount of the internal standard added to the samples. A volume of 0.5 ml of the specimen to be analyzed is pipetted into a vessel; 0.1 ml of the internal standard (a 0.2% w/v solution of *tert*-butanol in water) is added; the vessels are sealed with a rubber septum; and the covers are secured with aluminum caps to compensate for the eventuality of an excess pressure buildup. For standard samples, instead of the specimen, 0.5 ml of a known ethanol concentration solution is added. Finally, the vessels are placed into the turntable of the headspace analyzer, which is thermostatted at 60°C.[2]

The standard samples are run parallel to the investigated samples, and from them, the calibration factor is calculated via Eq. 1,

$$f = C_{\mathrm{E}} \frac{H_{\mathrm{B}}}{H_{\mathrm{E}}} \tag{1}$$

where C_{E} is the concentration of ethanol in the standard sample, and H_{B} and H_{E} are the heights of the *tert*-butanol and ethanol peaks, respectively. The concentration of ethanol in the investigated samples is calculated as

$$\%\ \text{Ethanol} = \frac{H'_{\mathrm{E}}}{H'_{\mathrm{B}}} \times fF, \tag{2}$$

where H'_{B} and H'_{E} are the respective heights of the *tert*-butanol and ethanol peaks when unknown samples are analyzed and F is a correction factor. The values of F have been determined experimentally and confirmed by calculation; for blood samples, $F = 1.08$, whereas for serum, $F = 1.26$.

Typical chromatograms for a standard sample and unknown blood samples in the presence, as well as in the absence, of alcohol are shown in Fig. 1.

Exactly the same technique (headspace GC) can be applied for the determination of alcohol concentration in other biological specimens (urine, spinal-column fluid, or fluid from the eyes), with the only difference being the standard solutions.

Finally, GC can be used to determine alcohol concentration in breath specimens obtained from living subjects. Appropriately modified GCs are used, and directly collected or field-collected breath can be analyzed. These chromatographs are equipped with an appropriate multisampling valve for injecting the sample and a flame ionization detector (FID).[1]

Detection of Ignitable Liquid Residues

Generally, it is accepted that when an incident of fire is investigated, the examiner first has to locate the fire's origin and then determine the accelerants used. Many fires are criminal actions (arsons), and in these cases, oil fuels or other organic solvents have often been used as accelerants. Arson can start in two ways: Either the place is impregnated with the ignitable liquids and the fire begins from a naked flame (matches, lighter, a flaming piece of textile, etc.), or an improvised incendiary device is used. In the latter case, the location of the arson's origin will reveal materials (parts of the device) where accelerant residues exist.

Contrary to popular myth, ignitable liquids or accelerants are not completely consumed by fire; small amounts will be absorbed by the material on which they were applied. This includes wood, concrete, tiles, textiles, and

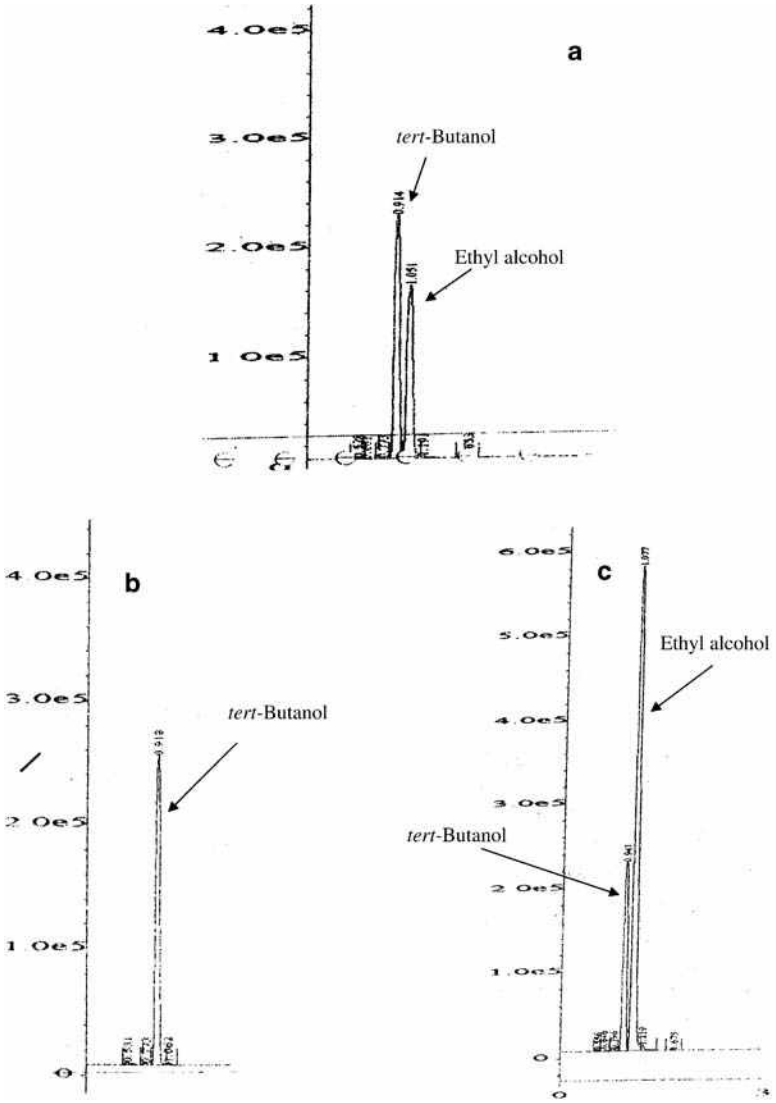

Fig. 1 GCs obtained from (a) a standard solution, (b) a blood sample without alcohol, and (c) a blood sample with alcohol. GC HP-5800 with FID, column HP-INNOWAX (15 m × 0.53 mm × 1 μm), injector temperature = 130°C, detector temperature = 220°C, oven temperature = 65°C. Automated headspace sampler, Perkin Elmer Turbomatix 40, syringe temperature = 85°C, transfer line temperature = 110°C, pressurizing time = 3 sec, inject time = 0.075 sec, and withdraw time = 0.15 sec. Carrier gas He with flow rate = 20 ml/min.

other common construction materials that have some porosity. Sometimes, a sufficient amount will be absorbed into the material, which then outgases after the fire. This may create a recognizable odor that is noticeable right after the fire has been extinguished. Most firefighters are instructed to remain alert for the existence of odors during overhaul after the fire. In "pour pattern" areas, some of the accelerants may have soaked into the material, especially if the material has significant porosity. With appropriate sampling and analysis, the accelerants can be identified via chemical analysis. The sampling and analysis must be performed properly to ensure that the evidence will stand up in court later.[3]

Sampling and Extracting Techniques

Samples of fire debris suspected of containing accelerants must be transported to the laboratory in a specific type of container. The most basic requirements are that the sample be protected from loss of accelerant residues and that it be protected from contamination. Cost and practicality are also important considerations. So glass jars, paint cans, and various plastic bags can be used. Polyester–polyolefin composite bags, however, are preferable.

The extraction of accelerants absorbed from fire debris can be conducted by supercritical fluid extraction (SFE), Soxhlet extraction, distillation after the addition of water and *n*-hexane, or adsorption onto activated charcoal. Of these procedures, SFE was found to have some advantages over conventional extraction procedures, whereas the adsorption techniques were found to be less time consuming, and the distillation method presented a higher degree of efficiency. The use of granular-activated charcoal to store extracts eluted using a dynamic headspace technique has also been examined. Activated charcoal may be used as an adsorbent for the long-term storage of as little as 1 μl of petroleum product from fire-debris samples.[4]

The introduction of commercially produced, activated charcoal strips into fire-debris analysis has provided an easy, efficient, and cost-effective method for accelerant extraction. However, several parameters require consideration to obtain a truly representative sample of accelerant. Newman, Dietz, and Lothridge[5] have investigated the effects of time, temperature, charcoal strip size, and sample concentration on the adsorption of common accelerants.

Carbon disulfide (CS_2) has long been the solvent of choice for the elution of adsorption packages (e.g., activated charcoal strips) used in fire-debris analysis. The selection of CS_2 stems from its efficiency at displacing materials adsorbed onto charcoal and its minimal response with the flame ionization detector. Unfortunately, CS_2 is highly flammable and extremely toxic, and possesses a strong, unpleasant odor. In laboratories that utilize mass selective detectors instead of the F.I.D., diethyl ether, a much friendlier solvent, can be used instead of CS_2.

Detection and Identification

For the detection of the accelerant's residues, which have been extracted by the one of the above techniques, a GC with an F.I.D. detector is used, and the pattern of peaks produced in the chromatogram is compared with the pattern produced by solutions of known accelerants, which have been analyzed separately.

Commercial products—unleaded gasoline, diesel, paraffin, white spirit, lighter fluid, etc.—are used as reference materials. Two characteristics of the accelerant chromatogram should be considered. First, the retention times over which peaks can be observed provides an indication of the boiling range; second, the detailed pattern of the peaks can permit an accelerant to be classified with more specificity. In Fig. 2, chromatograms from commercial products (diesel and unleaded gasoline) are illustrated.

An accelerant can be said to be of the same type as a reference material if the chromatograms produced show similar patterns (i.e., the major components are eluted over approximately the same range of retention times, and the proportions of the major components are similar).

Identification of Explosive Materials and Examination of Postexplosion Exhibits

Explosives can be divided into the following categories:

1. Mechanical explosives (water is instantaneously converted to gas, or gas is suddenly heated in a limited closed area)

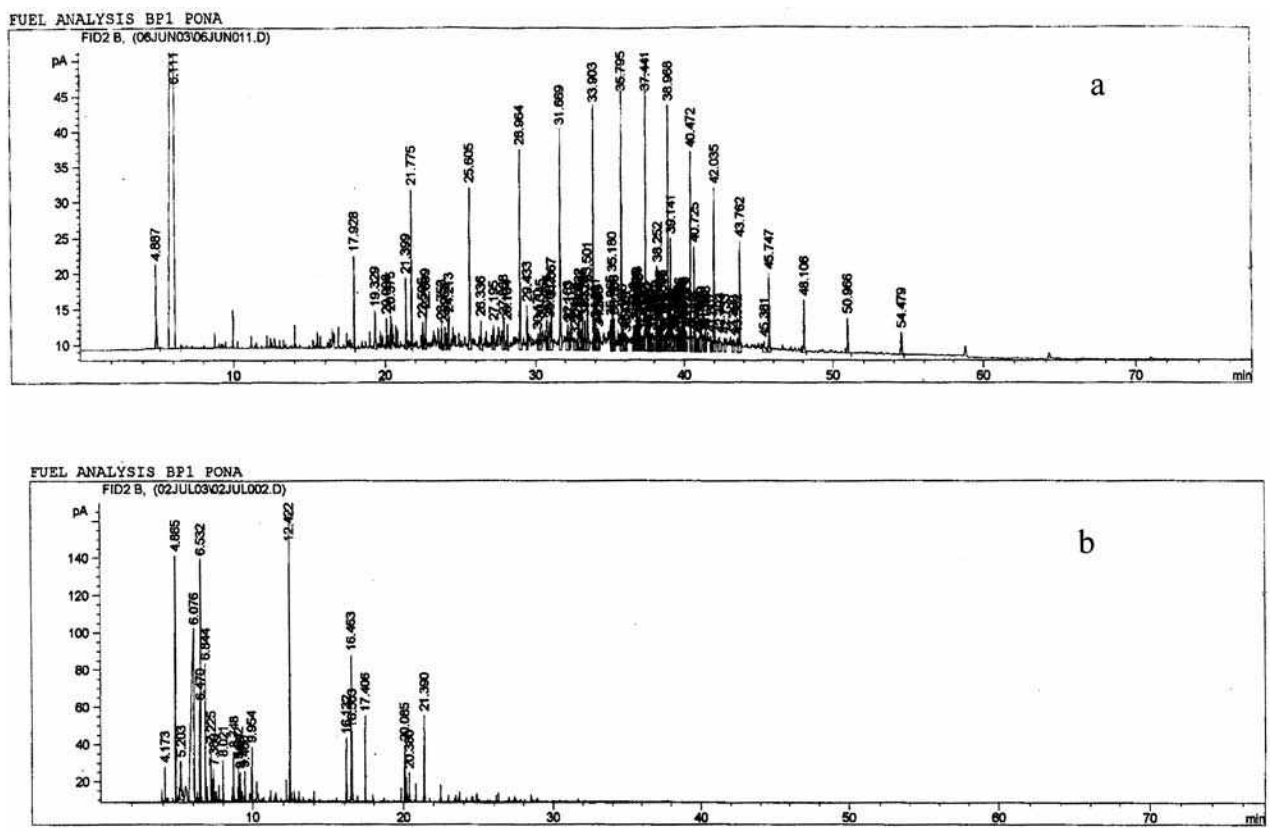

Fig. 2 GCs obtained after injecting 1 μl of (a) diesel and (b) unleaded gasoline. GC HP-6890 with FID, column BP1-PONA from SGE (50 m × 0.15 mm × 0.45 μm), injector temperature = 250°C, detector temperature = 300°C, oven temperature program = initial temp 40°C, rate 5°C/min, final temp 275°C. Carrier gas He with flow rate = 1 ml/min.

2. Nuclear explosives (introduced in 1945 as military weapons)
3. Chemical explosives.

Of the above three categories, the third one is the most interesting for forensic purposes. Every chemical explosive should have at least one oxidant and one reductant part. If these two parts coexist in the same substance, the explosive is called "one-substance explosive". In the other case (where both one oxidant and one reductant are present), we have mixtures. The majority of the one-substance explosives are organic compounds and are also the main substance of the mixtures.

The one-substance explosives are nitrobenzene, *m*-dinitrobenzene, 1,3,5 trinitrobenzene, *o*-nitrotoluene, *m*-nitrotoluene and *p*-nitrotoluene, 2,3-2,4-2,5-2,6-3,4 and 3,5 dinitrotoluene (DNT), 2,4,6 trinitrotoluene (TNT), mononitro- dinitro- and trinitro-naphthalene, trinitrochlorobenzene (Picrylchloride), 2,4,6 trinitrophenol (picric acid), ethyleneglycol dinitrate (EGDN), clycerol trinitrate (nitroglycerin, NG), penta erythritol tetranitrate (PETN), 2,4,6, *N*-tetranitro-*N*-methylamine (Tetryl), 1,3,5 trinitro-1,3,5-triazacyclohexane (RDX), and 1,3,5,7-tetranitro-1,3,5,7-tetrazacyclooctane (Octagen, HMX).[6]

Some of the above chemical explosives are exclusively used by the military; some others can be used with a license for demolition purposes in mines, construction, etc.

From all the above, it is obvious that the possession of any explosive material without the appropriate license is a criminal action and the penalty depends on the kind of explosives used. Except for the above, when abandoned explosives are discovered in police researches the possibility of their use in criminal action has to be investigated. In these cases, a forensic laboratory has to analyze them to determine their chemical composition, characterize them (for military or commercial use, their power, and their specialty), and estimate how dangerous they are. Furthermore, in a postblast investigation, the main objectives are the determination of the used explosives and the reconstruction of the explosive device that was utilized.

Detection and Identification

GC is used for the detection and identification of explosives, whether they are found as pure materials or postblast residues. According to Yinon and Zitrin,[7] GC detectors suitable for the determination of explosives are the F.I.D., mass spectrometer (MS), electron capture detector (ECD), nitrogen–phosphorus detector (NPD), and thermal energy analyzer (TEA). The most selective detector is the TEA, which detects only compounds that produce NO or NO_2.

Helium is used as a carrier gas with a flow rate of 2 ml/min; the temperatures of the detector and injector are held at 200°C and 175°C, respectively, while the temperature in the oven is started at 80°C and ramped at 20°C/min up to 200°C. Likewise, three different types of columns are usually applied for GC analysis: dimethylsiloxane, 5% diphenyl-dimethylsiloxane, and 7% cyanopropyl-7% phenyl-1% vinyl-dimethylsiloxane.

When pure explosives are analyzed, a small aliquot of the sample is diluted with ethyl acetate, and identification is based upon the comparison of relative retention times with those of explosives in a standard solution analyzed both before and after the sample. The standard solution is prepared by the dilution of the 11 most common explosives (EGDN, NG, PETN, RDX, 2,4-2,6-3,4 DNT, TNT, *o*, *m*, and *p* nitrotoluene) in ethyl acetate. Also, a mixture of two retention references markers is coinjected with every sample and standard solution, and retention times are measured relative to these substances. The markers commonly used to provide reference peaks in GC analyses are 2 fluoro-5-nitrotoluene (FNT) and 2,6 dinitro-3,4,5-trimethyl-*tert*-butylbenzene (MT).

In postblast investigations, the determination of the explosive material that was used depends mainly on the collection of appropriate debris from the scene. In a forensic laboratory, the debris is first viewed by the naked eye under low-power magnification. If there are any microscopic explosive particles, they are delivered by using acetone; the solution can be analyzed in the GC without further manipulation.

However, postexplosion analysis is usually characterized by small amounts of residues present in a complex, highly contaminated matrix. The exhibits are washed with acetone to dissolve the explosive residues, and the liquid phase is filtered through a 0.45 μm filter. A cleanup procedure based on SPE with C_{18}-bonded phase as adsorbent should be used prior to GC analysis.[8] Furthermore, the cleanup procedure is used to overcome difficulties in the GC analysis of postexplosion residues involving PETN. After the cleanup procedure and the evaporation of the acetone to increase the concentration of the solution, the analysis is similar to that described above.

Drug Analysis, Profiling, and Forensic Toxicology

For every drug seizure, part of the sample is sent to a forensic laboratory, which performs chemical analysis to determine either the type of drug or the origin of samples from different seizures. On the other hand, in many cases of forensic interest, body fluids and tissues have to be analyzed to quantify any drugs that are possibly found.

Drug analysis, either from seizure loads or biological-specimen extraction, is very difficult to describe in detail in this entry due to the different drug classes. Hereinafter, the main steps of the analysis of different drug classes are explained briefly.

Drug Analysis and Profiling

The application of GC for the analysis of illicit heroin samples can proceed after silylation of the samples, using

MSTFA (*N*-methyl-*N*-trimethylsilyl-trifluoracetamide) as the silylation reagent. The same procedure can be applied to the determination of morphine, cocaine, and opium.[9] Strömberg et al. introduced a system for the retrospective comparison of South Asian heroin; this system consisted of an improved GC profiling method and computerized data retrieval. The peaks from the GC profile were investigated for abundance, intensity, GC behavior (reproducibility), and correlations.[10] The basis of the chemical analysis was a capillary GC method for the analysis of heroin trace impurities, which has been described in detail elsewhere.[11,12]

Cannabis and its preparations (loose marijuana, kilobricks, buds, sinsemilla, Thai sticks, hashish, hash oil, etc.) represent the most widely used group of illicit drugs in the world. The various biological effects of cannabis are attributed to the complex chemical composition of the plant material. In addition, the chemical profiles of the variants of marijuana are certainly different and could contribute to the variability of results among investigators. El Sohly et al., investigated more than 35,000 samples of cannabis and its preparations to estimate their qualitative and quantitative determinations.[13]

Amphetamine (AM, *R*, *S*-1-phenyl-2-propanamine) and methamphetamine (MA, *R*, *S*-*N*-methyl-1-phenyl-2-propanamine) are powerful stimulants to the central nervous system. They are drugs of abuse, as well as doping agents in sports, and their abuse has a history as old as the drugs themselves. Amphetamine derivatives, or "designer drugs"—3,4-methylene-diaxyamphetamine (MDA), 3,4-methyl-enedioxymethamphetamine (MDMA), and 3,4-methyl-enedioxyethylamphetamine (MDEA)—are currently abused as psychedelics. Their mean "street" purity is around 5%, with caffeine, glucose, and other sugars being the main cutting agents. For intelligence profiling of amphetamine samples, GC with split/splitless injector and silica capillary column with BP-5 stationary phase can be applied.[14]

Finally, GC detection of the manufacturing impurities of cocaine can be enhanced by chemical derivatization via the use of an electron-capture detector. In this method, unadulterated cocaine hydrochloride samples were derivatized directly in acetonitrile with heptafluorobutyric anhydride (HFBA); the derivatives of the manufacturing impurities were extracted into isooctane. Then the isolated derivatives were subjected to GC-electron capture detection analysis.[15] This methodology is especially suitable for sample comparison analysis.

Determination of Drugs of Abuse in Biological Specimens

The area of toxicological analysis in the forensic field has been, and continues to be, extremely dynamic. When faced with a general unknown, it is normal for the toxicologist to begin with screening techniques that are amenable to mass screening, and if positive, drugs must be extracted, confirmed, and quantified. Immunoassay techniques [radioimmunoassay (RIA)], enzyme-multiplied immunoassay (EMIT), enzyme-linked immunosorbent assay (ELISA), etc. often form the first part of the toxicological analysis. Immunoassay screening for certain drug groups, however, constitutes only part of the total screening requirement. The remaining portion of the screening sequence, involving further extraction of drug groups, is then required and forms an ever-increasing array of screening procedures for particular analytes. The oldest method of extracting drugs from body fluids and tissues, termed liquid/liquid extractions, is still commonly used, although a more recent extraction process, SPE, has gained popularity. Further expansion of SPE involves the collection of a sample of fibers or membranes solid-phase microextraction (SPME), which leads to a cleaner extract for analysis.

Urine, blood, vitreous humor, and tissues were considered to be useful samples, whereas hair, nails, saliva, serum, sweat, and other biological matrices have been determined to be useful samples for drug analysis, as either alternatives or complements to other techniques.

Following initial immunoassay and extraction procedures, the extracts are subjected to various instrumental screening procedures designed to provide some indication of specific drug presence. Preliminary identification of drugs within the extracts is normally conducted via chromatographic techniques. Quantification is performed using GC or HPLC, with the incorporation of suitable quality-control procedures. Mass spectrometry is also used as a screening and quantification tool, as well as a confirmatory technology.

Liquid–liquid or solid-phase procedures for extraction are predominant in the determination of amphetamines, methamphetamines, and other designer drugs in blood and urine. Following the extraction, the derivatization and then the determination—GC–MS with electron impact (EI) ionization operated in the selected ion monitoring (SIM)—are performed.[16–18]

The most widespread abuse of cannabis is by smoking. It occasionally may be abused orally. When smoked, initial metabolism occurs in the lungs, whereas this takes place in the liver when marijuana is taken orally. The identification of 9-carboxy-tetrahydrocannabinol (THC) in urine is considered to be the best indication of previous cannabis consumption. Before SPE, alkaline hydrolysis of the sample is necessary to free the metabolite 9-carboxy-THC. Afterward, *N,O*-bis-trimethylsilyl-trifluoroacetamide (BSTFA) and trimethylchlorodilsne (TMCS) are added for derivatization; the product is analyzed by GC–MS in EI or negative-ion chemical ionization (NICI) mode.[16,17]

In the laboratory analysis of various biological specimens for heroin or related opiates, such as morphine and codeine, acid hydrolysis is required for the isolation of the drug from the urine; then SPE is used for cleanup. Derivatization is required to overcome the poor chromatographic behavior of morphine. Silylation or

fluoracetylation are the preferred methods. GC–NPD or GC–MS in EI mode is used for the determination of opiates in biological specimens.[16,17]

The conversion of cocaine to metabolites, benzoylecgonine (BE), and ecgonine methyl ester (EME) begins to occur soon after absorption. The coadministration of cocaine and ethanol leads to the formation of ethylbenzoylecgonine (EBE, also known as cocaethylene), a transesterification that is hydrolyzed to BE and ecgonine ethyl ester. Other metabolites are norcocaine and benzoylnorecgonine.

Anhydroecgonine methyl ester is produced when cocaine is smoked. The metabolic profiles and detection windows differ, depending on the biological matrix. After cocaine administration, the major compound found in blood and urine is BE, whereas the parent drug has been analyzed as the highest concentration in other matrices (hair, saliva, and sweat). With respect to the detection windows, BE can be detected in blood and saliva during one day; in urine, for several days; in sweat, for two or three weeks; and in hair, for months or years, depending on the length of the hair shaft. There is no need for hydrolysis, and to detect the metabolites of cocaine after SPE, the extract should be derivatized by alkylation/acylation (suitable for GC/FID and GC/NPD) or silylation (suitable for GC/FID or GC/MS).[16]

Benzodiazepines, used therapeutically as tranquilizers, hypnotics, anticonvulsants, and centrally acting muscle relaxants, rank among the most prescribed drugs. They are administered in a wide range of dosages, from less than 0.1 to 100 mg or more each day. Numerous benzodiazepines have been synthesized. They appear mainly as capsules and tablets; however, some are marketed in other pharmaceutical forms, such as injectable solutions. Abuse of benzodiazepines is internationally widespread, which means that any forensic laboratory may encounter a range of these compounds. Many benzodiazepines are hydrolyzed in acid solution to form the corresponding benzophenone; this can be capitalized on for analytical purposes. In the free base/acid form, benzodiazepines are generally soluble in most organic solvents, such as ethyl ether, ethyl acetate, chloroform, and methanol, but most are insoluble in water.

Benzodiazepines are metabolized through a variety of hydroxylation, desalkylation, reduction, and acetylation reactions, followed in many cases by conjugation to glucuronic acid prior to excretion. The most common specimens for the analysis of benzodiazepines are urine, blood, serum/plasma, and liver. Prior to liquid-liquid or SPE, samples should be hydrolyzed.

GC is a suitable technique for the analysis of benzodiazepines. Derivatization techniques are used, and silyl, acyl, and alkyl derivatives are formed. Electron capture detector gives the best detection limits ($\leq$1 ng/ml) for plasma, although NPD provides detection limits down to 5 ng/ml. GC-MS is an excellent confirmatory method for benzodiazepines. All the details for determination of benzodiazepines in biological specimens are provided elsewhere.[19,20]

Finally, GC is used for the determination of lysergic acid diethylamide (LSD) and phencyclidine (PCP) in biosamples. Lysergic acid diethylamide is difficult to detect and to quantify in biosamples because of its very low active dose, whereas there are well-established detection and quantitation procedures for PCP. An analytical approach for both is given in the literature.[21]

Examination of Paints and Paint Marks from Crime Scenes

The importance of paints as physical evidence has been recognized for quite some time. In fact, paints are among those forensic materials that have engaged the attention of crime investigators and concerned scientists since the inception of forensic science laboratories, and they have always played important and crucial roles in crime investigation.

Paint, as a physical clue, is frequently encountered in hit-and-run incidents, burglaries, art forgeries, and other offenses. A paint chip or a paint smear may be transferred to the victim or left at the scene of an accident, or a paint smear could be transferred to a tool during the commission of a burglary. There are numerous possibilities and situations in which the transfer of paint from one surface to another could occur. Routine forensic examination of paint allows for the identification of the organic and inorganic composition of each paint layer.

Automotive paint formulations undergo constant evolution and revision based on the needs of the industry, including appearance, longevity, repair, and economics. Formulation may also include a higher solid load, changed polymer chemistries, water-based products, and the results of other new technologies. The fragments of paint recovered during forensic investigations are often analyzed using pyrolysis-GC/MS (PyGC/MS). Pyrograms generated from intact fragments or separated layers are used to match paint evidence to known paint formulations in an effort to narrow the scope of the search, help identify involved vehicles, and exclude others. The peaks that appear in a pyrogram of automotive paint may be a complex mixture of polymer pyrolyzate, plasticizers, and other ingredients, each of which has a specific function in the performance of the paint as a coating product.[22]

Pyrograms, or the graphical output presentations of a PyGC system, are influenced by numerous sample characteristics and instrumental parameters, such as pyrolytic temperature, pyrolytic temperature ramp rates, preconditioning cycles, etc. This requires that the user maintain adequate reference sets of bulk polymers and copolymers for comparative analyses. Replicate sampling and analysis of each case item are necessary during PyGC testing to ensure pyrogram reproducibility and establish intrasample

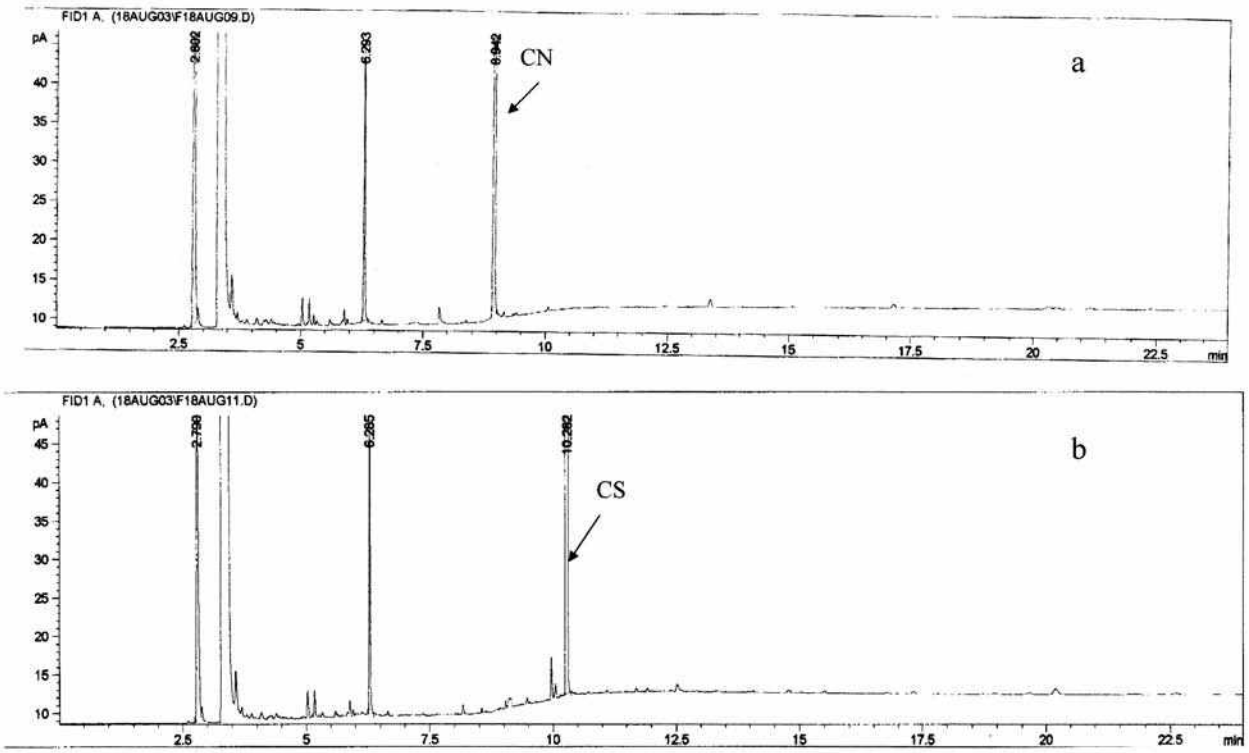

Fig. 3 GCs of tear gases (a) 2-chloroacetophenone (CN) and (b) *O*-chlorobenzylidene malononitrile (CS). Gas chromatograph, HP-6890 with FID, column CP-SIL-5 CB from CHROMPAC (25 m × 0.32 mm × 1.20 μm), injector temperature = 280°C, detector temperature = 300°C, oven temperature program = initial temp 50°C, rate 30°C/min, final temp 260°C. Carrier gas He with flow rate = 1.1 ml/min.

variations prior to pyrogram comparisons. Consideration must be given to the applicability of this procedure to each case, depending on the film's complexity and the amount of sample consumption that can be tolerated.[23]

Blank runs between samples, using all system components and full temperature-time profiles, are also essential to preventing sample carryover. Several pyrolysis systems and techniques are available and are discussed in an overview by Blackledge.[24]

Analysis of Tear Gases

Tear gases are used largely to control civil unrest. Their incapacitating effects involve the eyes, skin, and respiratory tract. Although aerosol sprays containing tear gases are available to the public in some countries, in others, tear-gas aerosols are classified as offensive weapons, and their possession is illegal. Because of the legal restrictions on these products, the identification of their active ingredients is of forensic interest.

The lachrymatory materials commonly used are 2-chloroacetophenone (CN), *O*-chloro-benzylidene malononitrile (CS), and oleoresin capsaicin. In commercial aerosol products, these materials are present with a propellant and a suitable organic solvent. From the above, CN and CS can be determined by GC; the procedure is as follows.

A short burst from the aerosol container is sprayed into a weighed beaker. After standing at room temperature for about 1 hr to allow all the propellant to evaporate, the beaker is reweighed. The residue is dissolved in acetone, and after suitable dilution, 1 μl is injected onto the chromatograph. Because of the vastly different volatilities of the compounds, a temperature program is used. Both flame ionization and ECDs can be used. In Fig. 3, chromatograms of CN and CS produced following the above procedure are illustrated.

Standard solutions of lachrymators can be prepared by diluting a known amount of pure CS and CN in acetone and, when kept refrigerated, remain stable for long periods.

Finally, another forensic application of GC is the determination of carboxyhaemoglobin (COHb) in blood. The carbon monoxide in blood can be identified by using headspace GC, as described in detail elsewhere.[25,26]

CONCLUSION

There isn't any forensic laboratory in the world without at least one GC. GC, a widespread analytical technique, is

used for the analysis of exhibits from crime scenes to obtain answers to questions that have arisen. GC is used for the detection of residues of explosive and inflammable materials, for the determination of the type and the common origin of seized drugs, for the analysis of biological specimens (blood, urine, saliva, etc.), to determine the use of drugs of abuse and alcohol (forensic toxicology), and for the analysis of tear gases and plastic materials derived from crime scenes.

REFERENCES

1. Garriott, J.C. *Medicolegal Aspects of Alcohol Determination in Biological Specimens*; PSG Publishing Co., Inc.: Littleton, MA, 1988; 36–73, 101–130.
2. Perper, J.A. Tolerance at high blood alcohol concentrations. A study of 110 cases and review of the literature. J. Forensic Sci. **1986**, *31*, 212–221.
3. Noon, R. *Engineering Analysis of Fires and Explosives*; CRC Press: Boca Raton, FL, 1995; 195–215.
4. Lennard, C. Fire (Determination of Cause) A Review 1995 to 1998. 12th Interpol Forensic Science Symposium;1998; Lyon; France; pp. 1–23.
5. Newman, R.T.; Dietz, W.R.; Lothridge, K. The use of activated charcoal strips for fire debris extractions by passive diffusion. Part I: The effects of time, temperature, strip size, and sample concentration. J. Forensic Sci. **1996**, *41*, 361–370.
6. Yallop, J.H. *Explosive Investigation*; The Forensic Science Society and Scottish Academic Press, Clark-Constable Ltd: Edinburgh, UK, 1980; 13–79.
7. Yinon, J.; Zitrin, S. *Modern Methods and Applications in Analysis of Explosives*; Wiley: Chichester, UK, 1993; 1–30, 163–208.
8. Kolla, P. Trace analysis of explosives from complex mixtures with a sample preparation and selective detection. J. Forensic Sci. **1991**, *36*, 1342–1359.
9. Gloger, M.; Neumann, H. Analysis of heroin samples by capillary gas-chromatography. Comparison of glass-capillary column and packed-column. Forensic Sci. Int. **1983**, *22*, 63–74.
10. Strömberg, L.; Lundberg, L.; Neumann, B.; Bobon, B.; Huizer, H.; van der Stelt, N.W. Heroin impurity profiling. A harmonization study for retrospective comparisons. Forensic Sci. Int. **2000**, *114*, 67–88.
11. Allen, A.C.; Cooper, D.A.; Moore, J.M.; Gloger, M.; Neumann, H. Illicit heroin manufacturing by—products: Capillary gas chromatographic determination and structural elucidation of narcotine—and non-laudanosine—related compounds. Anal. Chem. **1984**, *56*, 2940–2947.
12. Neumann, H.; Gloger, M. Profiling of illicit heroin samples by high-resolution capillary gas chromatography for forensic application. Chromatographia **1982**, *16*, 261–264.
13. El Sohly, M.A.; Ross, S.A.; Mehmedic, Z.; Arafat, R.; Yi, B.; Banahan, B.F. Potency trends of Δ^9—THC and other cannabinoids in confiscated marijuana from 1980–1997. J. Forensic Sci. **2000**, *45*, 24–30.
14. King, L.A.; Clarke, K.; Orpet, A.J. Amphetamine profiling in the UK. Forensic Sci. Int. **1994**, *69*, 65–75.
15. Moore, J.M.; Cooper, D.A. The application of capillary gas chromatography—electron capture detection in the comparative analyses of illicit cocaine samples. J. Forensic Sci. **1993**, *38*, 1286–1304.
16. UN document ID number: ST/NAR/31. *Recommended Methods for the Detection and Assay of Lysergide (LSD), Phencyclidine (PCP) and Methaqualone in Biological Specimens*; United Nations Drug Control Programme, 1999, http://www.unodc.org
17. Moeller, M.R.; Steinmeyer, S.; Kraemer, T. Determination of drugs of abuse in blood. J. Chromatogr. B, **1998**, *713*, 91–109.
18. Kraemer, T.; Maurer, H.M. Determination of amphetamine, methamphetamine and amphetamine-derived designer drugs or medicaments in blood and urine. J. Chromatogr. B, **1998**, *713*, 163–187.
19. *Recommended Methods for the Detection and Assay of Barbiturates and Benzodiazepines in Biological Specimens*; United Nations International Drug Control Program: Vienna, Austria, 1997; 93–98, http://www.unode.org/pdf/publications/report_assay_1997-01-01_1.pdf
20. Drummer, O.H. Methods for the measurements of benzodiazepines in biological samples. J. Chromatogr. B, **1998**, *713*, 201–225.
21. Schneider, S.; Kuffer, P.; Wenning, R. Determination of lysergide (LSD) and phencyclidine in biosamples. J. Chromatogr. B, **1998**, *713*, 189–200.
22. Singh, R.B. Evidence Type Paint and Glass. 12th Interpol Forensic Science Symposium; Lyon; France, 1988.
23. Standard Guide for Forensic Paint Analysis and Comparison. ASTM Standards, Designation: E 1610-95; ASTM: Philadelphia, PA, 1995.
24. Blackledge, R.D. Applications of pyrolysis gas chromatography in forensic science. Forensic Sci. Rev. **1992**, *4* (1), 2–15.
25. Goldbaum, L.R.; Chace, D.H.; Lappas, N.T. Determination of carbon monoxide in blood by gas chromatography using a thermal conductivity detector. J. Forensic Sci. **1986**, *31* (1), 133–142.
26. Van Dam, J.; Daenens, P. Microanalysis of carbon monoxide in blood by head-space capillary gas chromatography. J. Forensic Sci. **1994**, *39* (2), 473–478.

Forensic Ink: TLC Analysis

Joseph Sherma
Department of Chemistry, Lafayette College, Easton, Pennsylvania, U.S.A.

INTRODUCTION

Thin-layer chromatography (TLC) and high-performance TLC (HPTLC) have been important methods in forensic analysis since their inception, e.g., for the determination of drugs and pesticides. The analysis of inks for investigations of counterfeiting, fraud, forgery, and other crimes is the most important forensic application of TLC and HPTLC, and these are the most widely used chromatographic techniques for the analysis of inks. Major advantages of TLC in ink analysis are ease of use and low cost. Resolution of the components of ink formulations is high, especially for HPTLC, and the visual detection of the colored components allows convenient and rapid comparison of different ink formulations and batches. The use of densitometric scanning enhances the detection of zones on the layer and comparison of different samples and can provide quantitative data for separated components.

A review paper[1] included selected references on methods for extraction from paper, layers, mobile phases, and component characterization methods used in TLC and HPTLC for separation of ink components and identification and comparison of ink formulations from ballpoint, fountain, and fiber-tipped pens and typewriter ribbons published between 1960 and 1996. This entry describes standard TLC methods for ink analysis published by the ASTM International (West Conshohocken, Pennsylvania, U.S.A.) and advances in the field of forensic ink analysis using these and other TLC and HPTLC procedures published since 1996.

ASTM METHODS

ASTM Designations E-1422-05 and E-1789-04 are standard guides for forensic writing ink comparison and identification using TLC and additional methods. Ink comparisons by E-1422-05 can definitely determine whether an ink is the same (in formula) as that on other parts of the same document or on other documents, and may offer clues about whether two writings with similar ink came from the same writing instrument or ink well, and about the date of ink entries. Non-destructive optical examinations are specified with visible light, ultraviolet (UV) light, reflected infrared (RIR) radiation, and infrared luminescence (IRL) non-destructive optical examinations (Sections 7.1–7.5). Chemical examinations (Section 7.6) involve spot testing and solubility testing (e.g., to differentiate ballpoint and non-ballpoint ink) and TLC.

The TLC procedure is contained in Section 7.7 of Guide E-1422-05. The substrate (e.g., a paper sheet) is sampled by removing 7–10 plugs from a line using a hollow boring hypodermic needle (if a scalpel is used, about 1 cm of the line is removed). The plugs are placed in a vial and extracted by agitation for about 1 min with 3–5 μl of pyridine for ballpoint inks or ethanol–water (1:1) for non-ballpoint inks. A glass plate or plastic sheet commercially precoated with 60 Å particle size silica gel without fluorescent indicator is activated by heating in an oven at 100°C for 10–15 min and then cooled, and then the colored extract is immediately applied as a 2–3 mm spot onto the layer origin with a micropipet along with an extract from a control area of the substrate and a suitable calibration standard. The layer is air-dried and then developed in a previously equilibrated tank with the mobile phase ethyl acetate–ethanol–water (75:35:30). Evaluation is performed by viewing the chromatograms under shortwave (254 nm) and longwave (366 nm) UV light and in ambient light and recording the colors, R_f values, and relative concentrations of all bands in each ink sample. If more information is needed to distinguish similar inks, additional recommended TLC methods are the use of silica gel and a different mobile phase [*n*-butanol–ethanol–water (50:10:15); use of different layers and appropriate mobile phases; evaluation of chromatograms in RIR and IRL; and densitometric scanning of chromatograms to get relative concentrations of the components. Other analytical techniques suggested for obtaining additional information are Fourier transform infrared spectrometry, gas chromatography (GC) and GC/mass spectrometry (GC/MS), high-performance column liquid chromatography (HPLC), microspectrophotometry transmittance or reflectance curves, spectrofluorometry emission spectra, X-ray fluorescence spectrometry (for inorganic components), and capillary electrophoresis.

Guide E-1798-04 gives detailed interpretation procedures that allow an examiner to accurately discriminate between ink formulas, as well as significantly reducing false matches of ink samples from different sources or incorrectly differentiating ink samples from a common source. The results are based on the TLC procedures in Guide E-1422 and comparison against a library of standard inks.

VISUAL CHROMATOGRAM COMPARISON SOFTWARE

A software tool has just now become available for visual comparison of multiple thin layer chromatograms. The Image Comparison Viewer (ICV) from Camag (Muttenz, Switzerland) will greatly aid comparison of different ink sample chromatograms, and sample chromatograms with standard chromatograms.

Chromatogram images are obtained with a CCD (charge coupled device) camera in Camag's DigiStore 2 image documentation system controlled by WinCATS software. The ICV allows simultaneous display, side-by-side, of chromatogram images in separate tracks from the same TLC plate or different plates.

The process involves three steps: selecting the tracks, comparing samples, and printing a report. The tracks of interest are marked and transferred to the ICV with information such as position, width, length, and sample identification (I.D.) taken from the winCATS analysis file. During visual comparison, a table on top of the images automatically displays for each track important data such as sample I.D., original analysis file name, track number, source, etc. The printed report includes the images and the table, assuring traceability of the generated data.

RECENT APPLICATIONS OF TLC IN FORENSIC INK ANALYSIS

Dating Questioned Documents

TLC and GC/MS can be used to determine the age of writing inks on questioned documents.[2] Dating techniques that use TLC are based on analysis of ink dye components, while GC/MS can date inks based on detection, identification, and quantification of the residues of the vehicle solvents in ink lines. Capability to date most ballpoint, porous tip, roller pen, stamp pad, and jet printer inks by analyzing the single ink entry, stamp impression, or printed test in question was shown by testing in the Division of Identification and Forensic Science, Israel Police Headquarters.

Identification of Unknown Black Inks

A college organic chemistry laboratory experiment was devised to demonstrate forensic analysis by having students identify unknown black inks (liquid, ballpoint, and felt tip) by TLC comparison of zone colors and R_f values to standard inks.[3] Silica gel G (gypsum binder) plates are developed with two mobile phases: ethyl acetate–sec-butanol–*n*-propanol–absolute ethanol–water (1:1:1:1:1) and *n*-butanol–absolute ethanol–water–acetic acid (60:10:20:0.5). A second experiment was designed to introduce undergraduate chemistry students to forensic science by applying TLC to decide if more than one ballpoint pen was used to write signatures on a questioned will.[4]

TLC Separation of Pigments in Inks of Different Colors

Pigments in blue, black, green, and purple writing inks were separated into multiple bands on silica gel developed with 95% aqueous ethanol.[5] The inks were initially diluted 1:5 with 95% alcohol before spotting 5 μl initial zones. This is a simple system for comparing commercial inks based on observation of chromatograms under UV light and in visible light.

Analysis of Writing Inks in Changed Documents

Plates are usually developed by capillary flow in the ascending direction in a conventional, large volume glass chamber presaturated for ~15 min with mobile phase vapor. However, in a study of documents changed accidentally or on purpose, by staining with liquids (e.g., coffee) or by exposure to high temperature, a Type DS II horizontal sandwich chamber Type DS II (Chromdes, Lublin, Poland) was used for analysis of blue writing inks from 15 different ballpoint and roller pens.[6] The DS II gave advantages of a small volume of mobile phase and immediate development without vapor saturation. Lines (2 cm) of ink drawn on paper were cut with a scalpel and extracted for 10 min at 100°C in sealed capillaries with dimethylformamide–chloroform (9:1), the layer was Merck (Darmstadt, Germany) silica gel 60, and the mobile phase was ethyl acetate–isopropanol–water–acetic acid (30:25:10:1). The obtained chromatograms were examined in visible light and at 254 and 366 nm to assess the changes, which were greatest in samples treated with raised temperature.

Analysis of Thermal Transfer Inks

TLC with Merck silica gel 60 TLC plates and hexane–methyl ethyl ketone–ethyl acetate (80:3:17) mobile phase was used successfully to analyze 81 different samples, which included 54 thermal transfer printer samples (43 photographic prints on paper and 11 plastic card samples) and 27 printer ribbons, with excellent resolution of the colors.[7] Pyridine was used for extraction of 5 mm hole punches from paper samples, 5 × 5 mm cuttings from ribbons, and scalpel scrapings from cards. Developed plates were examined in daylight and under 254 and 366 nm UV light, and a Foster and Freeman, Ltd. (Evesham, Worcestershire, UK) Video Spectral Comparator 2000 High Resolution (VSC 2000 HR) was used to document and record the TLC plates in black and white and color modes, and to observe and record IRL properties on the TLC plate produced from the D2T2 (dye diffusion thermal transfer) process dyes and/or overlays.

Differentiation of Black Gel Inks

Black gel inks from 29 pens and 17 companies were differentiated by TLC on Merck silica gel 60 layers developed with ethyl acetate–ethanol–water (75:35:30) mobile phase. A VSC 2000 HR was used to examine and document the TLC plates in visible, UV, and near IR reflectance (IRR) modes. Written gel ink lines on filter paper were sampled by extracting 1.3 mm punch holes with 20 μl of ethanol–water (1:1). Spot tests and capillary column GC/MS were also used for ink analyses in this study.[8] A flowchart was developed allowing systematic determination of a questioned ink.

Analysis of Red Inks by TLC/MS

The direct analysis of separated extracts of ink from eight red pens on hydrophobic reversed phase (RP) octyl (C8) chemically bonded silica gel TLC plates using a surface sampling/electrospray emitter probe coupled with a triple quadrupole linear ion trap mass spectrometer was demonstrated.[9] Effects of the composition and flow rate of the eluting solvent and layer surface scan rate on sensitivity and preservation of TLC resolution were studied. The C8 layer was spotted with extracts of 1×1 cm squares of Whatman (Florham Park, New Jersey, U.S.A.) 3 mm chromatography paper covered with ink writing (sonication for 10 min with 0.5 ml of ethanol in a 1.5 ml Eppendorf tube). The mobile phase used for the separation was methanol–water (80:20) containing 200 m*M* ammonium acetate. This TLC/MS method has great potential for forensic ink analysis if it can be extended to the hydrophilic silica gel layers usually used.

Differentiation of Colored Inkjet Printer Cartridges

TLC and HPLC were combined for the differentiation of colored inks of 23 inkjet cartridges from the Canon, Epson, Xerox, and Hewlett Packard companies.[10] The yellow, cyan, and magenta inks stored in individual compartments of the cartridges used to produce a full color image were the target inks. Samples drawn from the cartridges were diluted with ethanol–water (1:1), while small areas of a paper color printout were cut and extracted with pyridine–water (4:1). TLC was on a Macherey-Nagel (Dueren, Germany) Alugran silica gel UV_{254} plate (0.2 mm layer thickness) developed with ethyl acetate–ethanol–water (70:35:30) or *n*-butanol–ethanol–water (10:2:3), and detection was made under white and long wavelength UV light. HPLC was on a chemically bonded C18 RP column with a mobile phase gradient composed of aqueous ammonium acetate and methanol, and detection was with a photodiode array (PDA) detector at 400, 540, and 650 nm. Data from the two methods provided a good tool for discriminating the brand of the cartridges, and a database of ink profiles was generated.

The U.S. International Ink Library

The U.S. Secret Service and Internal Revenue Service National Forensic Laboratory jointly maintain the largest known forensic collection of writing inks in the world, which is composed of over 8500 ink standards collected worldwide dating back to the 1920s. One hundred pens were randomly obtained from a variety of sources, and a study was conducted to evaluate the reliability of matching their respective ink concentrations with standards.[11] A writing sample from each pen was made on Whatman No. 2 filter paper, 5–10 hole punches of ~1 mm diameter were removed from each ink line, and the punches were extracted with an 5 μl of pyridine for ballpoint inks and ethanol–water (1:1) for fiber tip, roller ball, and gel inks in a glass vial by agitation for 20–30 sec. TLC was performed in accordance with Section 7.7 in the ASTM Standard Guide E-1422-05 (described above) using a silica-gel layer and the mobile phase ethyl acetate–ethanol–water (70:35:30). Optical comparison between samples and standards was made using a VSC 2000 HR according to ASTM Standard Guide E-1789-04 (described above). It was found that 15 of the 100 inks evaluated were unsuitable for identification because they lacked any extractable colored components necessary for comparison with standards in the library. The remaining 85 pens examined were categorized into 44 different ink formulations. Three of the inks did not match any specimen on record; one of these inks was similar to an ink from an identical brand of pen in the database, but had a modified formulation. The U.S. International Ink Library is an invaluable tool for reliable forensic ink analysis.

Differentiation of Blue Ballpoint Inks by HPTLC

In a study of 31 blue ballpoint pen inks,[12] Merck silica-gel HPTLC plates were used instead of the usual TLC plates. HPTLC plates are coated with a thinner layer having a smaller mean particle size and particle size distribution, leading in general to higher resolution and faster separations. Ink entries of about 1 cm in length were scraped from paper with a scalpel and extracted by standing in the dark for 24 hr in a sealed conical vial containing 15 μl of methanol. Aliquots of the extract (2.5 and 5 μl) were applied in 5 mm long bands to the plate using a Camag Linomat automated instrument. Development was carried out in a horizontal chamber with two sequential mobile phases: *n*-butanol–isopropanol–water (10:5:0.5) and *n*-butanol–ethanol–water–acetic acid (15:3:3.9:0.45). The resulting chromatograms were scanned at 590 nm with a Camag Scanner III, and detection and semiquantitative analysis were accomplished using the winCATS software. On the basis of number of spots, their R_f values, and their

colors, plus the semiquantitative data, 12 classes of ballpoint inks were distinguished on a qualitative basis. The tested samples could be further discriminated into 18 classes by calculating their relative scan peak intensities. Thirty-seven pairs were not discriminated.

Further classification was obtained by direct analysis of pen strokes on paper (without elution) using laser desorption ionization (LDI) time-of-flight (TOF) mass spectrometry. However, only basic dyes and pigments could be identified by positive mode LDI/MS.

Effect of Electronic Beam Radiation on Forensic Evidence

Since late-2001, when anthrax-tainted letters were discovered in the United States, the U.S. Postal Service began to use an electron beam irradiation process for destroying such biological agents. Some published reports indicated missing or additional dye bands in thin layer chromatograms of irradiated writing inks compared with control (non-irradiated) samples, so writings from 97 different black, blue, red, green, and yellow inks on paper, from ballpoint, gel, plastic/felt tip, and rollerball pens, were tested using TLC with a video spectral comparator and standard mail irradiation conditions.[13]

Extraction and TLC analysis on Merck silica gel 60 layers was carried out in accordance with ASTM Guide E-1422-01, which is essentially the same as E-1422-05 described above. The only deviation from the ASTM method was that the spotted plate was oven dried at 100°C for 10 min, instead of being air dried, before mobile phase development.

The study found that none of the irradiated inks showed significant optical or chemical differences from control samples based on thin layer chromatograms. Therefore, it was proven that evidence is conserved after the irradiation treatment.

CONCLUSION

TLC and HPTLC are the most widely used methods today for forensic analysis of ink formulations and their writings. The methods are simple to perform and inexpensive compared with the other spectrometric and chromatographic methods that have been applied less often. The availability of the International Ink Library is a great advantage for comparative purposes, and its value will increase as more samples are collected in the future. Combination of TLC with MS can give positive identification of ink components from molecular weight data.

REFERENCES

1. Zlotnick, J.A.; Smith, F.P. Chromatographic and electrophoretic approaches in ink analysis. J. Chromatogr. B, **1999**, *733*, 265–272.
2. Aginsky, V.N. An application of chromatographic methods for dating questioned documents. In *Chromatography*; Kaiser, O., Kaiser, R.E., Gunz, H., Gunther, W., Eds.; InCOM: Duesseldorf, Germany, 1997; 1–6.
3. Olsen, B.; Hopson, D. Identification of unknown black inks by thin layer chromatography. Int. J. Forens. Doc. Exam. **1999**, *5*, 354–355.
4. Quigley, M.N.; Qi, H. A chemistry whodunit: Forensic examination of pen inks. Intl. J. Forens. Doc. Exam. **1997**, *3*, 265–267.
5. Druding, L.F. TLC separation of ink pigments. Intl. J. Forens. Doc. Exam. **1999**, *5*, 356.
6. Trzcinska, B.M. Analysis of writing inks in changed documents. A preliminary study with thin layer chromatography. Chem. Anal. (Warsaw) **2001**, *46*, 507–513.
7. LaPorte, G.M.; Wilson, J.D.; Mancke, S.A.; Payne, J.A.; Ramotowski, R.S.; Fortunato, S.L. The forensic analysis of thermal transfer printing. J. Forens. Sci. **2003**, *48*, 1163–1171.
8. Wilson, J.D.; LaPorte, G.M.; Cantu, A.A. Differentiation of black gel inks using optical and chemical techniques. J. Forens. Sci. **2004**, *49*, 364–370.
9. Ford, M.J.; Kertesz, V.; Van Berkel, G.J. Thin layer chromatography/electrospray ionization triple quadrupole linear ion trap mass spectrometry system: Analysis of rhodamine dyes separated on reversed phase C8 plates. J. Mass Spectrom. **2005**, *40*, 866–875.
10. Poon, N.L.; Ho, S.S.H.; Li, C.K. Differentiation of colored inks of inkjet printer cartridges by thin layer chromatography and high performance thin layer chromatography. Sci. Justice **2005**, *45*, 187–194.
11. LaPorte, G.M.; Arredondo, M.D.; McConnell, T.S.; Stephens, J.C.; Cantu, A.A.; Shaffer, D.K. An evaluation of matching unknown writing inks with the United States International Ink Library. J. Forens. Sci. **2006**, *51*, 689–692.
12. Weyermann, C.; Marquis, R.; Mazzella, M.; Spengler, B. Differentiation of blue ballpoint pen inks by laser desorption ionization mass spectrometry and high performance thin layer chromatography. J. Forens. Sci. **2007**, *52*, 216–220.
13. Ramotowski, R.S.; Regen, E.M. The effect of electron beam irradiation on forensic evidence. 2. Analysis of writing inks on porous surfaces. J. Forens. Sci. **2007**, *52*, 604–609.

Forskolin Purification

Hiroyuki Tanaka
Yukihiro Shoyama
Graduate School of Pharmaceutical Sciences, Kyushu University, Fukuoka, Japan

INTRODUCTION

Forskolin, a labdane diterpenoid, was isolated from the tuberous roots of *Coleus forskohlii* Briq. (Lamiaceae).[1] *C. forskohlii* has been used as an important folk medicine in India. Forskolin was found to be an activator of adenylate cyclase,[2] leading to an increase of c-AMP, and now a medicine in India, Germany, and Japan. The production of forskolin is completely dependent on the commercial collection of wild and cultivated plants in India. We have already set up the production of monoclonal antibodies (MAbs) against forskolin.[3] The practical application of enzyme-linked immunosorbent assay (ELISA) for the distribution of forskolin contained in clonally propagated plant organs and the quantitative fluctuation of forskolin depend on the age of *C. forskohlii*.[4,5] As an extension of this approach, we present the production of the immunoaffinity column using antiforskolin MAb and its application.[6]

MATERIALS AND METHODS

Chemicals

Bovine serum albumin (BSA) was provided by Pierce (Rockford, Illinois, U.S.A.). Forskolin and 7-deacetylforskolin were isolated from the tuberous root of *C. forskohlii*, as previously reported.[1] 1-Deoxyforskolin, 1,9-dideoxyforskolin, and 6-acetyl-7-deacetylforskolin were purchased from Sigma Chemical Company (St. Louis, Missouri, U.S.A.). The mixture (approximately 20 mg) of forskolin and 7-deacetylforskolin, purified by the immunoaffinity column, was acetylated with pyridine and acetic anhydride mixture (each 100 ml) at 4°C for 2 hr to give pure forskolin.

Preparation of Immunoaffinity Column Using Anti-Forskolin Monoclonal Antibody[6]

Purified IgG (10 mg) in PBS was added to a slurry of CNBr-activated Sepharose 4B (600 mg; Pharmacia Biotech) in coupling buffer (0.1 *M* $NaHCO_3$ containing 0.5 *M* NaCl). The slurry was stirred for 2 hr at room temperature and then treated with 0.2 *M* glycine at pH 8.0 for blocking of activated groups. The affinity gel was washed four times with 0.1 *M* $NaHCO_3$ containing 0.5 *M* NaCl and 0.1 *M* acetate buffer (pH 4.0). Finally, the affinity gel was centrifuged and the supernatant was removed. The immunoaffinity gel was washed with phosphate buffer solution (PBS) and packed into a plastic mini-column in volumes of 2.5 ml. Columns were washed until the absorption at 280 nm was equal to the background absorption. The columns were stored at 4°C in PBS containing 0.01% sodium azide.

Direct Isolation of Forskolin from Crude Extractives of Tuberous Roots and Callus Culture of *C. forskohlii* by Immunoaffinity Column

The dried powder (10 mg dry weight) of tuberous root was extracted five times with diethyl ether (5 ml). After evaporation of the solvent, the residue was redissolved in MeOH and diluted with PBS (1 : 16), and then filtered by Millex-HV filter (0.45 μm filter unit; Millipore Products, Bedford, Massachusetts, U.S.A.) to remove insoluble portions. The filtrate was loaded onto the immunoaffinity column and allowed to stand for 90 min at 4°C. The column was washed with the washing buffer solution (10 ml). After forskolin disappeared, the column was eluted with PBSM (45%) at a flow rate of 0.1 ml/min. The fraction containing forskolin was lyophilized and extracted with diethyl ether. Forskolin was determined by TLC developed with C_6H_6–EtOAc (85 : 15) [Rf; forskolin (0.21), 7-deacetylforskolin (0.16)] and ELISA.

RESULTS AND DISCUSSION

We established a simple and reproducible purification method for forskolin using an immunoaffinity column chromatography method. Because forskolin is almost insoluble in water, various buffer solutions were tested for the solubilization of forskolin. It became evident that 6% MeOH in PBS was necessary for the solubilization of forskolin.[3,5] Next, the elution system for the immunoaffinity column was investigated by using various elution buffers based on PBS. Only 9% of bound forskolin can be recovered by the PBS supplemented with 10% of MeOH. The forskolin concentrations eluted increased rapidly from 20% of MeOH, and reached the optimum at 45% of MeOH.

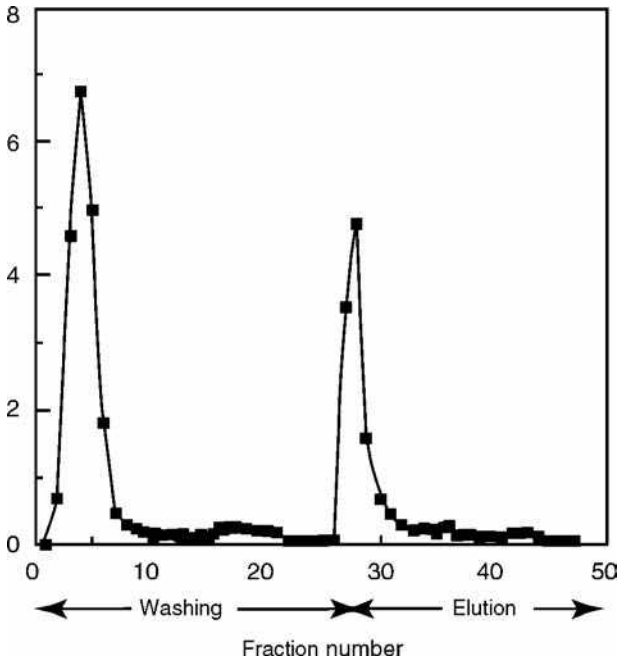

Fig. 1 Elution profile of forskolin in the tuberous root of *C. forskohlii* by purification on immunoaffinity column chromatography. The column was washed with PBSM, then eluted by PBS containing 45% of methanol after the forskolin disappeared. Individual fractions were assayed by ELISA.

To assess the capacity and the recovery of forskolin from the affinity column, 30 μg of forskolin was added and passed through the column (2.5 ml of gel), and the forskolin content was analyzed by ELISA. After washing with 5 column volumes of PBST, 22.5 μg of forskolin remained bound and was then completely eluted with the PBS containing 45% of MeOH. Therefore, the capacity of affinity column chromatography was determined to be 9.4 μg/ml.

The crude diethyl ether extracts of the tuberous root of *C. forskohlii* were loaded onto the immunoaffinity column chromatography system, washed five times with PBS containing 6% of MeOH, and eluted with the PBS containing 45% of MeOH. Fig. 1 shows a chromatogram detected by ELISA. Fractions 2–8 contained 45 μg of forskolin that were over the column capacity, together with the related compounds 1-deoxyforskolin, 1,9-dideoxyforskolin, 7-deacetylforskolin and 6-acetyl-7-deacetylforskolin, and other unknown compounds which were detected by TLC, as indicated in Fig. 2. The peak of fractions 26–30 shows the elution of forskolin (21 μg) eluted with the PBS containing 45% of MeOH. Forskolin eluted by washing solution (fractions 2–8) was repeatedly loaded and finally isolated. However, forskolin purified by the immunoaffinity column chromatography was still contaminated with a small amount of 7-deacetylforskolin (Fig. 2) because this compound has a 5.5% cross-reactivity against Mab, as previously indicated.[3]

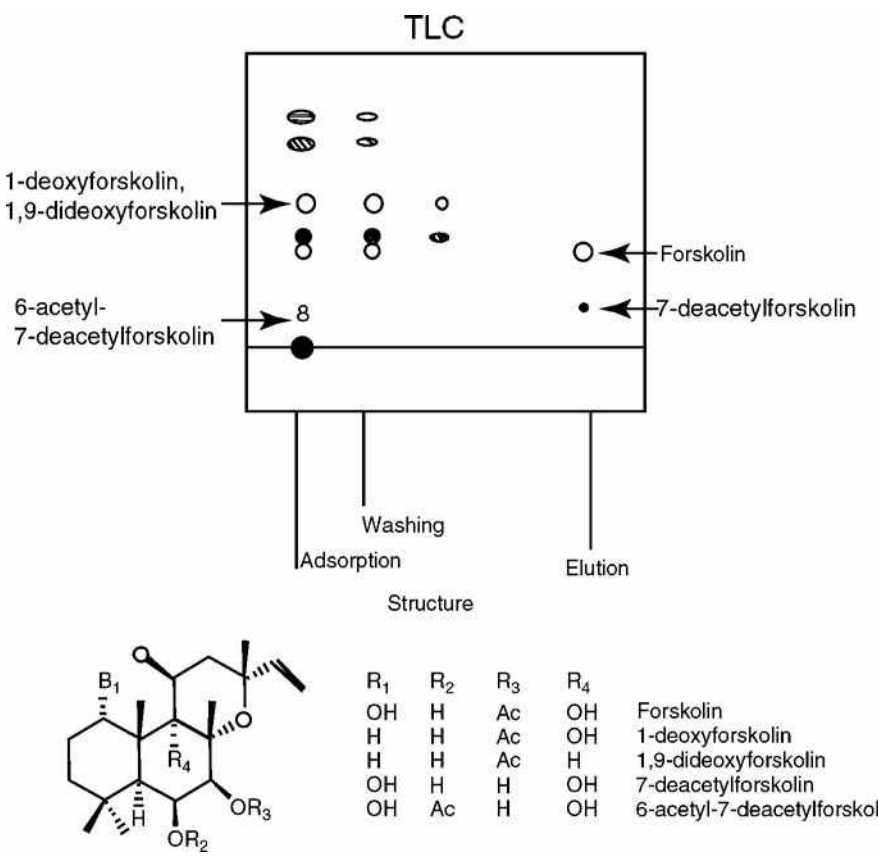

Fig. 2 TLC of adsorption, washing, and elution solutions, and structures of forskolin and the related compounds.

Therefore, the mixture was treated with pyridine and acetic anhydride at 4°C for 2 hr to give pure forskolin. In our case, the stability of antibody against PBS containing 45% MeOH is also quite high, because the immunoaffinity column has been used over 10 times, under the same conditions, without any substantial loss of capacity. Therefore, we concluded that the PBS supplemented with 45% MeOH can be routinely used as an elution buffer solution.

REFERENCES

1. Bhat, S.V.; Bajwa, B.S.; Dornauer, H.; de Sousa, N.J.; Fehlhaber, H.W. Structures and stereochemistry of new labdane diterpiniods from coleus forskohlii briq. Tetrahedron Lett. **1977**, *18* (19), 1669–1672.
2. Metzger, H.; Lindner, E. The positive inotropic-acting forskolin, a potent adenylatecyclase activator. Drug Res. **1981**, *31*, 1248–1250.
3. Sakata, R.; Shoyama, Y.; Murakami, H. Production of monoclonal antibodies and enzyme immunoassay for typical adenylate cyclase activator, Forskolin. Cytotechnology **1994**, *16* (2), 101–108.
4. Yanagihara, H.; Sakata, R.; Shoyama, Y.; Murakami, H. Relationship between the content of forskolin and growth environments in clonally propagated *Coleus forskohlii* Briq. Biotronics **1995**, *24*, 1–6.
5. Yanagihara, H.; Sakata, R.; Shoyama, Y.; Murakami, H. Rapid analysis of small samples containing forskolin using monoclonal antibodies. Planta Med. **1996**, *62*, 169–172.
6. Yanagihara, H.; Minami, H.; Tanaka, H.; Shoyama, Y.; Murakami, H. Immunoaffinity column chromatography against forskolin using an anti-forskolin monoclonal antibody and its application. Anal. Chim. Acta **1996**, *335*, 63–70.

Frontal Chromatography

Peter Sajonz
Merck Research Laboratories, Rahway, New Jersey, U.S.A.

INTRODUCTION

Frontal chromatography is a mode of chromatography in which the sample is introduced continuously into the column. The sample components migrate through the column at different velocities and eventually break through as a series of fronts. Only the least retained component exits the column in pure form and can, therefore, be isolated; all other sample components exit the column as mixed zones. The resulting chromatogram of a frontal chromatography experiment is generally referred to as a breakthrough curve, although the expression *frontalgram* has also been used in the literature.[1]

The exact shape of a breakthrough curve is mainly determined by the functional form of the underlying equilibrium isotherms of the sample components, but secondary factors such as diffusion and mass-transfer kinetics also have influence. The capacity of the column is an important parameter in frontal chromatography, because it determines when the column is saturated with the sample components and, therefore, is no longer able to adsorb more sample. The mixture then flows through the column with its original composition.

THE USE OF FRONTAL CHROMATOGRAPHY

Frontal chromatography can also be called *adsorptive filtration* because it can be used for the purpose of filtration. The purification of gases and solvents are two classical applications of frontal chromatography. Another important use is the purification of proteins, where a frontal chromatography step is used in the initialpurification procedure.[2,3]

One of the most important applications of frontal chromatography is the determination of equilibrium adsorption isotherms. It was introduced for this purpose by Shay and Szekely and by James and Phillips.[4,5] The simplicity as well as the accuracy and precision of this method are reasons why the method is so popular today and why it is often preferred over other chromatographic methods, for example, elution by characteristic points (ECP) or frontal analysis by characteristic points (FACP).[6,7] Frontal chromatography as a tool for the determination of single-component adsorption isotherms will be discussed in the following section.

FRONTAL CHROMATOGRAPHY FOR THE DETERMINATION OF ISOTHERMS

Theory

First, the column is filled only with sample at concentration C_n; then, a step injection is performed (i.e., sample with the concentration C_{n+1} is introduced into the column). This results in a breakthrough curve, as shown in Fig. 1. The amount adsorbed at the stationary phase Q_{n+1} can be calculated by

$$\begin{aligned} Q_{n+1} &= q_{n+1} Vs \\ &= (C_{n+1} - C_n)(V_{R,n+1} - V_0) + q_n V_s \end{aligned}$$

where q_n and q_{n+1} are the initial and final sample concentrations, respectively, in the stationary phase and C_n and C_{n+1} are the initial and final sample concentrations in the mobile phase, respectively. V_s is the volume of adsorbent in the column, V_0 is the holdup volume, and $V_{R,n+1}$ is the retention volume of the breakthrough curve. The retention volume is calculated from the area over the breakthrough curve:

$$V_R = \int_0^\infty \frac{(C_{n+1} - C)dV}{C_{n+1} - C_n}$$

The retention volume defined by the area method always gives the theoretically correct result for the amount adsorbed. In practice, it is, however, often easier and better to use the retention volume from half-height [i.e., at the concentration $(C_{n+1} + C_n)/2$] or the retention volume derived from the inflection point of the breakthrough curve. The reason for this is that the calculation of the area incorporates signal noise and it is very dependent on the integration limits. This is often a problem, especially when the mass transfer is slow, because, in this case, the plateau concentration C_{n+1} is only reached slowly and, therefore, systematic errors in the calculated area occur. It has been shown that the use of the retention volumes derived from the inflection point or the half-height gives satisfactory results. The half-height method is, however, easier to use and slightly more accurate than the inflection-point method.[5]

It has to be noted that the half-height and inflectionpoint methods do not give reliable results if the isotherm is

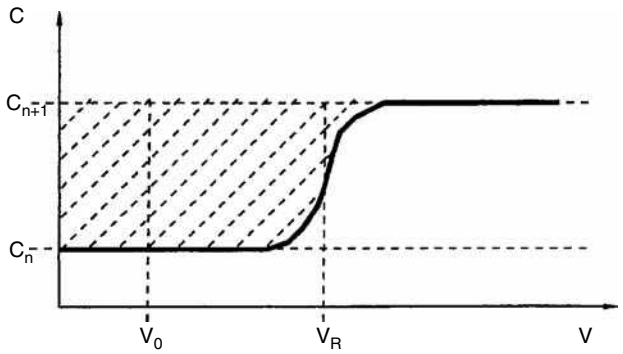

Fig. 1 Example of a frontal chromatography experiment; breakthrough curve of a single component.

concave upward and ascending concentration steps are performed. The same is true for a convex upward isotherm and descending concentration steps. The reason for this is that, in these cases, a diffuse breakthrough profile is obtained and, consequently, errors are made in the accurate determination of the retention volumes when they are derived from the half-height or the inflection point. The diffuse profile can, however, be used for the determination of isotherms by FACP.

MODES OF FRONTAL ANALYSIS

There are two possibilities for performing a frontal chromatography experiment for the purpose of the determination of equilibrium isotherms. The step-series method uses a series of steps starting from $C_n = 0$ to C_{n+1}. After each experiment, the column has to be reequilibrated and a new step injection with a different end concentration C_{n+1} can be performed. In the staircase method, a series of steps is performed in a single run with concentration steps from 0 to C_1, C_1 to C_2, ..., C_n to C_{n+1}. The column does not have to be reequilibrated after each step and, therefore, the staircase method is faster than the step-series method. Both modes of frontal analysis give very accurate isotherm results.

Determination of Multicomponent Isotherms by Frontal Analysis

It is possible to extend the frontal chromatography method for the measurement of binary and multicomponent isotherms. In this case, the profiles are characterized by successive elution of several steep fronts. The use of these profiles for the determination of competitive isotherms in the binary case has been developed by Jacobsen et al.[8]

Combination of Frontal Analysis with Chromatographic Models

Frontal chromatography can be used in combination with chromatographic models to study mass-transfer and dispersion processes (e.g., the equilibrium dispersive or the transport model of chromatography.[7])

CONSTANT PATTERN, SELF-SHARPENING EFFECT, SHOCK-LAYER THEORY

Frontal chromatography generally requires the adsorption isotherm to be convex upward if the step injection is performed with ascending concentration (i.e., $C_{n+1} > C_n$) because, in this case, the profile of a breakthrough curve tends asymptotically toward a limit. After this constant profile has been reached, the profile migrates along the column without changing its shape. This state is called constant pattern.[9] This phenomenon arises because the self-sharpening effect associated with a convex isotherm is balanced by the dispersive effect of axial dispersion and a finite rate of mass-transfer kinetics. If the equilibrium adsorption isotherm is linear or concave upward, no constant pattern behavior is observed and the breakthrough curve spreads constantly during its migration through the column. This case is unfavorable. If the adsorption isotherm is concave upward, then a descending concentration step (i.e., $C_{n+1} < C_n$) leads to the formation of a constant pattern.

A very detailed study of the combined effects of axial dispersion and mass-transfer resistance under a constant pattern behavior has been conducted by Rhee and Amundson.[10] They used the *shock-layer* theory. The shock layer is defined as a zone of a breakthrough curve where a specific concentration change occurs (i.e., a concentration change from 10% to 90%). The study of the shock-layer thickness is a new approach to the study of column performance in non-linear chromatography. The optimum velocity for minimum shock-layer thickness (SLT) can be quite different from the optimum velocity for the height equivalent to a theoretical plate (HETP).[9]

INSTRUMENTATION

There are many possibilities for performing frontal chromatography experiments. In general, standard chromatographic equipment can be used. The preparation of a series of solutions of known concentration can be easily accomplished by using a chromatograph with a gradient delivery system applied as a mobile-phase mixer. If this system is not available, then the solutions have to be prepared manually. Two pumps can be used to perform the step injections or a single pump with a gradient delivery system. An injector having a sufficient large loop can also

be used. Even a single pump without gradient delivery system can be used. In this case, the step injection has to be made by manually switching the solvent inlet line to the prepared sample reservoir. The choice of the system is dependent on the application. For fast and accurate measurements of adsorption isotherms, a multisolvent gradient system with two pumps and a high-pressure mixer is a very good choice.

REFERENCES

1. Parcher, J. In *Advances in Chromatography*, Giddings, J. C., Ed.; Marcel Dekker, Inc.: New York, 1978; Vol. 16, 151.
2. Antia, F.; Horváth, Cs. Operational modes of chromatographic separation processes. Ber. Bunsenges. Phys. Chem. **1989**, *93*, 968.
3. Lee, A.; Aliao; Horváth, Cs. Tandem separation schemes for preparative HPLC of proteins. J. Chromatogr. **1988**, *443*, 31.
4. James, D.; Phillips, C. The chromatography of gases and vapours. Part III. The determination of adsorption isotherms. J. Chem. Soc. **1954**, *1066*.
5. Shay, G.; Szekely, G. Gas adsorption measurements in flow systems. Acta Chim. Hung. **1954**, *5*, 167.
6. Guan, H.; Stanley, B.; Guiochon, G. Theoretical study of the accuracy and precision of the measurement of single component isotherms by the elution by characteristic points (ECP) method. J. Chromatogr. A, **1994**, *659*, 27.
7. Sajonz, P. *Ph.D. Thesis*; University Saarbrücken: Germany, 1996.
8. Jacobsen, J.; Frenz, J.; Horváth, Cs. Measurement of competitive adsorption isotherms by frontal chromatography. Ind. Eng. Chem. Res. **1987**, *26*, 43.
9. Guiochon, G.; Golshan-Shirazi, S.; Katti, A. *Fundamentals of Preparative and Nonlinear Chromatography*; Academic Press: Boston, 1994.
10. Rhee, H.; Amundson, N. A study of the shock layer in nonequilibrium exchange systems. Chem. Engng. Sci. **1972**, *27*, 199.

Fuel Cells: Reversed-Flow GC

Dimitrios Gavril
Physical Chemistry Laboratory, Department of Chemistry, University of Patras, Patras, Greece

Abstract
Fuel cells are developed as a viable alternative for clean energy generation. The rational operation of the fuel cell units is closely related to the development of very active, selective, and poison-resistant catalysts.

Reversed-flow gas chromatography (RF-GC) has been successfully used to characterize solid catalysts under conditions compatible with the operation of real catalysts. RF-GC is not limited to chromatographic separation; since RF-GC is accompanied by suitable mathematical analysis of the chromatographic data, the simultaneous determination of various physicochemical parameters is possible. Thus, various catalytic processes related to the operation of fuel cell units such as steam reforming, catalytic partial oxidation, autothermal reforming, as well as water-gas shift (WGS) reaction and selective CO oxidation can be studied.

The use of RF-GC methodologies has been successfully extended to the study of selective CO oxidation over various fuel processing candidate catalysts, such as monometallic Rh/SiO_2, bimetallic $Pt–Rh/SiO_2$, and nanosized $Au/\gamma\text{-}Al_2O_3$, under different conditions, compatible with the operation of fuel cell units. These studies concern: 1) activity/selectivity measurements; 2) the determination of kinetic rate constants; and 3) investigation of the surface topography.

INTRODUCTION

Fuel cell technology applications vary from portable/micro power and transportation through to stationary power for buildings and distributed generation. Various fuel cell applications operating at different temperatures have been developed:[1–3] solid polymer fuel cells also known as proton-exchange membrane (PEM) fuel cells operate at ~80°C, alkaline fuel cells (AFC) at ~100°C, phosphoric acid fuel cells (PAFC) at ~200°C, molten carbonate fuel cells (MCFC) at ~650°C, and solid oxide fuel cells (SOFC) at higher temperatures of 800–1,100°C. A series of advantages such as low operating temperature, low weight, compactness, long stack life, suitability to discontinuous operation, as well as potential for low cost make PEM fuel cells the leading candidates for mobile power and/or for small power applications.

The rational operation of the fuel cell units is closely related to the development of very active, poison-resistant catalysts, which result in small catalytic volumes, durability under steady-state and transient conditions, low cost, and versatility to variations in fuel/feed composition.

The method used to produce hydrogen for the fuel cell is a critical factor in the design of fuel processing catalysts. Chemical processes such as steam reforming, catalytic partial oxidation (CPO), and autothermal reforming (ATR) are used for reforming fuels and to produce syngas (a mixture of carbon monoxide and hydrogen); the water-gas shift reaction (WGS) consumes carbon monoxide and water vapors to produce more hydrogen and carbon dioxide. However, trace amounts of carbon monoxide in the hydrogen-rich stream deteriorate the efficiency of the PEM fuel cell by poisoning the platinum (or Pt–Ru) anode, accelerated at CO levels higher than 50 ppm. Another catalytic process such as selective carbon monoxide oxidation (SCO) is considered to be the most promising and the lowest-cost approach.[4] An efficient SCO catalyst must be highly active in CO oxidation at temperatures compatible with the operation of the PEM fuel cell (70–100°C) and very selective toward CO_2 formation.

The characterization of fuel processing catalysts is a necessary step following their design and it usually involves activity/selectivity tests, and investigation of the kinetics of the related reactions as well as of the nature of the active sites. All the above processes are closely related to diffusion, adsorption/desorption, and surface reaction phenomena. Chromatographic separation is also a physicochemical process based on diffusion, adsorption, and chemical kinetics. Based on the broadening factors embraced by the van Deemter equation, precise and accurate physicochemical measurements have been done during the last few decades by gas chromatography, using relatively cheap instrumentation and very simple experimental setup.[4,5]

In conventional GC a gaseous mobile phase flows in a defined direction over a stationary phase or packing, resulting in the selective retention of solute components. In reversed-flow gas chromatography (RF-GC) the system is modified; another column (diffusion column) is placed perpendicularly in the center of the chromatographic

column (sampling column). The carrier gas flows continuously through the sampling column, while it is stagnant in the diffusion column, as is shown in Fig. 1. The reversing of the carrier gas flow for short time intervals results in extra chromatographic peaks on the continuous concentration–time curve. Thus repeated sampling of the physicochemical phenomena occurring in the diffusion column is achieved, and by using appropriate mathematical analysis, the values of the relevant physicochemical quantities are determined. In contrast with conventional GC, where the mobile phase is the center of interest, in RF-GC the solid or liquid substance placed in the diffusion column is under investigation. Thus RF-GC can be assumed as an inverse gas chromatographic method.

EXPERIMENTAL

The experimental setup of RF-GC for the study of catalytic processes comprises[6–11] the "sampling cell," formed by the sampling column $l' + l$ and the diffusion column L, which is connected perpendicularly to the middle of the sampling column. The ends D_1 and D_2 of the sampling column are connected through a four-port valve to the carrier gas inlet and the detector, as shown in Fig. 1. A conventional gas chromatograph is equipped with the appropriate detector (e.g., flame ionization, thermal conductivity). A separation column L' may also be incorporated in the GC oven. This column can be filled with the appropriate material for the separation of the carrier gas constituents due to the reactants and possible reaction products, and it can be heated at the same or at a temperature different from that of the sampling cell.

Performing flow perturbations, negative and positive abrupt fronts appear in the chromatogram, forming the so-called sampling peaks like those shown in Fig. 2.[8] The volumetric carrier gas flow rate does not affect the physicochemical phenomena occurring in the diffusion column, but only the speed of the sampling procedure.

The fuel processing catalyst can be studied either under non-steady-state conditions, having placed it near the injection point at the closed end of the diffusion column, or under steady-state conditions by putting it in the middle of the sampling column, as is shown in Fig. 1. The input of the studied adsorbate under non-steady-state conditions is done by injecting a small amount (e.g., 1 ml of CO at atmospheric pressure) at the closed end of the diffusion column, L (c.f. Fig. 1).

The gas atmosphere of the hydrogen-rich fuel/feed stream (containing CO, O_2, H_2, CO_2, H_2O), which passes through the fuel processing catalyst, can be easily simulated either by using a flowing system with mass flow controllers or by using a carrier gas mixture. Thus, in order to examine the effect of various H_2-rich feed/stream compositions in CO adsorption, three hydrogen/helium mixtures with different compositions were prepared by B.O.C. Gases GmbH (Germany) and were used as carrier gases.[8]

THEORY

All determinations by RF-GC are based on experimental chromatographic data like the height or the area of the extra sample peaks that appear in the chromatogram after each flow reversal, forming the "sampling peaks" as in Fig. 2.[8] The whole treatment of experimental data is based on the fact that the heights of the "sampling peaks" are described by a clear function of time comprising the sum of four exponentials:[6–11]

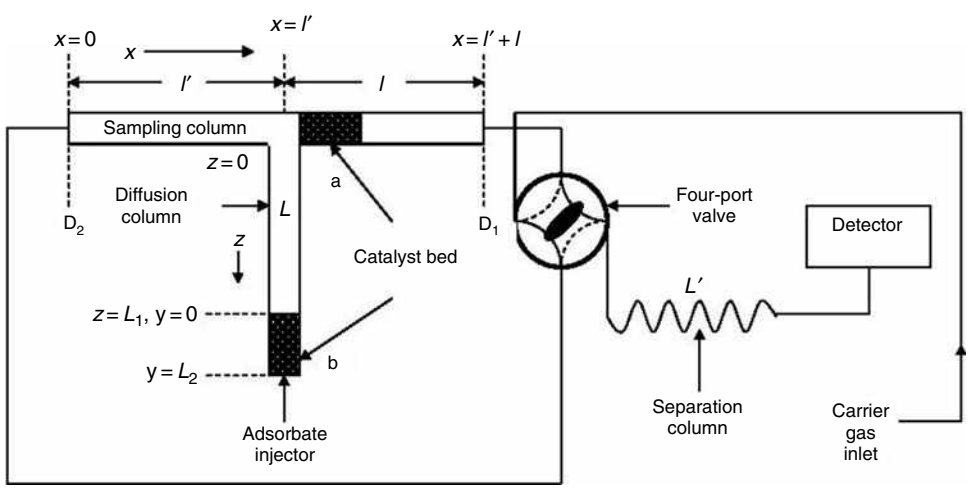

Fig. 1 Experimental setup used by reversed-flow gas chromatography for the characterization of solid catalysts: a) under steady-state conditions, with catalyst bed being put at a short length of sampling column l, near the junction of diffusion and sampling columns; b) under non-steady-state conditions, with catalytic bed being put at the top of diffusion column L.

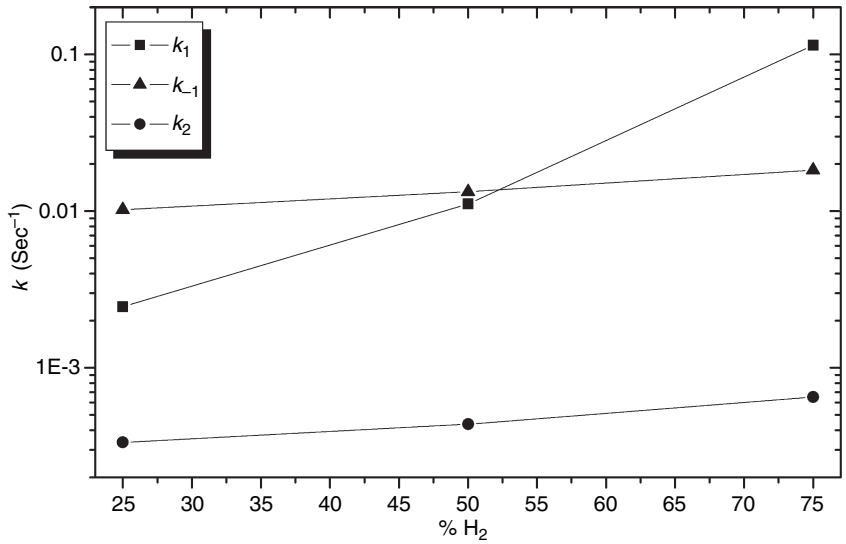

Fig. 2 Plots of the adsorption (k_1), desorption (k_{-1}), and irreversible surface binding (k_2), rate constants, at 373.2 K, over a Rh/SiO_2 catalyst, against carrier gas hydrogen percentage.
Source: From An inverse gas chromatographic instrumentation for the study of carbon monoxide's adsorption on Rh/SiO_2, under hydrogen-rich conditions, in Instrum. Sci. Technol.[8]

$$H^{1/M} = \sum_{i=1}^{4} A_i \exp\,(B_i t) \tag{1}$$

where H are the heights of the experimentally obtained chromatographic peaks, M the response factor of the detector and t the time from the beginning of the experiment. The values of the pre-exponential factors A_i and the corresponding coefficients of time B_i are easily determined from the chromatogram by using PC programs of non-linear least-squares regression (c.f. Appendix of Ref. 11).

POTENTIAL OF THE METHODOLOGY AND INDICATIVE RESULTS

Reversed-flow gas chromatography has all the advantages of a dynamic method such as GC and moreover it gives the opportunity for catalytic characterizations under either steady- or non-steady state conditions in a simple experiment under conditions compatible with the operation of real catalysts. All the catalytic processes related to the operation of PEM fuel cells, e.g., autothermal reforming or selective CO oxidation, can be studied. The hydrogen-rich fuel/feed stream atmosphere (CO, O_2, H_2, CO_2, H_2O, etc.) is easily and quantitatively achieved either by using a flowing system with mass-flow controllers or by using prepared carrier gas mixtures.

Chromatographic separation is widely used for conventional catalytic activity/selectivity measurements. RF-GC is not limited to chromatographic separation, since it is accompanied by suitable mathematical analysis of the chromatographic data (e.g., the height or the area of the experimentally obtained sampling peaks), which makes possible the simultaneous determination of various physicochemical parameters. Thus, 1) time-dependent, X_t, and overall, X, conversions, under either steady- or non-steady-state conditions;[6,7] 2) adsorption, k_1, desorption, k_{-1}, and surface reaction, k_2, rate constants and the respective activation energies, E_a;[8] 3) local adsorption energies, ε, local adsorption isotherms, $\theta(p,T,\varepsilon)$, local monolayer capacities, c^*_{max}, and adsorption energy distribution functions, $f(\varepsilon)$, for the adsorption of gases on heterogeneous surfaces;[9,10] 4) the energy of the lateral molecular interactions as well as the surface diffusion coefficients for physically adsorbed or chemisorbed species on heterogeneous surfaces;[10,11] and 5) the nature of the various groups of active sites of solid catalysts[10] have been determined.

Furthermore, the results derived by utilizing RF-GC methodologies for the investigation of the adsorption of CO, O_2, and CO_2 as well as the oxidation of CO over well-studied silica-supported Pt–Rh bimetallic catalysts are in agreement with those obtained by using different techniques and methodologies for the same catalysts, ascertaining the potential of RF-GC for reliable and accurate catalytic characterizations.

The utilization of RF-GC has been extended to CO adsorption under H_2-rich conditions (which is an elementary step of selective CO oxidation), initially over a silica-supported rhodium catalyst, which combines high selectivity and satisfactory activity.[8] The influence of the hydrogen amount in catalyst adsorptive behavior was studied by using three different composition carrier gas hydrogen/helium mixtures. Their compositions were 25.05% H_2 + 74.95% He (v/v, 99.999% pure), 49.95% H_2 + 50.05% He (v/v, 99.999% pure), and 75.05% H_2 + 24.95% He (v/v, 99.999% pure).

Rate constants for carbon monoxide's adsorption, desorption, and irreversible surface binding (e.g., its chemisorption), at different hydrogen compositions, over the

Table 1 Rate constants for CO adsorption (k_1), desorption (k_{-1}), and irreversible surface binding (k_2), at 373.2 K, for a silica-supported rhodium catalyst, under three different H_2-rich carrier-gas compositions.

% H_2	T (K)	$10^2\ k_1$ (sec^{-1})	$10^2\ k_{-1}$ (sec^{-1})	$10^4\ k_2$ (sec^{-1})
25.05	373.2	0.246	1.02	3.34
49.95	373.2	1.11	1.33	4.36
75.05	373.2	11.4	1.83	6.51

studied silica-supported rhodium catalyst at 373.2 K are referred in Table 1 and their variation against hydrogen percentage in the carrier gas mixture is shown in Fig. 2.

The values of the irreversible surface binding rate constants, k_2, increase with increasing carrier gas hydrogen content. Similarly, the desorption rate constants being two orders higher than those of irreversible surface binding are also found to increase with hydrogen amount. Moreover, the adsorption rate, k_1, was found to increase drastically with increasing hydrogen percentage compared to the increase of k_{-1} and k_2.

More quantitative information for the adsorption of carbon monoxide over the studied catalyst was extracted from the variation of local isotherms θ against the local adsorbed concentration of the adsorbate, c_s^*, shown in Fig. 3 of Ref. 8. The values of maximum local monolayer capacity (corresponding to $\theta = 1$) were easily determined from those plots. These values, referred in Table 2, also ascertained that higher amounts of carbon monoxide are present on catalyst surface as the hydrogen amount increases.

From the above results it is obvious that higher amounts of CO can be adsorbed on Rh/SiO_2 as the carrier gas hydrogen amount increases. The increase of the CO adsorption rate, k_1, indicated that the respective activation energy should decrease with increasing H_2 content and consequently higher amounts of CO should be bound less strongly on the studied catalyst active sites at 373.2 K. This fact explains the high selectivity of supported Rh catalysts observed at lower temperatures for SCO due to the almost entire coverage of catalyst surface by CO, which excludes the more weakly adsorbed species H_2 and O_2 from the active sites (CO inhibitive effect).[12,13] An entirely new observation of this preliminary work was that the selectivity of the studied catalyst is expected to increase at higher H_2 compositions of the feeding stream due to the above-mentioned CO inhibition. However, the increase of the desorption rate, k_{-1}, with H_2 amount is much lower than that of k_1, indicating that the studied Rh/SiO_2 catalyst may not be active enough for SCO at higher H_2 compositions, at low temperatures. This observation is consistent with literature information that at lower temperatures CO oxidation over noble metal catalysts (Pt, Pd, Rh) either in the presence or in the absence of hydrogen is CO desorption limited.[12,13]

Table 2 Maximum local monolayer capacities (c^*_{max}) estimated by the plots of the local isotherms θ, against the local adsorbed concentration, (c_s^*), for the adsorption of carbon monoxide over Rh/SiO_2 catalyst, at various H_2-rich carrier-gas compositions.

% H_2	c^*_{max}
25.05	12.1 μmol g^{-1}
49.95	83.5 μmol g^{-1}
75.05	1.98 mmol g^{-1}

CO sorption has been further studied over silica-supported monometallic Rh and $Rh_{0.50}$+$Pt_{0.50}$ alloy catalysts, in a wide temperature range, under various hydrogen atmospheres ranging from 25% to 75% H_2.[14] The variation of the experimentally determined rate constants and the activation energies against the nature of the used catalyst (monometallic or alloy) and the amount of hydrogen in the carrier gas gave useful information for the selectivity as well as the activity of SCO. At low temperatures and under H_2-rich conditions, compatible with the operation of PEM fuel cells, the activity of the monometallic and the alloy catalysts is expected to be similar; however, the selectivity of the $Rh_{0.50} + Pt_{0.50}$ alloy catalyst is expected to be higher, making Pt–Rh alloy catalyst a better candidate for CO preferential oxidation. The determined desorption barriers were in any case much lower than the respective activation energies found for CO desorption in the absence of hydrogen, indicating H_2-induced desorption, explains the rate enhancement of SCO oxidation given in the literature.

The study of the effect of hydrogen in the "topography" of the active sites related to CO adsorption focused on the Rh/Sio_2 catalyst, at 90°C.[15] The comparative presentation of the energy distribution function $\varphi(\varepsilon;t)$ against the lateral interaction energy β for CO adsorption on Rh/SiO_2 catalyst, at 90°C, is shown in Fig. 3, in the absence of hydrogen as well as with excess of hydrogen. These plots clearly indicate that the topography of the catalyst in the absence of hydrogen consists of both randomly and islands of CO bound over chemisorbed CO molecules (groups A, B, C, and D respectively). In contrast, under H_2-rich conditions, the observed topography was almost entirely patchwise because of long-range lateral attractions between adsorbate molecules (group B). Moreover, in excess of hydrogen, CO adsorption is shifted at higher lateral attraction values, β, which correspond to weaker adsorbate–adsorbent interactions and lower surface coverage. This indicated a H_2-induced desorption, which was attributed to the formation of an H–CO complex desorbing from the catalyst surface below the temperature required for CO desorption, in the absence of H_2, and it may explain the enhancement of the SCO rate by H_2, which is well-known in the literature.

Recently, novel studies giving further information on the mechanism of selective CO oxidation over γ-alumina-supported nanoparticle-sized gold catalysts were carried out, utilizing, among other techniques, RF-GC.[16,17] It was observed that: 1) CO_2 formation, increases with rising

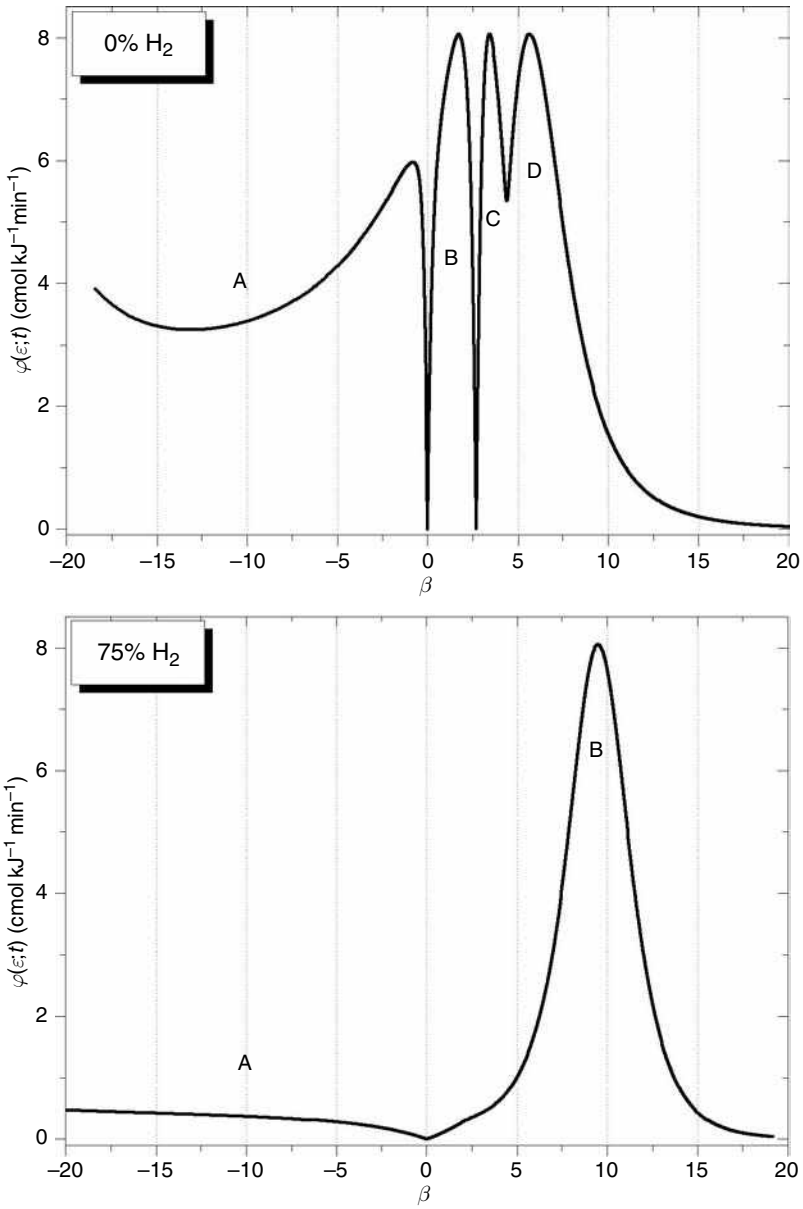

Fig. 3 Comparative presentation of the energy distribution function $\varphi(\varepsilon;t)$ against the lateral interaction energy β for CO adsorption on Rh/SiO_2 catalyst, at 90°C, in the absence of hydrogen (0% H_2) and in excess of hydrogen (75% H_2).
Source: From Inverse gas chromatographic investigation of the active sites related to CO adsorption over Rh/SiO_2 catalysts in excess of hydrogen, in J. Chromatogr. A.[15]

temperature, in the absence of hydrogen and oxygen, pointing to a model of active sites consisting of an ensemble of metallic Au atoms and a cationic Au with a hydroxyl group; 2) at high temperatures (>200°C) in the presence of excess of H_2, reversed water gas shift (RWGS) reaction results in the formation of CO and H_2O with consumption of CO_2; and 3) hydrogen strongly influences the interaction of CO on $Au/\gamma\text{-}Al_2O_3$ by weakening CO adsorption. It was concluded that the presence of hydrogen plays an important role in both decreasing the strength of CO bonding and preventing the deactivation and regeneration.

The nature of the active sites related to CO adsorption over $Au/\gamma\text{-}Al_2O_3$ both in the presence and in the absence of hydrogen in a wide temperature range has also been studied.[18] As has been shown, useful information concerning active sites topography can be extracted by plotting the energy distribution function $\varphi(\varepsilon;t)$ against the lateral interaction energy β, as shown in Fig. 4. The degree of surface heterogeneity increases with rising temperature, since new groups of active sites appear, in the presence as well as the absence of hydrogen. The topography of the $Au/\gamma\text{-}Al_2O_3$ catalyst concerning selective CO oxidation is patchwise at lower temperatures and becomes intermediate at higher temperatures.

Moreover, it was found that: 1) higher amounts of CO can be bound on the catalyst active sites, under conditions compatible with the operation of PEM-FCs; 2) at rising temperatures, catalyst adsorptive capacity decreases while the degree of surface heterogeneity increases since new groups of active sites appear, in the presence as well as in

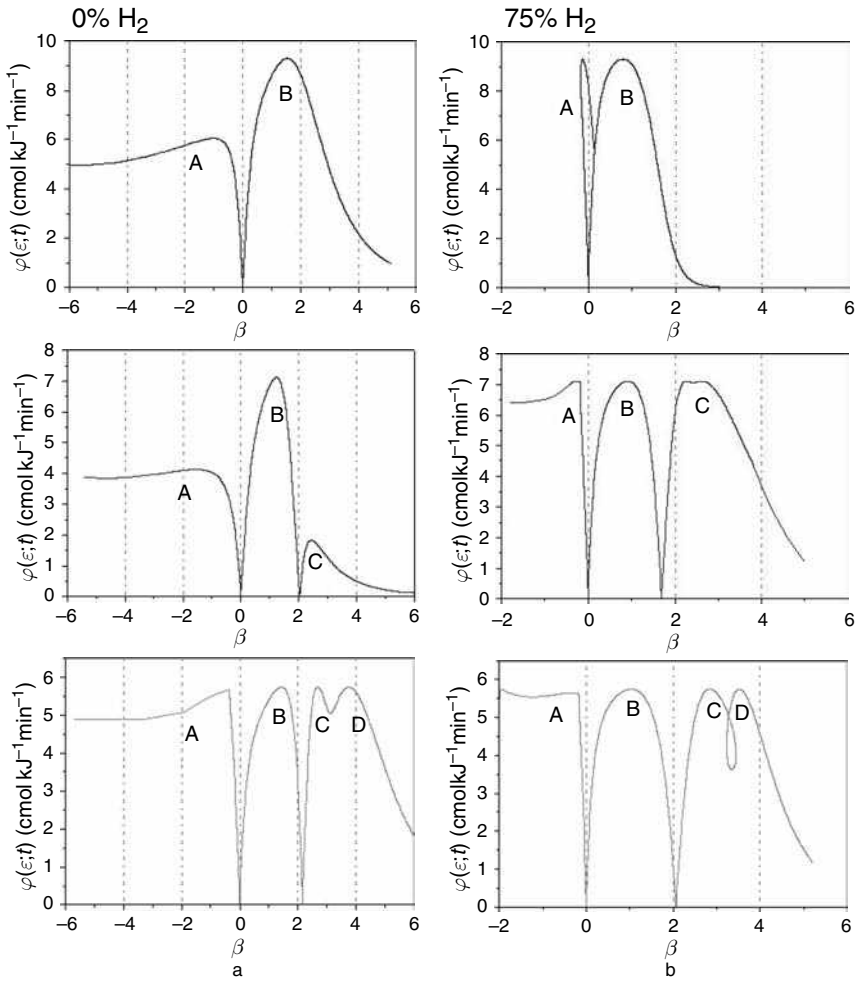

Fig. 4 Comparative presentation of the energy distribution function $\varphi(\varepsilon;t)$ against the lateral interaction energy β for CO adsorption on Au/γ-Al_2O_3 catalyst, at 50°C, 150°C, and 250°C, in the absence of H_2 (a) and under H_2-rich conditions (b). **Source:** From Gas chromatographic investigation of the effects of hydrogen and temperature on the nature of the active sites related to CO adsorption on nanosized Au/γ-Al_2O_3, in J. Chromatogr. A.[18]

the absence of hydrogen; and 3) the experimentally observed high activity of Au/γ-Al_2O_3 for SCO at ambient temperatures was explained as a consequence of weak CO bonding over metallic Au active sites in comparison to strong CO bonding taking place at active sites located on γ-Al_2O_3 support, which is related to deactivation.

CONCLUSIONS

RF-GC has been used to characterize solid catalysts under either steady- or non-steady-state conditions, compatible with the operation of real catalysts. RF-GC is not limited to chromatographic separation; since RF-GC is accompanied by suitable mathematical analysis of the chromatographic data, the simultaneous determination of various physicochemical parameters related to the kinetics of the elementary steps (adsorption, desorption, surface reaction) and the nature of the active sites is possible.

The use of RF-GC methodologies has been successfully extended to the study of selective CO oxidation over various fuel processing candidate catalysts, such as monometallic Rh/SiO_2, bimetallic Pt–Rh/SiO_2, and nanosized Au/γ-Al_2O_3, under different conditions, compatible with the operation of fuel cells units.

These studies concern: 1) activity/selectivity measurements; 2) the determination of kinetic rate constants (adsorption, desorption, surface bonding); and 3) investigation of the surface topography. Important questions answered in the last study are: 1) What amount of CO molecules is adsorbed on the catalyst surface; 2) Where are the molecules on the surface (e.g., Au particles or support); 3) What is the nature of the surface chemical bonds?

It should be noted that all the related catalytic processes such as steam reforming, catalytic partial oxidation, autothermal reforming, as well as WGS reaction and selective CO oxidation can be studied.

REFERENCES

1. Gray, P.G.; Frost, J.C. Impact on clean energy in road transportation. Energy Fuels **1998**, *4*, 1121–1129.

2. Brown, D.R. PEM fuel cells for commercial building. Office of Building technology, State and community programs, Document Number PNNL-12-51, prepared at the US Department of energy by the Pacific Northwest National Laboratory, November 1998.
3. Ghenciu, A.F. Review of fuel processing catalysts for hydrogen production in PEM fuel cell systems. Curr. Opin. Solid State Mater. Sci. **2002**, *6*, 389–399.
4. Conder, J.C.; Young, C.L. *Physicochemical Measurements by Gas Chromatography*. Wiley: Chichester, 1979.
5. Laub, R.J.; Pescok, R.L. *Physicochemical Applications of Gas Chromatography*. Wiley: New York, 1978.
6. Gavril, D. Reversed flow gas chromatography: A tool for instantaneous monitoring of the concentrations of reactants and products in heterogeneous catalytic processes. J. Liq. Chromatogr. Rel. Technol. **2002**, *25*, 2079–2099.
7. Gavril, D.; Loukopoulos, V.; Karaiskakis, G. Study of CO dissociative adsorption over Pt and Rh catalysts by inverse gas chromatography. Chromatographia **2004,** *59*, 721–729.
8. Loukopoulos, V.; Gavril, D.; Karaiskakis, G. An inverse gas chromatographic instrumentation for the study of carbon monoxide's adsorption on Rh/SiO_2, under hydrogen-rich conditions, Instrum. Sci. Technol. **2003**, *31*, 165–181.
9. Gavril, D. An inverse gas chromatographic tool for the experimental measurement of local adsorption isotherms, Instrum. Sci. Technol. **2002**, *30*, 397–413.
10. Gavril, D.; Nieuwenhuys, B.E. Investigation of the surface heterogeneity of solids from reversed flow inverse gas chromatography. J. Chromatogr. A, **2004**, *1045*, 161–172.
11. Katsanos, N.A.; Gavril, D.; Karaiskakis, G. Time–resolved determination of surface diffusion coefficients for physically adsorbed or chemisorbed species on heterogeneous surfaces, by inverse gas chromatography. J. Chromatogr. A, **2003**, *983*, 177–193.
12. Kahlich, M.J.; Gasteiger, H.A.; Behm, R.J. Kinetics of the selective CO oxidation in H_2-rich gas on Pt/Al_2O_3. J. Catal. **1997**, *171*, 93–105.
13. Oh, S.H.; Sinkevitch, R.M. Carbon monoxide removal from hydrogen-rich fuel cell feedstreams by selective catalytic oxidation. J. Catal. **1993**, *142*, 254–262.
14. Gavril, D.; Loukopoulos, V.; Georgaka, A.; Gabriel, A.; Karaiskakis, G. Inverse gas chromatographic investigation of the effect of hydrogen in carbon monoxide adsorption over silica supported Rh and Pt–Rh alloy catalysts, under hydrogen-rich conditions. J. Chromatogr. A, **2005**, *1087*, 158–168.
15. Gavril, D.; Georgaka, A.; Loukopoulos, V.; Karaiskakis, G. Inverse gas chromatographic investigation of the active sites related to CO adsorption over Rh/SiO_2 catalysts in excess of hydrogen. J. Chromatogr. A, **2007**, *1160*, 289–298.
16. Gavril, D.; Georgaka, A.; Loukopoulos, V.; Karaiskakis, G.; Nieuwenhuys, B. On the mechanism of selective CO oxidation on nanosized $Au/\gamma\text{-}Al_2O_3$ catalysts. Gold Bull. **2006**, *39*, 192–199.
17. Georgaka, A.; Gavril, D.; Loukopoulos, V.; Karaiskakis, G.; Nieuwenhuys, B. H_2 and CO_2 coadsorption effects in CO adsorption over nanosized $Au/\gamma\text{-}Al_2O_3$ catalysts. J. Chromatogr. A, **2008**, *1205*, 128–136.
18. Gavril, D.; Georgaka, A.; Loukopoulos, V.; Karaiskakis, G. Gas chromatographic investigation of the effects of hydrogen and temperature on the nature of the active sites related to CO adsorption on nanosized $Au/\gamma\text{-}Al_2O_3$, J. Chromatogr. A, **2007**, *1164*, 271–280.

Gas Sampling Systems for GC

Piotr Słomkiewicz
Zygfryd Witkiewicz
Institute of Chemistry, Jan Kochanowski University, Kielce, Poland

Abstract
The methods for the collection and introduction of gas samples in gas chromatography (GC) are described. Containers for sampling gases, sorption pipes, two- and three-position multiport valves and chambers capable of changing pressure with a mobile piston are presented. The methanizer in which the catalytic reduction of carbon monoxide and carbon dioxide to methane occurs is also presented.

INTRODUCTION

Gases analyzed by gas chromatography (GC) can be divided according to their origin into three large groups. The first group consists of gases occurring in the atmospheres of Earth and other planets, the second group consists of gases present in different types of holders, reactors, and other technological systems, and the third group consists of gases occurring in liquids and solids. Atmospheric gases of planets other than that of Earth are introduced into gas chromatographs automatically and ways of this type are not dealt with in this entry.

Atmospheric air can be injected into a chromatographic column automatically, directly into the place where analysis is performed, with the use of portable chromatographs. In this case, injection is done by means of sampling valves into which air is pressed or sucked. Air can also be injected into a chromatographic column with a gas-tight syringe prior to its direct uptake from the atmosphere.

GAS SAMPLING

Gases in installations and technological systems are under pressures that are usually different from the atmospheric pressure and can be injected into a chromatographic column automatically or manually by means of sampling valves or manually with syringes.

Gases present in liquids can be separated using the following methods:

1. By decreasing pressure above the liquid, which makes gases dissolved in the liquid pass into the gaseous phase whose samples are analyzed.[1]
2. By heating the liquid up to its boiling point. Increasing the temperature of the liquid results in decreasing the solubility of its dissolved gases, which then pass into the headspace phase.[1]
3. By blowing through the liquid containing inert gas; gases dissolved in the liquid are eluted with a stream of inert gas.[2]
4. By microextraction to the stationary phase, gases present in the liquid are adsorbed on to a sorbent from which they are thermally desorbed.[3]
5. By headspace analysis. In a closed container, above the liquid surface there is an equilibrium between a vapor of the liquid sample and gases dissolved in it. The samples of the gaseous phase are taken for analysis.[4]

Gases can be separated from solids by desorption under vacuum, melting under vacuum, and melting in an atmosphere of inert gas.[4]

A number of analyses are done, not in situ but in a laboratory provided with a sample of the gas under analysis. Containers made of glass or of Tedlar® are used in these cases.

Containers for Sampling Gases

Glass containers (Fig. 1) can be expendable (Fig. 1a) or multiusable (Fig. 1b) vacuum vessels or flow vessels called gaseous pipettes (Fig. 2). Vacuum vessels are spontaneously filled after opening, whereas gaseous pipettes are filled by suction or by pressing the gas through them (Fig. 2A). Tedlar containers are bags into which the gas is forced. They are superior to glass containers because they are light, transportable, unbreakable, and capacious.

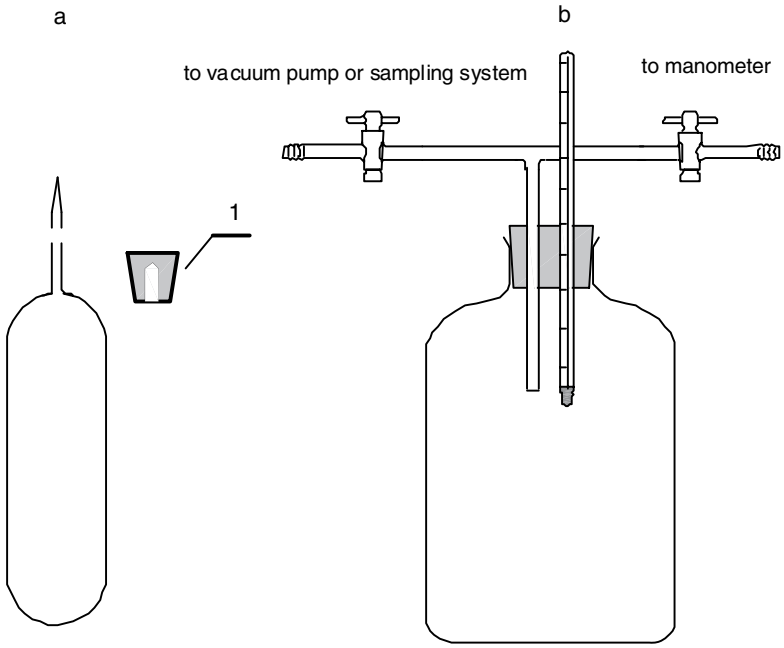

Fig. 1 Glass containers for taking samples of gases: a, expendable sampling ampoule; (1), rubber stopper; b, vacuum bottle.

Analytical samples are taken from containers through a rubber membrane using a syringe (Fig. 2B). When glass containers are used, each sampling decreases the pressure of gas in a container. Consequently, once a syringe needle is extracted, the laboratory atmospheric air gets into the container and changes the composition of the gas. This can be prevented by filling the container with a liquid that is resistant to absorbing analytes, for example, concentrated solution of NaCl, in the course of sampling. Such a problem does not arise when a Tedlar container is used, because an overpressure can be formed in it by exerting external pressure on its elastic walls.

ABSORPTION AND ADSORPTION OF GASEOUS ANALYTES

Gases can be analyzed immediately after sampling if the concentration of the analytes is sufficient for detecting and determining them by means of a detector. If the

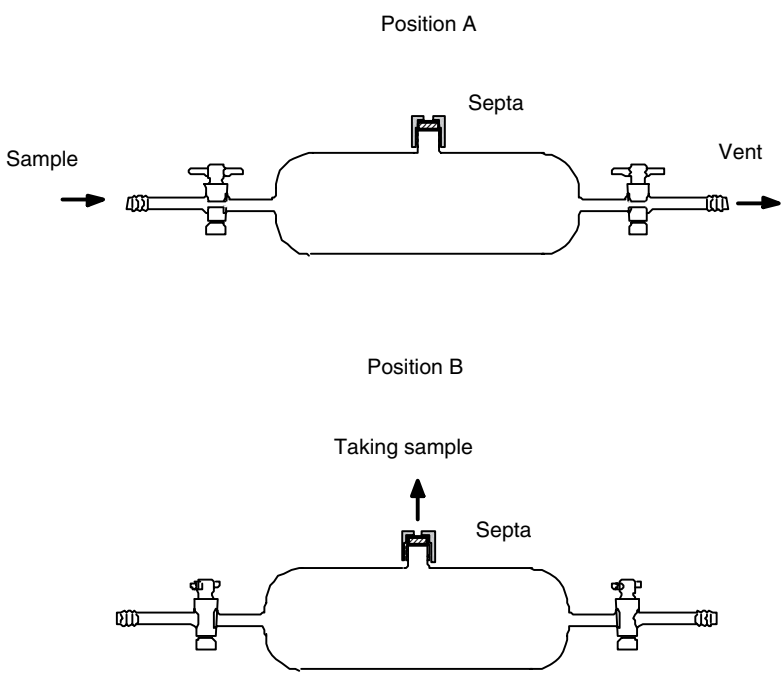

Fig. 2 Taking sample by gas pipette.

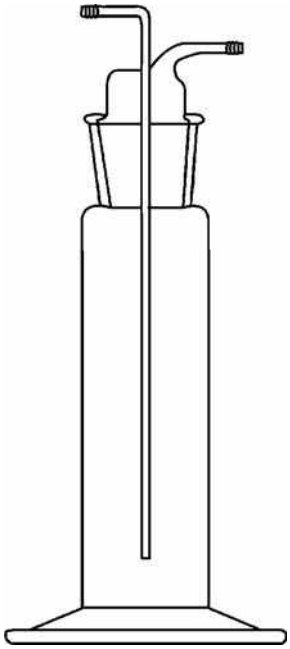

Fig. 3 Gas absorption bulb.

concentration of an analyte is too low, it should then be increased by absorption in a liquid or on to an adsorbent. Absorption in liquids is carried out in bulbs (Fig. 3). A bulb is filled with a solvent or a solution of reagent absorbing an analyte. In the second case, the derivation of the analyte is carried out. The solvent must absorb an analyte well, and the reagent must quantitatively react with the analyte. The liquid in a bulb cannot be readily volatile; cooling is used if necessary. An analysis of the liquid or its headspace phase is done according to the analytical task involved.

Samples of gases for chromatographic analysis can be taken by their adsorption on beds of sorbents. Among others, active carbons, silica gels, molecular sieves, carbon sieves, and graphitized carbon blacks are used as sorbents.[5] Sorption is carried out by pressing or sucking gas through a sorptive tube (Fig. 4). The adsorbed analytes are then subjected to desorption with a solvent or to thermal desorption. The sorption of analytes in sorptive tubes can be made in situ or in a laboratory by connecting a sorptive tube with a container of the gas under analysis. If gaseous analytes dissolved in liquids are to be analyzed, inert gas can be passed through these liquids to elute the analytes from the liquid matrix. The gas mixture obtained is directed into an injector of gas chromatograph or into a sorptive tube or a bulb and the further procedure is followed as described above. Sorptive tubes can be connected with sampling valves.

SAMPLING VALVES

The injection of gas samples into a chromatographic column can be done with gas-tight syringes through the membrane of a sample injector. The syringes of this type, with a capacity from a few cubic millimeters to a great many cubic centimeters, are made of glass. The advantage in using syringes is that a gas sample of chosen capacity can be injected, whereas their disadvantage is in injecting a gas sample of atmospheric or higher pressure and at room temperature.

Sampling valves provide much higher reproducibility of injected gas samples than do syringes. With them, it is possible to inject a sample of pressure different from atmospheric pressure and at elevated temperatures. Moreover, the membrane of a sample injector does not become perforated.

Despite their different construction, most sampling valves are based on the same principle of operation. It is based on switching streams of analyzed gases and carrier gas flowing through the sample loop connected to the valve. A sample loop is usually a section of capillary tubing having a particular capacity. A sample of gas at a particular pressure and at constant temperature is introduced into a sample loop, using its overpressure, and then, after switching the streams of gases, the sample loop is included in the stream of carrier gas and, together with it, the sample of gas is injected into a chromatographic column.

Based on their construction, sampling valves can be divided into rotary, membrane, and piston types. The switching of gas tracks in rotary valves occurs through

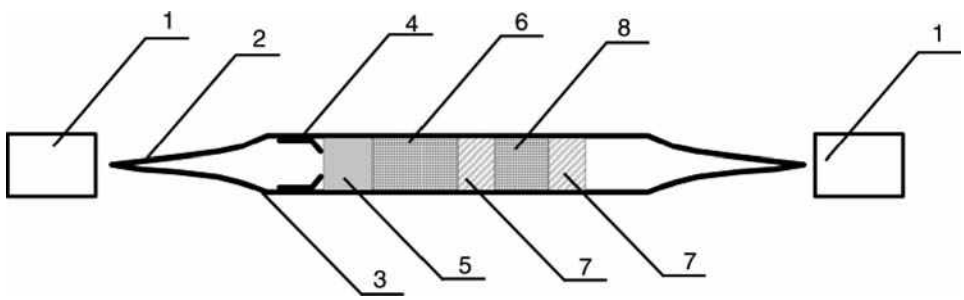

Fig. 4 Sorptive tube by National Institute for Occupational Safety and Health: (1) plastic cap; (2) sealed tube ends (broken before use); (3) glass sorptive tube, (4) spring; (5) glass wool; (6) sorbent; (7) stopper; and (8) protective layer of sorbent.

ducts cut in a rotating disk or in the cone of a rotor that is connected by slots situated in the subrotor plane and that are outlets of gas ducts in the valve body. In membrane valves, the flow of gases through individual ducts of the valve body is opened and shut down by the elastic membrane placed at their outlets, which is mechanically or pneumatically pressed down to these outlets. Piston-type valves assume the shape of a cylinder where individual outlets of gas ducts and the piston with toroidal packings are placed. The reciprocating motion of the piston switches individual outlets of gas ducts in the valve body.

The principle of taking samples of gas by different types of valves equipped with a number of sample loops is given in the following examples. Diagrams illustrating the principle of their operation take rotary valves, which are most frequently used.

Two-position, Multiport Valves

Multiport valves of two working positions are most widely used. One position serves to fill one or many sample loops with the gas under analysis, whereas the other one serves to inject a sample taken from a sample loop into a stream of carrier gas.

A two-position, six-port valve with one sample loop is the simplest one, and sampling from one gas duct is made possible here (Fig. 5). In position A, the gas to be analyzed flows through the sample loop and at the same time the stream of carrier gas flows through the valve into a chromatographic column bypassing the sample loop. When the rotor of the six-port valve is switched to position B, the sample present in the sample loop is introduced into the stream of carrier gas, and the sample, together with the carrier gas, is directed to a chromatographic column. In this position, the stream of gas being

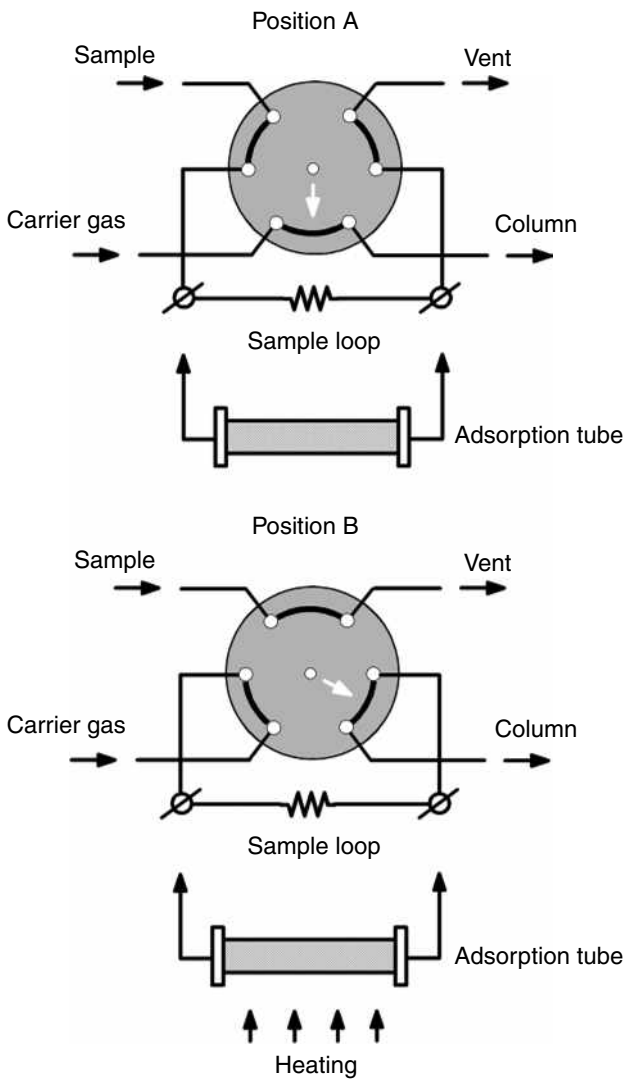

Fig. 5 Two-position, six-port valve with one sample loop, taking sample from one gas track, and an adsorption tube, taking sample from sorbent.

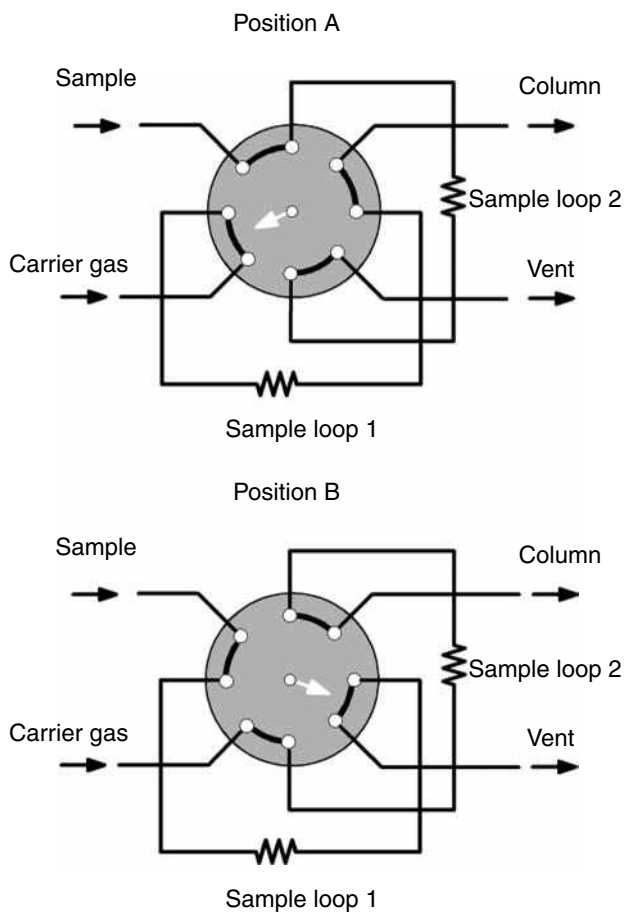

Fig. 6 Two-position, eight-port valve with two sample loops, taking sample from one gas track.

analyzed flows through the valve, bypassing the sample loop.

When the concentration of analytes in the gas is too low to be analyzed, the sample loop can be replaced with a sorptive tube (adsorber). In Fig. 5, the operational principle of a six-port valve equipped with an adsorber is shown. In position A, the gas to be analyzed flows through the sorbent bed into the adsorber, where it is adsorbed, and at the same time, a stream of carrier gas flows through the valve into a chromatographic column. When the six-port valve is switched to position B, a sample of the gas is thermally desorbed and is introduced into the stream of carrier gas, and the sample, together with the carrier gas, is directed to a chromatographic column. In this position, the stream of the analyzed gas flows through the six-port valve, bypassing the adsorber.

To inject two samples of different quantities from one duct of the gas under analysis, a two-position, eight-port valve with two sample loops is used (Fig. 6). In position A, the carrier gas flows through sample loop 1 into a chromatographic column and the gas under analysis flows through sample loop 2 into the outlet. The switching of the valve rotor to position B causes the sample of gas present in sample loop 2 to be injected into a chromatographic column and sample loop 1 is filled with gas. Another switching of the valve rotor to position A causes a sample of gas from sample loop 1 to be injected into a chromatographic column and sample loop 2 is filled with gas.

To inject samples from two ducts of gases under analysis, a two-position, ten-port valve with two sample loops is used (Fig. 7). In position A, the carrier gas flows through sample loop 1, the gas under analysis (gas 2) flows through sample loop 2, and gas 1 flows through the valve, omitting

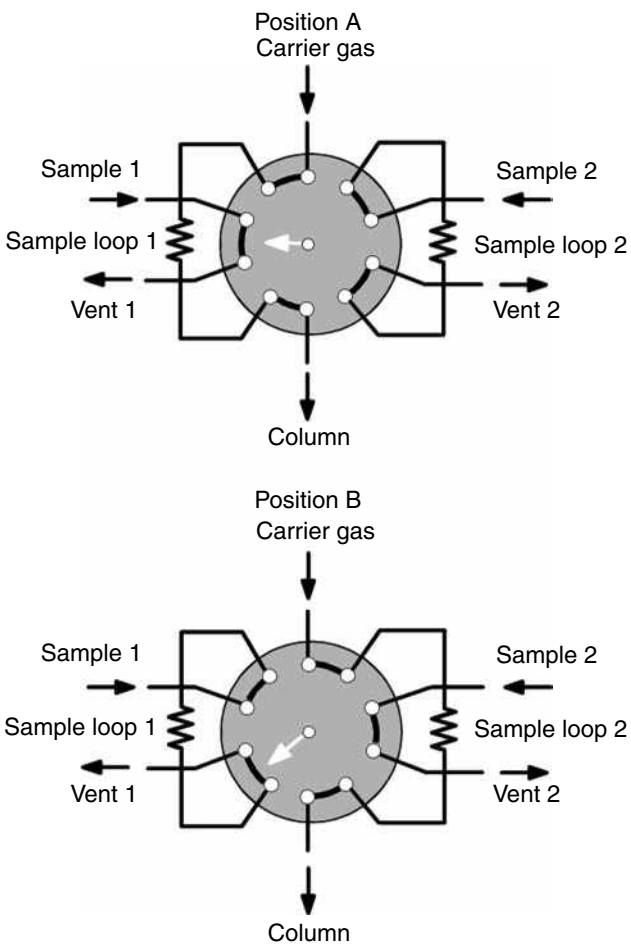

Fig. 7 Two-position, ten-port valve with two sample loops, taking sample from two gas tracks.

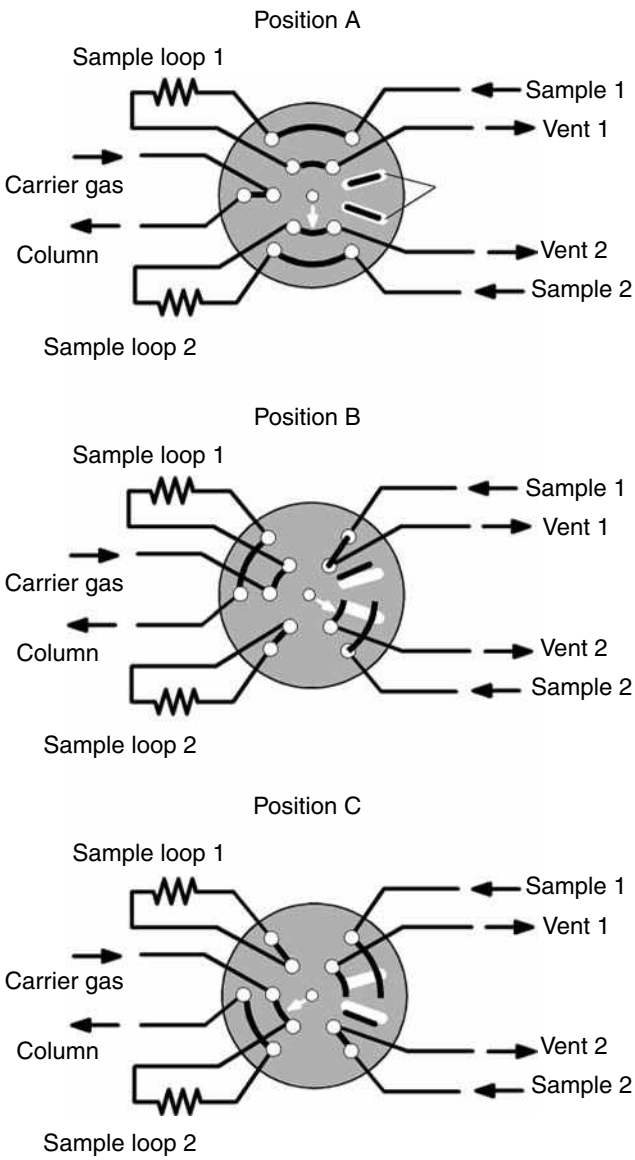

Fig. 8 Three-position, ten-port valve with two sample loops, taking sample from two gas tracks.

the sample loops. The switching of the valve rotor to position B causes the sample of gas 2 from sample loop 2 to be injected into a chromatographic column with carrier gas, and gas 2 flows through the valve, omitting the sample loops, and at the same time gas 1 flows through sample loop 1. Another switching of the valve rotor to position A causes a sample of gas 1 from sample loop 1 to be injected into a chromatographic column with carrier gas, such that gas 1 flows through the valve, omitting the sample loops, and gas 2 flows through sample loop 2.

Three-position, Multiport Valves

The above-mentioned sampling from two tracks of gases under analysis through the two-position, ten-port valve having two sample loops is limited to alternately successive operations.

This shortcoming is absent in the three-position, ten-port valve having two sample loops, which is used for taking samples from two gas tracks (Fig. 8).[6] This valve can be used to analyze two gases in any order. The constructional solution of this valve makes it possible to simultaneously take two samples of different gases into two sample loops and perform their chromatographic analyses.

In position A, the carrier gas flows through the valve, omitting the sample loops, gas 1 flows through sample loop 1, and gas 2 flows through sample loop 2. The switching of the valve rotor to position B injects a sample of gas 1 from sample loop 1 into a chromatographic column with carrier gas, and gas 1 flows through the valve (omitting the sample loops) and gas 2 flows through the duct placed in the valve body on the plane under its rotor and a sample of gas 2 is trapped in sample loop 2. The switching of the valve rotor to position C injects a sample of gas 2 from sample loop 2 into a chromatographic column with carrier gas, and simultaneously, gas 2 flows through the valve and gas 1 flows through the duct placed in the valve body on the plane under its rotor and a sample of gas 1 is trapped in sample loop 1.

Sampling by means of a valve with a sample loop has its own disadvantage, because it cannot adjust the pressure of gas in a sample loop to the pressure of carrier gas at the inlet of a chromatographic column. When the pressure of gas in the sample loop considerably exceeds the pressure of carrier gas, inserting such a sample loop into the circulation of carrier gas results in disturbing the flow that is caused by the impact of the pressure of the expanding gas from the sample loop. The pressure disorder goes through the chromatographic column and disturbs the operation of the detector of the chromatograph. When a flame ionization detector with a small flow of carrier gas and hydrogen is used, high pressure in a sample loop can extinguish the flame. Furthermore, the impacts of the expanding gas from the sample loop impair the efficiency of a chromatographic column.

A method of taking samples of gas of high pressure with a three-position, six-port valve connected with a chamber capable of changing pressure with a mobile piston is described (Fig. 9).[7] The wall of the chamber is provided with a hollow caved duct acting as a sample loop connected with a six-port valve. When the pressure of a sample placed in a duct is decreased with a piston, which increases the volume of a chamber while moving, the pressure of gases taken decreases and, regardless of the position of the piston, the flow of gases through the caved duct in the chamber is stable.

In position A, gas with high pressure flows through the duct of the chamber capable of changing pressure and carrier

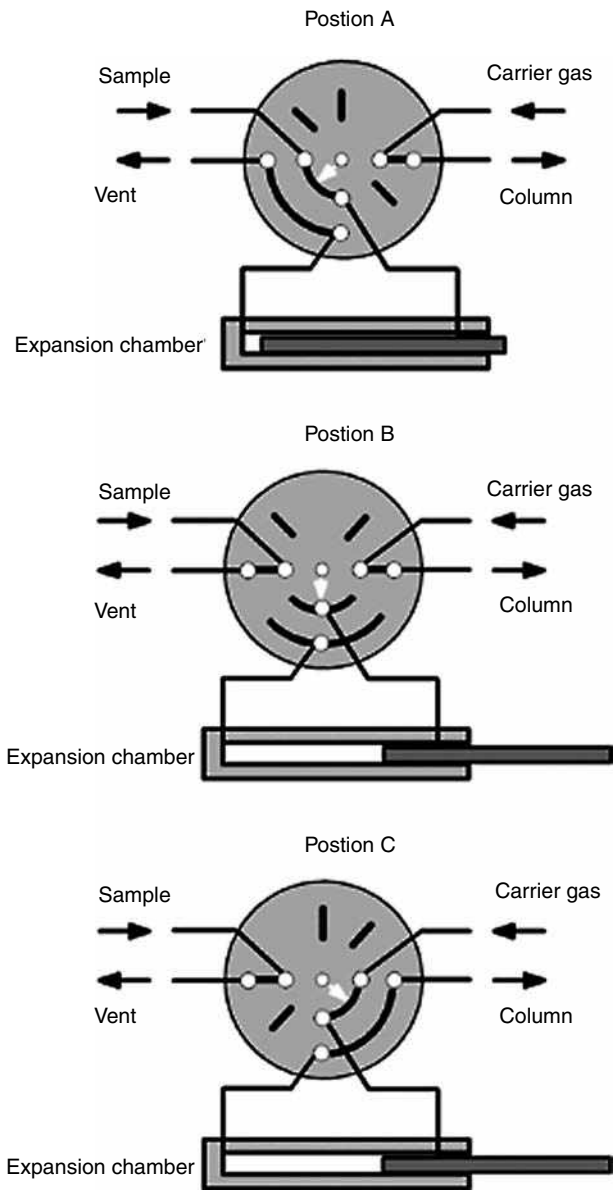

Fig. 9 Three-position, six-port valve with expansion chamber, taking sample from one gas track.

gas flows through the six-port valve, bypassing the chamber. In position B, both the gas under analysis and carrier gas flow through the six-port valve and the chamber is disconnected; therefore, the pressure of a gas sample in it can be decreased by shifting the piston. The switching of the valve rotor to position C injects a sample of the gas from the chamber capable of changing pressure into a chromatographic column with carrier gas, and simultaneously, the gas flows through the valve. The above-mentioned apparatus can also be used to take samples of gas whose pressure is lower than that of the carrier gas. The piston decreasing the volume of the chamber capable of changing pressure can increase the pressure of a sample of the gas taken. If the pressure of the gas under analysis is lower than the atmospheric pressure, its flow through the chamber capable of changing pressure must then be forced by a pump.

According to the quantitative composition of gas under analysis, sample loops of different volumes should be used. The replacement of a sample loop with another in the course of analysis necessitates the interruption of the flow of gases in the carrier gas track of a gas chromatograph or in the track of the gas under analysis. In the first case, air is injected into a chromatographic column, whereas in the second one, air is injected into the track of the gas under analysis, which can be disadvantageous in some cases. The serious disadvantage of valves with sample loops is that they make a quantitative analysis by the method of internal standard impossible.

An apparatus for injecting samples of gas different in size without replacing a sample loop and interrupting the operation of a gas chromatograph, with the possibility of

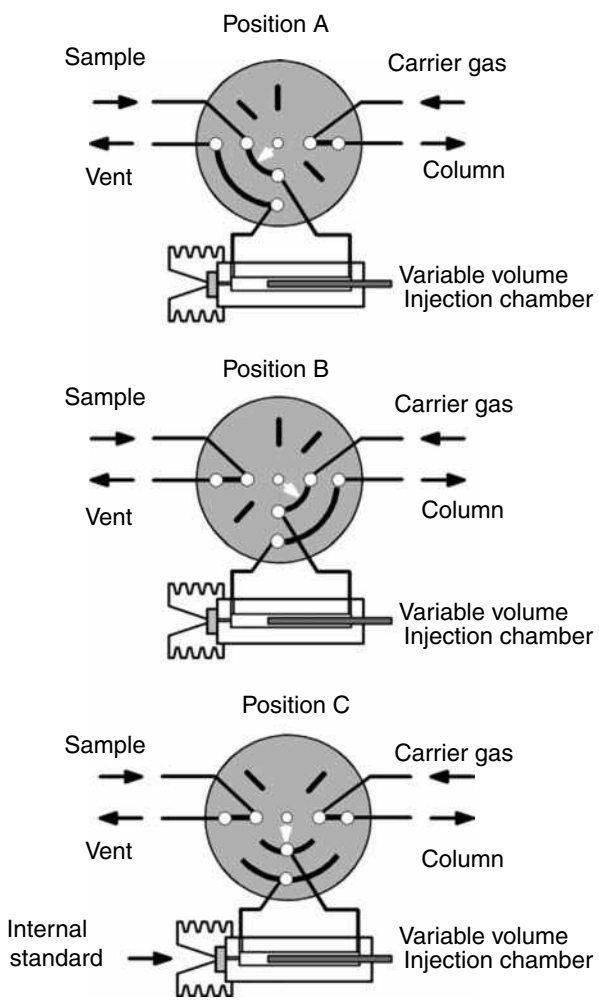

Fig. 10 Three-position, six-port valve with variable volume injection chamber, taking sample from one gas track.

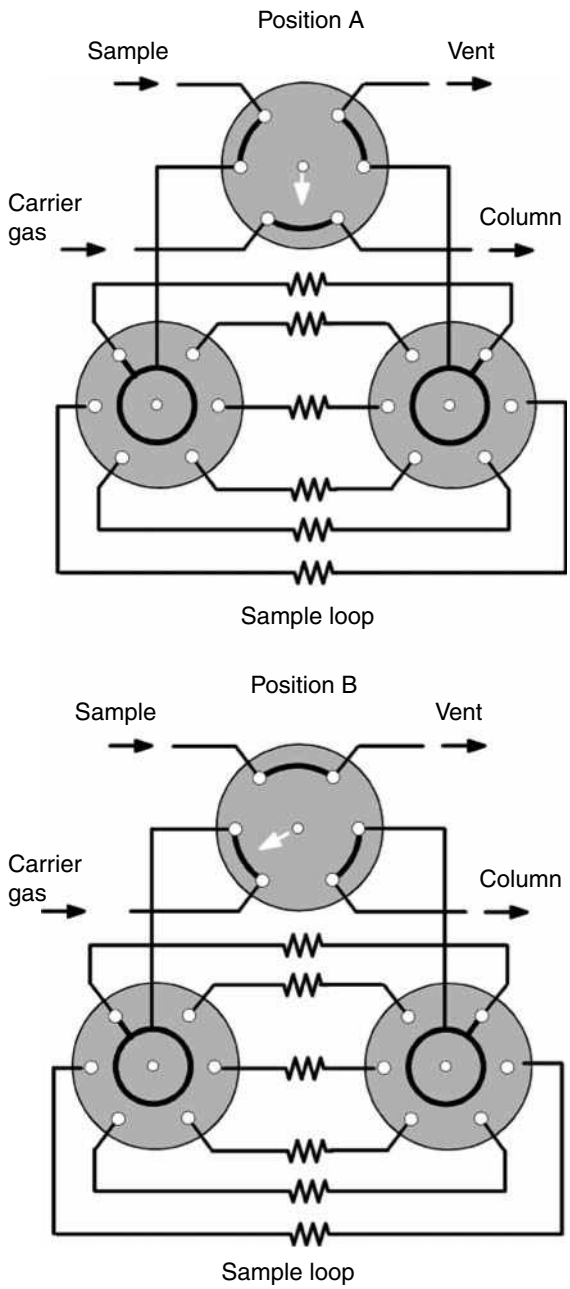

Fig. 11 Two-position, six-port valve with two distributing six-port valves with six sample loops, taking sample from one gas track.

adding the internal standard, is described.[8] It is a combination of a three-position, six-port valve and a chamber of changeable volume that acts as a sample loop (Fig. 10). The volume of a chamber is changed by a piston. In position A, the gas under analysis flows through the chamber and the carrier gas flows through the six-port valve. The switching of the valve rotor to position B results in injecting a sample of the gas under analysis from the chamber into a chromatographic column with carrier gas, and simultaneously, the gas under analysis flows through the valve. In position C, both the gas under analysis and carrier gas flow through the six-port valve and the chamber is disconnected. The internal standard can then be injected, using a syringe, into the sample taken and retained in the chamber with a syringe. The switching of the valve rotor to position B introduces the sample of the gas under analysis together with the internal standard into a chromatographic column.

Sets of Multiport Valves

The use of the above-mentioned multiport valves is limited because a subsequent sample can be injected into a column only after the previous sample has been analyzed. A solution to overcome this limitation and to take successive samples for analysis at shorter intervals is offered.[9]

The number of samples of gas was increased by replacing the sample loop in a two-position, six-port valve (as seen in Fig. 5) with two separate six-port valves combined by rotors with six sample loops (Fig. 11).

In position A (as seen in Fig. 11), the gas under analysis flows through the separating six-port valves and one of the six sample loops, and simultaneously, the carrier gas flows into a chromatographic column through the six-port valve. The switching of the rotors of the separating six-port valves to successive positions makes it possible to fill successive sample loops. When the rotor of the six-port valve is switched to position B, the sample placed in one of the sample loops is introduced into the stream of carrier gas. The switching of the rotors of the separating six-port valves to successive positions makes it possible to direct samples into a chromatographic column.

METHANIZER

A thermal conductivity detector cannot be used to detect low concentrations of carbon monoxide and carbon dioxide in gases because of its low sensitivity. These gases cannot be detected by a flame ionization detector. They can be analyzed by this detector after carbon monoxide and

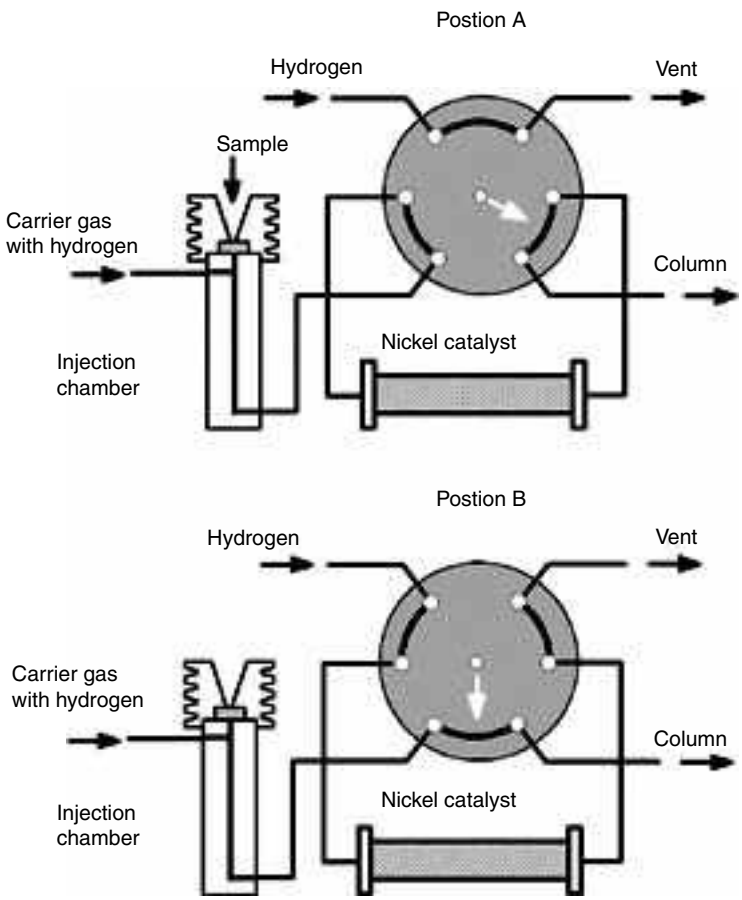

Fig. 12 Scheme of methanizer with six-port valve.

carbon dioxide are catalytically reduced with hydrogen to methane. The microreactors in which the catalytic reduction of carbon monoxide and carbon dioxide to methane occurs are called methanizers. A nickel catalyst in the atmosphere of hydrogen, heated to 350–400°C, is generally used for reduction in methanizers.

A methanizer for reducing carbon dioxide to methane with a catalyst obtained from $Ni(NO_3)_2 \cdot 6H_2O$ and SiO_2 is described.[10] The carrier gas containing hydrogen flows through the six-port valve to a microreactor containing a nickel catalyst (Fig. 12). In position A, a sample of gas containing carbon dioxide is injected into a methanizer, reduced on a nickel catalyst and injected into a chromatographic column. The switching of the six-port valve to position B makes a stream of pure hydrogen pass through the catalyst in the microreactor for its reduction.

REFERENCES

1. Bovijn, L.; Pirotte, J.; Berger, A. *Gas Chromatography*; Desty, D.H., Ed.; Butterworths: London, 1958; 310–320.
2. Arthur, C.L.; Chai, M.; Pawliszyn, J. Solventless injection technique for microcolumn separations. J. Microcol. **1993**, *5*, 51.
3. Arthur, C.L.; Killam, L.M.; Bucholz, K.D.; Pawliszyn, J. Analysis of dichlorobenzene in water by solid-phase microextraction. Anal. Chem. **1992**, *64*, 1960.
4. Guiochon, G.; Pommier, C. *La chromatographie en phase gazeuse en chimie inorganique*; Gauthier-Villars Editeur: Paris, 1971.
5. Witkiewicz, Z. *Podstawy chromatografii*; WNT: Warszawa, 2005.
6. Słomkiewicz, P.M. The Sample Injector for the Gas Chromatograph, Polish patent Pl 178,186, 24, February 2000.
7. Słomkiewicz, P.M. The Sample Injector for the Gas Chromatograph, Especially for High Pressure Samples. Polish patent Pl 177, 984, 18, February 2000.
8. Słomkiewicz, P.M. The Variable Volume Sample Injector with Six-port Valve for Gas Chromatograph. Polish patent Pl 177, 330, 5 November 1999.
9. VICI AG. In *Valco Catalog*; Valco International: Houston, TX, U.S.A., 1999.
10. Słomkiewicz, P.M. Injector for analysis the samples of carbon dioxide in the air with hydrogen reduction method. Works Stud. Inst. Environ. Eng. Polish Acad. Sci. **2000**, *53*, 201.

GC/MS Systems

Raymond P.W. Scott
Scientific Detectors Ltd., Banbury, Oxfordshire, U.K.

INTRODUCTION

Despite the speed and accuracy of contemporary analytical techniques, the use of more than one, separately and in sequence, is still very time-consuming. To reduce the analysis time, many techniques are operated concurrently, so that two or more analytical procedures can be carried out simultaneously. The tandem use of two different instruments can increase the analytical efficiency, but due to unpredictable interactions between one technique and the other, the combination can be quite difficult in practice. These difficulties become exacerbated if optimum performance is required from both instruments. The mass spectrometer was a natural choice for the early tandem systems to be developed with the gas chromatograph, as it could easily accept samples present as a vapor in a permanent gas.

BACKGROUND INFORMATION

The first GC/MS system was reported by Holmes and Morrell in 1957, only 4 years after the first description of GC by James and Martin in 1953. The column eluent was split and passed directly to the mass spectrometer. Initially, only packed GC columns were available and thus the major problem encountered was the disposal of the relatively high flow of carrier gas from the chromatograph (~25 ml/min or more). These high flow rates were in direct conflict with the relatively low pumping rate of the MS vacuum system. This problem was solved either by the use of an eluent split system or by employing a vapor concentrator. A number of concentrating devices were developed (e.g., the jet concentrator invented by Ryhage and the helium diffuser developed by Biemann).

The jet concentrator consisted of a succession of jets that were aligned in series but separated from each other by carefully adjusted gaps. The helium diffused away in the gap between the jets and was removed by appropriate vacuum pumps. In contrast, the solute vapor, having greater momentum, continued into the next jet and, finally, into the mass spectrometer. The concentration factor was about an order of magnitude and the sample recovery could be in excess of 25%.

The Biemann concentrator consisted of a heated glass jacket surrounding a sintered glass tube. The eluent from the chromatograph passed directly through the sintered glass tube and the helium diffused radially through the porous walls and was continuously pumped away. The helium stream enriched with solute vapor passed into the mass spectrometer. Solute concentration and sample recovery were similar to the Ryhage device, but the apparatus was bulkier although somewhat easier to operate. An alternative system employed a length of porous polytetrafluorethylene (PTFE) tube, as opposed to one of sintered glass, but otherwise functioned in the same manner.

The introduction of the open-tubular columns eliminated the need for concentrating devices as the mass spectrometer pumping system could cope with the entire column eluent. Consequently, the column eluent could be passed directly into the mass spectrometer and the total sample can enter the ionization source. The first mass spectrometer used in a gas chromatography GC/MS mass Spectrometry tandem system was a rapid-scanning magnetic sector instrument that easily provided a resolution of one mass unit. Contemporary mass spectrometers have vastly improved resolution and the most advanced system (involving the triple quadrupole mass spectrometer) gives high in-line sensitivity, selectivity, and resolution.

IONIZATION TECHNIQUES FOR GC/MS

There are a number of ionization processes that are used, probably the most important being electron-impact ionization. Electron-impact ionization is a harsh method of ionization and produces a range of molecular fragments that can help to elucidate the structure of the molecule. Nevertheless, although molecular ions are usually produced that are important for structure elucidation, sometimes only small fragments of the molecule are observed, with no molecular ion invoking the use of alternative ionizing procedures. A diagram showing the configuration of an electron-impact ion source is shown in Fig. 1. Electrons, generated by a heated filament, pass across the ion source to an anode trap. The sample vapor is introduced in the center of the source and the solute molecules drift, by diffusion, into the path of the electron beam. Collision with the electrons produce molecular ions and ionized molecular fragments, the size of which is determined by the energy of the electrons. The electrons are generated by thermal emission from a heated tungsten or rhenium filament and accelerated by an appropriate potential to the anode trap. The magnitude of the collection potential may range from 5 to 100 V, depending on the electrode geometry and the

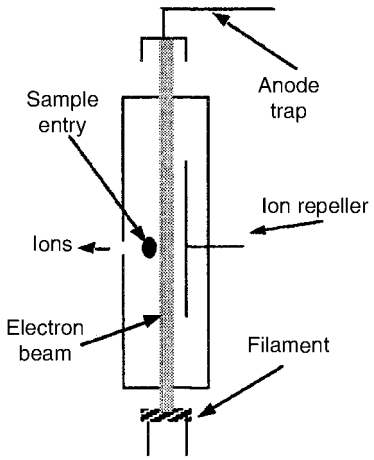

Fig. 1 An electron-impact ionization source.

ionization potential of the substances being ionized. The ions that are produced are driven by a potential applied to the ion-repeller electrode into the accelerating region of the mass spectrometer.

Unfortunately, with electron-impact ionization, there is a frequent absence of a molecular ion in the mass spectrum, which makes identification uncertain and complicates structure elucidation. One solution is to employ chemical ionization. If an excess of an appropriate reagent gas is fed into an electron-impact source, an entirely different type of ionization takes place. As the reagent gas is in excess, the reagent molecules are preferentially ionized and the reagent ions then collide with the sample molecules and produce sample + reagent ions or, in some cases, protonated ions. In this type of ionization, very little fragmentation takes place and parent ions + a proton or + a molecule of the reagent gas are produced. Little modification to the normal electron impact source is required and an additional conduit to supply the reagent gas is all that is necessary.

Chemical ionization was first observed by Munson and Field, who introduced it as an ionization procedure in 1966. A common reagent gas is methane and the partial pressure of the reagent gas is arranged to be about two orders of magnitude greater than that of the sample. The process is gentle and the energy of the most reactive reagent ions never exceeds 5 eV. Consequently, there is little fragmentation, and the most abundant ion usually has a *m*/*z* value close to that of the singly-charged molecular ion. The spectrum produced depends strongly on the nature of the reagent ion; thus, different structural information can be obtained by choosing different reagent gases. This adds another degree of freedom in the operation of the mass spectrometer. Using methane as the reagent ion, the following reagent ions can be produced:

$$CH_4 \rightarrow CH_4^+, CH_3, CH_2^+$$
$$CH_4^+ + CH_4 \rightarrow CH_5^+ + CH_3$$
$$CH_3^+ + CH_4 \rightarrow C_2H_4^+ + H_2$$

Other reactions can occur that are not useful for ionization but, in general, these are in the minority. The interaction of positively charged ions with the uncharged sample molecules can also occur in a number of ways, and the four most common are as follows:

1. Proton transfer between the sample molecule and the reagent ion

   $$M + BH^+ \rightarrow MH^+ + B$$

2. Exchange of charge between the sample molecule and the reagent ion

   $$M + X^+ \rightarrow M^+ + X$$

3. Simple addition of the sample molecule to the reagent ion

   $$M + X^+ \rightarrow MX^+$$

4. Anion extraction

   $$AB + X^+ \rightarrow B^+ + AX$$

As an example, ions, which are formed when methane is used as the reagent gas, will react with a sample molecule largely by proton transfer; that is,

$$M + CH_5^+ \rightarrow MX^+ + CH_4$$

Some reagent gases produce more reactive ions than others and will produce more fragmentation. For example, methane produces more aggressive reagent ions than isobutane. Consequently, whereas methane ions produce a number of fragments by protonation, isobutane, by a similar protonation process, will produce almost exclusively the protonated molecular ion. This is shown in the mass spectra of methyl stearate in Fig. 2. Spectrum (a) was produced using methane as the reagent gas and exhibits fragments other than the protonated parent ion. In contrast, spectrum b obtained with butane as the reagent gas, exhibits the protonated molecular ion only. Continuous use of a chemical ionization source causes significant source contamination, which impairs the performance of the spectrometer and thus the source requires cleaning by baking-out fairly frequently. Retention data on two-phase systems coupled with matching electron-impact mass spectra or confirmation of the molecular weight from chemical ionization spectra are usually sufficient to establish the identity of a solute.

The inductively coupled plasma (ICP) source is used largely for specific element identification and evolved from the ICP atomic emission spectrometer; it is probably more commonly employed in LC/MS than GC/MS. In GC/MS, the ICP ion source is used in the assay of

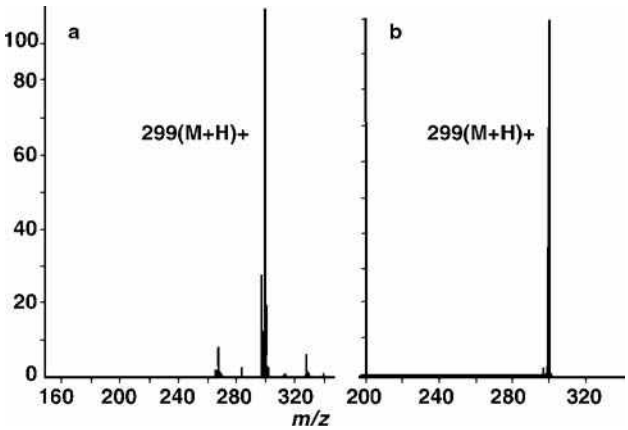

Fig. 2 Mass spectrum of methyl stearate produced by chemical ionization.

organometallic materials and in metal speciation analyses. The ICP ion source is very similar to the volatilizing unit of the ICP atomic emission spectrometer, and a diagram of the device is shown in Fig. 3. The argon plasma is an electrodeless discharge, often initiated by a Tesla coil spark, and maintained by radio-frequency (rf) energy, inductively coupled to the inside of the torch by an external coil, wrapped around the torch stem.The plasma is maintained at atmospheric pressure and at an average temperature of about 8000 K. The ICP torch consists of three concentric tubes made from fused silica. The center tube carries the nebulizing gas, or the column eluent, from the gas chromatograph. Argon is used as the carrier gas, and the next tube carries an auxiliary supply of argon to help maintain the plasma and also to prevent the hot plasma from reaching the tip of the sample inlet tube. The outer tube also carries another supply of argon at a very high flow rate that cools the two inner tubes and prevents them from melting at the plasma temperature. The coupling coil

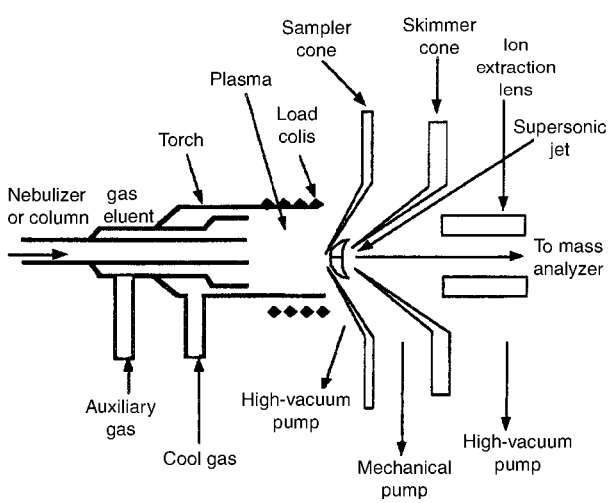

Fig. 3 ICP mass spectrometer ion source.

consists of two to four turns of water cooled copper tubing, situated a few millimeters behind the mouth of the torch. The rf generator produces about 1300 W of rf at 27 or 40 MHz, which induces a fluctuating magnetic field along the axis of the torch. Temperature in the induction region of the torch can reach 10,000 K, but in the ionizing region, close to the mouth of the sample tube, the temperature is 7000–9000 K.

The sample atoms account for less than of the total number of atoms present in the plasma region; thus, there is little or no self-quenching. At the plasma temperature, over 50% of most elements are ionized. The ions, once formed, pass through the apertures in the apex of two cones. The first has an aperture about 1 mm inner diameter (I.D.) and ions pass through it to the second skimmer cone. The space in front of the first cone is evacuated by a high-vacuum pump. The region between the first cone and the second skimmer cone is evacuated by a mechanical pump to about 2 mbar and, as the sample expands into this region, a supersonic jet is formed. This jet of gas and ions flows through a slightly smaller orifice into the apex of the second cone. The emerging ions are extracted by negatively charged electrodes (−100 to −600 V) into the focusing region of the spectrometer, and then into the mass analyzer.

The ICP ion source has the advantages that the sample is introduced at atmospheric pressure, the degree of ionization is relatively uniform for all elements, and singly-charged ions are the principal ion product. Furthermore, sample dissociation is extremely efficient and few, if any, molecular fragments of the original sample remain to pass into the mass spectrometer. High ion populations of trace components in the sample are produced, making the system extremely sensitive. Nevertheless, there are some disadvantages: the high gas temperature and pressure evoke an interface design that is not very efficient and only about 1% of the ions that pass the sample orifice pass through the skimmer orifice. Furthermore, some molecular ion formation does occur in the plasma, the most troublesome being molecular ions formed with oxygen. These can only be reduced by adjusting the position of the cones, so that only those portions of the plasma where the oxygen population is low are sampled.

Although the detection limit of an ICP/MS is about 1 part in a trillion, as already stated, the device is rather inefficient in the transport of the ions from the plasma to the analyzer. Only about 1% pass through the sample and skimming cones and only about 10^{-6} ions will eventually reach the detector. One reason for ion loss is the diverging nature of the beam, but a second is due to space-charge effects, which, in simple terms, is the mutual repulsion of the positive ions away from each other. Mutual ion repulsion could also be responsible for some non-spectroscopic interelement interference (i.e., matrix effects). The heavier ions having greater momentum suffer less dispersion than

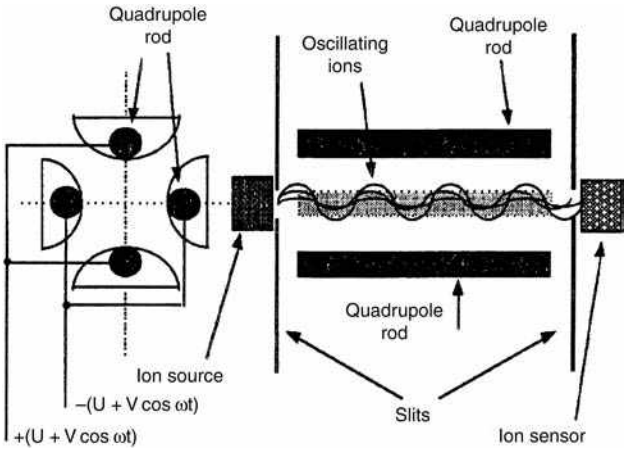

Fig. 4 Quadrupole mass spectrometer.

the lighter elements, thus causing a preferential loss of the lighter elements.

MASS SPECTROMETERS FOR MS/GC TANDEM OPERATION

The most common mass spectrometer used in GC/MS systems is the quadrupole mass spectrometer, either as a single quadrupole or as a triple quadrupole, which can also provide MS/MS spectra. A diagram of a quadrupole mass spectrometer is shown in Fig. 4. The operation of the quadrupole mass spectrometer is quite different from that of the sector instrument. The instrument consists of four rods which must be precisely straight and parallel and so arranged that the beam of ions is directed axially between them. Theoretically, the rods should have a hyperbolic cross section, but in practice, less expensive cylindrical rods are nearly as satisfactory. A voltage comprising a DC component (U) and a rf component (V_0 cos wt) is applied between adjacent rods, opposite rods being electrically connected. Ions are accelerated into the center, between the rods, by a potential ranging from 10 to 20 V. Once inside the quadrupole, the ions oscillate in the x and y dimensions induced by the high-frequency electric field. The mass range is scanned by changing U and V_0 while keeping the ratio U/V_0 constant. The quadrupole mass spectrometer is compact, rugged, and easy to operate, but its mass range does not extend to very high values. However, under certain circumstances, multiply-charged ions can be generated and identified by the mass spectrometer. This, in effect, increases the mass range of the device proportionally to the number of charges on the ion.

The quadrupole mass spectrometer can also be constructed to provide MS/MS spectra by combining three quadrupole units in series. A diagram of a triple quadrupole mass spectrometer is shown in Fig. 5. The sample enters

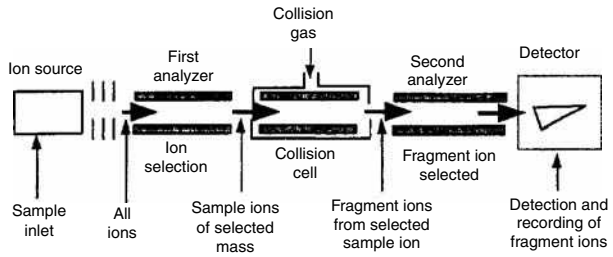

Fig. 5 Triple quadrupole mass spectrometer.

the ion source and is usually fragmented by either an electron-impact or chemical ionization process. In the first analyzer, the various charged fragments are separated in the usual way, which then pass into the second quadrupole section, sometimes called the collision cell. The first quadrupole behaves as a straightforward mass spectrometer. Instead of the ions passing to a sensor, the ions pass into a second mass spectrometer and a specific ion can be selected for further study. In the center quadrupole section, the selected ion is further fragmented by collision ionization and the new fragments pass into the third quadrupole, which functions as a second analyzer. The second analyzer resolves the new fragments into their individual masses producing the mass spectrum. Thus, the exclusive mass spectrum of a particular molecular or fragment ion can be obtained from the myriad of ions that may be produced from the sample in the first analyzer. This is an extremely powerful analytical system that can handle exceedingly complex mixtures and very involved molecular structures.

Another form of the quadrupole mass spectrometer is the ion trap detector, which has been designed more specifically as a chromatography detector than for use as a tandem instrument. The electrode orientation of the quadrupole ion trap mass spectrometer is shown in Fig. 6. The ion trap mass spectrometer has an electrode arrangement that consists of three cylindrically symmetrical electrodes comprised of two end caps and a ring. The device is small, the opposite internal electrode faces being only 2 cm apart. Each electrode has accurately machined hyperbolic internal faces. An rf voltage together with an additional DC voltage is applied to the ring, and the end caps are grounded. The rf voltage causes rapid reversals of field direction, so any ions are alternately accelerated and decelerated in the axial direction and vice versa in the radial direction. At a given voltage, ions of a specific mass range are held oscillating in the trap. Initially, the electron beam is used to produce ions, and after a given time, the beam is turned off. All the ions, except those selected by the magnitude of the applied rf voltage, are lost to the walls of the trap, and the remainder continue oscillating in the trap. The potential of the applied rf voltage is then increased, and the ions sequentially assume unstable trajectories and

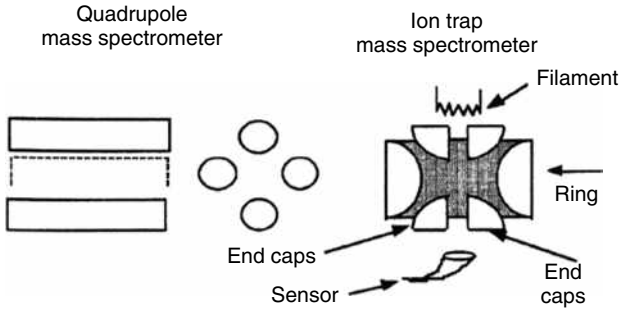

Fig. 6 Pole arrangement for the quadrupole and ion trap mass spectrometers.

leave the trap via the aperture to the sensor. The ions exit the trap in order of their increasing m/z values. The first ion trap mass spectrometers were not very efficient, but it was found that the introduction of traces of helium to the ion trap significantly improved the quality of the spectra. The improvement appeared to result from ion-helium collisions that reduced the energy of the ions and allow them to concentrate in the center of the trap. The spectra produced are quite satisfactory for solute identification by comparison with reference spectra. However, the spectrum produced for a given substance will probably differ considerably from that produced by the normal quadrupole mass spectrometer.

The time-of-flight mass spectrometer was invented many years ago, but the performance of the modern version is greatly improved. A diagram of the time-of-flight mass spectrometer is shown in Fig. 7. In a time-of-flight mass spectrometer, the following relationship holds:

$$t = \left(\frac{m}{2zeV}\right)^{1/2} L$$

where t is the time taken for the ion to travel a distance L, V is the accelerating voltage applied to the ion, and L is the distance traveled by the ion to the ion sensor.

The mass of the ion is directly proportional to the square of the transit time to the sensor. The sample is volatilized into the space between the first and second electrodes and a microsecond burst of electrons is allowed to produce ions. An extraction voltage is then applied for another short time period, which, as those further from the second electrode will experience a greater force than those closer to the second electrode, will focus the ions. After focusing, the accelerating potential (V) is applied for about 100 ns so that all the ions in the source are accelerated almost simultaneously. The ions then pass through the third electrode into the drift zone and are then collected by the sensor electrode. The particular advantage of the time-of-flight mass spectrometer is that it is directly compatible with surface desorption procedures. Consequently, it can be employed with laser-desorption and plasmadesorption techniques.

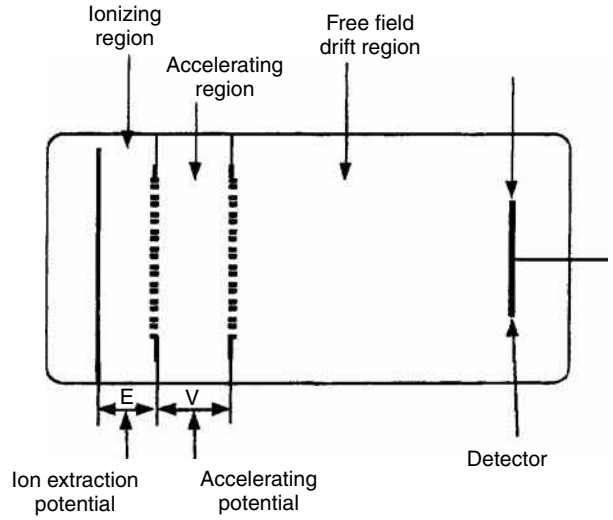

Fig. 7 The time-of-flight mass spectrometer.
Source: Courtesy of VG Organic Inc.

An excellent discussion on general organic mass spectrometry is given in *Practical Organic Mass Spectrometry* edited by Chapman.[1]

The combination of the gas chromatograph with the single quadrupole mass spectrometer or with the triple quadrupole mass spectrometer are the most commonly used tandem systems. They are used extensively in forensic chemistry, in pollution monitoring and control, and in metabolism studies. The quadrupole mass spectrometers provide both high sensitivity and good mass spectrometric resolution. They can be readily used with open-tubular columns, and an example of the use of the single quadrupole monitoring a separation from an open-tubular column is shown in Fig. 8. The column was 30 m long with a 0.25 mm I.D. and carried a 0.5 mm film of stationary

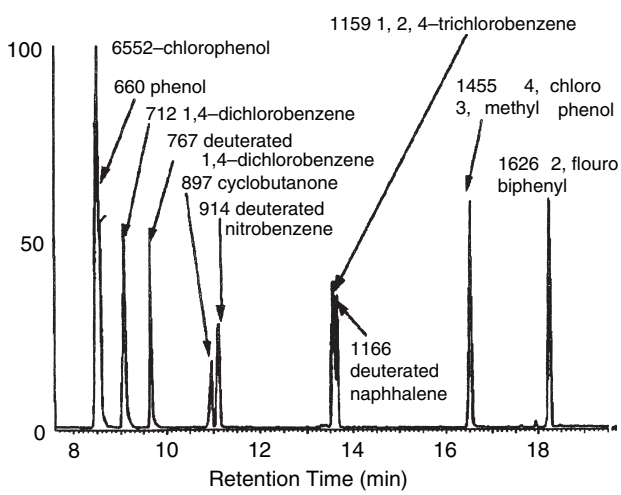

Fig. 8 A separation from an open-tubular column monitored by a single quadrupole mass spectrometer.

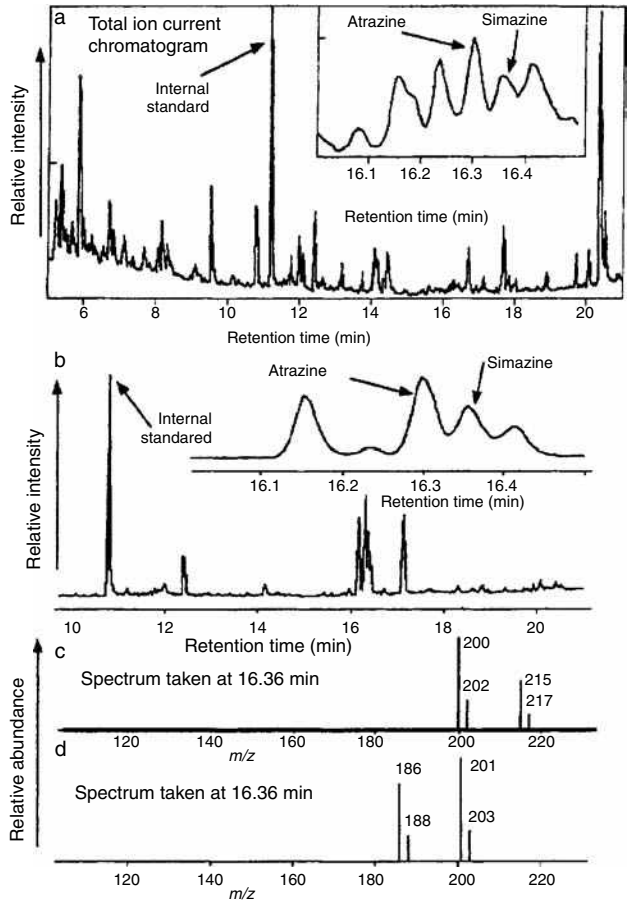

Fig. 9 Chromatogram and spectra from a sample of river water containing 200 ppt of atrazine and simazine.
Source: From On-line preconcentration of aqueous samples for gas chromatographic – mass spectrometric analysis, in Analyst.[2]

phase.A 1 ml sample was used and the column was programmed from 50°C to 300°C at 10°C/min.

An elegant example of the use of GC/MS in the analysis of pesticides in river water is given by Vreuls et al.[2] A 1-ml sample was collected in an LC sample loop and the internal standard added. The sample was then displaced through a short column 1 cm long with a 2 mm I.D. packed with 10 mm particles of a proprietary PLRP-S adsorbent (styrene–divinylbenzene copolymer) by a stream of pure water.The extraction column was then dried with nitrogen and the adsorbed materials displaced into a gas chromatograph with 180 ml of ethyl acetate. The sample was passed through a short retention gap column and then to a retaining column. The GC oven was maintained at 70°C so that the ethyl acetate passed through the retaining column and was vented to waste.The solutes of interest were held in the retaining column at this temperature during the removal of the ethyl acetate. The temperature was then increased and the residual material separated on an analytical column using an appropriate temperature program. The eluents from the analytical column passed to a quadrupole mass spectrometer. An example of the chromatograms and spectra obtained are shown in Fig. 9. Fig. 9a shows the total ion current chromatogram from a sample of Rhine River water containing 200 ppt of the herbicides atrazine and simazine. The pertinent peaks are shown enlarged in the inset. Fig. 9b shows a section of the same chromatogram presented in the selected ion mode. It is seen that the herbicide peaks are clearly and unambiguously revealed. In Fig. 9c and d, the individual mass spectra of atrazine (eluted at 16.30 min) and simazine (eluted at 16.36 min) are shown. The spectra are clear and more than adequate to confirm the identity of the two herbicides.

REFERENCES

1. Chapman, J.R., Ed.; *Practical Organic Mass Spectrometry*; John Wiley & Sons: New York, 1994.
2. Vreuls, J.J.; Bulterman, A.-J.; Ghijsen, R.T.; Brinkman, U.Th. On-line preconcentration of aqueous samples for gas chromatographic—mass spectrometric analysis. Analyst **1992**, *117* (11), 1701.

BIBLIOGRAPHY

1. Message, G.M. *Practical Aspects of GC/MS*; John Wiley & Sons: New York, 1984.
2. Scott, R.P.W. *Tandem Techniques*; John Wiley & Sons: New York, 1984.

GC: Fourier Transform Infrared Spectroscopy

Hui-Ru Dong
Peng-Yu Bi
College of Science, Beijing University of Chemical Technology, Beijing, China

INTRODUCTION

The combination of gas chromatography (GC) with Fourier transform infrared spectroscopy (FTIR) has gradually become the important analytical tool for qualitative and quantitative analysis of complex mixtures. Numerous applications have been reported in previous reviews.[1–3] Separation and identification of components in complex mixtures can be a daunting task. GC is the most common technique for separation of volatile and semivolatile mixtures. It is well accepted that when GC is coupled with spectral detection methods, such as MS, NMR, or FTIR spectrometry, the resulting combination is a powerful tool for the analysis of complex mixtures.

FTIR spectroscopy, used as a detector in GC, has many advantages. First, FTIR is the most universal of all detectors currently used in GC, because all organic compounds exhibit IR-active vibrations and, thus, absorb IR radiation. Moreover, these absorptions obey Beer's law so that the data can be used directly for quantification. Furthermore, FTIR can be used both as a selective and as a specific detector. Finally, the non-destructive character of GC/FTIR is an important advantage when compared with other detectors; it offers the opportunity to investigate GC eluates after FTIR analysis. However, despite these advantages, FTIR detection is not widely applied in GC analysis at present. This is, particularly, due to its lack of sensitivity; a second reason is the complexity of IR spectra. Yet, the power of GC/FTIR is the unique structural information that can be extracted from the spectral data and that cannot be obtained from any other method. It is, therefore, very likely that, in the next few years, this technique will attract much closer attention from analytical chemists.

Although GC/IR was first introduced in the 1960s, its use did not become widespread until the 1980s. Several factors were responsible for its application in GC analysis. That is, particularly, due to its lack of sensitivity and the interfaces.

INTERFACES

In GC/FTIR systems, three types of FTIR interfaces are currently in use: light pipe, matrix isolation (MI), and direct deposition (DD, also called cryotrapping or cryofocusing).

The light-pipe interface is the simplest design; it comprises a thin glass tube with IR-transparent windows at both ends. The entrance of the light pipe is connected to the end of the GC column by a heated transfer line. Cell and transfer line are operated at, typically, 300°C to prevent condensation. The cell is internally gold-coated to accomplish maximum light throughput. The dimensions are of the order of 0.3–1 mm in internal diameter (I.D.) and 5–10 cm in length to achieve a cell volume that matches the average peak volume of capillary-GC columns. Spectra obtained with a light-pipe interface are very similar to vapor-phase spectra. Therefore, spectra can be easily searched against commercially available collections of vapor-phase reference spectra.

DD-FTIR and MI-FTIR are very similar in that the sample is cryogenically frozen on a surface for FTIR analysis. The major difference between the two is that in the DD-FTIR interface, the surface is an IR-transparent window, usually ZnSe. GC effluent is deposited onto this window and absorption spectra are subsequently acquired. The DD technique is based on crystallization of the separated species on a moving IR-transparent window at liquid-nitrogen temperature (80 K). In a DD interface, the transfer line from the GC column is connected to an orifice (75–100 μm I.D.) that acts as a restrictor. The tip of the restrictor is located about 30 μm above the surface of the window, and eluates that leave the tip are immediately crystallized as a trace of about 100 μm wide. The window slowly moves in such a way that the immobilized spots pass through the external beam of an IR spectrometer a few seconds after deposition, thus providing chromatograms and spectra recorded on the fly. A major advantage of this interface is that the spectra are very much like conventionally recorded (KBr) spectra of solids and, herefore, can be compared with those in standard computer-readable KBr spectra, which are much larger than those available for both light–pipe- and MI-FTIR.

The MI technique is also based on cold-trapping of the GC eluates, but differs from DD in the addition of 1–2% of an inert matrix gas (typically argon) to the carrier gas. The effluent stream is sprayed onto the surface of a slowly rotating, gold-coated drum at a temperature of about

Table 1 Characteristics of various GC/FTIR interfaces.

Feature	Light-pipe	Direct deposition	Matrix isolation
Detection type	Online	At-line	At-line
Hardware	Accessory and stand-alone	Accessory	Stand-alone
Average LOD (ng)	10	0.1	0.3
Data acquisition	On-the-fly	On-the-fly and post-run	Post-run
Storage capacity	Infinite	50–100 hr	60 hr
Spectrum characteristics	Vapor phase	KBr-pellet like	Peak sharpening
Library search collections	Commercially available	Commercially available	Not available (home-made)

Source: From FT-IR detection in gas chromatography, in Trends Anal. Chem.[1]

10 K, and, in this way, the analytes are frozen into a cage of argon molecules, i.e., "matrix-isolated." The diameter of the spots is a little larger than that obtained with the DD technique, i.e., 200–300 μm. Matrix-isolated spectra maydiffer from spectra that have been recorded with conventional methods. In particular, relatively small molecules (MW $<$ 200) may exhibit considerable band-narrowing effects. As a consequence, identification of GC/MI-FTIR spectra demands special reference collections.

To prevent interfering crystallization of carbon dioxide and water vapor from the atmosphere, both DD and MI cold-trapping techniques require a high vacuum and a leak-tight interface housing.

Comparison studies of the different interfaces have been reported,[1,4] and the most important characteristics of different types of GC/FTIR interfaces are summarized in Table 1.

SENSITIVITY

The sensitivity of a GC/FTIR system depends on the type of interface and the molar absorbance index of the analyte. Comparative studies of the three interfaces have shown that the highest sensitivity is achieved with the DD interface. In general, the limit of detection (LOD) of the light-pipe GC/FTIR is about 10 ng on-column, while, the LODs of the DD/FTIR and MI/FTIR are 35 and 100 pg, respectively. In practice, the LODs of analytes in real samples are of the order of 0.5–25 ng on-column. To enhance the sensitivity of detection, additional clean-up and preconcentration methods are applied, such as headspace sampling, purge and trap, solid-phase extraction, and solid-phase micro-extraction. It would also be possible to achieve improved sensitivity by modifications of other parts of the analytical procedure, such as the use of large-volume sampling methods.

Heaps and Griffiths[5] have shown how the smallest quantity of molecules injected into a GC for which an identifiable infrared spectrum can be measured online has been reduced by a factor of 10 below the detection limit of the most sensitive current technique. In this entry, a commercial direct deposition interface between a GC and an FTIR spectrometer was modified by vapor-depositing an island film of silver on the surface of the ZnSe substrate; it can reduce the detection limit of the GC/FTIR interface to the point that it becomes comparable to those of GC/MS. Coating the ZnSe substrate that is used for GC/DD-FTIR measurements leads to a reduction in the limit at which molecules eluting from a GC can be identified in comparison with any other GC/FTIR technique.

Norton and Griffiths[4] studied the comparison of flow-cell and DD interfaces between GC and FTIR spectrometers. Seven barbiturates were separated on fused-silica GC capillary columns. Infrared spectra of the separated barbiturates were measured in real time by either a Hewlett-Packard infrared detector (flow-cell) interface or a Digilab Division of Bio-Rad Tracer (DD) interface. Without losing chromatographic resolution, the GC/DD-FTIR interface gave both detection limits and minimum identifiable quantities nearly two orders of magnitude lower than the flow-cell GC/FTIR interface.

Hankemeier et al.,[6] studied large-volume injection combined with GC/DD-FTIR. A loop-type injection interface was chosen because of its rather simple optimization. Large-volume injection by means of a loop-type interface can be carried out successfully in conjunction with GC/DD-FTIR. The hyphenation permits enhanced detectability of analytes by about two orders of magnitude when compared with conventional split/splitless ones. As demonstrated, the determination and identification of PAHs in river water is possible down to a level of 0.5 μg/L, even when using simple "micro" liquid–liquid extraction as a sample preparation technique. The present system may, therefore, be considered a viable approach to trace-level environmental analysis.

Auger et al.,[7] reported that GC/DD-FTIR permits coupling of GC to FTIR at a level of sensitivity of routine GC/MS coupling, but the presence of ice resulting from living organisms limits the usefulness of the system. Headspace solid-phase micro-extraction (SPME) coupled to GC/DD-FTIR leads to a rigorous absence of water and can be applied to unknown volatiles trapped in situ in combination with SPME–GC/MS. Coupling of SPME to

GC-IR can permit the development of a GC/DD-FTIR interface to-date limited by its water sensitivity. As SPME is a rapid sampling device and permits a significant reduction of the duration of GC analysis (solvent-free), SPME–GC is especially interesting for living organisms. For instance, the sensitivity of SPME–GC/DD-FTIR allows one to follow the kinetics of pheromonal emission of an individual insect "on-line."

APPLICATIONS

Analysis of Environmental Samples

The separation and characterization of environmental pollutants in aqueous samples is a demanding task. The concentration of contaminants is usually very low (typical < 10 μg/L) and the matrices may be complex. GC is necessary for analyte separation while, in most cases, IR is very suitable for this purpose because of its unique molecular fingerprinting properties. Applications of GC/FTIR are found in a wide variety of analytical fields. Most applications have been reported on the analysis of environmental samples. A representative example of what can be achieved nowadays is the identification of pesticides in water samples at the European alert and alarm levels of 0.1–1 ng/ml, as described by Hankemeier et al.,[8]

Visser et al.,[9] have developed an on-column interface to introduce large sample volume for GC/FTIR analysis and utilized it for trace analysis of environmental contaminants.

The feasibility of the technique is demonstrated by the identification of pesticides in water at a level of 0.5 μg/L using online desorption of presampled solid-phase extracted cartridges. The applicability of GC/FTIR to environmental trace analysis is largely enhanced by modification and optimization of chromatography and interfacing. Improvement of the detectability of analytes in terms of concentration by two to three orders of magnitude to the low μg/L level can be achieved by incorporation of trace-enrichment techniques. On-column interfacing LVI-GC with cryotrapping IR detection offers a selective method for monitoring and identifying contaminants in drinking water, particularly when used in conjunction with online desorption of presampled SPE cartridges.

Rodríguez et al.,[10] described a procedure for the identification and determination of structural isomers of polychlorinated phenols in drinking water. First, their acetylation and concentration on graphitized carbon cartridges were carried out. Detection is accomplished by GC/FTIR using a DD interface. In this way, it is possible to accurately identify and differentiate variably substituted isomers of chlorophenols, which is very difficult or even impossible to do by means of the widely used GC/MS instrumentation. The GC/DD-FTIR technique permits the differentiation of structural isomers of chlorophenols present in drinking water samples in quantities below the levels permitted by legislation (0.5 ng/ml). The most serious problem of the GC/DD-FTIR coupling is the presence of water as an interfering agent in the spectra; any trace of water reaching the interface is deposited as ice onto the ZnSe plate, thus interfering with the IR spectra of the analytes. This problem can be easily overcome by assuring leak-tight connections using metal ferrules.

Identification of Pharmaceutical Samples

Unequivocal identification is also very important in the analysis of forensic and pharmaceutical samples. The utility of GC/FTIR for this purpose has been widely demonstrated. Examples are the identification of drugs of abuse, such as amphetamines. Amphetamine (β-phenylisopropylamine) is the basic molecule of the amphetamines, a group of structurally related compounds with stimulating and mood-modifying properties. Despite overwhelming evidence of their dangerous effects, amphetamines remain significant drugs of abuse and addiction. So-called designer drugs are widespread drugs of abuse among recreational drug users. Therefore, many of these phenethylamines have become controlled substances. Unambiguous identification of these amphetamines is essential for the successful prosecution of these designer drug cases in a court of law. Although GC/MS spectra often yield complementary information for structure elucidation, identification of underivatized amphetamines with GC/MS alone can be difficult, owing to the very similar mass spectral fragmentation patterns of the analogues. GC/FTIR, however, is the most powerful hyphenated technique in the fingerprinting of isomeric structures and the identification of functional groups.

Dirinck et al.,[11] successfully applied GC/FTIR to the analysis of amphetamine-like compounds in judiciary exhibits. With light-pipe GC/FTIR, unique vapor-phase infrared spectra were generated, allowing the unambiguous differentiation between closely related amphetamines. The obtained vapor-phase spectra were submitted to a spectral search on a laboratory-made vapor-phase FTIR library. Several amphetamine analogues have been identified in confiscated powders and tablets using this approach.

Analysis of Food Samples

Important benefits of GC/FTIR are also found in the food industry. Compounds from natural origin, such as terpenes, isomeric sugars, and conjugated unsaturated oils, are difficult to identify by GC/MS alone, and additional GC/FTIR data appear to be very helpful in these cases. The unraveling of the molecular structures of flavors and fragrances present in, for instance, cherimoya fruit and strawberries, are largely based on the results obtained by light-pipe GC/FTIR.

The determination of the *cis*/*trans* geometry of the double bonds in natural oils is another example from the food

industry, although it is also important from the medical point of view. Knowledge of the *cis*/*trans* configuration is relevant, since the *trans*-conjugated, unsaturated fatty acids are believed to contribute to the prevention of heart attacks and cancer. Mossoba[12] studies of the determination of *cis*/*trans* double bonds were carried out by GC/DD-FTIR, and anticancer activity has been correlated with structural properties.

GC/FTIR data have also contributed to the structure elucidation of other compounds of biological origin, such as mycotoxins, which are formed by fungal activity in food products under specific environmental conditions of moisture, temperature, and host. Trichothecene mycotoxins, secondary fungal metabolites produced by species of mold, are a natural contaminant of feedstuffs and food. Because they can be toxic to humans and animals, their detection is important. Sehat et al.,[13] utilized GC/MI-FTIR and GC/MS to analyze grains for these contaminants.

The analysis of carbohydrates continues to be of considerable importance in the biological sciences. The diversity of structure and function of carbohydrates in organisms contributes to the difficulty of analysis of these materials. There exist a number of techniques for the analysis of carbohydrates, but no single technique has universal applicability. For the identification of carbohydrates, trimethylsilyl ethers are widely used in GC/MS. Veness and Evans[14] showed that GC/FTIR can also be used, with some advantages, for this purpose. A selection of 42 monosaccharides and related compounds were examined and, in each case, unique spectra were obtained for the differing compounds and their isomeric forms, allowing unambiguous identification. These results indicate that GC/FTIR of trimethylsilyl ethers of monosaccharides is a useful analytical technique for their identification. The resultant spectra are unique, easy to interpret, and stereoisomeric forms are readily differentiated.

Structural Analysis of Samples

As mentioned above, GC/FTIR is very useful for structural analysis; it may provide essential structural information for analytes, but the technique lacks the sensitivity needed to become competitive with GC/MS. In terms of data interpretation, however, IR spectra are more discriminative and provide greater confidence in identification than mass spectra. These properties make GC/FTIR a powerful tool for the discrimination of isomers and the identification of compounds with closely related structures, particularly in combination with GC/MS.

Wachholz et al.,[15] analyzed a mixture of linear and cyclic methylsiloxanes to characterize the different types of siloxane structures using GC/DD-FTIR. The main structural units are $(CH_3)_3SiO_{1/2}$, $(CH_3)_2SiO$, and $(CH_3)SiO_{3/2}$; GC–MS may provide molecular mass information, but it is not able to identify isomeric structures. Coupling GC with FTIR enables the determination of group frequencies to assign specific structures. Thus, combination of GC with MS and FTIR may be used in elucidating complex cyclosiloxane compounds.

Many natural products, particularly terpenes, bear vinyl groups conjugated to carbon–carbon double bonds. A number of these vinyl compounds are either disubstituted 1,3-butadienes with a methyl group (designated as α-type, 1, 2) or mono-substituted 1,3-butadienes (β-type, 3) with a large substituent group attached to the C-3 atom. Although ^{1}H NMR spectroscopy can be used to characterize these carbon skeletons, relatively large sample amounts (10–100 μg) in nearly pure form are required. Frequently, natural product chemists are frustrated by the unavailability of large samples. But, they can be characterized by GC/FTIR. Svatoš and Attygalle[16] have demonstrated that GC/FTIR data allow definitive deductions to be made about the stereochemistry of carbon–carbon double bonds conjugated to a vinyl group.

Yashitake and Furukawa[17] investigated the thermal degradation mechanism of α,γ-diphenyl alkyl allophanates and carbanilates as model compounds for crosslinking sites in polyurethane networks by pyrolysis-high-resolution GC/FTIR (Py-HR GC/FTIR). Pyrolysis was performed at 250°C, 350°C, 450°C, and 500°C.

Py-HRGC using a 25 ml capillary column coated with silicone OV-1 followed by FTIR was carried out. The products were identified by use of a reference system attached to the FTIR apparatus.

The primary degradation reaction was dissociation of allophanate into phenyl isocyanate and alkyl carbanilate, followed by dissociation of the alkyl carbanilate into phenyl isocyanate and alcohol. Decarboxylation of the ethyl carbanilate fragment also took place slowly. A small amount of diphenyl carbodimide was observed at the pyrolysis temperature of 450°C. In addition, decarboxylation of the isopropyl carbanilate fragment took place at 550°C. A small amount of diphenyl carbodimide was observed from 350°C to 550°C.

Sigrist, Manzardo, and Amado[18] investigated the behavior of 3-methyl-2,4-non-anedione under photooxidative conditions. The structure of main oxidation product, 3-hydroxy-3-methyl-2,4-non-anedione, was tentatively assigned based on mass (GC/MS) and vapor-phase infrared (GC/FTIR). The infrared spectrum showed the status of the OH group, and the structure was easily assigned to α-hydroxy-β-diketones.

CONCLUSION

GC/FTIR is very useful for identification analysis of volatile compounds. This technique produces excellent spectroscopic information and is best suited for discrimination of isomers and the identification of compounds with closely related structures. The GC/FTIR identification

obtained is complementary to the identification obtained from GC/MS. With the IR subtractive spectrum technique, the GC overlap peaks can be resolved without a separate step in the experiment.

It has been over 40 years since infrared spectroscopy was first applied to GC by identifying trapped effluents taken directly from the column. With the advances of FTIR spectrometers and computer techniques, these modern FTIR spectrometers and data systems provide rapid scanning, increased sensitivity, and endless disk space for data storage. All of these characteristics are necessary to merge FTIR with today's sensitive high-resolution capillary gas chromatography. Therefore, the reliability of qualitative analysis of GC/FTIR is greatly enhanced.

REFERENCES

1. Visser, T. FT-IR detection in gas chromatography. Trends Anal. Chem. **2002**, *21*, 627.
2. Sasaki, T.A.; Wilkins, C.L. Gas chromatography with Fourier transform infrared and mass spectral detection. J. Chromatogr. A, **1999**, *842*, 341.
3. Ragunathan, N.; Krock, K.A.; Klawun, C.; Sasaki, T.A.; Wilkins, C.L. Multispectral detection for gas chromatography. J. Chromatogr. A, **1995**, *703*, 335.
4. Norton, K.L.; Griffiths, P.R. Comparison of direct deposition and flow-cell gas chromatography-Fourier transform infrared spectrometry of barbiturates. J. Chromatogr. A, **1995**, *703*, 383.
5. Heaps, D.A.; Griffiths, P.R. Reduction of detection limits of the direct deposition GC/FT-IR interface by surface-enhanced infrared absorption. Anal. Chem. **2005**, *77*, 5965.
6. Hankemeier, Th.; van der Laan, H.T.C.; Vreuls, J.; Vredenbregt, M.J.; Visser, T.; Brinkman, U.A.Th. Detectability enhancement by the use of large-volume injections in gas chromatography-cryotrapping-Fourier transform infrared spectrometry. J. Chromatogr. A, **1996**, *732*, 75.
7. Auger, J.; Rousset, S.; Thibout, E.; Jaillais, B. Solid-phase microextraction-gas chromatography-direct deposition infrared spectrometry as a convenient method for the determination of volatile compounds from living organisms. J. Chromatogr. A, **1998**, *819*, 45.
8. Hankemeier, Th.; Hooijschuur, E.; Vreuls, R.J.J.; Brinkman, U.A.Th.; Visser, T. On-line solid phase extraction-gas chromatography-cryotrapping-infrared spectrometry for the trace-level determination of microcontaminants in aqueous samples. J. High Resol. Chromatogr. **1998**, *21*, 341.
9. Visser, T.; Vredenbregt, M.J.; de Jong, A.P.J.M.; Somsen, G.W.; Hankemeier, Th.; Velthorst, N.H.; Gooijer, C.; Brinkman, U.A.Th. Improvements in environmental trace analysis by GC-IR and LC-IR. J. Molec. Struct. **1997**, *408/409*, 97.
10. Rodríguez, I.; Bollaín, M.H.; García, C.M.; Cela, R. Analysis of structural isomers of polychlorinated phenols in water by liquid-nitrogen-trapping gas chromatography-Fourier transform infrared spectroscopy. J. Chromatogr. A, **1996**, *733*, 405.
11. Dirinck, I.; Meyer, E.; Van Bocxlaer, J.; Lambert, W.; De Leenheer, A. Application of gas chromatography-Fourier transform infrared spectrometry to the analysis of amphetamine analogues. J. Chromatogr. A, **1998**, *819*, 155.
12. Mossoba, M.M. Application of gas chromatography-infrared spectroscopy to the confirmation of the double bond configuration of conjugated linoleic acid isomers. Eur. J. Lipid Sci. Technol. **2001**, *103*, 624.
13. Sehat, N.; Rickert, R.; Mossoba, M.M.; Kramer, J.K.G.; Yurawecz, M.P.; Roach, J.A.P.; Radlof, R.O.; Morehouse, K.M.; Fritsche, J.; Eulitz, K.D.; Steinhart, H.; Ku, Y. Improved separation of conjugated linoleic acid methyl esters by silver-high performance chromatography. Lipids **1999**, *34*, 407.
14. Veness, R.G.; Evans, C.S. Identification of monosaccharides and related compounds by gas chromatography-Fourier transform infrared spectroscopy of their trimethylsilyl ethers. J. Chromatogr. A, **1996**, *721*, 165.
15. Wachholz, S.; Keidel, F.; Just, U.; Geissler, H.; Käppler, K. Analysis of a mixture of linear and cyclic siloxanes by cryo-gas chromatography-Fourier transform infrared spectroscopy and gas chromatography-mass spectrometry. J. Chromatogr. A, **1995**, *693*, 89.
16. Svatoš, A.; Attygalle, A.B. Characterization of vinyl-substituted, carbon-carbon double bonds by GC/FT-IR analysis. Anal. Chem. **1997**, *69*, 1827.
17. Yashitake, N.; Furukawa, M. Thermal degradation mechanism of α, γ-diphenyl alkyl allophanate as a model polyurethane by pyrolysis-high-resolution gas chromatography/FT-IR. J. Anal. Appl. Pyrol. **1995**, *33*, 269.
18. Sigrist, I.A.; Manzardo, G.G.G.; Amado, R. Aroma compounds formed from 3-methyl-2,4-nonanedione under photooxidative conditions. J. Agric. Food Chem. **2003**, *51*, 3426.

GC: System Instrumentation

Gunawan Indrayanto
Mochammad Yuwono
Faculty of Pharmacy, Airlangga University, Surabaya, Indonesia

INTRODUCTION

Gas chromatography (GC) was first described by Martin and James in 1952. It has become one of the most frequently used separation techniques for the analysis of gases and volatile liquids and solids. An important breakthrough in GC was the introduction of the open tubular column by Golay in 1958 and the adoption of fused silica capillary columns by Dandeneau and Zerenner in 1979.

Today, using of the capillary columns can solve many kinds of analytical problems, such as isomer separation and analysis of complex mixtures of natural products and biologicals.

The gas chromatograph involves volatilization of the sample in a heated inlet port (injector), separation of the component mixtures in a column, and detection of each component by a detector.

GC SYSTEM INSTRUMENTATION

GC, first described by James and Martin[1] in 1952, has become one of the most frequently used separation technique for the analysis of gases, volatile liquids, and solids. The major breakthrough of GC was the introduction of the open tubular column by Golay and Desty[2] in 1958 and the adoption of fused silica capillary columns by Dandeneau and Zerenner[3] in 1979. Today, using of the capillary columns can solve many analytical problems, such as isomeric separation and analysis of complex mixtures of natural products and biological samples.

The basic principle of a gas chromatograph involves volatilization of the sample in a heated inlet port (injector), separation of the component mixtures in a column, and detection of each component by a detector. Although the basic components remain the same, some improvements in gas chromatograph appeared in the commercial marketplace. GC with electronic integrators and computer-based data processing systems became common in 1970s, whereas in the 1980s, a computer was introduced to control all GC parameters automatically, such as column temperature, flow rates, inlet pressure, and sample injection, and to evaluate the data obtained. The automated equipment can be operated unattended overnight.[4,5]

Combinations of highly efficient separation columns, with specific or selective detectors, such as electron capture detector (ECD), GC/mass spectrometry (MS), and GC-Fourier transform infrared (FTIR) detector, make GC a more favorable technique. Multidimensional GC systems, which contain at least two columns operated in series, have also proved to be a powerful tool in the analytical chemistry of complex mixtures.

The dramatic advance in GC instrumentation is the introduction of portable gas chromatographs, which have been developed during 1990s to provide a field-based analysis. Recently, the micro high-speed GC portable has also appeared to carry out the analysis up to 10 times faster than conventional laboratory GCs.[6–8]

The GC system (Fig. 1) consists of a carrier gas supply system, an inlet to deliver sample to a column, the column where the separations occur, an oven as a thermostat for the column, a detector to register the presence of a chemical in the column effluent, and a data system to record, display, and evaluate the chromatogram.

CARRIER GAS

The carrier gas that is used as the mobile phase transfers the sample from the injector, through the column, and into the detector. For a laboratory gas chromatograph, the carrier gas is usually obtained from a commercial pressurized gas cylinder equipped with a two-stage regulator for coarse and fine flow control. In most instruments, provision is made for secondary fine-tuning of pressure and gas flow. In 1990, electronic pressure control was developed, which allows operation at constant pressure, constant flow, and pressure-programing modes. The gas flow can be read electronically on the instrument panel or measured using a soap-bubble flow meter at the outlet of the column. The carrier gas flow is directed through a sieve trap, or a series of traps to remove the moisture, organic matter, and oxygen, and then through frits to filter off any particulate matter.[9] It is also suggested to use copper tubing for the connection of the gas cylinder to the gas chromatographs. Polymer tubing should be avoided because the oxygen from the atmosphere can often permeate the tubing walls. The oxygen in the gas stream may cause degradation of some column stationary phases at elevated operating temperatures, thereby producing unstable baselines with the ECD and shortening filament lifetime for the thermal conductivity detector. To

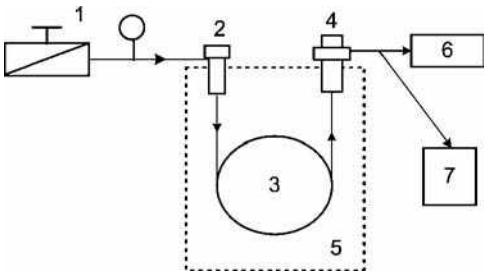

Fig. 1 Gas chromatography system schematic.

minimize contamination, high purity carrier gases are used, combined with additional chemical and or catalytic gas purifying devices. The gas chromatograph may have thermostatically controlled pneumatics to prevent drift, in which pressure regulators, flow controllers, and additional gas purifying traps and filters are housed. The carrier gas must be inert so that it reacts neither with the sample nor with the stationary phase at the operating temperature.[9] The choice of carrier gas requires consideration of the detector used, the separation problem to be solved, and the purity of the gases available. A further consideration in the selection of carrier gas is its availability and its cost. In practice, the choice of carrier gas will determine the efficiency of the GC system because the height equivalent to a theoretical plate depends on solute diffusivity in the carrier. The influence of the mobile-phase velocity on column efficiency and practical consequences of the carrier gas selection in capillary GC have been described in previous publications.[9,10] Normally, a compromise between inertness, efficiency, and operating cost make nitrogen or helium the most common GC carrier gases. The carrier gas flow can be determined by either linear velocity, expressed in cm/sec, or volumetric flow rate, expressed in ml/min. The linear velocity is independent of the column diameter, whereas the flow rate is dependent on the column diameter. For capillary columns, makeup gas is added at the column exit to obtain a total gas flow of 30–40 ml/min into the detector; it can be the same gas as the carrier gas or a different gas, depending on the type of detector being used.

SAMPLE INLET SYSTEMS

Sample introduction into the gas chromatograph is the first stage in the chromatographic process. It is of primary importance, especially in capillary GC, because its efficiency is reflected in the overall efficiency of the separation procedure and the quantitative results. The basic prerequisite of the sample injection system is that the sample should be introduced into the column as a narrow band, ideally with maintenance of constant pressure and flow. The specially designed inlet should be hot enough to flash-evaporate the sample and large enough in volume to allow the sample vapor to expand without blowing back through the septum. Care must be taken not to overheat the injector because the injection cell or the sample may decompose. The sample must be gaseous or an easily vaporized liquid or solid. Most organic compounds may be introduced onto the column in the form of a liquid sample, either as the neat compound or, in the case of a solid, as a solution. When the dilution of the solid sample would be undesirable, the solid may be encapsulated in glass capillaries and mechanically pushed into the heated injection block and crushed.[10,11]

For injecting gases and vapors, gas-tight syringes with Teflon-tipped plungers and syringe barrels are available. Many analysts favor using gas syringes for gas samples; however, the introduction of accurately measured volumes of gases remains a problem. In the alternative method, gas samples can be introduced onto a column using rotary gas switching valves, which generally consist of a rotating polymeric core, encased in a stainless-steel body. For repetitive or periodic injection of a large number of the same or different samples, auto samplers may be used.[10,12] The sample volume for analytical work depends on the dimensions of the column and on the sensitivity of the detector. For a packed column, sample size ranges from tenths of 1 μl up to 20 μl. Capillary columns need much less sample (0.01–1 μl). The most commonly used silicone-rubber septa may contain impurities that may bleed into the column above a certain temperature, resulting in unsteady baseline and ghost peaks. Recently, various kinds of septa have become available which can be used at very high temperatures.[13]

Packed and Open Tubular Column Inlet

Because of the variety of columns and samples that can be analyzed by GC, several injection techniques have been developed. The packed inlet system is designed mainly for packed and wide-bore columns. However, an adapter can be used to enable capillary columns to be used. When injection is carried out in the on-column mode, glass wool can be used for packing the injector. For capillary GC, split technique is most common, which is used for high concentration samples. This technique allows injection of samples virtually independent of the selection of solvent, at any column temperature, with little risk of band broadening or disturbing solvent effects. The splitless technique, on the other hand, is used for trace level analysis. The so-called cold injection techniques (on-column, temperature programed vaporization, cooled needle split) have also been recently developed.[4,14,15]

Pyrolysis GC

Pyrolysis involves the thermal decomposition, degradation, or cracking of a large molecule into smaller fragments. Pyrolysis GC is an excellent technique for identifying

certain types of compounds which cannot be analyzed by derivatization, e.g., polymers. The pyrolysis temperature is typically between 400°C and 1000°C. A number of analytical pyrolyzers have been introduced and are commercially available. The devices consist of platinum resistively heated and Curie point pyrolyzers. The carrier gas is directed through the system, and the platinum wire is heated to a certain temperature. The material decomposes, and the fragmentation products are analyzed.[16,17]

Headspace Analysis

Headspace analysis is an excellent technique for gas chromatography to analyze volatile samples in which the matrix is of no interest. It is readily applied to many analytical problems, such as monitoring of volatiles in soil and water, determination of monomers in polymers, aromas in food and beverages, etc. A variety of headspace auto samplers are commercially available, based on the principle of static or dynamic headspace. In static headspace, the sample is transferred to a headspace vial that is sealed and placed in a thermostat to drive the desirable component into the headspace sampling. An aliquot of the vapor phase is introduced into the GC system via a gas-tight syringe or a sample loop of a gas-sampling valve. Static headspace implies that the sample is taken from a single-phase equilibrium. To increase the detectability, dynamic headspace analysis has been developed. Driving the headspace out of the vial via an inert gas continuously displaces the phase equilibrium. A detailed discussion of headspace GC is reported in the previous work.[18]

Solid-Phase Microextraction

Solid-phase microextraction, first reported by Belardi and Pawliszyn in 1989, is an alternative sampling technique. The method has the advantages of convenience and simplicity, and it does not release environmentally polluting organic solvents into the atmosphere. The method is based on the extraction of analytes directly from liquid samples or from headspace of the samples onto a polymer- or adsorbent-coated fused silica fiber. After equilibration, the fiber is then removed and injected onto the gas chromatograph.[19–22]

Purge-and-Trap Methods

Purge and trap samplers have been developed for analysis of non-polar and medium-polarity pollutants in water samples. The commercially available systems are all based on the same principle. Helium is purged through the sample that is contained in a sealed system, and the volatiles are swept continuously through an adsorbent trap where they are concentrated. After a selected time, purging is stopped, the carrier gas is directed through the trap via a six-way valve, and the trap is heated rapidly to desorb the solutes.[4,9]

OVEN

The column is ordinarily housed in a thermostatically controlled oven, which is equipped with fans to ensure a uniform temperature. The column temperature should not be affected by changes in the detector, injector, and ambient temperatures. Temperature fluctuations in column ovens can decrease the accuracy of the measured retention times and may also cause the peak splitting effect. For conventional ovens, the oven wall is well insulated using a wire coil of high thermal capacity, which is able to radiate heat into the inner volume of the oven. The characteristics of a more efficient method can accurately control the temperature of a column and allow the operator to change the temperature conveniently and rapidly for temperature programing. It is designed by suspending the column in an insulated air oven through which the air circulated at high velocity by means of fans or pumps. Most commercial instruments employ this design and allow for the adjustment and control of temperature between 50°C and 450°C. Subambient temperature operation would normally require a cryogenic cooling system using liquid nitrogen or carbon dioxide.[4,9,10]

DETECTOR

The detector in a gas chromatograph senses the differences in the composition of the effluent gases from the column and converts the column's separation process into an electrical signal, which is recorded. There are many detectors that can be used in GC, and each detector gives a different type of selectivity. An excellent discussion and review on developments of GC detectors has been published.[23]

Detectors may be classified on the basis of selectivity. A universal detector responds to all compounds in the mobile phase except carrier gas. A selective detector responds only to a related group of substances, and a specific detector responds to a single chemical compound. Most common GC detectors fall into the selective designation. Examples include flame ionization detector (FID), ECD, flame photometric detector (FPD), and thermoionic ionization detector. The common GC detector that has a truly universal response is the thermal conductivity detector (TCD). Mass spectrometer is another commercial detector with either universal or quasi-universal response capabilities.

Detectors can also be grouped into concentration-dependent detectors and mass-flow-dependent detectors. Detectors whose responses are related to the concentration of solute in the detector cell, and do not destroy the sample, are called concentration-dependent detectors, whereas detectors whose response is related to the rate at which solute molecules enter the detector are called mass-flow-dependent detectors. Typical concentration-dependent detectors are TCD and GC/FTIR. Important

mass-flow-dependent detectors are the FID, thermoionic detector for N and P (N-, P-FID), FPD for S and P (FPD), ECD, and selected ion monitoring MS detector.

The FID is one of the most widely used GC detectors. The detection principle is based on the change in the electric conductivity of a hydrogen flame in an electric field when fed by organic compound(s). The resulting current is then directed into a high impedance operational amplifier for measurement. The FID is sensitive to all compounds which contain C–C or C–H linkages and considerably less sensitive up to insensitive to certain functional groups of organic compounds, such as alcohol, amine, carbonyl, and halogen. In addition, the detector is also insensitive toward non-combustible gases such as H_2O, CO_2, SO_2, and NO. A TCD, which was one of the earliest detectors for GC, is based on changes in the thermal conductivity of the gas stream caused by the presence of analyte molecules. This device is sometimes called a katharometer. Because the TCD reacts non-specifically, it can be used universally for the detection of either organic or inorganic substances. In the ECD, the column effluent passes over a beta-emitter, such as nickel-63 or tritium. The electrons from emitter bombard the carrier gas (nitrogen), giving rise to ions and a burst of electrons. In the absence of an analyte, the ionization process yields a constant standing current. However, this background current decreases in the presence of organic compounds that can capture electrons. The applications of the ECD illustrate the advantages of a highly sensitive special detector toward molecules that contain electronegative functional groups such as halogens, peroxide, quinines, or nitro groups.[22–24]

GC DATA SYSTEM

The GC data system performs the tasks of recording, handling, evaluation, and documentation of the chromatogram. In a modern gas chromatographic system, these can be performed by means of a computer with specialized software. Nowadays, software for calculating the quantitative results and for the method validation is available.[4]

CONCLUSIONS

Since the introduction of GC, the basic parts of a gas chromatograph have been unchanged in function and purpose, even though the improvement has been occurring in design and materials. One area of dramatic advance in GC instrumentation was the introduction of the open tubular columns. Consequently, most GC analyses in practice are performed in capillary columns that show the separation with high efficiencies and high resolution. The developments of GC instrumentation are occurring with sample handling techniques and refinements of detectors. The dramatic advance in GC instrumentation is the development of a small, high-speed, and portable gas chromatograph to provide a field-based analysis.

REFERENCES

1. James, A.T.; Martin, A.J.P. Gas–liquid partition chromatography: The separation and micro-estimation of volatile fatty acids from formic acid to dodecanoic acid. Biochem. J. **1952**, *50*, 679.
2. Golay, M.J.E.; Desty, D. *Gas Chromatography*; Butterworths: London, 1958.
3. Dandeneau, R.D.; Zerenner, E.H. An investigation of glasses for capillary chromatography. J. High Resolut. Chromatogr. **1979**, *2* (6), 351.
4. Schomburg, G. *Gas Chromatography, A Practical Course*; VCH Verlagsgesellschaft: Weinheimd, 1990.
5. Poole, C.F.; Poole, S.K. *Chromatography Today*; Elsevier: Amsterdam, 1991.
6. Eiceman, G.A.; Gardea-Torresdey, J.; Overton, E.; Carney, K.; Dorman, F. Gas chromatography. Anal. Chem. **2002**, *74*, 2771–2780.
7. See http://www.agilent.com/about/newsroom/pesrel/2002/30sep2002b.html.
8. See http://www.hnu.com/fpi/gc311.htm.
9. Sandra, J.F. Gas chromatography. *Ullmann's Encyclopedia of Industrial Chemistry*; Wiley-VCH Verlag GmbH: Weinheim, 2002.
10. Ravindranath, B. *Principles and Practice of Chromatography*; Ellis Horwood Limited: Chichester, UK, 1989.
11. Sandra, P. *Sample Introduction in Capillary Gas Chromatography*; Hüthig Verlag: Heidelberg, 1985.
12. Grob, K.; Neukom, H.P., Jr. The influence of syringe needle on the precision and accuracy of vaporizing GC injections. J. High Res. Chrom. Comm. **1979**, *2*, 15–21.
13. Olsavicky, V.M. A comparison of high temperature septa for gas chromatography. J. Chromatogr. Sci. **1978**, *16*, 197–200.
14. Grob, K. *Classical Split and Splitless Injection in Capillary GC*; Hüthig Verlag: Heidelberg, 1986.
15. Grob, K. *On Column Injection in Capillary GC*; Hüthig Verlag: Heidelberg, 1987.
16. Wang, F.C.Y.; Burleson, A.D. Development of pyrolysis fast gas chromatography for analysis of synthetic polymers. J. Chromatogr. A, **1999**, *833* (1), 111–119.
17. Haken, J.K. Pyrolysis gas chromatography of synthetic polymers: A bibliography. J. Chromatogr. A, **1998**, *825* (2), 171–187.
18. Joffe, B.V.; Vitenberg, A.G. *Headspace Analysis and Related Methods in Gas Chromatography*; John Wiley: New York, 1984.
19. See http://gc.discussing.info/gs/r_hs-gs/microextraction.html (accessed February 2002).
20. Scarlata, C.J.; Ebeler, S.E. Headspace solid-phase microextraction for the analysis of dimethyl sulfide in beer. J. Agric. Food Chem. **1999**, *47* (7), 2505–2508.
21. Mills, G.A.; Walker, V.; Mughal, H. Quantitative determination of trimethylamine in urine by solid-phase microextraction

and gas chromatography mass spectrometry. J. Chromatogr. B, **1999**, *723* (1–2), 281–285.
22. Pinho, O.; Ferreira, I.M.P.L.V.O.; Ferreira, M.A. Solid-phase microextraction in combination with GC/MS for quantification of the major volatile free fatty acids in ewe cheese. Anal. Chem. **2002**, *74*, 5199–5204.
23. Buffington, R.; Wilson, M.K. *Detectors for Gas Chromatography—A Practical Primer*; Hewlett-Packard Corporation, 1987, Part No. 5958-9433.
24. Hill, H.H., McMinn, D.G., Eds.; *Detectors for Capillary Chromatography*; John Wiley & Sons: New York, 1992.

GPC/SEC

Vaishali Soneji Lafita
Abbott Laboratories, Inc., Abbott Park, Illinois, U.S.A.

INTRODUCTION

The basic principle of chromatography involves the introduction of the sample into a stream of mobile phase that flows through a bed of a stationary phase. The sample molecules will distribute so that each spends some time in each phase. Size-exclusion chromatography (SEC) is a liquid column chromatographic technique which separates molecules on the basis of their sizes or hydrodynamic volumes with respect to the average pore size of the packing. The stationary phase consists of small polymeric or silica-based particles that are porous and semirigid to rigid. Sample molecules that are smaller than the pore size can enter the stationary-phase particles and, therefore, have a longer path and longer retention time than larger molecules that cannot enter the pore structure. Very small molecules can enter virtually every pore they encounter and, therefore, elute last. The sizes, and sometimes the shapes, of the mid-size molecules regulate the extent to which they can enter the pores. Larger molecules are excluded and, therefore, are rapidly carried through the system. The porosity of the packing material can be adjusted to exclude all molecules above a certain size. SEC is generally used to separate biological macromolecules and to determine molecular-weight distributions of polymers.

HISTORY

It is not obvious who was the first to use SEC. However, the first effective separation of polymers based on *gel filtration chromatography* (GFC) appears to be that reported by Porath and Flodin.[1] Porath and Flodin employed insoluble cross-linked polydextran gels, swollen in aqueous medium, to separate various water-soluble macromolecules. GFC generally employs aqueous solvents and hydrophilic column packings, which swell heavily in water. Moreover, at high flow rates and pressures, these lightly cross-linked soft gels have low mechanical stability and collapse. Therefore, GFC stationary phases are generally used with low flow rates to minimize high-back pressures. GFC is mainly used for biomolecule separations at low pressure.[2]

Moore described an improved separation technique relative to GFC and introduced the term gel permeation chromatography (GPC) in 1964.[3] GPC performs the same separation as GFC, but it utilizes organic solvents and hydrophobic packings. Moore developed rigid polystyrene gels, cross-linked with divinylbenzene, for separating synthetic polymers soluble in organic media. These extensively cross-linked gels are mechanically stable enough to withstand high pressures and flow rates. The more rugged GPC quickly flourished in industrial laboratories where polymer characterization and quality control are of primary concern. Since its introduction in the 1960s, the understanding and utility of GPC has substantially evolved. GPC has been widely used for the determination of molecular weight (MW) and molecular-weight distribution (MWD) for numerous synthetic polymers.[4]

Other names such as gel chromatography, exclusion chromatography, molecular sieve chromatography, gel exclusion chromatography, size separation chromatography, steric exclusion chromatography, and restricted diffusion chromatography have been utilized to reflect the principal mechanism for the separation. The fundamental mechanism of this chromatographic method is complex and certainly will not be readily incorporated into one term. Strong arguments have been made for many of the above-listed titles.[5] In an attempt to minimize the dispute over the proper name, the term SEC will be used in this entry, as it appears to be the most widely used.

MECHANISM

SEC is a liquid chromatography (LC) technique in which a polymer sample, dissolved in a solvent, is injected into a packed column (or a series of packed columns) and flows through the column(s) and its concentration as a function of time is determined by a suitable detector. The column packing material differentiates SEC from other LC techniques where sample components primarily separate by differential adsorption and desorption. The SEC packing consists of a polymer, generally polystyrene, which is chemically cross-linked so that varying size pores are created. Several models are discussed by Barth et al.[6] to illustrate SEC separation theory. A rather simplified separation mechanism is described here. A polymer sample dissolved in the SEC mobile phase is injected in the chromatographic system. The column eluent is monitored by a mass-sensitive detector, which responds to the weight concentration of polymer in the mobile phase. The most common detector for SEC is a differential refractometer. The raw data in SEC consists of a trace of detector response proportional to the amount of polymer in solution and the

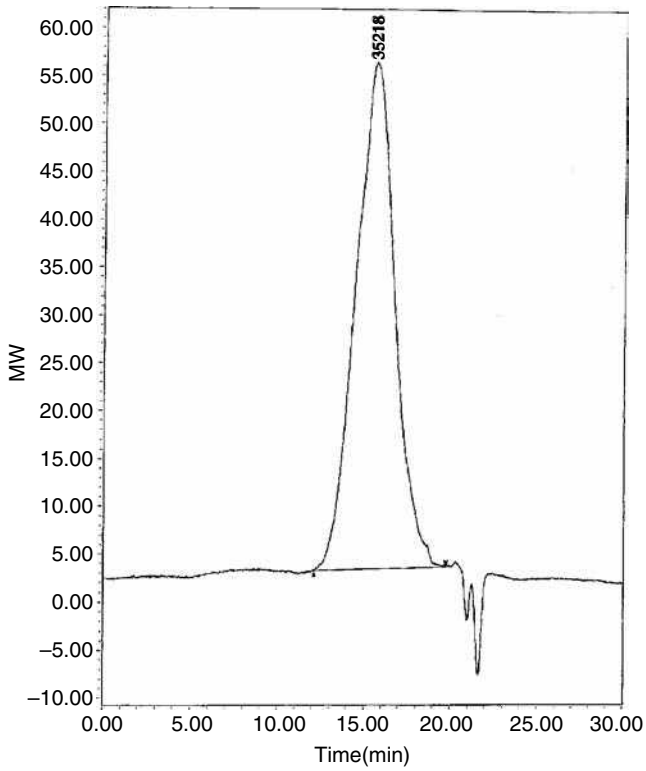

Fig. 1 Typical SEC of a polymer sample. SampleName: 6B Vial: 15 Inj: 1 Ch: 410 Type: Broad Unknown.

corresponding retention volume. A typical SEC sample chromatogram is depicted in Fig. 1. An SEC chromatogram generally is a broad peak representing the entire range of molecular weights in the sample. For synthetic polymers, this can extend from a few hundred mass units up to a million or more. The average molecular weight can be calculated in a number of ways. Both natural and synthetic polymers are molecules containing a distribution of molecular weights. The most commonly calculated molecular-weight averages using SEC are the weight-average molecular weight (M_w) and number-average molecular weight (M_n). These terms have been well defined by Cazes.[7]

The weight-average molecular weight is defined as

$$\bar{M}_w = \frac{\sum_{i=1}^{\infty} W_i M_i}{\sum_{i=1}^{\infty} W_i} \quad (1)$$

and the number-average molecular weight is defined as

$$\bar{M}_n = \frac{W}{\sum_{i=1}^{\infty} N_i} = \frac{\sum_{i=1}^{\infty} M_i N_i}{\sum_{i=1}^{\infty} N_i} \quad (2)$$

where W is the total weight of the polymer, W_i is the weight fraction of a given molecule i, N_i is the number of moles of each species i, and M_i is the molecular weight of each species i.

M_w is generally greater than or equal to M_n. The samples in which all of the molecules have a single molecular weight ($M_w = M_n$) are called monodisperse polymers. The degree of polydispersity (i.e., the ratio of M_w to M_n) describes the spread of the molecular-weight-distribution curve. The broader the SEC curve, the larger the polydispersity.

The detector response on the SEC chromatogram is proportional to the weight fraction of total polymer, and suitable calibration permits the translation of the retention volume axis into a logarithmic molecular-weight scale. Calibration of SEC is perhaps the most difficult aspect of the technique because polymer molecules are separated by size rather than by molecular weight. Size, in turn, is most directly proportional to the lengths of the polymer molecules in solution. A length, however, is proportional to molecular weight only within a single polymer type. An absolute SEC calibration would require the use of narrow molecular-weight range standards of the same polymer that is being analyzed. This is not always practical because a wide range of polymer types needs to be evaluated. SEC calibration is often achieved using the "universal calibration" technique, which assumes hydrodynamic volume is the sole determinate of retention time or volume.[8] A series of commercially available monodisperse molecular-weight polystyrenes are the most commonly used SEC calibration standards. If polystyrene standards are used to calibrate the analyses of any other type of polymer, the molecular weights obtained for a polymer sample are actually "polystyrene-equivalent" molecular weights. Numeric conversion factors are available for correlating "molecular weight per polystyrene length" to that of other polymers, but this approach only produces marginally better estimates of the absolute molecular weights. In addition, approaches such as these are usually invalid because the calibration curve for the polymer being analyzed does not often have the same shape as the curve generated with the polystyrene standards.

Size-exclusion chromatograms of narrow-distribution polystyrene standards along with a typical polystyrene calibration curve are shown in Fig. 2a and 2b. The peak retention volume and corresponding molecular weights produce a calibration curve. With a calibration curve, it is possible to determine M_w and M_n for a polymer. The SEC curve of a polymer sample is divided into vertical segments of equal retention volume. The height or area of each segment and the corresponding average molecular weight, calculated from the calibration curve, are then used for M_w and M_n calculations. There are several commercially available software packages that simplify the calculation process for molecular-weight determinations.

APPLICATION

Until the mid-1960s, molecular-weight averages were determined only by techniques such as dilute solution viscosity, osmometry, and light scattering. Most of these

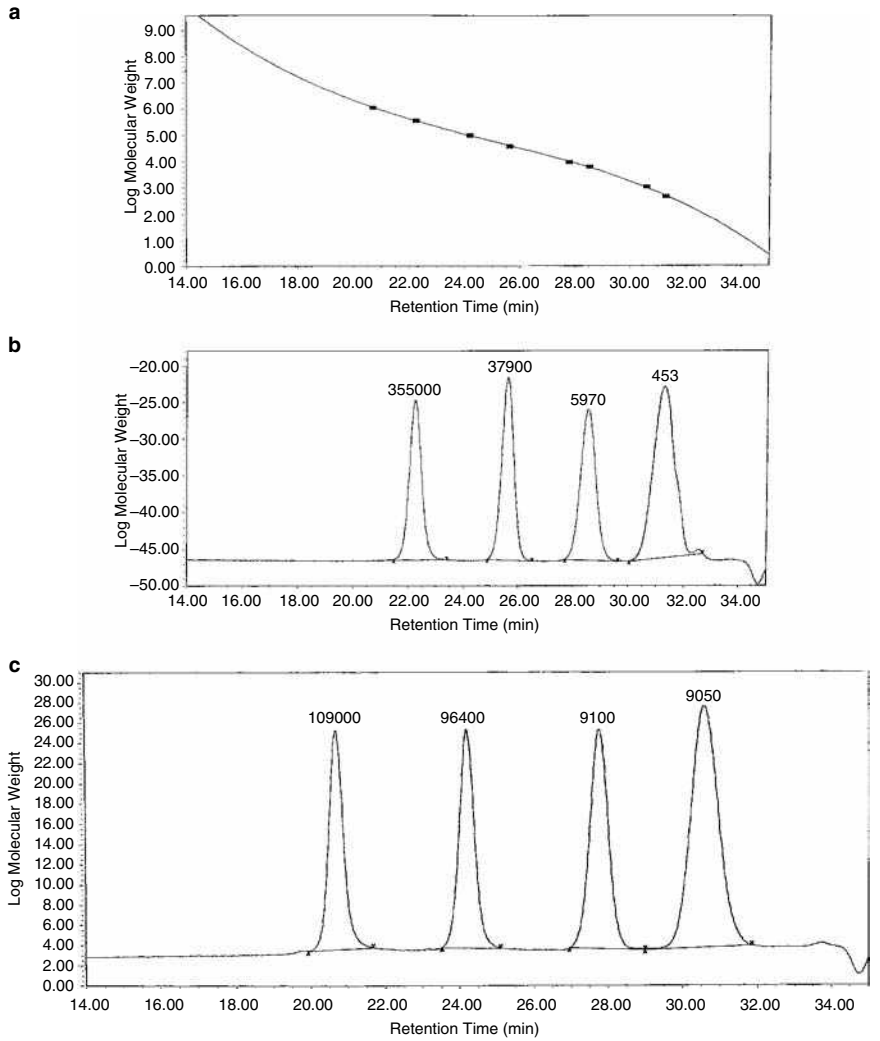

Fig. 2 Typical polystyrene narrow molecular-weight range standard chromatograms and calibration curve.

techniques work best for polymers with a narrow MWD. None of these techniques, either alone or in combination, could readily identify the range of molecular weights in a given sample. SEC was introduced in the mid-1960s to determine MWDs and other properties of polymers. During the first two decades of SEC acceptance, the emphasis was on improving the fundamental aspects of chromatography, such as column technology, optimizing solvents, and the precision of analysis. Over the past 10 years, there has been an increasing demand for deriving more information from SEC, driven by the need to characterize, more fully, an increasingly complex array of new polymers. Significant developments in SEC detection systems include light scattering, viscometry, and matrix-assisted laser desorption ionization time-of-flight (MALDI–TOF) mass spectrometry and, most recently, nuclear magnetic resonance (NMR) detection in conjunction with SEC for determining MW and chemical composition of polymers. The use of SEC for measuring physiological properties of polymers, especially biopolymers, has become an important area of research.

Finally, SEC is merely a separation technique based on differences in hydrodynamic volumes of molecules. No direct measurement of molecular weight is made. SEC itself does not render absolute information on molecular weights and their distribution or on the structure of the polymers studied without the use of more specialized detectors (e.g., viscometry and light scattering). With these detectors, a "self-calibration" may be achieved for each polymer sample while it is being analyzed by SEC. However, it is possible to calibrate the elution time in relation to molecular weight of known standards. With proper column calibration, or by the use of molecular-weight-sensitive detectors such as light scattering, viscometry, or mass spectrometry, MWD and average molecular weights can be obtained readily.[6] The combined use of concentration sensitive and molecular-weight-sensitive detectors has greatly improved the accuracy and precision of SEC measurements. Thus, SEC has become an essential technique that provides valuable molecular-weight information, which can be related to polymer physical properties, chemical resistance, and processability.

REFERENCES

1. Porath, J.; Flodin, P. Gel filtration: A method for desalting and group separation. Nature **1959**, *183*, 1657.
2. Danilov, A.V.; Vagenina, I.V.; Mustaeva, L.G.; Moshnikov, S.A.; Gorbunova, E.Y.; Cherskii, V.V.; Baru, M.B. Liquid chromatography on soft packing material, under axial compression: Size-exclusion chromatography of polypeptides J. Chromatogr. A, **1997**, *773*, 103.
3. Moore, J.C. Comments on "Gel permeation chromatography. I. A new method for molecular weight distribution of high polymers." J. Polym. Sci. Part A. **1964**, *2*, 835.
4. Lafita, V.S.; Tian, Y.; Stephens, D.; Deng, J.; Meisters, M.; Li, L.; Mattern, B.; Reiter, P. *Proc. Int. GPC Symp. 1998*; Waters Corp.: Milford, MA, 1998; 474–490.
5. Johnson, J.; Porter, R.; Cantow, M. Gel permeation chromatography with organic solvents. J. Macromol. Chem. Part C. **1966**, *1*, 393.
6. Barth, H.G.; Boyes, B.E.; Jackson, C. Size exclusion chromatography and related separation techniques. Anal. Chem. **1998**, *70*, 251R.
7. Cazes, J. Gel permeation chromatography. Part I. J. Chem. Educ. **1966**, *43*, A567.
8. Boyd, R.H.; Chance, R.R.; Ver Strate, G. Effective dimensions of oligomers in size exclusion chromatography. A molecular dynamics simulation study. Macromolecules **1996**, *29* (4), 1182–1190.

GPC/SEC Viscometry from Multi-Angle Light Scattering

Philip J. Wyatt
Ron Myers
Wyatt Technology Corp., Santa Barbara, California, U.S.A.

INTRODUCTION

Viscometric techniques have long been used in combination with gel permeation chromatography/size-exclusion chromatography (GPC/SEC) separations since the early discovery[1] that the elution of many classes of divers polymers follows a so-called "universal calibration" curve. A plot of the logarithm of the hydrodynamic volume, $M[\eta]$, where M is the molar mass and $[\eta]$ the intrinsic (or "limiting") viscosity, against the elution volume V yields a common curve (differing for each mobile phase, operating temperature, and column set) along which polymers of greatly differing conformation appear to lie. Neglecting the fact that the errors of such fits can be quite large (the results are usually presented on a logarithmic scale), the concept of universal calibration (UC) allows one to estimate (from the UC curve) the molar mass of an eluting fraction by measuring only the intrinsic viscosity, $[\eta]$, and the corresponding elution volume (time). Key to the measurement of $[\eta]$ is the determination of the specific, η_{sp}, or relative, η_{rel}, viscosity and the concentration c, both in the limit as $c \to 0$. These viscosities are defined by

$$\eta_{sp} = \frac{\eta \pm \eta_0}{\eta_0} \tag{1}$$

and

$$\eta_{rel} = \frac{\eta}{\eta_0} \tag{2}$$

where η is the solution viscosity and η_0 is the viscosity of the pure solvent. Because $\eta_{rel} = \eta_{sp} + 1$, it is easily shown for η_{sp} small compared to unity that

$$\lim_{c\to 0} = \frac{\ln(\eta_{rel})}{c} = \lim_{c\to 0}\frac{\eta_{sp}}{c} = [\eta] \tag{3}$$

For the case of GPC/SEC elutions, the concentration c following separation is generally so small that Eq. 3 is assumed to be valid.

THE MARK–HOUWINK–SAKURADA EQUATION

Even without the use of a UC curve (one must be generated for each series of measurements), measurement of $[\eta_0]$ is believed by some to yield an intrinsic viscosity-weighted molar mass.[2] Most importantly, there is a historic interest in the relation of $[\eta]$ to molar mass and/or size. Indeed, the study and explanation of UC has occupied the theorists for some time and, accordingly, there are various formulations describing such relationships.[2] For linear polymers, the most popular empirical relationship between $[\eta]$ and molar 1mass is the Mark–Houwink–Sakurada (MHS) equation

$$[\eta] = KM^a \tag{4}$$

where K and a are the MHS coefficients. For many polymer–solvent combinations, a plot of $\log([\eta])$ vs. $\log(M)$ is linear over a wide range of molar masses. In other words, both K and a are constant throughout the range. Thus, the equation may be used for such polymer–solvent combinations to determine molar mass by measuring $[\eta]$.

Unfortunately, for some solvent–polymer combinations, even for nearly ideal random coils such as polystyrene, the coefficients are not constant but vary with molar mass.

THE FLORY–FOX EQUATION

In the various theoretical attempts to explain the relation between $[\eta]$ and the molar mass M, a relation derived by Flory and Fox for random coil molecules is often applied to interpret viscometric measurements for even more general polymer structures. Although applicable to a broader range of polymers than the MHS equation, the Flory–Fox relation has its own shortcomings. Nevertheless, its frequent use and good correlation with experimental data over a wide range of polymer types confirms its potential for combination with light-scattering measurements to eliminate the need for separate viscometric determinations. In its most general form, the Flory–Fox equation is given by

$$M[\eta] = \Phi\left(\sqrt{6r_g}\right)^3 \tag{5}$$

where r_g is the root mean square radius (or "radius of gyration"). The excluded volume effect is taken into account by representing the Flory–Fox coefficient as $\Phi = \Phi_0(1 \pm 2.63\varepsilon + 2.86\varepsilon^2)$. The constant $\Phi_0 = 2.87 \times 10^{23}$ and ε is related to the MHS coefficient a by the relation $2a = 1 + 3\varepsilon$. Thus, ε ranges from 0 at the theta point to 0.2 for a good solvent. Eq. 5 is of particular interest because multiangle light-scattering (MALS) measurements [3] determine M and r_g directly. Thus, if a polymer–solvent combination is well characterized by Eq. 5, then this equation may be used directly to calculate the intrinsic viscosity without need for a viscometer.

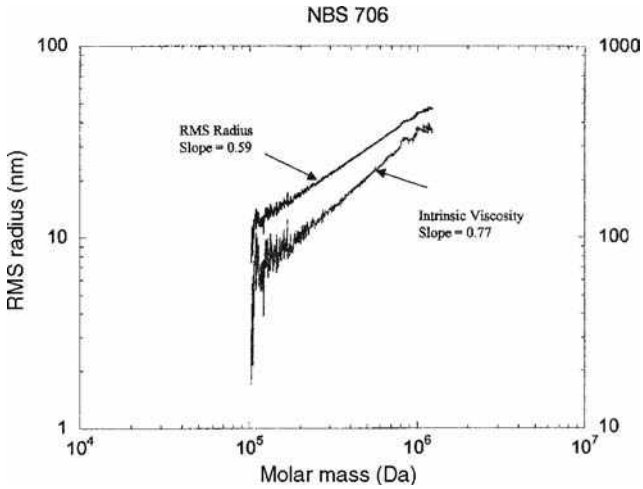

Fig. 1 Conformation plot for $\log(r_g)$ vs. $\log(M)$.

VISCOMETRY WITHOUT A VISCOMETER

As we have seen earlier, $[\eta]$ may be calculated directly from the (absolute) MALS measurements of M and r_g using Eq. 5. For linear polymers spanning a relatively broad molecular range (an order of magnitude or more), the measurement of M and r_g permits the determination of the molecular conformation defined by

$$r_g = kM^{\alpha} \tag{6}$$

where k and α are constants generally calculated from the intercept and slope of the least-squares fitted plot of $\log(M)$ against $\log(r_g)$. Combining Eqs. 4 and 5, we obtain

$$KM^{\alpha-1} = \left(\Phi\sqrt{6r_g}\right)^3 \tag{7}$$

Solving for r_g and substituting into Eq. 6 yields

$$\frac{K^{1/3}M^{(a-1)/3}}{\Phi\sqrt{6}} = kM^{\alpha} \tag{8}$$

Therefore, we have the following relations between the coefficients:

$$a = 3\alpha - 1 \quad \text{and} \quad K = \Phi\left(\sqrt{6k}\right)^3 \tag{9}$$

Eq. 9 show that we can obtain the MHS coefficients a and K directly from a MALS measurement and a determination from such measurements of the molecular conformation parameters α and k. Note that when long-chain branching becomes significant and the molecular conformation becomes more compact such that $\alpha \to {}^1/_3$, the MHS equation, Eq. 4, shows that the intrinsic viscosity no longer varies with molar mass, but becomes constant. This condition also represents a failure of the Flory–Fox equation and the concepts associated with the use of intrinsic viscosity as a means (through UC, for example) to determine molar mass. For linear polymers for which MALS measurements yield values for r_g and M at each eluting slice, all of the important viscometric parameters may be derived directly from the Flory–Fox relation and the MHS equation, as has been shown. For more complex molecular structures or solvent–solute interactions, the MHS coefficients are no longer constants and the empirical theory itself begins to fail.

It is well known,[3] however, that the MALS measurements begin to fail in the determination of r_g once r_g falls below about 8–10 nm, even though the M values generated still remain precise. This lack of precision is due to the limitations of the laser "ruler" to resolve a size much below about one-twentieth of the incident wavelength. The trouble with empirical relations, such as the relation between intrinsic viscosity and molar mass, is that they too are often limited to regions where such concepts are applicable. For very small molar masses, the conformation of a polymer molecule may be poorly described by the same theory applied for the larger constituents of a sample. Although MALS conformation measurements may be extrapolated in r_g for the case of linear polymers, such extrapolations must be used with great caution. Similar remarks apply, of course, to the use of viscometric measurements for characterizing complex molecules whose conformations (and, therefore, MHS coefficients) are changing with M.

Fig. 1 presents the conformation plot for $\log(r_g)$ vs. $\log(M)$ as obtained from a MALS measurement for the

polystyrene broad linear standard NIST706 in toluene. Superimposed thereon is a plot of the calculated $\log[\eta]$ as a function of $\log(M)$ for the same sample. From the latter plot, the MHS coefficients may be deduced by inspection of the slope and intercept to yield $a = 0.77$ and $K \approx 0.008$.

REFERENCES

1. Benoit, H.; Grubisic, Z.; Rempp, R. Reflections on "a universal calibration for gel permeation chromatography." J. Polym. Sci. B **1967**, *5*, 753.
2. Kamide, K.; Saito, M. *Determination of Molecular Weight*; Cooper, A.R., Ed.; John Wiley & Sons: New York, 1989.
3. Wyatt, P.J. Light scattering and the absolute characterization of macromolecules. Anal. Chim. Acta **1993**, *272*, 1.

BIBLIOGRAPHY

1. Billingham, N.C. *Molar Mass Measurements in Polymer Science*; John Wiley & Sons: New York, 1977.
2. Zimm, B.H. The Scattering of light and the radial distribution function of high polymer solutions. J. Chem. Phys. **1948**, *16*, 1093; *16*, 1099.

GPC/SEC/HPLC without Calibration: Multi-Angle Light Scattering

Philip J. Wyatt
Wyatt Technology Corp., Santa Barbara, California, U.S.A.

INTRODUCTION

Traditional size-exclusion chromatography (SEC) or gel permeation chromatography (GPC) as used to obtain molar masses and their distributions has been described elsewhere in this volume. The method suffers from three shortcomings:

1. The calibration standards generally differ from the unknown sample;
2. The results are sensitive to fluctuations in chromatography conditions (e.g., temperature, pump speed fluctuations, etc.); and
3. Calibration must be repeated frequently.

DISCUSSION

By adding a multiangle light-scattering[1] detector directly into the separation line, as shown schematically in Fig. 1, the eluting molar masses are determined *absolutely*, thus obviating the need for calibration and elimination of all of the three shortcomings listed. Fig. 1 illustrates also two most important elements associated with making quality light-scattering measurements: an inline degasser and an inline filter. The inline degasser is essential to minimize dissolved gases and, thereby, prevent the production of bubbles during the measurement process. Scattering from such bubbles can overwhelm the signals from the solute molecules or particles. Perhaps even more importantly, the system requires that the mobile phase be dust-free. The filter illustrated is placed between the pump and the injector. Usually, this filter station is comprised of two holders, holding, respectively, a 0.20 μm filter followed by a 0.02 or 0.01 μm filter. Although providing for such pristine operating conditions may seem bothersome, it has been shown that so-called "dirty" solvents, although rarely affecting the refractive index detector (RID) signal, do actually contribute significantly to the degradation of HPLC and SEC columns as well as resulting in the more frequent need to rebuild pumps. The additional solvent cleanup effort is well worth it!

An "absolute" light-scattering (LS) measurement is one that is independent of calibration standards which have "known" molar masses to which the unknown is compared. A LS measurement requires the chromatographer to determine the fundamental properties of the solution (refractive index, *dn/dc* value) and the detector response (field of view, sensitivity, solid angle subtended at the scattering volume). In addition, other factors must be determined, such as the light wavelength and polarization, geometry of the scattering cell, refractive index of all regions through which the scattered and incident light will pass, and the ratio of the scattered light to the incident light. Generally, these determinations are made in conjunction with appropriate multiangle light-scattering (MALS) software. The importance of light scattering's independence of a set of reference molar masses to determine the molar mass of an unknown cannot be overemphasized.

THEORY

As described in detail in Refs.,[1–3] the fundamental equation relating the quantities measured during a MALS detection and the quantities derived is, in the limit of "... vanishingly low concentrations...,"[2] given by

$$\frac{K^{*}c}{R(\theta)} \approx \frac{1}{MP(\theta)} + 2A_2c \tag{1}$$

where $K^{*} = 4\pi^2(dn/dc)^2 n_0{}^2(N_A\lambda_0{}^4)^{-1}$, M is the weight-average molar mass, N_A is Avogadro's number, dn/dc is the refractive index increment, λ_0 is the vacuum wavelength, θ is the angle between the incident beam and the scattered light, and n_0 is the refractive index of the solvent. The refractive index increment, dn/dc, is measured off-line (or looked up in the literature) by means of a differential refractive index (DRI) operating at the same wavelength as the one used for the MALS measurements. It represents the incremental refractive index change dn of the solution (solvent plus solute) for an incremental change dc of the concentration in the limit of vanishingly small concentration. Most importantly, the excess Rayleigh ratio, $R(\theta)$, and form factor $P(\theta)$ are defined respectively by

$$R(\theta) = \frac{f(\theta)_{\text{geom}}[I(\theta) - I_S(\theta)]}{I_0} \tag{2}$$

$$P(\theta) = 1 - \alpha_1 \sin^2(\theta/2) + \alpha_2 \sin^2(\theta/2) - \cdots \tag{3}$$

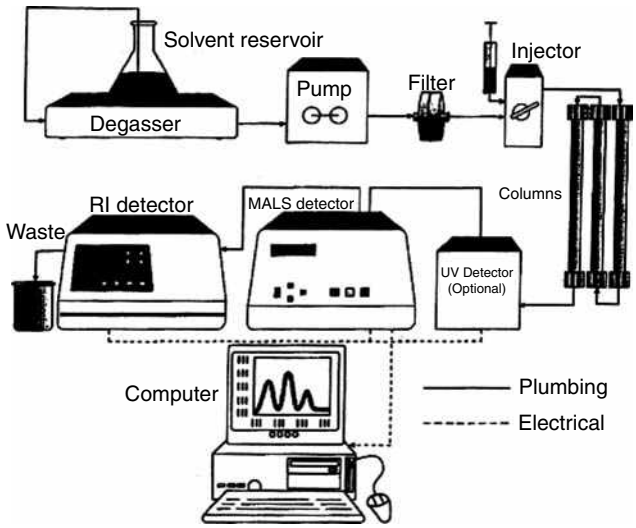

Fig. 1 Schematic diagram showing elements of traditional chromatograph with added MALS detector and dust- and bubble-reducing elements.

where

$$\alpha_1 = \frac{1}{3}\left(\frac{4\pi n_0}{\lambda_0}\right)\langle r_g{}^2\rangle \tag{4}$$

I_0 is the incident light intensity (ergs/cm^2/sec), $f(\theta)_{\text{geom}}$ is a geometrical calibration constant that is a function of the solvent and scattering cell's refractive index and geometry, and $I(\theta)$ and $I_S(\theta)$ are the normalized intensities respectively of light scattered by the solution and by the solvent per solid angle. The mean square radius is given by Eq. 5, where the distances r_i are measured from the molecule's center of mass to the mass element m_i:

$$\langle r_g{}^2\rangle = \frac{\sum_i r^2 m_i}{\sum_i m_i} = \frac{1}{M}\int r^2 dm \tag{5}$$

For MALS measurement following GPC separation, the sample concentration at the LS detector is usually diluted sufficiently that the term $2A_2c$ often may be safely dropped from Eq. 1. In some applications involving very high molar masses, it is often worthwhile to perform an off-line determination of the second virial coefficient from a Zimm plot[1–2] to confirm its negligible effect on the derived molar mass of Eq. 1.

BASIC PRINCIPLES

In the limit of vanishingly small concentrations, and the extrapolation of Eq. 3 to very small angles, the two basic principles of light scattering are evident:

1. The amount of light scattered (in excess of that scattered by the mobile phase) at $\theta \approx 0$ is directly proportional to the product of the weight-average molar mass and the concentration (ergo, measure the concentration and derive the mass!).
2. The angular variation of the scattered light at $\theta \approx 0$ is directly proportional to the molecule's mean square radius (i.e., size).

The successful application of absolute MALS measurements requires a sufficient number of resolved scattering angles to permit an accurate extrapolation to $\theta \approx 0$. Again, all required calculations are performed by the software. Whenever the mobile phase is changed, its corresponding refractive index must be entered into the software program, which should correct automatically for the resultant change of scattering geometry. Fig. 2 shows the normalized light-scattering signals at each scattering angle (detector) as a function of elution volume for a relatively broad sample. Also indicated is the corresponding concentration detector signal.

In conventional SEC measurements, it is necessary to calibrate the mass detector [DRI or ultraviolet (UV)] so that its response yields concentration directly. For example, a DRI detector, following calibration, should produce a response proportional to the refractive index change (Δn) detected. This is related to the concentration change Δc by the simple result $\Delta c = \Delta n/(dn/dc)$. Implicit in the use of a DRI detector, therefore, is that measurement of the concentration of the unknown requires that its differential refractive index, *dn/dc*, be measured, or otherwise determined.

Combining SEC with MALS to produce absolute molar mass data without molecular calibration standards also requires prior calibration of the concentration detector as well as calibration of the MALS detector itself. The latter calibration involves the determination of all geometrical contributions such that the MALS detector measures the Rayleigh excess ratio at each scattering angle. This is most

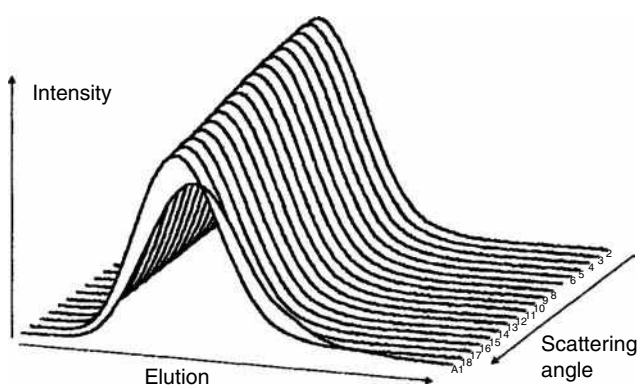

Fig. 2 Light-scattering and DRI signals from MALS setup shown in Fig. 1.

easily achieved by using a turbidity standard such as toluene. Details are found in Ref.[2] Once the refractive index of the mobile phase is entered, the software[4] performs the required calibration.

DERIVED MASS, SIZE, AND CONFORMATION

The MALS detector produces the absolute molar mass and mean square $\langle r_g^2 \rangle$ radius at each eluting slice. The *root mean square* (RMS) *radius* $r_g = \langle r_g^2 \rangle^{1/2}$ is often referred to by the misnomer "radius of gyration." There is a lower limit to its determination, which is generally about 8–10 nm. Below this value, MALS cannot generally produce a reliable value. Nevertheless, whenever both r_g and molar mass M are determined by MALS over a range of fractions present in an unknown sample, the sample's so-called conformation may be determined by plotting the logarithm of the RMS radius vs. the logarithm of the corresponding molar mass. A resultant slope of unity indicates a rodlike structure, a slope of 0.5–0.6 corresponds to a random coil, and a slope of 1/3 would indicate a sphere. Values below 1/3 generally suggest a highly branched molecular conformation.

Fig. 3 shows the MALS-derived molar mass and RMS radius as a function of elution volume for a broad polystyrene sample. Measurements were made in toluene at 690 nm.The value of *dn/dc* chosen was 0.11. From Fig. 3, it should be noted that the radius data begins to deteriorate around 10 nm, whereas the mass data extends to its detection limits. From the mass and radius data of Fig. 3, a conformation plot is easily generated with a slope of about 0.57 (i.e., corresponding to a random coil). These same data can also be used immediately to calculate the mass and size moments of the sample as well as its polydispersity as shown in the next section.

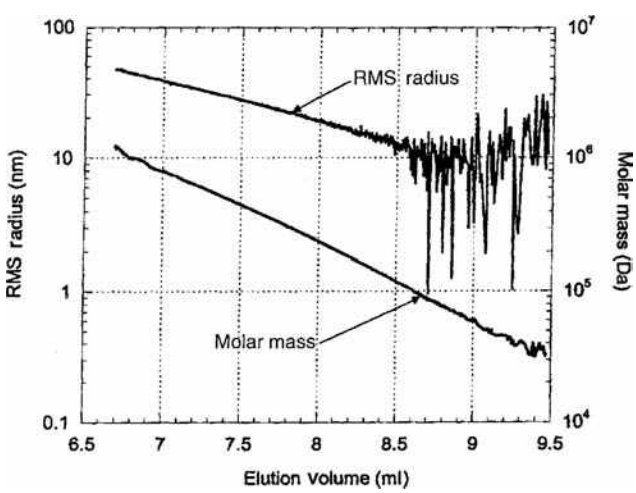

Fig. 3 Molar mass and RMS radius generated from data of Fig. 2 as a function of elution volume.

MASS AND SIZE MOMENTS

If we assume that the molecules in each slice, i, following separation by SEC, are monodisperse, the mass moments of each sample peak selected are calculated from the conventional definitions[3,5] by

$$M_n = \frac{\sum_i n_i M_i}{\sum_i n_i} = \frac{\sum_i c_i}{\sum_i c_i / M_i} \tag{6}$$

for the *number*-average molar mass, where n_i is the number of molecules of mass M_i in slice i and the summations are over all the slices present in the peak; the concentration c_i of the ith species, therefore, is proportional to $M_i n_i$;

$$M_w = \frac{\sum_i c_i M_i}{\sum_i c_i} = \frac{\sum_i n_i M_i^2}{\sum_i n_i M_i} \tag{7}$$

for the *weight*-average molar mass; and

$$M_z = \frac{\sum_i n_i M_i^3}{\sum_i n_i M_i^2} = \frac{\sum_i c_i M_i^2}{\sum_i c_i M_i} \tag{8}$$

for the z-average ("centrifuge") molar mass. Note how these "moments" are defined. In particular, the zaverage moment corresponds to "the next higher weighting" of both numerator and denominator by the factor Eqs. 6 and 7, of course, have a simple physical interpretation in terms of molecular numbers and concentration. From Eq. 8, it is a simple matter to write down expressions for the z + 1, z + 2, ... moments.

A similar set of expressions may be written down for the so-called size number and weight moments by replacing the mass terms M_i by the mean square radius values at each slice $\langle r_g^2 \rangle_i$ in Eqs. 6 and 7. A z-average term, on the other hand, takes on a more convoluted form.[5] For a random coil conformation under socalled theta conditions, the molar mass is directly proportional to $\langle r_g^2 \rangle$, and an expression that looks identical to Eq. 8 with one of the M_i of the numerator sum replaced by $\langle r_g^2 \rangle_i$ is obtained. However, in general, this "equivalence" is not the case and the "light-scattering" value LS is a better description, namely

$$\langle r_g^2 \rangle_{LS} = \frac{\sum_i c_i M_i \langle r_g^2 \rangle_i}{\sum_i M_i c_i} \tag{9}$$

Despite the non-random-coil-at-theta conditions, Eq. 9 is commonly referred to as the z-average mean square radius. The cross-term $M_i \langle r_g^2 \rangle_i c_i$ of Eq. 9 is a quantity measured directly by light scattering, at small $\sin^2(\theta/2)$, as clearly may be seen by expanding the term $1/P(\theta)$ in Eq. 1 using the expansion of $P(\theta)$ of Eq. 3.

POLYDISPERSITY

Within the peak selected, the sample polydispersity is simply the ratio of the weight to number average (viz. M_w/M_n) obtained from Eqs. 7 and 6, respectively.

DIFFERENTIAL MASS WEIGHT FRACTION DISTRIBUTION

The MALS measurements illustrated by Fig. 2 also may be used directly to calculate the differential mass weight fraction distribution, $x(M) = dW(M)/d(\log_{10}M)$ by using the measured $\log_{10}M$ as a function of the elution volume V. Thus, if the concentration detector's baseline subtracted response is $h(V)$, then $dW/dV = \pm h(V)/\int h(V)\,dV$, the integral representing the sum over all contributing concentrations to the peak. It is then easily shown[6] that

$$x(M) = -\frac{h(V)/\int h(V)dV}{d(\log_{10}M)/dV} \tag{10}$$

Note that for so-called "linear" column separations, the denominator $d(\log_{10}M)/dV$ is just a constant and, therefore, the differential weight fraction distribution will appear as a reflection (small mass first, from left to right) of the DRI signal. In general, column separations are not linear, so the DRI signal is not a good representation of the mass-elution distribution.

BRANCHING

The MALS measurements which eliminate the need for column calibration and all of its subsequent aberrations also permit the direct evaluation of branching phenomena in macromolecules because the basic quantitation of branching may only be achieved from such measurements as shown in the article by Zimm and Stockmayer.[7] Empirical approaches to quantitate branching, using such techniques as viscometry, have been shown to yield consistently erroneous results especially when long-chain branching becomes dominant.

REVERSED-PHASE AND OTHER SEPARATION TECHNIQUES

Because MALS determinations are independent of the separation mechanism, they may be applied to many types of HPLC. Reversed-phase separations are of particular significance because they cannot be calibrated, as sequential elutions do not occur in a monotonic or otherwise predictable manner. Again, as with all MALS chromatography measurements, all that is required is that the concentration and MALS's signals be available at each elution volume (slice).

Another separation technique of particular application for proteins, high-molar-mass molecules, and particles is the general class known as field-flow fractionation (FFF) in its various forms (cross-flow, sedimentation, thermal, and electrical). Once again, MALS detection permits mass and size determinations in an absolute sense without calibration. For homogeneous particles of relatively simple structure, a concentration detector is not required to calculate size and differential size and mass fraction distributions. Capillary hydrodynamic fractionation (CHDF) is another particle separation technique that may be used successfully with MALS detection.

REFERENCES

1. Wyatt, P.J. Light scattering and the absolute characterization of macromolecules. Anal. Chim. Acta **1993**, *272*, 1.
2. Zimm, B.H. The scattering of light and the radial distribution function of high polymer solutions. J. Chem. Phys. **1948**, *16*, 1093–1099.
3. Billingham, N.C. *Molar Mass Measurements in Polymer Science*; John Wiley & Sons: New York, 1977.
4. ASTRA®, software Wyatt Technology: Santa Barbara, CA, 1999.
5. Wyatt, P.J. *Analytical and Preparative Separation Methods of Biomacromolecules*; Aboul-Enein, H.Y., Ed.; Marcel Dekker, Inc: New York, 1999.
6. Shortt, D.W. Differential molecular weight distributions in high performance size exclusion. J. Liq. Chromatogr. & Relat. Techna. **1993**, *16*, 3371–3391.
7. Zimm, B.H.; Stockmayer, W.H. The dimensions of chain molecules containing branches and rings. J. Chem. Phys. **1949**, *17*, 1301.

BIBLIOGRAPHY

1. Huglin, M.B., Ed.; *Light scattering from Polymer Solutions*; Academic: London, 1972.

GPC/SEC: Calibration with Narrow Molecular-Weight Distribution Standards

Oscar Chiantore
Department of Inorganic, Physical, and Material Chemistry, University of Torino, Torino, Italy

INTRODUCTION

In size-exclusion chromatography (SEC), polymer solutions are injected into one or more columns in series, packed with microparticulate porous packings. The packing pores have sizes in the range between ~ 5 and 10^5 nm, and during elution, the polymer molecules may or may not, depending on their size in the chromatographic eluent, penetrate into the pores. Therefore, smaller molecules have access to a larger fraction of pores compared to the larger ones, and the macromolecules elute in a decreasing order of molecular weights. For each type of polymer dissolved in the chromatographic eluent, and eluting through the given set of columns with a pure exclusion mechanism, a precise empirical correlation exists between molecular weights and elution volumes. This relationship constitutes the calibration of the SEC system, which allows the evaluation of average molecular weights (MWs) and molecular-weight distributions (MWDs) of the polymer under examination.

Direct column calibration for a given polymer requires the use of narrow MWD samples of that polymer, with molecular weights covering the whole range of interest. The polydispersity of the calibration standards must be less than 1.05, except for the very low and very high MWs ($<10^3$ and $>10^6$), for which polydispersity can reach 1.20. The chromatograms of such standards give narrow peaks and to each standard is associated the retention volume of the peak maximum.

There is a limited number of polymers for which narrow MWD standards are commercially available: polystyrene, poly(methyl methacrylate), poly (α-amethyl styrene), polyisoprene, polybutadiene, polyethylene, poly(dimethyl siloxane), polyethyleneoxide, pullulan, dextran, polystyrene sulfonate sodium salt, and globular proteins. In some cases, the standards available cover a limited molecular weight range, so it may be impossible to construct the calibration curve over the complete column pore volume.

Standard methods for calibration of SEC columns with narrow MWD samples have been published by the American Society for Testing and Materials (ASTM D2596-97) and the Deutsches Institut for Normung (DIN 55672-1).

PROCEDURE

Fresh solutions of the standards are prepared in the solvent used as chromatographic eluent. Calibration solutions should be as dilute as possible, in order to avoid any concentration dependence of sample retention volumes. The concentration effect causes an increase of retention volumes with increased sample concentration. As a rule of thumb, when high efficiency microparticulate packings are used, the concentration of narrow standards should be $\leq 0.025\%$ (w/v) for MW over 10^6, $\leq 0.05\%$ for MW between 10^6 and 2×10^5, and $\leq 0.1\%$ for MW down to 10^4. With a lower MW and in the oligomer range, the sample concentration can be higher than the previously suggested values.

Two or more standards may be dissolved and injected together to determine several retention volumes with a single injection. In such a case, the MW difference between the samples in the mixture should be sufficient to give peaks with baseline resolution. A sufficient number of narrow MWD standards, with different MWs, are required for establishing the calibration of a SEC column system. At least two standards per MW decade should be injected, and a minimum of five calibration points should be obtained in the curve.

MW FRACTIONATION RANGE OF THE COLUMN SET

The maximum injection volume depends from column size and packing pore volumes, and for high-efficiency 300×8 mm columns, it is generally recommended not to exceed 100 μl per column.

The flow rate of the chromatographic apparatus must be extremely stable and reproducible: Flow rate fluctuations about the specified value should be lower than 3%, and long-term drift lower than 1%. Repeatability of flow rate setting is extremely important, as a 1% constant deviation of the actual flow rate from the required value may give 20% differences in calculated MW averages.

The systematic errors introduced by flow rate differences may be avoided by adding to the solutions a

minimum amount of a low-molecular-weight internal standard (*O*-dichloro benzene, toluene, acetone, sulfur) which must not interfere with the polymer peaks. Flow rate is monitored in each chromatogram by measuring the retention time of the internal standard, and eventual variations may be corrected accordingly.

The peak retention times for the narrow polymer standards are measured from the chromatograms and transformed into retention volumes according to the real flow rate. For each standard, the logarithm of nominal molecular weight is plotted against its peak elution volume. Often, retention times are directly employed and plotted as the measured variable, and in this case, the condition of equal flow rate elutions for all the standards and for any subsequent sample analysis is achieved by means of the internal standard elution.

The molecular weight of the standards is supplied by the producers, either with a single value which should correspond to that of peak maximum, or with a complete characterization data sheet containing the values of M_n and M_w determined by osmometry and light scattering. In the latter case, the peak molecular weight to be inserted in the calibration plot is the mean value $(M_n M_w)^{1/2}$. A typical calibration curve for a threecolumn set, 300×7.5 mm, packed with a mixture of individual pore sizes is shown in Fig. 1. The calibration curve has a central part which is essentially linear and becomes curved at the two extremes: on the high-MW side when it approaches the retention value of totally excluded samples; on the low-MW side with a downward curvature until it reaches the retention time of total pore permeation.

The calibration curve, therefore, defines the extremes of retention times (or volumes) for the specific column system, the useful retention interval for sample analysis, and the related MW range. Columns packed with a balanced mixture of different pore sizes are capable of giving linear calibrations over the whole MW range of practical interest, from the oligomer region to more than 10^6.

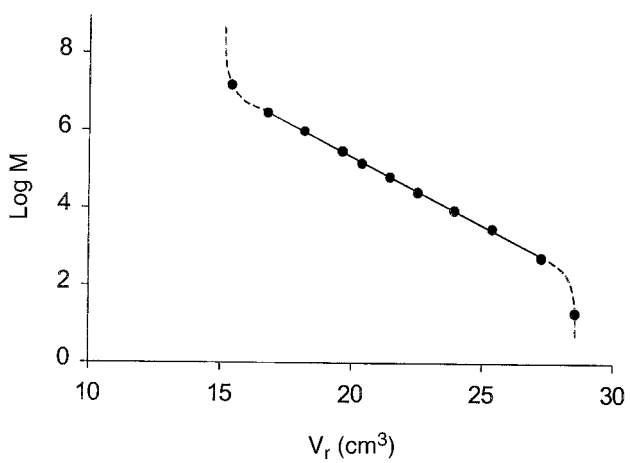

Fig. 1 Example of calibration curve with narrow MWD standards.

The plot of log M vs. peak retention volumes of narrow standards is represented in the more general form by a nth-order polynomial of the type

$$\log M = A + BV_r + CV_r^2 + DV_r^3 + \cdots$$

the coefficients of which are determined by regression on the experimental data. Most usually, when the linear plot is not sufficient to fit the points, a third-order polynomial will be adequate to represent the curve. Higher-order equations, although improving the fit, should be used with great care, as they can lead to unrealistic oscillations of the function.

The goodness of different equations fitted to the experimental data points is assessed by the results of statistical analysis or by simply considering the standard error of the estimate. It should be also considered that the adequacy of the calibration function for the determination of correct MW values is also dependent on the quality of the narrow MWD standards. Their nominal MWs are determined with independent absolute methods and are affected by experimental errors which may be different between samples with different MWs, or coming from different producers. A check of the quality of the narrow standards may be obtained by calculating the percent MW deviation of each standard from the calibration curve:

$$\Delta M(V_i)\% = \frac{M_{\text{pcak}}(V_i) - M_{\text{calc}}(V_i)}{M_{\text{pcak}}(V_i)} \times 100$$

A plot of $\Delta M(V_i)\%$ vs. log M results in positive and negative values scattered around the MW axis, which allows one to visualize the limits of percent error into which the MW of standards are estimated by the calibration curve. If the MW error of some standard is found to be significantly larger than all the others, it is likely that its nominal MW is incorrect. The point of such sample should be removed from the calibration and the regression recalculated.

The calibration curve should always cover the MW of the samples that must be analyzed. Extrapolation of the calibration outside the range of injected polymer standards should be avoided in MW determinations.

From the calibration curve, the resolution power of the column set may also be evaluated. Resolution between two adjacent peaks, 1 and 2, is defined in terms of their retention volumes, V_r, and peak widths, w:

$$R_S = \frac{2(V_{r2} - V_{r1})}{w_1 + w_2}$$

The calibration is often expressed in the form of ln M vs. V_r, and assuming a linear function, it may be written as

$$\ln M = \ln D_1 - D_2 V_r$$

By solving for V_r and substituting into the relationship for R_S, we obtain

$$R_S = \frac{\ln(M_1/M_2)}{wD_2} = \frac{\ln(M_1/M_2)}{4\sigma D_2}$$

valid for peaks of similar width or standard deviation σ, where $w_1 \approx w_2 = w = 4\sigma$. The above equation shows that the MW fractionation of SEC columns is linked to both their useful pore volume (slope D_2 of the calibration curve) and to packing quality (column efficiency or number of plate heights, determining peak widths). Working with columns having linear calibration in their whole fractionation range guarantees equal resolution power over several MW decades.

BIBLIOGRAPHY

1. ASTM D5296-97. Standard Test Method for Molecular Weight Averages and Molecular Weight Distribution of Polystyrene by High Performance Size-Exclusion Chromatography (1997).
2. DIN 55672-1. Gelpermeationschromatographie Teil 1: Tetrahydrofuran als Elutionsmittel (1995–02) (1995).
3. Janca, J., Ed.; *Steric Exclusion Liquid Chromatography of Polymers*; Marcel Dekker, Inc.: New York, 1984.
4. Mori, S.; Barth, H. *Size Exclusion Chromatography*; Springer-Verlag: Berlin, 1999.
5. Yau, W.W.; Kirkland, J.J.; Bly, D.D. *Modern Size-Exclusion Liquid Chromatography*; John Wiley & Sons: New York, 1979.

GPC/SEC: Calibration with Universal Calibration Techniques

Oscar Chiantore
Department of Inorganic, Physical, and Material Chemistry, University of Torino, Torino, Italy

INTRODUCTION

Direct calibration of (gel permeation chromatography/size exclusion chromatography) GPC/SEC columns requires well characterized polymer standards of the same type of polymer one has to analyze. However, narrow molecular-weight distribution (MWD) standards are available for a limited number of polymers only, and well-characterized broad MWD standards are not always accessible. The parameter controlling separation in GPC/SEC is the size of solute in the chromatographic eluent. Therefore, if different polymer solutes are eluted in the same chromatographic system with a pure exclusion mechanism, at the same retention volume, molecules with the same size will be found.

DISCUSSION

By plotting the logarithm of solute size vs. retention volume, the points of all different polymers will be represented by a unique curve—a universal calibration curve. Thus, by application of the universal calibration, average molecular weights (MWs) and MWDs of any type of polymer may be evaluated from the SEC, provided that the relationship between molecular size and polymer molecular weight is known.

Several size parameters can be used to describe the dimensions of polymer molecules: radius of gyration, end-to-end distance, mean external length, and so forth. In the case of SEC analysis, it must be considered that the polymer molecular size is influenced by the interactions of chain segments with the solvent. As a consequence, polymer molecules in solution can be represented as equivalent hydrodynamic spheres,[1] to which the Einstein equation for viscosity may be applied:

$$\eta = \eta_0(1 + 2.5\phi_s) \tag{1}$$

η and η_0 are the viscosities of solution and solvent, respectively, and ϕ_s is the volume fraction of solute particles in the solution.

By expressing the solute concentration c in grams per cubic centimeter, the relationship holds:

$$\phi_s = \frac{cN_AV_h}{M} \tag{2}$$

where N_A is Avogadro's number and V_h and M are the hydrodynamic volume and the molecular weight of the solute, respectively. Substituting in Eq. 1 and taking into account that

$$[\eta] = \lim_{c\to 0}\left(\frac{(\eta - \eta_0)/\eta_0}{c}\right) \tag{3}$$

we obtain

$$[\eta]M = 2.5N_AV_h \tag{4}$$

Eq. 4 states that the hydrodynamic volume of a polymer molecule is proportional to the product of its intrinsic viscosity times the molecular weight.

The use of $[\eta]M$ as size parameter for GPC/SEC universal calibration was first proposed by Benoit and coworkers[2] and shown to be valid for homopolymers and copolymers with various chemical and geometrical structures. Their data are reported in the semilogarithmic plot of Fig. 1.

The hydrodynamic volume parameter $[\eta]M$ has been proven to be applicable also to the cases of rodlike polymers[3] and to separations in aqueous solvents[4] where, however, secondary non-exclusion mechanisms often superimpose and affect the sample elution behavior. In the latter situation, careful choice of eluent composition must be made in order to avoid any possible polymer-packing interaction.

The application of universal calibration requires a primary column calibration with elution of narrow MWD standards. For SEC in tetrahydrofuran, polystyrene (PS) standards are generally used. Intrinsic viscosities of the standards are either known or calculated from the proper Mark–Houwink equation, so that the plot of $\log[\eta]_{PS}M_{PS}$ values vs. retention volumes V_r may be created. The universal calibration equation is obtained by polynomial regression, in the same way described for the calibration with narrow MWD standards.

Average-molecular weights and MWDs of any polymer sample eluted on the same columns with pure exclusion mechanism may be calculated by considering that, at any retention volume, the following relationship holds:

$$[\eta]_iM_i = [\eta]_{PS,i}M_{PS,i} \tag{5}$$

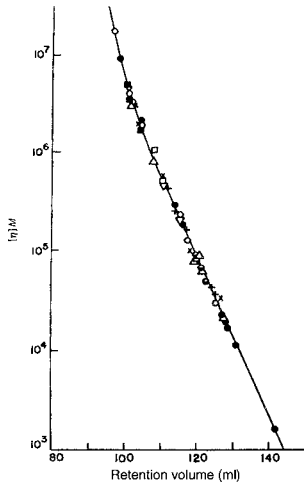

Fig. 1 Retention volume vs. $[\eta]M$.
Source: From A universal calibration for gel permeation chromatography, in J. Polym. Sci. B.[2]

from which

$$M_i = \frac{[\eta]_{\mathrm{PS},i} M_{\mathrm{PS},i}}{[\eta]_i} \tag{6}$$

To solve Eq. 6, the denominator must be known. Substituting into the denominator the Mark–Houwink expression $[\eta] = KM^a$ for the investigated polymer and rearranging, we obtain

$$M_i = \left(\frac{[\eta]_{\mathrm{PS},i} M_{\mathrm{PS},i}}{K} \right)^{1/1+a} \tag{7}$$

where K and a are the constants of the viscosimetric equation for that polymer, dissolved in the chromatographic eluent and at the temperature of analysis.

From Eq. 7, the molecular weight of each fraction in the chromatogram is obtained and average molecular weights may be calculated by application of the appropriate summations. The numerator in Eq. 7 is the value of the universal calibration at each retention volume.

The necessary conditions for application of the universal calibration method and for calculation of molecular weights through Eq. 6 is the knowledge of the $[\eta]_i$ values, which are obtained from the Mark–Houwink equations when the pertinent values of K and a constants are known. An alternative way is to make a continuous measurement of $[\eta]_i$ at the different elution volumes with an online viscometer detector coupled to the usual concentration detector system.

Methods for application of the universal calibration have been developed also for cases where K and a of the polymer of interest are not known and neither $[\eta]_i$ values are measured. Such methods are based on the availability of two broad MWD standards, having different molecular weights, of the polymer under examination.[5]

One important property of the universal calibration concept is that, in the SEC separation of complex polymers (i.e., polymers with different architectures or copolymers with non-constant chemical composition), at each retention volume, $V_{r,i}$, molecules with same hydrodynamic volume but possibly different molecular weights will elute. It has been demonstrated that, in such a case, the application of the hydrodynamic volume parameter, $[\eta]M$ gives the number-average molecular weight, M_n, of the polymer.[6] In fact, at each retention volume, the intrinsic viscosity of the eluted fraction is given by the weight average over the n different molecular species present:

$$[\eta]_i = w_1[\eta]_1 + w_2[\eta]_2 + \cdots + w_n[\eta]_n \tag{8}$$

Eq. 8 may be written as

$$[\eta]_i = \frac{[\eta]_1 M_1 w_1}{M_1} + \frac{[\eta]_2 M_2 w_2}{M_2} + \cdots + \frac{[\eta]_n M_n w_n}{M_n} \tag{9}$$

As the condition holds, at each retention volume

$$[\eta]_1 M_1 = [\eta]_2 M_2 = \cdots = [\eta]_{\mathrm{PS}} M_{\mathrm{PS}} \tag{10}$$

Eq. 9 becomes

$$[\eta]_i = [\eta]_{\mathrm{PS}} M_{\mathrm{PS}} \sum \left(\frac{w_i}{M_i} \right) = \frac{[\eta]_{\mathrm{PS}} M_{\mathrm{PS}}}{M_{n,i}} \tag{11}$$

$$[\eta]_i M_{n,i} = [\eta]_{\mathrm{PS}} M_{\mathrm{PS}} \tag{12}$$

By considering all the fractions of the chromatogram, the M_n value of the whole sample may be then calculated.

Experimental aspects for the determination of molecular weight averages and MWD distributions by GPC/SEC using universal calibration are described in a standard ASTM method.[7] Detailed discussion on the validity and limitations of the method may be also found in Ref.[8]

REFERENCES

1. Flory, P.J. *Principles of Polymer Chemistry*; Cornell University Press: Ithaca, NY, 1953.
2. Grubisic, Z.; Rempp, P.; Benoit, H. A universal calibration for gel permeation chromatography. J. Polym. Sci. B, **1967**, *5*, 753.
3. Dawkins, J.V.; Hemming, M. Polymer **1975**, *16*, 554.
4. Dubin, P.L. *Aqueous Size Exclusion Chromatography*; Elsevier: Amsterdam, 1988.
5. Coll, H.; Gilding, D.K. J. Polym. Sci. A-2. **1970**, *8*, 89.
6. Hamielec, A.E.; Ouano, A.C.; Nebenzahl, L.L. J. Liquid Chromatogr. **1978**, *1*, 111.
7. ASTM D 3593-80, Standard Test Method for Molecular Weight Averages and Molecular Weight Distribution of Certain Polymers by Liquid Size-Exclusion Chromatography (Gel Permeation Chromatography—GPC) Using Universal Calibration; 1980.
8. Dawkins, J.V. *Steric Exclusion Liquid Chromatography of Polymers*; Janca, J., Ed.; Marcel Dekker, Inc.: New York, 1984.

GPC/SEC: Experimental Conditions

Sadao Mori
PAC Research Institute, Mie University, Nagoya, Japan

INTRODUCTION

In order to calculate the molecular-weight averages of a polymer from the size-exclusion chromatography (SEC) chromatogram, the relationship between the molecular weight and the retention volume (called the "calibration curve") needs to be known, unless a molecular-weight-sensitive detector is used. The retention volume of a polymer changes with changing experimental conditions; therefore, when molecular-weight averages of the polymer are calculated using the calibration curve, care must be taken with the effect of experimental conditions.[1]

DISCUSSION

Sample concentration is one of the most important operating variables in SEC, because the retention volumes of polymers increase with increased concentration of the sample solution. The concentration dependence of the retention volume is a well-known phenomenon and the magnitude of the peak shift to higher retention volume is more pronounced for polymers with a higher molecular weights than for those with lower molecular weights. This phenomenon is almost improbable for polymers with a molecular weight lower than 10^4 and is observed ever at a low concentration, such as 0.01%, although the peak shift is smaller than that at a higher concentration.

In this sense, this concentration dependence of the retention volume should be called the "concentration effect," not "overload effect" or "viscosity effect." If a large volume of a sample solution is injected, an appreciable shift in retention volume is observed, even for low-molecular-weight polymers; this is called the "overload effect."

The retention volume increases with increasing concentration of the sample solution and the magnitude of the increase is related to the increasing molecular weight of the sample polymers.[2] The reason for the increase in retention volume with increasing polymer concentration is considered to result from the decrease in the hydrodynamic volume of the polymer molecules in the solution.

Molecular-weight averages calculated with calibration curves of varying concentrations may differ in value. As the influence of the sample concentration on the retention volume is based on the essential nature of the hydrodynamic volume of the polymer in solution, it is necessary to select experimental conditions that will reduce the errors produced by the concentration effect.

By rule of thumb, the preferred sample concentrations, if two SEC columns of 8 mm inner diameter (I.D.) $\times$ 25 cm in length are used, are as follows. The sample concentrations should be as low as possible and no more than 0.2%. For high-molecular-weight polymers, concentrations less than 0.1% are often required, and for low-molecular-weight polymers, concentrations of more than 0.2% are possible. The concentrations of polystyrene standards for calibration should be one-half of the unknown sample concentration. For polystyrene standards with a molecular weight over 10^6, it is preferable that they are one-eighth to one-tenth and for those with a molecular weights between 5×10^5 and 10^6, a quarter to one-fifth of the sample concentration.

The retention volume of a polymer sample increases as the injection volume increases.[3] In some cases, the increase in the retention volume from an injection volume increase from 0.1 to 0.25 ml was 0.65 ml, whereas that from 0.25 to 0.5 ml was only 0.05 ml, suggesting that a precise or constant injection is required even if the injection volume is as small as 0.1 or 0.05 ml. In view of the significant effect of the injection volume on the retention volume, it is important to use the same injection volume for the sample under examination as that used when constructing the calibration curve. The use of a loop injector is essential, and the same injection volume must be employed for all sample solutions including calibration standards, regardless of their molecular-weight values. The increase in the injection volume results in a decrease in the number of theoretical plates, due to band broadening, which means that the calculated values of the molecular-weight averages and distribution deviate from the true values (Fig. 1).

The retention volume in SEC increases with increasing flow rate.[3] This is attributed to non-equilibrium effects, because polymer diffusion between the intrapores and extrapores of gels is sufficiently slow that equilibrium cannot be attained at each point in the column. With a decreasing flow rate, the efficiency and the resolution are increased. Bimodal distribution of a PS standard (NBS706) with a narrow molecular weight distribution was clearly observed at the lower flow rate.

Separation of molecules in SEC is governed, mainly, by the entropy change of the molecules between the mobile phase and the stationary phase, and the temperature independence of peak retention can be predicted. However, an

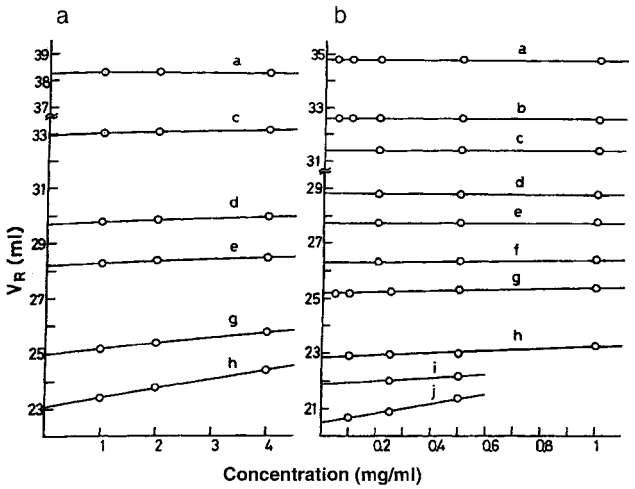

Fig. 1 Concentration dependence of retention volume for polystyrene in good solvents on polystyrene gel columns: (a) in toluene on microstyragel columns (3/8 in. × 1 ft × 4) (10^6, 10^5, 10^4, and 10^3 nominal porosity) at a flow rate 2 ml/min and injected volume 0.25 ml; (b) in Tetrahydrofuran on Shodex A 80 *M* columns (8 mm × 50 cm × 2) (mixed polystyrene gels of several nominal porosities) at a flow rate 1.5 ml/min and injected volume 0.25 ml. Molecular weight of polystyrene standards: (a) 2100; (b) 10,000; (c) 20,400; (d) 97,200; (e) 180,000; (f) 411,000; (g) 670,000; (h) 1,800,000; (i) 3,800,000; (j) 8,500,000.

increase in retention volume with increasing column temperature is often observed. A temperature difference of 10°C results in a 1% increase in the retention volume, which corresponds to a 10–15% change in molecular weight.[4]

Two main factors that cause retention-volume variations with column temperature are assumed: an expansion or a contraction of the mobile phase in the column and the secondary effects of the solute to the stationary phase. When the column temperature is 10°C higher than room temperature, the mobile phase (temperature of the mobile phase is supposed to be the same as room temperature in this case) will expand about 1% from when it entered the columns, resulting in an increase in the real flow rate in the column due to the expansion of the mobile phase and the decrease in the retention volume. The magnitude of the retention-volume dependence on the solvent expansion is evaluated to be about one-half of the total change in the retention volume. The residual contribution to the change in retention volume is assumed to be that due to gel–solute interactions such as adsorption.

In order to obtain accurate and precise molecular-weight averages, the column temperature, as well as the difference of both temperatures, the solvent reservoir and the column oven, must be maintained.

Other factors affecting retention volume are the viscosity of the mobile phase, the sizes of gel pores, and the effective size of the solute molecules. Of these, the former two can be ignored, because they exhibit either no effect or only a small effect. The effective size of a solute molecule may also change with changing column temperature. The dependence of intrinsic viscosity on column temperature for PS in chloroform, tetrahydrofuran, and cyclohexane were tested.[5] The temperature dependence of intrinsic viscosity of PS solutions was observed over a range of temperatures. The intrinsic viscosity of PS in tetrahydrofuran is almost unchanged from 20°C up to 55°C, whereas the intrinsic viscosity in chloroform decreased from 30°C to 40°C. Cyclohexane is a theta solvent for PS at around 35°C and intrinsic viscosity in cyclohexane increased with increasing column temperature.

Because the hydrodynamic volume is proportional to the molecular size, the intrinsic viscosity can be used as a measure of the molecular size and optimum column temperatures and solvents must be those where no changes in intrinsic viscosity are observed.

REFERENCES

1. Mori, S.; Barth, H.G. *Size Exclusion Chromatography*; Springer-Verlag: New York, 1999; Chap. 5.
2. Mori, S. Effect of experimental conditions. In *Steric Exclusion Liquid Chromatography of Polymers*; Janča, J., Ed.; Marcel Dekker, Inc.: New York, 1984.
3. Mori, S. High-speed gel permeation chromatography. A study of operational variables. J. Appl. Polym. Sci. **1977**, *21*, 1921.
4. Mori, S.; Suzuki, T. Effect of column temperatures on molecular weight determination by high performance size exclusion chromatography. Anal. Chem. **1980**, *52*, 1625.
5. Mori, S.; Suzuki, M. Hydronic volume fluctuation of polystyrene by column temperature and its effect to retention volume in size exclusion chromatography. J. Liquid Chromatogr. Relat. Technol. **1984**, *7* (9), 1841.

Gradient Development in TLC

Wojciech Markowski
Department of Inorganic and Analytical Chemistry, Medical University of Lublin, Lublin, Poland

INTRODUCTION

The main task of analytical TLC is separation of sample from matrix, separation of sample components, their identification, and the measurement of peak heights or areas for quantitative purposes. Finally, the peaks should be narrow and symmetrical. Two problems are related to the analysis: choice of suitable conditions of development, such that all components of the sample are eluted in optimal range of retention factor; and their separation, allowing for identification and quantitation.

GENERAL ELUTION PROBLEM

In practice, a problem that appears very often is components of widely differing retention properties being present in the sample.[1–3] For example, consider a model mixture composed of 15 components with capacity factors $k_0(j)$ forming a geometrical progression and exponentially dependent on the modifier concentration (molar or volume fraction φ), in accordance with the Snyder–Soczewiński model of adsorption (Fig. 1A–D).[4]

$$k_0(j) = \frac{25.6}{2^j}, \quad k(j,i) = \frac{k_0(j)}{c(i)^{m(j)}} \tag{1}$$

$$R_F(j,i) = \frac{1}{1 + k(j,i)} \tag{2}$$

where j is the code of the solute (1–15), i the number of elution step (elution fraction), $k(j, i)$ the capacity factor of solute j in the ith step, $R_F(j, i)$ the retardation factor of solute j in the fraction of eluent of concentration $\varphi(i)$, $\varphi(i)$ the concentration of modifier (mole/volume fraction) in the ith step, $v(i)$ the volume of eluent delivered in the ith step, and $m(j)$ the slopes of linear plots of $R_M(j,i) = R_M^0(j) - m(j)\log\varphi(i)$.

In Fig. 1 are presented chromatograms (simulated) to illustrate the "general elution problem" addressed to TLC. Consider a representative mixture for components of a wide range of polarity. If the elution conditions are suitable for weakly polar compounds, the strongly polar ones will remain at or near the start line. On the other hand, if the system is set up so that strongly polar components are separated, the weakly polar ones will accumulate at the mobile-phase front. It can be seen from the picture that no isocratic eluent can separate all components. A pure modifier of $\varphi = 1.0$ (100%) well separates solutes S3–S6, and the less polar solutes accumulate near the solvent front (Fig. 2A); for $\varphi = 0.5$ (50%), solutes S5–S8 are well separated, the remaining ones accumulating near either the start line or the front line (Fig. 2B); for $\varphi = 0.05$ (5.0%), solutes 1–11 accumulate near the start line; only solutes S12–S15 are separated in the optimal R_F window (Fig. 2C). Thus, only about one-third of the components can be satisfactorily separated by isocratic elution. This problem is named "the general elution problem" and is attacked in different ways in different modes of chromatography (Fig. 2D). Usually, some kind of change of parameters is done. This involves a stepwise or continuous change of chosen parameter. Both in column chromatography and in TLC, the isocratic mode is preferred unless the "general elution problem" is encountered. Its solution may consist of gradient elution (stepwise or continuous), gradation of stationary phase, development with a mixed eluent composed of solvents of different polarity (polyzonal TLC), or temperature programming.[3,5,6] When the strength of mobile phase delivered to the layer is programmed, this is called gradient development. One of advantages of gradient TLC is the feasibility of application of both simple and reversed gradients (decreasing modifier concentration) and a complex gradient—a combination of both types of gradient. The gradient of the mobile phase is both simple and practical in application. In a simple gradient, the eluent strength is increased from the beginning to the end of the development process. The reversed gradient can be applied in the case of multiple development (MD), and the eluent strength decreases with increase in number of developments.

DESCRIPTION OF THE MOBILE-PHASE GRADIENT

The gradient is defined by the variation of elution strength of a series of single solvents or a mixture of solvents, or by the variation of composition of the mobile phase, by the percentage content of the weaker component A and the stronger component B, called the modifier. The gradient is also characterized by its steepness, shape, and complexity. The steepness is defined by the concentration of the modifier of the first and last fractions of the eluent delivered to the adsorbent layer. When the differences in modifier concentrations between all steps are constant, the gradient is

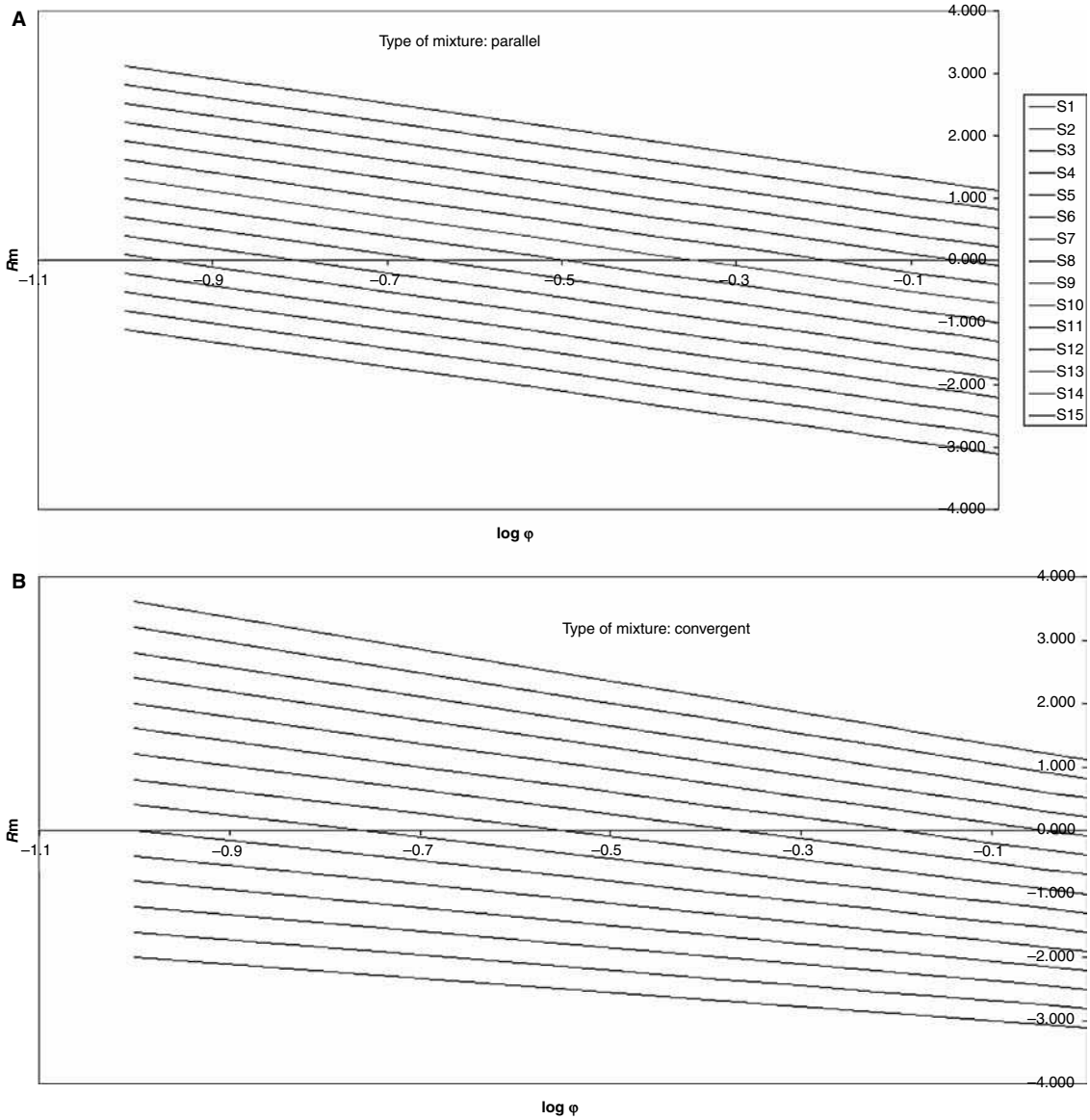

Fig. 1 Family of 15 $R_M(j,i) = R_M{}^0(j) - m(j)\ \log\ c(i)$ plots for model mixture of solutes S1–S15 according to adsorption model of Snyder–Soczewiński. A, Family of parallel lines; B, family of convergent lines; C, family of divergent lines; and D, family of crossing lines.

called linear. When these differences are large in the beginning and then decrease in the consecutive steps, it is known as a convex gradient program, and in the opposite case, as a concave gradient. The complexity of the gradient is related to the number of fractions of mobile phase delivered to the layer and combination of three basic profiles and dimensions of the volume of fractions. Fig. 3 illustrates different profiles of stepwise simple gradient use in TLC.

MIGRATION OF SOLUTES UNDER MOBILE-PHASE GRADIENT CONDITIONS

The use of a stepwise gradient of the mobile phase is well described by the theoretical models.[4–8] In the ideal situation, the spots of solutes are overtaken by consecutive fronts of increased modifier concentration, accelerating their migration so that even strongly retained solutes start to migrate. Depending on the polarities of the solutes, some migrate all the time in the first concentration zones [when the retardation factor of the solutes follow the condition $R_F(j,1) \geq 1 - v(1)$], or they are overtaken by the consecutive zones of higher concentration. It can be seen (Fig. 4) that both weakly polar (15–13) and strongly polar (1–5) compounds are well separated in the final chromatogram. The migration of the components under conditions of stepwise gradient with one void volume of mobile phase is describing by the following equations: In the case when solutes migrate only in the first zone, the final position $R_P(j)$ is specified by

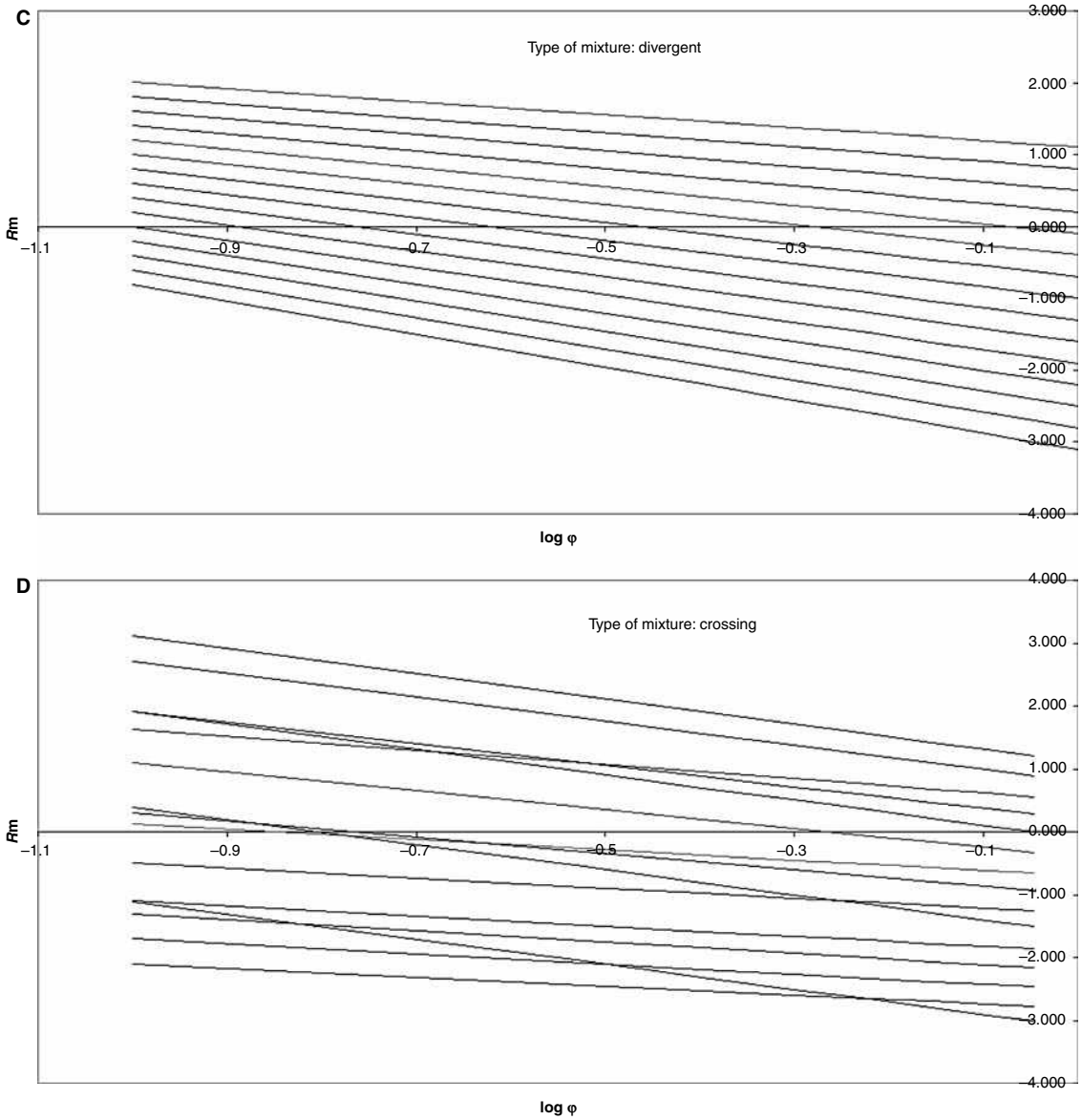

Fig. 1 (*Continued*).

$$R_{\mathrm{P}}(j) = R_{\mathrm{F}}(j,1) = \frac{1}{1 + k(j,1)} \tag{3}$$

and for other solutes migrating through different zones of concentration, the final position is specified by

$$R_{\mathrm{P}}(j) = \sum_{i=1}^{h-1} v(i) \frac{R_{\mathrm{F}(j,i)}}{1 - R_{\mathrm{F}(j,i)}} + R_{\mathrm{F}(j,h)} \left(1 - \sum_{i=1}^{h-1} v(i) \frac{1}{1 - R_{\mathrm{F}(j,i)}} \right) \tag{4}$$

(For detailed derivation and discussion, see Ref.[7]) Both equations could be applied to formulate computer programs (in any programming language or using a spreadsheet) that calculate the final spot position for a given gradient program and retention–eluent composition relationships. The retention–eluent composition relationships are obtained from preliminary isocratic runs. The experimental results obtained in Refs.[9,10] are in good agreement with the theoretical values calculated from Eqs. 1 and 2 (average error 1.5% and 0.17%). The simulation of gradient development can help considerably in the selection of an optimal program for a given system of adsorbent/mobile phase.[11] In the model, it is assumed that the stagnant mobile phase in the pores of the adsorbent is rapidly displaced and demixing does not occur. In reality, demixing takes place (especially in the first fractions of low concentrations of modifier) and the exchange of the stagnant solvent in the pores with the mobile phase is slow;

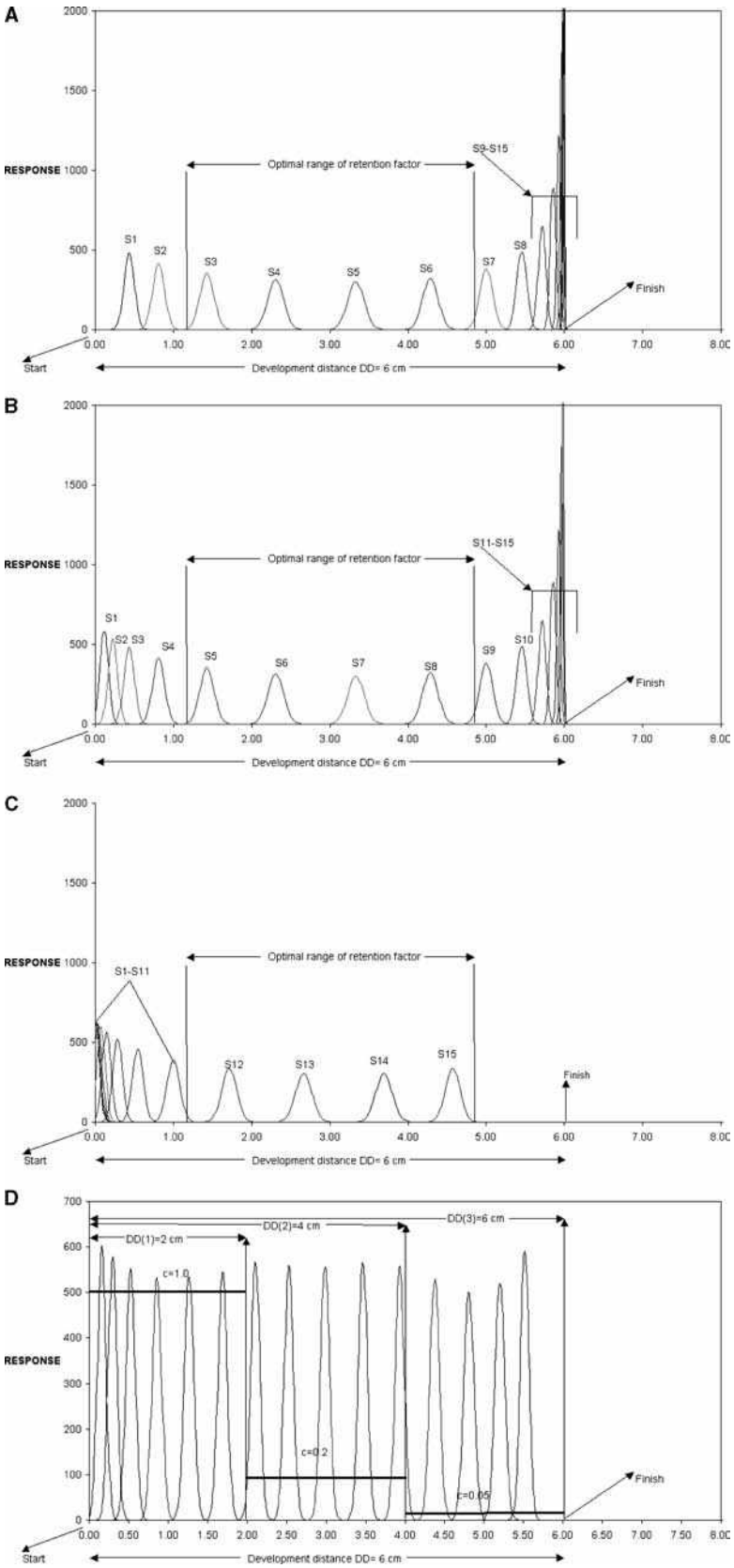

Fig. 2 Simulated chromatograms of hypothetical solutes S1–S15 (Fig. 1) for isocratic conditions of development. Concentration of modifier in volume fraction: A, $\varphi = 1.0$; B, $\varphi = 0.5$; C, $\varphi = 0.05$. Other conditions of simulation: development distance $DD = 6$ cm; spreading of zone (according to Eqs. 8–10 and Belenkii model of spot broadening.[5] D, Simulated chromatogram of hypothetical solutes S1–S15 for G IMD. Number of developments $n = 3$; increment of development distance $IDD = 2$ cm; total distance of development $DD = 6$ cm. Reverse gradient of mobile phase: $\varphi(1) = 1.0$; $\varphi(2) = 0.2$; $\varphi(3) = 0.05$.

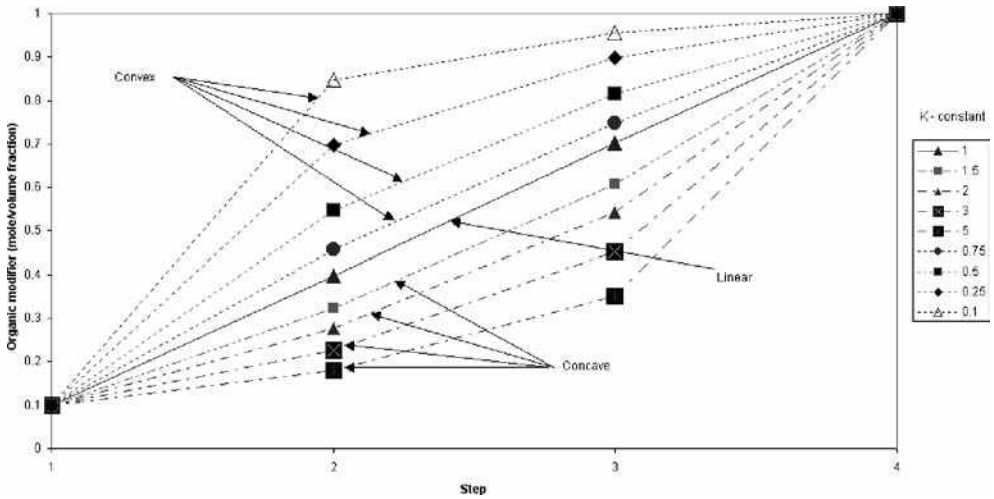

Fig. 3 Various stepwise gradient profiles used in simple gradient. Constant K is a measure of deviation from linearity by convex and concave profiles of gradient.

therefore, the boundaries of the concentration zones are not sharp but somewhat diffuse, and the solutes migrate in zones of intermediate properties. The demixing effect may cause deviation of the gradient profile from the planned one, especially for low concentration of modifier, and in consequence, the concentration fronts are delayed. For this reason, the distances of migration of solutes in lower concentration zones are smaller. The final relative position is lower in comparison to the position expected for ideal conditions. Because of the complexity of gradient development, only some rules of thumb can be given. In planning the gradient program, it is necessary to choose conditions under which the weakly retained components do not migrate with the front of the mobile phase and the strongly retained ones do not remain on the start line. After the choice of adsorbent (the first choice is silica gel), the next step is selection of the eluent. After Ref.,[8] the following series of solvents with increasing elution strength can be applied to TLC on silica gel: heptane, trichloroethylene, dichloromethane, diisopropyl ether, ethyl acetate, and isopropanol. They can be used as one-component mobile phases or as components of multiple-component mobile phases. These solvents can be replaced by other solvents with similar strength but different selectivity belonging to the eight groups exploited in the Prisma model of optimization.[12] The conditions of development depend on the type of mixture of components. Inspection of many experiments carried out on the relationships between retention parameter (R_M) and log φ or φ permits one to distinguish the following groups of solutes (Fig. 1): parallel, crossing, convergent, divergent.[13] The parameters that influence the separation are number of steps, volumes of steps, and profile of gradient including difference in concentration between the first and last step. Additionally, with the same number of steps of gradient, the volumes of eluent fractions can be equal or different. In Fig. 4, there are examples showing the influence of profile (linear, concave) and different volumes of the steps on the separation of an illustrative mixture of 15 solutes (parallel). In Table 1 are presented the minimal resolution (R_{Smin}—elementary criteria) and the multipeak criterion (MPC—product of the elementary criteria) values obtained for basic type of mixture and three programs of gradient (concave, linear, convex). These criteria were selected for estimation of the quality of chromatograms.[14] The R_{Smin} is given for the least resolved solute pair. The MPC is expressed as a percentage. When all compounds are equally spaced from each other and from the chosen boundaries, the function has a maximal value of 100%. It follows from the data presented in Table 1 that profiles can be ordered as follows: concave, linear, and convex. The application of the stepwise mobile-phase gradient greatly improves the separation of complex mixtures (e.g., plant extracts). In such cases, a gradient program with more steps of different concentrations is recommended; in many cases, the number of recognized spots is considerably increased in comparison to isocratic elution.[15] An example of practical application of a simple stepwise gradient is presented in Fig. 5, where separation of a quaternary alkaloid mixture is reported.[16] The application of a stepwise gradient using organic eluents allows one to avoid more time consuming systems, like cellulose powder and aqueous eluents.[17]

GRADIENT MULTIPLE DEVELOPMENT (MD)

In all techniques of MD, the plate is repeatedly developed in the same direction, with intermittent removal of the

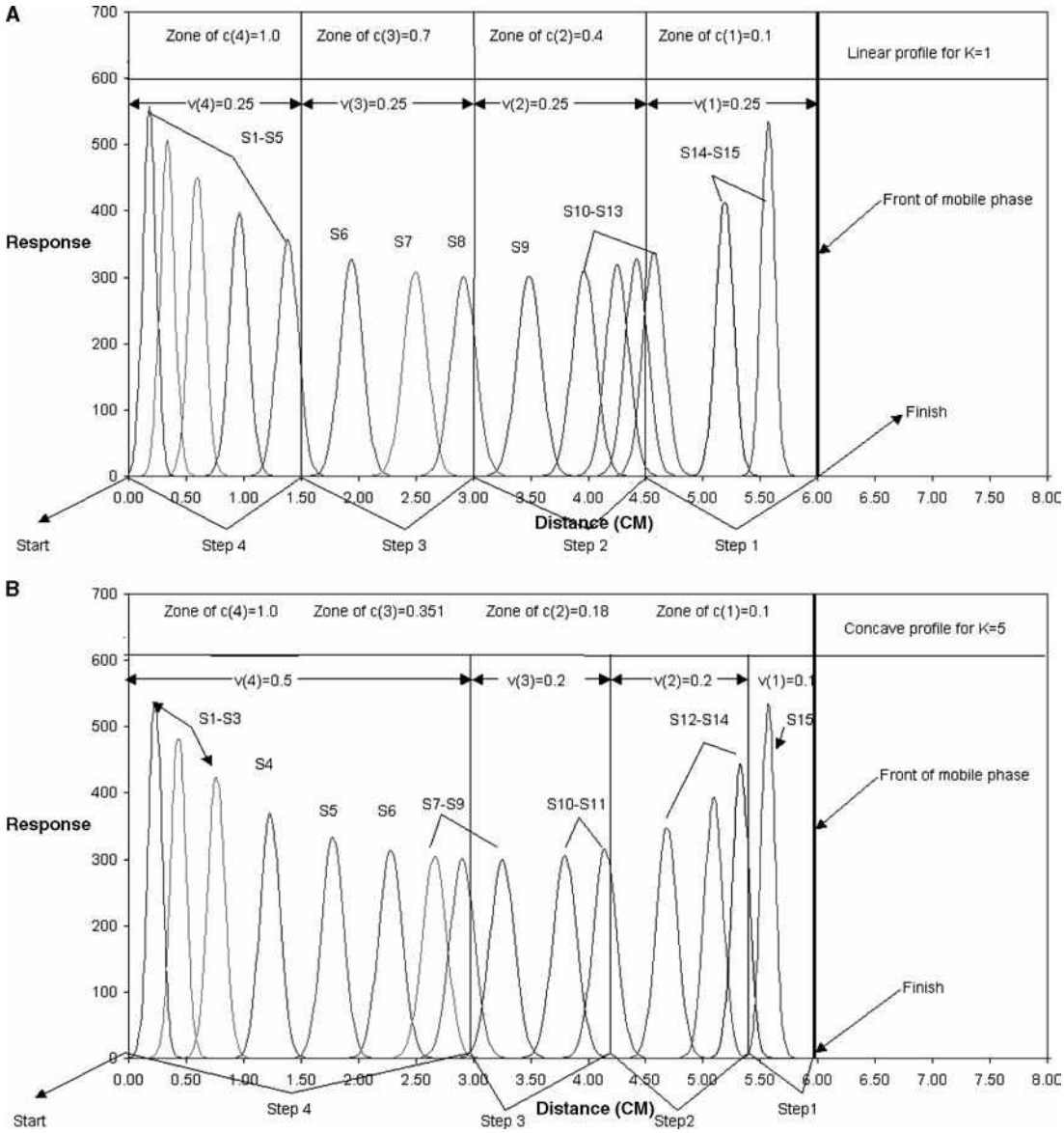

Fig. 4 Simulated chromatograms of hypothetical solutes S1–S15 for simple gradient development. A, Linear profile for $K = 1$; and B, concave profile for $K = 5$.

mobile phase between consecutive developments. Three basic criteria can be used to classify the methods of MD.[18–20] They are distance of development, properties of the mobile phase used in the process of development, and automation of the development and drying processes—automatic multiple development (AMD). The simplest version of MD is when the distances of development are identical in each step (unidimensional multiple development—UMD) and the mobile phase in each step is identical as well. A variation of this technique, called incremental multiple development (IMD), consists of stepwise change of the development distance, which is shortest in the first step and is then increased, usually by a constant increment (equal distance or time); the last development step corresponds to the maximum development distance. If, in the process of MD, the solvent strength of the mobile phase is varied, the technique is called gradient multiple development (G UMD or G IMD). The change in the mobile phase may concern several or all steps. The MD technique gives the possibility to use, in sequence, systems of mobile phase with very different selectivity and of increasing or, in most cases, decreasing elution strength. The process of MD with any variation of distance and mobile-phase composition can be described by the model and equations reported, modified to take into account the intermittent evaporation of solvents:[19]

Table 1 Influence of gradient profile on selected criteria for estimation of quality of separation of different types of mixtures in stepwise gradient development.

	Parallel		Convergent		Divergent		Crossing	
Profile of gradient	R_S[a]	MPC[b]	R_S	MPC	R_S	MPC	R_S	MPC
Linear	0.392	19.15	0.513	4.098	0.140	7.128	0.170	0.204
Convex	0.044	0.07	0.192	0.660	0.047	0.340	0.494	0.867
Concave	0.472	12.99	0.641	5.5	0.600	27.079	0.537	0.900

[a]Minimal values.
[b]Multipeak criterion in %.

$$SMD(j) = SMD(j, n-1) + [DD(n) - SMD(j, n-1)] \cdot R_F(j, n) \quad (5)$$

$$R_P(j) = \frac{SMD(j)}{DD(n)} \quad (6)$$

where $SMD(j)$ is the total migration distance of solute j after n steps, frequently expressed in millimeters, $SMD(j, n-1)$ the sum of the migration distances of solute j after $n-1$ steps, and $DD(n)$ the development distance in the last, nth step. $R_P(j)$ is the final position of the spot after n steps of gradient and is equal to the sum of distances traveled by a solute, divided by development distance corresponding to the distance between start and finish. Eqs. 5 and 6 are of typical recurrent type, in which the $(k-1)$th value for the sum of migration distances traveled by a solute is needed to calculate the kth value. In the simplest case, e.g., two groups of solutes with strong differences in polarity, the version of a decreasing stepwise gradient with two steps can be applied. The layer is developed 2/3 of the distance with a polar eluent that separates the most polar components in the lower part of the chromatogram; the less polar components are accumulated in the front area. Their separation occurs in the second stage, when the layer is developed to the full distance with a less polar eluent (Fig. 6).[21,22] The polar components are not significantly affected by the mobile phase used in the second step and keep their positions from the first step. The incremental, multistep version of this technique, with programmed, automated development and evaporation steps, is called automated multiple development (AMD) and the method is considered to be the most effective and versatile TLC technique.[23]

Eqs. 5 and 6 could be applied to formulate computer programs that calculate the final values of $R_P(j)$ for a given gradient program and the retention–eluent composition relationships for selected systems. The systems very often applied in MD contain thin layers of adsorbents with definite groups like diol, cyano, or amine.[24] The basic equation describing the retention of solutes in such systems has the form of Eq. 2 or the following formula:[25]

$$R_F(j, i) = \frac{1}{1 + k_0(j)/10^{m(j)\cdot c(i)}} \quad (7)$$

G IMD permits application of gradient profiles similar to those presented in Fig. 3. The gradient profiles begin with a high concentration of modifier and end with

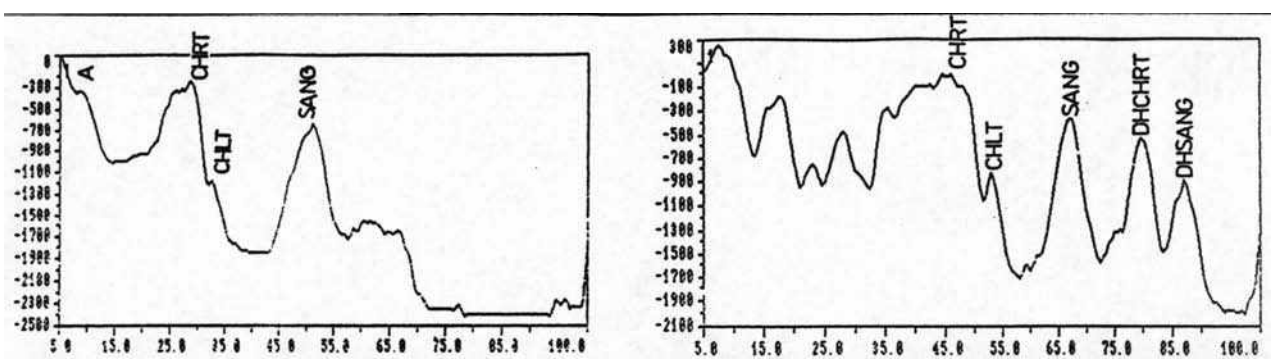

Fig. 5 (A) Densitogram obtained from micropreparative zonal chromatography of a mixture of quaternary alkaloids on silica plate with toluene/EtOAc/MeOH (83 : 15 : 2) as mobile phase. Detection by UV at $\lambda = 254$ nm. (B) Densitogram obtained from micropreparative zonal chromatography of a quaternary alkaloid mixture on silica plate. Gradient elution with T/EtOAc/MeOH, $n = 1$; 75 : 25 : 5, $n = 2$; 70 : 20 : 10, $n = 3$; 70 : 15 : 15, $n = 4$; EtOH/$CHCl_3$/AcOH (67 : 30 : 3) as mobile phases. Detection by UV at $\lambda = 254$ nm.
Source: From 4-Chloro-5,7-dinitrobenzofurazan and 7-chloro-4, 6-dinitrobenzofuroxan–new spray reagents for the detection of amino compounds on thin-layer plates, in J. Planar Chromatogr.[16] Copyright Research Institute for Medicinal Plants, Hungary.

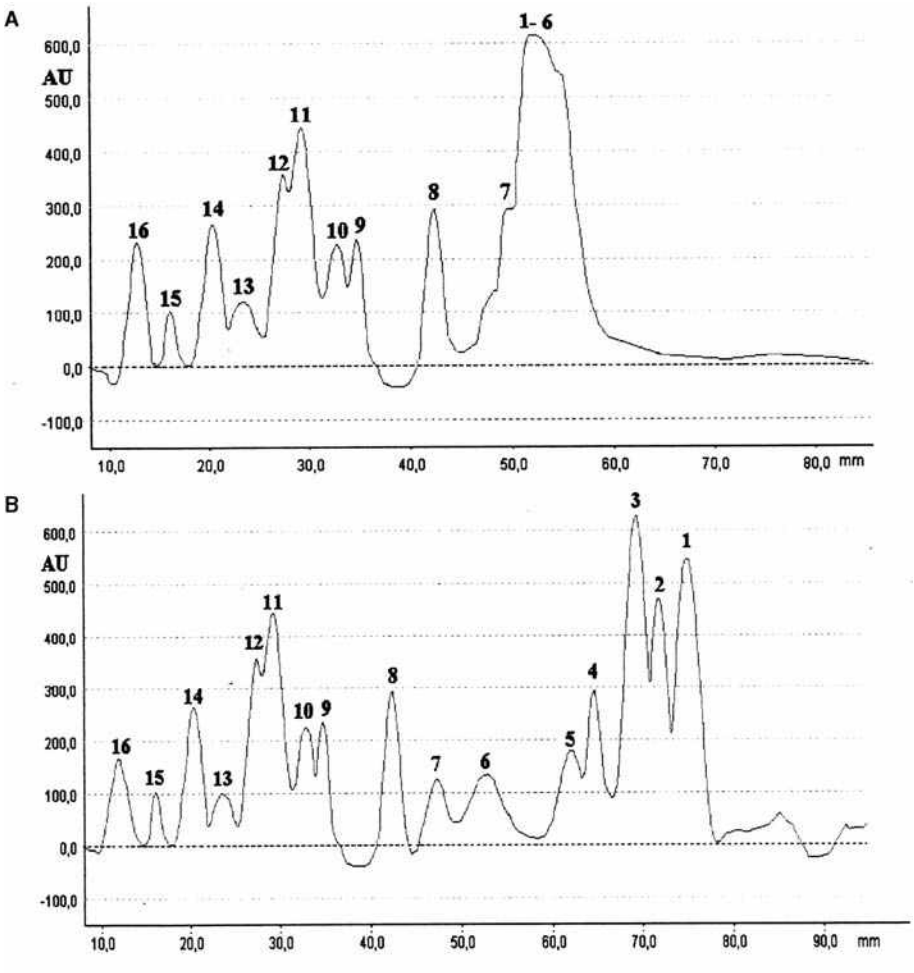

Fig. 6 Densitograms of flavonoids: (A) after first development with EtOAc/HCOOH/H_2O (85 : 15 : 0.5); (B) after second development with CH_2Cl_2/EtOAc/HCOOH (85 : 15 : 0.5). 1–7, Aglycones; 8–16, glycosides.
Source: From Simultaneous separation of aglycones and glycosides of flavonoids by double-development TLC, in J. Planar Chromatogr.[21] Copyright Research Institute for Medicinal Plants, Hungary.

a low concentration. In MD, it is also possible to create segmented gradients. In the majority of practical applications, the number of systems used in the program of development can be more than two. The chromatograms obtained in MD (G IMD) show mostly evenly distributed peaks between the start and finish line. Fig. 7 shows a densitogram of chamomile extract obtained in MD with improved separation compared to the isocratic mode. The marked fractions on the densitogram were recovered from the plate and further analyzed by GC/MS. Chromatograms obtained in this way are much simpler (compared to that of the extract), which simplifies their identification by GC/MS.[26]

The application of G IMD to the analysis of complex mixtures is based on the selection of mobile phases suitable to each group of solutes present in the mixture, e.g., polar, weakly polar, and/or non-polar. In the next step, it is possible to design a gradient program. The profile of the gradient can be adjusted to specific properties of the components of particular groups. The number of steps may be varied depending on the number of components—more components require more steps.

Considering the distance of development, it is possible to develop chromatogram on the total distance with a mobile phase of rather low elution strength and, after removal of the mobile phase, to develop on a shortened distance with a very strong mobile phase. Fig. 8 illustrates the separation of two groups of alkaloids by this method.[27] The condition for the second step of development was that solutes to be separated in the second step still be on or near the start line after the first step. In this mode of MD, the compression effect related to multiple passing of the mobile phase is absent. In UMD, the application of a simple gradient is possible as well. It is used to fractionate complex mixtures by separating just a few solutes in each step. In this case, the plate has to be scanned after some steps and the results recorded. This mode cannot be applied when the picture of the final separation is required as a single chromatogram.

The AMD technique finds application in various fields, such as, for example, the determination of pesticides in water,[28,29] herbicides in plants,[30] and biogenic amines in fish meal,[31] the separation of gangliosides,[32] and the analysis of plant material by coupling with other

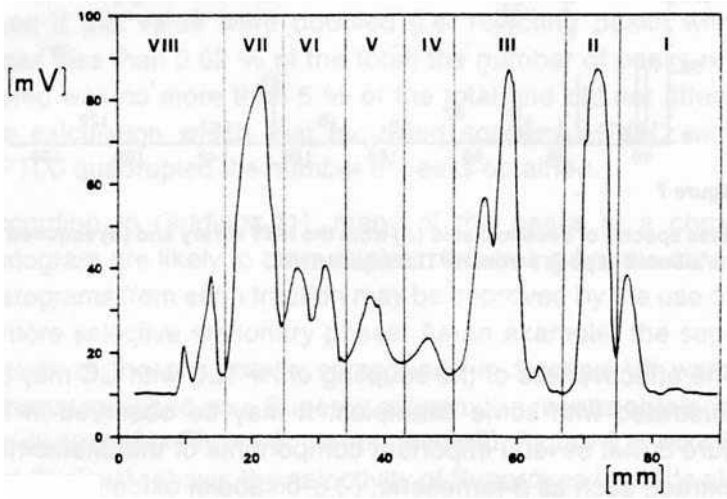

Fig. 7 Densitogram of chamomile extract obtained by MD.
Source: From On the role of planar multiple development in a multidimensional approach to TLC–GC, in J. Planar Chromatogr.[26] Copyright Research Institute for Medicinal Plants, Hungary.

chromatographic (reverse-phase HPLC, HPLC/MS) and spectroscopic methods (UV, FTIR).[33–35]

MECHANISM OF COMPRESSION OF CHROMATOGRAPHIC ZONES

One of the advantages of gradient elution is the compression of zones. Each passage of the front of the mobile phase or of the concentration of the multiple-component mobile phase through a spot leads to compression of the spot in the direction of development. This is due to the fact that the front of the increased eluent concentration first reaches the lower edge of the spot, so that the solute molecules in this region start to move (MD) or accelerate their migration (gradient) earlier than the molecules in the farther parts of the spot. When the front of the mobile phase or of the concentration zone overtakes the whole spot, the compressed spot continues to migrate and gradually becomes more diffuse, as in isocratic elution. If the two mechanisms, compression and diffusion, become counterbalanced, the spot may migrate through considerable distances without any marked broadening (Fig. 9). The final width of the spot can be calculated from the equation

$$\sigma_x{}^2 = \sigma_{\text{spotting}}{}^2 + \sigma_{\text{chrom}}{}^2 + \sigma_{\text{inst}}{}^2 + (-\Delta)_{\text{compression}} \qquad (8)$$

The last term of the equation is responsible for the compression effect. The contributions of particular terms of the equation can be estimated from the following equations. For spreading of the zone caused by the process of chromatography,

$$\sigma_{\text{chrom}}{}^2 = \overline{H \cdot MD(j,i)} \qquad (9)$$

where $\overline{H}$ is the average height equivalent to a theoretical plate and $MD(j, i)$ is migration distance for solute j in the ith step. The values of this term depend on the efficiency of chromatographic layer and on the velocity of the mobile phase associated with migration distance $MD(j, i)$.

The compression effect can be calculated from the formula

$$\Delta = [0.25 \cdot w(j, i-1) \cdot R_{\text{F}}(j,i)]^2 \qquad (10)$$

where $w(j, i–1)$ is the width of the zone at the end of the preceding step. The compression effect is most effective for zones with high R_{F} value. The contribution to zone broadening associated with the properties of the detection and recording devices are negligible. During the MD process, the migration distances of particular solutes are rather short; the contribution is not very high and decreases with the progress of development. Additionally, the effect of compression keeps the spots narrow. The formation of more compact spots causes an increase in sensitivity of detection, in comparison to the spots after single development, and an increase of peak capacity.[36]

Incremental multiple development provides superior separation in comparison to multiple chromatography, in this case, by minimizing zone broadening and enhancing the zone center separation by migrations of the sample components over a longer distance while maintaining a mobile-phase flow rate range close to the best value for the separation. This variant can also be achieved by change of the point of delivery of the eluent to the layer.[37] Not all compounds are suitable for separation by MD. Compounds with significant vapor pressure may be lost during the repeated solvent evaporation steps. Certain solvents of low volatility and/or high polarity, such as acetic acid, triethylamine, dimethyl sulfoxide, and so forth are unsuitable as mobile phases because of the difficulty of removing them from the layer by vacuum evaporation between development steps. Water can be used, but the drying steps are then lengthy. The solvent residues remaining after the drying step can modify the selectivity of mobile phases used in later

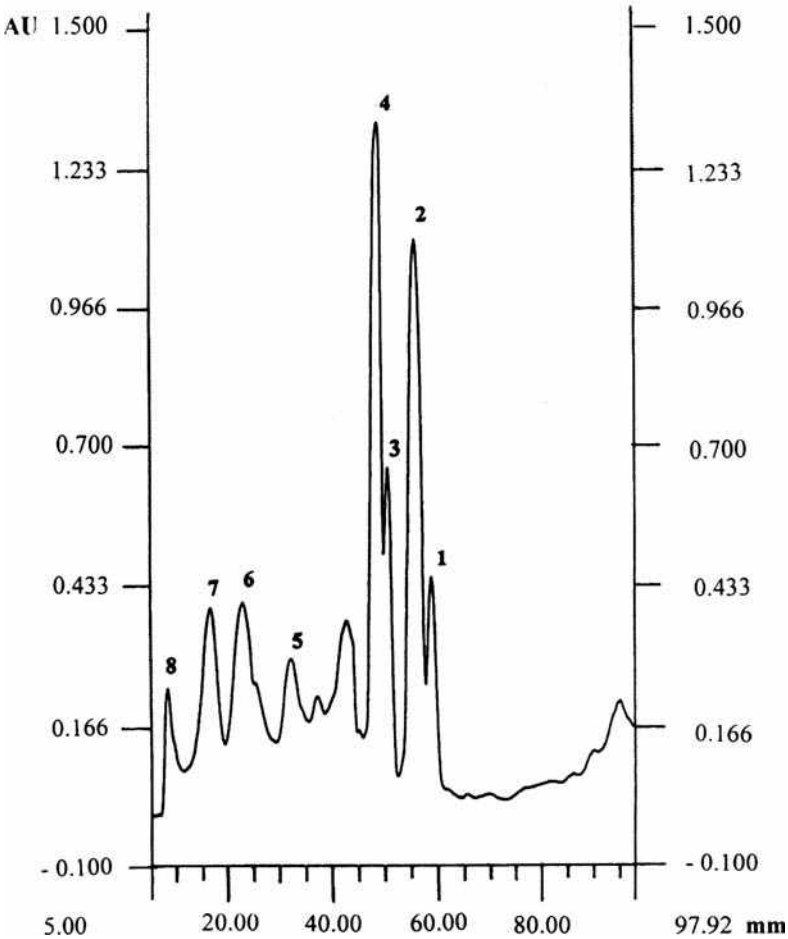

Fig. 8 Two-step gradient elution of the fraction of quaternary alkaloids of *Chelidonium majus* L. Stationary phase: Kieselgel Si 60. Mobile phase: first gradient step: T/EtOAc/MeOH (80 : 15 : 5, v/v), $DD(1) = 8$ cm; second gradient step: EtOH/$CHCl_3$/AcOH (67 : 30 : 3, v/v), $DD(2) = 4$ cm. Compounds: 1—chelirubine, 2—sanguinarine, 3—chelilutine, 4—chelerythrine, 5—corysamine, 6—berberine, 7—coptisine, 8—magnoflorine.
Source: From Isolation of some quaternary alkaloids from the extract of roots of *Chelidonium majus* L. by column and thin-layer chromatography, in Chromatographia.[27] Copyright Vieweg Verlag, Germany.

steps, resulting in irreproducible separations. Although precautions can be taken to minimize the production of artifact peaks in MD, the separation of light- and/or air-sensitive compounds is probably better handled by other techniques such as simple gradient development.

POLYZONAL TLC

Polyzonal TLC is the simplest method for formation of gradients in TLC. The main effect utilized is solvent demixing, which occurs in the case of the application of binary and polycomponent solvents, especially those of differentiated polarity. For an *n*-component mixed eluent, *n*–1 solvent fronts are formed, ordered in the sequence of polarity of the components. A gradient of eluent strength is thus formed along the layer; the solutes migrate in various zones, and the passage of fronts leads to compression of the TLC spots.[3,6]

EQUIPMENT FOR GRADIENT TLC

Depending on the type of gradient, various apparatuses are applied for its generation. Numerous gradient generators have been described.[3,5] The gradient of the mobile phase can be formed in some types of horizontal chambers (Fig. 10) (e.g., Camag, Muttenz, Switzerland; Chromdes, Lublin, Poland; Desaga, Wiesbaden, Germany). The generation of stepwise gradients is simple for sandwich chambers with distributors, which allow for complete absorption of the eluent fractions from the reservoir. For sandwich chambers, eluent fractions of increasing eluent strength (increasing concentrations of the polar modifier) are introduced under the distributor. After absorption of the preceding eluent fraction by the adsorbent layer, the next fraction of eluent of changed strength is delivered; the total volume of the eluent fractions corresponds to the development distance. Any gradient program, including continuous and multiple-component gradients, can be

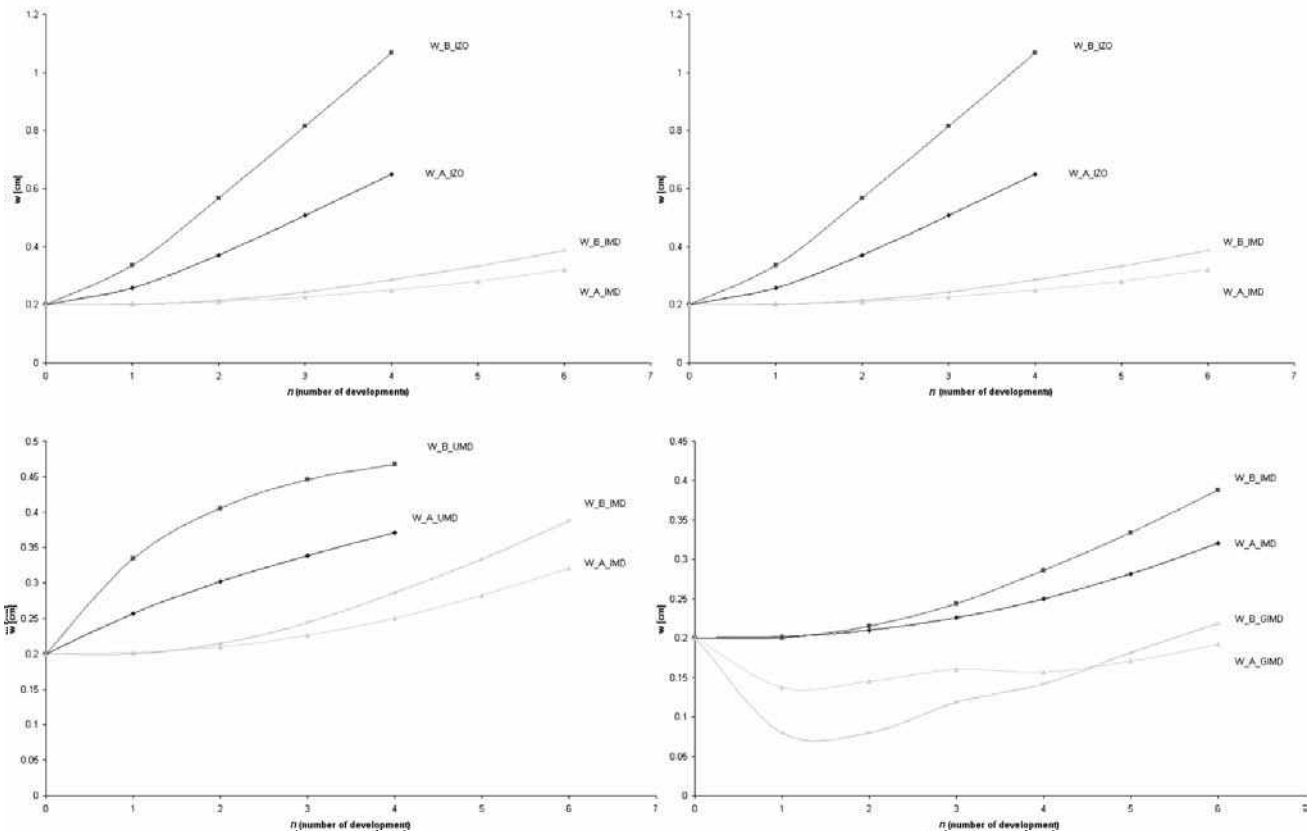

Fig. 9 Comparison of zone width in different modes of MD. (A) Zone width in a single isocratic development and unidimensional development. $R_F(A) = 0.091$, $R_F(B) = 0.288$, $\varphi = 0.05$. (B) Zone width in a single isocratic development and IMD. Increment of development distance $IDD = 1$ cm; number of developments $n = 6$; $\varphi = 0.5$. (C) Zone width in UMD and IMD. (D) Zone width in IMD and GIMD. Gradient: number of steps $n = 6$; concentration program: $\varphi(1) = 0.3$, $\varphi(2) = 0.2$, $\varphi(3) = 0.1$, $\varphi(4) = 0.05$, $\varphi(5) = 0.05$, $\varphi(6) = 0.05$; increment of development distance $IDD = 1$ cm.

generated in this way. The process of MD can be fully automated (Fig. 11) (AMD2 chamber, Camag Scientific; TLC–MAT, Desaga). An apparatus comprises an N-type chamber with connections for adding and removing solvents and gas phases. AMD2 involves the use of a stepwise gradient of different mobile phases with decreasing strength in 10–30 successive developments increasing in length by about 1–5 mm. The initial solvent, which is the strongest, focuses the zones during the first short run, and the solvent is changed for each, or most, of the following cycles. The mobile phase is removed from the chamber, the plate dried and activated by vacuum evaporation, and the layer conditioned with a controlled atmosphere of vapors prior to the next development. High resolution and improved detection limits are achieved because zones are focused during each development stage. The widths of the separated zones are approximately constant at 1–3 mm, and the separation capacity for baseline-resolved peaks is 25–40. Zones migrate different distances according to their polarity. The reproducibility of values is 1–2% (CV) for multiple spots on the same plate or different plates from

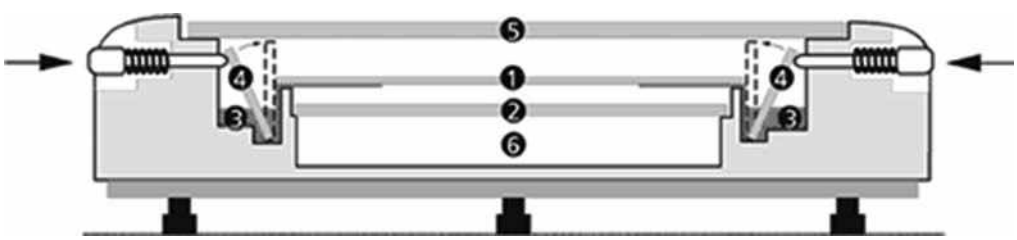

Fig. 10 Horizontal developing chamber (Camag). 1—HPTLC plate (layer facing down), 2—glass plate, 3—reservoir for developing solvent, 4—glass strip, 5—cover plate, 6—conditioning tray.
Source: Photo courtesy of Camag.

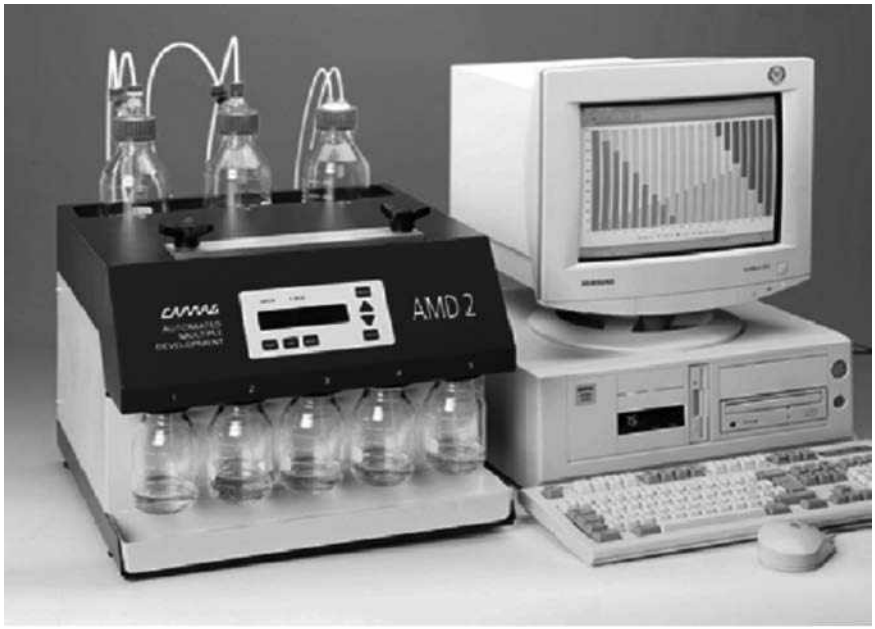

Fig. 11 Chamber for AMD (AMD2, Camag). AMD2 is controlled by winCats software through interface "EquiLink" or through keypad. Programmed gradient is displayed on screen of computer monitor or on screen of device. Dosage of solvents to generate gradient is created by piston pump following entered program. Solvent is completely removed from chamber, and plate with adsorbent is dried under vacuum. Solvent migration distances are monitored with a CCD sensor.
Source: Photo courtesy of Camag.

the same batch. A typical universal gradient for a silica gel layer involves 25 steps, with methanol, dichloromethane, or *tert*-butyl ether, and hexane as the component solvents.

A discontinuous gradient of the stationary phase can be obtained easily using an ordinary spreader. The trough is divided into separate chambers filled with suspensions of mixtures of adsorbents. The carrier plates are covered in the usual way.[3,5] Another method of formation of gradients of stationary-phase activity is the use of a Vario-KS chamber, which permits adsorption of various vapors on the adsorbent surface or control of the activity of the adsorbent.[6]

CONCLUSIONS

To sum up, the development process, applied as a simple gradient or combined with MD, can improve the separation power of planar chromatography in cases when transport of the mobile phase is controlled by capillary forces. The advantages of gradient development are as follows:

- More compact zones.
- Greater separation capacity.
- Greater sensitivity.

Other benefits of gradient follow:

- Possibility of separation of complex samples containing components with a wide spectrum of polarity or samples containing groups of solutes with different properties.
- More optimal use of solvents of different strength and selectivity.
- Possibility of coupling with HPLC and spectroscopic techniques

In the case gradient development is carried out, the following conditions need to be fulfilled:

- Application of sample by an automatic device.
- Development with use of an automatic developing chamber.
- Densitometric evaluation and documentation with image processing.

Then the technique can be recognized as a very powerful modern instrumental system that offers reproducible and accurate quantitation for a wide variety of applications.

REFERENCES

1. Jandera, P. On the way to a general theory of gradient elution. In *A Century of Separation, Science,* 1st Ed.; Issaq, H.J., Ed.; Marcel Dekker, Inc.: New York, 2002; 211–229.
2. Schoenmakers, P. Programmed analysis. In *Handbook of HPLC*; Katz, E. Eksteen, E. Schoenmakers, P., Miller, N., Eds.; Marcel Dekker, Inc.: New York, 1998; 193–232.
3. Gołkiewicz, W. Gradient development in thin-layer chromatography. In *Handbook of Thin-Layer Chromatography,* 3rd Ed.; Sherma, J., Fried, B., Eds.; Marcel Dekker, Inc.: New York, 1997; 135–154.
4. Soczewiński, E. Solvent composition effects in thin-layer systems of the type silica gel–electron donor solvent. Anal. Chem. **1969**, *41*, 179.
5. Geiss, F. Gradients. In *Fundamentals of Thin Layer Chromatography (Planar Chromatography)*; Huethig: Heidelberg, 1987; 388–397.

6. Snyder, L.R.; Saunders, D.L. Resolution in thin-layer chromatography with solvent or adsorbent programming. J. Chromatogr. **1969**, *44*, 1–13.
7. Soczewiński, E.; Markowski, W. Stepwise gradient development in thin-layer chromatography. III. A computer program for the simulation of stepwise gradient elution. J. Chromatogr. **1986**, *370*, 63–73.
8. Soczewiński, E. Stepwise gradient development in thin-layer chromatography. Optimization of gradient program. J. Chromatogr. **1986**, *369*, 11–17.
9. Wang, Q.-S.; Yan, B.-W.; Zhang, Z.-C. Computer-assisted optimization of mobile phase composition in stepwise gradient HPTLC. J. Planar Chromatogr. **1994**, *7*, 229–232.
10. Markowski, W.; Soczewiński, E.; Matysik, G. A microcomputer program for the calculation of R_F values of solutes in stepwise gradient thin-layer chromatography. J. Liquid Chromatogr. **1987**, *10*, 1261–1267.
11. Markowski, W. Computer-assisted selection of the optimum gradient program in thin-layer chromatography. J. Chromatogr. **1989**, *485*, 517–532.
12. Nyiredy, Sz. Planar chromatographic method development using the Prisma optimization system and flow charts. J. Chromatogr. Sci. **2002**, *40*, 553–563.
13. Felinger, A.; Guiochon, G. Multicomponent interferences in overloaded gradient elution chromatography. J. Chromatogr. **1996**, *724*, 27–37.
14. Siouffi, A.-M. Some aspects of optimization in planar chromatography. J. Chromatogr. **1991**, *556*, 81–94.
15. Matysik, G.; Markowski, W.; Soczewiński, E.; Polak, B. Computer-aided optimization of stepwise gradient profiles in thin-layer chromatography. Chromatographia **1992**, *34*, 303–307.
16. Evgen'ev, M.I.; Evgen'ev, I.I.; Levinson, F.S. 4-Chloro-5,7-dinitrobenzofurazan and 7-chloro-4,6-dinitrobenzofuroxan—new spray reagents for the detection of amino compounds on thin-layer plates. J. Planar Chromatogr. **2000**, *13*, 199–209.
17. Matysik, G. Separation of DABS derivatives of amino acids by multiple gradient development (MGD) in thin-layer chromatography. Chromatographia **1996**, *43*, 301–303.
18. Markowski, W. Past, present and future of multiple development in planar chromatography. The Application of Chromatographic Methods in Phytochemical and Biomedical Analysis4th International Symposium on Chromatography of Natural Products, Lublin–Kazimierz Dolny, Poland, June14–17, 2004; Skubiszewski Medical University of Lublin: Lublin, 2004; L-25, 41.
19. Markowski, W. Computer-aided optimization of gradient multiple development thin-layer chromatography. Part II. Multistage development. J. Chromatogr. **1993**, *653*, 283–289.
20. Szabady, B. The different modes of development. In *Planar Chromatography. A Retrospective View for the Third Millennium*; 1st Ed. Nyiredy, Sz., Ed.; Springer: Budapest: 2001; 88–102.
21. Soczewiński, E.; Wójciak-Kosior, M.; Matysik, G. Simultaneous separation of aglycones and glycosides of flavonoids by double-development TLC. J. Planar Chromatogr. **2004**, *17* (4), 261–263.
22. Johansson, L.A. Chromatographic analysis of epicuticular plant waxes. Sver. Utsadesforen. Tidskr. **1985**, *95*, 129–136.
23. Poole, C.F.; Belay, M.T. Progress in automated multiple development. J. Planar Chromatogr. **1991**, *4* (9/10), 345–358.
24. Lodi, G.; Betti, A.; Menziani, E.; Brandolini, V.; Tosi, B. Some aspects and examples of automated multiple development (AMD) gradient optimization. J. Planar Chromatogr. **1991**, *4* (3/4), 106–110.
25. Valko, K.; Snyder, L.R.; Glajch, J.L. Retention in reversed-phase liquid chromatography as a function of mobile-phase composition. J. Chromatogr. **1993**, *656*, 501–520.
26. Betti, A.; Lodi, G.; Fuzzati, N.; Coppi, S.; Benedetti, S. On the role of planar multiple development in a multidimensional approach to TLC–GC. J. Planar Chromatogr. **1991**, *4* (9/10), 360–364.
27. Gołkiewicz, W.; Gadzikowska, M. Isolation of some quaternary alkaloids from the extract of roots of *Chelidonium majus* L. by column and thin-layer chromatography. Chromatographia **1999**, *50* (1/2), 52–56.
28. de la Vigne, U.; Jaenchen, D. Determination of pesticides in water by HPTLC using automated multiple development (AMD). J. Planar Chromatogr. **1990**, *3* (1/2), 6–9.
29. Błądek, J.; Rostkowski, A.; Miszczak, M. Application of instrumental thin-layer chromatography and solid extraction to the analyses of pesticide residues in grossly contaminated samples of soil. J. Chromatogr. **1996**, *754*, 273–278.
30. Lautie, J.P.; Stankovic, V. Automated multiple development TLC of phenylurea herbicides in plants. J. Planar. Chromatogr. **1996**, *9* (3/4), 113–115.
31. Vega, M.H.; Saelzer, R.F.; Figueroa, C.E.; Rios, G.G.; Jaramillo, V.H. Use of AMD HPTLC for analysis of biogenic amines in fish meal. J. Planar Chromatogr. **1999**, *12* (1/2), 72–75.
32. Muthing, J.; Ziehr, H. Enhanced thin-layer chromatographic separation of G_{M1b}-type gangliosides by automated multiple development. J. Chromatogr. **1996**, *687*, 357–362.
33. Queckenberg, O.R.; Frahm, A.W. Chromatographic and spectroscopic coupling: a powerful tool for the screening of wild Amaryllidaceae. J. Planar Chromatogr. **1993**, *6* (1/2), 55–61.
34. Galand, N.; Pothier, J.; Viel, C. Plant drug analysis by planar chromatography. J. Planar Chromatogr. **2002**, *40* (11/12), 585–597.
35. Kovar, K.-A.; EnÔlin, H.K.; Frey, O.R.; Rienas, S.; Wolff, S.S. Applications of on-line coupling of thin layer chromatography and FTIR spectroscopy. J. Planar Chromatogr. **1991**, *4* (5/6), 246–250.
36. Essig, S.; Kovar, K.-A. The efficiency of thin-layer chromatographic systems: a comparison of separation numbers using addictive substances as an example. J. Planar Chromatogr. **1997**, *10* (3/4), 114–117.
37. Poole, S.K.; Poole, C.F. The influence of the solvent entry position on resolution in unidimensional multiple development thin layer chromatography. J. Planar Chromatogr. **1992**, *5*, 221–228.

Gradient Elution Fundamentals

J.E. Haky
D.A. Teifer
Department of Chemistry and Biochemistry, Florida Atlantic University, Boca Raton, Florida, U.S.A.

INTRODUCTION

The term *gradient elution* refers to a systematic, programmed increase in the elution strength of the mobile phase during the chromatographic run. Of all the techniques used to provide quality separations among complex mixtures, gradient elution offers the greatest potential.[1] Basically, the composition of the mobile phase is varied throughout the separation so as to provide a continual increase in solvent strength and, thereby, a more convenient elution time and sharper peaks for all sample components.[2] What makes this method so useful is the ability to choose from a variety of different eluents. Although most instruments permit gradients to be automatically prepared from various concentrations of only a two-eluent mixture, sample mixtures of a wide range of polarities can be separated efficiently.

DISCUSSION

The process of mixing eluents is a sensitive one. When two solvents with a large difference in their elution strengths are used, even a small increase in the polar component produces a sharp rise in elution strength. Such an effect is undesirable because the components are almost always eluted at the beginning of the analysis and displacement effects may result from demixing of eluent mixtures.[1] According to Poole et al.,[3] the most frequently used gradients are binary solvent systems with a linear, convex, or concave increase in the percent volume fraction of the stronger solvent, as depicted in the following equations:

Linear gradient

$$\theta_B = \frac{t}{t_G} \tag{1}$$

Convex gradient

$$\theta_B = 1 - \left(1 - \frac{t}{t_G}\right)^n \tag{2}$$

Concave gradient

$$\theta_b = \left(\frac{t}{t_B}\right)^n \tag{3}$$

In these equations, θ_B is the volume fraction of the stronger eluting solvent, t is the time after the gradient begins, t_G is the total gradient time, and n is an integer controlling gradient steepness.

Complex gradients can be constructed by combining several gradient segments (i.e., rates of increase of strong solvent composition) to form the complete gradient program.[3] Linear gradients are most commonly used, with convex and concave gradients employed only when necessary to optimize more complex separations. In a linear-solvent-strength gradient, the logarithm of the capacity factor for each sample component, k', decreases linearly with time, according to Eq. 4:

$$\log k = \log k_0 - b\frac{[t]}{[t_m]} \tag{4}$$

In this equation, k_0 is the value of k determined isocratically in the starting solvent, b is the gradient steepness parameter, t is the time after the start of gradient and sample injection, and t_m is the column dead time. Ideally, this equation shows that a linear-solventstrength gradient should result in equal resolution and bandwidths of all components. Unfortunately, this is not always possible. There are certain cases where linear- solvent-strength gradient is not the ideal method. In some cases, for example, b actually increases regularly with solute retention, which reduces the separation of late-eluting components. Such an effect is observed in the separation of polycyclic aromatic hydrocarbons.[3]

There are three things to consider when finding a suitable gradient for a separation: (a) the initial and final mobile-phase compositions, (b) the gradient shape, and (c) the gradient steepness.[3] A convex gradient leads to the elution of bands with a lower average capacity factor and a shorter total analysis time. In other words, the later-eluting bands appear wider and better resolved than the early eluting bands. A concave gradient resolves the early bands to a greater degree than the later bands.

Solvent selection is one of the most important facets of gradient elution. The choice of the first solvent influences the separation of the initial bands, whereas the strength of the final solvent influences the selectivity of the separation and the retention times and peak shapes of later-eluting

bands. If solvent B is too weak, the analysis time may become very long and the latereluting bands might broaden excessively; thus, a stronger solvent B may be required.[3]

Abbott et al.,[4] devised a method designed to predict the retention times in gradient elution under the assumption that the retention factor as determined under isocratic conditions is a log-linear function of solvent composition according to Eq. 5, where k_w is the retention factor obtained in water, φ_0 refers to the volume fraction of the organic component, and S refers to the solvent strength for which the values can be obtained as the negative slope of plots of log k vs. volume fraction:

$$\log k = \log k_w - S\varphi_0 \tag{5}$$

Engelhardt and Elgass[5] found that if the gradient volume is held constant and the initial and final compositions of the eluent are fixed, each component of a sample is eluted at a given solvent composition. Snyder et al.[6] derived a simple relationship between the elution time of a solute and the rate of change of solvent composition in gradient elution. Utilizing Eq. 6, they found that the elution time t_e is related to column dead time, t_0, and an experimental parameter b whereby k_0 is the retention factor that would be obtained in isocratic elution with mobile-phase composition used at the beginning of the gradient:[1]

$$t_e\left(\frac{t_0}{b}\right)\log(2.31k_0b + 1) + t_0 \tag{6}$$

The parameter b is defined as

$$b = \frac{\phi S t_0}{100} \tag{7}$$

where Φ is the rate of increase in the concentration of the solvent component having eluent strength S and given as volume percent of organic solvent component per minute.[1]

Many technical problems can occur with gradient elution, some of which can be avoided through various methods. To begin, gradient elution relies upon the purity of the solvents used. The high-performance liquid chromatography (HPLC) column can collect impurities, in the mobile phase, which may or may not elute as sharp peaks at a certain eluent composition. These can be mistaken for sample components. Such peaks are called "ghost peaks" and can result in inaccurate data. Water presents its own set of problems. Contaminated water can also result in ghost peaks. Even deionization of water by ion exchangers can leach out organics from the resin.[1] For this reason, it is advisable to run a gradient first without injecting the sample and use commercially available, purified solvents, including the water, to determine if they result in the elution of ghost peaks.

Another thing to consider with gradient elution is changes in the eluent viscosity. When gradient elution with a hydro-organic mobile phase is used (e.g., methanol-water), systematic variations in the flow rate are expected under conditions of constant-pressure operation, and systematic variations in the operating pressure will be found when a constant flow rate is used.[1] The compressibility of the solvent is species-specific.

In summary, gradient elution is a powerful method for the separation and analysis of complex mixtures containing components with a wide variety of polarities and hydrophobicities. It can also be used to help establish an isocratic mobile phase for the analysis of simpler mixtures. In either case, utmost care must be taken in the selection and use of solvents of high purity and selectivity.

ACKNOWLEDGMENT

The author wishes to thank D.A. Teifer for technical assistance.

REFERENCES

1. Horvath, C. *High Performance Liquid Chromatography: Advances and Perspectives*; Academic Press: New York, 1980; Vol. 2.
2. Kirkland, J.J.; Glajch, J.L. Optimization of mobile phases for multisolvent gradient elution liquid chromatography. J. Chromatogr. **1983**, *255*, 27.
3. Poole, C.F.; Schuette, S.A. *Contemporary Practice of Chromatography*; Elsevier: Amsterdam, 1984.
4. Abbott, S.R.; Berg, J.R.; Achener, P.; Stevenson, R.L. Chromatographic reproducibility in high-performance liquid chromatographic gradient elution. J. Chromatogr. **1976**, *126*, 421.
5. Englehardt, H.; Elgass, H. Optimization of gradient elution: Separation of fatty acid phenacyl esters. J. Chromatogr. **1978**, *158*, 249.
6. Snyder, L.R.; Dolan, J.W.; Gant, J.R. Gradient elution in high-performance liquid chromatography: I. Theoretical basis for reversed-phase systems. J. Chromatogr. **1979**, *165*, 3.

Gradient Elution in CE

Haleem J. Issaq
National Cancer Institute at Frederick (NCI-Frederick), National Institutes of Health (NIH), Frederick, Maryland, U.S.A.

INTRODUCTION

Gradient elution is routinely used in high-performance liquid chromatography (HPLC) to achieve the complete resolution of a mixture which could not be resolved using isocratic elution. Unlike isocratic elution, where the mobile-phase composition remains constant throughout the experiment, in gradient elution the mobile-phase composition changes with time. The change could be continuous or stepwise, known as the *step-gradient*. In the continuous gradient, the analyst can pick one of three general shapes: linear, concave, or convex.

DISCUSSION

Gradient elution in HPLC is achieved using two pumps, two different solvent reservoirs, and a solvent mixer. In capillary electrophoresis (CE), electro-osmotic flow controls the flow of the mobile phase, which is, in most cases, an aqueous buffer and is used in place of a mechanical pump.

A manual step-gradient was used by Balchunas and Sepaniak[1] to separate a mixture of amines by micellar electrokinetic chromatography (MEKC). Stepwise gradients were produced by pipetting aliquots of a gradient solvent to the inlet reservoir which was filled with 2.5 ml of running buffer. A small magnetic stirring bar was used to ensure thorough mixing of the added gradient solvent with the starting mobile phase. The gradient elution solvent was manually added, in four 0.5 ml increments, spaced 5 min apart, 5 min after start of the experiment.

Bocek and his group[2] developed a method for controlling the composition of the operational electrolyte directly in the separation capillary in isotachophoresis (ITP) and capillary zone electrophoresis (CZE). The method is based on feeding the capillary with two different ionic species from two separate electrode chambers by simultaneous electromigration. The composition and pH of the electrolyte in the separation capillary is thus controlled by setting the ratio of two electric currents.This procedure can be used, in addition to generating the mobile-phase gradient, for generating pH gradients.[3,4] Sepaniak et al.[5–7] produced continuous gradients of different shapes (linear, concave, or convex) by using a negative-polarity configuration in which the inlet reservoir is at ground potential and the outlet reservoir at a very high negative potential. This configuration allows two syringe pumps to pump solutions into and out of the inlet reservoir. Tsuda[8] used a solvent-program delivery system, similar to that used in HPLC, to generate pH gradients in CZE. A pH gradient derived from temperature changes has also been reported.[9] Chang and Yeung[10] used two different techniques (i.e., the dynamic pH gradient and electro-osmotic flow gradient) to control selectivity in CZE. A dynamic pH gradient from pH 3.0 to 5.2 was generated by a HPLC gradient pump. An electro-osmotic flow gradient was produced by changing the reservoirs containing different concentrations of cetylammonium bromide for injection and running.

Capillary electrochromatography (CEC) is a separation technique which combines the advantages of micro-HPLC and CE. In CEC, the HPLC pump is replaced by electro-osmotic flow. Behnke and Bayer[11] developed a micro-bore system for gradient elution using 50 and 100 μm fused-silica capillaries, packed with 5 μm octadecyl reversed phase silica gel and voltage gradients, up to 30,000 V, across the length of the capillary. A modular CE system was combined with a gradient HPLC system to generate gradient CEC. Enhanced column efficiency and resolution were realized. Zare and his coworkers[12] used two high-voltage power supplies and a packed fused-silica capillary to generate an electro-osmotically driven gradient flow in an automated manner. The separation of 16 polycyclic aromatic hydrocarbons was resolved in the gradient mode; these compounds were not separated when the isocratic mode was employed. Others[13–16] used gradient elution in combination with CEC to resolve various mixtures.

Multiple, intersecting narrow channels can be formed on a glass chip to form a manifold of flow channels in which CE can be used to resolve a mixture of solutes in seconds. Harrison and coworkers[17] showed that judicious application of voltages to multiple channels within a manifold can be used to control the mixing of solutions and to direct the flow at the intersection of channels. The authors concluded that such a system, in which the applied voltages can be used to control the flow, can be used for sample dilution, pH adjustment, derivatization, complexation, or masking of interferences. Ramsey and coworkers[18] used a microchip device with electrokinetically controlled solvent mixing for isocratic and gradient elution in MEKC. Isocratic and gradient conditions are controlled by proper setting of voltages applied to the buffer reservoirs of the microchip. The precision of such control was successfully tested for gradients of various shapes (linear, concave, or

convex) by mixing pure buffer and buffer doped with a fluorescent dye. By making use of the electro-osmotic flow and employing computer control, very precise manipulation of the solvent was possible and allowed fast and efficient optimization of separation problems.

ACKNOWLEDGMENT

This project has been funded in whole or in part with federal funds from the National Cancer Institute, National Institutes of Health, under Contract No. NO1-CO-56000.

REFERENCES

1. Balachunas, A.T.; Sepaniak, M.J. Gradient elution for micellar electrokinetic capillary chromatography. Anal. Chem. **1988**, *60*, 617.
2. Popsichal, J.; Deml, M.; Gebauer, P.; Bocek, P. Generation of operational electrolytes for isotachophoresis and capillary zone electrophoresis in a three-pole column. J. Chromatogr. **1989**, *470*, 43.
3. Bocek, P.; Deml, M.; Popsichal, J.; Sudor, J. Dynamic programming of pH—a new option in analytical capillary electrophoresis. J. Chromatogr. **1989**, *470*, 309.
4. Sustacek, V.; Foret, F.; Bocek, P. Simple method for generation of dymanic pH gradient in capillary zone electrophoresis. J. Chromatogr. **1989**, *480*, 271.
5. Sepaniak, M.J.; Swaile, D.F.; Powell, A.C. Instrumental developments in micellar electrokinetic capillary chromatography. J. Chromatogr. **1989**, *480*, 185.
6. Powell, A.C.; Sepaniak, M.J. Development of a model for predicting retention times in solvent-gradient micellar electrokinetic capillary chromatography. J. Microcol. Separ. **1990**, *2* (6), 278–284.
7. Powell, A.C.; Sepaniak, M.J. Anal. Instrum. **1993**, *21*, 25.
8. Tsuda, T. pH gradient capillary zone electrophoresis using a solvent program delivery system. Anal. Chem. **1992**, *64*, 386.
9. Wang, C.W.; Yeung, E.S. Temperature programming in capillary zone electrophoresis. Anal. Chem. **1992**, *64*, 502.
10. Chang, H.-T.; Yeung, E.S. Optimization of selectivity in capillary zone electrophoresis via dynamic pH gradient and dynamic flow gradient. J. Chromatogr. **1992**, *608*, 65.
11. Behnke, B.; Bayer, E. Pressurized gradient electro-high-performance liquid chromatography. J. Chromatogr. **1994**, *680*, 93.
12. Yan, C.; Dadoo, R.; Zare, R.N.; Rakestraw, D.J.; Anex, D.S. Gradient elution in capillary electrochromatography. Anal. Chem. **1996**, *68*, 2726.
13. Schmeer, K.; Behnke, B.; Bayer, E. Capillary electrochromatography-electrospray mass spectrometry: A microanalysis technique. Anal. Chem. **1995**, *67*, 3656.
14. Taylor, M.R.; Teale, P.; Westwood, S.A.; Perrett, D. Analysis of corticosteroids in biofluids by capillary electrochromatography with gradient elution. Anal. Chem. **1997**, *69*, 2554.
15. Taylor, M.R.; Teale, P. Gradient capillary electrochromatography of drug mixtures with UV and electrospray ionisation mass spectrometric detection. J. Chromatogr. A, **1997**, *768*, 89.
16. Gfrorer, P.; Schewitz, J.; Psecker, K.; Tseng, L.-H.; Albert, K.; Bayer, E. Gradient elution capillary electrochromatography and hyphenation with nuclear magnetic resonance. Electrophoresis **1999**, *20* (1), 3–8.
17. Seller, K.; Fan, Z.H.; Fluri, K.; Harrison, J. Electroosmotic pumping and valveless control of fluid flow within a manifold of capillaries on a glass chip. Anal. Chem. **1994**, *66*, 3485.
18. Kutter, J.P.; Jacobson, S.J.; Ramsey, J.M. Integrated microchip device with electrokinetically controlled solvent mixing for isocratic and gradient elution in micellar electrokinetic chromatography. Anal. Chem. **1997**, *69*, 5165.

Gradient Elution Program: Selection and Important Instrumental Considerations

Adriana Segall
Pharmacy and Biochemistry Faculty, University of Buenos Aires, Buenos Aires, Argentina

Abstract
A review of gradient elution chromatography application and instrumental considerations is presented. Gradient elution refers to any kind of intentional variation of mobile-phase composition with time during the course of an analysis. Solvent programing should take place in such a way that the solvent strength increases with time; in other words, the migration velocity of analytes increases as a result of the gradient. This entry describes the advantages and disadvantages of gradient elution. An initial gradient elution run is often the best starting point for liquid chromatography (LC) method development, even where a final isocratic method may be possible. Two kinds of equipment are used for gradient elution: high-pressure mixing systems and low-pressure mixing systems. With either of these devices, changes in the composition of the mobile phase during gradient elution can be stepwise or continuous, depending on the mode of control. One limitation is that many detectors cannot be used.

INTRODUCTION

Isocratic liquid chromatography (LC) is able to separate a limited number of peaks, typically 10 or 12. The general elution problem, which arises when a complex mixture of solutes having widely varying k' (capacity factor) values are required to be separated, is most conveniently solved by the use of gradient elution (Figs. 1 and 2). Gradient elution in LC is analogous to temperature programing in gas chromatography. While the advantages and disadvantages of gradient elution must be weighed for each application, many separations are only possible using gradient elution program.

The use of gradient elution for routine application is recommended for the following kinds of samples:

- Samples with a wide k' range (i.e., where no isocratic conditions result in $0.5 < k' < 20$ for all bands of interest).
- Samples composed of large molecules (e.g., with molecular weights above 1000 and especially samples of biological origin).
- Samples containing late-eluting interferences that can either foul the column or overlap subsequent chromatograms.
- Dilute solutions of the sample dissolved in a weak solvent (e.g., aqueous sample solutions for injection onto a reversed-phase column).

In addition, an initial gradient elution run is often the best starting point for LC method development, even where a final isocratic method may be possible.

INSTRUMENTAL CONSIDERATIONS

The disadvantages of gradient elution are the following:

- Gradient equipment is not available in some laboratories.
- Gradient elution cannot be used with some LC detectors (e.g., refractive index detectors).
- Gradient elution is more complicated, and it appears to make both method development and routine application more difficult.
- Gradient runs take longer, because it is necessary for column equilibration after each run.
- Gradient methods do not always transfer well, because differences in equipment can affect separation.
- Baseline problems are more common with gradient elution, and solvents must be of higher purity.
- Certain column–mobile-phase combinations are not recommended for gradient elution.

DISCUSSION

In LC, "gradient" is short for gradient elution and both terms are commonly used as synonyms for solvent programing. Solvent programing refers to any kind of intentional variation of mobile-phase composition with time during the course of an analysis. Solvent programing should take place in such a way that the solvent strength increases with time; in other words, the migration velocity of analytes increases as a result of the gradient.

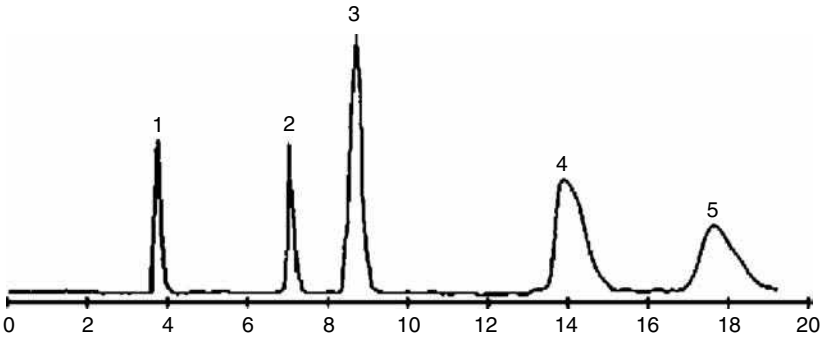

Fig. 1 Chromatogram obtained using isocratic LC: 1, Theophylline; 2, acetylsalicylic acid; 3, propanolol; 4, nortriptyline; 5, trimipramine. Column: C_{18}, 3 μm; mobile phase: 0.1% trifluoroacetic acid (TFA) in water; flow rate: 2.5 ml/min; detector: evaporative light-scattering detector (ELSD).

The initial conditions at the start of the run are chosen such that the retention factor of the first (relevant) component is within the optimal window (typically $1 < k' < 10$) or higher. Under these conditions, no relevant components are eluted too early in the chromatogram. However, some components may have very high k' values under initial conditions. When the solvent strength increases, the retention factors of these components start to become smaller. In gradient elution, mobile-phase strength (%B) increases during separation, which means that sample retention, measured as k', decreases for each band as it migrates through the column. It is assumed that band X is the first sample band that elutes, and band Z is the last band. At the beginning of the separation process, %B is low and k' for band X is large. After some time, however, the increase in %B results in a k' value for band X that is small enough ($k' < 10$) to allow it to start moving in the column. With time, k' for band X continues to decrease and X migrates faster and faster. Eventually, at the band retention time t_x, X reaches the outlet of the column and appears in the detector to be recorded as a peak in the chromatogram.

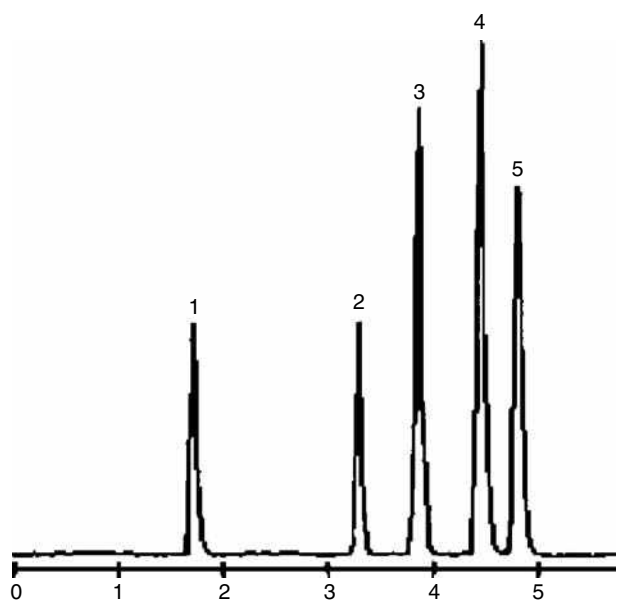

Fig. 2 Chromatogram obtained using gradient elution LC: 1, Theophylline; 2, acetylsalicylic acid; 3, propanolol; 4, nortriptyline; 5, trimipramine. Column: C_{18}, 3 μm; mobile phase: A, 0.1% TFA in water; B, 0.1% TFA in acetonitrile; gradient: time 6 min; %B 10–90; flow rate: 2.5 ml/min; detector: ELSD.

The value of k' for each band in isocratic elution is quite important in understanding and controlling LC separation. In gradient elution k' is equally important. The effective value of k' in gradient elution is equal to k' for the band when it has migrated halfway through the column. This average value of k' in gradient elution, defined as k^*, determines sample resolution and bandwidth, just as in isocratic separation.

The last band, Z, remains at the column inlet for a longer time, but eventually the mobile phase becomes strong enough for $k' < 10$. Band Z then migrates through the column in similar fashion as the first band, elutes at a retention time t_z, and its effective k' value, k^*, is also equal to 2. As a result, every band in a linear-gradient chromatogram will have similar widths, and sample resolution will not necessarily be poorer at the beginning of the chromatogram, as is so often the case in isocratic separation.

Gradients result from the mixing of two or more different solvents. The following restrictions apply to isocratic solvents: selectivity, safety, sample compatibility, column compatibility, detector compatibility, viscosity, corrosivity, purity, cost. The same restrictions apply to gradient solvents, as well as, miscibility, mutual compatibility, and insensitivity of detector for variations in composition.

In addition, certain considerations apply specifically when selecting gradient solvents. Miscibility of the different solvents is an obvious requirement. Even when solvents are considered to be well miscible, as in the case of methanol and water, there may be a significant heat effect on mixing. In this particular example, there is also a significant contraction (i.e., a mixture of methanol and water has a smaller volume than the sum of the individually measured components).

When buffers or salts are added to (one of) the solvents, miscibility considerations become more urgent. Buffer solubility is typically much higher in water than in organic solvents, methanol being better than acetonitrile. In organic solvents, organic buffers tend to be more soluble

than typical inorganic buffers. When using gradient elution, online mixing of solvents must take place and, during this process, local conditions may cause solubility problems. For example, when mixing an aqueous buffer with a pure organic solvent, buffer precipitation may occur more quickly than mixing. Some useful practical tips are listed below:

1. Always verify the miscibility of the individual solvents in an off-line (test tube) experiment, especially when using buffers, salts, or other solid additives.
2. Keep a safety margin relative to the verified solubility. For example, keep the buffer concentration in online mixing well below that tried in the off-line experiment.
3. Use partially mixed solvents in the reservoirs when possible. Mixing a solution of 10% A in B with one of 10% B in A is much safer than mixing pure A with pure B.

The column must be equilibrated, re-equilibrated to the initial high aqueous solvent composition before another analysis can be performed. Normally this re-equilibration is included at the end of the gradient. How much equilibration time is enough? In reality, it depends on the column length, flow rate, and the hydrophobicity of the sample peptides. Some chromatographers use 10 min as the standard equilibration time. Equilibration is all about fitness of purpose. One should determine the equilibration time experimentally; the criteria should be, does the analyte really stick to the column and chromatograph appropriately and reproducibly for subsequent analyses. If this part of the method development is taken care of, it will undoubtedly be rewarded with improved chromatography and better cycle time.

INSTRUMENTAL ASPECTS

Equipments for carrying out gradient elution in LC can be divided into two distinct types: low-pressure mixing systems and high-pressure mixing systems. With either of these systems, changes in the composition of the mobile phase during gradient elution can be stepwise or continuous, depending on the mode of control. Changes in solvent composition can be programed on a linear basis but, often, some type of exponential change (convex or concave) is preferred for optimum separation.

HIGH-PRESSURE MIXING SYSTEMS

This type of gradient device involves the high-pressure mixing of two solvents to generate a mobile-phase gradient by programing the delivery from the high-pressure system. In this type of LC system, the output from two or more high-pressure pumps is programed into a mixing chamber before it flows into the column. Both reciprocating- and displacement-type pumps have been used. Since the output of each pump can be separately controlled (electronically), it is possible to conveniently generate almost any kind of gradient; systems of this type are widely used in commercial instruments. However, this arrangement is expensive, as two or more high-pressure pumps plus a gradient controller are required. An important limitation is that reciprocating pumps operate with poor precision at low flow rates (e.g., less than 0.1 ml/min). This poses a problem at both extremes of the solvent program, where a small amount of one solvent is mixed with the other. As a result of this imprecision of solvent delivery at low flow rates by reciprocating pumps, the gradients that are formed at the initial and final stages of the program can be imprecise and the solute elution erratic. For example, to add 2% methanol to an otherwise aqueous eluent at a combined flow rate of 1 ml/min, the methanol pump is required to perform reliably at a level of 20 μl/min. Such a value is low for most common LC pumps. If a specifically designed micro-LC pump were to be used, problems might arise when methanol concentration would be increased to much higher values.

Another complication is that the delivered flow rate varies with the eluent. Different solvents have different compressibilities and viscosities. These properties may have a fundamental and an empirical effect (respectively) on the resulting flow rate. Often, pumps can be calibrated to compensate for such effects.

LOW-PRESSURE MIXING SYSTEMS

In this approach, solvent gradients are first formed by mixing two or more solvents at atmospheric pressure, then pumped via a single pump. The simplest arrangement of the low-pressure gradient systems involves adding the modifying stronger solvent to a stirred reservoir filled with the lower-strength initial solvent, which feeds the pump.

A more versatile and precise approach is used by several suppliers. In this approach, a series of reservoirs containing mobile phases of increasing solvent strength is used. Separation starts with the weakest solvent A. The gradient is produced by sequentially opening and closing valves leading to reservoirs containing solvents of increasing strength, B and C. The concentrations of these solvents can be selected by proportioning the time that the valves to the various reservoirs are opened and closed, using a microprocessor control system. After the desired solvent mixture is generated, it is mixed and fed to a single reciprocating pump for pressurization. Useful gradients can be generated with two reservoirs containing solvents of different strengths. However, by using additional solvents (e.g., up to 20) more sophisticated gradients can be generated that are capable of resolving mixtures containing compounds of widely differing chemical properties.

Low-pressure mixing systems require advanced software control for the opening and closing of the valves. This is mainly because LC pumps are designed to deliver a flow that is as constant as possible. The suction (input) flow, however, is extremely variable. For the delivery stroke to be smooth, the suction (refill) stroke has to be rapid. Yet, it is in this inlet flow stream that mixtures and gradients are being generated.

A typical pump head of an LC pump may have a volume of 100 μl. To generate mixtures with an accuracy of 0.1%, the composition of the solvent entering the pump has to be controlled to within 100 nl.

Degassing of solvents is the final subject that deserves attention. The heat effect of mixing solvents, especially water and organics, can be quite considerable. This may easily cause the emergence of dissolved gases in the form of bubbles, which in turn can affect the performance of the pump to a great extent. Extensive degassing of the individual solvents by helium purging has long been the method of choice, except for premixed mobile phases (mixtures of two or more solvents), salt or buffer solutions, etc. A quick burst of helium followed by leaving a helium cap (low flow of helium) in the bottle is then recommended. In recent years, in-line degassers have emerged, in which the mixed eluent passes alongside a membrane, the other side of which is pumped to a vacuum. In-line degassers allow effective degassing without affecting the composition of mixed eluents.

CONCLUSIONS

Some samples are well separated by isocratic elution, but they contain late-eluting interferences that either contaminate the column or interfere with subsequent separations. As gradient elution LC is an invaluable separation technique for complex mixtures of non-volatile solutes, it would solve this problem. Two kinds of equipment are used for gradient elution: high-pressure mixing systems and low-pressure mixing systems. One limitation is that many detectors cannot be used. In scouting separations of unknown samples, the flexibility and power of gradient elution will continue to make it a popular technique for solving the general elution problem.

BIBLIOGRAPHY

1. Katz, E.; Eksteen, R.; Schoenmakers, P.; Miller, N. Eds. *Handbook of HPLC*; Marcel Dekker, Inc: New York, 1998.
2. Snyder, L.R.; Kirkland, J.J.; Glajch, J.L. Eds. *Practical HPLC Method Development*; John Wiley & Sons Inc: New York, 1997.
3. Snyder, L.R.; Kirkland, J.J. Eds. *Introduction to Modern Liquid Chromatography*; John Wiley & Sons Inc: New York, 1979.
4. Schellinger, A.P.; Stoll, D.R.; Carr, P.W. High-speed gradient elution reversed-phase liquid chromatography of bases in buffered eluents Part I. Retention repeatability and column re-equilibration. J. Chromatogr. A, **2008**, *1192*, 41–53.
5. Schellinger, A.P.; Stoll, D.R.; Carr, P.W. High-speed gradient elution reversed-phase liquid chromatography of bases in buffered eluents Part II. Full equilibrium. J. Chromatogr. A, **2008**, *1192*, 54–61.
6. Fatemi, M.H.; Abraham, M.H.; Poole, C.F. Combination of artificial neural network technique and linear free energy relationship parameters in the prediction of gradient retention times in liquid chromatography. J. Chromatogr. A, **2008**, *1190*, 241–252.
7. Pavel, J.; Česla, P.; Hájek, T.; Vohralík, G.; Vyňuchalová, K.; Fischer, J. Optimization of separation in two-dimensional high-performance liquid chromatography by adjusting phase system selectivity and using programmed elution techniques. J. Chromatogr. A, **2008**, *1189*, 207–220.
8. Gritti, F.; Guiochon, G. The ultimate band compression factor in gradient elution chromatography. J. Chromatogr. A, **2008**, *1178*, 79–91.
9. Pappa-Louisi, A.; Nikitas, P.; Papageorgiou, A.; Optimisation of multilinear gradient elutions in reversed-phase liquid chromatography using ternary solvent mixtures. J. Chromatogr. A, **2007**, *1166*, 126–134.
10. Nikitas, P.; Pappa-Louisi, A.; Papageorgiou, A. Simple algorithms for fitting and optimization for multilinear gradient elution in reversed-phase liquid chromatography. J. Chromatogr. A, **2007**, *1157*, 178–186.
11. Coym, J.W.; Roe, B.W. Effect of temperature on gradient reequilibration in reversed-phase liquid chromatography. J. Chromatogr. A, **2007**, *1154*, 182–188.
12. Gritti, F.; Guiochon, G. The bandwidth in gradient elution chromatography with a retained organic modifier. J. Chromatogr. A, **2007**, *1145*, 67–82.
13. Pappa-Louisi, A.; Nikitas, P.; Balkatzopoulou, P.; Louizis, G. Fundamental equation of dual-mode gradient elution in liquid chromatography involving simultaneous changes in flow rate and mobile phase composition. Anal. Chem. **2007**, *79* (10), 3888–3893.
14. Gacía-Lavandeira, J.; Martínez-Pontevedra, J.A.; Lores, M.; Cela, R. Computer-assisted transfer of programmed elutions in reversed-phase high-performance liquid chromatography. J. Chromatogr. A, **2006**, *1128*, 17–26.
15. Pappa-Louisi, A.; Nikitas, P.; Agrafiotou, P. Column equilibration effects in gradient elution in reversed-phase liquid chromatography. J. Chromatogr. A, **2006**, *1127*, 97–107.
16. Piątkowski, W.; Kramarz, R.; Poplewska, I.; Antos, D. Deformation of gradient shape as a result of preferential adsorption of solvents in mixed mobile phases. J. Chromatogr. A, **2006**, *1127*, 187–199.
17. Pavel, J. Can the theory of gradient liquid chromatography be useful in solving practical problems? Review. J. Chromatogr. A, **2006**, *1126*, 195–218.
18. Nikitas, P.; Pappa-Louisi, A.; Agrafiotou, P. Multilinear gradient elution optimization in reversed-phase liquid chromatography using genetic algorithms. J. Chromatogr. A, **2006**, *1120*, 299–307.

19. Neue, U.; Marchand, D.H.; Snyder, L.R. Peak compression in reversed-phase gradient elution. J. Chromatogr. A, **2006**, *1111*, 32–39.
20. Schellinger, A.P.; Carr, P.W. Isocratic and gradient elution chromatography: A comparison in terms of speed, retention reproducibility and quantitation. J. Chromatogr. A, **2006**, *1109*, 253–266.
21. Hao, W.; Zhang, X.; Hou, K. Analytical solutions of the ideal model for gradient liquid chromatography. Anal. Chem. **2006**, *78* (22), 7828–7840.
22. Hendriks, G.; Franke, J.P.; Uges, G.R.A. New practical algorithm for modeling retention times in gradient reversed-phase high-performance liquid chromatography. J. Chromatogr. A, **2005**, *1089*, 193–202.
23. Gilroy, J.J.; Dolan, J.W. Gradient performance checks. LC-GC-Europe. **2004**, *17* (11), 566–572.
24. Schweitz, L.; Fransson, M.; Karlsson, L.; Torstensson, A.; Johansson, E. On-line process control of gradient elution liquid chromatography. Anal. Chem. **2004**, *76* (16), 4875–4880.
25. Nikitas, P.; Pappa-Louisi, A.; Papachristos, K. Optimisation technique for stepwise gradient elution in reversed-phase liquid chromatography. J. Chromatogr. A, **2004**, *1033* (2), 283–289.
26. Law, B. The effect of eluent pH and compound acid-base character on the design of generic-gradient reversed-phase high-performance liquid chromatography (PR-HPLC) methods for use in drug discovery. J. Pharm. Biomed. Anal. **2004**, *34* (1): 215–219.
27. Vivo Truyols, G.; Torres Lapasio, J.R.; Garcia Alvarez Coque, M.C. Enhanced calculation of optimal gradient programmes in reversed-phase liquid chromatography. J. Chromatogr. A, **2003**, *1018* (2), 183–196.
28. Dolan, J.W. The hazards of adjusting gradients. LC-GC-North-Am. **2002**, *20* (10), 940–946.
29. Jupille, T.; Snyder, L.; Molnar, I. Optimizing multilinear gradients in HPLC. LC-GC-Europe. **2002**, *15* (9), 596–601.
30. Dolan, J.W. Starting out right. Part VI—The scouting gradient alternative. LC-GC-North-Am. **2000**, *18* (5), 478–487.
31. Dolan, J.W.; Snyder, L.R.; Wolcott, R.G.; Haber, P.; Baczek, T.; Kaliszan, R.; Sander, L.C. Reversed-phase liquid chromatographic separation of complex samples by optimizing temperature and gradient times. III. Improving the accuracy of computer simulation. J. Chromatogr. A, **1999**, *857* (1–2), 41–68.
32. Dolan, J.W.; Snyder, L.R.; Djordjevic, N.M.; Hill, D.W.; Waeghe, T.J. Reversed-phase liquid chromatographic separation of complex samples by optimizing temperature and gradient time. II. Two-run assay procedures. J. Chromatogr. A, **1999**, *857* (1–2), 21–39.
33. Dolan, J.W.; Snyder, L.R.; Djordjevic, N.M.; Hill, D.W.; Waeghe, T.J. Reversed-phase liquid chromatographic separation of complex samples by optimizing temperature and gradient time. I. Peak capacity limitations. J. Chromatogr. A, **1999**, *857* (1–2), 1–20.
34. Wolcott, R.G.; Dolan, J.W. Column temperature effects in gradient elution. LC-GC. **1998**, *16* (12), 1080–1083.
35. Nelson, M.D.; Dolan, J.W. Gradient background peaks—a case study. LC-GC. **1998**, *16* (11), 992–996.
36. Molnar, I. Robust HPLC methods. Part 3: Robust isocratic and robust gradient methods. LaborPraxis. **1998**, *22* (11), 72–79.
37. Li, J.B.; Morawski, J. Strategies for faster gradient chromatography. LC-GC. **1998**, *16* (5), 468–476.
38. Dolan, J.W.; Snyder, L.R.; Saunders, D.L.; Van-Heukelem, L. Simultaneous variation of temperature and gradient steepness for reversed-phase high-performance liquid chromatography method development. II. The use of further changes in conditions. J. Chromatogr. A, **1998**, *803* (1–2), 33–50.
39. Dolan, J.W.; Snyder, L.R.; Djordjevic, N.M.; Hill, D.W.; Saunders, D.L.; Van-Heukelem, L.; Waeghe, T.J. Simultaneous variation of temperature and gradient steepness for reversed-phase high-performance liquid chromatography method development. I. Application to 14 different samples using computer simulation. J. Chromatogr. A, **1998**, *803* (1–2), 1–31.
40. Molnar, I.; Snyder, L.R.; Dolan, J.W. Reversed-phase gradient elution: How to get better results with less work. LC-GC-Int. **1998**, *11* (6), 374–387.
41. Dolan, J.W. Problems with gradient methods. LC-GC-Int. **1996**, *9*(5), 278–282.
42. Zhu, P.L.; Snyder L.R.; Dolan J.W. Improved baselines in gradient elution. J. Chromatogr. A, **1995**, *718*, 429–435.

Gradient Elution Techniques

Ioannis N. Papadoyannis
Kalliopi A. Georga
Laboratory of Analytical Chemistry, Chemistry Department, Aristotle University of Thessaloniki, Thessaloniki, Greece

INTRODUCTION

Gradient elution is the elution method in which the mobile-phase composition changes during time. It may be considered as an analogy to the temperature programming in gas chromatography (GC).

DISCUSSION

The main purpose of gradient elution is to move strongly retained components of a mixture faster, while having the least retained components well resolved. At the beginning of the analysis, the solvent used is appropriate to elute some of the components, but is "weak" in terms of its ability to remove other compounds from the column and separate them from one another.

Gradient elution operates on the principle that, under the initial mobile-phase conditions, many of the components have a k' (capacity factor) value of essentially infinity, in that these components are stopped in a narrow band near the head of the column. As the solvent composition is changed and its solvent strength is increased, sample components dissolve at a characteristic solvent strength and then migrate down the column, leaving the remaining components behind. Changes in the mobile-phase composition may be "continuous" with a predetermined set of conditions or may be done in "steps" of substantial solvent composition changes.

The typical gradients used in reversed-phase chromatography are linear or binary (i.e., involving two mobile phases). Convex and concave gradients are used occasionally for analytical purposes, particularly when dealing with multicomponent samples requiring extra resolution either at the beginning or at the end of the gradient (Fig. 1).

The concentration of the organic solvent is lower in the initial mobile phase (mobile phase A) than it is in the final mobile phase (mobile phase B). The gradient then, regardless of the absolute change in percent organic modifier, always proceeds from a condition of high polarity (high aqueous content, low concentration of organic modifier) to low polarity (higher concentration of organic modifier, lower aqueous content). Reversed-phase separations can be achieved using either a stepwise or a continuous gradient to elute sample components. Step gradients (i.e., a series of isocratic elutions at different percentages of B) are useful for applications such as desalting, but for separations requiring high resolution, a linear continuous gradient is required.

Step gradients are also ideal when performing process scale applications providing the desired resolution can be obtained; less complex instrumentation is required to generate step gradients. Additionally, step gradients can be generated more reproducibly than linear gradients.

Gradient shape (combination of linear gradient and isocratic conditions), gradient slope, and gradient volume are all important considerations in reversed-phase chromatography. Typically, when first performing a reversed-phase separation of a complex sample, a broad gradient is used for initial screening in order to determine the optimum gradient shape.

The ideal gradient shape and volume are empirically determined for a particular separation. Generally, the sample is chromatographed using a broad-range linear gradient to determine where the molecules of interest will elute. The initial conditions usually consist of mobile phase A containing 10% or less organic modifier and mobile phase B containing 90% or more organic modifier. The initial gradient runs from 0% B to 100% B over 10–30 column volumes. A blank gradient is usually run prior to injecting the sample, in order to detect any baseline disturbances resulting from the column or impurities originating in the mobile phase.

After the initial screening is completed, the gradient shape may be adjusted to optimize the separation of the desired components. This is usually accomplished by decreasing the gradient slope, where the desired components elute, and increasing it before and after. The choice of gradient slope will depend on how closely the contaminants elute to the target molecule. Generally, decreasing the gradient slope increases the resolution. However, the peak volume and retention time increase with decreasing gradient slope. Shallow gradients with short columns are generally optimal for high-molecular-weight biomolecules.

Gradient slopes are generally reported as change in percent B per unit time (% B/min) or per unit volume (% B/ml). When programming a chromatography system

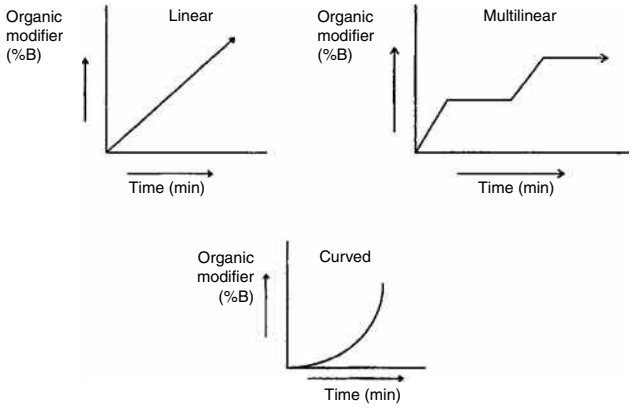

Fig. 1 Various gradient shapes.

in the time mode, it is important to remember that changes in flow rate will affect gradient slope and, therefore, resolution.

Resolution is also affected by the total gradient volume (gradient volume × flow rate). Although the optimum value must be determined empirically, a good rule of thumb is to begin with a gradient volume that is approximately 10–20 times the column volume. The slope can then be increased or decreased in order to optimize the resolution.

Except for optimizing gradient elution methods, which is a very important parameter in chromatographic analysis, another parameter of great significance is the mixing of the mobile-phase components.

There are two primary methods of mixing the mobile-phase components, known as "low-pressure mixing" and "high-pressure mixing." The first method employs electrically actuated solenoid valves located ahead of a single-solvent delivery system (pump). The precision of the gradient depends on the ability of the solenoid to reproducibly dispense solvents in segments of variable size (volume), depending on the composition desired. If reproducible retention times and stable detector baselines are to be obtained, these "segments of solvent plugs" must be well mixed into a homogenous mobile-phase stream before entering the chromatographic column.

The second method uses a separate solvent delivery device for each solvent, with each being capable of delivering smooth, precise flow rates of as low as a few microliters per minute. Gradients are formed by varying the delivery speeds and simply blending the concurrent solvent streams on the high-pressure side of the pumps.

Each method of gradient formation has advantages and disadvantages. The low-pressure gradient formation is preferred most of the time, because it uses only one pump, whereas the high-pressure method uses two pumps which might go wrong during use. Because low-pressure gradient systems have only one pump, they are, of course, less expensive. These systems require extensive degassing and have a large lag time (delay volume) in starting the gradient, whereas, in high-pressure systems, degassing is desired but not essential.

Moreover, low-pressure systems often use three or four solvents. This multiple-solvent blending might also be useful for the optimization of both isocratic and gradient elution methods. This is an advantage that the high-pressure system also has; when not using a gradient system, the operator has two independent isocratic pumps.

Gradient elution is ideal for separating certain kinds of sample which cannot be easily handled by isocratic methods, because of their wide k' range. Nevertheless, there is a strong bias against the use of gradient elution in many laboratories.

Some of the reasons for not preferring gradient elution are as follows: Gradient equipment is not available in some laboratories, because of its higher cost, and gradient elution is more complicated and makes both method development and routine analysis more difficult; the most important issue is that it is not compatible with some high-performance liquid chromatography (HPLC) detectors (e.g., refractive index detectors). Furthermore, gradient runs take longer, because of the need of column equilibration after each run. Baseline problems are more common with gradient elution and the solvent must be of high purity.

Although the disadvantages of gradient elution must be taken into serious consideration, many separations are only possible using gradient elution. The use of gradient elution for routine applications is suggested for the following kinds of sample:

1. Samples with a wide range of k'
2. Samples composed of large molecules >1000 in molecular weight
3. Samples containing late eluting interferences that can either foul the column or overlap subsequent chromatograms

Using gradient elution to develop HPLC methods has many advantages compared with using isocratic experiments. First, errors in solvent strength can be adjusted when changing from one solvent to another. Second, the ability to increase resolution during early exploratory runs is a distinct advantage when doing solvent mapping. Early bands often are severely overlapped in isocratic separations, so that it may not be clear how resolution is changing as separation conditions are varied. Gradient elution opens up the front of the chromatogram, allowing a better view of what is happening as conditions are varied (Fig. 2).

Third, using gradient elution runs during the initial stages of method development makes it easier to locate compounds that elute either very early or very late in the chromatogram. With isocratic separation, early-eluting compounds are often lost in the solvent front, whereas late-eluting compounds disappear into the baseline or

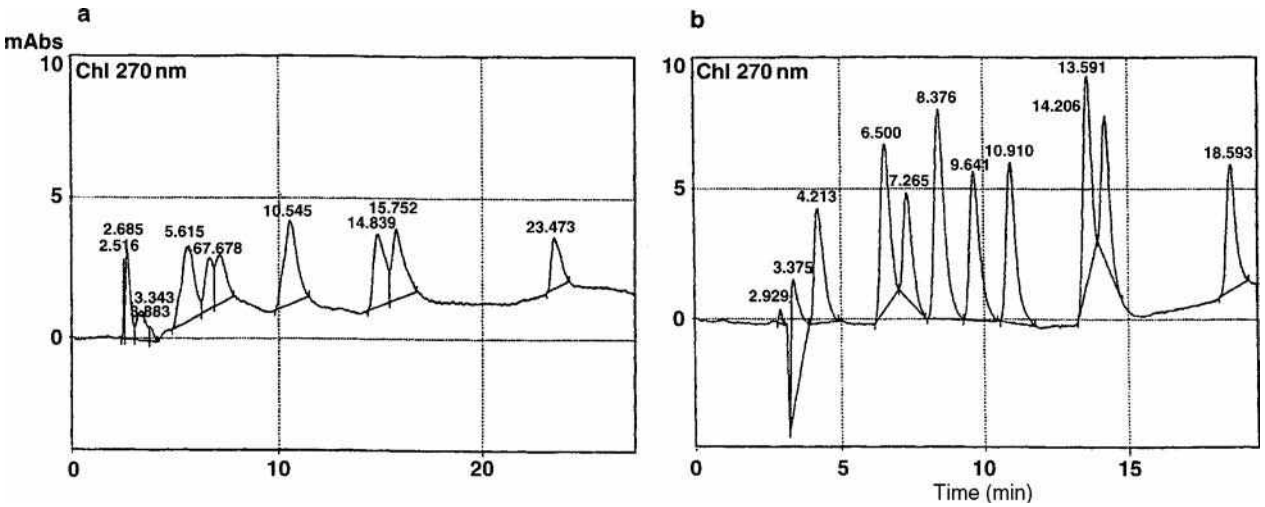

Fig. 2 HPLC analysis of eight methylxanthines: a, with isocratic elution; and b, with gradient elution.

overlap the next sample. Finally, gradient elution method development works for either gradient or isocratic elution.

In conclusion, gradient elution is not preferred as a quantitative technique because it is more complex than isocratic elution and, hence, more things can potentially go wrong. However, with proper control of operating parameters and good instrumentation, it is possible to obtain a separation with excellent quantitative results. This requires that the operator understand the hardware and determine that it is working correctly before attempting a separation. The ideal gradient system should be easy to operate, reproducible to provide consistent retention times, versatile to provide capability of generating various concave, convex, and linear gradient shapes, and convenient to provide a rapid turnaround time to initial eluent conditions (equilibration) for fast throughput from analysis to analysis.

BIBLIOGRAPHY

1. Bidlingmeyer, B.A. *Practical HPLC Methodology and Applications*; John Wiley & Sons, Inc.: New York, 1992.
2. Papadoyannis, I.; Samanidou, V.; Georga, K. Solid-phase extraction study and photodiode array RP-HPLC analysis of xanthine derivatives in human biological fluids. J. Liq. Chromatogr **1996**, *19* (16), 2559.
3. Pharmacia Biotech. *Reversed Phase Chromatography*; Pharmacia Biotech: Uppsala, Sweden, 1996.
4. Snyder, L.R.; Glajch, J.L.; Kirkland, J.J. *Practical HPLC Method Development*; John Wiley & Sons, Inc.: New York, 1988.
5. Snyder, L.R.; Kirkland, J.J.; Glajch, J.L. *Practical HPLC Method Development,* 2nd Ed.; John Wiley & Sons: New York, 1997.

Gradient HPLC: Gradient System Selection

Pavel Jandera
Department of Analytical Chemistry, University of Pardubice, Pardubice, Czech Republic

Abstract

Gradient elution is widely used for the separation of complex samples in reversed-phase high-performance liquid chromatography (HPLC) systems and ion-exchange systems. The theory of gradient elution has now been elaborated so that it allows predicting the retention and the resolution of sample compounds in reversed-phase, ion-exchange, and normal-phase systems for almost any combination of gradient profile and relationship between the retention and mobile-phase composition.

The most important sources of errors in the prediction and optimization of gradient elution are the gradient dwell volume and the preferential adsorption of the strong solvents, especially in normal-phase (adsorption) chromatography. The gradient dwell volume effects are more important in micro-LC techniques than in conventional analytical LC and may cause significant increase in the time of analysis, unless special instrumentation and (or) pre-column flow splitting is used, but their effects can be taken into account in predictive calculations. In normal-phase gradient HPLC, poor reproducibility may be caused by preferential adsorption of polar solvents from mixed mobile phases, which may cause significant deviations of the actual gradient profile from the preset program. Using carefully dried solvents and controlling the temperature, reproducibility of retention in normal-phase gradient elution can be largely improved.

The parameters of binary or ternary linear and non-linear gradients can be adjusted by predictive calculations to optimize the resolution and minimum separation time in various chromatographic systems. In addition to accurate calculations of the gradient elution data, simple procedures can be employed for rapid estimation of the effects of the gradient program, column geometry, or mobile-phase flow rate on the retention both in reversed-phase and in normal-phase gradient chromatography and for transfer of gradient methods between various instruments. In gradient elution, sample band broadening is largely suppressed with respect to isocratic operation, providing a higher number of separated peaks within the same separation time interval. Because of higher peak capacity, gradient elution is especially suitable for two-dimensional liquid chromatography, where increased peak capacity is of primary concern.

INTRODUCTION

Many high-performance liquid chromatography (HPLC) analyses can be performed at constant, isocratic, operating conditions using isocratic elution. However, isocratic elution with a mobile phase of fixed composition often does not yield a successful separation of complex samples containing compounds that differ widely in retention characteristics. To keep the time of analysis within acceptable limits, the retention factors [$k = (V_R/V_m - 1)$] of the most strongly retained sample components should usually be lower than 10 (V_R = retention volume, V_m = column holdup volume). For a satisfactory separation of both weakly and strongly retained sample compounds in a single run, operating conditions controlling retention, such as the composition or flow rate of the mobile phase, or the column temperature, should be varied during the chromatographic experiment. Flow programming in contemporary HPLC, using efficient small-particle columns, has only marginal effect on separation and is limited by the maximum instrumental pressure. Temperature programming is widely used in gas chromatography (GC), but rarely in HPLC, because a large rise in temperature during the run is required to significantly reduce retention. Solvent gradients are generally much more efficient to decrease the retention than programmed temperature. For example, retention factors k of low-molecular-weight analytes in reversed-phase LC (RPLC) decrease by a factor of 2–3 with a 10% increase in the concentration of organic solvent in aqueous–organic mobile phase, whereas an increase of temperature by 10°C usually leads to a decrease in k of non-ionic compounds by 10–20%. Furthermore, many commercial HPLC columns, especially with stationary phases bonded onto a silica gel support, are not stable at temperatures higher than 60°C. Also, only a few instruments that allow steep-enough temperature gradients are available because of a relatively slow response of the temperature inside the column to a change in the temperature setting in an air-heated thermostated compartment, especially with conventional analytical columns of 2 mm inner diameter or larger.

For these reasons, solvent gradients are most frequently used in contemporary HPLC. In gradient elution, the composition of the mobile phase is changed during the chromatographic run, either stepwise or continuously, to

increase the elution strength of the mobile phase, which allows decreasing the retention factors by 2 to 3 orders of magnitude in a single run. However, gradient elution requires more complicated equipment than isocratic HPLC, as two or more components of the mobile phase should be accurately mixed according to a preset time program; in addition, the selection of detectors is limited. Gradient runs generally take a longer time than isocratic elution because the column should be re-equilibrated to initial gradient conditions after each run.

The phenomena controlling gradient elution have often been misunderstood by many practicing chromatographers, who often consider it as subject to more experimental problems, less reproducible, slower, and more difficult to transfer from one instrument (laboratory) to another than isocratic elution, the reason being more complex equipment, more tedious method development, and more difficult interpretation of results. That is why some workers try to avoid gradient elution; however, by doing so they can miss undeniable benefits of this technique.

The main reasons for the use of gradient elution are the following:

- Improving the resolution of samples with wide range of retention.
- Increasing the number of peaks resolved within a fixed time of separation (increasing the peak capacity in single- or multidimensional LC).
- Separation of mixtures of compounds with high molecular weights such as synthetic polymers, proteins, and other biopolymers, whose retention changes markedly for small changes in the composition of mobile phases.
- Providing economic and fast generic separation methods that can be applied with confidence in development and control laboratories to a large number of samples of variable composition to provide important information in short time to synthetic chemists, either for fast sample screening or for generating impurity profiles.
- Using initial "scouting" gradient experiments for efficient development of final gradient or isocratic methods.
- Removing strongly retained interfering compounds in a separate sample pretreatment before analysis.
- Suppression of tailing peaks, especially for samples containing basic compounds.

Because of a higher number of experimental variables that may affect the retention, the effective use of gradient technique requires understanding how the gradient profile controls the separation. Some practitioners may be puzzled by observing that, for example, using a longer column or decreasing the flow rate of the mobile phase, while keeping other gradient conditions unchanged, may shorten the analysis time and decrease the resolution in gradient elution, contrary to the effects in isocratic HPLC. The theory developed in the past few decades can satisfactorily explain such "unexpected" results in gradient elution. Theoretical models describing the sample behavior under gradient conditions provide efficient tools for development and optimization of gradient HPLC methods.

PRINCIPLES OF GRADIENT ELUTION

Mobile-phase gradients can be formed outside the separation column by pumping and mixing the liquid components according to a preset time program (external gradients), or can be generated inside the column as a consequence of changing the equilibrium between the components adsorbed on the stationary phase and in the solution, induced by incoming mobile phase (internal gradients). Therefore, the second approach is suitable only for a limited number of separation cases and is generally not used, except for some ion chromatography systems with reagent-free eluent generators to produce hydroxide eluents for isocratic or gradient separations. The retention of non-ionic compounds in RPLC and normal-phase LC (NPLC) depends mainly on their polarities and the polarities of the stationary and mobile phases; hence, external polarity (solvent strength) gradients, prepared by mixing solvents of different polarities, are suitable for their separation. Solvent strength gradients are often useful for the separation of ionic compounds; however, the mobile phase should contain buffers or other ionic additives so that ionic strength or pH gradients can also be used for separations in ion-exchange (IE) or ion-pair gradient chromatography of ionic compounds.

Mobile-phase gradients in analytical HPLC can be classified using several criteria:

1. Number of mobile-phase components whose concentrations change with time:
   - Two-component (binary) gradients
   - Multicomponent (ternary, quaternary, etc.) gradients
   - Relay gradients, i.e., multicomponent gradients consisting of several subsequent steps with different solvents where the mobile phase changes from solvent A to solvent B in the first step, from solvent B to solvent C in the second step, etc.
2. Profile of the gradient:
   - Linear gradients
   - Non-linear gradients with curved profile (concave or convex, rarely used, mostly substituted by segmented gradients)
   - Step gradients, including several subsequent isocratic steps with increasing concentration of one or more strong eluting components of the mobile phase
   - Segmented gradients, including several subsequent steps, usually linear with different slopes

(ramps) or isocratic hold periods (most often at the end or at the beginning of elution, but also inserted between linear gradient steps)
- Reverse gradients with decreasing concentration of the strong mobile-phase component are often used to restore the initial conditions before the next sample injection.

3. Chromatographic mode and mobile phase:
   - RP solvent gradients—concentration(s) of one or more organic solvent(s) in water increase(s); nonpolar bonded columns
   - Non-aqueous RP solvent gradients—concentration(s) of one or more less polar organic solvent(s) in a more polar one increase(s)
   - Ion-pair RP solvent gradients in mobile phases containing ion-pair reagents
   - Ion-pair reagent concentration gradients in RP mode
   - RP pH gradients
   - RP decreasing ionic strength gradients (hydrophobic interaction chromatography, salting-out chromatography)
   - Ionic strength gradients in ion-exchange liquid chromatography (IELC) (may be combined with solvent gradients)
   - pH gradients in IELC (may be combined with solvent gradients)
   - NP solvent gradients—concentration(s) of one or more polar solvent(s) in a less polar one increase(s); non-aqueous mobile phases, polar adsorbent, or polar-bonded-phase columns
   - NP hydrophilic interaction chromatography gradients—concentration(s) of water (or of water and a more polar organic solvent) in a less polar solvent increase(s); aqueous mobile phases, polar adsorbent, or bonded-phase columns

Most frequent are simple continuous gradients, which can be characterized by three parameters: 1) the initial concentration; 2) the steepness (slope); and 3) the shape (curvature) of the gradient, which all affect the elution time and the spacing of the peaks in the chromatogram. A linear gradient profile is used almost exclusively in practice and can be described by Eq. 1:

$$\varphi = \mathrm{A} + \mathrm{B}'t = \mathrm{A} + \frac{\Delta\varphi}{t_G}t = \mathrm{A} + \frac{\mathrm{B}'}{\mathrm{F_m}}V = \mathrm{A} + \mathrm{B}V = \mathrm{A} + \frac{\Delta\varphi}{V_G}V \quad (1)$$

where A is the initial concentration φ of the strong solvent in the mobile phase at the start of the gradient, and B or B′ is the steepness (slope) of the gradient (i.e., the increase in φ in the time unit or in the volume unit of the mobile phase); V_G and t_G are the gradient volume and the gradient time during which the concentration φ is changed from the initial value A to the concentration $\varphi_G = \mathrm{A} + \Delta\varphi$ at the end of the gradient; and $\Delta\varphi$ is the gradient range. Curved gradients are often substituted by multiple linear segmented gradients consisting of several subsequent linear gradient steps with different slopes B.

The theory of gradient elution chromatography allows prediction of the elution behavior of sample compounds by calculating from their isocratic retention data (or from two initial gradient experiments) in RPLC, NPLC, and IELC systems. Unlike isocratic conditions, the retention factors change (decrease) during gradient elution and can be considered constant only in a very small (differential) volume of the mobile phase dV corresponding to migration along a differential part of the column holdup volume V_m, dV_m:

$$\mathrm{d}V = k \cdot \mathrm{d}V_m \quad (2)$$

The differential equation Eq. 2 can be solved after introducing the dependence of k on the volume of the eluate passed through the column from the start of the gradient run V. Any dependence of k on V can be divided into two parts: 1) a dependence of k on the concentration of a strong eluting component in the mobile phase φ controlled by the thermodynamics of the distribution process (the retention equation); and 2) the parameters of Eq. 1 describing the gradient profile, adjusted by the operator. A plethora of models for the description of retention in RPLC, IE, and NPLC have been suggested during the past 40 years, resulting in various retention Eqs. 1–3. For practical prediction and optimization of retention in gradient elution, the retention model can be rigorously theoretical, semiempirical or fully empirical.

RP GRADIENT LC

RP chromatography is, by far, the most widely used LC mode for the separation of complex mixtures based on different lipophilicities of sample compounds.[1] The effect of the volume fraction φ of the organic solvent in a binary aqueous–organic mobile phase on the retention factors k in RP chromatography can be very often described by a simple equation (Eq. 3):[1,2]

$$\log k = \log k_0 - m\varphi = a - m\varphi \quad (3)$$

Here, k_0 is the retention factor of the sample solute extrapolated to pure water as the mobile phase, and m characterizes the "solvent strength" (i.e., the change in log k per concentration unit of the organic solvent). Assuming the validity of Eq. 3, the retention volume V_R in RP gradient elution chromatography with linear gradients can be calculated from Eq. 4:[3]

$$V_R = \frac{1}{mB}\log\{2.31\ mB\ [V_m\ 10^{(a-mA)} - V_D] + 1\} + V_m + V_D \quad (4)$$

V_D is the so-called gradient dwell volume [i.e., the volume of the mobile phase contained in the instrument parts (mixer, filter, and tubing) between the pump and the column]. In an ideal case, linear concentration gradients in RPLC correspond to the linear solvent strength (LSS) gradients according to the model developed by Snyder and Dolan;[4] hence, Eq. 4 describes the retention data in LSS gradient elution.

In gradient elution of weak acids or bases, gradients of organic solvent (acetonitrile, methanol, or tetrahydrofuran) in buffered aqueous–organic mobile phases are most frequently used. The solvent affects the retention as in RP chromatography (RPC) of non-ionic compounds, except for some influence on the dissociation constants, but Eq. 4 is usually accurate enough for calculations of gradient retention volumes.

The pH gradients may be used for RPC separation of weak acids or bases, whose ionization and retention strongly depend on the pH of the mobile phase. The retention factor, k, of a non-dissociated acid or a base may be 10–20 times larger than that of their dissociated forms. However, pH gradients are generally less useful and more difficult to design than solvent gradients. Quasi-linear pH gradients can be accomplished by mixing universal buffers containing phosphoric, acetic, and boric acids as solvent A with sodium hydroxide as solvent B. An RP column should be stable over a wide range of pH; bidentate bonded silica columns, hybrid silica–organic polymer matrix columns, or columns based on modified zirconium dioxide support are generally suitable for pH gradients. Theoretical model of RP pH gradients enables numerical calculation of the retention times of weak acids or weak bases in LC with linear pH gradients.[5] The dependence of the dissociation constants on the concentration of organic solvent in the mobile phase may affect the accuracy of prediction.

Completely ionized substances can often be separated in ion-pair chromatography (IPC), where an ion-pair reagent with surface-active properties, containing a strongly acidic or strongly basic group and a bulky hydrocarbon part in their molecules, is added to aqueous–organic mobile phases to increase the retention and improve the peak symmetry of ionic samples. Adequate ion-pair reagent concentrations in IPC are between 10^{-4} and 10^{-3} mol. A major disadvantage of gradient IPC is slow column equilibration after changing the mobile phase. Complete washout of the adsorbed ion-pair reagent from the column may be difficult to achieve. Furthermore, increasing concentration of organic solvent during gradient elution affects the distribution equilibrium of the ion-pairing reagent between the stationary and the mobile phase, which may impair the accuracy of the predicted gradient data.

NP (ADSORPTION) GRADIENT LC

Normal-phase chromatography (NPC) is far less used than RPC, but it has several practical advantages: 1) because of lower viscosity, pressure drop across the column is lower than with aqueous–organic mobile phases used in RPC; 2) columns are usually more stable in organic than in aqueous–organic solvents; 3) columns packed with unmodified inorganic adsorbents are not subject to "bleeding," i.e., to gradual loss of the stationary phase, which decreases slowly the retention during the lifetime of a chemically bonded column; 4) some samples are more soluble or less likely to decompose in organic than in aqueous mobile phases; 5) because of fixed position of the adsorption sites, NPC is suitable for separation of various positional isomers or stereoisomers; 6) if sample pretreatment involves extraction into a non-polar solvent, direct injection onto an NPC column is less likely to cause problems than the injection onto an RPC column; 7) gradient NPC is more suitable than RPC for the separation of synthetic polymers insoluble in water, but it has lower selectivity for the separation of molecules differing in the hydrocarbon part. However, reproducible NP gradient operation requires strict control of temperature and of trace concentrations of water in non-aqueous mobile phases. Last but not the least, organic solvents are more expensive to purchase and dispose than water.

In NP chromatography, the elution strength of the mobile phase is proportional to its polarity, which is usually adjusted using binary mobile phases consisting of a weak (non-polar) solvent A and a stronger, more polar solvent B. Hence, the elution strength increases with increasing concentration of the polar solvent B. A simple equation (Eq. 5) can often adequately describe the experimental dependencies of the retention factors k of sample compounds on the volume fraction φ of a polar solvent B in a binary mobile phase consisting of two organic solvents with different polarities, if the sample solute is very strongly retained in the pure, less polar solvent:

$$k = k_0\ \varphi^{-m} \quad (5)$$

k_0 and m in Eq. 5 depend on the nature of the solute and on the chromatographic system, but are independent of the concentration of the strong solvent B in the mobile phase.

In NP gradient LC on polar adsorbents, the concentration of one (or more) polar solvent(s), B, in a non-polar solvent A increases. Assuming the validity of Eq. 5 in NP gradient chromatography with linear increase in the volume fraction of a polar solvent B, the elution volume V_R of a sample solute can be calculated from Eq. 6:[2]

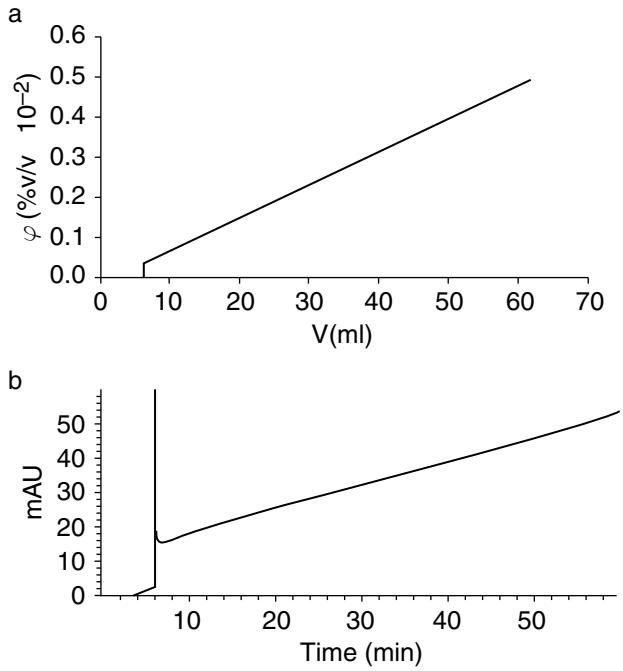

Fig. 1 Calculated breakthrough curves in NP gradient elution HPLC. Simulated calculation using the experimental isotherm data and assuming $N = 5000$. a) Gradient dwell volume = 0.50 ml. b) Record of the blank gradient detector trace showing the breakthrough of propan-2-ol at 6 min and a "ghost peak" of impurities displaced at the breakthrough volume. Column: silica gel Separon SGX (7.5 μm), 150 × 3.3 mm I.D., 1 ml/min, 40°C. Gradient: 0–50% 2-propanol in 30 min (φ = concentration of propan-2-ol in the eluate; V = volume of the eluate from the start of the gradient).

$$V_R = \frac{1}{B}\left[(m+1)B(k_0 V_m - V_D A^m) + A^{(m+1)}\right]^{\frac{1}{m+1}} - \frac{A}{B} + V_m + V_D \quad (6)$$

Here, as in Eq. 4, V_m is the column holdup volume and V_D is the gradient dwell volume.

Eq. 5 is applicable to systems where the solute retention is very high in the pure non-polar solvent. If this is not the case, the retention is better described by Eq. 7.[6]

$$k = (a + b\varphi)^{-m} \quad (7)$$

Here, a, b, and m are experimental constants depending on the solute and on the chromatographic system [$a = 1/(k_a)^m$, k_a is the retention factor in pure non-polar solvent]. Usually, Eq. 7 slightly improves the description of the experimental data with respect to Eq. 5. In NP systems where Eq. 7 applies under isocratic conditions, the elution volume V_R of a sample solute in NPLC with linear gradients described by Eq. 1 can be calculated using Eq. 8:[6]

$$V_R = \frac{1}{bB}\left[(m+1)bBV_m + (a + Ab)^{(m+1)}\right]^{\frac{1}{m+1}} - \frac{a + Ab}{bB} + V_m \quad (8)$$

In contrast to RP gradient elution, preferential adsorption of polar solvents from the mobile phase onto the surface of the polar adsorbent during a gradient run may lead to significant deviations of the actual gradient profile from the preset mobile-phase composition program and to a decrease in the reproducibility of the retention data (Fig. 1). Furthermore, because of the strong preferential adsorption of polar solvents, column re-equilibration times after the end of the gradient are often long in NPLC. This has been a reason for strong bias against the use of gradient elution in NP chromatography. To suppress these effects, which are most significant with gradients starting in pure non-polar solvents, gradients should be started, rather, at 3% or more than at a zero concentration of the polar solvent, if possible, and non-localizing polar solvents should be used, such as dichloromethane, dioxane, or *tert*-butyl methyl ether.

Water is much more strongly adsorbed than polar organic solvents on polar adsorbents; hence, even trace water concentrations in the mobile phase decrease the adsorbent activity and very significantly affect the retention. As the distribution equilibrium of water and other polar solvents between the polar adsorbent and an organic mobile phase is strongly affected by temperature, it is very important to work with a thermostated column. The reproducibility of the retention data in NP gradient LC can be considerably improved to the level comparable with RP gradient chromatography by keeping a constant temperature and adsorbent activity and by controlling the water content in the mobile phase best by using dehydrated solvents kept dry over activated molecular sieves and filtered before use.[6]

Aqueous–organic mobile phases are sometimes used in NP "hydrophilic interaction chromatography" (HILIC),[7] employing diol, aminopropyl, or specially designed HILIC (e.g., polyhydroxyethyl aspartamide)-bonded phases more often than unmodified silica. The retention increases as the polarity of analytes increases and as the amount of water, which is the most polar component in the mobile phase, decreases. This behavior is characteristic of NPC and opposite to RPC; Eq. 5 can often be used to describe the effect of the concentration of water in the mobile phase on the retention in HILIC. Hence, the retention in gradient HILIC with increasing concentration of water (usually starting at 1–10% water) can be described by Eq. 6. HILIC provides excellent separation selectivity for some strongly polar samples, such as some peptides and proteins, carbohydrates,

oligonucleotides, and so on, very weakly retained in RPC or very strongly retained in non-aqueous NPC.

IE GRADIENT LC

The IE process is based on the competition between the solute and the counterion in the mobile phase, which is essentially aqueous or aqueous–organic solution of a salt or buffer. Salt (ionic strength) gradients in IE chromatography are frequently used in the separation of complex peptides, proteins, and other biopolymer samples as a complementary technique to RP solvent gradient separations, often in a 2-D setup. The gradients usually start at a low salt (chloride, sulfate, etc.) concentration and typically run from 0.005 to 0.5 *M*. A buffer is used to control the pH; acetonitrile and methanol may be added to improve the resolution and urea to improve the solubility of proteins that are difficult to dissolve. Ion exchangers with weak hydrophobic matrices usually prevent protein denaturation in aqueous mobile phases.

The retention in IE chromatography can be described by a stoichiometric model as competition between the sample ions and the counterions in the mobile phase for IE sites in the stationary phase. Because this principle is similar to the competition between a non-ionic sample and a polar solvent for the adsorption centers in the competition/displacement model of NP chromatography on polar adsorbents, Eq. 5 can also be used to describe the effect of the ionic strength in the mobile phase on retention in isocratic IE chromatography, if φ has the meaning of the molar concentration of a salt (buffer) in the mobile phase. k_0 is the retention factor in the mobile phase containing 1 mol/L salt (buffer) and $m = x/y$ is the stoichiometric coefficient of IE, where x is the charge on the analyte and y is the charge of the eluent competing ion (counterion).[3] The exponent m is a measure of the decrease in retention for per unit change in concentration of counterions in the mobile phase and is proportional to the charge of analyte. k_0 depends on the IE capacity of the stationary phase and on the IE selectivity coefficient between the analyte ion and the competing counterion in the eluent, which is difficult to predict a priori. In practice, m and k_0 are determined on the basis of a limited number of experiments at different isocratic eluent compositions or scouting gradient runs.

Because of the validity of Eq. 5 in IE isocratic chromatography, elution times (volumes) in IE gradient chromatography can be predicted using Eq. 6, with A standing for the molar concentration of the counterion at the start of the gradient and B characterizing the gradient ramp as the change in the molar concentration of the counterion per volume unit of the mobile phase passed through the column. This gradient elution retention model for IE chromatography was proposed by Jandera and Churáček[2] and was later applied by Baba et al.[8] to the prediction and optimization in IE chromatography of polyphosphates and by Shellie et al.[9] in ion chromatography of various anions and cations.

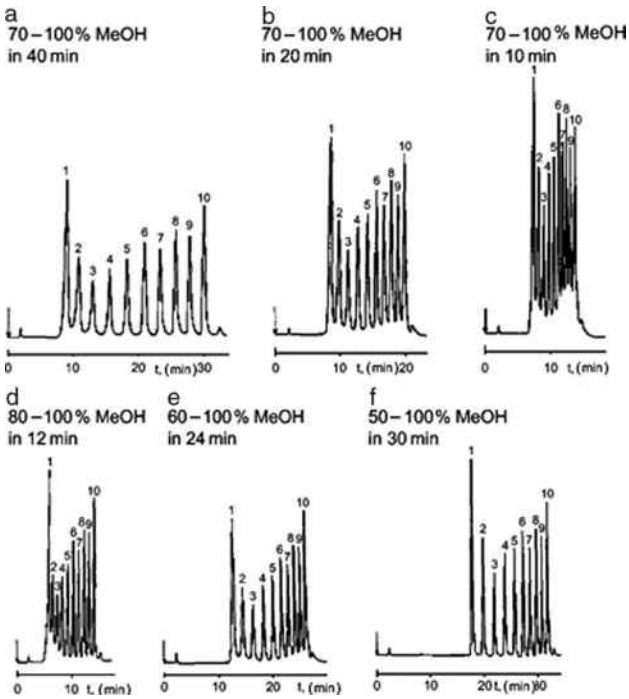

Fig. 2 RP gradient elution separation of 1,2-naphthoylenebenzimidazole alkylsulfonamides. Column: Lichrosorb RP-18, 10 μm (300 × 4 mm I.D.). Linear gradients of methanol in water with a constant gradient range but different gradient volumes (a–c), and with a constant gradient steepness (1.67% methanol/min) but different initial concentrations of methanol (d–f). Flow rate = 1 ml/min. The number of peaks agrees with the number of carbon atoms in alkyls.

The pH affects the degree of dissociation and hence the selectivity of separation of weak acids and bases. The change in ionization is greatest when pH is close to pK_a. If the pK_a values are known, the change in ionization and in retention of the sample compounds resulting from a change in pH can be predicted. The use of pH gradients to accomplish the separation of solutes differing in the degree of ionization is more frequently applied in IE than in RPC, especially for the separation of biopolymers such as proteins, which elute roughly in the order of their isoelectric points, p*I*. Protein molecules carry multiple negative charges and are strongly retained on an anion exchanger at a pH higher than p*I*, but as soon as the pH drops below the p*I* during gradient elution, the initially strongly retained protein gets positively charged and is released from the ion exchanger rapidly. Hence, proteins are focused in narrow bands during the separation and their elution occurs at the time when the instantaneous pH at the column outlet reaches the p*I* of the solute. The band shapes improve with respect to ionic strength gradients.

The formation of linear pH gradients in IE chromatography is more difficult than in RPLC, because the ion exchanger may show preferential adsorption for certain buffer components and consequently change the preset gradient. For this reason, IE materials with small IE capacities are required in combination with buffer components that are not adsorbed on the IE column. Ethanol is added to the buffer to reduce the adsorption. In combination with RP solvent gradient in second dimension, pH IE gradient in first dimension seems a promising emerging technique for 2-D separations of proteins. The dependence of the retention in gradient elution with pH gradients is less straightforward, so that the prediction of retention behavior is more difficult than with salt gradients.

EFFECTS OF GRADIENT PROFILE ON SEPARATION: COMPARISON WITH ISOCRATIC ELUTION

The gradient profile affects retention in a similar way as the concentration of the strong solvent in a binary mobile phase under isocratic conditions. This is illustrated in Fig. 2 for gradient elution RP chromatography separation of 10 homologous derivatives of *n*-alkylamines. At a constant gradient range (70–100% methanol), the steepness of the gradient decreases as the gradient time increases from 10 to 40 min; the resolution improves, but the retention times increase (the top three chromatograms). The bottom three chromatograms show the effect of the gradient range on the separation at a constant steepness of the gradient (1% methanol/0.6 min)—as the initial concentration increases from 50% to 80% methanol, both retention and resolution decrease. The retention times of early eluting compounds are affected more significantly by the initial concentration of the strong solvent (methanol) than by the gradient steepness. The examples in Fig. 2 illustrate the importance of appropriate adjustment of both the gradient range and the initial gradient concentration to keep the analysis time short.

Eqs. 4 and 6 show that, for comparable retention times, a less steep gradient should be used to compensate for a higher parameter m in Eqs. 3 and 4, which usually increases with increasing size of the molecule. This behavior has the following practical consequences for gradient elution of high molecular compounds: 1) macromolecules may have so large an m that a very small change in the concentration of the strong solvent may change the retention from very strong to practically no retention, so that isocratic separation of large molecules is difficult, if possible at all; 2) shallow gradients are usually required for separations of high molecular samples, so that the selection of a suitable combination of the gradient parameters A and B is more critical than for small molecules; and 3) samples with a broad range of molar masses may require a flatter gradient at the end of the chromatogram than at its start for regular band spacing (a convex gradient).

Under isocratic conditions, bandwidths increase for more strongly retained compounds, but the bandwidths in gradient elution chromatography are approximately constant for both early-eluting and late-eluting compounds. This is caused by increasing migration velocities of the bands along the column during gradient elution, so that all sample compounds are eventually eluted with very similar instantaneous retention factors k_e at the time they leave the column, which are approximately half the average retention factors (k^*) during the band migration along the column. The bandwidths decrease with steeper gradients (the three top chromatograms in Fig. 2). Because k_e values are usually significantly lower than the retention factors in isocratic LC, the peaks in gradient elution chromatography are generally narrower and higher, improving the detector response and the sensitivity of determination. However, the beneficial effect of gradient elution on increasing sensitivity is often counterbalanced by an increased baseline drift and noise in comparison with isocratic HPLC. To avoid this inconvenience, high-purity solvents and mobile-phase additives are generally used in gradient elution HPLC.

The bandwidths W_g in gradient elution can be determined by introducing the appropriate instantaneous retention factor k_e at the elution of the peak maximum calculated using an appropriate gradient retention equation (e.g., Eq. 4 or Eq. 6):

$$W_g = \frac{4V_m(1+k_e)}{\sqrt{N}}G \tag{9}$$

N is the number of theoretical plates determined under isocratic conditions; and V_m is the holdup volume of the column. It should be noted that the correct plate number value cannot be determined directly from a gradient elution chromatogram, as the retention factors k are continuously changing during the elution. G in Eq. 9 is the band compression factor, which accounts for additional band compression in gradient elution. This occurs because the trailing edge of the sample band moves along the column in a mobile phase with higher elution strength faster than the leading edge, migrating more slowly in a weaker mobile phase during gradient elution. Neglecting the additional band compression may lead up to 10–20% positive errors in the calculated bandwidths. A simplification adopted in the derivation of Eq. 9 by neglecting the effects of changing mobile-phase composition on the diffusion coefficients, which affects the band broadening, may cause errors in the calculated gradient bandwidths, which are generally estimated to be less than 1% for low molecular samples. For practical method development, neglecting band compression may be used as a "safety tolerance" to compensate for

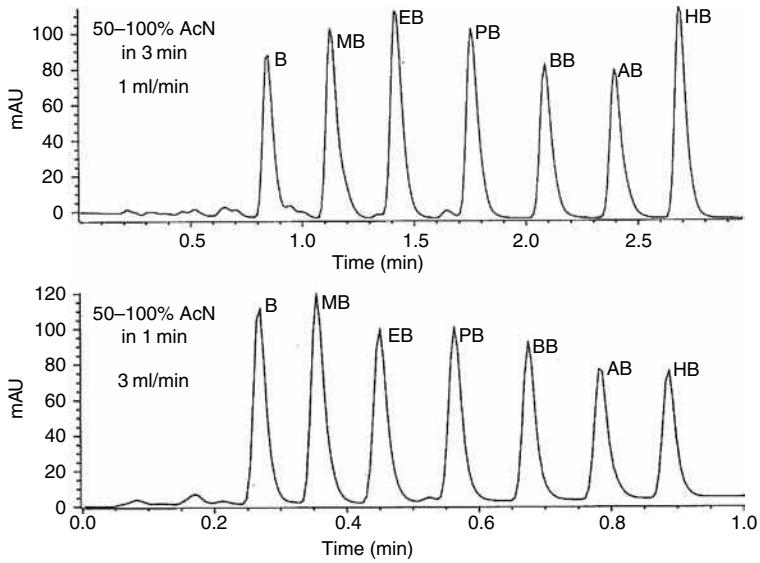

Fig. 3 Gradient elution RP separation of alkylbenzenes with gradient times adjusted to varying flow rate of the mobile phase. Linear gradients, 50–100% acetonitrile in 3 min at 1 ml/min (*top*) and 50–100% acetonitrile in 1 min at 3 ml/min (*bottom*). Conditions: Purospher Star RP-18e, 3 μm, column (30 × 4 mm I.D.), 40°C, detection UV, 254 nm; sample: B, benzene; MB, toluene; EB, ethylbenzene; PB, propylbenzene; BB, butylbenzene; AB, amylbenzene; HB, hexylbenzene.

additional band broadening effects caused by variation of the viscosity and diffusion coefficients during the gradient, or due to extracolumn band broadening.[10]

Combining the appropriate equations for the retention volumes of solutes 1 and 2 with adjacent bands and Eq. 9, for bandwidths, we can calculate the resolution in gradient HPLC as follows:

$$R_s = \frac{V_{R(2)} - V_{R(1)}}{W_g} \tag{10}$$

Here, $V_{R(1)}$ and $V_{R(2)}$ are the retention volumes of sample compounds with adjacent peaks.

TRANSFER OF GRADIENT METHODS BETWEEN DIFFERENT INSTRUMENTS, COLUMNS, AND SEPARATION CONDITIONS

Transfer of gradient methods between various instruments and columns with different geometry and/(or particle size is less straightforward than the transfer of isocratic HPLC methods, as changing column dimensions and flow rate affect the gradient volume (gradient ramp) and consequently not only the elution times and the column efficiency (plate number) but also the selectivity of separation may change. Hence, the gradient profile should be adapted to match any change in flow rate F_m, column length L, or diameter d_c by appropriate change in the gradient time t_G to keep the ratio V_m/V_G constant to obtain predictable results. The necessary changes in operation parameters can be calculated from Eq. 11 assuming a constant gradient concentration range [i.e., constant concentrations of the stronger solvent at the start (A) and at the end (φ_G) of the gradient]:

$$\frac{V_m}{V_G} = \frac{V_m}{t_G F_m} = \frac{d_c^2 l}{t_G F_m} = const \tag{11}$$

Eq. 11 shows that the number of column holdup volumes necessary to elute a sample compound, V_R/V_m, is directly proportional to the ratio of the gradient volume, V_G, and the holdup volume, V_m, which should be kept constant when changing column geometry or flow rate. This condition is similar to keeping a constant retention factor, k, at a constant mobile-phase composition and temperature. Hence, any change of column length, l, or diameter, d_c, at a constant gradient range $\Delta\phi$ should be compensated by appropriate change in the gradient time, t_G, or flow rate of the mobile phase, F_m, to keep the ratio V_m/V_G constant.[10] In this case, a change in operation conditions has the same impact on the column plate number, N, and time of separation as in isocratic chromatography. With two columns of different diameters, but the same length, the column holdup volumes are proportional to the second power of the column diameters.

Eq. 11 shows that the flow rate of the mobile phase should be adjusted in the proportion of changing V_m, to keep the separation time constant. Alternatively, the gradient time can be adjusted to keep the ratio $V_m/(t_G \times F_m)$ constant.[10] Clearly, the speed of separation increases at a higher flow rate, but to achieve the desired decrease in the separation time, the gradient time should be decreased in inverse proportion. Fig. 3 illustrates proportional decrease in the elution times with increasing flow rate at the gradient time adjusted in this way, in agreement with Eq. 11.

Fast generic gradient methods are required for high throughput in food safety control, in environmental analysis, and especially in pharmaceutical laboratories throughout the whole drug analysis process, including drug discovery screening, raw material analysis, impurity

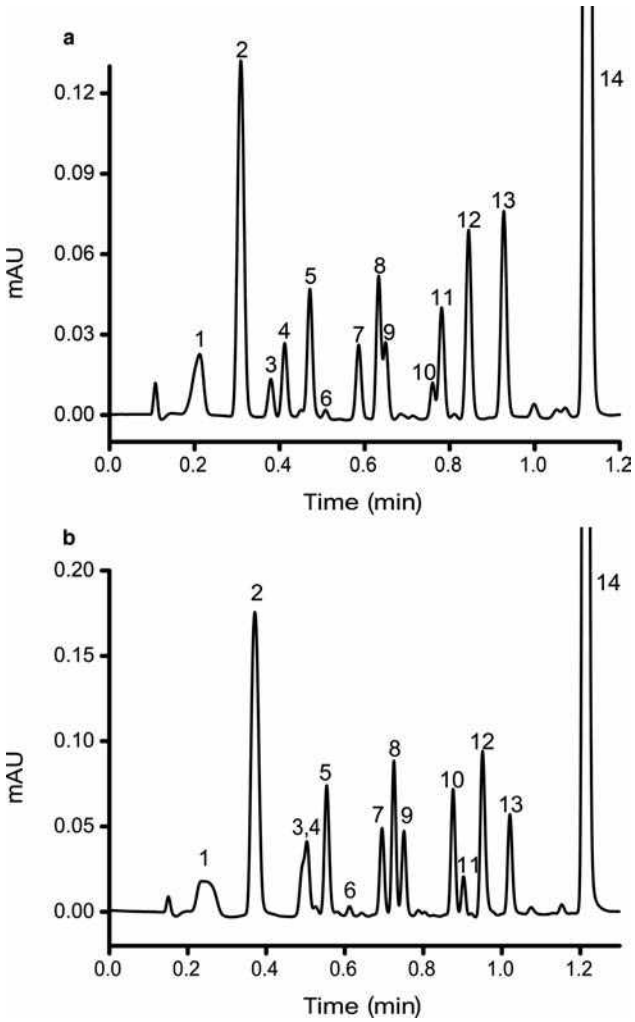

Fig. 4 High-pressure fast gradient separation of natural phenolic antioxidants. (a) Ascentis Express C18 column with fused core 2.7 μm C18 particles with a thin porous outer shell (0.5 μm), 30 × 3.0 mm I.D. at 1.5 ml/min, 53 MPa. (b) Acquity BEH Phenyl column with totally porous particles in 1.7 μm particles at 1.5 ml/min, 74 MPa, UV detection, 254 nm. Sample: 1, gallic acid; 2, protocatechine; 3, esculine; 4, chlorogenic acid; 5, caffeine; 6, epicatechine; 7, vanilline; 8, rutine; 9, sinapic acid; 10, hesperidine; 11, 4-hydroxycoumarine; 12, morine; 13, quercetine; 14, 7-hydroxyflavone.

profiling, pharmacokinetic studies, and final product stability tests. At a constant ratio of V_G/V_m, the resolution only slightly impairs when decreasing the column length, keeping a constant ratio of the column length to the mean particle diameter, l/d_p, but the time of separation decreases proportionally to l. Hence, much faster separations can be achieved on short columns packed with small particles, for example, with a 3 cm column packed with a 3 μm material, or even better with a 1 cm, 1 μm column, in comparison with conventional 5 cm, 5 μm columns. Very fast gradients with short columns require a modified LC instrument with minimized extracolumn volumes by using low-volume injectors and detector cells, fast autosamplers, detectors with a short time constant, high signal sampling rates, and flow splitting to decrease the effects of the gradient dwell volume. Over the last few years, instrumental systems suitable for fast gradient separations have become available, operating at considerably higher pressures up to 150 MPa. Monolithic columns or columns packed with non-porous or fused-core superficially porous particles offer decreased band broadening, yielding comparable efficiencies and separation times at lower operation pressures than fully porous particles of smaller particle size. Fig. 4 compares fast-gradient RP separation of 14 phenolic acids and flavones on a column with superficially porous fused-core particles (4a) and on a column with small totally porous particles, at a significantly higher pressure for comparable run time (4b). Separations can be further accelerated at high temperatures due to decreased viscosity of the mobile phase and lower pressure drop across the column.

The simple transfer rule of Eq. 11 does not take into account the differences between the instrumental gradient dwell volumes, V_D, in various commercial instruments, which may complicate the transfer of gradient methods, as more or less significant differences in the retention times and unexpected changes in the band spacing and sample separation may appear, due to the different migration of analytes along the column under isocratic conditions in the mobile phase contained in different dwell volumes before the actual start of the gradient. The effect of the dwell volume on the retention times of analytes increases with decreasing retention factor k_I at the start of gradient elution and with increasing ratio V_D/V_m and becomes very significant in the instrumental setup with the dwell volume comparable to or larger than the column holdup volume, which is more likely to occur in micro- or in capillary LC than in conventional analytical LC. Possibilities for correcting for different dwell volumes in the transfer of gradient methods are discussed in the section dealing with instrumental aspects of gradient elution.

TERNARY MOBILE-PHASE GRADIENTS

If the separation with binary gradients is unsatisfactory, ternary gradients can sometimes improve the selectivity by changing, simultaneously, the concentrations of two components with high elution strengths in a ternary mobile phase. For example, the early-eluting compounds show poor resolution with the gradients of methanol, but are better separated with gradients of acetonitrile in water, whereas the separation selectivity for the late-eluting compounds is better with a gradient of methanol than with gradients of acetonitrile in water.

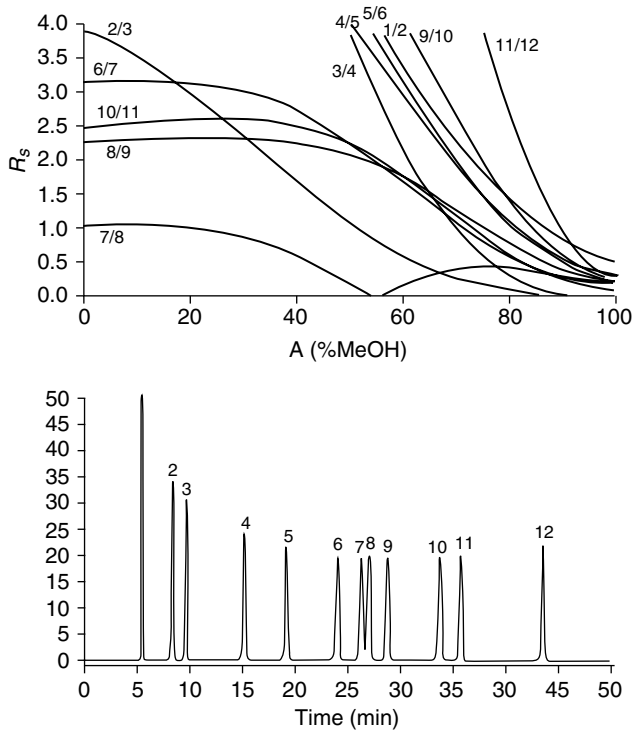

Fig. 5 *Top*: The resolution window diagram for RP gradient elution separation of phenylurea herbicides on a Separon SGX C18 7.5 μm column (150 × 3.3 mm I.D.) dependent on the initial concentration of methanol in water at the start of the gradient *A* with optimum gradient volume $V_G = 73$ ml. Column plate number $N = 5000$; sample compounds: 1, hydroxymetoxuron; 2, desphenuron; 3, phenuron; 4, metoxuron; 5, monuron; 6, monolinuron; 7, chlorotoluron; 8, metobromuron; 9, diuron; 10, linuron; 11, chlorobromuron; and 12, neburon. *Bottom*: The separation with optimized binary gradient from 24% to 100% methanol in water in 73 min. Flow rate = 1 ml/min; $T = 40°C$.

A ternary gradient with increasing concentration of methanol and simultaneously decreasing concentration of acetonitrile may improve the resolution of the sample.[6,11] Two specific types of ternary gradients are probably most useful in practice:

1. The "elution strength" (or "isoselective") ternary gradients, where the concentration ratio of two strong mobile-phase components is kept constant and the sum of their concentrations changes during the elution (so-called isoselective multisolvent gradient elution).
2. The "selectivity ternary gradients," where the sum of the concentrations of two strong mobile-phase components in the mobile phase is constant, but their concentration ratio changes during the elution.

OPTIMIZATION OF GRADIENT ELUTION

Gradient elution can be optimized using strategies common in isocratic HPLC. In RP gradient elution chromatography, the Dry-Lab G commercial software is probably the most popular tool for optimization of operating parameters.[7,12] Here, the retention data from two initial gradient runs are used to adjust, subsequently, the steepness and the range of the gradient, and, if necessary, other working parameters. This approach can be adapted to optimize segmented gradients.

Some parameters may show synergistic effects on the separation. Appropriate selection of the concentration of the strong solvent in the mobile phase at the start of the gradient A is equally important as adjusting the gradient steepness B because each parameter influences, very significantly, the resolution and the time of analysis. The gradient steepness and the initial concentration of the strong solvent can be optimized simultaneously, using the simplex method,[8,13] or a simple strategy employing a preset concentration of the strong solvent φ_G at the end of the gradient and gradient volume, V_G. Then, the steepness parameter B of the gradient depends on the initial concentration A, and the elution volumes V_R can be calculated as a function of a single parameter A:[6,11]

$$B = \frac{\varphi_G - A}{V_G} \tag{12}$$

The differences between the retention volumes of compounds with adjacent peaks or corresponding resolution R_s can be plotted vs. the initial concentration of the strong solvent A in the form of a "window diagram" to select the optimum A that provides the desired resolution for all adjacent bands in the chromatogram in the shortest time. With optimized A, the corresponding gradient steepness parameter *B* can be calculated for the preset gradient volume V_G and final concentration φ_G using Eq. 12. An example of the "window diagram" for optimization of NP gradient elution chromatography is shown in Fig. 5 (*top*), and the corresponding optimized separation is shown in Fig. 5 (*bottom*). In addition to the gradient steepness and initial concentration, the gradient shape can be adjusted for non-linear gradients or segmented gradients with several subsequent linear steps with different gradient steepness.

The composition of mixed mobile phases for ternary or quaternary "isoselective gradient elution" can be optimized using "overlapping resolution mapping" strategy to adjust optimum separation selectivity based on seven or more initial experiments with solvent mixtures of approximately equal elution strengths. Based on the retention data from the initial experiments, either 3-D diagrams or contour "resolution

maps" are constructed for all adjacent bands in a selectivity triangle space as a function of the concentration ratios of three solvents or two solvents and the pH of the mobile phase, from which the concentration ratio of the strong solvents that provides maximum resolution is selected.[14]

INSTRUMENTAL ASPECTS OF GRADIENT ELUTION CHROMATOGRAPHY

Even though the most common UV and fluorometric HPLC detectors can be used without problems in gradient elution if high-purity solvents are used as the mobile-phase components, some detectors are not compatible with gradient elution, such as the universal refractometric detector, which gives a response for almost all sample compounds, but also for the mobile-phase components. However, the only universal detector that can be used for gradient elution is the evaporative light-scattering (ELS) detector, which is less sensitive for UV-absorbing compounds than for the UV detector. As the ELS detector gives response to the stray light on solid particles of analytes after evaporation of the solvent from the nebulized column effluent, its use is restricted to volatile mobile phases and non-volatile analytes. Furthermore, this detector provides a non-linear concentration response. Mass spectrometric detection is ideally suited for gradient elution HPLC, as it combines the features of universality and specific detection, including possibilities of online mass spectral analysis of each peak.

Electrochemical detectors are generally incompatible with gradient elution, except for the multichannel coulometric CoulArray detector, which is controlled by a software compensating for the gradient baseline drift during the elution. This detector allows highly sensitive and selective detection of oxidizable or reducible compounds in gradient HPLC.

In micro-HPLC with narrow bore or capillary columns, lower flow rates should be used at comparable linear mobile-phase velocities. The flow rate should decrease in proportion

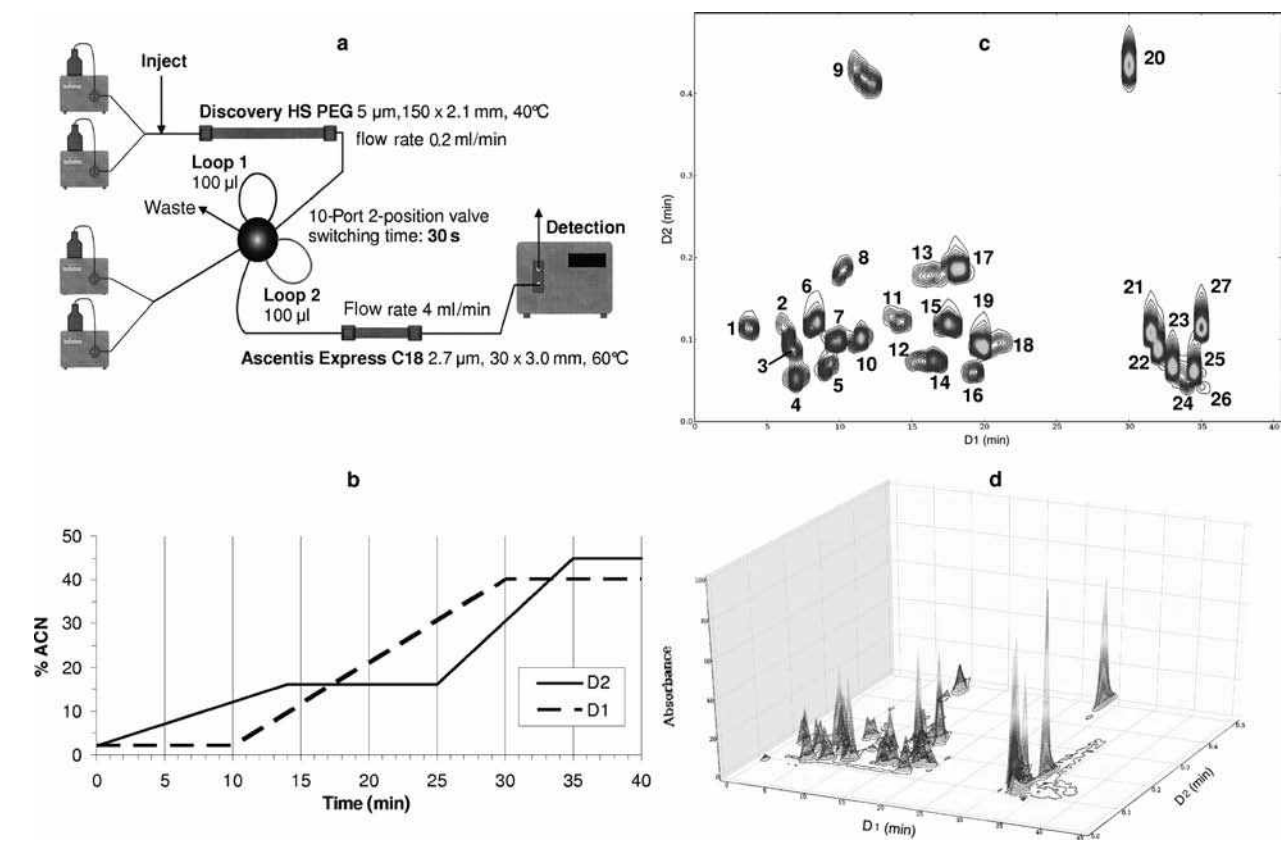

Fig. 6 Comprehensive LC × LC separation of phenolic acids and flavones using parallel gradients in the first and in the second dimension. (a) Instrumental setup; (b) parallel gradients in the first (D1) and in the second (D2) dimensions; (c) contour plot; and (d) 3-D presentations of 2-D chromatograms, UV detection at 280 nm. D2 pressure = 400 bar. Compounds: 1, esculine; 2, 4-hydroxyphenylacetic acid; 3, chlorogenic acid; 4, gallic acid; 5, protocatechuic acid; 6, syringic acid; 7, vanillic acid; 8, salicylic acid; 9, hesperidine; 10, *p*-hydroxybenzoic acid; 11, sinapic acid; 12, (–)-epicatechine; 13, naringin; 14, caffeic acid; 15, ferulic acid; 16, (+)-catechin; 17, 4-hydroxycoumarin; 18, *p*-coumaric acid; 19, rutine; 20, flavone; 21, 7-hydroxyflavone; 22, hesperetin; 23, naringenin; 24, luteolin; 25, apigenin; 26, quercetin; 27, biochanin A.

to the second power of the column inner diameter, so that micro-LC columns with 1 mm I.D. require flow rates in the range of 30–100 μl/min, whereas capillary columns with 0.3–0.5 mm I.D. require flow rates between 1 and 10 μl/min, and capillary or nano-LC columns with 0.075–0.1 mm I.D. require flow rates in the range of hundreds of nanoliters per minute. Special miniaturized pump systems are required to accurately deliver the mobile phase at very low flow rates in isocratic LC. It is technically much more difficult to keep very low flow rates constant during a gradient run than in isocratic LC, and to simultaneously change accurately the volume proportions of the mixed solvents according to a preset time program. In contemporary micro-LC and capillary LC practice, concentration gradients can be achieved using sophisticated LC pumping systems for the delivery of microliter-per-minute gradients that are either flow-split or sampled. High-precision microflow reciprocating pumps using precolumn flow splitting can be used for delivery of flow rates ranging down to 50 nl/min in micro-LC and capillary LC systems. If a precolumn flow splitter is used, only a small part of the mixed mobile phase from the pump flows through the column, whereas a larger part is diverted through a bypass capillary. To avoid some problems connected with flow splitting, splitless systems with large inner volume syringe pumps for each solvent can be used, which deliver smooth flow. Mobile phase is not wasted and the systems are less affected by a change of the column backpressure in gradient runs where solvents with different viscosities are mixed. However, a change of mobile phase contained in the pump inner volume is time-consuming and such devices are rarely used in modern HPLC practice.

The instrumental errors that can decrease the reproducibility of gradient elution data may originate from imperfect functioning of gradient pumps, especially when volatile or viscous solvents are mixed. These errors are usually most significant in the initial parts and the final parts of the gradient where the proportions of the solvents mixed are lower than 1:20 and rounding of the gradient is observed; this can reduce the retention times of the bands eluting near the start of the gradient and increase the retention times of bands eluting near the end of the gradient. It is usually more significant in the instruments with larger volumes between the gradient mixer and the column inlet, i.e., the "gradient dwell volume" V_D. The dwell volume may be as high as a few milliliters with some instruments and may differ from one instrument to another. It can be determined from a "blank" gradient. Much more important than contributing to the rounding of the gradient, dwell volume increases the retention times, as the sample bands migrate a certain distance along the column under isocratic conditions in a mobile phase with a low elution strength, before the front of the gradient gets to the actual position of the sample zone in the column. The gradient delay due to the dwell volume can be relatively very significant in microcolumn gradient operation, especially in the system using precolumn flow splitting with 0.1 mm or lower I.D. capillaries.

When transferring gradient methods between instruments with different dwell volumes, these differences can be compensated for experimentally by programmed delayed sample injection after the start of the gradient elution, or by insertion of a "mixing chamber"—an additional piece of tubing or a small precolumn packed with an inert material in front of the injector to obtain equal dwell volumes with different instruments. Unfortunately, some LC workstations do not allow using delayed injection. Furthermore, it is not always possible to merge a makeup initial holdup time into the equilibration time between the subsequent runs in a sequence of analyses. Finally, a makeup gradient delay contributes to the run time and may be impractical with narrow-diameter columns.

To avoid difficulties when a gradient HPLC method is transferred between the instruments with different V_D values and to improve the precision of predictive calculations of the gradient elution data, the correction for the gradient dwell volume should be accounted for in calculations, using equations such as Eqs. 4, 6, or 8, as appropriate.[10]

GRADIENT ELUTION IN 2-D LC

Two-dimensional LC × LC systems essentially represent programming of stationary phases. The separation selectivity in the first dimension should largely differ from that in the second dimension. "Comprehensive" LC × LC technique represents a new emerging specific 2-D mode, where all sample compounds eluting from the first dimension are subjected to separation in the second dimension. The whole effluent from the first dimension is transferred into the second-dimension separation system in subsequent aliquot fractions collected in two alternating sampling loops of a 10-port (or 8-port) switching valve in multiple repeated cycles. The record of the detector at the outlet from the second-dimension column is transformed into a 2-D chromatogram, which is usually represented as a contour plot with the separation time in the second dimension plotted vs. the separation time in the first dimension. The separation time in the second dimension in comprehensive LC × LC is strictly limited, as the whole separation in the second dimension should be accomplished while the next fraction is collected from the first dimension by the fraction transfer cycle time from the first dimension, and every peak eluting from the first-dimension column should be sampled in several (at least three or four) subsequent fractions, to avoid loss of resolution achieved in the first dimension.

Gradient elution operation is a useful mean to suppress the band broadening and to increase the number of sample compounds separated and should be applied, if possible, in both dimensions.[15] Fig. 6 shows an example of comprehensive LC × LC separation of natural antioxidants with

simultaneous gradients on a first-dimension microcolumn and on a second-dimension short column.

CONCLUSIONS

The elution with solvent gradients is the most efficient technique for improving the separation of complex samples by programmed change of retention during the HPLC separation run. Understanding of the theoretical principles of gradient elution is important for rational method development, optimization, and transfer between different instrumental systems and column geometries in RP, IE, and NP modes. The gradient dwell volume of the system is the main instrumental factor complicating the method transfer and limiting rapid high resolution in gradient micro-HPLC. The most important recent advances in the instrumentation for gradient elution HPLC have resulted in the development of sophisticated instrumentation for gradient micro-HPLC, and the availability of universal ELS detection for compounds that do not contain chromophores or fluorophores and of a sensitive multichannel coulometric detection for gradient HPLC of electroactive compounds. Gradient elution is well suited for HPLC/mass spectrometry applications and for 2-D HPLC, especially in comprehensive LC × LC mode.

REFERENCES

1. Snyder, L.R.; Dolan, J.W.; Gant, J.R. Gradient elution in high-performance liquid chromatography: I. Theoretical basis for reversed-phase systems. J. Chromatogr. **1979**, *165*, 3–30.
2. Jandera, P.; Churáček, J. Gradient elution in liquid chromatography: II. Retention characteristics (retention volume, bandwidth, resolution, plate number) in solvent-programmed chromatography—theoretical considerations. J. Chromatogr. **1974**, *91*, 223–235.
3. Jandera, P.; Churáček, J. Liquid chromatography with programmed composition of the mobile phase. Adv. Chromatogr. **1981**, *19*, 125–260.
4. Snyder, L.R.; Dolan, J.W. The linear-solvent-strength model of gradient elution. Adv. Chromatogr. **1998**, *38*, 115–187.
5. Kaliszan, R.; Wiczling, P.; Markuszewski, M.J. pH gradient reversed-phase HPLC. Anal. Chem. **2004**, *76*, 749–760.
6. Jandera, P. Gradient elution in normal-phase high-performance liquid chromatographic systems. J. Chromatogr. A, **2002**, *965*, 239–261.
7. Alpert, A.J. Hydrophilic-interaction chromatography for the separation of peptides, nucleic acids and other polar compounds. J. Chromatogr. **1990**, *499*, 177–196.
8. Baba, Y. Computer-assisted retention prediction for high-performance liquid chromatography in the ion-exchange mode. J. Chromatogr. **1989**, *485*, 143–168.
9. Shellie, R.A.; Ng, B.X.; Dicinoski, G.W.; Poynter, S.D.H.; O'Reilly, J.W.; Pohl, C.A.; Haddad, P.R. Prediction of analyte retention for ion chromatography separations performed using elution profiles comprising multiple isocratic and gradient steps. Anal. Chem. **2008**, *80*, 2474–2482.
10. Jandera, P. Can the theory of Gradient liquid chromatography be useful in solving practical problems? J. Chromatogr. A, **2006**, *1126*, 195–218.
11. Jandera, P. Predictive calculation methods for optimization of gradient elution using binary and ternary gradients. J. Chromatogr. **1989**, *485*, 113–141.
12. Dolan, J.W.; Snyder, L.R. Maintaining fixed band spacing when changing column dimensions in gradient elution. J. Chromatogr. A, **1998**, *799*, 21–34.
13. Schoenmakers, P.J. *Optimization of Chromatographic Selectivity*; Elsevier: Amsterdam, 1986.
14. Glajch, J.L.; Kirkland, J.J. Method development in high-performance liquid chromatography using retention mapping and experimental design techniques. J. Chromatogr. **1989**, *485*, 51–63.
15. Cacciola, F.; Jandera, P.; Hajdú, Z.; Cesla, P.; Mondello, L. Comprehensive two-dimensional LC × LC with parallel gradients for separation of phenolic and flavone antioxidants. J. Chromatogr. A, **2007**, *1149*, 73–87.

BIBLIOGRAPHY

1. Jandera, P.; ChuraEek, J. *Gradient Elution in Column Liquid Chromatography, Theory and Practice*; Elsevier: Amsterdam 1985.
2. Snyder, L.R.; Kirkland, J.J.; Glajch, J.L. *Practical HPLC Method Development*, 2nd Ed.; John Wiley & Sons: New York, 1997.
3. Snyder, L.R.; Dolan, J.W. *High-Performance Gradient Elution, The Practical Application of the Linear-Solvent-Strength Model*. Wiley-Interscience: Hoboken, NJ, 2007.
4. Jandera, P. Gradient elution in liquid column chromatography—prediction of retention and optimization of separation. Adv. Chromatogr. **2005**, *19*, 1–108.

Headspace Sampling

Raymond P.W. Scott
Scientific Detectors Ltd., Banbury, Oxfordshire, U.K.

INTRODUCTION

Headspace sampling is usually employed to identify the volatile constituents of a complex matrix without actually taking a sample of the material itself. There are three variations of the technique: (a) static headspace sampling, (b) dynamic headspace sampling, and (c) purge and trapping.

DISCUSSION

The first technique, commonly used to monitor the condition of foodstuffs, particularly for detecting food deterioration (food deterioration is often accompanied by the characteristic generation of volatile products such as low-molecular-weight organic acids, alcohols, and ketones, etc.), involves first placing the sample in a flask or some other appropriate container and warming to about 40°C. Raising the temperature increases the distribution of the volatile substances of interest in the gas phase. A defined volume of the air above the material is withdrawn through an adsorption tube by means of a gas syringe. Graphitized carbon is often used as the adsorbing material, although other substances such as porous polymers can also be employed. Carbon adsorbents having relatively large surface areas (~100 m^2/g) are used for adsorbing low-molecular-weight materials, whereas for large molecules, adsorbents of lower surface areas are used (~5 m^2/g). After sampling, the adsorption trap is placed in an oven and connected to the chromatograph. The column is maintained at a low temperature (50°C or less) to allow the desorbed solutes to concentrate at the beginning of the column. The trap is then heated rapidly to about 300°C and a stream of carrier gas sweeps the desorbed solutes onto the column. When desorption is complete, the temperature of the column is programed up to an appropriate temperature and the components of the headspace sample are separated and quantitatively assayed. The proportions of each component in the gas phase will not be the same as that in the sample, as they are modified by the distribution coefficient. Thus, analyses will be comparative or relative, but not absolute.

The second analytical procedure is somewhat similar, but a continuous stream of gas is passed over the sample and through the trap. This produces a much larger sample of the volatile substances of interest and, thus, can often detect trace materials. The adsorbed components are desorbed by heat in the same manner and passed directly onto a gas chromatography (GC) column. The results are still determined by the distribution coefficient of each solute between the sample matrix and the air and, thus, the quantitative results remain comparative or relative, but not absolute.

The third method (purge and trap) is used for liquids and, in particular, for testing for water pollution by volatile solvents. In this method, air or nitrogen is bubbled through the water sample and then through the adsorbent tube. In this way, the substances of interest can be completely leached from the water; the results will give the total quantity of each solute in the original water sample. Thus, with this method, the results can be actual and not relative or comparative. The solutes are desorbed by heat in exactly the same way as the previous two methods, but provision is usually made to remove the water that is also collected before developing the separation.

A good example of the use of headspace analysis is in the quality control of tobacco. Despite the health concern in the United States, tobacco is an extremely valuable export and its quality needs to be carefully monitored. Tobacco can be flue cured, air cured, fire cured, or sun cured, but the quality of the product can often be monitored by analyzing the vapors in the headspace above the tobacco.

The headspace over tobacco can be sampled and analyzed using a solid-phase microextraction (SPME) technique. The apparatus used for SPME is shown in Fig. 1. The basic extraction device consists of a length of fused-silica fiber, coated with a suitable polymeric adsorbent, which is attached to the steel plunger contained in a protective holder. The steps that are taken to sample a vapor are depicted in Fig. 1. The sample is first placed in a small headspace vial and allowed to come to equilibrium with the air in the vial.[1] The needle of the syringe containing the fiber is then made to pierce the cap, and the plunger pressed to expose the fiber to the headspace vapor. The fiber is left in contact with air above the sample for periods that can range from 3 to 60 min, depending on the nature of the sample.[2]

The fiber is then removed from the vial[3] and then passed through the septum of the injection system of the gas chromatograph into the region surrounded by a heater (4). The plunger is again depressed and the fiber, now protruding into the heater, is rapidly heated to desorb the

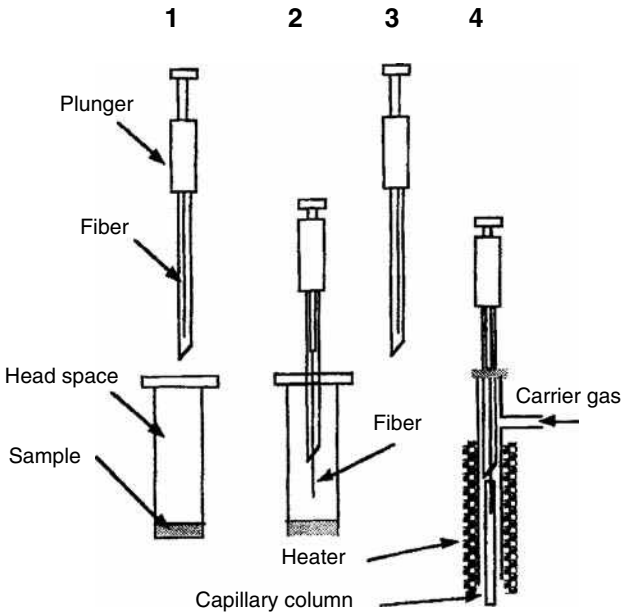

Fig. 1 The SPME apparatus.

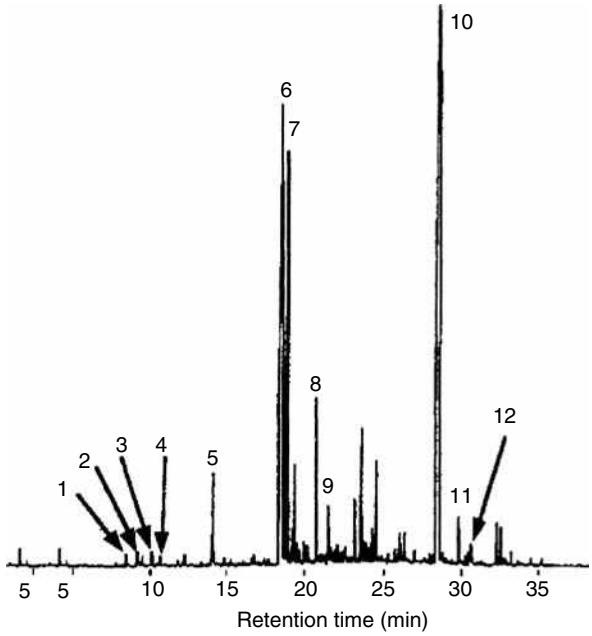

Fig. 2 A chromatogram of tobacco headspace. 1: Benzaldehyde; 2: 6-methyl-5-heptene-2-one; 3: phenylacetaldehyde; 4: ninanal; 5: menthol; 6: nicotine; 7: solanone; 8: geranyl acetone; 9: β-nicotyrine; 10: neophytadiene; 11: famesylacetone; 12: cembrene.

sample onto the GC column. In most cases, the column is kept cool so the components concentrate on the front of the column. When desorption is complete (a few seconds), the column can then be appropriately temperature programed to separate the components of the sample. A chromatogram of the headspace sample, taken over tobacco, is shown in Fig. 2. The actual experimental details were as follows. One gram of tobacco (12% moisture) is placed in a 20 ml headspace vial and 3.0 ml of 3 *M* potassium chloride solution is added. The fiber is coated with polydimethyl siloxane (a highly dispersive adsorbent) as a 100 μm film. The vial is heated to 95°C and the fiber is left in contact with the headspace for 30 min. The sample is then desorbed from the fiber for 1 min at 259°C. The separation can be carried out on a column 30 cm long with a 250 μm inner diameter, carrying a 0.25 μm-thick film of 5% phenylmethylsiloxane. The stationary phase is predominantly dispersive, with a slight capability of polar interactions with strong polarizing solute groups by the polarized aromatic nuclei of the phenyl groups. Helium can be used as the carrier gas, at 30 cm/sec. The column is held isothermally at 40°C for 1 min, then programed to 250°C at 6°C/min and held at 250°C for 2 min. It is seen that a clean separation of the components of the tobacco headspace is obtained and the resolution is quite adequate to compare tobaccos from different sources, tobaccos with different histories, and tobaccos of different quality.

REFERENCES

1. Grant, D.W. *Capillary Gas Chromatography*; Scott, R.P.W., Simpson, C.F., Katz, E.D., Eds.; John Wiley & Sons: Chichester, 1996.
2. Scott, R.P.W. *Introduction to Analytical Gas Chromatography*; Marcel Dekker, Inc.: New York, 1998.
3. Scott, R.P.W. *Techniques of Chromatography*; Marcel Dekker, Inc.: New York, 1995.

Headspace Sampling in GC

Clayton B'Hymer
National Institute for Occupational Safety and Health, Centers for Disease Control and Prevention, U.S. Department of Health and Human Services, Cincinnati, Ohio, U.S.A.

Abstract
Headspace sampling is an important technique for the analysis of volatile compounds from a sample matrix that cannot readily be sampled by means of direct injection into a gas chromatograph (GC). Non-volatile liquid and solid samples can contaminate the injector of a GC; thus, there is the need for the indirect sampling technique of headspace analysis for volatile components existing within the sample matrix. Headspace sampling is a mature technique, spanning several decades, but new variations of the technique plus the extensive variety of commercial equipment available allow for its extensive use in solving many analytical problems encountered today. The three main techniques of headspace sampling are static, dynamic, and solid-solid-phase microexraction (SPME); they are described and a discussion of their advantages and limitations is included. Applications of headspace sampling are extensive; specific examples included in this discussion are the analysis of volatile compounds from complex biological matrices for toxicological studies, the detection of volatile biomarkers from chemical exposure, and the analysis for volatile impurities remaining in pharmaceutical compounds and products.

INTRODUCTION

Headspace sampling is a type of analysis in which the volatile analytes are separated from a sample matrix prior to their introduction into a gas chromatograph (GC). The gaseous phase or "headspace" above the sample matrix within a sealed system is collected and then analyzed by the GC. Headspace sampling represents an indirect method to measure volatile components of the sample matrix; that is, the gaseous phase above a sample matrix is measured, not the sample matrix itself. In the general technique, an aliquot of gas (vapor) phase sampled is in equilibrium with the liquid or solid phase of the sample matrix. In equilibrium, the distribution of the analytes between the two phases is dependent upon their partition coefficients; thus, the quantity of the original analyte in the sample can be determined from the analytical results of the headspace aliquot. Dynamic (purge-and-trap, P&T) and static headspace are the two main classic types of headspace sampling techniques performed today. In the last decade, solid-phase microextraction (SPME) has also been developed to sample headspace volatile. An additional equilibrium is established between the gas phase above the sample matrix and the solid-phase of the SPME fiber. Applications of headspace sampling are extensive and include the analysis of volatile components in the food and flavor industry, pharmaceuticals, cosmetics, biomarkers of chemical exposure or ingestion, environmental testing, and volatile monomers from plastics. Headspace sampling and analysis represent a broad analytical field with continued growth in numerous applications.

HISTORICAL BACKGROUND

Since the inception of GC analysis, the need to analyze volatile components from a non-volatile sample matrix has often been encountered. When a non-volatile sample matrix is directly introduced into a GC, the sample remains within the injector, thus contaminating it. Headspace sampling was a logical development to avoid this sample matrix problem. Headspace sampling was initially applied to other analytical techniques before use with GC, and this chronological description has been reported elsewhere.[1] The first apparent reported combination of headspace sampling with GC analysis was by Bovijn, Pirotte, and Berger[2] in 1958; they used the technique to monitor trace concentrations of hydrogen in water present in a power plant high-pressure boiler. The terms "headspace," "headspace sampling," and "headspace analysis" have been attributed to the food packaging industry where the gas layer above the food in sealed containers was described as the headspace. This terminology was first used in the early 1960s by Stahl and his coworkers while at McCormick & Company, Incorporated (Baltimore, Maryland, U.S.A.). In Stahl's work, the oxygen content within the headspace gases of metal food cans was determined by headspace sampling GC, and Stahl's work has been described within the historical context of headspace sampling.[1] Headspace analysis gained wide use within the food industry with the development of more sensitive detectors for GC in the late 1950s. Initial headspace sampling was performed manually using syringes, but automated instrumentation was

quickly devised by major manufacturers for commercial sale. The needs of forensic analysis have been one of the main driving forces in accurate quantitative headspace sampling instrumentation; exacting quantitative results have been demanded by the court system for blood alcohol analysis. Blood alcohol analysis has been a common application for headspace sampling for several decades. Regulatory requirements by the Food and Drug Administration in the United States and by the European drug regulatory agencies have also generated demand within the pharmaceutical industry for accurate quantitative measurements of residual solvents and volatile components of drug products.[3,4]

THE TYPES OF HEADSPACE SAMPLING

As mentioned in "Introduction," there are basically three headspace sampling techniques. Dynamic or P&T headspace sampling and static headspace sampling are the two classical techniques. SPME is the third headspace sampling technique that will be discussed. These three methodologies have been described extensively in the literature[1,3–5] and their basic designs are diagramed in Fig. 1. The sample matrices can be gas, liquid, or solid. Most often, liquids or liquid/solid mixtures are used because of better sample homogeneity and the relatively quick establishment of equilibrium of the gas phase above the sample matrix. Solid samples may require additional time for a volatile component to diffuse out of the solid matrix; residual solvents may be entrapped within a solid crystal structure. (The use of a dissolution solvent to release the analytes within a solid is done frequently in headspace analysis.) Finally, derivatization/reaction headspace sampling is a variation of headspace sampling and will also be discussed.

Dynamic Headspace Sampling

In dynamic headspace analysis, a continuous flow of gas is swept over the surface of the sample matrix. The sample may be heated during this cycle. The volatile components of the sample are swept into a trap where these analytes are accumulated prior to GC analysis (Fig. 1a). The trap consists of a column containing a sorbent such as Tenex®, Chromosorb®, Porapak®, Amerlite®, XAD resins, or activated carbon. Tenex is most often used because of its superior thermal stability. A rapid thermal desorption cycle of the trap is initiated, and a carrier gas takes the desorbed analytes into a GC for analysis. Cold trapping can be used as an alternative to the sorbent trap in dynamic headspace sampling. After collection of the volatile components, the cold trap is then heated and the analytes are introduced into the GC by a carrier gas. Other terminology and variations of dynamic headspace sampling are thermal desorption sampling (TDS) or direct thermal extraction. The last two sampling methods can involve more extreme heating cycles of the sample matrix.

Dynamic headspace sampling has several advantages over static headspace analysis. Dynamic headspace analysis is particularly suitable for the determination of volatile analytes at very low concentrations from the sample matrix. Lower detection limits are obtained because the "total" amount of a volatile substance can be extracted, trapped, and analyzed at one time. The detection limits for dynamic headspace sampling have been noted as being substantially lower than those for static headspace sampling.[6] Also, dynamic headspace sampling has the advantage of avoiding an equilibrium between the gas phase and the sample matrix, as is required with static headspace and SPME techniques. In the specific case of solid samples being thermally decomposed, an advantage of dynamic headspace analysis is that the use of a dissolution solvent and thus its associated peak can be avoided in the chromatogram.[7] The most frequently cited disadvantage of

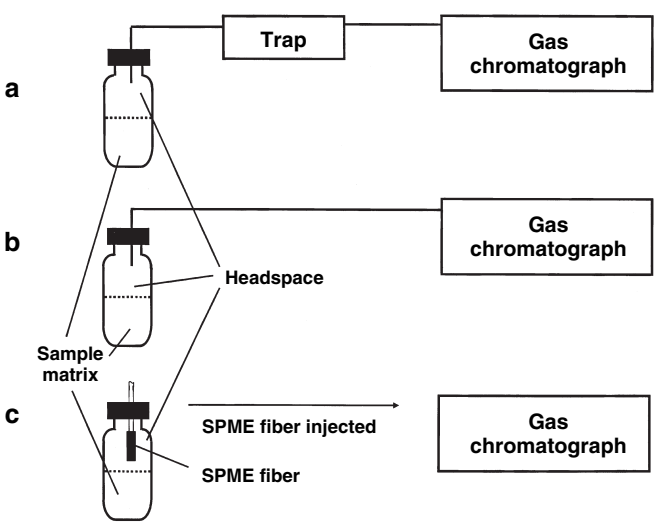

Fig. 1 Comparison of dynamic, static, and SPME headspace sampling. (a) Dynamic headspace sampling uses a sorbent or cold trap to concentrate volatile analytes before analysis by the GC. (b) Static headspace sampling uses direct transfer of a volume of gas from the headspace above the heated sample vial directly to the GC for analysis. Injection designs are illustrated in Fig. 2. (c) SPME headspace sampling uses a fiber support with solid-phase coating. The fiber is placed in the headspace and reaches equilibrium with the headspace volatile analytes. The SPME fiber is transferred by means of a syringe and thermally desorbed in the injector of the GC for analysis.

dynamic headspace sampling is the problem of artifact volatile collection in the trap. This is common for the P&T technique and can be minimized by complete desorption of the trap. This could include desorption cycles having higher temperatures or extending for longer periods to remove the artifacts. Numerous dynamic headspace sampling instruments are commercially available allowing for easy use of this technique.

Static Headspace Sampling

Static headspace analysis is probably the most widely practiced form of headspace analysis. In static headspace sampling, a liquid or solid sample is placed into a sealed vial. The vial is heated for a time until an equilibrium of the volatiles between the sample and the gas phase is reached. An aliquot of the headspace gas is sampled and injected into the GC for analysis. The basic physicochemical properties and gas laws are applied in this technique and need not be detailed in this entry. Higher temperatures will promote higher partial pressure and concentration of volatile compounds within the headspace of a given sample; polarity considerations of solutes vs. solvents will also come into play. In pharmaceutical testing, static headspace sampling is preferred when the liquid or solid samples are soluble (or extractable) in solvents such as water, benzyl alcohol, dimethyl formamide (DMF), or dimethyl sulfoxide (DMSO).[4,8] A liquid sample matrix offers a system in which the partitioning equilibrium is more readily established and reproducible. The repeated gas-extraction method first described by McAuliffe[9] can be used when the partition coefficients (the partition coefficient, *k*, equals the ratio of the concentration of the volatile analyte in the sample matrix divided by the concentration of the volatile in the gaseous headspace at equilibrium) and the equilibrium time are not well known. Kolb and Pospisil[10] popularized this technique, but referred to it as multiple-headspace extraction (MHE). In MHE, the headspace sample is extracted several times with a gas to obtain exponentially decreasing peak area responses. This allows for the calculation of the total residual solvent or volatile in the original sample, assuming that the thermodynamic equilibration was reached during the multiple extractions. Kolb and Pospisil[10] proposed MHE with solid or certain insoluble samples requiring external calibration. MHE as a headspace sampling technique has fallen out of current usage and is not very common today.

The main disadvantages of static headspace sampling over dynamic headspace sampling are in higher detection limits and lower sensitivity. Detection limits and sensitivity can be improved by pH control, salting-out or increasing the equilibrium temperature during sample heating.[11–15] Salting-out is done simply by adding an inorganic salt to an aqueous sample matrix. High salt concentrations in aqueous samples decrease the solubility of polar organic volatiles and thus promote their transfer into the headspace. Some common salts used for salting-out include ammonium chloride or sulfate, sodium chloride, citrate, or sulfate, magnesium sulfate, or potassium carbonate. The magnitude of the salting-out effect is not the same for all compounds. Generally, volatile polar compounds in aqueous matrices will experience the largest increase in partitioning into the gaseous headspace and have higher responses after the addition of a salt. Increasing the sample heating temperature will increase the analyte response until the boiling point temperature of the analytes is reached.[16] When water is chosen as the dissolution medium, non-polar analytes are enriched in the headspace and have higher GC responses, while polar analytes have lower GC responses. Dennis, Josephs, and Dokladalova[17] showed enrichment in the headspace up to a factor of 50 for trace non-polar solvents in water, while polar analyte responses in the headspace of polar sample matrices dropped by up to a factor of 4. Use of multiple internal standards may be necessary in static headspace sampling to match the solubility and partitioning of the analytes in the sample matrix. The purity of the dissolution solvent is another common problem encountered with static headspace sampling. A small impurity in the dissolution solvent might produce an interference peak in the chromatogram.

Instrumental design for static headspace samplers

Automated headspace systems have been offered by several manufacturers for many years, including Thermo Electron Corporation (San Jose, California, U.S.A.), PerkinElmer (Wellesley, Massachusetts, U.S.A.), Tekmar (Mason, Ohio, U.S.A.), and Agilent Technologies (Palo Alto, California, U.S.A.). There are essentially three injection techniques for static headspace sampling: gas-tight syringe, balanced-pressure, and pressure-loop injection (Fig. 2). All these techniques are used on commercial headspace systems and are described.

The gas-tight syringe injection technique can be done manually, although Thermo Electron-Finnigan offers some autosamplers that perform this technique. A syringe draws a sample of the headspace after equilibrium has been achieved above the sample; then the syringe is used to inject the headspace gases directly into a GC (Fig. 2A). Volatile sample loss can occur unless precautions are taken. The syringe must be heated correctly to ensure that no analytes condense inside the syringe; reproducibility problems can occur from sample loss using the syringe. Some sample loss may occur owing to the pressure changes between the heated headspace vial and the atmospheric conditions. Early static headspace analysis was performed manually using handheld gas-tight syringes, but reproducibility of injections and analyte condensation were significant problems until automated systems were available. The Finnigan TRACE model HS2000 headspace autosampler uses the gas-tight syringe design.

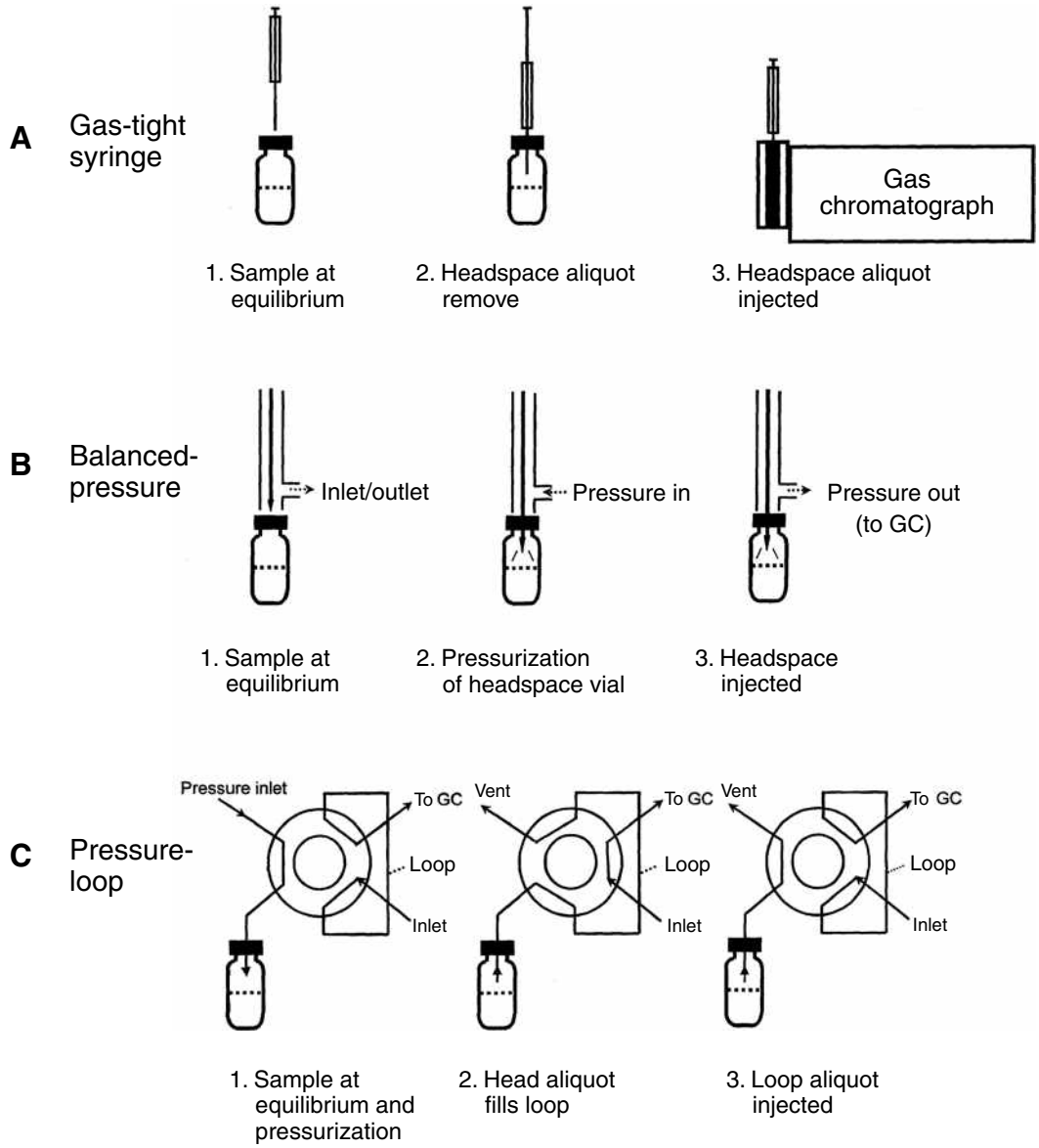

Fig. 2 The three designs of static headspace injection systems. (A) The gas-tight syringe system uses a syringe to collect and transfer a headspace aliquot to the GC. (B) The balanced-pressure system pressurizes the vial after thermal equilibrium, then releases the pressurized headspace into the GC. (C) The pressure-loop system pressurizes the headspace vial, fills a fixed-volume loop with a headspace aliquot, and then the loop contents are flushed into the GC.

The balanced-pressure injection entails the headspace vial being pressurized and allowed to reach an equilibrium; then a valve is switched to direct part of the sample into the transfer line and the GC for a specific time interval (Fig. 2B). The absolute volume of the sample injected into the GC is unknown because this technique uses a theoretical amount of time to inject the sample. A number of contact parts are minimized in this design which should in theory lessen the chance of analyte adsorption or condensation within the system. An example of an instrument utilizing the balanced-pressure technique is the Perkin-Elmer TurboMatrix model HS-40.

The pressure-loop system uses a known amount of sample, unlike the pressure-balance injection technique. After the sample vial has reached an equilibrium and has been pressurized, a fixed-volume loop is filled with an aliquot of the headspace gases. This sample loop is flushed with carrier gas and the volatile analytes are carried by means of the transfer line into the GC (Fig. 2C). Typically, this technique uses a six-port valve system much like those used on high-performance liquid chromatographic (HPLC) injection systems. Loop volumes are generally 1 ml or slightly larger. The loop is flushed between injections, but might cause ghost peaks because of sample carryover

from a previous analysis. Analyte condensation is minimized by heating the sample loop and transfer line, although adsorption problems are possible in the sample loop and various transfer lines. The pressure-loop system is noted for its good run-to-run reproducibility and precision of duplicate injections. The pressure-loop injection design is used by the Tekmar model 7000HT and by Agilent Technologies in their models G1888 and 7694E static headspace sampling systems.

SPME Headspace Sampling

In SPME headspace sampling, a small amount of extracting phase, a stationary phase (described as the solid phase), is coated on a support, most commonly a fused silica fiber. The extraction phase is placed in the headspace of a sealed vial containing the sample matrix and heated until a concentration equilibrium is reached. The analytes reach an equilibrium between the sample matrix, the headspace above the sample matrix, and the extraction solid phase of the SPME fiber (Fig. 1C). Once equilibrium is reached, continued exposure of the SPME fiber does not lead to any additional accumulation of the analytes. The fiber is usually attached to a sampling device, which is basically a syringe. The SPME fiber is attached to the plunger and is extended during sampling and withdrawn into the syringe before insertion into a GC. The fiber is extended into the inlet of a GC, and the volatile analytes are thermally desorbed from the extracting phase of the fiber and swept onto the GC column for analysis. The SPME sampling by direct contact or immersion with a liquid sample matrix has also been done to measure volatile components, but this technique is not true "headspace sampling" and will not be discussed here.

"Gas-tight" and "headspace injection" SPME are the two types of injection techniques used. In gas-tight SPME, only a small volume of headspace gas is removed from the sample vial for injection. In headspace injection SPME, a larger volume of headspace gas is removed from the sample vial along with the SPME fiber (see Fig. 3). Camarasu, Meqei-Szuts, and Varga[6] conducted extensive comparison tests of these techniques along with static headspace sampling of common solvents found in pharmaceutical products, which are listed in Table 1. Gas-tight SPME was found to be the most sensitive technique for acetonitrile, dichloromethane, and chloroform in the Camarasu study. This was attributed to the inherent selectivity of the SPME fiber (polydimethylsiloxane/divinylbenzene). Volatile residual solvents commonly found in pharmaceuticals were shown to have detection limits nearly two orders of magnitude lower when using gas-tight SPME over the detection limits determined for static headspace sampling GC.[6] The main limitation of SPME headspace sampling is in the capacity of the fiber itself. Overloading the SPME fiber is possible and the equilibrium time of both

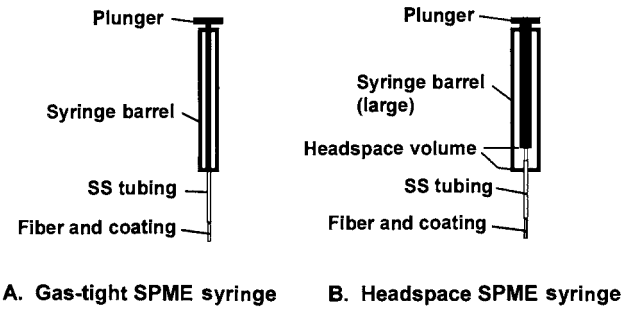

Fig. 3 Injection modes of solid-phase microextraction (SPME) using a manual syringe. (A) The gas-tight SPME samples a small volume of the sample headspace by using a small syringe. Most of the volatile analytes are collected on the coating of the SPME fiber. (B) Headspace SPME syringe collects a larger volume of the sample's headspace gases along with the volatile analytes collected on the SPME fiber. The headspace aliquot and the analytes adsorbed to the fiber are injected into the GC.

the headspace and the SPME fiber in the headspace must be experimentally determined.

Solid-phase microextraction headspace sampling has the advantage of concentrating the analytes, thus lowering detection limits of volatiles. In recent years, SPME headspace analysis has gained a solid reputation as a valid alternative to traditional headspace GC because of the simplicity of execution of the procedure and the low cost of the hardware.[18] Utilization of SPME headspace sampling is increasing with the availability of commercial devices. Supelco (Avondale, Pennsylvania, U.S.A.) has offered a manual syringe SPME system. Varian offers SPME capability in their Combi PAL autosampling system. Many autosampler designs can be adapted to SPME injection since it is analogous to the operation of a common hand held syringe. Another advantage of this technique is that SPME fibers can be cleaned easily and are ready for

Table 1 Detection limit comparison of headspace sampling methods (ng/ml).

Residual solvent	Headspace SPME (PDMS/DVB)	Gas-tight SPME (PDMS/DVB)	Static headspace
Acetonitrile	0.1	0.05	2
Benzene	0.01	0.01	0.1
Chloroform	0.01	0.007	7
1,2-Dichloroethylene	0.01	0.02	7
Dichloromethane	0.01	0.005	0.5
1,4-Dioxane	2	2	20
Trichloroethylene	0.01	0.01	7
Pyridine	0.05	0.7	30

PDMS/DVB, polydimethylsiloxane/divinylbenzene coated fiber; SPME, solid-phase microextraction.
Source: From Residual solvents in pharmaceutical products by GC–HS and GC–MS–SPME, in J. Pharm. Biomed.[6]

reuse after thermal desorption which simplifies their adaptation to automation. SPME has been reviewed in the literature.[19,20]

Derivatization/Reaction Headspace

Chemical derivatization is a technique that can be used to increase the headspace sampling/chromatographic response of specific compounds which may lack volatility if not derivatized. Compounds with the capability of hydrogen bonding (i.e., alcohols, acids, amines) are difficult to volatilize and analyze by direct GC. Derivatization can be performed in the actual headspace sample vial to form the more volatile derivatized analyte which can, in turn, be sampled in the gaseous headspace. One common example is the use of methanol and boron trifluoride to derivatize fatty acids to the corresponding methyl esters. The major disadvantage of this approach is that the derivatization reagents and associated by-products from the derivatization reaction may be volatile and can partition into the headspace along with the desired derivatized compounds. This may cause difficulties with interfering peaks which might coelute with the compounds of interest. Pressures within the headspace/reaction vial may also cause problems by exceeding the pressure sealing abilities of the septum or the vial's structure.

EXAMPLE APPLICATIONS OF HEADSPACE SAMPLING IN GC

There are many areas in analytical chemistry which utilize headspace sampling and headspace analysis with GC. The role of food analysis in the historical development of headspace analysis has been briefly discussed in this entry. Headspace analysis is widely practiced in environmental analytical chemistry; it is often used in the analysis of volatile organic chemicals in water, waste water, and soil. Plastic materials testing for volatile monomers in finished plastic products has been performed using headspace analysis. Forensic chemists are using SPME headspace sampling for use in testing traces of residual accelerants from residue ash or post fire debris. SPME fibers are replacing the activated charcoal strips previously used in sampling headspace of collected fire debris. Dynamic, static, and SPME headspace analysis, as well as cryogenic focusing, have been used in arson analysis.[21,22] The three examples that will be briefly discussed for this entry will be clinical/toxicological analysis, industrial health and hygiene exposure analysis, and pharmaceutical analysis. Many more applications obviously exist and can be readily found in the literature.

Clinical/Toxicological Analysis

Clinical/toxicological analysis is another important area for headspace sampling including blood alcohol analysis, although forensic analysis of blood alcohol levels for court cases is one of the most common uses of headspace sampling. Clinical testing and testing of blood for volatile alcohol in support of toxicology studies are equally significant. Fig. 4 displays a chromatogram of typical blood alcohol analysis; in this particular example, rat blood was analyzed using manual syringe headspace sampling.[23] In addition to ethanol, longer chain alcohols were analyzed simultaneously using this procedure. Blood alcohol testing, in general, has been reviewed in the literature,[24] and headspace sampling offers an ideal technique for the analysis of volatile components. This is also true for many toxicological analyses where it is not possible to inject blood, tissue, or sample matrix directly into a GC. The Doizaki and Levitt[23] procedure cited above was also

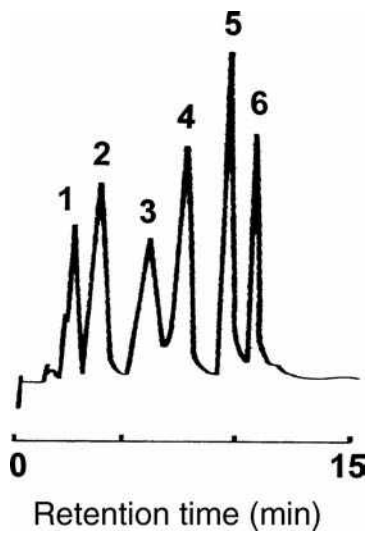

Fig. 4 Gas chromatogram of a standard alcohol mixture. The concentration of each alcohol is at 1000 nmol/ml aqueous solution. Peaks: 1) ethanol; 2) *n*-propanol; 3) 2-propen-1-ol (allyl alcohol); 4) *n*-butanol; 5) 3-methyl-1-butanol (isoamyl alcohol); 6) *n*-pentanol (*n*-amyl alcohol). Manual static headspace sampling was used with the following conditions: 0.2 ml aliquot of sample added to 9 ml serum bottle containing 200 mg of potassium carbonate and heated for 20 min at 70°C. A 0.2 ml headspace aliquot was injected. The Hewlett-Packard Model 5880 gas chromatograph was equipped with a cryogenic attachment (carbon dioxide cooling) and a 50 m × 0.2 mm (I.D.) Carbowax 20 *M* (HP) column. Initial column temperature was 20°C with a 6 min hold, then increased at a rate of 5–40°C/min, then increased at a rate of 10°C/min to a final temperature of 90°C and held for 5 min. A flame ionization detector (FID) was used.
Source: From Gas chromatographic method for the determination of the lower volatile alcohols in rat blood and in human stool specimens on a fused silica capillary column, in J. Chromatogr.[23]

applied in the determination of alcohols in human stool specimens.

Industrial Health and Hygiene Biomonitoring Exposure Analysis

Headspace sampling is being used to monitor the internal exposure of human subjects to chemicals in their work environment. Test methods have been devised to measure residual parent compounds or their metabolites (biomarkers for exposure) in human blood or urine samples taken from the exposed population. In one published work, a method to measure urinary 1- and 2-bromopropane was validated.[16] 1-Bromopropane is a commonly used industrial solvent, and 2-bromopropane is often found as an impurity component in industrial grade 1-bromopropane. 1-Bromopropane has numerous industrial applications including cleaning metal, optical instruments, and electronics, and as a component in spray adhesives. Both compounds are a health concern for exposed workers owing to their chronic toxicity. Because of the extensive use of 1-bromopropane in the industrial setting, workers can be exposed to 1-bromopropane in both vapor and liquid form, including by direct dermal contact. In the chromatogram displayed in Fig. 5, 1- and 2-bromopropane were analyzed using static headspace sampling of spiked urine samples.[16] Headspace sampling of adsorbent material used to monitor the workplace environment is also carried out. The other forms of headspace sampling are finding applications in the industrial health and hygiene monitoring field.

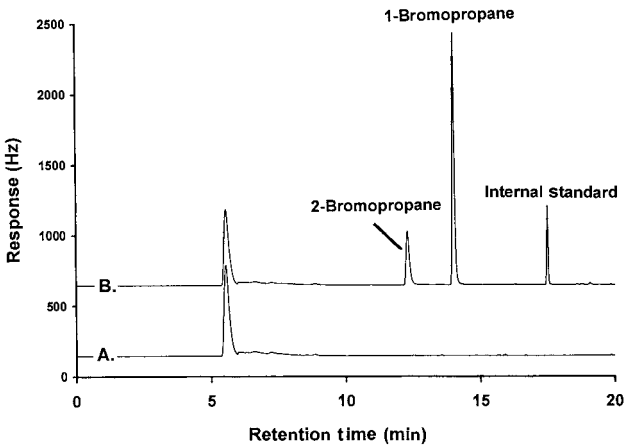

Fig. 5 Gas chromatograms of blank (a) and spiked (b) human urine samples containing 1-bromopropane, 2-bromopropane, and 1-bromobutane as the internal standard. Static headspace sampling was used with the following conditions: Tekmar model 7000 HT headspace sampler with a 1.0 ml sample loop and platen temperature of 75°C and a valve/loop temperature of 120°C. Sample equilibrium time was 34 min. The Agilent Technologies Model 6890 gas chromatograph was equipped with an Agilent J&W DB-1 (dimethylpolysiloxane) column with a 1 μm film thickness. Initial column temperature was 45°C with a 10 min hold, then increased at a rate of 12.5°C/min to a final temperature of 170°C. A microelectron capture detector (μ-ECD) was used.
Source: From Development of a headspace gas chromatographic test for the quantification of 1- and 2-bromopropane in human urine, in J. Chromatogr. B.[16]

Pharmaceutical Analysis

Pharmaceutical products are extensively tested for residual solvents, often using headspace analysis. Residual solvents in pharmaceuticals are generally volatile chemicals that are used in and are produced during the synthesis of drug substances or can exist in the excipients used in the production of drug formulations. These residual volatile chemicals can be remains from processing agents. Many of these volatile organic substances cannot be completely removed by standard manufacturing processes and are left behind, usually at low or trace levels. High levels of residual organic solvents can play a role in the physicochemical properties such as crystallinity of the bulk drug substance. Residual solvents also present a risk to human health because of their toxicity. Some odor problems have also been associated with finished drug products having high levels of residual volatiles. Therefore, the main purpose of pharmaceutical residual solvent testing is its use as a monitoring check for further drying of bulk drug substance or as a final check of a finished product. In Fig. 6, chromatograms from a headspace GC method to quantify the levels of various residual solvents in the bulk pharmaceutical product α-phenyl-1-(2-phenylethyl)-piperine methanol, a serotonin 5-HT2 receptor antagonist, are shown.[25] The solvents detected in this chromatogram are possibly present in bulk drugs since they were used in its synthetic route or used to recrystallize the final bulk product. Static headspace sampling was used for this specific chromatographic test method analysis, but dynamic headspace sampling has been applied to analytical problems within the pharmaceutical industry. SPME headspace sampling is a more recent development and has been applied to pharmaceutical residual solvent analysis.[6]

CONCLUSIONS AND FUTURE TRENDS

Headspace sampling in GC analysis is a highly useful technique and has been widely practiced in multiple analytical fields over the past four decades. The advantages of avoiding direct sampling of sample matrices that would contaminate the operation of a GC make headspace sampling a valuable technique. Coupling this sampling technique with today's greater availability of both more sensitive and more specific GC detectors including mass spectrometry will only lead to continued

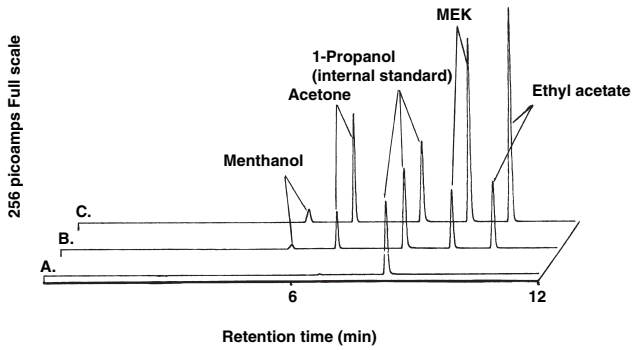

Fig. 6 Gas chromatograms of the drug substance α-phenyl-1-(2-phenylethyl)-piperine methanol, a serotonin 5-HT2 receptor antagonist, spiked with possible processing solvents. Three solvent levels are represented, a) 0% (w/w); b) 0.1% (w/w) spike; c) 0.3% (w/w) spike. Peaks: methanol; acetone; 1-propanol (internal standard); methyl ethyl ketone (MEK); ethyl acetate. The unspiked drug substance contained a low level of acetone of less than 0.01% (w/w). Static headspace sampling was used with the following conditions: Tekmar 7000 with 1.0 ml sample loop with a block temperature of 80°C and the loop temperature at 95°C. Sample equilibrium time was 40 min. The Hewlett-Packard Model 5890 gas chromatograph was equipped with a 60 × 0.32 mm (I.D.) Supelco SPB-1 (dimethylpolysiloxane) column with a 1 μm film thickness. The initial column temperature was 50°C with a 12 min hold, and then a post run at 100°C for 3 min. A flame ionization detector (FID) was used.
Source: From Development of a residual solvent test for bulk α-Phenyl-1-(2-phenylethyl)-piperine methanol using headspace sampling, in J. Chromatogr. Sci.[25]

use and growth in the future. The use of SPME headspace sampling will certainly increase as commercial instrumentation becomes more available and the technique becomes more accepted in the different fields of analysis. Recent applications of headspace SPME have included the detection of volatile liver cancer biomarkers from blood samples[26] as well as the determination of volatile plant protection agents from soil samples.[27] Headspace SPME, along with the traditional forms of headspace sampling,[1,3–5,11] will undoubtedly continue to grow in use in the future. For a more detailed description of the general theory of headspace sampling GC analysis, see Hachenburg and Schmidt[11] as well as the various review articles in the literature.[3,4]

DISCLAIMERS

The findings and conclusions in this report are those of the authors and do not necessarily represent the views of the National Institute for Occupational Safety and Health (NIOSH). The mention of company names and/or products does not constitute endorsement by NIOSH.

ACKNOWLEDGMENTS

The author would like to thank Anne P. Vonderheide, Dennis W. Lynch, Lisa S. Milstein, and David C. Ackley for their editorial comments and help during the preparation of this manuscript.

REFERENCES

1. Ettre, L.S. The beginnings of headspace analysis. LC–GC N. Am. **2002**, *20*, 1120–1129.
2. Bovijn, L.; Pirotte, J.; Berger, A. Determination of hydrogen in water by means of gas chromatography. In *Gas Chromatography, 1958*, Proceedings of the 2nd Symposium (Amsterdam), Desty, D.H., Ed.; Butterworths: London, 1958; 310–320.
3. B'Hymer, C. Residual solvent testing: A review of gas-chromatographic and alternative techniques. Pharmaceut. Res. **2003**, *20*, 337–344.
4. Witschi, C.; Doelker, E. Residual solvents in pharmaceutical products: acceptable limits, influences on physicochemical properties, analytical methods and documented values. Eur. J. Pharm. Biopharm. **1997**, *43*, 215–242.
5. Kolb, B.; Ettre, L.S. *Static Headspace Gas Chromatography: Theory and Practice*; Wiley-VCH, Inc.: New York, U.S.A., 1997.
6. Camarasu, C.C.; Meqei-Szuts, M.; Varga, G.B. Residual solvents in pharmaceutical products by GC–HS and GC–MS–SPME. J. Pharm. Biomed. **1998**, *18*, 623–638.
7. Wampler, T.P.; Bowe, W.A.; Levy, E.J. Dynamic headspace analysis of residual volatiles in pharmaceuticals. J. Chromatogr. Sci. **1985**, *23*, 64–67.
8. Mulligan, K.J.; McCauley, H. Factors that influence the determination of residual solvents in pharmaceuticals by automated static headspace sampling coupled to capillary GC–MS. J. Chromatogr. Sci. **1995**, *33*, 49–54.
9. McAuliffe, C.D. GC determination of solutes by multiple phase equilibration. Chem. Tech. **1971**, *1*, 46–51.
10. Kolb, B.; Pospisil, P. A gas chromatographic assay for quantitative analysis of volatiles in solid materials by discontinuous gas extraction. Chromatographia **1977**, *10*, 705–711.
11. Hachenberg, H.; Schmidt, A.P. *Gas Chromatographic Headspace Analysis*; Heyden Press: Rheine, Germany, 1977.
12. Drozd, J.; Novak, J. Headspace gas analysis by gas chromatography, J. Chromatogr. **1979**, *165*, 141–165.
13. Poole, C.F.; Schuette, S.A. Isolation and concentration techniques for capillary column gas chromatographic analysis. J. High Resolut. Chromatogr. **1983**, *6*, 526–549.
14. Nunez, A.J.; Gonzalez, L.F.; Janak, J. Pre-concentration of headspace volatiles for trace organic analysis by gas chromatography. J. Chromatogr. **1984**, *300*, 127–162.
15. Vitenberg, A.G. Methods of equilibrium concentration for the gas chromatographic determination of trace volatiles, J. Chromatogr. **1991**, *556*, 1–24.
16. B'Hymer, C.; Cheever, K.L. Development of a headspace gas chromatographic test for the quantification of 1- and 2-bromopropane in human urine. J. Chromatogr. B, **2005**, *814*, 185–189.

17. Dennis, K.J.; Josephs, P.A.; Dokladalova, J. Proposed automated headspace method for organic volatile impurities (467) and other residual solvents. Pharm. Forum **1993**, *19*, 5063–5066.
18. Croan, S.A.; Giannellini, V.; Furlanetto, S.; Banbagiotti-Alberti, M.; Pinznuti, S. Improving gas chromatographic determination of solvents in pharmaceuticals by combined use of headspace solid-phase microextraction and isotopic dilution. J. Chromatogr. A, **2001**, *915*, 209–216.
19. Kataoka, H.; Lord, H.L.; Pawliszyn, J. Application of solid-phase extraction in food Analysis. J. Chromatogr. A, **2000**, *880*, 35–62.
20. Lord, H.; Pawliszyn, J. Evolution of solid-phase microextraction technology. J. Chromatogr. A, **2000**, *885*, 153–193.
21. Reeve, V.; Jeffery, J.; Weihs D.; Jennings, W. Developments in arson analysis: A comparison of charcoal adsorption and direct headspace injection techniques using fused silica capillary gas chromatography. J. Forensic Sci. **1986**, *31*, 479–488.
22. Steffen, A.; Pawliszyn, J. Determination of liquid accelerants in arson suspected fire debris using headspace solid-phase microextraction. Anal. Commun. **1996**, *33*, 129–131.
23. Doizaki, W.M.; Levitt, M.D. Gas chromatographic method for the determination of the lower volatile alcohols in rat blood and in human stool specimens on a fused silica capillary column. J. Chromatogr. **1983**, *276*, 11–18.
24. Tagliaro, F.; Lubli, G.; Chielmi, S.; Franchi, D.; Marigo, M. Chromatographic methods for blood-alcohol determination. J. Chromatogr. Biomed. Appl. **1992**, *580*, 161–190.
25. B'Hymer, C. Development of a residual solvent test for bulk α-Phenyl-1-(2-phenylethyl)-piperine methanol using headspace sampling. J. Chromatogr. Sci. **2007**, *45*, 293–297.
26. Xue, R.; Dong, L.; Zhang, S.; Deng, C.H.; Liu, T.T.; Wang, J.; Shen, X. Investigation of volatile biomarkers in liver cancer blood using solid-phase microextraction and gas chromatography/mass spectrometry. Commun. Mass Spectrom. **2008**, *22*, 1181–1186.
27. Fernández-Alvarez, M.; Llompart, M.; Lamas, J.P.; Lores, M.; Garcia-Jares, C.; Cela, R.; Dagnac, T. Simultaneous determination of traces of pyrethroids, organochlorinated and other main plants protection agents in agricultural soils by headspace solid-phase microextraction-gas chromatography. J. Chromatogr. A, **2008**, *1188*, 154–163.

Helium Detector

Raymond P.W. Scott
Scientific Detectors Ltd., Banbury, Oxfordshire, U.K.

INTRODUCTION

The outer group of electrons in the noble gases is complete, and as a consequence, collisions between noble gas atoms and electrons are perfectly elastic. It follows that if a high potential is set up between two electrodes in a noble gas and ionization is initiated by a suitable radioactive source, electrons will be accelerated toward the anode and will not be impeded by energy absorbed from collisions with the noble gas atoms. However, if the potential of the anode is high enough, the electrons will develop sufficient kinetic energy that, on collision with the noble gas atom, energy can be absorbed and a *metastable* atom can be produced. A metastable atom carries *no* charge, but adsorbs energy from collision with a high-energy electron by displacing an orbiting electron to an outer orbit.

DISCUSSION

Metastable helium atoms have an energy of 19.8 and 20.6 eV and thus can ionize and, consequently, detect all permanent gas molecules and, in fact, the molecules of all other volatile substances. A collision between a metastable atom and an organic molecule will result in the outer electron of the metastable atom collapsing back to its original orbit, followed by the expulsion of an electron from the organic molecule. The electrons produced by this process are collected at the anode and produce a large increase in anode current. However, when an ion is produced by collision between a metastable atom and an organic molecule, the electron, simultaneously produced, is also immediately accelerated toward the anode. This results in a further increase in metastable atoms and a consequent increase in the ionization of other organic molecules.

This cascade effect, unless controlled, results in an exponential increase in ion current. It is clear that the helium must be extremely pure or the production of metastable helium atoms would be quenched by traces of any other permanent gases that may be present.

Originally, a very complicated helium-purifying chain was necessary to ensure the helium detector's optimum operation. However, with high-purity helium becoming generally available, the helium detector is now a more practical system.

The metastable atoms that must be produced in the argon and helium detectors need not necessarily be generated from electrons induced by radioactive decay. Electrons can be generated by electric discharge or photometrically, which can then be accelerated in an inert gas atmosphere under an appropriate electrical potential to produce metastable atoms. This procedure is the basis of a highly sensitive helium detector that is depicted on the left-hand side of Fig. 1. The detector does not depend solely on metastable helium atoms for ionization and, for this reason, is called the helium discharge ionization detector (HDID).

The sensor consists of two cavities, one carrying a pair of electrodes across which a potential of about 550 V is applied. In the presence of helium, this potential initiates a gas discharge across the electrodes. The discharge gas passes into a second chamber that acts as the ionization chamber and any ions formed are collected by two plate electrodes having a potential difference of about 160 V. The column eluent enters the top of the ionization chamber and mixes with the helium from the discharge chamber and exits at the base of the ionization chamber.

In this particular detector, ionization probably occurs as a result of a number of processes. The electric discharge produces both electrons and photons. The electrons can be accelerated to produce metastable helium atoms which, in turn, can ionize the components in the column eluent. However, the photons generated in the discharge have, themselves, sufficient energy to ionize many eluent components and so ions will probably be produced by both mechanisms. It is possible that other ionization processes may also be involved, but the two mentioned are likely to account for the majority of the ions produced. The response of the detector is largely controlled by the collecting voltage and is very sensitive to traces of inert gases in the carrier gas. Peak reversal is often experienced at high collecting voltages, which may also indicate that some form of electron capturing may take place between the collecting electrodes. This peak reversal appears to be significantly reduced by the introduction of traces of neon in the helium carrier gas.

The helium discharge ionization detector has a high sensitivity toward the permanent gases and has been used very successfully for the analysis of trace components in ultrapure gases. It would appear that the detector response is linear over at least two, and possibly three, orders of magnitude, with a response index probably lying between

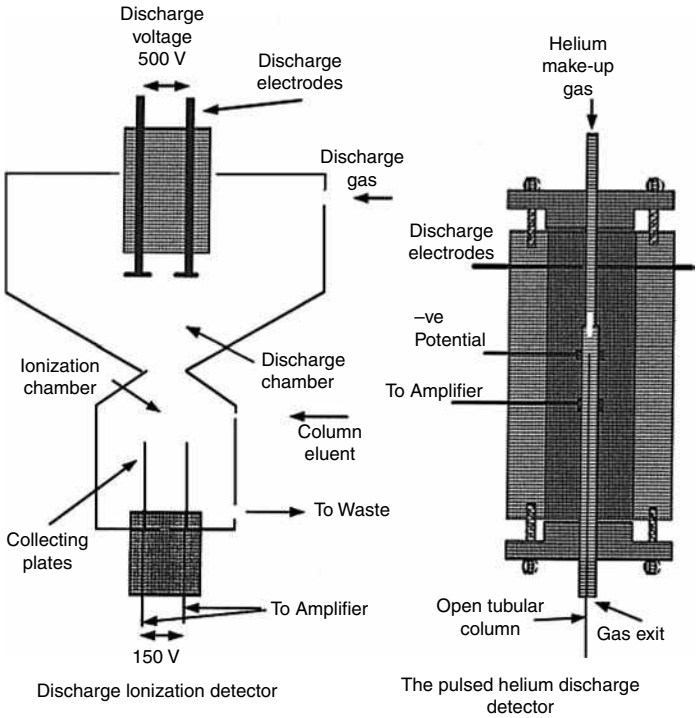

Fig. 1 The discharge ionization detector (courtesy of GOW-MAC Instruments) and the pulsed helium discharge detector (courtesy of Valco Instruments).

0.97 and 1.03. In any event, any slight non-linearity of the sensor can be corrected by an appropriate signal-modifying amplifier. The potential sensitivity of the detector to organic vapors appears to be about 1×10^{-13} g/ml.

THE PULSED HELIUM DISCHARGE DETECTOR

The pulsed helium discharge detector[1,2] is an extension of the helium detector, a diagram of which is shown on the right-hand side of Fig. 1. The detector has two sections: the upper section consisting of a tube 1.6 mm I.D. (where the discharge takes place) and the lower section, 3 mm I.D. (where reaction with metastable helium atoms and photons takes place). Helium makeup gas enters the top of the sensor and passes into the discharge section. The potential (about 20 V) applied across the discharge electrodes and for optimum performance is pulsed at about 3 kHz with a discharge pulse width of about 45 μs. The discharge produces electrons and high-energy photons (that can also produce electrons), and probably some metastable helium atoms. The photons and metastable helium atoms enter the reaction zone where they meet the eluent from the capillary column. The solute molecules are ionized and the electrons produced are collected at the lower electrode and measured by an appropriate high-impedance amplifier. The distance between the collecting electrodes is about 1.5 mm. The helium must be 99.9995 pure, otherwise permanent gas impurities quench the production of metastable atoms. The base current ranges from 1×10^{-9} to 5×10^{-9}A, the noise level is about 1.2×10^{-13}A, and the ionization efficiency is about 0.07%. It is claimed to be about 10 times more sensitive than the flame ionization detector and to have a linear dynamic range of 10^5. The pulsed helium discharge detector appears to be an attractive alternative to the flame ionization detector and would eliminate the need for three different gas supplies. It does, however, require equipment to provide specially purified helium, which diminishes the advantage of using a single gas.

REFERENCES

1. Wentworth, W.E.; Vasnin, S.V.; Stearns, S.D.; Meyer, C.J. Pulsed discharge helium ionization detector. Chromatographia **1992**, *34*, 219.
2. Wentworth, W.E.; Cai, H.; Stearns, S.D. Pulsed discharge helium ionization detector universal detector for inorganic and organic compounds at the low picogram level. J. Chromatogr. **1994**, *688*, 135.

BIBLIOGRAPHY

1. Scott, R.P.W. *Chromatographic Detectors*; Marcel Dekker, Inc.: New York, 1996.
2. Scott, R.P.W. *Introduction to Analytical Gas Chromatography*; Marcel Dekker, Inc.: New York, 1998.

Heterocyclic Bases: LC Analysis

Monika Waksmundzka-Hajnos
Department of Inorganic Chemistry, Medical University of Lublin, Lublin, Poland

INTRODUCTION

There are no absolute rules that formulate the influence of functional groups on pharmaceutical activities of compounds. However, it has been pointed out that an amine group or heterocyclic nitrogen atom possessing an aromatic ring causes an increase in a compound's biological activity. This is probably caused by the possibility of drug–receptor bonding, where electrostatic driving forces between ions present in the drug and receptor play the fundamental role. The presence of basic electron donor centers (amino group or heterocyclic nitrogen) makes possible their ionic interactions with acidic groups in proteins (–COOH), phospholipids, or nucleic acids (HPO_4^{2-}). Of course, other interactions, such as ion–dipole, dipole–dipole, induced dipole–dipole, H-bonds, and hydrophilic–hydrophobic specific interactions also play an important role in the fitting of drug molecules to the receptor. The chemical structures of drugs also play an important role in their solubility in body fluids and their transport through the lipid membranes of cells. Therefore, compounds possessing heterocyclic nitrogen are present in numerous drug groups. Examples of such drugs, their chemical structures, and pharmacological activities are presented in Table 1. Groups of alkaloids, which occur in plant organs with their pharmacological activities, are presented in Table 2.

STRUCTURE–CHROMATOGRAPHIC RETENTION RELATIONSHIPS

The relationship between the chemical structures of compounds and their chromatographic behavior has been considered by many scientists and was first reported by Martin in partition chromatography, where the partition coefficient is regarded as an additive value.[1] The hypothesis of the R_M additivity has raised worldwide discussion; hence, additivity rules were formulated. Deviation from the R_M additivity results from the complex character of the chromatographic process (change of a composition and volume proportions of phases), constitutional effects in molecules, because of reciprocal interactions of functional groups (internal hydrogen-bond effects, steric and electromeric effects) as well as ionization of substances.

Snyder[2] takes into consideration many factors influencing the value of adsorption energy of a molecule. Molecular planarity, steric hindrance, chemical interaction of adjacent functional groups (H-bonding), electronic interactions of some functional groups (induction and mesomeric effects), and simultaneous adsorption of two neighboring functional groups ("anchorage" effect of molecule on the adsorption sites especially on alumina surface) have been taken into account.

Retention in chromatographic systems can be connected with the properties of the chromatographed compounds. It should manifest itself in quantitative structure–retention relationships (QSRR) equations,[3] correlating retention parameters (log k) with the properties of analytes and chromatographic system revealed by molecular descriptors: dipolarity/polarizability, ability to donate H-bonds, measure of analyte H-bond accepting potency, analyte molecular volume, and others.

ADSORPTION CHROMATOGRAPHY

Silica Gel

The retention–mobile phase composition relationships for heterocyclic bases in systems involving silica/binary eluent can be expressed as the linear plots of log $k(R_M)$ vs. log X (X is the molar fraction of polar modifier in the eluent).[4] It proves a simple displacement model of retention of these substances in normal-phase systems. Slopes of log k vs. log X plots provide information about interactions of chromatographed substances with the adsorbent surface. Unit slopes, meaning single-point adsorption, are usually obtained for monofunctional heterocyclic bases (pyridine, quinoline, acridine without any functional groups). When unit slopes are obtained for bifunctional solutes, the complete delocalization of the weaker functional group takes place. It occurs for the apolar functional groups—for example, an alkyl chain. Sufficient adsorption energies of the two groups and suitable distance between the groups are two sufficient conditions of two-point adsorption for bifunctional heterocyclic bases (or other solutes). The experimental data indicate that for bases with two strongly polar functional groups, e.g., 4-aminopyridine, 5-hydroxyquinoline, 5-aminoquinoline, two-point adsorption on silica occurs.[4] When the functional groups in the solute molecule differ significantly in their adsorption energies, the localization of the stronger group and the resulting delocalization of the weaker group may cause a decrease of

Table 1 Structure and pharmacological activity of some heterocyclic base derivatives.

Drugs	Structure	Pharmacological activity
Benzodiazepine derivatives	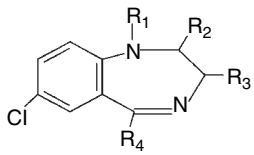	Sedative, antiepileptic, hypnotic, anesthetic
1,4-Dihydropyridine derivatives	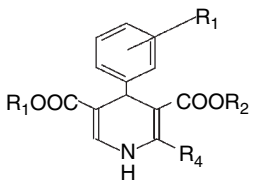	Ca-channel blocker, hypotensic
4-Aminoquinoline derivatives	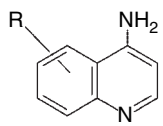	Antiinflammatory, antimalarial
8-Hydroxyquinoline derivatives	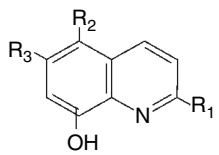	Antiseptic
Acridine derivatives	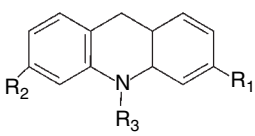	Antiseptic
Barbiturates	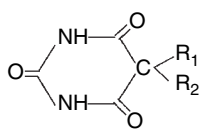	Hypnotic, sedative, anesthetic
Thiobarbiturates	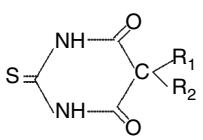	Anesthetic
Hydantoin derivatives	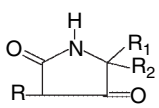	Antiepileptic
Quinoline derivatives	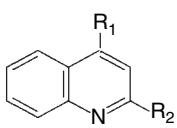	Anesthetic
Phenothiazine derivatives	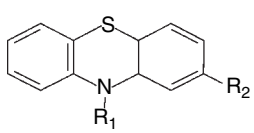	Sedative, spasmolytic, antihistaminic

(Continued)

Table 1 Structure and pharmacological activity of some heterocyclic base derivatives. *(Continued)*

Drugs	Structure	Pharmacological activity
Butyrophenone derivatives	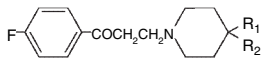	Sedative, psychotropic
5-Pyrazolone derivatives	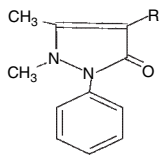	Analgetic, antipyretic
3,5-Pyrazolidinedione derivatives	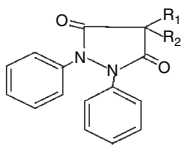	Analgetic, antiinflammatory
Imidazole derivatives	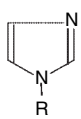	Fungicidal
Imidazoline derivatives	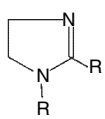	Antihistaminic
Pyridine derivatives	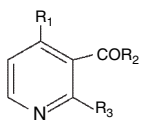	Hypotensic, cardiac
Pyridine derivatives	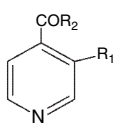	Tuberculostatic
Monobactams	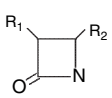	Antibiotic
Penicillins	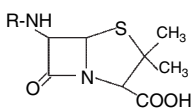	Antibiotic
Cephalosporins	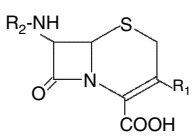	Antibiotic
Piperazine derivatives	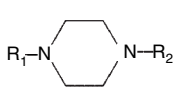	Antidepressive

(Continued)

Headspace – Human

Table 1 Structure and pharmacological activity of some heterocyclic base derivatives. *(Continued)*

Drugs	Structure	Pharmacological activity
Morpholine derivatives	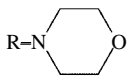	Analgetic, β-adrenolytic, antiepileptic
Piperidine derivatives	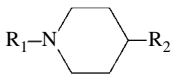	Neuroleptic, antidepressive, antihistaminic, psychotropic

Table 2 Alkaloids and their pharmacological activities.

Alkaloid type	Group of alkaloids	Main active alkaloids	Biological activity
Pyridine, piperidine	Nicotine and anabazine	Nicotine, anabazine, nornicotine	Synapotolytic, toxic
	Cortex granati	Isopelletierine and derivatives	Toxic, anthelmintic
	Lobeline group	Lobeline, isolobeline, sedamine	Synapsotropic, analeptic, secretolytic
	Arecoline	Arecoline	Anthelmintic, purgative
	Conium	Coniine, coniidine	Toxic, poisonous
	Lycopodium	Lycopodine and derivatives	Toxic, poisonous
	Quinolizidine	Lupanine, sparteine, cytisine, lobeline	Toxic, antiarrythmic
Tropane	Tropine	Tropine, hyoscyamine, atropine, scopolamine	Paraspasmolytic
	Ecgonine	Ecgonine, cocaine	Anesthetic
Isoquinoline	Benzylisoquinoline	Papaverine	Spasmolytic
	Aporphine	Glaucine, magnoflorine, boldine	Spasmolytic, hypotensic, choleretic
	Protoberberine	Berberine, narcotine, palmatine	Antibacterial, choleretic, analgetic, antiarrythmic
	Benzophenanthridine	Chelidonine, sanguinarine, chelerythrine	Choleretic, anesthetic, spasmolytic
	Protopine	Protopine, cryptopine	Antiarrythmic
	Morphinan	Morphine, codeine, thebaine	Narcotic, analgetic, spasmolytic
	Emetine	Emetine, cephaline	Antimicrobial (protozoa)
Indole	Indole alkaloids, *Catharanthus roseus*	Vincristine, vinblastine, vindesine	Anticancer, cytostatic
	β-carboline	Harman, harmine	Hallucinogenic, antiparkinsonian
	Yohimbine	Yohimbine, serpentine	Spasmolytic, hypotensic
	Reserpine	Reserpine, rescinnamine	Psychotropic, anxiolytic, antiarrythmic
	Eburamine	Vincamine	Hypotensic
	Strychnos	Strychnine, brucine	Analeptic, toxic, convulsant
	Ibogaine	Ajmaline, ibogaine	Antiarrythmic, psychotropic
	Secale cornutum	Ergotamine, ergocriptine, ergozine	α-Adrenolytic, spasmolytic, hypotensic
Purine		Caffeine, theophylline, theobromine	Analeptic, diuretic, spasmolytic
Steroidal	*Fritillaria* isosteroidal	Cevanine, jervine veratramine	Antitussive, tracheal, and bronchial relaxative
	Veratrum album	Protoveratrine A and B, veratramine, germine, veratrine, protoverine	Hypotensic, insecticidal
	Solanum	Solanine, tomatine, tomatidine, solanidine	Toxic, antifungal
Quinoline	*Cinchona*	Cinchonine, quinidine, quinine, cinchonidine	Antipyretic, antimalarial, antiarrythmic
Pyrrolizidine		Retronecine, heliotridine	Hepatotoxic, cancerogenic, cytotoxic

the slope, for example, for quinoline derivatives with a methoxy group in the meta or para position.

The slope of R_M vs. log c plots depends also on solvent strength. For the polar component of an eluent with low solvent strength (diethyl ether, methyl ethyl ketone), the slopes of methoxy and acetyl derivatives are greater than for stronger ones. The use of diethylamine as the eluent modifier leads to single-point adsorption of almost all heterocyclic bases investigated because the weaker group is unable to compete with the solvent for surface hydroxyl groups. Only basic groups such as $-NH_2$ in 4-aminopyridine, 3-aminopyridine, and 5-aminoquinoline can compete with diethylamine for surface hydroxyls, and the slopes for these solutes are approximately equal to 2.0.

Ortho substituted heterocyclic bases behave, on a silica surface, like monofunctional solutes and, in most cases, have slopes near unity [for example 2-acetylpyridine, 1-(pyridyl-2′)-ethan-1-ol], whereas the slope values for analogous para isomers are much higher. Also, 8-substituted derivatives of quinoline behave like ortho isomers (see 8-hydroxyquinoline). This is caused by the ortho effect—H-bond interactions of two neighboring polar groups (internally H-bonded groups), which cause their weaker adsorption and single-point interactions with surface silanols [compare slopes of 5-hydroxyquinoline and 8-hydroxyquinoline, 2-acetylpyridine and 4-acetylpyridine, 1-(pyridyl-2′)-ethan-1-ol and 1-(pyridyl-4′)-ethan-1-ol].[4]

Polar modifier influences separation selectivity of nitrogen bases on silica only to a small degree. Matyska and Soczewiński[5] compared separation selectivity of quinoline bases in equieluotropic eluent systems consisting of *n*-heptane and various modifiers (ethyl methyl ketone, ethyl acetate, diethyl ether, diisopropyl ether) and with chloroform and the same modifiers. They concluded that retention and separation selectivity of investigated nitrogen bases is, in most cases, similar. However, selectivity of separation of quinoline bases with two polar groups (hydroxy, amino derivatives) strongly depends on the modifier used as the eluent component.

Petrowitz compared adsorptive properties of alkyl- and halogen-derivatives of different solutes, and also heterocyclic bases. For example, methyl derivatives of pyridine behave in a different way on silica, depending on the group position. Thus, α- and γ-methylpyridine are strongly retained on silica because of hyperconjugation and formation of a double bond with increase of basicity of heterocyclic nitrogen, which does not occur in the β-isomer. It is also mentioned that in homologous series of pyridine alkyl-derivatives, a decrease of adsorption ability with the increase of the alkyl chain length is observed. When a pyridine or quinoline molecule has two functional groups (e.g., amino group in 2-position and methyl group in various positions), the adsorption affinity depends on steric hindrance of heterocyclic nitrogen by the neighboring methyl group. When retention behavior of quinolines with polar—hydroxy or amino group in the 8-position is observed, the methyl group in the 2-position significantly reduces the adsorption ability of molecules.

Retention behavior of halogenopyridines depends on the molecular mass of the halogen. The reduction of adsorption ability with an increase of halogen molecular mass is observed. The position of the halogen atom also has great meaning—a halogen neighboring the polar group or heterocyclic atom influences more adsorption ability and causes its decrease.

Alumina

Previous systematic investigations of organic compounds' adsorption from various chemical groups indicated analogies in the adsorption ability of silica and alumina.[6] However, alumina has heterogeneous surface active sites—electron donor oxygen atoms and electron acceptor aluminum ions. Numerous publications[7] have drawn attention to certain regularities in the adsorption onto alumina of the substituted pyridines and related aza aromatics. The contribution of the nitrogen atom in these adsorbates to total adsorption energy is markedly sensitive to the steric environment about the nitrogen atom. Klemm, Klopfstein, and Kelly stated[8] that the interaction between nitrogen and adsorbent is the result of charge-transfer complex formation. The presence of strong electron donor, as well as electron acceptor centers, favors especially considerable adsorption of molecules having, in adjacent positions, functional groups able to simultaneously interact with the surface aluminum ions produced by the formation of the chelate complex.[8] The same substances interact weakly with the silica surface. Retention behavior of hydroxyquinoline derivatives is quite different on alumina compared to silica.[1] 8-Hydroxyquinoline is strongly retained on the alumina surface due to anchorage of adjacent polar groups by the formation of a chelate with Al^{3+} ions, whereas, on a silica surface, it is weakly adsorbed. Rupture of an internal H-bond by methylation of the OH group leads to the increase of adsorption of methoxy derivative on silica, unlike alumina, on which 8-hydroxyquinoline is more strongly retained due to the anchorage effect than 8-methoxyquinoline (Table 3).[1] From the slopes of R_M

Table 3 R_F values of hydroxy and methoxy derivatives of quinoline on alumina and silica.

	R_F values in chromatographic systems			
	10% MeOH + B		40% AcOEt + Cx	
Substance	SiO_2	Al_2O_3	SiO_2	Al_2O_3
8-Hydroxyquinoline	0.60	0.04	0.50	0.0
5-Hydroxyquinoline	0.16	0.29	0.14	0.15
8-Methoxyquinoline	0.34	0.78	0.06	0.28
5-Methoxyquinoline	0.48	0.82	0.26	0.66

Abbreviations: MeOH—methanol, B—benzene, AcOEt—ethyl acetate, Cx—cyclohexane.

vs. log X plots obtained for alumina in binary eluents, it is visible that in the case of the covering of a heterocyclic nitrogen by a methyl group or by a condensed ring, flat adsorption of the molecule is possible.

Magnesium Silicate—Florisil

Linear dependencies of R_M vs. log c of heterocyclic bases on Florisil layers indicate the displacement model of retention. It has been confirmed[1] that quinolines (methyl or benzo derivatives) are more strongly adsorbed onto Florisil than onto silica in non-aqueous *n*-heptane and polar modifier eluent systems. In spite of this, separation selectivity is better when Florisil is used (methylquinolines can be separated from dimethylquinolines and from quinoline). The influence of the neighboring methyl group in 8-methylquinoline on the decrease of adsorption affinity on Florisil is observed, as in the case of silica. The heterocyclic bases with a second electron acceptor group (6-nitroquinoline, 2-chloro-3-nitropyridine, 2-chloro-5-nitropyridine) are adsorbed more strongly onto Florisil active centers (OH groups and Mg^{2+} ions) than onto silica.[9]

Table 4 shows ΔR_M values for substituted quinolines in isoeluotropic eluent systems on different adsorbents.[10] The isoeluotropic series obtained for quinoline on various adsorbents is developed with solvents from different selectivity groups (Table 4). It is clearly seen that the highest ΔR_M values were obtained for quinoline bases on Florisil with dichloromethane, 2-propanol, and other modifiers, which proves highest selectivity of separation in this system.

Polar-Bonded Stationary Phases

Polar-bonded stationary phases, such as cyanopropyl, diol, or aminopropyl, bonded to a silica matrix, have moderate polarity and can be used in normal- and reversed-phase (RP) systems. The retention behavior of heterocyclic bases was also examined using these adsorbents by determination of R_M (log k) values of solutes by the use of eluents with various modifier concentrations.[1] It was statistically found that the Snyder–Soczewiński equation and Scott theory describe the retention of quinolines on polar-bonded stationary phases in normal-phase systems sufficiently well. It seems that results are consistent with a displacement model. The dispersive interactions between solute molecules and the polar component of an eluent seem also to have an important role.[1] Similarly, the retention–

Table 4 ΔR_M ($R_{M(QX)} - R_{M(Q)}$) values for substituted quinolines in isoeluotropic eluent systems.[a]

Silica functional group	**5% iPrOH**	**40% DX**	**50% THF**	**60% AcOEt**	**80% EtMeCO**	**50% Me_2CO**	**100% iPr_2O**	**100% DCM**
CH_3	–0.05	–0.02	–0.02	0.04	0.00	0.02	0.07	0.12
CH_3O	0.04	0.13	0.09	0.14	0.04	0.07	0.27	0.41
NO_2	0.15	0.19	0.11	0.14	–0.04	0.00	0.37	0.12
C_9H_6N	–0.35	–0.20	–0.24	–0.56	–0.46	–0.15	–0.65	–0.33
C_6H_4	–0.23	–0.07	–0.15	–0.31	–0.24	–0.09	–0.26	0.27
Alumina functional group	**5% iPrOH**	**15% DX**	**20% THF**	**15% AcOEt**	**20% EtMeCO**	**20% Me_2CO**	**90% iPr_2O**	**90% DCM**
CH_3	–0.03	–0.02	–0.04	–0.03	–0.04	–0.08	0.04	0.04
CH_3O	0.05	0.23	0.15	0.19	0.13	0.08	0.28	0.21
NO_2	0.05	0.33	0.30	0.32	0.17	0.00	0.45	0.04
C_9H_6N	–0.20	–0.15	–0.23	–0.22	–0.29	–0.33	–0.32	–0.46
C_6H_4	–0.01	–0.02	0.00	–0.08	–0.07	–0.15	–0.04	0.00
Florisil functional group	**10% iPrOH**	**20% DX**	**30% THF**	**40% AcOEt**	**30% EtMeCO**	**30% Me_2CO**	**100% iPr_2O**	**100% DCM**
CH_3	–0.02	0.00	0.00	0.06	–0.02	–0.06	—	0.21
CH_3O	0.60	0.47	0.40	0.33	0.28	0.08	0.66	0.57
NO_2	0.70	0.59	0.32	0.19	0.09	–0.17	0.78	0.10
C_9H_6N	–0.26	–0.17	–0.21	–0.41	–0.39	–0.37	0.07	–0.69
C_6H_4	0.13	0.38	0.09	–0.04	0.00	–0.13	0.43	0.78

Abbreviations: iPrOH—2-propanol, DX—dioxane, THF—tetrahydrofuran, EtMeCo—ethylmethyl ketone, iPr_2O—diisopropyl ether, DCM—dichloromethane.
[a]The eluent strength of polar modifier—*n*-heptane binary mixtures was selected to give retention factor k, of 1 for quinoline.
Source: From Comparison of retention of phenols, aniline derivatives and quinoline bases in normal-phase TLC with binary isoeluotropic eluents, in J. Planar Chromatogr.[10]

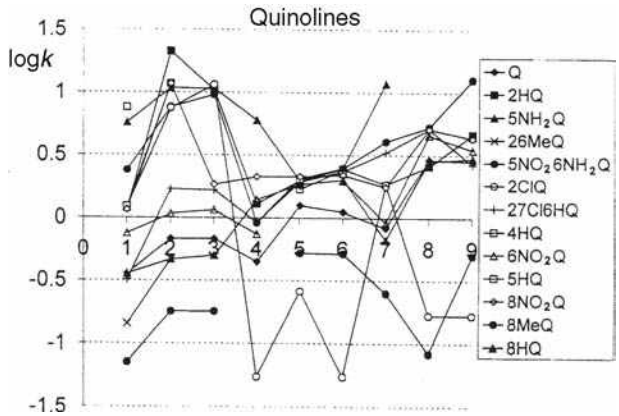

Fig. 1 Graphical comparison of log k values for quinoline bases in the following chromatographic systems. Diol phase: (1) 15% iPrOH, (2) 20% THF, (3) 20% DX; aminopropyl phase: (4) 10% iPrOH, (5) 10% THF, (6) 10% DX; cyanopropyl phase: (7) 10% iPrOH, (8) 5% THF, (9) 5% DX. All modifiers are dissolved in *n*-heptane. Q—quinoline, 2HQ—2-hydroxyquinoline, $5NH_2Q$—5-aminoquinoline, 26MeQ—2,6-dimethylquinoline, $5NO_26NH_2Q$—5-nitro-6-aminoquinoline, 2ClQ—2-chloroquinoline, 27Cl6HQ—2,7-dichloro-6-hydroxyquinoline, 4HQ—4-hydroxyquinoline, $6NO_2Q$—6-nitroquinoline, 5HQ—5-hydroxyquinoline, $8NO_2Q$—8-nitroquinoline, 8MeQ—8-methylquinoline, 8HQ—8-hydroxyquinoline.
Source: From Comparison of chromatographic properties of cyanopropyl-, diol- and aminopropyl–polar bonded stationary phases by the retention of model compounds in normal-phase liquid chromatography systems, in J. Chromatogr. A.[11]

eluent composition relationships for quinolines on such layers in RP systems using aqueous eluents can be represented by a semilogarithmic equation.[1]

The selectivity of separation of quinoline bases using normal-phase systems and polar-bonded stationary phases was compared by log k_1 – log k_2 correlations.[11] The values of regression coefficients for all correlation lines are relatively low. This results from different selectivities and mechanism of separation of the heterocyclic bases in the investigated systems. Fig. 1 is a graphical comparison of quinoline separation selectivity by the use of various systems as log k spectrum. It is seen that all polar-bonded stationary phases can be used for the separation of quinoline derivatives, especially with 2-propanol or tetrahydrofuran as eluent modifiers.

Application of Polar Adsorbents in Separation of Heterocyclic Bases

Polar adsorbents, especially silica, are widely used for the separation of alkaloids and basic drugs, such as barbiturates, benzodiazepines, and other pyridine and quinoline derivatives. Because of strong interactions of basic nitrogen with surface silanols, solvents with high eluent strength are used as mobile phases. In a review[12] describing thin-layer chromatography (TLC) analysis of benzodiazepines, there are more than 40 papers cited where the use of silica layers is reported. Mixtures of highly polar solvents—alcohols (MeOH, EtOH), chloroform, and mostly ammonium aqueous solutions or ethylenediamine as ionization suppressing agents are used as eluents. Moreover, basic components of an eluent can block the surface acidic silanols of silica. In a few cases, the use of a polyamide with various eluents and alkyl-bonded phases with aqueous eluents is reported. The use of similar chromatographic systems, e.g., silica/chloroform + alcohol (MeOH, EtOH, BuOH), is reported for analytical TLC of polyhydroxy–chromone and flavonoid alkaloids.[13] Cellulose, with multicomponent aqueous eluent, has also been used. There were no reports of high-performance liquid chromatography (HPLC) of flavonoid alkaloids until 2002. For the separation of polar chromone alkaloids, the use of silica with aqueous eluents containing ammonia is also reported.[13] Normal-phase systems can also be used for the isolation of chromone and flavonoid alkaloids using silica columns or preparative silica layers, mostly with gradient elution with chloroform + methanol. Because of the detection difficulty of polyhydroxy alkaloids (pyrrolidine, piperidine, pyrrolizidine, indolizidine, and nortropane classes) resulting from their lack of suitable chromophores for spectroscopic detection, analytical TLC is used for purity determination and detection in plant extracts and in pharmacokinetic studies.[14] Preparative planar chromatography has also been a separation method of choice for isolation of individual polyhydroxy alkaloids from mixtures. Silica gel, with combinations of chloroform, methanol, and aqueous ammonium, has been widely used for TLC in analytical, as well as on preparative, scale. *Cinchona*–quinoline alkaloids, mostly analyzed in RP systems, are also separated by normal-phase chromatography, mainly using bare silica columns or layers with mobile phases containing solvents such as chloroform, acetone, or ethyl acetate with alcohols as polarity adjusters and ammonia or diethylamine as ionization suppressors and silanol blockers.[15] Fig. 2 presents an example of the separation of isoquinoline alkaloids by use of two-dimensional TLC (2D-TLC) on a silica plate.[16]

RETENTION OF IONIZABLE WEAK BASES IN RPLC

HPLC separation of ionic samples is more complicated[17] than separation of non-ionic compounds. For regular ionic samples, three HPLC methods: reversed-phase, ion-pair, or ion-exchange chromatography (IEC) can be chosen. Because of its simplicity, reversed-phase chromatography (RPC) is usually the best starting point. If RPC separation proves inadequate, the addition of an ion-pairing reagent to the mobile phase or application of IEC can be considered.

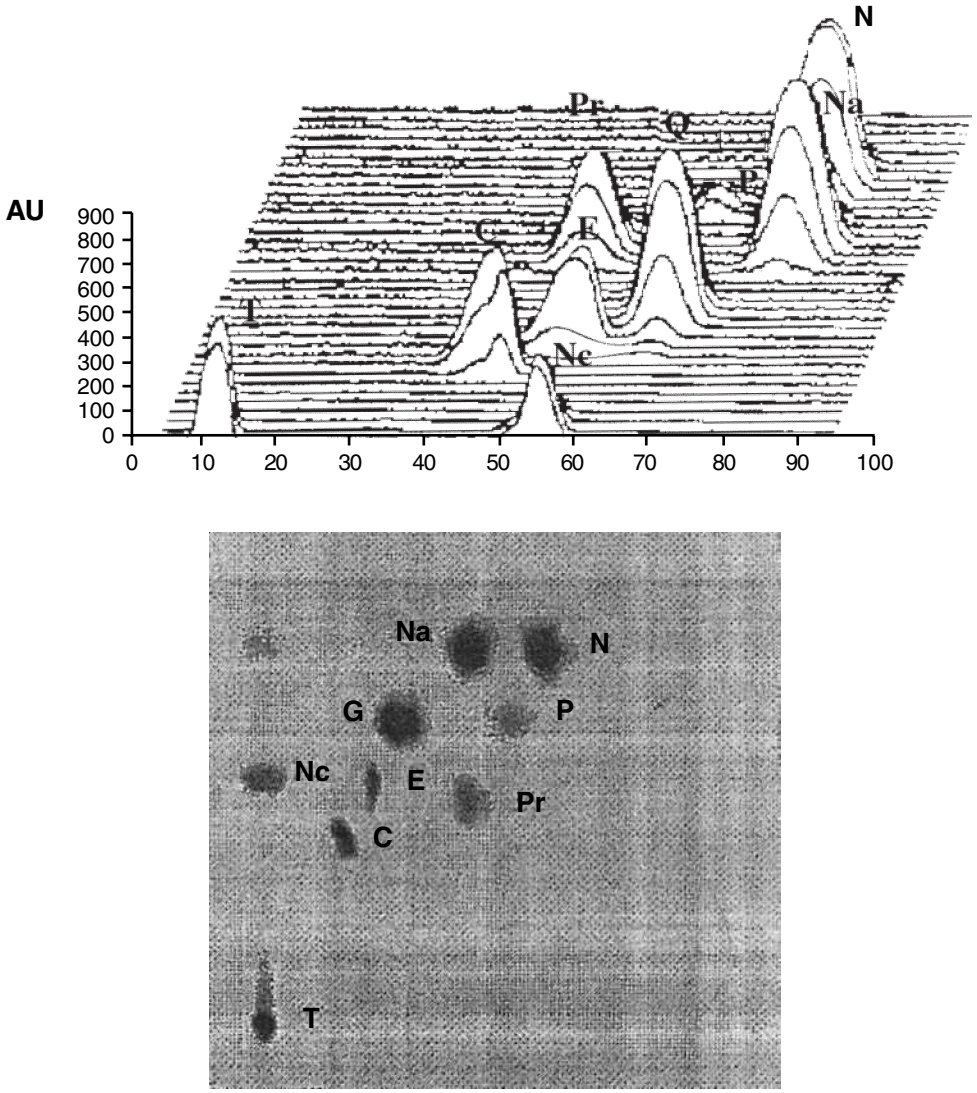

Fig. 2 Densitogram and videoscan from 2D-TLC of isoquinoline alkaloids separated on silica layer by use of aqueous methanol (8%) with 1% ammonia as the first direction eluent and multicomponent non-aqueous eluent with 0.1 *M* DEA as the second direction eluent. N—noscapine, Na—narcotine, Nc—narceine, G—glaucine, E—emetine, C—codeine, P—papaverine, Pr—protopine, T—tubocurarine. **Source:** From the effect of chromatographic conditions on the separation of selected alkaloids on silica layers, in J. Planar Chromatogr.[16]

Separation Selectivity as a Function of pH and Mobile-Phase Composition

From the theory[18] for RP retention of ionic (e.g., basic) compounds as a function of pH, it can be assumed that a given solute (e.g., a heterocyclic base) exists in ionized (+) and non-ionized forms and its capacity factor k is given by:

$$k = k^0(1 - F^+) + k_1F^+ \quad (1)$$

where k_0 and k_1 refer to k values for non-ionized and ionic forms and F^+ is the fraction of ionized solute molecules for the case of a basic solute:

$$F^+ = 1/\{1 + (K_a/[H^+])\} \quad (2)$$

The dependencies of log k (R_M) as a function of pH for selected alkaloids are given in Fig. 3.[19]

The potential errors in the use of Eqs. 1 and 2 result from the following facts:[18] retention of solutes, especially protonated bases, by processes other than solvophobic interactions, e.g., with exposed silanols or metal contaminants;[20] change in K_a values as a function of ionic strength; solvophobic effect of ionic strength on solute retention; ion-pair interaction of sample ions with ionized buffer species; change in the sorption properties of the stationary phase (C_8 or C_{18}) as a result of changing ionization of silanols; a

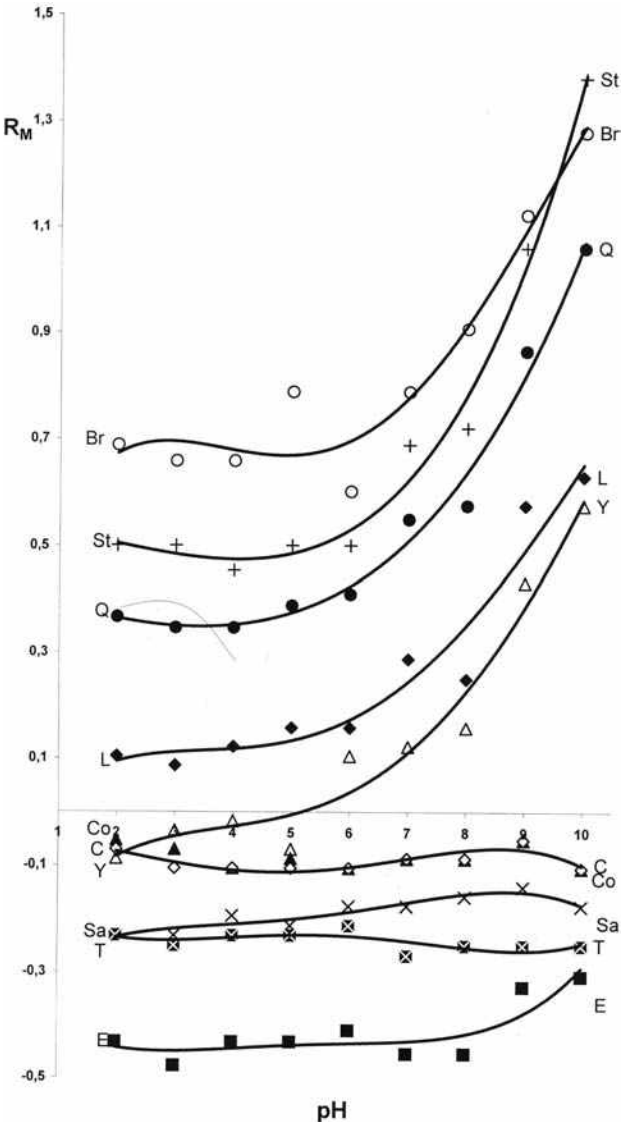

Fig. 3 Dependence of R_M vs. pH of mobile phase for investigated alkaloids. System: C18W/MeOH/water (8 : 2) buffered with phosphate buffer 0.01 *M*/L. E—emetine, T—theophylline, Sa—santonine, Co—colchicine, C—caffeine, Y—yohimbine, L—lobeline, Q—quinine, Br—brucine, St—strychnine.
Source: From The effect of chromatographic conditions on the separation of selected alkaloids in RP-HPTLC, in J. Chromatogr. Sci. [19]

change in buffer type, when more than one buffer type is needed to cover a given pH range.

It is maintained[18] that computer simulations based upon the theoretical model (Eqs. 1 and 2) are able to predict, accurately, retention and resolution of basic solutes as a function of pH. Predicted retention times and α values were significantly more difficult for the case of basic, rather than acidic, solutes, due to silanol effects (more significant for basic solutes).

As retention factors (k) can decrease by a factor of 10 or more for an ionized vs. a non-ionized compound, it is often necessary to combine pH optimization with variation of solvent strength (%B, φ) in order to maintain a reasonable k range for the effective separation ($1 < k < 20$).[18]

$$k = \mathrm{f}([\mathrm{H}^+], \varphi) \tag{3}$$

Because the capacity factor of a weak base is the average of capacity factors of individual forms BH^+ and B:

$$k = k_0\left(\frac{[\mathrm{BH}^+]}{[\mathrm{BH}^+] + [\mathrm{B}]}\right) + k_1\left(\frac{[\mathrm{B}]}{[\mathrm{BH}^+] + [\mathrm{B}]}\right) \tag{4}$$

it can be transformed to the equation:

$$k = \frac{k_0 + k_1[\mathrm{H}^+]/K_\mathrm{a}}{1 + [\mathrm{H}^+]/K_\mathrm{a}} \tag{5}$$

However, the problem is more complex because the acidity constant K_a as well as the retention factor of the protonated form k_0 and ionized form k_1 vary with the concentration of modifier in the aqueous mobile phase (φ), although the general form of Eq. 5 is maintained. This problem of the retention factor as the combined function of pH and modifier concentration in aqueous mobile phase has been analyzed by several researchers.[1]

Marques and Schoenmakers[21] took two approaches for weak acids; nevertheless, ionized base can be counted as cationic acid BH^+:

1. At constant pH, they describe k_0 and k_1 as a function of concentration of organic modifier in the mobile phase—φ, taking, from previous papers, the dependence of acidity constant as a function of φ:[22]

$$k = \delta + \frac{k_0(\varphi) + k_1(\varphi)[\mathrm{H}^+]/K_\mathrm{a}(\varphi)}{1 + [\mathrm{H}^+]/K_\mathrm{a}(\varphi)} \tag{6}$$

2. The second approach starts with:

$$\ln k = A + B\varphi + C\varphi^2 \tag{7}$$

where A is ln k for 0% modifier (methanol), which should be sigmoidal function of $[H^+]$, so that

$$A = \ln\left[\frac{k_0{}^\mathrm{w} + k_1{}^\mathrm{w}[\mathrm{H}^+]/K_\mathrm{a}{}^\mathrm{w}}{1 + [\mathrm{H}^+]/K_\mathrm{a}{}^\mathrm{w}}\right] \tag{8}$$

where $k_0{}^w$ is the capacity factor of B, $k_1{}^w$ is the capacity factor of BH^+, and $K_a{}^w$ is the acidity constant, all in pure water.

The first approach (Eq. 5) is realized assuming k_0, k_1, and K_a as different functions of mobile-phase composition: linear, quadratic, cubic (for K_a), and $\delta = 0$ or $\delta \neq 0$ (δ is the constant shift parameter). All the models (class 1 models) were verified experimentally. The model approaching ln k_0, ln k_1, and ln K_a as quadratic function of φ and $\delta = 0$

is, in the authors' opinion, the best compromise between precision and practicality.

The second approach is realized assuming k_0 as a sigmoidal function of $[H^+]$, the B parameter as quadratic, cubic, or sigmoidal function of $[H^+]$, and $C = 0$ or C as a linear function of $[H^+]$ and $\delta = 0$ or $\delta \neq 0$. All models were verified experimentally (class 2 models).

Models approaching k_0 as a sigmoidal function of $[H^+]$, B as cubic function of $[H^+]$, $C = 0$ and $\delta \neq 0$ or k_0 as sigmoidal function of $[H^+]$, B as quadratic, and C as a linear function of $[H^+]$ and $\delta \neq 0$ are adequate for practical purposes.

Retention as a Function of Ionic Strength of Eluent

The pH of the mobile phase is a major factor in the separation of ionizable compounds. As mentioned earlier, the most widely used model[18] considers the retention factor as an average of k_0 and k_1 according to the mole fraction of the neutral and ionic forms. The mole fraction depends on pK_a and pH of mobile phase. The pH of the mobile phase is taken to be the same as that of the aqueous fraction and this implies a false assumption. Even when pH is measured after mixing the buffer with the organic modifier, the potentiometric system, calibrated with aqueous standards, does not measure the true pH of the mobile phase.[23]

The second problem is that[21] pH should be taken from the activity of hydrogen ions, and the effect of activity coefficients γ can be neglected in water, but when the percentage of the organic modifier in the mobile phase increases, the activity coefficients decrease and cannot be neglected. Similarly, for the dissociation constant, the concentration should be changed by activities. From the Debye–Hückel definition, an activity coefficient depends on the ionic strength I of the solution.

The pH scale of any amphiprotic solvent is limited by zero and pK_{ap} values (K_{ap} is the autoprotolysis constant of medium); it differs in a mixed solvent, for example, methanol–water, where different proton-transfer equilibria occur. Ionizable solutes dissolved in these mixtures are differently solvated, show different dissociation constants, and the pH scale of the medium changes with mobile-phase composition.

Because the retention of ionic solutes depends on K_a, pH, and solvent strength, it depends on the activity coefficients of ions in the medium and, therefore, on its ionic strength.

Application of RP-HPLC Systems for Heterocyclic Base Analysis

Optimization in RP separation, and controlling the selectivity of basic samples, can be performed similarly as for non-ionic compounds by the variation of the solvent strength (%B) to obtain a satisfactory k range ($1 < k < 10$) or by change of the column type (C8, C18, phenyl, cyano). In applications of RP systems for the analysis of ionic compounds, the choice of suitable buffer is very important. Several properties such as buffer capacity, UV absorbance, and also solubility, stability, and interactions with the sample and chromatographic system, should be taken into account.

For RP separations when silica-based columns are used, the pH range of the mobile phase should be between 2 and 8. Therefore, for chromatographic analysis of heterocyclic bases, the following buffers may be used: phosphate buffer, (2.1–3.1, 6.2–8.2, and 11.3–13.3), acetate buffer (3.8–5.8), citrate buffer (2.1–6.4), carbonate buffer (3.8–5.8), formate buffer (2.8–4.8), and ammonia buffer (8.2–10.2) can be used.

Ionic samples, especially basic compounds, can interact with underivatized free silanols of silica-based alkyl-bonded columns. It appears that retention occurs by an ion-exchange process that involves protonated bases and ionized silanols. This case leads to increased retention, band tailing, and column-to-column irreproducibility. It is generally desirable to minimize these silanol interactions by an appropriate choice of experimental conditions. Silanol interactions can be reduced by selecting a column that is designed for basic samples with a reduced number of very acidic silanols that favor the retention process. The first method to reduce the silanol effect is the use of a low pH mobile phase ($2.0 < pH < 3.5$) to minimize the concentration of ionized silanols because, in this case, ionization of silanols is largely suppressed, giving rise to better peak shapes. The silanol effect can be further reduced by using a higher buffer concentration (> 10 mM) and the choice of buffer cations that are strongly held by the silanols ($Na^+ < K^+ < NH_4^+ <$ triethylammonium$^+ <$ dimethyloctylammonium$^+$) and, therefore, block sample retention by ionized silanols. Successful analysis of bases can be obtained even with classical RP-HPLC silicas by incorporation of amines into the mobile phases, which then compete with the analytes for column silanol sites. Working at high pH (e.g., $pH > 7.0$) for the separation of basic compounds is also recommended. Weak bases (e.g., pyridines) may be non-ionized at higher pH values and, thus, they may eliminate ionic interactions with acidic silanols. The problem, however, is with poor stability of silica-based columns, which are less stable for pHs over 6 and cannot be used at all for pH greater than 8. Only densely bonded alkyl end capped columns can be routinely used up to at least pH 11 when organic buffers and temperature under 40°C are used.

Reversed-phase HPLC is the method recommended for the screening of plant material, in which chromone alkaloids can be present.[13] Mostly C-18 columns were applied with aqueous mobile phases containing high concentrations of buffer at pH 4.5–6.5, modified with methanol or acetonitrile. Polyhydroxy alkaloids of the pyrrolidine, piperidine, pyrrolizidine, indolizidine, and tropane classes, because of their lack of a suitable chromophore, have rarely been analyzed

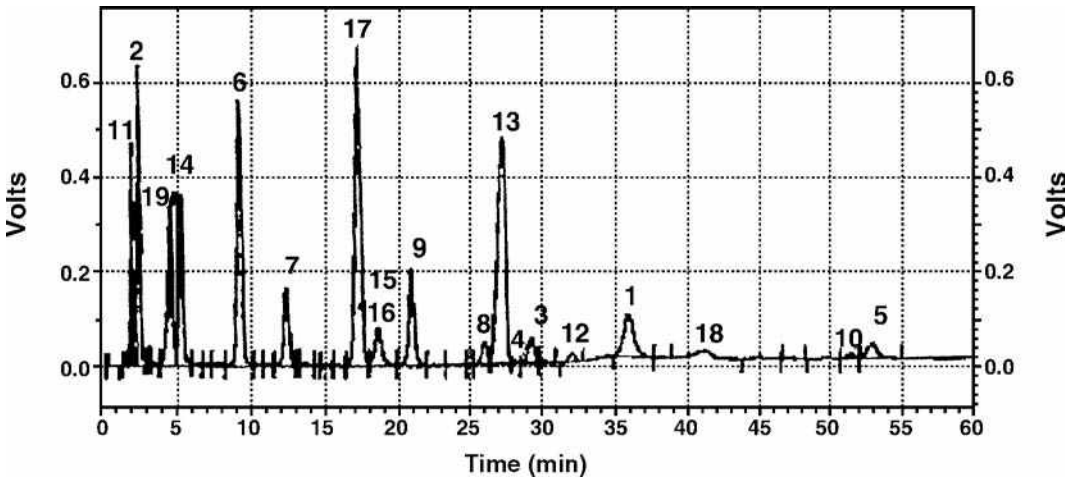

Fig. 4 HPLC chromatogram of the separation of alkaloids' standard mixture. Phenyl column, acetonitrile gradient 15–50%, acetate buffer at pH 3.5 + 0.05 *M*/L DEA. 1—berberine, 2—boldine, 3—chelidonine, 4—chelilutine, 5—chelerythrine, 6—codeine, 7—dionine, 8—emetine, 9—glaucine, 10—homochelidonine, 11—laudanosine, 12—noscapine, 13—narcotine, 14—narceine, 15—papaverine, 16—paracodine, 17—protopine, M. 18—sanguinarine, 19—tubocurarine.
Source: From Effect of chromatographic conditions on the separation of selected alkaloids on phenyl stationary phase by an HPLC method, in J. Liquid Chromatogr. Relat. Technol.[24]

by conventional HPLC with UV detection. The detection problem could be surmounted by derivatization of the hydroxyl groups or by the use of other detection methods.[14] Amino columns, eluted with acetonitrile–water, or C-18 columns with buffered aqueous methanol with MS detection, were used for these purposes. Analysis of *Cinchona* alkaloids can also be performed by RP-HPLC, which is still the first choice for their separation.[15] Mostly, C-18 columns with aqueous mobile phases modified with methanol, acetonitrile, or tetrahydrofuran at acidic pH, have been used. The eluents with competitive amines to mask silanol effects were also used for the separations of *Cinchona* alkaloids.[17] Isosteroidal alkaloids, the main bioactive ingredient of *Fritillaria* species, do not display strong UV absorption and cannot be analyzed by conventional HPLC/UV. Systems with C18 columns and aqueous methanol containing amines were used when evaporative light-scattering detection was applied. Fig. 4 presents separation of isoquinoline alkaloid standards on a phenyl stationary phase with an eluent containing diethyl amine (DEA).[24]

A review describing methods of measurement of benzodiazepines in biological samples[1,25] also reports a number of examples of the use of HPLC with alkyl-bonded phases and aqueous eluents. Mainly, C-18 columns eluted with aqueous acetonitrile or methanol at low pH and UV detection, were used in benzodiazepine analyses.

RETENTION OF HETEROCYCLIC BASES IN RP ION-PAIR LC

Ion-pair and RP-HPLC share several features. The columns and mobile phases used for these separations are generally similar, differing mainly in the addition of an ion-pairing reagent to the mobile phase for ion-pair chromatography (IPC). If RPC method development is unable to provide an adequate separation due to poor band spacing, IPC provides an important additional selectivity option.[1]

Parameters Influencing the Retention and Selectivity in IP Systems

For the analysis of basic compounds, anionic ion-pairing reagents, such as sulfonic acids, alkyl sulfonates, and other acids such as *bis*-(2-ethylhexyl)-ortho-phosphoric acid (HDEHP), have been employed. When the concentration of the ion-pairing reagent gradually increases, then a distinct increase in retention of the analytes is observed, and in a limited range of concentrations, a linear relationship of log k and log of concentration of counterion is obtained[26,27] at the moment of approaching the saturation of surface concentration of hydrophobic counterions. Further increase of concentration does not lead to significant changes in retention even a decrease of retention is sometimes observed[1] (Fig. 5)[28]. The change of type and concentration of the counterion often causes variation in selectivity of separation.[29]

Additionally, the retention and selectivity in IP–RP systems can be controlled by the change of type and concentration of the organic modifier in the aqueous mobile phase[29] and the pH of the mobile phase,[1] which should be selected to obtain maximal ionization of solute molecules and ion-pairing reagent molecules for the possibility of forming an ion pair. For the basic solutes, analyses of the pH range 7.0–7.5 are often applied.

The stationary phase (the length of the alkyl chains bonded to the silica support) also influences the retention of hydrophobic ion pairs.

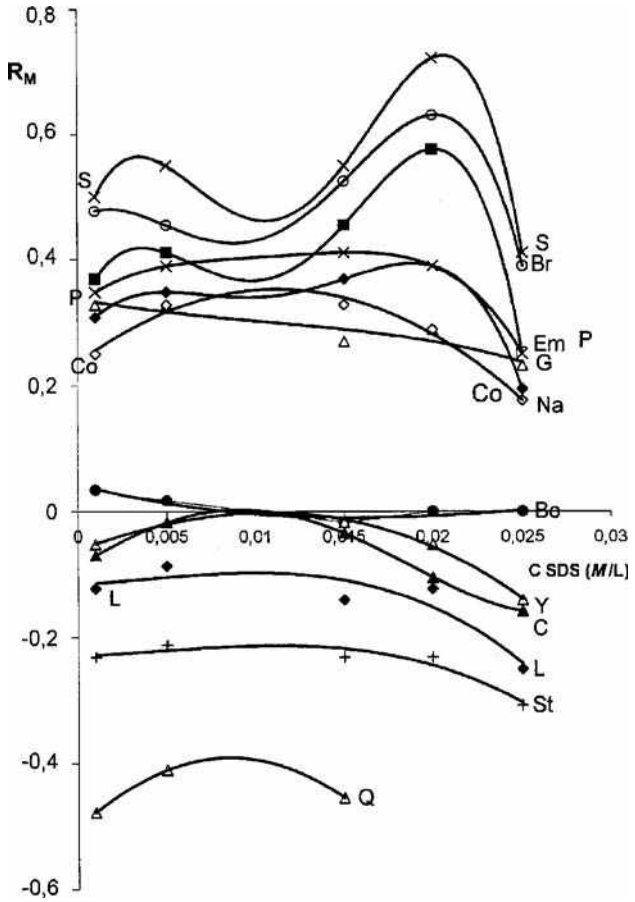

Fig. 5 Dependence of R_M vs. concentration of sodium dodecyl sulfate in mobile phase for investigated alkaloids. System: C18W/MeOH/water (8 : 2) buffered with phosphate buffer 0.01 *M*/L at pH 3. Em—emetine, S—santonine, Co—colchicine, C—caffeine, Y—yohimbine, L—lobeline, Q—quinine, Br—brucine, St—strychnine, P—papaverine, G—glaucine, Bo—boldine.
Source: From The effect of chromatographic conditions on the separation of selected alkaloids in RP-HPTLC, in J. Chromatogr. Sci.[28]

Similarly, as for RP-HPLC separations, selectivity can be additionally varied by solvent type (methanol, tetrahydrofuran, acetonitrile), buffer concentration, and temperature.[1]

RP–IP Systems in Analysis of Heterocyclic Bases

The comparison of separation of *Chelidonium majus* L. alkaloids on a cyanopropyl column, with a buffered aqueous mobile phase, without (a) and with IP reagent (b) is presented in Fig. 6.[30]

Some special problems for RP-IP-HPLC, such as positive and negative artifactual peaks appearing in a blank run, occur and can interfere in the development of the method and its routine use. Another problem in IP separations is slow column equilibration, which is slower when an ion-pair reagent is more hydrophobic. The slow equilibration of the column with many ion-pair reagents can create problems if a gradient elution is used under these conditions.

CHROMATOGRAPHY OF WEAK BASES USING ION-EXCHANGE SYSTEMS

Today, IEC is used infrequently in comparison with other chromatographic methods. In most cases, IPC is more convenient because of its higher column efficiency, more stable and reproducible columns, and easier control over selectivity and resolution. There are, however, cases for using IEC instead of RP- or IP-HPLC, especially when organic ions have poor UV absorbance and need other detection (conductivity or MS). Then, completely volatile components of mobile phase are required. In such cases, IEC with volatile buffers fulfil this requirement, whereas ion-pair reagents are not sufficiently volatile in most cases; also, when compounds are isolated or purified by HPLC separation, the removal of mobile phase is necessary. When multistep separation is required, the aqueous buffer–salt mobile phase used for ion-exchange allows direct injection of a sample fraction onto an RP column for the next step of separation. This may be difficult with IP systems.

For the separation of weak bases, cation-exchange columns are used, which have negatively charged groups (e.g., sulfonic or carboxylic) attached to the stationary phase. Two kinds of cation-exchange columns can be used: weak cation exchanger (WCX) or strong cation exchanger (SCX). The retention of basic compounds X^+ on such stationary phases (R^-) can be manifested by the equilibrium of an ion exchange:

$$X^+ + R^-K^+ \leftrightarrow X^+R^- + K^+ \quad (9)$$

where K^+ plays a role of counterion in mobile phase.

The increase of salt or buffer concentration in the mobile phase results in a decrease of the retention of sample compounds. Varying pH is usually a way to change the selectivity in IEC separations. Another way to change retention in IEC systems is the use of different counterions (displacers). Sometimes, the addition of organic modifiers, such as methanol or acetonitrile, is applied in IEC. This causes decreased retention of ionizable compounds.

There are several examples of the use of IEC systems for purification, isolation, and separation of heterocyclic bases. Based on ion-exchange SPE, a first and reliable procedure for the extraction of food tetrahydro-β-carboline, is accomplished on strong cation-exchange (SCX–benzenesulfonic acid cartridges) columns.[1] Water and/or alcoholic extracts of polyhydroxy alkaloids containing many other polar constituents are also purified by the use of resins.[14] The acidified aqueous solution is applied to the column and unretained neutral or acidic substances are eluted with water. The alkaloids, which

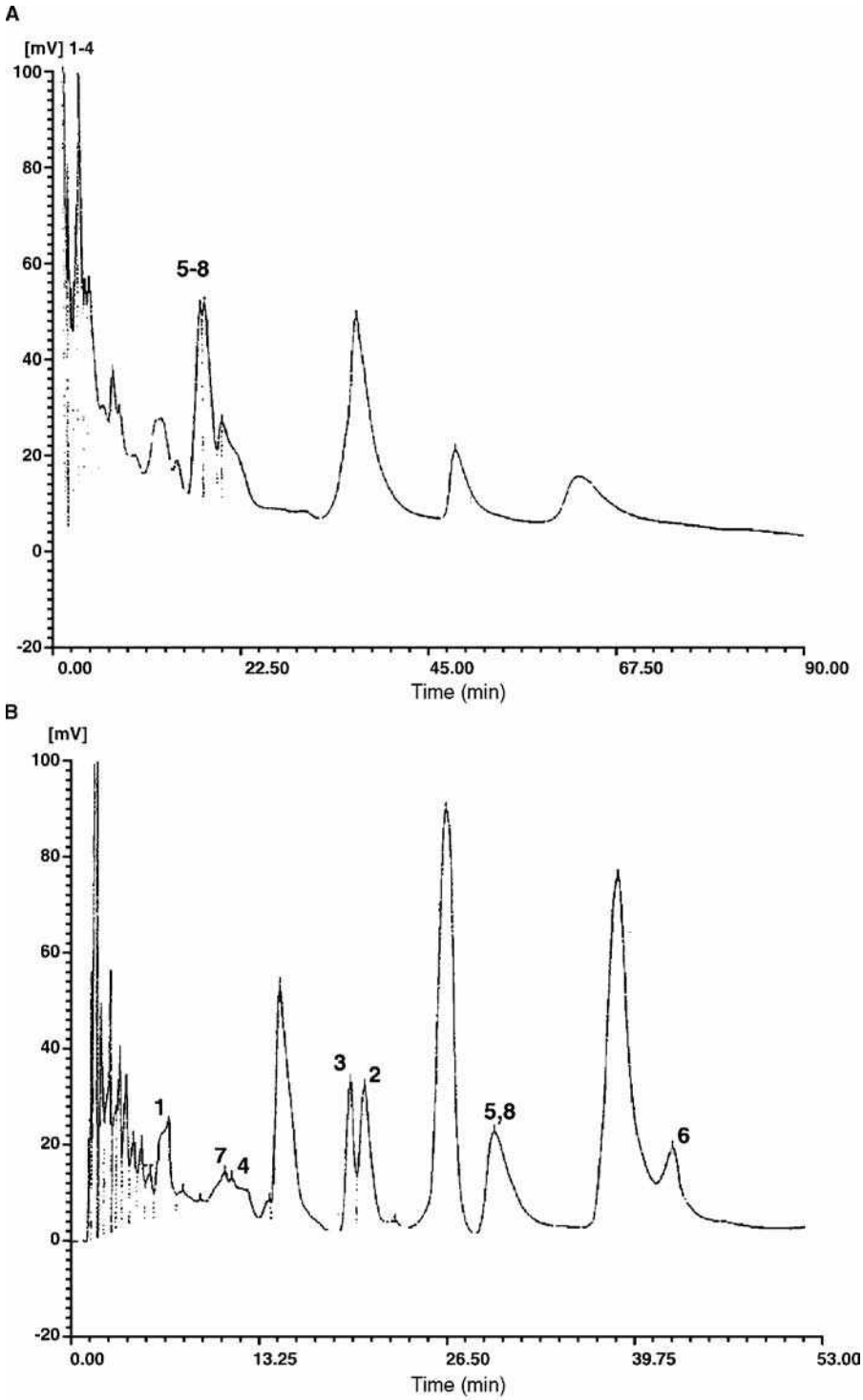

Fig. 6 Chromatogram of separation of *Chelidonium majus* L. extract in system: cyanopropyl–silica/20% MeCN + phosphate buffer pH 7.8 aqueous solution (A) and cyanopropyl–silica/20% MeCN + phosphate buffer pH 5.6 + 0.001 *M* octane-1-sulfonic acid sodium salt aqueous solution (B). 1—allocryptopine, 2—berberine, 3—chelerythrine, 4—chelidonine, 5—chelilutine, 6—chelirubine, 7—homochelidonine, 8—protopine.
Source: From Optimization of the separation of some Chelidonium maius L. alkaloids by reversed phase high-performance liquid chromatography using cyanopropyl bonded stationary phase, in Acta Pol. Pharm. Drug Res.[30]

are bound to the resin, accompanied by any other non-alkaloidal basic compounds, are then displaced with dilute ammonium hydroxide. Thus, an extension of the ion-exchange purification process—column chromatography—can be used for isolation of alkaloids on a preparative scale.[14] Also, with HPLC analysis, cation-exchange columns can be used; especially when UV detection is impossible because of lack of suitable chromophores, amperometric detection for the analysis of polyhydroxy alkaloids is applied. In such cases, a cation-exchange column, Dionex CS3, eluted with hydrochloric acid, was used for the separation and detection.[14] In the case of MS detection, the use of a separation process with a cation-exchange column, with the elution using volatile eluents, is also preferred.[14] Ion chromatography using a Dionex cation-

exchange column, with the aqueous HCl as eluent, was applied to the analysis of theobromine and theophylline in foods and pharmaceutical preparations.[1]

CONCLUSIONS

It has been shown that there are many approaches to the separation of heterocyclic bases by chromatographic techniques. Normal-phase adsorption, reversed-phase, ion-pairing, and ion-exchange chromatographic methods have been reported extensively in the cited literature.

REFERENCES

1. Waksmundzka-Hajnos, M. Retention behaviour of heterocyclic bases. Research trends. Trends Heterocycl. Chem. **2003**, *9*, 129–166.
2. Snyder, L.R. R_F values in thin-layer chromatography on alumina and silica. Adv. Chromatogr. **1967**, *4*, 3–11.
3. Kaliszan, R. *Quantitative Structure Chromatographic Retention Relationships*; John Wiley & Sons: New York, 1987.
4. Gołkiewicz, W.; Soczewiński, E. A simple molecular model of adsorption chromatography. VI. R_M—composition relationships of solutes with two functional groups. Chromatographia **1972**, *5*, 594–601.
5. Matyska, M.; Soczewiński, E. Computer-aided optimization of liquid solid systems in TLC. Comparison of selectivity of various silica–diluent + modifier systems. J. Planar Chromatogr. **1990**, *3*, 264–268.
6. Wawrzynowicz, T.; Kuczmierczyk, J. A comparison of adsorption of organic compounds of different molecular structure on silica and alumina from nonaqueous solvents. Chem. Anal. (Warsaw) **1985**, *30*, 63–75.
7. Snyder, L.R. Adsorption from solution. III. Derivatives of pyridine, aniline and pyrrole on alumina. J. Phys. Chem. **1963**, *67*, 2344–2353.
8. Klemm, L.H.; Klopfstein, C.E.; Kelly, H.P. Thin layer chromatography of azines and of aromatic nitrogen heterocycles on alumina. J. Chromatogr. **1966**, *23*, 428–435.
9. Waksmundzka-Hajnos, M. Comparison of adsorption properties of Florisil and silica in HPLC. II. Retention behaviour of bi- and tri-functional model solutes. J. Chromatogr. **1992**, *623*, 15–23.
10. Waksmundzka-Hajnos, M.; Hawrył, A. Comparison of retention of phenols, aniline derivatives and quinoline bases in normal-phase TLC with binary isoeluotropic eluents. J. Planar Chromatogr. **1998**, *11*, 283–294.
11. Waksmundzka-Hajnos, M.; Petruczynik, A.; Hawrył, A. Comparison of chromatographic properties of cyanopropyl-, diol- and aminopropyl–polar bonded stationary phases by the retention of model compounds in normal-phase liquid chromatography systems. J. Chromatogr. A, **2001**, *919*, 39–50.
12. Klimes, J.; Kastner, P. Thin layer chromatography of benzodiazepines. J. Planar Chromatogr. **1993**, *6*, 168–180.
13. Houghton, P.J. Chromatography of chromone and flavonoid alkaloids. J. Chromatogr. A, **2002**, *967*, 75–84.
14. Molyneux, R.J.; Garden, D.R.; James, L.F.; Colegate, S.M. Polyhydroxy alkaloids: Chromatographic analysis. J. Chromatogr. A, **2002**, *967*, 57–74.
15. McCalley, D.V. Analysis of the *cinchona* alkaloids by high performance liquid chromatography and other separation techniques. J. Chromatogr. A, **2002**, *967*, 1–19.
16. Petruczynik, A.; Waksmundzka-Hajnos, M; Hajnos, M.L. The effect of chromatographic conditions on the separation of selected alkaloids on silica layers. J. Planar Chromatogr. **2005**, *18* (101), 78–84.
17. Snyder, R.L. Role of the solvent in liquid solid chromatography—A review. Anal. Chem. **1974**, *46*, 1384–1393.
18. Lewis, J.A.; Lommen, D.C.; Raddatz, W.D.; Dolan, J.W.; Snyder, L.R.; Molnar, I. Computer simulation for the prediction of separation as a function of pH for reversed-phase high-performance liquid chromatography. J. Chromatogr. **1992**, *592*, 183–195.
19. Petruczynik, A.; Waksmundzka-Hajnos, M.; Hajnos, M.L. The effect of chromatographic conditions on the separation of selected alkaloids in RP-HPTLC. J. Chromatogr. Sci. **2005**, *43* (1), 183–194.
20. Scholten, A.B.; Claessens, H.A.; de Haan, J.W.; Cramers, C.A. Chromatographic activity of residual silanols of alkylsilane derivatized silica surface. J. Chromatogr. A, **1997**, *759*, 37–46.
21. Marques, R.M.L.; Schoenmakers, P.J. Modeling retention in reversed phase liquid chromatography as a function of pH and solvent composition. J. Chromatogr. **1992**, *592*, 157.
22. Rorabacher, D.B.; MacKellar, W.J.; Shu, F.R.; Bonavita, S.M. Solvent effects on protonation constants. Ammonia, acetate, polyamine and polyaminocarboxylate ligands in methanol–water mixtures. Anal. Chem. **1971**, *43*, 561–573.
23. Roses, M.; Bosch, E. Influence of mobile phases and acid–base equilibria on the chromatographic behaviour of protolytic compounds. J. Chromatogr. A, **2002**, *982*, 1–30.
24. Petruczynik, A.; Waksmundzka-Hajnos, M. Effect of chromatographic conditions on the separation of selected alkaloids on phenyl stationary phase by an HPLC method. J. Liquid Chromatogr. Relat. Technol. **2006**, *29* (19), 2807–2822.
25. Drummer, O.H. Methods for measurements of benzodiazepines in biological samples. J. Chromatogr. B, **1998**, *713*, 201–225.
26. Bidlingmeyer, B.A. J. Chromatogr. Sci. **1980**, *18*, 525.
27. Low, K.G.C.; Bartha, A.; Billiet, H.A.H.; de Galan, L. Systematic procedure for the determination of the nature of the solute prior to the selection of the mobile phase parameters for optimization of reversed-phase ion-pair chromatographic separations. J. Chromatogr. **1989**, *478*, 21–38.
28. Petruczynik, A.; Waksmundzka-Hajnos, M; Hajnos, M.L. The effect of chromatographic conditions on the separation of selected alkaloids in RP-HPTLC. J. Chromatogr. Sci. **2005**, *43* (1), 183–194.
29. Bieganowska, M.L.; Petruczynik, A. Thin-layer reversed phase chromatography of some alkaloids in ion-association systems. Part II. Chem. Anal. (Warsaw) **1994**, *39*, 445–454.
30. Petruczynik, A.; Gadzikowska, M.; Waksmundzka-Hajnos, M. Optimization of the separation of some Chelidonium maius L. alkaloids by reversed phase high-performance liquid chromatography using cyanopropyl bonded stationary phase. Acta Pol. Pharm. Drug Res. **2002**, *59*, 61–64.

Highly Selective RP/HPLC: Polymer Grafting to Silica Surface

Hirotaka Ihara
Atsuomi Shundo
Makoto Takafuji
Department of Applied Chemistry and Biochemistry, Kumamoto University, Kumamoto, Japan

Shoji Nagaoka
Kumamoto Industrial Research Institute, Kumamoto, Japan

INTRODUCTION

Reversed-phase high-performance liquid chromatography (RP-HPLC) with, simply, octadecylated silica (ODS) and similar hydrophobized silicas, is the most popular method for analytical separation because of its wide applicability, with only slight modification of a mobile phase system. The separation mode is quite simple. It is usually understandable by the hydrophobic effect and partition coefficients of solutes, while highly-dense packing of organic phase on silica often brings selectivity increase based on a molecular slot effect.[1,2] However, if further specific selectivity is desired, even in RP-HPLC, its simple solution may be to immobilize a functional organic phase onto the silica surface, i.e., to develop new organic stationary phases. A typical example is seen in macrocyclic compound-immobilized silicas, such as those modified with porphyrin, cyclodextrin, and calixarene. In the case of porphyrin, its selectivity in HPLC is truly based on original functions derived from porphyrin.[3,4] Another solution can be expected by immobilization of a polymeric organic phase on silica. In this case, unexpected selectivity increase can be realized by a multiple-interaction mechanism, even if a polymer does not possess any macrocyclic structure. A typical example can be seen in poly(4-vinylpyridine)-grafted silicas.[5,6] The molecular-planarity selectivity towards polycyclic aromatic hydrocarbons (PAHs) compares to that in a porphyrin-immobilized silica in a reversed phase mode. In this entry, we introduce polymer-grafting onto silica as an organic stationary phase for highly selective HPLC.

ADVANTAGE OF POLYMER GRAFTING

Polymer-grafting onto silica can be usually carried out by activation of silica surface and subsequent radical polymerization with a vinyl monomer. However, we recommend preparing a polymer with a reactive terminal group at one side, and then immobilizing it onto the silica surface, as schematically illustrated in Fig. 1. This method gives us many advantages.

1. A polymer with a terminal reactive group can be obtained by one-step telomerization. By choosing monomer, a function of the resultant polymer can be tunable.
2. Usual spectroscopy is applicable for determination of the chemical structure before immobilization onto silica. The stereoregularity is also estimated by NMR spectroscopy.
3. Telomerization usually leads narrow polydispersity of degree of polymerization. This promises homogeneity as an organic phase.
4. Polymerization degree can be controlled by the initial molar ratio of a vinyl monomer to a telogen. This is an essentially important feature because large polymers cannot penetrate into the pores of silica and, thus, this causes heterogeneity in surface modification.

The first successful result was seen in the grafting of poly(octadecyl acrylate) onto silica and its application for separation of PAHs in a reversed phase mode.[7] The polymer is obtained by telomerization of octadecyl acrylate, initiated with 3-mercaptopropyltrimethoxysilane (Fig. 1). The following immobilization is carried out by mixing with porous silica in a suitable solvent. The resultant polymer-grafted silica shows, not only extremely high separation of PAHs, but also specific temperature dependency on the selectivity, which is induced by an ordered-to-disordered transition of the grafted polymer.[7] The detail is described later.

GRAFTING OF DISORDERED POLYMERS

A simple application of our grafting method is seen for polymerization of styrene,[8] methyl acrylate,[9]

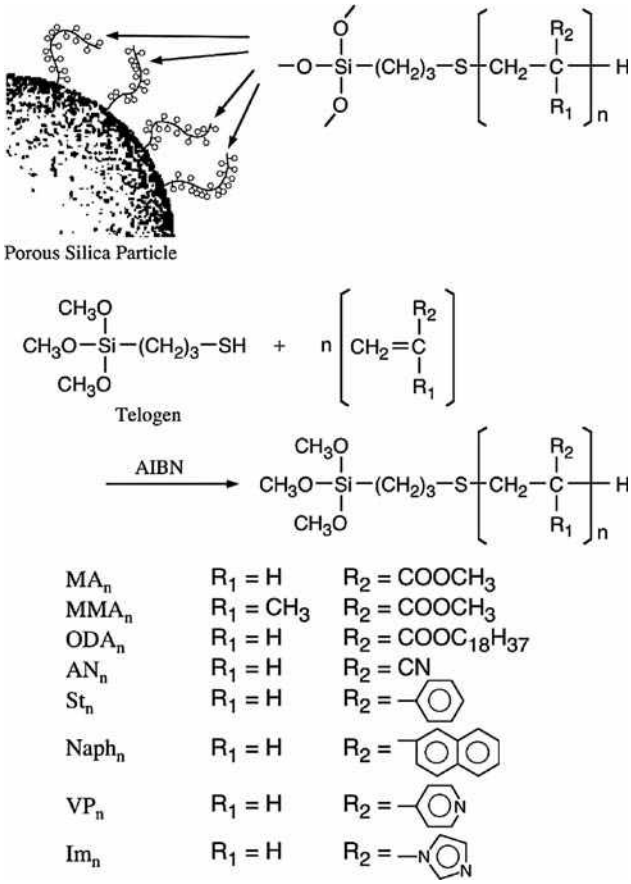

Fig. 1 Chemical structures of polymeric organic phases prepared by one-step telomerization. These polymers can be readily immobilized onto silica through the terminal methoxysilyl group.

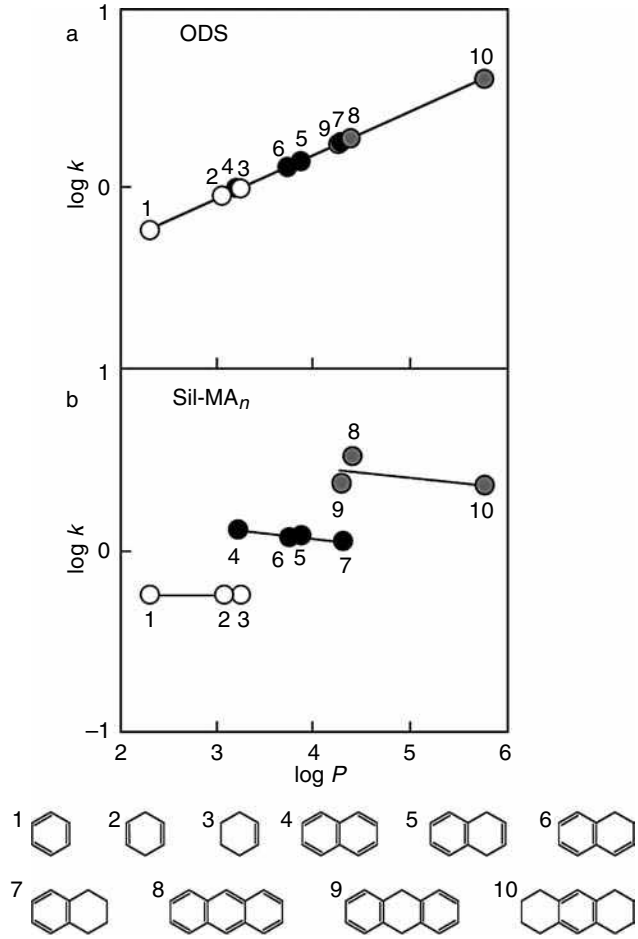

Fig. 2 Relationship between log k and log P with octadecylated silica (ODS) (a) and Sil-MA$_n$ (b). Mobile phases: (a) methanol–water (9:1); (b) methanol–water (7:3).

acrylonitrile,[5] etc. (Fig. 1). Radical polymerization of these monomers provides their random polymers. However, the polymer-grafted silicas showed unique features as RP-HPLC packing materials. For example, when the polystyrene-grafted silica (Sil-PSt$_n$, where n is the average degree of polymerization) is applied for separation of PAHs, both the retention and separation factors are higher than commercially available phenyl-bonded silicas. In addition, the elution peaks are comparably symmetrical, although conventional porous poly(styrene-divinylbenzene) packing materials showed remarkable peak-tailing. These desirable properties are attributable to the fact that Sil-PSt$_n$ does not include a cross-linking structure in the bonded phase, but rather fluid to be a liquid.

Poly(methyl acrylate)-grafted silica (Sil-MA$_n$) showed unexpectedly unique selectivity in a reversed phase mode.[9] The unusual nature of Sil-MA$_n$ is emphasized by Fig. 2. Octadecylated silica shows a good linearity in the log k–log P plots (Fig. 2a), indicating that the elution order is understandable by molecular hydrophobicity of solutes. On the other hand, Sil-MA$_n$ provides no similar result. As shown in Fig. 2b, it seems to show that Sil-MA$_n$, instead, recognizes the molecular size (i.e., the number of the rings). This unusual result should be explained by including π–π interaction derived from a carbonyl group of an acrylate moiety. This interaction is estimated by the ab initio MO/MP2 calculations[10,11] (Fig. 3) to be stronger than a benzene π–benzene π interaction,[12] and is also experimentally supported by a substitution effect.[13] Thus, it can be specified as a carbonyl-π interaction.

Similar specificities in HPLC have been realized with poly(4-vinylpyridine)[5,6] and poly(acrylonitrile).[5] The similarity of these polymers can be characterized by the fact that their residual groups include locally polarized moieties with π-electrons. Here, their uniqueness is summarized through the results of poly(4-vinylpyridine)-grafted silica (Sil-VP$_n$): Sil-VP$_n$ is less sensitive for molecular hydrophobicity of solutes, as shown in a typical chromatogram of Fig. 4A. This is proof of a great difference from ordinary ODS. On the contrary, higher retention and selectivity (Fig. 4C) are observed for PAHs or π-electron-containing substances, especially sensitive for difference of the molecular planarities of solutes

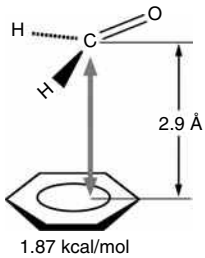

Fig. 3 Formaldehyde–benzene complex model by ab initio MO/MP2 calculations performed with the Gaussian 94 package.[11] The binding energy was calculated as a function of distance *R* between the carbon atom of formaldehyde and benzene plane, in which formaldehyde was removed perpendicularly to the benzene plane (plane-to-plane interaction) with the orientation fixed to that of the optimized geometry. A formaldehyde–benzene interaction (1.83 kcal/mol) is more effective than benzene–benzene[12] (0.49 kcal/mol in the parallel interaction) complex.

(Fig. 4E). In addition, Sil-VP$_n$ shows specificity for ortho-isomers[6] better than for para-isomers, as shown in Fig. 5A. This selectivity is often seen in adsorption chromatography, but it should be noted that a mobile phase is aqueous or composed of polar solvents. These uniquenesses will compensate us for limited applicability in ordinary ODS and other π-electron-containing stationary phases in a reversed phase mode. The simple application is cited in Fig. 5B and C, while ODS shows almost no separation for these substances.

When *N*-isopropylacrylamide (NIPAM) is chosen as a vinyl monomer and the resultant polymer is grafted onto silica, its HPLC behavior is temperature-dependent because poly(NIPAM) has a typically lower critical solution temperature (LCST) around 32°C in an aqueous solution (Fig. 6).[15,16] Above its LCST, the organic phase behaves as a hydrophobic surface, which is due to dehydration of the grafted polymer chain. Recently, the separations of amino acid phenylthiohydantoins[17] and bisphenol A[18] are achieved by using this temperature-responsive chromatography with an aqueous solution as the mobile phase.

GRAFTING OF ORDERED POLYMERS

Selectivity Increase Due to Ordering in Polymeric Organic Phase

It is difficult to control the stereoregularity of polymers in radical telomerization. However, the side chain ordering in the polymer can be realized if a long-chain alkyl compound is chosen as a vinyl monomer for telomerization. A preliminary example is reported with poly(octadecyl acrylate), ODA$_n$.[7] The resultant polymer can be easily grafted onto porous silica through a terminal trimethoxysilyl group. Toluene and tetrachloromethane are good solvents for this procedure.

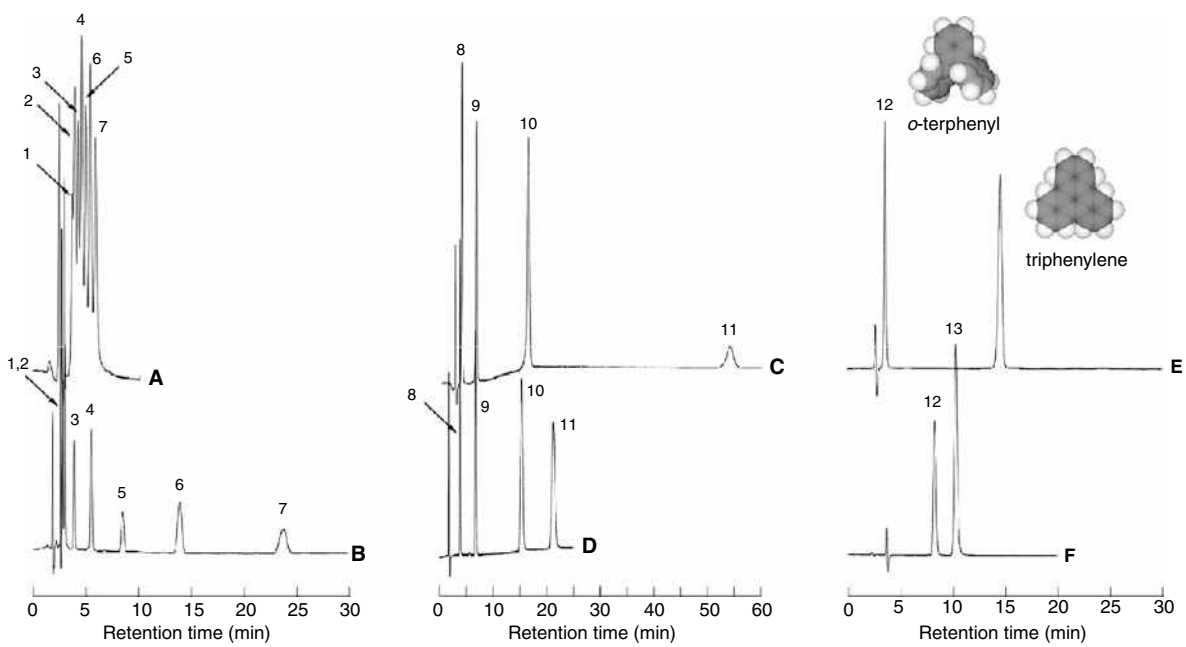

Fig. 4 Typical chromatograms with Sil-VP$_n$ (A, C and E) and ODS (B, D and F) at 30°C.[5] Mobile phase: (A), (B), (E) and (F), methanol–water (7:3); (C) and (D), methanol–water (7:3). Solutes: 1, toluene; 2, ethylbenzene; 4, hexylbenzene: 5, octylbenzene; 6, decylbenzene; 7, dodecylbenzene; 8, benzene; 9, naphthalene; 10, anthracene; 11, pyrene; 12, *O*-terphenyl; 13, triphenylene.

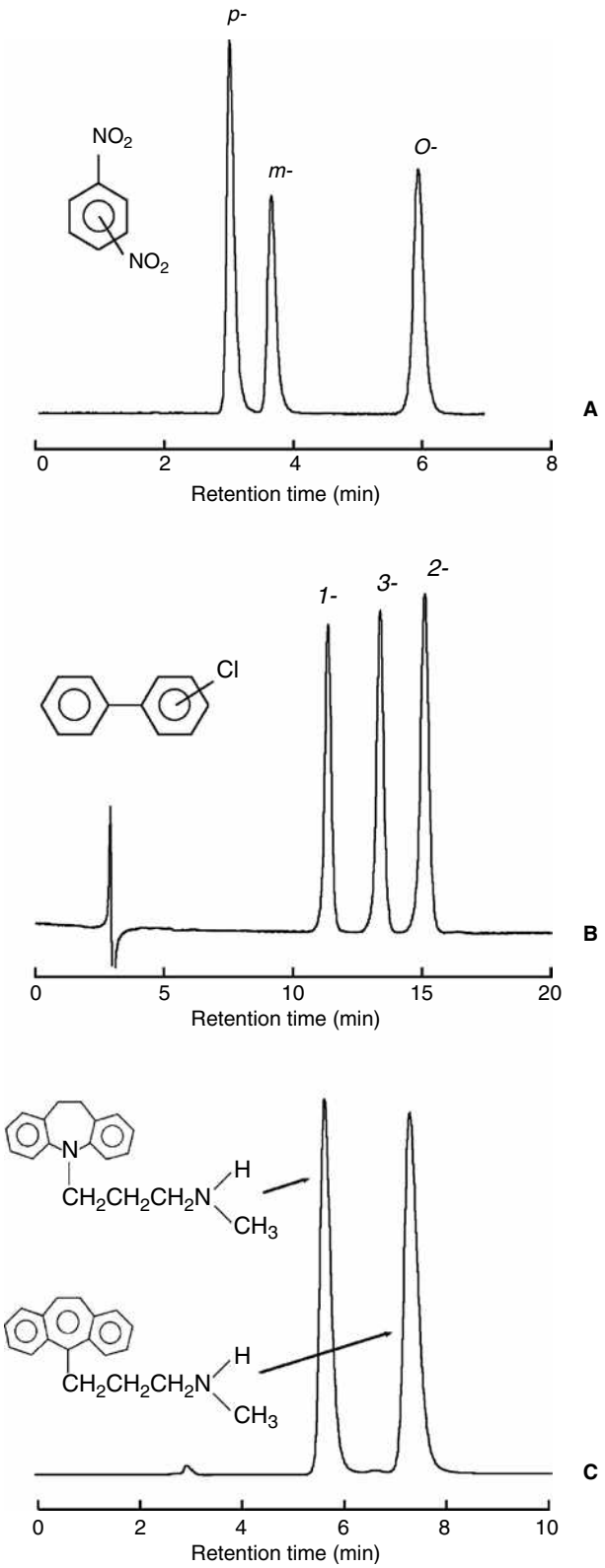

Fig. 5 Examples of chromatographic separation with Sil-VP$_n$ at 30°C. Mobile phase: (A) and (B), methanol–water (6:4); (C), methanol–0.01 *M* KH_2PO_4 (7:3). Sample: (A), *O*-, *m*-, and *p*-dinitrobenzenes; (B), 1-, 2-, and 3-chlorobiphenyls; (C), desipramine and protriptyline.

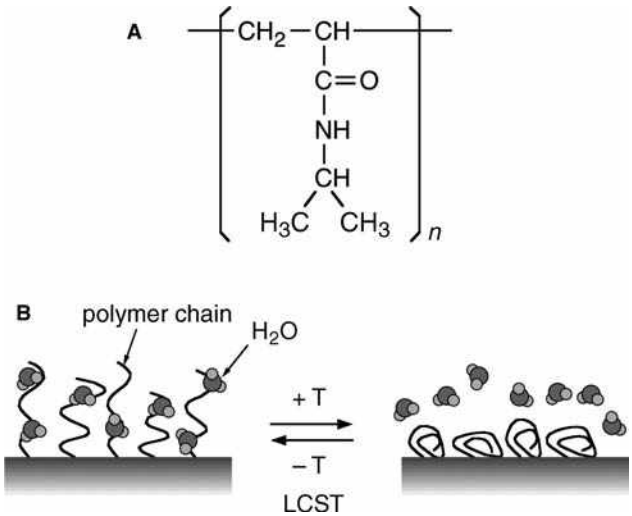

Fig. 6 A, Chemical structure of poly(*N*-isopropylacrylamide) and B, schematic illustration of temperature-responsive surface.

Poly(octadecyl acrylate) is characterized by differential scanning calorimetry (DSC)[19] and NMR spectroscopy.[20] The DSC thermogram shows a sharp endothermic peak (T_c) in both the heating and cooling processes. For example, the temperature of ODA_{27} (n=27) provides a peak around 49°C (T_{C_2}) with a shoulder (T_{C_1}) at 42–47°C in the heating process. Polarity microscopic observation indicated that T_{C_1} and T_{C_2} are assigned to crystalline-to-liquid crystalline and liquid crystalline-to-isotropic phase transitions, respectively. Similar phase transitions are also observed even after immobilization on silica. In a methanol–water (7:3) mixture as a mobile phase, a peak-top temperature (T_{C_2}) falls about 8°C, compared with the original T_{C_2}. This indicates that silica influences the orientation of bound ODA_{27}, but the bonded phase can maintain ordered structures and undergo crystalline-to-isotropic phase transition on silica, as illustrated in Fig. 7B.

The phase transition of ODA_n on silica can be also detected by a combination of suspension-state ^{1}H NMR and solid-state ^{13}C-CP/MAS-NMR spectroscopies.[20] For example, with a gradual increase in temperature, the intensity of proton signals (^{1}H NMR) of octadecyl moieties (mainly methylene groups) rises with a sharp inclination coincident with an endothermic peak in DSC thermogram, implying a relatively complete solid to liquid phase transition. In addition, the ratio of *trans*- to *gauche*-conformations can also be determined. This phase characterization method, in conjunction with conformation determination drawn from NMR spectroscopy, is important for a better understanding of the structure, dynamics, and separation behavior of organic layers grafted onto the silica surface. Interestingly, this method clarified that most of the octadecyl chains in the case of monomeric ODS, despite having

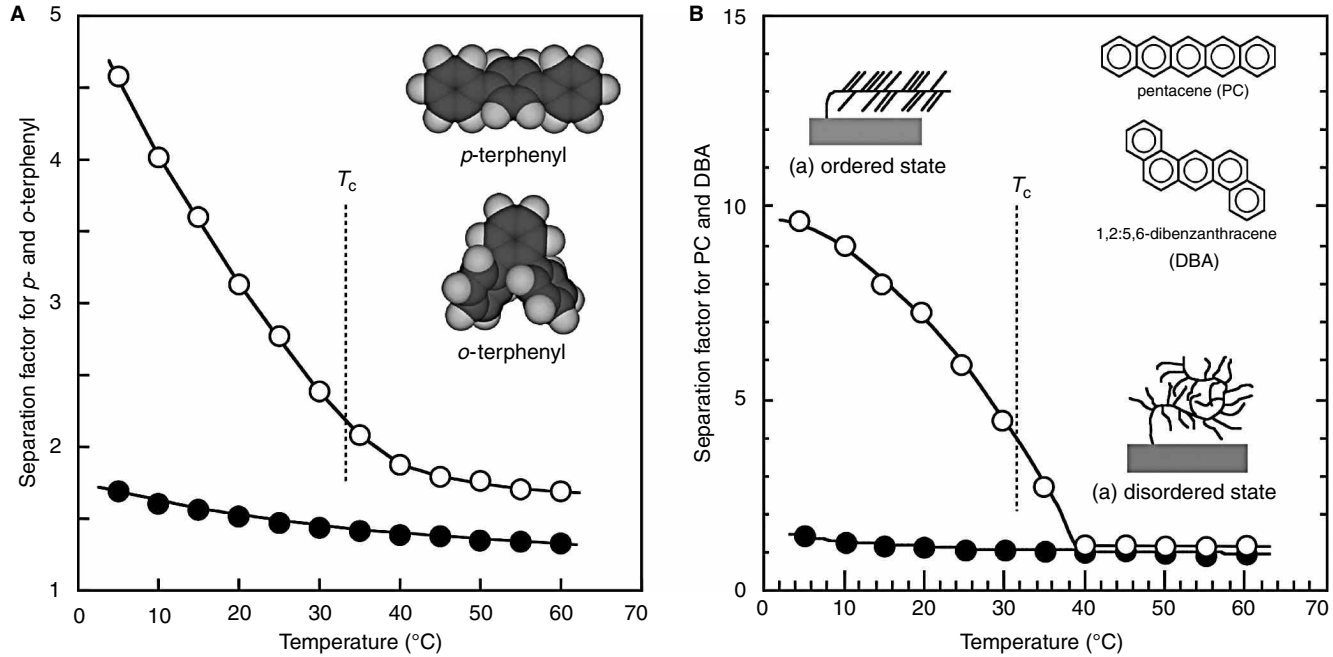

Fig. 7 Temperature dependencies on the separation factor with Sil-ODA$_n$ (open circles) and ODS (solid circles). Mobile phase: methanol (A); ethanol (B).

a gauche conformation, were still in a solid phase and only 12.3–18.5% of them have enough mobility to be considered as being in a liquid phase.[20]

Sil-ODA$_n$ shows ODS-related retention orders for usual hydrophobic solutes in a reversed phase mode, but the unique performance of Sil-ODA$_n$ is emphasized by temperature dependency. Sil-ODA$_n$ shows distinct bending in the plots of temperature vs. k in HPLC. T_c of Sil-ODA$_n$ observed completely agrees with the temperature of the bending point. This is accompanied by the remarkable selectivity change. A typical example is shown in Fig. 7. Both increases of the retention and separation factors always appear at temperature below T_c, where the physical state is in an ordered form. On the other hand, higher selectivity is clearly observed for PAHs vs. non-aromatic hydrocarbons. To clarify the separation mechanism of Sil-ODA$_n$, we have investigated the selectivity with geometrical isomers from various substituted azobenzene compounds.[13] As a result, it was found that the separation factor between the *trans*- and *cis*-isomers was remarkably dependent on the electron-donating property of the substituent group. This strongly suggests that bonded ODA$_n$ works as an electron-acceptor and a π–π interaction is brought by a carbonyl π moiety in ODA$_n$. As supporting this assumption, a carbonyl group-containing polymeric organic phase, Sil-MA$_n$ with neither a long-chain alkyl group nor any ordered structure shows no bending behavior in the temperature-selectivity plots, but also the separation factor is higher when compared with ODS.[13] In addition, the separation factor decreases with addition of acetone to a mobile phase, which can work as an inhibitor for a carbonyl π–benzene π interaction. No similar decrease is observed by 2-propanol. Theoretical study of a carbonyl π–benzene π interaction with a model system has also been done with ab inito calculation (Fig. 3).[10–12] Therefore, it is concluded that solute molecules are not incorporated into a crystalline (ordered) phase, but rather adsorbed onto the aligned carbonyl groups. On the other hand, the isotropic (disordered) bonded does not have such specificity. The solutes can partition into the bonded phase and, thus, the separation mode is similar to that of ODS.

Effect of Stereoregularity of Polymeric Organic Phase on Selectivity Increase

As briefly mentioned above, a stereoregularity of polymers is hardly controlled in a radical telomerization, although it would be an important factor to increase the selectivity. However, it is certain that stereoregularity can be influenced by solvent and temperature in a telomerization process. In support of this, when the telomerization is prepared in methanol, benzene, or cyclohexane, and then the resultant polymers, abbreviated as ODA$_n$-M, ODA$_n$-B and ODA$_n$-C respectively, are applied as organic stationary phases, significant selectivity difference is detected among them.[21] A typical example can be shown by the separation of a mixture of *m*- and *p*-terphenyls. These structural isomers are useful for evaluating the molecular shape selectivity because the molecular shape differs in planarity and length, but the hydrophobicity is similar. Therefore, a conventional RP-HPLC shows very low selectivity, e.g., α=1.1 and 1.3 in monomeric and polymeric ODSs, respectively, while complete separations (α=3.0–3.3) are observed in all Sil-ODA$_n$ at 0°C. Here, if the separation factor is compared with the results at 35°C, the solvent effect in the telomerization makes it clear. This difference can be explained by the fact that the phase transition temperature of ODA$_n$-M is a little higher (40°C in a peak-top temperature) than the others (35°C). This difference reflects the molecular orientation among the long-chain alkyl groups. The orientation of the side chain alkyl groups of ODA$_n$ can be also evaluated by the suspension-state ^{1}H NMR in methanol with the nanoprobe.[20] The octadecyl methylene peak is very small and broadened at 0°C, but the normalized intensity begins to increase distinctly around 30°C. This temperature is close to the phase transition temperature. This unusual increase of the intensity in ODA$_n$ can be explained by the fact that the mobility of octadecyl groups increases with the ordered-to-disordered transition, as shown in the DSC data. On the other hand, when ^{13}C NMR spectroscopy of ODA$_n$ is carried out in chloroform-d at room temperature, all ODA$_n$ provides nine distinct peaks in the range of 10–70 ppm. All peaks are assigned reasonably by considering electronegative forces of their neighboring moieties. On the basis of the assignment, it is estimated that ODA$_n$-C and ODA$_n$-B show relatively high polydispersity in the tacticity compared to ODA$_n$-M. This estimate agrees with the fact that the phase transition temperature of ODA$_n$-M is a little higher than the others. This study cannot confirm exact conformation of the carbonyl groups in ODA$_n$ but shows that the microenvironmental difference in polymer influences the resultant selectivity. Thisfinding is very valuable because it indicates that conformational control of the polymer main chain would lead to high selectivity in HPLC.

To discuss the effect of structural ordering of the polymer on selectivity, we have been focusing on secondary structures of poly(α-amino acid)s, i.e., polypeptides.[22,23] They provide rigid and exact conformations, such as α-helix and β-structure, spontaneously if polymerization is done with a purely chiral amino acid. The poly(L-alanine), poly(L-leucine), and poly(L-phenylalanine) with a terminal reactive trimethoxysilyl group can be prepared by the corresponding *N*-carboxyanhydrides and 3-aminopropyltrimethoxysilane as an initiator for polymerization. However, in this case, a

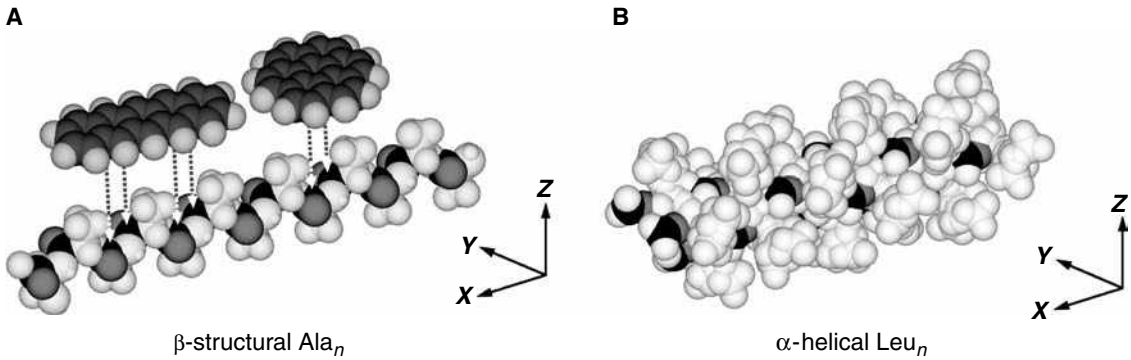

Fig. 8 CPK models of (A) β-structural Ala$_n$ and (B) α-helical Leu$_n$ derived from PEPCON. The black atoms present carbonyl carbons. A linear and planar solute such as pentacene provides more effective interaction area with the carbonyl groups one-dimensionally-aligned on the rigid main chain than a disk-like solute such as coronene (A). On the other hand, the carbonyl groups of Leu$_n$ are covered with their bulky residual groups (B).
Source: From Molecular-length and chiral discriminations by β-structural poly(L-alanine) on silica, in J. Chromatogr, A.[22]

serious problem is often accompanies the procedure. This is due to lower solubility of the resultant polypeptides and, particularly, becomes formidable with an increase of the polymerization degree. Therefore, grafting of polypeptides is usually carried out by immobilization of 3-aminopropyltrimethoxysilane onto porous silica and subsequent polymerization with *N*-carboxyanhydride initiated with the activated silica. The secondary structures of polypeptides on silica can usually be estimated by the absorption bands ascribed to an amide I and II in IR spectroscopy, because the strong absorption due to silica overlaps with that of an amide V. IR spectroscopy indicated that the main secondary structures of poly(L-alanine) and poly(L-leucine) on silica were the β-structure and the α-helix, respectively.[22]

When poly(L-alanine)-grafted silica is applied for separation of PAHs in a reversed phase mode, we can encounter various specific selectivities. For example, α=10.4 was obtained for a mixture of *p*- and *o*-terphenyls, while α=1.5 in ODS. Both *p*- and *o*-terphenyls possess the same numbers in carbon atoms and π-electrons, but the molecular planarity is entirely different. As indicated in the Corey-Pauling-Koltun (CPK) models of Fig. 7A, *p*-terphenyl is a little twisted (almost planar), but more slender (linear) than *o*-terphenyl. No similar enhancement of the selectivity is observed in poly(L-leucine)- and poly(L-phenylalanine)-grafted silica. These polypeptides show, rather, similarity to ODS: e.g., α=1.7 in poly(L-leucine)-grafted silica.

To explain the high selectivity of the poly(L-alanine) phase, we apply a multiple carbonyl π-to-benzene π interaction mechanism on highly-ordered structures. As shown in the schematic illustrations of Fig. 8, the carbonyl groups in the poly(L-alanine) main chain as a π-electron source are well-oriented because the peptide main chain is in a rigid β-form structure on silica. On the basis of these facts, we explain the multiple π–π interaction mechanism:

1. Polycyclic aromatic hydrocarbons can interact with the carbonyl groups. The methyl group of the poly(L-alanine) side chain does not prevent electrostatic interaction (Fig. 8A).
2. On the contrary, poly(l-leucine) does not offer a chance to provide this interaction because the residual isobutyl groups are too bulky to approach each other (Fig. 8B). Also, it should be noted that poly(L-leucine) provides only α-helices, even on silica and, thus, their carbonyl groups are absolutely covered with the bulky residual groups. As a result, the poly(L-leucine) phase showed only hydrophobicity recognition similar to ODS. The selectivity is close to that in ODS (α=1.5).
3. The carbonyl groups in poly(L-alanine) should be aligned unidimensionally along the β-structure form. This conformation promotes the multiple carbonyl-π interaction, which works more effectively with longer (slender and linear) PAHs than with shorter ones. Fig. 8A show that a longer and planar PAH, such as pentacene, yields higher contact points with poly(L-alanine) than a disk-like PAH such as coronene.

Multi-Anchoring Effect on Selectivity Increase

Porphyrin-derivatized bonded phases show unique shape selectivity, retaining planar PAHs.[3,4] Similar molecular-planarity selectivity is also observed in cholesteryl-10-undecenoate and 4,4′-dipentyldiphenyl bonded phases. These phases contain rigid structures and, thus, the limited mobility in their organic phases contributes to the molecular-shape selectivity. A similar effect on selectivity increase can be seen in the comparison of the retention behaviors between polymeric and

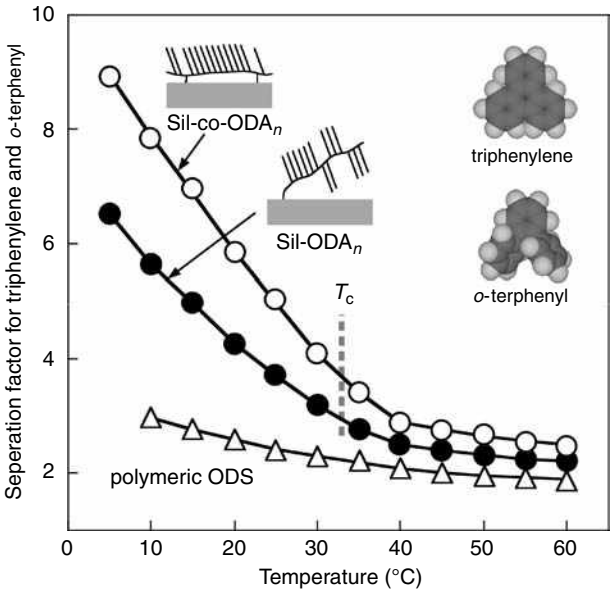

Fig. 9 Temperature dependencies of the separation factors between triphenylene and *o*-terphenyl with multi-anchored ODA$_n$ (open circles), Sil-ODA$_n$ (solid circles) and polymeric ODS (open triangles). Mobile phase: methanol–water=9:1.

monomeric ODSs.[2] Therefore, to increase the selectivity, decreasing molecular mobility of ODA$_n$ having plural reactive groups in the side chain has been synthesized and immobilized onto silica. This polymeric phase can be obtained by co-telomerization with γ-methacryloxypropyltrimethoxysilane. As expected, this polymer phase-immobilized silica showed better selectivity for PAHs: e.g., 1.4 times higher selectivity for the separation of triphenylene and *o*-terphenyl than Sil-ODA$_n$ (Fig. 9). This is a typical example that the immobilization method of polymer on support materials influences the resultant molecular-shape selectivity and, thus, this finding encourages us to investigate the multi-anchoring effect for various polymeric phases.

Application for Chiral Discrimination

It is well known that, for biologically active substances, one enantiomer shows different biological activity from the other. For example, the studies by Mori et al. on the relationship between optical purity and biological activity of insect pheromones have revealed that the biological activities were dramatically changed by their optical purities. Therefore, it is important to determine the absolute configuration and accurate optical purity of biologically active compounds.

For this purpose, a diastereomer method has been widely used for determination of the absolute configuration and optical purity and, thus, many diastereomerizing reagents have been developed for racemic amines, alcohols, and amino acids.[10,14] When this method is combined with RP-HPLC, it yields very convenient and quick analyses of enantiomer mixtures. Diastereomerizing reagents can be generally characterized by the fact that chromophoric groups are included for sensitive detection and chiral separation is realized by discriminating the hydrophobicity (or polarity) difference between the resulting diastereomers. Therefore, π–π interaction-supported RP-HPLC with ODA$_n$ would show much better discrimination for the resultant diastereomers, compared with ordinary ODS.

Fig. 10A shows a typical example for *N*-acyl amino acid diastereomerized with *N*-dansyl amino acid.[24] Diethyl phosphorocyanidate (DEPC) is adopted as a condensation reagent instead of conventional dicyclohexylcarbodiimide (DCC), to avoid racemization during the reaction. Fig. 10A shows the time course of chromatograms for the methyl ester of DL-phenylalanine diastereomerized by *N*-dansyl-L-proline with Sil-ODA$_n$. The chromatogram, a minute after addition of DEPC to the mixture of dl-phenylalanine and *N*-dansyl-L-proline, provided two new peaks with λ_{max} of 350 nm at 6.8 min and 8.5 min which are attributable to the absorption based on a dansyl group. It is also assigned that the first peak, at 6.8 min, has the same retention time as that obtained by the diastereomer of L-phenylalanine methyl ester with *N*-dansyl-L-proline. The selectivity in Sil-ODA$_n$ is temperature-dependent and much higher at temperature below T_c (α=1.45, −10°C) than that in ODS (α=1.16, −10°C).

Another good example is shown in Fig. 10B.[25] Ohrui et al., have developed the chiral labeling reagents, 2-(2,3-anthracenedicarboximide)cyclohexane carboxylic acid and 2-(2,3-anthracenedicarboximide)cyclohexanol to discriminate the diastereomers having chiral centers separated by more than four bonds. The use of these reagents made it possible to separate the branched fatty acids or alcohols having a branched methyl group by reversed phase HPLC with ODS. However, it was necessary to apply low column-temperature conditions (around −40°C) for their separation because the mobility of octadecyl groups in ODS should be remarkably reduced. To solve this problem, Sil-ODA$_n$ has been applied instead of conventional ODS because the ODA$_n$ phase is rigid and ordered in the side chain at temperatures below T_c.

Fig. 10B shows chromatograms for the diastereomers, *S,S,R*-**1** and *R,R,R*-**1** by HPLC with Sil-ODA$_n$ and ODS at 0°C.[25] No separation is observed in ODS, where it was necessary to apply lower column-temperature conditions for a substantial separation. Even each injection showed almost no separation at 0°C ($k_{R,R,R}$ and $k_{S,S,R}$=15.2 with ODS). On the contrary, complete separation is observed in Sil-ODA$_n$ ($k_{R,R,R}$=21.0, $k_{S,S,R}$=17.3, α=1.21). There is a

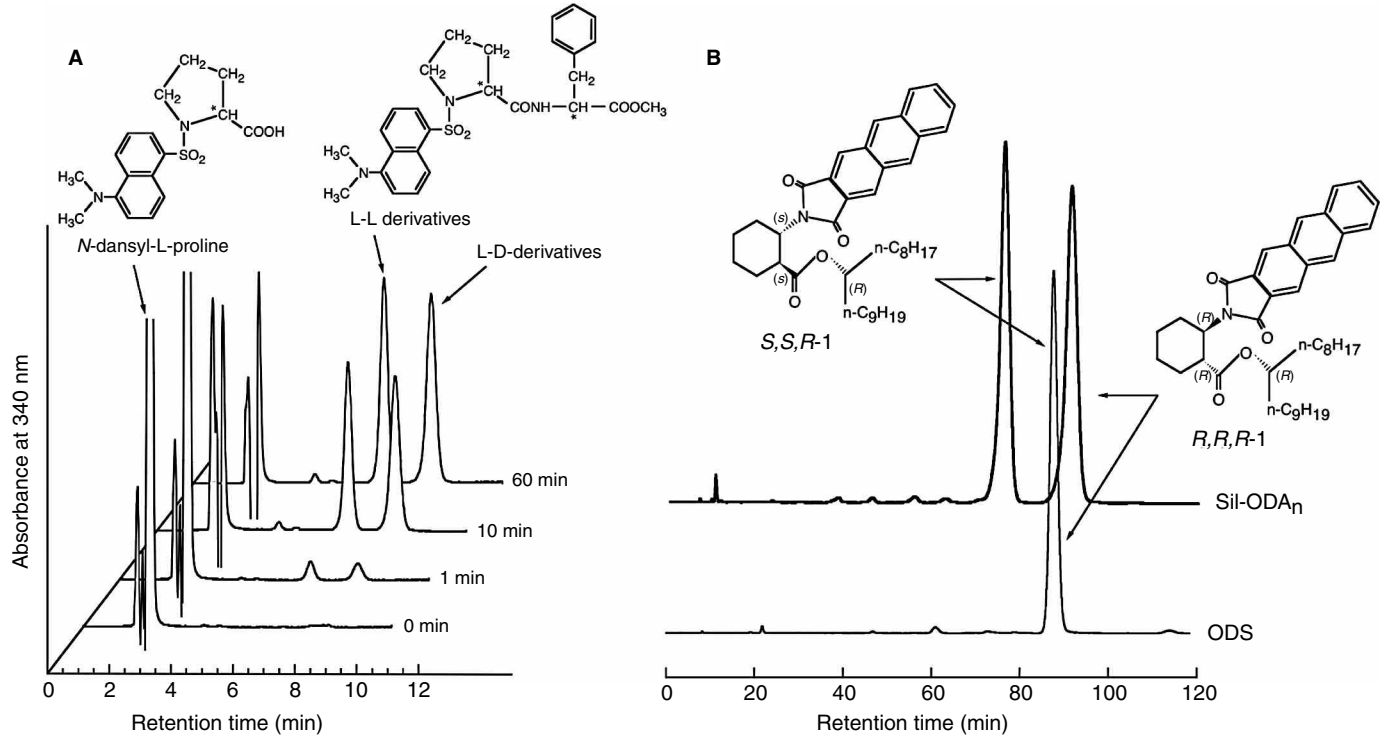

Fig. 10 (A) Time course of diastereomerization of dl-phenylalanine with *N*-dansyl-L-proline using DEPC[24] and (B) chromatograms of the mixture of *S*,*S*,*R*-**1** and *R*,*R*,*R*-**1** with Sil-ODA$_n$ and ODS.[25] Mobile phases: (A), methanol–water (7:3) at 25°C; (B), methanol at 0°C.

series of the Ohrui's reagents; then similar good results are always obtained with Sil-ODA$_n$, compared with ODS. This is due to the fact that the separation is supported with π–π interaction as well as a hydorophobic effect.

CONCLUSIONS

Lipid bilayer membrane systems, having gel (solvated crystalline state)-to-liquid crystalline phase transitions are attractive as specific organic media for separation chemistry. The first approach in HPLC was direct immobilization of a phosphatidylcholine lipid onto silica. This modified silica shows interesting selectivity against amino acids, but the separation mode is too complicated, due to the zwitterionic property of the immobilized molecule. In addition, no lipid membrane function is realized on the silica because of the direct immobilization with covalent bonding, which prohibits lateral diffusion of lipids from forming highly-ordered structures that lead to supramolecular functions of lipid membrane systems.

Sil-ODA$_n$ has been developed to address this question.[7] The ODA$_n$ phase does not make lipid membrane structures in an aqueous system, but it possesses similar functions, such as side-chain ordering and phase transition behavior between ordered and disordered states. However, the resultant selectivity in HPLC often excelled, better than expected. This is due to a sort of a side effect and, then, it may be called a polymeric effect, which promotes multiple interactions to increase the selectivity. Molecular ordering of functional groups particularly enhances it.

This entry has revealed that a grafting method is useful to direct a polymeric effect in HPLC. The advantage of this method is quite clear. Firstly, grafted polymers are not appreciably influenced by carrier particles. This feature is very important to maintain the original functions of polymers. For example, ODA$_n$ can undergo a phase transition, even after immobilization on silica. The other advantage is based on the fact that the functions of polymers are absolutely tunable by judicious selection of the monomer. Copolymerization would expand their versatility remarkably. Also, potential applicability of a polymer grafting method for surface modification must be limited to use in HPLC.

REFERENCES

1. Sander, L.C.; Wise, S.A. Synthesis and characterization of polymeric C18 stationary phases for liquid chromatography. Anal. Chem. **1984**, *56*, 5044.
2. Wise, S.A.; Sander, L.C. Factor affecting the reversed-phase liquid chromatographic separation of polycyclic aromatic hydrocarbon isomers. J. High Resol. Chromatogr. Chromatogr. Commun. **1985**, *8*, 248.
3. Chen, S.; Meyerhoff, M.E. Shape-selective retention of polycyclic aromatic hydrocarbons on metalloprotoporphyrin-silica phases: Effect of metal ion center and porphyrin coverage. Anal. Chem. **1998**, *70*, 2523.
4. Xiao, J.; Kibbey, C.E.; Coutant, D.E.; Martin, G.B.; Meyerhoff, M.E. Immobilized porphyrins as versatile stationary phases in liquid chromatography. J. Liq. Chromatogr. **1996**, *19*, 2901.
5. Ihara, H.; Dong, W.; Mimaki, T.; Poly(4-vinylpyridine) as novel organic phase for RP-HPLC. Unique selectivity for polycyclic aromatic hydrocarbons. J. Liq. Chromatogr. **2003**, *26*, 2473.
6. Ihara, H.; Fukui, M.; Mimaki, T.; Poly(4-vinylpyridine) as a reagent with silanol-masking effect for silica and its specific selectivity for PAHs and dinitropyrenes in a reversed phase. Anal. Chim. Acta **2005**, *548*, 51.
7. Hirayama, C.; Ihara, H.; Mukai, T. Lipid membrane analogs. Specific retention behavior in comb-shaped telomer-immobilized porous silica gels. Macromolecules **1992**, *25*, 6375.
8. Ihara, H.; Nakamura, N.; Nagaoka, S.; Hirayama, C. Linear polystyrene-grafted silica gels for high-performance liquid chromatography. Anal. Sci. **1995**, *11*, 739.
9. Ihara, H.; Tanaka, H.; Shibata, M.; Sakaki, S.; Hirayama, C. Detection of potential molecular recognition ability in linear poly(methyl acylate). Chem. Lett. **1997**, 113.
10. Ihara, H.; Sagawa, T.; Nakashima, K.; Mitsuishi, K.; Goto, Y.; Chowdhury, J. Enhancement of diastereomer selectivity using highly-oriented polymer stationary phase. Chem. Lett. **2000**, 128.
11. Ihara, H.; Takafuji, M.; Sakurai, T.; Sagawa, T.; Nagaoka, S. Self-assembled organic phase for RP HPLC. In *Enclyclopedia of Chromatography*, 3rd Ed. Cazes, J., Ed.; Marcel Dekker: New York, 2010; *3*, 2146–2156.
12. Sakaki, S.; Kato, K.; Miyazaki, T.; Structures and binding energies of benzene–methane and benzene–benzene complexes. An ab initio SCF/MP2 study. J. Chem. Soc. Faraday Trans. **1993**, *9*, 659.
13. Ihara, H.; Sagawa, T.; Goto, Y.; Nagaoka, S. Crystalline polymer on silica. Geometrical selectivity for azobenzenes through highly-oriented structure. Polymer **1999**, *40*, 2555.
14. Goto, Y.; Nakashima, K.; Mitsuishi, K.; Takafuji, M.; Sakaki, S.; Ihara, H. Selectivity enhancement for diastereomer separation in RPLC using crystalline-organic phase-bonded silica instead of simply-hydrophobized silica. Chromatographia **2002**, *56*, 19.
15. Kanazawa, H.; Yamamoto, K.; Matsushima, Y.; Temperature-responsive chromatography using poly(*N*-isopropylacrylamide)-modified silica. Anal. Chem. **1996**, *68*, 100.
16. Kanazawa, H. Temperature-responsive polymers for liquid-phase separations. Anal. Bioanal. Chem. **2004**, *378*, 46.
17. Kanazawa, H.; Sunamoto, T.; Matsushima, Y.; Kikuchi, A.; Okano, T. Temperature-responsive chromatographic separation of amino acid phenylthiohydantoins using aqueous media as the mobile phase. Anal. Chem. **2000**, *72*, 5961.
18. Yamamoto, K.; Kanazawa, H.; Matsushima, Y.; Oikawa, K.; Kikuchi, A.; Okano, T. Temperature-responsive

chromatographic separation of bisphenol A with water as a sole mobile phase. Environ. Sci. **2000**, *7*, 47.

19. Ihara, H.; Tanaka, H.; Nagaoka, S.; Sakaki, K.; Hirayama, C. Lipid membrane analogue-immobilized silica gels for separation with molecular recognition. J. Liq. Chromatogr. **1996**, *19*, 2967.
20. Ansarian, H.R.; Derakhshan, M.; Rahman, M.M.; Sakurai, T.; Takafuji, M.; Ihara, H. Evaluation of microstructural features of a new polymeric organic stationary phase grafted on silica surface: A paradigm of characterization of HPLC-stationary phases by a combination of suspension-state ^{1}H NMR and solid-state ^{13}C-CP/MAS-NMR. Anal. Chim. Acta **2005**, *547*, 179.
21. Takafuji, M.; Fukui, M.; Aansarian, H.R.; Derakhshan, M.; Shundo, A.; Ihara, H. Conformational effect of silica-supported poly(octadecyl acrylate) on molecular-shape selectivity of polycyclic aromatic hydrocarbons in RP-HPLC. Anal. Sci. **2004**, *20*, 1681.
22. Shundo, A.; Sakurai, T.; Takafuji, M.; Nagaoka, S.; Ihara, H. Molecular-length and chiral discriminations by β-structural poly(l-alanine) on silica. J. Chromatogr, A, **2005**, *1073*, 169.
23. Ihara, H.; Matsumoto, A.; Shibata, M.; Hirayama, C. Host-guest chemistry using α-helical poly(l-lysine). In *Polymeric Materials Encyclopedia*; Salamone, J.C., Ed.; CRC Press: New York, 1996; 3067–3074.
24. Ihara, H.; Takafuji, M.; Sakurai, T.; Facile enantiomer analysis by combination of *N*-dansyl amino acid as diastereomerizer and molecular-shape recognitive RP-HPLC. Using comb-shaped polymer-immobilized silica. J. Liq. Chromatogr. **2004**, *27*, 2559.
25. Fukui, M.; Shundo, A.; Nakashima, R.; Takafuji, M.; Akasaka, K.; Ohrui, H.; Ihara, H. Chromatographic separation of diastereomers using the comb-shaped polymer-grafted silica. International Chemical Congress of Pacific Basin Societies, Hawaii, USA, Dec15–20, 2005; Vol. ANYL-287.

High-Temperature High-Resolution GC

Fernando M. Lanças
Institute of Chemistry of São Carlos (USP), University of São Paulo, São Carlos, Brazil

J.J.S. Moreira
Chromatography Laboratory, University of São Paulo, São Carlos, Brazil

INTRODUCTION

Gas chromatography (GC), in its early days, used packed columns with chemically inert solid supports coated with stationary phases. These columns presented low efficiency due to the wide range of particle sizes used, causing inhomogeneity in the packed bed and, consequently, high instability due to a poor deactivation and thermal instability at high-temperature operations.[1] This characteristic limited the use of the GC to only volatile and low-mass molecular compounds. The later development of columns with a stationary phase coated on the inner wall of the capillary provided a more inert environment. In this form, columns with higher thermal stability and more efficiency (higher N) were produced, allowing the analysis of semivolatile and medium molecular mass compounds. This technique was named high-resolution gas chromatography (HRGC).[1] The possibility of using thermally stable, highly efficient columns, stimulated scientists to search for new stationary phases and chemical manufacturing processes to produce capillary columns with high thermal stabilities, capable of operating at higher temperatures[2] (to 360°C).

Lipsky and McMurray[3] suggested, in their pioneering work on high-temperature high-resolution gas chromatography (HT-HRGC), the use of column temperatures equal to, or higher than, 360°C. However, other column temperature values have also been reported for this technique.[4]

The thermal stability of the high-temperature capillary columns allowed the analysis of higher molecular masses (more than 600 Da) and non-volatile compounds never before directly analyzed by gas chromatography.[2]

INSTRUMENTATION FOR HT-HRGC

The instrumentation used for HT-HRGC is the same as used for conventional GC, with only minor modifications.

Columns

The columns utilized in HT-HRGC are short (usually equal to, or shorter than, 10 m) coated with thin films (~ 0.1 μm or less) and having an inner diameter (I.D.) around 0.2 mm.[5]

A smaller inner diameter (e.g., 0.1 mm) can also be used, but with the inconvenience of limiting the work to more diluted samples in order to avoid column overload. On the other hand, this type of column permits carrier gas speeds higher than with columns of inner diameters in the range 0.2–0.3 mm. Columns with inner diameters equal to 0.1 mm exhibit fewer plates with the increment of the carrier gas speed, in contrast to the columns with equivalent characteristics, but of 0.3 mm I.D.[5] The increase of the carrier gas speed in smaller-I.D. columns performs an analysis in a shorter time, without undermining the efficiency of separation.[6]

Capillary columns, to be suitable to HT-HRGC, must be extremely robust and must be coated with a thin film of the stationary phase with the purpose of reducing the retention of the less volatile compounds and preventing stationary-phase bleed at high temperatures.[7]

Using such proper columns, elution of substances with carbon numbers in excess of *n*-C_{130} has been reported, at column temperatures of up to 430°C.[8]

Tubing Material for HT-HRGC Columns

There are four major types of materials being utilized to prepare columns for high-temperature capillary columns:[2]

1. Glass (borosilicate)
2. Polyimide-clad fused silica
3. Aluminum-clad fused silica
4. Metal-clad fused silica

Columns of aluminum-clad fused silica,[2,4] and metal-clad fused silica support temperatures up to 500°C, representing an advantage in comparison with borosilicate glass columns, with a temperature limit to 450°C, and columns of polyimide-clad fused silica for high temperature,[2,9] limited temperature to 400–420°C. On the other hand, aluminum-clad fused silica columns present leakage, principally in the connections, after a short time of use.[2,9] Polyimide-clad fused-silica

capillaries, after prolonged exposure to temperatures above 380°C, tend to break spontaneously at many points, thus losing the polyimide coating.[9] Borosilicate columns are inexpensive, being an alternative to fused silica for high-temperature applications. However, these columns have been reported to leak when coupled with retention gap and to mass spectrometry detectors.[2] An important alternative for HT-HRGC are HT metal-clad fused-silica columns which resist temperatures above 500°C for long-term exposure.[9]

Stationary Phases

The first results on HT-HRGC[3,10] were published in 1983, dealing with stationary-phase immobilization (polysiloxane –OH terminated). Due to the column instability, when submitted to high temperature, stationary-phase loss was common at that time. These works can be considered to be the precursor of high-temperature gas chromatography, because the phase immobilization process developed resulted in a series of OH-terminated polysiloxane phases compatible with the inner surfaces of borosilicate glass and fused-silica tubing. These phases are thermally stable and capable of withstanding elevated temperatures[11] used in HT-HRGC. After this report, many other articles dealing with the ideal stationary phase for high-temperature gas chromatography appeared. Non-polar stationary phases of the carborane–siloxane-type bonded phase (temperature range >480°C) and siloxane–silarylene copolymers suitable for HT-GC were developed[7] around 1988.

A medium-polarity stationary phase based on fluoralkyl–phenyl substitution, which is thermally stable up to 400°C, was reported,[12] and a CH_3O-terminated polydimethyl siloxane, diphenyl-substituted stationary phase made possible the analysis of complex high-molecular-mass mixtures such as free-base porphyrins and triglycerides using narrow-bore capillary columns.[5] Since these developments, a variety of stationary phases for analysis of specific analytes by HT-HRGC were found.[2]

Sample Introduction

The sampling and elution of such high-molecular-weight materials requires careful attention in order to avoid quantitative sample losses during the sample introduction step. In general, "cold" injection techniques are required for accurate non-discriminative sample transfer into the column. Cold on-column and programmed temperature (PT) split/splitless injection have been used with success for a large number of HT-HRGC analyses. In certain cases, however, significant losses of compounds above *n*-C_{60} have been observed with PT splitless injection.[13] This effect was identified as a time-based discrimination process caused by purging the PT inlet too soon after injection, resulting in incomplete sample vaporization.[14]

Actually, same articles show the possibility of use split injection[8] in HT-HRGC analyses of substances up to C_{78}. However, volatile materials from the septum accumulate at the head of the column during the cool-down portion of the temperature program. When the columns are reheated to analyze the next sample, these accumulated volatiles are eluted, producing peaks, a baseline rise, or both. This difficulty can be solved using commercial septa already available for HT-HRGC, which exhibit very low bleed levels.

DETECTORS

High-temperature high-resolution GC is a technique similar to conventional GC; however, it presents high column bleeding due to the high temperature to which the column is submitted. Selective detectors, when used in HT-HRGC, require special attention. As an example, the electron-capture detector (ECD) is a very sensitive detector and should not be used in HT-HRGC because of its ability to detect column bleeding. This fact limits the detectors used to a few, such as the flame ionization detector (FID), alkali-flame ionization detector (AFID), and mass spectrometry detector (MS). In HT-HRGC, these detectors usually need small adjustments; for example, the MS detector requires a special interface when used for HT-HRGC.[2]

HT-HRGC APPLICATION

High-temperature high-resolution GC has opened to many scientists the opportunity to analyze compounds of high molecular mass (600 Da or more) with similar efficiency to conventional high-resolution gas chromatography (HRGC). Actually, HT-HRGC has been applied to the analyses of compounds from several different areas.[15–18] As a general rule, this will avoid the time-consuming and usually expensive step of derivatization. In natural products, underivatized triterpenic compounds found in medicinal plants can be analyzed by this technique. The HT-HRGC analysis of triterpenes in aqueous alcoholic extracts of *Maytenus ilicifolia* and *M. aquifolium* leaves clearly allows the detection of the presence of friedelan-3-ol and friedelin and, therefore, allows distinguishing between the two varieties;[15] this differentiation is very important in pharmacological studies, because they present different biological activities.

Cyclopeptidic alkaloids (molecular mass ~ 600 Da), a class of important alkaloids which present biological

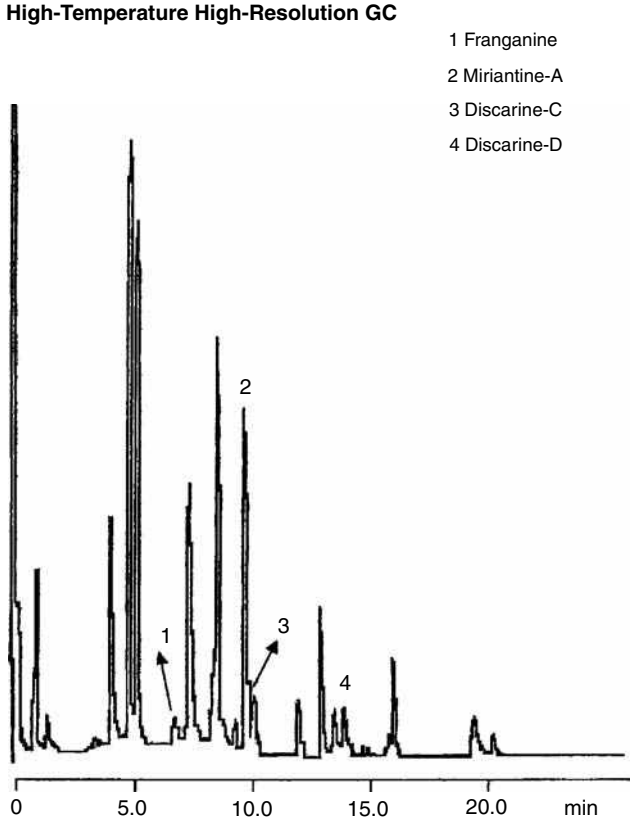

Fig. 1 Analysis of underivatized cyclopeptidic alkaloids in chloroform extract using HT-HRGC. Condition: fused-silica capillary column (6 m × 0.25 mm × 0.08 μm) coated with a LM-5 (5% phenyl, 95% polymethylsiloxane immobilized bonded phase) stationary phase. Temperature condition: column at 200°C (1 min), increased by 4°C/min, then 300°C (5 min); inlet: 250°C; FID detector: 310°C.

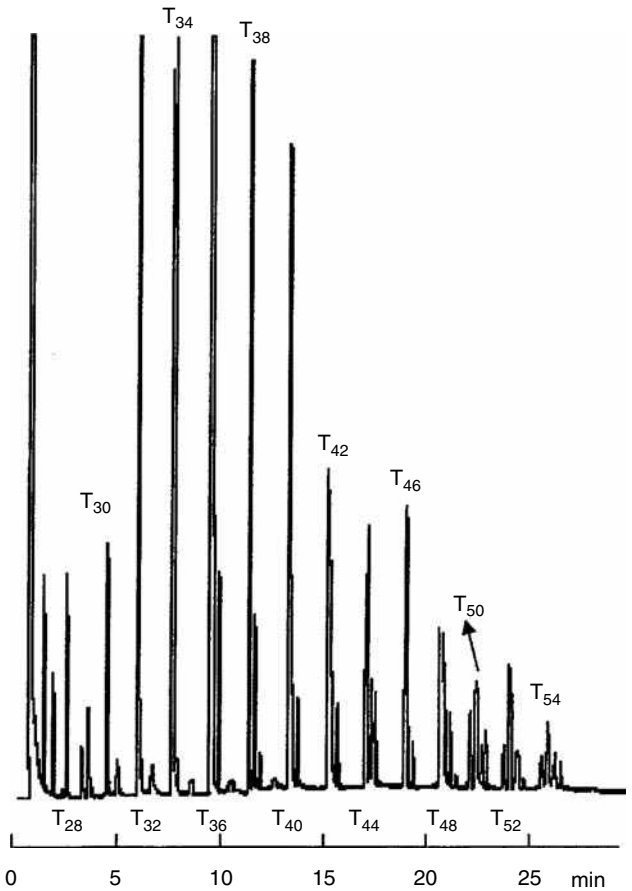

Fig. 2 Chromatogram of underivatized Palmist Oil (*Elaesis guineensis* L.) triacylglyceridic fraction using HT-HRGC. Condition: fused-silica capillary column (25 m × 0.25 mm × 0.1 μm) with the stationary phase OV-17-OH (50% phenyl, 50% methylpolysiloxane immobilized phase).Temperature condition: column at 350°C isothermic; injector: 360°C; FID detector: 380°C. T is the number of the underivatized triacilglyceride (e.g., T_{50} means a triacylglyceride having 50 carbon atoms).

activity,were analyzed by HT-HRGC without derivatization.[16] Fig. 1 illustrates the separation of cyclopeptidic alkaloids in the chloroform fraction. The following selected compounds were identified: (1) Franganine, (2) Miriantine-A, (3) Discarine-C, and (4) Discarine-D.

Triacylglycerides from animal and vegetable sources have been separated and identified by HT-HRGC and high-temperature gas chromatography coupled to mass spectrometry (HT-HRGC/MS). Fig. 2 shows the chromatographic profile of palm oil (*Elaeis guineensis* L.) by HT-HRGC, and the triacylglyceride compounds identification.[17]

The HT-HRGC/MS technique was also used as an important tool to identify and quantify cholesterol present in the total lipid extracts of archeological bones and teeth, constituents of a new source of paleodietary information.[19]

The detection of vanadium, nickel, and porphyrins in crude oils were analyzed by high-temperature gas chromatography–atomic emission spectroscopy (HT-GC–AES), presenting characteristic metal distributions of oils from different sources.[18] Other related applications of HT-HRGC, including the analysis of α, β, and γ cyclodextrins, antioxidants, and oligosaccharides.[2]

Considering that HT-HRGC is still a young separation technique and that it presents several attractive features, including the analysis of higher-molecular-weight compounds within short analysis times, without the necessity of sample derivatization, we can envisage a bright future for this technique, with many new applications being developed in the near future.

REFERENCES

1. Fowlis, I.A. *Gas Chromatography,* 2nd Ed.; John Wiley & Sons: New York, 1994; 1–11.

2. Blum, W.; Aichholtz, R. *Hochtemperatur Gas-Chromatographie*; Hüthing: Germany, 1991; 26–114.
3. Lipsky, S.R.; McMurray, W.J. Role of surface groups in affecting the chromatographic performance of certain types of fused-silica glass capillary columns: II. Deactivation by esterification with alcohols and deactivation with specially prepared high-molecular-weight stationary phases. J. Chromatogr. **1983**, *279*, 59.
4. Lanças, F.M.; Galhiane, M.S. High temperature capillary gas chromatography (HT-CGC) determination of limonin in citrus juice. J. High Resolut. Chromatogr. **1990**, *13* (9), 654–655.
5. Damasceno, L.M.P.; Cardoso, J.N.; Coelho, R.B. High temperature gas chromatography on narrow bore capillary columns. J. High Resolut. Chromatogr. **1992**, *15* (4), 256–259.
6. Grob, K.; Tschuor, R. Optimal carrier gas velocities at high temperatures in capillary GC. J. High Resolut. Chromatogr. **1990**, *13* (3), 193–194.
7. Hubball, J. LC/GC **1990**, *8*, 12.
8. Hinshaw, J.V.; Ettre, L.S. Apects of high-temperature capillary gas chromatography. J. High Resolut. Chromatogr. **1989**, *12* (4), 251–254.
9. Blum, W.; Damasceno, L. High temperature glass capillary gas chromatography using OH-terminated polysiloxane stationary phases. Separation of antioxidants and UV-stabilizers. J. High Resolut. Chromatogr. **1987**, *10* (8), 472–476.
10. Verzele, M.; David, F.; van Roelenbosch, M.; Diricks, G.; Sandra, P. In situ gummification of methylphenylsilicones in fused-silica capillary columns. J. Chromatogr. **1983**, *279*, 99–102.
11. Lipsky, S.R.; Duffy, M.L. High temperature gas chromatography: The development of new aluminum clad flexible fused silica glass capillary columns coated with thermostable nonpolar phases: Part 1. J. High Resolut. Chromatogr. **1986**, *9* (7), 376–382.
12. Aichholz, R.; Lorbeer, E. Use of methoxy-terminated poly(diphenyl/1H, 1H, 2H, 2H-perfluorodecylmethyl) siloxane as stationary phase for high temperature capillary gas chromatography and its application in the analysis of beeswax. J. Microcol. Separ. **1996**, *8* (8), 553–559.
13. Trestianu, S.; Zilioli, G.; Sironi, A.; Saravelle, C.; Munari, F.; Galli, M.; Gaspar, G.; Colin, J.; Jovelin, J.L. Automatic simulated distillation of heavy petroluem fractions up to 800°C TBP by capillary gas chromatography: Part I: Possiblities and limits of the method. J. High Resolut. Chromatogr. **1985**, *8* (11), 771–781.
14. Hinshaw, J.V. Modern inlets for capillary gas-chromatography. J. Chromatogr. Sci. **1987**, *25* (2), 49–55.
15. Lanças, F.M.; Vilegas, J.H.Y.; Antoniosi Filho, N.R. High temperature capillary GC analysis of phytopreparations of "espinheira santa" (Maytenus ilicifolia M. and Maytenus aquifolium M. – Celastraceae), a Brazilian antiulcer plant. J. Chromatogr. **1995**, *40* (5–6), 341.
16. Lanças, F.M.; Moreira, J.J.S. High temperature gas chromatography (HT-GC) analysis of underivatized cyclopeptidic alkaloids. In *Proc. of the 23rd Int. Symp. Capill. Chromatogr.*; 2000.
17. Antoniosi Filho, N.R. Analysis of the vegetable oils and fats using high resolution gas chromatography and computational methods. In *Ph.D. thesis*; University of São Paulo, Institute of Chemistry at São Carlos: Brazil, 1995; 140–152.
18. Zeng, Y.; Uden, P.C. High temperature gas chromatography—atomic emission detection of metalloporphyrins in crude oils. J. High Resolut. Chromatogr. **1994**, *17* (4), 223–229.
19. Stott, A.W.; Evershed, R.P. Analysis of cholesterol preserved in archaeological bones and teeth. Anal. Chem. **1996**, *68*, 4402.

Histidine in Body Fluids: HPLC Determination

Toshiaki Miura
College of Medical Technology, Hokkaido University, Sapporo, Japan

Naohiro Tateda
Kiichi Matsuhisa
Asahikawa National College of Technology, Asahikawa, Japan

INTRODUCTION

Amino acids in biological samples have been principally determined by high-performance liquid chromatography (HPLC) with pre- or postcolumn chemical derivatization selective for a primary amino group. Although HPLC methods are applicable to the assay of all commonly encountered amino acids in biological samples, they are time-consuming and inadequate for the assay of a large number of samples when a specific amino acid is required to be assayed. In such cases, a rapid assay can be achieved by the use of a chemical derivatization that is selective for the individual amino acid, which renders the HPLC separation conditions to be very simple. As an example of such a case, this paper describes a rapid HPLC method for the determination of histidine in body fluids. The method is based on the separation by a reversed-phase, ion-pair chromatography followed by the selective postcolumn detection of histidine with fluorescence derivatization using *O*-phthalaldehyde (OPA).

SELECTIVE FLUORESCENCE DETECTION OF HISTIDINE WITH OPA

OPA has been known to give a fluorescent adduct with most primary amines in the presence of a thiol compound, but only with several biogenic amines such as histidine, histamine, and glutathione in the absence of a thiol compound in a neutral or alkaline medium. In the case of histidine, it gradually reacts with OPA alone in an alkaline medium, to give a relatively stable fluorescent adduct showing excitation and emission maxima at 360 and 440 nm, respectively.[1] Håkanson et al. optimized these reaction conditions and showed that the fluorescence intensity due to histidine reached a maximum 10 min after initiation of the reaction at pH 11.2–11.5, at 40°C. This fluorescence reaction is relatively selective for histidine and has been used in a batch method for the assay of histidine.[1]

On the other hand, we revealed the mechanistic pathway of the OPA-induced fluorescence reaction of histidine, as shown in Fig. 1.[2] In addition, we found that the fluorescent adduct of histidine rapidly forms in a neutral medium, although its stability is low.[3] These findings led us to optimize this fluorescence reaction for a postcolumn detection of histidine in its HPLC determination. Under the optimized conditions (for 30 sec at pH 7 and at 40°C), no significant fluorescence was observed with other biological substances, except for histamine and glutathione. The relative fluorescence intensities of histamine and glutathione were 14.4% and 11.8% of that given by histidine on a molar base, respectively.[3] Such high selectivity of this fluorescence reaction was reasonably explained by the fact that both the primary amino group and imidazole ring of histidine participate in the formation of the fluorescent adduct (Fig. 1).

Because the reaction temperature markedly influences the rates of formation and degradation of the fluorescent adduct, its precise control is an essential factor for the reproducibility of the postcolumn fluorescence detection. Therefore preheating of both the eluent and OPA reagent to a constant temperature of 40°C is required before their mixing, and these was achieved by insertion of preheater tubes for both the eluent and OPA reagent into the line. As described in the section "HPLC System and Conditions," the preheater tubes, as well as columns, resistor tube, and the reactor tube were placed in a column oven maintained at 40°C.

HPLC CONDITIONS FOR SEPARATION OF HISTIDINE

As described above, histamine and glutathione also show significant fluorescence in the postcolumn detection with OPA. The levels of glutathione are comparable or higher than those of histidine in many biological samples, such as liver, kidney, and blood (mainly in the erythrocytes). On the other hand, most biological samples normally contain histamine at markedly lower levels than histidine; in particular, the level of histamine in human serum or plasma is 10,000-fold lower than that of histidine. These facts indicate that the interfering biological substance is limited to glutathione in the HPLC method in the postcolumn fluorescence detection using OPA. Thus HPLC separation conditions had only to separate histidine from

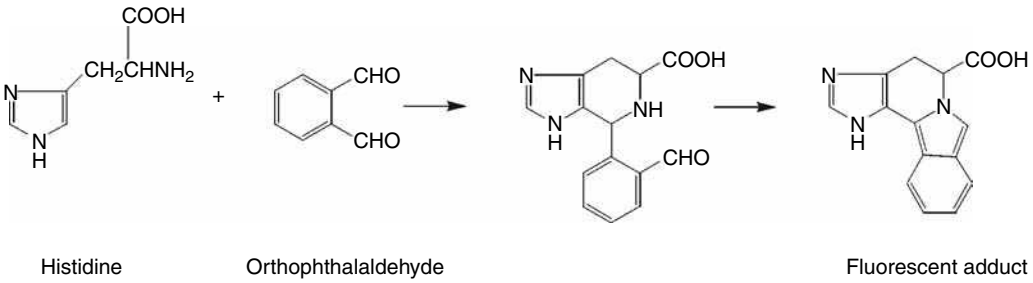

Fig. 1 Mechanistic pathway for the formation of fluorescent adduct in the reaction of histidine with *O*-phthalaldehyde.

glutathione, which was easily achieved by a reversed-phase ion-pair chromatography on an ODS short column with a 5 : 95 (v/v) mixture of methanol and sodium phosphate buffer (35 m*M*, pH 6.2) containing 5.3 m*M* sodium octanesulfonate, at a flow rate of 0.5 ml/min and at 40°C. Under these conditions, histidine and glutathione were eluted at 2.7 and 1.4 min, respectively (Fig. 2A).

DETERMINATION OF HISTIDINE IN BODY FLUIDS

HPLC System and Conditions

The HPLC system comprised an L-6000 pump (Hitachi, Tokyo, Japan) and an LC-9A pump (Shimadzu, Kyoto, Japan) for deliveries of an eluent and the OPA reagent, a DGU-12A degasser (Shimadzu), a Rheodyne Model 7725i sample injector (Rheodyne, Cotati, CA, USA), a CTO-10A column oven (Shimadzu), an F-1050 fluorescence detector equipped with a 12 μl square flow cell, and a D-2500 data processor (Hitachi). Separation was performed at 40°C with a Develosil ODS UG-3 column (30 × 4.6 mm I.D., 3 μm; Nomura Chemical, Seto, Japan) as an analytical column, which was protected by a guard-pak cartridge column (Develosil ODS UG-5, 10 × 4.0 mm I.D., 5 μm), and with a 1:19 (v/v) mixture of methanol and sodium phosphate buffer (35 m*M*, pH 6.2) containing 5.3 m*M* sodium octanesulfonate as an eluent. The OPA reagent was a 15:1 (v/v) mixture of 50 m*M* sodium phosphate buffer (pH 8.0) and 50 m*M* OPA in methanol. Both the eluent and OPA reagent were filtered through a 0.45 μm membrane filter (Millipore, Bedford, Massachusetts, U.S.A.) before use. The eluent was delivered to the column at a flow rate of 0.5 ml/min through a preheater tube (stainless-steel tube, 10 m × 0.8 mm I.D.). Ten microliters of the sample solution was introduced to the column. The eluate from the column was added with OPA reagent delivered at a flow rate of 0.5 ml/min to a mixing T-joint attached to the column through a preheater tube (stainless-steel tube, 10 m × 0.8 mm I.D.) and a resistor polytetrafluoroethylene (PTFE) tube (20 m × 0.25 mm I.D.). The mixture was passed through a reactor tube (coiled PTFE tube, 2.5 m × 0.5 mm I.D., coil diameter of 20 mm) and the generated fluorescence was detected at 435 nm with an excitation wavelength of 365 nm. All columns, preheater, resistor, and reactor tube were placed in the column oven which was maintained at 40°C.

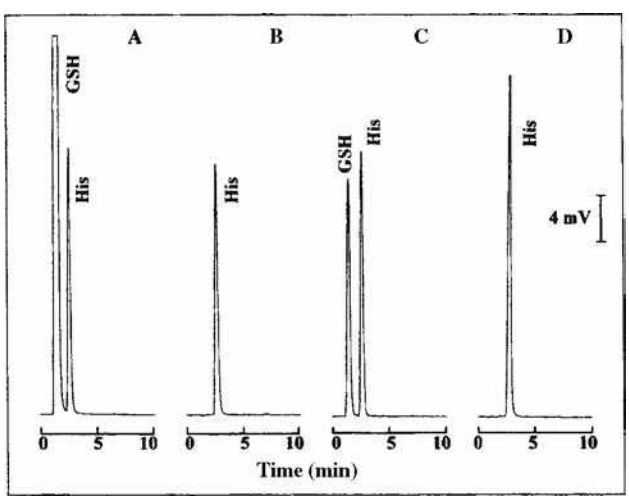

Fig. 2 Typical HPLC chromatograms of histidine. (A) Standard histidine and glutathione. Injected amounts: histidine (His), 5 pmol; glutathione (GSH), 500 pmol. (B) Human serum. (C) Human blood. (D) Human urine. (See the section "HPLC System and Conditions" for chromatographic conditions.)

Sample Preparation

Because of high selectivity of the postcolumn fluorescence detection with OPA, no sample pretreatment other than deproteinization was required for the assay of histidine in body fluids such as human serum, blood, and urine as follows:

- Human serum was mixed with an equal volume of 6% (w/v) perchloric acid and was vortexed several times. The mixture was centrifuged at 10,000 × *g* for 10 min at 4°C, then the supernatant was diluted 10-fold with water and was filtered through the 0.45 μm membrane filter. A portion of the filtrate was further diluted 10-fold with 0.01 *M* HCl for HPLC analysis.

- Heparinized human blood (1.0 ml) was mixed with water (0.9 ml) and 60% (w/v) perchloric acid (0.1 ml), vortexed, and then centrifuged at 4°C and 10,000 × *g* for 10 min. The supernatant (400 μl) was transferred to an Ultrafree-MC centrifugal filter unit (Durapore type, 0.22 μm) (Millipore) and centrifuged at 4°C and 10,000 × *g* for 1 min. A portion of the filtrate was diluted 200-fold with 0.01 *M* HCl and injected onto the HPLC column.
- Human urine was mixed with an equal volume of 6% (w/v) perchloric acid and was then filtered through the membrane filter. The filtrate was diluted 1000-fold with 0.01 *M* HCl and injected onto the HPLC column.

Evaluation of the Present HPLC Method

Fig. 2A shows the chromatogram of a 1:100 mixture of standard histidine and glutathione. The peak due to histidine was observed at 2.7 min with no interference from 100-fold excess of glutathione. The HPLC method gave a linear calibration curve ($r = 1.000$) over the range of 0.25–1000 pmol per injection (10 μl) with the coefficient of variation of 0.9% at 2 pmol ($n = 10$) and with the detection limit ($S/N = 8$) of 25 fmol.

Fig. 2B and D shows the typical chromatograms of deproteinized human serum and urine, respectively, which contain less glutathione than histidine. The high selectivity of the postcolumn detection made the chromatograms quite simple, where the peak due to histidine appeared as a sole peak. On the other hand, both glutathione and histidine were detected in human blood, which contains glutathione at a higher level than histidine (Fig. 2C).

Recoveries of the present HPLC method were tested by using a pooled human serum, blood, or urine, to which were added various amounts of histidine prior to the sample preparation. The mean recovery values were in the range of 101–104%. The values of histidine in human sera, blood, and urine, determined by the HPLC method, were 85.6 ± 15.0 μ*M* ($n = 47$, mean ± SD), 95.3 μ*M* ($n = 2$, 96.8 and 93.8 μ*M*), and 1.13 ± 0.48 mmol/mg of creatinine ($n = 10$, mean ± S.D.), respectively, which were in good agreement with their reported values. The coefficients of the day-to-day variation obtained with a pooled human serum, blood, or urine were below 1.0%.

CONCLUSIONS

Because of the high selectivity and sensitivity of the postcolumn fluorescence detection of histidine with OPA, the present HPLC method is applicable to a specific and rapid assay of histidine in human serum, blood, and urine after simple pretreatment. A recent paper demonstrated that the postcolumn detection with OPA was applicable to the simultaneous assays of histidine and its major metabolites (*cis*- and *trans*-urocanic acids) in human stratum corneum.[4] The postcolumn detection system was also applicable to the flow injection analysis (FIA) method for the assay of histidine in serum and urine. The FIA method enabled us to determine histidine in blood after pretreatment of the sample with *N*-ethylmaleimide (masking reagent of glutathione).[5] These methods are useful in the diagnosis of histidinanemia, one of hereditary metabolic disorders characterized by a virtual deficiency of histidine ammonia-lyase.

REFERENCES

1. Håkanson, R.; Rönnberg, A.L.; Sjölund, K. Improved fluorometric assay of histidine and peptides having NH_2-terminal histidine using *o*-phthalaldehyde. Anal. Biochem. **1974**, *59*, 98–109.
2. Yoshimura, T.; Kamataki, T.; Miura, T. Difference between histidine and histamine in the mechanistic pathway of the fluorescence reaction with *ortho*-phthalaldehyde. Anal. Biochem. **1990**, *188*, 132–135.
3. Tateda, N.; Matsuhisa, K.; Hasebe, K.; Kitajima, N.; Miura, T. High-performance liquid chromatographic method for rapid and highly sensitive determination of histidine using postcolumn fluorescence detection with *o*-phthaldialdehyde. J. Chromatogr. B, **1998**, *718*, 235–241.
4. Tateda, N.; Matsuhisa, K.; Hasebe, K.; Miura, T. Simultaneous determination of urocanic acid isomers and histidine in human stratum corneum by high-performance liquid chromatography. Anal. Sci. **2001**, *17*, 775–778.
5. Tateda, N.; Matsuhisa, K.; Hasebe, K.; Miura, T. Sensitive and specific determination of histidine in human serum, urine and stratum corneum by a flow injection method based on fluorescence derivatization with *o*-phthalaldehyde. J. Liq. Chromatogr. Relat. Technol. **2001**, *24*, 3181–3196.

HPLC Column Maintenance

Sarah S. Chen
Analytical Science, GlaxoSmithKline, King of Prussia, Pennsylvania, U.S.A.

COLUMN CONFIGURATION

The high-performance liquid chromatography (HPLC) column usually consists of a stainless steel tubing packed with porous particles for separation. These particles are sealed in the tubing by HPLC column end fittings at each end. Porous frits close the ends of columns and retain the packing particles. Typically, 2 μm and 0.5 μm pore size stainless steel frits are used for 5 and 3 μm particles, respectively.[1] Many problems arising from stainless steel columns can be traced to the inlet stainless steel frit, which has a higher surface area than the column walls and can lead to sample adsorption. High backpressure, poor peak shapes, and low sample yields are indications of possible frit problems.

COLUMN PACKING MATERIALS

Silica-based packings are the most popular HPLC column because of their favorable physical and chemical properties.[2,3] The silica particles have high mechanical strength, narrow pore size, and particle size distributions. The surface of silica can be chemically modified with a large variety of bonded molecules having various functionalities. Silica-based packings are compatible with water and all organic solvents, and exhibit no swelling with change in solvents, in contrast to most polymer-based stationary phases.

Columns packed with porous, polymeric particles, such as divinylbenzene-cross-linked polystyrene, substituted methacrylates, and polyvinyl alcohols can also be used for HPLC method development,[4] as can modified alumina and zirconia stationary phases.[5,6]

COLUMN MAINTENANCE

Proper column maintenance is very important to ensure optimal performance and prolonged column lifetimes. There are common procedures that apply to all columns, e.g., avoiding mechanical or thermal shock. And, there are procedures that are column-specific, such as avoiding chloride-containing mobile phases to prevent "halide cracking" if the column tubing and frits are made of stainless steel (especially at low pH). Nonetheless, columns made with stainless steel tubing and packed with silica-based stationary phases are the most commonly used in HPLC. Thus, problems associated with these columns and how to prevent such problems by proper column maintenance will be discussed here.

How to Ensure Retention and Resolution Reproducibility with HPLC Columns

Reproducible retention and resolution are very important when developing routine methods. Changes in resolution and retention can be a function of the column quality, its mode of operation, instrumental effects, or variations in separation conditions. The first important step in maintaining retention reproducibility is through selection of a good quality column with a less acidic and highly purified support. Choosing a favorable mobile-phase condition (pH, buffer type and concentration, additives, etc.) that can eliminate surface silanol interactions when separating basic compounds is also very important for column retention reproducibility. There should be minimal variation in laboratory temperature (or column temperature) for retention and resolution reproducibility. Proper laboratory instrumentation and column storage conditions cannot be neglected either.

Poor retention reproducibility and tailing peaks often occur in poorly buffered mobile phases, owing to an inappropriately selected buffer, too low a buffer concentration, or a pH out of the effective range of a buffer. Increasing buffer concentration can minimize some of the problems. However, the buffer concentration must not be too high; otherwise, the buffer may not be miscible with the organic portion of the mobile phase. Other factors, such as tailing peaks, high backpressure, or loss of stationary phase will also result in poor retention reproducibility and will be discussed later.

How to Avoid Band Tailing

Band tailing leads inferior separations and reduced precision. Thus, conditions resulting in tailing or asymmetrical peaks should be avoided. Peak asymmetry or band tailing can arise from several sources: plugged column frits, void in the column, buildup of "garbage" on the column inlet, sample overload, solvent mismatch with sample, chemical or secondary interaction (many times silanol effects),

contaminating heavy metals, and excess void volume in the HPLC system.

Tailing peaks are common with heavily used columns. During use, columns can develop severe band tailing or even split peaks for a single component. Such effects usually arise from a void in the inlet of the column and/or a dirty or partially plugged inlet frit. The cause of the void can be either poorly packed columns that settle during use or dissolution of silica packing at high pH. Excessive system backpressure or pressure surges caused by poorly operating pumps or sample injection valves can also cause voiding. Voids can be eliminated by the addition of new packing material at the inlet end of the column. This can be done by carefully removing the end fitting from the column inlet. Packing material is then added in a slurry form to the void space. For the best results, packing material of the same type should be used. Old frits should be replaced with new ones of the same type before the end fitting is put back onto the column inlet. However, sometimes it is difficult to achieve the same column efficiency after such procedures.

The presence of strongly retained materials in "real-world" samples can result in peaks that are eluted long after the normal run time is over. These peaks can cause three kinds of problems in later runs. If the peaks are large and well behaved, they can show up in a subsequent run as very broad peaks. If the peaks are very small, they can elute under a peak of interest and cause distortion. It is also possible that peaks eluted late in a run can be small enough or so strongly retained that they appear only as a baseline bump. The development of broader tailing peaks during use may also indicate the buildup of strongly retained sample components (garbage) on the column. Purging the column with a strong solvent may eliminate this buildup. For reversed-phase columns, a 20-column-volume purge (about 50 ml for a 250 × 4.6 mm I.D. column) with 100% acetonitrile is often adequate. In case a stronger solvent is needed, a mixture of 96% dichloromethane and 4% methanol with 0.1% ammonium hydroxide is often effective. Since dichloromethane is not miscible with aqueous mobile phases, it is necessary to flush the reversed-phase column with acetonitrile prior to and after the use of dichloromethane. Methanol is used for normal-phase columns. Sometimes, it may be sufficient to flush the column once a day. If strongly retained materials are known to exist in the sample, it is a good idea to flush the column with a strong solvent at the end of each run sequence so that any strongly retained materials are flushed out before the next sample is analyzed.

How to Avoid High Backpressure

High backpressure is one of the most commonly encountered problems when performing HPLC analysis. Normal column backpressure is observed after a new column has been installed and equilibrated with the mobile phase. Unfortunately, this pressure often will increase with time of use because of particles collecting on the column inlet or outlet frit. These particles can be sample impurities, mobile-phase contaminants, or materials from the injector or autosampler rotor seal. Unfavorable buffer conditions, such as high pH, can dissolve silica particles. After the breakdown, small particles can clog the frit at the outlet of the column. The presence of small particles in the system can result in increased backpressure, split peaks, tailing, and eventually over-pressure shutdown. Most times, plugged frits can be eliminated by back flushing the column with a strong solvent. If this does not work, the plugged inlet frit can be replaced with a new frit without disturbing the packing. When replacing the inlet frit, additional packing material may be needed if a void is noticed at the column inlet. To reduce backpressure problems, samples should be cleaned before being injected. Sample treatment may include filtering the samples to remove particulates or using solid-phase extraction techniques to remove highly retained sample or matrix components. Only HPLC grade or superior solvents should be used for the mobile phase, and buffer solutions should be filtered and prefilters should be installed at the buffer reservoir. Rotor seals should be changed on a routine basis. Along with these preventative measures, it is advisable to use column prefilters, such as a guard column protection systems. Particles then build up on the inexpensive, replaceable frit in the prefilter, instead of the permanent frit at the head of the column. To choose a guard column for HPLC, it is best to choose one with the same type of stationary phase to match the analytical column. The length of a guard cartridge is usually 1 or 2 cm, with typical diameters ranging from 2.0 to 4.6 mm.

How to Prevent Loss of Stationary Phases

Column lifetime can be reduced significantly by loss of stationary phases during separations. Stationary/mobile phase combinations that lead to a rapid loss of bonded phase should be avoided. Column manufacturer's recommendations should be followed when using the column for separations. Commonly, reversed-phase columns with short-chain silane groups are the least stable, since the silane groups can be easily hydrolyzed with aggressive mobile phases (e.g., pH <2.0). Reversed-phase columns with longer alkyl groups, such as C_8 or C_{18} (Fig. 1), are usually considered relatively stable because of the inaccessibility of the surface Si–O–R. Polymeric C_8 and C_{18} are considered to be more stable than their monomeric counterparts. However, over long periods at very low or high pH, these columns can also lose bonded molecules. Use of sterically protected silane stationary phases will provide additional stability in aggressive low-pH environments.

The stability of the bonded organic ligand on a reversed-phase column depends on the type and acidity

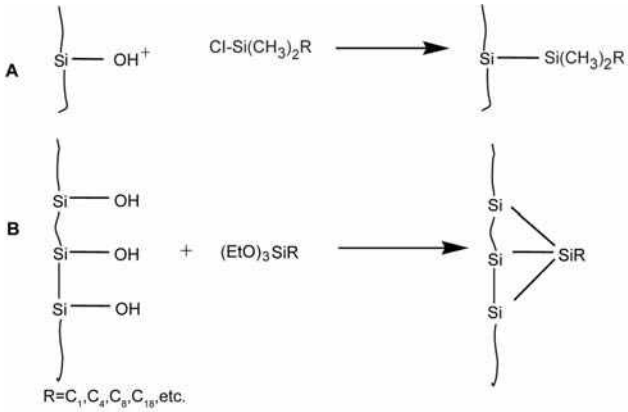

Fig. 1 Schematic diagram of monomeric (A) and polymeric (B) stationary phases for reversed-phase HPLC.

of the silica used as the support. Packings made with fully hydroxylated silicas with a homogeneous distribution of silanol groups show superior stability. Higher bonded-phase stability, apparently, can occur with columns made with highly purified silica supports having a lower surface acidity.

Loss of stationary phase from silica-based columns is accelerated at higher temperatures. Temperatures above ~40°C should be used with caution when operating at intermediate or high pH with phosphate buffers. Operation at pH < 3 and elevated temperatures can degrade the bonded stationary phase more rapidly and cause retention reproducibility problems. However, there are specially "end-capped" stationary phases available from several of column manufacturers that can withstand higher temperature with less hydrolysis.

Avoid using 100% aqueous mobile phase on reversed-phase columns

Unless specified by the manufacturer, 100% aqueous mobile phase should be avoided with a reversed-phase column such as C_{18} or C_8. Most reversed-phase columns exhibit decreased and poorly reproducible retention when operated with more than 98% aqueous conditions. This problem is explained as being the result of ligand collapse or incomplete wetting. When a C_{18} column is washed with water, the bonded phases are collapsed or incompletely wetted.[7] Subsequent flushing with mobile phase removes the wash solvent, but the stationary phase remains in the collapsed configuration, which causes a change in retention and selectivity. Therefore, it is advised that washing a reversed-phase column with water should be avoided. Furthermore, if the organic solvent content of a mobile phase is too low, the bonded material will tend to collapse onto itself to a low-energy conformation. This collapse/incomplete wetting could lead to abnormal chromatographic behavior and generally undesirable results. To avoid this phenomenon, scientists have used embedded polar phases, including amide or carbamate groups,[8–11] which presumably do not undergo phase collapse in 100% water and can withstand mobile phase with high aqueous content. If 100% aqueous mobile phase is needed for reversed-phase separation, columns with embedded polar groups should be used.

Other Factors in Column Maintenance

Storing a column in 100% organic solvent, such as acetonitrile, best preserves the performance and lifetime of bonded-phase columns. Storage with buffered solutions (particularly those containing high concentrations of water and alcohols) should be avoided. When buffers are used, columns should be flushed with 15–20 column volumes of the same aqueous/organic mobile phase without buffer before converting to 100% organic for storage. Columns should be capped tightly during storage, to prevent the packed bed from drying out. Bacterial growth often occurs in buffers and aqueous mobile phases that are prepared and stored at ambient temperature for more than a day. Particulates from this source can plug the column inlet and reduce column life significantly. As a result, mobile phases that are free of organic solvents should be discarded at the end of each day. Alternatively, 20% of organic modifier in the mobile phase retards bacterial growth. The organic modifier also assists in the mobile phase degassing process.

CONCLUSION

In general, mechanical and thermal shock of the column should be avoided to prevent disturbing column bed. Pressure surge in the system should also be avoided. Choosing a suitable buffer system is very critical to maintaining retention and resolution reproducibility, thus preventing the loss of stationary phase. Samples containing strongly retained components and particulates should be filtered before injection. The use of guard columns can reduce the "garbage" build-up at a column inlet and reduce the risk of high backpressure. It is good practice to flush the column frequently with a strong solvent after heavy use, and store in proper solvent.

REFERENCES

1. Snyder, L.R.; Kirkland, J.J.; Glajch, J.L. *Practical HPLC Method Development,* 2nd Ed.; John Wiley & Sons, Inc.: New York, 1997.
2. Iler, R.K. *The Chemistry of Silica*; Wiley: New York, 1979.

3. Unger, K.K. *Porous Silica, Journal of Chromatography Library*; Elsevier: Amsterdam, 1979; Vol. 16.
4. Tanaka, N.; Araki, M. Polymer-based packing materials for revese-phase liquid chromatography. Adv. Chromatogr. **1989**, *30*, 81.
5. Pesek, J.J.; Sandoval, J.E.; Su, M. New alumina-based stationary phases for high-performance liquid chromatography: Synthesis by olefin hydrosilation on a silicon hydride-modified alumina intermediate. J. Chromatogr. **1990**, *630* (1–2), 95–103.
6. Sun, L.; Annen, M.J.; Lorenzano-Porras, F.; Carr, P.W.; McCormick, A.V. Synthesis of porous Zirconia spheres for HPLC by polymerization-induced colloid aggregation (PICA). J. Coll. Interf. Sci. **1993**, *163* (2), 464–473.
7. Wolcott, R.G.; Dolan, J.W. Simple preparation of a C8 HPLC stationary phase with an internal polar functional group. LC-GC **1999**, *17* (4), 316.
8. O'Gara, J.E.; Alden, B.A.; Walter, T.H.; Petersen, J.S.; Niederlander, C.L.; Neue, U.D. Anal. Chem. **1995**, *67* (20), 3809–3813.
9. Cqajkwaka, T.; Hrabovsky, I.; Buszewski, B.; Gilpin, R.K.; Jaronieic, M. Comparison of the retention of organic acids on alkyl and alkylamide chemically bonded phases. J. Chromatogr. A, **1995**, *691* (1–2), 217–224.
10. Ascah, T.L.; Kallury, K.M.R.; Szafravski, C.A.; Corman, S.K.; Liu, F. Characterization and high performance liquid chromatographic evaluation of a new amide-functionalized reversed phase column. J. Liq. Chromatogr. & Relat. Technol. **1996**, *19* (7), 3409–3073.
11. Czajkowaka, T.; Jaronieic, M. Selectivity of alkylamide bonded-phases with respect to organic acids under reversed-phase conditions. J. Chromatogr. A, **1997**, *762* (1–2), 147–158.

HPLC Instrumentation: Troubleshooting

Ioannis N. Papadoyannis
Victoria F. Samanidou
Laboratory of Analytical Chemistry, Chemistry Department, Aristotle University of Thessaloniki, Thessaloniki, Greece

INTRODUCTION

Despite the advances in technology and instrumentation, problems still arise when practicing high-performance liquid chromatography (HPLC), which cause headaches to chromatographers. During several stages of analysis, such as method development or routine operation, a variety of separation artifacts may be noticed. Pressure abnormalities, sample recovery, poor reproducibility, loss of resolution, instability, leaks, etc. are common problems.

General problems can be detected by smell, sight, or sound, although major symptoms in the liquid chromatography (LC) system show up as changes in the chromatogram, such as irregular peak shapes, extra peaks, negative peaks, varying retention times, and many others. It is well known that, if a picture is worth a thousand words, then a chromatogram, to a chromatographer, is equally valuable. Any chromatographer who has injected many samples into an LC system has occasionally confronted more than one of the abovementioned problems. Some problems can be corrected by changes in the equipment, whereas others require modification of the assay procedure. However, many of the common LC problems can be prevented with routine preventive maintenance.

Guides for troubleshooting HPLC instrumentation provide analysts and laboratory technicians with a readily available, very useful aid for solving operational problems of equipment and techniques. In order that the chromatographer effectively solves an arising problem in HPLC, he/she should be aware of the role of operating parameters, as these are indicators of system performance. Step-by-step troubleshooting protocols for each system component should be followed to isolate the problem and its cause.

OVERVIEW

This entry covers problem identification and procedures for solving them, as well as practices to maintain HPLC systems in good operating condition. It also guides users of HPLC equipment to investigate the source of a malfunction through each system component, from sample preparation to detection and integration.

PROBLEMS: CAUSES AND SOLUTIONS

In an HPLC system, problems can arise from many sources. Malfunction can be allocated to various points. Chromatographers should use not only their experience to locate problems but also all their senses (obviously, except taste) to identify LC problems. For example, a leak can be noticed by smell before it is actually seen. A strange noise indicates some kind of malfunction and a "hot" smell indicates an overheating module. Most problems, however, are identified by sight, and they can mainly be observed as changes in the chromatogram. As soon as the problem has been defined, actions should be taken to correct the malfunctioning component. The incident should be recorded, in a log book kept for this purpose, to help with further failure problems at a later time.

The HPLC user should know or learn what to look for and what to do to prevent HPLC problems and, finally, what can and should be done before calling a service technician. User's manuals, manufacturer's advice, books, articles in scientific journals, computer programs, and network sites can be used as resources for troubleshooting. A general rule is that one can know that a problem exists only when one knows how the system operates when it is working well. This means that keeping detailed records of system performance (log book) is very helpful.

Dolan (refer to "Bibliography") has very effectually set forth five rules of thumb for HPLC troubleshooting.

1. Do not change more than one thing at a time.
2. A problem is considered as problem when it occurs more than once.
3. A questionable system component should be substituted/replaced with one that is known to be working properly. Known good parts should be put back into service while all failed parts should be thrown away.
4. An experienced chromatographer should try to anticipate what will fail next.
5. Good records of maintenance and troubleshooting actions should be kept.

In HPLC instrumentation troubleshooting, problems can be classified as follows. Major HPLC problems are discussed under this paragraph, while an extended

summary of problem causes and remedy actions are tabulated in the respective tables.

Problems with the Chromatogram

Peak shape

Broad peaks, ghost peaks, pseudo peaks, negative peaks, peak doubling, peak fronting, peak tailing, spikes, no peaks. The major causes and their solutions are tabulated in Table 1.

Variable retention times

Retention time inconsistency (changing, increasing, decreasing), change in separation (loss of resolution). Table 2 summarizes their causes and solutions.

Baseline

Short-term noise, long-term noise, and drift. The causes of the baseline problems and their remedies are discussed in Table 3.

Pressure abnormalities

These include increased pressure, decreased pressure, unstable/fluctuating pressure, and high backpressure. Table 4 lists the major causes and their solutions.

Leaks

Leaks at various points, such as the column, fittings, the detector, the injection valve, or the pump. Table 5 summarizes their causes and solutions.

Change in quantitation

Including imprecision, change in selectivity, change in peak height–lack of sensitivity, poor sample recovery. Table 6 summarizes their causes and solutions.

Fig. 1 illustrates some of the changes that appear in the chromatogram as a result of the various problems.

Changes in the Chromatogram

Baseline

Baselines in chromatograms are not always smooth. On the contrary, a baseline may have spikes, noise, and other disturbances, indicating existing problems. Indeed, by magnifying the baseline, chromatographers can obtain information to recognize the problem and correct it. For example, trace contaminants in water, buffer, and reagents may cause peaks when using gradient elution.

Very often baseline problems are related to detector problems. Many detectors are available for HPLC systems. The most common are fixed and variable wavelength ultraviolet spectrophotometers, refractive index, and conductivity detectors. Electrochemical and fluorescence detectors are less frequently used, as they are more selective. Detector problems fall into two categories: electrical and mechanical/optical. The instrument manufacturer should correct electrical problems. Mechanical or optical problems can usually be traced to the flow cell; however, improvements in detector cell technology have made them more durable and easier to use. Detector-related problems include leaks, air bubbles, and cell contamination. These usually produce spikes or baseline noise on the chromatograms or decreased sensitivity. Some cells, especially those used in refractive index detectors, are sensitive to flow and pressure variations. Flow rates or backpressures that exceed the manufacturer's recommendation will break the cell window. Old or defective source lamps, as well as incorrect detector rise time, gain, or attenuation settings will reduce sensitivity and peak height. Faulty or reversed cable connections can also be the source of problems.

Electronic noise from fluorescent lights and other common sources is often called 60-cycle noise because it coincides with the 60-Hz frequency of the alternating current servicing the laboratory.

To isolate the origin of the problem due to the detector, the chromatographer may perform the "dry cell test": by disconnecting the detector from the column and then blowing the cell dry with dry nitrogen. Under these conditions no drift should be observed.

Ghost peaks

These peaks appear in a chromatogram due to contamination of mobile phase, injector, column, or strongly retained compounds from previous sample injections. When an autosampler is used, the problem is often referred to as "carryover." Flushing the injector and the column with strong solvent will remove interfering or late eluting compounds. To correct carryover problems, the chromatographer should change injection size, check wash solvent, increase wash solvent volume, adjust its pH value, use a portion of organic solvent, change a needle seal, injection loop, and check fitting assembly.

Ghost peaks in gradient runs can be avoided by increasing the equilibration time between analyses.

No peaks and negative peaks

If no peaks are observed, then the chromatographer should check the detector, the connections, the flow (leaks, pump function, air bubbles), the sample (for its stability), and

Table 1 Peak shape problems and remedies.

Peak shape
Fronting
1. Column overloaded. → Decrease sample amount or dilute sample.
2. Sample solvent incompatible with mobile phase. → Adjust solvent.
3. Nonresolved peak from another component. → Improve resolution by altering mobile or stationary phase.
4. Wrong pH value of mobile phase. → Adjust pH.
5. Channeling in column. → Replace or repack column.
Tailing
1. Secondary retention effects; residual silanol interactions. → Use ion pair reagent, or competing base or acid modifier. Triethylamine for basic compounds, acetate for acidic compounds.
2. Wrong pH value of mobile phase. → Adjust pH. For basic compounds lower pH usually provides more symmetric peaks.
3. Wrong stationary phase. → Change column.
4. Void at column inlet. → Repack top of column with stationary phase.
5. Wrong injection solvent. → Dissolve sample in mobile phase.
6. Interference in sample. → Check column performance with standards. Change mobile phase or stationary phase. Check selectivity.
7. Chelating solutes—trace metals in base silica. → Use high purity silica-based column with low trace-metal content, add EDTA or chelating compound to mobile phase; use polymeric column.
8. Unswept dead volume. → Minimize number of connections; ensure injector rotor seal is tight: ensure all compression fittings are correctly scaled.
9. Silica-based column-degradation at high temperature. → Reduce temperature to less than 50°C.
Double (split) peaks
1. Column voided. → Repack top of column with stationary phase; replace column.
2. Partially blocked frit. → Clean or replace the plugged frit. Install an in-line filter between pump and injector to remove solids from mobile phase or between injector and column to filter particulates from sample.
3. If only one peak is split co-eluting interfering components. → Use sample cleanup.
4. Sample solvent incompatible with mobile phase. → Inject samples in mobile phase.
5. Blocked frit. → Replace or clean frit, install 0.5 um porosity in-line filter between pump and injector to eliminate mobile-phase contaminants or between injector and column to eliminate sample contaminants.
6. Co-elution of interfering compound from previous injection. → Use sample cleanup; adjust selectivity by changing mobile or stationary phase. Flush column with strong solvent at end of ran; end gradient at higher solvent concentration.
7. Column overloaded. Sample volume too large. → Use higher-capacity stationary phase, increase column diameter, decrease sample amount.
8. Column void or channeling. → Replace column, or, if possible, open top endfitting and clean and fill void with glass beads or same column packing; repack column.
9. Injection solvent too strong. → Use weaker injection solvent or stronger mobile phase.
Broad peaks (all)
1. Large injection volume; detector operating outside linear dynamic range. → Injection of smaller sample volume or diluted sample (1 : 10).
2. High viscosity of mobile phase. → Change mobile phase, or increase column temperature. Change to lower viscosity solvent.
3. Poor column efficiency due to column void or column contaminated/worn out. → Repack top of column; replace column.
4. Incorrect detector settings. → Check settings and adjust.
5. Low mobile phase flow rate. → Increase flow rate.
6. Tubing too long or too wide; large extra column volume. → Use right tubing, shorten path. Use low- or zero-dead-volume endfittings and connectors; use smallest possible diameter of connecting tubing (<0.10 in. i.d.); connect tubing with matched fittings.
7. Leaks between column and detector. → Check for leaks.
8. Guard column contaminated/worn out. → Replace guard column.

(Continued)

Table 1 Peak shape problems and remedies. *(Continued)*

Peak shape
9. Retention times too long. → Use gradient elution or a stronger mobile phase for isocratic elution.
10. Too large volume of detector cell. → Use smaller cell volume.
11. Slow detector time constant → Adjust time constant to match peak width.
Broad peaks (some)
1. Late eluted peak from previous run. → Flush the column with a strong eluent after each run or end gradient at a higher concentration of strong solvent.
2. High molecular weight sample. → Optimize sample clean up.
Negative peaks
1. Highly UV absorbing mobile phase. → Change detection wavelength taking into account the UV cutoff of mobile phase solvents.
2. Refractive index of mobile phase is very different from RI of sample. → Change eluent.
3. Recorder connections. → Check polarity.
Ghost peaks
1. Dirty mobile phase. → Use HPLC grade solvents.
2. Carryover. Retained compound from previous injection. → Flush column with strong solvent to remove late eluting compounds. End gradient at higher solvent concentration.
3. Contamination of injector. → Flush injector.
4. Contamination of column. → Flush column with strong solvent.
5. Unknown interferences in sample. → Use sample cleanup or prefractionation before injection.
Spikes
1. Bubbles in mobile phase. → Degas mobile phase. Sparge it with helium (3–5 psi) during use; ensure that all fittings are tight; store column tightly capped.
2. Bubbles in detector. → Use back-pressure regulator at detector outlet.
Extra column dispersion
1. Wrong tubing dimensions. → Use short, small internal diameter (narrower) tubing between injector and column and between column and detector.
2. Detector overloaded. Outside linear dynamic range. → Use a low volume detector cell.
3. Large sample volume. → Inject small sample volumes.
No peaks
1. Detector off. → Check detector.
2. No flow. Pump off. → Start pump.
3. No sample. Sample deteriorated. → Check injector. Check sample stability.
4. Wrong settings on recorder or detector. → Check attenuation, gain, and detector wavelength.
5. Flow interrupted. → Check reservoirs, loop, degassing of mobile phase, and compatibility of mobile phase components.
6. Leaks. → Check fittings and pump for leaks and pump seals.
7. Air trapped in the system. → Prime pump.

settings on the detector (e.g., wrong wavelength), or integration.

Negative peaks are due to wrong polarity of recorder, or absorbance or refractive index of mobile phase higher than that of solute.

Peak tailing and peak fronting

Peak tailing (peak asymmetry factor >1.2). This is attributed to the wrong pH value, wrong column, wrong sample solvent (mobile phase is better to be used), void volumes at

Table 2 Retention time inconsistency.

Variable retention times

1. Leaks. → Check for loose fittings, pump leaks, seals.
2. Change in mobile phase composition. → Prepare new. Ensure that gradient system is delivering correct composition. Prevent evaporation.
3. Air trapped in pump. → Prime pump. Degas mobile phase—Sparge it with helium (3–5 psi) during use.
4. Overloading. → Dilute sample.
5. Sample dissolved in a solvent that is incompatible with the mobile phase. → Dissolve sample in the mobile phase.
6. Temperature fluctuations. → Use column oven.
7. Isocratic elution: Insufficient equilibration time. → Pass 10–15 column volumes of mobile phase through column for equilibration.
8. Gradient elution: Insufficient column regeneration time. → Increase equilibrating time.

Loss of resolution

1. Leak. Pump flow problems. → Check for leaks.
2. Obstructed guard or analytical column. → Replace guard column. Reverse analytical column and flush disconnected from the detector. Change inlet frit. Replace the column.
3. Improperly prepared mobile phase; contaminated mobile phase. → Prepare fresh mobile phase. Check pump-proportioning valve for malfunction.
4. Sample overloaded. → Dilute sample and reinject.
5. Extra column dead volume. → Check system plumbing and all connections for dead volume.
6. Injector problem. → Leaking injection valve or a damaged or blocked needle has to be corrected.
7. Temperature fluctuations. → Use column oven.

Table 3 Baseline.

Baseline

Regular noise

1. Air bubbles. → Prime pump. Degas solvent. Sparge mobile phase with helium during use.
2. Pump pulsations. → Use a pulse dampener.
3. Incomplete mixing. Malfunctioning proportioning valves. → Ensure complete mixing. Clean or replace the proportioning valve; partially remix solvents.
4. Other electronic equipment on the same line. → Check electronic equipment in line. Correct as necessary.
5. Leaks. → Check pump for leaks, salt build-up. Check fittings and pump seals.
6. Continuous-detector lamp problem or dirty flow cell. → Replace UV lamp (each should last 2000 hr); clean and flush flow-cell.

Irregular noise

1. Leaks. → Check fittings, pump seals, and pump for leaks.
2. Electronics. → Locate problem. Get servicing. Isolate detector and recorder electronically. Use a voltage stabilizer for the LC system or use an independent electrical circuit for the chromatography equipment.
3. Insufficient grounding. → Establish sufficient grounding.
4. Flow cell contamination. → Clean detector cell.
5. Detector lamp failing. → Replace detector lamp.
6. Mobile phase mixer inadequate or malfunctioning. → Repair or replace the mixer or mix off-line in case of isocratic elution.
7. Air bubbles in detector. → Install backpressure regulator after detector.
8. Occasional sharp spikes—external electrical interference. → Use voltage stabilizer for LC system; use independent electrical circuit.
9. Periodic-pump pulses. → Service or replace pulse damper; purge air from pump; clean or replace check valves.
10. Random-contamination buildup. → Flush column with strong solvent; clean up sample; use HPLC grade solvent.

Drift

1. Strongly retained materials. → Flush column with strong solvent.

(Continued)

Table 3 Baseline. *(Continued)*

Baseline
2. Default mixing. → Check mixer. Check flow rate and composition.
3. Air in the detector cell. → Clean cell. Use backpressure regulator at detector outlet.
4. Contamination of mobile phase. → Flush column with strong solvent; use HPLC grade solvents; clean-up sample.
5. Fluctuation of column temperature. → Use column oven.
6. Gradient elution. A. Positive direction. Absorbance of mobile phase B. → Add UV absorbing compound to mobile phase A. Negative direction. Absorbance of mobile phase A. → Add UV absorbing compound to mobile phase B.
7. Temperature at RI detector unstable. → Control changes in room temperature. Insulate column, use column oven, cover RI detector keeping it out of air currents.
8. Mobile phase not in equilibrium with column. → Allow more time for column equilibration.

Table 4 Pressure abnormalities.

Increased pressure

1. Blocked flow lines: Pump. Injector. Tubing. → Locate obstruction, by systematic disconnection of system components. Replace or clean blocked components.
2. Obstructed column or guard column, from particulate buildup at top of column. → Replace guard column. Reverse analytical column and flush disconnected from the detector. Change inlet frit. Replace the column. Filter sample.
3. Salt precipitation. → Ensure mobile phase compatibility with buffer concentration.
4. High viscosity of mobile phase. → Use solvent of lower viscosity or increase temperature.
5. Microbial growth in the column. → Store column with at least 25% organic solvent. Add 0.02% sodium azide to aqueous mobile phases, or use a mobile phase with at least 10% organic solvent.

Decreased pressure

1. Leaks in the system: Fittings not tight. → Check all connection for leaks. Tighten or replace fittings. Replace or clean check valves.
2. Piston seal(s) worn. → Replace piston seal(s).
3. Air trapped in pump. → Prime pump.
4. Mobile phase interrupted. Insufficient flow from pump. → Check reservoirs, loop, degassing of mobile phase, and compatibility of mobile phase components.

Unstable-fluctuating pressure

1. Air bubbles in pump. → Degas mobile phase—Sparge it with helium (3–5 psi) during use. Prime pump.
2. Leaks in pump check valve or seals. → Replace or clean check valves; replace pump seals.

High backpressure

1. Plugged frit, pre-filter, guard column; plugged inlet frit. → Backflush column/cartridge. Replace frit, pre-filter, guard column; replace endfitting or frit assembly.
2. Irreversibly retained contaminants on the column head. → Column cleaning/regeneration.
3. Precipitation of buffer. → Flush with water at low flow rate.
4. Precipitation or aggregation of proteins in column, particulate matter trapped by the top and/or bottom filter build-up of lipids, DNA, or other macromolecules non-specifically bound to the column microbial contamination. → Clean column, following column instructions with appropriate solvents, change top and/or bottom filter.
5. Column blocked with irreversibly adsorbed sample. → Improve sample cleanup; use guard column; reverse-flush column with strong solvent to dissolve blockage.
6. Column particle size too small (for example, 3 μm). → Use larger particle size (for example, 5 μm).
7. Microbial growth on column. → Use at least 10% organic modifier in mobile phase; use fresh buffer daily; add 0.02% sodium azide to aqueous mobile phase: store column in at least 25% organic solvent without buffer.
8. Mobile phase viscosity too high. → Use lower viscosity solvents or higher temperature. Replace frit or guard column.

(Continued)

Table 4 Pressure abnormalities. *(Continued)*

9.	Plugged frit in in-line filter or guard column; plugged inlet frit. → Replace end-fitting or frit assembly.
10.	Polymeric columns—solvent change causes swelling of packing. → Use correct solvent with column; change to proper solvent composition! Consult manufacturer's solvent-compatibility chart; use a column with a higher percentage of cross-linking.
11.	Salt precipitation (especially in reversed-phase chromatography with high concentration of organic solvent in mobile phase). → Ensure mobile phase compatibility with buffer concentration; decrease ionic strength and water-organic solvent ratio; premix mobile phase.
12.	When injector disconnected from column-blockage in injector. → Clean injector or replace rotor.

column inlet (the column may need repacking), as well as to active sites within the column which can be solved with the use of a competing basic or acidic modifier.

If only some of the peaks tail, secondary retention effects, such as residual silanol interactions, may take place. Another possibility is that a small peak is eluting on the tail of a larger peak. If all peaks tail, this may be due to a bad column or build up of contamination on the column inlet frit.

Peak fronting (peak asymmetry factor <0.9). This indicates that a small band is eluting before a large band, a wrong pH value of the mobile phase is used, an

Table 5 Leaks.

Leaks
Injector leaks
Rotor seal failure → Replace rotor seal.
Blocked loop → Clean or replace loop.
Loose injection-port seal → Tighten.
Waste line siphoning → Keep waste line above surface waste.
Waste line blockage → Replace waste line.
Column leaks.
Loose endfitting → Tighten endfitting.
Improper frit thickness → Use proper frit.
Detector leaks
Cell gasket failure → Prevent excessive backpressure; replace gasket.
Cracked cell window → Replace window.
Leaky fittings → Tighten or replace.
Blocked waste line → Replace waste line.
Leaky fittings
Loose fitting → Tighten.
Stripped fitting → Replace.
Overtightened fitting → Loosen and retighten; replace.
Dirty fitting → Disassemble and clean; replace.
Mismatched parts → Use parts from the same brand so that they match.
Leaks at pump
Loose check valves or fittings → Tighten.
Mixer seal failure → Replace mixer seal; replace mixer.
Pump seal failure → Repair or replace.
Pressure transducer failure → Repair or replace.
Pulse damper failure → Replace pulse damper.
Proportioning valve failure → Check diaphragms, replace if leaky; check for fitting damage, replace.
Purge valve → Tighten valve; replace purge valve.

Table 6 Imprecision.

Change in selectivity

1. Not enough sample is injected. → Increase amount of injected sample.
2. Sample loop of injector is underfilled. → Overfill loop with sample.
3. Sample is lost during sample preparation. → Optimize sample preparation.
4. Autosampler line is blocked. → Clean blockage.
5. Detector attenuation is set too high. → Reduce detector attenuation.
6. Peaks are outside detector's linear range. → Dilute or enrich sample to reach linear range of detector.
7. Column is worn out. → Replace column.
8. Column temperature is altered. → Use column oven to maintain constant temperature.

Change in height–lack of sensitivity

1. Sample deterioration. → Use fresh sample.
2. Leak. → Check for pump leaks and fittings.
3. Nonreproducible sample volume. → Ensure loop is completely filled. Check autosampler. Check flow and clear any blockages.
4. Low detector response. → Check detector settings and operating conditions.
5. Detector attenuation is set too high. → Reduce detector attenuation.
6. Sample is lost during preparation. → Optimize sample preparation. Use internal standard during sample preparation.
7. Peaks are outside the linear range of the detector. → Dilute of enrich the sample until concentration is within the linear range of the detector.
8. First few sample injections—sample adsorption in injector sample loop or column. → Condition loop and column with concentrated sample.
9. Injector sample loop is underfilled. → Overfill loop with sample.
10. Not enough sample is injected. → Increase amount of sample injected.
11. Peaks are outside detector's linear range. → Dilute or concentrate sample to bring detector response into linear range.

Imprecision

1. Operator dependence during sample processing and clean-up. → Check all steps for errors.
2. Sample injection. → Check autosampler; fill loop completely.
3. Detection. → Clean flow-cell. Improve signal-to-noise ratio.
4. Separation. → Improve resolution.
5. Data processing and calibration. → Use internal standard. Calibrate frequently.

Poor sample recovery

1. Absorption or adsorption of proteins. → Reduce non-specific interactions by changing HPLC mode; add protein-solubilizing agent, strong acid or base (with polymeric columns only), or detergent such as SDS to mobile phase.
2. Adsorption or chemisorption on column packing or on different hardware components. → Increase mobile phase strength; add competing base (for basic compounds) or use base-deactivated packing; ensure no reactive groups are present; use inert tubing and flow-path components, e.g., PEEK.
3. Irreversible adsorption on active-sites (less than 90% yield). → For basic compounds use end-capped, base-deactivated, sterically protected, high coverage, or polymeric reversed-phase. → For acidic compounds use endcapped or polymeric packing; acidify mobile phase.

overloaded column, a void volume at the inlet, or that the sample solvent is incompatible with the mobile phase.

Double peaks, rounded peaks, and broad peaks

A void volume in the column, or a partially blocked frit can possibly cause double or split peaks. In case that only one peak is a doublet, then co-eluting compounds may be present.

Rounded peaks are attributed to high concentrations (the detector response being outside the linear dynamic range), wrong sample solvent, or too high a setting of the detector or integrator time constant.

Problem No. 1: No Peaks/Very Small Peaks

Normal

794-0747

1. Detector lamp off.	1. Tum lamp on.
2. Loose/broken wire between detector and integrator or recorder.	2. Check electrical connections and cables.
3. No mobile-phase flow.	3. See “No Flow” (Problem No. 2).
4. No sample/deteriorated sample/wrong sample.	4. Be sure automatic sampler vials have sufficient liquid and no air bubbles in the sample. Evaluate system performance with fresh standard to confirm sample as source of problem.
5. Settings too high on detector or recorder.	5. Check attenuation or gain settings. Check lamp status. Auto-zero if necessary.

Problem

794-0748

Problem

794-0749

Problem No. 2: No Flow

Normal

794-0747

1. Pump off.	1. Start pump.
2. Flow interrupted/obstructed.	2. Check mobile-phase level in reservoir(s). Check flow throughout system. Examine sample loop for obstruction or air lock. Make sure mobile phase components are miscible and mobile phase is properly degassed.
3. Leak.	3. Check system for loose fittings. Check pump for leaks, salt buildup, unusual noises. Change pump seals if necessary.
4. Air trapped in pump head. (Revealed by pressure fluctuations.)	4. Disconnect tubing at guard column (if present) or analytical column inlet. Check for flow. Purge pump at high flow rate (e.g., 5–10 ml/min), prime system if necessary. (Prime each pump head separately.) If system has check valve, loosen valve to allow air to escape. If problem persists, flush system with 100% methanol or isopropanol. If problem still persists, contact system manufacturer.

Problem

794-0748

Fig. 1 Typical changes that appear in the chromatogram as a result of various problems in HPLC.
Source: Reprinted with permission of Supelco, Bellefonte, PA, from Bulletin 826D, 1999.

Problem No. 3: No Pressure/Pressure Lower Than Usual

Normal

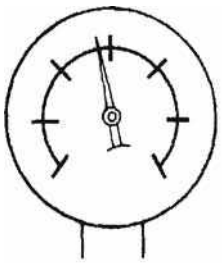

794-0750

Problem

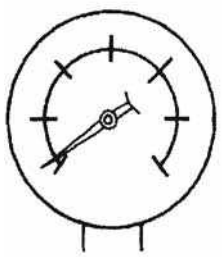

794-0751

1. Leak.	1. Check system for loose fittings. Check pump for leaks, salt buildup, unusual noises. Change pump seals if necessary.
2. Mobile-phase flow interrupted/ obstructed.	2. Check mobile phase level in reservoir(s). Check flow throughout system. Examine sample loop for obstruction or air lock. Make sure mobile phase components are miscible and mobile phase is properly degassed.
3. Ait trapped in pump head. (Revealed by pressure fluctuations.)	3. Disconnect tubing at guard column (if present) or analytical column inlet. Check for flow. Purge pump at high flow rate (e.g., 10 ml/min), prime system if necessary. (Prime each pump head separately.) If system has check valve, loosen valve to allow air to escape.
4. Leak at column inlet end fitting.	4. Reconnect column and pump solvent at double the flow rate. If pressure is still low, check for leaks at inlet fitting or column end fitting.
5. Air trapped elsewhere in system.	5. Disconnect guard and analytical column and purge system. Reconnect column(s). If problem persists, flush system with 100% methanol or isopropanol.
6. Worn pump seal causing leaks around pump head.	6. Replace seal. If problem persists, replace piston and seal.
7. Faulty check valve.	7. Rebuild or replace valve.
8. Faulty pump seals.	8. Replace seals.

Problem No. 4: Pressure Higher Than Usual

Normal

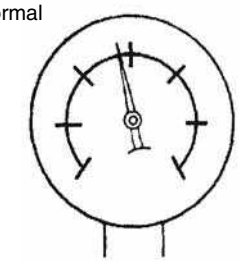

794-0750

Problem

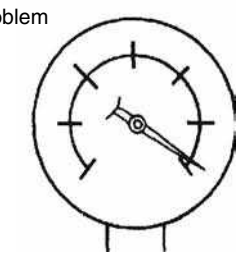

794-0752

1. Problem in pump, injector, in-line filter, or tubing.	1. Remove guard column and analytical column from system. Replace with unions and 0.010˝ I.D. or larger tubing to reconnect injector to detector. Run pump at 2–5 ml/min. If pressure is minimal, see Cause 2. If not, isolate cause by systematically eliminating system components, starting with detector, then in-line filter, and working back to pump. Replace filter in pump if present.
2. Obstructed guard column or analytical column.	2. Remove guard column (if present) and check pressure. Replace guard column if necessary. If analytical column is obstructed, reverse and flush the column, while disconnected from the detector (page 14). If problem persists, column may be clogged with strongly retained contaminants. Use appropriate restoration procedure (Table 2, page 14). If problem still persists, change inlet frit (page 16) or replace column.

Fig. 1 (*Continued*)

Problem No. 5: Variable Retention Times

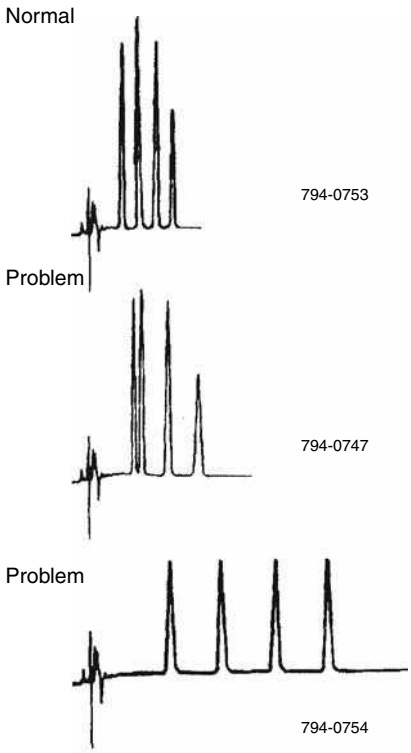

1. Leak.	1. Check system for loose fittings. Check pump for leaks, salt buildup, unusual noises. Change pump seals if necessary.
2. Change in mobile-phase composition. (Small changes can lead to large changes in retention times.)	2. Check make-up of mobile phase. If mobile phase is machine mixed using proportioning values, hand mix and supply from one reservoir.
3. Air trapped in pump. (Retention times increase and decrease at random times.)	3. Purge air from pump head or check valves. Change pump seals if necessary. Be sure mobile phase is degassed.
4. Column temperature fluctuations (especially evident in ion-exchange systems).	4. Use reliable column oven. (Note: higher column temperatures increase column efficiency. For optimum results, heat eluant before introducing it onto column.)
5. Column overloading. (Retention times usually decrease as mass of solute injected on column exceeds column capacity.)	5. Inject smaller volume (e.g., 10 µl vs. 100 µl) or inject the same volume after 1:10 or 1:100 dilutions of sample.
6. Sample solvent incompatible with mobile phase.	6. Adjust solvent. Whenever possible, inject samples in mobile phase.
7. Column problem. (Not a common cause of erratic retention. As a column ages, retention times *gradually* decrease.)	7. Substitute new column of same type to confirm column as cause. Discard old column if restoration procedures fail (see page 14).

Problem No. 6: Loss of Resolution

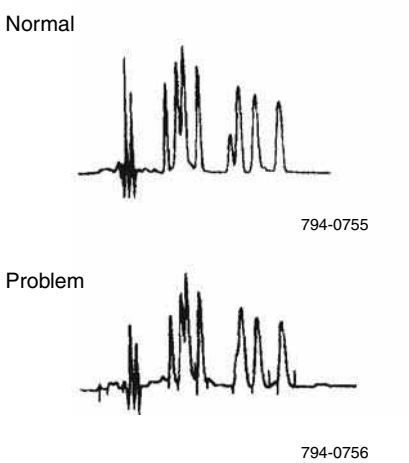

1. Mobile phase contaminated/ deteriorated (causing retention times and/or selectivity to change).	1. Prepare fresh mobile phase (page 2).
2. Obstructed guard or analytical column.	2. Remove guard column (if present) and attempt analysis. Replace guard column if necessary. If analytical column is obstructed, reverse and flush (page 14). If problem persists, column may be clogged with strongly retained contaminants. Use appropriate restoration procedure (Table 2, page 14). If problem still persists, change inlet frit (page 16) or replace column.

Fig. 1 (*Continued*)

Additionally, these peak-related problems may be attributed to column overload, too long or too wide tubing, column contamination, low flow rate, etc.

If all peaks are broadened, possible causes include a large sample volume injected, or a viscous mobile phase, or a column that has lost its efficiency, possibly due to the presence of a column void. If only some peaks are broadened, then a peak from a previous run may be eluted late, or a high molecular mass sample, e.g., a protein or a polymer is present.

Problem No. 7: Split Peaks

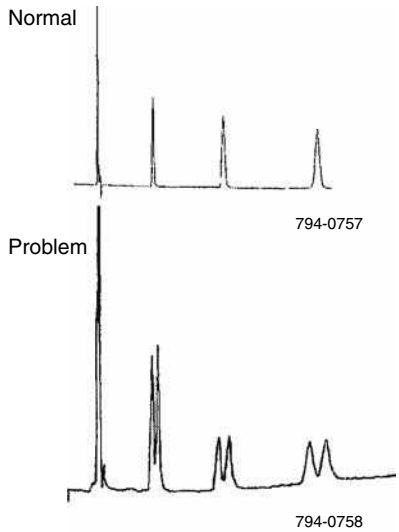

1. Contamination on guard or analytical column inlet.	1. Remove guard column (if present) and attempt analysis. Replace guard column if necessary. If analytical column is obstructed, reverse and flush (page 14). If problem persists, column may be clogged with strongly retained contaminants. Use appropriate restoration procedure (Table 2, page 14). If problem still persists, inlet frit is probably (partially) plugged. Change frit (page 16) or replace column.
2. Partially blocked frit.	2. Replace frit (see above)
3. Small (uneven) void at column inlet.	3. Repack top of column with pellicular particles of same bonded phase functionality. Continue using the column in reverse flow direction.
4. Sample solvent incompatible with mobile phase.	4. Adjust solvent. Whenever possible, inject samples in mobile phase.

Problem No. 8: Peaks Tail on Initial and Later Injections

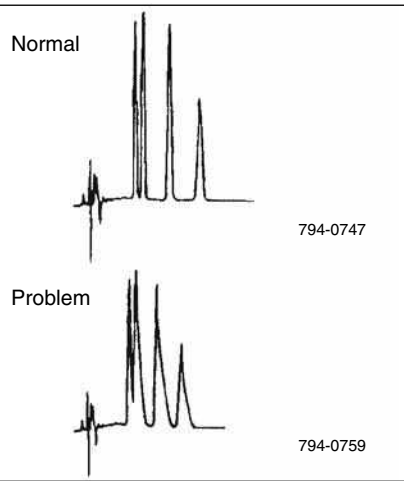

1. Sample reacting with active sites.	1. First check column performance with standard column test mixture. If results for test mix are good, add ion pair reagent or competing base or acid modifier (page 2).
2. Wrong mobile phase pH.	2. Adjust pH. For basic compounds, lower pH usually provides more symmetric peaks.
3. Wrong column type.	3. Try another column type (e.g., deactivated column for basic compounds).
4. Small (uneven) void at column inlet.	4. See Problem No. 7.
5. Wrong injection solvent.	5. Peaks can tail when sample is injected in stronger solvent than mobile phase. Dissolve sample in mobile phase.

Problem No. 9: Tailing Peaks

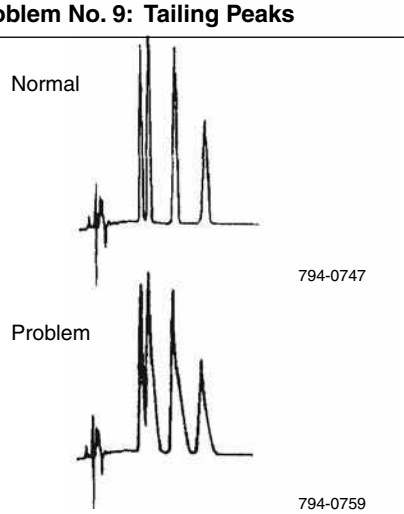

1. Guard or analytical column contaminated/worn out.	1. Remove guard column (if present) and attempt analysis. Replace guard column if necessary. If analytical column is source of problem, use appropriate restoration procedure (Table 2, page 14). If problem persists, replace column.
2. Mobile phase contaminated/ deteriorated.	2. Check make-up of mobile phase (page 2).
3. Interfering components in sample.	3. Check column performance with standards.

Fig. 1 (*Continued*)

Problem No. 10: Fronting Peaks

Normal

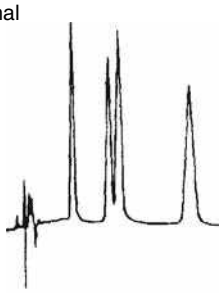

794-0760

1. Column overloaded.	1. Inject smaller volume (e.g., 10 µl vs. 100 µl). Dilute the sample 1:10 or 1:100 fold in case of mass overload.
2. Sample solvent incompatible with mobile phase.	2. Adjust solvent. Whenever possible, inject samples in mobile phase. Flush polar bonded phase column with 50 column volumes HPLC grade ethyl acetate at 2–3 times the standard flow rate, then with intermediate polarity solvent prior to analysis.
3. Shoulder or gradual baseline rise before a main peak may be another sample component.	3. Increase efficiency or change selectivity of system to improve resolution. Try another column type if necessary (e.g., switch from nonpolar C18 to polar cyano phase).

Problem

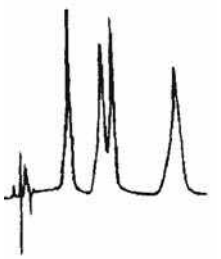

794-0761

Problem No. 11: Rounded Peaks

Normal

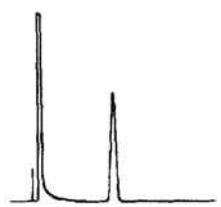

794-0762

1. Detector operating outside linear dynamic range.	1. Reduce sample volume and/or concentration.
2. Recorder gain set too low.	2. Adjust gain.
3. Column overloaded.	3. Inject smaller volume (e.g., 10 µl vs. 100 µl) or 1:10 or 1:100 dilution of sample.
4. Sample-column interaction.	4. Change buffer strength, pH, or mobile phase composition. If necessary, raise column temperature or change column type. (Analysis of solute structure may help predict interaction.)
5. Detector and/or recorder time constants are set too high.	5. Reduce settings to lowest values or values at which no further improvements are seen.

Problem

794-0763

Fig. 1 (*Continued*)

System peaks

A system peak is a peak that originates from the chromatographic system itself, i.e., mobile phase and column, and not from the sample. Its appearance and size are sensitive to the sample composition, but its origins are generally the mobile phase components.

When a mobile phase is introduced to a column, its components undergo distribution until equilibrium is attained. Injection of a sample different from the mobile phase causes a small equilibrium perturbation at the column head. The equilibrium of each component of the mobile phase can be disturbed and, thereby, manifested by one system peak for each mobile phase additive, using the appropriate detection conditions.

System peaks are most often recognized as a pair of peaks, one positive and the other negative, which represent enrichment and depletion zones eluted from the column. They may vary in retention time and size, depending on the sample matrix, injection volume, mobile-phase composition, and the stationary phase. Dissolving samples in the mobile phase is the best way to minimize system peak effects. System peaks are especially important in ion-pairing chromatography and in ion chromatography. In the latter, they are pH dependent and they often interfere with sample components.

Problem No. 12: Baseline Drift

Normal

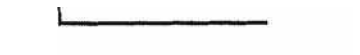

794-0748

Problem

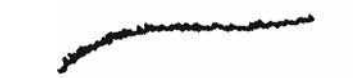

794-0764

1. Column temperature fluctuation. (Even small changes cause cyclic baseline rise and fall. Most often affects refractive index and conductivity detectors, UV detectors at high sensitivity or in indirect photometric mode.)	1. Control column and mobile-phase temperature, use heat exchanger before detector.
2. Non-homogeneous mobile phase. (Drift usually to higher absorbance, rather than cyclic pattern from temperature fluctuation.)	2. Use HPLC grade solvents, high purity salts, and additives. Degas mobile phase before use, sparge with helium during use.
3. Contaminant or air buildup in detector cell.	3. Flush cell with methanol or other strong solvent. If necessary, clean cell with 1 N HNO_3 (never with HCl and never use nitric acid with PEEK tubing or fittings.)
4. Plugged outlet line after detector, (High pressure cracks cell window, producing noisy baseline.)	4. Unplug or replace line. Refer to detector manual to replace window.
5. Mobile phase mixing problem or change in flow rate.	5. Correct composition/flow rate. To avoid problem, routinely monitor composition and flow rate.
6. Slow column equilibration, especially when changing mobile phase.	6. Flush column with intermediate strength solvent, run 10–20 column volumes of new mobile phase through column before analysis.
7. Mobile phase contaminated, deteriorated, or not prepared from high quality chemicals.	7. Check make-up of mobile phase (page 2).
8. Strongly retained materials in sample (high k') can elute as very broad peaks and appear to be a rising baseline. (Gradient analyses can aggravate problem.)	8. Use guard column. If necessary, flush column with strong solvent between injections or periodically during analysis.
9. Detector (UV) not set at absorbance maximum but at slope of curve.	9. Change wavelength to UV absorbance maximum.

Problem No. 13: Baseline Noise (regular)

Normal

794-0748

Problem

794-0765

1. Air in mobile phase, detector cell, or pump.	1. Degas mobile phase. Flush system to remove air from detector cell or pump.
2. Pump pulsations.	2. Incorporate pulse damper into system.
3. Incomplete mobile phase mixing.	3. Mix mobile phase by hand or use less viscous solvent.
4. Temperature effect (column at high temperature, detector unheated).	4. Reduce differential or add heat exchanger.
5. Other electronic equipment on same line.	5. Isolate LC, detector, recorder to determine if source of problem is external. Correct as necessary.
6. Leak.	6. Check system for loose fittings. Check pump for leaks, salt buildup, unusual noises. Change pump seals if necessary.

Fig. 1 (*Continued*)

Pressure abnormalities

Lower pressure than anticipated is observed due to leaks, insufficient flow from the pump, air bubbles, and worn pump seals. Fluctuating pressure is attributed to air trapped in the pump, or leaking pump check valves or seals. Higher pressure than anticipated is due to blocked flow lines, particulate build up at the head of the column, or buffer

Problem No. 14: Baseline Noise (irregular)

Normal

794-0748

Problem

794-0766

1. Leak.	1. Check system for loose fittings. Check pump for leaks, salt buildup, unusual noises. Change pump seals if necessary.
2. Mobile phase contaminated, deteriorated, or prepared from low quality materials.	2. Check make-up of mobile phase. (page 2).
3. Detector/recorder electronics.	3. Isolate detector and recorder electronically. Refer to instruction manual to correct problem.
4. Air trapped in system.	4. Flush system with strong solvent.
5. Air bubbles in detector.	5. Purge detector. Install back pressure regulator after detector. Check the instrument manual, particularly for RI detectors (excessive backpressure can cause the flow cell to crack).
6. Detector cell contaminated. (Even small amounts of contaminants can cause noise.)	6. Clean cell.
7. Weak detector lamp.	7. Replace lamp.
8. Column-leaking silica or packing material.	8. Replace column and clean system.

Problem No. 15: Broad Peaks

Normal

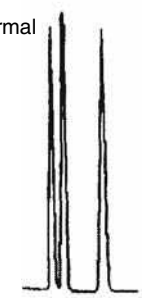

794-0767

Problem

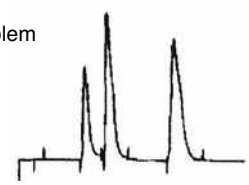

794-0768

1. Mobile-phase composition changed.	1. Prepare new mobile phase.
2. Mobile-phase flow rate too low.	2. Adjust flow rate.
3. Leak (especially between column and detector).	3. Check system for loose fittings. Check pump for leaks, salt buildup, and unusual noises. Change pump seals if necessary.
4. Detector settings incorrect.	4. Adjust settings.
5. Extra-column effects:	
a. Column overloaded	5. a. Inject smaller volume (e.g., 10 µl vs. 100 µl) or 1:10 and 1:100 dilutions of sample.
b. Detector response time or cell volume too large.	b. Reduce response time or use smaller cell.
c. Tubing between column and detector too long or I.D. too large.	c. Use as short a piece of 0.007–0.010" I.D. tubing as practical.
d. Recorder response time too high.	d. Reduce response time.
6. Buffer concentration too low.	6. Increase concentration.
7. Guard column contaminated/worn out.	7. Replace guard column.
8. Column contaminated/worn out.	8. Replace column with new one of same type. If new column does not provide narrow peaks, flush old column (Table 2, page 14), then retest.
9. Void at column inlet.	9. Replace column or open inlet end and fill void (page 16).
10. Peak represents two or more poorly resolved compounds.	10. Change column type to improve separation.
11. Column temperature too low.	11. Increase temperature. Do not exceed 75°C unless higher temperatures are acceptable to column manufacturer.

Fig. 1 (*Continued*)

salt precipitation. To locate blockage, components should be systematically disconnected, starting from the detector-end to column-end. Once the blocked component is located, it must be either cleaned or replaced. Back flushing of column will help to remove particulates at the top of column, thus reducing pressure. If buffers are used, their compatibility with the mobile phase should be checked to avoid precipitation within the system.

Problem No. 16: Change in Peak Height (one or more peaks)

Normal

794-0769

Problem

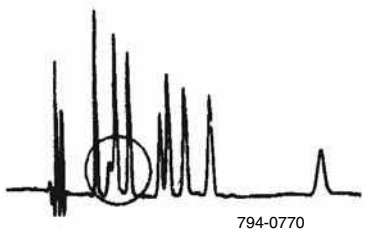

794-0770

1. One or more sample components deteriorated or column activity changed.	1. Use fresh sample or standard to confirm sample as source of problem. If some or all peaks are still smaller than expected, replace column. If new column improves analysis, try to restore the old column, following appropriate procedure (Table 2, page 14). If performance does not improve, discard old column.
2. Leak especially between injection port and column inlet. (Retention also would change.)	2. Check system for loose fittings. Check pump for leaks, salt buildup, unusual noises. Change pump seals if necessary.
3. Inconsistent sample Volume.	3. Be sure samples are consistent. For fixed volume sample loop, use 2–3 times loop volume to ensure loop is completely filled. Be sure automatic sampler vials contain sufficient sample and no air bubbles. Check syringe-type injectors for air in systems with wash or flushing step, be sure wash solution does not precipitate sample components.
4. Detector or recorder setting changed.	4. Check settings.
5. Weak detector lamp.	5. Replace lamp.
6. Contamination in detector cell.	6. Clean cell.

Problem No. 17: Change in Selectivity

Normal

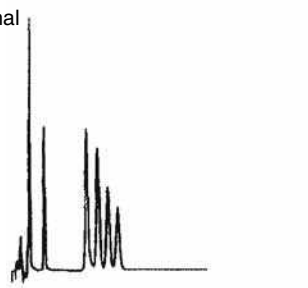

794-0771

Problem

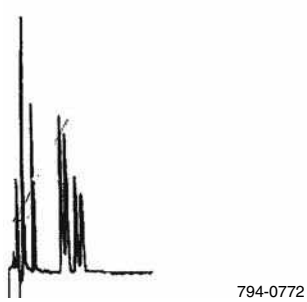

794-0772

1. Increase of decrease solvent ionic strength, pH, or additive concentration (especially affects ionic solutes).	1. Check make-up of mobile phase (page 2).
2. Column changed, new column has different selectivity from that of old column.	2. Confirm identity of column packing. For reproducible analyses, use same column type. Establish whether change took place gradually. If so, bonded phase may have stripped. Column activity may have changed, or column may be contaminated.
3. Sample injected in incorrect solvent or excessive amount (100–200 µl) of strong solvent.	3. Adjust solvent. Whenever possible, inject sample in mobile phase.
4. Column temperature change.	4. Adjust temperature. If needed, use column oven to maintain constant temperature.

Fig. 1 (*Continued*)

Change on separation (loss of resolution) and changes in height

Changes in separation, implying a loss of resolution, are attributed to leaks or an obstructed column. Change in height originates from sample deterioration, leaks, non-reproducible sample volumes, and low detector response. A fresh sample should be checked, as well as detector settings and operating conditions.

Problem No. 18: Negative Peak(s)

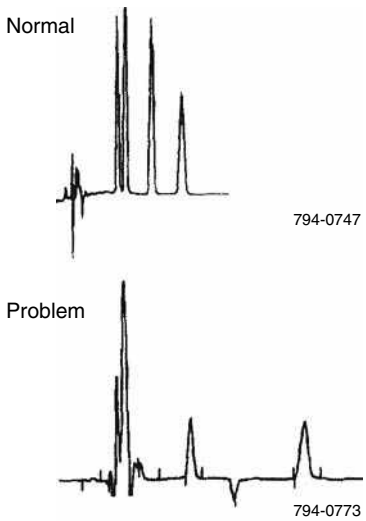

1. Recorder leads reversed.
2. Refractive index of solute less than that of mobile phase (RI detector).
3. Sample solvent and mobile phase differ greatly in composition (vacancy peaks).
4. Mobile phase more absorptive than sample components to UV wavelength.

1. Check polarity.
2. Use mobile phase with lower refractive index, or reverse recorder leads.
3. Adjust or change sample solvent. Dilute sample in mobile phase whenever possible.
4. a. Change polarity when using indirect UV detection, or
   b. Change UV wavelength or use mobile phase that does not adsorb chosen wavelength.

Problem No. 19: Ghost Peak

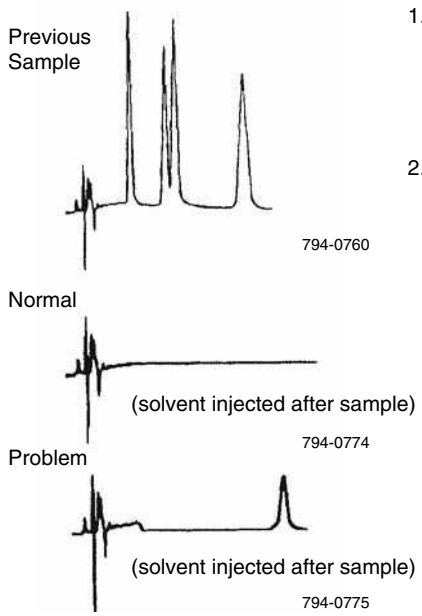

1. Contamination in injector or column.
2. Late-eluting peak (usually broad) present in sample.

1. Flush injector between analyses (a good routine practice). If necessary, run strong solvent through column to remove late eluters. Include final wash step in gradient analyses, to remove strongly retained compounds.
2. a. Check sample preparation.
   b. Include (step) gradient to quickly elute component.

Fig. 1 (*Continued*)

Leaks

Leaks can be detected visually or by smell before even a pressure decrease is noticed. They can take place in different positions in the LC system, such as the column, the pump, the injection valve, or the detector. In case of leaks at the column or fittings, a leaky fitting should be tightened or replaced. The detector seal should be replaced if there is a leak at the detector.

A worn or scratched valve rotor in the injection valve should be replaced to prevent leaks in the injection valve.

In case of pump seal failure, pump seals should be replaced, or the piston should be checked for scratches and should be replaced if necessary.

Sample introduction

Problems with the sample introduction may arise both in manual injection and during autosampling. Table 7 summarizes the problems related to sample introduction.

In the case of autosamplers, although they are considered as time saving devices, their function is associated with some

Table 7 Problems related to sample introduction.

Manual injector problems
Damaged rotor seal → Rebuild or replace valve.
Rotor too tight → Adjust rotor tension.
Valve misaligned → Adjust alignment.
Blocked loop → Replace loop.
Dirty syringe → Clean or replace syringe.
Blocked lines → Clean or replace lines.
Autoinjector problems
No air pressure → Supply proper pressure.
Rotor too tight → Adjust.
Valve misaligned → Adjust alignment.
Blockage → Clean or replace blocked portion.
Jammed mechanism → See service manual.
Faulty controller → Repair or replace controller.
Carryover problems → 1. Replace blank. 2. Change injection size. 3. Check fitting assembly and washing mechanism. 4. Use fresh wash solvent. 5. Increase wash volume. 6. Use more organic solvent in wash. 7. Adjust wash pH. 8. Change injection solvent. 9. Change needle seal, injection loop. 10. Replace valve.

common problems. For example, needle depth adjustment is very critical when there is not enough sample available; a needle blockage may occur from a septum. Another common problem related to the autosampler is carryover that causes the appearance of a peak in a blank injection following injection of a high concentration of sample. Sample stability is a figure of merit that certainly has to be evaluated to avoid imprecision and lack of sensitivity.

PREVENTIVE MAINTENANCE

Many of the problems that the chromatographer encounters can be avoided if preventive maintenance is performed in routine operation, in every step of chromatographic analysis, from sample preparation to the final step of an analysis.

Precautions regarding the use of the analytical columns, as well as the operation of each module, e.g., the pump, the detector, etc. may help keep away or postpone most of the abovementioned problems related to HPLC instrumentation.

Preventive Maintenance During Sample Preparation

As already mentioned, many problems concerning increased pressure and backpressure are due to plugged frits or system clogging from a sample matrix particulates or salt precipitation.

Preventive actions include the following:

1. Sample filtration to ensure it contains no solids.
2. Sample dissolution in the mobile phase or solvent weaker than the mobile phase.
3. Use of reduced sample volumes, whenever possible.

Mobile phase inlet filters, pre-injector and pre-column filters, saturator columns, and guard columns greatly reduce problems associated with complex separations.

Moreover, all solvents should be filtered through 0.2 μm filters, while particulates from samples can be removed by filtration through 0.45 or 0.2 μm syringe filters.

Bacterial Growth Precautions

Bacteria that grow in water reservoirs can yield by-products such as metabolites and dead bacteria, thus producing ghost peaks. Adding organic solvent to the aqueous part of the mobile phase, at a percentage of $> 20\%$ or sodium azide 0.04% will prevent bacterial growth.

Sources of Contamination

Numerous sources of contamination should be taken into account: air particles from the laboratory environment, phthalates from plastic stoppers, plasticizers from plastic containers, detergents and cleaning agents from sample containers and glassware, stabilizing agents and additives from solvents, reagents and chemicals solvent impurities, purified water, and microorganisms. The use of reagent blanks (sample matrix is water in this case) and matrix blanks may help to monitor an analysis on a day-to-day basis.

The compatibility of an organic solvent with a buffer in the mobile phase must be checked as the buffer salts can be easily precipitated when using online mixing, thus causing frit blockage, check valve malfunction, and other problems.

Good Column Practice: Column Protection

The most common problem associated with analytical columns is column deterioration. Deterioration may appear as poor peak shapes, split peaks, shoulders, loss of resolution, decreased retention times, and high backpressure. These symptoms indicate contaminants that have accumulated on the frit or column inlet, or there are voids, channels, or a depression in the packing bed. Deterioration is more evident in higher efficiency columns. For example, a column with 3 μm packing is more susceptible to plugging than one with 5 or 10 μm packing. Proper column protection and sample preparation are essential to prolong a column's life and obtain its best performance.

Filters and guard columns prevent particles and strongly retained compounds from accumulating on the analytical column. Silica particles in a saturator column dissolve in high pH mobile phases, protecting the silica-based packing in the analytical column. The useful life of these disposable products depends on mobile phase composition, sample purity, pH value within the recommended range, etc. As these devices become contaminated or plugged with particles, pressure increases and peaks broaden or split.

Keeping records of column backpressure and important chromatographic parameters [number of theoretical plates (N), peak asymmetry factor (As), retention factor (k'), resolution factor (Rs)] helps to monitor the required column performance, while storage in the appropriate organic solvent extends column lifetime. Table 8 presents the preventive actions for column protection.

Lamp Failure

Many detectors track the number of hours the lamp is ignited. Although the lamp life may vary, the detector's meter reading can be a helpful guide for troubleshooting. Lamps can sometimes operate for more than 2000 hr. To distinguish a lamp problem from air bubbles, one should stop the mobile-phase flow. A lamp problem will persist when the flow is stopped, whereas, if the problem is due to the presence of a bubble, the baseline remains steady on- or off-scale. If the bubble stops in the flow cell, it causes a dramatic baseline shift, usually off-scale.

Solvent degassing and backpressure regulators after the detector minimize bubble formation. It is a helpful practice to perform blank runs every day to provide reference data that can be consulted at a later date.

Spikes in chromatograms can come from many sources, such as aging detector lamps or bubbles in the flow cell; both

Table 8 Preventive maintenance for HPLC instrumentation.

Preventive maintenance for HPLC columns	Preventive maintenance to avoid high backpressures	General preventive maintenance
Filter solvents before use.	Use HPLC or analytical grade buffers, freshly prepared, filtered and degassed before use.	Filtering mobile phase prevents often replacing inlet frits and check valves.
Use in-line filters for all columns, and guard columns for dirty samples; pre-treat dirty samples, remove particulates.	Filter or centrifuge the sample to remove particulate matter. Turbid samples should not be injected onto column.	Degassing mobile phase prevents bubble formation.
Check samples for compatibility with mobile phase.	Set the maximum backpressure of the pumps at or slightly below the value suggested in the column instructions so that in case of increased pressure, the system will turn off before any damage occurs.	Inlet frits prevent check valve failure.
Avoid extreme column temperatures. Keep column temperature below 60°C.	Use the recommended flow rates for the column.	Rotor seal wear should not be over-tightened.
Flush column frequently/daily with strong solvent. Use stronger solvent protocol for dirty samples.	Ethanol, glycerol, high salt, urea, and cause increases in back pressure—reduce flow rate accordingly.	Sample filtration prevents injector function, frit blockage.
Keep the mobile phase pH between 3 and 7. If operating outside of this pH range use a precolumn.	When performing the separation at low temperatures, e.g., at 4°C, the recommended flow rate should be reduced by 50%.	In line filters or guard column prevent frit blockage.
Use fresh buffer solutions and aqueous mobile phases or treat them with sodium azide.	Wash the chromatography column thoroughly at the end of each separation.	Use of guard column or pre-column help avoiding void at top of column.
To prepare column for storage purge column of buffers and leave in appropriate solvent. Cap tightly.	Clean columns when needed, following the column instructions.	The use of restrictor after cell prevents bubble formation in cell.
Prevent microbial growth when storing columns by using 50–100 % organic/water mixtures or adding azide to gel filtration columns.	Maintain a log of each chromatographic run, including buffer composition, flow rate, observed back-pressure (before and after sample application), sample composition, binding, and elution conditions.	Flushing buffer from LC prevents corrosive abrasive damage.
Avoid physically mishandling columns: banging, dropping, or over-tightening fittings.	Monitor column efficiency via regular column testing (i.e., acetone tests, function tests).	Keeping spare parts in lab can reduce waiting time intervals.

can be easily corrected. External electrical noise sources, such as ovens, refrigerators, cellular telephones, and fluorescent lights, and other possible noise sources such as system electronics or from external electronic sources, and laboratory power feed may be beyond a chromatographer's control.

Having an unused spare detector lamp available makes checking the problems attributed to the lamp performance an easy task.

Preventing and Solving Common Hardware Problems

Special care can be taken to avoid high backpressure in the LC system. Preventive actions to this end, as well as general preventive maintenance practices that can generally help reduce the failure rate, are summarized in Table 8.

Preventing leaks

Leaks are a common problem in HPLC analysis. Their occurrence can be minimized by avoiding interchanging hardware and fittings from different manufacturers. Incompatible fittings can be forced to fit initially, but repeated connections may eventually leak. If interchanging is unavoidable, the appropriate adapters should be used and all connections should be checked for leaks before proceeding.

Highly concentrated salts (>0.2 *M*) and caustic mobile phases can reduce pump seal efficiency. The lifetime of injector rotor seals also depends on mobile phase conditions, e.g., operation at high pH. In some cases, prolonged use of ion pair reagents has a lubricating effect on pump pistons that may produce small leaks at the piston seal. Some seals do not perform well with certain solvents.

Instrument manufacturers' specifications should be consulted before using a pump under adverse conditions. To replace seals, refer to the maintenance section of the manufacturer's pump manual.

Unclogging the Column Frit

A clogged column frit is another common HPLC problem. To minimize this problem from the start, the use of a pre-column filter and/or guard column is recommended. To clean the clogged inlet frit, the column must be disconnected and reversed. Then it should be connected to the pump (but not to the detector), and solvent should be pumped through it at twice the standard flow rate. About 5–10 column volumes of solvent should be sufficient to remove small amounts of particulate material from the inlet frit. The performance of the cleaned column has to be evaluated by using a standard test mixture. It should be noted, however, that some columns are designated by the manufacturer as not to be used in a reverse flow mode. Of course, if the plugging prevents the column from being used anyway, then reverse flow treatment is an acceptable action.

Filling a Void/Replacing a Frit at the Column Inlet

Sometimes, neither solvent flushing nor restoration procedures restore a column's performance. If the column is proved to be the problem source, a void in the packing or a persistent obstruction on the inlet frit may exist. In this case, replacing the frit and/or topping the column with slurry of the sorbent material in a volatile solvent, e.g., acetone, to fill the void, may help.

Mobile Phase

Contamination of mobile-phase reservoirs can often become a possible source of problems such as blocked frits, irregular pump performance, extra peaks, or noise in the chromatogram. Mobile phase degassing by helium sparging, sonication, and vacuum or heating (mostly in case of electrochemical detection) prior to, or during, use prevents air bubble formation.

Manually mixed mobile phases can be adequately degassed before pumping. However, if mixing takes place in the LC equipment, solvents must be simultaneously degassed. Besides bubble formation, oxygen is the primary problem interfering with detector response. In UV detectors, oxygen can cause a significant baseline rise. In fluorescence detectors, oxygen can adversely affect sensitivity by quenching sample fluorescence. Also, oxygen-free mobile phase is required for electrochemical detectors in the reductive mode.

Degassing is not required only in some cases of normal phase LC or non-aqueous SEC due to not significantly different solubility of air in the solvents used (e.g., hexane, toluene, dichloromethane, etc.).

Another case where degassing is not necessary is when high-pressure mixing is performed, where mobile phase components are mixed after the pump, at the high pressure side of the pump, so that gas is kept dissolved in solution by the high pressure.

Keeping Accurate Records

Most problems do not occur suddenly; rather, they usually develop gradually. Accurate record keeping, then, is of paramount importance in detecting and solving many gradually developing problems. When using a new column for the first time, it should be evaluated initially and at regular intervals thereafter. By keeping a written history of column efficiency, mobile phases used, lamp current, pump performance, etc. the chromatographer can monitor a system's performance.

Records also help prevent mistakes, such as introducing water into a silica column, or precipitating buffer in the system by adding too much organic solvent. Many analysts occasionally modify their HPLC systems for a variety of reasons. Reliable records are the best way to ensure that a modification does not introduce problems. For problems relating to pumps, detectors, automatic samplers, and data systems, instrument manuals provide suitable troubleshooting guides.

Referring to the maintenance and troubleshooting sections of an instrument's manual is highly recommended. Many individuals consult manuals only after a catastrophic failure and then only when all other problem-solving approaches have been exhausted. Modern HPLC systems often have self-diagnostic capabilities that help isolate the problem area within the instrument.

CONCLUSIONS

The common problems in HPLC concern pressure (high, low, or unstable, or none), leaks, quantitation (detection problems, injection problems, sample problems or data-system problems), chromatogram (peak shape), and hardware.

Troubleshooting HPLC instrumentation guides provide a systematic approach to isolating and correcting common HPLC problems. Referring to the maintenance and troubleshooting sections of instrument manuals is strongly recommended. Modern HPLC systems often have simple self-diagnostic capabilities that help isolate the problem area within the instrument.

It is good practice to run quality control samples (samples spiked at known levels) randomly among samples of unknown assay levels.

Performing a system suitability test each day provides a good assay reference.

Preventive maintenance helps the chromatographer to reduce instrument downtime, allowing for more efficiency and cost effectiveness in the HPLC laboratory.

BIBLIOGRAPHY

1. Cooley, L.; Dolan, J. Reproducibility and carryover-A case study. LC GC Eur. **2001**, *11*, 209–214.
2. Dolan, J. Communicating with baseline. LC GC Eur. **2001**, *9*, 530–534.
3. Dolan, J. Attacking carryover problems. LC GC Eur. **2001**, *11*, 664–668.
4. Dolan, J. *Merck LC Troubleshooting Chrombook*; Merck: Rahway, NJ, USA.
5. Dolan, J. Problem isolation: Three more things. LC GC Int. **1993**, *6* (1), 14–17.
6. Dolan, J.; Snyder, L.R. *Troubleshooting LC Systems*; Humana Press: Clifton, NJ, USA.
7. Frasca, V. Troubleshooting high back pressure. Sci. Tools Pharm. Biotech. **1997**, *2*, 3.
8. HPLC Troubleshooting Technical Notes, 1st Ed.; Phenomenex Corp.: Torrance, CA, USA, 2 Feb, 1993.
9. http://kerouac.pharm.uky.edu/asrg/hplc/troubleshooting.html.
10. McDowall, R.D. Where did that peak come from? LC GC Int. **1997**, *6*, 358–359.
11. Nelson, M.; Dolan, J. UV detection noise. LC GC Int. **1995**, 64–70.
12. Supelco HPLC troubleshooting guide. Bulletin **1999**, *826D*,
13. http://www.chromatography.co.uk/TECHNIQS/HPLC/trouble1.html.
14. http://www.chromtech.com.
15. http://www.dq.fct.unl.pt/QOF/hplcts.html.
16. http://www.fortunecity.de/lindenpark/lilienthal/8/trouble.html.
17. http://www.hplc1.com/shodex/english/dd.htm.
18. http://www.metachem.com/tech/troubleshoot.
19. http://www.rheodyne.com/tsguide/tsg.html.

HPLC Instrumentation: Validation

Ioannis N. Papadoyannis
Victoria F. Samanidou
Laboratory of Analytical Chemistry, Chemistry Department, Aristotle University of Thessaloniki, Thessaloniki, Greece

INTRODUCTION

Validation is the process of providing documented evidence that an instrument, a system, a method, a product, or a procedure performs as expected within specified design parameters and requirements so that the obtained results are reliable. Validation efforts should be broken down into separate components addressing the equipment—both the instrument and the computer controlling it—and the analytical method run on that equipment. After these have been separately verified, they should be checked together to confirm the expected performance limits of the system (system suitability testing, SST). Fig. 1 illustrates the basic validation steps with regard to computerized high-performance liquid chromatography (HPLC) equipment.

The need for validation in analytical laboratories may originate from regulations such as current Good Manufacturing Practices (cGMP), Good Laboratory Practice (GLP), and Good Clinical Practices (GCP); or quality and accreditation standards such as the International Standardization Organization (ISO) 9000 series, ISO 17025, and the European Norm (EN 45001), *United States Pharmacopoeia* (USP), Food and Drug Administration (FDA), and Environmental Protection Agency (EPA). All regulations require instruments to be calibrated, well maintained, and suitable for their intended use. However, validation of equipment and analytical methods is necessary not only because of the regulations and accreditation standards, but also as a prerequisite in terms of any *good analytical practice*.

OVERVIEW

Validation is a regular process that starts before an instrument is placed online and continues long after method development and transfer. It consists of at least three stages, each being critical to the overall description of the process:

- Phase 1. Instrument or equipment qualification, including computer qualification. Individual modules of equipment (hardware and firmware) have to be separately validated, as well as the entire system. Validation of computer systems includes the evaluation of hardware and software.
- Phase 2. Analytical method validation prior to routine use and after changing method parameters.
- Phase 3. Analytical system suitability testing, which combines instrument, computer, and method. When the equipment and a particular method have been selected and validated, the equipment for that method goes through an SST prior to, and within, sample analyses, or practically on a day-to-day basis.

Information about validation procedures concerning HPLC instrumentation and guidelines are discussed in the following sections.

EQUIPMENT VALIDATION OR QUALIFICATION

Validation of HPLC instrumentation, also called "qualification," is the procedure that ensures that the instrument is qualified; that is, that its performance complies with the method's predetermined requirements, providing reliable and valid results. Modern HPLC systems are computerized, generally consisting of analytical hardware, computer hardware, peripherals, and software.

Validation of instrument hardware includes testing according to documented specifications. If HPLC instruments consist of several modules, individual modules (modular validation), as well as the entire system (holistic validation), should be validated. However, the latter is preferred, as individual module tests should be performed as part of the diagnosis if the system fails.

The equipment used in a study should be tested on site before it is used the first time, within certain time intervals, and after repairs. It should be periodically inspected, cleaned, maintained, and calibrated according to the standard operating procedures (SOPs). Records of these activities should be maintained.

Qualification of HPLC equipment (equipment qualification, EQ) begins at the vendor's site. During this stage, the instrument and software are developed, designed, and produced in a validated environment according to GLP, cGMP, and/or ISO 9000 standards, preferably ISO 9001; ISO 9002 or 9003 are insufficient because they do not cover development.

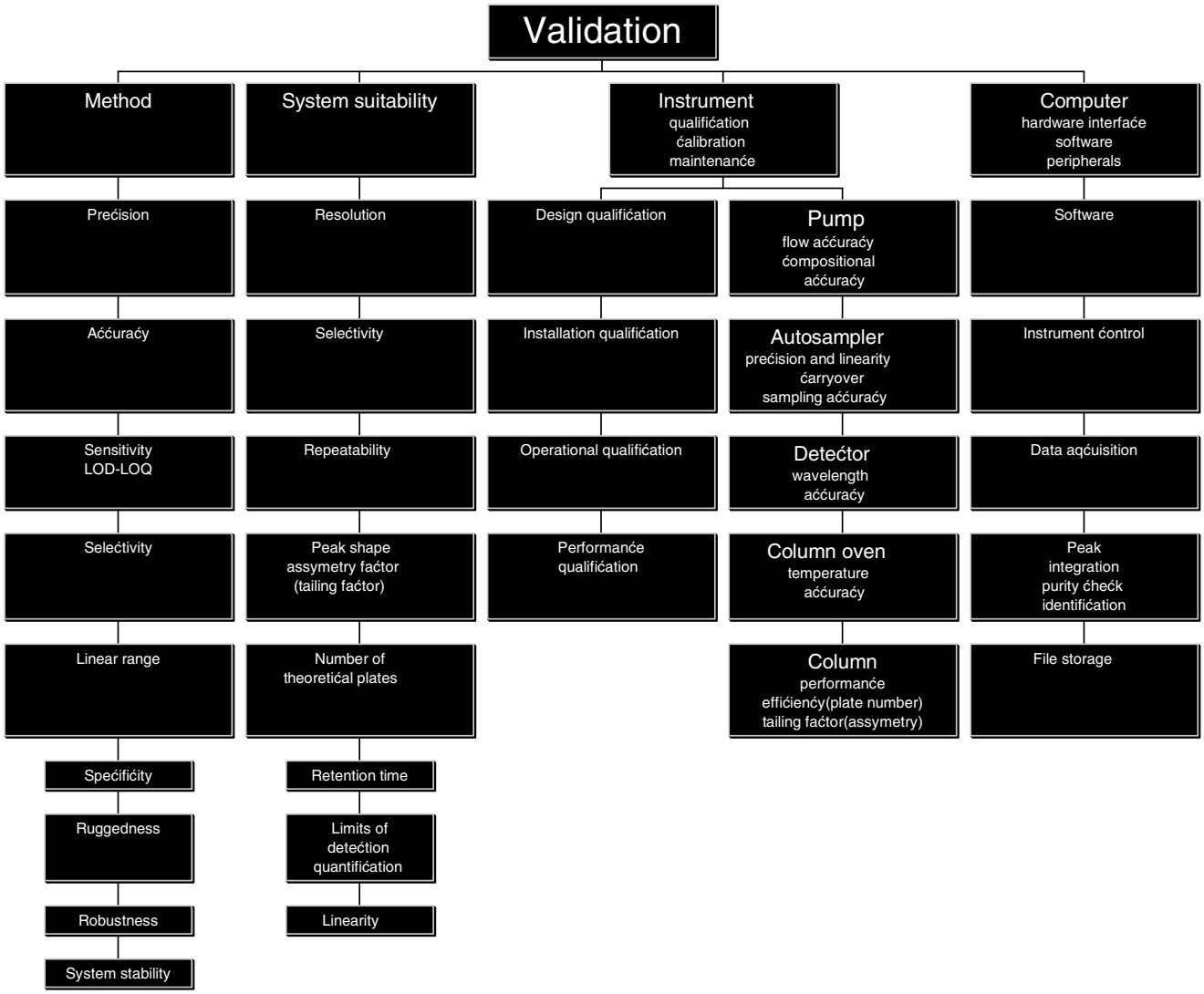

Fig. 1 Basic validation steps in an analytical laboratory.

Qualification can be subdivided into four stages: 1) design qualification (DQ); 2) installation qualification (IQ); 3) operational qualification (OQ); and 4) performance qualification (PQ).

Design Qualification (DQ)

DQ covers setting of user requirements, as well as functional and performance specifications. DQ should ensure that the instrument has all the necessary functions and performance criteria that will enable it to be successfully used for the intended application. DQ includes: 1) Description of the intended use of the equipment; 2) selection of the analysis technique, selection of the technical, environmental, and safety specifications, and final selection of the supplier and equipment; and 3) development and documentation of final functional and operational specifications.

Installation Qualification (IQ)

IQ establishes that the instrument is received as designed and specified, that it is properly installed in the selected environment, and that this environment is suitable for the operation and use of the instrument. During installation, one should: 1) Compare the equipment, as received, with the purchase order; 2) check documentation for completeness or for any damage; 3) install hardware (computer, equipment, fittings and tubings for fluid connections, columns in HPLC, power cables, and instrument control cables); 4) install software on the computer following the manufacturer's recommendation, and verify correct software installation; 5) make a backup copy of the software; 6) configure peripherals, e.g., equipment modules; 7) switch on the instrument and check for any error messages; 8) identify all hardwares and make a list with a description of each; 9) list equipment manuals and SOPs;

10) inject and qualitatively evaluate a standard; and 11) prepare an installation report describing how and by whom the instrument was installed.

Operational Qualification (OQ)

OQ, or acceptance testing, is the process of demonstrating that the whole instrument or its modules will function according to its operational specification, in the selected environment, according to previously defined functional and performance specifications ("acceptance criteria"). This procedure can be performed to the extent of the self-diagnostics routine test or to a more detailed procedure regarding flow-rate, injector precision, or wavelength accuracy. It can be carried out by the user or the vendor on behalf of the user.

Performance Qualification (PQ)

PQ is the process of testing and calibrating the instrument before and during routine use to verify system performance. This test is repeatedly executed to ensure that the entire system generates valid results and performs as intended, throughout representative or anticipated operating ranges. The criteria of PQ should also be used for revalidation later. After the instrument is placed online in the laboratory, and after a period of use, regulations require maintenance, followed by calibration and standardization. Each laboratory should have SOPs that define the period of use (usually a reasonable time interval in which the instrument properly operates). Records should be kept to track instrument maintenance.

The frequency of PQ depends on the type of instrument, on the stability of the performance parameters, on the specified acceptance criteria, and on the use of the equipment. The test frequency for PQ is much higher than for OQ. PQ is always performed under similar conditions to establish a routine sample analysis; that is, using the same column, the same analysis conditions, and the same test compounds. PQ should be performed on a daily basis or whenever the instrument is used. For a liquid chromatograph, the most important unit may be the chromatographic column or the detector's lamp condition. The test criteria and frequency should be determined during the development and validation of the analytical method. In practice, PQ can mean SST, where critical system performance characteristics are measured and compared with documented, preset limits. An example sequence for PQ includes: 1) definition of the performance criteria and test procedures; 2) selection of critical parameters: precision of the peak area/height, precision of retention times, resolution between two peaks, peak width at half height or peak tailing, limit of detection (LOD), and limit of quantitation (LOQ), wavelength accuracy of a UV/Visible detector; 3) definition of the frequency, e.g., every day, every time the system is used, before, between, and after a series of runs; 4) specification of corrective actions in case the system does not meet the criteria.

DQ should always be performed by the user, whereas IQ for large, complex, and high-cost instruments should be performed by the vendor. In some cases, warranty is lost if the user installs the system. OQ can be performed by either the user or the vendor. The decision mainly depends on the available resources at the user's site, and on the vendor's capability to offer such a service with high quality. PQ should always be performed by the user because it is very application-specific and the vendor may not be familiar with the method. As PQ should be performed on a daily basis, this practically limits this task to the user anyway. On completion of equipment qualification, detailed documentation should be available, considering qualification checklist, procedures for testing, qualification test reports with signatures and dates, PQ test procedures, and representative results.

Computer Validation/Qualification

Computer validation/qualification refers to computer hardware, peripherals, and software validation, the latter including operating software, e.g., Microsoft Windows, MS-DOS, and the application HPLC software. In the hardware, the most important unit to validate is the analog-to-digital converter (ADC) because it converts input voltage into numeric data. Software, however, is very difficult to validate because of its complex structure. For this reason, the vendor should check, validate, and document software according to Computer-Aided Software Engineering (CASE) principles. After installation, software validation can be performed with regard to the integrity of program code and data, as well as the data security, with special software packages; this can be automatically checked at power on. On the other hand, comprehensive validation of a data system is beyond the capability expected from many chromatography laboratories. The only parts of the software package that is created after installation are user-written programs (macros); they should be tested, ensuring security of data with restricted access to data and regular backup copies, documenting every change made either on the data acquisition system computer or software. Computer systems should be validated during, and at the end of, the development process and after software updates.

Equipment validated under a specified set of conditions must be revalidated whenever there is a change in those conditions. For example, changes in application software may influence the correct functioning of the computer system. Revalidation refers to those items of the system that are affected by the change.

HPLC INSTRUMENTATION QUALIFICATION

Instrument hardware should be validated for its intended use before and during its operation as part of the overall

validation process; that is, prior to routine use, after repair, and at regular time intervals.

The main qualification tests applied to HPLC instrumentation concern:

- The injection system (usually an autosampler). The parameters that have to be checked are precision and accuracy.
- The pump. The parameters that have to be checked are flow-rate precision, flow-rate accuracy, and stability regarding an isocratic pump. Gradient delay volume and gradient mixing volume, repeatability of the gradient, and mixing and proportioning accuracy are important when a gradient pump is used.
- The detector. The parameters that have to be checked are wavelength accuracy detection, refractive index sensitivity, linearity, spectral quality (PDAD) short-term or long-term noise, drift, and flow sensitivity.
- Column efficiency.
- Within-day and between-day reproducibility of the whole chromatographic system.

The first step is to establish internal specifications; then, compare the obtained results with the manufacturer's specifications; and, finally, interpret the differences. Within-day and interday reproducibility is the minimum test for routine use. Chromatographic systems should be tested for suitability to the performance criteria of the method on a daily basis before and during routine application. An HPLC system should be tested before each single sample analysis, or, if a series of samples are analyzed within a sequence, before each sequence.

Retention time, peak height or area, resolution, and peak shape are the data used to monitor the performance of the HPLC system. Peak shape is one of the first things that experienced chromatographers notice when looking at a chromatogram. Ideal chromatographic peaks are Gaussian-shaped; however, in practice, most peaks show some peak tailing, which is measured by using the asymmetry factor or the USP tailing factor as described in Fig. 2A. Column plate number, N, is the most common parameter to describe the shape of the peak. Resolution R_s, as described in Fig. 2B, is the measure of separation of two peaks, as well as of the efficiency of the column.

The frequency of the control sample analysis depends on the nature of the analysis. Successful analysis of the control samples assures that the system is performing as expected under the SOP. Validation of HPLC equipment assures that valid measurements are obtained. The quality of the analytical data can be maintained by keeping, in a safe place, records of the actual instrument conditions at the time the measurements were made. Backups should also be maintained.

The tests can be performed by using a typical C_{18} analytical column, 250 × 4 or 250 × 4.6 mm, and a mobile phase consisting of water–methanol or water–acetonitrile mixture. The analysis should concern compounds similar to those used for testing the performance of C_{18} columns (e.g., phenol) or compounds used for routine analysis in the laboratory. New columns must be checked for performance. Records of its chromatographic parameters must be kept.

Modular Calibration: Detector Performance

The refractive index sensitivity affects gradient analysis and should be checked by measuring the absorbance when the cell is filled with methanol ($n = 1.329$) and cyclohexane ($n = 1.427$) at 270 nm.

Noise and drift are measured in static (dry detector cell) and in dynamic mode at different wavelengths, e.g., 200, 254, and 390 nm. The change in the absorbance as a function of flow rate at the same wavelengths reflects flow sensitivity. Noise is expressed in AU/cm, drift in AU/hr, and flow sensitivity in AU min/ml. Some equipment units can automatically perform calibration for accuracy. For example, some HPLC/UV/Visible detectors include holmium oxide filters for measurement and calibration of the wavelength accuracy.

The characteristics of an equipment may change over time, e.g., UV detector lamps lose intensity, or pump piston seals abrade, or short-term noise affecting the LOD is increased because of flow cell contamination. These changes will have a direct impact on the performance of the HPLC instrument. The frequency of performance tests will be determined by experience and is based on need, type, and history of equipment performance. Intervals between the checks should be shorter than the time the instrument drifts outside acceptable limits. New instruments need to be checked more frequently, and, if the instrument meets the performance specifications, the time interval can be increased.

Long-term noise can be erroneously considered as late-eluting peaks, while drift affects the obtained data when the instrument is running over a long time period. Flow sensitivity affects flow rate and gradient programs using constant pressure pumps.

Photodiode array (PDA) or variable UV/Visible detector

A number of reference chemicals with well-defined UV spectra have been used for detector wavelength calibration, e.g., uracil, erbium perchlorate, holmium oxide, caffeine, etc.

Pump

The accuracy and stability of the pump flow rate can be checked at 1 ml/min, with the column in place, by measuring the time required to fill a 10 ml volumetric flask at the detector outlet. Other flow rates can be tested if

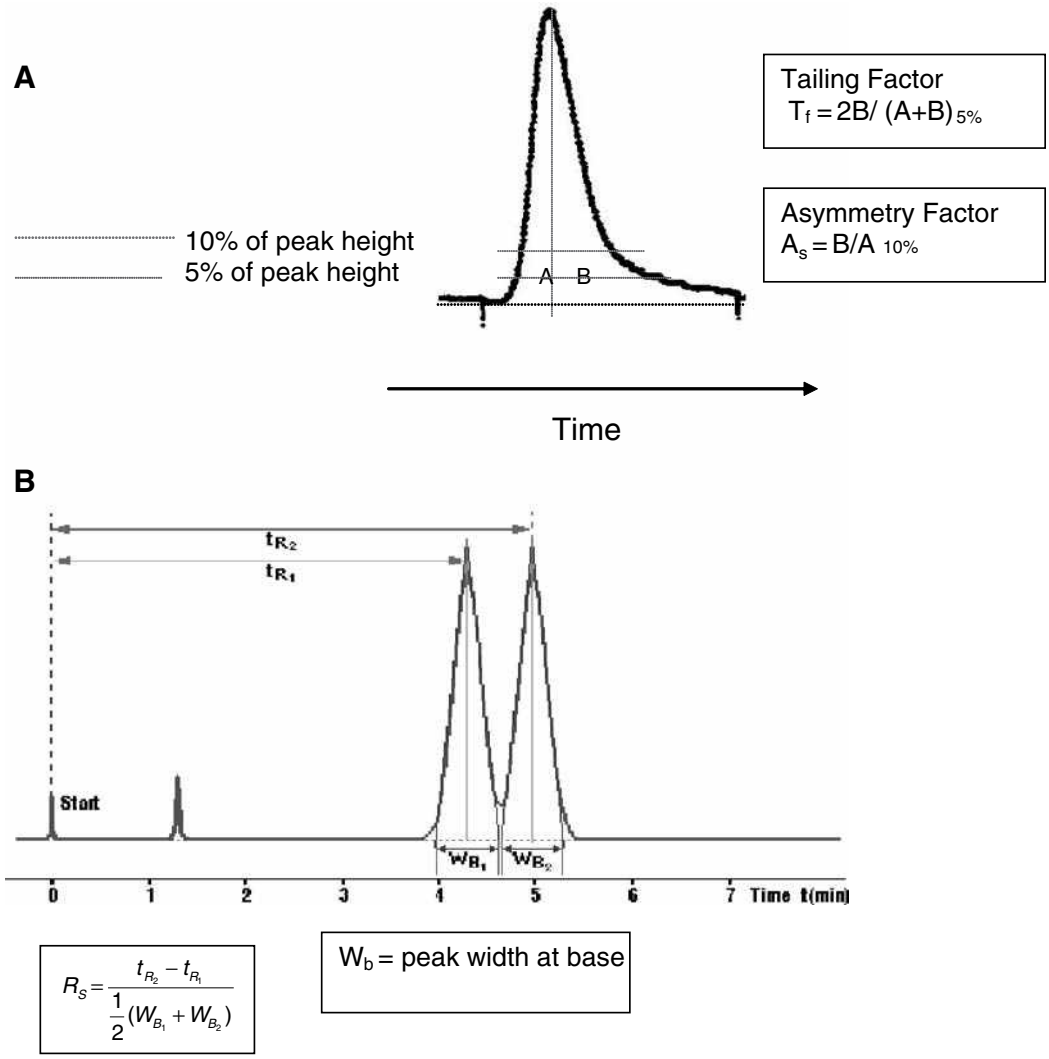

Fig. 2 (A) Measurement of peak tailing using USP tailing factor and peak asymmetry factor. (B) Peak resolution.
Source: From Merck HPLC Tutorial.

analyses with narrow bore or fast liquid chromatography (LC) are routinely performed. An acceptance criterion is 1.00 ± 0.05 ml/min. Flow-rate variations affect retention times.

Gradient pumps

Gradient delay volume, gradient mixing volume, and mixing and proportioning accuracy should be evaluated. These tests are executed by replacing the column with short tubing and filling the reservoirs with water and aqueous phenol solution. Increasing and decreasing steps must be used. The abovementioned parameters affect R_t and the selectivity of the separation. This is especially important when the gradient method has to be transferred from one system to another. Repeatability of the gradient analysis, important for the precision of the gradient method, is assessed by calculating the RSD of the peak area and retention times for replicate analysis of a control compound solution. Compositional accuracy is determined by making 5 min step gradients from water in one solvent line to 0.1% acetone in water in a second solvent line. The absorbance of each step against that of the 100% step is measured. A higher flow rate of 2 ml/min can be used to sharpen the step definition and increase test robustness. All four solvent lines are checked in a 1 hr solvent program.

Gradient methods in HPLC depend on the dwell volume, V_d, i.e., the volume between the point of mixing eluents A and B and the column inlet, including the loop of the injector. This volume differs from instrument to instrument, so that a method can be transferred only if this volume is well defined. When there is a significant difference in dwell volume between the two systems, retention times and resolution are dramatically different. So one must be state in which range of V_d the method is still valid.

Autosampler

Autosampler precision can be checked by replicate injections of a control sample, with wash injection intervals between every two sample injections. The repeatability of peak areas, mathematically expressed as RSD, is used as a criterion for autosampler precision. For example, when 10 consecutive injections of 10 μl of a solution are performed, the expected RSD for peak area precision ranges from 0.5% to 1.0%. Single injections of different volumes, such as 5, 10, 50, or 80 μl, can also be used, simultaneously checking the linearity of the injector, the detector, and the data system. Another approach to qualify the autosampler involves the gravimetric determination of the average volume of water per injection withdrawn from a tared vial after six 50 μl injections. The procedure takes less than 10 min and has an acceptance criterion of 50 ± 2 μl.

The same experiment can be used for the assessment of flow-rate precision by evaluating the repeatability of retention times for the examined compounds, expressed again as RSD. Both terms, flow-rate and injection volume precision, affect the precision of the results of the analysis. Carryover problems can be identified in the wash chromatograms at maximum detector sensitivity. They can be checked by multiple analyses of high-concentration samples followed by blank injections.

Column oven

A temperature accuracy test of the column oven, using a calibrated thermal probe, is used with an acceptance criterion of $35 \pm 2°C$.

Column

Two peaks are considered resolved if the R_s value is > 1.5. For multicomponent mixtures, a number of R_s values may have to be considered. The resolution between the most critical peaks may solely be considered as an indicator of the quality of the separation. Typical values for R_s range from 1.5 to 2.0 for critical resolution.

Computer

A computer associated with an HPLC equipment may control the instrument or part of it, e.g., the photodiode array detector, or acquire data generated by the instrument, such as the peak area of analytes.

- Software functions: For an automated HPLC analysis, required software functions include instrument control, data acquisition, peak integration, peak purity checks, compound identification through spectral libraries, quantitation, file storage and retrieval, and a printout of methods and data.
- Hardware interface: Determining the true performance of an electronic interface of a chromatography data system requires special instrumentation that is not generally found in a chromatographic laboratory. Testing procedure is similar to that of calibrating any electronic instrument.

The equipment hardware and computer software should be developed and validated according to a documented procedure, e.g., according to a product life cycle. The vendor should have a documented and certified quality system, e.g., ISO 9001. Quality must be designed and programmed into software prior to, and during, its development phases by following written development standards, including the use of appropriate test plans and methods.

Correct functioning of software and computer systems should be verified after installation and before routine use. Operational qualification for software and computer systems is more difficult than for hardware, as 1) it is more difficult to define specifications, test procedures, and acceptance criteria; and 2) there are hardly any guidelines available on OQ of software and computer systems. Because of these problems, there is even more uncertainty for software and computer systems than for equipment hardware.

The type of testing required for the qualification of software and computer systems depends very much on the type and complexity of software, i.e., if the software and computer hardware are supplied by one vendor, or computer systems that are interconnected and/or interfaced to analytical systems, or if the software are developed in the user's laboratory in addition to a vendor-supplied package (e.g., a macro).

ANALYTICAL METHOD VALIDATION

After equipment validation, the next step is analytical method validation, which covers testing of significant method characteristics according to good analytical practice guidelines. The validation of an HPLC method is the procedure that gives the chromatographer information to determine whether the system is operating as it should, providing accurate, precise, and reliable analytical data in a specific situation, meeting the preestablished specifications.

The validity of a specific method should be demonstrated in laboratory experiments by using samples or standards that are similar to the unknown samples that will be routinely analyzed. Chromatographic methods need to be validated before the first routine use. To obtain the most accurate results, all of the variables of the method should be considered, such as sampling, sample preparation, chromatographic separation, detection, and data

evaluation, using the same matrix as that of the intended sample. The proposed procedure must go through a rigorous process of validation. All validation experiments should be documented in a formal report.

Although the need to validate analytical methods is clear, the procedure for performing the validation is not clearly defined in terms of the validation parameters to be used, the specific procedures to be used in evaluating a particular parameter, and the appropriate acceptance criteria for a particular parameter.

Successful completion of the validation results in a method that can reliably be used to characterize "real samples." Ongoing validation activities may also be necessary during the routine utilization of an analytical procedure, as well as the revalidation of the analytical procedure, as certain operational aspects of the method are changed during its routine and continuous application.

Validation Parameter Guidelines for Method Validation

After the method has been developed, its performance must be validated with respect to different performance parameters. To determine which operational parameters should be included in a formal validation protocol, the chemical literature may be used to assess the practical state of the art among the practitioners of the desired methodology. Alternatively, existing guidelines published by organizations with recognized authority may be examined. Regulatory agencies and published literature provide the criteria for what constitutes a validated chromatographic method. The USP, for example, has published specific guidelines for method validation regarding pharmaceuticals. However, there are no official guidelines referring to biological fluids.

An attempt for harmonization was made at the International Conference on Harmonization (ICH) in 1995 and 1996 by representatives from the industry and regulatory agencies from the United States, Europe, and Japan, who defined parameters, requirements, and, to some extent, also methodology, for analytical methods validation.

In 1990, the USP 22 guideline listed eight individual parameters that must be investigated and documented in order to validate a method: 1) Accuracy; 2) precision; 3) limit of detection; 4) limit of quantification; 5) selectivity; 6) range; 7) linearity; and 8) ruggedness.

In 1995, USP 23 changed these parameters to some extent. Selectivity is now explicitly referred to as specificity, linearity and range were combined, and robustness was broken out of ruggedness. Ruggedness retains its original definition of day-to-day, instrument-to-instrument, operator-to-operator, etc. reproducibility. The robustness of an HPLC method is defined as a measure of its capacity to remain unaffected by small but deliberate variations in method parameters and provides an indication of its reliability during normal usage. So USP 23 includes: 1) Accuracy; 2) precision; 3) limit of detection; 4) limit of quantification; 5) specificity; 6) linearity and range; 7) ruggedness(*); 8) robustness(*). The asterisk is indicating that the terminology is included in an ICH publication, but they are not part of required parameters.

The definitions of these parameters and the indicative acceptance criteria are discussed in the following paragraphs. Each of the above-listed parameters is evaluated in terms of validating an HPLC method. The procedures for performing the validation must be presented in a complete, well-defined, practical, and understandable format. Once the validation is complete, an investigator must be able to interpret the results. The acceptance criteria allow the researcher to definitely determine, by comparing method performance data to the criteria, whether the method under evaluation is performing in a valid manner. These criteria should be universally applicable, numerically and mathematically explicit, complete, and achievable.

Accuracy and Recovery

The accuracy of an analytical method is the degree of agreement of results generated by the method to the true value or a conventional true value. Accuracy can be assessed by applying the analytical method to samples or mixtures of sample matrix components to which known amounts of the analyte have been added, above and below the normal levels expected in the samples. Method accuracy is the agreement between the difference in the measured analyte concentrations of the fortified (spiked) and unfortified samples and the known amount of analyte added to the fortified sample.

Comparison of the method's results can be performed by using an established reference method, assuming that the latter is free from systematic errors. Second, accuracy can be measured by analyzing a certified reference material, and comparing the measured value with the true value as supplied with the material. If such reference material is not available, a blank sample matrix can be spiked with a known concentration that should cover the range of concern, including one concentration close to the quantitation limit. The expected recovery depends on the sample matrix, on the sample processing procedure, and on the analyte concentration. Recoveries can be determined by either external or internal standard methods. Although it is desirable to attain a recovery close to 100%, other values such as not less than 50%, 80%, and 90% have been used as limits. Quantification by external standard is the most straightforward approach because the peak response of the standard is compared to the peak response of the sample. The standard solution concentration should be close to that expected in the sample solution. Precise control of the injection volume is mandatory because it influences the

accuracy. Peak response is measured as either peak height or peak area.

For the internal standard method, a substance is added at the earliest possible point in the analytical scheme to compensate for sample losses during extraction, cleanup, and final chromatographic analysis. The internal standard must be completely resolved from all other peaks in the chromatogram, having chemical and physical properties as similar as possible to those of the analyte of interest, so that the detector response is similar to the solute to be quantified. However, it is sometimes difficult to find the proper internal standard, as this must be stable over the time of the measurement period, absent from real samples, not reactive with the analytes, and eluted within a reasonable retention time. Analogs, homologs, and isomers are usually preferred. In the presence of analytes with different chemical or physical properties, two or more internal standards representing these analytes should be used.

Reagent blank, internal standard blank, solvent blank, and compound blank samples must also be analyzed for accurate qualitative and quantitative results.

Procedural guidelines for accuracy determination include replicate analysis, e.g., three to six assays, at five levels, over the range from 80% of the lowest expected assay value to 120% of the highest expected assay value, or from 75% to 125% of label claim, six samples of drug in the matrix spanning 50% to 150% of the expected content. At minimum, three concentrations must be used within the analytical range (extremes and midpoint of expected or near quantitation limit, center of range, and upper bound of standard curve).

For trace level analyses, acceptance criteria include 60–110% recovery for concentrations below 100 ppb, 80–100% recovery for concentrations above 100 ppb, and 70–120% for concentrations below 1 ppm. In biological samples, method accuracy for discovery phase investigations should be $\pm 20\%$ of actual, with recoveries of $\pm 10\%$ being necessary in preclinical and clinical studies. Alternatively, it is recommended that the mean recovery value should be within $\pm 15\%$ of actual, except at the quantitation limit where $\pm 20\%$ is acceptable.

Precision and Reproducibility

The precision of a method is the extent of agreement among individual test results, when the procedure is repeatedly applied to multiple samplings. Precision can be divided into three categories: 1) Repeatability; 2) intermediate precision; and 3) reproducibility.

Repeatability (intra-assay or within-day precision) is obtained when the analysis is carried out in one laboratory by one operator, using one piece of equipment over a relatively short time span. It reflects the variation in replicate procedures performed within a short time period, with the same operational conditions.

At least five or six determinations of three different matrices at two to three concentrations should be performed and expressed by the RSD. The acceptance criteria for precision depend on the type of analysis. While a precision of better than 1% RSD is easily achieved for compound analysis in pharmaceutical quality control, the precision may be at levels of 10–15% for biological samples. For environmental and food samples, the precision is very much dependent on the sample matrix, the analyte concentration, and the analysis technique, varying between 2% and 20%.

Intermediate precision is defined by ICH as "the long-term variability" of the measurement process, and is determined by comparing the results of a method run within a single laboratory over a number of weeks. A method's intermediate precision may reflect disagreement in results obtained by different operators, from different instruments, with standards and reagents from different suppliers, with columns from different batches, or a combination of these. The objective of intermediate precision validation is to verify that, in the same laboratory, the method will provide the same results after finishing the method development.

Reproducibility, as defined by ICH, represents the precision obtained between laboratories with the objective of verifying if the method will provide the same results in different laboratories. The reproducibility of an analytical method is determined by analyzing aliquots from homogeneous lots in different laboratories with different analysts, and by using operational and environmental conditions that may differ from, but are still within the specified, parameters of the method (interlaboratory tests). Various parameters affect reproducibility. These include differences in room environment (temperature and humidity), operators with different experience, equipment with different characteristics (e.g., delay volume of an HPLC system), variations in material and instrument conditions (e.g., in HPLC), mobile phases composition, pH, flow rate of mobile phase, columns from different suppliers or different batches, solvents, reagents, and other material with different quality.

Reproducibility is defined as the long-term variability of the measurement process, which may be determined for a method run, within a single laboratory, but on different days. Reproducibility also applies to a method, either run by different operators, different instruments, or a combination of the above. The reproducibility standard deviation is typically twofold to threefold larger than that for repeatability. Precision is often expressed relative to 1 day as intraday (within-day) precision or relative to a period of days, as interday (between days) precision. Reproducibility, in the sense of intralaboratory precision, is related to the procedure being performed at two or more laboratories as in, e.g., a collaborative study.

Precision in retention times and peak area or height is a major criterion of a separation system. Retention-time precision is important because R_t is the primary means

for peak identification. It is also an important performance criterion and diagnostic for an LC pump and a column.

Precision of peak areas or heights is important because they are used for calculating amounts during quantification. It is also the most important performance criterion for an LC injection system. Precision should be determined using a minimum of five replicate chromatograms. For bioanalytical samples, precision is studied at least at low, medium, and high concentrations. This is repeated on separate days to calculate intraday and interday precision.

Precision reflects a procedure's ability to reproduce the same, but not necessarily the correct or expected, result each time it is correctly performed. Precision is assessed by repetitively injecting a number of samples and statistically evaluating the resulting data. Important issues related to the precision determination include the number of replicates required and the type of sample to be tested. For the determination of repeatability, recommendations include: 1) Five to ten replicates for release or stability assays; 2) duplicate measurements made on 10 samples at each of three different analyte levels; 3) five replicates at three levels (limit of quantitation, midrange, and upper calibration bound); 4) replicate samples at analyte levels of 80–120% of expected for dosage forms and drug substance tests.

For intermediate precision, the repeatability experiments should be performed on 2, 3–5, or at least 10 separate days. To assess reproducibility, the experiments have to be performed in at least two laboratories.

System precision should be $\leq$1–2% relative standard deviation (RSD) (or higher for low-level impurities). The repeatability is generally 1/2 to 1/3 of the reproducibility. However, for biological samples, an RSD of 10–15% should be acceptable as the minimum precision.

Systematic errors result from sources traced to the methodology, the instrument, or the operator. These affect both the accuracy and the precision of the measurement. Random errors affect the precision and are difficult to eliminate as they result from random fluctuations in the measured signal because of noise and other factors. The imprecision of the entire procedure is often dominated by the random errors of the most imprecise step. The difference between an accurate and a precise method is illustrated in Fig. 3.

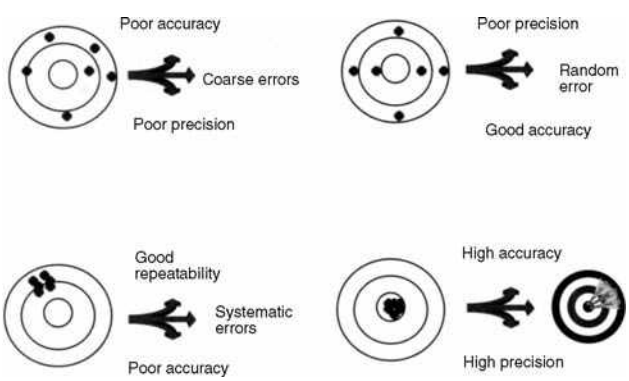

Fig. 3 Comparison of precision and accuracy parameters of an analytical method.

Selectivity–Specificity

The terms selectivity and specificity are often interchangeably used. The term specificity generally refers to a method that produces a response for a single analyte only, while the term selective refers to a method that provides responses for a number of chemical entities that may or may not be distinguished from each other. Because there are very few methods that respond to only one analyte, the term selectivity is usually more appropriate. The USP defines selectivity of an analytical method as its ability to accurately measure an analyte in the presence of interferences, such as synthetic precursors, excipients, enantiomers, and known (or likely) degradation products that may be expected to be present in the sample matrix.

Selectivity in HPLC is obtained by setting optimal chromatographic conditions, such as mobile phase composition, column temperature, and detector wavelength. There are a variety of ways to validate selectivity. One approach is to demonstrate a lack of response in the blank biological matrix. A second approach is to check whether the intercept of the calibration curve is significantly different from zero.

Peak purity is one important parameter in chromatography to determine whether the peaks within a sample chromatogram are pure or if it consists of more than one compound. To determine the homogeneity of a chromatographic analyte response, the use of UV/Visible photodiode-array detector (PDAD) and mass spectrometers is recommended, acquiring spectra during the entire chromatogram. The acquired spectra are normalized and overlaid for graphical presentation; if they are different, then the peak consists of at least two compounds. Usually, the simplest and most frequently used peak purity algorithm compares three spectra across a peak: On the upslope, at the peak apex, and on the downslope.

Specificity relates to the ability of a method to measure only what it is intended to be measured with a requisite level of accuracy and precision, although the sample may contain other related compounds. The most commonly cited specificity evaluation procedure is the analysis of a placebo, wherein the sample matrix without the analyte is analyzed and the resulting system response is examined for the presence of responses, which interfere or overlap with that of the analyte of interest. Other procedures for specificity include: 1) Peak reanalysis, wherein the peak of interest is collected and reanalyzed by different chromatographic conditions or with methods that are sensitive to analyte structure; 2) collaboration, in which the sample is quantitatively analyzed using two or more detection or

separation strategies, and the results compared; 3) use of detectors (e.g., MS or PDAD to assess peak purity).

Linearity and Range

The linearity of an analytical method is its ability to extract test results that are directly, or by means of well-defined mathematical transformations, proportional to the concentration of analytes in samples within a given range. In chromatography, peak parameters are related to analyte concentration via standardization procedures. This relationship is then used to convert a sample's peak parameter to its analyte concentration. Linearity is determined by a series of three to six injections of five or more standards, whose concentrations span over the range of expected concentrations, or 80% of the lowest expected level to120% of the highest expected level, or 50–150% or 10–200% of the expected working range, or 25–125% of the target range specified. The response should be directly or, by means of a well-defined mathematical calculation, proportional to the concentrations of the analytes. A linear regression equation applied to the results should have an intercept not significantly different from zero; otherwise, it should be demonstrated that there is no effect on the accuracy of the method. Frequently, the linearity is graphically evaluated in addition to, or alternatively to, mathematical evaluation.

The correlation coefficient of the best linear least squares regression model should be between 0.98 and 1.00 or greater than 0.999 with the slope and intercept reported. However, there is no rule stating that the relationship between instrumental response and analyte concentration must be directly linear for a procedure to be valid. The desire to have a linear relationship reflects the practical consideration that a linear relationship can be accurately described with fewer standards than a nonlinear relationship, and the subjective expectation that a linear relationship is more rugged than a more complicated, nonlinear relationship.

A method's range is linked to its linearity. The range is the interval between the lower and upper analyte concentration, for which it has been demonstrated that the analytical procedure has a suitable level of accuracy, precision, and linearity. The range is expressed in the same units as the analytical method's results (e.g., ng/μl, ppb, %, etc).

Limits of Sensitivity: Limit of Detection and Limit of Quantitation

Sensitivity is the ability of a method to reliably respond in a consistently recognizable manner to decreasingly smaller amounts of analyte. Frequently utilized measures of sensitivity are the limit of detection (LOD) and the limit of quantitation (LOQ). For chromatographic procedures, LOD is the lowest concentration of analyte that can be detected above the baseline detector noise at the most sensitive instrument setting, but not necessarily quantified. In chromatographic practice, the detection limit is the injected amount that results in a peak with a height twice or three times as high as the baseline noise.

The LOD can be determined either directly or from other validation data. Its direct measurement involves an analysis of the method's peak-to-peak baseline noise or an analysis of the variation in the method's blank response. In either case, LOD is calculated as either two or three times the variation in measured response, where the factors are associated with the 95% and 99% confidence intervals for a normal distribution. Practically, LOD can be measured by the serial dilution of samples until the peak can no longer be observed. LOD can be estimated as the value of the linear calibration curve's *y* intercept.

The LOQ is the minimum injected amount that gives precise measurements in chromatography, typically requiring peak heights 10 to 20 times higher than baseline noise. Another approach is the EURACHEM: A number of samples with decreasing amounts of the analyte are injected six times. The calculated RSD% of the precision is plotted against the analyte amount. The amount that corresponds to the previously defined required precision is equal to the LOQ. Alternatively, LOQ is the lowest injected amount of analyte, which results in a reproducible measurement of peak areas and can be reproducibly quantitated above the baseline noise. Peak heights are typically required to be about 10 to 20 times higher than baseline noise. Quantitation implies that the measurement possess a specified accuracy and precision. In some applications, LOQ is defined as the smallest concentration included in the standard curve.

The baseline response method for estimating LOQ involves the following procedure: The chromatogram resulting from a blank injection is examined over a range of 20 peak widths and the noise is measured as either the largest peak-to-peak fluctuation or as the largest deviation (positive or negative) from the mean response. The LOQ is then calculated as the product of 10 times the measured deviation and the calibration curve slope. The LOQ can also be determined as the lowest analyte concentration for which duplicate injections result in a $\%RSD \leq 2\%$. In routine applications, it has been recommended that LOQ should be within the working linear concentration range and that a specification limit should be no lower than twice the LOQ. For clinical applications, the LOQ should be at least 10% of the minimum effective concentration.

Ruggedness

It is generally expected that an analytical method will perform in an acceptable manner each time it is used. While a consideration of method ruggedness is a necessary part of any method's validation, it is a critical issue for compendial methods because of their widespread use in many different laboratories.

Ruggedness establishes a method's ability to effectively perform in the face of variations on operational and environmental conditions, which can reasonably be expected to occur whenever the method is applied. More specifically, ruggedness is the reproducibility of test results obtained by the analysis of samples under a variety of normal test conditions such as different laboratories, analysts, instruments, reagent lots, elapsed assay times, temperatures, etc. Thus, ruggedness addresses unintentional variation in the method introduced by its application, at different times, by different people, at different locations, using different instrumentation and materials. A rugged method will be able to withstand minor operating or performance changes and has built-in buffers against typical procedural abuses, such as differences in care, technique, equipment, and conditions.

For the determination of the method's ruggedness within a laboratory, a number of chromatographic parameters, e.g., flow rate, column temperature, detection wavelength, or mobile phase composition is varied within a realistic range, and the quantitative influence of the variables is determined. If the influence of the parameter is within a previously specified tolerance range, the parameter is said to be within the method's ruggedness range. Clearly, ruggedness is assessed by analyzing aliquots from homogeneous sample lots using operational and environmental conditions that differ, but are still within the method's specified operating range. The ruggedness test should be performed at several values of each operational parameter that affects method performance, e.g., mobile phase flow rate and composition, (pH, buffer concentration, ion pairing reagent concentration, percent organic phase, column temperature, injection volume, gradient dwell time, column lots or column manufacturers, different room temperature and humidity in separate laboratories, detection wavelength, analysts with different experience, instruments from various vendors, reagents from different suppliers, columns from different batches, sample and standard preparation procedures, and operating temperature. For operator-related ruggedness, a number of analysts, e.g., three to five, perform one assay per day for 3 days. The utilization of statistically designed experiments (e.g., nested ANOVA) to establish the ruggedness of an assay is recommended.

In ruggedness assessment regarding the column, the specificity (selectivity) of at least three columns, from three different batches, supplied by one column manufacturer must be checked. A similar column from another manufacturer should also be evaluated. Variability also arises from the degradation of the column over its lifetime. Even columns with the same material and dimensions may vary in performance and selectivity. If columns are packed in the laboratory, they should be tested before they are first used. Columns purchased from vendors should be supplied with test certificates.

The quantitative measure of a method's ruggedness is the precision behavior it exhibits over the course of the various operational scenarios, examined during the validation exercise. Generally, a rugged method's reproducibility is two to three times greater than the method's repeatability (inherent method precision under "normal" controlled operating conditions).

Robustness

Robustness tests examine the effect operational parameters have on the analysis results. For the determination of a method's robustness, a number of chromatographic parameters (e.g., flow rate, column temperature, injection volume, detection wavelength, or mobile phase composition) are varied within a realistic range and the quantitative influence of the variables is determined. If the influence of the parameter is within a previously specified tolerance, the parameter is said to be within the method's robustness range. Obtaining data on these effects will allow one to judge whether a method needs to be revalidated when one or more of parameters are changed, for example, to compensate for column performance over time.

The difference between ruggedness and robustness is that the former is related to unintentional variation in a method because of its use in varying analytical situations, although the latter is the procedure's capacity to remain unaffected by small but deliberate variations in method parameters. Thus, robustness is a measure of the procedure's reliability during normal usage. Although it is time-consuming, thorough robustness studies will help to avoid unexpected results in subsequent applications of the method. While data for robustness is not usually submitted in regulatory product applications, a robustness evaluation is recommended. Clearly, a robust method is one that is operationally immune to commonly encountered but relatively minor variations in its critical operating parameters.

It has been suggested that, in order to determine robustness, a method's critical operational variables should be identified by breaking the testing process into unit operations and then assessing the potential variability of each operation. Unit operations might include: 1) Analytical solution preparation—amount of material used, volumes of solvent used, dissolution times and conditions, and solvent used; 2) variation in the tested product (inhomogeneity, aging); 3) instrumental analysis—detection wavelength, mobile phase composition and flow rate, and column use history.

Stability

Many solutes readily decompose prior to chromatographic investigations, e.g., during the preparation of the sample solutions, during extraction, cleanup, phase transfer, and during storage of prepared vials (in refrigerators or in an automatic sampler). Under these circumstances, method

development should investigate the stability of the analytes.

The term "system stability" is a measure of the bias in assay results generated during a preselected time interval, e.g., every hour up to 10 hr, using a single solution. Stability should be determined by replicate analysis of the sample solution and the relative standard deviation calculated. The assay results obtained in different time intervals should not exceed more than 20% of the corresponding value of the system precision. If the value is higher on plotting the assay results as a function of time, the maximum duration of the usability of the sample solution can be calculated.

The effect of long-term storage and freeze–thaw cycles can be investigated by analyzing a spiked sample immediately upon preparation and on subsequent days of the anticipated storage period. A minimum of two cycles at two concentrations should be studied in duplicate. If the integrity of the drug is affected by freezing and thawing, spiked samples should be stored in individual containers and appropriate caution should be employed for study samples.

In most routine applications, solutions are not immediately used after preparation, but may be stored under specified conditions prior to use. Verifying solution stability is an important aspect of method validation; specifically, a valid method is one for which all related and analytical solutions are stable over the period typically required for their utilization or analysis. To address stability, the analytical solutions should be prepared, assayed, allowed to stand (in accordance with the method's protocol or specification) for a length of time equal to the anticipated maximum analysis time, and then reassayed. For analytical procedures involving overnight runs, up to three to four sample solutions over the working concentration range should be repetitively analyzed over the course of at least 16 hr. In such evaluations, the analytical solution is stable if all concentration values obtained before and after storage agree to within three times the system precision. Additionally, no new peaks should appear, nor should existing peaks be lost, from the chromatograms of the first and last sample injection. The stability of a solution must be checked for at least 16 hr, especially when an autosampler is used.

The preparation and execution should follow a validation protocol, preferably written in a step-by-step instructional format. Once the validation protocol is completed, the validation report should be prepared, including data listed in Table 1.

There are no official guidelines on the sequence of validation experiments and the optimal sequence can depend on the method itself. A potentially useful sequence for a liquid chromatographic method is: 1) Selectivity of standards (optimizing separation and detection of standard mixtures); 2) precision of retention times and peak areas; 3) linearity, limit of quantitation, limit of detection, range; 4) selectivity with real samples; 5) trueness or accuracy, at different concentrations; 6) ruggedness.

Table 1 Parameters to be included in a validation report.

1. Objective and scope of the method (applicability, type).
2. Type of compounds and matrix.
3. Detailed chemicals, reagents, reference standards, and control sample preparations.
4. Procedures for quality checks of standards and chemicals used.
5. Safety considerations.
6. Method parameters.
7. Critical parameters indicated from robustness testing.
8. Listing of equipment and its functional and performance requirements, e.g., cell dimensions, baseline noise, and column temperature range.
9. Detailed conditions on how the experiments were conducted, including sample preparation.
10. Statistical procedures and representative calculations.
11. Procedures for quality control in the routine (e.g., system suitability tests).
12. Representative plots, e.g., chromatograms, spectra, and calibration curves.
13. Method acceptance limit performance data.
14. The expected uncertainty of measurement results.
15. Criteria for revalidation.
16. Analyst who developed and initially validated the method.
17. Summary and conclusions.

Source: From Validation of analytical methods: Review and strategy, in LC GC Int.[1]

The more time-consuming experiments, such as accuracy and ruggedness, are put toward the end. Some of the parameters can be measured in combined experiments. For example, when the precision of peak areas is measured over the full concentration range, the data can be used to validate the linearity.

Revalidation

Once the method is validated, any modification requires revalidation to demonstrate that it still works as defined. If the new parameter is within the tolerance range of the method as specified during the ruggedness test of method validation, the method does not need to be revalidated. In other cases, it should go through revalidation. With the system suitability software frequently offered by analytical equipment vendors, methods can be automatically revalidated with little operator interaction. The validation can be performed overnight.

Operating ranges should be defined for each method based on experience with similar methods, or they should be investigated during robustness studies. Availability of such operating ranges makes it easier to decide when a method should be revalidated. Part or full revalidation may also be considered if SST or the results of quality control

Table 2 Method changes and revalidation tests required.

Method characteristics changed	Performance parameters to revalidate
Instrument changes	Linearity (working range), LOD, LOQ, system precision.
Product changes	Selectivity, accuracy, precision.
Sample preparation procedure (same solvent, same concentration range)	Accuracy, recovery, precision, ruggedness
Sample preparation procedure (different solvent, different concentration range)	Complete reassessment of all previously used validation parameters.
Analyst changes	Qualification testing (perform retests, side-by-side collaborative studies).
Chromatographic change (e.g., column, mobile phase)	Selectivity, linearity, LOD/LOQ, system precision.
Extraction solvent, buffer, back extraction, matrix or injection solvent	Linearity, recovery, LOQ, intrabatch precision and accuracy, in-process solution stability. Additionally, if injection solvent is changed, processed sample stability should be checked, but recovery or in-process stability checks are not necessary.
Chromatographic conditions [column, mobile phase composition, detector type or monitoring condition (e.g., wavelength) change]	Linearity, selectivity, and intrabatch precision and accuracy (recovery not necessary).
Extending the upper end or reducing calibration curve range	Linearity, LOQ (if reduced), lower end of the intrabatch precision and accuracy at revised upper or lower levels.
Internal standard.	Selectivity, intrabatch precision and accuracy, recovery.

Source: From Chromatographic method validation: A review of current practices and procedures. Part III. Ruggedness, revalidation and system suitability, in J. Liq. Chromatogr.[2]

sample analysis are out of preset acceptance criteria and the source of the error cannot be tracked back to instruments or anything else.

For HPLC methods, significant changes could occur, and the recommended parameters for revalidation are summarized in Table 2. For bioanalytical methods, precision, accuracy, and limit of quantitation are considered to be the minimum revalidation tests.

SYSTEM SUITABILITY TESTING

Daily, prior to the sample analyses, the analyst must establish that the HPLC system and procedure are capable of providing data of acceptable quality. The validation procedure of an analytical system combining the analytical method and instrument performance is referred to as system suitability testing. The objective of an SST is to assess if the chromatograph or its modules, i.e., the column, the mobile phase, the detector lamp, etc. perform as required for a particular analytical run and can generate results of acceptable accuracy and precision or should be replaced before samples are committed for analysis. System suitability testing provides the analyst with diagnostic information by warning that part of the process is likely to be out of control. It typically represents a subset of the method validation procedure.

The requirements for SST are usually developed after method development and validation have been completed, giving information about acceptable system operation by comparing observed performance vs. previously established criteria or guidelines.

Critical issues of concern include the identification of performance characteristics that need to be monitored and the frequency of test execution. In general, intervals between tests should be shorter than the observed time in which the system drifts outside of acceptable levels: In most cases, at the beginning and at the end of a run, or in a more thorough approach, a quality control sample is run for every 10 samples. Additionally, an SST evaluation is performed each time an instrument malfunction has been observed during the course of a run. The final decision is based on the experience of the analyst depending on need, as well as previous performance of the equipment. In case the system is in continuous use for the same analysis, it may be sufficient to perform an abbreviated SST check each day. Full SST should be performed each time the system is assembled for the assay.

Quality control samples at three concentrations (low, middle, and high) around the expected range can be used to assess accuracy by two to five injections. The acceptance criteria established for the SST evaluation must balance the need to ensure adequate performance with the practical reality of performing chemical analyses. This means that they must be sufficiently tight, but not so restrictive that acceptable systems fail to pass. Some examples of the acceptance criteria are summarized in Table 3.

Table 3 Recommended system suitability testing acceptance criteria.

Parameter	Assay type	Acceptance criterion
Capacity factor	General	2–8
factor	Trace	1–3
	Stability indicating	> 4
Selectivity	General	1.05–2.0
Retention time	General	< 0.1 min
Resolution	General	> 2.0
	Quantitative analysis	> 1.5
	Biologicals	> 1.2
Plate count (*N*)	General	> 2000
Precision	General	%RSD < 1.5%
	Biologicals	%RSD < 5%
	Trace	%RSD 5–15%
Tailing factor	General	1.5–2.0

Source: From Chromatographic method validation: A review of current practices and procedures. Part III. Ruggedness, revalidation and system suitability, in J. Liq. Chromatogr.[2]

System suitability testing parameters regarding HPLC methods reflect problems associated with the performance of chromatographic procedures, e.g., flow irregularity, injection irreproducibility, system plumbing problems, detector misalignment or malfunction, wavelength accuracy, oven temperature, column malfunction, and mispreparation of analytical solutions regarding mobile phase, standard solutions, or samples. Detailed records of maintenance and changes must be kept. Documentation can be accomplished by using software especially designed for the task. The same software can be used to troubleshoot the method.

To obtain a good and acceptable analytical result, two requirements must be met: 1) The method has to be adequate; and 2) the execution has to be adequate.

The simplest form of an HPLC SST involves comparison of the chromatogram with a standard one, allowing comparison of the peak shape and the peak width baseline resolution. Additional parameters that can be experimentally calculated to provide quantitative SST report include the number of theoretical plates, separation factor, resolution, tailing or peak asymmetry factor, accuracy, and precision (RSD of six measurements). Resolution may also be combined with a selectivity test to check the resolution of the analytes from components present in the sample matrix. If matrix components interfere with a method, a matrix blank may be included in the SST. Peak shape and asymmetry, or tailing factor, can have a major impact on the performance of a quantitative method, especially at low amounts or concentrations, and may vary over the lifetime of a column.

The number of theoretical plates can provide the historical data needed to determine if the column needs to be replaced, based on scientific reasoning, and not simply a by a judgment that the column does not work.

Retention times tend to vary over time because of a number of causes, e.g., differences between batches of mobile phase, column performance and different columns, and ambient temperatures of laboratories. The RSD of retention time, especially important because it is used for peak identification, is influenced by: 1) Pump flow; 2) composition precision; 3) mobile-phase composition of solvent delivery systems; and 4) column temperature. Imprecise retention time indicates problems within the HPLC system such as piston seals, check valves, etc.

Signal-to-noise (S/N) ratio may become important when measuring analytes at low concentrations. Related to this measurement may be the limits of detection (LOD) or quantification (LOQ), which may be of particular importance in trace analysis. For methods determining analytes over a large concentration range, a linearity test can be incorporated into the SST.

The RSD of the peak area is influenced by: 1) Injection mode and volume; 2) pump flow and pulsation; 3) detector noise, drift, and response; and 4) sampling rate and integration parameters of the data system.

Additional checks should be performed in some cases; this could be a routine check of the wavelength accuracy, the baseline noise, and the intensity of the UV lamp.

Automation of the System Suitability Testing

Modern data-acquisition systems can offer SSTs with the basic software, leaving the analyst to fill in the required parameters. Storing chromatograms and multiple plotting of chromatograms over time provides a chromatographer with the ability to see the historical performance of the analytical column for the past week, month, or even the column's lifetime.

CONCLUSIONS

A successful chromatographic analysis depends on the precise performance of the HPLC instrumentation, i.e., control of pressure, the composition of mobile phase, the performance of the analytical column, the detector, the injector or autosampler, and the electronic data handling system.

Validation is the process of confirming that the analytical equipment, method, or system for a specific test is suitable for its intended use. Methods need to be validated before their introduction into routine use and revalidated whenever there is a change (outside the original scope of the method) in any parameter of the method.

In accordance with GLP, a chromatographic procedure must 1) exactly follow a protocol; 2) be conducted by a qualified personnel; 3) be controlled by standard operating procedures (SOPs); 4) use proper and adequate facilities;

5) use calibrated and well maintained equipment; and 6) provide fully retrievable raw data.

Satisfactory results for a method can only be obtained with properly performing equipment that is periodically inspected, cleaned, maintained, and calibrated according to SOPs. Records of those activities should be maintained.

A laboratory applying a specific method should have documentary evidence that the method has been appropriately validated; this holds for methods developed in-house as well as for standard methods, to demonstrate the validity of the method in the laboratory environment.

For routine use, relevant tests should be selected, depending on the use of the equipment, in order to verify that the instrument is performing in a regulated, controlled manner.

Instrument hardware should be validated prior to routine use, after repair, and at regular time intervals. Computer systems should be validated during, and at the end of, the development process and after software updates. Computer systems with complex software are frequently gradually developed over many years. It is critical to note that quality cannot be tested into a product or system at the final testing stages. To ensure quality during the development process, the life cycle concept has been developed.

Analytical methods should be validated prior to routine use and after changing method parameters.

Analytical systems should be tested for system suitability prior to, and during, routine use, practically on a day-to-day basis.

However, validation and verification of an HPLC equipment are not one-time events. They are on-going processes, covering the entire life of the instrument.

REFERENCES

1. Huber, L. Validation of analytical methods: Review and strategy. LC GC Int. **1998**, *11* (2), 96–105.
2. Jenke, J.R. Chromatographic method validation: A review of current practices and procedures. Part III. Ruggedness, revalidation and system suitability. J. Liq. Chromatogr. **1996**, *19* (12), 1873–1891.

BIBLIOGRAPHY

1. Currie, L. Nomenclature in evaluation of analytical methods including detection and quantification capabilities (IUPAC recommendations 1995). Anal. Chim. Acta **1999**, *391*, 105–126.
2. Dong, M.; Paul, R.; Roos, D. Committeeing to calibrate HPLC. Today's Chem. Work **2001**, 42–48 (February).
3. Hearn, G.M. *A Guide to Validation in HPLC*; Perkin Elmer: England, 1991; 1–20.
4. Hokanson, G.C. A life cycle approach to the validation of analytical methods during pharmaceutical product development. Part I: The initial validation process. Pharm. Technol. September, **1994**, *9*, 118–130.
5. Huber, L. *Good Laboratory Practice and Current Good Manufacturing Practice*; Hewlett-Packard: Germany, 1994; 152.
6. Huber, L. Laboratory accreditation. Part 3: Validation and calibration of equipment. Int. Lab. **1995**, *25* (9), 8–12.
7. Huber, L. Validation of computerized analytical systems. Part I: Overview, regulations and terminology. LC GC Int. **1996**, *9* (9), 564–572.
8. Huber, L. Validation of computerized analytical systems, Part 3: Installation and operational qualification. LC GC **1996**, *14* (9), 806–812.
9. http://www.labcompliance.com.
10. Jenke, J.R. Chromatographic method validation: A review of current practices and procedures. Part I. General concepts and guidelines. J. Liq. Chromatogr. **1996**, *19* (4), 719–736.
11. Jenke, J.R. Chromatographic method validation: A review of current practices and procedures. Part II. Guidelines for primary validation parameters. J. Liq. Chromatogr. **1996**, *19* (5), 737–757.
12. McDowall, R.D. A suitable system for chromatography? LC GC Int. **1995**, *8* (4), 196–206.
13. Molnar, I. Validation of robust chromatography methods using computer-assisted method development for quality control. LC GC Int. **1996**, *9* (12), 800–808.
14. Ouchi, G.I. Data file monitoring chromatography system performance. LC GC Int. **1993**, *6* (6), 356–360.
15. Snyder, L.R.; Kirkland, J.J.; Glajch, J.L. *Practical Method Development*, 2nd Ed.; John Wiley & Sons, Inc.: New York, 1997; 685–713 Chapter 15.
16. Swartz, M.E.; Krull, I.S. *Analytical Method Development and Validation*; Marcel Dekker, Inc.: New York, 1997; 92.
17. van der Voet, H.; van Rhijn, J.A.; van de Wiel, H.J. Inter-laboratory, time, and fitness-for-purpose aspects of effective validation. Anal. Chim. Acta **1999**, *391*, 159–171.

Human Exposure to Endocrine-Disrupting Chemicals: LC/MS for Risk Assessment

Hiroyuki Nakazawa
Rie Ito
Yusuke Iwasaki
Koichi Saito
Department of Analytical Chemistry, Faculty of Pharmaceutical Sciences, Hoshi University, Tokyo, Japan

Abstract
It has been emphasized that certain chemicals incorporated in daily life products, including plastic materials having wide industrial and consumer applications, may have endocrine-disrupting effects. There are in vitro and in vivo data showing that such chemicals are weak agonists of nuclear receptors and influence embryonic and/or fetal development of laboratory animals. The association between exposure to endocrine-disrupting chemicals (EDCs) and an increased incidence of endocrine disease in humans has underscored the need for accurate analytical techniques that would relate exposure to these compounds to an individual's risk of developing diseases. The development of highly sensitive and reliable analytical methods is required to assess human exposure to related chemicals. To acquire as much information as possible from limited amounts of samples, hyphenated analytical methods that use liquid chromatography–mass spectrometry (LC–MS) and LC–tandem mass spectrometry (MS/MS) for the determination of EDCs, such as bisphenol A (BPA), phthalate esters (PEs), and perfluorinated chemicals (PFCs), were developed. These simple, accurate, reliable, and high-sensitivity methods have been applied to the trace analysis of biological and environmental samples. By using LC–MS/MS, BPA, PEs, and PFCs were determined in human biological samples for the assessment of human exposure.

INTRODUCTION

Many reports of phenomena in humans and wildlife that were difficult to explain with existing biological, toxicological, and medical knowledge emerged in the 1960s and the 1970s. One report concerns the development of vaginal cancer in girls born to women who took diethylstilbestrol (DES) to prevent miscarriage during pregnancy. Abnormal reproductive function and behavior, demasculinization, and deleterious effects on the immune and nervous systems of fish, reptiles, birds, and other wildlife were reported as well. In 1962, Carson sent a reminder[1] concerning the biogeocenosis effect of agrichemicals, including dichlorophenyl trichloroethane (DDT), in her book entitled "Silent Spring." In 1996, Colborn, Dumanoski, and Peterson, analyzing the risks associated with chemicals that affect human health even at minute levels, published a warning[2] regarding chemicals existing in materials expelled into the environment. Those chemicals disrupt hormonal secretion by the endocrine system, which is important for the maintenance of homeostasis in living organisms. That finding sparked a series of local and international studies that focused on those chemicals as endocrine-disrupting chemicals (EDCs). In July 2007, the U.S. Environmental Protection Agency (EPA) published a final list.[3] The list included the chemicals that are the first to be considered for screening under the Federal Food, Drug, and Cosmetic Act. This final list was not to be construed as a list of known or likely endocrine disruptors. On the final list are 73 agrichemicals that humans are very likely exposed to. Our group has published several papers[4–8] as well as a review paper[9] on various residual agrichemicals, including those on that list. Modern society has created a large number of chemicals that we have come to depend on for a comfortable and convenient lifestyle. Many chemicals are used in daily commodities and materials, including toys, food container packing materials, cosmetic products, and building materials, as well as in specialized areas, such as laboratory equipment and medical devices. Plasticizers, monomers, and heavy metals eluted from such daily commodities have endocrine-disrupting effects. In fact, when human blood was analyzed, chemicals that may have been derived from high-molecular-weight molecules were detected.[10] However, the amounts of minute chemicals, such as EDCs, that destabilize complex body functions were not clarified. In addition, the extent of the endocrine-disrupting effects of chemicals on successive generations of living organisms ("low" dosage problem), which is a dose–behavior relationship, remains to be known.[11–14] For bisphenol A (BPA), the National Toxicology Program (NTP) reported in the draft NTP brief on BPA (April 14, 2008) that despite recognition of the lack

of data on the effects of BPA on humans and the limited evidence of the "low" dose effects on laboratory animals, as will be discussed in detail below, the possibility that BPA may alter human development cannot be dismissed. As mentioned above, we are living in times[15] where the danger has not yet been accurately exposed.

By citing cases demonstrated through various research projects, we will discuss the analysis and risk factors of minute amounts of EDCs, namely, BPA, phthalate esters (PEs), and perfluorinated chemicals (PFCs).

ANALYSIS OF BPA

BPA is widely used as an ingredient of polycarbonate and epoxide resins. BPA disposition[16] was examined in a cynomolgus monkey that was orally and intravenously (IV) administered radioisotope-labeled BPA (^{14}C-BPA). BPA half-life was approximately 10 hr (oral administration) and most of the BPA was converted into glucuronic acid conjugate that was excreted into the urine within 24 hr. It is assumed that BPA disposition in the human body is the same as that in cynomolgus monkey. Völkel et al. administered 5 mg of deuterium-labeled BPA (BPA-d_{16}) per os to healthy volunteers, monitored the pharmacokinetics and metabolism, and found that BPA half-life inside the human body was approximately 6 hr and that most of the BPA was excreted into the urine[17] as glucuronic acid conjugate, similar to the case of cynomolgus monkey. Glucuronic acid conjugation with BPA has been detected[18,19] in animal tests and it is assumed[20] that glucuronic acid conjugate is a useful biomarker. In BPA metabolism in humans, the discovery of sulfate conjugate[21] as well as the glucuronic acid conjugate indicated the need to consider various metabolic processes. When BPA metabolism was examined using rat or mouse liver S9, chemical species that exhibited higher estrogenic activity than BPA, dimers, and other chemical species were observed[22,23] although it was difficult to say if they were the major BPA metabolites in humans. Thus, the mono- or di-glucuronic acid conjugate may also exist.

BPA is widely incorporated in products used in our daily lives, such as canned beverages, etc.[24] The amount of BPA in the environment, food, and biological samples is still controversial and should be monitored. In this section, we will introduce examples of the analysis of BPA exposure that we conducted.

ANALYSIS OF BPA IN HUMAN BLOOD PLASMA SAMPLES

Since BPA exists in trace amounts in biological samples, highly sensitive methods are required for its analysis. In addition, the pretreatment process for the removal of other components is important for the analysis. Because of its chemical structure, liquid chromatography–electrochemical detection (LC–ECD) is applied[25] to the analysis of human blood plasma samples. However, it is essential to discuss the pretreatment method for the biological sample used in BPA analysis because the sample contains many other compounds. When human blood plasma is used for analysis, the plasma sample is initially purified with a solid-phase extraction (SPE) cartridge and then subjected to LC–ECD. In this case, the quantitative limit of 0.6 ng/ml(blood plasma) was established.[26] On the contrary, the quantitative limit of 0.5 ng/ml (seminal plasma) was established[27] for BPA in human seminal plasma pretreated with SPE cartridge. Watanabe et al. reported the utility of LC with fluorescence detection using 4-(4,5-diphenyl-1H-imidazol-2-yl) benzoyl chloride as labeling reagent for the determination of BPA in plasma samples.[28] Recently, mass spectrometry (MS) has become popular as it has increased the reliability of compound identification. Currently, LC–MS and LC–tandem mass spectrometry (MS/MS) are mainly used in the analysis of BPA in biological samples. LC–MS was developed for the determination of BPA in serum and plasma samples.[29] Gas chromatography (GC)–MS method was also developed.[30,31]

ANALYSIS OF BPA AND BADGE-4OH IN HUMAN URINE SAMPLES

Ionization was enhanced by adding an appropriate amount of acid to the mobile phase of LC–MS.[32] Therefore, we studied the influence of adding a small amount of acid to the mobile phase on the ionization efficiency. The standard product of BPA and the hydrolysis product of BPA diglycidyl ether (BADGE-4OH) to which ammonium acetate was added were measured, and their multiple reaction monitoring (MRM) response ratios were compared. When 0.5 m*M* ammonium acetate was added, chromatograms having sufficient sensitivity and selectivity were obtained. The method of analysis was validated to determine the reliability of the established analytical method. The limit of detection (LOD) was 1.0 ng/ml and the correlation coefficient was 0.999. In the recovery test using human urine samples, 95% or higher recovery was obtained. The method is useful for the determination of BPA and BADGE-4OH in urine samples.

Völkel, Kiranoglu, and Fromme monitored free and total BPA in human urine samples to assess daily uptake. Using LC–MS/MS, an LOD of 0.3 μg/L was determined.[33] Literature on the determination of urinary BPA using LC–MS or LC–MS/MS is available.[34–36] Moreover, the pretreatment method as well as the method to concentrate and/or purify BPA in urine samples were examined. For example, coacervative microextraction,[37] hollow fiber-assisted liquid-phase microextraction,[38] and

SPE based on molecularly imprinted polymers[39] were examined as the pretreatment method of BPA in urine samples.

ANALYSIS OF PEs

Polyvinyl chloride (PVC) resin is widely used in our daily lives and is essential for the production of plastics used in the manufacture of food gloves,[40,41] medical devices,[42,43] furniture, flooring, and so on. PEs, particularly di(2-ethylhexyl)phthalate (DEHP), are extensively used as plasticizers to increase the flexibility of PVC products; however, it has been reported that DEHP was easily eluted from PVC products into food, drugs, and body fluids. DEHP is considered to exhibit reproductive and developmental toxicity,[44,45] carcinogenicity, and testicular toxicity.[46–48] It was also found to affect the reproductive organs and fertility.[49]

As PEs are rapidly metabolized, measurement of the metabolites is generally accepted when the amount of exposure to humans is evaluated. PEs are mainly metabolized into phthalate monoesters and excreted into the urine (Fig. 1). Albro and Lavenhar reported[50] 30 or more metabolites of DEHP metabolism. The exposure amount[51,52] of mono(2-ethylhydroxyhexyl) phthalate (MEHHP) in which mono(2-ethylhexyl) phthalate (MEHP) is subjected to oxidation by ω-1 and mono(2-ethyl-5-oxohexyl) phthalate (MEOHP) that is an oxide of MEHHP, etc. has been reported. MEHP oxides such as MEHHP and MEOHP were excreted into the urine at a high ratio compared to MEHP, when they were measured after DEHP exposure.[53–55] It is known that PEs other than DEHP are metabolized into the mono form.[56] The rate of metabolism is 69% when dibutyl phthalate is metabolized into monobutyl phthalate and 73% when dibutyl benzyl phthalate is metabolized into monobutyl benzyl phthalate. Because it is considered that PE, the parent compound (di form), is a ubiquitous compound, its metabolites are frequently monitored during exposure evaluation. Various pretreatments have been discussed[57,58] to avoid contamination of PEs during analysis. Kato et al. developed[57] the method without DEHP contamination, using essential oil quantitative equipment for measurement of blood plasma samples. Ito et al. developed the column-switching method to avoid DEHP contamination.[43,58]

The U.S. Centers for Disease Control and Prevention (CDC) has continuously promoted studies on human exposure to PE. The National Health and Nutrition Examination Survey (NHANES) project of CDC conducted a large-scale investigation of human exposure to PEs.[59] This project reported the analysis[60] of 8 phthalate monoesters, which are the metabolites of PEs, and the simultaneous analysis[52] of 11 PE metabolites when another metabolite is added using LC–atmospheric pressure chemical ionization (APCI)–MS/MS. In addition, electrospray ionization (ESI) and the use of LC–MS/MS for the simultaneous analysis of 15–16 materials related to PEs, including phthalic acid (PA) and an isomer, were reported.[61,62] Fig. 2 shows the main chemicals used as biomarkers for the evaluation of the amount of exposure to PA. Epidemiologic analysis of exposure levels in healthy individuals and the effects on the human body was conducted[63–65] using such exposure reports as those published by CDC.[66] However, there are many unsolved problems, including the identification of exposure levels on a nationwide level and the evaluation of exposure in medical practice. Clearly, much work needs to be done.

With regard to the studies of PEs conducted to date, we will introduce: 1) the evaluation of exposure to DEHP using human urine samples; 2) the measurement of DEHP and related compounds in human blood samples; and 3) the measurement of exposure to DEHP eluted from medical devices made of PVC, in this section.

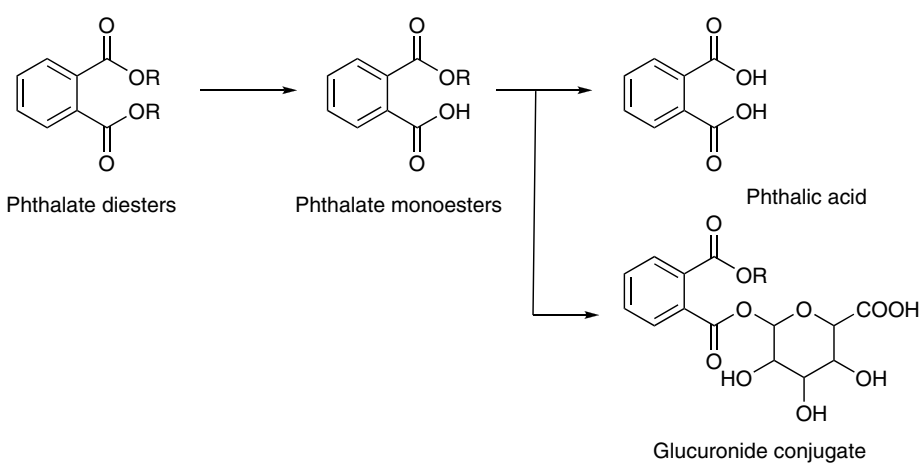

Fig. 1 Metabolic pathway of phthalate. Phthalates with R and R groups are metabolized into phthalate monoesters, which are found in urine as glucuronide conjugates or free acids.

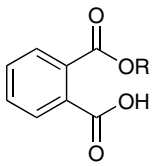

Fig. 2 Structures of PEs for exposure assessment. R=CH_3: MMP, monomethyl phthalate; R=CH_2CH_3: MEP, mono-ethyl phthalate; R=$(CH_2)_3CH_3$: MBP, mono-butyl phthalate; R=C_6H_{11}: MCHP, mono-cyclohexyl phthalate; R=$CH_2C_6H_5$: MBzP, mono-benzyl phthalate; R=$CH_2(C_2H_5)(CH_2)_3CH_3$: MEHP, mono(2-ethylhexyl) phthalate; R=$(CH_2)_7CH_3$: MOP, mono-*n*-octyl phthalate; R=$(CH_2)_2CH(CH_3)CH_2C(CH_3)_3$: MNP, mono-isononyl phthalate; R=$(CH_2)_2CH(CH_3)CH_2(CH_2)_2CH(CH_3)_2$: MDP, mono-3-methyl-7-methyloctyl phthalate; R=$CH_2CH(C_2H_5)(CH_2)_2CH(OH)CH_3$: MEHHP, mono(2-ethylhydroxyhexyl) phthalate; R=$CH_2CH(C_2H_5)(CH_2)_2COCH_3$: MEOHP, mono(2-ethyl-5-oxohexyl) phthalate; R=$(CH_2)_3COOH$: MCPP, mono(3-carboxypropyl) phthalate; R=H: PA, phthalic acid; R=$CH_2CH(C_2H_5)(CH_2)_3COOH$: MECPP, mono(2-ethyl-5-carboxypentyl) phthalate.

Evaluation of Exposure to DEHP Using Human Urine Samples

As has been described earlier, evaluation of the amount of exposure to PEs using human urine samples is frequently performed by measuring the metabolites. In our monitoring study,[51] where we monitored MEHP, MEHHP, and MEOHP, the metabolites of DEHP, in urine, we performed SPE easily and rapidly by introducing online automation. In addition, we established a highly sensitive and accurate method[51] that uses LC–MS/MS and a deuterated surrogate standard. As a result of applying the above method to the determination of DEHP metabolites in the urine samples of 70 healthy volunteers, we found that the urinary concentration of MEHHP is 9.5–320.8 ng/ml, that of MEOHP is 13.9–187.5 ng/ml, and that of MEHP is not determined (ND) to 13.9 ng/ml. The urinary concentrations of MEHHP and MEOHP are higher than that of MEHP and their detection rates are 100%. Accordingly, MEHHP and MEOHP are as useful as MEHP as biomarkers for the measurement of the amount of exposure to DEHP using urine samples.

In addition to the evaluation of healthy individuals, studies on workers who were exposed to PEs in a plastic factory were carried out. We measured urinary MEHP and MBP concentrations of workers ($n = 246$) in a factory that manufactures PEs in China. MEHP was detected in all but three workers. The exposure levels after correction for creatinine was conducted were 12.4–22836.9 μg/g for MBP and 1.1–9753.2 μg/g for MEHP. The average values are 776 μg/g for MBP and 423 μg/g for MEHP. Compared to the exposure levels of previously described healthy individuals, it is clear that the workers are exposed to PEs at notably high levels.[67] This is a proof that urine samples are suitable for the assessment of DEHP exposure.[68–71]

Measurement of DEHP in Human Blood Samples

As DEHP metabolism in human blood is accelerated by blood enzymes, such as esterase, its metabolites are frequently measured. In the study[72] where the metabolites of deuterium-substituted DEHP in urine and in blood serum were compared after oral administration of DEHP, MEHP was found to be the main metabolite in blood serum, existing in greater quantities than MEHHP and MEOHP detected in urine. Therefore, we decided to measure DEHP and MEHP in blood serum. Four healthy volunteers were asked to consume food in containers that were made in part of plastic, and DEHP and MEHP concentrations in blood sera were measured. The concentration of DEHP was equal to or less than the quantitative lower limit (trace level) in all the volunteers. The concentration of MEHP was trace in three of the four volunteers and was lower than the quantitative lower limit in one volunteer.[73] In addition, we measured DEHP and MEHP in human blood plasma samples using LC–MC with the column-switching system as pretreatment. DEHP and MEHP concentrations in blood plasma sampled from six healthy volunteers were equal to or less than the quantitative limit (DEHP <25 ng/ml, MEHP <5 ng/ml).[74] The results prove that DEHP is rapidly metabolized so that the blood concentration is low and quantification is difficult at normal exposure levels. Urine samples are more suitable for the evaluation of the exposure index of PEs than blood samples.

Measurement of DEHP Eluted from Medical Devices Made of PVC

As medical practice with devices made of PVC has many advantages, the risk of exposure to DEHP tends to be ignored. Therefore, it is important that the amount of exposure be determined accurately. Studies that used PE exposure models in medical practice have been conducted.[75–77]

What should be considered in the elution of DEHP from PVC medical devices are fat-soluble agents and blood products into which DEHP may be eluted at high concentrations. The amount of DEHP that eluted into blood products stored in PVC bags was measured. When the amounts of DEHP in red blood cell products, whole blood products, blood platelet products, and blood plasma products were compared, a high concentration of DEHP was detected in whole blood products. This means that the sample matrix affects the elution of DEHP.[78] We also analyzed blood products stored in PVC bags and found that the amount of DEHP eluted increased with the storage period, and the exposure to DEHP in an amount that exceeded tolerable dairy intake (TDI) value was noted after only one blood transfusion even if the blood product had not reached the expiration date.[78] In addition, we established a method for the simultaneous analysis of DEHP and MEHP with high sensitivity and accuracy and

applied it to an elution test using drugs from medical containers. MEHP that is not used as plasticizer was detected and it was verified in a material test[43] that MEHP is indeed present. It is known that DEHP is metabolized into MEHP in the presence of blood enzymes; however, no blood enzymes existed in this case. We then decided to examine whether or not the sterilization process, which is essential for medical devices, affects the elution behavior of DEHP and MEHP. Using unsterilized products as control, we measured the elution of DEHP and MEHP from PVC products that were subjected to autoclave sterilization, gamma sterilization, and ethylene oxide gas sterilization (EOG) and found that high concentrations of MEHP were eluted from PVC products subjected to gamma sterilization. The material test also showed that MEHP was detected only from the samples subjected to gamma sterilization. The results suggest the possibility that DEHP is decomposed into MEHP during gamma sterilization.[79]

PERFLUORINATED CHEMICALS

Recently, PFCs have been focused on as new EDCs. Perfluorooctanesulfonic acid (PFOS), perfluorooctanoic acid (PFOA), perfluorooctane sulfonylamide (PFOSA), perfluorononanoic acid (PFNA), and perfluorohexanesulfonic acid (PFHxS) are examples of PFCs. They are widely used in daily commodities, such as water repellents for fabric, surfactants, leveling agents, fire-extinguishing agents, lubricants, and anticoagulants. PFCs are characterized by the attachment of several fluorine atoms to all the carbon atoms in a straight chain and a sulfonate group or a carboxylic group at the ends of the carbon atoms (Fig. 3). As the bonds between carbon atoms and fluorine atoms are extremely strong, PFCs are very stable. PFCs are relatively stable in the environment, such as in river water. On the contrary, endocrine-disrupting effects, including teratogenesis, influence on thyroid hormone,[80,81] and norepinephrine-enhancing action,[82] were found in experimental animals.[82–84] Therefore, PFCs are considered to have an adverse effect on future generations.

As an example of PFC contamination, Giesy and Kannan reported[85] the worldwide contamination by PFOS, PFHxS, and PFOSA, which are used in plastic materials and additives. PFCs remain intact in marine mammals, fishes, and birds for long periods as PFC metabolism and elimination occur very slowly. As PFCs[86] easily bond to human blood plasma protein, it is assumed that PFCs tend to remain in the blood, and therefore, PFC monitoring in blood is very useful for the evaluation of human exposure.[87–89] Methods for the analysis of PFOS, PFOA, PFOSA, and PFHxS in human blood samples have been reported.[90] PFOS was detected[90] at a rate of 100% (65 samples) in the concentration range of 6.7–81.5 ng/ml (blood serum). This indicates that human contamination with PFCs is widespread and their effects on the human body should be carefully studied. Our study suggested that PFOS and PFOA may be transported into the human fetus in the uterus through maternal blood.[91] Therefore, strict surveillance is necessary to evaluate the risk posed by PFCs to biogeocenosis and humans, especially children. Regarding chemicals related to PFOS, monitoring on a nationwide level remains to be accomplished and therefore, analytical methods with high sensitivity and reliability are required for human biological samples.

In this section, we will introduce our studies of PFCs, including: 1) the development of analytical methods to detect PFCs in blood; 2) the correlation between PFCs in maternal blood and cord blood to evaluate human exposure and their influence on future generations; and 3) the analysis of house dust and carpet dust as room environment media, to discover the source of exposure to PFCs.

Development of Analytical Methods to Detect PFCs in Human Blood Samples

The first analysis of PFOS and related chemicals in human blood serum involved the use of LC–MS/MS after liquid–liquid extraction with methyl *tert*-butyl ether (MTBE).[90]

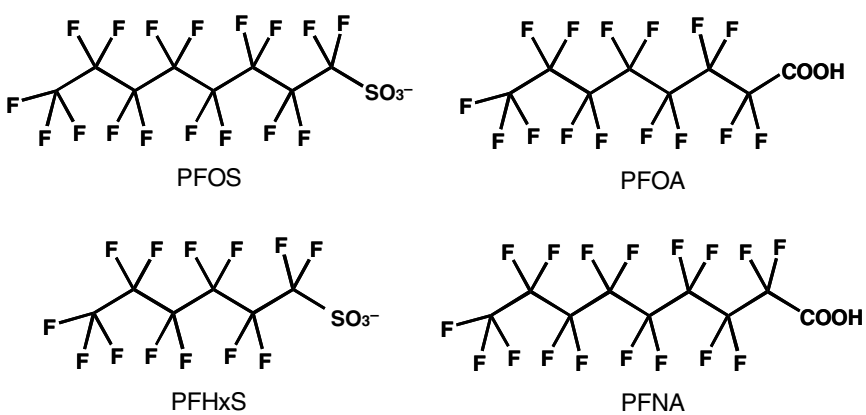

Fig. 3 Structures of PFCs: PFOS, perfluorooctanesulfonic acid; PFOA, perfluorooctanoic acid; PFNA, perfluorononanoic acid; PFHxS, perfluorohexanesulfonic acid.

This method is widely used[92] in the analysis of human blood samples in the United States. A screening analysis in which LC–MS with ESI is applied to human blood serum after the same pretreatment has been reported.[93] CDC has reported[94] the analysis of 13 PFCs in blood and maternal milk with automated SPE and LC–MS/MS. In Japan, environmental monitoring of PFCs has been performed.[95] However, investigation of human exposure has seldom been done. Currently, LC–MS or LC–MS/MS is used[91,94,96–99] to determine PFCs in biological samples. However, it is said that the use of LC–MS/MS that has high accuracy is favorable to correctly evaluate human exposure. As sample pretreatment methods, the liquid–liquid extraction method,[95–97] the SPE method,[94,98] and the column-switching method[91,99] have been reported. However, the liquid–liquid extraction method and the manual SPE method are tedious and time-consuming.

To develop a rapid, highly sensitive, and highly accurate method for the analysis of exposure in biological samples, we established the SPE LC–MS/MS method[99] in which the column-switching method and LC–MS/MS[100] that has superior selectivity are adopted. The column-switching method used in DEHP measurement (as mentioned in the preceding section) was applied to PFC measurement. As a result, pretreatment was easily achieved and contamination was reduced during measurement. This system concentrated and cleaned up analytes on the SPE cartridge after a sample from which protein was removed with acetonitrile was injected into the LC with an auto sampler and ammonium acetate buffer (pH = 4.7) and methanol (90/10, v/v) of 50 m*M* were infused for 5 min. The hexagonal valve was switched and gradient elution of a mixture of water/acetonitrile at 1 m*M* to which ammonium acetate was added was performed with the backflushing method. The analytes were eluted from the SPE cartridge and introduced into the analytical column. The ESI negative ion mode was adopted as MS/MS condition and the calibration curve and actual samples were measured in the MRM mode.

Using the online SPE pretreatment, PFCs in human blood plasma samples can be measured easily only by removing proteins. The background can be reduced by applying MS/MS. LOD is 0.08–0.14 ng/ml (S/N = 3) and the limit of quantitation (LOQ) is 0.50 ng/ml. Using an internal standard, a calibration curve was obtained with good linearity (correlation coefficient of 0.999 or higher) in the range of 0.5–100 ng/ml. In the spike recovery test of blood plasma samples, the average recovery was 93.3% or higher ($n = 6$). To validate the reliability of the proposed method, we conducted internal quality control and participated in an international accuracy control project. As internal quality control, we evaluated the reproducibility of the measured values of four samples for 20 days using PFOS standard solution at 10 ng/ml and drew control charts. As a result, the measured values were within the action lines for all 20 days. As regards external accuracy control, we participated in the international accuracy control project held in August 2005 and evaluated the validity of the values[101,102] measured using the proposed method. The measured values were all in the range of Z scores, proving the high reliability of this method.

Correlation between PFC Concentrations in Maternal Blood and Cord Blood

Blood sampled from 447 pregnant volunteers living in Hokkaido was analyzed. PFOS was detected in all samples, and PFOA and PFNA were detected at the rates of 93.1% and 43.9%, respectively. The detection range was 1.3–16.2 ng/ml for PFOS, ND (<0.5 μg/ml) to 5.2 ng/ml for PFOA, and ND (<0.5 ng/ml) to 1.6 ng/ml for PFNA. PFOS and PFOA concentrations were measured to determine the relationships between PFC concentration in blood and such parameters as the duration of pregnancy, fetal growth, and complications during pregnancy. It was verified that PFOS and PFOA concentrations were significantly higher in pregnant women suffering from fetal distress, weakness, or rigidity of the soft birth canal, than in healthy pregnant women. These new findings clarified the influence of PFOS and PFOA on the fetal growth stage. Meanwhile, PFOSA and PFDA were hardly detected.

Then, maternal blood and cord blood of 15 healthy pregnant volunteers were analyzed[91] to evaluate the transport of PFOA, PFOSA, and PFOS to the fetus in the uterus. PFOS was found in all maternal blood and cord blood samples whereas PFOA was detected in three maternal blood samples. PFOSA concentration in all maternal blood samples and PFOA and PFOSA concentrations in all cord blood samples are equal to or less than the LOQ levels. The detection range of PFOS in maternal blood and cord blood was 4.9–17.6 ng/ml and 1.6–5.3 ng/ml, respectively. A strong correlation was found between them, and the transport rate was assumed to be 30% from the obtained linear slope (Fig. 4). Accordingly, the possibility that PFCs are transported to the fetus in the uterus through cord blood was suggested.

We also analyzed blood and seminal plasma of 50 male volunteers (age: 18–24 years old). We investigated the

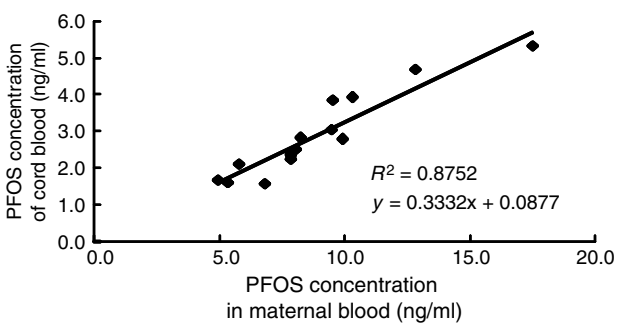

Fig. 4 Correlation between PFOS concentrations in maternal blood and cord blood.

influence of PFOS on sperm count and sperm physical properties. As PFOS was detected at low levels in seminal plasma, it is unlikely that PFOS affects the male reproductive organ.

Investigation of source of exposure to PFCs

Studies of the source of exposure to PFCs have rarely been conducted. Thus, studies of the source of contamination with PFC, the source of exposure, the diffusion path, the accumulated form, and toxicity are necessary. Currently, environmental contaminant of PFCs were mainly reported in polluted mud,[103] environmental water,[104] and atmosphere.[105] However, the concentrations of detected PFCs are extremely low, and it is not sufficient to evaluate them as an exposure source. Therefore, we focused on house and carpet dust,[106] which exists in our daily lives and contains many chemicals, to clarify the source of exposure to PFCs, and discussed[107] a highly sensitive and accurate method for the analysis of PFCs in house and carpet dust. The analytes were PFOS, PFOA, PFNA, and PFHxS, which are frequently detected in human blood, and surrogate standards were $^{13}C_4$-PFOS and $^{13}C_2$-PFOA. The supercritical fluid extraction (SFE) method was used for house and carpet dust. Effective extraction is expected when supercritical liquid is used as the extraction solvent, as the elution ability of supercritical liquid is similar to that of conventional liquid and supercritical fluid can permeate every corner of the sample, as air does.

Accurate analysis was achieved using optimum LC–MS/MS conditions: LOD was 0.58 ng/ml or higher and LOQ was 2.5 ng/ml in all the analytes. The spike recovery test was conducted with internal standards and the average recovery was 97.9% or higher [relative standard deviation (RSD) 5.8%, $n = 6$], thereby suggesting that this method is useful to quantitatively determine PFCs in house and carpet dust. This method revealed that PFC concentration in house dust was extremely high compared to that in environmental samples, including environmental water and air.

Then, PFC concentration in the blood of 20 healthy volunteers was measured and compared to that in house dust collected from each volunteer's house. PFOS and PFOA were detected from all human blood samples (plasma). PFNA and PFHxS were also detected at high frequencies. When PFC concentrations in blood plasma and house dust were compared, weak correlation was found for PFOA (Fig. 5). Accordingly, it is assumed that house dust is one of the sources of exposure to PFCs in humans.

RISK ASSESSMENT

One of the ultimate goals is to clarify how trace amounts of harmful chemicals affect human health. We need to know how much of the subject chemical humans take in through an intake medium, such as water, air, or food (evaluation of the amount of exposure), and to measure the concentration of the subject chemical in each medium. To calculate the amount of human exposure to EDCs, two exposure routes are considered. One is the calculation of the exposure amount from the intake medium, and the other is the estimation of exposure amount by analyzing human biological samples.

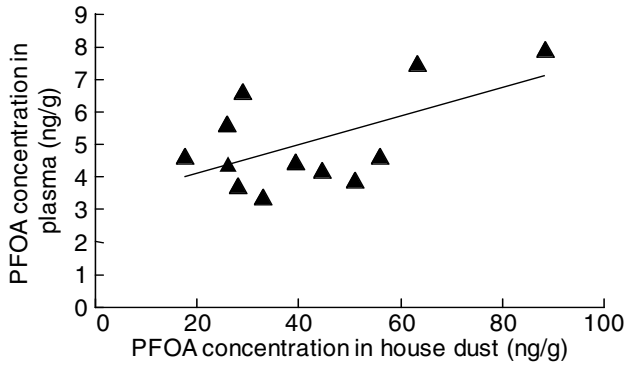

Fig. 5 Correlation between PFOA concentrations in human plasma and house dust.

PEs and PFCs detected in human urine and blood samples are chemicals that we may be constantly exposed to. Thus, evaluation of the amount of exposure and the toxicity using various assays including animal experiments is necessary to assess the risk. In the case of EDCs, many problems exist, such as "low" dosage and the multigeneration influence in the safety assessment (toxicity test), and no concrete conclusion has been reached so far. Therefore, it is necessary to evaluate the amount of human exposure to EDCs and to perform safety assessment based on the evaluation results.

This section focuses on the fact that there is irregular exposure to PEs eluted from medical devices and the exposure level is high compared to that of BPA and PFCs, to which humans are constantly exposed. Therefore, we evaluated the risk of exposure to PEs eluted from medical devices. We evaluated: 1) the exposure to DEHP when a PVC blood bag is used and 2) the exposure to DEHP from medical devices subjected to gamma sterilization.

DEHP EXPOSURE EVALUATION WHEN BLOOD BAG IS USED[78]

Evaluation of the elution of DEHP and MEHP into blood products revealed that DEHP was eluted at the highest concentration into human whole blood products. Accordingly, risk assessment was conducted with whole blood products that contained the highest concentration of DEHP. When 400 ml of whole blood was transfused at one time to a patient (50 kg), the total amount of DEHP exposure was 0.7 mg/kg/time. This value was compared to that[108] reported by the U.S. Food and Drug Administration (FDA). According to the U.S.

FDA, DEHP exposure through blood transfusions to a trauma patient is 8.5 mg/kg/day when the patient's weight is 70 kg. This confirmed that the exposure level in our study was very low. In addition, the combined amount of exposure of DEHP and MEHP was calculated. When 400 ml of whole blood was transfused at one time to a human patient, the amount of MEHP exposure was 10 μg/ml × 400 ml = 4 mg. If the patient's weight were 50 kg, the amount of exposure to MEHP would be 4 mg $(50\ \text{kg})^{-1}$/time = 0.08 mg/kg/time in one blood transfusion. Because MEHP is also eluted, we decided to conduct risk assessment of the joint exposure to DEHP and MEHP.

The U.S. FDA reported[108] the relative testicular toxicity of MEHP to DEHP as relative potency factor (RPF) = 10; that is, MEHP toxicity is 10 times higher than DEHP toxicity. The U.S. EPA performed risk assessment of a mixture using RPF, which is also known as the toxic equivalency factor (TEF), and the concentration of the mixture of MEHP and DEHP is calculated with the following formula:

$$C_{\text{mixture}} = C_{\text{index}} + \sum [\text{RPF}_i \times C_i]$$

where C is the concentration and RPF_i is the relative potency factor of the index compound.

To perform risk assessment of the combined amount of exposure of DEHP and MEHP, first, DEHP was adopted as the index compound (C_{index}: DEHP concentration) and RPF was multiplied by the amount of exposure to MEHP (C_i: MEHP concentration). Then, the value obtained was converted into the amount of exposure to DEHP, namely, 0.8 mg/kg/time. Similarly, when the amount of exposure to DEHP (when 400 ml of blood was transfused to a human weighing 50 kg) was calculated, the total amount of DEHP was 0.7 mg/kg/time (0.66 mg/kg/time); that is, the exposure amount in the combined exposure to DEHP and MEHP is 1.5 mg/kg/time with DEHP conversion. The TDI of DEHP via non-oral administration is 600 μg/kg/day, and it is suggested that patients are exposed to DEHP twice as much as TDI at one time during the blood transfusion.

DEHP EXPOSURE EVALUATION[79] FROM MEDICAL DEVICES WITH GAMMA STERILIZATION

The concentration of MEHP that was eluted from a PVC sheet subjected to gamma sterilization was approximately 600 ng/ml. In this analysis method, a piece of PVC sheet measuring 1 × 3 cm was soaked in 5 ml of polyoxyethylated hydrogenated castor oil, a pharmaceutical additive, and MEHP was extracted. The amount of MEHP that eluted into the 5 ml solution was 3 μg (=600 ng/ml × 5 ml). The surface area of the PVC sheet used in the extraction was 6 cm^2 for both sides, and the amount of MEHP eluted per unit area was 0.5 μg/cm^2. The surface area of gamma ray-sterilized infusion set (tube) having the largest surface area among commercially available PVC medical devices was 101.3 cm^2. The amount of MEHP that was eluted from the medical device is 50.7 μg (=0.5 μg/cm^2 × 101.3 cm^2).

When this medical device was used for two days, the amount of MEHP a patient weighing 50 kg was exposed to at one time was 0.51 μg/kg/day. The amount of DEHP exposure per day (approximately 35 ng/ml was eluted from samples subjected to gamma sterilization) was similarly calculated to be approximately 0.03 μg/kg/day (29.5 ng/kg/day). When this value was substituted into the formula for the exposure evaluation described before, risk evaluation of the concentration with combined exposure to DEHP and MEHP is calculated. DEHP concentration + [10 × MEHPconcentration] = 0.03 + [10 × 0.51] = 5.13 (μg/kg/day).

TDI of DEHP is 40 μg/kg/day in the case of oral administration, and it is 600 μg/kg/day in the case of non-oral administration. According to the risk evaluation of the joint exposure to DEHP and MEHP eluted from PVC with gamma sterilization, the exposure amount was 5.13 μg/kg/day as DEHP, which is below TDI.[79]

As "medical treatment" with blood products, etc. is not conducted on a daily basis and many advantages are gained from medical care, it is considered that the risk is underestimated. When medical devices are applied to pregnant women and newborn, both of whom are high-risk patients, it may be necessary to pay close attention to the DEHP exposure.

It is necessary to evaluate the amounts of human exposure to EDCs and to perform safety assessment based on those values.

CONCLUSION

EDCs have generated complex and wide-ranging issues. To this end, it is important to evaluate (risk assessment) risk as trace amounts of harmful chemicals affect our health from various perspectives. One of the issues that need to be discussed immediately is how accuracy control and analysis method validation should be performed to secure and guarantee the reliability of results.

It is necessary to not only depend on the latest analytical equipment, but to obtain reliable data, achieve reproducibility of the experiment, and analyze and disclose obtained data.

REFERENCES

1. Carson, R. *Silent Spring*. Houghton Mifflin: Boston, 1962.
2. Colborn, T.; Dumanoski, D.; Peterson, J. *Our Stolen Future*. Dutton: NY, 1996.
3. U.S. Environmental Protection Agency: EPA Federal Register Notice, http://www.epa.gov/scipoly/oscpendo/

pups/prioritysetting/final_listfacts.htm (accessed April 2009).
4. Horie, M.; Saito, K.; Nakazawa, H. Determination of kitasamycin and josamycin in meat by HPLC. Bunseki Kagaku **1996**, *45*, 1089.
5. Yamaguchi, S.; Eto, S.; Eguchi, Y.; Kido, K.; Hisamatsu, Y.; Nakazawa, H. Screening analysis for multiple pesticide residues in agricultural products with the GC/MS-SCAN method. Bunseki Kagaku **1997**, *46*, 905.
6. Nakazawa, H.; Kanzaki, Y.; Takahashi, N.; Oka, H. The rapid analysis for residual pesticides by tandem mass spectrometry with immunoaffinity extraction. Bunseki Kagaku **2004**, *53*, 1295.
7. Takagami, H.; Horie, M.; Nakazawa, H. Determination of macrolide antibiotics in milk by high-performance liquid chromatography/mass spectrometry. Bunseki Kagaku **2006**, *55*, 651.
8. Iwasaki, Y.; Ito, T.; Kitamura, W.; Kato, M.; Kodaira, T.; Horie, M.; Ito, R.; Saito, K.; Nakazawa, H. Analysis of fluoroquinolones in meat samples by enzyme-linked immunosorbent assay and HPLC. Bunseki Kagaku **2006**, *55*, 943.
9. Horie, M.; Nakazawa, H. Analysis of residual chemicals in food. Bunseki Kagaku **1996**, *45*, 279.
10. Inoue, K.; Kawaguchi, M.; Ito, R.; Saito, K.; Nakazawa, H. Analytical methods of endocrine disrupting chemicals released from plastic materials. Bunseki, Kagaku **2005**, *361*, 35.
11. Andrade, A.J.M.; Grande, S.W.; Talsness, C.E.; Grote, K.; Chahoud, I. A dose-response study following in utero and lactational exposure to di-(2-ethylhexyl)-phthalate (DEHP): Non-monotonic dose-response and low dose effects on rat brain aromatase activity. Toxicology **2006**, *227*, 185.
12. Takano, H.; Yanagisawa, R.; Inoue, K.-I.; Ichinose, T.; Sadakano, K.; Yoshikawa, T. Di-(2-ethylhexyl) phthalate enhances atopic dermatitis-like skin lesions in mice. Environ. Health Perspect. **2006**, *114*, 1266.
13. Welshons, W.V.; Thayer, K.A.; Judy, B.M.; Taylor, J.A.; Curran, E.M.; vom Saal, F.S. Large effects from small exposures. I. Mechanisms for endocrine-disrupting chemicals with estrogenic activity. Environ. Health Perspect. **2003**, *111*, 994.
14. Wetherill, Y.B.; Petre, C.E.; Monk, K.R.; Puga, A.; Knudsen, K.E. The xenoestrogen bisphenol A induces inappropriate androgen receptor activation and mitogenesis in prostatic adenocarcinoma cells. Mol. Cancer Ther. **2002**, *1*, 515.
15. Ministry of Health, Labour and Welfare in Japan: ISBN4-87326-387-5 (2005).
16. Kurebayashi, H.; Harada, R.; Stewart, R.K.; Numata, H.; Ohno, Y. Disposition of a low dose of bisphenol A in male and female cynomolgus monkeys. Toxicol. Sci. **2002**, *68*, 32.
17. Völkel, W.; Colnot, T.; Csanády, G.A.; Filser, J.G.; Dekant, W. Metabolism and kinetics of bisphenol A in humans at low doses following oral administration. Chem. Res. Toxicol. **2002**, *15*, 1281.
18. Yokota, H.; Iwano, H.; Endo, M.; Kobayashi, T.; Inoue, H.; Ikushiro, S.; Yuasa, A. Glucuronidation of the environmental oestrogen bisphenol A by an isoform of UDP-glucuronosyltransferase, UGT2B1, in the rat liver. Biochem. J. **1999**, *340*, 405.
19. Inoue, H.; Yokota, H.; Makino, T.; Yuasa, A.; Kato, S. Bisphenol A glucuronide, A major metabolite in rat bile after liver perfusion. Drug Metab. Dispos. **2001**, *29*, 1084.
20. Brock, J.W.; Yoshimura, Y.; Barr, J.R.; Maggio, V.L.; Graiser, S.R.; Nakazawa, H.; Needham, L.L. Measurement of bisphenol A levels in human urine. J. Expo. Anal. Environ. Epidemiol. **2001**, *11*, 323.
21. Kim, Y.H.; Kim, C.S.; Park, S.; Han, S.Y.; Pyo, M.Y.; Yang, M. Gender differences in the levels of bisphenol A metabolites in urine. Biochem. Biophys. Res. Commun. **2003**, *312*, 441.
22. Yoshihara, S.; Mizutare, T.; Makishima, M.; Suzuki, N.; Fujimoto, N.; Igarashi, K.; Ohta, S. Potent estrogenic metabolites of bisphenol A and bisphenol B formed by rat liver S9 fraction: Their structures and estrogenic potency. Toxicol. Sci. **2004**, *78*, 50.
23. Philippejaeg, J.; Perdu, E.; Dolo, L.; Debrauwer, L.; Cravedi, J.-P.; Zalko, D. Characterization of new bisphenol A metabolites produced by CD1 mice liver microsomes and S9 fractions. J. Agric. Food Chem. **2004**, *52*, 4935.
24. Horie, M.; Yoshida, T.; Ishii, R.; Kobayashi, S.; Nakazawa, H. Determination of bisphenol A in canned drinks by LC/MS. Bunseki Kagaku **1999**, *48*, 579.
25. Inoue, K.; Kato, K.; Yoshimura, Y.; Makino, T.; Nakazawa, H. Determination of bisphenol A in human serum by high-performance liquid chromatography with multi-electrode electrochemical detection. J. Chromatogr. B, **2000**, *749*, 17.
26. Inoue, K.; Yamaguchi, A.; Wada, M.; Yoshimura, Y.; Makino, T.; Nakazawa, H. Quantitative detection of bisphenol A and bisphenol A diglycidyl ether metabolites in human plasma by liquid chromatography–electrospray mass spectrometry. J. Chromatogr. B, **2001**, *765*, 121.
27. Inoue, K.; Wada, M.; Higuchi, T.; Oshio, S.; Umeda, T.; Yoshimura, Y.; Nakazawa, H. Application of liquid chromatography–mass spectrometry to the quantification of bisphenol A in human semen. J. Chromatogr. B, **2002**, *773*, 97.
28. Watanabe, T.; Yamamoto, H.; Inoue, K.; Yamaguchi, A.; Yoshimura, Y.; Kato, K.; Nakazawa, H.; Kuroda, N.; Nakashima, K. Development of sensitive high-performance liquid chromatography with fluorescence detection using 4-(4,5-diphenyl-1H-imidazol-2-yl)-benzoyl chloride as a labeling reagent for determination of bisphenol A in plasma samples. J. Chromatogr. B, **2001**, *762*, 1.
29. Liu, M.; Hashi, Y.; Pan, F.; Yao, J.; Song, G.; Lin, J.-M. Automated on-line liquid chromatography-photodiode array-mass spectrometry method with dilution line for the determination of bisphenol A and 4-octylphenol in serum. J. Chromatogr. A, **2006**, *1133*, 142.
30. Kawaguchi, M.; Ito, R.; Okanouchi, N.; Saito, K.; Nakazawa, H. Miniaturized hollow fiber assisted liquid-phase microextraction with in situ derivatization and gas chromatography-mass spectrometry for analysis of bisphenol A in human urine sample. J. Chromatogr. B, **2008**, *870*, 98.
31. Moors, S.; Blaszkewicz, M.; Bolt, H.M.; Degen, G.H. Simultaneous determination of daidzein, equol, genistein and bisphenol A in human urine by a fast and simple

method using SPE and GC-MS. Mol. Nutrition Food Res. **2007**, *51* 787.
32. Wu, Z.; Gao, W.; Phelps, M.A.; Wu, D.; Miller, D.D.; Dalton, J.T. Favorable effects of weak acids on negative-ion electrospray ionization mass spectrometry. Anal. Chem. **2004**, *76*, 839.
33. Völkel, W.; Kiranoglu, M.; Fromme, H. Determination of free and total bisphenol A in human urine to assess daily uptake as a basis for a valid risk assessment. Toxicol. Letter, **2008**, *179*, 155.
34. Ye, X.; Kuklenyik, Z.; Needham, L.L.; Calafat, A.M. Quantification of urinary conjugates of bisphenol A, 2,5-dichlorophenol, and 2-hydroxy-4-methoxybenzophenone in humans by online solid phase extraction-high performance liquid chromatography–tandem mass spectrometry. Anal. Bioanal. Chem. **2005**, *383*, 638.
35. Völkel, W.V.; Bittner, N.; Dekant, W. Quantitation of bisphenol A and bisphenol A glucuronide in biological samples by high performance liquid chromatography–tandem mass spectrometry. Drug Metabol. Dispos. **2005**, *33*, 1748.
36. Itoh, H.; Iwasaki, M.; Hanaoka, T.; Sasaki, H.; Tanaka, T.; Tsugane, S. Urinary bisphenol-A concentration in infertile Japanese women and its assocation with endometriosis: A cross-sectional study. Environ. Health Prevent. Med. **2007**, *12*, 258.
37. García-Prieto, A., Lunar, M.L., Rubio, S., Pérez-Bendito, D. Determination of urinary bisphenol A by coacervative microextraction and liquid chromatography-fluorescence detection. Anal. Chim. Acta **2008**, *630*, 19.
38. Kawaguchi, M., Ito, R., Okanouchi, N., Saito, K., Nakazawa, H. Miniaturized hollow fiber assisted liquid-phase microextraction with in situ derivatization and gas chromatography–mass spectrometry for analysis of bisphenol A in human urine sample. J. Chromatogr. B, **2008**, *870*, 98.
39. Zhang, J.-H.; Jiang, M.; Zou, L.; Shi, D.; Mei, S.-R.; Zhu, Y.-X.; Shi, Y.; Dai, K.; Lu, B. Selective solid-phase extraction of bisphenol A using molecularly imprinted polymers and its application to biological and environmental samples. Anal. Bioanal. Chem. **2006**, *385*, 780.
40. Tsumura, Y.; Ishimitsu, S.; Kaihara, A.; Yoshii, K.; Nakamura, Y.; Tonogai, Y. Di(2-ethylhexyl) phthalate contamination of retail packed lunches caused by PVC gloves used in the preparation of foods. Food Addit. Contam. **2001**, *15*, 569.
41. Tsumura, Y.; Ishimitsu, S.; Saito, I.; Sakai, H.; Tsuchida, Y.; Tonogai, Y. Estimated daily intake of plasticizers in 1-week duplicate diet samples following regulation of DEHP-containing PVC gloves in Japan. Food Addit. Contam. **2003**, *20*, 317.
42. Inoue, K.; Higuchi, T.; Okada, F.; Iguchi, H.; Yoshimura, Y.; Sato, A.; Nakazawa, H. The validation of column-switching LC/MS as a high-throughput approach for direct analysis of di(2-ethylhexyl) phthalate released from PVC medical devices in intravenous solution. J. Pharm. Biomed. Anal. **2003**, *31*, 1145.
43. Ito, R.; Seshimo, F.; Miura, N.; Kawaguchi, M.; Saito, K.; Nakazawa, H. High-throughput determination of mono- and di(2-ethylhexyl)phthalate migration from PVC tubing to drugs using liquid chromatography-tandem mass spectrometry. J. Pharm. Biomed. Anal. **2005**, *39*, 1036.
44. Koizumi, M.; Ema, M.; Hirose, A.; Hasegawa, R. Recent studies on toxic effects of phthalate esters on reproduction and development: Focus on di(2-ethylhexyl)phthalate and di-n-butyl phthalate. Jpn. J. Food Chem. **2000**, *7*, 65.
45. Koizumi, M.; Ema, M.; Hirose, A.; Kurokawa, Y.; Hasegawa, R. No observed adverse effect levels of phthalate esters on reproductive and developmental toxicity, the differences with age and species in testicular toxicity, and tolerable daily intake of DEHP. Jpn. J. Food Chem. **2001**, *8*, 1.
46. Tickner, J.A.; Schettler, T.; Guidotti, T.; McCally, M.; Rossi, M. Health risks posed by use of Di-2-ethylhexyl phthalate (DEHP) in PVC medical devices: A critical review. Am. J. Ind. Med., **2001**, *39*, 100.
47. Yakubovich, M.; Vienken, J. Is there a need for plasticizer-free biomaterials in dialysis therapy? Med. Device Technol. **2000**, *11*, 18.
48. Hill, S.; Shaw, B.; Wu, A. The clinical effects of plasticizers, antioxidants, and other contaminants in medical polyvinylchloride tubing during respiratory and non-respiratory exposure. Clin. Chim. Acta **2001**, *304*, 1.
49. Thomas, J.A.; Northup, S.J. Toxicity and metabolism of monoethylhexyl phthalate and diethylhexyl phthalate: A survey of recent literature. Toxicol. Environ. Health **1982**, *9*, 141.
50. Albro, P.W.; Lavenhar, S.R. Metabolism of di(2-ethylhexyl)phthalate. Drug Metabol. Rev. **1989**, *21*, 13.
51. Kato, K.; Yamauchi, T.; Higashiyama, K.; Nakazawa, H. High throughput analysis of di-(2-ethylhexyl)phthalate metabolites in urine for exposure assessment. J. Liq. Chromatogr. Rel. Technol. **2003**, *26*, 2151.
52. Silva, M.J.; Malek, N.A; Hodge, C.C.; Reidy, J.A.; Kato, K.; Barr, D.B.; Needham, L.L.; Brock, J.W. Improved quantitative detection of 11 urinary phthalate metabolites in humans using liquid chromatography–atmospheric pressure chemical ionization tandem mass spectrometry. J. Chromatogr. B, **2003**, *789*, 393.
53. Albro, P.W.; Corbett, J.T.; Schroeder, J.L.; Jordan, S.; Matthews, H.B.: Pharmacokinetics, interactions with macromolecules and species differences in metabolism of DEHP. Environ. Health Perspect. **1982**, *45*, 19–25.
54. Schmid, P.; Schlatter, C. Excretion and metabolism of di(2-ethylhexyl)-phthalate in man. Xenobiotica **1985**, *15*, 251.
55. Elcombe, C.R.; Mitchell, A.M. Peroxisome proliferation due to di(2-ethylhexyl) phthalate (DEHP): Species differences and possible mechanisms. Environ. Health Perspect. **1986**, *70*, 211.
56. Anderson, W.A.C.; Castle, L; Scotter, M.J.; Massey, R.C.; Springall, C. A biomarker approach to measuring human dietay exposure to certain phthalate diesters. Food Addit. Contam. **2001**, *18*, 1068.
57. Kato, K.; Yoshimura, Y.; Ito, Y.; Oka, H.; Nakazawa, H. Preparation of samples for gas chromatography/mass spectrometry analysis of phthalate and adipate esters in plasma and beverages by steam distillation and extraction. AOAC Int. **2002**, *85*, 719.
58. Ito, R.; Seshimo, F.; Miura, N.; Kawaguchi, M.; Saito, K.; Nakazawa, H. Effect of sterilization process on the

formation of mono(2-ethylhexyl)phthalate from di(2-ethylhexyl)phthalate. J. Pharm. Biomed. Anal. **2006**, *41*, 455.
59. David, R.M. Exposure to phthalate esters. Environ. Health Perspect. **2000**, *108*, A440.
60. Blout, B.C.; Milgram, K.E.; Silva, M.J.; Malek, N.A.; Reidy, J.A.; Needham, L.L.; Brock, J.W. Quantitative detection of eight phthalate metabolites in human urine using HPLC–APCI-MS/MS. Anal. Chem. **2000**, *72*, 4127.
61. Silva, M.J.; Slakman, A.R.; Reidy, J.A.; J.L. Preau Jr., Herbert, A.R.; Samandar, E.; Needham, L.L.; Calafat, A.M. Analysis of human urine for fifteen phthalate metabolites using automated solid-phase extraction. J. Chromatogr. B, **2004**, *805*, 161.
62. Kato, K.; Silva, M.J.; Needham, L.L.; Calafat, A.M. Determination of 16 Phthalate metabolites in urine using automated sample preparation and on-line preconcentration/high-performance liquid chromatography/tandem mass spectrometry. Anal. Chem. **2005**, *77*, 2985.
63. Silva, M.J.; Barr, D.B.; Reidy, J.A.; Malek, N.A.; Hodge, C.C.; Caudill, S.P.; Brock, J.W.; Needham, L.L.; Calafat, A.M. Urinary levels of seven phthalate metabolites in the U.S. population from the National Health and Nutrition Examination Survey (NHANES) 1999–2000. Environ. Health Perspect. **2004**, *112*, 331.
64. Duty, S.M.; Silva, M.J.; Barr, D.B.; Brock, J.W.; Ryan, L.; Herrick, R.F.; Christiani, D.C.; Hauser, R. Phthalate exposure and human semen parameters. Epidemiology **2003**, *14*, 269.
65. Hoppin, J.A.; Brock, J.W.; Davis, B.J.; Baird, D.D. Reproducibility of urinary phthalate metabolites in first morning urine samples. Environ. Health Perstpect. **2002**, *110*, 515.
66. Blount, B.C.; Silva, M.J.; Caudill, S.P.; Needham, L.L.; Pirkle, J.L.; Sampson, E.J.; Lucier, G.W.; Jackson, R.J.; Brock, J.W. Levels of seven urinary phthalate metabolites in a human reference population. Environ. Health Perspect. **2000**, *108*, 979.
67. Yoshimura, M.; Inoue, K.; Hanaoka, T. Pan, G.; Takahashi, K.; Yamano, Y.; Iwasaki, Y.; Ito, R.; Saito, K.; Tsugane, S.; Nakazawa, H. Development of simultaneous determination method of phthalate monoester metabolites in urine by LC/MS/MS and its application to assessment of phthalate-ester exposure. Bunseki Kagaku **2006**, *55*, 661.
68. Adibi, J.J., Whyatt, R.M., Williams, P.L., Calafat, A.M., Camann, D., Herrick, R., Nelson, H., Bhat, H.K., Perera, F.P., Silva, M.J., Hauser, R. Characterization of phthalate exposure among pregnant women assessed by repeat air and urine samples. Environ. Health Perspect. **2008**, *116*, 467.
69. Fromme, H.; Gruber, L.; Schlummer, M.; Wolzb, G.; Böhmera, S.; Angererc, J.; Mayerd, R.; Liebld, B.; Boltea, G. Intake of phthalates and di(2-ethylhexyl)adipate: Results of the integrated exposure assessment survey based on duplicate diet samples and biomonitoring data. Environ. Int. **2007**, *33*, 1012.
70. Itoh, H.; Yoshida, K.; Masunaga, S. Quantitative identification of unknown exposure pathways of phthalates based on measuring their metabolites in human urine. Environ. Sci. Technol. **2007**, *41*, 4542.
71. Calafat, A.M.; McKee, R.H. Integrating biomonitoring exposure data into the risk assessment process: Phthalates [diethyl phthalate and di(2-ethylhexyl) phthalate] as a case study. Environ. Health Perspect. **2006**, *114*, 1783.
72. Koch, H.M.; Bolt, H.M.; Angerer, J. Di(2-ethylhexyl)phthalate (DEHP) metabolites in human urine and serum after a single oral dose of deuterium-labelled DEHP. Arch. Toxicol. **2004**, *78*, 123.
73. Takatori, S.; Kitagawa, Y.; Kitagawa, M.; Nakazawa, H.; Hori, S. Determination of di(2-ethylhexyl)phthalate and mono(2-ethylhexyl)phthalate in human serum using liquid chromatography-tandem mass spectrometry. J. Chromatogr. B, **2004**, *804*, 397.
74. Inoue, K.; Kawaguchi, M.; Okada, F.; Yoshimura, Y.; Nakazawa, H. Column-switching high-performance liquid chromatography electrospray mass spectrometry coupled with on-line of extraction for the determination of mono- and di-(2-ethylhexyl) phthalate in blood samples. Anal. Bioanal. Chem. **2003**, *375*, 527.
75. Hanawa, T.; Muramatsu, E.; Asakawa, K.; Suzuki, M.; Tanaka, M.; Kawano, K.; Seki, T.; Juni, K.; Nakajima, S. Investigation of the release behavior of diethylhexyl phthalate from the polyvinyl-chloride tubing for intravenous administration. Int. J. Pharm. **2000**, *210*, 109.
76. Haishima, Y.; Matsuda, R.; Hayashi, Y.; Hasegawa, C.; Yagami, T.; Tsuchiya, T. Risk assessment of di(2-ethylhexyl)phthalate released from PVC blood circuits during hemodialysis and pump–oxygenation therapy. Int. J. Pharm. **2004**, *274*, 119.
77. Venkataramanan, R.; Burckart, G.J.; Ptachcinski, R.J.; Blaha, R.; Logue, L.W.; Bahnson, A.; C.S. Giam., Brady, J.E. Leaching of diethylhexyl phthalate from polyvinyl chloride bags into intravenous cyclosporine solution. Am. J. Hosp. Pharm. **1986**, *43*, 2800.
78. Inoue, K.; Kawaguchi, M.; Yamanaka, R.; Higuchi, T.; Ito, R.; Saito, K.; Nakazawa, H. Evaluation and analysis of exposure levels of di(2-ethylhexyl) phthalate from blood bags. Clin. Chim. Acta **2005**, *358*, 159.
79. Ito, R.; Seshimo, F.; Miura, N.; Kawaguchi, M.; Saito, K.; Nakazawa, H. Effect of sterilization process on the formation of mono(2-ethylhexyl)phthalate from di(2-ethylhexyl)phthalate. J. Pharm. Biomed. Anal. **2006**, *41*, 455.
80. Thibodeaux, J.R.; Hanson, R.G.; Rogers, J.M.; Grey, B.E.; Barbee, B.D.; Richards, J.H.; Butenhoff, J.L.; Stevenson, L.A.; Lau, C. Exposure to perfluorooctane sulfonate during pregnancy in rat and mouse. I: Maternal and prenatal evaluations. Toxicol. Sci. **2003**, *74*, 369.
81. Lau, C.; Thibodeaux, J.R.; Hanson, R.G.; Rogers, J.M.; Grey, B.E.; Stanton, M.E.; Butenhoff, J.L.; Stevenson, L.A. Exposure to perfluorooctane sulfonate during pregnancy in rat and mouse. II: Postnatal evaluation. Toxicol. Sci. **2003**, *74*, 382.
82. Austin, M.E.; Kasuri, B.S.; Barber, M.; Kannan, K.; MohanKumar, P.S.; MohanKumar, S.M.J. Neuroendocrine effects of perfluorooctane sulfonate in rats. Environ. Health Perspect. **2003**, *111*, 1485.
83. Renner, R. Growing Concern Over Perfluorinated Chemicals. Environ. Sci. Technol. **2001**, *35*, 154A.
84. Renner, R. Concerns over common perfluorinated surfactant. Environ. Sci. Technol. **2003**, *37*, 201A.
85. Giesy, J.P.; Kannan, K. Global distribution of perfluorooctane sulfonate in wildlife. Environ. Sci. Technol. **2001**, *35*, 1339.

86. Han, X.; Snow, T.A.; Kemper, R.A.; Jepson, G.W. Binding of perfluorooctanoic acid to rat and human plasma proteins. Chem. Res. Toxicol. **2003**, *16*, 775.
87. Reagen, W.K.; Ellefson, M.E.; Kannan, K.; Giesy, J.P. Comparison of extraction and quantification methods of perfluorinated compounds in human plasma, serum, and whole blood. Anal. Chim. Acta **2008**, *628*, 214.
88. Kärrman, A.; Ericson, I.; VanBavel, B.; Ola Darnerud, P.; Aune, M.; Glynn, A.; Ligneli, S.; Lindström, G. Exposure of perfluorinated chemicals through lactation: Levels of matched human milk and serum and a temporal trend, 1996-2004, in Sweden. Environ. Health Perspect. **2007**, *115*, 226.
89. Ehresman, D.J.; Froehlich, J.W.; Olsen, G.W.; Chang, S.-C.; Butenhoff, J.L. Comparison of human whole blood, plasma, and serum matrices for the determination of perfluorooctanesulfonate (PFOS), perfluorooctanoate (PFOA), and other fluorochemicals. Environ. Res. **2007**, *103*, 176.
90. Hansen, K.J.; Clemen, L.A.; Elefson, M.E.; Johnson, H.O. Compound-specific, quantitative characterization of organic fluorochemicals in biological matrices. Environ. Sci. Technol. **2001**, *35*, 766.
91. Inoue, K.; Okada, F.; Ito, R.; Kato, S.; Sasaki, S.; Nakajima, S.; Uno, A.; Saijo, Y.; Sata, F.; Yoshimura, Y.; Kishi, R.; Nakazawa, H. Perfluorooctane sulfonate (PFOS) and related perfluorinated compounds in human maternal and cord blood samples: Assessment of PFOS exposure in a susceptible population during pregnancy. Environ. Health Perspect. **2004**, *112*, 1204.
92. Olsen, G.W.; Church, T.R.; Miller, J.P.; Burris, J.M.; Hansen, K.J.; Lundberg, J.K.; Armitage, J.B.; Herron, R.M.; Medhdizadehkashi, Z.; Nobiletti, J.B.; O'Neill, E.M.; Mandel, J.H.; Zobel, L.R. Perfluorooctanesulfonate and other fluorochemicals in the serum of American Red Cross adult blood donors. Environ. Health Perspect. **2003**, *111*, 1892.
93. Harada, K.; Sato, N.; Inoue, K.; Yoshinaga, T.; Watanabe, T.; Sasaki, S.; Kamiyama, S.; Koizumi, A. The influence of time, sex and geographic factors on levels of perfluorooctane sulfonate and perfluorooctanoate in human serum over the last 25 years. J. Occup. Health **2004**, *46*, 141.
94. Kuklenyik, Z.; Reich, J.A.; Tully, J.S.; Needham, L.L.; Calafat, A.M. Automated solid-phase extraction and measurement of perfluorinated organic acids and amides in human serum and milk. Environ. Sci. Technol. **2004**, *38*, 3698.
95. Taniyasu, S.; Kannan, K.; Horii, Y.; Hanari, N.; Yamashita, N. A survey of perfluorooctane sulfonate and related perfluorinated organic compounds in water, fish, birds, and humans from Japan. Environ. Sci. Technol. **2003**, *37*, 2634.
96. Olsen, G.W.; Hansen, K.J.; Stevenson, L.A.; Burris, J.M.; Mandel, J.H. Human donor liver and serum concentrations of perfluorooctanesulfonate and other perfluorochemicals. Environ. Sci. Technol. **2003**, *37*, 888.
97. Kannan, K.; Corsolini, S.; Falandysz, J.; Fillmann, G.; Kumar, K.S.; Loganathan, B.G.; Mohd, M.A.; Olivero, J.; Yang, J.H.; Aldous, K.M. Perfluorooctanesulfonate and related fluorochemicals in human blood from several countries. Environ. Sci. Technol. **2004**, *38*, 4489.
98. Karrman, A.; Van, B.B.; Jarnberg, U.; Hardell, L.; Lindstrom, G. Development of a solid-phase extraction—HPLC/single quadrupole MS method for quantification of perfluorochemicals in whole blood. Anal. Chem. **2005**, *77*, 864.
99. Inoue, K.; Okada, F.; Ito, R.; Kawaguchi, M.; Okanouchi, N.; Nakazawa, H. Determination of perfluorooctane sulfonate, perfluorooctanoate and perfluorooctane sulfonylamide in human plasma by column-switching liquid chromatography–electrospray mass spectrometry coupled with solid-phase extraction. J. Chromatogr. B, **2004**, *810*, 49.
100. Nakata, H.; Nakata, A.; Okada, F.; Ito, R.; Inoue, K.; Saito, K.; Nakazawa, H. Development of online solid-phase extraction—HPLC/MS/MS method for the determination of perfluorochemicals in human plasma. Bunseki Kagaku **2005**, *54*, 877–884.
101. van Leeuwen, S.P.J.; Karrman, A.; van Bavel, B.; de Boer, J. Lindstrom, G. Struggle for quality in determination of perfluorinated contaminants in environmental and human samples. Environ. Sci. Technol. **2006**, *40*, 7854–7860.
102. Rivo report C070/05 "1st worldwide interlaboratory study on perfluorinated compounds in human and environmental matrices—Final report."
103. Schroder, H.F. Determination of fluorinated surfactants and their metabolites in sewage sludge samples by liquid chromatography with mass spectrometry and tandem mass spectrometry after pressurised liquid extraction and separation on fluorine-modified reversed-phase sorbents. J. Chromatogr. A, **2003**, *1020*, 131.
104. Hansen, K.J.; Johnson, H.O.; Eldridge, J.S.; Butenhoff, J.L.; Dick, L.A. Quantitative characterization of trace levels of PFOS and PFOA in the tennessee river. Environ. Sci. Technol. **2002**, *36*, 1681.
105. Sasaki, K.; Harada, K.; Saito, N.; Tsutsui, T.; Nakanishi, S.; Tsuzuki, H.; Koizumi, A. Impact of airborne perfluorooctane sulfonate on the human body burden and the ecological system. Bull. Environ. Contam. Toxicol. **2002**, *71*, 408.
106. Roinestad, K.; Louis, J.; Rozen, J. Determination of pesticides in indoor air and dust. J. AOAC Int. **1993**, *76*, 1121.
107. Katsumata, T.; Nakata, A.; Iwasaki, Y.; Ito, R.; Saito, K.; Nakazawa, H. Determination of perfluorochemicals in house-dust by LC/MS/MS after supercritical fluid extraction. Bunseki Kagaku **2006**, *55*, 955–961.
108. Center for Devices and Radiological Health, U.S. Food and Drug Administration (FDA), September 4 (2001), http://www.fda.gov/cdrh/ost/dehp-pvc.pdf (accessed May 2009).

Hybrid Micellar Mobile Phases

M.C. García-Alvarez-Coque
J.R. Torres-Lapasio
M.J. Ruiz-Angel
Department of Analytical Chemistry, University of Valencia, Valencia, Spain

Abstract
Micellar liquid chromatography (MLC) is a reversed-phase liquid chromatographic (RPLC) mode with mobile phases containing a surfactant with either ionic or non-ionic head groups above the critical micellar concentration. An organic solvent (usually a short-chain alcohol or acetonitrile) is also added to decrease the retention and improve peak shape. Surfactant monomers are adsorbed on the RPLC bonded stationary phase, giving rise to a stable modified surface, whereas the mobile phase contains micelles in addition to surfactant monomers. Solute interactions with the mobile and stationary phases are mainly governed by hydrophobic forces, but electrostatic attraction and repulsion between ionic groups may be important. The combination of the surfactant-modified stationary phase, micelles, and the hydro-organic medium determines the retention, efficiency, and selectivity of the separation, which are affected by a variety of experimental factors, such as the nature and concentration of surfactant and organic solvent, temperature, ionic strength, and pH. The retention behavior is highly stable and can be described through mechanistic models, taking into account the solute interactions with the mobile and stationary phases. In addition to the particular selectivity, the most relevant features of MLC are the elution of compounds in a wide range of polarities (neutral and ionic) using isocratic elution, and the feasibility of direct injection of physiological fluids.

INTRODUCTION

The first report on the use of an aqueous solution of a surfactant above its critical micellar concentration (CMC) as the mobile phase in reversed-phase liquid chromatography (RPLC) was published in 1980.[1] The technique named micellar liquid chromatography (MLC) is an interesting example of the modification of the chromatographic behavior taking advantage of a secondary equilibrium with the micelles in the mobile phase. Micelles alter solute partitioning between the bulk solvent (i.e., water or hydro–organic mixture) and the stationary phase that is coated with surfactant monomers (Fig. 1). This is translated into a major impact on both retention and selectivity.[2]

Solutes in the mobile phase can remain in the bulk water, be associated to the free surfactant monomers or micelle surface, be inserted into the micelle palisade layer, or penetrate into the micelle core. The surface of the surfactant-modified stationary phase is similar to an opened micelle and can give rise to similar interactions with the solutes. With non-ionic surfactants, the interactions are mainly hydrophobic in nature. Charged heads of ionic surfactants in both micelles and monomers adsorbed on the stationary phase are in contact with the polar solution, producing additional electrostatic interactions with charged solutes. Finally, the association of solutes with the non-modified bonded stationary phase and free silanol groups still exists.

The most serious limitations of pure micellar solutions are their poor efficiencies and weak elution strength. As early as 1983, the addition of a small percentage of 1-propanol was found to enhance both the efficiency and symmetry of chromatographic peaks, and decrease the retention.[3] Later, the term "hybrid micellar mobile phases" was given to the ternary eluents of water/organic solvent/micelles. Although 1-propanol is still the most frequent additive, other alcohols (methanol, ethanol, 1-butanol, and 1-pentanol) and organic solvents common in conventional RPLC (acetonitrile and tetrahydrofuran) have also been used. It should be noted that micellar solutions increase the solubility of butanol and pentanol in water to reach concentration levels useful in chromatography.

In the hybrid system, solute partition equilibria are significantly displaced away from the micelle and the stationary phase toward the bulk hydro–organic phase, which is more non-polar (Fig. 1). However, as long as the integrity of micelles is maintained, the addition of organic solvent to micellar mobile phases will not create a hydro–organic system. The chromatographic behavior of alkyl homologous series has been used to demonstrate that the separation mechanism in hybrid MLC is

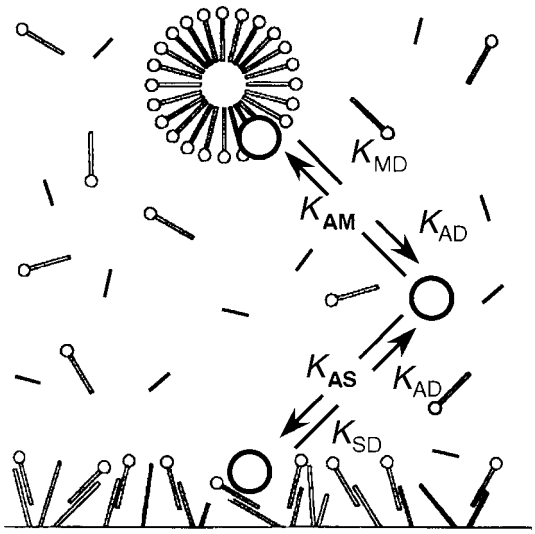

Fig. 1 Solute–micelle and solute–stationary phase interactions in hybrid micellar mobile phases (see text for meaning of equilibrium constants).

more similar to pure MLC than to conventional RPLC.[4] In hydro–organic systems, the retention of homologue compounds is described as follows:

$$\log k = \log \alpha(CH_2) n_C + \log \beta \quad (1)$$

where n_C is the number of carbon atoms in the homologue, $\alpha(CH_2)$ is the non-specific selectivity of a methylene group, and β is the contribution of the series functional group to the retention. In contrast to this behavior, a linear relationship between k and n_C is observed either with pure or hybrid micellar mobile phases.

NATURE OF THE MOBILE AND STATIONARY PHASES

Most MLC procedures use micelles of the anionic surfactant sodium dodecyl sulfate (SDS). Other useful surfactants include the cationic cetyltrimethylammonium bromide or chloride (CTAB or CTAC) and the non-ionic Brij-35.[2,5] The separations are usually carried out in C_{18} or C_8 columns.

The presence of a small amount of an organic solvent in the mobile phase produces changes in the micellization process which depend on the nature of the additive. A progressive increase in the CMC of SDS (8.2×10^{-3} *M* in water at 25°C) is observed by adding methanol and acetonitrile; the reverse is observed when ethanol, propanol, butanol, and pentanol are added. As an example, the CMC of SDS in the presence of 4% (v/v) organic solvent is 8.7×10^{-3} *M* (methanol), 9.2×10^{-3} *M* (acetonitrile), 7.4×10^{-3} *M* (ethanol), 5.9×10^{-3} *M* (propanol), 2.7×10^{-3} *M* (butanol), and 2.0×10^{-3} *M* (pentanol).[6]

Methanol, which has the shortest carbon chain, is more polar and soluble than other alcohols. SDS monomers are more easily solvated in an aqueous–methanol medium. This inhibits them from interacting and forming micelles. A similar behavior is expected for acetonitrile. Ethanol and propanol, which are also miscible with water, remain outside the micelles, dissolved in the bulk liquid, but interact with the micelle surface. Repulsion among the ionic heads of surfactant monomers is reduced in the presence of these two alcohols, thus aiding the formation of micelles.

As the length of the alcohol alkyl chain increases, its affinity for the SDS micelle is enhanced. Butanol and pentanol are inserted in the intermonomer spaces of the micelle palisade aligned with the surfactant molecules, the polar hydroxyl group oriented toward the Stern layer, and the alkyl chains located in the non-polar micelle core. A swollen mixed micelle is thus formed. Such micelles are geometrically hindered to allocate additional surfactant monomers, which is translated into a CMC reduction. However, above 4% butanol and 1.5% pentanol, the decay rate in the CMC values slows down. An explanation for this behavior is that above a given concentration, the amount of alcohol entering the palisade is not significant and the excess is solubilized in the core of the swollen micelle. Further additions of alcohol lead to a dramatic change in the mobile-phase microstructure, yielding a microemulsion.

Surfactant coating masks the stationary phase. In the case of C_8 and C_{18} columns, the hydrophobic tail of surfactants associates to the alkyl chain bonded to the silica stationary phase, with the polar head groups oriented away from the surface (Figs. 1, 2A and B). For SDS and CTAB, this creates negatively and positively charged layers, respectively, which affect the penetration depth of solutes into the bonded phases. For CTAB, surfactant adsorption leads to a more hydrophobic stationary phase, because the cationic trimethylammonium head group is partially incorporated into the bonded phase, associated to free silanols. In contrast, on cyano columns, both charged surfactants (SDS and CTAB) are adsorbed head down with their tails projected outward, thus creating pseudoalkyl-bonded phases (Fig. 2C and D).[7]

Organic solvents induce changes in the properties of surfactant-coated stationary phases, such as polarity, surface area, or pore volume. Several studies have demonstrated that *n*-alcohols interpenetrate the C_{18}-bonded alkyl chains to form a single monolayer, i.e., the hydroxyl group oriented toward the aqueous phase. The competition between organic solvent and surfactant molecules for the active sites on the column explains the reduction of adsorbed surfactant at increasing concentration of organic solvent in the mobile phase. For ionic surfactants, this reduction is linear with slopes that depend on the strength of the solvent (methanol<ethanol<propanol<butanol<pentanol).[2]

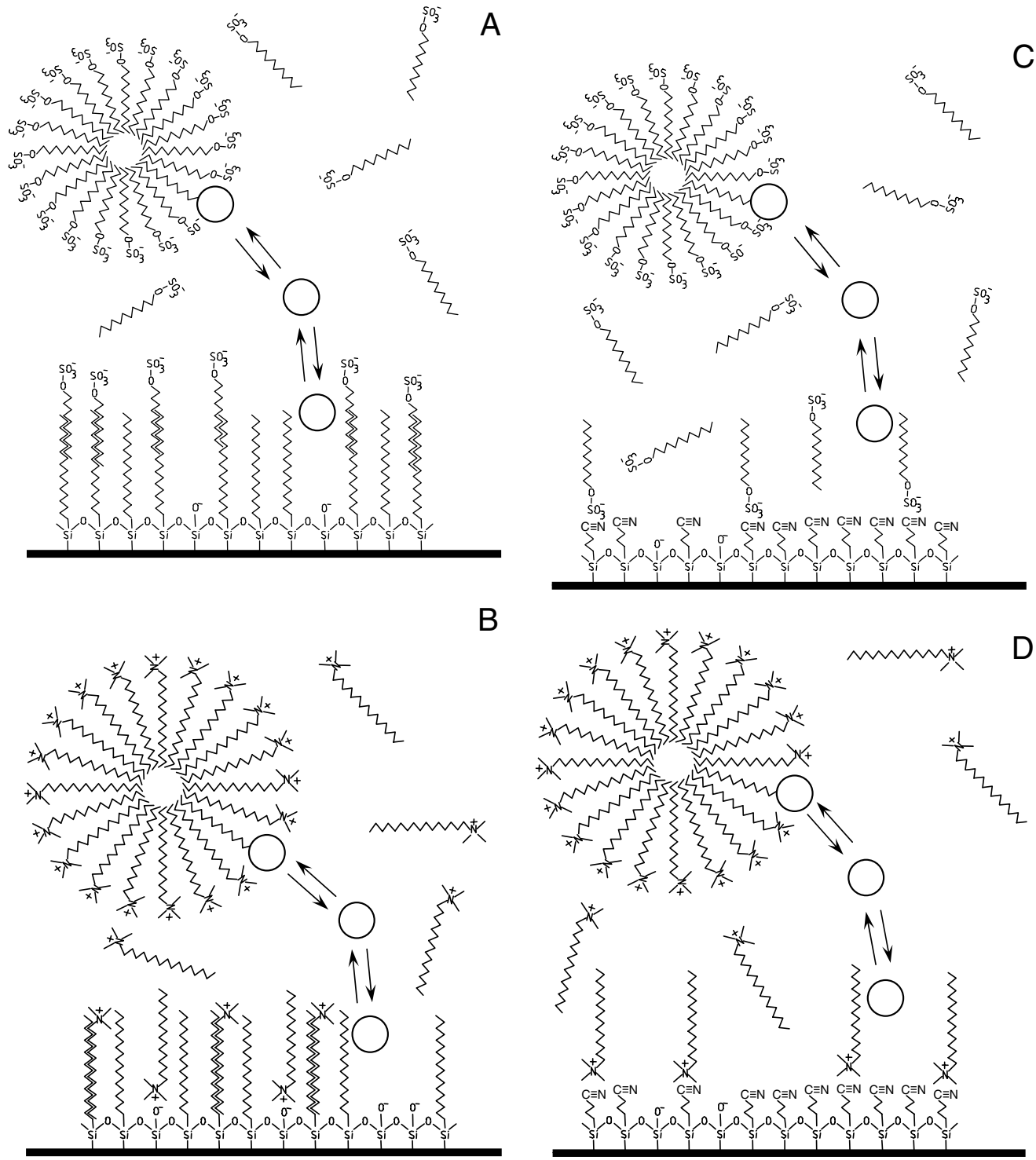

Fig. 2 Schematic representation of separation microenvironments in MLC using octadecyl- (A,B) and cyanopropyl-(C,D)-bonded phases, and mobile phases containing the anionic SDS (A,C) and the cationic CTAB (B,D).

Solute retention varies with the concentration of propanol, butanol, and pentanol in the mobile phase, in the same way as CMC does. This means that the collateral effects which change the CMC in an organic–micellar system are, at least partially, those that induce shorter retention with hybrid mobile phases: the modification of bulk water and micelle. As noted, another important issue that affects retention is the modification of the

structure of the stationary phase. The analogous effects on both microenvironments (micelle and stationary phase) are evidenced in the parallel variation of solute–micelle and solute–stationary phase association constants, as the concentration of organic solvent changes.[8]

RETENTION MECHANISMS

In MLC, solutes are separated on the basis of their differential partitioning between bulk solvent and micelles in the mobile phase or surfactant-coated stationary phase.[9] For water-insoluble species or for species strongly bound to micelles, partitioning can also occur via direct transfer between the micellar pseudophase and the modified stationary phase. Partition equilibria are affected by a variety of factors, such as the nature and concentration of surfactant and organic modifiers, temperature, ionic strength, and pH.

Neutral solutes eluted with all types of surfactants and charged solutes eluted with non-ionic surfactants will only be affected by non-polar, dipole–dipole, and proton donor–acceptor interactions. Besides these interactions, charged solutes interact electrostatically with ionic surfactants. In any case, the steric factors can be important, owing to the difficult access of micelles to the bonded-phase pores.

For charged solutes eluted with ionic surfactants, two situations are possible: repulsion or attraction, depending on the mutual charges of solutes and surfactant. In the case of electrostatic repulsion with the stationary phase, charged solutes cannot be retained and elute at the dead volume, unless significant hydrophobic interactions with the modified bonded layer exists. In contrast, combined electrostatic attraction and hydrophobic interactions with the modified stationary phase may give rise to strong retention.

According to their elution behavior, solutes can be classified into those binding to micelles, non-binding, and antibinding. Binding solutes show decreased retention when the concentration of micelles in the mobile phase is increased. For solutes that do not associate with micelles, the retention may remain unaltered upon changes in micelle contents (non-binding), or increase with the micelle concentration (antibinding). The most common behavior is binding to micelles, while antibinding is uncommon, and has only been observed with stationary phases that do not adsorb large quantities of surfactant (such as C_1), or with cyano-bonded phases, where the surfactant charge is buried close to the bonded phase. In both cases, charged solutes are strongly excluded or repelled from the micelle, which forces them to bind to the stationary phase, where they are retained due to hydrophobic forces. The change in the antibinding behavior to non-binding and further to binding upon the addition of salts reveals the electrostatic nature of the interactions.

Electrostatic interactions between solutes and charged stationary phase and micelles are also the main factors responsible for the shifts in the dissociation constants and retention of ionizable solutes. In alkyl-bonded stationary phases with SDS, both weak acids and bases show the largest retention in acidic solution (descending k vs. pH curves). Mirror curves (i.e., ascending) are found with CTAB: the largest retention is observed in basic solution. This behavior contrasts with that observed in conventional RPLC, where the k vs. pH curves are descending for weak acids and ascending for weak bases.

DESCRIPTION OF THE RETENTION BEHAVIOR

In pure micellar mobile phases, retention is described by a hyperbolic relationship.[10]

$$k = \frac{\phi P_{AS}}{1 + \upsilon(P_{AM} - 1)[M]} = \frac{K_{AS}}{1 + K_{AM}[M]} \quad (2)$$

where k is the retention factor, ϕ is the phase ratio, P_{AS} and P_{AM} are the solute–stationary phase and solute–micelle partition coefficients, υ is the specific volume of surfactant monomers, and $[M]$ is the concentration of surfactant forming micelles (total surfactant concentration minus the CMC). The right term with K_{AS} and K_{AM} is often used for simplicity.

The same model is valid for hybrid micellar mobile phases at fixed concentration of organic solvent, although both constants, K_{AS} and K_{AM}, decrease when the modifier concentration increases especially for non-polar solutes. An extended model, including the effect of changes in organic solvent concentration, has also been proposed:[11]

$$k = \frac{K_{AS}\frac{1 + K_{SD}\varphi}{1 + K_{AD}\varphi}}{1 + K_{AM}\frac{1 + K_{MD}\varphi}{1 + K_{AD}\varphi}[M]} \quad (3)$$

where φ is the volume fraction of organic solvent, K_{AS} and K_{AM} are the association constants in pure micellar eluents, and K_{AD}, K_{MD}, and K_{SD} measure the relative changes in solute concentration in bulk water, micelle, and stationary phase, respectively, in the presence of organic solvent, taking the pure micellar solution as reference (see also Fig. 1). The last three constants increase with the organic solvent strength. For polar and moderately polar solutes eluted with propanol, K_{SD} can be disregarded and Eq. 3 is simplified as follows:

$$\frac{1}{k} = c_0 + c_1[M] + c_2\varphi + c_{12}[M]\varphi \quad (4)$$

Chromatographic optimization is usually performed at a preselected pH. However, the simultaneous consideration of the three factors (i.e., surfactant, organic solvent, and pH) expands the separation capability for some problems. The retention can be predicted from (see below)

$$k = \frac{K_{AS}\frac{1+K_{SD}\varphi}{1+K_{AD}\varphi} + K_{HAS}\frac{1+K_{HSD}\varphi}{1+K_{HAD}\varphi}K_H[H]}{\left(1 + K_{AM}\frac{1+K_{MD}\varphi}{1+K_{AD}\varphi}[M]\right) + \left(1 + K_{HAM}\frac{1+K_{HMD}\varphi}{1+K_{HAD}\varphi}[M]K_H[H]\right)} \quad (5)$$

where K_{AS}, K_{AM}, K_{AD}, K_{MD}, and K_{SD} are the equilibrium constants associated to the basic species; and K_{HAS}, K_{HAM}, K_{HAD}, K_{HMD}, and K_{HSD} correspond to the acidic species. K_H is the protonation constant in the hydro–organic bulk solvent, and $[H]$ is the proton concentration.[12]

Eqs. 2–5 give accurate predictions of the retention with several types of surfactant (anionic, cationic, and nonionic) and organic solvents (alcohols and acetonitrile), and solutes of diverse charge and polarity, with errors usually below 3–5%.

ELUTION STRENGTH

One of the most serious problems of pure micellar eluents is their weak elution strength. Shorter retention times are obtained by increasing the surfactant concentration, but the chromatographic efficiency usually deteriorates. Ultrawide pore or shorter chain-length-bonded stationary phases constitute other alternatives, but the most practical solution seems to be the addition of a small amount of an organic solvent to the mobile phase. This strategy may result in adequate elution strengths, together with improved chromatographic efficiencies and selectivities, which will produce favorable effects on both the resolution and the analysis time. However, the addition of an organic solvent is unsuitable for low-retained solutes because the retention level may fall below the optimal retention range. In other instances, adequate retention times are achieved, but the efficiencies remain low.

The elution strength of the organic solvent in MLC has been described according to Eq. 3.[13] However, a simple logarithmic relationship (similar to that used in conventional RPLC) is customary:[14]

$$\log k = \log k_0 - S\varphi \quad (6)$$

where S is the sensitivity of solute retention to changes in the volume fraction of organic solvent and $\log k_0$ is the retention in a pure aqueous micellar solution. A similar equation has been used for the surfactant:

$$\log k = \log k'_0 - S'[M] \quad (7)$$

If Eq. 2 is rewritten in the logarithmic form:

$$\log k = \log K_{AS} - \log\left(1 + K_{AM}[M]\right) \quad (8)$$

and linear relationships are assumed between $\log K_{AS}$ and $\log (1+K_{AM}[M])$ with φ, the following results:

$$S = S_s - S_m \quad (9)$$

S_s and S_m represent the sensitivity of variations in solute partitioning from bulk solvent into the stationary phase and micelles, respectively, with changes in φ. The negative sign in Eq. 9 reflects the competing nature of the two partition equilibria. In the absence of micelles, $S_m = 0$ and $S = S_s$, which represents the solvent strength parameter in conventional hydro-organic RPLC. Eq. 9 also shows that the elution strength in hybrid micellar systems will generally be smaller. The magnitude of the reduction depends on the interaction degree of solutes and organic solvents with micelles.

Longer length alcohols, which are more hydrophobic, are able to shorten the retention to a larger extent. Retention times are smaller for micellar solutions containing greater amounts of modifier, but even relatively low amounts can produce dramatic effects. These are attenuated as the surfactant concentration is increased. Finally, the decrease in retention times is more intense for more hydrophobic solutes. Depending on the strength of the interactions, the surfactant or the organic solvent has a prevalent effect on the elution strength of the micellar systems. In the case of basic drugs eluted with SDS micellar mobile phases, changes in retention with the surfactant concentration are larger due to the high affinity of these compounds for the anionic micelles.

The elution strength of hybrid micellar mobile phases was measured for a number of organic additives (alcohols, alkane diols, alkanes, alkylnitriles, and dipolar aprotic solvents, such as dimethyl sulfoxide and dioxane) added to micellar SDS, CTAC, and Brij-35.[15] Benzene and 2-ethylanthraquinone were used as probe compounds. The presence of alcohols, alkane diols, alkylnitriles, and dipolar aprotic solvents produced a diminution of the retention times, reaching remarkable levels for the most hydrophobic compound (2-ethylanthraquinone). The observed elution strength order roughly correlated the octanol–water partition coefficients of the additives, $P^{a}_{o/w}$ (Fig. 3), or their ability to bind to micelles (not shown). In contrast, alkanes (pentane, hexane, and cyclohexane) had relatively little effect on the retention.

In MLC, highly hydrophobic solutes are removed from the column more effectively with regard to conventional RPLC, transported by micelles. Also, when compounds in a wide range of polarities are eluted with hybrid micellar mobile phases at increasing volume fraction of organic

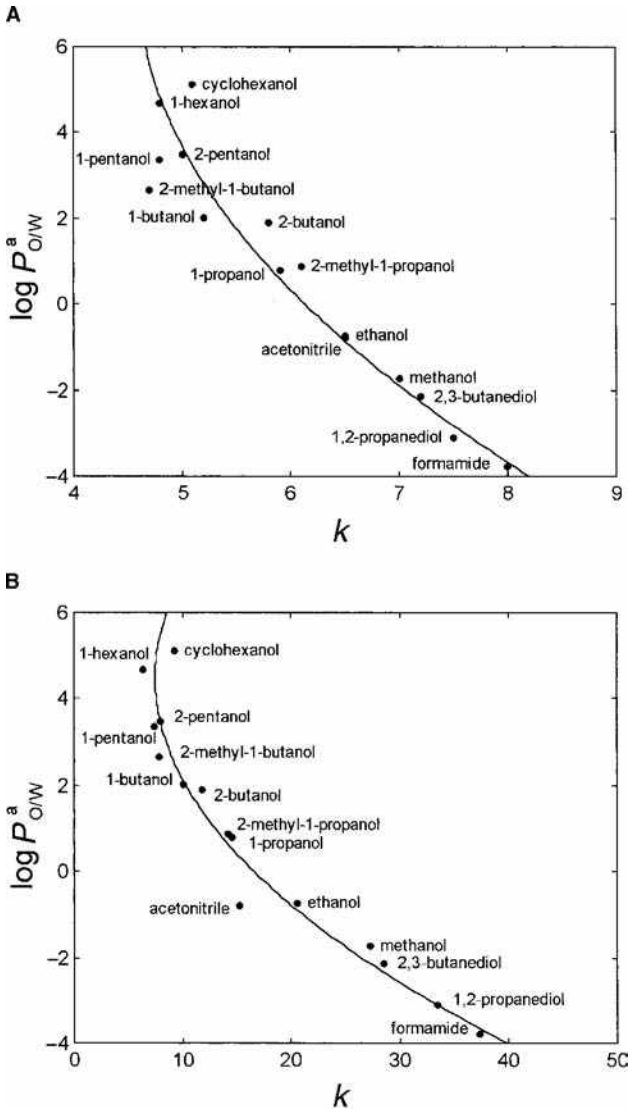

Fig. 3 Correlation between octanol–water partition coefficients of the organic solvents (log $P^a_{o/w}$), and the retention factors for: A, benzene and B, 2-ethylanthraquinone in hybrid SDS micellar mobile phases. The concentration of surfactant and organic solvent was 0.285 *M* and 5%(v/v), respectively.
Source: From Effect of a variety of organic additives on retention, and efficiency in micellar liquid chromatography, in Anal. Chem.[15]

solvent, the retention times of late-eluting compounds are reduced to a larger extent than earlier peaks.

EFFICIENCY

Low efficiencies are observed for highly hydrophobic solutes eluted with pure micellar mobile phases. This fact hindered the initial development of MLC. The addition of a small amount of organic solvent at least partially remedied this situation.[16] Efficiency enhancements—dramatic in some cases—have been reported for solutes eluted with SDS micellar mobile phases in the presence of alcohols, alkane diols, alkylnitriles, and dipolar aprotic solvents. In some instances, efficiencies are comparable or even superior in MLC with regard to conventional RPLC, using the same column and instrument. Concomitant with the enhanced efficiencies, improvements in peak symmetry have been observed. The reason for these effects is an increased solute mass transfer between micelles/stationary phase and aqueous phase due to the greater solute–micelle exchange rate constants, lower stationary phase viscosity, and smaller amount of adsorbed surfactant.

The case of basic drugs is particularly interesting, with large efficiency enhancements and peak-tailing suppression in SDS systems.[17] This makes the use of special columns less necessary. The surfactant layer adsorbed on the column prevents the interaction of basic compounds with free silanol groups, which accounts for the low efficiencies observed with conventional columns in hydro–organic RPLC. Cationic basic drugs interact with the negatively charged surfactant layer in a fast process, without penetrating too deep in the alkyl-bonded layer to interact with the buried silanols (slow process).

Plots of log $P^a_{o/w}$ vs. plate count for benzene and 2-ethylanthraquinone eluted with micellar SDS, in the presence of several alkanols and alkane diols, show an initial steep increase in efficiency, after which an approximately constant value is reached (Fig. 4). Among the alcohols, maximal efficiency for benzene and 2-ethylanthraquinone is obtained with butanols and pentanols, with enhancement factors of 2.5 and 25, respectively (compared to pure SDS). However, final efficiencies for 2-ethylanthraquinone are much lower compared to benzene. Dipolar aprotic modifiers (acetonitrile or dimethylsulfoxide) appear to be somewhat more effective in enhancing efficiencies than alcohols with comparable $P^a_{o/w}$. The advantage of using acetonitrile as additive in MLC for the analysis of sulfonamides, tetracyclines, and most polar steroids has been reported.[18]

Chromatographic efficiency seems to be linked to the additive-to-surfactant concentration ratio in the micellar mobile phase. The plate count increases with this ratio, and reaches a maximal level (e.g., at pentanol/SDS = 6 and acetonitrile/CTAC = 12).[16] The organic solvent/surfactant ratio affects the exchange rates of the solute between micelle/stationary phase and micelle/aqueous phase. It also controls the extent of the surfactant coverage and the fluidity of the organic layer on the stationary phase.

RESOLUTION PERFORMANCE

The rate of change in retention at varying surfactant and organic solvent concentration depends on the solute charge and polarity, and on the nature of both surfactant and

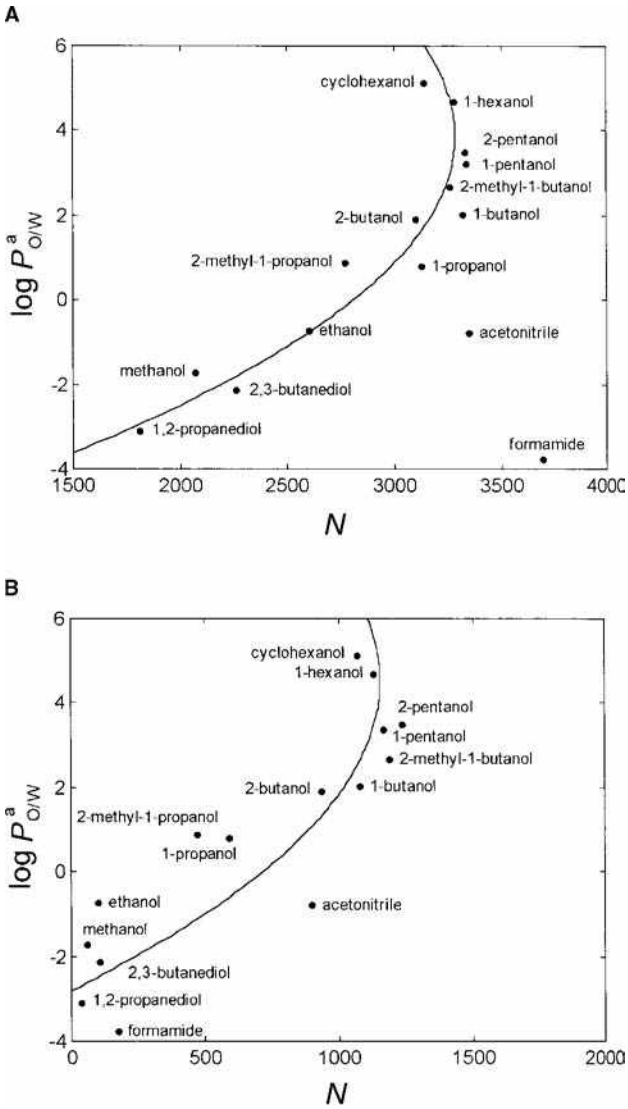

Fig. 4 Correlation between octanol–water partition coefficients of the organic solvents and the efficiencies (plate count) for A, benzene and B, 2-ethylanthraquinone in hybrid SDS micellar mobile phases.
Source: From Effect of a variety of organic additives on retention, and efficiency in micellar liquid chromatography, in Anal. Chem.[15]

organic solvent in the mobile phase. Although the elution strength increases with the concentration of the micelle and the organic solvent, their effect on peak resolution can be quite different, even opposite. The resolution behavior of solutes depends on the relative change of the apparent solute–micelle and solute–stationary phase association constants. These usually decrease with an increase in volume fraction of organic solvent. The magnitude of the diminution is, however, not equal for each solute.

Improving the resolution and simultaneously reducing the analysis time are the two most important goals in optimization strategies. Several examples have been published where a hybrid micellar mobile phase was able to achieve an acceptable separation—impossible with pure micellar eluents—within much shorter analysis times. The first decision in method development in MLC concerns the selection of a surfactant/organic solvent system. The second step consists of the optimization of the selectivity. The separation can be improved by varying only one factor (i.e., proton, surfactant, and/or organic solvent concentration), or by modifying one after optimizing the other. However, operating like this, the best separation conditions can be easily missed.

Typically, resolution diagrams in MLC are complex, with several local maxima, frequently denoting interaction between factors. For this reason, reliable optimal conditions require considering all factors simultaneously, by applying an interpretive optimization strategy (i.e., based on the description of the retention behavior and peak shape of solutes). In this task, the product of free peak areas or purities has proved to be the best optimization criterion.[19] An interactive computer program is available to obtain the best separation conditions in MLC.[20]

GUIDELINES AND SCOPE

The routine work with hybrid micellar mobile phases requires keeping some cautions usually not described in scientific reports or specialized manuals. The experimental procedure comprises two main stages: the mobile phase preparation and the column conditioning.[21]

The surfactant concentration range in the mobile phase is usually relatively narrow. The lowest concentration should be well above the CMC. Usual values are 0.05 *M* for SDS and 0.04 *M* for CTAB. Concentrations exceeding 0.20 *M* are not convenient due to the high viscosity of the mobile phase and degradation of the efficiencies. Most separations are performed in a buffered medium, phosphoric, and citric acid systems being the most appropriate. It should be taken into account that potassium salts are not compatible with SDS (which is used in more than 60% of the work involving MLC), since potassium dodecyl sulfate may precipitate from aqueous solution at room temperature.

The concentration of organic solvent must be low enough to guarantee the existence of micelles. Such maximal amount depends on the type of surfactant and organic solvent. For SDS, the maximal volume fractions of acetonitrile, propanol, butanol, and pentanol that seem to guarantee the presence of micelles are 30%, 15%, 10%, and 7% (v/v), respectively. However, analytical reports where authors claim the use of hybrid micellar mobile phases and these maximal values are exceeded—micelles do not exist—are not unusual.

Selection of the most suitable organic solvent should consider the polarity of analytes and the strength of their association with the surfactant. Solute log $P_{o/w}$ values can be used, in most cases, as a guide to make this decision.[18] Thus, with SDS as surfactant, a low concentration of propanol (1%v/v) is useful to separate compounds with log $P_{o/w} < 1$ as amino acids. A greater concentration of this solvent (5–7%) is needed for

compounds in the range $1 < \log P_{o/w} < 2$ as diuretics and sulfonamides. Pentanol (2–6%) is more convenient for low polar compounds with $\log P_{o/w} > 3$ as steroids. For basic compounds, such as phenethylamines with $0 < \log P_{o/w} < 2$ and β-blockers with $1 < \log P_{o/w} < 3$, propanol is however too weak, due to the strong electrostatic interaction between the cationic solutes and the anionic surfactant adsorbed on the stationary phase. In this case, a high concentration of propanol (15%), or preferably a moderate concentration of butanol (<10%) should be used. Methanol and ethanol are scarcely used in practice, owing to their weak elution strength.

Working in MLC involves coating the column with a layer of surfactant, and its further regeneration before stopping the system or removing it for storage. Before flushing the micellar mobile phase, removing any organic solvent contained in the column with water is recommended. Once the mobile phase is flushed, about 1 hr is required to assure complete surfactant coverage. In order to avoid any column damage, the micellar mobile phase should be continuously flushed through the system. To reduce the cost, it can be recycled even during the analysis, as long as a low number of injections are performed. Regeneration should be carried out by removing first the micellar mobile phase with pure water (10–20 volumes), and next replacing water by 100% methanol (at least 10 volumes). The complete cleaning procedure takes about half an hour.

Applications are mainly focused on the determination of drugs (e.g., anticonvulsant agents, barbiturates, β-blockers, diuretics, corticoids, stimulants) in formulations of physiological fluids, such as serum, plasma, or urine.[2,5,22] In this case, the direct injection capability of MLC is especially appreciated. Simple filtration of the sample permits the direct injection of the physiological fluids in the chromatographic system, with no noticeable damage after repetitive injections. MLC has also been extended to the analysis of samples of industrial, environmental, veterinarian, and nutritional interest.

MLC has revealed as an interesting way to simulate different systems. It has been demonstrated that RPLC with micellar mobile phases of Brij-35 can emulate in vitro partitioning processes in biomembranes, better than the conventional RPLC.[23] The therapeutic action of diuretics has been attributed to their hydrophobic character, among other properties. It has been shown that MLC with SDS mobile phases and C_{18} columns offers a scale for hydrophobicity that leads to a further correlation between the retention and the sites of action of diuretics within the nephron.[24] MLC has also served to model the behavior of environmental pollutants in ground water. In this case, the stationary phase and the micellar mobile phase simulate soil particles containing organic matter and groundwater carrying a surfactant, respectively.[25]

CONCLUSIONS

Pure micellar mobile phases are certainly attractive, considering the increasing restrictions in the use of organic solvents in laboratories. Hybrid micellar mobile phases were first belittled because some of MLC's appeal was considered to be lost. However, most reported analytical procedures in MLC utilize hybrid eluents. For most analytes, retention with pure micellar mobile phases is too high, which necessitates the addition of an organic solvent to achieve adequate retention times. This makes peak shape to improve as well.

Procedures that use the hybrid eluents still have the advantage of requiring significantly smaller amounts of organic solvent with respect to conventional RPLC. In MLC, the organic solvent is also highly retained in micellar solution, which reduces the risk of evaporation. The mobile phases can therefore be kept stable for a long time. The toxicity, flammability, environmental impact, and cost of RPLC are consequently reduced.

Micellar mobile phases are compatible with a wide range of solutes (ionic to water-insoluble). The decrease in the strength of acids in the SDS micellar system expands the pH range where the acidic species is dominant to more basic medium with regard to hydro–organic mixtures. This gives rise to three advantages: maximal retention is more often observed within the operable limits of silica-based columns, column life is extended as working at less stressing pH is possible, and measurements are more reproducible since these are made in a region of constant retention, where only one species dominates. Regarding basic compounds, their retention is increased by attraction to the stationary phase of the cationic species, which is dominant in acidic medium. This allows an improved control of selectivity. Peak tailing is also eliminated due to the effective masking of silanol groups.

Chromatographic peaks in MLC appear usually more evenly distributed with regard to those obtained with conventional hydro–organic mixtures. Owing to this compression effect, the use of gradients is less necessary. The above features have allowed the development of multiple applications that are competitive against conventional RPLC.

ACKNOWLEDGMENTS

This work was supported by Project CTQ2007–61828/BQU (Ministerio de Educación y Ciencia of Spain, MEC) and FEDER funds. M.J.R.-A. thanks the MEC for a Ramón y Cajal research contract.

REFERENCES

1. Armstrong, D.W.; Henry,S.J. Use of an aqueous mobile phase for separation of phenols and PAHs via HPLC. J. Liq. Chromatogr. **1980**, *3*, 657–662.
2. Berthod, A.; García-Álvarez-Coque, C. *Micellar Liquid Chromatography*; Cazes J. Ed.; Marcel Dekker, Inc.: New York, U.S.A., 2000.
3. Dorsey, J.G.; DeEchegaray, M.T.; Landy, J.S. Efficiency enhancement in micellar liquid chromatography. Anal. Chem. **1983**, *55*, 924–928.
4. Khaledi, M.G.; Breyer, E.D. Quantitation of hydrophobicity with micellar liquid chromatography. Anal. Chem. **1989**, *61*, 1040–1047.
5. Ruiz-Ángel, M.J.; García-Álvarez-Coque, M.C.; Berthod, A. New insights and recent developments in micellar liquid chromatography: A review. Sep. Purif. Rev. **2009**, *38*, 1–32.
6. López-Grío, S.; Baeza-Baeza, J.J.; García-Álvarez-Coque, M.C. Influence of the addition of modifiers on solute–micelle interaction in hybrid micellar liquid chromatography. Chromatographia **1998**, *48*, 655–663.
7. Lavine, B.K.; Hendayan, S.; Cooper, W.T.; He, Y. Selectivity in micellar liquid chromatography: Surfactant-bonded phase associations in micellar reversed phase liquid chromatography. ACS Symp. Ser. **1999**, *740*, 290–313.
8. Marina, M.L.; García, M.A. Evaluation of distribution coefficients in micellar liquid chromatography. J. Chromatogr. A, **1997**, *780*, 103–116.
9. Ruiz-Ángel, M.J.; Carda-Broch, S.; Torres-Lapasió, J.R.; García-Álvarez-Coque, M.C. Retention mechanisms in micellar liquid chromatography. J. Chromatogr. A, **2008**, doi:10.1016/j.chroma.2008.09.053.
10. García-Álvarez-Coque, M.C.; Torres-Lapasió, J.R.; Baeza-Baeza, J.J. Modelling of retention behavior of solutes in micellar liquid chromatography. A review. J. Chromatogr. A, **1997**, *780*, 129–148.
11. López-Grío, S.; Baeza-Baeza J.J.;García-Álvarez-Coque, M.C. Modelling of the elution behavior in hybrid micellar eluents with different organic modifiers. Anal. Chim. Acta **1999**, *381*, 275–285.
12. Ruiz-Ángel, M.J.; Torres-Lapasió, J.R.; García-Álvarez-Coque, M.C. Effect of pH and the presence of micelles on the resolution of diuretics by reversed-phase liquid chromatography. J. Chromatogr. A, **2004**, *1022*, 51–65.
13. Lopez-Grio, S.; Baeza-Baeza, J.J.; García-Álvarez-Coque, M.C. Evaluation of the elution strength of organic modifier, and surfactant in micellar mobile phases. J. Liq. Chromatogr. Rel. Technol. **2001**, *24*, 2765–2783.
14. Kord, A.S.; Khaledi, M.G. Controlling solvent strength and selectivity in MLC: Role of organic modifiers and micelles. Anal. Chem. **1992**, *64*, 1894–1900.
15. Lopez-Grío, S.; García-Álvarez-Coque, M.C.; Hinze, W.L.; Quina, F.H.; Berthod, A. Effect of a variety of organic additives on retention, and efficiency in micellar liquid chromatography. Anal. Chem. **2000**, *72*, 4826–4835.
16. Berthod, A. Causes and remediation of reduced efficiency in micellar liquid chromatography. J. Chromatogr. A, **1997**, *780*, 191–206.
17. Ruiz-Ángel, M.J.; Carda-Broch, S.; Torres-Lapasió, J.R.; Simó-Alfonso, E.F.; García-Álvarez-Coque, M.C. Micellar–organic versus aqueous–organic mobile phases for the screening of β-blockers. Anal. Chim. Acta **2002**, *454*, 109–123.
18. Caballero, R.D.; Ruiz-Ángel, M.J.; Simó-Alfonso, E.; García-Álvarez-Coque, M.C. Micellar liquid chromatography: A suitable technique for screening analysis. J. Chromatogr. A, **2002**, *947*, 31–45.
19. Carda-Broch, S.; Torres-Lapasió, J.R.; García-Álvarez-Coque, M.C. Evaluation of several global resolution functions for liquid chromatography. Anal. Chim. Acta **1999**, *396*, 61–74.
20. Torres-Lapasió, J.R. *Michrom Software*, Cazes, J. Ed.; Marcel Dekker, Inc.: New York, U.S.A., 2000.
21. Ruiz-Ángel, M.J.; García-Álvarez-Coque, M.C. Micellar liquid chromatography: How to start. LC-GC Europe **2008**, *21*, 420–429.
22. Esteve-Romero, J.; Carda-Broch, S.; Gil-Agustí, M.; Capella-Peiró, M.J.; Bose, D. Micellar liquid chromatography for the determination of drug materials in pharmaceutical preparations and biological samples. Trends Anal. Chem. **2005**, *24*, 75–91.
23. Quiñones-Torrelo, C.; Martín-Biosca, Y.; Martiñnez-Pla, J.J.; Sagrado, S.; Villanueva-Camañas, R.M. QRAR models for central nervous system drugs using biopartitioning micellar chromatography. Mini Rev. Med. Chem. **2002**, *2*, 145–161.
24. Medina-Hernández, M.J.; Bonet-Domingo, E.; Ramis-Ramos, G.; García-Álvarez-Coque, M.C. On the retention of diuretics in micellar liquid chromatography and their site of action within the nephron. Anal. Chem. **1993**, *26*, 1881–1889.
25. Simmons, R.N.; McGuffin, V.L. Modeling transport effects of perfluorinated and hydrocarbon surfactants in groundwater by using micellar liquid chromatography. Anal. Chim. Acta **2007**, *603*, 93–100.

Hydrodynamic Equilibrium in CCC

Petr S. Fedotov
Boris Ya. Spivakov
Vernadsky Institute of Geochemistry and Analytical Chemistry, Russian Academy of Sciences, Moscow, Russia

INTRODUCTION

In all cases, countercurrent chromatography (CCC) utilizes a hydrodynamic behavior of two immiscible liquid phases through a tubular column space which is free of a solid support matrix. The most versatile form of CCC, called the hydrodynamic equilibrium system, applies a rotating coil in an acceleration field (either in the unit gravity or in the centrifuge force field). Two immiscible liquid phases confined in such a coil distribute themselves along the length of the coil to form various patterns of hydrodynamic equilibrium.[1]

DISCUSSION

According to the hypothesis proposed by Ito,[2] the multitude of hydrodynamic phenomena observed in the rotating coils can be attributed to the following types of liquid distribution.

1. The basic hydrodynamic equilibrium (the two liquid phases are evenly distributed from one end of the coil, called the head, and any excess of either phase is accumulated at the other end, called the tail). Here, the tail–head relationship of the rotating coil is defined by the direction of the Archimedean screw force which drives all objects toward the head of the coil.
2. The unilateral hydrodynamic equilibrium [the two solvent phases are unilaterally distributed along the length of the coil, one phase (head phase) entirely occupying the head side and the other phase (tail phase) the tail side of the coil]. The head phase can be the lighter or the heavier phase and also can be the aqueous or the non-aqueous phase, depending on the physical properties of the liquid system and the applied experimental conditions. This type of equilibrium may also be called bilateral, indicating the distribution of the one phase on the head side and the other phase on the tail side.[3]

To illustrate the process of establishing the hydrodynamic equilibrium, it is worthwhile to begin with the distribution of two immiscible solvent phases in the "closed" coil, simply rotated around the horizontal axis in the unit gravitational field. The coil is filled with equal volumes of the lighter and heavier phase and then sealed at both ends. At a slow rotation of 10–20 revolutions per minute (rpm), two liquid phases are evenly distributed in the coil (basic hydrodynamic equilibrium) due to the Archimedean screw force. As the rotational speed increases, the heavier phase quickly occupies more space on the head side of the coil and, at the critical speed range of 60–100 rpm, the two phases are completely separated along the length of the coil, with the heavier phase on the head side and the lighter phase on the tail side (unilateral hydrodynamic equilibrium).

After this critical speed range, the amount of the heavier phase on the head side decreases sharply, reaching substantially below the 50% level at about 160 rpm. Further increase of the rotational speed again distributes the two phases fairly evenly throughout the coil, apparently due to the strong radial centrifugal force field produced by the rotation of the coil. The phase distribution described can be observed in many solvent systems [chloroform-acetic acid-water (2/2/1), hexane-methanol, *n*-butanol-water, etc.], glass coils [10–20 mm inner diameter (I.D.)] with different helical diameters (5–20 cm) being applied.

As a first approximation, the complex hydrodynamic phenomenon taking place in the rotating coil may be explained by the interplay between two force components acting on the fluid. The tangential force component (F_t) generates the Archimedean screw effect to move two phases toward the head of the coil, and the radial force component (F_r) which acts against the Archimedean force. The critical speed range is the most interesting. An increase of the rotational speed up to 60–100 rpm alters the balance of the hydrodynamic equilibrium by an enhanced radial centrifugal force field that increases the net force field acting at the bottom of the coil and decreases that acting at the top. Under this asymmetrical force distribution, the movement of the heavier phase toward the head is accelerated, whereas the movement of the lighter phase toward the head is retarded. This results in a unilateral hydrodynamic phase distribution in the rotating coil.

The hydrodynamic equilibrium condition may be used for performing CCC as follows. First, the coil is completely filled with the stationary phase, either the lighter or the heavier phase, and the other phase is introduced from the

head end of the coil while the coil is rotated around its axis. Then, the two liquid phases establish equilibrium in each turn of the coil and the mobile phase finally emerges from the tail end of the coil, leaving some amount of the stationary phase permanently in the coil. Solutes locally introduced at the head of the coil are subjected to a partition process between two phases and eluted in order of their partition coefficients. In general, higher retention of the stationary phase significantly improves the peak resolution. Consequently, the unilateral hydrodynamic equilibrium condition provides a great advantage in performing CCC, because the system permits retention of a large amount of stationary phase in the coil if the lighter phase is eluted in a normal mode (head-to-tail direction) or the heavier phase in a reversed mode (tail-to-head direction).

In general, the retention of the stationary phase in the coil rotated in the unit gravity field entirely relies on relatively weak Archimedean screw force. In this situation, application of a high flow rate of the mobile phase would cause a depletion of the stationary phase from the column. This problem can be solved by the utilization of synchronous planetary centrifuges, free of rotary seals, which enable one to increase the rotational speed and, consequently, enhance the Archimedean screw force. The seal-free principle can be applied to various types of synchronous planetary motion. In all cases, the holder revolves around the centrifuge axis and simultaneously rotates about its own axis at the same angular velocity ω.

When the coil is mounted coaxially around the holder, which revolves around the central axis of the device and counterrotates about its own axis, two axis being parallel (Type I), two solvent phases are distributed along the length of the coil according to the basic hydrodynamic equilibrium. It does not favor the stationary-phase retention. Another, similar planetary motion, except that the holder revolves around the central axis of the centrifuge and rotates about its own axis in the same direction (Type J), produces, regardless of the rotational speed, a totally different phase-distribution pattern which is typical for the unilateral hydrodynamic equilibrium. The unilateral distribution can also be attained in the coaxially mounted coils in cross-axis planetary centrifuges.[4] It is important to note that all the planetary motions providing the unilateral distribution form an asymmetrical centrifuge force field that closely resembles that observed in the coil rotating at the critical speed in the unit gravity.

The unilateral hydrodynamic equilibrium conditions provide the basis for high-speed CCC (HSCCC, $\omega = 800$ rpm or more) which has mainly gained acceptance for CCC separations. The stroboscopic observation on two-phase flow through the running spiral column of a Type J system reveals the following pattern. When the lower phase (chloroform) is eluted through the stationary lighter phase (water) from the head toward the tail of the spiral column, a large volume of the stationary phase is retained in the column and the spiral column is divided into two distinct zones: the mixing zone in about one-fourth of the area near the center of the centrifuge and the settling zone showing a linear interface between the two phases in the rest of the area. The mixing zone is always fixed at the vicinity of the central axis of the centrifuge while the spiral column undergoes the planetary motion. In other words, the mixing zone in each loop is traveling through the spiral column toward the head at a rate equal to the column rotation. Consequently, at any portion of the column, the two liquid phases are subjected to a typical partition process of repetitive mixing and settling at a high frequency, over 13 times per second at 800 rpm of column revolution, while the mobile phase is being continuously pumped through the stationary phase.[3]

At a first approximation, the hydrodynamic phenomenon observed also may be explained by the interplay between two force components acting on the fluid. At the distal portion of the coil, both the strong radial force field and the reduced relative flow of the two phases establish a clear and stable interface between the two liquid phases. At the proximal portion of the spiral column, where the strength of the radial-force component is minimized, the effect of the Archimedean screw force becomes visualized as agitation at the interface caused by the relative movement of two liquid layers.[2]

It should be noted that the centrifuge force field acts on the fluid in the rotated coil in parallel with other forces of different nature[5]:

- F_A, buoyancy force due to the difference between the stationary and mobile phases
- F_i, inertial force caused by coil motion, comprises components of centrifugal force field
- F_η, viscosity force due to the overflow of the stationary phase along the coil tube walls
- F_γ, interfacial tension force
- F_W, adhesion force
- F_h, hydraulic resistance force caused by moving of two immiscible phases relative to each other

HYDRODYNAMIC EQUILIBRIUM IN CCC

The following balance of these forces of a different nature is considered:

$$F_i = F_A + F_\eta + F_\gamma + F_W + F_h$$

From this, the basic equation of the stationary-phase retention process can be derived, a number of assumptions and complex theoretical treatments being required. Taking as example the planetary centrifuge of Type J, the average cross-sectional area of a stationary-phase layer has been estimated for hydrophobic liquid systems, which are characterized by high values of interfacial tension γ, low values

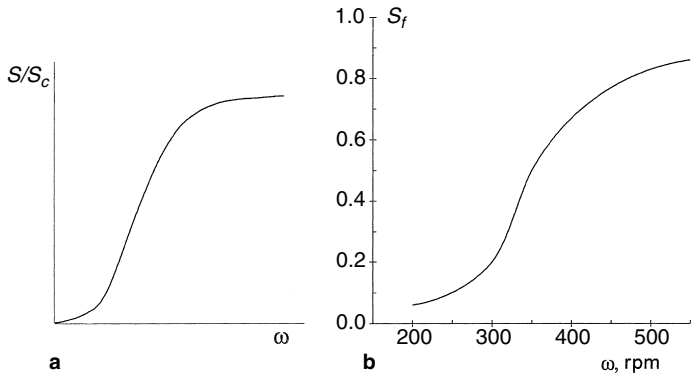

Fig. 1 a, Theoretical ω-dependence of S/S_c; and b, Experimental ω dependence of S_f for the *n*-decane–water system. Planetary centrifuge of Type J; $\beta = 0.37$; flow rate = 1 ml/min.

of viscosity η, and low hydrodynamic equilibrium settling times:

$$\left(\sqrt{\frac{S_c}{S}} - 1\right)(S_c - S) \approx \frac{v_m^{1/2} r^{1/2} \eta_s}{\rho_m \Delta\rho R \omega^{3/2}}$$

where S and S_c are the cross-sectional areas of the stationary-phase layer and the spiral column, respectively, v_m is the linear speed of the mobile phase flow, η_s is the viscosity of the stationary phase, and r and R are rotation and revolution radii, respectively; ρ_m is the density of the mobile phase and $\Delta\rho$ is the density difference between two phases. After a few assumptions, it can be rewritten as

$$\frac{S}{S_c} \approx 1 - k_1 \frac{\beta^{1/4}}{\omega^{3/4} R^{1/4}} \approx 1 - k_2 \frac{1}{\omega^{3/4}}$$

where $\beta = r/R$, is a proportional coefficient characterizing peculiarities of the liquid system (it is dependent on the interfacial tension, viscosity of the stationary phase, and density difference between two phases); $k_2 = k_1(r^{1/4}/R^{1/2})$.

The ratio of the cross-sectional area of the stationary-phase layer to that of the coil tube (S/S_c) governs the volume of the stationary phase retained in the column. The theoretical dependence of S/S_c on the rotation speed ω and the experimental dependencies of the S_f value (ratio of the volume of the stationary phase retained in the column to the total column volume) on ω for *n*-decane-water and chloroform-water liquid systems are in good agreement (Fig. 1).

Hence, an approach based on considering the balance of forces of a different nature acting on the fluid in the rotating coil may give some correlation among the peculiarities of the liquid system, operation conditions, design parameters of the planetary centrifuge, and the stationary-phase retention. However, any rigorous mathematical model describing the complex hydrodynamic equilibrium of two liquid phases in the rotating coiled column has not been yet elaborated. This issue remains open.

REFERENCES

1. Conway, W.D. *Countercurrent Chromatography. Apparatus, Theory and Application*; VCH: New York, 1990.
2. Ito, Y. Speculation on the mechanism of unilateral hydrodynamic distribution of two immiscible solvent phases in the rotating coil. J. Liq. Chromatogr. Relat. Technol. **1992**, *15* (15–16), 2639–2675.
3. Ito, Y. Principle, apparatus, and methodology of high-speed countercurrent chromatography. In *High-Speed Countercurrent Chromatography*; Ito, Y., Conway, W.D., Eds.; John Wiley & Sons: New York, 1996; 3–44.
4. Menet, J.-M.; Shimomiya, K.; Ito, Y. Studies on new cross-axis coil planet centrifuge for performing counter-current chromatography: III. Speculations on the hydrodynamic mechanism in stationary phase retention. J. Chromatogr. **1993**, *644*, 239.
5. Fedotov, P.S.; Kronrod, V.A.; Maryutina, T.A.; Spivakov, B.Ya. On the mechanism of stationary phase retention in rotating coil columns. J. Liq. Chromatogr. Relat. Technol. **1996**, *19* (19), 3237.

Hydrophilic Vitamins: TLC Analysis

Fumio Watanabe
Emi Miyamoto
Department of Health Science, Kochi Women's University, Kochi, Japan

INTRODUCTION

The benefit of using thin-layer chromatography (TLC) for the identification of unknown vitamins and related compounds by comparing R_f values of the unknown compounds with authentic vitamins is beyond doubt. The quantification of the separated vitamins can be performed by the use of modern densitometry. TLC [or high-performance thin-layer chromatography (HPTLC)], as a powerful separation and analytic tool, is used particularly with pharmaceutical preparations and food products. Because amounts of most hydrophilic vitamins are low, or very low, in tissues or body fluids, bioautography or derivatization is used before densitometry.

In this section, we summarize the recent advance of TLC analysis for hydrophilic vitamins.

THIAMINE (VITAMIN B_1)

To investigate thiamine metabolism in mammals, thiamine (R_f values: 0.16, 0.04, and 0.03), urinary excretion of thiamine metabolites [thiochirome (R_f values: 0.31, 0.28, and 0.33), thiazole (R_f values: 0.85, 0.79, and 0.81), and 2-methyl-4-amino-pyrimidinecarboxylic acid (R_f values: 0.42, 0.21, and 0.26)], and related compounds [pyrimidinesulfonic acid (R_f values: 0.48, 0.39, and 0.46), α-hydroxyethylthiamine (R_f values: 0.23, 0.09, and 0.06), N'-methylnicotinamide (R_f values: 0.31, 0.06, and 0.05)] were analyzed and identified by TLC on silica gel with acetonitrile–water (40:10 vol/vol) adjusted to a pH of 2.54, 4.03, and 7.85 with formic acid as solvents, respectively.[1] Although N'-methylnicotinamide and thiochrome could not be separated in single-phase chromatography at pH 2.54, a second phase at right angle, with a pH 4.03 solvent, separated these quite clearly without affecting the resolution of the other compounds.[1]

The quantitative analysis of thiamine hydrochloride (vitamin B_1), using HPTLC on silica gel plates with two different mobile phases, was elaborated.[2] After TLC separation, vitamin B_1 was derivatized by the use of *tert*-butyl hypochlorite or potassium hexacyanoferrate (III)–sodium hydroxide as reagents. The *tert*-butyl hypochlorite reagent formed yellow-fluorescing derivatives with a limit of detection of less than 3 ng per chromatogram zone. The potassium hexacyanoferrate (III)–sodium hydroxide reagent led to a bluish-fluorescing derivative with a limit of detection of 500 ng per chromatogram zone.

RIBOFLAVIN (VITAMIN B_2)

TLC on silica gel 60 plates was used in various TLC solvent systems for both determination and identification of flavin derivatives in baker's yeast[3] and foods (plain yogurt and bioyogurt, raw egg white, and egg powder).[4,5] The R_f values of two unknown compounds found in plain yogurt were identical to those of 7α-hydroxyriboflavin (R_f values: 0.32 and 0.21) and riboflavin-β-galactoside (R_f values: 0.14 and 0.10), but not to those of other flavin compounds [flavin adenine dinucleotide or FAD (R_f values: 0 and 0), flavine mononucleotide or FMN (R_f values: 0 and 0.05), 10-hydroxyethylflavin (R_f values: 0.71 and 0.40), riboflavin (R_f values: 0.55 and 0.32), and 10-formylmethylflavin (R_f values: 0.86 and 0.76)] by TLC on silica gel with chloroform–methanol–ethyl acetate (5:5:2) and 1-butanol–benzyl alcohol–glacial acetic acid (8:4:3) as solvents, respectively.[4]

7α-Hydroxyriboflavin was identified in blood plasma from humans, following oral administration of riboflavin supplements, by fluorescence after TLC [benzene–1-butanol–methanol–water (1:2:1:1 vol/vol)]and by its spectrum.[6]

PYRIDOXINE (VITAMIN B_6)

TLC of vitamin B_6 compounds, on various layers in different solvents, was studied.[7] The R_f values of pyridoxine, pyridoxal, pyridoxamine, pyridoxal ethyl acetate, 4-pyridoxic acid, 4-pyridoxic acid lactone, pyridoxine phosphate, pyridoxal phosphate, and pyridoxamine phosphate were 0.62, 0.68, 0.12, 0.54, 0.91, 0.91, 0.95, 0.95, and 0.86, respectively, by TLC on silica gel HF_{254} with 0.2% NH_4OH in water as solvent. When adsorbents containing fluorescent indicators are used, all forms and derivatives of vitamin B_6 can be detected

through fluorescence, or through quenching of indicator fluorescence in ultraviolet (UV) light (254 nm).

When radioactive pyridoxine hydrochloride was orally supplemented to evaluate vitamin B_6 metabolism in adult domestic cats, two unknown radioactive compounds (compounds X and Y) were excreted in the urine.[8] The R_f values of compound X (R_f values: 0.95, 0.83, 0.2, 0.5, and 0.62) and compound Y (R_f values: 0.35, 0.20, 0.22, 0.32, and 0.25) were identical to those of pyridoxine-3-sulfate and *N*-methylpyridoxine, respectively, but not to those of pyridoxine (R_f values: 0.73, 0.83, 0.78, 0.52, and 0.62) in various solvent systems [0.5% ammonium hydroxide, 95% ethanol, chloroform–methanol (3:1 vol/vol), isoamyl alcohol–acetone–triethylamine–water (24:18:8:6 vol/vol), and 2-butanol–1.5 N ammonium hydroxide (3:1 vol/vol), respectively] by TLC on silica gel plates.

COBALAMIN (VITAMIN B_{12})

Usual dietary sources of vitamin B_{12} are animal food products (meat, milk, eggs, and shellfish), but not plant food products. To evaluate whether foods contain true vitamin B_{12} or inactive corrinoids, vitamin B_{12} compounds were purified and characterized using TLC on silica gel.[9] The R_f values of the unknown vitamin B_{12} compound, purified from an algal health food (Spirulina tablets) were identical to those of pseudovitamin B_{12} (R_f values: 0.14 and 0.42), but not to those of vitamin B_{12} (or 5,6-dimethylbenzimidazolyl cyanocobamide) (R_f values: 0.23 and 0.56), benzimidazolyl cyanocobamide (R_f values: 0.18 and 0.52), 5-hydroxybenzimidazolyl cyanocobamide (R_f values: 0.20 and 0.47), and *p*-cresolyl cyanocobamide (R_f values: 0.38 and 0.62) by TLC on silica gel 60 with 1-butanol–2-propanol–water (10:7:10 vol/vol) and 2-propanol–NH_4OH (28%)–water (7:1:2 vol/vol) as solvents, respectively. The results indicate that an inactive vitamin B_{12} compound (pseudovitamin B_{12}) is predominant in Spirulina tablets.[10]

Because amounts of vitamin B_{12} are very low in foods, tissues, and body fluids, bioautography is used before densitometry. A selected strain of *Escherichia coli* is used as a micro-organism for the bioautography. Growth spots are enhanced by the addition of 2,3,5-triphenyltetrazolium chloride, which is converted to the red-colored formazan by *E. coli* growth. Determination of vitamin B_{12} in human plasma and erythrocytes was accomplished by one-dimensional bioautography.[11] A sensitive two-dimensional bioautography was also developed to investigate B_{12} metabolism in health and a wide range of diseases.[12]

NICOTINIC ACID AND NICOTINAMIDE

Nicotinic acid and nicotinamide and their derivatives were analyzed by TLC on MN 300G cellulose plates in various solvent systems (K. Shibata, personal communications, October 16, 2001). The R_f values of nicotinamide adenine dinucleotide phosphate or $NADP^+$ (R_f values: 0.03, 0.50, and 0.70), nicotinamide adenine dinucleotide or NAD^+ (R_f values: 0.13, 0.61, and 0.58), nicotinic acid adenine dinucleotide (R_f values: 0.15, 0.52, and 0.57), nicotinamide mononucleotide (R_f values: 0.11, 0.63, and 0.73), nicotinic acid mononucleotide (R_f values: 0.13, 0.47, and 0.75), nicotinamide (R_f values: 0.87, 0.88, and 0.45), and nicotinic acid (R_f values: 0.77, 0.82, and 0.55) are shown in various solvent systems [1 *M* ammonium acetate–95% ethanol (3:7), pH 5.0; 2-butyric acid–ammonia–water (66:1.7:33), and 600 g of ammonium sulfate in 0.1 *M* sodium phosphate–2% 1-propanol (pH 6.8), respectively]. The detection is performed by illumination under short-wavelength (257.3 nm) UV light. Urinary metabolites of the vitamin could be analyzed by TLC.[13]

PANTOTHENIC ACID

A rapid, simple, and specific TLC method has been developed for the estimation of panthenol and pantothenic acid in pharmaceutical preparations containing other vitamins, amino acids, syrups, enzymes, etc.[14] The vitamin was extracted with ethanol (from tablets and capsules) or benzyl alcohol (from liquid oral preparations) and isolated from other ingredients by TLC on silica gel 60 plates with 2-propanol–water (85:15 vol/vol) as a solvent. β-Alanine (panthothenate) or β-alanol (panthenol) was liberated by heating for 20 min at 160°C. The liberated amines were visualized with the ninhydrin reaction and estimated by spectrodensitometry at 490 nm. Recoveries for panthenol and pantothenic acid were 99.8 ± 2.25% and 100.2 ± 1.7%, respectively.

BIOTIN

Unidentified biotin metabolites were analyzed and identified in urine from healthy adults by TLC.[15,16] Three unknown biotin metabolites were identified as biotin sulfone (R_f values: 0.49 and 0.17), bisnorbiotin methyl ketone (R_f values: 0.78 and 0.29), and tetranorbiotin-*l*-sulfoxide (R_f values: 0.22 and 0.01) by derivatization with *p*-demethylaminocinnamaldehyde after TLC on microcellulose with 1-butanol–acetic acid–water (4:1:1) and 1-butanol as solvents, respectively.[15]

FOLIC ACID

Folates [pteroylmonoglutamates (PteGlu)] and related compounds were separated by TLC on cellulose powder (MN300 UV_{254}) with 3.0% (wt/vol) NH_4Cl and 0.5%

(vol/vol) 2-mercaptoethanol as solvents.[17] The R_f values of PteGlu (R_f value: 0.24), H_2-PteGlu (R_f value: 0.1), 5,10-CH=H_4-PteGlu (R_f value: 0.32), H_4-PteGlu (R_f value: 0.56), 5-CHO-H_2-PteGlu (R_f value: 0.72), 5-HCNH-H_4-PteGlu (R_f value: 0.72), 5,10-CH_2-H_4-PteGlu (R_f value: 0.75), 5-CH_3-H_4-PteGlu (R_f value: 0.8), 10-CHO-H_4-PteGlu (R_f value: 0.82), 5-CH_3-H_2-PteGlu (R_f value: 0.87), 10-CHO-PteGlu (R_f value: 0.7), and 10-CHO-H_2-PteGlu (R_f value: 0.73) were shown in this TLC system, which is applied to evaluate the transport and metabolism of reduced folates in blood.

A TLC densitometric method could be applied to evaluate the purity of folic acid preparations for the final purpose of determination of the *N*-(4-aminobenzol)-L-glutamic acid content as an impurity.[18] The separation was performed in 1-propanol–NH_4OH (25%)–ethanol (2:2:1) and toluene–methanol–glacial acetic acid–acetone (14:4:1:1) as solvents. The silica gel plates developed were scanned at 278 nm.

ASCORBIC ACID (VITAMIN C)

TLC has been widely used to determine ascorbic acid concentrations in foods,[19–21] pharmaceutical preparations,[21–23] and biological materials.[21,24,25] Isomers of ascorbic acid and their oxidation product, dehydroascorbic acid, were separated by TLC on sodium borate-impregnated silica gel and cellulose plates.[21] This TLC method has been adapted to separate and identify ascorbic acid and dehydroascorbic acid in fresh orange and lime juices, pharmaceutical preparations (ascorbic acid), and guinea pig tissues (liver, kidney, and eye lens) and fluids (plasma and urine).

The components of an analgesic mixture (paracetamol, ascorbic acid, caffeine, and phenylephrine hydrochloride) were separated by HPTLC on silica gel plates with methylene chloride–ethyacetate–ethanol–formic acid (3.5:2:4:0.5 vol/vol) as the mobile phase.[22] The plates were scanned at 264 nm for ascorbic acid (R_f value: 0.53), 254 nm for paracetamol (R_f value: 0.87), and 274 nm for phenylephrine hydrochloride (R_f value: 0.22) and caffeine (R_f value: 0.69).

Ascorbic acid and dipyrone (metamizole) are sometimes combined in pharmaceutical dosage forms to relive pain and fever. Simultaneous determination of ascorbic acid and dipyrone was done by TLC on silica gel using water–methanol (95:5 vol/vol) as the solvent.[23] The developed plates were directly scanned at 260 nm. The R_f values for ascorbic acid and dipyrone were 0.92 and 0.65, respectively.

MULTIVITAMIN COMPLEX

Vitamin B_1, vitamin B_2, and nicotinic acid, all of which frequently occur together in foods, were separated by TLC and fluorimetrically determined by using a commercially available fiber optic-based instrument.[26] A fluorescent tracer (fluoresceinamine, isomer II) was used to label the nicotinic acid. Vitamin B_1 was converted to fluorescent thiochrome by oxidizing with potassium ferricyanide solution in aqueous sodium hydroxide. These vitamins were separated by HPTLC on silica gel using methanol–water (70:30 vol/vol) as mobile phase. Under these conditions, the R_f values of the vitamin B_1, vitamin B_2, and nicotinic acid derivatives were 0.73, 0.86, and 0.91, respectively.

A vitamin B complex (vitamin B_1, vitamin B_2, vitamin B_6, vitamin B_{12}, and folic acid) was also separated into its components using TLC plates impregnated with different transition metal ions.[27] $CuSO_4$ at 0.4% impregnation in all the employed solvent systems resulted in the simultaneous resolution of constituents of the vitamin B complex with appreciable differences in R_f values.

Water-soluble vitamins (vitamin B_1, vitamin B_6, vitamin B_{12}, and vitamin C) in "Kombucha" drink (a curative liquor) were separated by TLC on silica gel plates with water as the solvent.[28] The plates were visually examined under UV light at 254- and 366-nm wavelengths. The four vitamins were identified and determined by comparing the R_f values with the reference values (vitamin B_1, 0.21; vitamin B_6, 0.73; vitamin B_{12}, 0.34; and vitamin C, 0.96).

An overpressured layer chromatographic procedure, with photodensitometric detection for the simultaneous determination of water-soluble vitamins in multivitamin pharmaceutical preparations, was developed and evaluated.[29] HPTLC on silica gel plates with 1-butanol–pyridine–water (50:35:15 vol/vol) as mobile phase was used. The quantitation was carried out without derivatization [vitamin B_2 (R_f value: 0.30), vitamin B_6 (R_f value: 0.64), folic acid (R_f value: 0.37), nicotinamide (R_f value: 0.80), and vitamin C (R_f value: 1.02)] or after spraying ninhydrin reagent [calcium panthothenate (R_f value: 0.72)] or 4-demethylaminocinnamaldehyde [vitamin B_{12} (R_f value: 1.84) and biotin (R_f value: 0)].

CONCLUSIONS

TLC is used as a powerful separation tool particularly for the analysis of pharmaceutical preparations and food products. The separated vitamins can be quantified by the use of densitometry. In biological materials (tissues and body fluids), which contain only trace amounts of vitamins, bioautography or derivatization is used before densitometry.

TLC offers great advantages (simplicity, flexibility, speed, and relative low expense) for the separation and analysis of hydrophilic vitamins.

REFERENCES

1. Ziporin, Z.Z.; Waring, P.P. Thin-layer chromatography for the separation of thiamine, *N′*-methylnicotinamide, and related compounds. Methods Enzymol. **1970**, *18A*, 86–87.
2. Funk, W.; Derr, P. Characterization and quantitative HPTLC determination of vitamin B_1 (thiamine hydrochloride) in a pharmaceutical product. J. Planar Chromatogr. **1990**, *3*, 149–152.
3. Gliszczynska, A.; Koziolowa, A. Chromatographic determination of flavin derivatives in baker's yeast. J. Chromatogr. A, **1998**, *822*, 59–66.
4. Gliszczyłska-Swigło, A.; Koziołowa, A. Chromatographic determination of riboflavin and its derivatives in food. J. Chromatogr. A, **2000**, *881*, 285–297.
5. Gliszczynska, A.; Koziołowa, A. Chromatographic identification of a new flavin derivative in plain yogurt. J. Agric. Food Chem. **1999**, *47*, 3197–3201.
6. Zempleni, J.; Galloway, J.R.; McCormick, D.B. The identification and kinetics of 7α-hydroxyriboflavin (7-hydroxymethylriboflavin) in blood plasma from humans following oral administration of riboflavin supplements. Int. J. Vitam. Nutr. Res. **1996**, *66*, 151–157.
7. Ahrens, H.; Korytnyk, W. Pyridoxine chemistry: XXI. Thin-layer chromatography and thin-layer electrophoresis of compounds in the vitamin B_6 group. Anal. Biochem. **1969**, *30*, 413–420.
8. Coburn, S.P.; Mahuren, J.D. Identification of pyridoxine 3-sulfate, pyridoxal 3-sulfate, and *N*-methylpyridoxine as major urinary metabolites of vitamin B_6 in domestic cats. J. Biol. Chem. **1987**, *262*, 2642–2644.
9. Watanabe, F.; Miyamoto, E. TLC separation and analysis of vitamin B_{12} and related compounds in food. J. Liq. Chromatogr. Relat. Technol. **2002**, *25*, 1561–1577.
10. Watanabe, F.; Katsura, H.; Takenaka, S.; Fujita, T.; Abe, K.; Tamura, Y.; Nakatsuka, T.; Nakano, Y. Pseudovitamin B_{12} is the predominant cobamide of an algal health food, Spirulina tablets. J. Agric. Food Chem. **1999**, *47*, 4736–4741.
11. Gimsing, P.; Nexo, E.; Hippe, E. Determination of cobalamins in biological material: II. The cobalamins in human plasma and erythrocytes after desalting on nonpolar adsorbent material, and separation by one-dimensional thin-layer chromatography. Anal. Biochem. **1983**, *129*, 296–304.
12. Linnell, J.C.; Hoffbrand, A.V.; Peters, T.J.; Matthews, D.M. Chromatographic and bioautographic estimation of plasma cobalamins in various disturbances of vitamin B_{12} metabolism. Clin. Sci. **1971**, *40*, 1–16.
13. Shibata, K.; Taguchi, H. Nicotinic acid and nicotinamide. In *Modern Chromatographic Analysis of Vitamins,* 3rd Ed.; De Leenheer, A.P. Lambert, W.E., Van Bocxlaer, J.F., Eds.; Marcel Dekker, Inc.: New York, 2000; 325–364.
14. Nag, S.S.; Das, S. Identification and quantitation of panthenol and pantothenic acid in pharmaceutical preparations by thin-layer chromatography and densitometry. J. AOAC Int. **1992**, *75*, 898–901.
15. Zempleni, J.; McCormick, B.; Mock, D.M. Identification of biotin sulfone, bisnorbiotin methyl ketone, and tetranorbiotin-*l*-sulfoxide in human urine. Am. J. Clin. Nutr. **1997**, *65*, 508–511.
16. Zempleni, J.; Mock, D.M. Advanced analysis of biotin metabolites in body fluids allows a more accurate measurement of biotin bioavailability and metabolism in humans. J. Nutr. **1999**, *129*, 494S–497S.
17. Brown, J.P.; Davidson, G.E.; Scott, J.M. Thin-layer chromatography of peteroglutamates and related compounds. Application to transport and metabolism of reduced folates in blood. J. Chromatogr. **1973**, *79*, 195–207.
18. Krzek, J.; Kwiecien, A. Densitometric determination of impurities in drugs: Part IV. Determination of *N*-(4-aminobenzoyl)-L-glutamic acid in preparations of folic acid. J. Pharm. Biomed. Anal. **1999**, *21*, 451–457.
19. Beljaars, P.R.; Horrock, W.V.S.; Rondags, T.M.M. Assay of L(+)-ascorbic acid in buttermilk by densitometric transmittance measurement of the dehydroascorbic acid. J. Assoc. Off. Anal. Chem. **1974**, *57*, 65–69.
20. Okamura, M. Distribution of ascorbic acid analogs and associated glycorides in mushrooms. J. Nutr. Sci. Vitaminol. **1994**, *40*, 81–94.
21. Roomi, M.W.; Tsao, C.S. Thin-layer chromatographic separation of isomers of ascorbic acid and dehydroascorbic acid as sodium borate complexes on silica gel and cellulose plates. J. Agric. Food Chem. **1998**, *46*, 1406–1409.
22. El-Sadek, M.; El-Shanawany, A.; Aboul Khier, A. Determination of the components of analgesic mixture using high-performance thin-layer chromatography. Analyst **1990**, *115*, 1181–1184.
23. Aburjai, T.; Amro, B.I.; Aiedeh, K.; Abuirjeie, M.; Al-Khalil, S. Second derivative ultraviolet spectrophotometry and HPTLC for the simultaneous determination of vitamin C and dipyrone. Pharmazie **2000**, *55*, 751–754.
24. DiMattio, J. A comparative study of ascorbic acid entry into aqueous and vitreous tumors of the rat and guinea pig. Invest. Ophthalmol. Vis. Sci. **1989**, *30*, 2320–2331.
25. Chatterjee, I.B.; Banerjee, A. Estimation of dehydroascorbic acid in blood of diabetic patients. Anal. Biochem. **1979**, *98*, 368–374.
26. Diaz, A.N.; Paniaqua, A.G.; Sanchez, F.G. Thin-layer chromatography and fibre-optic fluorimetric quantitation of thiamine, riboflavin and niacin. J. Chromatogr. A, **1993**, *655*, 39–43.
27. Bhushan, R.; Parshad, V. Improved separation of vitamin B complex and folic acid using some new solvent systems and impregnated TLC. J. Liq. Chromatogr. Relat. Technol. **1999**, *22*, 1607–1623.
28. Bauer-Petrovska, B.; Petrushevska-Tozi, L. Mineral and water soluble vitamin content in the Kombucha drink. Int. J. Food Sci. Technol. **2000**, *35*, 201–205.
29. Postaire, E.; Cisse, M.; Le Hoang, M.D.; Pradeau, D. Simultaneous determination of water-soluble vitamins by over-pressure layer chromatography and photodensitometric detection. J. Pharm. Sci. **1991**, *80*, 368–370.

Hydrophobic Interaction

Karen M. Gooding
Eli Lilly and Company, Indianapolis, Indiana, U.S.A.

INTRODUCTION

Hydrophobic-interaction chromatography (HIC) is a mode of separation in which molecules in a high-salt environment interact hydrophobically with a non-polar bonded phase. HIC has been predominantly used to analyze proteins, nucleic acids, and other biological macromolecules by a hydrophobic mechanism when maintenance of the three-dimensional structure is a primary concern.[1–4] The main applications of HIC have been in the area of protein purification because the recovery is frequently quantitative in terms of both mass and biological activity.

In HIC, a high-salt environment causes the association of hydrophobic patches on the surface of an analyte with the non-polar ligands of the bonded phase. Elution is generally effected by an "inverse" gradient to lower salt concentration. This is considered "inverse" because it is the opposite of gradients used for ion-exchange chromatography. Effective salts for HIC are those which are "antichaotropic"; that is, they promote the ordering of water molecules at interfaces. Because interaction is only with the surface of a macromolecule such as a protein, the number of amino acids involved in the chromatography is relatively small, and changes in surface structure can cause differential binding and, hence, separation.

Reversed-phase chromatography (RPC) and HIC are both based on interactions between hydrophobic moieties, but the operational aspects of the techniques render selectivities totally different. The physical properties and selectivities of the two methods are contrasted in Fig. 1. The bonded phase of HIC supports consists of a hydrophilic matrix into which hydrophobic chains are inserted, generally in low density. This can be contrasted with the higher-density organosilane chemistry used in RPC. The chromatograms illustrate that both the selectivity and the number of peaks obtained for a protein mixture vary between the two modes. Cytochrome c is not retained at all by HIC and myoglobin is split into two peaks by RPC. A primary reason for the vast difference is the mobile-phase environment for each method. The organic solvents and generally acidic conditions used in RPC cause denaturation of most proteins and even splitting into subunits, whereas the high-salt concentrations at neutral pH used in HIC result in stabilization of globular or three-dimensional structures for biological macromolecules. The hydrophobic amino acid residues of globular proteins are generally folded inside the structure or located in a few patches on the surface. As a protein is denatured, the buried amino acids are exposed, yielding more sites for hydrophobic binding. The hydrophobic interaction system thus encounters primarily surface amino acids—far fewer hydrophobic residues than the reversed phase.

SUPPORTS

Bonded phases for HIC consist of a hydrophilic polymeric layer into which hydrophobic ligands are inserted. The hydrophilic layer totally covers the silica or polymer matrix, providing a wettable and non-interactive surface which is neutral to the protein. In HIC, even short ligands cause substantial binding and there is a definite relationship between ligand chain length and retention, contrary to the minimal effect of chain length observed in the RPC of proteins and peptides. The ligand chains are postulated either to interact with hydrophobic surface patches on the proteins or to be inserted into their hydrophobic pockets; it is the latter interaction which is strengthened by and related to chain length. The strength of the binding causes some proteins to bind irreversibly if the ligand is too long; therefore, most ligands are either aromatic or 1–3 carbon alkyl chains.

Because HIC supports are designed for macromolecules, they either possess pore diameters of at least 300 Å to allow inclusion or are non-porous. Both silica and polymer matrices are used because the hydrophilic polymeric coating minimizes or eliminates most matrix—based effects. The absolute retention and selectivity of an HIC support may be affected by the specific composition of the bonded phase, as well as the ligand. For example, protein mixtures have shown distinct selectivity on different HIC columns which have propyl functional groups.[5]

OPERATION

Mobile Phase

In HIC, the concept of weak and strong solvents is different than in other modes because the weak solvent, or the one

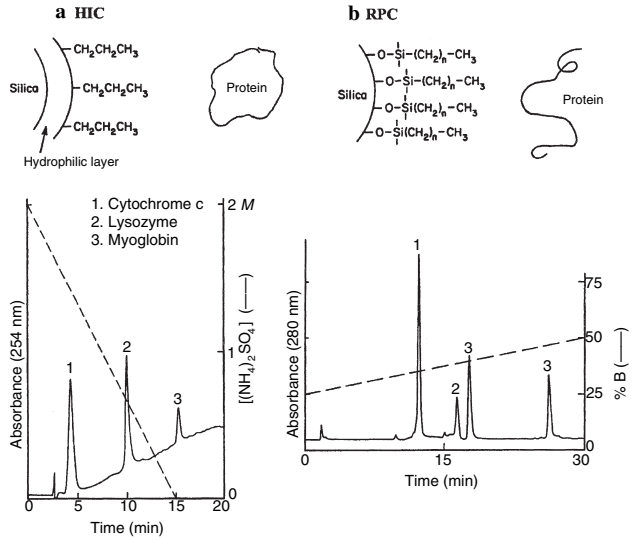

Fig. 1 (a) SynChropak Propyl; 15 min gradient from 2–0 *M* $(NH_4)_2SO_4$ in 0.1 *M* potassium phosphate, pH 6.8. (b) SynChropak RPP (C_{18}); 30 min gradient from 25% to 50% ACN with 0.1% TFA.
Source: Used with permission of Eichrom.

which promotes binding, is that containing high-salt concentration. The strong solvent, or one which causes elution, is that with low-salt concentration.

Salt

The most important variable in HIC retention, other than the ligand chain, is the composition of the salt used to promote binding. The effectiveness is based on the molal surface tension increment, which is parallel to the Hofmeister salting-out series for precipitation of proteins. The strength of HIC binding for some commonly used salts is K_3citrate > Na_2SO_4 > $(NH_4)_2SO_4$ > Na_2HPO_4 > NaCl.

Although potassium citrate and sodium sulfate cause stronger retention, ammonium sulfate is probably the most popular choice for HIC. Besides being effective for retention, it is highly soluble, stabilizing for enzymes, and resistant to microbial growth. Ammonium sulfate is available in high purity because of its use for salt fractionation. Sodium sulfate is less soluble and may precipitate under conditions of high concentration. The initial concentration of salt must be at a level high enough to cause binding of all the proteins to the bonded phase to avoid variable retention of early eluting peaks, which may also be broad.[6] Most proteins will bind when 2 *M* ammonium sulfate is used. In HIC, the concentration of antichaotropic salt is proportional to log *k*, as has been shown for conalbumin in four different salts.[7] The exact relationship varies for each salt, as well as for the specific protein.

pH

In HIC, the mobile phase should be buffered to provide control of ionization because amino acids which are not ionized are more hydrophobic than those which are charged. The effect of pH on hydrophobicity produces some variation of retention with pH; however, it is not directly related to the p*I* of the analyte because only surface amino acids interact with the ligands. In a study of the effect of pH on retention by HIC for a series of lysozymes from different bird species, those containing histidine residues in the hydrophobic contact region exhibited deviation for pH values of 6–8, which is near the p*K* of histidine (pK = 6).[7]

Additives

Because HIC is based on surface-tension phenomena, changing those characteristics by the addition of surfactants affects retention. In a study of the effects of surfactants on retention of proteins by HIC, the addition of CHAPS {3-[(3-cholamidopropyl) dimethylammonio]-1-propane sulfonate} to the mobile phase resulted in shortened retention, improvement of peak shape, and a change in peak order for enolase and bovine pancreatic trypsin inhibitor.[8] The effects were dependent on the concentration of the surfactant. Surfactants can usually be washed easily from hydrophobic interaction columns because the bonded phases are neither highly hydrophobic nor ionic.

The hydrophobic basis of HIC means that alcohols may reduce interaction with supports; however, disruption of protein conformation may also occur. Because of the high salt concentrations used in HIC, organic solvents should only be added after compatibility with the mobile phase has been tested to ensure that precipitation will not take place. Generally, no more 2 Hydrophobic Interaction Chromatography than 10% organic is added. Other additives that increase the stability of a given protein can often be included in the mobile phase for HIC without adversely changing the separation.

Flow Rate and Gradient

Almost all HIC separations are performed in the gradient mode because proteins bind with multipoint interactions. The flow rate and gradient have an effect on retention in HIC because HIC follows the linear solvent strength model.[9] The time of the gradient is another determinant in improving resolution in that longer gradients provide increased resolution. Generally, a 20–60 min gradient from 2–0 *M* ammonium sulfate in

0.02 *M* buffer at neutral pH, with a moderate flow rate (1 ml/min for a 4.6 mm I.D.), will provide a satisfactory starting point for an HIC analysis.[1]

Temperature

Hydrophobic interaction chromatography is different than other modes of chromatography in that it is an entropy-driven process, characterized by increased retention with increased temperature. This is a major benefit when subambient temperatures must be used to preserve the structure and biological activity of labile proteins. Retention is usually decreased rather than increased as temperatures are lowered. In one study, the retention of lysozyme was relatively unchanged throughout a temperature range 0–45°C, whereas bovine serum albumin exhibited two peaks which changed in proportion with temperature, as well as increased in retention.[10] Some of the increase in retention with elevated temperatures, in this or other studies, can be attributed to protein unfolding and the increased exposure of internal hydrophobic residues, especially when peak broadening also occurs.

Loading

Loading capacities for proteins on HIC columns are quite high because proteins retain their globular forms during the procedure.[1,4] High loading is generally accompanied by high recoveries of biological activity. Dynamic and absolute loading capacities of HIC supports are in the range of 10 mg/ml and 30 mg/ml, respectively. Loading is also related to the relative sizes of the pore diameter and the solute, with 300 Å giving maximum capacity for many proteins.

APPLICATIONS

The primary application for HIC has been in protein analysis and purification due to the good selectivity and preservation of biological activity.[1–4] Because of the major differences in selectivity, HIC can be used as an orthogonal technique to RPC, as well as to ionexchange and size-exclusion chromatography.

Although the best high-performance liquid chromatography (HPLC) method for peptide analysis is RPC, HIC offers a different selectivity for those peptides possessing three-dimensional conformations under high-salt conditions. When the separations of peptide mixtures by HIC and RPC have been compared, peaks were generally narrower on RPC due to the organic mobile phase. In a study of calcitonin variants, it was seen that peptides with certain amino acid substitutions could not be resolved by RPC, but were separated by HIC.[11] The main utility of HIC for peptide separations seems to lie in applications for extremely hydrophilic or hydrophobic peptides, or those with three-dimensional structures stable in high salt.

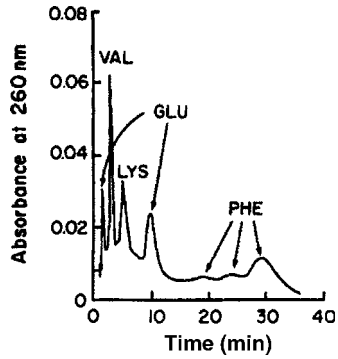

Fig. 2 Column: Polyol HIC, 100 nm; mobile phase: 0.7 *M* disodium hydrogen phosphate, pH 6.3.
Source: From High-performance liquid chromatography of tRNAs on novel stationary phases, in J. Chromatogr.[12]

The separation of nucleic acids, particularly t-RNA, has been another useful application of HIC for biological macromolecules. The tertiary structure of t-RNA has made analysis under the gentle conditions of HIC very feasible.[12] Fig. 2 shows an example of the purification of t-RNA molecules specific for different amino acids on a 100 nm polyol HIC column. Separation of t-RNA molecules has also been accomplished successfully by using HIC conditions on supports with alkylamino ligands, which are functionally similar to those traditionally used to separate nucleic acids.[1]

CONCLUSIONS

Hydrophobic interaction chromatography is a mode of chromatography particularly effective for the analysis of proteins and other macromolecules. The hydrophobic interactions are primarily with non-polar groups on the surface of the analytes due to maintenance of the tertiary structure. High loading and recovery of both mass and biological activity are achieved.

REFERENCES

1. Cunico, R.L.; Gooding, K.M. Hydrophobic interaction chromatography. In *Basic HPLC and CE of Biomolecules*; Bay Bioanalytical Laboratories: Richmond, CA, 1998.

2. Shansky, R.E.; Wu, S.-L.; Figueroa, A.; Karger, B.L. Hydrophobic interaction chromatography of proteins. In *HPLC of Biological Macromolecules*; Gooding, K.M., Regnier, F.E., Eds.; Marcel Dekker, Inc.: New York, 1990; 95.
3. Aguilar, M.I.; Hearn, M.T.W. Reversed-phase and hydrophobic-interaction chromatography of proteins. In *HPLC of Proteins, Peptides and Polynucleotides*; Hearn, M.T.W., Ed.; VCH: New York, 1991; 247.
4. Ingraham, R.H. Hydrophobic interaction chromatography of proteins. In *High-Performance Liquid Chromatography of Peptides and Proteins*; Mant, C.T., Hodges, R.S., Eds.; CRC Press: Boca Raton, FL, 1991; 425.
5. Alpert, A.J. High-performance hydrophobic-interaction chromatography of proteins on a series of poly(alkyl aspart-amide)-silicas. J. Chromatogr. **1986**, *359*, 85.
6. Kato, Y.; Kitamura, T.; Nakatani, S.; Hashimoto, T. High-performance hydrophobic interaction chromatography of proteins on a pellicular support based on hydrophilic resin. J. Chromatogr. **1989**, *483*, 401.
7. Fausnaugh, J.L.; Regnier, F.E. Solute and mobile phase contributions to retention in hydrophobic interaction chromatography of proteins. J. Chromatogr. **1986**, *359*, 131.
8. Wetlaufer, D.B.; Koenigbauer, M.R. Surfactant-mediated protein hydrophobic-interaction chromatography. J. Chromatogr. **1986**, *359*, 55.
9. Snyder, L.R. Gradient elution separation of large biomolecules. In *HPLC of Biological Macromolecules*; Gooding, K.M., Regnier, F.E., Eds.; Marcel Dekker, Inc: NewYork, 1990; 95.
10. Goheen, S.C.; Engelhorn, S.C. Hydrophobic interaction high-performance liquid chromatography of proteins. J. Chromatogr. **1984**, *317*, 55.
11. Heinitz, M.L.; Flanigin, E.; Orlowski, R.C.; Regnier, F.E. Correlation of calcitonin structure with chromatographic retention in high-performance liquid chromatography. J. Chromatogr. **1988**, *443*, 229.
12. El Rassi, Z.; Horvath, Cs. High-performance liquid chromatography of tRNAs on novel stationary phases. J. Chromatogr. **1985**, *326*, 79.

Hydroxy Compounds: Derivatization for GC Analysis

Igor G. Zenkevich
Chemical Research Institute, St. Petersburg State University, St. Petersburg, Russia

Abstract
The hydroxyl group is one of the most propagated functional groups in organic compounds, including numerous biogenic substances. The determination of OH compounds has been one of the important problems of gas chromatography (GC) analysis in more than half a century that this method has been in existence.

The main classes of hydroxy compounds are aliphatic alcohols with OH groups attached to sp^3 hybridized carbon atoms and phenols, in which the OH groups are attached to sp^2 carbon atoms located in the aromatic systems. Another group of hydroxy compounds—namely, the carboxylic acids, having the structural fragment COOH—is discussed separately.

Even the simplest bifunctional compounds of these classes being analyzed on non-polar phases show broad non-symmetrical peaks on chromatograms. This leads to low detection limits and bad reproducibility of RIs (the position of the peaks' maxima strongly depends on the quantities of analytes) as compared with non-polar compounds. The general method to avoid all of the above-mentioned problems is based on the conversion of hydroxy compounds to less polar and thermally stable volatile derivatives. The less polar products typically yield narrower chromatographic peaks, which provide better signal-to-noise ratio and, hence, lower detection limits. Non-polar derivatives have much better interlaboratory reproducibility of RIs compared with initially polar compounds.

Most important types of organic reactions used in derivatization of hydroxy compounds are silylation (a kind of etherification), acylation (esterification), and alkylation (preferably used for phenols).

INTRODUCTION

The hydroxyl group is one of the most propagated functional groups in organic compounds. Important biogenic substances (carbohydrates, phenolic acids, flavones, etc.) belong to the class of hydroxy compounds. One of the principal methods of metabolism of different ecotoxicants and drugs in vivo is their hydroxylation followed by the formation of conjugates with carbohydrates, sulfuric, or amino acids. For example, the bio-oxidation of the widespread environmental pollutants polychlorinated biphenyls (PCBs) leads to hydroxy-PCBs.[1] The determination of OH compounds has been one of the important challenges in gas chromatographic (GC) analysis for more than half a century that this method has been in existence.

The main classes of hydroxy compounds are aliphatic alcohols with OH groups attached to sp^3-hybridized carbon atoms, and phenols, in which the OH groups are located in the aromatic systems attached to sp^2 carbon atoms. Some carbonyl compounds (preferably having a few C═O groups, like 2,4-alkanediones, ketocarboxylic acids and their esters, 1,2- and 1,3-cycloalkanediones) exist in equilibrium with their corresponding enols in accordance with the general scheme $-CH_2-CO- \rightleftarrows -CH{=}C(OH)-$, which implies the presence of hydroxyl groups in these molecules as well. Another type of hydroxy compounds, namely, the carboxylic acids—having the structural fragment CO_2H—are discussed separately in another entry (see *Acids: Derivatization for GC Analysis*, p. 3).

A simple rule for predicting the possibility of GC analysis of organic compounds is based on the reference data on their boiling points. If any compound can be distilled without decomposition at pressures ranging from atmospheric to 0.01–0.1 Torr, it can be subjected to GC analysis at least on standard non-polar polydimethyl siloxane stationary phases. Thus, most of the monofunctional hydroxy compounds, as well as their *S*-analogues (thiols, thiophenols) can be analyzed directly. The confirmation of chromatographic properties of any analyte should not only be verbal (at the binary "yes/no" level) but also indicate its GC retention index (RI) as the most objective criteria, as illustrated in Table 1.

The chemical properties of hydroxy compounds depend on the presence of active hydrogen atoms in the molecule. The pK_a values of aliphatic alcohols are 70 comparable to that of water (≈16), but phenols having weak acidic properties are characterized by $pK_a \approx 9–10$. Enols of carbonyl compounds are also usually weak acids.

An increase in the number of polar functional groups in the molecules leads to an increase in the strength of intermolecular interactions. This is manifested as a rise in melting and boiling points of compounds. For example, some aliphatic diols and triols have boiling points at atmospheric pressure and, hence, are volatile enough for GC analysis. Similar compounds with four or more hydroxyl groups have

Table 1 Physicochemical (boiling point) and chromatographic (RI) characteristics of some compounds with single hydroxy group and their thio-analogs.

Compound	T_b, °C	$RI_{non\text{-}polar}$
1-Tetradecanol	290.8	1664 ± 12
4-Methyl-2,6-di-*tert*-butyl phenol	265	1491 ± 10
1-Decanethiol	239.2	1320
2-Methylbenzenethiol	194	1061 ± 11

no boiling points at atmospheric pressure, which means that their GC analysis is impossible. The same restrictions are valid for the series of polyfunctional phenols Table 2.

Even the simplest bifunctional compounds of these classes when analyzed on non-polar phases show broad non-symmetrical peaks on chromatograms. This leads to low detection limits and bad reproducibility of RIs, because the position of the peaks' maxima strongly depend on the quantity of the analyte relative to the quantity of the non-polar compound. A general method to avoid all of the above-mentioned problems is based on the conversion of hydroxy compounds to their thermally stable and less polar volatile derivatives. This task is one of the most important prerequisites to GC analysis. This chemical treatment may be used not only for non-volatile compounds, but also for the so-called semivolatile substances. The less polar products typically yield narrower chromatographic peaks, which provide better signal-to-noise ratios and, hence, lower detection limits. Non-polar derivatives have much better interlaboratory reproducibility of RIs compared with initially polar compounds.

METHODS OF DERIVATIZATION OF HYDROXY COMPOUNDS

The principal methods used for the derivatization of hydroxy compounds may be classified on the basis of the following types of chemical reactions:

Table 2 Physicochemical and chromatographic characteristics of some polyhydroxy compounds.

Compound	Number of OH groups	T_b, °C	$RI_{non\text{-}polar}$
Glycerol	3	290.5	1196 ± 28
meso-Erythrol	4	329–331	≈1320
Xylitol	5	None	None
Hydroquinone	2	287	1338 ± 14
Pyrogallol	3	309	1420–1550
1,2,4-Benzenetriol	3	None	None

$$\text{Sylilation}: R(OH)_n + XSi(CH_3)_3 \rightarrow R(OTMS)_3 + nXH[TMS = Si(CH_3)_3]$$
$$\text{Acylation}: R(OH)_n + nR'COX + nB \rightarrow R(OCOR')_n + nBH^+X^-$$
$$\text{Alkylation}: R(OH)_n + nR'X \rightarrow R(OR')_n + nXH$$

where the generally accepted codification of structural fragment *X* is as the carrier of the target silyl, acyl, or alkyl chemical functions.

The experimental details of these derivatization reactions are presented in some well-known specialized texts.[2–5] The first two reactions mentioned are sensitive to the presence of water in the samples (typical silylation and acylation reagents react with water more quickly than with the target organic compounds) and usually cannot proceed in aqueous media. The analysis in these conditions typically requires special sample preparation (drying before derivatization).

The large group of silylation reactions [trimethylsilyl (TMS) derivatives are the most widely used] involve the replacement of active hydrogen atoms in molecules of analytes by silyl groups donated by different *O*-, *N*-, or *C*-silylating reagents. The reaction order of the OH compound's reactivity in general is *prim*-OH > *sec*-OH > *tert*-OH ≈ Ar-OH > R-SH. The first part of Table 3 includes physicochemical and GC constants of different reagents in the approximate order of increasing silyl donor strength. The second part of this table presents compounds later introduced into analytical practice, with still unestimated relative silylation activity, as well as a few non-TMS reagents. Besides the individual chemicals, their different combinations are known as the so-called silylating mixtures, e.g., hexamethyldisilazane (HMDS) + trimethyl chlorosilane (TMCS) or HMDS + dimethyl formamide (DMFA). The triple mixture *bis*-TMS-acetamide (BSA)/TMS-imidazole (TMSI)/TMCS (1:1:1 v/v) seems to be the most active currently known silylating agent. It can be used for the derivatization of all types of substances with active hydrogen atoms, including enols of carbonyl compounds and even *aci*-forms of aliphatic nitro compounds. To illustrate the "popularity" of silylating mixtures, it should be mentioned that more than a dozen such mixtures are presented in Sigma-Aldrich catalogs at present.[6]

Some reagents in Table 3 are characterized not only by their own RI, but also by the RI values of the principal by-products of the reaction. This permits us to predict the possible overlapping of their chromatographic peaks with signals of derivatives of the target analytes.

The list of recommended silylating compounds is constantly changing. Some older reagents get replaced by more effective ones. Most of them, depending on the chemical nature of the carrier of TMS groups, are classified as *N*- or *O*-silylating agents. At the same time it is important to note the increasingly frequent application of different *C*-silylating agents, like ethyl(trimethylsilyl)acetate (ETSA) or allyl trimethyl silane (Allyl-TMS). The

Table 3 Physicochemical and gas chromatographic properties of some silylating derivatization reagents.

Reagent	Abbreviation	MW	T_b, °C (P)	$RI_{non\text{-}polar}$	By-products ($RI_{non\text{-}polar}$)[a]
Most widely used reagents (in order of increasing silyl donor strength)					
Hexamethyldisilazane	HMDS	161	126	817 ± 29	NH_3 (ND)[b]
Trimethylchlorosilane	TMCS	108	57.7	560 ± 8	HCl (ND)
N-Methyl-*N*-trimethylsilyl acetamide	MSA	145	159–161	947 ± 14	$CH_3CONHCH_3$ (816 ± 22)
N-Trimethylsilyl diethylamine	TMSDEA	145	125–126	817 ± 11[c]	$(C_2H_5)_2NH$ (548 ± 8)
N-Trimethylsilyl dimethylamine	TMSDMA	117	84	660 ± 4[c]	$(CH_3)_2NH$ (425 ± 16)
N-Methyl-*N*-trimethylsilyl trifluoroacetamide	MSTFA	199	130–132	826 ± 3[c]	$CF_3CONHCH_3$ (540)
N,*O-bis*-Trimethylsilyl acetamide	BSA	203	71–73 (35)	1008[c]	CH_3CONH_2 (711 ± 19)
N,*O-bis*-Trimethylsilyl trifluoroacetamide	BSTFA	257	145–147	887[c]	CF_3CONH_2 (675 ± 11)
N-Trimethylsilyl imidazole	TMSI	140	222–223	11786 ± 18[c]	Imidazole (1072 ± 17)
Later-proposed and special reagents (in order of increasing molecular weights)					
Allyl trimethyl silane	Allyl-TMS	114	85–86	650 ± 2	Propene (290 ± 3)
2-(Trimethylsilyloxy)propene	IPOTMS	130	—	675 ± 12	Acetone (472 ± 12)
Chloromethyldimethyl chlorosilane	CMDCS	142	114	755 ± 8[c]	HCl (ND)
N-Trimethylsilyl pyrrolidine	TMSP	143	139–140	862 ± 5[c]	Pyrrolidine (686 ± 10)
Dimethyl-*tert*-butyl chlorosilane	TBDMS-Cl	150	125	729 ± 11[c]	HCl (ND)
Ethyl trimethylsilylacetate	ETSA	160	156–159	930 ± 5[c]	$CH_3CO_2C_2H_5$ (602 ± 9)
bis-Trimethylsilyl methylamine	BSMA	175	144–147	903 ± 18[c]	CH_3NH_2 (348 ± 12)
Trimethylsilyl trifluoroacetate	TNSTFA	186	88–90	674 ± 5[c]	CF_3CO_2H (744 ± 6)
Bromomethyldimethyl chlorosilane	BMDMS	186	—	842 ± 14[c]	HCl (ND)
bis-Trimethylsilyl formamide	BSFA	189	158	948 ± 14[c]	$HCONH_2$ (637 ± 6)
bis-Trimethylsilyl urea	BSU	204	—	1237 ± 11	$CO(NH_2)_2$ (ND)
N,*O-bis*-Trimethylsilyl carbamate	—	205	77–78 (mp)[d]	—	H_2NCO_2H[e], NH_3, CO_2 (ND)
N-methoxy-*N*,*O-bis*-TMS carbamate	BSMOC	235	—	1156 ± 18[c]	CH_3ONHCO_2H (ND)
Trimethylsilyl trifluoromethanesulfonate	—	222	77 (80)	—	CF_3SO_2OH (ND)
Dimethyl-*tert*-butylsilyl trifluoroacetamide	MTBSTFA	241	168–170	996 ± 13[c]	CF_3CONH_2 (675 ± 11)
Dimethylpentafluorophenyl chlorosilane (in the mixture with dimethylpentafluorophenylsilyl amine, 1:1 v/v)[f]	—	260	88–90 (10)	—	HCl (ND)
N-Methyl-*N*-trimethylsilyl heptafluorobutanamide	MSHFBA	299	148	906 ± 11[c]	$C_3F_7CONH_2$ (750 ± 18)

[a] Common hydrolysis by-products for all reagents are trimethylsilanol $(CH_3)_3SiOH$ (RI 584 ± 8) or dimethyl-*tert*-butyl silanol (RI 753 ± 18[c]).
[b] ND: by-product is not detectable after formation of non-volatile salts with bases (HCl) or acids (NH_3).
[c] Estimated RI values.
[d] Melting point.
[e] Semisilylated by-products like $H_2NCO_2Si(CH_3)_3$ can be observed.
[f] An example of silylating mixtures.

last-mentioned reagent, in the silylation reaction, forms a single gaseous product: propene. Besides that, this reagent indicates highest chemical selectivity in relation to substrates of different chemical origin: it reacts only with alcohols and acids, but has no influence on phenols, thiols, and amines.

Keeping in mind the possible variety of substrates used for silylation, it is not so simple to reliably characterize the differing activity of various silylation reagents. So far the typical form of presentation of such information includes a semiquantitative description (e.g., "++"—good silylation; "+"—silylation is possible, "−"—no reaction

Table 4 Some examples of the recommendations on the use of some silylating reagents.

Reagent (abbreviation)	Special comments	Applicability for different classes of compounds				
		Alcohols	Phenols	Acids	Thiols	Amines
BSA	Reactive, universal	++	++	++	+	++
BSTFA	Highly reactive	++	++	++	+	++
HMDS	Gaseous by-product formed	++	++	+	+	+
MSA	Can act as a solvent for polar compounds	++	++	++	−	+
MSTFA	Highly reactive	++	++	++	+	++
TMCS	Universal	++	++	++	+	+
TMSDEA	Volatile by-products formed, selective for equatorial hydroxyl groups	++	++	++	+	++
TMSA	Highly reactive, discriminates amino groups	++	++	++	++	−
Allyl-TMS	Only propene formed as by-product	++	−	++	−	−

Symbolism: "++" represents good silylation,"+" represents silylation is possible, "−" represents no reaction observed.
Source: From Derivatization reagents, in Sigma-Aldrich Analytix.[6]

observed) supplemented by some verbal comments, as demonstrated by Table 4.[6]

Another way of simplifying the visual perception of information about derivatization reaction for users is to list recommended reagents for different classes of organic compounds, supplemented by short comments on important details of the processes. Some examples of this form, for selected hydroxy compounds, are presented in Table 5.[7]

Standard electron impact (EI) mass spectra of TMS derivatives of aliphatic hydroxy compounds register no peaks of molecular ions M^+, but in many cases, signals of ions $[M\text{-}CH_3]^+$ are reliably registered. The same derivatives of phenols and enols of carbonyl compounds with –p conjugated system C═C–O in the molecules register the signals of M^+ or higher intensities. Typical base peaks in the mass spectra of *O*-TMS derivatives are $[Si(CH_3)_3]^+$ (*m*/*z* 73) and, sometimes, $[Si(CH_3)_2OH]^+$ (*m*/*z* 75). For example, in Fig. 1, the mass spectrum of *tris*-TMS ether of glycerol (Fig. 1a) is compared with that of *bis*-TMS derivative of acetoacetic acid ($CH_3COCH_2CO_2H$, enol form, Fig. 1b). The signal of molecular ions with MW 308 is absent in the former, while signal with MW 246 is distinctly registered in the latter.

The principal disadvantage of TMS derivatives is their easy postreaction hydrolysis. Most of these compounds cannot exist in aqueous media. If stability is important, another type of derivatives, namely dimethyl-*tert*-butylsilyl, that has approximately 10^3 times lower hydrolysis constants owing to sterical hindrance of Si–O bonds by

Table 5 Some examples of the form of presentation of the recommendations on the selection of derivatization reagents for different classes of organic compounds.

Class of compounds or type of functional groups	Type of derivatization	Reagent(s) (abbreviation)	Additional notes
Hydroxyl groups in alcohols and phenols	Silylation	BSA, BSTFA, BSTFA + TMCS, HMDS, MSTFA, MSTFA + TMCS	Most often used derivatives; Good thermal stability
		TMCS	Usually used in combination with HMDS; can be used for salts
		TMSI	Can be used with some syrups
		MTBSTFA	More stable than TMS, good MS fragmentation patterns
	Acylation	MBTFA, TFAA, TFAI, PFAA, HFBI, HFAA	Good for trace analysis with ECD
	Alkylation	PFB-Br	With alkoxides only
Carbohydrates	Silylation	MSTFA, TMSI	Can be used with some syrups
	Acylation	MBTFA,TFAI	Applicable to *mono*-, *di*-, and *tri*-saccharides

Source: From *Chromatography Catalog and Handbook*.[7]

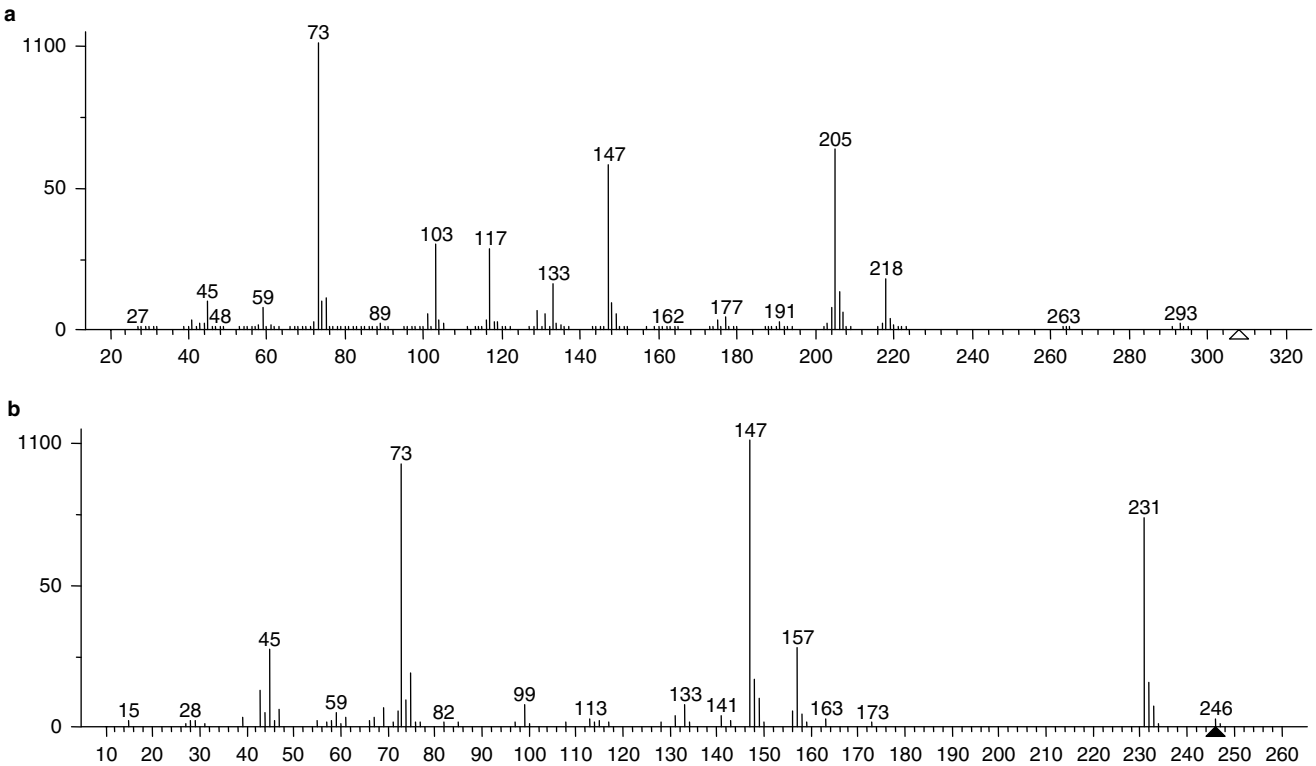

Fig. 1 Comparison of the mass spectrum of (a) *tris*-TMS ether of glycerol; (b) *bis*-TMS derivative of acetoacetic acid ($CH_3COCH_2CO_2H$, enol form).
Source: From NIST Chemistry Webbook, in NIST Standard Reference Database.[17]

tert-butyl groups, seems preferable.[8] Unfortunately, mass spectra of such derivatives are not very informative for the elucidation of structures of unknown analytes; the base peaks for most of them belong to non-characteristic ions $[C_4H_9]^+$ (*m/z* 57) and $[M\text{-}C_4H_9]^+$, but they are considered as "good MS fragmentation patterns" for identification of compounds with known mass spectra using MS library search techniques. Other trialkyl derivatives were

Table 6 Some reagents used for the analytical acylation of hydroxy compounds.

Reagent	Abbreviation	Derivatives
Acetic anhydride in the presence of (H^+) or bases	AA	$R(Ar)OCOCH_3$
Trifluoroacetic anhydride	TFAA	$R(Ar)OCOCF_3$
bis-Trifluoroacetyl methylamine	MBTFA	$R(Ar)OCOCF_3$
Trifluoroacetyl imidazole	TFAI	$R(Ar)OCOCF_3$
Pentafluoropropionic anhydride	PFPA	$R(Ar)OCOC_2F_5$
Heptafluorobutyric anhydride	HFBA	$R(Ar)OCOC_3F_7$
Pentafluorobenzoyl chloride	PFB-Cl	$R(Ar)OCOC_6F_5$
Chloroacetic anhydride	—	$R(Ar)OCOCH_2Cl$
Dichloroacetic anhydride or trichloroacetyl chloride	—	$R(Ar)OCOCHCl_2$
N-Trifluoroacetyl-L-prolyl chloride	*N*-TFA-L-Pro-Cl	*N*-TFA-L-Prolyl esters
Diethyl chlorophosphate	—	$R(Ar)OP(O)(OC_2H_5)_2$
2-Chloro-1,3,2-dioxaphospholane	—	2-Alkoxy(aryloxy)-1,3,2-dioxaphospholanes
$NaNO_2$ in the presence of (H^+); special derivatization of simplest C_1–C_4 aliphatic alcohols into volatile alkyl nitrites for head-space analysis	—	RONO

Source: From *Head-Space Analysis and Related Methods in Gas Chromatography*.[13]

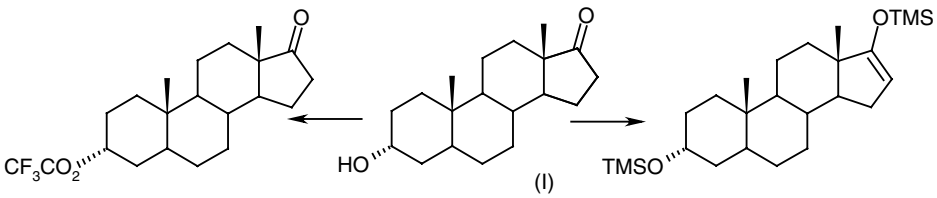

Fig. 2 Formation of *mono*- and *bis*-TMS derivatives by silylation of androsterone.

recommended for the derivatization of hydroxy compounds, but in practice, they are not easily available and are used rarely.[9]

Some halogenated silylating reagents are used in the synthesis of derivatives for GC analysis with selective (element-specific) detectors, e.g., $ClCH_2SiMe_2Cl$, $BrCH_2SiMe_2Cl$, and $C_6F_5SiMe_2Cl$ in electron capture detection. In nitrogen/phosphorus (NP)-selective flame photometric detectors, the conversion of hydroxy compounds into 2-cyanoethyldimethylsilyl derivatives using $(C_2H_5)_2N–Si(CH_3)_2–CH_2CH_2CN$ (2-cyanoethyldimethyl-silyl diethylamine) as reagent is recommended.[10]

Polyfunctional hydroxy compounds, according to the general principles of derivatization, require the modification of all functional groups in their molecules. For instance, within the important group of hydroxy carbonyl compounds, the steroids, all carbonyls prior to silylation should be converted to alkoxyimino fragments $C{=}O \rightarrow C{=}N–OR$ or hydroxylamino fragments with following silylation: $C{=}O \rightarrow C{=}N–OH \rightarrow C{=}N–O–SiMe_3$ (the same methods are used for carbohydrates). Besides, there is a single-step method for the derivatization of steroids in which treatment with the most active silylation reagents leads to the formation of *per*-TMS derivatives of enols. For selective derivatization of hydroxyl and carbonyl groups with varying reactivities in steroids, a great variety of reagents have been proposed.[2–5] These complex organic compounds with large retention parameters require fewer restrictions on the chemical origin of reagents. For example, one of them, namely *N*-methoxy-*N*,*O*-*bis*-TMS carbamate (BSMOC) [$CH_3O–N(TMS)CO_2TMS$], has an RI on standard non-polar phase of 1146 ± 9 and has been used for the derivatization of only carboxylic acids, selected sugars,[11] and steroids.[12]

The second group of hydroxy compound derivatization reactions includes acylation of OH groups with the formation of esters. The most important are listed in the Table 6.

It is recommended that these reactions be conducted in the presence of bases without active hydrogen atoms (pyridine, triethyl amine, etc.). These basic media are necessary for the conversion of acidic by-products into non-volatile salts to protect the acid-sensitive analytes from decomposition and to avoid the appearance of extra peaks of by-products on the chromatograms. Exceptions are indicated by "reagent/(H^+)." Phenols can be converted into Na salts before acylation. A large variety of anhydrides of perfluorinated carboxylic acids are recommended for derivatization because of the favorable chromatographic properties of perfluoroacyl derivatives.

The possible enolization of carbonyl compounds explains the significant discrepancies in the formation of different derivatives of polyfunctional compounds like hydroxy ketones (a typical combination of functional groups in steroids). For example, androsterone [androstan-3-ol-17-one (I)] after treatment by trifluoroacetylating reagents forms only *mono*-TFA derivatives, whereas after silylation it may form both *mono*- and *bis*-TMS derivatives (depending on the silylating strength of the reagent), as illustrated in Fig. 2.

The third group of derivatization reactions of hydroxy compounds for GC analysis involves the formation of their alkyl or substituted benzyl ethers (Table 7). A more comprehensive list of alkylating reagents is presented in *Acids: Derivatization for GC Analysis*.

Methylation by diazomethane is a simple method of derivatization of relatively acidic compounds like phenols (pK_a 9–10) or carboxylic acids (pK_a 4.4 ± 0.2). The

Table 7 Some reagents used for the alkylation of hydroxy compounds.

Reagent	Abbreviation	Derivatives
Diazomethane (as diethyl ether solution) in the presence of HBF_4	—	$ArOCH_3$
Methyl iodide in the presence of dimethylformamide (DMFA), K_2CO_3, BaO, etc.	—	$R(Ar)OCH_3$
Pentafluorobenzyl bromide	PFB-Br	$ArOCH_2C_6F_5$
3,5-*bis*-Trifluoromethylbenzyl dimethylanilinium fluoride (only for phenols during on-column injection)	BTBDMA-F	$ArOCH_2C_6H_3(CF_3)_2$

Source: From Development of 3,5-*bis*-(trifluoromethyl)benzyl-dimethylphenylammonium fluoride, an efficient new on-column derivatization reagent, in J. Chromatogr. A.[14]

Table 8 Some reagents used for the derivatization of polyhydroxy compounds.

Class of polyfunctional compounds	Reagent(s)	Derivatives
1,2-Diols	Acetone/(H^+)	2,2-Dimethyl-1,3-dioxolanes
	Methane (R = CH_3), butane (R = C_4H_9), or benzene (R = C_6H_5), boronic acids, $RB(OH)_2$	2-Methyl(butyl, phenyl)-1,3,2-dioxaborolanes (methyl, butyl, or phenyl boronates)
2-Amino alcohols	Methane (R = CH_3), butane (R = C_4H_9), or benzene (R = C_6H_5), boronic acids, $RB(OH)_2$	2-Methyl(butyl, phenyl)-1,3,2-oxazaborolanes
1,2-Benzenediols	Di-*tert*-butyl dichlorosilane	Di-*tert*-butyl silylene derivatives

Source: From Cyclic di-*tert*-butyl silylene derivatives of substituted salicylic acids and related compounds. A study by gas chromatography–mass spectrometry, in J. Chromatogr.[15]

application of this reagent for methylation of aliphatic alcohols needs additional acid catalysis. Methyl iodide is the most suitable reagent for the synthesis of permethylated derivatives of polyols (including carbohydrates) and phenols. Dimethyl sulfate $(CH_3O)_2SO_2$ can be used in basic media for the methylation of phenols, but the yields of methyl ethers in this case are not sufficient for the quantitative determination of initial compounds by GC.

Some special derivatization methods that lead to the formation of cyclic products were recommended for alcohols with more than two hydroxyl groups in the molecule (polyols including carbohydrates), amino alcohols, and polyfunctional aromatic hydroxy compounds. An appropriate arrangement of two functional groups [$(OH)_2$, (OH) + (NH_2) or (OH) + (CO_2H)] in 1,2 (*vic*); 1,3; or *ortho* (in aromatic series) positions is necessary for their realization (Table 8).

The simplest reagent of this type, widely used for the derivatization of *vic*-polyols, is acetone in the presence of water-coupling additives. The resultant isopropylidene derivatives (2,2-dimethyl-1,3-dioxolanes), similar to TMS ethers, usually indicate no signals of molecular ions, but signals of $[M\text{-}CH_3]^+$ ions are informative. As an example, the standard mass spectrum of *tris*-1,2:3,4:5,6-isopropylidene derivative of mannitol (Fig. 3) (MW 302) is presented in Fig. 4.

The choice of chemical reactions available for the derivatization of hydroxy compounds in aqueous samples (when it is impossible to remove the large excess of water) is relatively limited compared with the whole range of derivatization reactions. For example, hydrophilic and polar compounds such as monoethanolamine (MEA), $HOCH_2CH_2NH_2$, require derivatization prior to GC analysis, but can be preconcentrated from the air of industrial areas only as a mixture with water (owing to air humidity). A suitable method for the derivatization of MEA is based on its interaction with benzaldehyde in water media. This reaction produces the corresponding Schiff base $HOCH_2CH_2N{=}CHC_6H_5$, which can exist in the tautomeric cyclic form, namely, 2-phenyloxazolidine.[16]

The number of proposed methods of derivatization for alcoholic and phenolic *S*-analogues in GC analysis is significantly smaller than that for alcohols, because, in actual practice, the former compounds are analyzed less frequently. As per general recommendations, thiols and thiophenols may be converted into TFA (PFP, HFB) esters, or PFB ethers (*S*-TMS derivatives seem not to be as stable as *O*-TMS ethers). Derivatization of these compounds is necessary not only for the optimization of their chromatographic parameters, but also to prevent their easy oxidation by atmospheric oxygen dissolved in the liquid samples before analysis.

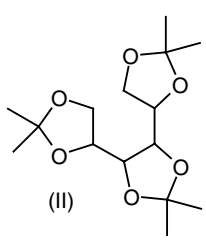

Fig. 3 Molecular structure of *tris*-1,2:3,4:5,6-isopropylidene derivative of mannitol (MW 302).

CONCLUSIONS

The simplest monofunctional hydroxy compounds are stable and volatile enough for direct GC analysis. However, the polyfunctional compounds of this class, owing to their high polarity and low volatility, usually cannot be analyzed in their native form. Hence their derivatization by various reagents is not only strongly recommended, but it is a generally accepted and routine procedure of sample preparation for GC analysis at present.

Besides the optimization of retention parameters and peak shaping, an additional function of derivatization is the protection of analytes from chemical transformation, which is most important for *S*-analogues of hydroxy compounds.

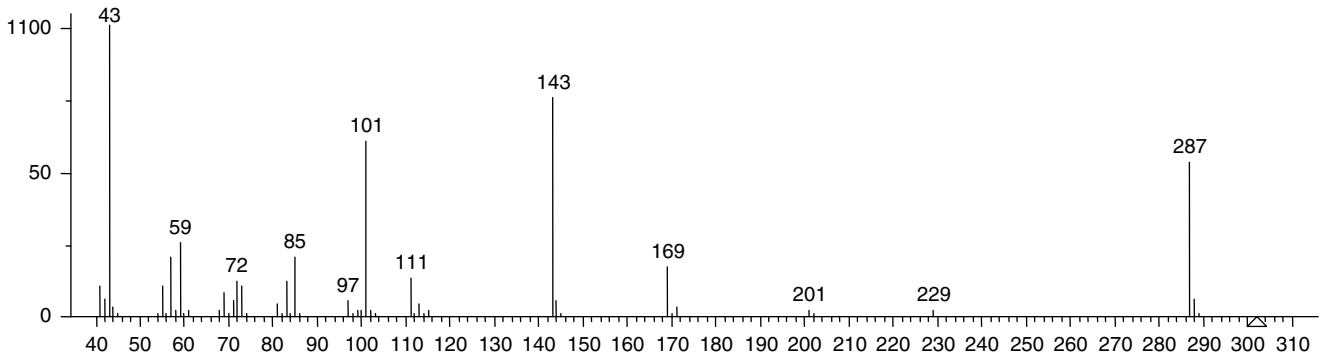

Fig. 4 Standard mass spectrum of *tris*-1,2:3,4:5,6-isopropylidene derivative of mannitol.
Source: From NIST Chemistry Webbook, in NIST Standard Reference Database.[17]

REFERENCES

1. Zenkevich, I.G.; Moeder, M.; Koeller, G.; Schrader, S. Using new structurally related additive schemes in the precalculation of GC retention indices of polychlorinated biphenyls on HP-5 stationary phase. J. Chromatogr. A, **2004**, *1025*, 227–236.
2. Blau, K.; King, G.S., Eds.; *Handbook of Derivatives for Chromatography*; John Wiley & Sons: Chichester. U.K., 1978; 576.
3. Knapp, D.R. *Handbook of Analytical Derivatization Reactions*; John Wiley & Sons: New York, 1979; 741.
4. Drozd, J. Chemical derivatization in gas chromatography. In *Journal of Chromatography Library; Elsevier: Amsterdam, 1981; Vol. 19, 232.*
5. Blau, K.; Halket, J.M., Eds.; *Handbook of Derivatives for Chromatography*, 2nd Ed.; John Wiley & Sons: New York, 1993; 369.
6. Derivatization reagents. In Sigma-Aldrich Analytix. **2002**, *3*, 8. http://www.sigma-aldrich.com/new (accessed September 2008).
7. Chromatography Catalog and Handbook. Pierce Biotechnology Inc., Illinois, U.S.A, 2003; 89.
8. Schoene, K.; Bruckert, H.-J.; Steinhanses, J.; Konig, A. Two-stage derivatization with *N-tert*-butyldimethylsilyl/-*N*-methyl-trifluoroacetamide—MTBSTFA—and *N*-methyl-*bis*-/trifluor-oacetamide—MBTFA—for the gas chromatographic analysis of OH-, SH- and NH-compounds. Fresenius J. Anal. Chem. **1994**, *348*, 364–370.
9. Poole, C.F.; Zlatkis, A.Trialkylsilyl ether derivatives (other than TMS) for gas chromatography and mass spectrometry. J. Chromatogr. Sci. **1979**, *17* (3), 115–123.
10. Bertrand, M.J.; Stefanidis, S.; Sarracin, B. 2-Cyano ethyl dimethyl(diethyl)amino silane, a silylating reagent for selective GC analysis using a nitrogen-phosphorus detector. J. Chromatogr. **1986**, *351*, 47–56.
11. Morvai-Vitanyi, M.; Molnar-Perl, I.; Knausz, D.; Sass, P. Simultaneous GC derivatization and quantification of acids and sugars. Chromatographia **1993**, *36*, 204–206.
12. Szederkenyi, F.; Ambrus, G.; Horvat, G.; Ilkov, E. *N*-Methoxy *N*,*O-bis*-TMS carbamate as a derivatization reagent for the gas chromatography of sitosterol degradation products. J. Chromatogr. **1988**, *446*, 253–257.
13. Ioffe, B.V.; Vitenberg, A.G. *Head-Space Analysis and Related Methods in Gas Chromatography*; Wiley-Interscience Publishers: New York, 1984; 276.
14. Amijee, M.; Cheung, J.; Wells, R.J. Development of 3,5-*bis*-(trifluoromethyl)benzyl-dimethylphenylammonium fluoride, an efficient new on-column derivatization reagent. J. Chromatogr. A, **1996**, *738*, 57–72.
15. Brooks, C.J.W.; Cole, W.T. Cyclic di-*tert*-butyl silylene derivatives of substituted salicylic acids and related compounds. A study by gas chromatography–mass spectrometry. J. Chromatogr. **1988**, *441*, 13–29.
16. Zenkevich, I.G.; Chupalov, A.A. Gas chromatographic determination of monoethanolamine in air of industrial areas. Rus. J. Anal. Chem. **1996**, *51* (6), 642–646.
17. Linstrom, P.J; Mallard, W.G., Eds.; NIST Chemistry Webbook, NIST Standard Reference Database No. 69. National Institute of Standards and Technology: Gaitherburg, MD, http://webbook.nist.gov (accessed June 2009).

Immobilized Antibodies: Affinity Chromatography

Monica J.S. Nadler
Beth Israel Deaconess Medical Center, Harvard Medical School, Boston, Massachusetts, U.S.A.

Tim Nadler
Applied Biosystems, Inc., Framingham, Massachusetts, U.S.A.

INTRODUCTION

Antibodies are serum proteins that are generated by the immune system which bind specifically to introduced antigens. The high degree of specificity of the antibody–antigen interaction plays a central role in an immune response, directing the removal of antigens in concert with complement lysis (humoral immunity). Importantly, this high degree of specific binding has been exploited as an analytical tool: Antigens can be detected, quantified, and purified from sources in which they are in low abundance with numerous contaminants. Examples include enzyme-linked immunosorbent assays (ELISAs), Ouchterlony assays, and Western blots. Antibodies that are specifically immobilized on high-performance chromatographic media offer a means of both detection and purification that is unparalleled in specificity, versatility, and speed.

We will focus, here, on the use of immobilized antibodies for analytical affinity chromatography, which offers a number of advantages over standard partition chromatography. The first advantage is the specificity imparted by the antibody itself, which allows an antigen to be completely separated from any contaminants. During a chromatographic run with an antibody affinity column, all of the contaminants wash through the column unbound, and the bound antigen is subsequently eluted, resulting in only two peaks generated in the chromatogram (contaminants in the flowthrough step and antigen in the elution step). With antibodies which are immobilized on high-speed media such as perfusive media,[1,2] typical analytical chromatograms can be generated in less than 5 min and columns can last for hundreds of analyses. In Fig. 1, an example of 5 consecutive analytical affinity chromatography assays are shown, followed by the results of the last 5 assays of a set of 5000. Note that, here, the cycle time for loading, washing out the unbound material, eluting the bound material, and reequilibration of the affinity column is only 0.1 min (6 sec). Also note that the calibration curve has changed little between the first analysis and after 5000 analyses, demonstrating both the durability and reproducibility of this analytical technique. Although many soft-gel media are also available for antibody immobilization, these media do not withstand high linear velocity and, therefore, are not suited for high-performance affinity chromatography.

Affinity chromatography using immobilized antibodies offers several advantages over conventional chromatographic assay development. First, assay development can be very rapid because specificity is an inherent property of antibody and solvent mobilephase selection is limited to a capture buffer and an elution buffer, which is often the same from one antibody to the next. Therefore, there is less "column scouting" for appropriate conditions. In addition, the assays are fast (see above) and chromatograms yield only two peaks instead of multiple peaks. Furthermore, the two peaks in the affinity chromatogram indicate both antigen concentration (from the eluted peak) and purity (from the ratio of the eluted peak to the total peak area). Thus, affinity chromatography with immobilized antibodies allows both fast assay development and rapid analysis times.

The limitations of immobilized antibody affinity chromatography are few. First, plentiful amounts of antibody, usually milligram quantities, are required to get reasonable ligand density on a useful amount of chromatographic media. Also, it is optimal if the antibody is antigen affinity purified, so that when it is immobilized, no other contaminating proteins with competing specificity dilute the antibody's concentration. Finally, the antibody must be amenable to affinity chromatography such that it is not irreversibly denatured by the immobilization process and can withstand many cycles of antigen capture and elution. Both monoclonal and polyclonal antibodies have been used successfully.

IMMOBILIZATION CHEMISTRIES

Many different chemistries can be used to immobilize antibodies onto chromatographic media and only a few will be discussed. In most cases, the chromatographic media is coated with the active chemistry, which will then react with the antibody. These include amine reactive chemistries such as epoxide-, aldehyde-, and cyanogen bromide (CNBr)-activated media, carboxyl reactive chemistries such as carbodiimides, aldehyde-reactive chemistries such as amino and hydrazide, and thiol-reactive chemistries such as iodoacetyl and reduce thiol media. Although there are several antibody isotypes (IgA, IgE, IgG, IgM), the most

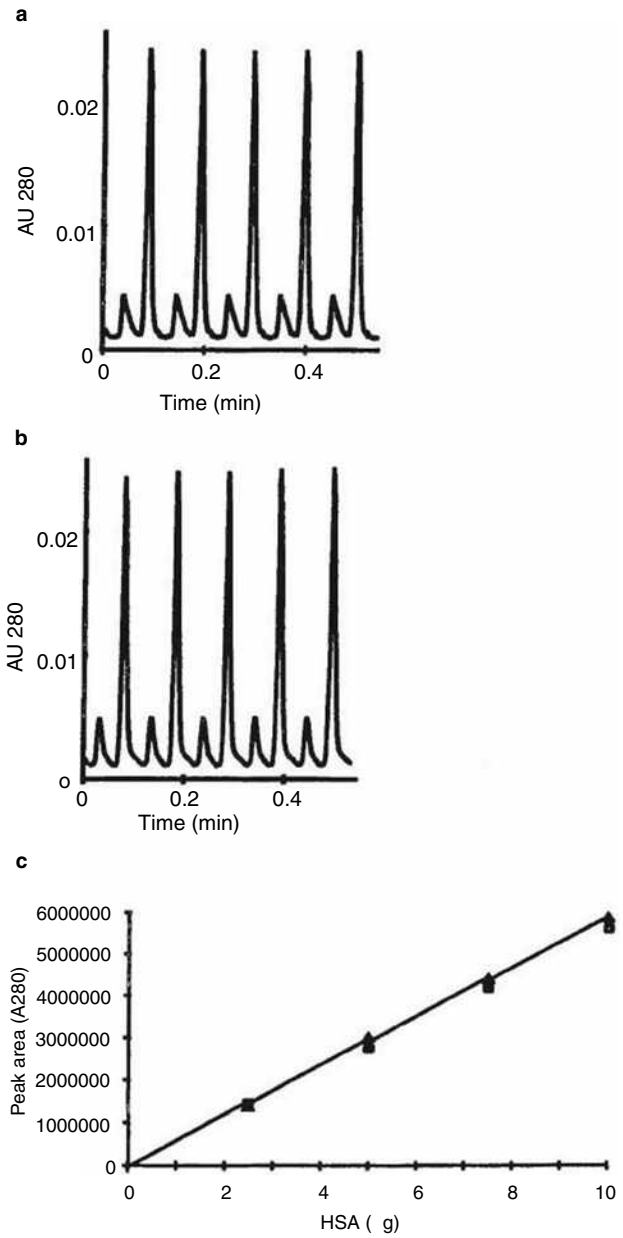

Fig. 1 Examples of affinity chromatography with an epoxyimmobilized polyclonal anti-human serum albumin (HSA) antibody in a 2.1 mm I.D. × 30 mm POROS CO column run at 5 ml/min (8000 cm/hr) using phosphate-buffered saline for loading and 12 m*M* HCl with 150 m*M* NaCl for elution. The sample was 10 μg HSA at 1 mg/ml. Part (a) shows the first five analyses of a relatively pure sample of HSA, where the first small peak is the unbound contaminant and the larger peak is the elution of the HSA from the affinity column; (b) shows the results of the last 5 analyses from a set of 5000; and (c) shows the calibration curve before (squares) the 5000 analyses and after (triangles).

common antibody immobilized for affinity chromatography is IgG, which is composed of four polypeptide chains (two heavy and two light) which are disulfide linked to form a Y-shaped structure capable of binding two antigens. For best results, it is also important to antigen affinity purify the antibody prior to immobilization to yield optimum binding capacity and a wider dynamic range for analytical work. Also note that the antibody may be digested with pepsin or papain to separate the constant region from the antigenbinding domains, which may then be immobilized.

Antibodies are very often immobilized through their amino groups either through the *N*-terminal amines or the epsilon amino groups of lysine. Reactions with epoxide-activated media are performed under alkaline conditions and lead to extremely stable linkages between the chromatographic support and the antibody. Similarly, immobilization using an aldehyde-activated media first proceeds through a Schiff base intermediate which must then be reduced (often by sodium cyanoborohydride) to yield a very stable carbon–nitrogen bond linking the antibody to the media. *N*-Hydroxy-succinimide-activated media also couples via primary amines and leads to a stable linkage in a single-step reaction. The major advantage of these chemistries is that they are extremely stable due to the formation of covalent bonds to the media. Although less stable but easy to use is CNBr-activated media, which also immobilizes antibodies through their primary amines.

Antibodies can also be immobilized through their carboxyl groups by first treating them with a carbodiimide such as EDC (1-ethyl-3-[3-dimethlaminopropyl]-carbodiimide) followed by immobilization on an amine-activated chromatographic resin. It is important to note that EDC does not add a linker chain between the antibody and the media, but simply facilitates the formation of an amide bond between the antibody's carboxyl and the amine on the media. Coupling through sulfhydryls on free cysteines can be accomplished with thiol-activated media by formation of disulfide bonds between the media and the antibody. However, this coupling is not stable to reducing conditions and a more stable iodoacetyl-activated media is often preferred because the resulting carbon–sulfur bond is more stable. Free cysteines can be generated in the antibody by use of mild reducing agents (e.g., 2-mercaptoethylamine), which can selectively reduce disulfide bonds in the hinge region of the antibody. Alternatively, antibodies may also be immobilized through their carbohydrate moieties. One method involves oxidation of the carbohydrate with sodium periodate to generate two aldehydes in the place of vicinyl hydroxyls. These aldehydes may then be coupled either directly to hydrazide-activated media or through amine-activated media with the addition of sodium cyanoborohydride to reduce the Schiff base. The primary advantages of these chemistries is to offer alternative linkages to the antibody beyond primary amines.

In addition, antibodies may also be coupled to other previously immobilized proteins. For example, the antibody may be first captured on protein A or protein G media and then cross-linked to the immobilized protein A or G with reagents such as glutaraldehyde or dimethyl pimelimidate. The advantage here is that the antibody need not be

pure prior to coupling because the protein A or protein G will selectively bind only antibody and none of the other serum proteins. The disadvantage is that free protein A or protein G will still be available to cross-react with any free antibody in samples to be analyzed, which will only be problematic with serum-based samples. Antibody coupling does not need to be covalent to be effective. For example, biotinylated antibodies can be coupled to immobilized streptavidin. The avidin–biotin interaction is extremely strong and will not break under normal antigen elution conditions. The advantage of this immobilization protocol is that many different biotinylation reagents are available in a wide range of chemistries and linker chain lengths. Once biotinylated and free biotin are removed, the antibody is simply injected onto the streptavidin column and it is ready for use. Immobilization can be accomplished through hydrophobic interaction by simply injecting the antibody onto a reversed-phase column and then blocking with an appropriate protein solution such as albumin, gelatin, or milk. This is analogous to techniques used to coat ELISA plates and perform Western blots, and although this noncovalent coupling is not stable to organic solvents and detergents, it can last for hundreds of analyses under the normal aqueous analysis conditions. The advantage of this immobilization is that it can be done very quickly (in several minutes) by simply injecting an antibody first and then a blocking agent.

OPERATION

A wide range of buffers can be used for loading the sample and eluting the bound antigen; however, for best analytical performance, a buffer system that has low a low ultraviolet (UV) cutoff and rapid reequilibration properties is desirable. One of the better examples is phosphate-buffered saline (PBS) for loading and 12 m*M* HCl with 150 m*M* NaCl. The NaCl is not required in the elution buffer but helps to minimize baseline disturbances due to the refractive index change between the PBS loading buffer and the elution buffer because both will contain about 150 m*M* NaCl. UV detection is well suited for these assays and wavelengths at 214 or 280 nm are commonly used.

For analytical work, large binding capacities are not required, but increased capacity does increase the dynamic range of the analysis. However, the dynamic range can be increased by injecting a smaller volume of sample onto the column at the expense of sensitivity at the low end of the

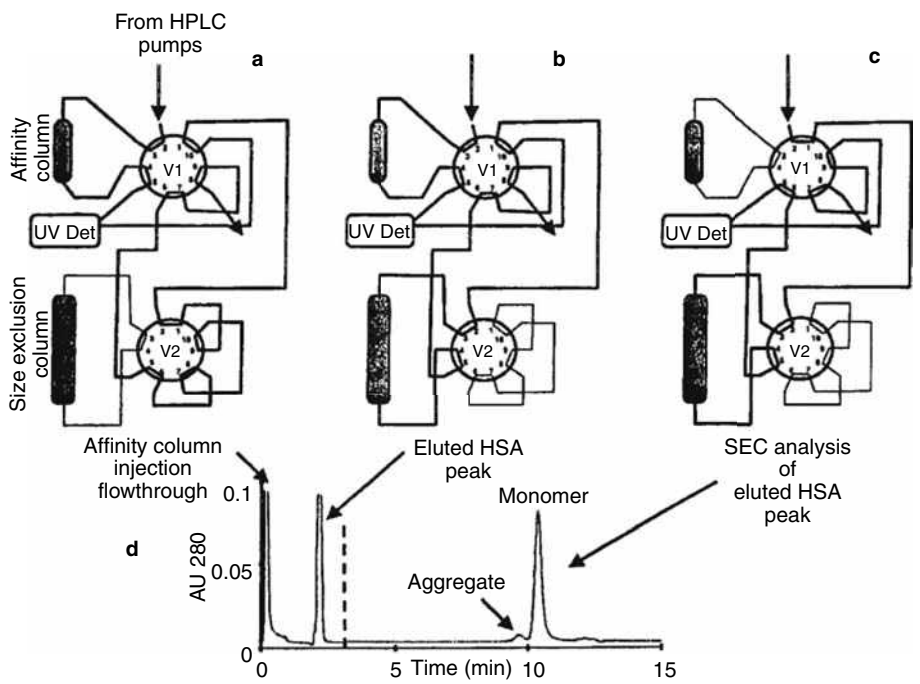

Fig. 2 Example of a multidimensional LC analysis for albumin aggregates using immobilized antibody affinity chromatography with SEC. Part (a) shows the flow path during the loading of the sample to capture the albumin monomer and aggregates while allowing all other proteins to elute to waste. Part (b) shows the transfer of the albumin and its aggregates to the size-exclusion column. Part (c) shows the flow path used to elute the size-exclusion column to separate the aggregate and monomer. Part (d) shows the UV trace from this analysis. Note that in this plumbing configuration, the albumin passes through the detector twice, once as it is transferred from the affinity to the size-exclusion column and again as the albumin elutes from the size exclusion column.The affinity column is a 2.1 mm I.D. × 30 mm POROS XL column to which anti-human serum albumin has been covalently cross-linked, run at 1 ml/min, loaded in PBS, and eluted with 12 m*M* HCl. The size-exclusion column is a 7.5 mm I.D. × 300 mm Ultrasphere OG run at 1 ml/min with 100 m*M* potassium phosphate with 100 m*M* sodium phosphate, pH 7.0. The sample was 100 μg heat-treated albumin.

calibration curve. Likewise, sensitivity can be increased by injecting more sample volume.

APPLICATION EXAMPLES

The most obvious way to use immobilized antibodies for analytical affinity chromatography is to simply use it in a traditional single-column method to determine an antigen's concentration and/or purity. However, there are a number of ways this technique can be advanced to more sophisticated analyses. For example, instead of immobilizing an antibody, the antigen may be immobilized to quantify the antibody as has been done with the Lewis Y antigen.[3] However, the analysis is still a single-column method.

Immobilized antibodies have also been used extensively in multidimensional liquid chromatography (MDLC) analyses. As shown in Fig. 2, an affinity column with immobilized anti-HSA is used to capture all of the human serum albumin in a sample, allowing all of the other components to flow through to waste. Then, the affinity chromatography column is eluted directly into a size-exclusion column where albumin monomers and aggregates are separated and quantified. In this example, neither mode of chromatography would be sufficient by itself. The affinity media does not distinguish between monomer and aggregate, and the size-exclusion column would not be able to discriminate between albumin and the other coeluting proteins in the sample. Other MDLC applications employing immobilized antibodies include an acetylcholine esterase assay utilizing SEC,[4] combinations of immobilized antibodies with reversed-phase analysis,[5–7] protein variant determination using immobilized antibodies to select hemoglobin from a biological sample followed by oncolumn proteolytic digestion, and LC/MS peptide mapping.[8]

There are many more examples of immobilized antibodies used for affinity chromatography which are not mentioned here, but it was the goal of this section to present some of the capabilities of this technique for analytical chromatographic applications.

REFERENCES

1. Afeyan, N.B.; Gordon, N.F.; Mazsaroff, I.; Varady, L.; Fulton, S.P.; Yang, Y.B.; Regnier, F.E. Flow-through particles for the high-performance liquid chromatographic separation of biomolecules: Perfusion chromatography. J. Chromatogr. **1990**, *519* (1), 1.
2. Afeyan, N.B.; Gordon, N.F.; Regnier, F.E. Automated real-time immunoassay of biomolecules. Nature **1992**, *358* (6387), 603.
3. Schenerman, M.A.; Collins, T.J. Determination of a monoclonal antibody binding activity using immunodetection. Anal. Biochem. **1994**, *217* (2), 241.
4. Vanderlaan, M.; Lotti, R.; Siek, G.; King, D.; Goldstein, M. Perfusion immunoassay for acetylcholinesterase: Analyte detection based on intrinsic activity. J. Chromatogr. A, **1995**, *711* (1), 23.
5. Cho, B.Y.; Zou, H.; Strong, R.; Fisher, D.H.; Nappier, J.; Krull, I.S. Immunochromatographic analysis of bovine growth hormone releasing factor involving reversed-phase highperformance liquid chromatography-immunodetection. J. Chromatogr. A, **1996**, *743* (1), 181.
6. Battersby, J.E.; Vanderlaan, M.; Jones, A.J. Purification and quantitation of tumor necrosis factor receptor immunoadhesin using a combination of immunoaffinity and reversed-phase chromatography. J. Chromatogr. B, **1999**, *728* (1), 21.
7. Holtzapple, C.K.; Buckley, S.A.; Stanker, L.H. Determination of four fluoroquinolones in milk by on-line immunoaffinity capture coupled with reversed-phase liquid chromatography. J. AOAC Int. **1999**, *82* (3), 607.
8. Hsieh, Y.L.; Wang, H.; Elicone, C.; Mark, J.; Martin, S.A.; Regnier, F. Automated analytical system for the examination of protein primary structure. Anal. Chem. **1996**, *68* (3), 455.

Immobilized Metal Affinity Chromatography (IMAC)

Roy A. Musil
Althea Technologies, Inc., San Diego, California, U.S.A.

INTRODUCTION

The foundations for immobilized metal affinity chromatography (IMAC) were first laid in 1961 when Helferich introduced "ligand-exchange chromatography".[1] The modern-day usage of this technique and its practical applications as a purification tool did not emerge, however, until 1975 and the seminal work by Porath et al.[2]

Among the many new protein purification approaches introduced in recent years, IMAC stands out for its ease of use and widespread applicability. This highly versatile and efficient technique is based on the interaction between biological molecules and covalently bound chelating ligands immobilized on a chromatographic support. Indeed, because the popularization of the Qiagen Qiaexpress® bacterial expression and one-step purification system,[3] the use of IMAC has become nearly ubiquitous as tool for molecular biologists.

DISCUSSION

The principle behind IMAC lies in the fact that many transition metal ions [i.e., Ni(II) and Cu(II)] can coordinate to the amino acids histidine, cysteine, and tryptophan via electron-donor groups on the amino acid side chains.

An IMAC column may be loaded with a given metal–ion by perfusing the column with a metal–ion solution until equilibrium is reached between the metal chelated to the stationary phase and the metal ion in solution. The solid support (typically agarose, crosslinked dextran, or silica) is covalently linked to a metal-chelating ligand. The two most common ligands are iminodiacetic acid (IDA) and nitrilotriacetic acid (NTA).[4] All major chromatography suppliers now offer their own brands of IMAC supports, with IDA typically the ligand of choice. The IDA residue is very suitable as an immobilized chelating agent because a bidentate chelating moiety remains free after immobilization, to which a metal ion can be coordinated. The NTA ligand contains an additional chelating site for metal ions, which can minimize metal leakage on the column. Free coordination sites of the metal ion are then used to bind different proteins and peptides.

Pearson systematized metal ions into three categories according to their reactivity toward nucleophiles: hard, intermediate, and soft.[5] Hard metal ions, such as Fe(III), prefer oxygen, whereas soft metal ions prefer sulfur. Intermediate types of ions such as Cu(II), Zn(II), Ni(II), and Co(II) coordinate nitrogen but also oxygen and sulfur. All the metals mentioned have been successfully employed for use in IMAC.[6] The immobilized metal–ion adsorbents may be prepared by charging the chelating gels with a slightly acid solution of the metal salt (pH 3–5). Charging the gel under acidic conditions is essential in the case of Fe(III) to avoid the formation of ferric hydroxide particles in solution. The use of colored Ni(II) or Cu(II) ions facilitates checking of leakage and the possible presence of metal ions bound to the protein eluate.

In his pioneering contribution, Porath postulated that the histidine, cysteine, and tryptophan residues of a protein were most likely to form stable coordination bonds with chelated metal ions at near neutral pH.[2] To date, an analysis of several protein models[7] lend full to his original theory. Having said that, histidine, by far and away, plays the most prominent role in IMAC binding. In a very real sense, IMAC has subtly become synonymous as a histidine affinity technique. The absence of a histidine residue on a protein surface correlates with the lack of retention of that protein on any IDA–metal column. The presence of even a single histidine on a protein surface, available for coordination, results in retention of that protein on an IDA–Cu(II) column. Also, a protein needs to display at least two histidine residues on its surface to be retained on an IDA–Ni(II) column. Thus, beyond its role as a purification technique, IMAC has been used as a tool to probe the surface topography of proteins.[6]

The Qiaexpress® system is based on the selectivity of Ni–NTA for proteins with an affinity tag of six consecutive histidine residues: the 6x His tag. The 6x His tag is much smaller than such affinity tags as glutathione *S*-transferase, protein A, and maltose-binding protein and is uncharged at physiological pH. It has been shown to rarely contribute to a protein's immunogenicity, interfere with protein structure, function, or affect secretion from its expression system.[3]

As in any chromatography technique, one can break down the separation process to its two most fundamental aspects: adsorption and elution. On a more practical level, the execution of an IMAC experiment involves five discrete steps which can be readily automated: column equilibration (charging of the gel), sample loading, removal of unbound material (washing), elution, and regeneration.

Adsorption of a protein to an IMAC column has to be performed at a pH at which an electron-donor group(s) on the protein's surface is at least partially unprotonated. Because the pK_a value of histidine groups (which supply the strongest metal interactions) lies in the neutral range, the binding of protein samples to the column should normally occur at a pH value of approximately 7. However, the actual pK_a value of an individual amino acid varies strongly depending on the neighboring amino acid value. Various experiments show that depending on the protein structure, pK_a the value of an amino acid can deviate from the theoretical value up to one pH unit.[4] Therefore, an application buffer of pH 8 often achieves improved binding. In order to eliminate any non-specific electrostatic interactions, it is common to include salt in the equilibrating buffer. Typically, sodium chloride is used in concentrations between 0.1 *M* and 1.0 *M*.[8]

The buffer itself should not effectively compete with a protein for coordination to the metal ligand. Sodium phosphate or sodium acetate are recommended buffers (depending on the pH choice) and the presence of ethylenediaminetetraacetic acid (EDTA) or sodium citrate should be avoided. The presence of detergents (Triton X-100, Tween-20, urea, etc.) in the buffer does not normally affect the adsorption of proteins.[4]

Elution of proteins can be achieved by one of three methods: protonation, ligand exchange, or column stripping. Protonation is the most common method and probably the simplest. The pH is reduced by either a linear gradient or step-gradient in the range of pH 8 to 3 or 4, reflecting the titration of the histidyl residues. Most proteins elute between pH 6 and 4. Again, sodium phosphate or sodium acetate are the buffers of choice. Competitive elution with ammonium chloride (0–2.0 *M*), imidazole (0–0.5 *M*) or its analogs histidine (0–0.05 *M*) and histamine yield similar selectivity.[8] Competitive elution with a linear gradient or step-gradient is best run at a constant nearly neutral pH. The final method of elution is to use chelating agents such as EDTA or ethylene glycol tetraacetic acid (EGTA) (0.05 *M* solutions) which will strip the metal ions from the gel and cause the proteins to elute. Unless the protein of interest is the only one still bound on the column, this method will result only in recovery and not in purification or resolution.[3] Another undesirable feature of this protocol is that the eluate will contain a high concentration of free metal ion. Most resin manufacturers recommend that to maintain reproducibility and consistency, IMAC columns should be stripped of their metal ligands after each use and subsequently recharged with metal before the next run.[6] Recently, Fe(III)–IMAC has found specific application in the separation of phosphorylated macromolecules and other biological substances.[9] Unlike Cu(II)–IDA complexes which have no formal charge, the metal–ligand complex Fe(III)–IDA has a net positive charge. In terms of use, the highest protein capacity is reached at low pH (< 6) rather than at or above neutrality and at low ionic strength rather than at high salt concentrations. Electrostatic interactions for Fe(III) complexes play an important in protein binding.[2] However, Fe(III)–IMAC systems do not interact with phosphoproteins in the same way as ordinary ionexchange resins. Fe(III)–IMAC can be employed to resolve proteins with a wide range of isoelectric points (p*I* 4–11) something that is not generally possible in a simple, single ion-exchange chromatographic step.

Immobilized metal affinity chromatography has been shown to be effective for isolating proteins from crude mixtures, as well as for selective separations of closely related proteins.[2] With respect to separation efficiency, IMAC compares well with biospecific affinity chromatography and the immobilized metalion complexes are much more robust than antibodies or enzymes. These factors make IMAC particularly well suited for scale-up to process scale chromatography. The main scale-up points to be aware of are the degree to which the column is metal saturated, the chelating agent content of the sample, and the potential of leached metal (or its interactions) within the product eluate.

Leakage of metals from the column during elution can be the most significant problem due to their toxicity, but there are several ways to avoid this pitfall. Some references suggest the precaution of underloading IMAC columns (by as much as 20%) with the metal ion to begin with.[8] Another precaution is to add EDTA with imidazole, histidine, or histamine to the column fractions. EDTA competitively blocks formation of coordination complexes between protein carboxyl clusters and divalent metal cations, whereas the imidazolium groups block histidyl–metal complexation. For best reproducibility and general ease of use, a two-column format is preferred for process scale. A second scavenging column with 5% of the volume of the metal saturated purification column is simply placed in line.

Besides accommodating raw feedstreams, the relative independence of protein binding from salt concentration offers a great deal of flexibility for process sequencing. IMAC can follow virtually any other technique without the requirement for buffer exchange. The main exception is hydrophilic interaction chromatography (HIC) with ammonium sulfate. IMAC can also be used as the initial capture step enabling purification up to a 1000-fold[4] and subsequent preequilibration for downstream low-ionic-strength methods. Although high salt loading improves IMAC-binding specificity,[5] its concentration can be reduced after the major contaminants are washed through the column. Even with sodium chloride concentrations of up to 0.1 *M*, just a minor dilution can allow for the following charge-based chromatography method. This flexibility reveals IMAC as a valuable tool for streamlining the overall process design.

REFERENCES

1. Helferich, F. 'Ligand exchange': A novel separation technique. Nature **1961**, *189* (4769), 1001.
2. Porath, J.; Carlsson, J.; Olsson, I.; Belfrage, G. Metal chelate affinity chromatography, a new approach to protein fractionation. Nature **1975**, *258* (5536), 598.
3. *The Qiaexpressionist,* 2nd; Qiagen Inc.: Chatsworth, CA, 1992.
4. Porath, J. Immobilized metal ion affinity chromatography. Protein Express. Purif. **1992**, *3* (4), 263–281.
5. Sulkowski, E. Purification of proteins by IMAC. Trends Biotechnol. **1985**, *3* (1), 1–7.
6. Sulkowski, E. The saga of IMAC and MIT. BioEssays **1989**, *10* (5), 170.
7. Johnson, R.D.; Arnold, F.H. Review: Multipoint binding and heterogeneity in immobilized metal affinity chromatography. Biotechnol. Bioeng. **1995**, *48* (5), 437.
8. Porath, J.; Olin, B. Immobilized metal affinity adsorption and immobilized metal affinity chromatography of biomaterials. Serum protein affinities for gel-immobilized iron and nickel ions. Biochemistry **1983**, *22* (7), 1621.
9. Holmes, L.D.; Schiller, M.R. Immobilized iron(III) metal affinity chromatography for the separation of phosphorylated macromolecules: Ligands and applications. J. Liq. Chromogr. Relat. Technol. **1997**, *20* (1), 123.

Immobilized Metal Ion Affinity Chromatography (IMAC): Chelating Sorbents

Radovan Hynek
Anna Kozak
Jirí Sajdok
Jan Kás
Department of Biochemistry and Microbiology, Institute of Chemical Technology, Prague, Czech Republic

INTRODUCTION

Immobilized metal ion affinity chromatography (IMAC) is a collective term that includes all kinds of affinity chromatography, where metal atoms or ions immobilized on polymer cause or dominate the interaction at the sorption site.

DISCUSSION

Metal-chelate affinity chromatography was introduced as a specific method for fractionation of proteins by Porath et al., in 1975.[1] The principle of this type of chromatographic method is that certain amino acid residues, such as histidine, cysteine, lysine, tryptophan, aspartic acid, glutamic acid, or phosphorylated amino acids, which are accessible on the protein surface, can interact through non-bonding lone-pair electron coordination with some metal ions. Metal cations Cu^{2+}, Ni^{2+}, Zn^{2+}, Co^{2+}, Fe^{3+}, Al^{3+}, and Cr^{3+}, and which have been chelated to ligands immobilized on support material, have already been used for such specific interactions.[2,3] The most widely used chelating ligands for the isolation of proteins are iminodiacetic acid (IDA) and its analogs, such as tricarboxyethylenediamine (TED). IDA is covalently coupled to an insoluble matrix (e.g., agarose or Sepharose) and forms stable coordinate compounds with a variety of divalent metal ions. These chelates create bases for the above-mentioned specific adsorption. Elution of adsorbed solutes from immobilized metal ion affinity adsorbents can be provided by changing the pH of the elution buffer or by a specific competing solute, such as histidine, imidazole, or sodium phosphate, depending on the interaction types involved.

Ligands coupled to agarose gels were commonly used at the beginning of IMAC application; however, these sorbents were not suitable for high-performance liquid chromatography (HPLC). Then, Small et al.,[4] used a silica-based matrix and demonstrated that such IMA sorbents can be used in HPLC techniques. The metal-chelate adsorbent "TSK gel chelate-5PW," suitable for HPLC, which was prepared by coupling IDA to a hydrophilic resin-based matrix (TSK gel G 5000 PW), later became commercially available (Fig. 1).

Since the introduction of metal ion affinity sorbents for the fractionation of proteins,[1] the method became popular for the purification of a wide variety of biomolecules. Metal ion affinity sorbents are also widely used for the immobilization of enzymes. At present, IMAC is a powerful method for separation of phosphorylated macromolecules, particularly proteins and peptides. The significance of techniques for separation and characterization of phosphorylated biomolecules is now increasing, because phosphorylation modulates enzyme activities and mediates cell membrane permeability, molecular transport, and secretion. Phosphorylated peptides can be separated from a peptide mixture on IDA–Sepharose with Fe^{3+} ions (Fig. 2). The majority of peptides pass freely through an IMAC column, whereas acidic peptides, including phosphorylated ones, are retained and can be released by a pH gradient.

Acidic peptides are released in the pH range 5.5–6.2 and phoshorylated peptides are eluted in the pH range 6.9–7.5.[5] Elution of retained peptides can also be performed with sodium phosphate. IMAC has been successfully used for the characterization of casein phosphopeptides in cheese extracts.[6] Phosphoproteins can be separated under very similar conditions as phosphopeptides. IMA sorbents were already used for fractionation of proteins

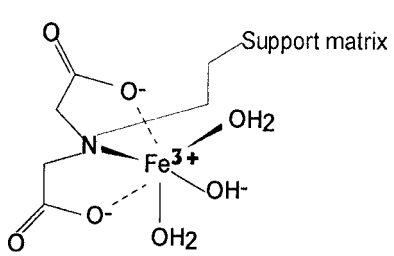

Fig. 1 Complex of water with IDA–$Fe3^{3+}$.

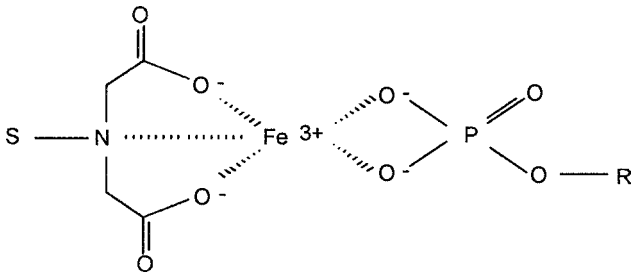

Fig. 2 Interaction of phosphate group with Fe^{3+} ion on IDA-Sepharose.

according to the number of phosphate groups contained in their molecules.

Separations of biomolecules on IMA sorbents achieved significant advances in the past few years, but detailed analyses of the mechanism of adsorption of molecules should be completed. Various factors, such as support matrix, chelating ligands, buffer composition, temperature, and so forth should be investigated in order to optimize analysis on metal-chelate ion affinity sorbents.

REFERENCES

1. Porath, J.; Carlsson, J.; Olsson, I.; Belfrage, G. Metal chelate affinity chromatography, a new approach to protein fractionation. Nature **1975**, *258* (5536), 598.
2. Sulkowski, E. Purification of protein by IMAC. Trends Biotechnol. **1985**, *3*, 1.
3. Hemdan, E.S.; Zhoa, Y.J.; Sulkowski, E.; Porath, J. Surface topography of histidine residues: A facile probe by immobilized metal ion affinity chromatography. Proc. Natl. Acad. Sci. USA. **1989**, *86*, 1811–1815.
4. Small, D.A.P.; Atkinson, T.; Lowe, C.R. *Affinity Chromatography and Biological Recognition*; Chaiken, I.M. Wilchek, M., Parikh, I., Eds.; Academic Press: New York, 1983; 267.
5. Muszyńska, G.; Doborrowolska, G.; Medin, A.; Ekman, P.; Porath, J.O. Model studies on iron(III) ion affinity chromatography. II. Interaction of immobilized iron(III) ions with phosphorylated amino acids, peptides and proteins. J. Chromatogr. **1992**, *604*, 19–28.
6. Hynek, R.; Kozak, A.; Dráb, V.; Sajdok, J.; Káš, J. Charecterization of Casein phosphopeptides in cheese extracts using a combination of immobilized metal chelate affinity and reversed-phase high-performance liquid chromatography. Adv. Food Sci. (CMTL) **1999**, *21* (5/6), 192.

Immunoaffinity Chromatography

David S. Hage
Department of Chemistry, University of Nebraska-Lincoln, Lincoln, Nebraska, U.S.A.

Abstract
The general principles of immunoaffinity chromatography (IAC) are discussed in this entry. The term IAC refers to any chromatographic method in which the stationary phase consists of antibodies or antibody-related binding agents. The highly selective binding of antibodies has made IAC a popular purification tool for the isolation of many biological and non-biological substances, as well as a specific means for chemical measurement. In this entry, several formats of IAC are described, including the on-off elution mode for the purification or direct detection of chemicals and the indirect detection modes based on chromatographic immunoassays. The use of antibodies as a means for selective sample extraction or as part of a postcolumn detection scheme in combination with other chromatographic methods is also discussed.

INTRODUCTION

Immunoaffinity chromatography (IAC) refers to any chromatographic method in which the stationary phase consists of antibodies or antibody-related binding agents. Antibodies, or immunoglobulins, are a diverse class of glycoproteins that are produced by the body in response to a foreign agent, or antigen. Antibodies are highly selective in their interactions with other molecules and can be produced against a wide range of substances. These properties have made IAC popular as a purification tool for the isolation of targets that include hormones, peptides, enzymes, proteins, receptors, viruses, and subcellular components. The high selectivity of IAC has also made it appealing as a means for developing specific analytical methods. This entry will examine the basic principles of IAC and the various formats in which it can be used.

HISTORY OF IAC

The use of an immobilized ligand for the purification of antibodies was first reported in 1935, when antigens adsorbed on kaolin and charcoal were employed for the isolation of antibodies associated with syphilis and tuberculosis.[1] In 1936, Landsteiner and van der Scheer began to immobilize targets for antibodies by using a diazo coupling method and chicken erythrocyte stroma as the support material.[2] However, the first modern use of IAC is generally credited to Campbell et al., who in 1951 coupled serum albumin to *p*-aminobenzylcellulose for use in antibody purification.[3] There are now thousands of methods based on IAC that have been reported for the isolation of chemicals and biochemicals,[4–11] with a growing number of applications also using this method for chemical analysis.[5,8–19]

ANTIBODY STRUCTURE

The key component of any IAC method is the preparation of the antibody used as the stationary phase. The basic structure of a typical antibody (such as immunoglobulin G or an IgG-class antibody) consists of four polypeptides that are linked by disulfide bonds to form a Y- or T-shaped structure (see Fig. 1). The two upper arms of this structure are called the F_{ab} fragments and contain two identical antigen-binding regions. The lower stem region is known as the F_c fragment and has a structure that is highly conserved between antibodies that belong to the same class. Other classes of antibodies (e.g., IgA, IgM, IgD, and IgE) have the same basic structure as that of IgG but may contain multiple units that are cross-linked through the presence of additional peptide chains. The amino acid composition within the F_{ab} fragments is highly variable from one type of antibody to the next. It is this variability that allows the body to produce antibodies with a variety of affinities and binding specificities for foreign agents.

Typical antigens in nature include bacteria, viruses, and foreign proteins from animals or plants. All of these agents are fairly large in size compared to the binding sites on an antibody. As a result, these antigens usually have many different locations on their surfaces to which an antibody can bind; each of these locations is called an epitope. Smaller antigens (i.e., those with a molecular mass below several thousand daltons) are too small to produce an immune response by themselves. These substances can result in antibody production if they are first coupled to a larger species such as a carrier protein.

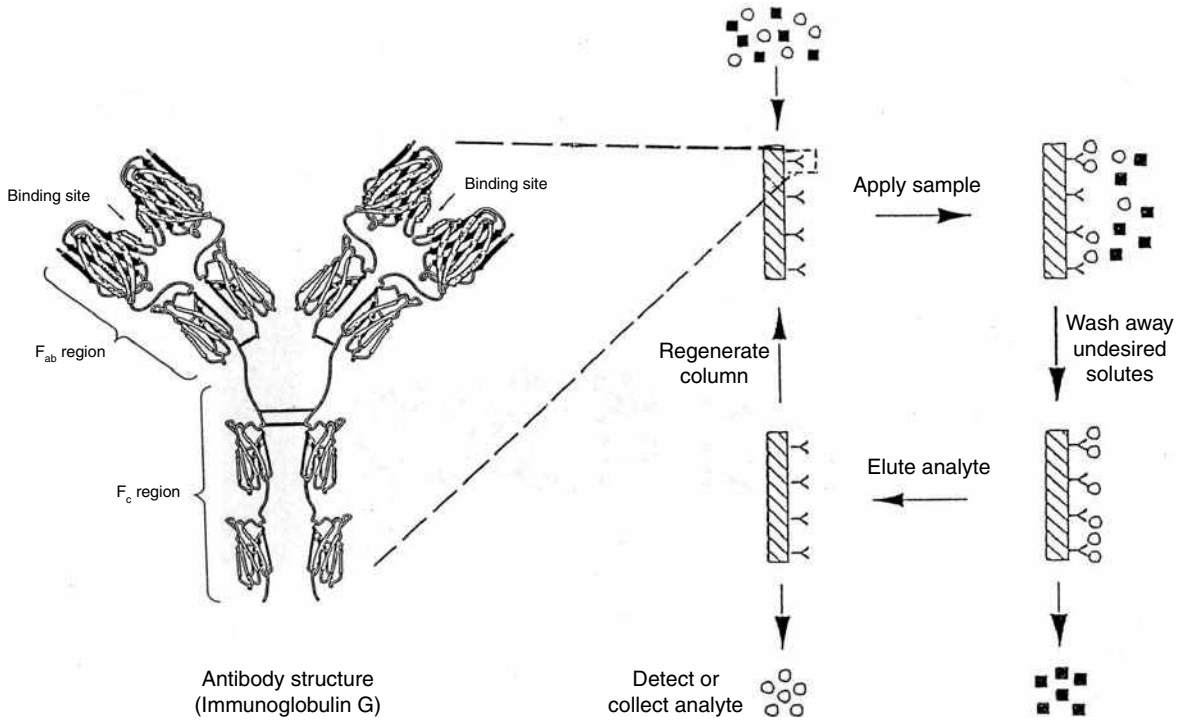

Fig. 1 Basic structure of an antibody and an example of the use of antibodies in the on-off mode of immunoaffinity chromatography.
Source: From Chromatographic immunoassays, in Anal. Chem.[14]

The agent that is coupled to the carrier protein in this situation is called a hapten.

ANTIBODY PRODUCTION

One way to produce antibodies that are directed against a given target is to inject the corresponding antigen or hapten–carrier conjugate into an animal such as a mouse or a rabbit. Samples of the animal's blood are then taken at specified intervals to collect any antibodies that are produced against the injected foreign agent. This method results in a heterogeneous mixture of antibodies that bind with a range of strengths and to various epitopes on the antigen or the hapten–carrier conjugate. These antibodies are called polyclonal antibodies because they are produced by several different immune system cell lines. Techniques have also been developed that allow for the isolation of single antibody-producing cells and their subsequent hybridization with cancer cells to produce combined cell lines that are stable and relatively easy to grow over long periods of time. These combinations of immune system/cancer cells are called hybridomas, and their product is a single type of well-defined antibody known as a monoclonal antibody. Both polyclonal and monoclonal antibodies have been used in IAC methods.[8,12]

IMMUNOAFFINITY SUPPORTS

The support material is an important factor to consider in the development of a successful IAC method. Originally, most IAC applications were based on low-performance supports that consisted of non-rigid media that could be operated under gravity flow or in the presence of peristaltic flow or a small applied vacuum. The supports were typically based on carbohydrate-related materials like agarose and cellulose, or synthetic organic supports, such as acrylamide-based polymers. However, IAC has also been used in high-performance liquid chromatography (HPLC), where more rigid and higher efficiency materials are employed. Some examples of HPLC supports that have been utilized for IAC include derivatized glass, silica, polystyrene-based perfusion media, azalactone beads, and monolithic supports.[8,12,18] When these types of supports are used in IAC, the resulting method is often referred to as high-performance immunoaffinity chromatography (HPIAC). Of these two approaches, low-performance IAC is the method most often employed for the purification of solutes or for use in sample pretreatment prior to analysis by other techniques. HPIAC can also be used for sample pretreatment or compound isolation, but it is more commonly employed as an analytical tool for measuring specific chemicals in complex mixtures.[5,8,12]

ANTIBODY IMMOBILIZATION

One common approach for antibody immobilization involves direct covalent attachment between the support and the free amine groups on the antibodies. Examples include reductive amination (i.e., the Schiff base method) or the reaction of antibodies with supports that have been activated with reagents such as 1,1′-carbonyldiimidazole or *N*-hydroxysuccinimide. Antibodies or antibody fragments can also be immobilized through more site-selective methods. For instance, free sulfhydryl groups that are generated during the production of F_{ab} fragments can be used to couple these fragments to thiol-activated supports. In addition, mild oxidation of the carbohydrate residues in the F_c region of antibodies can be used for coupling to a support by reacting these oxidized residues with amine- or hydrazide-activated materials. The main advantage of site-selective immobilization is that it produces immobilized antibodies or antibody fragments that have fairly well-defined points of attachment and greater accessibility of their binding regions to analytes, thus resulting in higher binding activities than are obtained by more general coupling methods.

Non-covalent immobilization can also be used for the site-selective coupling of antibodies to supports. This approach typically involves absorbing the antibody to a secondary ligand such as protein A or protein G, both of which bind to the F_c region of many antibody classes. This binding is quite strong under physiological conditions but can be disrupted by decreasing the pH of the surrounding solution. This method is useful when high antibody activity is needed or when it is desirable to have frequent replacement of antibodies in the IAC column. Other secondary ligands that can be used to adsorb antibodies in affinity columns are avidin or streptavidin, which bind to antibodies that have been labeled with biotin tags.[8]

APPLICATION AND ELUTION CONDITIONS

The mobile phase used in IAC is another factor to be considered in this method. The application buffer that is present during sample injection should facilitate quick and efficient binding of the analyte to the immobilized antibodies. This mobile phase is usually selected so that it mimics the natural environment of the antibody (e.g., a buffer with a physiological pH and ionic strength). The association equilibrium constants for antibody–antigen interactions under such conditions are often in the range of 10^6–10^{12} M^{-1}. This generally results in extremely strong binding between the analyte and the immunoaffinity column during sample application.

Although it is possible to use isocratic elution for IAC columns that contain low-affinity antibodies (i.e., those with association equilibrium constants below 10^6 M^{-1}), isocratic elution is not practical when working with high-affinity antibodies. The only way solutes can be quickly eluted from high-affinity antibodies is to change the column conditions to lower the effective strength of the antibody–analyte interaction. This change is effected by applying an elution buffer to the column. Usually an acidic buffer (pH 1–3) or a solution that contains a chaotropic agent (e.g., sodium thiocyanate) is used for analyte elution in such situations. Occasionally a competing agent, an organic modifier, a temperature change, or a denaturing agent is also employed. The elution buffer is typically applied in a step gradient, but more gradual linear or non-linear gradients have been reported as well.[5,8,12]

TRADITIONAL IAC

There are a variety of ways by which IAC can be carried out. The simplest format (shown in Fig. 1) is the on-off mode. In this technique, the sample is first injected onto the IAC column in the presence of an application buffer. As the analyte is being retained, other compounds in the sample pass through non-retained and are washed from the column. After these non-retained solutes have been removed, the elution buffer is applied. The analyte is then collected or detected as it elutes from the column. Later, the initial application buffer is reapplied and the antibodies are allowed to regenerate before the next sample is injected.

The on-off mode is the format most commonly used in IAC for the purification of compounds. This format has been used with a broad array of compounds, ranging from proteins and glycoproteins to carbohydrates, lipids, bacteria, viral particles, drugs, and environmental agents.[4–11] IAC has been especially popular in the isolation of specific antibodies or antigens, where an appropriate ligand (i.e., either an antibody or a purified antigen) is used to isolate its counterpart from a sample. This approach allows the isolation of an immunologically specific agent, regardless of its chemical or biochemical nature. The on-off mode is also used in analytical applications that involve analytes that are labeled or that occur at sufficiently high levels to allow their direct detection as they pass through an IAC column. In this type of application, the on-off mode of IAC is sometimes referred to as the direct detection mode.[12]

IMMUNOEXTRACTION METHODS

Another type of IAC is immunoextraction.[12–14] This term refers to the use of IAC for the removal of a specific solute or group of solutes from a sample prior to the determination of these targets by a second analytical method. Off-line immunoextraction is the easiest way for combining IAC with techniques such as gas chromatography (GC) or HPLC. In this method, antibodies are typically immobilized onto a low-performance support that is packed into a small disposable syringe or solid-phase extraction

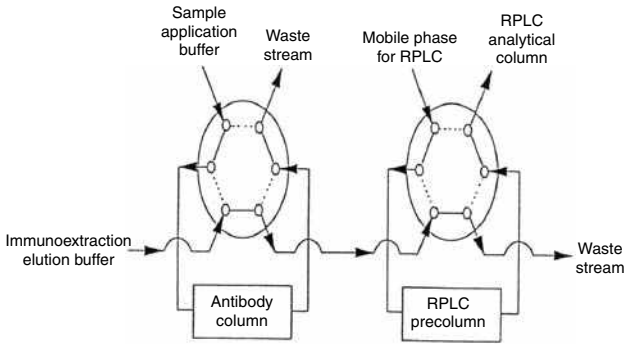

Fig. 2 Typical scheme for the online coupling of immunoextraction with reversed-phase liquid chromatography (RPLC).
Source: From Analysis of atrazine and its degradation products in water by tandem high-performance immunoaffinity chromatography and reversed-phase liquid chromatography, in *Immunochemical Technology for Environmental Applications*.[19]

cartridge. After the sample has been applied to the immunoaffinity column and undesired sample components have been washed away, an elution buffer is passed through the IAC support and the analyte is collected. In some situations, the collected fraction is dried and reconstituted in a solvent that is more suitable for later analysis, such as by adding a volatile solvent for compound analysis by GC. Off-line immunoextraction is quite common and has been used to analyze substances in samples that range from plasma and urine to food, water, and soil extracts. Immunoextraction has also gained popularity in recent years for the removal of high-abundance proteins from samples for proteomics studies; this approach is sometimes referred to as immunoaffinity depletion.[9]

The relative ease with which IAC can be directly coupled to an HPLC system makes online immunoextraction appealing as a means for automating and reducing the time required for sample pretreatment in HPLC. Direct coupling of IAC with size-exclusion and ion-exchange chromatography has also been accomplished, but the vast majority of online immunoextraction has involved coupling IAC with reversed-phase liquid chromatography (RPLC).[12–14] An example of an HPLC system that can be used for this purpose is shown in Fig. 2.[19] Part of the reason for the popularity of this combination is the widespread use of RPLC in chemical separations. Another reason is that the elution buffer for an IAC column is an aqueous solvent with little or no organic modifier, which makes this buffer act as a weak mobile phase for reversed-phase columns. Online immunoextraction coupled with RPLC has been used to measure compounds in food extracts, bodily fluids, enzyme digests, cell extracts, and environmental samples. Online IAC has also been coupled with capillary electrophoresis,[20–24] mass spectrometry,[25] and microfluidic devices.[16,26] In addition, coupling of immunoextraction with GC has also been investigated.[27]

CHROMATOGRAPHIC IMMUNOASSAYS

Another important technique in IAC is the use of immobilized antibody columns to create a chromatographic (or flow-injection) immunoassay.[12,14,28] One way this technique can be carried out is by employing a competitive binding format (see Fig. 3). The simplest competitive binding scheme is to mix the sample and a labeled analyte analogue (often called the "label"), which are then applied simultaneously to the IAC column; this method is known as a simultaneous injection competitive binding immunoassay. An alternative method is to first apply the sample to the IAC column and later make a separate injection of the label, a technique that is called a sequential injection competitive binding immunoassay. In both of these formats, an indirect measure of the analyte is obtained by examining the amount of label that elutes in either the non-retained or in the retained IAC fractions.

An alternative format for a chromatographic immunoassay is the displacement competitive binding immunoassay. In this format, the IAC column is first saturated with the labeled analogue, followed by application of sample to the column. As the analyte travels through the column, it is able to bind to any antibody sites that are momentarily unoccupied by the label as the analyte and antibodies undergo local dissociation and reassociation. This situation results in competition between the analyte and the label

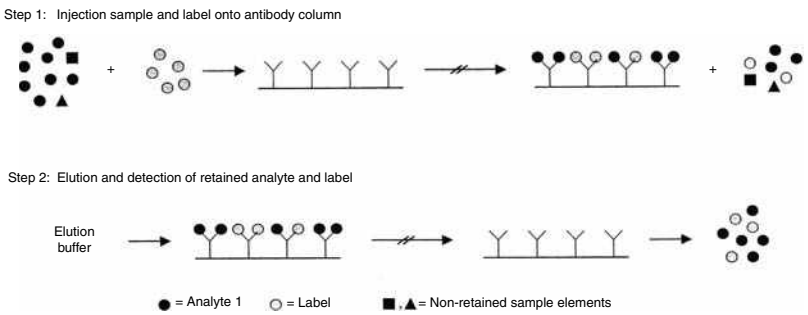

Fig. 3 Typical scheme for a chromatographic competitive binding immunoassay. This particular example is for the simultaneous format.
Source: From Chromatographic Immunoassays, in *Handbook of Affinity Chromatography*.[28]

and displacement of the label from the column, the degree of displacement being directly proportional to the amount of injected analyte.

A sandwich immunoassay in IAC uses two groups of antibodies that bind to different regions on the analyte of interest. The first group of antibodies is immobilized within the IAC column and is used for the extraction of an analyte from the sample. The second group of antibodies contains an easily measured label and is added in solution to bind the analyte either before or after sample extraction. This label allows the analyte to be measured by providing a final signal that is proportional to the amount of analyte that has been extracted by the IAC column.

In a one-site immunometric assay, the sample is first incubated with a known excess of labeled antibodies (or F_{ab} fragments) that are specific for the analyte of interest. After this binding has occurred, the resulting mixture is applied to a column that contains an immobilized analogue of the analyte; this column is used to extract any antibodies or antibody fragments that are not bound to the analyte. Those antibodies/antibody fragments that are bound to the analyte will pass through the column in the non-retained peak. Detection is accomplished either by examining the non-retained labeled antibodies or by monitoring the amount of excess antibodies that later dissociate from the column during the elution step.

A variety of detection schemes have been used with chromatographic immunoassays. The detection can be based on chemical tags that act as chromophores, fluorophores, chemiluminescent agents, or electrochemically active species. Enzymes like β-galactosidase, alkaline phosphatase, and horseradish peroxidase have also been employed as labels to generate products for detection by absorbance, fluorescence, chemiluminescence, electrochemical, or thermometric measurements. Liposomes, radiolabels, and bioassays have also been used for detection in chromatographic immunoassays.[14,28]

POSTCOLUMN IMMUNODETECTION

The technique of postcolumn immunodetection uses an IAC column that is attached to the exit of an analytical HPLC system. The IAC column in this approach serves to collect and retain a specific analyte from the HPLC column eluent for later detection.[12,29] The direct detection mode of IAC is the simplest approach for postcolumn immunodetection if the analyte of interest is capable of generating a sufficiently strong signal for detection. For instance, this approach has been used to measure the enzyme acetylcholinesterase by capturing it by IAC after elution from a size exclusion column, and later applying a chromogenic substrate to the IAC column for the detection of the enzyme.[30]

One factor that must be considered in postcolumn immunodetection is the need to adjust the eluent of the HPLC analytical column to a pH, ionic strength, and polarity that are appropriate for an IAC application buffer.[31] This factor is especially important when using immunodetection with RPLC because an appreciable amount of organic modifier may be present in the mobile phase leaving the reversed-phase analytical column, which may damage the IAC column. One way to avoid this problem is to combine the analytical column eluent with a dilution buffer prior to sample application onto the IAC column. Immunodetection by the on-off mode also requires that the eluting analyte be present in a conformation that is recognized by the antibodies in the IAC column.

Chromatographic sandwich immunoassays have been used for postcolumn immunodetection;[31] however, the one-site immunometric assay is a more common approach.[12,29,32] The use of a one-site immunometric assay in this application involves taking the analytical column eluent and combining it with a solution of labeled antibodies or antibody fragments that will bind to the analyte of interest. The column eluent and the antibody/antibody fragment mixture are then allowed to react in a mixing coil and are passed through an immunodetection column that contains an immobilized analogue of the analyte. The antibodies or antibody fragments that are bound to the analyte will pass through this column and on to the detector, where they will provide a signal that is proportional to the amount of bound analyte. If desired, the immunodetection column can later be washed with an eluting solvent to dissociate the retained antibodies or antibody fragments. However, a sufficiently high binding capacity is generally used in the immunodetection column so that a large amount of the analytical column eluent can be analyzed before the immunodetection column must be regenerated.

CONCLUSION

IAC is a powerful method for the selective binding of targets from samples. This method makes use of antibodies as specific binding agents within a column. There are several ways in which antibodies can be used in IAC. The first of these is the on-off mode, which can be employed for the purification of compounds by immunoaffinity columns or for the direct detection of such agents. It is also possible to use IAC for the indirect detection of chemicals, as is accomplished through the use of chromatographic immunoassays in which a labeled antibody or a labeled analogue of the target provides a signal that is related to the amount of a given chemical in the sample. In addition, IAC can be utilized for the postcolumn detection of analytes as they elute from other types of chromatographic columns. These formats have appeared in numerous applications and fields ranging from biotechnology, clinical analysis, and pharmaceutical testing to environmental work and food analysis.[4–17]

REFERENCES

1. d'Allesandro, G.; Sofia, F. The adsorption of antibodies from the sera of syphilitics and tuberculosis patients. Z. Immunitats **1935**, *84*, 237–250.
2. Landsteiner, K.; van der Scheer, J. Cross reactions of immune sera to azoproteins. J. Exp. Med. **1936**, *63*, 325–339.
3. Campbell, D.H.; Luescher, E.; Lerman, L.S. Immunologic adsorbents. I. Isolation of antibody by means of a cellulose-protein antigen. Proc. Natl. Acad. Sci. U.S.A. **1951**, *37*, 575–578.
4. Calton, G.J. Immunosorbent separations. Methods Enzymol. **1984**, *104*, 381–387.
5. Phillips, T.M. High performance immunoaffinity chromatography. An introduction. LC Mag. **1985**, *3*, 962–972.
6. Ehle, H.; Horn, A. Immunoaffinity chromatography of enzymes. Bioseparation **1990**, *1*, 97–110.
7. Nakajima, M.; Yamaguchi, I. Purification of plant hormones by immunoaffinity chromatography. Kagaku to Seibutsu **1991**, *29*, 270–275.
8. Hage, D.S.; Phillips, T.M. Immunoaffinity chromatography. In *Handbook of Affinity Chromatography*, 2nd Ed.; Hage, D.S., Ed.; Taylor & Francis: New York, 2006; Chapter 6.
9. Zolotarjova, N.; Boyes, B.; Martosella, J.; Yang, L.-S.; Nicol, G.; Zhang, K.; Szafranski, C.; Bailey, J. Immunoaffinity depletion of high-abundant proteins for proteomic sample preparation. In *Separation Methods in Proteomics*; CRC Press: Boca Raton, 2006; 63–79.
10. Gallant, S.R. Immunoaffinity chromatography of proteins. Methods Mol. Biol. **2004**, *251*, 103–109.
11. Weller, M.G. Immunochromatographic techniques—A critical review. Fres. J. Anal. Chem. **2000**, *366*, 635–645.
12. Hage, D.S. Survey of recent advances in analytical applications of immunoaffinity chromatography. J. Chromatogr. B, **1998**, *715*, 3–28.
13. de Frutos, M.; Regnier, F.E. Tandem chromatographic-immunological analyses. Anal. Chem. **1993**, *65*, 17A–25A.
14. Hage, D.S.; Nelson, M.A. Chromatographic immunoassays. Anal. Chem. **2001**, *73*, 198A–205A.
15. Hage, D.S.; Clarke, W. Immunoaffinity chromatography in clinical analysis. In *Separation Techniques in Clinical Chemistry*; Aboul-Enein, H.Y., Ed.; Marcel Dekker: New York, 2003; 361–387.
16. Peoples, M.C.; Karnes, H.T. Microfluidic immunoaffinity separations for bioanalysis. J. Chromatogr. B, **2008**, *866*, 14–25.
17. Nelson, M.A.; Hage, D.S. Environmental analysis by affinity chromatography. In *Handbook of Affinity Chromatography*, 2nd Ed.; Taylor & Francis: New York, 2006; Chapter 19.
18. Jiang, T.; Mallik, R.; Hage, D.S. Affinity monoliths for ultrafast immunoextraction. Anal. Chem. **2005**, *77*, 2362–2372.
19. Hage, D.S.; Rollag, J.G.; Thomas, D.H. Analysis of atrazine and its degradation products in water by tandem high-performance immunoaffinity chromatography and reversed-phase liquid chromatography. In *Immunochemical Technology for Environmental Applications*; Aga, D.S.; Thurman, E.M., Eds.; ACS Press: Washington, DC, 1997; Chapter 10.
20. Heegaard, N.H.H.; Schou, C. Affinity ligands in capillary electrophoresis. In *Handbook of Affinity Chromatography*, 2nd Ed.; Taylor & Francis: New York, 2006; Chapter 26.
21. Amundson, L.K.; Siren, H. Immunoaffinity CE in clinical analysis of body fluids and tissues. Electrophoresis **2007**, *28*, 99–113.
22. Guzman, N.A.; Phillips, T.M. Immunoaffinity CE for proteomics studies. Anal. Chem. **2005**, *77*, 60A–67A.
23. Guzman, N.A. Immunoaffinity capillary electrophoresis applications of clinical and pharmaceutical relevance. Anal. Bioanal. Chem. **2004**, *378*, 37–39.
24. Moser, A.C.; Hage, D.S. Capillary electrophoresis-based immunoassays: Principles and quantitative applications. Electrophoresis **2008**, *29*, 3279–3295.
25. Briscoe, C.J.; Clarke, W.; Hage, D.S. Affinity mass spectrometry. In *Handbook of Affinity Chromatography*, 2nd Ed.; Taylor & Francis: New York, 2006; Chapter 27.
26. Phillips, T.M. Microanalytical methods based on affinity chromatography. In *Handbook of Affinity Chromatography*, 2nd Ed.; Taylor & Francis: New York, 2006; Chapter 28.
27. Farjam, A.; Vreuls, J.J.; Cuppen, W.J.G.M.; Brinkman, U.A.T.; de Jong, G.J. Direct introduction of large-volume urine samples into an online immunoaffinity sample pretreatment-capillary gas chromatography system. Anal. Chem. **1991**, *63*, 2481–2487.
28. Moser, A.C.; Hage, D.S. Chromatographic Immunoassays. In *Handbook of Affinity Chromatography*, 2nd Ed.; Taylor & Francis: New York, 2006; Chapter 29.
29. Irth, H.; Oosterkamp, A.J.; Tjaden, U.R.; van der Greef, J. Strategies for online coupling of immunoassays to HPLC. Trends Anal. Chem. **1995**, *14*, 355–361.
30. Vanderlaan, M.; Lotti, R.; Siek, G.; King, D.; Goldstein, M. Perfusion immunoassay for acetylcholinesterase: Analyte detection based on intrinsic activity. J. Chromatogr. A, **1995**, *711*, 23–31.
31. Cho, B.Y.; Zou, H.; Strong, R.; Fisher, D.H.; Nappier, J.; Krull, I.S. Immunochromatographic analysis of bovine growth hormone releasing factor involving reversed-phase high-performance liquid chromatography-immunodetection. J. Chromatogr. A, **1996**, *743*, 181–194.
32. Irth, H.; Oosterkamp, A.J.; van der Welle, W.; Tjaden, U.R.; van der Greef, J. Online immunochemical detection in liquid chromatography using fluorescein-labeled antibodies. J. Chromatogr. **1993**, *633*, 65–72.

Immunodetection

E.S.M. Lutz
Bioanalytical Chemistry Department, AstraZeneca R&D Mölndal, Mölndal, Sweden

INTRODUCTION

Monitoring a liquid chromatography (LC) effluent by means of an immunoassay provides sensitive and selective detection in combination with the separation of cross-reactive compounds.[1,2] When implementing the immunoassay as a postcolumn reaction detection system after LC, it is frequently referred to as immunodetection.[3,4] Automation and assay speed are the main advantages of immunodetection over off-line coupling of immunoassays to LC by means of fraction collection.[5,6]

The typical setup of immunodetection is illustrated in Fig. 1.[5,6] The column effluent is mixed with labeled antibodies which will bind selectively to the analytes while passing through a reaction coil. This binding is based on the affinity between analyte and antibody and is characterized by the association and dissociation rate constants of the affinity reaction. Whereas the association rate constant (k_{+1}) is diffusion controlled, the dissociation rate constant (k_{-1}) depends on the interactions between the antibody and its antigen. Generally, k_{+1} lies in the range of 10^7–10^8 L/ml sec, whereas k_{-1} is comparably slow (10^3–10^5/sec). The volume of the reaction coil and the flow rates used determine the reaction time during which the labeled antibodies can bind to analyte molecules. Typical reaction times lie in the range of a few minutes and thus allow the fast association reaction to take place, whereas the dissociation reaction can practically be neglected. Quantification of the analyte concentration is then possible by distinguishing labeled antibody which has bound to analyte from free antibody. For that purpose, the free and the bound antibody needs to be separated (e.g., by means of an affinity column which traps free antibody), whereas the analyte–antibody complex passes the affinity column unretained for detection in a conventional flow through the detector. Using this setup, both analyte recognition and quantification occurs through the labeled antibody.

Alternatively, it is possible to use untreated antibodies in combination with a labeled antigen; see Fig. 2.[5,6] Under these circumstances, a two-step reaction is performed after the analytical separation. First, the column effluent is mixed with antibodies to allow the recognition of analyte(s). In the second step, the labeled antigen is added to saturate the fraction of free antibodies and allow quantification. When binding of labeled antigen to the antibody causes a change in detection properties, the reaction mixture can be monitored directly for quantification (homogeneous assay). However, generally the labeled antigen which has reacted with the antibody needs to be separated from the free labeled antigen to allow quantification. Again, affinity columns can be used for this purpose. Other forms of separating free and bound labeled antigens comprise restricted access columns, free-flow electrophoresis, and cross-flow filtration.

REAGENTS

So far, primarily antibodies and their Fab fragments have been implemented in immunodetection for analyte recognition. Antibodies can be raised against virtually any compound of interest; accordingly, their implementation into detection for LC provides a general approach. Antibody affinity and selectivity can be modulated by appropriate design of the hapten, by adequate screening of the antibodies, and by site-directed mutagenesis. Because the chemical structure and properties of antibodies against different antigens is comparatively homogenous, immobilization, stabilization, calibration, and storage procedures can be standardized.

The approach of implementing a biological assay as a postcolumn reaction detection system after LC can not only be applied to antibodybased assays (immunoassays) but also to assays employing other affinity interactions with high association and low dissociation rate constants, such as receptors. Information obtained from such a detection system not only provides quantitative results but also indicates the biological activity of the detected compound.

Requirements with respect to the label used to mark one of the immunoreagents are comparable to those in other postcolumn reaction detection systems.[4] The label should preferably allow sensitive and rapid detection and be non-toxic, stable, and commercially available. So far, mainly fluorescence labels have been employed (e.g., fluorescein), although, in principle, also liposomes, time-resolved fluorescence, and electrochemical or enzymatic labels are feasible. On the other hand, labels providing a slow response, including radioactive isotopes and glow-type chemiluminescence, are less suitable for immunodetection. When attaching the label to the immunoreagent, care has to be taken not to affect the affinity reaction between the antibody and its antigens and thus deteriorate assay performance.

A concern in recent research involving immunodetection has been availability, quality, and cost of reagents,

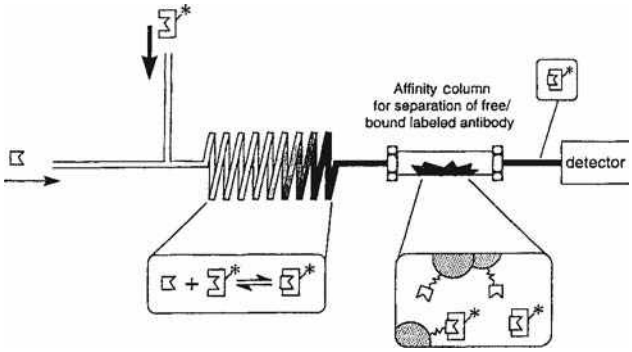

Fig. 1 Scheme of the immunodetection system employing labeled antibodies ( ) and an affinity column for separating labelled antibodies which have reacted with an analyte ( ) from free-labeled antibodies.

especially of antibody and receptor preparations. In the future, this concern may be overcome with novel cloning techniques providing possibilities to drastically reduce the cost of producing proteins as well as to develop proteins for specific applications.

INTERFACING LC/IMMUNODETECTION

The attractiveness of immunodetection consists in its on-line coupling to a separation step, such as liquid chromatography. Parameters to consider are band broadening caused by the postcolumn reaction and interference of the LC mobile phase with the immunoreaction.[4,7]

In conventional immunoassays with long incubation times, the environment in which the affinity reaction is taking place needs to be strictly controlled with respect to, for example, pH, salt, and organic modifier content. In contrast, immunodetection takes place within a few minutes, entailing less stringent requirements with respect to reaction conditions. Nevertheless, the mobile phase needs to be consistent with the affinity reaction; that is, the mobile phase should not denature the immunoreagents or compete with the analyte for the available binding sites. Mobile-phase compatibility has mainly been evaluated with reversed-phase LC, as it is a frequently used analytical separation technique and constitutes the greatest challenges in interfacing to biological assays. The crucial consideration is the organic-modifier content in the reversed- phase LC mobile phase. Investigations have shown that up to 15–25% (v/v) of organic modifier can be used in immunodetection without affecting the antibody–antigen interaction.[5] These results are in concurrence with immunodetection systems which have been coupled to reversedphase LC. At higher concentrations of organic modifier, the affinity reaction can be hampered seriously, which typically is overcome by dilution of the column effluent.[8,9]

However, many interesting analytes (e.g., peptides and proteins) are commonly separated by means of a gradient. The challenge of coupling immunodetection to gradient LC is twofold: On the one hand, the affinity interaction will be affected; on the other hand, the detection properties of the label will vary. For example, using a gradient of organic modifier affects the conformation of the antibody and, thus, its affinity characteristics, as well as the detection properties of a fluorescence label. When acceptance of an increasing baseline[10,11] is out of the question, additional interfacing between the separation step and the immunodetection is required. One approach is to introduce a buffer-exchange step after the separation (e.g., with on-line dialysis[12] or an ion-exchange column[7]). However, this will introduce extra band broadening as well as affect robustness with yet another part in the system.

APPLICATIONS

Feasibility of LC/immunodetection has been shown for quantitative analysis and for screening for biological activity, as summarized in Table 1. For analytical purposes, immunodetection in combination with LC is most promising in those cases when conventional immunoassays or conventional LC methods by themselves do not suffice for accurate analytical determinations. Being an approach offering high selectivity and sensitivity, applications are directed toward measurement of trace levels of compounds which lack appropriate detection properties in complex matrices. This is illustrated, for example, by measuring endogenous levels of the protein granulocyte colony-stimulating factor (GCSF) in biological matrices.[10] Affinity chromatography for sample preparation introduces high selectivity into the system but does not provide

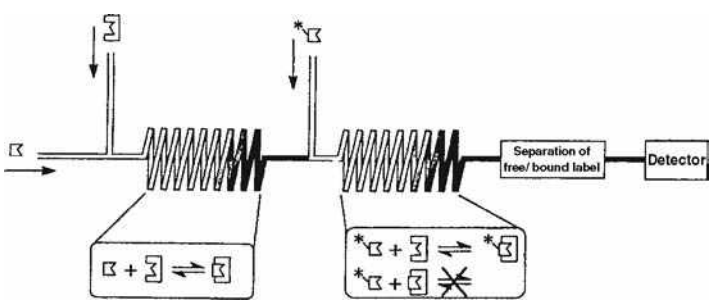

Fig. 2 Scheme of the immunodetection system employing untreated antibodies ( ) and a labeled antigen ( ).

Table 1 Review of immunodetection applications.

Application area	Compound	Matrix	Immunodetection type	Detection limit	Refs.
Protein bioanalysis	Granulocyte colony-stimulating factor (GCSF)	Plasma	Fluorescence-labeled antibodies, affinity chromatography	0.6 nmol/L	[10]
	Growth-hormone-releasing factor (GHRF)	Plasma	Fluorescence and enzyme-labeled antibodies, affinity chromatography, interface for dilution between LC and immunodetection for compatibility	0.2 ng/ml	[9]
	Urokinase	Plasma	Fluorescence-labeled receptor, affinity column	40 nmol/L	[11]
	Interleukine 4	?	Fluorescence-labeled antibodies, affinity chromatography	2 fmol	[16]
Drug bioanalysis	Diogoxin	Plasma	Fluorescence-labeled antibodies, affinity chromatography	0.2 nmol/L	[8]
Biomarker analysis	Sulfodipeptide Leukotrienes	Urine, human cell culture extract	Untreated antibodies and fluorescence-labeled ligand, reversed-phase restricted-access chromatography	0.4 nmol/L	[15]

a means to improve detection properties of the protein. By combining the affinity chromatography for sample preparation with an analytical separation by means of reversed-phase LC and immunodetection, levels of GCSF were determined in plasma.

In other bioanalytical applications, the emphasis lies more on overcoming cross-reactivity. For example, the heart glycoside digoxin is cross-reactive with several of its metabolites as well as with plasma constituents, thus hampering approaches solely based on immunoassays. By treating plasma samples with solid-phase extraction on a restricted access column, coupled online to reversed-phase LC/immunodetection, digoxin and two of its cross-reactive metabolites were analyzed in patients treated with the heart glycoside.[8]

A key to successful drug development is the identification of new lead compounds. Lead compounds can be identified through receptor assays, where the receptor–ligand interaction reflects the biomolecular mechanism associated with a disorder. By implementing the receptor interactions into postcolumn reaction detection systems, biologically active compounds can be separated and detected with high sensitivity and selectivity. This concept has been described for the analysis of estrogens using a recombinant steroid-binding domain of the human estrogen receptor for analyte recognition and coumestrol, a fluorescent estrogen, as reporter molecule.[13] Prior to detection samples were treated online and automated by reversed-phase solid-phase extraction and reversed-phase LC. Selectivity of this system is demonstrated for analysis in urine samples, which shows the feasibility of using this method in the determination of the abuse of steroid hormones in performance doping or cattle breeding. When performing both LC/immunodetection and mass spectrometry, information on biological activity is combined with structure elucidation.[11]

Recently, also direct recognition of active ligands attached to bead surfaces has been achieved with immunodetection.[14] This provides a rapid and automated screening tool which is compatible with solidphase bound compounds originating from solid-phase chemistry in combinatorial chemistry. However, this approach has so far only been published for a model system.

CONCLUSIONS

Immunodetection coupled online to LC as a tool for quantitative analysis has been developed for model compounds as well as been applied in relevant applications. The approach is particularly appealing for trace analysis in complicated matrices and for identifying ligands for certain receptors in drug discovery. However, each application still requires a fair amount of method development and optimization, and obtaining the desired, pure immunoreagents still is a concern, although advances in recombinant protein production are providing us with an increased choice and availability of affinity reagents at reduced cost.

In parallel with miniaturization of LC, immunodetection will be downscaled, thus lowering reagent consumption and, consequently, cost. However, increased challenges with respect to band broadening in a postcolumn reaction detection system and non-specific binding to capillary walls will need to be addressed. The trend toward miniaturization will simultaneously give the opportunity to couple immunodetection to other analytical separation methods, such as capillary electrophoresis. Combination of immunodetection with mass spectrometry enables the combination of information of biological activity with structure elucidation. Other developments in immunodetection concern the separation of free and bound labels, enabling the implementation of suspended materials in detection LC, including, for example, suspended membrane receptors, whole cells, and molecularly imprinted polymers serving as artificial receptors. Consequently, immunodetection potentially conquer new

application areas, such as the evaluation of absorption profiles of drugs and the investigation of drug metabolism on a cellular level.

REFERENCES

1. Mattiasson, B.; Nilsson, M.; Berdén, P.; Håkansson, H. Flow-ELISA: Binding assays for process control. Tr. A. C. **1990**, *9*, 317.
2. De Frutos, M.; Regnier, F.E. Tandem chromatographic immunological analyses. Anal. Chem. **1992**, *65*, 17.
3. Hage, D.S. Survey of recent advances in analytical applications of immunoaffinity chromatography. J. Chromatogr. B, **1998**, *715*, 3.
4. Krull, I.S.; Cho, B.-Y.; Strong, R.; Vanderlaan, M. LC/GC Int. May **1997**, *278.*
5. Irth, H.; Oosterkamp, A.J. Tjaden, U.R.; van der Greef, J. Strategies for on-line coupling of immunoassays to high-performance liquid chromatography. Tr. A. C. **1995**, *14* (7), 355.
6. Lutz, E.S.M.; Oosterkamp, A.J.; Irth, H. On-line coupling of liquid chromatography to biological assays. Chim. Oggi **1997**, *15*, 11.
7. Shahdeo, K.; March, C.; Karnes, H.T. Postcolumn immunodetection following conditioning of the HPLC mobile phase by on-line ion-exchange extraction. Anal. Chem. **1997**, *69*, 4278.
8. Oosterkamp, A.J.; Irth, H.; Beth, M.; Unger, K.K; Tjaden, U.R.; van der Greef, J. Bioanalysis of digoxin and its metabolites using direct serum injection combined with liquid chromatography and on-line immunochemical detection. J. Chromatogr. B, **1994**, *653*, 55.
9. Cho, B.-Y.; Zou, H.; Strong, R.; Fisher, D.H.; Nappier, J.; Krull, I.S. Immunochromatographic analysis of bovine growth hormone releasing factor involving reversed-phase high-performance liquid chromatography-immunodetection. J. Chromatogr. A, **1996**, *743*, 181.
10. Miller, K.J.; Herman, A.C. Affinity chromatography with immunochemical detection applied to the analysis of human methionyl granulocyte colony stimulating factor in serum. Anal. Chem. **1996**, *68*, 3077.
11. Oosterkamp, A.J.; van der Hoeven, R.; Glässgen, W.; König, B.; Tjaden, U.R.; van der Greef, J.; Irth, H. Gradient reversed-phase liquid chromatography coupled on-line to receptor-affinity detection based on the urokinase receptor. J. Chromatogr. B, **1998**, *715*, 331.
12. Kaufmann, M.; Schwarz, T.; Batholmes, P. Continuous buffer exchange of column chromatographic eluates using a hollow-fibre membrane module. J. Chromatogr. A, **1993**, *639*, 33.
13. Oosterkamp, A.J.; Villaverde Herraiz, M.T.; Irth, H.; Tjaden, U.R.; van der Greef, J. Reversed-phase liquid chromatography coupled on-line to receptor affinity detection based on the human estrogen receptor. Anal. Chem. **1996**, *68*, 1201.
14. Lutz, E.S.M.; Irth, H.; Tjaden, U.R.; van der Greef, J. Biochemical detection for direct bead surface analysis. Anal. Chem. **1997**, *69*, 4878.
15. Oosterkamp, A.J.; Irth, H.; Heintz, L.; Marko-Varga, G.; Tjaden, U.R.; van der Greef, J. Simultaneous determination of cross-reactive leukotrienes in biological matrices using on-line liquid chromatography immunochemical detection. Anal. Chem. **1996**, *68*, 4101.
16. Schenk, T.; Irth, H.; Heintz, L.; Marko-Varga, G.; Tjaden, U.R.; van der Greef, J.

Industrial Applications of CCC

Alain Berthod
Laboratory of Analytical Sciences, University of Lyon I, Villeurbanne, France

Serge Alex
Center for Chemical Process Studies of Quebec (CEPROCQ), Montreal, Quebec, Canada

Abstract
Countercurrent chromatography (CCC) is a separation technique using a biphasic liquid system. Since the stationary phase is liquid, the injected solutes have access to its volume rather than only its surface like with a solid stationary phase in classical liquid chromatography (LC). Column overload is much less of a problem in CCC than in LC. It is shown that 24 g of 98% pure glucoraphanin could be produced from a methanolic broccoli seed extract in 4 hr using about 10 L of solvent. The simple liquid–liquid partitioning of the injected material offers an original and unique new approach to any difficult separation. Therefore, CCC should deserve a try in the industrial environment. The modern reliable CCC columns are presented.

INTRODUCTION

For human consumption, industry has to produce material products and goods. The chemical industry produces millions of metric tons of basic chemicals such as soda, ethylene, sulfuric acid, and urea, as well as a few kilograms or less of fine and/or complicated chemicals such as chiral drugs, catalysts, antibiotics, and delicate perfumes.

Countercurrent chromatography (CCC) is useful in the production of the latter class of chemicals. This entry explains the role that CCC can play in industrial processes, revealing concepts and ideas and giving some examples of real large-scale purification performed by the CCC technique. In recent years, significant developments occurred in the preparative side of CCC and modern, large-volume, reliable CCC instruments appeared. At the moment, only a handful of chemical companies are using CCC in commercial processes. Often, they are apparently very successful with the technique, because they purchase more CCC systems and CCC becomes part of the production process. The word is slowly spreading: CCC works.

THE LIQUID STATIONARY PHASE

Defining CCC in few words is easy: CCC is a chromatographic separation technique that uses a support-free liquid stationary phase.[1] The mobile phase must be a solvent or a mixture of solvents immiscible with the liquid stationary phase.

It is the liquid nature of the stationary phase in CCC that renders it useful for three reasons:

1. The solutes can access the whole volume of the stationary phase, not only the surface of a solid stationary phase as in most other chromatographic techniques. Column overload is much more difficult with a CCC column than with a classical preparative liquid chromatography (LC) column of similar volume. Large amounts of a substance can be processed in a single run. Countercurrent chromatography is truly a preparative technique.
2. The retention mechanism is very simple. The only physicochemical parameter responsible for solute retention is the liquid–liquid distribution coefficient, K_D, also called partition coefficient. The retention volume of a given solute is

$$V_R = V_M + K_D V_S = V_C + (K_{D-1})V_S \qquad (1)$$

   where V_M and V_S are the volumes of the mobile and stationary phases respectively, inside the CCC system. The sum of these two volumes always corresponds to the CCC system volume, V_C, because there is absolutely no solid support inside the column.
3. It is possible to use the liquid nature of the stationary phase to gain advantages that have no equivalent in classical LC. For example, the roles of the phases can be switched during a run: the mobile phase becomes the stationary phase, and vice versa. This way of working with a CCC column is called the dual mode method (see *Octanol–Water Distribution Constants Measured by CCC*, p.1616). It is also possible to flush the content of a CCC column, ensuring a complete recovery of all parts of the injected sample.

A combination of these three points produces the following advantages.

A study and optimization of a separation of a complex mixture can be accomplished with a low-volume CCC column by injecting small amounts of the sample and using reduced solvent volumes. The biphasic liquid system composition is *optimized rapidly and efficiently*.

If the retention volumes of some constituents of the sample are too large, different methods using the liquid stationary phase can be employed to speed up the separation. For example, the dual mode method can be used. The retained constituents are eluted in the reversed mode. It is absolutely certain that *no part of the sample can stay trapped* inside the CCC column.

Once the separation is optimized, the distribution coefficient of each constituent is then calculated using Eq. 1. The very same liquid system must be used in a large-volume CCC column so that the distribution coefficients remain identical. So, the *retention volumes of each component can be predicted* because the distribution coefficients depend only and entirely on the liquid–liquid system. The scaling-up is straightforward.[2]

LARGE-SCALE SEPARATION OR PURIFICATION

Industrial CCC Equipment

In the twentieth century, only the Japanese company Sanki Engineering Ltd. marketed industrial CCC columns based on the hydrostatic CCC scheme (interconnected channels). Recently, new large-scale CCC columns based on the hydrodynamic scheme (open tubes coiled in rotating spools) were developed in the United Kingdom and China, and modern and reliable hydrostatic preparative CCC columns were developed in France (Fig. 1 and Table 1). These twenty-first-century machines are much more efficient, well designed, and reliable than previously proposed large-volume CCC columns. On industrial determination, they could definitively prove the CCC capability in terms of purity of the produced compounds, solvent saving, and throughput.

Classical Use of the CCC Column

In a recent work, 1 kg of glucoraphanin was isolated from raw broccoli seed using a 5 L Midi column (Dynamic Extraction, Berkshire, U.K.) (Table 1).[3] Glucoraphanin is a promising cancer preventive and antioxidant drug of the glucosinolate family. This potassium salt of β-thioglucoside-*N*-hydroxysulfate is highly polar and is always present in the seed along with its glucosinolate homologue, glucoiberin, differing from glucoraphanin shorter by a methylene group. Eight kilograms of broccoli seed were extracted by boiling methanol to produce about 4.8 kg of crude extract that was processed in 42 CCC runs done in 7 days. The biphasic liquid system used was a mixture of 1-propanol/acetonitrile/31% ammonium sulfate solution in the 1/2/4 v/v ratio. The lower aqueous phase was selected to be the stationary phase. The upper organic phase was the mobile phase flown in the tail-to-head direction at 40 ml/min. A total of 115 g of methanolic crude extract was dissolved in 240 ml of a 1/1 upper/lower phase mixture. The injection volume corresponded to about 5% of the whole column volume. The full CCC run needed about 10 L of mobile phase eluted in 4 hr, producing about 24 g of 98% pure glucoraphanin. The production of 1 kg of 98% pure glucoraphanin needed 420 L of solvents and 170 working hours. The average throughput of this purification was an impressive 6 g of glucoraphanin per hour meaning that 0.42 L of solvent was used to purify one gram of glucoraphanin.

The production of 1 kg of 98% pure glucoraphanin is the largest published CCC purification procedure to date. The high loading capability of large-volume CCC systems is commonly used in industry. Large amounts (in the scale of several grams) of natural products with high added values are separated by CCC. Alkaloids, antibiotics, enzymes, macrolides, peptides, rare fatty acids, saponins, tannins, taxoids and/or precursors of Taxol®, and other fine chemicals have been isolated, separated, and/or purified by preparative CCC.[1,2]

The specificities of CCC that could promote its use rather than the use of classical preparative liquid chromatography purification are as follows:

- An original or unique selectivity obtained with a subtle polarity difference between the two liquid phases.
- The possibility of injecting heavily concentrated, viscous, or even polyphasic samples (e.g., fermentation broths).
- The gentle interactions during the separation process that preserve delicate molecules (e.g., proteins) from denaturation.

Displacement Chromatography

In displacement chromatography, the sample to be purified is injected in a large volume, or even continuously, into the CCC machine. The sample components have different affinities for the stationary phase in an exclusive way: The component with a higher affinity for the stationary phase displaces another one with a lower affinity. Bands of pure components form. This method of using CCC offers the maximum throughput capability.[1,2] Displacement CCC can be done using the solute ionization capability (pH zone refining) or complexation capability (ion-exchange CCC).

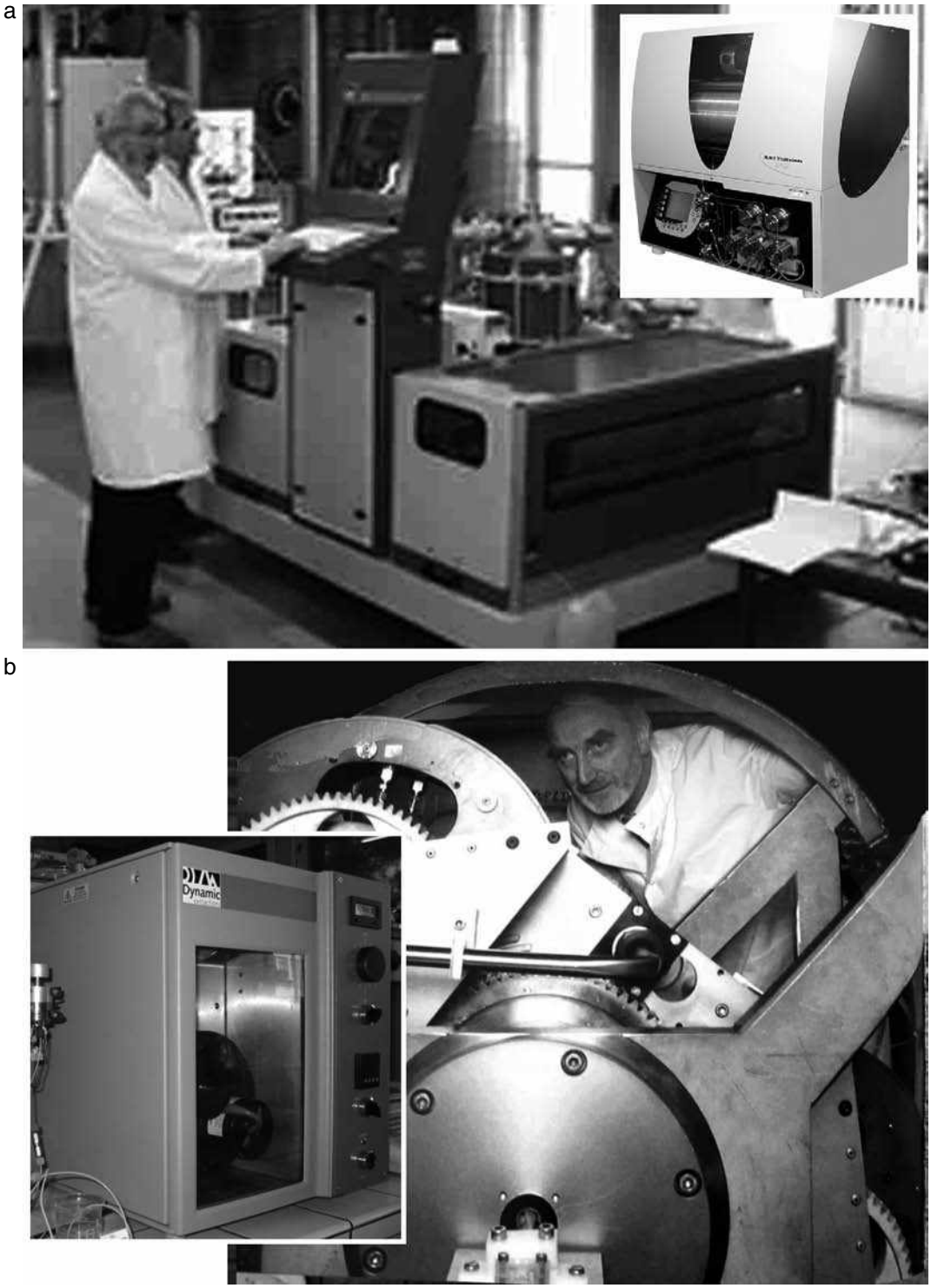

Fig. 1 Countercurrent chromatography columns. a, The hydrostatic Armen Elite CPC12L with two 6 L rotors. The inset shows the small Elite CPC250 (0.25 L column) (http://www.armen-instrument.com and Table 1); b, The hydrodynamic Maxi 5 L column. Pr. Ian Sutherland (Brunel University, Uxbridge, U.K.) poses inside the rotor to give the scale. The inset shows the Spectrum 20 ml column (http://www.dynamicextractions.com and Table 1).

pH Zone Refining

pH zone refining is a form of displacement chromatography for ionizable compounds. It sorts compounds by their ionization constants, K_a, using a stationary phase with a different pH from the mobile phase.[4] For example, the stationary phase is an acidic organic phase [e.g., methyl *tert*-butyl ether (MTBE) with 1% acetic acid] and the

Table 1 Commercially available CCC columns and their typical characteristics.

Model name	Volume (L)	Size (L × W × H, cm)	Weight (kg)	Maximum rotation (rpm)	Maximum pressure (kg/cm^2)	Maximum flow rate (ml/min)	Maximum sample load (g)	Typical run time (min)	Price level (U.S. $ in thousands)[a]
Hydrodynamic columns									
Dynamic Extractions: 890, Plymouth Rd, Slough, Berkshire, SL1 4LP, U.K.; Tel: +44 1753 696979; Fax: +44 1753 696976 (http://www.dynamicextractions.com)									
Spectrum	0.02					1	0.1	20	
	0.05	46 × 52 × 48	65	2100	8	5	0.5	20	~100
	0.125					10	1.2	30	
Midi	0.04					1	0.2	40	
	0.5	58 × 66 × 56	85	1400	6	100	5	10	~130
	1					100	20	20	
Maxi	5	200 × 270 × 150	500	850	6	1500	1500	30	—
Quattro AECS: P.O. Box 80, Bridgend, South Wales, CF31 4XZ, U.K.; Tel: +44 1656 782985; Fax: +44 1656 789 282 (http://www.ccc4labprep.com)									
Quickprep	0.02					1	0.5	40	
MK5	0.1	42 × 42 × 45	80	860	8	5	4	40	~30
	0.85					30	30	80	
Tauto Biotech: Aidisheng Road, Zhangjiang High-Tech Park, 201203 Shanghai, China; Tel: +86 21 51320588; Fax: +86 21 51320502 (http://www.tautobiotech.com)									
TBE 20A	0.02	33 × 60 × 50	60	1500	15	1	0.5	40	~30
TBE 300A	0.26	53 × 52 × 33	95	900	10	2	5	200	~35
TBE 1000A	1	62 × 91 × 104	400	600	12	10	20	200	~45
Hydrostatic columns									
Armen Instruments: 15 rue Ampère, Z.I. de Kermelen, 56890 Saint Ave, France; Tel: +33 297 618 400: Fax: +33 297 618 500 (http://www.armen-instrument.com)									
Elite CPC250	0.25	48 × 48 × 47	60	2500	140	25	5	20	~50
Elite CPC2X500[b]	2 × 0.5	56 × 68 × 56	80	2500	140	40	10[b]	20	~100
Elite CPC1000	1	56 × 68 × 56	80	2500	140	100	20	20	~100
Kromaton SEAB: 9 rue Alexander Fleming, 49066 Angers, France, Tel +33 241 774 148, Fax: +33 241 739 623 (http://www.kromaton.com)									
FCPC C50	0.05	33 × 52 × 60	45	2000	60	10	1	10	~35
FCPC A200	0.2	72 × 68 × 48	65	2000	60	20	5	20	~50
FCPC A1000	1	72 × 68 × 48	80	1500	50	30	30	60	~65
FCPC A5000	5	100 × 67 × 117	410	1200	50	150	150	60	~250

[a]U.S. prices are indicative only and were obtained from the CCC Web site http://www.cherryinstruments.com for delivery in continental United States (May 2008).
[b]The Armen CPC2X500 has two 0.5 L columns that could perform the TMB continuous separation way (see text).

mobile phase is an aqueous basic buffer (e.g., 0.015 *M* NH_3 solution, pH 10). The acid in the stationary phase is considered as the retainer and the base in the mobile phase is the displacer.

Up to 60% of the CCC system volume of a mixture of organic acids can be introduced into the apparatus (in their ammonium salt form at pH 10).[4] As the mixture contacts the acidic stationary MTBE phase, the injected organic salts are protonated: these ions take their molecular form. A very large polarity difference exists between the ionic form and the molecular form of these solutes. The protonated molecular forms stay in the organic phase, and the ionized basic forms prefer the aqueous phase. The weaker acid is protonated first, and so it is the most retained. Bands of pure and concentrated organic acids form in the order of decreasing pK_a values.[4]

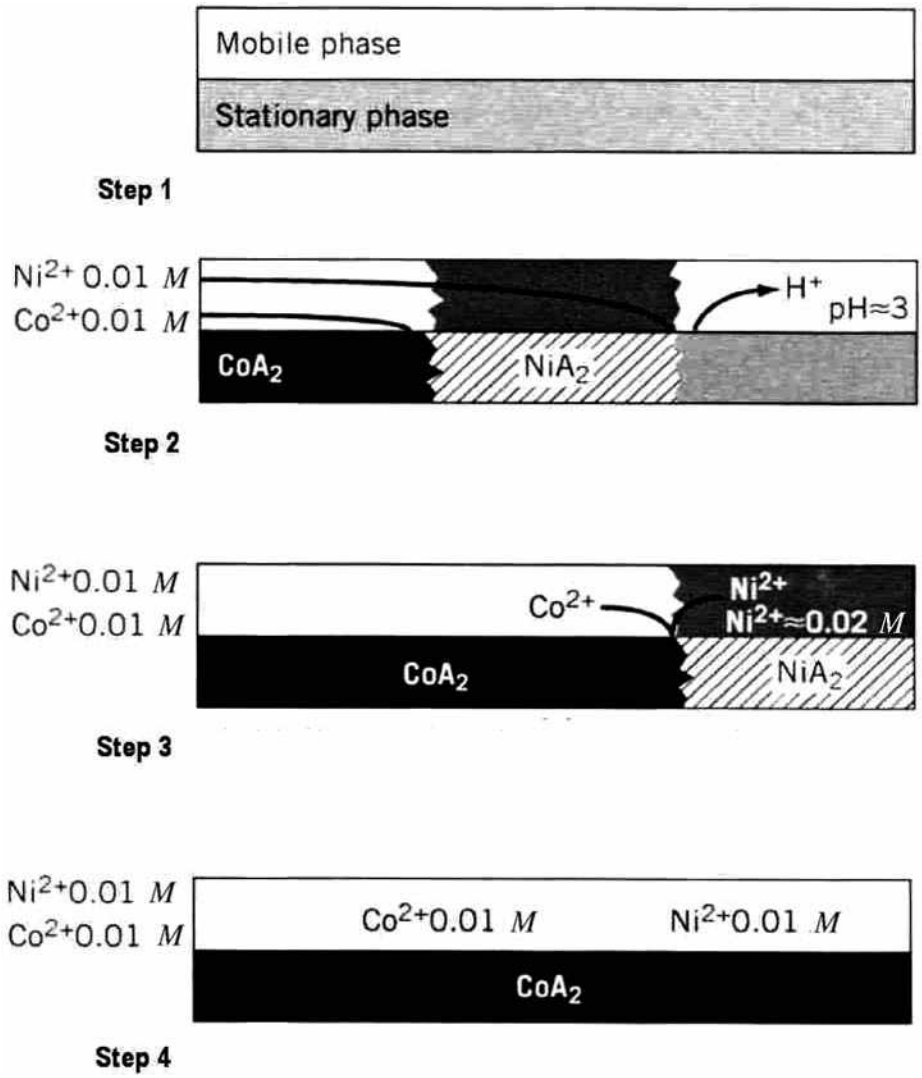

Fig. 2 Removal and separation of cobalt and nickel ions by CCC. Stationary phase: heptane + diethyl hexyl phosphoric acid (noted HA, concentration 0.5 *M*); mobile phase: aqueous solution of cobalt and nickel acetate (0.01 *M* each). Step 1: The CCC machine is equilibrated with water. Step 2: The ionic solution is introduced into the machine; the ions are extracted into the stationary phase; and the cobalt complex displaces the nickel one, which is less stable. Deionized water at pH 3 exits the column because all ions are replaced by protons. Step 3: The stationary phase is saturated in nickel ions. The greenish effluent leaving the machine contains only nickel ions, which is 2 times more concentrated than the entering solution. Cobalt ions are still extracted, displacing nickel ions. Step 4: End of the process—the stationary phase is saturated in cobalt ions. The machine is stopped; the dark blue stationary phase is collected; and cobalt ions are recovered by an acid wash.
Source: From Chromatographie a contre courant et micelles inverses pour la separation et l'extraction de cations metalliques, in Can. J. Chem.[5]

Ion-Exchange CCC

Complexation can be used to separate metallic ions on an industrial scale. Fig. 2 illustrates the process in the case of the separation of nickel and cobalt ions.[5] A chelating agent (e.g., diethyl hexyl phosphoric acid) is added to a heptane stationary phase. A large volume (up to 20 times the CCC machine volume V_C) of the ionic solution is introduced into the CCC column. The nickel ions are displaced in the aqueous phase, and the cobalt ions can be collected in the stationary phase. More than two ions can be separated in bands of increasing complexation constants order.[5] Because no ions can stay trapped inside the CCC machine, it could be a very potent tool in the separation of radionuclides in the processing of nuclear wastes.

Extraction

Countercurrent chromatography can be used to extract and to concentrate, in a low volume of the stationary phase, a component present in large volumes of the mobile phase. It was shown that a 60 ml CCC instrument was able to extract 285 mg of a non-ionic surfactant contained in 20 L of water (at 16.5 ppm or mg/L) and was able to concentrate it into 30 ml of ethyl acetate (at 9500 ppm or 9.5 g/L).[6]

CONCLUSION

At the moment, CCC is scarcely used in industry, the reason being that the technique is not well known because only a few small companies market good and reliable CCC systems. However, the capabilities of a

liquid stationary phase in industrial environment are very large. The CCC technique could be of great help in many industrial processes such as classical ones, extraction, purification, and separation of fragile compounds, as well as in novel ones such as the use of a CCC system as a powerful liquid–liquid reactor.

REFERENCES

1. Berthod, A. *Countercurrent Chromatography: The Support-Free Liquid Stationary Phase*; Comprehensive Analytical Chemistry; Elsevier: Amsterdam, 2002; Vol. XXXVIII.
2. Berthod, A. CCC: From the milligram to the kilogram. Adv. Chromatogr. **2009**, *47*, 323–352.
3. Sutherland, I.A. Recent progress on the industrial scale-up of CCC. J. Chromatogr. A, **2007**, *1151*, 6–13.
4. Ito, Y.; Shinomiya, K.; Fales, H.M.; Weisz, A. pH-Zone refining CCC. A new technique for preparative separation. In *Modern Countercurrent Chromatography*; Conway, W.D.; Petroski, R.J., Eds.; ACS Symposium Series No. 368; American Chemical Society: Washington, D.C., 1995; 156–183.
5. Berthod, A.; Xiang, J.; Alex, S.; Collet-Gonnet, C. Chromatographie a contre courant et micelles inverses pour la separation et l'extraction de cations metalliques. *Can. J. Chem.* **1996**, *74*, 277–286.
6. Berthod, A. High speed CCC in environmental analysis. In *Encyclopedia of Environmental Analysis and Remediation*; Meyers, R.A., Ed.; John Wiley & Sons: New York, 1998; 1312–1327.

Injection Techniques for CE

Robert Weinberger
CE Technologies, Inc., Chappaqua, New York, U.S.A.

INTRODUCTION

In liquid chromatography (LC), a loop containing a defined volume is used to introduce the sample into the flowing mobile phase. Injection in high-performance capillary electrophoresis (HPCE) differs in two ways: (a) the injection volume is not as well defined and (b) injection is performed with the electric field turned off. Both of these features can contribute to quantitative errors of analysis. In addition, the length of the injection plug must be kept quite small to maintain the efficiency of the electrophoretic process.[1] The use of stacking electrolytes permits large injections to be made.[2] This is necessary to achieve acceptable limits of detection.

There are two modes of injection in capillary electrophoresis (CE): hydrodynamic injection and electrokinetic injection. In hydrodynamic injection, pressure or vacuum are placed on the inlet sample vial or the outlet waste vial, respectively. For electrokinetic injection, the voltage is activated for a short time with the capillary and electrode immersed in the sample.

The general process of performing an injection and run is as follows:

1. The capillary is rinsed with 0.1 N sodium hydroxide or 0.1 N phosphoric acid for 1–2 min.
2. A second rinse with background electrolyte (BGE) is performed for 2–3 min.
3. The inlet side of the capillary is immersed in the sample.
4. Injection is performed for 1–30 sec.
5. The voltage is ramped up (15 sec) to the designated value and the separation is performed.
6. The process repeats for the next sample.

VOLUMETRIC CONSTRAINTS ON INJECTION SIZE

Because the entire internal volume of a 50 cm × 50 μm-inner diameter (I.D.) capillary is only 981 nl, the injection volume must be kept quite small. The contribution to band broadening (variance) from a plug injection is given by

$$\sigma_{\text{inj}}{}^2 = \frac{l_{\text{inj}}{}^2}{12} \tag{1}$$

where l is the length of the injection plug. To calculate the band broadening from the injection process, the diffusion-limiting case can be considered using the Einstein equation:

$$\sigma_{\text{diff}}{}^2 = 2D_m t \tag{2}$$

Because the squares of the variances are additive, the contributions to band broadening from injection and diffusion can be inserted into the theoretical plate equation:

$$N = \left(\frac{L_d}{\sigma_{\text{tot}}}\right)^2 \tag{3}$$

For a 50 cm capillary and a solute migration time of 600 sec, the impact of the injection size for a small molecule ($D_m = 10^{-5}$ cm^2/sec) and large molecule ($D_m = 10^{-6}$ cm^2/sec) is shown in Fig. 1.

As illustrated in Fig. 1, injection of 1% (0.5 cm) of the capillary volume with sample produces a 92% loss of efficiency for a large molecule and an 8% loss of efficiency for a small molecule. Because diffusion is a limiting cause of efficiency, the large molecule provides a higher number of theoretical plates. The more efficient the separation process, the more difficult it is to maintain that inherent efficiency.

This model assumes that the sample is dissolved in BGE. Through the use of a low-ionic-strength solution as the sample diluent, sample stacking permits large-volume injections to be made.

In a well-controlled separation, injection can be the greatest source of band broadening.[1] This is one of the reasons that micromachined systems may become important for high-resolution DNA separations. In this case, it is possible to inject minute amounts of sample and use shortened separation channels.[3] Sensitivity does not suffer because laser-induced detection is employed.

HYDRODYNAMIC INJECTION

The volume of material injected per unit time (V_t, nl/sec) is determined by the Poiseuille equation.

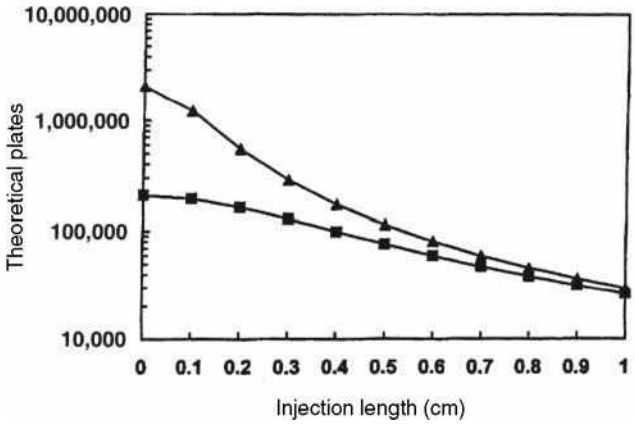

Fig. 1 Effect of the injection zone length on the number of theoretical plates for a small molecule and large molecule (■, $D_m = 10^{-5}$ cm^2/sec) and large molecule (▲, $D_m = 10^{-6}$ cm^2/sec) as solved by Eq. 3. Conditions: capillary length = 50 cm to detector; migration time = 600 sec.

$$V_t = \frac{PD^4\pi}{128\eta L} \tag{4}$$

where ΔP equals the pressure drop, D is the capillary internal diameter, η is the viscosity, and L is the length of the capillary. On some instruments, the pressure is generated by raising the capillary inlet side (siphoning).

The problems generated using an open-ended injection system as shown by the Poiselle equation dictate that changes in the experimental conditions will result in variations of the amount of material injected. Internal standards are best used to compensate for some of the experimental variables.

Pressure-driven systems are preferred compared to vacuum-driven systems for two reasons: (a) Generation of pressures over 1 atm is important when viscous polymer networks are used for size separations and (b) interface to the mass spectrometer is simpler.

ELECTROKINETIC INJECTION

The quantity (Q) of a solute injected is given by

$$Q = (\mu_{ep} + \mu_{eo})\pi r^2 ECt \tag{5}$$

where μ_{ep} and μ_{eo} are the electrophoretic and electro-osmotic mobilities, respectively, r is the capillary radius, E is the field strength, t is the time of injection, and C is the concentration of each solute.

As illustrated in Fig. 2, solutes with high mobility are preferably injected compared to those with low mobility.[4] Note the smaller peak heights for lithium and arginine compared to rubidium when electrokinetic injection is employed. Solutes that have identical mobility in free solution show no such bias (e.g., oligonucleotides and DNA fragments). This is fortunate because it is often necessary to use electrokinetic injection with gel-filled capillaries or when high-viscosity polymer networks are employed.

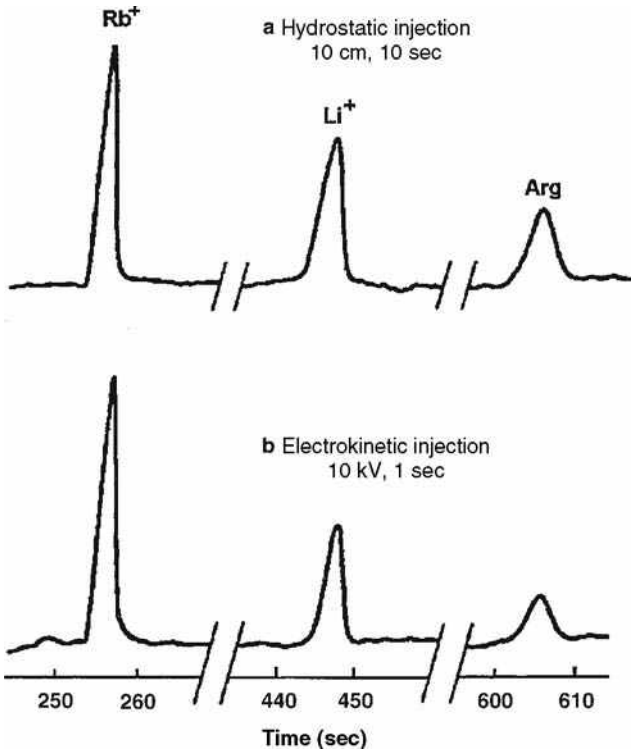

Fig. 2 Hydrostatic vs. electrokinetic injection. Buffer: 20 mM MES adjusted with histidine to pH 6.0; solutes: Rb^+, Li^+, and arginine, 5×10^{-5} M injection: (top) hydrostatic, $\Delta h = 10$ cm, $t = 10$ sec; (bottom) electrokinetic, 1 sec at 10 kV; detection: conductivity.
Source: Reprinted with permission from Bias in quantitative capillary zone electrophoresis caused by electrokinetic sample injection, in Anal. Chem.[4]

The problem with electrokinetic injection is that the field strength at the point of injection is inversely proportional to the sample conductivity. Calibration curves for ionic solutes show negative deviations from linearity because of this. Internal standards are necessary unless it is certain that the sample conductivities are identical. Low-conductivity samples are preferable because they stack.

The advantage of electrokinetic injection is that extreme trace enrichment is possible.[5] If the electro-osmotic flow approaches zero, it is possible to inject only solute ions, omitting the sample diluent.

"SHORT-END" INJECTION

The section of capillary between the outlet vial and the detector can be used for high-speed separations if sufficient selectivity is designed into the separation.[6] The process is

as follows. (1) Equilibrate the capillary in BGE as usual. (2) Place the sample at the capillary outlet. (3) Inject by pressuring the outlet vial or with electrokinetic injection using negative polarity (inlet-side negative). (4) Set the power supply to negative polarity and perform the usual voltage ramp. Because the capillary length is short, the injection should also be kept small and stacking buffers should be used. Be sure to set the detector time constant to 10–20% of the peak width to minimize that form of band broadening. Depending on the instrument, the short-end of the capillary usually ranges from 6 to 10 cm.

INJECTION ARTIFACTS, PROBLEMS, AND SOLUTIONS

No Injection

A plugged capillary is the usual culprit. Cut a few millimeters of the inlet or pressurize the outlet with a syringe to unplug it. When plugged, the observed current is usually zero. No injection can also occur if an empty or incorrect sample vial is used, if an incorrect vial is called for in the method, if the vial cap is missing or badly leaking, or if the external pressure source (if required) is not activated. It is possible that the capillary is broken. Breaks usually occur at the detection window. Check that the voltage polarity is correctly set.

Peak Tailing

Peak tailing can result from a poorly cut capillary inlet. If the capillary is not cut squarely, a concentration gradient can occur upon injection.[7]

Peak Splitting

Artifactual-injection-related peak splitting can occur under certain conditions. When the sample diluent contains organic solvents and micellar electrokinetic capillary electrophoresis or cyclodextrin containing electrolytes are employed, splitting can occur due to the distribution of the solute between two phases moving at different speeds at the point of injection.[8] The problem is solved by dissolving the solute in aqueous media. If the sample is insoluble in totally aqueous solvents, 6 *M* urea can be added both to the BGE and the sample diluent.

A fracture near the capillary inlet can also cause peak splitting. The break can occur if the capillary hits a vial wall or seal. The polyimide coating keeps the cracked portion intact. During injection, the sample moves into the capillary from both the open end of the tube and through the crack. The split peak is usually smaller than the main component and always has a migration time that is a little shorter. This is confirmed by examining the capillary inlet. If fractured, a small piece often detaches and the peak splitting is resolved.

REFERENCES

1. Huang, X.; Coleman, W.F.; Zare, R.N. Analysis of factors causing peak broadening in capillary zone electrophoresis. J. Chromatogr. **1989**, *480*, 95.
2. Burgi, D.; Chien, R.-L. Optimization in sample stacking for high-performance capillary electrophoresis. Anal. Chem. **1991**, *63*, 2042.
3. Jacobson, S.C.; Hergenroder, R.; Koutny, L.B.; Warmack, R.J.; Ramsey, M.J. Effects of injection schemes and column geometry on the performance of microchip electrophoresis devices. Anal. Chem. **1994**, *66*, 1107.
4. Huang, X.; Gordon, M.J.; Zare, R.N. Bias in quantitative capillary zone electrophoresis caused by electrokinetic sample injection. Anal. Chem. **1988**, *60*, 375.
5. Zhang, C.-X.; Thormann, W. Head-column field-amplified sample stacking in binary system capillary electrophoresis. 2. Optimization with a preinjection plug and application to micellar electrokinetic chromatography. Anal. Chem. **1998**, *70*, 540.
6. Euerby, M.R.; Johnson, C.M.; Cikalo, M.; Bartle, K.D. Short-end injection—rapid analysis capillary electrochromatography. Chromatographia **1998**, *47*, 135.
7. Guttman, A.; Schwartz, H.E. Artifacts related to sample introduction in capillary gel electrophoresis affecting separation performance and quantitation. Anal. Chem. **1995**, *67*, 2279.
8. Weinberger, R. Am. Lab. **1997**, *29*, 24.

Inorganic and Organic Cations: Ion Chromatographic Determination

Rajmund Michalski
Institute of Environmental Engineering, Polish Academy of Science, Zabrze, Poland

Abstract
Ion chromatography is an analytical technique that has changed the analysis of inorganic and organic ions, and has revolutionized analytical chemistry. Recently, there is a significant number of ion chromatography methods developed for the determination of cations in a wide variety of sample matrices. A short review of application of ion chromatography for the determination of inorganic and organic cations of alkali, alkaline earth, ammonia, heavy and transition metals as well as lanthanides and actinides is described.

INTRODUCTION

A variety of methods have been used for the analysis of inorganic and organic cations: traditional spectroscopic techniques such as colorimetry, wet chemical methods such as gravimetric analysis, turbidimetry, and titrimetry, and electrochemical techniques such as use of an ion-selective electrode and amperometric titrations. Some of these methods suffer from interferences and limited sensitivity; they can be labor-intensive and are often difficult to automate.

The most popular instrumental methods available for cation analysis are rapid and sensitive spectroscopic methods like AAS (Atomic Absorption Spectroscopy), ICP–AES (Inductively Coupled Plasma–Atomic Emission Spectroscopy), and ICP–MS (Inductively Coupled Plasma–Mass Spectrometry), as well as electrochemical methods such as polarography and anodic stripping voltammetry.[1]

In some cases they are unsuitable for direct trace analysis in complex matrix samples, because of spectral and chemical interferences, or for studies on metal speciation. Due to strong environmental impact, metal ion determination and speciation have been given significant attention in the last few years.[2,3]

An alternative to spectroscopic methods in the analysis of cations are liquid chromatography methods, which can be divided into:

1. Ion chromatography (ion exchange: cation, anion, and ion exclusion).[4]
2. Reversed-phase ion interaction chromatography.[5]
3. Chelation chromatography.[6]
4. Multidimensional and multimode chromatography (e.g., ion exchange coupled with ion exclusion).

Acceptance of ion chromatography for anion analysis was very rapid mainly due to the lack of alternative methods that could quickly and accurately determine several anions in a single analysis. However, the situation regarding analysis of cations was quite different because of many alternative rapid and sensitive methods available. Nevertheless, ion chromatography has advantages over spectroscopic techniques for cation analysis because it allows metal speciation and simultaneous determination of many ions, thus the total ionic composition is known using a single analytical technique.[7]

Division of ion chromatography methods regarding separation mechanism and detection mode used is given in Table 1. Taking into consideration analytical conditions and equipment necessary for the determination of inorganic and organic cations (separation column, eluent, detection mode), analytes determined by means of ion chromatography methods can be divided into three groups:

- alkali and alkaline earth metals, and ammonium[8]
- heavy and transition metals; lanthanides and actinides[9,10]
- organic cations.[11]

Determination of alkali metals, alkaline earth metals, and ammonia is the most often used application of ion chromatography in the range of cation analysis. The key advantage of this method is the ability to determine ammonia in complex samples that contain both inorganic cations and organic amines, as the latter compounds can interfere with the conventional colorimetric or ion selective electrode methods used for ammonia analysis.

Cation exchangers are usually made of organic polymers (styrene-divinylbenzene, ethylvinylbenzene-diviniylbenzene, polymethacrylate, and polyvinyl), however, a variety of other substrate materials are also available (e.g., latexed cation exchangers, silica-based exchangers).

Table 1 Cations determined by ion chromatography methods.

Analyte groups		Examples of analytes	Separation mechanism	Detection mode
Inorganic	Alkali, alkaline earth metals and ammonia	Li^+, Na^+, K^+, NH_4^+, Rb^+, Cs^+, Mg^{2+}, Ca^{2+}, Sr^{2+}, Ba^{2+}	Cation exchange	Suppressed and non-suppressed conductivity
	Heavy and transition metals	Cu^{2+}, Ni^{2+}, Zn^{2+}, Co^{2+}, Cd^{2+}, Pb^{2+}, Mn^{2+} Fe^{2+}, Fe^{3+}, Sn^{2+}, Sn^{4+}, Cr^{3+}, V^{4+}, V^{5+}, UO_2^{2+}	Anion exchange ion exclusion,	Ultraviolet and visible spectrometry (UV/Vis), AAS, ICP, ICP–MS, ICP–AES
	Lanthanides, actinides	La^{3+}, Ce^{3+}, Pr^{3+}, Nd^{3+}, Sm^{3+}, Eu^{3+}, Gd^{3+}, Tb^{3+}, Dy^{3+}, Ho^{3+}, Er^{3+}, Tm^{3+}, Yb^{3+}, Lu^{3+}, Am^{3+}, Cm^{3+}, Pu^{3+}	Anion exchange, cation exchange	UV/Vis, AAS, ICP, ICP–MS, ICP–AES
Organic	Low-molecular-weight amines, alkylamines, mono-, di-, tri-, tetramethylamine, alkanolamines, monoethanolamine, diethanolamine		Cation exchange, ion pair	Suppressed and non-suppressed conductivity
	High-molecular-weight amines alkylamines, aromatic amines, cyclohexamines, quaternary ammonium ions, polyamines		Cation exchange, ion pair	Suppressed and non-suppressed conductivity, UV/Vis

Elution order of alkali and alkaline earth metals and ammonia cations depends on many factors (e.g., column selectivity, eluent type) but is usually as follows: Li^+, Na^+, NH_4^+, K^+, Mg^{2+}, Ca^{2+}, and Ba^{2+}.

Type of eluent for cation-exchange chromatography depends on the detection method being used.[12] In suppressed and non-suppressed ion chromatography for the separation of alkali metals, ammonium and small aliphatic amines on strong cation exchangers, and mineral acids (e.g., HCl, H_2SO_4, HNO_3) are typically used as eluents.

Divalent cations such as alkaline earth metals exhibit a much higher affinity with stationary phase of strong acid cation exchangers and thus cannot be eluted with diluted mineral acids. Therefore, application of another eluent is necessary.

Simultaneous analysis of alkali and alkaline earth metals can only be performed with weak acid cation exchangers, using carboxylic groups as ion-exchange functionality group and usually with methanesulfonic acid as the eluent.

In non-suppressed ion chromatography, mixtures of ethylenediamine and aliphatic carboxylic acids (such as tartaric acid or oxalic acid) are typically employed. In suppressed ion chromatography, the required reduction of background conductivity would only be possible by using high-capacity membrane-based suppressor systems.

In spite of strong competition from atomic spectrometric techniques, ion chromatography of heavy and transition metal cations is now well established as the relative cheapness, ease of automation, and online capability is particularly attractive in a wide variety of routine trace analysis.

Unlike spectroscopic methods, ion chromatography can distinguish different metal oxidation states such as Cr(III)/Cr(VI), Fe(II)/Fe(III), or As(III)/As(V).[13,14] Moreover, ion chromatography has also been used to determine stable metal complexes. A further advantage of ion chromatography over spectroscopic methods is its relatively wide dynamic range, which means that it is possible to determine low analyte concentrations in the presence of high levels of other species, which would tend to cause problems in nebulizers used in atomic spectrometry.

There is a significant number of ion chromatography methods developed for the determination of metal pollutants in a wide variety of environmental samples.[15] Review of current state of research and progress in ion chromatography as an analytical tool for trace metal analysis in environmental samples is described by Shaw and Haddad.[16]

Separation of heavy and transition metals with ion exchangers requires complexation of metal ions in the mobile phase to reduce their effective charge density. Because selectivity coefficients for heavy and transition metals of the same valency are so similar, a selectivity change is obtained only by the introduction of a secondary equilibrium such as a complexation equilibrium established by adding appropriate complexing agents to the mobile phase.

When selecting a ligand for the separation and elution of heavy and transition metal ions from cation exchangers, the following guidelines should be taken into account:

- Metal ions and ligands must form neutral or anionic complexes.
- Different complex formation constants for the various metals increase the selectivity.
- Transition metal complexes being formed should be thermodynamically stable and kinetically labile.

Table 2 Examples of ion chromatography methods for inorganic and organic cations analysis established by ISO, US EPA, and ASTM.

Method number	Method name	Analytes	Matrices
	ISO methods		
ISO 14911 (1998)	Water quality—determination of dissolved Li^+, Na^+, NH_4^+, K^+, Mn^{2+}, Ca^{2+}, Mg^{2+}, Sr^{2+}, and Ba^{2+} using ion chromatography method	Li^+, Na^+, NH_4^+, K^+, Mn^{2+}, Ca^{2+}, Mg^{2+}, Sr^{2+}, Ba^{2+}	Drinking water, wastewater, ground water
	US EPA methods		
US EPA method 200.10 (1997)	Determination of trace elements in marine waters by online chelation preconcentration and inductively coupled plasma–mass spectrometry	Cd^{2+}, Co^{2+}, Cu^{2+}, Pb^{2+}, Ni^{2+}, VO^{2+}, VO_2^{2+}, UO_2^{2+}	Brines, seawater, marine water, estuarial water
US EPA method 200.13 (1997)	Determination of trace elements in marine waters by off-line chelation preconcentration with graphite furnace atomic absorption	Cd^{2+}, Co^{2+}, Cu^{2+}, Pb^{2+}, Ni^{2+}	Brines, seawater, marine water, estuarial water
US EPA method 300.7 (1995)	Dissolved sodium, ammonium, potassium, magnesium, and calcium in wet deposition by chemically suppressed ion chromatography	Na^+, NH_4^+, K^+, Mg^{2+}, Ca^{2+}	Wet deposition, rain water, snow, dew, sleet, hail
	ASTM methods		
D 6504–00	Standard practice for on line determination of cation conductivity in high purity water	Li^+, Na^+, NH_4^+, K^+, Mg^{2+}, Ca^{2+}	High purity water
D 6919–03	Standard test method for determination of dissolved alkali and alkaline earth cations and ammonium in water and wastewater by ion chromatography	Li^+, Na^+, NH_4^+, K^+, Mg^{2+}, Ca^{2+}	Reagent water, surface water, ground water, wastewater
UOP 959–98	Ammonium determination in aqueous solutions by ion chromatography	NH_4^+	Drinking water, wastewater
WK653	New determination of dissolved alkali and alkaline earth cations and ammonium in water and wastewater by ion chromatography	Li^+, Na^+, NH_4^+, K^+, Mg^{2+}, Ca^{2+}	Reagent water, surface water, ground water, wastewater

Among many ligands used for simultaneous ion chromatography of metals, the most common eluents used are oxalic acid, tartaric acid, citric acid, 4-(2-pirydylazo)resorcinol (PAR), pyridine-2,6-dicarboxylic acid (PDCA), α-hydroxyisobutyric acid (HIBA), 1,2-diaminocyclohexanetetraacetic acid (DCTA), diethylenetriaminepentaacetic acid (DTPA), and ethylenediaminetetraacetic acid (EDTA).

While non-suppressed and suppressed conductivity detection modes are suitable for detection of alkali and alkaline earth metals, for detection of other metal ions only non-suppressed conductivity detection can be used, because these metals would mostly be transferred by the suppressor reaction into insoluble hydroxides. Thus, spectrometric detection after suitable post- or precolumn derivatization is usually carried out.[17]

Transition metal ions may also be separated via ion-pair chromatography on macroporous polystyrenedivinylbenzene (PS/DVB) resins or chemically bonded silica. Elution of cations is achieved by their complexation with the eluent ligand and ion-pairing of negatively charged complex formed with ion-pair chromatography or their cation exchange with counterion.

Ion chromatography is increasingly used for the separation of lanthanides and actinides. Cation exchange of lanthanides has been performed in peculiar, latex-agglomerated columns in the presence of appropriate chelating agents. Usually it is α-hydroxyisobutyric acid (HIBA) that forms complexes with lanthanides whose order of elution is correspondent to their stability.

In case of anion-exchange separation mechanism, lanthanides have been predominantly separated using a mixed bed column containing both anion and cation-exchange sites.

Analysis of certain sample matrices can be difficult because of coelution problems occurring when some transition metals are present in much higher concentrations. Luckily, while transition metals form stable monovalent and divalent complexes with PDCA, lanthanides complexes with PDCA are trivalent.

Review concerning the determination of lanthanides in metallurgical, environmental, and geological samples is presented by Rao, Metilda, and Gladis.[18]

Analysis of organic cations such as amines is an application of ion chromatography of great significance. Short-chain aliphatic amines such as methylamines or ethanoloamines are used as organic neutralization agents or buffer substances. They are also used as corrosion inhibitors. Higher amines such as selected biogenic amines play a decisive role in the food analysis.

Another significant application of ion chromatography is the determination of organic amines in the petrochemical industry. Wastewaters from oil refineries, for example, contain these amines and their concentration levels may significantly vary.

The latest development in carboxylic-based weak acid cation exchangers are columns designed for the determination of hydrophobic and polyvalent amines, including biogenic amines, alkylamines, and diamines, using simple aqueous eluent and elevated column temperature.[19]

Because many amines elute under chromatographic conditions that are suitable for the separation of alkali and alkaline earth metals, direct conductivity detection is possible. However, amperometric and UV/Vis detection modes are much more selective and sensitive.

While addition of organic solvents to the mobile phase is of great importance for the analysis of organic amines, retention behavior of inorganic cations is not significantly affected by organic solvents.

Application of ion chromatography for the determination of inorganic and organic cations mostly concerns the following areas: environmental analysis, power plant chemistry, semiconductor industry, metal processing, pharmaceutics, biotechnology, mining, agriculture, food and beverages, electroplating, and pulp and paper industry.

In the middle of 1980s, the United States Environmental Protection Agency (US EPA) approved ion chromatography for the analysis of alkali and alkaline earth cations and ammonium in rain water and wet precipitation. In 1998, International Standard Organization (ISO) published Method 14911[20] for the simultaneous determination of dissolved alkali and alkaline earth cations, ammonia and manganese in water and wastewater using suppressed ion chromatography.

Recently, ion chromatography has become well established as a regulatory method for the analysis of inorganic ions in water and wastewater.[21] Regulatory ion chromatographic methods for environmental samples of both inorganic and organic cations recommended by ISO, US EPA, and American Society for Testing and Materials (ASTM) are listed in Table 2.

CONCLUSION

Currently, there is a significant number of ion chromatography methods developed for the determination of inorganic and organic cations in wide variety of sample matrices. Moreover, it has become one of the most widely applied analytical tools for the analysis of complex matrices and for the speciation studies in the field of metal analysis.

Ion chromatography gained general acceptance as fast and sensitive multielement detection method for the determination of alkali and alkaline earth metals, heavy and transition metals, actinides and lanthanides, as well as selected organic cations, allowing detection limits in the range of microgram per liter and analysis time of less than 20 min.

REFERENCES

1. Kuban, P.; Guchardi, R.; Hauser, P.C. Trace-metal analysis with separation methods. Trend. Anal. Chem. **2005**, *24*, 192–198.
2. Das, A.K.; Guardia, M.; Cervera, M.L. Literature survey of on-line elemental speciation in aqueous solutions (Review). Talanta **2001**, *55*, 1–28.
3. Kot, A.; Namiesnik, J. The role of speciation in analytical chemistry. Trend. Anal. Chem. **2000**, *19*, 69–79.
4. Weiss, J. *Handbook of Ion Chromatography*; Wiley-VCH: Weinheim, Germany, 2004; 279–357.
5. Sun, H.-L.; Liu, H.-M.; Tsai, S.-J. Quantitative analysis of manganese, chromium and molybdenum by ion-pair reversed-phase high-performance liquid chromatography with pre-column derivatization and UV-visible detection. J. Chromatogr. A, **1999**, *857*, 351–357.
6. Nesterenko P.N.; Jones, P. Recent developments in the high-performance chelation ion chromatography of trace metals. J. Sep. Sci. **2007**, *30*, 1773–1793.
7. Nesterenko P.N. Simultaneous separation and detection of anions and cations in ion chromatography. Trend. Anal. Chem. **2001**, *20*, 311–319.
8. Thomas, D.H.; Rey, M.; Jackson, P.E. Determination of inorganic cations and ammonium in environmental waters by ion chromatography with a high-capacity cation-exchange column. J. Chromatogr. A, **2002**, *956*, 181–186.
9. Ammann, A.A. Speciation of heavy metals in environmental water by ion chromatography coupled to ICP-MS. Anal. Bioanal. Chem. **2002**, *372*, 448–452.
10. Perna, L.; Bocci, F.; Heras, L.A.; Pablo, J.; Betti, M. Studies on simultaneous separation and determination of lanthanides and actinides by ion chromatography inductively coupled plasma mass spectrometry combined with isotope dilution mass spectrometry. J. Anal. Atom. Spectrom. **2002**, *17*, 1166–1171.
11. Zhu, Y.; Wang, M.H.; Du, H.Y. Organic analysis by ion chromatography 1. Determination of aromatic amines and aromatic diisocyanates by cation-exchange chromatography with amperometric detection. J. Chromatogr. A, **2002**, *956*, 215–220.
12. Gjerde, D.T. Eluent selection for determination of cations in ion chromatography. J. Chromatogr. A, **1988**, *439*, 49–61.
13. Sarzanini, C.; Bruzzoniti, M.C. Metal species determination by ion chromatography. Trends Anal. Chem. **2001**, *20*, 304–310.
14. Guierin, T.; Astruc, A.; Astruc, M. Speciation of arsenic and selenium compounds by HPLC hyphenated to specific

detectors: A review of the main separation techniques. Talanta **1999**, *50*, 1–24.
15. Montes-Bayon, M.; DeNicola, K.; Caruso, J.A. Liquid chromatography—inductively coupled plasma mass spectrometry (Review). J. Chromatogr. A, **2003**, *1000*, 457–476.
16. Shaw, M.J.; Haddad, P.R. The determination of trace metal pollutants in environmental matrices using ion chromatography. Environ. Int. **2004**, *30*, 403–431.
17. Santoyo, E.; Santoyo-Gutiérrez, S.; Verma, S.P. Trace analysis of heavy metals in groundwater samples by ion chromatography with post-column reaction and ultraviolet-visible detection. J. Chromatogr. A, **2000**, *884*, 229–241.
18. Rao, T.P.; Metilda, P.; Gladis, J.M. Overview of analytical methodologies for sea water analysis: Part I—Metals. Crit. Rev. Anal. Chem. **2005**, *35*, 247–288.
19. Borai, E.H.; Lasheen, Y.F.; Seliman, A.F. Gradient elution method for successive separation of common cations and hydrophobic amines using suppressed ion chromatography. J. Liq. Chromatogr. Rel. Technol. **2008**, *6*, 838–849.
20. ISO 14911:1998. Water Quality—Determination of Dissolved Li^+, Na^+, NH_4^+, K^+, Mn^{2+}, Ca^{2+}, Mg^{2+}, Sr^{2+} and Ba^{2+} Using Ion Chromatography Method.
21. Michalski, R. Ion Chromatography as a reference method for the determination of inorganic ions in water and wastewater. Crit. Rev. Anal. Chem. **2006**, *36*, 107–127.

Inorganic Elements: CCC Analysis

Eiichi Kitazume
Faculty of Humanities and Social Sciences, Iwate University, Iwate, Japan

Abstract
The unique feature of countercurrent chromatography (CCC) applied to the separation and enrichment of inorganic elements is described. A highly efficient enrichment of metal ions was achieved by pH-peak-focusing high-speed countercurrent chromatography (HSCCC) that is developed by the variation of the pH-zone-refining high-speed CCC. In this method, Ca, Cd, Cu, Mg, Mn, and Zn are chromatographically extracted in a basic organic stationary phase containing ammonia and a complex-forming reagent such as di(2-ethylhexyl) phosphoric acid, by introducing the sample solution into the column rotated at 800–1200 rpm. When the column is eluted with the acidified mobile phase containing hydrochloric acid, metal ions are trapped and concentrated around the sharp pH border formed in between the acidic and the basic zones, moving toward the outlet of the column. Enriched metal ions are finally eluted with the sharp pH border as a highly concentrated peak into a small amount of eluate. The pH of the border is determined by the kinds of base and acid, and it shows the neutralization point. At this pH, trapped solute is moved toward the outlet of the column, based on its distribution ratio in each phase. The movement of this pH border through the column is determined by the molar ratio between the base in the stationary phase and the acid in the mobile phase. By selecting appropriate experimental conditions, such as acidity of the sample, bore of the column, and volume of the sample, each metal separation was achieved due to a longitudinal pH gradient on both sides of the pH border. Metal ions were concentrated at different positions in the moving pH border. When the pH border was sufficiently wide in the final stage of the elution, each concentrated metal could be separated mutually. The present method can be successfully applied to trace determination of cadmium in tap water, with coexisting relatively large amounts of magnesium. Also, the process of metal enrichment and separation is described.

INTRODUCTION

Countercurrent chromatography (CCC) was being applied to preconcentration and separation of inorganic elements since the end of the 1980s. During the early 1990s, certain inorganic elements, including rare earths, have been separated using high-speed countercurrent chromatography (HSCCC). In addition, preconcentration and separation of inorganics from geological samples have been studied. Many of the features of HSCCC have convinced us that this method can be successfully used in the separation of inorganic elements and in inorganic analytical chemistry. However, the liquid systems for inorganics are somewhat complicated as compared with those for the separation of organics because they usually contain significant amounts of an extracting reagent, which influences the kinetic properties and viscosity of the two-phase system.

To achieve high sensitivity when analyzing trace inorganic elements in a sample solution using an atomic absorption spectrometry (AAS) or Inductively coupled plasma (ICP) atomic-emission spectrometry (ICP–AES), conventional preconcentration methods such as evaporation, ion exchange, and solvent extraction techniques have been used. However, there are several problems in their methodologies for the determination of ultra-trace elements; e.g., peak broadening in the ion exchange technique and low enrichment factor in the solvent extraction techniques are encountered. It is difficult to directly work with under 0.5 ml concentrated sample solution by conventional methods. If there were effective methods for concentrating traces into 0.1 ml or lower solution volume, absolute detection limits for trace analysis using techniques such as AAS, ICP/AES, and ICP–mass spectrometry (ICP/MS) would be considerably lowered, as well as matrix effects would be eliminated.

pH PEAK FOCUSING

pH-peak-focusing countercurrent chromatography (pH-PFCCC) is a unique technique, based on neutralization between mobile and stationary phases.[1,2] It has been applied to the separation and enrichment of organic compounds such as indole auxins, bromoacetyl thyroxine and its analogs, dinitrophenyl amino acids, transretinoic acid, and diazepam. Neutralization is initiated at the mobile-phase front, but

advances through the column at a slow pace, forming a sharp border between basic and acidic zones. Trace impurities in the sample solution are concentrated at this narrow pH boundary in the column. This effect offers great potential for online enrichment and subsequent analysis of trace inorganic elements by interfacing HSCCC with analytical instruments such as non-flame atomic absorption spectrometry (NFAAS), ICP/AES, and ICP/MS.

Recently, the feasibility of an HSCCC centrifuge in enriching several metallic elements was demonstrated using pH-PFCCC. Under optimum conditions, an excellent enrichment factor of over 100 was achieved with good recovery of Ca, Cd, Mg, Mn, Pb, and Zn at a concentration of several parts per billion by online detection using a direct-current plasma atomic emission spectrometer (DCP-AES) as the detector.[3] In addition, many metal ions were efficiently enriched into an eluent volume of 100 μl or lower by HSCCC, resulting in a greater than 100-fold increase in peak intensities for a 10 ml sample solution. Preconcentrating the sample solution by substantially improving detection limits facilitates conventional trace determination of inorganic elements by instrumental analysis; however, more often the metals could not be separated from each other. If the pH border is sufficiently broad, and the order of the elements in the column is maintained until the final stage of the elution, each concentrated metal ion may be separated individually, as in displacement chromatography.

Under appropriate experimental conditions in pH-PFCCC, major matrix elements such as Ca and Mg in enriched tap water were found to be separated from trace elements.[4] Trace Cd, which appears between the chromatographic bands of Mg and Ca when using di(2-ethylhexyl) phosphoric acid (DEHPA) as an extracting reagent, was well determined without interference from alkali metals that are main components of biological and environmental samples.

EXTRACTION REAGENT FOR THE SEPARATION OF INORGANIC ELEMENTS

The existence of an extracting reagent in the mobile phase is an essential factor to be considered in the separation and enrichment of inorganic elements. It complicates the determination of several important parameters, e.g., distribution coefficients, peak resolution, and separation efficiency. Some basic researches revealed that kinetic properties of specific systems used in HSCCC affect the separation efficiency. Moreover, mass transfer rates into organic stationary phases are significantly responsible for the separating mode, i.e., stepwise or isocratic elution. In addition, the values of the distribution coefficients, determined by the batch extraction measurements in the systems, are sometimes considerably different from those of the dynamic distribution coefficients calculated from elution curves plotted from experimental data. Further theoretical and basic investigations are necessarily concerned with extraction kinetics as well as hydrodynamic behavior of the two phases in the HSCCC column.

In Table 1, typical extracting reagents used for separation and enrichment of inorganic elements are summarized. Organophosphorus extractants are often used because of their solubility properties. Di(2-ethylhexyl) phosphoric acid is commonly applied to industrial separations because of its high extractability and high separation factors between many inorganic elements, especially rare earth elements. Other metal ions are extracted as well as the trivalent metal ions.

ENRICHMENT ANALYSIS IN THE EFFLUENT

Large-Scale Enrichment Followed by Conventional Eluent

Enrichment of the desired trace elements prior to their determination cannot simply overcome problems such as interference and toxic or radioactive samples, but can facilitate highly sensitive determination of trace elements.

The parts-per-billion level of metal ions in 500 ml of the mobile phase was continuously concentrated into small volumes of the stationary phase retained in the column. Concentrated metal ions were simultaneously eluted with nitric acid and determined by the emission intensity with a DCP–AES. The recoveries of Ca, Cd, Mg, Mn, Pb, and Zn

Table 1 Typical extracting reagent for separation and enrichment of inorganic elements using HSCCC.

Extracting reagent	Two-phase system	Inorganic element
Di(2-ethylhexyl) phosphoric acid (DEHPA)	HCl, organic acid–heptane	Rare earth, heavy metals
2-Ethylhexylphosphonic acid mono-2-ethylhexyl ester (EHPA)	Carboxylic acid–toluene	Rare earth
Dinonyltin dichloride	HCl, HNO_3–Methylisobutylketone (MIBK)	Orthophosphate and pyrophosphate
Cobalt dicarbolide	HNO_3–nitrobenzene	Cs and Sr
Tetraoctylethylenediamine (TOEDA)	HCl, HNO_3, organic acid–chloroform	Alkali, alkaline earth, rare earth, heavy metals, Hf, Zr, Nb, Ta

ranged over 88% at the concentration, of each, of 10 ppb in 500 ml of the sample solution. Versatility of this method was further demonstrated in the determination of trace metals in tap water and deionized water.

Rare earth elements have been enriched into a stationary phase composed of toluene including 2-ethylhexylphosphonic acid mono-2-ethylhexyl ester (EHPA) from 1 L of aqueous solution and eluted with a stepwise pH gradient. As many elements remained in the column head because of their high partition coefficients to the stationary phase, they could be eluted with a mobile phase and also separated from each other.

A large-scale enrichment technique is very useful for determining extremely low level concentrations of metals in solution when a large amount of sample such as natural water is available.

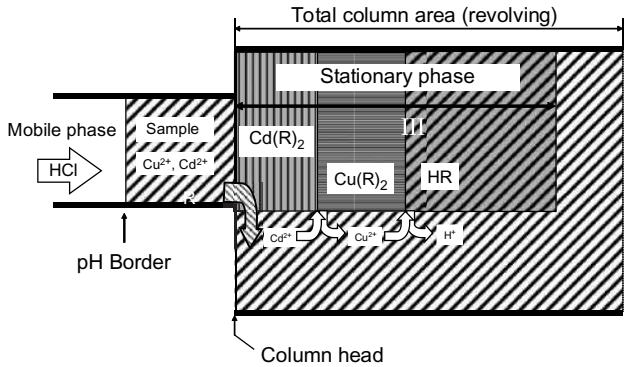

Fig. 2 Metal displacement process in stationary phase.

Enrichment Using pH-Zone-Refining Technique as Preconcentration Method of Inorganic Analysis for Subsequent Determination

Even if sufficient sample size, in volume, may not be available, enrichment techniques that concentrate trace metals in microliter samples are sometimes quite useful because modern instrumental detection systems such as AAS, ICP–AES, and ICP–MS do not need a large sample size. Moreover, if trace metals that have been separated from other major substances can be concentrated in an extremely small area of the polytetrafluoroethylene (PTFE) tube in HSCCC, this would be an ideal flow injection analysis system for the determination of inorganics. From this point of view, the recently developed pH-zone refining technique has great potential for enrichment, especially for instrumental inorganic trace analysis.

In the pH-zone refining technique, a basic organic solution containing a complex-forming reagent, such as DEHPA, is used as the stationary phase. After the sample solution is introduced into the column, metal ions stay close to the sharp pH-border region in the small-bore PTFE tube. Then, the trace inorganic ions in the sample are moved by the acid eluent (diluted hydrochloric, nitric acid, etc.) to the tail of the column while concentrating at the sharp moving pH "interface," and finally eluted as small fractions containing concentrated inorganic ions. This enrichment method for trace organic impurities is called "pH-peak-focusing countercurrent chromatography (pH-PFCCC)."

The concentration procedure is modeled in Figs. 1–3. In Fig. 1, the sample ion is concentrated into the column head immediately after the concentration procedure is started. (After the stationary phase has been introduced into the system, the HSCCC is started at an appropriate rotational rate, followed by the sample and the mobile-phase pumps.) For example, monovalent metal or inorganic ions (M^+) are concentrated into the stationary phase as MR in Fig. 1. The dark-shaded zone shows an organic stationary phase, which includes organophosphorus extractants (HR) and an alkali such as ammonia. The bright-shaded zone shows the sample phase with its pH adjusted by ammonia. When the column rotation is started, as the organic stationary phase is lighter than the mobile phase (diluted acid solution, HCl in Fig. 1), it

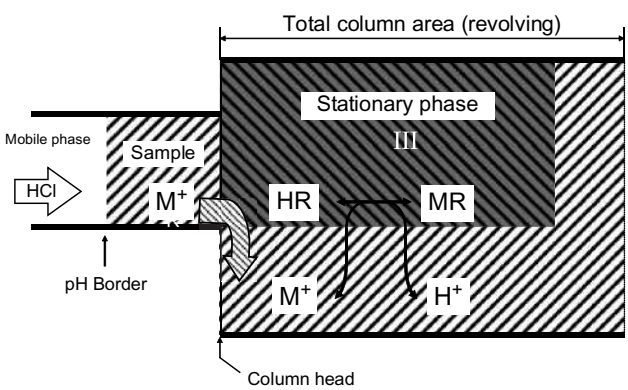

Fig. 1 Metal extraction into stationary phase.

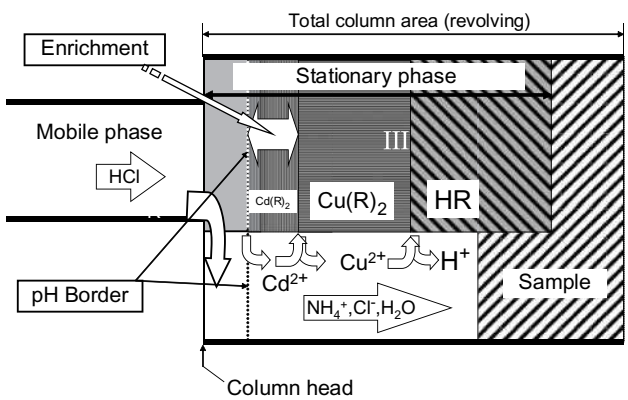

Fig. 3 Metal enrichment process after sample injection.

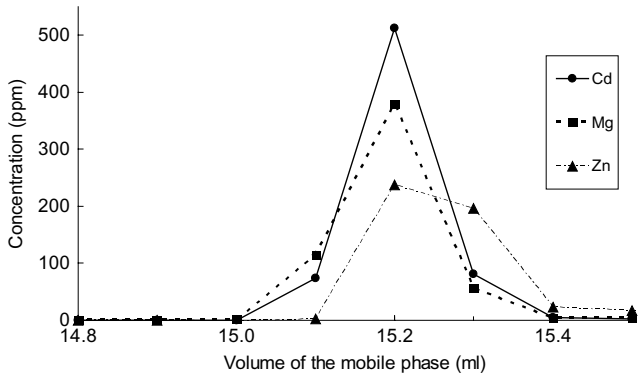

Fig. 4 Typical concentration results for a 10 ppm solution of Cd, Mn, and Zn. Experimental conditions: Apparatus: HSCCC centrifuge with 10.0 cm revolution radius; column: one multilayer coil, 0.5 mm I.D. × 32 m; sample: 5 ml of each 10 ppm solution (pH 9.25) in 0.1 *M* tartaric acid; mobile phase: 0.1 *M* HCl saturated with ether; stationary phase: 6 ml of 0.2 *M* DEHPA and 0.18 *M* ammonia in ether; flow rate: 0.05 ml/min; rotational speed: 950 rpm.

moves to the head of the column by Archimedean screw effect (ASE). The driving force, based on ASE, increases with the rotational speed of the column. Therefore the stationary phase can be retained in the column by selecting an appropriate rotational rate and pump rate, even if the mobile phase is introduced from the head direction (left side in Fig. 1) into the column. The retention ratio of the stationary phase to the whole column varies from 20% to 70%, but is stable when all conditions including pump speed and rotational speed are constant. So the position of the mobile phase is stable in a column while in operation. Inorganic ions (M^+) form complexes with ligand ions (R^-) and are mainly concentrated on the column head, shown as MR in Fig. 1. A proton is transferred into the mobile phase when the inorganicion is extracted into the stationary phase.

Fig. 2 shows the displacement procedure as well as the concentration procedure in the HSCCC column after most of the ions in the sample are extracted onto the stationary phase. If the sample contains two kinds of divalent metalions (Cu and Cd) in a large amount of solution, each metal might be arranged by the difference of its affinity or partition rate to the stationary phase. As Cd ion is usually more extractable than Cu ion, Cd can displace Cu at the end (left) of the Cu band in the stationary phase. However, the bandwidth of Cd increases until the entire sample is introduced into the column.

Metal-focusing process after the sample injection is shown in Fig. 3. After all the ions in the sample are extracted onto the stationary phase, mobile phase is introduced in to the column. Ammonia in the stationary phase begins to be neutralized with hydrochloric acid in the mobile phase. The neutralization area, where reaction between the acid and the base has just finished, is shown as pH border in Fig. 3. The pH border moves from left to right (the same direction as the mobile phase); however, its flow rate is lower than that of the mobile phase because of the delay caused by the neutralization of the acid in the mobile phase by the base in the stationary phase. Therefore the flow rate of the pH border may be controlled by adjusting the concentration of base and acid in the respective phase.

As a result, the Cd zone will be enriched despite an increase in its retention time of chromatogram. On the other hand, as the border between Cd and Cu also move as a result of proceeding elution of Cd, Cu zone also moves to the tail with enrichment.

If the concentration of hydrochloric acid just adjacent to the sample is very low or in case of using gradient elution mode, pH border shown as dotted line in Fig. 3 will move more slowly.

If the speed of the pH border is relatively high as compared with the movement of the Cu zone, its moving rate is as shown in the concentration stage in Fig. 2; pH border will catch up with the border between Cu zone and

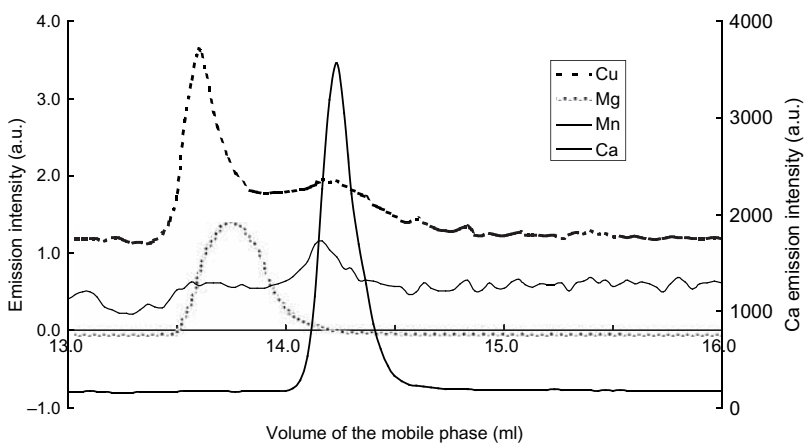

Fig. 5 Enrichment profiles of Mg, Cu, Mn, and Ca in 10 ml of tap water. Experimental conditions: column: one monolayer coil, 0.5 mm I.D. × 10 m (2 ml); sample: 10 ml of tap water (pH 8.0) in 0.1 *M* tartaric acid; mobile phase: 0.1 *M* HCl including 0.1 *M* tartaric acid; stationary phase: 0.22 *M* DEHPA and 0.20 *M* ammonia in heptane; flow rate: 0.1 ml/min at enrichment stage and 1.0 ml/min at detection stage; rotational speed: 1200 rpm; Sf: 7.5%.

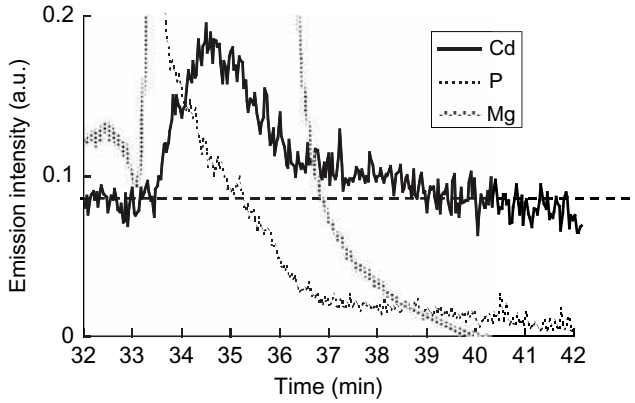

Fig. 6 Enrichment profiles of Cd and Mg in 30 ml of tap water. Experimental conditions: column: one monolayer coil, 1.6 mm I.D. × 0.86 m (2 ml); sample: 30 ml of tap water (pH 7.1) in 0.1 *M* tartaric acid; mobile phase: 0.1 *M* HCl including 0.1 *M* tartaric acid; stationary phase: 2 ml of 0.22 *M* DEHPA and 0.20 *M* ammonia in heptane; flow rate: 1.0 ml/min; rotational speed: 800 rpm; Sf: 20%.

reagent zone shown as HR in Fig. 3. Then the two peaks cannot be separated well in such relatively quick movement of the pH border. However, the peak height of each element will be increased by enrichment in small volume. In that case, both peaks will appear simultaneously.

In concentration mechanisms described above, there is little diffusion process observed as in usual elution procedures with ion exchange or other chromatographic separation methods, such as conventional HSCCC and HPLC. If there is no basic compound such as ammonia in the stationary phase, ions move to the tail with a different flow rate which is a function of the distribution ratio between the stationary phase and the mobile phase. Many ions can be separated from each other in that case, but as there is no pH border in the column, concentration is not affected, but the separation is affected by diffusion.

Fig. 4 shows the typical concentration results for a 10 ppm solution of Cd, Mg, and Zn. The injected sample solution contained 50 μg of each in 5 ml of 0.1 *M* tartaric acid solution, adjusted to a pH of 9.25. The mobile phase was pumped at a flow rate of 0.05 ml/min. Rotational speed was 950 rpm. The eluate was collected every 2 min (0.1 ml fractions). The fractions were diluted with water (1:10), and the emission intensity of each element was measured by plasma atomic emission spectrometer. The emission intensity of each element was found increased 20-fold as compared with the original sample solution. The results of this study demonstrated the high-performance capabilities of the pH-zone refining technique. Trace elements in the sample solution could be successfully concentrated into a small volume, almost under 0.1 ml with an enormous level of enrichment.

On the other hand, if the speed of the pH border is relatively low as in Fig. 3, so that the pH border cannot catch up with the border between the Cu zone and the reagent zone until the border passes through the stationary phase, both peaks would be separated. This phenomenon would be observed when the length of the stationary phase would be too small to allow the pH border to catch up with the Cu zone. Therefore, the Cu zone will be eluted before the enriched Cd zone comes close to it. In that case, the order of the elements will be maintained until the final stage of elution at the tail of the stationary phase in the column. Whereas the use of a large-bore column may accelerate the appearance of the peak owing to the short longitudinal distance of the stationary phase, each metal may be separated well as compared with the case of using a small-bore column. As well as enrichment, good chromatographic separation would be essential for exact measurement. The unilateral speed of the pH border can be controlled by choosing appropriate experimental conditions, such as bore size of the column and the molar ratio between acid and base.

When a small-bore column, e.g., 0.5 mm I.D., was used, all peaks appeared simultaneously if the volume of the retained stationary phase was over 15%.[3] However, if the retention volume of the stationary phase was less than 10% in a small-bore column, peak separation was observed as shown in Fig. 5.[4] Each peak was detected by plasma atomic emission spectrometry. This peak profile shows enrichment profiles with separation of Mg, Cu, Mn, and Ca in tap water. The intensity of Ca is shown on the right axis, 3 orders higher than that of the other elements, while the intensity of Mn is amplified 10 times. The spectral interference of Ca to the signal of Cu is observed. This separation phenomenon is considered to be quite useful for the exact determination of trace metals.

On the other hand, with a large-bore column, e.g., 1.6 mm I.D., for the same volume of stationary phase, peak separation was observed even if there was sufficient retention volume (more than 15%). This phenomenon may be explained by the shorter longitude of the stationary phase in a large-bore column, as compared with a small-bore column. Fig. 6 shows the signals of Mg, P, and Cd for 30 ml of tap water. The large peak of the Cd emission line may be the result of spectral interference caused by the scaled-out peak of Mg. On the shoulder of the Cd peak, a small peak was observed. This may be the real emission signal of Cd. When the large peak was used in the determination of Cd, the result was 3 ppb. On the other hand, the result determined using the small peak was about 1 ppb. Using the pH-PFCCC system, precision results for the determination of Cd or other elements that are influenced by matrix elements could be obtained.

CONCLUSIONS

In contrast to HPLC, the unique feature of CCC is that there is no solid support in the column. As the distribution abilities, including the capacity of the stationary phase, are easy to control, CCC can be applied to the separation, enrichment, and purification of inorganics over a wide range of concentration. In particular, enrichment of trace elements using pH-PFCCC will be an ideal preconcentration method[5,6] for subsequent determination of inorganics using modern instrumental analytical methods. Countercurrent chromatography can be combined directly with the flow injection technique, and it shows great potential for preconcentration of selected desired trace inorganic elements prior to their final detection and quantitation. Online enrichment and subsequent analysis, based on a simple and high-performance enrichment system for inorganics, may take the place of conventional sample preparation using a beaker and a separatory funnel in future investigations in this field.

REFERENCES

1. Ito, Y.; Conway, W.D., Eds.; *High-Speed Countercurrent Chromatography*; John Wiley & Sons: New York, 1996.
2. Ito, Y.; Shibusawa, Y.; Fales, H.M.; Cahnmann, H.J. Studies on an abnormally sharpened elution peak observed in countercurrent chromatography. J. Chromatogr. A, **1992**, *625*, 177.
3. Kitazume, E.; Higashiyama, T.; Sato, N.; Kanetomo, M.; Tajima, T.; Kobayashi, S. On-line microextraction of metal traces for subsequent determination by plasma atomic emission spectrometry using pH peak focusing countercurrent chromatography. Anal. Chem. **1999**, *71*, 5515.
4. Kitazume, E.; Takatsuka, T.; Sato, N.; Ito, Y. Mutual metal separation system with enrichment using pH-peak focusing countercurrent chromatography. J. Liq. Chromatogr. Relat. Technol. **2003**, *27*, 427.
5. Kitazume, E. High-speed countercurrent chromatograph device and analysis method. Jpn. Kokai Tokkyo Koho JP. **2005**, 315731 A.
6. Kitazume, E. Countercurrent chromatography. Bunseki **2008**, 287.

Inorganic Oxyhalide By-Products in Drinking Water: Ion Chromatographic Methods

Rajmund Michalski
Institute of Environmental Engineering, Polish Academy of Science, Zabrze, Poland

Abstract
In an effort to protect the public from potentially hazardous microorganisms, drinking water supplies are routinely disinfected with a variety of treatment regimes. This entry describes some ion chromatography (IC) methods for the determination of inorganic disinfection by-products such as bromate, chlorite, and chlorate.

INTRODUCTION

The first documentation of drinking water treatment, describing procedures used for purifying water, can be found in Egyptian hieroglyphics. The basic methods were the same as they are today, i.e., boiling, chemical treatment, and filtration. The importance of drinking water quality and its influence on human health were known, but the specific contaminants would not be identified for centuries to come.

This situation changed in the nineteenth century when chlorine was introduced as a chemical disinfectant for water treatment. The introduction of chlorination to drinking water was followed by a remarkable reduction of cholera, dysentery, and typhoid worldwide.

Water treatment by disinfection processes is considered a major public health achievement of the twentieth century. Consequently, there has been a shift in the identification methods of water contaminants from microbiological to chemical. The number of chemicals determined in drinking water has grown exponentially; however, out of hundreds of them, only very few have been studied or have documented proof of their health effects.

In the 1970s, it was discovered that chlorination of drinking water produced carcinogens, such as trihalomethanes and haloacetic acids.[1] Since 1974, the presence of more than 500 disinfection by-products has been determined in drinking water.[2] Since that time, environmental regulatory agencies as well as drinking water treatment technologists have been carrying out extensive research for alternative disinfection methods that minimize the generation of by-products with significant health risks.

FORMATION, TOXICITY, AND REGULATION OF INORGANIC DISINFECTION BY-PRODUCTS IN DRINKING WATER

Many drinking water utilities are replacing chlorine, as their primary disinfectant, with alternative disinfectants, such as ozone, chlorine dioxide, and chloramines, which reduce regulated trihalomethane and some organochlorine compound levels but, at the same time, often increase the level of other potentially toxic compounds.

Ozonization has emerged as one of the most promising alternatives to chlorination. In the last decade, the use of ozone in the treatment of drinking water to improve taste and odor and to remove organic and inorganic micropollutants has been visibly spreading. In the early 1980s, it became obvious that the application of ozonization in drinking water treatment resulted not only in the formation of oxygenated compounds but also in bromide-containing water; brominated organic compounds and bromate were formed as well.

Recently, bromate has become the most important inorganic oxyhalide by-product, and its concentration in drinking water has to be controlled. Furthermore, the subjects of interest and advanced research are chlorite and chlorate. Bromates are formed when water containing bromide is ozonated. The concentration of bromide in natural waters varies, typically, between 10 and 1000 μg/L. From the theoretical and practical point of view, it can be seen that bromate formation can be influenced by many parameters, such as ozone dose, water pH, temperature, and indigenous concentration of bromide.[3]

Bromate formation can be restricted by careful adaptation of the ozone dosage to disinfectant demand. Other options include lowering of the pH, the use of ozone and hydrogen peroxide, addition of ammonia, removal of bromide before ozonization, and the use of membrane filtration or anaerobic processes.[4]

Chlorite (ClO_2^-) is a disinfection by-product that is formed when chlorine dioxide (ClO_2) is used for disinfecting drinking water, while chlorate (ClO_3^-) is formed when chlorine dioxide or chloramine is used.[5] Chlorination using hypochlorite acid solutions, which contain some ClO_3^- as a product of HClO disproportionation, may also contribute to ClO_3^- contamination in disinfected water. Even at low levels, chlorite may lead to hemolytic anemia

and can have dangerous effects on the nervous system in infants and young children.

Bromate has been identified as an animal, and possibly human, carcinogen. The International Agency for Research on Cancer (IARC) has classified bromate in group B-2 (the agent is possibly carcinogenic for humans).[6] In 1993, bromate was judged, by the World Health Organization (WHO), as a potential carcinogen, initially at a 25 μg/L level, which was associated with an excessive lifetime cancer risk of 7×10^{-5} on account of the limitations in the available analytical and treatment methods. Soon, health effects research indicated that it can be a human carcinogen that poses a potential 10^{-4} risk of cancer after a lifetime exposure in drinking water at a 5.0 μg/L level and a potential 10^{-5} risk at a 0.5 μg/L level.

The U.S. Environmental Protection Agency (U.S. EPA),[7] as well as the Commission of the European Communities,[8] has recently issued new rules that require public water suppliers to control some of the previously unregulated microorganisms and cancer-causing disinfection by-products in drinking water. According to these regulations, the maximum admissible level (MAL) is 10 μg/L for bromate and 1000 μg/L for chlorite.

No limit has been specified for chlorate, on account of the limited knowledge about its toxicity; however, the WHO recommends minimizing the level of chlorate as much as possible for as long as there is no reliable toxicological data. The MAL for bromate is primarily based on current analytical capability (not on toxicological considerations—the target concentration for bromate in drinking water is zero); thus, there is a need for ongoing development and refinement of analytical technologies to allow rapid and reliable determinations at the submicrogram-per-liter level.

Global and national agencies are continually striving to monitor bromate, chlorite, and chlorate levels in drinking water to establish appropriate regulatory limits. Based on the results of further research, a risk model could indicate a better-defined guideline value for oxyhalides in drinking water. Higher limits are set mainly on account of the non-availability of sensitive analytical methods in routine laboratories. Thus, there is a need for improving existing methods in terms of sensitivity, cost, and reliability.

The problem of bromate also concerns bottled water, which has become a healthier choice than tap water for many people, because they believe that bottled water contains fewer contaminants or they dislike the taste of chlorinated tap water. Therefore, the annual consumption of bottled drinking water in the world is substantial. Nevertheless, it is well known that significant amounts of bottled drinking water pass through treatment processes such as filtration, deionization, reverse osmosis, or ozonization to ensure its quality.[9]

APPLICATION OF ION CHROMATOGRAPHY IN THE DETERMINATION OF BROMATE, CHLORATE, AND CHLORITE IN DRINKING WATER ANALYSIS

Numerous techniques including colorimetry, wet chemical methods (e.g., titrimetry), electrochemical techniques (e.g., amperometry, polarography, ion-selective electrodes), UV spectrophotometry, capillary electrophoresis, and gas chromatography are used to determine inorganic oxyhalide compounds. Many of these methods suffer from interferences and limited sensitivity; they can be labor-intensive and are often difficult to automate. A very useful analytical technique for the determination of inorganic anions and cations is ion chromatography (IC). Since its introduction, IC has seen phenomenal growth in most areas of analytical chemistry; it has become a versatile and powerful technique for the analysis of a vast number of ions present in the environment and in biological tissues and fluids.

Modern IC is faster, more convenient, and has a greater separating ability than classical wet methods. The IC methods for determination of inorganic disinfection by-products can be divided into three groups. All of them are based on IC separation, but their detection methods are different. The first one, which is the most popular, uses conductivity detection; the second is based on UV/Vis detection after post-column derivatization; and the third is based on mass spectrometric detection.

Initially, application of IC for the analysis of inorganic disinfection by-products using conductivity detection was based on low-capacity ion exchangers. Therefore, injection volume and ionic strength of the sample were strictly limited to avoid column overloading. Also, the removal of interfering ions, such as chloride and sulfate, was necessary. Unfortunately, these methods are not well suited for routine analysis at levels below 1 μg/L because of the high cost of sample pretreatment, as well as the time spent on preconcentration and cleanup steps.

In the mid-1990s, ISO was working on Method 15061 for bromate[10] and Method 10304-4[11] for chlorite, chloride, and chlorate determination. The ISO 15061 standard specifies a method for the determination of dissolved bromate in drinking water, raw water, surface water, partially ozonated water, and swimming-pool water. Measurement of bromate is done in the range from 0.5 to 1000 μg/L, with or without sample preconcentration. If preconcentration is necessary, 6 ml of the sample is passed through three cation-exchange cartridges, in the Ba, Ag, and H forms, to reduce the total ionic strength.

The ISO 10304-4 standard specifies a method for the determination of dissolved chlorite, chloride, and chlorate anions in water at low levels of contamination (e.g., drinking water, raw water, swimming-pool water). An appropriate sample pretreatment and detection using conductivity, UV, or amperometric method ensures working ranges from 0.03–10 μg/L (chlorate) to 0.01–1000 μg/L (chlorite).

In 1987, the U.S. EPA presented a draft of Method 300.0, which was recommended for the determination of common anions (fluoride, chloride, nitrate, and sulfate) at milligram-per-liter levels using standard, low-capacity anion-exchange columns and conductivity detection.

Soon, this method was updated to include Part B for the determination of bromate and other inorganic disinfection by-products using modern high-capacity anion-exchange columns with a carbonate/bicarbonate eluent. The limit of detection using this column was still at a less-than-adequate level. In 1997, the U.S. EPA Method 300.1 was published as an update to Method 300.0, which was developed as a more sensitive method by identifying specific parameters (columns, eluent, and injection volume) that could be utilized to provide quantification of lower concentrations of bromate in drinking water, even in the presence of up to 50 mg/L of chloride ions. This method incorporated a new high-capacity anion-exchange column with higher efficiency for resolving trace bromate from the common anions.

By using a high-capacity anion-exchange column, it is possible to determine bromate at levels lower than 1 μg/L by directly injecting a very large volume (up to 1 ml) without any sample preconcentration or pretreatment.[12]

The interferences of chlorite create a significant problem during bromate determination. A number of procedures have been investigated for removing chlorite without adversely affecting bromate levels. Of these, the procedure that employs Fe(II) in acidic solution was found to be the most effective. The elimination of these interfering compounds was the final step toward the development of EPA Method 317.0.[13]

Considering these drawbacks, methods based on postcolumn derivatization and UV/Vis detection are found to be very attractive alternatives. The use of UV/Vis detection with a variety of postcolumn reagents, including chlorpromazine, *O*-dianisidine, fuchsine, or excess bromide (or iodide) under acidic conditions, has been shown to allow submicrogram per liter detection limits for bromate.

However, it is not easy to select one postcolumn derivatization method for bromate analysis from the various options, because each option has its own advantages and disadvantages. For example, the method that uses a mixture of nitric acid, potassium bromide, and *o*-dianisidine is the simplest one among the postcolumn derivatization techniques currently proposed. Nevertheless, the *o*-dianisidine used in this method is a possible carcinogen that requires special handling of waste from the system.

Chiu and Eubanks[14] reported a simple and rapid method based on the strong absorption of the tribromide generated from bromide under an excess of hydrobromic acid. This procedure was used for the determination of bromate by using IC with postcolumn derivatization.[15] Stable tribromide compounds were formed and detected by UV at 267 nm. The commonly occurring anions in typical drinking water are invisible to the detector and, therefore, do not interfere with analyzed bromate ions.[16]

Sensitivity for bromate determination has been improved by more than a factor of 10 through the use of a postcolumn derivatization reaction in which HI is generated in situ from KI and reacts with bromate to form the triiodide anions (I_3^-). In 2000, the U.S. EPA published Method 317.0, which uses postcolumn derivatization with *o*-dianisidine; this reacts with the eluting bromate to form a chromophore, which is then measured with a UV/Vis detector. This method offers excellent limits of detection, below 1 μg/L, for bromate, as well as for chlorite and chlorate.

The U.S. EPA Method 321.8 specifies the use of an anion-exchange column and detection of bromate using inductively coupled plasma–mass spectrometry (ICP–MS) in the atmospheric pressure mode. The U.S. EPA Method 326.0 has been developed for the analysis of ultra trace bromate concentrations in drinking water using a postcolumn derivatization reaction with Mo(VI). A review of the methods of IC determination of inorganic disinfection by-products published by U.S. EPA has been conducted by Hautman et al.[17] The ISO standards for the determination of inorganic oxyhalides in water are summarized in Table 1, and U.S. EPA methods recommended are listed in Table 2.

Table 1 ISO standards for the determination of inorganic oxyhalides in water.

Standard number	Standard name	Inorganic oxyhalide ion determined	Detection mode	Range (μg/L)
ISO 15061 (2001)	Water quality. Determination of dissolved bromate—method by liquid chromatography of ions	BrO_3^-	Conductivity. A UV detector (λ = 190–205 nm) is suitable for confirming the conductivity results only	0.5–1000
ISO 10304-4 (1997)	Water quality. Determination of dissolved anions by liquid chromatography of ions—Part 4: determination of chlorate, chloride, and chlorite in water with low contamination	ClO_3^-	Conductivity	0.03–10
		ClO_2^-	Conductivity	0.05–1
			UV (λ = 207–220 nm)	0.1–1
			Amperometry (0.4–1.0 V)	0.01–1

Table 2 U.S. EPA methods recommended for the determination of inorganic oxyhalides in water.

Method number	Method name	Oxyhalide ions determined	Columns	Eluent	Injection volume (μl)	Detection mode	Limit of detection (μg/L)
300.0—Part B (1993)	Determination of inorganic anions in water by ion chromatography	$BrO_3^-ClO_2^-ClO_3^-$	Dionex IonPac AG9 + AS9 (or equivalent)	1.7 m*M* $NaHCO_3$ + 1.8 m*M* Na_2CO_3	50	Suppressed conductivity	
300.1 (1997)	Determination of inorganic anions in water by ion chromatography	$BrO_3^-ClO_2^-ClO_3^-$	Dionex IonPac AG9-HC + AS9-HC	9.0 m*M* Na_2CO_3	200	Suppressed conductivity	
317.0 (2000)	Determination of inorganic oxyhalide disinfection by-products in drinking water using ion chromatography with the addition of a postcolumn reagent for trace bromate analysis	$BrO_3^-ClO_2^-ClO_3^-$	Dionex IonPac AG9-HC + AS9-HC (or equivalent)	9.0 m*M* Na_2CO_3	225	Suppressed conductivity followed in series with UV postcolumn derivatization with *O*-dianisidine	Conductivity
321.8 (1997)	Determination of bromate ions in water using ion chromatography with inductively coupled plasma-mass spectrometry	BrO_3^-	Dionex PA-100	5.0 m*M* HNO_3 25.0 m*M* NH_4NO_3	580	ICP–MS	
326.0 (2002)	Determination of inorganic oxyhalide disinfection by-products in drinking water using ion chromatography incorporating the addition of a suppressor acidified postcolumn reagent for trace bromate analysis	$BrO_3^-ClO_2^-ClO_3^-$	Dionex IonPac AG9-HC AS9-HC (or equivalent)	9.0 m*M* Na_2CO_3	225	Suppressed conductivity followed in series with UV postcolumn derivatization with Mo(VI)	Conductivity

Besides the methods recommended by ISO and U.S. EPA, there exist many methods developed by manufacturers of chromatography equipment, such as Metrohm, Dionex, and Shimadzu. Much lower detection limits are obtained using hyphenated techniques such as IC coupled with MS detection.[18] ICP–MS coupled with IC offers the capability of speciation with multielemental detection, excellent sensitivity and detection limits, and a wide dynamic range. Other combinations are IC combined with negative thermal ionization isotope dilution mass spectrometric (IC–NTI-IDMS) analysis[19] and electrospray IC coupled with tandem MS (IC–MS/MS).[20] The application of atmospheric pressure ionization–mass spectrometry (API–MS), coupled with IC, showed a performance comparable to that of IC–MS/MS and IC–ICP–MS.[21] In contrast to IC–API–MS, IC–ICP–MS can tolerate a higher salt concentration in the eluent, which allows the use of high-capacity columns and larger sample volumes. This lowers the detection limits by one order of magnitude for the ICP–MS detection mode, as compared to API–MS. The obvious disadvantages of MS-based detection techniques are that all of them add considerable complexity and significant cost to the analysis and that, to date, no international IC method-based ion MS or ICP–MS detection has been promulgated for the regulatory monitoring of bromate or any other disinfection by-product anions. Hyphenated techniques are very sensitive and the operating cost of a single analysis is low, but they are highly sophisticated, and the instrumentation is very expensive. Hence, these methods are not used for routine analysis.

In 2000, an interlaboratory trial was organized, involving 26 laboratories using the draft standard ISO 15061 IC method with conductivity detection and/or alternative methods. Three alternative laboratory methods based on IC coupled with different detection systems were developed: ICP–MS, colorimetry, and fluorimetry. The performance data of these three methods are comparable to the respective data of standard IC with conductivity detection.[21]

The comparison of three postcolumn methods for the analysis of bromate in drinking water (potassium iodide–ammonium heptamolybdate; *o*-dianisidine; and sodium bromide–sodium nitrate methods) shows that all of them are compatible with conductivity detection; detection limits for bromate were 0.17, 0.24, and 0.19 μg/L, respectively.[22]

All IC methods used for bromate, chlorite, and chlorate analyses have some advantages and disadvantages. Nevertheless, at present IC is the only accepted standard method for the analysis of inorganic oxyhalide disinfection by-products. The choice of the most convenient and the best method for the determination of specific oxyhalides depends on many factors, such as expected concentration of analyte, sample matrix, limit of determination obtainable by the method used, and its availability.[23]

CONCLUSION

All the three groups of IC methods recently developed (based on conductivity, UV/Vis, and MS detection modes, respectively) yield comparable results and comply with the requirements of the international directives concerning inorganic oxyhalide by-products in drinking water.[24,25] The future application and choice of a method will depend on the equipment available in the laboratories, as well as the number and kinds of samples to be analyzed.

REFERENCES

1. Boorman, G.A.; Dellarco, V.; Dunnick, J.K.; Chapin, R.E.; Hunter, R.S.; Hauchman, F.; Gardner, R.H.; Cox, M.; Sills, R.C. Drinking water disinfection by-products: Review and approach to toxicity evaluation. Environ. Health Perspect. **1999**, *107*, 207–216.
2. Richardson, S.D. Drinking water disinfection by-products. In *The Encyclopedia of Environmental Analysis and Remediation*; Meyers, R.A., Ed.; Wiley: New York, 1998; 1398–1421.
3. Gunten, U. Ozonation of drinking water: Part II. Disinfection and by-product formation in presence of bromide, iodide or chlorine. Wat. Res. **2003**, *37*, 1469–1487.
4. Camel, V.; Bermond, A. The use of ozone and associated oxidation process in drinking water treatment (review). Wat. Res. **1998**, *32*, 3208–3216.
5. Veschetti, E.; Cittadini, B.; Maresca, D.; Citi, G.; Ottaviani, M. Inorganic by-products in waters disinfected with chlorine dioxide. Microchem. J. **2005**, *79*, 165–170.
6. IARC. Some naturally occurring and synthetic food components, furocoumarins and ultraviolet radiation: Potassium bromate. In *Monographs on the Evaluation of the Carcinogenic Risk to Human*. Lyon, 1986; Vol. 40, 207–220.
7. U.S. EPA, *Stage 1: Disinfectants and Disinfection By-Products Rule. A Quick Reference Guide*, EPA 816-F-01-010. 1998.
8. *Council Directive Concerning the Quality of Water Intended for Human Consumption* Directive 98/89/CE Commission of the European Union: Brussels. 1998.
9. Matsis, V.M.; Nikolaou, E.C. Determination of inorganic oxyhalide disinfection by-products in bottled water by EPA Method 326.0 for trace bromate analysis. Desalination **2008**, *224*, 231–239.
10. ISO 15061, *Water Quality—Determination of Dissolved Bromate—Method by Liquid Chromatography of Ions*. 2001.
11. ISO 10304-4, *Water Quality—Determination of Dissolved Anions by Liquid Chromatography of Ions—Part 4: Determination of Chlorate, Chloride, and Chlorite in Water with Low Contamination*. 1997.
12. Valsecchi, S.; Isernia, A.; Polesello, S.; Cavalli, S. Ion chromatography determination of trace level bromate by large volume injection with conductivity and spectrometric detection after post column derivatisation. J. Chromatogr. A, **1999**, *864*, 263–270.

13. Wagner, H.P.; Pepich, B.V.; Hautman, D.P.; Munch, D.J. Performance evaluation of a method for the determination of bromate in drinking water by ion chromatography (EPA Method 317.0) and validation of EPA Method 324.0. J. Chromatogr. **2000**, *884*, 201–212.
14. Chiu, G.; Eubanks, E.D. Rapid determination of bromide ions in sea water by spectrometric method. Microchim. Acta **1989**, *11*, 145–149.
15. Delcomyn, C.A.; Weinberg, H.S.; Singer, P.C. Use of ion chromatography with post-column reaction for the measurement of tribromide to evaluate bromate levels in drinking water. J. Chromatogr. **2001**, *920*, 213–217.
16. Yamanaka, M.; Sakai, T.; Kumagai, H.; Inoue, Y. Specific determination of bromate and iodate in ozonized water by ion chromatography with post column derivatization and inductively-coupled plasma mass spectrometry. J. Chromatogr. **1997**, *789*, 259–264.
17. Hautman, D.P.; Munch, D.J.; Frebis, Ch.; Wagner Pepich, B.V. Review of the methods of the U.S. environmental protection agency for the bromate determination and validation of Method 317.0 for disinfection by-product anions and low-level bromate. J. Chromatogr. **2001**, *920*, 221–226.
18. Zwiener, C.H.; Richardson, S.D. Analysis of disinfection by-products in drinking water by LC–MS and related MS techniques. Trends Anal. Chem. **2005**, *24*, 613–621.
19. Diemer, J.; Heumann, K.G. Bromide–bromate speciation by NTI-IDMS and ICP-MS coupled with ion exchange chromatography. Fresenius J. Anal. Chem. **1997**, *357*, 72–75.
20. Charles, L.; Pepin, D. Electrospray ion chromatography–tandem mass spectrometry of bromate at sub-ppb levels in water. J. Chromatogr. **1998**, *804*, 105–108.
21. Seubert, A.; Schminke, G.; Nowack, M.; Ahrer, W.; Buchberger, W. Comparison of on-line coupling of ion-chromatography with atmosphere pressure ionisation mass spectrometry and with inductively coupled plasma mass spectrometry as tools for the ultra-trace analysis of bromate in surface water samples. J. Chromatogr. **2000**, *884*, 191–196.
22. EC contract SMT4-CT96-2134, EUR report, European Commission, No. 1960, ISBN 92-828-9401-0 Brussels. 2000.
23. Thompson, K.C.; Guinamant, J.L.; Ingrand, V.; Elwaer, A.R.; McLeod, D.C.; Schmitz, F.; Swaef, G.; Queauviller, P. Interlaboratory trial to determine the analytical state-of-the-art of bromate determination in drinking water. J. Environ. Monit. **2000**, *2*, 416–422.
24. Echigo, S.; Minear, R.A.; Yamada, H.; Jackson, P.E. Comparison of three post column reaction methods for the analysis of bromate and nitrite in drinking water. J. Chromatogr. **2001**, *920*, 205–211.
25. Laubli, M.; Proost, R.; Seifert, N.; Unger, S; Wille, A. Bromate in drinking water—which method to use in ion chromatography. LC GC. **2003**, *6*, 17–22.

Inverse GC

Zygfryd Witkiewicz
Institute of Chemistry, Jan Kochanowski University, Kielce, Poland

Henryk Grajek
Institute of Chemistry, Military University of Technology, Warsaw, Poland

Abstract
Inverse gas chromatography (IGC) has been characterized as a method for determining the physicochemical magnitudes characterizing properties of solids and low-volatile liquids. The methods of determination of isotherms and specific surface areas of adsorbents and catalyzers are presented. The dependencies used to estimate the thermodynamic parameters characterizing surface energy and acceptor–donor properties of solids have been precisely presented. Rudimentary information about testing polymeric materials, volatile substances, and diffusion in gases is given.

THE ESSENCE OF INVERSE GAS CHROMATOGRAPHY

Gas chromatography is commonly known as a method for the separation of components of homogeneous mixtures. The chromatographic method is based on the differences in the drift rates of the concentration zones of mixture components, which are in dynamic equilibrium in mobile and stationary phases. The separation of mixture components results from different types of interactions of the chromatographed substances mainly with the stationary phase. These interactions depend on the physicochemical properties of the stationary phase and of the components of the mixture, and have a decisive influence on the retention values. Conversely, chromatographic effects can be used for investigating the intensity of interactions and the type and properties of the stationary phases in a chromatographic system. This type of chromatography is known as inverse gas chromatography (IGC) (Fig. 1). It is a dynamic method of testing, as opposed to the majority of methods for physicochemical investigations, which are static. Static methods yield plausible results, but they are time-consuming. On the other hand, IGC is less time-consuming, and the results obtained are also plausible. During one IGC run it is possible to determine many physicochemical quantities. Also, a commercial chromatograph can easily be adapted for physicochemical investigations.

Attempts for employing gas chromatography for testing the properties of liquids and solids were made in the 1950s. Smidsrød and Guillet[1] and Kiselev (working independently)[2] are thought to be the creators of the aforesaid separation method. The properties of high-boiling liquids, solids, volatile substances, and systems comprising a volatile substance and a high-boiling liquid or a volatile substance and a solid can be easily tested by the IGC method. A chromatographed substance with precisely defined physicochemical properties may be employed as a reference *probe* for testing the properties of the column filling material. The shape of the chromatographic peak and the retention time of the reference probe are dependent on its dispersive, polar, and ionic interactions with atoms (or their groups) in the outermost layer as well as in the bulk of the column filling.

Depending on the type of components in the chromatographic system, the following phenomena can occur in the column: dissolution, adsorption, phase transitions, diffusion, and non-specific or specific intermolecular interactions (including chemical reactions). The analysis of these effects, appearing in the form of an elution peak of the chromatographed substance with a defined shape and retention time, enables the determination of the properties of the stationary phase in a chromatographic system. In practice, the properties of adsorbents, catalyzers, polymers, and asphaltenes are often tested using IGC. Neutral and polar substances are employed for testing acidity, basicity, acceptor and donor properties, polarity, and dissolution and diffusion parameters of the column filling.

All physicochemical parameters derived from chromatographic measurements are related to the concentration profile of the eluted substance. To make measurements plausible, it is important to know the determinants of the substance's concentration profile. The elution peak always has a finite width, and, although often approximately Gaussian in shape, it is actually asymmetrical to a greater or lesser degree. In such cases, the theory of statistical moments has to be employed for characterizing the peaks of any shape, whether Gaussian or non-

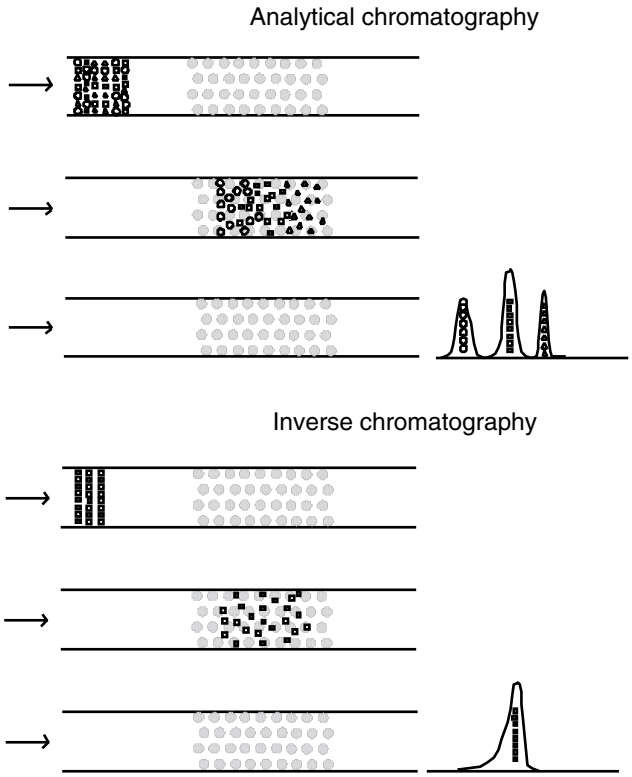

Fig. 1 Schematic representation of the principle of analytical chromatography and inverse chromatography.

Gaussian. The statistical moments approach directly gives the expressions for retention and plate height.

In linear chromatography, the equilibrium concentrations of admolecules in the stationary phase and in the mobile phase are proportional, so the equilibrium isotherms are straight lines beginning at the origin. In contrast, in non-linear chromatography, the equilibrium concentrations of admolecules in the stationary phase and in the mobile phase are not proportional, so the equilibrium isotherms are non-linear.

In ideal chromatography, it is assumed that the axial dispersion is negligibly small and the rate of the mass transfer kinetics is infinite; in other words the column efficiency is infinite. In non-ideal chromatography the column efficiency is a defined and measurable value.

The specific, $V_{g(T)}$, and the net, V_N, retention volumes are the chromatographic values most frequently employed in the calculation of thermodynamic quantities:

$$V_{g(T)} = \frac{V_N}{m} \tag{1a}$$

$$V_N = (t_R - t_M) j \frac{(p_o - p_{H_2O})T}{p_o T_{fm}} F_{fm} \tag{1b}$$

where m is the mass of the tested adsorbent or the mass of the liquid stationary phase deposited on the inert support; t_R is the total retention time of the chromatographed substance; t_M is the holdup time; j is the James–Martin compressibility factor; p_o is the gas pressure at the column outlet; p_{H_2O} is the pressure of water vapor; T is the column temperature; T_{fm} is the temperature of the flow meter; F_{fm} is the uncorrected flow rate of carrier gas through the bed.

DETERMINATION OF ISOTHERMS AND SPECIFIC AREAS OF ADSORBENTS AND CATALYZERS

One of the most important applications of IGC is in the testing of adsorbents and catalyzers. It is possible to determine the adsorption isotherms of volatile substances, the specific surface areas, the different potential functions for adsorbate–adsorbent interaction, and the diffusion coefficients of gases in porous solids.

There is a dependency between the shape of the chromatographic peak and the profile of the adsorption isotherm on the stationary phase. Symmetric peaks for which retention time does not depend on the volume of probe injected onto the column, which imply a linear adsorption (partition) isotherm, are usually obtained in the case of non-specific (dispersive) adsorbate–adsorbate and adsorbate–adsorbent interactions. The convex isotherm is usually obtained when the diffusive parts of the dependent peaks overlap and the adsorbate–adsorbent interactions are relatively stronger in comparison with the adsorbate–adsorbate interactions. The concave isotherm is usually obtained when the self-sharpening parts of the dependent peaks superimpose and the adsorbate–adsorbate interactions are relatively stronger in comparison with the adsorbate–adsorbent interactions.

Elution and frontal methods are commonly employed for the determination of adsorption isotherms of different probes on ground solids. The application of the elution techniques is more widespread. The use of one of these methods involves several injections for different amounts of the probe and overlapping of the obtained peaks to check whether the diffusive parts of them superimpose, which is a characteristic feature of the equilibrium conditions of ideal, non-linear models. It is mandatory to select an inert gas with a relatively small kinetic diameter, which is not adsorbed under the chromatographic conditions applied.

The areas of the peaks, S_{peak}, with the superimposed diffusive parts, are inversely proportional to the amount of admolecules, a:

$$a = \frac{n_a S_{ads}}{m S_{peak}} \tag{2}$$

where n_a is the amount of adsorbate injected onto the column; S_{ads} is the area on a chromatogram bounded by the peak height h between the outflow of the non-adsorbing substance and the extended profile of the chromatogram, cm^2; m is the mass of adsorbent in the column; S_{peak} is the peak area, cm^2.

The equilibrium pressure, p, corresponding to the determined adsorption, is calculated from the following equation:

$$p = \frac{n_a whRT}{F_c S_{peak}} \tag{3}$$

where w is the recording speed of the chromatogram, cm/min; h is the height of the peak, cm; R is the universal gas constant, J/mol·K; T is the column temperature, K; F_c is the carrier gas flow rate, cm^3/min.

The elution by characteristic point method (named also as peak profile method) enables the determination of an adsorption isotherm from a single chromatogram. The method gives good results for ideal, linear, and non-linear chromatographic conditions, for example, if the front or rear profiles of the elution peaks for various sample sizes superimpose.

Adsorption isotherms can be determined by the heat desorption method. This method was worked out by Nelsen and Eggertsen,[3] and it is widely employed because of the simplicity of its measurement apparatus and its great sensitivity. The principle of the method is based on the adsorption of nitrogen by a solid in the column from a stream of a gas mixture (usually H_2–N_2 or N_2–He) at the temperature of liquid nitrogen and then on its desorption after the removal of the liquid nitrogen. The quantity of adsorbed nitrogen, a, at an appropriate relative pressure, is estimated from the desorption peak, because it is more symmetrical. Each experiment performed for a given concentration of the adsorbate in the mixture gives one point on the adsorption isotherm. The most important characteristic of solids is their specific surface area. There are a few methods for the determination of specific surface area of solids based on chromatographic measurements.[4]

In one method adsorption isotherms are determined first and the specific surface areas are calculated from these isotherms by means of the BET method. The specific surface area of the solid, S, can be determined at ideal, non-linear chromatographic conditions, if the magnitude of monolayer adsorption, a_m, and the area occupied by a molecule of the adsorbate in the monolayer, ω, are known:

$$S = a_m N_A \omega \tag{4}$$

where N_A is the Avogadro number.

Methods in which the specific surface areas are calculated directly from the retention volume are based on the ideal, linear chromatographic conditions. The principle of these methods are derived from the theory of ideal, linear chromatography, which states that the specific retention volume, $V_{g(T)}$, of a substance is proportional to the magnitude of the surface area, S, of the adsorbent in the column:

$$S = V_{g(T)} \frac{S^{st}}{V^{st}_{g(T)}} \tag{5}$$

where $V_{g(T)}$ is the specific retention volume of an adsorbate on the investigated adsorbent; S^{st} is the specific surface area of the standard adsorbent; $V^{st}_{g(T)}$ is the specific retention volume of the adsorbate on the standard adsorbent.

Methods in which the specific surface area is calculated from the second (B_{2s}) and third (B_{3s}) gas–solid virial coefficients are valid if the values of B_{2s} [$=V_{g(T)}$] and B_{3s} are known. In such cases, the specific surface area can be calculated from the following equation:

$$S = -\pi D^2 \frac{B_{2s}^2}{B_{3s}} \tag{6}$$

where D is the diameter of the collision area of the adsorbate with the tested adsorbent, calculated on the basis of the density and dimensions of the adsorbate molecule.

DETERMINATION OF THERMODYNAMIC PARAMETERS

Thermodynamic parameters, excluding the highly precise parameters, of a chromatographic process may be determined if helium, whose properties are those of a perfect gas, is employed as the carrier gas.

The isosteric enthalpy of adsorption, ΔH_{ads}, can be determined by IGC, based on the changes in retention times or retention volumes with column temperature, employing the Clausius–Clapeyron equation for calculations, or, alternatively, using the second adsorption virial coefficient B_{2s}:[5]

$$\Delta H_{ads} = -RT^2 \frac{d \ln\left(\frac{V_{g(T)}}{T}\right)}{dT} \text{ or } \Delta H_{ads} = -RT^2 \frac{d \ln\left(\frac{B_{2s}}{T}\right)}{dT} \tag{7}$$

It is reasonable to use the Clausius–Clapeyron equation for calculating the isosteric enthalpy of adsorption as long as the equilibrium pressures are low (within Henry's law region) and the measurement temperatures are fairly close. Isothermal chromatographic measurements must be undertaken with changes of column temperature of 10 K at most.

Retention volumes are commonly used for the determination of enthalpy and entropy of adsorption, but Kováts retention indices can also be successfully used for such

calculations. Grajek[6] and Grajek, Witkiewicz and Jankowska[7] have suggested that if the number of carbon atoms of the adsorbate, $n \geq 5$, the following equation can be derived:

$$\frac{b(I_x - 100n)}{100} = \frac{-\Delta H^{I}_{ads(x)} + \Delta H^{V}_{ads(n)}}{2.303RT} + \frac{\Delta S^{I}_{ads(x)} - \Delta S^{V}_{ads(n)}}{2.303R} \quad (8)$$

where the differences $\left(\Delta H^{V}_{ads(n)} - \Delta H^{I}_{ads(x)}\right)$ and $\left(\Delta S^{I}_{ads(x)} - \Delta S^{V}_{ads(n)}\right)$ in Eq. 8 were directly proportional to the slope of the straight line and the intercept on the ordinate at $(1/T) = 0$, respectively. The $\Delta H_{ads(n)}$ and $\Delta S_{ads(n)}$ values were calculated from the specific retention volumes for *n*-alkanes employed as the reference "molecular probes" for adsorbates other than *n*-alkanes.[7]

The IGC at infinite dilution can also be employed for the determination of dispersive properties of solids. In the case where the tested solid adsorbent is covered with liquid, it is necessary to consider the interaction of the adsorbate with both the solid and the deposited liquid. The free energy of adsorption of one mole of adsorbate for a reference state of adsorption, ΔG_{ads}, is given by:[8]

$$\Delta G_{ads} = -RT \ln\left(V_{g(T)} \cdot \frac{P_o}{S\pi_o}\right) \quad (9)$$

where S is the specific area of the solid; π_o is the spreading pressure defined at the standard pressure P_o.

The reference states proposed by de Boer[8] are the most commonly employed ones for defining π_o and P_o.[9] Belgacem and Gandini[10] assumed the free energy of adsorption to be related to the work of adhesion, W_{adh}, mainly between the adsorbate molecules and the outermost layer of solid atoms and the atoms in bulk as well, and to the surface area of the adsorbate molecule, ω, in contact with the column filling:

$$\Delta G_{ads} = N_A \cdot \omega \cdot W_{adh} \quad (10)$$

According to Fowkes, the work of adhesion between an adsorbent surface (S) and a liquid (L), considering only dispersive interactions (D), can be described by the geometric mean of the surface free energy:[10]

$$W_{adh} = 2\sqrt{\left(\gamma^{D}_{S} \cdot \gamma^{D}_{L}\right)} \quad (11)$$

where γ^{D}_{S} and γ^{D}_{L} are the dispersive components of the surface energy of the solid and the liquid, respectively. From Eqs. 9–11 Schultz and Lavielle derived the equation:[11]

$$RT \ln V_{g(T)} = 2N_A\sqrt{\gamma^{D}_{S}} \cdot \omega\sqrt{\gamma^{D}_{L}} + K_3 \quad (12)$$

where K_3 is a constant term. Eq. 12 is usually plotted as $RT \ln V_{g(T)}$ vs. $\omega\sqrt{\gamma^{D}_{L}}$ and the values of the γ^{D}_{S} parameter are calculated.

Eq. 12 is developed for liquid adsorption on solid, although the molecules adsorbed at infinite dilution do not form an adsorbed liquid film. Schultz et al.[12] demonstrated the validity of this equation, and of the assumptions made, under certain conditions, by comparing the surface energy measured by contact angle method with that determined by gas–solid adsorption on solid surfaces; the dispersive component of the surface energy of the liquid equals the surface tension of the alkane probe at the same temperature, i.e., $\gamma^{D}_{L} = \gamma_H$, and ω represents the surface area that the probe covers when adsorbed onto the solid surface.

The values of these interactions appear as a deviation from the straight line of the reference alkane and can be quantified by the free energy, ΔG_{ads}, of adsorption–desorption of the specific polar adsorbate:[13]

$$\Delta G_{ads} = \Delta G^{D}_{ads} + \Delta G^{SP}_{ads} = N_A\omega W^{D}_{adh} + N_A\omega W^{SP}_{adh} \quad (13)$$

W^{D}_{adh} and W^{SP}_{adh} are the dispersive and the specific (non-dispersive) contributions in the work of adhesion.

The dispersive free energy of adsorption can be estimated by employing the following dependency:

$$\Delta G^{D}_{ads} = N_A\omega W^{D}_{A} = RT \ln V^{ref}_{N} \quad (14a)$$

And the specific free energy of adsorption can be estimated by employing the following dependency:

$$\Delta G^{SP}_{ads} = N_A\omega W^{SP}_{A} = RT \ln V_N \quad (14b)$$

In a plot of $RT \ln V^{ref}_{N}$ vs. $\omega\sqrt{\gamma^{D}_{L}}$, i.e., the product of the molecular surface area of the molecular probes, ω, and the *dispersive* component of the surface tension of the molecular probes, γ^{D}_{L}, the coordinates for a series of *n*-alkanes define a reference line (see Fig. 2).

All other polar probes exhibit higher net retention volumes, V_N, and the difference between their net retention volume and that of the *n*-alkanes for the same value of the dispersive component of surface energy leads to the value of the free energy of desorption, ΔG_{sp}, corresponding to the specific acid–base interaction, expressed as:

$$\Delta G_{SP} = RT \ln\left(\frac{V_N}{V^{ref}_{N}}\right) \quad (15)$$

Different approaches have been suggested for estimating the acidic/basic characteristics of the surfaces studied by IGC. In the simplest one the specific interactions between

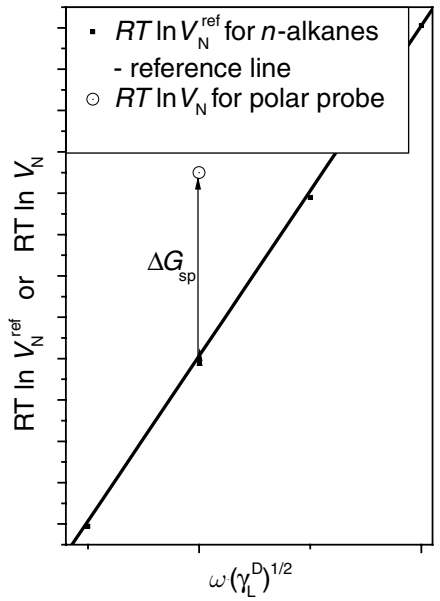

Fig. 2 Schematic representation of $RT \ln V_N$ vs. $\omega\left(\gamma_L^D\right)^{\frac{1}{2}}$ for an unknown probe.

the surface tested and two chromatographed reference polar adsorbates, i.e., a donor adsorbate and an acceptor one, are studied. The ΔG_{ads} values determined for the donor and the acceptor are related to the corresponding values of acceptor number, AN_S, and donor number, DN_S, for the solid:[14]

$$\Delta G^{SP}_{donor} \equiv AN_S \tag{16}$$

$$\Delta G^{SP}_{acceptor} \equiv DN_S \tag{17}$$

Lara and Schreiber[14] assumed that Eqs. 16 and 17 describe the acidic and the basic character of the surface, respectively. The donor number, DN_S, is a measure of the electron-donor (basicity) ability of the "molecular probe", while the acceptor number, AN_S, is a measure of the electron-acceptor (acidity) ability of "molecular probe": Based on the values of AN_S and DN_S, surfaces are characterized as follows:

$$\frac{AN_S}{DN_S} \geq 1.1 \quad \text{acidic surface}$$

$$\frac{AN_S}{DN_S} \leq 0.9 \quad \text{basic surface}$$

$$0.9 < \frac{AN_S}{DN_S} < 1.1 \quad \text{amphoteric surface}$$

$$AN_S \approx DN_S \approx 0 \quad \text{neutral(non-polar)surface}$$

The second approach, was proposed by Schultz and Lavielle.[11] It is based on the Gutmann's acid–base theory. The authors elaborated a semiquantitative approach to characterize the acidic/basic properties of solid surfaces based on the correlation of the enthalpy of desorption corresponding to specific interactions, ΔH_{SP}, with the acidic/basic properties of chromatographed polar adsorbates (acceptor number, AN_S, and donor number, DN_S, for the adsorbate):

$$\Delta H_{SP} = K_A DN_S + K_B AN_S \tag{18}$$

where K_A and K_B describe the acidic and basic characteristics of the solid surface, respectively, and are the slope and the intercept of the linear dependency $\frac{\Delta H_{SP}}{AN_S} = f\left(\frac{DN_S}{AN_S}\right)$, which enables the determination of the acidic and basic characteristics of the solid surface tested.

The third approach was developed by Boluk and Schreiber on the basis of Drago's acid–base concept.[15] In this case a homologous series of alcohols and amines were employed as the acidic and the basic probes, respectively. The interaction parameter, Ω, reflects the acidic/basic properties of the solid surface and is defined as follows: for acidic surfaces, the specific retention volume, $\left[V^o_{g(T)}\right]_b$, of basic adsorbate exceeds the $\left[V^o_{g(T)}\right]_a$ value for the acidic alcohol. In this case *n*-butylamine and *n*-butyl alcohol are commonly employed to calculate the interaction parameter, Ω:

$$\Omega = 1 - \frac{\left[V^o_{g(T)}\right]_b}{\left[V^o_{g(T)}\right]_a} < 0 \tag{19}$$

$$\Omega = 1 - \frac{\left[V^o_{g(T)}\right]_a}{\left[V^o_{g(T)}\right]_b} > 0 \tag{20}$$

where $\left[V^o_{g(T)}\right]_a$ and $\left[V^o_{g(T)}\right]_b$ are the specific retention volumes for the acidic and basic adsorbate, respectively.

DETERMINATION OF PROPERTIES OF LIQUIDS

The partition coefficient at infinite dilution of the solute, K^∞, between the carrier gas and the stationary phase can be defined as[9]

$$K^\infty = \lim_{x_i \to 0} \frac{c_S}{c_G} = \frac{V_N}{V_{Lm}} \tag{21}$$

where x_i is the mole fraction of chromatographed substance; c_S is the concentration of adsorbate in the stationary phase; c_G is the concentration of adsorbate in the gas phase; V_{Lm} is the molar volume of the stationary phase.

The partition coefficient, K, of the solute between a mobile (gas) phase and a stationary phase is the concentration ratio:

$$K = \frac{c_S}{c_G} = \frac{RT}{p_{ia}\gamma_s V_{Lm}} \tag{22}$$

p_{ia} is the pressure of saturated vapor of the adsorbate at the column temperature, T; γ_s is the activity coefficient of adsorbate in stationary phase.

If volume partition of the test substance is the only retention mechanism between the liquid deposited on the solid carrier and a gas phase, then the K value can be calculated using the specific retention value, $V_{g(T)}$:

$$K = V_{g(T)}\frac{T}{273.15}\frac{m}{V_L} = V_{g(T)}\frac{T\cdot\rho_L}{273.15} \tag{23}$$

The thermodynamic partition constant, K_i, has to be employed for calculating the free energy of adsorption of any adsorbate, which differs in nature from the chromatographic partition constant, K. Actually, the thermodynamic partition coefficient, K_i, is the ratio of the partial pressure of the chromatographed solute p_i to its molar fraction in the stationary phase, x_i. For designing chemical processes the thermodynamic K_i values are usually expressed as:

$$K_i = \frac{p_i}{x_i} \tag{24}$$

By the aforesaid reasoning, K_i can be expressed as $K_i = \gamma_i p_{i(o)}$. The K_i and activity coefficient values are used for calculating other magnitudes and thermodynamic quantities.

The partition coefficient K_i can be correlated to the thermodynamic parameters of the stationary phase via the following equations:

$$\Delta G_{ads} = RT\ln V_N + C_1 \tag{25}$$

$$\frac{-\Delta G_{ads}}{RT} = \ln K_i + C_2 \tag{26}$$

$$\frac{d\ln(K_i)}{d\left(\frac{1}{T}\right)} = \frac{-\Delta H_{ads}}{R} \tag{27}$$

$$\Delta S_{ads} = -\left(\frac{\Delta H_{ads} + \Delta G_{ads}}{T}\right) \tag{28}$$

where ΔG_{ads} is the standard free energy of adsorption; C_1 and C_2 are the constants on the reference state of the probe; ΔH_{ads} is the standard enthalpy of adsorption; ΔS_{ads} is the standard entropy of adsorption.

The partition and activity coefficients are used for determining the excess thermodynamic functions of the mixing of chromatographed substances on stationary phase: free energy, ΔG_E, enthalpy, ΔH_E, and entropy, ΔS_E. The values of these thermodynamic functions characterize the intermolecular interactions in the dissolution process. They can be calculated by using the following dependencies:

$$\Delta G_E = RT\ln K_i \tag{29}$$

$$\Delta H_E = R\frac{d\ \lg\ \gamma_i}{d\left(\frac{1}{T}\right)} \tag{30}$$

$$\Delta S_E = \frac{(\Delta H_E - \Delta G_E)}{T} \tag{31}$$

The IGC technique can be employed for the identification of asphaltenes. In this case the relative coefficients of interaction of standard substances with the stationary phase, I_g, are used:

$$I_g = 100\ \lg\frac{V_R^o}{V_{RP}^o} \tag{32}$$

where V_R^o and V_{RP}^o are the retention volumes of a standard substance and an n-alkane with molecular weight equal to that of the test substance. This parameter hardly depends on chromatographic conditions and therefore can be used in comparing properties of different asphaltenes.

The IGC technique is also useful for characterizing the properties of liquid crystals.[16] The melting and clearing temperatures of liquid crystals and their ability to overcool can be determined based on the dependency $t_R = f(T_c)$. Retention values differ in different physical states of the liquid crystal substance. The retention of chromatographed substance usually decreases with increasing column temperature within a temperature range for the solid state of the liquid crystal stationary phase. After achieving a minimum, and on further increase in temperature, retention significantly increases and achieves the maximum at the melting point, and a mesophase structure appears. In the mesophase the retention times decrease and they may increase again before the transition point to isotropic liquid, but to a small extent. Sometimes this cycle is visible during transition from one to another kind of mesophase. After finishing the transition to isotropic liquid, retention decreases.

The IGC technique can be employed for investigating the phenomenon of complex formation, especially for the following applications:

- Determination of the stability constants for complexing reactions.
- Testing the energy-related effects for the complexing reactions.[9]

By employing IGC, it is possible to test donor–acceptor molecular complexes and the stability of hydrogen bonds.

The main advantages of using IGC in the study of equilibrium constants of complexes are the following:

- There is the possibility of determining the equilibrium constants directly from retention data, without the necessity of the estimation of equilibrium concentrations.
- The method is relatively rapid and technically simple.
- Very small amounts of rare or even impure compounds can be used.
- By employing mixtures of solutes, measurement of many parameters can be made in a single experiment.
- Hydroxylable or water-insoluble complexes may be studied in non-aqueous media.

CHROMATOGRAPHIC TESTING OF POLYMERIC MATERIALS

Polymers can be tested by means of IGC technique. The following parameters and phenomena can be determined or investigated: molecular masses of polymers, phase transitions, glass transition temperatures, kinetics of reaction with polymers, values of thermodynamic functions of dissolution of different substances in polymers, and acidic/basic properties of polymers.

The determination of the crystallinity of polymer stationary phases is based on the differential solubility of the "molecular probe" in crystalline and amorphous domains. In effect the adsorbate "senses" only the amorphous regions, leading to an increase in retention volume with decreasing crystallinity.

The retention diagrams through the melting transitions of semicrystalline polymers (see Fig. 3) could be analyzed quantitatively to yield the crystallinity and the melting curve of a polymer. It was found that both above and below the melting point, T_m, retention proceeded by bulk sorption, thus allowing for a comparison of the specific retention volumes. Above T_m the polymer is completely amorphous and a linear retention diagram is obtained. By extrapolating this straight line to lower temperatures the specific retention volume for the amorphous polymer can be computed theoretically. A comparison with the experimentally determined specific retention volume yields the amorphous fraction of the stationary phase, x:

$$x = \frac{V_{g(T)}}{V_{g(T)}'} \tag{33}$$

where $V_{g(T)}$ is the specific retention volume of the chromatographed substance; $V_{g(T)}'$ is the specific retention volume of the chromatographed substance extrapolated to the dashed line.

The studies on polymer stationary phases revealed that retention diagrams exhibited certain singularities, such as those depicted in Fig. 3, corresponding to the transitions of the polymer stationary phase. Both glass (B) and melting (F) transitions were thus detected. These transitions of the stationary phase are of paramount importance in IGC for determining the nature of the information that can be derived from any one experiment.

In the region corresponding to segment AB of Fig. 3, the polymer is below its glass transition temperature, T_g, and penetration of the "molecular probe" molecules into the bulk of the polymer phase is precluded. Retention proceeds exclusively by surface adsorption, and the corresponding retention diagram is linear. At point B, corresponding to the glass transition, penetration of the "molecular probe" into the bulk of the polymer begins, causing an increase of specific retention volume with temperature. Owing to the initially slow rate of diffusion of the "molecular probe" into and out of the stationary phase, non-equilibrium conditions prevail. As the temperature increases in region BC, the diffusion coefficient rises sharply, leading to equilibrium conditions at point C.

At temperatures below the melting point of the polymer, in region CD, retention proceeds by bulk sorption, but the tested polymer–"molecular probe" interaction is restricted to the amorphous domains of the stationary phase. Upon melting, in region DF, the fraction of amorphous material increases, leading to an increase in retention volume. At temperatures above the melting point, segment FG, a linear retention diagram corresponding to bulk sorption into the completely amorphous polymer, is obtained. By extrapolation of this line to lower temperatures (i.e., dashed line FE), the crystalline content of the stationary phase can be determined by comparing the

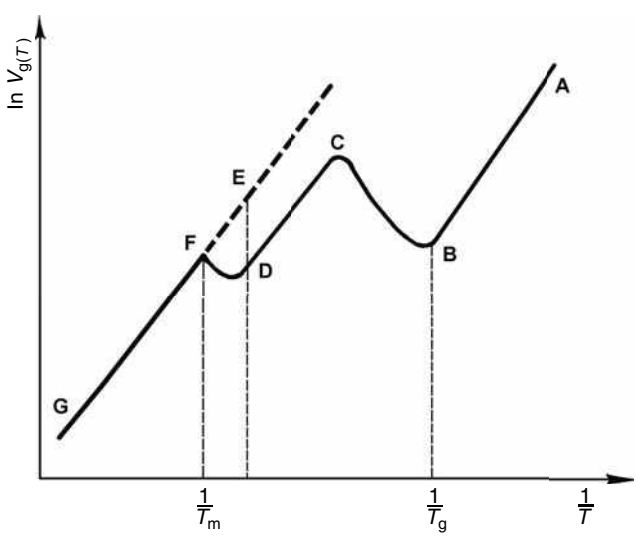

Fig. 3 The variation of the $\ln V_{g(T)}$ vs. $\frac{1}{T}$ for a semicrystalline polymer.

experimentally determined specific retention volume with the extrapolated value.

In region FG the polymer is completely amorphous and the properties of the tested polymer–"molecular probe" solution can be investigated. Care must be taken to ensure that any contribution from surface adsorption is taken into account. For non-crystalline polymers, liquid-like behavior is observed from point C onward. The location of point C on the temperature axis depends both on the tested polymer–"molecular probe" system considered and on chromatographic conditions, film thickness, and flow rate.

INVESTIGATION OF VOLATILE SUBSTANCES AND DIFFUSION IN GASES

The dependencies in plate theory, describing the efficiency of chromatographic columns, can be used in diffusion tests. It is possible to determine the diffusion coefficient of any volatile solute in the carrier gas by means of gas chromatograph apparatus. In this case a capillary column without any stationary phase, of length L and internal diameter d, with u being the flow rate of the carrier gas, is employed. Vapors of a volatile substance are injected into the column, and a peak of the substance is registered. The retention time, t_R, and the base width of Gaussian peak in units of chart distance,w_b, are measured. The plate height can be calculated from the following dependency:

$$H = \frac{L}{16}\left(\frac{w_b}{t_R}\right)^2 \tag{34}$$

The H values can be inserted into the Van Deemter equation for capillary columns, and the diffusion coefficient, D_f, can be estimated:

$$H = \frac{2D_f}{u} + \frac{d^2 u}{24D_f} \tag{35}$$

where d is the diameter of the column; D_f is the coefficient of molecular diffusion of the solute in carrier gas; u is the linear velocity of carrier gas.

The D_f values can be calculated from the linear relationship between Hu and u^2. If the method is to be successful, laminar flow must be maintained throughout the experiment.

REFERENCES

1. Smidsrød, O.; Guillet, J.E. Study of polymer-solute interactions by gas chromatography. Macromolecules **1969**, *2*, 272–277.
2. Kiselev, A.V.; Yashin, Y.I. *Gas-Adsorption Chromatography*; Plenum Publ.: New York, 1967.
3. Nelsen, F.M.; Eggertsen, F.T. Determination of surface area: Adsorption measurements by a continuous flow method. Anal. Chem. **1958**, *30*, 1387–1392.
4. Paryjczak, T. *Gas Chromatography in Adsorption and Catalysis*; PWN, Warszawa—Ellis Horwood Limited Publisher: Chichester, 1986.
5. Grajek, H. Investigations of the dependencies between the retention data in the inverse gas chromatography and the adsorption parameters of active carbons. Maria Curie-Skłodowska University Press: Lublin, Poland, 2003 (in Polish).
6. Grajek, H. Rediscovering the problem of interpretation of chromatographically determined enthalpy and entropy of adsorption of different adsorbates on carbon materials. Critical appraisal of literature data. J. Chromatogr. A, **2007**, *1145*, 1–50.
7. Grajek, H.; Witkiewicz, Z.; Jankowska, H. Application of Kovats retention indices for investigation of adsorption properties of activated carbons. J. Chromatogr. **1997**, *782*, 87–98.
8. de Boer, J.H. *The Dynamical Character of Adsorption*; Oxford University Press: London, 1953.
9. Conder, J.R.; Young, C.L. *Physicochemical Measurement by Gas Chromatography*; John Wiley & Sons: Chichester, U.K., 1979.
10. Belgacem, M.N.; Gandini, A. *Inverse Gas Chromatography as a Tool to Characterize Dispersive and Acid-Base Properties of the Surface of Fibers and Powders—Surfactant Science Series—Vol. 80*; Pefferkorn, E., Ed.; Marcel Dekker, Inc.: New York, 1999, 41–124.
11. Schultz, J.; Lavielle, L. Interfacial Properties of Carbon Fiber-Epoxy Matrix Composites. In *Inverse Gas Chromatography*; ACS Symposium Series; Lloyd, D.R.; Ward, T.C.; Schreiber, H.P.; Pizaña, C.C., Eds.; American Chemical Society: Washington, DC, 1989, Vol. 391, Chapter 14.
12. Schultz, J.; Lavielle, L.; Martin, C. The role of the interface in carbon fibre-epoxy composites. J. Adhesion **1987**, *23*, 45–53.
13. Garnier, G.; Glasser, W.G. Measurement of the surface free energy of amorphous cellulose by alkane adsorption: a critical evaluation of inverse gas chromatography (IGC). J. Adhesion **1994**, *46*, 165–180.
14. Lara, J.; Schreiber, H.P. Specific interactions and adsorption of film-forming polymers. J. Coating Technol. **1991**, *63*, 81–88.
15. Boluk, Y.M.; Schreiber, H.P. Interfacial interactions and the properties of filled polymers: I. Dynamic-mechanical responses. Polym. Comp. **1986**, *7*, 295–301.
16. Witkiewicz, Z.; Oszczudłowski, J.; Repelewicz, M. Liquid-crystalline stationary phases for gas chromatography. J. Chromatogr. **2005**, *1062*, 155–174.

Iodine-Azide Reaction as a Detection System in TLC

Robert Zakrzewski
Witold Ciesielski
Department of Instrumental Analysis, University of Łódź, Łódź, Poland

Abstract
The possibilities of application of iodine-azide reaction as a detection system has been presented. In this method, the developed plates are sprayed with a mixture of sodium azide and iodine solution. A modified procedure includes spraying the developed plate with sodium azide and starch solution and afterward exposing it to iodine vapor. In reversed-phase high-performance thin-layer chromatography (RP-HPTLC) mode, sodium azide becomes a constituent of the mobile phase. The catalytic effect of C–S, C=S, P–S, and P=S bonds results in white spots emerging on the violet–gray background. It has been found that the detection limits are as low as a picomol per dot, and the factors leading to such low values have been explored. The method has been used to distinguish different thiols in biological samples, such as urine or blood serum, pesticides, and drugs. The outcome of the derivatization process with phenyl isothiocyanate or butyl isothiocyanate is the transformation of the amino acids, biogenic amines, and amphetamines into inductors [phenylthiocarbamyl (PTC), butylthiocarbamyl (BTC), or phenyl thiohydantoin (PTH) derivatives] of the iodine-azide reaction.

INTRODUCTION

There are numerous methods for sulfur(II) detection in thin-layer chromatography (TLC). Most of them are based on general, rather than specific, techniques. The iodine-azide reaction takes place only in the presence of a sulfur(II) compound (selective induction), and only these compounds are visible on the thin-layer plate after treating with an iodine-azide reagent. The detection limits are as low as a picomol per spot. The factors that have an impact on the detection limits are discussed in this entry. The developed method has been applied to detect various thiols in biological samples (urine and blood serum), pesticides, and drugs.

IODINE-AZIDE REACTION

The iodine-azide reaction, $2N_3^- + I_2 \xrightarrow{\text{sulfur(II) compound}} 3N_2 + 2I^-$ introduced by Rashing,[1] has been explored extensively for decades in analytical chemistry. Sulfur(II) compounds act rather as inductors than as catalysts. Compounds such as sulfide, thiosulfate, thiocyanate, and polythionates and elemental sulfur (after cleavage of S_8 ring) are inductors of the iodine-azide reaction. Among the organic compounds, thiols, thionates, disulfides, organophosphorus compounds containing a P=S, or a P–S bond, and compounds with sulfur in the ring (after cleavage with iodide azide) have induction properties. Nitrogen evolved during the reaction, heat changes generated, and iodine consumed in the reaction are proportional to the amount of sulfur(II) compound present in a sample, and the quantity of the sulfur(II) compound is determined based on these changes.

The iodine-azide reaction has been widely applied for the determination of sulfur(II) compounds using various techniques, e.g., titration, spectrophotometry, coulometry, flow injection analysis, TLC, and high-performance liquid chromatography.

The iodine-azide reaction mechanism was introduced by Strickland, Mack, and Childs[2] and modified by Kurzawa and Kurzawa.[3] The reaction of iodine with azide ion, induced by the sulfur(II) compound, takes place in solution, as shown in Fig. 1. Azide ion reacts neither with iodine nor with a sulfur(II) compound directly, or these reactions are very slow (reaction 1). The equilibrium of reaction 1 shifts strongly to the left. If it were possible to remove iodide ions I^-, the reaction between $I_2N_3^-$ complex and the azide ion would take place (reaction 2).[4] In the presence of a sulfur(II) compound, the intermediate compound RSI is formed (reaction 3). The induction cycle starts with the reaction of intermediate compound RSI with an azide ion or a sulfur(II) compound involved in the induction cycle (reaction 4). The reaction ends when the entire amount of sulfur(II) compound is deactivated in the iodimetric reaction (reaction 5). Induced and iodimetric reactions are competitive. In the iodimetric reaction, the inductor is oxidized by iodine and removed from the induction cycle.

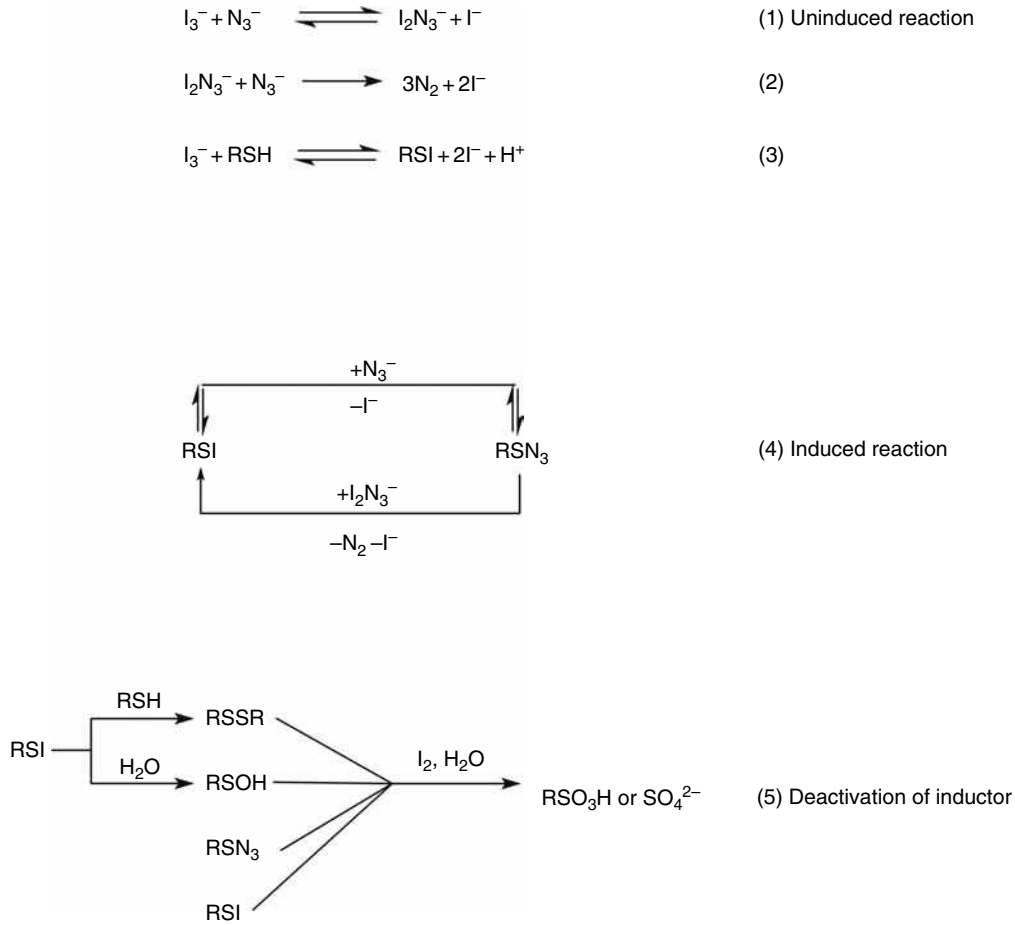

Fig. 1 Mechanism of iodine-azide reaction.

DETECTION OF SULFUR COMPOUNDS

The developed TLC plates were sprayed with different iodine-azide solutions as shown in Table 1. Generally, it can be stated that the sprayed reagents were prepared by mixing the two solutions: sodium azide and iodine (in potassium iodide to dissolve iodine in water)[5–20] (procedure 1). Sometimes starch solution was applied[21–27] (procedure 2), and in another procedure the developed TLC plates were sprayed with sodium azide and starch solution and then exposed to iodine vapor[28–40] (procedure 3). In the reversed-phase (RP) mode, sodium azide was incorporated into the mobile phase (procedure 4).[31,32,34]

In all the procedures, the chromatographic bands became visible as white spots on a yellow background or as white spots on a violet–gray background when starch was used. The spots appear because of the induction effect of the C–S, C=S, P–S, or P=S bonds. However, after some time, the background starts to disappear owing to iodine sublimation.

The method was applied to detect the various sulfur(II) compounds listed in Table 1. As can be seen, the lowest detection limits are obtained when the TLC plates are sprayed with azide/starch solution and exposed to iodine vapor (procedures 3 and 4). In procedures 1 and 2 (spraying TLC plates with azide and iodine and/or starch solution), the detection limits are in nanomol per spot levels.

Influence of Varied Factors on Detection Limit

Several parameters have to be determined for achieving the optimum conditions when using iodine-azide reaction as the detection system in TLC: pH (Fig. 2), the concentration of spray solution, and the influence of iodine and iodide ions on the course of iodine-azide reaction.

To optimize the postchromatographic reaction, the conditions should lead to the highest consumption of iodine in the induced reaction. This consumption of iodine is reflected in the induction coefficient, defined by the equation:

$$F_i = \frac{n_I}{n_S}$$

where n_I is the moles of iodine consumed in the inducted reaction and n_S is the moles of the inductor. From the

Table 1 Composition of iodine-azide solution and detection limits for different sulfur(II) compounds.

No.	Detected compounds	Spray solution	Detection limit		Refs.
			μg/spot	nmol/spot	
		Procedure 1			
1	PTH derivatives of amino acids[a]	Aqueous mixture of 0.5 *M* sodium azide, 0.01 *M* iodine, 0.5 *M* potassium iodide	0.5		[5]
2	Cysteine, cystine, methionine[a]	Aqueous mixture of 0.2% sodium azide, 0.02 *M* iodine	—		[6]
3	Thiophoshoric esters	Aqueous mixture of 3–5% sodium azide, 0.05–0.1 *M* iodine	1–2		[7]
	Thiophosphoryl compounds, mercaptoacetic acid, thiourea and its derivatives, thiocyanate, thiosulfate		0.08–180		[8]
4	Penicillins[a]	Aqueous solution of 3.5% sodium azide in 0.1 *M* iodine	5–10		[9,10]
5	Free sulfur	Aqueous solution of 3% sodium azide in 0.1 *M* iodine	0.2		[11]
6	1,4-Oxathiins	Aqueous mixture of 0.5 *M* sodium azide and 0.1 *M* iodine	0.2		[12]
7	Free sulfur	0.1 *M* iodine solution in a mixture of ethanol:water (3:7, v/v) with the addition of 3% sodium azide solution	5		[13, 14]
8	Heavy metal dithiocarbamates and related compounds	Aqueous mixture of 3% sodium azide, 0.05 *M* iodine	10–20		[15]
9	Thiophosphoryl compounds	Aqueous mixture of 0.5 *M* sodium azide, 0.5 *M* iodine, 0.5 mol potassium iodide adjusted to pH 6.0		0.1–160	[16]
	Thiophosphoryl nucleotides			0.3–25	[17]
	Biologically oriented thiophosphoryl compounds			0.5–100	[18]
	Sulfur-containing amino acids and their aminophoshonic analogs			20–30	[19]
	Thioureas, isothiouronium bases; isothiobiurets; imidazo-, pyrimido-, diazepino-triazines; isothiocyanates		—		[20]
		Procedure 2			
10	PTH derivatives of amino acids	Aqueous mixture of 0.1% sodium azide, 0.01 *M* iodine, 0.75% starch	0.01–0.02		[21–23]
11	PTH derivatives of amino acids	Aqueous mixture of 0.1 *M* sodium azide, 0.1 *M* iodine, 0.4% starch	1		[24]
12	Thiuram[a]	Aqueous mixture of 1.5% sodium azide, 0.5 *M* iodine, 1% starch	0.25		[25]
	Diphenylthiourea[a]		0.5		
13	Thiophosphoric esters (pesticides)	Aqueous mixture of 0.5 *M* sodium azide, 0.5 *M* iodine, 0.5 *M* potassium iodide adjusted to pH 6.0. Then the second spray solution was used: 1% aqueous starch solution	0.5–10		[26]
14	β-Lactam antibiotic drugs	Aqueous mixture of 3.5% sodium azide, 0.1 *M* iodine in 0.1 *M* potassium iodide, 1% starch	100		[27]

(Continued)

Table 1 Composition of iodine-azide solution and detection limits for different sulfur(II) compounds. *(Continued)*

No.	Detected compounds	Spray solution	Detection limit		Refs.
			μg/spot	nmol/spot	
		Procedure 3			
15	Carbimazole	Aqueous mixture of 4% sodium		0.08	[28]
	PTC derivatives of amino acids	azide and 0.5% starch adjusted to		0.001–0.1	[29–32]
	BTC derivatives of amino acids	pH 5.5–6.0 and then the TLC/		0.002–0.09	[33]
	PTC derivatives of biogenic amines	HPTLC plate was exposed to iodine vapor for 5 sec.		0.01–0.11	[34]
	PTC amphetamine and its analogs			0.08–0.19	[35]
	PTC dipeptide			0.001–0.1	[36]
	Thiouracils			0.001–0.01	[37]
	Mercaptopyridines and mercaptopyrimidines			0.001–0.02	[38]
	Heterocyclic thiols			0.001–0.08	[39]
	Thiuram			0.0005	[40]
		Procedure 4			
16	PTC derivatives of amino acids	2% starch solution and then the		0.007–0.25	[31–32]
	PTC derivatives of biogenic amines	TLC plate was exposed to iodine vapor for 5 sec (sodium azide at proper pH was incorporated into the mobile phase).		0.030–0.45	[34]

Dash indicates not stated.
[a]Paper chromatography was used.

analytical point of view, the value of the induction coefficient is a measure of the determination sensitivity of a given sulfur(II) compound in volumetric, coulometric, spectrophotometric, and flow injection analysis determination. The induction coefficient can be applied for predicting detection limits in various methods. This implies a direct relationship: the higher the induction coefficient, the more sensitive the determination of a given inductor is. There is a good correlation between the induction potency of thiouracils and their detectability in TLC methods using the iodine-azide reaction as a visualization step.[37]

Iodine and Iodide Ions

Procedure 3 (spraying with sodium azide and starch solution and exposing to iodine vapor)[28–40] yields lower detection limits as compared with spraying using the mixture of the solutions sodium azide, iodine, and/or iodide ions (procedures 1 and 2).[5–20] Excess of iodine, which is difficult to avoid in procedure 1, raises the detection limits because it makes the white spots vanish (see Table 4 of Ref. 37 or Table 6 of Ref. 29). The phenomenon does not generally occur with other visualization techniques in planar chromatography: an excess of visualization solution does not raise the detection

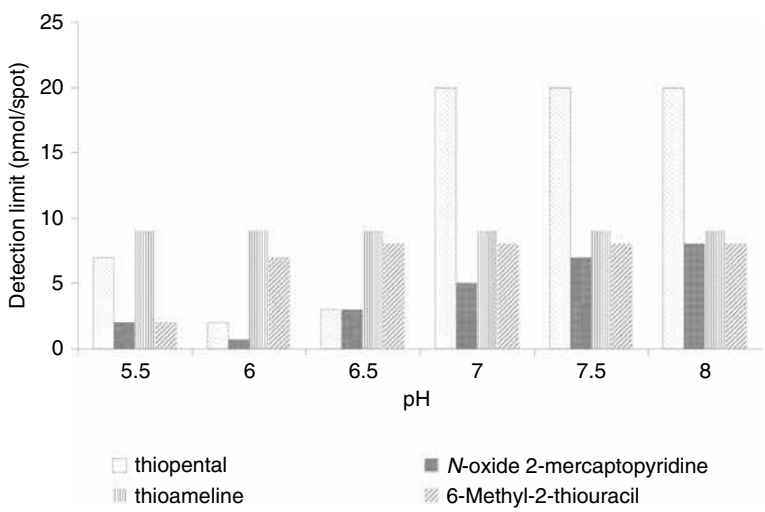

Fig. 2 The dependence of detection limits in TLC on pH of the spray solution.

limit. The use of iodine vapor, however, lowers the detection limits considerably by avoiding the excess of iodine, and it enables iodine to be dispersed evenly onto TLC plates.

The hampering effect of the iodide ions on the iodine-azide reaction induced with some organothiophosphorus compounds increases with increasing iodide-ion concentration.[29,41] Presence of high concentration of potassium iodide (0.5 mol/L) in the spray solution totally prevents the course of the iodine-azide reaction (for details see table 1 in Ref. 16 and Table 1 in Ref. 17). In this case, the rate of iodimetric reaction is higher than that of the induced reaction. This is the reason for the appearance of brown spots (these dots are similar to the ones obtained with iodine vapor) instead of white dots corresponding to a particular organothiophosphorus compound.

The presence of iodide ions raises the detection limits for many thiols (e.g., thiouracils[37]) when sprayed with iodine in potassium iodide solution; however, the detection limits are not raised to the same extent for some PTC derivatives of amino acids[30] for the same concentration of iodide ions. The iodine-azide reaction takes place at a lower rate in the presence of iodide ions, and white spots take longer to appear, particularly for higher concentrations of iodide ions.

Sometimes a small amount of iodide ions in the spray solution in the improved iodine-azide procedure had a positive impact on the detection limits (e.g., 2,4-dimercaptopyrimidine, 2-thioorotic acid, 2-mercapto-3,4,5,6-tetrahydropyrimidine).[38] For ethyl 4-amino-2-mercaptopyrimidine 5-carboxylate, increasing the concentration of iodide ions in the spray solution in the improved iodine-azide procedure enhanced the detection limits.[39] Fig. 3 shows instances of the reliance of the detection limits in TLC on iodide ions solution concentration.

pH of Spray Solution

For many compounds, the detection limit was found to be dependent on the pH of the reagent (sodium azide solution). A solution with pH lower than 5.5 is not recommended because of the emission of the poisonous, volatile hydrazoic acid HN_3. On the contrary, when the pH is over 8.0, the catalytic reaction does not proceed, as iodine forms hypoiodite (IO^-), which is not a reagent in the iodine-azide reaction. Therefore, a suitable pH should be chosen within the range 5.5–8. The pH chosen for spray solutions in TLC corresponds to the pH of the reaction medium in other techniques using iodine where the iodine-azide reaction is applied as a measurement method.

Concentration of Azide Ions

Increasing the sodium azide concentration in the spray reagent, up to 4% (procedure 3), causes a slight decrease in detection limits.[28–40] Beyond the 4% limit, further increase in the concentration of sodium azide solution does not influence the detection limits.

Induction Time

The spots become visible after a time lag on account of the induction time (i.e., time required for the induction reaction to complete) conditioned by induction properties of the particular compound. The induction time should not be too long because it may cause disappearance of the background owing to iodine sublimation.

QUANTITATIVE ANALYSIS

Densitometric analysis coupled with iodine-azide reaction as a detection system is relatively difficult to conduct owing to background disappearance. There are two processes behind this: iodine sublimation from a plate area and uninduced iodine-azide reaction proceeding outside a spot. Addition of potassium iodide to the spray solution lowers

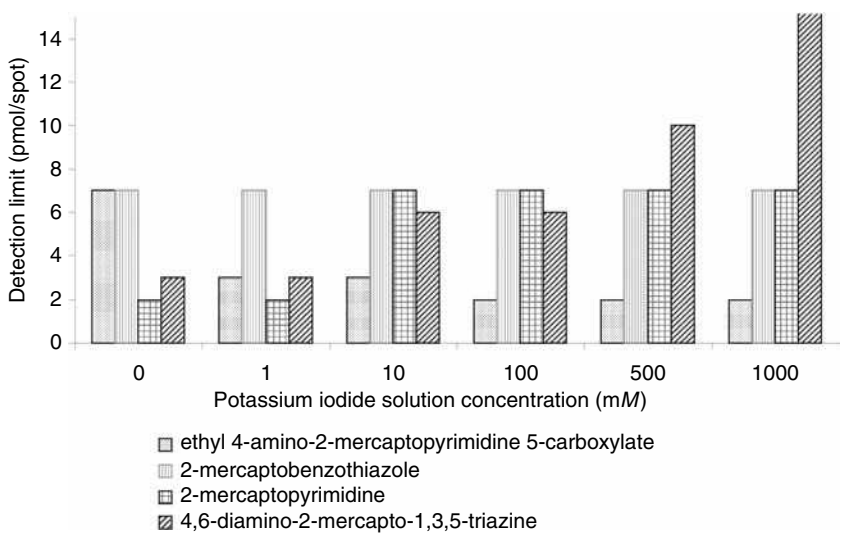

Fig. 3 The dependence of detection limits in TLC on potassium iodide concentration in the spray solution.

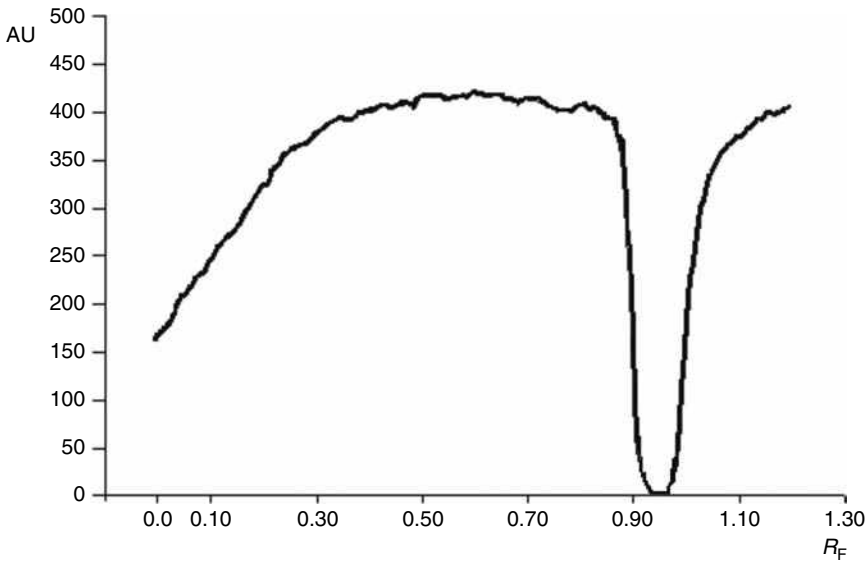

Fig. 4 Scan of TLC plate for the dot corresponding to 5 pmol/dot with TLC densitometer at 483 nm.

iodine volatility. At higher concentration of iodide ions, the background is stable because the concentration of the nonvolatile triiodide ions increases as a result of a further shift in the equilibrium of iodine–iodide ions ($I_2 + I^- \rightleftarrows I_3^-$) to the right. High concentration of potassium iodide in the spray solution also results in hampering the uninduced iodine-azide reaction;[4] moreover, the amount of iodine is constant on a specific area of the plate. The higher the concentration of iodide ions, the more stable the background obtained.

The background color changes from violet–gray (corresponding to iodine–starch complex) to brown (iodine–iodide–starch complex) as the iodide ion concentration increases. This color transformation is the consequence of the hypsochromic shift of background maximum absorption wavelength from 550 to 483 nm. Plates were covered with sodium azide (in the spray solution) and iodine (plates were placed in an iodine chamber). Thanks to the presence of starch and iodide ions plates change color from violet–gray to brown. In the case of TLC plate where thiuram is present, iodine-azide reaction induced by thiuram takes place, and a white spot appears, which makes densitometric analysis possible.[40]

In procedure 3, the plate is scanned at 483 nm, which corresponds to the maximum absorption of iodine–iodide–starch complex (Fig. 4). As the plate is covered with iodine, a constant absorbance is maintained and recorded as a background from iodine–iodide–starch complex. When the light passes a white dot, the signal decreases owing to the consumption of iodine in the iodine-azide reaction induced by thiuram within this spot. Outside the thiuram spot, the absorbance signal gets restored to its initial value and a negative peak is recorded. Calibration plots were constructed by plotting spot area (calculated from end and start R_F value) against the corresponding amount (in picomols) of thiuram. In an alternate method, a PC scanner was also applied as an analytical instrument. The chromatograms were stored in the form of 24-bit true-color images (Fig. 5). The pixels of white chromatographic bands were counted and calibration plots were constructed by plotting the number of pixels against the corresponding amount (in picomols) of thiuram. Results obtained with the PC scanner are similar to those obtained with TLC densitometry coupled with iodine-azide detection procedure.

APPLICATION OF THE METHOD

The evaluated methods were applied to detect thiols in blood serum, urine,[28,37,38,39] and food samples;[40] aspartic acid in drugs;[29] free sulfur traces in chemical reagents that include sulfur in their structure;[14] ores and products of their flotation;[13] tire treads;[13] and rubber vulcanizates[11] (Table 2).

β-Lactam antibiotic drugs,[27] amino acids,[31,32] and biogenic amine[34] as a PTC derivative, BTC amino acids,[33] thiouracils,[37] pyrimidines, and pyridines[38] were separated in HPTLC and detected with the suggested method.

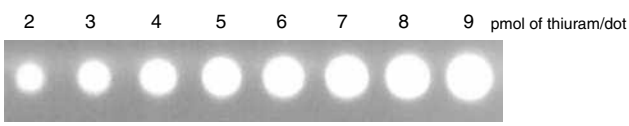

Fig. 5 Detection of thiuram (2–9 pmol/dot) using iodine-azide reaction method; Experimental conditions: TLC plate; mobile phase: methanol; development distance: 5 cm.

Table 2 Application of iodine-azide reaction.

Compound	Matrix	Detection limit	Refs.
Thioguanine	Blood serum	35 nmol/ml of blood serum	[39]
Thioguanine	Urine	20 nmol/ml of urine	[39]
6-Merkaptopurine	Urine	50 nmol/ml of urine	[39]
Thiopental	Blood serum	30 nmol/ml of blood serum	[38]
Thiopental	Urine	0.5 nmol/ml of urine	[38]
6-Methyl-2-thiouracil	Blood serum	0.75 nmol/ml of blood serum	[37]
6-Methyl-2-thiouracil	Urine	3 nmol/ml of urine	[37]
6-Propyl-2-thiouracil	Blood serum	2.5 nmol/ml of blood serum	[37]
6-Propyl-2-thiouracil	Urine	3 nmol/ml of urine	[37]
6-Benzyl-2-thiouracil	Blood serum	2.5 nmol/ml of blood serum	[37]
6-Benzyl-2-thiouracil	Urine	3 nmol/ml of urine	[37]
Carbimazole	Blood serum	0.75 nmol/ml of blood serum	[28]
Thiuram	Apples	10 nmol/g of apples	[40]
Thiuram	Apple juice	1.25 nmol/ml of juice	[40]
Thiuram	Carrot juice	10 nmol/ml of juice	[40]
Aspartic acid	Drug	—	[29]
Free sulfur traces	Chemical reagents which include sulfur in their structure	—	[14]
Free sulfur traces	Ores and product of their flotation	—	[13]
Free sulfur traces	Tire treads	—	[13]
Free sulfur traces	Rubber vulcanizates		[11]

Dash indicates not stated.

CONCLUSION

The discussed results confirm the potential and beneficial effects of iodine-azide reaction as a detection system in planar chromatography. The proposed detection system allows selective and sensitive detection for thiol or thione at picomol per spot level (procedures 3 and 4). The other detection methods routinely used in TLC—iodine vapor, UV—gave a positive but less sensitive test. Iodine-azide detection system is inexpensive; the reagents are readily available chemicals; and the analysis times are short. The non-improved iodine-azide method (procedures 1 and 2) has not been widely applied on account of the relatively high detection limits obtained with the procedure.

It was found that the results obtained using a PC scanner were as good as those recorded by the more conventional measurements using TLC densitometer.

REFERENCES

1. Rashing, F. Neue Reactionen der Stickstoffwasserstoffsäure. Chem. Ztg. **1908**, *32*, 1203.
2. Strickland, R.D.; Mack P.A.; Childs, W.A. Determination of cystine by its catalytic effect on the iodine–azide reaction. Anal. Chem. **1960**, *32*, 430–436.
3. Kurzawa, J.; Kurzawa, Z. A new determination technique of divalent sulphur compounds by induced iodine–azide reaction. Chem. Anal. (Warsaw) **1986**, *31*, 45–52.
4. Kurzawa, Z.; Kurzawa, J. Uninduced reaction of sodium azide with iodine. Pol. J. Chem. **1984**, *58*, 373–376.
5. Sjöquist, J. Paper strip identification of phenyl thiohydantoins. Acta Chem. Scand. **1953**, *7*, 447–448.
6. Ave, W.; Reinecke, I.; Thum, J. Die Anwendung der Jod-Azid-Reaktion im Papierchromatogramm. Natureissenschaften **1954**, *41*, 41.
7. Fisher, R.; Otterbeck, N. Zum Nachweis von Thiophosphorsäureestern. Sci. Pharm. **1959**, *27*, 1–6.
8. Petschik, H.; Steger, E. Zum Nachweis von Thiophosphorsäurederivaten und ähnlichen Verbindungen auf Chromatogrammen. J. Chromatogr. **1962**, *7*, 135–136.
9. Ave, W.; Neuwald, F.; Ulex, G.A. Die Anwendung der Jod-Azid-Reaktion im Papierchromatogramm. Natureissenschaften **1954**, *41*, 41.
10. Fischer, R.; Lautner, H. Zum papierchromatographischen Nachweis von Penicillinpräparaten. Archiv. Pharm. **1961**, *294*, 1–7.
11. Davies, J.R.; Thuraisingham, S.T. Quantitative determination of free elemental Sulphur in rubber vulcanizates by thin-layer chromatography. J. Chromatogr. **1968**, *35*, 513–518.
12. Onuska, F.I.; Comba, M.E. Sodium azide–iodine reagent for the detection of 1,4-oxathiin derivatives by thin-layer chromatography. J. Chromatogr. **1974**, *100*, 247–248.

13. Banaszkiewicz, S.; Śliwok, M. Determination of free sulfur in selected natural and industrial products by means of thin-layer chromatography. Chem. Anal. (Warsaw) **1973**, *18*, 1013–1018.
14. Banaszkiewicz, S. Determination of free sulphur in chemical reagents by means of thin-layer chromatography. Microchim. J. **1976**, *21*, 306–308.
15. Futter, J.E. A simple and rapid high-performance thin-layer chromatographic method for the separation and identification of heavy metal dithiocarbamates and related compounds. In *Recent Advances in Thin-Layer Chromatography*; Dallas, F.A.A., Read, H., Ruane, R.J., Wilson, I.D., Eds.; Plenum Press: New York, 1988; 231–235.
16. Kudzin, Z.H.; Kotyński, A.; Kiełbasiński, P. Application of the iodine–azide reagent for selective detection of thiophosphoryl compounds in thin-layer chromatography. J. Chromatogr. **1991**, *588*, 307–313.
17. Kotyński, A.; Kudzin, Z.H.; Okruszek, A.; Krajewska, D.; Olesiak, M.; Sierzchała, A. Iodine–azide reagent in detection of thiophosphoryl nucleotides in thin-layer chromatography systems. J. Chromatogr. A, **1997**, *773*, 285–290.
18. Kotyński, A.; Ciesielski, W.; Kudzin, Z.H.; Okruszek, A.; Krajewska, D.; Lipka, P. Iodine–azide reagent for the detection of biologically oriented thiophosphoryl compounds in thin-layer chromatography systems. J. Chromatogr. A, **1998**, *813*, 135–143.
19. Kudzin, Z.H.; Saganiak, M.; Kotyński, A.; Ciesielski, W. Comparison of the thin-layer chromatographic properties of sulfur-containing amino acids and their aminophosphonic analogues. J. Chromatogr. A, **2000**, *888*, 335–339.
20. Di Bello, C.; Celon, E. Chromatographic behaviour of ureas, thioureas, biuret derivatives and related compounds. J. Chromatogr. **1967**, *31*, 77–81.
21. Cherbuliez, E.; Baehler, Br.; Rabinowitz, J. Etude de structures peptidiques à l'aide du phénylisothiocyanate. Chromatographie sur couche mince de phénylthiohydantoïnes dérivées d'acides aminés. Hel. Chim. Acta **1964**, *47*, 1350–1353.
22. Cherbuliez, E.; Baehler, Br.; Rabinowitz, J. Etude de structures peptidiques à l'aide du phénylisothiocyanate. Sur l'emploi de la microchromatographie d'adsorption sur couches mines des phénylthiohydantoïnes. Hel. Chim. Acta **1960**, *43*, 1871–1873.
23. Cherbuliez, E.; Baehler, Br.; Rabinowitz, J. Etude de structures peptidiques à l'aide du phénylisothiocyanate-[^{35}S]. Hel. Chim. Acta **1960**, *43*, 896–900.
24. Kulbe, K. Rapid separation of phenylthiohydantoin (PTH) amino acids by thin-layer chromatography on polyamide glass plates. Anal. Biochem. **1971**, *44*, 548–558.
25. Piechocka, J. Detection of thiuram and diphenylthiourea by means of paper chromatography. Roczniki PZH **1966**, *17*, 529–533.
26. Cserhati, T.; Orsi, F. The application of the iodine–azide reaction in thin-layer chromatography studies of pesticide preparations. Periodica Polytechnica **1982**, *26*, 111–119.
27. Thangadural, S.; Shukla, S.K.; Anjaneyulu, Y. Separation and detection of certain lactam and fluoroquinolone antibiotic drugs by thin-layer chromatography. Anal. Sci. **2002**, *18*, 97–100.
28. Ciesielski, W.; Zakrzewski, R.; Skowron, M. Determination of carbimazole with the use of the iodine–azide reaction. Chem. Anal. (Warsaw) **2001**, *46*, 873–881.
29. Zakrzewski, R.; Ciesielski, W.; Kaźmierczak, D. Application of the iodine–azide procedure for the detection of glycine, alanine, and aspartic acid in planar chromatography. J. Liq. Chromatogr. Relat. Technol. **2002**, *25*, 1599–1614.
30. Zakrzewski, R.; Ciesielski, W.; Kaźmierczak, D. Detection of proline, arginine, and lysine using iodine–azide reaction in TLC and HPTLC. J. Sep. Sci. **2003**, *26*, 1063–1066.
31. Kaźmierczak, D.; Ciesielski, W.; Zakrzewski, R. Detection of amino acids using iodine–azide reaction in TLC and HPTLC. Ann. Pol. Chem. Soc. **2003**, *2*, 323–327.
32. Kaźmierczak, D.; Ciesielski, W.; Zakrzewski, R. Application of iodine–azide reaction for detection of amino acids in thin-layer chromatography. J. Chromatogr. A, **2004**, *1059*, 171–174.
33. Kaźmierczak, D.; Ciesielski, W.; Zakrzewski, R. Detection and separation of amino acids as butylthiocarbamyl derivatives by thin-layer chromatography with the iodine–azide detection system. J. Liq. Chromatogr. Relat. Technol. **2005**, *28*, 2261–2271.
34. Kaźmierczak, D.; Ciesielski, W.; Zakrzewski, R. Application of the iodine–azide procedure for detection of biogenic amine in TLC. J. Liq. Chromatogr. Relat. Technol. **2006**, *29*, 2425–2436.
35. Zakrzewska, A.; Parczewski, A.; Kaźmierczak, D.; Ciesielski, W.; Kochana, J. Visualization of amphetamine and its analogues in TLC. Acta Chim. Slov. **2007**, *54*, 106–109.
36. Kaźmierczak, D.; Ciesielski, W.; Dyńska K.; Zakrzewski, R. Iodine–azide detection system for dipeptides in thin-layer chromatography. J. Liq. Chromatogr. Relat. Technol. **2008**, *31*, 752–762.
37. Zakrzewski, R.; Ciesielski, W. Application of improved iodine–azide procedure for the detection of thiouracils in blood serum and urine with planar chromatography. J. Chromatogr. B, **2003**, *784*, 283–290.
38. Zakrzewski, R.; Ciesielski, W. Detection of mercaptopyridines and mercaptopyrimidines in planar chromatography with iodine–azide reaction as a detection system. J. Chromatogr. B, **2005**, *824*, 222–228.
39. Zakrzewski, R.; Ciesielski, W. Planar chromatography of heterocyclic thiols with detection by use of the iodine–azide reaction. J. Planar Chromatogr. **2006**, *19*, 4–9.
40. Zakrzewski, R.; Ciesielski W. Thin layer chromatography with post-chromatographic iodine–azide reaction for thiuram analysis in food samples. J. Liq. Chromatogr. Relat. Technol. **2008**, *31*, 2657–2672.
41. Ciesielski, W.; Kudzin, Z.H.; Kiełbasiński, P. Organothiophosphorus compounds as inductors of the iodine–azide reaction. Analytical application. Talanta **1994**, *41*, 1493–1498.

Iodine–Azide Reaction: HPLC Analysis

Robert Zakrzewski
Witold Ciesielski
Department of Instrumental Analysis, University of Łódź, Łódź, Poland

Abstract
A postcolumn detection system based on the reaction between azide ions and iodine, induced by sulfur(II) compounds, is presented. The method involves separation of sulfur(II) compounds using varied chromatographic systems, followed by spectrophotometric measurement of the residual iodine from the postcolumn reaction after mixing with the iodine–azide reagent. The obtained chromatograms show a negative peak as a result of the decrease in background absorbance. Various factors that have an impact on the determination of sulfur(II) compounds are discussed.

INTRODUCTION

High-performance liquid chromatography (HPLC) is a powerful tool for the separation of different classes of compounds. However, detection sensitivity remains an important issue, particularly when dealing with minor components in complex mixtures. Both the selectivity and the sensitivity of these detectors can be further enhanced by using suitable derivatization techniques. This has led to the use of procedures that render the substances more readily detectable by chemical reaction either before (precolumn) or after chromatography (postcolumn). The main advantages of the postcolumn approach include separation of analytes in their original form. So far postcolumn reactions are not so widely used in HPLC, although such reaction detectors have been available for several years. The reason for this may be caused by the problem in adjusting this continuous detection system to the chromatographic apparatus without destroying the achieved chromatographic separation. One requirement for postcolumn reaction is to store the column effluent and the added reagent after thorough mixing during the reaction time and to transport both into detectors without destroying the once-achieved separation.

Postcolumn detection by reaction uses a chemical or photochemical reaction to generate a detectable product species (P) from the analyte (A) by addition of a reagent or photons:

$$A + R \rightarrow P$$

Iodine–azide detection system is very selective because the reaction between iodine and azide ions takes place only in the presence of sulfur(II) compounds:

$$2N_3^- + I_2 \xrightarrow{\text{sulfur(II) compound}} 3N_2 + 2I^-$$

Sulfur(II) compounds act as inductors rather than as catalysts. Both inorganic (sulfide, thiosulfate, thiocyanate, polythionates, and elemental sulfur after cleavage of the S_8 ring) and organic (thiols, thionates, disulfides, organophosphorus derivatives with a P═S or P═S bond, and compounds containing a sulfur element in a ring) sulfur(II) compounds have induction properties. The mechanism of the iodine–azide reaction is discussed elsewhere in the literature.[1,2]

Under predetermined conditions, the amount of iodine consumed in the induced reaction, the heat changes generated, [3] and the amount of evolved nitrogen[4] are proportional to the amount of the sulfur(II) compound present. The most widely used method for sulfur(II) compound determination is the evaluation of iodine consumption in the induced reaction. These parameters are monitored by volumetric,[5] coulometric,[6] or spectrophotometric[7] analysis; slow titration with biamperometric detection of the end point;[8] a stopped-flow technique;[9] or detection by HPLC[10–12] and thin-layer liquid chromatography (TLC).[13,14]

DETECTION OF SULFUR(II) COMPOUNDS

Currently, three modes of separation (ion,[11] ion-pair,[12] and reversed-phase[15–19] chromatography) for the detection of sulfur(II) compounds using the iodine–azide detection system are available.

In ion-pair[11] and ion[12] chromatography, a proper mobile phase is pumped through the chromatographic column at an optimal flow rate. A sulfur(II) compound sample is injected into the HPLC system. The effluent from the column containing separated analytes is allowed to flow

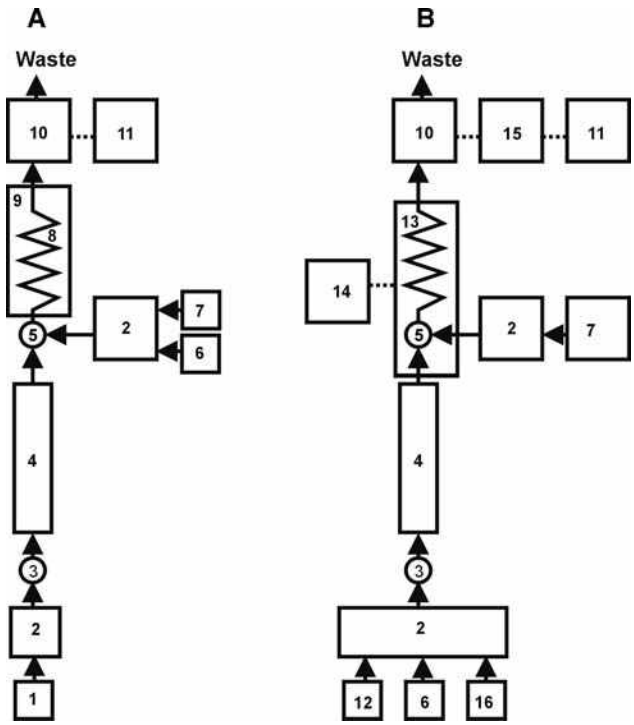

Fig. 1 Flow diagram of an HPLC system with postcolumn iodine–azide reaction detection. A, Ion and ion-pair chromatography, and B, reversed-phase chromatography 1, mobile phase; 2, pump; 3, injection valve; 4, HPLC column; 5, mixing tee; 6, sodium azide solution; 7, iodine solution; 8, reaction tube; 9, thermostat; 10, LC spectrophotometer; 11, recorder or computer as a recorder; 12, acetonitrile; 13, postcolumn reaction module; 14, temperature control system; 15, bus Sat/In module; 16, water.

through a T-union where the iodine in potassium iodide ions and acetic acid solution as well as sodium azide are delivered at a suitable flow rate. The resultant stream is passed through a mixing tee. The iodine–azide reaction induced by a single analyte takes place in the postcolumn reaction tube (Fig. 1A). For the reversed-phase mode,[15–19] sodium azide is a constituent of the mobile phase and the effluent is mixed with iodine in potassium iodide solution; the iodine–azide reaction takes place in the postcolumn reaction module maintained at an appropriate temperature (Fig. 1B). A UV/Vis detector at $\lambda = 350$ nm is applied in all separation modes.

Thus, in the absence of sulfur(II) compounds, a constant absorbance of iodine is recorded when the HPLC system is supplied with azide ions from the mobile phase and iodine solution from postcolumn reagents. Moreover, a decrease in the signal is observed when a sulfur(II) compound is present in the chromatographic band. This is attributed to iodine consumption in the iodine–azide reaction and is detected as a negative peak at 350 nm. The peak is quantitatively dependent on the amount of the sulfur(II) compound present. Fig. 2 shows the chromatogram obtained for 2-thiobarbituric acid.

INFLUENCE OF VARIOUS FACTORS ON DETECTION WITH A POSTCOLUMN IODINE–AZIDE REACTION

To establish optimal conditions for HPLC determination with a postcolumn iodine–azide reaction, a wide range of parameters that can lead to high iodine consumption should

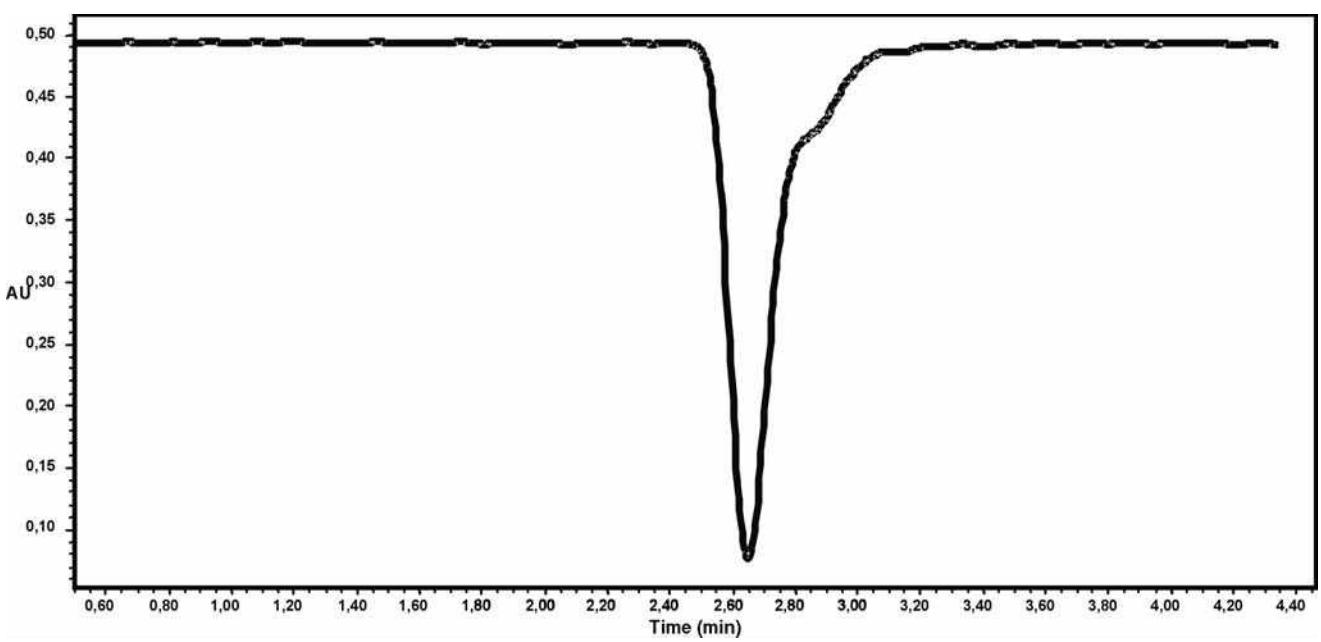

Fig. 2 Chromatogram of 2-thiobarbituric acid 10 n*M* (for chromatographic conditions, see Tables 1–3).

be taken into consideration. Among them are those with an effect upon the separation process alone (i.e., stationary phase) and those that influence the iodine–azide detection process (i.e., concentration of iodine and potassium iodide solution, and its flow rate, as well as postcolumn reaction module temperature). However, there are also a great number of factors that have an impact on both the processes mentioned above. Successful HPLC determination means a separate evaluation procedure for each parameter. The highest consumption of iodine in the induced reaction is the critical indicator when it comes to optimal conditions for postcolumn reaction. The optimal determination conditions of detection, chromatographic separation, and postcolumn reaction, and the results of sulfur(II) compound determination are listed in Tables 1–4, respectively.

Organic Modifier of the Mobile Phase

The main goal of applying an organic solvent into the mobile phase is to acquire the proper resolution of separated sulfur(II) compounds. However, the type and concentration of the organic solvent have an impact on the course of the iodine–azide reaction. Generally, it has been observed that the addition of an organic solvent lowers the consumption of iodine in the induced reaction, with some exceptions (e.g., thiopental, vitamin B1).

Sodium Azide Concentration

Buffer sodium azide of neutral pH is an inhibitor of bacterial growth. In addition, it neither modifies the chromatographic performance of proteins nor exhibits any affinity for them. On account of its activity toward anion exchangers and binding sites, buffer sodium azide is usually excluded from ion-exchange chromatography; also, it finds no application in the determination of sulfur anions forming part of a mobile phase.[11,12] However, in reversed-phase HPLC (RP-HPLC), sodium azide is incorporated into the mobile phase as one of the reagents in the iodine–azide reaction, which substantially simplifies the determination procedure. To complete the postcolumn reaction, sodium azide solution at higher concentrations is introduced into the ion chromatographic technique. On account of the poisoning properties of sodium azide, it is recommended that it should be used in small quantities. In an RP-HPLC study, sodium azide was used as a buffer for pumping the separation column. Its use was based on two main facts: first, it was important to stop the dilution of sodium azide, which could lead to a decrease in iodine consumption in the induced reaction; second, the same buffer solution could be used for the separation process and the postcolumn detection system.

pH of the Postcolumn Reaction Medium

Both the separation process and the iodine–azide reaction are influenced by the pH of the sodium azide solution. The effect of pH is mainly found in the level of iodine consumption. Some restrictions on pH need to be imposed when it comes to sodium azide solution. In solutions of pH lower than 5.5, the emission of poisonous, volatile hydrazoic acid is detectable, and at pH values over 8.0 the formation of iodate(I) obstructs the iodine–azide reaction.

In ion and ion-pair chromatography, pH of the postcolumn reaction solution is adjusted by the acetic acid solution in the postcolumn reaction module because the separation pH is different from the pH of the iodine–azide reaction course (for details see Table 3). In reversed-phase chromatography, sodium azide solution plays two roles: as a constituent of the mobile phase and as the reaction medium for the iodine–azide reaction. Therefore, pH adjustment for thiol determination is performed only once in the mobile phase without any additional pH correction of the postcolumn reaction solutions. Consequently, the procedure is simplified and no extra operations concerning the introduction of other solutions are required.

Influence of the Mobile Phase and Iodine Solution Flow Rates on Induction Properties

Induction properties depend not only on the reaction solution (concentration of acetonitrile and sodium azide, pH) but also on the reaction time, which is called the induction time. This is the time required for the iodine–azide reaction induced by a sulfur(II) compound to get completed.

Table 1 Detection conditions of sulfur(II) compound determination.

Compound	Column	Injection value (μl)	Wavelength of detection (nm)
Sulfur anion	TSK-gel IC-Anion-PW 50 × 4.6 mm	50	350
Polythionates and thiosulfate	TSK-gel ODS-Ts 150 × 4.6 mm	300	350
2-Thiobarbituric acid	Nova-Pak CN HP 150 × 3.9 mm	20 or 200	350
Thiopental	Nova-Pak CN HP 150 × 3.9 mm	20 or 200	350
Methimazole	Symmetry C18 150 × 3.9 mm	20	350
Thioguanine	Symmetry C18 150 × 3.9 mm	20	350
6-Propyl-2-thiouracil	Symmetry C18 150 × 3.9 mm	20	350

Table 2 Chromatographic conditions of sulfur(II) compound determination.

Compound	Composition	Mobile pH	Column temperature (°C)	Flow rate (ml/min)	Sodium azide solution concentration (%)	Sodium azide solution pH
Sulfur anion	Acetonitrile:6 m*M* sodium carbonate solution (15:85, v/v)	—	—	0.5	—	—
Polythionates and thiosulfate	Acetonitrile:water (20:80, v/v) containing 3 m*M* tetrapropylammonium hydroxide	5.0	23	0.6	—	—
2-thiobarbituric acid	Acetonitrile:sodium azide solution (11:89, v/v)	—	—	0.75	0.4	6.9
Thiopental	Acetonitrile:sodium azide solution (16:84, v/v)	—	—	1	0.3	7.8
Methimazole	Acetonitrile:sodium azide solution:water (1:50:49, v/v)	—	—	0.5	2.5	5.5
Thioguanine	Acetonitrile:sodium azide solution:water (1:50:49, v/v)	—	—	0.5	1.5	6.0
6-Propyl-2-thiouracil	Acetonitrile:sodium azide solution:water (24:50:26, v/v)	—	—	1.4	2.5	5.5

In chromatography using the iodine–azide detection system, the induction time is the contact time between the eluate [containing sulfur(II) compounds and optional azide ions] and the postcolumn reaction solution (containing the iodine and optional azide ions). The induction time can be increased either by lengthening the postcolumn reaction tube or by increasing the flow rates of the mobile phase and the iodine solution. An excessive increase in the reaction time leads to peak broadening. Hence, it is necessary to optimize the reaction time by exploiting its dependence on the flow rate of the mobile phase and postcolumn reaction solutions as well as on the distance from the column tip to the detector cell.

It has been observed that the peak height of most sulfur(II) compounds decreased with increasing flow rate of the iodine solution, as the inductor does not get enough time for inducing the iodine–azide reaction. To slow down the iodimetric reaction in the postcolumn module, application of small amounts of iodine is recommended. Under such conditions, the iodine consumption in the iodine–azide reaction as well as the peak height increase.[1,5] Too low a flow rate of the iodine solution may lead to significant band broadening and lower peak heights. The influence of flow rate of the iodine solution on the ratio of sulfur(II) compound peak height to noise peak height for 2-thiobarbituric acid and thiopental is illustrated in Fig. 3.

Table 3 Postcolumn conditions of sulfur(II) compound determination.

Compound	Postcolumn reaction solution flow rate (ml/min)	Iodine solution concentration (μ*M*)	Iodide solution concentration (m*M*)	Sodium azide solution concentration	Acetic acid concentration (*M*)	Postcolumn reaction module temperature (°C)
Sulfur anion	0.25	5	100	10%	0.8	40
Polythionates and thiosulfate	0.3	10	100	2 *M*	1	30
2-Thiobarbituric acid	0.3	200	20	—	—	25
Thiopental	0.3	200	20	—	—	30
Methimazole	0.2	200	20	—	—	25
Thioguanine	0.3	200	10	—	—	30
6-Propyl-2-thiouracil	0.3	400	20	—	—	35

Table 4 Results of sulfur(II) compound determination.

Compound	Calibration range	Detection limit	Quantification limit	R.S.D.
Sulfur anion	Up to:17.6 ppb for sulfide 56.9 11.6 ppb for thiosulfate11.6 ppb for thiocyanate	Up to: 0.14 ng for sulfide 0.16 ng for thiosulfate 0.05 ng for thiocyanate		
Polythionates and thiosulfate	Up to: 0.1 μ*M* for thiosulfate 200 μ*M* for trithionate 8.0 μ*M* for tetrathionate 0.2 μ*M* for pentathionate 0.4 μ*M* for hexathionate 5 n*M*	Up to:1.1 n*M* for thiosulfate 4.3 μ*M* for trithionate 0.1 μ*M* for tetrathionate 2.7 n*M* for pentathionate 5.0 n*M* for hexathionate		
2-thiobarbituric acid	20–200 n*M* (for 20 μl loop) 1–10 n*M* (for 200 μl loop)	0.8 n*M* (for 20 μl loop) 0.7 n*M* (for 200 μl loop)	20 n*M* (for 20 μl loop)1 n*M* (for 200 μl loop)	3.9% (quantification limit)
Thiopental	40–1000 n*M* for standard solution 0.05–2.5 nmol/ml urine	20 n*M* for standard solution 0.025 nmol/ml urine	40 n*M* for standard solution 0.05 nmol/ml urine	6.7% for standard solution 3.5% for thiopental in urine (quantification limit)
Methimazole	2–10 nmol/ml urine	1 nmol/ml urine	2 nmol/ml urine	3.2% (quantification limit)
Thioguanine	0.8–1.7 nmol/ml urine	0.4 nmol/ml urine	0.5 nmol/ml urine	4.3% (quantification limit)
6-Propyl-2-thiouracil	0.4–1.0 nmol/ml urine	0.3 nmol/ml urine	0.4 nmol/ml urine	0.9% (quantification limit)

The concentration of iodine and iodide ions influences the course of the iodine–azide reaction. The iodine in iodide ion solutions or a mixture of iodine, iodide ions, and acetic acid solutions is delivered to the HPLC system after the separation step.

In an RP-HPLC determination, the concentration of iodine solution within the range 0.1–0.4 m*M* did not influence the course of postcolumn reaction for a constant potassium iodide solution concentration and a constant flow rate.

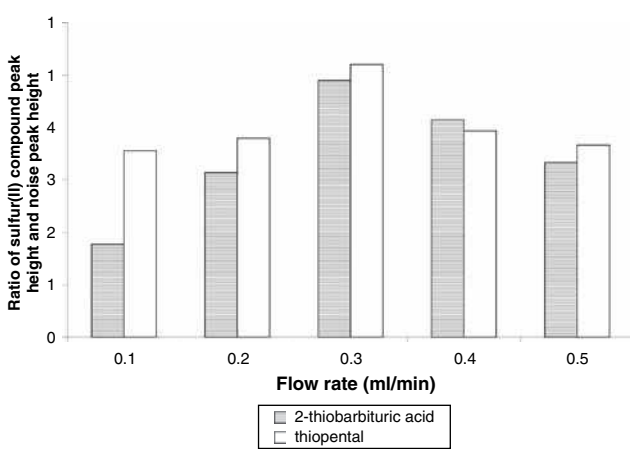

Fig. 3 The influence of iodine solution flow rate on the ratio of peak height to noise peak height for 2-thiobarbituric acid and thiopental (for chromatographic conditions, see Tables 1–3; 2 pmol on-column for 2-thiobarbituric acid and thiopental).

In the case of thiosulfate determination, the peak height increased with the iodine solution concentration within the range of 1–3 μ*M*; then the peak height stayed constant within the range of 3–6 μ*M*. The peak height decreased with increase in the iodine solution concentration above 6 μ*M*. The decrease in peak height is caused by the iodimetric reaction that competes with the induced postcolumn reaction for thiosulfate. The optimal iodide concentration was chosen to obtain an absorbance level at ~0.5 AU.

Addition of potassium iodide is necessary for dissolving iodine in water. Then the following equilibrium condition is attained

$$I_2 + I^- \rightleftarrows I_3^-$$

and the triiodide ion concentration is monitored. The degree to which the iodide ions may influence the course of the iodine–azide reaction depends on the inductor's properties. In the case of many sulfur compounds, it can be stated that an excess of iodide ions increases the consumption of iodine in the iodine–azide reaction with consequent lengthening of induction time. The influence of iodide ions on the course of the iodine–azide reaction applied as a postcolumn detection system in HPLC can be divided into three steps (Fig. 4):

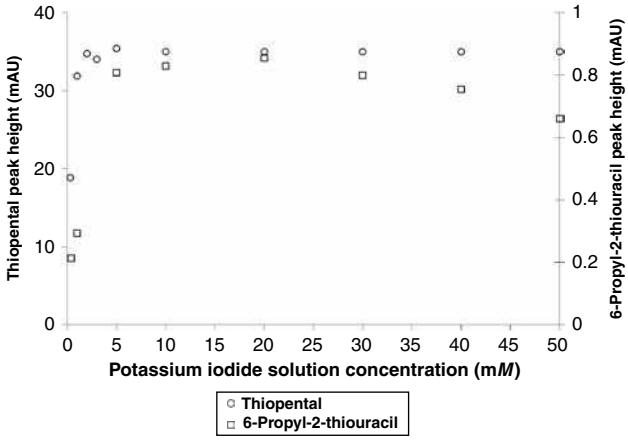

Fig. 4 The influence of potassium iodide solution concentration on peak height of thiopental and 6-propyl-2-thiouracil (2 pmol on-column for thiopental 0.2 pmol on-column for 6-propyl-2-thiouracil; for chromatographic conditions, see Tables 1–3).

1. The sulfur(II) compound peak height increases with the rise in the iodide ion concentration owing to the shift in the iodine–triiodide equilibrium that results in the growing concentration of triiodide ions.
2. The peak height is at its maximum value.
3. The peak height remains constant with the increase of the iodide ion concentration when the iodide ions do not have any impact on the course of the iodine–azide reaction induced by a particular sulfur(II) compound; or the peak height decreases with the increase of iodide ion concentration when the iodide ions hampered the course of iodine–azide reaction induced by a particular sulfur(II) compound (e.g., 6-propyl-2-thiouracil).

Postcolumn Reaction Module Temperature

An increase in postcolumn reaction temperature accelerates the oxidation reaction rate of a sulfur(II) compound to a non-inducing level. It has been found that a temperature maintained at 30–40°C level gives the highest sensitivity of determination.

Interferences

It is possible to eliminate matrix interferences by shifting the detection wavelength from the UV region (corresponding to sulfur(II) compound absorption) to the region corresponding iodine adsorption ($\lambda = 350$ nm). In general, the iodine–azide detection system allows only sulfur(II) compounds to be visible on chromatograms. However, four groups of additional peaks may be found on account of certain other compounds:

1. Iodine–azide reaction inductors (e.g., cysteine or cystine), which generate negative peaks.
2. Compounds that react with iodine under experimental conditions (e.g., ascorbic acid), which generate negative peaks.
3. Compounds that react with iodide ion [e.g., bromate(V), iodate(V), nitrate(III)], which generate positive peaks.
4. Compounds that absorb at 350 nm (e.g., sulfasalazine).

ANALYTICAL APPLICATION OF THE METHOD

The evaluated technique has been applied for the determination of sulfur ions (S^{2-}, $S_2O_3^{2-}$, SCN^-) and polithionates in hot-spring water and river water (at nanomolar level for thiosulfate, micromolar level for polithionates, and parts per billion level for sulfide ions).

Application of the elaborate HPLC method for the determination of thiopental, methimazole, thioguanine, and 6-propyl-2-thiouracil using the iodine–azide reaction detection system has been extended to include patient urine samples at the nanomol per milliliter level (Table 5). The chromatogram of a patient urine sample is shown in Fig. 5.

CONCLUSION

The discussed results confirm the potential and the beneficial effects of iodine–azide reaction as a detection reaction in HPLC. The proposed detection system allows

Table 5 Application of the method.

Compound	Matrix	Refs.
Sulfur anion	Hot spring water; river water	[11]
Polythionates and thiosulfate	Hot spring water	[12]
Thiopental	Human urine	[16]
Methimazole	Human urine	[17]
Thioguanine	Human urine	[18]
6-Propyl-2-thiouracil	Human urine	[19]

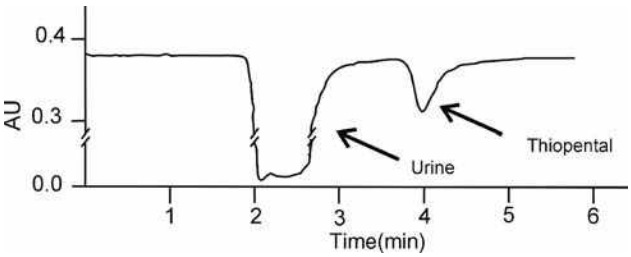

Fig. 5 Chromatogram of thiopental in patient urine sample (3.49 nmol/ml urine) (for chromatographic conditions, see Tables 1–3).

selective determination of various sulfur(II) compounds with high sensitivity. A postcolumn detection system using the iodine–azide reaction in HPLC is a fast, reliable, and inexpensive method; the required reagents are readily available chemicals and the analysis time is short.

The sensitivity of this method is comparable to, or better than, those of LC separation techniques for urine. The technique overcomes the limitations of and obstacles in conventional methods such as the use of expensive and frequently contaminated organic solvents and of tedious and time-consuming sample preparation [e.g., derivatization procedure, solid-phase extraction (SPE)] with satisfactory levels of sensitivity.

Moreover, the postcolumn reaction is compatible with the mobile phase of HPLC. The results from this study indicate that the proposed HPLC with the iodine–azide postcolumn reaction can potentially be used for routine clinical monitoring and in pharmacokinetic studies of thiols.

REFERENCES

1. Kurzawa, J.; Kurzawa Z. A new determination technique of divalent sulphur compounds by induced iodine–azide reaction. Chem. Anal. (Warsaw) **1986**, *31*, 45–52.
2. Zakrzewski, R.; Ciesielski W.; Kaźmierczak, D. Iodine–azide reaction as a detection system in TLC. In *Encyclopedia of Chromatography*, 3rd Ed.; Cazes, J., Ed.; Taylor & Francis: New York, 2010, 1226–1233.
3. Wroński, M.; Goworek, W. Identification of divalent sulphur compounds by an enthalpimetric approach to the iodine–azide reaction. Analyst **1987**, *112*, 333–334.
4. Atkinson, L.P.; Natoli, J.G. Gas chromatographic determination of inorganic sulfide and organic thiol compounds using the catalyzed azide–iodine reaction. Anal. Chem. **1974**, *46*, 1316–1319.
5. Kurzawa, J. The iodine–azide reaction induced by mercaptopyrimidines and its application in chemical analysis. Chem. Anal. **1987**, *32*, 875–890.
6. Ciesielski, W. Coulometric determination of sulphur compounds using the induced iodine–azide reaction. Acta Univ. Lodz. Folia Chimica **2004**, *13*, 171–177.
7. Ciesielski, W. Simultaneous spectrophotometric determination of cysteine, glutathione, and ascorbic acid with the use of the iodine–azide reaction. Chem. Anal. **1986**, *31*, 99–103.
8. Kurzawa, J. Determination of sulphur(II) compounds by flow injection analysis with application of the induced iodine–azide reaction. Anal. Chim. Acta **1985**, *173*, 343–348.
9. Kurzawa, J.; Wiśniewska, A.; Janowicz, K. Stopped-flow determination of 2-mercaptopyrimidines as inductors of the iodine–azide reaction. Anal. Chim. Acta **2006**, *567*, 286–292.
10. Miura, Y. Ion chromatography for rapid and sensitive determination of inorganic sulfur anions in their mixtures. Bunseki Kagaku **2005**, *54*, 651–664.
11. Miura, Y.; Fukasawa, K.; Koh, T. Determination of sulfur anions at the ppb level by ion chromatography utilizing their catalytic effects on the post-column reaction of iodine with azide. J. Chromatogr. A, **1998**, *804*, 143–150.
12. Miura, Y.; Watanabe, M. Ion-pair chromatography of polythionates and thiosulfate with detection based on their catalytic effects on the post-column azide–iodine reaction. J. Chromatogr. A, **2001**, *920*, 163–171.
13. Kudzin, Z.H.; Saganiak, M.; Kotyński, A.; Ciesielski, W. Comparison of the thin-layer chromatographic properties of sulphur-containing amino acids and their aminophosphoric analogues. J. Chromatogr. A, **2000**, *888*, 335–339.
14. Zakrzewski, R.; Ciesielski, W. Iodine–azide detection system in planar chromatography. Trends Chromatogr. **2007**, *3*, 1–10.
15. Zakrzewski, R.; Ciesielski, W. Application of iodine–azide reaction as post-column reaction in HPLC for determination of 2-thiobarbituric acid. Chromatography **2004**, *59*, 683–689.
16. Zakrzewski, R.; Ciesielski, W. Determination of thiopental in urine sample with high-performance liquid chromatography using iodine–azide reaction as a post-column detection system. J. Chromatogr. B, **2005**, *824*, 327–332.
17. Zakrzewski, R. Determination of methimazole in urine following its separation by RP-HPLC with iodine–azide detection system. J. Chromatogr. B, **2008**, *869*, 67–74.
18. Zakrzewski, R. Application of the iodine–azide postcolumn reaction in RP-HPLC for determination of thioguanine in urine. J. Sep. Sci. **2008**, *31*, 2199–2205.
19. Zakrzewski, R. High-performance liquid chromatographic determination of propylthiouracil in human urine by post-column iodine–azide reaction. J. Pharm. Biomed. Anal. **2008**, *48*, 145–150.

Ion Chromatography: Modern Stationary Phases

Rajmund Michalski
Institute of Environmental Engineering, Polish Academy of Science, Zabrze, Poland

Abstract
Because of the better understanding of the processes taking place at the surface of stationary phases, the number of ion-exchange materials for ion chromatography has increased significantly over recent years. As a result, the multitude of commercially available columns with their different selectivities for anion and cation separations and their determination is almost confusing. This entry is a review of stationary phases used in modern ion chromatography.

INTRODUCTION

Ion chromatography is based on an ion-exchange process taking place between the mobile phase and the ion-exchange groups bonded with the support material. The stationary phase used in ion chromatography consists of polystyrene (PS), ethylvinylbenzene (EVB), or methacrylate resins copolymerized with divinylbenzene (DVB) and modified with ion-exchange groups. Furthermore polyvinyl, silica-based, and many other materials are used. Stationary phases used in ion chromatography differ, not only in the type of support material, but also according to their different pore sizes and ion-exchange capacities. Improvements in eluent methodologies, novel detection modes, and particularly new highly selective and efficient stationary phases make ion chromatography a significant and competitive technique for solving analytical problems in many fields of interest. A review of modern stationary phases used for ion chromatography is given by Weiss and Jensen.[1] A comparison and critical appraisal of particle-packed columns and monolithic columns in high-performance liquid chromatography (HPLC) is described by Unger, Skudas, and Schulte.[2] In general there are three major criteria in characterizing an HPLC (including IC) column: hydrodynamic, kinetic, and thermodynamic properties. There are several major variables that distinguish ion-exchange stationary phases, such as structure of the bonded phase, including the chemistry of the functional group, charge density and related nominal capacity, and properties of the support matrix, including composition and pore diameter.

COLUMNS FOR ANION DETERMINATION

The application of ion-exchange phenomena in analytical chemistry is described by Walton and Rocklin.[3] Throughout many years in the past, a large variety of stationary phases with various selectivities and capacities have been developed for both anion- and cation-exchange chromatography.[4]

The major differences between classical ion-exchange chromatography and modern high-performance ion chromatography are the methods of sample introduction and the types of separation and detection systems used. In classical ion-exchange chromatography, columns are filled with anion- or cation-exchange resins having particle sizes between 75 and 250 μm. Earlier suppressed and non-suppressed ion chromatography required low column capacities. These columns were easily overloaded by high sample concentrations. Increasing suppression capacity has enabled ever-increasing eluent concentrations and, in turn, increasing column capacities.

At the beginning, with ion chromatography, column materials utilized particles greater than 40 μm and generated only about 120 and 300 theoretical plates efficiency. In the first commercial column used for IC (Dionex AS-1), the particle size was reduced to 25 μm and efficiencies increased to ~700 theoretical plates. Modern high-capacity columns have efficiencies over 5000 plates (for 4 × 250 mm column dimensions) and 5 μm particle size.[5]

Anion exchangers contain alkanol or alkyl quaternary amine functional groups, and their selectivity variation has been obtained by modifying the structures of the ion-exchange sites. Anion exchangers are divided into polymer-based anion exchangers [styrene–divinylbenzene (PS–DVB), ethylvinylbenzene-divinylbenzene EVB–DVB, polymethacrylate and polyvinyl copolymers], latex-agglomerated anion exchangers, silica-based, and others.[6]

Polymer-Based Anion Exchangers

In contrast to silica-based column packings usually used in classical high-performance liquid chromatography, in ion chromatography, organic polymers are often employed as the predominant support material. These resins show a

Table 1 Selected columns based on the surface-aminated styrene–divinylbenzene (PS–DVB) resins.

	Column				
Parameter	**PRP-X100**	**LCA A01**	**ExcelPak ICS-A23**	**Metrosep A supp 8**	**Star ion A 300 IC anion**
Manufacturer	Hamilton	Sykam	Yokogawa	Metrohm	Phenomenex
Column dimensions (mm)	250 × 4.1	200 × 4	75 × 4.6	150 × 4.0	100 × 4.6
pH range	1–13	1–14	2–12	0–14	1–12
Solvent compability (%)	100	<10	<50	<5	<5
Capacity (mequiv/column)	0.096	0.04	0.7	Not specified	Not specified
Particle diameter (μm)	10	12	5	5	Not specified

much higher stability over an extreme pH range, between 0 and 14, compared to silica-based materials (pH 2–8). Common carbonate eluents used with ion chromatography have a pH around 10, whereas hydroxide eluents have pH close to 12.

PS–DVB Copolymers

These copolymers are the most widely used packing materials for ion chromatography. In general, these kinds of columns can be divided into two groups, i.e., surface-aminated PS–DVB, and surface-aminated EVB–DVB copolymers.

A surface-functionalized polymer-based EVB–DVB is produced by grafting technology, which was first used for the preparation of stationary phases by Schomburg.[7] Various monomers are attached to the support material via cografting, and each of these monomers contributes its specific properties to the selectivity of the stationary phase, which can be modulated by varying the percentages of the comonomers. Surface-functionalized polymer-based EVB–DVB columns are produced by Dionex (Sunnyvale, U.S.A.).

The percentage of DVB in the resin is indicated as "percent cross-linking," which determines the porosity of the resin. The distinction is made between microporous and macroporous resins. Examples of commercially available PS–DVB and EVB–DVB columns used in anion-exchange chromatography are given in Tables 1 and 2, respectively.

Polymethacrylate and Polyvinyl Anion Exchangers

Methacrylate-based resins with quaternary amine functional groups are stable at pH 1–12. Anions can be separated using weak organic and inorganic acids. Macroporous polyvinyl resins are stable at pH 0–14, thus allowing the use of a large number of eluents. When compared with methacrylate materials, they exhibit lower chromatographic efficiency; however, these phases are suitable for separating analytes from complex samples. Examples of anion-exchange columns with polymethacrylate and polyvinyl phases are given in Tables 3 and 4, respectively.

Latex-Agglomerated Resins

A special type of peculiar anion exchanger was first introduced in 1975. These stationary phases, which are called latex-based anion exchangers, have been further developed by Dionex.[8] They comprise a surface-sulfonated PS–DVB substrate with particle diameters between 5 and 25 μm and are fully aminated, high-capacity, porous polymer beads made of poly(vinylbenzyl chloride) or polymethacrylate, which are called latex

Table 2 Selected columns based on the surface-aminated ethylvinylbenzene–divinylbenzene (EVB–DVB) resins.

	Column: Dionex IonPac				
Parameter	**AS14**	**AS15**	**AS20**	**AS22**	**AS24**
Column dimensions (mm)	250 × 4	250 × 4	250 × 4	250 × 4	250 × 4
pH range	2–11	0–14	0–14	0–14	0–14
Solvent compability (%)	100	100	100	100	100
Capacity (mequiv/column)	0.065	0.225	0.31	0.21	0.14
Particle diameter (μm)	9	9	7.5	6.5	7

Table 3 Selected columns based on the surface-aminated polymethacrylate resins.

Parameter	Column				
	Metrosep anion dual 2	**TSK-Gel IC-PW**	**Shimpack IC-A1**	**Polyspher IC AN-1**	**Universal anion**
Manufacturer	Metrohm	Toyo soda	Shimadzu	Merck	Alltech
Column dimensions (mm)	75 × 4.6	50 × 4.6	100 × 4.6	100 × 4.6	150 × 4.6
pH range	1–12	1–12	2–11	2–10	2–12
Solvent compability (%)	<20	<20	<10	<20	<5
Capacity (mequiv/g)	0.034	0.03	Not specified	Not specified	0.1
Particle diameter (μm)	6	10	10	12	10

particles. The latex particles have a diameter of about 0.1 μm and are agglomerated to the surface by electrostatic and van der Waals interactions.

By changing the degree of cross-linking and by varying the functional groups bonded to the latex it is possible to moderate the properties of final materials. Since the introduction of gradient elution in ion chromatography, in 1987, hydroxide-selective latex-based anion exchangers have also been developed.[9] Example of latex-agglomerated anion-exchange columns produced by Dionex are given in Table 5.

Silica-Based Anion Exchangers

The application of inorganic ion exchangers in chemical analysis is given by Quereshi and Varshney.[10] Contrary to organic polymers, silica-based substrates have the advantage of high mechanical stability. Moreover, chromatographic efficiencies of silica-based phases are very high (up to 20,000 theoretical plates), but they can only be used with eluents in the pH range between 2 and 8. Nevertheless, newer silica-based stationary phases have been developed.[11] The characteristics of some commercially available silica-based columns are given in Table 6.

Other Materials for Anion Separations

Inorganic and organic anions can also be separated on cross-linked polymers modified with cyclic ethers. Pioneering work in the field of adsorbing crown ethers onto chemically bonded reversed phases and PS–DVB polymers has been carried out by Kimura et al.[12] The number of applicable crown ethers is limited because of their limited solubility and high price. Moreover, crown ether resins are mechanically unstable and are therefore operated with low flow rates, thus resulting in long analysis times.

In 1994, Lamb et al.[13] developed a series of cryptand-based anion separators. The biggest advantage of cryptand columns, used in gradient elution mode, is the ability to elute non-polarizable and polarizable anions in the same run, which is very difficult (or even impossible) with latex-agglomerated anion exchangers and aminated grafted polymers.[14]

Although Al_2O_3 is one of the most common adsorbents used in liquid chromatography, it has seldom been used in the past for ion chromatography, because of the low ion-exchange capacity and the inadequate stability against strong acids and bases. Anion-exchange properties of aluminia can occur at pH values below the isocratic point, which depends on the type of eluent.

Table 4 Selected columns based on the surface-aminated polyvinyl resins.

Parameter	Column			
	Metrosep anion supp 4	**Metrosep anion supp 5**	**Metrosep anion supp 7**	**ION-100**
Manufacturer	Metrohm	Metrohm	Metrohm	Interaction chemicals
Column dimensions (mm)	250 × 4	250 × 4	250 × 4	250 × 3
pH range	3–12	3–12	3–12	0–14
Solvent compability (%)	100	100	100	<10
Capacity (mequiv/g)	0.071	0.107	0.140	0.1
Particle diameter (μm)	9	5	5	10

Table 5 Selected columns based on the latex-agglomerated resins.

	Column: Dionex IonPac									
Parameter	**AS4-SC**	**AS5**	**AS7**	**AS9-SC**	**AS9-HC**	**AS10**	**AS11**	**AS16**	**AS17**	**AS18**
Column dimensions (mm)	250 × 4	250 × 4	250 × 4	250 × 4	250 × 4	250 × 4	250 × 4	250 × 4	250 × 4	250 × 4
pH range	0–14	0–14	0–14	2–11	0–12	0–14	0–14	0–14	0–14	0–14
Solvent compability (%)	100	<3	<5	100	100	100	100	100	100	100
Capacity (mequiv/g)	20	20	100	35	190	170	45	170	30	285
Particle diameter (μm)	13	10	10	13	9	8.5	13	9	10.5	7.5
Size of latex particle (nm)	160	120	530	110	90	65	85	80	75	65
Degree of cross-linking (%)	55	2	2	55	55	55	55	55	55	55

COLUMNS FOR CATION DETERMINATION

Like anion exchangers, cation exchangers are divided into polymer-based cation exchangers (PS–DVB, EVB–DVB, polymethacrylate, and polyvinyl copolymers), latex-agglomerated cation exchangers, silica-based, and other (e.g., crown ether, aluminia materials).[15] Modern cation exchangers contain sulfonic, carboxylic, carboxylic–phosphonic, and carboxylic–phosphonic–crown ether functional groups.

Polymer-Based Cation Exchangers

Styrene–divinylbenzene copolymers

These types of polymer resins are widely used as substrate materials for the manufacture of cation exchangers. Simultaneous analysis of mono- and divalent cations is not possible with surface-sulfonated cation exchangers; thus, they are used for sequential analysis of alkali and alkaline earth metals. The ion-exchange capacity is determined by the degree of PS–DVB sulfonation. The characteristic structural and technical properties of selected surface-sulfonated PS–DVB columns are summarized in Table 7.

EVB–DVB Copolymers

Because of various affinities toward strong acid cation exchangers, alkali and alkaline earth metals can only be analyzed sequentially on sulfonated PS–DVB. Simultaneous analysis of alkali and alkaline earth metals, as well as aliphatic amines, can be realized with acid cation exchangers using carboxyl groups as the ion-exchange functionality. Examples of cation-exchange columns produced by Dionex are given in Table 8.

Latex Cation Exchangers

Latex cation exchangers were introduced by Dionex Corp. 10 years later than latex-agglomerated anion exchangers. These types of cation exchangers consist of a weakly sulfonated PS–DVB substrate with latex beads with a very small diameter agglomerated on its surface by both electrostatic and van der Waals interactions.

Table 6 Silica-based anion-exchange columns.

	Column			
Parameter	**Wescan 269-001**	**Nucleosil 10 anion**	**TSK-Gel IC-SW**	**Vydac 302 IC**
Manufacturer	Wescan	Macherey & Nagel	Toyo soda	Separations group
Column dimensions (mm)	250 × 4.6	250 × 4	250 × 4.6	50 × 4.6
Capacity (mequiv/g)	0.08	0.06	0.4	0.1
Particle diameter (μm)	13	10	5	10

Table 7 Selected cation-exchange columns based on the surface-sulfonated styrene–divinylbenzene (PS–DVB).

	Column					
Parameter	**IonPac CS2**	**LCA-K01**	**MCI Gel**	**PRO-X200**	**Shimpack IC-C1**	**TSK-Gel IC cation**
Manufacturer	Dionex	Sykam	Mitsubishi	Hamilton	Shimadzu	Toyo soda
Column dimensions (mm)	250 × 4.6	125 × 4	150 × 4.6	250 × 4	150 × 5	50 × 4.6
Solvent compability (%)	0	<5	<5	100	<10	<10
Capacity (mequiv/g)	0.05	0.05	0.05	0.035	0.05	0.012
Particle diameter (μm)	15	10	10	10	10	10

In contrast to surface-sulfonated phases, latex cation exchangers exhibit a significantly higher chromatographic efficiency. Examples of Dionex latex cation-exchange columns are given in Table 9.

Other Cation-Exchange Resins

Although organic polymers are predominantly used for cation-exchange chromatography, silica-based exchangers are also used. These cation exchangers are only of minor importance, despite their comparatively high chromatographic efficiencies. Cross-linked polymers, modified with cyclic ethers, are also used in cation-exchange columns.[16]

NEW PERSPECTIVES AND CHALLENGES

The following general trends in the development of new stationary phases for ion chromatography can be identified: new stationary phases matrices and bonding chemistries; improvement of column efficiency, trend toward reduction in the diameter of separation column, and new chemistry of the bonded functional groups/layers.[17,18]

New directions in the development of stationary phases for various modes of ion chromatography are, among other things, zwitterionic ion exchangers. The combination of positively and negatively charged sites in a single particle, or within the functional groups of a single molecule attached to the surface of an absorbent, provides unique opportunities to vary the selectivity of separation.[19] This results in reduced shrinking and swelling, and improved mechanical stability of zwitterionic ion exchangers, in comparison to traditional ion exchangers. Moreover, these types of ion exchangers demonstrate unique separation selectivities and, often, simultaneous separation of anions and cations with a single column is possible.

In recent years, the interest in using porous silica and polymer-based monolithic stationary-phase media for ion chromatographic separations of inorganic and organic ions has increased.[20,21] As compared to particle bed columns, monolithic columns represent a single piece of porous cross-linked polymer or porous silica. Monoliths are made in different formats as porous rods, generated in thin capillaries or made as thin membrane or disks.

Ion exchangers based on polymeric monoliths have made an appearance, mainly for biomolecule separations; it will be of interest to see if such columns will be useful for the separation of smaller molecules. Monoliths, compared with packed columns, have recently decreased pressure drop requirements, allowing the use of longer columns.

The interest in monoliths appears to be the greatest in preparative and analytical chromatography, where high-throughput (short and fast columns) and/or high-efficiency (long columns) separations are required.[22]

Monolithic columns are applied in low- and medium-pressure ion chromatography, ultrafast ion chromatography, capillary chromatography, flow gradients, and double-gradient ion chromatography, and, also, multi-column/multidimensional ion chromatography.[23] Monolithic columns are considered, by many, to be a

Table 8 Selected columns of carboxylate-based weak acid cation exchangers.

	Column: Dionex IonPac					
Parameter	**CS12**	**CS14**	**CS15**	**CS16**	**CS17**	**CS17**
Column dimensions (mm)	250 × 4	250 × 4	250 × 4	250 × 4	250 × 4	250 × 2
Solvent compability (%)	100	100	100	100	100	<20
Capacity (mequiv/column)	2800	1300	2800	8400	1450	290
Particle diameter (μm)	8	8.5	8.5	5	7	6

Table 9 Selected columns of latexed cation exchangers.

	Columns: Dionex IonPac		
Parameter	**CS3**	**CS10**	**CS11**
Column dimensions (mm)	250 × 4	250 × 4	250 × 4
pH range	1–12	0–14	0–14
Solvent compability (%)	<5	100	100
Capacity (mequiv/column)	100	80	35
Particle diameter (μm)	10	8.5	8
Size of latex particle (nm)	300	200	200

more practical alternative to packed columns because they offer many advantages like packed columns, but without problems typical of packed columns.[24] The further expansion of monolithic columns is expected, both in classical ion chromatography and in microchip and capillary ion chromatography.[25]

CONCLUSION

The central and most essential part of an IC system is the separation column, and its stationary phase. The number of commercially available ion-exchange columns that have been developed for ion chromatography has increased impressively. The diversity of anion- and cation-exchange columns available today allows the ion chromatography user selection of stationary phase that is best suited for the required application. Nevertheless, the potential of packing and stationary phase design and development has not been explored to the full extent.

REFERENCES

1. Weiss, J.; Jensen, D. Modern stationary phases for ion chromatography. Anal. Bioanal. Chem. **2003**, *375*, 81–98.
2. Unger, K.K.; Skudas, R.; Schulte, M.M. Particle packed columns and monolithic columns in high-performance liquid chromatography—comparison and critical appraisal. J. Chromatogr. A, **2008**, *1184*, 393–415.
3. Walton, H.F.; Rocklin, R.D. *Ion Exchange in Analytical Chemistry*; CRC Press: Boca Raton, FL, MA, 1990.
4. Fritz, J.S.; Gjerde, D.T.; Pohlandt, C. *Ion Chromatography*; Verlag: New York, 1982; 7–20.
5. Sarzanini, C.; Bruzzoniti, M.C. New materials: Analytical and environmental applications in ion chromatography, *Anal. Chim. Acta* **2005**, *540*, 45–53.
6. Weiss, J. *Handbook of Ion Chromatography*; Wiley-VCH: Weinheim, Germany, 2004, 35–98.
7. Schomburg, G. Stationary phases in high performances liquid chromatography. Chemical modification by polymer coating. LC–GC **1988**, *6*, 36–50.
8. Jackson, P.E.; Pohlandt, C. Advances in stationary phase development in suppressed ion chromatography. Trend. Anal. Chem. **1997**, *16*, 393–400.
9. Jackson, P.E.; Weigert, C.; Pohl, C.A.; Saini, C. Determination of inorganic anions in environmental waters with a hydroxide-selective column. J. Chromatogr. **2000**, *884, 175*–184.
10. Quereshi, M.; Varshney, K.G. *Inorganic Ion Exchangers in Chemical Analysis*. CRC Press: Boston, MA, 1991.
11. Auler, L.M.; Silva, C.R.; Collins, K.E.; Collins, C.H. New stationary phase for anion-exchange chromatography. J. Chromatogr. **2005**, *1073*, 147–153.
12. Kimura, K.; Harino, H.; Hajatta, E.; Shono, T. Liquid chromatography of alkali- and alkaline-earth metal ions using octadecylsilanized silica columns modified in situ with lipophilic crown ethers. Anal. Chem. **1986**, *58*, 2233–2237.
13. Lamb, J.D.; Smith, R.D.; Anderson, R.C.; Mortensen, M.K.J. Anion separations on columns based on transition metal–macrocycle complex exchange sites. J. Chromatogr. **1994**, *671*, 55–62.
14. Chiou, Ch.-S.; Shih, J.-S. Fullerene C_{60}-cryptand chromatographic stationary phase for separations of anions/cations and organic molecules. Anal. Chim. Acta **2000**, *416*, 169–175.
15. Weiss, J. *Handbook of Ion Chromatography*. Wiley-VCH: Weinheim, Germany, 2004, 280–308.
16. Ohta, K. Indirect ultraviolet spectrophotometric detection in the ion chromatography of common mono- and divalent cations on an aluminum adsorbing silica gel column with tyramine-containing crown ethers as eluent. J. Chromatogr. **2000**, *884*, 113–122.
17. Haddad, P.R.; Nesterenko, N.; Buchberger, W. Recent developments and emerging directions in ion chromatography. J. Chromatogr. A, **2008**, *1184*, 456–473.
18. Buchmeiser, M.R. Stationary phases for chromatography prepared by ring opening metathesis polymerization. J. Sep. Sci. **2008**, *31*, 1907–1922.
19. Nesterenko, P.N.; Haddad, P.R. Zwitterionic ion-exchangers in liquid chromatography. Anal. Sci. **2000**, *16*, 565–575.
20. Wu, R.; Hu, L.; Wang, F.; Ye, M.; Zou, H. Recent development of monolithic stationary phases with emphasis on microscale chromatographic separation. J. Chromatogr. A. **2008**, *1184*, 369–392.
21. Nunez, O.; Nakanishi, K.; Tanaka, N. Preparation of monolithic silica columns for high-performance liquid chromatography. J. Chromatogr. A, **2008**, *1191*, 231–252.
22. Pohl, C. Recent developments in ion-exchange and low molecular weight molecules. LC–GC **2003**, 1–4.
23. Paull, B.; Nesterenko, P.N. New possibilities in ion chromatography using porous monolithic stationary-phase media. Trend. Anal. Chem. **2005**, *24*, 295–303.
24. Svec, F.; Peters, E.C.; Sýkora, D.; Fréchet, J.M. Design of the monolithic polymers used in capillary electrochromatography columns. J. Chromatogr. **2000**, *887*, 3–29.
25. Sarzanini, C. Recent developments in ion chromatography. J. Chromatogr. **2002**, *956*, 3–13.

Ion Chromatography: Suppressed and Non-suppressed

Ioannis N. Papadoyannis
Victoria F. Samanidou
Laboratory of Analytical Chemistry, Chemistry Department, Aristotle University of Thessaloniki, Thessaloniki, Greece

INTRODUCTION

Ion chromatography (IC) is a mode of high-performance liquid chromatography (HPLC) in which ionic analyte species are separated on cationic or anionic sites of the stationary phase. The separation mechanisms can be broadly compared to ion exchange, using fixed-site exchange resins of various composition and ion-interaction methods, using a variety of columns as substrates to support dynamically exchanged or permanently bonded ionic groups. Alternative approaches of minor significance also exist. The mobile phase is an aqueous buffer solution. The rate of migration of the ion (inorganic ions and organic acids and bases) through the column is directly dependent on the type and concentration of eluent ions. Retention is based on the affinity of different ions for the ion-exchange sites and on the competition between eluent buffer ions and analyte ions, which is dependent on the ionic strength of the buffer and can be adjusted by altering the pH of the mobile phase or the concentration of any organic modifier in it.

DISCUSSION

Ion chromatography operates at pressures ranging from several hundred to several thousand pounds per square inch. In most cases, the same chromatographic components (pumps, injectors, etc.) can be employed in both HPLC and IC. Most of the chromatographic principles developed in HPLC stand for IC also, with possible minor modifications. Injection volumes in ion chromatography are generally somewhat larger than those normally in HPLC, typically in the range 50–100 μl, in contrast to HPLC, where 5–20 μl are injected.

It was in 1975 when Small and his co-workers introduced the high-pressure operation mode of ion chromatography. In their original paper, they described a novel system for the chromatographic determination of inorganic ions, in which a resin was used for the separation and a second ion-exchange column was combined to chemically suppress the background conductance of the eluent, thus improving detection limits for eluted ions. Since 1975, IC has grown rapidly and ion chromatographic methods for ions are currently among the best available and have been applied to a wide range of inorganic species. This can be attributed to concurrent advances in separation technology and detection methods.

Detection techniques can be subdivided into three broad categories:

1. Electrochemical detection (using conductivity, amperometry, or potentiometry).
2. Spectroscopic detection (using ultraviolet/visible (UV/Vis) absorbance, refractive index, fluorescence, atomic absorption or atomic emission).
3. Techniques based on postcolumn reactions.

Conductivity detectors provide the advantage of universal detection, as all ions are electrochemically conducting. Thus, the majority of ion chromatography detectors rely upon conductivity measurements.

The principle of conductivity-detector operation is the differential measurement of conductance of the eluent, prior to and during elution of the analyte ion. The detector response depends on analyte concentration, the degree of ionization of both eluent and analyte (governed by the eluent pH), and limiting equivalent conductances of the eluent cation and of the eluent and analyte anions (where an anion-exchange system is considered). If the eluent and analyte are fully ionized, the signal is proportional to the analyte concentration and to the difference (positive or negative) in limiting equivalent conductances which determines sensitivity.

Conductivity detection provides a sensitive measure of ion concentrations in solution, but its measurement is hampered by high conductivity of the eluent, as ion exchange requires a competing electrolyte to displace the analytes from the column. In order to eliminate background conductivity and thus to improve the analyte signal, *H*, Smith et al., proposed the use of a second ion-exchange column. In this way, two different ion chromatography techniques are distinguished: eluent suppressed and non-suppressed (also called single-column ion chromatography) using different packing

materials and different eluents, leading to specific advantages and disadvantages for each technique.

ELUENT SUPPRESSED ION CHROMATOGRAPHY

Various schemes have been devised to improve the signal-to-noise ratio (S/N) by decreasing the background signal of the eluent/displacer or increasing the conductance of the analyte, or both.

The principle of conductivity suppression is the reduction of background conductivity by converting the eluent to a less conductive medium (H_2O) through acid–base neutralization while the analyte ions' conductivity is increased, by converting them to a more conductive medium: Anions are converted to their acid forms and cations to their hydroxide forms. These reactions lead to higher S/N ratios, thus significantly improving baseline stability and detection limits.

Suppressor devices include packed column suppressors, hollow-fiber membrane suppressors, micromembrane suppressors, suspension postcolumn reaction suppressors, autoregenerated electrochemical suppressors, and so forth.

The packed column suppressor, originally introduced by Small et al., suffers from a number of drawbacks, such as time shifts due to Donnan exclusion effects, band broadening (due to a large dead volume and high dispersion), and oxidation of nitrite, which is easily oxidized to nityrate, due to the formation of nitrous acid in the suppressor. Because of these limitations, they were only practical for isocratic elution. However, the main disadvantage of the method is the necessity for periodical regeneration of the suppressor (also called stripper) to restore its ion-exchange capacity.

For anion analysis, the regenerant must supply a source of hydrogen ions to convert the eluent anions to a less conductive form. The most common regenerant is dilute sulfuric acid, whereas for cation analysis, the most common regenerant is hydroxide (sodium, potassium, or tetramethylammonium hydroxide).

The preferred eluents for anions are dilute carbonate–bicarbonate mixture, sodium hydroxide and, for common alkali metals and simple amines, dilute mineral acids (HCl, HNO_3, $BaCl_2$, $AgNO_3$, amino acids, alkyl and aryl sulfonic acids). The most common choice is HCl, but in the case of divalent ions, an eluent of much higher affinity for the ion-exchange resin, such as $AgNO_3$, must be used.

Typical neutralization reactions for chemical suppressors are as follows:

Anion-exchange chromatography:

Eluent reaction: $NaOH + resin\text{–}SO_3^-H^+ \rightarrow Resin\text{–}SO_3^-Na^+ + H_2O$

Analyte reaction: $NaX + resin\text{–}SO_3^-H^+ \rightarrow Resin\text{–}SO_3^-Na^+ + HX$, where X = anions ($Cl^-$, Br^-, NO_2^-, etc.).

Cation-exchange chromatography:

Eluent reaction: $HCl + resin\text{–}NR_3^+OH^- \rightarrow Resin\text{–}NR_3^+Cl^- + H_2O$

Analyte reaction: $MCl + resin\text{–}NR_3^+OH^- \rightarrow Resin\text{–}NR_3^+Cl^- + MOH$, where M = cations ($Na^+$, K^+, etc.).

The reaction, in the case of bicarbonate, yields the largely undissociated carbonic acid that does not contribute significantly to the conductivity.

Without chemical suppression, the contribution to the total measured conductivity from the eluent is many orders of magnitude higher than that from the analyte, leading to low sensitivity (Fig. 1).

Some of the drawbacks that packed column suppressors have were eliminated when hollow-fiber membrane suppressors were introduced in 1981. These were found to be even more convenient and efficient, with low dead volume and high capacity, and they are dynamically regenerated. Eluent passes through the core of the fiber and regenerant washes the outside. However, they have also limited suppression capacity and are restricted only to isocratic operation.

Micromembrane suppressors introduced in 1985 use thin, flat ion-exchange membranes to enhance ion transport while maintaining a very low dead volume, providing a high suppression capacity, with low dispersion.

Later, electrochemically regenerated suppression modules were introduced, where an electrochemical process is used to regenerate a solid-phase chemical suppressor for continuous reagent-free operation. Self-regenerating suppressors are similar to micromembrane suppressors, except that regenerant hydronium and hydroxide ions are produced, *in situ*, by electrolysis of water supplied by recycle or an external source.

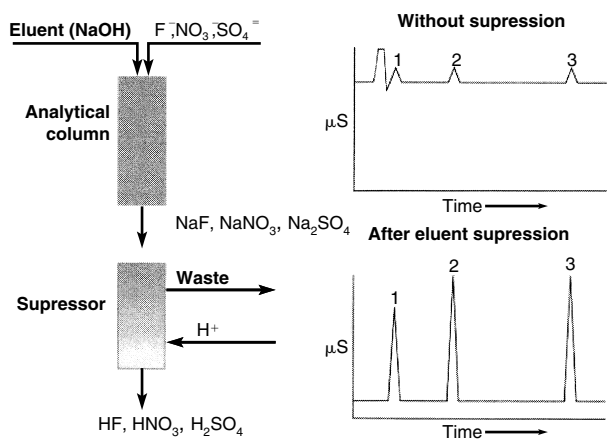

Fig. 1 The effect of the background conductivity suppression on the monitored signal of the analyte anions, after separation by means of ion chromatography. Peaks: 1 = fluoride, 2 = nitrate, 3 = sulfate.

This is achieved by incorporating electrodes inside the regenerant chambers; thus, external acid or base supply are unnecessary. The two electrolysis reactions taking place are

Anode: $2H_2O \rightarrow 4H^+ + O_2 + 4e$

Cathode: $2H_2O + 2e \rightarrow H_2 + 2OH^-$

Another technique of improving the S/N ratio is the one that uses postcolumn addition of a solid-phase reagent (SPR), which is a colloidal suspension of ultrafine ion-exchange particles. The SPR reacts with the analyte to increase its conductivity. Additionally, the SPR has a low electrophoretic mobility and, hence, conductance. This technique avoids the dead time due to suppressor column and also eliminates the regeneration cycle.

NON-SUPPRESSED SINGLE-COLUMN ION CHROMATOGRAPHY

Another approach of ion chromatography is the non-suppressed single column, in which no suppressor device is used. In this case, the only method for improving the sensitivity is to maximize the difference between mobile-phase conductivity and analyte conductivity.

Non-suppressed single-column ion chromatography (SCIC) was introduced in 1979 by Gierde and coworkers, based on a two-principal innovation:

1. The use of a special anion-exchange resin of very low capacity (0.007–0.007 mEq/g).
2. The adoption of an eluent having a very low conductivity, which can be passed directly through the conductometric detector. Typical eluents used are benzoate, phthalate, or other aromatic acid salts, with low limiting equivalent conductances (leading to direct detection) or potassium hydroxide eluent, with high conductivity for anions or dilute nitric acid for cations, leading to indirect detection mode (decrease of conductivity as the analyte is eluting).

The major limitation of non-suppressed conductivity detection is that gradient systems cannot be used; thus, the background conductivity remains constant.

Virtually every type of HPLC detector can be combined with SCIC: refractive index, UV absorbance (direct and indirect), electrochemical, and so forth.

A typical non-suppressed SCIC separation obtained with a low-capacity resin-based strong anion exchanger (PRP-X100 Hamilton) used as the analytical column is illustrated in Fig. 2 for the simultaneous determination of eight inorganic anions (F^-, Br^-, NO_2^-, Cl^-, NO_3^-, PO_4^{3-}, SO_4^{2-}, CO_3^{2-}), with conductometric detection, using a mixture of 2.0 m*M* sodium benzoate and 2.5 m*M* *p*-hydroxybenzoic acid (pH 9.0 adjusted with 1*N* NaOH) as eluent, with the organic modifier methanol 8% v/v, at a flow rate of 0.7 ml/min. The detection limits (S/N = 3) were 100 μg/L for carbonate and 50 μg/L for the rest of the cited anions, when 50 μl of the samples were injected onto the analytical column.

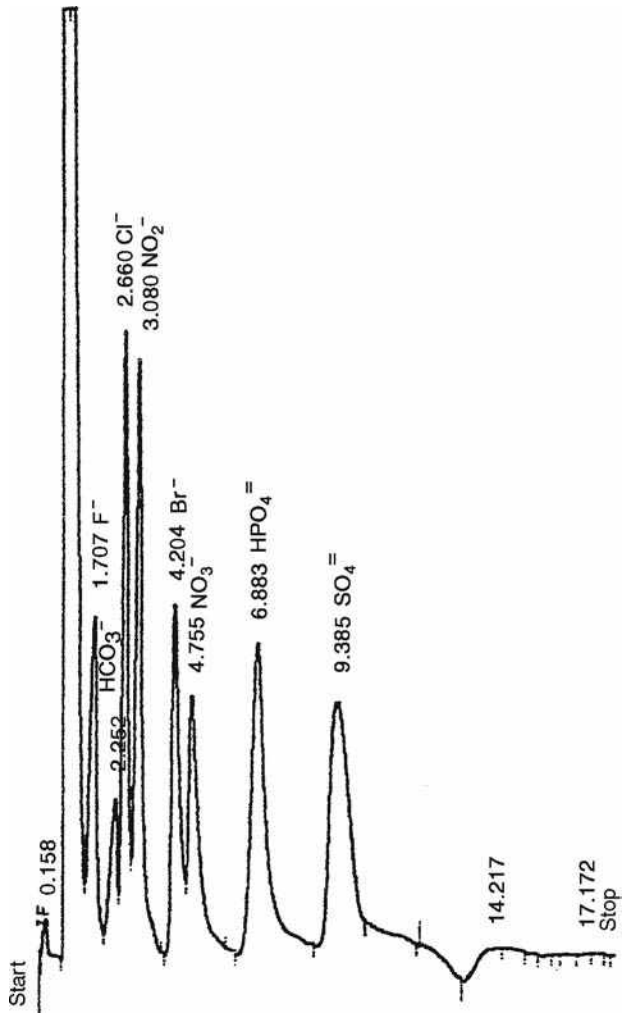

Fig. 2 Non-suppressed SCIC determination of eight inorganic anions.

COLUMNS

Two types of packing materials are commonly used for ion chromatography: silica-based and polymer-based ion exchangers. The polymer-based ion exchangers typically contain a PSDVB (polystyrenedivinylbenzene) backbone, lightly sulfonated (cation exchanger) or lightly aminated (anion exchanger), whereas the silica-based ion exchangers use a porous silica bead, chemically prepared to form

the anion or cation exchanger. The resins have the advantage that they can be used over the entire pH range, whereas silica based materials can be used in a narrow working pH range (2–6.5).

Detection limits for ions vary with the sensitivity of the detector, with the volume of sample injected, and with the identity, concentration, and pH of the eluent, as well as with chromatographic factors, such as column efficiency and so forth.

COMPARISON OF ESIC AND SCIC

The main advantages of eluent suppressed ion chromatography (ESIC) are that a wide range of eluents and columns can be used, the wide dynamic range, and the higher sensitivity; the main disadvantage is the periodical necessity for suppressor-column regeneration.

On the other hand, SCIC is rapid, sensitive, with easy sample preparation, and simple instrumentation; however, it requires a significant difference in conductance between eluent and analyte ions and the temperature stability is crucial. The answer to the question of which IC technique is most efficient is dependent on several considerations, such as the nature of sample analytes, the concentration of the solute ions, the sensitivity required, the equipment available, and so forth.

APPLICATIONS

Ion chromatography, suppressed and non-suppressed, can be applied both to anion and cation analysis. The current situation is that the methods for anion determination have far outnumbered those for cation analysis, for the reason that there are available methods for the latter, which are rapid and sensitive (e.g., AAS, ICP, ASV). It is difficult to mention all the ionic species detectable by this analytical technique. Practically, any compound that can be converted to an ionic form is amenable to analysis by IC. Among the inorganic ions determined are (F^-, Br^-, NO_2^-, Cl^-, NO_3^-, PO_4^{3-}, SO_4^{2-}, CO_3^{2-}, CrO_4^{2-}, I^-, IO_3^-, $C_2O_4^{2-}$, BrO_3^-, SCN^-, Na^+, K^+, Mg^{2+}, Ca^{2+}, NH_4^+, at the ppm or ppb levels, in drinking water, food samples, food additives, beverages, environmental samples (soil extracts, rain water, surface water or groundwater), cosmetics, pharmaceuticals, biomedical, plating bath analysis, biological fluids, industrial process products, wastewater, and so forth. IC is also capable of speciation analysis of polyvalent anions or transition metal ions with multiple oxidation states, at levels lower than those possible with ICP or AAS. Organic species of biological and biochemical interest can also be determined.

BIBLIOGRAPHY

1. Dasgupta, P. Ion chromatography: The state of the art. Anal. Chem. **1992**, *64* (15), 775A–783A.
2. Gierde, D.; Fritz, J.; Schmuckler, G. Anion chromatography with low-conductivity eluents. J. Chromatogr. **1979**, *186*, 509–519.
3. Gierde, D.; Schmuckler, G.; Fritz, J. Anion chromatography with low-conductivity eluents. II. J. Chromatogr. **1980**, *187*, 35–45.
4. Haddad, P.; Heckenberg, A. Determination of inorganic anions by high-performance liquid chromatography. J. Chromatogr. **1984**, *300*, 357–394.
5. Henderson, I.; Saari-Nordhaus, R.; Anderson, J., Jr. Sample preparation for ion chromatography by solid-phase extraction. J. Chromatogr. **1991**, *546*, 61–71.
6. Henshall, A.; Rabin, S.; Statler, J.; Stilian, J. Int. Chromatogr. Lab. **1993**, *12*, 7–14.
7. Papadoyannis, I.; Samanidou, V.; Moutsis, K. Determination of silver iodide by high pressure ion chromatography in soil and water matrices after solid phase extraction. J. Liquid Chromatogr. Relat. Technol. **1998**, *21* (3), 361–379.
8. Papadoyannis, I.; Samanidou, V.; Zotou, A. Highly selective simultaneous determination of eight inorganic anions by single column high pressure anion chromatography in drinking water. J. Liquid Chromatogr. **1995**, *18* (7), 1383–1403.
9. Pietrzyk, D.; Iskandarani, Z.; Schmitt, G. Anion-exchange adsorption on low capacity anion exchangers: Separation of organic acids, amino acids, small chain peptides. J. Liquid Chromatogr. Relat. Technol. **1986**, *9* (12), 2633–2659.
10. Saari-Nordhaus, R.; Anderson, J., Jr. Int. Chromatogr. Lab. **1994**, *18*, 4–10.
11. Schmuckler, G. Recent developments in ion chromatography. J. Chromatogr. **1984**, *313*, 47–57.
12. Small, H.; Stevens, T.; Bauman, W. Novel ion exchange chromatographic method using conductimetric detection. Anal. Chem. **1975**, *47* (11), 1801–1809.
13. Tarter, J. *Ion Chromatography*; Chromatographic Science Series; Marcel Dekker, Inc.: New York, 1987; Vol. 37.
14. Walker, T.; Akbari, N.; Ho, T. Comparison of silica-based strong ion exchangers and low-capacity polymer-based strong ion exchangers for the separation of organic analyte ions using indirect UV detection. J. Liquid Chromatogr. Relat. Technol. **1991**, *14* (4), 619–641.

Ion Chromatography: Water and Waste Water Analysis

Rajmund Michalski
Institute of Environmental Engineering, Polish Academy of Science, Zabrze, Poland

INTRODUCTION

Water and waste water are important areas of chemical analysis. The development of new methods and improvement of existing ones are major tasks for analytical chemists. There is a need for strict control and monitoring of many substances present in water and waste water to prevent contamination and to protect our natural resources.

Substances present in various types of water may be classified as biological, chemical (both inorganic and organic), physical, and radiological impurities. In many laboratories within the confines of routine analysis, the most frequently determined species are inorganic anions and cations.

Until 1975, only a small range of analytical parameters could be measured automatically; therefore, it was necessary to develop and validate new methods to extend the scope of such parameters. An alternative, introduced in 1975, that has almost replaced most of the wet chemical methods used in water analysis is ion chromatography.

Ion chromatography is an attractive technique, especially for laboratories that need to determine numerous anions and cations in several thousand samples but do not have the throughput to justify the purchase of large automatic analyzers that are usually based on colorimetric procedures. Ion chromatography eliminates the need to use the hazardous reagents that are often integral to wet chemical methods.

Regulator demands for justifiable analytical results and laboratories' needs for validated methods have led to the necessity for standardized ion chromatography methods. This entry reviews standard ion chromatography methods for determination of inorganic anions (F^-, Cl^-, NO_2^-, NO_3^-, BrO_3^-, ClO_2^-, ClO_3^-, PO_4^{3-}, SO_3^{2-}, SO_4^{2-}, CrO_4^{2-}, I^-, SCN^-, and $S_2O_3^{2-}$) and cations (Li^+, Na^+, NH_4^+, K^+, Mn^{2+}, Ca^{2+}, Mg^{2+}, Sr^{2+}, and Ba^{2+}) in water and waste water.

ION CHROMATOGRAPHY AS A REFERENCE METHOD

Water is considered to be one of the basic substances supporting life and the natural environment, a primary component for industry, a consumer item for both humans and animals, and a vector for domestic and industrial pollution. Various directives provide a framework for the control of aquatic substances, the quality of bathing, surface, and drinking water and effluents.

The number of species determined in water has grown exponentially during the past 50 years. However, very few have been studied or have led to documented proof of their health effects.

Nearly half of the monitored parameters are being measured for operational reasons (e.g., iron, ammonium, pH, chloride, dissolved organic carbon) and for reasons of customer satisfaction (e.g., color, taste, total hardness).[1] Of the health-related substances, a number of metals and small groups of organic compounds and pesticides, in most countries, are being measured on a regular basis. They include such metals as antimony, arsenic aluminum, chromium, magnesium, magnum, cadmium, copper, nickel, lead, mercury, and iron, as well as inorganic ions (ammonium, fluoride, nitrite, nitrate, and cyanide) and organic compounds (e.g., benzo(a)pyrene, trihalomethanes, chlorobenzenes, pesticides). Recently, inorganic oxyhalide disinfection by-products such as bromate, chlorite, and chlorate have also begun to be measured.

The United States Environmental Protection Agency (USEPA) has established regulations and methodology for inorganic contaminants under the Safe Drinking Water Act. Fluoride, nitrate, and nitrite are limited as primary pollutants because they can cause adverse health effects. For instance, high levels of fluoride cause skeletal and dental fluorosis and nitrite and nitrate overexposure can cause methemoglobulinemia that can be fatal to infants. Other common inorganic anions, e.g., chloride and sulfate, are considered as secondary contaminants and are responsible for water taste, odor, color, and certain other aesthetic effects.

The determination of common inorganic anions (fluoride, chloride, nitrite, bromide, nitrate, phosphate, and sulfate) and cations (sodium, potassium, magnesium, and calcium) was traditionally carried out using wet chemical methods such as gravimetry, titration, photometry, turbidimetry, and colorimetry.

Many of these methods suffer from interferences and limited sensitivity and they can be labor intensive and difficult to automate. Although performance criteria (accuracy, precision, and limit of detection) can be specified for analytical methods, it is still difficult to obtain similar results in different laboratories. For example, there are over 200 available methods to assay for

sulfate and nitrate. Unfortunately, most of those methods are characterized by a lack of sensitivity or selectivity and they are difficult and cumbersome to use.

One of the prime analytical chemists of the twentieth century, Professor Harvey Diehl of Iowa State University, proposed that the Nobel Price should be given to the scientist that develops a better method for sulfur analysis than gravimetry or nephelometry. Today, we can say that ion chromatography has met this challenge.[2]

In 1975, Small et al.[3] described a novel ion-exchange chromatographic method for the separation and conductometric detection of ionic species. They employed a low-capacity ion-exchange stationary phase for the separation of analyte ions, in conjunction with a second ion-exchange column and conductivity detector that allowed for continuous monitoring of eluent.

In September 1975 ion chromatography was publicly presented at a meeting of the American Chemical Society where the Dionex Corporation exhibited the first commercially available instrument for performing ion chromatography.[4] Several years later, Gjerde et al.[5] developed a variety of ion chromatography, a non-suppressed ion chromatography techniques.

Ion-exchange is the primary separation mode used with modern ion chromatography, although other approaches used for separation of inorganic anions and cations include ion interaction, ion exclusion, and chelation chromatography. Ion chromatography, with suppressed conductivity detection, is the most widely used and generally offers the best performance.

Analyzed ions are separated on the ion-exchange column and these ions, together with the eluent, are moved to the suppressor. In the suppressor, the conductance of the eluent is lowered, or suppressed, and the conductance of the sample ions is increased, leading to a large increase in the signal-to-noise ratio of the detection signal.[6] The conceptualization of suppressed conductivity by Small et al.[3] was the seminal idea in the development of ion chromatography. The development and use of suppression devices for the conductometric detection of inorganic ions by ion chromatography was described by Haddad et al.[7]

In recent years, a large variety of stationary phases, with different selectivities and capacities, have been developed for both anion-, and cation-exchange chromatography. The stationary phases used in ion chromatography have usually been polystyrene–divinylbenzene (PS–DVB), polymethacrylate, and polyvinyl resins. Recently, there has been an increasing interest in using porous monolithic stationary phases for high-performance separation of inorganic and organic ions.[8]

A variety of eluents can be used in the separation of anions; although bicarbonate eluents have been used as the mainstay eluent in suppressed ion chromatography. The ideal eluent seems to be hydroxide since, after suppression, it forms water that has virtually zero conductance and, therefore, provides the perfect conductivity baseline. However, hydroxide eluent is difficult to use because it readily absorbs carbon dioxide and forms carbonate.[9] The most popular eluents used in cation analysis are low concentration mineral acids such as HCl, HNO_3, and H_2SO_4, also containing organic modifiers (e.g., ethylenediamine, 2,3-diaminopropionic acid).[10]

Through the choice of stationary phase and eluent composition, the selectivity can be modulated, but the eluent must meet the requirements of the detection system. Although the conductivity detector is still the most popular, other types of detection can be applied for different analytes. These include electrochemical (amperometric, pulsed and integrated amperometric, potentiometric), photometric (UV–Vis, indirect photometric following post column derivatisation, chemiluminescence, refractive index), and fluorescence.

Ion chromatography plays a very important role in hyphenated techniques used in species analysis.[11] Coupling techniques represent the link of ion chromatography systems with an independent analytical detection method, usually spectroscopic (AAS-Atomic Absorption Spectroscopy, ICP-AES-Inductively Coupled Plasma Atomic Emission Spectroscopy, ICP-MS-Inductively Coupled Plasma-Mass Spectrometry[12]).

Ion chromatography can be used for the determination of ionic solutes such as inorganic anions, inorganic cations (including alkali metals, alkaline earth metals, transition metals, and rare earth metals), carboxylic, phosphonic and sulfonic acids, detergents, carbohydrates, low molecular weight organic bases, and ionic metal complexes.

It is applicable for the determination of ions in many sample matrices although the determination of inorganic ions in water continues to be the most widely used application. Ion chromatography offers several advantages over conventional methods for determination of inorganics:

- short time of analysis;
- sensitivity at the μg/L level;[13]
- high selectivity in samples with complex matrices;[14]
- simple water sample pretreatment;[15]
- small sample volume;
- simultaneous determination of anions and cations, or inorganic and organic ions;[16]
- species analysis (e.g., $NO_2^-/NO_3^-/NH_4^+$; $SO_3^{2-}/SO_4^{2-}/S^{2-}$; $H_2PO_4^-/HPO_4^{2-}/PO_4^{3-}$; Br^-/BrO_3^-; $Cl^-/ClO_2^-/ClO_3^-/ClO_4^-$;Cr(III)/Cr(VI); Fe(II)/Fe(III));[17]
- use of cheap, safe, and environment friendly chemicals.

Acceptance of ion chromatography for anion analysis was very rapid, primarily due to the lack of alternative methods that could determine multiple anions in a single analysis. However, the situation regarding the analysis

of cations was quite different because of many rapid and sensitive spectroscopic methods such as AAS, ICP-AES, ICP-MS, as well as polarography and stripping voltammetry.

Ion chromatography provides a straightforward method for the simultaneous determination of alkali and alkaline earth cations and ammonia. A key benefit of this approach is the ability to detect ammonia in complex samples that contain both inorganic cations and organic amines, as the latter compounds can interfere with the conventional colorimetric or ion selective electrode methods used for ammonia analysis.

More than 15 years ago, capillary electrophoresis appeared as a promising substitute for ion chromatography, mainly because of its higher speed of separation. Comparison of ion chromatography and capillary electrophoresis has shown that these techniques can be considered as being complementary rather than competitive.[18] Nevertheless, until now there were no international standards applied for capillary electrophoretic methods.

Standardization of Ion Chromatographic Methods

Regulators and clients expect to receive accurate and comparable results from a laboratory. Legislators generally define which of various validated methods should be applied to analyze environmental water samples. In general, standard methods can be chosen to serve as reference methods, but the laboratory serving a public client should apply official reference methods.

The best methods for inorganic anion and cation determinations should meet the following criteria:

- determination of target ions with limit of determination of 25% of maximum acceptable concentration;
- simple sample treatment;
- short analysis time;
- low cost of single analysis;
- method availability.

Ion chromatography methods meet these requirements and can be used for routine applications in environmental laboratories. Considering that several individual wet chemistry methods for common inorganic anions or cations could be replaced by one fast and reliable chromatographic separation, it is not surprising that ion chromatography has quickly become accepted worldwide by regulatory bodies to be used for the analysis of anions and cations in water and waste water. However, there are relatively few regulatory methods for cations analysis that use ion chromatography.

Standardization on the international level is the responsibility of International Standardization Organization (ISO). ISO Technical Committee 147, founded in 1971, is responsible for the standardization in the field of water quality. Ion chromatography methods have been developed, especially for drinking and waste water analyses; however, other applications (e.g., rain water, swimming pool water) are acceptable as well. During the standardization process, the draft standard methods have to go through a validation procedure, including checks for accuracy, precision, recovery, and, finally, an interlaboratory trial before they are published as standard methods.

The normative part of an analytical standard method in ISO includes at least the following clauses: scope, normative references, interferences, principle, essential minimum requirements, reagents, apparatus, quality requirements for the separator column, sampling and sample pretreatment, procedure, calculation, expression of results, and test report.

Methods can be deleted from the standards system if they do not pass the approval stage successfully, a confirmation after 5 years is refused, or there is a replacement of an existing standard by a new one.[19] The philosophy of setting standards in ISO and the US EPA is different. ISO prefers documents that do not specify trademarks or equipment produced by a single manufacturer.

In 1993, the USEPA published Method 300.0—the first USEPA method widely accepted as the standard for common inorganic anions.[20] Soon, this method was updated to include part B for the determination of bromate and other inorganic disinfection by-products using a modern high-capacity anion exchange column with carbonate/bicarbonate eluent.

Many different regulatory agencies use the same methodology as USEPA Method 300.0; however, each agency has a unique method format and style. Also, differences exist in the methods of quality control.[21]

Standard methods can be adopted as recommended on a voluntary basis by any laboratory around the world. Governments can decide to incorporate existing standards into their national standards.

After the publication of USEPA and, particularly, ISO ion chromatography standards concerning ion chromatography, the number of laboratories applying this technique has increased dramatically. For those laboratories, ion chromatography is a reliable and economical supplement to existing wet chemical methods.

Ion chromatography can be considered to be a well-established, mature technique for the analysis of anions and cations and many organizations, such as ISO, US EPA, ASTM (American Society for Testing and Materials), and AOAC (Association of Official Analytical Chemists) base their standards or regulatory methods of analysis upon it.

From 1992 to 2005, five ion chromatography standards concerning ion determination in water and waste water have been published. Only one standard concerns cation determination. All ISO ion chromatography standards are

Table 1 The characteristics of ISO standard 10304-1 and 10304-2.

Standard number	ISO 10304-1		ISO 10304-2	
Published	1992		1995	
Standard name	Water quality—determination of dissolved fluoride, chloride, nitrite, orthophosphate, bromide, nitrate, and sulfate ions using liquid chromatography of ions. Part 1: Method for water with low contamination		Water quality—determination of dissolved anions by liquid chromatography of ions. Part 2: Determination of bromide, chloride, nitrate, nitrite, orthophosphate, and sulfate in waste water	
Sample matrix	Drinking water, rain water, ground water, surface water		Waste water	
	Ions	**Range (mg/L)**	**Ions**	**Range (mg/L)**
Determined ions and working range	Fluoride (F^-)	0.01–10	—	—
	Chloride (Cl^-)	0.1–50	Chloride (Cl^-)	0.1–50
	Nitrite (NO_2^-)	0.05–20	Nitrite (NO_2^-)	0.05–20
	Orthophosphate (PO_4^{3-})	0.1–20	Orthophosphate (PO_4^{3-})	0.1–20
	Bromide (Br^-)	0.05–20	Bromide (Br^-)	0.05–20
	Nitrate (NO_3^-)	0.1–50	Nitrate (NO_3^-)	0.1–50
	Sulfate (SO_4^{2-})	0.1–100	Sulfate (SO_4^{2-})	0.1–100
Detection mode	Suppressed conductivity			

based on suppressed conductivity detection, although two of them (ISO 10304 part 3, and part 4) allow the use of UV–Vis and amperometry detection modes.

The USEPA published seven ion chromatography methods, three of which (Methods: 317.0, 321.8, and 326.0) concern determination of oxyhalide disinfection by-products (bromate, chlorite, and chlorate). It is noteworthy that two USEPA Methods (314.1, and 332.0) published the analysis of perchlorate, which is a new challenge for analytical chemistry.

The review of ISO and USEPA methods for the determination of inorganic anions and cations in water and

Table 2 The characteristics of ISO standard 10304-3 and 10304-4.

Standard number	ISO 10304-3			ISO 10304-4		
Published	1997			1997		
Standard name	Water quality—Determination of dissolved anions by liquid chromatography of ions. Part 3: Determination of chromate, iodide, sulfite, thiocyanate and thiosulfate			Water quality—Determination of dissolved anions by liquid chromatography of ions. Part 4: Determination of chlorate, chloride and chlorite in water with low contamination		
Sample matrix	Waste water			Drinking water, raw water, swimming pool water		
	Ion	**Range (mg/L)**	**Detection**	**Ion**	**Range (mg/L)**	**Detection**
Determined ions, working range and detection mode	Chromate (CrO_4^{2-})	0.05–50	UV (λ=365 nm)	Chlorate (ClO_3^-)	0.03–10	Suppressed conductivity
	Iodide (I^-)	0.1–50	CD or UV (λ=205 to 236 nm); AD (0.7 to 1.1 V)	Chloride (Cl^-)	0.1–50	Suppressed conductivity
	Sulfite (SO_3^{2-})	0.1–50	CD	Chlorite (ClO_2^-)	0.05–1	Suppressed conductivity
	Thiocyanate (SCN^-)	0.5–50	UV (λ=205 to 220 nm)		0.1–1	UV (λ=207 to 220 nm)
	Thiosulfate ($S_2O_3^{2-}$)	0.1–50	CD or UV (λ=205 to 236 nm); AD (0.7 to 1.1 V)		0.01–1	AD (0.4 to 1.0 V)

CD = conductivity detection; AD = amperometric detection; UV = UV–Vis detection.

Table 3 The characteristics of ISO standard 15061 and 14911.

Standard number	ISO 15061		ISO 14911	
Published	2001		1998	
Standard name	Water quality—Determination of dissolved bromate. Method by liquid chromatography of ions		Water quality—Determination of dissolved Li^+, Na^+, NH_4^+, K^+, Mn^{2+}, Ca^{2+}, Mg^{2+}, Sr^{2+} and Ba^{2+} using ion chromatography method. Method for water and waste water	
Sample matrix	Drinking water, raw water, surface water, partially treated water and swimming pool water		Waste water	
	Ion	**Range (mg/L)**	**Ion**	**Range (mg/L)**
Determined ions and working range	Bromate (BrO_3^-)	0.0005–1	Lithium (Li^+)	0.01–1
			Sodium (Na^+)	0.1–10
			Ammonium (NH_4^+)	0.1–10
			Potassium (K^+)	0.1–10
			Manganese (Mn^{2+})	0.5–50
			Calcium (Ca^{2+})	0.5–50
			Magnesium (Mg^{2+})	0.5–50
			Strontium (Sr^{2+})	0.5–50
			Barium (Ba^{2+})	1–100
Detection mode	Suppressed conductivity. UV detector ($\lambda = 190$–205 nm) is suitable to confirm the conductivity results only.		Suppressed conductivity	

waste water is given in Tables 1–3 (ISO Standards), and Tables 4 and 5 (USEPA Methods).

CONCLUSIONS

Ion chromatography is an innovative analytical technique that has significantly improved analysis of ions in water and waste water. The most routine ion chromatography methods have been standardized over the last 20 years.

The most important advantages of ion chromatography are: a broad range of applications, well-developed hardware, many detection options, reliability (good accuracy and precision), high selectivity, high speed, high separation efficiency, good tolerance to sample matrices, and low cost of consumables. With this included, ion

Table 4 The characteristic of USEPA Methods 300 and 300.1.

Method number	300.0		300.1	
Published	1993		1997	
Method name	The determination of inorganic anions in water by ion chromatography		The determination of inorganic anions in water by ion chromatography	
Sample matrix	Drinking water, surface water, waste water			
	Ions	**Limit of detection (μg/L)**	**Ions**	**Limit of detection (μg/L)**
	Fluoride (F^-)	9	Fluoride (F^-)	9
	Chloride (Cl^-)	4	Chloride (Cl^-)	4
	Nitrite (NO_2^-)	1	Nitrite (NO_2^-)	1
	Bromide (Br^-)	14	Bromide (Br^-)	14
	Nitrate (NO_3^-)	11	Nitrate (NO_3^-)	8
	Phosphate (PO_4^{3-})	19	Phosphate (PO_4^{3-})	19
	Sulfate (SO_4^{2-})	19	Sulfate (SO_4^{2-})	19
	Bromate (BrO_3^-)	20	Bromate (BrO_3^-)	1.44
	Chlorite (ClO_2^-)	10	Chlorite (ClO_2^-)	0.89
	Chlorate (ClO_3^-)	3	Chlorate (ClO_3^-)	1.31
Detection mode	Suppressed conductivity			

Table 5 The characteristic of USEPA Methods: 314.1; 317.0; 321.8; 326.0; and 332.0.

Method number	314.1	317.0	321.8	326.0	332.0
Published	Revised in 2005	2001	1997	2002	Revised 2005
Method name	Determination of perchlorate in drinking water using inline column concentration /matrix elimination ion chromatography with suppressed conductivity detection	Determination of inorganic oxyhalide disinfection by-products in drinking water using ion chromatography with the addition of a postcolumn reagent for trace bromate analysis	Determination of bromate ions in waters using ion chromatography with inductively coupled plasma mass spectrometry	Determination of inorganic oxyhalide disinfection by-products in drinking water using ion chromatography incorporating the addition of a suppressor acidified postcolumn reagent for trace bromate analysis	Determination of perchlorate in drinking water by ion chromatography with suppressed conductivity and electrospray ionization mass spectrometry
Sample matrix	Raw and drinking water	Drinking water			

	Ions	**Limit of detection (μg/L)**	**Ions**	**Limit of detection (μg/L)**	**Ions**	**Limit of detection (μg/L)**	**Ions**	**Limit of detection (μg/L)**	**Ions**	**Limit of detection (μg/L)**
Determined ions and limit of detection ($\mu g/L^{-1}$)	ClO_4^-	0.03	Conductivity detection		BrO_3^-	0.3	Conductivity detection		ClO_4^-	0.02
			ClO_2^-	0.45			ClO_2^-	20		
			ClO_3^-	0.92			ClO_3^-	17		
			BrO_3^-	0.98			BrO_3^-	12		
			UV/Vis detection				UV/Vis detection			
			ClO_2^-	0.89			BrO_3^-	0.17		
			ClO_3^-	0.62			—	—		
			BrO_3^-	0.12			—	—		
Detection mode	Suppressed conductivity		Suppressed conductivity followed in series with UV post column derivatisation with *O*-dianisidine		ICP-MS		Suppressed conductivity or UV/Vis		ESI/MS	

chromatography is widely accepted as the standard reference methodology for water and waste water analysis. Ion chromatography separation will continue to be developed as more and more inorganic contaminants (e.g., perchlorate, chromate, cyanide) become regulated at lower and lower levels in the future.

REFERENCES

1. Richardson, S.D. Water analysis: Emerging contaminants and current issues. Anal. Chem. **2003**, *75*, 2831–2857.
2. Koch, W.F. Ion chromatography and the certification of standard reference materials. J. Chromatogr. Sci. **1989**, *27*, 418–421.
3. Small, H.; Stevens, T.S.; Bauman, W.C. Novel ion exchange chromatographic method using conductometric detection. Anal. Chem. **1975**, *47*, 1801–1886.
4. Small, H.; Bowman, B. Ion chromatography: A historical perspective. Am. Lab. **1998**, *10*, 1–8.
5. Gjerde, D.T.; Fritz, J.S.; Schmuckler, G. Anion chromatography with low-conductivity eluents. J. Chromatogr. **1979**, *186*, 509–519.
6. Liu, Y.; Srinivasan, K.; Pohl, C.; Avdalovic, N. Recent developments in electrolytic devices for ion chromatography. J. Biochem. Biophys. Methods **2004**, *60*, 205–232.
7. Haddad, P.R.; Jackson, P.E.; Shaw, M.J. Developments in suppressor technology for inorganic ion analysis by ion chromatography using conductivity detection. J. Chromatogr. **2003**, *1000*, 725–742.
8. Paull, B.; Nesterenko, P.N. New possibilities in ion chromatography using porous monolithic stationary-phase media. Trends Anal. Chem. **2005**, *24*, 295–303.
9. Liu, Y.; Kaiser, E.; Avdalovic, N. Determination of trace-level anions in high-purity water samples by ion chromatography with an automated on-line eluent generation system. Microchem. J. **1999**, *62*, 164–173.
10. Gjerde, D.T. Eluent selection for determination of cations in ion chromatography. J. Chromatogr. **1988**, *439*, 49–61.
11. Das, A.K.; Guardia, M.; Cervera, M.L. Literature survey of on-line elemental speciation in aqueous solutions. Talanta **2001**, *55*, 1–28.
12. Buchberger, W.W. Detection techniques in ion chromatography of inorganic ions. Trends Anal. Chem. **2001**, *20*, 296–303.
13. Marchetto, A.; Mosello, R.; Tartari, G.A. et al. Precision of ion chromatographic analyses compared with that of other analytical techniques through intercomparison exercises. J. Chromatogr. **1995**, *706*, 13–19.
14. Singh, P.R.; Abbas, N.M.; Smesko, S.A. Suppressed ion chromatography analysis of anions in environmental waters containing high salt concentration. J. Chromatogr. **1996**, *733*, 73–91.
15. Slingby, R.; Kiser, R. Sample treatment techniques and methodologies for ion chromatography. Trends Anal. Chem. **2001**, *20*, 288–295.
16. Nesterenko, P.N. Simultaneous separation and detection of anions and cations in ion chromatography. Trends Anal. Chem. **2001**, *20*, 311–319.
17. Sarzanini, C.; Bruzzoniti, M.C. Metal species determination by ion chromatography. Trends Anal. Chem. **2001**, *20*, 304–310.
18. Haddad, P.R. Comparison of ion chromatography and capillary electrophoresis for the determination of inorganic anions. J. Chromatogr. **1997**, *770*, 281–290.
19. Hecq, P.; Hulsmann, A.; Hauchman, F.S.; McLain, J.L.; Schmitz, F. Drinking water regulations. In *Analytical Methods for Drinking Water. Advances in Sampling and Analysis*; Quevauviller, P., Thompson, K.C., Eds.; Wiley: Chichester, UK, , 2006; 16–35.
20. US Environmental Protection Agency. In *USEPA Method 300.0. The Determination of Inorganic Anions in Water by Ion Chromatography;* USEPA: Cincinnati, OH, 1993.
21. Jackson, P.E. Determination of inorganic ions in drinking water by ion chromatography. Trends Anal. Chem. **2001**, *20*, 320–329.

Ion Exchange: Mechanism and Factors Affecting Separation

Karen M. Gooding
Eli Lilly and Company, Indianapolis, Indiana, U.S.A.

INTRODUCTION

Ion-exchange chromatography (IEC) is a technique in which ionic solutes bind to charged functional groups on the bonded phase. The power and versatility of IEC as an analytical and preparative technique is due in large part to the ability to drastically change the selectivity through manipulation of the mobile phase. Although it is obvious that the pH determines the charge on the support and the analytes, the nature of the salt is an equally important parameter. The constituent ions of the salt associate with the support functional groups and/or those of the solute, yielding distinct ionic interactions. Mobile-phase additives, temperature, and gradient conditions also contribute to the separation in IEC.

MOBILE PHASE

pH

Adjustment of the pH is a critical factor in IEC because the pH dictates the charge of both the solutes and the ion exchanger, thus controlling their affinity for one another or their ability to release from a bound state. The essential nature of pH in the process necessitates its exact control; therefore, any mobile phase used for IEC should contain an effective buffer (0.02–0.1 *M*) within its optimum pH range. Some common buffers which cover much of the range of pH used in IEC are phosphate, citrate, acetate, and tris(hydroxymethyl) aminomethane (Tris).[1,2] The pH should be selected to yield ionization of the functional groups on the support as well as those on the analytes. For molecules with a single charge, the pH should be at least two units from the p*K* in the direction of ionization. The guideline for zwitterions is that the pH be at least two units from the isoelectric point (p*I*). A pH near neutrality is often effective for complex mixtures of diverse substances. Even carbohydrates, whose hydroxyl groups do not ionize until the pH is greater than 12, can be separated by IEC when the pH is adjusted to a high enough value with low concentrations of base as the mobile phase.[3]

The choice of pH for IEC of proteins or other macromolecules is not as simplistic as it is for small molecules. Although using the p*I* as a guide frequently yields an adequate separation, the p*I* encompasses all the charged groups in the molecule, whereas, because of their defined tertiary structures, only the surface amino acids of proteins are actually involved in the binding. Under denaturing conditions, more amino acids are likely to be exposed to the bonded phase.

Salt Concentration

IEC is a very predictable technique because the mechanism is well defined. The capacity factor (k) for the binding of an ionic solute to an ion-exchange functional group in IEC is directly related to the concentration (c) of salt in the mobile phase:

$$\log k = \log K_0 + Z_c \log\left(\frac{1}{c}\right)$$

where K_0 is the distribution coefficient and Z_c is an experimentally determined parameter that reflects the apparent number of ionic charges associated with the process of a specific solute with a specific surface.[4] For isocratic separations of simple molecules with up to several charges, the analysis time can be optimized along with resolution by adjustment of the salt concentration. For more complex analytes or mixtures, salt gradients are often necessary to achieve acceptable separations. Generally, a gradient from 0 to 1 *M* salt in a buffer at a suitable pH will yield a preliminary separation.

An opposite mechanism to ion exchange occurs when the ionic strength is too low. Ion exclusion is a phenomenon in which a charged analyte is repelled by the like charges within a pore. This is very likely to occur if water is used alone as the mobile phase with ion-exchange supports or with other modes of silica-based columns. Adding buffer and salt usually eliminates the problem.

Salt Composition

Elution with increased concentrations of salt is the most common and readily controlled method of achieving displacement of molecules which are strongly bound by an ion exchanger. The salt counterions competitively displace solute ions from the charged sites on the stationary phase. Smaller, more highly charged ions are most effective at this displacement. Specifically, the strength of displacement for cations

$$Mg^{2+} > Ca^{2+} > NH_4^+ > Na^+ > K^+$$

is and for anions, it is

$$SO_4^{2-} > HPO_4^{2-} > Cl > CH_3COO^-$$

The strength of the ions for displacement is not necessarily related to optimum selectivity or resolution. Selectivity is dictated by the effect of the salt on both the solute and the bonded phase. Besides displacing the solute from the support, either of the ions of the salt can complex with the ion-exchange functional group or the solute, alter the tertiary structure of the solute, or enhance hydrophobic properties. It is this combination of effects which results in selectivity. For example, when a mixture of proteins was run on a polyethyleneimine (PEI) weak anion-exchange column with gradients formed with 1.0 *N* salt, substitution of sodium acetate for sodium phosphate produced not only longer retention but also much better resolution of the proteins.[5] Sodium phosphate produced narrower peaks with less tailing, but the peaks had only slight differences in retention. In this case, the short retention was proven to be due to a special affinity of phosphate for PEI, which did not occur with anion-exchange supports having quaternary (*Q*) or diethylaminoethanol (DEAE) functional groups. The salt effects on selectivity encompass anions and cations in both anion-exchange and cation-exchange chromatography, as illustrated in Fig. 1, implying that the selectivity occurs because of ionic interactions with the functional groups of both the support and the solute. In the case of adenosine 5-diphosphate (ADP), divalent ions like calcium can bridge between the oxygens in the phosphate and thus reduce the ionic properties. Phosphate salts reduce the retention of ADP on PEI supports due to the phosphate–PEI affinity discussed earlier. Another example of ion-based selectivity is the excellent resolution obtained for sugars when a calcium salt is used with a cation-exchange resin. This ability to change selectivity so dramatically by varying the salt significantly broadens the utility of IEC.

The only restrictions on the choice of salt are those involving analyte solubility or stability. Volatile salts such as ammonium acetate even allow IEC to be interfaced with

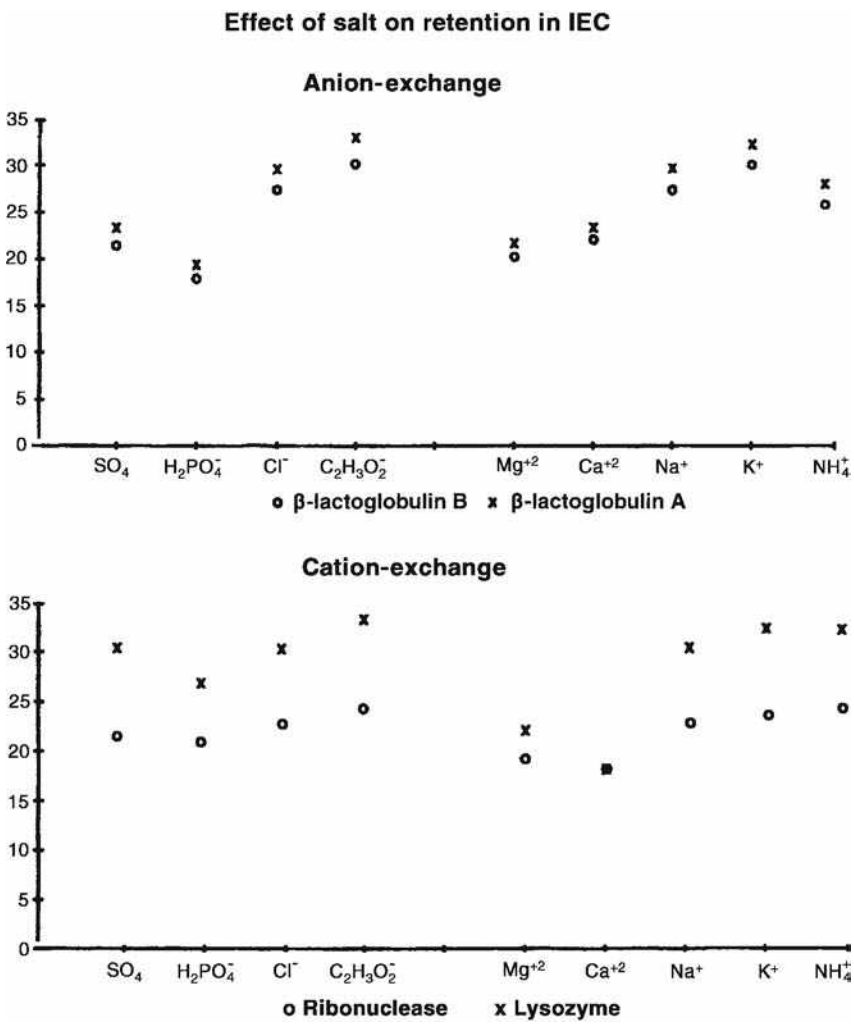

Fig. 1 Anion-exchange chromatography (AEX): SynChropak AX300 (polyethyleneimine, 300 Å, 6 μm); cation-exchange chromatography (CEX): SynChropak CM300 (carboxymethyl, 300 Å, 6 μm); 30 min gradient (0–1*N*) of sodium or chloride salts in 0.02 *M* Tris, pH 7.
Source: Reprinted with permission of MICRA Scientific.

mass spectrometry or evaporative lightscattering detection. It is very important that a given salt be totally stripped from a support before changing to other ions to avoid mixed ion effects. An acid such as trifluoroacetic acid is often effective as a bridge/washing solvent for this purpose.

SURFACTANTS AND ORGANIC SOLVENTS

Secondary separation which may be present in IEC is generally size exclusion or hydrophobicity. Size exclusion will occur if macromolecules are larger than the pores in a support. Hydrophobic interactions are most often observed under conditions of high salt for solutes with significant non-polar characteristics, such as certain peptides. The hydrophobicity of an ion-exchange support is due to either the matrix or the cross-linking agents which were employed in the synthesis of the bonded phase. Any hydrophobic interactions are fundamentally undesirable and can be minimized by the addition of 1–10% of an organic solvent, such as methanol, ethanol, or acetonitrile, to the running buffer. The solubility of the salt in the organic mobile phase should always be verified to avoid precipitation.

Non-ionic detergents may also reduce hydrophobic interactions with a column. These detergents, such as CHAPS or urea, can also be added to ion-exchange mobile phases to aid in the solubilization of membrane or other insoluble proteins. Such detergents are easy to equilibrate and remove from ion-exchange columns; however, ionic detergents should be avoided because of their very strong binding to the column or the solutes.

FLOW RATE AND GRADIENT

Small molecules can often be effectively separated isocratically by IEC; however, due to multipoint interactions, isocratic IEC of proteins and most biological macromolecules is not usually feasible, yielding no resolution and extreme tailing. Such complex molecules are generally separated by gradient elution.

As a salt gradient proceeds to higher levels in IEC, molecules elute at a specific salt concentration, generally without binding from secondary effects. The relationship of gradient conditions to elution (k^*) can be described by

$$k^* = 0.87 t_G \frac{F}{V_M} \left(\log \frac{C_2}{C_1} \right) Z$$

where C_1 and C_2 are the total salt concentrations (salt plus buffer) at the beginning and the end of the gradient, respectively, Z is the effective charge on the solute molecule, F is the flow rate; V_M is the total mobile-phase volume, and t_G is the gradient time.[6] The Z number will vary with solute and pH. An initial ion-exchange protocol of a 20–30 min linear gradient from 0–1 M salt in a buffer at a suitable pH will usually yield a separation which can be later optimized, if necessary. For shortest analysis times, a gradient should begin at the highest salt concentration where the analytes are bound and it should end at the lowest ionic strength that causes elution. The pH gradients may also be used to elicit elution during IEC, although this has been a less popular strategy than salt gradients. Ion-exchange columns can be effectively washed with a mobile phase of higher ionic strength than the upper gradient limit or with low pH. For gradients, intermediate flow rates of 1 ml/min for a 4.6 mm inner diameter column are usually satisfactory.

TEMPERATURE

The use of elevated temperature in IEC reduces the mobile-phase diffusion coefficient and concomitantly

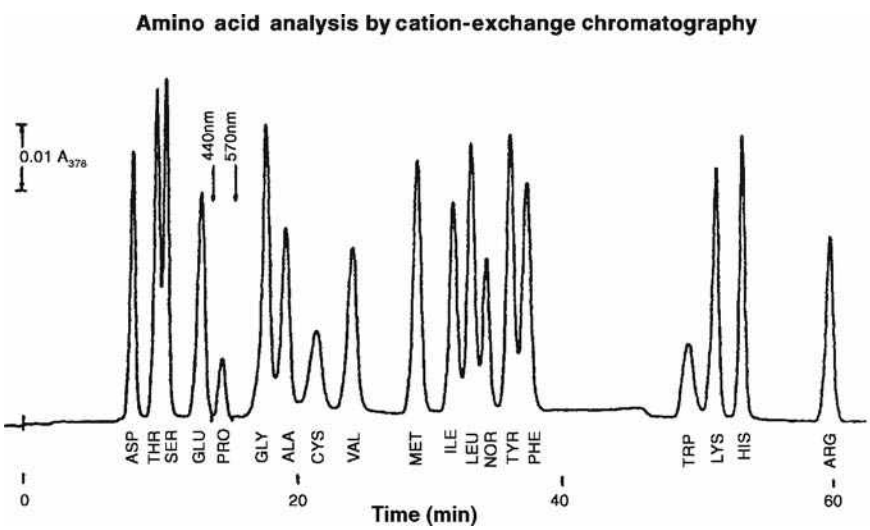

Fig. 2 Column: Micropak AA (sulfonated polystyrene); solvent A: 0.2 M sodium citrate, pH 3.25; solvent B: 1 M sodium citrate, pH 7.40. Gradient: 5 min 100% A; 100–75% A in 20 min; 75–70% A in 5 min; 70–35% A in 5 min; 10 min 35%; 35–0% A in 1 min. $T = 50°C$ for 25 min, then 90°C. Detection after ninhydrin postcolumn reaction.
Source: Reprinted from Amino acid analysis with ninhydrin postcolumn derivatization, *LC at Work*, Varian Associates, with permission.

decreases band spreading. Most mobile phases in IEC are composed of water with salts and thus produce efficiencies which are less than those obtained in modes using organic solvents. Because increased temperatures decrease retention, they may permit the use of lower salt concentrations. Elevated temperatures have been especially effective in amino acid analyses by cation-exchange chromatography, as illustrated in Fig. 2.

CONCLUSIONS

The effectiveness of IEC as a method for separating charged species is enhanced by the ability of many operational factors to change the selectivity and resolution. Salt concentration, salt composition, and pH are the most important operational parameters which strengthen the versatility of the technique.

REFERENCES

1. Cunico, R.L.; Gooding, K.M.; Wehr, T. Ion-exchange chromatography. In *Basic HPLC and CE of Biomolecules*; Bay Bioanalytical Laboratories: Richmond, VA, 1998.
2. *Ion-Exchange Chromatography, Principles and Methods*; Pharmacia Biotech: Sweden, 1998.
3. Townsend, R.R. High-pH anion exchange chromatography of recombinant glycoprotein glycans. In *High Performance Liquid Chromatography: Principles and Methods in Biotechnology*; Katz, E.D., Ed.; John Wiley & Sons: New York, 1996.
4. Aguilar, M.I.; Hodder, A.N.; Hearn, M.T.W. HPIEC of proteins. In *HPLC of Proteins, Peptides and Polynucleotides*; Hearn, M.T.W., Ed.; VCH: New York, 1991; 199.
5. Nowlan, M.P.; Gooding, K.M. HPIEC of proteins. In *High-Performance Liquid Chromatography of Peptides and Proteins*; Mant, C.T., Hodges, R.S., Eds.; CRC Press: Boca Raton, FL, 1991.
6. Snyder, L.R. Gradient elution separation of large biomolecules. In *HPLC of Biological Macromolecules: Methods and Applications*; Gooding, K.M., Regnier, F.E., Eds.; Marcel Dekker, Inc.: New York, 1990.

Ion-Exchange Buffers

J.E. Haky
H. Seegulum
Department of Chemistry and Biochemistry, Florida Atlantic University, Boca Raton, Florida, U.S.A.

INTRODUCTION

Ion-exchange chromatography is a separation method based on the exchanging of ions in a solution with ions of the same charge present in a porous insoluble solid. The method is used for the deionization of water.[1,2] It is often employed for the separation and identification of the rare earth and transuranium elements.[2] Additionally, ion-exchange chromatography is also used in clinical laboratories for the automated separation and analysis of amino acids and other physiologically important amines used for pharmaceutical purposes.[3]

DISCUSSION

In ion-exchange chromatography, ions are separated on the basis of their differences in relative affinity for ionic functional groups on the stationary phase. Anionic and cationic functional groups are covalently attached to the stationary phase, usually resins, which are amorphous particles of organic material.[1–3] Sulfonated styrene-based polymers are the most widely used cation-exchange resin, and similar polymers containing quaternary ammonium groups are the most widely used anion exchangers.[4] Oppositely charged solute ions are attracted to ionic functional groups on the stationary phase by electrostatic forces. Retention is based on the attraction between solute ions and charged sites bound to the stationary phase.[4,5]

Due to the desirable solvent and ionizing properties of water, most ion-exchange chromatographic separations are carried out in aqueous media. Once the selection of the column type has been made, the resolution of components in the sample can be optimized by adjusting ionic strength, temperature, flow rate, and, most importantly, the pH and concentration of buffer or organic modifier in the mobile phase.

Solvent strength, which is defined as the ability of the solvent to elute a given solute from the stationary phase, increases with increased ionic strength of the mobile phase. Selectivity is generally not affected by changes in ionic strength, except for samples containing solutes with different valence charges. With increased temperature, the rate of solute exchange between the stationary phases and mobile phases increases, and the viscosity of the mobile phase decreases, resulting in increased solvent strength. Solvent strength also increases with the volume percent of organic modifier for hydrophobic solutes. However, most ion-exchange chromatography is performed in totally aqueous mobile phases, due to the hydrophilic nature of most ionic solutes. Flow rates of the mobile phase can change resolution in ion-exchange chromatography, but the effects are often minimal.[5]

Increases in mobile-phase pH cause decreases in solute retention in cation-exchange chromatography and increases in retention in anion-exchange chromatography. Separation selectivity can also be greatly influenced by small changes in pH. In ion-exchange chromatography with aqueous mobile phases, buffers are used to maintain the pH in the mobile phase. A buffered solution can resist the changes in pH when an acid or base is added or when dilution is occurring. The pH of a buffer is given by the Henderson–Hasselbalch equation:

$$\mathrm{pH} = \mathrm{p}K_a + 109\,\frac{[\mathrm{A}^-]}{[\mathrm{HA}]} \tag{1}$$

where $\mathrm{p}K_a$ refers to the acid dissociation constant of the species in the denominator, HA, and A refers to the conjugate base of the acid HA. Buffer capacity, the measure of how well a solution resists changes in pH when a strong acid or base is added, increases as the concentration of the buffer increases. However, the pH of a buffer solution is virtually independent of dilution. When the $\mathrm{pH} = \mathrm{p}K_a$ the maximum buffer capacity is met and a good working range of the buffer is approximately when the $\mathrm{pH} = \mathrm{p}K_a = 1 \pm 1$.[1] A buffer is very easy to make. For example, to prepare 1.00 L of buffer containing 0.100 M tris(hydroxymethyl)aminomethane hydrochloride at pH of 7.4, simply weigh out 0.100 mol of its hydrochloride salt and dissolve it in a beaker containing about 900 ml of water. Then, add a base (e.g., NaOH), until the pH is exactly 7.4. Then, quantitatively transfer the solution to a volumetric flask. Finally, dilute to the volumetric mark and mix.[1]

By increasing the buffer concentration, the concentration of the counterions are increased in the mobile phase and stronger competition is provided between the sample components and the counterions for the exchangeable ionic centers, resulting in reduced solute retention.[5] As stated

Table 1 Typical buffers for ion-exchange chromatography.

Buffer salt	pH Range
Ammonia	8.2–10.2
Ammonium acetate	8.6–9.8
Ammonium phosphate	2.2–6.5
Citric acid	2.0–6.0
Disodium hydrogen citrate	2.6–6.5
Potassium dihydrogen phosphate	2.0–8.0/9.0–13
Potassium hydrogen phthalate	2.2–6.5
Sodium acetate	4.2–5.4
Sodium borate	8.0–9.8
Sodium dihydrogen phosphate	2.0–6.0/8.0–12
Sodium formate	3.0–4.4
Sodium perchlorate	8.0–9.8
Sodium nitrate	8.0–10.0
Triethanolamine	6.7–8.7

earlier, selectivity and retention can also be adjusted by changing the pH of the mobile phase. This occurs because such a change in pH modifies the character of both the ionexchange medium and the acid–base equilibrium as well as the degree of ionization of the sample.[3] A pH gradient in which the pH of the mobile phase is changed during the chromatographic analysis can also be used to control the solvent strength and retention of ionic solutes. Such gradients can also be used to control selectivity.[6]

The working pH range for a separation can be estimated from the pK_a values of the sample components. If such pK_a values are not available, they can often be estimated by considering the number and types of functional groups present and the molecular structures of the components in the sample.[1] In order to ensure that solutes are ionized and retained by the ion exchanger, the optimum buffer pH of the mobile phase should be 1 or 2 pH units above the pK_a of acids and 1 or 2 pH units below the pK_a of bases.[3]

Two criteria should be met when choosing the components of the buffer. First, the buffer must be able to maintain the operating pH for the separation to be performed. Second, the exchangeable buffer counterion must yield the desired eluent strength.[3] Some common buffer salts used in ion-exchange chromatography and their usable pH ranges are summarized in Table 1. Examples of their use includes the chromatography of amino acids, polymeric, cation exchanger using various combinations of citrate and borate buffer.[3] Additionally, carbohydrates can be separated by anion-exchange chromatography using an aqueous solution of sodium hydroxide–sodium acetate as the eluent.[3] Being weak acids, the ion-exchange behavior of such compounds is significantly affected by the pH of the mobile phase. Similar separations of ionizable compounds through the use of ion-exchange chromatography with these and other buffers have been reported.[1–7]

ACKNOWLEDGMENT

The author wishes to thank H. Seegulum for technical assistance.

REFERENCES

1. Harris, D.C. *Quantitative Chemical Analysis,* 5th Ed.; W.H. Freeman: New York, 1998; 755–766.
2. Walton, H.F. *Ion-Exchange Chromatography*; Hutchinson and Ross: Dowden, U.K., 1976.
3. Poole, C.F.; Poole, S.K. *Chromatography Today*; Elsevier: New York, 1991; 422–439.
4. Small, H. *Ion Chromatography*; Plenum: New York.
5. Gjerde, D.T.; Fritz, J.S. *Ion Chromatography,* 2nd Ed.; Huthig: New York, 1987.
6. Snyder, L.R.; Kirkland, J.J. *Introduction to Modern Liquid Chromatography,* 2nd Ed.; John Wiley & Sons: New York, 1979; 410–452.
7. Rieman, W.; Walton, H.F. *Ion Exchange in Analytical Chemistry*; Pergamon Press: New York, 1976.

Ion-Exchange Resins: Inverse GC

Piotr Słomkiewicz
Zygfryd Witkiewicz
Institute of Chemistry, Jan Kochanowski University, Kielce, Poland

INTRODUCTION

Over the last 20 years ion exchange resins have been used more and more frequently as active catalysts of a number of reactions on a commercial and a laboratory scale.[1] Investigations need defining adsorption equilibrium constants of reactants and adsorption model, as well as determining equilibrium constants of these reactions. In this paper, measuring methods that favor the investigation of catalytic reactions on ion exchange resins using inverse gas chromatography are described.

DETERMINATION OF ADSORPTION ISOTHERMS OF REAGENTS ON ION EXCHANGE RESINS

Being active catalysts of a number of reactions, ion exchange resins are also adsorbents. The determination of adsorption isotherms of reactants on ion exchange resins can be made by the peak profile method, using inverse gas chromatography. It is also possible to determine whether a catalytic reaction likely to accompany adsorption occurs during the measurement of adsorption.

Apparatus

The apparatus for determining the isotherm of adsorption using gas chromatography is shown in Fig. 1. In the apparatus, two gas chromatographs are used, one with a thermoconductivity detector for adsorption investigation and the other with a flame ionization detector for analytical purpose. The apparatus contains three identical carrier gas tracks. Each gas track contains an electromagnetic valve (1), a flow stabilizer (2), and a needle valve (3). These gas tracks supply the detectors in two gas chromatographs. The injector (4) is used to introduce adsorbate samples into a sorption pipe (5) containing the investigated ion exchange resin. The carrier gas flowing out of the sorption pipe is introduced to the thermoconductivity detector (8). The comparative chamber of the thermoconductivity detector is supplied with the carrier gas from the other injector (6) and the tube (7) containing reference sample of exchange resin.

The second gas chromatograph was used for detecting possible products of a catalytic reaction of adsorbate on the surface of ion exchange resin. The carrier gas containing desorbed adsorbate, and possible products of the catalytic reaction on adsorbent, flows out of the thermoconductivity detector and can be flowed through the six-port valve (10) and the four-port valve (11) immediately to a sample injector (12) and a chromatographic column (13) for

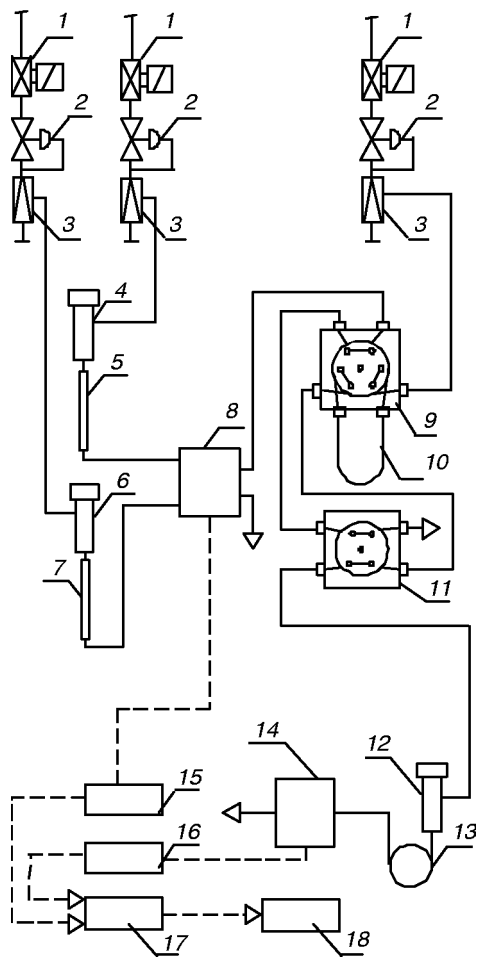

Fig. 1 Scheme of apparatus for adsorption measurement. (1) Electromagnetic valve; (2) flow stabilizer; (3) needle valve; (4), (6), (12) injector; (5), (7) sorption pipe; (8) thermal conductivity detector; (9), (11) six-port valve; (10) freezing capillary; (13) chromatography column; (14) flame ionization detector; (15) amplifier; (16) electrometer; (17) analog-to-digital converter; (18) computer.

analysis. A six-port valve (10) with a freezing capillary (10) for taking samples of adsorbate and products of the above-mentioned catalytic reactions can also be used before their injection into a chromatographic column (13). This column is connected to the flame ionization detector (14). Voltage from the amplifier (15) and the electrometer (16) are directed to the analog-to-digital converter (17) and the computer (18).

The measurement of adsorption is taken by injecting with a syringe a sample of adsorbate through the injector (4) into the sorption pipe (5), containing ion exchange resin and the adsorbate peak is recorded after it flows through the adsorbent by the thermoconductivity detector (8) (Fig. 2). The adsorbate flowing out of the detector is collected in a freezing capillary connected to the six-port valve (10). The heating of the capillary and its inclusion in the carrier gas track of a gas chromatograph with a flame ionization detector by means of the six-port valve (10) make it possible to analyze the composition of the sample collected in the capillary. When products of its catalytic reaction on ion exchange resin are found in a sample of adsorbate, the results of adsorption measurement are incorrect.

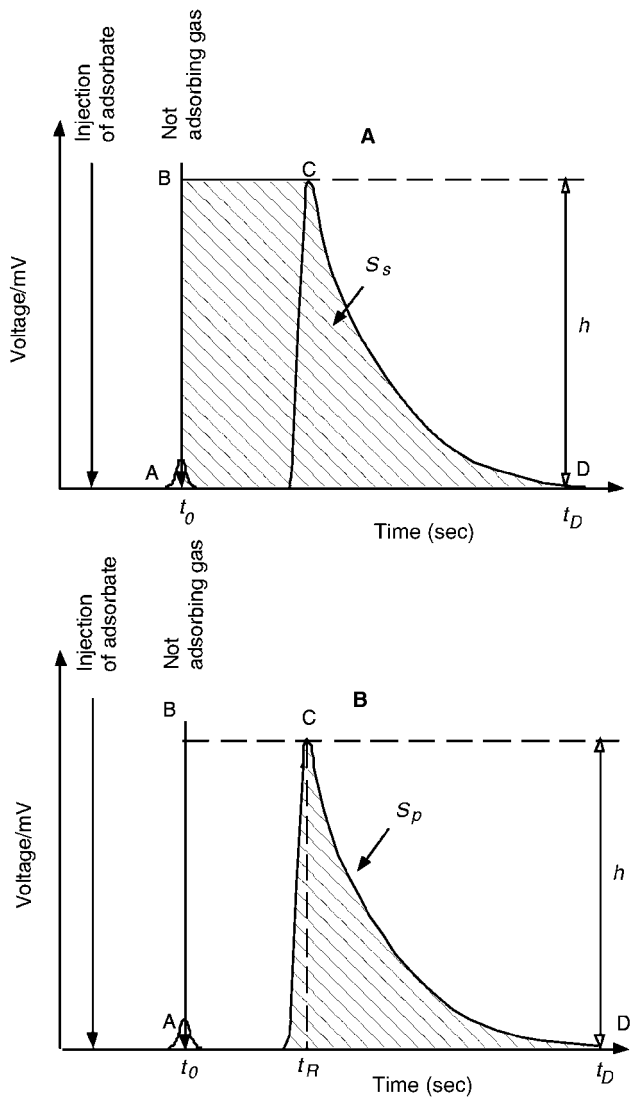

Fig. 2 The method of determination of adsorption data from chromatographic peak. (A) S_s, total adsorption area ABCD; (B) S_p, area of adsorption peak.

Method of Calculations

The method of measuring the quantities of adsorption and partial pressure of adsorbates is described in the work.[2]

The quantity of the adsorption a_i of the substance I, at the equilibrium concentration of adsorbate c_i in the gas phase, is expressed by the following equation:

$$\frac{da_i}{dc_i} = \frac{V_R}{m} \tag{1}$$

where a_i, quantity of moles of adsorbate i [mol/g]; c_i, equilibrium concentration of substance i in gas phase [mol/cm]; m, mass of adsorbent [g]; V_R, retention volume [cm^3].

From Eq. 1 it can be written:

$$a_i = \frac{1}{m}\int_0^{c_i} V_R dc_i \tag{2}$$

Retention volume V_R is expressed by the equation:

$$V_R = t_R F \tag{3}$$

where F, flow rate of carrier gas [cm^3/sec]; t_R, retention time of adsorbate peak [sec].

Detector constant k [mol/cm/mV] necessary for calculations is expressed by the following equation:

$$k = \frac{c_i}{h} \tag{4}$$

where h, height of peak [mV].

The total adsorption surface S_s is the area between points ABCD in Fig. 2.

The area of adsorption surface S_s [mV sec] is defined by the equation:

$$S_s = \int_0^h (t_D - t_0)dh \tag{5}$$

where t_0, hold up time [sec]; t_D, time from the introduction of adsorbate onto the adsorbent to the completion of recording the peak [sec].

After introducing Eqs. 3 and 4, transformed to form $dc_i = kdh$ into Eq. 2, it may be obtained:

$$a_i = \frac{kF}{m}\int_0^h (t_D - t_0)dh \tag{6}$$

And after the integration of Eq. 6 and introducing Eq. 5, it may be obtained:

$$a_i = \frac{kF}{m}S_s \tag{7}$$

The dependence between the quantity of moles n of the injected substance i and the area of chromatographic peak surface corresponding to it (Fig. 2) is expressed by the equation:

$$n = kF\int_0^t hdt = kFS_p \tag{8}$$

where n, quantity of moles of substance i injected on adsorbent [mol]; S_p, total surface of chromatographic peak [mV sec].

Determining the constant of the detector k from Eq. 8 and putting it into Eq. 7, it may be obtained:

$$a_i = \frac{nS_s}{mS_p} \tag{9}$$

Eq. 9 is used to determine from a chromatogram the value of adsorption at specific temperature.

Determining the constant of the detector k from Eq. 8 and putting it into Eq. 4, it may be obtained:

$$c_i = \frac{nh}{FS_p} \tag{10}$$

which can be transformed into the form, making it possible to calculate the equilibrium pressure p_i:

$$p_i = \frac{nh}{FS_p}RT \tag{11}$$

where p_i, partial pressure of adsorbate i [Pa]; R, gas constant [cm^3 Pa/K/mol]; T, temperature of measurement, [K].

As a result, the dependence $a_i = f(p_i)$ being the function of the adsorption isotherm may be obtained. For the determination of this isotherm points the introduction series of samples of adsorbate of different quantity into a sorption pipe is given. One sample of definite quantity of adsorbate corresponds with one point of the isotherm. The method of determining adsorption isotherms mentioned above is a general method used in investigating a great number of adsorbents.

THE VERIFICATION OF THE ADSORPTION MODEL OF REAGENTS ON ION EXCHANGE RESINS

The determination of the number of adsorption sites by the adsorption of adsorbate on ion exchange resin by inverse gas chromatography consists in saturating this resin with vapors of adsorbate under definite conditions of temperature and pressure. Next, an excess of adsorbate is removed from the ion exchange resin by blowing inert gas through its bed and the desorption of adsorbate during the programmed increase of temperature.[3]

Apparatus

The apparatus for investigation is presented in Fig. 3. The carrier gas of the measurement track flows through the electromagnetic valve (1), the flow stabilizer (2) and the needle valve (3). A six-port valve (4) serves to change over the flow of carrier gas and the flow of auxiliary gas, which contains vapors of adsorbate. Both of these flows could be directed through the chamber of the injector (5) to the sorption pipe (6), in which the investigated sample of ion exchange resin is placed. Auxiliary gas flowed by electromagnetic valve (7), flow stabilizer (8), and needle valve (9), is saturated with vapors of adsorbate in the reservoir for vaporizing (10). The reservoir is switched on in the auxiliary gas track by the six-port valve (11). The reference system is made by the parallel track of carrier gas flowed by electromagnetic valve (12), flow stabilizer (13), needle valve (14), and the chamber of the injector (15) with the pipe (16), in which the reference sample of ion exchange resin is placed. From the sorption pipes (6), (16), the carrier gases of the measurement track and of the reference track are introduced into the thermal conductivity detector (17). The electric signal from detector is amplified in the amplifier (18), and is directed to the analog-to-digital converter (19) and the computer (20).

The chromatographic analysis is used to control whether, in desorbed gases, the products of the possible catalytic reaction on ion exchange resin occur or not. The analytical gas chromatograph, is supplied with carrier gas by electromagnetic valve (21), flow stabilizer (22), and needle valve (23). The desorbed gases from thermal conductivity detector (17) are flown immediately by four-port valve (24) to the sample injector (25) and the chromatography column (26) connected with flame ionization detector (27). The six-port valve (24) with freezing capillary (28) is used to improve the conditions of chromatography analysis in the case of considerably stretched desorption peaks. Electric signals from the electrometer (29) are directed to the analog-to-digital converter (19) and the computer (20).

The measurement of adsorption on ion exchange resin needs preparing a samples series of this resin with different quantities of deactivated functional groups. The deactivation of functional groups consists in their blocking so as not to let them participate in adsorption. The deactivation of sulfonic groups of ion exchange resin can be quantitatively made by a base, (e.g., NaOH). Each sample of the series should be introduced into the sorption pipe (6). Once ion exchange resin is saturated with adsorbate steams at a given temperature, the sorption pipe should be blown through with

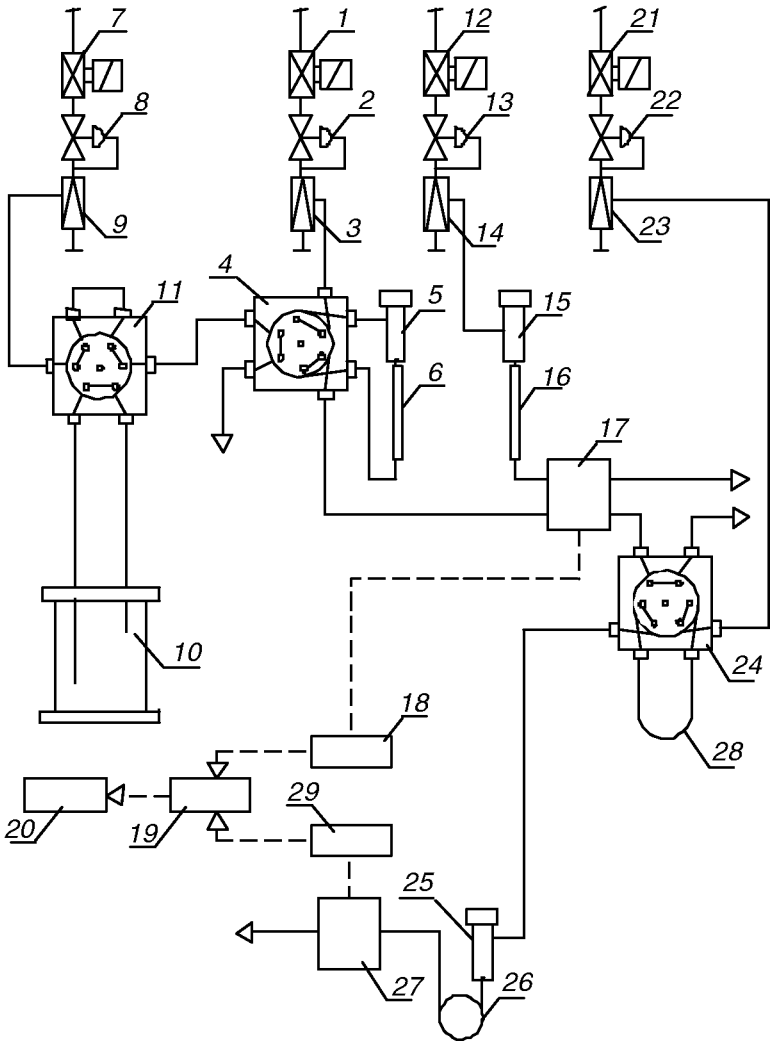

Fig. 3 Apparatus set for the determination of the adsorption model of adsorbate on ion exchange resin by inverse gas chromatography. (1), (7), (12), (21) Electromagnetic valve; (2), (8), (13), (22) flow stabilizer; (3), (9), (14), (23) needle valve; (4), (11), (24) six-port valve; (5), (15), (25) injector; (6), (16) sorption pipe; (10) reservoir for vaporizing; (17) thermal conductivity detector; (18) amplifier; (19) analog-to-digital converter; (20) computer; (26) chromatography column; (27) flame ionization detector; (28) freezing capillary; (29) electrometer.

inert gas as long as adsorbate excess is removed from the resin bed. The thermoconductivity detector (17) is used to check whether the adsorbate is completely rinsed out of the sorption pipe (6) with carrier gas. Next, the thermodesorption of adsorbate from the resin bed is carried out using a programmed increase of temperature. Desorbed adsorbate is collected in a freezing capillary (28) connected to the six-port valve (24). The heating of the capillary, and its inclusion in the gas carrier track of a gas chromatograph with a flame ionization detector by the six-port valve (24), makes it possible to analyze the composition of the sample collected in the capillary. When products of its catalytic reaction on ion exchange resin are found in a sample of adsorbate, the results of adsorption measurement are incorrect.

Method of Calculations

The adsorption of a single molecule of adsorbate (A) without dissociation through a number (n) of functional groups (s) of ion exchange resin proceeds in accordance with the reaction:

$$A + ns \rightleftharpoons A - ns \tag{12}$$

whose course can be shown by the equation:

$$\frac{c_A}{c_L} = \frac{(K_A p_A)^{1/n}}{[1 + (K_A p_A)^{1/n}]} \tag{13}$$

where c_A, concentration of adsorbate adsorbed by functional groups of ion exchange resin (mmol/g); p_A, mean partial pressure of adsorbate (kPa); K_A, constant of adsorption of adsorbate (kPa^{-1}); c_L, ion-exchange capacity of ion exchange resin after partial deactivation (mmol/g), and the deactivation degree of functional groups x of ion exchange resin is expressed by the following formula:

$$x = \frac{c_L}{c_L^0} \tag{14}$$

where c_L^0, total ion-exchange capacity of ion exchange resin [mmol/g].

Changes of concentration of the adsorbate, adsorbed by functional groups in the function of the change of the partial pressure of the adsorbate, for a series of ion exchange resins of the different content of functional groups can be expressed as the following function:

$$\frac{dc_A}{dp_A} = f(K_A, x^n) \tag{15}$$

The number of functional groups n formed an adsorption complex with one molecule of the adsorbate can be determined from this function after its differentiation in relation to dp_A and linear representation.

After the differentiation of Eq. 13 in relation to dp_A within the range of $p_A \rightarrow 0$ and the introduction of

$$m = \frac{1}{n} \tag{16}$$

instead of n, it is obtained:

$$dc_A = c_L(K_A p_A)^m dp_A = x c_L^0 K_A^m (p_A)^m dp_A \tag{17}$$

Assuming that $K_A^m = \text{const.}$ within the range of small partial pressures of adsorbate:

$$\frac{dc_A}{m(p_A)^{m-1} dp_A} = K_A^m c_L^0 x \tag{18}$$

and after taking a logarithm of both members of the equation, for $m = 1$ it is obtained:

$$log(c_A) = m\ log(x) + log\left(K_A^m c_L^0\right) \tag{19}$$

for $m = 2$ it is obtained:

$$log\left(\frac{c_A}{p_A}\right) = m\ log(x) + log\left(K_A^m c_L^0\right) \tag{20}$$

for $m = 3$ it is obtained:

$$log\left(\frac{c_A}{p_A^2}\right) = m\ log(x) + log\left(K_A^m c_L^0\right) \tag{21}$$

The mean equilibrium pressure p_A corresponding with the concentration of adsorbate in the gas phase during the thermal desorption at the temperature range ΔT can be determined by the following formula:

$$p_A = \frac{Rf(S_i)\Delta T}{V} \tag{22}$$

where R, gas constant; ΔT, the temperature range where the thermal desorption peak appears [K]; V, the retention volume of the peak [cm^3]; $f(S_i)$, the quantity of adsorbate moles calculated on the basis of the surface of the peak from the calibration curve [mmol].

According to Eq. 12 it was assumed that the quantity of adsorbate moles adsorbed by ion exchange resin depends on the number of functional groups participating in adsorption. Therefore, the dependence between the quantity of adsorbed adsorbate and the deactivation degree of functional groups of ion exchange resin can be searched for. The independent variable in Eqs. 19–21 is a logarithm of the deactivation degree of functional groups x (Eq. 14), and the dependent variable is a logarithm of the concentration c_A of the adsorbate adsorbed by functional groups of ion exchange resin (Eq. 19) or the quotient of adsorbate concentration c_A and the mean partial pressure p_A raised to a definite power (Eqs. 20 and 21). Eqs. 19-21 are equations of straight lines. The verification of the adsorption model consists in checking which of these equations correlates with the results of adsorption measurements on a series of samples prepared from ion exchange resin with partially deactivated functional groups. The correctness of the adsorption model assumed can be determined by the slope of straight line.

DETERMINATION OF EQUILIBRIUM CONSTANT OF CATALYTIC REACTION ON ION EXCHANGE RESINS

The method described here is used for determining the equilibrium constant of the reaction catalyzed by ion exchange resin. It consists in preparing a reaction mixture of definite molar composition and in introducing it into a reactor (column) with ion exchange resin. Once the equilibrium between reactants of the catalytic reaction is obtained, carrier gas is passed through the column and the composition of the equilibrium mixture is analyzed by gas chromatograph.

Apparatus

The method used relay on introducing into an injector with syringes the standard of substrates and products of the catalytic reaction at the stoichiometric ratio. The injection of reactants with syringes makes it possible to proportion the composition of the mixture freely and to obtain high-composition reproducibility of prepared mixtures. During the injection of reactants, the injector is disconnected from the carrier gas flow (i.e., reactants are arrested in it). The scheme of the injection method is shown in Fig. 4. The injector (1) is connected to the three position six-port valve (2). This valve is fed through two gas tracks—carrier gas track and auxiliary gas track. In position A, the six-port valve (2) disconnects the injector (1) from the carrier gas track and the auxiliary track. In this particular position, samples of reactants can be injected with a syringe. Position B of the six-port valve (2) is used to introduce

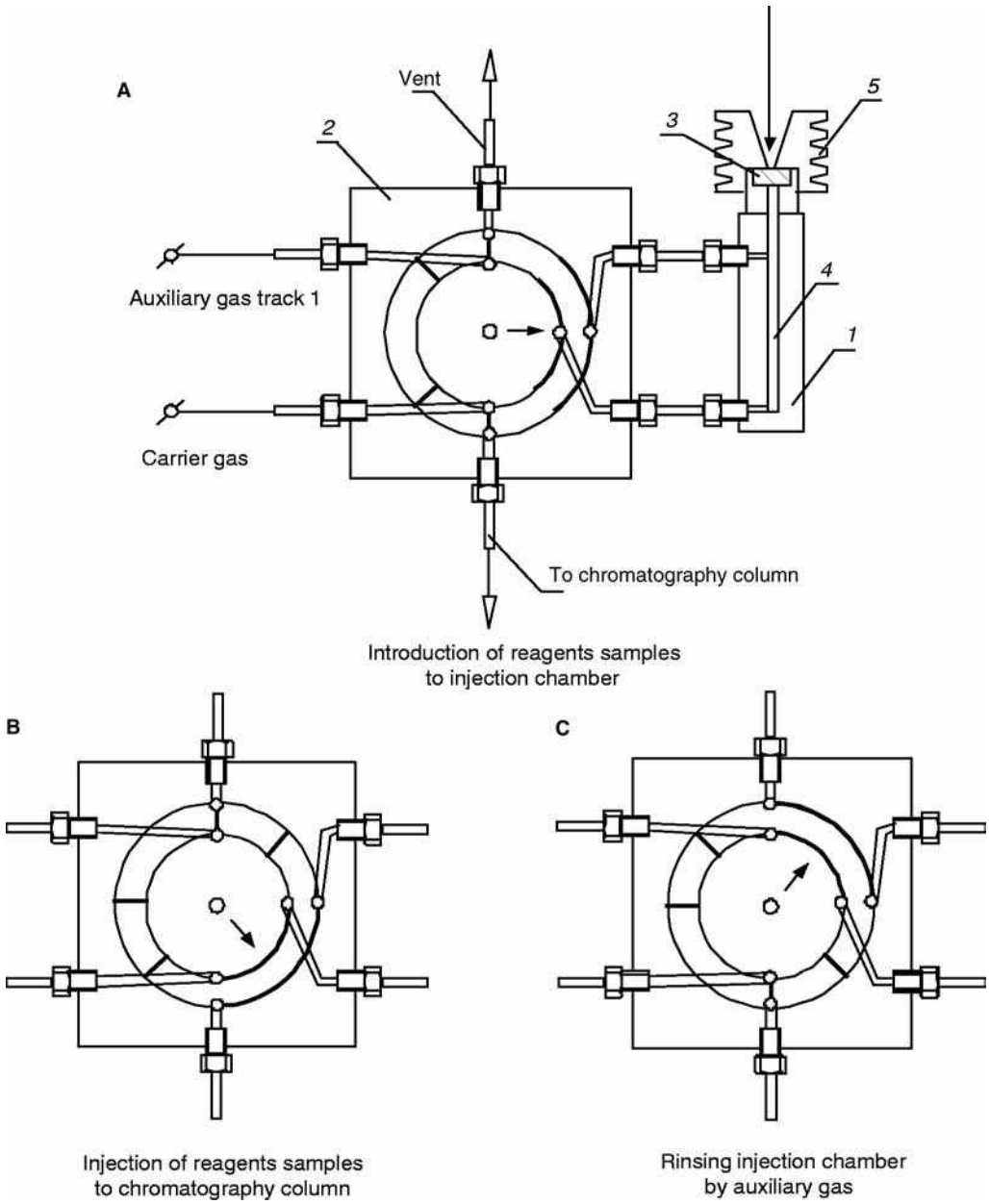

Fig. 4 Three position six-port valve with injection chamber. (1) Injector; (2) three position six-port valve; (3) septa; (4) injector chamber; (5) nut.

reactants from the injector (1) into the carrier gas of the chromatograph, and position C is used to wash the injector with auxiliary gas from track (1). The scheme of apparatus for determining equilibrium constants is given in Fig. 5. Reactants from the injector (5) (1 in Fig. 4) flow together with carrier gas into the column (10) containing ion exchange resin through the three position six-port valve (4) (2 in Fig.4) and through the six-port valve (9). By means of the six-port valve (9) it is possible to disconnect the flux of carrier gas from the column (10). This procedure makes it possible to specify the conditions under which the equilibrium between the injected reactants of the catalytic reaction taking place on ion exchange resin is attained. The switch-over of the six-port valve (9) makes it possible to transfer reactants in the flow of carrier gas through the thermoconductivity detector (16) into the freezing capillary (17) with the six-port valve (18) where the reactants are arrested. The thermoconductivity detector (16) is used to check whether the reactants are completely rinsed out of the column (10) with carrier gas. The electromagnetic valve (11), the flow stabilizer (12), the needle valve (13), the injector (14), and the column with ion exchange resin (15) make up the gas track supplying the comparative chamber of the thermoconductivity detector (16) with

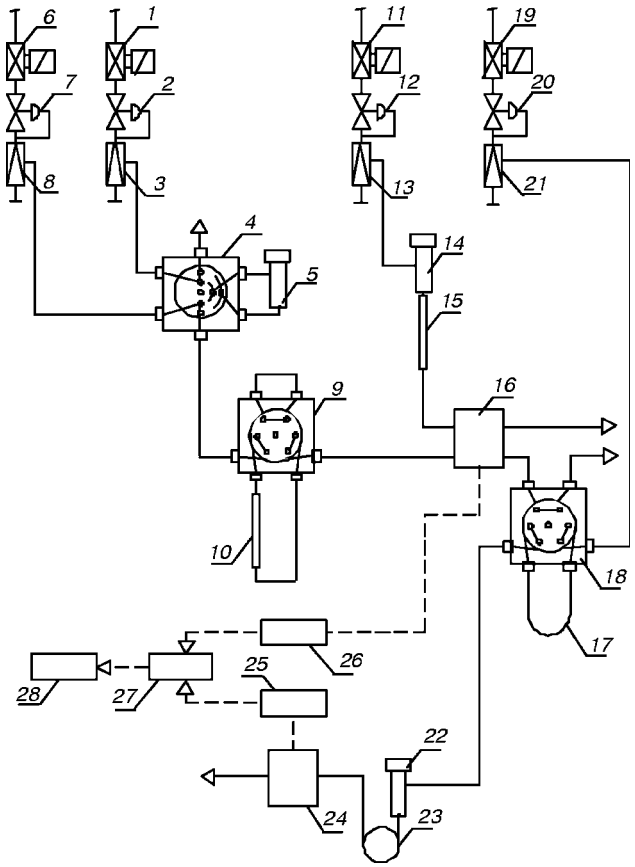

Fig. 5 Scheme of apparatus for the determination of reaction equilibrium constant. (1), (6), (11), (19) Electromagnetic valve; (2), (7), (12), (20) flow stabilizer; (3), (8), (13), (21) needle valve; (4) three position six-port valve; (5), (14), (22) injector; (10), (15) column with catalyst; (9), (18) six-port valve; (16) thermal conductivity detector; (17) freezing capillary; (23) chromatography column; (24) flame ionization detector; (25) electrometer; (26) amplifier; (27) analog-to-digital converter; (28) computer.

carrier gas. The analytical gas chromatograph is supplied with carrier gas by the electromagnetic valve (18), the flow stabilizer (20), and the needle valve (21). The switch-over of the six-port valve (18) makes it possible to direct the reactants from the capillary (17), together with carrier gas, through the injector (22) into the chromatographic column (23) and the flame ionization detector (24). The electric signals from the electrometer (25) of the flame ionization detector and from the amplifier (26) of the thermoconductivity detector are directed into the analogue-to digital converter (27) and the computer (28).

When the reactants are introduced into the column (10) containing ion exchange resin and the flow of carrier gas is cut off, the column acts as a stationary catalytic reactor and the attainment of the equilibrium in it is a time function. It is important to check whether there is equilibrium between the reactants of the reaction taking place on ion exchange resin. It can be done by comparing the results of measurements of reactant concentrations obtained for different times of the catalytic reaction taking place in the column. If the results of measurements are the same, it can be assumed that the reactants of the catalytic reaction taking place on ion exchange resin have reached equilibrium and the results obtained can be used to calculate the equilibrium constant of the reaction.

Method of Calculations

The equation of the reaction between the substrates A and B, as well as the products C and D, can be expressed as follows:

$$aA + bB \rightleftharpoons cC + dD \tag{23}$$

The quantities of reactants used to measure equilibrium are as follows: n_A^0, quantity of substrate moles A [mol]; n_B^0, quantity of substrate moles B [mol]; n_C^0, quantity of product moles C [mol]; n_D^0, quantity of product moles D [mol].

The total quantity of reactant moles present in the column is expressed by the equation:

$$n_T = n_A^0 + n_B^0 + n_C^0 + n_D^0 \tag{24}$$

The quantities of reactants determined when equilibrium has been reached: n_A, quantity of reactant moles B [mol]; n_B, quantity of reactant moles B [mol]; n_C, quantity of reactant moles C [mol]; n_D, quantity of reactant moles D [mol].

The equilibrium constant of the reaction can be calculated from the equation:

$$K = \frac{\left(\frac{n_C}{n_T}\right)^c \left(\frac{n_D}{n_T}\right)^d}{\left(\frac{n_A}{n_T}\right)^a \left(\frac{n_B}{n_T}\right)^b} \tag{25}$$

REFERENCES

1. Chakrabarti, A.; Sharma, M.M. Cationic ion-exchange resins as catalyst. React. Polym. **1993**, *20*, 1–45.
2. Paryjczak, T. *Gas Chromatography in Adsorption and Catalysis*; Halsted Press: New York, 1986.
3. Słomkiewicz, P.M. Determination of the adsorption model of alkenes and alcohols on sulfonic copolymer by inverse gas chromatography. J. Chromatogr. A, **2004**, *1034*, 169.

Ion-Exchange Stationary Phases

Karen M. Gooding
Eli Lilly and Company, Indianapolis, Indiana, U.S.A.

INTRODUCTION

In ion-exchange chromatography (IEC), molecules bind by the reversible attraction of electrostatic charges located on the outer surface of a solute molecule with dense clusters of groups with an opposite charge on an ion-exchange support. To maintain electrical neutrality, the charges on both the analytes and the matrix are associated with ions of opposite charge, termed counterions, which are either provided by preequilibration with the mobile phase or during manufacturing. Because a solute must displace the counterions on the matrix during attachment, the technique is termed "ion exchange." If the support possesses a positive charge, it is used for anion-exchange chromatography, whereas if it carries a negative charge, it is for cation exchange. Generally, the molecule of interest will have a charge that is opposite (positive or negative) to that on the support and the same as the competitively displaced counterions.

There are several major variables which distinguish ion-exchange packings and determine their utility for specific classes of solutes and for analytical or preparative applications. Those variables are as follows:

1. Structure of the bonded phase, including the chemistry of the functional group, its p*K*, and the properties of the spacer arm and/or bonded phase layer.
2. Charge density and related nominal capacity.
3. Properties of the support matrix, including composition and pore diameter.

BONDED PHASE

Functional Groups

The functional groups of an ion-exchange bonded phase are ionizable under specific pH conditions. The extent of their charge dependence on pH is the basis for distinguishing two types of ion exchangers—strong and weak. These designations do not refer to the strength of binding or to the capacity of the gel, but simply to the p*K* of the ionizable ligand group, similar to the designations for acids and bases. The structures and approximate p*K* and pH ranges of some typical strong and weak ion-exchange groups are shown in Table 1.[1–5]

Generally, strong ion-exchange groups retain their charge over a wide range of pH, with binding capacity dropping off at the extremes. For example, quaternary ammonium (Q) resins are strong anion-exchange groups which are effective throughout the pH range of about 2–12. Similarly, sulfonyl groups are strong cation-exchange groups that remain negatively charged until acidic pH levels are used. Strong ion-exchange groups can be considered to possess a permanent positive or negative charge.

The diminished ionization of weak ion-exchange groups near neutral pH result in less predictable separations if operation in this range is necessary for analyte stability, as in the case of many proteins. In these cases, the use of a strong ion exchanger allows the pH of the mobile phase to be manipulated to protonate or deprotonate the analytes without changing the ionic properties of the packing. For example, certain amino acids are most highly charged at pH less than 4, where a weak cation-exchange support would not be fully charged, but a strong cation-exchange group would.

Because weak ion-exchange groups are not fully charged in certain pH ranges, column equilibration may require more mobile phase or time under those conditions. Conversely, highly bound molecules may release more easily from supports which are not totally ionized. Clearly, careful consideration of the titration curves for an ion-exchange support is an essential aspect of designing appropriate conditions for a separation. A complete description of the charged group of an ion exchanger is necessary to understand its pH characteristics because they are dependent on the exact chemical composition of the bonded phase and the matrix. Convenient descriptions such as "strong," "S," "stable weak ion-exchange," and so forth do not sufficiently describe the ionic characteristics of the packing. The exact p*K* and functional pH range are also affected by the chemistry of the remainder of the bonded phase and of the matrix. For example, a silica matrix may ion-pair with cationic functional groups or a polymeric layer with amines may ion-pair with anionic functional groups. The actual titration curves, p*K*, and/or pH range for a given support should always be consulted.

Hydrophobic Spacer Arms

Ion-exchange functional groups are chemically bonded to the support, often through a polymeric layer which totally

Table 1 Properties of ion-exchange groups.

	Functional group	Type	p*K*	pH Range (approximate)
Anion exchange				
DEAE (diethylaminoethyl)	$–O–CH_2–CH_2–N^+ H(CH_2CH_3)_2$	Weak	15–9	2–9
PEI (polyethyleneimine)	$(–NHCH_2CH_2)_n–N(CH_2CH_2–)_{n'}$ $CH_2CH_2NH_2$	Weak	15–9	2–9
Q (quaternary ammonium)	$–CHOH–CH_2–N^+(CH_3)_3$	Strong	>13	2–12
Cation exchange				
CM (carboxymethyl)	$–O–CH_2–COO^-$	Weak	14–6	6–10
SP (sulfopropyl)	$–CH_2–CH_2–CH_2SO_3^-$	Strong	<1	4–13
S (sulfonate)	$–R–CH_2SO_3^-$ (R may be methyl with hydroxyl or amide groups)	Strong	<1	3–11

covers the matrix. The chemical nature of this coupling chemistry and its spatial characteristics can affect the chromatographic properties. Hydrophobic linkages may impart a non-polar aspect to the separations. Spacer arms make the functional groups more accessible by distancing them from the support surface. Tentacle IEC bonded phases are a spacer design incorporating a hydrophilic ligand arm.[6]

Charge Density

The number of charges, as measured by titration, defines the nominal capacity of a support. the charge density of an ion-exchange support is determined by the number of ionic groups divided by the surface area or the volume. Typical values range from 3 to 370 μEq/ml of support. The lower values are generally found in non-porous supports. High loading capacities are associated with IEC, especially for porous supports. Weak ion-exchange groups only have maximum capacity in the pH range where they maintain charge -pH less than 9 for DEAE supports and pH greater than 6 for CM.

Counterions

In certain cases, ion-exchange columns are preequilibrated with distinct counterions by the manufacturer. These ions, such as calcium for amino acids, impart a specific selectivity (see *Ion Exchange: Mechanism and Factors Affecting Separation*, p. 1258). Alternatively, a layer of counterions is applied by the user by conditioning a column with the salt of interest. An intermediate step of washing with a weak acid may accelerate the equilibration process.

MATRIX

Composition

Ion-exchange supports based on derivatized cellulose and agarose have been popular since the 1960s, particularly for protein analysis. For high-performance liquid chromatography (HPLC), less compressible supports, such as silica and cross-linked polymers, are most commonly used.

Carbohydrate Matrix

Carbohydrate supports such as dextran or agarose are very hydrophilic and easily derivatized with ionic functional groups. They have been very popular for analysis and purification of biological molecules like proteins. One major drawback to these supports is that their volume changes with mobile-phase composition. This has been alleviated in part by higher cross-linking.

Silica Matrix

In silica-based ion exchangers, the silica is bonded through a polymeric layer to a charged ligand group. Operating pH is generally limited to pH 2–8 due to the silica backbone. Although some small-pore silica-based ion exchangers have been synthesized with silane bonding, large-pore supports ($\geq$ 300 Å) designed for protein analysis have polymeric layers containing ionic functional groups which are very stable and even protect the silica matrix from erosion. Silica columns have several advantages:

1. High mechanical stability
2. Minimal shrinkage or swelling with changes in counterions
3. Stability to organic modifiers (with the restriction of salt solubility)
4. High capacity
5. Good mass transfer
6. Large variety of particle and pore sizes.

Polymeric Matrix

Polymeric matrices are also widely available for IEC. Polystyrene cross-linked with divinylbenzene (PSDVB) is one such polymer, typically available with pore diameters of

at least 1000 Å. The repetitive structure of polystyrene permits reproducible coupling of both strong and weak ion-exchange groups; cross-linking adds the rigidity required for high-pressure applications. These polymeric supports have most of the same advantages as silica for IEC. Methacrylate copolymers, which are also used as matrices in IEC, are more hydrophilic than PSDVB.

Pellicular Matrix

A third group of ion-exchange supports are pellicular, consisting of a solid inert core made of PSDVB agglomerated with 350 nm functionalized latex. The quaternary amine groups are closely and uniformly bound on the microbeads, improving flow and reducing non-specific retention. These pellicular supports are primarily used for carbohydrate analysis.[7]

Pore Diameter

Pore diameter is a major determinant in ion-exchange capacity because as the pore diameter decreases, there is a tremendous increase in surface area. Nominal loading capacity is directly related to the surface area and the ligand density; consequently, matrices with the smallest pores exhibit the highest ion-exchange capacities for small, totally included solutes.

The ion-exchange capacities of picric acid correlate with surface area. For example, that of a 100 Å pore was seen to be 1415 μmol/g, whereas that of a 300 Å pore was only 656 μmol/g.[8] The capacities for macromolecules such as proteins do not relate directly to surface area because they are excluded by size from portions of small pores and are effectively prevented from reaching all the reactive exchange sites.[5,8] Consequently, larger pores exhibit maximum capacity for macromolecules. For example, a 300Å pore exhibited maximum capacities of 98 and 130 mg/g for ovalbumin (45,000 MW) and bovine serum albumin (65,000 MW) respectively, because they were able to permeate and bind to the optimum available surface area.[5,8]

REFERENCES

1. Cunico, R.L.; Gooding, K.M.; Wehr, T. Ion-exchange chromatography. In *Basic HPLC and CE of Biomolecules*; Bay Bioanalytical Laboratories: Richmond, VA, 1998.
2. *Ion-Exchange Chromatography Principles and Methods;* Pharmacia Biotech.: Sweden.
3. Katz, E.D., Ed.; In *High Performance Liquid Chromatography: Principles and Methods in Biotechnology*; John Wiley & Sons: New York, 1996.
4. Aguilar, M.I.; Hodder, A.N.; Hearn, M.T.W. HPIEC of proteins. In *HPLC of Proteins, Peptides and Polynucleotides*; Hearn, M.T.W., Ed.; VCH: New York, 1991; 199.
5. Mant, C.T., Hodges, R.S., Eds.; In *High-Performance Liquid Chromatography of Peptides and Proteins*; CRC Press: Boca Raton, FL, 1991.
6. Muller, W. New ion exchangers for the chromatography of biopolymers. J. Chromatogr. **1990**, *510*, 133.
7. Analysis of Carbohydrates by HPAE-PAD, Technical Note 20, Dionex. 1993.
8. Vanecek, G.; Regnier, F.E. Variables in the high-performance anion-exchange chromatography of proteins. Anal. Biochem. **1980**, *109*, 345.

BIBLIOGRAPHY

1. Nowlan, M.P.; Gooding, K.M. HPIEC of proteins. In *High-Performance Liquid Chromatography of Peptides and Proteins*; Mant, C.T., Hodges, R.S., Eds.; CRC Press: Boca Raton, FL, 1991; 203.

Ion-Exclusion Chromatography

Ioannis N. Papadoyannis
Victoria F. Samanidou
Laboratory of Analytical Chemistry, Chemistry Department, Aristotle University of Thessaloniki, Thessaloniki, Greece

INTRODUCTION

Ion exclusion is the term that describes the mechanism by which ion-exchange resins are used for the fractionation of neutral and ionic species. Ionic compounds are rejected by the resin, due to Donnan exclusion, and they are eluted in the void volume of the column. Non-ionic or weakly ionic substances penetrate into the pores of the packing, they are retained and, thus, separation is achieved, as they partition between the liquid inside and outside the resin particles.

Ion-exclusion chromatography is a mode of high-performance liquid chromatography (HPLC) and, thus, the same equipment can be used, with the proper eluent, column, and detection technique. The technique is mostly used for the analysis of organic acids, sugars, alcohols, phenols, and organic bases. It provides a convenient way to separate molecular acids from highly ionized substances. Ionized acids pass rapidly through the column while molecular acids are held up to varying degrees. A conductivity detector is commonly used. Carboxylic acids can be separated by using water, a dilute mineral acid, or a dilute benzoic or succinic acid as eluent.

DISCUSSION

As neutral species, rather than ions, are being separated, ion-exclusion chromatography cannot be considered as a form of ion chromatography; although ion-exchange polymers are used, ion-exchange mechanisms are not involved.

Anions, most commonly simple carboxylic acids (e.g., tartaric, malic, citric, lactic, acetic, succinic, formic, propionic, butyric, etc.), are separated on cation-exchange resins in acidic form. Salts of weak acids can also be analyzed, as they are converted to the corresponding acid by the hydrogen ions in the exchanger. Cations (weak bases and their salts) are separated on anion-exchange resins in the hydroxide form.

In order to understand the mechanism of ion-exclusion chromatography, the behavior of the resin, in an aquatic medium, must be taken into account. In this case, three parts can be distinguished:

1. The resin network.
2. The liquid inside the resin particles.
3. The liquid between the resin particles.

The first acts as a semipermeable membrane between the stationary liquid phase within the resin and the mobile-liquid phase between the resin beads.

Ionic groups are fixed on the resin and movement of ions across the membrane takes place as predicted by Donnan theory. The ion-exclusion mechanism involves interaction between partially ionized species and fully ionized polymer matrix. Electrostatic repulsive forces, between strong electrolytes (e.g., chloride, in the case of using HCl as eluent) and the ionic groups fixed on the resin (e.g., sulfonate), prevent them from entering into the resin, due to high ionic concentration inside the resin. Because ionized analytes are not retained, they are excluded from the polymer, migrate rapidly through the column, and are eluted at the column void volume. Partially ionized and neutral species (e.g., the undissociated forms of the analyte acids), as they penetrate into the pores of the resin, are distributed between the mobile phase in the column and the immobilized liquid in the pores of the packing. Separation is accomplished by differences in acid strength, size, and hydrophobicity.

The degree of retardation increases with the decrease of the ionization degree and, additionally, depends on polar attractions between analyte and fixed functional groups and on different van der Waals forces between an analyte and the hydrocarbon part of the resin. Elution order is related to pK_a values for ionic species and to the molecular size for neutral compounds.

Members of a homologous series, such as formic, acetic, and propionic acids, elute in the order of increasing pK_a (decreasing acid strength). Dibasic acids elute sooner than monobasic acids of the same carbon number. Isoacids elute earlier than normal acids. Double bonds retard elution, whereas keto groups increase elution rate.

Microporous polystyrene divinylbenzene resins are used, operating at pressures sometimes exceeding 3000 psi; unlike silica-based packings, they are stable from pH 0 to 14. For ion-exclusion separation of organic acids and weakly acidic compounds, strongly acidic, high-capacity, sulfonated styrene divinylbenzene in the hydrogen form are used. For organic bases, separation columns are packed with strongly basic copolymer with a quaternary ammonium functional group. The degree of cross-linking (the percentage of divinylbenzene in the copolymer) affects the retention of weakly ionized species; the lower

the degree of cross-linking, the longer the retention time of acid, either strong or weak. This is due to the fact that as cross-linking decreases, ions more readily penetrate the resin, where they are held up.

As aforementioned, a large number of organic and weak inorganic acids can be eluted from the hydrogen form of cation-exchange resin using water as the eluent. However, the addition of mineral acid to the water eluent suppresses the ionization of strong and moderately strong organic acids, allowing them to partition into the resin phase and, thus, improve selectivity, as retention times on the resin are increased. The addition of inorganic salts, such as $(NH_4)_2SO_4$ or organic modifiers (acetonitrile, isopropanol, ethanol, methanol), to the eluent may improve separation. Acetonitrile, for example, decreases the retention time of relatively non-polar compounds.

Ion-exclusion chromatography can couple to ion chromatography to improve the chromatographic resolution of inorganic anions and organic acids in complex matrices. The dual system can be either in the order ion-exchange chromatography (IEC)/ion chromatography (IC) or IC/IEC.

Various detection systems can be used in ion-exclusion chromatography, among them ultraviolet (UV)/vis spectrophotometry, conductivity, electrochemistry, fluorometry, refractive index (RI) measurement, are the most common techniques. Additionally, combined detection systems (e.g., UV/amperometry, UV/RI) may be used, leading to enhanced selectivity.

Ultraviolet detection is useful, especially when water or sulfuric acid, which do not absorb in the UV region, are used. Detection for most non-aromatic carboxylic acids is accomplished at 210 nm.

Conductivity detection is preferred when water is used as eluent; then ionizable analytes are readily detected. However, in the case where HCl is used as the eluent, the analytical column is followed by a suppressor column, packed with a cation-exchange resin in the silver form. The hydrogen ions of the eluent are exchanged for silver ions, which then precipitate chloride ions, thus removing the ions contributed by the eluent and enhancing the analyte's signal.

Electrochemical detectors (coulometric and amperometric) are used when the analytes are electrochemically active or capable of being coupled to an electrochemical reaction.

Refractive index monitors are used in food analysis, for detecting carbohydrates, alcohols, and other substances with weak or no UV absorption.

With the combination of RI and UV, simultaneous detection of organic acids, carbohydrates, and alcohols with one sample injection can be achieved. Postcolumn reactions can be used for fluorometric detection of amino acids, with excellent sensitivity and selectivity.

Ion-exclusion chromatography finds numerous applications for identification and determination of acidic species in complex matrix materials, such as dairy products, coffee, wine, beer, fruit juice, and other commercial products which can be quickly analyzed with minimal sample preparation before injection (usually only filtration, dilution, or centrifugation). Organic acid determination is also of great importance in biomedical research [e.g., physiological samples, in which most of the Krebs cycle acids (tricarboxylic acid cycle) are present].

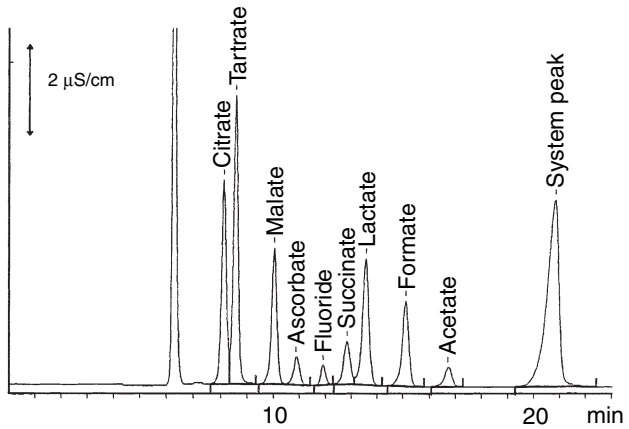

Fig. 1 Determination of organic acids and fluoride using ion-exclusion chromatography with direct conductivity detection, using mmol/L H_2SO_4, and 10% acetone as eluent.
Source: From Metrohm Ltd., with permission.

Organic acids can be detected in the parts per billion range. With preconcentration, this limit can be further decreased. A typical ion-exclusion chromatogram of organic acids separation is presented in Fig. 1.

BIBLIOGRAPHY

1. Gierde, D.; Fritz, J. *Ion Chromatography,* 2nd Ed.; Alfred Huethig Verlag: New York, 1987.
2. Gierde, D.; Mehra, H. *Advances in Ion Chromatography*; Jandik, P., Cassidy, R., Eds.; Century International: Franklin, MA, 1989; Vol. 1.
3. Haddad, P.; Jackson, P. *Ion Chromatography, Principles and Application*; Elsevier: Amsterdam, 1990.
4. Kaine, L.; Crowe, J.; Wolnic, K. Forensic applications of coupling non-suppressed ion-exchange chromatography with ion-exclusion chromatography. J. Chromatogr. **1992**, *602*, 141–247.
5. Metrohm IC Application Note No. O-5, Application Notes, Metrohm, Herisau (1996).
6. Small, H. *Ion Chromatography*; Plenum Press: New York, 1989.
7. Tanaka, K.; Fritz, J. Determination of bicarbonate by ion-exclusion chromatography with ion-exchange enhancement of conductivity detection. Anal. Chem. **1987**, *59*, 708–712.
8. Tarter, J. *Ion Chromatography*; Chromatographic Science Series; Marcel Dekker, Inc.: New York, 1987; Vol. 37.
9. Togami, D.; Treat-Clemons, L.; Hometchko, D. Int. Lab. **1990**, *2*, 29–33.

Ion-Interaction Chromatography

Teresa Cecchi
Department of Chemical Science, University of Camerino (UNICAM), Camerino, Italy

INTRODUCTION

Under reversed-phase (RP) high-performance liquid chromatography (HPLC) conditions, ionic compounds are weakly retained. On the contrary, when an ion-interaction reagent (IIR), which is a large lipophilic ion, is added to the mobile phase, ionized species of opposite charge are separated on RP columns with adequate retention. This is the chromatographic approach of RP ion-interaction chromatography (IIC). It has become a widely used separation mode in analytical HPLC because it provides a useful and flexible alternative to ion-exchange chromatography. Better selectivity, enhanced resolution, and retention are usually gained by this separation strategy.

According to the qualitative retention model of Bidlingmeyer, the lipophilic IIR, flowing under isocratic conditions, dynamically adsorbs onto the alkyl-bonded apolar surface of the stationary phase, forming a primary charged ion layer. The corresponding counterions are found in the diffuse outer region to form an electrical double layer. This charged stationary phase can then more strongly retain analyte ions of the opposite charge.

Unlike conventional ion exchange, IIC can be used to separate non-ionic and ionic or ionizable compounds in the same sample, because retention of an analyte involves its transfer trough the electrical double layer and depends on both electrostatic interactions and adsorptive (RP) effects.

In recent's, many examples of applications of IIC have been reported. They essentially concern the separation of organic and inorganic ions in the environmental, pharmaceutical, food, and clinical fields.

RETENTION MECHANISM

The larger number of names (e.g., ion-pair chromatography, dynamic ion-exchange chromatography, hetaeric chromatography, soap chromatography) which have been given to the IIC mode sheds light on the uncertainty concerning the retention mechanism. A majority of the proposed models are stoichiometric. They suggest that the oppositely charged analyte and IIR form a complex, according to a clear reaction scheme, either in the mobile-phase (ion-pair model) or at the stationary-phase surface (dynamic ion-exchange model). According to the first theory, the uncharged ion pair between oppositely charged analyte and IIR, which is formed in the mobile phase, is then more strongly retained by the stationary phase. The second theory presumes that solute ions undergo an ion-exchange process, at exchange sites dynamically generated by the adsorption of the IIR at the stationary phase. Knox and Hartwick demonstrated that both models lead to identical retention equation.

These models, although of practical and intuitive value, are not well founded in physical chemistry. The pioneeristic, even if qualitative, work of Bidlingmayer demonstrated that IIRs adsorb onto the stationary phase. It follows that stoichiometric equilibrium constants, which depend on the change in free energy of adsorption of the analyte, cannot be considered constant if the IIR concentration in the mobile phase increases, because the stationary phase surface properties (including its charge density) are modified. The multibody interactions and long-term forces involved in IIC can better be described by a thermodynamic approach.

A quantitative non-stoichiometric model was developed by Ståhlberg and coworkers. The model applies the Gouy–Chapman electrostatic theory to describe the interactions between charged species and it does not assume the formation of any chemical complexes: The adsorption of the IIR onto the stationary phase establishes a certain electrostatic surface potential, because its counterion has a lower adsorption tendency. An electrical double layer develops and a difference in electrostatic potential is created between the electroneutral bulk of the mobile phase and the net charged surface. The intuitive view of the effect of the IIR on retention is an electrostatic repulsion or attraction of the analyte to the charged stationary-phase surface, according to the analyte and IIR charge status. However, the adsorptive (RP) effects are also considered, to evaluate the total free energy of adsorption of the solute: The latter is partitioned into a "chemical" and an electrostatic free energy. This is a first approximation: The "chemical" part depends on the concentration of the IIR, as it determines a dynamic modification of the stationary-phase properties. This electrostatic theory of IIC has been implemented by taking into account the competition between IIR and analyte for a limited surface area, and the different surface area requirements of analyte and IIR (multisite occupancy model). However, the main drawback of this powerful electrostatic theory is the complex algebraic form of the resulting equations; hence, a series of approximations has to be made to obtain a relationship between the analyte capacity factor and

mobile-phase concentration of IIR, which is of interest for practical work.

Cantwell and coworkers proposed a surface adsorption, diffuse-layer ion-exchange double-layer model in which they underlined the role of the diffuse part of the double layer by assigning a stoichiometric constant for the exchange of ions.

Stranahan and Deming proposed a thermodynamic model for IIC in which the distribution a sample between the mobile and the stationary phase is discussed in terms of chemical potentials in both phases.

Additional peaks relative to the number of components injected are often obtained in IIC. These so-called "system peaks" confirm the proposed mechanism of dynamic functionalization of the stationary phase. They can be explained by taking into account that IIR ions are locally adsorbed onto (desorbed from) the stationary phase by injection of adsorbophilic solute ion of the opposite charge (of same charge). This change in the eluent composition, created by the sample injection, migrates along the column and give a signal if at least one of the eluent components can be detected. The same rationale provides the explanation for the indirect ultraviolet (UV) visualization (or amplification) of otherwise non-UV-absorbing samples, when a UV-absorbing lipophilic ion is added to the eluent.

INFLUENCE OF EXPERIMENTAL PARAMETERS ON RETENTION

The optimization of separations performed with IIC and the rationalization of analytes retention behavior are not easy tasks because they are influenced by many interdependent factors. This allows a fine modulation of their effects to achieve tailor-made separations.

Experimental design can be very helpful, and a number of chemometric optimization methods are present in the literature. Neural network models provided a good prediction power and a great versatility, without the need to develop any equations.

The following presents the effect of varying some individual factors on analyte retention.

ION-INTERACTION REAGENT

Type

The hydrophobic character of the IIR increases with increasing its chain length. More lipophilic reagents have higher adsorption constants, hence the effect of increasing chain length is qualitatively similar to the effect of increasing IIR concentration (see below) with regard to the degree of stationary-phase coverage. The use of multiply-charged IIRs allows the chromatographer to obtain larger changes of analyte retention. If chiral compounds are used as the IIR, the separation of the enantiomeric forms of the analyte may be achieved. The most popular IIRs are listed in Table 1.

Table 1 Commonly used ion-interaction reagents.

Cationic IIRs	Anionic IIRs
Tetramethylammonium	Butanesulfonate
Tetraethylammonium	Pentanesulfonate
Tetrabutylammonium	Hexanesulfonate
Cetyltrimethylammonium	Octanesulfonate
Octylammonium (from octylamine)	Dodecanesulfonate

Concentration

If the eluent concentration of the IIR increases, the amount of the adsorbed IIR also increases, according to its adsorption isotherm. This induces a higher surface potential on the stationary phase but also adsorption competes between analyte and IIR for the available stationary phase sites. Therefore, the following hold:

1. If the charge status of analyte and the IIR is the same, a decrease in retention is observed because of electrostatic repulsion between solute and charged stationary phase, and because of adsorption competition.
2. If the charge status of analyte and the IIR is the opposite, an increase in retention is expected because of electrostatic attraction between solute and charged stationary phase. A parabola-like dependence of analyte capacity factors on IIR concentration is observed if the investigated concentration range is broad. For narrower ranges, a linear increase may hold. Some authors have emphasized that analyte retention passes through a maximum because if the ionic strength is not kept constant when increasing the IIR concentration, there is a competition between analyte ion and IIR counterion; this competition counteracts the retention increase. However, a foldover of the plot may still occur even if the ionic strength is kept constant, because there is a critical value of the IIR concentration at which the positive effect of the electrostatic attraction is balanced by the negative effect of adsorption competition for the available stationary-phase surface area.
3. If the analyte is uncharged, a very weak decrease in retention is usually observed, primarily because of adsorption competition for the stationary phase.

Increasing the IIR above its critical micelle concentration leads into the field of micellar chromatography in

which analyte may partition between the mobile phase and both the stationary phase and the micelle.

MOBILE-PHASE COMPOSITION

Organic-Modifier Concentration

In IIC, the logarithm of the analyte capacity factor is described as a linear function of the organic-modifier concentration in the mobile phase. When the sample ion is in the same charge status as the IIR, the slope of the linear relationship, if compared to the original RP slope, becomes steeper (the contrary is observed for oppositely charged combinations). This can be explained by taking into account that the organic modifier, through desorption effects, decreases the retention of ionic solutes via the simultaneous decrease of the free energy of adsorption of both the analyte and IIR.

Ionic Strength

An increase in salt concentration in the bulk mobile phase provides those counterions which are able to reduce, according to the Gouy–Chapman electrostatic theory, the electrostatic stationary-phase surface potential. Hence, the adsorption of the IIR may increase, even if its concentration in the eluent is the same, because of lower electrostatic "self"-repulsion. However, the net effect is a reduced surface potential: The ion interactions decrease, and analyte retention may be modulated.

From an intuitive point of view, the inorganic ions are eluting agents because they limit the interaction of oppositely charged analyte and IIR, via a competing equilibrium for adsorbed lipophilic ions. This view gives the rationale for the use of mobile-phase additives, such as sodium carbonate, to avoid the unnecessarily high resolution which may be obtained between analytes of different charge.

It has to be emphasized that the nature of the electrolyte ions influences the surface potential value because the effective surface charge concentration is reduced if slight hydrophobic, adsorbophilic electrolytic counterions are included in the eluent.

The influence of moderate increase of ionic strength on the "chemical" part of the free energy relative to the analyte transfer from the mobile to the stationary phase has been usually neglected.

MOBILE-PHASE pH

The eluent pH value affects the degree of ionization of the species involved in ion interaction. Hence, the greatest retention is obtained for completely dissociated species. This is the opposite of what is observed in RP chromatography.

Unexpected pH dependencies were explained by (a) competition between negative analyte ions and OH^- ions for interaction with the electrical double layer and (b) a mixed retention mechanism in which RP partition or interaction with unreacted silanols from the stationary-phase base may play a significant role.

RP STATIONARY PHASE

A number of different packings were used in IIC, including the newly developed graphitized carbon column, which has excellent chemical and physical resistance. The use of polymeric material has the drawback of poor physical resistance. However, a wider pH range is investigable and the affinity for certain IIR is higher, by comparison with the silica-based RP columns. However, discordant results are present in literature reports with regard to the chromatographic efficiency.

With regard to the silica-based RP stationary phase, unreacted residual silanol groups may play a significant role in IIC because it was shown that they are ion-exchange sites not only for analyte cations but also for alkylammonium IIR. The higher retentions that were noticed for the silica-based stationary phase if compared to end-capped or polymer-based packings supports this.

The reproducibility of results obtained with silica-based RP, of the same declared characteristics but from different manufacturers, was sometimes poor, probably because of the properties of the silica used and the different reaction conditions in the alkylation of the support.

Stationary phases with higher hydrophobicities and adsorption capacities show increased retention of both solute and IIR. Hence, an increased capacity factor value should be expected, even if anomalies can be due to direct competition of solute and IIR for the available stationary phase.

TEMPERATURE

Temperature control is very important for obtaining reproducible separations. Indeed, the adsorption of the IIR onto the stationary phase follows an adsorption isotherm; hence, an increase of the column temperature leads to a decreased amount of the adsorbed IIR, even if its concentration in the mobile phase is constant. This, in turn, determines a decreased absolute surface potential and a modification of the solutes' capacity factors. Usually, a temperature increase results in an improved resolution and faster separation, even if a reversal of the

elution sequence of the components of a mixture may sometimes be observed, because of the interplay of electrostatic and RP interaction which are characterized by different enthalpies.

BIBLIOGRAPHY

1. Bartha, A.; Ståhlberg, J. Electrostatic retention model of reversed-phase ion-pair chromatography. J. Chromatogr. A, **1994**, *668* (2), 255–284.
2. Bidlingmeyer, B.A. Separation of ionic compounds by reversed-phase liquid-chromatography—an update of ion-pairing techniques. J. Chromatogr. Sci. **1980**, *18* (10), 525–539.
3. Chen, J.C.; Weber, S.G.; Glavina, L.L.; Cantwell, F.F. Electrical double-layer models of ion-modified (ion-pair) reversed-phase liquid chromatography. J. Chromatogr. **1993**, *656*, 549–576.
4. Gennaro, M.C. Reversed-phase ion-pair and ion-interaction chromatography. In *Advances in Chromatography*, Brown, P., Grushka, E., Eds.; Marcel Dekker, Inc.: New York, 1995, Vol. 35, 343–381.
5. Knox, J.H.; Hartwick, R.A. Mechanism of ion-pair liquid chromatography of amines, neutrals, zwitterions and acids using anionic hetaerons. J. Chromatogr. **1981**, *204*, 3–21.
6. Okamoto, T.; Isozaki, A.; Nagashima, H. Studies on elution conditions for the determination of anions by supressed ion-interaction chromatography using a graphitized carbon column. J. Chromatogr. A, **1998**, *800*, 239–245.
7. Pietrzy, D. J. Chromatogr. Sci. **1998**, *78*, 413–462.
8. Sacchero, G.; Bruzzoniti, M.C.; Sarzanini, C.; Mentasti, E.; Metting, H.J.; Coenegracht, P.M.J. Comparison of prediction power between theoretical and neural-network models in ion-interaction chromatography. J. Chromatogr. A, **1998**, *799*, 35–45.
9. Stranahan, J.; Deming, S.N. Thermodynamic model for reversed-phase ion-pair liquid chromatography. Anal. Chem. **1982**, *54*, 2251–2256.
10. Weiss, J. *Ion Chromatography,* 2nd Ed.; VCH: Weinheim, 1995; 239–289.

Ion-Interaction Chromatography: Comprehensive Thermodynamic Approach

Teresa Cecchi
Department of Chemical Science, University of Camerino (UNICAM), Camerino, Italy

INTRODUCTION

Reverse-phase (RP) chromatography is, by far, the most widely used separation mode in high-performance liquid chromatography (HPLC). A wide variety of mobile-phase additives that may also modify the surface of the packing material are used in optimization procedures. Ion-interaction chromatography (IIC) is an RP technique that involves the use of ion-interaction reagents (IIRs) that are large lipophilic ions; they are retained much more than their non-adsorbophilic counterions. An electrostatic potential difference between the stationary phase and the bulk mobile phase develops and influences ionic solute retention. When IIR is used, conventional RP columns are able to retain oppositely charged analytes with adequate retention. Improved resolution and selectivity broaden the scope of separation of organic and inorganic ions.

IIC analyses are challenging because of the high number of easily tunable but interdependent mobile-phase variables. Retention models are often sought because there is a need for a detailed understanding of the underlying phenomena that govern solute distribution between the two phases. The retention equations of a theoretical model can also be advantageously used during method development, involving the setup of custom modes in computer-supported software tools.

ION INTERACTION INTERPRETATION

To obtain a simple interpretation of the experimental findings in IIC, theoretical chromatographers first adopted a stoichiometric strategy that pioneered this separation mode. Unfortunately, the reaction schemes of stoichiometric models in both the mobile phase (ion pair model)[1] and stationary phase (dynamic ion exchange model)[2] lack a firm foundation in physical chemistry[3] because they are not able to account for the stationary-phase modification that results from the addition of the IIR to the eluent, and they fail to properly describe experimental results, as pointed out by Bidlingmeyer et al.[4] Key insights on these retention models were also provided by Knox and Hartwick.[5] The contrast between the simplicity and practicality of stoichiometric relationships, and the complexities of the thermodynamics solutes undergo is an important underlying theme of meditation for a model maker. Later, electrostatic theories[3,6] tried to pattern chromatographic findings according to electrostatic interactions between charged IIRs and an analyte, thereby disregarding chemical equilibria in the IIC system, but some predictions of theirs are at variance with experimental evidence.[7–9] Conversely, the recently developed extended thermodynamic approach to IIC[7–18] considers that a major contribution to the distribution of charged solutes between phases is the electrostatic potential difference between them, but also capitalizes on the importance of complex formation at a thermodynamic level, and not a stoichiometric level, to take into account the stationary-phase electrostatic potential that results from IIR adsorption. In the following, we will discuss in detail how this retention model may help the chromatographer to make educated guesses and to simplify the complex task of a successful optimization in the parameter space of IIC separations.

THEORY

Influence of IIR Concentration on the Retention Behavior of Charged, Neutral, and Zwitterionic Analytes

Amphiphilic IIR ions (H) dynamically adsorb onto the stationary phase, forming a primary charged ion layer, and counterions in the diffuse outer region form an electrical double layer. The adsorption isotherm of an IIR can be described by the Freundlich equation:

$$[\mathrm{LH}] = a[\mathrm{H}]^b \tag{1}$$

where a and b are constants; [H] and [LH] are, respectively, the mobile-phase and the stationary-phase concentrations of the IIR. The use of the Freundlich adsorption isotherm is not empirical[19] because it is related to the potential modified Langmuir adsorption isotherm, which holds for the adsorption of ions that have a substantial hydrophobic moiety. Because IIR counterions have a negligible adsorbophilic aptitude, an electrical potential difference Ψ° develops between the surface and the bulk solution. This potential is given by the rigorous Gouy–Chapman theory equation: if the ionic strength is high enough and the Debye

length is low, we are allowed to use a planar surface geometry;[3] we have the following relationship:[3,7]

$$\Psi = \frac{2RT}{F}\ln\left\{\frac{[\mathrm{LH}]|z_\mathrm{H}|F}{\left(8\varepsilon_0\varepsilon_\mathrm{r}RT\sum_i c_{0i}\right)^{\frac{1}{2}}} + \left[\frac{([\mathrm{LH}]z_\mathrm{H}F)^2}{8\varepsilon_0\varepsilon_\mathrm{r}RT\sum_i c_{0i}} + 1\right]^{\frac{1}{2}}\right\} \quad (2)$$

where F is the Faraday constant, R is the gas constant, T is the absolute temperature, z_H is the charge of the IIR, ε_r is the dielectric constant of the medium, ε_0 is the vacuum permittivity, and $\sum c_{0i}$ is the mobile-phase concentration of singly charged electrolytes. For the sake of simplicity, we will indicate the following:

$$f = \frac{|z_\mathrm{H}|F}{\left(8\varepsilon_0\varepsilon_\mathrm{r}RT\sum_i c_{0i}\right)^{\frac{1}{2}}} \quad (3)$$

where f (m^2/mol) is a constant, which can be evaluated from experimental conditions.

The complex equation Eq. 2 can be advantageously approximated, for high surface potential, by the following very simple expression:[10,12,14,19]

$$\Psi = \alpha + \beta\ln[\mathrm{LH}] \quad (4)$$

where α and β are constants[10] that depend on experimental conditions.

For surface potential below 25 mV, Eq. 2 can be linearized[3,11,15] and approximated by the following:

$$\Psi = \frac{z_\mathrm{H}[\mathrm{LH}]F}{\kappa\varepsilon_0\varepsilon_\mathrm{r}} \quad (5)$$

where κ is the inverse Debye length.

It has been demonstrated[7] that the course of analyte retention on the mobile-phase and stationary-phase concentrations of the IIR can be described, respectively, by the following two expressions

$$k = \phi[\mathrm{L}]_\mathrm{T}\frac{K_\mathrm{LE}\frac{\gamma_\mathrm{L}\gamma_\mathrm{E}}{\gamma_\mathrm{LE}}\exp(-z_\mathrm{E}F\Psi/RT) + K_\mathrm{EHL}\frac{\gamma_\mathrm{E}\gamma_\mathrm{H}\gamma_\mathrm{L}}{\gamma_\mathrm{EHL}}[\mathrm{H}]}{\left(1 + K_\mathrm{EH}\frac{\gamma_\mathrm{E}\gamma_\mathrm{H}}{\gamma_\mathrm{EH}}[\mathrm{H}]\right)\left(1 + K_\mathrm{LH}\frac{\gamma_\mathrm{L}\gamma_\mathrm{H}}{\gamma_\mathrm{LH}}\exp(-z_\mathrm{H}F\Psi/RT)[\mathrm{H}]\right)} \quad (6)$$

$$k = \phi\frac{K_\mathrm{LE}\frac{\gamma_\mathrm{L}\gamma_\mathrm{E}}{\gamma_\mathrm{LE}}\exp(-z_\mathrm{E}F\Psi/RT) + \frac{K_\mathrm{EHL}}{a^{1/b}}\frac{\gamma_\mathrm{E}\gamma_\mathrm{H}\gamma_\mathrm{L}}{\gamma_\mathrm{EHL}}[\mathrm{LH}]^{1/b}}{\left(1 + \frac{K_\mathrm{EH}}{a^{1/b}}\frac{\gamma_\mathrm{E}\gamma_\mathrm{H}}{\gamma_\mathrm{EH}}[\mathrm{LH}]^{1/b}\right)} \times([\mathrm{L}]_\mathrm{T} - [\mathrm{LH}]) \quad (7)$$

where ϕ is the phase ratio of the column; K_EL, K_EHL, K_EH, and K_HL, are the thermodynamic equilibrium constants for adsorption of the analyte E onto the stationary phase, ion pair formation in the stationary phase, ion pair formation in the eluent, and adsorption of the IIR onto the stationary phase, respectively; γ represents the activity coefficient for each species; z_E is the charge of the analyte; and $[\mathrm{L}]_\mathrm{T}$ estimates the total ligand surface concentration.

The first term in the numerator of Eqs. 6 and 7 describes the electrostatic interaction between the analyte and the charged stationary phase. This interaction will be attractive (repulsive) if the analyte is oppositely (similarly) charged to the IIR; hence, its retention increases (decreases) with increasing IIR concentration. The second term in the numerator of Eqs. 6 and 7 accounts for ion pair formation at the stationary phase that results in a retention increase. The left factor of the denominator of Eq. 6 and the denominator of Eq. 7 accounts for ion pair formation in the mobile phase that tends to reduce retention because the analyte is withdrawn from the stationary phase toward the eluent. Both terms concerning ion pair formation are missing if the analyte and IIR are similarly charged, or if the analyte is neutral. The right-hand factor of the denominator of Eq. 6 and the right-hand factor of Eq. 7 describe adsorption competition between the analyte and the IIR. From Eq. 6, it is clear that Ψ° always runs counter to further adsorption of the IIR because Ψ° is of the same sign as z_H. From Eq. 7, it is evident that adsorption competition, if it applies, shows only if [LH] is high, compared to $[\mathrm{L}]_\mathrm{T}$.

Eluent pH is an important optimization parameter because it influences the analyte ionization, which, in turn, controls the magnitude of electrostatic interactions.

When Eqs. 1–3 are substituted into Eqs. 6 and 7, the following two expressions are obtained:

$$k = \frac{c_1\left(a[\mathrm{H}]^b f + \left((a[\mathrm{H}]^b f)^2 + 1\right)^{\frac{1}{2}}\right)^{(\pm 2|z_\mathrm{E}|)} + lc_2[\mathrm{H}]}{(1 + c_3[\mathrm{H}])\left(1 + c_4[\mathrm{H}]\left(a[\mathrm{H}]^b f + \left((a[\mathrm{H}]^b f)^2, +1\right)^{\frac{1}{2}}\right)^{(-2|z_\mathrm{H}|)}\right)} \quad (8)$$

$$k = \frac{d_1\left([\mathrm{LH}]f + \left(([\mathrm{LH}]f)^2 + 1\right)^{\frac{1}{2}}\right)^{\pm 2|z_\mathrm{E}|} + d_2[\mathrm{LH}]^{1/b}}{(1 + d_3[\mathrm{LH}]^{1/b})} \times (d_4 - [\mathrm{LH}]) \quad (9)$$

In the exponent of the first term of the numerator, the plus sign applies for oppositely charged analytes and IIRs, whereas the minus sign applies for similarly charged analytes and IIRs, as expected according to the electrostatic behavior; Eqs. 8 and 9 are also able to take into account, via the magnitude of z_E in the exponents, that the electrostatic interaction is stronger for multiply charged analytes.

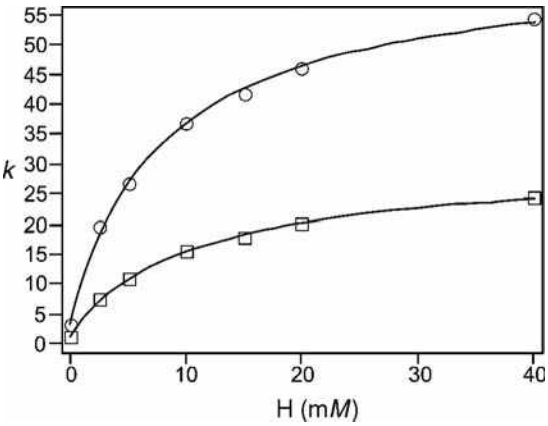

Fig. 1 Dependence of k on adrenaline (squares) and L-tyrosine hydrazide (circles), on mobile-phase concentration of 1-hexanesulfonate. Column: Synergi Hydro-RP (Phenomenex) 150 × 4.6 mm I.D., particle size 4 μm, and bonded phase coverage 4.05 μmol/m^2. Eluent: phosphate buffer 37.10 m*M* KH_2PO_4 and 4.29 m*M* Na_2HPO_4 calculated to provide a pH of 6.0. After addition of the desired amount of sodium 1-hexanesulfonate, NaCl was added so that the total sodium concentration was 50 m*M* (constant ionic strength). Experimental data were fitted by Eq. 8.

When Eqs. 8 and 9 are fitted to experimental data, excellent results are obtained, as shown in Figs. 1 and 2 for analytes charged oppositely to the IIRs; in Figs. 3 and 4 for analytes charged similarly to the IIRs; and in Fig. 5 for a doubly charged analyte, as detailed in the captions. Tables 1 and 2 detail parameter estimates and their standard deviations, correlation coefficients, and sum of square errors obtained from the best fit of these experimental data by Eqs. 8 and 9, respectively. Fitting parameters $c_1 - c_4$ and $d_1 - d_4$ are not simple adjustable constants, but have a clear physical meaning,[7] and this allows the parameter estimates to be commented on. As expected, $c_2 - c_3$ and

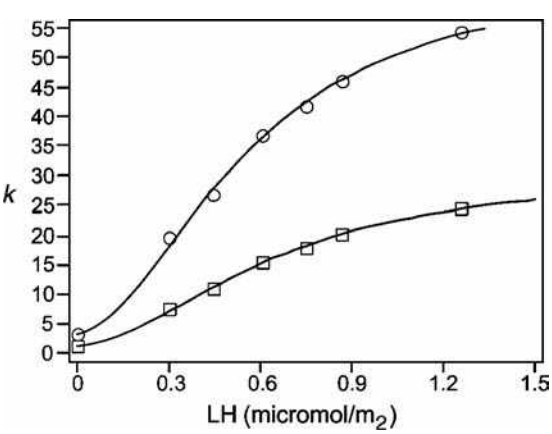

Fig. 2 Dependence of k on adrenaline (squares) and L-tyrosine hydrazide (circles), on stationary-phase concentration of 1-hexanesulfonate. Conditions as in Fig. 1. Experimental data were fitted by Eq. 9.

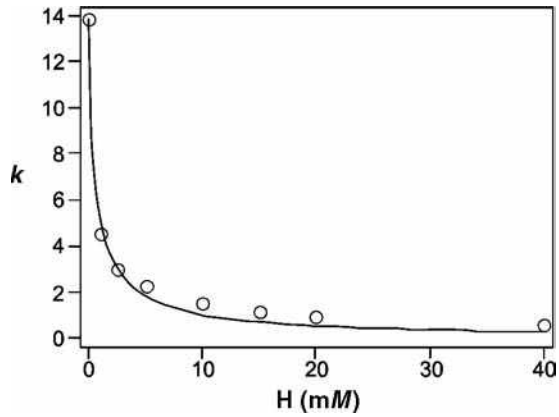

Fig. 3 Dependence of k on sodium *p*-toluenesulfonate, on mobile-phase concentration of 1-hexanesulfonate. Conditions as in Fig. 1. Experimental data were fitted by Eq. 8.
Source: From Extended thermodynamic approach to ioninteraction chromatograph: Effect of the electrical charge of the solute ion, in J. Liq. Chromatogr. Relat. Technol.[18]

$d_2 - d_3$, which are related to ion pair equilibrium constants, decrease with decreasing analyte lipophilicity; d_4, which represents the total ligand concentration, compares well with the bonded phase coverage of the column (4.05 μmol/m^2), as expected; from the estimated c_4, which represents the equilibrium constant for the IIR adsorption, we obtain an averaged $\Delta G^\circ = -15.6$ kJ/mol, which is a very reasonable value for the standard free energy of adsorption of hexanesulfonate.[19,20] In Table 1, c_1 is missing for all analytes except 2,6-naphthalenedisulphonate because it was not considered an optimization parameter, since it represents k_0 that is analyte retention without the IIR in the mobile phase and it can

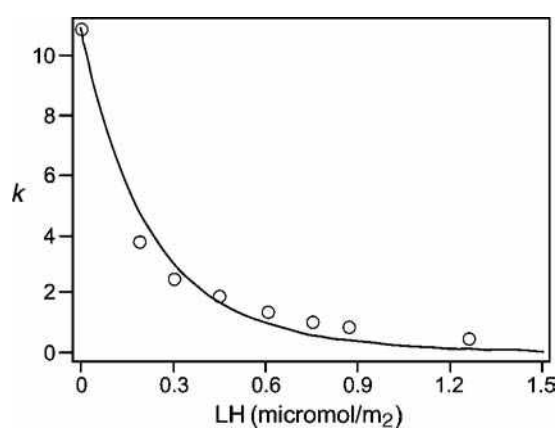

Fig. 4 Dependence of k sodium salicylate on the stationary-phase concentration of 1-hexanesulfonate. Conditions as in Fig. 1. Experimental data were fitted by Eq. 9.
Source: From Extended thermodynamic approach to ioninteraction chromatograph: Effect of the electrical charge of the solute ion, in J. Liq. Chromatogr. Relat. Technol.[18]

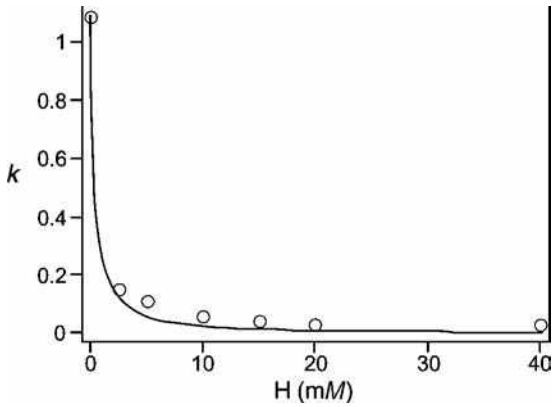

Fig. 5 Dependence of k on 2,6-naphthalenedisulfonate, on mobile-phase concentration of 1-hexanesulfonate. Conditions as in Fig. 1. Experimental data were fitted by Eq. 8.
Source: From Extended thermodynamic approach to ioninteraction chromatograph: Effect of the electrical charge of the solute ion, in J. Liq. Chromatogr. Relat. Technol.[18]

be obtained from experimental results. When c_1 was estimated by the model (as for the doubly charged 2,6-naphthalendisulphonate, for which other fitting parameters do not apply because electrostatic repulsion entirely models its retention behavior), the percent error is very low (0.6%).

When Eq. 4 is used to obtain the surface potential that has to be substituted into Eq. 6, we obtain[10] the following expression (a parallel expression can also be obtained from Eq. 7 to model retention data as a function of the stationary-phase concentration of the IIR):

$$k = \frac{c_1[\mathrm{H}]^{z_\mathrm{E}/z_\mathrm{H}(b-1)} + c_2[\mathrm{H}]}{(1 + c_3[\mathrm{H}])(1 + c_4[\mathrm{H}]^b)} \qquad (10)$$

For a detailed description of $c_1 - c_4$ in Eq. 10, the reader is referred to Ref.[10] Fig. 6 details how this equation properly describes the retention of neutral analytes in IIC;[12] in this case the above expression can be simplified because z_E, c_2, and c_3 are all zero and only adsorption competitions model the retention decrease with increasing IIR concentration.

The surface potential is easily predicted to alter the retention behavior of zwitterions.[13–15,21] The molecular electrical dipole is subjected to a torque moment that arranges it parallel to the lines of the non-homogeneous electrical field, with the head oppositely charged to the electrostatic surface potential facing the stationary phase. Hence, the electrical force is always attractive and it pushes the dipole toward the interphase, where the field is stronger. This force was used to calculate the electrostatic contribution to the electrochemical potential of the analyte, and to the thermodynamic equilibrium constant for its adsorption. It was demonstrated that, from Eq. 6, the following relationship is quantitatively able to model zwitterions retention and can be advantageously used in life science chromatography:

$$k = \frac{c_1\left(a[\mathrm{H}]^b f + \left((a[\mathrm{H}]^b f)^2 + 1\right)^{\frac{1}{2}}\right)^{2c_2\kappa/F}}{1 + c_4[\mathrm{H}]\left(a[\mathrm{H}]^b f + \left((a[\mathrm{H}]^b f)^2 + 1\right)^{\frac{1}{2}}\right)^{-2|z_\mathrm{H}|}} \qquad (11)$$

In Eq. 11, c_1 and c_4 are the already discussed parameters, whereas c_2 is related to the molecular dipole: the higher it is, the stronger is the retention increase on IIR addition. A parallel expression can also be obtained from Eq. 7 to model retention data as a function of the stationary-phase concentration of the IIR.[13] A fractional charge approach to the IIC of zwitterions was also recently put forward.

Influence of Organic Modifier Concentration

A bivariate treatment of the simultaneous effects of IIR mobile-phase concentration and organic modifier percentage in the eluent on analyte retention gives the following relationship[16]

Table 1 Summary of parameter estimates and their standard deviation, correlation coefficient (r), and sum of square errors (SSE) for the best fit of experimental retention data (some of which are shown in Figs. 1, 3, and 5) as a function of the mobile-phase concentration of the IIR by Eq. 8.

Analyte	c_1	c_2 (m/M)	c_3 (m/M)	c_4 (m/M)	r Eq. 8	SSE Eq. 8
L-Tyrosine hydrazide	—	4.627 ± 0.295	0.111 ± 0.006	—	0.999	2.531
Adrenaline	—	1.368 ± 0.084	0.090 ± 0.004	—	0.999	0.321
Octopamine		0.989 ± 0.087	0.085 ± 0.005	—	0.999	0.380
Sodium *p*-toluenesulfonate	—	—	—	0.629 ± 0.144	0.995	1.337
Sodium salicylate	—	—	—	0.488 ± 0.140	0.994	1.064
2,6-Naphthalenedisulfonate	1.097 ± 0.035	—	—	—	0.996	0.007

Conditions as in Fig. 1.
Source: From Extended thermodynamic approach to ioninteraction chromatograph: effect of the electrical charge of the solute ion, in J. Liq. Chromatogr. Relat. Technol.[18]

Table 2 Summary of parameter estimates and their standard deviation, correlation coefficient (r), and sum of square errors (SSE) for the best fit of experimental retention data (some of which are shown in Figs. 2 and 4) as a function of the stationary-phase concentration of the IIR by Eq. 9.

Analyte	d_1	d_2 ($m^2/\mu mol)^{(1/b)}$	d_3 ($m^2/\mu mol)^{(1/b)}$	d_4 ($\mu mol/m^2$)	r Eq. 9	SSE Eq. 9
L-Tyrosine hydrazide	—	101.829 ± 10.444	3.011 ± 0.229	—	0.999	4.587
Adrenaline	—	35.116 ± 2.971	2.350 ± 0.146	—	0.999	0.606
Octopamine	—	25.396 ± 2.300	2.204 ± 0.144		0.999	0.408
Sodium *p*-toluenesulfonate	—	—	—	1.311 ± 0.393	0.987	3.380
Sodium salicylate	—	—	—	1.616 ± 0.595	0.987	2.085
2,6-Naphthalenedisulfonate	1.097 ± 0.036	—	—	—	0.996	0.008

Conditions as in Fig. 1.
Source: From Extended thermodynamic approach to ioninteraction chromatograph: Effect of the electrical charge of the solute ion, in J. Liq. Chromatogr. Relat. Technol.[18]

$$k = \frac{c_{1_0}e^{-m_1\varphi}\left(\frac{a_o e^{-m_2\varphi}[H]^{(b_0+m_3\varphi)}}{\left(h(\varepsilon_{H_2O}-(\varepsilon_{H_2O}-\varepsilon_{MeOH})\varphi)\right)^{\frac{1}{2}}}+\left(\left(\frac{a_o e^{-m_2\varphi}[H]^{(b_0+m_3\varphi)}}{\left(h(\varepsilon_{H_2O}-(\varepsilon_{H_2O}-\varepsilon_{MeOH})\varphi)\right)^{\frac{1}{2}}}\right)^2+1\right)^{\frac{1}{2}}\right)^{(\pm 2|z_E|)}+c_{2_0}e^{-m_4\varphi}[H]}{(1+c_{3_0}e^{-m_5\varphi}[H])\left(1+c_{4_0}e^{-m_6\varphi}[H]\left(\frac{a_o e^{-m_2\varphi}[H]^{(b_0+m_3\varphi)}}{\left(h(\varepsilon_{H_2O}-(\varepsilon_{H_2O}-\varepsilon_{MeOH})\varphi)\right)^{\frac{1}{2}}}+\left(\left(\frac{a_o e^{-m_2\varphi}[H]^{(b_0+m_3\varphi)}}{\left(h(\varepsilon_{H_2O}-(\varepsilon_{H_2O}-\varepsilon_{MeOH})\varphi)\right)^{\frac{1}{2}}}\right)^2+1\right)^{\frac{1}{2}}\right)^{(-2|z_H|)}\right)} \quad (12)$$

where φ is the percentage (% vol/vol) of methanol in the mobile phase; $c_{1_0} - c_{4_0}$ are the already discussed parameters $c_1 - c_4$ when the organic modifier is not present in the eluent; a_o and b_0 are a and b when the organic modifier is not present in the eluent; and h is a parameter that accounts for the eluent ionic strength. If the latter is not constant and the dependence of h on total ionic concentration is explicitly introduced in Eq. 12, (see above) allows a multivariate approach to IIC; m_1, m_2, m_3, m_4, m_5, and m_6 are parameters that depend on experimental conditions: m_1 depends on the analyte characteristic, m_2, m_3, and m_6 depend on the peculiarity of IIR, whereas m_4 and m_5 depend on the nature of both the analyte and the IIR. For analytes oppositely charged to the IIR, the active fitting parameters are m_1, m_4, m_5, c_{2_0}, and c_{3_0} because m_2, m_3, a_0, and b_0 are readily obtained from the fitting of the Freundlich constants as functions of the organic modifier concentration in the eluent. The bivariate non-linear regression of the retention of a typical analyte oppositely charged to the IIR gives parameter estimates that were used to graphically present Eq. 12 in Fig. 7: it is rewarding to observe that retention decreases with increasing organic modifier concentration and increases with increasing IIR concentration. This increase is steeper at low organic modifier percentages because the organic modifier reduces analyte retention both directly (it decreases the analyte free energy of adsorption) and indirectly (it decreases the IIR free energy of adsorption: a lower surface concentration of the IIR results in a lower electrostatic attraction of the analyte and hence in a lower retention).

Noteworthy, in the absence of the IIR, Eq. 12 reduces to one which describes the influence of the organic modifier on RP-HPLC retention. A relationship similar to Eq. 12 can be obtained to describe the simultaneous effects of the IIR stationary-phase concentration and organic modifier percentage in the eluent on analyte retention.[16]

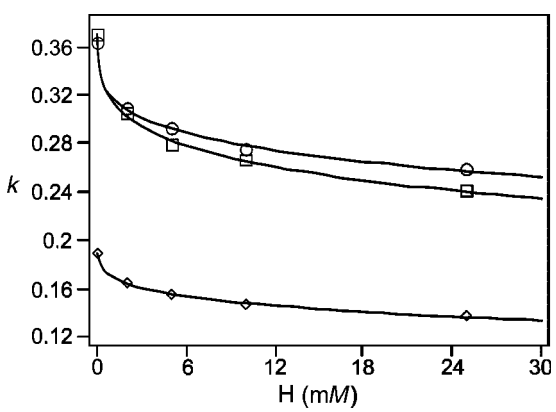

Fig. 6 Dependence of k on dimethylformamide (squares), dimethylchetone (circles), and dimethylsulfoxide (rhombs), on mobile-phase concentration of tetrabutylammonium bromide. Column: Res Elut 5 C_{18} (Varian), 25 cm × 4.6 mm I.D., 5 μm. Eluent: 81.6 m*M* phosphate buffer, pH 7.2—methanol, 85:15, vol/vol containing tetrabutylammonium bromide. Experimental data were fitted by Eq. 10 with all z_E, c_2, and c_3 equal to zero.
Source: From Ion interaction chromatography of neutral molecules: A potential approximation to obtain a simplified retention equation, in J. Liq. Chromatogr. Relat. Technol.[12]

Influence of Ionic Strength

In IIC method development, when a compensatory electrolyte is not added to the eluent, the ionic strength is not constant; hence, the dependence of f Eq. 3 on the ionic

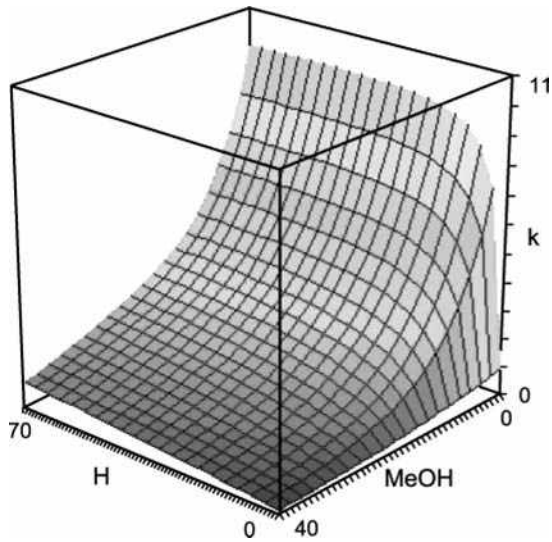

Fig. 7 Retention behavior of a typical analyte in IIC as a function of IIR mobile-phase concentration and organic modifier percentage in the eluent, according to Eq. 12.

concentration must be explicitly addressed.[17] At a fixed IIR surface concentration, the electrostatic potential decreases with increasing electrolyte concentration because counterions in the diffuse layer shield the surface charge. However, with increasing ionic strength, there is an increased surface concentration of the IIR because counterions lower the self-repulsion forces between the similarly charged adsorbed IIR ions. Yet, this Donnan effect is not able to compensate the decreased surface potential due to a higher concentration of counterions in the diffuse layer. The strong interplay between these issues can be easily taken into account using the adsorption isotherm of the IIR obtained when its counterion concentration is not kept constant in the eluent.[17] The retention of a solute oppositely (similarly) charged to the IIR is predicted to decrease (increase) with increasing ionic strength because of the lower net electrostatic attraction (repulsion).

CONCLUSIONS

The distinguishing features that set this retention model apart are the following:[7–18,21]

1. It is general. From two equations, quantitative predictions can be made for the retention behavior of charged, multiply charged, neutral, and zwitterionic solutes in IIC as a function of both the mobile-phase and the stationary-phase concentrations of the IIR. Retention equations can also quantitatively take into account the influence of the organic modifier concentration and the ionic strength; in the absence of IIR, they reduce to the well-known relationships of RP-HPLC.
2. It reduces to the relationships of stoichiometric or electrostatic approaches in IIC, respectively, if the surface potential or ion pairing equilibria are disregarded.
3. It is able to rationalize experimental behaviors that cannot be explained by other outstanding electrostatic retention models: 1) different theoretical curves when k is plotted as a function of the stationary-phase concentration of the IIR, for different IIRs; 2) dependence of the ratio of the retention of two different analytes on the IIR concentration; 3) dependence of the k/k_0 ratio on the analyte nature if the experimental conditions are the same; and 4) better agreement between electrostatic retention model predictions and experimental findings for analytes similarly charged as the IIR.
4. It is able to explain why the electrostatic approach is sometimes at variance with experimental evidence (this happens if experimental data underscore and involve complex formation).
5. Adjustable parameters have a clear physical meaning and their estimates are reliable because they compare well with literature estimates and with direct experimental measurements.
6. It is able to rationalize, in a quantitatively unprecedented way, with very low percent errors, experimental evidence qualitatively or semiquantitatively explained by other models.

As a concluding remark, it has to be emphasized that every acceptable retention theory must be consistent with fundamental physics, as well as describe experimental findings. The complex multiplicity of phenomena involved in an IIC system requires a complex description of the thermodynamics solutes have undergone: this description is epistemologically acceptable if the model is well founded in physical chemistry and if it is able to describe experimental data better than previous models.

REFERENCES

1. Horvath, C.; Melander, W.; Molnar, I.; Molnar, P. Enhancement of retention by ion-pair formation in liquid chromatography with nonpolar stationary phases. Anal. Chem. **1977**, *49* (14), 2295–2305.
2. Kissinger, P.T. Comments on reverse-phase ion-pair partition chromatography. Anal. Chem. **1977**, *49* (6), 883.
3. Bartha, A.; Stahlberg, J. Electrostatic retention model of reversed-phase ion-pair chromatography. J. Chromatogr. A, **1994**, *668*, 255–284.
4. Bidlingmeyer, B.A.; Deming, S.N.; Price, W.P., Jr.; Sachok, B.; Petrusek, M. Retention mechanism for reversed-phase ion-pair liquid chromatography. J. Chromatogr. **1979**, *186*, 419–434.

5. Knox, J.H.; Hartwick, R.A. Mechanism of ion-pair liquid chromatography of amines, neutrals, zwitterions and acids using anionic heterons. J. Chromatogr. **1981**, *204*, 3–21.
6. Cantwell, F.F. Retention model for ion-pair chromatography based on double-layer ionic adsorption and exchange. J. Pharm. Biomed. Anal. **1984**, *2* (2), 153–164.
7. Cecchi, T.; Pucciarelli, F.; Passamonti, P. Extended thermodynamic approach to ion-interaction chromatography. Anal. Chem. **2001**, *73* (11), 2632–2639.
8. Cecchi, T. Extended thermodynamic approach to ion-interaction chromatography: A thorough comparison with the electrostatic approach and further quantitative validation. J. Chromatogr. A, **2002**, *958* (1–2), 51–58.
9. Cecchi, T.; Pucciarelli, F.; Passamonti, P. Ion interaction chromatography of neutral molecules. Chromatographia **2001**, *53* (1–2), 27–34.
10. Cecchi, T.; Pucciarelli, F.; Passamonti, P. An extended thermodynamic approach to ion-interaction chromatography for high surface potential: Use of a potential approximation to obtain a simplified retention equation. Chromatographia **2001**, *54* (9–10), 589–593.
11. Cecchi, T.; Pucciarelli, F.; Passamonti, P. Extended thermodynamic approach to ion-interaction chromatography for low surface potential: Use of a linearized potential expression. J. Liq. Chromatogr. Relat. Technol. **2001**, *24* (17), 2551–2557.
12. Cecchi, T.; Pucciarelli, F.; Passamonti, P. Ion interaction chromatography of neutral molecules: A potential approximation to obtain a simplified retention equation. J. Liq. Chromatogr. Relat. Technol. **2001**, *24* (3), 291–302.
13. Cecchi, T.; Pucciarelli, F.; Passamonti, P.; Cecchi, P. The dipole approach to ion interaction chromatography of zwitterions. Chromatographia **2001**, *54* (1–2), 38–44.
14. Cecchi, T.; Cecchi, P. The dipole approach to ion interaction chromatography of zwitterions: Use of a potential approximation to obtain a simplified retention equation. Chromatographia **2002**, *55* (5–6), 279–282.
15. Cecchi, T.; Cecchi, P. The dipole approach to ion interaction chromatography of zwitterions: Use of the linearized potential expression for low surface potential. J. Liq. Chromatogr. Relat. Technol. **2002**, *25* (3), 415–420.
16. Cecchi, T.; Pucciarelli, F.; Passamonti, P. Extended thermodynamic approach to ion-interaction chromatography. The influence of the organic modifier concentration. Chromatographia **2003**, *58* (7–8), 411–419.
17. Cecchi, T.; Pucciarelli, F.; Passamonti, P. Extended thermodynamic approach to ion-interaction chromatography. A mono- and bivariate strategy to model the influence of ionic strength. J. Sep. Sci. **2004**, *27*.
18. Cecchi, T.; Pucciarelli, F.; Passamonti, P. Extended thermodynamic approach to ion-interaction chromatograph: Effect of the electrical charge of the solute ion. J. Liq. Chromatogr. Relat. Technol. **2004**, *27* (1), 1–15.
19. Davies, J.T.; Rideal, E.K. Adsorption at liquid interfaces. In *Interfacial Phenomena*; Academic Press: New York, 1961; 154–216.
20. Rosen, M.J. Adsorption of surface-active agents at interfaces: the electrical double layer. In *Surfactant and Interfacial Phenomena,* 2nd Ed.; John Wiley & Sons: New York, 1978; 33–106.
21. Cecchi, T.; Pucciarelli, F.; Passamonti, P. Ion-Interaction Chromatography of Zwitterions. The Fractional Charge Approach to Model the Influence of the Mobile Phase Concentration of the Ion-Interaction Reagent The Analyst. 2004; Vol. 129, 1037–1046. (article B404721D available: DOI 10.1039/b404721d, http://www.rsc.org/is/journals/current/analyst/anlpub.htm).

Ion-Pairing Techniques

Ioannis N. Papadoyannis
Anastasia Zotou
Laboratory of Analytical Chemistry, Chemistry Department, Aristotle University of Thessaloniki, Thessaloniki, Greece

INTRODUCTION

Ion-pair chromatography (IPC) is of relatively recent origin, being first applied in the mid-1970s. Much of the development work in both theory and practice was performed by Schill and coworkers. At various times, IPC has also been called extraction chromatography, chromatography with a liquid ion exchanger, soap chromatography, paired-ion chromatography and ion-pair partition chromatography.

BACKGROUND INFORMATION

When solute ions (A^-) are added to a chromatographic system containing pairing ions (B^+) and associated counter ions (C^-), the degree of retention of (A^-) depends on the following equilibrium:

$$A^-_{aq} + B^+_{aq} = AB_{org} \tag{1}$$

with an extraction constant

$$E_{AB} = \frac{[AB_{org}]}{[A^-_{aq}][B^+_{aq}]} \tag{2}$$

In the simplest case of IPC, it can be assumed that the sample and counterions are soluble only in the aqueous mobile phase and the ion pair formed is soluble only in the organic stationary phase.

Assuming that the concentration of the pairing ion in the aqueous phase is high compared to that of the solute ion, the *distribution coefficient* of A^-, D^-_A, is given by

$$D^-_A = \frac{[AB_{org}]}{[A^-_{aq}]} = E_{AB}[B^+_{aq}] \tag{3}$$

The *capacity factor* k' is related to E_{AB} as follows (in the reversed-phase mode):

$$k' = \frac{V_S}{V_m}\left(\frac{[AB_{org}]}{[A^-_{aq}]}\right) \tag{4}$$

$$= \frac{V_S}{V_m}(E_{AB}[B^+_{aq}]) \tag{5}$$

or

$$k' = D^-_A \frac{V_S}{V_m} \tag{6}$$

Because the capacity factor k' is proportional to $1/D$ in normal-phase chromatography and to D in reversed-phase chromatography, it follows that k' in IPC is inversely proportional to the pairing ion concentration in the normal-phase situation but directly proportional in the reversed-phase case.

When the pairing ion is very hydrophobic, B^+ will be extracted into the organic phase with its normal counterion C^-, according to

$$C^-_{aq} + B^+_{aq} = CB_{org}(\text{ion pair}) \tag{7}$$

Subtracting it from Eq. 1 gives

$$A^-_{aq} + CB_{org} = AB_{org} + C^-_{aq} \tag{8}$$

This is very similar to ion-exchange chromatography with an equilibrium constant:

$$K_{IE} = \frac{[AB_{org}][C^-_{aq}]}{[CB_{org}][A^-_{aq}]} \tag{9}$$

This gives

$$D^-_A = \frac{[AB_{org}]}{[A^-_{aq}]} = K_{IE}\frac{[CB_{org}]}{[C^-_{aq}]} \tag{10}$$

from which it follows that k' is inversely proportional to the concentration of the counterion in the aqueous phase.

The latter situation is usual in the reversed-phase mode, where the hydrophobic ion is adsorbed onto the bonded

hydrocarbon of the packing material. Thus, we can distinguish three different techniques:

1. Normal-phase IPC, where the support is coated with an aqueous stationary phase containing the pairing ion and the ion pairs are partitioned between the stationary phase and an organic mobile phase.
2. Reversed-phase IPC, where the liquid stationary phase is organic and the pairing ion is introduced in the aqueous mobile phase.
3. Reversed-phase IPC, using a chemically bonded stationary phase and a hydrophobic pairing ion in the aqueous mobile phase.

The use of bonded-phase partition systems is generally preferred over mechanically held stationary phases; this gives advantage to technique 3.

NORMAL-PHASE ION-PAIR CHROMATOGRAPHY

The support is loaded with the aqueous stationary phase containing the pairing ion by one of the following three methods:

1. The stationary phase or a concentrated solution of the stationary phase in acetone is pumped through the packed column bed. The excess is then removed by passing eluent or hexane, followed by eluent saturated with stationary phase, until equilibrium is reached. Equilibrium is normally achieved when stable k' values are obtained for a series of representative solutes. This usually requires passage of several hundred milliliters of eluent.
2. The stationary phase can be loaded onto the column in several large plugs (0.1–1.0 ml) using a stopped-flow technique and equilibrium is achieved in the same way as previously.
3. The eluent, which has been preequilibrated with the stationary phase, is pumped through the column until stable k' values are obtained. The stationary phase is adsorbed onto the support surface, but at equilibrium, the pores of the support are not as completely filled as they are in the columns obtained by the first two methods. The equilibration can be a very time-consuming procedure, but the columns thus obtained are stable and reproducible.

Because the columns are in an equilibrium situation, it is obvious that gradient elution is not possible. In the normal-phase situation, the k' value of a solute is inversely proportional to the pairing ion concentration. Because the pairing ion is in the stationary phase, this concentration is not readily changed, and for this reason, retention is normally controlled by modification of the eluent. Hydrocarbon or chlorinated hydrocarbon solvents are usually employed with a small percentage of alcohol as a modifier. Varying the concentration or nature of the alcohol can produce the required changes in retention or selectivity.

Very high efficiencies have not usually been achieved with normal-phase IPC; the advantage of the reversed-phase mode, where the pairing ion concentration can be easily altered, has led to almost total takeover in the ion-pair field. The normal phase has two advantages compared to the reversed-phase mode:

1. The use of ultraviolet (UV) absorbing or fluorescent ions to enhance or enable the detection of non-absorbing solutes.
2. The possibility of varying selectivity by varying the organic-phase composition.

REVERSED-PHASE ION-PAIR CHROMATOGRAPHY

Most often, pentanol or butyronitrile is used as the stationary phase loaded onto a hydrophobic support such as silanized silica.

The equilibration time depends on the hydrophobicity of the support (the coating of pentanol on a hydrocarbon-bonded silica takes no longer than 2 hr at a flow rate of approximately 1 ml/min).

The retention of analytes can be regulated by varying the following factors:

1. The capacity factor increases with the hydrophobicity of the pairing ion. For hydrophilic solutes, hydrophobic pairing ions are chosen, and vice versa.
2. The capacity factor increases linearly with pairing ion concentration. Alternatively, gradient elution can be performed by decreasing the pairing ion concentration.
3. The choice of the organic phase affects the selectivity of the system.

REVERSED-PHASE ION-PAIR CHROMATOGRAPHY USING A CHEMICALLY BONDED STATIONARY PHASE

This is, by far, the most commonly used form of reversed-phase IPC. This technique has been also called *soap chromatography* although, in soap chromatography, the use of detergents as counterions is introduced. Here, the columns (with C_8 or C_{18} packings) are prepared by equilibrating the stationary bonded phase with the mobile phase containing the pairing ion. The ion-pair reagent is attracted to the stationary phase because of its hydrophobic alkyl group

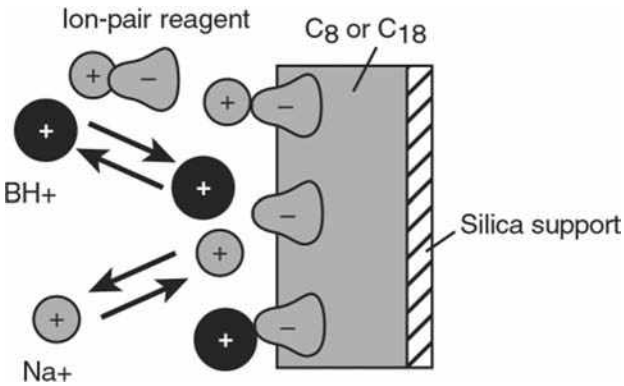

Fig. 1 Pictorial representation of IPC retention of a protonated base (BH^+); Na^+ is the mobile-phase cation; the IPC reagent is hexane sulfonate.
Source: From *Practical HPLC Method Development*,[1] by permission of John Wiley & Sons, Inc.

and the charge carried by the reagent thereby attaches to the stationary phase.

The surface of a C_8 or C_{18} column packing is shown in Fig. 1 as a rectangle covered by sorbed molecules of a negative ion-pair reagent (e.g., hexane sulfonate, C_6-SO_3^-).[1] The negative charge on the stationary phase is balanced by the positive ions (Na^+) from the reagent and/or buffer. A positively charged sample ion (protonated base BH^+) can exchange with a Na^+ ion as shown (arrows), resulting in the retention of the sample ion by an ion-exchange process.

For each ion-pair reagent, the column uptake increases for a higher reagent concentration in the mobile phase, but then levels off as the column becomes saturated with the reagent. The more hydrophobic reagents are retained more strongly and saturate the column at a lower mobile-phase reagent concentration ($10^{-5}M$), but equilibration may take several hours. Less hydrophobic ion-pair reagents are added at a slightly higher concentration (10^{-4}–$10^{-3}M$) and equilibrium is reached much faster (1–2 hr at a flow rate of 1ml/min). This is shown in Fig. 2a, where the concentration of reagent in the stationary phase $(P^-)_S$ is plotted vs. the concentration of reagent in the mobile phase $(P^-)_m$ for two reagents of different hydrophobicity.

The change in sample retention, as the ion-pair reagent concentration increases, is shown in Fig. 2b for a hydrophilic sample compound BH^+. Once the column becomes saturated with the reagent, the sample retention levels off. Because IPC retention involves an ion-exchange process, further increases in reagent concentration lead to an increase in the counterion concentration (Na^+), which competes with the retention of the sample ion on the column.

In practice, when very hydrophobic pairing ions are used, the columns are irreversibly altered, because the ions can never be completely removed. Once equilibrium

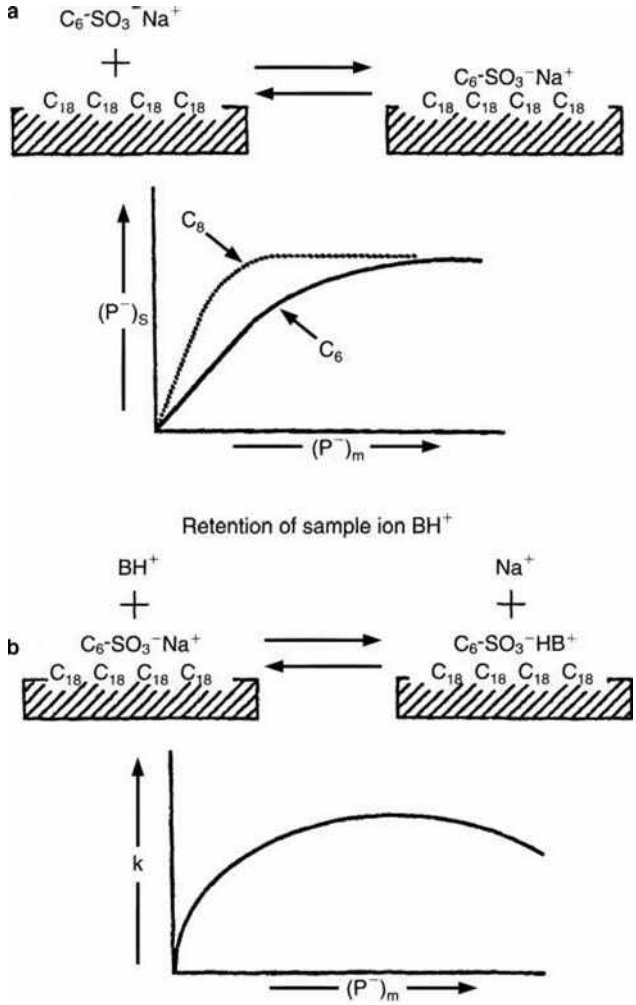

Fig. 2 Effect of ion-pair reagent concentration on separation. (a) Sorption of the ion-pair reagent as a function of concentration for reagents of different hydrophobicity (C_6- and C_8-sulfonates); (b) retention as a function of reagent concentration.
Source: From *Practical HPLC Method Development*,[1] by permission of John Wiley & Sons.

is reached, the columns are stable and can be used for several months. The columns should be stored in the mobile phase because of the lengthy equilibration times. Only if the column is not used for an extended period of time should one consider storing the column in an organic solvent.

DESIGN OF AN ION-PAIR SEPARATION

Unless there is a specific reason to choose a normal-phase system, IPC should be carried on in the reversed-phase mode, using chemically bonded stationary phases.

The best counterion and pH depend on the kind of sample to be separated. Most ion-pair reagents used today

are either alkyl sulfonates or tetraalkyl ammonium salts, either of which allow UV detection above 210 nm. The IPC aqueous phase must be adequately buffered with respect to both pH and concentration of the counterion.

Inadequate buffering of the aqueous phase is a source of band tailing in IPC. Conventional buffers, such as citrate and phosphate, have been used and, in some cases, the counterion itself is an adequate buffer. For separations at low pH, 0.1–0.2 *M* solutions of a strong acid provide adequate buffering. Inadequate buffering of the aqueous phase is a source of band tailing in IPC.

In reversed-phase IPC, maximum k' values are obtained at intermediate values of pH, where the sample compounds are completely ionized and ion-pair formation is at a maximum. As the pH of the mobile phase is lowered, sample anions A^- begin to form the unionized acids HA, leading to a smaller number of sample ion pairs in the stationary phase. Acids are usually separated at a pH of 7–9, whereas bases are separated at a pH of 1–6.

In reversed-phase systems, the solvent strength is readily varied by changing the counterion or its concentration. When all sample ions are fully ionized, a change in solvent strength via a change in counterion concentration leads to minimal changes in separation selectivity. The concentration of the counterion is usually 0.005–0.05 *M*, except for perchlorate (0.5–1 *M*) or the detergents used in soap chromatography (e.g., 1 wt% of counterion). Buffer concentrations are similar to those used in ion-exchange chromatography (0.001–0.5 *M*).

An increase in the alkyl chain length of the counter-ion increases retention in reversed-phase IPC by up to 2.5 times per added $-CH_2-$ group in the counterion.

Apart from an increase in the counterion concentration, an increase in ionic strength of the aqueous phase generally reduces the formation of ion pairs, as a result of the competition of secondary ions in forming ion pairs with the counterion. One study showed a twofold to threefold change in k' for each doubling of ionic strength.

For reproducible separations by IPC, it is important to thermostat the column. Temperature effects in IPC are more important than in some other methods.

REFERENCE

1. Snyder, L.R.; Kirkland, J.J.; Glajch, J.L. *Practical HPLC Method Development,* 2nd Ed.; John Wiley & Sons: New York, 1997; 317–341.

BIBLIOGRAPHY

1. Bidlingmeyer, B.A. *Practical HPLC Methodology and Applications*; John Wiley & Sons: New York, 1992; 157–165.
2. Gilbert, M.T. *High Performance Liquid Chromatography*; IOP Publishing, Wright: Bristol, U.K., 1987; 227–253.
3. Snyder, L.R.; Kirkland, J.J. *Introduction to Modern Liquid Chromatography,* 2nd Ed.; John Wiley & Sons: New York, 1979; 454–482.
4. Su, S.C.; Hartkopf, A.V.; Karger, B.L. High-performance ion-pair partition chromatography of silfa drugs study and optimization of chemical parameters. J. Chromatogr. **1976**, *199*, 523.

Isocratic HPLC: System Selection

Pavel Jandera
Department of Analytical Chemistry, University of Pardubice, Pardubice, Czech Republic

Abstract
The effects of various factors on the separation in isocratic high-performance liquid chromatography (HPLC) are discussed. Various separation modes, including aqueous-organic and non-aqueous reversed-phase (RP) chromatography, adsorption normal-phase liquid chromatography (NPLC), hydrophilic interaction liquid chromatography (HILIC), ion-exchange, ion-pair, and size-exclusion chromatography (SEC) for non-ionic samples differing in the size and polarities and for partially or fully ionized acidic or basic compounds are addressed. Selection of the column length, inner diameter (I.D.), character of the column bed, and the type of stationary phase are discussed, using the information on the sample properties, such as solubility, polarity, presence of specific functional groups in sample compounds, sample amount and concentration, and so on. Empirical and model-based approaches to the optimization of the operation parameters controlling the separation selectivity, efficiency, and resolution in HPLC are outlined, including column characteristics, selectivity of the stationary phase, composition of binary or more complex mobile phases, and operation temperature.

INTRODUCTION

Any new sample type delivered for high-performance liquid chromatography (HPLC) analysis requires an adequate separation method. Previous experience with similar samples is very useful, and many methods can be looked up in the literature; however, it is often necessary to modify earlier established methods to suit laboratory equipment or sample matrices, or to improve sample throughput in the laboratory. In many cases, a desired separation can be achieved with a few experiments, but some separation problems are more difficult and their solution may require considerable experimental effort. Nowadays, effects of experimental conditions on HPLC separations are well understood, and this knowledge can be used for effective method development. First, the objective of the separation should always be kept in mind. Any information available on the sample is very helpful in HPLC method development: the matrix, the approximate number of sample components and their chemical structures, concentrations, solubilities, and other properties provide clues for the selection of sample pretreatment approach (if necessary), suitable detection conditions, and a separation system. Most often, variable-wavelength or diode array ultraviolet (UV) absorbance detectors are used, but mass spectrometry (MS) coupled to HPLC is becoming increasingly popular because it offers valuable structural information for unknown samples. Other detection techniques are used less frequently—mainly fluorimetric and electrochemical detection for sensitive and selective environmental, biological, and food analyses, or light-scattering detection for the analysis of compounds that do not absorb in the UV region and can neither be oxidized nor reduced. For adequate separation, suitable chromatographic mode, stationary phase, mobile phase, flow rate, column dimension, and temperature should be selected. Many analyses can be performed at constant operating conditions using the so-called isocratic elution.

SELECTION OF A COLUMN AND PACKING MATERIAL

Many HPLC separations are performed with conventional analytical columns, which are 10–25 cm long and 3–4.6 mm in diameter. The column plate number, the pressure drop across the column, and the separation time at a constant flow rate are directly proportional to the column length. With short (2–6 mm), high-speed columns of the same diameter, simple separations can be accomplished in 1–3 min, so that the productivity of the laboratory increases considerably and solvent consumption per analysis is reduced.

The flow rate, consumption of the mobile phase at a constant flow rate, and the pressure drop increase with the second power of the column diameter. Separations on microbore columns (15–25 cm long and 1–2 mm I.D.) need less mobile phase and allow high mass sensitivity of detection, which is useful for analyses of small sample amounts with mass spectrometric detection. Separations on high-speed microbore, and especially on capillary HPLC columns of 0.1–0.5 mm internal diameter, are subject to more significant extracolumn contributions of the injector, detector, and connecting tubing to band broadening in comparison to conventional analytical columns, so that miniaturized HPLC requires specially designed

low-volume injectors and detectors, often at the cost of decreased sensitivity of detection. Hence, microbore and capillary HPLC columns have so far been more frequently used for HPLC–MS trace analysis than for other routine quantitative analytical applications.

Usually, HPLC columns contain spherical particle packings which are carefully sorted to fractions with narrow size distribution to provide high separation efficiency. Totally porous packing materials most frequently used for separation of small molecules in contemporary HPLC have pore sizes of 7–12 nm and specific surface area of 150–400 m^2/g, but wide-pore particles with pore sizes of 15–100 nm and relatively low specific surface area of 10–150 m^2/g, or non-porous materials are used for separation of macromolecules. Perfusion materials, designed especially for the separation and isolation of biopolymers, contain very broad pores (400–800 nm) throughout the whole particle, which are interconnected by smaller pores. Column efficiency and flow resistance increase with small particles, and a high pressure has to be applied for maintaining the required flow rate and keeping the time of analysis within an acceptable limit. However, the maximum operating pressure is 30–40 MPa with the common instrumentation for HPLC. Hence, short columns should be used with small-diameter particles. Five-micrometer particles are most often used in conventional analytical columns, and particles of 3–4 μm are common in short, high-speed columns for rapid separations (columns packed with 1–2 μm particles are employed in ultrahigh-pressure liquid chromatography, UHPLC, with instrumentation designed for maximum operation pressures up to 150 MPa).

Unlike packed columns, monolithic (continuous bed), analytical, or capillary columns in the form of a rod with flow-through pores offer high porosity and improved permeability. Silica-based monolithic columns are generally prepared by gelation of a silica sol to a continuous sol–gel network, onto which a C18 or another stationary phase is subsequently chemically bonded. Such columns provide efficiency and sample capacity comparable to those of conventional columns packed with 5 μm particle materials, but have 3 to 5 times lower flow resistance, thereby allowing higher flow rates and faster HPLC analysis. Rigid polyacrylamide, polyacrylate, polymethacrylate, or polystyrene monolithic columns are prepared by in situ polymerization in desired column format.

SELECTION OF HPLC SEPARATION MODE

The first step in HPLC method development consists of selecting an appropriate separation mode. Many neutral compounds can be separated either by reversed-phase (RP) or by normal-phase (NP) chromatography. An RP system is usually the best first choice because it is likely to result in a satisfactory separation of a great variety of non-polar, polar, and even ionic compounds. Lipophilic samples often can be separated either by non-aqueous RP chromatography or by NP chromatography. Weak acids or weak bases can be analyzed by RP chromatography with buffered mobile phases, and strong acids or strong bases by ion pair or ion exchange chromatography (IEC). Special chiral columns or chiral selector additives to the mobile phase can be used for separation of optical isomers (enantiomers).

Macromolecules are usually separated and characterized by size-exclusion chromatography (SEC) on columns packed with inert materials (gels) characterized by controlled pore distributions, based on different accessibilities of the pores for molecules of different sizes, with the larger molecules eluting first. For some lower polymers with molecular masses in the range 10^3–10^4 Da, interactive (i.e., RP-HPLC or NP-HPLC) modes provide better selectivity of separation than SEC. Many ionizable biopolymers such as peptides, proteins, oligonucleotides, and nucleic acids can be separated by IEC or RP chromatography on wide-pore packing materials, with the mobile phases containing trifluoroacetic acid or triethylammonium acetate as ion pair reagents.

REVERSED-PHASE LIQUID CHROMATOGRAPHY (RPLC)

The stationary phase in RP chromatography—usually an alkyl immobilized on an inorganic support—is less polar than the aqueous–organic mobile phase. Non-polar samples are more strongly retained than the polar ones, and the retention increases with increasing polarity of the mobile phase, so that very lipophilic samples may require non-aqueous mobile phases.

Silica gel-based materials for RP chromatography with non-polar (most often C8 or C18 alkyls) or moderately polar stationary phases covalently bonded via Si–O–Si–C bonds are prepared by chemical modification of the silanol (Si–OH) groups on the silica gel surface by chloro-silane or alkoxy-silane reagents, and are relatively stable to hydrolysis. The retention in RP increases with increasing surface coverage and length of the bonded alkyl chains, so that C18 phases show greater retention than C8-bonded phases.

Monofunctional silane reagents yield efficient stationary phases with flexible fur-like or brush-like structure of the chains bonded on the silica surface. When bifunctional or trifunctional silanes are used for modification, Cl or alkoxy groups are introduced into the stationary phase, which are subject to hydrolysis and react with excess molecules of reagents to form a polymerized sponge-like bonded phase structure. Stationary phases prepared in this way usually show stronger retention but lower separation efficiency (plate number) than do monomerically bonded stationary phases.

Bonded phases prepared by modification of silica gel type A, in turn prepared by gelation of soluble silicates, are acidic because of contamination with certain metals that activate surface silanol groups, and can complex with some chelating solutes, causing strong retention or asymmetrical peaks. They are not stable in mobile phases with pH > 8, where the silica gel slowly dissolves. However, chemically bonded groups on silica support can hydrolyze at pH < 3, causing stationary phase bleeding. The hydrolysis is enhanced at higher temperatures, so that many bonded phases are not stable at temperatures higher than 60°C. Newer, highly purified, less acidic silgel spherical silica particles (type B) are formed by the aggregation of silica sols in the air; they contain only low amounts of metals; and are more stable than the type A silica materials at intermediate and higher pH, up to at least pH 9. They generally provide better separations, especially of basic samples. Silica gel type C with a hydrosilated surface populated with non-polar silicon hydride Si-H groups (instead of silanol groups) may have up to 95% of original silanols removed, so that it is less polar than silica gels with higher population of silanol groups.

Rather bulky silanization reagents can chemically modify no more than 50% of the original silanol groups. The residual silanol groups may interact with polar solutes, especially basic solutes, often causing strong and irreversible retention and poor separation with tailing or distorted peaks. Some residual silanol groups can be removed by a subsequent end-capping reaction with small-molecule trimethylchlorosilane or hexamethyldisilazane reagents. Another approach relies on using an alkyl di-isopropyl monochlorosilane or an alkyl di-tert-bertyl monochlorosilane reagents in a single silanization step to provide steric shielding of residual silanols.

Stationary phases prepared by modification of the silica gel surface with bidentate silanes containing C18 or C8 alkyls and two reactive groups separated by a $–CH_2–CH_2–$ or a $–CH_2–CH_2–CH_2–$ bridging group show high bonding density and improved stability over a broad pH range. With alkenes used in the silanization/hydrosilation process, bonded phases attached to the surface of the hydrosilated silica type C by one point are produced, whereas double-point attachment of a bidentate bonded phase occurs when an alkyne is used instead. Bridged bidentate bonded phases efficiently shield the non-reacted silanol groups and protect the surface of the silica gel support from direct contact with the mobile phase, thus improving the column stability over a broad pH range.

In highly aqueous mobile phases, which are often necessary for RPLC separations of polar compounds, non-polar bonded alkyls are poorly solvated and may collapse and stick together, changing significantly the properties of the bonded stationary phases. The so-called aqua bonded phases are designed to improve the solvation of the bonded material and to improve the retention of hydrophilic compounds when using highly aqueous mobile phases. Incorporating amide or carbamate groups between the alkyl chain and the surface of the silica gel support improves the retention behavior in highly aqueous mobile phases. Another approach for improving the performance of bonded phases in highly aqueous media relies on end capping of the non-reacted residual silanol groups with polar hydrophilic ligands instead of hydrophobic short alkyl groups.

Stationary phases with methyl groups incorporated into the silica gel structure contain lower concentrations of silanol groups and show improved pH stability. Hybrid particles with both inorganic (silica) components and organic (organosiloxanes) components such as 1,2-bis(siloxy)ethane incorporated in their skeleton, chemically modified with the desired functionality and endcapped in separate steps, possess ethylene bridge moieties shielding residual silanol groups and show improved pH and mechanical stability.

Stationary phases with chemically bonded branched hydrocarbons, perfluoroalkanes, polyethylene glycol, cholesterol, or alkylaryl groups show different separation selectivities which can be useful for specific separations. For example, chemically bonded phenyl groups show preferential retention of aromatic compounds and increased shape selectivity for planar and rigid rod-like molecules.

Materials with inorganic or porous hydrophobic or (less frequently) hydrophilic organic polymer matrices and graphitized carbon are stable over a broad pH range from 0 to 12–14; hence, they are useful in separations of basic compounds. Reversed phases on aluminum and zirconium oxide supports exhibit hardness and mass transfer properties comparable to silica, and can be prepared by forming a cross-linked polystyrene, polybutadiene, or alkylated polymethylsiloxane layer on the support surface to which alkyls are attached. The inorganic surface, encapsulated by a non-polar stationary phase, does not come into contact with the mobile phase or with the analyte; so these materials can be used in the pH range 1–14.

Porous graphitized carbon adsorbents with sufficient hardness and well-defined and stable pore structures without micropores are now available with increased affinity for aromatic and polar substances, allowing difficult separations of some hydrophilic or isomeric compounds.

Chromatographic tests of the properties of chemically bonded phases usually are intended to determine the hydrophobic selectivity (relative retention of two hydrocarbons), hydrogen-bonding acceptor and donor selectivity (e.g, relative retention of butyl paraben and dipropyl phthalate) and silanol activity (relative retention of basic vs. neutral compounds); metal chelating activity can be measured, e.g., as the relative retention of 2,2′dipyridyl to 4,4′dipyridyl.

The mobile phase in RP chromatography contains water and one or more organic solvents, most frequently acetonitrile, methanol, tetrahydrofuran, or propanol. By the choice

of the organic solvent, selective polar interactions (dipole–dipole, proton–donor, or proton–acceptor) with analytes can be either enhanced or suppressed, and the selectivity of separation can be adjusted. Binary mobile phases are usually well suited for the separation of a variety of samples, but ternary or, less often, quaternary mobile phases may offer improved selectivity for some difficult separations. The retention times t_R are controlled by the concentration of the organic solvent in the aqueous–organic mobile phase. Eq. 1 is widely used to describe the effect of the volume fraction of methanol or acetonitrile ϕ on the retention factors $k = (t_R/t_0) - 1$ where t_0 is the column dead (holdup) time. [1]

$$k = k_0 \times 10^{-m\varphi} \quad (1)$$

The constants m and k_0 in Eq. 1 increase as the polarity of the solute decreases, or as its size increases. Furthermore, the constant m increases with decreasing polarity of the organic solvent.

NORMAL-PHASE LIQUID CHROMATOGRAPHY (NPLC)

In NP chromatography (also called adsorption or liquid–solid chromatography), the stationary phase is more polar than the mobile phase. The retention increases as the polarity of the mobile phase decreases, and polar analytes are more strongly retained than non-polar ones (i.e., the opposite of RP chromatography; Fig. 1). The column packing is

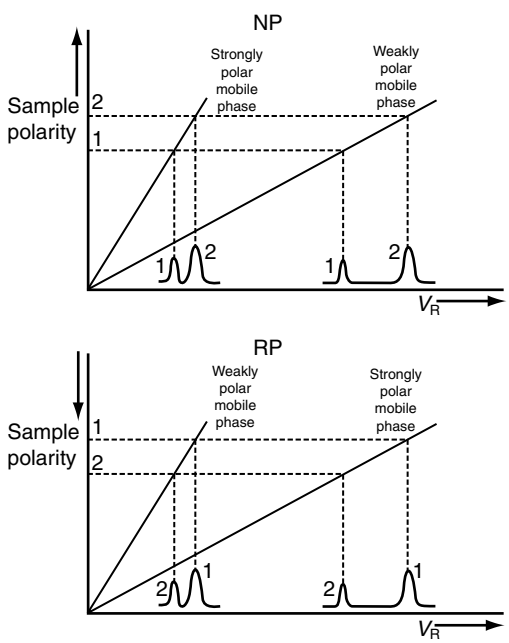

Fig. 1 Schematic diagram of the effects of sample and mobile phase polarities on retention in NPLC and RPLC. V_R = retention volume.

either an inorganic adsorbent (silica gel or, less often, aluminum oxide) or a moderately polar bonded phase [cyanopropyl–$(CH_2)_3$–CN, diol –$(CH_2)_3$–O–CH_2–CHOH–CH_2–OH, or aminopropyl–$(CH_2)_3$–NH_2] chemically bonded onto the silica gel, and the mobile phase usually is a mixture of a non-polar solvent and one or more strongly or moderately polar solvents. Normal-phase behavior can be sometimes observed also in non-aqueous RP liquid chromatography (NARPLC), probably because of the activity of polar residual silanol groups.

For the separation of molecules differing in their hydrophobic parts, RP chromatography generally offers a better selectivity than NPLC, but there are some practical reasons for selecting NP chromatography methods in specific cases, as follows:

1. A lower organic-mobile-phase viscosity offers a lower pressure drop across the column than that obtained in aqueous–organic mobile phases used in RPLC at a comparable flow rate.
2. HPLC columns are usually more stable and have longer lifetimes in organic solvents than in aqueous–organic mobile phases.
3. Many samples are more soluble or less prone to decompose in organic mobile phases than in aqueous mobile phases and do not cause injection problems in NPLC, as is occasionally observed in RPLC.
4. Unlike RP chromatography, NP chromatography enables the direct injection of samples extracted into a non-polar solvent.
5. NPLC is usually better suited for the separation of positional isomers or stereoisomers than RPLC.

Very large changes in separation selectivity are possible by changing either the mobile phase or the stationary phases in NPLC. Proton donor–acceptor interactions cause strong retention of basic compounds on silica gel in non-aqueous mobile phases, whereas acidic compounds show higher affinities to aminopropyl columns. The elution strength is proportional to the polarity of the mobile phase. Wide variations in the selectivity of NP chromatography separations can be achieved by selecting solvents with appropriate types of selective polar interactions. Usually, binary organic mobile phases, comprised of a less polar solvent A (a hydrocarbon such as hexane) and a more polar solvent B (propanol, dioxane, dichloromethane, acetonitrile, etc.), are employed in NP chromatography. With some simplification, the dependence of the retention factor k on the volume fraction φ of the polar solvent B in binary mobile phases can be described by Eq. 2:[2]

$$k = k_0\varphi^{-m} \quad (2)$$

The constants k_0 and m depend on the nature of the solute and on the chromatographic system, but are independent of the concentration, φ, and k_0 is the retention factor in pure

solvent B. The parameter *m* theoretically corresponds to the number of molecules of the strong solvent B necessary to displace one adsorbed sample molecule.

Highly hydrophilic samples are usually too weakly retained in RPLC to allow their separation, whereas they are often retained too strongly in non-aqueous mobile phases used in conventional adsorption NPLC and/or are not sufficiently soluble in the non-aqueous mobile phases. This problem can be solved by using polar stationary phases, such as silica gel with decreased surface concentration of silanol groups, or chemically bonded amino-, amido-, cyano-, carbamate-, diol-, polyol-, poly(2-sulphoethyl aspartamide), zwitterionic sulfobetaine, etc. ligands in aqueous–organic mobile phases rich in organic solvents (usually acetonitrile). This separation mode is called hydrophilic interaction liquid chromatography (HILIC) and can be characterized as NPLC with conventional RP mobile phases. Since its introduction in the early 1980s, HILIC has been successfully applied in the analysis of carbohydrates, amino acids, peptides, polar drugs, toxins, natural compounds in plant extracts, and other compounds important to food and pharmaceutical industries.

In contrast to RP chromatography, water is the stronger solvent in HILIC mobile phases, where it is usually contained in concentrations of 1–30%. Hence it forms an adsorbed layer on the surface of a polar adsorbent, which is thick enough to induce liquid–liquid partition between the bulk mobile phase and the adsorbed aqueous liquid layer. Consequently, the retention in HILIC is often due to the combination of adsorption and liquid–liquid partition mechanisms with possible additional effects of ion exchange (especially on bonded amino, zwitterionic, or weak ion exchange columns). The transition between the adsorption and partition retention mechanisms is probably continuous as the water concentration in the mobile phase gradually increases.

In RP chromatography with binary mobile phases (methanol–water or acetonitrile–water), retention decreases as the concentration of the less polar organic solvent increases, whereas in aqueous NP (HILIC) chromatography retention decreases with increasing concentration of the more polar water. Consequently, U-shape plots of the retention times vs. the concentration of the organic solvent are often observed on HILIC columns over the full composition range of the mobile phase, with the minimum corresponding to the transition from the RP to the NP mechanism. The U-turn mobile-phase composition shifts to higher concentrations of water in the mobile phase when less polar stationary phases are used, allowing HILIC separations in mobile phases with higher water concentrations. Stationary phases with various functionalities show significant differences in retention and separation selectivity. Silica gel has the least retention, but often has higher selectivity differences for small polar compounds such as carboxylic acids, nucleosides, and nucleotides, with respect to other polar bonded stationary phases commonly used in HILIC (amide, amino, aspartamide, or sulfobetaine).

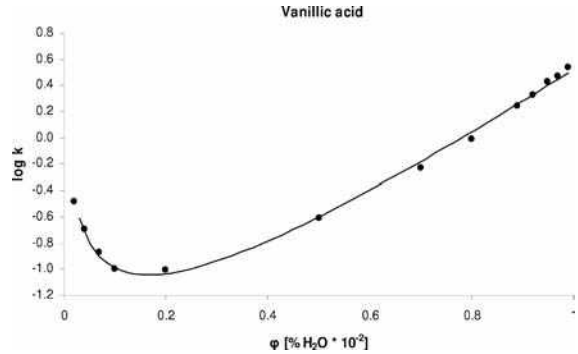

Fig. 2 Effects of the volume fraction of water, ϕ, in binary acetonitrile–water mobile phases on the retention factor, k, of vanillic acid on a bonded polyethylene glycol column. HILIC mode at $\phi < 0.2$, RP mode at $\phi > 0.2$.

The retention dependence on the volume fraction of water ϕ can be described by Eq. 2 in the HILIC range to a first approximation. To characterize the effects of water on the retention over the full composition range of binary mobile phases, as described in Eq. 3 can be obtained by combining Eqs. 1 and 2 for the RP and HILIC range, respectively:

$$\log k = a + m_1 \cdot \varphi_w - m_2 \cdot \log \varphi_w \quad (3)$$

ϕ_w is the volume fraction of water in the mobile phase. Fig. 2 shows an example of the validity of Eq. 3 for vanillic acid on a bonded polyethylene glycol column.

Suitability of a HILIC system for particular samples can be evaluated using a gradient of increasing concentration of water in acetonitrile (from 2–10% to 50% in 10 min). Increasing concentration of the organic solvent or of a salt in the mobile phase enhances the retention of polar compounds, except for the bonded amino phase, where the retention of the acid compounds decreases with increasing concentration of salts due to the ion exchange effects. In HILIC, mobile phases should be buffered, as pH affects the ionization and hence the retention of weakly acidic or weakly basic polar compounds.

LC SEPARATION OF IONIC COMPOUNDS

Ionized compounds are usually much less retained than non-charged compounds; their separation in RP chromatography is usually possible only with ionic additives to the mobile phase. Basic compounds can interact with residual silanols in alkyl silica-bonded phases ionized to SiO^- anions; consequently, strong retention and tailing peaks are observed. Alkylamine additives to the mobile phase sometimes improve peak shape by blocking the silanol groups. Repulsive interactions with the negatively charged

residual-SiO^- groups in the alkyl silica-bonded phases cause ionic exclusion, owing to which a part of the inner pore volume is not accessible to anionic samples. Ion exclusion may result in poor separation of strong acids, which elute close to, or even before the column holdup time, usually as asymmetrical peaks. Ion exclusion may be suppressed at a higher ionic strength of the mobile phase, which decreases the negative surface zeta potential of the residual silanol groups on the surface of silica-based chemically bonded phases. Hence, addition of salts to the mobile phase often improves separations of anionic compounds.

In mobile phases containing 5–50 m*M* phosphate or acetate buffers of pH 2–8.5, the ionization of weak acids (at pH < 7) or weak bases (at pH > 7) can be more or less suppressed to improve separation and peak symmetry. By adjusting the pH in the range ± 1.5 around the pK_a, differences in the degree of ionization of the individual sample components can often be utilized to control the separation selectivity. The retention is usually adjusted by the addition of up to 30–40% acetonitrile, methanol, or tetrahydrofuran to the mobile phase.

Strong acids and strong bases are completely ionized over a broad pH range and their chromatographic behavior is usually affected very little by adding a buffer to the mobile phase. Such compounds can be separated by RP ion pair or IEC. In ion pair chromatography (IPC), ion pair reagents whose molecules contain a strongly acidic or strongly basic group and a bulky hydrocarbon part are added to the mobile phase. Basic substances can usually be separated using C6–C8 alkanesulphonates, and acidic substances using tetralkylammonium salts. Ion pair additives significantly increase retention and improve peak symmetry through the formation of neutral ionic-associated species, called ion pairs, with increased affinity to a non-polar stationary phase. The retention in IPC can be controlled by the type and concentration of the ion pair reagent or of the organic solvent in the mobile phase. Increasing the number and size of alkyls in the reagent molecules enhance retention in the reagent concentration range between 10^{-4} and 10^{-2} *M*.

Nowadays, IEC is used mainly for the separation of small inorganic ions or ionic biopolymers such as oligonucleotides, nucleic acids, peptides, and proteins, rather than in the analysis of small organic ions, for which RP chromatography and IPC usually offer higher efficiency and better resolution. The columns in IEC are packed with fine particles of ion exchangers, which contain charged ion exchange groups covalently attached to a solid matrix (either an organic cross-linked styrene–divinylbenzene or ethyleneglycol–methacrylate copolymer), or inorganic support to which a functional group is chemically bonded via a spacer (a propyl, or phenylpropyl moiety). Strong cation exchangers contain $-SO_3^-$ sulfonate groups and strong anion exchangers contain $-N(CH_3)_3+$ quaternary ammonium groups, completely ionized over a broad pH range (pH = 2–12). Weak cation exchangers contain carboxylic or phosphonic acid groups, which are ionized only in alkaline solutions, and tertiary or secondary amino groups (e.g., diethyl aminoethyl) in weak anion exchangers are ionized only in acidic mobile phases. Ion exchange separations require aqueous or aqueous–organic mobile phases containing counterions (10^{-2}–10^{-1} *M* salts, buffers, ionized acids, or bases), which compete with the sample ions for the ion exchange groups. The retention in IEC decreases with increasing concentration of counterions in the mobile phase and with decreasing ion exchange capacity of the column (1–5 mEq/g for organic polymer ion exchangers and 0.3–1 mEq/g for silica-based ion exchangers). Weak acids are usually separated by anion exchange chromatography at pH > 6, and weak bases are separated by cation exchange chromatography at pH < 6; their retention increases with increasing ionization. By varying the pH of the mobile phase the separation selectivity can be adjusted, whereas the retention is controlled by the ionic strength.

STRATEGIES FOR SELECTING AND OPTIMIZING ISOCRATIC SEPARATION CONDITIONS

Once a suitable HPLC separation mode has been selected, experimental conditions can be adjusted using either an empirical method or a systematic method development approach. The separation of two sample compounds is conveniently characterized by resolution R_S:[4]

$$R_s \cong \frac{\sqrt{N}}{4}(r_{1,2}-1)\frac{k}{1+k} \quad (4)$$
$$= \text{Efficiency} \times \text{Selectivity} \times \text{Capacity}$$

Here, N is the column efficiency expressed in terms of plate number; $r_{1,2}=k_2/k_1$ is the separation factor, which characterizes the selectivity of separation; and k is the average retention factor of the two sample compounds 1 and 2 as a measure of capacity contribution to the resolution. The three terms contributing to the resolution depend on many experimental conditions which can be adjusted either simultaneously or in consecutive steps.

For accurate quantitative analysis the resolution usually should be 1–1.5. However, too high a resolution may result in excessive analysis time. The chromatogram in Fig. 3A schematically illustrates adequate separation of a three-component sample. If the separation is not satisfactory, it can be improved according to the following strategy:

1. Poorly resolved peaks appearing close to the column holdup volume, such as the one in the example in Fig. 3B, show that the retention is too low and should be increased; this is best done by decreasing the elution strength of the mobile phase, whereas the elution strength should be increased if the retention volumes are too large (Fig. 3C).

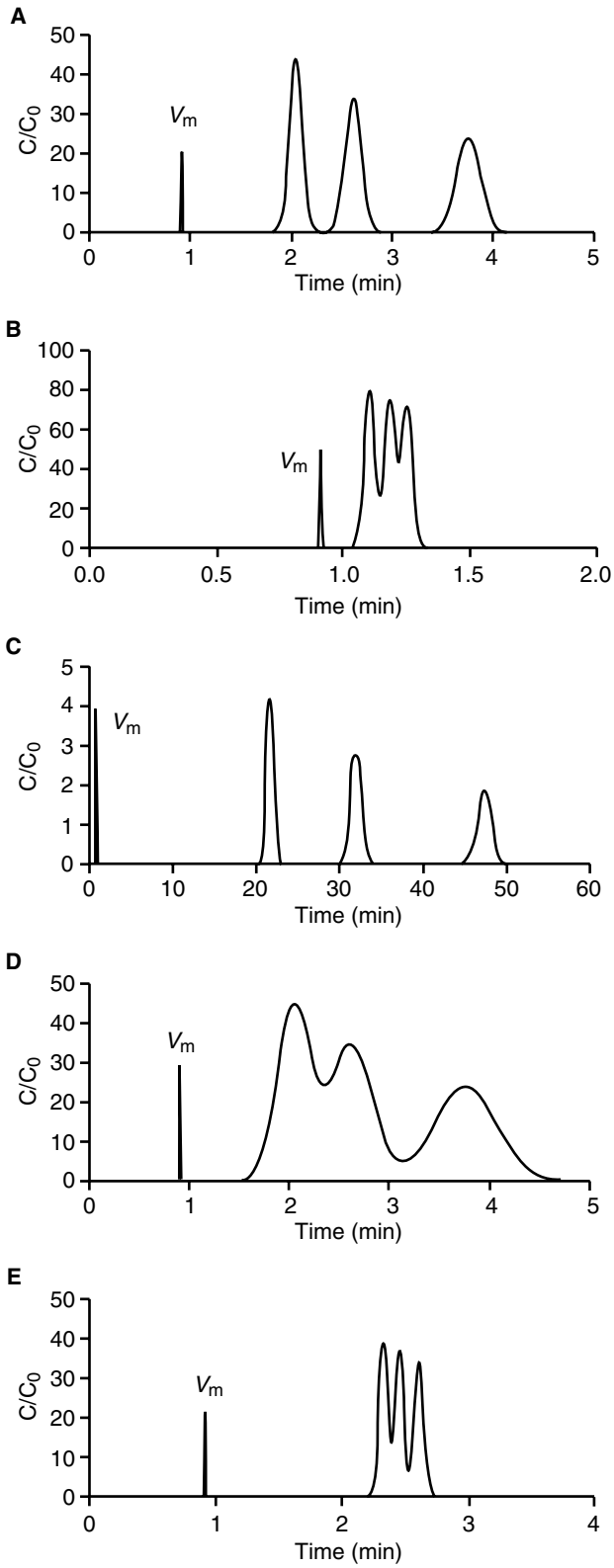

Fig. 3 Examples of chromatographic separation of a three-component sample. (A) Satisfactory separation. (B) Unsatisfactory separation, too low retention. (C) Good resolution, but too long time of separation. (D) Unsatisfactory separation, too low column efficiency. (E) Unsatisfactory separation, good retention and column efficiency, but too low separation selectivity.

2. If the retention times are adequate and partial separation of the bands is apparent but the bands are relatively broad (Fig. 3D), the resolution can possibly be improved by increasing the efficiency (i.e., the plate number of the column).
3. If the bands are narrow, but are not well-separated from each other, such as in Fig. 3E, the selectivity should be improved

    a. By changing the components of the binary mobile phase.
    b. By using ternary or more complex mobile phases or mobile phase additives inducing specific interactions with sample components.
    c. By using another HPLC column with a different stationary phase.

4. If the resolution of early eluted bands is unsatisfactory and the separation time is long, the sample separation is usually improved by temperature or solvent gradients.

CONTROL OF SEPARATION EFFICIENCY

The efficiency contribution to the resolution (i.e., the column plate number, N) is directly proportional to column length, and increases with decreasing particle size of the column packing. Further, column efficiency often improves as the temperature increases because of decreasing viscosity of the mobile phase and increasing diffusion coefficient.

The efficiency contribution to the resolution, i.e., the column plate number, N, is directly proportional to the column length, L, and increases with decreasing particle size of the column packing and—to a lesser extent—with decreasing flow rate of the mobile phase. The dispersion of a solute band as it migrates along the column is characterized by the height equivalent to theoretical plate, $H = L/N$, and depends on experimental conditions, such as the velocity of the mobile phase, u, described to a first approximation by the well-known van Deemter equation:

$$H = A + \frac{B}{u} + Cu = \lambda d_p + 2\gamma\left(\frac{D_M}{u}\right) + c\left(\frac{d_p^2}{D_M}\right)u \quad (5)$$

A, B, and C represent three additive contributions to band broadening. The velocity-independent term A represents the contribution of eddy (radial) diffusion to band broadening and is a function of the size and distribution of interparticle channels and the possible non-uniformities

in the packed bed (coefficient λ); it is directly proportional to the mean diameter of the column-packing particles, d_p. The term B describes the effect of molecular (longitudinal) diffusion in the axial direction and is directly proportional to the solute diffusion coefficient in the mobile phase, D_M. The obstruction factor γ takes into account the hindrance to the rate of diffusion caused by the particle skeleton.

The third term, C, is a measure of the resistance to mass transfer between the stationary phase and the mobile phase. To a first approximation, it is inversely proportional to the diffusion coefficient, D_M, and directly proportional to the second power of the distance a solute molecule should travel from the mobile phase to reach the interaction site in the particle. For a totally porous particle, this distance is proportional to the mean particle diameter, d_p. More exactly, average pore depth should be used instead, but this quantity is difficult to determine.

The minimum on the H–u plot (Eq. 5) corresponds to the best separation efficiency, but separations are often performed at a higher-than-optimum flow rate to decrease the run time. The speed vs. efficiency characteristics of various HPLC columns can be optimized using kinetic plots proposed by Poppe.[3] There, the minimum column holdup time, t_0, necessary to produce the desired number of theoretical plates, N, can be determined from the diagonal line at the point on the plots of H/u, characterizing the speed of separation vs. N in logarithmic coordinates.[3] The plots are charted for different column types assuming a maximum allowed instrumental pressure, $\Delta P_{max} = 40$ MPa, as is usual in conventional LC, and at the optimum flow velocity, u, corresponding to the minimum height equivalent to theoretical plate, H, on the van Deemter H–u curve (Eq. 5). An example of the kinetic plots for columns packed with materials of different mean particle diameter is shown in Fig. 4.

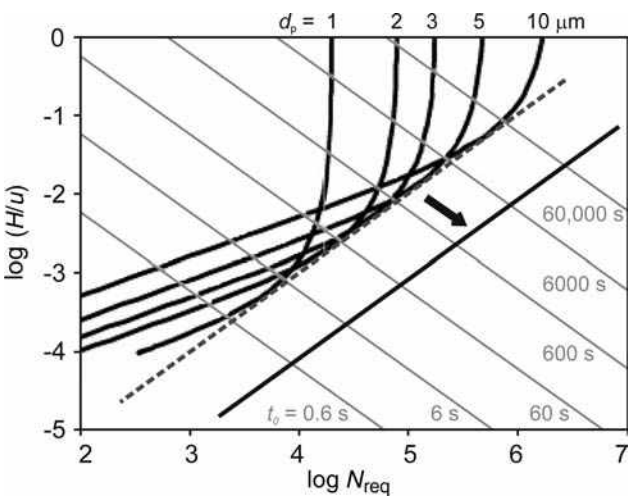

Fig. 4 Kinetic plots for columns packed with different particle sizes, d_p, at a maximum instrumental operation pressure of 40 MPa and optimum flow velocity, u, at the minima of H–u plots; t_0 is column holdup time, N_{req} is the maximum number of theoretical plates.

The kinetic plots divide the plane into two regions. The part on the right side below the dashed envelope line corresponds to the forbidden region, where the desired N vs. t_0 performance cannot be accomplished within the experimental pressure limits. The plots show that very high numbers of theoretical plates can be achieved in long columns packed with relatively large-diameter particles (>10 μm), however at the cost of very long separation times. On the other hand, fast separations in less than 1 min require short columns packed with particles of diameters less than 2 μm, with relatively low N at 40 MPa. To achieve the efficiency of several thousands of theoretical plates with particle diameters of 1–2 μm, longer columns are necessary. This means that the kinetic plots should be moved deeper to the forbidden region, as indicated by the full line in Fig. 4. This can be accomplished using instrumentation for UHPLC technique, with pressure limits up to 150 MPa. Another way to achieve this goal, using the conventional equipment, is decreasing the flow resistance of the columns. Monolithic columns with large flow pores and better permeabilities or columns packed with fused-core particles of small size (2.7 μm) with a thin porous shell (0.5 μm), which provide shorter diffusion paths inside the particles and reduced axial dispersion of solutes, have less stringent pressure limitations and offer faster separations at the same pressure drop in comparison to the columns with totally porous structure. Column permeability is also enhanced at high temperatures, owing to reduced viscosity of mobile phases.

CONTROL OF RETENTION AND SEPARATION SELECTIVITY: STATIONARY PHASE

The retention and the selectivity of separation in RP and NP chromatography depend primarily on the chemistry of the stationary phase and the mobile phase, which control the polarity of the separation systems. There is no generally accepted definition of polarity, but it is agreed that it includes various selective contributions of dipole–dipole, proton–donor, proton–acceptor, π–π electron, or electrostatic interactions. Linear Free-Energy Relationships (LFER) widely used to characterize chemical and biochemical processes were successfully applied in liquid chromatography to describe quantitative structure–retention relationships (QSRR) and to characterize the structural contributions to the retention and selectivity, using multiple linear correlation, such as Eq. 6:[4]

$$\log k = (\log k)_0 + \frac{m_1 V_X}{100} + s_1\pi_2^* + a_1\alpha_2 + b_1\beta_2 \qquad (6)$$

The molecular structural descriptors in Eq. 6 characterizing various structural effects influencing the retention are molar volume of a solvated solute, V_X, polarity, π_2*, hydrogen

bonding basicity, β_2, and hydrogen bonding acidity, α_2. Eq. 6 allows predictions of retention of different solutes on the same column and in the same mobile phase using these molecular descriptors, which can be found in published data bases of properties.[4] The parameters of the LFER equation (Eq. 6), m_1, s_1, a_1 and b_1, obtained using multivariate simultaneous least squares regressions of the experimental retention data for selected standard compounds are characteristic for specific combinations of mobile and stationary phases and can be therefore used for HPLC method development. Stationary phases providing large differences in the LFER parameters for the individual sample components are likely to provide high specific polar selectivity for the separations of specific sample types.

To better distinguish the contributions of polar interactions to retention, the LFER model was transformed into the so-called hydrophobic subtraction model (HSM) for RPLC, where the hydrophobic contribution to retention is compensated for by relating the solute retention to a standard nonpolar reference compound. This approach was applied to characterize more than 300 stationary phases for RPLC, including silica gel supports with bonded alkyl-, cyanopropyl-, phenylalkyl-, and fluoro-substituted stationary phases and columns with embedded or end-capping polar groups. The QSRR models can be used to characterize and compare the suitability of columns not only for reversed-phase, but also for NP and HILIC systems.

Recently, phase optimized liquid chromatography (POPLC) strategy was introduced for selecting the suitable column for specific RP separations. The principle is basically similar to the PRISMA approach suggested earlier by Nyiredy[5] for the selection of optimum composition of ternary mobile phases (see below). A sample is injected under the same isocratic conditions on five bonded-phase columns with different chemistries: 1) an end-capped C18 column with predominant hydrophobic interactions, 2) a C18 column with an embedded amide group providing, in addition, preferential interactions with carbonyl, carboxylic acid, and amino compounds, 3) a phenyl column with preferential adsorption of aromatic compounds on account of π–π interactions, 4) a nitrile column with enhanced dipole–dipole interactions, and 5) a C30 column with enhanced retention of planar compounds in comparison to non-planar ones. Based on the experimental retention data, software calculations are performed to design a POPLC column comprising combinations of various lengths of the five basic stationary phases in up to 25 segments of 10 mm each, tailor-made to provide optimum resolution of a specific sample.

CONTROL OF RETENTION AND SEPARATION SELECTIVITY: MOBILE PHASE

For a successful HPLC separation, the appropriate selection of a mobile phase is equally important as the correct choice of a separation column. Single-component mobile phases do not allow a fine adjustment of the elution strength, as there is only a limited selection of solvents compatible with UV and other common detection techniques, so mixed mobile phases composed of solvents with different elution strengths should be used. Increasing the concentration of the strong solvent in a mixed mobile phase speeds up the elution. The retention of weak acids and weak bases in RPLC increases when the pH of the mobile phase is adjusted to suppress their ionization. A change in the retention, induced by an increase or decrease in the concentration of the strong solvent, is often accompanied by a change in the separation selectivity. The effects of the mobile phase on separation can be predicted, and the separation can be optimized using either a commercial software such as Dry Lab I or simple predictive calculations employing, e.g., Eq. 1 or Eq. 2.

Ternary and more complex mobile phases contain at least two different strong solvents with different predominant selective polar contributions (dipole–dipole, proton–donor, and proton–acceptor) in a weak solvent. Fine selectivity tuning is often possible by appropriate selection of the concentration ratios of the strong solvents.[6] In RP chromatography, acetonitrile with dipole–dipole properties, tetrahydrofuran with proton–acceptor properties, and methanol with both proton–donor and proton–acceptor properties are used as strong solvents in water; in NP chromatography, a non-localizing solvent (dichloromethane), a basic localizing solvent (methyl-*t*-butyl ether), and a non-basic localizing solvent (acetonitrile or ethyl acetate) are mixed and diluted with hexane or heptane to adjust the elution strength. For any three-component or four-component mobile phase, the proportions of the individual selective contributions to the polarity are determined by the concentration ratios of the three strong solvents, whereas the elution strength is controlled by the concentration of water in RPLC and of alkane in NPLC, e.g., using the PRISMA optimization approach.

Single-parameter optimization employs several experiments at preselected values of the optimized parameter (such as the concentration of the strong solvent in a binary mobile phase, pH, temperature) to predict the resolution as a function of the optimized parameter using empirical or simple model-based calculations. Then, plots are constructed (the window diagrams [7]) in which the range of the optimized parameter is searched for the value that provides the desired resolution for all adjacent bands in the chromatogram in the shortest time. An example of a window diagram (Fig. 5) illustrates the approach adopted for the optimization of a binary mobile phase in NPLC.

Some parameters may show synergistic effects on separation. In this case, simultaneous optimization of two or more parameters can provide better results than their sequential optimization. Simple methods can be used for sequential multiparameter optimization in HPLC.

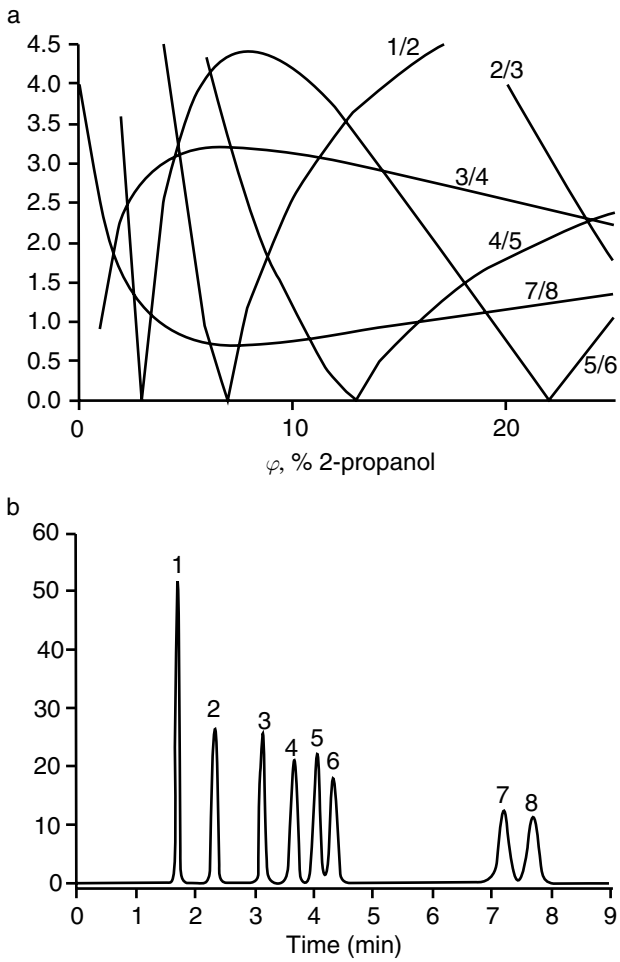

Fig. 5 (a) The window diagram (the dependence of the resolution on the concentration) of 2-propanol in *n*-heptane as the mobile phase, for a mixture of eight phenylurea herbicides on a Separon SGX 7.5 μm silica gel column (150 × 3.3 mm I.D.). (b) The separation with an optimized concentration of 19% 2-propanol in the mobile phase for maximum resolution. Column plate number $N = 5000$, $T = 40°C$, flow rate 1 ml/min. Sample compounds: neburon (1), chlorobromuron (2), 3-chloro-4-methylphenylurea (3), desphenuron (4), isoproturon (5), diuron (6), metoxuron (7), and deschlorometoxuron (8).

Alternatively, the composition of mixed mobile phases can be optimized using an overlapping resolution mapping strategy to adjust the optimum separation selectivity based on seven or more initial experiments with solvent mixtures of approximately equal elution strength. Based on the retention data from the initial experiments, either 3-D diagrams or contour resolution maps are constructed for all adjacent bands in the selectivity triangle space as a function of the concentration ratios of three solvents or two solvents and the pH of the mobile phase, from which the composition of the mobile phase that provides maximum resolution is selected.

Structure-based commercial optimization software (e.g., Chromdream, Chromsword, or Eluex) incorporate some features of the expert system, as the retention is predicted based on the additive contributions of the individual structural elements and, consequently, the optimum composition of the mobile phase is suggested. Such predictions are only approximate and do not take into account stereochemical and intramolecular interaction effects.

TEMPERATURE AS A TOOL FOR CONTROLLING EFFICIENCY, RETENTION, AND SELECTIVITY IN HPLC

The regulation of temperature is convenient and simple, but is usually less effective for improving HPLC separations than is varying the composition of the mobile phase. Further, thermal instability of some solutes can limit the use of high temperatures in HPLC. Another limiting factor is the limited practical temperature range, dictated by the poor stability of many HPLC stationary phases chemically bonded on silica gel supports at temperatures above 60°C (except for some new polydentate bonded phases with bridged structure showing improved resistance against hydrolysis and dissolution). Organic polymer, carbon, or the newly developed zirconium dioxide (zirconia) adsorbents with carbon deposited on the surface or modified with C18, polybutadiene, polystyrene, and other ligands are now commercially available, which show excellent long-term chemical and thermal stability and withstand extended exposure to column temperatures as high as 200°C, unfortunately, often at the cost of inferior efficiency in comparison to bonded silica gel columns.

High-temperature liquid chromatography (HTLC) offers distinct advantages with respect to ambient temperature operation for thermally stable compounds, because mobile phase viscosity and, hence, operating pressure decrease at elevated temperatures, allowing small particle size columns to be used at relatively high flow rates, with improved efficiency. Increased temperature usually affects favorably the separation selectivity of ionic or partially ionized compounds. High temperature enhances the high-speed potential of UHPLC, so that separations of a large variety of samples, such as drugs and chiral compounds, are possible in less than 2 min. At elevated temperatures water polarity decreases, so that pure water can be often used as mobile phase providing retention comparable to aqueous–organic solvent mixtures containing methanol or acetonitrile.

Linear relationships between ln k and the reciprocal value of the thermodynamic temperature T (in Kelvins), have been observed in many chromatographic systems, according to van't Hoff equation (Eq. 7):

$$\ln k = -\frac{\Delta H}{RT} + \frac{\Delta S}{R} + \ln \Phi \qquad (7)$$

where R is the universal gas constant; $-\Delta H$ and ΔS are the enthalpy and entropy, respectively, connected with the solute transfer from the mobile phase to the stationary phase; and Φ is the ratio of the volumes of the stationary to the mobile phase, $\Phi = V_s/V_m$ in the column. Eq. 7 can be used to distinguish the enthalpic and entropic contributions to the retention. However, if the molecular conformation changes with changing temperature, non-linear ln k vs. $1/T$ plots may be observed, such as with biopolymers (proteins). The retention factors, k, of small molecules usually decrease by approximately 1–2% when the column temperature increases by 1°C, but for the same change in temperature, the retention factors of solutes with large $-\Delta H$ are more strongly affected. A change in temperature may be accompanied by a change in separation selectivity, $r_{1,2}$, when sample molecules have different functional groups, relative size, or shape, or if the conformation of the stationary phase changes at increased temperatures. Temperature regulation can be used for optimizing the resolution, e.g., using window diagram strategy, as in the optimization of the composition of the mobile phase.

Column temperature together with mobile phase composition can be optimized simultaneously in RPLC using the optimization software based on Eq. 8:

$$\ln k = a_1 + \frac{a_2}{T} + m\,\varphi\left(1 - \frac{T_C}{T}\right) \quad (8)$$

where ϕ is the volume fraction of the organic solvent in the aqueous–organic mobile phase, T_C is the enthalpy–entropy compensation temperature and a_1, a_2, and m are parameters depending on solutes and stationary phase. For a given sample, four initial experiments should be run at two different temperatures and mobile phase compositions to allow designing of the resolution map as a function of both temperature and mobile phase composition.

Simultaneous optimization of temperature and stationary phase can be carried out for two tandem columns with different selectivities for the sample compounds by adjusting the temperature individually for each column at a constant composition of the mobile phase.

CONCLUSIONS

Suitable detection conditions, separation mode, appropriate column dimensions, and packing materials (stationary phase) in isocratic LC should be selected keeping in mind the objective of separation, using the information on sample properties, such as solubility, polarity, and presence of specific functional groups in sample compounds, sample amount, concentration., etc. For the control of separation selectivity, resolution, and time of analysis, appropriate selection of the mobile phase is as important as the choice of the stationary phase. Isocratic separations can be optimized using single-parameter or multiparameter strategies, using either commercial software or simple computer-aided predictive calculations.

REFERENCES

1. Snyder, L.R.; Dolan, J.W.; Gant, J.R. Gradient elution in high-performance liquid chromatography: I. Theoretical basis for reversed-phase systems. J. Chromatogr. **1979**, *165*, 3–30.
2. Jandera, P.; Kučerová, M.; Holíková, J. Description and prediction of retention in normal-phase high-performance liquid chromatography with binary and ternary mobile phases. J. Chromatogr. A, **1997**, *762*, 15–26.
3. Poppe, H. Some reflections on speed and efficiency of modern chromatographic methods. J. Chromatogr. A, **1997**, *778*, 3–21.
4. Du, C.M.; Valkó, K.; Bevan, C.; Reynolds, D.; Abraham, M.H. Characterizing the selectivity of stationary phases and organic modifiers in reversed-phase high-performance liquid chromatography systems by a general solvation equation. J. Chromatogr. Sci. **2000**, *38*, 503–511.
5. Nyiredy, S.; Szucs, Z.; Szepesy, L. Stationary phase optimized selectivity liquid chromatography: Basic possibilities of serially connected columns using the "PRISMA" principle. J. Chromatogr. A, **2007**, *1157*, 122–130.
6. Glajch, J.L.; Kirkland, J.J.; Snyder, L.R. Practical optimization of solvent selectivity in liquid–solid chromatography using a mixture-design statistical technique. J. Chromatogr. **1982**, *238*, 269–280.
7. Price, W.P.; Deming, S.N. Optimized separation of scopoletin and umbelliferone and *cis–trans* isomers of ferulic and *p*-coumaric acids by reverse-phase high-performance liquid chromatography. Anal. Chim. Acta **1979**, *108*, 227–231.

BIBLIOGRAPHY

1. Neue, U.D.; *HPLC Columns: Theory, Technology and Practice*. Wiley-VCH: New York, 1997.
2. Schoenmakers, P.J. *Optimisation of Chromatographic Selectivity*. Elsevier: Amsterdam, 1986.
3. Snyder, L.R.; Kirkland, J.J.; Glajch, J.L. *Practical HPLC Method Development 2nd*. John Wiley & Sons: New York, 1997.

Katharometer Detector for GC

Raymond P.W. Scott
Scientific Detectors Ltd., Banbury, Oxfordshire, U.K.

INTRODUCTION

The katharometer detector [sometimes spelled "catherometer" and often referred to as the *thermal conductivity detector* (TCD) or the *hot-wire detector* (HWD)] is the oldest commercially available gas chromatography (GC) detector still in common use. Compared with other GC detectors, it is a relatively insensitive detector and has survived largely as a result of its almost universal response. In particular, it is sensitive to the permanent gases to which few other detectors have a significant response. Despite its relatively low sensitivity, the frequent need for permanent gas analysis in many industries probably accounts for it still being the fourth most commonly used GC detector. It is simple in design and requires minimal electronic support and, as a consequence, is also relatively inexpensive compared with other detectors.

DISCUSSION

In the late 1940s and early 1950s, the katharometer was developed for measuring the amount of carbon dioxide in flue gases. However, with the advent of GC, its use as a detector was investigated by Ray.[1] It was soon established as a very effective GC detector and was found to be simpler to fabricate than the gas density bridge, but had about the same sensitivity and linearity. For a while, it was the only detector that was commercially available. At the time, its mode of action was the subject of some controversy, as it was not clear whether it responded to changes in the *thermal conductivity* or the *specific heat* of the column eluent. The response of the detector was examined in detail by Mellor[2] and Harvey and Morgan[3] in 1956 and it would appear that no such detailed studies have been carried out since that time. It was concluded that the katharometer responded to both changes in thermal conductivity *and* to changes in the specific heat of its surroundings. In any particular system, depending on the operating conditions employed, one or the other property may dominate in controlling the response of the detector. The relationship, however, is not simple and it was not found possible to accurately predict the response of the detector from a knowledge of the specific heat and thermal conductivity of the gases or vapors involved.

The basic design of a katharometer is as follows. A filament carrying a current is situated in the column eluent. Under equilibrium conditions, the heat generated in the filament will equal the heat lost by conduction, convection, and radiation and the filament will assume a constant temperature. The filament is constructed from a metal, such as platinum, that has a high temperature coefficient of resistance, and at the equilibrium temperature, the resistance of the filament and, thus, the potential across it will be constant. The heat lost from the filament will depend on the thermal conductivity of the gas, its specific heat, and the thermal emissivity of the filament surface. Both the thermal conductivity and the specific heat of the gas will change in the presence of a different gas or solute vapor. As a result, the temperature of the filament will change, causing a change in potential across the filament. This potential change is amplified and either fed to a suitable recorder or regularly sampled by an appropriate data acquisition system.

As the device responds to the heat lost from the filament, the katharometer detector is extremely *flow* and *pressure* sensitive. Consequently, all katharometer detectors must be carefully thermostatted and must be fitted with reference cells to help compensate for changes in pressure or flow rate. There are two basic katharometer designs: the "in-line" cell, where the column eluent actually passes directly over the filament, and the "off-line" cell, where the filaments are situated away from the main carrier gas stream and the gases or vapors only reach the sensing element by diffusion. Due to the high diffusivity of vapors in gases, the diffusion process can be considered as almost instantaneous. Diagrams of the two katharometer designs are shown in Fig. 1.

The sensitivity of the katharometer is only about 10^{-6} g/ml (probably the least sensitive of all GC detectors) and has a linear dynamic range of about 500 (the response index lying between 0.98 and 1.02). It is, however, a general detector and will sense all permanent gases and vapors other than the gas that is used as the carrier gas. Its universal response is one reason for its survival as a GC detector, despite its very limited sensitivity. Although the least glamorous, this detector can be used in most GC analyses that utilize packed columns and where there is no limitation to sample availability. Although small-volume katharometers have been designed for use with capillary columns, the katharometer is rarely used with such columns, again due to its relatively low sensitivity. The device is simple, reliable, rugged, and, as already stated, comparatively inexpensive. As a consequence, it has found use in less than ideal environments where GC

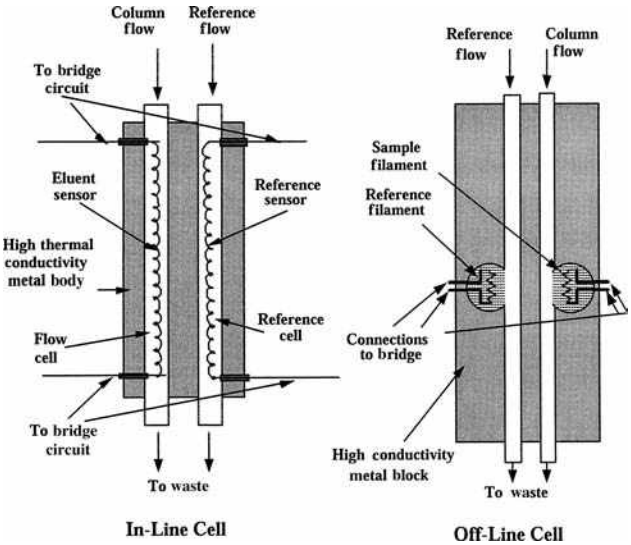

Fig. 1 Katharometer cells.

is employed for process monitoring and process control. If constructed of platinum and Teflon, the katharometer is one of the few detectors that can be used for detecting very corrosive materials such as the halogens, uranium hexafluoride, volatile inorganic acids, and so forth.

REFERENCES

1. Ray, N.H. Gas chromatography. I. The separation and estimation of volatile organic compounds by gas-liquid partition chromatography. J. Appl. Chem. **1954**, *4* (1), 21.
2. Mellor, N. *Vapor Phase Chromatography*; Desty, D.H., Harbourn, C.L.A., Eds.; Butterworths: London, 1957; 63.
3. Harvey, D.; Morgan, G.O. *Vapor Phase Chromatography*; Desty, D.H., Harbourn, C.L.A., Eds.; Butterworths: London, 1957; 74.

BIBLIOGRAPHY

1. Scott, R.P.W. *Chromatographic Detectors*; Marcel Dekker, Inc.: New York, 1996.
2. Scott, R.P.W. *Introduction to Gas Chromatography*; Marcel Dekker, Inc.: New York, 1998.

Kovats' Retention Index System

Igor G. Zenkevich
Chemical Research Institute, St. Petersburg State University, St. Petersburg, Russia

INTRODUCTION

In "classical" chromatographic methods (excluding hyphenated techniques), analytical signals are two dimensional. Each chromatographic peak may be characterized by two parameters: area, which is proportional to the quantity of substance being eluted from column, and its position on the chromatogram (retention time, t_R), which reflects the interaction between the sorbate (analyte) and sorbent (stationary phase). This interaction is the principal source of information about the chemical nature and structure of the analytes.

However, the "raw" retention times by themselves are not useful for any chemical interpretation owing to their dependence on numerous conditions of analysis. In Gas Chromatography, for example, these conditions include type of stationary phase, its content in packed columns or film thickness in the capillary columns, length of the column, oven temperature (constant temperature in isothermal conditions or initial temperature and ramp at temperature programming), carrier gas flow, and even the pressure gradient between the inlet and outlet of the chromatographic system. The characterization of analytes in chromatography by net retention times may be compared to the measurements of temperature by thermometers with different arbitrary scales or even without any scales at all. Thus, the standardization of chromatographic retention parameters is a problem of extremely high importance.

One possible solution is based on the complete interlaboratory standardization of all above-mentioned experimental conditions. The realization of the so-called retention time locking (RTL) concept became possible only during the mid-1990s by using high precision chromatographic equipment. At present, it is rarely used for determination of only restricted sets of analytes (typical examples of confirmatory analysis), for instance, pesticides or drugs.[1] The second most widely used and conventional approach requires the recalculation of the raw retention data, which are measured at different conditions using an interlaboratory comparable scale. The mathematical method suitable for this recalculation—linear interpolation—has been known long before the appearance of chromatography.

Given pairs of function (y) and argument (x) values—$y_1(x_1)$, $y_2(x_2)$,..., $y_n(x_n)$—that are connected by a known or unknown functional dependence $y = f(x)$, we can estimate the unknown values y_i, which are located between the known values $y_k < y_i < y_{k+1}$ from the value $x_i (x_k < x_i < x_{k+1})$ by following a simple linear interpolation relationship:

$$y_i = y_k + (y_{k+1} - y_k) \times (x_i - x_k)/(x_{k+1} - x_k) \quad (1)$$

In the case of a non-linear or unknown dependence $y = f(x)$, the application of a simple linear interpolation leads to some uncertainty in the results. However, if the equation for non-linear dependence $f(x)$ is known, a transformation of Eq 1 into Eq. 2 can be used to remove the non-linearity and, hence, errors of interpolation. This approach gives results of the same precision as that of direct calculation with $y = f(x)$:

$$y_i = y_k + (y_{k+1} - y_k) \times \{[f(x_i) - f(x_k)]/[f(x_{k+1}) - f(x_k)]\} \quad (2)$$

The application of this concept in chromatography requires the introduction of some extra components with previously known (postulated) retention indices (RIs) into the samples being analyzed. Their peaks form a "mobile" co-ordinate system for the recalculation of t_R data of the target analytes. Hence, the establishment of any retention index system needs the following:

1. The choice of set of reference compounds (most often they are members of the same homologous series that differ by a homologous difference CH_2).
2. The attribution of standard (conventional) RI values for these compounds.
3. The choice of a formula for the calculation of RI values for all other analytes.

The basis of RI systems in chromatography is similar to the mode of the definition of commonly used temperature (T) scales, namely centigrade (Celsius), where:

1. Reference points for this scale are melting and boiling temperatures (T) of water.
2. Standard (conventional) T values for these reference points are 0°C (melting) and 100°C (boiling).
3. The formula for calculation of other T values between and outside accepted reference points is that for linear interpolation (1).

KOVATS' RETENTION INDICES

The first RI system was proposed by Kovats in 1958[2] for isothermal conditions of gas chromatography (GC) analysis.

The easily accepted *n*-alkanes (*n*-C_nH_{2n+2}), with postulated RI values $RI = 100 \times n_C$ [e.g., methane (CH_4)—100, *n*-non-ane (C_9H_{20})—900, *n*-hentriacontane ($C_{31}H_{64}$)—3100, etc.], were recommended as reference compounds. This is because, under isothermal conditions of GC analysis, a linear dependence of logarithms of corrected retention times $t_R' = t_R - t_0$ (t_0 is the hold up time of chromatographic system) on the number of carbon atoms in the molecule of homolog is observed, i.e., $\log t_R' = an_C + b$. Keeping in mind that (by definition) $100n_C = RI$, the existence of the following linear dependence is implied:

$$RI = a \log t_R' + b \tag{3}$$

If we consider the last relationship as the function $y = f(x)$ in Eq. 2, we come to the final equation of Kovats' Retention Index (KRI) System:

$$RI_x = RI_k + (RI_{k+1} - RI_k) \times \{[\log(t_{R,x}') - \log(t_{R,k}')]/[\log(t_{R,k+1}') - \log(t_{R,k}')]\} \tag{4}$$

where $t_{R,\,x}' < t_{R,\,k}' < t_{R,\,k+1}'$ are the corrected retention times of reference *n*-alkanes with k and $k + 1$ the number of carbon atoms being eluted immediately before ($t_{R,\,k}'$) and after ($t_{R,\,k+1}'$) the target compound ($t_{R,\,x}'$).

Because the basis of formula (4) is linear dependence (Eq. 3), it is possible to use retention times of those reference *n*-alkanes that differ not by one, but by a greater number of carbon atoms, i.e., RI_{k+m} and RI_k with $t_{R,k+m}$ and $t_{R,k}$ ($m > 1$). In the original publication of Kovats[2] the difference $m = 2$ was only used. But when $m = 1$, Eq. 3 may be simplified to the various seemingly different, but same, relationship formulas. For example:

$$RI_x = 100 \times \{k + [\log(t_{R,x}'/t_{R,k}')]/[\log(t_{R,k+1}'/t_{R,k}')]\} \tag{5}$$

where k is the number of carbon atoms in the *n*-alkane that elutes before the compound undergoes characterization, and 100 is the RI equivalent of homologous difference CH_2.

The numerical coefficient 100 included in the formula for calculation of RIs has only conventional sense. The same relationships can be used for presentation of retention data without this coefficient in the form of the so-called MU (molecular units) values. In this form, reference *n*-alkanes are characterized by standard values $MU = n_C$, and, hence, MU equivalent of homologous difference CH_2 is equal to 1. Other relationships that need to be calculated are the same as those in KRI. Organic compounds of some selected groups (for instance, steroids and their derivatives[3]) are historically often characterized not by RIs, but just by MU values.

The proposed form of data presentation has become highly popular and useful in GC. To date, thousands of citations have been made to Ref.[2] The RI values are proportional to the free energies of sorption, that is their thermodynamic interpretation. However, the principal restriction of KRI seems to be that they can be applied only in isothermal conditions of GC separation, whilst most of the real analyses of complex mixtures need temperature programming (linear programming used preferably), or, in general cases, non-isothermal regimes. The generalization of RI concept on these conditions implies using the same linear interpolation relationship (1).

LINEAR AND OTHER RETENTION INDICES

For linear temperature programming regimes [which are characterized by two variables: initial temperature, T_0, and rate of its increase (ramp), r, deg/min], linear relationship (3) does not hold. In some partial cases, another linear dependence seems more precise for retention time approximation:

$$RI \approx at_R + b \tag{6}$$

This is a reason to change the formula for RI calculation (the set of reference compounds and their attributed RI values remain the same). This version of RIs especially for linear temperature programming regime (linear RIs) had been proposed by Van den Dool and Kratz in 1963:[4]

$$RI_x = RI_k + (RI_{k+1} - RI_k) \times (t_{R,x} - t_{R,k})/(t_{R,k+1} - t_{R,k}) \tag{7}$$

Or after the same simplifications as those that were used for Eq. 4, one gets:

$$RI_x = 100 \times [k + (t_{R,x} - t_{R,k})/(t_{R,k+1} - t_{R,k})] \tag{8}$$

Owing to the approximate character of dependence (6), Eqs. 7 and 8 give less comparable results for the same compounds in different temperature programming regimes. As a consequence, the replacement of k, $k + 1$ pair of reference *n*-alkanes on the k, $k + m$ ($m > 1$) also increases the errors to an unpredictable extent and is usually not recommended.

At any non-isothermal conditions of GC analysis, all analytes can be characterized not only by retention times (t_R), but also by the so-called retention temperatures, T_R, especially those that are directly proportional to the retention times at linear temperature programming ($r = \text{const}$), $T_R = T_0 + rt_R$, where T_0 is the initial temperature. Hence, relationships (7) and (8) can be rewritten by including T_R values instead of t_R, for example:

$$RI_x = 100 \times [k + (T_{R,x} - T_{R,k})/(T_{R,k+1} - T_{R,k})] \tag{9}$$

However, this replacement of variables is only in the theoretical sense, because of less precision of T_R value measurement in comparison with that for retention times.

Complex dependencies $RI = f(t_R)$ in non-isothermal conditions of GC analysis may be described by polynomials of different degrees (up to 13 have been tested) or splines (cubic splines seem most convenient[5]). However, the calculation of coefficients of an N-degree polynomial needs t_R data for at least $N + 1$ reference compounds instead of only two t_R values in "classical" RI systems. In connection with this fact, it is interesting to mention the combined lin-log RI system, which was proposed in 1984.[6,7] If both dependencies (3) and (6) are non-linear at temperature programming, each local window of retention times of reference compounds may be precisely approximated by linear and logarithmic addends in variable proportion:

$$RI = a(t_R + q \log t_R') + c \quad (10)$$

and

$$RI_x = RI_k + (RI_{k+m} - RI_k) \times \{[f(t_{R,x}') - f(t_{R,k}')]/[f(t_{R,k+m}') - f(t_{R,k}')]\} \quad (11)$$

where $f(t_R') = t_R + q \log t_R'$. The variable parameter q may be calculated in different ways, but in the simplest case it only needs t_R data for three successive reference compounds with retention times $t_{R,k-1}$, t_R, and $t_{R,k+1}$:

$$q = (2t_{R,k} - t_{R,k-1} - t_{R,k+1})/(\log t_{R,k-1}' + \log t_{R,k+1}' - 2 \log t_{R,k}') \quad (12)$$

This formula for the calculation of parameter q can be generalized on the various sets of reference n-alkanes.

The most convenient advantage of lin-log RI system is the possibility of its application in any temperature regime of GC analysis without special choice of formulas for calculations. Under isothermal conditions, the logarithmic contribution in the total dependence $RI = f(t_R)$ exceeds the linear one by many times, which automatically reflects on the value of $q(|q| \to \infty)$. Only lin-log RI system provides the most comparable results in different temperature conditions of analyses.

The last statement can be illustrated by the following example. The analytical problem is the characterization of 2,4,4-trimethyl-2-pentene (diisobutylene, *I*) by RI values on packed column with polar inorganic sorbent Silipor-600 (LaChema, Czech Republic) in temperature programming regime from 50 up to 220°C (ramp 8 deg/min). Raw retention times of (*I*) and reference *n*-alkanes (min) are: (*I*)—20.16; C_6—12.70; C_7—15.94; C_8—18.73; C_9—none; C_{10}—23.74; $t_0 \approx 1.01$. The results of RI calculation with various sets of *n*-alkanes illustrate the maximal reproducibility of just lin-log RIs in the absence of the influence of the choice of reference compounds. The negative value of parameter q is typical for temperature programming regimes with high ramps (8 deg/min in the case under consideration).

Set of reference n-alkanes	RI_{linear}	$RI_{logarithmic}$
7,8	851	846
7,10	862	877
8,10	857	862
Average RI values	857 ± 6	862 ± 15
Set of reference n-alkanes (q)	$RI_{lin\text{-}log}$	
6,7,8 (–6.14)	855	
6,8,10 (–6.15)	855	
7,8,10 (–6.09)	855	
Average RI values	855	

These large differences in the reproducibility are caused by principal non-linearity of the dependencies $RI = f(\log t_R')$ and $RI = f(t_R)$, whilst the appropriate choice of parameter q provides the real linear dependence $RI = f(t_R' + q\log t_R')$ in any temperature programming regimes, as is illustrated in Fig. 1 for the example of retention times of reference *n*-alkanes C_6, C_8, and C_{10} presented above.

Retention indices of various systems sometimes are considered as different characteristics of chemical compounds. However, it is rational to neglect the differences in these parameters for the same compounds, measured in unequal conditions (in various laboratories) with the same stationary phases. Statistical processing of all of them (so-called randomization) gives averaged RI values (together with corresponding standard deviations), which can be considered as GC constants of organic compounds, as well as their other physicochemical parameters (Table 1).

Retention indices values of all systems can be calculated using the simplest auxiliary computer programs, even with those used for pocket programmable calculators. Unfortunately, this very fact (the necessity of additional calculations) is often declared as the principal reason for restricted application of these GC parameters in real analytical practice.

PROPERTIES AND APPLICATIONS OF RETENTION INDICES

The maximal influence on RI values is the nature of stationary phase in the chromatographic column (few hundred phases are recommended in contemporary analytical practice). Use of these parameters as the constants of chemical compounds (similar to other known physicochemical constants like boiling point, T_b, refractive index, n_D^{20}, density, d_4^{20}, etc.) implies the choice of standard phases for their determination. In accordance with the criteria of most common application, two types of phases may be classified as standard ones:

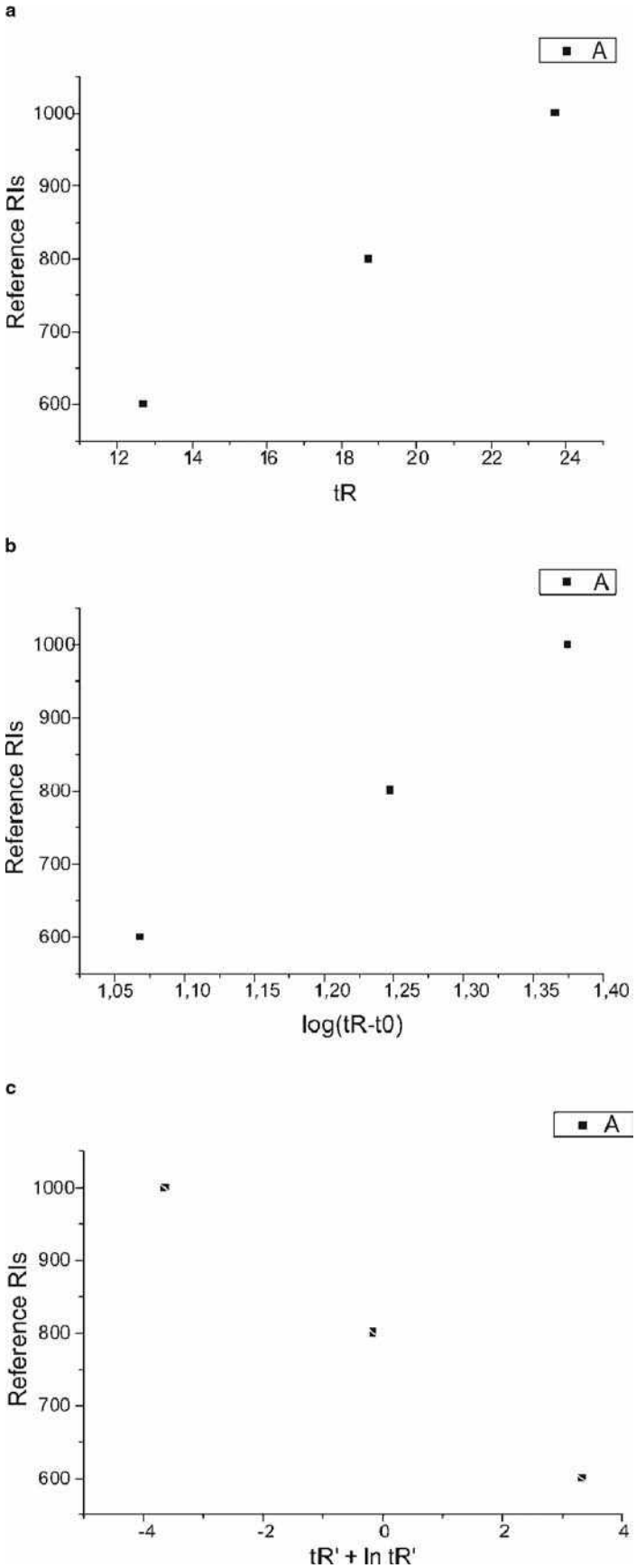

Fig. 1 Graphical illustration of the linearity of the interpolation of retention times of reference *n*-alkanes in temperature programming regime by various functions: (a) $RI = f(t_R)$ (non-linear); (b) $RI = f(\ln t_R')$ (non-linear) and (c) $RI = t_R' + q\ln t_R'$ (linear, $\rho = -1.0000$, $q = -6.15$).

Table 1 GC retention indices as constants of some organic compounds.

Molecular weight	Molecular formula	Compound	RI $\pm$ s_{RI} (N)[a]
137	$C_9H_{15}N$	Pyridine-1,2-dihydro-2,2,4,6-tetramethyl	942 $\pm$ 4 (3)
138	$C_{10}H_{18}$	Cyclodecene	1114 $\pm$ 6 (6)
140	C_8H_9Cl	Benzene-1-chloro-2-ethyl	1016 $\pm$ 6 (3)
140	$C_3H_9O_4P$	Trimethylphosphate	902 $\pm$ 10 (5)
142	$C_7H_{10}O_3$	2,4-Pentanedione-2-acetyl	1045 $\pm$ 3 (4)
148	$C_{11}H_{16}$	Benzene-1-ethyl-2,3,5-trimethyl	1184 $\pm$ 2 (5)
149	$C_{10}H_{15}N$	Benzenemethanamine-*N*-(1-methylethyl)	1148 $\pm$ 5 (3)

[a]N is the number of initial RI values taken for statistical processing.
All data are taken from the author's database.

1. Polydimethyl siloxanes $[–Si(CH_3)_2–O–]_n$ (standard non-polar phases) (maximal temperature of application ≈300–350°C).
2. Polythylene glycols $[–CH_2CH_2–O–]_n$ (standard polar phases) (maximal temperature of application ≈225–250°C).

Each of these groups of phases includes numerous items of various trade names, different average molecular weights, viscosity, thermal stability, and so forth, but having similar polarity. Up to the mid-1970s, the preferred non-polar phase was squalane (isoprenoid alkane $C_{30}H_{62}$), but this phase is no longer used because of its low thermal stability (only about 110°C). However, this obsolete phase maintains its importance as a non-polar standard in GC. Other phases are characterized by differences of RI values (so-called Rohrschneider constants,[8] later generalized by McReynolds) of specially selected 5 or 10 test compounds between the phase under consideration and squalane, for example:

Test compounds	ΔRI
Benzene	16 $\pm$ 1
1-Butanol	53 $\pm$ 2
2-Pentanone	44 $\pm$ 1
Nitropropane	65 $\pm$ 2
Pyridine	42 $\pm$ 1

The comparison of RI values of the same compounds measured with the same stationary phase but at different conditions of analysis indicates some deviations. Most significant of them are temperature dependence of RIs, non-controlled sorption of analytes in GC columns and variations of ratio of analytes and reference alkanes,[9] and, of course, the features of RI approximation in temperature programming regimes (see above). The first of these seems to make the most important contribution (coefficient β is a measure of this dependence; typically $\beta > 0$):

$$\beta = dRI/dT \approx [RI(T_2) - RI(T_1)]/(T_2 - T_1) \quad (13)$$

Among the multitude of organic compounds, there is a small number of objects with $\beta \approx 0$ (all types of acyclic compounds most topologically relevant to *n*-alkanes). The increase in number of cycles in the molecules leads to the increase of β up to 0.3–0.5 (cycloalkanes, arenes, etc.), 0.5–0.8 (naphthalenes, biphenyl, etc.), and 1.0 and more retention index units per degree (i.u./deg) for tri- and polycyclic structures. Hence, it is not surprising that RI data for isoalkanes, ethers, esters, etc. being measured at different conditions, are in good accordance with each other (standard deviations of randomized interlaboratory values are not more than 1–3 i.u.). The same statistical characteristics for substituted benzenes is about 8 i.u., and for naphthalenes and other condensed arenes, it may exceed 10–15 i.u.

The choice of *n*-alkanes as a reference set of compounds for the determination of RI values has been accepted up to the present. Meanwhile, numerous other homologous series have been recommended for different specific applications. For example, GC analysis with electron capture detectors (selective to halogenated compounds) needs other reference compounds of similar chemical origin. These series are alkyl trichloroacetates $(CCl_3CO_2C_nH_{2n+1})$,[10] trialkylamines,[11] alkyl methyl phosphonofluoridates $[CH_3P(O)(F)OC_nH_{2n+1}]$ (so called P series), *O*-alkyl *bis*(trifluoromethyl)phosphinothionates $[(CF_3)_2P(S)\ OC_nH_{2n+1}]$ (A series), alkyl *bis*(trifluoromethyl)thiophosphines $[(CF_3)_2P(S)\ C_nH_{2n+1}]$ (M series), and others (see review[12]). The last two series seem most universal for different types of GC detectors owing to the simultaneous presence of various elements in the molecule (Hal, P, S, CH). A special set of reference objects has been proposed by Lee, Novotny, and Bartle[13,14] for the analysis of polycyclic aromatic compounds to eliminate the strong temperature dependence of their RIs in the *n*-alkane scale. This system is based on benzene (postulated RI value 100 = 100 × number of cycles), naphthalene (200), phenanthrene (300), chrysene (400), picene (500), benzo[b]-picene (600) and dinaphtho[2,1-a : 2,1-h]anthracene (700) (i.e., condensed aromatic hydrocarbons) and formulas of

linear RI system (7) and (8). Of course, RI values, being measured with different reference series, are not directly comparable to each other; but, if necessary, they may be recalculated.

As can be seen, reference compounds in Lee's RI system belong not to the same homologous series, but rather to the special group of structural analogs. In fact, all formulas for RI calculation [(4), (5), (7), and (8)] do not include mathematical restrictions on the choice of reference compounds. However, the non-equidistant choice of reference points decreases the precision of recalculation of these indices into other scales. Another example of the similar choice of non-homologous reference compounds is, for instance, the system presented in he work[15] and based on trifluoroacetic esters of 4-fluorophenol (100), 1-naphthol (200), 4-phenanthrol (300), and 3-hydroxybenzo[c]phenanthrene (400).

Since the 1980s, some applications of the RI system have been reported for reversed phase HPLC (RP-HPLC). The principal requirement for the reference compounds in this method with UV detection is the presence of chromophores in the molecules. The most widely accepted RI system in HPLC is based on homologous alkyl phenyl ketones $PhCOC_nH_{2n+1}$ (so called Smith's system of RIs; by analogy with GC, the RI values, attributed for reference compounds, are $100 \times n_C$).[16] Other RI scales imply the use of homologous monoalkylbenzenes (PhC_nH_{2n+1}), 1-nitroalkanes ($C_nH_{2n+1}NO_2$), glycerol-1-(4-acylphenyl) ethers [4-$C_nH_{2n+1}CO$–C_6H_4–OCH_2–CH(OH)–CH_2OH], and so forth. The last set of substances is convenient for determination of RIs of most hydrophilic organic compounds; the first member of this set is eluted before the simplest reference components of other series. In the isocratic regimes of HPLC separation, which are analogous to isothermal conditions in GC, linear dependence (3) is correct and RIs must be calculated with formulas (4) and (5). With gradient elution, by analogy with temperature programming, formulas (7) and (8), which are based on dependence (6), are preferable. Of course, lin-log RI system may be used in any regimes of RP-HPLC as well as in GC.

Statistical processing of these RIs similar to that in GC gives values, which can be considered as chromatographic constants in RP-HPLC (Table 2).

It is interesting to note that by analogy with chromatographic retention parameters, the values of some other properties of organic compounds may be presented in the linear interpolated form relative to the set of reference compounds. Those equivalent to indices' forms have values known for boiling points,[17] molecular weights,[18] and molar refractions, $MR_D = (MW/d) \times (n^2–1)\ /(n^2 + 2)$, where MW is the molecular weight, n_D^{20} is the refractive index, and d_4^{20} is the density.[19] For example:

$$I(T_b) = 100\times[k + (\log(T_{b,x}/T_{b,k})/(\log(T_{b,k+1}/T_{b,k})] \quad (14)$$

where $T_{b,k} < T_{b,x} < T_{b,k+1}$ are the boiling points of *n*-alkanes with k and $k + 1$ carbon atoms in the molecule and the target compound.

For non-polar compounds, the values $I(T_b)$ are close to experimental RI data being measured on non-polar stationary phases, which is an important feature for their precalculation.

The possibility of precalculation of RIs both from other physicochemical parameters and molecular topological parameters[20] and by different additive schemes, which is impossible for net retention times, seems to be their most significant feature. The methods of RI precalculation form complex algorithms, and as very simple but useful rules. For instance, it is interesting to note that even in the first publication of Kovats,[2] the rule for precalculation of RIs for compounds of general type A–B by arithmetic averaging of data for compounds A–A and B–B has been recommended, i.e., RI(A–B) = [RI(A–A) + RI(B–B)]/2. However, this

Table 2 Retention indices as constants of some organic compounds in reversed phase HPLC with *n*-alkylphenyl ketones as reference compounds.

Molecular weight	Molecular formula	Compound	RI ± s_{RI}
94	C_6H_6O	Phenol	688 ± 16
96	$C_5H_4O_2$	Furfurol	593 ± 9
135	C_8H_9NO	Acetanilide	689 ± 10
146	$C_9H_6O_2$	Coumarin	791 ± 13
148	$C_{10}H_{12}O$	Anethol	1142 ± 10
150	$C_{10}H_{14}O$	Thymol	1027 ± 10
152	$C_8H_8O_3$	Methyl salicylate	934 ± 9
152	$C_8H_8O_3$	Vanillin	702 ± 22
164	$C_{10}H_{12}O_2$	Eugenol	910 ± 14
165	$C_9H_{11}NO_2$	Benzocaine	823 ± 11
194	$C_8H_{10}N_4O_2$	Caffeine	633 ± 27

All data are taken from the author's database.

rule can be used in the mathematically transformed form, namely RI(B–B) = 2RI(A–B) –RI(A–A). If B is a more complex structural fragment than A, this is the simplest way to precalculate RIs of high molecular weights compounds from data for simpler precursors.

This general statement may be illustrated by following example: The estimation of unknown RI value of 1,1,1,3,3,3-hexachloropropane CCl_3–CH_2–CCl_3 needs the data of 1,1,1-trichloropropane and non-substituted propane, as $2 \times CCl_3$–CH_2–$CH_3 - C_3H_8 = CCl_3$–CH_2–CCl_3, namely $2 \times (736 \pm 3) - 300 = 1172 \pm 4$. The same logical scheme of evaluation starting from 1,1,1-trichloroethane and methane, $2 \times CCl_3$–$CH_3 - CH_4 = CCl_3$–CH_2–CCl_3, gives a similar RI value of $2 \times (638 \pm 9) - 100 = 1176 \pm 13$.

CONCLUSIONS

The Kovats Retention Index System, which was proposed in the early period of the development of GC (1958), has become a useful tool for retention data processing, presentation, and interpretation. Use of these analytical parameters at present should be considered as obligatory in the reliable identification of analytes in contemporary hyphenated techniques, especially GC/MS. There are a lot of complex mixtures of organic compounds, whose identification of components cannot be made without taking into account the reference RI data, namely petroleum products, essential oils, flavors and fragrances, pharmaceutical metabolites, and so forth. As a confirmation of this conclusion, the following fact may be noted: The rules of paper presentation in some journals like *Journal of Essential Oil Research*, *Flavor and Fragrance Journal*, *Agricultural and Food Chemistry*, etc. imply the obligatory presentation of retention parameters, preferably in the form of RIs.

The real contemporary problems in perfecting GC retention index system seem to be the formation of available and representative databases by analogy with well-organized databases in mass spectrometry and improvement in the methods of their precalculation. It means at first obtaining the higher precision of the results and then expanding the domains of chemical determination of corresponding algorithms, i.e., their applicability to the larger multitudes of organic compounds of various chemical origin.

REFERENCES

1. Rasanen, I.; Kontinen, I.; Nokua, J.; Ojanpera, I.; Vuori, E. Precise gas chromatography with retention time locking in comprehensive toxicological screening for drugs in blood. J. Chromatogr. B, **2003**, *788*, 243–250.
2. Kovats, E. Gas chromatographische Charakterisierung organischer Verbindungen. Helv. Chim. Acta **1958**, *41*, 1915–1932.
3. Iida, T.; Hikosaka, M.; Goto, G.; Nambara, T. Capillary gas chromatographic behavior of *tert*.-hydroxylated steroids by trialkylsilylation. J. Chromatogr. A, **2001**, *937*, 97–105.
4. Van den Dool, H.; Kratz, P.D. A generalization of the retention index system including linear temperature programmed gas–liquid partition chromatography. J. Chromatogr. **1963**, *11*, 463–471.
5. Halang, W.A.; Langlais, R.; Kugler, E. Cubic spline interpolation for the calculation of retention indices in temperature programming gas–liquid chromatography. Anal. Chem. **1978**, *50* (13), 1829–1832.
6. Zenkevich, I.G. Generalized retention indices for gas chromatographic analysis with linear temperature programming. Zh. Anal. Khim. (Russ.) **1984**, *42* (7), 1297–1307.
7. Zenkevich, I.G.; Ioffe, B.V. System of retention indices for linear temperature programming regime. J. Chromatogr. **1988**, *439*, 185–194.
8. Rohrschneider, L. Eine Methode zur Charakterisierung von gas chromatographischen Trennflussigkeiten. J. Chromatogr. **1966**, *22*, 6–22.
9. Zenkevich, I.G.; Tsibulskaya, I.A. Influence of relative quantities of components of mixtures on the precision of measurements of GC retention indices. Zh. Anal. Khim. (Russ.) **1989**, *44* (7), 90–96.
10. Schwarts, T.R.; Petty, J.D.; Kaiser, E.M. Preparation of *n*-alkyl trichloroacetates and their use as retention index standards in gas chromatography. Anal. Chem. **1983**, *55*, 1839–1840.
11. Hall, S.L.; Whitehead, W.E.; Mourer, C.R.; Shibamoto, T. A new GC retention index for pesticides and related compounds. J. High Resolut. Chromatogr. Chromatogr. Commun. **1986**, *9* (3), 266–271.
12. Castello, G. Retention index systems: Alternatives to the *n*-alkanes as calibration standards. J. Chromatogr. A, **1999**, *842*, 51–64.
13. Lee, M.L.; Vassilaros, D.L.; White, C.M.; Novotny, M. Retention indices for programmable temperature capillary column gas chromatography of polycyclic aromatic hydrocarbons. Anal. Chem. **1979**, *51* (6), 768–774.
14. Lee, M.L.; Novotny, M.V.; Bartle, K.D. In *Analytical Chemistry of Polynuclear Aromatic Hydrocarbons*; Academic Press: New York, 1981.
15. Green, G.B.; Yu, S.; K.-T.; Vrana, R.P. GC–MS analysis of carboxylic acids in petroleum after esterification with fluoroalcohols. J. High Resolut. Chromatogr. **1994**, *17* (6), 427–438.
16. Smith, R.M., Ed.; *Retention and Selectivity in Liquid Chromatography*; Journal of Chromatography Library, Elsevier: Amsterdam, 1995; Vol. 57, 462.
17. Robinson, P.G.; Odell, A.L. A system of standard retention indices and its uses. The characterization of stationary phases and the prediction of retention indices. J. Chromatogr. **1971**, *57*, 1–10.
18. Evans, M.B.; Haken, J.K.; Toth, T.J. Solute characterization in gas chromatography by an extension of Kovats retention index system. Dispersion and selectivity indices. J. Chromatogr. **1986**, *351*, 155–164.
19. Zenkevich, I.G.; Kuznetsova, L.M. A new approach to the prediction of GC retention indices from physico-chemical constants. Collect. Czech Chem. Commun. **1991**, *56* (10), 2042–2054.
20. Kaliszan, R. In *Quantitative Structure–Chromatographic Retention Relationships*; Wiley & Sons: New York, 1987; 303.

Lanthanides: HPLC Separation

P.R. Vasudeva Rao
N. Sivaraman
T.G. Srinivasan
Chemistry Group, Indira Gandhi Center for Atomic Research (IGCAR), Kalpakkam, India

INTRODUCTION

Lanthanides are a series of elements ($Z = 57$–71), starting with lanthanum, in which the 4f orbitals are being filled. Lanthanide chemistry is dominated mainly by the +3 oxidation state. Lanthanides have common chemical properties, because of their same charge and similarity in size. The lanthanide cations are prototypical hard acids, bonding preferentially with hard bases such as oxygen donor ligands. They have coordination numbers between 6 and 12. The chemistry of lanthanides is well documented.[1] Lanthanides are extensively used in commercial applications, such as alloys for aeronautical components, permanent and superconducting magnets, catalysts, phosphors, lasers, batteries, chemicals, ceramics, glass, glazes, lighting, medical imaging, thermal spray powders, etc.[2] The separation and the determination of lanthanides are very important for measuring the burn-up of nuclear reactor fuels[3] and in geological studies.[4]

LANTHANIDE SEPARATIONS

Perhaps the most striking feature of lanthanide chemistry is the similarity in the properties of the lanthanide ions, owing to the small differences in the sizes of their hydrated lanthanide ions. The size of the trivalent lanthanide ion decreases gradually from 1.032 Å for lanthanum to 0.861 Å for lutetium (effective ionic radii in crystals for Ln^{3+}, CN: 6) owing to the well-known "lanthanide contraction."[5] The similarity in properties makes the isolation of pure lanthanide elements challenging; conventional separation techniques do not yield individual lanthanides of very high purity. Nuclear fuel cycle studies, such as burn-up measurements on highly radioactive solutions, also demand rapid and high-resolution separation of lanthanides to ensure minimization of the radiation dose to the operator. Major advantages of high-performance liquid chromatography (HPLC) techniques are their ability to provide rapid, high performance separations and the ability to extend the separations and purifications from laboratory scale to large scale. Developments and advances in the process of lanthanide separation by liquid chromatography have been reviewed in the literature.[6,7] To complement these excellent resources, this entry will focus mainly on the methods for individual separation of lanthanides using dynamic ion-exchange chromatographic methods employing HPLC.

Separation of Lanthanides—Need for a Complexing Reagent

It is possible to use the differences in the stabilities of the complexes formed by lanthanides to effect their separation. Lanthanides form complexes with weak organic acids, such as α-hydroxy isobutyric acid (α-HIBA), citrate, lactate, tartrate, and α-hydroxy-α-methyl butyric acid, to name a few. The decreasing ionic size across the lanthanide series results in increasing ionic potential; consequently, the stabilities of the complexes formed by lanthanides with the ligands mentioned above increase as we proceed across the series. This difference in the stabilities of the complexes of lanthanides can be effectively used to enhance the separation of the lanthanides in chromatography. In the presence of the complexing agent, e.g., α-HIBA, lutetium is eluted first and lanthanum last, because of the formation of complexes of high stability in the case of Lu as compared with the case of La. Among the various organic acids which have been used, α-HIBA has been shown to provide a good degree of separation between adjacent lanthanides, and hence is the most extensively used complexing reagent for individual separation of lanthanides.

Any factor that influences the stability of the complex formed would obviously affect the retention behavior in a cation exchange column. Thus, retention of lanthanides from a column will decrease when the mobile phase pH is increased (typically from 3 to 4.5). This effect occurs until the dissociation of the protonated ligand is complete, beyond which further increase in pH does not significantly alter retention times. In a similar manner, the changes in concentration of the mobile phase containing the complexing reagent can be used to alter the retention time; increasing the concentration of complexant in the mobile phase generally results in reduction of retention time. The separation efficiencies can be improved by operating at elevated temperatures (40–60°C). However, most dynamic ion-exchange separations have been carried out at ambient temperatures.

Development of Dynamic Ion-Exchange Methods

An average separation factor of 1.28 was reported for separation of lanthanides on polystyrene-divinylbenzene (PS-DVB) based cation exchange resin.[8] The separation efficiency was improved later with an ion exchanger of lower cross linkage.[9] In both cases, α-HIBA was used as the eluent. The HPLC technique was applied in the early 1970s to separate lanthanides.[10] The bonded phase ion-exchange columns that were subsequently developed were quite rigid and exhibited good mass transfer properties, compared with the PS-DVB cation exchange resins.[11] Subsequently, dynamic ion-exchange (also referred to as ion-pair/ion-interaction) chromatographic techniques using coated columns have been developed for the rapid separation of lanthanides[3,12–17] and they offer several advantages when compared to traditional ion-exchange techniques; they are described in detail in the following sections.

Principle of Lanthanide Separation Using Dynamic Ion-Exchange Chromatography

In this technique, a hydrophobic stationary phase, generally a C_{18} column, is used with a suitable ion-pairing reagent (IPR) for metal ion separations.[3,12,13] Some examples of ion-pairing reagents used for cation exchange separation include pentanesulfonate, hexanesulfonate, and octanesulfonate (Table 1). The stationary phase provides a neutral surface, which can be modified to form an ion-exchange support, with both cation as well as anion exchangers by the use of suitable modifiers. The modifiers can be continuously passed through the column or coated "permanently" onto a column, depending on their aqueous solubility. Passing a solution of a water-soluble modifier, e.g., octanesulfonate (10^{-2} to 10^{-3} *M*) through a C_{18} support results in the formation of a cation exchange surface. This method is generally referred to as a "dynamic ion-exchange" technique. Lanthanides can be subsequently separated by exchange with the hydrogen ions (or sodium) present in the modifier, similar to the exchange that takes place in the conventional cation exchange resins. Use of a suitable complexing reagent, e.g., α-HIBA, leads to the elution and separation of lanthanides. The water insoluble modifiers, e.g., dodecylsulfate ($C_{12}H_{25}SO_4^-$), are dissolved in methanol–water mixtures and are passed through a C_{18} column.[18,19] Depending on the concentration of the modifier, the methanol content is varied, generally between 50 and 70 vol.%. A solution of about 10^{-3} to 10^{-4} *M* of modifier is used for modifying the column by passing about a liter through the column, to establish an ion-exchange support. The volume required for the equilibration varies with the solvent composition and the concentration of the modifier. After the modification step, a mobile phase containing the complexing reagent is passed for achieving the separation. The ion-exchange columns prepared by these methods are generally referred to as "permanently" coated columns in which separation of lanthanides occurs through an ion-exchange mechanism.

The following effects on retention are observed in the dynamic ion-exchange separation: The total concentration of the IPR adsorbed onto the stationary phase is dependent on 1) its concentration in the mobile phase; 2) concentration of organic solvent such as methanol in the mobile phase (higher concentration of methanol results in lower concentrations of IPR on the stationary phase); and 3) hydrophobicity of the IPR (the larger the hydrophobicity, greater will be the adsorption onto the stationary phase). However, for a given eluent composition, the concentration of the adsorbed IPR remains constant. The retention of lanthanides increases with an increase in the concentration of the ion-pairing reagent and retention of solute decreases with increasing content of methanol in the mobile phase.

Advantages of Dynamic System over Conventional Ion-Exchange System

The important features of dynamically modified columns are their high column efficiency (height equivalent to a theoretical plate (HETP) is approximately 0.02–0.03) and easily variable ion-exchange capacity.[3] The high column efficiency is a result of thin layer of modifier being coated onto the surface of the stationary phase, leading to significant reduction in stationary phase mass transfer. The ion-exchange capacity depends on the surface concentration of the sorbed modifier and this concentration can be

Table 1 Some ion-pairing reagents used for separation of metal ions.

Name	Structure	Number of carbon atoms
1-Pentanesulfonate	$CH_3(CH_2)_4SO_3^-$	C_5
1-Hexanesulfonate	$CH_3(CH_2)_5SO_3^-$	C_6
1-Octanesulfonate	$CH_3(CH_2)_7SO_3^-$	C_8
1-Dodecylsulfate	$CH_3(CH_2)_{11}SO_4^-$	C_{12}
1-Eicosylsulfate	$CH_3(CH_2)_{19}SO_4^-$	C_{20}
Camphor-10-sulfonic acid	$C_{10}H_{15}SO_3H$	C_{10}
Di-(2-ethylhexyl)phosphoric acid (liquid cation exchanger)	$C_{16}H_{34}O_3POH$	C_{16}

"quickly" changed over a wide range, by changing the mobile phase concentration. This feature is not available with conventional ion-exchange resins. The variation of ion-exchange capacity can be effectively used to optimize the column efficiency and the selectivity. Another important advantage of this technique is that the column can be reused for other reverse phase applications after washing it with water (in the case of dynamic ion-exchange) or with methanol (in the case of "permanently" coated columns).

Separation Mechanism

The mechanisms of separation using ion-pairing reagents are discussed in the literature.[20,21] In the dynamic ion-exchange mode, the modifier is assumed to be adsorbed onto the C_{18} support to create an ion-exchange surface. The adsorbed IPR imparts a charge to the stationary phase, causing it to behave as an ion exchanger. A constant interchange of IPR occurs between the eluent and stationary phase and the stationary phase can be considered to be a dynamic ion exchanger. The sample ions are then exchanged between the stationary phase and the mobile phase by an ion-exchange process. The ion-pair model leads to the formation of ion-pair complex between analyte ion and modifier, which is subsequently partitioned between stationary phase and mobile phase. Retention, therefore, results mainly as a consequence of interaction taking place in the eluent between solute and IPR and the subsequent partition of the complex to the stationary phase. The degree of retention of the ion-pair is dependent on its hydrophobicity, which in turn depends on the hydrophobicity of the ion-pairing reagent. An increase in the percentage of methanol in the eluent generally decreases the interaction of the ion-pairs with the stationary phase. The ion-interaction model may be viewed as an intermediate between the dynamic ion-exchange and ion pairing models. It incorporates both the adsorptive effects, which forms the basis of dynamic ion-exchange, and the electrostatic effects, which are the basis of the ion-pair model. The schematic of ion-pair, dynamic ion-exchange, and ion-interaction models for the retention of anionic solutes is shown in Fig. 1. Although many of these models define the solute retention under certain conditions, it is likely that the exact mechanism could be a combination of dynamic ion exchange, ion-pair formation, etc.

EXPERIMENTAL METHODS

The HPLC technique, with postcolumn derivatization, is well discussed in the literature.[3,13,22] In brief, the HPLC technique employs columns that contain stationary phase materials of small and uniformly sized particles, necessitating high operating pressures. These columns provide high efficiency, as well as faster and high-resolution separations. Some typical stationary phase and mobile phase systems used for lanthanide separations are given next.

Stationary Phase

The dynamic ion-exchange separations are performed successfully on a wide range of stationary phases, which include PS-DVB copolymers (e.g., Hamilton PRP columns), and chemically bonded silica materials (C_{18}, C_8, and phenyl groups). C_{18} supports are the most popular choice (e.g., hypersil, merck, and phase separation). Columns packed with 3 or 5 μm particles are used for analytical scale separation of lanthanides.

Mobile Phase

Aliphatic sulfonic acids and their salts (Table 1) are used as water-soluble ion-pairing reagents in dynamic ion-exchange chromatography, e.g., sodium octanesulfonate. The complexing reagent, e.g., α-HIBA, is dissolved along with the ion-pairing reagent in HPLC grade water. The pH of the mobile phase is generally adjusted using dilute ammonia/sodium hydroxide. The mobile phase solution is passed through the reverse phase column (typically 100–125 ml) to establish a dynamic ion-exchange surface, after which samples are introduced into the HPLC system for separation. In the case of "permanently" coated columns, about 60 ml of the mobile phase containing the complexing reagent is passed through the coated column prior to the introduction of sample.

Injection of Lanthanide Samples

Generally, lanthanide samples in the form of their nitrates are injected into the HPLC system. For preparing a calibration, lanthanide samples over the concentration range of about 1–10 ppm (injected amount 20 μl) are introduced into the system, though the linear dynamic range exceeds well beyond this region.

Detection of Lanthanides

Postcolumn derivatization has been an extensively used technique for the detection of lanthanides.[3,13] Commonly used chromogenic reagents are Arsenazo I, Arsenazo III, and 4-(2-Pyridylazo)-resorcinol (PAR); the lanthanide complexes are detected at 590, 658, and 520 nm, respectively. Arsenazo III is generally employed in the aqueous as well as in acetic acid medium. The postcolumn reagents are added to the eluate with a reciprocating pump/peristaltic pump. The rapid and efficient mixing of color-producing reagent with eluent is essential and dead volume must be minimized for achieving better resolution and sensitivity. The molar absorptivity of the complexes is generally in the region of 30,000–60,000 L/mol/cm, which permits a detection limit as low as 10–20 ng for various lanthanides.

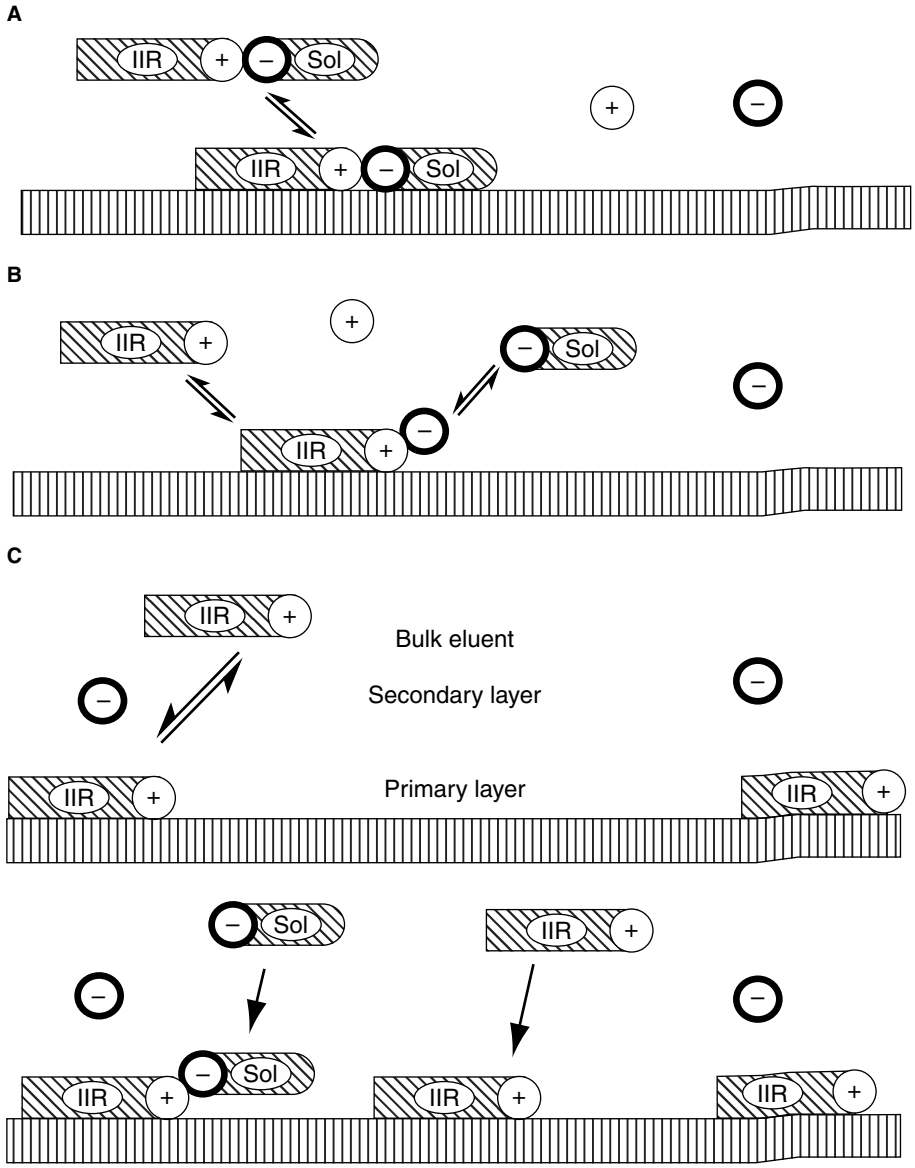

Fig. 1 Schematic of (A) the ion-pair model; (B) the dynamic ion-exchange model; and (C) the ion-interaction model for the retention of anionic solutes in the presence of a lipophilic cationic IIR. The solute and the IIR are labeled on the diagram. The large hatched box represents the lipophilic stationary phase, the black circle with the negative charge represents the counter–anion of the IIR, whilst the white circle with the positive charge represents the counter cation of the solute.
Adapted from Haddad & Jackson[20] and Snyder & Kirkland.[21]

Some Typical Separations of Lanthanides

In this section, detailed descriptions of typical procedures involving dynamic ion-exchange and "permanently" coated columns are given.

Separation of lanthanides using dynamic ion-exchange HPLC

An efficient separation of mixtures of lanthanide ions using sodium octanesulfonate as the ion-pairing reagent and α-HIBA as the complexing reagent was reported.[3] A 15 cm reverse phase column was employed with sodium octanesulfonate (0.01 *M*) and α-HIBA (0.05–0.4 *M*); the pH of the mobile phase was kept at 4.6. Complete separation of lanthanides was obtained before 9 min (Fig. 2). The lanthanides could be eluted with sharp symmetrical peaks, reflecting the rapid mass transfer characteristics with high column efficiencies, i.e., HETP of about 0.02–0.03 mm. An average detection limit of approximately 2.5 ng was obtained for lanthanides in this study. A dynamic ion-exchange technique using sodium octanesulfonate-α-HIBA has also been employed for the individual separation from a mixture containing the lanthanides yttrium, uranium, and thorium.[23] It was also demonstrated that the peak positions of Th(IV) and U(VI) in the lanthanide elution chromatogram could be optimized by appropriate adjustments in the concentration of octanesulfonate, methanol, and eluent pH. In another study, the performance of α-hydroxycarboxylic acids, such as α-HIBA, α-hydroxy-α-methylbutyric acid, and lactic acid were compared for the separation of lanthanides using octanesulfonate as the ion-pairing reagent.[16] It is also understood that a longer alkyl group in the hydroxycarboxylic acids improves the resolution, particularly for the lighter

lanthanides. In another study, mandelic acid was employed instead of α-HIBA, with octanesulfonate as the ion-pairing reagent for the separation.[15] Using a mandelic acid gradient, all 14 lanthanides were separated. The Th(IV) and U(VI) were well separated from lanthanides. The separation of lanthanides obtained, however, is inferior to that obtained with α-HIBA. This is possibly because of the fact that, with α-HIBA, the lanthanides are retained mainly through an ion-exchange mechanism; however, with mandelic acid, lanthanides may be retained through a hydrophobic interaction mechanism in addition to an ion-exchange mechanism. A rapid separation procedure for the isolation of individual lanthanides using camphor-10-sulfonic acid (CSA) as the ion-pairing reagent has also been developed.[17] A binary gradient with a mobile phase composition of 0.05 *M* CSA and 0.07–0.3 *M* α-HIBA (pH 3.8) was employed and the lanthanides could be separated in about 8 min (Fig. 3). Excellent peak profiles with baseline resolution for individual lanthanides have been achieved with this method.

Separation of lanthanides using "permanently" coated columns

The separation of lanthanides on a reverse phase column modified with eicosylsulfate was reported, with α-HIBA (0.025–0.25 *M*, pH 3.8) as the mobile phase.[18] The lanthanides could be eluted within approximately 32 min with this method (Fig. 4). In another study, a column coated with Di-(2-ethylhexyl)-phosphoric acid (HDEHP) was employed for the individual separation of lanthanides.[19] A binary gradient in concentration of α-HIBA (0.07–0.3 *M*, pH 3.5) was employed in that study for the separation (Fig. 5). The separation of the entire lanthanide series was completed in about 20 min. It was reported that these coated columns are quite stable and can be employed for longer periods.[19]

Some Applications of Determination of Lanthanides by HPLC

Lanthanides in silicate rocks, commercial phosphoric acid, geological materials, refractory alloys, steel alloys, minerals, ores, monazite, and luminescent phosphors have been determined by HPLC. Determination of trace lanthanide impurities in nuclear grade uranium has been studied.[18] An HPLC technique using the dynamic ion-exchange approach was also employed for the determination of ^{147}Pm in urine.[24] A typical application of lanthanide assay in nuclear industry is described next.

Burn-up measurements on nuclear reactor fuels

Lanthanides (La, Ce, Pr, Nd, Sm, and Eu) constitute about one-fourth of the total fission products produced in nuclear fission of uranium or plutonium. Thus, accurate estimation of Nd or La in the dissolver solution of spent fuel can be used to determine the number of fissions that have occurred in nuclear reactor fuel. The burn-up or atom percent fission (number of fissions per 100 initial heavy element atoms such as U and Pu) is an important parameter and the

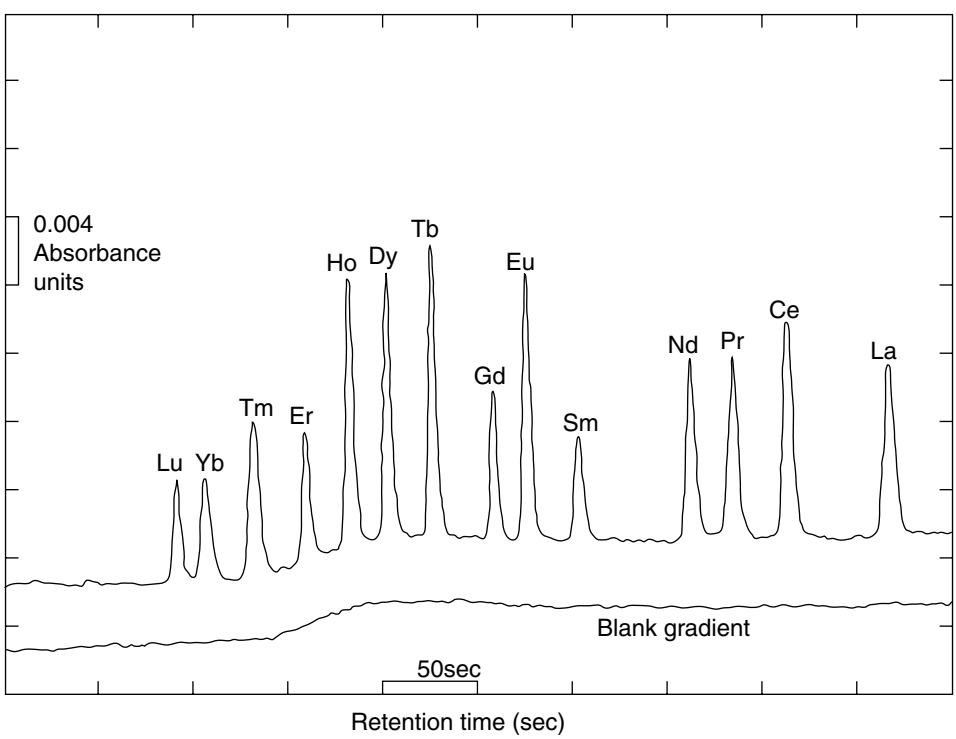

Fig. 2 Gradient separation of the lanthanides. Supelco LC18 column; linear program at pH 4.6 from 0.05 mol/L α-HIBA to 0.4 mol/L α-HIBA over 10 min at 2.0 ml/min; modifier, 1-octanesulfonate at 1×10^{-2} mol/L; detection at 653 nm after post-column reaction with Arsenazo III; sample 5 μl of a solution containing approximately 10 μg/ml of each lanthanide.
Source: From Dynamic ion exchange chromatography for determination of number of fissions in thorium–uranium dioxide fuels, in Anal. Chem.[3]

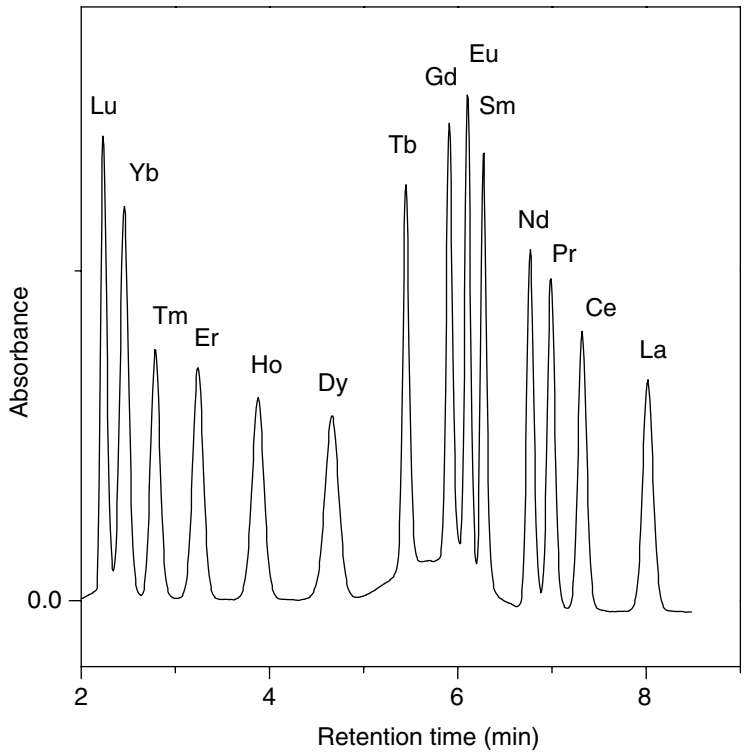

Fig. 3 Separation of lanthanides using gradient elution. Experimental conditions: column, reverse phase C_{18}; mobile phase, camphor-10-sulfonic acid (0.05 *M*); α-HIBA varied from 0.07 to 0.3 *M*, pH 3.8; flow rate: 2 ml/min. Postcolumn reagent: Arsenazo III (1.8×10^{-4} *M*); flow rate: 1.5 ml/min; detection: 655 nm.

experimental methods have been found to be more accurate and reliable for determining this parameter. High performance liquid chromatography based techniques have been developed for determining the number of fissions in uranium dioxide, thorium–uranium dioxide, and fast reactor fuels such as mixed carbides of uranium and plutonium.[3,13,17] Ion-pair HPLC techniques using CSA–α-HIBA/sodium octanesulfonate–α-HIBA systems were employed for separation and assay of lanthanide fission products. In one of the studies, the HPLC method was used to separate and estimate a lanthanide fission product, e.g., lanthanum and a heavy element, e.g., uranium.[3] The burn-up obtained was found to be in good agreement with the conventional mass spectrometric method. In another study,

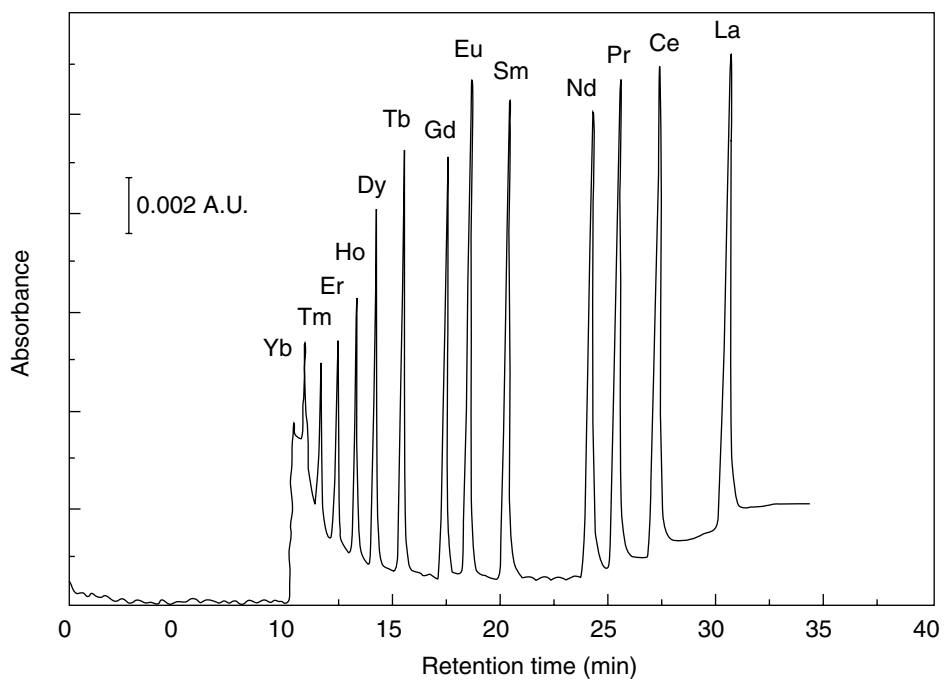

Fig. 4 Separation of lanthanides by HPLC. Experimental conditions: reversed phase column, 4.6 × 150 mm 5 μm Supelcosil LC-18 coated with 2.5×10^{-4} *M* $C_{20}SO_4^-$ in 25% acetonitrile–water; eluent, 0.025 *M* α-HIBA (pH 3.8) for 9 min followed by linear gradient from 0.025 to 0.25 *M* α-HIBA (pH 3.8) over 20 min; detection, 658 nm after postcolumn reaction with Arsenazo III.
Source: From Determination of trace lanthanide impurities in nuclear grade uranium by coupled-column liquid chromatography, in Anal. Chem.[18]

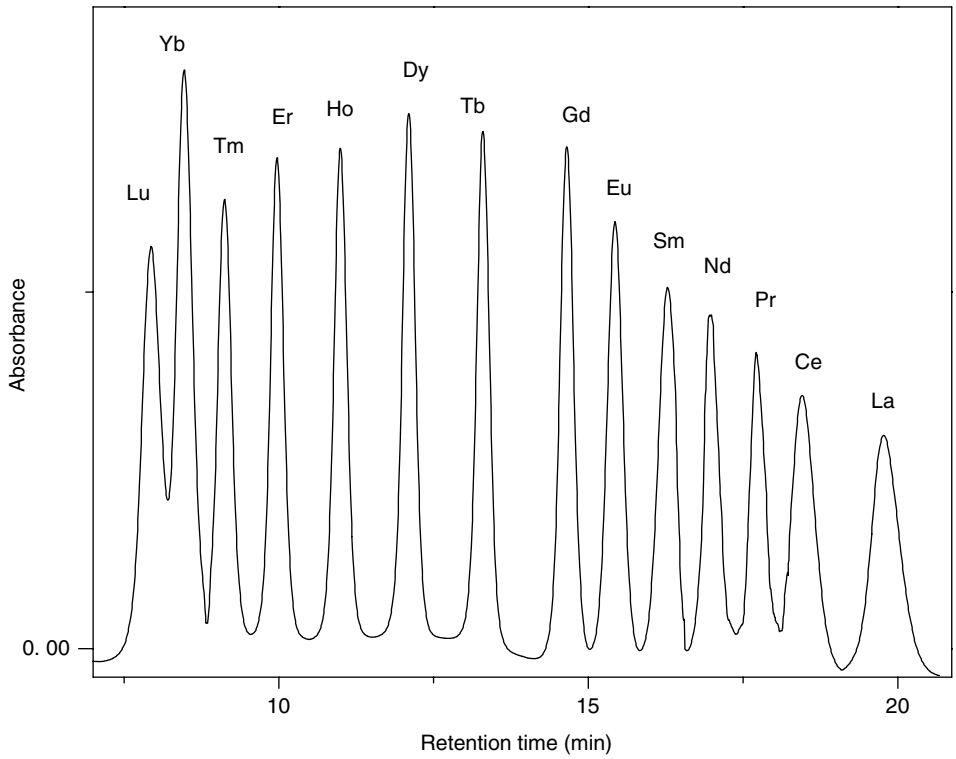

Fig. 5 Separation of lanthanides using HDEHP coated column. Experimental conditions: reverse phase C_{18} column coated with HDEHP (0.27 m*M*); mobile phase, α-HIBA varied from 0.07 to 0.3 *M*; pH 3.5; flow rate, 1.5 ml/min; postcolumn reagent, Arsenazo III; flow rate, 2 ml/min; detection, 655 nm; lanthanide, 5 μg/ml, 100 μl injected.
Source: From Separation of lanthanides using ion-interaction chromatography with HDEHP coated columns, in J. Radioanal. Nucl. Chem.[19]

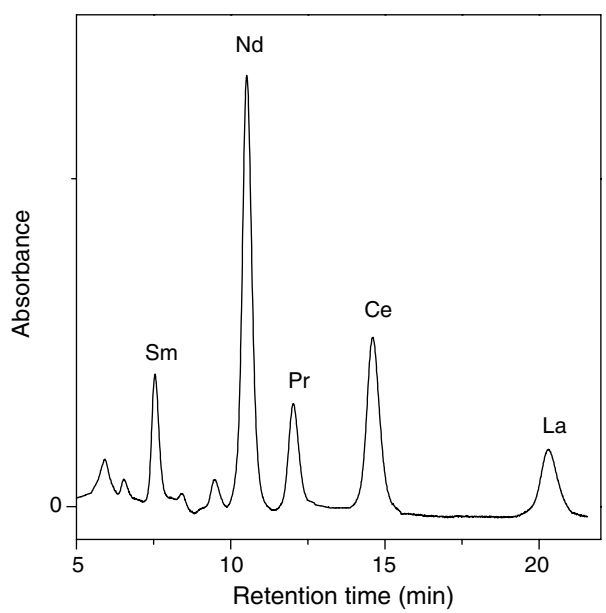

Fig. 6 Separation of lanthanide fission products present in dissolver solution of thermal reactor fuel. Column: reverse phase C_{18}, mobile phase: camphor-10-sulfonic acid (0.05 *M*), and α-HIBA: (0.1 *M*); pH 3.85, flow rate: 1 ml/min. Postcolumn reaction with Arsenazo III; detection: 655 nm.
Source: From Burn-up measurements on nuclear reactor fuels using high performance liquid chromatography, in J. Radioanal. Nucl. Chem.[17]

terbium (which is not a fission product) was employed as an internal standard for the quantitative determination of fission products such as Nd, Sm, and La.[17] An HPLC method has also been developed for determining the fractional fissions from uranium and plutonium by the measurement of the Nd/Sm ratio.[17] High performance liquid chromatography techniques have been employed for the rapid isolation of lanthanide fractions for their isotopic composition using mass spectrometric measurements.[25] The separation of lanthanide fission products present in dissolver solution of a thermal reactor fuel by HPLC is illustrated in Fig. 6. An important advantage of employing the HPLC technique for determining the number of fissions is the reduction in analysis time and, hence, a considerable reduction in radiation exposure to the personnel.

CONCLUSIONS

The increasing technological significance of lanthanides will continue to pave the way for development of rapid and efficient separation methods with sensitive detection. Several reviews on lanthanide analysis indicate the importance of these materials and the need for the development of new and better techniques. Many HPLC based techniques have been developed for the separation of individual lanthanides using cation exchange, dynamic ion-exchange methods, etc. The selection of gradient elution techniques has been

commonly identified as an important factor for achieving rapid and high-resolution separations. It is to be noted that α-HIBA is being used as the most efficient complexing agent during a period of 40 yr, since its early use for discovery of trans-plutonium elements. There is still scope for understanding the nature of α-HIBA complexes of lanthanides and its interaction with the support. Complexing reagents alternate to α-HIBA and the development of better stationary phase supports may continue to offer excitement in the years to come.

REFERENCES

1. Gschneidner, K.A.; Eyring, L. *Handbook on the Physics and Chemistry of Rare Earths*; Elsevier: Amsterdam, 1987; Vol. 9.
2. Spedding, F.H.; Daane, A.H. *The Rare Earths*; Wiley: New York, 1961.
3. Knight, C.H.; Cassidy, R.M.; Recoskie, B.M.; Green, L.W. Dynamic ion exchange chromatography for determination of number of fissions in thorium–uranium dioxide fuels. Anal. Chem. **1984**, *56* (3), 474–478.
4. Henderson, P. *Rare Earth Element Geochemistry*; Elsevier: Amsterdam, 1984.
5. Shannon, R.D. Revised effective ionic radii and systematic studies of interatomic distances in halides and chalcogenides. Acta Cryst. **1976**, *A32*, 751–767.
6. Robards, K.; Clarke, S.; Patsalides, E. Advances in the analytical chromatography of the lanthanides. A review. Analyst **1988**, *113*, 1757–1779.
7. Nash, K.L.; Jensen, M.P. Analytical-scale separations of the lanthanides: A review of techniques and fundamentals. Sep. Sci. Technol. **2001**, *36*, 1257–1282.
8. Sisson, D.H.; Alan Mode, V.; Campbell, D.O. High-speed separation of the rare earths by ion exchange. Part II. J. Chromatogr. A, **1972**, *66* (1), 129–135.
9. Campbell, D.O. Rapid rare earth separation by pressurized ion exchange chromatography. J. Inorg. Nucl. Chem. **1973**, *35* (11), 3911–3919.
10. Schadel, M.; Trautmann, N.; Herrmann, G. Fast separation of lanthanides by high pressure liquid chromatography. Radiochim. Acta **1977**, *24*, 27–31.
11. Elchuk, S.; Cassidy, R.M. Separation of the lanthanides on high-efficiency bonded phases and conventional ion-exchange resins. Anal. Chem. **1979**, *51* (9), 1434–1438.
12. Cassidy, R.M.; Elchuk, S. Dynamically coated columns for the separation of metal ions and anions by ion chromatography. Anal. Chem. **1982**, *54* (9), 1558–1563.
13. Cassidy, R.M.; Elchuk, S.; Elliot, N.L.; Green, L.W.; Knight, C.H.; Recoskie, B.M. Dynamic ion exchange chromatography for the determination of number of fissions in uranium dioxide fuels. Anal. Chem. **1986**, *58* (6), 1181–1186.
14. Karunasagar, D.; Joseph, M.; Saha, B.; Mathews, C.K. Rapid determination of burn-up of nuclear fuel—a possible approach. Sep. Sci. Technol. **1988**, *23* (12 and 13), 1949–1957.
15. Elchuk, S.; Burns, K.I.; Cassidy, R.M.; Lucy, C.A. Reversed-phase separation of transition metals, lanthanides and actinides by elution with mandelic acid. J. Chromatogr. **1991**, *558*, 197–207.
16. Raut, N.M.; Jaison, P.G.; Aggarwal, S.K. Comparative evaluation of three α-hydroxycarboxylic acids for the separation of lanthanides by dynamically modified reversed-phase high performance liquid chromatography. J. Chromatogr. A, **2002**, *959*, 163–172.
17. Sivaraman, N.; Subramaniam, S.; Srinivasan, T.G.; Vasudeva Rao, P.R. Burn-up measurements on nuclear reactor fuels using high performance liquid chromatography. J. Radioanal. Nucl. Chem. **2002**, *253* (1), 35–40.
18. Lucy, C.A.; Gureli, L.; Elchuk, S. Determination of trace lanthanide impurities in nuclear grade uranium by coupled-column liquid chromatography. Anal. Chem. **1993**, *65* (22), 3320–3325.
19. Sivaraman, N.; Kumar, R.; Subramaniam, S.; Vasudeva Rao, P.R. Separation of lanthanides using ion-interaction chromatography with HDEHP coated columns. J. Radioanal. Nucl. Chem. **2002**, *252* (3), 491–495.
20. Bidlingmeyer, B.A. Separation of ionic compounds by reversed-phase liquid chromatography: An update of ion-pairing techniques. J. Chromatogr. Sci. **1980**, *18*, 525–539.
21. Haddad, P.R.; Jackson, P.E. *Ion Chromatography—Principles and Applications*; J. Chromatogr. Libr., Elsevier: New York, 1990; Vol. 46, Chapter 6.
22. Snyder, L.R.; Kirkland, J.J. *Introduction to Modern Liquid Chromatgraphy,* 2nd Ed.; John Wiley & Sons, Inc.: New York, 1979.
23. Barkley, D.J.; Blanchette, M.; Cassidy, R.M.; Elchuk, S. Dynamic chromatographic systems for the determination of rare earths and thorium in samples from uranium ore refining processes. Anal. Chem. **1986**, *58* (11), 2222–2226.
24. Elchuk, S.; Lucy, C.A.; Burns, K.I. High-resolution determination of ^{147}Pm in urine using dynamic ion-exchange chromatography. Anal. Chem. **1992**, *64* (20), 2339–2343.
25. Cassidy, R.M.; Miller, F.C.; Knight, C.H.; Roddick, J.C.; Sullivan, R.W. Evaluation of dynamic ion exchange for the isolation of metal ions for characterization by mass and α spectrometry. Anal. Chem. **1986**, *58* (7), 1389–1394.

Large Volume Injection for GC

Yong Cai
Department of Chemistry, Florida International University, Miami, Florida, U.S.A.

INTRODUCTION

Trace or ultratrace analyses for environmental and biological samples require sensitive methods, including sample preparation and detection techniques, to be used. The enhancement of the detectability of analytical procedure is often brought about by some form of preconcentration, such as Soxhlet extraction, liquid–liquid extraction, and solid–phase extraction. Capillary gas chromatography (GC) coupled with different detectors is one of the most frequently employed techniques for trace analysis of micropollutants. However, because of the limited sample capacity of the capillary column, only a small portion (1–5 μl) of the final sample extract is introduced into the gas chromatographic system. This means that after careful workup, which often comprises analyte isolation by extraction and changing to a GC-compatible solvent, a maximum few percent could be injected and reach the detector.[1] The concentration detection limit of the method can be improved by increasing the concentration factor of the extraction and cleanup procedure. This is generally achieved by using a larger amount of sample or/and by reducing the volume of final extract through evaporation. Both methods have limitations for practical application. Extraction of a large amount of sample is very time consuming and requires a large volume of toxic organic solvents. Sampling a large amount of sample is sometimes difficult or even impossible. Although solvent evaporation is frequently used, it is a rather critical step in which the more volatile compounds may be lost from the sample because of the coevaporation with the solvent.[1,2] Recently, there has been increased interest in the introduction of large sample volumes in capillary GC.[1–6] Several hundred microliters of sample can be introduced by using these techniques. Among the several techniques for the introduction of a large volume of sample, on-column injection and programed-temperature vaporization (PTV) injection are best developed.

ON-COLUMN INJECTION

The on-column injection techniques, in which the solvent is generally vaporized in a few meters of uncoated deactivated capillary (retention gap) and vented via an early vapor exit valve, are of good accuracy and reproducibility.[3–5] A schematic diagram for on-column injection is shown in Fig. 1. The on-column large-volume injection system generally consists of a regular gas chromatograph equipped with an on-column injector, a retention gap, a retaining precolumn, an analytical column, and a heated early solvent vapor exit.

The introduction of a large volume of sample can be performed using a technique called partially concurrent solvent evaporation (PCSE). With PCSE, some 90% of the solvent injected is evaporated during the injection through the early solvent vapor exit.[1] The injection rate of the sample is controlled based on the length of the retention gap and the boiling points of the analytes. If the sample volume exceeds the capacity of the uncoated retention gap to retain liquid (it is true for most large-volume injection applications), the injection speed should be adjusted to result in a sufficiently large proportion of concurrent evaporation to prevent liquid solvent from spreading into the analytical column.[2] Most of the vapor escapes through the open solvent vapor exit. After large-volume on-column injection, the analytes are spread out over several meters of the uncoated retention gap. Solvent evaporation continues, removing solvent from the rear to the front of the sample film. Relatively volatile analytes evaporate and are reconcentrated by the liquid ahead. This process is described as the solvent-trapping effect. Less volatile components do not evaporate with the solvent and remain on the dry retention gap surface. The vapor exit valve is closed shortly before the end of solvent evaporation when the residual liquid still remains the volatile components. The rest of the solvent is discharged through the analytical column. Reconcentrations of the less volatile compounds are carried out by phase-ratio focusing; that is, the difference in migration speed in the retention gap and in the coated column causes the rear end of the zone to catch up with the front end at an appropriately increased oven temperature.[1,2] As soon as the front end of the zone reaches the stationary phase, its migration speed reduces dramatically, while the remaining part, which is still in the retention gap, continues to migrate at a higher speed.

With on-column large-volume injection, the selection of appropriate experimental conditions is complicated.[2] Generally, the following parameters need to be carefully optimized.

1. The sample must be introduced at a rate slightly exceeding the evaporation rate. Slower injection causes the loss of solvent trapping because all solvent evaporate concurrently, whereas a too high introduction

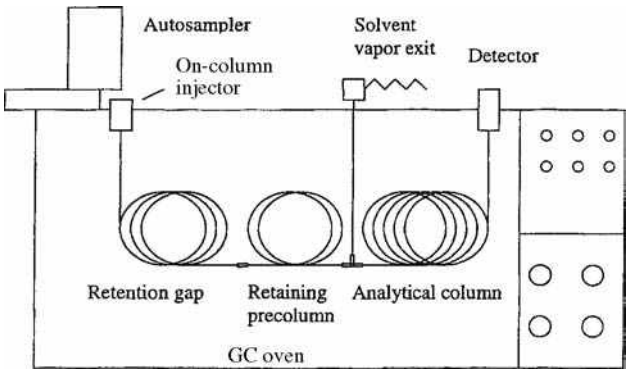

Fig. 1 Schematic diagram of GC with on-column large-volume injection.

rate results in flooding of the solvent into the retaining precolumn and, eventually, the analytical column and the vapor exit.

2. The temperature of the column oven during injection should be set slightly below the pressure-corrected boiling point of the solvent used. At too high temperatures, the solvent starts to boil and causes the backflush of solvent into the injector.
3. The vapor exit valve must be closed at a right time. Early closing of the valve may cause the remaining solvent in the retention gap to exceed the capacity of the analytical column. However, delayed closure will result in the loss of volatile components.

On-column large-volume injection has wide applications in terms of volatility and thermostability of the analytes.[4] If the solvent exit valve is operated carefully, compounds with boiling points only slightly above that of the solvent can be recovered quantitatively. However, the technique is generally not very suitable for dirty samples. Frequent analysis of samples with high contents of matrix compounds can rapidly decrease the column performance.[3–6]

PROGRAMED-TEMPERATURE VAPORIZATION

Vogt and co-workers in 1979 described an injector that allowed the injection of up to 250 μl into a cold glass insert filled with glass wool.[7,8] This technique has been modified and refined in the recent years.[3–6,9,10] In fact, the large-volume sampling technique using PTV injectors is modified from a conventional split/splitless injector.[1] The main differences between the conventional split/splitless and the PTV injectors are the temperature control of the injector and the solvent venting capacity of the split/splitless valve. In PTV injectors, the injection port should be heated or cooled rapidly, and the split/splitless valve should be large enough to be able to vent the solvent vapor produced during injection. Before a large volume of sample is introduced, the temperature of the injection port is reduced to below the boiling point of the solvent. The sample is injected into the liner of the injector at a controlled rate. Upon introduction, the solvent is selectively eliminated and solvent vapor is vented via the split/splitless valve. The less volatile components are retained in the cold liner. When solvent elimination is finished, the components retained in the liner are transferred to the analytical column by rapid temperature-programed heating of the injector.

In order to obtain a quantitative analysis for the analytes with a wide range of volatility using the PTV injection technique, the following parameters are of great importance: injection speed, liner packing material, solvent venting temperature, and solvent venting time. The speed of sample introduction should roughly equal the rate of solvent elimination.[1] If the sample is injected at a rate exceeding the evaporation rate, the sample will accumulate in the liner, which eventually will result in overloading of the liner. This will cause flooding of the analytical column and severe losses of both volatile and non-volatile components via the split exit. On the other hand, a too slow sample introduction rate will cause losses of volatile sample components. The use of liners packed with an absorbent is an efficient means to retain the liquid sample and minimize losses of volatile compounds.[1,10] A number of packing materials, such as glass wool, quartz wool, cup liner, Tenax TA, PTFE wool, have been investigated in terms of their interaction with different types of analytes.[10] An unsuitable choice of the packing material can cause degradation of the analyte in the liner. The solvent venting temperature and solvent venting time must be carefully optimized. The liner temperature is held below the boiling point of the solvent during the solvent venting time. The split/splitless valve must be closed at the right time. Early closing will cause accumulation of the solvent, which may exceed the capacity of the column, whereas delayed closure can result in losses of the volatile sample components.

It has been shown that the PTV injector is a very useful technique for large-volume injection, especially for the analysis of a dirty sample. Because the vaporization of the solvent is carried out at a low temperature, nonvolatile matrix constituents remaining in the liner will not contaminate the GC column. However, the PTV injection technique is less suited when analyzing volatile compounds because only components with volatility significantly below that of the solvent are trapped in the cold liner, unless liners packed with a selective adsorbent is used.[4]

REFERENCES

1. Mol, H.G.J.; Janssen, H.G.M.; Cramers, C.A.; Vreuls, J.J.; Brinkman, U.A.Th. Trace level analysis of micropollutants in aqueous samples using gas chromatography with on-line

sample enrichment and large volume injection. J. Chromatogr. A, **1995**, *703*, 277.
2. Grab, K. Development of the transfer techniques for on-line high-performance liquid chromatography-capillary gas chromatography. J. Chromatogr. A, **1995**, *703*, 265.
3. Mol, H.G.J.; Althuizen, M.; Janssen, H.G.; Cramers, C.A.; Brinkman, U.A.Th. Environmental applications of large volume injection in capillary GC using PTV injectors. J. High Resolut. Chromatogr. **1996**, *19* (2), 69–79.
4. Bosboom, J.C.; Janssen, H.G.; Mol, H.G.J.; Cramers, C.A. Large-volume injection in capillary gas chromatography using a programmed-temperature vaporizing injector in the on-column or solvent-vent injection mode. J. Chromatogr. A, **1996**, *724*, 384.
5. Stan, H.J.; Linkerhagner, M. Large-volume injection in residue analysis with capillary gas chromatography using a conventional autosampler and injection by programmed-temperature vaporization with solvent venting. J. Chromatogr. A. **1996**, *727*, 275.
6. Munari, F.; Colombo, P.A.; Magni, P.; Zilioli, G.; Trestianu, S.; Grab, K. GC instrumentation for on-column injection of large volumes: Automated optimization of conditions. J. Microcol. Separ. **1995**, *7* (4), 403–409.
7. Vogt, W.; Jacob, K.; Obwexer, H.W. Sampling method in capillary column gas-liquid chromatography allowing injections of up to 250 1. J. Chromatogr. **1979**, *174*, 437.
8. Vogt, W.; Jacob, K.; Ohnesorge, A.B.; Obwexer, H.W. Capillary gas chromatographic injection system for large sample volumes. J. Chromatogr. **1979**, *186*, 197.
9. Ramalho, S.; Hankemeier, T.; de Jong, M.; Brinkman, U.A.Th.; Vreuls, R.J.J. Large-volume on-column injections for gas chromatography. J. Microcol. Separ. **1995**, *7* (4), 383–394.
10. Mol, H.G.J.; Hendriks, P.J.M.; Janssen, H.G.; Cramers, C.A.; Brinkman, U.A.Th. Large volume injection in capillary GC using PTV injectors: Comparison of inertness of packing materials. J. High Resolut. Chromatogr. **1995**, *18* (2), 124–128.

Large Volume Sample Injection in FFF

Martin Hassellöv
Department of Chemistry, Analytical and Marine Chemistry, Göteborg University, Göteborg, Sweden

INTRODUCTION

Field-flow fractionation (FFF) techniques are used for a range of sample types including polymers, macrobiomolecules, glass beads, silica, and other inorganic particles due to their good separation characteristics (e.g., high molecular weight, separation selectivity, and large dynamic operating range). These analytes are dissolved or suspended in an appropriate liquid, and small aliquots of the suspensions (typically 10–50 μl) are injected into the FFF channel. For these applications, it has usually been possible to adjust the analyte concentration to ensure an acceptable signal-to-noise ratio, given detector sensitivity and the dilution in the FFF system. However, there are a number of applications where the solutes are very dilute, and any preconcentration may cause perturbation of the size distribution or other changes of the sample characteristics. Such applications could include most of the groups of sample types mentioned earlier, and especially environmental particles and colloids, which are often present in low concentrations and are easily disturbed. Here, we discuss approaches taken to counteract the dilution effect in FFF to overcome detection problems.

Schure[1] had recently evaluated dilution factors and detection limits for FFF in comparison with LC and capillary electrophoresis. It is obvious that samples are subject to much higher dilution in FFF channels (~200–1000 times) compared with most LC techniques (~3–25) due to the rather low efficiency and large elution volumes. A more narrow and thin channel than that with more conventional dimensions would improve the dilution factors. But there are practical problems involved in the production and maintenance of such a channel. There is the option of using any of the outlet flow splitting devices that have been developed. These are different approaches having in common removal of some of the overlying liquid at the end of the channel and thus reducing the dilution. The principles build on horizontal flow splitters, capillaries exiting both above and below the channel, a second porous frit section (frit outlet), or a so-called slot outlet in the overlying channel wall letting out excess liquid. There had been difficulties in accurate production, maintenance, and precision of some of these technical solutions. But there are now systems commercially available using the frit-outlet system in symmetrical flow FFF (FlFFF) and a slot-outlet system in asymmetrical FlFFF for removal of excess liquid,[2] with which up to a 10-fold reduction in dilution can be achieved.

SAMPLE INJECTION

The injection volume of the conventional stop–flow sample injection technique is limited typically to 10–100 μl. This procedure is carried out using a sample loop and injecting the sample plug just onto the channel carried with the channel flow before stopping that flow and letting the sample attain its equilibrium distribution relative to the accumulation wall (relaxation). Sedimentation FFF (SedFFF) is the only technique where the field is not applied during the complete stop–flow procedure; however, the centrifuge is started as soon as the sample is injected and the channel flow is switched off for practical reasons.

Kirkland, Yau, and Doerner[3] introduced an injection technique for SedFFF where the sample is slowly injected with the centrifuge spinning at a high field thereby retaining the analytes in a narrow band at the entrance of the channel. When the sample is injected, the flow is stopped, the centrifuge speed is decreased to the initial elution speed, and an appropriate relaxation time is allowed. This technique has been further refined and developed by Giddings, Karaiskakis, and Caldwell[4] into an on-channel preconcentration step for concentrating dilute particulate samples in SedFFF.

Another injection technique, which involves a sample injection port a small distance downstream of the channel inlet, where the sample was injected and relaxed between two focusing flows with a reversed flow from the channel outlet, was first employed for asymmetrical FlFFF.[5] The theoretical basis of the horizontal transport was derived and fundamental practical aspects were discussed. This procedure is now standard for asymmetrical FlFFF, partly due to the difficulties of adapting the stop–flow injection mode. This was further optimized by Wahlund and Litzén[6] to include injection of up to 5 ml of sample in a 0.8 ml channel.

This approach has been subsequently used in symmetrical FlFFF[7,8] where the sample is injected in either the forward or backward focusing flow streams (Fig. 1). Lyvén et al.[7] showed a virtually quantitative recovery for preconcentration of 1.7 to over 100 ml of low-

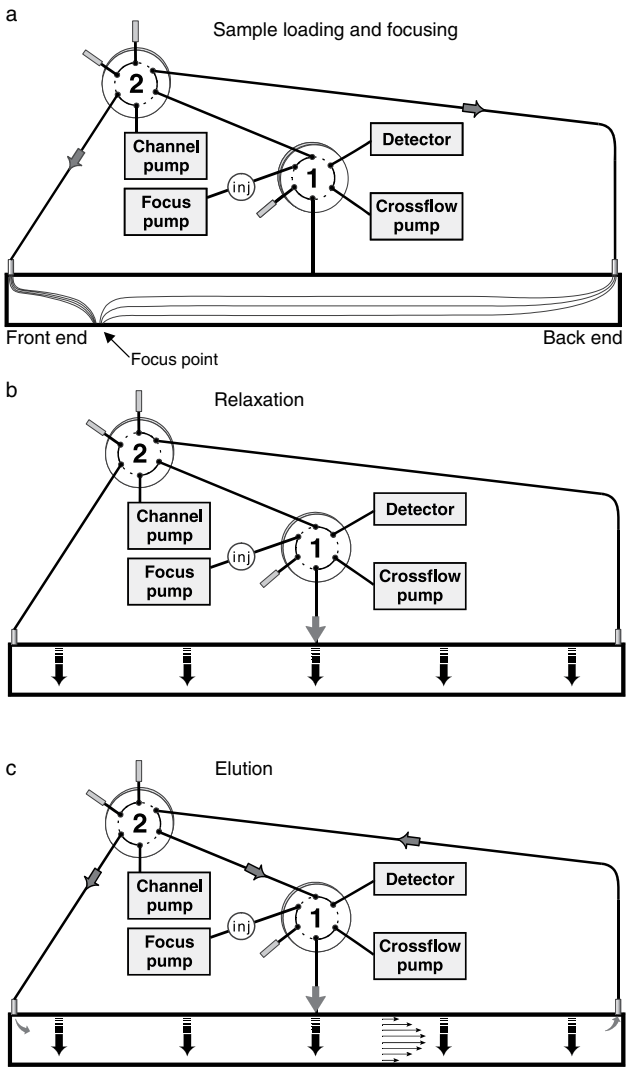

Fig. 1 Instrumental schematics of FlFFF with on-channel preconcentration showing the three different steps. The first involves emptying of the sample loop into either the forward or backward flows and subsequent focusing of the sample material at the focusing point. In the next step, the samples are allowed to relax at the equilibrium position by applying cross-flow only, and then the channel flows are switched on and elution is commenced.
Source: From Optimisation of on-channel preconcentration in flow field-flow fractionation for the determination of size distributions of low molecular weight colloidal material in natural waters, in Anal. Chim. Acta.[7]

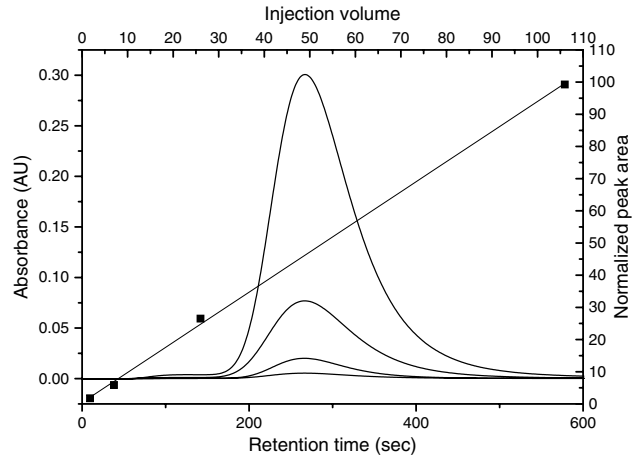

Fig. 2 Results showing preconcentration of 1.7–106 ml of a natural freshwater sample using the procedure in Fig. 1. The solid lines show the UV detector response while the squares with regression line (slope 0.94 and R^2 0.9993) represent peak area vs. injection volume. The samples were first diluted in order not to exceed the overloading point.
Source: From Optimisation of on-channel preconcentration in flow field-flow fractionation for the determination of size distributions of low molecular weight colloidal material in natural waters, in Anal. Chim. Acta.[7]

molecular-weight polymers and natural water colloids (Fig. 2) with a molecular weight of the same order as the membrane cut-off by optimizing injection flows, membrane, and carrier. Injection in both the forward and backward focusing flow stream was evaluated. An experimental approach was used to determine the minimum time for sample loading and focusing. In order to ensure sufficient focusing time for all colloids, the focusing time was increased until a stabile retention time was attained for the largest reference standard. This on-channel preconcentration method has been later used in an FlFFF coupling with inductively coupled plasma mass spectrometry for trace element size distributions for natural water colloids[9,10] The colloids and the associated metals would have been impossible to study without the preconcentration procedure due to the very low concentrations of both colloids and trace metals often found in natural waters. Lee, Ratanathanawongs Williams, and Giddings[8] presented a method for preconcentrating 10 ml samples of dilute polystyrene latex beads, river sediment particles, and proteins, which are injected in the channel inlet stream with an opposed focusing flow from the channel outlet. Results of recoveries are shown for different membrane materials. On-channel preconcentrations for FlFFF and SedFFF are rather simple to incorporate in a conventional instrument, just with the addition of a second switching valve and a liquid pump. The sample is exposed to the same media as in the separation step, and the preconcentration step is carried out just prior to analysis, which is not always the case for external preconcentration techniques such as ultrafiltration or centrifugation.[11,12]

Precautions must be taken in all FFF analyses when injecting large amounts of material with any injection technique. During the sample relaxation, local concentrations of analytes can become very high, and at some point the

sample components start affecting each other. Then, conformational changes or intermolecular repulsion can occur, preventing the analytes from attaining a true equilibrium distribution in the channel. This phenomenon is often referred to as overloading and is usually indicated by a earlier eluting peak with a fronting peak shape.

Overloading in polymer analysis using flow and thermal FFF is thoroughly described by Caldwell et al.,[13] where different overloading mechanisms during relaxation and elution are theoretically and experimentally evaluated. Usually, for FFF separations, the detector sensitivity is sufficiently high to detect the separated components at sample concentrations well below the overloading concentration. For further characterization of the particulate material by other detection systems, e.g., mass spectrometry, or subsequent analysis of collected fractions, it is often necessary to inject large amounts of sample material to exceed the detection limits, and then it is essential to be observant of overloading effects. The best way of investigating the elution behavior in order to rule out overloading is to inject various amounts of the sample and follow the retention time as well as the shape of the peak. The applied field in stop–flow relaxation or focusing flows in on-channel preconcentration could also have an effect on non-ideal behavior, e.g., the sample components are compressed during high fields, causing both higher local concentrations and potential interaction with the accumulation wall. When working with sample amounts near the overloading point, varying the field strength acting on the analytes can be used to find conditions where overloading starts and thereby avoid it.

CONCLUSIONS

To lower the detection limits of an FFF analysis, it is best to first apply one of the postchannel flow splitters (e.g., slot outlet or frit outlet) to remove excess liquid and thus reduce the dilution. If this is still not enough, a preconcentration method has to be applied. On-channel preconcentration by the opposing flow focusing injection of large sample volumes is the standard method in asymmetrical FlFFF and is easily modified in symmetrical FlFFF. The method utilizes the FlFFF channel as an ultrafiltration cell in a step just prior to elution. For Sedimentation FFF, external preconcentration methods are more practical even though examples of large volume injections have been shown.

REFERENCES

1. Schure, M.R. Limit of detection, dilution factors, and technique compatibility in multidimensional separations utilizing chromatography, capillary electrophoresis, and field-flow fractionation. Anal. Chem. **1999**, *71*, 1645–1657.
2. Li, P.; Hansen, M.; Giddings, J.C. Advances in frit-inlet and frit-outlet flow field-flow fractionation. J. Microcol. Sep. **1998**, *10*, 7–18.
3. Kirkland, J.J.; Yau, W.W.; Doerner, W.A. Sedimentation field flow fractionation of macromolecules and colloids. Anal. Chem. **1980**, *52*, 1944–1954.
4. Giddings, J.C.; Karaiskakis, G.; Caldwell, K.D. Concentration and analysis of dilute colloidal samples by sedimentation field-flow fractionation. Sep. Sci. Technol. **1981**, *16*, 725–744.
5. Wahlund, K.-G.; Giddings, J.C. Properties of an asymmetrical flow field-flow fractionation channel having one permeable wall. Anal. Chem. **1987**, *59*, 1332–1339.
6. Wahlund, K.-G.; Litzén, A. Application of an asymmetrical flow field-flow fractionation channel to the separation and characterization of proteins, plasmids, plasmid fragments, polysaccharides and unicellular algae. J. Chromatogr. **1989**, *461*, 73–87.
7. Lyvén, B.; Hassellöv, M.; Haraldsson, C.; Turner, D.R. Optimisation of on-channel preconcentration in flow field-flow fractionation for the determination of size distributions of low molecular weight colloidal material in natural waters. Anal. Chim. Acta **1997**, *357*, 187–196.
8. Lee, H.; Ratanathanawongs Williams, S.K.; Giddings, J.C. Particle size analysis of dilute environmental colloids by flow field-flow fractionation using an opposed flow sample concentration technique. Anal. Chem. **1998**, *70*, 2495–2503.
9. Hassellöv, M.; Lyvén, B.; Haraldsson, C.; Sirinawin, W. Determination of continuous size and trace element distribution of colloidal material in natural water by on-line coupling of flow field-flow fractionation with ICP-MS. Anal. Chem. **1999**, *71*, 3497–3502.
10. Lyvén, B.; Hassellöv, M.; Turner, D.R.; Haraldsson, C.; Andersson, K. Competition between iron- and carbon-based carriers for colloidal trace metals in freshwater. Geochim. Cosmochim. Acta **2003**, *67* (20), 3791–3802.
11. Saal, C.; Kammer, F.v.d. Comparison of different filtration techniques for the pre-concentration of natural colloidal dispersions for field-flow-fractionation (FFF). Vom Wasser **2002**, *98*, 193–202 (In German).
12. Beckett, R.; Nicholson, G.; Hart, B.T.; Hansen, M.; Giddings, J.C. Separation and size characterization of colloidal particles in river water by sedimentation field-flow fractionation. Water Res. **1988**, *22* (12), 1535–1545.
13. Caldwell, K.C.; Steven, L.B.; Gao, Y.; Giddings, J.C. Sample overloading effects in polymer characterization by field-flow fractionation. J. Appl. Polym. Sci. **1988**, *36*, 703–719.

Laser-Induced Fluorescence Detection in CE

Huan-Tsung Chang
Tai-Chia Chiu
Chih-Ching Huang
Department of Chemistry, National Taiwan University, Taipei, Taiwan

INTRODUCTION

Separations of small solutes and macromolecules by capillary electrophoresis (CE) have been widely accepted by the scientific community, mainly due to its inherent advantages such as high resolution, compatibility with smaller samples, consumption of less buffer, rapidity, and ease of automation. Some of these advantages stem from the use of capillaries with inner diameters of 1–100 μm. With such small diameters, injection volumes are typically 0.1–10 nl, leading to a difficulty of detection. For detecting an analyte present at 1 n*M* concentration, with a 0.1-nl injection volume, extremely sensitive detection systems, providing a detection limit below 100 zmol for the analyte, are needed. Over the past 20 years, a number of nanoscale detectors, based on mass spectrometry, amperometry, chemiluminescence, raidochemistry, and fluorescence, have been developed to meet the extraordinary sensitivity challenges posed by CE. Of these, laser-induced fluorescence (LIF) has been the most successful and has been applied to single-cell analysis, DNA sequencing and separations, protein analysis, single-molecule detection, etc. One good example is that LIF, in conjunction with capillary array electrophoresis (CAE), has been successfully used for DNA sequencing, which has considerably assisted in the rapid progress of the Human Genome Project.

FLUORESCENCE

Fluorescence is the process of emission of light after absorption; its intensity is generally small, which depends on the extinction coefficient and quantum efficiency of the analyte, optical length, power of the light source, and light collection efficiency. In fluorescence measurements, one molecule can be reexcited thousands of times during the measurement to generate sufficient numbers of photons for detection. Thus it is essential to minimize the stray light from the optics and Rayleigh and Raman scattering of the solvent molecules. Once stray light and background signals are under control, a laser can be used to increase the excitation intensity, leading to larger signals and improved limit of detection (LOD) in fluorescence. To prevent photobleaching of analytes and damages of capillaries, lasers with 1–10 mW power are commonly used in CE; some are listed in Table 1.

Instrumentation

Since the first successful use of LIF for CE by Gassmann et al.,[1] several designs have been tested, including cross-beam excitation, epi-illumination, axial-beam excitation, and sheath-flow cuvette. Of these, the design of cross-beam excitation has been most commonly adopted in CE. Because laser light is well collimated, it can be focused to a beam diameter smaller than any practical capillaries used in CE. Thus the maximum photon flux can be delivered to the interior of a capillary to allow efficient excitation of analytes and to reduce the scattering from the capillary wall. With the capillary tilted at an angle to the laser beam, and the emitted fluorescence collected in a direction perpendicular to the plane of the capillary and excitation beam, the background from refracted light is minimized after appropriate spatial and spectral filtering. One basic instrumental setup of CE/LIF is shown in Fig. 1. With such a simple system, Tseng et al. were able to detect 11.1 n*M* human serum albumin labeled with albumin blue 580, using a low-cost He–Ne laser.[2]

A novel LIF detector, which uses a sheath flow cuvette developed by Wu and Dovichi, provides better sensitivity than the design of cross-beam excitation.[3] For example, LOD values as low as 1.7 zmol for fluorescein derivatives of amino acids have been achieved when injecting a 1.3 nl sample. Briefly, a sheath flow cuvette uses a flowing jacket of refractive index-matching buffer to hydrodynamically focus solutes as they exit from the capillary, leading to a thin stream in the center of the flow chamber. Thus it is easy to excite fluorophores migrating in such a thin stream by a focused laser beam, with a minimum Rayleigh scattering from the capillary wall and Raman scattering from water.

Fluorescence Signal

Compared to absorption, fluorescence is highly selective and sensitive. However, only very few solutes of interest have excellent photophysical properties, including high molar absorptivity, quantum yield, and photostability. Some solutes that can be detected by laser-induced native

Table 1 Lasers commonly used in CE/LIF.

Wavelength (nm)	Type	Representative applications	Derivitizing agent	Comments
248	KrF	Proteins and DNA	none	pulsed, KrF gas used
266	Nd:YAG	Proteins, PAHs, and catecholamines	none	pulsed
275	Ar^+	Proteins, PAHs, and catecholamines	none	continuous
305	Ar^+	PAHs and catecholamines	none	continuous
325	He–Cd	Proteins PAHs	NBD none	short lifetime
334	Ar^+	Proteins PAHs	DNS, OPA none	continuous
355	Nd:YAG	Enzyme assay	NAD^+ + substrate → NADH + product	pulsed
363	Ar^+	Enzyme assay PAHs	NAD^+ + substrate → NADH + product none	continuous
442	He–Cd	Proteins PAHs	NBD none	short lifetime
488	Ar^+	Proteins and amino acids	FITC	continuous
543.6	He–Ne	DNA	YOYO-1	cheap, stable, low power

PAHs: polycyclic aromatic hydrocarbons. FITC: fluorescein isothiocyanate. DNS: dansyl halide. OPA: *O*-phthaldialdehyde. NBD: 4-clair-7-nitrobenz-2-oxa-1,3-diazole. YOYO-1: benzoxazolium-4-quinolinium dimer. NAD^+: nicotinamide adenine dinucleotide.

fluorescence (LINF) in CE, using mid- to deep-UV lasers, include proteins, nucleic acids, polycyclic aromatic hydrocarbons, and catecholamines. Most commonly used UV lasers include a continuous frequency-doubled Ar^+ laser as well as pulsed excimer lasers and quadruplet Nd:YAG laser. Although the analyses of proteins within single human erythrocytes and enzyme activity in cancer cells have been demonstrated by using a continuous UV laser,[4] high costs and maintenance of the laser are problematic.

For those without native fluorescence, two common approaches have been employed, namely, derivatization and indirect fluorescence. Derivatizing agents should be pure, low fluorescent, and stable, as well as react quickly and uniquely with the analytes and, thus, formed compounds should be strongly fluorescent and stable. These include dansyl chloride, fluorescamine, 4-clair-7-nitrobenz-2-oxa-1,3-diazole (NBD), *O*-phthaldialdehyde (OPA), fluorescein isothiocyanate (FITC), and naphthalene-2,3-dicarboxaldehyde (NDA), which have been used for the analyses of amino acids, peptides, proteins, thiols, and sugars with LOD in 1–100 n*M* range. Compared to LINF, approaches based on derivatization provide the

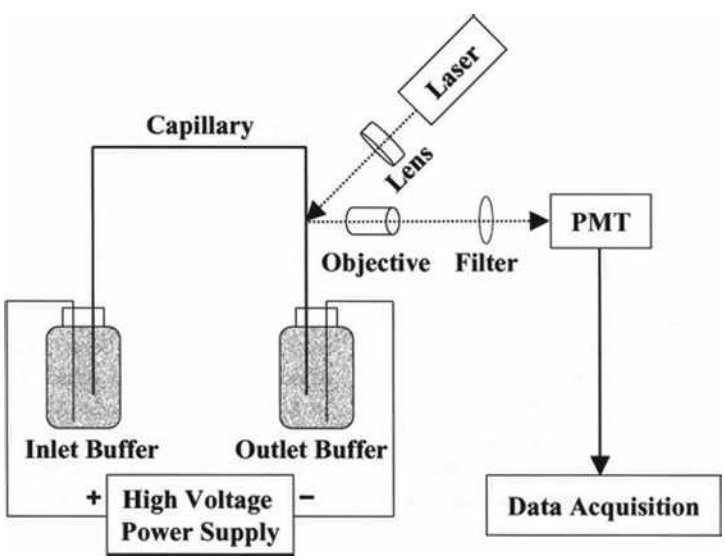

Fig. 1 Instrumental setup of CE-LIF.

advantages of relatively low cost and versatility in instrumentation, but they may suffer from contamination and loss of temporal information.

Indirect LIF (ILIF), in conjunction with CE, has been widely used for the analysis of ionic solutes, including organic acids, inorganic anions, carbohydrates, amino acids, and metal ions.[5] To optimize sensitivity, the use of an ionic dye with a greater fluorescent quantum yield and a very stable laser is essential, according to Eq. 1:

$$C_{\mathrm{LOD}} = C_{\mathrm{m}}/(\mathrm{DR} \times \mathrm{TR}) \quad (1)$$

where C_{LOD} is the concentration limit of detection; C_{m} is the concentration of relevant mobile-phase components; DR is the ability to measure a small change on top of a large signal and is equal to a signal-to-noise ratio (*S*/*N*) of the background signal; and TR refers to transfer ratio, which is the degree of displacement of the probe (co-ion) by the analyte. A system providing a high TR is also required for optimum sensitivity, as shown in Eq. 1, which can be realized by the use of fluorophores with a high charge density and a comparable mobility with analytes. By carefully controlling these factors, an LOD down to submicromolar for an analyte is easily achieved. As a result, the analysis of metal ions in single human erythrocytes by ILIF-CE has been demonstrated,[6] but its use for macromolecules such as proteins and DNA has been limited. Owing to the use of low ionic-strength buffers for achieving a high TR, matrix interference is a common problem.

APPLICATIONS

With high resolution, rapidity, and sensitivity, CE/LIF has become one of the most important separation tools in many fields. Most exciting research goals target at DNA sequencing, analysis of polymerase chain reaction products, single-cell analysis, single-molecule analysis, monitoring trace peptides and proteins in clinical analysis, determination of toxic chemicals, enantiospecific analyses in the fields of pharmaceutical drug research and production, etc. Herein we show some examples focusing on the analyses of DNA, proteins, and single cells.

DNA Sequencing and Separation

Although CE-LINF, using a UV Ar^+ laser, has been applied to the analysis of DNA, the majority has been performed by using visible lasers such as Ar^+ at 488 nm and He–Ne laser at 543.6 nm. These visible lasers are employed to excite DNA labeled covalently with fluorophores, such as modified fluorescein and rhodamine or intercalated DNA complexes. Some intercalating dyes, such as ethidium bromide (EtBr), benzothiazolium-4-quinolinium dimer (TOTO-1), benzoxazolium-4-quinolinium dimer (YOYO-1), and quinolinium-4-[(3-methyl-2(3*H*)-benzothiazolylidene)methyl]-1-[3-(trimethylammonio)-propyl]-diodide (TOPRO-1), have been developed that fluoresce weakly unless they insert inside a DNA strand, resulting in a low background and strong fluorescence. Detection limits in the level of zeptomole for these intercalated complexes have been demonstrated. Owing to high quantum yields, greater stability of these intercalated complexes, and multiple labeled capability, single-molecule detection for large DNA molecules has been achieved.[7] Moreover, some novel single-molecule-detection techniques have been developed and used to monitor the changes in DNA conformation (U-J-I) when migrating through gel matrices at applied electric fields.

Although DNA separation in CE relies on a sieving mechanism, like that in slab gel electrophoresis, polymer solutions prepared from linear polymers, such as linear polyacrylamide, poly(ethylene oxide), and cellulose derivatives, are commonly used, simply because they are of relatively low viscosity and are replaceable between runs. Polymer solutions can be filled into capillaries either under the influence of pressure prior to analysis in the absence of electro-osmotic flow (EOF), or by electrokinetic means during analysis in the presence of EOF. By taking advantage of EOF, Huang et al. have demonstrated gradient CE techniques for optimizing resolution, sensitivity, and speed in the analysis of DNA,[8] and online concentration techniques for DNA analysis with more than 400-fold improvement in the sensitivity, as shown in Fig. 2.[9] One should note that the migration order is the reverse of that observed in conventional CE methods (in the absence of EOF), because of DNA migrating against EOF.

The speed of CE is excellent compared to slab gel electrophoresis, but it is not throughput comparable to DNA sequencing. To overcome this disadvantage, the concept of high-throughput DNA analyzers, using an array of capillaries, has been realized and tested for DNA sequencing. One representative example is shown in Fig. 3.[10] Parallel separations result in significant challenges, such as reproducibility among capillaries, detecting DNA migrating through as many as 1000 capillaries at one time, cross talk between capillaries, and signal procession. So far, some novel CAE systems utilizing multiple sheath flow, line focus illumination, confocal fluorescence scanner, rotary confocal fluorescence scanner, fiber optic array illumination, together with charged coupled device (CCD) detection, have been developed and tested for DNA sequencing, forensic short tandem repeats, and genotyping.

Single-Cell Analysis

Generally, capillaries with inner diameters of 5–25 μm are used to inject and analyze single cells in CE. With such small capillaries, several features can be achieved, including low risk of injection of more than one cell at a time, low dilution factors after cell lysis, high resolving power, and

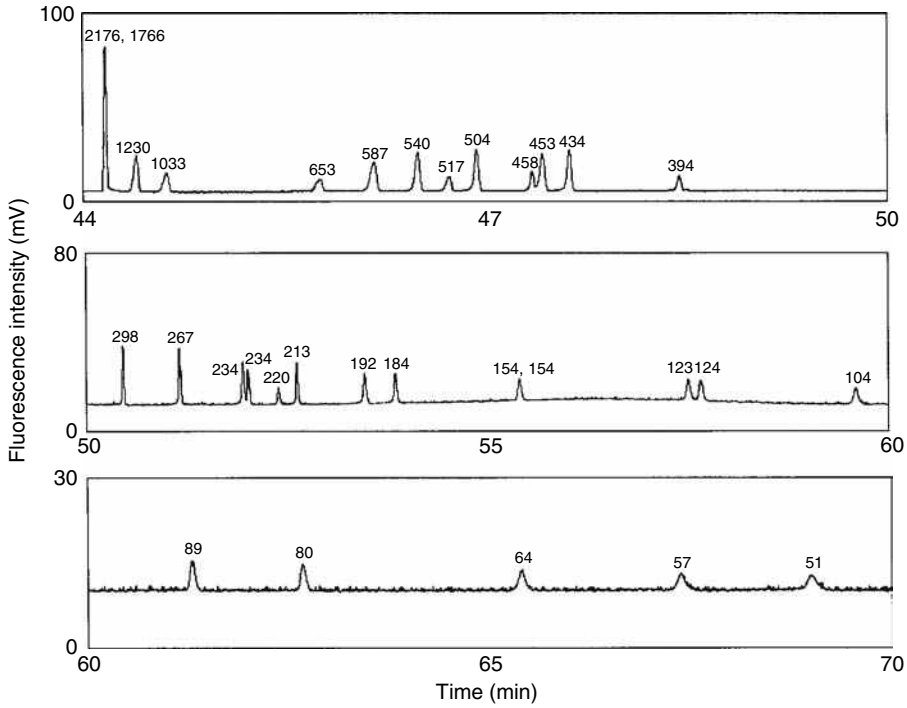

Fig. 2 Separation of 5 μl 0.1 μg/ml DNA markers V and VI prepared in 10 mm Tris-Borate (TB), pH 10.0, containing 2.5 mm NaCl at 444 V/cm for 30 min and, subsequently, at 222 V/cm for the rest using 2.5% PEO prepared in 200 mm TB, pH 9.0. Capillary: 45 cm in total length, 35 cm in effective length, 150 μm I.D., filled with 400 mm TB, pH 10.0.
Source: From Maximization of injection volumes for DNA analysis in capillary electrophoresis, in Electrophoresis.[9]

rapidity at high electric field strengths. It is important to keep a very small dilution factor, as the amounts of important markers in single cells are extremely low, mostly in the range of atomole–yoctomole. Besides, high resolving power is needed in order to separate a number of markers from a complicated cell environment. Although CE, in conjunction with mass spectrometry or amperometry, has been tested for single-cell analysis, most successful examples were conducted by CE/LIF. After injection of a cell into a capillary by pressure or electrokinetic means, lysis by osmosis, detergents, high voltage, or light takes place. When CE/LINF, using an Ar^+ laser at 275 nm is applied to detect proteins in erythrocytes, insulin contents in single islet cells, or catecholamines in adrenal medullary cells, the lysis components are directly subject to separation and detection. The success of these methods relies on the high sensitivity of LINF, with LOD values for proteins and catecholamines lower than nanomolar. For example, the determination of epinephrine and norepinephrine in individual bovine adrenal medullary cells, under acidic conditions, has been demonstrated.[11] Using a 285 groove/mm holographic grating and a CCD camera for detection, identification of ~ 30 compounds within single-neuron cells has been demonstrated using a frequency-doubled Ar^+ laser at 257 nm. When derivatization is required, background electrolytes containing suitable derivatizing agents are commonly used to perform on-column reaction. Compared to off-column derivatization, on-column reaction provides the advantages of low risk of contamination, low dilution factors, simplicity, and rapidity. One example is the use of naphthalene-2,3-dicarboxaldehyde and CN^- for the determination of dopamine and five amino acids in individual rat pheochromocytoma cells.[12] To increase the sensitivity and specificity, capillary affinity electrophoresis, in conjunction with immunoassay using antibody-fluorescein, has been developed for the determination of insulin in single islet cells.[13] In addition, the application of online enzyme assay, using an Ar^+ laser at 366 nm, has been demonstrated in the comparison of the activity of lactate dehydrogenase (LDH) in lymphoblastic cells and leukemia cells. With a high turnover number and low LOD for NADH, the same strategy has also been applied to the determination of the activity of single LDH molecules.

Protein Analysis

Proteomics is becoming increasingly important following the human genome era because proteins are the main catalysts, structural elements, signaling messengers, and molecular machines of biological tissues. A proteome represents the protein pattern of an organism, a cell, an organelle, or even a body fluid determined quantitatively at a certain time under precisely defined conditions. With high sensitivity and resolution, CE/LIF has shown high potential for quantification of proteins and exploration of their localization, modification, interaction, activity, and, ultimately, their function. In addition to separations based on a sieving mechanism, capillary zone electrophoresis using fused-silica capillary at low pH, high pH, or in high-conductivity background electrolytes, or using coated capillaries under mild conditions has been applied to the analysis of proteins. Besides, isotachophoresis and

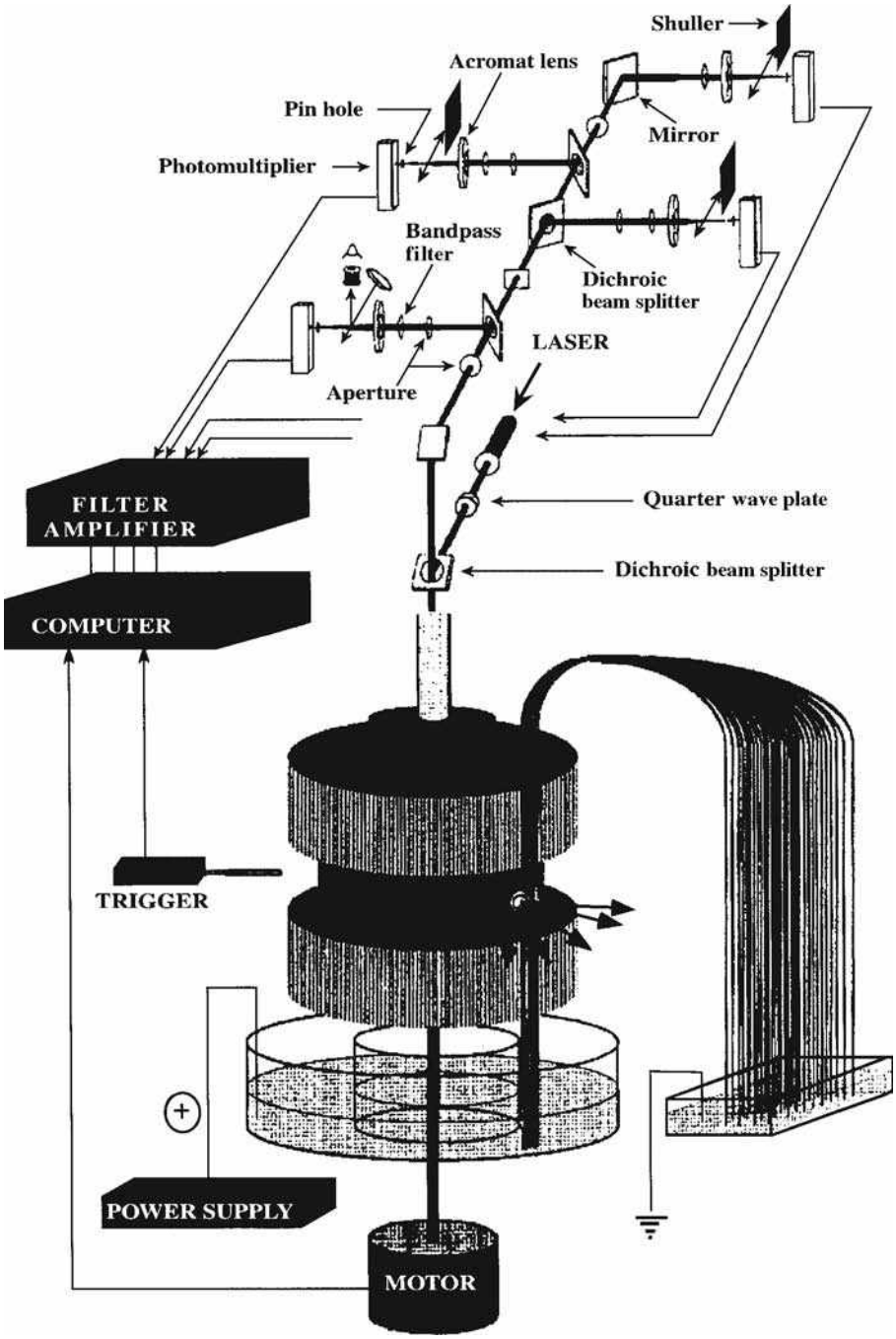

Fig. 3 Schematic representation of a 1000-capillary rotary scanner and a four-color confocal fluorescence detection system.

Source: From Ultra-high throughput rotary capillary array electrophoresis scanner for fluorescent DNA sequencing and analysis, in Electrophoresis.[10]

isoelectric focusing in capillaries have shown to be useful for separation of proteins. Although an Ar^+ laser at 275 nm and Kr^+ laser at 280 nm have been commonly used for protein analysis in CE/LINF, relatively inexpensive Nd:YAG pulsed laser at 266 nm and KrF excimer laser at 248 nm have also been employed. Generally speaking, pulsed lasers provide about 10 times higher LOD than continuous laser sources (former case). In spite of this, the LOD values down to picomolar for proteins have been achieved using a Nd:YAG laser when applying an online concentration technique.[14] When performing CE/LINF for protein analysis, a great effort must be made to minimize interferences, photobleaching, and quenching that may occur at low pH, high pH, high salt concentrations, and the existence of detergents. On the other hand, these problems can be minimized or prevented by careful selection of visible lasers, such as He–Ne lasers and dyes such as 3-(2-furoyl)quinoline-2-carboxaldehyde (FQ), NDA, Sypro Red, and Nile Red. Lee et al. have demonstrated protein analysis by on-column reaction using FQ, with a LOD of picomolar when excited with Ar^+ laser at 488 nm.[15] One drawback of performing derivatization is that multiple derivatization and byproducts might occur, leading to difficulty of separation.

CONCLUSIONS

With high sensitivity, rapidity, and high efficiency, CE/LIF has proved to be a powerful tool in the analysis of DNA, proteins, amino acids, glycoproteins, and single cells. To prevent photobleaching, as well as to reduce autofluorescence background and the cost of lasers, the use of diode lasers in the near-infrared region, together with suitable dyes, as well as sensitive detectors such as avalanche photodiode, has attracted much interest, which has been demonstrated in DNA sequencing and single-molecule detection. As the analyses of a single DNA molecule and single enzyme activity by CE/LIF have been demonstrated, its role in disease diagnosis and fundamental research, such as the interactions between DNA and proteins, will soon be recognized in many realms, such as in the life sciences. Recently, micrototal-analysis systems with LIF have become increasingly important in modern science and have been applied to the analysis of polymerase chain reaction (PCR) products or enzyme activity in a chip. Thus it is our belief that, despite LIF, some other laser techniques such as thermal lens absorption and Raman scattering spectroscopy will continue to play a strong role in the life sciences.

ACKNOWLEDGMENT

This work was supported by the National Science Council of the Republic of China under contract number NSC 90-2113-M002-058.

REFERENCES

1. Gassmann, E.; Kuo, J.E.; Zare, R.N. Electrokinetic separation of chiral compounds. Science **1985**, *230* (4727), 813–814.
2. Tseng, W.-L.; Chiu, T.-C.; Weng, J.-M.; Chang, H.-T. Analysis of albumins using albumin blue 580, by capillary electrophoresis and laser-induced fluorescence. J. Liq. Chromatogr. Relat. Technol. **2001**, *24* (19), 2971–2982.
3. Wu, S.; Dovichi, N.J. High-sensitivity fluorescence detector for fluorescein isothiocyanate derivatives of amino acids separated by capillary zone electrophoresis. J. Chromatogr. **1989**, *480* (1), 141–155.
4. Yeung, E.S. Study of single cells by using capillary electrophoresis and native fluorescence detection. J. Chromatogr. A, **1999**, *830* (2), 243–262.
5. Chiu, T.-C.; Huang, M.-F.; Huang, C.-C.; Hsieh, M.-M.; Chang, H.-T. Indirect fluorescence of aliphatic carboxylic acids in non-aqueous capillary electrophoresis using merocyanine 540. Electrophoresis **2002**, *23* (2), 449–455.
6. Hogan, B.L.; Yeung, E.S. Determination of intracellular species at the level of a single erythrocyte via capillary electrophoresis with direct and indirect fluorescence detection. Anal. Chem. **1992**, *64* (22), 2841–2845.
7. Ma, Y.; Shortreed, M.R.; Yeung, E.S. High-throughput single-molecule spectroscopy in free solution. Anal. Chem. **2000**, *72* (19), 4640–4645.
8. Huang, M.-F.; Hsu, C.-E.; Tseng, W.-L.; Lin, Y.-C.; Chang, H.-T. Separation of dsDNA in the presence of electroosmotic flow under discontinuous conditions. Electrophoresis **2001**, *I* (11), 2281–2290.
9. Huang, C.-C.; Hsieh, M.-M.; Chiu, T.-C.; Lin, Y.-C.; Chang, H.-T. Maximization of injection volumes for DNA analysis in capillary electrophoresis. Electrophoresis **2001**, *22* (20), 4328–4332.
10. Scherer, J.R.; Kheterpal, I.; Radhakrishnan, A.; Ja, W.W.; Mathies, R.A. Ultra-high throughput rotary capillary array electrophoresis scanner for fluorescent DNA sequencing and analysis. Electrophoresis **1999**, *20* (7), 1508–1517.
11. Chang, H.-T.; Yeung, E.S. Determination of catecholamines in single adrenal medullary cells by capillary electrophoresis and laser-induced native fluorescence. Anal. Chem. **1995**, *67* (6), 1079–1083.
12. Gilman, S.D.; Ewing, A.G. Analysis of single cells by capillary electrophoresis with on-column derivatization and laser-induced fluorescence detection. Anal. Chem. **1995**, *67* (1), 58–64.
13. Tao, L.; Kennedy, R.T. On-line competitive immunoassay for insulin based on capillary electrophoresis with laser-induced fluorescence detection. Anal. Chem. **1996**, *68* (22), 3899–3906.
14. Tseng, W.-L.; Chang, H.-T. On-line concentration and separation of proteins by capillary electrophoresis using polymer solutions. Anal. Chem. **2000**, *72* (20), 4805–4811.
15. Lee, I.H.; Pinto, D.; Arriaga, E.A.; Zhang, Z.; Dovichi, N.J. Picomolar analysis of proteins using electrophoretically mediated microanalysis and capillary electrophoresis with laser-induced fluorescence detection. Anal. Chem. **1998**, *70* (21), 4546–4548.

LC/MS

Ioannis N. Papadoyannis
Georgios A. Theodoridis
Laboratory of Analytical Chemistry, Chemistry Department, Aristotle University of Thessaloniki, Thessaloniki, Greece

INTRODUCTION

In the few years that have passed since the first version of this entry, the field of liquid chromatography/mass spectrometry (LC/MS) has changed dramatically. We had quoted then that "The coupling of liquid chromatography and mass spectrometry (LC–MS) was initially considered impossible and actually is still characterized as a hyphenated technique." The situation now looks very different due to the remarkable increase of the magnitude of this subject and the massive expansion of the application of LC/MS, which are now driven by life sciences. The finalization of the human genome project (where the "shotgun approach" and hyphenated technologies were central) shifted the interest of a massive research and development sector toward the analysis and identification of macromolecules (genes, proteins, polysaccharides, etc.) in biological samples. These new needs are practically approached by a few rapidly evolving methodologies such as array techniques, LC/MS, and matrix-assisted laser desorption ionization/surface-enhanced laser desorption ionisation (MALDI/SELDI/MS). In addition, revolutionary developments in instrumentation (linear ion traps, quadrupole time-of-flight/MS, TOF/TOF/MS) continue to push instrument features and application possibilities even further. As a result, it is no surprise that LC/MS is now adapted by many different disciplines, and a greater scope of the technique's applicability and overall turnover is thus projected. In fact, in recognition of his innovative contributions for the coupling of LC with MS (electrospray technique), Prof. John Fenn was awarded a part of the Nobel Prize for Chemistry for the year 2002.

LC/MS

The coupling of LC with MS requires an appropriate interface due to the incompatibilities of the two methods. In order to introduce a conventional LC flow (0.5–1.5 ml/min) into the mass spectrometer, one should evaporate it, producing a vapor with a volume far beyond the capacity of the mass spectrometer pump systems. The selection of the interface is the key decision and a limiting factor in the utilization of the instrument. Some years ago, LC/MS systems were state-of-the-art, space-occupying machines, accessible only to specialists. In the last years, evolution in technology and electronics, together with stronger cooperation of LC with MS manufacturers (often in the form of company acquisition or merging and strategic alliances), brought to the market bench top, low price, dedicated systems that require less handling and are often used for routine analysis.

The advantages of an online LC/MS approach are many. Both techniques show high separation power and their on line combination is a powerful tool for identification purposes and quantitative studies. Many detectors are available for high-performance liquid chromatography (HPLC): ultraviolet (UV), conductivity, electrochemical, fluorescence, refractometer, etc. Unfortunately, most of them lack specificity, selectivity, and sensitivity. Hence, identification of unknown compounds is actually impossible.

An ideal detector for HPLC should combine optimum sensitivity with maximum identification capability. It should also respond to all the solutes and increase its signal linearly with the amount of the solute, but at the same time be unaffected by changes in the mobile phase. Finally, it should be reliable and robust and should not contribute to extracolumn peak broadening. Of the detectors used with HPLC, the mass spectrometer is the closest to these above requirements. A mass spectrometer offers many attractive features as a chromatographic detector. Low detection limits down to picogram range can be accomplished in optimized configurations. Mass spectrometry offers high specificity and mass distinction according to nominal mass (low-resolution MS). The specificity is much more increased in high-resolution MS where mass distinction is made according to accurate mass. This enables the resolution of compounds with the same nominal mass but with different elemental composition. Mass spectrometry provides compound specific information by fragmentation obtained either by hard ionization or by tandem MS. Fragmentation patterns greatly increase identification power in the analysis of unknown compounds in complex matrices. Finally, a mass spectrometer is potentially a universal detector.

A diagram of a typical mass spectrometer scheme is depicted in Fig. 1. The simplest form of an MS system should perform the following fundamental tasks:

1. Vaporize compounds of varying volatility. This is accomplished in the inlet system. Introduction of

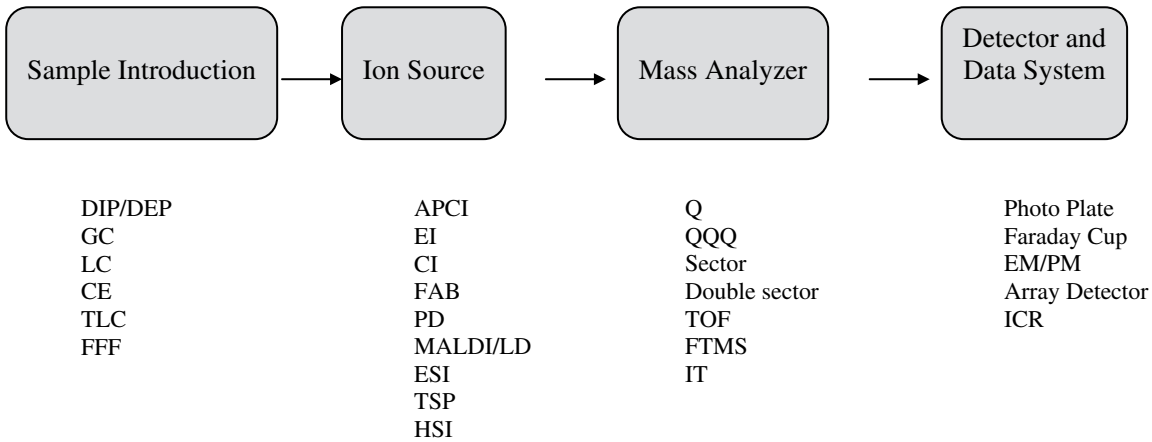

Fig. 1 Schematic representation of a mass spectrometer depicting its main components and the different modes used. DIP: direct insertion probe, DEP: direct exposure probe, CE: capillary chromatography, FFF: field flow fractionation, APCI: atmospheric pressure ionization, EI: electron impact, CI: chemical ionization, FAB: fast atom bombardment, PD: plasma desorption, MALDI: matrix-assisted laser desorption ionization, LD: laser desorption, TSP: thermospray, ESI: electron spray ionization, HSI: hyperthermal surface ionization, Q: quadrupole, QQQ: triple quadrupole, TOF: time-of-flight, FTMS: Fourier transform mass spectrometer, IT: ion trap, EM: electron multiplier, PM: photo multiplier, ICR: ion cyclotron resonance.

the sample is done by direct insertion probe, reservoir inlet, or following a separation step (GC, HPLC, or capillary electrophoresis (CE)). In the latter case to introduce on line the LC/CE flow to the mass spectrometer, one needs an appropriate interface. Development of appropriate interfaces was utmost for evolution of the LC/MS coupling.

2. Produce ions from neutral molecules in the vapor phase. This occurs in the ion source. As seen in Fig. 1, there are several modes of ion sources. Of those, the most used in LC/MS are: electrospray ionization (ESI), chemical ionization (CI), thermospray ionization (TSP), fast atom bombardment (FAB) and electron impact (EI).
3. Separate the formed ions according to their mass-to-charge ratio (m/z ratio). This takes place in the mass analyzer. By far the most used analyzer is the quadrupole either as single or as triple quadrupole combined with a soft ionization technique. In the latter configuration, tandem MS can be accomplished. The magnetic sector is also coupled to LC when there is a need for higher-resolution power or higher sensitivity.
4. Detect and record the separated ions. Multipliers are the most common detectors used in LC/MS instruments. Proper fully computerized data manipulation systems are required to handle the massive information flux from the detector.

Interfacing

Interfacing LC and MS benefits both techniques. An obvious question could be why does one need such a seemingly unorthodox coupling, when other robust and well-established techniques (GC/MS) are already available. The great potential of the LC/MS approach is its applicability in the analysis of thermolabile or non-volatile compounds; this is of enormous interest in bioanalysis. Despite its high-resolution power, GC is actually suitable only for the analysis of volatile compounds of low molecular mass. LC/MS analysis gave a real boost to bioanalysis enabling the positive identification and low level detection of peptides, proteins, carbohydrates, polar analytes, and many other types of synthetic or naturally occurring compounds. Lately, it has been stated by eminent mass spectrometrists that MS alone can handle most samples and provide adequate information (both qualitative and quantitative). Claims were made that chromatography could be disregarded since the mass spectrometer could operate as a perfect powerful separator and detector. This could be true in ideal situations or in pure "academic samples." The truth is that in real samples and most importantly in life sciences' applications, the separation power of chromatographic or electrophoretic techniques is still necessary. A big obstacle for the direct introduction of complex samples in MS is ion suppression: In such a case, the presence of interfering sample components would dominate the MS spectra and also hinder the ionization of important target analytes (in the ion source), which thus could not be seen by the analyzer. Due to such reasons, efficient methods for sample fractionation and analyte purification and enrichment are sought. As a result, more and more research groups are focused on the development of multidimensional separation modes. Hence, the future of LC and also LC/MS should not be regarded as vague. In contrast, in our opinion, LC/MS seems to dominate several routine analysis fields. LC/MS will hold a stronger grip in several fields such as forensic analysis, metabolite identification, or lead

Table 1 General features and applicability of various LC/MS interfaces.

Type	Solvent	Flow rate (μl/min)	Ionization	Analyte type
MB	NP	<2000	EI, CI, FAB	Non/slightly polar
	RP (< 50% H_2O)	<500	EI, CI, FAB	RV
DLI	RP (< 50% H_2O)	<50	Solvent-CI	Non/medium polar, MV
PB	RP, NP	100–500	EI, CI, FAB	Non/medium polar, MV
TSP	RP, NP	500–2000	TSP, solvent-CI	Non-polar to polar, V to RIV
ESI	RP, NP	1–1000	IE, API	Polar, IV
ISP	RP, NP	10–1000	IE, API	Polar, IV
HNI	RP, NP	1–2000	APCI	Non/medium polar, RV
cfFAB	RP, NP	<20	FAB	Polar, IV

MB: moving belt, DLI: direct liquid introduction, ISP: ionspray, HNI: heated nebulizer interface, cfFAB: continuous flow FAB, RP: reversed phase, NP: normal phase, IE: ion evaporation, API: atmospheric pressure ionization. RV: relatively volatile, RIV: relatively involatile, IV: involatile. The rest of the abbreviations as in Fig. 1.

finding and will continue to lead the proteome–genome–metabolome research.

Numerous types of LC/MS interfaces have been developed. Early attempts were focused on methods of overcoming the incompatibility of the liquid flow rate and maintenance of the MS high vacuum. Recent approaches pay more attention to the practical use of ionization techniques that do not require sample volatilization. The main approaches to overcome incompatibilities are:

1. Splitting of the flow. A high proportion of the sample is wasted this way.
2. Increasing the source housing pump speed, usually with the addition of a cryo-pump.
3. Miniaturizing the LC dimensions.
4. Removal of the solvent prior to the introduction in the MS. This approach is used in transport interfaces (MB) and PB.
5. Attaching additional pump to the ion source, which can then accept higher flow rates. This approach is used in TSP.
6. Atmosphere pressure ionization (ESI, APCI, ISP).

The main features of LC/MS interfaces are illustrated in Table 1.

The first commercially available LC/MS system (Finnigan 1976) used a moving belt interface. This was a straightforward approach based on the 1960s instrument design of moving wires and cords. An endless continuous moving belt transports the analytes from the LC system to the MS. The LC flow is deposited on a polyimide belt, and the mobile phase is removed by heating and subsequent evaporation in two consecutive vacuum chambers. Next, the analyte is desorbed from the belt and is introduced into the ion source. On the return path, the belt passes over a clean-up heater to remove residual solvent and sample and finally through a waterbath to remove any involatile material.

More robust, sensitive, and user-friendly devices soon replaced the first type of interfaces (MB and DLI). During the 1980s, a lot of effort was put on the development of TSP and PB. Since the last decade, ESI has been by far the most used interface for LC/MS, with APCI ranking second in applicability. Recently the two modes have been combined in a single interfacing device that can alternate from ESI to APCI eliminating the need for ion source replacement.

In ESI, the column effluent is passed through a small jet maintained at high voltage (kV range). Due to electronic charging, the liquid is broken into very small droplets. Desolvation of the droplets increases the electric field strength at the surface and leads to the ejection of charged compounds by ion evaporation (Fig. 2).

ESI demonstrates three major advantages:

1. It is a gentle technique and leads to less thermal degradation compared to other techniques.
2. Since it is an atmospheric pressure ionization technique, up to 100% ionization can be achieved, thus enhancing method sensitivity.
3. Multiple ions (sometimes up to 70–100 charges) are often formed, thus lowering the m/z ratio and permitting the analysis of high molecular weight compounds.

Despite its great advantages, LC/MS has also a number of limitations, apart from the interfacing need:

1. Incompatibility with some of the non-volatile buffers and other mobile phase additives. Hence, phosphates, ion pairing agents, and amine modifiers are replaced by ammonium acetate, ammonium formate, etc.
2. Special care has to be taken to ensure that no connection will introduce peak broadening.
3. Interfaces are not compatible with all the ionization modes, and, in general, although the MS is a universal detector, the fact remains that not all compounds can be analyzed with any configuration.
4. Instrument price still remains high (i.e., compared to GC/MS and MS/MS).

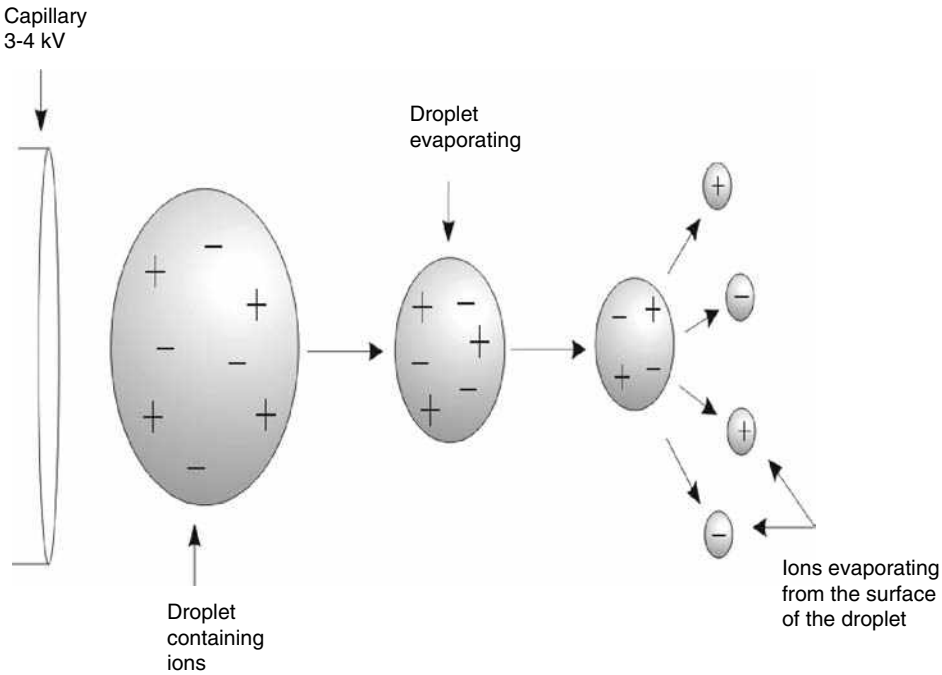

Fig. 2 Ion evaporation in the ESI mode.

ADVANCEMENTS

In the last years following the nanotechnology trend, great efforts have been put towards miniaturization and the developments of nano-LC. This is actually mandated from the end needs of the MS detection in genome–proteome research: Tiny amounts of the biomacromolecule are present in complex samples of limited volume and availability. Thus, miniaturization is a one-way road in proteomics, and microbore/capillary LC has become more popular. It is also believed that new bioanalytical LC/MS methods will be developed aiming at capillary or nano-LC dimensions. New, truly nano-LC pumps have now been commercialized to cover the niche. However, this has not yet passed into the bulk of the LC/MS reported works, where conventional LC columns still dominate the field. Reversed-phase (RP) LC is still by far the method of choice in LC/MS schemes, but more and more multidimensional schemes are reported employing size exclusion, ion exchange, or affinity modes and RP (Table 2).

The immense interest and the increasing needs for the application of LC/MS in various life science riddles motivated and pushed developments in mass analyzing technologies. Notable recent developments from the coupling and MS perspective include the development of interfaces for LC/MALDI/MS coupling, the LC/qTOF schemes, the expansion of LC/ion trap MS, and developments toward linear ion traps, Fourier transform ion cyclotron resonance MS, and TOF/TOF/MS schemes. Such developments result in enhanced versatility and dynamic span in method development. For example, LC/MALDI/MS schemes enable the simultaneous analysis (separation, identification, and quantitation) of a large number of very high molecular compounds (more than a 1,000,000 Da), and at the same time they improve detection sensitivity and scanning speed. The combination of LC with MALDI/MS is accomplished off-line as described at the end of this entry. The LC/TOF combination is practically realized via an APCI/ESI LC interface, introduction to a quadrupole MS, and subsequent orthogonal introduction to TOF/MS. Recent enhancement in the resolution power of TOF analyzers (reaching resolution values of 20,000 and 5–10 ppm mass accuracy) rendered LC/qTOF schemes as an attractive alternative of the bulky high-resolution

Table 2 Characteristics of various LC modes.

LC mode	I.D.	Injection volume	Flow rate
Conventional	3–6 mm	10–50 μl	0.5–2 ml/min
Microbore	0.5–2 mm	0.5–2 μl	10–300 μl/min
Packed microcapillary	0.2–0.5 mm	0.1 μl	1–10 μl/min
Drawn packed capillary	50–200 μm	10 nl	<0.1 μl/min
Open tubular	5–25 μm	1 nl	<0.1 μl/min

double/triple sector configurations. The LC/TOF/MS, when combined with ion traps or quadrupoles, provides also MS/MS capabilities with very high mass accuracy, improved resolution power, and wide dynamic range. LC/linear ion trap MS utilizes a quadrupole functioning as a linear trap (often in a triple quadrupole configuration). This scheme results in the accumulation of a higher number of ions, thus providing high-sensitivity full-scan MS and simultaneously improving MS/MS possibilities and time throughput.

APPLICATIONS

The application area of LC/MS is rapidly growing. LC/MS is now regularly used for the analysis of many different types of compounds: drugs and metabolites, herbicides–pesticides and metabolites, surfactants, dyes, saccharides, lipids–phospholipids, steroids, and many others. Obviously, the area that profits more from the development of LC/MS is life sciences: genomics and proteome research, bioanalysis, therapeutic drug monitoring, lead finding, natural products, and many other sectors rely on the unparalleled separation and identification possibilities of LC/MS. This is the field where a rapid expansion is progressing now and an even greater expansion is projected for the future. Needs in life sciences for the recognition of key elements (disease biomarkers, inherent compounds or metabolites and also drug metabolites) push more and more researchers to adopt LC/MS or MALDI/MS schemes in their protocols. Perhaps no tool has been more instrumental to proteomics revolution than the mass spectrometer. Due to its capacity to deconvolute highly complex matrices, MS instruments facilitate the identification and quantitation of proteins. Apart from the cartography of the proteome (estimates are from 300,000 to several millions of proteins in the human body), MS and LC/MS methods are the key elements in determining the dynamic state of proteins. In contrast to the more or less static genome, proteins are subject to several post-translational modifications, protein–protein interactions (including oligomerization and polymerization) and cell localization. In addition, many proteins exist in minute amounts and no multiplication tool is at hand. Thus, MS detection is absolutely necessary for both unambiguous identification and determination of proteins or peptides. Finally, peptide/protein sequencing is a broad field where again MS machines are instrumental.

LC/MS is penetrating many other scientific research sectors and is becoming widely used by various scientists: toxicologists, physicians, environmental scientists, veterinary scientists, and so forth. This becomes more evident in fields where unambiguous identification of banned or toxic substances is required. In clinical and forensic toxicology, LC/MS "competes" with GC/MS, the working horse of the field. Identification and quantitation of several drugs of abuse, pharmaceuticals, and doping agents is now performed with LC/MS or LC/MS/MS with equal or better specificity and sensitivity than GC/MS. Functional utilities used in GC/MS such as the MS libraries (obtained by electron impact ionization) are not at hand for LC/MS. Despite the developments and the ongoing efforts, reaching such high levels of validation and assurance in LC/MS seems a very difficult target.

The overwhelming amount of data generated and collected, produces what is now perceived as the bottleneck: the information manipulation. New software (bioinformatics) tools are being produced to cope with these rapidly expanding needs. In our opinion, this is the field where critical progress should be expected. The best software tools, which could rapidly and precisely identify minor amounts of complex peptide fragments in real samples or enable faster gene/protein identification, will probably be key elements in decision making.

Finally, an aspect that should not be left out of consideration is the off-line combination of LC with MS. A great advantage of the online methods is the integration of the evaluation systems used. In online LC/MS systems, identification of not completely resolved peaks is easily and unambiguously accomplished, taking advantage of the mass spectrometer separation power. In contrast in off-line LC/MS, complete resolution of the peaks is essential. Moreover, fraction collection, evaporation, and sample introduction may result in sample loss or contamination. However, off-line LC/MS can still be of great value, for preparative purposes or in cases where a special MS technique is required. For example, characterization of biopolymers or proteins by MALDI/TOF cannot be performed on line with a chromatographic separation method due to the nature of the two techniques (LC is a continuous flow technique whereas MALDI/MS is a pulsed technique). In this case, off-line LC/MS is the method of choice, and new interfaces have been recently produced. The LC effluent is robotically deposited onto precoated MALDI targets ("peak parking"). One by one, the spots on the target are subsequently shot by laser to ionize the molecules and introduce them to the MS. This orthogonal scheme has its own advantages as species can be selected to be analyzed again, whereas in online flow through modes this is not possible and a second LC/MS run is necessary.

CONCLUSIONS

In the past years, LC/MS has progressed and spread immensely and evolved from a high-end technology to a mature, indispensable technique applied both to research and routine analysis. The field continues to change dynamically as it remains in the forefront of contemporary research and development. Remarkable advancements have been made in both the LC field and the MS analyzing field; however, the interfacing principles and technologies

remain more or less more concentrated on the ESI/APCI schemes that have been developed more than a decade ago. It should be pointed out that new advancements and technologies seem to be driven by the pharmaceutical industry, which has invested heavily on hyphenated techniques (LC/NMR, LC/MS, and so forth) for bioanalytical purposes and the identification of disease biomarkers. Hence, important developments may not be disclosed for propriety purposes, whereas at the same time we see small instrumentation companies producing novel tools to cover interfacing niches mostly aiming at a higher throughput (multi-ESI needles). It should be expected that the chromatographic-separation element of several LC/MS methods and schemes will be significantly altered in the coming years. But we strongly believe that chromatography cannot and will not be displaced. In contrast, further expansion of the LC/MS can be expected: Miniaturization of both modes (LC and MS) will remain a major goal. Sample purification needs in proteome research render LC an integral part in the analysis of proteins. The absence of a multiplication method for proteins (as PCR functions for the genes) necessitates analyte separation and enrichment prior to the introduction to the MS for peptide identification and/or sequencing. The coupling is certainly a win–win situation from both perspectives and methods, and practitioners may greatly benefit by understanding and taking advantage of the additional features of the coupled methodology. LC/MS continues to be an exciting field, and now it is at the service of an ever-expanding number of scientists.

BIBLIOGRAPHY

1. Niessen, W.M.A.; Van der Greef, J. *Liquid Chromatography–Mass Spectrometry*; Chromatographic Science Series; Marcel Dekker: New York, 1991.
2. Niessen, W.M.A. *Liquid Chromatography–Mass Spectrometry;* 2nd Ed. (revised and expanded); Marcel Dekker: New York, 1998.
3. Yergey, A.L.; Edmonds, C.G.; Lewis, I.A.S.; Vestal, M.L. *Liquid Chromatography–Mass Spectrometry. Techniques and Applications*; Plenum Press: New York, 1990.
4. Chapman, J.R. Mass spectrometry as an LC detection technique. In *A Practical Guide to HPLC Detection*; Parriott, D., Ed.; Academic Press: San Diego, CA, 1993.
5. Verheij, E.R. Strategies for compatibility enhancement in liquid chromatography–mass spectrometry. Ph.D. Thesis, Leiden University, 1993.
6. Arpino, P.J. Combined liquid chromatography/mass spectrometry. A review. In *Mass Spectrometry in Biological Sciences: A Tutorial*; Gross, M.L., Ed.; Kluwer: Dordrecht, 1992.
7. Tomer, K.B. HPLC detection by mass spectrometry. In *HPLC Detection Newer Methods*; Patonay, G., Ed.; Weinheim: VCH, 1992.
8. Lee, M.S. *LC/MS Applications in Drug Development*; 2002.
9. Barcelo, D. *Applications of LC–MS in Environmental Chemistry*; Elsevier Science: Amsterdam, 1996.
10. Dass, C., Ed.; *Principles and Practice of Biological Mass Spectrometry*; John Wiley & Sons: NY, 2000.
11. Chapman, J.R., Ed.; *Mass Spectrometry of Proteins and Peptides*; Humana Press: Totowa, 2000.
12. Cole, R.B., Ed.; *Electrospray Ionization Mass Spectrometry: Fundamentals Instrumentation and Applications*; John Wiley & Sons: NY, 1997.
13. Pramanik, B.N.; Ganguly, A.K.; Gross, M.L. *Applied Electrospray Mass Spectrometry*; Marcel Dekker: NY, 2002.
14. Ardrey, R.E. *Liquid Chromatography–Mass Spectrometry: An Introduction*; Analytical Techniques in the Sciences; John Wiley & Sons: NY, 2003.
15. Niessen, W.M.A. Progress in liquid chromatography–mass spectrometry instrumentation and its impact on high-throughput screening. J. Chromatogr. **2003**, *1000*, 413–436.
16. Gelpi, E. Contributions of liquid chromatography–mass spectrometry to "highlights" of biomedical research. J. Chromatogr. **2003**, *1000*, 567–581.
17. Erickson, B.E. HPLC and the ever popular LC/MS. Bioanalytical applications drive the market. Anal. Chem. **2000**, *72*, 711A–716A.
18. Ferrer, I.; Thurman, E.M. Liquid chromatography/time-of-flight/mass spectrometry (LC/TOF/MS) for the analysis of emerging contaminants. TRAC Trends Anal. Chem. **2003**, *22*, 750–756.
19. Marquet, P. Progress in liquid chromatography–mass spectrometry in clinical and forensic toxicology. Ther. Drug Monitor. **2002**, *24*, 255–276.

LC/NMR and LC/MS/NMR

Maria Victoria Silva Elipe
Analytical Research and Development Department, AMGEN, Thousand Oaks, California, U.S.A.

Abstract
A general overview of the recent technological advancements and applications of nuclear magnetic resonance (NMR) hyphenated with other analytical techniques is given from a practical point of view. Details of the pros and cons of the hyphenation of NMR with liquid chromatography (LC) as LC/NMR and also with mass spectrometry (MS) as LC/MS/NMR are demonstrated with two examples. Current developments of NMR and MS/NMR with other analytical separation techniques are discussed, especially with solid-phase extraction (SPE) as SPE/NMR and SPE/NMR/MS and capillary liquid chromatography (capLC) as capLC/NMR.

INTRODUCTION

During the last decade, hyphenated analytical techniques have grown rapidly to solve complex analytical problems. The combination of separation technologies with spectroscopic techniques is extremely powerful in carrying out qualitative and quantitative analysis of unknown compounds in complex matrices. High-performance liquid chromatography (HPLC) is the most widely used analytical separation technique for the qualitative and quantitative determination of compounds in solution. Mass spectrometry (MS) and nuclear magnetic resonance (NMR) are the primary analytical techniques that provide structural information for the analytes. The physical connection of HPLC and MS (LC/MS) or NMR (LC/NMR) increases the capability of analysts to solve structural problems of mixtures of unknown compounds. LC/MS has been the more extensively applied hyphenated technique because MS has higher sensitivity than NMR.[1–3] Advances in NMR, LC/NMR, and even LC/MS/NMR have enabled these techniques to become routine analytical tools in many laboratories. This entry provides an updated overview for the LC/NMR and LC/MS/NMR (or LC/NMR/MS) techniques with a description of their limitations, together with an example for LC/NMR and another for LC/MS/NMR to illustrate the data generated by these hyphenated techniques. This entry is not meant to imply that LC/MS/NMR will replace LC/MS, LC/NMR, or NMR techniques for structural elucidation of compounds. LC/MS/NMR, together with LC/MS, LC/NMR, and NMR, are techniques that should be available and applied to appropriate cases based on their advantages and limitations.

PRACTICAL ISSUES OF LC/NMR

NMR is one of the most powerful techniques for elucidating the structures of organic compounds. Before undertaking the NMR analysis of a complex mixture, separation of the individual components by chromatography is required. LC/MS is routinely used to analyze mixtures without prior isolation of their components. In many cases, however, NMR is needed for the identification of ambiguous structures. Although hyphenated LC/NMR has been known since the late 1970s,[4–6] it has not been widely implemented until the last decade.[7–11] The major technical considerations of LC/NMR are NMR sensitivity, NMR and chromatographically compatible solvents, solvent suppression, NMR flow-probe design, and compatibility of the volume of the chromatographic peak with the volume of the NMR flow cell.

NMR is a less sensitive technique compared to MS and hence requires much larger samples for analysis. MS analysis is routinely carried out in the picogram range. Modern high-field NMR spectrometers (400 MHz and higher) can detect proton signals from pure demonstration samples well into the nanogram range (MW 300 Da). For real world samples, however, purity problems become more intrusive with diminishing sample size and can be overwhelming in the submicrogram domain. This places a practical lower limit for most structural elucidation by NMR, which is estimated by the author to be close to 500 ng (MW 300 Da).

Although several other important nuclides can be detected by NMR, proton (^{1}H) NMR remains the most widely used because of its high sensitivity, high isotopic natural abundance (99.985%), and its ubiquitous presence in organic compounds. Of comparable importance

is carbon (^{13}C), with 1.108% abundance, which, because of substantial improvements in instrument sensitivity, is now utilized as routinely as proton. Fluorine (^{19}F) with 100% abundance is used less often because it is present in only about 10% of pharmaceutical compounds. Another consequence of the intrinsic low sensitivity of NMR is that virtually all samples require signal averaging to reach an acceptable signal-to-noise level. Depending on the sample size, signal averaging may range anywhere from several minutes to several days. For metabolites in the 1–10 μg range, overnight experiments are generally necessary.

Liquid NMR requires the use of deuterated solvents. Conventionally, the sample is analyzed as a solution using a 5 or 3 mm NMR tube depending on the NMR probe, which requires ~500 or 150 μl, respectively, of deuterated solvents. The increased solvent requirement for LC/NMR makes this technique highly expensive. Deuterium oxide (D_2O) is the most readily available, reasonably priced solvent (over $300/L). The price of deuterated acetonitrile (CD_3CN) is dropping and varies depending on the percentage of included D_2O, but still exceeds $1000/L. Deuterated methanol (CD_3OD) is even more expensive. Deuterated solvents for normal-phase columns are not readily available, but those that are available have even more prohibitive price tags. This necessitates the use of reversed-phase columns. Another factor that raises concern is the compatibility of the HPLC gradient–solvent system with NMR operations. An HPLC gradient–solvent system greater than 2–3%/min causes problems in optimizing the magnetic field homogeneity (shimming) because of solvent mixing in the flow cell.

During the LC/NMR run, the solvent signal in the chromatographic peak is much larger than those of the sample and needs to be suppressed. Even with deuterated solvents, the residual proton solvent signals need to be suppressed. In the case of acetonitrile, the two ^{13}C satellite peaks of either the protonated or residual protonated methyl group for CH_3CN or CD_3CN need to be suppressed because they are typically much larger than signals from the sample. In 1995, Smallcombe et al.[12] optimized the WET (water suppression enhanced through T1 effects) solvent suppression technique, which greatly improves the quality of spectra generated during LC/NMR. One disadvantage of suppressing the solvent lines is that any nearby analyte signal will also be suppressed, resulting in loss of structural information.

Conventional NMR flow cells have an active volume of 60 μl (i.e., corresponds to the length of the receiver coil) and a total volume of 120 μl. This means that NMR will only "see" 60 μl of the chromatographic peak. If the flow rate in the HPLC system is 1 ml/min, when 4.6 mm columns are used, only 3.6 sec of the chromatographic peak will be "seen" by NMR. Chromatographic peaks are generally much wider than 4 sec, indicating that less than half of the chromatographic peak will be detected. This is one of the disadvantages of LC/NMR compared with conventional 3 mm NMR probes where the amount of sample "seen" by NMR receiver coil is independent of the width of the chromatographic peak. There are other sizes commercially available for the NMR flow cells with active volume of 10, 30, 60, and 120 μl. For applications using solid-phase extraction (SPE) as SPE/NMR, the more appropriate sizes are 10 or 30 μl flow cells. Microcoil NMR flow cells for capillary LC/NMR (capLC/NMR) or microflow NMR have a flow cell with an active volume of 1.5 μl, which is appropriate for applications with samples in low concentrations.

Because NMR is a low-sensitivity technique that requires samples in the order of several micrograms, analytical HPLC columns have to be saturated when injecting samples in that range. This will affect the chromatographic resolution and separation because resolution is often degraded when sample injection is scaled up to that level. Another factor that can affect chromatographic performance is the use of deuterated solvents. In many cases, analytes show different retention times from non-deuterated solvents, resulting in occasional peak broadening. When this occurs, more study is required in order to obtain reasonable resolution. Decreasing the flow rate to less than 1 ml/min will increase the LC/NMR sensitivity, and a greater portion of the chromatographic peak will be "seen" by NMR. However, it requires an accurate LC pump for flow rates lower than 1 ml/min. For the SPE/NMR application, the LC/NMR sensitivity is increased by concentrating the chromatographic peak into the SPE cartridge when injecting the sample several times. In the case of capLC/NMR or microflow NMR, the LC/NMR sensitivity is improved by concentrating the sample to 5 μl volume.

There are many examples in the literature of LC/NMR applications in natural products,[13–19] food analysis,[20,21] metabolites,[22–29] degradation products,[30–32] drug impurities,[33–35] and drug discovery.[36–38]

Other chromatographic techniques have been coupled online to NMR for additional applications, such as size-exclusion chromatography (SEC), as SEC/NMR;[39] capillary electrophoresis (CE), as CE/NMR;[40,41] capillary electrochromatography (CEC), as CEC/NMR;[42–45] capillary zone electrophoresis (CZE), as CZE/NMR;[42,45] gel-permeation chromatography (GPC), as GPC/NMR;[46] and supercritical fluid chromatography (SFC), as SFC/NMR.[46] CE/NMR, CEC/NMR, and CZE/NMR are techniques that work with very small-volume NMR probes, with capillary separations. SPE/NMR has become a common technique for trace analysis.[47] In SPE/NMR, the chromatographic peaks are trapped into cartridges through multiple injections to concentrate the analytes of interest. The cartridges are dried with nitrogen to remove any residual solvent and the analyte(s) in each cartridge is flushed to the NMR flow cell with deuterated solvents, creating a sharp eluting band (25–30 μl eluting volume) appropriate for small NMR flow cells, such as 10 or 30 μl flow cells.[48,49] Recently,

more developments have been carried out to hyphenate capillary-based HPLC with NMR (capLC/NMR) and the use of commercial microcoil NMR probes.[50–52] With microcoil NMR probes, the range of sample used in capLC/NMR could reach the nanogram level (low nanogram level only for detection limit, but not for structural analysis).[50,51] With this technique, the volume of the chromatographic peak is comparable with the volume of the microcoil NMR flow cell.

OPERATIONAL MODES OF LC/NMR

HPLC is connected by red polyether ether ketone (PEEK) tubing to the NMR flow cell, which is inside the magnet. With shielded cryomagnets, the HPLC can be as close as 30–50 cm to the magnet as compared to 1.5–2 m with conventional magnets. Normally, a UV detector is used in the HPLC system to monitor the chromatographic run. Radioactivity or fluorescent detectors can also be used to trigger the chromatographic peak of interest.[10,11,26]

There are four general modes of operation for LC/NMR: on-flow, stop-flow, time-sliced, and loop collection.

On-flow or continuous-flow experiments require more sample to analyze "on the fly," because the resident time in the NMR flow cell is very short (3.6 sec at 1 ml/min) during the chromatographic run.

Stop-flow requires the calibration of the delay time, which is the time required by the sample to travel from the UV detector to the NMR flow cell, which depends, in turn, on the flow rate and the length of the tubing connecting HPLC with NMR. Because the chromatographic run is automatically stopped when the chromatographic peak of interest is in the flow cell, the amount of sample required for the analysis can be reduced and 2-D NMR experiments, such as correlation spectroscopy (COSY), total correlation spectroscopy (TOCSY), and others can be obtained because the sample can remain inside the flow cell for days. It is possible to obtain NMR data on a number of chromatographic peaks in a series of stops during the chromatographic run without on-column diffusion that causes loss of resolution, but only if the NMR data for each chromatographic peak can be acquired in a short time (30 min or less).

"Time-sliced" operation involves a series of stops during the elution of a chromatographic peak of interest. Time-sliced is used when two analytes elute together or have close retention times, or when the separation is poor.

Loop collection can be used when there is more than one chromatographic peak of interest. Chromatographic peaks are stored in loops for later off-line NMR study. In this case, the analytes must be stable inside the loops during the extended period of the analysis. Capillary tubing should be used to avoid peak broadening with concomitant loss of analyte "seen" by the NMR spectrometer.

Stop-flow is the preferred mode of operation to analyze the structure of metabolites when the chromatography is reasonable or the metabolite is unstable or volatile. The following example illustrates the application of LC/NMR for a volatile metabolite with a small molecular weight.[26] Conventional NMR was not doable because the radioactivity of the fraction containing the metabolite of interest was lost during evaporation to dryness prior the NMR analysis. In this case

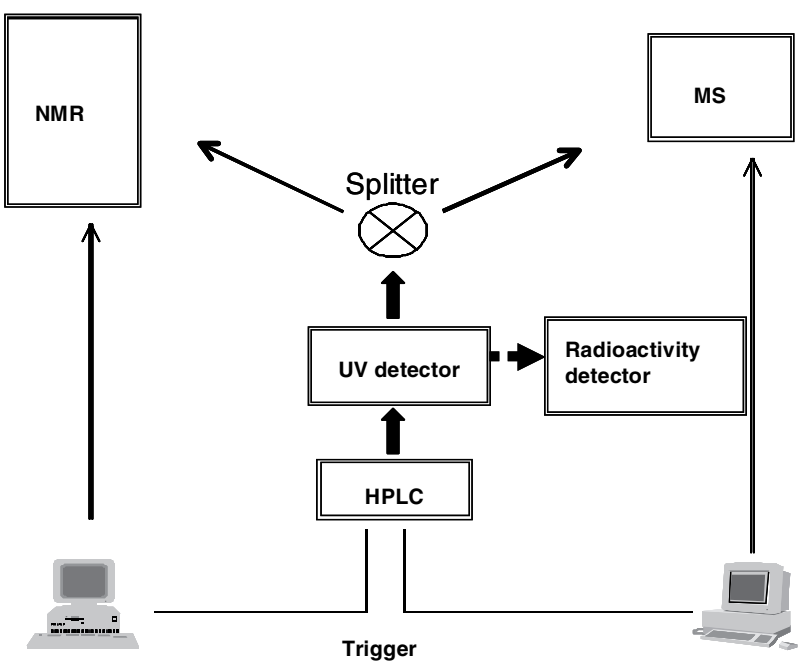

Fig. 1 Schematic setup for the LC/MS/NMR system.

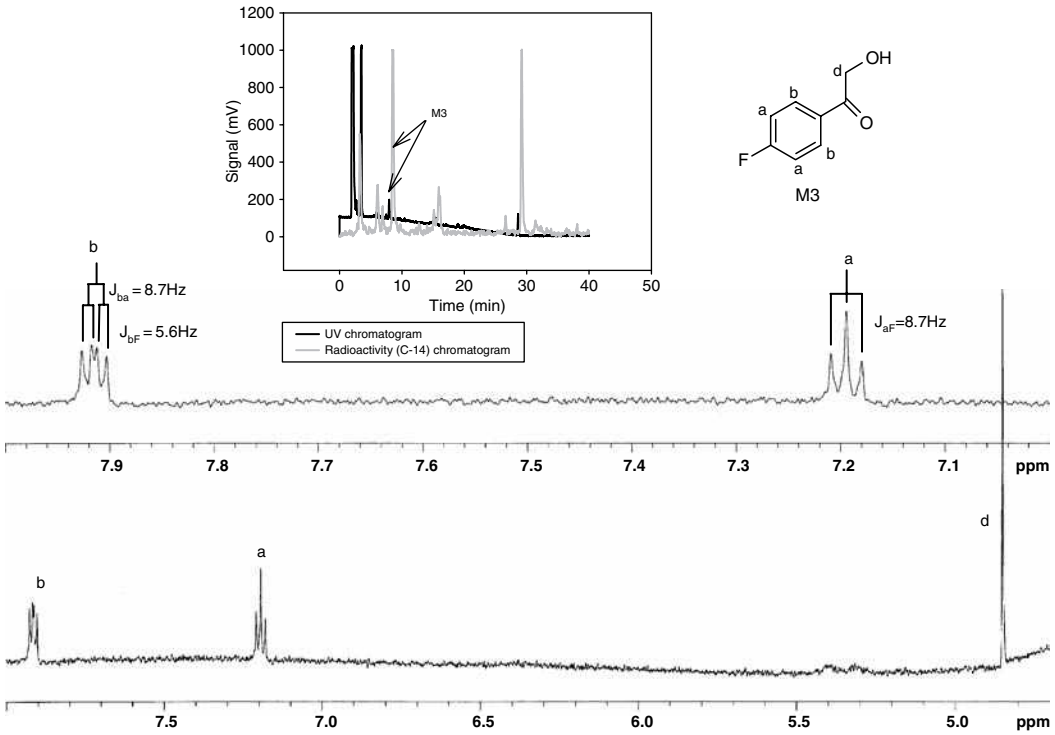

Fig. 2 UV and radioactive (C-14) chromatograms of the fraction containing the metabolite M3 (top), and the aromatic section (from 7.0 to 8.0 ppm) (middle) and the expanded section (from 4.7 to 8.0 ppm) (bottom) of the ^{1}H NMR spectrum of the metabolite M3.

LC/MS was not informative, suggesting a molecular weight less than 200 Da. LC/NMR was the alternative to solve the structural problem. A radioactive detector equipped with a liquid scintillation cell (Radiomatic C150TR, Packard, Meriden, Connecticut, U.S.A.) was connected online to the LC/UV system of the LC/NMR to identify the UV chromatographic peak corresponding to the radioactive metabolite, as shown in Fig. 1. For an initial identification of the metabolite of interest, small injections were carried out to identify the UV chromatographic peak associated with the radioactive peak of the metabolite prior the stop-flow experiment (Fig. 2). Because of the shorter transfer delay from the UV to the NMR than from the radioactive to the NMR because of the thicker tubing in the scintillation cell, UV was used to trigger the stop-flow experiments. ^{1}H NMR spectrum showed the presence of the *p*-fluorophenyl ring, with its characteristic splitting pattern indicating that the compound was drug related. The downfield shift of the *ortho* protons (δ 7.91 ppm) suggested the presence of a carbonyl substituent (Fig. 2). The presence of a singlet (δ 4.85 ppm) that integrated for approximately two protons was consistent with a methylene flanked by the carbonyl and a hydroxyl group (Fig. 2). The structure of *p*-fluoro-α-hydroxyacetophenone for the M3 metabolite was proposed based on these features (Fig. 2).

PRACTICAL ISSUES OF LC/MS/NMR (OR LC/NMR/MS)

NMR and MS data for the same analyte are crucial for structural elucidation. When different isolates are analyzed by NMR and MS, one cannot always be certain that the NMR and the MS data apply to the same analyte. To avoid this ambiguity, LC/MS and LC/NMR are combined. MS data should be obtained initially because with NMR, data collection in the stop-flow mode can take hours or days, depending on the complexity of the structure and the amount of sample. This is why it is preferable to designate this operation as LC/MS/NMR rather than LC/NMR/MS.

Because MS is considerably more sensitive than NMR, a splitter is incorporated after the HPLC to direct the sample to the MS and NMR units separately. In the example below, the MS used in these studies is an LCQ Classic instrument (ThermoFinnigan, California, U.S.A.). A custom-made splitter was used with a splitting ratio of 1:100 (Acurate^{TM}, LC Packings, California, U.S.A.). It was designed to deliver 1% of the sample initially to the MS and the balance 20 sec later to the NMR. With a flow rate of 1 ml/min, the final flow rate going to the NMR will be 0.990 ml/min and to the MS will be 0.010 ml/min. Electrospray is the only source of ionization that will work

with such a low flow rate (10 μl/min) in LCQ. Fig. 1 depicts the scheme of our LC/MS/NMR system.[10,11]

Another consideration for the LC/MS/NMR is the use of deuterated solvents needed for NMR. Analytes with exchangeable or "active" hydrogens can exchange (i.e., equilibrate) with deuterium (^{2}H) at different rates. The analyst should be alerted to this possibility because it could result in the appearance of several closely spaced molecular ions.

There are examples in the literature for the application of LC/MS/NMR in natural products,[53–55] drug metabolism,[55–63] combinatorial chemistry,[64] pharmaceutical research,[8,65] drug discovery,[66] degradation products,[67] and food analysis.[68,69] LC/NMR/MS (or LC/MS/NMR as described in this entry) has also been integrated with SPE as LC/SPE/NMR/MS combined with cryogenic NMR probes in the areas of natural products[70] and drug metabolism.[71]

OPERATIONAL MODES OF LC/MS/NMR (OR LC/NMR/MS)

As mentioned in the section "Operational Modes of LC/NMR," with the use of shielded cryomagnets the location of the MS instrument will follow the same rule as for the HPLC. The most common modes of operation for LC/MS/NMR are on-flow and stop-flow. With stop-flow, the MS instrument can also be used to stop the flow on the

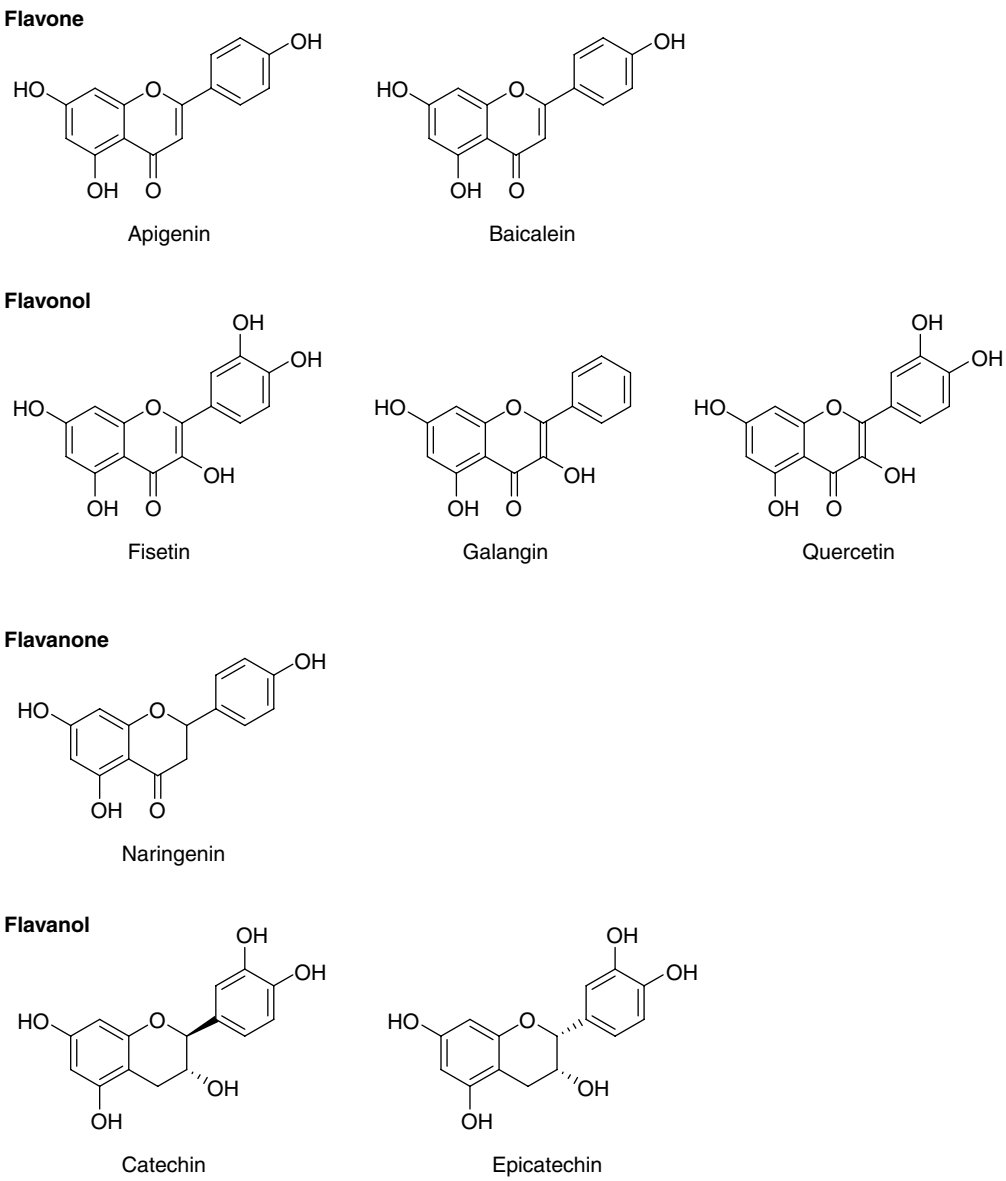

Fig. 3 Structures of eight flavonoids used for the LC/MS/NMR technology development studies.

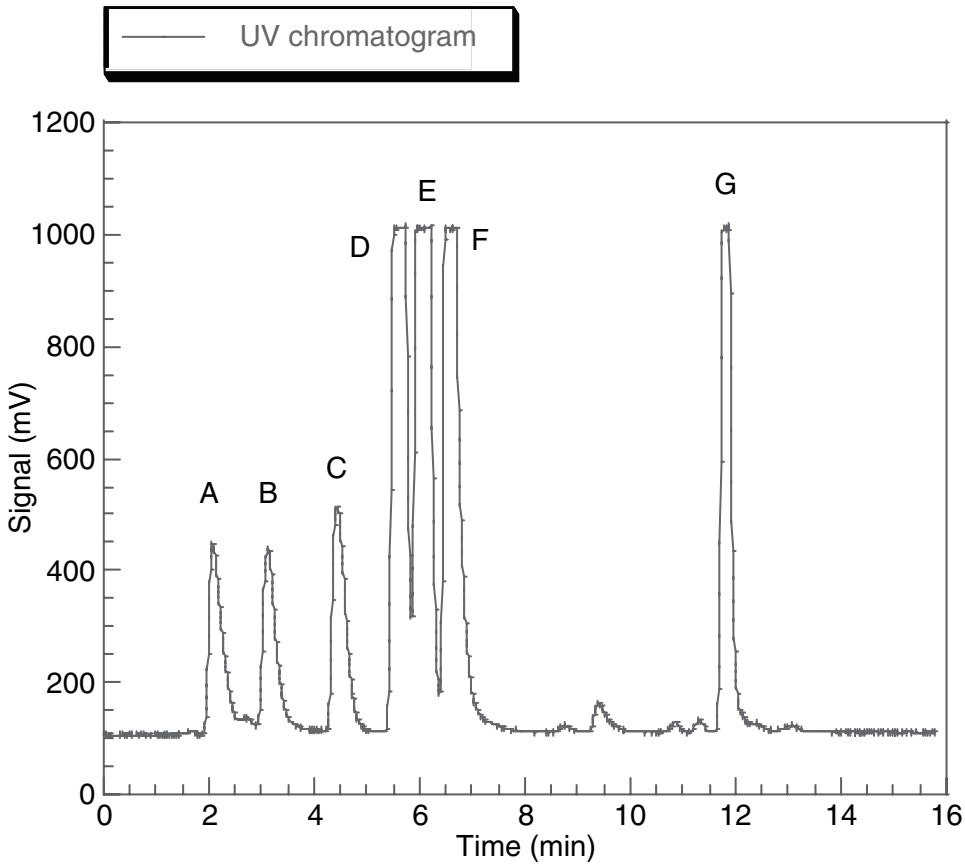

Fig. 4 UV chromatogram of the on-flow experiment injecting a mixture of eight flavonoids: a, catechin + epicatechin; b, fisetin; c, quercetin; d, apigenin; e, naringenin; f, baicalein; g, galangin.

chromatographic peak of interest that is to be analyzed by NMR.

In the last few years, there have been relatively few more examples in the literature that deal with the application of LC/MS/NMR. We have been interested in evaluating this technology to determine the pros and cons and to decide which cases are suitable for this application. To illustrate these modes of operation, a group of flavonoids was chosen. These compounds have simple structures with primarily aromatic protons; some have low-field aliphatic protons, which would not be hidden under the NMR solvent peaks. Phenolic protons exchange fast enough with D_2O so that each compound will only show one molecular ion. Flavonoids are natural products with important biological functions, acting as antioxidants, free-radical scavengers, and metal chelators, and are related to the food industry. Fig. 3 shows the group of eight flavonoids chosen for these studies.

The chromatographic conditions used for these studies were as follows: 35–50% B 0–10 min, 50–80% B 10–15 min; A: D_2O, B: acetonitrile (ACN), 1 ml/min, 287 nm, Discovery C18 column 15 × 4.6 cm, 5 μm. Stock solutions of each compound were prepared at 1 μg/μl in ACN/MeOH (1:1).

A Varian Unity Inova 600 MHz NMR instrument (Palo Alto, California, U.S.A.) equipped with a $^{1}H[^{13}C/^{15}N]$ pulse field gradient triple resonance microflow NMR probe (flow cell 60 μl; 3 mm O.D.) was used. Reversed-phase HPLC of the samples was carried out with a Varian modular HPLC system (a 9012 pump and a 9065 photodiode array UV detector). The Varian HPLC software was also equipped with the capability for programmable stop-flow experiments based on UV peak detection. An LCQ

Table 1 MS data of flavonoids in negative mode from the on-flow run in the LC/MS/NMR mode of operation.

Peak	Compound	MW[a]	MW[b]	*m/z*[c]
A	Catechin + Epicatechin	290	295	293
B	Fisetin	286	290	288
C	Quercetin	302	307	305
D	Apigenin	270	273	271
E	Naringenin	272	275	273
F	Baicalein	270	273	271
G	Galangin	270	273	271

[a]Molecular weight.
[b]Molecular weight with all the hydroxyl protons deuterated.
[c]$[M\text{-}^{2}H]^{-}$.

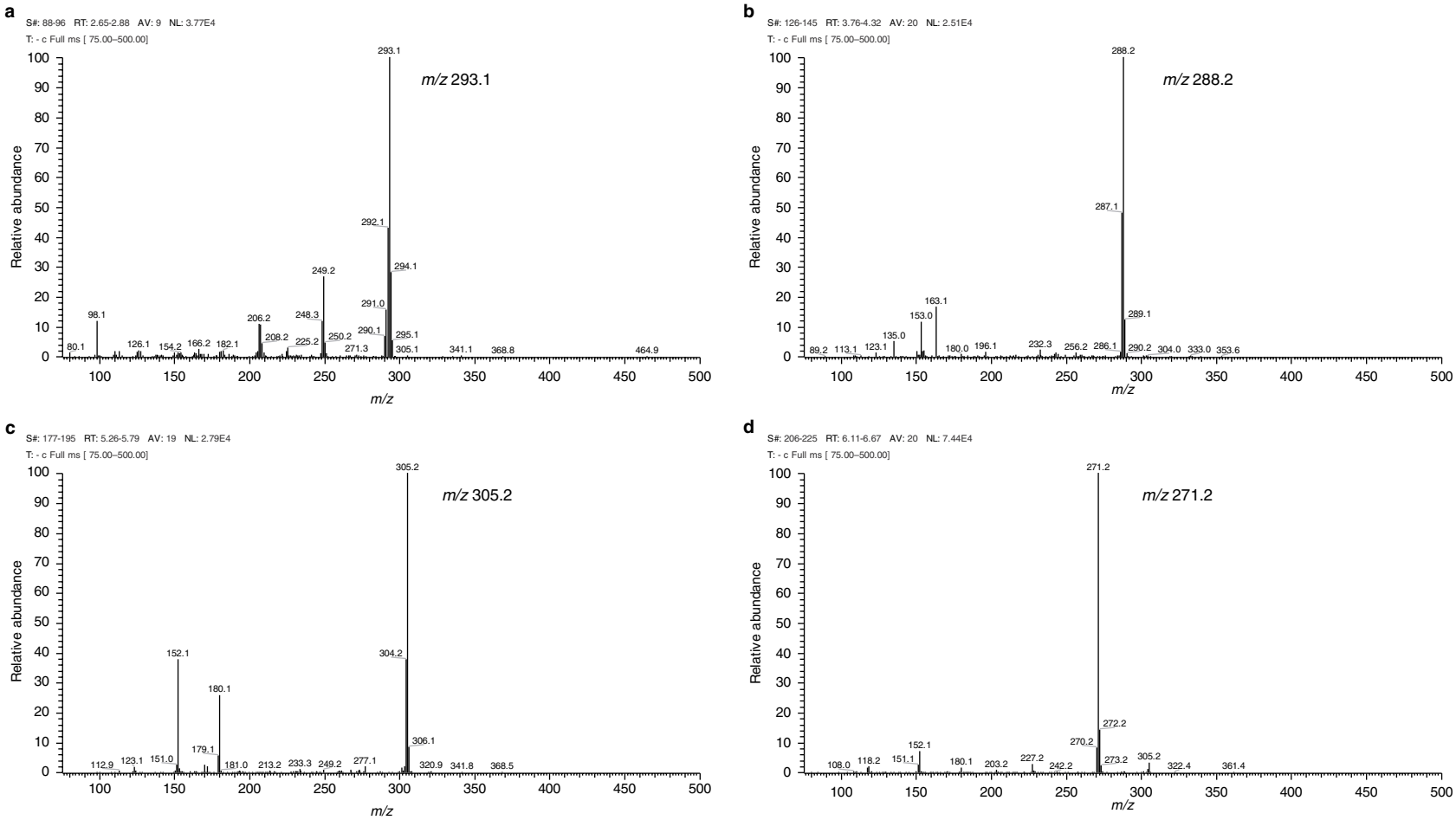

Fig. 5 MS data on the on-flow experiment of the eight flavonoids: a, catechin + epicatechin; b, fisetin; c, quercetin; d, apigenin; e, naringenin; f, baicalein; g, galangin.

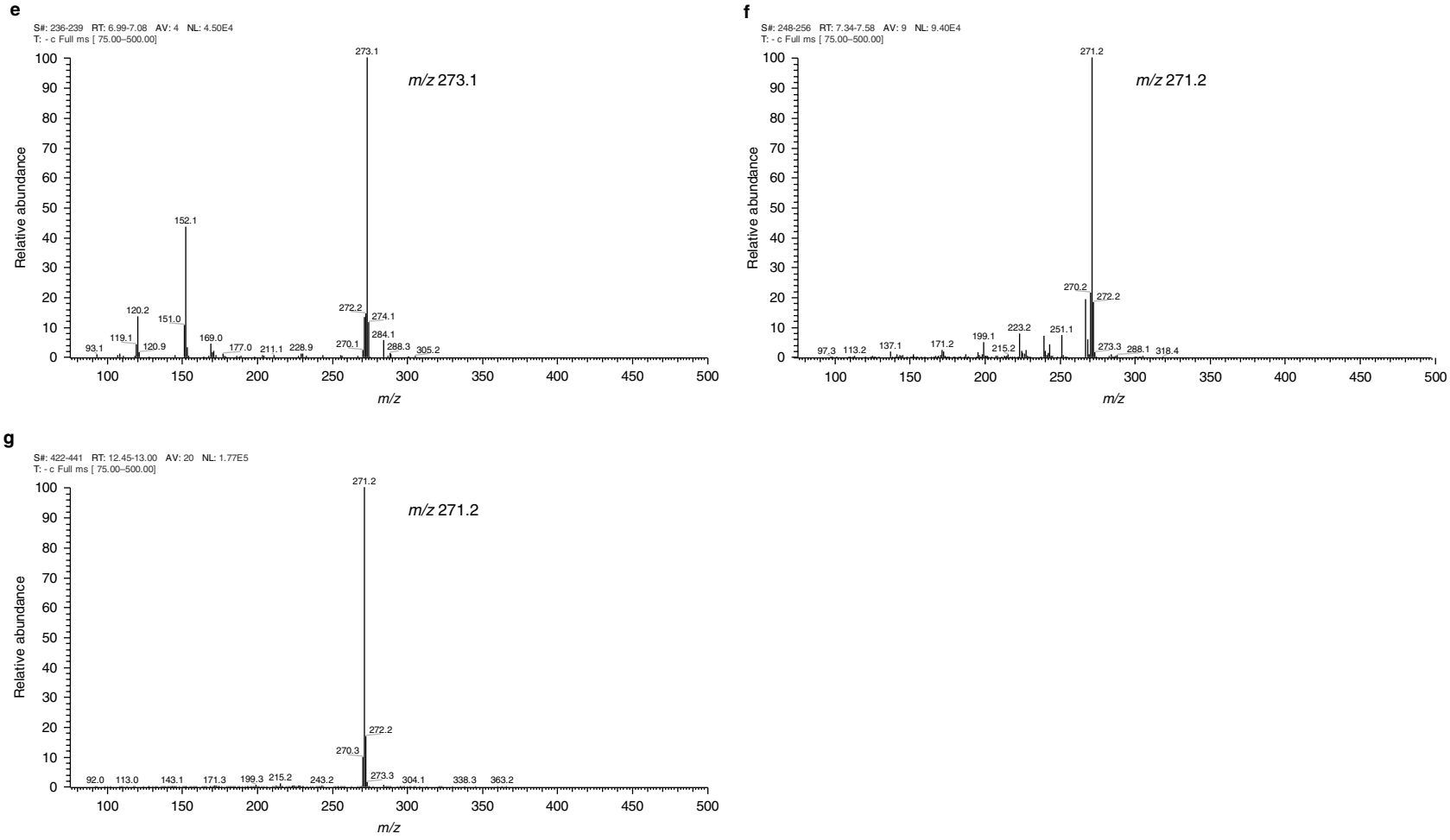

Fig. 5 (*Continued*)

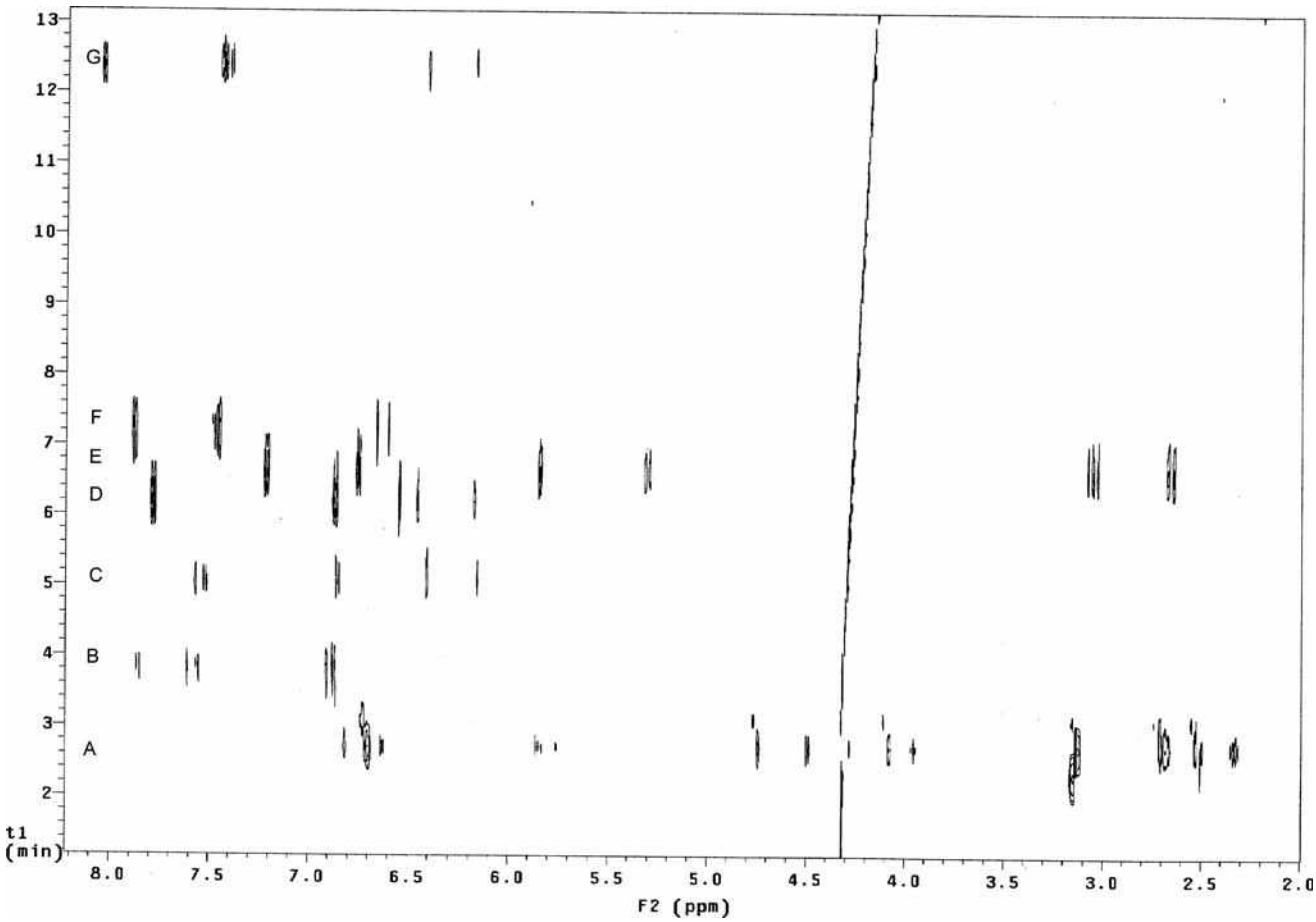

Fig. 6 2-D data set (time vs. chemical shift) for the on-flow experiment injecting a mixture of eight flavonoids: A, catechin + epicatechin; B, fisetin; C, quercetin; D, apigenin; E, naringenin; F, baicalein; G, galangin.

classic MS instrument, mentioned in the previous section, was connected online to the HPLC/UV system of the LC/NMR by contact closure. The ^{2}H resonance of the D_2O was used for field-frequency lock and the spectra were centered on the ACN methyl resonance. Suppression of resonances from HOD (the residual protonated signal of D_2O) and the methyl of ACN and its two ^{13}C satellites was accomplished by means of a train of four selective WET pulses, each followed by a B_0 gradient pulse and a composite 90° read pulse.[12]

The on-flow experiment was carried out on a mixture of eight flavonoids (20 μg each) (Fig. 3). MS and NMR data were obtained during this on-flow experiment. The UV chromatogram is depicted in Fig. 4. Table 1 and Fig. 5 show the pseudo-molecular ion information $[M\text{-}^{2}H]^{-}$ (where M is the molecular weight with all the hydroxyl protons deuterated, in negative mode) for the eight flavonoids obtained in this on-flow experiment. Fig. 6 is the 2-D data set (time vs. chemical shift) where each ^{1}H NMR spectrum was acquired for 16 scans and decreasing the delays (total time per spectrum of 20 sec). Fig. 7 depicts the ^{1}H NMR traces of each flavonoid extracted from the 2-D data set. It is notable that catechin and epicatechin coelute under these conditions (peak A of the UV chromatogram of Fig. 4). Distinguishing these diastereomers by MS alone is not feasible. Differences in the NMR spectra would be expected, and are in fact observed. The ability of LC/MS/NMR to distinguish signals from individual diastereomers is illustrated in Figs. 6 and 7A.

Two stop-flow experiments were carried out on apigenin (10 μg) (Fig. 3) by using, independently, the UV peak maximum or the molecular ion chromatographic peak seen in the MS instrument to trigger the stop-flow. The Varian software triggers the stop-flow automatically with the UV peak, so this mode was used as a reference point. When the MS was used to trigger the stop-flow, it was carried out manually with a chronometer while the molecular ion of apigenin was being monitored in negative mode (*m/z* 271). After peak detection in the UV or MS and a time delay of about 52 or 20 sec, respectively, the HPLC pump was stopped, trapping the peak of interest in the LC/NMR microprobe. ^{1}H NMR stop-flow spectra were acquired using an acquisition time of 1.5 sec, a delay between the successive pulses of 0.5 sec, a spectral width of 9000 Hz, and 32 K time-domain data points. The

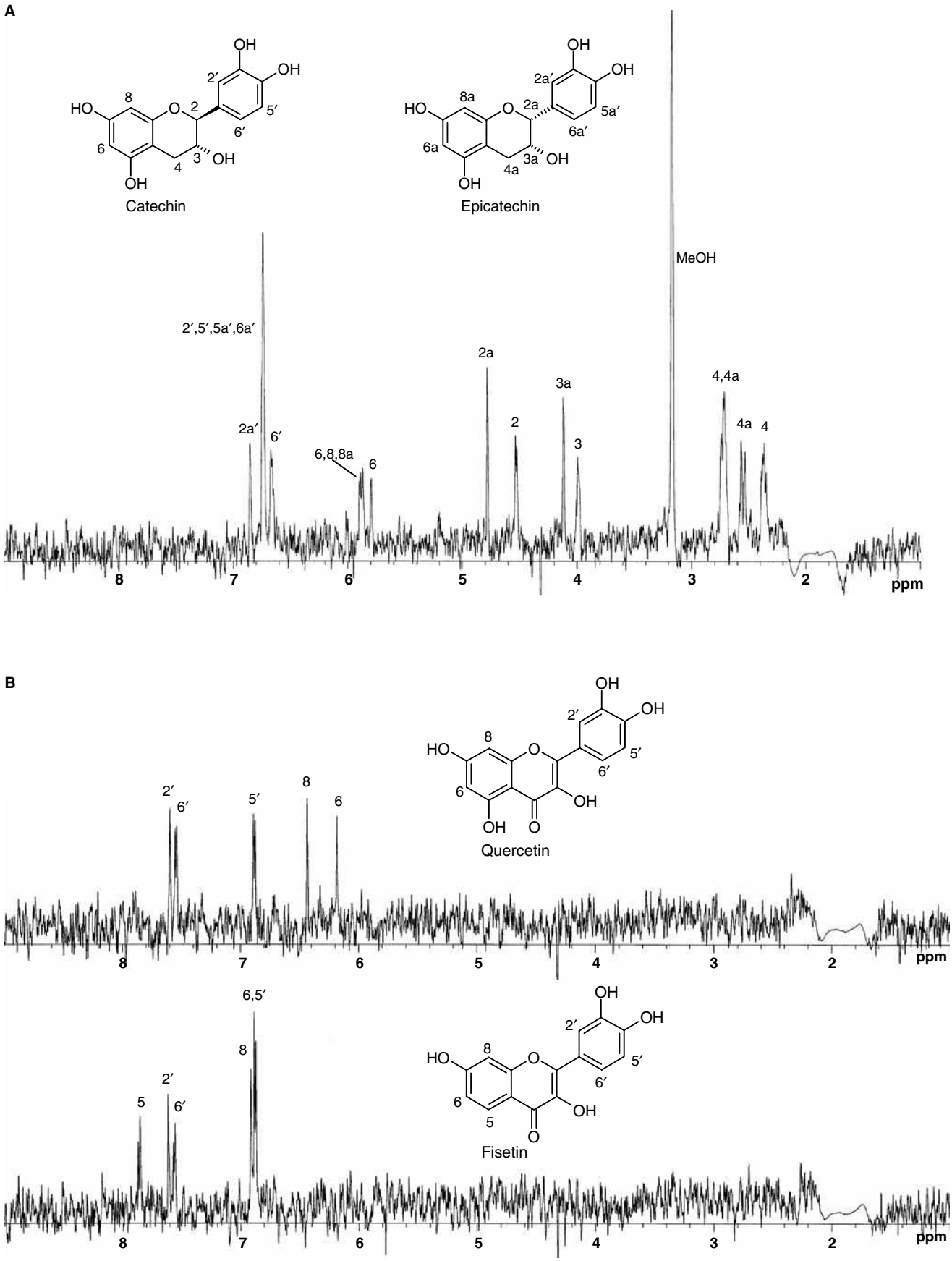

Fig. 7 ^{1}H NMR spectra from the 2-D data set of the on-flow experiment of (A) catechin and epicatechin, (B) quercetin (top) and fisetin (bottom), (C) naringenin (top) and apigenin (bottom), and (D) galangin (top) and baicalein (bottom).

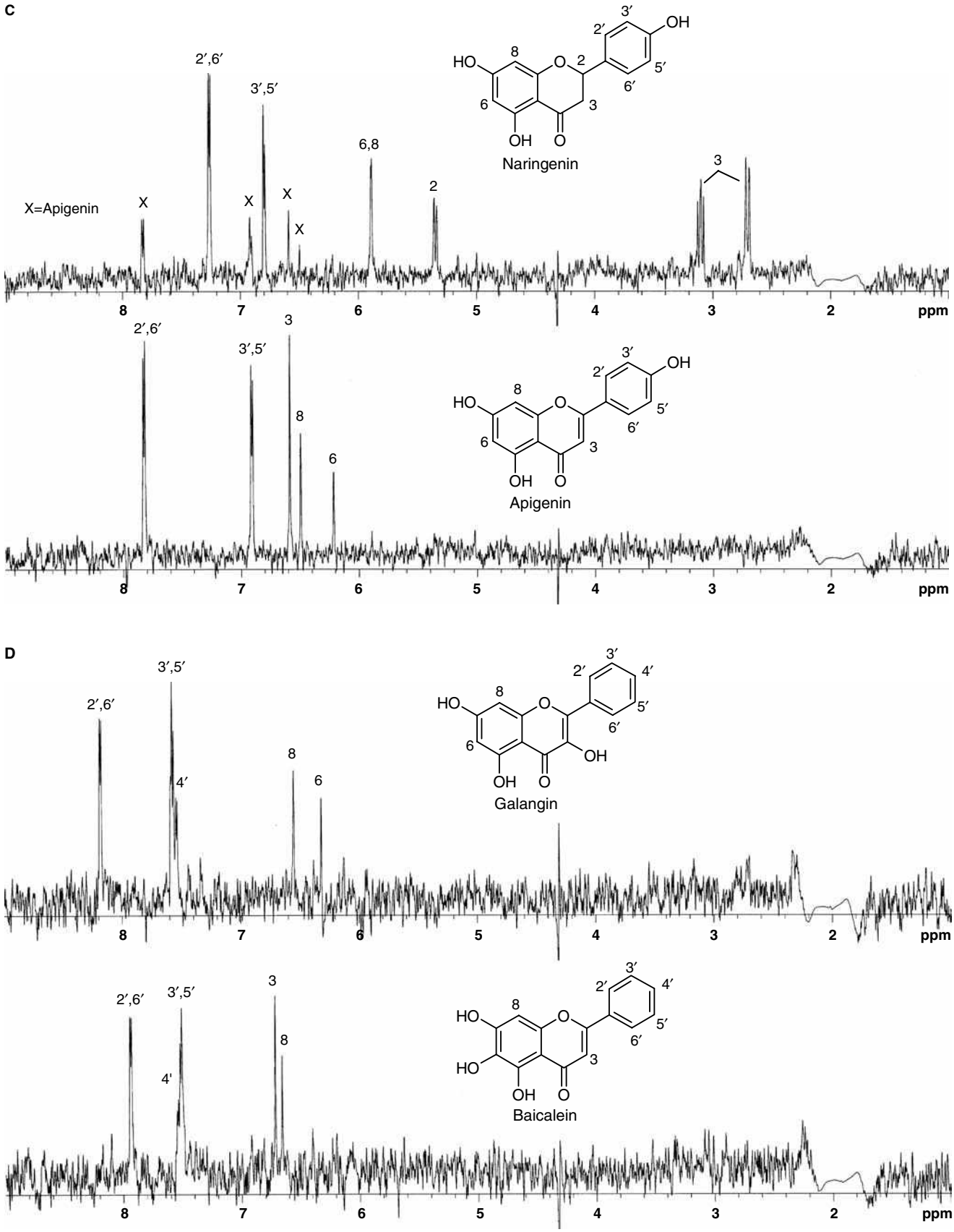

Fig. 7 (*Continued*)

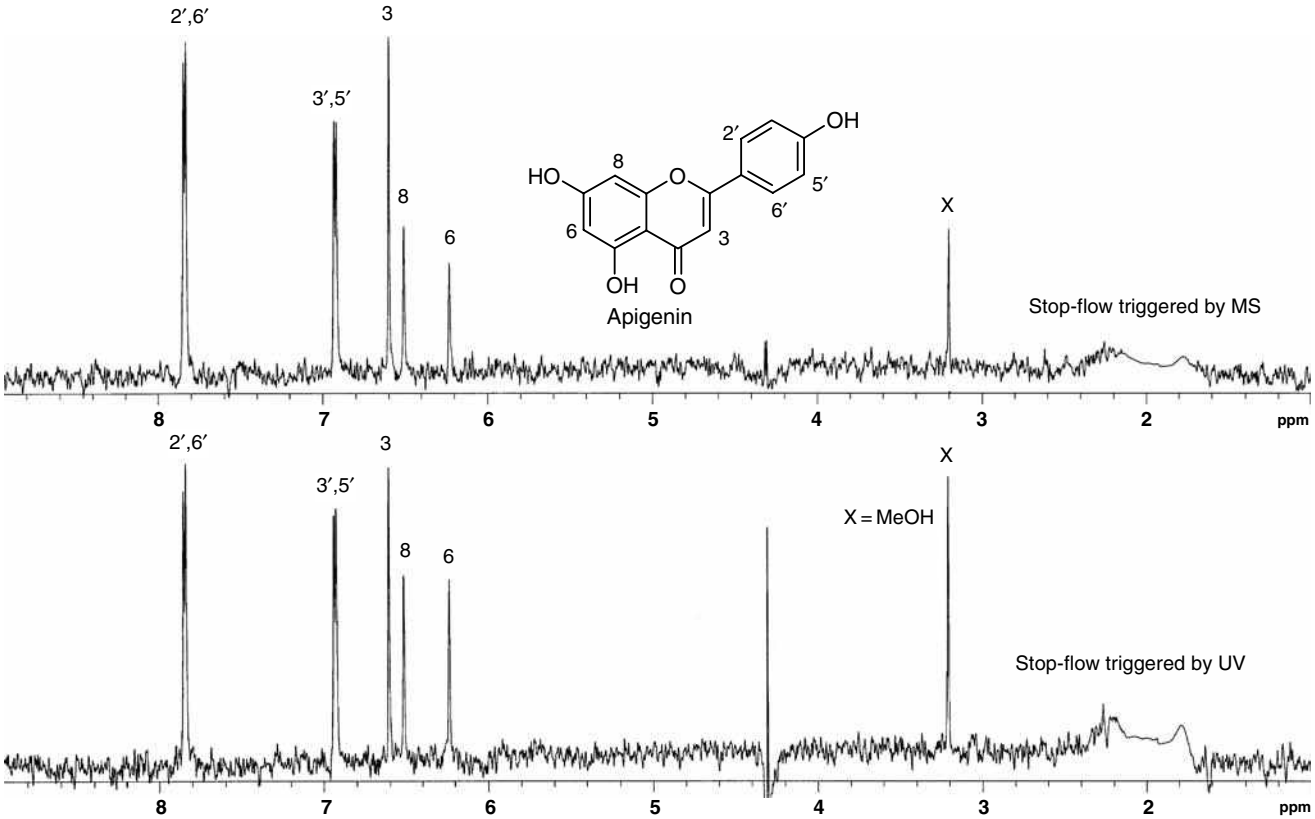

Fig. 8 ^{1}H NMR spectra of apigenin triggering the stop-flow by MS (top) and by UV (bottom).

methyl resonance of ACN was referenced to 1.94 ppm. These two experiments were carried out by injecting 10 μg of apigenin and acquiring ^{1}H NMR spectra for approximately 4.5 min (128 scans), giving rise to the same quality of ^{1}H NMR spectra of apigenin (Fig. 8).

These experiments indicate that for sample mixtures, the on-flow mode of LC/MS/NMR is useful in obtaining structural information for the major components. If a more detailed analysis is required, or the amount of sample is small and the compound(s) cannot be isolated because of instability, stop-flow is the mode of choice. LC/MS and LC/NMR chromatographic conditions must be compatible; in addition, prior evaluation of the LC conditions on the LC/MS/NMR system needs to be carried out to ensure consistency with the chromatographic resolution needed in the LC/NMR part of the system. The sample must ionize well by electrospray to obtain MS data. To use MS to trigger halting the flow in the stop-flow mode, prior MS information of the chromatographic peak(s) of interest in deuterated solvent(s) is needed to evaluate the suitability of the system in providing structural information.

CONCLUSIONS

Hyphenated analytical and spectroscopic techniques have enhanced the ability of analysts to solve structural problems. Until the advent of recent developments in NMR, LC/MS had been the only hyphenated technique for qualitative analysis of structures on mixtures. NMR could only be applied to reasonably pure compounds until the last decade. LC/NMR has expanded the capability of solving structural problems in complex mixtures. LC/NMR, however, is not comparable to LC/MS because of its lower sensitivity, the need of expensive deuterated solvents, the need of solvent suppression of the residual protonated solvents, and the compatibility of the volume of the chromatographic peak with the volume of the NMR flow cell. To overcome some of these problems, more development has led to the hyphenation of capillary HPLC (capLC) and NMR (capLC/NMR), where the amount of solvent used is minimal and the volume of the chromatographic peak is comparable to the volume of the NMR flow cell, but the suppression of the residual protonated solvents must still be carried out. SPE/NMR has been demonstrated to be another option for the analysis of minor components by concentrating them into cartridges through numerous injections and flush them to the NMR flow cell with deuterated solvents, and so minimum solvent suppression is required.

Within the last decade, hyphenated LC/MS, LC/NMR, and LC/MS/NMR (or LC/NMR/MS) techniques have become available. Because MS is destructive (in contrast to NMR) and requires far less sample than NMR, a splitter

is incorporated online, to direct the bulk of the sample to the less sensitive technique. In addition to the advantage of having MS and NMR information for the same chromatographic peak, the combination of these two techniques with different sensitivities must deal with other issues, such as the effect of deuterated solvents on the MS, the limitation of source of ionization on the MS compatible with low flow rates, and the timing that depends on the slower NMR technique. SPE/NMR/MS has been developed to analyze low-concentrated analytes. However, there is still room for improvement for LC/MS/NMR (or LC/NMR/MS) and the next decade will define the areas where this hyphenated technique is best suited.

LC/MS/NMR cannot replace LC/MS, LC/NMR, or even NMR techniques for the structural elucidation of compounds. There will always be cases where purification of the analyte(s) is required when the structural problem is too complex or the separation of the chromatographic peak is not suitable. LC/MS/NMR (or LC/NMR/MS), LC/MS, LC/NMR, and NMR have to be available so that the analyst can choose the appropriate technique for each structural problem. The success rate of problem solution will depend on choosing the right technique, depending on the difficulty and nature of the problem. Each technique has its own advantages and limitations.

ACKNOWLEDGMENTS

The author is thankful to Dr. Ray Bakhtiar (Drug Metabolism of MRL at Rahway) for the preparation of Fig. 1 and his support and encouragement in writing this manuscript; to Dr. Byron H. Arison (Drug Metabolism of MRL at Rahway) for his interest, support, encouragement, and constructive discussions during the course of this work; and David Knapp and Uresh Parikh (Medicinal Chemistry of MRL at Rahway) for technical help connecting the MS detector online to the LC/NMR system.

REFERENCES

1. Lee, M.S.; Kerns, E.H. LC/MS applications in drug development. Mass Spectrom. Rev. **1999**, *18*, 187–279.
2. Wu, Y. The use of liquid chromatography–mass spectrometry for the identification of drug degradation products in pharmaceutical formulations. Biomed. Chromatogr. **2000**, *14*, 384–396.
3. Clarke, N.J.; Rindgen, D.; Korfmacher, W.A.; Cox, K.A. Systematic LC/MS metabolite identification in drug discovery. Anal. Chem. **2001**, *73* (15), 430A–439A.
4. Watanabe, N.; Niki, E. Direct-coupling of FT–NMR to high performance liquid chromatography. Proc. Jpn. Acad. Ser. B. Phys. Biol. Sci. **1978**, *54*, 194–199.
5. Bayer, E.; Albert, K.; Nieder, M.; Grom, E.; Keller, T. On-line coupling of high-performance liquid chromatography and nuclear magnetic resonance. J. Chromatogr. **1979**, *186*, 497–507.
6. Haw, J.F.; Glass, T.E.; Hausler, D.W.; Motell, E.; Dorn, H.C. Direct coupling of a liquid chromatograph to a continuous flow hydrogen nuclear magnetic resonance detector for analysis of petroleum and synthetic fuels. Anal. Chem. **1980**, *52*, 1135–1140.
7. Albert, K. Liquid chromatography–nuclear magnetic resonance spectroscopy. J. Chromatogr. A, **1999**, *856*, 199–211.
8. Lindon, J.C.; Nicholson, J.K.; Wilson, I.D. Directly coupled HPLC–NMR and HPLC–NMR–MS in pharmaceutical research and development. J. Chromatogr. B. Biomed. Sci. Appl. **2000**, *748*, 233–258.
9. Albert, K. *On-line LC–NMR and Related Techniques*; John Wiley & Sons: England, 2002.
10. Silva Elipe, M.V. Advantages and disadvantages of nuclear magnetic resonance spectroscopy as hyphenated technique. Anal. Chim. Acta **2003**, *497*, 1–25.
11. Silva Elipe, M.V. LC–NMR overview and pharmaceutical applications. In *HPLC for Pharmaceutical Scientists*; Kazakevich, Y., LoBruto, R., Eds.; John Wiley & Sons: New Jersey, 2007; 901–936.
12. Smallcombe, S.H.; Patt, S.L.; Keifer, P.A. WET solvent suppression and its applications to LC NMR and high-resolution NMR spectroscopy. J. Magn. Reson. Ser. A, **1995**, *117*, 295–303.
13. Bobzin, S.C.; Yang, S.; Kasten, T.P. Application of liquid chromatography–nuclear magnetic resonance spectroscopy to the identification of natural products. J. Chromatogr. B. Biomed. Sci. Appl. **2000**, *748*, 259–267.
14. Bobzin, S.C.; Yang, S.; Kasten, T.P. LC/NMR: A new tool to expedite the dereplication and identification of natural products. J. Ind. Microbiol. Biotech. **2000**, *25*, 342–345.
15. Bringmann, G.; Wohlfarth, M.; Rischer, H.; Heubes, M.; Saeb, W.; Diem, S.; Herderich, M.; Schlauer, J. A photometric screening method for dimeric naphthylisoquinoline alkaloids and complete on-line structural elucidation of a dimer in crude plant extracts, by the LC–MS/LC–NMR/LC–CD triad. Anal. Chem. **2001**, *73*, 2571–2577.
16. Wolfender, J.-L.; Ndjoko, K.; Hostettmann, K. The potential of LC–NMR in phytochemical analysis. Phytochem. Anal. **2001**, *12*, 2–22.
17. Hostettmann, K.; Marston, A. Twenty years of research into medicinal plants: Results and perspectives. Phytochem. Rev. **2002**, *1*, 275–285.
18. Chen, P.; Li, C.; Liang, S.; Song, G.; Sun, Y.; Shi, Y.; Xu, S.; Zhang, J.; Sheng, S.; Yang, Y. Li, M. Characterization and quantitation of eight water-soluble constituents in tubers of *Pinellia ternate* and in tea granulated form Chinese multiherb remedy Xiaochaihu-tang. J. Chromatogr. B, **2006**, *843*, 183–193.
19. Qu, J.; Wang, Y.-H.; Li, J.-B.; Yu, S.-S.; Li, Y.; Liu, Y.-B. Rapid structural determination of new trace cassaine-type diterpenoid amides in fractions from *Erythrophleum fordii* by liquid chromatography–diode-array detection/electrospray ionization tandem mass spectrometry and liquid chromatography/nuclear magnetic resonance. Rapid Commun. Mass Spectrom. **2007**, *21*, 2109–2119.

20. Careri, M.; Mangia, A. Multidimensional detection methods for separations and their application in food analysis. *Trends Anal. Chem.* **1996**, *15* (10), 538–550.
21. Albert, K.; Schlotterbeck, G.; Tseng, L.-H.; Braumann, U. Application of on-line capillary high-performance liquid chromatography–nuclear magnetic resonance spectrometry coupling for the analysis of vitamin A derivatives. J. Chromatogr. A, **1996**, *750*, 303–309.
22. Mutlib, A.E.; Strupczewski, J.T.; Chesson, S.M. Application of hyphenated LC/NMR and LC/MS techniques in rapid identification of in vitro and in vivo metabolites of iloperidone. Drug Metab. Dispos. **1995**, *23* (9), 951–964.
23. Lindon, J.C.; Nicholson, J.K.; Sidelmann, U.G.; Wilson, I.D. Directly coupled HPLC–NMR and its application to drug metabolism. Drug Metab. Rev. **1997**, *29* (3), 705–746.
24. Zhang, K.E.; Hee, B.; Lee, C.A.; Liang, B.; Potts, B.C.M. Liquid chromatography–mass spectrometry and liquid chromatography–NMR characterization of in vitro metabolites of a potent and irreversible peptidomimetic inhibitor of rhinovirus 3C protease. Drug Metab. Dispos. **2001**, *29* (5), 729–734.
25. Singh, R.; Chen, I.-W.; Jin, L.; Silva Elipe, M.V.; Arison, B.H.; Lin, J.H.; Wong, B.K. Pharmacokinetics and metabolism of *RAS* farnesyl transferase inhibitor in rats and dogs: In vitro–in vivo correlation. Drug Metab. Dispos. **2001**, *29*, 1578–1587.
26. Silva Elipe, M.V.; Huskey, S.-E. W.; Zhu, B. Application of LC–NMR for the study of the volatile metabolite of MK-0869, a substance P receptor antagonist. J. Pharma. Biomed. Anal. **2003**, *30*, 1431–1440.
27. Sohda, K.-Y.; Minematsu, T.; Hashimoto, T.; Suzumura, K.-I.; Funatsu, M.; Suzuki, K.; Imai, H.; Usiu, T.; Kamimura, H. Application of LC–NMR for characterization of rat urinary metabolites of zonampanel monohydrate (YM872). Chem. Pharm. Bull. **2004**, *52* (11), 1322–1325.
28. Murai, T.; Iwabuchi, H.; Ikeda T. Identification of gemfibrozil metabolites, produced as positional isomers in human liver microsomes, by on-line analyses using liquid chromatography/mass spectrometry and liquid chromatography/nuclear magnetic resonance spectroscopy. J. Mass. Spectrom. Soc. Jpn. **2004**, *52* (5), 277–283.
29. Tang, C.; Subramanian, R.; Kuo. Y.; Krymgold, S.; Lu, P.; Kuduk, S.D.; Ng, C.; Feng, D.-M.; Elmore, C.; Soli, E.; Ho, J.; Bock, M.G.; Baillie, T.A.; Prueksaritanont, T. Bioactivation of 2,3-diaminopyridine-containing bradykinin B_1 receptor antagonists: Irreversible binding to liver microsomal proteins and formation of glutathione conjugates. Chem. Res. Toxicol. **2005**, *18*, 934–945.
30. Peng, S.X.; Borah, B.; Dobson, R.L.M.; Liu, Y.D.; Pikul, S. Application of LC/NMR and LC/MS to the identification of degradation products of a protease inhibitor in dosage formulations. J. Pharm. Biomed. Anal. **1999**, *20*, 75–89.
31. Novak, P.; Tepeš, P.; Cindrić, M.; Ilijiaš, M.; Dragojević, S.; Mihaljević, K. Combined use of liquid chromatography–nuclear magnetic resonance and liquid chromatography–mass spectrometry for the characterization of an acarbose degradation product. J. Chromatogr. A, **2004**, *1033*, 299–303.
32. Fukutsu, N.; Kawasaki, T.; Saito, K.; Nakazawa, H. Application of high-performance liquid chromatography hyphenated techniques for identification of degradation products of cefpodoxime proxetil. J. Chromatogr. A, **2006**, *1129*, 153–159.
33. Potts, B.C.M.; Albizati, K.F.; O'Neil Johnson, M.; James, J.P. Application of LC/NMR to the identification of bulk drug impurities in GART inhibitor AG2034. Magn. Reson. Chem. **1999**, *37*, 393–400.
34. Sharma, G.J.; Jones, I.C. Critical investigation of coupled liquid chromatography–NMR spectroscopy in pharmaceutical impurity identification. Magn. Reson. Chem. **2003**, *41*, 448–454.
35. Novak, P.; Tepeš, P.; Fistrić, I.; Bratoš, I.; Gabelica, V. The application of LC–NMR and LC–MS for the separation and rapid structure elucidation of an unknown impurity in 5-aminosalicylic acid. J. Pharm. Biomed. Anal. **2006**, *40*, 1268–1272.
36. Peng, S.E. Hyphenated HPLC–NMR and its applications in drug discovery. Biomed. Chromatogr. **2000**, *14*, 430–441.
37. Eldridge, G.R.; Vervoort, H.C.; Lee, C.M.; Cremin, P.A.; Williams, C.T.; Hart, S.M.; Goering, M.G.; O'Neil-Johnson, M.; Zeng, L. High-throughput method for the production and analysis of large natural product library for drug discovery. Anal. Chem. **2002**, *74*, 3963–3971.
38. Sing, S.K.; Reddy, M.S.; Shivaramakrishna, S.; Kavitha, D.; Vasudev, R.; Babu, J.M.; Sivalakshmidevi, A.; Rao, Y.K. Modified reaction conditions to achieve high regioselectivity in the two component synthesis of 1,5-diarylpyrazoles. Tetrahedron Lett. **2004**, *45*, 7679–7682.
39. Ludlow, M.; Louden, D.; Handley, A.; Taylor, S.; Wright, B.; Wilson, I.D. Size-exclusion chromatography with on-line ultraviolet, proton nuclear magnetic resonance and mass spectrometric detection and on-line collection for off-line Fourier transform infrared spectroscopy. J. Chromatogr. A, **1999**, *857*, 89–96.
40. Wu, N.; Peck, T.L.; Webb, A.G.; Magin, R.L.; Sweedler, J.V. Nanoliter volume sample cells for ^{1}H-NMR: Application to on-line detection in capillary electrophoresis. J. Am. Chem. Soc. **1994**, *116* (17), 7929–7930.
41. Schewitz, J.; Pusecker, R.; Gfrörer, P.; Gotz, U.; Tseng, L.-H.; Albert, K.; Bayer, E. Direct coupling of capillary electrophoresis and nuclear magnetic resonance spectroscopy for the identification of a dinucleotide. Chromatographia **1999**, *50*, 333–337.
42. Pusecker, K.; Schewitz, J.; Gfrörer, P.; Tseng, L.-H.; Albert, K.; Bayer, E.; Wilson, I.D.; Bailey, N.J.; Scarfe, G.B.; Nicholson, J.K.; Lindon, J.C. On-flow identification of metabolites of paracetamol from human urine using directly coupled CZE–NMR and CEC–NMR spectroscopy. Anal. Commun. **1998**, *35*, 213–215.
43. Gfrörer, P.; Schewitz, J.; Pusecker, K.; Tseng, L.-H.; Albert, K.; Bayer, E. Gradient elution capillary electrochromatography and hyphenation with nuclear magnetic resonance. Electrophoresis **1999**, *20*, 3–8.
44. Gfrörer, P.; Tseng, L.-H.; Rapp, E.; Albert, K.; Bayer, E. Influence of pressure upon coupling pressurized capillary electrochromatography with nuclear magnetic resonance spectroscopy. Anal. Chem. **2001**, *73*, 3234–3239.
45. Schewitz, J.; Gfrörer, P.; Pusecker, K.; Tseng, L.-H.; Albert, K.; Bayer, E.; Wilson, I.D.; Bailey, N.J.; Scarfe, G.B.; Nicholson, J.K.; Lindon, J.C. Directly coupled CZE–NMR and CEC–NMR spectroscopy of metabolite analysis: Paracetamol metabolites in human urine. Analyst **1998**, *12*, 2835–2837.

46. Korhammer, S.A.; Bernreuther, A. Hyphenation of high-performance liquid chromatography (HPLC) and other chromatographic techniques (SFC, GPC, GC, CE) with nuclear magnetic resonance (NMR): A review. Fresen. J. Anal. Chem. **1996**, *354*, 131–135.
47. De Koning, J.A.; Hogenboom, A.C.; Lacker, T.; Strhoschein, S.; Albert, K.; Brinkman, U.A.Th. On-line trace enrichment in hyphenated liquid chromatography–nuclear magnetic resonance spectroscopy. J. Chromatogr. A, **1998**, *813*, 55–61.
48. Onaka, T.; Kobayashi, M.; Ishii, Y.; Okumura, K.; Suzuki, M. Applications of solid-phase extraction to the analysis of the isomers generated in biodesulfurization against methylated dibenzothiophenes. J. Chromatogr. A, **2000**, *904*, 193–202.
49. Nyberg, N.T.; Baumann, H.; Kenne, L. Solid-phase extraction NMR studies of chromatographic fractions of saponins from *Quillaja saponaria*. Anal. Chem. **2003**, *75*, 268–274.
50. Lacey, M.E.; Subramanian, R.; Olson, D.L.; Webb, A.G.; Sweedler, J.V. High-resolution NMR spectroscopy of sample volumes from 1 nl to 1 μl. Chem. Rev. **1999**, *99*, 3133–3152.
51. Lacey, M.E.; Tan, Z.J.; Webb, A.G.; Sweedler, J.V. Union of capillary high-performance liquid chromatography and microcoil nuclear magnetic resonance spectroscopy applied to the separation and identification of terpenoids. J. Chromatogr. A, **2001**, *922*, 139–149.
52. Rehbein, J.; Dietrich, B.; Grynbaum, M.D.; Hentschel, P.; Holtin, K.; Kuehnle, M.; Schuler, P.; Bayer, M.; Albert, K. Characterization of bixin by LC–MS and LC–NMR. **2007**, *30*, 2382–2390.
53. Sandvoss, M.; Weltring, A.; Preiss, A.; Levsen, K.; Wuensch, G. Combination of matrix solid-phase dispersion extraction and direct on-line chromatography–nuclear magnetic resonance spectroscopy–tandem mass spectrometry as a new efficient approach for the rapid screening of natural products: Application to the total asterosaponin fraction of the starfish *Asterias rubens*. J. Chromatogr. A, **2001**, *917*, 75–86.
54. Fritsche, J.; Angoelal, R.; Dachtler, M. On-line liquid chromatography–nuclear magnetic resonance spectroscopy–mass spectrometry coupling for the separation and characterization of secoisolariciresinol diglucoside isomers in flaxseed. J. Chromatogr. A, **2002**, *972*, 195–203.
55. Yang, Z. Online hyphenated liquid chromatography–nuclear magnetic resonance spectroscopy–mass spectrometry for drug metabolite and nature product analysis. J. Pharma. Biomed. Anal. **2006**, *40*, 516–527.
56. Burton, K.I.; Everett, J.R.; Newman, M.J.; Pullen, F.S.; Richards, D.S.; Swanson, A.G. On-line liquid chromatography coupled with high-field NMR and mass spectrometry (LC–NMR–MS): A new technique for drug metabolite structure elucidation. J. Pharm. Biomed. Anal. **1997**, *15*, 1903–1912.
57. Dear, G.J.; Ayrton, J.; Plumb, R.; Sweatman, B.C.; Ismail, I. M.; Fraser, I.J.; Mutch, P.J. A rapid and efficient approach to metabolite identification using nuclear magnetic resonance spectroscopy, liquid chromatography/mass spectrometry and liquid chromatography/nuclear magnetic resonance spectroscopy/sequential mass spectrometry. Rapid Commun. Mass Spectrom. **1998**, *12*, 2023–2030.
58. Scarfe, G.B.; Wilson, I.D.; Spraul, M.; Hofmann, M.; Braumann, U.; Lindon, J.C.; Nicholson, J.K. Application of directly coupled high-performance liquid chromatography–nuclear magnetic resonance–mass spectrometry to the detection and characterisation of metabolites of 2-bromo-4-(trifluoromethyl)aniline in rat urine. Anal. Commun. **1997**, *34*, 37–39.
59. Scarfe, G.B.; Wright, B.; Clayton, E.; Taylor, S.; Wilson, I.D.; Lindon, J.C.; Nicholson, J.K. ^{19}F–NMR and directly coupled HPLC–NMR–MS investigations into the metabolism of 2-bromo-4-(trifluoromethyl)aniline in rat: A urinary excretion balance study without the use of radiolabelling. Xenobiotica **1998**, *28* (4), 373–388.
60. Scarfe, G.B.; Wright, B.; Clayton, E.; Taylor, S.; Wilson, I.D.; Lindon, J.C.; Nicholson, J.K. Quantitative studies on the urinary metabolic fate of 2-chloro-4-trifluoromethylaniline in the rat using ^{19}F NMR spectroscopy and directly coupled HPLC–NMR–MS. Xenobiotica **1999**, *29* (1), 77–91.
61. Shockcor, J.P.; Unger, S.E.; Savina, P.; Nicholson, J.K.; Lindon, J.C. Application of directly coupled LC–NMR–MS to the structural elucidation of metabolites of the HIV-1 reverse-transcriptase inhibitor BW935U83. J. Chromatogr. B. Biomed. Sci. Appl. **2000**, *748*, 269–279.
62. Scarfe, G.B.; Nicholson, J.K.; Lindon, J.C.; Wilson, I.D.; Taylor, S.; Clayton, E.; Wright, B. Identification of the urinary metabolites of 4-bromoaniline and 4-bromo-[carbonyl-^{13}C]-acetaniline in rat. Xenobiotica **2002**, *32*, 325–337.
63. Stűlten, D.; Lamshõft, M.; Zűhlke, S.; Spiteller, M. Isolation and characterization of a new human urinary metabolite of diclofenac applying LC–NMR–MS and high resolution mass analyses. J. Pharm. Biomed. Anal. **2008**, *47*, 371–376.
64. Holt, R.M.; Newman, M.J.; Pullen, F.S.; Richards, D.S.; Swanson, A.G. High-performance liquid-chromatography/NMR spectrometry/mass spectrometry: Further advances in hyphenated technology. J. Mass Spectrom. **1997**, *32*, 64–70.
65. Pullen, F.S.; Swanson, A.G.; Newman, M.J.; Richards, D.S. On-line liquid chromatography/nuclear magnetic resonance/mass spectrometry—A powerful spectroscopic tool for the analysis of mixture of pharmaceutical interest. Rapid Commun. Mass Spectrom. **1995**, *9*, 1003–1006.
66. Corcoran, O.; Spraul, M. LC–NMR–MS in drug discovery. Drug Discov. Today **2003**, *8*, 624–631.
67. Wilson, I.D.; Griffiths, L.; Lindon, J.C.; Nicholson, J.K. HPLC/NMR and related hyphenated NMR methods. Progress Pharma. Biomed. Anal. **2002**, *4*, 299–322.
68. Duarte, I.F.; Spraul, M.; Godejohann, M.; Braumann, U.; Gil, A.M. Application of NMR and hyphenated NMR spectroscopy for the study of beer components. Magn. Reson. Food Sci. **2002**, *286*, 151–157.
69. Gil, A.M.; Duarte, I.F.; Godejohann, M.; Braumann, U.; Maraschin, M.; Spraul, M. Characterization of the aromatic composition of some liquid foods by nuclear magnetic resonance spectrometry and liquid chromatography with nuclear magnetic resonance and mass spectrometric detection. Anal. Chim. Acta **2003**, *488*, 35–51.
70. Exarchou, V.; Godejohann, M.; Van Beek, T.A.; Gerothanassis, I.P.; Vervoort, J. LC–UV–solid-phase extraction–NMR–MS combined with cryogenic flow probe and its application to the identification of compounds present in Greek oregano. Anal. Chem. **2003**, *75*, 6288–6294.
71. Godejohann, M.; Tseng, L.-H.; Braumann, U.; Fuchser, J.; Spraul, M. Characterization of a paracetamol metabolite using on-line LC–SPE–NMR–MS and a cryogenic NMR probe. J. Chromatogr. A, **2004**, *1058*, 191–196.

Lewis Base-Modified Zirconia as Stationary Phases for HPLC

Y.-L. Hu
Y.-Q. Feng
S.-L. Da
Department of Chemistry, Wuhan University, Wuhan, China

INTRODUCTION

The developments of the Lewis base-modified zirconia and mixed-oxide containing zirconia as stationary phases for high-performance liquid chromatography (HPLC) are reviewed. In this context, the preparation methods of porous spherical zirconia, and zirconia supports for HPLC based on modification with fluoride, phosphate, phosphonate, carboxylic acid, phenols, and protein, as well as cyclodextrin derivative, are covered. The application of modified-zirconia in capillary electrochromatography (CEC) is also discussed.

ALTERNATIVES TO SILICA AS HPLC SUPPORTS

Over the past few years, there has been considerable interest expressed in materials that can serve as alternatives to silica as the basis of supports in different mode of HPLC. Zirconia is chemically and mechanically stable relative to silica and polymeric phases. It is resistant to chemical degradation from pH 1 to pH 14. The material's thermal stability is excellent over any liquid chromatographically accessible temperature, leading to increased flexibility when designing separation.[1]

However, the surface of zirconia is much more complex than silica. A number of distinct classes of sites exist which can significantly contribute to the retention of a given solute. These sites include Brönsted acid sites, Brönsted base sites, and Lewis acid sites. Among these, the most chromatographically troublesome sites on the zirconia surface are the Lewis acid sites. These sites arise from the surface discontinuity in bonding between metal and oxygen atoms. They can form coordinate complexes with a number of Lewis bases and are responsible for the irreversible adsorption for proteins and other solutes. However, these sites can be blocked by adsorption with competing Lewis bases. This can be compared to adding amines to the mobile phase when silica-based stationary phases are used to decrease peak tailing due to silanophilic interaction. The effective candidates for modification of the zirconia surface are those species that interact strongly with these hard surface Lewis acid sites, such as fluoride, inorganic phosphate, organic phosphonate, and carboxylic acid. When the surface of zirconia was modified by these species, they exhibited quicker kinetics in the chromatographic process, as well as different selectivity and separation mechanism. This review will cover some aspects of Lewis base-modified zirconia as stationary phases for HPLC.

Preparation of Porous Zirconia Spheres for HPLC

The preparation of porous zirconia with narrow particle size distribution is the foundation for further Lewis base modification. There are several methods reported for the preparation of spherical zirconia. Among these, an oil emulsion method is most widely used in several laboratories for its simplicity and good reproducibility.[2–4] The method involves mechanically dispersing micrometer-scale droplets of an aqueous zirconia sol in an oil phase, in the presence of surfactants. Simultaneous gelation of the colloids within the droplets and extraction of water from the droplets yields zirconia aggregates that are further strengthened by sintering. The oil emulsion method has also been successfully applied for the synthesis of zirconia-containing mixed oxides in our laboratory.[5–7] Sun et al.[8] and Reeder et al.[9] developed another promising method referred as the polymerization-induced colloid aggregation (PICA) for the preparation of spherical, porous zirconia. In this method, an aqueous zirconia sol is mixed with urea and formaldehyde, which are polymerized by the acidic sol. The oligomer so formed adsorbs on the surface of colloids, causing the colloids to aggregate. Zirconia prepared by the PICA method usually has a relatively narrow particle size distribution. Techniques based on a spray-drying process have also been used for the preparation of porous zirconia.[2,10] In this process, a zirconia sol, which may contain a reactive binder, is forced through a nozzle. Droplets of zirconia solution are dried to yield rigid particles. Zirconia spheres prepared by this method usually have a broad size distribution; so size classification is necessary to make them useful for HPLC.

Fluoride-Modified Zirconia as a Biocompatible Stationary Phase

Because fluoride ion forms some of its strongest coordination compounds with zirconium ion in solution, it should be a very powerful displacing agent toward any Lewis base

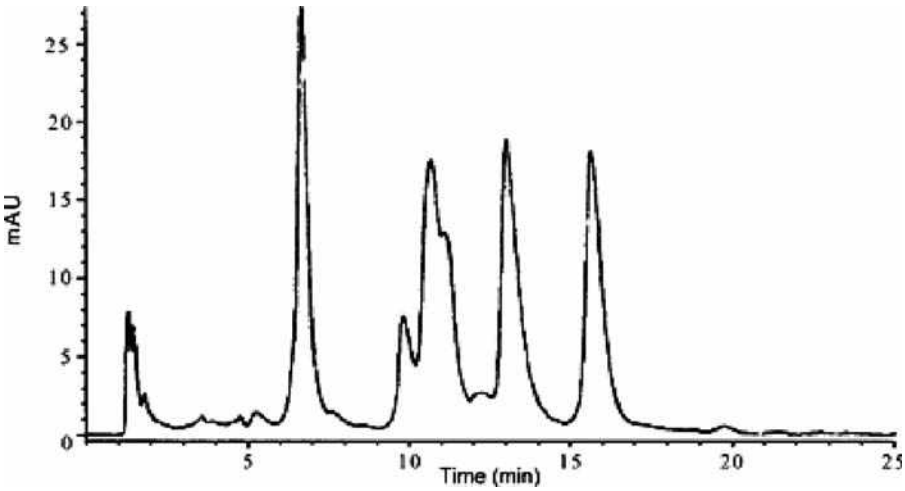

Fig. 1 Protein separation on fluoride modified zirconium oxide. A linear gradient of 0–0.75 *M* Na_2SO_4 in 100 m*M* NaF and 20 m*M* MES at pH 5.5 was used. Flow-rate was 0.5 ml/min at 35. Protein loadings were 4.4 μg lysozyme, 15.4 μg α-chymotrypsin, 13.6 μg myoglobin and 15.4 μg cytochrome *c*.
Source: From Fluoride-modified zirconium-oxide as a biocompatible stationary phase for high-performance liquid-chromatography, in J. Chromatogr.[12]

on a zirconium oxide surface. Blackwell and Carr[11] have studied the fluoride adsorption characteristics of porous zirconium oxide. They found that the composition of fluoride coordinated to the surface of zirconia is pH and ionic strength dependent. At low pH, the fluoride was more easily adsorbed onto the surface, due to less effective competition from hydroxide ion. Washing the zirconia particles with 0.1 M sodium hydroxide quantitatively desorbs bound fluoride. To maintain chromatographic reproducibility, a small amount of fluoride is added to the mobile phase for separation of proteins.[12] The fluoride-modified zirconia is very biocompatible. The unique overall retention properties of this material are operationally analogous to those of calcium hydroxyapatite. However, the system does not have the chemical and physical weaknesses that limit the use of hydroxyapatite. Fig. 1 shows that very efficient separation can be implemented in any of the number of elution schemes.[12] In addition, the substantial base stability allows sterilization of the packing material and stripping of irreversibly bound proteins with sodium hydroxide solution.

Inorganic Phosphate and Organic Phosphonate as Modifiers

The Lewis acid of zirconia can be blocked by other than fluoride. The effectiveness of the blocking of the Lewis acid sites should be related to the strength of the interaction between the Lewis base used and the zirconium ion coordination site. Blackwell and Carr[13] have developed the relative eluotropic strength of a number of Lewis bases in terms of their ability to elute a wide variety of benzoic acid derivatives. Phosphate ranks at the top of the elution series. It brought about elution of the benzoic acid derivatives in the column dead volume. This proves that phosphate binds strongly to the surface of zirconia. The strong affinity of zirconia for phosphate suggested that a phosphate modification of the surface should be a reasonable approach. Schafer et al.[14] used several spectroscopic techniques to characterize the surface species on phosphate-modified zirconia particles. Their results show that phosphate merely adsorbs on the surface of zirconia under the "mildest" phosphate concentration, i.e., neutral pH, room temperature, and short contact times. However, at acidic pH and higher temperatures, esterification of the phosphate with surface hydroxyls takes place as the kinetic barriers are overcome. The solid ^{31}P NMR studies clearly show the presence of covalently bound phosphate. This phosphate modification effectively blocks the sites responsible for the strong interaction of certain Lewis bases with the zirconia surface, resulting in a more biocompatible stationary phase.[15] Unlike fluoride-modified zirconia, phosphate-modified zirconia behaves as a classic cation exchanger and not as a mixed-mode medium analogous to hydroxyapatite, despite spectroscopic evidence of zirconium phosphate formation on the surface. This limits the applicability of the supports, as most proteins and enzymes are anionic at neutral pH. Nevertheless, its ability to separate proteins with high p*I* values still deserves much attention. The preparative-scale separation of murine IgGs from a fermentation broth demonstrates the utility of the supports for solutes that are retained.

Porous zirconia particles were also treated with polyphosphates of chain lengths between 3 and 100 for affinity chromatography of nucleic acids and proteins.[16] The affinity matrix was stable in the pH range of 3 to 11 during a 120 hr incubation period. It is demonstrated that polyphosphate-modified zirconia not only is a useful support for the separation of cationic proteins as is phosphate-modified zirconia, but also can be used for the binding of neutral proteins (e.g., DNase I) and anionic proteins (e.g., alkaline phosphatase). Applying both HPLC and batch procedures can perform protein separation on this packing. The polyphosphate-modified zirconia can also be used in the effective purification of nucleic acids. It was found that 1) double-stranded DNA does not bind to the zirconia

either in the absence or presence of Mg^{2+} ions, and 2) single-stranded DNA and RNA, in the absence of Mg^{2+} ions, also does not bind to the matrix; however, after addition of Mg^{2+} or other divalent cations, they bind strongly to the matrix. Elution of DNA and RNA can be performed with ethylenediaminetetraacetic acid (EDTA).

Based on the successful utility of phosphate-modified zirconia for protein separation, Clausen and Carr[17] have extended their investigation to include the study of ethylenediamine-*N*,*N*′-tetramethylphosphonic acid (EDTPA), a phosphonate analog of EDTA, as a surface modifier for zirconia. They compared EDTPA-modified zirconia (PEZ) with inorganic phosphate-modified zirconia ($ZrPO_4$). Similar to $ZrPO_4$, cation-exchange is the dominant mechanism of protein retention on zirconia. However, PEZ showed increased efficiency, as well as unique selectivity for chromatography of proteins on the chelator-modified surface. Fig. 2[17] shows the chromatogram of the protein mixture on the PEZ and the $ZrPO_4$ phases using the same elution conditions. It can be seen that PEZ is less retentive for all proteins but lysozyme relative to the $ZrPO_4$ phase, but PEZ is able to better resolve proteins especially for α-chymotrypsin and ribonuclease A. This can be accounted for by a mix of lower surface coverage of EDTPA and a change in the chemical nature of the modifier ligand. The presence of ionizable nitrogens in EDTPA should render the zirconia surface less negatively charged than orthophosphate-modified zirconia, resulting in the decrease in retention for all proteins other than lysozyme, as well as to serve, in part, to change the selectivity. It is important, as with $ZrPO_4$, to maintain a small concentration of EDTPA in the mobile phase to keep the stability. Subramanian et al.[18] have used the spray-dried zirconia microsphere (20–30 μm) modified with EDTPA for the isolation of monoclonal antibodies (MAbs) from cell culture supernatant. The selectivity between MAb and bovine serum albumin (BSA), which are the main constituents in the sample matrix, is very high. Analysis by enzyme-linked immunosorbent assay (ELISA) and gel electrophoresis demonstrates that MAbs can be recovered from a cell culture supernatant at high yield (92–98%) and high purity (95%) in a single chromatographic step.

As reversed-phase HPLC is the most common mode of HPLC, many efforts have been made by chromatographers to introduce hydrophobic moieties on the zirconia surface. Polybutadiene-coated zirconia (PBD-ZrO_2) was proven to be an excellent reversed-phase packing material.[19] PBD-ZrO_2 has excellent pH and thermal stability and is efficient for the separation of some small molecules. However, the separation of peptides and proteins on PBD-ZrO_2 has not been successful, due to irreversible adsorption. The addition of phosphate to the mobile phase can alleviate interaction between the Lewis acid sites on zirconia and carboxyl groups on proteins.[20] The phosphate-modified PBD-ZrO_2 phase has both reversed-phase and cation-exchange characteristics under acidic mobile-phase conditions. The PBD

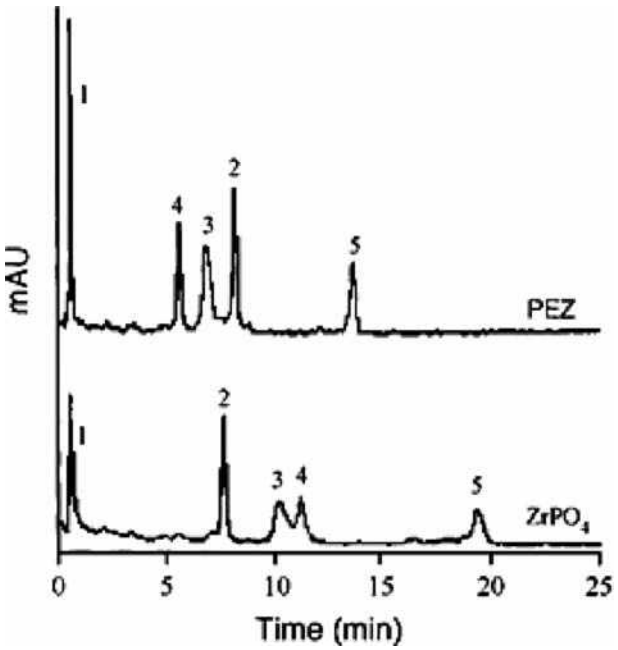

Fig. 2 Chromatographic comparison of protein elution profiles from PEZ and $ZrPO_4$ phases. Particles (4.5 μm) were packed in 50 mm times; 4.6 mm I.D. columns. Mobile phase: 30 min linear gradient from 50 to 500 m*M* potassium phosphate dibasic, pH 7.0; 0.5 ml/min; ambient temperature; detection at 280 nm. Peaks: 1—myoglobin, 2—lysozyme, 3—R-chymotrypsin, 4—ribonuclease A, 5—cytochrome *c*.
Source: From Chromatographic characterization of phosphonate analog EDTA-modified zirconia support for biochromatographic applications, in Anal. Chem.[17]

coating provides hydrophobic moieties, and the phosphate ions adsorbed on zirconia's surface provide cation-exchange sites. The phosphate-modified PBD-ZrO_2 performs satisfactorily for both hydrophobic peptides and positively charged peptides. The limitation of the phase is the reduced efficiency due to secondary equilibrium in the mixed-mode retention mechanism. As an alternative to adding Lewis bases to the eluent, Trammell et al.[21] also studied the effect of permanently modifying PBD-ZrO_2 by covalently attaching vinylphosphonic acid (VPA) to PBD which was predeposited in the pores of zirconia. The resultant stationary phase allows catechol and carboxylates to elute with 100% recovery, without the use of mobile-phase additives. Although this is a tremendous improvement over previous PBD-ZrO_2 phases, a mobile-phase Lewis base additive is still required to provide acceptable peak shapes and plate counts. Evaluation of the cation exchange characteristic of VPA-PBD-ZrO_2 shows that it is significantly more negatively charged than is PBD-ZrO_2 in the presence of phosphate or phosphonate eluent additive. A tremendous improvement in the separation of peptides is achieved when ultralow-pH eluents are used.

Particle pore characteristics are crucial factors for chromatographic performance. Recently, other metal oxides,

such as magnesia and ceria, were introduced into zirconia for improvement of its physicochemical properties in our laboratory.[5–7] The mixed-oxides demonstrate higher specific surface area, large specific pore volume, and better pore connectivity than pure zirconia. Increased surface basicity was also observed on magnesia–zirconia and ceria–zirconia, but especially on magnesia–zirconia, which led to stronger affinity toward Lewis base solutes. In the consequent study, alkylphosphonate with 15 carbons, which was synthesized in our laboratory, was adopted to modify magnesia–zirconia[22] and ceria–zirconia.[23] The new materials illustrated satisfactory pH stability, even in the absence of alkylphosphonic acid in the mobile phase. Alkylphosphonic acid–modified magnesia–zirconia is very stable against extreme pH conditions, e.g., from pH 2 to pH 11.[22] This might be ascribed to be the existence of magnesia on the surface of magnesia–zirconia. The chromatographic performance of the new materials was studied by using polycyclic aromatic hydrocarbons (PAHs) and basic compounds as probes. PAHs were retained on alkylphosphonic acid–modified mixed oxides by typical reversed-phase mechanism in the entire pH range studied. Basic solutes were retarded on stationary phases, mainly by hydrophobic interaction at higher pH, whereas they also showed cation-exchange interaction with the stationary phase at relatively lower pH conditions.[24] It is found that the alkylphosphonic acid–modified magnesia–zirconia and ceria–zirconia are more viable supports for reversed-phase chromatography of basic solutes, relative to silica-based hydrophobic stationary phases, for less peak tailing of these solutes.[22–25] The separations of PAHs and basic solutes on alkylphosphonic acid–modified magnesia–zirconia are illustrated in Fig. 3[26] and Fig. 4,[25] respectively. Application of this material to the separation of nucleosides and nucleobases was also confirmed successful.[27] However, acidic compounds still exhibit strong interaction with alkylphosphonic acid–modified magnesia–zirconia and ceria–zirconia using a typical reversed-phase mobile phase.

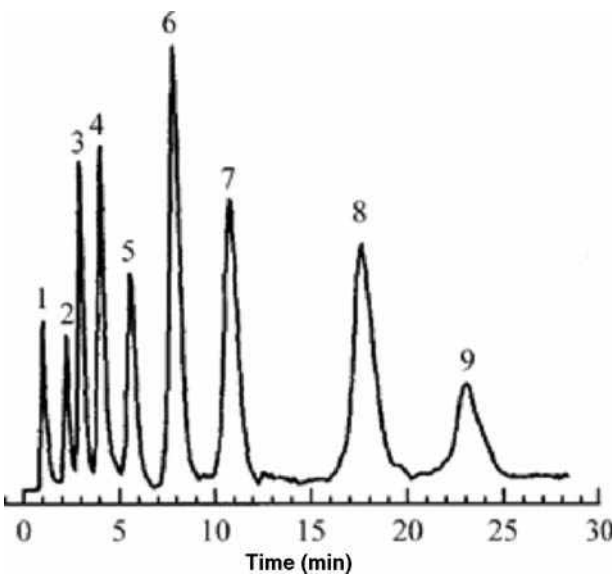

Fig. 3 PAHs separation on alkylphosphonate-modified magnesia–zirconia composite (4–6 μm, 150 mm × 4.6 mm I.D. column). Mobile phase: methanol-water (75 : 25, v/v). 1—Solvent; 2—Benzene; 3—Toluene; 4—Naphthalene; 5—Biphenyl; 6—Fluorene; 7—*O*-terphenyl; 8—*M*-terphenyl; 9—*P*-terphenyl.
Source: From Retention behavior of some polycyclic aromatic hydrocarbons on alkylphosphonate-modified magnesia–zirconia composite stationary phase for reversed-phase liquid chromatography, in Chin. J. Chromatogr.[26]

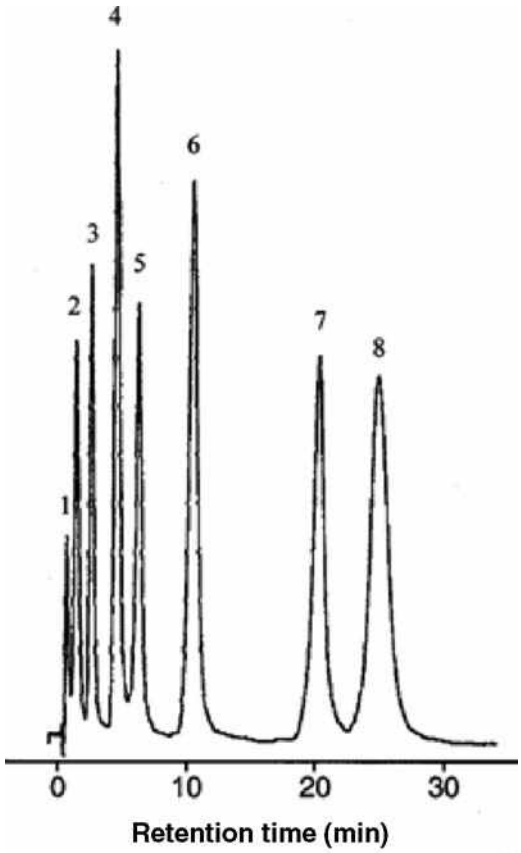

Fig. 4 Separation of basic compounds on the alkylphosphonate-modified magnesia–zirconia composite column with 35 : 65 (v/v) methanol-TRIS buffer (5.0 m*M* TRIS and 50 m*M* NaCl, pH 10.0) as mobile phase at a flow rate of 1.0 ml/min. 1—Solvent; 2—Caffeine; 3—Aniline; 4—*O*-toluidine; 5—*N*-methylaniline; 6—*O*-nitroaniline; 7—*N*,*N*′-dimethylaniline; 8—β-aminonaphthalene.
Source: From Retention behavior of basic compounds on alkylphosphonate-modified magnesia–zirconia composite stationary phase in RPHPLC, in Chromatographia.[25]

Stearic Acid-Modified Zirconia and Ceria–Zirconia for RP-HPLC

Octadecyl-silica stationary phases (ODS) are among the most widely used packing materials in all modalities of

HPLC, owing to their applicability to the separation of solutes of very different polarity, molecular weight, and chemical functionality. Yu and Rassi[28] have investigated the expansion of chemical bonding octadecylsiliane on the zirconia's surface. The resulting octadecyl-zirconia was quite useful in the separation of PAHs, alkylbenzenes, alkylalcohol homologous series, oligosaccharides, and peptides. However, this method has its limitation for lower stability of Zr–O–Si–R relative to Si–O–Si–R bonds. As zirconia and zirconia-containing mixed-oxides have strong affinity toward carboxyl acid derivatives, we[7,29] developed a simple method to dynamically modify zirconia and ceria–zirconia with stearic acid, a fatty acid with 18 carbons, and comparable to octadecylsilane. Stearic acid–modified ceria–zirconia illustrates better chromatographic properties than stearic acid–modified zirconia, owing to its improved column efficiency and hydrophobicity. PAHs and basic compounds are well resolved on the material. Better selectivity of basic compounds was obtained on stearic acid–modified ceria–zirconia than on an ODS column. However, the stability of the stationary phases is worse than for alkylphosphonic acid–modified mixed-oxides in higher pH eluents. This is predictable, since phosphates are stronger Lewis bases than carboxyl acids.

Zirconia-Containing Mixed-Oxides Modified with Phenol Derivatives for Separation of Fullerene Compounds

Chromatographic separation of fullerene compounds has been of great interest during the past few years. Silica-based stationary phases were the most widely used materials for fullerene purification. As synthesis of new silica bonded stationary phase is always time-consuming, we have recently attempted to prepare a useful stationary phase for fullerene separation by a simple method. As mentioned previously, Lewis bases, including some phenol derivatives, strongly adsorb onto the surface of zirconia-containing mixed-oxides. Although these phenol derivatives can be gradually stripped from the matrix in polar solvents, they exhibit high stability while exposed to non-polar solvents which are commonly used as the mobile phase for fullerene separation. Therefore, zirconia-containing mixed-oxides were modified with various phenolic compounds to test their ability for separation of fullerene compounds.[30] A consequence of the retention behavior of fullerene compounds on these stationary phases was that charge–transfer interaction was the main retention mechanism. Based on the results of a column loading capacity test, 2,4,6-trinitrophenol-modified ceria–zirconia and alumina–zirconia are considered as a potential material for the separation of C_{60} and C_{70} in large amounts.[31] Fig. 5 illustrated their separation under the overloaded condition on an analytical column.

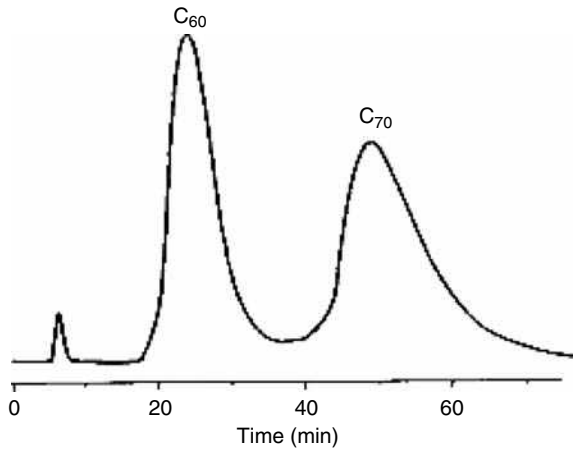

Fig. 5 Separation of C_{60} and C_{70} on 2,4,6-trinitrophenol-modified zirconia–ceria stationary phase (4–6 μm, 150 mm × 4.6 mm I.D. column). Mobile phase: toluene–cyclohexane (30 : 70, v/v). Sample: 11.4 mg/ml of C_{60}, C_{70} mixture in toluene. Injection volume: 0.8 ml. Flow rate: 0.25 ml/min. UV detection at 380 nm.

Other Lewis Bases as Modifier

The results of Blackwell and Carr's study show that the chromatographic properties of the zirconia surface in aqueous media are highly dependent upon the chemical composition of the eluent.[32] They investigated the retention of various small solutes in the presence of glycolic acid, malic acid, succinic acid, citrate, or borate, and concluded that these Lewis base eluent components act to control retention in two ways. They modify the net ligand exchange contribution to retention, and they serve as sites for secondary interactions, such as hydrogen bonding and hydrophobic interaction between solutes and the dynamic stationary phase.

Whitman et al.[33] also evaluated the effect of pretreatments of zirconia with a number of Lewis bases on normal phase selectivity. Chemometric methodology was used to characterize the similarities and differences between the "acid"- and "base"-washed supports. Hydrogen bonding interactions are quite pronounced for the Lewis base-modified zirconia, the extent of which differs greatly among the various Lewis bases used to modify the zirconia.

The irreversible binding of many proteins to bare zirconia can be modulated by addition of some weaker Lewis bases other than phosphate and fluoride.[34] Phosphate and fluoride are able to bring about elution of nearly all proteins, as they are the strongest Lewis bases. On the other hand, there is not much leeway for modulating the strength of the competitive ligand exchange interaction through adjustments of their concentrations for the ease of saturation of their adsorption isotherm. In contrast, weaker Lewis bases such as borate, sulfate, and bromide are able to elute only those proteins retained primarily by ionic interaction. Proteins that contain a large number of accessible Lewis base sites cannot be eluted from zirconia in weak eluents.

Blackwell and Carr investigated the ligand exchange chromatography of free amino acids on copper-loaded zirconia.[35,36] It was shown that the use of Lewis base buffers in this system improved the operating efficiency. Acetate, sulfate, fluoride, and phosphate are the effective competing ions.

Park et al.[37] reported a method to modify zirconia by adsorption with BSA and, subsequently, crosslinked by glutaraldehyde. The BSA-zirconia showed good enantioselectivity for some enantiomers and could be used for RPLC separation in mobile phases of alkaline pH. They also developed a carboxymethyl-β-cyclodextrin-coated zirconia stationary phase for the separation of racemic 2,4-dinitrophenyl amino acids.[38]

Lewis Base-Modified Zirconia–Magnesia in Capillary Electrochromatography (CEC)

Capillary electrochromatography (CEC) is a relatively new technique for chemical analysis. It brings together the advantages of the capillary electrophoresis (CE) and HPLC. CEC can be performed in open tubes or packed structures. To date, the most commonly used packing materials for CEC are the silica-based stationary phases. Recently, zirconia and zirconia–magnesia were successfully utilized as packing or coating material for CEC in our laboratory.[39–41] As mentioned above, alkylphosphonic acid–modified zirconia–magnesia has exhibited excellent chromatographic properties in HPLC. In the subsequent study, Xia et al.[39] demonstrated its usefulness as packing material in CEC. The alkylphosphonic acid–modified zirconia–magnesia shows distinct electro-osmotic flow (EOF), compared with the unmodified zirconia–magnesia for its negative surface at lower pH. Successful separation of polycylic aromatic hydrocarbons can be obtained within a shorter time in the CEC mode than in the HPLC mode, due to the higher column efficiency in CEC. A zirconia–magnesia coating was also fabricated inside fused-silica capillaries for open tubular capillary electrochromatography (OTCE).[40] The capillaries coated with zirconia–magnesia exhibited switchable EOF at pH 5.2. Then, its surface was further modified with SO_4^{2-} and alkylphosphonic acid, respectively, and the isoelectric point of the capillary shifted accordingly. The capillary coated by SO_4^{2-} modified zirconia–magnesia shows better chromatography toward basic compounds than unmodified zirconia–magnesia, with less peak tailing; the alkylphosphonate-modified magnesia–zirconia coated capillary can separate six PAHs within 13 min.

REFERENCES

1. Nawrocki, J.; Rigney, M.P.; McCormick, A.; Carr, P.W. Chemistry of zirconia and its use in chromatography. J. Chromatogr. **1993**, *657*, 229–282.
2. Carr, P.W.; Funkenbusch, E.F.; Rigney, M.P.; Coleman, P.L.; Hanggi, D.L.; Schafer, W.A. High stability porous zirconium oxide spherules. U.S. Patent 5015373, 1991.
3. Trudinger, U.; Muller, G.; Unger, K.K. Porous zirconia and titania as packing materials for high-performance liquid-chromatography. J. Chromatogr. **1990**, *535*, 111–125.
4. Yu, J.; El-Rassi, Z. Reversed-phase liquid-chromatography with microspherical octadecyl-zirconia bonded stationary phases. J. Chromatogr. **1993**, *631*, 91–106.
5. Zhang, Q.H.; Feng, Y.Q.; Da, S.L. Characterization and evaluation of magnesia–zirconia supports for normal-phase liquid chromatography. Chromatographia **1999**, *50*, 654–660.
6. Zhang, Q.H.; Feng, Y.Q.; Da, S.L. Preparation and characterization of silica-zirconia supports for normal-phase liquid chromatography. J. Liq. Chromatogr. Relat. Technol. **2000**, *23*, 1461–1470.
7. Hu, Y.L.; Feng, Y.Q.; Wan, J.D.; Da, S.L.; Hu, L. Native and stearic acid modified ceria–zirconia supports in normal and reversed-phase HPLC. Talanta **2001**, *54*, 79–88.
8. Sun, L.; Annen, J.; Lorenzano-Porras, C.F.; Carr, P.W.; McCormick, A.V. Synthesis of porous zirconia spheres for HPLC by polymerization-induced colloid aggregation (pica). J. Colloid Interf. Sci. **1994**, *163*, 464–473.
9. Reeder, D.H.; Clausen, M.J.; Annen, M.J.; Carr, P.W.; Flickinger, M.C.; McCormick, A.V. An approach to hierarchically structured porous zirconia aggregates. J. Colloid Interf. Sci. **1996**, *184*, 328–330.
10. Wax, M.J.; Grasselli, R.K. EP Patent 0 490 226 A1, 1991.
11. Blackwell, J.A.; Carr, P.W. Study of the fluoride adsorption characteristics of porous microparticulate zirconium-oxide. J. Chromatogr. **1991**, *549*, 43–57.
12. Blackwell, J.A.; Carr, P.W. Fluoride-modified zirconium-oxide as a biocompatible stationary phase for high-performance liquid-chromatography. J. Chromatogr. **1991**, *549*, 59–75.
13. Blackwell, J.A.; Carr, P.W. Development of an eluotropic series for the chromatography of lewis-bases on zirconium-oxide. Anal. Chem. **1992**, *64*, 863–873.
14. Schafer, W.A.; Carr, P.W.; Funkenbusch, E.F.; Parson, K.A. Physical and chemical characterization of a porous phosphate-modified zirconia substrate. J. Chromatogr. **1991**, *587*, 137–147.
15. Schafer, W.A.; Carr, P.W. Chromatographic characterization of a phosphate-modified zirconia support for biochromatographic applications. J. Chromatogr. **1991**, *587*, 149–160.
16. Lorenz, B.; Marmé, S.; Muller, W.E.G.; Unger, K.; Schroeder, H.C. Preparation and use of polyphosphate-modified zirconia for purification of nucleic-acids and proteins. Anal. Biochem. **1994**, *216*, 118–126.
17. Clausen, A.M.; Carr, P.W. Chromatographic characterization of phosphonate analog EDTA-modified zirconia support for biochromatographic applications. Anal. Chem. **1998**, *70*, 378–385.
18. Subramanian, A.; Carr, P.W.; McNeff, C.V. Use of spray-dried zirconia microspheres in the separation of immunoglobulins from cell culture supernatant. J. Chromatogr. A, **2000**, *890*, 15–23.
19. Rigney, M.P.; Weber, T.P.; Carr, P.W. Preparation and evaluation of a polymer-coated zirconia reversed-phase

chromatographic support. J. Chromatogr. **1989**, *484*, 273–291.
20. Sun, L.F.; Carr, P.W. Mixed-mode retention of peptides on phosphate-modified polybutadiene-coated zirconia. Anal. Chem. **1995**, *67*, 2517–2523.
21. Trammell, B.C.; Hillmyer, M.A.; Carr, P.W. A study of the Lewis acid-base interactions of vinylphosphonic acid-modified polybutadien-coated zirconia. Anal. Chem. **2001**, *73*, 3323–3331.
22. Feng, Y.Q.; Zhang, Q.H.; Da, S.L.; Zhang, Y. Preparation and characterization of alkylphosphonate-modified magnesia–zirconia composite for reversed-phase liquid chromatography. Anal. Sci. **2000**, *16*, 579–583.
23. Hu, Y.L.; Feng, Y.Q.; Da, S.L. Chromatographic evaluation of alkylphosphonic acid-modified ceria–zirconia in reversed-phase HPLC. J. Liq. Chromatogr. Relat. Technol. **2001**, *24*, 957–971.
24. Hu, Y.L.; Feng, Y.Q.; Da, S.L. Comparison of chromatographic properties of Lewis base-modified mixed oxides as stationary phases for HPLC. J. Liq. Chromatogr. Relat. Technol. **2002**, *25*, 83–99.
25. Feng, Y.Q.; Fu, H.J.; Zhang, Q.H.; Da, S.L.; Zhang, Y.J. Retention behavior of basic compounds on alkylphosphonate-modified magnesia–zirconia composite stationary phase in RPHPLC. Chromatographia **2000**, *52*, 165–168.
26. Fu, H.J.; Feng, Y.Q.; Zhang, Q.H.; Da, S.L.; Zhang, Y.J. Retention behavior of some polycyclic aromatic hydrocarbons on alkylphosphonate-modified magnesia–zirconia composite stationary phase for reversed-phase liquid chromatography. Chin. J. Chromatogr. **2000**, *18*, 194–197.
27. Fu, H.J.; Feng, Y.Q.; Zhang, Q.H.; Da, S.L.; Zhang, Y.J. High-performance liquid chromatography of some bases and nucleosides on alkylphosphonate-modified magnesia–zirconia column. Anal. Lett. **1999**, *32*, 2761.
28. Yu, J.; Rassi, Z.E. Reversed-phase liquid-chromatography with microspherical octadecyl-zirconia bonded stationary phases. J. Chromatogr. **1993**, *631*, 91–106.
29. Zhang, Q.H.; Feng, Y.Q.; Yan, L.; Da, S.L.; Wang, Z.H. Retention behavior of solutes on liquid chromatographic column packed with dynamically modified zirconia. Chin. J. Chromatogr. **1999**, *17*, 229–231.
30. Hu, Y.L.; Feng, Y.Q.; Wan, J.D.; Da, S.L. Phenol-modified ceria–zirconia and calcia–zirconia as chromatographic packings for separation of C_{60} and C_{70}. Anal. Sci. **2001**, *17*, Supplement a321–a324.
31. Wan, J.D.; Feng, Y.Q.; Hu, Y.L.; Da, S.L.; Wang, Z.H. Preparation and evaluation of 2,4,6-trinitrophenol-modified zirconia–alumina for high performance liquid chromatography and its application in the separation of fullerenes. Chem. J. Chin. Univ. **2002**, *23*, 1259–1263.
32. Blackwell, J.A.; Carr, P.W. A chromatographic study of the Lewis acid-base chemistry of zirconia surfaces. J. Liq. Chromatogr. **1991**, *14*, 2875–2889.
33. Whitman, D.A.; Weber, T.P.; Blackwell, J.A. Chemometric characterization of Lewis base–modified zirconia for normal-phase chromatography. J. Chromatogr. A, **1995**, *691*, 205–212.
34. Blackwell, J.A.; Carr, P.W. Ion-exchange and ligand-exchange chromatography of proteins using porous zirconium-oxide supports in organic and inorganic Lewis base eluents. J. Chromatogr. **1992**, *596*, 27–41.
35. Blackwell, J.A.; Carr, P.W. Ligand-exchange chromatography of free amino-acids and proteins on porous microparticulate zirconium-oxide. J. Liq. Chromatogr. **1992**, *15*, 1487–1506.
36. Blackwell, J.A.; Carr, P.W. Ligand-exchange chromatography of free amino-acids on phosphated zirconium-oxide supports. J. Liq. Chromatogr. **1992**, *15*, 727–751.
37. Park, J.H.; Ryu, J.K.; Park, J.K.; McNeff, C.V.; Carr, P.W. Separation of enantiomers on bovine serum albumin coated zirconia in reversed-phase liquid chromatography. Chromatographia **2001**, *53*, 405–408.
38. Park, S.Y.; Park, J.K.; Park, J.H.; McNeff, C.V.; Carr, P.W. Separation of racemic 2,4-dinitrophenyl amino acids on carboxymethyl-beta-cyclodextrin coated zirconia in RPLC. Microchem. J. **2001**, *70*, 179–185.
39. Xia, D.; Feng, Y.Q.; Da, S.L. Capillary electrochromatography with alkylphosphonate-modified magnesia–zirconia as the chromatographic support material. J. Liq. Chromatogr. Relat. Technol. **2001**, *24*, 1881–1894.
40. Xie, M.J.; Feng, Y.Q.; Da, S.L.; Meng, D.Y.; Ren, L.W. Capillary electrophoresis and open tubular capillary electrochromatography using a magnesia–zirconia coated capillary. Anal. Chim. Acta **2001**, *428*, 255–263.
41. Xie, M.J.; Feng, Y.Q.; Da, S.L. Capillary electrophoresis using zirconia-coated fused silica capillaries. J. Sep. Sci. **2001**, *24*, 62–66.

Lignins and Derivatives: GPC/SEC Analysis

Wenshan Zhuang
Taro Pharmaceuticals, Inc., Brampton, Ontario, Canada

INTRODUCTION

Lignins are a group of naturally occurring organic polymers that are present in all dry-land arborescent and herbaceous plants as one of three major structural materials of cell walls (the other two are cellulose and hemicelluloses). Among all biopolymers, lignins are second only to cellulose in abundance; they are readily available in massive quantities from chemical pulping processes, which convert wood chips into cellulosic fibers (pulps) by removing lignins. Presently, these byproducts are consumed mostly as fuel. Intensive research is underway, worldwide, for the full utilization of this valuable resource for polymeric materials. Such materials have a clear advantage in terms of environmental management over the widely used synthetic plastics such as polyethylene, polypropylene, and polystyrene; if suitably formulated, they are completely biodegradable.

LIGNINS

Molecular weight distribution (MWD) and average molecular weights are important macromolecular properties of lignins. In this regard, size-exclusion chromatography (SEC) has been the most convenient and widely used technique for lignin determination. The technique was originally termed differently in different scientific branches; some examples are gel filtration chromatography (GFC) for separating water-soluble biopolymers and gel permeation chromatography (GPC) for determining the average molecular weights and MWDs of synthetic polymers, which are mostly soluble in organic solvents; the latter term is still commonly used today. Although SEC has other applications in lignin research, such as purification, desalting, and kinetic studies, this entry focuses on its usage for the determination of MWD and average molecular weights, with a brief introduction to the chemical structures, preparations, and associative properties of lignins, which is necessary knowledge for understanding and practicing SEC of these compounds.

Structures of Native Lignins

Lignins are phenylpropane-type polymers, formed by enzyme-catalyzed dehygrogenative polymerization of one to three types of monolignols, viz., coniferyl, sinapyl, and *p*-coumaryl alcohols (Fig. 1). The corresponding building blocks in the resulting lignin molecular structure are often referred to as guaiacylpropane (G), syringylpropane (S), and *p*-hydroxyphenylpropane (H) units, respectively. The proportion of these three types of units is dependent on the plant species. As a rule of thumb, gymnosperm (softwood) lignins are almost exclusively built from G units; angiosperm (hardwood) lignins are composed of both G and S units, while lignins of Gramineae (grasses) contain all three types of units. The three-carbon side chain of the units is essentially of the glycerol type if the interunit linkages are ignored. The structural elements comprising lignins are linked by both ether and carbon–carbon bonds, mainly β–O–4 (around 50–65%), α–O–4, 4–O–5, β–5, 5–5, β–1, and β–β. These linkages are denoted by the positions involved in creating the bonds between the phenylpropane units in question. Thus, lignins are basically copolymers, not only in terms of monomers (in the case of hardwood and grass lignins), but also because of interunit linkages (for all three types of lignins). It should be pointed out that lignins, even within a plant species, exhibit considerable variations in their monomer composition and frequency of interunit linkages with age, cell type, and morphological region of the cell wall.

Although the basic concepts of lignin structure described above have been firmly established, many structural details are still vague and remain to be revealed, such as the nature and extent of chain branching and/or cross-linking, and the sequence of building units. Consensus has not been reached on the most fundamental question—whether the native biopolymers possess random or regular structures.

Lignin Preparations

Even though many techniques have been invented for isolating lignins, it has not been possible to obtain intact lignins from source materials, where lignins coexist with carbohydrates, not only in physical proximity, but also through chemical bonding. For structural study, lignins are usually isolated as milled wood lignins (MWLs), with a yield of about 50% of total lignins. The preparation involves extensive milling of wood meals followed by extraction with a neutral organic solvent, typically aqueous dioxane. Milling increases the yield, but causes rupture of some covalent bonds. Nevertheless, MWL has

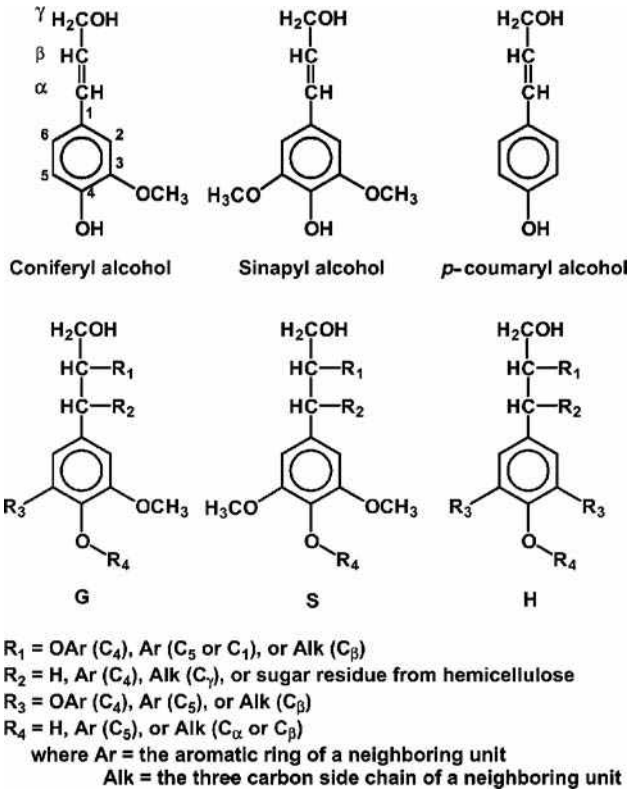

Fig. 1 Three *p*-hydroxycinnamyl alcohols (lignin precursors) and corresponding structural units in lignin molecular structure.

been frequently touted as being most closely related to the native biopolymer.

Isolated lignins available in the largest quantity are those derived from pulp production as byproducts, i.e., kraft lignins from kraft pulping (approximately 45 million metric tons each year globally) and lignosulfonates from sulfite pulping (2 million metric tons per annum). In pulping processes, nucleophilic reagents (OH^- and HS^- in kraft pulping or HSO_3^- in sulfite pulping) react with native lignins in wood chips at high temperature, resulting in the cleavage of some interunit alkyl aryl ether bonds with concomitant generation of hydrophilic groups (phenolic hydroxyl group and sulfhydryl or sulfonic group) in the resultant lignin fragments, which are thus made soluble in the aqueous pulping liquor. The yield of soluble lignins is about 70–90% of the total lignins in wood chips. These industrial lignins are characterized by decreased average molecular weights, decreased frequency of interunit ether bonds with correspondingly increased phenolic hydroxyl content, increased interunit carbon–carbon linkages, and the presence of some functional groups that are absent in the native macromolecules from which they are derived.

It is still a mystery as to what the true molecular weights and polydispersities of native lignins are. Isolated lignins have molecular weights ranging from hundreds to millions, with varying polydispersities, depending on the plant species and the isolation method. Despite significant differences in their chemical structures and molecular sizes, native lignins, isolated lignins and lignin derivatives, are often indiscriminately referred to as "lignins" or simply "lignin."

Non-covalent Intermolecular Interaction

One of the difficulties encountered in the measurement of MWDs and average molecular weights of lignin samples is that lignin components generally exhibit a strong tendency to form associated complexes in solution. Before this associative phenomenon was recognized in the field, people were often frustrated by their inconsistent and irreproducible results when determining average molecular weights and MWDs of lignin preparations. It has now become quite clear that there are two distinct mechanisms responsible for intermolecular lignin associations, i.e., non-covalent interactions, presumably between the aromatic rings, and hydrogen bonding. Which mechanism prevails in the system is dependent on solution conditions such as pH and the type of solvent.[1]

For example, in aqueous alkaline solutions, kraft lignin preparations with concentrations greater than 100 g/L readily undergo a slow, but well-defined, associative process; conversely, dissociation occurs in diluted preparations (< 1 g/L).[1] Fig. 2 illustrates the

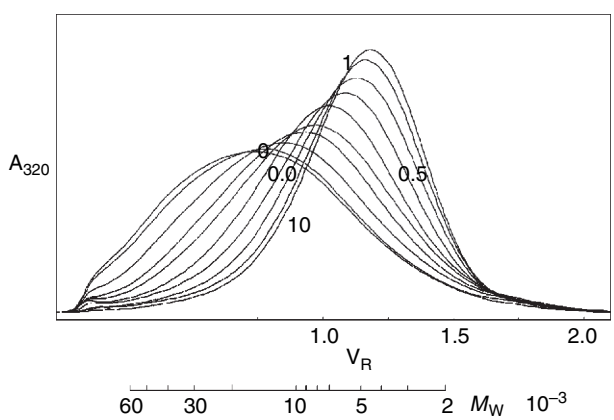

Fig. 2 Apparent MWDs representing homologous series of an aspen kraft lignin preparation secured by fractionation/desalting through Sephadex LH-20 in aqueous 35% dioxane after incubation of parent preparation at 203 g/L in 1.0 *M* ionic strength aqueous 0.40 *M* NaOH for (1) 7215 hr, (2) 4600 hr, (3) 1930 hr, (4) 1116 hr, (5) 542 hr, and (6) 252 hr, and at 0.10 g/L in aqueous 0.10 *M* NaOH for (7) 74 hr, (8) 382 hr, (9) 1167 hr, and (10) 2728 hr. Sephadex G-100/aqueous 0.10 *M* NaOH elution profiles monitored at 320 nm.
Source: From Hardwood kraft lignin: Molecular weight dependent structural properties and non-covalent interactions between constituent species, in M.S. Thesis; University of Minnesota.[2]

dependence of degree of association of a lignin sample on the lignin concentration and incubation time. It is presumed that intermolecular non-bonded orbital interactions, dominated by those of the HOMO–LUMO type involving the π-orbitals of the aromatic moieties, govern the underlying mechanism of these processes. The reported findings suggest that association/dissociation is a reversible process, involving at least two kinetically distinguishable steps.[1] Two coupled steps have been identified as a rapid equilibrium between associated complexes and dissociated components, and a slow (and thus rate determining) equilibrium between the conformation of a (dissociated) discrete species which is ready to associate with complementary complexes and that of one for which association is not directly accessible:[1]

$$\begin{array}{c}\text{Associated complex with } n \text{ components}\\ \uparrow\downarrow \text{ fast}\\ \text{Associated complex with } n-1 \text{ components}\\ +\ \text{Conformationally compatible component}\\ \uparrow\downarrow \text{ slow}\\ \text{Discrete component}\end{array}$$

On the other hand, the rapid and extensive association facilitated by protonation of kraft lignin phenoxide moieties as the pH of the aqueous solution is lowered, or when they are present in non-aqueous solvents, is presumably mediated by hydrogen bonding and/or dipolar interactions, with non-bonded orbital interactions remaining the primary intermolecular forces. It has been shown that the absolute molecular weights of associated kraft lignin complexes encountered in *N*,*N*-dimethylformamide (DMF) could exceed values 1000 times larger than those observed in aqueous alkaline solutions.[3]

Therefore, precaution should be taken in interpretation of the average molecular weights and MWDs reported in the literature. Depending on the sample history (e.g., isolation method, solution conditions, and storage/incubation time) and SEC conditions, the reported measurements may represent those of totally discrete lignin components or those of mixtures of discrete components and complexes with varying degrees of association.

SEC OF LIGNINS AND THEIR DERIVATIVES

Unlike other forms of chromatography that are driven by enthalpy terms in thermodynamic equilibrium, SEC is an entropy-controlled chromatographic separation technique that is, under ideal conditions, based solely on solute size. Although SEC is a relatively rapid and simple method for determining the MWDs and average molecular weights of macromolecular lignins, there are some strict requirements that must be met for proper use of this technique.

Column Packing Material/Eluent

The "ideal conditions" for lignin SEC are those under which energetic interactions between the solute and the column packing material (typically adsorption) and between solute species (mainly association) are negligible. Thus, the selection of appropriate eluting solvent and column packing material for the SEC of lignins is a critical step, and, in practice, it is the most difficult task. From a chromatographic point of view, the main selection criteria for eluent are: high solubility for lignins, inactivity toward lignin solute, packing materials, and other components of the chromatograph, hindrance of solute–matrix and solute–solute interactions, and suitability for the chosen detector type. The choice of column packing materials is based largely on the nature of the eluting solvent and lignin solute. A literature survey shows that solvents popularly used for eluting lignins and their derivatives are tetrahydrofuran (THF), DMF, dimethylsulfoxide (DMSO), and aqueous alkaline solutions. Frequently used packing materials are cross-linked polysaccharides and poly(styrene–divinylbenzene) (PSDVB). Some typical examples are shown in Table 1. Polysaccharide-based gels, such as the Sephadex G series, function very well in aqueous SEC, i.e., in those SEC systems that, as the term suggests, use aqueous solvent as the mobile phase. Conversely, PSDVB columns can be used only in non-aqueous SEC. When THF, a relatively non-polar solvent, is employed as the eluent, lignin samples usually have to be derivatized, typically by silylation, methylation, and/or acetylation, since most underivatized lignins are sparsely soluble in this solvent. On the other hand, both DMF and DMSO dissolve most underivatized lignin preparations, but they tend to elicit pronounced association between lignin components. A common solution is to add LiCl or LiBr, as it is generally believed that lithium halide can interfere with the molecular association by shielding dipoles in individual molecules or by blocking proton uptake from solution, which presumably occurs before anionic lignin molecules undergo association—the negative charge density on the resulting complexes would otherwise be prohibitively large.[1] The effect of LiCl is observable only when its concentration is above 0.1 m*M*, and a concentration of 0.1 *M* is needed for effectively defeating molecular association.[1] However, absolute molecular weight determinations have not been carried out to clarify whether the effect of lithium halides arises really from promotion of dissociation of the macromolecular lignin complexes or largely from enhancement of reversible adsorption to the column packing material.[23,24] Serious adsorption onto the packing material was noted in several SEC systems; for instance, it was reported that the recovery of acetylated lignin samples from PSDVB columns was

Table 1 Typical packings/eluents used in the SEC of lignins and derivatives.

Packing material	Brand name	Eluent	Sample	Refs.
Dextran cross-linked with epichlorohydrin	Sephadex G	Aqueous 0.1 *M* or 0.5 *M* NaOH	Kraft lignin	[1,4]
		Dioxane/H_2O (1 : 1, v/v)	MWL	[5]
		DMSO	MWL	[6,7]
Hydroxypropylated cross-linked dextran	Sephadex LH	Dioxane/H_2O (7 : 3, v/v)	Low-MW lignin in bleachery effluent	[8]
		DMF/0.1 *M* LiCl	Kraft lignin	[1]
Agarose cross-linked with 2,3-dibromopropanol	Sepharose CL	DMF/0.1 *M* LiCl	Kraft lignin	[1]
		Aqueous 50% DMSO/0.1 *M* Tris buffer, pH 7.1	Kraft lignin	[9]
Highly cross-linked agarose	Superose	Aqueous 0.1 *M* NaOH	MWL	[10]
Methacrylate-based polymer	Ultrahydrogel	Aqueous 0.05 *M* NaOH	Lignin reaction products	[11]
Hydrophilic cross-linked polymer gel of $(–CH_2CHOHCH_2O–)_n$ with residual carboxylate functionality on packing surface	TSK-gel GMPW	Aqueous 0.1 *M* $NaNO_3$/CH_3CN (4 : 1, v/v)	Lignosulfonate	[12]
Silica gel chemically bonded with hydrophilic compounds that have primary alcohols on surface	TSK SW	Aqueous 0.2 *M*NaAc adjusted to pH 7 by HNO_3	Lignosulfonate	[13]
PSDVB gel with polar-bonded phase	DVB Glucose BR	DMSO/0.1 *M* LiCl	Lignins	[14]
Cross-linked PSDVB	Styragel	Dioxane/water (9 : 1)	Exploded lignin	[15]
	Styragel HR	*N,N*-Dimethylacetamide/0.1 *M* LiCl, DMF/0.1 *M* LiCl	Kraft lignin and its acetylated derivative	[6,17]
	Ultrastyragel	THF	Kraft lignin, and its acetylated and silylated derivatives	[18]
		DMF/0.1 *M* LiBr	Superfluid-extracted lignin	[19]
	μStyragel	THF or THF/0.05 *M* LiBr	Acetylated MWL and its fractions	[20,21]
	μSpherogel	THF	Acetylated MWL, organosolv lignin, etc.	[20,21]
	TSK HXL	THF/20 m*M* methyltrioctyl ammonium chloride	Kraft lignin, lignosulfonate, organosolv lignins	[22]
	TSK H	DMF	Acetylated methylated kraft lignin	[23,24]
	PLgel	DMF	Acetylated methylated kraft lignin	[23,24]
	PLgel MIXED	DMF/0.1 *M* LiCl	Kraft lignins	[25]
		THF	MWL, organosolv and alkaline lignins	[26]
	LiChrogel PS	THF	Organosolv lignin	[27]

incomplete in both THF and DMF (pure or containing dissolved electrolyte).[23,24]

It appears that SEC with the Sephadex G series/aqueous 0.1 *M* NaOH solution is remarkably reliable:[23,24] Lignin samples are totally recovered from the column, and fast associations through hydrogen bonding or dipolar interactions are completely defeated. However, more stable lignin complexes held by non-bonded orbital interactions can be disassembled completely in aqueous alkaline solution only after prolonged incubation at low concentrations, since the association/dissociation via this mechanism is a considerably slow process. It should be also noted that, with soft Sephadex G series gels, formed in the 30–80 μm particle size range, which are packed manually in open columns, resolution is inherently lower than that offered by high-resolution SEC columns, e.g., those packed with rigid PSDVB gels of smaller particle size. Thus, a continuing search for better column/eluent systems for the SEC of lignins is needed.

It is equally important to choose an appropriate sample concentration, injection or loading volume, flow rate, column temperature, pore size, particle size, and detection method in order to obtain MWDs with high fidelity and adequate resolution. The effects of these parameters are relatively straightforward, except for pore size and detection method, which are discussed later in "Error Analysis". The choices of those parameters are based on the same considerations as for commonly known polymers, which are discussed in several excellent monographs, one of which is listed in the Bibliography (Yau, Kirkland, and Bly).

Standardization of Elution Profiles

Raw elution profiles are expressed as detection response vs. elution volume. To facilitate comparison of elution profiles of various samples, elution profiles need to be normalized to a common area through rescaling of the *y*-axis.

When the SEC of lignins is performed on an open column packed with soft gels, such as Sephadex G, the elution volume of the same solute size varies slightly between runs due to small fluctuations in the flow rate and ambient temperature that may disturb the void volume and total permeation volume of the gel bed. Moreover, a new column has to be packed every three months for a Sephadex G gel/aqueous 0.1 *M* NaOH system because reproducible column performance can be maintained only for a finite period of time as a result of slow decomposition of the packing material. Thus, the variation in the elution volume between columns can be considerably large because of variation in the height of the gel bed from one column to another. To overcome uncertainty arising from these potential sources, the elution volume is often converted to a dimensionless variable prior to *y*-axis rescaling. This variable is termed the distribution function $K = (V - V_0)/(V_T - V_0)$, where V is the elution volume of the sample, and V_T and V_0 are the total permeation volume and the void volume, respectively. The value of K represents the fraction of the internal volume (the total volume of pores in the gel bed) accessible to a particular solute in a given column and, thus, is directly related to molecular size. The variable K is insensitive to the small changes in V_T and V_0 caused by fluctuations of pressure and temperature and to the bed height variation in columns packed with the same batch of gel if the packing technique is consistent.

The values of V_T and V_0 are usually determined by the respective standard markers. For example, in the Sephadex G-100/aqueous 0.1 *M* NaOH system, blue dextran (BD) and *p*-nitrophenol (*p*NP) are often used as standard markers for V_0 and V_T, respectively. In the standardized elution profiles depicted in Fig. 2, the elution volume has been converted to a slightly different dimensionless parameter, termed relative retention volume (V_R), which is operationally defined as $V_R = V_r \times$ scaling factor, where $V_r = (V - V_0)/V_0$. The V_0 is taken as the starting, rather than the apex position, of the BD peak.[23,24] The "scaling factor" normalizes V_r, which may vary slightly from run to run due to experimental background variations, by setting the V_R value of *p*NP to 2 (since the V_r value of *p*NP eluted from a 2.5 × 100 cm column packed with Sephadex G-100 with aqueous 0.1 *M* NaOH is close to 2). Thus, an equivalent expression is $V_R = 2 \times (V - V_0)/(V_{pNP} - V_0)$, where V_{pNP} is the elution volume of *p*NP.[23,24]

Determination of V_0 and V_T is not always straightforward. Since elution profiles of lignins often cover almost the whole elution volume range (between V_0 and V_T) a column can offer, V_0 and V_T standard markers added would coelute with sample components. Under this circumstance, the sample may be eluted twice, once with and once without markers. Corresponding points with respect to the shapes of both profiles can be found according to a constant concentration ratio. Since baseline fluctuations have relatively small effects at the maximum of the largest peak, due to high signal levels in that region, and since changes in the concentration in the vicinity of this position are relatively small, the ratio of the concentrations at the respective peak maxima in the two profiles can be conveniently used to find the corresponding points between them: The concentration ratio at each pair of corresponding points must always be the same.

Since the values of V_R at each pair of corresponding points between the two profiles must be the same, it follows that

$$\frac{V_i - V_0}{V_T - V_0} = \frac{V_i' - V_0'}{V_T' - V_0'} \quad (1)$$

Rearranging gives

$$V_i = \frac{V_T - V_0}{V_T' - V_0'} V_i' - \frac{V_T - V_0}{V_T' - V_0'} V_0' + V_0 \quad (2)$$

where $i = 1, 2, 3, \ldots$ for the pairs of corresponding points, and the prime ($'$) refers to the profile with standard markers. Hence, V_0 and V_T can be derived from the values of the slope and the intercept obtained by a linear regression for a plot of V_i vs. V_i':

$$\begin{aligned} V_0 &= \text{slope} \times V_0' + \text{intercept} \\ V_T &= \text{slope} \times (V_T' - V_0') + V_0 \end{aligned} \quad (3)$$

The validity of the pairing between both profiles can be evaluated by the ratios of calculated relative retention volume in the profile with markers, V_R', to the corresponding one in the profile without markers, V_R; they should be centered at unity and show no systematic changes with increasing retention volume (e.g., the 90% confidence interval of the slope should encompass zero).

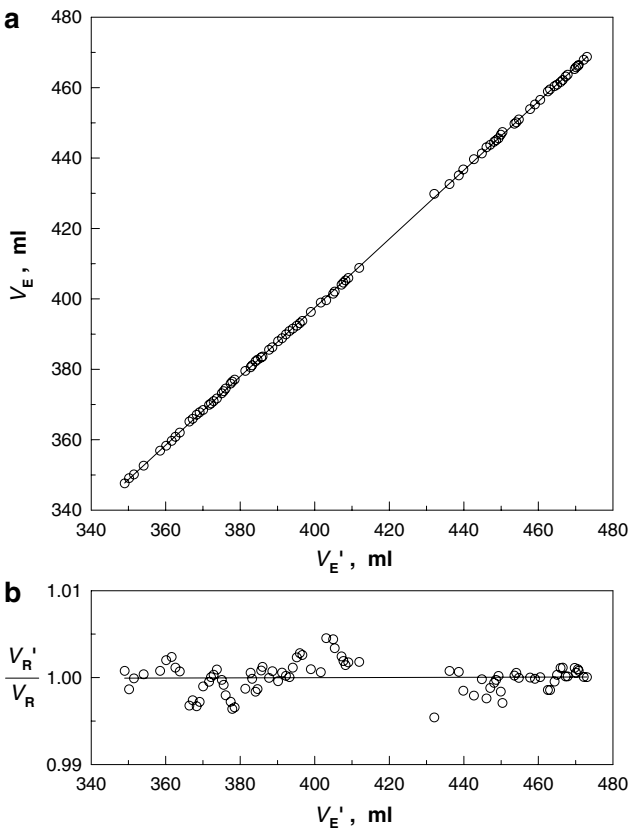

Fig. 3 Linear regression for (a) determination of V_0 and V_T and (b) evaluation of validity of calculated V_R in sample profile. Regression results: Plot A: slope $= 0.976 \pm 0.002$, intercept $= 7.0 \pm 0.6$, and $R^2 = 0.9999$; Plot B: slope $= 9 \times 10^{-7} \pm 8 \times 10^{-6}$, intercept $= 1.000 \pm 0.003$, and $R^2 = 0.0005$. Uncertainties following $\pm$ are calculated at 90% confidence level.
Source: From Hardwood kraft lignin: Molecular weight dependent structural properties and non-covalent interactions between constituent species, in M.S. Thesis; University of Minnesota.[2]

Taking a dissociated aspen kraft lignin preparation as an example, Fig. 3a shows a plot of V_i vs. V_i' with a linear regression line, and Fig. 3b illustrates a plot of V_R'/V_R vs. V_i' with a least-squares fit. Regression lines in both plots fit to the data very well. The V_R'/V_R values have an average of 1.0000 ± 0.0003 and the regression gives a slope of $9 \times 10^{-7} \pm 8 \times 10^{-6}$, indicating that corresponding points between the two profiles have been satisfactorily found.

CALIBRATION

Since the size-exclusion phenomenon depends not really on molecular weight but rather on hydrodynamic volume, calibration is needed for making reliable measurements of average molecular weights and for making meaningful comparisons of MWDs reported by different authors. The purpose of calibration is to correctly establish the quantitative relationship between elution volume and molecular weight for a particular SEC system and sample type under study. Several calibration methods can be used in the SEC of lignins.

Peak Position Calibration with Paucidisperse Standards

This is the most reliable method to obtain the true calibration curve and, thus, is frequently used in the lignin field. The standards should be conformationally close to lignins, preferably those narrow fractions collected from the elution profile of the lignin sample under study. The fractions should be characterized independently by an absolute method such as ultracentrifuge sedimentation equilibrium or velocity, light-scattering photometry, osmometry, or mass spectrometry with soft ionization (matrix-assisted laser desorption/ionization or electrospray ionization). Fig. 4 illustrates a molecular weight calibration curve for a Sephadex G-100 column with aqueous 0.1 *M* NaOH as the eluent for an aspen kraft lignin. The calibration curve was constructed using paucidisperse standards obtained by chromatographic fractionation of parent, associated, and dissociated lignin preparations. The relative elution volume of each standard was based on its peak position in the elution profile obtained from the SEC system being calibrated, and the weight-average molecular weight of each standard was determined by ultracentrifuge sedimentation equilibrium analysis. The standard having the highest molecular weight was collected near the void volume from the elution profile of the associated kraft lignin. The linear calibration curve was established by least-squares fitting to the data points of the remaining standards. The drawback of this type of calibration is that these absolute methods are time-consuming and expensive.

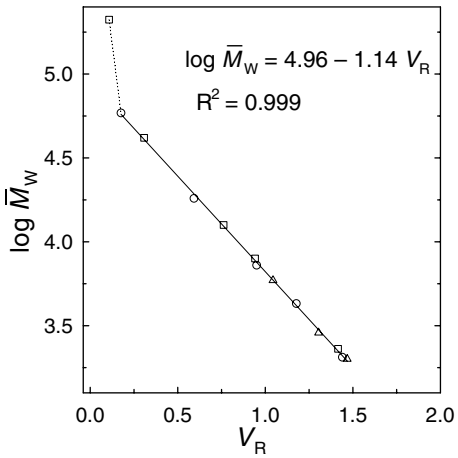

Fig. 4 Molecular weight calibration curve for Sephadex G-100/aqueous 0.10 *M* NaOH of aspen kraft lignins, constructed based on paucidisperse fractions of aspen kraft lignin samples differing in degree of association. ○ Parent preparation; □ associated sample obtained from a 7215 hr incubation of parent preparation at 200 g/L in 1.0 *M* ionic strength aqueous 0.40 *M* NaOH at room temperature; Δ dissociated sample obtained from ultrafiltration with water through Amicon YC05 membrane (to remove NaOH and to concentrate sample solution) following a 5640 hr incubation of parent preparation at 0.10 g/L in aqueous 0.10 *M* NaOH at ambient temperature. Data point with highest $\overline{M}_w$ value was excluded for least-squares linear regression.
Source: From Hardwood kraft lignin: Molecular weight dependent structural properties and non-covalent interactions between constituent species, in M.S. Thesis; University of Minnesota.[2]

Universal Calibration

The SEC of lignins reported in the past has been dominated by calibration with the commercially available well-characterized paucidisperse standards of polystyrene. However, the hydrodynamic volume of a lignin solute is generally not the same as that of polystyrene of the same molecular weight. Furthermore, when the solvent or temperature is changed, the extent to which the molecular size of a lignin solute changes is often different from that for polystyrene. Hence, the measurements based on conventional polystyrene calibration not only do not represent the true molecular weights of a lignin sample, but also depend on the given eluting solvent and temperature. An elegant solution to this difficulty is universal calibration. It was shown more than 30 years ago that the effective hydrodynamic specific volume of a molecule, expressed by the product $[\eta]M$, is uniquely related to the elution volume.[28] Thus, by measurement of the intrinsic viscosities of polystyrene standards and of selected sample fractions, or by the use of an online differential viscometer with SEC, a calibration curve constructed from a homologous series of polystyrene can be converted to a lignin calibration curve with little effort and simple equipment.

Calibration with One or More Polydisperse Standards

An effective calibration curve can be constructed based on any two known values of $\overline{M}_n$ and/or $\overline{M}_w$ of one or two polydisperse standards of the lignin of interest. A nonlinear regression method is used to find the two unknown coefficients in the linear calibration equation such that the calculated $\overline{M}_n$ and/or $\overline{M}_w$ of the broad chromatogram(s) based on this calibration curve agree with the known values, which have been obtained by independent methods such as osmometry and light-scattering photometry. Obviously, the accuracy of this type of calibration depends on the accuracy of the known values of $\overline{M}_n$ and $\overline{M}_w$ as well as the validity of the assumption that the molecular weights of all constituent species of the polydisperse standard are within the linearity ranges of the column being calibrated. In addition, significant deviation from the true calibration curve can occur unless a low-dispersion SEC column is employed or correction for column band dispersion is incorporated into the method.[29] This method is of practical convenience for routine calibration, though its application in the lignin field is only scarcely reported.

Online Calibration

A recent advance in the SEC of lignins is the online molecular weight measurement of macromolecules eluting from the column using molecular-weight-sensitive detectors such as differential viscometers and light-scattering photometers. Among several types of light-scattering detectors, the low-angle laser light-scattering (LALLS) photometer is favored for online measurement, since the incident laser beam is very intense to allow for measurement of very dilute eluate with reasonably good signal-to-noise ratios and can be focused extremely well to allow for reliable measurement of scattered light at an angle very close to zero (typically 2–7°), thus avoiding any uncertainty that arises from data extrapolation and fitting that would have to be performed in multiangle light-scattering detection to obtain the excess Rayleigh ratio at 0°.

ERROR ANALYSIS

Several factors may affect the accuracy of lignin elution profiles and, thus, that of the calculated average molecular weights. Some important sources of errors are discussed below.

Enthalpic Interactions

It is well understood that any kind of energetic interaction of the solute with the stationary phase would cause

non-SEC behaviors. The proper choice of mobile and stationary phases is critical to eliminate this type of error or reduce it to insignificant levels. An appropriate mobile phase is also needed to suppress instant association between lignin components, which often results in misleading SEC results.

Pore Size

Separation of solutes by SEC is regulated by the selection of the pore size of the packing material. Most lignin preparations have very wide ranges of molecular weights. It has been pointed out that the bimodal distributions reported in many cases were due to insufficient pore size of the packing material used, which resulted in a high-molecular-weight peak that merely represents the accumulation of all macromolecules of hydrodynamic volume greater than the total exclusion limit of the column.[6] Apparently, use of inappropriate pore size causes considerable error in molecular weight analysis. Any peak appearing at the void volume or at the total permeation volume is an alarming sign of this problem.

Detector Response to Heterogeneous Polymeric Solutes

Ideally, an SEC detector for measuring mass concentration should have a constant response factor (response per solute concentration) for all polymeric solutes so that the elution profile recorded represents the true concentration (or weight fraction) change with elution volume. This is true for homogeneous polymers, but not so for heterogeneous polymers, since the response factor generally changes with the chemical composition of eluate. For example, it is well known that the absorptivities of H, G, and S units at a given wavelength are considerably different and that some local structure features, such as the ionized phenolic hydroxyl group, have significant influence on the absorptivity. Notwithstanding this, the ultraviolet detector, being highly sensitive to aromatic structures and yet insensitive to temperature variation, is the most frequently used detector in the SEC of lignins and their derivatives. However, in publications dealing with lignin SEC, the absorptivity at a chosen detection wavelength has been commonly assumed to be the same for all lignin molecules in the sample. Thus, lignin elution profiles generally contain a certain degree of error. This may be especially true for hardwood and grass lignin preparations, which are built up from more than one type of structural unit. The second most frequently used concentration detector is the differential refractometer (though far less popular than the UV detector) for the SEC of lignins; however, it fares no better. Since the specific refractive index increment (dn/dc) is sensitive to the heterogeneous nature of lignin macromolecules, the response factor of this detector type is likely to fluctuate, to some degree, during the course of elution. Indeed, ideal concentration-sensitive detectors for lignins have yet to be found. Interestingly, SEC can be undertaken without any concentration detector, and thus free of the foregoing source of error, to determine number-average molecular weights. The method uses a universal calibration curve and needs only an online differential viscometer in the SEC system.[30–32] This measurement, however, is quite sensitive to baseline noise.

Compositional Local Polydispersity

For compositionally heterogeneous polymers, macromolecules of different molecular weights may possess the same hydrodynamic volume; thus, their SEC elution profile exhibits local polydispersity in the molecular weight at each elution volume where different molecular weights coelute. Since conventional interpretation of SEC elution profiles assumes no local polydispersity, the MWDs derived via column calibration can be misleading if significant coelution of different molecular weights occurs in the SEC of lignins. Conceivably, the problem is more serious for hardwood and grass lignins.

Column Axial Dispersion (Band Broadening)

Axial dispersion impairs the chromatographic resolving power, causing local polydispersity in molecular size (and thus, in molecular weight as well) at each elution volume, even for homogeneous polymers. As a result, the elution profile obtained is broader than it should be, calculated average molecular weights deviated from the true values, and polydispersity ($\overline{M}_w/\overline{M}_n$) is usually overestimated. Obviously, the error is more significant for low-resolution columns, which are often employed in aqueous SEC of lignins. Fortunately, band broadening can be assessed by the standard deviation of a narrow standard peak obtained under the same SEC conditions as for samples, and local polydispersity due to this source can be corrected for by published mathematical treatments.[29]

ACKNOWLEDGMENTS

The author thanks Dr. Ontai Leung, Frank Roth, and Phil van den Heuvel for their critique of the manuscript.

REFERENCES

1. Dutta, S.; Garver, T.M.; Sarkenen, S. Modes of association between kraft lignin components. In *Lignin: Properties and Materials*; ACS Symposium Series 397; Glasser, W.G., Sarkenen, S., Eds.; ACS: Washington, 1989; 155–176.

2. Zhuang, W. Hardwood kraft lignin: Molecular weight dependent structural properties and non-covalent interactions between constituent species. M.S. Thesis; University of Minnesota, 1996; 114, 178, 195.
3. Dutta, S.; Sarkenen, S. A new emphasis in strategies for developing lignin-based plastics. In *Materials Interactions Relevant to the Pulp, Paper, and Wood Industries*; Materials Research Society Symposium Proceedings 197; Caulfield, D.F. Passaretti, J.D., Sobczynski, S.F., Eds.; Materials Research Society: Pittsburgh, PA, 1990; 31–39.
4. Forss, K.; Kokkonen, R.; Sågfors, P.-E. Determination of the molar mass distribution of lignins by gel permeation chromatography. In *Lignin: Properties and Materials*; ACS Symposium Series 397; Glasser, W.G., Sarkenen, S., Eds.; ACS: Washington, DC, 1989; 124–133.
5. Farrington, A.; Nelson, P.F.; Vanderhoek, N. The effect of anthraquinone on the alkaline degradation of lignin: Gel filtration studies. Appita **1979**, *32* (4), 300–304.
6. Obiaga, T.I.; Wayman, M. Improved calibration procedure for gel permeation chromatography of lignins. J. Appl. Polym. Sci. **1974**, *18*, 1943–1952.
7. Mbachu, R.A.D.; Manley, R.S.J. Degradation of lignin by ozone. II. Molecular weights and molecular weight distributions of the alkali-soluble degradation products. J. Polym. Sci. Polym. Chem. Ed. **1981**, *19* (8), 2065–2078.
8. Ristolainen, M.; Alen, R.; Knuutinen, J. Characterization of TCF effluents from kraft pulp bleaching. I. Fractionation of hardwood lignin-derived material by GPC and ultrafiltration. Holzforschung **1996**, *50* (1), 91–96.
9. Huettermann, A. Gel permeation chromatography of water insoluble lignins on controlled pore glass and Sepharose CL-6B. Holzforschung **1978**, *32* (3), 108–111.
10. Himmel, M.E.; Oh, K.K.; Quigley, D.R.; Grohmann, K. Alkaline size-exclusion chromatography of lignins and coal extracts using cross-linked dextran gels. J. Chromatogr. **1989**, *467*, 309–314.
11. Rittstieg, K.; Suurnakki, A.; Suortti, T.; Kruus, K.; Guebitz, G.; Buchert, J. Investigations on the laccase-catalyzed polymerization of lignin model compounds using size-exclusion HPLC. Enzyme Microb. Technol. **2002**, *31* (4), 403–410.
12. Kato, Y.; Matsuda, K.; Hashimoto, T. New gel permeation column for the separation of watersoluble polymers. J. Chromatogr. **1985**, *332*, 39–46.
13. van der Hage, E.R.E.; van Loon, W.M.G.M.; Boon, J.J.; Lingeman, H.; Brinkman, U.A.Th. Combined high-performance aqueous size-exclusion chromatographic and pyrolysis–gas chromatographic–mass spectrometric study of lignosulphonates in pulp mill effluents. J. Chromatogr. **1993**, *634*, 263–271.
14. Jordi, H. Jordi gel columns for size exclusion chromatography. In *Column Handbook for Size Exclusion Chromatography*; Wu, C.-s., Ed.; Academic Press: New York, 1999; 367–423.
15. Jakobsons, J.; Hortling, B.; Erins, P.; Sundquist, J. Characterization of alkali soluble fraction of steam exploded birch wood. Holzforschung **1995**, *49* (1), 51–59.
16. Sjöholm, E.; Gustafsson, K.; Colmsjö, A. Size exclusion chromatography of lignins using lithium chloride/*N*,*N*-dimethylacetamide as mobile phase. I. Dissolved and residual birch kraft lignins. J. Liq. Chromatogr. Rel. Technol. **1999**, *22*, 1663–1685.
17. Sjöholm, E.; Gustafsson, K.; Colmsjö, A. A. Size exclusion chromatography of lignins using lithium chloride/*N*,*N*-dimethylacetamide as mobile phase. II. Dissolved and residual pine kraft lignins, **1999**, *22*, 2837–2854.
18. Pellinen, J.; Salkinoja-Salonen, M. High-performance size-exclusion chromatography of lignin and its derivatives. J. Chromatogr. **1985**, *328*, 299–308.
19. Li, L.; Kiran, E. Supercritical fluid extraction of lignin from wood. In *Lignin: Properties and Materials*; ACS Symposium Series 397; Glasser, W.G., Sarkenen, S., Eds.; ACS: Washington, DC, 1989; 42–57.
20. Himmel, M.E.; Tatsumoto, K.; Grohmann, K.; Johnson, D.K.; Chum, H.L. Molecular weight distribution of aspen lignins from conventional gel permeation chromatography, universal calibration and sedimentation equilibrium. J. Chromatogr. **1990**, *498*, 93–104.
21. Himmel, M.E.; Tatsumoto, K.; Oh, K.K.; Grohmann, K.; Johnson, D.K.; Chum, H.L. Molecular weight distribution of aspen lignins estimated by universal calibration. In *Lignin: Properties and Materials*; Glasser, W.G., Sarkenen, S., Eds.; ACS Symposium Series 397; ACS: Washington, DC, 1989; 82–99.
22. Majcherczyk, A.; Hüttermann, A. Size-exclusion chromatography of lignin as ion-pair complex. J. Chromatogr. A, **1997**, *764*, 183–191.
23. Himmel, M.E.; Mlynár, J.; Sarkenen, S. Size exclusion chromatography of lignin derivatives. In *Handbook of Size Exclusion Chromatography*; Wu, C.-S., Ed.; Chromatographic Science Series 69 Marcel Dekker, Inc.: New York, 1995; 353–379.
24. Mlynár, J.; Sarkenen, S. Renaissance in ultracentrifugal sedimentation equilibrium calibrations of size exclusion chromatographic elution profiles. In *Strategies in Size Exclusion Chromatography*; Potschka, M. Dubin, P.L., Eds.; ACS Symposium Series 635; ACS: Washington, DC, 1996; 379–400.
25. Pinto, P.C.; Evtuguin, D.V.; Pascoal Neto, C.; Silvestre, A.J.D.; Amado, F.M.L. Behaviour of *Eucalyptus globulus* lignin during kraft pulping. Part 2. Analysis by NMR, ESI/MS and GPC. J. Wood Chem. Technol. **2002**, *22* (2 & 3), 109–125.
26. Lawther, J.M.; Sun, R.-C.; Banks, W.B. Extraction and comparative characterization of ball-milled lignin (LM), enzyme lignin (LE) and alkali lignin (LA) from wheat straw. Cellulose Chem. Technol. **1996**, *30* (5–6), 395–410.
27. Lindner, A.; Wegener, G. Characterization of lignins from organosolv pulping according to the Organocell process, Part 3. Molecular weight determination and investigation of fractions isolated by GPC. J. Wood Chem. Technol. **1990**, *10* (3), 331–350.
28. Grubisic, Z.; Rempp, P.; Benoit, H. A universal calibration for gel permeation chromatography. J. Polym. Sci. B **1967**, *5*, 753.
29. Yau, W.W. The Chevron approach to GPC axial dispersion correction. In *Chromatography of Polymers: Hyphenated and Multidimensional Techniques*; Provder, T., Ed.; ACS Symposium Series 731 ACS: Washington, DC, 1999; 35–43.

30. Goldwasser, J.M. Absolute M_n determined by gel permeation chromatography—differential viscometry. In *Chromatography of Polymers: Characterization by SEC and FFF*; Provder, T., Ed.; ACS Symposium Series 521 ACS: Washington, 1993; 243–251.
31. Balke, S.T.; Mourey, T.H.; Harrison, C.A. Number-average molecular weight by size exclusion chromatography. J. Appl. Polym. Sci. **1994**, *51*, 2087–2102.
32. Yau, W.W. Axial dispersion correction for the Goldwasser method of absolute polymer M_n determination using SEC-viscometry. In *Chromatography of Polymers: Hyphenated and Multidimensional Techniques*; Provder, T., Ed.; ACS Symposium Series 731; ACS: Washington, DC, 1999; 44–51.

BIBLIOGRAPHY

1. Bo, H.; Turunen, E.; Kokkonen, P. Molar mass and size distribution of lignins. In *Handbook of Size Exclusion Chromatography and Related Techniques*; Wu, C.-S., Ed.; Chromatographic Science Series 91; Marcel Dekker, Inc.: New York, 2004; 355–383.
2. Gellerstedt, G. Gel permeation chromatography. In *Methods in Lignin Chemistry*; Lin, S.Y., Dence, C.W., Eds.; Springer-Verlag: Berlin, 1992; 487–497.
3. Yau, W.W.; Kirkland, J.J.; Bly, D.D. *Modern Size-Exclusion Liquid Chromatography: Practice of Gel Permeation and Gel Filtration Chromatography*; John Wiley & Sons: New York, 1979; 476 pp.

Lipids: CCC Separation

Kazuhiro Matsuda
Pharmacology Division, National Cancer Center Research Institute, Tokyo, Japan

Sachie Matsuda
Department of Dermatology, Horikiri Central Hospital, Tokyo, Japan

Yoichiro Ito
National Heart, Lung, and Blood Institute (NHLBI), National Institutes of Health (NIH), Bethesda, Maryland, U.S.A.

INTRODUCTION

We demonstrate the separation of human brain lipids by using toroidal-coil countercurrent chromatography (TC-CCC). It becomes possible to select the suitable two-phase solvent systems because retention of a stationary phase is much more stable in TC-CCC than in high-speed countercurrent chromatography (HS-CCC). Optimizing the solvent systems, we succeeded in separating major brain lipids. The two-phase solvent, consisting of chloroform/methanol/water (5:4:3), was suitable for the separation of acidic phospholipids (phosphatidic acid [PA], phosphatidylserine [PS], phosphatidylinositol [PI], lysophosphatidylinositol [lysoPI], and lysophosphatidylserine [lysoPS]). By using hexane/ethylacetate/ethanol/0.1% aqueous ammonia (5:5:5:4), neutral phospholipids (phosphatidylcholine [PC], sphingomyelin [SPM], and lysophosphatidylcholine [lysoPC]) were separated. Nonpolar lipids (cholesterol, alkali-labile glycoglycerolipids, and cerebrosides [CS]) were separated by using the solvent of hexane/ethanol/water (10:15:4). Sphingomyelin (SPM), cerebrosides, and phosphatidylcholine are each reported to have more than 100 molecular species, which are derived from variations of the hydrophobic tail group in mammalian tissues. For this reason, SPM was further separated into two groups (SPM-I and SPM-II). Cerebrosides were separated into several groups by using hexane/ethanol/water (5:4:3). It was clearly shown that synthesized PC (distearoyl phosphatidylglycerol and dipalmitoyl phosphatidylglycerol) was completely separated. Because the partition behavior of molecules in the two-phase solvent system can be measured, TC-CCC could be useful not only for the separation, but also for the biological analysis of mammalian cell-membrane lipids.

COUNTERCURRENT CHROMATOGRAPHY

Phospholipids, glycolipids, and cholesterol are the major components of mammalian cell-membrane lipids. They play important roles in cell-signaling transduction and cell-to-cell recognition or modification of enzyme functions. All of these lipids have amphipathic properties, and contain hydrophobic and hydrophilic regions. In the cell membrane, the hydrophobic and hydrophilic residues and their behavior play an important role in cell functions. The amphipathic property disturbs the separation of these compounds via a countercurrent distribution method because the vigorous mixing of the two solvent phases causes the formation of an emulsion.

Countercurrent chromatography (CCC) is a liquid partition chromatographic technique which eliminates the use of a solid support.[1,2] CCC utilizes two immiscible solvent phases. The partition process takes place in an open column in which one phase (the stationary phase) is retained while the other phase (the mobile phase) is continuously equilibrating with the stationary phase. To retain the stationary phase in the column, the system uses various combinations of column configuration and force fields (gravitational and centrifugal). Countercurrent liquid partition chromatography is a system without a solid phase. Therefore it may become a useful method for analyzing the hydrophobicity and the behavior of lipids, avoiding the influence of a solid phase or spacers.

Previously, we showed that HS-CCC could separate alkali-labile glycolipids (ALGLs), which were isolated from the human brain, into several groups.[3] In that experiment, HS-CCC could finely separate the molecular species in the final step of purification. Nevertheless, the retention of a stationary phase is poor in HS-CCC. Therefore the available two-phase solvent systems have their limitations. Moreover, it was actually difficult to separate them from crude materials because of severe emulsification and the subsequent loss of the stationary phase from the column. To overcome this problem, we developed an analytical-scale TC-CCC, which has the advantage of using centrifugal force to retain the stationary phase.[4] In this system, a stable two-phase separation can be obtained by increasing the rotational speed (centrifugal force) and/or decreasing the flow rate to avoid emulsification. We can use most of the two-phase solvent systems for this TC-CCC.

In this study, the TC-CCC system was applied to solve the problem of emulsification, and satisfactory stationary phase retention was obtained. Human brain lipids could then be separated. We established the solvent systems that are used for the separation of most of the phospholipids, glycolipids, and less-polar lipids of the human brain. Furthermore, we demonstrated that molecular species, which are derived from variations of the hydrophobic tail group, were separated by optimizing the composition of the solvents. TC-CCC is available for analyzing the hydrophobicities of various lipid molecules in biomembranes.[5]

EXPERIMENTAL APPROACH

Apparatus

The present studies employ a commercial model of the toroidal coil centrifuge (TC-CCC 1000) purchased from Pharma-Tech Research (Baltimore, Maryland, U.S.A.). The apparatus is a compact tabletop unit measuring 30 × 630 × 640 cm. It is equipped with a flow-through device without the use of rotary seals, according to a previously described principle.[6] In this implement, rotation speed is continuously adjustable up to 3000 rpm, having a speed regulator equipped with a digital display. The toroidal coil separation column was prepared by winding a 0.4 mm I.D. 15–100 m polytetrafluoroethylene (PTFE) tubing (Zeus Industrial Products, Raritan, New Jersey, U.S.A.) onto a nylon pipe of 1.5 mm O.D. thus making a right-handed coil. Next, the coiled tube was affixed to the inner wall of the cylindrical centrifuge bowl (diameter: 12 cm and height: 5 cm), thus forming a doughnut-shaped configuration (toroidal coil) consisting of two to three coiled layers. The toroidal coil is about 6 m in length (made from 60 m-long PTFE tubing) and consists of 12,000 helical turns with a total capacity of about 8 ml. The inlet and outlet flow lines were made of thick-wall PTFE tubes (0.35 mm I.D.) to withstand constant flexing movements. A chromatographic metering pump (model 515 HPLC pump, Waters, U.S.A.) was used for pumping in the mobile phase, and a fraction collector (Ultrorac, LKB Instruments, Stockholm, Sweden) was used to collect the eluate into test tubes.

Reagents

Phospholipid standards (Phospholipid kit) were purchased from Funakoshi (Tokyo, Japan). Cerebroside (bovine), D-α-phosphatidylcholine dipalmitoyl, and D-α-phosphatidylcholine distearoyl were purchased from Sigma (St. Louis, Missouri, U.S.A.). Chloroform and methanol, both of glass-distilled chromatographic grades were purchased from Burdick and Jackson Labs. (Muskegon, Michigan, U.S.A.), and a reagent-grade glacial acetic acid, water, hexane, and ethyl acetate from Fisher Scientific (Fair Lawn, New Jersey, U.S.A.). Ethanol was purchased from Pharmaco Products (Brookfield, Connecticut, U.S.A.). Trifluoroacetic acid (TFA) was from Pierce Chemical (Rockford, Illinois, U.S.A.). Ammonium hydroxide was from J.T. Baker (Philipsburg, New Jersey, U.S.A.).

Lipid Extraction and Purification

Human brain tissue (200 g, wet weight) was homogenized, and the total lipids were successively extracted with 3 L each of mixtures composed of chloroform/methanol, 2:1, 1:1, and 1:2 (v/v). The lipid extracts were combined and evaporated to dryness in a rotary evaporator, then suspended and dialyzed against distilled water, and, finally, lyophilized. Unbound (neutral) lipids and bound (acidic) lipid fractions were separated with a column packed with DEAE Sephadex A-25 (Pharmacia LKB Biotechnology, Uppsala, Sweden) (bed volume, 200 ml).

Preparation of Two-Phase Solvent System and Sample Solution

Each solvent system was thoroughly equilibrated in a funnel at room temperature. The sample solution was prepared by dissolving 1–5 mg of lipids in 0.05 ml each of the upper and lower phases.

CCC Procedure

In each separation, the toroidal coil was first entirely filled with a stationary phase (either the upper or the lower phase), and a sample solution was injected into the coil. Next, the mobile phase (organic phase) was pumped into the column while the column was rotated at the desired rate. The effluent from the outlet of the column was collected in test tubes at a rate of 0.2 ml/tube, and at a flow rate of 0.1 ml/min. After the desired peaks eluted, the centrifuge run was terminated and the column contents were fractionated into test tubes at 0.5 ml/tube by eluting the column with the solvent initially used as the stationary phase, at a flow rate of 0.25 ml/min.

High-Performance Thin-Layer Chromatography

The lipids were separated on a high-performance thin-layer chromatography (HPTLC) plate. The developing solvent was a mixture of chloroform, methanol, and 0.2% aqueous $CaCl_2$. Orcinol reagent[7] and Dittmer's reagent[8] were used to detect glycolipids and phospholipids.

RESULTS

Fig. 1A shows the procedure for acidic and neutral lipid preparation. Human brain tissue was homogenized and extracted by using a mixture of chloroform and methanol. Next, the lipid extract was dialyzed and applied to the

anion exchange column. Then, the binding fraction (acidic fraction) and the non-binding fraction (neutral fraction) were separated. Cholesterol, phospholipids, and glycolipids were the main components of these fractions. The general structures of these lipids are summarized in Fig. 1B. There are two types of glycolipids and phospholipids. One is a sphingo type and the other is a glycero type. In humans, sphingomyelin is only one sphingo type of phospholipid. In glycosphingolipids, X represents various carbohydrates. The carbohydrate containing sialic acid is called a ganglioside, which is eluted as a binding fraction by using anion-exchange column chromatography. We tried various solvent systems and various compositions for each solvent system. We then determined that the following conditions are the most appropriate for the separation of the lipids.

Separation of Acidic Fraction

A chloroform/methanol/water system is appropriate for the separation of an acidic fraction. If the solvent compositions are not optimized, the phospholipids and glycolipids are eluted at the solvent front or in the column contents. When we chose a suitable solvent, acidic phospholipids (phosphatidic acid, phosphatidylserine, phosphatidylinositol, lysophosphatidyl-inositol, and lysophosphatidylserine) were satisfactorily separated between the solvent front and the column contents (Fig. 2A). Samples (2 mg each) of the acidic fraction of human brain lipids was applied to TC-CCC by using the chloroform/methanol/water (5:4:3) solvent system. Aliquots of each fraction were spotted and developed by HPTLC.

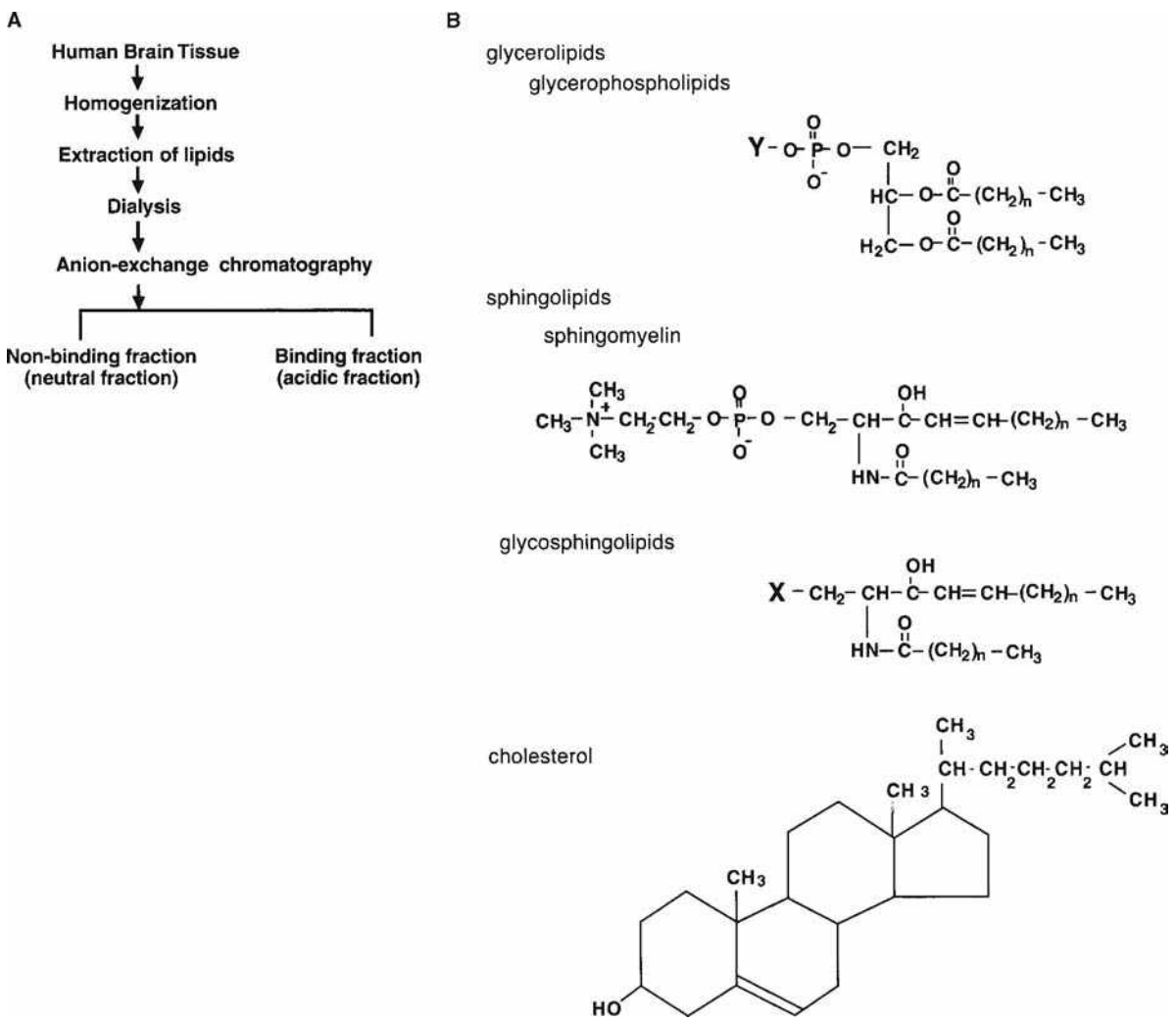

Fig. 1 A, Procedure to obtain acidic and neutral fractions; B, General structures of lipids analyzed in this study. Glycosphingolipid is composed of a ceramide (a hydrophobic-tail group) and a carbohydrate (X). X represents various sugar chains. If the X contains sialic acid, it is called a ganglioside. The gangliosides are eluted as acidic fraction in anion-exchange column chromatography. A glycerophospholipid is composed of diacylglycerol (a hydrophobic-tail group) and Y. Y is a hydrophilic head group. Phospholipid classes show differences in Y residue as follows: –H, PA; $–CH_2CH_2NH_3$, PE; $–CH_2CHN(CH3)_3$, PC; $–CH_2CHNH_3 + COO–$, PS; myo-inositol, PI.

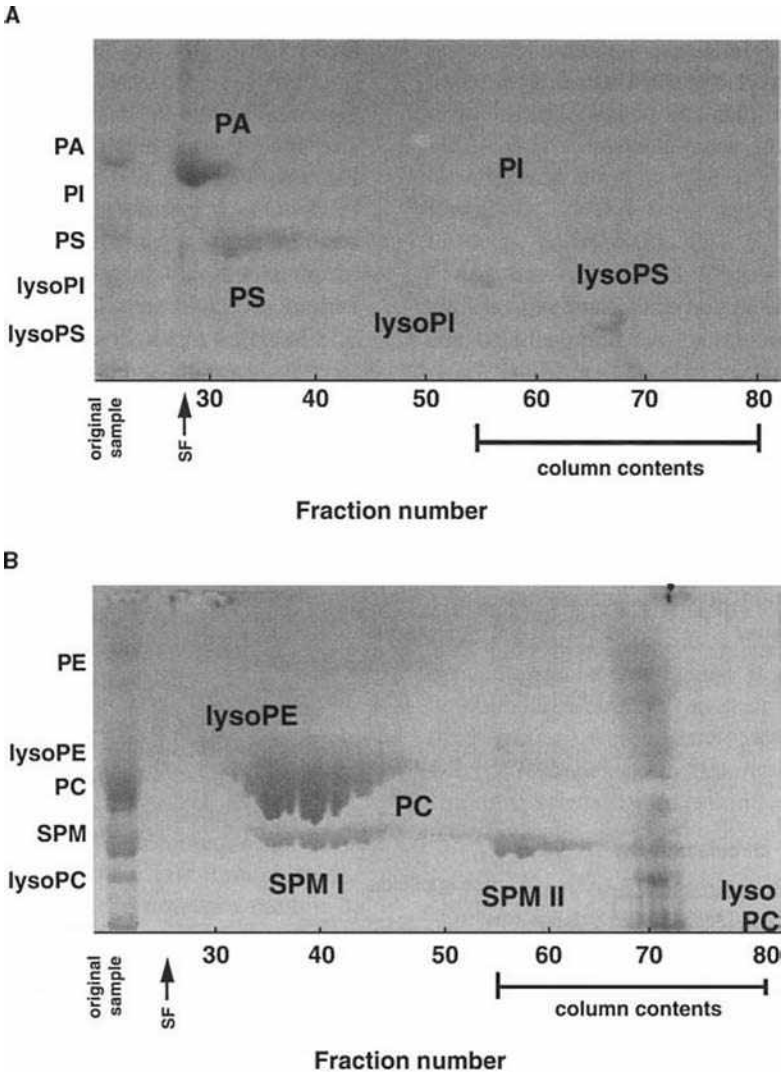

Fig. 2 Separation of acidic phospholipids in the human brain. A, The solvent system used for TC-CCC was chloroform/methanol/water (5:4:3). The lower phase (organic phase) was mobile. The revolution speed was maintained at 1500–700 rpm. The highest column pressure was 350 psi. A 2 mg portion of the acidic fraction of human brain lipids was loaded. Each fraction was spotted and developed on the HPTLC using chloroform/methanol/0.2% $CaCl_2$ (60:32:4). Phospholipids were stained with Dittmer's reagent. PA, phosphatidic acid; PS, phosphatidylserine; PI, phosphatidylinositol; lysoPI, phosphatidylinositol; lysoPS, lyso phosphatidylserine. SF, solvent front. (B) Separation of neural phospholipids in the human brain. The solvent system used for the TC-CCC was hexane/ethyl acetate/ethanol/0.1% aqueous ammonia (5:5:5:4). The upper phase (organic phase) was mobile. The revolution speed was controlled to run from 1500 to 700 rpm. The highest column pressure was 350 psi. A total of 5 mg of a neutral fraction of human brain lipids was loaded. Each fraction was spotted and developed on the HPTLC sing chloroform/methanol/0.2% $CaCl_2$ (60:32:4). Phospholipids were stained with Dittmer's reagent. PC, phosphatidylcholine; SPM, sphingomyelin; PE, phosphatidylethanolamine; lysoPE, lysophosphatidylethanolamine; lysoPC, lysophosphatidylcholine. SF, solvent front.

Phospholipids were visualized as blue-colored bands by using Dittmer's reagent, which specifically stains phospholipids. Phosphatidylinositol is completely separated from phosphatidic acid (PA) and phosphatidylserine (PS). The PA, which is the most hydrophobic phospholipid in this solvent system, eluted first, followed by PS, PI, lysoPI, and lysoPS. These phospholipids were identified by using phospholipid standards. The minor phospholipid components (fr. 65–68) may either be phosphatidylinositol phosphate (PIP) or phosphatidylinositol bisphosphate (PIP2). Each phospholipid (e.g., PS or PI) was further separated into some groups, because each phospholipid has various molecular species, which are derived from variations of hydrophobic tails (ceramide or diacylglycerol). Glycolipids were visualized as pink- or purple-colored bands by using orcinol reagent (data not shown). Sulfatides (fractions [frs.] 40–64) and gangliosides (GM1, GD1a, and GD1b) (frs. 68–70) were eluted. The abbreviations for gangliosides (GM1, GD1a, and GD1b) are according to Svennerholm's nomenclature. The sulfatides and phospholipids were eluted in the same fraction by TC-CCC.

Separation of the Neutral Fraction

Most of the lipids of the neutral fraction were eluted at the solvent front when the chloroform/methanol/water solvent system, which is suitable for the separation of the acidic fraction, was used. We then tried solvent systems which can separate more hydrophobic lipids. Using the hexane/ethyl acetate/ethanol/0.1% aqueous ammonia solvent system, we could separate phospholipids (Fig. 2B) and glycolipids (data not shown). A 5 mg amount of a neutral fraction from human brain lipids was applied to TC-CCC by using hexane/ethyl acetate/ethanol/0.1% aqueous ammonia (5:5:5:4). Phosphatidylcholine (PC), sphingomyelin (SPM), and lysophosphatidylcholine (lysoPC) were successively eluted. Phosphatidylethanolamine (PE) and lysophosphatidylethanolamine (lysoPE) and other minor phospholipid components were retained as the column contents with this solvent system. Cerebroside (fr. 28/36) and some other neutral glycolipids (frs. 35–43 and 55–63) were visualized on HPTLC when we used orcinol staining (data not shown). Cholesterol (Chol) is eluted at the solvent front (frs. 28–32)

and non-specifically stained (a brown color). It should be noted that SPM, which is usually difficult to separate into two groups with a silica bead column, is completely separated into two groups (SPM I and SPM II) (Fig. 2).

Separation of Less-Polar Neutral Lipids

Cholesterol and cerebrosides were difficult to separate via the hexane/ethyl acetate/ethanol/0.1% aqueous ammonia system. Therefore we used another solvent system to separate less hydrophobic lipids. A 5 mg amount of a neutral fraction from human brain lipids was applied to TC-CCC by using hexane/ethanol/water at a volume ratio of 10:15:4 (Fig. 3). In Fig. 3, the orcinol staining shows the specific purple color for cerebroside (CS) and ALGLs,[3] and a non-specific brown color for other lipids (not identified). Most of the phospholipids and glycolipids were retained in the column contents. Cholesterol was isolated from other lipids (frs. 38–43) (Fig. 3A). Cerebroside is eluted at frs. 60–72.

We changed the composition of the solvent system to determine whether TC-CCC could separate molecular species of CS. Fig. 3B shows the result when we used hexane/ethanol/water at a volume ratio of 5:4:3. It has been reported that CS is composed of more than 100 molecular species. The difference in intensity in the two bands represents the different molecular species. To show more clearly that TC-CCC can separate molecular species, the following studies were carried out.

Separation of Molecular Species

To assess the ability of the TC-CCC molecular species, two molecular species of phosphatidylcholine, which weresynthesized, were subjected to TC-CCC. Dipalmitoyl phosphatidylcholine (PC C16:0) and distearoyl phosphatidylcholine (PC C18:0), two of the major molecular species of phosphatidylcholine, were completely separated as shown in Fig. 4. Distearoyl phosphatidylcholine contains 2 mol of esterified stearic acids and dipalmitoyl phosphatidylcholine contains 2 mol of esterified palmitic acid. The structures of these compounds are shown in Fig. 4. These two compounds were completely separated. This result indicates that the TC-CCC system can separate molecular species in both phospholipids and glycolipids categories.

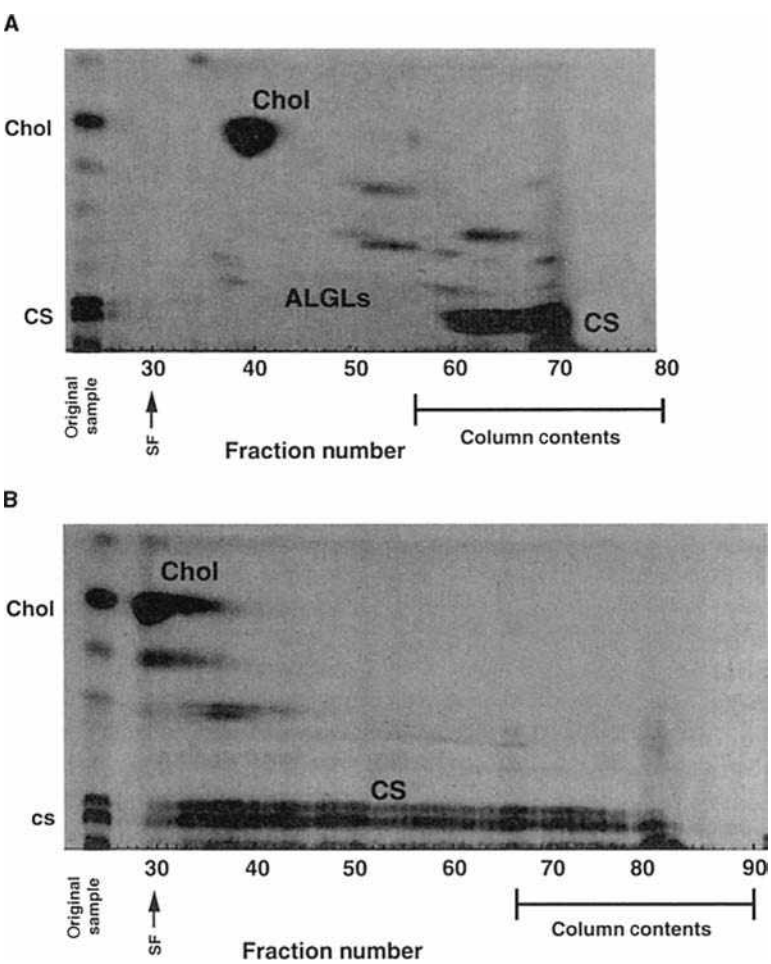

Fig. 3 Separation of highly non-polar neutral glycolipids in the human brain. The solvent system used for the TC-CCC was hexane/ethanol/water (10:15:4) (A) and (5:4:3) (B). The upper phase (organic phase) was mobile. The revolution speed was controlled to run from 1500 to 700 rpm. The highest column pressure was 350 psi. A total of 5 mg of a neutral fraction of human brain lipids was loaded. Each fraction was spotted and developed on the HPTLC using chloroform/methanol/0.2% $CaCl_2$ (90:12:1). Chol, cholesterol; CS, cerebroside. SF, solvent front.

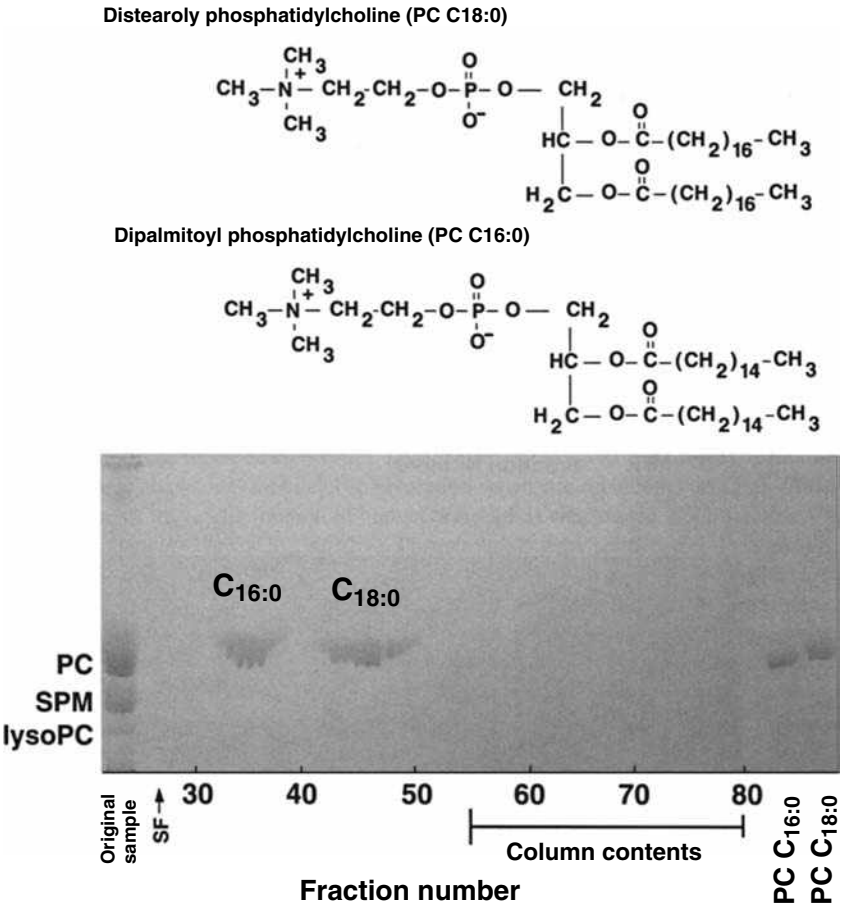

Fig. 4 Separation of dipalmitoyl phosphatidylcholine and distearoyl phosphatidylcholine. The solvent system used for the TC-CCC was hexane/ethyl acetate/ethanol/1% trifluoroacetic acid (5:5:5:4). The upper phase (organic phase) was mobile. The rotational speed was maintained at 1500–700 rpm. The highest column pressure was 360 psi. Amounts (100 μg each) of phosphatidylcholine dipalmitoyl and phosphatidylcholine distearoyl were loaded. Each fraction was spotted and developed on the HPTLC using chloroform/methanol/0.2% $CaCl_2$ (60:32:4). Distearoyl phosphatidylcholine contains 2 mol of esterified stearic acids and dipalmitoyl phosphatidylcholine contains 2 mol of esterified palmitic acids. PC C16:0, dipalmitoyl phosphatidylcholine; PC C18:0, distearoyl phosphatidylcholine. SF, solvent front.

DISCUSSION

Advantages of TC-CCC

Applications of countercurrent distribution to lipid purification were already reported in the 1950s. These included the isolation of PC, SPM, or cerebrosides from brain tissue,[9,10] or the placenta.[11] It was then mentioned that lipids easily emulsify, and this adversely affects the ability to separate them. Therefore these methods were only used for crude separation. The method also requires a long time for phase separation before each phase transfer, and this procedure needs to be repeated 500–3000 times. Otsuka and Yamakawa[12] reported the application of droplet CCC to the purification of phospholipids and glycolipids. Because the stationary phase retention is much more stable in TC-CCC than with HS-CCC, it has become possible to select appropriate two-phase solvent systems. In this study, we showed the successful separation of human brain lipids by using TC-CCC. Additionally, if an isolated band can be observed on HPTLC, the lipid can be purified by using silica column chromatography after TC-CCC crude separation.

Reverse-phase column chromatography using HPLC can be used to separate these compounds according to their hydrophobicities. However, the reported solvent systems contain salt. The TC-CCC system has an advantage in that lipids can be separated without the use of salted buffer. We plan to monitor the eluted lipids from TC-CCC by using a mass spectrometer, and this can be achieved employing salted, buffer-free solvent systems.

Separation of Molecular Species

In this paper, we have shown that this system can separate molecular species. One example is shown for cerebrosides (Fig. 3B). Human phospholipids and glycolipids have many forms (molecular species) because of the variation in fatty acids or ceramides. Phosphatidylcholine, sphingomyelin, and cerebroside are each reported to consist of more than 100 molecular species.[13] As shown in Fig. 4, it is possible to obtain better resolution by changing the flow rate and the volumes of the fractions. Furthermore, better conditions can be optimized by changing the composition of the solvents to target one lipid, as shown.

It should be emphasized that the SPM was completely separated into at least two groups (SPM I and SPM II). It was reported that there are two forms of dihydrosphingomyelin (DHS) and sphingomyelin (SPM) in commercially available bovine brain SPM;[14] SPM I and SPM II may correspond to these. TC-CCC is still in the prototype stage because there

are many factors that still need to be improved, e.g., the flow volume, the flow rate, and the tube length, as previously described. In addition, the injection system and the detection system could be improved. If these elements can be enhanced, resolution may dramatically improve.

Applications for Biological Analysis

There is a possibility that TC-CCC can be useful not only for the separation of lipids, but also as an instrument for showing the hydrophobic behavior of lipids in cell membranes. Both phospholipids and glycolipids are important components of cell membranes, in which molecular interactions between hydrophilic or hydrophobic molecules play an important role in a cell's physiology. Avoiding the effects of hydrophobicity in a solid phase system, we are able to study molecular interactions between lipids and hydrophobic molecules. The advantage of the present system is that the net partition behavior of molecules in the two-phase solvent system can be measured by monitoring the retention volumes of eluted molecules. As a result, we can obtain the partition coefficient (K) of molecules in the two-phase solvent system. This may provide a method for measuring the lipid–protein interaction in a cell membrane. This method may be useful for purifying and analyzing of caveolae, lipoprotein, or such hydrophobic microdomains in biomembranes.

Next, we determined appropriate solvent systems, and showed the hydrophobicity of lipids. In other words, most of the major human brain lipids were mapped with HPTLC using TC-CCC. Calcium plays an important role in a biomembrane. It is interesting to note that calcium improves the separation of lipids by the HPTLC.[15] In this system, it is possible to see the effect of either calcium or pH on the elution profiles of lipids.

CONCLUSIONS

Phospholipids, glycolipids, and cholesterol are the major components of mamalian cell-membrane lipids. They play important roles in cell-signaling transduction and cell-to-cell recognition or modification of enzyme functions. In this study, the TC-CCC system was applied to solve the problem of emulsification, and satisfactory stationary phase retention was obtained. Human brain lipids could then be separated. We established the solvent systems that are used for the separation of most of the phospholipids, glycolipids, and less-polar lipids of the human brain. Furthermore, we demonstrated that molecular species, which are derived from variations of the hydrophobic tail group, were separated by optimizing the composition of the solvents. TC-CCC is available for analyzing the hydrophobicities of various lipid molecules in biomembranes.

ACKNOWLEDGMENT

The authors thank Dr. Henry M. Fales of the National Institutes of Health for editing the manuscript with valuable suggestions.

REFERENCES

1. Ito, Y.; Bowman, R.L. Countercurrent chromatography: Liquid-liquid partition chromatography without solid support. Science **1970**, *167*, 281–283.
2. Ito, Y.; Bowman, R.L. *Countercurrent Chromatography*; Mandava, N.B., Ito, Y., Eds.; Marcel Dekker, Inc: New York, 1988; 79.
3. Matsuda, K.; Ma, Y.; Baughout, V.; Ito, Y.; Chatterjee, S. Isolation of less polar alkali-labile glycolipids of human brain by high-speed countercurrent chromatography. J. Liq. Chromatogr. Relat. Technol. **1998**, *21*, 103–110.
4. Matsuda, K.; Matsuda, S.; Ito, Y. Toroidal coil countercurrent chromatography: Achievement of high resolution by optimizing flow-rate, rotation speed, sample volume and tube length. J. Chromatogr. A, **1998**, *808*, 95–104.
5. Matsuda, K.; Matsuda, S.; Saito, M.; Ito, Y. Separation of phospholipids and glycolipids using analytical toroidal-coil countercurrent chromatography. I. Separation of human brain lipids. J. Liq. Chromatogr. Relat. Technol. **2002**, *25*, 1255–1269.
6. Ito, Y.; Suaudeau, J.; Bowman, R.L. New flow-through centrifuge without rotating seals applied to plasmapheresis. Science **1975**, *189*, 999–1000.
7. Svennerholm, L. The quantitative estimation of cerebrosides in nervous tissue. J. Neurochem. **1956**, *1*, 42–53.
8. Dittmer, J.C.; Lester, R.L. A simple, specific spray for the detection of phospholipids on thin-layer chromatograms. J. Lipid Res. **1964**, *5*, 126–127.
9. Nielsen, K. A preliminary note on the composition of the non-hydratable soyabean phosphatide. Acta Chem. Scand. **1955**, *9*, 173.
10. Cole, P.; Lathe, G.; Ruthven, C. The application of countercurrent methods to the fractionation of lipid material from brain. Biochem. J. (London) **1953**, *54*, 449–458.
11. Lovern, J. The application of counter-current distribution to the separation of phospholipids. Biochem. J. (London) **1952**, *51*, 464–470.
12. Otsuka, K.; Yamakawa, T. The application of droplet counter-current chromatography (DCC) for the separation of acidic glycolipids. J. Biochem. (Tokyo) **1981**, *90*, 247–254.
13. Kim, Y.; Wang, T.C.; Ma, Y.C. Liquid chromatography/mass spectrometry of phospholipids using electrospray ionization. Anal. Chem. **1994**, *66*, 3977.
14. Byrdwell, Y.C. Dual parallel mass spectrometers for analysis of sphingolipid, glycerophospholipid and plasmalogen molecular species. Rapid Commun. Mass Spectrom. **1998**, *12*, 256–272.
15. Svennerholm, L. Chromatographic separation of human brain gangliosides. J. Neurochem. **1963**, *10*, 613–623.

Lipids: HPLC Analysis

Jahangir Emrani
Department of Civil and Environmental Engineering, North Carolina A & T State University, Greensboro, North Carolina, U.S.A.

INTRODUCTION

Lipids are mixtures of fatty molecules that contain polar and non-polar groups. Polar lipids include phospholipids and glycolipids, whereas non-polar lipids include fatty acids and their esters, cholesterol and its esters, essential oils, wax esters, and squalene. Lipids are important ingredients in the production of modern food and play key roles in physiological systems. The role of lipids in certain cardiovascular and dermotological conditions has been established. Understanding the roles of lipids in cellular and physiological systems have been the driving force behind recent developments in lipid analysis. Historically, thin-layer chromatography (TLC) and gas chromatography (GC) have been used for the analysis of lipids. Due to the limitations of these techniques and the advances in high-performance liquid chromatography (HPLC) detection technology, HPLC is gaining popularity for lipid analysis. The high temperatures used in the GC causes degradation of some molecules, whereas many fat molecules are not volatile enough to go through the GC. On the other hand, detection of fats on TLC is somewhat cumbersome.

Today, HPLC is the dominant analytical technique used for the analysis of most classes of compounds. The analyses can be carried out at room temperature and the collection of fractions for reanalysis or further manipulation is straightforward. The main reason for the slow acceptance of the HPLC technique for lipid analysis has been the detection system. Traditionally, HPLC used ultraviolet/visible (UV/Vis) detection, which requires the presence of a chromophore in the analyte. Most lipid molecules do not contain chromophores and therefore would not be detected by UV/Vis. Modern HPLC detection techniques, such as the use of a mass spectrometer as the detector, derivatization techniques to introduce chromophores, and the availability of pure solvents to reduce interference, have allowed HPLC to compete with and/or complement GC and other traditional methods of lipid analysis. In addition to analytical HPLC, preparative HPLC has been used extensively to collect pure samples of the lipids for the derivatization or synthesis of new compounds.

MODES OF SEPARATION OF LIPIDS BY HPLC

The mode of separation in the HPLC depends on the selection of the stationary and mobile phases. In HPLC of lipids, normal- and reversed-phase modes are primarily used, with the reverse phase being more common than the normal phase. Separation in the reversed-phase mode is mainly by partition chromatography, whereas separation in the normal phase mode is primarily by adsorption chromatography. Normal-phase HPLC is used for the separation of the lipids into classes of lipids.[1] Reversed-phase HPLC (RP-HPLC), on the other hand, is mainly used to separate each lipid class into individual species.[2,B1] For example, several triglycerides were separated from each other via non-aqueous reversed-phase HPLC, involving an octadecyl (ODS) column and a non-polar (non-aqueous) mobile phase. RP-HPLC alone can be used to separate the fat molecules into classes and species.[2,B1]

In reversed-phase chromatography of lipids,[B2] the lipophilic interaction between the octadecyl chains of the column and the fatty molecules of the analyte determines the retention. For this reason, the retention times of the lipid molecules depend on the stationary-phase chain length and number of double bonds in each lipid structure. In general, the retention time increases as the number of double bonds decrease. Glycerides with the shortest acyl chain length and highest number of double bonds elute first. This general rule applies if the column contains a stationary phase. Using such a general correlation and knowing the relative retention time of a reference compound such as a phospholipid on ODS columns, the retention time of other phospholipids can be calculated.[B1]

In addition to normal- and reversed-phase chromatography, silver ion HPLC, RP ion-pair HPLC, chiral separation, and supercritical fluid chromatography (SFC) have been used for analysis of lipids.[3] In silver-ion HPLC, the counterion of an ion-exchange column such as sulfonate is exchanged with silver ions. Only the degree of unsaturation in the lipid molecule determines retention. In RP ion-pair HPLC, different ion-pairing agents, such as alkylamonium phosphates, are added to the ODS column for molecular species separation. In SFC, which is used in combination with flame ionization detection (FID), solubility of lipids in carbon dioxide allows the separation to be performed. This mode of analysis is not widely used.

SELECTION OF THE STATIONARY PHASE

The type of packing in the HPLC column is the most important factor affecting the HPLC separation. Silica is

the most common packing material for normal-phase chromatography because it is stable under pressure and has a neutral pH. Silica-bonded and on the other hand, are the most common packing materials for RP chromatography because they are stable to pressure and low pH. Diol-bonded phases are also used as polar column packing.[4] In cases where gradient elution is necessary, diol-bonded stationary phases are more suitable than silica. For lipid classes found in plants, chemically bonded phases have produced better resolution than silica gel.[5] Cyanopropyl, amino, and other stationary phases have all been used. Aminopropyl phases are suitable for acidic and non-polar lipids. These columns are compatible with commonly used solvents and modifiers. Florisil is another stationary phase used for the separation of lipids; however, irreversible retention may occur.

The method of stationary-phase preparation has a major effect on the resolution, column stability, retention time, reproducibility, and peak shape. When preparing or for example, it is important that the residual silanol groups are capped to prevent peak tailing. The extent of capping must be consistently maintained between different batches of the stationary phase for reproducible results.

In terms of particle size and column dimensions, stationary phases with particle sizes of 5–10 μmm in 250×4.6 mm analytical columns are most common. HPLC columns with smaller particle sizes (2–3 mm) have also been prepared and used. Such columns have the advantages of higher efficiency, better resolution, and shorter analysis times. For example, the triglycerides of cocoa butter were baseline separated with columns that contained 2–3 mm particles. Research and development of columns with smaller particles is very active.

SELECTION OF THE MOBILE PHASE

The mobile phase consists of one or more solvents that are pumped through the chromatographic system, resulting in the separation of analytes. Mobile phases may also contain modifiers. Examples of frequently used solvents include hexane, methanol, 2-propanol, acetonitrile (ACN), and water. Examples of modifiers include tri-fluoroacetic acid, acetic acid, or formic acid. In general, the composition of the mobile phase should be kept simple. Factors that influence the choice of mobile phase include the solubility of the sample in the mobile phase, the polarity of the mobile phase, ultraviolet absorption wavelength, refractive index, and viscosity of the solvents. The purity of the solvents in the mobile phase is also important because the region of UV that is used for the detection of lipids (200–215 nm) must be free of interferences. For phospholipids, the most popular solvent systems are transparent to UV in the range of 200–215 nm; they include hexane–2-propanol–water and acetonitrile–methanol–water. Variations include hexane–methanol–isopropanol or water–methanol. The ratios of these solvents in the mobile phase depends on the nature of the lipid substances being separated. Several examples of mobile phases commonly used in the analysis of lipids are listed in the general references.

In order to separate the molecular species of lipids that have very close characteristics, small differences such as the number of double bonds in each molecule can occasionally be used as a guide to devise a solvent system to separate the molecules. This method is not always successful and may have to be further optimized for a good separation.

DETECTION

No single HPLC detector has all the characteristics of a good detector, which include sensitivity, specificity, detectability, linearity, repeatability, and dependability. Detection by UV/Vis is widely used for the analysis of lipids; it is simple, concentration sensitive, and non-destructive. However, the analyte to be monitored by UV/Vis absorption must contain a chromophore, and because many fat molecules do not contain a chromophore, this detection system cannot be used in many cases. Fortunately, in cases where no chromophore is present in the molecule, a chromophore can be introduced through derivatization. If the derivatization is done before the analyte enters the column, it is called precolumn derivatization, whereas if it is done after the elution of analyte, it is called postcolumn derivatization.

For the detection of phospholipids, UV/Vis at 205 nm is often used. In cases where the molecules contain several lipid groups, UV detection in the range of 205–215 nm has been used. Vitamin E, α-, β-, δ-, and γ-tocopherols have been analyzed by RP-HPLC using UV at 215[B1] and 280 nm. In other cases, UV diode-array detection at 190–350 nm or 200–400 nm has been used. Tocopherols and triglycerides from vegetable oils and human lipoproteins were analyzed by RP-HPLC using a UV/Vis diode-array detector. With diode-array detection, UV spectra of the peaks can be collected during the analysis. In many analyses, the UV absorption of the lipid analyte is due to the carbonyl group in the actyl group of the molecules.

More recently, a less sensitive detection technique, refractive index (RI) detection, has been used. The disadvantage of RI is that one is limited to isocratic elution, because RI detection is affected by changes in the pressure and temperature of the mobile phase. On the other hand, infrared (IR) detection can be used when the solvents in the mobile phase do not absorb infrared light, which can create interference. Because of these limitations, RI and IR have not been used as widely as UV detection.

In contrast, newer techniques such as FID and evaporative light-scattering detection (ELSD, "Universal Detector") are more sensitive and have been used for the analysis of many lipids, including the polar and neutral lipid classes.[6] For preparative scale separations, if the UV absorbance is more than what the detector can handle, an ELSD is used.[B2]

Fluorescence (FL) detection is another selective and sensitive technique. Vitamin E, α-, β-, δ-, and γ-tocopherols have been analyzed by RP-HPLC using FL as well as UV detection. In addition, a newer technique, electrochemical detection, has been reported in the analysis of phenolic compounds of olive oil.[7]

Finally, the detection by liquid chromatography/mass spectrometry (LC/MS), which has been largely dependent on the price, mode of ionization, and ease of operation of the mass spectrometer, is becoming popular.[8] It is predicted that LC/MS will become the method of choice for lipid analysis in coming years.

DERIVATIZATION

Samples of lipids may be derivatized either before they are injected into the HPLC or after they emerge from the HPLC column. The purpose of derivatization is either to make the lipid molecules detectable or to improve peak shape during the analysis. The addition of functional groups, such as phenyl, 2,4-dinitrophenyl, or anisyl to the molecule enhances the detectability by changing the absorption wavelength of a lipid molecule. On the other hand, making derivatives such as acetates or methyl esters help to improve the peak shape. To make the lipid molecules fluorescent, groups such as anthroyl, 7-methoxycoumaryl, naproxen, and naphthyl[B1] are added to the lipid molecules. The reactions are carried out postcolumn and the derivatized molecules can be detected by both excitation and emission. For the detection of fatty acids, they are derivatized by reacting with either *p*-bromophenacylbromide, 9-anthryldiazomethane, or bromomethyl-methoxy-cumarin. These derivatizations also make the molecules UV absorbers. Fatty acids have also been analyzed directly without derivatization using conductivity for detection (Fig. 1).[9] Many examples of derivatization techniques have been tabulated in Ref.[B1] Phosphatidilic acids, which result from the enzymatic reaction of phospholipase D with phospholipids, are derivatized to the methyl ester by treatment with diazomethane. In the reaction, the phosphate salt is converted to a neutral organophosphate, thereby changing its chromatographic behavior without affecting UV absorption of the lipid. Several commercially available phosphatidylethanolamines (PEs) have been derivatized for HPLC analysis as dansyl, pyrenesulphonyl, and fluoresceinthiocarbomoyl derivatives. Diacylglycerol acetates, from bovine brain ethanol-amineglycerophospholipid (EGP), were separated into molecular species using an ODS column. The chromatograms of derivatized phospholipids showed better resolution when compared with the chromatograms of underivatized phospholipids.

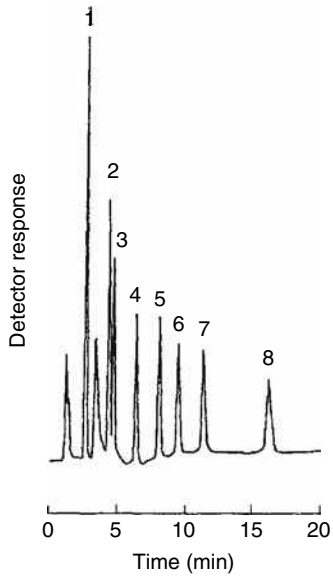

Fig. 1 Separation of free fatty acids by HPLC with conductivity detection. Mobile phase is methanol–5 m*M* tetrabutylammonium salt (75:25, v/v; pH 7.5) at a flow rate of 0.8 ml/min. Peaks: 1, lauric (12:0); 2, myristic (14:0); 3, linolenic (18:3); 4, linoleic (18:2); 5, palmitic (16:0); 6, oleic (18:1); 7, margaric (17:0); 8, stearic acids (18:0).
Source: From High-performance liquid chromatography of phosphatidic acid, in J. Chromatogr. B.[9]

SAMPLE CLEANUP

Before analysis, lipids are extracted from biological matrices with either a single organic solvent or a mixture of several organic solvents, such as chloroform–methanol or 2-propanol–hexane. Some lipids that contain several double bonds are easily oxidized by air during extraction. To prevent oxidation of such lipids, it is best to perform the extraction in an atmosphere of nitrogen and/or at low temperature. Prior to extraction, an antioxidant, such as BHT, may be added to inhibit oxidation. After the extraction, the extracts are cleaned up by solid-phase extraction (e.g., aminopropyl), column chromatography, or TLC.[10] Then, one-dimensional or two-dimensional TLC is used to separate the lipids. The separated lipids are eluted from the silica gel by scraping the zones of interest from the plate and extracting the lipids with a solvent.

In many cases, HPLC can replace TLC in this step. HPLC has the advantage that, during the analysis, oxygen-sensitive lipids are not exposed to air and autoxidation is limited. After the cleanup steps, samples are analyzed by GC or HPLC. Analysis of triglycerides often involves saponification before the HPLC analysis. Because samples of lipids may originate from a variety of different sources,

the specific cleanup steps prior to analysis depend largely on the sample and the original sample matrix. For analysis of cholesterol in blood plasma, a sample of plasma was mixed with isopropanol and centrifuged. After centrifugation, the supernatant was directly analyzed by HPLC.[10] For analysis of monoglycerides in emulsifiers, the sample was dissolved in hexane–2-propanol (90:10), diluted, and injected into the HPLC. For analysis of vegetable oils, a dilute solution of oil in hexane–2-propanol is prepared and analyzed.

For quantitation of cholesterol and its derivatives in muscle and liver tissues, the extracts of the tissue homogenates are evaporated, dissolved in a mobile phase such as hexane–isopropanol, and injected onto a normal-phase column. For analysis of soybean oil by reversed-phase HPLC, after extraction with chloroform–methanol (9:1), the neutral lipids, chlorophyls, and the phospholipids are separated by TLC. The lipids recovered from the TLC are analyzed by HPLC.

EXAMPLES OF LIPID ANALYSIS BY HPLC

For examples of separation of lipids see general references. For tabulated examples, see Ref.[B1] for separation of molecular species of phospholipids by HPLC, Ref.[I] for separation of lipids in food by HPLC, Ref.[H] for HPLC of phosphatidic acid, and Ref.[B2] for preparative HPLC of lipids.

For separation of intact polar lipids by HPLC and detection by mass spectrometer, see Ref.[8] For triglycerides and fatty acids, see Ref.[B4] For separation of neutral lipids into classes and species, see Ref.[2]

ACKNOWLEDGMENTS

The author wishes to thank Sue Hammer for preparation of the manuscript, Andrea Wong for reviewing the manuscript, and Peter Austin for library searches.

REFERENCES

1. Hamilton, J.G.; Comai, K. Separation of neutral lipid, free fatty acid and phospholipid classes by normal phase HPLC. Lipids **1988**, *23*, 1150–1158.
2. Antonopoulou; Andrikopolos, N.K.; Demopoulos, C.A. Separation of the main neutral lipids into classes and species by RP-HPLC and UV detection. J. Liquid Chromatogr. **1994**, *17* (3), 633–648.
3. Christie, W.W. Some recent advances in the chromatographic analysis of lipids. ANALUSIS Mag. **1998**, *26* (3), M34–M40.
4. Elfman-Borjesson, I.; Harrod, M. Analysis of nonpolar lipids by HPLC on a diol column. J. High Resolut. Chromatogr. **1997**, *20*, 516.
5. Christie, W.W.; Anne Urwin, R. Separation of lipid classes from plant tissues by HPLC on chemically bonded stationary phases. J. High Resolut. Chromatogr. **1995**, *18*, 97.
6. Liu; Lee, T.; Bobik, E., Jr.; Guzman-Harty, M.; Hastilow, C. Quantitative determination of monoglycerides and diglycerides by HPLC and evaporative light-scattering detection. J. Am. Oil Chem. Soc. **1993**, *70*, 343.
7. Seta, K.; Nakamura, H.; Okuyama, T. Determination of a-tocopherol, free cholesterol, esterified cholesterols and triacylglycerols in human lipoproteins by HPLC. J. Chromatogr. **1990**, *515*, 585–595.
8. Karlsson, A.A. Analysis of intact polar lipids by HPLC mass spectrometry/tandem mass spectrometry with use of thermospray or atmospheric pressure ionization. In *Lipid Anal. Oils Fats*; Hamilton, R.J., Ed.; Blackie: London, 1998; 290–316.
9. Abidi, S.L.; Mounts, T.L. High-performance liquid chromatography of phosphatidic acid. J. Chromatogr. B, **1995**, *671*, 281–297.
10. Nissen, H.P.; Kreysel, H.W. The use of HPLC for determination of lipids in biological samples. Chromatographia **1990**, *30* (11/12), 686.

GENERAL REFERENCES

For important references in lipid analysis see Appendices in *Advances in Lipid Methodology, Volumes 1–4* (W.W. Christie, ed.), The Oily Press, Dundee (1990, 1992, 1994, 1997).

For more detailed description of the subjects consult the following:

- The following chapters in *Advances in Lipid Methodology, Volume 4*: (B1) Chapter 2, Separation of molecular species of phospholipids by high-performance liquid chromatography, M.V. Bell; (B2) Chapter 3, Preparative high-performance liquid chromatography of lipids, P. Van der Meeren and J. Vanderdeelen; (B3) Chapter 4: Structural analysis of fatty acids, W.W. Christie; (B4) Chapter 6: Reverse-phase high-performance liquid chromatography: General principles and application to the analysis of fatty acids and triglycerols, B. Nikolova-Damyanova.
- The following chapters in *Advances in Lipid Methodology, Volume 3*: (C1) Chapter 3, Separation of phospholipid classes by high-performance liquid chromatography. W.W. Christie; (C2) Chapter 6, Plant glycolipids: Structure, isolation and analysis, E. Heinz.
- The following chapters in *Advances in Lipid Methodology, Volume 2*: (D1) Chapter 2, Preparation of ester derivatives of fatty acids for chromatographic analysis, W.W. Christie; (D2) Chapter 3, Size

exclusion chromatography in the analysis of lipids, M.C. Dobarganes and G. Marquez-Ruiz; (D3) Chapter 5, Capillary isotachophoresis in the analysis of lipoproteins, G. Schmitz, G. Nowicka, and C. Mollers; (D4) Chapter 6, Preparation of lipid extracts from tissues, W.W. Christie.

- The following chapters in *Advances in Lipid Methodology, Volume 1*: (E1) Chapter 1, Solid-phase extraction columns in the analysis of lipids, W.W. Christie; (E2) Chapter 3, Supercritical fluid chromatography of lipids, P. Laakso; (E3) Chapter 4, The chromatographic resolution of chiral lipids, W.W. Christie; (E4) Chapter 6, Silver ion chromatography and lipids, B. Nikolova-Damyanova; (E5) Chapter 7, Detectors for high-performance liquid chromatography of lipids with special reference to evaporative light-scattering detection, W.W. Christie.

BIBLIOGRAPHY

1. Tsuyama, Y.; Uchida, T.; Goto, T. Analysis of underivatized C12-C18 fatty acids by reverse phase ion-pair high-performance liquid chromatography with conductivity detection. J. Chromatogr. **1992**, *596*, 181–184.
2. Berg, K.A.; Canessa, C.E. HPLC applications in food and nutritional analysis. In *Chromatographic Science*; Nollet, L.M.L., Ed.; Marcel Dekker, Inc.: New York, 1998; Vol. 78, 753–787.
3. Christie, W.W. Lipid class separations using high performance liquid chromatography. In *New Trends in Lipid and Lipoprotein Analyses*; Sebedio, J.L., Perkins, E.G., Eds.; AOCS Press: Champaign, IL, 1995; 1934 pp.
4. Shulka. High performance liquid chromatography, normal phase, reverse phase detection methodology. In *New Trends in Lipid and Lipoprotein Analyses*; Sebedio, J.L., Perkins, E.G., Eds.; AOCS Press: Champaign, IL, 1995; 38 pp.

Lipids: Solid-Phase Extraction Purification

Jacques Bodennec
Department of Biological Chemistry, Weizmann Institute of Science, Rehovot, Israel

Jacques Portoukalian
Laboratory of Tumor Glycobiology, University Claude Bernard Lyon I, Oullins, France

INTRODUCTION

In recent years, solid-phase extraction (SPE) has emerged as an important tool for the purification of compounds in various fields of chemistry and biochemistry. This technique is taking place with others such as thin-layer chromatography (TLC) and high-performance liquid chromatography (HPLC) in the wide range of preparative tools available to the analyst. SPE technology is relatively new, as the first applications were published during the past two decades, and its real development occurred only in the nineties. The advantages of SPE, as compared to other methods, makes it an attractive method of choice for purification of molecules. Among these advantages are less time and lower solvent consumption when compared to classical liquid–liquid extraction, low cost, and excellent reproducibility of SPE products. Moreover, SPE is easily automated, so that numerous samples can be processed at the same time. SPE is frequently used in lipid chemistry and biochemistry for the isolation of particular compounds or groups of molecules for analytical or preparative purposes.[1–3] Here, we will focus on the applications of SPE in the field of lipid biochemistry, and, primarily, on the use of the aminopropyl-bonded silica gel matrix for lipid fractionation.

GENERAL PRINCIPLES AND METHODOLOGY OF SPE

SPE is a technique which is used for concentration and purification of analytes from solution by adsorption onto a disposable solid-phase-containing cartridge, disk, or syringe barrel, followed by elution of analytes with an appropriate solvent. From a general point of view, the principles of SPE are the same as conventional LC and HPLC, so that the retention and elution depend on interactions of the analyte with the stationary solid and mobile liquid phases. Retention mechanisms include normal and reversed phases and ion exchange. The SPE procedure begins by sorbent conditioning to remove cartridge impurities and to wet the functional groups at the surface of the matrix. Then, the sample is loaded onto the SPE matrix and the sorbent is rinsed to remove the components which are not desired. In a final step, the analytes are eluted from the SPE matrix and recovered in an appropriate solvent for further analysis. A wide variety of solid phases are available. Most applications are performed on the silica gel solid phase, which can be bonded with the same substituents used for HPLC or conventional LC columns. SPE principles are described in detail in adhoc reviews or books.[1,4] This method (as with all chromatographic methods) requires an accurate determination of the conditions of column preparation, sample loading, and stepwise elution. Hence, incomplete elution or analyte breakthrough can occur if optimal conditioning or elution parameters are not well defined. A good choice of solid sorbent must be made according to the nature of the analytes that are to be recovered. The choice of solvents and their volumes, as well as flow rates, must also be carefully determined to ensure optimal recovery of analytes. An understanding of the interactions between sorbent and analytes is needed to develop and optimize SPE procedures.[4]

Its advantages and ease of use have made SPE an appropriate method for concentration and fractionation of lipid classes.[2,3] Many different solid-phase types have been used in lipid fractionation on silica, alumina, porous carbon, and ion-exchange resins. Various bonded phases have been used, particularly with the silica gel matrix.

SEPARATION OF LIPID CLASSES BY REVERSED-PHASE SPE

The reversed-phase procedure has been applied in some cases for the isolation of lipid classes on SPE columns. This procedure is mainly suitable for the isolation of lipids dissolved in polar solvents, such as aqueous samples. The mechanism involves partitioning of organic solutes from the polar mobile phase to a non-polar sorbent phase, which can be C_2, C_4, C_8, and C_{18} aliphatic chains, or cyclohexyl and phenyl groups. Elution of analytes is accomplished by choosing a solvent that will disrupt the van der Waals forces retaining the molecules on the matrix. Methanol, ethyl acetate, and acetonitrile are often used for this purpose, as they can overcome van der Waals forces and they succeed in bonding to free silanol groups of the column and dissolve residual water coming from the aqueous matrix sample. Reversed-phase separations are not as common as

normal-phase separation of lipids by SPE. C_{18} SPE tubes have been often used in the isolation of phosphatidylcholine, cerebrosides, sulfatides, and gangliosides from water-soluble compounds (Figlewicz et al. 1985, quoted in Ref.[2]). C_{18} has been shown to be an efficient tool for the purification of these lipids and is easier to use than other liquid–liquid methods. Reversed-phase SPE columns have also been used for the isolation of short- and long-chain fatty acids from distilled water and seawater (Pempkoviak 1983, quoted in Ref.[2]). For more information on the use of SPE in the reverse phase, references cited at the end of this entry should be consulted.

SEPARATION OF LIPID CLASSES BY NORMAL-PHASE SPE

Most of applications deal with silica gel sorbent and with aminopropyl-bonded silica sorbents. Silica is a sorbent of choice for lipid fractionation, because these analytes are first recovered in non-polar solvents as chloroform. The polar silanol groups present at the surface of the silica sorbent will more strongly adsorb polar compounds such as phospholipids, rather than neutral lipids such as sterols and triglycerides. The retention of analytes and their elution will depend on solvent polarity. The mildly acidic nature of silica can also interfere with the separation mechanism by ion-exchange effects. Silica matrix solid-phase extraction has been used to purify some individual lipid classes, such as phosphatidylcholine (PC) or phosphatidylethanolamine (PE) from total lipids. More complex separations are also possible with silica SPE columns. Hence, a procedure for isolating cholesterol esters, triglycerides, free fatty acids (FFAs), cholesterol, acidic phospholipids such as phosphatidylinositol (PI) and phosphatidylethanolamine (PE) from a neutral phospholipid fraction containing PC, lyso-PC, and sphingomyelin (SPH) has been described.[5] This procedure was modified and adapted for further isolation of specific classes of molecules such as the choline phospholipid platelet-activating factor (PAF).

Numerous chemically bonded stationary phases can be formed by reacting the silanol groups of silica with various organic reagents. These can be successfully used for the isolation of specific lipid classes, because the bonded phases will have greater bonding potential for some specific molecules according to their functional groups. This is the case for aminopropyl-bonded phases whose primary amine group can develop a strong interaction by hydrogen-bonding with molecules having functional groups such as hydroxyl. The amino group can also be used to separate molecules on the basis of an ion-exchange mechanism, because it can also have weak anion-exchange properties.[2]

As with silica gel sorbent, neutral lipids will be poorly retained as compared to polar lipids such as phospholipids or glycosphingolipids. Aminopropyl-bonded silica gel SPE sorbent can be used according to its chemical properties, compared to an unbonded silica matrix. Surprisingly, relatively few procedures have been described for lipid fractionation and purification using aminopropyl-bonded silica SPE columns. Kaluzny et al.[6] first described a detailed procedure which allows the fractionation of neutral lipids into different classes. In this procedure, all neutral lipids were eluted from the column with a mixture of chloroform–methanol (2:1, v/v) and transferred for further fractionation onto a second column to obtain cholesterol esters, triacylglycerols, cholesterol, diacylglycerols, and monoacylglycerols to separate fractions, with good yields. With such elution, FFAs and phospholipids still bind to the column. They are then eluted in a stepwise manner by washing this column with 2% acetic acid in diethyl ether (FFA) followed by methanol to elute neutral phospholipids such as PC and SPH. Aminopropyl columns show, here, some advantage compared to unbonded silica matrix to isolate FFA, since these molecules are firmly bound to the amino group of the column and with relative selectivity compared to other neutral lipids. In the case of an unbonded silica matrix, FFAs would have been eluted before monoacylglycerols, with the other neutral lipids.

Elution of FFAs from the aminopropyl-bonded column requires a change in pH of the elution solvent to weaken the interaction between the FFA carboxyl and the column's amino groups. This is achieved by washing the column with diethyl ether containing 2% acetic acid. This example shows the advantage which can be realized by adapting the nature of the solid phase to the kind of molecule to be recovered. This is particularly useful with molecules which tend to elute together on an unbonded silica sorbent. This is often the case with free ceramides and FFAs, which will tend to migrate close to each other on a silica gel matrix; thus, it can sometimes be difficult to individually purify these compounds, particularly when high levels of FFAs are present in the sample. By choosing aminopropyl SPE tubes, this problem can be avoided, as FFA will be firmly retained, allowing further efficient elution and purification of these compounds.

However, Hamilton and Comai described a procedure which allows good recovery and separation of the neutral lipids from FFA on a silica SPE matrix.[5] Separation of the different phospholipids can be also achieved on an aminopropyl column. These polar compounds are tightly bound to the matrix, so they are retained while eluting neutral lipids and FFAs. Then, the different phospholipids can be washed from the column by changing the pH and the ionic strength of the solvent. Stepwise elution of phospholipids was obtained (PC, PE, PS, and PI) by increasing, progressively, the polarity of the solvent and its pH.[7]

Suzuki et al. also separated phospholipids by using a combination of aminopropyl-bonded silica and an unbonded silica SPE to recover PC, PE, cardiolipin, phosphatidylglycerol, and phosphatidylserine. Phospholipids

were recovered with good purity and high yields.[8] The present procedure allows the optimized use of the advantages of each kind of column. Such a combination of two SPE tubes with different matrices was already successfully used by Prietto et al. (1992, in Ref.[2]). Steryl esters, TGs, FFAs, diglycerides, monoglycerides, monogalactosylmonoglycerides, and monogalactosyldiglycerides and their digalactosyl derivatives were separated from PC and lyso-PC onto a silica gel SPE tube by different solvents of increasing polarity. Then, phosphatidylethanolamine and its lyso derivatives, which were coeluting from the silica tube, were separated on an aminopropyl-bonded SPE.

Recovery of phospholipids, as well as the various neutral lipids, is obtained with good yields on aminopropyl tubes. Hence, Kaluzny's procedure was shown to recover up to 100% of all the lipid classes studied, giving better results than the TLC procedure.[6] This latter procedure has been extensively used by many workers to separate lipid mixtures from different origins. It has been slightly modified and adapted for particular use with poorer fractionation of lipid samples.[2] This SPE procedure has been used to achieve partial fractionation of phospholipids by various researchers[2] and, particularly, to recover acidic phospholipids, which can only be eluted from an aminopropyl matrix by changing the ionic strength of the solvent.

Surprisingly, the development of SPE procedures for fractionation of lipid samples has attracted relatively little attention as compared to conventional methods, such as TLC. However, because of its qualities and advantages, it promises to be applied much more in the future. The development of such separation methods is still in progress, as new sorbents and enhanced quality of packing will become available in the near future, from the more than 50 manufacturers currently making SPE products.[9]

REFERENCES

1. Christie, W.W. Solid-phase extraction columns in the analysis of lipids. In *Advances in Lipid Methodology, Volume 1*; Christie, W.W., Ed.; The Oily Press: Arly, Scotland, 1992; 1–17.
2. Ebeler, S.E.; Shibamoto, T. Overview and recent developments in solid-phase extraction for separation of lipid classes. In *Lipid Chromatographic Analysis*; Shibamoto, T., Ed.; Marcel Dekker, Inc.: New York, 1994; 1–49.
3. Ebeler, S.E.; Ebeler, J.D. SPE methodologies for the separation of lipids. INFORM **1996**, *7*, 1094–1103.
4. Thurman, E.M.; Mills, M.S. *Solid-Phase Extraction. Principles and Practice*; Winefordner, J.D., Ed.; John Wiley & Sons: New York, 1998.
5. Hamilton, J.G.; Comai, K. Rapid separation of neutral lipids, free fatty acids and polar lipids using prepacked silica Sep-Pak columns. Lipids **1988**, *23*, 1146–1149.
6. Kaluzny, M.A.; Duncan, L.A.; Merritt, M.V.; Epps, D.E. Rapid separation of lipid classes in high yield and purity using bonded phase columns. J. Lipid Res. **1985**, *26*, 135–140.
7. Pietsch, A.; Lorenz, R.L. Rapid separation of the major phospholipid classes on a single aminopropyl cartridge. Lipids **1993**, *28*, 945–947.
8. Suzuki, E.; Sano, A.; Kuriki, T.; Miki, T. Improved separation and determination of phospholipids in animal tissues employing solid phase extraction. Biol. Pharm. Bull **1997**, *20* (4), 299–304.
9. Majors, R.E. Current trends and developments in sample preparation. LC–GC Int. **1998**, *11* (Suppl.), 8–16.

Lipids: TLC Analysis

Boryana Nikolova-Damyanova
Institute of Organic Chemistry, Bulgarian Academy of Sciences, Sofia, Bulgaria

INTRODUCTION

The term lipids in this entry is restricted (according to Christie) to esters and amides of the long-chain aliphatic monocarboxylic acids, the fatty acids, and to their biosynthetically or functionally related compounds. The most abundant lipids are the esters of fatty acids with glycerol (1,2,3-trihydroxypropane), which are denoted as glycerolipids. Lipids are classified according to the number of hydrolytic products per mol.

Simple (or *neutral*) lipids release two types of products, e.g., fatty acids and glycerol. The most abundant simple lipids are the triacylglycerols.

Complex (or *polar*) lipids give three or more products, such as fatty acids, glycerol, phosphoric acid, and an organic base. Typical complex lipids include the glycerophospholipids (phospholipids), glycoglycerolipids (galactolipids), and the sphingolipids. A natural lipid mixture comprises different types (denoted as lipid classes) of simple and complex lipids.

LIPIDS

Lipids are important constituents of all living organisms. Thus, for example, triacylglycerols serve as an energy reserve while complex lipids are structural components of the cell membranes with substantial role in cell functions. Lipids are also important components of the human and animal diet. Disturbances in the lipid metabolism of the organism leads to various disorders and malfunctions. In humans, these are unambiguously related to the development of cardiovascular disease.

The complexity of natural lipids requires relevant methods for examination. Adequate approaches for separation and isolation of lipid components are mandatory and, among these, the chromatographic techniques are of primary importance. Among the different chromatographic methods, thin-layer chromatography (TLC) occupies a special place, being one of the first separation methods applied to lipid analysis. Most of the present basic knowledge on the structure and biological role of lipids has been achieved by using various TLC techniques.

The first description of TLC goes back to 1938, but Kirchner (in the fifties) and later Stahl (1965) were those who converted the idea into a full-scale analytical technique. In the early 1960s, Kaufmann and coworkers in Germany and the group of Privet in the United States introduced TLC to lipid analysis.

TLC is a powerful tool in the analysis of lipids.[1–7] It is easy to perform, versatile, and relatively cheap, and it allows for direct quantitative measurements of the separated compounds via scanning densitometry. An important feature is that the analyst obtains a full picture of the examined sample.

The General TLC Technique for Lipids

TLC is a separation technique in which the components of a lipid mixture are differentially distributed between a solid stationary phase, spread as a thin layer on a plate made of inert material, and a solvent mobile phase. Depending on their type, the components are retained with different strengths on the layer to give distinctive spots or bands. The migration of a band is presented quantitatively by the corresponding R_f value. The stronger the retention, the lower the R_f value becomes.

Three modifications of TLC are in use for lipid analysis: 1) separation on unmodified silica gel layer, silica gel TLC; 2) separation on a layer impregnated with silver ions, silver ion-TLC (Ag-TLC); and 3) separation on a layer modified with silanes or long-chain hydrocarbons to give a nonpolar stationary phase, reverse-phase TLC (RP-TLC).

The universal TLC facilities are utilized: plates, adsorbents, microcapillaries, or micropipettes for sample application, development tanks, detection spray reagents, devices for spraying, and densitometers for quantification. Plates are either commercially precoated or handmade. Silica gel G (G, for gypsum as a binding substance), silica gel H (no binding substance) and, rarely, alumina and kieselguhr, form the thin-layer stationary phases. Complete sets of devices necessary for the preparation of handmade plates are commercially available. After the silica gel slurry is spread on the plates, they are left to dry in the air for at least 24 hr and shortly in an oven at 110°C. The plates are then ready for either direct use or for modification of the layer. From the great variety of precoated plates, which are commercially available and preferred nowadays, silica gel plates and plates with layers modified with carbon chains from C_2 to C_{18} are of interest in lipid analysis. Understandably, precoated plates for Ag-TLC are not commercially available. Preparative TLC is performed mostly on 20×20 cm plates with layer thickness of

1 mm. Analytical separations are usually performed on 5 × 20 cm plates with layer thickness of 0.2 mm.

The preparation of a lipid sample includes extraction of the lipid material from the examined object (seeds, tissues, food, etc.) and choosing which among the several widely accepted procedures should be used. Extraction with chloroform–methanol, 2 : 1 (the Folch extraction) is the most popular. A solution of known concentration in hexane or dichloroethane is prepared and a suitable aliquot is applied onto the plate as a small spot or, better yet, as a narrow band. Two, three, or more solvents, mixed in different proportions, comprise the mobile phase. Development is performed in common tanks (Desaga-type, for example), in the ascending mode. For fine separations, cylindrical or sandwich-type tanks provide better results.

In preparative TLC, detection is performed by spraying the plate with 2,7-dichlorofluorescein and viewing the plate under UV light. The spraying reagent does not affect the lipid and it can be easily removed during the isolation process, if necessary. Non-specific destructive reagents are used in analytical TLC. The most widely used of these are the alcoholic solutions of sulfuric (up to 50%) or phosphomolybdic (5%) acid, applied as spraying reagents. They are equally suitable for non-modified, as well as for modified layers. Reliable results are also obtained by saturating the layer with vapors of sulfuryl chloride (for silica gel TLC and Ag-TLC only). To visualize the separated components, the plate is heated at 180–220°C. The substances carbonize to give intensively stained spots, contrasting well with the background. The concentration of the lipid substance in the spots can be directly measured on the plate by using scanning densitometry.

Separation by Silica Gel TLC

Silica gel TLC is used for the identification of lipid classes in the sample (analytical TLC) and for isolation of a given lipid class for further examination (preparative TLC). Silica gel TLC is a good aid in checking both the identity and purity of individual components and different derivatives.

Separation is based on the interaction (hydrogen bonding, van der Waals forces, and ionic bonding) between the lipid molecules and the silica gel. Lipid classes with free hydroxyl-, keto-, and carboxyl groups are held stronger than those containing only fatty acid residues.

Mobile phases of hexane or light petroleum ether as main components and acetone or diethyl ether as polar modifiers are used for the separation of simple lipids. Acetic or formic acid is often added to keep the free fatty acids in the fully protonated form. The retention of simple lipids increases in the order: waxes, sterol esters, methyl esters, triacylglycerols, free fatty acids, sterols, diacylglyerols, monoacylglycerols (Fig. 1A). If no acid is present in the mobile phase, the free fatty acids migrate between diacylglyerols and monoacylglycerols. Complex lipids remain at the starting point. Retention of phospholipids depends on the nature of the polar "head" and increases in the order: cardiolipin, phosphathidylethanolamine, phosphathidylserine, phosphatidylinositol, phosphatidylcholine [silica gel H, mobile-phase chloroform–methanol–acetic acid–water, 25 : 15 : 4 : 2 (v/v/v/v)]. Galactolipids can be separated with the same solvent system after the solvent proportions are changed to increase the polarity. Predictably, monogalactosyl diacylglycerols migrate ahead of digalactosyl diacylglycerols.

Identification of the lipid components is easily performed by applying a standard lipid mixture on the same plate prior to the development.

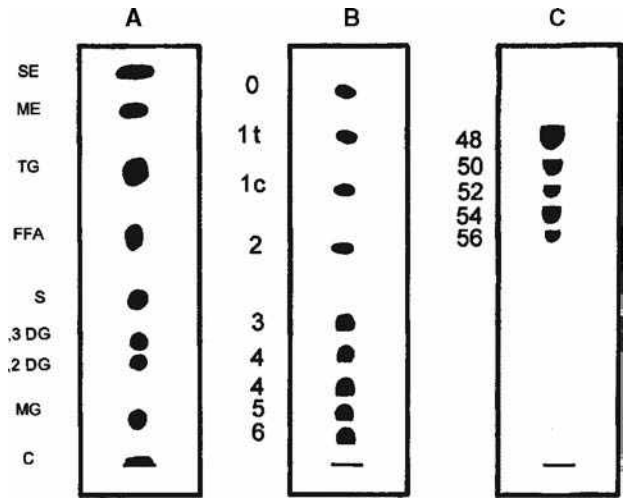

Fig. 1 Schematic presentation of lipid separation by TLC. (A) Reference mixture of simple lipid classes, silica gel TLC, mobile phase: hexane–ethyl ether–acetic acid, 80 : 20 : 2 (v/v/v); SE, sterol esters; ME, fatty acid methyl esters; TG, triacylglycerols; FFA, free fatty acids; S, sterols; 1,3-DG, 1,3-diacylglycerols; 1,2-DG, 1,2-diacylglycerols; MG, monoacylglycerols; C, complex lipids; detection by spraying with 5% ethanolic phosphomolibdic acid and heating for several minutes at 180°C. (B) Reference mixture of fatty acid methyl esters, Ag-TLC on silica gel layer impregnated with 0.5% methanolic solution of silver nitrate, mobile phase 5 ml of light petroleum ether–acetone–formic acid, 92 : 2 : 1 (v/v/v), development in open cylindrical tank; detection by treatment for 30 min with sulfurylchloride vapors and heating for 5 min at 180°C; the figures denote the number of double bonds, t, for a *trans* double bond, c, for a *cis* double bond. (C) triacylglycerols of the 001 class (0 for zero and 1 for one double bond in the molecule), RP-TLC on kieselguhr layer silanized by treatment with dimethyldichlorosilane vapors, mobile phase acetone–acetonitrile–water, 70 : 30 : 12 (v/v/v), detection by spraying with 50% ethanolic sulfuric acid and heating at 220°C for 10 min; the figures denote the partition number of the triacylglycerol species.

Separation by Ag-TLC

Ag-TLC is the modification with the most important impact on the development of lipid chemistry and has been of immense importance for the understanding of

lipid structure. The separation is based on the ability of unsaturated fatty acid residues in lipid molecules to form weak, reversible charge-transfer complexes with silver ions. Thus Ag-TLC separates lipid classes into molecular types depending on the number, configuration, and occasionally, on the position of the double bonds in the fatty acid residues.

The impregnation of the layer is performed by immersing the plate in a solution of the silver salt in methanol, acetone, or acetonitrile, or by spraying the plate with one of these solutions. Preparative plates are usually treated with 1–20% silver nitrate solutions. For analytical Ag-TLC, the concentration of silver nitrate varies in the range 0.5–10%. The impregnation procedures must be standardized to provide reproducible separation. Plates are left in the air for the solvent to evaporate and are usually activated prior to use (between 5 min and 1 hr depending on the purpose) by heating at 110°C.

The separation is affected by the dimensions of the tank, the volume of the mobile phase, the development mode (covered or "open" tanks, with or without saturation of the atmosphere, respectively), the atmospheric humidity, and the temperature. Ag-TLC plates are normally developed at ambient temperature.

Hexane or light petroleum ether, chloroform, benzene, and toluene are most often the major components of the mobile phase, while smaller proportions of diethyl ether, acetone, methanol, ethanol, or acetic acid are added as modifiers. Chloroform–methanol and hexane–acetone mobile phases reportedly provide very good separations. Often, more than one development is required for reliable resolution. The separation starts with the most polar phase and proceeds, after drying between runs, with mobile phases of gradually decreasing polarity. Highly unsaturated components are resolved first and do not move further with subsequent developments when the more saturated components are separated.

In general, the migration order of any lipid class is determined by the overall number of double bonds in the molecule. Thus the retention of common fatty acids (chain lengths of 16–22 carbon atoms, methylene interrupted double bonds) increases with increasing number of double bonds from 0 to 6 (Fig. 1B). For the triacylglycerols, which contain the above type of acyl residues, the order of increasing retention is: 000, 001, 011, 002, 111, 012, 112, 003, 112, 013, 113, 222, 023, 123, 223, 133, 233, 333 (the figures indicate the number of double bonds in the fatty acid residue but not the position in the glycerol backbone). The same order of retention is valid for complex lipids but, because of different technical difficulties, Ag-TLC is only rarely applied in the analysis of these lipids. Species with *cis*-double bonds are held stronger than those with *trans*-double bonds, and this differentiation is of great practical importance. Ag-TLC is capable, under specific conditions, of differentiating fatty acids and triacylglycerols according to the position of the double bond in the carbon chain.

Both handmade and precoated plates provide reliable separation of fatty acids. Successful separation of triacylglycerols has been achieved on handmade plates only.

Ag-TLC offers an effective means of fractionation of lipid mixtures into distinct fractions differing in the number of double bonds, thus ensuring unambiguous results by further chromatographic and spectral characterization. Ag-TLC serves also as an enrichment procedure for minor components and allows for a more accurate identification and quantification. Quantitative procedures have been developed for the determination of fatty acids and triacylglycerols by using Ag-TLC and densitometry.

Separation by RP-TLC

RP-TLC is less popular and has been applied, so far, only for the resolution of fatty acids and triacylglycerols. It is based on the distribution of lipid molecules between a non-polar stationary phase and a relatively polar mobile phase. Lipids are, therefore, separated according to their overall polarity, expressed by the Partition Number (PN). PN relates the migration of a component to the total number of carbon atoms, CN (in the acyl residues only) and the total number of double bonds, n, so that $PN = CN - n$; the higher is the PN, the stronger the component is retained in the non-polar layer (the lower the R_f value becomes).

RP-TLC also uses the common supporting facilities. In the laboratory, the non-polar stationary phase can be produced by impregnating the layer (kieselguhr G or silica gel G) with long-chain hydrocarbons or liquid paraffin or by treatment with dimethyldichlorosilane (DMCS). Although commercial RP-TLC plates are available, so far, experiments have only employed C_{18} plates.

Mobile phases that provide good separation for triacylglycerols include: 1) acetone–acetonitrile water, 70 : 30 : X (v/v/v, the water proportion, X, increases with the increasing unsaturation of the lipid class), which is suitable for handmade kieselguhr layers, treated with DMCS; and 2) acetonitrile-2-butanone-chloroform, 50 : 35 : 15 (by volume), which is suitable for precoated C_{18} plates.

At present, RP-TLC finds application only as a quantitative technique, complementary to the analytical and preparative Ag-TLC of triacylglycerols. The triacylglycerol mixture is first fractionated into classes according to the unsaturation, and then each class is subjected to RP-TLC to give a series of species with different PN. An example is shown in Fig. 1C.

Quantification

The most widely applied procedure is indirect quantification by extracting the fractions from the adsorbent layer in the presence of an internal standard, transmethylating, and

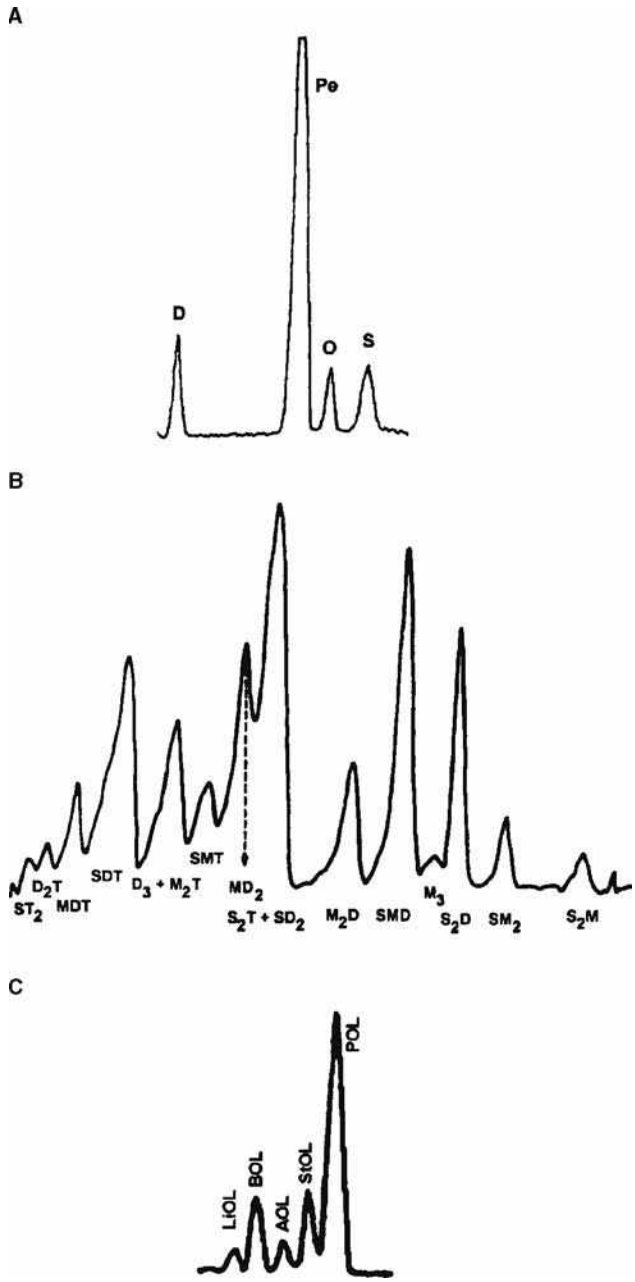

Fig. 2 Densitograms for quantitative determination of fatty acid and triacylglycerol in lipid samples produced on Shimadzu CS-930 scanner in zigzag reflection mode at 450 nm, beam slit varies depending on the sample. A) Determination of fatty acids, as phenacyl esters, in *Petroselinum sativum* seed oil by Ag-TLC, 4 × 19 cm glass plate covered with 0.2 mm thick silica gel layer; layer was impregnated by dipping with 1.0% methanolic silver nitrate and the plate was developed twice in closed cylindrical tank with 3 ml of chloroform–acetone, 100 : 0.25 (v/v); visualization by successive treatment with bromine (30 min) and sulfuryl chloride (30 min) vapors and heating on a hot plate at 180–200°C; scanning with beam slit 0.4 × 0.4 mm; S, saturated, O, oleic, Pe, petroselinic, D, dienoic fatty acid. B) Determination of lemon seed oil triacylglycerols by Ag-TLC, TLC plate as in panel A, impregnated by dipping with 0.5% methanolic silver nitrate and developed with 8 ml petroleum ether–acetone, 100 : 6 (v/v) in open cylindrical tank; visualization by successive treatment with bromine (30 min) and sulfuryl chloride (30 min) vapors and heating on a hot plate at 180–200°C; scanning with beam slit 1.2 × 1.2 mm; S, saturated, M, monenoic, D, dienoic, T, trienoic acyl residues. C) Determination of triacylglycerols by RP-TLC on kieselguhr layer silanized by treatment with dimethyldichlorosilane vapours, mobile phase acetone–acetonitrile–water, 70 : 30 : 18 (v/v/v), visualization by spraying with 50% ethanolic sulfuric acid and heating at 220°C for 10 min; P, palmitic, St, stearic, A, arachidic, B, behenic, Li, lignoceric, O, oleic, L, linoleic acyl residues.

subjecting the methyl esters of the fatty acids to GC analysis. Information is simultaneously obtained on the composition of the fractions and their absolute amounts. In practice, the sample is resolved on a preparative plate, each distinct zone is carefully scraped off, a standard solution of the internal standard (usually an odd-chain fatty acid methyl ester) is added, and the material is extracted with a suitable polar solvent such as diethyl ether or a chloroform–methanol mixture. More complicated extraction procedures are sometimes needed for polar complex lipids. Fatty acid methyl esters are directly subjected to GC while triacylglycerols and other lipids are usually transmethylated with the internal standard before analysis by GC. Indirect quantification is the method of choice in the determination of lipid classes.

Direct, in situ, quantification by scanning photodensitometry (a technique developed especially for TLC) is more advantageous. Densitometric measurements are based on the difference in optical response between the blank part of the plate and regions where the analytes are present. Nowadays, excellent instrumentation is available and the problems that arise are rarely a function of the densitometer and depend mainly on the properties of the chromatogram. A uniform layer, a clean background, well-resolved, distinct, and evenly stained zones, and good contrast between spots and background are required. Zigzag (or flying spot) scanning is greatly superior to linear scanning and should be preferred. Modern instruments are fully computerized and quantify the peaks in the most accurate, reproducible, and convenient manner.

The problem in applying scanning photodensitometry is that lipids do not possess any chromogenic groups and are usually visualized for direct quantification by charring and carbonization. Although charring is a sensitive detection procedure, all steps, including treatment of the plate with the charring reagent, and the temperature and duration of heating must be standardized as far as possible to obtain reproducible results. In most instances, the charring procedure is therefore the critical step. However, efforts to replace charring by another visualization procedure have not led to satisfactory results. An important requirement is that the charring reagent should react in an equal manner with all components, and in particular, staining should not be influenced by the different degree of unsaturation of the separated species. Spraying of the layer with charring reagents (50–70% aqueous, methanolic, or ethanolic solutions of sulfuric acid) or treatment with vapors of such charring reagents such as sulfuryl chloride have been tested, and which one to choose depends on the specific application of TLC.

The recommended procedure for densitometric quantification of fatty acid esters and triacylglycerol separated by Ag-TLC is the successive treatment of the plate with bromine and sulfuryl chloride vapors, followed by heating at 180–200°C (Fig. 2a and b). Correction factors are not required because the quantitative results do not depend on the unsaturation. Spraying with a 50% ethanolic solution of sulfuric acid is suitable for densitometric quantification of triacylglycerols separated by RP-TLC (Fig. 2c).

Lipid analysts have often been skeptical about the possibilities for quantification offered by densitometry, their opinions generally being formed by earlier experience when the instrumentation was quite primitive. Today, however, the situation is greatly changed and laboratories whose staff are well trained in silver ion TLC methods can successfully apply densitometry. It can be claimed that the overall procedure is cheaper and more suitable for routine analysis of large numbers of samples compared to any alternative technique, while providing results of the same range of accuracy and reproducibility.

ACKNOWLEDGMENTS

Partial financial support of the Bulgarian National Scientific Fund, Contract No X-1009, is gratefully acknowledged.

REFERENCES

1. Ackman, R.G. Application of thin-layer chromatography to lipid separation. In *Analysis of Fats, Oils and Lipoproteins*; Perkins, G.E., Ed.; Amer. Oil Chem. Soc.: Champaign, IL, 1991; 60–82.
2. Christie, W.W. *Lipid Analysis;* 2nd Ed.; Pergamon Press: Oxford, 1982.
3. Fried, B.; Sherma, J. *Thin-Layer Chromatography, Techniques and Applications*; Marcel Dekker, Inc.: New York, 1994.
4. Hamilton, R.J. Thin-layer chromatography and high-performance liquid chromatography. In *Analysis of Oils and Fats*; Hamilton, R.J., Rossel, J.B., Eds.; Elsevier: London, 1986; 243–311.
5. Kuksis, A. Lipids. In *Chromatography. Part B—Application;* 5th Ed.; Heftman, E., Ed.; Elsevier: Amsterdam, 1992; B171–B227.
6. Nikolova-Damyanova, B. Silver ion chromatography of lipids. In *Advances of Lipid Methodology—One*; Christie, W.W., Ed.; The Oily Press Ltd.: Ayr, Scotland, 1992; 181–237.
7. Nikolova-Damyanova, B. Quantitative thin-layer chromatography of triacylglycerols: Principles and application. J. Liq. Chromatogr. Relat. Technol. **1999**, *22*, 1513–1537.

Lipophilic Vitamins: TLC Analysis

Alina Pyka
Department of Analytical Chemistry, Medical University of Silesia, Sosnowiec, Poland

INTRODUCTION

Vitamins are organic compounds that have biochemical and physiological proprieties. Because of these qualities, they have been the subject of numerous scientific investigations. Vitamins are classified according to their solubility in water and in fats. Lipophilic (hydrophobic) vitamins are vitamins A, D, E, and K. Chromatography is useful in the identification and determination of vitamins in pharmaceutical preparations, the identification and determination of vitamins and related substances in natural materials and foodstuffs, and the chemical and biochemical determination of vitamins and their metabolites in fats and tissues.

Vitamins that are soluble in fat (lipophilic vitamins) are the subject of wide investigations because of their biological proprieties. High-performance liquid chromatography (HPLC), thin-layer chromatography (TLC), and gas chromatography (GC) are the principal techniques used for qualitative and quantitative investigations of lipophilic vitamins. Analysis of lipophilic vitamins by liquid chromatography (LC) (TLC and HPLC) is the subject of many scientific publications.

Generally, TLC is useful for the investigation of a wide range of lipophilic vitamin applications, i.e., purification of samples, qualitative detection, quantitative determination, and the use of new visualizing agents, and also for separation of some optical isomers.[1,2]

The aim of this entry is to present selected works that describe the analytical separation of lipophilic vitamins by means of TLC.

VITAMIN A

Physiological forms of vitamin A include retinol (vitamin A_1) and its esters, 3-dehydroretinol (vitamin A_2) and its esters, retinal (retinene, vitamin A aldehyde), 3-dehydroretinal (retine-2), retinoic acid, neovitamin A, and neo-β-vitamin A_1. Active analogs and related compounds known as vitamin A are α-, β-, and γ-carotene, neo-β-carotene B, cryptoxanthine, myxoxanthine, torularhodin, aphanicin, and echinenone. Kitol, xanthophyll, and others are inactive analogs and related compounds of vitamin A. Vitamin A supports the formation of the cells of the skin and is essential for vision. It is involved in the viability of the reproductive system by acting as a hormone and regulating the expression of specific genes. Good sources of vitamin A are fish liver oil from cod, salmon, halibut, and shark, chicken, eggs, milk, cheese, butter, and liver. Vitamin A occurs as retinyl esters in foods of animal origin. Vitamin A_1 is susceptible to oxidation and degradation. Therefore, control of the vitamin A level in foodstuffs is recommended. Foods of plant origin do not contain vitamin A, but are rich sources of previtamin A. About 50 of the 500 known carotenoids may be converted to vitamin A. β-Carotene is the most important of the carotenoids that occur in nature. β-Carotene (provitamin A), precursor of vitamin A, is found in plants. Good sources are yellow-orange fruits and vegetables, and green leafy vegetables (carrots, apricots, collard green, sweet potatoes, spinach, mangoes, mustard greens, turnip, and sweet red peppers). Both vitamin A and carotenoids with and without provitamin A activity appear to show anticancer effects. Vitamin A plays an essential role in protecting the body from infection.

Sliwiok, Podgorny, and Siwek[3] used TLC and HPLC to compare the hydrophobicity of vitamin A derivatives. TLC was performed on RP-2 F_{254} and Kieselguhr F_{254} (impregnated with 10% paraffin oil in cyclohexane) with methanol–water (95 : 5, v/v). R_M values were –0.60, –0.51, –0.37, and 0.09 on RP-2F_{254} plates and –1.59, –0.84, –0.22, and 1.18 on paraffin oil-impregnated Kieselguhr for all-*trans*-retinic acid, all-*trans*-retinal, vitamin A acetate, and vitamin A palmitate, respectively. The separations of the vitamin A derivatives on the paraffin oil-impregnated plates were better than those on the RP-2 plates. The log *P* values calculated from fragmental constants by Rekker for all-*trans*-retinic acid, all-*trans*-retinal, vitamin A acetate, and vitamin A palmitate are 4.85, 6.48, 7.92, and 15.30. The relationship obtained by the authors on the basis of R_M and log *P* values confirms the following sequence of increasing hydrophobicity: all-*trans*-retinic acid < all-*trans*-retinal < vitamin A acetate < vitamin A palmitate.

Two separate methods all-*trans*- and 13-*cis*-retinoic acids, one for gel and one for cream samples, were described by De Paolis.[4] A methanol extract of the gel formulation may be analyzed directly on high-performance TLC (HPTLC) silica gel plates eluted with diethyl ether–cyclohexane–acetone–glacial acetic acid (40 : 60 : 2 : 1, v/v/v/v). This method gives fast and complete resolution of the two isomers with a detection limit

of about 20 ng for each of them. Methanol extracts of the cream samples contain interfering excipients, which require cleaning prior to chromatography. This was accomplished conveniently on a reversed-phase C_{18} and normal-phase silica gel, two-dimensional TLC plate. The C_{18} reversed phase separated the cream excipients from the isomers of retinoic acid using ethanol–distilled water (80 : 20, v/v) as mobile phase. The normal phase on silica gel resolved both isomers all-*trans*- (R_F 0.34) and 13-*cis*-retinoic acid (R_F 0.39). This two-dimensional separation of all-*trans*- and 13-*cis*-retinoic acid is shown in Fig. 1.[4]

Recent publications concern the qualitative and the quantitative determination of β-carotene by TLC. Isomerization of α- and β-carotene was catalyzed by iodine according to the method of Zechmeister.[5] Fig. 2A illustrates typically developed TLC plates for a mixture of α- and β-carotene isomers.[5] Two-dimensional TLC was done on calcium hydroxide plates with 1.2% acetone in petroleum ether as mobile phase. Expected isomers from the iodine-catalyzed reaction are neoisomers U and B for β-carotene and neoisomers U, W, and B for α-carotene.[5] Photoisomerization of all-*trans*-α- and β-carotene solutions was also conducted by Nyambaka and Ryley.[6] This photoisomerization of individual all-*trans*-α- and β-carotene solutions produced several isomers each. Nyambaka and Ryley[6] applied the separation TLC method, which was done by Schwartz and Patroni-Killam,[5] to isolate and collect major isomers of β-carotene (13-*cis*-, all-*trans*-, 9-*cis*-, and 7-*cis*-). Fig. 2B illustrates a typical plate obtained by Nymbaka and Ryley[6] for β-carotene isomers from iodine-catalyzed photoisomerization. After extraction of the zones by TLC, the isomers were identified by their behavior in UV–Vis absorbance spectra. This method was applied to dark green leafy vegetables (Italian spinach, sprig cabbage, and cowpea leaves).

The carotenoid composition, including β-carotene, of *Rosa canina* fruits was determined by TLC with densitometric analyses and also by HPLC. The peaks of the extracts obtained from TLC densitograms were identified as β-carotene, lycopene, β-cryptoxanthin, rubixanthin, and zeaxanthin mixed with lutein (R_F 0.96, 0.90, 0.62, 0.53, and 0.32, respectively) on silica gel with 15% (v/v) acetone in petroleum ether. The distribution of these compounds was reproducible by TLC as well as by HPLC.[7]

Small amounts of intensely colored pigments can be detected in UV light and also in visible light; the limit of detection is 0.01 μg of the carotenoids. Retinal (0.02–0.03 μg) can be detected after spraying rhodamine (orange-red spot of retinal). Many vitamin A compounds fluoresce yellow-green in light at 365 nm (limit of detection 0.05 μg). Vitamin A compounds can be detected with antimony(III) chloride (Carr–Price reagent) and antimony(V) chloride (blue spots), with concentrated sulfuric acid (blue color of spot),[4,8] with molybdophosphoric

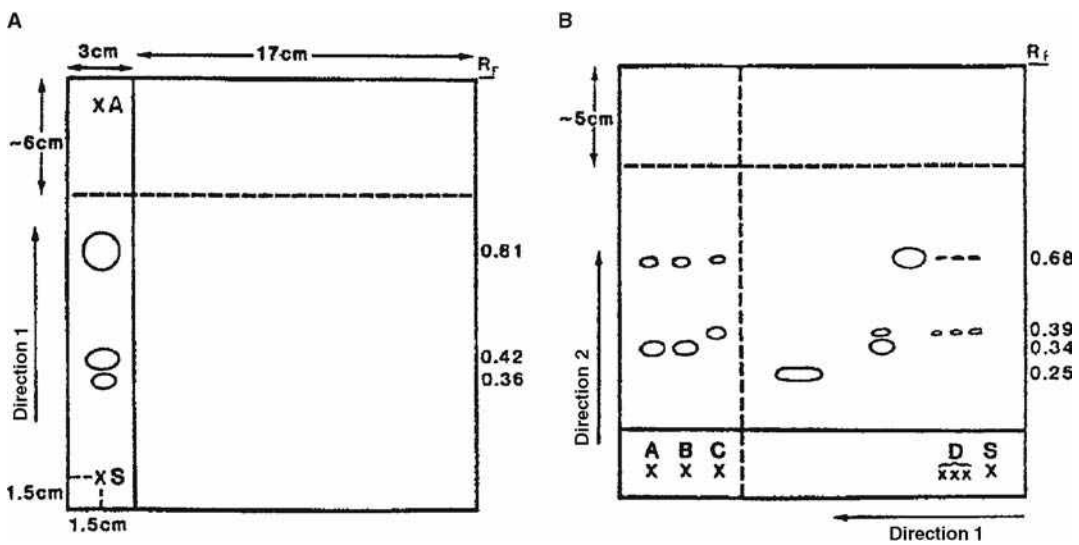

Fig. 1 Typical chromatograms of (A) the cream sample on the Multi-K CS5 TLC plate after development in solvent system B (80% ethanol in water), and (B) the cream sample and standards, tretinoin and 13-*cis*-retinoic acid (13-*cis*-Ra), after development in solvent system A (diethyl ether–cyclohexane–acetone–glacial acetic acid, 40 : 60 : 2 : 1). The spotting areas are designated as follows: S = sample; A and B = tretinoin standard stock solution at the beginning of analysis and just before development in direction 2, respectively; C and D = 13-*cis*-RA standard test solutions. The broken lines represent solvent fronts. The R_F values in (A) are 0.81 for plar excipients, 0.42 for tretinoin and 13-*cis*-RA, and 0.36 for butylated hydroxytoluene (bHT). In (B), the R_F values are 0.25 for polar excipients, 0.34 for tretinoin, 0.39 for 13-*cis*-RA, and 0.68 for BHT.

Source: From Determination of all-*trans*- and 13-*cis*-retinoic acids by two-phase, two-dimensional thin layer chromatography in creams and by high-performance thin-layer chromatography in gel formulations, in J. Chromatogr.[4]

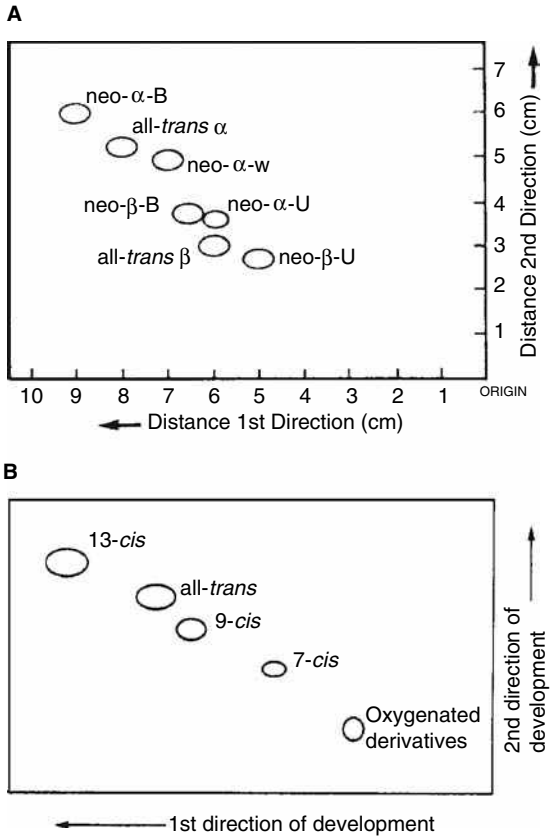

Fig. 2 Two-dimensional TLC chromatogram of (A) *cis–trans* α-and β-carotene isomers. (B) β-Carotene isomers from iodine-catalyzed photoisomerization.
Adapted from Schwartz & Patroni-Killam[5] and Nyambaka & Ryley.[6]

acid (green-blue spots), and with potassium dichromate in sulfuric acid (limits of detection 0.1–0.3 μg). The limit of detection of retinol isomers converted to 2,4-dinitrophenylhydrazones of retinals is 1 μg.[1,2,8] Bromophenol blue was also used for detection of vitamin A (3 μg) after adsorption TLC.[9]

VITAMIN D

Physiological forms of vitamin D include vitamin D_2 (calciferol, ergocalciferol), vitamin D_3 (cholecalciferol), phosphate esters of D_2, D_3, 25-hydroxycholecalciferol, 1,25-dihydroxycholecalciferol, and 5,25-dihydroxycholecalciferol. Vitamins D_2 and D_3 are 9,10-secosteroids, which differ structurally in the degree of saturation of an isoprenoid side chain. The biological activity of vitamin D_3 is greater than that of vitamin D_2. Vitamin D_2 is of vegetable origin, whereas D_3 is formed in the skin of humans and animals. From the chemical standpoint, ergocalciferol (vitamin D_2) is a relatively stable vitamin. Active analogs and related compounds known as vitamin D include 22-dihydroergosterol (vitamin D_4), 2-dehydrostigmasterol (vitamin D_6), and 7-dehydrositosterol (vitamin D_5). Lumisterol, tachysterol, ergosterol, and 7-dehydrocholesterol are inactive analogs and related compounds of vitamin D. Vitamins D_2 and D_3 are photochemically derived from their precursors ergosterol (provitamin D) and 7-dehydrocholesterol, respectively. Vitamins D_2 and D_3 are precursors of hormones. Vitamin D_3, which has little biological activity is converted into biologically active metabolites by oxidation.

Kocjan and Śliwiok[10] determined the hydrophobicity of vitamins D_2 and D_3 by RPTLC, thin-layer adsorption chromatography, and IR spectrometry. Partition TLC separations of vitamins D_2 and D_3 were done on TLC plates precoated with Kieselguhr F_{254} (E. Merck) impregnated with 10% paraffin oil in benzene and developed to 10 cm with binary mixtures of methanol–water (9.5 : 0.5, v/v; R_F values 0.56 and 0.48, respectively) and acetonitrile–water (9.5 : 0.5, v/v; R_F values 0.50 and 0.41, respectively). Adsorption TLC was done on glass plates precoated with activated silica gel 60 F_{254} (E. Merck), with a mobile phase of benzene–methanol (9 : 1, v/v). Measurement of the surface of chromatographic spots (141.0 and 99.5 mm^2 for vitamins D_2 and D_3, respectively) obtained by adsorption TLC gave hydrophobicity coefficients (h_f values are 6.09 and 9.05 for vitamins D_2 and D_3, respectively). The results indicate that the hydrophobicity of vitamin D_3 is greater than that of vitamin D_2. This conclusion was proved by the lower R_F values for vitamin D_3 obtained by partition chromatography, the higher values of the respective hydrophobicity coefficients, and by the greater relative decreases in the ratio of free to bonded OH groups (obtained by spectrometry measurement). It was apparent from the literature that the biological activity of vitamin D_3 is greater than that of vitamin D_2. The authors concluded that the molar weight of vitamin D_2 is greater than that of vitamin D_3; the double bond in the hydrocarbon chain of vitamin D_2 results in its lower hydrophobicity.[10]

Justova and Starka[11] described TLC separations of vitamin D_3 and its hydroxymetabolites. They tested three stationary phases [Kieselgel 60F_{254} (E. Merck), Silufol UV 254 (Kavalier, Sávaza, Czech Republic), and silica gel 6061 (Eastman-Kodak, Rochester, U.S.A.)] and one relatively polar mobile phase (chloroform–ethanol–water, 183 : 16 : 1, v/v/v). The optimal separation was achieved on Kieselgel 60F_{254} foils produced by E. Merck; the R_F values were 0.69, 0.35, 0.56, 0.20, 0.41, and 0.30 for D_3, 1-OH-D_3, 25-OH-D_3, 1,25-$(OH)_2$-D_3, 24,25-$(OH)_2$-D_3, and 25,26-$(OH)_2$-D_3, respectively.[11] In biological samples, the vitamin D_3 hydroxymetabolite contents are at nanogram levels, which is below the limit of sensitivity of the applied visualization methods (UV light and the anisaldehyde reagent). Therefore, the

hydroxycholecalciferols were localized with corresponding metabolites used as markers. The vitamin D_3 metabolites were then scraped off and extracted with ethanol, and eluates were examined for radioactivity. The complete chromatographic procedure on the accuracy and precision of the determination was presented. The recovery of the markers in five replicate determinations was 97.8 ± 2.9% for vitamin D_3 and 98.7 ± 1.5% for 25-OH-D_3.

Thierry-Palmer and Kenney-Gray[12] compared HPTLC and TLC methods for the analysis of vitamin D_3 as well as the mono- and dihydroxylated metabolites of vitamin D_3. TLC was performed on silica gel HPTLC-HLF and GHLF plates (Analtech, Newark, Delaware, U.S.A.) without previous activation. The mixtures dichloromethane–isopropanol (90 : 10, v/v), hexane–isopropanol (85 : 15, v/v), and chloroform–ethyl acetate (50 : 50, v/v) were applied as mobile phases. Migration distances were 7 cm for HPTLC plates and 14 cm for the conventional TLC plates. Generally, the effectiveness of separation by conventional TLC was very similar to that by HPTLC (Table 1).[12] 23,25-Dihydroxyvitamin D_3 and 24,25-dihydroxyvitamin D_3 separate faintly using dichloromethane–isopropanol (90 : 10, v/v) and HPTLC and conventional TLC plates as well as using chloroform–ethyl acetate (50 : 50, v/v) and conventional TLC plates. Therefore, the system of choice would depend on the metabolite of interest. However, the separations by HPTLC were faster (developing times were 11–12 min) than those by conventional TLC (developing times were 35–45 min).[12]

Spots of vitamin D derivatives can be inspected in short-wavelength UV light (limit of detection 0.025–0.5 μg). The mono- and dihydroxycholecalciferols can be visualized under UV light at 254 nm or by spraying the foil with a solution of anisaldehyde in sulfuric acid (2%, w/v) mixed with glacial acid (1 : 10, v/v) at 40°C. Vitamins D_2 and D_3 can be detected with antimony(III) chloride (Carr–Price reagent) and antimony(V) chloride (gray-blue and orange-red spots, respectively; limit of detection 0.025–0.3 μg), with concentrated sulfuric acid (brown and green spots, respectively, of vitamins D_2 and D_3; limit of detection 30 μg), with tungstophosphoric acid (gray-brown spots; limit of detection 0.2 μg), with molybdophosphoric acid (gray-blue spots; limit of detection 0.3 μg), and with trichloroacetic and trifluoroacetic acids (limit of detection 0.1–0.2 μg).[1,2,8] Vitamins D_2 and D_3 separated by adsorption TLC were visualized with 0.005% aqueous new fuchsine solution.[10] A densitogram of vitamin D_3 after a spraying of antimony(III) chloride (Carr–Price reagent) is given by Jork et al.[8] Vitamin D_3 was also detected with sodium hydroxide (yellow and orange spots in visible and UV light, respectively; limit of detection 1–8 μg), with iron(III) chloride (brown-red spot in visible light; limit of detection 8 μg), with iodoplatinate (black and brown spots in visible and UV light, respectively; limit of detection 1–8 μg), and with phosphomolybdate (pinkish brown spot in visible light; limit of detection 8 μg).[13] Bromocresol green, bromothymol blue, and helasol green can be used for detection of vitamins D_2 and D_3 after adsorption TLC (limit of detection 5 μg) and partition TLC (limit of detection 50 μg), respectively.[9]

VITAMIN E

The known physiological forms of vitamin E are D-α-tocopherol, tocopheronolactone, and their phosphate esters. Active analogs and related compounds known as vitamin E are DL-α-tocopherol, L-α-tocopherol, esters (succinate, acetate, phosphate), β, ζ_1, and ζ_2-tocopherols. δ-, ε-, and η-Tocopherols are inactive analogs and related to vitamin E.[1,2] In nature, vitamin E occurs in eight different forms (α-, β-, γ-, and δ-tocopherols and α-, β-, γ- and δ-tocotrienols) with varying biological activities. The biological properties of α-tocopherol are of particular importance. Of these eight compounds, α-tocopherol has the highest biological activity. Tocopherol possesses three asymmetric carbon atoms, and there are eight possible stereoisomeric tocopherols. Natural α-tocopherol occurs as the enantiomer about the configuration 2*R*, 4′*R*, 8′*R*.

Table 1 Comparison of separations of the hydroxylated metabolites of vitamin D_3 and vitamin D_3 by HPTLC and TLC methods.

	R_F values					
	Dichloromethane–isopropanol (90 : 10, v/v)		Chloroform–ethyl acetate (50 : 50, v/v)		Hexane–isopropanol (85 : 15, v/v)	
Compound	HPTLC	TLC	HPTLC	TLC	HPTLC	TLC
$1,24,25(OH)_3D_3$	0.21	0.17	0.05	0.05	0.14	0.12
$1,25(OH)_2D_3$	0.37	0.29	0.19	0.14	0.26	0.22
$25,26(OH)_2D_3$	0.44	0.35	0.29	0.19	0.35	0.28
$24,25(OH)_2D_3$	0.61	0.49	0.44	0.33	0.46	0.40
$23,25(OH)_2D_3$	0.64	0.53	0.51	0.36	0.51	0.46
$25(OH)D_3$	0.73	0.62	0.71	0.55	0.59	0.55
Vitamin D_3	0.89	0.76	0.87	0.71	0.66	0.69

Source: From Separation of the hydroxylated metabolites of vitamin D_3 by high-performance thin-layer chromatography, in J. Chromatogr.[12]

Semisynthetic α-tocopherol is a mixture of the diasteroisomers about configuration 2*R*/*S*, 4′*R*, and 8′*R*. The antioxidative effect of the different tocopherols may not be identical. It has been shown in antioxidation tests with foodstuffs that the antioxidative activity of the tocopherols increases in the order γ-, δ-, β-, and α-tocopherol. Vitamin E occurs principally in wheat germ, vegetable oil, and vegetables.

α-, β-, γ-, and δ-Tocopherols were separated (R_M values 0.438, 0.037, 0.008, and –0.275, respectively) on Kieselguhr G plates impregnated with a 10% solution of paraffin oil in hexane and a mobile phase of methanol–water (9.5 : 0.5, v/v) by Sliwiok and Kocjan.[14] They correlated their results with those of quantum-mechanical calculations and respective steric effects. Hydrophobic constants h_f were determined by adsorption TLC and partition coefficient by Rekker as well as the sum of the net electron charges ($\sum$ NEC) on the tocopherols' –C–O–H groups were calculated for the investigated tocopherols (Table 2).[14] It was established that the investigated tocopherols can be arranged with respect to their lipophilic properties in the order α-tocopherol > β-tocopherol > γ-tocopherol > δ-tocopherol. But, enantiomers of DL-α-tocopherol were separated on Chiralplates (Machery-Nagel, Germany) with 2-propanol–water–methanol (17 : 2 : 1, v/v/v) as mobile phase.[15] Under these conditions, two bands were generated with R_F values of 0.72 and 0.62.

α-, β-, γ-, and δ-Tocopherols were also separated by reversed-phase high-performance TLC (RP-C18-HPTLC), normal-phase HPLC, reversed-phase HPLC (RP-C18-HPLC), and GC.[16] R_M values of the α-, β-, γ- and δ-tocopherols investigated by RP-18-HPTLC and ethanol–water as mobile phase are shown in Table 2.[16] The chromatographic conditions can be used to allow for the separation of the four tocopherols in various biological samples. The selected topological indices based on connectivity–adjacency matrix (M^{ν}, $^1\chi^{\nu}$), on distance matrix (W, ^0B, MTI) and on information theory (I_{AC}, $\bar{I}_{AC}$) were calculated for these tocopherols. The observed chromatographic separations of investigated tocopherols were compared. The comparison indicated that RP-C18-HPTLC, HPLC, and GC are the best techniques for the separation of these tocopherols. Topological index ^0B was the most significant. A definite dependence between the numerical values of the topological index ^0B and the chromatographic separation of the investigated tocopherols was obtained.[16] α-, β-, γ-, and δ-Tocopherols were also separated by RP-TLC on C_{18} plates using seven different mobile phases (methanol, ethanol, *n*-propanol, and mixtures containing ethanol and water, and *n*-propanol and water in the volume proportions 9.5 : 0.5, and 9 : 1, v/v).[17] The R_M values obtained are presented in Table 2.[17] The R_M values of the compounds were correlated with the numerical values of the topological indexes, the sum of the net electron charge ($\sum$ NEC) on the tocopherols' –C–O–H groups, the moment dipoles (μ_{mph}), and the permittivities (ε_{mph}) of the mobile phases. Most accurate prediction of the R_M values of the tocopherols in all the mobile phases investigated was achieved by the use of two parametric equations employing the dipole moments of the mobile phases, and one topological index from among the topological indexes $^2\chi^{\nu}$, ^0B, C, or the sum of the net electron charge ($\sum$ NEC).[17] For example:

$$R_{M(all)} = -25.3626(\pm 2.4142) + 11.1984(\pm 0.5350)\mu_{mph} + 3.1933(\pm 1.0329)^0B \quad (1)$$

($n = 28$; $R^2 = 94.70\,\%$ $F = 223.5$; $s = 0.114$; $P < 0.0001$.)

Ruggeri et al.[18] investigated DL-α-, DL-γ-, and DL-δ-tocopherol, DL-α-tocotrienol, and DL-tocol by TLC and HPLC. TLC was performed on silica gel GF plates (Analtech, Newark, Delaware, U.S.A.) using hexane–isopropyl ether (85 : 15, and 80 : 20, v/v) as mobile phase, and a scanning densitometer operating at 350 nm. Fig. 3 illustrates the chromatogram obtained by Ruggeri et al.[18] for analysis of the

Table 2 Hydrophobic constants (h_f) obtained by NP-TLC, partition coefficient (log *P*) by Rekker, and the sum of the net electron charge ($\sum$NEC) on the tocopherols' –C–O–H groups as well as R_M values of the α-, β-, γ-, and δ-tocopherols investigated by RP-18-HPTLC.

				R_M[b]						
Compound	h_f[a]	**log *P* by Rekker**	**ΣNEC**	**S1**	**S2**	**S3**	**S4**	**S5**	**S6**	**S7**
α-Tocopherol	20.5	12.37	0.0039	0.661	0.017	0.314	0.647	–0.589	–0.466	–0.265
β-Tocopherol	17.2	11.86	0.0223	0.565	–0.054	0.226	0.591	–0.653	–0.489	–0.302
γ-Tocopherol	16.6	11.86	0.0327	0.520	–0.124	0.154	0.540	–0.723	–0.512	–0.337
δ-Tocopherol	14.8	11.36	0.0432	0.477	–0.237	0.050	0.489	–0.803	–0.537	–0.414

[a]Kieselgel G 0.25 mm; mobile phase: benzene–acetone, 9 : 1 (v/v).
[b]Mean values, $n = 5$. RP18 plates; S1 contained 100% methanol; S2, S3, S4 contained ethanol and water in the volume proportions 10 : 0, 9.5 : 0.5, and 9 : 1 (v/v); and S5, S6, S7 contained *n*-propanol and water in the volume proportions 10 : 0, 9.5 : 0.5, and 9 : 1 (v/v), respectively.
Adapted from Sliwiok & Kocjan,[14] Pyka & Sliwiok,[16] and Pyka & Niestrój.[17]

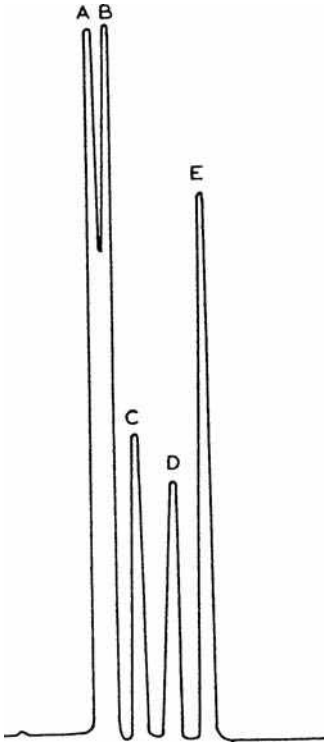

Fig. 3 TLC chromatogram of tocopherol isomers and related compounds. Conditions: plates: silica gel GF; solvent: hexane–isopropyl ether (85 : 15, v/v); detection: $\lambda = 350$ nm, D_2 lamp: 10 mV range; visualizing agent: 10% $CuSO_4$–8% H_3PO_4. Peak identities: A = D,L-tocol (0.46 μg); B = D,L-δ-tocopherol (0.4 μg); C = D,L-γ-tocopherol (0.4 μg); D = D,L-α-tocotrienol (0.4 μg); E = D,L-α-tocopherol (0.4 μg). R_F values: A, 0.27; B, 0.29; C, 0.33; D, 0.37; E, 0.42.
Source: From Comparative analysis of tocopherols by thin-layer chromatography and high-performance liquid chromatography, in J. Chromatogr.[18]

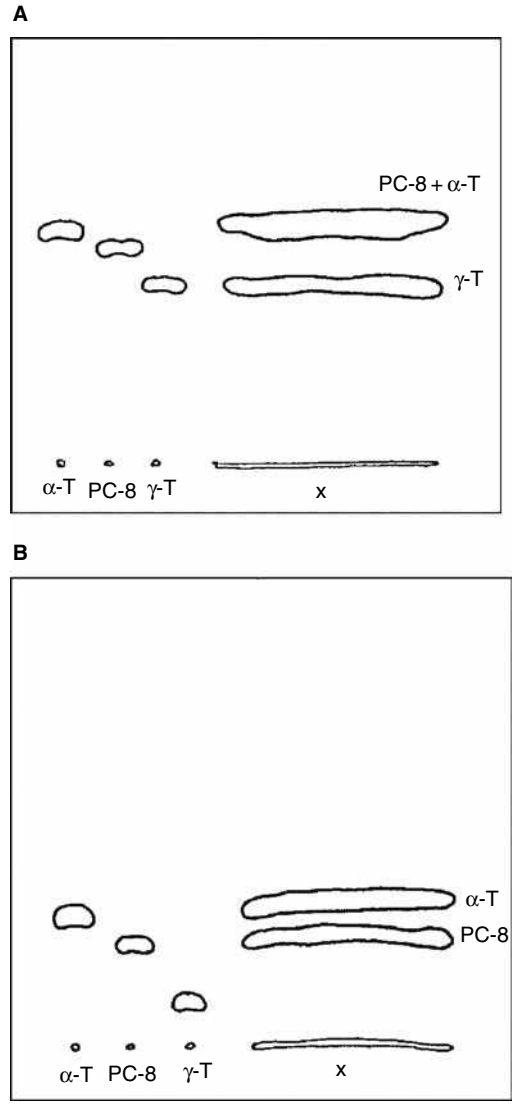

Fig. 4 (A) Preparative separation of plastochromanol-8 (PC-8) and α-tocopherol (α-T) on TLC (silica gel G, $CHCl_3$); α-T, PC-8, γ-T standards; *x*-sample (the unsaponifiable fraction of linseed oil). (B) Rechromatography of PC-8 and α-T on TLC (silica gel G, hexane–diethyl ether, 19 : 1); α-T, PC-8, γ-T standards; *x*-sample (the unsaponifiable fraction of linseed oil).
Source: From Isolation and some properties of plastochromanol-8, in Nahrung.[19]

standard compounds. The HPLC system used a Varian MCH 10 C18 Micropak column (30 cm × 4 mm), methanol–water (95 : 5, v/v) as mobile phase (2 ml/min), and detection at 296 nm. The two systems (TLC and HPLC) were considered comparable in sensitivity, reproducibility, recovery (~ 91%), and ease of application.[18]

Olejnik, Gogolewski, and Nogala-Kałucka[19] have determined α- and γ-tocopherols and plastochromanol-8 in linseed oil. TLC was applied for purification of unsaponifiable fraction of linseed oil. TLC was carried out on silica gel G. Chromatograms were developed by means of chloroform, which separated PC-8 and α-tocopherol from γ-tocopherol (Fig. 4A).[19] After reapplication, hexane–diethyl ether (19 : 1, v/v) separated PC-8 from α-tocopherol (Fig. 4B).[19]

Vitamin E compounds can be detected (about 20 μg) as dark spots in UV light. They appear violet, and detection is more sensitive (0.02 μg) on layers that contain 0.02% Na-fluorescein. Moreover, these are visible in daylight as red spots (limit of detection 2 μg). Spraying with fluorescein or dichlorofluorescein reagent produces the same effect. Non-specific visualization procedures for tocopherols and tocotrienols are based on spraying with sulfuric acid, molybdophosphoric acid, antimony(V) chloride, dipyridyliron reagent, nitric acid, copper(II) sulfate–phosphoric acid, and bathophenanthroline. α-Tocopherol was also visualized by a coupled redox–complexation reaction with iron (III), phenanthroline, and bromophenol blue.[1,2,8] Aniline blue, alkaline blue, and bromothymol blue can be also used for detection of vitamin E (1 μg)

after adsorption TLC.[9] When β-carotene was used as a TLC spray reagent, tocopherols (10 μg) appeared as yellow spots against a white background.[1,2,8] The densitogram of D-α-tocopherol after spraying dipyridyliron reagent was given by Jork et al.[8]

VITAMIN K

Physiological forms of vitamin K are vitamin K_1 (phylloquinone, phytonadione) and vitamin K_2 (farnoquinone). Active analogs and related compounds known as vitamin K are menadiol diphosphate, menadione (vitamin K_3), menadione bisulfite, phthiocol, synkayvite, menadiol (vitamin K_4), menaquinone-*n* (MK-*n*), ubiquinone (Q-*n*), and plastoquinone (PQ-*n*). Reduced vitamin K is an inactive analog. Dicoumarol, sulfonamides, antibiotics, α-tocopherol quinone, dihydroxystearic acid glycide, salicylates, iodinin, and warfarin are antagonists of vitamin K. Vertebrates and some bacteria (intestinal bacteria in humans) are exogenous sources of vitamin K. Endogenous sources of vitamin K are plants, bacteria, and all other organisms that require it. Phylloquinone (K_1), and menaquinone-4 (MK-4) are natural K vitamins and are often used as medicine to prevent intracranial hemorrhage in the newborn. Vitamin K contributes to the formation and regulation of numerous proteins in the body, but most significantly to prothrombin, a protein essential for blood clotting. Vitamin K is also necessary for converting prothrombin to thrombin, which is also required for blood clotting. Vitamin K is a key factor in the creation of many important nutrients and proteins necessary for essential body functions.

Argentation TLC (on silver nitrate-impregnated silica gel plates) and hexane–ethyl acetate–diisopropyl ether (2 : 2 : 1, v/v/v) as mobile phase were used to separate vitamins K_1, K_2, K_3, ubiquinone-6, ubiquinone-9, and ubiquinone-10 (R_F values 0.71, 0.63, 0.57, 0.42, 0.21, and 0.28, respectively).[20]

Hachuła[21] developed a sensitive spectrophotometric method for determination of vitamin K_4 in drugs (Styptobion, E. Merck) after chromatographic separation on silica gel with benzene–acetone (9 : 1, v/v) as mobile phase. Beer's law was obeyed for 0.3–1 μg/ml vitamin K_4 ($\varepsilon = 196{,}000$). No detection limit was given. The results obtained from proposed analytical procedure were in accordance with those expected and the precision of the measurement was satisfactory. The proposed method is rapid and has rather low analysis costs. Pharmaceutical preparations, including tablets, coated tablets, and injection solution, containing vitamin K_1 (I), vitamin K_3 (II), or vitamin K_4 (III), were analyzed by TLC/spectrophotometry.[22] TLC was done on silica gel HF_{254} (E. Merck) with the following mobile phases: benzene–ethyl acetate (97 : 3, v/v) for K_1, cyclohexane–chloroform–methanol–glacial acetic acid (2 : 15 : 3 : 1, v/v/v/v) for K_2, and benzene–acetone lpar;9 : 1, v/v) for K_3. The spots, located with 254-nm radiation, were scraped off, extracted with ethanol (for I), water (for II) or methanol (for III), and the vitamins were determined at 251, 234, or 225 nm, respectively, by using suitable calibration graphs.[22]

All lipoquinones at levels of 0.5 μg or more are visible as dark spots on layers containing inorganic fluorescent material when illuminated with UV light, after adding Na-fluorescein or rhodamine B or 6G to the adsorbent or by spraying the chromatographed layer with fluorescein or dichlorofluorescein reagents. These compounds can be detected in daylight and, with high sensitivity, in UV light. Vitamin K compounds can be detected with iodine vapor (brown spots), with concentrated sulfuric acid followed by heating (violet spots, limit of detection 3 μg), with molybdophosphoric acid (gray-blue spots, limit of detection 0.5 μg), and with potassium hexaiodoplatinate reagent. Long and shortwave UV light were used to detect vitamin K; under shortwave UV light, vitamin K showed an intense purple color. Vitamin K_1 was also detected with antimony(III)chloride (pink spots in visible light, limit of detection 8 μg), with iron(III) chloride (blue spot in visible light; limit of detection 8 μg), with sulfuric acid (green-brown spot in visible light; limit of detection 8 μg), with iodoplatinate (yellow and brown spots in visible and UV light, respectively; limit of detection 1–8 μg), and with phosphomolybdate (black spot in visible light; limit of detection 8 μg).[1,2,8]

SEPARATION OF MIXTURES OF LIPOPHILIC VITAMINS AND OF LIPOPHILIC VITAMINS FROM OTHER COMPOUNDS

Chromatographic systems have been developed for the reversed-phase TLC separation of lipophilic vitamins on RP-18 as stationary phase.[23] A mixture of lipophilic vitamins (A acetate, E, E-acetate, and D_3) was separated using acetonitrile–benzene–chloroform (10 : 10 : 1, v/v) as mobile phase (Table 3).[23] The applied chromatographic conditions do not permit the separation of vitamin E and vitamin E-acetate. Derivative spectrometry was used to determine vitamin A acetate in mixtures of other lipophilic or water-soluble vitamins. Spectrophotometric analysis of lipophilic vitamins enables determination of vitamin A-acetate in the presence of vitamins E, E-acetate, and D_3 and also C, B_1, and nicotinamide.

The satisfactory separation of D-α-, D-β-, D-γ-, and D-δ-tocopherol, and vitamin A acetate (R_F values 0.362, 0.287, 0.255, 0.165, and 0.635, respectively) was obtained on silica gel G using cyclohexane–*n*-hexane–isopropyl ether–ammonium hydroxide (40 : 40 : 20 : 2, v/v/v/v) as mobile phase.[24]

Perisic-Janjic, Petrovic, and Hadzić[25] described a method for the quantitative analysis of lipophilic vitamins

Table 3 R_F values of hydrophobic vitamins separated on various supports.

Support Vitamin	RP-18	Starch	Cellulose	Talc
A-acetate	0.86[a]	0.82[b]	0.85[b]	0.86[b]
A-palmitate	—	0.25[b]	0.33[b]	0.27[b]
K_1	—	0.40[b]	0.53[b]	0.45[b]
E	0.80[a]	0.63[b]	0.72[b]	0.67[b]
E-acetate	0.80[a]	0.52[b]	0.63[b]	0.56[b]
D_2	—	0.79[b]	0.82[b]	0.83[b]
D_3	0.62[a]	0.79[b]	0.82[b]	0.83[b]
K_3	—	0.45[c]	0.57[c]	0.60[c]
K_4	—	0.84[c]	0.77[c]	0.47[c]
K_5	—	0.26[c]	0.18[c]	0.09[c]

[a]Mobile phase: acetonitrile–benzene–chloroform (10 : 10 : 1, v/v/v).
[b]Mobile phase: acetone–concentrated acetic acid (3 : 2, v/v); stationary phase impregnated with paraffin oil.
[c]Mobile phase: water–dioxane–acetone–formaldehyde (85 : 20 : 15 : 25, v/v/v/v).
Adapted from Baranowska & Kadziolka[23] and Perisic-Janjic, Petrovic, & Hadzić.[25]

by TLC on starch, cellulose, and talc impregnated with paraffin oil. Vitamin A acetate, A palmitate, K_1, DL-α-tocopherol, DL-α-tocopherol acetate, D_2, and D_3 were separated with acetone–concentrated acetic acid (3 : 2, v/v), while vitamins K_3, K_4, and K_5 migrate to the front (Table 3).[25] Vitamins K_3, K_4, and K_5 can be separated on starch, cellulose, and talc using mixture of water–dioxane–acetone–formaldehyde (85 : 20 : 15 : 25, v/v/v/v) as mobile phase (Table 3).[25] Differences between the R_F values were satisfactory (except vitamins A-acetate, D_2, and D_3) and allowed for accurate identification. However, identification was still possible. Vitamin A-acetate gives blue color with $SbCl_5$ indicator, while vitamins D_2 and D_3 give reddish brown color seen as two connected spots of different colors.[25]

Most of the prenyllipids, such as chlorophylls, carotenoids, and prenylquinones, as well as tocopherols and vitamin K_1, which occur in plant lipid extracts, can be separated by TLC using silica gel plates or special mixtures of silica gel with other adsorbents.[20] But the compounds with one double bond per isoprene and others with a partially or fully unsaturated isoprenoid chain can be separated efficiently by argentation TLC. The R_F values of selected lipophilic vitamins, their provitamins, and related compounds separated by argentation TLC using different mobile phases are listed in Table 4.[20]

Wardas and Pyka[9] separated vitamins D_2, D_3, acid of vitamin A, and DL-α-tocopherol by NP-TLC and RP-TLC. Vitamins D_2 and D_3 could not be separated by NP-TLC and RP-TLC. Eleven visualizing reagents were used for detection of vitamins on TLC plates. It was found that more advantageous visualizing effects for all investigated vitamins were

Table 4 R_F values of selected lipophilic vitamins, provitamins, and related compounds separated by argentation TLC.

	$R_F \times 100$[a]				
	S1	S2	S3	S4	S5
β-Carotene (provitamin A)	7	10	64	35	—
α-Tocopherol	60	70	68	56	54
α-Tocotrienol (ξ-tocopherol)	48	58	55	45	—
β-Tocopherol	58	69	64	52	—
β-Tocotrienol (ε-tocopherol)	46	55	49	40	—
Vitamin K_1 (phylloquinone)	67	71	76	73	70
Vitamin $K_{2(20)}$ (menaquinone-4)	50	63	62	50	49
Desmethylvitamin K_1	63	70	73	63	—
Vitamin K_3 (menadion)	48	57	56	47	46
Plastoquinone-9	18	31	50	41	—
Ubiquinone-6	25	42	48	40	—
Ubiquinone-9	5	21	35	24	—
Ubiquinone-10	9	28	38	30	—
α-Tocoquinone	—	—	—	59	50
Vitamin A alcohol	—	—	—	62	51
Vitamin A aldehyde	—	—	—	62	51
Vitamin A palmitate	—	—	—	82	77
Vitamin D_2	—	—	—	32	19
Vitamin D_3	—	—	—	39	25
Ergosterol	—	—	—	28	15

[a]Solvents: S1 = hexane–ethyl acetate–diisopropyl ether (2 : 1 : 2, v/v/v); S2 = hexane–ethyl acetate–diisopropyl ether (2 : 2 : 1, v/v/v); S3 = light petroleum (b.p. 50–70°C)–chloroform–acetone (50 : 10 : 24, v/v/v); S4 = light petroleum (b.p. 50–70°C)–chloroform–acetone (50 : 10 : 17, v/v/v); S5 = hexane–ethyl acetate–diisopropyl ether (2 : 1 : 1, v/v/v).
Source: From Separation of prenylquinones, prenylvitamins and prenols on thin-layer plates impregnated with silver nitrate, in J. Chromatogr.[20]

obtained on adsorption TLC compared with partition TLC. In adsorption TLC, the limits of detection found for the vitamins followed the pattern DL-α-tocopherol > acid of vitamin A > vitamin D_2 and D_3. After separation using adsorption TLC, the best results were obtained with aniline blue, alkaline blue, phenol red, bromocresol green, and brilliant-cresyl blue, and bromophenol blue. After separation using partition TLC, the best results were obtained with bromothymol blue and helasol green. The R_F values and color formation of vitamins D_2, D_3, acid of vitamin A, DL-α-tocopherol with selected visualizing reagents are listed in Table 5.[9]

On silica gel plates (LK6DF Linear-K silica gel), diphacinone, pindone, valone, warfarin, bromadiolone, vitamins K_1 and D_3 were separated with three tested mobile phases (1,2-dichloroethane–methanol–glacial acetic acid, 90 : 8 : 2, v/v/v; chloroform–methanol, 97 : 3, v/v; and cyclohexane–1,2-dichloroethane–glacial acetic acid (75 : 25 : 0.6, v/v/v). No single phase used could separate all seven compounds. However, vitamins

Table 5 Color formation of vitamins D_2, D_3, acid of vitamin A, DL-α-tocopherol, and vitamin K_1 with spray reagents.

Vitamin	Refs.	Chromatographic plate	R_F		Color formed with visualizing reagent: Alkaline blue	Bromothymol blue	Helasol green	Bromocresol green	$SbCl_3$	$FeCl_3$	Iodo-platinate	Phospho-molybdate
D_2	[9]	Silica gel 60[a]	0.26	I	White-blue	Light blue	White	White	ns	ns	ns	ns
				II	Celadon	Blue	Light pink	Light celadon				
D_2	[9]	Silica gel 60/Kieselguhr F_{254} + paraffin oil[b]	0.39	I	—	—	—	—	ns	ns	ns	ns
				II	—	Light beige	Light orange	—				
D_3	[9]	Silica gel 60[a]	0.26	I	White-blue	Light blue	White	White	ns	ns	ns	ns
				II	Celadon	Blue	Light pink	Light celadon				
D_3	[9]	Silica gel 60/Kieselguhr F_{254} + paraffin oil[b]	0.37	I	—	—	—	—	ns	ns	ns	ns
				II	—	Light beige	Light orange	—				
A	[9]	Silica gel 60[a]	0.10	I	White	Light blue	Pink-yellow	White	ns	ns	ns	ns
				II	Light blue	Light blue	Light yellow	Light celadon				
A	[9]	Silica gel 60/Kieselguhr F_{254} + paraffin oil[b]	0.81	I	Yellow	—	Yellow	Yellow-green	ns	ns	ns	ns
				II	Yellow	Light beige	Yellow-pink	Yellow				
E	[9]	Silica gel 60[a]	0.76	I	Dark blue	Blue	Dark pink	Green	ns	ns	ns	ns
				II	Navy blue	Dark blue	Pink	Gray-celadon				
E	[9]	Silica gel 60/Kieselguhr F_{254} + paraffin oil[b]	0.31	I	—	—	—	—	ns	ns	ns	ns
				II	—	Light beige	Orange-pink	—				
K_1	[13]	Silica gel G[c]	0.92	III	ns	ns	ns	ns	Brown	Blue	Yellow	Black
				IV		—	Brown	—	Black	—	Brown	—
D_3	[13]	Silica gel G[c]	0.68	III	ns	ns	ns	ns	Pink	Brownish red	Black	Pinkish brown
				IV					—	—	Brown	—

I = evaluation 20 min after spraying of the plates with visualizing agents; II = evaluation after heating at 110°C for 15 min; III = visible evaluation; IV = evaluation in UV.
ns, not studied.
[a]Mobile phase: chloroform.
[b]Mobile phase: methanol—water, 9 : 1, v/v.
[c]Mobile phase: chloroform—methanol, 97 : 3, v/v.
Adapted from Wardas & Pyka[9] and Opong-Mensah & Porter.[13]

K_1 and D_3 were separated with a mixture of 1,2-dichloromethane–methanol–glacial acetic acid (90 : 8 : 2, v/v/v), and with a mixture of chloroform–methanol (97 : 3, v/v).[13] The R_F values obtained using chloroform–methanol (97 : 3, v/v) and color formation of vitamins D_3, and K_1 with spay reagents are listed in Table 5.[13]

Densitometrical analysis is the most important method of detection of organic compounds including lipophilic vitamins. Jork et al.[8] investigated vitamin D_3 and D-α-tocopherol on HPTLC Kieselgel 60 (Merck) plates using cyclohexane–diethylether (40 : 20, v/v) and toluene–chloroform (10 : 10, v/v), respectively. Fluorescence scan of a chromatogram track with 50 ng vitamin D_3 per chromatogram zone is presented in Fig. 5A.[8] Reflectance scan of a chromatogram track with 200 ng D-α-tocopherol per chromatogram zone is presented in Fig. 5A.[8]

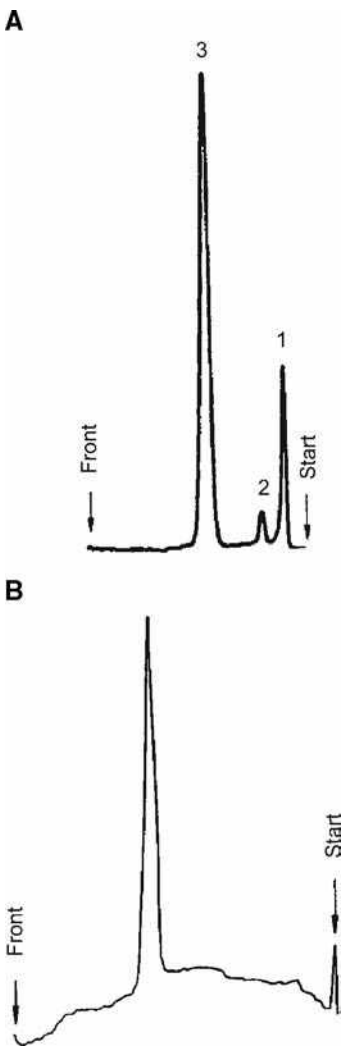

Fig. 5 a, Fluorescence scan of a chromatogram track with 50 ng vitamin D_3 per chromatogram zone: contraries (1, 2), vitamin D_3 (3). b, Reflectance scan of a chromatogram track with 200 ng D-α-tocopherol per chromatogram zone.
Source: From *Dünnschicht-Chromatographie, Reagenzien und Nachweismethoden, Physikalische und Chemische Nachweismethoden: Grundlagen, Reagenzien I*.[8]

CONCLUSIONS

In the present entry, TLC in the investigation of lipophilic vitamins was shown. It was shown that TLC as the separation method assures qualitative and quantitative investigation of lipophilic vitamins. Considering the development of densitometry and spectrodensitometry, the analysis of these vitamins is becoming more common. The application of TLC techniques, together with a densitometric scanning apparatus, now allows precise and sensitive quantification of vitamins A, D, E, and K compounds on TLC plates. The application of TLC to the separation of mixtures of fatty vitamins as well as their derivatives was introduced simultaneously. Generally, we can say that TLC stands up as the important investigative technique in relation to different chromatographic techniques. The presented data indicate that TLC can be further developed to investigate lipophilic vitamins.

REFERENCES

1. Pyka, A. Lipophilic vitamins: TLC Analysis. In *Encyclopedia of Chromatography*, 3rd Ed.; Cazes, J., Ed.; Taylor & Francis: New York, 2010; 1389–1399.
2. Pyka, A. Lipophilic vitamins. In *Handbook of Thin-Layer Chromatography*, 3rd Ed.; Sherma, J., Fried, B., Eds.; Revised and Expanded Marcel Dekker, Inc.: New York, 2003; 671–696.
3. Sliwiok, J.; Podgorny, A.; Siwek, A. Chromatographic comparison of the hydrophobicity of vitamin A derivatives. J. Planar Chromatogr.-Mod. TLC **1990**, *3*, 429–430.
4. DePaolis, A.M. Determination of all-*trans*- and 13-*cis*-retinoic acids by two-phase, two-dimensional thin layer chromatography in creams and by high-performance thin-layer chromatography in gel formulations. J. Chromatogr. **1983**, *258*, 314–319.
5. Schwartz, S.J.; Patroni-Killam, M. Detection of *cis–trans* carotene isomers by two-dimensional thin-layer and high performance liquid chromatography. J. Agric. Food Chem. **1985**, *33*, 1160–1163.
6. Nyambaka, H.; Ryley, J. An isocratic reversed-phase HPLC separation of the stereoisomers of the provitamin A carotenoids (α- and β-carotene) in dark green vegetables. Food Chem. **1996**, *55*, 63–72.
7. Hodisan, T.; Socaciu, C.; Ropan, I.; Neamtu, G. Carotenoid composition of *Rosa canina* fruits determined by thin-layer chromatography and high-performance liquid chromatography. J. Pharm. Biomed. Anal. **1997**, *16*, 521–528.
8. Jork, H.; Funk, W.; Fischer, W.; Wimmer, H. *Dünnschicht-Chromatographie, Reagenzien und Nachweismethoden, Physikalische und Chemische Nachweismethoden: Grundlagen, Reagenzien I*; VCH: Weinheim, Germany, 1989; 1a, 206, 208, 216, 217, 218, 342, 402, 418.

9. Wardas, W.; Pyka, A. New visualizing agents for fatty vitamins in TLC. Chem. Anal. (Warsaw) **1995**, *40*, 67–72.
10. Kocjan, B.; Śliwiok, J. Chromatographic and spectroscopic comparison of the hydrophobicity of vitamins D_2 and D_3. J. Planar Chromatogr.-Mod. TLC **1994**, *7*, 327–328.
11. Justova, V.; Starka, L. Separation of functional hydroxymetabolites of vitamin D_3 by thin-layer chromatography. J. Chromatogr. **1981**, *209*, 337–340.
12. Thierry-Palmer, M.; Kenney-Gray, T. Separation of the hydroxylated metabolites of vitamin D_3 by high-performance thin-layer chromatography. J. Chromatogr. **1983**, *262*, 460–463.
13. Opong-Mensah, K.; Porter, W.R. Separation of some rodenticides and related compounds by thin-layer chromatography. J. Chromatogr. **1988**, *455*, 439–443.
14. Sliwiok, J.; Kocjan, B. Chromatographische Untersuchungen der hydrophoben Eigenschaften von Tocopherolen. Fat. Sci. Technol. **1992**, *94*, 157–159.
15. Sliwiok, J.; Kocjan, B.; Labe, B.; Kozera, A.; Zalejska, J. Chromatographic studies of tocopherols. J. Planar Chromatogr.-Mod. TLC **1993**, *6*, 492–494.
16. Pyka, A.; Sliwiok, J. Chromatographic separation of tocopherols. J. Chromatogr. A, **2001**, *935*, 71–77.
17. Pyka, A.; Niestrój, A. The application of topological indexes for prediction of the R_M values of tocopherols in RP-TLC. J. Liq. Chromatogr. Relat. Technol. **2001**, *24*, 2399–2413.
18. Ruggeri, B.A.; Watkins, T.R.; Gray, R.J.H.; Tomlins, R.I. Comparative analysis of tocopherols by thin-layer chromatography and high-performance liquid chromatography. J. Chromatogr. **1984**, *291*, 377–383.
19. Olejnik, D.; Gogolewski, M.; Nogala-Kałucka, M. Isolation and some properties of plastochromanol-8. Nahrung **1997**, *41*, 101–104.
20. Lichtenthaler, H.K.; Börner, K.; Liljenberg, C. Separation of prenylquinones, prenylvitamins and prenols on thin-layer plates impregnated with silver nitrate. J. Chromatogr. **1982**, *242*, 196–201.
21. Hachuła, U. Determination of vitamin K_4 and B_1 in pharmaceutical preparations after chromatographic separation. J. Planar Chromatogr.-Mod. TLC **1997**, *10*, 131–132.
22. Marciniec, B.; Stachowicz, M. Analysis of products of drugs decomposition. XLII. Determination of vitamins K in pharmaceuticals in the presence of decomposition products. Acta Pol. Pharm. **1989**, *46*, 138–145.
23. Baranowska, I.; Kądziolka, A. RPTLC and derivative spectrophotometry for the analysis of selected vitamins. Acta Chromatogr. **1996**, *6*, 61–71.
24. Lovelady, H.G. Separation of β- and γ-tocopherols in the presence of α- and δ-tocopherols and vitamin A acetate. J. Chromatogr. **1973**, *78*, 449–452.
25. Perisic-Janjic, N.; Petrovic, S.; Hadzić, P. Separation of fat-soluble vitamins by thin-layer chromatography. Chromatographia **1976**, *9*, 130–132.

Lipophilicity: Assessment by RP/TLC and HPLC

Anna Tsantili-Kakoulidou
Department of Pharmaceutical Chemistry, University of Athens, Athens, Greece

INTRODUCTION

The purpose of this review is to summarize the conditions used to derive chromatographic lipophilicity indices, to appraise associated difficulties, and to provide an overview of their relation with octanol–water partition coefficients. In this aspect, both techniques will be discussed in parallel.

LIPOPHILICITY

The major importance of lipophilicity in drug design has been well established since the pioneering work of Hansch in the 1960s. Penetration across biological membranes during drug transport, hydrophobic interactions with receptors, as well as toxic aspects of drug actions are governed, to a great extent, by this property.[1,2] The most widely accepted measure of lipophilicity is the octanol–water partition coefficient, which is expressed in its logarithmic form as log P. A variety of experimental protocols for the determination of log P are reported in the literature.[3,4] The classical shaking flask method, via direct partition experiments, is tedious and time-consuming, while presenting limitations concerning the log P range, which can be reliably measured. Partition chromatographic techniques, in particular high-performance liquid chromatography (HPLC) and reversed-phase thin-layer chromatography (RP-TLC), permit an easy and rapid measurement of various indices that provide information on the lipophilic behavior of chemicals and offer a popular alternative, combining the possibility of automation, high dynamic range, and low sensitivity to impurities, while being compound-sparing.[5,6] Extrapolated capacity factors to pure water as mobile phase, expressed as log k_w and R_{Mw}, are considered as more representative lipophilicity indices compared to isocratic log k and R_M.[5–8] Literature is rich in research articles investigating similarities/dissimilarities between octanol–water partitioning and chromatographic retention. The selection of either technique is associated with the state of the art concerning their technology. Moreover, all assumptions dealing with the complex nature of lipophilicity as the outcome of intermolecular and intramolecular interactions, involving electronic, steric, or conformational effects, embrace chromatographic retention as well.[9,10]

STATIONARY PHASES IN PARTITION CHROMATOGRAPHY

In RP-TLC, silica gel plates impregnated with a strong hydrophobic agent (paraffin oil or silicone oil, usually 5%) have been extensively used in the past as non-polar stationary phases. Nowadays, plates covered with octadecyl-silanized (ODS) silica gel are available. In this material, the silanol groups are etherified with alkyls containing 8 (C_8) or 18 (C_{18}) carbon atoms. The low wettability of high-pressure TLC (HPTLC) plates coated with highly etherified silica gel poses limitations in the water content of the mobile phase. This problem is circumvented by the use of RP-C_{18} plates with 50% etherification. However, the presence of free silanol groups may lead to undesirable silanophilic interactions, especially with low water content in the mobile phase.[11]

ODS silica gel is, in most cases, the filling material in HPLC columns. Because the columns in HPLC are not disposable, one should take into account the pH limitations of this material (i.e., outside the pH range 2–7.5). The second problem is associated with the presence of free silanol groups, which may be responsible for silanophilic interactions, as already mentioned.[5,12–14] Nowadays, end-capped BDS or ABZ columns are available, which are treated with secondary silanization using small alkyls or zwitterionic fragments to bind the free silanol groups, thus suppressing their contribution to retention.[13]

Octadecyl–polyvinylalcohol copolymer gel, ODP, offers an alternative as a non-polar stationary phase in HPLC.[12,13] With this material, no silanophilic interactions take place and there are no pH limitations. Drawbacks of ODP columns are the large retention times observed and the longer equilibration time required.

Octanol-coated ODS columns have also been used in an effort to better simulate octanol–water partitioning. However, retention times were less reproducible due to instability and column bleeding.[13]

Recently, immobilized artificial membrane (IAM) tationary phases are becoming more popular for membrane simulation.[15] In IAM columns, silica gel is chemically bonded to phospholipids. There are various types of IAM columns. Among them, the most frequently used is IAMPC, which contains phosphatidylcholine.

MOBILE PHASES USED IN PARTITION CHROMATOGRAPHY

The mobile phases in RP-TLC and HPLC are mixtures of water or buffer with organic modifiers. With an octanol-coated stationary phase, no organic modifier is added to the mobile phase, whereas in IAM chromatography, the organic modifier is necessary only in the case of highly retained solutes.[13,15]

The most common organic modifiers are methanol, acetonitrile, and tetrahydrofuran. Acetonitrile may not be suitable for use with an ODP stationary phase,[12] whereas this solvent is the modifier of choice in IAM chromatography.[15]

The buffer composition of the aqueous component may affect the retention of ionizable solutes. Some authors suggest the use of morpholinepropanesulfonic acid (MOPS). The zwitterionic nature of this buffer offers the advantage that it does not lead to any interactions with the solutes.[12,13]

The addition of a masking agent to the mobile phase may be necessary when silanophilic interactions interfere with the partition mechanism. Silanophilic interactions are important in the case of protonated amines, or with solutes containing strong hydrogen bond acceptor groups, especially when mobile phases poor in water content are used.[12,14] Hydrophobic amines (e.g., *n*-decylamine) are suitable masking agents; however, their addition to the mobile phase adds an extra component to chromatographic conditions.

CAPACITY FACTORS AS LIPOPHILICITY INDICES

The lipophilicity indices measured by RP-TLC and HPLC are derived from the retardation factor R_f and the retention time t_r, respectively. R_f and t_r are converted to the logarithm of the capacity factor (R_M/log k') via Eqs. 1 and 2:

$$R_M = \log(1/R_f - 1) \quad (1)$$

$$\log k = [\log(t_r - t_o)/t_o] \quad (2)$$

where t_o is the retention time of an unretained compound, usually the solvent front or an inorganic salt such as potassium bichromate.

The less polar a solute is, the stronger will be its interaction with the stationary phase, which is expressed by decreasing R_f values and increasing R_M values in RP-TLC and by increasing retention times and log k' values in HPLC. Thus R_M and log k' values are directly correlated to octanol–water log P via Collander-type equations:

$$\log P = aR_M + b \quad (3)$$

$$\log P = a' \log k' + b' \quad (4)$$

where the coefficients a,b and a',b' are derived by regression analysis. The quality of the equations depends on the chromatographic conditions and the solutes.

For lipophilicity assessment, calibration equations with types similar to Eqs. 3 and 4 should be constructed using compounds with known log P values. These calibration equations are applied for further log P calculations. According to the author, it is recommended to measure more than one set of isocratic R_M or log k' values to construct the corresponding calibration equations and to calculate the average log P.[16]

Instead of isocratic capacity factors derived for a selected mobile phase composition, one can use extrapolated R_{Mw} and log k_w' values, which correspond to 100% aqueous mobile phase.[5–8,11–13]

Eqs. 5 and 6 describe the relationship between retention and fraction φ of the organic modifier present in the mobile phase:

$$R_M = A\varphi^2 - B\varphi + C \quad (5)$$

$$\log k' = A'\varphi^2 - B'\varphi + C' \quad (6)$$

The intercepts C and C' correspond to R_{Mw} and log k_w', respectively.

For a certain φ range, the quadratic term in Eqs. 5 and 6 may not be significant. In that case, R_{Mw} and log k_w' are obtained by linear extrapolation according to Eqs. 7 and 8:

$$R_M = -S\varphi + R_{Mw} \quad (7)$$

$$\log k' = -S'\varphi + \log k_w' \quad (8)$$

Linearly extrapolated capacity factors should be preferred because quadratic extrapolation may lead to erroneous overestimated values. The linearity range depends on the organic modifier as well as on the solutes. Methanol does not disrupt, substantially, the hydrogen bonding network of water and, usually, a wide linearity range is achieved relative to acetonitrile or tetrahydrofuran.

However, in the case of protonated amines, quadratic relationships were obtained with MeOH.[17] In general, for polar solutes, linearity holds within a limited range using mobile phases rich in aqueous component. In contrast, for more hydrophobic solutes, linear extrapolation is still possible with mobile phases rich in organic modifier. It has been suggested that linearity holds better for modifier concentrations that produce $0 < \log k' < 1$.[18]

ISOCRATIC VS. EXTRAPOLATED CAPACITY FACTORS

Extrapolated capacity factors, R_{Mw} and log k_w', are in the same order as the octanol–water log P values and are

considered as more general lipophilicity indices. Because the slopes in Eqs. 7 and 8 may vary considerably, the extrapolation lines may intersect each other, thereby leading to an inversion of lipophilicity in a higher percentage of organic modifiers (Fig. 1). In this aspect, a proper expression of the lipophilicity actually is found only at 100% aqueous phase composition. However, some authors argue that extrapolated capacity factors can predict log P only for compounds that do not contain strong hydrogen bond acceptor substituents.[19] Nevertheless, the problem of non-hydrophobic interactions can be faced by the proper selection of the stationary phase and the protection of the silanophilic sites.

However, extrapolated capacity factors may be affected by the nature of the organic modifier. In a study concerning the measurement of lipophilicity indices for monosubstituted benzenes by HPLC, the log k_w' values of the more polar derivatives appeared to be lower when methanol was used as an organic modifier, compared to the log k_w values obtained with acetonitrile.[12] In contrast, for non-polar derivatives, acetonitrile led to lower log k_w' values. An analogous decrease in the log k_w values for a series of lipophilic 9*H*-xanthene and 9*H*-thioxanthene derivatives was observed when tetrahydrofuran was used instead of methanol.[20] The differences in the extrapolated capacity factors described above may be attributed to changes in the hydrophobic character of the stationary phase caused by organic modifiers and water molecules dragged onto the reversed-phase material during equilibration.

It is the opinion of the author that the best simulation of the octanol–water system is achieved with (end-capped) silanized octadecylsilica gel stationary phase, methanol as the organic modifier, and a masking agent, if necessary. Depending on the structure of the solutes, in many such cases, a good correlation between the chromatographic data and log P is obtained with the coefficients a,a' and b,b' close to 1 and 0, respectively.

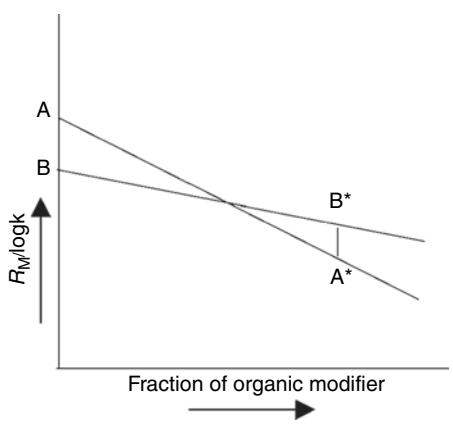

Fig. 1 Plot of R_M/log k vs. fraction of organic modifier. Inversion of lipophilicity occurs for organic modifier concentrations higher than the intersection point of the lines.

$$\log P = aR_{Mw} + b \quad (9)$$

$$\log P = a' \log k_w' + b' \quad (10)$$

Far from being a general rule, Eqs. 11–13 represent three examples of 1 : 1 correlation between log P and extrapolated capacity factors obtained under the above-recommended conditions:

$$R_{Mw} = 0.959(\pm 0.011) \log P + 0.067(\pm 0.147) \quad (11)$$

[$n = 121$, $r = 0.967$, $s = 0.353$, $F = 1703$ (RP-18 plates; from Ref.[11])]

$$\log P = 1.01(\pm 0.08) \log k_w - 0.43(\pm 0.25) \quad (12)$$

[$n = 19$, $r = 0.947$ (ABZ column; from Ref.[13])]

$$\log P = 0.91(\pm 0.03) \log k_w + 0.18(\pm 0.12) \quad (13)$$

[$n = 28$, $r = 0.983$, $s = 0.181$, $F = 763$ (ODS column + n-decylamine as masking agent; from Ref.[12])].

EFFECT OF IONIZATION ON RETENTION

To correct capacity factors for ionization, the same equations are used as for the corresponding correction of the apparent partition coefficients. Thus for monoprotic acids and bases, Eqs. 13 and 14 are suggested for extrapolated, as well as isocratic, capacity factors derived from HPLC and RP-TLC:

$$\log k_w = \log k_{w(app)} + \log(1 + 10^{pH - pK_a}) \quad \text{acids} \quad (14)$$

$$\log k_w = \log k_{w(app)} + \log(1 + 10^{pK_a - pH}) \quad \text{bases} \quad (15)$$

However, whether the effects of ionization in the octanol–water partition systems in HPLC and TLC are similar remains to be clarified. The stationary phase material and, especially the presence of the acidic silanol sites, may have an active role. Moreover, concerning the two chromatographic techniques, even in the case of identical stationary phases, an essential difference between HPLC and TLC is the fact that, in HPLC, the column is equilibrated with the mobile phase before runs are conducted. Thus the stationary phase is adjusted to the mobile phase pH, whereas on a TLC plate, a pH gradient is formed.

EFFECT OF CONFORMATION IN RETENTION

Conformational effects in lipophilicity have been well established.[9] Analogous effects, although not necessarily to the same extent, may be expected in retention. In such

cases, differences in the partitioning behavior in the octanol–water system and the chromatographic system may be manifested, thus affecting the quality of equations.

OTHER CHROMATOGRAPHIC DATA AS LIPOPHILICITY-RELEVANT EXPRESSIONS

The slope S of the regression curve used to obtain $\log k_w'$ or R_{Mw} (Eqs. 7 and 8) is considered to encode significant information on the lipophilic behavior of the solute. In a simplified aspect, the slope is thought to express, mainly, the solute/solvent interactions, whereas the intercept value is rather associated with solute stationary phase interactions. Some authors relate the slope S to the specific hydrophobic surface area.[21] Basically, the retention mechanism consists of two components: the size of the solute (reflected by its volume or surface area), and its hydrogen-bonding capacity. If there are no considerable differences in hydrogen-bonding capacity within a series of compounds, a good relationship between the slope and the intercept is anticipated:

$$S = aR_{Mw} + b$$

$$S' = a' \log k_w + b'$$

Thus slope analysis may unravel differences in hydrogen bonding within a series of compounds.[13]

The organic modifier concentration φ_o, which produces an equal molar distribution between the stationary phase and the mobile phase, leading to $\log k = 0$, has also been proposed as a measure to rank lipophilicity.[22] φ_o indices have been mainly developed for HPLC. They correspond to the quotient:

$$\varphi_o = \log k_w / S$$

Based on the φ_o concept, a fast gradient method RP-HPLC has been proposed to determine the chromatographic hydrophobicity index (CHI) as a high-throughput alternative to other lipophilicity measures.[23] For this purpose, gradient retention times (t_g) are measured and converted to CHI values by means of a calibration equation, derived by a set of standards with well-determined CHI (φ_o) values:

$$\text{CHI} = \text{slope} \times t_g + \text{intercept}$$

The absolute magnitude of the CHI parameter depends on the values assigned to the set of standards. The method has the advantage that, once the calibration equation has been established, the retention parameter is obtained from a single fast gradient run, thus saving time and solvents. The CHI parameter has been reported to correlate satisfactorily with log P.

CONCLUSIONS

RP-TLC and HPLC provide a variety of descriptors that can be used as lipophilicity indices. Among them, extrapolated capacity factors often lead to 1 : 1 correlation with octanol–water log P. On the other hand, isocratic capacity factors need fewer experiments to be determined; however, they depend strongly on chromatographic conditions. The CHI combines easy and rapid measurements with a uniform lipophilicity scale. However, both lipophilicity and reversed-phase chromatographic retention are composite phenomena and, consequently, their resemblance cannot always be anticipated. Because standard reference sets cannot be available for all structurally diverse compounds, a comparison between chromatographic indices and octanol–water log P within the series of the investigated compounds is still indispensable.

REFERENCES

1. van de Waterbeemd, H.; Testa, B. The parameterization of lipophilicity and other structural properties in drug design. In *Advances in Drug Research*; Testa, B., Ed.; Academic Press: New York, 1987; Vol. 16, 85–227.
2. Conradi, R.A.; Burton, P.S.; Borchard, R.T. Physico-chemical and biological factors that influence a drug's cellular permeability by passive diffusion. In *Lipophilicity in Drug Action and Toxicology*; Pliska, V., Testa, B., van de Waterbeemd, H., Eds.; VCH: Weinheim, 1996; 233–252.
3. Leo, A.; Hansch, C.; Elkins, D. Partition coefficients and their uses. Chem. Rev. **1973**, *71*, 525–616.
4. Hersey, A.; Hill, A.P.; Hyde, R.M.; Livingstone, J. Principles of method selection in partition studies. Quant. Struct.-Act. Relatsh. **1989**, *8*, 288–296.
5. Kaliszan, R. High performance liquid chromatographic methods and procedures of hydrophobicity determination. Quant. Struct.-Act. Relat. **1990**, *9*, 83–87.
6. Dross, K.P.; Mannhold, R.; Rekker, R.F. Drug lipophilicity in QSAR practice: II. Aspects of R_M-determinations; critics of R_M-corrections; interrelations with partition coefficients. Quant. Struct.-Act. Relat. **1992**, *11*, 36–44.
7. Tsantili-Kakoulidou, A.; El Tayar, N.; van de Waterbeemd, H.; Testa, B. Structural effects in the lipophilicity of di- and poly-substituted benzenes as measured by reversed phase high-performance liquid chromatography. J. Chromatogr. **1987**, *389*, 33–45.
8. Biagi, G.L.; Barbaro, A.M.; Recanatini, M. Determination of lipophilicity by means of reversed-phase thin layer chromatography: 3. Study for the TLC equations for a series of ionizable quinolone derivatives. J. Chromatogr. A, **1994**, *678*, 127–137.
9. Testa, B.; Carrupt, P.-A.; Gaillard, P.; Tsai, R.-S. Intramolecular interactions encoded in lipophilicity: their nature and significance. In *Lipophilicity in Drug Action and Toxicology*; Pliška, V., Testa, B., van de Waterbeemd, H., Eds.; VCH: Weinheim, 1996; 49–71.
10. Tsantili-Kakoulidou, A.; Varvaresou, A.; Siatra-Papastaikoudi, Th.; Raevsky, O. A comprehensive investigation of the

partitioning and hydrogen bonding behavior of indole containing derivatives of 1,3,4-thiadiazole and 1,2,4-triazole by means of experimental and calculative approaches. Quant. Struct.-Act. Relat. **1999**, *18*, 482–489.
11. Mannhold, R.; Dross, K.; Sonntag, C. Estimation of lipophilicity by reversed-phase thin-layer chromatography. In *Lipophilicity in Drug Action and Toxicology*; Pliška, V., Testa, B., van de Waterbeemd, H., Eds.; VCH: Weinheim, 1996; 141–156.
12. Bechalany, A.; Tsantili-Kakoulidou, A.; El Tayar, N.; Testa, B. Measurement of lipophilicity indices by reversed-phase high-performance liquid chromatography: Comparison of two stationary phases and various eluents. J. Chromatogr. **1991**, *541*, 221–229.
13. van Waterbeemd, H.; Kansy, M.; Wagner, B.; Fischer, H. Lipophilicity measurement by reversed-phase high-performance liquid chromatography (RP-HPLC). In *Lipophilicity in Drug Action and Toxicology*; Pliška, V., Testa, B., van de Waterbeemd, H., Eds.; VCH: Weinheim, 1996; 73–87.
14. El Tayar, N.; Tsantili-Kakoulidou, A.; Roethlisberger, T.; Testa, B.; Gal, J. Different partitioning behavior of sulphonyl-containing compounds in reversed-phase high-performance liquid chromatography and octanol–water systems. J. Chromatogr. **1988**, *439*, 237–244.
15. Geetha, T.; Singh, S. Applications of immobilized stationary-phase liquid chromatography: A potential in vitro technique. PSTT **2000**, *3*, 406–416.
16. Tsantili-Kakoulidou, A.; Antoniadou-Vyza, A. Determination of the partition coefficients of adamantyl derivatives by reversed phase TLC and HPLC. In *QSAR: Quantitative Structure–Activity Relationships in Drug Design*; Alan R. Liss, Inc.: New York, 1989; 71–74.
17. El Tayar, N.; van de Waterbeemd, H.; Testa, B. Measurements of protonated basic compounds by reversed-phase high-performance liquid chromatography: II. Procedure for the determination of a lipophilic index by reversed-phase high-performance liquid chromatography. J. Chromatogr. **1985**, *320*, 305–312.
18. Schoenmakers, P.J.; Billiet, H.A.H.; de Galan, L. Influence of organic modifiers on the retention behavior in reversed-phase liquid chromatography and its consequences for gradient elution. J. Chromatogr. **1979**, *185*, 179–195.
19. Yamagami, C.; Yokota, M.; Takao, N. Hydrophobicity parameters determined by reversed-phase liquid chromatography: 9. Relationship between capacity factor and water–octanol partition coefficient of monosubstituted pyrimidines. J. Chromatogr. A, **1994**, *662*, 49–60.
20. Tsantili-Kakoulidou, A.; Filippatos, E.; Todoulou, O.; Papadaki-Valiraki, A. Use of reversed phase high-performance liquid chromatography in lipophilicity studies of 9*H*-xanthene and 9*H*-thioxanthene derivatives containing an amino alkanamide or a nitrosoureido group. Comparison between capacity factors and calculated octanol–water partition coefficients. J. Chromatogr. A, **1993**, *654*, 43–52.
21. Horvath, C.; Melander, W.; Molnar, I. Solvophobic interactions in liquid chromatography with non polar stationary phases. J. Chromatogr. **1976**, *125*, 129–156.
22. Perišic-Janjić, N.U.; Acanski, M.M.; Janjić, N.J.; Lazarević, M.D.; Dimova, V. Study of the lipophilicity of some 1,2,4-triazole derivatives by RP-HPLC and TLC. JPC, J. Planar Chromatogr. **2000**, *13*, 281–284.
23. Valko, K.; Bevan, C.; Reynolds, D. Chromatographic hydrophobicity index by fast-gradient RP-HPLC: A high-throughput alternative to log *P*/log *D*. Anal. Chem. **1997**, *69*, 2022–2029.

Lipoproteins: CCC and LC Separation

Yoichi Shibusawa
Division of Pharmaceutical and Biomedical Analysis, School of Pharmacy, Tokyo University of Pharmacy and Life Science, Tokyo, Japan

Yoichiro Ito
National Heart, Lung, and Blood Institute (NHLBI), National Institutes of Health (NIH), Bethesda, Maryland, U.S.A.

Abstract
High-density, low-density, and very-low-density lipoproteins (HDLs, LDLs, and VLDLs) were purified from human serum by the combined use of countercurrent chromatography (CCC) and hydroxyapatite chromatography. Polymer-phase CCC of human serum using the cross-axis coil-planet centrifuge (cross-axis CPC) yielded two lipoprotein fractions, one containing HDLs and LDLs and the other VLDLs and serum proteins. Each fraction was concentrated and subjected to hydroxyapatite chromatography to obtain three lipoprotein fractions, all free from serum proteins. Each lipoprotein was confirmed by agarose gel electrophoresis.

INTRODUCTION

Polymer phase systems were first introduced by Albertsson[1] in the 1950s for partitioning macromolecules and cell particles. One of these two-phase solvent systems consists of one polymeric component, such as polyethylene glycol (PEG), and a high concentration of a salt such as potassium phosphate in water. Being free from any organic solvents, the system can preserve a natural structure of proteins if the pH of the system is kept within physiological range. In the past, polymer phase systems composed of PEG and potassium phosphate were most successfully used for protein separations. In these systems, proteins are distributed according to their partition coefficients; this forms the basis for their purification. For example, relatively hydrophobic proteins distribute more into the PEG-rich upper phase and hydrophilic proteins into the phosphate-rich lower phase.

Chromatographic partitioning of proteins using polymer phase systems can be performed by countercurrent chromatography (CCC)[2] using a centrifugal device: the cross-axis coil-planet centrifuge (cross-axis CPC) is mainly used for preparative-scale separations. Because of the protective effects of high polymer-salt concentrations, proteins can maintain their integrity at room temperature for a relatively long period of time, and, usually, the purification can be performed without cooling the column or collecting fractions. Combined with liquid chromatography (LC), this method has been successfully applied to separation of lipoproteins directly from human serum, as described below.[3]

APPARATUS

A photograph of the cross-axis CPC is shown in Fig. 1. The apparatus consists of a pair of horizontal rotary shafts, symmetrically mounted, one on each side of the rotary frame, at a distance of 10 cm from the centrifuge axis. A spool-shaped column holder is mounted on each rotary shaft at an off-center position 10 cm from its midpoint. The large multilayer coil separation column was prepared from polytetrafluoroethylene (PTFE) tubing with 2.6 mm I.D. by winding it on a 15.2 cm diameter holder hub, forming a single layer of left-handed coils between a pair of flanges spaced 5 cm apart. The pair of columns mounted on the rotary frame are connected in series using a flow tube to give a total capacity of 60 ml. Both inflow and outflow tubes exit together at the center of the top plate of the centrifuge case where they are tightly supported by a pair of clamps equipped with silicone rubber pads. The speed of the apparatus is regulated at 500 rpm using a speed control unit.

PARTITION COEFFICIENTS OF LIPOPROTEINS AND SERUM PROTEINS

CCC is a two-phase procedure where the separation is based on the difference in partition coefficients of solutes

Encyclopedia of Chromatography, Third Edition DOI: 10.1081/E-ECHR3-120045285

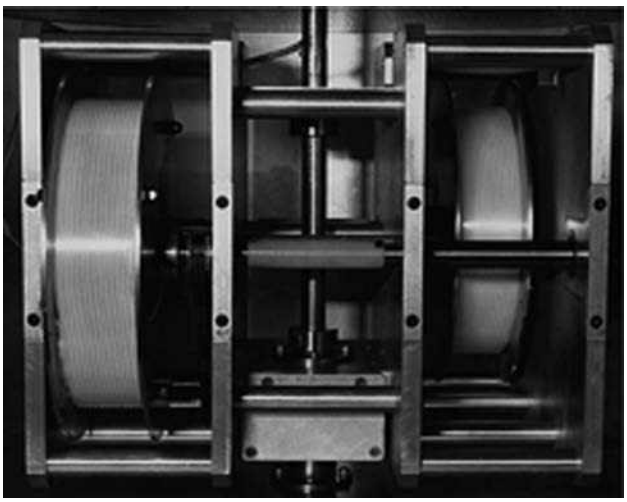

Fig. 1 Photograph of the type XL cross-axis coil-planet centrifuge.

within the phases. To achieve efficient separation of lipoproteins from human serum, it is essential to optimize the partition coefficient of each component by selecting an appropriate pH for the polymer phase system.

Fig. 2 shows the partition coefficients of three lipoproteins and three serum proteins plotted on a logarithmic scale against the pH of 16% PEG 1000–12.5% potassium phosphate buffer. The partition coefficients of serum proteins and very-low-density lipoprotein (VLDL) show an increase from 6.8 to 9.2 with increased pH, while those of high-density lipoprotein (HDL) and low-density lipoprotein (LDL) display quite different trends, i.e., they become less than 1.0 at pH 9.2, indicating that these lipoproteins are mainly distributed in the potassium phosphate-rich lower phase at high pH.

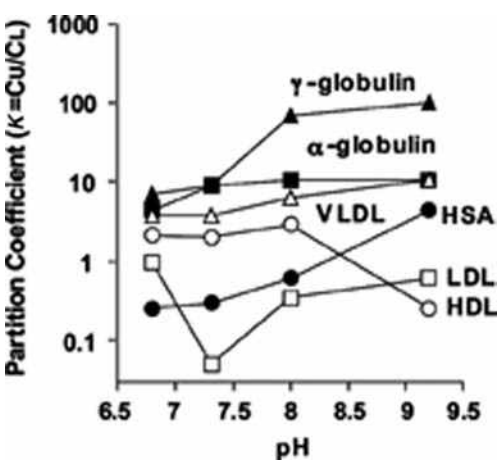

Fig. 2 Partition coefficients (K) of HDLs, LDLs, VLDLs, and serum proteins in polymer phase systems composed of 16% PEG 1000 and 12.5% potassium phosphate buffers.

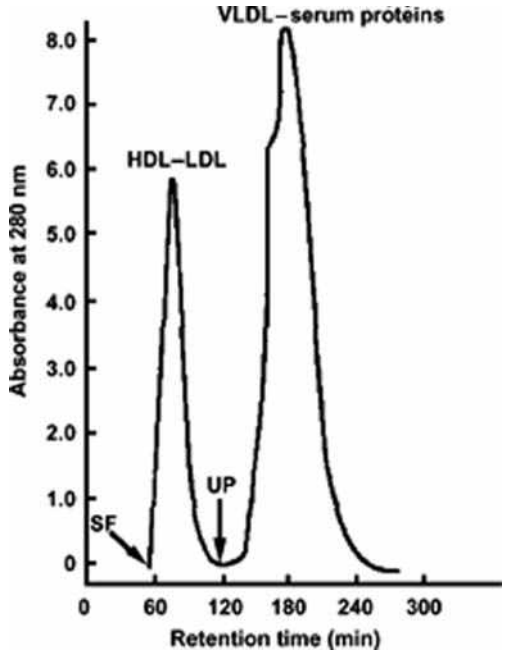

Fig. 3 CCC separation of HDL–LDL and VLDL–serum protein fractions from human serum with an aqueous polymer phase system. Column: 2.6 mm I.D. PTFE single-layer coil (×2) with 60 ml capacity; sample: 4 ml of human serum; solvent system: 16% PEG 1000–12.5% dibasic potassium phosphate at pH 9.2; mobile phase: lower phase; flow rate: 0.5 ml/min; revolution speed: 500 rpm. SF = solvent front, UP = starting point of the reversed elution mode with the upper phase.

CCC OF HUMAN SERUM

Two lipoprotein fractions (HDL–LDL and VLDL–serum proteins) from human serum were obtained using the cross-axis CPC equipped with a small-capacity column (60 ml). Fig. 3 shows a chromatogram of human serum (4 ml) obtained with the cross-axis CPC using 16% PEG 1000–12.5% potassium phosphate buffer (pH 9.2). The separation was performed at 500 rpm and at a flow rate of 0.5 ml/min using the lower phase as the mobile phase where HDLs and LDLs were eluted together near the solvent front (SF), while other proteins were retained in the column for a much longer period of time. After collecting the HDL–LDL fraction, VLDL was eluted together with serum proteins (VLDL–serum proteins fraction) by pumping the upper phase in the reverse direction (marked "UP" in Fig. 3). The separation was completed within 4.5 hr. The lipoprotein in each peak fraction was confirmed by agarose gel electrophoresis with Oil Red 7B staining, and the serum proteins were also detected by SDS–PAGE with Coomassie Brilliant Blue protein staining. The first peak contained HDLs and LDLs but no serum proteins, and the second peak contained VLDLs mixed with serum proteins.

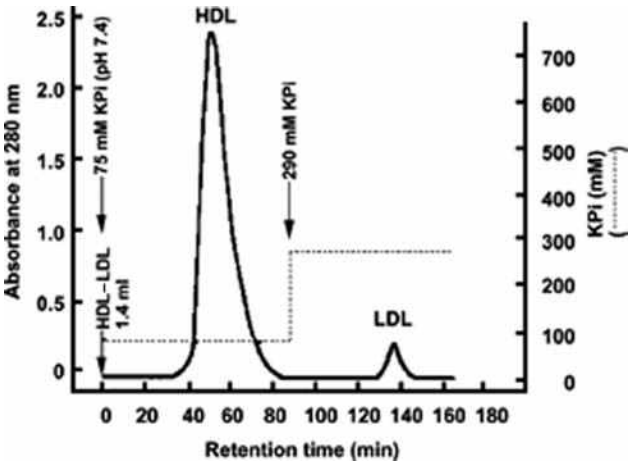

Fig. 4 Stepwise elution profile of HDLs and LDLs by hydroxyapatite chromatography. Column: Biogel HTP DNA-grade hydroxyapatite (5.0 × 2.5 cm I.D.); eluents: 75 and 290 m*M* potassium phosphate buffers at pH 7.4; flow rate: 1.0 ml/min; sample: 1.4 ml concentrated HDL–LDL CCC fraction.

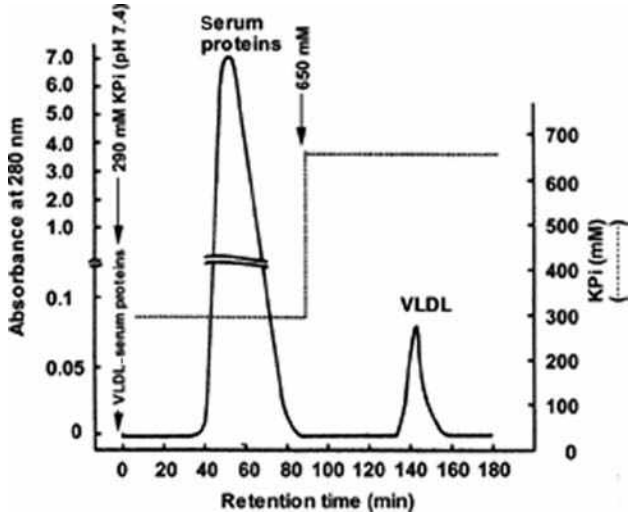

Fig. 5 Stepwise elution profile of serum proteins and VLDLs by hydroxyapatite chromatography. Column: Biogel HTP DNA-grade hydroxyapatite (5.0 × 2.5 cm I.D.); eluents: 290 and 650 m*M* potassium phosphate buffers at pH 7.4; flow rate: 1.0 ml/min; sample: 1.5 ml concentrated VLDL–serum protein CCC fraction.

HYDROXYAPATITE CHROMATOGRAPHY OF CCC FRACTIONS

The CCC fractions, HDL–LDL and VLDL–serum proteins, were each separately dialyzed against distilled water until the concentration of potassium phosphate was decreased to the level in the starting buffer used for the hydroxyapatite chromatography. These two fractions were concentrated separately by ultrafiltration. The concentrates of both fractions were chromatographed on the hydroxyapatite column. Fig. 4 shows the elution profile on hydroxyapatite obtained from the HDL–LDL fraction. A 1.4 ml volume of the concentrate was loaded onto a Biogel HTP DNA-grade column (5.0 × 2.5 cm I.D.) and eluted at 1.0 ml/min with 75 and 290 m*M* potassium phosphate buffer at pH 7.4. Two lipoprotein peaks were eluted: the first peak contained HDLs and the second peak contained LDLs.

The concentrate (1.5 ml) of the VLDL–serum proteins fraction was similarly chromatographed (Fig. 5). The separation was performed in a two-step elution process with 290 and 650 m*M* potassium phosphate buffer at pH 7.4. Most of the serum proteins, including albumin and globulins, were eluted with 290 m*M* potassium phosphate buffer at pH 7.4. The VLDLs, on the other hand, were retained in the column for a much longer period of time and were eluted with a 650 m*M* potassium phosphate buffer. Lipoproteins in the hydroxyapatite chromatographic fractions were confirmed by agarose gel electrophoresis.

CONCLUSIONS

CCC is a very useful technique for the separation and fractionation of human serum lipoproteins. The HDL–LDL and VLDL–serum protein fractions were directly obtained from human serum using a solvent system composed of 16% PEG 1000–12.5% potassium phosphate at pH 9.2. The separated HDL–LDL and VLDL–serum protein fractions were loaded onto hydroxyapatite columns and separated into HDLs, LDLs, VLDLs, and serum proteins, respectively. The combination of CCC and hydroxyapatite chromatography is a useful method for the separation of the three main classes of lipoproteins from human serum, without prior ultracentrifugation.

REFERENCES

1. Albertsson, P.A. *Partition of Cell Particles and Macromolecules*, 3rd Ed.; Wiley-Interscience: New York, **1986**.
2. Ito, Y. Principle and instrumentation of countercurrent chromatography. In *Countercurrent Chromatography: Theory and Practice*; Ito, Y., Mandava, N.B., Eds.; Marcel Dekker: New York, **1988**; 79–442.
3. Shibusawa, Y.; Mugiyama, M.; Matsumoto, U.; Ito, Y. Complementary use of counter-current chromatography and hydroxyapatite chromatography for the separation of three main classes of lipoproteins from human serum. *J. Chromatogr. B,* **1997**, *664*, 295–301.

Liquid Crystal GC Phases

Zygfryd Witkiewicz
Jerzy Oszczudlowski
Institute of Chemistry, Jan Kochanowski University, Kielce, Poland

INTRODUCTION

The search for new and highly selective stationary phases is one of the trends in gas chromatography (GC) development. Among them are chiral phases, cyclodextrins, and liquid crystals. Liquid crystals are materials with anisotropic properties. While being liquids, they maintain an ordered state of molecules, characteristic of crystals within the range of melting and clarifying points. Among several types of liquid crystals of primary importance are rod-like and thermotropic liquid crystals whose occurrence and properties depend on temperature. These liquid crystals are mainly used in displays, but as solvents with anisotropic properties they are also used for syntheses of certain chemical compounds and as chromatographic stationary phases.

The use of liquid crystals as stationary phases in gas chromatography has been described in the literature.[1,2] A survey of uses of liquid crystal applications as stationary phases in gas chromatography has been given in Refs.,[3–7] whereas a survey of uses of analytical liquid crystals as stationary phases in liquid chromatography has been presented in Refs.[8,9] The use of side-chain liquid-crystalline polymers as stationary phases in GC, high-performance liquid chromatography (HPLC), and supercritical fluid chromatography (SFC) has been described by Chain-Shu-Hsu.[10]

CHARACTERISTICS OF LIQUID CRYSTALS

The molecular structure of thermotropic, rod-like liquid-crystalline substances can be shown as a scheme:

$$\text{Substituent}_1 - [\text{Cyclic system-joining bridge}]_n - \text{Cyclic system} - \text{Substituent}_2$$

Alkyl, acyl, ester, etheric, cholesteryl, nitrile, nitro, rhodanate, and halogen groups are substituents. Terminal substituents affect the polarities of the mesophase and thermotropic properties of a liquid crystal. The cyclic system consists of aromatic, cycloalkane, and heterocyclic rings. Such groups of chemical compounds as olefin and Schiff's base and those that contain groups like nitro, azo, azoxo, and ester make the central group (the joining bridge).

Liquid crystals are substances which attain the mesomorphic state, called the mesophase, after melting. This state is maintained within a certain range of temperatures, from the melting to the clarifying points, where ordinary isotropic liquid is formed. The mesophase can range from a few degrees to about 200°C.

According to the character and the degree of the ordering of molecules in the mesophase, liquid crystals are divided into nematics, smectics, and cholesterics (Figs. 1–3). Smectics are the most ordered phases, whereas nematics are the least ordered ones.

The ordering of rod-like molecules of liquid crystals affects the various ways in which chemical compounds, whose molecules are different in shape, dissolve in them. This was employed in chromatography using liquid crystals as stationary phases.

EXAMPLES OF LIQUID-CRYSTALLINE STATIONARY PHASES

About 60,000 liquid crystals are known, and over 250 have been investigated as stationary phases in gas chromatography, high-pressure liquid chromatography, and supercritical chromatography.

In gas chromatography, thermotropic liquid crystals belonging to such groups of chemical compounds as Schiff's base, azo- and azoxy-compounds, esters, derivatives of biphenyls and terphenyls, organic complexes with transition metals, and organic polymers are used. Siloxane polymers of liquid-crystalline properties are stable within the wide range of temperatures from 50°C to 300°C.

As conventional stationary phases, liquid-crystalline stationary phases (LCSPs) are used in columns packed after depositing onto supports or, more widely, in capillary columns generally used with temperature programming. In columns of this type, a high stability of liquid-crystalline stationary phases is required within the wide temperature range where the mesophase should occur. Among such LCSPs are monomeric liquid crystals of high molecular weight and liquid-crystalline polymers.

Monomeric liquid crystals of low-molecular weight and low-melting temperatures are successfully employed to

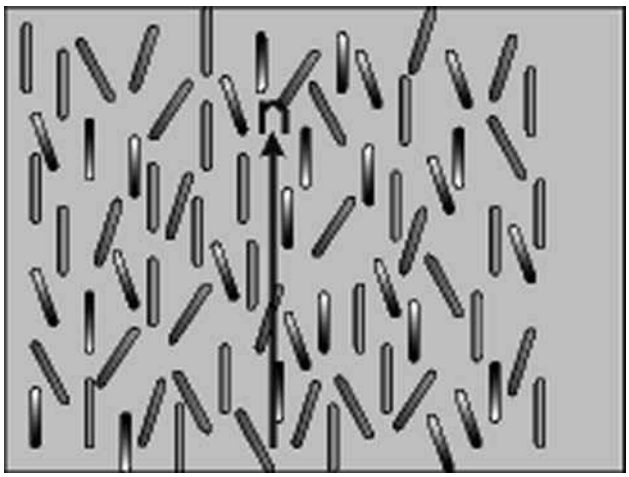

Fig. 1 Molecules are oriented parallel in average to an axis called director in the nematic phase.

separate volatile organic compounds, including their isomers (e.g., alkanes, and derivatives of benzene and naphthalene). Liquid-crystalline stationary phases of high-molecular weight and polymeric liquid crystals are employed to separate high-boiling compounds (e.g., polycyclic aromatic hydrocarbons, polychlorinated biphenyls, polychlorinated dibenzodioxines, and polychlorinated dibenzofuranes).

Examples of Polymeric Liquid-Crystalline Phases

1. Mesogenic polymeric methyl poly-siloxane (MPMS)—commercially available.
2. Mesomorphic polysiloxane (MEPSIL)—commercially available.
3. Liquid-crystalline polymer (LCP) (Scheme 1).

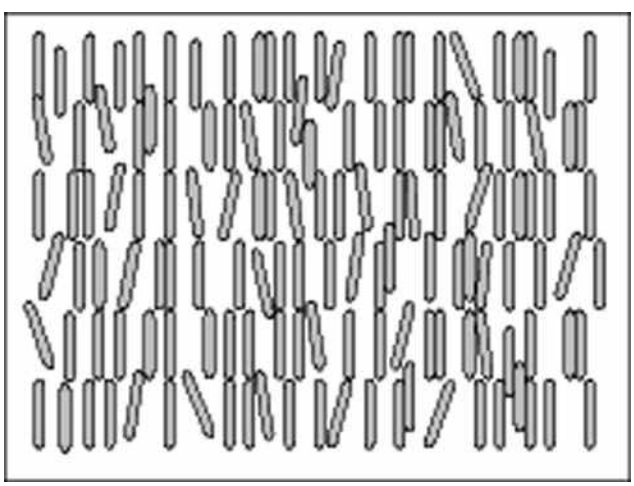

Fig. 2 Layered structure in smectic A phase.

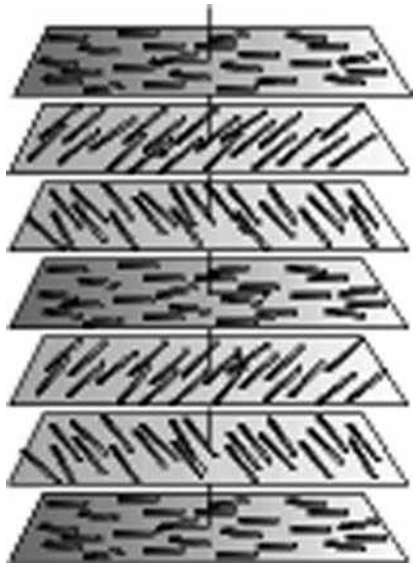

Fig. 3 Molecular structure in chiral nematic (cholesteric) phase.

Examples of Monomeric Liquid-Crystalline Phases

1. 4,4′-Azoxyanizole (PAA) with temperature of phase transition: crystalline; 119.5°C, nematic; 136.5°C, isotropic (Scheme 2).
2. bis-(Methoxybenzylidineanil-chloroaniline) $(MBCA)_2$—commercially available (Scheme 3).
3. SB-smectic—commercially available, where R_1 is $C_{10}H_{21}$ and R_2 is C_8H_{16} (Scheme 4).

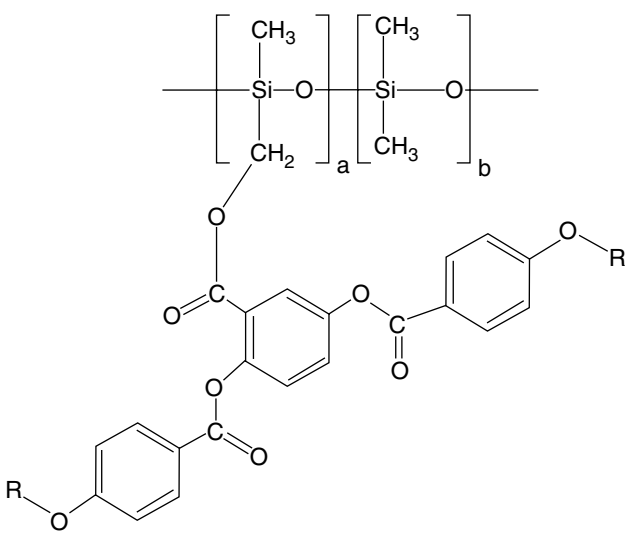

Scheme 1

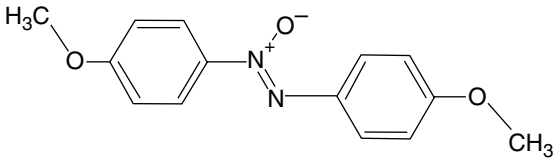

Scheme 2

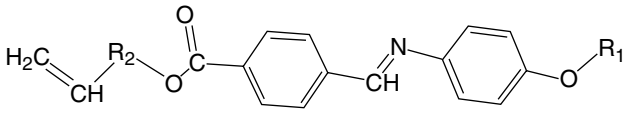

Scheme 4

4. TBBA with temperature of phase transition: crystalline; 113.0°C, smectic G; 144.5°C, smectic A; 199.0°C, nematic; 235.0°C, isotropic (Scheme 5).
5. Liquid-crystalline complex with transition metal ion [e.g., Cu(II)] (Scheme 6).

MECHANISM OF SEPARATION ON LIQUID-CRYSTALLINE STATIONARY PHASES

The chromatographic separation of components of mixtures, using most of the conventional stationary phases, is associated with the polarities of these phases, and with the polarities and polarizabilities of chromatographed substances as well as with subsequent intermolecular interactions.

The mechanism of chromatographic separation on LCSPs is mainly connected with the differentiation of the structures of molecules of chromatographed substances with the so-called stereoselectivity or stereospecificity. The differentiation of the structures of molecules of the chromatographed substances results from the ordering of the liquid crystal structure and depends on the type of mesophase and on thermodynamic effects of dissolving components of the chromatographed mixture in LCSP.[11] The effect of the separation of components of mixtures on LCSPs is associated with the different energies of the interactions of components of these mixtures with liquid crystals.

On the basis of the dependence of the selectivity coefficients (α) of the tested substances on temperature: $\ln \alpha = f(1/T)$, it is possible to determine the selectivities of liquid crystals in relation to the substances of molecules that are different in shape. However, on the basis of the dependence: $\ln \alpha = -\Delta(\Delta G_{a,b})/(RT)$, it is possible to determine, quantitatively, the differences of partial molar free energies of the substances a and b that are chromatographed on liquid crystals.

Liquid-crystalline stationary phases are particularly useful to separate isomers. Isomers that are more elongated in shape (e.g., *p*-xylene) are retained in a column filled with LCSPs longer than isomers that are less elongated in shape (e.g., *m*-xylene). The retention of isomers of chromatographed substances considerably depends on the type of the mesophase of the liquid-crystalline stationary phase. This results from the fact that the type of mesophase affects the dissolution and diffusion of isomers of the chromatographed substance to a different degree. On the whole, nematic liquid crystals show the best separation properties in relation to isomers but, in some cases, very good separation can be obtained on smectic and cholesteric stationary phases.

Diffusion and dissolution of substances chromatographed on stationary phases are determined by the mass transfer resistance, which affects the efficiencies of chromatographic columns. Efficiencies of columns with LCSPs are generally lower than those of columns with conventional stationary phases. Therefore, mixtures of LCSPs with conventional stationary phases can be advantageous. The mixture of a liquid crystal with a conventional stationary phase increases the efficiency of a column by improving the homogeneity of the stationary phase film on the wall of a capillary column. The mixture of two liquid crystals can also prove advantageous. The properties of combined stationary phases are described elsewhere.[12]

Some monomeric LCSPs of high-molecular weight have been found to separate high-boiling chemical compounds at temperatures corresponding to the solid of a liquid

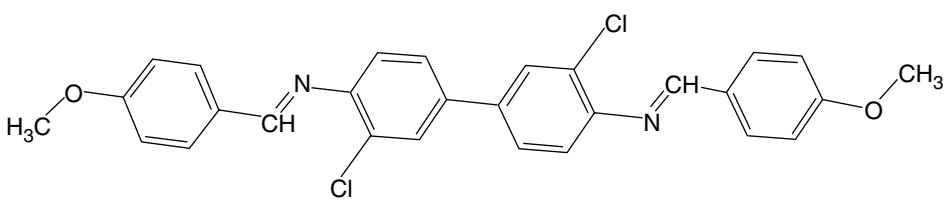

Scheme 3

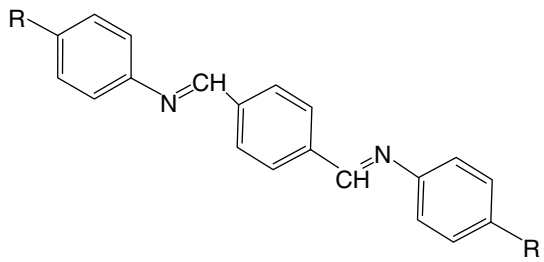

Scheme 5

crystal.[13] In such conditions, a good separation is obtained in a shorter time than during the separation in the mesophase range. This phenomenon can probably be accounted for by the local transition of a liquid crystal to liquid under the influence of the chromatographed substance interacting with it.

With a view to obtaining stationary phases of the wide temperature range of the mesophase, of high stability in columns, and of good separation properties, more attention is paid to polymeric liquid crystals, including those in the form of complexes with transition metal ions [e.g., Cu(II), Zn(II), and Ni(II)]. The separation ability of the latter is considered to be connected with both their ordered structures and the possibility of exchanging organic ligands of a liquid crystal with organic substances.[14] The separation on these LCSPs is complex and, in the case of mixtures whose components can interact with LCSPs according to both mechanisms, the separations obtained can be very good.

While investigating interdependences between general physico-chemical properties of liquid crystals and their separation ability, apart from traditional methods of physico-chemical investigations, methods of inverse gas chromatography are also used.[15]

APPLICATION EXAMPLES

Liquid-crystalline stationary phases are used to analyze a great number of chemical compounds such as polycyclic aromatic hydrocarbons, polychlorinated biphenyls, polychlorinated dibenzodioxins, polychlorinated dibenzofurans, polychlorinated naphthalenes, terpenes, steroids, pesticides, pheromones, etc.

On the monomeric LCSP called 4,4′-biphenylene-bis (4-*n*-butyloxy-benzoate) placed in a capillary column, 12 polynuclear aromatic hydrocarbon (PAHs) were separated in the mixture derived from coal tar (Fig. 4). The chromatogram of selected PAHs on metallomesogen stationary phase is presented in Fig. 5. Chromatograms of selected volatile aromatics compounds on monomeric stationary phases are presented in Figs. 6 and 7.

CONCLUSIONS

It is possible to achieve good separation of drugs, environmental pollutants, and components of biological liquids having electron donor properties on liquid-crystalline complexes with ions of transition metals. In recent years, remarkable progress in research on the use of liquid-crystalline compounds as stationary phases, in both gas

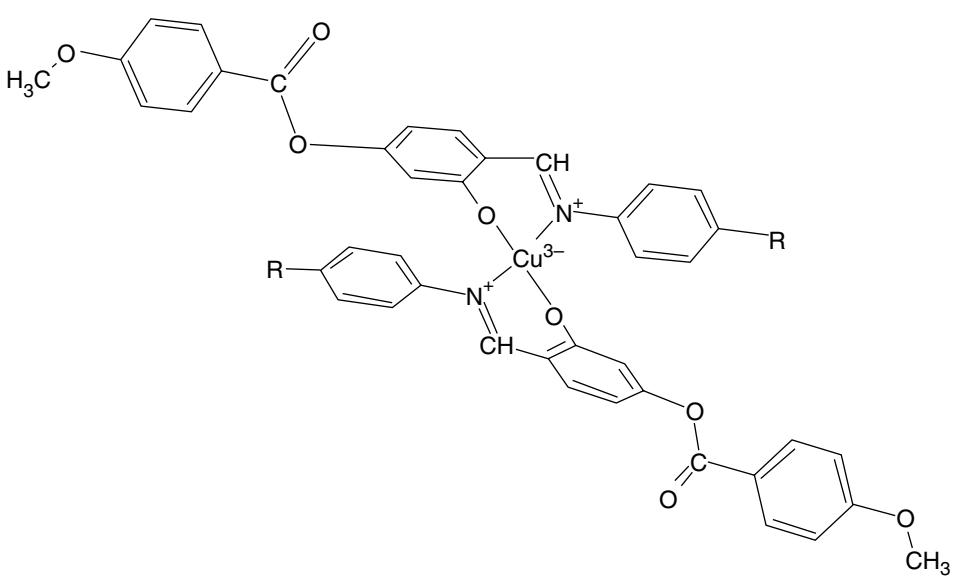

Scheme 6

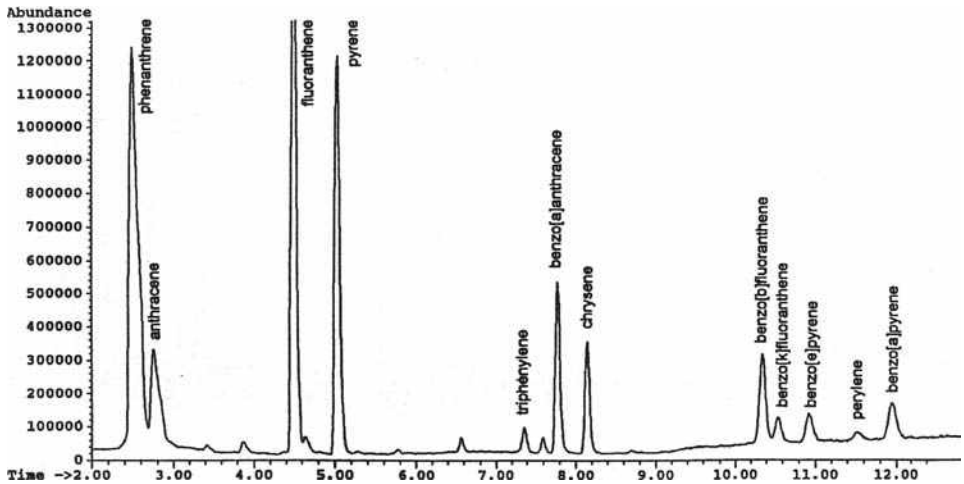

Fig. 4 Chromatogram of the separation of PAHs contained in coal tar on monomeric liquid crystal.
Source: From Separation of polycyclic aromatic hydrocarbons by capillary gas chromatography using high temperature liquid crystalline stationary phases, in Chem. Anal.[16]

chromatography and liquid chromatography, has been observed. However, it is noteworthy that the commercialization of research achievements is still of little importance, and liquid-crystalline stationary phases are not so popular

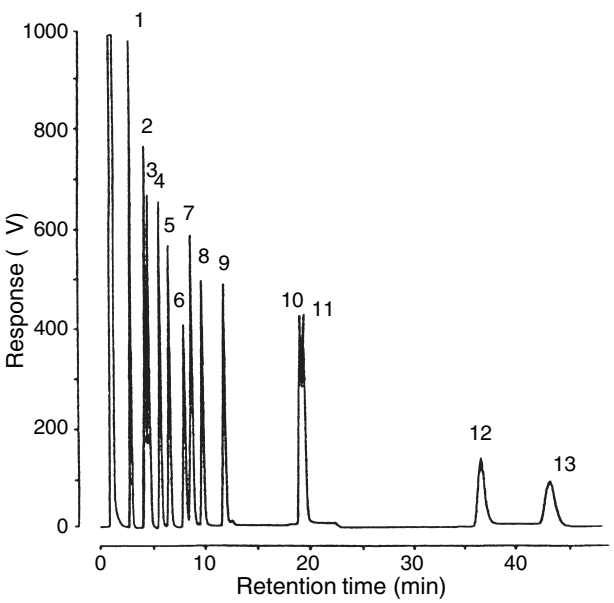

Fig. 5 Chromatogram of selected PAHs on metallomesogen phase. Temperature programmed from 150°C to 190°C at 3°C/min. 1) naphthalene; 2) 2-methylnaphthalene; 3) 1-methylnaphthalene; 4) biphenyl; 5) diphenylmethane; 6) acenaphthylene; 7) acenaphthene; 8) dibenzofuran; 9) fluorine, 10) phenanthrene; 11) anthracene; 12) fluoranthene; and 13) pyrene.
Source: From Synthesis and characterization of the novel wall coated capillary column for the separation of polycyclic aromatic hydrocarbons, in J. Chromatogr. A.[14]

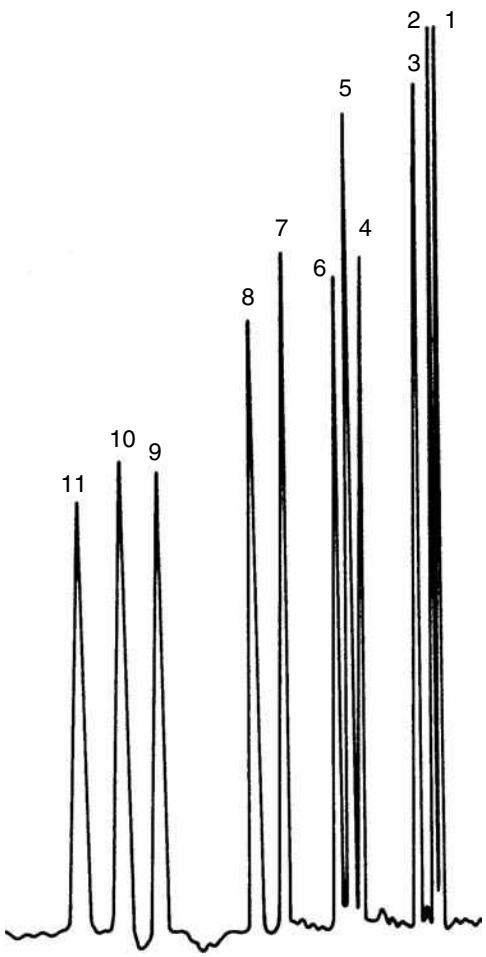

Fig. 6 Chromatogram of the separation of selected hydrocarbons on monomeric liquid-crystalline stationary phases.[3] Temperature of capillary column: 50°C. Time of separation: 14 min. 1) hexane; 2) heptane; 3) octane; 4) *m*-xylene; 5) *p*-xylene; 6) *O*-xylene; 7) *m*-ethyltoluene; 8) *p*-ethyltoluene; 9) *m*-diethylbenzene; 10) *O*-diethylbenzene; and 11) *p*-diethylbenzene.

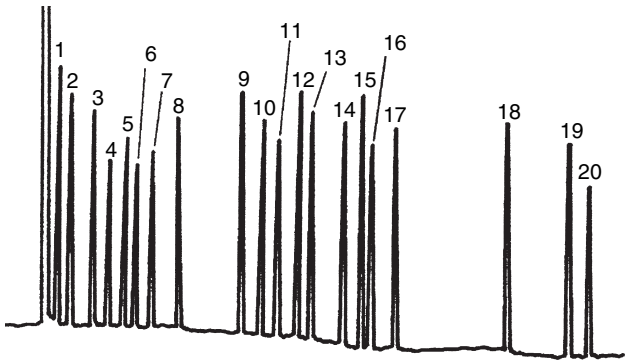

Fig. 7 Chromatographic separation of volatile aromatic compounds on LCSP. *N,N′*-diphenyl-[4-(2,3,4-*tri*-(2-methoxyethoxy)-ethoxy)benzylidene) imine]-piperidine in the nematic state. 1) α-pinene; 2) β-pinene; 3) eucalyptol; 4) limonene; 5) D-camphor; 6) linalool; 7) linalyl acetate; 8) citronellal; 9) terpineol; 10) menthol; 11) borneol; 12) nerol; 13) citronellol; 14) geraniol; 15) estragole; 16) thymol; 17) carvacrol; 18) *cis*-isoeugenol; 19) anethole; and 20) *trans*-isoeugenol.
Source: From Synthesis and properties of two new liquid crystals: an analytical and thermodynamic, in J. Chromatogr. A.[17]

as conventional stationary phases, and that the tradeoff related to liquid-crystalline stationary phases is still low.

REFERENCES

1. Kelker, H. Kristallin-Flussige schmelzen als stationare Phasen in der Gas-Flussigkeits-Verteilungschromatographie. Z. Anal. Chem. **1963**, *198*, 254.
2. Dewar, M.J.S.; Shroeder, J.P. Liquid crystals as solvents. I. The use of nematic and smectic phase in gas-liquid chromatography. J. Am. Chem. Soc. **1964**, *86*, 5235.
3. Witkiewicz, Z. Liquid-crystalline stationary phases for gas chromatography. J. Chromatogr. **1982**, *251* (3), 311–337.
4. Witkiewicz, Z. Application of liquid crystals in chromatography. J. Chromatogr. **1989**, *466* (1), 37–87.
5. Witkiewicz, Z. Liquid crystals in chromatography. In *Liquid Crystals—Applications and Uses*; World Scientific Publishing: Singapore, 1991.
6. Witkiewicz, Z.; Mazur, J. Liquid-crystal stationary phases in capillary columns. LC-GC **1990**, *8* (3), 224–234.
7. Witkiewicz, Z.; Oszczudłowski, J.; Repelewicz, M. Liquid-crystalline stationary phases for gas chromatography. J. Chromatogr. A, **2005**, *1062* (2), 155–174.
8. Gritti, F.; Felix, G. Application of liquid crystals in liquid chromatography. From low- to high-molecular-weight liquid crystals. Chromatographia **2002**, *55*, 523–532.
9. Witkiewicz, Z.; Oszczudłowski, J.; Repelewicz, M. Liquid crystalline stationary phases for high-performance liquid chromatography. Chem. Anal. (Warsaw) **2003**, *48*, 397–412.
10. Chain-Shu-Hsu The application of side-chain liquid-crystalline polymers. Progr. Polym. Sci. **1997**, *22*, 829–871.
11. Ammar-Khodja, F.; Guermouche, S.; Guermouche, M.H.; Rogalska, E.; Rogalski, M.; Judeinstein, P.; Bayle, J.P. A thermodynamic approach to understanding liquid crystal selectivity in gas chromatography. Chromatographia **2003**, *57*, 249–254.
12. Sied, M.B.; Lopez, D.O.; Tamarit, J.L.I.; Bario, M. Liquid crystal binary mixtures 8CB + 8OCB: Critical behaviour at the smectic a—nematic transition. Liq. Cryst. **2002**, *29*, 57–66.
13. Berdague, P.; Perez, F.; Courtieu, J.; Bayle, J.P.; Abdelhadi, O.; Guermouche, S. Investigation of thermal and analytical properties of two nematic liquid crystals by gas chromatography. Chromatographia **1995**, *40*, 581–586.
14. Chen-Ying Liu; Cho-Chum Hu; Cheng-Lung Yang Synthesis and characterization of the novel wall coated capillary column for the separation of polycyclic aromatic hydrocarbons. J. Chromatogr. A, **1997**, *773*, 199–208.
15. Price, G.J.; Shillcock, I.M. Inverse gas chromatography study of the thermodynamic behaviour of thermotropic low molar mass and polymeric liquid crystals. Phys. Chem. Chem. Phys. **2002**, *4*, 5307–5316.
16. Kraus, A.; Kraus, G.; Kubinec, R.; Ostrovsky, L.; Sojak, L. Separation of polycyclic aromatic hydrocarbons by capillary gas chromatography using high temperature liquid crystalline stationary phases. Chem. Anal. (Warsaw) **1997**, *42*, 497–502.
17. Judeinstein, P.; Berdague, P.; Bayle, J.P.; Rogalska, E.; Rogalski, M.; Petit-Jean, D.; Guermouche, M.H. Synthesis and properties of two new liquid crystals: an analytical and thermodynamic. J. Chromatogr. A, **1999**, *859*, 59–67.

Liquid–Liquid Partition Chromatography

Anant Vailaya
Merck Research Laboratories, Rahway, New Jersey, U.S.A.

INTRODUCTION

Liquid–liquid partition chromatography (LLPC), employing an organic–aqueous two-phase solvent system and a silica support to separate amino acids, was pioneered by Martin and Synge,[1] for which they received the Nobel Prize. Its invention presented a significant advancement over conventional adsorption-based chromatographic processes that were rather unfavorable, due to the energetic heterogeneity of the adsorbent surface. By replacing the solid surface with a layer of an immiscible liquid to retain the solutes, much higher separation efficiencies could be obtained with LLPC. Its scope was later expanded to resolve water-insoluble sample mixtures as well as to isolate biopolymers by introducing organic–organic and aqueous–aqueous two-phase systems, respectively, and by extending the range of supports to include cellulose, dextran, and polymerbased supports.

The rapid development of hydrocarbonaceous bonded phases (non-polar stationary phases with hydrocarbon chains covalently attached to the silica support) in the 1970s and 1980s for the popular reversed-phase chromatographic (RPC) technique has, however, eclipsed this technique somewhat, lately. Nevertheless, LLPC has become one of the most powerful separation techniques for the isolation of natural products and biopolymers.

FUNDAMENTAL PRINCIPLES AND THEORETICAL BACKGROUND

Martin and Synge provided the first theoretical treatment of LLPC by adapting the concept of theoretical plates which had been developed, mainly, for distillation and countercurrent extraction. According to the theory, a chromatographic column is considered to consist of a number of theoretical plates, within each of which perfect equilibrium occurs between the mobile and the stationary phases. Unlike in RPC employing hydrocarbonaceous bonded stationary phases where the retention mechanism is still the subject of controversy,[2] three distribution processes contributing to the total retention of the solute may be clearly identified in LLPC systems. They are (a) partitioning between the two bulk liquid phases, (b) adsorption at the surface of the support, and (c) adsorption at the liquid–liquid interface. Assuming an inert support with large pores that minimize solute adsorption at the support surface and weak adsorption at the liquid–liquid interface, solute retention associated with undesirable adsorption effects may be neglected. Thus, separation in LLPC may be visualized as a multistep partition process, similar to countercurrent distribution, in which the differential migrations of various sample constituents are governed by their partition coefficients and by the volume ratio of the two phases. Then, the magnitude of solute retention in LLPC, measured under isocratic condition by the retention factor, k', is given by

$$k' = \frac{KV_s}{V_m} \tag{1}$$

where K is the partition coefficient of the solute in the two-phase system employed, V_m is the volume of the mobile phase, measured by an inert tracer and V_s is the volume of the stationary phase.The retention factor is evaluated directly from the chromatogram as

$$k' = \frac{V_r - V_m}{V_m} \tag{2}$$

where is the retention volume of the solute.

Shake-flask measurements are often employed to design a suitable LLPC system for a given sample mixture by assisting in the selection of the two phases in which the compound of interest shows a partition coefficient sufficiently different from those of the impurities. One of the two phases is then immobilized on a suitable support that is packed into the column, and the second phase is used as the mobile phase. In general, partition coefficients of solutes obtained from static experiments compare favorably with those obtained from chromatographic experiments.[3] A comprehensive thermodynamic treatment of LLPC can be found in Ref.,[4] and the prediction and control of zone migration is discussed extensively in Ref.[5] Liquid–liquid partition chromatography systems have been used with or without stationary-phase support. Support-free LLPC has been classified as countercurrent chromatography (CCC). High-speed CCC techniques, based on planetary motion and coaxial orientation of the coiled column, have been developed that achieve both high partition efficiency and excellent retention of the stationary phase, thus circumventing the need for stationary-phase supports.[6]

Encyclopedia of Chromatography, Third Edition DOI: 10.1081/E-ECHR3-120040039

Liquid–liquid partition chromatography systems employing stationary-phase supports have been applied in both paper and column chromatographic modes. Paper strips impregnated with the liquid stationary phase are employed as supports for paper chromatography.[5] Column supports for LLPC bind the liquid stationary phase selectively enough to immobilize it and thus prevent its bleeding by the mobile phase. The support surface is homogeneously coated with the stationary phase and is sufficiently large to generate an interface for solute partitioning. Given these considerations, macroporous supports of average pore diameter greater than 50 nm are most suitable as column packings. Supports with smaller pores might contribute to retention by adsorption of solutes. In principle, both organic- and inorganic-based column packings can be employed in LLPC. Soft packings, such as cellulose, dextran, polymers, and diatomaceous earth, which do not withstand high pressures, are preferably used as larger particles at low pressures. On the other hand, microparticulate and bonded silicas are the supports of choice in the high-performance mode.

In the separation of large biopolymers, such as proteins and nucleic acids, specific supports characterized by large pores and bonded structure have been developed for LLPC employing poly(ethylene glycol) (PEG)–dextran two-phase aqueous–aqueous system. Bonded silica [e.g., LiChrospher® Diol (typically 1000 Å pore size and 10 μm particle size)] or a hydrophilic methacrylate polymer (e.g., Fractogel®) are chemically modified to form polyacrylamide chains of defined lengths that facilitate the selective binding of a dextran-rich aqueous phase. Polymer-based materials serve frequently as phase supports insensitive to high pH systems.

Columns for LLPC are prepared by using solvent evaporation, direct coating, precipitation, or a dynamic coating technique.[3] In the solvent-evaporation technique, the non-volatile liquid stationary phase is dissolved in a volatile solvent and mixed with the dry support. Then, the solvent is slowly removed by rotating the suspension in a rotary evaporator until the coated support remains as a dry, free-flowing powder. In the direct coating technique, the liquid stationary phase is pumped through the column, and then the excess is displaced by elution with a mobile phase saturated with the stationary phase. In the precipitation technique, the liquid stationary phase precipitates in the support pores when a solvent, which is not miscible with the liquid stationary phase, is pumped through the column. Finally, the liquid-mobile phase saturated with a liquid stationary phase is pumped through the prepacked column in the dynamic coating technique. The liquid stationary phase is adsorbed at the surface of the support until it builds a multilayer and completely fills the pore volume.

LIQUID–LIQUID SYSTEMS

Binary and sometimes ternary systems employing phases of different polarity, which is characterized by Hildebrand's solubility parameter[7] or Snyder's polarity index,[8] are used for LLPC separations. Applying the solubility parameter concept, various organic–organic, organic–aqueous, and aqueous–aqueous LLPC systems have been utilized to modulate solute retention. Based on polarity differences, LLPC can be operated in both normal phase (polar stationary phase, non-polar mobile phase) and reversed-phase (polar mobile phase and non-polar stationary phase) modes. Mobile phases typically used in the normal-phase mode are aliphatic hydrocarbons such as hexane, heptane and isooctane, alcohols, tetrahydrofuran (THF), methylene chloride, dioxane, and aromatic solvents. Stationary phases in the normal-phase mode include water, formamide, glycerol, and glycols. In the reversed-phase mode, hydro-organic mixtures such as acetonitrile–water and methanol–water are employed as mobile phases, whereas non-polar solvents such as squalane, octanol, and aliphatic hydrocarbons are used as stationary phases. For the separation of large biopolymers based on aqueous–aqueous LLPC systems, a PEG-rich aqueous phase forms the mobile phase, and the dextran-rich aqueous phase is immobilized on the polyacrylamide support to form the stationary phase.

APPLICATIONS

A number of advantages of current LLPC systems make them attractive for widespread application in the separation and isolation of low-molecular-weight compounds as well as macromolecules. Among them are simple preparation of bulk liquid phases, high reproducibility of retention and selectivity under isothermal conditions and lesser contamination, higher efficiency, and longer lifetime compared to adsorbent columns. Some of the most common applications of LLPC are now described.

Small Molecules

Liquid–liquid partition chromatography employing organic–organic, organic–aqueous, and aqueous–organic binary systems with column support have been used to separate small molecules of wide polarity.[3] A majority of applications involve the use of LLPC systems in the normal-phase mode (e.g., the separation of polyaromatic hydrocarbons, alcohols, esters, alkylated and chlorinated aromatic derivatives, pesticides, herbicides, and steroids). Several nitrogen-containing compounds, radionuclides, derivatives of aromatic carboxylic acids, benzodiazepines, aromatic compounds, and naphthalenesulfonic acids have successfully been separated in the reversedphase mode. Many ternary LLPC systems in both the normal-phase and reversed-phase modes have also been employed in the separation of polyaromatic hydrocarbons, benzodiazepines, steroids, metal chelates, glycosides, metabolites, dansyl amino acids, herbicides, aliphatic carboxylic and dicarboxylic acids, sulfonic acids, nucleosides, barbiturates,

chlorinated phenols, and alkylbenzenes. Support-free high-speed CCC has been employed in the separation of dyes, rare earth and certain inorganic elements, as well as in the preparative and analytical applications of medicinal herbs and other natural products, such as alkaloids, tannins, flavonoids, marine compounds, and anthraquinones.[6]

Biopolymers

Classical LLPC using aqueous–aqueous polymer systems based on Albertsson's[9] PEG–dextran system has provided a versatile tool for the separation of proteins and nucleic acids, thus increasing the arsenal of biopolymer purification methods currently dominated by gel filtration, ion-exchange chromatography, and affinity chromatography RPC.The technique operates on the basis of the biopolymers partitioning between the top PEG-rich aqueous mobile phase and the bottom dextran-rich aqueous stationary.[10] Factors that depend on the nature of the protein, such as size, surface area, and hydrophobicity, determine their partition in the PEG–dextran systems. Other factors associated with the nature of the two-phase system that strongly influence protein retention in LLPC are the size of the phase-forming polymers, the pH of the system, and the presence of salts, zwitterions, detergents and organic solvents.

Liquid–liquid partition chromatography techniques based on aqueous–aqueous systems have successfully been employed in the fractionation of crude human serum, purification of steroid hormone-binding proteins from human serum, isolation of basic proteins from crude bacterial extracts, purification of immunoglobulins and monoclonal antibodies, DNA fractionations by size, topology and base sequence, as well as the isolation of soluble and ribosomal RNAs in preparative amounts from bulky mixtures.[10] High-speed CCC using PEG–dextran system has also been employed in the separation of proteins.[6]

REFERENCES

1. Martin, A.J.P.; Synge, R.L.M. A new form of chromatogram involving two liquid phases. Biochem. J. **1941**, *35*, 1358–1368.
2. Vailaya, A.; Horváth, Cs. Retention in reversed-phase chromatography: partition or adsorption? J. Chromatogr. A, **1998**, *829*, 1–27.
3. Kraak, J.C.; Crombeen, J.P. *Practice of High Performance Liquid Chromatography*; Engelhardt, H., Ed.; Springer-Verlag: Berlin, 1986; 182–194.
4. Locke, D.C. In *Advances in Chromatography*; Calvin, J., Keller, R., Eds.; Marcel Dekker: New York, **1969**, Vol. 8, 47–89.
5. Soczewinski, E. In *Advances in Chromatography*; Calvin, J., Keller, R., Eds.; Marcel Dekker: New York, **1968**, Vol. 5, 3–78.
6. Ito, Y.; Conway, W.D. *High Speed Countercurrent Chromatography*; Wiley–Interscience: New York, 1996.
7. Horváth, Cs.; Synder, L.R.; Karger, B.L. *Introduction to Separation Science*; Wiley–Interscience: New York, 1974; 49–55, 268–276.
8. Snyder, L.R. Classification of the solvent properties of common liquids. J. Chromatogr. Sci. **1978**, *16*, 223–234.
9. Albertsson, P.Å. *Partition of Cell Particles and Macromolecules,* 2nd Ed.; Wiley–Interscience: New York, 1971.
10. Müller, W. Liquid-liquid partition chromatography of biopolymers in aqueous two-phase systems. Bioseparation **1990**, *1*, 265–282.

Long-Chain Branching Macromolecules: SEC Analysis

Andre M. Striegel
Department of Chemistry, Florida State University, Tallahassee, Florida, U.S.A.

INTRODUCTION

Long-chain branching (LCB), generally thought of as when the length of the branch or branches is comparable to (or is a substantial fraction of) that of the main macromolecular backbone, can influence a variety of chemical, physical, processing, and end-use properties of polymers and polymer solutions. The multiplicity of end-groups that is created as a result of an increase in branches can affect the chemical reactivity of the molecule, while the changes that LCB brings about in space-filling physical properties affect the viscosity and elasticity of melts as well as the viscosity, sedimentation behavior, and angular distribution of scattered radiation of dilute polymer solutions.[1]

In an size-exclusion chromatography (SEC) also known as gel permeation chromatography (GPC) experiment, a branched macromolecule elutes from the column later than a linear macromolecule of equal chemistry and molar mass. As the branched polymer occupies a smaller solvodynamic volume in solution than does its linear counterpart, the former experiences a longer statistical path in its passage through the porous column packing than does the linear analyte.[2] This, of course, assumes that we are operating within the separation range of the column and that the separation proceeds by a strict size-exclusion mechanism (i.e., that the enthalpic contribution to the separation process is minimal).

In this chapter, the analysis of LCB in macromolecules using SEC with multiple detection is described.[3] While the qualitative information obtained from this type of analysis is mentioned, particular attention is paid to the requirements necessary for accurate, quantitative determination of LCB, of the long-chain branching distribution (LCBD), and of the fractal dimension (d_f) of macromolecules.

QUANTITATING THE MACROMOLECULAR LCBD BY SEC/MALS

Virtually every chromatographic method of quantifying the LCB of macromolecules harkens back to the classic 1949 publication by Zimm and Stockmayer.[4] There, the authors derived the root-mean-square (rms) radius of a polymer in a near-infinitely dilute solution, $\langle r^2 \rangle^{1/2}$, and showed how the ratio of the mean-square radius of a branched polymer, $\langle r^2 \rangle_B$, to that of a linear polymer, $\langle r^2 \rangle_L$, may be used as the basis for branching calculations. This ratio, termed the ratio of the mean-square radii, has been given the symbol g and is defined by Eq. 1, with the subscript M referring to values obtained for the same molar mass:

$$g = \left(\frac{\langle r^2 \rangle_B}{\langle r^2 \rangle_L} \right)_M \tag{1}$$

Strictly speaking, it is the z-average radii that are being compared, though, in the case of an SEC separation, it is usually assumed that each slice eluting from the column is monodisperse within the limits of experimental accuracy.

The assumptions inherent in the branching calculations were well-recognized at the time:[4] Only materials of equal chemistry should be compared, their molar mass distributions (MMDs) should overlap in the region of interest, and the type (functionality, f) of the branch points should remain uniform throughout the molecule. The calculations were shown to be invariant to changes in the length of the branches throughout the MMD. The number-average number of branch points (B_n) per molecule for a monodisperse system is given by Eq. 2 for the case of trifunctional ($f = 3$) branching and by Eq. 3 for the case of tetrafunctional ($f = 4$) branching. The weight-average number of branch points (B_w) for a trifunctionally branched polydisperse species is given by Eq. 4, while B_w for a tetrafunctionally branched polydisperse species is given by Eq. 5:

$$g = \left[\left(1 + \frac{B_{3n}}{7} \right)^{1/2} + \left(\frac{4B_{3n}}{9\pi} \right) \right]^{-1/2} \tag{2}$$

$$g = \left[\left(1 + \frac{B_{4n}}{6} \right)^{1/2} + \left(\frac{4B_{4n}}{3\pi} \right) \right]^{-1/2} \tag{3}$$

$$g = \frac{6}{B_{3w}} \left\{ \frac{1}{2} \left(\frac{2 + B_{3w}}{B_{3w}} \right)^{1/2} \times \ln \left[\frac{(2 + B_{3w})^{1/2} + {B_{3w}}^{1/2}}{(2 + B_{3w})^{1/2} - {B_{3w}}^{1/2}} \right] - 1 \right\} \tag{4}$$

$$g = \frac{\ln\,(1 + B_{4w})}{B_{4w}} \tag{5}$$

It should be noted that the symbols used here are those that have found favor in the literature over the years and

Encyclopedia of Chromatography, Third Edition DOI: 10.1081/E-ECHR3-120040040

that are presently being used; as such, they may differ from the symbols used in the original publication. It is also important to realize that, excluding the backbone, one branch emanates from each branch point when $f = 3$, whereas two branches emanate from each branch point when $f = 4$. Zimm and Stockmayer[4] and, later, Stockmayer and Fixman[5] showed how to calculate the number of arms (f) for various types of star polymers by first determining the g parameter.

The rms radius of the polymeric species in each slice eluting from the SEC column can be measured by using an online multiangle light-scattering (MALS) detector, in combination with a concentration-sensitive detector (most often, though not exclusively, a differential refractometer, here abbreviated DRI).[3] This combination also allows measurement of the weight-average molar mass (M_w) of the polymer in each eluting slice. Thus, combining the molar mass results for all the slices yields the MMD, while comparing the molar mass and radius data produces the so-called "conformation plot" of $\log \langle r^2 \rangle^{1/2}$ vs. $\log M$. Comparing the conformation plot of the branched species with that of its linear counterpart allows the determination of g at each molar mass slice and, thence, calculation of the number of branches as a continuous function of the molar mass of the branched macromolecule, the LCBD (these calculations necessitate an a priori knowledge of the branching functionality, f, as do the calculations using g' and the "mass method," both described below). One may also obtain the fractal dimension, d_f, of macromolecules from the conformation plot, as d_f is inversely related to the slope, α, of the plot ($d_f \equiv 1/\alpha$).[3,6] Changes in d_f across the MMD are normally related to architectural variations in the polymer, though they may also be caused by thermodynamic changes in the polymer solution, the latter being a less likely scenario.

Recently,[6] SEC/MALS measurements were used to obtain approximate measures of the average molar mass of a long-chain branch and of the average molar mass between branch points, both as a continuous function of the molar mass of the macromolecule. Though the particular experiments applied to the study of cross-link-induced branching well below the percolation threshold, the theory and measurements extend naturally to the study of "native" branching.

QUALITATIVE AND SEMIQUANTITATIVE DESCRIPTIONS OF THE LCBD BY SEC/VISC

If an online viscometer (VISC) is used instead of a MALS detector in SEC (again, in conjunction with a concentration-sensitive detector),[3] the ratio, g', of the intrinsic viscosities of the branched molecule ($[\eta]_B$) and of the linear standard ($[\eta]_L$), at the same molar mass (M), has been used for the branching calculations:[7,8]

$$g' = \left(\frac{[\eta]_B}{[\eta]_L}\right)_M \tag{6}$$

The relationship between g and g' is given by Eq. 7, where ε is known as the viscosity shielding ratio:

$$g' = g^{\varepsilon} \tag{7}$$

This ratio was defined by Debye and Bueche[9] as the distance within the hydrodynamic sphere occupied by the molecule in solution over which the flow of solvent decreases by a factor $1/e$ of that in the free solution, divided by the radius of said hydrodynamic sphere. It should be noted that even though this definition applied strictly to the Debye–Bueche linear-density pearl-string model of a polymer in solution, the authors demonstrated its suitability to the more accurate Kirkwood–Riseman Gaussian-density polymer model. The value of ε is dependent upon a number of factors, including solvent, temperature, and branching. ε has been found to fall in the range of 0.5–1.5, with the smaller value determined by Zimm and Kilb[10] to correspond to non-free draining, high molar mass, and regular stars, and the larger value determined by Berry[11] for comb-shaped polystyrenes in good solvents. (For a table of ε values, see Ref.[12]) ε can be determined, as a continuous function of molar mass, in a single SEC/DRI/MALS/VISC experiment. It is precisely this type of measurement that has shown the viscosity shielding ratio to be non-constant across the MMD of certain low-density polyethylenes.[13] As such, quantitation of the LCBD by SEC/VISC should be approached with extreme caution.

One may alternatively calculate g by what is known as the "mass method,"[14] by comparing the molar masses of the branched molecule (M_B) and of the linear standard (M_L) at the same elution volume (V), via

$$g = \left(\frac{M_L}{M_B}\right)_V^{(a+1)/\varepsilon} \tag{8}$$

Here, a is the exponent in the Mark–Houwink relationship ($[\eta] = KM^a$). As results from the mass method are also dependent upon the value of the viscosity shielding ratio, the same caveat expressed in the previous paragraph applies.

While generally less accurate than SEC/MALS measurements, SEC/VISC measurements are usually both more precise and extend to lower molar masses. The increased precision stems from the relatively higher signal-to-noise ratio in viscometric measurements than in dissymmetry experiments. The lack of sufficient angular dissymmetry for medium- to small-size polymers means that it is extremely difficult to determine their rms radius precisely, especially for the low molar mass species of a broad polydispersity sample; employing high concentrations is out of the question for these types of sample due to column overloading effects as well as to the possibility of

no longer operating in the dilute, non-entangled viscoelastic regime.[15] As a rule of thumb, an approximate cut-off in the determination of the rms radius occurs when $\langle r^2 \rangle^{1/2} \leq \lambda/20$, where $\lambda = \lambda_0/n$, and λ_0 is the vacuum wavelength of the incident radiation and n is the refractive index of the solvent.

An example of the type of qualitative comparison that SEC/VISC permits is shown in Fig. 1 for two polyolefin molecules, one linear and one branched.[7,8] In this overlay of Mark–Houwink plots, the slope of the plot of the linear polyethylene is constant as a function of increasing molar mass, reflecting the constancy in chain density at different sizes. At any given molar mass, the intrinsic viscosity of the branched polyethylene is lower than that of its linear counterpart, as a result of the more compact nature of the former with respect to the latter caused by LCB. Moreover, the slope of the Mark–Houwink plot of the branched polyethylene is seen to decrease with increasing molar mass, indicating an increase in LCB with increasing molar mass. It is important to realize that these types of qualitative assessments, as well as the quantitative measures obtained by SEC/MALS, are contingent upon the thermodynamics of the polymer solution remaining constant at different molar masses, i.e., it is assumed that the second virial coefficient does not change with molar mass.

Calculation of the fractal dimension is also possible from SEC/VISC measurements. Here, d_f is determined from[3,16]

$$d_f = \frac{3}{1+a} \tag{9}$$

where a, once again, is the exponent in the Mark–Houwink equation. This way of calculating d_f presupposes a constancy in the polymer draining (Φ) and coil interpenetration (Ψ^*) parameters across the MMD.[3,6,17]

BRANCHING AND SEC/QELS

In 1953, Stockmayer and Fixman[5] observed that the ratio, h, of hydrodynamic or Stokes radii (R_H) of the branched and linear macromolecules could also be used as a measure of branching. The relatively recent introduction of online quasielastic light scattering (QELS, also known as dynamic light scattering and as photon correlation spectroscopy) detectors for SEC[3,18] permits direct determination of h by

$$h = \left[\frac{(R_H)_B}{(R_H)_L}\right]_M \tag{10}$$

To date, this relation has not been used extensively in SEC/QELS to measure branching as a continuous function of molar mass, chiefly because it is not clear how to correlate measured values of h to calculations of B, the number of branch points. Nonetheless, the ratio of hydrodynamic to rms radii, ρ, and the distribution of ρ as a function of molar mass, has proven fruitful in demonstrating either constancy or changes in architecture across the MMD of polymers.[17,18]

CONCLUSIONS

The study of LCB in macromolecules by means of multi-detector SEC has been described. Calculations of LCB, of the LCBD, and of fractal dimensions are performed most

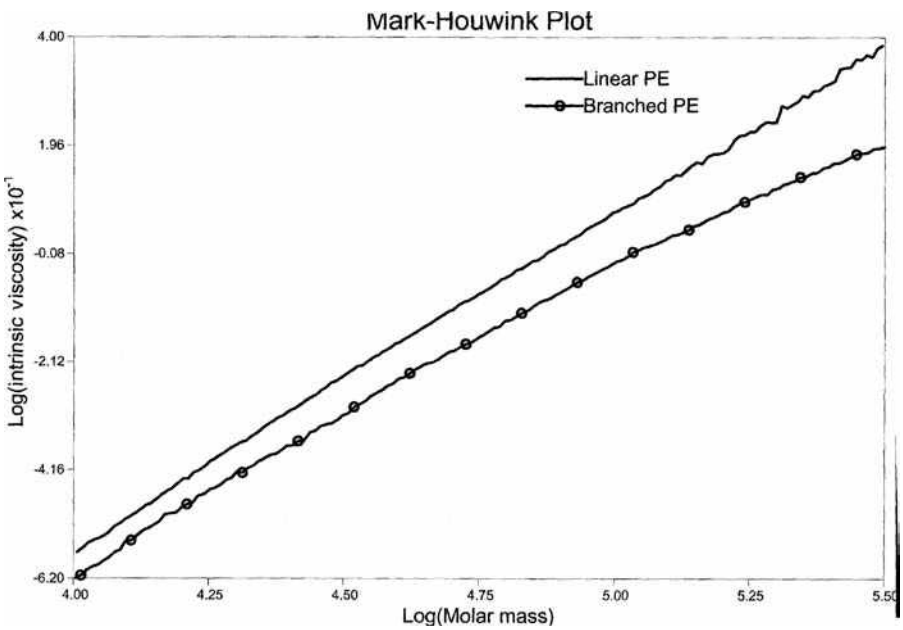

Fig. 1 Overlay of the Mark–Houwink plots of linear and branched polyethylene (PE) samples. See Ref.[7,8] for experimental details.
Adapted from Striegel & Krejsa.[7,8]

accurately using SEC/MALS, though SEC/VISC appears to provide higher precision, more distinct qualitative comparisons, and discrimination between branching levels to lower molar masses than does SEC/MALS. Large errors can result from the branching calculations based on Zimm–Stockmayer theory, however, if careful attention is not paid to a number of parameters.[7,8] Various metrics exist for gauging macromolecular branching and architecture, and an excellent way of determining these is by SEC/DRI/VISC/MALS/QELS, as demonstrated recently by Cotts.[18] As SEC detectors, VISC, QELS, and even nuclear magnetic resonance (NMR) spectroscopy all have the potential to determine the short-chain branching distribution (SCBD) in polymers.[3] Though not the topic of this entry, measurement of the SCBD is complementary to that of the LCBD. Currently, some of the most elegant work on measuring the SCBD in polyolefins is being performed using SEC coupled to Fourier-transform infrared spectroscopy detection (SEC/FT-IR).[19]

Additional support to the chromatographic determination of the LCBD in polymers can be provided by rheological experiments,[20] by a variety of computer modeling techniques,[21,22] and even by enzymology.[23]

REFERENCES

1. Striegel, A.M., Ed.; *Multiple Detection in Size-Exclusion Chromatography*; ACS Symposium Series 893; American Chemical Society: Washington, DC, 2005.
2. Yau, W.W.; Kirkland, J.J.; Bly, D.D. *Modern Size-Exclusion Liquid Chromatography*; John Wiley & Sons: New York, 1979.
3. Striegel, A.M. Multiple detection in size-exclusion chromatography of macromolecules. Anal. Chem. **2005**, *77*, 104A–114A.
4. Zimm, B.H.; Stockmayer, W.H. The dimensions of chain molecules containing branches and rings. J. Chem. Phys. **1949**, *17*, 1301–1314.
5. Stockmayer, W.H.; Fixman, M. Dilute solutions of branched polymers. Ann. N.Y. Acad. Sci. **1953**, *57*, 334–352.
6. Striegel, A.M. Mid-chain grafting in PVB–*graft*–PVB Polym. Int. **2004**, *53*, 1806–1812.
7. Striegel, A.M.; Krejsa, M.R. Complementarity of universal calibration SEC and ^{13}C NMR in determining the branching state of polyethylene. J. Polym. Sci. B, Polym. Phys. **2000**, *38*, 3121–3135.
8. Striegel, A.M.; Krejsa, M.R. In International GPC Symposium 2000 Proceedings; 2001; 1–14.
9. Debye, P.; Bueche, A.M. Intrinsic viscosity, diffusion and sedimentation rate of polymers in solution. J. Chem. Phys. **1948**, *16*, 573–579.
10. Zimm, B.H.; Kilb, R.W. Dynamics of branched polymer molecules in dilute solution. J. Polym. Sci. **1959**, *37*, 19–42.
11. Berry, G.C. Thermodynamic and conformational properties of polystyrene III. Dilute solution studies on branched polymers. J. Polym. Sci. A-2. **1971**, *9*, 687–715.
12. Roovers, J. *Encyclopedia of Polymer Science and Engineering*; John Wiley & Sons: New York, 1985; Vol. 2, 478–499.
13. Beer, F.; Capaccio, G.; Rose, L.J. High molecular weight tail and long-chain branching in low-density polyethylenes. J. Appl. Polym. Sci. **2001**, *80*, 2815–2822.
14. Yu, L.-P.; Rollings, J.E. Low-angle laser light scattering–aqueous size exclusion chromatography of polysaccharides: molecular weight distribution and polymer branching determination. J. Appl. Polym. Sci. **1987**, *33*, 1909–1921.
15. Graessley, W.W. Polymer chain dimensions and the dependence of viscoelastic properties on concentration, molecular weight and solvent power. Polymer **1980**, *21*, 258–262.
16. de Gennes, P.-G. *Scaling Concepts in Polymer Physics*; Cornell University Press: Ithaca, NY, 1979.
17. Burchard, W. Solution properties of branched macromolecules. Adv. Polym. Sci. **1999**, *143*, 113–194.
18. Cotts, P.M. *Multiple Detection in Size-Exclusion Chromatography*; ACS Symposium Series 893; Striegel, A.M., Ed.; American Chemical Society: Washington, DC, 2005; 52–75.
19. DesLauriers, P.J. *Multiple Detection in Size-Exclusion Chromatography*; ACS Symposium Series 893; Striegel, A.M., Ed.; American Chemical Society: Washington, DC, 2005; 210–229.
20. Lusignan, C.P.; Mourey, T.H.; Wilson, J.C.; Colby, R.H. Viscoelasticity of randomly branched polymers in the vulcanization class. Phys. Rev. E. **1999**, *60*, 5657–5669.
21. Freire, J.J. Conformational properties of branched polymers: theory and simulations. Adv. Polym. Sci. **1999**, *143*, 35–112.
22. Striegel, A.M.; Plattner, R.D.; Willett, J.L. Dilute solution behavior of dendrimers and polysaccharides: SEC, ESI–MS, and computer modeling. Anal. Chem. **1999**, *71*, 978–986.
23. Catley, B.J.; Whelan, W.J. Observations on the structure of pullulan. Arch. Biochem. Biophys. **1971**, *143*, 138–142.

Longitudinal Diffusion in LC

J.E. Haky
Department of Chemistry and Biochemistry, Florida Atlantic University, Boca Raton, Florida, U.S.A.

INTRODUCTION

Longitudinal diffusion refers to the natural spreading of a solute band from regions of high concentration to those of lower concentration as it passes through a chromatographic system.[1] It is a simple process which is dependent on the time that the solute spends on the chromatographic system, which, in turn, is related to the flow rate of the mobile phase.

DISCUSSION

As an extreme illustration of the longitudinal diffusion process, consider a situation in which a solute is put onto a liquid chromatographic column and the flow of the mobile phase is shut off prior to any of the solute eluting from the column. The column is then sealed. Under these conditions, the solute molecules in the column would begin to diffuse from a concentrated band outward to regions of lower concentrations in the column. Given enough time, this diffusion would continue until the solute concentration throughout the mobile phase in the sealed column is constant. Although this is an extreme example of band broadening caused by this phenomenon, such longitudinal diffusion occurs to a lesser extent even when the mobile phase is flowing.

The degree of band broadening of any chromatographic peak may be described in terms of the height equivalent to a theoretical plate, H, given by

$$H = \frac{L}{N} \tag{1}$$

where L is the length of the column (usually in cm) and N is the number of theoretical plates, which can be calculated from Eq. 2,

$$N = 16\left(\frac{t_R}{W}\right)^2 \tag{2}$$

where t_R and W are the retention time and width of the peak of interest, respectively. Because higher values of N correspond to lower degrees of band broadening and narrower peaks, the opposite is true for H. Therefore, the goal of any chromatographic separation is to obtain the lowest possible values for H.

The contribution of longitudinal diffusion and other factors to band broadening in liquid chromatography can be quantitatively described by the following equation, which relates the column plate height H to the linear velocity of the solute, μ:

$$H = A\mu^{0.33} + \frac{B}{\mu} + C\mu + D\mu \tag{3}$$

In this equation, A, B, C, and D are constants for a given column.[2] The linear velocity μ is related to the mobile-phase flow rate and is determined by

$$\mu = \frac{L}{t_0} \tag{4}$$

where t_0 (the so-called "dead time") is determined from the retention time of a solute which is known not to interact with the stationary phase of the column.

The second term in Eq. 3, B/μ, describes the contribution of longitudinal diffusion to band broadening of the solute as it passes through the chromatographic system. This is the only term in the equation inversely proportional to the linear velocity of the mobile phase; the other terms increase in value as the linear velocity increases. Giddings and others have also shown that this term is also directly proportional to the diffusion coefficient D_m of the solute in the mobile phase according to the following equation, where C_d is a constant:[3]

$$\frac{B}{\mu} = \frac{C_d D_m}{\mu}$$

Encyclopedia of Chromatography, Third Edition DOI: 10.1081/E-ECHR3-120040041

Fortunately, the mobile-phase flow rates used in most modern liquid chromatography (LC) separations are sufficiently high enough to minimize the effects of longitudinal diffusion on chromatographic band broadening under usual conditions. Other factors, such as solute mass transfer, are usually more important contributors to band broadening in LC. However, longitudinal diffusion can be an important factor in situations where the flow rate of the mobile phase is either stopped or significantly reduced during a chromatographic separation. Additionally, because it occurs throughout the path of a solute passing through a chromatographic system, efforts should be made to minimize longitudinal diffusion effects by minimizing open space ("extracolumn volume") in the chromatographic system before and after the column.

REFERENCES

1. Harris, D.C. *Quantitative Chemical Analysis*; W.H. Freeman: New York, 1999; 662.
2. Snyder, L.R.; Kirkland, J.J. *Introduction to Modern Liquid Chromatography;* 2nd Ed.; John Wiley & Sons: New York, 1979; 168–173.
3. Giddings, J.C. *Dynamics of Chromatography*; Marcel Dekker, Inc.: New York, 1965; 47–61.

Magnetic FFF and Magnetic SPLITT

Maciej Zborowski
P. Stephen Williams
Department of Biomedical Engineering, Cleveland Clinic Foundation, Cleveland, Ohio, U.S.A.

Jeffrey J. Chalmers
Department of Chemical and Biomolecular Engineering, Ohio State University, Columbus, Ohio, U.S.A.

Abstract
The addition of magnetic force to the family of field-flow fractionation (FFF) and split-flow thin-channel (SPLITT) techniques expands their application to characterization and separation of magnetic nanoparticles, microparticles, and magnetizable particular matter, such as biological cells. A combination of the well-established analytical principles of FFF and information about the material properly of the particles subjected to analysis allows one to probe for the magnetic properties of particulate matter on a micro- and nanoscale. A highly regular SPLITT separation process provides the basis for a rational design of new magnetic separation for difficult separations, such as rare circulating tumor cells from blood. Well-established principles of FFF and SPLITT provide foundations for continuing development of better magnetic separation and microanalytical techniques.

INTRODUCTION

Magnetic field-flow fractionation (FFF) employs static or quasi-static magnetic fields and excludes electromagnetic fields. Electromagnetic fields having frequencies in the kilohertz to megahertz range are used in dielectrophoretic FFF. Static electric fields are used in electrical FFF (see *FFF Fundamentals*, p. 849). In this Chapter, a review of magnetic separation fundamentals is provided together with a selection of recent applications of magnetic FFF, SPLITT, and related techniques.

MAGNETOPHORETIC MOBILITY AND MAGNETIC FIELD ENERGY DENSITY GRADIENT

The magnetic field is described by two vectors: magnetic field strength, **H** and magnetic flux density (also called magnetic induction or simply magnetic field), **B**, described by Maxwell's equations. The magnetic field is solenoidal; that is, its sources are electric currents or magnetic dipoles (but not "magnetic charges").[1] The magnetic property of matter is described by its magnetic permeability, μ, which for an isotropic medium is a scalar. The difference between the external, applied field **H** and the induced field **B** is the magnetization of the matter, which is a vector quantity **M**. An external magnetic field always induces magnetization in matter and, in this sense, all matter is magnetic. (The microscopic basis of magnetization is provided by quantum physics and is beyond the scope of this entry.) For a large class of materials, magnetization is a linear function of the applied external magnetic field strength and it always consists of a diamagnetic contribution and, less often, a paramagnetic contribution. In the International System of Units, we have

$$\mathbf{B} = \mu\mu_0\mathbf{H},\ \mathbf{M} = \frac{1}{\mu_0}\mathbf{B} - \mathbf{H},\ \mathbf{M} = \chi\mathbf{H}$$

where **B** is measured in tesla (T), **H** is measured in A/m, $\mu_0 = 4\pi \times 10^{-7}$ Tm/A is a constant called the magnetic permeability of a vacuum, and χ is the volumetric susceptibility of the material (dimensionless). The vector quantities are indicated by boldface type, **B**, their magnitude by italics, **B**, etc. Note that $\mu = 1 + \chi$. Diamagnetic magnetization is antiparallel to the applied field ($\chi < 0$) and paramagnetic magnetization is parallel to the applied field ($\chi > 0$). Diamagnetic effects are very weak (with the notable exceptions of bismuth and graphite) and are dominated by much stronger paramagnetic effects.

Typical fluid media encountered in magnetic separation are diamagnetic (for water, $\chi = -9.05 \times 10^{-6}$). For certain metals, their alloys and oxides, the coordinated behavior of the neighboring atoms or molecules (the totality of which is referred to as a magnetic domain) gives rise to very strong magnetic effects known as ferromagnetism and ferrimagnetism.[2] For such material, magnetization increases very rapidly with the applied field strength H, and the value of the magnetization depends on the history of the material (hysteresis effect). In particular, the magnetization does not disappear with the removal of the external field (residual magnetization) and requires

application of an opposite field to be brought down to zero (coercive force). For convenience, diamagnetics and paramagnetics are characterized by their magnetic susceptibility, χ (typically, the absolute value of $\chi = 10^{-2}$–10^{-5}), whereas ferromagnetics are characterized by their magnetic permeability, μ (typically, $\mu = 10^5$). For particles having a size not larger than that of the magnetic domain, the hysteresis curve reduces to a straight line and such particles are referred to as superparamagnetic particles. Paramagnetic and superparamagnetic particles and colloids are used to tag (or label) weakly magnetic particles and biological cells for their selective separation.[3]

The fluid dynamic properties of continuous magnetic media, including liquid ferromagnetic media (ferrofluids), are described by the Navier–Stokes equations with the addition of terms describing the interaction with the magnetic field and are the subject of a considerable number of studies.[1] The motion of discrete magnetic particles in a very weakly magnetic ("non-magnetic") medium can be described by a combination of long-range magnetic body forces and local shear stresses due to the resulting motion through the viscous medium. In the case of colloidal particles for which inertial effects are much lower than the viscous effects (low-particle Reynolds number), and for laminar flows (low-channel Reynolds number), the equation of motion reduces to

$$0 = 6\pi\eta R\mathbf{v} - \Delta\chi V\nabla\left(\frac{B^2}{2\mu_0}\right)$$

from which

$$\mathbf{v} = \frac{\Delta\chi V}{6\pi\eta R}\nabla\left(\frac{B^2}{2\mu_0}\right)$$

where η is the viscosity of the medium, R is the particle radius, V is the particle volume, $\mathbf{v}$ is the particle linear velocity vector relative to the medium, and $\Delta\chi$ is the difference between the particle magnetic susceptibility and that of the medium. The operand acted on by the nabla operator (resulting in a gradient of scalar quantity), is the external magnetic field energy density, $B^2/2\mu_0$, in a non-magnetic medium. The expression for the field-induced velocity can be conveniently presented as a product of the particle magnetophoretic mobility, m, and the magnetic field energy density gradient, $\mathbf{S}_\mathrm{m}$,

$$\mathbf{v} = m \cdot \mathbf{S}_m$$

where

$$m \equiv \frac{\Delta\chi V}{6\pi\eta R} \text{ and } \mathbf{S}_m \equiv \nabla\left(\frac{B^2}{2\mu_0}\right)$$

For paramagnetic (and diamagnetic) particles in diamagnetic media, $\Delta\chi$ is independent of S_m and the magnetophoretic mobility depends entirely on the intrinsic properties of the particle and those of the continuous medium.[4] For a ferromagnetic particle, $\Delta\chi$ is, in general, a function of H, and therefore the magnetophoretic mobility depends on the properties of the particle, the medium, and the field strength.[5] Particle magnetophoretic mobility provides the basis of magnetic separation, and its role is analogous to the electric and sedimentation mobilities encountered in the electrical and sedimentation split-flow thin-channel (SPLITT) separations, respectively.

The order-of-magnitude analysis of the magnetophoretic mobility of weakly paramagnetic particles, 10 μm in diameter, acted on by the body forces available for the magnetic separation, returns the following numerical values: $\Delta\chi = 10^{-3}$, $V = 524\ \mu\mathrm{m}^3$, $\eta = 10^{-3}$ kg/ms, $R = 5$ μm, $B = 1$ T, gradient of $B = 200$ T/m, $m = 5.6 \times 10^{-15}$ (m/sec)/(N/m^3), and $S_\mathrm{m} = 1.6 \times 10^8$ N/m^3. It follows that the particle velocity induced by the magnetic field is $\nu = 9 \times 10^{-7}$ m/sec, or about 1 μm/sec.

Advantages of the magnetostatic or quasi-static field as compared to the oscillating electromagnetic fields in application to separation include the following: no interaction with the suspending fluid, which typically is diamagnetic or very weakly paramagnetic, and therefore no Joule heating, no convective effects and no need for a cooling system; no electro-osmotic effects; long range of the magnetic interactions (as compared to dielectrophoresis); the possibility of using permanent magnets for the magnetic field and thus no requirement for power supply; high specificity in targeting the separands by using magnetic labels as ligands to specific receptors; and no demonstrated biological effects in the practical range of magnetic fields and gradients. The limitations of the magnetic separation include a requirement for magnetic labels for non-magnetic separands and, generally, a complex geometry of the magnetic force field, which tends to make it difficult to control the separation process.

MAGNETIC FFF

The majority of publications concerning magnetic field-flow fractionation (magnetic FFF or MgFFF) describe different technical approaches for achieving a uniformly high magnetic field and gradient over the entire channel volume. In this sense, MgFFF has not achieved the level of maturity of other FFF techniques for which the field and flow geometries are well established. The separation mechanism of FFF requires a laminar fluid flow in a thin channel with a field or field gradient applied across the channel thickness, perpendicular to the direction of flow. The field or field gradient need not be constant across the channel thickness, but there should not be strongly localized forces on particles that might induce capture. As in chromatography, separation is achieved by differential rates of migration of the sample components along the

separation column (or channel, as it is referred to in FFF), leading to different elution times. Unlike in chromatography, there is no partition between phases in FFF and the different migration rates of the sample components depend on their different steady-state distributions across the fluid velocity profile.

The simplest approach to implementing magnetic FFF is to use a capillary tube as the separation channel. The tube may be coiled against the face of a circular pole piece as proposed by Vickrey and Garcia-Ramirez in 1980.[6] A similar approach was taken by Mori in 1986.[7] High field strengths may be generated in the tube, but field gradients tend to be small for this approach. Latham et al.[8] more recently wound a capillary tube along the edge of a circular magnet pole piece where the field gradient is highest and were able to obtain a separation between 6 nm Fe_2O_3 and 13 nm $CoFe_2O_4$ particles. Tubular channels with transverse fields or field gradients are far from ideal for achieving FFF separation,[9] although some continue their study.[10,11] Semenov and Kuznetsov[12] proposed in 1986 the mounting of a ferromagnetic wire on the axis of a tubular separation channel. The channel was to be placed perpendicular to a magnetic field that magnetized both the wire and the particles to be separated. They presented calculations that suggested retention of both paramagnetic and diamagnetic particles would be possible in such a system. However, the force on the particles may be expected to increase rapidly as they approach the wire and this may lead to particle capture. The small surface of the wire would also have to serve as the accumulation wall which would mean that the system would be susceptible to overloading effects.

In the same year (1986), Semenov[13] proposed a parallel plate magnetic FFF channel in which the field gradient was provided by an array of ferromagnetic wires embedded in one of the walls. The wires were to be magnetized by a magnetic field applied across the channel thickness. The channel geometry was much better suited to FFF, but the field gradient would still vary rapidly with distance from the magnetized wires. From 1994, Ohara et al.[14–21] have pursued an approach to magnetic FFF similar in concept to that proposed by Semenov.[13]

The magnitude of the quadrupole magnetic field is axisymmetric and increases in proportion to the radial distance from the axis. The gradient in field is therefore directed radially outward from the axis and is of constant magnitude within the aperture. This is a great advantage for the purposes of implementing magnetic FFF, as there is no strong variation in field gradient that can induce particle capture. A quadrupole field was considered by Takahashi et al.[10] but with a tubular FFF channel offset from the quadrupole axis. A better exploitation of the axisymmetric magnetic field gradient uses an annular FFF channel,[22] as for the magnetic SPLITT devices described below. A drawback of using an annular channel for achieving FFF separations is the requirement of very uniform mean fluid velocity around the full circumference. Very slight variation in annular thickness will strongly influence the fluid distribution. Also, the fluid must be distributed evenly around the circumference at the channel inlet and be collected uniformly around the outlet. The distribution and collection of fluid was accomplished using several inlet and outlet ports around the circumference. Any flow variation in the ports, including that caused by their partial or complete blockage, would also disturb the fluid flow uniformity. It must be pointed out that these disturbances to flow would greatly reduce the efficiency of separation by FFF, but are far less critical for continuous separation by SPLITT fractionation in an annular channel.

The disturbance to flow arising out of the use of multiple inlet and outlet ports can be avoided by using single inlet and outlet ports and making use of just a fraction of the annulus for the channel. A better approach is to use single inlet and outlet ports and a helical path for the channel in the annular space. The channel is machined into the surface of a polyoxymethylene rod (Delrin™ from DuPont) that fits tightly into an internally polished stainless steel tube.[23–25] The constant thickness of the channel is maintained by the tight fit of the rod within the steel tube. The helical path taken by the channel also exposes all of the migrating species to any slight variations in the magnetic field gradient around the circumference. In an annular channel, such variations would also contribute to loss of separation efficiency.

The FFF retention theory for quadrupole magnetic FFF (QMgFFF) is developed in an analogous way to that of the other FFF techniques. The magnetic force on a single particle due to its interaction with the magnetic field is given by

$$\mathbf{F}_m = V_m M \nabla B$$

where V_m is the volume of the magnetized component of the particle, M is the magnetization of this component, and ∇B is the gradient in magnetic field. It is common for magnetic nanoparticles used for cell labeling or for magnetic drug targeting to have a core of magnetite or some other magnetizable material and a hydrophilic coating to stabilize the particles in aqueous suspension. Other materials such as antibodies or drugs may also be included. The coating also reduces the particle magnetic dipole–dipole interaction between particles in a magnetic field and reduces the tendency for chaining and aggregation. To a good approximation, only the magnetic component has a significant response to the magnetic field. A steady-state concentration profile is quickly established in the thin FFF channel where the drift toward the outer channel wall and consequent buildup of concentration against the wall is countered by diffusion. As in other forms of FFF, the concentration c decays exponentially away from this wall according to the equation

$$c = c_0 \exp\left(-\frac{x}{l}\right) = c_0 \exp\left(-\frac{1}{\lambda}\frac{x}{w}\right)$$

where c_0 is the concentration at the outer wall (the so-called accumulation wall), x is the distance from the wall, l is the mean layer thickness of the steady-state particle zone, w is the channel thickness, and $\lambda = l/w$ is the FFF retention parameter. It may be shown that

$$\lambda = \frac{kT}{F_m w}$$

For a parallel plate channel and to a good approximation for a thin helical channel, the elution time for a monodisperse sample of particles is obtained from the equation

$$R = \frac{t^0}{t_r} = 6\lambda(\coth(1/2\lambda) - 2\lambda) \approx 6\lambda(1 - 2\lambda)$$

in which R is the so-called retention ratio, t^0 is the time for a non-retained material to pass through the channel, and t_r is the elution time for the retained particles. The elution time is therefore directly related to the volume of magnetic material in the particles.

The magnetic nanoparticles used for cell labeling and for magnetic drug targeting have been found to be polydisperse in terms of their magnetic content. Because of the relatively high selectivity of magnetic FFF (i.e., elution time increases with the cube of magnetic core diameter), it is necessary to carry out particle elution under conditions of magnetic field gradient decay. A quadrupole electromagnet with computer control of the current is required for this.[23–25] The quantitative relationship between the amount of magnetic material contained in the nanoparticles and their elution times, even under conditions of field gradient decay,[26] allow the characterization of a sample in terms of not only the mean magnetic content but also the distribution in the magnetic content of the particles.[25]

MAGNETIC SPLITT

The requirement of a highly regular field and flow geometries is even more stringent in SPLITT separations because they often rely on the transport, rather than the equilibrium, separation mechanism. The solenoidal character of the magnetic field requires modification of the usual rectangular geometry of the SPLITT channel. This has led to the design of an annular channel around an axisymmetric magnetic quadrupole field (similar to that used in quadrupole mass spectroscopy).[27] Quadrupole magnetic SPLITT offers the advantages of a highly regular S_m, which is a linear function of the distance from the axis of symmetry and directed along the radial position vector, and of an edgeless flow channel. The theory of the quadrupole magnetic SPLITT separation has been developed and its experimental verification in biological applications is ongoing.[28]

A SPLITT system based on a quadrupole magnetic field combined with annular channel geometry possesses an axial symmetry that lends itself to the mathematical description of the separation process. Given the magnetophoretic mobility of a paramagnetic particle, m, the magnetic field energy gradient in the annular channel, S_m, the system dimensions, and flow rates, it is possible to predict particle trajectory through the system as a function of starting position. It follows that it is possible to calculate the flow rate conditions required to continuously separate particles within a given window of the magnetophoretic mobilities. All particles having mobilities higher than a certain characteristic upper critical m value are collected at one channel outlet, and those having mobilities lower than a lower critical m value are collected at another outlet. The resolution of the fractionation increases with the increasing size of the mobility window separating the two outlet fractions. The volumetric throughput is inversely proportional to the separation resolution.

The availability of monoclonal antibodies conjugated to magnetic micro- and nanoparticles from commercial sources makes it possible to purify or isolate certain specific biological cell types using magnetic SPLITT.[28] These procedures are designed for applications in cancer treatment, cancer treatment prognosis, and various other cell therapies. Unlabeled biological cells tend to be only very weakly influenced by magnetic fields. Flow conditions may be selected so that when a mixture of labeled and unlabeled cells is passed through the magnetic SPLITT system, the labeled cells are selectively drawn toward the outer channel wall and are retained inside the channel (removed from the flow of cell suspension). An example of this type of separation is shown in Fig. 1. For that particular application, the SPLITT system was reduced to a single inlet-single outlet configuration.

The magnetophoretic mobility of a cell labeled with a monoclonal antibody–magnetic particle conjugate (or more generally, a magnetic ligand) is directly proportional to the number of magnetic particles attached to the cell. An important question in magnetic SPLITT is this: Given the upper and lower limit of the number of the antibody receptors on a cell and the size of the cell, how many different fractions may one separate the magnetically labeled cell sample into? For a simple model of a cell as a sphere of a diameter distributed normally in the cell sample population, the theoretical number of the magnetically fractionated subpopulations is given by

$$n = \ln\left(\frac{\alpha_n}{\alpha_0}\right)\left[\ln\left(\frac{1 + z\sigma}{1 - z\sigma}\right)\right]^{-1}, \; 0 < |z\sigma| < 1$$

where α_n and α_0 are the high and low values of the magnetic receptor density on a cell, respectively, and σ is the relative

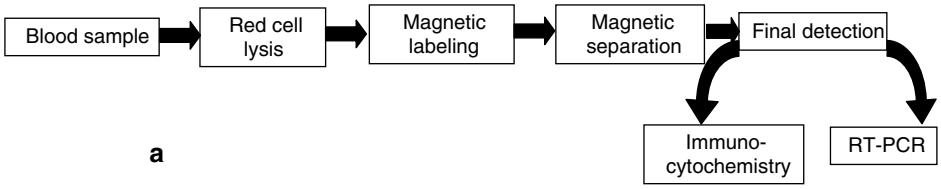

a

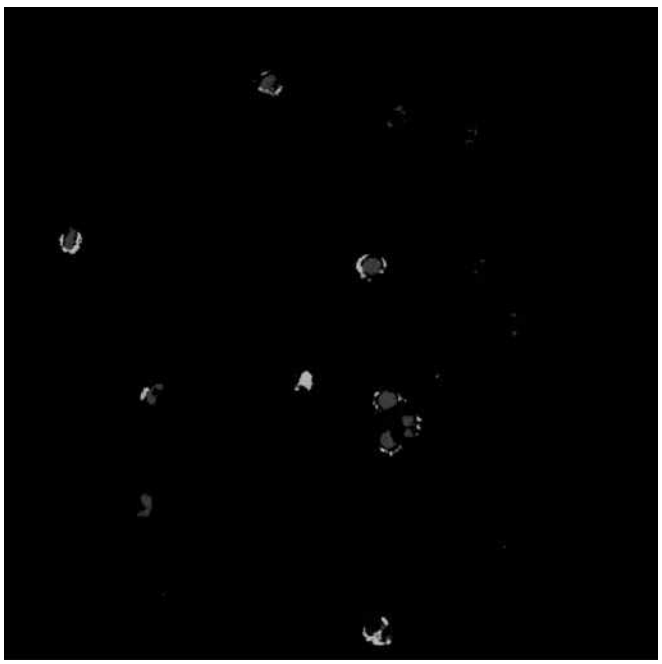

b ~10 m

Fig. 1 Circulating tumor cell (CTC) detection in the peripheral blood of cancer patients by magnetic SPLITT technique. a, Flow diagram of the CTC enrichment protocol. Magnetic labeling step consisted of targeting white blood cells expressing CD45 cell surface marker with a commercial antibody and magnetic labeling reagent. These cells were removed from the sample, effectively enriching the CTC's in the final preparation by a factor of ~10,000. b, Confocal microphotograph of an enriched CTC preparation from a head and neck cancer patient. The dark gray color indicates DAPI stained cell nuclei, the light gray indicates FITC stained intracellular cytokeratin (here used as a CTC marker). Note high fraction of CTC's in the magnetically enriched preparation (stained both by DAPI and FITC).

standard deviation in the cell diameter. The parameter z is an independent variable of the standard normal distribution (with a mean of zero and a variance of one). The number z is chosen according to the desired confidence level of including cells of a given receptor density in a sorted fraction. For instance, at a level of 95.5%, the corresponding value of $z = 2$. As an example, assuming $\alpha_0 = 100$, $\alpha_n = 100{,}000$, and $\sigma = 0.3$ (representative of white blood cells) one obtains $n = 5$ at a confidence level of 95.5%. A more complete discussion of this relationship can be found in the work done by Chalmers et al.[29]

RELATED TECHNIQUES

There are significant advantages in miniaturizing channels and magnets used for magnetic FFF and magnetic SPLITT. These include the ability to generate high fields and high magnetic gradients at moderate magnet costs and an increased flexibility in testing various field and flow configurations.[30] The advances in channel microfabrication methods and permanent magnet material technologies led to an increasing number of publications on magnetophoretic separations in flowing suspensions during the past several years.[31–37] Although the field and flow configurations used for miniaturization rarely fit the narrow definition of the FFF and SPLITT geometries, they nevertheless share many important properties, in particular, the independence of solid phase (substrate) for accomplishing separation and the well-defined laminar flow conditions. It is likely that the basic concepts of the (magnetic) FFF and SPLITT such as, resolving power and the interdependence of the resolving power and throughput will be adapted with time to quantitative analysis of separations based on microfluidics and the micromagnetics.

REFERENCES

1. Rosensweig, R.E. *Ferrohydrodynamics*. Cambridge University Press: Cambridge, MA, 1985.
2. Bozorth, R.M. Magnetism. Rev. Mod. Phy. **1947**, *19* (1), 29–86.
3. Pankhurst, Q.A.; Connolly, J.; Jones, S.K.; Dobson, J. Applications of magnetic nanoparticles in biomedicine. J. Phys. D: Appl. Phys. **2003**, *36* (13), R167–R181.
4. Moore, L.R.; Milliron, S.; Williams, P.S.; Chalmers, J.J.; Margel, S.; Zborowski, M. Control of magnetophoretic

mobility by susceptibility-modified solutions as evaluated by cell tracking velocimetry and continuous magnetic sorting. Anal. Chem. **2004**, *76* (14), 3899–3907.
5. Zborowski, M.; Chalmers, J.J. *Magnetic Cell Separation*. In *Laboratory Techniques in Biochemistry and Molecular Biology*. Elsevier Science: Amsterdam, 2008; Vol. 32.
6. Vickrey, T.M.; Garcia-Ramirez, J.A. Magnetic field-flow fractionation: Theoretical basis. Sep. Sci. Technol. **1980**, *15* (6), 1297–1304.
7. Mori, S. Magnetic field-flow fractionation using capillary tubing. Chromatographia **1986**, *21* (11), 642–644.
8. Latham, A.H.; Freitas, R.S.; Schiffer, P.; Williams, M.E. Capillary magnetic field flow fractionation and analysis of magnetic nanoparticles. Anal. Chem. **2005**, *77* (15), 5055–5062.
9. Giddings, J.C., The field-flow fractionation family: Underlying principles. In *Field-Flow Fractionation Handbook*; Schimpf, M.E., Caldwell, K.D., Giddings, J.C., Eds.; Wiley-Interscience: New York, 2000; 3–30.
10. Takahashi, M.; Fukui, S.; Takahashi, Y.; Abe, R.; Ogawa, J.; Yamaguchi, M.; Sato, T.; Imaizumi, H.; Ohara, T. Numerical study on magnetic chromatography using quadrupole magnetic field. IEEE Trans. Appl. Supercond. **2006**, *16* (2), 1116–1119.
11. Fukui, S.; Shoji, Y.; Abe, R.; Ogawa, J.; Yamaguchi, M.; Sato, T.; Imaizumi, H.; Ohara, T. Numerical simulation of flow fractionation characteristics of magnetic chromatography using an HTS bulk magnet. IEEE Trans. Appl. Supercond. **2008**, *18* (2), 828–831.
12. Semenov, S.N.; Kuznetsov, A.A. Flow fractionation in a transverse high-gradient magnetic field. Russ. J. Phys. Chem. **1986**, *60* (2), 247–250.
13. Semenov, S.N. Flow fractionation in a strong transverse magnetic field. Russ. J. Phys. Chem. **1986**, *60* (5), 729–731.
14. Ohara, T.; Mori, S.; Oda, Y.; Yamamoto, K.; Wada, Y.; Tsukamoto, O. FFF using high gradient and high intensity magnetic field: Process analysis. Presented at *Fourth International Symposium on Field-Flow Fractionation (FFF94)*, Lund, Sweden, 1994.
15. Tsukamoto, O.; Ohizumi, T.; Ohara, T.; Mori, S.; Wada, Y. Feasibility study on separation of several tens nanometer scale particles by magnetic field-flow-fractionation technique using superconducting magnet. IEEE Trans. Appl. Supercond. **1995**, *5* (2 Part 1), 311–314.
16. Ohara, T.; Mori, S.; Oda, Y.; Wada, Y.; Tsukamoto, O. Feasibility of using magnetic chromatography for ultra-fine particle separation. Proc. IEE Japan **1995**, 161–166.
17. Ohara, T.; Mori, S.; Oda, Y.; Wada, Y.; Tsukamoto, O. Feasibility of magnetic chromatography for ultra-fine particle separation. Trans. IEE Japan **1996**, *116-B* (8), 979–986.
18. Ohara, T., Feasibility of using magnetic chromatography for ultra-fine particle separation. In *High Magnetic Fields: Applications, Generations, Materials*; Schneider-Muntau, H.J., Ed.; World Scientific: New Jersey, 1997; 43–55.
19. Ohara, T.; Wang, X.; Wada, H.; Whitby, E.R. Magnetic chromatography: Numerical analysis in the case of particle size distribution. Trans. IEE Japan **2000**, *120-A* (1), 62–67.
20. Karki, K.C.; Whitby, E.R.; Patankar, S.V.; Winstead, C.; Ohara, T.; Wang, X. A numerical model for magnetic chromatography. Appl. Math. Model. **2001**, *25* (5), 355–373.
21. Mitsuhashi, K.; Yoshizaki, R.; Ohara, T.; Matsumoto, F.; Nagai, H.; Wada, H. Retention of ions in a magnetic chromatograph using high-intensity and high-gradient magnetic fields. Sep. Sci. Technol. **2002**, *37* (16), 3635–3645.
22. Williams, P.S.; Moore, L.R.; Chalmers, J.J.; Zborowski, M. The potential of quadrupole magnetic field-flow fractionation for determining particle magnetization distributions. Eur. Cells Mater. **2002**, *3* (Suppl. 2), 203–205.
23. Carpino, F.; Moore, L.R.; Chalmers, J.J.; Zborowski, M.; Williams, P.S. Quadrupole magnetic field-flow fractionation for the analysis of magnetic nanoparticles. J. Phy.: Conf. Series **2005**, *17*, 174–180.
24. Carpino, F.; Moore, L.R.; Zborowski, M.; Chalmers, J.J.; Williams, P.S. Analysis of magnetic nanoparticles using quadrupole magnetic field-flow fractionation. J. Magn. Magn. Mater. **2005**, *293* (1), 546–552.
25. Carpino, F.; Zborowski, M.; Williams, P.S. Quadrupole magnetic field-flow fractionation: A novel technique for the characterization of magnetic nanoparticles. J. Magn. Magn. Mater. **2007**, *311* (1), 383–387.
26. Williams, P.S.; Giddings, M.C.; Giddings, J.C. A data analysis algorithm for programmed field-flow fractionation. Anal. Chem. **2001**, *73* (17), 4202–4211.
27. Williams, P.S.; Zborowski, M.; Chalmers, J.J. Flow rate optimization for the quadrupole magnetic cell sorter. Anal. Chem. **1999**, *71* (17), 3799–3807.
28. Jing, Y.; Moore, L.R.; Schneider, T.; Williams, P.S.; Chalmers, J.J.; Farag, S. S.; Bolwell, B.; Zborowski, M. Negative selection of hematopoietic progenitor cells by continuous magnetophoresis. Exp. Hematol. **2007**, *35* (4), 662–672.
29. Chalmers, J.J.; Zborowski, M.; Moore, L.; Mandal, S.; Fang, B.B.; Sun, L. Theoretical analysis of cell separation based on cell surface marker density. Biotechnol. Bioeng. **1998**, *59* (1), 10–20.
30. Xia, N.; Hunt, T.P.; Mayers, B.T.; Alsberg, E.; Whitesides, G.M.; Westervelt, R.M.; Ingber, D.E. Combined microfluidic-micromagnetic separation of living cells in continuous flow. Biomed. Microdev. **2006**, *8* (4), 299–308.
31. Han, K.H.; Frazier, A.B. Paramagnetic capture mode magnetophoretic microseparator for blood cells. IEE Proc. Nanobiotechnol **2006**, *153* (4), 67–73.
32. Pamme, N. Magnetism and microfluidics. Lab Chip **2006**, *6* (1), 24–38.
33. Mikkelsen, C.; Bruus, H. Microfluidic capturing-dynamics of paramagnetic bead suspensions. Lab Chip **2005**, *5*, 1293–1297.
34. Ramadan, Q.; Samper, V.D.; Puiu, D.P.; Yu, C. Fabrication of three-dimensional magnetic microdevices with embedded microcoils for magnetic potential concentration. J. Microelectromech. Syst. **2006**, *15* (3), 624–638.
35. Choi, J.-W.; Liakopoulos, T.M.; Ahn, C.H. An on-chip magnetic bead separator using spiral electromagnets with semi-encapsulated permalloy. Biosens. Bioelectron. **2001**, *16* (6), 409–416.
36. Smistrup, K.; Kjeldsen, B.G.; Reimers, J.L.; Dufva, M.; Petersen, J.; Hansen, M.F. On-chip magnetic bead microarray using hydrodynamic focusing in a passive magnetic separator. Lab Chip **2005**, *5* (11), 1315–1319.
37. Yellen, B.B.; Er, R.M.; So, H.S.; Hewlin, J.R.; Shan, H.; Le, G.U. Traveling wave magnetophoresis for high resolution chip based separations. Lab Chip **2007**, *7* (12), 1681–1688.

Mark–Houwink Relationship

Oscar Chiantore
Department of Inorganic, Physical, and Material Chemistry, University of Torino, Torino, Italy

INTRODUCTION

The molecular weight of polymer molecules can be determined by the measurement of the viscosity of dilute polymer solutions.[1] The relationship used is the so-called Mark–Houwink (MH) empirical equation:

$$[\eta] = KM^a \tag{1}$$

where the intrinsic viscosity $[\eta]$, also called the limiting viscosity number, is proportional to the polymer molecular weight, M, through the constants K and a, valid for each polymer–solvent system at a given temperature.

APPLICATIONS

The constants of Eq. 1 are obtained by measuring the intrinsic viscosities, in the solvent and at the temperature of choice, of a series of polymer samples having different and known molecular weights.

For flexible macromolecules, the exponent a takes values between 0.5 and 0.8, whereas, for rigid chains, it can reach values higher than 1, up to 2.

The intrinsic viscosity of a polymer is obtained from the viscosities η and η_0 of solution and solvent, respectively, through the following transformations. The relative viscosity is the ratio $\eta_{rel} = \eta/\eta_0$. By assuming that the viscosity η of a dilute solution is given by the sum of viscosities from solvent and solute molecules, the specific viscosity, η_{sp}, represents the polymer contribution to viscosity:

$$\eta_{sp} = \frac{\eta - \eta_0}{\eta_0} = \eta_{rel} - 1 \tag{2}$$

and dividing by the concentration, c, the reduced viscosity η_{sp}/c is obtained. The intrinsic viscosity is the value of reduced viscosity at infinite dilution:

$$\eta = \lim_{c \to 0} \frac{\eta_{sp}}{c} \tag{3}$$

Experimentally, the viscosity of dilute polymer solutions is, in most cases, determined with glass capillary viscometers, making application of the Hagen–Poiseuille's law for laminar flow of liquids. The time required for a specific volume of a liquid to flow through a capillary of defined length and radius is proportional to the ratio of the viscosity by the density of the liquid itself. As the density of a dilute solution may be considered practically equal to that of the pure solvent, the ratio of efflux time of the solution, t, to that of solvent t_0, gives the relative viscosity:

$$\eta_{rel} = \frac{t}{t_0} = \frac{\eta}{\eta_0} \tag{4}$$

The relative viscosities of polymer solutions are measured at different concentrations and a plot of the reduced viscosity vs. concentration is made, in order to extrapolate to zero concentration. The concentration dependence of the viscosity of polymer solutions, in the dilute regime, may be expressed by several linear equations. For practical extrapolation to zero concentration, the most commonly employed are the Huggins equation:

$$\frac{\eta_{sp}}{c} = [\eta] + k_H[\eta]^2 c \tag{5}$$

and the Kraemer equation, where a new quantity, the inherent viscosity η_{inh}, is defined:

$$\eta_{inh} = \ln\left(\frac{\eta_{rel}}{c}\right) = [\eta] + k_K[\eta]^2 c \tag{6}$$

The constants of the two equations are connected by the relationships $k_K = k_H - 0.5$. Given that, for flexible polymers, the k_H values vary between 0.3 and 0.5, the slope of Kraemer equation is generally negative, with absolute values lower than the Huggins slope. This helps in the extrapolation procedure which is conveniently made, in order to reduce experimental uncertainties, by plotting in the same graph the viscosity data according to Eqs. 5 and 6, as shown in the example of Fig. 1.

The combination of Eqs. 5 and 6 with the assumption that $k_H + k_K = 0.5$ leads to the Solomon–Ciuta equation:

$$[\eta] = \frac{[2(\eta_{sp} - \ln \eta_{rel})]^{0.5}}{c} \tag{7}$$

which may be used to obtain intrinsic viscosity by a single measurement performed at reasonably low concentration. Eq. 7 finds application also in the evaluation of data from viscometer absolute detectors in gel permeation chromatography/size-exclusion chromatography (GPC/SEC).[2]

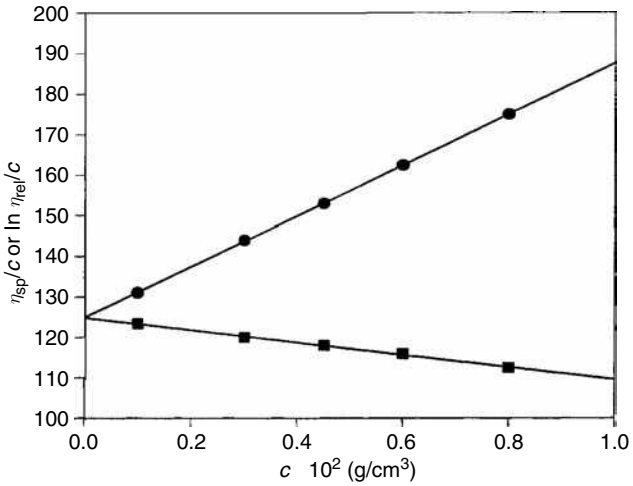

Fig. 1 Double extrapolation of viscometric data according to the Huggins and Kraemer equations: ●: reduced viscosity; ■: inherent viscosity.

In the case of polymers with different chain lengths, the molecular weight obtained from the Mark–Houwink equation is a viscosity-average molecular weight, M_v, whereas the intrinsic viscosity is the weight average. In fact, at infinite dilution, one may write

$$[\eta] = \Sigma\left(\frac{\eta_{sp,i}}{c_i}\right) = \Sigma\left(\frac{c_i[\eta]_i}{c_i}\right) = \Sigma\ w_i[\eta]_i = [\eta]_w \tag{8}$$

where $w_i = c_i/\Sigma\ c_i$ is the weight fraction of the ith component.

The expression for M_v is immediately derived by combining Eq. 8 with the Mark–Houwink relationship:

$$[\eta]_w = \Sigma\ w_i[\eta]_i = K\ \Sigma\ w_i M_i^{\ a} = KM_v^a \tag{9}$$

$$M_v = (\Sigma\ w_i M_i^{\ a})^{1/a} \tag{10}$$

The viscosity-average molecular weight is located between the number- and weight-average values but is, in any case, closer to the weight average. From Eq. 10, it may be seen that viscosity and weight averages coincide for $a = 1$. It is also worth noting that the M_v of a polymer is not a unique definite value because, depending on the exponent a, it varies with the solvent, where the polymer is dissolved.

Mark–Houwink relationships are also important for the application of the universal calibration procedure in GPC/SEC of polymer molecules, where the calibration curve is expressed in terms of the size of fractionated molecules against retention volumes. The intrinsic viscosity of a polymer (expressed in cm^3/g) is, in practice, a measure of the

Table 1 Literature values for Mark–Houwink constants K and a in tetrahydrofuran.

Polymer	Temp. (°C)	$K \times 10^2$ (cm^3/g)	a	Refs.
Polystyrene	23	1.11	0.723	[4]
Poly(methyl styrene)	25	4.2	0.608	[5]
Poly(vinyl chloride)	25	1.50	0.77	[4]
Poly(vinyl acetate)	25	3.50	0.63	[6]
Poly(methyl methacrylate)	23	0.93	0.69	[7]
	25	1.08	0.702	[8]
Poly(ethyl methacrylate)	25	1.549	0.679	[9]
Poly(butyl methacrylate)	25	0.503	0.758	[9]
Poly(methyl acrylate)	25	0.388	0.82	[10]
Polyisobutylene)	40	5.79	0.593	[11]
Polycarbonate	25	3.99	0.77	[12]
Polybutadiene	30	2.56	0.74	[13]
Polyisoprene	25	1.77	0.753	[14]
Butyl rubber	25	0.85	0.75	[12]
Poly(vinyl butyral)	25	1.4	0.80	[15]
Poly(2-vinyl pyridine)	25	2.23	0.66	[16]
Poly(dimethyl siloxane)	25	0.65	0.77	[17]
Cellulose nitrate	25	25.0	1.00	[18]
Poly(DL-lactic acid)	31.15	5.49	0.639	[19]
Poly(ethylene-*co*-vinyl acetate) (27–29% VA)	20	9.7	0.62	[20]
Poly(ethylene-*co*-propylene-*co*-ethylidene norbornene) (EPDM: 27% PP, 11.5%: ENB)	35	27.4	0.54	[21]

volume occupied by a unit weight of the macromolecules in the solution. From the Flory–Fox equation for viscosity of flexible chain molecules and from the Einstein relationship for viscosity of a dispersion of spheres,[3] it turns out that the product $[\eta]M$ can be used to represent the dimension of polymer molecules in the solution:

$$[\eta]M = \phi'\alpha^3\langle s_0^2\rangle^{3/2} = 2.5N_AV_h \quad (11)$$

ϕ' is the so-called Flory's constant, α is the expansion factor of the polymer molecule, which depends from the thermodynamic quality of the solvent ($\alpha = 1$ in ideal solvent), $\langle s_0^2\rangle$ is the mean-square radius of gyration, N_A is Avogadro's number, and V_h is the volume of the equivalent hydrodynamic sphere.

In GPC/SEC with universal calibration, at each retention volume i of the chromatogram, a value of $[\eta]_i/M_i$ is read, and for molecular-weight and molecular-weight-distribution calculations the values of $[\eta]_i$ are needed. These are obtained, whenever the equation is known, from the Mark–Houwink constants of the polymer in the solvent and at the temperature of chromatographic elution.

A selection of literature values for Mark–Houwink constants K and a in tetrahydrofuran, which is the eluent most commonly used in size-exclusion chromatography, is collected in Table 1 for the principal polymer structures. An accurate, more extensive compilation of the same constants for homopolymers and copolymers may be found in Ref.[22]

REFERENCES

1. Billingham, N.C. *Molar Mass Measurements in Polymer Science*; John Wiley & Sons: New York, 1977.
2. Yau, W.W.; Abbot, S.D.; Smith, G.A.; Keating, M.Y. A new stand-alone capillary viscometer used as a continuous size exclusion chromatographic detector. ACS Symp. Ser. **1987**, *352*, 80.
3. Flory, P.J. *Principles of Polymer Chemistry*; Cornell University Press: Ithaca, NY, 1953.
4. Kolinsky, M.; Janca, J. Some applications of gel-permeation chromatography in investigations of structure and the solution properties of radical-initiated poly(vinyl chloride). J. Polym. Sci. A-1 **1974**, *12* (6), 1181–1191.
5. Schroder, U.K.O.; Ebert, K.H. Makromol. Chem. **1987**, *188*, 1415.
6. Goedhar, D.; Opshoor, A. Polymer characterization by coupling gel-permeation chromatography and automatic viscometry. J. Polym. Sci. A-2 **1970**, *8* (7), 1227–1233.
7. Grubisic, Z.; Rempp, P.; Benoit, H. A universal calibration for gel permeation chromatography. J. Polym. Sci. B **1967**, *5*, 753.
8. Chen, Y-J.; Li, J.; Hadjichristidis, N.; Mays, J.W. Mark-Houwink-Sakurada coefficients for conventional poly (methyl methacrylate) in tetrahydrofuran. Polym. Bull. **1993**, *30* (5), 575.
9. Samay, G.; Kubin, M.; Podesva, Reliability of universal calibration for calculating molecular weights from GPC data. J. Angew. Makromol. Chem. **1978**, *72* (1), 185.
10. Szesztay, M.; Tuedoes, F. GPC calibration for poly(methyl acrylate) Polym. Bull. **1981**, *5* (8), 429.
11. Xie, J. Viscometric constants for small polystyrenes and polyisobutenes by gel permeation chromatography. Polymer **1994**, *35*, 2385.
12. Evans, J.M. Gel permeation chromatography: A guide to data interpretation. Polym. Eng. Sci. **1973**, *13* (6), 401.
13. Zhongde, X.; Minghsi, S.; Hadjichristidis, N.; Fetters, L. Method for gel permeation chromatography calibration and the evaluation of Mark-Houwink-sakurada constants. J. Macromolecules **1981**, *14* (5), 1591–1594.
14. Kraus, C.; Stacy, C.J. Molecular weight and long-chain branching distributions of some polybutadienes and styrene-butadiene rubbers. Determination by GPC and dilute solution Viscometry. J. Polym. Sci. A-2 **1972**, *10* (4), 657–672.
15. Mrkvickova, L.; Danhelka, J.; Pokorny, S. Characterization of commercial polyvinulbutyral by gel permeation chromatography. J. Appl. Polym. Sci. **1984**, *29* (3), 803–808.
16. Hugelin, C.; Dondos, A. Makromol. Chem. **1969**, *126*, 207.
17. Mrkvickova, L.; Radhakrisnan, N. The SEC estimation of [η]-M relationship for linear poly-(dimethylsiloxane) in tetrahydrofuran. Eur. Polym. J. **1997**, *33*, 1403.
18. Rudin, A.; Hoegy, H.W. J. Polym. Sci. A-1 **1972**, *10*, 217.
19. van Dijk, J.A.P.P.; Smit, J.A.M.; Kohn, F.E.; Feijten, J. Characterization of poly(d,l-lactic acid) by gel permeation chromatography. J. Polym. Sci., Polym. Chem. Ed. **1983**, *21*, 197.
20. Echarri, J.; Iruin, J.J.; Guzman, G.M.; Amsorena, J. Makromol. Chem. **1979**, *180.*
21. Chiantore, O.; Cinquina, P.; Guaita, M. Fractionation and molecular characterization of EPDM rubbers. Eur. Polym. J. **1994**, *30*, 1043.
22. Mori, S.; Barth, H. *Size Exclusion Chromatography*; Springer-Verlag: Berlin, 1999.

Mass Transfer between Phases

J.E. Haky
D.A. Teifer
Department of Chemistry and Biochemistry, Florida Atlantic University, Boca Raton, Florida, U.S.A.

INTRODUCTION

Chromatography is a separation method which involves two phases—one stationary and one mobile. A mixture is introduced into the mobile phase and is carried through the system by it. At some point, the mobile phase passes over and through the stationary phase. The components of the mixture partition between the two phases, resulting in different migration rates through the system.[1] At any given point, an analyte molecule will either be moving along the mobile phase or be held immobile in the stationary phase. A separation results as the molecules emerge from the bed at different times, which are called retention times.

BACKGROUND INFORMATION

The retention time of a solute is partially controlled by how effectively it interacts with the stationary phase as it passes through the column. As a solute molecule moves through a chromatographic system, it is carried through the mobile phase to a new solution site in the stationary phase. Simultaneously, other solute molecules are moving from the stationary phase and are being conducted through the column by the mobile phase. In any separation of components of a mixture by, liquid chromatography (LC) the rate at which this repeated transfer of solutes between the stationary phase and the mobile phase is an important factor affecting retention, peak shape, and resolution.

Mass transfer in both the stationary and mobile phases are not instantaneous and, consequently, complete equilibrium is not established under normal separation conditions.[2] The result is that the solute concentration profile in the stationary phase is always displaced slightly behind the equilibrium position and the mobile-phase profile is slightly in advance of the equilibrium position.[2] A high degree of displacement will lead to wider peaks and reduced resolution. In fact, the largest problem associated with mass transport in the packed column revolves around moving the solute from the stationary phase to the mobile phase.

The degree of band broadening of any chromatographic peak may be described in terms of the height equivalent to a theoretical plate, H, given by

$$H = \frac{L}{N} \tag{1}$$

where L is the length of the column (usually in cm) and N is the number of theoretical plates, which can be calculated from

$$N = 16\left(\frac{t_R}{W}\right)^2 \tag{2}$$

where t_R and W are the retention time and width of the peak of interest, respectively.

Because higher values of N correspond to lower degrees of band broadening and narrower peaks, the opposite is true for H. Therefore, the goal of any chromatographic separation is to obtain the lowest possible values for H.

The contribution of mass transfer and other factors to band broadening in LC can be quantitatively described by the following equation, which relates the column plate height H to the linear velocity of the solute, μ:

$$H = A\mu^{0.33} + \frac{B}{\mu} + C\mu = D\mu \tag{3}$$

In this equation, A, B, C, and D are constants for a given column[3]. The linear velocity μ is related to the mobile-phase-flow rate and is determined by

$$\mu = \frac{L}{t_0} \tag{4}$$

where t_0 (the so-called "dead time") is determined from the retention time of a solute, which is known not to interact with the stationary phase of the column.

The first term in Eq. 3, $A\mu^{0.33}$, includes the contribution of eddy diffusion to band broadening as well as that of mass transfer of the solute through the mobile phase. This contribution of this mobile-phase mass transfer to this term, H_i, increases with the square of the stationary-phase particle diameter d_p. It is also inversely proportional to the diffusion coefficient of the solute in the mobile phase, D_m, according to

$$H_i = \frac{C_m d_p{}^2 \mu}{D_m} \tag{5}$$

where C_m is a constant.

The third and fourth terms of Eq. 3 also relate to mass transfer. The third term, $C\mu$, describes the contribution of mass transfer of solutes to and from areas in the column where the mobile phase is stagnant (e.g., within the pores of the packing). The size of this term is related to stationary-phase particle diameter and solute diffusion coefficient according to

$$C\mu = \frac{C_{sm} d_p{}^2 \mu}{D_m} \tag{6}$$

where C_{sm} is a constant.

Finally, the fourth term in Eq. 3, $D\mu$, describes the contribution of mass transfer of solutes to and from the stationary phases. This term is related to the thickness d_f of the phase that coats the stationary phase and the diffusion coefficient D_s of the solute in the stationary phase according to

$$D\mu = \frac{C_s d_s{}^2 \mu}{D_s} \tag{7}$$

where C_s is a constant.

To minimize band broadening in LC, conditions must be established to minimize each of the terms described by Eqs. 5–7. Because each of these terms is directly proportional to mobile-phase linear velocity, employing the lowest possible mobile-phase flow rates would seem to serve this purpose. However, use of extremely low flow rates [$<$ 0.5 ml/min for a standard high-performance liquid chromatography (HPLC) column] can increase solute retention times to impractical levels and may actually increase band broadening due to increased longitudinal diffusion (described by the second term in Eq. 3). For this reason, other factors are usually adjusted to minimize these mass transfer terms. Such adjustments include (a) using monomerically bonded stationary phases with small particle diameters [this reduces the size of d_f and d_p terms in Eqs. 5–7, which, in turn, has an exponential effect on reducing the size of the mass transfer terms]; (b) employing mobile phases of low viscosity at high temperatures (this increases the sizes of the diffusion coefficients D_s and D_m in the equations, resulting in fast mass transfer and narrow chromatographic bands.[4])

Column manufacturers and researchers have optimized the above parameters to produce LC columns of remarkably high selectivities and efficiencies. However, there are practical limitations to adjustments of these parameters. For example, stationary phases with particle diameters below 3 μm generally cannot be routinely used, owing to excessively high back-pressures and short column lifetimes. Additionally, for obvious reasons, operating temperatures must be kept below the boiling points of the components of the mobile phase. Use of non-porous pellicular column packings has also been attempted in an effort to eliminate any areas of stagnant mobile phase in the chromatographic system, thus reducing the size of the third term in Eq. 3 to zero. However, such pellicular stationary phases have very low sample capacities, and diffusion coefficients of many solutes on their polymeric coatings are often low, which, of course, results in increased band broadening.[3]

At commonly used mobile-phase flow rates, mass transfer of solutes through and between the stationary phase and the mobile phase is generally the most important factor controlling the widths of chromatographic bands in LC. Although manufactures have designed packings and columns to minimize their effects, consideration of solute mass-transfer effects are extremely important in the development of any chromatographic method.

ACKNOWLEDGMENT

The author wishes to thank D.A. Teifer for technical assistance.

REFERENCES

1. Miller, J.M. *Chromatography: Concepts and Contrasts*; John Wiley & Sons: New York, 1988; Chap. 2.
2. Giddings, J.C. *Dynamics of Chromatography*; Marcel Dekker, Inc.: New York, 1965; 95–118.
3. Snyder, L.R.; Kirkland, J.J. *Introduction to Modern Liquid Chromatography,* 2nd Ed.; John Wiley & Sons: New York, 1979; Chap. 5.
4. Snyder, L.R.; Kirkland, J.J.; Glajch, J.L. *Practical HPLC Method Development,* 2nd Ed.; John Wiley & Sons: New York, 1997; Chap. 2.

McReynolds Method for Stationary Phase Classification

Barbara Gawdzik
Faculty of Chemistry, MCS University, Lublin, Poland

Abstract
McReynolds constants were introduced for selectivity characterization of liquid stationary phases in partition gas chromatography (GC). They were soon applied to solid stationary phases, mainly of synthetic polymer nature, in adsorption GC.

INTRODUCTION

McReynolds constants were introduced for selectivity characterization of liquid stationary phases in partition gas chromatography (GC).[1,2] They were soon applied to solid stationary phases, mainly of synthetic polymer nature, in adsorption GC.

The system based on characteristic phase constants, known as the McReynolds constants, proved to be the most successful for describing phase selectivity. A similar system was introduced simultaneously by Rohrschneider,[3] but his characteristic phase constants have not become so popular.

Applying these systems, the phase selectivity, defined as its relative capacity to enter into specific intermolecular interactions, such as dispersion, induction, orientation, hydrogen-bond formation, and charge-transfer complexation, can be characterized by 5 or 10 constants. These constants represent differences in the Kováts retention indices[4] of test substances on the phase under study and on a reference column containing a non-polar phase, at the same temperature. McReynolds proposed 120°C as a standard reference temperature. As a standard non-polar phase, Rohrchneider introduced squalane.[3]

To choose proper test substances, McReynolds studied the behavior of a large number of substances of the following compound classes: alcohols, glycols, aldehydes, ketones, esters, acetals, ethers, oxides, hydrocarbons, chloro compounds, difunctional and polyfunctional compounds, and other miscellaneous substances.[1] For the stationary phase classification, he eventually proposed benzene, *n*-butanol, 2-pentanone, 1-nitropropane, and pyridine to represent compounds of different chemical interactions.[2] McReynolds' characteristic phase constants for these five compounds describe the selectivity of the phase.

The founding principle of both systems was that intermolecular forces were assumed to be additive, and that their individual contributions to retention can be evaluated from the differences in retention index values for a series of test solutes on the phase to be characterized and on a nonpolar reference phase.

This approach was immediately appreciated by scientists throughout the world. During the Symposium of the Biochemical Society in 1970, James stressed achievements of McReynolds and Rohrschneider, saying,

> This enables us to clarify our minds as to how to exploit interaction forces in solution and showed that since, in the nonpolar stationary phases such as long chain paraffin hydrocarbons, where London dispersion forces were operative, that the molecular weight (rather than BP) was the major factor controlling separation, with molecular configuration as the secondary, though still important, effect. In solvents such as alcohols and polyethers, hydrogen bonding with donor or acceptor solutes occurred in addition to London dispersion interactions.[5]

The studies of McReynolds and Rohrschneider had fundamental importance for chromatography. At present, the sum of five McReynolds constants is the most commonly accepted criterion for the overall polarity of the stationary phase.[6–10]

CHARACTERIZATION OF THE METHOD

McReynolds' characteristic phase constants are usually found in the contemporary scientific and commercial literature for characterization of liquid stationary phase selectivity. This method allows for direct comparison of the GC columns (both packed and capillary), provided the data for standard test compounds are obtained at the same temperature.

Such conditions were chosen by McReynolds after measuring and listing the retention data of more than 300 compounds on 74 liquid stationary phases at 100°C, 120°C, 140°C, and 160°C.[1] The solid support used in all columns was Celite® 545. The retention data were given as specific retention volumes (V_g) and retention index values (I). For determination of retention data of the studied

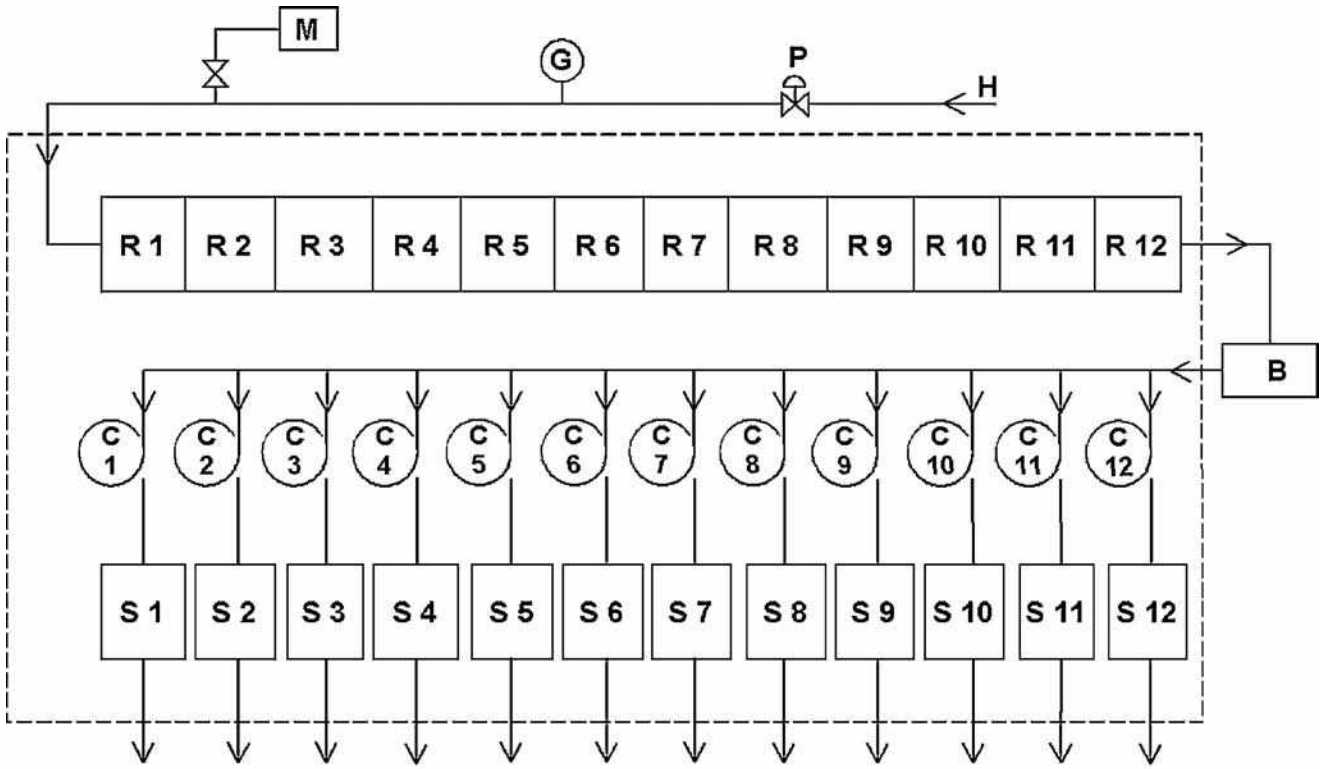

Gas flow of instrument used for determining retention data. Broken line indicates portion of instrument within thermostatted oven.

B Sample injection block
C1 to C12 Columns 1 to 12
H Inlet helium
M Mercury manometer
P Pressure regulator

R1 to R12 Reference side of detectors 1 to 12
S1 to S12 Sensing side of detectors 1 to 12

Fig. 1 Schematic for determination of retention data.

compounds, McReynolds used a specially constructed chromatograph.[2] The instrument permitted as many as 12 columns to be run simultaneously. This apparatus is presented in Fig. 1.

From the obtained data, 10 compounds representing different classes of organic compounds were selected in order to test correlation between the various sets of stationary phase constants and the retention data at 120°C.

To characterize liquid stationary phases in partition GC, McReynolds used benzene, 1-butanol, 2-pentanone, 1-nitropropane, and pyridine as test compounds. In their selection, he applied regression analyses to determine which compounds could be best for calculation of the retention indices of other compounds. These compounds had the same chemical nature as those proposed by Rohrschneider, but their BP were higher. In the approach of Rohrschneider, benzene, ethanol, methyl ethyl ketone, nitromethane, and pyridine were used. An inconvenience of this method is that since ethanol, methyl ethyl ketone, and nitromethane give index numbers near or below 500 with some liquid phases, it was necessary to use, for their determination, hydrocarbons, which were gases at ambient temperature and pressure, for their determinations.

McReynolds also studied the behavior of an additional five compounds: 2-methyl-2-pentanol, 1-iodobutane, 2-octyne, 1,4-dioxane, and *cis*-hydrindane. In the case of 2-methyl-2-pentanol and 1-iodobutane, he observed some improvements in prediction of retention indices of branched compounds, especially alcohols and halogen-containing compounds. For 2-octyne, 1,4-dioxane, and *cis*-hydrindane, only minor improvement was achieved. Finally, the latter five compounds were neglected.

The main assumption of their methods was that the retention index of a substance on a non-polar phase, such as

squalane, is associated only with dispersive interactions and that any differences in the retention index values for a polar phase (ΔI) are due to polar interactions. These interactions can be of different nature, e.g., induction, orientation, hydrogen-bond formation, and charge-transfer complexation.

In the approach of Rohrschneider, the difference in the retention index value for polar phase (ΔI) is represented as a series of terms composed of solute-specific contributions ($a,\ldots,e$) and the stationary phase characteristic term ($x',\ldots,s'$), which can be written as:[3,11]

$$\Delta I = ax' + by' + cz' + du' + es',$$

where a, b, c, d, and e are the coefficients determined by the multiple regression of the compound retention index on several characterized phases. In consequence, the characteristic phase constants represent mixed retention and intermolecular interactions.

The concept of McReynolds used five solutes (benzene = x, 1-butanol = y, 2-pentanone = z, 1-nitropropane = u, and pyridine = s) that are considered to represent typical chemical interactions.[2]

For each of them, the constants x', y', z', u', and s' are defined accordingly. They are shown in Table 1.

The sum of the retention index differences on a certain phase relative to squalane is a measure of the polarity of this phase (),

$$\sum = x' + y' + z' + u' + s',$$

where

$$x' = I_{\text{benzene}} - I^{\text{sq}}_{\text{benzene}},$$
$$y' = I_{1-\text{butanol}} - I^{\text{sq}}_{1-\text{butanol}},$$
$$z' = I_{2-\text{pentanone}} - I^{\text{sq}}_{2-\text{pentanone}},$$
$$u' = I_{1-\text{nitropropane}} - I^{\text{sq}}_{1-\text{nitropropane}},$$
$$s' = I_{\text{pyridine}} - I^{\text{sq}}_{\text{pyridine}}.$$

If, for example, the solute is an alcohol, it can be formally divided into the alkyl residue (which interacts only by weak dispersion forces with all phases) and the OH group, which is able to donate a hydrogen bond. Interaction with a stationary phase will lead to stronger retention on the polar phase and therefore a large increase in the retention index. This increase is represented by the constant y'.

Characteristic phase constants describe the liquid stationary phase accurately if differences in the retention data between stationary phases are accompanied by corresponding differences in the characteristic phase constants.

The McReynolds constants for liquid stationary phases, most commonly used in practice, are given by Kenndler.[12] These data are presented in Table 2. In his opinion, polarity of two phases can be considered as nearly equal if the sums of their indices differ by more than about 200. In general, it is not meaningful to use two such phases. This does not mean, however, that their selectivities concerning one special type of interaction are probably negligible.

The McReynolds method was also used for characterization of solid porous adsorbents in GC. Negative values of the McReynolds constants on solid porous polymeric phases of styrene-divinylbenzene led Smith, Tameesh, and Waddington[13] to introduce thermally graphitized carbon black (GTCB) as the standard non-polar phase for this kind of chromatographic solid stationary phase. He also increased the temperature for McReynolds constants determination to 140°C. After these modifications, the method, with the use of the sum of only three constants for benzene, *n*-butanol, and 2-pentanone, becomes the most convincing technique for solid porous polymeric stationary phase characterization. It was also used in the works reported by Gawdzik et al.[14] and Gawdzik[15].

The system of McReynolds constants inspired many researchers to carry out more extensive explorations. Based on this system, Tacács[16] constructed a unified system for the prediction of retention data in gas–liquid chromatography.

Table 1 McReynolds five solutes representing typical chemical interactions.

		Type of interaction				
Reference solute	**McReynolds constant**	**Dispersion**	**Dipole**	**H-donor**	**H-acceptor**	**Typical for**
Benzene	x'	+	−	−	+	Olefins, aromatic compounds
Butanol-1	y'	+	+	*Strong donor*	−	Alcohols, phenols, acids, amides
2-Pentanone	z'	+	+	−	*Acceptor*	Ketones, aldehydes, esters, ethers, epoxides
1-Nitro propane	u'	+	*Strong dipole*	−	+	Nitro-, nitrilo- compounds
Pyridine	s'	+	+	−	*Strong acceptor*	Aromatic amines

Table 2 McReynolds constants and their sum, $=x' + y' + z' + u' + s'$, used for characterization of liquid stationary phase polarity.

Stationary phase	Composition	x′	y′	z′	u′	s′	Σ
Squalane	Hydrocarbon	0	0	0	0	0	0
Dimethyl silicone	100% Methyl	17	57	45	67	43	229
Phenyl methyl	5% Phenyl	32	72	65	98	67	334
silicone	50% Phenyl	119	158	162	243	202	884
	75% Phenyl	178	204	208	305	208	1,103
Cyanopropyl	6% cpph	50	115	107	164	103	539
phenyl (cpph)	50% cpph	227	373	336	489	398	1,823
dimethyl silicone	100% cpph	523	757	659	942	801	3,682
PEG 20 mol/L	Polyglycol	322	536	368	572	510	2,308

Source: From *Gas Chromatography*, in Version 19/01/2004.[12]

To achieve a detailed classification of the possible interaction of solid porous non-polar polymeric phases with different functional groups of solute molecules, Castello and D'Amato[17] used the following polarity reference substances: ethanol, 2-butanone, nitromethane, benzene, pyridine, *n*-butanol, 2-pentanone, and 1-nitropropane. The first five represent the test substances proposed by Rohrschneider, while the last three were recommended by McReynolds. The retention indices of these substances enable evaluation of the polarity of any solid porous polymeric stationary phase. In their studies Porapak Q, as the least polar commercially available porous polymer, was used as the reference stationary phase.

Some authors[18] raise the question of experimental inaccuracy of McReynolds constants determination associated with inaccurate determination of retention times for *n*-alkanes on polar stationary phases. In such cases, retention depends on the amount of the analyte sample. To avoid such errors in the determination of McReynolds constants, Smith, Tameesh, and Waddington[19] proposed the use of trace amounts of the test solutes by dipping a 1 μl syringe needle (at the zero position of the piston) in the sample for 1 sec.

Kersten, Poole, and Furton[20] found that many ambiguities in the determination of the polarity with the McReynolds stationary phase constants are due to the use of *n*-alkanes as the reference series, and estimated on 15 columns spanning a wide polarity range the 2-alkanones as the universal retention index markers to replace the *n*-alkanes which do not partition with polar phases. Ketones were also suggested by many authors as a good alternative series to *n*-alkanes; however, Mathiasson et al.[21] found that, because of variation in retention volume with the amount injected, alkanols and 2-alkanones are unsuitable on both polar and non-polar columns. He suggested the use of alkylbenzenes as reference compounds, as these compounds seem to behave almost ideally on liquid phases of different polarities.

Some authors[22–24] proposed use of other homologous series as reference compounds for index calculation, or even other reference stationary phases.

In spite of some critical opinions, connected mainly with incorrect determination of retention indices of standard substances, the McReynolds constants system gave logical basis for stationary phase classification and allowed for selection of the proper gas chromatographic column. Until now, it has been the most common approach employed for stationary phase selectivity ranking in GC.

CONCLUSIONS

The system of McReynolds constants is a useful tool for characterization of the selectivity of stationary phases in GC. The founding principle of this approach is that intermolecular forces are additive and their individual contributions to retention can be evaluated from the difference in retention index values of selected test probes measured on a liquid phase to be characterized, and on the non-polar reference phase, i.e., squalane. To characterize the stationary phase polarity, the concept uses five special solutes (benzene, *n*-butanol, 2-pentanone, 1-nitropropane, and pyridine) that are considered to represent typical chemical interactions.

The simplicity of this method makes it the most commonly employed approach for liquid stationary phase selectivity ranking. The attempts to replace it by another system have been unsuccessful so far. It even inspired construction of an analogous system allowing for characterization of stationary phases in liquid chromatography.[25]

It is noteworthy that the method introduced by McReynolds has not only significant scientific but also practical importance.

REFERENCES

1. McReynolds, W.O. Gas chromatographic retention data. In *Gas Chromatographic Retention Data*; Preston Technical Abstracts Co.: Evanston, IL, 1966.
2. McReynolds, W.O. Characterization of some liquid phases. J. Chromatogr. Sci. **1970**, *8*, 685–691.

3. Rohrschneider, L. Eine Methode zur Charakterisierung von Gaschromatographischen Trennflussigkeiten. J. Chromatogr. **1966**, *22* (1), 6–22.
4. Kováts, E. Retentionsindices Aliphatischer Halogenide, Alkohole, Aldehyde und Ketone. Helv. Chim. Acta **1958**, *41*, 1915–1932.
5. James, A.T. Notion de phases polaire et non polaire. Biochem. Soc. Symp. **1970**, *30*, 199.
6. Berezkin, V.G.; Korolev, A.A.; Malyukova, I.V. Pressure effects on relative retention in capillary gas-liquid chromatography. J. High Resolut. Chromatogr. **1997**, *20*, 333–336.
7. Voelkel, A.; Kopczyński, T. Inverse gas chromatography in the examination of organic compounds. J. Chromatogr. A, **1998**, *795*, 349–357.
8. Dallos, A.; Sisak, A.; Kulcsár, Z.; Kováts, E. Pair-wise interactions by gas chromatography. VII. Interaction free enthalpies of solutes with secondary alcohol groups. J. Chromatogr. A. **2000**, *904*, 211–242.
9. Héberger, K. Evaluation of polarity indicators and stationary phases by principal component analysis in gas-liquid chromatography. Chemom. Intell. Lab. Syst. **1999**, *47*, 41–49.
10. Varian. Chromatography & Spectroscopy Supplies; Varian: Walnut Creek, CA, 2001–2002.
11. Rohrschneider, L. Explanatory coefficients for stationary phases in gas chromatography from McReynolds phase constants. Chromatographia **1994**, *38* (11/12), 679–688.
12. Kenndler, E. Gas Chromatography, Version 19/01/2004; Institute of Analytical Chemistry, University of Vienna: Vienna, 2004; p. 22–25.
13. Smith, J.R.L.; Tameesh, A.H.H.; Waddington, D.J. Porous polyaromatic beads. III. A method for classifying the selectivity of porous polyaromatic beads. J. Chromatogr. **1978**, *151*, 21–26.
14. Gawdzik, B.; Zuchowski, Z.; Matynia, T.; Gawdzik, J. Studies of chromatographic packings consisting of porous polymers. II. Separation properties of a porous styrene polymer cross-linked by di(methacryloyloxymethyl) naphthalene. J. Chromatogr. **1982**, *234*, 365–372.
15. Gawdzik, B. Studies on selectivity of porous polymers based on polyaromatic esters. J. Chromatogr. **1990**, *503*, 41–49.
16. Tacács, J.M. Unified system for the prediction of retention data in gas-liquid chromatography. J. Chromatogr. A. **1998**, *799*, 185–205.
17. Castello, G.; D'Amato, G. Effect of solute polarity on the performance of porapak type porous polymers. Chromatographia **1987**, *23* (11), 839–844.
18. Abraham, M.H.; Poole, C.F.; Poole, S.K. Classification of stationary phases and other materials by gas chromatography. J. Chromatogr. A **1999**, *842* (1/2), 79–114.
19. Smith, J.R.L.; Tameesh, A.H.H.; Waddington, D.J. The preparation, characterization and use in gas chromatography of chemically modified porous polyaromatic beads. J. Chromatogr. **1978**, *148*, 353–363.
20. Kersten, B.R.; Poole, C.F.; Furton, K.G. Influence on concurrent retention mechanisms on the determination of stationary phase selectivity in gas chromatography. J. Chromatogr. **1987**, *411*, 43–59.
21. Mathiasson, L.; Jönsson, J.A.; Olsson, A.M.; Haraldson, L. Sensitivity of retention index to variations in column liquid loading and sample size. J. Chromatogr. **1978**, *152*, 11–19.
22. Castello, G.; D'Amato, G. Classification of the "polarity" of porous polymer bead stationary phases by comparison with squalane and apolane standard liquid phases. J. Chromatogr. **1983**, *269*, 153–160.
23. Castello, G. Retention index systems: Alternatives to the *n*-alkanes as calibration standards. J. Chromatogr. A. **1999**, *842*, 51–64.
24. Heldt, U.; Köser, H.J.K. Different bases for the gas chromatographic retention index system. J. Chromatogr. **1980**, *192*, 107–116.
25. Smith, R.M. Retention and selectivity in liquid chromatography. Anal. Chem. **1984**, *56* (2), 256–262.

Metal Ions: CPC Separation

Subra Muralidharan
Chemistry Department, Western Michigan University, Kalamazoo, Michigan, U.S.A.

INTRODUCTION

Centrifugal partition chromatography (CPC), a multistage countercurrent liquid–liquid distribution technique employing discrete stages and two immiscible bulk liquid phases, is ideally suited for the detailed examination through separation factors and efficiencies, the influence of bulk aqueous and liquid–liquid interfacial equilibria and kinetics, on the separations of metal ions. This has been demonstrated by separations of transition metals, platinum group metals, and trivalent lanthanides; the significant findings are as follows: (a) Separation efficiencies are mainly limited by back-extraction kinetics which occur in the bulk aqueous phase and at the organic–aqueous interface as indicated by a direct linear correlation between the half-lives ($t_{1/2}$) of the dissociation reactions and the reduced plate height. (b) The interfacial areas calculated through this correlation are much larger in many cases than those generated in highly stirred two-phase mixtures. (c) The addition of surfactants and interfacial catalysis of the formation and dissociation of the complexes dramatically improve efficiencies. Examples of the separation of platinum group metal and trivalent lanthanides and the kinetic information that can be derived from their chromatograms are discussed.

CENTRIFUGAL PARTITION CHROMATOGRAPHY

The CPC apparatus, manufactured by Sanki Engineering Company, Japan,[1] consists of a series of cartridges, with each cartridge containing 40–400 channels, depending on the desired internal volume. These channels serve as stages in the separation experiment and the total number of channels is sometimes 400–4800, depending on the number of cartridges employed. The cartridges are arranged in a rotor which is rotated at 700–1200 rpm and the centrifugal force generated keeps one of the two phases (usually the organic phase) stationary while the other phase (usually the aqueous phase) is moved through it at a constant flow rate. The injected analyte mixture is carried by the aqueous mobile phase into the cartridges where they are extracted into the organic stationary phase by simple distribution if they are organic or by complexation with a suitable ligand if they are metals. When the mobile phase is depleted of the analytes, further flow of the mobile phase of the same (isocraticelution) or different (gradient elution) composition causes the back-extraction of the analytes, which can be detected by a suitable method. If the analytes are completely separated, they appear as discrete peaks similar to conventional chromatographic methods such as high-performance liquid chromatography (HPLC), and, hence, it is called centrifugal partition chromatography. CPC has these unique features: a large number of discrete stages (400–4800 depending on the operational volume chosen); high loading capacity for extractants and analytes; negligible loss of stationary phase due to "bleeding"; flexible organic–aqueous phase volume ratios; high stationary phase to mobile phase ratio; and ready adaptability to the process scale.

The basic parameters employed in the analysis of the CPC chromatograms are the retention volume V_r, which is related to the stationary phase and mobile phase volumes V_s and V_m, respectively, and the distribution ratio of the analyte D (Eq. 1), the chromatographic efficiency, as measured by the number of theoretical plates N, which is calculated from the retention volume V_r and the width of the chromatogram w, (Eq. 2), the chromatographic inefficiency represented by the channel equivalent of a theoretical plate (CETP), which is analogous to reduced plate height and is the ratio of the number of channels (CH) (2400 in our experiments) to N (Eq. 3), and the selectivity I achieved in the separation of two analytes (1 and 2), which is the ratio of their distribution ratios D_1 and D_2 (Eq. 4)[2]:

$$V_r = V_m + DV_s \tag{1}$$

$$N = 16\left(\frac{V_r}{w}\right)^2 \tag{2}$$

$$\mathrm{CERP_{obs}} = \frac{\mathrm{CH}}{N} \tag{3}$$

$$\alpha = \frac{D_2}{D_1}\ (D_2 > D_1) \tag{4}$$

SEPARATION OF PLATINUM GROUP METALS

Separation, extraction, and purification of the platinum group metals (PGM) Pt, Pd, Ir, and Rh in their various oxidation states continues to be challenging and represent

interesting areas of research. The separation of PGM from chloride media by solvent extraction can be achieved either by complexation with a suitable ligand or through ion-pair formation with a large cation. Complexation with a ligand is more selective but generally suffers from slow complex formation and dissociation kinetics. By contrast, ion-pair formation is diffusion controlled and not very selective, but it is necessary to separate kinetically inert species such as $PtCl_6^{2-}$ and $IrCl_6^{2-}$.

Trioctylphosphine oxide (TOPO) is an organophosphorus compound and is a stable and inexpensive extractant. TOPO, as we have shown,[3–5] is unique in that it can function as a monodentate ligand and as a cation for ion-pair extraction when protonated and the extraction equilibrium for the neutral ligand is shown in Eq. 5, indicating the extraction of the neutral complex $MCl_2(TOPO)_2$ [M = Pd(II), Pt(II); $n = 2$–4]:

$$MCl_n^{(n-2)-} + 2TOPO_0 \underset{\longleftarrow}{\overset{k_{ex}}{\longrightarrow}} MCL_2(TOPO)_{2,0} + (n-2)Cl^- \quad (5)$$

The K_{ex} values for $PdCl_2$, $PdCl_3^-$ and $PdCl_4^{2}$ are 794.3 M^{-2}, 2.75 M^{-1} and 0.14 respectively. A single peak was observed in the CPC chromatogram of Pd(II) at any concentration of Cl^-, as its hydrolytic equilibria are rapid. The corresponding values for the three Pt(II) chloro species are 48 M^{-2}, 0.047 M^{-1} and 0.018, clearly indicating the better extractibility of Pd(II) over Pt(II). The difference in the K_{ex4} values for the MCl_4^{2} species can be exploited to obtain an efficient separation of Pt(II) and Pd(II) from Rh(III) and Ir(III).

Formation of $HTOPO^+$, at HCl concentrations of 0.1 M, resulted in the extraction of $(HTOPO)_2MCl_4$ (M = Pt or Pd):

$$MCl_4^2 + 2H^+ + 2TOPO_0 \underset{\longleftarrow}{\overset{k_{ex}}{\longrightarrow}} (HTOPO)_2MCl_{4,0} \quad (6)$$

The chromatogram of the separation of $RhCl_6^{3-}$, $PdCl_4^{2-}$, and $PtCl_4^{2-}$ by $HTOPO^+$ is shown in Fig. 1. The K_{ex} values of Pd(II) and Pt(II) are 93.3 M^{-4} and 1961 M^{-4} respectively, indicating that Pd(II) elutes ahead of Pt(II) in the ion-pair separation, whereas the opposite is true in the separation by complexation. While the chromatogram of Pt(II) involves only the formation of $(HTOPO)_2PtCl_4$, the chromatogram of Pd(II) also involves the formation of In fact, under the experimental conditions employed in these separations, this is the major Pd ion pair that is extracted. The extraction equilibrium constant for $(HTOPO)PdCl_3$ is 18.25 M^{-1}. Similarly, Pt(IV) and Ir(IV) could be separated $HTOPO^+$ by by ion-pair formation with their MCl_6^{2-} species. The K_{ex} values for the Pt(IV) and Ir(IV) species are 1576 M^{-4} and 8035 M^{-4} respectively.

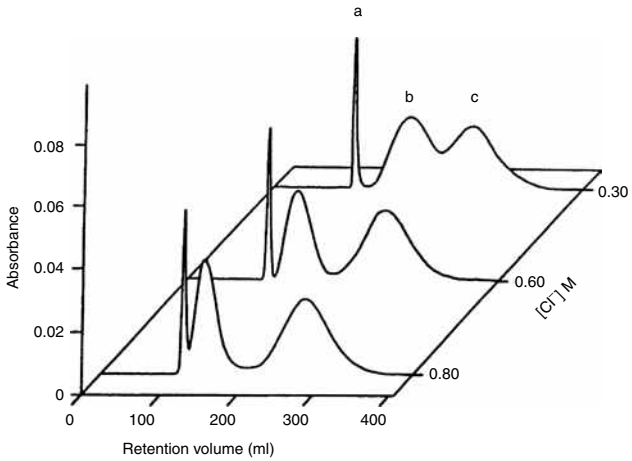

Fig. 1 Separation of 10^{-4} M $IrCl_6^{2-}$, $PtCl_4^{2-}$, and 10^{-3} M $PdCl_4^{2}$ as their ion pairs with $HTOPO^+$ as a function of $[Cl^-]$ with 0.5 MTOPO at 0.1 M HCl and 4.0 ml/min flow rate. Eluting species are (a) $IrCl_6^{2-}$, (b) $PdCl_4^{2-}$, and (c) $PtCl_4^{2-}$.

SEPARATION EFFICIENCIES OF PLATINUM GROUP METALS

We observed, early on, that CETP values are significantly larger for metal-ion separations than those for simple organic analytes under the same conditions. They are far larger than could be explained in terms of mass-transfer and diffusion factors. Moreover, they increase more rapidly with increasing flow rate than those of organic analytes, indicating a chemical kinetic component affecting the CETP. The CETP values observed with metal ions, after correction for mass transport and diffusion (achieved using an organic analyte with similar distribution characteristics), reflect the half-lives of chemical reactions causing the added inefficiencies. Metal-complex formation and dissociation reactions with half-lives of milliseconds (i.e., rapid enough that in batch experiments they reach equilibrium "instantaneously") will lower the efficiencies of CPC chromatograms. Conversely, CETP values can be used to study rapid reaction kinetics if this relationship is found to be generally valid. Thus, CPC is a useful tool not only for uncovering kinetics of metals separations but also for obtaining detailed mechanisms of those reactions responsible for inefficiencies in multistage metals separations. This demonstrates the utility of CPC for examining the kinetics of metal-complex formation and dissociation reactions in two-phase systems that are too rapid for the automated membrane extraction system (AMES).

It was evident, from the separations of PGM, that their experimental CETP values were much larger compared to that for an organic analyte at identical distribution ratios. These results indicated that factors other than mass transfer and diffusion were responsible for the additional bandwidths in the case of the metal ions. The most likely factor is the slow kinetics of back-extraction of the metal ions as

the forward extraction reactions are usually rapid. To test this hypothesis, 3-picoline was used as the model compound for the determination of the CPC bandwidth due to mass transfer and diffusion ($CETP_{dif}$), and the CETP value due to slow chemical kinetics ($CETP_{ck}$) was derived by expressing the experimental CETP ($CETP_{obs}$) as a sum of $CETP_{dif}$ and $CETP_{ck}$:

$$CETP_{obs} = CETP_{dif} + CETP_{ck} \quad (7)$$

The $CETP_{ck}$ values determined by varying the concentrations of the species in the aqueous and organic phases clearly showed that the slow back-extraction kinetics of the metal complexes were indeed responsible for the broad bands in the CPC chromatograms. On the basis of these results, a mechanism of the dissociation step could be deduced, which indicated that the dissociation of $MCl_2(TOPO)$ is rate limiting in the back-extraction of $MCl_2(TOPO)_2$ (M = Pd, Pt). A plot of the $CETP_{ck}$ values for $MCl_2(TOPO)_2$ against the $t_{1/2}$ values yielded a straight line. Further, these points and those for the Pd(II) system fall on a single line, indicating a general correlation for the separation of these two metals using TOPO in the heptane–H_2O phase pair.

Dissociation reactions with half-lives ranging from milliseconds to seconds can adversely affect the CPC efficiencies. It is important to realize the consequence of these findings: Extraction and back-extraction reactions that appear to be rapid in single-stage equilibrations may still be slow enough to reduce the efficiencies of multistage separations. A further significant finding of this work is that a direct linear correlation exists between $CETP_{ck}$ and $t_{1/2}$ for the Pd(II)–TOPO system and several other systems. Because the $CETP_{ck}$ values are a measure of the half-lives of the slow dissociation steps in metal-complex dissociation reactions, CPC is a useful tool for examining the kinetic and the equilibrium aspects of such reactions.

SEPARATION OF TRIVALENT LANTHANIDES

The trivalent lanthanides have been separated using acidic organophosphorous ligands and the acylpyrazolones.[6–8] The phosphinic acid bis(2,4,4-trimethylpentyl)phosphinic acid (Cyanex 272) in the heptane–water phase pair is dimeric and provides excellent separations of the adjacent light lanthanides at a fixed pH and a mixture of light and heavy lanthanides using a pH gradient (Fig. 2). Cyanex 272 is a chelating ligand that extracts the trivalent lanthanides by chelating them in its dimeric form (Eq. 8). The acylpyrazolones, 1-phenyl-3-methyl-4-benzoyl-5-pyrazolone (HPMBP) and 1-phenyl-3-methyl-4-capryloyl-5-pyrazolone (HPMCP, see structure below) have also been used in the toluene–H_2O phase pair for the extraction and separation of the

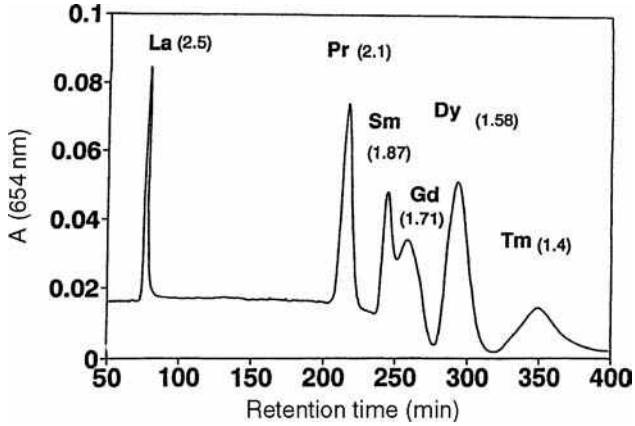

Fig. 2 Separation of lanthanides by use of a pH gradient with 0.1 *M* Cyanex 272 at $V_s/V_m = 0.18$ and flow rate of 1 ml/min. The concentrations and pH of elution are as follows: La (2 ppm; 2.5), Pr (6 ppm; 2.1), Sm (4 ppm; 1.87), Gd (4 ppm; 1.71), Dy (10 ppm; 1.58), and Tm (8 ppm; 1.4).

trivalent lanthanides. The extraction equilibrium constant for are given in Eq. 9.

$$M^{3+} + 3(HL)_{2(0)} \underset{\longleftarrow}{\overset{K_{ex}}{\longrightarrow}} M(HL_2)_{3(0)} + 3H^+ \quad (8)$$

$$M^{3+} + 3HL_0 \underset{\longleftarrow}{\overset{K_{ex}}{\longrightarrow}} ML_{3(0)} + 3H^+ \quad (9)$$

Significant differences are seen between Cyanex 272 and the acylpyrazolones. The extractibility of the trivalent lanthanides is higher with Cyanex 272 than with the acylpyrazolones, where HPMBP shows better extraction than HPMCP. The stability constants of the lanthanides increases from the light to heavy, and the values for the Cyanex 272 and HPMCP complexes are larger than those of HPMBP. The separation factor (or selectivity) for a pair of lanthanides is much better with Cyanex 272 than with HPMBP or HPMCP, which have similar separation factors.

The lanthanide complexes lack distinct ultraviolet–visible spectra and, hence, kinetic information on their complex formation and dissociation reactions was obtained indirectly by the metallochromic indicator method.[9] These studies indicate that in the case of the Cyanex 272 complexes, the CPC efficiencies are mainly limited by the slow dissociation of the $M(HL_2)HL^+$ complex at the heptane–H_2O interface. In the case of the complexes of the acylpyrazolones, the CPC efficiencies are again limited by the dissociation of the lanthanide–pyrazolone complexes at the organic–aqueous interface with the rate-limiting step being the dissociation of the ML^{2+} complex. It was also shown that because the dissociation reactions are interfacial separations, efficiencies can be dramatically improved by the addition of surfactants like Triton X-100 to the organic phase and by

interfacial catalysis by the addition of a aqueous soluble metallochromic indicator, which formed highly interfacially active lanthanide–indicator complex. The adsorption of this complex at the organic–aqueous interface catalyzed the metal-complex formation and dissociation reactions leading to high efficiencies in CPC separations.[10]

Two significant results have emerged from the CPC separations of metals ions, namely (a) separation efficiencies are significantly reduced by slow metal-complex formation and dissociation kinetics and (b) CPC separations can be entirely interfacially driven analogous to conventional liquid chromatography.

REFERENCES

1. Foucault, A.P., ed.; *Centrifugal Partition Chromatography*; Marcel Dekker, Inc., New York, 1994.
2. Berthod, A.; Armstrong, D.W. Centrifugal partition chromatography II. Selectivity and efficiency. J. Liquid Chromatogr. **1988**, *11*, 567.
3. Surakitbanharn, Y.; Muralidharan, S.; Freiser, H. Separation of palladium(II) from platinum(II), iridium(III) and rhodium(III) using centrifugal partition chromatography. Solvent Extract. Ion Exchange **1991**, *9*, 45.
4. Surakitbanharn, Y.; Muralidharan, S.; Freiser, H. Centrifugal partition chromatography of palladium(II) and the influence of chemical kinetic factors on separation efficiency. Anal. Chem. **1991**, *63*, 2642.
5. Surakitbanharn, Y.; Freiser, H.; Muralidharan, S. Centrifugal partition chromatographic separations of platinum group metals by complexation and ion pair formation. Anal. Chem. **1996**, *68*, 3934.
6. Cai, R.; Muralidharan, S.; Freiser, H. Improved separation of closely related metal ions by centrifugal partition chromatography. J. Liquid Chromatogr. **1990**, *13*, 3651.
7. Inaba, K.; Freiser, H.; Muralidharan, S. Effect of kinetic factors on the efficiencies of centrifugal partition chromatographic separations of tervalent lanthanides with bis(2,4,4,-trimethylpentyl)phosphinic acid as extractant. Solvent Extract. Res. Dev. Japan **1994**, *1*, 13.
8. Ma, G.; Freiser, H.; Muralidharan, S. Centrifugal partition chromatographic separation of tervalent lanthanides using acylpyrazolone extractants. Anal. Chem. **1997**, *69*, 2835.
9. Inaba, K.; Muralidharan, S.; Freiser, H. Simultaneous characterization of extraction equilibria and back-extraction kinetics: Use of arsenazo III to characterize lanthanide–bis(2,4,4-trimethylpentyl)phosphinic acid complexes in surfactant micelles. Anal. Chem. **1993**, *65*, 1510.
10. Ma, G.; Freiser, H.; Muralidharan, S. Interfacial catalysis of formation and dissociation of tervalent lanthanide complexes in two phase systems. Anal. Chem. **1977**, *69*, 827.

Metal Ions: Silica Gel Surface Modification for Selective Extraction

Mohamed E. Mahmoud
Medical Chemistry Department, King Abdullaziz University, Jeddah, Saudi Arabia

INTRODUCTION

Silica gel is the most commonly used inorganic solid support in the field of chromatographic applications. Silica gel is a polymeric type of silicic acid (H_4SiO_4), which is synthesized from the hydrolysis reactions of alkoxysilanes or sodium silicate, in the presence of an acid or a base; there are also other known routes of preparation and manufacturing.[1] The structure of silica gel is characterized by the presence of certain functional moieties owing to the presence of some groups such as siloxane, ≡Si–O–Si≡, with the oxygen located on the surface, as well as silanol groups, ≡Si–OH. Active silica gel is mostly characterized by the surface silanol groups that are known to exist in several forms,[2] as shown in Scheme 1.

Several other arrangements of the silanol groups are also known; they are dependent upon the possible interactions between them, as shown in Scheme 2.

The surface silanol groups are the major contributing factors that are responsible for binding, adsorption, and extraction processes with the target analytes of interest such as metal ions or their more complex species. The weak ion-exchange properties of silanol groups are to favor their low interaction behavior with the various species. Therefore, improvements of the adsorption efficiency and extraction power of the sorbent are always aimed via surface modification with certain functional groups. This objective can be accomplished by application of either physical adsorption or chemical immobilization methods.

MODIFICATION OF THE SILICA GEL SURFACE

Two principle methods of surface modification are well known; they can be summarized as the physical adsorption method and the chemical immobilization technique of the organic modifier.[3] Each method is experienced with certain advantages and disadvantages over the other. For example, the physical adsorption approach is commonly accomplished in a single-step reaction; this requires less time for obtaining the final modified solid extractor, but the active donor centers or atoms in the physically modified phases may be consumed in the adsorption process. In addition, these modified phases were found to suffer from leaching or desorption processes under the influence of strong acidic or basic media.[4] The modified phases that are synthesized on the basis of a chemical immobilization method are characterized by good stability characteristics in acidic and basic media, but the disadvantage of this technique is the multistep reactions needed to obtain the modified solid extractors. The active donor atoms or groups in the modified sorbents, prepared by the chemical immobilization method, are well defined in such phases. The types of compounds that can be loaded onto the surfaces of solid phases are unlimited; these include:

1. Long chain and short chain hydrocarbons
2. Polar and non-polar organic compounds
3. Inorganic and organometallic compounds
4. Simple and macromolecular compounds
5. Chelating compounds.

Chelating compounds are the most important class of compounds that can be used and applied in the processes of solid-phase extraction (SPE) of transition and non-transition metal ions. The reason for this interest and conclusion is the presence of certain donor atoms, mainly nitrogen, oxygen, sulfur, and phosphorus in these compounds. The donor atoms are the active centers and are known to be responsible for the incorporation of certain selectivity characteristics into the newly modified solid phases. However, the reported rules controlling such incorporated selectivity toward certain metal ions are mainly based on several important factors:

1. The size of the organic chelating modifiers as reported for crown ether derivatives
2. The reactivity and activity of the loaded surface group
3. The nature of the interacting donor atoms and metal ions
4. The length of hydrocarbon chain in separation of some rare earth elements
5. The reported formula of hard–soft acids-bases.

Metal ions and their species, either essential or toxic for living organisms, are finding their routes into the various samples, matrices, and environments from many sources. The accurate determinations, qualitative or quantitative, of the target metal ions or their species, especially in the environmental, biological, and industrial samples are considered of

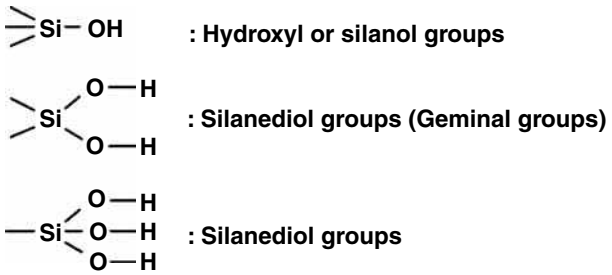

Scheme 1

great challenge to the analytical chemist because of the huge number of interfering species and compounds. The determination procedure is principally started with an important step, i.e., extraction and/or preconcentration. Several available techniques are commonly used and applied in metal ion extraction; these include the direct precipitation of metal ions as hydroxides. Liquid or solvent extraction techniques are routinely used in this respect. Although this technique is a simple method for the extraction and preconcentration of the analyte of interest, it is always plagued with several major disadvantages such as the inability to directly apply it for poorly soluble species in the conventional non-polar organic solvents. In addition, the amount of organic solvent used in this technique, either in a single or multistep analysis, is commonly high and leads to a direct impact on environmental pollution, owing to the problem of waste generation and destruction. The problems of time, effort, and money consumption are also evident in practicing this technique.[5] The other alternative technique to liquid extraction is now known as SPE. This affords several advantages over the classical liquid extraction technique, including:

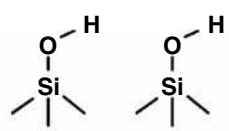

Free Silanol groups

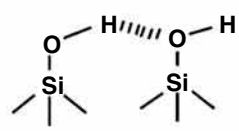

Hydrogen-bonded silanol groups

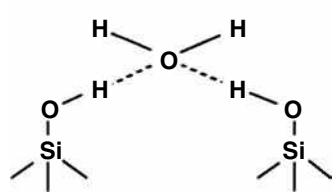

Water hydrogen-bonded silanol groups

Scheme 2

1. No waste generation in the experimental process owing to non-dependence on extraction solvents.
2. Allows direct, simple, and fast sample applications in very small (microliter) or large (liter) volume sizes without sample loss.
3. Can be directly applied for different matrices without prior treatments.
4. The ability of SPE to be online or off-line, interfaced with major analytical instrumentation, is considered as another dimension and an advantage over the classical liquid extraction.

Solid-phase extraction is mainly based on the utilization of a solid support instead of an organic solvent onto which the target metal ion or analyte is loaded onto the surface. Solid-phase extractors are materials derived from organic or inorganic origins. The organic solid supports include polyurethane foams, filter paper, cellulose, naphthalene, ion exchange resins, and polymeric species. On the other hand, silica gel, alumina, magnesia, zirconia, and metal oxides are the major inorganic solid supports. The simple comparison between inorganic and organic solid-phase extractors such as silica and ion exchange resins, respectively, mainly points out the following:[6]

1. High ability and superiority of the inorganic ones for binding, extraction, removal, and preconcentration of transition metal ions already present with high concentrations of interfering alkali and alkaline earth metal ions.
2. Inorganic solid extractors can afford higher mechanical, chemical, and thermal stability.
3. Fast time of binding with the target metal ions as well as good kinetic properties.
4. Non-swelling properties as reported for organics.

EXAMPLES OF MODIFIED SILICA GEL PHASES, CLASSIFIED ACCORDING TO THE DONOR ATOMS AND THEIR APPLICATIONS

Silica Gel Phases with Nitrogen Donor Atom

Silica gel functionalized by reaction with γ-aminopropyltriethoxysilane was prepared and its selective adsorption characteristics for various metal ions such as Au(III), Pt(IV), and Pd(II) chlorocomplex ions from sample solutions containing Fe(III) and Cu(II) ions by ion exchange were studied.[7] The structure of the modified silica gel phase is shown in Scheme 3.

Silica gel phases modified via covalent bonding of γ-aminopropyltriethoxysilane, ethylenediamine, diethylenetriamine, and triethylenetetramine were synthesized and

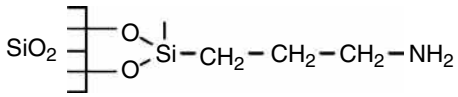

Scheme 3

the surfaces of these modified phases were characterized by secondary ion mass spectrometry and infrared spectrophotometry. The thermal stability from electron impact-mass spectrometry (EI-MS) as well as the potentiometric titration of these phases with Cu(II) was studied and evaluated. The selectivity properties incorporated into these phases via immobilization of the nitrogen donor atom were also reported for a series of metal ions.[8] The structures of these modified silica gel phases are given in Scheme 4.

Preconcentration of metal ions from ethanolic solution by a packing material based on silica gel functionalized with 3-(1-imidazolyl) propyl groups for column chromatographic application was performed. The modified silica gel was applied to preconcentrate Cu, Ni, Fe, Zn, and Cd ions from commercial ethanol. The method is suitable for quantitative determination of these metals at low μg/L levels.[9]

Ir(IV), Rh(III), Pt(IV), Os(VIII), Pd(II), and Au(III) were sorbed from aqueous solution by silica gel, which was chemically modified with nitrogen-containing organic ligands. This was performed as a function of hydrochloric acid concentration, time of contact, concentration of the element, and the ionic strength. Extraction, followed by determination on the sorbent surface by x-ray fluorescence of Ir(IV), and Rh(III), from 10^{-8} to 10^{-7} *M* solutions, were achieved. An atomic emission method was used to determine Au(III) on the surface of the sorbent containing bonded diethylenetriamine groups.[10]

Preconcentration and removal of Co, Cu, Zn, Cd, and Hg by silica gel modified with pyridinium ions was developed and applied by using the column technique. Selective elution of these metals was accomplished by a

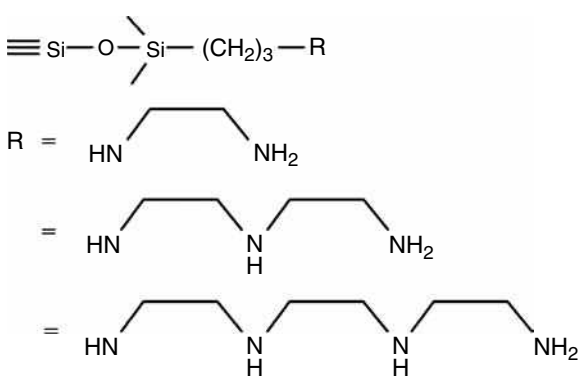

Scheme 4

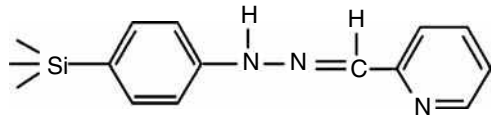

Scheme 5

C_2H_5OH–H_2O binary mixture. For the elution mixture with a mole fraction of 0.5, the observed order was Co ~ Cd (~ 96%) > Cu ~ Zn (~ 30%) > Hg (not eluted).[11]

Metal ions sorption by 2-pyridine carboxaldehyde phenylhydrazone supported by chemical binding on a silica surface were confirmed to the Langmuir isotherm. The modified phase was used and applied as a metal-ion extractant for determination of trace amounts of iron, cobalt, nickel, and copper. The relative orders of the Langmuir constants *K* and the column retention capacity factors *K′* for the four transition metal ions are the same as the natural order of the stability constants for their metal chelates: Fe(II) < Co(II) < Ni(II) < Cu(II).[12] The structure is given in Scheme 5.

A silica-based sorbent-anion complexone polymer coating [24]ane-N_6 macrocycle was prepared. The chelation properties of this material were investigated for Cu(II), Cd(II), Co(II), and Zn(II). Oxalic acid was found to be the most effective eluent for the separation of these metal ions from seawater. The limits of these metal ions were identified to be 5×10^{-7} *M*, 1×10^{-5} *M*, 3×10^{-5} *M*, and 2×10^{-6} *M* for Cu(II), Cd(II), Co(II), and Zn(II), respectively.[13]

Silica Gel Phases with Oxygen Donor Atoms

The effect of pH of the sample, eluent flow rate, and the amount of silica on sorption and elution experimental parameters were investigated by a new phase, which was synthesized from a high surface area silica gel with a 3-trimethoxysilyl-1-propanol group. In addition, both batch and column techniques were applied to identify the characteristics of this modified silica and its application to the preconcentration and separation of Co and Ni prior to determination by graphite furnace atomic absorption spectrometry (GFAAS).[14]

Column preconcentration of alkali metal cations by the newly synthesized silica gel phases-with chemically modified-pentadentate carboxylic acid groups were described.

1. The cavity size of the crown ether unit.
2. Conformational positioning of the proton-ionizable side arm with respect to the crown ether cavity.
3. Capping of residual silanol surface with trimethylsilyl was found to influence the selectivity and efficiency properties incorporated into these

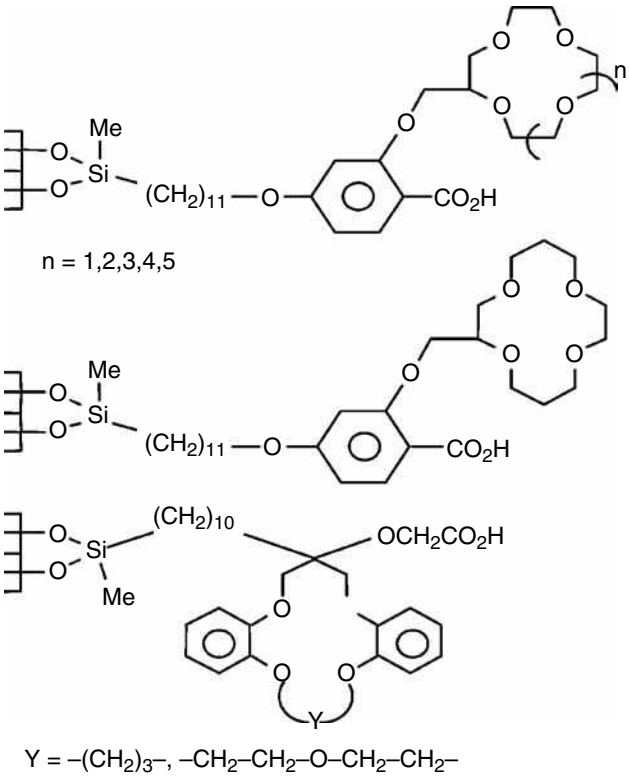

Scheme 6

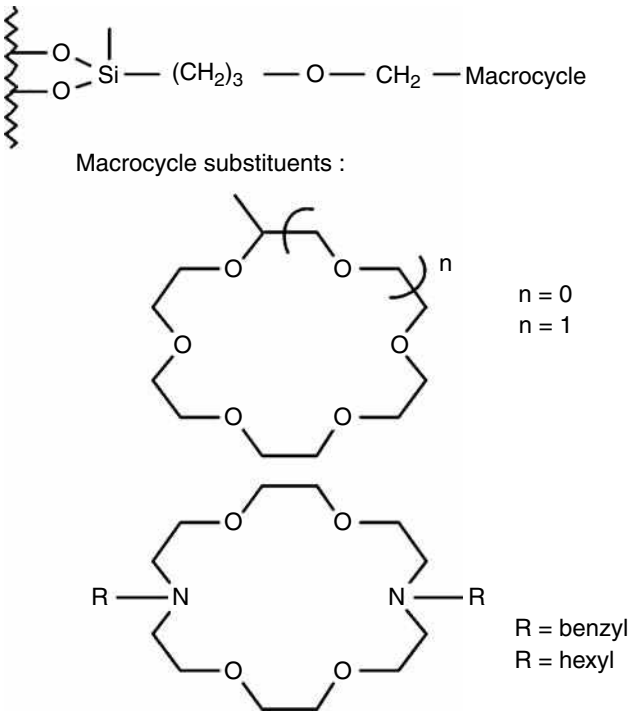

Scheme 7

newly modified silica phases.[15] The structures of the modified silica gel phases are shown in Scheme 6.

Macrocyclic substituents attachment to silica gel phases via hydrocarbon type linkage were reported. These modified phases were found to be capable of selective and quantitative removal of Ag(I), Hg(II), Tl(I), and Pb(II) from aqueous solutions.[16] The structures of these modified silica gel phases are shown in Scheme 7.

1,8-Dihydroxyanthraquinone anchored on silica gel was synthesized and used as a solid-phase extractant for Pb(II), Zn(II), and Cd(II) prior to their determination by flame atomic absorption spectrometry (FAAS).[17]

A highly selective solid phase for Fe(III) was synthesized and was based on chemically modified silica gel with purpurogallin as an oxygen donor atom-chelating compound. The modified phase was applied for selective extraction and preconcentration Fe(III) in the presence of other interfering metal ions from various matrices.[18]

Silica Gel Phases with Sulfur Donor Atom

Selective preconcentration of arsenite from natural waters was reported by the application of a surface-modified mercapto silica gel. Both column and batch preconcentration techniques were employed by this material for selective removal of arsenite from samples that also contain arsenite, monomethylarsonate, and dimethylarsinate.[19]

Silica modified by the addition of mercapto-chelating groups was developed for the preconcentration of trace amounts of Cd, Cu, Pb, and Zn from aqueous solution and natural waters. This material was found to remove and preconcentrate these metals by both column and batch techniques. Under column and batch conditions, recoveries larger than 95% were reported. For batch extraction of Cd, Zn, Cu, and Pb from seawater, recoveries of 96 ± 5% were obtained.[20]

Silica Gel Phases with Nitrogen and Oxygen Donor Atoms

The interaction of silica gel phases-modified-diethylenetriamine, with naphthaldehyde and salicylaldehyde, was found to produce four new solid-phase extractors. Characterization of these modified silica gel phases and their capability toward selective extraction and separation of six metal ions: Fe(III), Ni(II), Cu(II), Zn(II), Cd(II), and Pb(II), were studied and evaluated by both the batch and the column techniques as a function of pH and time of contact. The reactivity of metal ion sorption was discussed on the basis of effects of bulk as well as orientation of immobilized chelate on sorbent reactivity. Other aspects of synthesis,

characterization, and structural effects on metal ion(s) selectivity of these newly synthesized silica gel phases are also reported.[21]

A simple method was described for the extraction and determination of ultratrace amounts of Cu(II) ions using octadecyl-bonded silica membrane disks modified with a recently synthesized Schiff's base {2,2′-[1,2-ethanediyl-*bis*-(nitriloethylidyne)]-*bis*-(1-naphthalene)}. The pH effect, nature and amount of counter anions, flow rates, and type of stripping acid were evaluated as the important factors of extraction efficiency of metal ions. The capacity was found to be 396 μg of copper for the membrane disks modified by 5 mg of the ligand. The limit of detection of the proposed method is 4 ng/1000 ml.[22] The structure of the organic modifier is given in Scheme 8.

Separation, preconcentration, and purification of metal ions from dilute aqueous solutions were accomplished by silica gel impregnated with a mixture of Calcon and Aliquat 336 as chelating sorbents. The relative capacities of 33 metal ions were determined in different experimental conditions of pH range as well as the concentrations of hydrochloric acid and perchloric acid.[23]

Sorption of metal ions such as Ca, Mg, Al, Cu, Fe, Ni, Co, Cd, Zn, Pb, Hg, and Cr on silica gel impregnated with a mixture of Aliquat 336 and Titan Yellow was investigated in the pH range 1–9. The column extraction chromatography application of the sorbent to the separation of solutions of analytical reagent grade sodium, potassium, calcium, magnesium, and ammonium chloride from traces of Cu, Pb, Cd, and Zn, and the separation of some metal ion mixtures were also reported.[24]

The chemical immobilization of formylsalicylic acid derivatives on the surface of amino group-containing silica gel phases was reported. The resulting phases were examined for the extraction of Fe(III) and showed an exchange capacity of 0.95–0.96 mmol/g. The other tested metal ions showed lower metal capacity than Fe(III). The selectivity incorporated into these silica gel phases for the extraction of Fe(III) from a mixture containing several other interfering metal ions was studied and evaluated by atomic absorption spectrophotometric analysis. In addition, a method for the recycling of the immobilized silica gel phases after metal extraction was also described on the basis of using ethylenediaminetetraacetic acid as a regeneration reagent.[25]

New silica gel phases were synthesized by a single-step reaction via immobilization of 5-formyl-3-arylazosalicylic acid derivatives on the surface of silica gel. These phases proved to show an excellent improvement in the Fe(III) extraction; the determined mmol/g is in the range 1.24–1.32. The process of selective extraction of Fe(III) in the presence of an interfering ion was studied by both column and batch equilibrium techniques. Cr(III) was found to cause interference based on the affinity for binding to the chelation centers of the salicylic acid moiety of the silica gel phase. Mg, Ca, and Mn ions exhibited minimum interference in Fe(III) extraction. A group of six divalent metal ions (Co, Ni, Cu, Zn, Cd, and Pb) were found to show a specific interference based on the availability and participation of arylazo-moiety.[26] The structures of these silica gel phases-immobilized-5-formyl-3-arylazosalicylic acids are shown in Scheme 9.

A batch equilibrium method, as a function of pH and shaking time, was performed to characterize the metal uptake properties of silica gel-immobilized-aminophenol and aminobenzoic acid. Studies were made and evaluated on the basis of column application of immobilized chelating sorbents for the removal of various metal ions from sugar cane molasses. These revealed that they have higher preference toward Mn(II), Fe(III), Co(II), Cu(II), and Zn(II) rather than alkali and alkaline earth metals.[27] The structures of the modified silica gel phases are shown in Scheme 10.

Modification of aliphatic mono- and poly-amine sorbents by incorporation of hard oxygen donor ligands, through Schiff's base reaction with carbonyl containing compounds, was found to significantly improve the uptake of Fe(III), known to act as hard acid.[28]

Physical adsorption and chemical immobilization techniques were used for the modification of silica gel surface by 1-aminoanthraquinone to produce three modified silica gel phases. These modified phases were studied for their metal sorption and extraction properties. The chemically modified silica phases were applied for selective extraction and preconcentration of Cu(II) and Cr(III) from seawater samples.[29]

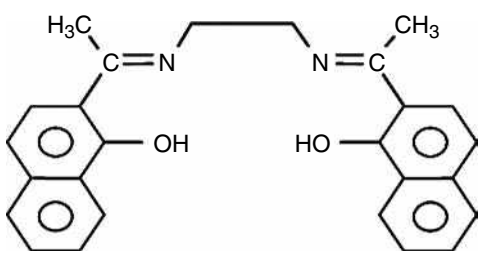

Scheme 8

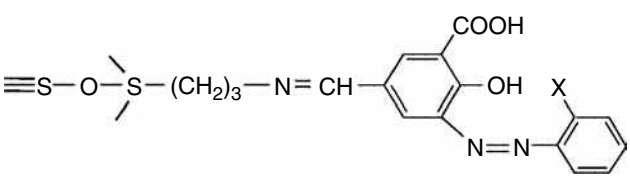

Scheme 9

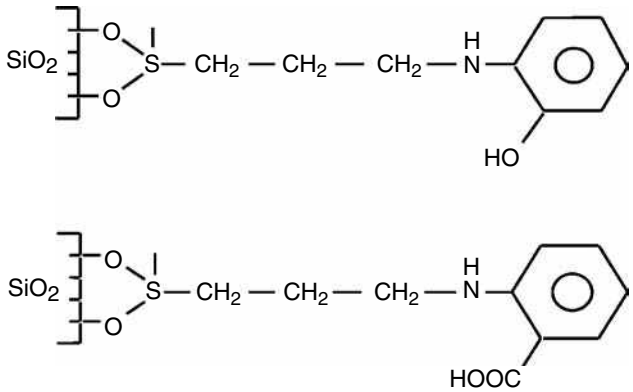

Scheme 10

Iminosalicyl groups attached to a silica gel surface were used for the adsorption of metal ions from ethanol (Scheme 11). Extraction of iron, nickel, cobalt, copper, zinc, and cadmium from ethanol by batch and column techniques was reported. The average distribution coefficient determined was: Fe(III), 4.5×10^2; Co(II), 1.4×10^2; Ni(II), 1.1×10^2; Cu(II), 3.6×10^2; Zn(II), 3.0×10^2; and Cd(II), 2.2×10^2.[30]

Immobilization of 2,3-dihydroxybenzoyl and 3,4,5-trihydroxybenzoyl amide functional groups on the surface of silica was reported. Significant affinity for preconcentration of transition metal ions and no affinity toward uptake of Ca, Mg, Na, and K ions from dilute aqueous solutions were identified by the synthesized phases.[31] The structures of these modified phases are shown in Scheme 12.

A successful method was applied for the determination of (parts per billion (ppb) levels of aluminum ion in tap water, river water, and tea samples by O, O′-dihydroxyazobenzene (dhab) via a selective and sensitive visual method. In this method, octadecylsilyl (ODS) - silica thin layer was used and a positively charged fluorescent 1 : 1 Al(III) chelate $[Al(dhab)]^+$ was retained at a spotting position. The immobilization of $[Al(dhab)^+]$ was attributed to the electrostatic interaction between it and the anionic charge of silanol groups on the ODS-silica plate.[32]

A combination of C_{18} reversed phase, Dowex anion-exchange resin, and the chelating resin, chelamine, in a three columns system, was described for the simultaneous preconcentration and differentiation between natural

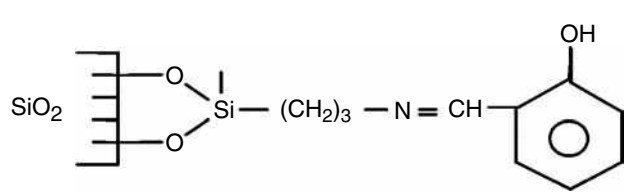

Scheme 11

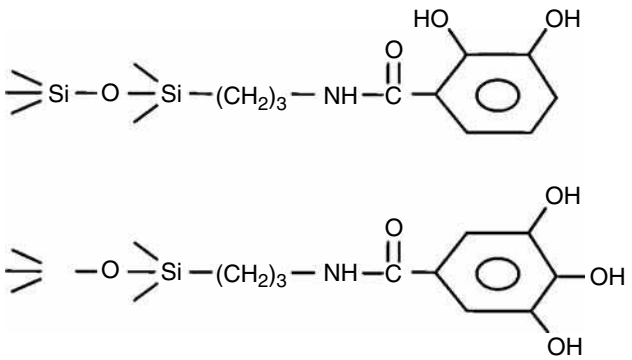

Scheme 12

hydrophobic organic metal complexes, anionic complexes, and the free ion concentration of the transition metals in water samples with complex matrices. The method showed excellent reproducibility for the determination of Cu(II), Cd(II), Pb(II), and Mn(II) in several freshwater and seawater samples.[33]

Attachment of crown ethers and their derivatives to silica gel via a hydrocarbon-type linkage was applied for selective and quantitative removal of cations from aqueous solutions. The modified phases were found to be of potential value in preconcentration of nanogram per milliliter levels of some cations. In addition, these phases were operated without loss of the macrocycle and maintained the same selectivity toward metal ions in aqueous solution by the particular macrocycle in the free state.[34–36]

Immobilization of polyaza as well as mixed-donor (O, N) and (O, S) macrocycles to a silica gel matrix was described. These phases were used to investigate their selectivity toward preconcentration and separation of transition metal ions. A 17-membered O_2N_3-donor macrocycle exhibited a remarkable selectivity toward Cu(II) retention in presence of Ni(II), Zn(II), and Cd(II). The polyaza-macrocycles 1,4,7,10-tetraaza-18-crown-6, pentaaza-15-crown-5, and hexaaza-18-crown-6 were synthesized with macrocycles covalently bonded to silica gel via one of the nitrogen donor atoms. These bound macrocycles were found to have strong and selective interaction with soft heavy metal ions. Separation of ppb levels of these cations from concentrated mixtures of other cations such as alkali and alkaline earth cations were accomplished (Scheme 13).[37]

A number of methods for the immobilization of 8-hydroxyquinoline (8HQ) onto silica substrates have been proposed, characterized, and optimized. Examples of these modified silica gel phases with 8HQ as well as their applications are also reviewed in the following section.

A simple method for the preparation of silica immobilized 8HQ was described and investigated for its affinity for Cu, Ni, Co, Fe, Mn, Cr, Zn, Cd, Pb, and Hg. The metal uptake capacities for these metal ions were

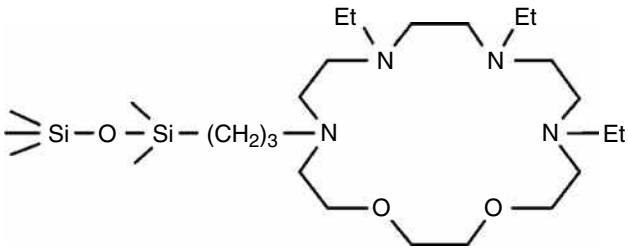

Scheme 13

found to be in the range of 0.2–0.7 mmol/g. The distribution coefficients were found to be in the range from 1000 up to >90,000.[38] The structure of this modified sorbent is given in Scheme 14.

Silica-immobilized-8-hydroxyquinoline (SG-8HOQ) was reported for the purpose of solid–liquid extraction of metals. The separation of metals as their chelates by batch equilibrium or column chromatography was performed for trace amounts of Al(III), Cd(II), Co(II), Cu(II), Fe(III), Mn(II), Mg(II), Ni(II), and Zn(II) in solid-liquid back extraction.[39] The structure of SG-8HOQ is shown in Scheme 15.

Procedures based on the application of immobilized quinoline-8-ol silica and stripping voltammetry were developed for the determination of copper, lead, cadmium, bismuth, indium, and zinc in seawater. Better sensitivity and lower detection limits were achieved with the application of smaller sample volumes. The feasibility and reliability of the developed procedures were confirmed by the analysis of a near shore seawater sample and CASS-2 reference seawater.[40]

A flow-system utilizing a miniature column packed with SG-8HOQ was used for the preconcentration of Cd, Pb, Zn, Cu, Fe, Mn, Ni, and Co from seawater prior to their determination by GFAAS. A preconcentration factor sufficient to permit the analysis of an open seawater reference material, using a 50 ml sample, was obtained. Recoveries of the above elements from seawater averaged 93% (range 87–97%) with absolute blanks ranging between 0.04 ng (Ni) and 4.0 ng (Fe).[41]

Several 8-quinolinol silica gel columns were used with metal-uptake capacities 10–156 μmol/g. Various transition and heavy metal ions were used in the form of nitrate, sulfate, phosphate, citrate, tartarate, oxalate, phthalate, and maleate mobile phases. Column capacity and pH were found to influence the metal ion retention.

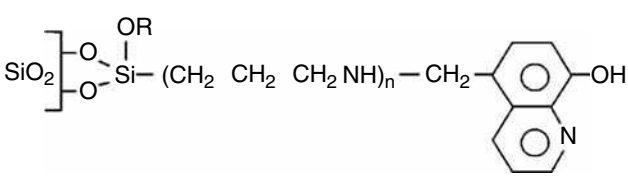

Scheme 14

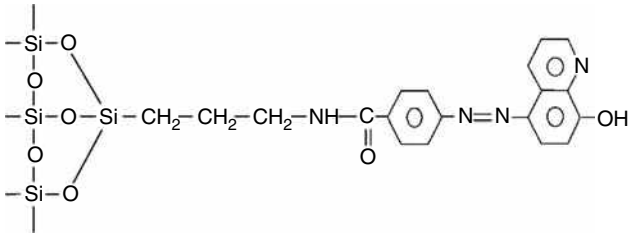

Scheme 15

Optimum capacity factors were obtained on columns of intermediate capacity (27 and 46 μmol/g). Retention times decreased with an increase in eluent buffer concentration, typically by half with a doubling of buffer concentration.[42]

8-hydroxyquinoline, 8-hydroxy-5-sulphonic acid quinoline, and 2-amino-1-cyclopentene-1-dithiocarboxylic acid silica gels, loaded with Cu(II), Ni(II), or Zn(II), were examined for the separation of some aromatic amines in the normal phase mode. All phases studied interact strongly with the sample compounds, but the presence of cations increases the selectivity of the column. Ni(II) or Zn(II) loading proved to be better than Cu(II) loading, because with these ions, strong peak broadening and disturbances of the base line are avoided. End capping of the chelating silica gels was indispensable to obtain good efficiencies.[43]

Silica Gel Phases with Nitrogen and Sulfur Donor Atoms

Selective solid-phase extractors and preconcentrators of Hg(II) were synthesized and studied. These modified silica gel phases are based on chemical immobilization and physical adsorption of dithizone as well as chemical immobilization of dithiocarbamate on some amine-modified silica gel phases. The mmol/g values as the metal capacities of these modified silica gel phases were determined for a series of metal ions under the effect of pH of metal ions and the equilibration shaking times by the batch equilibrium technique. The modified silica gel phases were found to exhibit excellent affinity toward selective extraction of Hg(II) in presence of other interfering metal ions. The potential applications of these modified silica gel phases as selective solid-phase extractors and preconcentrators for Hg(II) from natural water samples were also studied and the results indicated excellent extraction of Hg(II) with insignificant contributions by matrix effects.[6,44]

2-Mercaptobenzothiazole-modified silica gel was used for the flow injection (FI) online preconcentration, separation, and determination of silver by FAAS. The results showed that Ag(I) was selectively adsorbed from 0.05 to 6 M HNO_3 solution and was readily desorbed by thiourea solution. The ions coexisting with Ag(I) exhibit virtually

no interference in the determination, with only the exception of Cl^-. Silver in a geological sample, a copper metal sample, and a lead nitrate sample were determined satisfactorily (Scheme 16).[45]

A method was presented for the immobilization of a thioglycolic acid moiety on the surface of active silica gel via a simple and direct synthetic route based on a single-step reaction for the formation of two solid-phase extractors. The selective removal and preconcentration of some heavy metal ions, viz. Cu(II), Zn(II), and Hg(II) from natural seawater was successfully accomplished.[46]

Diethyldithiocarbamate, pyrrolidin-1-yldithioformate, and diphenylthiocarbazone (dithizone), as three mercury chelate forming reagents, were used for the preconcentration of ultratrace amounts of inorganic mercury and methyl mercury in silica C_{18} minicolumn as the solid sorbent. Sample FI online sorbent extraction was coupled with continuous cold vapor atomic absorption spectrometry (CVAAS) for detection. The results showed the superiority of the carbamate type reagents over the dithizone for the online formation and preconcentration of the corresponding mercury chelate. The detection limit was found to be 16 ng/L of mercury.[47] The structures of these organic chelate modifiers are shown in Scheme 17.

Chemical immobilization of 2-amino-1-cyclopentene-1-dithiocarboxylic acid as a chelating compound on the surface of silica gel was prepared. This showed great affinity for removal of Ag(I), Hg(II), and Pd(II) from dilute matrices, with exchange capacities in the range of 0.98–0.90 mmol/g. Fast equilibration times for these metal ions were determined (Scheme 18).[48]

Studies of the selective separation of Pd(II) from Rh(III) and Ir(III), in the presence of high concentrations of base metal ions, at pH 1, as well as preconcentration from dilute aqueous solutions, were performed using a column packed with silica gel-immobilized-2-[(2-triethoxysilyl) -ethyl thio] aniline. A quantitative elution of Pd (II) was effective with acidic 5% thiourea solution.[49]

Silica gel phases modified with aminopropyltriethoxysilane, ethylenediamine, diethylenetriamine, and triethylenetetramine were modified to the corresponding

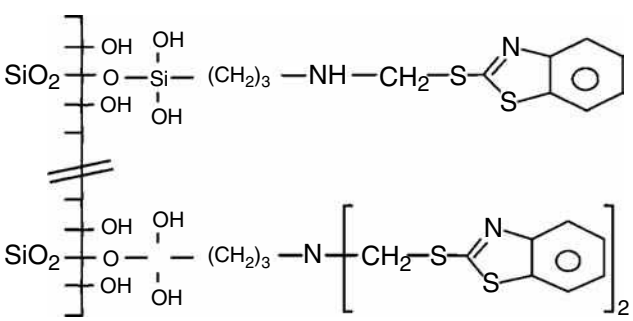

Scheme 16

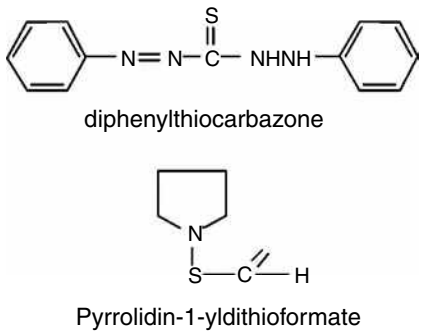

Scheme 17

dithiocarbamate derivatives. The surfaces of these modified phases were characterized by elemental analysis and infrared spectrophotometry. The thermal stability from EI-MS and the selectivity properties incorporated into these phases via immobilization of the nitrogen and sulfur donor atoms were also reported for a series of metal ions.[50]

A flow-injection online preconcentration and separation system with microwave-assisted desorption is proposed for the efficient determination of trace amounts of Pt by FAAS. A microcolumn packed with thiourea modified silica, placed in a microwave oven, was used to collect Pt from the sample solutions. The detection limit was 0.060 μg/ml. The results obtained by the proposed method for three metallurgical samples, a secondary nickel alloy, anode slim, and a $CoCl_2$ solution, were in good agreement with the recommended values.[51]

A new silica gel-based chelating sorbent, with thiourea as a functional group, was used for the FI online preconcentration and separation of trace levels of silver, gold, and palladium. The selected metal ions were adsorbed onto a column packed with thiourea-modified silica gel (TuSG). The sorbent exhibited excellent stability and the sorption properties of TuSG did not change after 1000 cycles of use. The selected metals in a secondary nickel alloy, an anode slim, an electrolytic solution, and three national certified ore samples were determined satisfactorily using the proposed method.[52]

A FI online sorbent extraction system was studied in conjunction with FAAS to determine cadmium, copper, and lead in a digest solution of solid environmental sample using octadecyl functional groups (C_{18})-bonded silica gel as sorbent with diethyl

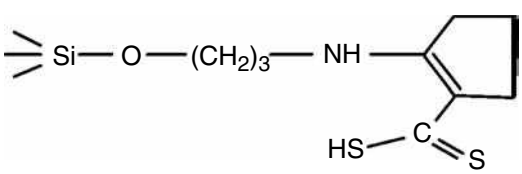

Scheme 18

ammonium-*N*,*N*,diethyldithiocarbamate or ammonium diethyldithiophosphate as complexing agent and methanol as eluent. The results of the analysis of five environmental standard reference materials were in good agreement with the certified values, with the exception of cadmium. The detection limits were 0.8, 1.4, and 10.0 μg/L, respectively for cadmium, copper, and lead.[53]

Silica Gel Phases with Nitrogen, Oxygen, and Sulfur Donor Atoms

Para-substituted, X = H, CH_3, OCH_3, Cl, and NO_2, dithioacetal derivatives were synthesized and chemically immobilized onto the surface of silica gel for the formation of five newly modified silica gel phases. The metal sorption properties of these silica gel phases were studied and the results revealed a general rule of excellent affinity for the selective extraction of Hg(II) in the presence of other interfering metal ions, giving rise to a range of 94–100% extraction of the spiked Hg(II) in the metal ion mixture. The potential applications of these modified silica gel phases for selective extraction of Hg(II) from two different natural water samples by a column technique, followed by cold vapor atomic absorption analysis, were also studied. The substituent effect on the process of selective extraction of Hg(II) by the modified silica gel phases was also presented.[5] The structures of silica gel-immobilized-dithioacetals are given in Scheme 19.

Silica gel-chemically immobilized-Eriochrome black T was synthesized and the surface coverage was found to be 0.38 mmol/g. The stability toward hydrolysis of this silica gel phase in various buffer solutions (pH 1.0–10.0) was studied and evaluated. The applicability of silica gel phase-immobilized-Eriochrome black T as a solid-phase extractor for Zn(II), Mg(II), and Ca(II) was performed by the batch equilibrium technique and was found to show an order similar to the formation constant values of the three metal ions with the indicator. The separation and selectivity of this modified silica gel for these metal ions, based on a column technique, were found to afford a reasonable performance of the three studied metal ions.[54] The structure of silica gel-chemically immobilized-Eriochrome black T is given in Scheme 20.

Azo dyes supported on silica gel were prepared and their adsorption behavior toward metal ions were investigated. The 1-(2-pyridylazo-2-naphthol)-immobilized silica gel and 2-(2-thiazolylazo)-*p*-cresol-immobilized silica gel showed greater affinity for UO(III) compared with Cu, Cd, Fe, and alkaline earths. Trace uranyl was quantitatively retained on the column at neutral pH. Matrix components in seawater did not interfere and the spiked recovery of uranyl in artificial seawater was found to average 98.6% with a relative standard deviation of 1.08%.[55]

Preconcentration and separation of trace Hg(II) with aminopropylbenzoylazo-2-mercaptobenzothiazole-bonded

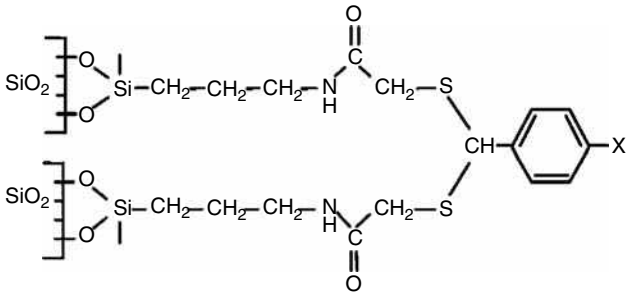

X = H, CH_3,OCH_3,Cl,NO_2

Scheme 19

to silica gel (ABMBT-SG) was reported. This phase was found to show an exchange capacity of 41.4 μmol/g. Determination of trace Hg(II) in environmental samples was accomplished by UV–Vis spectrophotometry. The described method is simple and efficient and can be applied for polluted soil (2 μg/L), incinerated biological material (18 ng/L), and spiked natural water (5 μg/L).[56] The structure of ABMBT-SG is given in Scheme 21.

5-Methylene-2-(2′-thiazolylazo)-anisole was immobilized on silica gel via an Si–O–Si–C moiety. The capacity for palladium is about 0.070 mmol/g; this chelating silica was used to preconcentrate and separate palladium from a synthetic solution containing traces of palladium and large amounts of copper. Distribution coefficient studies of platinum metals, gold, and base metals showed that the chelating silica gel was found to be selective for Pd(II).[57] The structure of the modified silica gel phase is shown in Scheme 22 4-Amino-3-hydroxy-2-(chlorobenzene)-azo-1-naphthalene sulfonic acid was used as a chelating compound to improve the reactivity of silica gel surface toward selective extraction and binding with heavy metal ions. The modified silica gel phases showed high affinity and selectivity characteristics for binding with heavy metal ions, compared to alkali and alkaline earth metals.[58]

Silica Gel Phases with Oxygen and Sulfur Donor Atoms

Octadecyl-bonded-silica membrane disks modified with hexathia-18-crown-6-tetraone (Scheme 23) was synthesized

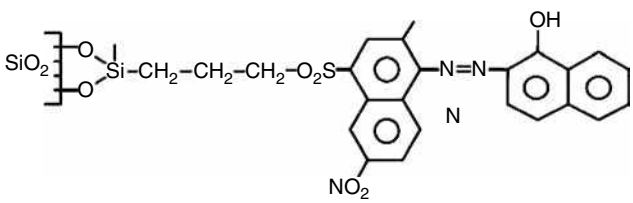

Scheme 20

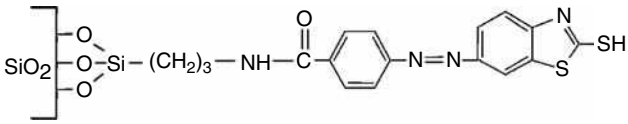

Scheme 21

and applied as a rapid extraction and determination method of ultratrace amounts of Hg(II) ion by CVAAS. This method was used for the recovery of Hg(II) ions from synthetic samples and four different water samples.[59]

The macrocycles, 1,5-dithia-19-crown-6 ($T_2$19C6) and 1,4,7,10-tetrathia-18-crown-6 ($T_4$18C6), were chemically bonded to silica gel. The interaction of Pd(II), Au(III), Ag(I), and Hg(II) with the immobilized macrocycles was evaluated on the basis of determination of the binding constants (*K*). Other binding constants for Cu(II), Fe(III), and other base metals were at least 10 orders of magnitude less than constants for Pd(II), Au(III), Ag(I), and Hg(II). Values of *K* were higher for $T_4$18C6 than for $T_2$19C6. Immobilized thiamacrocycles effectively removed Au(III) and Pd(II) from 1L of 1*M*-HCl and 1*M*-$FeCl_3$. Palladium was also removed from an industrial silver electrolyte solution with 99.9% purity, in one pass through the column.[60] Structures of ($T_2$19C6) and ($T_4$18C6) are shown in Scheme 24.

Poly (crown ether) as well as the corresponding monocyclic crown ethers was immobilized on silica surface by covalent bonding. The chromatographic behavior of the modified silica gel phases for alkali metal salts was demonstrated. Poly (crown ether)-modified silica provided better separation of the metal salts compared to the corresponding monocyclic crown ether-modified one.[61] Other examples of modified silica and their applications (Table 1).

CONCLUSIONS

Silica gel is characterized by the presence of certain functionalities resulting from the presence of groups such as siloxane, ≡Si–O–Si≡, with the oxygen located on the surface, as well as silanol groups, ≡Si–OH. Surface silanol groups are the major contributing factors that are responsible for binding, adsorption, and extraction processes with the target analytes of interest such as metal ions or their more complex species. Improvements of the adsorption efficiency and extraction power of the sorbent are accomplished by surface modification with certain functional groups. The types of compounds that can be loaded onto the surfaces of solid phases are unlimited; these include long chain and short chain hydrocarbons, polar and non-polar organic compounds, inorganic and organometallic compounds, simple and macromolecular compounds, and chelating agents.

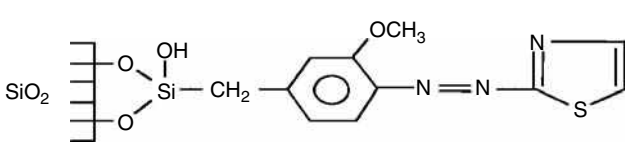

Scheme 22

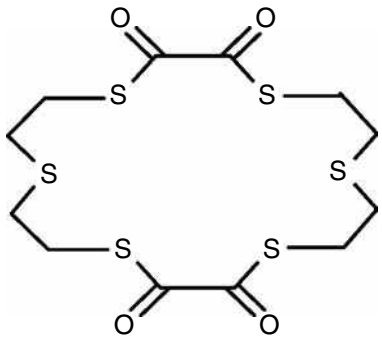

Scheme 23

REFERENCES

1. Unger, K. *Porous Silica, Its Properties and Use as a Support in Column Liquid Chromatography*; Elsevier: Amsterdam, 1979.
2. Ong, S.W.; Zhao, X.L.; Eisenthal, K.B. Polarization of water molecules at a charged interface: second harmonic studies of the silica/water interface. Chem. Phys. Lett. **1992**, *191* (3–4), 327.
3. Jal, P.K.; Patel, S.; Mishra, B.K. Chemical modification of silica surface by immobilization of functional groups for extractive concentration of metal ions. Talanta **2004**, *62* (5), 1005–1028.
4. Filho, N.L.D.; Gushikem, Y. 2-Mercaptoimidazole covalently bonded to a silica gel surface for the selective separation of mercury(II) from an aqueous solution. Sepn. Sci. Technol. **1997**, *32* (15), 2535–2545.

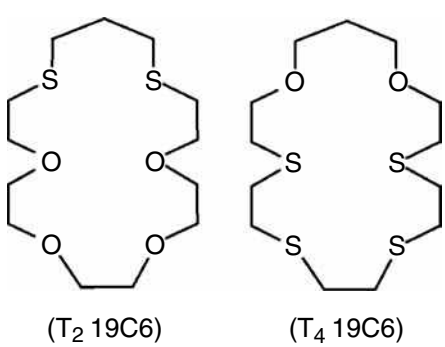

Scheme 24

Table 1 Examples of modified silica and their applications.

Modified silica gel	Possible applications	Refs.
Silica gel chemically modified with Zr(IV) phosphate	Preconcentration of lead and copper and their sequential determination by FAAS	[62]
Silica gel modified with 3-mercaptopropyltrimethoxy silane	Selective separation and preconcentration of selenite [Se(IV)] from aqueous solutions containing Se(IV) and Se(VI)	[63]
Octadecyl silica membrane disks modified by pentathia-15-crown-5	Selective concentration and determination of μg/L levels of Au(III) ions in aqueous solution by FAAS	[64]
Silica gel-modified-thioglycolic acid	Determination of copper ions in aqueous/ ethanolic solutions	[65]
Silica gel functionalized with methylthiosalicylate (TS-gel)	Online preconcentration of lead by flow injection system	[66]
Octadecyl silica membrane-modified-*bis* (2-hydroxyl phenyl amino) glyoxime	Selective adsorption and quantitative determination of the Cu^{2+} ions	[67]
Palladium-dimethylglyoxime complex on silica gel	Determination of palladium at trace levels by atomic absorption spectrometry	[68]
Reverse-phase C18 column	Determination of arsenite [As(III)], dimethyl arsenic acid, monomethyl arsenic and arsenate [As(V)] in Chinese brake fern by ion-pair reverse-phase HPLC–inductively coupled plasma (ICP) MS	[69]
Silica-immobilized brown alga *Pilayella littoralis*	Online metal preconcentration procedure in a flow-injection system for determination of Al, Co, Cu, and Fe in lake water samples by (ICP-OES)	[70]
Bis-naphthaldehyde and salicylaldehyde Schiff's base ligands immobilized on silica	Metal ions determination and preconcentration by atomic absorption analysis	[21]
Octadecyl (C_{18})-bonded silica gel	Separation and preconcentration of platinum group metals (Ru, Rh, Pd, Os, Ir, and Pt) as ion associates of their chlorocomplexes	[71]
C_{18}-bonded silica membrane disk modified with hexathia-18-crown-6	Selective separation and concentration of trace amounts of silver ion from aqueous samples for the subsequent measurement by atomic absorption spectrometry	[72]
Octadecyl-bonded silica membrane disks modified with pentathia-15-crown-5	Solid-phase extraction of gold	[64]
Octadecyl silica membrane disks with Schiff base ligand, thiophene-2-carbaldehyde (ethanamine 2,2′-[1,2-ethylene *bis*(oxy)]*N*,*N*′-*bis*(2-thienylmethylene))	Separation and preconcentration of trace amount of Pb^{2+} from aqueous solution and selective extraction and determination of ultra trace amounts of mercury	[73]
Octadecyl-bonded silica membrane disks modified with piroxicam	Extraction of uranium from aqueous solution using	[74]
2-Mercaptobenzothiazole impregnated on silica	Preconcentration of inorganic and organic mercury compounds from seawater and other metal ions from aqueous solution	[75]
Silica gel impregnated with 2-mercapto-*N*-2-naphthylacetamide	Extraction of Pd(II) from dilute solution	[76]
A chelating sorbent prepared by adsorption of 3,3′,4′,5, 7-pentahydroxyflavone on to a silica surface	Preconcentration and sorption-spectroscopic determination of Sn(IV) from aqueous solution at pH 1.8–2.2	[77]
Silica-based strongly basic anion exchanger with octadecyl silica Separon SGX C18 and Separon SGX RPS	Molybdenum was separated and preconcentrated as molybdate on microcolumns	[78]
Silica gel modified with 2-hydroxy-1-naphthaldehyde	Metal sorption and solid-phase extraction and their preconcentration properties	[79]
Physically immobilized-2-thiouracil	Selective extraction and pre concentration of heavy metals from seawater	[80]
Poly(benzo-15-crown-5) and *bis*(benzo-15-crown-5) modified silica gel	Extraction and chromatographic separation of alkali and alkaline earth metal ions	[81]
2-[(2-(Triethoxysilyl) ethyl) thio] aniline immobilized silica	Separation and preconcentration of Pd(II) from a matrix rich in Rh(III) and Ir(III)	[82]
Covalent grafting of 3-(2-aminoethyl-amino) propyl trimethoxysilane onto mesoporous sol–gel silica	Extraction of Cu(II) ions from aqueous solutions.	[83]
Silica gel phases-chemically immobilized-4-amino antipyrene	Selective extraction of heavy metal ions from natural waters	[84]
Silica gel-immobilized aliphatic amines 2-thiophenecarboxaldehyde Schiff's bases	Selective solid-phase extraction of Hg(II) from aqueous solutions at low pH values	[85]

5. Mahmoud, M.E.; Gohar, G.A. Silica gel-immobilized derivatives as potential solid phase extractors for mercury(II). Talanta **2000**, *51* (1), 77–87.
6. Mahmoud, M.E.; Osman, M.M.; Amer, M.E. Selective preconcentration and solid phase extraction of mercury(II) from natural water by silica gel-loaded dithizone phases. Anal. Chim. Acta **2000**, *415*, 33.
7. Tong, A.; Akama, Y.; Tanaka, S. Selective preconcentration of Au(III), Pt(IV) and PD(II) on silica get modified with γ-aminopropyltriethoxysilane. Anal. Chim. Acta **1990**, *230*, 179.
8. Mahmoud, M.E.; El-Essawi, M.M.; Kholeif, S.A.; Fathallah, E.I. Aspects of surface modiciation, structure characterization, thermal stability and metal selectivity properties of silica gel phases-immobilized-amine derivatives. Anal. Chim. Acta **2004**, *525*, 123.
9. Moriera, J.C.; Gushikem, Y. Preconcentration of metal ions on silica gel modified with 3(1-imidazolyl)propyl groups. Anal. Chim. Acta **1985**, *176*, 263.
10. Tikhomirova, T.I.; Fadeeva, V.I.; Kurdyavtsev, G.V.; Nesterenko, P.N.; Ivanov, V.M.; Savitchev, A.T.; Smirrova, N.S. Sorption of noble-metal ions on silica with chemically bonded nitrogen-containing ligands. Talanta **1991**, *38* (3), 267–274.
11. Imamoto, M.S.; Gushikem, Y. Adsorption and preconcentration of some metal ions from ethanol on silica gel modified with pyridinium ion. Analyst **1989**, *114* (8), 983.
12. Watanesk, S.; Schilt, A.A. Separation of some transition-metal ion on silica-immobilized 2-pyridinecarboxaldehyde phenylhydrazone. Talanta **1986**, *33* (11), 895–899.
13. Hsu, J.C.; Chang, C.H.; Liu, C.Y. Preparation and evaluation of a functionalized polymer-coated silica based sorbent for metal ion separation. Fresenius J. Anal. Chem. **1998**, *362* (6), 514–521.
14. Koklu, U.; Akman, S.; Gocer, O.; Doner, G. Separation and preconcentration of cobalt and nickel with 3-(trimethoxysilyl)-1-propanethiol loaded on silica gel. Anal. Lett. **1995**, *28*, 357.
15. Hankins, M.G.; Hayashita, T.; Kasprzyk, S.P.; Bartsch, R.A. Immobilization of crown ether carboxylic acids on silica gel and their use in column concentration of alkali metal cations from dilute aqueous solutions. Anal. Chem. **1996**, *68* (17), 2811–2817.
16. Izatt, R.M.; Bruening, R.L.; Breuning, M.L.; Tarbet, B.J.; Krakowiak, K.E.; Bradshaw, J.S.; Christensen, J.J. Removal and separation of metal ions from aqueous solutions using a silica-gel-bonded macrocycle system. Anal. Chem. **1988**, *60* (17), 1825–1826.
17. Goswami, A.; Singh, A.K. 1,8-Dyhydroxyanthraquinone anchored on silica gel: synthesis and application as solid phase extractant for lead(II), zinc(II) and cadmium(II) prior to their determination by flame atomic absorption spectrometry. Talanta **2002**, *58* (4), 669–678.
18. Mahmoud, M.E.; Al Saadi, M.S.M. Selective solid phase extraction and preconcentration of iron(III) based on silica gel-chemically immobilized purpurogallin. Anal. Chim. Acta **2001**, *450*, 229.
19. Howard, A.G.; Volkan, M.; Ataman, D.Y. Selective preconcentration of arsenite on mercapto-modified silica gel. Analyst **1987**, *112* (2), 159.
20. Volkan, M.; Ataman, O.Y.; Howard, A.G. Pre-concentration of some trace metals from sea water on a mercapto-modified silica gel. Analyst **1987**, *112* (10), 1409.
21. Soliman, E.M.; Mahmoud, M.E.; Ahmed, S.A. Synthesis, characterization and structure effects on selectivity properties of silica gel covalently bonded diethylenetriamine mono- and bis-salicyaldehyde and naphthaldehyde Schiff's bases towards some heavy metal ions. Talanta **2001**, *54* (2), 243–253.
22. Shamsipur, M.; Ghiasvand, A.R.; Sharghi, H.; Naeimi, N. Solid phase extraction of ultra trace copper(II) using octadecyl silica membrane disks modified by a naphthol-derivative Schiff's base. Anal. Chim. Acta **2000**, *408*, 271.
23. Kocjan, R.; Przeszlakowski, S. Calcon-modified silica gel sorbent. Application to preconcentration or elimination of trace metals. Talanta **1992**, *39* (1), 63–68.
24. Kocjan, R. Silica gel modified with Titan Yellow as a sorbent for separation and preconcentration of trace amounts of heavy metals from alkaline earth or alkali metal salts. Analyst **1992**, *117* (4), 741.
25. Mahmoud, M.E.; Soliman, E.M. Silica-immobilized formyl-salicylic acid as a selective phase for the extraction of iron(III). Talanta **1997**, *44* (1), 15–22.
26. Mahmoud, M.E.; Soliman, E.M. Study of the selective extraction of iron(III) by silica-immobilized 5-Formyl-3-Arylazo-salicylic acid derivatives. Talanta **1997**, *44* (6), 1063–1071.
27. Soliman, E.M.; Mahmoud, M.E. Metal uptake properties of silica gel-immobilized aminophenol and aminobenzoic acid and their application for heavy metal removal from sugar cane molasses. Analusis **1997**, *25* (5), 148.
28. Soliman, E.M. Synthesis, characterization and metal sorption studies of isatin and ninhydrin reagents immobilized on silica gel amine surface. Anal. Lett. **1998**, *31*, 299.
29. Mahmoud, M.E. Comparison of metal sorption properties of three silica gel phases—physically adsorbed and chemically immobilized-1-aminoanthraquinone. Anal. Lett. **2002**, *35*, 1251.
30. Kubota, L.T.; Morira, J.C.; Gushikem, Y. Adsorption of metal ions from ethanol on an iminosalicyl-modified silica gel. Analyst **1989**, *114* (11), 1385.
31. Seshadri, T.; Dietz, H.-J.; Haupt, G. Synthesis of silica-bound complexing agents containing 2,3-dihydroxybenzoyl and 3,4,5-trihydroxybenzoylamide functional groups and analytical studies of metal uptake. Fresenius Z. Anal. Chem. **1984**, *319* (4), 403–409.
32. Mizuguchi, H.; Kaneko, E.; Yosuyanagi, T. Visual fluorimetry of trace aluminium by specific immobilization with o,o-dihydroxyazobenzene on an octadecylsilanized silica thin layer. Analyst **2000**, *125* (9), 1667.
33. Groschner, M.; Appriou, P. Three-column system for preconcentration and speciation determination of trace metals in natural waters. Anal. Chim. Acta **1994**, *297*, 369.
34. Zaporozhets, O.A.; Tsyukato, Y. Xylenol orange adsorbed on silica surface as a solid phase reagent for lead determination using diffue reflectance spectroscopy. Talanta **2002**, *58* (5), 861–868.
35. Izatt, R.M.; Clark, G.A.; Bradshaw, J.S.; Lamb, J.D.; Christensen, J.J. Macrocycle-facilitated transport of ions in liquid membrane systems. Sepn. Purif. Meth. **1986**, *15* (1), 21–72.

36. Bartsch, R.A.; Czech, B.F.; Kang, S.I.; Stewart, L.E.; Walkwiak, W.; Charewicz, W.A.; Heo, G.S.; Son, B. High lithium selectivity in competitive alkali metal solvent extraction by lipophilic crown carboxylic acids. J. Am. Chem. Soc. **1985**, *107* (17), 4997–4998.
37. Dudler, V.; Lindoy, L.F.; Sallin, D.; Sclaaepfer, C.W. An oxygen-nitrogen donor macrocycle immobilized on silica gel. A reagent showing high selectivity for copper(II) in the presence of cobalt(II), nickel(II), zinc(II) or cadmium(II). Aust. J. Chem. **1987**, *40* (9), 1557.
38. Luhrmann, M.; Shelter, N.; Kettrup, A. Synthesis and properties of metal collecting phases with silica immobilized 8-Hydroxyquinoline. Fresenius Z. Anal. Chem. **1985**, *322* (1), 47.
39. Honjo, T.; Kitayama, H.; Terada, K.; Kiba, T. Fresenius J. Anal. Chem. **1988**, *330*, 159.
40. Daih, B.J.; Huang, H.J. Determination of trace elements in sea water by flow-injection anodic stripping voltammetry preceded by immobilized quinolin-8-ol silica gel preconcentration. Anal. Chim. Acta **1992**, *258*, 245.
41. Nakashima, S.; Sturgeon, R.E.; Willie, S.N.; Berman, S.S. Determination of trace metals in seawater by graphite furnace atomic absorption spectrometry with preconcentration on silica-immobilized 8-hydroxyquinoline in a flow-system. Fresenius Z. Anal. Chem. **1988**, *330* (7), 592.
42. Risner, C.H.; Jezorek, J.R. The chromatographic interaction and separation of metal ions with 8-Quinolinol stationary phases in several aqueous eluents. Anal. Chim. Acta **1986**, *186*, 233.
43. Pyell, U.; Stork, G. High-performance ligand-exchange liquid-chromatography (hplec) of aromatic-amines with copper(ii), nickel(ii) and zinc(ii) loaded chelating silica-gel columns. Fresenius J. Anal. Chem. **1992**, *343* (7), 576–581.
44. Mahmoud, M.E. Selective solid phase extraction of mercury(II) by silica gel-immobilized-dithiocarbamate derivatives. Anal. Chim. Acta **1999**, *398*, 297.
45. Pu, Q.; Sun, Q.; Hu, Z.; Su, Z. Application of 2-mercaptobenzothiazole-modified silica gel to on-line preconcentration and separation of silver for its atomic absorption spectrometric determination. Analyst **1998**, *123* (2), 239.
46. Soliman, E.M.; Mahmoud, M.E.; Ahmed, S.A. Reactivity of thioglycolic acid physically and chemically bound to silica gel as new selective solid phase extractors for removal of heavy metal ions from natural water samples. Int. J. Environ. Anal. Chem. **2002**, *82*, 403.
47. Garcia, M.F.; Garcia, R.P.; Garcia, N.B.; Medel, A.S. On-line preconcentration of inorganic mercury and methylmercury in sea-water by sorbent-extraction and total mercury determination by cold vapour atomic absorption spectrometry. Talanta **1994**, *42* (11), 1833–1839.
48. Seshadri, T.; Kettrup, A. Synthesis and characterization of silica gel ion-exchanger bearing 2-amino-1-cyclopentene-1-dithio-carboxylic acid (ACDA) as chelating compound. Fresenius Z. Anal. Chem. **1982**, *311* (1–2), *18*, 1.
49. Seshadri, T.; Haupt, H.-J. Silica immobilized 2-[(2-(triethoxysily)ethyl)thio]aniline as a selective sorbent for the separation and preconcentration of palladium. Anal. Chem. **1988**, *60* (1), 47–52.
50. Mahmoud, M.E.; El-Essawi, M.M.; Fathallah, E.I. J. Liq. Chromatogr. Rel. Technol. **2004**, *27*, 1.
51. Liu, P.; Pu, Q.; Hu, Z.; Su, Z. On-line preconcentration and separation of platinum using thiourea modified silica gel with microwave assisted desorption for FAAS determination. Analyst **2000**, *125* (6), 1205.
52. Liu, P.; Pu, Q.; Su, Z. Synthesis of silica gel immobilized thiourea and its application to the on-line preconcentration and separation of silver, gold and palladium. Analyst **2000**, *125* (1), 147.
53. Ma, R.; Mol, W.V.; Adams, F. Determination of cadmium, copper, and lead in environmental samples. An evaluation of flow injection on-line sorbent extraction for flame atomic absorption spectrometry. Anal. Chim. Acta **1994**, *285*, 33.
54. Mahmoud, M.E. Silica gel-immobilized Eriochrome black-T as a potential solid phase extractor for zinc(II) and magnesium(II) from calcium(II). Talanta **1997**, *45* (2), 309–315.
55. Ueda, K.; Koshino, Y.; Yamamoto, Y. Preconcentration of uranium in seawater with heterocyclic azo dyes supported on silica gel. Anal. Lett. **1985**, *18*, 2345.
56. Ma, W.X.; Liu, F.; Li, K.A.; Chen, W.; Tang, S.Y. Preconcentration, separation and determination of trace Hg(II) in environmental samples with aminopropybenzoy-lazo-2-mercaptobenzothiazole bonded to cilica gel. Anal. Chim. Acta **2000**, *416*, 191.
57. Sutthivaiyakit, P.; Kettrup, A. Immobilization of 5-methylene-2-(2'-thiazolylazo)-anisole on silica and its application in preconcentration of palladium. Anal. Chim. Acta **1985**, *169*, 331.
58. Mahmoud, M.E.; Soayed, A.A.; Hafez, O.F. Selective solid phase extraction and pre-concentration of heavy metals from seawater by physically and chemically immobilized 4-amino-3-hydroxy-2-(2-chlorobenzene)-azo-1-naphthalene sulfonic acid silica gel. Microchim. Acta **2003**, *143* (1), 165.
59. Yamini, Y.; Alizadeh, N.; Shamsipur, M. Solid phase extraction and determination of ultra trace amounts of mercury(II) using octadecyl silica membrane disks modified by hexathia-18-crown-6-tetraone and cold vapour atomic adsorption. Anal. Chim. Acta **1997**, *335*, 69.
60. Bruening, R.L.; Tarbet, B.J.; Krakowiak, K.E.; Bruening, M.L.; Izatt, R.M.; Bradshaw, J.S. Quantitation of cation binding by silica gel bound thiamocrocycles and the design of highly selective concentration and purification columns for palladium(II), gold(III), silver(I), and mercury(II). Anal. Chem. **1991**, *63* (10), 1014–1017.
61. Kimura, K.; Nakajima, M.; Shono, T. Poly(crown ether)-modified silica for stationary phase of liquid chromatography. Anal. Lett. **1980**, *13*, 741.
62. Matoso, E.; Kubota, L.T.; Cadore, S. Use of silica gel chemically modified with zirconium phosphate for preconcentration and determination of lead and copper by flame atomic absorption spectrometry. Talanta **2003**, *60* (6), 1105.
63. Sahin, F.; Volkan, M.; Howard, A.G.; Ataman, OY. Selective pre-concentration of selenite from aqueous samples using mercapto-silica. Talanta **2003**, *60* (5), 1003.
64. Bagheri, M.; Mashhadizadeh, M.H.; Razee, S. Solid phase extraction of gold by sorption on octadecyl silica membrane disks modified with pentathia-15-crown-5 and determination by AAS. Talanta **2003**, *60* (4), 839.
65. El-Kemary, M.A.; El-Mehasseb, I.M. Global and distribution analysis of fluorescence decays and spectrofluorimetric determination of stoichiometry and association constant of

the inclusion complex of 2-amino-5,6-dimethyl-benzimidazole with β-cyclodextrin. Talanta **2004**, *62* (2), 317.
66. Zougagh, M.; García de Torres, A.; Vereda Alonso, E.; Cano Pavón, J.M. Automatic on line preconcentration and determination of lead in water by ICP-AES using a TS-microcolumn. Talanta **2004**, *62* (3), 503.
67. Ghiasvand, A.R.; Ghaderi, R.; Kakanejadifard, A. Selective preconcentration of ultra trace copper(II) using octadecyl silica membrane disks modified by a recently synthesized glyoxime derivative. Talanta **2004**, *62* (2), 287.
68. Tokalloglu, S.; Oymak, T.; Kartal, S. Determination of palladium in various samples by atomic absorption spectrometry after preconcentration with dimethylglyoxime on silica gel. Anal. Chim. Acta **2004**, *511* (2), 255.
69. Pizarro, I.; Gómez, M.; Cámara, C.; Palacios, M.A. Arsenic speciation in environmental and biological samples: Extraction and stability studies. Anal. Chim. Acta **2003**, *495*(1), 85.
70. Carrilho, E.N.; Nóbrega, J.A.; Gilbert, T.R. The use of silica-immobilized brown alga (Pilayella littoralis) for metal preconcentration and determination by inductively coupled plasma optical emission spectrometry. Talanta 2003, *60* (6), 1131.
71. Vlaánkova, R.; Otruba, V.; Bendl, J.; Fiera, M.; Kanický, V. Preconcentration of platinum group metals on modified silicagel and their determination by inductively coupled plasma atomic emission spectrometry and inductively coupled plasma mass spectrometry in airborne particulates. 1999, *48* (4), 839.
72. Wittstock, Tim Asmus and Thomas Wilhelm. Investigation of ion-bombarded conducting polymer films by scanning electrochemical microscopy (SECM). Fresenius J. Anal. Chem. **2000**, *367* (4), 246.
73. Hashemi, O.R.; Raoufi, F.; Ganjali, M.R.; Moghimi, A.; Kargar-Razi, M.; Aghabozorg, H.; Shamsipur, M. Separation and preconcentration of trace amounts of lead on octadecyl silica membrane disks modified with a new *O*, *S*-containing schiff's base and its determination by flame atomic absorption spectrometry. Anal. Sci. **2000**, *16* (11), 1221.
74. Sadeghi, S.; Mohammadzadeh, D.; Yamini, Y. Solid-phase extraction-spectrophotometric determination of uranium(VI) in natural waters. Anal. Bioanal. Chem. **2003**, *375* (5), 698.
75. Terada, K.; Morimoto, V.; Kiba, T. The chromatographic concentration of mercury in sea water with 2-mercaptobenzothiazole supported on silica gel. Bull. Chem. Soc. Jpn. **1980**, *53* (6), 1605.
76. Terada, K.; Matsumoto, K.; Taniguchi, Y. Preconcentration of palladium(II) from water with thionalide loaded on silica gel. Anal. Chim. Acta **1983**, *147*, 411.
77. Zaporozhets, O.A.; Ivanko, L.S.; Marchenko, I.V.; Orlichenko, E.V.; Sukhan, V.V. Quercetin immobilized on silica gel as a solid phase reagent for tin(IV) determination by using the sorption-spectroscopic method. Talanta **2001**, *55* (2), 313.
78. Martynková, K.; Komendová, R.; Fišera, M.; Sommer, L. Solid phase extraction of molybdenum on modified octadecyl silica sorbents in the presence of cationic surfactants and on silica-based anionic exchanger and its determination by inductively coupled plasma emission spectrometry. Microchimica Acta **2004**, *147* (1–2), 65.
79. Osman, M.M.; Kholeif, S.A.; Abou Al-Maaty, N.A.; Mahmoud, M.E. Metal sorption, solid phase extraction and preconcentration properties of two silica gel phases chemically modified with 2-hydroxy-1-naphthaldehyde. Microchimica Acta **2003**, *143* (1), 25.
80. Almendral, M.J.; Alonso, A.; Porras, M.J.; García, M.A.; Curto, Y. Determination of iron in tap and waste water using liquid-liquid extraction in a flow-injection system. Microchimica Acta **2004**, *147*, 117.
81. Moberg, C.; Muhammed, M.; Svensson, G.; Weber, M. Novel quinaldic acids for selective chelation of cadmium(II). X-Ray crystal structure of $[Cd(C18H12NO_4)2](Me_2SO).2H_2O$. J. Chem. Soc. Chem. Commun. **1988**, *12*, 810.
82. Seshadri, T.; Haupt, H.J. Silica-immobilized 2-[(2 (triethoxysily)ethyl)thio]aniline as a selective sorbent for the separation and preconcentration of palladium. Anal. Chem. 1988, *60* (1), 47.
83. Lee, H.; Yi, J. Removal of copper ions using functionalized mesoporous silica in aqueous solution. Sep. Sci. Technol. 2001, *36* (11), 2433.
84. Osman, M.M.; Kholeif, S.A.; Abou-Almaaty, N.A.; Mahmoud, M.E. Synthesis, characterization of silica gel phases-chemically immobilized-4 aminoantipyrene and applications in the solid phase extraction, preconcentration and potentiometric studies. Anal. Sci. **2004**, *20* (5), 847.
85. Soliman, E.M.; Saleh, M.B.; Ahmed, S.A. New solid phase extractors for selective separation and preconcentration of mercury (II) based on silica gel immobilized aliphatic amines 2-thiophenecarboxaldehyde Schiff's bases. Anal. Chim. Acta **2004**, *523* (1), 133.

BIBLIOGRAPHY

1. Barby, D.; Parfitt, G.D.; Sing, G.S.W. *Silicas in Characterization of Powder Surfaces*; Academic Press: London, 1976.
2. Brinker, C.J.; Scherer, G.W. *Sol–Gel Science*; Academic Press: New York, 1989.
3. Iler, R.K. *The Chemistry of Silica Solubility, Polymerization, Colloid and Surface Properties and Biochemistry*; Wiley: New York, 1979.
4. Leyden, D.E.; Collins, W.T. *Chemically Modified Surfaces in Science and Industry*; Gordon and Breach: London, 1988.
5. Leyden, D.E.; Collins, W. *Silylated Surfaces*; Gordon and Breach: New York, 1980.
6. Mottola, H.A.; Steimetz, J.R. *Chemically Modified Surfaces*; Elsevier: New York, 1992.
7. Scott, R.P.W. *Silica Gel and Bonded Phases, Their Production Properties and Uses in LC*; Wiley: Chichester, 1993.
8. Unger, K. *Packing and Stationary Phases in Chromatographic Techniques*; Marcel Dekker: New York, 1990.

Metal–Ion Enrichment by CCC

Eiichi Kitazume
Faculty of Humanities and Social Sciences, Iwate University, Iwate, Japan

INTRODUCTION

Countercurrent chromatography (CCC) is a useful method for separating metal ions as well as organic compounds. In addition, highly efficient chromatographic separation has been achieved using a multilayer coil system and strong force field by applying over several hundred revolutions per minute. However, there have been no applications to the enrichment of inorganic elements until quite recently.

The latest study has revealed that CCC has great potential in the ultratrace determination of metals, because it can concentrate minute amounts of metal prior to instrumental multielement analysis, such as by atomic absorption spectrometry (AAS), inductively coupled plasma–atomic emission spectrometry (ICP–AES), and inductively coupled plasma–mass spectrometry (ICP–MS).[2,6,9]

Enrichment of the desired trace elements would not only allow highly sensitive determination of trace elements but also alleviate various problems, including interference, high risk of exposure to toxic chemicals and radiation from radioactive samples, and so forth.

EXTRACTION OF METAL IONS IN THE STATIONARY PHASE

The existence of an extracting reagent in the stationary phase is one of the essential factors in the enrichment of inorganic elements as well as in their separation. However, the values of the distribution ratios, determined by batch extraction measurements in a two-phase system, are sometimes considerably different from those of the dynamic distribution ratios calculated from elution curves. Further theoretical and basic investigations are necessarily concerned with extraction kinetics, as well as the hydrodynamic behavior of two phases in the high-speed CCC (HSCCC) column.[1]

Organophosphorus extractants such as di(2-ethylhexyl)-phosphoric acid (DEHPA), 2-ethylhexylphosphonic acid mono-2-ethylhexyl ester (EHPA), *N*-benzoyl-*N*-phenylhydroxylamine (BPHA), and tetraoctylethylenediamine (TOEDA) are often used due to their solubility properties in the stationary organic phase.[1–3]

ENRICHMENT IN THE EFFLUENT BY CONVENTIONAL ELUTION

After metal ions are enriched in the organic stationary phase, including the extracting reagent in the CCC column, they can be eluted simultaneously or chromatographically into the eluent stream by conventional elution mode.

It has been demonstrated that systems with DEHPA can extract and preconcentrate Zr(IV), Hf(IV), and Nb(V) into the organic stationary phase and can separate them from the majority of other elements.[1] The preconcentration of Zr(IV) and Hf(IV) and subsequent back-extraction, as well as the selective extraction of Zr(IV), Hf(IV), Nb(V), and Ta(V) into a 4 ml volume of the organic phase, can be performed with a mixture of DEHPA and BPHA.

A method has been developed for the separation of the entire group of rare-earth elements from high-purity calcium chloride by CCC, and subsequent determination of the elements by ICP–MS.[2] A solution of diphenyl [dibutylcarbamoylmethyl]phosphine oxide in chloroform (0.5 mol/L) was chosen as reagent for the extraction and preconcentration of trace rare-earth elements from aqueous 5% $CaCl_2$ solution, 3 mol/L in HNO_3, and 0.1 mol/L in $HClO_4$. The analytes are back-extracted into a small volume of water and the aqueous eluent is analyzed by ICP–MS. The performance characteristics of the procedure developed were checked by use of the standard addition technique and a real $CaCl_2$ sample was analyzed. The results obtained demonstrate the applicability of CCC to the determination of ultra trace elements.

The capability of HSCCC was also studied for enrichment and determination of metal ions at trace levels. Separation of selected divalent metal ions was performed using a small coiled column.[3] A hexane solution of EHPA was employed as the stationary phase. Loaded divalent metal ions such as Ni, Co, Cu, and Zn were chromatographically eluted in the order of increasing extractability by passing a mobile phase buffered at a desired pH. Each metal ion showed good linearity between concentrations and chromatographic peak areas of absorbance, as detected by postcolumn reaction with 4-(2-pyridylazo)resorcinol (PAR). Metal ions enriched in the stationary phase from a sample solution were separated into individual metal ions. A trace quantity of Zn in natural mineral water was determined by enrichment separation through an HSCCC column.

A 1000 ml sample solution containing 5×10^{-7} *M* of each rare-earth element was effectively enriched onto the CCC column head using carboxylic acid–toluene including EHPA system.[4] Then, each concentrated element on the column head was eluted chromatographically by the mobile phase with stepwise pH gradient.

Separation of selected lanthanoid elements was performed by HSCCC equipped with a small coiled column of 10 ml capacity.[5] A hexane solution of DEHPA was retained in the tubing column as the stationary phase. The stationary phase retention increased with increasing rotational speed and with decreasing flow rate of the aqueous mobile phase. Mixtures of lanthanoids (Gd, Tb, and Dy) were eluted in increasing order of extractability by introducing the buffered mobile phase. Lanthanoids (Sm through Er) and yttrium were simultaneously enriched in the stationary phase from a large volume of a sample solution, and then separated from each other with reasonable resolution.

Apart from this, the sample preconcentration capability of procedures such as AAS, ICP–AES, ICP–MS, etc. was studied.[6] After metal ions were enriched, they were eluted almost simultaneously by inorganic acid at low pH, because their diffusion in the column is disadvantageous for improvement of the detection limits. It has been demonstrated that metal ions such as Ca, Cd, Mg, Mn, Pb, and Zn were enriched with good recovery at a concentration of 10 ppb each in 500 ml of the sample solution. However, the final enriched sample volume eluted from the CCC column was as large as several milliliters due to longitudinal diffusion as the sample band in the retained stationary phase.[1,6] An additional band spreading occurred in the flow tube when the concentrated solution was eluted with an acid solution for the subsequent analysis.

Also, the mechanism of separation based on displacement chromatography followed by enrichment in a CCC column was studied, and a tenfold enrichment of the transition metal ions was observed in the stationary phase.[7] However, diffusion of the sample is an inherent process in chromatographic elution; spreading of the sample bands in the column is unavoidable in CCC as it is in conventional LC.

Therefore, it may be difficult to obtain highly concentrated metal ions in an extremely small volume of effluent, such as of under-milliliter order, even if a small-bore column is used with higher concentration efficiency.

ENRICHMENT IN THE EFFLUENT BY PH-PEAK FOCUSING TECHNIQUE

Recently, pH-zone refining countercurrent chromatography (pH-ZRCCC), which is a quite unique technique based on neutralization reaction between mobile and stationary phase, has been developed for preparative scale separation and enrichment of various organic compounds.[8] pH-ZRCCC can realize chemical reactions in a quite limited thin area (i.e., the interface between organic and aqueous phase, where there is spreading over a wide area in a small-bore tube). If the pH between two phases in the column is reversed, the stationary phase is continuously neutralized with the mobile phase. Therefore, the pH border, where neutralization has just finished, moves to the tail (outlet) from the head (inlet) of the column. The moving rate of the pH border in the column can be controlled by adjusting the pH in each phase. This means that "another flow rate," concerned with pH, different from the "real flow rate of the eluent," can be realized in the column. Impurities in the sample solution can be quantitatively trapped and enriched in the pH border at a specific condition of the moving rate. This enrichment method for trace organic impurities has been called pH-peak-focusing countercurrent chromatography (pH-PFCCC).

It has been shown that pH-PFCCC can be successfully applied to the enrichment of inorganic trace elements in solution.[9,10] It has great potential for on-line enrichment and subsequent analysis, when CCC is combined with another analytical instrument for solution. The peak intensities for a 10 ml standard sample in the effluent stream were increased over 100-fold, compared with the conventional plasma atomic emission spectrometry. In this method, Ca, Cd, Cu, Mg, Mn, and Zn are chromatographically extracted, in a basic organic stationary phase containing a complex-forming reagent such as DEHPA, by introducing the sample solution into a column rotated at 1200 rpm. When the column is eluted with the acidified mobile phase, metal ions are trapped and concentrated around the sharp pH border formed between the acidic and the basic zones, moving toward the outlet of the column. Enriched metal ions are finally eluted with the sharp pH border as a highly concentrated peak into a less than 100 μl volume.[9]

By selecting appropriate experimental conditions, such as the acidity of the sample, bore of the column, and volume of the sample, each metal separation was achieved due to a longitudinal pH gradient on both sides of the pH border. Metal ions were concentrated at different positions in the moving pH border. When the pH border was sufficiently wide in the final stage of the elution, each concentrated metal could be separated. This method can be successfully applied to trace determination of Cd in tap water, which coexists with relatively large amounts of magnesium.[10]

The conditions of distribution ratio (K) for a two-phase solvent for pH-PFCCC are shown in Fig. 1. In a relatively basic environment at the first stage of sample injection, the metal ion present in the aqueous phase forms a complex with the ligand and partitions into the organic phase with a distribution ratio of K_b, whereas in an acidic environment,

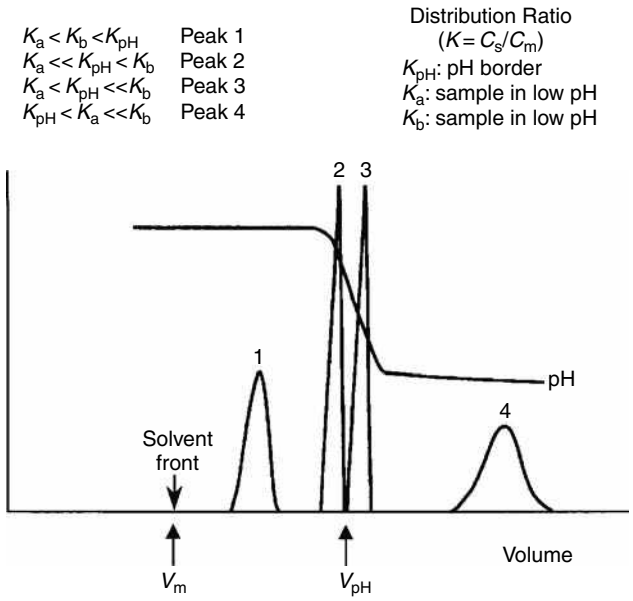

Fig. 1 Conditions of distribution ratio between two-phase solvent for pH-peak focusing.

the metal ion is mainly distributed into the aqueous phase with distribution ratio K_a.

As the elution proceeds, acid (e.g., HCl) present in the mobile phase steadily neutralizes the base (e.g., NH_3) in the stationary phase forming a narrow pH border between the basic front zone and the acidic rear zone. The traveling rate of this sharp pH border through the column is determined mainly by the molar ratio between the base in the stationary phase and acid in the mobile phase, but it is substantially lower than the flow rate of the mobile phase. The metal ion present in the acidic zone quickly moves with the mobile phase passing through the pH border into the basic zone, where it forms a metal–ligand complex and is transferred into the stationary phase. As the pH border moves forward, the complex is exposed to a lower pH, and the metal is displaced by proton (H^+) and released into the aqueous phase in its ionic form (M^+) to repeat the above cycle. Consequently, the metal element is always confined to a narrow region around the sharp pH border and finally eluted as highly concentrated sharp peaks (peaks 2 and 3) in the pH slope as shown in Fig. 1. Thus, the system eliminates longitudinal spreading of the sample band due to the separation process, which is inherent in other liquid chromatographic methods.

In the above method, trapping the metal element by the sharp pH border is essential, and this requires a relationship between the distribution ratios of the metal element and the traveling rate of the pH border through the column, as illustrated in Fig. 1. The distribution ratio is shown as K_a and K_b in the acidic and the basic zones, respectively. V_{pH} shows the volume of the eluent when the pH border comes out on the chromatogram. K_{pH} is assumed as a temporary distribution ratio when the solute peak appears at the retention volume V_{pH}. K_{pH} is adjustable by changing the molarity between the basic phase and the acidic phase. If K_{pH} is greater than K_a and K_b, the metal ion elutes earlier than the sharp pH border (peak 1), and if K_{pH} is smaller than K_a and K_b, the metal ion elutes after the sharp pH border (peak 4). Peak trapping takes place only when K_{pH} falls between K_a and K_b (peaks 2 and 3). The two metal peaks (peaks 2 and 3) may be resolved within a narrow range if there is a substantial difference between the K_a and K_b values, as shown in Fig. 1.

CONCLUSIONS

In contrast to high-performance liquid chromatography (HPLC), CCC has the unique feature that there is no solid support in the column. Because the distribution abilities, including the capacity of the stationary phase, are easy to control, CCC can be applied to the treatment of various inorganics, such as enrichment as well as separation and purification over a wide range of concentration. Moreover, the reproducibility of the enrichment operation has a substantial advantage over other enrichment systems, such as ion-exchange, because the absorber system in CCC is always "fresh" in each operation. In particular, enrichment of trace elements using pH-PFCCC is an ideal preconcentration method for subsequent inorganic determination by modern instrumental analytical methods. It can be combined directly with the flow injection technique, so that there is great potential for a new enrichment (preconcentration) system for the desired trace element prior to determination. Online enrichment and subsequent analysis may take the place of conventional sample preparation using a beaker and separating funnel in future investigations in this field.

REFERENCES

1. Fedotov, P.S.; Maryutina, T.A.; Grebneva, O.N.; Kuz'min, N.M.; Spivakov, B.Ya. Use of countercurrent partition chromatography for the preconcentration and separation of inorganic compounds: group extraction of Zr, Hf, Nb, and Ta for their subsequent determination by inductively coupled plasma atomic emission spectrometry. J. Anal. Chem. **1997**, *52*, 1034.
2. Ignatova, S.N.; Maryutina, T.A.; Spivakov, B.Ya.; Karandashev, V.K. Group separation of trace rare-earth elements by countercurrent chromatography for their determination in high-purity calcium chloride. Fresenius J. Anal. Chem. **2001**, *370* (8), 1109.
3. Hosoda, A.; Tsuyoshi, A.; Akiba, K. Enrichment and determination of zinc by high-speed countercurrent chromatography. Anal. Sci. **2002**, *18*, 897.
4. Nakamura, S.; Hashimoto, H.; Akiba, K. Purification of yttrium by high-speed countercurrent chromatography. J. Liq. Chromatogr. A, **1997**, *789*, 381.

5. Tsuyoshi, A.; Ogawa, H.; Akiba, K.; Hoshi, H.; Kitazume, E. High-speed countercurrent chromatography using a small coiled column. J. Liq. Chromatogr. Relat. Technol. **2000**, *23*, 1995.
6. Kitazume, E.; Sato, N.; Ito, Y. Concentration of heavy metals by high-speed countercurrent chromatography. J. Liq. Chromatogr. Relat. Technol. **1998**, *21*, 251.
7. Talabardon, K.; Gagean, M.; Marmet, J.M.; Berthod, A. Original uses of the liquid nature of the stationary phase in CCC. I. Extraction and separation of transition metal ions. J. Liq. Chromatogr. Relat. Technol. **1998**, *21*, 231.
8. Ito, Y.; Ma, Y. pH-zone-refining countercurrent chromatography. J. Chromatogr. A, **1996**, *753*, 1.
9. Kitazume, E.; Higashiyama, T.; Sato, N.; Kanetomo, M.; Tajima, T.; Kobayashi, S.; Ito, Y. On-line microextraction of metal traces for subsequent determination by plasma atomic emission spectrometry using pH peak focusing countercurrent chromatography. Anal. Chem. **1999**, *71* (24), 5515.
10. Kitazume, E.; Takatsuka, T.; Sato, N.; Ito, Y. Mutual metal separation system with enrichment using pH-peak focusing countercurrent chromatography. J. Liq. Chromatogr. Relat. Technol. **2004**, *27*, 437.

Metal-Ion Separation by Micellar HPLC

Subra Muralidharan
Chemistry Department, Western Michigan University, Kalamazoo, Michigan, U.S.A.

INTRODUCTION

The separation of target metal ions from a complex mixture is an extremely important area of research for the purpose of recovery of metal values from wastes and for environmental remediation and restoration. Conventional approaches to metal-ion separation and recovery fall into two broad classes, namely (a) solid–liquid and (b) liquid–liquid separations.

Solid–liquid methods include ion-exchange resins, which involve electrostatic interaction between the positively charged metal ions in solution and a negatively charged functional group on a polymer backbone such as SO_3^-, chelating polymers containing complexing ligands such as iminodiacetic acid, and membrane-mediated separations using solid membranes.

Liquid–liquid methods include solvent extraction with immiscible liquid–liquid systems in which a suitable ligand is dissolved in an organic phase and contacted with a metal ion containing an aqueous phase and liquid membranes. Separations can also be achieved with pseudo-phase systems such as micelles, microemulsions, and vesicles. Such separations can be solid–liquid or liquid–liquid and include separations with normal- and reversed-phase silica, and polymeric supports where the mobile phase contains the organized molecular assembly (OMA) of micelles, microemulsions, or vesicles. Separation of metal ions using the pseudo-phase systems is still in its infancy and a brief account will be provided here.

OMAs

OMAs are inherently capable of providing greater selectivities in separations of both organic compounds and metal ions mainly due to the ability of the organized microenvironments to discriminate among analytes with similar properties. Selectivities in metal-ion separation are best achieved through complexation rather than through ion-pair formation, and, in general, chelating ligands provide higher selectivities than monodendate ligands. The selectivities of the chelating ligands are limited in the conventional approaches using chelating resins and solvent extraction because the ligands are present in random macroenvironments. The incorporation of these ligands into organized microsturcutres such as micelles can provide dramatic improvements in their metal-ion selectivities. The factors that influence metal-ion selectivities are the stability constants of their complexes, the geometry and coordination number of the complexes, and the equilibrium and kinetics of metal complex formation and dissociation reactions, especially in the interfacial region. It is evident that these factors can be better exploited to achieve metal-ion selectivities in an organized microenvironment compared to a random macroenvironment. High-metal-ion selectivities are needed for the separation of target metal ions from complex matrices such as spent catalysts and electrochemical baths, geothermal brines, and nuclear wastes. Organized microenvironments will be key to achieving the selectivities demanded by such complex and difficult matrices.

MICELLES

Separations of metal ions mediated by the OMA micelles will be the focus of this entry. Micelles are formed from surfactants in aqueous solutions above a certain concentration of the surfactants called the critical micelle concentration (CMC).[1] These surfactants can be neutral, such as Triton X-100 and Brij 35, which have the general structure $R(OCH_2CH_2)_nOH$, where R is a long-chain alkyl group (C_{12} and above) and n the number of oxyethylene groups ($n = 9$ for Triton X-100 and 23 for Brij 35), or anionic such as sodium dodecyl sulfate (SDS; $C_{12}H_{25}SO_4^-Na$), or cationic such as cetyltrimethylammonium bromide [CTAB; $C_{16}H_{33}N(CH_3)_3^+Br^-$]. The CMC values of Triton X-100, SDS, and CTAB at an ionic strength of 0.1 are $2 \times 10^{-4}M$, $2 \times 10^{-3}M$, and $1.8 \times 10^{-4}M$, respectively, and their aggregation numbers are 100, 40, and 60, respectively. The neutral micelles in addition to the CMC are also characterized by the cloud point, which is the temperature at which a solution of the neutral micelle separates into two phases, namely the surfactant-rich phase and the water-rich phase. This property has been exploited to achieve cloud point separations analogous to separations employing two immiscible liquid phases. When the micelles are formed in the aqueous phase, the polar head groups of the surfactants, namely OH, SO_4^-, and $C_{16}H_{33}N(CH_3)_3^+$, are present on the surface of the micelles, and the interior of the micelle is hydrophobic like an organic phase in the case of the anionic and cationic micelles. In the case of the neutral micelles, the interior is composed of the oxyethylene groups terminating in an alkyl chain which form the

hydrophobic interior called the corona. Neutral surfactants form reverse micelles in non-polar solvents where the OH group is in the interior and the R group is on the surface. The presence of polar groups on the surface of the normal micelles in the aqueous phase results in an electrical double layer and an interfacial potential, which have significant influence on metal-ion selectivities. This potential is close to zero for neutral micelles, negative for anionic micelles, and positive for cationic micelles.

ADSORPTION OF SURFACTANTS ON SILICA AND REVERSED-PHASE SILICA

The neutral, anionic, and cationic surfactants will adsorb on silica and reversed-phase silica such as octadecylsilanized silica (ODS) from an aqueous solution to form a monolayer of the surfactant on the surface. The adsorption of surfactants on silica surface is more complex than their adsorption on ODS surface. The SiO_2 surface is polar due to the presence of surface silanol groups, and, as a result, the surfactants will adsorb with the polar group on the surface, namely the OH, SO_4^-, and $C_{16}H_{33}N(CH_3)_3^+$, with the alkyl groups pointed away from the surface. The adsorption of the surfactants on SiO_2 is pH dependent as the surface charge changes with pH. This adsorption is also dependent on the concentration of the surfactant with monolayers being formed at low surfactant concentrations and bilayers being formed at high surfactant concentrations. The bilayers are formed when a second layer of the surfactant adsorbs on the initial monolayer through its alkyl chains and the bilayer has the polar head groups pointing toward the bulk aqueous phase. Due to the complex adsorption phenomenon associated with adsorption of surfactants on SiO_2 surface, it is not a useful stationary phase for performing micellar chromatography.

The adsorption of surfactants onto ODS is more straightforward and well understood. Here, the formation of the monolayer of the surfactant on the ODS surface proceeds through the adsorption of the surfactant through its alkyl chain with the polar head group pointing into the bulk aqueous phase. Such an adsorption only results in a monolayer coverage, and the chromatographic behavior of these adsorbed monolayers can be discerned with established principles. The absorbed monolayers of surfactants on reversed-phase silica have been characterized by several spectroscopic methods [2] and will not be discussed here.

MICELLAR CHROMATOGRAPHIC SEPARATIONS OF METAL IONS

The adsorbed monolayers of surfactants on reversed-phase silica can be utilized as stationary phases and an aqueous solution of the same surfactant above its CMC as the mobile phase to separate both organic and inorganic analyte mixtures.[3] In the case of organic analytes, the selectivity between analyte components can be improved dramatically by employing micellar chromatography. The mechanism of separation, as in reversed-phase chromatography, is the distribution of the analyte between the micellar pseudo-phase and the stationary phase containing the adsorbed monolayer of the surfactant. Because the partitioning of the analyte now occurs between the organized microstructure of the micellar pseudo-phase and the adsorbed monolayer, the selectivity between closely related analytes is significantly improved. The separation of metal ions requires the addition of a complexing ligand in order to discriminate among the various metal ions. The SDS adsorbed on ODS as shown in Fig. 1 can function as an ion-exchange column but will not possess any selectivity between metal ions with similar charges analogous to a cation-exchange resin. Metal-ion separations can be achieved, in principle, on neutral, anionic, and cationic surfactants adsorbed on ODS columns, but only the separation with anionic surfactants adsorbed on ODS columns has been studied so far because of its complementary nature to conventional cation-exchange resins. The separations with neutral and cationic surfactants adsorbed are more complex and their behavior needs to understood before they will be useful for the separation of metal ions.

METAL-ION SEPARATIONS ON THE ODS–SDS COLUMN

The separation on the ODS–SDS column is achieved by the addition of a suitable complexing ligand to the mobile phase to discriminate between the various metal ions. The selectivity between two metal ions is achieved through two competing equilibria, namely the complexation equilibrium of the free metal ion in the micellar pseudo-phase and the complexation equilibrium of the metal ion adsorbed on the SDS monolayer and this is shown in Fig. 1. It is evident from this equilibrium that the distribution ratio (capacity factor) of the metal ion M^{2+} is given by Eq. 1, where the subscripts *a* and *s* represent the concentration of the free metal ion in the bulk aqueous phase and the adsorbed monolayer, respectively:

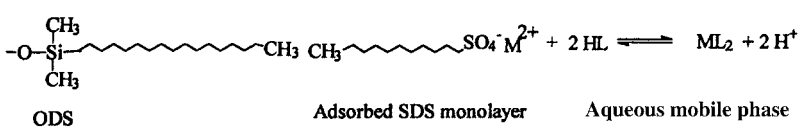

Fig. 1 Mechanism of separation of metal ions by micellar chromatography employing sodium dodecyl sulfate micelles in the mobile phase and octadecylsilanized silica as the stationary phase.

$$D = \frac{[M^{2+}]s}{[M^{2+}]s} \quad (1)$$

The associated equilibrium constant is defined in Eq. 2, where HL represents the ligand, and the relationship between log D and log[HL] and pH is given in Eq. 3:

$$K_{eq} = \frac{D[HL]^2}{[H^+]^2} \quad (2)$$

$$\log D = \log K_{eq} - 2\log[HL] - 2pH \quad (3)$$

As is evident from Eq. 3, a plot of log D as a function of log[HL] at constant pH and as a function of pH at constant [HL] will yield the stoichiometry of the equilibrium involved in the separation of the metal ion and the associated equilibrium constants.

The above-mentioned separation principle can be understood by the separation of Co(II), Ni(II), Cu(II), and Zn(II) by micellar chromatography employing SDS above its CMC in the mobile phase, ODS as the stationary phase, and 8-quinolinol-5-sulfonic acid ($pK_1 = 3.84$; $pK_2 = 8.35$) as the ligand:[4]

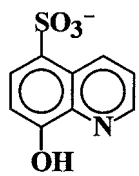

The logarithm of the stability constant for the 1:2 metal: ligand complex of this ligand with Co(II), Ni(II), Cu(II), and Zn(II) are 16.1, 16.77, 21.9, and 14.3, respectively. This separation employing a pH gradient is shown in Fig. 2, from which it is evident that the metal ions are eluted in the reverse order of their stability constants with 8-quinolinol-5-sulfonic acid. This elution order is readily understood from the equilibrium in Fig. 2, which indicates that the metal ion with the larger stability constant will be stripped from the adsorbed SDS monolayer more easily compared to the metal ion with a smaller stability constant. It may also be noted that the chromatographic bandwidths are much larger than those encountered with organic analytes and this is a direct consequence of slow metal complex formation and dissociation kinetics. Information on such kinetics can be obtained by studying the dependence of HETP on the concentrations of ligand and pH. This indicates that in the case of Co(II), Cu(II), and Zn(II), the dissociation of the metal complex is mainly responsible for the band broadening, whereas in the case of Ni(II), both metal complex formation and dissociation affect the efficiency.

Several simple water-soluble chelating ligands such iminodiacetic acid have been employed for the separation of a variety of metal ions. Okada demonstrated the

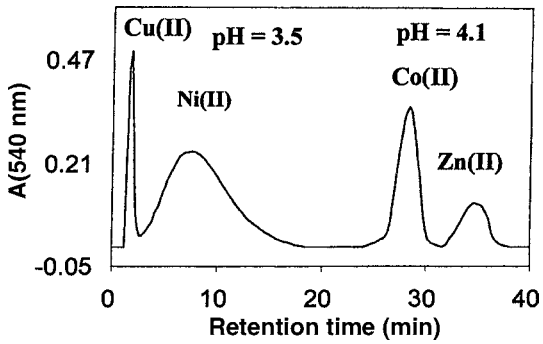

Fig. 2 Separation of Co^{2+}, Ni^{2+}, Cu^{2+}, and Zn^{2+} by micellar chromatography employing a pH gradient. Experimental conditions: mobile phase: [SDS] = 0.004 *M*, [8-quinolinol-5-sulfonic acid] = 0.002 *M*, ionic strength = 0.1; ODS stationary phase. 10 μl of the metal-ion mixture containing 0.002 *M* of each ion was injected at a mobile-phase flow rate of 1 ml/min. Cu^{2+} and Ni^{2+} elute at pH = 3.5 and Co^{2+} and Zn^{2+} elute at pH = 4.1.

separation of several divalent metal ions (Mn^{2+}, Co^{2+}, Ni^{2+}, Cu^{2+}, Zn^{2+}, Cd^{2+}) on ODS column with SDS micelles in the mobile phase and tartaric acid as the ligand.[5] The selectivity between the various divalent metal ions is much smaller than that observed with 8-quinolinol-5-sulfonic acid, which forms complexes with much larger stability constants than does tartaric acid. The stability constants of the metal complexes with a given ligand as mentioned earlier is one of the factors that affect selectivity. Karcher and Krull have published a review of the use of simple water-soluble ligands such as acetic acid, oxalic acid, hydroxyisobutyric acid, citric acid, tartaric acid, oxalic acid, and EDTA in micellar chromatography and with simple ion-exchange columns.[6] The selectivities obtained with these simple ligands is not as large as with ligands of the 8-quinolinol, acylpyrazolone, and aromatic oxime families, which are yet to be extensively investigated. Inorganic anions such as nitrate, nitrite, and phosphate can be separated by micellar chromatography using cationic micelles in the mobile phase and ODS as the stationary phase, as shown by Cassidy and Elchuk.[7]

CHELATING MICELLES

The studies that have been conducted so far have involved the addition of a suitable ligand to the micellar pseudo-phase in order to separate the mixture of metal ions. The location of the ligand in this pseudo-phase is a function of the hydrophilic and hydrophobic nature of the ligand. If the ligand is hydrophilic simple ones such as tartaric acid, then they will be present predominantly in the bulk aqueous phase, and if the ligand is hydrophobic such as 8-quinolinols, then they will distribute into the micellar pseudo-phase. The location of the ligands in the micellar

pseudo-phase is a function of the hydrophobicity of the ligand. Thus, the distribution of the ligand between the bulk aqueous phase and the micellar pseudo-phase introduces uncertainty in the location of the ligand and does not fully exploit the organized microenvironment. The aqueous-micelle interfacial region has a very high-interfacial area and possesses an electrical double layer with an interfacial potential. These can be effectively exploited to achieve even higher selectivities in metal-ion separations if the ligand can be specifically located at the interfacial region. We have recently achieved this by chemically derivatizing neutral surfactants such as Brij 35 such that a chelating ligand like 8-quinolinol or acylpyrazolone is the head group instead of OH. Such chelating surfactants form chelating micelles at CMC values much lower than Brij 35. The charge of the micelle is pH and ligand dependent and can be neutral, anionic, or cationic. In these chelating micelles, the ligand is exclusively present on the surface of the micelle and its chelating properties and metal-ion selectivities are strongly influenced by the interfacial region. We have synthesized chelating surfactants containing 2-methyl-8-quinolinol and 1-phenyl-3-methyl-4-benzoyl-5-pyrazolone as the head groups.[8] We have been able to obtain very large selectivities in the separation of divalent transition metal ions and trivalent lanthanide ions using these chelating micelles. The selectivities that we have achieved in the separation of the trivalent lanthanide metal ions are unprecedented and clearly indicate the tremendous gains in selectivities that can be achieved by the incorporation of ligands into organized microstructures. We have also shown that the mixed system of chelating surfactants with the 8-quinolinol and acylpyrazolone head groups form vesicles which also exhibit unique selectivities in the separation of transition and lanthanide metal ions on an ODS stationary phase. The chelating micelles are also interesting candidates for the separation of metal ions by electrokinetic chromatography, where the interfacial properties of the chelating micelles can be further exploited to achieve very high-metal-ion selectivities.

REFERENCES

1. Rosen, M.J. *Surfactants and Interfacial Phenomena,* John Wiley & Sons: New York, 1989.
2. Piasecki, D.A.; Wirth, M.A. Spectroscopic probing of the interfacial roughness of sodium dodecyl sulfate adsorbed to a hydrocarbon surface. Langmuir **1994**, *10*, 1913.
3. Hinze, W.L., Armstrong, D.W., Eds.; In *Ordered Media in Chemical Separations*; American Chemical Society: Washington, DC, 1987.
4. S. Muralidharan, unpublished results.
5. Okada, T. Interpretation of retention behavior of transition-metal cations in micellar chromatography using anion-exchange model. Anal. Chem. **1992**, *64*, 589.
6. Karcher, B.D.; Krull, I.S. The use of complexing eluents for the high performance liquid chromatographic determination of metal species. In *Trace Metal Analysis and Speciation*; Krull, I.S., Ed.; Journal of Chromatography Library Series Elsevier: Amsterdam, 1991; Vol. 47, 123–166.
7. Cassidy, R.M.; Elchuk, S. Dynamically coated columns for the separation of metal ions and anions by ion chromatography. Anal. Chem. **1982**, *54*, 1558.
8. S. Muralidharan, unpublished results.

Metalloproteins: Characterization Using CE

Mark P. Richards
Livestock and Poultry Sciences Institute (LPSI), Agricultural Research Service, U.S. Department of Agriculture (USDA-ARS), Beltsville, Maryland, U.S.A.

INTRODUCTION

Metalloproteins constitute a distinct subclass of proteins that are characterized by the presence of single or multiple metal ions bound to the protein by interactions with nitrogen, sulfur, or oxygen atoms of available amino acid residues or are complexed by prosthetic groups, such as heme, that are covalently linked to the protein. These metals function either as catalysts for chemical reactions or as stabilizers of the protein tertiary structure. Protein-bound metals may also be labile and, as such, be subject to transport, transient storage, and donation to other molecular sites of requirement within tissues and cells.

BACKGROUND INFORMATION

Metalloproteins play critical roles in a wide variety of basic cellular functions, including respiration, gene expression, reproduction, and metabolism. Isolation, characterization, and quantification of individual metalloproteins are each necessary and important steps toward understanding their unique biological functions. Alone or in combination, various types of chromatography, electrophoresis, and spectrometric techniques have been employed to study many unique aspects of metalloprotein structure and function. However, no one technique currently offers the ability to isolate, characterize, and quantify individual metalloproteins in a single step from complex matrices such as tissue extracts or physiological fluids. Therefore, there is an ongoing need for new and more capable methodologies. Because of the small-sample volume requirement, high degree of resolution, and advanced instrument automation capabilities, capillary electrophoresis (CE) has gained increasing popularity in the analysis of proteins.[1,2] In fact, many of the CE-based techniques developed for general protein separations are directly applicable to metalloprotein analyses.[2,3] This entry will emphasize some recent applications of CE and CE-related methodologies and their utility in providing new insight into the structure and function of a variety of metalloproteins.

Table 1 summarizes some of the ways CE has been applied to metalloprotein characterization. Altering capillary temperature, buffer ionic strength and pH, electric field strength (i.e., voltage), and capillary internal surface coating are but a few of the ways that CE conditions can be varied to influence the efficiency and selectivity of metalloprotein separations. Furthermore, different CE separation modes can be applied to gain new information about a specific metalloprotein.[3] For instance, capillary zone electrophoresis (CZE) can indicate a protein's net charge at a given pH; capillary isoelectric focusing (CIEF) gives a rapid estimate of its isoelectric point (*pI*); capillary gel electrophoresis (CGE), in the presence of sodium dodecyl sulfate (SDS), can be used to estimate its apparent molecular mass; and micellar electrokinetic chromatography (MEKC) can be useful in characterizing its surface hydrophobicity.

PROCEDURES

Varying CE separation conditions has been shown to be a particularly effective approach for improving the isolation and characterization of metallothioneins, a heterogeneous family of low-molecular-weight, cysteine-rich, heavy-metal-binding proteins.[4] It was found that (a) phosphate and borate buffers enhanced the sensitivity of detection at 200 nm by significantly reducing ultraviolet (UV) absorption of the background electrolyte, (b) the alkaline borate buffer (pH 8.4) gave rapid analysis times with reasonably high resolution, (c) the acidic phosphate buffer (pH 2.5) completely stripped zinc and cadmium from the proteins, yielding higher resolution and more reproducible separations of the apothioneins (metal-free proteins), (d) capillaries coated on their inner surface with a polyamine polymer that reversed electro-osmotic flow (EOF) or polyacrylamide that greatly suppressed EOF significantly improved resolution, (e) the MEKC mode of CE improved separation selectivity, and (f) photodiode array scanning detection to monitor UV absorption spectra of individual protein peaks separated at neutral pH was useful in determining both the presence and the type of metal associated with each.

CE is a useful tool for monitoring the purity of metalloproteins isolated from either natural or recombinant sources.[3] CZE was used to follow the purification progress of metallothioneins in samples subjected to gel filtration chromatography and reversed-phase high-performance liquid chromatography (HPLC).[3,4] Detection of a unique chromophore arising from the interaction of metal ions

Table 1 Characterization of metalloproteins using CE.

Identification and Purity Assessments
General characteristics (i.e., net charge, molecular weight, isoelectric point, etc.)
Monitoring purification steps
Separation of impurities or degradation products
Detection of unique UV/Visible absorbance (chromophore)
Structural information
Separation of molecular forms (i.e., isoforms, metalloforms, glycoforms, etc.)
Study of macromolecular assembly
Determination of metal-binding sites
Peptide mapping
Stability determinations
Effects of temperature and pH
Buffer additives (i.e., metals and metal chelators)
Activity measurements
Enzymatic activity
Electrophoretically mediated microassay (EMMA)
Isozyme profiling
Metal-binding/electrophoretic mobility shift
Affinity CE (ACE)
Immobilized metal-ion affinity CE (IMACE)
Metal-chelate coated capillaries
REDOX
Oxidation state of protein-bound metal
Elemental analyses
Indirect detection methods
Unique UV/Visible absorbance spectra (chromophore)
Mass spectrometry (CE/MS)
Direct (element-specific) detection methods
Inductively coupled plasma–mass spectrometry (CE/ICP–MS)
Proton-induced X-ray emission (PIXE)

and specific amino acid residues in the protein or with a prosthetic group attached to the protein can be useful. The selectivity achieved under such conditions can greatly reduce or even eliminate the need to purify metalloproteins prior to their analysis by CE. Two good examples of this are the detection of hemoglobin variants separated from red blood cell lysates by monitoring absorbance at 415 nm and the detection of transferrin in serum at 460 nm.[3] Absorbance at these characteristic wavelengths reflects the presence of iron atoms complexed by the heme moiety (hemoglobin) or by iron-binding sites located at the amino and carboxyl ends of the transferrin protein molecule. CE has also been used to characterize surface metal-binding sites on cytochrome-*c* and myoglobin modified with ruthenium-bis (bipyridine) imidazole, which imparts a strong absorbance at 292 nm to the modified proteins or peptides derived from a tryptic digest of the modified proteins.[3]

CE has proven to be useful in characterizing different molecular forms of various metalloproteins like metallothionein, transferrin, and conalbumin.[2–5] Molecular forms arise from differences in the amino acid sequence of proteins (isoforms), differences in the amount or type of metal bound (metalloforms), or from differences in the type and amount of carbohydrate side chains linked to the protein (glycoforms). CZE was used to follow the formation of the oligomeric iron core and its incorporation into ferritin, to detect and quantify ferritin species or ferritin subunit proteins in purified or partially purified states, and to study the interaction of different metal ions with ferritin.[2,3]

Structural stability of metalloproteins can be quickly assessed by CE under different conditions.[2,3] For example, thermally induced conformational changes in calcium-depleted α-lactalbumin and urea-induced unfolding of serum albumin were studied using CZE. The oxidation state of cysteine sulfhydryl groups in the zinc-containing protein, ribonuclease A, has been assessed using CZE to determine the presence or absence of a disulfide bond. Elevated capillary temperature altered the structure of myoglobin, which, in turn, resulted in reduction of the valence state of the iron atom bound to heme associated with this protein. Similarly, CIEF was used to separate and characterize different heme–iron valence hybrids of hemoglobin.[6]

Buffer additives, especially metals and metal chelators, can have dramatic effects on CE-based separations of metalloproteins by causing shifts in their electrophoretic mobility.[3] This observation forms the basis for a unique CE method referred to as affinity capillary electrophoresis or ACE. When a protein forms a complex with a charged metal-ion ligand, there can be a resulting change in electrophoretic mobility of the complexed protein relative to that of the metal-free protein. Scatchard analysis of the change in electrophoretic mobility of the protein as a function of the metal ion concentration in the separation buffer allows for the calculation of a metal-binding constant (K_b). ACE has been used to characterize K_b values for several metalloproteins, including (a) calcium affinity for calmodulin and C-reactive protein[3] and (b) the binding affinity of zinc for two separate sites in a highly basic, zinc-finger protein (NCp7) from the human immunodeficiency virus.[7] Haupt et al.[8] reported the development of an alternative CE affinity method based on immobilized metal affinity chromatography, which they called immobilized metal-ion affinity capillary electrophoresis or IMACE. In IMACE, metal ions (e.g., Cu^{2+}) are fixed to a soluble polyethylene glycol replaceable polymer matrix support added to the CE separation buffer. IMACE was used to study surface-related affinity

characteristics (number and accessibility of histidine residues and histidine microenvironment) for particular immobilized metal-ion chelate ligands in such proteins as cytochrome-*c*, ribonucleases A and B, chymotrypsin, and kallikrein.[8]

Some of the most promising advances in our understanding of unique characteristics of metalloprotein structure and function come from continuing developments in detection methodologies and from further development and refinement of coupled (hyphenated) systems such as CE/MS and CE/ICP/MS. The major difficulties restraining the routine use of such systems, aside from cost, arise from problems in interfacing the CE instrument with MS and ICP–MS instrumentation, although much progress is being made in this area.[9] CE/MS has been used to characterize metallothionein isoforms and metalloforms, the structures of which were deduced from discrete differences detected in molecular mass of the species separated by CE.[10] Using molecular masses calculated from the amino acid sequence and the type and amount of associated metals, it was possible to unequivocally identify distinct molecular forms.

The most definitive assessment of the metal composition of metalloproteins comes from the application of element-specific detection methods. CE/ICP–MS provides information not only about the type and quantity of individual metals bound to the proteins but also about the isotopes of each element as well.[11,12] Elemental speciation has become increasingly important to the areas of toxicology and environmental chemistry. Such analytical capability also opens up important possibilities for trace element metabolism studies. Fig. 1 depicts the separation of rabbit liver metallothionein containing zinc, copper, and cadmium (the pre-dominant metal) using CE/ICP–MS with a high-sensitivity, direct injection nebulizer (DIN) interface. UV detection (200 nm) was used to monitor the efficiency of the CE separation of the protein isoforms (MT-1 and MT-2), whereas ICP–MS detection made it possible to detect and quantify specific zinc, copper (not shown), and cadmium isotopes associated with the individual isoform peaks.

There are a number of emerging CE-based techniques that will greatly benefit the field of metalloprotein analysis in the near future. Major advances in interfacing instrumentation that will result in more efficient separations and more sensitive detection in coupled systems, especially for CE/MS and CE/ICP–MS, are occurring now.[9] Further development of capillary electrochromatography (CEC), new column packing materials, and commercial systems that allow for gradient elution CEC will have a major impact on improving CE separations of metalloproteins. Moreover, coupling CEC to MS or ICP–MS detectors will offer new and more powerful ways to isolate and characterize metalloproteins. The ability to accurately detect and quantify elemental isotopes offers the promise of being able to conduct isotope dilution experiments involving human and animal subjects in which metal metabolism will be studied and the molecular (metalloprotein) level. Finally, the push toward miniaturization of CE instrumentation (CE on a chip) will find increasing application in the analysis of metalloproteins. This will be especially true in clinical/diagnostic laboratories, where sample size may be severely limited.

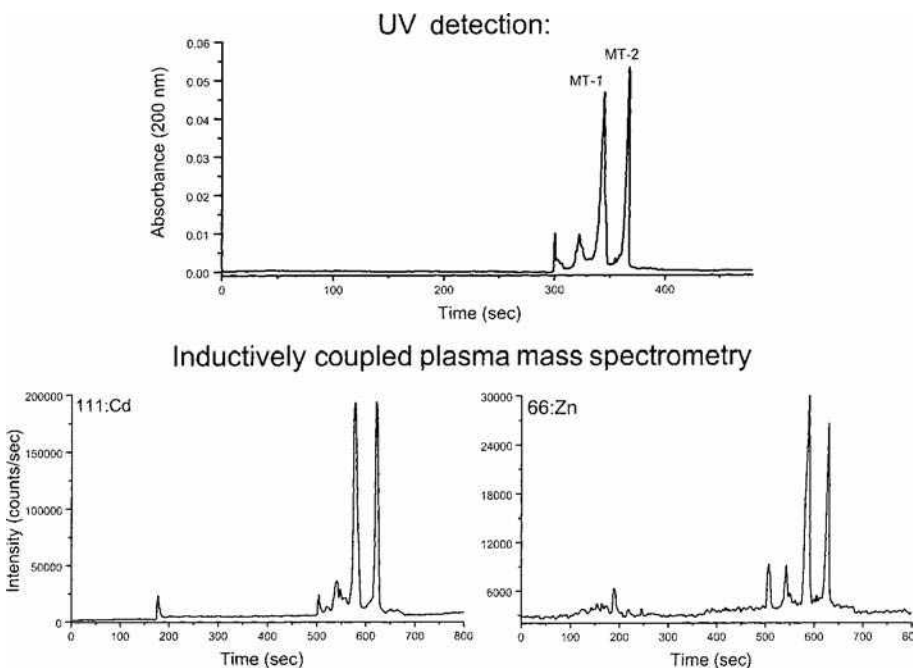

Fig. 1 Separation of rabbit liver metallothionein using CE–ICP–MS. The protein sample (1 mg/ml dissolved in deionized water) was first subjected to CZE with UV detection to optimize CE separation parameters for the major metallothionein isoforms (MT-1 and MT-2) shown in the upper panel. The CE instrument was then coupled to an ICP–MS instrument using a specially modified direct injection nebulizer (CETAC Technologies Inc., Omaha, NB) which enabled the entire capillary effluent from the CE to be directly injected into the ICP plasma torch, thus avoiding postcolumn dilution and band-broadening effects of conventional spray chamber nebulizers. Specific isotopes of cadmium (^{111}Cd) and zinc (^{66}Zn) associated with each isoform peak were monitored as shown by the figures in the lower panel.

REFERENCES

1. Landers, J.P., Ed.; *Handbook of Capillary Electrophoresis*; 2nd Ed.; CRC Press: Boca Raton, FL, 1997.
2. Wehr, T.; Rodriguez-Diaz, R.; Zhu, M. Capillary electrophoresis of proteins. In *Chromatographic Science Series*; Cazes, J., Ed.; Marcel Dekker, Inc.: New York, 1999; Vol. 80.
3. Richards, M.P.; Beattie, J.H. J. Capillary Electrophoresis **1994**, *1*, 196.
4. Richards, M.P.; Beattie, J.H. Comparison of different techniques for the analysis of metallothionein isoforms by capillary electrophoresis. J. Chromatogr. B, **1995**, *669*, 27.
5. Richards, M.P.; Huang, T.L. Metalloprotein analysis by capillary isoelectric focusing. J. Chromatogr. B, **1997**, *690*, 43.
6. Shih, M.L.; Korte, W.D. Analysis of hemoglobin derivatives by capillary isoelectric focusing and its application in the antidotal research of cyanide poisoning. Anal. Biochem. **1996**, *238*, 137.
7. Guszczynski, T.; Copeland, T.D. A binding shift assay for the zinc-bound and zinc-free HIV-1 nucleocapsid protein by capillary electrophoresis. Anal. Biochem. **1998**, *260*, 212.
8. Haupt, K.; Roy, F.; Vijayalakshmi, M.A. Immobilized metal ion affinity capillary electrophoresis of proteins–A model for affinity capillary electrophoresis using soluble polymer-supported ligands. Anal. Biochem. **1996**, *234*, 149.
9. Sutton, K.L.; Caruso, J.A. Interfacing capillary electrophoresis with inductively coupled plasma mass spectrometry. LC GC **1999**, *17*, 36.
10. Knudsen, C.B.; Bjornsdottir, I.; Jons, O.; Hansen, S.H. Detection of metallothionein isoforms from three different species using on-line capillary electrophoresis-mass spectrometry. Anal. Biochem. **1998**, *265*, 167.
11. Lu, Q.; Bird, S.M.; Barnes, R.M. Interface for capillary electrophoresis and inductively coupled plasma mass spectrometry. Anal. Chem. **1995**, *67*, 2949.
12. Michalke, B.; Schramel, P. Hyphenation of capillary electrophoresis to inductively coupled plasma mass spectrometry as an element-specific detection method for metal speciation. J. Chromatogr. A, **1996**, *750*, 51.

Metals and Organometallics: GC for Speciation Analysis

Yong Cai
Weihua Zhang
Department of Chemistry, Florida International University, Miami, Florida, U.S.A.

INTRODUCTION

There has been increasing interest in speciation information of elements present in environmental and biological samples since the toxicological and biological importance of many metals and metalloids greatly depends upon their chemical forms. Frequently, the lack of the speciation information is the major limitation to our understanding of the biogeochemical cycling of an element. Coupling of chromatographic techniques gas chromatography and high-performance liquid chromatography (GC and HPLC) with a highly sensitive and selective atomic spectrometry detector has been widely exploited and accepted for the speciation of metals and organometals. GC has enjoyed particular attention because of its high resolution for separation and simplicity of coupling. In this entry, the sample preparation and derivatization techniques for speciation and analysis of metal and organometallic ions are first discussed. Coupling of GC with atomic spectroscopic techniques and their applications are then reviewed.

BACKGROUND

Speciation analysis of an element is usually defined as the determination of the concentrations of the individual physico-chemical forms of the element in a sample that together constitute its total concentration. The International Union for Pure and Applied Chemistry (IUPAC) has recently recommended the definition of speciation as the distribution of an element amongst defined chemical species in a system.[1] IUPAC defines chemical species as the specific forms of an element defined as to isotopic composition, electronic or oxidative state, and/or complex or molecular structure.

Recently, there has been increasing interest in speciation information of elements present in environmental and biological samples since the toxicological and biological importance of many metals and metalloids greatly depends upon their chemical forms.[2–4] The determination of the total amount of an element is important but is not sufficient to assess its toxicity. Information about concentrations of the individual species of an element, including its organic derivatives, is particularly crucial. Frequently, the lack of the speciation information is the major limitation to our understanding of the biogeochemical cycling of the element.

The identification of the chemical forms of an element has become an important and challenging research area in environmental and biomedical studies. Two complementary techniques are necessary for trace element speciation. One provides efficient and reliable separation, and the other provides adequate detection and quantitation.[5] In its various analytical manifestations, GC is a powerful tool for separation of a vast variety of chemical species. Atomic spectroscopy offers the possibility of selectively detecting a wide range of metals and non-metals. The use of detectors responsive only to selected elements in a multicomponent mixture drastically reduces the constraints placed on the separation step, as only those components in the mixture that contain the element of interest will be detected.[6]

It is not surprising that the coupling of chromatographic techniques (GC and HPLC) with a highly sensitive and selective atomic spectrometry detector has been widely exploited and accepted for the speciation of metals and organometals. GC has enjoyed particular attention because of its high resolution for separation and simplicity of coupling. Multicapillary GC (MCGC) provides an attractive alternative for the conventional capillary GC (CGC). Multicapillary GC offers higher separation speed and a larger sample injection volume without sacrificing efficiency and resolution of separation. For example, the run time for separation of organomercury species using MCGC is up to a factor of 10 faster than CGC without loss of resolution.[7] Of selective atomic spectrometers coupled with GC, atomic absorption spectrometer (AAS) has been successfully used for the speciation of metal(loid)s and organometal(loid)s. Various plasma spectrometry methods, such as inductively coupled plasma mass spectrometry (ICP–MS), microwave-induced plasma atomic emission spectrometry (MIP–AES), furnace atomization plasma emission spectrometry (FAPES), and inductively coupled plasma optical emission spectrometry (ICP–OES), have also been widely investigated for speciation analysis of metallic and non-metallic elements. Details about GC coupled with AAS, MIP–AES, and ICP–MS are discussed here.

SAMPLE PREPARATION

The native species of most metals and metalloids, such as mercury, lead, tin, arsenic, and selenium, are generally present as ionic forms in sample matrices. For GC-based

coupling techniques, these compounds need to be extracted from the sample matrices and be converted to volatile and thermally stable derivatives. Frequently, the derivatives are then concentrated by solid-phase microextraction (SPME),[8] purge and (cryo) trapping,[2,9] stir bar sorptive extraction (SBSE),[10] or extracting into an organic solvent prior to injection onto a GC column.[2] Among these preconcentration methods, SPME is a simple, fast, and solvent-free technique and has been employed for single or multielemental speciation of organometallic compounds of mercury, lead, and tin.[11]

Grignard Reaction

Grignard reaction is one of the most widely used derivatization techniques for speciation of a number of elements.[12,13] The main advantage of this reaction is that different alkyl groups can be chosen to make fully alkylated species. Reactions for mercury analysis can be described as follows:

$$RMgX + R'Hg^{+} \rightarrow RHgR' \quad (1)$$

$$RMgX + Hg^{2+} \rightarrow R_2Hg \quad (2)$$

where R indicates propyl, butyl, or pentyl groups and R′ for methyl or ethyl groups. However, Grignard reagents are very sensitive to water. As a consequence, metals and organometallic compounds have to be extracted prior to derivatization into an organic solvent with the assistance of complexing reagents, such as dithiocarbamates and tropolone. The whole sample preparation can be tedious and time consuming.

Hydride Generation

Several elements (Hg, Ge, Sn, Pb, Se, As, Te, Sb, Bi, and Cd) can be transformed into volatile hydrides, providing the basis of their analysis.[2,4] Sodium borohydride ($NaBH_4$) is commonly used as a derivatization reagent. The reaction for methylarsenicals is shown below:

$$Me_nAsO(OH)_{3-n} + NaBH_4 \rightarrow Me_nAsH_{3-n} \quad (n = 1-3) \quad (3)$$

The usefulness of this procedure for speciation analysis, however, is restricted by either the thermodynamic inability of hydride formation for some species, or considerable kinetic limitation to hydride formation. Nevertheless, the technique is still essential for some classes of compounds.[2]

Aqueous Derivatization with Tetraalkyl(aryl)borates

The restricted versatility of using $NaBH_4$ can, to a certain degree, be overcome by replacing $NaBH_4$ by alkyl or arylborates.[2] The most common derivatization procedure relies on ethylation with sodium tetraethylborate, which was initiated for determining methyllead ionic compounds.[14]

$$Me_nPb^{(4-n)+} + NaBEt_4 \rightarrow Me_nPbEt_{(4-n)} \quad (n = 1-4) \quad (4)$$

$NaBEt_4$ acts as an aqueous-phase ethylation reagent, quantitatively transferring Et^{-} ions to ionic metals and organometals. Direct aqueous-phase ethylation with $NaBEt_4$ has been used for speciation of a variety of metals, such as lead, mercury, and tin in different environmental and biological samples. This reaction has significant advantages since the derivatization reaction is performed in aqueous phase, subsequently reducing the analysis time and eliminating the need for organic solvent extraction. However, this method cannot be used for the speciation of the natively occurring ethylated species, such as ethyllead and ethylmercury.[13]

Several efforts have been carried out to develop alternative aqueous derivatization reagents. The use of sodium tetrapropylborate ($NaBPr_4$) as an alkylation reagent represents the most recent advance. Compared to ethylation, propylation has equivalent or even higher sensitivity and has the advantages of occurring within a wider pH range and with less interferences for analysis of some elements (e.g., for Hg).[15] In spite of the limitation of its commercial availability, $NaBPr_4$ has been used to determine organolead, tin, and mercury compounds.[2,9,15] Phenylation with sodium tetraphenyl borate ($NaBPh_4$) is also a promising technique for the speciation of several metals. Compared to $NaBEt_4$ and $NaBPr_4$, $NaBPh_4$ is much more stable under ambient conditions and is a low cost and commercially available chemical. Its application in organomercury analysis has been comprehensively studied.[16]

COUPLING GC WITH ATOMIC SPECTROMETRIC DETECTION

GC/AAS

GC coupled with AAS has been the most popular hyphenated technique for the speciation of metals and organometals. Among different atomizer designs employed in coupling GC with AAS, electrothermal atomization, especially the electrothermally heated quartz tube, is preferred due to its high sensitivity, simple operation, and low cost.[6] The quartz tube (~100 × 10 mm I.D.) is usually constructed in-house and wrapped with Nichrome resistance wire and ceramic isolation material. A thermocouple is attached to the surface of the quartz burner for temperature control (Fig. 1). If necessary, hydrogen and air can be supplied from side arms of the burner. The furnace can be heated to more than 1000°C by means of a variable transformer.

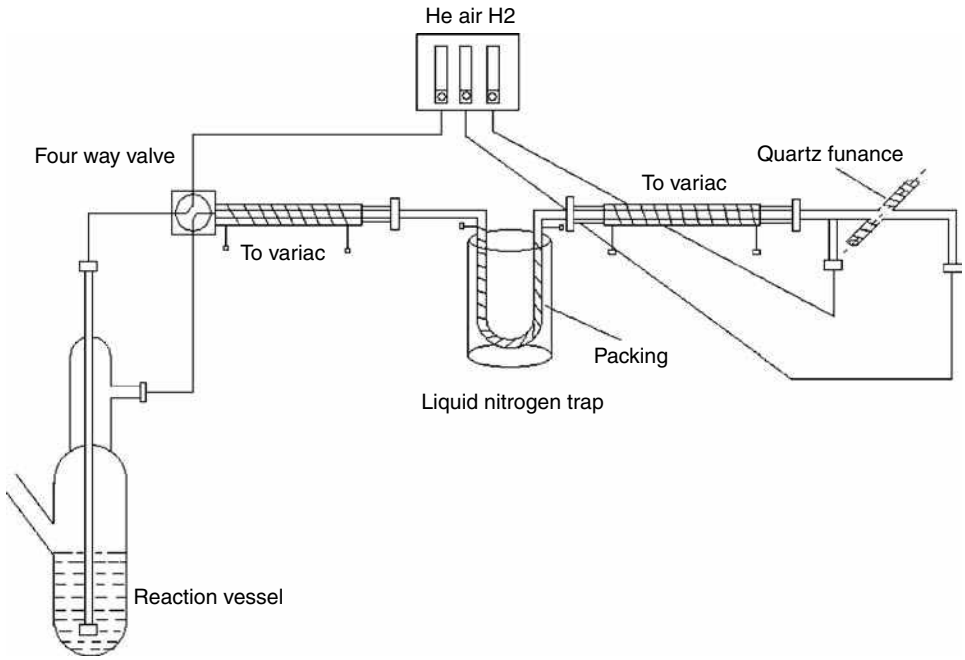

Fig. 1 Schematic diagram of a purge-and-trap GC/AAS system.

Two types of sample introduction/interface coupling GC and quartz furnace have been generally used. Fig. 1 shows a schematic representation of the first design, often called purge-and-trap. The instrumental set-up consists of a reaction vessel where the sample is brought in contact with a reagent, such as $NaBH_4$ or $NaBEt_4$, and a U-tube filled with a GC sorbent. During the reaction, the U-tube is maintained in liquid nitrogen, and the produced derivatives are purged with helium, and then trapped on the sorbent. Once the reaction is completed, the liquid nitrogen is removed and the U-tube is heated electrically. The trapped compounds are then separated according to their volatility and measured by AAS. The principal advantages of this set-up are its very high sensitivity and online aqueous derivatization. However, it suffers from water condensation problem in the U-trap, which limits the length of purge time. A water trap is often instaled upstream from the sorbent tube to avoid its blocking with ice crystals.[2]

The second design is actually modified from a regular GC device equipped with either a packed or a capillary column. The outlet of the GC is directly connected to the entrance of the quartz furnace through a piece of stainless steel tubing, which is electrically heated to avoid condensation of the compounds of interest. In order to use this technique, the target compounds have to be extracted from sample matrices, derivatized with an appropriate reagent, and back extracted into organic solvent before injection. Absolute detection limits obtained with this system are similar to those using purge-and-trap since they use the same detection technique. However, the concentration detection limits can be different as large as several orders of magnitude. With the purge-and-trap system, all target compounds in the sample are online preconcentrated and analyzed at once, while with the regular GC only a small portion of the sample extract is injected for analysis. The regular GC method offers a high versatility because of the possibility of using different Grignard reagents.

GC/MIP–AES

MIP–AES has two basic characteristics that can be utilized when coupling with a GC instrument.[6] The low gas temperature of the MIP allows small amounts of samples, compatible with those of GC solutes, to be introduced without extinguishing the plasma. In addition, sample introduction is easily facilitated as the carrier and plasma gases are the same (helium). These advantages have made the coupled GC/MIP–AES a popular technique and many applications have been reported.[6,16,17] Commercial instrument is currently available.

Helium plasma is maintained within a "cavity," which serves to focus power from a microwave source (usually operated at 2.45 GHz) into a discharge cell (usually a quartz capillary tube). The cavity that has been most used for GC detection, has been the atmospheric pressure TM_{010} cylindrical resonance cavity developed by Beenakker.[18] The effluent from a GC is connected directly to the discharge tube via a heated transfer line to prevent analyte condensation. The GC/MIP–AES requires a consistent supply of high purity gases for optimal performance. Hydrogen and oxygen are often used as plasma gases for metal and metalloid analysis. In addition, the AED spectrometer requires a continuous nitrogen purge.

Advantages of MIP–AES are low cost, simple operation, and high sensitivity. Its sensitivity for mercury analysis is compatible with that using GC coupled with atomic fluorescence detection,[16] which is currently recognized as the most sensitive method for determining mercury. The main drawback is the low tolerance for organic solvents. A venting system has to be used to prevent the solvent from getting into plasma tube.

GC/ICP–MS

Over the last decade, ICP–MS has proven to be a highly sensitive and selective technique for the determination of trace and ultratrace amounts of metals in various samples. It allows multielement detection in a single run and offers isotopic information of the elements of interest.[19–21] Solvent venting to prevent plasma instability is unnecessary, unlike in GC/MIP–AES, and no carbon accumulates as it does on MIP discharge tube. These features make the hyphenation GC/ICP–MS unique.

Coupling GC with ICP–MS is easily accomplished by connecting a column to the inner tube of the torch using a transfer line between the GC oven and the plasma torch (Fig. 2). The transfer line usually consists of an electrically heated stainless steel tube through which a piece of deactivated fused silica is passed. The transfer line capillary ends at the tip of the ICP injector. Generally, the stainless steel tubing is maintained at a temperature that prevents the condensation of the GC effluent in the transfer line. Fluctuation in the transfer line temperature can affect GC peak shape and resolution.

The ICP–MS instrument requires a carrier gas flow rate of approximately 1 L/min, while the capillary GC effluent is less than 5 ml/min. It is, therefore, necessary to introduce argon as a makeup gas. The makeup gas produces a central channel in the plasma and helps to carry analytes from GC column to the plasma. The makeup gas must be heated to avoid condensation of the column effluent, and this has been done by passing the argon gas through heated stainless steel tubing and adding it at the beginning of the transfer line.[19] However, a high flow rate of argon makeup gas results in an undesirable dilution effect. This is not the case for MCGC/ICP–MS since the dilution effect may be minimized or even eliminated due to large carrier gas flow without the need of an additional makeup gas.[7]

This hyphenated technique has been successfully applied to the speciation of a number of metals, including lead,[22] mercury,[23] and tin,[24] The advantages of determining multielements simultaneously and a wide dynamic linear range are obvious.[20] The high resolving capacity of GC and the high sensitivity and multielemental analysis capability of ICP–MS have made the combination most efficient and attractive for speciation analysis.[9] More recently, the remarkable developments in plasma sources, such as the low power plasma and glow discharge (GD) sources, as well as mass analyzers such as the use of collision/reaction cell, time-of-flight (TOF), and double-focusing sector field, have widened the window for elemental speciation using this technique.[9–24]

In addition, ICP–MS offers a unique characteristic of being able to provide isotopic information of an element. By utilizing isotope dilution (ID), GC/ICP–MS has been applied for accurate and precise determination of organotin and organomercury species. Not only is it possible to significantly improve the precision of determination, but it is also competent for studying transformation of species during analysis process by species-specific ID/GC/ICP–MS.[9]

CONCLUSIONS

Speciation analysis of metals and organometallics is a challenging analytical task. Because the native species of most metals and metalloids, such as mercury, lead, tin, arsenic, and selenium, are generally present as ionic forms in sample matrices, these compounds need to be extracted from the

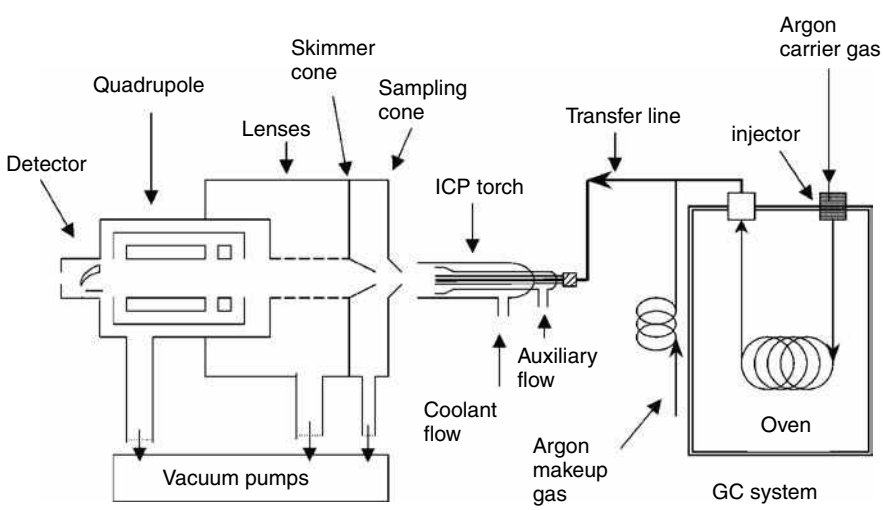

Fig. 2 Schematic diagram of a GC/ICP–MS system.

sample matrices and be converted to volatile and thermally stable derivatives for GC analysis. Hydride generation with $NaBH_4$, aqueous alkylation with $NaBEt_4$, $NaBPr_4$, and $NaBPh_4$ are the most widely used methods for derivatization. Coupling GC with ICP–MS has proven to be a highly sensitive and selective technique for the speciation of trace and ultratrace amounts of metals in various samples. It allows multielement detection in a single run and offers isotopic information of the elements of interest. With the rapid development and improvement of ICP–MS and the substantially reduced cost of using this instrument, coupling GC with ICP–MS will be one of the most powerful tools for metal and organometalloid speciation.

REFERENCES

1. Templeton, D.; Ariese, F.; Cornelis, R.; Danielsson, L.G.; Muntau, H.; van Leeuwen, H.P.; Lobinski, R. Guidelines for terms related to chemical speciation and fractionation of elements. Definitions, structural aspects, and methodological approaches (IUPAC recommendations 2000). Pure Appl. Chem. **2000**, *72*, 1453–1470.
2. Lobinski, R.; Adams, F.C. Speciation analysis by gas chromatography with plasma source spectrometric detection. Spectrochim. Acta B. **1997**, *52*, 1865–1903.
3. Sutton, K.; Sutton, R.M.C.; Caruso, J.A. Inductively coupled plasma mass spectrometric detection for chromatography and capillary electrophoresis. J. Chromatogr. A. **1997**, *789*, 85–126.
4. Cai, Y. Speciation and analysis of mercury, arsenic, and selenium by atomic fluorescence spectrometry. Trends Anal. Chem. **2000**, *19*, 62–66.
5. Vela, N.P.; Olson, L.K.; Caruso, J.A. Elemental speciation with plasma mass spectrometry. Anal. Chem. **1993**, *65*, 585A–597A.
6. Ebdon, L.; Hill, S.; Ward, R.W. Directly coupled chromatography–atomic spectroscopy. Part 1. Directly coupled gas chromatography–atomic spectroscopy. A review. Analyst **1986**, *111*, 1113–1138.
7. Rosenkranz, B.; Bettmer, J. Rapid separation of elemental species by multicapillary GC. Anal. Bioanal. Chem. **2002**, *373*, 461–465.
8. Botana, J.C.; Rodriguez, R.R.; Diaz, A.M.C; Derreira, R.A.L; Torrijos, R.C.; Pereiro, I.R. Fast and simultaneous determination of tin and mercury species using SPME, multicapillary gas chromatography and MIP–AES detection. J. Anal. At. Spectrom. **2002**, *17*, 904–907.
9. Wuilloud, J.C.A; Wuilloud, R.G.; Vonderheide, A.P.; Caruso, J.A. Gas chromatography/plasma spectrometry—an important analytical tool for elemental speciation studies. Spectrochim. Acta B. **2004**, *59*, 755–792.
10. Vercauteren, J.; Peres, C.; Devos, C.; Sandra, P.; Vanhaecke, F.; Moens, L. Stir bar sorptive extraction for the determination of ppq-level traces of organotin compounds in environmental samples with thermal desorption–capillary gas chromatography–ICP mass spectrometry. Anal. Chem. **2001**, *73*, 1509–1514.
11. Centineo, G.; González, E.B.; Sanz-Medel, A. Multielemental speciation analysis of organometallic compounds of mercury, lead and tin in natural water samples by headspace-solid phase microextraction followed by gas chromatography– mass spectrometry. J. Chromatogr. A. **2004**, *1034*, 191–197.
12. Chau, Y.K.P.; Wong, T.S.; Bengert, G.A.; Dunn, J.L. Determination of dialkyllead, trialkyllead, tetraalkyllead and lead(II) compounds in sediment and biological samples. Anal. Chem. **1984**, *56*, 271–274.
13. Cai, Y.; Jaffe, R.; Jones, R.D. Ethylmercury in the soils and sediments of the Florida Everglades. Environ. Sci. Technol. **1997**, *31*, 302–305.
14. Rapsomanikis, S.; Donard, O.F.X.; Weber, J.H. Speciation of lead and methyllead ions in water by chromatography/atomic absorption spectrometry after ethylation with sodium tetraethylborate. Ana1. Chem. **1986**, *58*, 35–38.
15. Bravo-Sanchez, L.R.; Encinar, J.R.; Martinez, J.I.F; Sanz-Medel, A. Mercury speciation analysis in sea water by solid phase microextraction–gas chromatography–inductively coupled plasma mass spectrometry using ethyl and propyl derivatization. Matrix effects evaluation. Spectrochim. Acta B. **2004**, *59*, 59–66.
16. Monsalud, S. *Determination of organomercury compounds in environmental and biological samples by using derivatization and gas chromatographic detection*; M.S. Thesis, Florida International University, 1999.
17. Dietz, C.; Landaluze, J.S.; Ximénez-Embun, P.; Madrid-Albarrán, Y.; Cámara, C. Volatile organo-selenium speciation in biological matter by solid phase microextraction–moderate temperature multicapillary gas chromatography with microwave induced plasma atomic emission spectrometry detection. Anal. Chim. Acta **2004**, *501*, 157–167.
18. Beenakker, C.I.M. Evaluation of a microwave-induced plasma in helium at atmospheric pressure as an element-selective detector for gas chromatography. Spectrochim. Acta B. **1977**, *32*, 173–187.
19. De Smaele, T.; Moens, L.; Dams, R.; Sandra, P. ICP–MS—a sensitive detection method for metal speciation with capillary GC. LC–GC **1996**, *14*, 876–880.
20. De Smaele, T.; Vercauteren, J.; Moens, L.; Dams, R.; Sandra, P. Coupling HP 6890 series GC to HP 4500 benchtop ICP–MS: higher sensitivities for metal speciation. Hewlett–Packard Peak **1999**, *2*, 10.
21. Byrdy, F.A.; Caruso, J.A. Elemental analysis of environmental samples using chromatography coupled with ICP–MS detection. Environ. Sci. Technol. **1994**, *28*, 528A–534A.
22. Pelaez, M.V.; Costa-Fernandez, J.M.; Sanz-Medel, A. Critical comparison between quadrupole and time-of-flight inductively coupled plasma mass spectrometers for isotope ratio measurements in elemental speciation. J. Anal. At. Spectrom. **2002**, *17*, 950–957.
23. Jitaru, P.; Adams, F.C. Speciation analysis of mercury by solid-phase microextraction and multicapillary gas chromatography hyphenated to inductively coupled plasma–time-of-flight-mass spectrometry. J. Chromatogr. A. **2004**, *1055*, 197–207.
24. Tao, H.; Rajendran, R.B.; Quetel, C.R.; Nakazato, T. Tin speciation in the femtogram range in open ocean seawater by gas chromatography/inductively coupled plasma mass spectrometry using a shield torch at normal plasma conditions. Anal. Chem. **1999**, *71*, 4208–4215.

Metformin and Glibenclamide: HPLC Determination

B.L. Kolte
B.B. Raut
Department of Chemical Technology, Dr. Babasaheb Ambedkar Marathwada University, Aurangabad, India

A.A. Deo
M.A. Bagool
Wockhardt Research Centre, Aurangabad, India

D.B. Shinde
Department of Chemical Technology, Dr. Babasaheb Ambedkar Marathwada University, Aurangabad, India

INTRODUCTION

A HPLC method was developed for the simultaneous determination of metformin and glibenclamide in a combined dosage form using a Zorbax XDB C_{18}, 15 cm column. The mobile phase was composed of the buffer and acetonitrile in the ratio 68 : 32, vol/vol; pH was adjusted to 7.5 with orthophosphoric acid. The buffer used in the mobile phase contains 10 m*M* disodium hydrogen phosphate and 10 m*M* sodium dodecyl sulphate (SDS) in double-distilled water. The mobile phase flow rate was 1 ml/min, column oven temperature was maintained at 40°C, and analytes were detected at a wavelength of 226 nm. The developed method was validated and shown to be linear. The correlation coefficients for metformin and glibenclamide were 1.0 and 0.9999, respectively. The relative standard deviations for six replicate measurements intwo sets of each drug in the tablets were always less than 2%.

OVERVIEW

Metformin HCl is 1,1-dimethyl biguanide hydrochloride and glibenclamide is 5-chloro-*N*-[2-[4-(cyclohexylamino)carboxyl]amino]sulfonyl]phenyl]ethyl]-2-methoxybenzamide. A combination of 500 mg of metformin HCl and 5 mg of glibenclamide is available commercially as tablets.[1] It has been concluded, from the comparative study, that combined treatment with metformin and sulphonylurea is more effective than these drugs alone for improving glycemic control in type II diabetes, while also allowing a reduction of the dosage of each drug.[2]

A literature survey revealed that few methods are reported for the individual estimation of metformin and glibenclamide. Both of these drugs are official in the IP[3] and BP;[4] glibenclamide is also reported in the United States Pharmacopeia (USP).[5] The methods for metformin[6–11] and glibenclamide[12–15] are reported for the estimation of these drugs in tablets and plasma. One method is reported for the estimation of metformin and glibenclamide in a combined dosage form.[16] In the reported method,[16] glibenclamide was estimated at 300 nm and metformin was estimated at 232 nm. The estimation of the analytes was performed by preparing two different sample preparations.

In the present article, attempts have been made to develop a simple and rapid method for the simultaneous determination of metformin and glibenclamide. Adequate separation was achieved by using a mobile phase containing 10 m*M* SDS and 10 m*M* disodium hydrogen phosphate in double-distilled water and acetonitrile in the ratio of 68 : 32, vol/vol, with pH adjusted to 7.5 with orthophosphoric acid. In the present developed method, the analytes of the combined dosage form were analyzed using the same sample preparation and were detected at a wavelength of 226 nm. In the reported method,[16] the recovery values for metformin HCl and glibenclamide were 99.37% and 101.57%, respectively. In the present method, the recovery values for metformin HCl and glibenclamide were 99.2% and 100.0%, respectively. The method is validated and shown to be linear, accurate, and precise. The method has been applied for the analysis of the ingredients of the combined dosage forms available in the commercial market.

EXPERIMENTAL TECHNIQUES

Materials and Reagents

Metformin HCl and glibenclamide were obtained from Wockhardt Research Centre (Aurangabad, Maharashtra State, India). SDS and disodium hydrogen phosphate were obtained from E. Merck (India) Ltd. (Worli,

Mumbai, India). Orthophosphoric acid and acetonitrile (HPLC grade) were obtained from Qualigens Fine Chemicals (Dr. Annie Besant Road, Mumbai, India). The 0.45 μm nylon filter was obtained from Advanced Microdevices Pvt., Ltd. (Ambala Cantt, India) and Whatman filter paper 41 was obtained from Whatman International Ltd. (Maidstone, England, UK). The tablets containing a combination of metformin and glibenclamide were purchased from the Indian market. Double-distilled water was used throughout the experiments. Other chemicals were of analytical or HPLC grade.

Chromatographic Conditions

A Thermoseparation Products Company high-performance liquid chromatography (HPLC) was utilized, consisting of the following components: Constametric 3500 pump, AS 3000 autosampler, and UV 1000 detector. A Zorbax XDB C_{18} (5 μm, 4.6 × 150 mm; Agilent Technologies) column was used. The mobile phase flow rate was 1 ml/min and the column oven temperature was maintained at 40°C; the analytes were detected at a wavelength of 226 nm. The injection volume was 25 μl. Data acquisition was performed with the software, PC 1000. Peak purity was checked with a photodiode array detector (UV6000 LP; Thermoseparation Products Co.).

Preparation of Solutions

Mobile phase

The mobile phase was composed of a buffer and acetonitrile in the ratio of 68 : 32, vol/vol. The pH of the mobile phase was adjusted to 7.5 with orthophosphoric acid. The buffer used in the mobile phase consisted of 10 m*M* disodium hydrogen phosphate and 10 m*M* SDS in double-distilled water. The mobile phase was premixed and filtered through a 0.45 μm nylon filter and degassed.

Standard stock solutions

Standard solutions were prepared by dissolving the drugs in the diluents and diluting them to the desired concentration. The buffer and diluents used for the standard preparation and sample preparation were prepared as follows:

- Buffer: contained 10 m*M* disodium hydrogen phosphate in double-distilled water; pH was adjusted to 4.0 with orthophosphoric acid.
- Diluent: contained the buffer and acetonitrile in the ratio 60:40, vol/vol.

Metformin HCl

A 125 mg portion of metformin HCl standard was accurately weighed and transferred to a 50 ml volumetric flask; it was dissolved and diluted to 50 ml with the diluent.

Glibenclamide

A 25 mg portion of glibenclamide standard was accurately weighed and transferred to a 50 ml volumetric flask; 30 ml of acetonitrile was then added and sonication was applied for 5 min. After sonication, 10 ml of the buffer was then added and the volume was made up to 50 ml with the diluent. From this solution, 2.5 ml was transferred into a 50 ml volumetric flask and diluted to the mark with the diluent.

Mixed standard preparation

For mixed standard solution, 2 ml of a metformin standard solution and 2 ml of glibenclamide standard solution were transferred to a 50 ml volumetric flask and diluted to the mark with the diluent. This solution contains 100 μg/ml metformin HCl and 1.0 μg/ml glibenclamide.

Assay preparation

Ten tablets were weighed and finely powdered. A quantity of powder equivalent to one tablet, containing 500 mg of metformin HCl and 5 mg of glibenclamide, was transferred to a 100 ml volumetric flask; 50 ml of acetonitrile was then added and sonication was applied for 5 min. After sonication, 20 ml of buffer was added and further sonication was applied for 20 min with swirling. The solution was cooled to ambient temperature and diluted to the desired volume with the diluent and mixed well. The solution was filtered through Whatman filter paper 41. The first 5 ml portion of the filtrate was rejected and then 1 ml of the filtered solution was transferred into a 50 ml volumetric flask and diluted with the diluent.

RESULTS AND DISCUSSION

Chromatography

A reverse-phase HPLC procedure was proposed as a suitable method for the simultaneous determination of metformin and glibenclamide in a combined dosage form. The chromatographic conditions were adjusted to provide adequate retention and resolution of metformin and glibenclamide. A mixture of buffer and acetonitrile, in the ratio of 68:32, vol/vol, with pH adjusted to 7.5 with orthophosphoric acid at a flow rate of 1 ml/min, was

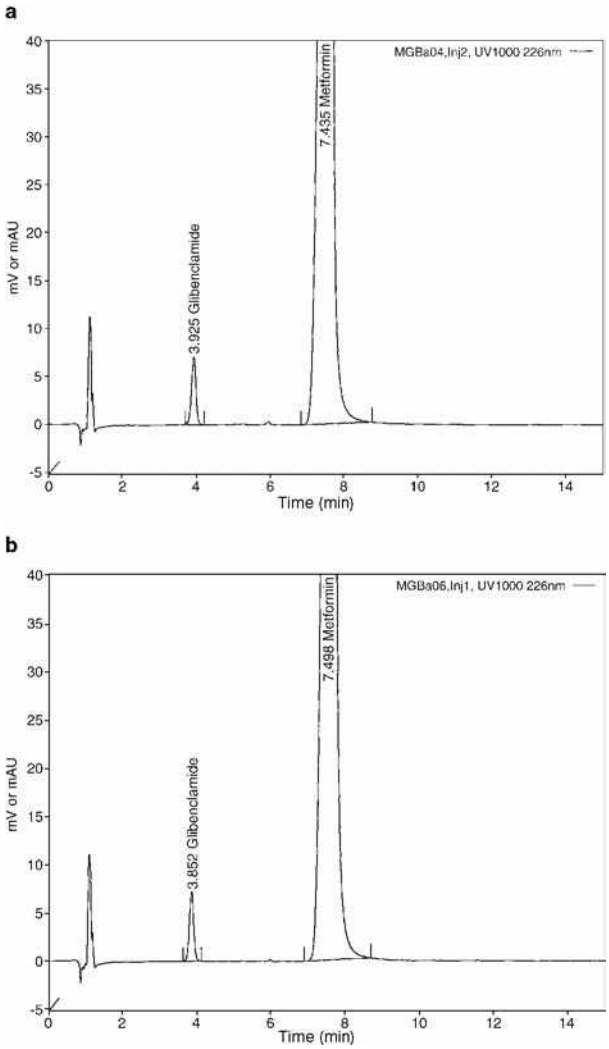

Fig. 1 a, A typical chromatogram of a mixed standard preparation; and b, A typical chromatogram of an assay preparation.

found to be an appropriate mobile phase, allowing adequate separation of active substances of the combined dosage form. Typical chromatograms obtained by using the aforementioned mobile phase, from 25 μl of the mixed standard preparation and assay preparation, are illustrated in Fig. 1A and B, respectively. The retention times of glibenclamide and metformin were 3.9 and 7.4 min, respectively.

Specificity

The specificity of the method was checked with a peak purity test of the assay preparation performed with a photodiode array detector. The peak purity values for metformin and glibenclamide were observed to be 995 and 999, respectively. The results of the peak purity analysis show that the peaks of the analytes were pure and that the formulation excipients did not interfere with the analyte peaks.

Linearity

Linearity of the method was tested from 25% to 150% of the targeted level of the assay concentration (100 μg/ml metformin HCl and 1.0 μg/ml glibenclamide) for the two analytes. The mixed standard solutions containing 25–150 μg/ml metformin HCl and 0.25–1.50 μg/ml glibenclamide were prepared from the standard stock solutions of metformin and glibenclamide. Linearity test solutions were injected and analyzed in triplicate. The calibration graphs were plotted by using peak areas of the analytes against the concentration of the drug (in micrograms per milliliter). In the simultaneous determination, the calibration graphs were found to be linear for both the analytes in the mentioned concentration ranges. The regression equations for metformin and glibenclamide were found to be $y = 74{,}383x + 22{,}660$ and $y = 60{,}424x - 150.79$, and the correlation coefficients for the regression lines were 1.0 and 0.9999, respectively.

Accuracy

The accuracy of the method was studied by recovery experiments. The recovery experiments were performed by adding known amounts of the drugs into a placebo. The recovery was performed at three levels (80%, 100%, and 120%) of the label claim per tablet (500 mg of metformin HCl and 5 mg of glibenclamide). Three samples were prepared for each recovery level. The recovery values for metformin HCl and glibenclamide ranged from 98.5% to 99.9% and from 99.3% to 101.2%, respectively (Table 1). The average recovery of three levels (nine determinations) for metformin HCl and glibenclamide were 99.2% and 100.0%, respectively.

Table 1 Results of the recovery tests for the drugs.

Level of addition (%)	Ingredient	Amount added (mg)	Amount recovered (%) (±SD)	Overall recovery (%) ($n = 9$)
80	Metformin HCl	400.0	99.8 (±0.08)	99.2 (±0.5)
	Glibenclamide	4.0	100.7 (±0.36)	100.0 (±0.6)
100	Metformin HCl	500.0	99.1 (±0.05)	
	Glibenclamide	5.0	99.6 (±0.08)	
120	Metformin HCl	600.0	98.7 (±0.17)	
	Glibenclamide	6.0	99.8 (±0.34)	

Table 2 Assay results of active ingredients in tablets.

Set	Ingredient	Label claim (mg)	Found (mg) (n = 6)	% Label claim (±SD)
Repeatability	Metformin HCl	500	498.0	99.6 (±1.6)
	Glibenclamide	5	5.12	102.3 (±1.6)
Intermediate	Metformin HCl	500	496.0	99.2 (±1.3)
Precision	Glibenclamide	5	5.07	101.3 (±1.5)

Precision

The precision (repeatability and intermediate precision) of the method was determined from one lot of the combined dosage form.

Repeatability

For repeatability of the method, six determinations of the concentrations of each ingredient in the tablets were performed. The results are shown in Table 2.

Intermediate Precision

Intermediate precision of the method was assessed by analyzing the samples six times on different days, by different chemists, by using different analytical columns of the same manufacture and different HPLC systems. The percentage assay was calculated using the area of the mixed standard preparation. The assay results are shown in Table 2.

Determination of the Limit of Detection and Limit of Quantitation

To determine the limit of detection (LOD) and the limit of quantitation (LOQ), the method based on the residual standard deviation of a regression line and slope was adopted. To determine the LOD and LOQ, a specific calibration curve was studied by using samples containing the analytes in the range of the detection limit and the quantitation limit. The limits of detection for metformin and glibenclamide were 0.013 and 0.007 μg/ml, respectively, and the limits of quantitation were 0.040 and 0.021 μg/ml, respectively.

Stability of Analytical Solutions

The stability of the analytical solutions was determined in terms of the assay of the drugs in the standard preparation and the assay preparation at room temperature. These solutions were analyzed at 0, 24, 48, and 72 hr against a freshly prepared standard at each time interval. The relative standard deviations for the assay values, determined up to 72 hr for metformin and glibenclamide in assay preparation and standard preparation, were 0.75% and 0.62%, respectively. The assay values were within ± 2% after 72 hr. The results indicate that the solutions were stable for 72 hr at room temperature.

Table 3 System suitability.

Analyte	RSD (%)	Tailing factor	Theoretical plates	Resolution
Metformin	0.61	1.04	9193	13.6
Glibenclamide	0.62	1.03	6395	

System Suitability

For system suitability studies, five replicate injections of mixed standard solutions were injected and parameters such as relative standard deviation of peak area, column efficiency, resolution, and tailing factors of the peaks were calculated. Results are shown in Table 3.

CONCLUSIONS

The described isocratic HPLC method is validated and shown to be precise and accurate. This method can be used in quality control departments for the simultaneous determination of metformin and glibenclamide in the combined dosage form.

ACKNOWLEDGMENTS

The authors are grateful to the Wockhardt Research Centre and to the Head of the Department of Chemical Technology, Dr. Babasaheb Ambedkar Marathwada University, Aurangabad, Maharashtra State, India, for providing the facilities for this research work.

REFERENCES

1. Indian Drugs Review (IDR); Sanjiv, M., Ed.; Mediworld Publications Pvt. Ltd.: New Delhi, 2003; Vol. *9* (4), 514.
2. Tosi, F.; Muggeo, M.; Brun, E.; Spiazzi, G.; Perobelli, L.; Zanolin, E.; Gori, M.; Coppini, A.; Moghetti, P. Combination treatment with metformin and glibenclamide versus single-drug therapies in type 2-diabetes mellitus: A randomized, double blind, comparative study. Metabolism **2003**, *52* (7), 862–867.
3. Indian Pharmacopoeia; The Controller of Publications: New Delhi, 1996.

4. British Pharmacopoeia; The Stationery Office: London, 1998.
5. The United States Pharmacopeia; U.S. Pharmacopeial Convention: Rockville, MD, 2002.
6. Vasudevan, M.; Ravi, J.; Ravisankar, S.; Suresh, B. Ion-pair liquid chromatography technique for the estimation of metformin in its multicomponent dosage forms. J. Pharm. Biomed. Anal. **2001**, *25*, 77–84.
7. Zarghi, A.; Foroutan, S.M.; Shafaati, A.; Khoddam, A. Rapid determination of metformin in human plasma using ion-pair HPLC. J. Pharm. Biomed. Anal. **2003**, *31* (1), 197–200.
8. Zhang, M.; Moore, G.A.; Lever, M.; Gardiner, S.J.; Kirkpatrick, C.M.; Begg, E.J. Rapid and simple high performance liquid chromatographic assay for the determination of metformin in human plasma and breast milk. J. Chromatogr. B Analyt. Technol. Biomed. Life Sci. **2002**, *766* (1), 175–179.
9. Cheng, C.L.; Chou, C.H. Determination of metformin in human plasma by high performance liquid chromatography with spectrophotometric detection. J. Chromatogr. B Biomed. Sci. Appl. **2001**, *762* (1), 51–58.
10. Bonfigli, A.R.; Manfrini, S.; Gregorio, F.; Testa, R.; De Sio, G.; Coppa, G. Determination of plasma metformin by a new cation exchange HPLC technique. Ther. Drug Monit. **1999**, *21* (3), 330–334.
11. Veterqvist, O.; Nabbie, F.; Swanson, B. Determination of metformin in plasma by high performance liquid chromatography after ultrafiltration. J. Chromatogr. B Biomed. Sci. Appl. **1998**, *716* (1–2), 299–304.
12. Han, F.M.; Cheng, Z.Y.; Chen, Y. Separation and determination of glibenclamide in xiaotangling tablets by micellar electrokinetic capillary chromatography. Se Puede **2000**, *18* (5), 456–458.
13. Niopas, I.; Daftsios, A.C. A validated high-performance liquid chromatographic method for the determination of glibenclamide in human plasma and its application to pharmacokinetic studies. J. Pharm. Biomed. Anal. **2002**, *28* (3–4), 653–657.
14. Khatri, J.; Qassim, S.; Abed, O.; Abraham, B.; Al-Lami, A.; Masood, S. A novel extractionless HPLC fluorescence method for the determination of glyburide in the human plasma: Application to a bioequivalence study. J. Pharm. Pharm. Sci. **2001**, *4* (2), 201–206.
15. Valdes Santurio, J.R.; Gonzalez Porto, E. Determination of glibenclamide in human plasma by solid-phase extraction and high-performance liquid chromatography. J. Chromatogr. B Biomed. Appl. **1996**, *682* (2), 364–370.
16. Khanolkar, D.H.; Shinde, V.M. RP/HPLC method for the estimation of glibenclamide and metformin HCl from combined dosage form. Indian Drugs **1999**, *36* (12), 739–742.

Microcystins: CE Determination

Dorota Szydlowska
Marek Trojanowicz
Department of Chemistry, Warsaw University, Warsaw, Poland

INTRODUCTION

Determination of microcystins (MC) has gained, in last two decades, a great interest because of the related ecological and public health risks. They are toxins which are produced and accumulated within the freshwater cyanobacterial algae during their blooming, and then enter the aquatic environment after cell lysis.[1–3] Over 70 different analogs of microcystins have been isolated from natural blooms and laboratory cultures of cyanobacteria.[4] Chemically, MC are cyclic heptapeptides, composed of five invariable and two variable amino acids (Scheme 1).

The general structure is cyclo(-D-Ala-L-X-D-erythro-β-methyliso Asp-L-Z-Adda-D-iso-Glu-*N*-methyldehydro Ala), where X and Z represent two variable L-amino acids, and Adda stands for 3-amino-9-methoxy-2,6,8-trimethyl-10-phenyldeca-4,6-dienoic acid. The main differences in variants are based on different variable amino acids in positions 2 and 4 of heptapeptide. Most commonly occurring MC contain leucine (L) and arginine (R) or tyrosine (Y), and their names are abbreviated as MC-LR, MC-RR, and MC-YR, respectively. Microcystins with different structure of Adda (in position 5), such as stereoisomers or 9-*O*-desmethyl-Adda, were also identified. Production of MC by cyanobacteria depends on different factors such as intensity and wavelength of light, temperature, pH, concentration of nutrients such as phosphorus and nitrogen. Their synthesis is an energy (ATP)-dependent process that can be also affected by the presence of some trace metals. Reported occurrences of most common MC in different environmental samples, where different MC are produced by different cyanobacteria are shown in Table 1.[5]

Among different toxins produced during the blooming of cyanobacteria, MC attracted the largest attention, as they have been involved in numerous intoxication cases with humans and domestic animals. They are hepatotoxins, and their related illness spreads through water contact and water consumption and through air. Besides their ability to cause acute poisonings, they can also promote cancer by chronic exposure of humans to low concentration of MC in drinking water. Microcystins are inhibitors of protein phosphatases from animals and higher plants, so they can act as tumor promoters. Regarding the water quality and the public health a maximum level of 1 ppb of MC-LR is recommended in drinking water.[6] Because of this serious health risk caused by these algal toxins, sensitive and specific analytical methods of determination are needed for warning and routine monitoring. At the present stage of development, besides high-performance separation methods discussed in detail here, mostly various type of bioassays are employed, including animal and plant bioassays, enzyme-linked immunosorbent assay (ELISA) using monoclonal or polyclonal antibodies radiometric or colorimetric and fluorimetric protein phosphatase inhibition assays.[7] The best detection limit was reported for inhibition-based enzyme assays, ELISA immunoassay, and high-performance liquid chromatography (HPLC) with fluorimetric and chemiluminescence detection.

HPLC OF MC

Because of the development of analytical methods for determination of MC, especially in last decade, the most widespread analytical techniques for their determination are commercialized; enzyme-linked immunosorbent assays and HPLC with diode array detectors of anion-exchange columns for this purpose were only sporadically reported with UV detection and isocratic[8,9] or gradient[10] elution. For anion-exchange stationary phase functionalized with diethylaminoethylene groups, better resolution for LR and YR was reported than for C18 columns.[8] For separation of cyanobacterial toxins, including MC-LR and -RR, hydrophilic interaction HPLC with gel Amide-80 column[11] and amide C16 column[12] providing comparable resolution to that of conventional reversed-phase C18 columns were applied.

Most commonly used HPLC protocols for the determination of MC rely on the use of high-resolution reversed-phase C18 columns, 15 or 25 cm of length, and 3 to 5μm particles to obtain sufficient resolution of MC. Both isocratic and gradient elution are equally employed, usually with addition of 0.05–0.1% trifluoroacetic acid (TFA), acting as pH modifier and ion-pairing reagent. For isocratic elution, eluents such as water with acetonitrile (ACN) containing TFA[13] or formic acid,[14] ammonium acetate with ACN,[15,16] and phosphate buffer with methanol[17] or ACN have been reported.[18] In gradient elution, most often gradient of ACN is employed,[12,19–22] and also the use of

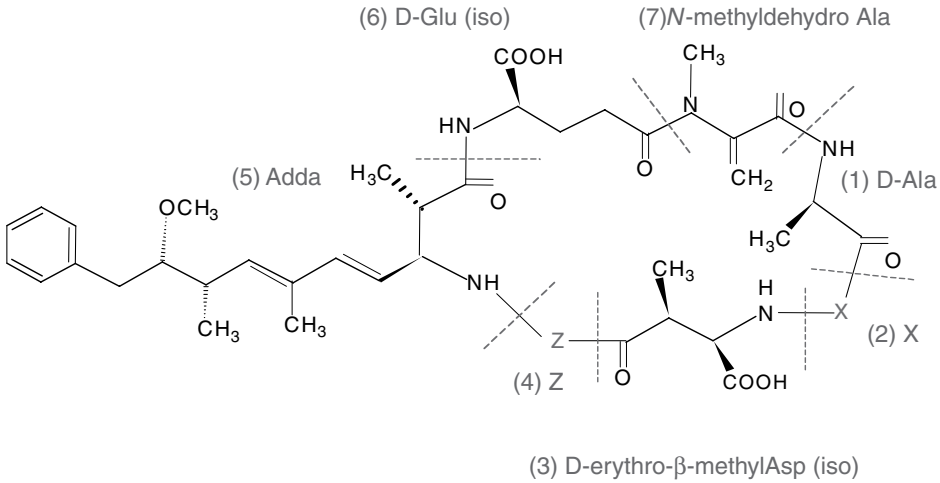

Scheme 1 General structure of microcystins.

methanol gradient was recently reported; however, for both conventional C18 column and monolithic silica C18 column the best combination of overall performance and high throughput was achieved with ACN gradient.[12] For HPLC separation of polar desmethyl MC and their main variants and also hydrophobic MC, several C18 columns and different eluents and elution modes have been compared[23] (see example recordings in Fig. 1).

Both commonly used elution methods with ammonium acetate/ACN and water/ACN with TFA were suitable for determination of MC, but performance of these methods was strongly dependent on the analytical column used. Addition of water to methanolic standard solutions of MC significantly increased the sensitivity of UV detection and resulted in better chromatography.

Besides various commercial, conventional reversed-phase C18 columns, including microbore columns for HPLC with mass spectrometry detection,[14,18,19] recently for determination of MC a monolithic silica C18 column has been employed.[12] The Chromolith column allowed a reduction in the time of analysis to 2.5 min at a flow-rate 4 ml/min compared to 45–60 min in commonly used chromatographic systems. The elution order of most MC was as predicted by the retention values of the variable amino acid residues. The observed higher limit of detection observed with UV detection with Chromolith column was attributed to the higher background noise resulting from an imperfect mixing of mobile phase components at high flow-rates. The best obtained combination of overall performance and rapid throughput with 2.5 min gradient of ACN is illustrated by chromatogram in Fig. 2.

The most commonly used detection for HPLC of MC is UV at 238 nm, usually performed with photodiode–array detectors,[12,17,18,21–23] which is also employed as reference method, e.g., for MC determination using a novel indirect competitive ELISA method[24] or for a time-resolved fluoroimmunometric assay.[20] The detection limit of MC in HPLC system without any preconcentration or clean-up is too high for practical applications (300–1000 ppb[12]). In the system with UV detection after sample clean-up employing immunoaffinity chromatography (IAP), for detection of main MC—RR, YR, LR, and LA—the limit of detection about 0.02 ppb was reported for determination in tap water.[21] The HPLC system with UV detection was also employed in studies on adsorption of MC-LR on surface of polymers and effect of methanol and ACN used in solutions of MC-LR on quantitative determination with UV detection.[22] The concentration of MC-LR measured by UV detection was found to be strongly affected by the content of mentioned solvents in solutions that was interpreted by changing availability of chromophores of MC-LR for detection by interaction in aqueous solutions.

The second most widely used detection in HPLC system for determination of MC is mass spectrometry, mostly used for the identification of MC, but also for their quantification. Since the middle of 1980s accurate mass measurements and tandem mass spectrometry (MS–MS) are employed to obtain empirical formulae and structural information. Applications of liquid chromatography with MS using frit-FAB ionization technique[25] and nebulizer-assisted electrospray (ion-spray)[26] were used for the identification of MC in cyanobacterial extracts. The tandem mass spectrometry combined with liquid chromatography was employed for analysis of purification MC with demonstration of the possibility of incorporating precursor-ion scans of *m/z* 135, a fragment of the Adda side chain into LC/MS–MS screening method.[27] Atmospheric pressure ionization in ion-spray mode was employed for the analysis of MC isolated from toxic strains of *Microcystis aeruginosa*.[19] The identity of suspected MC was confirmed by LC-tandem MS analysis with collisional activation achieved using argon target gas in the second quadrupole. The assignment of structures of fragment ions was confirmed by comparison of *m/z* values with those obtained from MS–MS spectra of ^{15}N labeled analogs, isolated after stable-isotope feeding experiments. Detailed list of assignment of fragment ions in product spectra of example MC,

Table 1 Occurrence of microcystins in different environmental samples.

Microcystin variant (MC-XZ)	Variable amino acid X	Variable amino acid Z	Cyanobacterial species	Different environmental samples		
				Aqueous samples	Animal tissue samples	Blue-green alga biomass samples
MC-LR	Leucine (L)	Arginine (R)	*Microcystis wesenbergii*, *Morelia viridis*, *M. aeruginosa*, *Anabaena flos-aquae bv. Radiocystis fernandoi*, *Oscillatoria*	Drinking water[17,24] Surface water[14,15,18,36,39]	Rat (liver) Mouse (liver) Fish (liver, kidney, blood, muscle)[21] Mussels (gills, muscle, digestive tract)[44] Crayfish (intestine, heptopancres)[43]	Field samples[11,13,21,23,31,35,39,45] Culture samples[10–12,14,19,20,22–24,30]
MC-RR	Arginine (R)	Arginine (R)	*M. aeruginosa*, *M. viridis*, *Anabaena*, *Oscillatoria*	Drinking water[17] Surface water[14,15,18,36]	Fish (liver blood, muscle)	Field samples[11,13,23,31,35,39,45] Culture samples[11,12,14,23,30]
MC-YR	Tyrosine (Y)	Arginine (R)	*M. aeruginosa*, *M. viridis, Oscillatoria*	Drinking water[17] Surface water[14,15,18]	Not identified	Field samples[14,45] Culture samples[12,13,19,30,31,39]
MC-LA	Leucine (L)	Alanine (A)	*M. aeruginosa*, *M. viridis*	Not identified	Not identified	Field samples[21] Culture samples
MC-LF	Leucine (L)	Phenylalanine (F)	*M. aeruginosa*	Not identified	Not identified	Field samples[45] Culture samples[12,19,23]
MC-LY	Leucine (L)	Tyrosine (Y)	*M. aeruginosa*	Not identified	Not identified	Field samples[45] Culture samples[12,19,23]

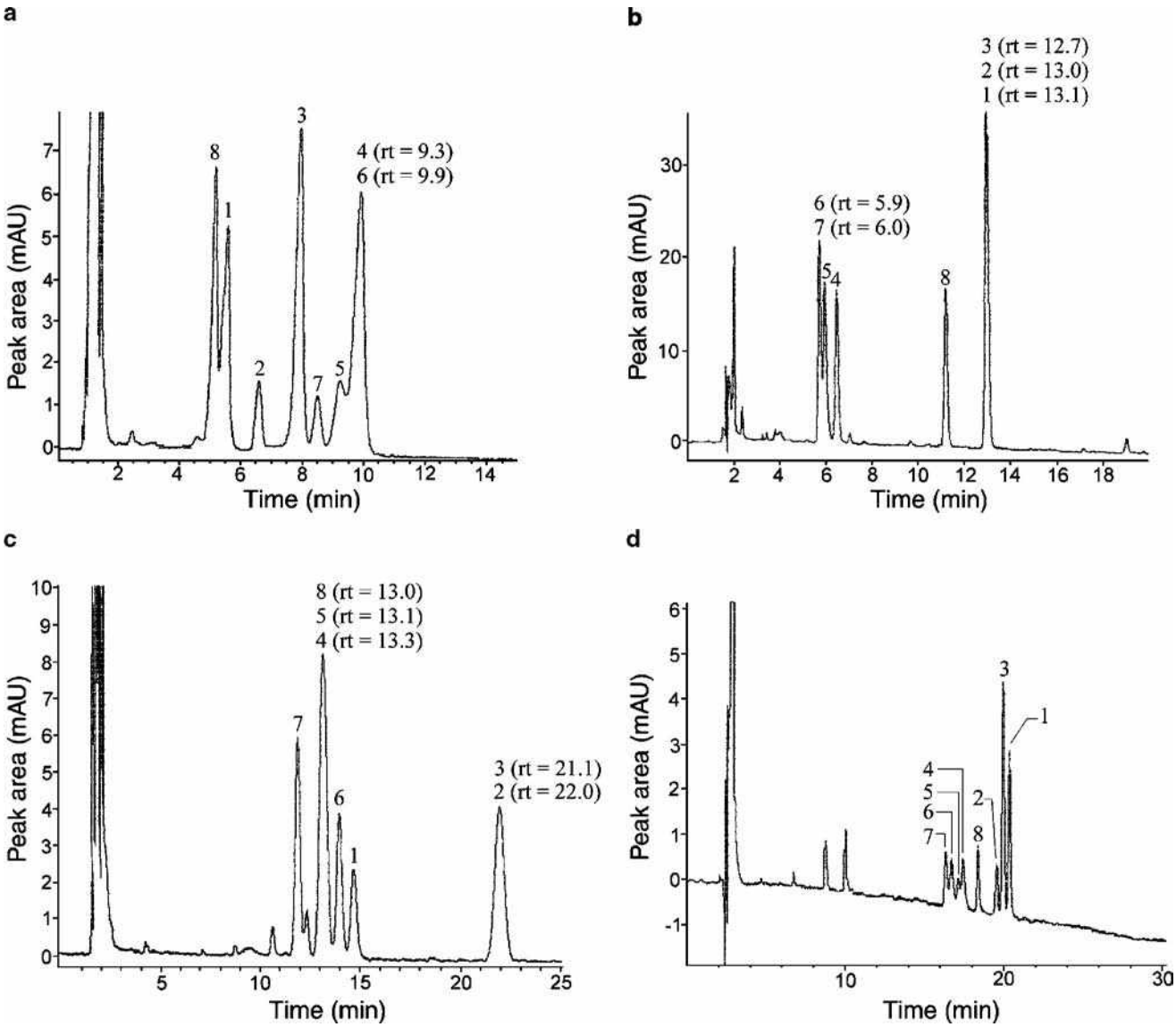

Fig. 1 Chromatograms obtained for mixture of microcystins using different commercial reversed-phase columns and different elution conditions.[23] (a) ODS Hypersil column 100 × 4.6 mm, elution with 10 m*M* ammonium acetate : acetonitrile (77 : 23) at 1 ml/min; (b) Zorbax Eclipse XDB-C18 250 × 3.0 mm, eluent as in A at 0.6 ml/min; (c) the same column as B, elution with 0.05% TFA : acetonitrile (70 : 30) at 0.6 ml/min and then programmed gradient of ACN, (d)-Lichrosper PAH 250 × 3.0 mm, elution as in C. Peaks assignment: 1-MC-LR, 2-[D-Asp^3]MC-LR, 3-[Dha^7]MC-LR, 4-MC-RR, 5-[D-Asp^3]MC-RR, 6-[Dha^7]MC-RR, 7-[D-Asp^3, Dha^7]MC-RR, 8-MC-YR.

namely for natural and ^{15}N enriched MC-LR and desmethyl MC-LR. Fragment ions in MS–MS of MC result mainly from consecutive cleavages of peptide bonds, hence they provide information concerning different peptide segments. A list of *m*/*z* values for characteristic fragment ions for six different MC is also provided. As shown in Table 2, the MS detection provides enhanced detection limit compared to UV detection without analyte preconcentration. Reported studies have shown evidence for two unknown MC-LW and -VF in extracts of *M. aeruginosa*, with Trp and Leu, and with Phe and Val, respectively. The comparison of chromatograms of extract obtained with non-specific UV detection at 214 nm, with detection at 238 nm corresponding to the chromophore of the unconjugated diene of the Adda, and total ion chromatogram obtained by LC–MS is shown in Fig. 3A where MC-LR can be observed as intense peak with retention time 17.4, whereas in Fig. 3B are shown mass spectra taken from LC–MS chromatogram shown in Fig. 3A.

The use of microbore columns in LC–MS system with positive electrospray ionization allowed enhanced sensitivity of MC determination.[14] In the system developed for determination of MC in water samples with 1 mm I.D. column and selected ion monitoring mode, and using sample preconcentration reported earlier on C18 cartridges,[28] detection limits for MC-LR, -RR, and -YR were reported

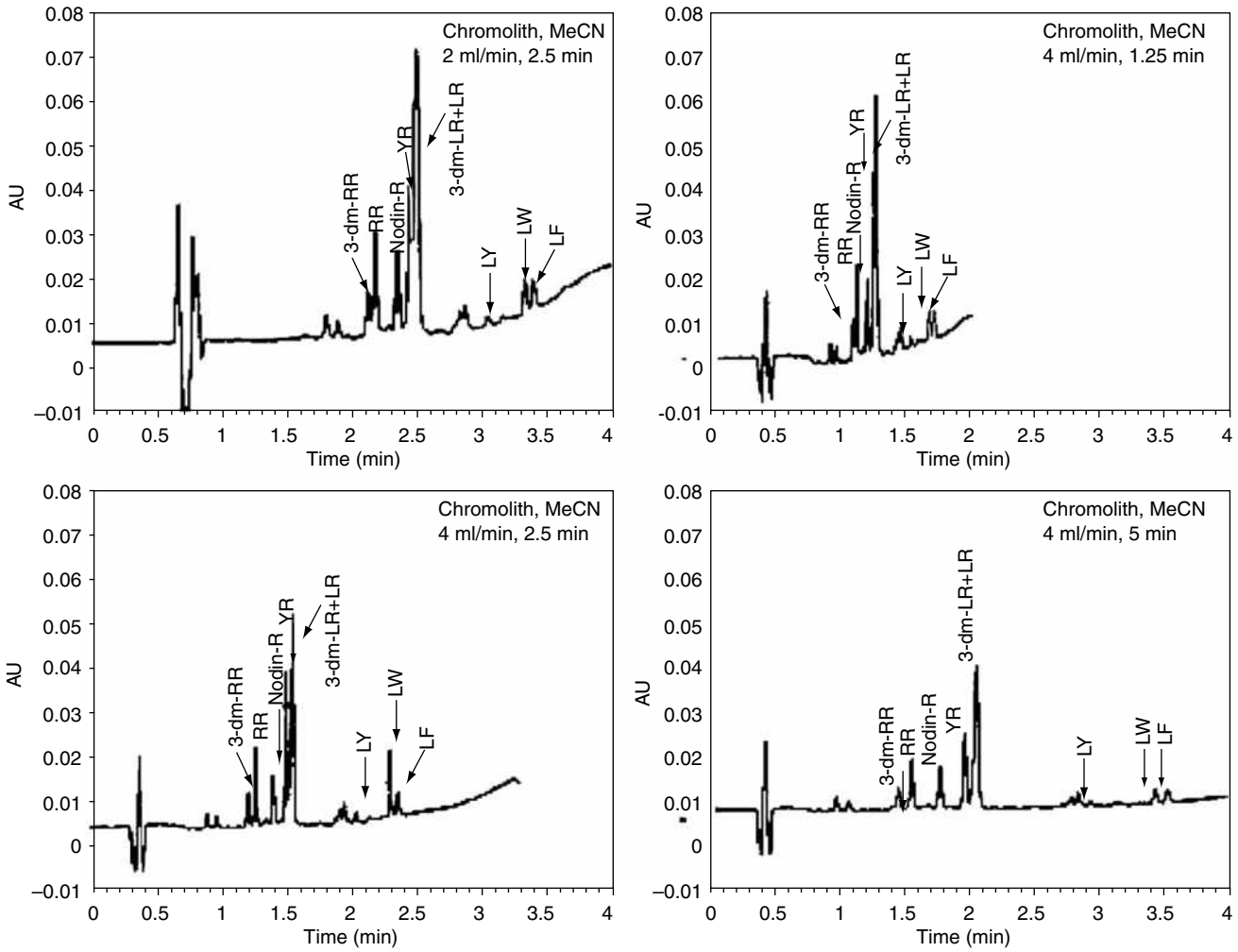

Fig. 2 Chromatograms obtained for mixture of MC with monolithic C18 column Chromolith with TFA-ACN phase (25–70% ACN) with flow rate 4 ml/min and length of gradient 2.5 min.[12] Detection at 238 nm.

in the range from 2 to 14 ppb. In examined natural water samples, MC-LR and -RR have been detected and determined in concentrations from 0.2 to 270 ppb. In LC–MS determination of MC in lake water samples, peaks of MC observed in HPLC with UV detection were successfully and reliably identified by excluding a few of non-MC peaks appearing even after the immunoaffinity purification.[18]

A similar detectability for dansyl-cysteine adducts of most common MC has been archived in HPLC system with peroxyoxalate chemiluminescence detection.[13] For this purpose dansyl-cysteine adducts of MC have to be produced off-line by nucleophilic addition of the thiol group in cysteine to the α,β-unsaturated carbonyl of the *N*-methyldehydroalanine moiety. High-performance liquid

Table 2 Limits of detection reported for determination of microcystins in HPLC systems with different detections.

Method of detection	Species detected	Limit of detection (μg/L)	Refs.
UV at 238 nm	Various	300–1000	[12]
	Various	0.02[a]	[21]
Mass spectrometry	MC-LR	50	[19]
	MC-LR	2[a]	[14]
	MC-RR	14[a]	[14]
	MC-YR	4[a]	[14]
Chemiluminescence	Dansyl-cysteine adducts of MC	<3	[13]
Electrochemical (amperometric)	MC-LR derivatized with Fe-C6-SH	360	[16]

[a]With preconcentration.

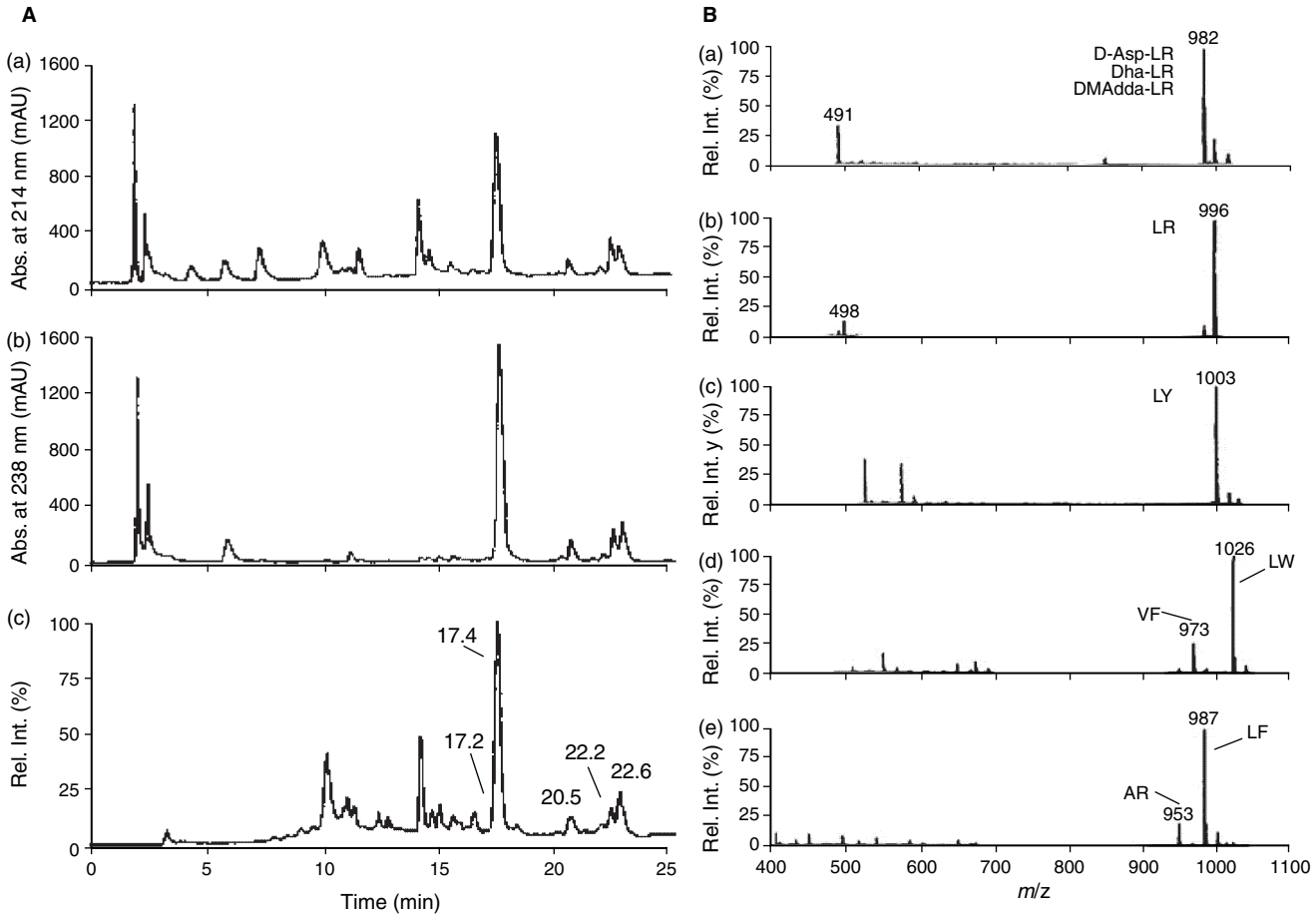

Fig. 3 A) Chromatograms of extract from *M. aeraginosa* at a) 214 nm, b) 238 nm, and c) with MS detection under full mass scan acquisition (*m/z* 400–1000).[19] B) Extracted mass spectra for peaks eluting at a) 17.2, b) 17.4, c) 20.5, d) 22.2, and e) 22.6 min corresponding to MC marked in spectra. Conditions: Vydac Z18TP52 column, linear gradient 10–60% aqueous acetonitrile (0.1% TFA), 0.2 ml/min flow-rate, injected 10 μl of methanolic extract.

chromatography determination is carried out in the system with two additional pumps for postcolumn addition of imidazole-nitrate buffer and peroxyoxalate reagent.

The electrochemical amperometric detection can be also applied in HPLC for determination of MC, LE, YR, and RR, and also to other species containing electroactive arginine, tyrosine, or tryptophan.[15] In the system with glassy carbon working electrode polarized at +1.2 V vs. Ag/AgCl determination can be carried out using ammonium acetate/ACN mobile phase, however, determinations in natural samples require effective way of sample pretreatment to lower the amounts of impurities. In another published approach, amperometric detection has been applied for determination of MC-LR off-line derivatized with redox-active 6-ferrocenylhexanethiol (Fe-CG-SH). The detection was carried out using a glassy carbon working electrode at +0.3 V vs. Ag/AgCl, and detection limit for determination of MC-LR was only 0.36 ppm.

Data listed in Table 2 indicate that any detection method used in HPLC can be used for determination of MC in sub-ppb level without preconcentration.

CAPILLARY ELECTROPHORESIS

Owing to its outstanding high-performance separation potential also capillary electrophoresis has been employed in different modes and with different detection methods for separation and determination of MC. Both capillary zone electrophoresis (CZE) and micellar electrokinetic chromatography (MEKC), which employs a surfactant above the critical micelle concentration to separate neutral and uncharged molecules based on electromigration principle, have been employed for determination of MC.[19,29–34]

In the simplest CZE system with UV detection as background electrolyte (BGE) a Tris buffer of pH 6 was employed with detection at 200 nm,[29] or with 40 m*M* acetate buffer at pH 4.0 and with detection at 238 nm.[30] The first conditions were employed for determination of MC in fractions from preparative HPLC with detection limit reported for MC-LR as 3 ppm.[29] For the same purpose also, the second-mentioned conditions were suitable, showing impurity of [D-dsp^3]MC-LR in MC-LR samples.[30] Capillary zone electrophoresis with UV detection

can be also carried out with capillaries coated with 5% hexadimethrine bromide and 2% ethylene glycol using as BGE 1 *M* formic acid.[19] To improve detectability of CZE determination of MC, a laser-induced fluorescence (LIF) detection was employed with two-step derivatization process carried out off-line prior to the sample injection into measuring system.[33] In the first step MC were converted into cysteine conjugates, and then labeled with fluorophore fluorescein 5-isothiocyanate. Capillary zone electrophoresis separation was carried with 25 m*M* borate of pH 9.0 as BGE. The electropherograms of derivatized three MC with LIF detection are shown in Fig. 4 together with response observed for mixture of MC.

Especially outstanding separation of 10 MC variants has been reported in MEKC mode of capillary electrophoresis with UV detection.[30] This is preferable method for electrophoretic determination of MC as their separation can be impeded by adsorption of analytes onto the capillary wall, hence separation conditions in basic media with micelles should prevent such interaction. As BGE for such separation 40 m*M* β-(cyclohexylamino)-1-propanesulfonate buffer of pH 10.6, containing acetate and 15 m*M* sodium dodecyl sulfate (SDS), was used and UV detection was carried out at 238 nm. The electropherogram obtained for a mixture of MC isolated with a preparative HPLC from cyanobacterial *Anabaena* 90 strains is shown in Fig. 5.

The identification of the isolated MC was made with an off-line electrospray mass spectrometry. The reported detection limits for MC-LR were 10 ppb with MEKC mode and 1 ppm in CZE mode in both cases at 238 nm. The MEKC measurements with UV detection were also carried out with borate buffer containing SDS and satisfactory separation of MC-LR, -YR, and -RR was reported within 6 min.[32] The migration window can be enlarged about 30% in the presence of 5% ACN or 10% methanol in BGE. The limit of detection for MC-LR in optimized condition was reported as 0.12 ppb without any preconcentration step and UV detection at 230 nm. In similar MEKC system using borate buffer with SDS, a base-line separation of the same MC was reported within 13 min.[31] In the same work CE–MS hyphenated system with formic acid BGE was additionally employed for confirmatory purposes in analysis of extracts of blue-green algae after immunoaffinity chromatography (IAC) clean-up.

The separation conditions mentioned above for CZE with dynamically coated capillaries UV detection and formic acid were also compatible with the operative of electrospray ionization in CE–MS system and CE–MS–MS analyses.[19] It was shown that an essential advantage of CE–MS over LC–MS was the possibility of separation and identification of three desmethyl isomers of MC-LR differing in the Adda, Masp, and Mdha residues.

Preconcentration of MC and Clean-Up of Analyzed Samples

There are two main areas where analytical determination of MC is needed and employed. One of them is identification and quantitation for preparatory purposes in extracts from laboratory-cultivated cyanobacteria. Another one is their determination in environmental samples. Depending on concentration level of MC in analyzed samples various methods of isolation (extraction), preconcentration or

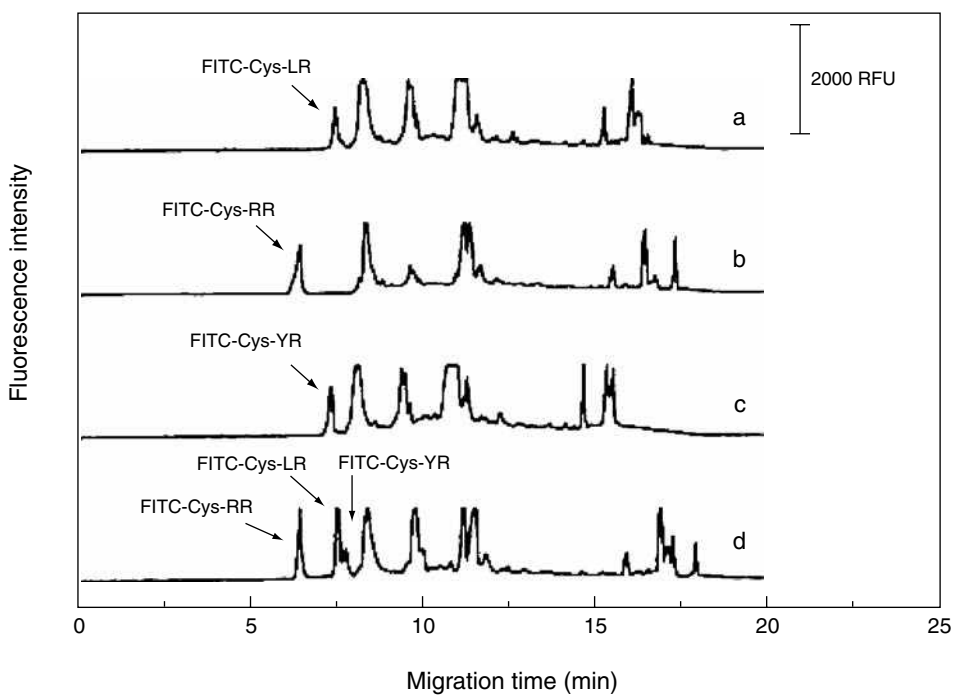

Fig. 4 Electropherograms obtained with LIF detection for MC conjugated with cysteine and derivatized with FITC.[33] Signals for derivatized MC marked in the figure. Capillary 47 cm × 75 μm, separation voltage 15 kV, BGE: 25 m*M* borate pH 9.0.

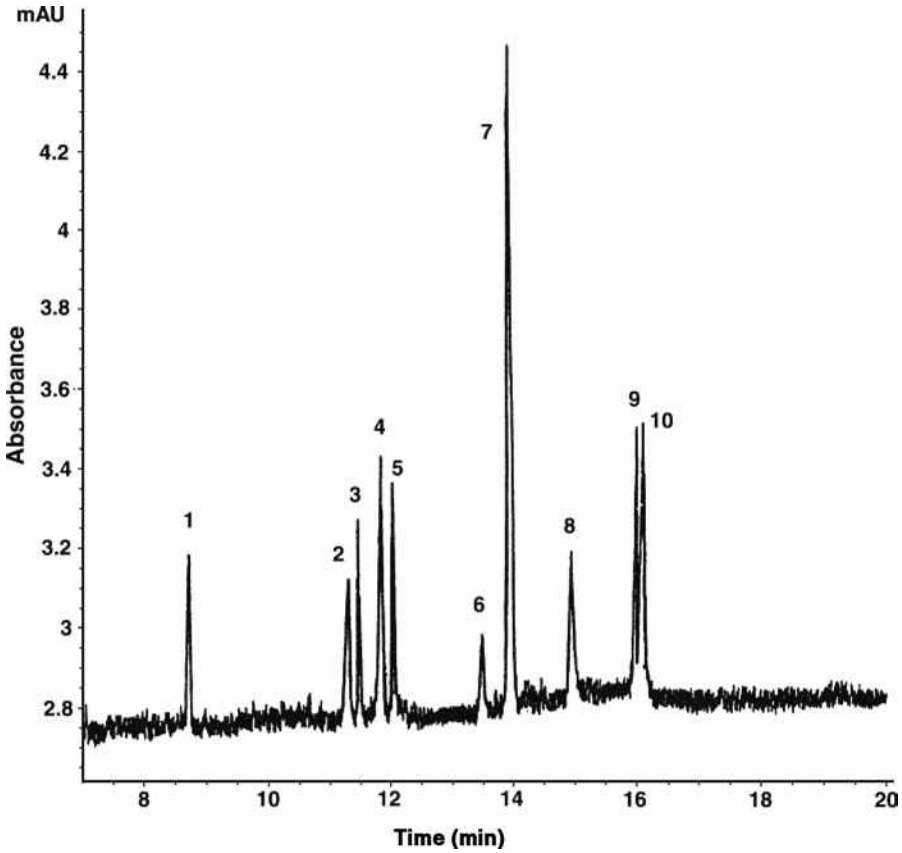

Fig. 5 Electropherogram for MC mixture obtained with MEKC mode using 40 m*M* CAPS buffer with 15 m*M* SDS at pH 10.6 as BGE[30] with UV detection at 238 nm. Peaks assignment: 1-[D-Asp^3, Dha^7]MC-LR, 2-MC-LR, 3-MC-YR, 4-[Dha^7]MC-LR, 5-MC-RR, 6-[Dha^7]MC-RR, 7-[D-Asp3, Dha^7]MC-RR, 8-[D-Asp3]MC-LR, 9-[D-Asp3]MC-RR, 10-MC-YA.

clean-up of analyzed samples can be employed and they have been already quite widely examined. Many of them have been applied in analytical procedures involving at the end the determination with HPLC or capillary electrophoresis with various detection, which were already discussed.

The most commonly used method for extraction and preconcentration of uncharged organic species is solid-phase extraction (SPE) on non-polar sorbents such as silica or polymers functionalized with octadecyl groups C18. On such sorbents MC were extracted from aqueous solutions and then eluted with methanol.[14,19,28,33] For the same purpose also a commercially available C18 disks were used with elution of extracted MC with methanol containing 0.1% TFA.[31] In some cases, a poor recovery of extracted MC from C18 sorbents has been reported, hence it was replaced by Waters Oasis HLB sorbent that can be used both for non-polar and polar analytes.[23] A more polar AccuBond cyano sorbent has been also successfully employed for extraction of MC with elution of preconcentration species with 70% ACN, which was reported to be more efficient than octadecylsilica (ODS) sorbents.[35] Ion-exchange cellulose sorbent functionalized with diethylaminoethyl groups was also applied for this purpose.[10] In a secondary clean-up process after initial clean-up with ODS cartridges, sorbents of various polarity have been reported.[36]

A solventless technique of solid-phase microextraction (SPME) has been also employed for HPLC determination of MC in a natural *Microcystins* sp. bloom in a freshwater, where three dominant MC variants MC-LR, -YR, and -RR were quantified.[37] For this purpose a measuring system with commercial SPME–HPLC interface was employed. Microcystins were sorbed from acidified solutions using SPME fibers with carbowax/templated resin and polydimethylsiloxane/divinylbenzene coating and desorbed at dynamic mode with HPLC eluent, which was used in isocratic elution mode and consisted of water and methanol with 0.05% TFA. For each toxin partition equilibrium was achieved within 60 min and example response obtained in SPME–HPLC system is shown in Fig. 6. The detection limits for all examined MC for 5 ml samples were reported at about 7 ppb.

A more selective extraction of MC from environmental samples or extracts from cyanobacteria can be achieved using IAC, with the use of solid sorbents with immobilized anti-MC antibodies. For this purpose both polyclonal anti-MC-LR antibody can be used[21,24,38,39] exhibiting cross-reactivity to other MC or also monoclonal antibodies.[17,18] Antibodies are immobilized on various supports such as activated silica gel, functionalized Sepharose, or less common ones such as Affi-Gel 10[17] or Formyl-Cellulofione.[18] Some of these immunoaffinity sorbents are also commercially available.[38,39] The preconcentration and clean-up

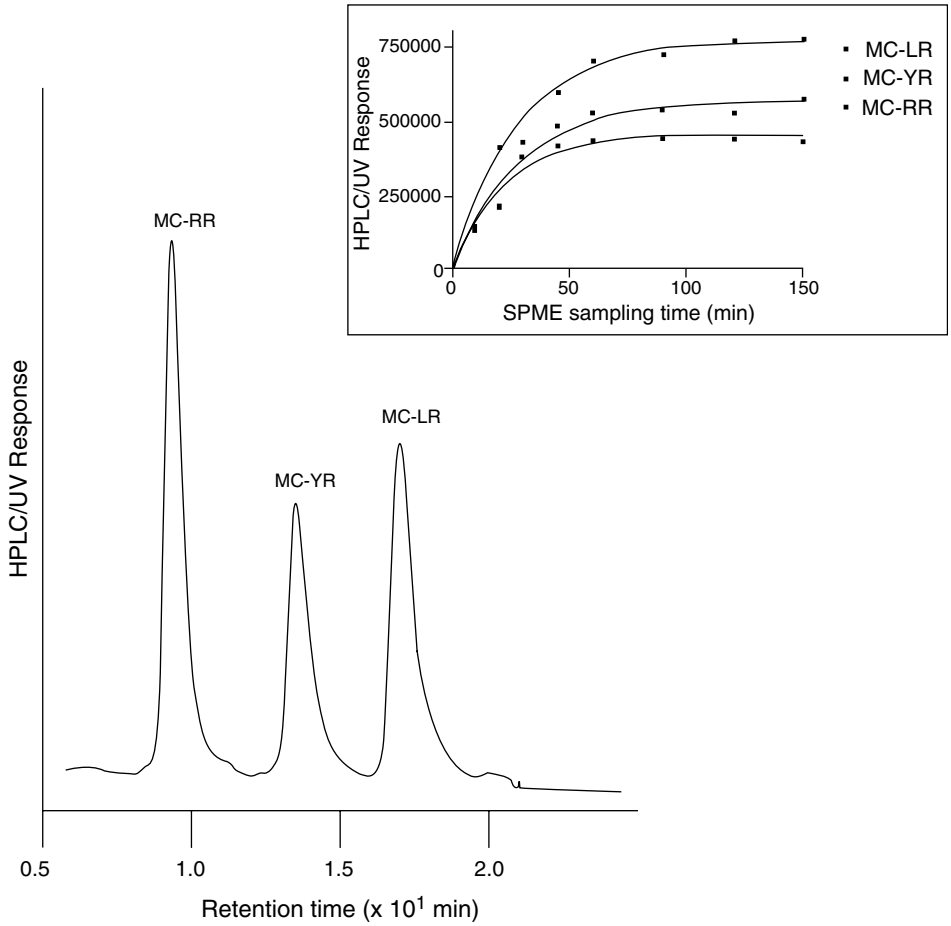

Fig. 6 Chromatogram of mixture of MC (0.6 μg each in 5 ml freshwater) obtained in HPLC system interfaced with solid-phase microextraction.[37] Absorption–time profiles of MC are shown in inset.

with IAC columns are mostly employed for determination of trace amounts of MC in natural waters, but also for extracts from cyanobacterial samples[21,24,39] and fish tissues.[21] The preconcentration is carried out from aqueous solutions, while for elution mostly methanol is used, without or with small content of water and acetic acid. For antibodies coupled to activated immunoaffinity support Formyl-Cellulfine, the elution of retained MC with 100% dimethylformamide was employed.[18] Reversability of IAC columns was reported from up to three times[18] to 43 extractions claimed for commercial silica-based ImmunoSep column.[38] The detection limits for water samples in procedures involving preconcentration and clean-up on IAP columns depend on numerous factors such as, e.g., initial sample volume or capacity of sorbent, and they were reported to be in the range from 0.002[39] to 0.05 ppb.[38]

The efficiency of sample clean-up of IAC columns in determination of MC has been compared by several authors to conventional SPE sorbents.[17,38,39] For clean-up of tap water samples, the use of C18 sorbent did not remove numerous coconcentrated impurities that make identification of MC signals more difficult.[17,39] The functioning of two different IAC columns, silica-based and Sepharose-based ones, has been compared to that of hydrophilic–lipophilic balanced Waters Oasis HPLC extraction cartridge, which contains a porous polymer sorbent consisting of a poly(divinylbenzene-co-*N*-vinylpyrrolidone) skeleton.[38] Chromatograms recorded for the same water samples using extraction with mentioned sorbents are shown in Fig. 7.

In quantitative analysis, results were similar for those of the Oasis HLB cartridge and Sepharose-based IAC. Results for silica-based IAC were lower, particularly for the less polar MC such as LA, WR, and AK. Good recovery was reported for Oasis HLB cartridge when several different sorbents for SPE have been compared.[23] Detection limits for IAC systems were about 0.5 ppb, while for system with SPE 0.1 ppb.

Determination of MC in cyanobacteria, algae, or tissues requires the optimization of additional step in analytical procedure—liquid extraction from these materials. In analysis of cyanobacterial cells, they are most often lyophilized and then extracted with 75% methanol[31,39] or with 80% ACN with addition of formic acid.[11] Double extraction with 75% methanol was also employed for homogenates of algae and fish tissue.[21] In another procedure, extraction of cells with 25% methanol[19] or 5% acetic acid[10] is assisted by sonication. The use of acetic acid instead of methanol is advantageous because of more

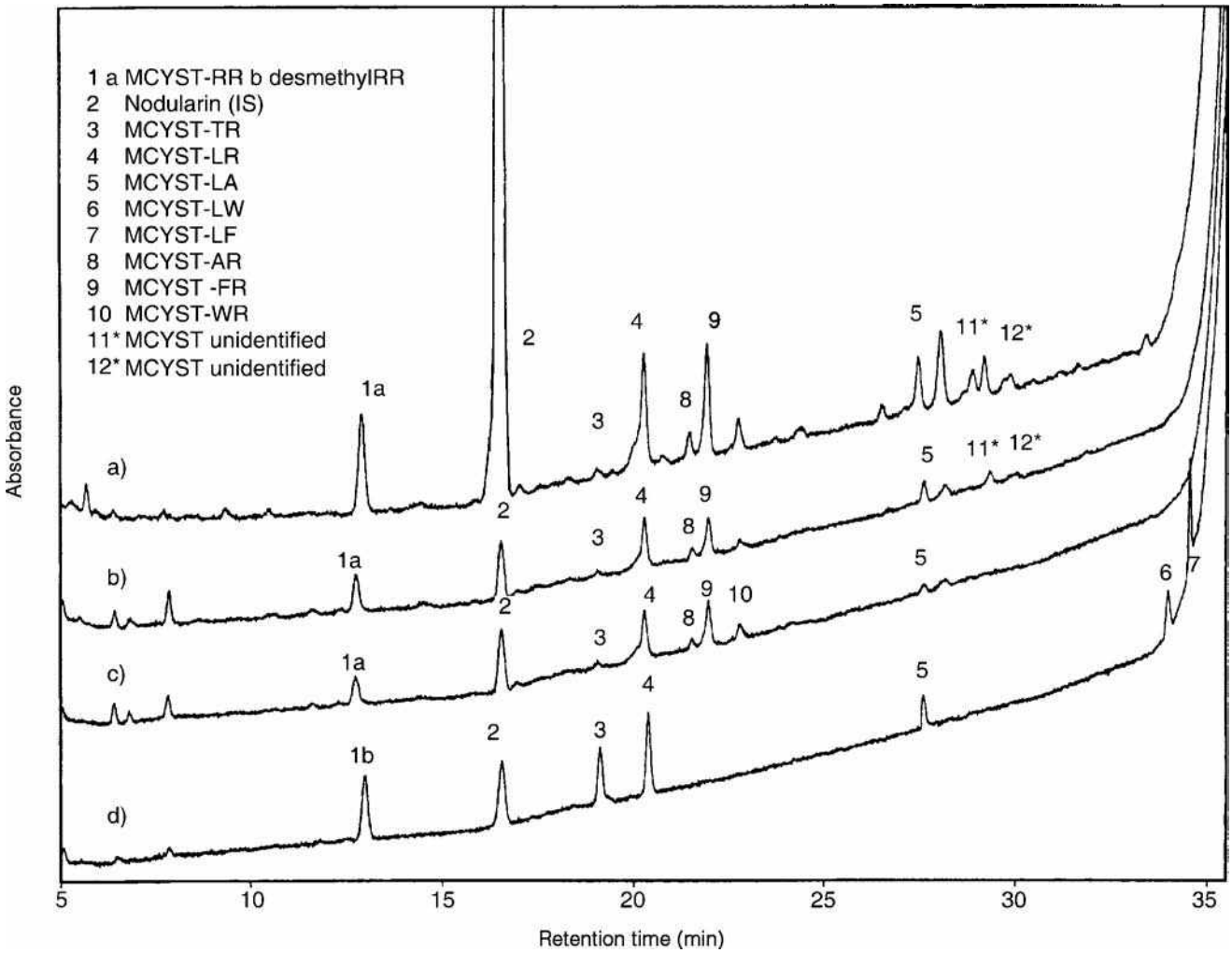

Fig. 7 Chromatograms obtained for water sample a–c) and standard mixture of MC d) in HPLC system with UV detection at 238 mm.[38] Chromatograms for water obtained using extraction with different sorbents: a) SPE with Waters Oasis HLB (50 × concentrated), b) with Sepharose-based immunoaffinity column (10 × concentrated), and c) with silica-based immunoaffinity column (10 × concentrated).

efficient elimination of proteins and possibility of direct use of extracts for preconcentration on C18 sorbents. With methanol solutions, however, a better extraction yield has been reported. In some procedures, aqueous methanol solutions were used for extraction with some content of *n*-butanol. Often methanolic extracts are preconcentrated by evaporation prior to the clean-up with SPE or IAC columns. It has been also observed that long sonication in plastic tubes gives some decrease in extraction yield, hence twice freezing at –20°C and then triple extraction with 5% acetic acid was recommended.[10]

A thorough comparison of sample pretreatment for determination of MC in cyanobacteria cells was reported recently by Rapala et al.[23]. Freezing and thawing (two or three times) and sonication in a water bath were compared for extraction of MC from cells in the water samples, and both were found ineffective. Extraction from water samples by disrupting the cells using a probe sonicator without addition of organic solvents was found to be effective for MC studied, including the hydrophobic variants. During pretreatment procedure the contact of samples with propylene should be avoided because of adsorption of MC on its surface, resulting in loss of analytes compared to the use of glass vessels.

CONCLUSIONS

Numerous HPLC and capillary electrophoresis methods for separation and determination of MC have been developed with various detection. They cannot be used, however, directly for trace determination of MC in natural waters without additional preconcentration and sample clean-up steps. The most promising in lowering the detection limits seem to be HPLC and CE methods with luminescence methods of detection, but further studies on

improvement of derivatization procedures are needed. Hyphenation of HPLC and CE instrumentation with MS or tandem MS setups are methods of choice for identification of MC variants in various samples.

The most effective method of preconcentration and clean-up of samples in determination of MC is IAP; however, sorbents with immobilized antibodies have limited repetitive use and they are expensive for routine monitoring. In some cases they can be replaced by SPE sorbents, but especially promising seems to be the use of imprinted polymers developed for selective binding of MC molecules.[40] With a comparable selectivity to antibodies they should exhibit longer life-time for repetitive use.

For high-performance separation methods suffering of insufficient detectability in determination of MC in environmental samples for routine applications the most effective is preconcentration on immunosorbents. The new advantageous competitors in this field might be enzymatic assays and biosensors based on inhibition of protein phosphatase activity by MC. Some successful attempts in this field have been reported recently as colorimetric assays or electrochemical biosensors.[41,42]

REFERENCES

1. Skulberg, O.M.; Carmichael, W.W.; Codd, G.A.; Skulberg, R. *Algal Toxins in Seafood and Drinking Water*; Falconer, I., Ed.; Academic Press: London, 1993; 145–164.
2. Codd, G.A. Cyanobacterial toxins: occurrence, properties and biological significance. Water Sci. Technol. **1995**, *32*, 149–156.
3. *Toxic Microcystins*; Watanabe, M.F. Harada, K.I., Carmichael, W.W., Eds.; CRC Press: Boca Raton, 1996.
4. Utkilen, H.; Gjolme, N. Iron-stimulated toxin production in *Microcystis aeruginosa*. Appl. Environ. Microbiol. **1995**, *61*, 797–800.
5. de Figueiredo, D.R.; Azeiteiro, U.M.; Esteves, S.M.; Goncalves, F.J.M.; Pereira, M.J. Microcystin-producing blooms—a serous global public health issue. Ecotoxicol. Environ. Saf. **2004**, *59*, 151–163.
6. World Health Organization. Guidelines for Drinking-Water Quality, 2nd Ed.; Geneva, 1998; Addendum to Vol. 1.
7. Lam, P.K.S.; Yang, M.; Lam, M.H.W. Toxicology and evaluation of microcystins. Therapeut. Drug Monitoring **2000**, *22*, 69–72.
8. Gathercole, P.S.; Thiel, P.G. Liquid chromatographic determination of the cyanoginosis, toxins produced by the cyanobacterium *Microcystis aeruginosa*. J. Chromatogr. A, **1987**, *408*, 435–440.
9. Watanabe, M.M.; Kaya, K.; Takamura, N. Fate of toxic cyclic heptapeptides, the microcystins from blooms of *Microcystis* (cyanobacteria) in a hypertrophic lake. J. Phycol. **1992**, *28*, 761–767.
10. Kos, P.; Gorzo, G.; Suranyi, G.; Borbely, G. Simple and efficient method for isolation and measurement of cyanobacterial hepatotoxins by plant tests (*Sinapis alba* L.). Anal. Biochem. **1995**, *225*, 49–53.
11. Dell-Aversano, C.; Eaglesham, G.K.; Quilliam, M.A. Analysis of cyanobacterial toxins by hydrophilic interaction liquid chromatography—mass spectrometry. J. Chromatogr. A, **2004**, *1028*, 155–164.
12. Spoof, L.; Meriluoto, J. Rapid separation of microcystins and nodularin using a monolithic silica C18 column. J. Chromatogr. A, **2002**, *947*, 237–245.
13. Murata, H.; Shoji, H.; Oshikata, M.; Harada, K.I.; Suzuki, M.; Kondo, F.; Gota, H. High-performance liquid chromatography with chemiluminescence detection of derivatization microcystins. J. Chromatogr. A, **1995**, *693*, 263–270.
14. Baraco, M.; Rivera, J.; Caixach, J. Analysis of cyanobacterial hepatotoxins in water samples by microbore reversed-phase liquid chromatography-electrospray ionization mass spectrometry. J. Chromatogr. A, **2002**, *959*, 103–111.
15. Meriluoto, J.; Kincaid, B.; Smyth, M.R.; Wasberg, M. Electrochemical detection of microcystins, cyanobacterial peptide hepatotoxins, following high-performance liquid chromatography. J. Chromatogr. A, **1998**, *810*, 226–230.
16. Lo, K.K.; Ng, D.C.; Lau, J.S.; Wu, R.S.; Lam, P.K. Derivatisation of microcystin with a redox-active label for high-performance liquid chromatography/electrochemical detection. New J. Chem. **2003**, *27*, 274–279.
17. Tsutsumi, T.; Nagata, S.; Hasegawa, A.; Ueno, Y. Immunoaffinity as clean-up tool for determination of trace amounts of microcystins in tap water. Food Chem. Toxicol. **2000**, *38*, 593–597.
18. Kondo, F.; Ito, Y.; Oka, H.; Yamada, S.; Tsuji, K.; Imokawa, M.; Niimi, Y.; Harada, K.; Ueno, Y.; Miyazaki, Y. Determination of microcystin in lake water using reusable immunoaffinity column. Toxicon **2002**, *40*, 893–899.
19. Bateman, K.P.; Thibault, P.; Douglas, D.J.; White, R.L. Mass spectral analyses of microcystin from toxic cyanobacterial using on-line chromatographic and electrophoretic separations. J. Chromatogr. A, **1995**, *712*, 253–268.
20. Mehto, P.; Ankelo, M.; Hinkkanen, A.; Mikhailor, A.; Eriksson, J.E.; Spoof, L.; Meriluoto, J. A time-resolved fluoroimmunometric assay for the detection of microcystins, cyanobacterial peptide hepatotoxins. Toxicon **2001**, *39*, 831–836.
21. Lawrence, J.F.; Menard, C. Determination of microcystins in blue-green algae, fish and water using liquid chromatography with ultraviolet detection after sample clean-up employing immunoaffinity chromatography. J. Chromatogr. A, **2001**, *922*, 111–117.
22. Hyenstrand, P.; Metcalf, J.S.; Beattie, K.A.; Codd, G.A. Effects of adsorption to plastic and solvent conditions in the analysis of the cyanobacterial toxin microcystin-LR by high performance liquid chromatography. Wat. Res. **2001**, *35*, 3508–3511.
23. Rapala, J.; Erkomaa, K.; Kukonen, J.; Sivonen, K.; Lahti, K. Detection of microcystins with protein phosphatase inhibition assay, high-performance liquid chromatography-UV detection and enzyme-linked immunosorbent assay. Comparison of methods. Anal. Chim. Acta **2002**, *466*, 213–231.
24. Metcalf, J.S.; Bell, S.G.; Codd, G.A. Production of novel polyclonal antibodies against the cyanobacterial toxin microcystin-LR and their application for the detection and quantification of microcystins and nodularin. Wat. Res. **2000**, *34*, 2761–2769.
25. Kondo, F.; Ukai, Y.; Oka, H.; Ishikawa, N.; Watariabe, M.F.; Watanabe, M.; Harada, K.; Suzuki, M. Separation

and identification of microcystins in cyanobacteria by frit-fast atom bombardment liquid chromatography/mass spectrometry. Toxicon **1992**, *30*, 227–237.
26. Poon, G.K.; Griggs, L.J.; Edwards, C.; Beattie, K.A.; Codd, G.A. Liquid chromatography-electrospray ionization mass spectroscopy of cyanobacterial toxins. J. Chromatogr. **1993**, *628*, 215–233.
27. Edwards, C.; Lawton, L.A.; Beattie, K.A.; Codd, G.A.; Pleasance, S.; Dear, G.J. Analysis of microcystins from cyanobacteria by liquid chromatography with mass spectroscopy using atomospheric-pressure ionization. Rapid Commun. Mass Spectrom. **1993**, *7*, 714–721.
28. Lawton, L.A.; Edwards, C.; Codd, G.A. Extraction and high-performance liquid chromatographic method for the determination of microcystins in raw and treated waters. Analyst **1994**, *119*, 1525–1530.
29. Boland, M.P.; Smillie, M.A.; Chen, D.Z.X.; Holmes, C.F.B. A unified bioscreen for the detection of diarrhetic shellfish toxins and microcystins in marine and freshwater environments. Toxicon **1993**, *31*, 1393–1405.
30. Siren, H.; Jussila, M.; Liu, H.; Peltoniemi, S.; Sivonen, K.; Riekkola, M.L. Separation, purity testing and identification of cyanobacterial hepatotoxins with capillary electrophoresis and electrospray mass spectrometry. J. Chromatogr. A, **1999**, *839*, 203–215.
31. Gago-Martinez, A.; Pineiro, N.; Aguette, E.C.; Vaquero, E.; Nogueiras, M.; Leao, J.M.; Rodriguez-Vazques, J.A.; Dabek-Zlotorzynska, E. Further improvements in the application of high-performance liquid chromatography, capillary electrophoresis and capillary electrochromatography to the analysis of algal toxins in the aquatic environment. J. Chromatogr. A, **2003**, *992*, 159–168.
32. Onyewuenyi, N.; Hawkins, P. Separation of toxic peptides (microcystins) in capillary electrophoresis, with the aid of organic mobile phase modifiers. J. Chromatogr. A, **1996**, *749*, 271–277.
33. Li, P.C.H.; Hu, S.; Lam, P.K.S. Development of a capillary zone electrophoretic method for the rapid separation and detection of hepatotoxic microcystins. Marine Poll. Bull. **1999**, *39*, 250–254.
34. Vasas, G.; Gaspar, A.; Pager, C.; Suraryi, G.; Mathe, C.; Hamras, M.; Borbely, B. Analysis of cyanobacterial toxins (anatoxin-a, cylindrospermopsin, microcystin-LR) by capillary electrophoresis. Electrophoresis **2004**, *25*, 108–115.
35. Pyo, D.; Shin, H. Extraction and analysis of microcystins RR and LR in cyanobacteria using a cyano cartridge. J. Biochem. Biophys. Meth. **2002**, *51*, 103–109.
36. Tsuji, K.; Naito, S.; Kondo, F.; Watanabe, M.F.; Suzuki, S.; Nakazawa, H.; Suzuki, M.; Shimada, T.; Harada, K. A clean-up method for analysis of trace amounts of microcystins in lake water. Toxicon **1994**, *32*, 1251–1259.
37. Poon, K.F.; Lam, M.H.W.; Lam, P.K.S.; Wong, B.S.F. Determination of microcystins in cyanobacterial blooms by solid-phase microextraction-high-performance liquid chromatography. Environ. Toxicol. Chem. **2001**, *20*, 1648–1655.
38. Aranda-Rodriguez, R.; Kubwabo, C.; Benoit, F.M. Extraction of 15 microcystins and nodularin using immunoaffinity columns. Toxicon **2003**, *42*, 587–599.
39. Aguete, E.C.; Gago-Martinez, A.; Leao, J.M.; Rodriguez-Vazquez, J.A.; Menard, C.; Lawrence, J.F. HPLC and HPCE analysis of microcystins RR, LR and YR present in cyanobacteria and water by using immunoaffinity extraction. Talanta **2003**, *59*, 697–705.
40. Chianella, I.; Lotierzo, M.; Piletsky, S.A.; Tothill, I.E.; Chen, B.; Karim, K.; Turner, A.P.F. Rational design of a polymer specific for microcystin-LR using a computational approach. Anal. Chem. **2002**, *74*, 1288–1293.
41. Robillot, C.; Hennion, M.-C. Issues arising when interpreting the results of the protein phosphatase 2A inhibition assay for the monitoring of microcystins. Anal. Chim. Acta **2004**, *512*, 339–346.
42. Campas, M.; Szydłowska, D.; Trojanowicz, M.; Marty, J.L. Towards the protein phosphatase-based biosensor for microcystins detection. Biosens. Bioelectron. **2005**, *20*, 1520–1530.
43. Vasconcelos, V.; Oliveira, S.; Teles, F.O. Impact of a toxic and a non-toxic strain of *Microcystins aeruginosa* on the crayfish *Procambarus* clarkii. Toxicon **2001**, *39*, 1461–1470.
44. Vasconcelos, V.M. Uptake and depuration of the heptapeptide toxin microcystin-LR in *Mytilus galloprovincialis*. Aquat. Toxicol. **1995**, *32*, 227–237.
45. Spoof, L.; Vesterkvist, P.; Lindholm, T.; Meriluoto, J. Screening for cyanobcteril hepatotoxins, microcystins and nodulrin in environmental water samples by reversed-phase liquid chromatography-electrospray ionization mass spectrometry. J. Chromatogr. A, **2003**, *1020*, 105–119.

Microcystins: Isolation by Supercritical Fluid Extraction

Huwei Liu
Institute of Analytical Chemistry, Peking University, Beijing, China

INTRODUCTION

Microcystins are an increasingly important group of bioactive compounds, produced mainly by planktonic cyanobacteria. They are a family of cyclic heptapeptides that cause both acute and chronic toxicity. Purified microcystins are utilized in a range of research applications. This review summarizes the isolation of microcystins from the cyanobacteria by supercritical fluid extraction (SFE). The microcystins can be successfully extracted when a modifier is used in supercritical carbon dioxide fluid. The advantage of the method is that the sample handling steps are minimized, thus reducing possible losses of microcystin and saving extraction and purification time.

MICROCYSTINS

Microcystins are a family of more than 50 structurally similar hepatotoxins produced by species of freshwater cyanobacteria (blue-green algae), primarily *Microcystis aeruginosa*.[1] Microcystins are potent toxins that inhibit the regulatory enzymes protein phosphatase 1 and 2A (PP1 and PP2A).[2–4] It is reported that liver is the target organ that shows the greatest degree of histopathological change when animals are poisoned by these cyclic peptides. Therefore their presence in water bodies has caused the death of wild and domestic animals worldwide,[5] and, more recently, they have been implicated in human fatalities.[6,7]

Microcystins are cyclic heptapeptides that share a general structure, as shown in Fig. 1 and Table 1, containing g-linked D-glutamicacid (D-Glu), D-alanine (D-Ala), β-linked D-*erythro*-b-methylaspartic acid (D-MeAsp), *N*-methyldehydroalanine (Mdha), and a unique C20 β-amino acid, (2*S*,3*S*,8*S*,9*S*)-3-amino-9-methoxy-2,6,8-trimethyl-10-phenyldeca-4(*E*), 6(*E*)-dienoic acid (Adda). The other two L-amino acids are variable (denoted X and Z) and are found in positions 2 and 4 of the cyclic structure. The single-letter abbreviation of the variable amino acids is used to distinguish different microcystins; for example, the most commonly occurring microcystin contains leucine and arginine in these positions and is therefore called microcystin LR.[8] Variation in these two amino acids accounts for many of the microcystin variants that have been characterized; however, other minor modifications, such as demethylation, increase the number of microcystin variants to at least 60.[5] The need for extensive research into their detection, toxicology, and the investigation of water-treatment strategies requires the availability of purified microcystins. Therefore the isolation of microcystins is very important and urgent.

ISOLATION AND PURIFICATION MODES

Microcystins were first purified by Botes et al.[9] in 1982, and, since then, many different approaches[10–14] have been adopted for the isolation of microcystins from cyanobacterial cells. The most widely used procedures[13,15–17] are as follows: The lyophilized cyanobacterial cells which contain microcystins are extracted with organic solvents several times, and then the extracts are applied to multistep column chromatography and thin-layer chromatography (TLC).[15] For example, Harada et al.[13] established an effective analysis method for microcystins RR and LR. They used 5% aqueous acetic acid solution as an extracting solvent and isolated microcystins by using preparative or semipreparative liquid chromatography (LC) with octadecyl-silanized (ODS), silica gel, or gel permeation columns.

In this review, we provide an in-depth survey of a rapid method for isolation of microcystin LR from cyanobacterial

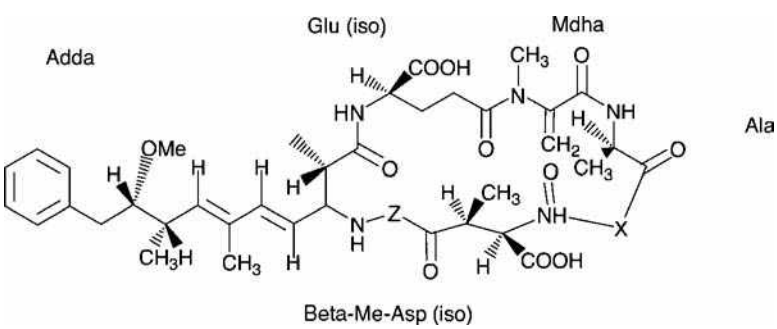

Fig. 1 General struacture of microcystrin where X and Z represent variable amino acids as presented in Table 1.

Table 1 Microcystins characterized to date indicating the molecular mass of each variant.

	Variable amino acid X										
Z compound	**Ala (A)**	**Arg (R)**	**Glu (E)**	**E (OMe)**	**Homo IsoL**	**Leu (L)**	**Methionine -S-oxide**	**Phe (F)**	**Try (W)**	**Tyr (Y)**	**Val (V)**
Alanine						909				959	
Aminoisobutyric acid						923					
Arginine	952	1037			1008	994	1028	1028	1067	1044, 1048^{t}, 1058^{hY}	
D-Asp^{3}, Dha^{7}		1099				966				1030^{hY}	
D-Asp^{3}		1023				980		1014, 1028^{hF}		1030, 1044^{hY}	
Dha^{7}		1023				980				1030, 1044^{hY}	
L-Ser^{7}		1041				998				1062^{hY}	
DMAdda^{5}						980					
D-Asp^{3}, D-Glu(OCH$_3$)^{6}						994					
(6Z)-Adda^{5}		1037				994					
D-Asp^{3}, ADMAdda^{5}						1008, 1022^{hR}					
D-Glu(OCH)^{6}						1008					
D-Asp^{3}, ADMAdda^{5}, Dhb^{7}		1052				1009				1073^{hY}	
L-MeSer^{7}						1012					
D-Asp^{3}, L-MeSer^{7}		1041									
ADMAdda^{5}						1022, 1036^{hR}					
D-Ser^{1}, ADMAdda^{5}						1038					
D-Glu-OC$_2$H$_3$(CH$_3$)OH^{6}						1052					
ADMAdda^{5}, MeSer^{7}						1040					
N-Methyllanthionine						1115					
E(OMe)											
D-Asp^{3}, Dha^{7}			969	983							
Dha^{7}			983	997							
L-Ser^{7}			1001	1015							
D-Asp^{3}, Ser^{7}				1001							
Leucine						951					
Methionine-S-oxide										1035	
Phenylalanine						985					971
Tryptophan						1024					
Tyrosine						1001					

Abbreviations and superscripts: ^{h}Homo variant of the amino acid indicated by single letter; ^{t}Tetrahydrotyrosine; ADMAdda, 6 *O*-Acetyl-*O*-demethylAdda; DMAdda, *O*-demethylAdda; (6*Z*)-Adda, stereoisomer of Adda at the Δ^{6} double bond; Dha, dehydroalanine; Dhb, dehydrobutyrine; MeSer, *N*-methylserine; E(OMe), glutamic acid methyl ester.

cells. The unique feature of the method is that it uses a one-step SFE and a one-step chromatography, instead of multiple extractions with organic solvents and multistep column chromatography.

PRINCIPLE AND INSTRUMENTATION FOR SFE

SFE is a well-recognized alternative to conventional solvent-based extraction techniques, which has the main advantages of being environmentally benign and available as fully automated instruments. Because SFE can minimize organic solvent consumption and increase sample throughput,[18] extraction with supercritical fluids has received wide attention in recent years.

From the chromatographic point of view, the physicochemical properties of a supercritical fluid are intermediate between those of the gases and liquids, and they are dependent upon the fluid composition, pressure, and temperature. Obviously, SFE possesses the following properties:

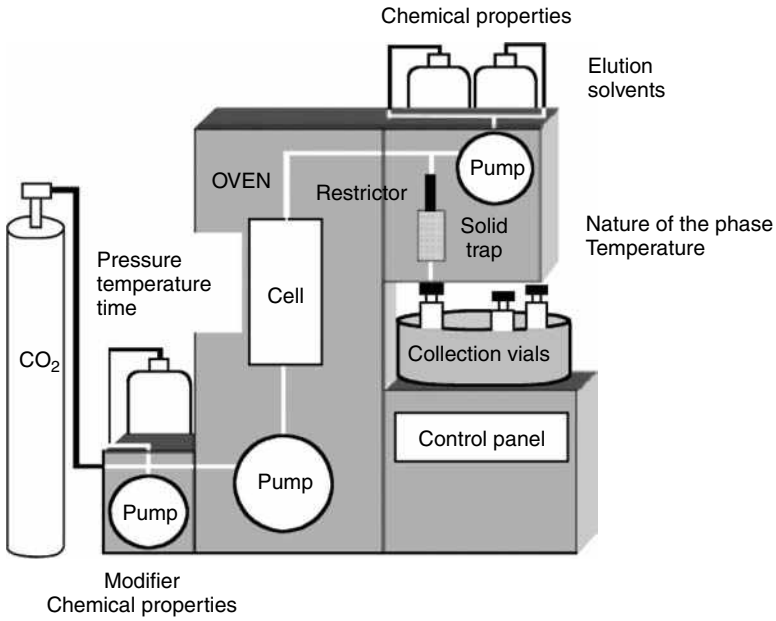

Fig. 2 Principle of an SFE system and influencing parameters.
Source: From Recent extraction techniques for solid matrices—supercritical fluid extraction, pressurized fluid extraction and microwave-assisted extraction: Their potential and pitfalls, in Analyst.[24]

low viscosity of gases, higher diffusion coefficients, higher compressibility, and solubilization power of liquids. Therefore SFE possesses a number of advantages including more rapid extraction rates, more efficient extractions, higher selectivity, and easy coupling online to other analytical technologies. In particular, the solvating strength of a supercritical fluid is related to its density, which may be adjusted by varying both the pressure and the temperature.[19] Consequently, the pressure and the temperature of the supercritical fluid are the two most important parameters to be optimized for most SFE experiments.

A typical SFE system comprises three integrated parts (Fig. 2): fluid delivery system, extraction cell of the analytes from the sample matrix, and subsequent collection (trapping) of the analytes.[18,20]

MICROCYSTINS ISOLATED BY SFE

From Fig. 1, both microcystins RR and LR contain a strongly basic functional group (NHCNH–NH_2), i.e., a guanidine moiety. (Microcystin LR contains one guanidine moiety and microcystin RR contains two guanidine moieties.) These microcystins would be present mainly in the following cationic form:[20]

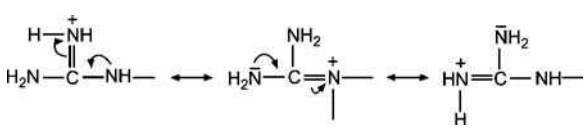

The poor extraction result obtained with neat CO_2 is probably caused by the fact that microcystins consist of fairly polar functional groups. The use of cosolvents can have a profound effect on increasing the solubility levels of polar solutes in supercritical fluids. In addition, water plays an important role in the SFE of microcystins. Dongjin Pyo[21] used aqueous acetic acid modified CO_2 for the extraction of microcystins from cyanobacteria. One of the difficulties with using aqueous acetic acid as a cosolvent was the high fluctuation of the pressure gauge which results from the clogging of the extraction line. Subsequently, Dongjin Pyo used aqueous methanol as a cosolvent, which could avoid the clogging and maintain the pressure of the extracting fluid fairly constant during SFE. Therefore the most suitable medium for the SFE of microcystins is a ternary mixed fluid (90% CO_2, 9.0% methanol, and 1.0% water). When 90% aqueous methanol was used as a cosolvent at 40°C and 250 atm. and the flow rate of the cosolvent and supercritical CO_2 fluid were 0.2 and 2.0 ml/min, respectively, 95% of microcystin RR and 94% of microcystin LR were extracted.[21–23]

PURIFICATION PROCEDURE FOR MICROCYSTIN BY HPLC SYSTEM

The extracts collected from SFE were treated according to the isolation procedures shown in Fig. 3.

Purification of Microcystin LR

Dongjin Pyo also reported some other procedures: The extraction by SFE was performed with a Beckman 116 pump (System Gold programmable solvent module 126), a 15 cm × 10 mm I.D. ODS column and Agilent high-performance liquid chromatography (HPLC) 1100 series diode-array detector. Methanol/0.05 *M* phosphate buffer

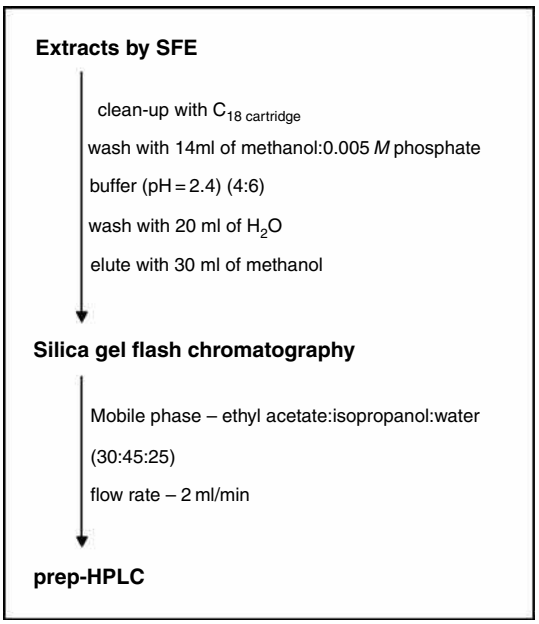

Fig. 3 Purification procedure for microcystin LR.
Source: From Rapid purification of microcystin-LR using supercritical fluid extraction and flash chromatography, in Anal. Lett.[23]

(52 : 48), pH 3, was used as a mobile phase at a flow rate of 2 ml/min. The analytical results obtained from real lake samples indicate the viability of the method for the determination of microcystins in real samples.[20]

CONCLUSIONS

SFE is very suitable for extracting thermolabile compounds, as it allows the possibility to perform fast extractions at moderate temperatures (around 40°C).[24] Therefore numerous applications of the technique have been reported. A large field has been covered: environmental matrices, plants, foods and fats, and polymers. As legislation will tend to restrict, or even ban, the use of many common solvents, recent extraction techniques will, in the future, undoubtedly supercede the traditional methods, as SFE considerably reduces the solvent volumes required, along with a reduction in the time devoted to the extraction step. SFE appears, undoubtedly, to be the most potentially selective extraction technique.

The isolation of microcystins by SFE is effective and successful. However, the main drawbacks of SFE are the difficulties in a tedious optimization of SFE methods, as several parameters need to be considered with this technique. In addition, because of the high investment cost of the technique, economic considerations will, in practice, also influence the choice of the extraction technique. Yet future trends will depend on the availability of commercial apparatus.

REFERENCES

1. Dawson, R.M. The toxicology of microcystins. Toxicon **1998**, *36* (7), 953–962.
2. Carmichael, W.W. In *Toxins of Freshwater Algae: Handbook of Natural Toxins*; Marcel Dekker, Inc.: New York, 1988; Vol. 3, 121–127.
3. Namikoshi, M.; Rinehart, K.L.; Sakai, R.; Sivonen, K.; Carmichael, W.W. Structures of three new cyclic hepatotoxins produced by the cyanobacterium (blue-green algae) *Nostoc* sp. strain 152. J. Org. Chem. **1990**, *55*, 6135–6141.
4. Sivonen, K.; Carmichael, W.W.; Namikoshi, M.; Rinehart, M.L.; Dahlem, A.M.; Niemela, S.I. Isolation and characterization of hepatotoxic microcystin homologues from the filamentous freshwater cyanobacterium *Nostoc* sp. strain 152. Appl. Environ. Microbiol. **1991**, *56*, 2650–2657.
5. Sivonen, K.; Jones, G. In *Toxic Cyanobacteria in Water*; Chorus, I., Bartram, J., Eds.; E&FN Spon: London, 1999; 41.
6. Bell, S.G.; Codd, G.A. Cyanobacterial toxins and human health. Rev. Med. Microbiol. **1994**, *5*, 256–264.
7. An, J.; Carmichael, W.W. Use of a colorimetric protein phosphatase inhibition assay and enzyme linked immunosorbent assay for the study of microcystins and nodularins. Toxicon **1994**, *32*, 1495–1507.
8. Lawton, L.A.; Edwards, C. Purification of microcystins. J. Chromatogr. A, **2001**, *912*, 191–209.
9. Botes, D.P.; Kruger, H.; Viljoen, C.C. Isolation and characterization of four toxins from the blue green alga *Microcystis aeruginosa*. Toxicon **1982**, *20*, 945–954.
10. Brooks, W.P.; Codd, G.A. Extraction and purification of toxic peptides from natural blooms and laboratory isolate of the cyanobacterium *Microcystis aeruginosa*. Lett. Appl. Microbiol. **1986**, *2*, 1–7.
11. Krishnamarty, T.; Carmichael, W.W.; Sarver, E.W. Investigations of freshwater cyanobacteria (blue-green algae) toxic peptides: I. Isolation, purification and characterization of peptides from *Microcystis aeruginosa* and *Anabaena* flos-aquae. Toxicon **1986**, *24*, 865–872.
12. Berg, K.; Carmichael, W.W.; Skulberg, O.M.; Benestad, C.; Underdal, B. Investigation of a toxic water-bloom of *Microcystis aeruginosa* (Cyanophyceae) in Lake Akersvatn, Norway. Hydrobiologia **1987**, *144*, 97–103.
13. Harada, K.I.; Matsuura, K.; Suzaki, M.; Oka, H.; Watanabe, M.F.; Oishi, S.; Dahlem, A.M.; Beasley, V.R.; Carmichael, W.W. Analysis and purification of toxic peptides from cyanobacteria by reversed-phased high-performance liquid chromatography. J. Chromatogr. **1988**, *448*, 275–281.
14. Poon, G.K.; Priestley, I.M.; Hunt, S.M.; Fawell, J.K.; Cood, G.A. Purification procedure for peptide toxins from the cyanobacterium *Microcystis aeruginosa* involving high-performance thin-layer chromatography. J. Chromatogr. **1987**, *387*, 551–558.
15. Pravda, M.; Kreuzer, M.P.; Guilbault, G.G. Analysis of important freshwater and marine toxins. Anal. Lett. **2002**, *35*, 1–15.
16. Namikoshi, M.; Sivonen, K.; Evans, W.R.; Carmichael, W.W.; Sun, F.; Rouhiainen, L.; Luukkainen, R.; Rinehart, K.L. Two new L-serine variants of microcystins-LR and -RD from *Anabaena* sp. strains. Toxicon **1992**, *30*, 1457–1462.

17. Meriluoto, J. Chromatography of microcystin. Anal. Chim. Acta **1997**, *352*, 277–298.
18. Turner, C.; Eskilsson, C.S.; Bjorklund, E. Collection in analytical-scale supercritical fluid extraction. J. Chromatogr. A, **2002**, *947*, 1–22.
19. McHugh, M.A.; Krukonis, V.J. In *Supercritical Fluid Extraction: Principles and Practice*; Butterworth: Boston, MA, 1986.
20. Dongjin, P.; Shin, H. Supercritical fluid extraction of microcystins from cyanobacteria. Anal. Chem. **1999**, *71*, 4772–4775.
21. Pyo, D.; Park, K.; Shin, H.; Moon, M. Extraction of microcystin from the cyanobacteria by acetic-acid modified supercritical CO_2. Chromatographia **1999**, *49* (9/10), 539–542.
22. Dongjin, P.; Yonsook, K. Rapid and efficient method for extraction and isolation of microcystin RR from the cyanobacterium. J. Liq. Chromatogr. Relat. Technol. **2001**, *24* (17), 2685–2696.
23. Dongjin, P.; Soyoung, L. Rapid purification of microcystin-LR using supercritical fluid extraction and flash chromatography. Anal. Lett. **2002**, *35* (9), 1591–1602.
24. Camel, V. Recent extraction techniques for solid matrices—supercritical fluid extraction, pressurized fluid extraction and microwave-assisted extraction: Their potential and pitfalls. Analyst **2001**, *126*, 1182–1193.

Micro-ThFFF

Josef Janca
Department of Chemistry, University of La Rochelle, La Rochelle, France

INTRODUCTION

Thermal field-flow fractionation (TFFF) is the oldest of all FFF methods.[1] It is based on the general principle invented by Giddings.[2] In this entry, miniaturization of this technique is discussed.

DISCUSSION

Thermal field-flow fractionation[1] was invented by Giddings.[2] The universal applicability of thermal FFF for the analysis of various polymers had been already demonstrated in 1979.[3] Several applications of TFFF to the analysis of polymers and colloidal particles were published (see Refs.[4,5] for a review); but the contemporary TFFF channels have practically the same dimensions (roughly $50 \times 2 \times 0.01$ cm) as those constructed at the very beginning. Giddings[6] concluded, in 1993, that the miniaturization of the FFF channels could provide only some limited advantages. The experimental study[7] dealt only with the effect of the reduced channel thickness on the performance of TFFF.

Contrary to the conclusions,[6] it has been shown[8] that the miniaturization of the TFFF channel is meaningful; it results in reduced carrier liquid and energy consumption and in an extended range of the operational conditions that can be utilized.

Theoretical and Practical Aspects of the Miniaturization of TFFF

Miniaturization of the FFF channel can be useful only if the resulting performance is higher in comparison with the conventional size FFF channel. The crucial parameter is, thus, the resolution R_s which, for TFFF, is given by:[9]

$$R_s = \left(\frac{1}{8w}\right)\sqrt{\frac{LD_T{}^3\Delta T^3}{6\langle v\rangle}}\left|\frac{1}{D_1}-\frac{1}{D_2}\right| \qquad (1)$$

where $D_{1,2}$ are the diffusion coefficients of two retained species, D_T is the thermal diffusion coefficient, $\langle v\rangle$ is the mean linear velocity of the carrier liquid inside the channel, w is the thickness of the channel, L is its length, and ΔT is the temperature drop across the channel. The mean linear velocity of the carrier liquid, $\langle v\rangle$, and the channel dimensions, L, w, are inter-related. This means that a shortening of the channel, accompanied by a corresponding decrease in $\langle v\rangle$, does not modify the resolution. Consequently, the energy flux can be reduced, proportionally to the shortening of the channel length.[8,9] The other gain can be achieved by the reduction of the thickness w of the channel and its breadth b (the aspect ratio w/b does not change). Such modification leads to an increase in resolution and maintains the same total heat flow across the channel. Reduced w, however, results in a proportional increase in the heat flow across the channel because the temperature drop has to be maintained to obtain the same retentions. A more elegant way is to increase the temperature drop without changing the thickness of the channel, because an increase in ΔT has a more pronounced effect on the resolution in comparison with a reduction of w for the same heat flow increase (see Eq. 1).[8] From a practical point of view, shortening of the channel length L, accompanied by an appropriate decrease in $\langle v\rangle$, maintains the resolution but the total heat flow across the channel is reduced for a given temperature drop ΔT due to the reduced surface area of the main channel walls. Thus, Eq. 1 simplifies to:

$$R_s = \text{const}\sqrt{\frac{\Delta T^3}{\langle v\rangle}} \qquad (2)$$

The validity of Eq. 2 was proven experimentally[9] and the result is shown in Fig. 1.

Limits of Miniaturization

The size ratio of the fractionated macromolecules or particles to the channel thickness must be taken into account. A decrease in channel thickness can lead to an important contribution of steric-exclusion to the mechanism of separation whenever the distance of the center of gravity of the concentration distribution of the retained species from the accumulation wall, l, becomes commensurable with the size of the retained species.[4,5] Whereas the elution order in normal (polarization mode) TFFF is from the small to the large species, it is inverted in purely steric-exclusion mode. Consequently, the fractionation deteriorates in the vicinity of the inversion point. The dependence of the retention ratio R on the particle radius r can be

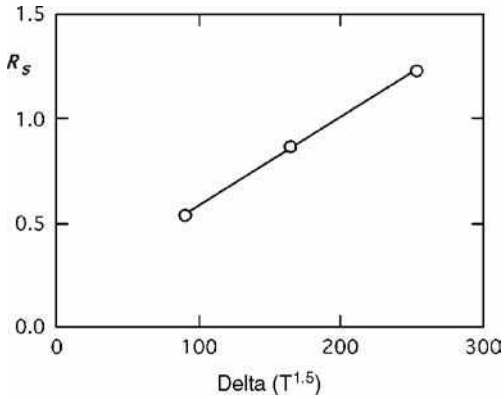

Fig. 1 Dependence of the resolution R_s on the $\Delta T^{1.5}$ in micro-TFFF.
Source: From Micro-thermal field-flow fractionation: new challenge in experimental studies of thermal diffusion of polymers and colloidal particles, in Phil. Mag.[9]

calculated from the theory of FFF for the case when only the polarization mechanism is effective and for the cases when both polarization and steric modes participate in the separation mechanism.[10] The theoretical calculations were compared with the experimental results obtained for a series of polystyrene (PS) standard latex samples.[10,11] The theoretically calculated curves and the experimental data, demonstrated in Fig. 2 and obtained for three temperature drops $\Delta T = 5$ K, $\Delta T = 10$ K, and $\Delta T = 20$ K, agree quite well. Obviously, the resolution is low in the vicinity of the inversion point and passes through zero at this point. Consequently, the optimal w must be carefully chosen in order to avoid undesirable simultaneous action of polarization and steric-exclusion mechanisms within the required size range of the fractionated species.

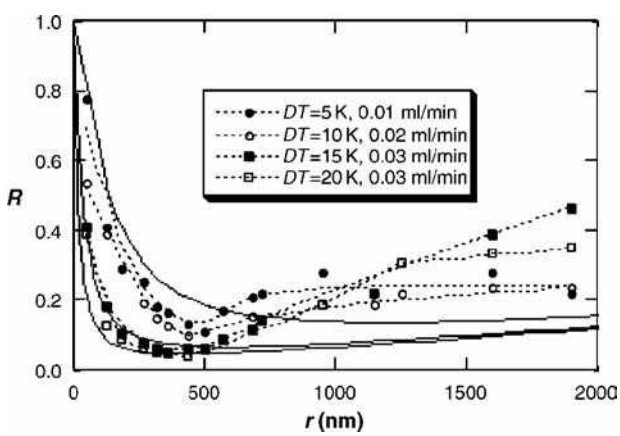

Fig. 2 Comparison of the experimental retention data with the theoretical R vs. particle radius r curves calculated for different temperature drops ΔT and different mean linear velocities of the carrier liquid.
Source: From Micro-thermal focusing field-flow fractionation, in J. Chromatogr. B.[11]

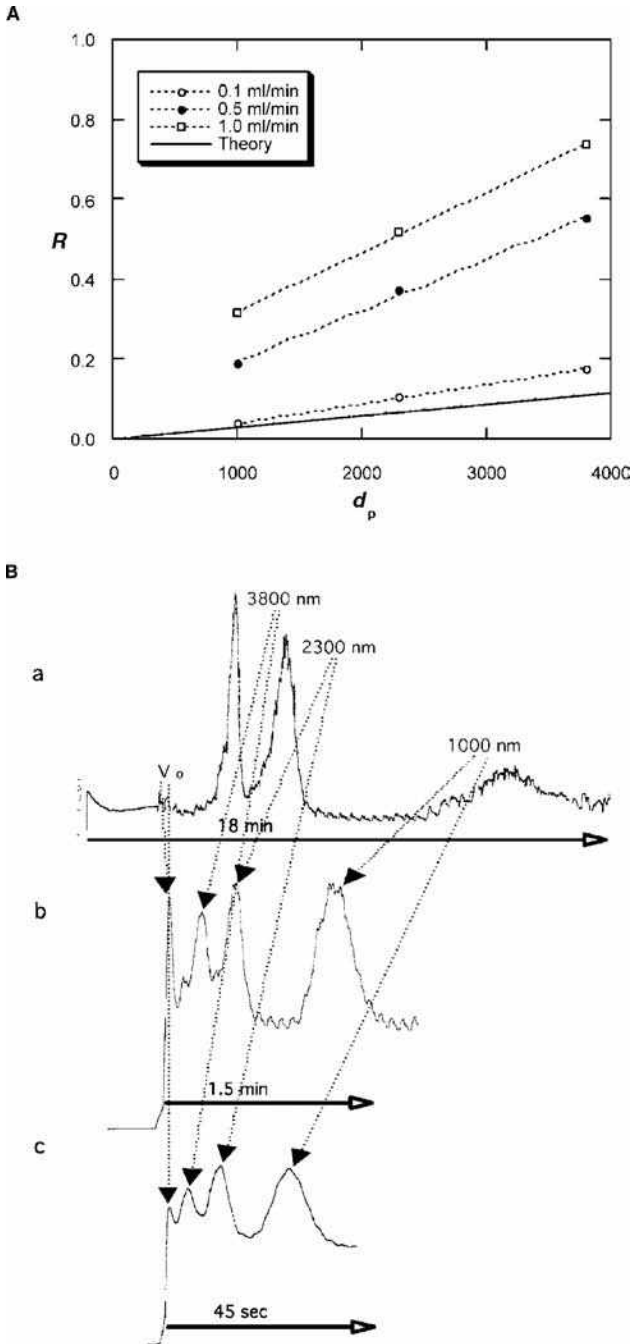

Fig. 3 A, Theoretical and experimental dependence of the retention ratio R on the particle diameter d_p. Theoretical curve corresponds to the pure steric exclusion mechanism, experimental data were obtained at different flow rates of the carrier liquid. B, Fractograms of a mixture of three PS latex samples obtained under different flow rates: 0.1 ml/min (a), 0.5 ml/min (b), 1.0 ml/min (c).
Source: From High-speed micro-thermal focusing field-flow fractionation of micron-size particles, in Coll. Czech. Chem. Commun.[12]

Extension of Micro-TFFF to Focusing Mode

When increasing the linear velocity of the carrier liquid, lift forces can appear that contribute actively to the

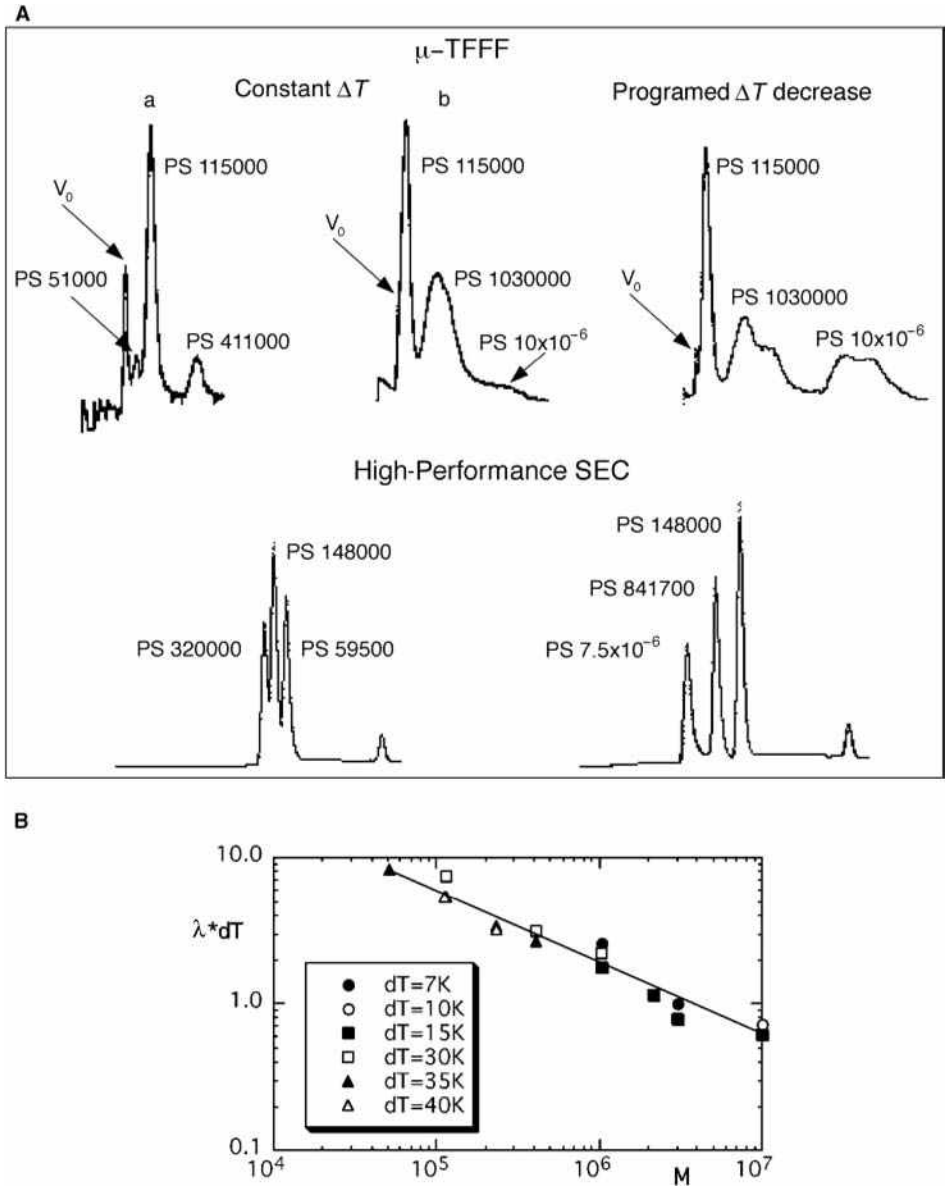

Fig. 4 A, Comparison of the separations of polystyrene standards carried out by micro-TFFF at constant temperature drop ΔT and programed decrease in ΔT with the chromatograms from high-performance size-exclusion chromatography. B, Dependence of the product of retention parameter λ and of the temperature drop ΔT on the molar mass M of polystyrene standards.
Adapted from Janča.[9,13]

separation. Such a transition from steric to focusing mechanism of separation can be seen in Fig. 3,[12] which shows progressive deviation of the experimental dependence of the retention ratio R on the particle size from the theoretical one, calculated for a dominating steric-exclusion mechanism. This deviation increases with increasing flow rate, due to the lift forces. It can be seen from Fig. 3 that "steric" FFF represents rather an exceptional case of the separation. In other words, whenever lift forces participate in FFF processes, it is a focusing mechanism and not a steric-exclusion mechanism that governs the retention in FFF.

The focusing mechanism was actively used in microthermal focusing FFF. The result of high-speed separation of micron-sized PS latex particles is an example of such an application.[11,12] Fig. 3 demonstrates that a substantial increase in the flow rate resulted in high-speed microthermal focusing FFF separation without an important loss of the resolution.

APPLICATIONS

Polystyrene standards were used as model samples to check the performance of micro-TFFF,[8] to compare the results with those obtained previously with the use of a standard size TFFF channel,[13] and to confirm that the ultrahigh molar mass (UHMM) PSs do not undergo shear degradation, observed frequently when separated by SEC.[14,15] The fractogram of three PSs of different molar

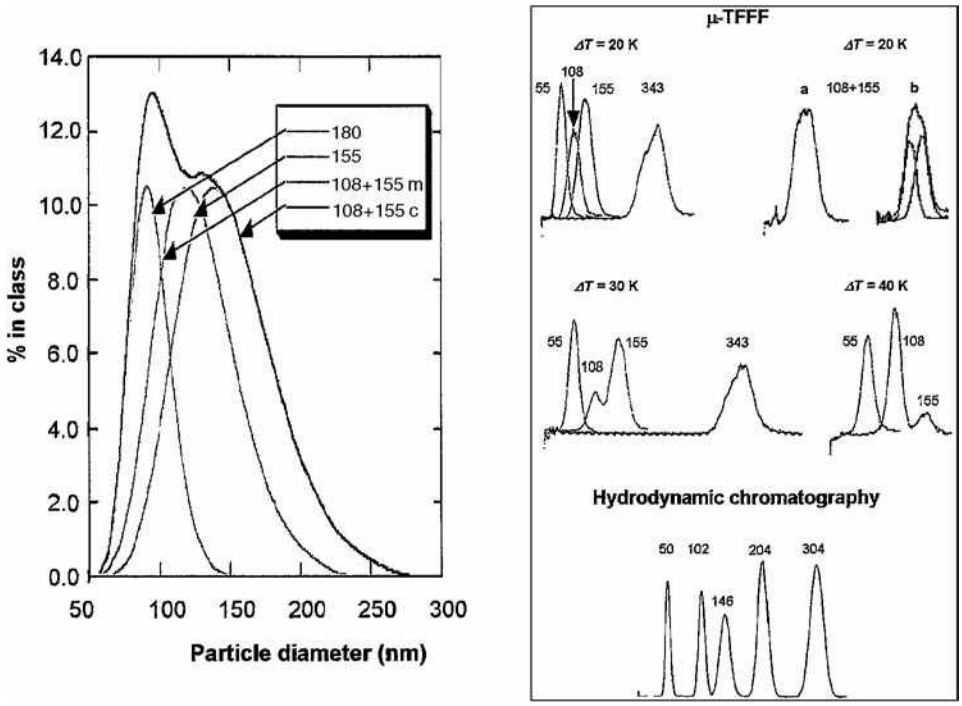

Fig. 5 Comparison of various methods of particle size analysis: Quasielastic light scattering, micro-TFFF, and hydrodynamic chromatography.
Source: From Microthermal field-flow fractionation: New highperformance method for particle size distribution analysis, in J. Coll. Interf. Sci.[18]

masses in Fig. 4 shows good resolution achieved by micro-TFFF, which is comparable with that obtained on a standard size TFFF channel.[13] Higher resolution, in comparison with SEC, was achieved by applying programed decrease in ΔT for a separation of ultrahigh molar mass PS in micro-TFFF.[13] The plot of $\lambda\Delta T$ vs. M, shown in Fig. 4, confirms the linearity of this dependence in log–log scale, found already by Gao et al.,[16] within an extended range of molar masses. A decrease in retention with increased cold wall temperature was found for dissolved polymers[13] as well as for suspended colloidal particles,[17] but higher cold wall temperature should be preferred due to the accelerated transport and relaxation processes.

Micro-TFFF was also applied to separate colloidal particles.[14] The experimental conditions were optimized with respect to the relaxation phenomena and related stop-flow procedure, and to the accumulation wall temperature.[17] An original method was proposed for the determination of the sign of the Soret coefficient,[17] based on the comparison of the retentions of the studied species in horizontally and vertically positioned micro-TFFF channels. The change of the retention in these two positions of the channel is due to the appearance of a convective flow, superposed to the forced flow of the carrier liquid, in the vertical channel.

Comparison of transmission electron microscopy, quasielastic light scattering, hydrodynamic chromatography, and micro-TFFF, applied to the determination of the particle size distribution, demonstrated specific performances of these methods.[18] Some of the results are shown in Fig. 5. The optimization of the operational variables resulted in high-speed micro-TFFF of colloidal particles.[19]

Micro-TFFF was used to characterize micrometer-sized (3–10 μm) silica chromatographic beads. In comparison with the retentions observed when only gravity was acting as the effective field ($\Delta T = 0$ K), the retentions of all studied particles substantially increased when a temperature drop was applied. As a result, micro-TFFF was found to be a rapid and easily applicable method for the characterization of the mean particle size and particle size distribution of the chromatographic beads.[20] Fig. 5 shows one result of this study.

CONCLUSIONS

Miniaturization of the FFF channel can be useful. The size ratio of the fractionated macromolecules or particles to the channel thickness must be taken into account. When increasing the linear velocity of the carrier liquid, lift forces can appear that contribute actively to the separation. Several useful applications of micro-TFFF have been described here.

REFERENCES

1. Thompson, G.H.; Myers, M.N.; Giddings, J.C. An observation of a field-flow fractionation effect with polystyrene samples. Sep. Sci. **1967**, *2*, 797.

2. Giddings, J.C. A new separation concept based on a coupling of concentration and flow nonuniformities. Sep. Sci. **1966**, *1*, 123.
3. Giddings, J.C.; Myers, M.N.; Janča, J. Retention characteristics of various polymers in thermal field-flow fractionation. J. Chromatogr. **1979**, *186*, 37.
4. Janča, J. *Field-Flow Fractionation: Analysis of Macromolecules and Particles*; Marcel Dekker, Inc.: New York, 1988.
5. Schimpf, M.E.; Caldwell, K.D.; Giddings, J.C. *Field-Flow Fractionation Handbook*; John Wiley & Sons: New York, 2000.
6. Giddings, J.C. Micro-FFF: theoretical and practical aspects of reducing the dimensions of field-flow fractionation channels. J. Microcol. Sep. **1993**, *5*, 497.
7. Giddings, J.C.; Martin, M.; Myers, M.N. High speed polymer separations by thermal field-flow fractionation. J. Chromatogr. **1978**, *158*, 419.
8. Janča, J. Micro-channel thermal field-flow fractionation: New challenge in analysis of macromolecules and particles. J. Liq. Chromatogr. Relat. Technol. **2002**, *25*, 683.
9. Janča, J. Micro-thermal field-flow fractionation: New challenge in experimental studies of thermal diffusion of polymers and colloidal particles. Phil. Mag. **2003**, *83*, 2045.
10. Janča, J.; Ananieva, I.A. Micro-thermal field-flow fractionation in the characterization of macromolecules and particles: Effect of the steric exclusion mechanism. e-Polymers **2003**, No. 034.
11. Janča, J.; Ananieva, I.A.; Menshikova, A.Y.; Evseeva, T.G. Micro-thermal focusing field-flow fractionation. J. Chromatogr. B, **2004**, *800*, 33.
12. Ananieva, I.A.; Menshikova, A.Y.; Evseeva, T.G.; Janča, J. High-speed micro-thermal focusing field-flow fractionation of micron-size particles. Coll. Czech. Chem. Commun. **2004**, *69*, 322.
13. Janča, J. Micro-thermal field-flow fractionation. Coll. Czech. Chem. Commun. **2002**, *67*, 1596.
14. Janča, J. Micro-channel thermal field-flow fractionation: Analysis of ultra-high molar mass polymers and colloidal particles with constant and programmed field force operation. J. Liq. Chromatogr. Relat. Technol. **2002**, *25*, 2173.
15. Janča, J.; Strnad, P. Micro- and frontal thermal field-flow fractionation: On the shear degradation of ultra-high molar mass polymers. J. Liq. Chromatogr. Relat. Technol. **2004**, *27*, 193.
16. Gao, Y.S.; Caldwell, K.D.; Myers, M.N.; Giddings, J.C. Extension of field-flow fractionation to ultra high (20×10^6) molecular weight polystyrenes. Macromolecules **1985**, *18*, 1272.
17. Janča, J. Micro-thermal field-flow fractionation of colloidal particle: Effect of temperature on retention and relaxation processes. Coll. Czech. Chem. Commun. **2003**, *68*, 672.
18. Janča, J.; Berneron, J.-F.; Boutin, R. Micro-thermal field-flow fractionation: New high-performance method for particle size distribution analysis. J. Coll. Interf. Sci. **2003**, *260*, 317.
19. Janča, J. Micro-channel thermal field-flow fractionation: High-speed analysis of colloidal particles. J. Liq. Chromatogr. Relat. Technol. **2003**, *26*, 849.
20. Ananieva, I.A.; Minarik, M.; Boutin, R.; Shpigun, O.A.; Janča, J. Characterization of chromatographic beads by micro-thermal field-flow fractionation. J. Liq. Chromatogr. Relat. Technol. **2004**, *27*, 2313.

Migration Behavior: Reproducibility in CE

Jetse C. Reijenga
Department of Chemical Engineering and Chemistry, Eindhoven University of Technology, Eindhoven, The Netherlands

INTRODUCTION

Identification of sample components based solely on migration time in capillary electrophoresis (CE) requires reproducibilities not normally obtained. These are caused, mainly, by two effects: temperature effects and electro-osmotic affects. Migration times in CE are determined by the electro-osmotic velocity υ_{EOF} and effective electrophoretic migration velocity υ_{EFF}; the net migration velocity υ_i is the vector sum of both velocities:

$$\upsilon_i = \upsilon_{EFF} + \upsilon_{EOF}$$

In terms of mobilities, this relationship becomes

$$\upsilon_i = \left(-\frac{\zeta\varepsilon}{\eta} + \mu_i \right) \cdot E$$

in which ζ is the zeta-potential of the capillary, ε is the dielectric constant of the liquid, η is the viscosity of the liquid, μ_{eff} is the effective mobility of the sample component, and E is the electric field strength. From this relationship, it is obvious that migration time reproducibility depends on the reproducibility of a number of parameters. In addition to the ones mentioned, sample matrix effects can also play a significant role.

ELECTROPHORETIC EFFECTS

The reproducibility of the effective mobility is governed by temperature and pH effects. An acceptable run-to-run pH reproducibility can usually be assured, at least in equipment where the effects of possible electrode reactions can be avoided. Again, temperature plays a leading role: The effective mobility has a temperature coefficient of 2–3% per degree. Most buffer solutions, incidentally, have a temperature-dependent pH value, so that changing the temperature in the capillary will, for weak ions, even lead to changing degrees of dissociation and, hence, effective mobility. These effects are, by definition, different for different buffers and different sample components.

SAMPLE MATRIX AND INJECTION EFFECTS

When injecting very dilute sample solutions, a relatively large proportion of the total voltage drop across the capillary will take place over this sample plug, resulting in a proportionally lower field strength in the remainder of the separation capillary. This will lead to systematically longer migration times. In this case, also, identification on the basis of effective mobilities is better than on migration times alone.

Another effect takes place when injecting different sample volumes in the capillary: This may systematically change the migration length and, thus, migration times. A constant injection volume is, therefore, advised in cases of required high migration time reproducibility.

ELECTRO-OSMOTIC EFFECTS

In coated capillaries, the $\zeta\varepsilon E/\eta$ term is small, possibly close to zero, compared to the $\mu_{EFF} \cdot E$ term. If, however, one works with unsuppressed electro-osmosis, the reproducibility of the $\zeta\varepsilon E/\eta$ term plays an important role. Both ζ and η depend on temperature, and in some equipment, thermostating is not perfect, at least not in all parts of the capillary. The viscosity alone accounts for an $\sim$2% per degree dependence. Another effect that might take place is the gradual change in ζ-potential due to adsorption of sample matrix components on the inner capillary surface. The good news is that run-to-run change in electro-osmotic velocity is directly obvious from the electro-osmotic flow (EOF) marker peak in the detection signal, so that changes in EOF can be accounted for in cases where they cannot be avoided. However, this also means that measures have to be taken to assure a clear EOF marker peak [e.g., by addition to the sample of a neutral ultraviolet (UV)-absorbing component, such as mesityloxide]. In complicated samples, such an EOF marker peak may not be possible. For reasons of EOF reproducibility, identification is preferentially based not on migration time but on effective mobility calculation by means of

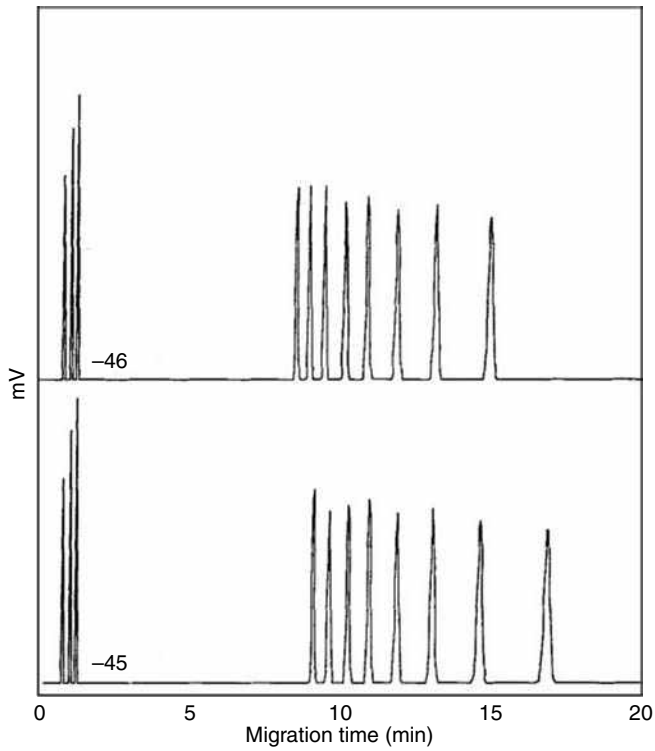

Fig. 1 Effect of capillary ζ-potential on the analysis of a mixture of anions in an uncoated fused-silica capillary in a 10 m*M* Tris/acetate buffer of pH 8. Normal ζ-potentials are around 50 mV at this pH.

$$\mu_{EFF} = \frac{L_d}{t_i E} - \mu_{EOF}$$

in which L_d is the capillary length to the detector and t_i is the migration time of the component i.

For quantitation under conditions of changing migration velocity, peak areas are usually divided by corresponding migration times to make them more independent of run-to-run differences in EOF. Migration times are especially susceptible to small EOF variations in the case of opposite signs for EOF and sample mobility (i.e., usually for anions). This is illustrated in Fig. 1, a separation of three cations before and eight anions after the EOF marker (not indicated in the figure). The traces given are for a ζ-potential of –46 and –45 mV, respectively. This 2% EOF change corresponds to the equivalent of only 1 degree temperature effect.

REFERENCES

1. Jorgenson, J.W.; Lucaks, K.D. Capillary zone electrophoresis. Science **1983**, *222*, 266.
2. Li, S.F.Y. *Capillary Electrophoresis—Principles, Practice and Applications*; Elsevier: Amsterdam, 1992.
3. Kenndler, E. Effect of electroosmotic flow on selectivity, efficiency, and resolution in capillary zone electrophoresis expressed by the dimensionless reduced mobility. J. Capillary Electrophor. **1996**, *3* (4), 191–198.

Milk Proteins: RP/HPLC Separation

I.M.P.L.V.O. Ferreira
Service of Bromatologia, Pharmacy College, University of Porto, Porto, Portugal

Abstract
Milk proteins in soluble and dispersed form are widely valued owing to their nutritional and technological value. Caseins represent about 80–85% of milk proteins, and they play a key role in human nutrition, in dairy industry, and as additives in food, paints, and glues because of their emulsifying properties. The remaining milk protein fraction is composed of the whey proteins, of which β-lactoglobulin and α-lactoalbumin are the main components. Analysis of milk proteins can be used to detect and quantify milk adulterations. Additionally, many bioactive peptides derived from milk proteins, latent in the primary sequences of proteins, and released during proteolysis have been identified. Reverse-phase (RP) high-performance liquid chromatographic (HPLC) methods for application on quality control and detection of species adulteration in dairy products are summarized.

INTRODUCTION

Controlling the quality of milk and its derivatives is a very demanding field with a great need for development of more economical, time-saving, and accurate methods of ensuring product quality. This entry presents various reversed-phase (RP) high-performance liquid chromatography, HPLC/UV methods for analysis of milk proteins, and describes how these techniques are used in the study of bovine, ovine, and human native milk proteins, casein fractions, cheese proteolysis evaluation, detection of product adulteration, enzyme hydrolysis of whey proteins, and peptide separation.

MILK PROTEINS

Proteins are important components in food, for both their nutritional and functional values. Dietary proteins provide amino acids and nitrogen needed by many organisms. In addition, they are believed to have other specific functions, owing to the presence of bioactive peptides in their primary sequences, making them potential health-promoting ingredients. Besides having this biological function, protein components play a major role in species identification and in determining the textural characteristics of food products. A certain number of food proteins, such as milk proteins, are characterized by great heterogeneity with the presence of several molecular forms, more or less phosphorylated or glycosylated, combined with a high degree of polymorphism.

Bovine milk proteins (3.2%) can be divided, according to their solubility at pH 4.6 and 20°C, into two major groups: about 79.5% of caseins that are insoluble at this pH and about 19.3% of whey proteins that are soluble. Another group exists as a minor fraction (about 1.2%), which includes proteins associated with the membrane of fat globules, enzymes, and proteins arising from blood and a polypeptide fraction (named proteose–peptone). The molecular weights of the individual milk protein monomers range from 15,500 to 67,000 Da.[1]

Caseins are quantitatively the most important protein components in bovine milk. This protein complex, known as a micelle, comprises four different caseins (α_{s1}-, α_{s2}-, β-, and κ-caseins), which are held together by non-covalent interactions and appear as a highly stabilized dispersion in milk.[1] During the classical cheese making process, it is the casein fraction that constitutes the cheese curd after the enzyme-triggered milk coagulation step.

The determination of individual proteins, and their degradation products in milk, cheese and other dairy products has been a major task for several years, since it can provide valuable information. Analysis of milk protein has been carried out using 1) classical gel electrophoretic methods, such as polyacrylamide gels with urea (urea–PAGE)[2–8] or sodium dodecyl sulfate (SDS) (SDS–PAGE)[9,10] and isoelectric focusing (IEF);[11] 2) HPLC by ion-exchange,[12,13] hydrophobic interactions,[14,15] gel filtration,[12,16] and reversed-phase[5,17–22] modes; 3) immunological methods;[23] and, more recently, 4) capillary electrophoresis.[24–27] Each method has its own merits, but the use of HPLC has resulted in the development of rapid and automated analyses with good separations and very high resolution, which gave accurate and reproducible results.

This entry describes RP-HPLC/UV methods for analysis of milk proteins that were developed with different

purposes, namely, to study the protein fraction of bovine, ovine, and human milk, characterize genetic polymorphisms, follow the extension of whey protein denaturation by heating, study the evolution of cheese proteolysis, detect milk and cheese adulterations, follow the enzymatic hydrolysis of whey proteins with different enzymes separated, and quantify bioactive peptides. The column was a reversed-phase column, Chrompack P 300 RP, which contains a polystyrene–divinylbenzene copolymer based packing material. In this type of column, separation is based on differences in surface hydrophobicity between the protein molecules and the stationary phase. Hydrophobic amino acid residues of proteins are bonded through hydrophobic interactions to a stationary matrix composed of a non-polar surface. Protein retention is controlled by increasing the concentration of organic solvents such as acetonitrile, thereby altering the polarity of the aqueous mobile phase.

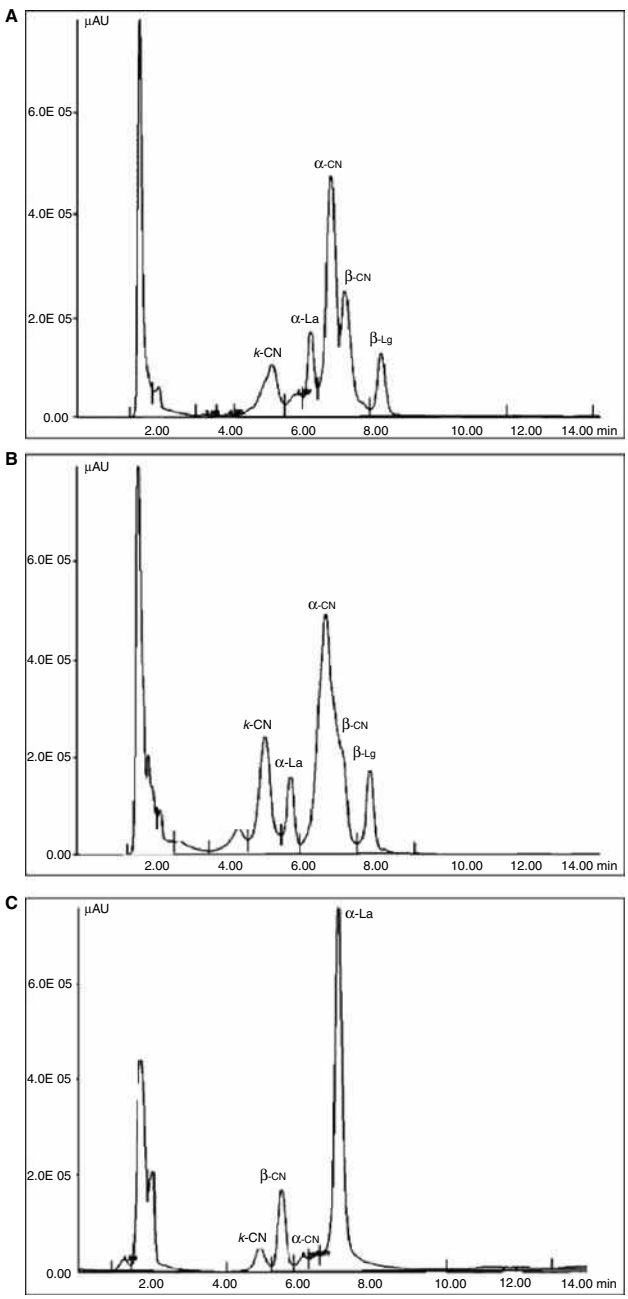

Fig. 1 Typical chromatographic profiles of (A) bovine, (B) ovine, and (C) human milk proteins, obtained by RP-HPLC. Detection at 280 nm.

RP-HPLC SEPARATION AND QUANTIFICATION OF BOVINE, OVINE, AND HUMAN NATIVE MILK PROTEINS

RP-HPLC simultaneous separation of the casein fraction and whey proteins, β-lactoglobulin and α-lactalbumin in bovine, ovine, and human raw milk was performed using gradient elution with a mixture of two solvents:[15,20,21] solvent A consisted of 0.1% trifluoroacetic acid (TFA) in water and solvent B consisted of 0.1% TFA in 95% (v/v) aqueous acetonitrile. Proteins were eluted as follows: 0–5 min, 36–47% B; maintaining 47% B for 2 min; 7–12 min, 47–52% B; 12–14 min, returning to initial conditions 52–36% B. The flow rate was 1.0 ml/min. The column was used at ambient temperature, and detection was at 280 nm. The total run time was 14 min.

Milk samples were skimmed by centrifugation for 5 min, filtered, and diluted with deionized water prior to injection. Different chromatographic patterns were obtained, as shown in Fig. 1. Peak identification was performed by comparison of retention times with those of standards from bovine, ovine, and human milk proteins.

Validation of the HPLC method was performed. The external standard method was used to calibrate the chromatographic system for protein quantification. Linearity between the concentration of casein fraction, β-lactoglobulin, and α-lactalbumin in bovine and the UV absorbance at 280 nm was maintained over the concentration ranges of 0.001–0.2, 0.004–0.6, and 0.002–0.2 g/100 ml, respectively. Repeatability of the injection was performed by 10 consecutive injections of bovine, ovine, and human milks. The relative standard deviation (RSD) values for peak areas were all below 2.3%. Recovery studies were carried

Table 1 Casein, β-lactoglobulin, and α-lactalbumin contents of bovine, ovine, and human mature milks (10 samples of each, with 90 ± 10 days of lactation).

Milk type	α-Lactalbumin (mg/ml)	β-Lactoglobulin (mg/ml)	Casein content (mg/ml)
Bovine	2.3 ± 0.10	4.7 ± 0.2	29.3 ± 0.60
Ovine	3.8 ± 0.20	5.9 ± 0.3	35.5 ± 0.50
Human	3.54 ± 0.03	n.d.	3.02 ± 0.01

Results are presented as mean ± standard deviation values; n.d., not detected.
Adapted from Ferriera, Mendes, & Ferriera,[15] Ferriera,[20] and Santos & Ferriera.[21]

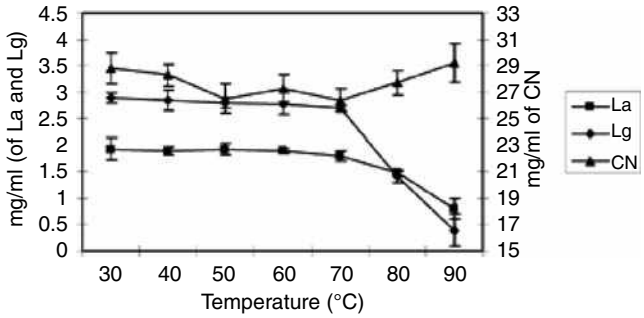

Fig. 2 Evolution of casein (CN), α-lactalbumin (α-La), and β-lactoglobulin (β-Lg) contents in raw milk heated for 5 min at defined temperatures ($n = 5$).

out to determine the accuracy of the method. Recoveries ranged between 96.3 and 99.8%.

Table 1 presents the mean contents of major proteins in bovine, ovine, and human mature milks.

Analysis of protein content in a variety of commercially processed milk and in raw milk samples showed that the Chrompack P 300 RP column enabled quantification of only "native" proteins;[15] thus, it can be used for the evaluation of the degree of heat-induced denaturation of milk proteins during processing by monitoring the remaining native milk proteins (Fig. 2). α-Lactalbumin and β-lactoglobulin were significantly affected by heat denaturation at 80°C ($p < 0.05$), whereas casein content did not present significant differences ($p > 0.05$).

RP-HPLC on polystyrene–divinylbenzene column was used for simultaneous separation and quantification of the major bovine whey proteins including proteose–peptone and caseinomacropeptide (CMP).[28] The optimized method allowed separation of proteins in 30 min and could be applied to the analysis of soluble proteins in a variety of commercial and laboratory whey products. Additionally, some information on protein heterogeneity and quality could be derived from the RP-HPLC analyses, with additional data available from on-line electrospray mass spectrometry. Within- and between-day repeatability over a wide range of concentrations was excellent (RSD < 5%) for all proteins except immunoglobulin G and bovine serum albumin where the RSD value was 7–10%. Analysis of grouped data from whey protein concentrate and whey protein isolate samples gave a detection limit of <0.3% powder mass and a quantitation limit of <1.0% powder mass for all proteins except immunoglobulin G. The detection and quantitation limits were 0.6 and 2.0%, respectively, for immunoglobulin G. Quantitative data obtained by the RP-HPLC method compared very favorably with data obtained by alternative methods of whey protein analysis.[28]

The protein composition of human milk is different from that of bovine milk.[29,30] One major difference is the level of protein, with mature milk containing less than 9 g/L in contrast to bovine milk which contains around more than 33 g/L. Although some of the protein components of human and bovine milk are similar, sequence homology and concentrations are often different.

α-Lactalbumin is the protein in highest concentration in human milk.[31] Human milk α-lactalbumin is not identical to bovine milk α-lactalbumin, although there is a 72% sequence homology[32] (Fig. 1). Concentration of this protein changes during lactation. Published values for the concentration of α-lactalbumin are highly variable, not only because of genetic, environmental, and dietary factors, but also because of the use of analytical methods with different reliability.[20,21,32,33]

RP-HPLC was applied to separate and characterize β-casein and α-lactalbumin fractions of human milk and to quantify milk protein contents.[20] The determinations were performed in the linear range of 0.09–1.5 and 0.45–3.6 g/L for β-casein and α-lactalbumin, respectively. Analysis of variance (ANOVA) showed significant differences ($p < 0.05$) between protein content in milk from different mothers at the same lactation time (1½ months). A significant decrease ($p < 0.05$) was observed for the casein and α-lactalbumin concentrations during the first 6 months of lactation.[20]

RP-HPLC SEPARATION OF CASEIN FRACTIONS: EVALUATION OF CHEESE PROTEOLYSIS

Caseins from milk and cheese samples were extracted prior to injection into an RP-HPLC column.[5] The samples were homogenized in a mortar and 1 *M* HCl was added until pH 4.3 was achieved. The resulting suspension was centrifuged at 4°C for 15 min at 3000 × *g* to recover the precipitated caseins. In order to remove the remaining fat, the sample was washed with acetone and left to dry in a fume hood at room temperature. Finally, the dried powdered casein was stored in a desiccator at 8°C until analysis was performed.

The casein powder was dissolved in a mixture of water and acetonitrile (70:30 v/v) for HPLC analyses. The solution was filtered through a 0.45 μm TR-200104 filter, composed of a mixture of cellulose esters (Teknokroma), and then was stored at –20°C until use.

Gradient elution was carried out with a mixture of two solvents: solvent A consisted of 0.1% TFA in water and solvent B was acetonitrile–water–TFA (95:5:0.1 v/v). Proteins were eluted with a series of linear gradients by increasing the proportion of solvent B from 29% to 100% over 35 min: 1–5 min, 29% B; 5–10 min, 29–37% B; 10–12 min, 37–41% B; 12–14 min, 41–42.5% B; 14–16 min, 42.5% B; 16–17 min, 42.5–43% B; 17–19 min, 43% B; 19–21 min, 43–47% B; 21–23 min, 47% B; 23–25 min, 47–54% B; 25–27 min, 54% B; 27–28 min, 54–100% B; 28–30 min, 100–29% B; 30–35 min, 29% B. The flow rate was 1 ml/min, the column temperature was 46 ± 0.1°C,

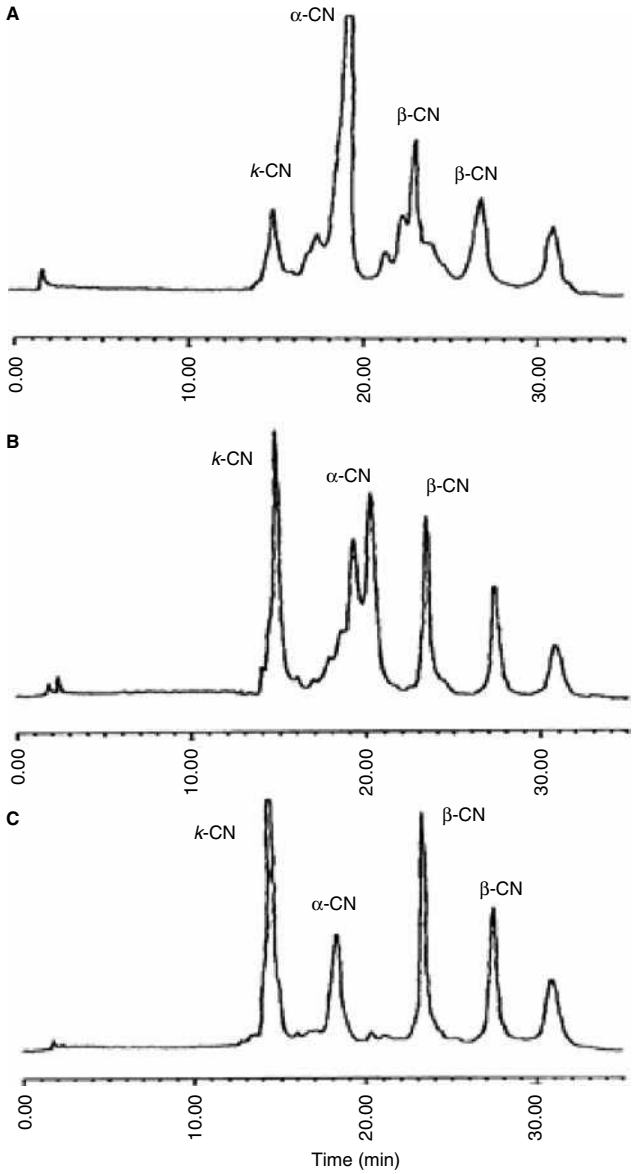

Fig. 3 Typical chromatographic profiles obtained for casein fraction from milk samples: (A) bovine, (B) ovine, and (C) caprine caseins, obtained by RP-HPLC. Detection at 280 nm.

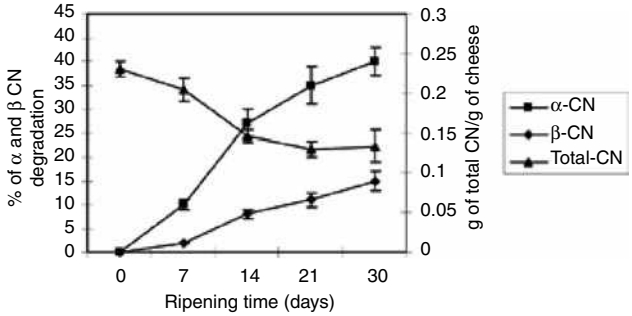

Fig. 4 Evolution of total casein content together with α- and β-casein degradation for 30 days of ripening of ewe cheese.

and the eluate was monitored at 280 nm.[5] This procedure is suitable for separation and quantification of κ-, α-, and β-caseins in raw and processed milks and cheeses because separation of the casein fraction in the three types of milk yielded good chromatographic separations (Fig. 3). Appropriate accuracy, precision, and rapidity are characteristics of the method; thus, it can be used to follow the evolution of casein content during cheese ripening and evaluate the degradation of casein fractions due to proteolysis (Fig. 4).

RP-HPLC separation can be used to evaluate the complexity and specificity of proteolytic development during cheese ripening, namely, the evolution of the four major caseins α_{s1}-, α_{s2}-, β-, and *para*-κ-caseins and its proteolytic products. RP-HPLC resolved not only proteins but also peptides, and provided proteolytic profiles that gave useful information about proteolysis extension and ripening time.[5,7,22,34,35]

The proteolytic process during 30 days of ripening of Terrincho ovine cheese based on the protein patterns obtained by HPLC from the insoluble fractions (at pH 4.3) was evaluated.[8] For that purpose gradient elution was carried out with a mixture of two solvents: solvent A consisted of 0.1% TFA in water and solvent B consisted of 0.1% TFA in 80% (v/v) aqueous acetonitrile. Proteins were eluted with a series of linear gradients: 29% of solvent B during 5 min, from 29% to 37% of B over 5 min, and from 37% to 54% of B over 15 min, keeping these conditions during

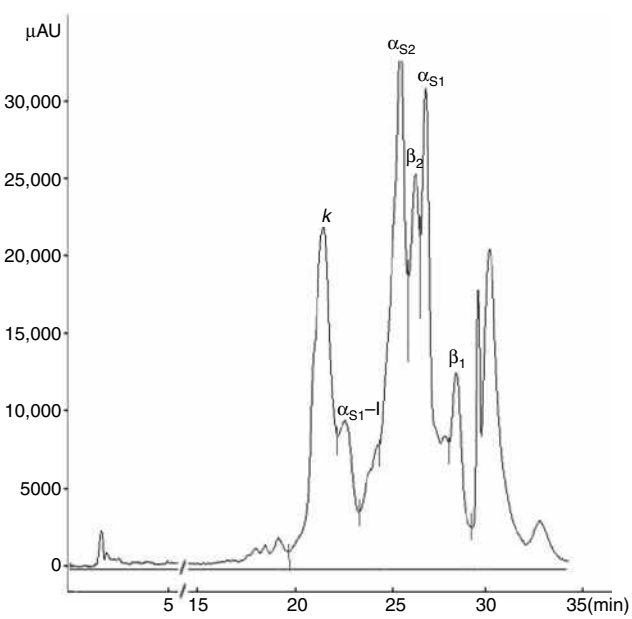

Fig. 5 Chromatographic patterns of Terrincho cheese from the pH 4.3 insoluble fractions at 1 day of ripening. κ, *para*-κ-casein; α_{s2}, α_{s2}-casein; α_{s1} α_{s1}-casein; α_{s1}-I, α_{s1}-I peptide; β_2, β_2-casein; β_1, β_1-casein.

2 min, finishing with 54–100% of B in 3 and 5 min for column re-equilibration. The flow rate was 1.0 ml/min, the column temperature was 46 ± 0.1°C, and the detection was made at a wavelength of 280 nm. Peaks were characterized using caseins from bovine and ovine milks identified according to Visser et al.[36] The areas under the five most representative peaks on the chromatogram, designated *k*-CN (*para-k*-casein), α_{s1}-I (α_{s1}-I peptide), α_{s2}-CN (α_{s2}-casein), β_2-CN (β_2-casein), α_{s1}-CN (α_{s1}-casein), and β_1-CN (β_1-casein) in order of elution (Fig. 5), were used to study the evolution of proteolytic process. It was concluded, with 95% confidence, that there were significant differences in the effect of ripening time of all quantified fractions (κ-CN, α_{s1}-I, α_{s2}-CN; α_{s1}-CN, β_1-CN, and β_2-CN). A significant reduction in the κ-CN, α_{s1}-CN, and α_{s2}-CN contents depending on the ripening time was observed, together with an increase of α_{s1}-I peptide.

Chemometric analysis of the HPLC data was also used to predict cheese ripening time[8] by multiple linear regression analysis with stepwise variable selection; two variables, α_{s1}-casein and α_{s1}-I peptide, and a constant were used. The estimation error was 2.5 days.

RP-HPLC DETECTION OF DAIRY PRODUCTS ADULTERATION

RP-HPLC of milk proteins can also be a useful tool to detect and quantify milk and cheese adulterations. For example, the substitution of bovine milk for caprine milk is a fraudulent practice; RP-HPLC analyses of the casein fraction can be used to detect bovine milk in caprine milk, with a detection limit of 5%.[5]

Adulteration of traditional ovine cheeses with bovine milk presents a problem for food monitoring, and the analysis of milk proteins is a solution for this problem.[35] However, the proteolysis that occurs during cheese ripening incurs a risk of complex formation, i.e., the formation of insoluble new compounds and smaller peptides that can interfere. Examples of these compounds are γ-casein, proteose–peptone fragments of β-casein originating from the action of plasmin, λ-caseins, presumably fragments of α_{s1}-caseins, glycomacropeptides, and *para*-κ-caseins as a result of chymosin action.[35] Discriminant analysis was applied to data from Terrincho, mixture, and bovine cheeses with 30 days of ripening obtained by RP-HPLC.[8] Peaks corresponding only to κ-CN, α_{s1}-I, α_{s2}-CN, and β_1-CN were selected; the peaks that were overlapped in mixture cheeses were excluded. The discriminant analysis indicated that three variables contributed significantly to explaining the variability among the different types of cheeses: κ-CN, α_{s1}-I, and β_1-CN. Differences between Terrincho and mixture cheeses result from higher β_1-CN content in mixture cheeses because this fraction is higher in bovine milk and more resistant to enzyme hydrolysis until 30 days of ripening.

Actually, some types of cheeses, especially protected denomination of origin cheeses, are manufactured from defined amounts of ovine, caprine, and bovine milks; thus, quantitative determination of each type of milk in mixed cheeses is an important issue. RP-HPLC separation of β-lactoglobulin can be used for detecting and quantifying bovine, ovine, and caprine milk mixtures in raw milk and cheeses.[37]

Binary mixtures of bovine and ovine or bovine and caprine raw milks containing 5, 10, 20, 30, 50, 75, and 95% (v/v) of bovine milk as well as ovine and caprine milk mixtures containing 5, 10, 20, 30, 50, 75, and 95% (v/v) of ovine milk were used for cheesemaking.[37] Cheeses were prepared with rennet whey and ripened for 4 weeks. Milk mixtures and fresh and ripened cheeses were analyzed. The whey protein fractions were obtained from the cheese samples (5 g) by extraction with water (15 ml), in a sonicator prior to centrifugation (4000 rpm, 10 min), or from 15 ml of skimmed milk. The supernatant was precipitated by addition of 1 *M* HCl until pH 4.6. After centrifugation (4000 rpm, 10 min), the resultant supernatant was filtered prior to HPLC analysis. All the samples were stored at 4°C.

Gradient elution was carried out with a mixture of two solvents:[37] solvent A consisted of 0.1% TFA in water and solvent B consisted of 0.1% TFA in 80% (v/v) aqueous acetonitrile. Proteins were eluted with a series of linear gradients, increasing the proportion of solvent B from 36% to 56% over 20 min, from 56% to 60% of B over 10 min, finishing with 60–36% of B in 5 min. The flow rate was 0.5 ml/min, the column temperature was 45 ± 0.1°C, and the detection was performed at a wavelength of 215 nm. Different chromatographic profiles were obtained for each type of milk in binary mixtures, as shown in Fig. 6.

A linear relationship was established between the $\log_{10}$ of β-lactoglobulin peak ratio (calculated as peak area ratio) and the $\log_{10}$ of the relative percentage of bovine or ovine milk (Figs. 7–9). The ratio between β-lactoglobulin peaks was not affected by the degree of ripening ($p < 0.05$), thus enabling the quantification of milk type percentage. The detection limit was 2%. This technique allowed quantification of milk species within the concentration range of 5–95%.

Dairy products, such as milk powder, should be prepared exclusively from milk and should not contain solids from whey. The absence of rennet whey solids from milk powder is required according to legislation. Considering the lower price of rennet whey, it can be an attractive adulterant of milk powder. Thus, the presence of CMP can be a good marker to evaluate milk powder authenticity.[38] Whey powders contain about 12% protein and 75% lactose. Caseinomacropeptide can account for more than 16% of the protein content. RP-HPLC can be used to detect rennet whey in milk powder by CMP measurement.[38] For this purpose, powdered milks were reconstituted with deionized water. Skim milks were prepared by separating the fat from the whole milk by centrifugation at 700 × *g* (at 4°C) for 10 min. Caseinomacropeptide and

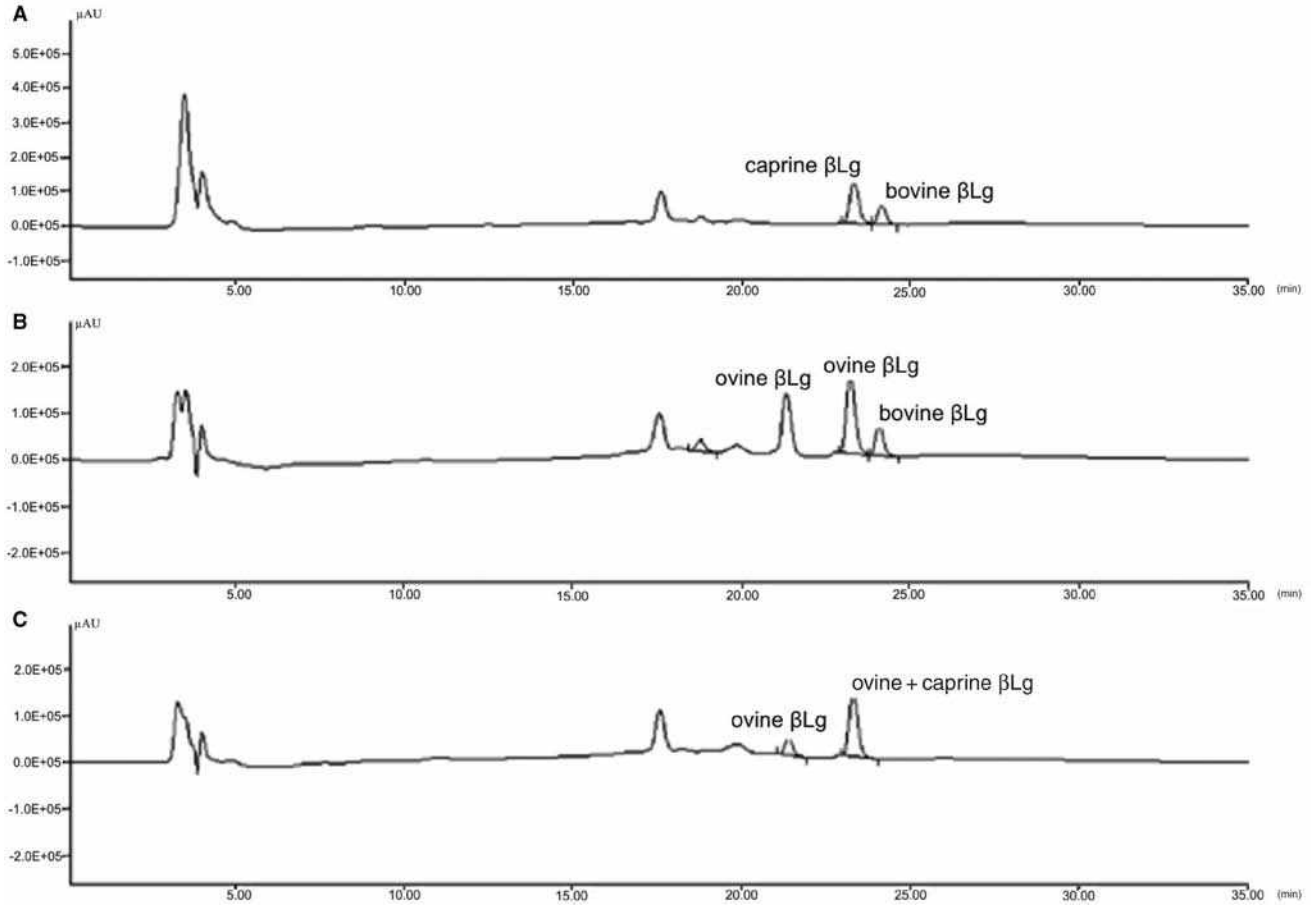

Fig. 6 Typical chromatographic profiles of whey proteins extracted from cheeses manufactured with binary milk mixtures: (A) 20% bovine milk and 80% caprine milk; (B) 20% bovine milk and 80% ovine milk; (C) 20% ovine milk and 80% caprine milk.

other whey protein fractions were extracted after casein precipitation with 1 *M* HCl until pH 4.6, centrifugation at $700 \times g$ (10 min), and filtration of the supernatant.

The column was equilibrated in 80% solvent A [0.1% (v/v) TFA in water] and, after sample injection, a series of linear gradients was applied to 100% solvent B [0.1% (v/v) TFA in 80% (v/v) aqueous acetonitrile] as follows: 1–6 min, 20–40% B; 6–16 min, 40–45% B; 16–19 min, 45–50% B; 19–20 min, 50% B; 20–23 min, 50–70% B; 23–24 min, 70–100% B. The column was re-equilibrated after a 1 min hold at 100% B by a 2 min linear gradient to 20% B, followed by an isocratic period of 3 min. The flow rate was 1 ml/min at room temperature, and the detection was at 214 nm.[38]

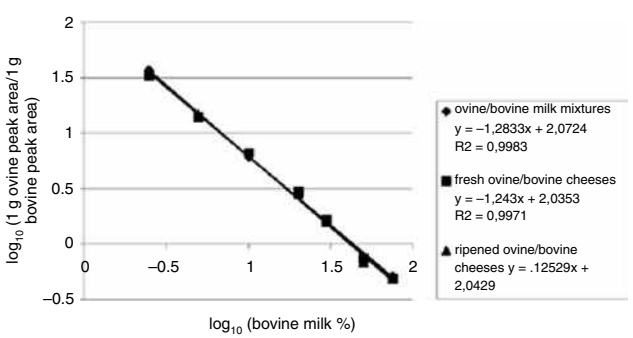

Fig. 7 Relationship between $\log_{10}$ of the ratio ovine β-lactoglobulin peak/bovine β-lactoglobulin peak (calculated as peak area ratio) and $\log_{10}$ of bovine milk percentage.

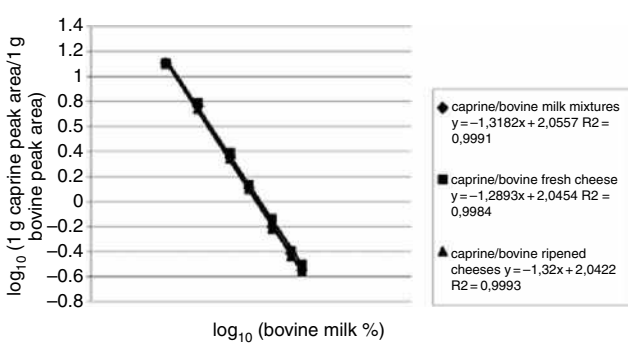

Fig. 8 Relationship between $\log_{10}$ of the ratio caprine β-lactoglobulin peak/bovine β-lactoglobulin peak (calculated as peak area ratio) and $\log_{10}$ of bovine milk percentage.

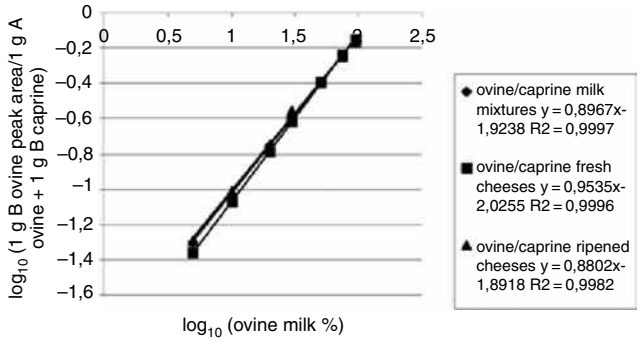

Fig. 9 Relationship between $\log_{10}$ of the ratio ovine β-lactoglobulin peak/ovine + caprine β-lactoglobulin peak (calculated as peak area ratio) and $\log_{10}$ of ovine milk percentage.

Two peaks, corresponding to the aglyco components of the two principal genetic variants (A and B) of CMP, eluted after less-resolved glyco-CMP components.[38] Calibration curves with concentrations ranging from 15 to 200 mg/ml were constructed. The detection limit was 2 mg/ml. Recoveries of 93% and 97% were obtained for concentration levels 0.10 and 0.20 mg/ml, respectively. The RSD was less than 4.87% ($n = 10$). Thus, the HPLC/UV procedure is suitable for detection of adulteration of powdered milk with rennet whey.

RP-HPLC CHARACTERIZATION OF ENZYMATIC HYDROLYSIS OF WHEY PROTEINS

In recent years there has been growing interest in bioactive peptides derived from whey proteins; such peptides have been found to exert various bioactivities both in vitro and in vivo, e.g., protective functions, regulation of digestion and nutrient uptake, and metabolic or physiological regulation of the body.[39] From a dietary point of view, protein hydrolysates can also be used, e.g., to reduce allergenicity or to improve digestibility of foodstuffs. In any case, it has been shown that protein hydrolysates should be rich in low-molecular-weight peptides with dietary advantages.[39] Depending on the type of product in which peptides will be incorporated, the degree of hydrolysis need is different. So far, the most common way to produce bioactive peptides has been through enzymatic digestion. Enzymes such as trypsin, pepsin, and Alcalase® have been used for identification of many known bioactive peptides.[39]

RP-HPLC can be used to determine the extent of degradation of native whey proteins (β-lactoglobulin and α-lactalbumin) by enzymes and to study their kinetics of degradation by monitoring both the disappearance of α-lactalbumin and β-lactoglobulin and the appearance of peptide products.[40] It can also be used to evaluate whether the chromatographic profile obtained is affected by temperature and pH conditions of the environment or is only dependent on the enzyme type.[40]

Gradient elution was carried out with a mixture of two solvents: solvent A consisted of 0.1% TFA in water and solvent B consisted of 0.1% TFA in 80% (v/v) aqueous acetonitrile. Proteins and peptides can be eluted as follows: 0–1 min, 90% A; 1–10 min, 90–80% A; 10–15 min, 80–75% A; 15–20 min, 75–60% A; 20–30 min, 60–50% A; 30–33 min, 50–40% A; 33–36 min, 40–30% A; 36–39 min, 30–20% A; 39–41 min, 20–0% A, and then returning to initial conditions in 4 min. Hydrolysis of whey protein concentrates at different temperatures and pHs using different enzymes, e.g., pepsin, trypsin, and Alcalase, was monitored.[40] The hydrolysis catalyzed by each enzyme results in different peptide profiles that can be used as fingerprints of the type of enzyme used (Fig. 10).

RP-HPLC using a polystyrene–divinylbenzene column was used for separation and quantification of angiotensin-converting enzyme (ACE) inhibitory peptides.[41,42] ALPMHIR, the most potent β-lactoglobulin-derived ACE inhibitory peptide was assayed during hydrolysis of whey protein concentrates with trypsin, and a correlation curve was constructed for the formation of this peptide as a function of hydrolysis time.[41] Two casein peptides (IPP Iso-Pro-Pro, VPP Val-Pro-Pro) presenting potent inhibitory activity of ACE and casein were simultaneously separated and quantified in commercial fermented milks labeled as presenting antihypertensive properties.[42] The detection limits were 0.004 mg/ml for VPP, 0.002 mg/ml for IPP, and 0.02 mg/ml for casein. The RSD values for concentration were below 5.08%, and recoveries ranged between 88% and 98.2%.

CONCLUSIONS

This work reports the results of the examination of the utility of RP-HPLC, using a polystyrene–divinylbenzene packing as stationary phase, for separation of milk proteins and peptides. In this type of column, separation is based on hydrophobicity, a phenomenon of great biological significance, because it is the main force that stabilizes the three-dimensional structure of proteins. Protein retention is controlled by increasing the concentration of acetonitrile, thereby altering the polarity of the aqueous mobile phase. Thus, different chromatographic conditions were used to separate and quantify milk proteins and to follow the extension of whey protein denaturation by heating or the evolution of cheese proteolysis. Detection of dairy product adulteration and study of the kinetics of whey protein enzymatic hydrolysis are other useful applications of RP-HPLC.

No loss in performance of the method or the column due to matrix contamination (e.g., by sugars) was observed during these studies. Also, the use of TFA in the mobile phase did not have adverse effects on the long-term stability of the column and increased peak resolution.

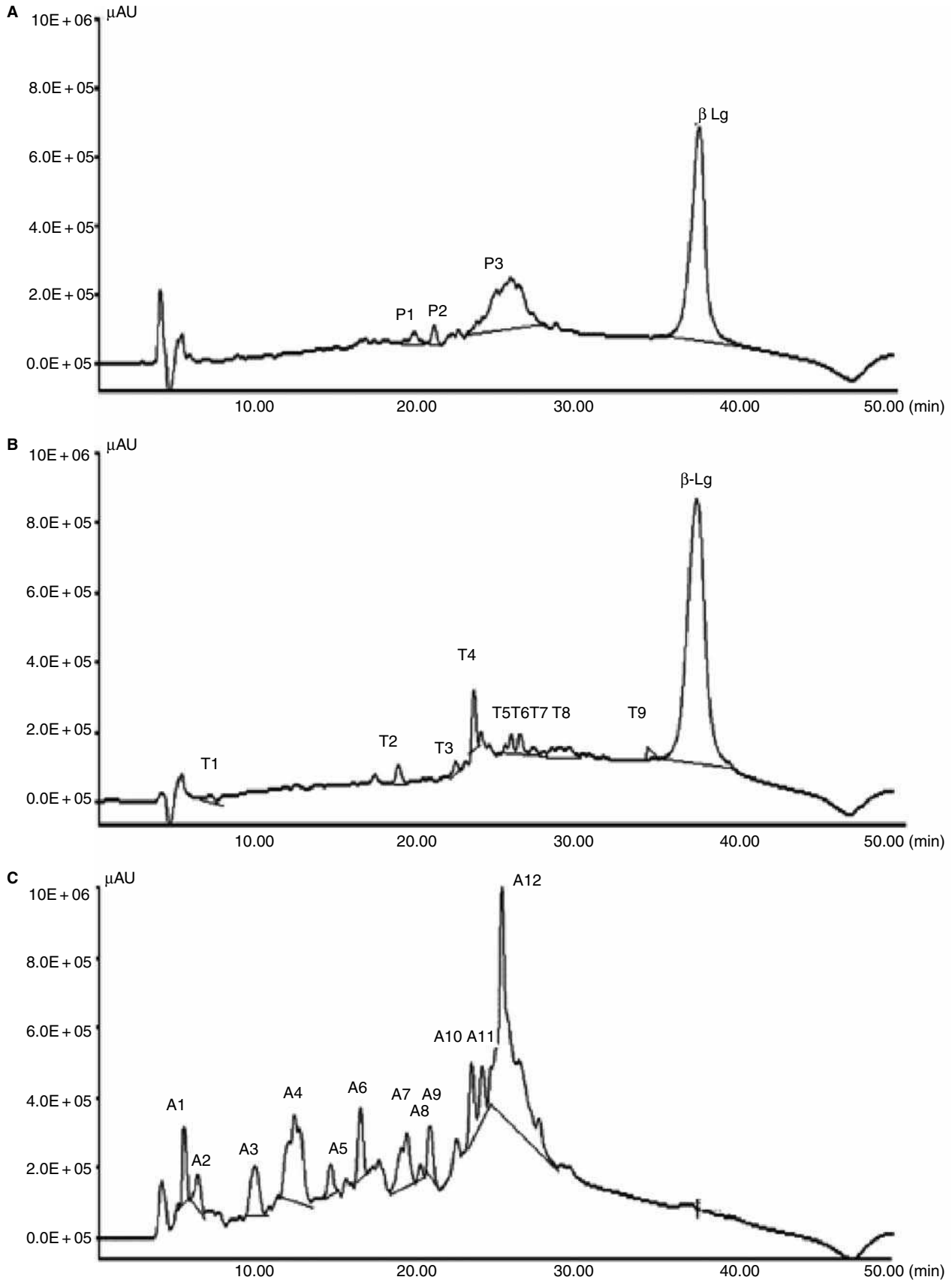

Fig. 10 Typical RP-HPLC profiles of whey protein hydrolysates ($T = 37°C$, 60 min hydrolysis time): (A) pepsin hydrolysis, pH2, three major fractions were designated P1 P3; (B) trypsin hydrolysis, pH 8, nine major fractions were designated T1–T9; (C) Alcalase hydrolysis, pH8, 12 major fractions were designated A1–A12.

REFERENCES

1. Belitz, H.D.; Grosch, W.; Schieberle, P. Milk and dairy products. In *Food Chemistry*, 3rd Ed. (revised); Belitz, H.D.; Grosch, W.; Schieberle, P., Eds.; Springer-Verlag: Berlin, 2004; 505–549.
2. Farkye, N.Y.; Kiely, L.J.; Allshouse, R.D.; Kindstedt, P.S. Proteolysis in mozzarella cheese during refrigerated storage. J. Dairy Sci. **1991**, *74*, 1433–1438.
3. Mayer, W.; Hörtner, H. Discontinuous electrophoresis of β-casein for the determination of bovine caseins in milk and dairy products. Electrophoresis **1992**, *13*, 803–804.
4. Carretero, C.; Trujillo, A.J.; Mor-Mur, M.; Pla, R.; Guamis, B. Electrophoretic study of casein breakdown during ripening of goat's milk cheese. J. Agric. Food Chem. **1994**, *42*, 1546–1550.
5. Veloso, A.C.A.; Teixeira, N.; Ferreira, I.M.P.L.V.O. Separation and quantification of the major casein fractions by reverse-phase liquid chromatography and urea–polyacrylamide gel electrophoresis: Detection of milk adulterations. J. Chromatogr. A, **2002**, *96*, 209–218.
6. Gobbetti, M.; Morea, M.; Baruzzi, F.; Corbo, M.R.; Matarante, A.; Considine, T.; Di Cagno, R.; Guinee, T.; Fox, P.F. Microbiological, compositional, biochemical and textural characterisation of Caciocavallo Pugliese cheese during ripening. Int. Dairy J. **2002**, *12* (6), 511–523.
7. Veloso, A.C.A.; Teixeira, N.; Peres, A.M.; Mendonça, A.; Ferreira, I.M.P.L.V.O. Evaluation of cheese authenticity and proteolysis by HPLC and urea–polyacrylamide gel electrophoresis. Food Chem. **2004**, *87*, 289–295.
8. Ferreira, I.M.P.L.V.O.; Veiros, C.; Pinho, O.; Veloso, A.C.A.; Peres, A.M.; Mendonça, A. Casein breakdown in Terrincho ovine cheese: Comparison with bovine cheese and with bovine/ovine cheeses. J. Dairy Sci. **2006**, *89*, 2397–2407.
9. Basch, J.J.; Douglas, F.W.; Procino, L.G.; Holsinger, V.H.; Farrell, H. Quantification of caseins and whey proteins of processed milks and whey protein concentrates application of gel electrophoresis and comparison with Harland–Ashworth procedure. J. Dairy Sci. **1985**, *68*, 23–31.
10. Jin, Y.K.; Park, Y.W. SDS–PAGE of proteins in goat milk cheeses ripened under different conditions. J. Food Sci. **1996**, *61*, 490–494.
11. Kim, H.-H.Y.; Jimenez-Flores, R. Comparison of milk proteins using preparative isoelectric focusing followed by polyacrylamide gel electrophoresis. J. Dairy Sci. **1994**, *77*, 2177–2190.
12. Andrews, A.T.; Taylor, M.D.; Owen, A.J. Rapid analysis of bovine milk proteins by fast protein liquid chromatography. J. Chromatogr. **1985**, *348*, 177–185.
13. Kaminarides, S.E.; Anifaantakis, E.M. Comparative study of the separation of casein from bovine, ovine and caprine milks using HPLC. J. Dairy Res. **1993**, *60*, 495–504.
14. Ferreira, I.M.P.L.V.O.; Mendes, E.; Marques, J.; Ferreira, M.A. Development, validation and application of an HPLC/UV method for quantification of casein in infant formulae and follow-up milks. J. Liq. Chromatogr. Rel. Technol. **2000**, *23*, 2057–2065.
15. Ferreira, I.M.P.L.V.O.; Mendes, E.; Ferreira, M.A. HPLC/UV analysis of proteins in dairy products using a hydrophobic interaction chromatographic column. Anal. Sci. **2001**, *17*, 499–501.
16. Gupta, B.B. Determination of native and denatured milk proteins by high-performance size exclusion chromatography. J. Chromatogr. **1983**, *282*, 463–475.
17. Visser, S.; Slangen, C.J.; Rollema, H.S. Phenotyping of bovine milk proteins by reversed-phase high-performance liquid chromatography. J. Chromatogr. **1991**, *548*, 361–370.
18. Bobe, G.; Beitz, D.C.; Freeman, A.E.; Lindberg, G.L. Separation and quantification of bovine milk proteins by reversed-phase high-performance liquid chromatography. J. Agric. Food Chem. **1998**, *46*, 458–463.
19. Michaelidou, A.; Alichanidis, E.; Urlaub, H.; Polychroniadou, A.; Zerfiridis, G.K. Isolation and identification of some major water-soluble peptides in feta cheese. J. Dairy Sci. **1998**, *81*, 3109–3116.
20. Ferreira, I.M.P.L.V.O. Chromatographic separation and quantification of major human milk proteins. J. Liq. Chromatogr. Rel. Technol. **2007**, *30*, 1–9.
21. Santos, L.H.L.M.L.M.; Ferreira, I.M.P.L.V.O. Quantification of α-lactalbumin in human milk: Method validation and application. Anal. Biochem. **2007**, *362*, 293–295.
22. Trujillo, A.J.; Isidre, C.; Buenaventura, G. Analysis of major ovine milk proteins by reversed-phase high-performance liquid chromatography and flow injection analysis with electrospray ionization mass spectrometry. J. Chromatogr. A, **2000**, *870*, 371–380.
23. Haza, A.I.; Morales, P.; Martín, R.; García, T.; Anguita, G.; González, I.; Sanz, B.; Hernández, P.E. Development of monoclonal antibodies against caprine α_{s2}-casein and their potential for detecting the substitution of ovine milk by caprine milk by an indirect ELISA. J. Agric. Food Chem. **1996**, *44*, 1756–1761.
24. Recio, I.; Amigo, L.; López-Fandiño, R. Assessment of the quality of dairy products by capillary electrophoresis of milk proteins. J. Chromatogr. B, **1997**, *697*, 231–242.
25. Cartoni, G.; Coccioli, F.; Jasionowska, R.; Masci, M.D. Determination of cows' milk in goats' milk and cheese by capillary electrophoresis of the whey protein fractions. J. Chromatogr. A, **1999**, *846*, 135–141.
26. Miralles, B.; Ramos, M.; Amigo, L. Application of capillary electrophoresis to the characterization of processed cheeses. J. Dairy Res. **2000**, *67*, 91–100.
27. Molina, E.; Frutos, M.; Ramos, M. Capillary electrophoresis characterization of the casein fraction of cheeses made from cows', ewes' and goats' milks. J. Dairy Res. **2000**, *67*, 209–216.
28. Elgar, D.F.; Norris, C.S.; Ayers, J.S.; Pritchard, M.; Otter, D.E.; Palmano, K.P. Simultaneous separation and quantification of the major bovine whey proteins including proteose peptone and caseinomacropeptide by reversed-phase high-performance liquid chromatography on polystyrene–divinylbenzene. J. Chromatogr. A, **2000**, *878*, 183–196.
29. Cavaletto, M.; Cantisani, A.M.; Napolitano, L.; Giuffrida, M.G.; Calderone, V., Fabris, C.; Bertino, E.; Prandi, M.G.; Conti, A. Comparative study of casein content in human colostrum and milk. Milchwissenschaft **1994**, *49*, 303–305.
30. Kroening, T.A.; Mukerji, P.; Hards, R.G. Analysis of beta-casein and its phosphoforms in human milk. Nutr. Res. **1998**, *18*, 1175–1186.

31. Lönnerdal, B. Nutritional and physiologic significance of human milk proteins. Am. J. Clin. Nutr. **2003**, *77*, 1537S–1543S.
32. Jackson, J.G.; Janszen, D.B.; Lonnerdal, B.; Lien, E.L.; Pramuk, K.P.; Kuhlman, C.F. A multinational study of α-lactalbumin concentrations in human milk. J. Nutr. Biochem. **2004**, *15*, 517–521.
33. Montagne, P.M.; Cuillière, M.L.; Molé, C.M.; Béné, M.C.; Faure, G.C. Dynamics of the main immunologically and nutritionally available proteins of human milk during lactation. J. Food. Comp. Anal. **2000**, *13*, 127–137.
34. Restani, P.; Velonà, T.; Carpen, A.; Duranti, M.; Galli. C.L. γ-Casein as a marker of ripening and/or quality of Grana Padano cheese. J. Agric. Food Chem. **1996**, *44*, 2026–2029.
35. Borková, M.; Snáselová, J. Possibilities of different animal milk detection in milk detection in milk and dairy products—A review. Czech J. Food Sci. **2005**, *23*, 41–50.
36. Visser, S.; Slengen, C.J.; Rollema, H.S. Phenotyping of bovine milk proteins by reversed-phase high-performance liquid chromatography. J. Chromatogr. **1991**, *548*, 361–370.
37. Ferreira, I.M.P.L.V.O.; Caçote, H. Detection and quantification of bovine, ovine and caprine milk percentages in protected denomination of origin cheeses by reversed-phase high-performance liquid chromatography of beta-lactoglobulins. J. Chromatogr. A, **2003**, *1015*, 111–118.
38. Ferreira, I.M.P.L.V.O.; Oliveira, M.B.P.P. Determination of caseinomacropeptide by an RP-HPLC method and monitoring of the addition of rennet whey to powdered milk. J. Liq. Chromatogr. Rel. Technol. **2003**, *26* (1), 99–107.
39. Clare, D.A.; Swaisgood, H.E. Bioactive milk peptides: A prospectus. J. Dairy Sci. **2000**, *83*, 1187–1195.
40. Mota, M.V.T.; Ferreira, I.M.P.L.V.O.; Oliveira, M.B.P.; Rocha, C.; Teixeira, J.A.; Torres, D.; Gonçalves, M.P. Enzymatic hydrolysis of whey protein concentrates: peptide HPLC profiles. J. Liq. Chromatogr. Rel. Technol. **2004**, *26* (16), 2625–2639.
41. Ferreira, I.M.P.L.V.O.; Pinho O.; Mota, M.V.; Tavares, P.; Pereira, A.; Gonçalves, M.P.; Torres, D.; Rocha, C.; Teixeira, J.A. Preparation of ingredients containing an ACE-inhibitory peptide by tryptic hydrolysis of whey protein concentrates. Int. Dairy J. **2007**, *17*, 481–487.
42. Ferreira, I.M.P.L.V.O.; Pinho O.; Tavares, P.; Pereira, A.; Roque, A.C. Development and validation of an HPLC/UV method for quantification of bioactive peptides in fermented milks. J. Liq. Chromatogr. Rel. Technol. **2007**, *30*, 1–9.

Minimum Detectable Concentration or Sensitivity

Raymond P.W. Scott
Scientific Detectors Ltd., Banbury, Oxfordshire, U.K.

INTRODUCTION

Detector sensitivity or the minimum detectable concentration (MDC) is defined as the minimum concentration of solute passing through the detector that can be unambiguously distinguished from the noise. The size of the signal that will be distinct from the noise (the signal-to-noise ratio) will be an arbitrary choice. In electronic measuring systems, it is generally accepted that a signal can be differentiated from the noise when the signal-to-noise ratio is 2. This criterion has been generally adopted for physical–chemical measurements and is used to define detector sensitivity in chromatography.

DISCUSSION

For a concentration-sensitive detector, the detector sensitivity or MDC is given by

$$X_D = \frac{2N_D}{R_c}\left(\frac{\text{g}}{\text{ml}}\right)$$

where R_c is the response of the detector (i.e., the voltage output for unit change in concentration (V/g/ml) and N_D is the detector noise level (V).

The sensitivity or MDC of a detector is *not* the same as the minimum mass that can be detected. This would be the *system mass sensitivity*, which will depend on the characteristics of the column and the chromatographic properties of the solute, as well as the detector specifications. In all chromatographic systems, the peak becomes broader as the retention increases. Consequently, a given mass may be detected if eluted as a narrow peak early in the chromatogram, but if eluted later, its peak height may be reduced to such an extent that it is impossible to discern it from the noise. Thus, detector sensitivity quoted as the "minimum mass detectable" must be carefully examined and related to the chromatographic system and, particularly, the column with which it is to be used. If the data to do this are not available, then the sensitivity must be calculated from the detector response and the noise level in the manner described earlier.

Some manufacturers have taken the minimum detectable concentration and multiplied it by the sensor volume and defined the product as the minimum detectable mass. This gives values that are very misleading. For example, a detector having a true sensitivity of 10^{-6} g/ml and a sensor volume of 10 μl would be attributed to a mass sensitivity of 10^{-8}g. This is grossly incorrect, as it is the *peak volume* that controls the mass sensitivity, not the *sensor volume*. Conversely, if the peak volume does approach that of the sensor, then a very serious peak distortion occurs with loss of resolution; thus, this way of specifying sensitivity remains meaningless.

BIBLIOGRAPHY

1. Scott, R.P.W. *Chromatographic Detectors*; Marcel Dekker, Inc.: New York, 1996.
2. Scott, R.P.W. *Introduction to Gas Chromatography*; Marcel Dekker, Inc.: New York, 1998.

Mixed Stationary Phases in GC

Raymond P.W. Scott
Scientific Detectors Ltd., Banbury, Oxfordshire, U.K.

INTRODUCTION

The desired interactive character of a gas chromatography (GC) stationary phase is usually obtained by choosing a thermally stable substance that contains the appropriate polar and dispersive groups that can provide the necessary molecular interactions for sample resolution.

BACKGROUND INFORMATION

Purnell and coworkers[1] pioneered an alternative approach to stationary-phase polarity control for GC. These workers demonstrated that for a wide range of stationary phases made up of binary mixtures, the corrected retention volume of a solute was linearly related to the volume fraction of either one of the two phases. At the time of discovery, this was quite an unexpected relationship, as it was generally accepted that the expression for the retention volume would take the form of the exponent of the stationary-phase composition. The results of Purnell and his co-workers can be summarized by

$$V_{r(A)}{}' = K_A \alpha V_S + K_B(1-\alpha)V_S$$

where $V_{r(AB)}{}'$ is the retention volume of the solute on a mixture of stationary phases A and B, K_A is the distribution coefficient of the solute with respect to the pure stationary phase A, K_B is the distribution coefficient of the solute with respect to the pure stationary phase B, V_S is the total volume of the stationary phase in the column, and α is the volume fraction of phase A in the stationary-phase mixture; that is,

$$V_{r(AB)}{}' = \alpha V_A{}' + (1-\alpha)V_B{}' \quad (1)$$

where $V_A{}'$ is the retention volume of the solute on the same volume of pure phase A and $V_B{}'$ is the retention volume of the solute on the same volume of pure phase B.

Rearranging Eq. 1,

$$V_{AB}{}' = \alpha(V_A{}' - V_B{}') + V_B{}' \quad (2)$$

This remarkably simple relationship is depicted in Fig. 1.

Purnell carried out three experiments to examine the effect of the composition of binary mixtures of stationary phases on solute retention. In the first experiment, the two fractions were mixed, coated on some support, and packed into the column. In the second experiment, each of the two fractions was coated on separate aliquots of support and the coated supports mixed and packed in a column. In the third experiment, each fraction was coated on a support and each support packed into separate columns and the columns joined in series. Purnell demonstrated that all three columns gave exactly the same corrected retention volume for a given solute.

It was found, however, that where strong association occurred between the two phases, there were exceptions to this relationship. If a strong association took place, the blend would no longer be a simple binary mixture but would contain the associate of the two phases as a third component. It is clear that for a ternary mixture, the simple linear relationship obtained for a binary mixture would not hold. The simple linear relationship for the binary mixture is not surprising. The distribution coefficient of the solute with either pure component is a constant. It follows that the volume fraction of each phase will determine the probability that a solute molecule will interact with a molecule of that phase. This is analogous to the partial pressure of solute determining the probability that a solute molecule will collide with a gas molecule.

Doubling the volume fraction of one phase doubles the probability of solute interaction and, consequently, doubles its contribution to retention. There is another interesting outcome from the results of Purnell and his co-workers. Where a linear relationship existed between the retention volume and the volume fraction of the stationary phase, the linear functions of the distribution coefficients could be summed directly, but their logarithms could *not*. In many classical thermodynamic descriptions of the effect of the stationary-phase composition on solute retention, the stationary-phase composition is often taken into account by including an extra term in the expression for the standard free energy of distribution. The results of Purnell indicate that this is not acceptable, as the solute retention or distribution coefficient is *linearly* not exponentially related to the stationary-phase composition. The stationary phases of intermediate polarities can easily be constructed from binary mixtures of a strongly dispersive stationary

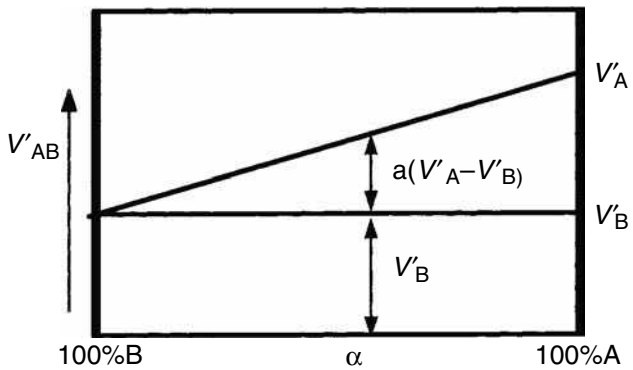

Fig. 1 Graph of corrected retention volume vs. volume fraction of the stationary phase.

phase and one that is strongly polar. This procedure is not commonly used for commercial columns, although it is a simple and economic method for constructing columns having intermediate polarities. Mixed phases are always worth considering as a flexible alternative to the use of a specific proprietary material.

REFERENCE

1. McCann, M.; Purnell, J.H.; Wellington, C.A. Proceedings of the Faraday Symposium, Chemical Society, 1980, 83.

BIBLIOGRAPHY

1. Scott, R.P.W. *Techniques of Chromatography*; Marcel Dekker, Inc.: New York, 1995.
2. Scott, R.P.W. *Introduction to Gas Chromatography*; Marcel Dekker, Inc.: New York, 1998.

Mixed Stationary Phases: Synergistic Effects in GC

L.M. Yuan
Department of Chemistry, Yunnan Normal University, Kunming, China

INTRODUCTION

It is generally believed that multicomponent stationary phases, or mixed stationary phases, show the average effect of individual pure phases in gas chromatography (GC). Investigations have shown the existence of a synergistic effect in some mixed GC stationary phases and about 18 entries have been published since 1996.[1,2] Some chromatographic properties of the mixtures, such as separation factor (α), retention factor (k'), elution order of Grob test regent, and McReynolds constants, are not the simple addition of the chromatographic properties of the two pure phases. These values of mixed stationary phases may be greater or less than either of the pure stationary phases. It is different from general experimental results. The positive synergistic effect is very useful in the separation of some substance pairs.

SYNERGISTIC EFFECT

The synergistic effect was first discovered in 1957 by Blake in the study of extraction of U(VI).[3] It has been widely studied in the extraction of inorganic and organic compounds. Generally, mixed stationary phases prepared from polar or non-polar stationary phases show the average effect of the corresponding individual pure phases. But for a few isomers, the separation factor (α) obtained by the use of the capillary columns coated with side-chain crown ether polysiloxane (PDB-14-C4) + heptakis(2,3,6-tri-*O*-ethyl)-β-cyclodextrin (PE-β-CD) was greater or smaller than those obtained from the individual columns coated with either PDB-14-C4 or PE-β-CD; a new term, the "coordination effect" was suggested to describe this unexpected and puzzling phenomenon.[1] Yuan et al. studied it carefully and used the "synergistic effect" to describe it because gas–liquid chromatography is actually partition chromatography and its principle is similar to solvent extraction.[4] The purpose of the present paper is to investigate this phenomenon using packed columns containing heptakis(2,3,6-tri-*O*-pentyl)-β-cyclodextrin + $AgNO_3$, heptakis(2,3,6-tri-*O*-pentyl)-β-cyclodextrin + $TlNO_3$, and xylene isomers as sample compounds.[3] They have positive synergistic effects for the separation of *m*- and *p*-xylene isomers, but negative synergistic effects for the *m*- and *O*-isomers (see Figs. 1 and 2).

The packed column gas chromatographic separations of some other aromatic compounds using special selectivity mixed stationary phase consisting of heptakis(2,3,6-tri-*O*-pentyl)-β-cyclo-dextrin + $AgNO_3$, heptakis(2,3,6-tri-*O*-pentyl)-β-cyclodextrin + $TlNO_3$, bentone + $AgNO_3$, and heptakis(2,3,6-tri-*O*-pentyl)-β-cyclodextrin + *O*-methyl-*p*-phenylene-bis-(*p*-heptoxy benzoate) liquid crystalline (BPBHpB) were investigated too. Most of the separations deviated from the additivity, and the synergistic effect was observed.[5] The synergistic effects of packed columns, by mixing the stationary phases before coating the support, were more pronounced than those from columns mixing the two packings.

A great deal of research about the synergistic effect of GC was reported using capillary column GC. Based on the experiences developed in Ref.[3] ethylhexylresorcarene + heptakis(2,6-di-*O*-pentyl-3-*O*-trifluoroacetyl)-β-CD mixed stationary phase was used for isomer separation.[6] Heptakis(2,3,6-tri-*O*-butyl)-β-cyclodextrin + $AgNO_3$ was used for some enantiomer and isomer separations.[7] Synergistic effects were observed on those phases. By investigating the chromatographic properties of the mixed stationary phase containing heptakis(2,3,6-tri-*O*-pentyl)-β-cyclodextrin + PEG-20M, the synergistic effect was observed in this mixed stationary phase.[8] Several similar synergistic effects were shown for the phases mixed with heptakis(2,3,6-tri-*O*-pentyl)-β-cyclodextrin + MPBHpB,[9] BPBHpB + heptakis(2,6-di-*O*-pentyl-3-allyl)-β-cyclodextrin, heptakis(2,3,6-tri-*O*-pentyl)-β-cyclodextrin + Dibenzo-18-crown-6, heptakis(2,3,6-tri-*O*-pentyl)-β-cyclodextrin + resorcarene derivative, and 25,27-dibutoxy-5,11,17,23-tetra-*tert*-butyl-26,28-diundecenyloxy cali[4]arene + permethyl-β-cyclodextrin.[9,10] Mixed cyclodextrin derivatives such as permethylated β-CD + heptakis(2,6-di-*O*-butyl-3-*O*-butyryl)-β-CD and permethylated β-CD + heptakis(2,6-di-*O*-nonyl-3-*O*-trifluoroacetyl)-β-CD had synergistic effects in the separation of enantiomers.[11] Our recent investigation has also shown the existence of a synergistic effect in mixed perpentylated-β-CD + permethylated β-CD stationary phase for the separation of enantiomers.

Besides cyclodextrin derivatives, other mixed special selectivity stationary phases also had synergistic effects in the separation of isomers. Those reported include dibenzo-18-crown-6 + MPBHpB,[12] dibenzo-18-crown-6 and resorcarene derivative,[2] MPBHpB + resorcarene derivative,[13] and 25,27-dibutoxy-5,11,17,23-tetra-*tert*-butyl-26,

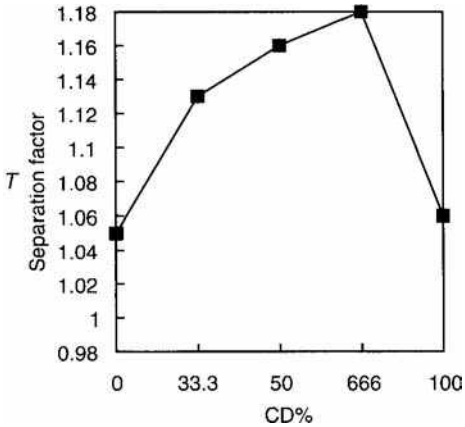

Fig. 1 Plot of $\alpha_{p,m}$ vs. CD% on mixed stationary phases.
Source: From U.S. Atomic Energy Commission.[3]

28-diundecenyloxy cali[4]arene + ω-undecylomethyl-18-crown-6 polysiloxane.[10]

The effects of temperature, linear velocity of carrier gas, and relative amounts of the individual phases in the mixed stationary phase were also examined.[2,4,5,8,9,12,13] These facts show that the synergistic effect is dependent upon the above three factors.

The synergistic effect was only found in mixed stationary phases that have a special selectivity. Those stationary phases were CD, crown ether, liquid crystalline, resorcarene, calixarene, $AgNO_3$, and others. Crown ether, CD, calixarene, and resorcarene possess cyclic moieties with cavity-like structures that are able to form inclusion complexes with metal ions and organic molecules. Liquid crystalline stationary phases have temperature-dependent ordered structures and the retention is governed by the solute's length-to-breadth ratio. $AgNO_3$ retards olefins by the formation of loose adducts. Together with the above special selectivity stationary phases, they have already been the focal point of supramolecular chemistry.

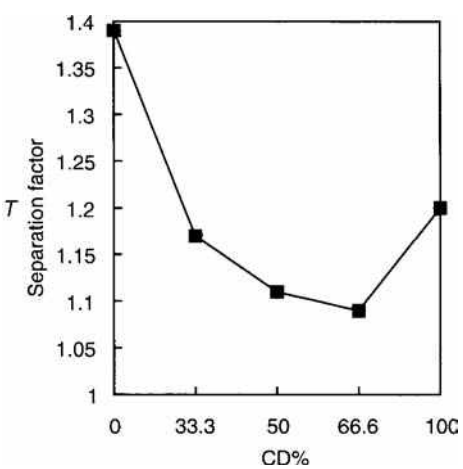

Fig. 2 Plot of $\alpha_{o,m}$ vs. CD% on mixed stationary phases.
Source: From U.S. Atomic Energy Commission.[3]

CONCLUSIONS

A synergistic effect of mixed stationary phases that have special selectivity exists in GC. It is based on the "steric fit" and on the probability of simultaneous interaction of mixed stationary phases with the solute pair. It can be assumed that the largest synergistic effect is attained with maximum steric fit and simultaneous interaction probability. This probability may depend on temperature, mixing ratio, linear velocity of carrier gas, and how mixing is accomplished.

ACKNOWLEDGMENTS

The work is supported by the National Natural Science Foundation, Yunnan Province's Natural Science Foundation, and TRAPOYT of China.

REFERENCES

1. Jing, P.; Fu, R.N.; Dai, R.J.; Gu, J.L.; Huan, Z.; Chen, Y. Consequence of diluting modified β-cyclodextrins in a side-chain crown ether polysiloxane and in a side-chain liquid-crystalline polysiloxane-containing crown ether as stationary phases in capillary gas chromatography. Chromatographia **1996**, *43*, 546–550.
2. Yuan, L.M.; Lin, Y.; Fu, R.N. Synergistic effect of dibenzo-18-crown-6 and resorcarene derivative mixed stationary phase in gas chromatography. Chem. J. Chin. Univ. **2000**, *21* (2), 213–215.
3. Blake, C.A.; Crouse, D.J.; Coleman, C.F.; Brown, K.B.; Kelmers, A.D. *U.S. Atomic Energy Commission, ORNL-2172 (1957), CA. 51: 8391e (1957).*
4. Yuan, L.M.; Fu, R.N.; Gui, S.H.; Xie, X.T.; Dai, R.J.; Chen, X.X.; Xu, Q.H. Synergistic effect in mixed gas chromatographic stationary phases containing Heptakis(2,3,6-tri-*O*-pentyl)-β-cyclodextrin and $AgNO_3$ or $TlNO_3$ in the separation of xylene isomers. Chromatographia **1997**, *46* (5/6), 291–294.
5. Yuan, L.M.; Fu, R.N.; Gui, S.H.; Chen, X.X.; Dai, R.J. Synergistic effect in special selectivity mixed gas chromatographic stationary phase in the separation of aromatic compounds. Chin. Chem. Lett. **1998**, *9* (2), 151–155.

6. Xiao, D.Q.; Lin, Y.; Wen, Y.X.; Fu, R.N.; Gu, J.L.; Dai, R.J.; Luo, A.Q. Synergistic effect of resorcarene and cyclodextrin mixed stationary phase in gas chromatography. Chromatographia **1997**, *46* (3/4), 183–188.
7. Chen, F.; Mo, W.M. Study of pebutylated-β-CD and $AgNO_3$ mixed stationary phase in capillary gas chromatography. Chin. J. Chromatogr. **2000**, *18* (3), 247–251.
8. Yuan, L.M.; Fu, R.N.; Chen, X.X.; Gui, S.H.; Dai, R.J. Synergistic effect of PEG-20M and Heptakis(2,3,6-tri-*O*-pentyl)-β-cyclodextrin mixed stationary phase in gas chromatography. Chem. Lett. **1998**, 141–142.
9. Yuan, L.M.; Ai, P.; Zi, M.; Fu, R.N.; Gui, S.H.; Chen, X.X.; Dai, R.J. Synergistic effect of heptakis(2,3,6-tri-*O*-pentyl)-β-cyclodextrin and *o*-methyl-*p*-phenylene-bis-(*p*-heptoxy benzoate) mixed stationary phase in capillary gas chromatography. J. Chromatogr. Sci. **1999**, *37*, 395–399.
10. Yu, X.D.; Lin, L.; Wu, C.Y. Synergistic effect of mixed stationary phase in gas chromatography. Chromatographia **1999**, *49* (9/10), 567–571.
11. Nie, M.Y.; Zhou, L.M.; Wang, Q.H.; Zhu, D.Q. Gas chromatographic enantiomer separation on single and mixed cyclodextrin derivative chiral stationary phases. Chromatographia **2000**, *51* (11/12), 736–740.
12. Yuan, L.M.; Fu, R.N.; Chen, X.X.; Gui, S.H. Synergistic effects in mixed gas chromatographic stationary phases consisting of dibenzo-18-crown-6 and MPBHpB. Chromatographia **1998**, *47* (9/10), 575–578.
13. Yuan, L.M.; Lin, Y.; Fu, R.N. Synergistic effect of liquid crystalline and resorcarene mixed stationary phase. Chin. J. Chem. **1999**, (2), 52–54.

Mobile Phase Modifiers for SFC: Influence on Retention

Yu Yang
Department of Chemistry, East Carolina University, Greenville, North Carolina, U.S.A.

INTRODUCTION

Carbon dioxide has been the most common mobile phase in supercritical fluid chromatography (SFC) due to its low critical point, non-toxicity, and wide availability in pure form. However, the polarity and solvating power of carbon dioxide are fairly low, which prevents polar and high-molecular-weight compounds to elute by using pure CO_2 as the mobile phase. Therefore, a small amount of organic or inorganic solvents are often added to CO_2 to enhance the solvating power of the mobile phase, so that polar and high-molecular-weight solutes can be eluted. Both polar and non-polar modifiers have been added to carbon dioxide to alter the chromatographic retention and selectivity.The modifiers and CO_2 can be either premixed in a compressed cylinder, mixed using a saturator column (device), or mixed by using two delivery pumps. Among many modifiers tested in SFC, methanol has been the most popular additive for carbon dioxide. Although binary systems have been used in many applications, ternary systems have also been investigated and found to be very successful in separating organic acids and bases. The modifier influence on chromatographic retention and the mechanism of modifier effect in SFC are also discussed in this entry.

PREPARATION OF THE MODIFIED MOBILE PHASE

There are a number of ways to mix modifiers with CO_2. A mixture of modifier and CO_2 can be purchased as premixed cylinders. Because the modifier is premixed with CO_2 in a cylinder, a modifier gradient cannot be carried out by this approach. Another drawback of this premixing method is that the concentration of the modifier may be increased as the cylinder is evacuated. Modifiers can also be directly introduced into an empty syringe pump that is then filled with CO_2. Again, similar limitations exist in this method. Another way to mix the modifier with CO_2 is to use a saturator column, usually a silica column saturated with polar modifiers. However, because the modifier-holding capacity of the silica column is limited, the amount of modifier dissolved in the mobile phase varies as the mobile phase passes through the saturator column. An improved mixing device in which highly porous stainless-steel filters were used to generate a modified CO_2 mobile phase has been developed to substitute for the saturator column. Although this mixing device can maintain the amount of modifiers dissolved in supercritical CO_2 for a long time, the performance of the modifier gradient remains impossible with this system. The best and most effective (also the most expensive) way of delivering a modifier in SFC is by using two supply pumps. One pump is used for CO_2 delivery and the other for modifier delivery. The modifier and CO_2 meet inside a mixing chamber that mixes the modifier with CO_2 and equilibrates the mixture in a thermostated zone, and then the mixed fluid is delivered to the SFC injection port and column.

METHANOL AS THE MODIFIER

Among the published articles regarding modifiers in SFC, methanol has been involved in at least two-thirds of the works. Therefore, methanol has been the most popular modifier for CO_2 in SFC.The mole fraction of methanol in the mobile phase is generally low, ranging from 1% to 10%. However, methanol concentrations up to 45% have also been tested. Due to the high cost of dual-pump systems, a constant concentration of methanol has normally been used to modify carbon dioxide. Once a dual-pump system is available, a programmed concentration of the modifier is preferred, as better separations can be achieved by using the modifier gradient technique. The methanol-modified mobile phase has been used to successfully separate phenols and their derivatives, amines and their derivatives, carboxylic acids, carbohydrates and their derivatives, herbicides and pesticides, alkylbenzenes, chlorobenzenes, chlorophenyls, higher-molecular-weight *n*-alkanes, polycyclic aromatic hydrocarbons (PAHs) and their derivatives, polychlorinated biphenyls (PCBs), pharmaceutical compounds, active ingredients in natural products, explosives, and other solutes.

TERNARY SYSTEMS

Because methanol is not very polar, the elution of strong organic acids and bases requires a mobile phase with even greater polarity. This has normally been done by adding a very low concentration of acids or bases into methanol, and then the modified methanol is mixed with CO_2 for separation. Citric, acetic, and chlorinated acetic acids have been

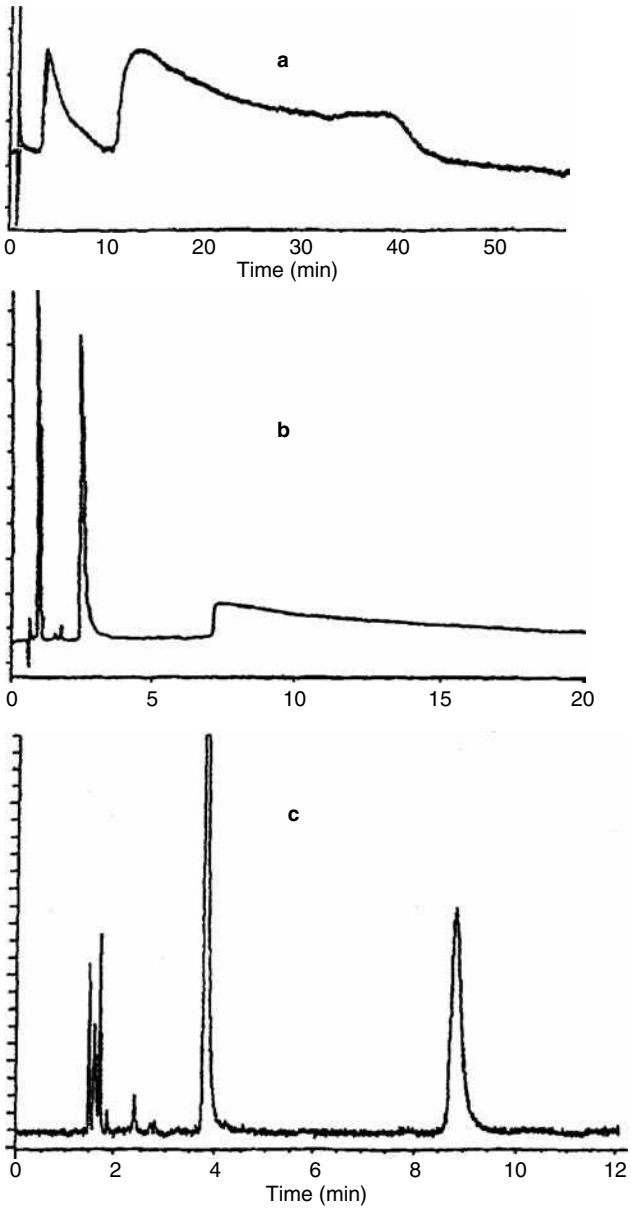

Fig. 1 Separation of benzylamines: a, On a Deltabond Octyl column (100 × 2 mm, 5 μm) using pure carbon dioxide (0.5 ml/min) at 40°C and 180 bar; b, on a Diol column (100 × 2 mm, 7 μm) using 5% methanol in carbon dioxide (0.5 ml/min) at 40°C and 182 bar; c, on a Diol column (250 × 4.6 mm, 5 μm) using 10% methanol (containing 0.6% isopropylamine) in carbon dioxide (2 ml/min) at 40°C and 200 bar.

Source: Reprinted from Separation of polar solutes by packed column supercritical fluid chromatography, in J. Chromatogr. A.[1] Copyright © 1997, with permission from Elsevier Science.

used as acidic secondary modifiers, whereas isopropylamine, triethylamine, and tetrabutylammonium hydroxide have been served as basic secondary modifiers. A good example with ternary systems is the separation of benzylamines, as shown in Fig. 1. None of the three tested amines were effectively eluted by pure CO_2 (Fig. 1a); however, some of these amines were eluted with very poor peak shapes when methanol was added to the CO_2 (Fig. 1b). However, the addition of isopropylamine to the methanol-modified mobile phase effectively eluted all of the three benzylamines and dramatically improved the peak shapes, as shown in Fig. 1c.

OTHER MODIFIERS

Besides methanol, many other polar and non-polar modifiers have also been used to successfully improve the separation in SFC. These modifiers include acetone, acetonitrile, acetic acid, butane, butanol, *n*-butyl chloride, carbon tetrachloride,dioxane, ethanol, formic acid, heptane, hexane, *n*-hexylamine, methylene chloride, nitromethane, propanol, proprionitrile, tetrahydrofuran, toluene, triethanolamine, trifluoroacetic acid, trifluoroethanol, trimethyl phosphate, and water.

FID-COMPATIBLE MODIFIERS

One of the major advantages of SFC over highperformance liquid chromatography (HPLC) is its compatibility with the flame ionization detector (FID), a universal and sensitive detector for carbon compounds. Unfortunately, most modifiers used in SFC are incompatible with FID. Therefore, a search for polar modifiers that have less response to FID led to the use of water, formic acid, and formamide. These modifiers produce acceptably low background noise and enable the use of FID. Because both water and formic acid have poor solubilities in carbon dioxide, they have been used as modifiers at very low concentrations. However, the modifier effect is significant even at this low level. For example, when water or formic acid was used as modifiers, the resolution of free fatty acids was significantly improved.

Very recently, the separation of polar analytes has also been performed by using pure water under subcritical conditions. Subcritical water has several unique characteristics. For example, the dielectric constant, surface tension, and viscosity of water are dramatically decreased by raising the water temperature while a moderate pressure is applied to keep water in the liquid state. At 200–250°C, the values of these physical properties are similar to those of pure methanol or acetonitrile at ambient conditions. Therefore, subcritical water may be a potential mobile phase for polar analytes. SFC mobile phases other than CO_2 are reviewed separately in this encyclopedia.

MODIFIER EFFECT ON RETENTION

It is very clear that chromatographic retention is changed by adding modifiers into carbon dioxide. However,

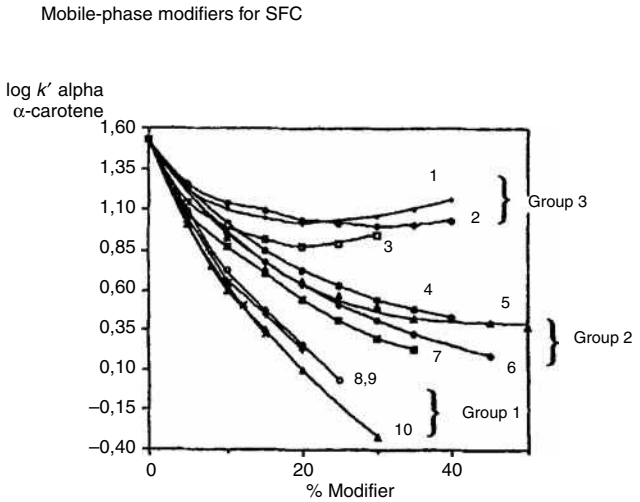

Fig. 2 Variation of the log *k* for α-carotene vs. the percentage of modifier in carbon dioxide.Temperature: 25°C (subcritical); outlet pressure: 150 bar; flow rate: 3 ml/min; UV at 450 nm; column: UB 225 (250 × 4.6 nm; 5 μm). 1. Acetonitrile; 2. methanol; 3. nitromethane; 4. ethanol; 5. proprionitrile; 6. acetone; 7. 1- propanol; 8. heptane; 9. tetrahydrofuran; 10. methylene chloride.
Source: Reprinted from Influence of the modifiers on the nature of the stationary phase and the separation of carotenes in sub-critical fluid chromatography, in J. Chromatogr.,[2] with permission from Friedr Vieweg und Sohn Verlagsgesellschaft mbH.

modifiers used in SFC can be classified in three groups, depending on the retention behavior of the solutes. Fig. 2 shows a good example of the modifier effect on the retention of α-carotene. For separations using heptane-, tetrahydrofuran-, and methylene chloride-modified CO_2 (group 1), the retention of α-carotene was decreased rapidly and almost inversely proportional to the modifier concentration, as shown in Fig. 2. The second group of modifiers include ethanol, proprionitrile, acetone, and 1-propanol. A more gradual decrease in the retention of α-carotene was obtained by using modifiers in this group. Methanol, acetonitrile, and nitromethane are in the third group. Even though the retention decreased significantly with increasing modifier percentage up to ~10% for all three modifiers in this group, the retention reached a minimum with acetonitrile- and nitromethane-modified carbon dioxide. For separation using the methanol-modified CO_2 the retention remained almost unchanged at higher methanol concentrations. A similar behavior was observed for separations of many other solutes with methanol as the modifier.

MECHANISM OF THE MODIFIER EFFECT

Although the exact mechanism is not very clear, the following factors may contribute to the modifier effect on chromatographic retention. Polar modifiers may cover the active sites of the stationary phase (deactivation) so that solute retention is reduced. This can be explained by the differences in retention change between packed and open-tubular columns when small amounts of modifiers were used. Open-tubular columns normally do not show the drastic changes in retention or efficiency upon the addition of small amounts (<2%) of modifier as most packed columns do. These less drastic differences were caused by the differences in the degree of deactivation of the packed column stationary phase as compared with the opentubular- column stationary phase. An open-tubular column has fewer active sites present and, thus, fewer active sites are present for the modifier to deactivate.

Modifiers may also swell the stationary phase, causing retention change of solutes.The density of the mobile phase can be increased by most polar and non-polar modi- fiers so that the solvating power of the mobile phase is enhanced. The polarity of the mobile phase is definitely increased by adding polar modifiers; thus, the retention of polar analytes is reduced. Specific intermolecular interactions between the solute and the modifier in the mobile phase may be additional factors for the modifier effect.

In conclusion, both polar and non-polar modifiers can be added to the SFC mobile phase to increase the solvent strength. Unlike pure carbon dioxide, the modified CO_2 can elute polar and high-molecularweight solutes due to its enhanced solvating power. The retention factors are reduced and peak shapes greatly improved by using binary or ternary mobile phases. Although ultraviolet detection can be applied for separations with many modifiers, only water, formic acid, and formamide are compatible with FID.

REFERENCES

1. Berger, T.A. Separation of polar solutes by packed column supercritical fluid chromatography. J. Chromatogr. A. **1997**, *785* (1–2), 3–33.
2. Lesellier, E.; Krstulovic, A.M.; Tchapla, A. Influence of the modifiers on the nature of the stationary phase and the separation of carotenes in sub-critical fluid chromatography. J. Chromatographia **1993**, *36* (1), 275.

BIBLIOGRAPHY

1. Berger, T.A.; Deye, J.F. Efficiency in packed column supercritical fluid chromatography using a modified mobile phase. J. Chromatographia **1991**, *31* (11–12), 529–534.
2. Cantrell, G.O.; Stringham, R.W.; Blackwell, J.A.; Weckwerth, J.D.; Carr, P.W. Effect of various modifiers on selectivity in packed-column subcritical and supercritical fluid chromatography. Anal. Chem. **1996**, *68* (20), 3645–3650.

3. Francis, E.S.; Lee, M.L.; Richter, B.E. Modifier addition in microcolumn supercritical fluid chromatography with a high pressure pulsed valve. J. Microcol. Separ. **1994**, *6* (5), 449–457.
4. Janssen, H.-G.; Schoenmakers, P.J.; Cramers, C.A. Effects of modifiers in packed and open-tubular supercritical fluid chromatography. J. Chromatogr. **1991**, *552*, 527–537.
5. Kuepper, S.; Grosse-Ophoff, M.; Klesper, E. Influence of linear velocity and multigradient programming in supercritical fluid chromatography. J. Chromatogr. **1993**, *629*, 345–359.
6. Lesellier, E.; Tchapla, A. Supercritical fluid chromatography with organic modifiers on octadecyl packed columns: recent developments for the analysis of high molecular organic compounds. In *Supercritical Fluid Chromatography with Packed Columns*; Anton, K., Berger, C., Eds.; Marcel Dekker, Inc.: New York, 1998; 195–221.
7. Morrissey, M.A.; Giorgetti, A.; Polasek, M.; Pericles, N.; Widmer, H.M. Pressure and modifier programming in packed-column supercritical fluid chromatography. J. Chromatogr. Sci. **1991**, *29* (6), 237–242.
8. Pyo, D.; Ju, D. Simple method for the preparation of water-modified or methanol-modified carbon dioxide as the mobile phase in supercritical fluid chromatography. Anal. Sci. **1994**, *10* (1), 171–174.
9. Pyo, D.; Li, W.; Lee, M.L.; Weckwerth, J.D.; Carr, P.W. Addition of methanol to the mobile phase in packed capillary column supercritical fluid chromatography retention mechanisms from linear solvation energy relationships. J. Chromatogr. A. **1996**, *753*, 291–298.
10. Roth, M. Thermodynamics of modifier effects in supercritical fluid chromatography. J. Phys. Chem. **1996**, *100* (6), 2372–2375.
11. Smith, R.M.; Briggs, D.A. Separation of homologous aromatic alcohols and carboxylic acids by packed column supercritical fluid chromatography. J. Chromatogr. A. **1994**, *688*, 261–271.
12. Taylor, L.T. Trends in supercritical fluid chromatography. J. Chromatogr. Sci. **1997**, *35*, 374–381.
13. Upnmoor, D.; Brunner, G. Packed column supercritical fluid chromatography with light-scattering detection (Part I or II?). J. Chromatographia **1992**, *33* (5–6), 261–266.

Molecular Interactions in GC

Raymond P.W. Scott
Scientific Detectors Ltd., Banbury, Oxfordshire, U.K.

INTRODUCTION

The retention of a solute is directly proportional to the magnitude of its distribution coefficient (K) between the mobile phase (gas) and the stationary phase. The magnitude of K depends on the relative affinity of the solute for the two phases; thus, the stronger the forces between the solute molecule and the molecules of the stationary phase, the larger the distribution coefficient and the more the solute is retained. It follows that the stationary phase must interact strongly with the solutes to be retained and to achieve a separation. Molecular interaction results from *intermolecular forces*, of which there are only two types effective in gas chromatography (GC).

In total, there are three different basic types of molecular force, all of which are electrical in nature. These forces are called *dispersion forces*, *polar forces*, and *ionic forces*. Despite there being many different terms used to describe molecular interactions (e.g., hydrophobic forces, π–π interactions, hydrogen-bonding, etc.), all interactions between molecules are the result of composites of these three different types of molecular force.

DISPERSION FORCES

Dispersion forces[1] arise from charge fluctuations throughout a molecule, resulting from electron/nuclei vibrations. Glasstone[2] described them in the following way:

> Although the physical significance probably cannot be clearly defined, it may be imagined that an instantaneous picture of a molecule would show various arrangements of nuclei and electrons having dipole moments. These rapidly varying dipoles, when averaged over a large number of configurations, would give a resultant of zero. However, at any instant, they would offer electrical interactions with another molecule, resulting in interactive forces.

Dispersion forces are those that occur between hydrocarbons and other substances that have either no permanent dipoles or can have no dipoles induced in them. In biotechnology and biochemistry, dispersive interactions are often referred to as "hydrophobic" or "lyophobic" interactions, apparently because dispersive substance such as the aliphatic hydrocarbons do not dissolve readily in water. To a first approximation, the interaction energy (U_D) involved with dispersive forces has been deduced to be

$$U_D = \frac{3h\nu_0\alpha^2}{4r^6}$$

where α is the polarizability of the molecule, ν_0 is a characteristic frequency of the molecule, h is Planck's constant, and r is the distance between the molecules. The dominant factor that controls dispersive force is the polarizability (α) of the molecule, which for substances that have no dipoles is given by

$$\frac{D-1}{D+2} = \frac{4}{3}\pi n\alpha$$

where D is the dielectric constant of the material and n is the number of molecules per unit volume.

If ρ is the density of the medium and M is the molecular weight, then the number of molecules per unit volume is N_ρ/M, where N is Avogadro's number. Thus,

$$\frac{4}{3}\pi N\alpha = \frac{D-1}{D+2}\frac{M}{\rho} = P$$

where P is called the molar polarizability. It is seen that the molar polarizability is proportional to M/ρ, the molar volume.

POLAR FORCES

Polar interactions arise from electrical forces between localized charges such as permanent or induced dipoles. Polar forces are always accompanied by dispersive interactions and may also be combined with ionic interactions. Polar interactions can be very strong and produce molecular associations that approach, in energy, that of a weak chemical bond (e.g.,"hydrogen-bonding").

DIPOLE–DIPOLE INTERACTIONS

The interaction energy (U_P) between two dipoles molecules is given, to a first approximation, by

$$U_P = \frac{2\alpha\mu^2}{r^6}$$

where α is the polarizability of the molecule, μ is the dipole moment of the molecule, and r is the distance between the

molecules. The energy depends on the square of the dipole moment, which can vary widely in strength. The numerical value of the dipole moment does not always give an indication of the strength of any polar interactions, as there is often internal electric field compensation when more than one dipole is present in the molecule. Although, the *polarizability* of a substance containing no dipoles may give an indication of the *strength of the dispersive* interactions, due to possible self-association or internal compensation, the *dipole moment* of a substance will *not* always give an indication of the *strength of any polar interaction* that might take place with another molecule.

DIPOLE–INDUCED-DIPOLE INTERACTIONS

Compounds, such as those containing the aromatic nucleus and thus π electrons, are polarizable. When such molecules are in close proximity to a molecule with a permanent dipole, the electric field from the dipole induces a counter-dipole in the polarizable molecule. This induced dipole acts in the same manner as a permanent dipole and, thus, polar interactions occur between the molecules. Induced-dipole interactions are, as with polar interactions, always accompanied by dispersive interactions. Aromatic hydrocarbons can be retained and separated in GC purely by dispersive interactions when using a hydrocarbon stationary phase or they can be retained and separated by combined induced-polar and dispersive interactions using a poly(ethylene glycol) stationary phase. Molecules can possess different types of polarity, phenyl ethanol, for example, will possess both a permanent dipole as a result of the hydroxyl group and also be polarizable due to the aromatic ring. More complex molecules can have many different interactive groups.

IONIC FORCES

Ionic interactions arise from permanent negative or positive charges on the molecule and, thus, usually occur between ions. Ionic interactions are exploited in ion-exchange chromatography, where the counterions to the ions being separated are situated in the stationary phase; ionic interactions are rarely active in GC separations.

To achieve the necessary retention and selectivity between the solutes for complete resolution, it is necessary to select a stationary phase that will provide the optimum balance of dispersive, polar, and induced-polar interactions between the solute molecules and those of the mobile phase.

REFERENCES

1. London, F. Phys. Z, **1930**, *60*, 245.
2. Glasstone, S. In *Textbook of Physical Chemistry*; D. Van Nostrand: New York, 1946, 298, 534.

BIBLIOGRAPHY

1. Scott, R.P.W. *Techniques of Chromatography*; Marcel Dekker, Inc.: New York, 1995.
2. Scott, R.P.W. *Introduction to Analytsical Gas Chromatography*; Marcel Dekker, Inc.: New York, 1998.

Monolithic Disk Supports for HPLC

Aleš Podgornik
M. Barut
A. Strancar
BIA Separations d.o.o., Ljubljana, Slovenia

INTRODUCTION

Chromatographic columns are typically several centimeters in length, resulting in a high number of column plates, and, consequently, such columns have high efficiency. These properties allow even very similar molecules to be separated. This is especially true for smaller molecules, where the separation is based on selective migration. For large molecules, a different separation mechanism is usually required. Large molecules normally interact with the matrix at several binding sites. Consequently, their adsorption isotherms are very steep, almost rectangular. For such molecules, there exists only a very narrow mobile phase range within which they interact with the active moieties on the stationary phase, but are not irreversibly retained. To elute them from the matrix, a change of the mobile phase composition is required. Therefore the separation is based upon the selective elution and requires the use of gradient chromatographic methods. For this type of separation, the column length is less important and the efficient separations can be achieved even with extremely short columns.

Because it is possible to use short columns, high flow rates can be used because of the low-pressure drop on the column. When this is accompanied with a steep gradient, extremely fast separations of large molecules can be achieved. However, to obtain efficient, fast separation, the mass transfer between the mobile and the stationary phase should also be fast. This might be a problem for large molecules having a very low mobility. Therefore suitable stationary phases should be used. In order to decrease the diffusion limitations, which are especially pronounced for large molecules, convection must be a significant part of the materials' mass transfer characteristics. To overcome a diffusion bottleneck, several types of stationary phases have been proposed, e.g., non-porous and perfusion particles. Despite significantly improved mass transfer in comparison to porous particles, preparation of short columns, as a result of the problems connected with column packing, can be problematic.

An alternative approach is represented by membranes. They are, by definition, very thin and seem ideally suited for the preparation of short columns. In fact, several successful large molecule separations were reported.[1] Membranes possess excellent mass transfer characteristics, enabling the fast exchange of molecules between the mobile and stationary phases. Because of their extreme thinness, several membranes are normally stacked to achieve acceptable binding capacity. This inherently introduces voids between the membranes that decrease the continuous nature of the matrix.

A decade ago, a new type of stationary phase was developed. It is commonly referred to as a monolith to emphasize that the matrix consists of a single piece of a highly porous material. Similar to the membranes, the monoliths have open pores that form a highly interconnected network of channels which are uniformly distributed in all directions. In contrast to the membranes, however, they can be prepared in various shapes and dimensions. The porous structure enables very good hydrodynamic characteristics. The mobile phase flows through the channels, and convection is the predominant transport mechanism. In this way, the mass transfer of large molecules is increased by at least an order of magnitude and, consequently, the analysis times can be significantly shortened without loss of resolution. In addition, chromatographic characteristics such as column efficiency and dynamic binding capacity are practically flow-independent. Similar to other chromatographic supports, monoliths can be prepared with different active groups. It is beyond the scope of this entry to describe in detail the characteristics of monoliths, but those interested in the subject are referred to a recent book entitled "Monolithic Separation Media."[2] Because the monoliths combine the advantageous hydrodynamic characteristics of the membranes with a flexible geometry, they are an ideal matrix for short chromatographic columns.

EFFECT OF THE COLUMN LENGTH ON THE RESOLUTION UNDER THE CONDITIONS OF A LINEAR GRADIENT ELUTION

Several decades ago, the theory of gradient elution was proposed by Snyder and Stadalius.[3] In this work, it was shown that the column length does not influence the resolution. This is especially true for steep gradients, where the separation is entirely based on selective elution. In contrast to isocratic separations, where a longer column normally

results in better separations, the elution time for gradient elutions depends upon the composition of the mobile phase. As a consequence, only a small part of the column is used for the separation. This conclusion is based upon the assumption of instantaneous equilibrium between the sample and the mobile phase. For large molecules, however, this assumption is hardly justified because of the significantly different mobilities of large and small molecules. Indeed, a detailed work by Dubinina, Kurenbin, and Tennikova[4] demonstrated that the gradient should be adjusted to the column length. Furthermore, they demonstrated that longer columns might even decrease the resolution because of pronounced band spreading. They introduced a term of gradient length, which depends on mobile phase velocity, concentration at which the molecule is eluted, steepness of the gradient, and the *Z* factor. The theoretical analysis showed that there is an increase in band spreading in the area where the gradient length is shorter than the column length. The spreading, together with the resolution, increases while the column length approaches the calculated gradient length. When the gradient and the column length are comparable, the bandwidth remains constant. Further increases in the column length result in a pronounced band spreading without improving the separation. The reason for this behavior lies in the equilibrium between the sample and the mobile phase. Once the molecules are released from the active groups, they start to move through the column with the mobile phase. Because of the lower mobility, however, their velocity is lower than the velocity of the eluting mobile phase. Therefore they become surrounded by the mobile phase with higher ionic strength, which, consequently, accelerates them. This results in a so-called sharpening effect resulting in lower bandwidth. When the gradient approaches the physical length of the column, the equilibrium between the sample molecules and the mobile phase composition is achieved at the end of the column. Therefore the mobile phase composition determines the band spreading and, in this way, preserves the resolution efficiency. A longer column does not contribute to a better separation, but only to additional band spreading because of axial dispersion, resulting in decreased resolution. Therefore for molecules that require a steep gradient for an efficient separation, short columns are not only a method of choice, but can even be superior to longer columns.

DEVELOPMENT AND CHARACTERISTICS OF DISK MONOLITHIC COLUMNS

The concept of monolithic columns in the shape of disks was first introduced at the beginning of the 1990s by Tennikova, Belenkii, and Svec.[5] They prepared hydrophobic methacrylate-based monolithic disks with a diameter of 20 mm and a thickness of 1 mm which demonstrated a very efficient separation of a protein mixture. After this initial research, monolithic disks of different diameters and thicknesses were prepared and used for various chromatographic separations. The smallest monolith had a diameter of only 1.8 mm, while the largest had a diameter of 50 mm. The thickness was between 0.3 and 7 mm.[6] In this way, the monolith volume differed by several orders of magnitude. The monolithic disks contained different chemical moieties which were used for separations in ion exchange, hydrophobic, and affinity interactions, as well as reversed phase modes.

Along with the development of the monolithic disks, a suitable housing had to be designed. The housing needed to facilitate the usage of the monolithic disks and enable the connection of the disk monolithic columns to an HPLC/LC or flow injection analysis (FIA) system. In addition, it needed to provide a uniform sample distribution over the entire monolith surface, ensure the mechanical stability of the monolithic disk when a high flow rate is applied, and prevent any bypass of the mobile phase. Furthermore, the peak spreading and the dead volume of such a unit should be as low as possible. Historically, this represented a major challenge. Several attempts to fulfill these requirements have been reported over the last several years.[7] In the initial experiments, the monolith was simply installed at the bottom of a filtration device. Despite the simplicity of such an approach, the large dead volume limited its wide applicability. To overcome this problem, a special housing with optimized sample distribution was constructed. This device enabled excellent separation of proteins within several minutes. The monolithic disk was placed between two sample distributors, and o-rings created a seal around the monolith. Because of the way the monoliths were fixed in the housing, the replacement often damaged the monolith. In 1998, a commercial product under the trademark CIM Convective Interaction Media® was launched.[8] The housing enables highly efficient separations and easy exchange of the monolithic disks. Along with the construction of the housing, the dimensions of the monolithic disks were standardized to have a diameter of 12 mm and a thickness of 3 mm. To provide additional mechanical stability to the monolith, a self-sealing non-porous ring was fixed around the monolith. These commercially available units are shown in Fig. 1.

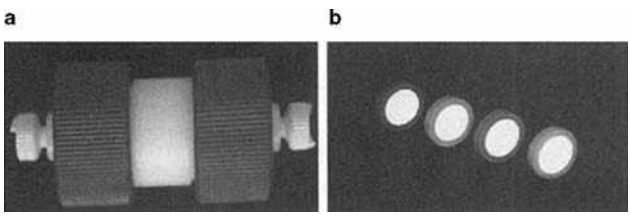

Fig. 1 The outlook of (a) the CIM® Disk Monolithic Column and (b) the CIM® Disks from BIA Separations, Ljubljana, Slovenia.

CHROMATOGRAPHIC CHARACTERISTICS OF MONOLITHIC DISKS

Despite the existing theory claiming that, under the conditions of a gradient elution, resolution does not improve with increased column length, very short chromatographic columns were not routinely used for separations in a gradient mode at the time the monolithic disks were introduced. To evaluate the chromatographic characteristics of the monolithic disks, a detailed analysis of their properties under gradient elution was published in 1993 by Tennikova and Svec.[9] They prepared monolithic disks with different chemistries, enabling ion-exchange (IEX), HIC, and RP separation modes. They investigated the effect of the gradient volume on the separation efficiency and concluded that the monolithic disks obey the same chromatographic rules as conventional particulate chromatographic columns. On the other hand, because of the enhanced transport mechanism, the separation characteristics were almost independent of the applied flow rate. Furthermore, the resolution increased even with the increases in linear velocity, which was explained by the narrowing of the peaks. They estimated that the apparent diffusivity of the proteins, as a result of the convective flow through the pores of the monolithic disk, was four magnitudes higher than the free diffusivity of proteins in solution.

In 1999, a similar analysis was performed for an isocratic separation.[10] The investigators examined the effect of the mobile phase composition and the monolithic disk thickness on band spreading. Again, it was found that, despite an extremely short column length and the monolithic structure, all conclusions for the conventional HPLC columns were applicable to these columns. Separation of oligonucleotides gave a height equivalent of theoretical plate (HETP) value of 18 μm, which is comparable to the chromatographic columns filled with 5–7 μm particles. Investigation of the effects of flow rate demonstrated a slightly improved separation at a higher flow rate. This surprising conclusion was explained by the increased flow through the small pores, which are not "permeable" at lower flow rates.[10] Both works demonstrated that the monolithic disks should be considered as "real" chromatographic columns.

All monolithic disks reported so far were methacrylate- or styrene-based. Because of that, they have a rigid structure, which minimizes compression when high flow rates are applied. This is confirmed by a linear correlation between the pressure drop and the linear velocity. For the commercially available CIM® disks of 12 mm diameter and 3 mm thickness, it was found that there is a pressure drop of about 0.5 bar per each ml/min. A low-pressure drop is very important for working at high flow rates. Because the mass exchange is not a limiting factor, the gradient can be adjusted in a way to optimally match the thickness of the monolithic disk. In this way, efficient separations in a very short time can be obtained. The extremely short separation times were investigated by Strancar et al.[11] (Fig. 2). The authors were able to separate a mixture of proteins within a few seconds at room temperature. For even faster separations, current HPLC equipment becomes a bottleneck.

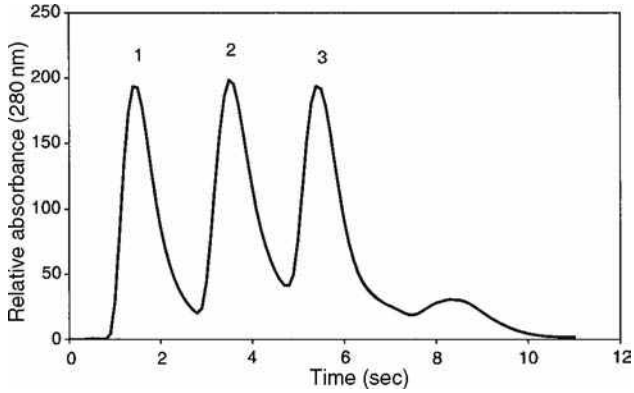

Fig. 2 Separation of test proteins in seconds on a CIM® QA disk monolithic column. Conditions—buffer A: 20 m*M* Tris–HCl buffer, pH 7.4; buffer B: 1 *M* NaCl in buffer A, pH 7.4; flow rate: 10 ml/min; detection: UV at 280 nm; gradient: step gradient at 0%, 20%, and 50% buffer B for 2 sec each; sample: (1) myoglobin (0.5 mg/ml), (2) conalbumin (1.5 mg/ml), (3) soybean trypsin inhibitor (2 mg/ml); injection volume: 20 μl.
Source: From Application of compact porous disks for fast separations of biopolymers and in-process control in biotechnology in Anal. Chem.[11]

Another consequence of the very fast mass exchange between the mobile and the stationary phase are the flow-independent characteristics of these units. In Fig. 3a, the comparison of a protein separation performed at flow rates from 2 up to 8 ml/min is shown. As can be seen, the chromatograms overlap, indicating no loss of separation efficiency. Similar results were achieved for the dynamic binding capacity. In Fig. 3b, breakthrough curves are presented. Again, they match closely, indicating a constant binding capacity.

Because of their small thickness, one might speculate that the monolithic disks can only separate a few substances during a chromatographic run. However, by precise gradient adjustments, more than 10 substances can be separated in a few minutes. In Fig. 4, a separation of 14 oligonucleotides was performed in 3 min at room temperature[12]—a feat hardly achievable with a conventional particulate column.

Monolithic structures enable two additional interesting features. Because of their defined dimension, several monolithic disks can be stacked together forming a single chromatographic column. Such a column has much better performance in comparison to a group of several columns in series comprising a single monolithic disk.[13] In this way, the capacity of the column increases linearly. It is important to note that this can be performed by the user without any additional equipment. Several disks also increase the column length, resulting in an increased number of theoretical plates and, consequently, better

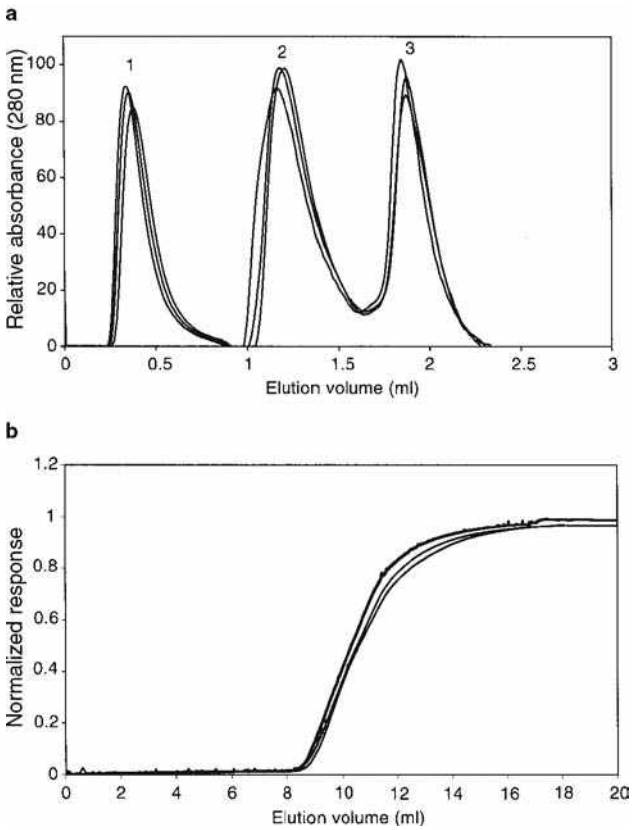

Fig. 3 Flow characteristics of the monolithic disks: (a) flow-independent resolution and B flow-independent dynamic binding capacity. A Conditions—buffer A: 20 m*M* Tris–HCl buffer, pH 7.4; buffer B: 1 *M* NaCl in buffer A, pH 7.4; flow rate: 10 ml/min; detection: UV at 280 nm; gradient: 0–70% buffer B in 30 sec; sample: (1) myoglobin (0.5 mg/ml), (2) conalbumin (1.5 mg/ml), (3) soybean trypsin inhibitor (2 mg/ml); injection volume: 20 μl. (b) Conditions—binding buffer: 20 m*M* Tris–HCl buffer, pH 7.4; flow rate: 2, 4, and 8 ml/min; detection: UV at 280 nm; sample: human serum albumin dissolved in buffer A (1 mg/ml).

efficiency in isocratic separation. In Fig. 5, a separation of organic acids with a monolithic column consisting of four monolithic disks is presented.

A similar approach using monolithic disks of different chemistries enables multidimensional separations. This approach, using monolithic disks, was called conjoint liquid chromatography (CLC).[13] The main advantage is that these columns can be reconstructed by placing the disks in a different order or exchanging some of the disks. This is possible because the stationary phases bearing different chemistries do not mix. An example of such a separation is shown in Fig. 6, applying affinity and ion-exchange disks in a single column.

The features clearly indicate that the monolithic disks enable efficient separations and purification of different types of molecules. This is demonstrated in a number of examples where these columns were used in the separation of complex biological mixtures.

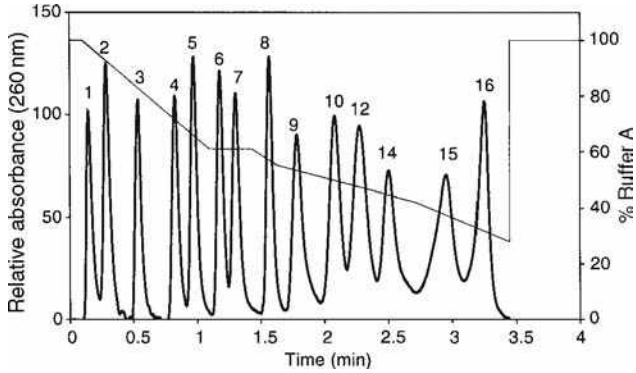

Fig. 4 Separation of oligomers using optimized gradient conditions. Conditions: mobile phase—buffer A: 20 m*M* Tris–HCl buffer, pH 8.5; buffer B: 1 *M* NaCl in 20 m*M* Tris–HCl buffer, pH 8.5; flow rate: 4 ml/min; stationary phase—CIM disk monolithic column comprising of a single disk; sample: oligonucleotides of different lengths (see the section, "Chromatographic Characteristics of Monolithic Disks"). Number near the peak represents the oligonucleotide length. Gradient: as shown in the figure; injection volume: 20 μl; detection: UV at 260 nm.
Source: From Application of very short monolithic columns for separation of low and high molecular mass substances, in J. Liq. Chromatogr. Relat. Technol.[12]

APPLICATION OF MONOLITHIC DISKS

Monolithic disks have been successfully used in the separation of different types of molecules. Most of the applications, however, deal with the separation of proteins. Initially, the studies were conducted with test solutions to

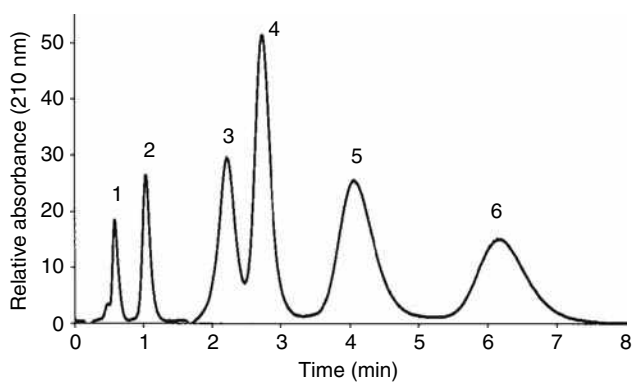

Fig. 5 Separation of the organic acid on CIM disk monolithic column. Conditions—mobile phase: 130 m*M* NaCl in 20 m*M* phosphate buffer, pH 8.0; separation unit: CIM® disk monolithic column comprising of four CIM® QA disks; flow rate: 5 ml/min; sample: (1) 0.03 g/L pyruvic acid, (2) 0.5 g/L malic acid, (3) 0.2 g/L α-ketoglutaric acid, (4) 0.007 g/L fumaric acid, (5) 2 g/L citric acid, and (6) 2 g/L isocitric acid; injection volume: 20 μl; detection: UV at 210 nm.
Source: From Application of convective interaction media (CIM®) disk monolithic columns for fast separation and monitoring of organic acids, in JCS.[17]

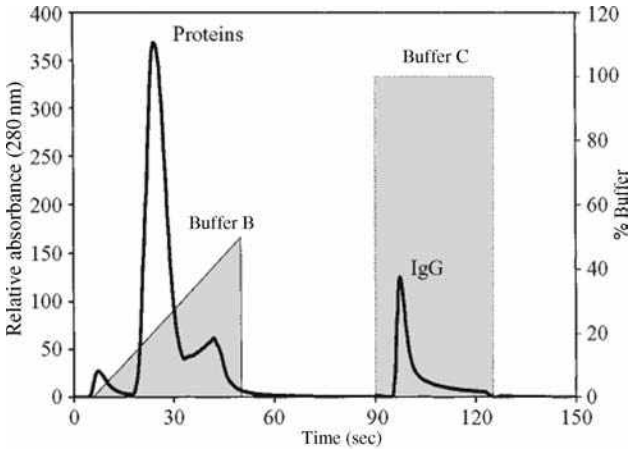

Fig. 6 Conjoint liquid chromatography (CLC): separation of proteins from mouse ascites and isolation of monoclonal antibody IgG in one step obtained by a combination of CIM® QA and CIM® Protein A Disks. Conditions—separation mode: CLC (first disk: CIM® QA; second disk: CIM® Protein A, inserted in one-disk monolithic column housing); instrumentation: gradient HPLC system with extra low dead volume mixing chamber; sample: mouse ascites; injection volume: 20 μl; mobile phase: buffer A—20 m*M* Tris–HCl, pH 7.4; buffer B—buffer A + 1 *M* NaCl; buffer C—0.1 *M* acetic acid; conditions: gradient—0–50% B in 50 sec, 100% A for 40 sec, and 100% C for 30 sec; flow rate—4 ml/min; detection—UV at 280 nm.
Source: From Convective interaction media: polymer-based supports for fast separation of biomolecules, in LC GC.[13]

prove the power of the separation media, but many applications with real samples have also been reported. All of these separations were performed in a short period of time, typically a few minutes or even less. Some of the representative ones are described.

Ion-Exchange, Hydrophobic, and Reverse Phase High-Performance Liquid Chromatography Disk Monolithic Columns

Separation of proteins

There are several reports about the application of the disk monolithic columns for the separation and purification of plasma proteins.[14,15] Purification and monitoring of clotting Factor IX (FIX) from human plasma were performed using the ion-exchange monolithic disks. In addition, separation of vitronectin from FIX was possible. A similar system was used for the separation of a complex between clotting Factor VIII and von Willebrand factor (FVIII–vWF). Another application was the monitoring of α_1-antitrypsin production. Separation of impurities such as human serum albumin and transferrin was achieved in a few minutes.

Another well-studied system was the monitoring and purification of extracellular ligninolytic enzymes from the fermentation broth of fungus *Phanerochaete chrysosporium*. Again, the ion-exchange disk monolithic columns were used. The different enzyme isoforms present in a fermentation broth have similar molecular weights. An efficient separation was achieved in a few minutes, thus reducing the required separation time by an order of magnitude, as compared with a conventional column. The purities of the isoforms were comparable using monolithic vs. conventional columns. The method was also used for monitoring the isoenzyme profiles during the fermentation process.[16]

Separation of polynucleotides

Monolithic disks seem to be very efficient columns for the separation of polynucleotides. They enabled not only the separation of pDNA from RNA, but also the separation of pDNA isoforms: supercoiled, open circular, and linear forms.[14] Besides a separation time of only a few minutes, the most outstanding characteristic of the monolithic disks is their high dynamic binding capacity for pDNA, which is in the range of 10 mg/ml of support.[6] In addition, the monolithic disks seem to be very attractive for the purification of even larger molecules, e.g., viruses.[6]

Small molecules

While most of the papers deal with the separation of large molecules, a few successful separations of small molecules were recently reported.[14] By stacking several disks of the same chemistry into a single monolithic column, it was possible to apply it for monitoring the organic acid formation during the fermentation of yeast *Yarrowia lypolitica*.[17] A similar column was used for the determination of Mn^{3+} tartrate complex in a fermentation medium of *P. chrysosporium*. Very recently, the separation of Zn complexes of citrate, oxalate, and EDTA, as well as hydrated Zn^{2+} species, was compared on an ion-exchange disk monolithic column and Mono Q. The former was found to be more efficient.[18]

More information about the applications of the monolithic disk columns can be found in several reviews.[14,15,17,19]

Affinity Monolithic Columns

Methacrylate-based monolithic disks are very suitable for the immobilization of various ligands because they contain epoxy groups which form very stable covalent bonds with the amino or sulfhydryl groups of the ligand. Recently, an extensive description of different immobilization procedures was published.[20]

Low molecular mass ligands

The first report about the immobilization of a small affinity ligand on monolithic disks was published in 1991.[21]

Immobilized *p*-(amino methyl) benzol sulfonamide, a carbonic anhydrase inhibitor, was used for the purification of carbonic anhydrase. The immobilization of various peptides, including the hormone bradykinin, on a CIM® disk monolithic column, was performed to investigate the possibility of purifying monospecific polyclonal antibodies in serum. Several disks, each with a different immobilized peptide, were placed in a single housing. This CLC approach demonstrated that the simultaneous loading of immunoglobulins can be performed in a few minutes. The specific immunoglobulins were then released from each monolithic disk separately.[21]

An important issue related to the small affinity ligands is their utilization (capacity per unit of ligand) on the matrix. Because of their size, they are more sensitive toward matrix composition and immobilization chemistry in comparison to large affinity ligands. A detailed study of the characteristics of a model peptide with affinity to chicken egg lysozyme immobilized to different supports such as agarose, cellulose, and methacrylate-based supports and via different immobilization chemistries revealed that the highest utilization of the ligand was achieved with the methacrylate-based monolithic disks.[15] This means that the ligand is optimally presented on the matrix surface, which additionally facilitates mass transfer between the mobile and stationary phases.

High molecular mass ligands

Different high molecular mass affinity ligands were successfully immobilized to monolithic disks.[14,20,21] Monolithic disks with immobilized heparin and collagen were used for the purification of membrane proteins and annexins. The heparin unit was also used in the quality control of the preparation of the plasma proteins Antithrombin III and clotting Factor IX. Purification of IgG was successfully performed by immobilizing Protein A, Protein G, and Protein L.[14,20] Because the elution is carried out under harsh conditions, which might cause denaturation, the fast separation enabled by the monolithic disks decreased such a risk. Indeed, the separation on a monolithic disk was performed within a few seconds.

Affinity monolithic disks were not only used in combination with an HPLC system, but also for the monitoring of specific compounds as part of an FIA system. The use of the monolithic disks is beneficial because it is compatible with high flow rates at low to medium pressure, has little to no dependency on the flow rate, is compatible with typical bioprocess samples, has long-term stability, and performs stable immobilization of highly active biologicals such as antibodies and enzymes.[20] The monitoring of recombinant protein G concentrations from a cell lysate of *E. coli* was performed using monolithic disks with immobilized IgG. A similar approach, this time with the enzyme glucose oxidase immobilized, was used for the monitoring of the glucose concentration in a fermentation broth.

Monolithic Disks as Bioreactors

Enzymes immobilized to monolithic disks were not applied only as biosensors, but also as bioreactors.[20,21] The first report, in 1991, describes the immobilization of carbonic anhydrase. Interestingly, an increase in enzyme activity with the increase of flow rate through the bioreactor was observed. Recently, the immobilization of trypsin was reported. Contrary to the previous work, increased flow rate diminished the extent of protein degradation. In contrast to the previously mentioned experiments, where the immobilized enzyme was used for substrate degradation, the synthesis of polyriboadenylate from ADP was studied by polynucleotide phosphorylase immobilized on a monolithic disk.

SCALE-UP OF MONOLITHIC DISK

An obvious approach for scaling-up the monolithic disks is by increasing their diameter. Because of the mechanical properties, however, this approach seems not to be the most appropriate one. The problem of increasing the volume while preserving the short column length was solved with the introduction of the tubular monolithic columns. Furthermore, with the introduction of the tube-in-tube approach, the CLC approach can also be scaled. Detailed information about the preparation and characteristics of the tube monolithic columns can be found elsewhere.[6,22]

CONCLUSIONS

Monoliths represent a novel stationary phase with advantageous chromatographic characteristics. Monolithic disks have proven to be very efficient separation media despite their short column length. Their main advantage is an extremely short separation time. This makes them a promising tool for the in-process monitoring of, for example, preparative chromatographic purification or bioprocesses, where fast analyses of complex mixtures are required to perform real-time actions. In addition, they are well suited for the very fast purification of small quantities of labile compounds, as well as in the fast development of chromatographic methods adapted to a preparative purification on larger monolithic columns.

REFERENCES

1. Tennikova, T.B.; Freitag, R. High-performance membrane chromatography of proteins. In *Analytical and Preparative Separation Methods of Biomacromolecules*; Aboul-Enein, H.Y., Ed.; Marcel Dekker, Inc.: New York-Basel, 1999; 255–300.

2. Svec, F., Tennikova, T.B., Deyl, Z., Eds.; *Monolithic Materials: Preparation, Properties and Applications*; Elsevier: Amsterdam, 2003.
3. Snyder, L.R.; Stadalius, M.A. High-performance liquid chromatography separations of large molecules: A general model. In *High-Performance Liquid Chromatography, Advances and Perspectives*; Horvath, Cs., Ed.; Academic Press: Orlando, 1986; Vol. 4, 195.
4. Dubinina, N.I.; Kurenbin, O.I.; Tennikova, T.B. Peculiarities of gradient ion-exchange high-performance liquid chromatography of proteins. J. Chromatogr. **1996**, *753*, 217–225.
5. Tennikova, T.B.; Belenkii, B.G.; Svec, F. High-performance membrane chromatography. A novel method of protein separation. J. Liquid Chromatogr. **1990**, *13* (1), 63–70.
6. Štrancar, A.; Podgornik, A.; Barut, M.; Necina, R. Short monolithic columns as stationary phases for biochromatography. In *Advances in Biochemical Engineering/ Biotechnology; Modern Advances Chromatography*; Freitag, R., Ed.; Springer-Verlag: Heidelberg, 2002; 49–85.
7. Josić, Dj.; Strancar, A. Application of membranes and compact, porous units for separation of biopolymers. Ind. Eng. Chem. Res. **1999**, *38* (2), 333–342.
8. http://www.biaseparations.com (accessed March 2002).
9. Tennikova, T.B.; Svec, F. High-performance membrane chromatography: Highly efficient separation method for proteins in ion-exchange, hydrophobic interaction and reversed-phase modes. J. Chromatogr. **1993**, *646*, 279–288.
10. Podgornik, A.; Barut, M.; Jancar, J.; Strancar, A. Isocratic separations on thin glycidyl methacrylate-ethylenedimethacrylate monoliths. J. Chromatogr. A, **1999**, *848*, 51–60.
11. Strancar, A.; Koselj, P.; Schwinn, H.; Josic, Dj. Application of compact porous disks for fast separations of biopolymers and in-process control in biotechnology. Anal. Chem. **1996**, *68* (19), 3483–3488.
12. Podgornik, A.; Barut, M.; Jaksa, S.; Jancar, J.; Strancar, A. Application of very short monolithic columns for separation of low and high molecular mass substances. J. Liquid Chromatogr. Relat. Technol. **2002**, *25*, 3099–3116.
13. Strancar, A.; Barut, M.; Podgornik, A.; Koselj, P.; Josic, Dj.; Buchacher, A. Convective interaction media: Polymer-based supports for fast separation of biomolecules. LC GC **1998**, *11*, 660–669.
14. Tennikova, T.B.; Freitag, R. An introduction to monolithic disks as stationary phases for high performance biochromatography (review). J. High Resol. Chromatogr. **2000**, *23*, 27–38.
15. Josic, Dj.; Buchacher, A. Monoliths as stationary phases for separation of proteins and polynucleotides and enzymatic conversion. (Review). J. Chromatogr. B Biomed. Sci. Appl. **2001**, *752* (2), 191–205.
16. Podgornik, H.; Podgornik, A.; Perdih, A. A method of fast separation of lignin peroxidases using convective interaction media disks. Anal. Biochem. **1999**, *272*, 43–47.
17. Vodopivec, M.; Podgornik, A.; Berovic, M.; Strancar, A. Application of convective interaction media (CIM®) disk monolithic columns for fast separation and monitoring of organic acids. JCS **2000**, *38* (11), 489–495.
18. Svete, P.; Milacic, R.; Mitrovic, B.; Pihlar, B. Potential for the speciation of Zn using fast protein liquid chromatography (FPLC) and convective interaction media (CIM®) fast monolithic chromatography with FAAS and electrospray (ES)–MS–MS detection. Analyst **2001**, *126*, 1346–1354.
19. Barut, M.; Podgornik, A.; Merhar, M.; Strancar, A. Rigid discs. In *Monolithic Materials: Preparation, Properties and Applications*; Svec, F., Tennikova, T.B., Deyl, Z., Eds.; Elsevier: Amsterdam, 2003.
20. Berruex, L.G.; Freitag, R. Affinity-based interactions on disks for fast analysis, isolation and conversion of biomolecules. In *Methods for Affinity-Based Separations of Enzymes and Proteins*; Gupta, M.N., Ed.; Birkhauser: Basel, 2002; Chapter 7.
21. Josic, Dj.; Buchacher, A. Application of monoliths as supports for affinity chromatography and fast enzymatic conversion. J. Biochem. Biophys. Methods **2001**, *49*, 153–174.
22. Podgornik, A.; Barut, M.; Mihelic, I.; Strancar, A. Tubes. In *Monolithic Materials: Preparation, Properties and Applications*; Svec, F., Tennikova, T.B., Deyl, Z., Eds.; Elsevier: Amsterdam, 2003.

Monolithic Stationary Supports: Preparation, Properties, and Applications

Aleš Podgornik
J. Jancar
M. Barut
A. Strancar
BIA Separations d.o.o., Ljubljana, Slovenia

INTRODUCTION

Chromatographic monoliths are a specific type of chromatographic stationary phase. In contrast to conventional, particle shaped supports, they consist of a single piece of porous material. The pores form a highly interconnected network of open channels through which the mobile phase flows. Therefore, the main transport mechanism of the molecules to be separated is convection. Because of this, mass exchange between the mobile and stationary phase is very fast, similar to that in the membrane supports. In contrast to the membranes, however, monoliths can be prepared in various shapes and dimensions. Besides convective transport, monoliths also exhibit several other unique features:

- Their dynamic porosity greatly exceeds the porosity of the particle shaped supports, reaching values up to 90%.
- Due to their surface accessibility, their dynamic binding capacity is high, especially for very large molecules.
- Their separation, resolution, and dynamic binding capacity are unaffected by the linear velocity, at least within the applicable flow rates.
- Preparation of monolithic columns is easy since there is no need for sieving as is generally required for particles; also, there is no need for column filling, since the monoliths can be prepared in situ in the column housing.

MONOLITHS

Because of their many advantages, monoliths have been implemented in several areas of separation science. Since they can be easily covalently bound to a surface, they are an almost ideal matrix for the preparation of flow-through microchips or capillaries. In fact, several excellent applications in this field have appeared recently.[1–7]

Monoliths are also extensively used on an analytical scale. Silica-based monoliths, commercialized under the trade name Chromolith® (Merck, Darmstadt, Germany), exhibit high resolving power, combined with a very low pressure drop and seem to be an ideal support for many small molecule applications.[8] On the other hand, methacrylate based monoliths, commercialized by BIA Separations (Ljubljana, Slovenia) under the trademark CIM Convective Interaction Media®, are widely used for separation and purification of large molecules such as proteins, DNA, or even viruses.[9]

Despite the significant success of the monoliths on a micro- and analytical scale, few reports in the literature describe applications of large volume monoliths. This is rather surprising, since one would expect that the combination of low pressure drop and flow, unaffected resolution, and especially, dynamic binding capacity, resulting in high productivity, are attractive features for any purification process. The lack of large monolithic units may therefore be attributed to the difficulties related to their preparation.

In fact, very few reports can be found about the preparation of large monolithic columns. Basically, scaling-up of three types of monoliths has been attempted. Silica monoliths have been scaled in the format of conventional chromatographic columns. The largest reported silica monolith has a dimension of 100 × 25 mm, with the volume close to 50 ml.[10] This seems to be close to the upper limit of thickness, since no further scale-up is reported. Preparation of silica monoliths consists of several steps, including the heating of the skeleton up to several hundred degrees Celsius to obtain a proper monolithic structure. For large monoliths, this is a challenging task, since any significant temperature gradients inside the monolith, occurring during heating or cooling, might cause formation of cracks in the structure. Such deformations inevitably cause irregularities in the flow of the mobile phase passing through the monolith, thereby resulting in a decrease of column efficiency. Despite these difficulties, 50 ml silica monolithic columns were successfully implemented in several processes, including simulated moving bed (SMB) technology.[11]

Other reports concerning preparation of large monoliths are related to agarose and methacrylate monoliths. Both types of monoliths are prepared by polymerization, which is an exothermic process that releases significant amounts of heat during the reaction. Temperature gradients formed inside the polymerization mixture during the polymerization process cause deformations in pore size distribution. Consequently, the efficiencies of such units are significantly decreased. There are basically two approaches reported in the literature, suggesting possible solutions for this problem. Peters, Švec, and Frechet[12] suggested preparation of the methacrylate monoliths via slow addition of the polymerization mixture to avoid a temperature increase inside the monolith during the polymerization itself. By properly adjusting polymerization conditions, they were able to prepare monoliths with uniform pore size distribution. Unfortunately, no information about the chromatographic properties or applications of the obtained monolith is given, and there are no reports about further development of the proposed method.

An alternative approach was suggested by Podgornik et al.[13] They implemented radial flow mode and introduced monolithic columns of a well defined thickness. A similar idea was later implemented for the preparation of agarose monolithic columns,[14] which were applied to pseudoaffinity chromatography using Cibacron Blue 3GA as a ligand and as bioreactors with the immobilized enzyme β-galactosidase.

In the following section, details about large volume radial flow methacrylate monolithic columns and the strategy for their preparation are presented.

DESIGN OF LARGE VOLUME RADIAL METHACRYLATE MONOLITHIC COLUMNS

Currently, there is still an ongoing discussion about the proper ways for scaling up the chromatographic columns. To preserve constant quality of the product, as an ultimate goal, several criteria have been proposed, among them constant column height or length, constant residence time, constant L/d_p ratio, etc.[15] Although proposed for conventional chromatographic columns, they can also be applied for the monolithic columns. For some of them, as for the L/d_p criterion, for which the particle diameter should be determined, implementation on the monoliths is not obvious, since it is difficult to define a particle diameter. However, there are still some characteristic dimensions that can be used instead of d_p. For the silica monoliths, Tallarek, Leinweber, and Siedel-Morgenstern[16] described a phenomenological approach, i.e., introducing an equivalent of the particle diameter based on the estimation of friction factor. For methacrylate monoliths, effective d_p was estimated from the measurement of peak broadening and pressure drop.[17]

Besides the abovementioned approaches, methacrylate based monoliths were scaled up following two additional ideas:

- They are mainly intended for the separation and purification of large molecules.
- Their structure should be similar regardless of the size.

Separation of macromolecules has several peculiarities that significantly influence the design of the chromatographic columns. Large molecules normally interact with the surface via several points. Consequently, their adsorption isotherm is extremely steep, almost rectangular. Because of this, there is only a very narrow mobile-phase window within which they can be eluted under isocratic conditions. Therefore, mobile phase gradients are normally applied. For this type of elution, the column length does not play a significant role. In fact, there is an optimal column length for a given system and gradient slope, which can be very short for large molecules,[18] and one can be flexible regarding the column length as well as the design.

The main reason to preserve the structure of the monolith on different scales is to make the transfer of chromatographic methods very simple and straightforward. Keeping a constant structure, the resin efficiency, normally measured in terms of height equivalent of theoretical plate (HETP), is also kept constant. Therefore, method transfer time can be significantly shortened since fewer experiments are required.

The structure of the methacrylate monoliths depends on several factors, e.g., the composition of the polymerization mixture and the polymerization temperature. The latter parameter, especially, is a very powerful tool, since different structures can be obtained without changing the chemical composition of the monolith. The main reason for such a significant influence of the temperature on the monolith's structure is the initiator degradation rate. During degradation, free radicals are released. The higher the temperature, the more radicals are formed per unit time, initiating formation of a larger number of nuclei that grow continuously. Because the total amount of monomer is limited, the larger number of the nuclei means that they are smaller, resulting in smaller pores. This process is extremely sensitive, since change of the polymerization temperature, e.g., 8°C, shifts pore size by almost an order of magnitude.[9] Being an excellent tool for tailoring monolith structure, temperature also represents one of the main problems in the preparation of large volume methacrylate monolithic columns.

Methacrylate polymerization is a highly exothermic reaction, releasing, in the particular case of methacrylate monoliths, around 190 J/g of heat.[19] Since preparation of the monoliths proceeds through bulk polymerization, the heat generated cannot be dissipated fast enough;

therefore, an increase of temperature occurs inside the polymerization mixture during the polymerization. At the maximal polymerization rate, the increase can be as high as 80°C.[9] Taking into account that even one-tenth of this value dramatically changes the pore diameter, it is clear that such increase results in extremely non-homogeneous pore distribution.[9]

To obtain uniform monolithic structure, the temperature increase should be small and well controlled. Since one cannot enhance heat dissipation by stirring, because it would destroy the monolithic structure, or change the physical properties of the polymerization mixture, the monolith thickness is limited.

The appropriate maximal monolith thickness was determined by mathematical modeling. Heat is released through chemical bond formation during polymerization. Therefore, the amount of heat released should be proportional to the reaction kinetics. By measuring the heat release, we were able to determine the reaction order as well as heat release per unit volume of polymerization mixture. Details about determination of reaction kinetics and mathematical modeling can be found elsewhere.[19,20] The outcome of the model is the maximal allowed monolith thickness providing uniform monolith structure, together with the time required to complete polymerization over the entire monolith volume.

As already stated, CIM monoliths were developed to be used for purification of large molecules, typically proteins, oligo- or polynucleotides, or viruses. Therefore, columns with rather short beds can be used. Since we are no longer bound to a chromatographic column of substantial length, different scale-up designs are possible. Especially, three seem to be suitable: rod format, disk format, and tube format. As described in detail elsewhere,[21] the tube format was found to be the most advantageous, since it gives a high degree of flexibility (tube diameter as well as tube height can be varied) combined with a low pressure drop. This is the main reason for the construction of tubular shaped, large volume methacrylate monolithic columns. Currently, four different volumes, specifically 8, 80, 800, and 8000 ml monolithic columns, are constructed, comprising the monoliths shown in Fig. 1. Details about the column features are described elsewhere.[22]

Despite the limitation of the monolith thickness related to the preparation problems, cylindrically shaped monoliths of desired thickness can be easily constructed, by polymerizing several cylinders of appropriate dimensions and inserting one into another, the so-called "tube-in-tube" approach, as shown in Fig. 2. Furthermore, each of the cylinders can have a different chemistry; therefore, a multidimensional chromatographic column, named the conjoint liquid chromatography

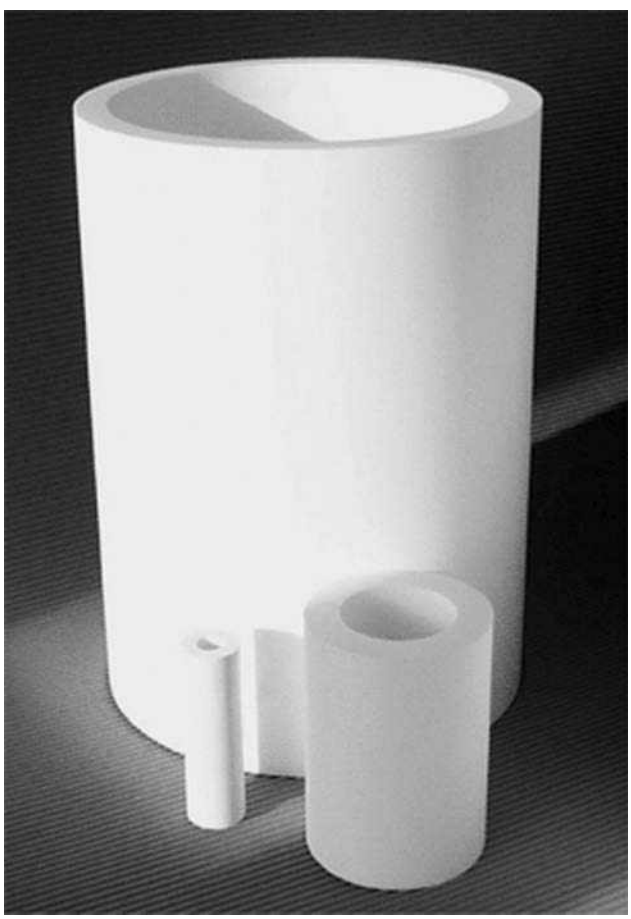

Fig. 1 Large volume cylindrical shaped methacrylate monoliths of volume 80, 800, and 8000 ml. The largest, the 8000 ml monolith, has a height of 41.5 cm and an outer diameter of 30 cm.

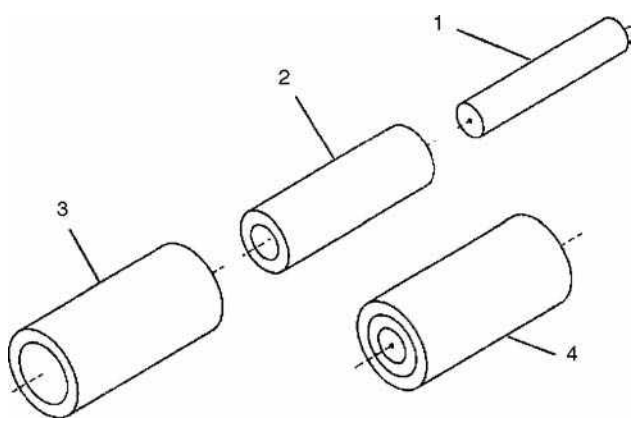

Fig. 2 Construction of a large volume methacrylate monolithic unit of desired thickness. The monolithic unit (4) consists of three monolithic cylinders (1, 2, and 3). The total thickness of the unit (4) is the sum of the thicknesses of monoliths 1, 2, and 3.
Source: From Construction of large-volume monolithic columns, in Anal. Chem.[13]

(CLC) column for the methacrylate monoliths, can be prepared. In this way, extracolumn broadening, which occurs when several columns are connected in series, is significantly reduced.[23]

RADIAL, LARGE VOLUME METHACRYLATE MONOLITHIC COLUMNS AND THEIR PROPERTIES

To exploit all benefits of the tubular approach, the commonly applied axial flow of the mobile phase has to be changed to a radial one. Entering into the chromatographic column, the mobile phase is directed into the channel extending over the entire outer surface of the monolith. In this way, the mobile phase is uniformly spread over the monolith. Since the monolith is sealed between two plates, the only possible course for the mobile phase is to penetrate into the monolith pores. After passing through the monolith, the mobile phase is collected in the middle hole and directed into the capillary connected with the column exit. The construction is shown in Fig. 3. In this way, the entire monolithic bed is uniformly used. This can be concluded from the capacity per monolith unit, which is the same as that for the monolithic disks of 0.34 ml volume operating in an axial mode.

As already mentioned, tubular shaped monolith can be prepared in various thicknesses by using a "tube-in-tube" approach. Since a radial chromatographic mode is applied, the linear velocity of the mobile phase increases when passing through the monolith.[13] In the case of particle shaped supports, change of linear velocity results in a change of column efficiency, according to the Van Deemter equation. For the monoliths, due to extremely fast exchange between the mobile and stationary phase, diffusion limitations can be neglected, thereby resulting

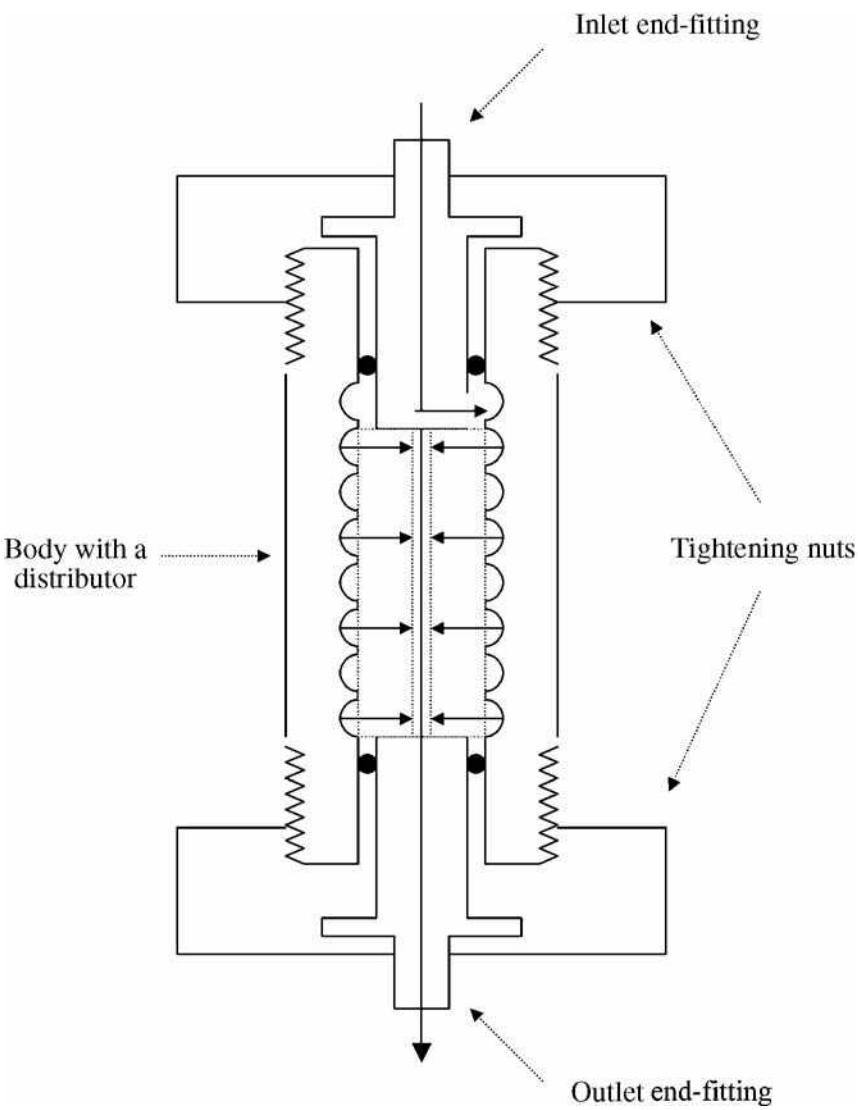

Fig. 3 Schematic representation of the housing for a radial monolithic column. A housing comprises inlet and outlet end-fittings, two tightening nuts and a body with distributor. Four O rings (black circles) assure proper sealing. Solid arrows indicate the direction of the mobile phase.
Source: From Construction of large-volume monolithic columns, in Anal. Chem.[13]

in flow-independent resolution and dynamic binding capacity. Jungbauer and Hahn[15] investigated the bed usage for the 8 ml tubular shaped monolithic column, assuming a certain linear velocity (critical velocity) beyond which diffusion restrictions become significant. They showed that, for a critical velocity of 1500 cm/hr, which is equivalent to 40 CV/min, over 99% of the bed is used. Such a high flow rate cannot be employed in practice since pressure drop becomes a process bottleneck. These theoretical findings are also experimentally confirmed. Fig. 4 shows that the change of the linear velocity, indeed, does not change either the resolution or the dynamic binding capacity. Therefore, although radial flow is implemented, one cannot distinguish, by performance, a radial monolithic column from an axially operating column.

So far, radial monolithic columns have been successfully implemented for purification of various types of macromolecules. In the field of proteins, anion exchange tubular monolithic columns were used for purification of lignin peroxidase isoforms,[24,25] having very similar molecular masses and isoelectric points, as shown in Fig. 5. Using a combination of pH and salt gradient, purification of manganese peroxidases was also possible.[25] There are several reports describing implementation of radial monolithic columns for purification of clotting factors from human plasma. A quaternary amine (QA) 8 ml unit was used for purification of factor VIII,[26] while an up to 500 ml. DEAE unit was used for purification of clotting factor IX,[27,28] as demonstrated in Fig. 6. All purifications were completed in a shorter time in comparison to those

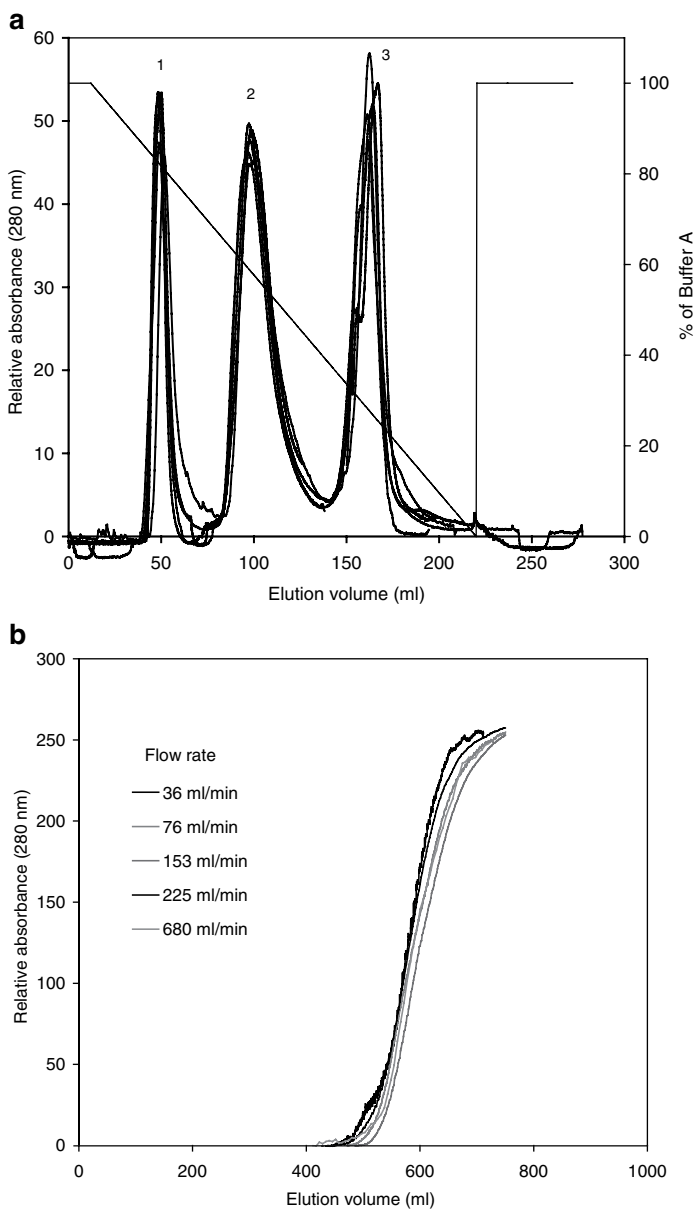

Fig. 4 Effect of flow rate on separation efficiency (a) and dynamic binding capacity (b). Conditions for (a): separation of a protein mixture at six different flow rates (40, 80, 120, 160, 200, and 240 ml/min) normalized to the elution volume. Stationary phase: CIM diethylaminoethyl (DEAE) 80 ml column. Conditions: mobile phase: buffer A: 20 m*M* Tris–HCl buffer, pH 7.4; buffer b: 20 m*M* Tris–HCl buffer + 1 *M* NaCl, pH 7.4; gradient: 0–100% buffer B in 200 ml; sample: 2 mg/ml of myoglobin (peak 1), 6 mg/ml of conalbumin (peak 2), and 8 mg/ml of soybean trypsin inhibitor (peak 3) dissolved in buffer A; injection volume: 1000 μl; detection: UV at 280 nm. Conditions for (B): stationary phase: CIM DEAE 80 ml column; flow rate: 36, 76, 153, 225, and 680 ml/min; sample: 3 mg/ml of BSA in 20 m*M* Tris–HCl buffer, pH 7.4; detection: UV at 280 nm.
Adapted from Podgornik et al.[13,22]

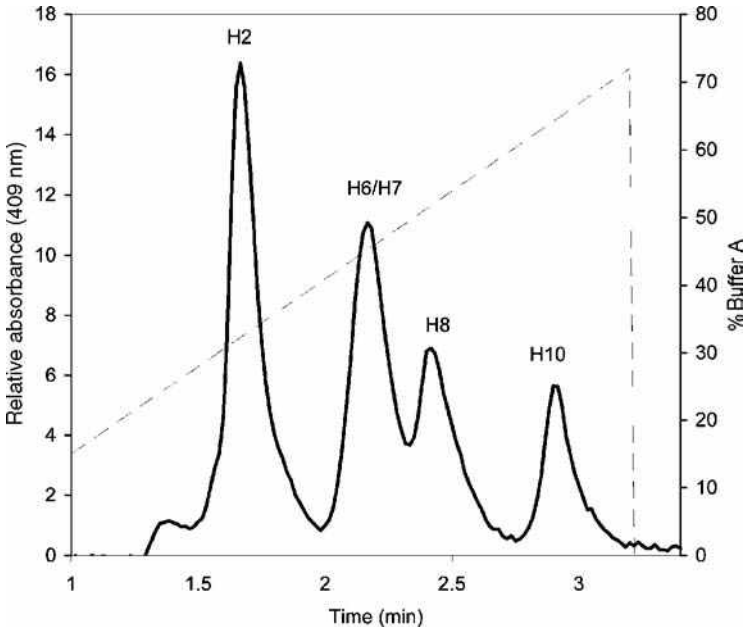

Fig. 5 Separation of lignin peroxidase isoenzymes using the 8 ml radial methacrylate monolithic columns. Stationary phase: CIM DEAE 8 ml column. Conditions: buffer A: 10 m*M* acetic buffer, pH 6.0; buffer B: 1 *M* acetic buffer, pH 6.0; flow rate: 8 ml/min; gradient: 10–70% buffer B in 2.25 min; sample: supernatant from *Phanerochaete chrysosporium* cultivation; injection volume: 500 μl; detection: UV at 409 nm.
Source: From Fast separation of biomolecules using polymer-based monolithic supports, in Am. Biotechnol. Lab.[24]

performed with conventional particle based supports. Large monolithic columns were also successfully used for purification of pDNA.[29] In this case, speed is also accompanied by an extremely high binding capacity,[30] making these columns an attractive option for the purification of polynucleotides.

CONCLUSIONS

Monolithic columns combine several features, such as high porosity, flow-independent resolution, and dynamic binding capacity, which make them very suitable for purification of large molecules. Although preparation of large volume monoliths with uniform structure is a challenging task, using a mathematical modeling approach and appropriate column design, this problem has been successfully solved. Such columns, with volumes up to 8 L, operate at low pressure drop and have already been successfully implemented in an industrial process for pDNA purification. Because of their useful properties, it is expected that they will also be applied in other processes involving macromolecule purification, including purification of viruses.

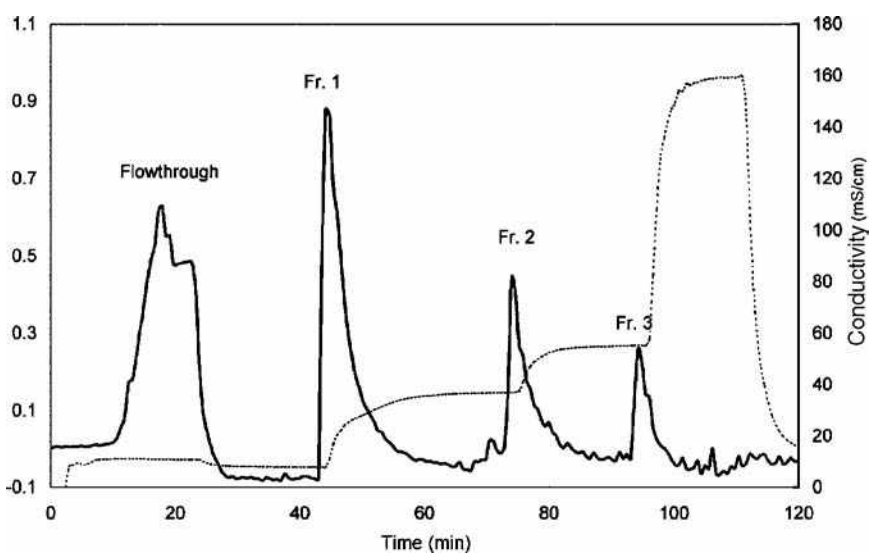

Fig. 6 Separation of DEAE-Sephadex eluate of cryo-poor human plasma on 500 ml radial DEAE monolithic column. Fraction 2 (Fr. 2) is rich in factor IX. Conditions: 50 ml/min; pressure drop less than 0.2 MPa, room temperature. Absorbance: —, conductivity: · · · · · · ·.
Source: From Application of semi-industrial monolithic columns for downstream processing of clotting factor IX, in J. Chromatogr.[28]

REFERENCES

1. Tanaka, N.; Motokawa, M.; Kobayashi, H.; Hosoya, K.; Ikegami, T. Monolithic silica columns for capillary liquid chromatography. In *Monolithic Materials: Preparation, Properties, and Applications*; Švec, F., Tennikova, T.B., Deyl, Z., Eds.; Elsevier: Amsterdam, 2003; 173–196.
2. Endres, H.N.; Johnson, J.A.C.; Ross, C.A.; Welp, J.K.; Etzel, M.R. Evaluation of an ion-exchange membrane for purification of plasmid DNA. Biotechnol. Appl. Biochem. **2003**, *37*, 259–266.
3. Iberer, G.; Hahn, R.; Jungbauer, A. Monoliths as stationary phases for separation of biopolymers: the fourth generation of chromatography sorbents. LC–GC **1999**, *17*, 998–1005.
4. Mihelič, I.; Koloini, T.; Podgornik, A.; Štrancar, A. Dynamic capacity studies of CIM (Convective Interaction Media)® monolithic columns. J. High Resolut. Chromatogr. **2000**, *23*, 39–43.
5. Švec, F.; Frechet, J.M.J. Molded rigid monolithic porous polymers: an inexpensive, efficient, and versatile alternative to beads for the design of materials for numerous applications. Ind. Eng. Chem. Res. **1999**, *38*, 34–38.
6. Lämmerhofer, M.; Lindner, W. Capillary electrochromatography. In *Monolithic Materials: Preparation, Properties, and Applications*; Švec, F., Tennikova, T.B., Deyl, Z., Eds.; Elsevier: Amsterdam, 2003; 489–556.
7. Fintschenko, Y.; Kirby, B.J.; Hasselbrink, E.F.; Singh, A.K.; Shepodd, T.J. Miniature and microchip technologies. In *Monolithic Materials: Preparation, Properties, and Applications*; Švec, F., Tennikova, T.B., Deyl, Z., Eds.; Elsevier: Amsterdam, 2003; 659–682.
8. Cabrera, K.; Lubda, D.; Eggenweiler, H.-M.; Minakuchi, H.; Nakanishi, K. A new monolithic-type HPLC column for fast separations. J. High Resolut. Chromatogr. **2000**, *23*, 93–99.
9. Štrancar, A.; Podgornik, A.; Barut, M.; Necina, R. Short monolithic columns as stationary phases for biochromatography. In *Advances in Biochemical Engineering/ Biotechnology; Modern Advances Chromatography*; Freitag, R., Ed.; Springer-Verlag: Heidelberg, 2002; Vol. 76, 49–85.
10. Schulte, M.; Lubda, D.; Delp, A.; Dingenen, J. Preparative monolithic silica sorbents (PrepRODs®) and their use in preparative liquid chromatography. J. High Resolut. Chromatogr. **2000**, *23*, 100–105.
11. Schulte, M.; Dingenen, J. Monolithic silica sorbents for separation of diastereomers by means of simulated moving bed chromatography. J. Chromatogr. A. **2001**, *923*, 17–25.
12. Peters, E.C.; Švec, F.; Frechet, J.M.J. Preparation of large-diameter "molded" porous polymer monoliths and the control of pore structure homogeneity. Chem. Mater. **1997**, *9*, 1898–1902.
13. Podgornik, A.; Barut, M.; Štrancar, A.; Josić, Dj.; Koloini, T. Construction of large-volume monolithic columns. Anal. Chem. **2000**, *72*, 5693–5699.
14. Gustavsson, P.-E.; Larsson, P.-O. Continuous superporous agarose beds in radial flow columns. J. Chromatogr. A. **2001**, *925*, 69–78.
15. Jungbauer, A.; Hahn, R. Large scale separations. In *Monolithic Materials: Preparation, Properties, and Applications*; Švec, F., Tennikova, T.B., Deyl, Z., Eds.; Elsevier: Amsterdam, 2003; 173–196.
16. Tallarek, U.; Leinweber, F.C.; Siedel-Morgenstern, A. Fluid dynamics in monolithic adsorbents: phenomenological approach to equivalent particle dimension. Chem. Eng. Technol. **2002**, *25*, 1177–1181.
17. Hahn, R.; Jungbauer, A. Peak broadening in protein chromatography with monoliths as very fast separations. Anal. Chem. **2000**, *72*, 4853–4858.
18. Dubinina, N.I.; Kurenbin, O.I.; Tennikova, T.B. Peculiarities of gradient ion-exchange high-performance liquid chromatography of proteins. J. Chromatogr. **1996**, *753*, 217–225.
19. Mihelič, I.; Krajnc, M.; Koloini, T.; Podgornik, A. Kinetic model of A methacrylate-based monolith polymerization. Ind. Eng. Chem. Res. **2001**, *40*, 3495–3501.
20. Mihelič, I.; Koloini, T.; Podgornik, A. Temperature distribution effects during polymerization of methacrylate-based monoliths. J. Appl. Polym. Sci. **2003**, *87*, 2326–2334.
21. Podgornik, A.; Barut, M.; Mihelič, I.; Štrancar, A. Tubes. In *Monolithic Materials: Preparation, Properties, and Applications*; Švec, F., Tennikova, T.B., Deyl, Z., Eds.; Elsevier: Amsterdam, 2003; 77–102.
22. Podgornik, A.; Jančar, J.; Merhar, M.; Kozamernik, S.; Glover, D.; Čuček, K.; Barut, M.; Štrancar, A. Large scale methacrylate monolithic columns: design and properties. J. Biochem. Biophys. Meth. **2004**, *60*, 179–189.
23. Štrancar, A.; Barut, M.; Podgornik, A.; Koselj, P.; Josić, Dj.; Buchacher, A. Convective interaction media: polymer-based supports for fast separation of biomolecules. LC–GC **1998**, *11*, 660–669.
24. Barut, M.; Podgornik, A.; Podgornik, H.; Štrancar, A.; Josić, Dj.; Mac Farlane, J. Fast separation of biomolecules using polymer-based monolithic supports. Am. Biotechnol. Lab. **1999**, *17*, 48–51.
25. Milavec Žmak, P.; Podgornik, H.; Jančar, J.; Podgornik, A.; Štrancar, A. Transfer of gradient chromatographic methods on CIM monolithic columns. J. Chromatogr. A. **2003**, *1006*, 195–205.
26. Štrancar, A.; Barut, M.; Podgornik, A.; Koselj, P.; Schwinn, H.; Raspor, P.; Josić, Dj. Application of compact porous tubes for preparative isolation of clotting factor VIII from human plasma. J. Chromatogr. A. **1997**, *760*, 117–123.
27. Branović, K.; Buchacher, A.; Barut, M.; Štrancar, A.; Josić, Dj. Application of monoliths for downstream processing of clotting factor IX. J. Chromatogr. A. **2000**, *903*, 21–32.
28. Branović, K.; Buchacher, A.; Barut, M.; Štrancar, A.; Josić, Dj. Application of semi-industrial monolithic columns for downstream processing of clotting factor IX. J. Chromatogr. B. **2003**, *790*, 175–182.
29. Necina, R.; Urthaler, J.; Štrancar, A.; Jančar, J.; Merhar, M.; Barut, M.; Podgornik, A. Method and device for isolating and purifying a polynucleotide of interest on a manufacturing scale. PCT Int. Appl. WO 03/051483, 2003.
30. Benčina, M.; Podgornik, A.; Štrancar, A. Characterization of methacrylate monoliths for purification of DNA molecules. J. Sep. Sci. **2004**, *27*, 801–810.

Multidimensional Separations

Haleem J. Issaq
National Cancer Institute at Frederick (NCI-Frederick), National Institutes of Health (NIH), Frederick, Maryland, U.S.A.

Abstract
Chromatography in all its formats is capable of resolving a simple mixture using one procedure. However the resolution of a complex mixture requires the use of two orthogonal procedures. Here we discuss two-dimensional thin-layer chromatography (TLC), gas chromatography (GC), and high-performance liquid chromatography (HPLC) that have been used for the separation of plant extracts, environmental samples, and cell and serum protein digests to mention a few. Mainly the first dimension is fractionation to simplify the complexity of the mixture while the second dimension is used to enhance the separation of the fractions. Both dimensions have different mechanisms of separation, i.e., they are orthogonal.

INTRODUCTION

Since the separation of a complex mixture is not possible using a single chromatographic or electrophoretic procedure, researchers investigated multidimensional strategies using two-dimensional (2-D) electrophoresis (2DE), 2-D chromatography, or a combination of both. Though we tend to think of multidimensional separations as a recent venture, analytical and bioanalytical chemists began developing better methods to achieve maximum resolution of a complex mixture over half a century ago. Scientists realized the significant advantages of multidimensional separations using one chromatographic mode for fractionation, normally the least resolving mode, followed by a second orthogonal (different selectivity) mode to separate the resulting fractions. Fractionation of a mixture by chromatography or electrophoresis is achieved by manipulations of: 1) the mobile-phase properties, such as slope (time) of the gradient, organic modifier, buffer pH, salt concentration; 2) column chemistry, such as reversed phase, ion exchange, size exclusion, normal phase (e.g., silica), hydrophobic interaction (HILIC), or affinity (e.g., antibody, lectin, aptamer, metal, DNA, etc.); and 3) ampholyte pH range and gel properties in electrophoresis.

The basis for developing multidimensional chromatographic approaches to separate complex mixtures is the work of Martin and his colleagues,[1] using paper chromatography to separate wool hydrolysate. The hydrolysate was applied at one corner of the square filter paper and developed in collidine for 3 days, taken out and dried, turned 90°, and then developed in phenol for 27 hr. A similar approach was also used to separate a mixture of the hydrochlorides of 22 amino acids.

In 1956, Smithies and Poulik[2] realized that "a combination of two electrophoretic processes on a gel at right angles should give a much greater degree of separation than is possible with either separately." Giddings defined 2-D separations as "those techniques in which a sample is subject to two displacement processes oriented at right angle to one another."[3] He also stated that "multidimensional chromatography, or generally multidimensional separation, provides a means of greatly enhancing the peak capacity and thus the resolution of the components of a complex mixture, and that the peak capacity of a multidimensional separation is the product of the peak capacities of its component one-dimensional methods."[4] The multidimensional system selected should allow analysis of the whole sample, and not just selected parts of the first-dimensional fraction, as in heart-cutting procedures that are used in high-performance liquid chromatography (HPLC)[5] and gas chromatography (GC)[6] where only regions of interest are transferred from the first column to a second column for enhanced separation.

OVERVIEW

Multidimensional separations are carried out online or off-line. In an off-line approach, samples are collected as they emerge from the first-dimension column at a specified time and are analyzed using a second orthogonal dimension. There are advantages and limitations to each. An online approach does not generally allow specific fractions to be reanalyzed by complementary techniques. While off-line methods do not approach the speed of online methods, they are typically easier to perform, large samples can be readily analyzed, many different column chemistries and sizes can be used, and collected fractions can be reanalyzed as needed.

Multidimensional chromatographic analyses have been carried out by: 1) thin-layer chromatography (TLC); 2) GC; and 3) HPLC. A few selected examples are presented for each.

1. **Thin-Layer Chromatography (TLC × TLC)**
   TLC is amenable to 2-D separations, preferably by either changing the mobile phase or using a plate that has two different chemistries side by side on the same plate. The 2-D experiment is achieved by successive developments in two perpendicular directions, using two retention mechanisms.[7] Multimodal multidimensional TLC separations are achieved by using plates that have two side-by-side different selectivity groups where the compounds are developed in the same mobile phase or two different mobile phases, or by using plates coated with a single stationary phase such cyano-, amino-, or phenyl-modified silica, which can be developed in two different mobile phases.[8] For example, multimodal TLC separations on a cyano-modified silica gel plate were reported for the separation of Taxol and cephalomannine in a methylene chloride extract of *Taxus brevifolia*.[8] In the first-dimension separation (adsorption), using a mobile phase of methylene chloride:hexane:acetic acid (9:10:1), the plate was dried, turned 90°, and developed in the second dimension (reversed phase) in a mobile phase made of water:acetonitrile:methanol:tetrahydrofuran (8:5:7:0.1). Two side-by-side stationary phases (silica and C-18 reversed phase) plate was used to separate a natural product extract.[9] The first development was done on the silica side, using hexane:acetone (3:2), and the second development was done on the C-18 side, using (85:15) acetonitrile:water.[9]
2. **Gas Chromatography (GC × GC)**
   Separation in GC is achieved by taking advantage of the differences in solute polarity or vapor pressure (i.e., by changing the column temperature). Most of the commercially available columns work on this principle. Another property of the solute that can be used to separate a mixture is the geometry of the molecule (i.e., the length-to-breadth ratio), using a liquid-crystal column. Solutes that elute together on a column that is based on polarity or vapor pressure are resolved on a liquid-crystal column because of differences in their geometry. GC × GC can be done using the heart-cutting technique, whereby selected regions of interest from the first-dimension separation are transferred to the second dimension, or by continuous comprehensive 2-D separation, whereby the total effluent of the first column is transferred to a second column of different selectivity for maximum resolution.

   Issaq, Fox, and Muschik[6] used a low-polarity column (DB-1) in the first dimension and a smectic liquid-crystal column in the second dimension for the separation of coeluting congeners of Aroclor 1242, 1254, and 1260, using the heart-cutting technique. This procedure requires the use of a gas chromatograph equipped with two independent ovens for optimizing the temperature conditions of each column. Excellent baseline separations of the congeners were achieved on multicuts, up to six cuts, of the same injection. This unique 2-D/multimodal capillary GC system, in which the two separation modes of vapor pressure and molecule geometry are employed, is a powerful analytical technique for the separation of complex volatile organic mixtures.

   Comprehensive GC × GC was first introduced in 1991 by Phillips and Liu.[10] In this 2-D GC approach, after completing the separation on the first column, the chromatographer, performs the separation on a different column. The critical, practical part of this approach is the ability to preserve the separation from the first-dimension column while enhancing the separation on the second column. The advantage of GC × GC is that the total mixture is subjected to two orthogonal separation procedures. These procedures result in maximum separation and give every component in the mixture two retention times, which enhances identification based on retention times. The principles and applications of comprehensive GC × GC were discussed by Marriott and Shellie.[11] Comprehensive 2-D GC was applied to the analysis of urban aerosols.[12] Samples were collected onto a glass-fiber filter, extracted by *n*-hexane/acetone, cleaned up on a silver-impregnated silica column, and analyzed by comprehensive GC × GC. A 20 m × 0.25 mm I.D. 5% phenyldimethyl-polysiloxane column was used for the first dimension and a 1 m × 0.1 mm I.D. 14% cyanopropyldiphenylmethylpolysiloxane column was used in the second dimension. Columns were connected to each other by specially made low-volume press fit connectors. A few polycyclic aromatic hydrocarbons and oxygenated polycyclic aromatic hydrocarbons were identified and quantified.
3. **HPLC (HPLC × HPLC)**
   HPLC, with all its different modes of separation [normal phase, reversed phase, ion exchange, size exclusion chromatography (SEC), and HILIC], is well suited for 2-D, or even 3-D. The separation can be carried out online by connecting two different selectivity columns in series or by packing a single column with two different selectivity materials.

   Opiteck et al.[13] and Opiteck and Jorgenson[14] described the 2-D HPLC system for separating complex protein mixtures that used two columns connected in series—the SEC column for the first dimension and the RP column for the second dimension. Peaks eluting from the SEC column were automatically introduced into the RP column to separate similarly sized proteins on the basis of their hydrophobicity.

   A second approach to an online 2-D HPLC separation is the use of a single column packed with two different materials at opposite ends. Washburn

et al. used a single capillary packed with strong cation exchanger (SCX) and RP particles to separate a complex mixture of peptides.[15] A major advantage of this separation technology is that the entire system is coupled directly online with a mass spectrometer (MS), enabling a large number of peptides to be directly identified in a high-throughput manner.

A third approach to 2-D HPLC is an off-line approach that uses two different selectivity columns. In this approach, fractions are collected at specific periods as they elute from the first column and then the fractions are each injected into the head of a different selectivity column and separated. Blonder et al. described a 2-D HPLC procedure for the identification of membrane proteins from mammalian cell/tissue.[16] After extraction, the proteins were digested with trypsin. The resulting peptides were analyzed by SCX in the first dimension, and fractions eluting from the column were collected every minute with the aid of a fraction collector, and were injected on an RP column and detected by MS.

Although 2-D strategies are the most popular methods of enhancing the separation of complex mixtures, there have been experiments that employed a 3-D approach. For example, a protein extract of mouse serum was first fractionated by ion exchange (IEX). Protein fractions were collected, digested with trypsin, and were subfractionated using SCX. The resulting subfractions of peptides were analyzed by RPLC/MS.[17]

CONCLUSIONS

Chromatography in all its formats is capable of resolving a simple mixture using one procedure. However the resolution of a complex mixture requires the use of two orthogonal procedures. Two-dimensional TLC, GC, and HPLC have been used for the separation of plant extracts, environmental samples, and cell and serum protein digests to mention a few. Many approaches have been employed in which the first dimension is fractionation (to simplify the complexity of the mixture) while the second dimension is used to enhance the separation of the fractions.

ACKNOWLEDGMENTS

This project has been funded in whole or in part with federal funds from the National Cancer Institute, National Institutes of Health, under Contract N01-CO-12400. The content of this publication does not necessarily reflect the views or policies of the Department of Health and Human Services, nor does mention of trade names, commercial products, or organizations imply endorsement by the U.S. government.

REFERENCES

1. Consden, R.; Gordon, A.H.; Martin, A.J.P. Qualitative analysis of proteins: A partition chromatographic method using paper. Biochem. J. **1984**, *38*, 224–232.
2. Smithies, O.; Poulik, M.D. Two-dimensional electrophoresis of serum proteins. Nature **1956**, *177*, 1033–1038.
3. Giddings, J.C. Two-dimensional separations: concepts and promise. Anal. Chem. **1984**, *56*, 1258A–1270A.
4. Giddings, J.C. Concepts and comparisons in multidimensional separations. J. High Resolut. Chromatogr. Chromatogr. Commun. **1987**, *10*, 319–323.
5. Erni, F.; Frei, R.W. Two-dimensional column liquid chromatographic technique for resolution of complex mixtures. J. Chromatogr. **1978**, *149*, 561–569.
6. Issaq, H.J.; Fox, S.D.; Muschik, G.M. The simultaneous use of solute vapor pressure and geometry in multidimensional capillary gas chromatography of polychlorinated biphenyls. J. Chromatogr. Sci. **1989**, *2*, 172–175.
7. Guiochon, G.; Beaver, L.A.; Gonnord, M.F.; Siouffi, A.M.; Zakaria, M. Theoretical investigation of the potentialities of the use of a multidimensional column in chromatography. J. Chromatogr. **1983**, *255*, 415–437.
8. Issaq, H.J. Recent advances in multimodal thin layer chromatography. TrAC Trends Anal. Chem. **1990**, *9*, 36–40.
9. Issaq, H.J.; Seburn, K.; Andrews, P.; Schaufelberger, D. Multimodal thin layer chromatographic separation of bryostatins 1 and 2 from marine organism extract employing side-by-side silica gel/C_{18} plates. J. Liq. Chromatogr. **1989**, *12*, 3121–3128.
10. Phillips, J.B.; Liu, Z. Comprehensive two-dimensional gas chromatography using an on-column thermal modulator interface. J. Chromatogr. Sci. **1991**, *29*, 227–231.
11. Marriott, P.; Shellie, R. Principles and applications of comprehensive two-dimensional gas chromatography. TrAC Trends Anal. Chem. **2002**, *21*, 573–583.
12. Kallio, M.; Hyotylainen, T.; Lehtonen, M.; Jussila, M.; Hartonen, K.; Shimmo, M.; Riekkola, M.L. Comprehensive two-dimensional gas chromatography in the analysis of urban aerosols. J. Chromatogr. A, **2003**, *1019*, 251–260.
13. Opiteck, G.J.; Ramirez, S.M.; Jorgenson, J.W., Moseley, M.A. Comprehensive two-dimensional high-performance liquid chromatography for the isolation of overexpressed proteins and proteome mapping. Anal. Biochem. **1998**, *258*, 349–361.
14. Opiteck, G.J.; Jorgenson, J.W. Two-dimensional SEC/RPLC coupled to mass spectrometry for the analysis of peptides. Anal. Chem. **1997**, *69*, 2283–2291.
15. Washburn, M.P.; Wolters, D.; Yates, J.R. Large-scale analysis of the yeast proteome by multidimensional protein identification technology. Nat. Biotechnol. **2001**, *19*, 242–247.
16. Blonder, J.; Chan, K.C.; Issaq, H.J.; Veenstra, T.D. Identification of membrane proteins from mammalian cell/tissue using methanol-facilitated solubilization and tryptic digestion coupled with 2D-LC-MS/MS. Nat. Protoc. **2007**, *1*, 2784–2790.
17. Hood, B.L.; Zhou, M.; Chan, K.C.; Lucas, D.A.; Kim, G.J.; Issaq, H.J.; Veenstra, T.D.; Conrads, T.P. Proteomic investigation of the mouse serum proteome. J. Proteome Res. **2005**, *4*, 1561–1568.

Multidimensional TLC

Simion Gocan
Department of Analytical Chemistry, Babes-Bolyai University, Cluj-Napoca, Romania

INTRODUCTION

Since the introduction of thin-layer chromatography (TLC), there has been great interest regarding the increase of separation capacity (spot capacity). This interest was motivated by the separation of complex mixtures that contain a great number of compounds. Some of them are difficult to separate because they have similar properties.

TWO-DIMENSIONAL DEVELOPMENT

Two-dimensional thin-layer chromatography (2D TLC) involves the application of a single sample to one corner of a TLC plate, which is subjected to two development processes. The TLC plate is developed with the first mobile phase, dried, and redeveloped in an orthogonal (the plate rotated through 90°) direction with a second mobile phase having different selectivity characteristics. Thus, the components migrate from the point of application into a two-dimensional thin layer, ensuring more space for resolution compared to one-dimensional separation.

Two-dimensional TLC is an analytical separation technique recommended for the separation of sample of compounds that are difficult to separate in a single dimension. This technique has been mostly used for qualitative clinical and biochemical analysis, where high selectivity separation is required.

In 2D TLC, any spot can be defined by a pair of x and y coordinates; the quality of a separation can be established by comparing the distance between all pairs of spots in the chromatogram. High resolution will be obtained when the selectivity between the two directions will be significantly different. In practice, several methods have been used to achieve this purpose. The potential methods for obtaining two different separation mechanisms in orthogonal directions are the following:

1. Two eluent systems of different selectivities for the sample components are used and a single sorbent thin layer for two dimensions is developed.
2. Two sorbent layers (e.g., silica gel and reversed phase) as adjacent zones with different selectivities can be used. The sorbent layer for the first development is a narrow strip (reversed phase), and for the second development, it is a large surface (normal phase). A suitable eluent system has to be used for each sorbent layer.

There are other possibilities, but all of them have the same principle (i.e., the selectivities to be different in the two orthogonal developments). If the selectivities are close to each other, the 2D separation effect will be a diagonal arrangement of the spots. A separation will be considered better when the spots will be uniformly spread along the entire surface of the plate.

2D TLC is used for a great number of compounds. When spot capacity in the first direction is n_1 and is n_2 in the orthogonal direction, then the total spot capacity will be equal to $n_1 n_2$. Refs.,[1,2] should also be consulted for routine procedures.

MULTIPLE UNIDIMENSIONAL DEVELOPMENT

Multiple unidimensional development (MUD) is the simplest approach for enhancement of the separation capacity in TLC.[2] In this approach, the TLC plate is developed for a selected distance, then the plate is withdrawn from the developing chamber and the adsorbed solvent is evaporated before repeating the development process. MUD is a very versatile strategy for the separation of complex mixtures. The main feature of MUD is that it leads to an increase in the spot reconcentration mechanism. There is an optimum number of developments that provide maximum separation.

PROGRAMMED MULTIPLE DEVELOPMENT

The term *programmed multiple development* (PMD) was introduced by Perry et al.[3] for a TLC developing technique and defined as follows: A TLC plate is repeatedly developed in the same direction with the same solvent. Each development run is longer than the previous development step. Following each run, the layer is dried by radiant heat, optionally assisted by a flow of inert gas. The lower edge of the layer remains, at all times, in the contact with the solvent in the reservoir, which is shielded from the radiant heat. The solvent migration distance is controlled, programmed via the lengths of intervals between the heating cycles.

AUTOMATED MULTIPLE DEVELOPMENT

Automated multiple development (AMD) combines the advantages of MUD and mobile-phase gradient elution. This multiple development approach was improved by Burger,[4] who maintained the basic idea of development. The chromatogram is developed in the same direction, stepwise, over an increasing solvent migration distance, but changes all other characteristics. The characteristics of the AMD system, according to Burger, are as follows: An HPTLC plate is developed several times in the same direction with eluents differing in elution power. In general, the polarity of the eluent is decreased step by step over the solvent migration distance. Between each run, the plate is completely dried by vacuum.

Gradient elution in AMD starts with the most polar eluent and is varied toward decreasing polarity. Fig. 1a shows a typical universal elution gradient, made up of the three solvents: methanol, dichloromethane, and hexane. Fig. 1b illustrates the increasing duration of the development cycles. Time increments are chosen to obtain uniform increases of the running distance of ~3 mm/step.

Automated multiple development causes sample fractions to become concentrated into narrow bands. The eluent flows over the lower part of a sample before reaching the upper part, concentrating the sample in the top to bottom direction. This is due to the fact that molecules in the lower part of the sample zone start their upward movement earlier than those in the upper part of that sample zone each time the eluent front passes through that area. A strong solvent used at the beginning of AMD causes concentration effects similar to a plate with a concentration zone. The separation power is increased by factor of 3, as compared with regular highpressure TLC (HPTLC). The combination of the focusing effect and gradient elution results in extremely narrow bands. Their typical peak width is about 1 mm. This means that with the available separation distance of 80 mm, up to 40 components can be completely resolved (i.e., with a resolution greater than 1).

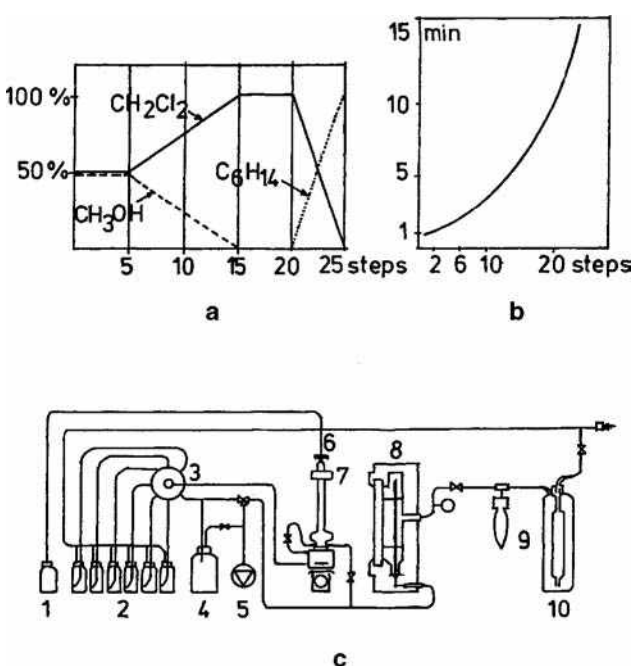

Fig. 1 (a) Typical universal elution gradient; (b) time of development vs. number of steps; (c) AMD system flow diagram.

DESIGN AND OPERATION OF AN AMD SYSTEM[5]

The Camag AMD system consists of two main components: the AMD developing unit (Fig. 1c) and the microprocessor-based controller. This system provides an AMD under reproducible conditions. For the AMD microprocessor-based controller, the following parameters may be chosen: the eluent composition, by selecting the number of solvent reservoir; the number of developing steps; the developing time for each step; the number of preconditions; the option of emptying the mixer after a selected step.

FUNCTIONAL PRINCIPLE OF THE AMD DEVICE

During the development process, the system is controlled by computer. The main component is an enclosed developing chamber (8), which is connected for introducing and withdrawing the developing solvent and for pumping the gas phase in and out. The six reservoir bottles (2) contain the individual solvent components. The gradient mixer (6) is connected, via motor valve (3), to reservoir bottles (2). The gas phase is made up externally by passing nitrogen through the wash bottle (l0) into the gas-phase reservoir (9). At the same time, the mixer is filled with solvent from the solvent reservoir bottle (1). Then, the chamber is equilibrated for 15 s with gas from the reservoir (9). The first step of development can start after filling the chamber (8) with the contents (8 ml) of the upper part of the gradient mixer (6), which is controlled by a light barrier (7).

Migration of the solvent in the layer starts immediately. At the end of the programmed time (determining the migration distance), the liquid solvent is removed by vacuum from the chamber (8) into the waste-collecting container (4). Then, after all liquid solvent has been removed, vacuum is applied by pump (5), thus drying the layer. The drying period is time programmed. Before the next developing cycle is started, the chromatographic thin layer is reconditioned by feeding the gas phase from the blender (9) into the chamber. After reconditioning the chamber, the next development step can start. While

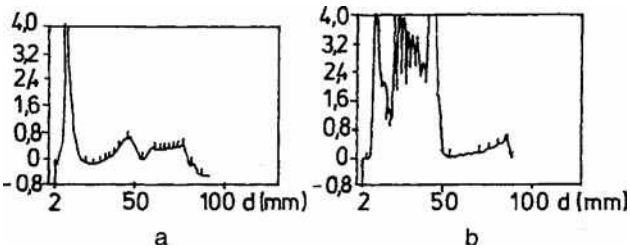

Fig. 2 Densitograms: (a) isocratic development TLC; (b) AMD-TLC.

the drying phase is carried out, the solvent for the next step is made up in the gradient mixer (6).

APPLICATION

When the sample components differ widely in their polarities, they can be separated by using a universal elution gradient. With AMD, it is possible to simultaneously analyze 12 samples. AMD-HPTLC has been applied for screening of pesticides from groundwater or drinking water and soil. A universal gradient based on dichloromethane was used to detect the presence of pesticides from different classes such as organochlorine, organophosphorus, carbamate, phenylureas, triazines, phenoxycarboxylic acids, and others. In this way, 283 pesticides were analyzed using this universal gradient.[6,7]

Plant extracts have a widespread application in the drug and cosmetic industries. For the separation of plant extracts, the AMD-HPTLC method is the most suitable because it has a higher separating power. Isocratic and AMD development are shown in Fig. 2.[8]

ON-LINE COUPLING OF HPLC/AMD-TLC

Combining different separation methods, governed by different separation mechanisms, to multidimensional methods is suitable for multiplying the potential of the individual techniques. Reversed-phase chromatography high-performance columns (RP-HPLC) can be coupled with normal phase TLC.[9,10]

PRINCIPLE

The system for mass transfer HPLC/TLC consists of a column filled with RP-C_{18} sorbent and a modified Linomat (Camag) sample spray unit for TLC. The effluent is transferred, via a capillary tubing, to a TLC applicator unit. While the effluent of the HPLC column is sprayed onto the thin layer with nitrogen, the plate is moved. The separation of 56 pesticide residues in drinking water in a single sample using RP-HPLC coupled with TLC and AMD has been demonstrated. For example, by AMD, a chromatogram of RP-HPLC cut no. 13 was separated and over 10 pesticides were detected through multiwavelength scanning by absorbance between 200 and 300 nm.[11]

REFERENCES

1. Grinberg, N., Ed.; *Modern Thin-Layer Chromatography*; Marcel Dekker, Inc.: New York, 1990.
2. Poole, C.F.; Poole, S.K. *Chromatography Today*; Elsevier: Amsterdam, 1991.
3. Perry, J.A.; Haag, K.W.; Glunz, L.J. Programmed multiple development in thin-layer chromatography. J. Chromatogr. Sci. **1973**, *11* (9), 447–453.
4. Burger, K. TLC-PMD, thin-layer chromatography with gradient-elution in comparison to HPLC. Fresenius. Z. Anal. Chem. **1984**, *318* (3–4), 228.
5. Jaenchen, D.E. *Proceedings 3rd International Symp. on Instrumental HPTLC*; Kaiser, R.E., Ed.; Institute for Chromatography: Bad Duerkheim, Germany, 1985; 71.
6. Butz, S.; Stan, H.J. Screening of 265 pesticides in water by thin-layer chromatography with automated multiple development. Anal. Chem. **1995**, *67*, 620.
7. Koeber, R.; Niessner, R. Screening of pesticide-contaminated soil by supercritical fluid extraction (SFE) and high-performance thin-layer chromatography with automated multiple development (HPTLC/AMD). Fresenius J. Anal. Chem. **1996**, *354* (4), 464–469.
8. Gocan, S.; Cimpan, G.; Muresan, L. Automated multiple development thin layer chromatography of some plant extracts. J. Pharm. Biomed. Anal. **1986**, *14*, 1221.
9. Jaenchen, D.E. *Proceedings 4th International Symposium on Instrumental High Performance Thin-Layer Chromatography*; Traitler, H., Studer, A., Kaiser, Eds.; Institute for Chromatography: Bad Duerkheim, Germany, 1987; 185.
10. Hofstraat, J.W.; Engelsman, M.; Van De Nesse, R.J.; Gooijer, C.; Velthorst, N.H.; Brinkman, U.A.Th. Coupling of narrow-bore liquid chromatography to thin-layer chromatography: Part I. Interfacing. Anal. Chim. Acta **1986**, *186*, 247.
11. Protze, B. Diploma thesis. Fachhochschule Niederrnein Krefeld: Germany, 1986.

Mycotoxins: TLC Analysis

Philippe J. Berny
Toxicology Unit, National Veterinary School of Lyon, Marcy L'Etoile, France

INTRODUCTION

Thin-layer chromatography (TLC) is a widely used analytical technique for many investigative purposes. Detection of mycotoxins by means of TLC has been in use for many years. Official methods of analysis often rely on these techniques for both identification and quantification of several mycotoxins.[1]

Mycotoxins are natural toxins produced by fungi contaminating foods and feeds. They may be extremely toxic [e.g., aflatoxin (*Aspergillus flavus*), which is a potent carcinogen].[2] They may be found in plant-derived products, but also in the tissues of exposed animals, where they can accumulate and, thus, be a serious health hazard for human beings. Consequently, many analytical methods have been developed in order to assess the potential contamination of food derived either from plants or from food-producing animals. A third group of analytical techniques has been developed for diagnostic purposes in animals without any direct public health hazard. In this entry, we will briefly review some of the techniques available to address these three goals.

ANALYSIS OF PLANTS AND PLANT-DERIVED PRODUCTS FOR MYCOTOXINS

Analysis of plants may yield very interesting results, because they are the major carrier of fungi and of mycotoxins. The presence of a genus of fungus may or may not be associated with the production of mycotoxins, depending on the climatic conditions at the time of harvest, for instance.[3] Therefore, it is extremely interesting to have qualitative as well as quantitative methods for the determination of mycotoxins in these matrices. Numerous techniques have been developed to determine the nature and degree of contamination of plants with mycotoxins; it would not be possible to present all of them in a single article.

Extraction and cleanup procedures usually require solid-phase extraction based on commercially available C_{18} cartridges, for instance, after liquid extraction with common organic solvents (methylene dichloride, chloroform, acetonitrile).[3–5] This step appears to be necessary to remove most of the interfering components such as carotenoids or chlorophyls, which are highly abundant in plants. Table 1 gives a list of some of the mycotoxins which can be analyzed by TLC, together with analytical features (plate material, elution, detection/visualization, limit of detection). Of particular interest are the following products: aflatoxins B1, B2, G1, and G2, zearalenon, ochratoxin, and fumonisins B1 and B2 in maize. Recently, high-performance TLC (HPTLC) techniques have also been applied to forage samples commonly infected with an endophyte considered as symbiotic but responsible for disorders in animals.[5] These mycotoxins include lolitrems and ergot alkaloids.

TLC plates used are generally silica gel plates, although C_{18} reversed-phase TLC plates may occasionaly be used.[4] Elution may be monodimensional or bidimensional.[3] The former is more common. Recent automated gradient techniques appear promising for the simultaneous determination of several mycotoxins in a single sample. Solvents used for elution depend on the type of plate used. Most of the time, organic solvents (ethanol chloroform, acetone) are used. One feature of HPTLC is that it uses much less solvent than HPLC and permits analysis of many samples in a very short time.[5]

Detection may be based on several techniques; older systems used postelution derivatization[7] and observation of colored spots. It is more common now to use either ultraviolet (UV)[5] or even fluorescence[3,4] because these techniques allow quantification of mycotoxin residues. More complex systems have been tested (computer imaging[6]) for particular applications, but these techniques are not applied to routine analysis of plants.

ANALYSIS OF ANIMAL TISSUES

Because animals may accumulate mycotoxins in their tissues, and considering the high toxicity of some products, it is a public health concern to have analytical techniques available for routine detection and quantitation of residues of these compounds in edible tissues of food-producing animals. Analysis of animal tissues may be difficult for several reasons:

1. Mycotoxins are poorly concentrated in many tissues or biological fluids (e.g., muscle or milk) and the analytical method employed should be sensitive enough to detect down to a few micrograms mycotoxins per kilogram sample or even less (aflatoxins in muscle samples, for instance).[2]

Table 1 Examples of HPTLC methods for the determination of mycotoxins in biological samples.

Mycotoxin	Plate	Matrix	Elution	Detection	Results	Refs.
Aflatoxins	Si60	Muscle, liver, kidney	1-Hexane/tetrahydrofuran/ethanol	Fluorescence	LOD[a]: 0.01 μg/kg	[2]
B1, G1, M1			2-$CHCl_3$/methanol		(B1, M1) LOD: 0.005 μg/kg (G1)	
Fumonisin	C18	Corn	Methanol/KCl 4% in water	Fluorescamin	LOD : 0.1 (B2), 0.5	[4]
B1, B2				Fluorescence	(B1) μg/kg, recovery > 80%	
Lolitrem	Si60	Forage	CH_2Cl_2/acetonitrile	UV (268 nm)	LOD : 0.1 mg/kg, recovery > 90%	[5]
Patulin	Si60	Fruit	1-Hexane/diethylether, 2-diethylether	UV (273 nm)	LOD : 40–100 μg/kg	[6]
Zearalenon	Si60	Corn	Toluene/ethylacetate/formic acid	Fluorescence	LOD : 2.6 μg/kg, recovery > 63%	[9]

[a]LOD = limit of detection.

2. Tissues and organs may contain interfering substances on chromatograms or densitograms.

For extremely toxic compounds like aflatoxins, acceptable daily intakes (ADI) have been defined and it is, therefore, necessary to check suspected tissues to monitor residues at this level.

TLC and HPTLC offer many advantages over other conventional methods gas chromatography (GC), high-performance liquid chromatography (HPLC), such as rapidity, simplicity, and sensitivity. However, it is usually necessary to extract and purify samples before spraying them onto TLC plates. In the case of aflatoxins, for instance, a commonly employed technique is based on liquid extraction by an organic solvent (chloroform), followed by purification on a silica gel column. The column has to be washed to elute interfering substances (with hexane and ether) and aflatoxins are eluted individually or all together with a specific combination of solvents (chloroform and acetone).[2]

If the purpose of the TLC technology is only to screen samples, the results may be merely qualitative. Older methods were usually based on the visual determination of dark spots on a bright fluorescent plate under UV light. Another use of TLC in the determination of mycotoxin residues is as preparative TLC, in which specific spots are visualized, scraped, and resolubilized for further analysis (Association of Official Analytical Chemistry).

More and more, however, quantitative analysis can be performed by means of scanners (UV, fluorescence), and HPTLC does not need to be completed by another analytical technique for the precise determination of residues. Today, most official methods of analysis for the detection of mycotoxins in foods are based on TLC technology.

DIAGNOSTIC PURPOSES

Mycotoxicoses may induce various pathological disorders in animals as well as in human beings. Considering the poor specificity of the signs observed and the very low concentrations of the toxic compounds in most biological tissues or fluids, it is necessary to be able to analyze, promptly and efficiently, biological samples to evaluate the risk of mycotoxicosis. The most common mycotoxins involved include aflatoxins, fumonisins, ochratoxin, zearalenon, and T2 toxin.[8] Analysis is usually based on foods and feeds (cereals, etc.). In swine, for instance, an epidemiological study conducted on feed samples detected ochratoxin (mean 58.3 μg/kg) and zearalenon (mean 30.3 μg/kg) in corn. These concentrations were associated with respiratory disorders and also infertility.[9] The advantage of TLC/HPTLC in such a situation is that it provides rapid and specific analysis of food samples at a low cost and, therefore, a reasonable cost/benefit ratio for breeders. If the diagnosis has to be confirmed on animal/human tissues or fluids, depending on the compound of interest, HPTLC techniques may also be available and convenient (see above).

CONCLUSIONS

TLC and HPTLC offer many possibilites for the determination of mycotoxins in plant or animal samples. Plant samples usually contain higher concentrations of mycotoxins, but analysis of animal tissues may be necessary either to confirm a suspected mycotoxicosis or to detect potential residues for human food. Many official methods are available, based on TLC, and the recent development of HPTLC also offers many possibilities for

the detection and quantitation of several mycotoxins in various biological samples.

REFERENCES

1. Stubblefield, R.; Honstead, J.P.; Shotwell, O.L. An analytical survey of aflatoxins in tissues from swine grown in regions reporting 1988 aflatoxin-contaminated corn. J. Assoc. Off. Anal Chem. **1991**, *74* (6), 897.
2. Fernandez, A.; Belio, R.; Ramos, J.J.; Sanz, M.C.; Saez, T. Aflatoxins and their metabolites in the tissues, faces and urine from lambs feeding on an aflatoxin-contaminated diet. J. Sci. Food Agric. **1997**, *74* (2), 161–168.
3. Phillips, S.I.; Wareing, P.W.; Dutta, A.; Panigrahi, S.; Medlock, V. Mycopathology **1996**, *133*, 15.
4. Rottinghaus, G.E.; Coatney, C.E.; Minor, H.C. A rapid, sensitive thin layer chromatography procedure for the detection of fumonisin B1 and B2. J. Vet. Diagn. Invest. **1992**, *4* (3), 326.
5. Berny, P.; Jaussaud, P.; Durix, A.; Ravel, C.; Bony, S. Rapid determination of the mycotoxin lolitrem B in endophyte-infected perennial ryegrass by high-performance thin-layer chromatography: A validated assay. J. Chromol. **1997**, *769*, 343.
6. Ross, P.F.; Rice, L.G.; Plattner, R.D.; Osweiler, G.D.; Wilson, T.M.; Owens, D.L.; Nelson, H.A.; Richard, J.L. Mycopathology **1991**, *114* (3), 129.
7. Osweiler, G.D.; Carson, T.L.; Buck, W.B.; Van Gelder, G.A. *Clinical and Diagnostic Veterinary Toxicology,* 3rd ed.; Ed.; Kendall/Hunt: Dubuque, 1988.
8. Ewald, C.; Rehm, A.; Haupt, C. Berlin. Münch. Tierärtzlich. Wochen. **1991**, *104* (5), 161.
9. Dawlatana, M.; Coker, R.D.; Nagler, M.L.; Bluden, G.; Oliver, G.W.O. An HPTLC method for the quantitative determination of zearalenone in maize. Chromatographia **1998**, *47*, 215.

BIBLIOGRAPHY

1. Liang, Y.; Baker, M.E.; Todd Yeager, B.; Bonner Denton, M. Quantitative analysis of aflatoxins by high-performance thin-layer chromatography utilizing a scientifically operated charge-coupled device detector. Anal. Chem. **1996**, *68*, 3885.

Natural Phenolic Compounds: Planar Chromatography Separation

Maged S. Abdel-Kader
Department of Pharmacognosy, King Saud University, Riyadh, Saudi Arabia

Mohamed M. Hefnawy
Abdul-Rahman A. Al-Majed
Department of Pharmaceutical Chemistry, King Saud University, Riyadh, Saudi Arabia

INTRODUCTION

Plant phenolic compounds probably constitute one of the most widespread and diverse groups of secondary metabolites.[1] This term embraces an embarrassingly large array of chemical compounds possessing an aromatic ring bearing one or more hydroxyl groups, together with a number of other substituents. In plants, all phenolic compounds are derived biogenetically from phenolic precursors through skimate pathway and phenylpropanoid metabolism.[2] Phenolic compounds have provoked much interest among chemists, biochemists, botanists, and food technologists.[3]

Phenolic compounds are of great taxonomic significance, owing to their widespread stability, in addition to the fact that they can be detected easily.[4] Plants produce phytotoxic phenolic compounds to suppress the growth of other plant species.[3] The anti-microbial and anti-fungal activities of phenolic compounds, pointed out to their role in plant disease resistance, is a hypothesis supported by many studies and has been formulated into the Phytoalexin Theory of Disease Resistance in Plants.[3,5] Plants respond to different elicitors by production of phytoalexins, which are mainly phenolic in nature.[6] The tannins, a well-known class of these compounds, have been employed since ancient times in tanning skins and manufacturing of ink.[4] Plant phenolic compounds are of great importance in food technology, since they affect the colors and flavors of our food and drink.[3]

Many plant phenolics are of pharmaceutical interest. Flavonoids, lignans, flavolignans, coumarins, phenyl propanoids, and other phenolic compounds show a wide variety of biological and pharmacological activities, such as anti-oxidant, anti-hepatotoxic, spasmolytic, cytotoxic, anti-fungal, and anti-bacterial. Some flavonoids improve capillary resistance while isoflavonoids found in soy and other legumes have estrogenic activity.[7–9]

The important applications of plant phenolics attracted natural product chemists to look for new compounds in plant species with interesting activities. Identification of compounds, usually preceded by obtaining them in a pure form. Different chromatographic techniques were applied for the purification of plant phenolics, as well as other plant constituents or products of chemical reactions.

Planar chromatography is a term originally used to describe techniques including thin-layer chromatography (TLC), paper chromatography, and zone electrophoresis. In all these techniques, the stationary phase is used in the form of a flat thin layer.[10,11]

TLC is regarded as an indispensable tool in both quality control and research laboratories. The technique is easy, fast, and the required apparatus is relatively inexpensive. TLC is widely used to check purity of compounds, monitor chemical reactions, monitor column chromatography, and explore the complexity of mixtures and choice of proper mobile phase for column chromatography. In most of these applications, in addition to the TLC plates, only capillaries and chromatographic tanks are required. Advances in analytical methods led to the development of more sophisticated instruments based on TLC, used for quantitative analyses. Plates with much smaller particle size stationary phases are usually employed in conjunction with these instruments for better results and are described as high-performance thin-layer chromatography (HPTLC).[10,11]

Another important application of planar chromatography is in the use of different types of flat layer stationary phases to obtain pure materials from mixtures. This application is regarded as preparative planar chromatography and it mainly includes preparative thin-layer chromatography (PTLC), preparative paper chromatography (PPC), and centrifugal preparative thin-layer chromatography (CPTLC). Of the three types, the latter only (CPTLC) requires relatively more complex instrumentation.[10,11] However, preparative planar chromatography can take advantages from the recent developments in planar chromatography, such as automated sample application, over pressured layer chromatography, alternatively described as optimum performance laminar chromatography (OPLC) and automated multiple development (AMD).[11,12] Literature survey reveals that these techniques are still of very limited use in preparative work, most likely due to the lack of instrumentation required and the predominance of

HPLC when talking about expensive sophisticated instruments.

One of the serious problems in preparative planar chromatography is the detection of zone locations on the chromatogram. In this regard, one cannot use destructive methods of detection. The great advantage of dealing with phenolic compounds in this regard is their ease of detection. With no exceptions, all phenolic compounds can be detected by the widely used UV lamps, since they all have UV-absorbing chromophores.

CLASSIFICATION OF PLANT PHENOLS

Plant phenols are not only widespread among plants, but also comprise a wide variety of structural diversity. Classification of plant phenols is based on structural similarities, as well as biogenetic pathways from which they originate. Brief notes are given here about the major classes of natural phenolics and their biological importance. Under each class, some structures for corresponding compounds in Table 1 are given.

SIMPLE PHENOLS, PHENOLIC ACIDS, AND RELATED COMPOUNDS

Compounds of this group usually contain one aromatic ring in their structures, and they often possess alcoholic, aldehydic, and carboxylic groups. The occurrence of these compounds in the form of glycosides (linked with one or more sugar unites) is common in nature. Vanillin (Vanilla pods, flavoring agent), capsaicin (*Capsicum*, Counter irritant), salicin (Willow barks, analgesic, and anti-inflammatory), and benzyl benzoate (Peru balsam, anti-parasitic) are examples of this class.[2,9]

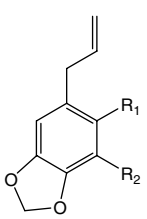

[1] $R_1=R_2=OCH_3$
[2] $R_1=OCH_3$, $R_2=H$
[3] $R_1=H$, $R_2=OCH_3$
[4] $R_1=R_2=H$

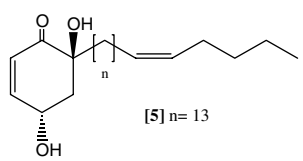

[5] n= 13

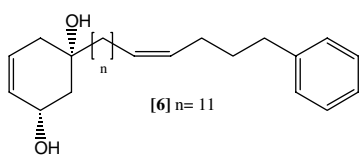

[6] n= 11

COUMARINS AND COUMARIN DERIVATIVES

Members of this group biogenetically originate from cinnamic acid derivatives via the shikimic acid pathway. They are all C-9 compounds having the 2H-1-benzopyran-2-one moiety in their skeleton. Coumarin itself has an unsubstituted basic skeleton. Compounds with hydroxyl or methoxyl substituents are described as simple coumarins. More complex are those bearing prenyl substituents or alkyl groups. In many natural coumarins, a third ring is fused to the benzopyran-2-one nucleus. The most common compounds with third ring are the furanocoumarins, e.g., psoralens used in the treatment of vitiligo.[2,9,13]

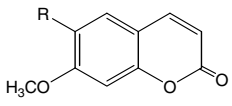

[7] R= 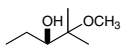

[8] R= 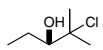

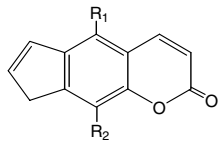

[9] $R_1=OCH_3$ $R_2=H$
[10] $R_1=$ $R_2=$ OCH_3
[11] $R_1=H$ $R_2=OCH_3$

FLAVONOIDS

Flavonoids (C-15 compounds) are the largest group of plant phenols. They occur either in the free state or in the form of glycosides. Ring-B of flavonoids is formed from phenylpropane via the shikimate pathway, while rings A and C arise from condensation of acetate units via malonlyl CoA. Flavonoids are classified into several subclasses according to their structural variations (Fig. 1).

Flavonoids and their derivatives, especially anthocyanidines and their glycosidic anthocyanins, are responsible for the colors of plant flowers. In addition to their value as chemotaxonomic markers, recent researches have demonstrated their involvement in the medicinal action of many drugs such as liquorice, chamomile, and gingko. Some flavonoids have anti-tumor, anti-viral, anti-bacterial, anti-fungal, anti-inflammatory, anti-allergic, anti-thrombitic, anti-oxidant, anti-hepatotoxic, vasoprotective, gastric protective, and estrogenic activity.[2,9,14,15]

LIGNANS

Lignans are C-18 natural compounds formed essentially by the union of two molecules of phenylpropene (C-6, C-3) formed from cinnamate derivatives. Lignans are optically active compounds and the union takes place between the middle carbons of the monomers' side chains. Important pharmaceutical examples are the lignans of *Podophyllum*

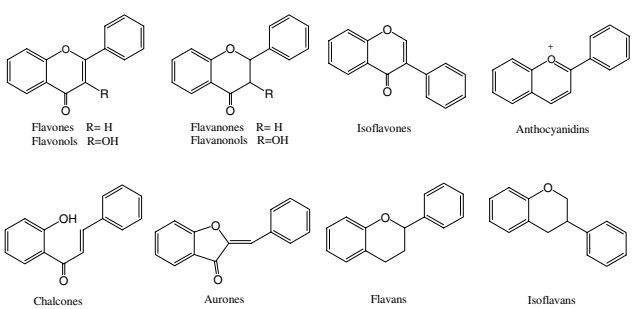

Fig. 1 Structures of flavonoids and their derivatives.

Table 1 Phenolic compounds isolated by PTLC.

Name	Mobile phase*	Refs.
Simple Phenols		
Dillapiole **[1]**	Petrol–EtOAc (49 : 1)	[19,20]
p-Hydroxybenzaldehyde	Petrol–$CHCl_3$	[21]
3-Hydroxy-3′-methoxy-4′-hydroxypropiophenone	Petrol–$CHCl_3$ (2 : 3)	[21]
Isoelemicin	Hexane–EtOAc (9 : 1)	[20,22]
5-Methoxy-6-(2-propenyl)-1,3-benzodioxol **[2]**	Petrol–EtOAc (49 : 1)	[19]
Myristicin **[3]**	Petrol–EtOAc (49 : 1)	[19,20]
Safrole **[4]**	Petrol–EtOAc (49 : 1)	[19]
trans-Sinapaldehyde	Petrol–$CHCl_3$ (2 : 3)	[21]
Syringaldehyde	Hexane–EtOAc (9 : 1) Petrol–$CHCl_3$ (2 : 3)	[22] [21]
Vanillin	Petrol–$CHCl_3$ (2 : 3)	[21]
Chlorogenic acid	EtOAc–HCOOH–AcOH–H_2O (100 : 11 : 11 : 26)	[23]
3,4-Di-*O*-caffeoylquinic acid	EtOAc–HCOOH–AcOH–H_2O (100 : 11 : 11 : 26)	[23]
3,5-Di-*O*-caffeoylquinic acid	EtOAc–AcOH–HCOOH–H_2O–toluene–$HCOOC_2H_5$ (50 : 5.5 : 13.5 : 2.5 : 2) EtOAc–HCOOH–AcOH–H_2O (100 : 11 : 11 : 26)	[24] [23]
4-Hydroxy-3,5-dimethoxybenzoic acid	Petrol–EtOAc (4 : 6, 3 runs)	[25]
4-Hydroxy-3-methoxybenzoic acid	Petrol–EtOAc (4 : 6, 3 runs)	[25]
Leiocarpic acid	$CHCl_3$–Me_2O–HCOOH (90 : 10 : 0.5)	[26]
Rosmarinic acid	$CHCl_3$–MeOH–H_2O (4 : 1 : 0.1)	[27]
3,4,5-Trimethoxybenzoic acid	Hexane:EtOAc (9 : 1)	[22]
4*S*,6*S*-Dihydroxy-6-(14′-nonadecenyl)-2-cyclo-hexanone **[5]**	Hexane:EtOAc (6 : 4)	[28]
1-Hydroxy-3-[14′-phenyldodecyl]benzene	Hexane–EtOAc (9 : 1)	[28]
1-Hydroxy-3-[14′-phenyltetradecyl]benzene	Hexane–EtOAc (9 : 1)	[28]
1-(16′-Phenyl-12′*Z*-hexadecenyl)-4-cyclohexene-(1*S*,3*S*)-diol. **[6]**	Hexane–EtOAc (6 : 4)	[28]
p-Coumaric ethyl ester	Hexane–EtOAc (8.5 : 1.5)	[29]
4-Methoxyphenylumbellate	MeOH–H_2O (7 : 3) RP18	[30]
Scandione	Hexane–CH_2Cl_2 (1 : 1)	[31]
Acetophenones		
2-Hydroxy-6-methyl-acetophenone	Et_2O–Petrol (1 : 3)	[32]
Ethuliaconyzophenone	Et_2O–Petrol (1 : 1)	[32]
Benzofurans		
Bolusanthin IV	Hexane–$CHCl_3$–Me_2CO (6 : 3 : 1)	[33]
2-(p-Hydroxy-benzyl)-6-methoxybenzofuran	$CHCl_3$–MeOH (97 : 3)	[34]
Maginaldehyde	MeOH–H_2O (7 : 3) RP18	[35]
Benzophenones		
18-Ethyloxy-17-hydroxy-17,18-dihydroscrobiculatone A	Hexane–Et_2O (1 : 1)	[36]
18-Ethyloxy-17-hydroxy-17,18-dihydroscrobiculatone B	Hexane–Et_2O (1 : 1)	[36]
4-O-β-D-Glucopyranosyl-2,6,4′-trihydroxybenzophenone	AcOH–H_2O (15 : 85) cellulose	[37]
Pseudoguttiaphenone A	Hexane–EtOAc (8 : 2)	[38]
Scrobiculatones A & B	Hexane–Et_2O (1 : 1)	[36]

(Continued)

Table 1 Phenolic compounds isolated by PTLC. *(Continued)*

Name	Mobile phase*	Refs.
2′,3′,6-Trihydroxy-2,4-dimethoxy-benzophenone	$CHCl_3$–MeOH (20 : 1)	[39]
Vismiaphenone C	Hexane.EtOAc (85 : 15)	[38]
Coumarins		
Aesculetin dimethyl ether	Hexane:$CHCl_3$ (2 : 1)	[30]
Coumarin	Cyclohexane–Me_2CO (9 : 1)	[40]
5,7-Dihydroxycoumarin	$CHCl_3$–MeOH (96 : 4)	[41]
Dipetalolactone	Hexane–EtOAc (8 : 2)	[42]
Fraxetin	EtOAc–benzene (1.5 : 8.5)	[29]
Scoparone	Hexane–EtOAc–MeOH (9 : 4.5 : 0.5)	[43]
Scopoletin	Petrol–EtOAc–MeOH (9 : 4 : 1) C_6H_6–EtOAc (8.5 : 1.5)	[44] [29]
Umbelliferone	Hexane–EtOAc (8 : 2) $CHCl_3$–Me_2CO (96 : 4)	[42] [41]
Dispardiol B	$CHCl_3$–EtOAc (9 : 1)	[45]
Disparinol D	$CHCl_3$–EtOAc (9 : 1)	[45]
Disparpropylinol B	Pentane–Me_2CO (93 : 7)	[45]
Epoxysuberosin	Hexane–EtOAc (3 : 2) CH_2Cl_2–Me_2CO (97 : 3)	[46]
Isodispar B	Hexane–EtOAc (9 : 1)	[45]
Mammea A/AB cyclo E	$CHCl_3$–EtOAc (9 : 1)	[45]
Mammea A/AB dioxalanocyclo F	Pentane–Me_2CO (93 : 7)	[45]
(+) Trachypleuranin A **[7]**	Hexane–EtOAc (3 : 2) CH_2Cl_2–Me_2CO (97 : 3)	[46]
(±) Trachypleuranin B **[8]**	Hexane–EtOAc (3 : 2)	[46]
Clauslactone A	$CHCl_3$–MeOH (30 : 1)	[41]
Clauslactone B	$CHCl_3$–Me_2CO (3 : 1)	[41]
Clauslactone E	$CHCl_3$–MeOH (20 : 1)	[41]
5′-*Epi*-isoethuliacoumarins A & B	Et_2O–petrol (1 : 1)	[32]
5-Geranyloxy-7-hydroxycoumarin	Hexane–Me_2CO (2 : 1)	[41]
7-Geranyloxy-6-methoxycoumarin	Benzene–Me_2CO (96 : 4)	[41]
Isoethuliacoumarins A & B	Et_2O–petrol (1 : 1)	[32]
Murrayacoumarins A & B & C	$CHCl_3$–MeOH (96 : 4)	[41]
Umbelliprenin	Hexane–EtOAc (8 : 2)	[47]
4-Hydroxy-5,6,7-trimethoxy-3-(3′,4′-methylenedioxy)phenylcoumarin	Petrol–EtOAc (3 : 2)	[48]
Graveolone	Hexane:$CHCl_3$ (2 : 1)	[30]
Montroumarin	CH_2Cl_2–Me_2CO (50 : 1)	[49]
3-(1′-1′-Dimethylallyl)-xanthyletin	Hexane–EtOAc (85 : 15)	[50]
Columbianetin acetate	C_6H_6–Me_2CO (96 : 4)	[41]
Furanocoumarins		
Alloxanthoxyletin	Hexane–EtOAc (8 : 2)	[42]
Avipirin	Hexane–EtOAc (8 : 2)	[47]
Baykangelicin	Hexane–EtOAc (8 : 2)	[47]
Bergopten **[9]**	Hexane–EtOAc (8 : 2) Hexane–$CHCl_3$ (2 : 1)	[47] [30]
Chalepin	C_6H_6–EtOAc (65 : 35)	[50]
Imperatorin	Hexane–EtOAc (8 : 2)	[47]

(Continued)

Table 1 Phenolic compounds isolated by PTLC. *(Continued)*

Name	Mobile phase*	Refs.
Isoimperatorin	Hexane–EtOAc (8 : 2)	[47]
Isopimpinellin **[10]**	Hexane–$CHCl_3$ (2 : 1)	[30]
2′-Isopropyl-psoralene	C_6H_6–EtOAc (99 : 1) Hexane–$CHCl_3$ (1 : 1)	[50]
Oxypeucedanin	CH_2Cl_2–Me_2CO (97 : 3)	[46]
Pimpinellin	Hexane–EtOAc (8 : 2)	[42]
Saxalin	Hexane–EtOAc (3 : 2)	[46]
Xanthotoxin **[11]**	Hexane:$CHCl_3$ (2 : 1)	[30]
Xanthotoxol	Hexane–EtOAc (8 : 2)	[47]
Xanthoxyletin	Hexane–EtOAc (8 : 2)	[42]
Coumestans		
Flemichapparin C	Hexane–CH_2Cl_2 (1 : 1)	[31]
3-Hydroxy-4,9-dimethoxy-coumestan	$CHCl_3$–MeOH (19 : 1)	[35]
Flavones		
Apigenin	EtOAc–CH_2Cl_2–HCOOH (8 : 12 : 1) $CHCl_3$:MeOH (9 : 1)	[51] [52]
Apigenin-7-*O*-glucuronide	EtOAc–HCOOH–AcOH–H_2O (100 : 11 : 11 : 26)	[23]
Apigenin-7-*O*-β-D(6″-*trans*-p-coumaroyl)glucoside	$CHCl_3$:MeOH (9 : 1, 2 runs)	[53]
Apigenin-7-xylosyl (1 → 2)glucoside	EtOAc–EtMeCO–HOAc–H_2O (20 : 3 : 1 : 1)	[54]
Artelasticin	Petrol–EtOAc (13 : 7)	[55]
Artelastinin	Petrol–EtOAc (3 : 2)	[55]
Carpachromene **[12]**	C_6H_6–EtOAc (9 : 1, 2 runs)	[56]
Crisilineol	$CHCl_3$–MeOH (9 : 1)	[57]
Crisimaritin	$CHCl_3$–MeOH (9 : 1)	[57]
Cyclocommunin (isocyclomulberrin)	Petrol–EtOAc (11 : 9)	[55]
5,4′-Dihydroxy-3′-methoxy-(6 : 7)-2,2-dimethylpyranflavone **[13]**	C_6H_6–EtOAc (9 : 1, 2 runs)	[56]
5,8-Dihydroxy-7,4′-dimethoxyflavone	$CHCl_3$–EtOAc (5 : 1)	[27]
5,4′-Dihydroxy-3′,5′-dimethoxy-6,7-(2″,2″-dimethylpyran) flavone	CH_2Cl_2–MeOH (99 : 1)	[58]
3,5-Dihydroxy-6,7-8,4′-tetramethoxyflavone	Toluene–EtMeCO (9 : 1)	[59]
5,4′-Dihydroxy-3′-methoxy-(6 : 7)-2,2-dimethylpyranoflavone	C_6H_6–EtOAc (9 : 1, 2 runs)	[56]
5,7-Dihydroxy-3′-methoxy-4′-acetoxy -flavone-8-C-β-D-xylopyrano-side-2″-*O*-glucoside	MeOH–H_2O (1 : 1) RP18	[60]
3,5-Dimethoxy-2″,2″-dimethylpyrano-(5″, 6″:8,7)-flavone	Petrol–EtOAc (8 : 2)	[61]
5,4′-Dimethoxy-(6 : 7)-2,2-dimethylpyrano-flavone **[14]**	C_6H_6–EtOAc (9 : 1, 2 runs)	[56]
Gnaphaliin	$CHCl_3$–MeOH (30 : 1, 2 runs)	[62]
3,5,6,7,3′,4′,5′-Heptamethoxylflavone	Hexane–Me_2CO (3 : 1)	[63]
3,5,7,8,3′,4′,5′-Heptamethoxylflavone	Hexane–CH_2Cl_2–MeOH (10 : 10 : 1)	[63]
5,7,8,3′,4′,5′-Hexamethoxyflavone	Hexane–CH_2Cl_2–MeOH (10 : 10 : 1)	[63]
Hispidulin	AcOH–H_2O (30 : 70) Cellulose	[23]
5-Hydroxy-3,7,8,3′,4′,5′-hexamethoxyflavone	Hexane–CH_2Cl_2–MeOH (10 : 10 : 1)	[63]
8-Hydroxy-3,5,7′,8,3′,4′,5′-hexamethoxyflavone	Hexane–CH_2Cl_2–MeOH (10 : 10 : 1)	[63]
5-Hydroxy-3,7,8,3′,4′,5′-pentamethoxyflavone	Hexane–Me_2CO (3 : 1)	[63]
Karanjin **[15]**	Petrol–EtOAc (8 : 2)	[61]
Luteolin-3′-*O*-β-xylosyl (1 → 2)glucoside	EtOAc–EtMeCO–HOAc–H_2O (20 : 3 : 1 : 1)	[54]

(Continued)

Table 1 Phenolic compounds isolated by PTLC. *(Continued)*

Name	Mobile phase*	Refs.
3,5,6,7,8-Pentahydroxy flavone	$CHCl_3$–MeOH (30 : 1, 2 runs)	[62]
3,5,6,7,8-Pentahydroxy flavone	EtOAc–CH_2Cl_2–HCOOH (8 : 12 : 1)	[51]
3,5,6,7,8-Pentahydroxy-4′-methoxy flavone	EtOAc–CH_2Cl_2–HCOOH (8 : 12 : 1)	[51]
Pongaglabrone **[16]**	Petrol–EtOAc (8 : 2)	[61]
Tricetin-3′-di-*O*-α-L-rhamnoside	$CHCl_3$–MeOH–H_2O (65 : 45 : 12)	[64]
Tricetin-3′-*O*-β-D-glucoside-5′-*O*-α-L-rhamnoside	$CHCl_3$–MeOH–H_2O (65 : 45 : 12)	[64]
Tricetin-7-*O*-methylether-3′-*O*-β-D-glucoside-5′-*O*-α-L-rhamnoside	$CHCl_3$–MeOH–H_2O (65 : 45 : 12)	[64]
5,7,4′-Trihydroxy-3′-methoxyflavone-8-C-β-D-xylopyranoside-2″-*O*-glucoside	MeOH–H_2O (1 : 1) RP18	[60]
Flavonols		
Artemetin	CH_2Cl_2–MeOH (99 : 1)	[65]
Gossypetin-8,3′-dimethylether-3-rutinoside **[17]**	MeOH–H_2O (7 : 3) RP18	[66]
Herbacetin-8-methylether-3-rutinoside **[18]**	MeOH–H_2O (7 : 3) RP18	[66]
Kaempferol	CH_2Cl_2–MeOH (9 : 1)	[40]
Karanjachromene	Petrol–EtOAc (8 : 2)	[61]
Lanceolatin B	Petrol–EtOAc (8 : 2)	[61]
Penduletin	Petrol–Et_2O (15 : 85)	[65]
Pongachromene	Petrol–EtOAc (8 : 2)	[61]
Ponganpin	Petrol–EtOAc (8 : 2)	[61]
Quercetin	AcOH–H_2O (3 : 7) cellulose	[65]
3,5,8,4′-Tetrahydroxy-7,3′-dimethoxy-6-(3-methylbut-2-enyl)flavone	$CHCl_3$–MeOH (9 : 1)	[67]
Flavanones & Isoflavanone		
Lysisteisoflavanone	CH_2Cl_2–MeOH (9 : 1)	[68]
Naringenin	CH_2Cl_2–MeOH (9 : 1)	[40]
3-Methoxy-(2″,3″:7,8) furanoflavanone **[19]**	Petrol–EtOAc (8 : 2)	[61]
3,4-Methylenedioxy-(2″,3″:7,8)-furanoflavanone **[20]**	Petrol–EtOAc (8 : 2)	[61]
Tetrapterols F, H, I **[21]**	Hexane–Me_2CO–EtOH (8 : 1 : 1)	[69]
Flavans & Isoflavans		
Caloflavans A, B	CH_2Cl_2–MeOH (4 : 1)	[70]
Bolusanthin III	Hexane–$CHCl_3$–Me_2CO (6 : 3 : 1)	[33]
2,3-*trans*-3,4-*trans*-3,4-dimethoxy-(2″,3″:7,8)-furanoflavan **[22]**	Petrol–EtOAc (8 : 2)	[61]
Neocandenatone	EtOAc–EtOH (5 : 1)	[71]
Chalcones		
2′,4′-Dihydroxydihydrochalcone **[23]**	Petrol–Me_2CO (5 : 1)	[62]
2′-Hydroxy-4,4′-dimethoxy-5′,6′-(2″,2″-dimethylpyrano)chalcone	Hexane–CH_2Cl_2–MeOH (10 : 10 : 1)	[72]
3,5,6,7,8-Pentahydroxychalcone **[24]**	EtOAc–CH_2Cl_2–HCOOH (8 : 12 : 1)	[51]
Isoflavones		
7-Acetoxy-6-methoxy-3′,4′-methylenedioxyisoflavone **[25]**	Petrol–EtOAc (7 : 3)	[73]
Auriculatin	Hexane–EtOAc–MeOH	[74]
Carpachromene	Hexane–EtOAc–MeOH	[74]
Derrone	Hexane–$CHCl_3$–Me_2CO (6 : 3 : 1)	[33]
Diacetate of 7,8-dihydroxy-4′-methoxyisoflavone	Petrol–EtOAc (7 : 3, 8 runs)	[25]
2,3-Dihydroauriculatin	Hexane–EtOAc–MeOH	[74]
7,3′-Dihydroxy-4′-methoxy-isoflavone	Hexane–$CHCl_3$–Me_2CO (7 : 2 : 1)	[33]
3′,4′-Dihydroxy-7-*O*-[(E)-3,7-dimethyl-2,6-octadienyl]-isoflavone	Petrol–EtOAc (3 : 2)	[48]

(Continued)

Table 1 Phenolic compounds isolated by PTLC. *(Continued)*

Name	Mobile phase*	Refs.
6,8-Diprenylgenistein	Hexane–EtOAc–MeOH	[74]
Gancaonin C	Hexane–$CHCl_3$–Me_2CO (6 : 3 : 1, 5 runs)	[33]
Genistein	Hexane–$CHCl_3$–Me_2CO (7 : 2 : 1, 2 runs)	[33]
	$CHCl_3$–Me_2CO (98 : 2)	[31]
	CH_2Cl_2:MeOH (20 : 1)	[75]
Griffonianone A	Petrol–EtOAc (4 : 6)	[73]
Griffonianone B	Petrol–EtOAc (6 : 4)	[73]
Griffonianone C	C_6H_6–Petrol–EtOAc (3 : 6 : 1)	[73]
Heptaacetate of diadzein-7-*O*-[α-rhamno-pyranosyl(1 → 6)-β glucopyranoside.	Petrol–EtOAc (55 : 45, 7 runs)	[25]
Heptaacetate of 7,8-dihydroxy-4′-methoxyisoflavone-7-*O*-[α-rhamno-pyranosyl-(1 → 6)]-β-glucopyranoside.	$CHCl_3$–MeOH (99 : 1, 7 runs)	[25]
Hexaacetate of afromosin 7-*O*-[α-rhamno-pyranosyl-(1 → 6)-β-glucopyranoside	Petrol–EtOAc (1 : 1, 3 runs)	[25]
Hexaacetate of 8-hydroxy-4′,7-dimethoxyisoflavone 8-*O*-[α-rhamno-pyranosyl-(1 → 6)-β-glucopyranoside	Petrol–EtOAc (1 : 1, 4 runs)	[25]
Hexaacetate of irisolidone 7-*O*-[α-rhamno-pyranosyl-(1 → 6)-β-glucopyranoside.	MeOH–H_2O (67 : 33) RP18	[25]
Isoderrone	$CHCl_3$	[76]
Isogacaonin C	Hexane–$CHCl_3$–Me_2CO (6 : 3 : 1, 5 runs)	[33]
Isosenegalensein **[26]**	MeOH–H_2O (8 : 2) RP18	[68]
Limonianin	Hexane–EtOAc–MeOH	[74]
Lupinwighteone	Hexane–$CHCl_3$–Me_2CO (6 : 3 : 1)	[33]
Lysisteisoflavone	Petrol–Et_2O (1 : 1)	[68]
Maximaisoflavone G acetate **[27]**	Petrol–EtOAc (7 : 3)	[73]
4-Methoxy-7-*O*-(*E*)-3-methyl-7-hydroxy-methyl-2,6-octadienyl]isoflavone	Petrol–EtOAc (3 : 2)	[48]
7-*O*-Methylluteone	CH_2Cl_2–MeOH (20 : 1)	[75]
8-Prenylluteone	CH_2Cl_2–MeOH (20 : 1)	[75]
	Hexane–EtOAc–MeOH	[74]
Tetraacetate of 7,8-dihydroxy-4′-methoxy-isoflavone-7-*O*-[α-rhamnopyramosyl-(1 → 6)-β-glucopyranoside.	$CHCl_3$–MeOH (99 : 1)	[25]
Tetraacetate of formononetin 7-*O*-β-glucopyranoside	Petrol–EtOAc (55 : 45, 3 runs)	[25]
Tetraacetate of 7-hydroxy-4′,8-dimethoxy-isoflavone 7-*O*-β-glucopyranoside	Petrol–EtOAc (55 : 45, 3 runs)	[25]
Vogelins H, I, J	Hexane–EtOAc–MeOH	[74]
Warangalone	Hexane–EtOAc–MeOH	[74]
Wighteone	CH_2Cl_2–MeOH (9 : 1)	[68]
	Hexane–$CHCl_3$–Me_2CO (6 : 3 : 1)	[33]
Pterocarpans		
Maackiain	$CHCl_3$ (2 runs)	[76]
Medicarpin	Hexane–$CHCl_3$–Me_2CO (6 : 3 : 1)	[33]
(-)-2-Methoxymaackiain	$CHCl_3$ (2 runs)	[76]
(-)-4-Methoxymaackiain	$CHCl_3$ (2 runs)	[76]
(-)-2,3,4-Trimethoxy-8,9-methylene-dioxypterocarpan	$CHCl_3$, 2 runs	[76]
3,4,9-Trimethoxypterocarpan	$CHCl_3$–MeOH (19 : 1)	[35]

(Continued)

Table 1 Phenolic compounds isolated by PTLC. *(Continued)*

Name	Mobile phase*	Refs.
Anthocyanins		
Cyanidin-3-*O*-[2-*O*-(6-*O*-*E*-caffeoyl-β-D-gluco -pyranosyl)]-{6-*O*-[4-*O*-*E*-3,5-dihydroxy-cinnamoyl-β-D-glucopyranosyl)-*E*-caffeoyl]-β-Dglucopyranosyl}-5-*O*-[β-D-glucopyranoside	EtOAc–AcOH–HCOOH–H_2O (10 : 11 : 11 : 26)	[77]
Cyanidin-3-*O*-[2-*O*-(6-*O*-*E*-coumaroyl-β-D-gluco -pyranosyl)]-{6-*O*-[4-*O*-(6-*O*-*E*-coumaroyl-β-D-glucopyranosyl)-*E*-caffeoyl]-β-D-gluco-pyranosyl}-5-*O*-[β-D-glucopyranoside	EtOAc–AcOH–HCOOH–H_2O (100 : 11 : 11 : 26)	[77]
3,7,8-Trimethyl-2-[(3*E*, 7*Z*)-4,12-dimethyl-8-carboxyl-3,7,11-tridecatrienyl]-3-chromen-6-ol	Hexane–EtOAc (8 : 2)	[78]
Lignans		
Ashantin	Hexane–Et_2O (1 : 1), 7 runs.	[79]
Boehenan	$CHCl_3$–Petrol (3 : 2)	[21]
Boehenans D, H, K.	$CHCl_3$–isoPrOH (25 : 1)	[21]
De-4′-*O*-methylmagnolin **[28]**	Hexane–$CHCl_3$–MeOH (1 : 1 : 0.5)	[80]
7-*O*-(3,3-Dimethylallyl)isodaurinol	Cyclohexane–Et_2NH (9 : 1, 2 runs)	[81]
Epieudesmin	Hexane–Et_2O (1 : 1)	[79]
Episesartemin B	Hexane–Et_2O (1 : 1)	[79]
Epiyangmbin	Hexane–Et_2O (1 : 1)	[79]
Erythro-carolignans E, F	$CHCl_3$–isoPrOH (25 : 1)	[21]
Fargesin	Hexane–EtOAc (85 : 15)	[50]
Grandisin **[29]**	Hexane–EtOAc (8 : 2)	[22]
Kaerophyllin	CH_2Cl_2–Me_2CO (50 : 1)	[49]
4-Ketopinoresinol	Petrol–$CHCl_3$ (2 : 3)	[21]
Lariciresinol	$CHCl_3$–MeOH (8 : 2)	[82]
Lintetralin	Petrol–EtOAc (4 : 1)	[83]
Longipedunin C	Petrol–EtOAc (1 : 1)	[84]
Lyoniresinol	Hexane–$CHCl_3$–MeOH (1 : 1 : 0.5) MeOH–H_2O (4.5 : 5.5) RP18	[80]
(+) Lyniresinol-3α-*O*-β-D-glucoside	$CHCl_3$–MeOH (85 : 15)	[85]
Medioresinol	$CHCl_3$–Petrol (3 : 2)	[21]
(7*R*,8*R*, 7′S,8′R)-3′,4′-Methylenedioxy-3,4,5,5′-tetramethoxy-7,7′-epoxylignan **[30]**	Hexane–EtOAc (7 : 3)	[20]
Paulownin	Hexane–EtOAc (9 : 1)	[86]
Pinoresinol	$CHCl_3$–EtOAc (4 : 1)	[21]
Pyramidatin A **[31]**	$CHCl_3$–EtOAc (9 : 1, 2 runs)	[87]
Pyramidatins B, C **[32]**, D	$CHCl_3$–EtOAc (9 : 1, 4 runs)	[87]
Pyramidatin H	$CHCl_3$–EtOAc (19 : 1)	[87]
rel-(7*R*,8*R*, 7′R,8′R)-3,4,3′,4′-Dimethylene-dioxy-5,5′-dimethoxy-7,7′-epoxylignan **[33]**	Hexane–EtOAc (8 : 2)	[22]
rel-(7*R*,8*R*,7′R,8′R)-3′,4′-Methyllene-dioxy-3,4,5,5′-tetramethoxy-7,7′-epoxylignan **[34]**	Hexane–EtOAc (8 : 2)	[22]
Sesamin	C_6H_6–EtOAc (9 : 1) Hexane–EtOAc (9 : 1)	[65] [86]
Sesartermin B	Hexane–Et_2O (1 : 1), 7 runs.	[79]
Syringaresinol **[35]**	$CHCl_3$–isoProH (25 : 1) Hexane–$CHCl_3$–MeOH (1 : 1 : 0.5)	[21] [80]
Taxiresinol	$CHCl_3$–MeOH (8 : 2)	[82]

(Continued)

Table 1 Phenolic compounds isolated by PTLC. *(Continued)*

Name	Mobile phase*	Refs.
threo-Carolignans E, H, K	$CHCl_3$–IsoPrOH (25 : 1)	[21]
Xanthones		
Ananixanthone	Hexane–EtOAc (85 : 15)	[88]
Brasillixanthone	CH_2Cl_2–Petrol (7 : 3)	[89]
Caloxanthones A, B	Cyclohexane–Me_2CO (7 : 3)	[90]
2-Carbomethoxy-6-methoxyxanthone	Toluene–EtOAc–HCOOH (65 : 35 : 1)	[91]
Cowagarcinone A	CH_2Cl_2–hexane (4 : 6)	[92]
Cowagarcinones B **[36]**, C **[37]**, D	CH_2Cl_2 (3 runs)	[92]
Cowagarcinone E	$CHCl_3$	[92]
Cowanol	CH_2Cl_2	[92]
6-Deoxyjacreubin	CH_2Cl_2–petrol (6 : 4)	[89]
6-Deoxy-γ-mangostin	Hexane–EtOAc (7 : 3)	[93]
1,5-Dihydroxy-6′-6′-dimethylpyrano[2′,3′:3,2]xanthone	CH_2Cl_2–petrol (6 : 4)	[89]
1,7-Dihydroxy-4-methoxyxanthone (Gentisin) **[38]**	$CHCl_3$–Me_2CO–HCOOH (85 : 15 : 1)	[55]
2,8-Dihydroxy-1-methoxyxanthone	$CHCl_3$–Me_2CO–HCOOH (95 : 5 : 1)	[55]
3,8-Dihydroxy-1,2,4-trimethoxyxanthone	$CHCl_3$–Me_2CO–HCOOH (80 : 20 : 1)	[26]
1,7-Dihydroxyxanthone	$CHCl_3$–Me_2CO–HCOOH (95 : 5 : 1) CH_2Cl_2–MeOH (99.5 : 0.5)	[55] [94]
1,2-Dimethoxy-3,8-dihydroxyxanthone	Petrol–EtOAc–HCOOH (70 : 30 : 1)	[91]
Dombakinaxanthene	Tolune–Et_2O (8 : 2)	[93]
Euxanthone **[39]**	Petrol–EtOAc–HCOOH (70 : 30 : 1)	[91]
Fucaxanthone A	CH_2Cl_2–Hexane (4 : 6)	[92]
3-Hydroxy-2,4-dimethoxyxantone	Toluene–EtOAc–HCOOH (65 : 35 : 1)	[26]
5-Hydroxy-1,3-dimethoxyxanthone	CH_2Cl_2–MeOH (95.5 : 0.5)	[94]
2-Hydroxy-1-methoxyxanthone	Petrol–EtOAc–HCOOH (70 : 30 : 1)	[91]
5-Hydroxy-1-methoxyxanthone	Hexane–Me_2CO (7 : 3)	[94]
7-Hydroxy-1,2,3,8-tetramethoxyxanthone	$CHCl_3$–Me_2CO–HCOOH (85 : 15 : 1)	[55]
6-Hydroxy-1,2,5-trimethoxyxanthone	Toluene–EtOAc–HCOOH (65 : 35 : 1)	[26]
7-Hydroxy-1,2,8-trimethoxyxanthone	Toluene–EtOAc–HCOOH (65 : 35 : 1)	[26]
Latisxanthone D	Petrol–CH_2Cl_2 (6 : 4)	[89]
Macluraxanthone	Hexane–EtOAc (7 : 3)	[94]
Mangostinone	CH_2Cl_2	[92]
1-Methoxy-2,8-dihydroxyxanthone	Petrol–EtOAc–HCOOH (70 : 30 : 1)	[91]
Morusignin C	CH_2Cl_2–petrol (7 : 3)	[89]
Nigrolineaxanthones A-G	Hexane–EtOAc (4 : 1)	[89]
Nigrolineaxanthones H, I **[40]**	Petrol–CH_2Cl_2 (5 : 1)	[89]
Rheediaxanthone A	Petrol–CH_2Cl_2 (3 : 7)	[89]
Scriblitifolic acid	$CHCl_3$–Me_2O–HCOOH (70 : 30 : 0.5)	[91]
1,3,5,7-Tetramethoxyxanthone	$CHCl_3$–Me_2O–HCOOH (70 : 30 : 0.5)	[91]
1,3,5-Trihydroxy-4-(3-hydroxy-3-methylbutyl)xanthone	Hexane–EtOAc (4 : 1)	[89]
1,3,7-Trihydroxy-2-(3-hydroxy-3-methylbutyl)xanthone	Hexane–EtOAc (4 : 1)	[89]
Naphthalenes		
4-Hydroxy-5-methoxy-2-naphthaldehyde	Petrol–$CHCl_3$ (1 : 4)	[95]
5-Hydroxy-4-methoxy-2-naphthaldehyde	Petrol–$CHCl_3$ (1 : 4)	[95]

(Continued)

Table 1 Phenolic compounds isolated by PTLC. *(Continued)*

Name	Mobile phase*	Refs.
Quinones		
Anhydrophlegmacin-9,10-quinones A_2 & B_2	$CHCl_3$–EtOAc (9 : 1)	[96]
2,3-Dimethyl-6-[(2*E*,6*E*,10*Z*)-3,7,15-trimethyl-11-carboxyl-2,6,10,14-hexa-decatetraenyl]-2,5-cyclohexadiene-1,4-dione	Hexane–EtOAc (8 : 2)	[78]
Diosindigo A	C_6H_6	[95]
Diospyrin **[41]**	$CHCl_3$–MeOH (99 : 1)	[95,97]
8′-Hydroxyisodiospyrin	$CHCl_3$–MeOH (99 : 1)	[97]
Isodiospyrine	$CHCl_3$–MeOH (99 : 1)	[95]
Isosengulone	$CHCl_3$	[96]
2-Methylnaphthoquinone **[42]**	Hexane–$CHCl_3$ (4 : 1)	[95]
Presengulone **[43]**	$CHCl_3$–EtOAc (9 : 1)	[96]
Sengulone	$CHCl_3$	[96]
Stilbenes		
(–) Ampelopsin A	$CHCl_3$–EtOAc–Me_2CO (2 : 1 : 1)	[98]
(+) Balanocarpol **[44]**	$CHCl_3$–EtOAc–Me_2CO (2 : 1 : 1)	[98]
Gnemonol M	$CHCl_3$–EtOAc–MeOH–H_2O (10 : 20 : 12 : 5)	[99]
Gnetifolin E	$CHCl_3$–EtOAc–MeOH–H_2O (15 : 15 : 9 : 2)	[99]
Gnetin D	$CHCl_3$–EtOAc–MeOH–H_2O (20 : 14 : 6 : 1)	[100]
Isorhapontigenin-3-*O*-β-D-glucopyranoside	$CHCl_3$–EtOAc–MeOH–H_2O (15 : 15 : 9 : 2)	[99]
Latifolol	$CHCl_3$–EtOAc:MeOH:H_2O (20 : 14 : 6 : 1)	[100]
Lirioresinol	$CHCl_3$–EtOAc–MeOH–H_2O (15 : 15 : 9 : 2)	[99]
Parviflorol **[45]**	$CHCl_3$–EtOAc–Me_2CO (2 : 1 : 1)	[89]
Piceid	$CHCl_3$–EtOAc–MeOH–H_2O (8 : 15 : 4 : 1)	[101]
Resveratrol	C_6H_6–EtOAc–MeOH (5 : 3 : 1)	[101]
Stilbostemin G **[46]**	$CHCl_3$–MeOH (97 : 3)	[102]
ϵ-Viniferin	$CHCl_3$–EtOAc–Me_2CO (2 : 1 : 1) C_6H_6–EtOAc–MeOH (10 : 3 : 1)	[98] [101]
Isoquinoline Alkaloids		
11-*O*-Acetylambelline	Me_2CO Hexane–EtOAc (1 : 1)	[103] [104]
11-*O*-Acetyl-1,2,-β-epoxyambelline	Hexane–EtOAc (1 : 1)	[104]
Ambelline	EtOAc–NH_3 atm. Me_2CO	[104] [103]
Armoline	C_6H_6–Me_2CO–NH_3 (10 : 10 : 0.3)	[105]
Ayuthianine **[47]**	CH_2Cl_2–MeOH (96 : 4)	[106]
Baluchistanamine	C_6H_6–Me_2CO–NH_3 (10 : 10 : 0.3)	[105]
Berbamine	C_6H_6–Me_2CO–NH_3 (10 : 10 : 0.3)	[105]
Buphanidrine	CH_2Cl_2–MeOH (24 : 1) NH_3 atm. Me_2CO	[104] [107]
Buphanisine	EtOAc–NH_3 atm.	[104]
Cherylline	Me_2CO	[107]

(Continued)

Table 1 Phenolic compounds isolated by PTLC. *(Continued)*

Name	Mobile phase*	Refs.
Chilenine	C_6H_6–Me_2CO–NH_3 (10 : 10 : 0.3)	[105]
Corydalmine	CH_2Cl_2–MeOH (96 : 4)	[106]
Crebanine **[48]**	CH_2Cl_2–NH_3 atm.	[106]
Crinamidine	Me_2CO	[107]
Crinine	Me_2CO EtOAc–MeOH (1 : 1)	[107] [104]
9-*O*-Demethylpluviine	EtOAc–NH_3 atm.	[104]
6′-Desmethylthalifaboramine	Cyclohexane–EtOAc–Et_2NH (6 : 4 : 1 to 4:8:1)	[108]
3,5′-Dihydroxythalifaboramine	Cyclohexane–EtOAc–Et_2NH (6 : 4 : 1 to 4:8:1)	[108]
1,2β-Epoxyambelline	CH_2Cl_2–MeOH (24 : 1) NH_3 atm	[104]
Flexinine	EtOAc–NH_3 atm	[104]
6α-Hydroxybuphanidrine	Me_2CO	[103]
3-Hydroxy-6′-desmethoxy-thalifaboramine **[49]**	Cyclohexane–EtOAc–Et_2NH (6 : 4 : 1 to 4:8:1)	[108]
3-Hydroxy-6′-desmethyl-9-*O*-methylthalifaboramine **[50]**	Cyclohexane–EtOAc–Et_2NH (6 : 4 : 1 to 4:8:1)	[108]
3-Hydroxythalifaboramine	Cyclohexane–EtOAc–Et_2NH (6 : 4 : 1 to 4 : 8 : 1)	[108]
5′-Hydroxythalifaboranine	Cyclohexane–EtOAc–Et_2NH (6 : 4 : 1 to 4 : 8 : 1)	[108]
Isocorydine	$CHCl_3$–MeOH–NH_3 (97 : 3 : few drops)	[109]
Isotetrandrine	C_6H_6–Me_2CO–NH_3 (10 : 10 : 0.3)	[105]
Krepowine	Me_2CO	[107]
Liriodenine	$CHCl_3$–MeOH–NH_3 (97 : 3 : few drops)	[109]
Lycorine	CH_2Cl_2–MeOH (24 : 1) NH_3 atm	[104]
Norcorydine	$CHCl_3$–MeOH–NH_3 (97 : 3 : few drops)	[109]
Obaberine	C_6H_6–Me_2CO–NH_3 (10 : 10 : 0.3)	[105]
Obamegine	C_6H_6–Me_2CO–NH_3 (10 : 10 : 0.3)	[105]
8-Oxyacanthine	C_6H_6–Me_2CO–NH_3 (10 : 10 : 0.3)	[105]
Oxyberberine	C_6H_6–Me_2CO–NH_3 (10 : 10 : 0.3)	[105]
Powelline	EtOAc–Me_2CO (1 : 1) Me_2CO	[104] [107]
Reticuline	$CHCl_3$–MeOH–NH_3 (97 : 3 : few drops)	[107]
Sternbergine	EtOAc–NH_3 atm	[104]
Tejedine	C_6H_6–Me_2CO–NH_3 (10 : 10 : 0.3)	[105]
Thalifoline	C_6H_6–Me_2CO–NH_3 (10 : 10 : 0.3)	[105]
Thaligrisine	C_6H_6–Me_2CO–NH_3 (10 : 10 : 0.3)	[105]
Undulatine	Me_2CO	[103,107]
Other Nitrogenous compounds		
Dictamnine	C_6H_6–$CHCl_3$–EtOAc–MeOH (57 : 30 : 10 : 3)	[81]
Arberinine	$CHCl_3$–MeOH (95 : 5)	[67]
Belladine	Me_2CO	[103]
6-Hydroxybenzoxazolinone	$CHCl_3$–MeOH (8 : 2)	[53]
Koenigine-quinones A **[51]**, B **[52]**	Hexane–C_6H_6–EtOAc (2 : 2 : 1)	[110]

*If not stated the stationary phase is silica gel.

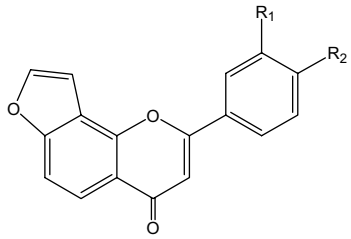

[15] R_1=R_2= H
[16] R_1, R_2 = OCH_2O

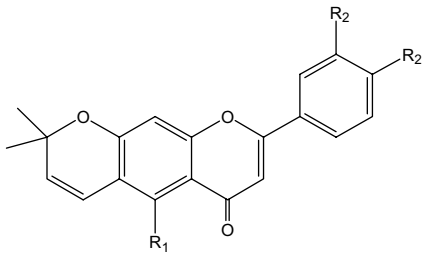

[12] R_1= OH, R_2=H, R_3=OH
[13] R_1= OH R_2= OCH_3, R_3= OH
[14] R_1= OCH_3, R_2=H, R_3 = OCH_3

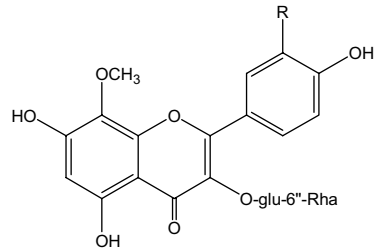

[17] R= H
[18] R= OCH_3

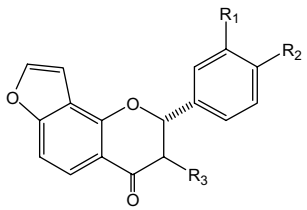

[19] R_1=R_2= H, R_3= OCH_3
[20] R_1, R_2 = OCH_2O, R_3=H

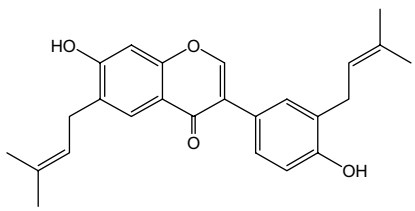

[21]

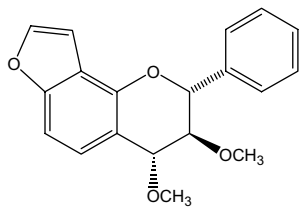

[22]

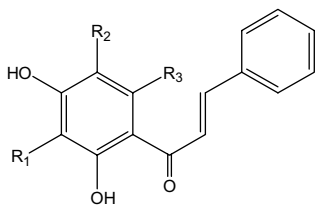

[23] R_1=R_2= R_3= H
[24] R_1=R_2= R_3= OH

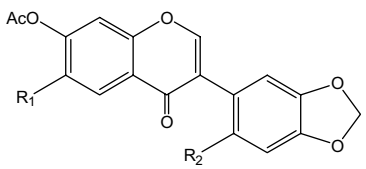

[25] R_1= OCH_3, R_2= H
[27] R_1=H, R_2= OCH_3

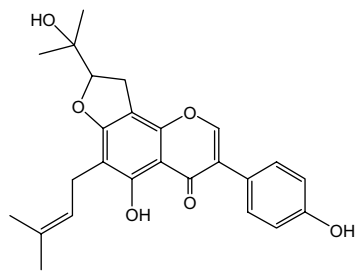

[26]

species. The anti-tumor lignan podophyllotoxin is the major active compounds of *Podophyllum hexandrum*.[2,9]

XANTHONES

Xanthones are benzo-γ-pyrone derivatives. Plant derived xanthones are of mixed shikimate-acetate origin. Mangiferin, a *C*-glycosyl xanthone present in the *Hypericum* species possesses anti-inflammatory, anti-hepatotoxic, and anti-viral properties.[9]

NAPHTHALENES

Naphthalenes are a small group of plant phenols formed from mixed shikimate-mevalonate pathways.[2]

QUINONES

Plant quinones show a diversity in their structures and origins, although they share the presence of two conjugated

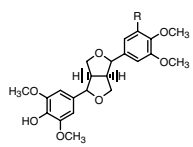

[28] R= H
[34] R= OCH_3

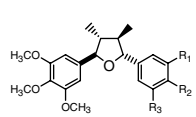

[29] R_1=R_2=R_3= OCH_3
[30] R_1= OCH_3, R_2, R_3= OCH_2O
[33] R_1, R_2= OCH_2O, R_3= OCH_3

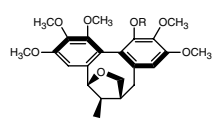

[31] R= CH_3
[32] R= H

carbonyl groups. Naphthoquinones are oxidation derivatives of naphthalenes **[41]**. Some highly oxidized diterpenoids with quinonoid moieties are described as diterepene quinones. An important class of quinones is the anthraquinone derivatives present in purgative drugs like *Senna*, *Aloes*, and *Cascara*. Biosynthetically, they are derived from polyketides resulting from the acetate pathway **[42, 43]**.[2,9]

STILBENES

Stilbenes are produced by the coupling of cinnamoyl-CoA with three malonyl-CoAs under the control of the enzyme

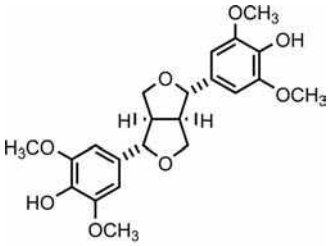

[35]

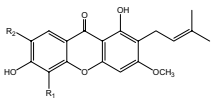

[36] R_1= H, R_2= OCH_3
[37] R_1= OCH_3, R_2= H

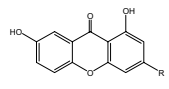

[38] R= OCH_3
[39] R= H

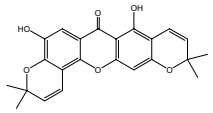

[40]

stilbene synthase, e.g., resveratrol. Resveratrol is a constituent of grapes and other food products, with anti-inflammatory, anti-platelet, and cancer-preventive properties.[2]

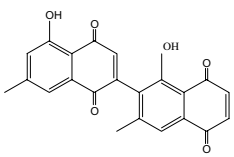

[41]

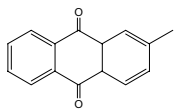

[42]

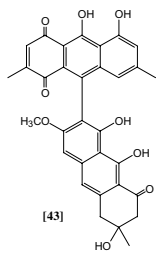

[43]

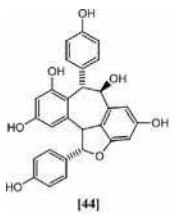

[44]

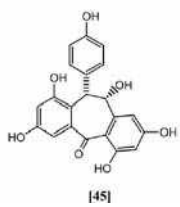

[45]

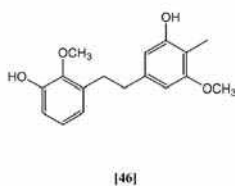

[46]

PHENOLIC NITROGENOUS COMPOUNDS

These include alkaloids and non-alkaloids that have phenolic functions in addition to a nitrogen atom. Even the alkaloids containing phenolic functions cannot be classified under one group. They may be phenyl alkyl amines, quinolines, isoquinolines, benzylisoquinolines **[47–50]**, carbazole **[51, 52]** and others. However, they are included in this entry owing to their phenolic nature. Some of these compounds, like opium alkaloids, are of great medicinal importance.[2,9]

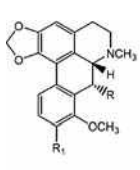

[47] R= OH, R_1= H
[48] R= H, R_1= OCH_3

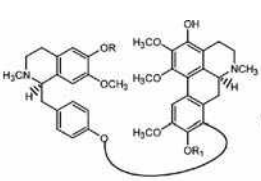

[49] R= CH_3, R_1= H
[50] R= H, R_1= CH_3

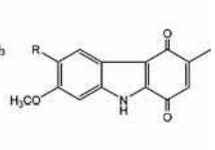

[51] R= H
[52] R= OCH_3

PREPARATIVE PLANAR CHROMATOGRAPHY

PTLC

This is the most widely used type of preparative planar chromatography, because of many factors. In PTLC, large plates (20 × 20), usually with thick layers (0.5–4 mm), are used, although, in some cases, researchers prefer to use thin layers (0.1–0.2 mm). The choice of the layer thickness is a compromise between the quality of separation and the amount of material that can be obtained from each plate. All TLC sorbents can be used in PTLC; thus, different mechanisms of separation can be utilized. Commercially available PTLC plates are homogenous and give excellent results. Some of these plates are prepared with a concentration zone for sample application to enhance separation. In addition to the cost issue, these plates are limited to certain types of sorbents and definite thicknesses. The alternative use of homemade plates overcomes these limitations and cuts the cost; however, the quality of the separation may be affected. The simplest form of PTLC requires only chromatographic tanks with suitable dimensions. Although TLC is generally more sensitive than other chromatographic methods, detection may be problematic if the materials to be isolated are not UV absorbing. This is, fortunately, not the case when dealing with phenolic compounds, as they are all UV active.[10,11,16] Manual application of samples is usual; however, automatic sample application is available to provide more accurate volumes and homogenous bands. OPTLC, introduced by Tyihak, Mincsovics, and Kalasz in 1979, greatly shortens the required time for separation, with greater resolution.[17] AMD also may be used to improve separation and allow multiple developments with different mobile phases, in a shorter time.[11,12,18]

PPC

PPC is currently of very limited application, in view of the great advances in separation techniques. PPC is generally used for more polar components. The separation is limited to partition and commercially available types of paper for chromatography. The cellulose fibers forming the paper matrix have larger sizes than the adsorbents used in TLC. Moreover, TLC has higher capacity than PC. These two factors make separations on TLC, in most cases, superior to those on PC. Although some development methods can only be used with PC, e.g., descending and horizontal developments, the flow rate is much slower when compared with TLC. The average time for development of a 10 cm TLC with silica gel as stationary phase is 20–30 min, while the same development in PC takes at least 2 hr.[10]

CPTLC

In this method, centrifugal force is used to accelerate the development with the mobile phase. The plates are circular and fixed on a rotor attached to a spindle; they are rotated using a motor. The mobile phase is introduced to the center of the plates by a pump. The instrument used for this type of chromatography is called Chromatotron. The samples are applied to the center of the plate. Mixture components move out radially, forming circles of increasing diameters. The instrument can be used along with a fraction collector. UV detection of zones is possible, thus facilitating the collection of different components in a pure form. Chromatotron plates are commercially available and can also be prepared in the laboratory. The layer thickness ranges from 2 to 8 mm, thus allowing the application of samples up to 4 g at once.[10,11,16] In CPTLC, the plates can be used several times after proper washing with more polar solvents. This gives CPTLC more advantages over PTLC, where plates can be used only once.

CONCLUSION

Different classes of natural phenols have the advantage of bearing chromophores that can absorb UV light. This characteristic makes their non-destructive detection an easy task and that, to some extent, may explain the popularity of their isolation using planar chromatography. Some adsorbents, e.g., alumina, are not used in their isolation since chemical reactions may take place between the acidic phenolic hydroxyl groups and the basic alumina. Normal silica gel is still the most popular adsorbent used for PTLC and is almost the only one used for CPTLC. Among PTLC separations included in this entry, RP 18 (C-18 reversed-phase silica gel) was used in seven references, while powdered cellulose was used in only two references (Table 1). It is worth mentioning that 14 references that used PTLC were excluded, owing to the lack of information about the mobile phase used in the separations. Among the benefits that one can gain from this entry is the convenient presentation of different mobile phases used for various separations. This

Table 2 Phenolic compounds isolated by Preparative Paper Chromatography (PPC).

Name	Mobile Phase	Refs.
Flavones		
Hispidulin	15% HOAc and BAW[a] 4 : 1 : 5 (upper phase)	[111]
Hispidulin 7, 4′-glycoside	15% HOAc and BAW[a] 4 : 1 : 5 (upper phase)	[111]
Hispidulin-7-*o*-methylglucuronide	15% HOAc and BAW[a] 4 : 1 : 5 (upper phase)	[112]
Nepetin	15% HOAc and BAW[a] 4 : 1 : 5 (upper phase)	[111]
Vicenin-2	15% HOAc and BAW[a] 4 : 1 : 5 (upper phase)	[111]
Flavonols		
Isorhamnetin-3-*o*-neohesperidoside	15% HOAc, BAW[a] 4 : 1 : 5 (upper phase) and BEW[b] 4 : 1 : 2.2	[111]
Isorhamnetin-3-*o*-robinobioside	15% HOAc, BAW[a] 4 : 1 : 5 (upper phase) and BEW[b] 4 : 1 : 2.2	[111]
Kaempferol 3-*O*-α-L-rhamnoside-7-*O*-β-D-xylosyl (1 → 2)-*O*-α-L-rhamnoside	15% HOAc	[113]
Quercetin 3-*O*-sophoroside	15% HOAc, BAW[a] 4 : 1 : 5 (upper phase) and BEW[b] 4 : 1 : 2.2	[111]
Chalcones		
Chalcononarigenin 2′,4′-*di*-*O*-glucoside	15% HOAc, BAW[a] 4 : 1 : 5 (upper phase) and BEW[b] 4 : 1 : 2.2	[114]
Chalcononarigenin 4-*O*-glucoside	15% HOAc, BAW[a] 4 : 1 : 5 (upper phase) and BEW[b] 4 : 1 : 2.2	[114]
Chalcononarigenin 4,2′,4′-*tri*-*O*-glucoside	15% HOAc, BAW[a] 4 : 1 : 5 (upper phase) and BEW[b] 4 : 1 : 2.2	[114]
Aurones		
Aureusidin 4,6-*di*-*O*-glucoside	15% HOAc, BAW[a] 4 : 1 : 5 (upper phase) and BEW[b] 4 : 1 : 2.2	[114]
Flavanones		
Naringenin 5,7-*di*-*O*-glucoside	15% HOAc, BAW[a] 4 : 1 : 5 (upper phase) and BEW[b] 4 : 1 : 2.2	[114]

[a]BAW = *n*-BuOH–AcOH–H_2O.
[b]BEW = *n*-BuOH–EtOH–H_2O.

Table 3 Phenolic compounds isolated by Centrifugal Chromatography (Chromatotrone).

Name	Mobile Phase	Refs.
Flavones		
Artoindonesianins U, V	Hexane–$CHCl_3$ 1 : 1 and 1 : 2	[115]
Artoindonesianins Q, R, S, T	Petrol–$CHCl_3$, $CHCl_3$, $CHCl_3$–Me_2CO	[116]
Artonin B	Hexane–$CHCl_3$ 1 : 1 and 1 : 2	[115]
Cyclocommunin	Hexane–$CHCl_3$ 1 : 1 and 1 : 2	[115]
5′-Hydroxycudraflavone A	Hexane–$CHCl_3$ 1 : 1 and 1 : 2	[115]
Isoflavones		
Kraussianone 2	CH_2Cl_2	[117]
Kraussianone 5	CH_2Cl_2–Et_2O 8 : 2	[117]
Benzoquinones		
3-Hydroxy-2-methyl-5-(3 methyl-2-butenyl)benzo-1,4-quinone	$CHCl_3$	[118]
2-Methyl-6-(3 methyl-2-butenyl)benzo-1,4-quinone	$CHCl_3$	[118]
Isoquinoline Alkaloids		
Adlumine	Hexane–EtOAc 9 : 1 → 1 : 1	[119]
Bicuculine	Hexane–EtOAc 9 : 1 → 1 : 1	[119]
Capnoidine	Hexane–EtOAc 9 : 1 → 1 : 1	[119]
Protopine	Hexane–EtOAc 9 : 1 → 1 : 1	[119]
Scoulerine	Hexane–$CHCl_3$ 1 : 1 → $CHCl_3$–MeOH 19 : 1	[119]
Tetrahydropalmatine	Hexane–EtOAc 9 : 1 → 1 : 1	[119]
Phenolic Amides		
Feruloyl-tyramine	Hexane–EtOAc 9 : 1 → 1 : 1	[119]

can greatly help in selecting the mobile phases suitable for different separations, based on the nature of compounds to be purified.

In the case of dealing with highly polar compounds, silica gel is not recommended. The earlier alternative is the use of paper chromatography. Only three references in this paper used PPC (Table 2), which have many disadvantages, including the relatively large particle sizes of the cellulose fibers and the slow movement of mobile phases. RP 18 is recommended for polar compounds; however, in the case of PTLC, the choice of mobile phase is limited in the percentage of water that can be used. If the percent in the mobile phase exceeds 50%, the development will not be homogeneous and will be at a very slow rate. The best solution in such cases is to use HPLC with a reversed phase column bearing different chain lengths of hydrocarbons (C-4, C-8, C-18). The composition of the mobile phase in this case is not restricted to 50% water. The highly polar anthocyanins are mainly purified by HPLC. In only two cases, silica gel PTLC was used for separation of three anthocyanins (Table 1).

Although CPTLC has many advantages over PTLC, its application is limited (3 references when compared with 99 for PTLC in this entry) (see Table 3). This is mainly due to the cost of the instrumentation required, as well as the wide spread of HPLC. The chromatotron used for CPTLC can be used only for separation and purification, while HPLC can also be used for both qualitative and quantitative analyses. The resolution in CPTLC is comparable with that of PTLC, since the stationary phases used are of the same particle sizes. HPLC gives much better resolution, however, owing to the use of stationary phases with smaller particle sizes.

REFERENCES

1. Macheix, J.J.; Fleuriet, A. *Fruit Phenolics*; CRC Press: Boca Raton, FL, 1990.
2. Dewick, P.M. *Medicinal Natural Products: A Biosynthetic Approach,* 2nd Ed.; John Wiley & Sons, Ltd: New York, 2002;
3. Walker, J.R.L. *The Biology of Plant Phenolics*; William Clowes & Sons Ltd: London, Cokhester and Beccles, 1975;
4. Ribérean-Gayon, P. *Plant Phenolics*; Oliver & Boyd: Edinburgh, 1972.
5. Geibel, M.; Treutter, D.; Feucht, W. *International Symposium on Natural Phenols in Plant Resistance*; ISHS Acta Horticulturae: Weihenstephan, Germany, 1994.
6. Grayer, R.; Kokubun, T. Plant-fungal interactions: the search for phytoalexins and other antifungal compounds from higher plants. Phytochemistry **2001**, *56*, 253–263.
7. Harborne, J.B. *Plant Phenolics*; Academic Press: London, San Diego, 1989.
8. Williamson, E.M.; Okpako, D.T.; Evans, F.J. *Pharmacological Methods in Phytotherapy Research Selection, Preparation and Pharmacological Evaluation of Plant Material*; John Wiley & Sons: Chichester, New York, Brisbane Toronto, Singapore, 1996.

9. Evans, W.C. *Trease and Evans Pharmacognosy* 14th Ed.; WB Saunders Company Ltd: London, 1996; Philadelphia, Toronto, Sydney, Tokyo, 1996.
10. Braithwaite, A.; Smith, F.J. *Chromatographic Methods,* 4th Ed.; Chapman and Hall: London, New York, 1990.
11. Gibbons, S.; Gray, A.I. Isolation by planar chromatography. In *Natural Products Isolation*; Cannell, R.J.P., Ed.; Humana Press: Totowa, New Jersey, 1998.
12. Galand, N.; Pothier, J.; Dollet, J.; Viel, C. OPLC and AMD, recent techniques of planar chromatography: their interest for separation and characterization of extractive and synthetic compounds. Fitoterapia **2002**, *73*, 121–134.
13. El-Mofty, A.M. Observation on the use of *Ammi majus* Linn in vitiligo. Brit. J. Dermatol. **1952**, *64* (12), 431–441.
14. Andersen, Ø.M.; Markham, K.R. *Flavonoids Chemistry, Biochemistry and Applications*; CRC Press, Taylor & Francis Group: Boca Raton, FL, 2006.
15. Bohm, B.A. *Introduction to Flavonoids*; Harwood Academic Publishers: New York, 1998.
16. Nyiredy, S. Thin-layer (planar)/preparative thin-layer (planar) chromatography. In *Chromatography*; Cook, M., Poole, C.F., Eds.; Academic Press: New York, 2000; Vol. 2.
17. Tyihak, E.; Mincsovics, E.; Kalasz, H. New planar liquid chromatographic technique: overpressured thin-layer chromatography. J. Chromatogr. **1979**, *174*, 75–81.
18. Nyiredy, S. Thin-layer (planar)/modes of development: forced flow, overpressured layer chromatography and centrifugal. In *Chromatography*; Cook, M., Poole, C.F., Eds.; Academic Press: New York, 2000; Vol. 2.
19. Parmar, V.S.; Jain, S.C.; Gupta, S.; Talwar, S.; Rajwanshi, V.K.; Kumar, R.; Azim, A.; Malhotra, S.; Kumar, N.; Jain, R.; Sharma, N.K.; Tyagi, O.D.; Lawrie, S.J.; Errington, W.; Howarth, O.W.; Olsen, C.E.; Singh, S.K.; Wengel, J. Polyphenols and alkaloids from *piper* species. Phytochemistry **1998**, *49*, 1069–1078.
20. Martins, R.C.C.; Latorre, L.R.; Sartorelli, P.; Kato, M.J. Phenylpropanoids and tetrahydrofuran lignans from *Piper solmsianum*. Phytochemistry **2000**, *55*, 843–846.
21. Seca, A.M.L.; Silva, A.M.S.; Silvestre, A.J.D.; Cavaleiro, J.A.S.; Domingues, F.M.J.; Pascoal-Neto, C. Phenolic constituents from the core of Kenaf (*Hibiscus cannabinus*). Phytochemistry **2001**, *56*, 759–767.
22. Martins, R.C.C.; Lago, J.H.G.; Albuquerque, S.; Kato, M.J. Trypanocidal tetrahydrofuran lignans from inflorescences of *Piper solmsianum*. Phytochemistry **2003**, *64*, 667–670.
23. Pavlović, M.; Kovâcević, N.; Couladis, M.; Tzakou, O. Phenolic constituents of *Anthemis triumfetti*(L.) DC. Biochem. Syst. Ecol. **2006**, *34*, 449–452.
24. Petrović, S.D.; Gorunović, M.S.; Wray, V.; Merfort, I. A taraxasterol derivative and phenolic compounds from *Hieracium gymnocephalum*. Phytochemistry **1999**, *50*, 293–296.
25. Rukachaisirikul, V.; Sukpondma, Y.; Jansakul, C.; Taylor, W.C. Isoflavone glycosides from *Derris scandens*. Phytochemistry **2002**, *60*, 827–834.
26. Kijjoa, A.; Gonzalez, M.J.; Afonso, C.M.; Pinto, M.M.M.; Anantachoke, C.; Herz, W. Xanthones from *Calophyllum teysmannii* var. inophylloide. Phytochemistry **2000**, *53*, 1021–1024.
27. Chen, W.; Tang, W.; Lou, L.; Zhao, W. Pregnane, coumarin and lupine derivatives and cytotoxic constituents from *Helicteres angustifolia*. Phytochemistry **2006**, *67*, 1041–1047.
28. Correia, S.de J.; David, J.M.; David, J.P.; Chai, H.-B.; Pezzuto, J.M.; Cordell, G.A. Alkyl phenols and derivatives from *Tapirira obtuse*. Phytochemistry **2001**, *56*, 781–784.
29. Almeida, E.X.; Conserva, L.M.; Lemos, R.P.L. Coumarins, coumarinolignoids and terpenes from *Protium heptaphyllum*. Biochem. Syst. Ecol. **2002**, *30*, 685–687.
30. Abdel-Kader, M.S. New ester and furocoumarins from the roots of *Pituranthos tortuosus*. J. Braz. Chem. Soc. **2003**, *14*, 48–51.
31. Mahabusarakam, W.; Deachathai, S.; Phongpaichit, S.; Janakul, C.; Taylor, W.C. A benzyl and isoflavone derivatives from *Derris scandens* Benth. Phytochemistry **2004**, *65*, 1185–1191.
32. Mahmoud, A.A.; Ahmed, A.A.; Iinuma, M.; Tanaka, T. Further monoterpene 5-methylcoumarins and an acetophenone derivative from *Ethulia conyzoides*. Phytochemistry **1998**, *48*, 543–546.
33. Erasto, P.; Bojase-Moleta, G.; Majinda, R.R.T. Antimicrobial and antioxidant flavonoids from the root wood of *Bolusanthus speciosus*. Phytochemistry **2004**, *65*, 875–880.
34. Franke, K.; Porzel, A.; Masaoud, M.; Adam, G.; Schmidt, J. Furanocoumarins from *Dorstenia gigas*. Phytochemistry **2001**, *56*, 611–621.
35. Abdel-Kader, M.S. Phenolic constituents of *Ononis vaginalis* roots. Planta Med. **2001**, *67*, 388–390.
36. Trusheva, B.; Popova, M.; Naydenski, H.; Tsvetkova, I.; Rodriguez, J.G.; Bankova, V. New polyisoprenylated benzophenones from Venezuelan propolis. Fitoterapia **2004**, *75*, 683–689.
37. Rancon, S.; Chaboud, A.; Darbour, N.; Comte, G.; Bayet, C.; Simon, P.-N.; Raynaud, J.; Di Pietro, A.; Cabalion, P.; Barron, D. Natural and synthetic benzophenones: interaction with the cytosolic binding domain of P-glycoprotein. Phytochemistry **2001**, *57*, 553–557.
38. Ali, S.; Goundar, R.; Sotheeswaran, S.; Beaulieu, C.; Spino, C. Benzophenones of *Garcinia pseudoguttifera* (Clusiaceae). Phytochemistry **2000**, *53*, 281–284.
39. Minami, H.; Hamaguchi, K.; Kubo, M.; Fukuyama, Y. A benzophenone and a xanthone from *Garcinia subelliptica*. Phytochemistry **1998**, *49*, 1783–1785.
40. Yang, L.; Wang, Z.; Xu, L. Phenols and a triterpene from *Dendrobium aurantiacum* var. *denneanum* (Orchidaceae). Biochem. Syst. Ecol. **2006**, *34*, 658–660.
41. Ito, C.; Itoigawa, M.; Onoda, S.; Hosokawa, A.; Ruangrungsi, N.; Okuda, T.; Tokuda, H.; Nishino, H.; Furukawa, H. Chemical constituents of *Murraya siamensis*: three coumarins and their anti-tumor promoting effect. Phytochemistry **2005**, *66*, 567–572.
42. Chlouchi, A.; Muyard, F.; Girard, C.; Waterman, P.G.; Bévalot, F. Coumarins from the twigs of *Diplolaena mollis*. Biochem. Syst. Ecol. **2005**, *33*, 967–969.
43. Um, B.H.; Lobstein, A.; Weniger, B.; Spiegel, C.; Yice, F.; Rakotoarison, O.; Andriantsitohaina, R.; Anton, R. New coumarins from *Cedrelopsis grevei*. Fitoterapia **2003**, *74*, 638–642.
44. Vardamides, J.C.; Azebaze, A.G.B.; Nkengfack, A.E.; Van Heerden, F.R.; Fomum, Z.T.; Ngando, T.M.; Conrad, J.; Vogler, B.; Kraus, W. Scaphopetalone and scaphopetalumate,

a lignan and a triterpene ester from *Scaphopetalum thonneri*. Phytochemistry **2003**, *62*, 647–650.
45. Guilet, D.; Séraphin, D.; Rondeau, D.; Richomme, P.; Bruneton, J. Cytotoxic coumarins from *Calophyllum dispar*. Phytochemistry **2001**, *58*, 571–575.
46. Guz, N.R.; Lorenz, P.; Stermitz, F.R. New coumarins from *Harbouria trachypleura*: isolation and synthesis. Tetrahedron Lett. **2001**, *42*, 6491–6494.
47. Murphy, E.M.; Nahar, L.; Byres, M.; Shoeb, M.; Siakalima, M.; Rahman, M.M.; Gray, A.I.; Sarker, S.D. Coumarins from the seeds of *Angelica sylvestris* (Apiaceae) and their distribution within the genus *Angelica*. Biochem. Syst. Ecol. **2004**, *32*, 203–207.
48. Yankep, E.; Fomum, Z.T.; Bisrat, D.; Dagne, E.; Hellwig, V.; Steglich, W. *O*-Geranylated isoflavones and a 3-Phenylcoumarin from *Millettia griffoniana*. Phytochemistry **1998**, *49*, 2521–2523.
49. Ito, C.; Mishina, Y.; Litaudon, M.; Cosson, J.-P.; Furukawa, H. Xanthone and dihydroisocoumarin from *Montrouziera sphaeroidea*. Phytochemistry **2000**, *53*, 1043–1046.
50. Anaya, A.L.; Macias-Rubalcava, M.; Cruz-Ortega, R.; Garcia-Santana, C.; Sánchez-Monterrubio, P.N.; Hernández-Bautista, B.E.; Mata, R. Allelochemicals from *Stauranthus perforatus*, a Rutaceous tree of the Yucatan Peninsula, Mexico. Phytochemistry **2005**, *66*, 487–494.
51. Ponce, M.A.; Scervino, J.M.; Erra-Balsells, R.; Ocampo, J.A.; Godeas, A.M. Flavonoids from shoots, roots and roots exudates of *Brassica alba*. Phytochemistry **2004**, *65*, 3131–3134.
52. Pistelli, L.; Chiellini, E.E.; Morelli, I. Flavonoids from *Ficus pumila*. Biochem. Syst. Ecol. **2000**, *28*, 287–289.
53. Amer, M.E.; Abou-Shoer, M.I.; Abdel-Kader, M.S.; El-Shaibany, A.M.S.; Abdel-Salam, N.A. Alkaloids and flavone acyl glycosides from *Acanthus arboreus*. J. Braz. Chem. Soc. **2004**, *15* (2), 262–266.
54. Parveen, M.; Shafiullah, M.S.K.; Ilyas, M. Luteolin 3α-xylosyl(1 → 2)glucoside from *Viburunum grandifolium*. Phytochemistry **1998**, *49*, 2535–2538.
55. Kijjoa, A.; Cidade, H.M.; Gonzalez, M.J.T.G.; Afonso, C.M.; Silva, A.M.S.; Herz, W. Further prenylflavonoids from *Artocarpus elasticus*. Phytochemistry **1998**, *47*, 875–878.
56. Borges-Argáez, R.; Peña-Rodriguez, L.M.; Waterman, P.G. Flavonoids from two *Lonchocarpus species* of the Yucatan Peninsula. Phytochemistry **2002**, *60*, 533–540.
57. Azam, M.M.; Ghanim, A. Flavones from leaves of *Tecomella undulate* (Bignoniaceae). Biochem. Syst. Ecol. **2000**, *28*, 803–804.
58. da Silva, I.G.; Barbosa-Filho, J.M.; da Silva, M.S.; de Lacerda, C.D.G.; da Cunha, E.V.L. Coclaurine from *Ocotea duckei*. Biochem. Syst. Ecol. **2002**, *30*, 881–883.
59. Wollenweber, E.; Stevens, J.F.; Ivancic, M. Flavonoid aglycones and a thiophene derivative from *Helichrysum cassianum*. Phytochemistry **1998**, *47*, 1441–1443.
60. Yayli, N.; Seymen, H.; Baltaci, C. Flavone C-glycosides from *Scleranthus uncinatus*. Phytochemistry **2001**, *58*, 607–610.
61. Magalhäes, A.F.; Tozzi, A.M.A.; Magalthäes, E.G.; Nogueira, M.A.; Queiroz, S.C.N. Flavonoids from *Lonchocarpus latifolius* roots. Phytochemistry **2000**, *55*, 787–792.
62. Su, B.-N.; Park, E.J.; Vigo, J.S.; Graham, J.G.; Cabieses, F.; Fong, H.H.S.; Pezzuto, J.M.; Kinghorn, A.D. Activity-guided isolation of the chemical constituents of *Muntingia calabura* using a quinine reductase induction assay. Phytochemistry **2003**, *63*, 335–341.
63. Ferracin, R.J.; da Silva, M.F. d.-G.F.; Fernandes, J.B.; Vieira, P.C. Flavonoids from the fruits of *Murraya paniculata*. Phytochemistry **1998**, *47*, 393–396.
64. Sharaf, M.; El-Ansari, M.A.; Saleh, N.A.M. Flavone glycosides from *Mentha longifolia*. Fitoterapia **1999**, *70*, 478–483.
65. Trifunović, S.; Vajs, V.; Juranić, Z.; Žižak, Ž.; Tešević, V.; Macura, S.; Milosavljević, S. Cytotoxic constituents of *Achillea clavennae* from Montenegro. Phytochemistry **2006**, *67*, 887–893.
66. Abdel-Kader, M.S.; El-Lakany, A.M. Two 8-methoxyflavonol rutinosides from *Gagonia boulosi* growing in Egypt. Alex. J. Pharm. Sci. **2002**, *16*, 103–105.
67. Sultana, N.; Hartley, T.G.; Waterman, P.G. Two novel prenylated flavones from the aerial parts of *Melicope micrococca*. Phytochemistry **1999**, *50*, 1249–1253.
68. El-Masry, S.; Amer, M.E.; Abdel-Kader, M.S.; Zaatout, H.H. Prenylated flavonoids of *Erythrina lysistemon* grown in Egypt. Phytochemistry **2002**, *60*, 783–787.
69. Shirataki, Y.; Matsuoka, S.; Komatsu, M.; Ohyama, M.; Tanaka, T.; Iinuma, M. Four isoflavanones from roots of *Sophora tetraptera*. Phytochemistry **1999**, *50*, 695–701.
70. Messanga, B.B.; Kimbu, S.F.; Sondengam, B.L.; Bodo, B. Triflavonoids of *Ochna calodendron*. Phytochemistry **2002**, *59*, 435–438.
71. Barragan-Huerta, B.E.; Peralta-Cruz, H.; Gonzalez-Laredo, R.F.; Karchesy, J. Neocandenatone, an isoflavan-cinnamylphenol quinine methide pigment from *Dalbergia congestiflora*. Phytochemistry **2004**, *65*, 925–928.
72. Tomazela, D.M.; Pupo, M.T.; Passador, E.A.P.; da Silva, M.F. d.-G.F.; Vieira, P.C.; Fernandes, J.B.; Fo, E.R.; Oliva, G.; Pirani, J.R. Pyrano chalcones and a flavone from *Neoraputia magnifica* and their *Trypanosoma cruzi* glycosomal glyceraldehydes-3-phosphate dehydrogenase-inhibitory activities. Phytochemistry **2000**, *55*, 643–651.
73. Yankep, E.; Mbafor, T.J.; Fomum, Z.T.; Steinbeck, C.; Messanga, B.B.; Nyasse, B.; Budzikiewicz, H.; Lenz, C.; Schmickler, H. Further isoflavonoid metabolites from *Millettia griffoniana* (Bail). Phytochemistry **2001**, *56*, 363–368.
74. Waffo, A.F.K.; Coombes, P.H.; Mulholland, D.A.; Nkengfack, A.E.; Fomum, Z.T. Flavones and isoflavones from the west African Fabaceae *Erythrina vogelii*. Phytochemistry **2006**, *67*, 459–463.
75. Yenesew, A.; Irungu, B.; Oerese, S.; Midiwo, J.O.; Heydenreich, M.; Peter, M.G. Two prenylated flavonoids from the stem bark of *Erythrina burttii*. Phytochemistry **2003**, *63*, 445–448.
76. Maximo, P.; Lourenço, A. A pterocarpan from *Ulex parviflorus*. Phytochemistry **1998**, *48*, 359–362.
77. Pale, E.; Kouda-Bonafos, M.; Nacro, M.; Vanhaelen, M.; Vanhaelen-Fastré, R Two triacylated and tetraglucosylated anthocyanins from *Ipomoea asarifolia* flowers. Phytochemistry **2003**, *64*, 1395–1399.
78. Silva, D.H.S.; Pereira, F.C.; Zanoni, M.V.B.; Yoshida, M. Lipophyllic antioxidants from *Iryanthera juruensis* fruits. Phytochemistry **2001**, *57*, 437–442.
79. Ahmed, A.A.; Mahmoud, A.A.; Ali, E.T.; Tzakou, O.; Couladis, M.; Mabry, T.J.; Gáti, T.; Tóth, G. Two highly

oxygenated eudesmanes and 10 lignans from *Achillea holosericea*. Phytochemistry **2002**, *59*, 851–856.
80. Kim, M.-R.; Jung, H.-J.; Min, B.-S.; Oh, S.-R.; Kim, C.-S.; Ahn, K.-S.; Kang, W.-S.; Lee, H.-K. Constituents from the stems of *Actinodaphne lancifolia*. Phytochemistry **2002**, *59*, 861–865.
81. Saĝlam, H.; Gözler, T.; Gözler, B. A new prenylated arylnaphthalene lignan from *Haplophyllum myrtifolium*. Fitoterapia **2003**, *74*, 564–569.
82. Erdemoglu, N.; Sahin, E.; Sener, B.; Ide, S. Structural and spectroscopic characteristics of two lignans from *Taxus baccata* L. J. Mol. Struct. **2004**, *692*, 57–62.
83. Chang, C.-C.; Lien, Y.-C.; Liu, K.C.S.C.; Less, S.-S. Lignans from *Phyllanthus urinaria*. Phytochemistry **2003**, *63*, 825–833.
84. Sun, Q.-Z.; Chen, D.-F.; Ding, P.-L.; Ma, C.-M.; Kakuda, H.; Nakamura, N.; Hattori, M. Three new lignans, longipedunins A_VC, from *adsura longipedunculata* and their inhibitory activity against HIV-I protease. Chem. Pharm. Bull. **2006**, *54*, 129–132.
85. Ul-Haq, A.; Malik, A.; Khan, M.T.H.; Ul-Haq, A.; Khan, S.B.; Ahmad, A.; Choudhary, M.I. Tyrosinase inhibitory lignans from the methanol extract of the roots of *Vitex negundo* Linn. and their structure-activity relationship. Phytomedicine **2006**, *13*, 255–260.
86. Silvester, A.J.D.; Evtuguin, D.V.; Sousa, A.P.M.; Silva, A.M.S. Lignans from a hybrid *Paulownia* wood. Biochem. Syst. Ecol. **2005**, *33*, 1298–1302.
87. Song, Q.; Fronczek, F.R.; Fischer, N.H. Dibenzocyclooctadiene-type lignans from *Magnolia pyramidata*. Phytochemistry **2000**, *55*, 653–661.
88. Bayma, J.C.; Arruda, M.P.; Neto, M.S. A prenylated xanthone from the bark of *Symphonia globulifera*. Phytochemistry **1998**, *49*, 1159–1160.
89. Rukachaisirikul, V.; Ritthiwigrom, T.; Pinsa, A.; Sawangchote, P.; Taylor, W.C. Xanthones from the stem bark of *Garcinia nigrolineata*. Phytochemistry **2003**, *64*, 1149–1156.
90. Yimdjo, M.C.; Azebaze, A.G.; Nkengfack, A.E.; Meyer, A.M.; Bodo, B.; Fomum, Z.T. Antimicrobial and cytotoxic agents from *Caliphyllum inophyllum*. Phytochemistry **2004**, *65*, 2789–2795.
91. Kijjoa, A.; Gonzalez, M.J.; Pinto, M.M.M.; Silva, A.M.S.; Anantachoke, C.; Herz, W. Xanthones from *Calophyllum teysmannii* var. *inophylloide*. Phytochemistry **2000**, *55*, 833–836.
92. Mahabusarakam, W.; Chairerk, P.; Taylor, W.C. Xanthones from *Garcinia cowa* Roxb. latex. Phytochemistry **2005**, *66*, 1148–1153.
93. Hay, A.-E.; Hélesbeux, J.-J.; Duval, O.; Labaïed, M.; Grellier, P.; Richomme, P. Antimalarial xanthones from *Calophyllum caledonicum* and *Garcinia vieillardii*. Life Sci. **2004**, *75*, 3077–3085.
94. Prachyawarakorn, V.; Mahidol, C.; Ruchirawat, S. Siamenols A & D, four new coumarins from *Mammea siamensis*. Chem. Pharm. Bull. **2006**, *54*, 884–886.
95. Ganapaty, S.; Thomas, P.S.; Fotso, S.; Laatsch, H. Antitermitic quinines from *Diospyros sylvatica*. Phytochemistry **2004**, *65*, 1265–1271.
96. Alemayehu, G.; Abegaz, B.; Kraus, W. A 1,4-anthraquinone-dihydroanthracenone dimer from *Senna sophera*. Phytochemistry **1998**, *48*, 699–702.
97. Ganapaty, S.; Thomas, P.S.; Karagianis, G.; Waterman, P.G.; Brun, R. Antiprotozoal and cytotoxic naphthalene derivatives from *Diospyros assimilis*. Phytochemistry **2006**, *67*, 1950–1956.
98. Tanaka, T.; Ito, T.; Ido, Y.; Son, T.-K.; Nakaya, K.; Iinuma, M.; Ohyama, M.; Chelladurai, V. Stilbenoids in the stem bark of *Hopea parviflora*. Phytochemistry **2000**, *53*, 1015–1019.
99. Iliya, I.; Ali, Z.; Tanaka, T.; Iinuma, M.; Furusawa, M.; Nakaya, K.-I.; Murata, J.; Darnaedi, D.; Matsuura, N.; Ubukata, M. Stilbene derivatives from *Gnetum gnemon* Linn. Phytochemistry **2003**, *62*, 601–606.
100. Iliya, I.; Ali, Z.; Tanaka, T.; Iinuma, M.; Furusawa, M.; Nakaya, K.-I.; Murata, J.; Darnaedi, D. Stilbenoids from the stem of *Gnetum latifolium* (Gnetaceae). Phytochemistry **2002**, *61*, 959–961.
101. Tanaka, T.; Ito, T.; Nakaya, K.; Iinuma, M.; Riswan, S. Oligostilbenoids in stem bark of *Vatica rassak*. Phytochemistry **2000**, *54*, 63–69.
102. Kostecki, K.; Engelmeier, D.; Pacher, T.; Hofer, O.; Vajrodaya, S.; Greger, H. Dihydrophenanthrenes and other antifungal stilbenoids from *Stemona* cf. *pierrei*. Phytochemistry **2004**, *65*, 99–106.
103. Nair, J.J.; Campbell, W.E.; Brun, R.; Viladomat, F.; Codina, C.; Bastida, J. Alkaloids from *Nerine filifolia*. Phytochemistry **2005**, *66*, 373–382.
104. Machocho, A.; Chhabra, S.C.; Viladomat, F.; Codina, C.; Bastida, J. Alkaloids from *Ammocharis tinneana*. Phytochemistry **1999**, *51*, 1185–1191.
105. Suau, R.; Rico, R.; López-Romero, J.M.; Najera, F.; Cuevas, A. Isoquinoline alkaloids from *Berberis vulgaris* subsp. *Australis*. Phytochemistry **1998**, *49*, 2545–2549.
106. Blanchfield, J.T.; Sands, D.P.A.; Kennard, C.H.L.; Byriel, K.A.; Kitching, W. Characterisation of alkaloids from some Australian *Stephania* (Menispermaceae) species. Phytochemistry **2003**, *63*, 711–720.
107. Nair, J.J.; Machocho, A.K.; Campbell, W.E.; Brun, R.; Viladomat, F.; Codina, C.; Bastida, J. Alkaloids from *Crinum macowanii*. Phytochemistry **2000**, *54*, 945–950.
108. Lin, L.-Z.; Hu, S.-F.; Chu, M.; Chan, T.-M.; Chai, H.; Angerhofer, C.K.; Pezzuto, J.M.; Cordell, G.A. Phenolic aporphine-benzylisoquinoline alkaloids from *Thalictrum faberi*. Phytochemistry **1999**, *50*, 829–834.
109. Jumana, S.; Hasan, C.M.; Rashid, M.A. Alakaloids from the stem bark of *Miliusa velutina*. Biochem. Syst. Ecol. **2000**, *28*, 483–485.
110. Saha, C.; Chowdhury, B.K. Carbazoloquinones from *Murraya koenigii*. Phytochemistry **1998**, *48*, 363–366.
111. Iwashina, T.; Kamenosono, K.; Ueno, T. Hispidulin and nepetin 4α-glucosides from *Cirsium oligophyllum*. Phytochemistry **1999**, *51*, 1109–1111.
112. Akkal, S.; Benayache, F.; Benayache, S.; Medjroubi, K.; Jay, M.; Tillequin, F.; Seguin, E. A new flavone glycoside from *Centaurea furfuracea*. Fitoterapia **1999**, *70*, 368–370.

113. El-Sayed, N.H.; Awaad, A.S.; Hifnawy, M.S.; Mabry, T.J. A flavonol triglycoside from *Chenopodium murale*. Phytochemistry **1999**, *51*, 591–593.
114. Iwashina, T.; Kitajima, J.; Shiuchi, T.; Itou, Y. Chalcones and other flavonoids from *Asarum* sensu lato (Aristolochiaceae). Biochem. Syst. Ecol. **2005**, *33*, 571–584.
115. Syah, Y.M.; Achmad, S.A.; Ghisalberti, E.L.; Hakim, E.H.; Mujahidin, D. Two new cytotoxic isoprenylated flavones, artoindonesianins U and V, from the heartwood of *Artocarpus champeden*. Fitoterapia **2004**, *75*, 134–140.
116. Syah, Y.M.; Achmad, S.A.; Ghisalberti, E.L.; Hakim, E.H.; Makmur, L.; Mujahidin, D. Artoindonesianins Q & T, four isoprenylated flavones from *Artocarpus champeden* Spreng. (Moraceae). Phytochemistry **2002**, *61*, 949–953.
117. Drewes, S.; Horn, M.M.; Munro, O.Q.; Dhlamini, J.T.B.; Meyer, J.J.M.; Rakuambo, N.C. Pyranoisoflavones with erectile-dysfunction activity from *Eriosema kraussianum*. Phytochemistry **2002**, *59*, 739–747.
118. Drewes, S.E.; Khan, F.; van Vuuren, S.F.; Viljoen, A.M. Simple 1,4-benzoquinones with antibacterial activity from stems and leaves of *Gunnera perpensa*. Phytochemistry **2005**, *66*, 1812–1816.
119. Majak, W.; Bai, Y.; Benn, M.H. Phenolic amides and isoquinoline alkaloids from *Corydalis sempervirens*. Biochem. Syst. Ecol. **2003**, *31*, 649–651.

Natural Pigments: TLC Analysis

Tibor Cserháti
Esther Forgács
Institute of Chemistry, Chemical Research Center, Hungarian Academy of Sciences, Budapest, Hungary

INTRODUCTION

Various natural pigment classes, such as flavonoids, anthocyanins, carotenoids, chlorophylls and chlorophyll derivatives, porphyrins, quinones, anthraquinones, betalains, and so forth are abundant in many families of the vegetable and animal kingdoms. As consumers generally dislike the color of synthetic dyes, the concentration and composition of pigments in foods and food products exert a considerable impact on the consumer acceptance and, consequently, on the commercial value of the products. It has been proven many times that one of the main properties employed for the commercial evaluation of the quality of products is their color; that is, an adequate color is an important requirement of marketability.

DISCUSSION

Spectroscopic methods for measuring the absorbance of pigment solutions or the adsorbance of the color of product surfaces on one or more wavelengths in the visible range are excellent tools for the accurate determination of the quantity of pigments; however, they do not contain any useful information on the concentration of the individual pigment fractions.

As the stability of the various pigments against hydrolysis, oxidation, and other environmental conditions shows marked differences, the assessment of the pigment composition may help for the prediction of the shelf life of products and the elucidation of the impact of various technological steps on the individual pigment fractions resulting in more consumer-friendly processing methods. Moreover, the exact knowledge of the pigment composition may facilitate the identification of the origin of the product. The advantageous characteristics of TLC (easy to use, low operating costs, no need for complicated instrumentation, manyfold possibilities of detection, etc.) make it a method of preference for the separation and, to a lesser extent, for the quantitative analysis of natural pigments.

The earlier results in the application of thin-layer chromatography (TLC) for the analysis of natural color pigments, in general,[1] and especially in plants,[2] have been reviewed. Pigments are more or less strongly bonded to cellulose, protein, cell-wall components, and so forth in both plant and animal issues; therefore, the efficaceous extraction sometimes is difficult and time-consuming with the traditional extraction methods, and the recoveries sometimes are inadequate. Depending on the character of the accompanying matrix and the solubility of the pigment, a considerable number of extraction solvents or solvent mixtures were proposed and used in the TLC analysis of natural pigments.

Thus, ethanol–water (7:3, v/v) and methanol–water in various ratios for flavonoids, methanol–25% HCl (9:1, v/v), methanol–acetic acid (5%), methanol–trifluoroacetic acid (3%) for unstable anthocyanins, acetone, methanol–acetone mixtures for carotenoids, acetone and petroleum ether for chlorophylls, and so forth. The pigments are fairly stable in their natural environment, but they generally become unstable in extracts; this has to be taken into consideration in the development of new, more efficaceous extraction procedures.

The impact of the extraction conditions using various solvents on the recoveries has never been studied in detail, and the results have never been compared. The introduction of modern extraction methods, such as microwave-assisted extraction, supercritical fluid extraction, and solid-phase extraction, probably will improve the efficiency of extraction, even in the instance of unstable pigments and pigment mixtures. The majority of TLC separations were carried out on traditional silica layers. As the chemical structures and, consequently, the retention characteristics of pigments are highly different, a wide variety of eluent systems has been employed for their separation, consisting of light petroleum, ethyl formate, ethyl acetate, benzene, toluene, chloroform, methanol, *n*-butanol, formic or acetic acid, and so forth.

Besides silica, other direct phase supports such as alumina, diatomaceous earth, cellulose, MgO–diatomaceous earth, and sucrose layers were employed for the separation of various pigment mixtures. Mixed-mode supports (cyano, diol, and aminosilica layers) were also employed in both the direct and reversed-phase elution modes for the separation of natural pigments, but their performance was markedly lower that those of traditional silica layers. Reversed-phase supports (polyamide, octadecylsilica, alumina, silica, and diatomaceous earth impregnated with paraffin oil) were also applied for the separation of color pigments (carotenoids from *Capsicum annuum*, anthocyanins from red wines) and it was found that their separation

Table 1 The R_f values obtained for carotenoids by use of different mobile phases.

No.	Carotenoid	R_f value in mobile phase 1	2	3
1	β-Carotene	0.93	0.92	0.93
2	α-Cryptoxanthin	0.76	0.83	0.80
3	β-Cryptoxanthin	0.75	0.83	0.80
4	Zeaxanthin	0.46	0.72	0.51
5	Lutein	0.46	0.73	0.52
6	Nigroxanthin	0.52	0.78	0.63
7	α-Carotene monoepoxide	0.92	0.92	0.91
8	β-Carotene monoepoxide	0.92	0.90	0.91
9	β-Carotene diepoxide	0.91	0.90	0.91
10	Lutein epoxide	0.46	0.58	0.47
11	Antheraxanthin	0.45	0.55	0.47
12	Violaxanthin	0.41	0.46	0.44
13	Cycloviolaxanthin	0.58	0.74	0.77
14	Cucurbitaxanthin A	0.50	0.72	0.63
15	Capsanthin 3,6-epoxide	0.43	0.61	0.55
16	Capsanthin	0.38	0.60	0.44
17	Capsanthin 5,6-epoxide	0.35	0.47	0.39
18	Capsorubin	0.32	0.42	0.38
19	Capsanthol (6′*R*)	0.25	0.26	0.23
20	Capsanthol (6′*S*)	0.38	0.68	0.49
21	5,6-Diepikarpoxanthin	0.35	0.36	0.39
22	6-Epikarpoxanthin	0.26	0.38	0.24
23	5,6-Diepilatoxanthin	0.36	0.45	0.33
24	5,6-Diepicapsokarpoxanthin	0.28	0.30	0.30

Note: Mobile phase 1: petroleum ether–acetone (6:4, v/v). Mobile phase 2: petroleum ether-tert-butanol (8:2, v/v). Mobile phase 3: methanol–benzene–ethyl acetate (5:75:25, v/v/v).
Source: Reprinted with permission from Planar Chromatogr.—Mod, in TLC.[5]

capacity was commensurate with those of direct phase layers. The separation of 22 pigment fractions extracted from paprika powders on diatomaceous layers impregnated with paraffin oil, using mixtures of acetone–water, was reported and it was established that baseline separation of each fraction cannot be achieved in one run and at a single mobile-phase composition.[3]

Unconventional layers have also been employed in the TLC analysis of pigments of sour cherry and blueberry. Baseline separations were carried out on corn and rice starch layers in the *n*-butanol–glacial acetic acid–water–benzene (30:20:10:0.5, v/v) mobile phase.[4] A considerable number of carotenoid standards can be separated in one run as demonstrated in Table 1, showing the R_f values of carotenoids in various eluent systems.[5]

Pigment extracts either derived from one plant or one part of a plant generally contain a considerable number of fractions with highly different retention characteristics. The separation of these extracts cannot be successfully achieved by the traditional TLC techniques. Elution methods similar to gradient elution in high-performance liquid chromatography were developed to overcome this difficulty. Stepwise gradient elution can be carried out by introducing eluent fractions with increasing eluent strength to the layer without interrupting the separation process. In programmed multiple-gradient development, the plate is developed to different distances with mobile phases of decreasing elution strength.

The plate is first developed for a given distance with the eluent having the highest elution strength and then the plates are dried. Pigments with the lowest mobility are separated. Then, a new eluent with a lower elution strength is applied for the separation of pigments with a higher mobility. The procedure can be repeatedly employed up to 25 times using eluents with decreasing elution strength. The advantages of programed multiple development were exploited in the separation of complex plant extracts of *Radix rhei* and *Cortex frangulae*.[6] Due to the considerable number of pigment fractions in an extract, the identification of the individual pigments separated by TLC is extremely difficult. Pigments can be identified by spotting an authentic standard on the neighboring track; however, in the instance of natural pigment mixtures, authentic standards are generally not available.

Coupled spectroscopic methods such as TLC–UV (ultraviolet) and visible spectroscopy, TLC/MS, and TLC–FTIR (Fourier transform infrared) have been developed to overcome this difficulty.[7] Their future application in the TLC analysis of natural pigments will markedly increase the information content of this simple and interesting separation technique. The automation of the various steps of TLC analysis (sample application, automated developing chambers, TLC scanners, etc.) greatly increased the reliability of the method, making it suitable for official control and legislative purposes.[8]

REFERENCES

1. Andersen, O.M.; Francis, G.W. *Handbook of Thin-Layer Chromatography*; Sherma, J., Fried, B., Eds.; Marcel Dekker, Inc.: New York, 1996; 715–752.
2. Pothier, J. *Practical Thin-Layer Chromatography*; CRC Press: Boca Raton, FL, 1996; 33–49.
3. Cserháti, T.; Forgács, E.; Holló, J. J. Planar Chromatogr.-Mod. TLC **1998**, *6*, 472.
4. Perisic-Janjic, N.; Vujicic, B. J. Planar Chromatogr.-Mod. TLC **1998**, *10*, 447.
5. Deli, J. J. Planar Chromatogr.-Mod. TLC **1998**, *11*, 311.
6. Matysik, G. Modified programmed multiple gradient development (MGD) in the analysis of complex plant extracts. Chromatographia **1996**, *43* (1), 39.
7. Pastene, E.; Montes, M.; Vega, M. J. Planar Chromatogr.-Mod. TLC **1997**, *10*, 362.
8. Brockmann, R. Fleischwirtschaft **1998**, *78*, 143.

Natural Products: CE Analysis

Noh-Hong Myoung
Seoul Metropolitan Government, Institute of Health and Environment, Seoul, South Korea

INTRODUCTION

Natural products chemistry is a science that investigates the identification, metabolism, biosynthesis, distribution, and biological activity of various organic compounds derived from living things. It concerns, essentially, the separation, purification, and structural determination of each compound. It was not until the late 1700s that, in plants or animals, the separation of natural products was carried out; for example, tartaric acid was extracted from grapes, citric acid from lemons, and malic acid from the apple by Scheele, a pharmacist in Sweden. In the nineteenth century, most of the compounds, alkaloid, terpenoid, and glycoside, were first isolated in pure form and elucidated structurally, since morphine was extracted from opium by Serturner. In the twentieth century, natural products chemistry achieved a great promotion through development of micro element analysis and column chromatography, which allowed physiological activity materials in crude form to be isolated with ease. Natural products are the organic and inorganic compounds found in nature: in plants (leaves, roots, barks, rhizoma, flowers, and seeds), in marine organisms (plants, animals, and microbes), in the fungi found in highly diverse and sometimes extreme environments, and in soil.[1]

DISCUSSION

There are two major classes of natural products: primary and secondary metabolites. Primary metabolites are compounds that exist in all organisms and are involved in basal and vital metabolism (e.g., glucose, fatty acids, amino acids, etc.). Secondary metabolites, alkaloids, terpenoids, and flavonoids, are unique to a particular species and vary in their basic structures. Secondary metabolites are usually accumulated, as most of their end metabolites are in plants, but are excreted in animals and microorganisms and some of these are proven to have pharmacological and ecological significance.

The pharmaceutical industry, in its drug discovery efforts, has relied heavily on natural products. Not all natural products are bioactive; in fact, most have little or no measurable activity at all. Simple sugars, lipids, amino acids, flavonoids, and so forth are nature's essential building blocks, and measurements of their quantities are needed for the study of metabolism, disease processes, and aging. In today's public maketplace, there is a growing interest in the so-called crude drugs, where an increasing number of herbal products claimed as health aids, bodybuilding supplements, nutrients, vitamin supplements, cosmetics, and so forth are being sold.

In Asia, plants have been applied in various diseases and studied with their components for many years. For research of their components, at first, fresh plants are dried at low temperature, for short times, in well-ventilated places so as to minimize chemical change of components, and then they are extracted. They are generally finely ground and extracted first with an organic solvent, then by water, to remove the widest possible range of compounds, from the hydrophilic to the most hydrophobic. The solvent is then removed and the crude extracts are tested for biological activity. If they are found to be active, fractionation by a variety of chromatographic techniques is initiated. At each step, the fractions are reevaluated, and only those fractions in which bioactivity is increasing are fractionated further. Finally, a pure chemical and structural identity of the molecule is determined by a combination of nuclear magnetic resonance (NMR), infrared (IR), ultraviolet (UV), mass spectrometry (MS), x-ray crystallography, and other analytical tools. Once the structure and chemical properties of an active compound are known, quantitative and qualitative analytical methods are employed to detect and quantify it. Recently, the pharmacological significance of the crude drugs is highlighted in terms of the suitability of their medicinal value and low number of side effects. Most crude drugs are comprised of more than one component and their number is determined through the analysis of major components.

Although high-performance liquid chromatography (HPLC) and gas chromatography (GC) have been mainly applied in quantitative method of analysis, they have difficulty with simultaneous quantitative analysis of crude drugs and have problems concerning the instability of experimental conditions, poor reproducibility because of pretreatment of crude drugs, efficacy of columns, and delay of separation time. GC has a limitation that components must be volatile. HPLC requires longer times for simultaneous analysis of samples, although gradient could be used advantageously for shortening analysis times.

With capillary electrophoresis (CE), it is possible to carry out simultaneous quantitative analysis with small sample volumes (1–10 nl); the amount of solvent waste generated is in the order of 1–2 ml/day and requires much less analysis time, with outstanding resolution. CE may be able to resolve a component of interest more quickly and with less

effort invested in sample preparation than alternative techniques, because it can resolve neutral as well as ionic compounds using the same column in the same analytical run. Although CE is an excellent micro-analytical technique, its use in a preparative format is limited at the present time. CE in its capillary zone electrophorsis (CZE) and micellar electrokinetic chromatography (MEKC) formats allows the analyst to resolve both ionic and neutral compounds on the same column using simple buffers, with or without an organic modifier, a micelle, a cyclodextrin, or a mixture of all of these. The reproducibility of migration time is the factor requiring improvement with CE, as the longer the migration time is, the more the peak area increases.

The velocity of a solute in the capillary is determined by its electrophoretic mobility and electro-osmotic flow (EOF), which are affected by temperature, and which is influenced by the diameter and length of the capillary, its contents, concentration, and pH of running buffer, applied voltage, current, viscosity, and zeta-potential. The subtle variation of EOF is also a main factor in maintaining high reproducibility if CE is automated by the constant temperature of the capillary and running buffer with proper buffering capacity. However, it is difficult to keep the temperature constant, as EOF depends on the condition of the fused silica.

The zeta-potential present on the silica surface is changed by the cleaning, preconditioning, storage method, and use time. Therefore, it is important to keep the surface condition reproducible. Usually, herb drugs are made of several crude drugs, as extracts, powders, or pills. The components of herb drugs are so varied that their quality control is applied to just one or two of their index components. CE has been applied to the analytical study of various components ever since it was applied to individual components in glycyrrhizin of an herb drug by Iwagami in 1991.[2] Presently, new analysis methods that are combinations of MEKC have been developed for the distribution of samples in an interfacially active agent by Terabe. CZE is able to analyze components with and/or without electric charge.[3]

Micellar electrokinetic chromatography was originally developed for the separation of electrically neutral substances by capillary electrophoresis and has proven to be a highly efficient separation method for various kinds of analyte. Although various ionic substances can be separated by CE alone, the separation of many components in complex mixtures is not always succesful. For example, a number of drugs are ionic, but some of them are not easily separated by CE. MEKC has been shown to be a powerful technique for the separation of complex drug mixtures. Although most of these drugs can be separated by HPLC, MEKC usually gives a better resolution in shorter analysis times.

Compared to HPLC, CE is simpler, faster, more convenient, and has a higher resolution power, which is a necessity when analyzing complex multicomponent mixtures.

A literature search reveals that CE has been used for the analysis of widely different natural compounds from

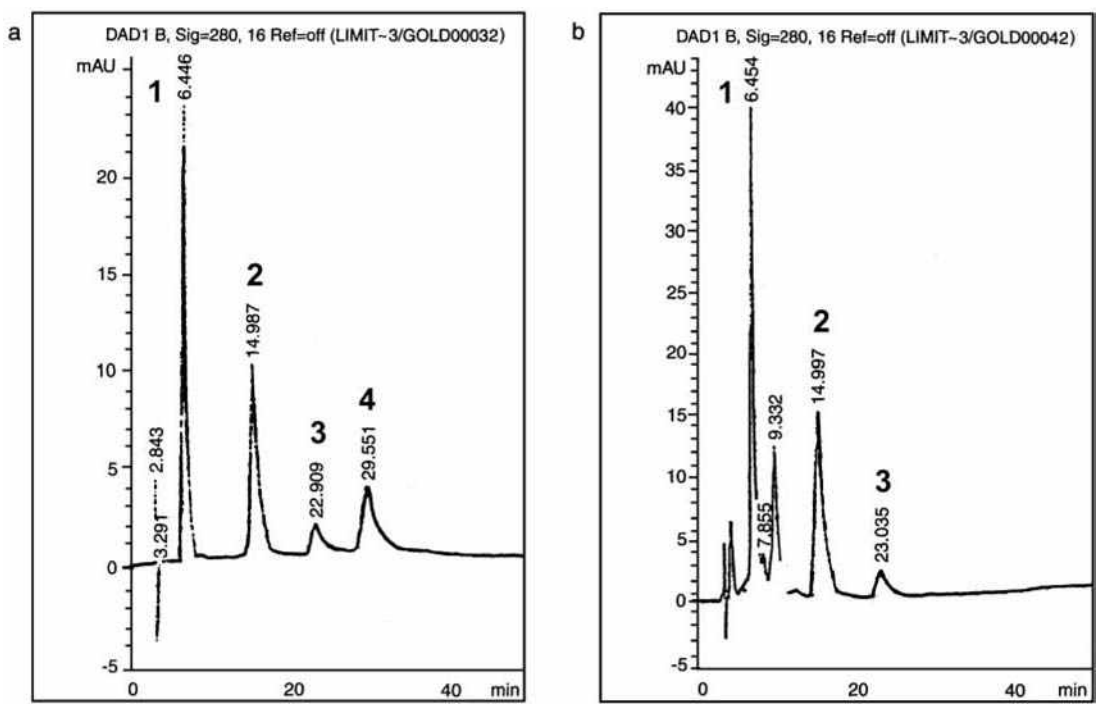

Fig. 1 HPLC chromatogram of standard mixtures (a) and a *Scutellaria radix* extract (b). *Key*: 1, baicalin; 2, baicalein; 3, wogonin; 4, chrysin.

extracts of leaves and needles, bark, roots, marine organisms, moss, soils, and so forth. To illustrate the problems associated with analyzing natural product extracts, especially from plant materials, by chromatography and to demonstrate how CE can overcome some of these problems as a consequence of its high resolving power, we compared the separation of an extract from the radix of the *Scutellaria baicalensis* Georgi by HPLC and CE. *Scutellaria radix* is the root of *Scutellaria baicalensis* Georgi. It is well known and is frequently used in oriental pharmaceutical preparations as a remedy for inflammation, suppurative dermatitis, allergic diseases, hyperlipidemia, and arteriosclerosis.[4]

Flavonoids are major components of *S. radix*, and about 40 kinds of flavonoids have been identified in it so far.[5] These flavonoids are known to have a broad range of physiological activities. The activities of baicalin, which is the main component, baicalein, and wogonin, in particular, have been investigated. From the results, it has been concluded that the most potent antiallergic material is baicalein, and the other flavonoids have low activities. Therefore, the quantitative analysis of individual flavonoids is important for evaluating the quality of *S. radix*. Figs. 1 and 2 show the HPLC chromatogram and CE electropherogram of a crude drug radix extract (*S. baicalensis* Georgi). These samples were obtained by first extracting with 50% ethanol. In the ethanol extract, many compounds are left. It is clear from Fig. 1 that HPLC is not the method of choice in this case. Important characteristics of an analytical procedure are sufficiently high precision and accuracy and also the time of analysis. Therefore, often it is not relevant in method development to simply maximize the resolution of the sample components without fulfilling the demands on analysis time. Decreasing the pH of the buffer leads to an increase in the degree of dissociation of baicalin, baicalein, wogonin, and chrysin. However, crude drugs have many components. As *S. radix* has about 40 kinds of flavonoid, it is very difficult to simultaneously separate baicalin, baicalein, wogonin, chrysin, and other flavonoids in a short time. Based on the dependence of the migration times and resolution on pH and phosphate buffer concentration (Fig. 2), it can be concluded that the most favorable electrolyte system is that with pH 7.0, 35 m*M* phosphate buffer. This

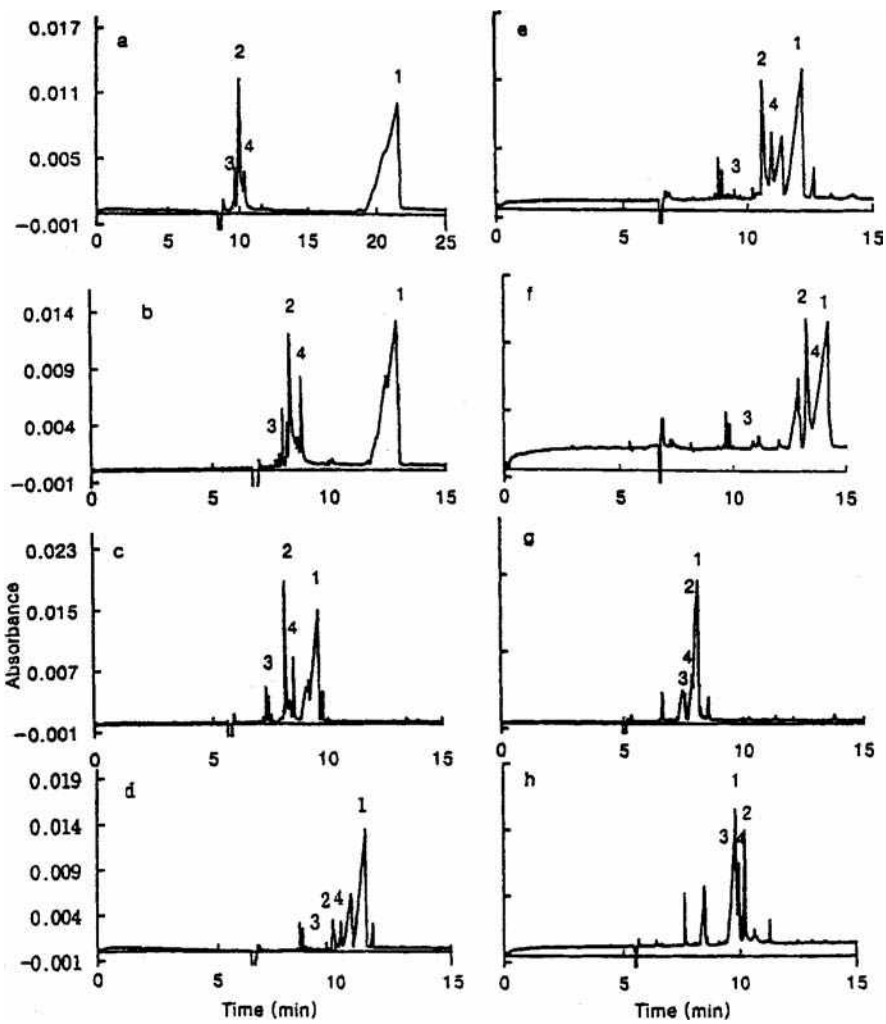

Fig. 2 Effect of running buffer pH and phosphate concentration on the separation of four components in the *Scutellaria radix* CE (1, baicalin; 2, bicalein; 3, chrysin; 4, wogonin). (a) pH 6.0 sodium citrate buffer (20 m*M*), (b) pH 6.5 sodium phosphate buffer (20 m*M*), (c) pH 7.0 sodium phosphate buffer (20 m*M*), (d) pH 7.0 sodium phosphate buffer (35 m*M*), (e) pH 7.0 sodium phosphate buffer (50 m*M*), (f) pH 7.0 sodium phosphate buffer (100 m*M*), (g) pH 7.5 sodium phosphate buffer (50 m*M*), (h) pH 8.0 sodium phosphate buffer (35 m*M*).

system was applied for the determination of baicalin, baicalein, wogonin, and chrysin in the extracts of *S. radix*. A typical HPLC chromatogram obtained from the extract of *S. radix* with a Korea Food and Drug Association (KFDA) regulation is shown in Fig. 1. Baicalin is not clearly distinguished from other components and the analysis time is greater than 35 min.

By comparing the records of Figs. 1 and 2 for the results of HPLC and CE analysis, it is seen that (a) CE provides higher sensitivity than HPLC and (b) the CE analysis time is shorter than HPLC.

CONCLUSIONS

The proposed method is well suited for the rapid and simultaneous determination of baicalin, baicalein, wogonin, and chrysin. The data presented in this report indicates that CE has application for crude drugs. The separation by CE is completed within 15 min and is much faster than HPLC. A comparision of the analysis time for both techniques is made. Resolution, recovery, and reproducibility for four flavonoids in *S. radix*, separated by CE, are greatly improved in crude drug analysis.

REFERENCES

1. Issaq, H.J. Capillary electrophoresis of natural products. Electrophoresis **1997**, *18*, 2438.
2. Iwagami, S.; Sawaba, Y.; Nakagawa, T. Micellar electrokinetic chromatography for the analysis of crude drugs. Determination of glycyrrhizin in oriental pharmaceutical preparations. Shoykugaku Zasshi **1991**, *45* (3), 233.
3. Terabe, S.; Otsuka, K.; Ichikawa, K.; Tsuchiya, A.; Ando, T. Electrokinetic separations with micellar solutions and open-tublar capillaries. Anal. Chem. **1984**, *56*, 111.
4. Lee, S.I.; An, D.G. *Natural Herb Products Sciences*; Young Lim Co.: Seoul, 1992; 178.
5. Yoon, H.S. Flavonoid components in plants of the Genus Scutellarin. Korean J. Pharmacogen. **1992**, *23*, 201.

Natural Rubber: GPC/SEC Analysis

Frederic Bonfils
C. Char
French Agricultural Research Center for International Development (CIRAD-CP), Montpellier, France

INTRODUCTION

Natural rubber (NR), produced from *Hevea brasiliensis*, a very high molar mass polymer, differs from most of its synthetic counterparts through its more complex structure, due to the interactions of non-isoprene compounds (proteins,[1] lipids[2]) with the polyisoprene chains. This "associative" structure is gradually destroyed, and partly when the polyisoprene is dissolved in a conventional solvent. However, in very many cases, a proportion of the NR remains insoluble in such solvents; this fraction is commonly called the gel phase or *macrogel*,[3] and is usually eliminated and quantified by centrifugation. The soluble fraction contains the polyisoprene macromolecules, and a variable quantity of microaggregates between 1 and 15 μm in diameter,[4] forming the *microgel*.

Numerous *Hevea* varieties, referred to as "clones" in professional jargon, can be found in estates. Subramaniam[5] was the first to study NR from different clone by size-exclusion chromatography (SEC) and to know about the native molar mass distribution (MMD_0). MMD_0 is the molar mass distribution of polyisoprene leaving the tree, without any treatments (drying, shearing) that could modify it. As we see later, MMD_0 is a very important clonal parameter for prediction of some properties of raw commercial NR.

This entry describes the different stages of NR analysis by SEC, concentrating on the points that distinguish NR from other more conventional polymers. The second part of the paper focuses on the evolution of macromolecular structure according to different agronomic or processing parameters.

SEC METHODOLOGY

Dissolving an Eluant

In most cases, tetrahydrofuran (THF) has been used as the mobile phase, except by Bartells et al.,[6] who used cyclohexane. However, using THF to analyze NR by SEC can raise certain problems.[7] As a general rule in our laboratory, the samples of NR are dissolved in cyclohexane (HPLC grade) stabilized with 2,6-di-*tert*-butyl-4-methylphenol (internal standard), at a rate of 60 mg for 30 ml of solvent. The solutions, stored at 30°C, are gently stirred for 1 hr periodically for 14 days.

Equipment

The equipment used consisted of a conventional SEC system [gas extractor, a pumping system, an injector, column(s), and detector(s)]. It is important to use a column oven. At room temperature, injecting NR solutions in SEC can block the columns. The oven temperature depends on the solvent used as the mobile phase. With cyclohexane, the oven temperature must be 65°C to overcome adsorption phenomenon due to the very low polarity of this solvent. When using THF, the oven is heated to 50°C.

Using columns with a porosity of 20 μm is also recommended, in order to shear at least the long chains of the polyisoprene.[8] As molar mass distribution (MMD) in NR is quite wide ($3 < I < 10$), the columns need to offer a considerable separation range.

As cyclohexane does not require an added stabilizer in the mobile phase, it means UV detection at 220 nm can be used. This is important as this type of detector is more sensitive than a refractometer. In fact, as NR is a polymer with a very high molecular weight, it is recommended that low-concentration solutions of maximum 0.2 mg/ml are injected, so as to overcome viscosity effects and avoid excessive shearing of the macromolecules.[9,8] Of course, a light scattering detector or a viscometer can be added to the system to access the branching rate.[10,11]

Calibration

Cyclohexane as the mobile phase requires the use of polyisoprene standards, as polystyrene standards are not soluble in this solvent. It should be noted that calibration by polystyrenes results in an overestimation of molar masses by a factor of around 2 compared to the use of polyisoprene standards.[12] It is therefore necessary to carry out universal calibration or convert molar masses using the Mark Houvink coefficients relative to synthetic or natural polyisoprene.[5,6,10,13,14]

Filtering the Solution Prior to Injection

The solution obtained after centrifugation is diluted to 0.2 mg/ml. It is left to stand for 24 hr and filtered through a disposable filter (glass fiber) with a porosity of 1 μm to eliminate the microgel. The filter porosity is very

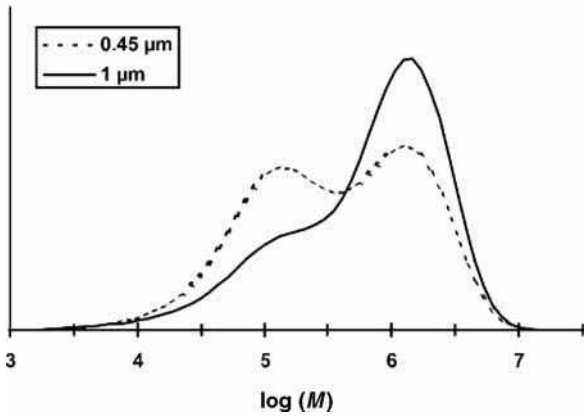

Fig. 1 Influence of the filter porosity on the molar mass distribution.

important, as the MMD observed after filtration through 0.45 or 1 µm is very different (Fig. 1). By filtering through 0.45 µm, shearing is considerable in the case of NR.

Macrogel Quantification

Once solubilization is complete, the solution is centrifuged (35,000 g—1 hr—17°C). The quantity of macrogel is determined by weighing the centrifugation residue after drying.

Microgel Quantification

The determination of microgel rate is possible by knowing the initial concentration of injected solution and the part eliminated by filtration. The latter can be determined from the polyisoprene peak area of the chromatogram.

Using UV detection with SEC, the Beer–Lambert law:

$$A = \varepsilon l C \tag{1}$$

with A being the absorbance, ε the molar extinction coefficient, l the cell length (cm), and C the concentration (mg/ml), implies that the area of the rubber peak, in a given chromatogram, is proportional to the concentration of the injected solution. For a given sample injected into the SEC apparatus, a calibration curve $S = f(C)$ (S is the area of the rubber peak and C is the concentration of the injected solution) gave the concentration of the solution after filtration. The calibration curve $S = f(C)$ is obtained from polyisoprene standards. Thus, the concentration of the solution was known before and after filtration, and the fraction eliminated by filtration, i.e., the percentage of microgel, could be determined.

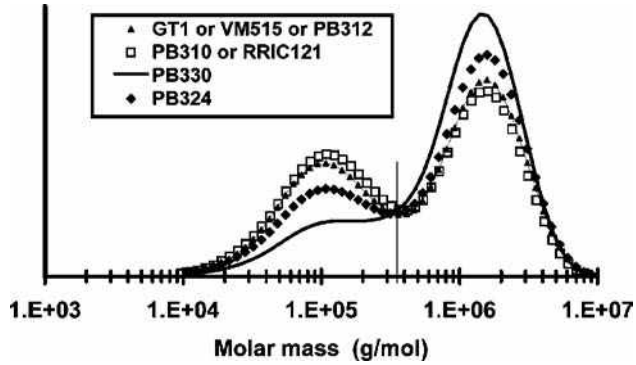

Fig. 2 Native molar mass distribution for different *Hevea* clones.

EVOLUTION OF MMD ACCORDING TO CLONALE ORIGIN OR PROCESSING

Natural rubber is a product of biological origin. This gives to it a structure particularly complex, and variable, according to agronomical parameters, as many polymers from natural origin. The main factor of influence is the *Hevea* clone from which the latex comes (Fig. 2). The MMD_0 show the presence of two main populations of variable relative amounts according to the clone: One of long chains (350–10,000 kg/mol, eq PI) and the other of short chains(10–350 kg/mol, eq PI). According to Angulo-Sanchez and Caballero-Mata,[10] the proportion of low molar masses would be principally linear macromolecules and the high molar masses would be mainly branched macromolecules. However, results of Tanaka, Kawahara, and Tangpakdee[2] allow to doubt this because after methanolysis of NR, a reaction that eliminates interactions involved in macrogel structuring, the bimodal distribution is maintained.

The MMD_0 is an important criterion to predict some properties of NR obtained after processing. The special

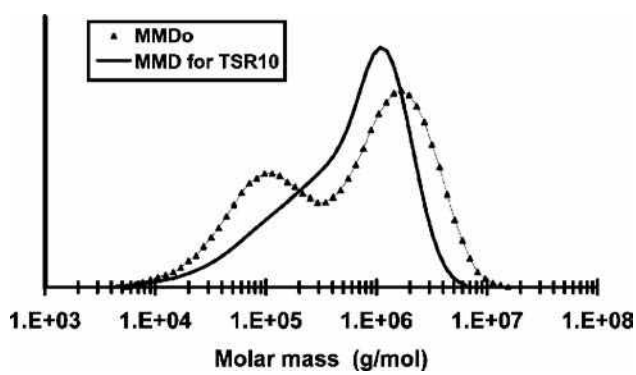

Fig. 3 Native molar mass distribution and molar mass distribution of TSR10 from clone PR107.

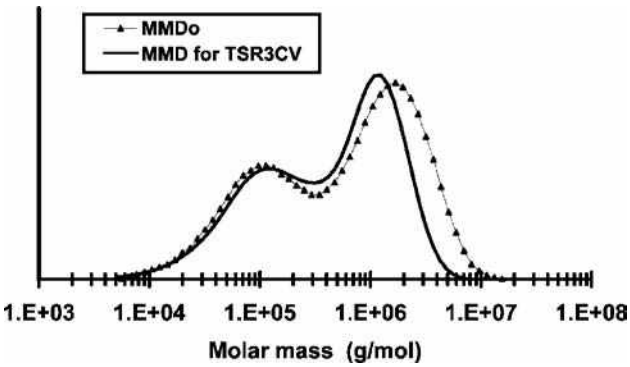

Fig. 4 Native molar mass distribution and molar mass distribution of TSR3CV from clone PR107.

feature of a MMD_0 "bimodal" or "unimodal with shoulder" will condition processed NR properties.[15] The natural coagulation of the latex and the maturation of the coagulum obtained (several days, commercial rubber type TSR10) will modify the macromolecular structure of NR. During these biological processes, the MMD of the dry processed NR lost the initial bimodal distribution of MMD_0 (Fig. 3). On the other hand, if the latex is stabilized with neutral hydroxylamine sulfate and coagulated with acid, with a minimum maturation of the coagulum (<16 hr, commercial rubber type TSR3CV), the bimodal distribution is maintained (Fig. 4).

CONCLUSIONS

Macromolecular structure of NR, as with any synthetic or natural polymers, needs to be known for several aspects (properties, biosynthesis mechanisms, etc.). SEC is probably still the best technique today but with certain obligations, especially the use of columns with high porosity (20 μm). SEC can be used not only for macromolecular analysis but also to determine microgel rate, an important parameter for NR.

REFERENCES

1. Grechanovskii, V.A.; Dmitrieva, I.P.; Zaitsev, N.B. Separation and preliminary characterisation of the protein component from commercial varieties of hevea rubber. Int. Polym. Sci. Technol. **1987**, *14*, 1–4.
2. Tanaka, Y.; Kawahara, S.; Tangpakdee, J. Structural characterization of natural rubber. Kautschuk und Gummi Kunststoff **1997**, *50*, 6–10.
3. Allen, P.W.; Bristow, G.M. The gel phase in natural rubber. Rubber Chem. Technol. **1963**, *36*, 1024–1034.
4. Voznyakovskii, A.P.; Dmitrieva, I.P.; Klyubin, V.V.; Tumanova, S.A. A dynamic light scattering study of natural rubber in solution. Polym. Sci. Ser. A, **1995**, *38*, 1153–1157.
5. Subramaniam, A. Gel permeation chromatography of natural rubber. Rubber Chem. Technol. **1972**, *45*, 346–358.
6. Bartells, H.; Hallensleben, M.L.; Pampus, G.; Scholz, G. Molar mass distribution determination of natural rubber and masticated natural rubber by gel permeation chromatography. Angew. Makromol. Chem. **1990**, *180*, 73.
7. Bonfils, F.; Sainte Beuve, J.; Laigneau, J.; Koman Achi, A.; Alledon, A.; Sylla, S. Steric exclusion chromatography study of natural rubber film prepared from fresh field latex. J. Nat. Rubber Res. **1995**, *10*, 143.
8. Parth, M.; Aust, N.; Lederer, K. SEC of ultra-high molar mass polymers: Optimization of experimental conditions to avoid molecular degradation in the case of narrow polystyrene standards. Int. J. Polym. Anal. Character. **2001**, *6*, 245–260.
9. Edwards, A. In *Natural Rubber Science and Technology*; Roberts, A.D., Ed.; Oxford University Press: London, 1988; 995–997.
10. Angulo-Sanchez, J.L.; Caballero-Mata, P. Longchain branching in natural hevea rubber: Determination by gel permeation chromatography. Rubber Chem. Technol. **1981**, *54*, 34.
11. Parth, M.; Aust, N.; Lederer, K. Distribution of molar mass and branching index of natural rubber from *Hevea brasiliensis* trees of different ages by SEC coupled with online viscometry. Macromol. Symp. **2002**, *181*, 447–455.
12. Swanson, C.L.; Carr, M.E.; Nielsen, H.C. Calibration of GPC columns for rubber analysis: Polystyrene vs. polyisoprene molecular weight standards. J. Polym. Mater. **1986**, *3*, 211–216.
13. Bhowmick, A.K.; Cho, J.; McArthur, A.; McIntyre, D. Influence of gel and molecular weight on the properties of natural rubber. Polymer **1986**, *27*, 1889.
14. Fuller, K.N.G.; Fulton, W.S. The influence of molecular weight distribution and branching on the relaxation behaviour of uncrosslinked natural rubber. Polymer **1990**, *31*, 609.
15. Bonfils, F.; Char, C.; Garnier, Y.; Sanago, A.; Sainte-Beuve, J. Inherent molar mass distribution of clones and properties of crumb natural rubber. J. Rubber Res. **2000**, *3*, 164–168.

Neuropeptides and Neuroproteins by CE

E.S.M. Lutz
Bioanalytical Chemistry Department, AstraZeneca R&D Mölndal, Mölndal, Sweden

INTRODUCTION

Neuropeptides comprise peptide neurotransmitters and neuromodulators occurring primarily in the central nervous system (CNS), but may also be found in peripheral tissues. In order to study their physiological effects and their role in a variety of physiological functions (e.g., sensory information, food intake control, regulation of hormone secretion, and control of the sleep–waking cycle), methods for accurate determination of neuropeptides in biological tissues and fluids are required. Typically, immunoassays are used for this purpose, but cross-reactivity, especially with unknown fragments and matrix components, compromises quantitative analysis. In addition, immunoassays are generally designed for a single analyte, whereas neuropeptide research regularly aims to separately determine several neuropeptides in the same sample. One approach to inducing selectivity and allowing multiple neuropeptide analysis is to employ high-performance separations such as capillary electrophoresis (CE) in combination with appropriate sample handling and sensitive detection.

CAPILLARY ELECTROPHORESIS OF NEUROPEPTIDES AND NEUROPROTEINS

Because peptides and proteins are zwitterionic substances whose charge can be controlled through the pH, CE is well suited to provide high-speed separations with high efficiency, good mass sensitivity, low sample consumption, and high resolution. Differences relative to CE of low-molecular-mass compounds are due to the larger size of peptides and proteins, their secondary and tertiary structures, and their tendency to interact with the wall of bare fusedsilica capillaries. This is valid for peptides and proteins occurring primarily in the CNS and for other peptide and protein analytes. For further reading, see the entry on Capillary Isoelectric Focusing of Peptides, Proteins, and Antibodies as well as to more extensive reviews (e.g., CE on opioid peptides by Lee et al).[1]

Briefly, CE of peptides and proteins is often performed in uncoated fused-silica capillaries. In order to reduce interactions with the wall and to ensure that all peptides and proteins are charged, a buffer with a low pH (e.g., 50 mmol/L phosphate pH 2.5) is commonly used. Consistent rinsing protocols are required between runs, such as 0.1 mol/L NaOH followed by rinsing with the running buffer in order to remove adsorbed contaminants. When such rinsing procedures are not in compliance with the total analytical system or when adsorption of the analyte and/or matrix components hampers analysis, coating of the capillaries may prove useful. Adsorption phenomena can also be influenced by pH adjustment, temperature control, or by adding ionic and non-ionic surfactants, organic solvents, or ion-pairing reagents to the running buffer. Both capillary coating and use of buffer additives affect the electro-osmotic flow leading to a reduction or a reversal of the flow, which, in turn, will affect the time required for separation.

Concentration sensitivities achieved in CE typically lie in the micromoles per liter or nanograms per liter range and are limited by sample loadability and detector path length (often 20–100 μm). Whether such concentration sensitivity is sufficient for a certain biochemical or pharmacological investigation depends primarily on the application. Complexity of the sample, concentration range of the analyte, and sample volume are all factors determining whether CE can be applied to analyze neuropeptides and neuroproteins in real-life samples. Plasma concentrations often are in the picomoles per liter range and can, accordingly, only be analyzed by CE after rigorous sample concentration. For instance, average concentrations of β-endorphin, methionin and leucine–enkephalin in 20 human plasma samples were determined to be 20 ng/ml, 2 ng/ml, and 2 ng/ml, respectively.[2] On the other hand, sampling of discrete areas in the brain can provide small samples with considerably higher concentrations of neuropeptides, and clear differences in concentrations may exist in the healthy and diseased states. For example, base levels of vasoactive intestinal peptide, substance P, and neuropeptide Y in nasal tissue of normal individuals are 28, 16, and 12 pg/μg protein, whereas patients suffering from allergy may have concentrations of 63, 165, and 98 pg/μg protein in perivascular lesion areas in the nasal tissue.[3]

Even though free-solution CE is most commonly used for neuropeptides and neuroproteins, other forms of CE have also been employed. For instance, as an alternative to conventional slab-gel electrophoresis, a method using sodium dodecyl sulfate (SDS) capillary gel electrophoresis was developed. It was applied to low-molecular-mass proteins (β-trace protein, β_2-microglobulin, φ-trace protein, and myelin basic protein) in cerebrospinal fluid.[4]

Advantageous features of capillary gel electrophoresis over slab-gel electrophoresis are compatibility with small sample volumes, shorter analysis times, and more accurate quantification of the analytes.

Generally, integration of sample collection, preparation, and introduction with the analytical separation and detection is decisive for successful application of CE to neuropeptide analysis; why both sample handling and detection will be discussed in this context.

SAMPLE HANDLING

Sample collection and preparation are crucial issues for any bioanalytical application in order to address the complexity of samples originating from biological tissues and fluids. It is necessary to cope with the lack in concentration sensitivity typical for capillary separation techniques, to avoid interference from matrix components as well as to ensure analyte stability. In peptide analysis, a strong focus exists on handling small-volume samples and on selective concentration of the analyte in order to overcome limitations with respect to loadability. In addition, loss of analyte frequently occurs due to degradation by proteases and due to adsorption to surfaces, which accordingly needs to be minimized.

In brain research, microdialysis sampling employing a miniaturized dialysis unit (probe) containing a dialysis membrane of a few millimeters length has become popular. The probe is implanted into the tissue or organ of the test animal and is infused with an isotonic solution (typically at 0.5–25 μl/min). A steady-state osmotic flux across the membrane removes molecules with a mass below the cutoff of the membrane from the extracellular matrix. Microdialysis yields relatively clean samples of volumes in the range 20–100 μl. However, the recovery of neuropeptides can be as low as 0.5–15%, leading to a low neuropeptide concentration in the samples.[5,6]

Problems with recovery are avoided when sampling the extracellular brain tissue by means of a push–pull cannula. A push–pull cannula consists of two coaxial assembled hollow needles (cannulae) which are implanted into the brain. Artificial cerebrospinal fluid is infused through the inner cannula and withdrawn through the outer cannula.[5–8]

In addition, a whole-tissue sample can be taken by means of routine pathological biopsy. Tissue samples are typically homogenized under denaturating conditions (0.1 mol/L HCl), centrifuged, and the supernatant is then used for further analysis.[5] When of interest, even morphologically defined areas can be investigated after being isolated by means of microdissection prior to further sample treatment. For example, nasal tissue biopsies were taken and perivascular lesion tissue or normal tissue 5 mm from the lesion were isolated by means of microdissection preceding further analysis.[3]

As discussed in-depth elsewhere in this encyclopedia, sample composition is important with respect to peak efficiencies achieved in CE. When the sample has a lower conductivity than the running buffer, focusing occurs, which often is referred to as sample stacking. This is a convenient way of increasing concentration sensitivity 5–10-fold. However, when the sample has a higher conductivity than the running buffer, uneven migration of the analyte(s) and zone spreading will occur, resulting in lower concentration sensitivities. Biological samples therefore need to be desalted prior to submitting them to capillary electrophoretic separation.

Desalting of biological samples can be achieved with traditional sample preparation methods, including ultrafiltration, liquid–liquid extraction, and solidphase extraction (SPE). Sample preparation, especially of plasma samples, involves, most often, protein precipitation by means of an acid or an organic solvent (e.g., acetonitrile), followed by SPE. After evaporation of the eluate and reconstitution in the running buffer used for CE, [D-Pen^{2,5}]enkephalin was analyzed in rat serum in this way.[9] These traditional sample preparation methods usually include deproteination, which reduces the protease content of the sample and improves analyte stability. Another option to reduce peptide degradation during sample handling is to add a protease inhibitor (e.g., 1 m mol/L leupeptin).[3]

Even under ideal circumstances, samples that are ready for CE analysis are in the microliter range, whereas typical injection volumes in CE are a few nanoliters. In order to take full advantage of the sample, increased injection volumes without column overload are desirable and can be achieved by coupling (transient) isotachophoresis (ITP) to CE. During ITP, the concentration of the sample introduced into the capillary is adapted to the concentration of the leading buffer, thus focusing the sample in a discrete zone. A discontinuous buffer is used during ITP, and after a change in conditions, separation by capillary zone electrophoresis continues. On-column ITP enables focusing of 10–100 times higher injection volumes (100–1000 nl), but it is limited to the total volume of the analytical system.

Another approach to increase the loadability is to enrich the analyte at the capillary inlet by means of an adsorptive phase, as reviewed in detail in Ref.[10] Reversed-phase materials such as octadecyl-bonded silica have regularly been used in the form of membranes or column materials, thus, in principle, performing miniaturized SPE (μSPE) in-line with CE, allowing injections of 10–15 μl. More selective sample concentration is obtained when using antibodies or Fab fragments for coating the inner wall of the capillary inlet.[3,5]

Often a combination of techniques is used to achieve a sufficient concentration of the sample in combination with selective cleanup—for instance, a combination of microdialysis and immunoaffinity CE,[11] microdissection and SPE,[7] or microdialysis and μSPE.[12]

DETECTION

Detection of neuropeptides in CE is usually performed by ultraviolet (UV) absorbance, fluorescence and mass spectrometry (MS). UV absorbance is widely used for detection in CE, often at 214 nm, because it is inexpensive, robust, and widely available on commercial instruments. Typically, concentration sensitivities lie in the micromoles per liter range, as shown in an application starting from 2.5-ml lumbar cerebrospinal fluid, where detection limits of neuroproteins with UV absorbance detection at 214 nm between 5 and 10 μg/ml, corresponding to 0.1–1 μmol/L, were reported.[4] In order to address the lack of sensitivity achieved with UV absorbance detection, path lengths in the detection window have been increased threefold by means of the bubble cell and 10-fold by applying the so-called *z*-cell.

Tryptophan and tyrosine are intrinsic fluorophores that are present in many peptides, which then can be identified with fluorescence detection. However, most peptides have no native fluorescence, thus making derivatization a prerequisite for fluorescence detection. Derivatization has been described with naphthalene-2,3-dicarboxaldehyde-β-mercaptoethanol for determination of substance P and its metabolites,[6] fluorescamine,[5] and 5-carboxyfluorescein succinimidyl ester[8] for luteinizing hormone-releasing hormone (LHRH), neuropeptide Y, and β-endorphin. Kostel and Lunte[6] compared various postcolumn reactor designs, whereas Advis et al.[5,8] employed precolumn derivatization, among others. In order to improve sensitivity, laser light is frequently employed for exciting the fluorescent molecules referred to as laserinduced fluorescence (LIF) and provides a 500–1000 times improved sensitivity compared to UV detection.

Mass spectrometry is another detection technique widely used in neuropeptide analysis. Concentration sensitivities in CE/MS do not reach those obtained by CE/LIF; nevertheless, tedious derivatization procedures are avoided. In addition, CE/MS has proven to be a powerful tool for structure elucidation as illustrated by the investigation of the in vivo metabolic fate of peptide E by Caprioli's group.[12] After microdialysis and in-line SPE, neuropeptides migrating out of the electrophoresis capillary were deposited directly onto a precoated cellulose target used in matrix-assisted laser desorption–time of flight (MALDI–TOF) MS subsequently. Structural information is then obtained along with the mass of the peptide(s).

More extensive structural information is obtained when using MS-MS, where information on the peptide sequence can be extracted from the fragmentation pattern. So far, CE/MS-MS has predominantly been performed with electrospray ionization (ESI)-triple quadrupole and ESI-ion trap instruments, as reviewed in Ref.[13] The advent of ESI-TOF and ESI-quadrupole-TOF instruments is believed to have a strong impact on CE/MS. TOF instruments require an extremely short time to produce a full mass spectrum and are especially attractive as a detection device for a separation technique producing sharp peaks, as illustrated by the separation of three enkephalins in a time window of 6 sec with detection by means of ESI-TOF.[14]

CONCLUSIONS

In this entry, an overview is given over the implementation of CE in neuropeptide and neuroprotein analysis. So far, relatively few applications in biological matrices, including cerebrospinal fluid, plasma, and neural tissue, have been published; nevertheless, the potential of this approach has been demonstrated over the past years and the number of publications is growing steadily. Accordingly, it is expected that more research groups will be enticed to use CE for neuropeptide and neuroprotein analysis.

REFERENCES

1. Lee, H.G.; Desiderio, D.M. Analytical and preparative capillary zone electrophoresis of opioid peptides. Anal. Chim. Acta **1999**, *383*, 79–99.
2. Ban, E.; Kim, D.; Yoo, E.A.; Yoo, Y.S. Anal. Sci **1997**, *13*, 489.
3. Phillips, T.M. Determination of in situ tissue neuropeptides by capillary immunoelectrophoresis. Anal. Chim. Acta **1998**, *372*, 209–218.
4. Hiraoka, A.; Arato, T.; Tominaga, I.; Eguchi, N.; Oda, H.; Urade, Y. Analysis of low-molecular-mass proteins in cerebrospinal fluid by sodium dodecyl sulfate capillary gel electrophoresis. J. Chromatogr. B, **1997**, *697*, 141–147.
5. Advis, J.P.; Iqbal, K.; Malick, A.W.; Guzman, N.A. *Handbook of Endocrine Research Techniques*; Academic Press: San Diego, CA, 1993; 127.
6. Kostel, K.L.; Lunte, S.M. Evaluation of capillary electrophoresis with post-column derivatization and laser-induced fluorescence detection for the determination of substance P and its metabolites. J. Chromatogr. B, **1997**, *695*, 27–38.
7. Advis, J.P.; Hernandez, L.; Guzman, N.A. Peptide Res. **1989**, *2*, 389.
8. SungAe, S.P.; Hung, W.-L.; Schaufelberger, D.E.; Guzman, N.A.; Advis, J.P. *Methods in Molecular Biology, Neuropeptide Protocols*; Irvine, G.B., Williams, C.H., Eds.; Humana Press: Totowa, NJ, 1997; Vol. 73, 101.
9. Chen, C.; Jeffery, D.; Jorgenson, J.W.; Moseley, M.A.; Pollack, G.M. Sensitive analysis of [-Pen2,5]enkephalin in rat serum by capillary electrophoresis and laser-induced fluorescence detection. J. Chromatogr. B, **1997**, *697*, 149–162.
10. Tomlinson, A.J.; Bensson, L.M.; Guzman, N.A.; Naylor, S. Preconcentration and microreaction technology on-line with capillary electrophoresis. J. Chromatogr. A, **1996**, *744*, 3–15.

11. Phillips, T.M.; Kennedy, L.M.; De Fabo, E.C. Microdialysis-immunoaffinity capillary electrophoresis studies on neuropeptide-induced lymphocyte secretion. J. Chromatogr. B, **1997**, *697*, 101–109.
12. Zhang, H.; Stoeckli, M.; Andren, P.E.; Caprioli, R.M. Combining solid-phase preconcentration, capillary electrophoresis and off-line matrix-assisted laser desorption/ionization mass spectrometry: intracerebral metabolic processing of peptide E in vivo. J. Mass Spectrom. **1999**, *34* (4), 377–383.
13. Figeys, D.; Aebersold, R. High sensitivity analysis of proteins and peptides by capillary electrophoresis-tandem mass spectrometry: Recent developments in technology and applications. Electrophoresis **1998**, *19* (6), 885–892.
14. Lazar, I.M.; Lee, E.D.; Rockwood, A.L.; Lee, M.L. General considerations for optimizing a capillary electrophoresis-electrospray ionization time-of-flight mass spectrometry system. J. Chromatogr. A. **1998**, *829*, 279–288.

Neurotransmitter and Hormone Receptors: Affinity Chromatography Purification

Terry M. Phillips
Ultramicro Analytical Immunochemistry Resource (UAIR), DBEPS, ORS, OD, National Institutes of Health, Bethesda, Maryland, U.S.A.

INTRODUCTION

The isolation of membrane receptors has great application in a number of fields ranging from structural biochemistry to pharmacology and the medicinal sciences. Although many biochemical approaches to receptor purification are available, the application of affinity techniques holds perhaps the greatest promise. The use of selective receptor ligands promises isolation not only of a specific receptor but also possibly in a bioactive form. The use of immobilized receptor ligands often ensures that the integrity of the receptor structure is maintained during the isolation process due to protection of the receptor binding domains by the ligand itself. Additionally, receptors can be isolated either via a chromatographic system or by batch technology. The application of ligand-coated magnetic beads offers a quick and relatively simple approach to receptor isolation and its use is now becoming a standard approach.

AFFINITY LIGANDS

The application of biotinylated receptor substrates is a useful approach, incubating the biotinylated substrates with their specific receptors prior to isolation on an avidin-coated support.[1] In such cases, biotinylation with a cleavable reagent such as Sulfo-NHS-SS-biotin or NHS-Iminobiotin is essential for recovery of the isolated receptor. Alternatively, the receptor can be recovered by substrate competition.

One of the major drawbacks to the application of affinity techniques is the relative low molecular weight or small size of receptor ligands, which makes them difficult to immobilize. However, this factor has not stopped affinity procedures from being applied to the purification of a number of different receptors, although relatively little work has been reported on those involved in the processing of neurotransmitters, neuropeptides, and hormones.[2,3]

Ligands used to isolate neurotransmitter and hormone receptors have ranged from immobilized receptor substrates to immobilized antireceptor antibodies, the latter being used extensively in recent years. This marks the increased availability of specific monoclonal antibodies to specific receptors and/or receptor domains and the increasing popularity of solid-phase extraction techniques over more physicochemical ones. The use of antibodies also circumvents problems arising from the immobilization chemistry required to maintain not only the integrity of receptor ligands but also their correct orientation. The rise of molecular biological techniques has opened a new approach to studying receptor structure and function. Cloning and expression of recombinant receptors in bacterial, yeast, or insect cells allows the investigator to engineer the receptor structure as well as the quantity of materials available for study. This situation has also increased the use of antibodies for the isolation of these recombinant receptors from culture medium.[4]

DISCUSSION

Cosgrove et al.[5] described studies that isolated a recombinant ectodomain of the human insulin receptor using immobilized insulin as an affinity ligand for chromatographically isolating the receptor domain. The efficiency of this system was shown by close similarities between the isolated receptor domain and the native form isolated by physicochemical techniques. The process also allowed for the receptor to be isolated in a bioactive form, as shown by its ability to bind insulin with a K_d of approximately 2×10^{-9} M. Feng et al.[6] approached the isolation of a recombinant human estrogen α-receptor in a different manner. They used a sequential heparin and 17-β-estradiol–17-hemisuccinate–bovine serum albumin affinity chromatography system to first remove the majority of the contaminating materials in the culture medium, followed by selective binding of the receptor to its substrate. This approach easily isolated the receptor, yielding 100-fold purification of a bioactive receptor. Ohtaki et al.[7] employed a biotinylated substrate to isolate a recombinant human pituitary adenylate cyclase-activating polypeptide (PACAP) receptor expressed in both insect cells and Chinese hamster ovary cells. The biotinylated ligand was immobilized on an avidin-coated support, allowing the receptor to be isolated by affinity chromatography.

The use of immobilized antibodies is perhaps the most popular approach to receptor isolation. Andersen and Stevens[8] employed a combination of immobilized metal affinity and immunoaffinity chromatography to isolate a functional recombinant human D_{1A} dopamine receptor

expressed in *Saccharomyces cerevisiae*. This was achieved by engineering both a FLAG and a His6 tag to the C-terminus of the receptor. The histamine tag was used to perform a primary selection via metal affinity chromatography, while immobilized antibodies directed against the FLAG tag were used in the second purification step. In this way, a bioactive recombinant receptor could be isolated in a relatively pure form. Recombinant human β-1 thyroid hormone receptors were isolated using a one-step immunoaffinity chromatography procedure.[9] Antibodies directed against the receptor were immobilized to a suitable chromatographic support, enabling the recovery of a bioactive receptor capable of binding 3,3′,5-triiodo-L-thyronine with a $K_a = 2 \times 10^{-9}$ *M*.

Eckard, Beck-Sickinger, and Wieland[10] isolated a series of rhodopsin-like, G-protein-coupled neuropeptide Y receptors (Y1, Y2, Y4, and Y5) using immunoaffinity chromatography. Antibodies were raised against synthetic fragments of the second (E2) and third (E3) extracellular loops of the Y receptors and used to recover the receptors of interest. In a similar manner, murine glucocorticoid receptors have been isolated from a lymphoma cell line by immunoaffinity chromatography using an immobilized monoclonal antibody.[11] The antibody called BUGR-2 was coupled to protein A-coated Sepharose 4B beads and used in a chromatography system. Recovery of the bound receptors was achieved by epitope competition. This procedure released not only multiple receptors but also the heat shock proteins 70 and 90, suggesting that the murine receptor interacts with these proteins, which may act as chaperones under physiological conditions. Repa et al.[12] also employed immunoaffinity chromatography for the isolation of members of the steroid/thyroid hormone receptor superfamily. Isolation of recombinant retinoic acid receptors expressed in an insect cell line was achieved by immunoaffinity chromatography using a monoclonal antibody to the human γ-retinoic acid receptor. The immunoaffinity-purified receptor was found to be biochemically greater than 90% pure, as revealed by silver-stained electrophoretic gels, as well as functional, binding its ligand with a K_d of approximately 2 n*M*.

REFERENCES

1. Santos-Alvarez, J.; Sanchez-Margalet, V. Affinity purification of pancreastatin receptor–Gq/11 protein complex from rat liver membranes. Arch. Biochem. Biophys. **2000**, *378*, 151.
2. Azzi, A.; Brodbeck, U.; Zahler, P. *Membrane Proteins. A Laboratory Manual.* Springer-Verlag: New York, NY, 1981.
3. Venter, J.C. Evolution and structure of neurotransmitter receptors. Recept. Biochem. Methodol. **1984**, *4*, 117.
4. Liitti, S.; Matikainen, M.T.; Scheinin, M.; Glumoff, T.; Goldman, A. Immunoaffinity purification and reconstitution of human α_2-adrenergic receptor subtype C2 into phospholipid vesicles. Protein Expression Purif. **2001**, *22*, 1.
5. Cosgrove, L.; Lovrecz, G.O.; Verkuylen, A.; Cavaleri, L.; Black, L.A.; Bentley, J.D.; Howlett, G.J.; Gray, P.P.; Ward, C.W.; McKern, N.M. Purification and properties of insulin receptor ectodomain from large-scale mammalian cell culture. Protein Expression Purif. **1995**, *6*, 789.
6. Feng, W.; Graumann, K.; Hahn, R.; Jungbauer, A. Affinity chromatography of human estrogen receptor-α expressed in *Saccharomyces cerevisiae*: Combination of heparin- and 17β-estradiol-affinity chromatography. J. Chromatogr. A, **1999**, *852*, 161.
7. Ohtaki, T.; Ogi, K.; Masuda, Y.; Mitsuoka, K.; Fujiyoshi, Y.; Kitada, C.; Sawada, H.; Onda, H.; Fujino, M. Expression, purification, and reconstitution of receptor for pituitary adenylate cyclase-activating polypeptide. Large-scale purification of a functionally active G protein-coupled receptor produced in SF9 insect cells. J. Biol. Chem. **1998**, *273*, 15464.
8. Andersen, B.; Stevens, R.C. The human D_{1A} dopamine receptor: Heterologous expression in *Saccharomyces cerevisiae* and purification of the functional receptor. Protein Expression Purif. **1998**, *13*, 111.
9. Park, J.-B.; Ashizawa, K.; Parkinson, C.; Cheng, S.-y. One-step immunoaffinity purification of human β1 thyroid hormone receptor with DNA and hormone binding activity. J. Biochem. Biophys. Meth. **1993**, *27*, 95.
10. Eckard, C.P.; Beck-Sickinger, A.G.; Wieland, H.A. Comparison of antibodies directed against receptor segments of NPY-receptors. J. Recept. Signal Transduct. Res. **1999**, *19*, 379.
11. Powell, C.E.; Watson, C.S.; Gametchu, B. Immunoaffinity isolation of native membrane glucocorticoid receptors from S-49 mGR++ cells: biochemical characterization and interactions with hsp 70 and 90. Endocrine **1999**, *10*, 271.
12. Repa, J.J.; Berg, J.A.; Kaiser, M.E.; Hanson, K.K.; Strugnell, S.A.; Clagett-Dame, M. One-step immunoaffinity purification of recombinant human retinoic acid receptor γ*[1]. Protein Expression Purif. **1997**, *9*, 319.

Neurotransmitters: HPLC Analysis

Joseph J. Pesek
Maria T. Matyska
Department of Chemistry, San Jose State University, San Jose, California, U.S.A.

INTRODUCTION

High-performance liquid chromatography (HPLC) has proven to be a valuable tool for the analysis of many metabolically important compounds. Neurotransmitters represent a class of compounds that have physiological and clinical significance. Their analysis in biological samples has often been done by gas chromatography/mass spectroscopy but gas chromatography/mass spectrometry (GC/MS) is only possible after extraction and/or derivatization. Because many neurotransmitters lack a suitable chromophore for detection in the UV–Visible spectral range, analysis by HPLC most often utilizes other means, such as electrochemical methods. Mass spectroscopy is a particularly useful detection mode for neurotransmitters when combined with HPLC, since it provides both good sensitivity and positive identification of the analyte. Both electrospray and atmospheric pressure chemical ionization (APCI) have been used as ionization methods for the LC/MS analysis of several of these types of compounds.

APPLICATIONS OF NEUTOTRANSMITTER ANALYSIS BY HPLC

Electrochemical Detection

The absence of a sensitive chromophore for many neurotransmitters has led to the use of other types of detection for these compounds. Because of the presence of an amine functionality in these analytes, electrochemical detection (ECD) is a viable and sensitive approach. Numerous examples of such analyses exist in the literature and, until recently, it was the most frequently used detector for neurotransmitters. ECD is generally done in the amperometric mode where very small currents can be measured, owing to the presence of a low background signal. For example, extracts of biological tissue were analyzed by μHPLC under reversed phase conditions, 82.5 : 17.5 citrate buffer (pH 3.2)/acetonitrile, using a C_{18} stationary phase.[1] Currents were in the low nanoamp range and detection limits on the order of 10 ng/ml. Under similar pH conditions, with a mixed citrate/acetate buffer/methanol 85 : 15 mobile phase, neurotransmitters from rat brain tissue were also analyzed with a C_{18} column.[2]

In addition to standard amperometric analysis on conventional electrodes, several other options exist for ECD. Electrodes can be chemically modified to increase both selectivity and sensitivity for the analytes. Poly(para-aminobenzoic acid) (P-pABA) was used for the analysis of monoamines and their metabolites.[3] These types of neurotransmitters were detected in nerve cells using the P-pABA modified electrode. An example of a separation of these compounds using a C_{18} column and a 5 : 95 methanol/0.1 *M* phosphate buffer (pH 5.0) mobile phase is shown in Fig. 1, using both a modified and a bare carbon electrode for detection. Further improvements in sensitivity and selectivity can be obtained by combining chemically modified electrodes with other electrochemical modes of operation. Neurotransmitters in cerebrospinal fluid were detected after separation by HPLC using cyclic voltammetry and differential pulse voltammetry.[4] It was shown that linear responses of over three orders of magnitude were obtained in these modes with the chemically modified electrodes. Other coatings have included ion-exchange polymers and a gold colloid that included the protein glucose oxidase[5] with detection by differential pulse voltammetry. These electrodes were found to be suitable for monitoring separations of both neurotransmitters and glucose in rat brain tissue.

Mass Spectrometric Detection

Mass spectroscopy is rapidly becoming the universal detector of choice because of its excellent sensitivity and specificity in identifying analytes. Costs for MS detectors have dropped considerably and they are more affordable to a greater number of laboratories. Operation of mass spectrometers is more straightforward and interfaces to HPLC systems are more rugged. Thus, it is logical that an increasing number of studies, as well as established methods for neurotransmitters, utilized MS detection. The analysis (total ion chromatogram) of a four-component catecholamine mixture on two hydride-based stationary phases in the reversed phase mode is shown in Fig. 2.[6] The elution order on the two columns is the same, but with higher retention on the cholesterol column. The identity of each peak in the chromatogram was verified from the mass spectral data.

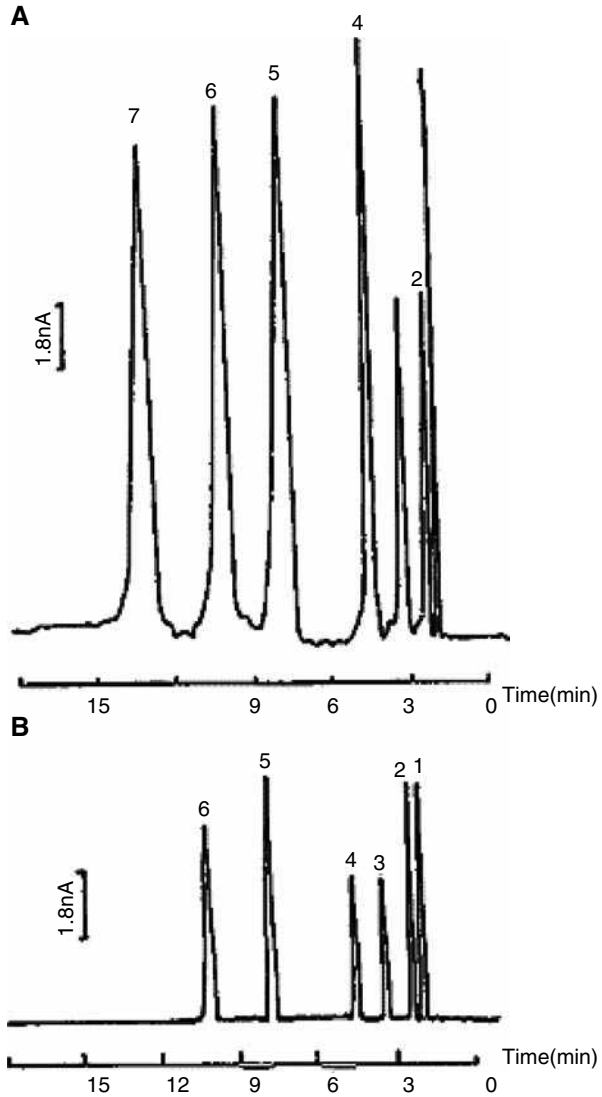

Fig. 1 Chromatograms of a standard solution of monoamine transmitters and their metabolites at (A) a poly(para-aminobenzoic acid) modified electrode and (B) a bare glassy carbon electrode. (1) Norepinephrine, (2) epinephrine, (3) dopamine, (4) 3,4-dihydroxyphenol acetic acid, (5) serotonin, (6) 5-hydroxyindole acetic acid, and (7) homovanillic acid.
Source: From Study on the effect of electromagnetic impulse on neurotransmitter metabolism in nerve cells by high performance liquid chromatography-electrochemical detection coupled with microdialysis, in Anal. Biochem.[3]

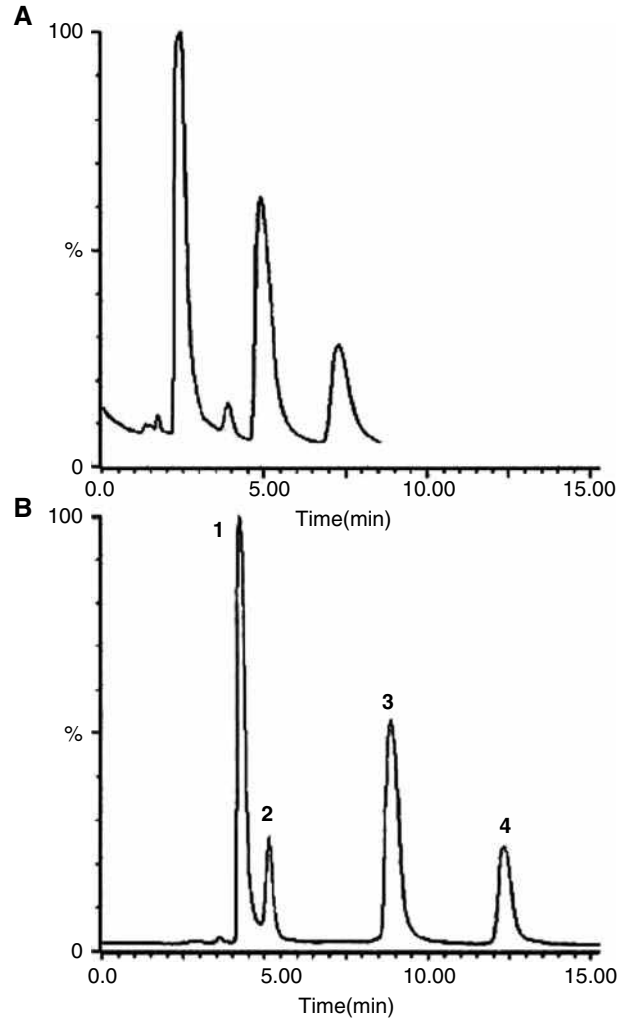

Fig. 2 Total ion chromatograms for the separation of a catecholamine mixture on (A) a hydride-based bidentate C_{18} column (15 cm × 4.6 mm) and (B) a hydride-based cholesterol column (7.5 cm × 4.6 mm). Mobile phase 5 : 95 acetonitrile/25 m*M* ammonium formate. Solutes: **1** = l-methyl-dopa (10 μg/ml); **2** = norepinephrine (3 μg/ml); **3** = epinephrine (10 μg/ml); **4** = dopamine (10 μg/ml).
Source: From Evaluation of hydride-based stationary phases for LC/MS, in Chromatographia.[6]

When trying to analyze more complex samples, the versatility, sensitivity, and the more extensive positive identification power of tandem mass spectroscopy (MS/MS) is increasingly being utilized for the analysis of neurotransmitters. These capabilities were highlighted for the measurement of several neurotransmitters and cocaine in brain fluids.[7] A rapid, sensitive, and positive identification method was developed for these analytes. The analysis of the target compounds was completed in 4 min and detection limits were in the pM range for the neurotransmitters and sub-pM for cocaine. A specific assay for the inhibitory neurotransmitter γ-aminobutyric acid was developed by a combination of HPLC and MS/MS.[8] The method encompassed a linear calibration curve of over two orders of magnitude and the detection limit was approximately a factor of 10 below the concentrations encountered in physiological samples. Similar LC/MS/MS methods have been, and are continuing to be, developed for many neurotransmitters using a variety of biological sources and preparative methods.

Other Detection Modes

Despite the apparent advantages of using electrochemical or mass spectroscopic methods of detection, other

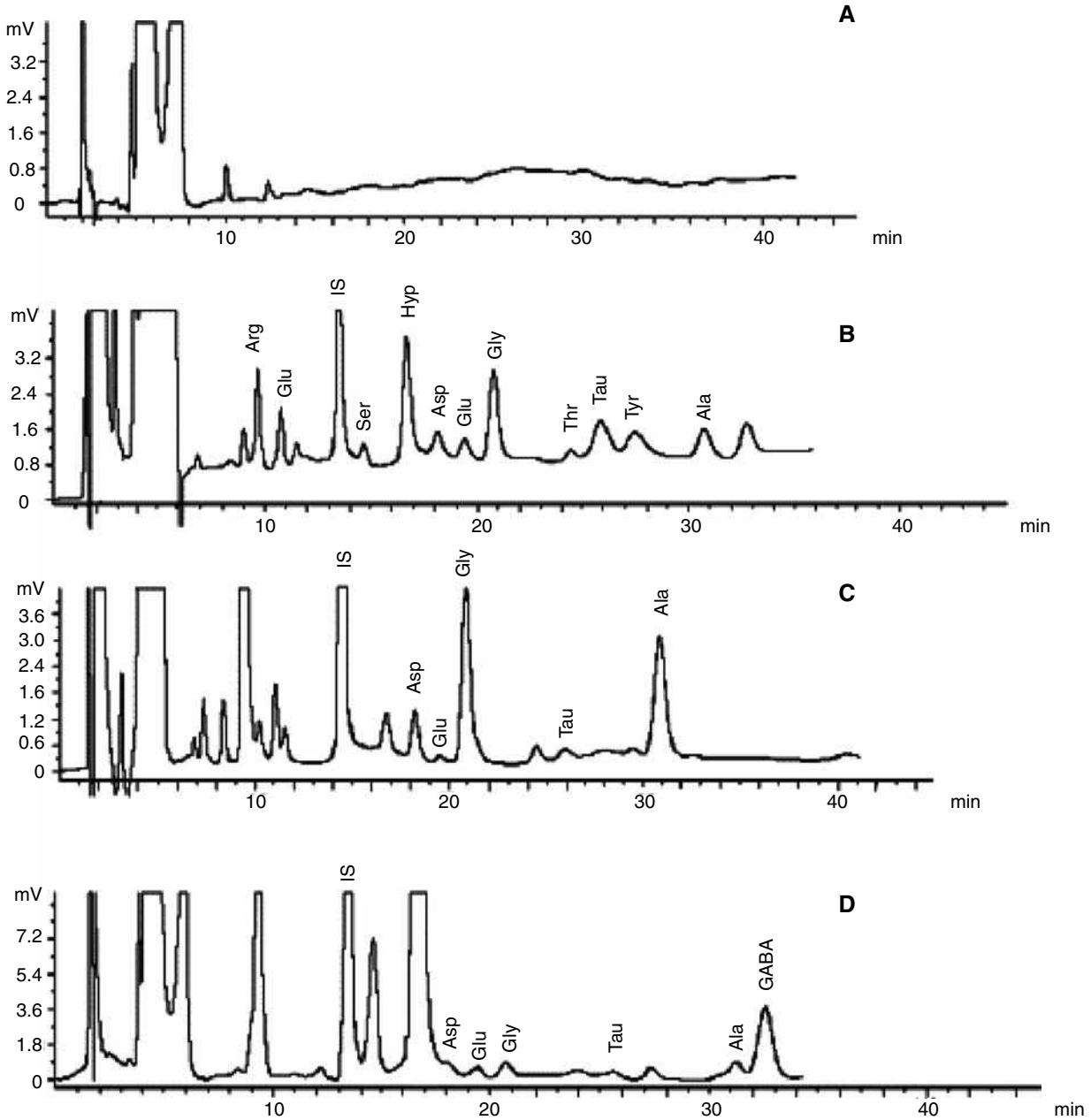

Fig. 3 HPLC separations of target amino acids: A, a blank (derivatization solution with no analyte); B, 12 amino acid standards (labeled) and the internal standard (IS); C, rabbit plasma sample; and D, rat brain sample. Experimental conditions: standards were roughly 45 ng of each amino acid in a 20 μl injection volume.
Source: From Optimization of dansyl derivatization and chromatographic conditions in the determination of neuroactive amino acids of biological samples, in Clin. Chim. Acta.[9]

approaches have been developed for those laboratories not possessing these types of equipment or, in some instances, for the specific analysis of a particular neurotransmitter. Similar to other types of analyses, improved detectablity and, hence, sensitivity is provided by derivatizing the analyte. Fluorescence spectroscopy is one mode of detection that is often used to improve sensitivity with respect to the more commonly used UV–Visible absorption technique. In the case of neurotransmitters based on amino acids, derivatization with dansyl chloride has been shown to be an effective means for determining these particular analytes.[9] Fig. 3 illustrates the separation of the derivatized amino acid standards, as well as target analytes in biological samples. Derivatization usually occurs before separation so that the HPLC properties of the target molecules are altered. In the case of dansyl modification of amino acids, the compounds become more hydrophobic and, hence, more amenable to

separation by reversed phase methods. Some derivatives, such as the dansyl moiety, allow a choice of either fluorescence or absorbance for detection.[9] In certain cases, specific reagents have been developed for targeted compounds in biological samples. One example is the use of *O*-phthaldialdehyde-mercaptoethanol derivatization for the analysis of glutamate and aspartate.[10] Depending on the reagent used and the desired analyte(s), the chromatographic method can be either isocratic[9] or gradient.[10] Other variables that must be considered in optimizing the method include choice of organic modifier, buffer, and pH. The latter is particularly important, since most of the neurotransmitters have ionizable groups, usually bases.

For physiological studies, it has been demonstrated that the use of radioactively labeled compounds can be used to follow the fate of a neurotransmitter and its metabolites. Dopamine metabolism can be elucidated through the use of a tritiated derivative, which was followed in vivo in rats.[11] The samples are extracted, from biological tissue by microdialysis and subsequently separated by standard HPLC methods (generally reversed phase on a C_{18}-bonded stationary phase). Detection of analytes via liquid scintillation measurement offers high sensitivity that, in most instances, is equal to or greater than that obtained from fluorescence spectroscopy or mass spectroscopy.

CONCLUSIONS

The analysis of neurotransmitters is a challenging and rapidly changing application area of HPLC. In most cases, conventional reversed phase methods are used for the separation aspect of the analysis. Because of the polar and, in many cases, basic character of these compounds, other options do exist, such as normal phase (organic and aqueous) and ion-exchange, which are also possible. The crucial feature in developing new methods for neurotransmitters often depends on the method of detection. Owing to the lack of strong chromophores in most neurotransmitters, conventional optical detection by UV–Visible absorption is usually not a viable option. Since the analysis of neurotransmitters often involves extracts from biological tissue or clinical samples, high sensitivity is an important criterion. Therefore, other methods of detection have been preferred, particularly for practical applications. Electrochemical methods and, more recently mass spectroscopy, have dominated method development for these compounds. In the case of ECD, the technique has high sensitivity with some selectivity. MS offers both high sensitivity and selectivity. Fluorescence spectroscopy and radiochemical methods are other options that can provide the sensitivity required for biological samples.

REFERENCES

1. Patel, B.A.; Arundell, M.; Parker, K.H.; Yeoman, M.S.; O'Hare, D. Simple and rapid determination of serotonin and catecholamines in biological tissue using high performance liquid chromatography with electrochemical detection. J. Chromatogr. B, **2005**, *818*, 269–276.
2. Kang, J.-S.; Mun, M.-S.; Shin, H.-S.; Lee, S.-C. The optimum conditions for the simultaneous determination of neurotransmitters in rat brain striatum by high performance liquid chromatography. Anal. Sci. Technol. **1995**, *8*, 215–220.
3. Xu, F.; Gao, M.; Wang, L.; Jin, L. Study on the effect of electromagnetic impulse on neurotransmitter metabolism in nerve cells by high performance liquid chromatography-electrochemical detection coupled with microdialysis. Anal. Biochem. **2002**, *307*, 33–39.
4. Zhang, W.; Wan, F.; Xie, Y.; Gu, J.; Wang, J.; Yamamoto, K.; Jin, L. Amperometric determination of (*R*)-salsolinol, (*R*)-*N*-methylsalsolinol and monoamine neurotransmitters with liquid chromatography using functionalized multiwall carbon nanotube modified electrode in Parkinson's patients cerebrospinal fluid. Anal. Chim. Acta **2004**, *512*, 207–214.
5. Zhang, W.; Cao, X.; Xie, Y.; Ai, S.; Jin, Y.; Jin, J. Simultaneous determination of the monoamine neurotransmitters and glucose in rat brain by microdialysis sampling coupled with liquid chromatography-dual electrochemical detection. J. Chromatogr. B, **2003**, *785*, 327–336.
6. Pesek, J.J.; Matyska, M.T.; Dalal, L. Evaluation of hydride-based stationary phases for LC/MS. Chromatographia **2005**, *62*, 595–601.
7. Hows, M.E.P.; Lacroix, L.; Heidbreder, C.; Organ, A.J.; Shah, A.J. High performance liquid chromatography/tandem mass spectrometric assay for the simultaneous measurement of dopamine, norepinephrine, 5-hydroxytryptamine and cocaine in biological samples. J. Neurosci. Meth. **2004**, *138*, 123–132.
8. Song, Y.; Shenwu, M.; Dhossche, D.M.; Liu, Y.-M. A capillary liquid chromatographic/tandem mass spectrometric method for the quantification of γ-aminobutyric acid in human plasma and cerebrospinal fluid. J. Chromatogr. B, **2005**, *814*, 295–302.
9. Kang, X.; Xiao, J.; Huang, X.; Gu, Z. Optimization of dansyl derivatization and chromatographic conditions in the determination of neuroactive amino acids of biological samples. Clin. Chim. Acta **2006**, *366*, 352–356.
10. Rabouan, S.; Olivier, J.C.; Guillemin, H.; Barthes, D. Validation of HPLC analysis of aspartate and glutamate neurotransmitters following *O*-phthaldiadehyde-mercaptoethanol derivatization. J. Liq. Chromatogr. Relat. Technol. **2003**, *26*, 1797–1808.
11. Niazi Shahabi, H.; Bergquist, F.; Nissbrandt, H. An investigation of dopaminergic metabolites in the striatum and in the substantia nigra in vivo utlizing radiolabeled L-DOPA and high performance liquid chromatography: A new approach in the search for transmitter metabolites. Neuroscience **2003**, *120*, 425–433.

Nitrofurans: HPLC Analysis

Mochammad Yuwono
Gunawan Indrayanto
Faculty of Pharmacy, Airlangga University, Surabaya, Indonesia

INTRODUCTION

Nitrofurans are a class of synthetic, broad-spectrum antibiotics which have been widely used in the form of feed additives for the prophylactic and therapeutic treatment of infections caused by bacteria and protozoa in food-producing animals, (e.g., cattle, pigs, poultry, cultured fish, and shrimps). Nitrofurans have also been used as animal growth stimulants, as well as for increasing egg production in layers.[1–3] The most common nitrofurans are furazolidone, furaltadone, nitrofurantoin, and nitrofurazone, which are characterized by the presence of a 5-nitro group. These drugs are rapidly metabolized by animals with in vivo half lives of a few hours, generating related metabolites that are stable during weeks as residues bound to tissue proteins. The metabolites of furazolidone, furaltadone, nitrofurantoin, and nitrofurazone are 3-amino-2-oxazolidinone (AOZ), 3-amino-5-methylmorpholino-2-oxazolidinone (AMOZ), 1-aminohydantoin (AH), and semicarbazide (SC), respectively (Fig. 1).

Furazolidone and its related compounds are used in human medicine for the treatment of urinary tract infections and gastrointestinal diseases. In veterinary practice, the use of nitrofurans can leave drug residues that can be found as contamination in foods of animal origin and in the environment. Residues of these drugs can cause serious health problems for humans, leading to increased drug resistance of microorganisms. Several reports have indicated that nitrofurans have a mutagenic effect, which has been observed in fungi, bacteria, and in submammalian systems. It has also been stated that furazolidone and AOZ, which is the main metabolite of furazolidone, are genotoxic and carcinogenic.[1,4] Therefore, nitrofurans have been banned for food-producing animals by the European Union, the United States, and some other countries. The EU Commission Decision of March 13, 2003 has set minimum required performance limits (MRPLs) at 1 μg/kg for each nitrofuran metabolite.[5]

Numerous analytical methods have been developed for the analysis of nitrofurans in various samples. These include microbiological,[6] thin-layer chromatography (TLC),[7,8] and high-performance liquid chromatography (HPLC) techniques. HPLC is the most widely used technique for determining nitrofurans of food sample origin, such as shrimps,[9] fish,[10] milk,[11] egg and chicken tissues,[12,13] honey,[14] plasma and urine,[15] and animal feeds.[16] One difficulty in the analyses of nitrofurans in biological samples is the complexities of the sample matrices. In addition, the use of nitrofurans in veterinary practice results in trace levels of the parent compound in edible products, due to a rapid metabolism of the compound in the animal. With HPLC techniques, it is possible to reduce interfering background peaks on chromatograms and increase specificity. The combination of HPLC separation and mass spectrometric (MS) detection is a valuable analytical technique that is increasingly being applied to identify nitrofuran in complex matrices, because it offers high sensitivity and selectivity in the analysis of nitrofurans based on its metabolites.

SAMPLE PREPARATION AND HPLC CONDITIONS

Several approaches to sample preparation for nitrofuran analysis have been reported, including using a single solvent to extract the analyte(s) from samples, followed by a single or several clean-up steps. The drugs have been extracted from samples primarily with acetonitrile, ethyl acetate, or dichlormethane. Liquid–liquid extraction using ethyl acetate, followed by evaporation and reconstitution in the mobile phase was reported by Muth et al.[15] for the determination of nitrofurantoin in plasma and urine. The reported recovery of nitrofurantoin was 84%–86% over the concentration range of 0.12–0.24 μg/ml. Hormazabal et al.[17] used acetonitrile for the extraction of furazolidone in meat tissues. The organic layer was separated and evaporated to dryness and then injected into the HPLC system. The recovery was reported to range from 97 to 100%. Liquid–liquid partition procedures are frequently applied as a clean-up step prior to solid–liquid partition using a column or cartridge. Solid phase extraction (SPE) with C_{18} cartridges is generally used in clean-up procedures, where they provide high recovery of the analyte(s). Degroodt et al.[10] reported a method for simultaneous determination of the nitrofuran derivatives furazolidone, furaltadone, nitrofurazone, and chloramphenicol residues in meat and fish. The samples were extracted with ethyl acetate, then purified with petroleum ether and *n*-pentane. The recoveries were reported in the range of 69–88%. A two-stage SPE clean-up was used by Cooper et al.[18] for the multi-residue determination of some veterinary drugs, including nitrofuran

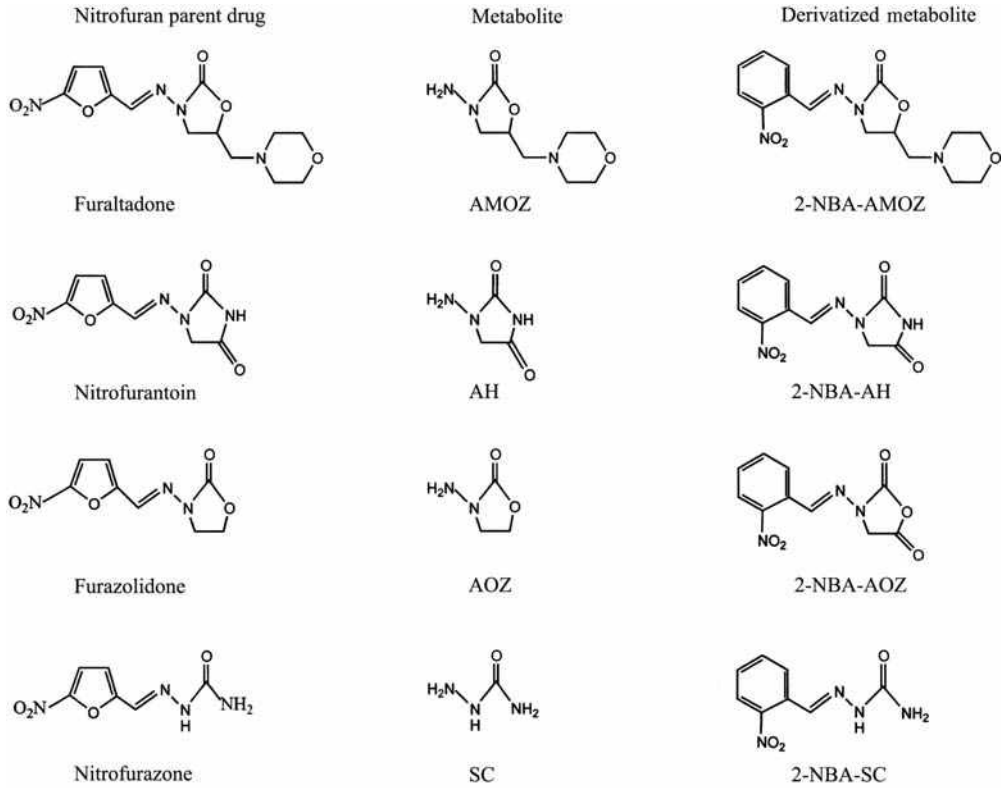

Fig. 1 Chemical structures of nitrofuran parent drug compounds, the metabolites, and their 2-NBA nitrophenyl derivatives.

derivatives, using C_{18} and silica cartridges. The proposed method was applied for screening pig kidney samples, achieving a limit detection of 2–18 μg/kg at recoveries of 40–70%. A one-step extraction/derivatization, followed by SPE clean-up using polymeric cartridges, was described by Edder et al.[9] for the analysis of nitrofuran metabolites in food. Gel permeation chromatography (GPC) has also been reported as the clean-up procedure for the determination of nitrofurans and their cyanometabolites, after liquid–liquid extraction with acetonitrile.[19]

The separations of nitrofurans have been carried out, in most instances, with a reversed phase (RP) column. As summarized in Table 1, C_{18} columns were selected as the analytical column for LC in most reports; however, the use of a C_8, CN, and cyanopropyl-modified silica analytical column has also been described. The parent compounds, as well as their metabolites, are satisfactorily separated by C_{18} columns with commonly used mobile phases, such as mixtures of acetonitrile with phosphate buffer, acetate buffer, or water. The mobile phase elution for HPLC analysis can be isocratic or as a gradient system. Acetonitrile-0.1 *M* aqueous solution of sodium perchlorate (28:72), with 0.5% glacial acetic acid, was reported by Galeano Diaz[20] as an optimum mobile phase for the separation of the three nitrofuran derivatives: nitrofurantoin, furazolidone, and furaltadone in milk. Lin et al.[16] used an acetonitrile gradient with an initial hold time of 1 min at 0% acetonitrile, followed by an increase to 50% acetonitrile over 10 min for the simultaneous separation of furazolidone, nitrofurazone, carbadox, olaquindox, and nitrovin in feed.

UV detection and diode-array detection (DAD) have been widely used, coupled to HPLC, for the analysis of the parent compounds of nitrofurans. The detection wavelengths of nitrofurans have been set at 368 nm,[19] 365 nm,[21] 360 nm,[10,22] 270 nm,[23] or at 254 nm.[24] An HPLC method, with electrochemical detection, has also been described for the monitoring of furazolidone and furaltadone hydrochloride in chicken tissues and eggs.[11]

Typical HPLC chromatograms and UV-spectra, obtained by injecting standard mixtures of nitrofurans (furazolidone, furaltadone, nitrofurazone, and nitrofurantoin) and standard mixtures of nitrofuran metabolites (AOZ, AMOZ, AH, and SC), are presented in Figs. 2 and 3, respectively. Fig. 4 shows a typical chromatogram and UV-spectra of standard mixtures of nitrofuran and its metabolites. Unfortunately, nitrofurantoin and furazolidone, as seen in Fig. 4, cannot be well separated. The optimization to separate the peaks at our laboratory is in progress.[25]

CONFIRMATION PROCEDURES

As described above, the nitrofurans used in veterinary practice are quickly metabolized by the animal,

Table 1 High-performance liquid chromatography (HPLC) conditions of the analysis of nitrofurans.

Column	Mobile phase	Detector	Substance	Refs.
Nova-Pak C_{18}	MeCN-0.1 *M* $NaClO_4$ + 0.5% HOAc (28:72)	ELCD	Nitrofurantoin, furazolidone, furaltadone in milk	[11]
C_{18}	MeCN–H_2O (1 m*M* NH_4OAc + 1% HOAc (50:50)	UV–DAD and MS	Nitrofurazone, furazolidone, furaltadone in egg	[13]
C_{18}	MeCN–HOAc/NaOAc 0.1 *M*, pH 3.2 (10:90)	UV 360 nm	Nitrofurantoin, furazolidone, furaltadone in milk feed formulation	[20]
Zorbax CN	Buffer 0.01 *M* NaOAc–MeOH (3:2)	UV 365 nm	Nitrofuran derivatives in animal substrates	[21]
C_{18}	A: 0.1 *M* NH_4OAc pH. 4.6; B: MeCN 100% A to 30% A in 8 min	UV 360 nm	Nitrofurazone, furazolidone, furaltadone in meat and lever poultry	[22]
Nova-Pak C_{18}	MeCN–Phosphate buffer	UV 254 nm	Furazolidone, berberine HCl, carbenoxolone Na in tablets	[24]
Cyanopropyl-modified silica	MeCN–Acetate buffer, pH 5 (20:30)	UV spectrometry	Nitrofurans derivatives from milk and meat	[26]
Luna C_{18}	MeCN-0.05 *M* NaH_2PO_4 gradient elution	UV DAD	Furazolidone and other antibacterial substances in chicken and swine	[27]
C_{18}	MeCN–Buffer pH 4.5 (15:85)	UV 230 nm	Furazolidone, metronidazole in tablets	[28]
Bondapack C_{18}	Water-MeCN-Triethyl amine (80:20:0.1)	UV 335 nm	Nitrofurazone, furazolidine, chloramphenicol in muscle, liver and kidney	[29]
C_{18}	Acetate buffer–MeCN (80:20)	UV DAD	Nitrofurans compounds	[30]
C_{18}	MeOH–Water–Buffer pH 3 (40:55:5)	UV 350 nm	Furazolidone, nefuroxime in dosage form	[31]
C_{18}	5 m*M* Oxalic acid–MeCN (55:45)	UV 265 nm	Furazolidone and other antibacterials in fish	[32]
C_{18}	H_3PO_4–MeCN (30:20)	UV 365 and DAD	Furazolidone in milk	[33]
C_{18}	Phosphate buffer (pH 4.5)-tetrahydrofuran (97:3)	UV 265 nm	Nitrofurantoin, nitrofurazone	[34]
C_{18}	0.5 mol/L KH_2PO_4 pH 4.3–4.4-MeOH (50:50)	UV 260, 289 nm	Salicylic acid, benzoic acid, resorcinol and nitrofurazone in powder	[35]
C_{18}	0.02 *M* sodium acetate buffer–MeCN (80:20)	370 nm	Nitrofurans, sulfonamides and chloramphenicol in milk	[36]
C_8	MeCN–H_2O–HOAc (3:97:1)	340 nm	Furazolidone, nitrofurantoin, carbadox, olaquindox, morantel in swine muscles	[37]

generating protein-bound metabolites that are detectable for several weeks after administration. Consequently, methods for the analysis of nitrofuran based on the parent drugs are inappropriate. Recently, the analysis of nitrofuran drug residues has been based on the detection of the protein-bound metabolites of their nitrofuran parents. Since the protein-bound metabolites cannot be separated from the tissue protein by liquid–liquid extraction, a hydrolysis step using aqueous hydrochloric acid is usually applied in the sample preparation to hydrolyze the metabolites from the tissue protein. After hydrolysis, it is also necessary to derivatize the nitrofuran metabolites, owing to their small molecular weights. For this purpose, the most commonly used derivatizing reagent is 2-nitrobenzaldehyde (2-NBA), which forms a nitrophenyl derivative (Fig. 1).

Particularly, in a residue analysis, identification of detected analytes is required to confirm a result. For nitrofurans analysis, there are a few confirmatory methods reported, including the use of the photodiode-array system and MS detection. The use of a photodiode array detector coupled to HPLC (HPLC–DAD) offers advantages that the target peak can be identified by its retention time and absorption spectrum. In this case, the continuous spectral data generated during the analysis are collected to check for interfering substances by comparing the spectra of samples with those of the standards. However, the specificity and the limit of detection are not sufficient to determine or identify

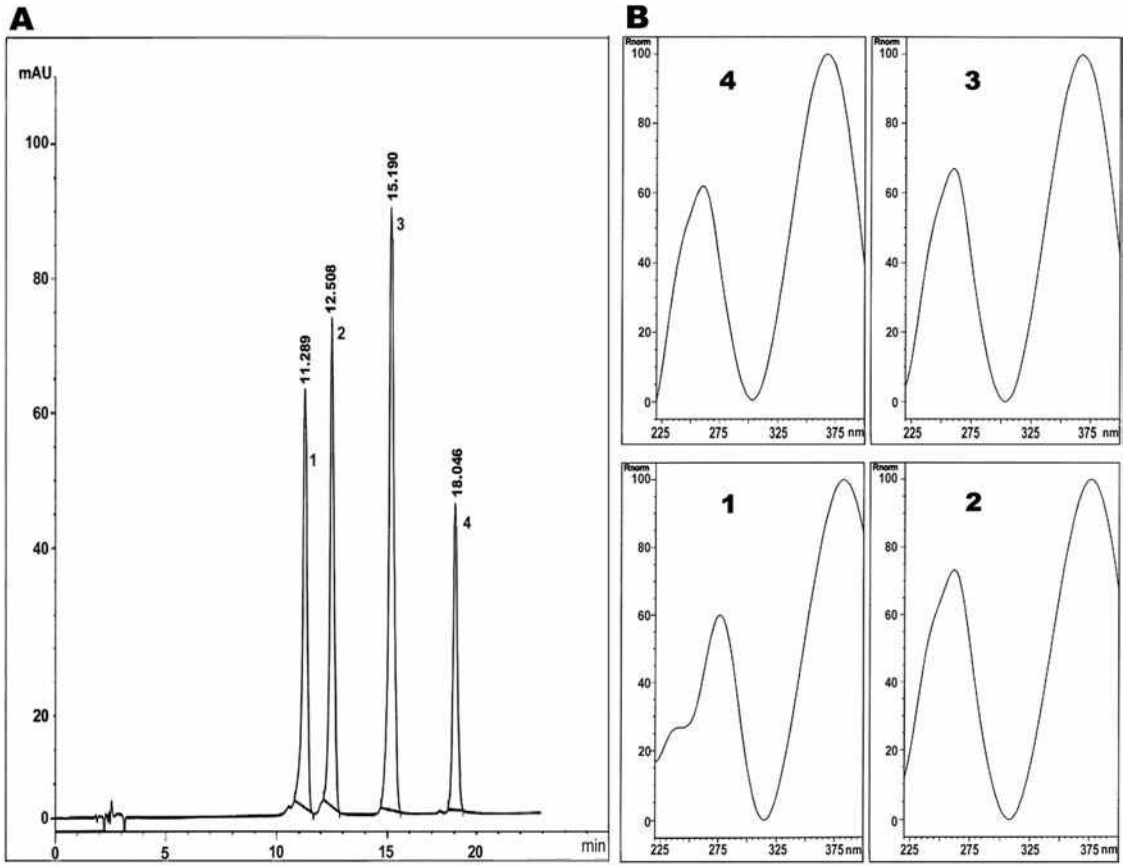

Fig. 2 High-performance liquid chromatography (HPLC) chromatograms (A) and UV-spectra (B) of standard mixtures of nitrofuran parent drugs nitrofurantoin (1), nitrofurazone (2), furazolidone (3), and furaltadone (4).

trace levels of the nitrofuran metabolites in samples. Considerable progress has been made recently in the detection of nitrofuran metabolites by the use of MS techniques[38] and tandem MS, owing to its high sensitivity and specificity. Draisci et al.[39] presented HPLC–DAD and HPLC–MS methods for the confirmation of the identities of nitrofurazone, furazolidone, and furaltadone residues. The HPLC–DAD limit of detection, based on a signal-to-noise ratio (S/N) of 3, was estimated to be 2.5 μg/kg for nitrofurazone and furazolidone and 5.0 μg/kg for furaltadone, whilst the HPLC–MS limits of detection were estimated to be 3.2, 1.6, and 1.0 μg/kg for nitrofurazone, furazolidone, and furaltadone, respectively. Recently, Leitner et al.[40] described a liquid chromatography-electrospray ionization tandem mass spectrometry (LC–ESIMS/MS) procedure for the simultaneous analysis of four nitrofuran metabolites in animal muscle tissues, at limit of detection of 0.5–5 ng/g. The bound metabolites are released from samples by acidic hydrolysis and subsequently derivatized using 2-NBA freshly prepared in DMSO. In this study, SC, as its 4-nitrobenzaldehyde derivative, was used as internal standard. Further sample preparation was improved by the use of SPE, leading to an effective sample clean-up with recoveries of 92–105%. Finzi et al.[41] proposed a similar LC–ESIMS/MS method that allows the simultaneous analysis of the metabolites of four commonly used nitrofuran drugs (AOZ, AMOZ, AH, and SC) in poultry muscle and eggs. The procedure involves an acid-catalyzed release of protein-bound metabolites, followed by their derivatization as described by Leitner et al.[40] A single step liquid–liquid extraction was performed for the sample clean-up before LC–MS/MS analysis. Two deuterated internal standards (AOZ-d4 and AMOZ-d5) were used during the study to mimic the analyte extraction. Limits of quantification of 0.5 ng/g were achieved using electrospray ionization in positive mode in an analytical run of 5 min. Mottier et al.[42] developed a confirmatory and quantitative method based on isotope dilution LC–ESIMS/MS for the determination of four nitrofuran metabolites in meat, e.g., furazolidone, furaltadone, nitrofurantoin, and nitrofurazone. Four isotope-labeled internal standards were used during this study. Liquid–liquid extraction and a polymeric SPE were carried out, after acid hydrolysis and derivatization into 2-NBA imine type derivatives. The method was fully validated following the European Union criteria and applied for monitoring nitrofuran residues in food. The author reported that the method is robust with decision limits ranged between 0.11 and 0.21 μg/kg.

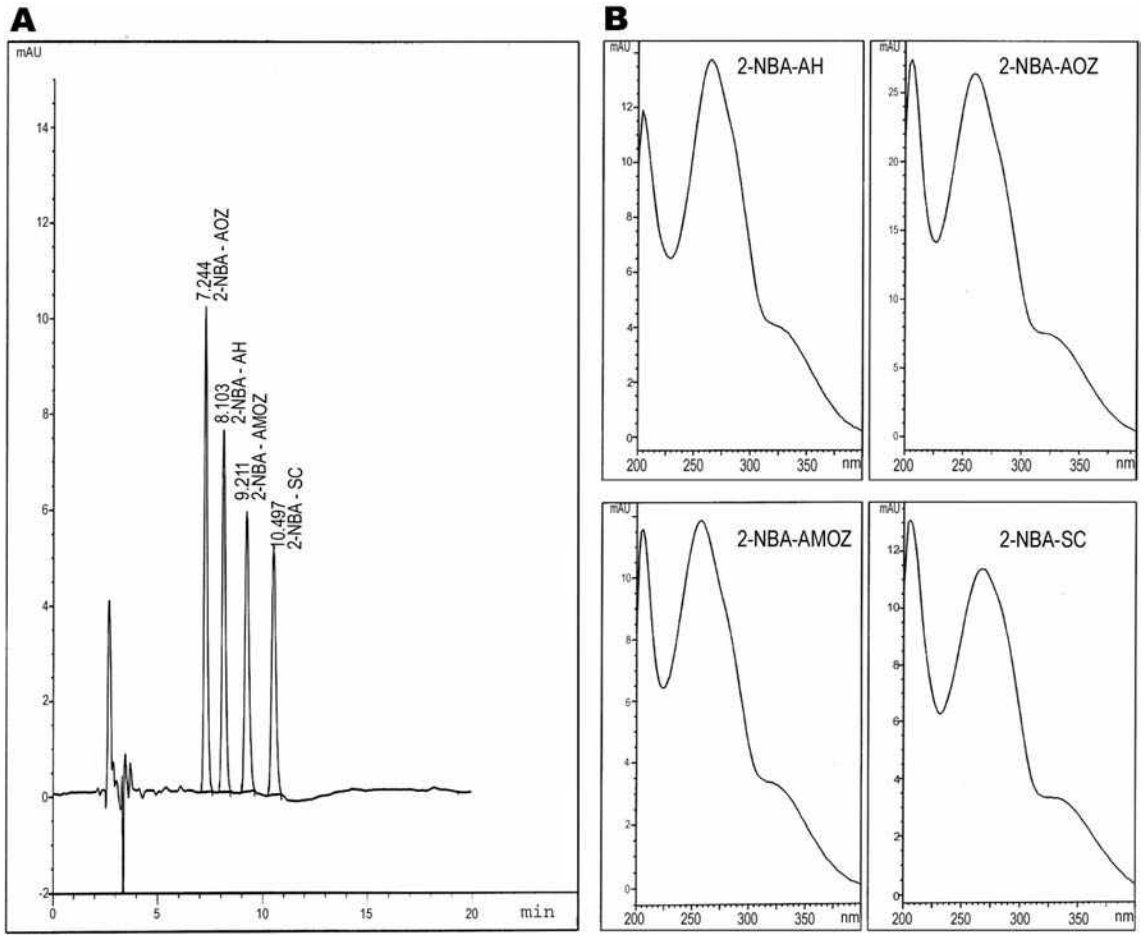

Fig. 3 High-performance liquid chromatography (HPLC) chromatograms (A) and UV-spectra (B) of standard mixtures of nitrofuran metabolites AOZ, AMOZ, SC, and AH after derivatization with 2-NBA.

CONCLUSIONS

High-performance liquid chromatography is the method of choice for the analysis of nitrofuran antibiotics furazolidone, furaltadone, nitrofurantoin, and nitrofurazone in food animal origin. The drugs are characterized by rapid metabolism, leading to trace levels of parent drugs found in samples. However, the metabolites (AOZ, AMOZ, AH, and SC), bound to protein tissues, are toxic and more stable within several weeks. Therefore, some authors have recently focused on the detection of protein-bound metabolites for the analysis of nitrofurans. For this purpose, LC–MS/MS is presently the most modern and promising method, due to its high sensitivity, reproducibility, and specificity.

ACKNOWLEDGMENTS

The authors wish to thank Prof. Dr. Rainer Ebel and Mr. Arnulf Diesel (Institute of Pharmaceutical Biology and Biotechnology, University of Düsseldorf, Germany) for the providing of recent references; DAAD (Deutscher Akademischer Austauschdienst), Bonn, Germany for the financial support during our short visit at some German universities in 2005; Ms. Nur Yanti S.Si, Apt and Mr. Fadjar Zulkarnaen Lubis (Assessment Service Unit, Faculty of Pharmacy Airlangga University, Surabaya-Indonesia) for the valuable technical assistance. Optimization of HPLC procedures for nitrofurans presented in this work is financed by the Indonesian Ministry of Education, DP2M through the research grant "Penelitian Hibah Bersaing XIV.1/2006."

REFERENCES

1. The European Agency for the Evaluation of Medicinal Products, Committee for Veterinary Medicinal Products. Furazolidone summary report at http://www.emea.europa.eu/pdfs/vet/mrls/Furazolidone.pdf. Accessed January 2006.
2. *United States Pharmacopoeia 28,* Rockville, MD: United States Pharmacopoeial Convention, Inc., 2005, 875, 1380–1384.

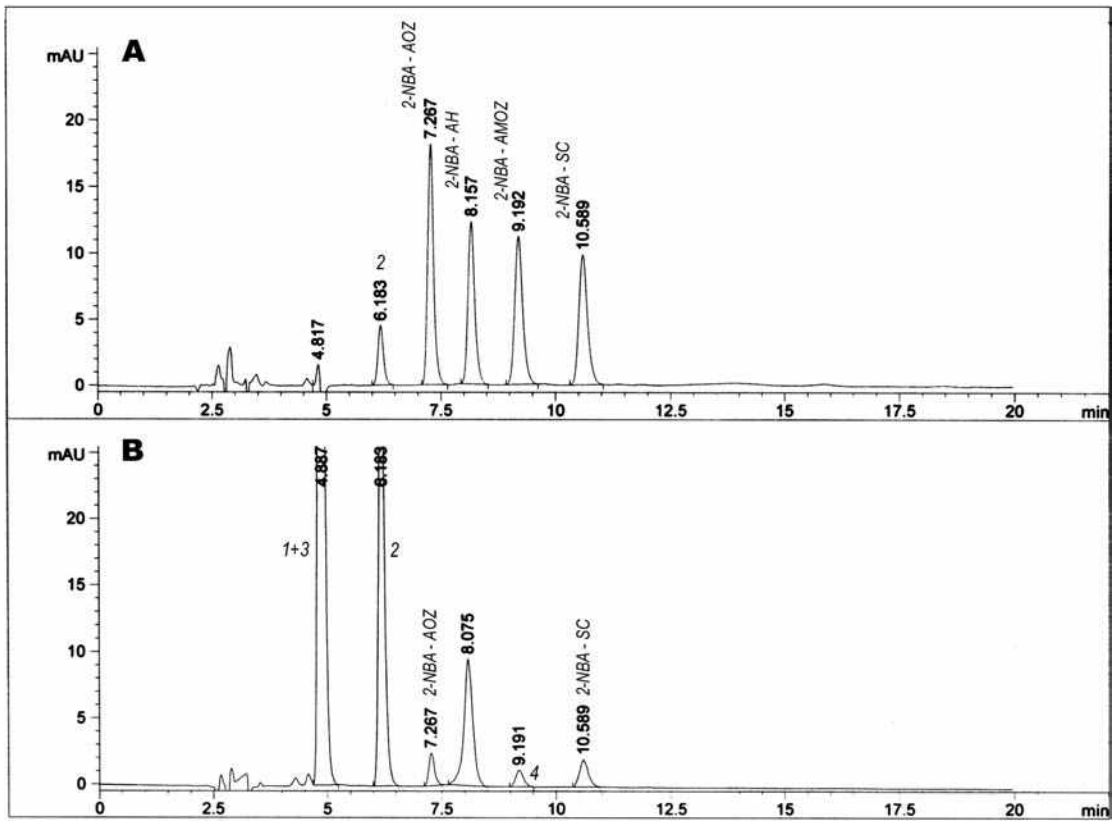

Fig. 4 High-performance liquid chromatography (HPLC) chromatograms and UV-spectra at 260 nm (A) and at 365 nm (B) obtained by injecting all standard mixtures of nitrofuran parent drugs and derivatized metabolites.

3. Alawi, M.A. Analysis of furazolidone and furaltadone in chicken tissues and eggs using modified HPLC/ELCD method. Fresenius Environ. Bull. **2000**, *9*, 508–514.
4. McCracken, R.J.; Kennedy, D.G. Bioavailability of residues of the furazolidone metabolite 3-amino-2-oxazolidinone in porcine tissues and the effects of cooking upon residue concentrations. Food Addit. Contam. **1997**, *14*, 507–513.
5. Commission Decision 2003/181/EC 13 March 2003, amending decision 2002/657/EC as regards the setting of minimum performance limits (MRPLs) for certain residues in food animal origin. Off. J. Eur. Commun. **2003**, *L71*, 17.
6. Franek, M.; Hruska, K. Antibody based methods for environmental and food analysis: A review. Vet. Med. Czech. **2005**, *50*, 1–10.
7. Kaniou, I.; Zachariadis, G.; Kalligas, G.; Tsoukali, H.; Stratis, J. Separation and determination of carbadox, nitrofurazone, nitrofurantoin, furazolidone, and furaltadone in their mixtures by thin layer and high performance liquid chromatography. J. Liq. Chromatogr. **1994**, *17*, 1385–1398.
8. Tendolkar, N.M.; Desai, B.S.; Gaudh, J.S.; Shinde, V.M. Simultaneous determination of tinidazole and furazolidone in suspension by HPTLC and HPLC. Anal. Lett. **1995**, *28*, 1641–1653.
9. Edder, P.; Vargas, S.; Ortelli, D.; Claude, C. Analysis of nitrofuran metabolites in food by high-performance liquid chromatography with tandem mass spectrometry detection. Clin. Chem. Lab. Med. **2003**, *41*, 1608–1614.
10. Degroodt, J.M.; Wyhowski de Bukanski, B.; De Groof, J.; Beernaert, H.; Srebrnik, S. Chloramphenicol and nitrofuran residue analysis by HPLC and photodiode array detection in meat and fish. J. Liq. Chromatogr. **1992**, *15*, 2355–2371.
11. Galeano Diaz, T.; Guibertau Cabanillas, A.; Acedo Valenzuela, M.I.; Salinas, C.A. Determination of nitrofurantoin, furazolidone and furaltadone in milk by high-performance liquid chromatography with electrochemical detection. J. Chromatogr. A, **1997**, *764*, 243–248.
12. Alawi, M.A. Determination of furazolidone and furaltadone in Jordanian local eggs using a modified HPLC method. Fresenius Environ. Bull. **1999**, *8*, 86–93.
13. Bellomonte, G.; Filesi, C.; Macri, A.; Mosca, M.; Sanzini, E. High-performance liquid chromatographic determination of nitrofurans and free chloramphenicol in poultry muscle, liver and eggs, Ital. J. Food Sci. **1993**, *5*, 247–253.
14. Khong, S.-P.; Gremaud, E.; Richoz, J.; et al. Analysis of matrix-bound nitrofuran residues in worldwide-originated honeys by isotope dilution high-performance liquid chromatography-tandem mass spectrometry. J. Agric. Food Chem. **2004**, *52*, 5309–5315.
15. Muth, P.; Metz, P.; Siems, B.; Bolten, W.W.; Vergin, H. Sensitive determination of nitrofurantoin in human plasma

and urine by high-performance liquid chromatography. J. Chromatogr. A, **1996**, *729*, 251–258.
16. Lin, S.-Y.; Jeng, S.-L. High-performance liquid chromatographic determination of carbadox, olaquindox, furazolidone, nitrofurazone, and nitrovin in feed. J. Food Prot. **2001**, *64*, 1231–1234.
17. Hormazabal, V.; Yndestad, M. Simple and rapid method of analysis for furazolidone in meat tissues by high-performance liquid chromatography. J. Liq. Chromatogr. **1995**, *18*, 1871–1877.
18. Cooper, A.D.; Creaser, C.S.; Farrington, W.H.H.; Tarbin, J.A.; Shearer, G. Development of multi-residue methodology for the HPLC determination of veterinary drugs in animal tissues. Food Addit. Contam. **1995**, *12*, 167–176.
19. Schmid, P.; Mooser, A.E.; Koch, H. Determination of nitrofuran derivatives and their cyanometabolites in the tissues of swine. Mitt. Gebiete Lebensm. Hyg. **1990**, *81*, 461–483.
20. Galeano Diaz, T.; Lopez Martinez, L.; Martinez Galera, M.; Salinas, F. Rapid determination of nitrofurantoin, furazolidone and furaltadone in formulations, feed and milk by high performance liquid chromatography. J. Liq. Chromatogr. A, **1994**, *17*, 457–475.
21. Laurensen, J.J.; Nouws, J.F.M. Simultaneous determination of nitrofuran derivatives in various animal substrates by high-performance liquid chromatography. J. Chromatogr. **1989**, *472*, 321–326.
22. Testa, C.; Calaresu, G.; Pulina, C. Simultaneous determination of nicarbazin, chloramphenicol, nitrofurazone, furazolidone, and furaltadone in meat and liver of poultry by HPLC. Boll. Chim. Igien. Parte Sci. **1991**, *42*, 335–342.
23. Pietsch, J.; Ricordel, D.; Imhof, L.; Trace analysis of veterinary chemotherapeutic residues in water by high-performance liquid chromatography. Vom. Wasser **1999**, *92*, 51–59.
24. Zhang, Y. Determination of furazolidone, carbenoxolone sodium and berberine hydrochloride in WeiKang tablets by reversed-phase high performance liquid chromatography (RP-HPLC). Sepu **2002**, *20*, 350–352.
25. Yuwono, M.; Rahman, A.; Indrayanto, G. Method validation for the analysis of nitrofuran residues in shrimps by HPLC–DAD, Penelitian Hibah Bersang XIV.1/2006. Research grant of Indonesian ministry of education, DP2M (unpublished result).
26. Petz, M. Method for determination of residues of furazolidone and four other nitrofurans in eggs, milk, and meat by HPLC. Deutsche Lebensmitt. Rund. **1982**, *78*, 396–401.
27. Kao, Y.-M.; Chang, M.-H.; Cheng, C.-C.; Chou, S.-S. Multiresidue determination of veterinary drugs in chicken and swine muscles by high performance liquid chromatography. J. Food Drug Anal. **2001**, *2*, 84–95.
28. Argekar, A.P.; Shah, S.J. A fast and accurate HPLC method for the simultaneous determination of metronidazole (MET) and furazolidone (FURA) in tablets. Indian Drugs **1998**, *35*, 71–74.
29. Gips, M.; Bridzy, M.; Barel, S.; Soback, S. A high performance liquid chromatography method for detection of chloramphenicol, nitrofurazone, and furazolidone residues in muscle, liver, and kidney. Residues Vet Drugs Food Proc. EuroResidue Conf. **1993**, *1*, 313–317.
30. Juszkiewicz, T.; Posyniak, A.; Semenjuk, S.; Niedzielska, J. Determination of 5-nitrofuran compounds in meat by high-performance thin layer and liquid chromatography. Residues Vet Drugs Food Proc. EuroResidues Conf. **1993**, *2*, 401–403.
31. Hassan, S.M.; Ibrahim, F.A.; Hefnawy, M.M. Simultaneous high-performance liquid chromatographic determination of furazolidone and nifuroxime in dosage forms. Anal. Lett. **1990**, *23*, 599–606.
32. Horie, M.; Saito, K.; Hoshino, Y.; Nose, N.; Nakazawa, H.; Yamane, Y. Simultaneous determination of residual synthetic antibacterials in fish by high-performance liquid chromatography. J. Chromatogr. A, **1991**, *538*, 484–491.
33. Long, A.R.; Hsieh, L.C.; Malbrough, M.S.; Short, C.R.; Barker, S.A. Method for the isolation and liquid chromatographic determination of furazolidone in milk. J. Agric. Food Chem. **1990**, *38*, 430–432.
34. Sun, T.; Ge, Z. Determination of related substances in nitrofurantoin by HPLC. Zhongguo Yiyao Gongye Zazhi **2003**, *34*, 28–30.
35. Ha, Y.; Kang, Z.; Liang, C.; Zhang, L.; Wang, C. Determination of salicylic acid, benzoic acid, resorcinol and nitrofurazone in Zujunqing powder by HPLC. Shenyang Yaoke Daxue Xuebao **2001**, *18*, 276–278.
36. Perez, N.; Guiterrez, R.; Noa, M.; Liquid chromatographic determination of multiple sulfonamides, nitrofurans, and chloramphenicol residues in pasteurized milk. J. AOAC Int. **2002**, *85*, 20–24.
37. Nagata, T.; Saeki, M. Simultaneous determination of five antibacterials in swine muscle by high performance liquid chromatography. J. Liq. Chromatogr. **1991**, *14*, 2551–2561.
38. McCracken, R.J.; Kennedy, D.G. Detetermination of the furazolidone metabolites, 3-amino-2-oxazolidinone, in porcine tissues using liquid chromatographic-thermospray mass spectrometry and the occurrence of residues in pigs produced in Northern Ireland. J. Chromatogr. B, **1997**, *691*, 87–94.
39. Draisci, R.; Giannetti, L.; Lucentini, L.; Determination of nitrofuran residues in avian eggs by liquid chromatography-UV photodiode array detection and confirmation by liquid chromatography-ionspray mass spectrometry. J. Chromatogr. A, **1997**, *777*, 201–211.
40. Leitner, A.; Zöllner, P.; Lindner, W. Determination of the metabolites of nitrofuran antibiotics in animal tissue by high-performance liquid chromatography-tandem mass spectrometry. J. Chromatogr. A, **2001**, *939*, 48–49.
41. Finzi, J.K; Donato, J.L.; Sucupira, M.; Nucci, G.D. Determination of nitrofuran metabolites in poultry muscle and eggs by liquid chromatography-tandem spectrometry. J. Chromatogr. B, **2005**, *824*, 30–35.
42. Mottier, P.; Khong, S.-P.; Gremaud, E.; Quantitative determination of four nitrofuran metabolites in meat by isotope dilution liquid chromatography-electrospray ionisation-tandem mass spectrometry. J. Chromatogr. A, **2005**, *1067*, 85–91.

Nitrogen Chemiluminescence: SFC Detection

William P. Farrell
Pfizer Global Research and Development, Pfizer Inc., La Jolla, California, U.S.A.

INTRODUCTION

Supercritical fluid chromatography (SFC) with nitrogen chemiluminescence detection (NCD or CLND) is a chromatographic technique that can be used to obtain quantitative results for nitrogen-containing analytes without the use of matching standards. For industries where sample throughput is an issue, such as combinatorial chemistry, SFC/NCD could reduce the need to isolate large numbers of standards and improve the speed of chromatographic characterization of synthetic reaction products. This entry will discuss the fundamental parameters that need to be considered to make SFC and NCD interfacing successful. Two other forms of nitrogen detection used with SFC will also be mentioned, but they fall outside the scope of this entry.

DISCUSSION

Supercritical fluid chromatography utilizes a compressed or dense gas as a mobile phase (i.e., carbon dioxide) and has been shown to be a powerful separation technique. The low viscosity and high diffusivity of supercritical fluids allow for the use of longer columns than in high-performance liquid chromatography (HPLC) without increasing runtimes. The increased number of theoretical plates available, combined with optimum linear velocities (μ_0) three to five times greater than in LC, can provide more separations per unit time. Berger has written a more detailed description of the functionality of packed column SFC.[1]

Supercritical fluid chromatography has some of the same characteristics of both HPLC and gas chromatography (GC). Packed column SFC uses the same column technology as HPLC, and when used with binary or tertiary solvents, has a broad range of applicability.[1] This range is much broader than GC, because compounds need not be volatile or thermally stable. As in GC, SFC can be coupled to most modern chromatographic detectors, such as element-specific detectors. These detectors are often very selective for the element under study, with detection limits below parts per billion.[1] Coupled to an SFC, an element-specific detector can become a powerful tool that offers selectivity, sensitivity, and speed.

Two other types of element-specific detector for nitrogen currently in use coupled to SFCs are the nitrogen phosphorus detector (NPD) and the thermal energy analyzer (TEA). The NPD uses a hot, catalytically active solid surface immersed in a layer of dissociated and to form electronegative N and P ions which are detected on a nearby electrode.[2] NPD has been shown to have broad application in SFC, especially in the agrochemical industry.[3] The TEA, as described by Fine et al.[4] uses low-temperature pyrolysis, followed by ozone-induced chemiluminescence, for the detection of compounds containing groups. The TEA has been used for the determination of tobacco-specific nitrosamines and explosives.[5] Both of these detectors require specific standards of the analytes of interest for quantitation.

The use of NCD, especially in pharmaceutical applications, have focused on exploiting the chemiluminescence properties of nitrogen dioxide (NO_2) formed from the high-temperature combustion of nitrogenous compounds.[6–8] This type of detector, originally developed for GC by Parks and Marietta,[9] forms nitric oxide followed by ozone-induced chemiluminescence. The reaction is characterized as follows:

$$\begin{aligned} R - N + O_2 &\rightarrow NO + \text{or other compounds} \\ NO + O_3 &\rightarrow NO_2{}^* + O_2 \\ NO_2{}^* &\rightarrow NO_2 + \text{light } (600 - 3200\,\text{nm}) \end{aligned} \quad (1)$$

Excited-state nitrogen-dioxide-mediated chemiluminescence occurs on a 1:1 molar ratio with solute nitrogen, provided that the combustion products form NO (and not). With complete combustion of the solute, the NCD can directly provide a quantitative measure of the amount of nitrogen in a chromatographic peak. This means that a single calibration curve using a stable nitrogen-containing compound can be used to quantify nitrogen content of any unknown peak in a chromatogram.[6] With a linear range of at least three orders of magnitude and picogram detection limits, SFC/CLND can provide an efficient technique for the quantification of nitrogen-containing compounds.[6]

The basic setup of a NCD system is shown in Fig. 1. In almost all cases, only a portion of the entire SFC mobile phase is diverted to the CLND detector using a fused-silica capillary or restrictor.[6–8,10,11] Use of a restrictor minimizes the effects of the SFC decompressed carbon dioxide (CO_2) and solvent composition on the pyrolysis reaction and chemiluminescence. The CO_2 flow rate, dictated largely by the SFC outlet pressure, can affect the residence time of the solute in the pyrolysis chamber and the

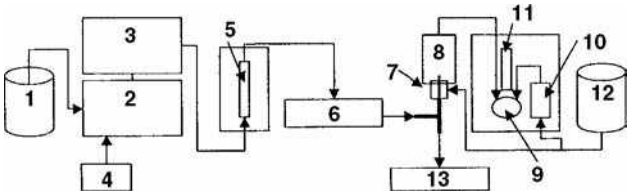

Fig. 1 Schematic diagram of SFC/CLND system: (1) CO_2 tank, (2) SFC pumping system, (3) autosampler, (4) modifier pump, (5) column, (6) UV detector, (7) pyrolysis inlet with linear restrictor, (8) pyrolysis chamber, (9) reaction cell, (10) ozone generator, (11) photomultiplier tube, (12) O_2 tank, (13) back-pressure regulator.

efficiency of the ozone reaction. The addition of modifiers to the SFC mobile phase (e.g., methanol) can compete for the available pyrolysis oxygen and can reduce signal response. High concentrations of modifier can dramatically affect the detection limits of some compounds.[7] Moreover, the sample concentration also appears to be limited by competition for oxygen, resulting in incomplete combustion.

The parameters that need special consideration for the successful coupling on an SFC to a CLND are restrictor position, ozone generation, combustion efficiency (temperature and oxygen flow rate), and quenching. Each of these will be discussed in detail.

RESTRICTOR POSITION

An important aspect for maintaining peak integrity using any split flow into a detector is the position of the restrictor tip relative to the detector source. Because SFC utilizes a gas under pressure, the rapid release of that pressure causes localized adiabatic cooling at the restrictor tip. On the other hand, at high temperatures, the mobile phase expands while the fluid density drops dramatically, resulting in precipitation of solutes at the end of the restrictor.[1] Careful attention to the restrictor placement should eliminate solute precipitation, maintain peak integrity, and provide sufficient mixing with oxygen for combustion. Several articles have discussed optimized placement of the restrictor for the Antek 705D CLND.[6,7,10] Inserting the restrictor beyond the inlet oxygen port to the pyrolysis chamber appears to provide both adequate solute nebulization and mixing prior to introduction into the furnace.[7]

OZONE GENERATION

Because ozone is very expensive to obtain in pure form and is quite unstable over long periods of time, CLND detectors utilize an ozone generator. Some of the oxygen flow is diverted over an electric arc to form ozone, which is then fed directly into the reaction cell. Because chemiluminescence occurs on a 1:1 molar ratio with NO, as described in Eq. 1, there must be excess ozone for chemiluminescence of NO independent of the other combustion products. Inlet oxygen flows of 5–10 ml/min appear to be adequate for most of the SFC/CLND experiments reported.[6,10,12]

COMBUSTION EFFICIENCY

Because detection is based on the formation of NO, the combustion conditions must be sufficient to completely convert the nitrogenous analytes to NO in the presence of mobile-phase modifiers. Temperatures ranging from 1050°C to 1100°C appear to provide the best environment for combustion. The amount of available oxygen for combustion is also highly dependent on the application. Table 1 outlines some of the conditions that have been reported. These conditions cover a wide range of mobile-phase flow rates (as decompressed CO_2) and modifier percentages. Shi et al. reported that too high an oxygen flow may reduce the residence time of the solute in the pyrolysis chamber and can negate any increase in combustion efficiency.[7]

QUENCHING

Nitrogen chemiluminescence takes place in a reaction cell, under vacuum, where the emitted light is measured using a photomultiplier tube. The primary combustion products from a methanol-modified SFC mobile phase are CO_2 and H_2O. Excessive CO_2 and water can increase the total number of colliding molecules in the reaction cell and reduce the signal. The addition of a membrane drier to selectively remove water has been shown to increase the detection limit of sulfamethazine by an order of magnitude.[11]

Table 1 Reported oxygen flow rates for several SFC/CLND applications.

CO_2 flow rate (ml/min)	Restrictor inner diameter (mm)	Modifier (%)	Oxygen flow (ml/min)	Refs.
3	0.025[a]	0	48	[5]
1200	0.025	8	185–200	[11]
600	0.075	10	50	[3]
150	0.075	15	50	[4]

[a]Open-tubular SFC.

Careful attention to the above-described parameters should allow for the successful interfacing of a CLND detector to an SFC system. Combining the separation efficiency of SFC with the specificity and sensitivity of CLND results in a powerful analytical technique for the quantification of nitrogenous solutes.

REFERENCES

1. Berger, T.A. *Packed Column SFC*; Royal Society of Chemistry: Cambridge, 1995.
2. Patterson, P. *Detectors for Capillary Chromatography*; John Wiley & Sons: New York, 1992; Chap. 7.
3. Berger, T.A. Feasibility of screening large aqueous samples for thermally unstable pesticides using high efficiency packed column supercritical fluid chromatography with multiple detectors. J. Chromatographia **1995**, *41* (7/8).
4. Fine, D.H.; Rufeh, F.; Gunther, B. A group specific procedure for the analysis of both volatile and nonvolatile N-nitroso compounds in pico gram amounts. Anal. Lett. **1973**, *6*, 731.
5. Francis, E.S.; Eatough, D.J.; Lee, M.L. Capillary supercritical fluid chromatography with nitro- and nitroso-specific-chemiluminescence detection. J. Microcol. Separ. **1994**, *6* (4), 395–401.
6. Shi, H.; Strode, J.T.B., III; Taylor, L.T.; Fujinari, E.M. Chemiluminescence nitrogen detection for packed-column supercritical fluid chromatography with methanol modified carbon dioxide. J. Chromatogr. A, **1997**, *757*, 183–191.
7. Shi, H.; Strode, J.T.B., III; Taylor, L.T.; Fujinari, E.M. Feasibility of supercritical fluid chromatography-chemiluminescent nitrogen detection with open tubular columns. J. Chromatogr. A, **1996**, *734*, 303–310.
8. Shi, H.; Strode, J.T.B., IIII; Taylor, L.T.; Fujinari, E.M. *Instrumental Methods in Food and Beverage Analysis*; Elsevier: Amsterdam, 1998.
9. Parks, R.E.; Marietta, R.L. Chemiluminescent nitrogen detection apparatus and method. U.S. Patent 4,018,562, October 24, 1975.
10. Strode, J.T.B., III; Loughlin, T.P.; Dowling, T.M.; Bicker, G.R. Packed-column supercritical fluid chromatography with chemiluminescent nitrogen detection at high carbon dioxide flow rates. J. Chromatogr. Sci. **1998**, *36*, 511–515.
11. Combs, M.T.; Ashraf-Khorassani, M.; Taylor, L.T. Optimization of chemiluminescent nitrogen detection for packed-column supercritical fluid chromatography with methanol-modified CO_2. Anal. Chem. **1997**, *69*, 3044–3048.
12. Shi, H.; Taylor, L.T.; Fujinari, E.M. Open-tubular supercritical fluid chromatography with simultaneous flame ionization and chemiluminescent nitrogen detection. J. High Resolut. Chromatogr. **1996**, *19* (4), 213–216.

Nitrogen/Phosphorus Detector

Raymond P.W. Scott
Scientific Detectors Ltd., Banbury, Oxfordshire, U.K.

INTRODUCTION

The nitrogen/phosphorus detector (NPD) is extremely sensitive [more so than the flame ionization detector (FID)] but is also highly selective. As its name suggests, it responds strongly to substances containing nitrogen and/or phosphorus. Physically, the design appears very similar to that of the FID but, in fact, operates on an entirely different principle. A diagram of an NPD detector is shown in Fig. 1.

DISCUSSION

The essential change that differentiates the NPD sensor from that of the FID is a rubidium or cesium bead contained inside a heater coil and situated close to the hydrogen flame. The bead, heated by a current through the coil, is situated above a jet, through which passes the helium carrier gas from the column mixed with hydrogen from a separate supply. If the detector is to respond to both nitrogen and phosphorus, then the hydrogen flow is arranged to be minimal so that the gas does not ignite at the jet. If the detector is to respond to phosphorus only, a large flow of hydrogen can be used and the mixture burned at the jet.

The detector functions in the following manner. The heated alkali bead emits electrons by thermionic emission, which are collected at the anode, providing a base current across the electrode system. When a solute that contains nitrogen or phosphorus is eluted, the partially combusted nitrogen and phosphorus materials are adsorbed on the surface of the bead. This adsorbed material *reduces* the work function of the surface and, as a consequence, the emission of electrons is increased, which *increases* the current collected at the anode. The sensitivity of the NPD is very high and only about an order of magnitude less than that of the electron capture detector ($\sim 10^{-12}$ g/ml for phosphorus and 10^{-11} g/ml for nitrogen).

A significant disadvantage of this type of detector is that its performance deteriorates gradually with time and eventually does not function at all. Reese[1] examined the performance of the NPD in great detail. The alkali salt employed as the bead is usually a silicate and Reese demonstrated that the loss in response was due to water vapor from the burning hydrogen converting the alkali silicate to the hydroxide and free silica. Unfortunately, at the normal operating temperature of the bead, the alkali hydroxide has a significant vapor pressure and, consequently, the rubidium or cesium is continually lost during the operation of the detector. Eventually, all the alkali is evaporated, leaving a bead of inactive silica. This is an inherent problem with all NPDs and, as a result, the bead needs to be replaced regularly if the detector is in continuous use. The detector can be made "linear" over three orders of magnitude, although no values for the response index appear to have been reported. Like the FID, it is relatively insensitive to pressure, flow rate, and temperature changes but is usually thermostatted at 260°C or above.

The specific nature of the NPD response to nitrogen and phosphorus, coupled with its relatively high sensitivity, makes it especially useful for the

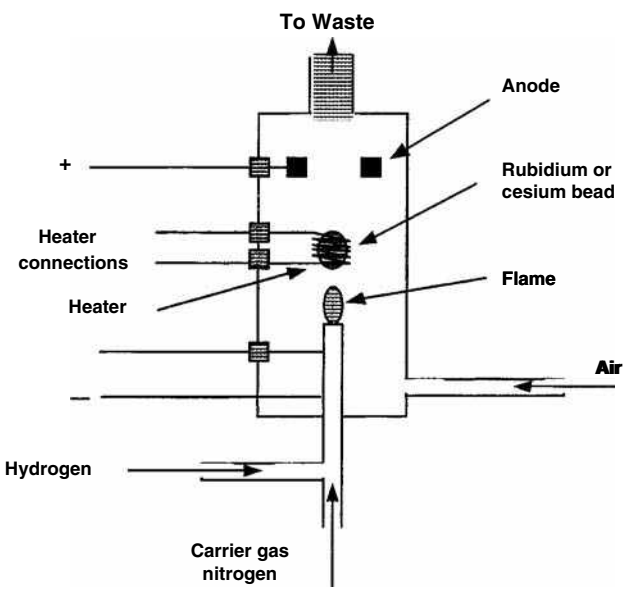

Fig. 1 The nitrogen/phosphorus detector.

analysis of many pharmaceuticals and, in particular, in environmental analyses of samples containing herbicides. Employing appropriate column systems, traces of herbicides at the 500 pg level can easily bedetermined. Virtually all the basic drugs presently employed in medicine contain nitrogen. Consequently, the specific detection of the NPD allows these drugs to be selectively monitored and quantitatively assayed, even when they are eluted among a large number of other unresolved compounds not containing nitrogen.

REFERENCE

1. Reese, C.H. *Ph.D. thesis*; University of London (Birkbeck College), 1992.

BIBLIOGRAPHY

1. Scott, R.P.W. *Chromatographic Detectors*; Marcel, Dekker, Inc.: New York, 1996.
2. Scott, R.P.W. *Introduction to Analytical Gas Chromatography*; Marcel Dekker, Inc.: New York, 1998.

Nonionic Surfactants: GPC/SEC Analysis

Ivan Gitsov
College of Environmental Science and Forestry, State University of New York, Syracuse, New York, U.S.A.

INTRODUCTION

Non-ionic surfactants are one of the most important and largest surfactant groups. They are amphiphilic molecules composed, in most cases, of poly(oxyethylene) blocks (PEO) as the water-soluble fragment and fatty alcohols, fatty acids, alkylated phenol derivatives, or various synthetic polymers as the hydrophobic part.[1] This class of surfactants is widely used as surface wetting agents, emulsifiers, detergents, phase-transfer agents, and solubilizers for diverse industrial and biomedical applications.[2] Several of them have been used for many years under different trade names: Brij (ethoxylated fatty alcohols), Synperonic (PEO copolymers) and Tween (ethoxylated sorbitan esters) by ICI Surfactants; Igepal (PEO copolymers) by Rhone-Poulenc, Rhodia; Pluronic [poly(oxyethylene)-*block*poly (oxypropylene) copolymers] by BASF; Triton DF (ethoxylated fatty alcohols) and Triton X (ethoxylated octylphenols) by Union Carbide; and others. The exploitation characteristics of non-ionic surfactants depend on the oligomer distribution, the molecular weight characteristics of the constituent blocks, and the hydrophilic/hydrophobic ratio of their chemical composition. Therefore, the quantitative determination of these factors is of primary importance for their performance evaluation.

DISCUSSION

Several high-performance liquid chromatography (HPLC) separation techniques have been used in combination with different detection methods to characterize poly(ethylene glycol)s and their amphiphilic derivatives.[3] SEC is a particularly attractive analytical tool for the investigation of non-ionic surfactants because it can provide information for their composition, molecular weight, and molecular-weight distribution along with their micellization in selective solvents. This entry will survey briefly both applications with major emphasis on the choice of the most appropriate eluent and stationary phase.

Molecular-weight determinations are performed in good solvents for both blocks of the PEO copolymers. The most widely used analysis conditions are as follows: eluents–tetrahydrofuran (THF) and chloroform (CHL); flow rate—1.0 ml/min; detection—differential refractive index (dRI) detector. The temperature interval is between 20°C and 40°C. The stationary phase is typically a polystyrene–divinylbenzene cross-linked matrix supplied by different vendors: Phenogel (Phenomenex, USA); PL Gel (Polymer Laboratories, U.K.), PSS Gel (Polymer Standards Service, Germany), TSKgel (tosoHaas, U.S.A.); Ultra Styragel (Waters Corporation, U.S.A.); and others. The pore size range of the column set should be adjusted to the molecular-weight range of the investigated materials. The SEC analysis in THF requires low-dRI response correction factors (1.66 for $M_n = 106$ and 1.00 for $M_n = 20{,}000$),[4] whereas the low-molecular-weight PEO derivatives are almost invisible in CHL. On the other side, the solubility of PEO in THF decreases with the molecular weight, as evidenced by steeper calibration curves and broadening of the peaks in the eluograms (Fig. 1). This complicates the precise molecular weight calculations of PEO copolymers and the choice of calibration standards becomes crucial.[5] The increasing content of PEO in the copolymer results in lower hydrodynamic volumes in THF and, consequently, yields lower apparent molecular weights, regardless of the macromolecular architecture of the analytes.[6–8] The problems with calibration mismatch can be avoided to some extent by using the universal calibration approach with online differential viscometry. This method provides accurate molecular-weight information for most linear and comb-graft PEO copolymers but has been proved less precise for copolymers with complex linear-dendritic or hyperbranched architecture. Online laser-light-scattering detection eliminates the need for a calibration curve and yields correct M_w values for macromolecules with molecular weights higher than 500 g/mol. The precision of the method depends largely on accurate *dndc* values that need to be measured for each copolymer investigated.

The self-assembly process of non-ionic surfactants in aqueous media differs in several aspects from the micellization of amphiphilic copolymers:

1. Micelles constructed of low-molecular-weight surfactants have much lower molecular weights than that of polymeric ones.
2. The critical micelle concentration (CMC) is much lower for polymer surfactants.
3. The vast majority of polymer micelles have spherical shape in dilute or semidilute solutions, whereas low-molecular-weight surfactants form structures that are

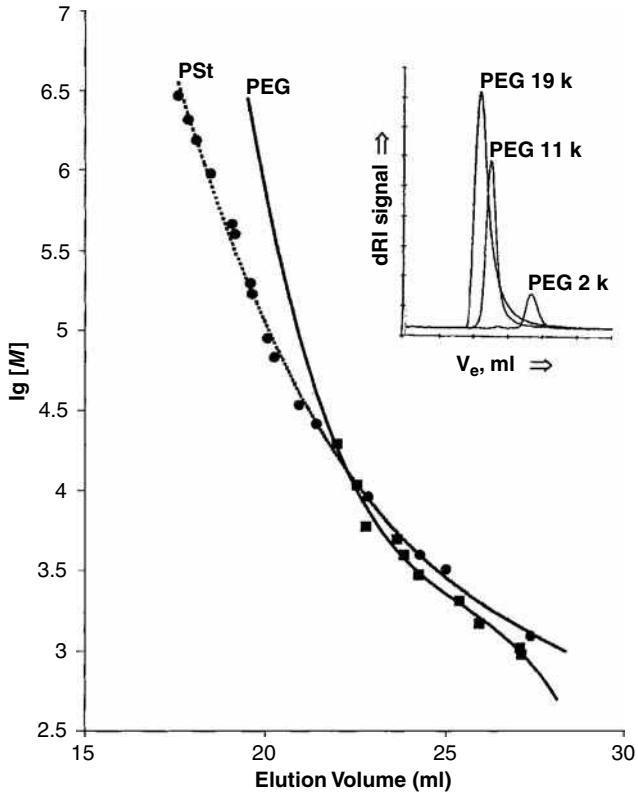

Fig. 1 Polystyrene, PSt, and poly(ethylene glycol), PEG, calibration curves obtained on PL Gel column set (Mixed C, 10^3 Å, 5×10^2 Å, and 10^2 Å). Eluent: THF; flow rate: 1 ml/min; temperature: 40°C. Inset: SEC elution profiles of poly(ethylene glycol)s (PEGs) at the same analysis conditions.

strongly concentration dependent: lamellae, sheets, rods, and spheres.

4. The kinetics of micelle formation and the dynamics of the micelle–unimer equilibrium are considerably slower for polymeric surfactants.

The last factor is particularly important for the successful utilization of aqueous SEC in the investigation of the micellization process. In order to provide a realistic picture for the micellization equilibrium, the chromatographic system needs to meet several strict requirements: The packing material and the eluent should be appropriately chosen to prevent the occurrence of non-size-exclusion phenomena and adsorption of micelles in the stationary phase. In all cases, mass balance of the material injected and recovered from the columns must be performed in order to verify the absence copolymer entrapment. Cross-linked copolymers containing either poly(vinyl alcohol) or poly(glycidyl methacrylate) as the hydrophilic component are the most widely used column packing materials for aqueous SEC. Both Shodex Protein KW (Showa Denko, Japan) and Micropak TSK-gel PW (Toyo Soda, Japan) columns have been reported to afford good information on the micellization behavior of PEO copolymers without interference of side effects.[9,10] The mobile phase is methanol-water (1 : 1, v/v) or pure water eluting at 1.0 ml/min. The analysis temperature is between 22°C and 40°C. Historically, the major concern for the use of SEC in the investigation of micellar systems has always been the lack of suitable calibration and, consequently, the inability of the method to furnish accurate information for the size (hydrodynamic volume) of the micelles and their molecular weight. The incorporation of light-scattering and viscosity detectors for online measurement seems to eliminate this problem. With no solute-column interaction present and slow unimer-micelle equilibrium, a multiangle light-scattering detector (DAWN-DSP, Wyatt Technology, U.S.A.) provides accurate information for the molecular weight and radius of gyration of the micelle using Zimm's formalism:

$$\frac{R_\theta}{K^* c} = kM_w P(\theta) - 2A_2 c M_w^2 P^2(\theta)$$

where R_θ is the excess Rayleigh ratio, K^* is an optical constant that includes the differential refractive index increment (*dndc*) of the solvent–solute mixture, c is the concentration of the solute molecules in the analyzed solution, M_w is the weight-average molecular weight, $P(\theta)$ is a form factor, and A_2 is the second virial coefficient. If the *dndc* value for the copolymer above CMC is known, the extrapolation to zero concentration and zero angle will yield the *Z*-average of the radius of gyration and A_2, respectively. The double extrapolation to zero angle and zero concentration will afford M_w. The hydrodynamic radii can be calculated using an online viscometric detector (Viskotek, U.S.A., and Waters) and the following relationship:

$$R_\eta^{\ 3} = \frac{3[\eta]M}{10\pi N_A}$$

where the value of $[\eta]M$ could be extracted directly from the universal calibration and is Avogadro's number (6.022×10^{23}). It should be pointed out, however, that this formula is strictly valid only for spherical structures. The hydrodynamic radius can also be measured by a combination of SEC and dynamic light scattering (Precision Detectors, U.S.A.) or NMR spectroscopy.[11] However, the same assumption for a spherical shape of the investigated macromolecules has to be made.

In conclusion, modern SEC is a versatile technique for the investigation of non-ionic surfactants in aqueous and organic media. In combination with different spectroscopic and viscometric detectors it will provide useful information for the molecular weight characteristics, chemical composition and solution behavior of this important class of materials.

REFERENCES

1. Jönsson, B.; Lindman, B.; Holmberg, K.; Kronberg, B. *Surfactants and Polymers in Aqueous Solution*; John Wiley & Sons: New York, 1998
2. Glass, J.E., Ed.; *Hydrophilic Polymers: Performance with Environmental Acceptability*; Advances in Chemistry Series; American Chemical Society: Washington, DC, 1996; Vol. 248.
3. Rissler, K. High-performance liquid chromatography and detection of polyethers and their mono(carboxy)alkyl and-arylalkyl substituted derivatives. J. Chromatogr. A, **1996**, *742*, 1.
4. Mori, S. Response correction of differential refractometer for polyethylene glycols in size exclusion chromatography. Anal. Chem. **1978**, *50*, 1639.
5. Trathnigg, B.; Feichtenhofer, S.; Kollroser, M. Quantitation in liquid chromatography of polymers: Size-exclusion chromatography with dual detection. J. Chromatogr. A, **1997**, *786*, 75.
6. Taton, D.; Cloutet, E.; Gnanou, Y. Novel amphiphilic branched copolymers based on polystyrene and poly(ethylene oxide). Macromol. Chem. Phys. **1998**, *199*, 2501.
7. Berlinova, I.V.; Dimitrov, I.V.; Gitsov, I. J. Polym. Sci., Part A: Polym. Chem. **1997**, *35*, 673.
8. Berlinova, I.V.; Amzil, A.; Vladimirov, N.G. J. Polym. Sci., Part A: Polym. Chem. **1995**, *33*, 1751.
9. Berlinova, I.V.; Vladimirov, N.G.; Panayotov, I.M. Makromol. Chem. Rapid Commun. **1989**, *10*, 163.
10. Xu, R.; Hu, Y.; Winnik, M.A.; Riess, G.; Crocher, M.D. J. Chromatogr. **1991**, *547*, 434.
11. Newkome, G.R.; Young, J.K.; Baker, G.R.; Potter, R.L.; Audoly, L.; Cooper, D.; Weis, C.D.; Morris, K.; Johnson, C.S., Jr. Cascade polymers. 35. pH dependence of hydrodynamic radii of acid-terminated dendrimers. Macromolecules **1993**, *26*, 2394.

Normal-Phase Chromatography

Fred M. Rabel
EMD Chemicals, Inc., Gibbstown, New Jersey, U.S.A.

INTRODUCTION

There are four basic separation modes in liquid chromatography (LC)—adsorption, normal-phase partition, reversed-phase partition, and ion exchange. Of these, normal-phase partition is the least practiced based on published references. Although similar to the well-known adsorption mode, both this and the normal-phase modes have been relegated to positions of decreased use by the ever-popular reversed-phase mode. Each mode, however, has to be evaluated on its own merits and what successes it could bring to the analysis problem.

As practiced, normal phase is very much like the adsorption mode (polar stationary-phase surface and non-polar mobile phase), the only difference being that the normal-phase separation is done on a less-polar surface. This is because the sorbent used in normal-phase separations is bonded with a polar-bonded phase, such as propyl cyano, propyl amino, or organo-diol (from a reagent derived from glycerol). Although selectivities are similar to the adsorption mode, the reproducibility is greatly increased due to less sensitivity to moisture in the mobile phase due to a lower silanol content.

The normal-phase mode, like the adsorption mode, is able to separate components that vary greatly in polarity. Samples of wide polarity are often found when natural products or biological system samples need to be analyzed. Often, this adsorption or normal phase is a first cleanup step, when it is necessary to fractionate the sample into more manageable parts for subsequent analyses. Other separations for which the adsorption mode is known to perform well (geometric isomers, *cis–trans* isomers) can also be done in the normal-phase mode with fewer reproducibility problems.

DESCRIPTION

There are a number of modes or mechanisms into which chromatography is divided. These include adsorption, normal-phase partition, reversed-phase partition, and ion exchange. Often, the term "partition" is deleted from the discussions of the differences and similarities of these modes. The inclusion of the word "partition" began to be used when supports had to be coated with liquid phase (and the mobile phases saturated with them) to accomplish separations with these two modes. Today, bonded-phase versions of these liquid phases are available, making them easier to use with greater reproducibility. Perhaps it has been the use of these bonded supports that have allowed the name of these modes to be simplified.

The reasons for distinguishing between these modes are as follows:

1. To better understand the operating parameters of each mode.
2. To understand what type of separations (isomers, equal polarity, different polarity) each is able to do better than another mode.

Often the modes can be complementary, allowing various types of selectivity. This is advantageous when doing separations of unknown substances, as different mechanisms will allow unique selectivities, thereby guaranteeing more complete separation. Applying different modes of chromatography to a single-separation problem is often called "multidimensional" chromatography.

Before bonded phases became available, all normal-phase partition—and reversed-phase partition—separations were done on silica and other supports, which were only "coated" with different polar and non-polar phases or oils. Obviously, their use presented many problems since it was absolutely necessary to keep both the mobile phase and the stationary phase saturated with these phases. The saturation level in both, of course, changes with temperature; hence, this had to be carefully controlled for reproducibility. The laboratory work of the analytical chemist was made infinitely simpler with the introduction of bonded phases, which this entry addresses.

Normal-phase (NP) chromatography is a close parallel to adsorption chromatography. Briefly, adsorption chromatography most often uses polar silica gel as the stationary phase and a mobile phase that is predominately non-polar, possibly with some polar modifier. An example of such a mobile phase would be hexane with 2% ethanol. When increasing the percentage of the polar modifier, the elution times decrease. When a sample containing a wide range of polarities (i.e., a lipid mixture) is encountered, then the normal-phase mode can be used with a gradient to separate the sample into fractions that are easier to analyze.

Normal-phase chromatography generally uses the same types of mobile phases as for the adsorption mode. The difference, however, is the nature of the stationary phase.

Table 1 The usual structures of polar-bonded phases.

Cyano	$Si–O–SiR_2–(CH_2)_3–CN$
Amino	$Si–O–SiR_2–(CH_2)_3–NH_2$
Nitro	$Si–O–SiR_2–(CH_2)_3–NO_2$
Diol	$Si–O–Si–O–CH_2OH–CHOH$

The R groups may be $–OCH_3$–OCH_2CH_3,–H,–CH_3,–CH_2CH_3, or others. Combinations of reagents or active groups are also possible. One manufacturer, for instance, offers a polar aminocyano (PAC)-bonded phase.

In NP chromatography, the packing is silica gel that has been bonded with a polar phase. The usual polar phases widely available from many manufacturers include cyano, amino, nitro, and diol phases. These are illustrated in Table 1. The first three often have a propyl group between the Si–O– and the X groups. The diol phase is derived from glycerol bonded to the silane reagent. Of course, each manufacturer uses a different silica, reagents, reaction conditions, and final workup; thus, any given polar-bonded phase from the various suppliers can differ in relative selectivity and/or retention times.

There are two major differences between using silica gel (for adsorption) and a polar-bonded phase (for normal phase) for a separation. First, the polar-bonded phase adds a different surface to the silica gel, which can impart unique selectivities (i.e., separation characteristics) to an analysis. This is because the stationary-phase surface is no longer as polar as it was before bonding. Many of the silanols are replaced with the organo-polar groups. As with any bonded phase, perhaps only 50% of the available silanols are actually bonded, because of their incomplete accessibility to any reagent. It is possible to also endcap (a second-step bonding reaction, with a trimethylsilyl reagent) more of the remaining silanols. This is not generally done; hence, there is often some definite silanol interaction, and, also, with amino and diol phases, where they would themselves react with the reagent, silanizing them. This would defeat the purpose of trying to produce a different selectivity packing.

The second difference comes from the fact that if there are fewer silanols available on the surface of the packing, it will be less sensitive to any moisture that gets into the mobile phase. One of the biggest problems observed by the uses of silica gel separations in the absorption mode is the control of the separation's reproducibility. Unless one is very careful in using dry solvents, or "controlled water content" mobile phases, the retention times of their compounds can change dramatically from analysis to analysis. If more water gets onto the silanols, they are deactivated, and any sample component elutes more rapidly. Removing water, with an exhaustively dried solvent combination, for instance, removes moisture from the silanol groups, and components are then retained longer. As a result, with less silanols available for deactivation by water, the polar-bonded phases are more reproducible and often preferred by chromatographers.

If variable retention times become a problem in the absorption mode, a switch to a polar-bonded phase column is often the simplest solution. When using the same solvent mixture as was used on the bare, unbonded silica gel column, it is often found that the elution order is often the same or very similar. Of course, a switch in mode would necessitate identifying the sample components, to guarantee that their elution order is, indeed, unchanged. With fewer silanols, however, the components of the mixture will elute faster; hence, readjusting the mobile phase is required to insure adequate resolution. As mentioned earlier, this polar-bonded-phase separation will be much less sensitive to small moisture variations in the mobile phase. Moisture in the mobile phase should, nevertheless, be controlled, but will present few, if any, problems over the time the samples in a study are being run.

As with adsorption chromatography, the normal-phase mode is separated on the basis of solubility in the mobile phase (so it dissolves relatively non-polar compounds) and the differences in the polarities of the components in the mixture and their attraction to the solvated polar-bonded phase. Relatively non-polar components elute first; more polar components elute later. These relative polarities and elution orders are summarized in Table 2.

At the non-polar end of the elution scheme, the elution of alkanes to ethers with perhaps only hexane or heptane would be expected. For elution of moderate-to-polar compounds, a polar modifier has to be added to the major non-polar component of the mobile phase. Much of the guesswork as to which solvent combinations to use has been simplified by the work of Snyder and Kirkland.[1] Their work has grouped solvents of similar selectivities (i.e., alcohols give identical elution order sequences; only the elution times change from one alcohol to another). As a result of their studies, the recommended solvents to be mixed with hexane or heptane to effect the greatest possible selectivity differences are diethyl ether, chloroform, and methylene dichloride.

It is possible to separate more polar components by introducing a gradient from a low concentration

Table 2 Relative group polarity and elution order in normal-phase partition chromatography.

$RH < RX < RNO_2 < ROR < RCOOR < RCONHR < RNH_2 < ROH$
RCRO R_2NH
RCHO R_3N
Increasing polarity of organic structures/groups → →
Increasing retention of compounds containing these structures/groups → →

The more functional groups in the compound, the greater its polarity. For polyfunctional compounds, the *most polar* groups determines the retention of the compound.

(0–10%) of a polar modifier to a higher concentration of this same polar solvent (to 90%, for example). The important consideration is the solubility limits of the polar component in the non-polar component. Thus, methanol is only soluble in hexane to about 5%, but ethanol can be brought up to 20% before reaching maximum solubility. If more polar samples are to be separated, then hexane can be replaced by ethyl acetate or chloroform. One constraint with the normal-phase mode, as with the adsorption mode, is that certain solvents are not transparent in the ultraviolet range most used in standard LC systems. The refractive index detector or the evaporative light-scattering detector can, of course, be used with any solvent(s) but are not standard components in most LC laboratories. With the growing use of LC/MS systems, which are compatible with less-polar-mobile phases, this detection problem is not as great a concern as in the past.

Using the normal-phase mode does not limit the chromatographer to only relatively non-polar-mobile phases. Much work with these bonded phases is also done with polar solvent mixtures, such as methanol–water or acetonitrile–water. They might appear to be reversed-phase separations, but this may not be the case. Often, when a CN (cyanopropyl) phase is used, it is used as a slightly more polar-bonded phase than would be a C4-bonded phase. Then, the polar organic–water combinations used almost always invoke the reversed-phase mode.

One widely used application using NP chromatography in which the mobile-phase composition is deceptive in the actual mode being used is the separation of sugars (carbohydrates) and oligosaccharides. The packing used is an NH_2 (aminopropyl, most often) bonded phase and the mobile phase is acetonitrile–water in the ratio of 20–35% water. This mobile phase might lead one to suspect a reversed-phase mechanism at work, but, in fact, adding more water (the polar component) to the mobile phase decreases the retention times of the sugars, proving it is, indeed, a normal-phase partition mode being used (if it were reversed-phase mode, the addition of more water would increase the retention of the compounds).[a]

It is also possible to use an NH_2-bonded phase as an ion exchanger, since it will form the quaternary ion, $-NH_3^+$ in buffers between pHs of 2 and 6 (i.e., a weak cation exchanger). This can also be a problem when doing the sugar separation described earlier, if acidic components in the mixture inadvertently transform the NH_2 to the $-NH_3^+$ form. The separation will not work as well, if at all. This, fortunately, is reversible by taking the column to pure water, then passing through 10 column volumes ($V_M \times 10$) of 0.01 *M* NH_4OH, and later pure water, to regenerate the free base.

Other possible problems with this reactive-bonded phase is that it can form Schiff bases with aldehydes and ketones; hence, samples containing these should be avoided. The NH_2 group can also be easily oxidized; hence, peroxides in any easily oxidizable solvents (i.e., diethyl ether, dioxane, and tetrahydrofuran) should be avoided.[2]

The types of compounds that can be separated in the normal-phase mode is as vast as for the adsorption mode. Likewise, because the range of solvents that can be used in this mode is virtually unlimited, it will lend itself to even more sample types. Unfortunately, not as many references exist for normal-phase separations as for reversed-phase separations. As a guide to the types of solvents to be used in the normal-phase mode, one may refer to the many studies on silica gel or the adsorption mode. As mentioned, usually only minor changes, if any, need be made to the mobile phase when adapting to the normal bonded-phase column.

CONCLUSIONS

Normal-phase chromatography and the bonded-phase sorbents that are used for this mode of chromatography have been discussed. It can be used with fewer reproducibility problems than the adsorption mode simply because the bonded sorbents used for NP chromatography have fewer silanols. Fewer silanols mean less sensitivity to water than is often found in variable amounts in the solvents used for high-performance liquid chromatography (HPLC).

Depending on the polar-bonded phase used, different selectivities can be found for the same mixture. This allows subtle optimization should the different bonded phases be tried during the method development phase.

Although the adsorption and normal-phase modes are not often used by many chromatographers, both have great potential for solving HPLC problems. Although mostly used with non-polar solvents with a polar modifier, polar-bonded-phase HPLC columns can also be used with organic/water combinations for additional unique selectivities.

REFERENCES

1. Snyder, L.R.; Kirkland, J.J. *Introduction to Modern Liquid Chromatography,* 2nd Ed.; John Wiley & Sons: New York, 1979; 247–264.
2. Meyer, V.R. *Practical High Performance Liquid Chromatography,* 2nd Ed.; John Wiley & Sons: New York, 1994; 166.

[a]If this column is supplied by the manufacturer in heptane or hexane, use an intermediate solvent like ethyl acetate, on going to the acetonitrile–water mobile phase to prevent immiscibility of one solvent in another.

Nucleic Acid Derivatives: TLC Analysis

M.L. Soran
National Institute of Research and Development for Isotopic and Molecular Technology, Cluj-Napoca, Romania

C. Marutoiu
Department of Chemistry, Lucian Blaga University of Sibiu, Sibiu, Romania

INTRODUCTION

In nature, the macromolecules of nucleic acids are found either free or as nucleoproteins with various topochemical distributions in the acellular (i.e., viral) and cellular (i.e., prokaryotes, eukaryotes) structures. The presence of these macromolecules in prokaryotes is not necessarily correlated with a defined morphologic structure. The localization in eukaryotes is generally in the cellular nucleus, but it is also present in the cellular cytoplasm, mitochondria, and plasmids.[1]

In slightly alkaline medium, the macromolecules of nucleic acids are broken into fragments named oligonucleotides, or even mononucleotides (often simply referred as "nucleotide") by advanced hydrolysis. These mononucleotides are, in fact, the structural blocks of the nucleic acids.

Further hydrolysis (acidic, basic, or enzymatic) of the mononucleotides leads to the corresponding nucleosides and phosphoric acid. The nucleosides can be hydrolyzed in nucleobases and pentose.[2]

SEPARATION OF NUCLEIC ACIDS

The nucleosides have been separated on cellulose plates (Avicel 1440, Schleicher & Schuell) using various mobile phases:

- *n*-butanol–*iso*-butyric acid–ammonium hydroxide conc.–water (75:37.5:2.5:25, v/v);
- ammonium sulfate (saturated solution)–0.1 *M* sodium acetate (pH 6)–isopropanol (79:19:2, v/v);
- *iso*-butyric acid–0.5 *M* ammonium hydroxide–0.1 *M* EDTA (100:60:1.6, v/v);
- *tert*-butanol–0.08 *M* formic acid–isoamyl alcohol (50:50:2, v/v);
- acetonitrile–ethyl acetate–*n*-butanol–isopropanol–0.04 *M* ammonium formiate (pH 7.6) (7:2:1:1:2.7, v/v);
- *tert*-amyl alcohol–methyl-ethyl-ketone–acetonitrile–ethyl acetate–water–formic acid, conc. (4:2:1.5:2:1.5:0.18, v/v).

The development of the spots was performed at 20–21°C, and the migration distance was 15 cm from the start. The nucleosides were visualized in UV light at 254 nm.

The nucleosides obtained by enzymatic digestion of t-RNA were separated by bidimensional chromatography using Merck cellulose layered on 20×50 cm^2 aluminum sheets. The elution in the first direction was performed with *n*-butanol–isobutyric acid–ammonium hydroxide, conc.–water (75:37.5:2.5:25, v/v) mixture for 24 hr at 20–21°C, in an unsaturated chamber. The chromatographic plate was dried with a fan for 3 hr at 20°C, after the first elution. Elution in the second direction was performed for 4 hr with the mixture ammonium sulfate (saturated solution)–0.1 *M* sodium acetate (pH 6)–isopropanol (79:19:2, v/v). The separated compounds were visualized in UV light at 254 nm.

The separated nucleosides were quantitatively determined by elution from spots with 0.5 ml water and then analyzed with a Beckman spectrophotometer (25 Model) at pH = 6, 1, and 13.[3]

The thin-layer chromatography (TLC) method was used for purifying the intermediary products obtained from the synthesis of the oligonucleotide dendrimers. The separations were performed on silica gel plates using various solvent mixtures as mobile phases, e.g., methanol–methylene chloride (1:9, v/v), methanol–chloroform (1:30, 1:9, v/v), hexane–dichloromethane (1:3, v/v), hexane–ethyl acetate (3:1, 1:1, 4:1, v/v). The separated compounds were visualized in an iodine atmosphere.[4]

Inosine monophosphate (IMP) can be detected in nucleotides following TLC purification. In the first stage, the sample is introduced into a mixture of water (10 μl) and 100 m*M* non-radioactive 5 IMP (1 μl); 2.5 μl from this mixture is spotted onto the chromatographic plate at 2.5 cm from the side of the plate. After drying of the spots, the plate is introduced into a methanol atmosphere (10 min), dried, and then bidimensionally developed on polyethyleneimide (PEI)–cellulose.[5]

The spots on the developed chromatographic plates were visualized in UV light. In the second stage of the purification, the sample is redeveloped with 1 *M* sodium formiate (buffer solution, pH 3.4) and it is dried in an anhydrous methanol atmosphere. The next step for the purification was the development of the plate with

saturated ammonium sulfate solution–isopropanol–0.1 *M* sodium acetate, pH 6.0 (79:2:19, v/v) mixture. The compounds were visualized in UV light and [^{32}P]IMP was identified by autoradiography, after drying of the plates.[6]

In the diagnosis and classification of brain tumors, TLC is used for the separation and identification of nucleotides obtained by DNA hydrolysis, according to the following procedure: the dried sample of DNA (1 μg) was dissolved in succinate buffer (pH 6) containing $CaCl_2$ (10 m*M*) and digested with spleen phosphodiesterase II (0.001 units) and micrococcal nuclease (0.02 units) in 3.5 μl total volume for 5 hr at 37°C. The DNA digest (0.17 μg) was labeled with 2 μCi [γ-^{32}P]ATP (4500 Ci/mmol; ICN, Irvine, CA; in stoichiometric amounts) and T_4 polynucleotide kinase (1.5 units) in 3 μl of 10 m*M* bicine–NaOH (pH 9.7) buffer containing $MgCl_2$ (10 m*M*), DTT (10 m*M*), and spermidine (1 m*M*). After incubation for 35 min at 37°C, 3 μl apyrase in bicine–NaOH (10 m*M*; 10 units/ml; pH 9.7) was added and incubation was continued for 35 min. The 3′-phosphate of a nucleotide was cleaved off with RNaseP1 (0.2 μg) in ammonium acetate buffer (500 m*M*; pH 4.5). Separation and identification of [γ-^{32}P]m^{5}dC was performed by a two-dimensional chromatography on cellulose TLC plates (Merck, Germany) using isobutyric acid–NH_4OH–H_2O (66:1:17, v/v) in the first dimension and 0.1 *M* sodium phosphate (pH 6.8)–ammonium sulfate–*n*-propyl alcohol (100 ml/60 g/1.5 ml) in the second dimension. Intensity analysis was done with the PhosphorImager Typhoon (Pharmacia, Uppsala, Sweden) and Image Quant Software.[7]

The nucleotides were separated on PEI-cellulose in 0.9 *M* guanidinium chloride. After separation, the plate was introduced, for 10 min, into absolute methanol and then dried in air. The plate was irradiated in a nuclear reactor for 96 hr, with a 4×10^{12} neutrons/cm/sec flux. The nucleotides with phosphorus (^{31}P) are activated at ^{32}P by this irradiation and can be detected by autoradiography. By this technique, nucleotides series such as ATP, ADP, AMP, GMP, GDP, and GTP were separated and identified. This method allows the quantitative determination of the separated and neutron-activated compounds.

CONCLUSION

TLC analysis of nucleotides by several unidimensional and bidimensional methods has been described. Optimal solvent systems were given.

REFERENCES

1. Darnell, J.; Lodish, H.; Baltimore, D. *Molecular Cell Biology*; Scientific American Book, Inc.: New York, 1986.
2. Garban, Z. *Biochimie. Comprehensive Treaty,* 2nd Ed.; Didactica si Pedagogica, R.A.: Bucharest, 1999.
3. Rogg, H.; Bramhilla, R.; Keith, J.; Staehelin, M. An improved method for the separation and quantitation of the modified nudeosides of transfer RNA. Nucleic Acids Res. **1976**, *3* (1), 285.
4. Shchepinov, M.S.; Udalova, I.A.; Bridgman, A.J.; Southern, E.M. Oligonucleotide dendrimers: synthesis and use as polylabelled DNA probes. Nucleic Acids Res. **1997**, *25* (22), 4447.
5. Gupta, R.C.; Randerath, E.; Randerath, K. A double-labeling procedure for sequence analysis of picomole amounts of non-radioactive RNA fragments. Nucleic Acids Res. **1976**, *3* (11), 2915.
6. Paul, M.S.; Bass, B.L. Inosine exists in mRNA at tissue specific levels and is most abundant in brain mRNA. EMO J. **1998**, *17*, 1120.
7. Zukiel, R.; Nowak, S.; Barciszewska, A.-M.; Gawronska, I.; Keith, G.; Barciszewska, M.Z. Molecular Cancer Res. **2004**, *2*, 196.

Nucleic Acids, Oligonucleotides, and DNA: CE

Feng Xu
Yuriko Kiba
Yoshinobu Baba
Department of Medicinal Chemistry, University of Tokushima, Tokushima, Japan

INTRODUCTION

As one of the basic analytical techniques in the modern molecular biology laboratory, capillary electrophoresis (CE) plays a prime role in nucleic acid separation. CE is carried out through a simple system that consists of a high-voltage power supply, one capillary or several capillaries, and an online detector. The separation is performed by applying a high voltage in narrow capillary tubes (10–300 μm inner diameter) filled with a gel or a polymer solution as the separation matrix. The high surface-to-volume ratio of the small tube can efficiently dissipate the Joule heat generated during electrophoresis. Thereby, the electric field strength can be very high, only limited by the onset of biased reptation. The solutes are detected by either Ultraviolet (UV) or laser-induced fluorescence (LIF) detection. Nowadays, more than 96 capillaries can be mounted in an electrophoresis apparatus to provide parallel analysis of multiple DNA samples at a time; thus, the running cost is considerably reduced. CE in a microfabricated chip (chip-CE) was developed in the early 1990s.[1] Its goal is to constitute truly automated micrototal analysis systems (μTAS), incorporating genomic DNA extraction from cells, polymerase chain reaction (PCR) amplification, electrophoretic sizing, and detection in a single unit. The technique has the benefits of low sample/reagent consumption, high throughput, fast separation, full automation, and portability.

Due to the fact that nucleic acids have nearly the same charge-to-mass ratio when they are larger than 400 bp,[2] separation in free solutions is difficult. By using some special techniques to break the charge-to-mass symmetry, e.g., attaching an uncharged, friction-generating large label such as protein streptavidin at the end of all DNA molecules, nucleic acids can be separated in free solutions, the so-called end-labeled free-solution electrophoresis (ELFSE).[3] The label has no charge and is easily attached to DNA via a biotin complex. In order to extend the read lengths of DNA fragments for practical use, larger friction-generating labels are still needed.

Most nucleic acids are separated by using sieving matrices. Cross-linked gels like polyacrylamide, directly coming from slab gel electrophoresis, were employed in early CE.[4] The capillary is prepared by in situ polymerization to form a cross-linked and three-dimensional network, which provides high-efficiency DNA separation. But several detrimental factors hinder the large-scale application of the gels. Bubble formation, clogging of pores, and gel degradation by hydrolysis in the alkaline buffer pH make the capillary lifetime short and the reproducibility low. Nowadays, gel-filled capillaries are gradually replaced by non-cross-linked polymer solution-filled capillaries, though the former are still used in some limited areas, such as separation of oligonucleotides and sequencing of reaction products,[5] in which the column can be thrown away after use.

Polymer solution-filled channels have the advantages of ease of replacement. Because bonded microfluidic devices cannot withstand high matrix loading pressure, viscosity is an important property to be considered. The recently developed viscosity-adjustable thermoresponsive polymer solutions are attractive. They can switch between low and high viscosity state through a modest temperature change, and have high separation ability. Another recent development is artificial sieving networks, such as entropic trapping (ET) techniques,[6] for the separation of long DNA fragments. Several hundred kilobases of DNA can be quickly separated by using only a direct circuit field in a solution containing no polymer matrix, which shows promise for use in μTAS platforms.

This review gives an overview of current advances in nucleic acid separation by CE and microchip electrophoresis. The focus is on the separation mechanisms during CE, conventional separation matrices and thermoresponsive polymers solutions, UV and fluorescence detection, microchip-based CE, and entropic trapping networks.

THEORY

Separation in Semidilute Regime Polymer Solutions

For a polymer solution, the intrinsic viscosity, $[\eta]$, is fitted to the empirical Mark–Houwink–Sakarada equation:[7]

$$[\eta] \simeq KM_w{}^a \quad (1)$$

Table 1 Characteristic constants for some polymers used in CE.

Polymer	K (ml/g)	a
Polyacrylamide	6.31×10^{-3}	0.80
Poly-*N,N*-dimethylacrylamide	2.32×10^{-2}	0.81
Polyoxyethylene	1.25×10^{-2}	0.78
Hydroxyethylcellulose	9.53×10^{-3}	0.87
Methylcellulose	0.316	0.55
Dextran	4.93×10^{-2}	0.60

Source: From Viscosity–molecular weight relationships and unperturbed dimensions of linear chain molecules, in Polymer Handbook.[7]

where K and a are characteristic constants for a given polymer–solvent system (Table 1) and M_w the molecular weight.

In a dilute polymer solution, polymer chains are hydrodynamically isolated and do not interact. As the concentration is increased, the polymer chains begin to interact and overlap. If the polymer concentration is too high (concentrated regime), the viscosity is so high that the polymer cannot be used in CE. In the semidilute regime, the polymer concentration is raised sufficiently for polymer coils to begin to interact and overlap in solution. The transition from dilute to semidilute regime occurs at an overlap threshold concentration, c^*, where the polymer chains begin to be densely entangled, and the bulk concentration equals the local concentration inside a polymer chain (Fig. 1). Only dilute and semidilute regimes are utilized for nucleic acid separation by CE. The entanglement threshold can be determined by[8]

$$c^* = \left(\frac{1.5}{K}\right) M_w{}^{-a} \tag{2}$$

For example, methylcellulose has a K value of 0.316 ml/g and an a value of 0.55 (Table 1), so the c^* value of methylcellulose (M_w 400 kDa) can be estimated to be 0.4%.

An entangled solution can be characterized as a network with an average mesh size, ξ_b. The mesh size is expressed as a function of the polymer concentration, c:

$$\xi_b = 1.43 \left[\frac{1.5^{1+1/a}}{2.5 N_A}\right]^{1/3} K^{-1/3a} c^{-(a+1)/3a} \tag{3}$$

where N_A is Avogadro's number. The higher the polymer concentration, the narrower the mesh size. For example, the mesh sizes of methylcellulose at various concentrations are estimated to be: $\xi_b = 48$ nm (if $c = 0.4\%$), 39 nm (0.5%), 33 nm (0.6%), 28 nm (0.7%), 25 nm (0.8%), 22 nm (0.9%), and 20 nm (1.0%).

Eqs. (2) and (3) seem to suggest that two solutions of the same polymer type with the same concentration but different molecular weights have the same mesh size, as long as

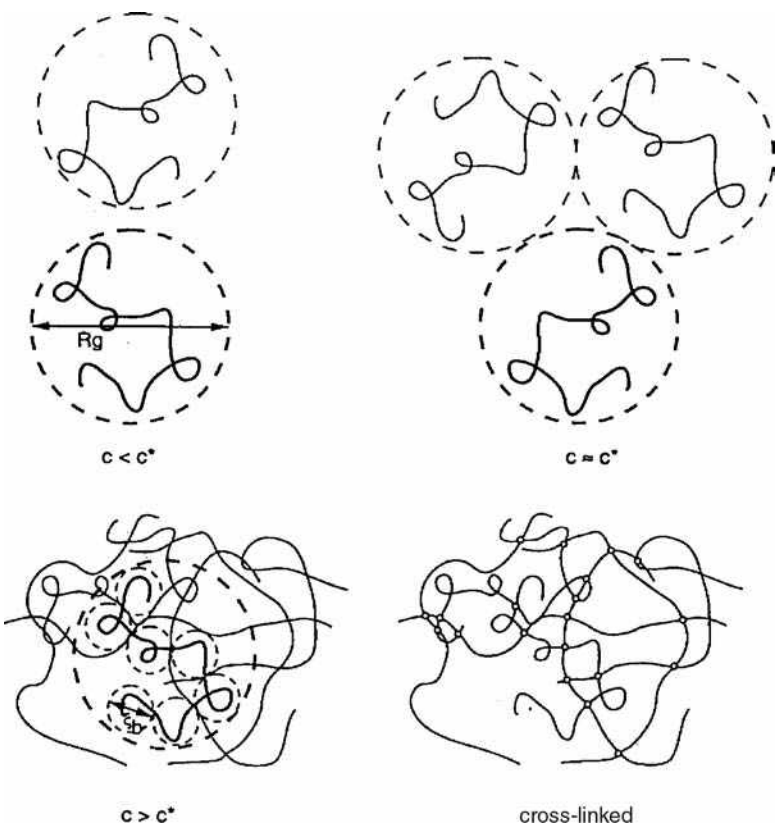

Fig. 1 Illustration of flexible polymers in dilute solution ($c < c^*$), entanglement threshold ($c = c^*$), and semidilute solution ($c > c^*$) regimes, as well as cross-linked chain. One chain is drawn as a thick line for easier visualization. The small circle in the semidilute solution regime represents the "blobs" of size ξ_b.
Source: From The separation matrix, in *Analysis of Nucleic Acids by Capillary Electrophoresis*.[41]

they are entangled. However, their viscosities are different, dependent on their molecular weights. Thus, one can choose the low-viscosity polymer as the separation matrix. For example, separation of oligonucleotides needs a polymer mesh size of about 8–10 nm. If a number of linear polyacrylamides (LPAs) are candidates, through Eq. 3, we obtain the corresponding concentration of LPA to be about 5–6%. Then, from Eq. 2, the LPA that can form an entangled solution at the concentration should have a molecular weight > 50 kDa. Above this limit, all degrees of polymerization give the same mesh size. If one wants to keep the viscosity low, one can choose the smallest possible M_w of 50 kDa.

The Ogston and the reptation models are commonly used to explain the electrophoretic behavior of DNAs. On the basis of the Ogston model, the separation matrix is treated as a random network of fibers, having a distribution of pore sizes and an "average pore radius." A DNA molecule is assumed to be an undeformable spherical particle that migrates through the network, diffusing laterally until it encounters a pore large enough to allow it to pass through. The network of the polymer matrix is a round pore. The DNA mobility, μ, is expressed as:

$$\frac{\mu}{\mu_0} = \exp(-CTN) \tag{4}$$

where T is the polymer concentration, N is the length of the DNA chain expressed in nucleotide units, C is a constant, and μ_0 is the DNA mobility in free solution. This formula predicts the existence of a linear relation between the logarithm of mobility and the DNA size (N) and polymer concentration (T). The Ogston model is successful in fitting experimental data for small DNA fragments with radius of gyration (R_g) much smaller than average pore size (ξ_b) in the limitation of low electric fields. The smaller fragments migrate faster as they can easily access the pores. For larger molecules with $R_g > \xi_b$, the Ogston model predicts that the DNA mobility will rapidly approach zero. But the fact is that they can still migrate even when $R_g \gg \xi_b$. This implies that the assumptions in the Ogston model are invalid for larger DNA molecules.

Reptation theory is another important model. The large DNA molecule is assumed to be an unraveled coil, unfolded from head to tail in a snakelike fashion. DNA chains move through the "tubes" in the polymer network, and the friction coefficient, ξ, is proportional to chain length (L), $\xi = \xi_0 L$, where ξ_0 is the friction coefficient per unit length. DNA is assumed to consist of N units of nucleotides (length of each unit $= a$). The total length of the DNA equals Na. In the model, only the force along the DNA chain (longitudinal force) is taken into account in the electric field. The DNA mobility, μ, is then expressed by

$$\mu = \frac{Q\langle x^2\rangle}{\xi_0 a L^2} \tag{5}$$

where Q is the total DNA charge, and x is the head-to-tail distance of the molecule in the direction of the electric field.

At low electric fields, a DNA molecule of medium size can be considered as a random coil with some degree of flexibility. Electrophoretic mobility is expressed as

$$\frac{\mu}{\mu_0} \propto \frac{1}{N}, \quad N < N^* \tag{6}$$

This is the so-called reptation-without-stretching, which is the typical phenomenon for DNA size shorter than a critical length, N^*, needed to pass through a gel at a low electric field. In this case, the mobility is inversely proportional to the DNA size.

Under a high electric field, DNA is no longer considered to move as a random-polymer coil, but moves with extended rod-like conformation. If DNA is completely extended, it moves in a straight fashion in the electric field direction, $\langle x^2\rangle = L^2$; then

$$\frac{\mu}{\mu_0} \propto N^0, \quad N > N^* \tag{7}$$

This regime is the so-called reptation-with-stretching. A mobility plateau is observed for large DNA (above the critical length, N^*) in the case of high electric field and resolution approaching 0. Fig. 2 shows the dependence of DNA mobility on its size.

Separation in Dilute Regime Polymer Solutions

Barron, Sunada, and Blanch[9] found that DNA fragments can be separated in a polymer solution at a concentration well below its entanglement threshold ($c \ll c^*$), and put forward a transient entanglement coupling mechanism. Such separation is believed to be impossible within the framework of the existing Ogston and reptation models. The new transient coupling mechanism explains that the DNA molecule undergoes collisions with neutral polymers, and the average number of polymers that the DNA drags along is dependent on the molecular weight of the DNA. So long DNA molecules have a higher probability of encountering polymer chains, and experience a greater decrease in mobility.

It should be noted that although the separation of DNA can occur in dilute polymer solutions, semidilute solutions give better resolution than dilute ones. In dilute solutions, a narrow ratio of mobility exists between small and large DNA fragments. Therefore, for high-resolution applications, semidilute solutions are preferred. However, if high resolution is not a necessity, dilute (and therefore less viscous) polymer solutions could be used, permitting easier

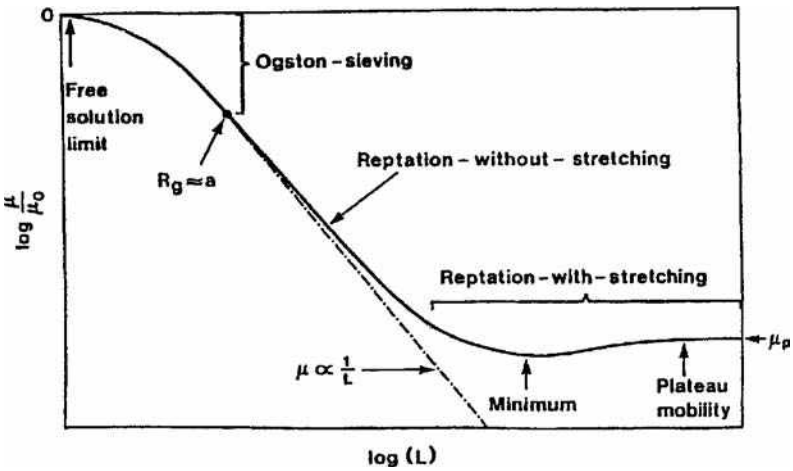

Fig. 2 Electrophoretic behavior of DNA in CE.

filling in microchannels and faster separation. By using dilute solutions of high-M_w polymers, it is also possible to separate large DNA and supercoiled DNA molecules.

DETECTION

UV and LIF are two common CE detection methods. UV detection of DNA fragments is based on the UV absorption of the nucleotide bases. The wavelengths for the UV absorption maxima of DNA bases are 260 nm for adenine, 254 nm for guanine, 267 nm for thymine, and 271 nm for cytosine. Nucleic acids are commonly detected in the UV region from 250 to 280 nm. The sensitivity of UV detection still suffers in CE because of the short optical path length provided by the internal diameter of the separation channel.[10] Laser-induced fluorescence detection is more sensitive than UV; however it requires fluorescent intercalating dyes added to the CE sieving matrix or chemically labeling fluorescent dyes to label nucleic acids. Ethidium bromide is the most common intercalating dye in CE. There are a number of other intercalating dyes, either monomeric or dimeric molecules. Thiazole orange (TO), TO-PRO-1, oxazole yellow (YO), YO-PRO-1, SYBR Green I, etc. are monomeric dyes. TOTO-1, YOYO-1, YOYO-3, etc. are dimeric dyes. These dyes have low background and high sensitivity. Regarding the aspect of detection sensitivity, the monomeric dyes TO, YO-PRO-1, and SYBR Green I are better than most dimeric dyes. Another LIF detection scheme for nucleic acid analysis in CE involves direct labeling of analytes with a suitable fluorophore. The most widely used fluorescent labels are the so-called ABI dyes, viz., FAM, JOE, TAMRA, and ROX. Fluorescently labeled probes and primers are used in many molecular biology applications involving PCR, DNA sequencing, and multicolor detection. New types of labeled agents, such as the energy-transfer (ET) primer, now have widespread application in DNA sequencing.

To make CE useful in high-throughput applications, scanning detection and multisheath flow confocal fluorescence detection have been used in commercial 96-capillary array electrophoresis devices. They have greatly facilitated the completion of the Human Genome Project.

SEPARATION MATRICES

Buffers and Additives

High-viscosity gels (e.g., the high-M_w LPA) require either in situ polymerization or very high pressure to replace them in the capillary. In contrast, many of the low-viscosity polymer solutions do not require polymerization by the user. It is necessary only to dissolve a known amount of the polymer in basic buffers, such as tris-borate-EDTA (TBE) or 3-[[tris(hydroxymethyl)methyl]amino] propanesulfonic acid (TAPS) (pH 8–9), or isoelectric buffers, such as His or Lys. Because the low conductivity of the isoelectric buffers minimizes Joule heating, high electric fields can be used for rapid separation.[11] For oligonucleotide separation, where the DNA is single stranded, denaturation by urea and formamide are also utilized.

Adding polyhydroxy compounds,[12,13] such as glycerol, mannitol, and glucose, to hydroxypropylmethylcellulose (HPMC) matrix can remarkably enhance the resolution of DNA fragments. Some intercalating dyes (e.g., ethidium bromide, YOYO, TOTO, and 9-aminoacridine)[14] can also enhance the resolution of DNA separation by modifying the DNA helix or persistence length.

Non-Cross-Linked Polymer Solutions

The separation matrix is the most important factor in CE separation of nucleic acids. Different polymers have different optimal concentration ranges for the separation of DNA fragments (Table 2). For DNA fragments ranging from 300 to 5000 bp, 0.5% cellulose derivative solution could be

Table 2 Proposed concentration range of polymer matrices for separation of DNA fragments.

	Polymer concentration (%, w/v)		
DNA size (bp)	**LPA**	**HEC, MC**	**PEG, PEO**
1–100	8.0–12	1.0–3.0	6.0–8.0
100–300	7.0–8.0	0.7–1.0	3.0–6.0
300–1000	5.0–7.0	0.5–0.7	2.0–3.0
1000–10,000	3.0–5.0	0.3–0.5	0.5–2.0
10,000–30,000	2.0–3.0	0.01–0.3	

LPA = linear polyacrylamide; MC = methylcellulose; HEC = hydroxyethylcellulose; PEG = poly(ethylene glycol); PEO = poly(ethylene oxide).

selected. For short DNA fragments smaller than 300 bp, the concentration of cellulose derivative should be higher. A more dilute polymer solution (less than 0.3%) is suitable for the separation of DNA fragments larger than 5000 bp. Most commercially available CE instruments are able to fill and empty capillaries with such solutions. An electric field strength between 50 and 800 V/cm is commonly used. When dilute polymer solutions are applied, wall-coated capillaries are usually needed to eliminate electro-osmotic flow (EOF). The inner wall is covalently coated by LPA,[15] polyvinyl alcohol (PVA),[16] etc. Some coated capillaries are commercially available (e.g., DB-17 from J&W Scientific). In contrast, coating the inner wall of microchips, especially in plastic substrates, is not easy. So the use of sieving matrices that do not necessitate wall coating is advantageous, such as poly-*N*,*N*-dimethylacrylamide (pDMA), poly(ethylene oxide) (PEO), and poly(-vinyl pyrrolidone) (PVP).

Linear polyacrylamide has the longest read length in DNA sequencing, due to its high hydrophilicity and thermostability. Solutions of high-molar-mass LPA are extremely viscous and need special loading facilities for injection into precoated separation channels. Short-chain LPA may provide low viscosity. For a given LPA, a higher LPA concentration improves the resolution of short DNA fragments, while a lower LPA concentration favors long DNA fragments. Copolymers of LPA with allyl-β-D-glucopyranoside, allylamide gluconic acid, and allylamide lactobionic acid have self-coating, low viscosity, and good separation abilities for oligonucleotides and small DNA molecules.[17]

Poly-*N*,*N*-dimethylacrylamide has good self-coating and separation abilities at low viscosity (75 cP).[18] Without surface reconditioning between runs, the uncoated capillary is quickly ready for use after replacing pDMA, and allows > 100 runs. Increasing the molar mass of pDMA beyond 98 kDa only slightly improves the resolution but adversely increases the viscosity. The performance of pDMA is a little lower than that of LPA, due to its slightly lower hydrophilicity. The performance can be improved by a copolymer of pDMA and LPA, which combines the excellent performance of LPA with the good self-coating property of pDMA.[19]

Poly(vinyl pyrrolidone) also has better self-coating, low viscosity, and DNA separation abilities. A mixture of polyacrylamide and PVP can form good interpenetrating networks for DNA separation.[20]

Poly(ethylene oxide) has self-coating property. The PEO-filled capillary is regenerated by flushing with HCl and PEO solutions for 2 hr. Low-molar-mass PEO solution provides higher efficiency for smaller DNA fragments, while high-molar-mass PEO solution favors larger DNA fragments. Mixing short and long PEO chains strikes a balance between high resolving power and low viscosity. A mixture of 0.5% PEO 1 MDa and 0.1% PEO 8 MDa successfully separates a range of DNA fragments from 80 to 40 kb (Fig. 3). Xu, Jabasini, and Baba[21] utilized an orthogonal designing technique to quickly optimize a series of mixtures of four PEO matrices, each PEO with a narrow but different range of molecular mass, through only 25 experimental runs in bare polymethylmethacrylate

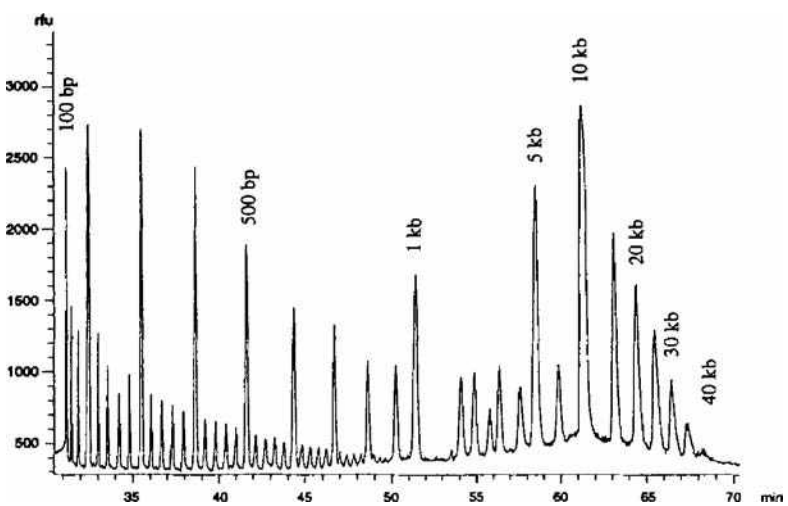

Fig. 3 Capillary electrophoretic separation of DNA fragments from a mixture of 20 bp, 100 bp, 1 kbp, and 5 kbp ladders (65 fragments ranging from 20 bp to 40 kbp) in a mixed matrix consisting of 0.5% PEO (M_n 1 MDa) and 0.1% PEO (M_n 8 MDa). Electrophoretic conditions: PEO in 1 × TBE with 2 nm TO-PRO-3 and 10 μ*M* 9-aminoacridine; 108 V/cm.
Source: From Versatile low-viscosity sieving matrices for non-denaturing DNA separations using capillary array electrophoresis, in Electrophoresis.[42]

(PMMA) microchips. The matrices are suitable for the analysis of DNA fragments ranging from 20 bp to 40 kbp.

Celluloses are described by the type of substituent carried by the cellulose backbone and the viscosity. They can separate DNAs at low concentrations (<2%). Hydroxyethylcellulose (HEC) is a linear derivative with bulky ethylene oxide side chains terminating in hydroxyl groups. In aqueous solutions, it has a stiff, extended conformation. It has relatively high viscosities at the entanglement concentration. A mixture of HEC of different sizes offers a wide range of DNA separation from 100 bp to 23 kbp.[22] Hydroxypropylcellulose (HPC) solution provides similar separation ability, and it has 2–3 times lower viscosity than HEC solution.

DNA separation by CE has been applied to many studies, such as PCR product and digested fragment analysis, restriction fragment length polymorphism analysis, single-stranded conformational polymorphism analysis, variable number of tandem repeat analysis, microsatellite analysis, hybridization, monitoring of DNA-based drugs,[23] etc. Capillary affinity gel electrophoresis, which combines the high specificity of affinity ligands with the high separation power of capillary gel electrophoresis, has been developed for the recognition of specific DNA bases.[24]

Oligonucleotides are generally short single-stranded DNA (<150 bases). Denatured cross-linked polyacrylamide gels, in which the concentration varies from 3% to 8% T and the degree of cross-linking varies from 3% to 5% C (% T is the monomer concentration; % C is the cross-linker concentration), have been used for the separation of oligonucleotides by CE. High-concentration polymer solutions with short M_w have also been adopted, which do not increase the viscosity much. Antisense DNAs are in generally rather small molecules (12–15 bases) and their separation is commonly performed at 13–18% LPA concentration under denaturing conditions (7 *M* urea and 30% formamide).[25] RNA molecules are single-stranded nucleic acids that can form complicated second and tertiary structures. Using CE, total RNA and ribosomal RNA extracted from cells or at the single-cell level (without extraction) are successfully separated with semidilute polymer solutions as the separation matrix.[26]

Thermoresponsive Polymer Solutions

Thermoresponsive matrices have different viscosities at varying temperatures. So they are "ideal" polymers that allow rapid microchannel loading under low viscosity and provide high separation power at high viscosity. The matrices can be classified into two categories: thermoassociating and thermothinning solutions.

Thermoassociating Polymer Solutions

At room temperature or below, thermoassociating polymer solutions have low viscosities. Elevation of temperature leads to hydrophobic association and higher viscosities, suitable for DNA separation. For example, a low-M_w triblock copolymer, $PEO_{99}PPO_{69}PEO_{99}$ [M_w 12.7 kDa, where PEO is poly(ethylene oxide), and PPO is poly(propylene oxide)], demonstrates viscosity-adjusting and self-coating properties. At 5°C, the 25% w/v matrix has a low viscosity of 50 cP (suitable for loading). At 20°C, the viscosity reaches 250 cP and a gel-like structure is formed. The PPO blocks form the core and the PEO blocks dangle outside to form a corona.[27] The effective pore size of the matrix is small due to high PEO concentration (above 20%), which is particularly suitable for small DNA molecule separation. Another similar copolymer solution, $PEO_{106}PPO_{70}PEO_{106}$ (M_w 13 kDa), can flow easily into capillaries at 0°C (100 cP, 20% w/v solution), but rapidly transform into a gel-like, liquid-crystalline phase of spherical micelles at room temperature, suitable for the resolution of oligonucleotides.[28]

A blended copolymer of 4% $PBO_6PEO_{46}PBO_6$ (M_w 2.9 kDa) and 4% $PBO_{10}PEO_{271}PBO_{10}$ [M_w 13 kDa, where PBO is poly(butylene oxide)] also shows thermoassociating and self-coating properties.[29] A resolution of 1.3 could be achieved for the separation of a 123 bp/124 bp doublet. Another copolymer, comprising an LPA backbone and poly(*N*-isopropylacrylamide) (pNIPA) comblike side-chains, has low injection viscosity at room temperature (<300 cP, 3–5% solution), and high viscosity (10,000 cP) at 66°C. It provides better resolution than pDMA solutions.[30] pNIPA-*g*-PEO ($M_w > 10$ MDa) is a different comblike copolymer, which uses long-chain pNIPA as the backbone densely grafted by short PEO chains.[31] When the temperature is raised above 36°C, the copolymer chains become insoluble and then collapse to nanoparticles, with pNIPA inside the core and the hydrophilic PEO chains on the shell. A resolution of 1.4 for the separation of 123 bp/124 bp fragments in pBR322/*Hae*III DNA digest is achieved within 12.5 min in an effective separation length of 10 cm at 200 V/cm by using 8% w/v copolymer.

Thermothinning Polymer Solutions

Polymer solutions of this category are opposite in temperature response compared with thermoassociating solutions. Because the moderately hydrophobic copolymers in the matrices may form an entangled network in aqueous solution, they have high viscosity at room temperature; however, at an elevated temperature, the solution viscosity drops quickly due to a solubility-to-insolubility phase transition. For example, the copolymer of *N*,*N*-dimethylacrylamide (DMA) and *N*,*N*-diethylacrylamide (DEA) has both self-coating ability and a low viscosity of 10 cP at 70°C. Single-base resolution of DNA is observed at 40°C, at which the solution becomes re-entangled. The temperature-dependent viscosity behavior is thermally reversible, facilitating easy medium replacement at low

viscosity. Another blended matrix of thermoresponsive polymer (1.4% w/v HPC) and non-thermoresponsive polymers (0.5% w/v HEC) has a low viscosity of 30 cP at 50°C, and a high viscosity of 1000 cP at 20°C. The matrix provides a thermally tunable mesh size, i.e., "dynamic porosity." Maximum selectivity is observed at 31°C for small DNA separation, while a significant increase of selectivity of large DNA molecules occurs at 36°C. In a temperature ramping experiment, high-resolution separation of both small and large DNA fragments has been achieved in a single run due to the changeable mesh properties of the matrix.

Thermoresponsive matrices appear to be quite promising for DNA separation, though their performance still lags behind that of the non-thermoresponsive LPA matrix, mainly due to the hydrophobicity of the former, which causes them to form less stable networks than LPA.

MICROCHIP ELECTROPHORESIS SEPARATION

Microchips are fabricated using either photolithography, chemical wet-etching methods on glass/silicone substrates, or molded plastic for a micromachined template. Then the channel plate is thermally bond with a top plate. By providing a set of intersecting channels and applying high voltages in reservoirs, it is possible to control the flow direction and flow rate of analytes. The microchip channels are commonly several centimeters in length, 10–100 μm in width, and 10–100 μm in depth. Although silicon can act as a substrate material for microchips, its semiconductor property is incompatible with the high voltage used in microchip electrophoresis. At present, glass, quartz, and various plastics, such as PMMA, polydimethylsiloxane (PDMS), polyacrylate, and polycarbonate are common substrates.

The use of microfabrication and array technologies for DNA separation has undergone quick development. The first DNA separation was carried out on a microchip channel in 1994.[5] Later, with the success of both chip and detection designs, microfabricated capillary array electrophoresis (μCAE) of 12-channel to 96-channel chips[32] appeared. PCR and μCAE can be functionally integrated on a single chip, where the DNA sample is amplified in a microfabricated PCR chamber and then injected electrophoretically into an electrophoresis chip. The total time of PCR and electrophoresis is only 20 min for a β-globin gene target and 45 min for a *Salmonella* genomic DNA target.[33] Rapid detection of deletion, insertion, and substitution mutations by combining allele-specific DNA amplification with heteroduplex analysis by microchip electrophoresis has been accomplished within 130 sec.[34] A 96-lane radial microchannel plate layout together with a rotary four-color confocal fluorescence scanning detector has been used for high-throughput genotyping.[35] Compared to the traditional CE methods, the analytical speed of microchip electrophoresis shows more than tenfold improvement. It is quite important for clinical diagnosis.

SEPARATION OF LARGE DNA MOLECULES

Field-Inversion Capillary Electrophoresis

Conventional CE in continuous electric fields cannot separate DNAs above 40 kb, due to reptation and loss of resolution. One has to resort to pulsed-field gel electrophoresis. This technique makes use of periodically varied direction and strength of an electric field (the net field direction is forward). The DNA molecules not only migrate in the direction of the field but also stretch out lengthwise. The time required for relaxation is directly proportional to the molecule length. Longer molecules relax less than shorter ones when the current is changed. DNA molecules are forced to reorient and are separated according to their sizes.

Nevertheless, the pulsed field run commonly takes longer than 10 hr. The pulsed field is also not easily implemented in CE, except for periodical reversion of field direction (the so called field-inversion CE, FICE). The technique uses alternating electric fields with a frequency >100 Hz. Equal pulse durations in FICE provide the best resolution, while dilute polymer solutions provide the fastest separation. DNA fragments of 200 kbp–1.6 Mbp are separated within 13 min in a dilute methylcellulose solution.[36]

Entropy-Based Separation

During the electrophoresis of long DNA molecules, aggregation of the DNA is a serious problem due to electrohydrodynamic instability triggered by dipole–dipole interaction.[37] In addition, the constituting multiplexed capillaries are also complicated. These problems can be solved by artificially microfabricated obstacles, which mimic polymer gels. Internal conformation entropy is one of the dominant properties of flexible DNA macromolecules, and is directly proportional to the molecular length. Electrophoretic "entropic trapping" (ET) separation is based on nanofluidic channels with narrow constrictions to create mobility differences for separating long DNA molecules (>5 kbp) without the use of polymer solutions and pulsed electric fields. Entropic trapping occurs when the radius of gyration (R_g) of the DNA molecule is comparable to the mean pore size of a separation "gel," e.g., one of the dimensions of a channel is smaller than R_g. Craighead's group designed several entropic devices (one is shown in Fig. 4). When driven by a d.c. field, DNA molecules in the 5–160 kbp range migrate through the periodic deep and shallow regions and become trapped at the entrance of the shallow constrictions before they manage to escape. In the thick region, DNA molecules can form spherical

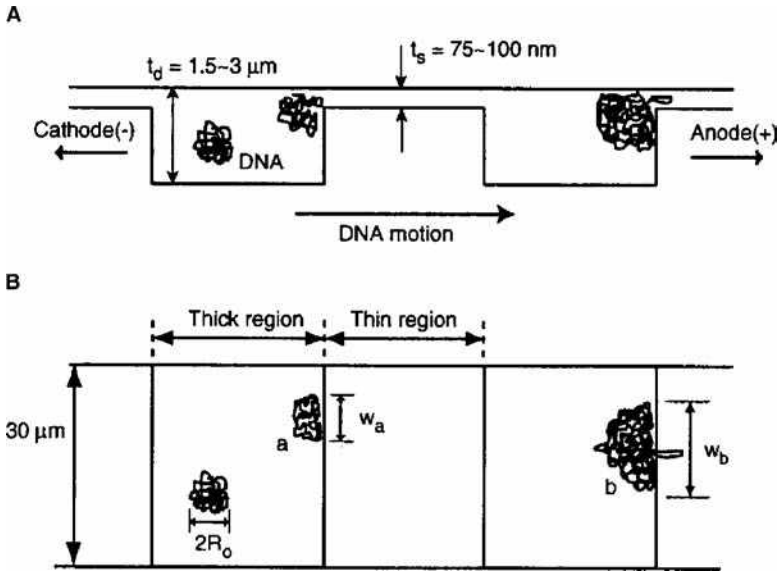

Fig. 4 Nanofluidic separation device with many entropic traps. A, Cross-sectional schematic diagram of the device. DNA molecules are trapped whenever they meet a thin region, because their R_g is much larger than the thin region depth. B, Top view of the device. Trapped DNA molecules eventually escape, with a probability of escape proportional to the length of the slit that the DNA molecule covers (w_a and w_b). Larger molecules have a higher escape probability because they cover wider regions of the slit ($w_b > w_a$).
Source: From Separation of long DNA molecules in a microfabricated entropic trap array, in Science.[6]

equilibrium shapes because the thickness here is larger than R_g, whereas in the thin region, DNA molecules are deformed. DNA molecules repeatedly change their conformation, and consume entropic free energy. The mobility becomes length dependent. Ueda et al.[38] investigated the electrophoretic behavior of large DNA based on the curvature effect of a nanofabricated chip with a curved channel. The DNA chain must endure deformation in the narrow and curved channel, and the ET effect is related to the problem of barrier crossing for flexible DNA molecules to pass through.

Turner, Cabodi, and Craighead[39] fabricated a quasi-two-dimensional nanofluidic structure, in which some regions are populated with a dense array of nanopillars of 35 nm diameter. The height of the fluid gap between the floor and ceiling is determined by the thickness of a sacrificial layer. Long DNA molecules can be electrophoretically driven through the closely spaced pillared region (160 nm apart). The DNA must elongate in order to migrate downfield, at a great cost of conformational entropy. When the field is turned off, molecules that have partially entered this pillar region quickly recoil in the pillar-free region to maximize their conformational entropy. Longer DNA molecules take longer to enter the pillared region than shorter molecules, thus making separation possible.

Fractionation of long DNA molecules is also demonstrated in microfabricated hexagonal arrays and asymmetric structures.[40] Statistical data show that nanopores can distinguish between DNA molecules of similar length and composition that differ only in sequence. Nanopores can quickly discriminate and characterize unlabeled DNA molecules at low copy number. Artificial gel on microchips alleviates the difficulties associated with the irreproducible architecture of gels and viscous polymer solutions. It is able to optimize the geometry of the system to both increase the separation speed and reduce the diffusion by the use of the deformation that the chain endures in the narrow passages. The main disadvantage of the promising technique is that the production of entropic trapping devices is a sophisticated and costly procedure with little tunability after construction.

CONCLUSIONS

We hope that this brief review has given the reader a general feeling of the development and application of CE in the separation of nucleic acids. With the advent of capillary array electrophoresis and microchip electrophoresis, as well as remarkable improvements in separation matrices, CE has become a standardized and cost-effective technique in the separation of nucleic acids. Novel thermoresponsive polymer solutions combine the merits of different monomers, and offer the possibility to fine-tune the desirable properties of polymer molecular architecture and chemical composition. Artificial entropic trapping systems obviate the use of viscous polymer solutions, and even offer fast, unattended, miniaturized, and multiplexed platforms. Optimizing the geometry of these electrophoretic systems to both increase the separation and reduce the diffusion (band broadening) is the main topic for future research.

ACKNOWLEDGMENTS

This work was partially supported by the CREST program of the Japan Science and Technology Corporation (JST); a grant from the New Energy and Industrial Technology Development Organization (NEDO) of the Ministry of Economy, Trade, and Industry, Japan; a Grant-in-Aid for

Scientific Research from the Ministry of Health and Welfare, Japan; a Grant-in-Aid for Scientific Research from the Ministry of Education, Science, and Technology, Japan; a Grant-in-Aid of the 21st Century COE Program, Human Nutritional Science on Stress Control, from the Ministry of Education, Science, and Technology, Japan; and a Grant-in-Aid from Shimadzu Corp., Japan.

REFERENCES

1. Harrison, D.J.; Manz, A.; Fan, Z.; Luedi, H.; Widmer, H.M. Capillary electrophoresis and sample injection systems integrated on a planar glass chip. Anal. Chem. **1992**, *64* (17), 1926–1932.
2. Stellwagen, N.; Gelfi, C.; Righetti, R.G. The free solution mobility of DNA. Biopolymers **1997**, *42* (6), 687–703.
3. Ren, H.; Karger, A.E.; Oaks, F.; Menchen, S.; Slater, G.W.; Drouin, G. Separating DNA sequencing fragments without a sieving matrix. Electrophoresis **1999**, *20* (12), 2501–2519.
4. Baba, Y.; Matsuura, T.; Wakamoto, K.; Morita, Y.; Nishitsu, Y.; Tsuhako, M. Preparation of polyacrylamide gel filled capillaries for ultrahigh resolution of polynucleotides by capillary gel electrophoresis. Anal. Chem. **1992**, *64* (11), 1221–1225.
5. Effenhauser, C.S.; Paulus, A.; Manz, A.; Widmer, H.M. High-speed separation of antisense oligonucleotides on a micromachined capillary electrophoresis device. Anal. Chem. **1994**, *66* (18), 2949–2953.
6. Han, J.; Craighead, H.G. Separation of long DNA molecules in a microfabricated entropic trap array. Science **2000**, *288* (5468), 1026–1029.
7. Kurata, M.; Tsunashima, Y. Viscosity–molecular weight relationships and unperturbed dimensions of linear chain molecules. In *Polymer Handbook*; Brandrup, J., Immergut, E.H., Eds.; John Wiley & Sons: New York, 1989.
8. Viovy, J.-L.; Heller, C. Principles of size-based separations in polymer solutions. In *Capillary Electrophoresis in Analytical Biotechnology*; Righetti, P.G., Ed.; CRC Press: Boca Raton, 1996; 477–508.
9. Barron, A.E.; Sunada, W.M.; Blanch, H.W. The use of coated and uncoated capillaries for the electrophoretic separation of DNA in dilute polymer solutions. Electrophoresis **1995**, *16* (1), 64–74.
10. Xu, F.; Jabasini, M.; Zhu, B.; Ying, L.; Cui, X.; Arai, A.; Baba, Y. Single-step quantitation of DNA in microchip electrophoresis with linear imaging UV detection and fluorescence detection through comigration with a digest. J. Chromatogr. A, **2004**, *105* (1–2), 147–153.
11. Gelfi, C.; Perego, M.; Righetti, P.G. Capillary electrophoresis of oligonucleotides in sieving liquid polymers in isoelectric buffers. Electrophoresis **1996**, *17* (9), 1470–1475.
12. Cheng, J.; Mitchelson, K.R. Glycerol-enhanced separation of DNA fragments in entangled solution capillary electrophoresis. Anal. Chem. **1991**, *66* (23), 4210–4214.
13. Xu, F.; Jabasini, M.; Baba, Y. DNA separation by microchip electrophoresis using low-viscosity hydroxypropylmethylcellulose-50 solutions enhanced by polyhydroxy compounds. Electrophoresis **2002**, *23* (20), 3608–3614.
14. Rye, H.S.; Glazer, A.N. Interaction of dimeric intercalating dyes with single-stranded DNA. Nucleic Acids Res. **1995**, *23* (7), 1215–1222.
15. Hjertén, S. High-performance electrophoresis: elimination of electroendosmosis and solute adsorption. J. Chromatogr. **1985**, *347*, 191–198.
16. Salas-Solano, O.; Carrilho, E.; Kotler, L.; Miller, A.W.; Goetzinger, W.; Sosic, Z.; Karger, B.L. Routine DNA sequencing of 1000 bases in less than one hour by capillary electrophoresis with replaceable linear polyacrylamide solutions. Anal. Chem. **1998**, *70* (19), 3996–4003.
17. Chiari, M.; Cretich, M.; Riva, S.; Casali, M. Performances of new sugar-bearing poly(acrylamide) copolymers as DNA sieving matrices and capillary coatings for electrophoresis. Electrophoresis **2001**, *22* (4), 699–706.
18. Madabhushi, R.S. Separation of 4-color DNA sequencing extension products in noncovalently coated capillaries using low viscosity polymer solutions. Electrophoresis **1998**, *19* (2), 224–230.
19. Song, L.; Liang, D.; Kielescawa, J.; Liang, J.; Tjoe, E.; Fang, D.; Chu, B. DNA sequencing by capillary electrophoresis using copolymers of acrylamide and *N*,*N*-dimethylacrylamide. Electrophoresis **2001**, *22* (4), 729–736.
20. Song, L.; Liu, T.; Liang, D.; Fang, D.; Chu, B. Separation of double-stranded DNA fragments by capillary electrophoresis in interpenetrating networks of polyacrylamide and polyvinylpyrrolidone. Electrophoresis **2001**, *22* (17), 3688–3698.
21. Xu, F.; Jabasini, M.; Baba, Y. Fast screening reduced-viscosity mixed polymer solutions using an orthogonal designing approach for microchip separation of specific DNA. In *Proceedings of Micro Total Analysis Systems 2003*; Northrup, M.A., Jensen, K.F., Harrison, D.J., Eds.; Transducers Research Foundation, Inc.: Ohio, 2003; 259–262.
22. Bunz, A.P.; Barron, A.E.; Prausnitz, J.M.; Blanch, H.W. Capillary electrophoretic separation of DNA restriction fragments in mixtures of low- and high-molecular-weight hydroxyethylcellulose. Ind. Eng. Chem. Res. **1996**, *35* (9), 2900–2908.
23. Baba, Y. Analysis of disease-causing genes and DNA-based drugs by capillary electrophoresis towards DNA diagnosis and gene therapy for human diseases. J. Chromatogr. B, **1996**, *687* (2), 271–302.
24. Baba, Y.; Tsuhako, M.; Sawa, T.; Akashi, M.; Yashima, E. Specific base recognition of oligonucleotides by capillary affinity gel electrophoresis using polyacrylamide-poly(9-vinyladenine) conjugated gel. Anal. Chem. **1992**, *64* (17), 1920–1925.
25. DeDionisio, L. Capillary gel electrophoresis and the analysis of DNA phosphorothioates. J. Chromatogr. A, **1993**, *652* (1), 101–108.
26. Han, F.; Lillard, S. In-situ sampling and separation of RNA from individual mammalian cells. Anal. Chem. **2000**, *72* (17), 4073–4079.
27. Wu, C.; Liu, T.; Chu, B. Viscosity-adjustable block copolymer for DNA separation by capillary electrophoresis. Electrophoresis **1998**, *19* (2), 231–241.

28. Liu, Y.; Locke, B.R.; Van Winkle, D.H.; Rill, R.L. Optimizing capillary gel electrophoretic separations of oligonucleotides in liquid crystalline Pluronic F127. J. Chromatogr. A, **1998**, *817* (1–2), 367–375.
29. Liu, T.; Liang, D.; Song, L.; Nace, V.M.; Chu, B. Spatial open-network formed by mixed triblock copolymers as a new medium for double-stranded DNA separation by capillary electrophoresis. Electrophoresis **2001**, *22* (3), 449–458.
30. Bokias, G.; Durand, A.; Hourdet, D. Molar mass control of poly(*N*-isopropylacrylamide) and poly(acrylic acid) in aqueous polymerizations initiated by redox initiators based on persulfates. Macromol. Chem. Phys. **1998**, *199* (7), 1387–1392.
31. Liang, D.; Zhou, S.; Song, L.; Zaitsev, V.S.; Chu, B. Copolymers of poly(*N*-isopropylacrylamide) densely grafted with poly(ethylene oxide) as high-performance separation matrix of DNA. Macromolecules **1999**, *32* (19), 6326–6332.
32. Paegel, B.M.; Emrich, C.A.; Wedemayer, G.J.; Scherer, J.R.; Mathies, R.A. High throughput DNA sequencing with a microfabricated 96-lane capillary array electrophoresis bioprocessor. Proc. Natl. Acad. Sci. U.S.A. **2002**, *99* (2), 574–579.
33. Woolley, A.T.; Hadley, D.; Landre, P.; deMello, A.J.; Mathies, R.A.; Northrup, M.A. Functional integration of PCR amplification and capillary electrophoresis in a microfabricated DNA analysis device. Anal. Chem. **1996**, *68* (23), 4081–4086.
34. Tian, H.; Brody, L.C.; Fan, S.; Huang, Z.; Landers, J.P. Capillary and microchip electrophoresis for rapid detection of known mutations by combining allele-specific DNA amplification with heteroduplex analysis. Clin. Chem. **2001**, *47* (2), 173–185.
35. Shi, Y.; Simpson, P.C.; Scherer, J.R.; Wexler, D.; Skibola, C.; Smith, M.T.; Mathies, R.A. Radial capillary array electrophoresis microplate and scanner for high-performance nucleic acid analysis. Anal. Chem. **1999**, *71* (23), 5354–5361.
36. Kim, Y.; Morris, M.D. Rapid pulsed field capillary electrophoretic separation of megabase nucleic acids. Anal. Chem. **1995**, *67* (5), 784–786.
37. Mitnik, L.; Heller, C.; Prost, J.; Viovy, J.L. Segregation of DNA solutions induced by electric fields. Science **1995**, *267* (5195), 219–222.
38. Ueda, M.; Hayama, T.; Takamura, Y.; Horiike, Y.; Baba, Y. Investigation of the possibility of geometrical electrophoresis. Electrophoresis **2002**, *23* (16), 2635–2641.
39. Turner, S.W.; Cabodi, M.; Craighead, H.G. Confinement-induced entropic recoil of single DNA molecules in a nanofluidic structure. Phys. Rev. Lett. **2002**, *88* (12), 128103.
40. Chou, C.F.; Bakajin, O.; Turner, S.W.; Duke, T.A.; Chan, S.S.; Cox, E.C.; Craighead, H.G.; Austin, R.H. Sorting by diffusion: an asymmetric obstacle course for continuous molecular separation. Proc. Natl. Acad. Sci. U.S.A. **1999**, *96* (24), 13,762–13,765.
41. Heller, C. The separation matrix. In *Analysis of Nucleic Acids by Capillary Electrophoresis*; Heller, C., Ed.; Vieweg Verlagsgesellschaft: Wiesbaden, 1997; 9.
42. Madabhushi, R.S.; Vainer, M.; Dolnik, V.; Enad, S.; Barker, D.L.; Harris, D.W.; Mansfield, E.S. Versatile low-viscosity sieving matrices for nondenaturing DNA separations using capillary array electrophoresis. Electrophoresis **1997**, *18* (1), 104–111.

Octanol–Water Distribution Constants Measured by CCC

Alain Berthod
Laboratory of Analytical Sciences, University of Lyon I, Villeurbanne, France

Abstract
The octanol–water partition coefficient ($P_{o/w}$) of a compound is the most universally accepted physicochemical parameter related to its polarity and/or hydrophobicity. $P_{o/w}$ can be measured directly without any approximation by countercurrent chromatography (CCC). CCC uses two liquid phases to separate mixtures. When the stationary phase is octanol and the mobile phase is water, the retention volume of all injected components is directly proportional to their respective $P_{o/w}$ coefficient.

INTRODUCTION

Hydrophobicity, from the Greek *hydro* (water) and (*phobia*) aversion, is a term referring to the way a molecule "likes" or "does not like" water. A compound with a high hydrophobicity will not be water soluble. It is apolar. Conversely, a compound with low hydrophobicity is said to be hydrophilic or polar. It is likely to be water soluble. In between the two extremes, hydrophobicity varies. A scale is needed. The problem is that hydrophobicity, or the polarity of a compound, depends on several parameters such as the dipole moment, the dielectric constant, the polarizability, the proton donor or acceptor character, or even the boiling point to molecular mass ratio. Since the end of the nineteenth century, the *octanol–water partition coefficient*, which should preferably be termed *distribution constant*, $P_{o/w}$, has been used with success as a measure of molecular hydrophobicity. The log $P_{o/w}$ is a convenient scale. Compounds with a positive log $P_{o/w}$ value are more and more hydrophobic or apolar as the value increases. Compounds with a negative log $P_{o/w}$ value are hydrophilic or polar.[1]

It is of paramount importance to be able to measure accurately the $P_{o/w}$ and log $P_{o/w}$ value of a compound, because they are the accepted parameters used by the Food and Drug Administration (FDA) and the Environmental Protection Agency (EPA) and many other international drug and environmental agencies to estimate the tendency of an organic chemical to bioconcentrate into living cells. A new drug cannot be considered by the FDA and EPA without the $P_{o/w}$ parameter.

Countercurrent chromatography (CCC) is a liquid chromatography (LC) technique in which the stationary phase is a support-free liquid phase.[2] Since the mobile phase is also a liquid, a two-phase liquid system must be used (see *CCC/MS*, p. 323). Octanol and water are two solvents very partly miscible. They form a biphasic liquid system. Octanol can be used as the stationary phase in CCC with the aqueous phase, saturated in octanol, being the mobile phase.

DISTRIBUTION CONSTANT, PARTITION COEFFICIENT, AND DISTRIBUTION RATIO

The first step is to define clearly the terms used. The *distribution constant* (K_D) is the ratio of the concentration of a solute in a single definite form in the organic phase to its concentration in the same form in the aqueous phase at equilibrium, e.g., for a solute A:

$$(K_D)_A = \frac{[A]_{org}}{[A]_{aq}} \quad (1)$$

A good synonym for K_D is *partition ratio.* The term *partition coefficient* is not recommended by IUPAC.[3] The *distribution constant* is proportional to the retention time in CCC if and only if the solute exists in a single definite form (no ionization, no complexation, no chemical reaction possible). In that case, $K_D = D$, the *distribution ratio.* The *distribution ratio* (D) is the ratio of the *total* analytical concentration of a solute in the liquid stationary phase, regardless of its chemical form, to its total analytical concentration in the mobile phase. As defined, the *distribution ratio* can vary with experimental conditions, e.g., pH, presence of complexing agents. It should not be confused with *distribution constant*, K_D (or *partition coefficient*, P, the term not recommended but still commonly used, especially as $P_{o/w}$), which applies to a particular chemical species and is by definition invariable. The *distribution ratio* of a solute is directly proportional to its CCC retention time or volume, not necessarily the *distribution constant*.

Let's make this delicate point clear using benzoic acid as an example. Benzoic acid does partition between octanol and water. However, in the aqueous phase, benzoic

acid can ionize, becoming the benzoate anion with very little or no affinity for the octanol liquid phase. Also, in the octanol phase, two molecules of benzoic acid can associate, forming a dimer. To make things simple, it is assumed that there are no benzoate anions in the octanol phase and no dimers in the aqueous phase. According to Eq. 1, the octanol–water distribution constant or partition coefficient of benzoic acid, φCOOH, is:

$$P_{o/w} = \frac{[\varphi\text{COOH}]_{oct}}{[\varphi\text{COOH}]_{aq}} \tag{2}$$

The distribution ratio that is measured by the retention time of benzoic acid observed in CCC is expressed by:

$$D_{o/w} = \frac{\left([\varphi\text{COOH}]_{oct} + [\varphi\text{COOH}_2]_{oct}\right)}{\left([\varphi\text{COOH}]_{aq} + [\varphi\text{COO}^-]_{aq}\right)} \tag{3}$$

Using the acid dissociation constant, K_a, and the dimerization constant, k_2, of benzoic acid, the relationship between the distribution ratio, $D_{o/w}$, and the distribution constant, $P_{o/w}$, is given as:

$$D_{o/w} = P_{o/w}\left(\frac{1 + k_2[\varphi\text{COOH}]_{oct}}{1 + \frac{K_a}{[H^+]}}\right) \tag{4}$$

From a practical point of view, the octanol–water partition coefficient of benzoic acid is 74 ($\log P_{o/w} = 1.87$), its acid dissociation constant is 6.3×10^{-5} ($pK_a = 4.2$), and its dimerization constant, k_2, is about 0.04.[2] At physiological pH of 7.4, benzoic acid is exclusively in the benzoate anion form. Eq. 4 gives a $D_{o/w}$ value of 0.05 whatever be the benzoic acid concentration injected (the buffer capacity is assumed to be high). When 1 *M* benzoic acid is injected in a pH 1 buffered aqueous phase, the measured $D_{o/w}$ value will be 77. A 0.1 *M* injection at pH 1 would produce a $D_{o/w}$ value of 74.3. In all cases, the $P_{o/w}$ coefficient is 74. The peak position of benzoic acid in the CCC chromatogram critically depends on the aqueous phase pH and marginally on the injected concentration.

CLASSICAL $P_{O/W}$ MEASUREMENT METHODS

The most extensive and useful sets of $P_{o/w}$ data were obtained by simply shaking a solute with the two immiscible octanol and water phases and then analyzing the solute concentration in one or both phases. For many solutes, when there is repeated inversion (say ~100) of a 25 ml tube ~0.01 *M* solute, the two phases establish equilibrium in ~15 min. Very vigorous shaking can produce troublesome emulsions. The solute can be analyzed in only one phase and the concentration in the other can be obtained by the difference. The phase analysis is most often done by gas chromatography, liquid chromatography, or ultraviolet (UV)–Visible spectroscopy. The shake flask method gives reliable results over the wide 10^{-4}–10^4 range. However, it requires highly pure solutes and is very sensitive to the smallest contamination.

Reversed-phase liquid chromatography (RPLC), capillary electrophoresis (CE), micellar liquid chromatography (MLC), and electrochromatography (EC) can be used to estimate values of $\log P_{o/w}$ from the corresponding $\log k$ values; k is the retention factor directly related to the retention parameter of the solute of interest. Good correlations are generally found between $\log k$ and $\log P_{o/w}$ for structural congeners. Unfortunately, the correlations are much poorer with dissimilar compounds. Trace amounts of octanol were added in the mobile phase to enhance $\log k$ – $\log P_{o/w}$ correlations with a wide variety of solutes. The range is 1–$10^{5.5}$. The advantages of the RPLC method are its relative simplicity and the fact that it does not need highly pure solutes. At the moment, the correlation remains the main drawback. Today, CE with micellar mobile phases is becoming a commonly used tool in industry to rapidly obtain a good estimation of the $\log P_{o/w}$ of a particular solute.[4]

DIRECT $P_{O/W}$ MEASUREMENT BY CCC

The decisive advantage of CCC in measurement is that there is no correlation at all. Water saturated with octanol is the mobile phase. Octanol saturated with water is the stationary phase. The octanol–water distribution constant of a given solute is the only physicochemical parameter responsible for the solute retention. If the solute is not highly pure, it is likely that the impurities will have differing values. This means that if the impurities have differing retention volumes, they are separated during the measurement from the solute of interest.

The $P_{o/w}$ value is easily derived from the CCC retention equation:

$$V_R = V_M + PV_S \tag{5}$$

using

$$P_{o/w} = \frac{(V_R^- V_M)}{V_S} = 1 + \frac{(V_R^- V_C)}{V_S} \tag{6}$$

In these equations, the volume subscripts R, M, S, and C stand for retention, mobile phase, stationary phase, and column volume, respectively.

If octanol is the stationary phase and water the mobile phase, $P_{o/w}$ is the octanol–water distribution constant (partition coefficient) without any assumption but with the condition that no chemical change can affect the

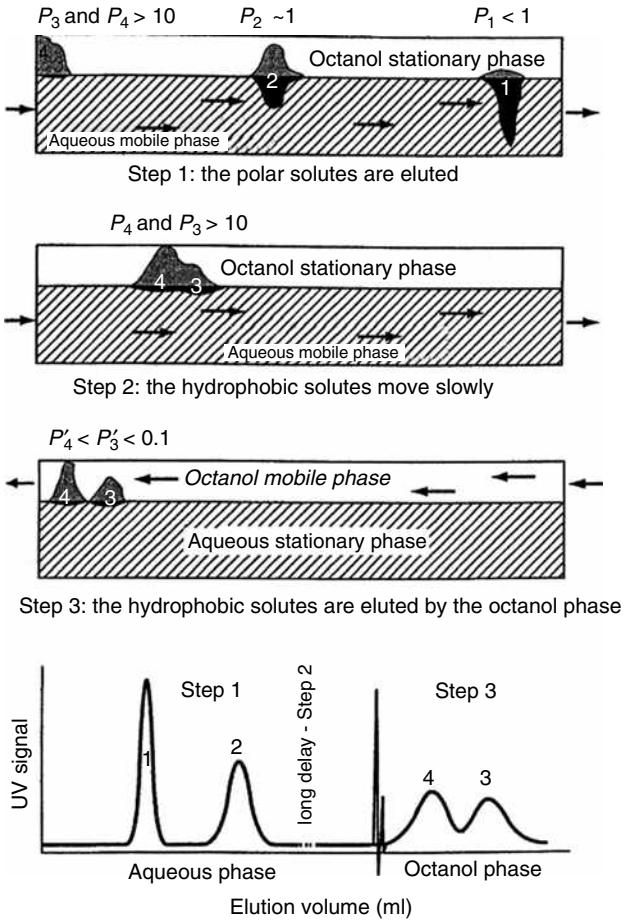

Fig. 1 Dual-mode CCC: Steps 1 and 2, classical elution mode. Step 3, both the nature and flowing direction of the mobile phase are changed.

solute (especially no ionization). Correlations of the $P_{o/w}$ or log $P_{o/w}$ values obtained with the same liquid system by the shake flask method and by CCC produce straight lines with a slope of unity and a negligible intercept. The validity and solidity of the method were assessed by Gluck and Martin for $P_{o/w}$ coefficients.[5] The $P_{o/w}$ range that can be obtained directly by CCC is limited to 0.05–200.[1,2] It is limited on the high side by the experiment duration. A value of 200 corresponds to a V_R retention volume of 6 L with a V_S value of only 30 ml (Eq. 5). This is 1200 min or 20 hr with a 5 ml/min flow rate. The lower-side limitation is due to experimental precision. The difference between the retention volume V_R and the dead volume V_M is equal to PV_S (Eq. 5). With a 30 ml V_S volume, the $P_{o/w}$ value of 0.05 corresponds to a $V_R - V_M$ value of only 1.5 ml. Such a low value may be difficult to evaluate with an acceptable accuracy. To increase the measurable range, the fact that the CCC stationary phase is a liquid can be used. This led to the dual-mode use of CCC and the cocurrent operation.

DUAL-MODE CCC

The idea is simple: Solutes with very high $P_{o/w}$ values move very slowly in the octanol phase; they need too long a time to emerge from the apparatus. To force them out of the CCC apparatus, the role of the aqueous and octanol phases and their flow directions are reversed after some reasonable flowing time in the normal direction. The dual-mode operation is illustrated in Fig. 1. It was demonstrated that the $P_{o/w}$ value can be simply expressed by

$$P_{o/w} = \frac{V_{aq}}{V_{oct}} \tag{7}$$

in which V_{aq} is the aqueous-phase volume passed in the normal way (descending or head to tail, Steps 1 and 2) and V_{oct} is the octanol-phase volume passed in the reversed way (ascending or tail to head, Step 3). The highest $P_{o/w}$ value that can be measured is again limited by the lowest volume that can be accurately determined. Because of band broadening, the practical minimum V_{oct} value is about 3 ml.[1] Then, with a 6000 ml V_{aq} volume, the corresponding $P_{o/w}$ value is 2000. Table 1 shows the experimental conditions corresponding to the dual-mode measurement of some $P_{o/w}$ values in the 40–3000 range. It was shown that the error on the $P_{o/w}$ determination was minimized when the octanol flow rate in the reversed mode was very low.[1]

COCURRENT CCC

The cocurrent CCC operation takes advantage of the liquid nature of the stationary phase. If a lipophilic solute stays too long inside the CCC apparatus, why not push it out, pushing the liquid stationary phase slowly in the same direction as the mobile phase? The theoretical treatment[6] and the practical promise of the method were established.[7] Three pumps are needed. Pump 1 allows the adjustment of the aqueous-phase flow rate in the few milliliters per minute range. Pump 2 governs the octanol phase flow rate in the microliter per minute range. Pump 3 is used to add a clarifying agent to the phase mixture leaving the CCC apparatus. The clarifying agent can be 2-propanol; it solubilizes the trace amounts of octanol present in the aqueous phase. The method is interesting in that there is no abrupt change; that is, it is continuous. The octanol volume retained in the CCC system is very stable, more stable than with other methods, because there is a constant input of octanol. The octanol volume changes, due to dissolution that was noted in the direct method or due to phase reversal as noted in the back-flushing method, do not exist with the cocurrent CCC method. The volume was determined using a test solute (2-chlorophenol, $P_{o/w} = 147$ in Ref. 7). Another very important effect that was experimentally observed is the increased peak efficiency due to the octanol flow rate. The measurable $P_{o/w}$ range was

Table 1 Octanol–water distribution ratio measured using different CCC methods.

Direct measurements						
Solute	$V_{R\ (ml)}$	$t_{R\ (hr)}$		$P_{o/w}$	log $P_{o/w}$	Literature
Benzamide	240	0.8		4.4 ± 0.1	0.64 ± 0.01	0.64 ± 0.02
Acetophenone	1,020	3.4		40 ± 0.8	1.60 ± 0.01	1.6 ± 0.02
2-Chlorobenzoic acid	2,280	7.6		97 ± 2	2.00 ± 0.01	2.0 ± 0.02
2-Chlorophenol	3,370	10.9		145 ± 2	2.16 ± 0.01	2.15 ± 0.03
Dual-mode measurements						
Solute	$V_{aq\ (ml)}$	$t_{R\ (hr)}$	$V_{oct\ (ml)}$	$P_{o/w}$	log $P_{o/w}$	Literature
Benzoic acid	178	0.8	2.36	74 ± 1.8	1.87 ± 0.02	1.85 ± 0.02
2-Chlorophenol	487	2.2	2.7	180 ± 2	2.24 ± 0.05	2.15 ± 0.03
Toluene	2,627	9.0	5.5	478 ± 5	2.68 ± 0.02	2.71 ± 0.06
Biphenyl	19,600	65	1.0	$19{,}600 \pm 140$	4.29 ± 0.02	3.8 ± 0.2
Cocurrent measurements						
Solute	$V_{oct\ (ml)}$	$t_{R\ (hr)}$	$V_{R\ (ml)}$	$P_{o/w}$	log $P_{o/w}$	Literature
Benzene	29.7	10.5	2,530	107 ± 5	2.03 ± 0.01	2.14 ± 0.03
Toluene	20.2	12	6,520	490 ± 10	2.69 ± 0.01	2.71 ± 0.06
Naphthalene	20.2	28.6	15,500	$5{,}100 \pm 100$	3.7 ± 0.03	3.2 ± 0.2
Phenanthrene	22.2	18.1	9,790	$20{,}000 \pm 1{,}000$	4.3 ± 0.1	4.4 ± 0.3

Adapted from Berthod,[1] Berthod & Carda-Broch,[4] and Berthod & Hassoun.[7]

extended up to 20,000 (log $P_{o/w} = 4.3$). Table 1 lists the actual conditions of some measurements by the cocurrent CCC method. The CCC methods presented here were extensively used to measure the value of molecular compounds.

IONIZABLE COMPOUNDS

The method was recently adapted to measure the $P_{o/w}$ values of ionizable compounds using buffered octanol-saturated aqueous phases.[8] Charged entities may well partition somewhat with octanol so that the $P_{o/w}$ coefficient for the molecule is associated to a K_D^- constant for its anion. In the case of an ionizable AH compound giving the A^- anion, the distribution ratio, D, can be expressed by modifying Eq. 3 as:

$$D = \frac{[AH]_{oct} + [A^-]_{oct}}{[AH]_{aq} + [A^-]_{aq}} \quad (8)$$

Using the AH dissociation constant K_a, the distribution constant can be expressed as:

$$D = \frac{P_{o/w} + K_D^- \left(\frac{K_a}{[H^+]}\right)}{1 + \frac{K_a}{[H^+]}} \quad (9)$$

K_D^- is the $P_{o/w}$ distribution constant of A^-, the anionic form of AH. Eq. 9 clearly shows that the D value measured by CCC for an ionizable compound is not $P_{o/w}$. It is highly dependent on the pH and solute pK$_a$. It was demonstrated[8] that three measurements at three pH values around the pK$_a$ value allows the determination of the molecular $P_{o/w}$ value of the solute as well as the $P_{o/w}$ value of its corresponding anion. Even though the $P_{o/w}$ values of the ions were always small as expected for such hydrophilic entities, they were not nil. CCC may be the only experimental method allowing estimation of the hydrophobicity of ions.[4,8]

ACKNOWLEDGMENTS

The French Centre National de la Recherche Scientifique, UMR5180 (P. Lanteri), is gratefully acknowledged for continuous support.

REFERENCES

1. Berthod, A. Liquid–liquid partition coefficients. In *Centrifugal Partition Chromatography*; Foucault, A.P. Ed.; Chromatographic Science Series; Marcel Dekker Inc.: New York, 1995; Vol. 68, 167–198.
2. Berthod, A. *Countercurrent Chromatography: The Support-free Liquid Stationary Phase*, Comprehensive Analytical Chemistry Series; Elsevier: Amsterdam, 2002; Vol. XXXVIII.

3. Rice, N.M.; Irving, H.M.N.H.; Leonard, M.A. Nomenclature for liquid-liquid distribution. Pure & Appl. Chem. **1993**, *65*, 2373–2396.
4. Berthod, A.; Carda-Broch, S. J. Determination of liquid-liquid partition coefficients by separation methods. Chromatogr. A, **2004**, *1037*, 3–14.
5. Gluck, S.J.; Martin, E.J. Assessment of CCC for determination of octanol-water partition coefficients. J. Liq. Chromatogr. **1990**, *13*, 2529–2551.
6. Berthod, A. Mesure de coefficients de partage par CCC. Analusis **1990**, *18*, 352–358.
7. Berthod, A.; Hassoun, M. Using the liquid nature of the stationary phase in CCC. IV-the Cocurrent CCC method. J. Chromatogr. A, **2006**, *1116*, 143–148.
8. Berthod, A.; Carda-Broch, S.; Alvarez-Coque, M.C.G. Hydrophobicity of ionizable compounds. A theoretical study and measurements of diuretic octanol-water partition coefficients by CCC. Anal. Chem. **1999**, *71*, 879–888.

On-Column Injection for GC

Mochammad Yuwono
Gunawan Indrayanto
Faculty of Pharmacy, Airlangga University, Surabaya, Indonesia

INTRODUCTION

The injection system in a gas chromatography (GC) analysis provides a means of introducing the sample onto the column. This is normally a simple injector design when packed columns are used. Capillary or open tubular columns require, however, more sophisticated design than do packed columns, because of their very low capacities and small internal diameters. A number of different injector designs have been recently developed. Unfortunately, no universal injector has so far been commercially available to handle all sample types. This entry will discuss various approaches to sample injection.

SELECTION OF INJECTION MODE

The selection of the most suitable injection system becomes important, especially when samples containing widely different boiling point components and different concentrations are to be analyzed.[1,2] Today, the most commonly used injectors for capillary GC fall into one of four techniques, i.e., split, splitless, on-column injection, and programmed-temperature vaporizers (PTV). The split injection mode was the first sample introduction system developed for capillary GC which, as the name signifies, splits the vaporized sample into two unequal portions, allowing only the smaller portion of it into the column and venting the larger from the system. The injector involves a heated chamber including a glass liner, into which the sample is introduced through an injection septum. For many applications, it is the most convenient sampling method, as it is very easy to operate, producing perfect peak shapes and good resolution after injecting concentrated samples in the same manner as for packed column systems.[3] A major drawback of the split injection technique is the so-called sample discrimination due to the uneven flash vaporization of the sample. The discrimination means that not all components of the vaporized samples are brought quantitatively into the column. When a sample containing compounds with widely different boiling points is analyzed with the split sampling technique, the less volatile components are discriminated. Consequently, the resultant chromatogram does not truly describe the real composition of the sample components; so the quantitative analysis becomes unreliable.[3,4] To minimize or prevent this, the use of other injection techniques is suggested, such as cooled needle injection, very fast injection, cold on-column or programmable vaporization.[5] Using an internal standard or an autosampler can also greatly enhance the accuracy of the results. With split techniques, problems arise also in analyzing thermally labile compounds which may decompose at the injection operating temperature. Introducing the samples using cold on-column injection technique is the best solution to solve this problem.[5,6] Because the split technique is beneficial for analysis of samples containing compounds at high concentration, the splitless injection mode was then developed for analyzing trace-level compounds. In this splitless technique, the entire vaporized sample volume is directed into the column by closing the split vent (purge off mode). In this way, the sample is transferred completely and slowly into the column; this ensures quantitative and representative sample introduction. Most split injectors today can operate in the splitless mode. These injectors are normally called split/splitless injectors, which can be operated first in a splitless mode (usually less than 1 min), allowing to gradually force the majority of the vaporized sample to the column inlet. The mode is then operated in split mode to purge the excess solvent. The method does not need fast vaporization, so that it is advantageous for the analysis of thermally unstable compounds. However, the solvent focusing techniques and other parameters must be gently optimized; otherwise, the results obtained are not reproducible and are low in accuracy.[5,7] The splitless injection technique is still used for the routine determination of trace-level compounds, such as for pesticide residues, drug impurities, etc. Direct and on-column flash vaporization injection has also been applied recently, which offers some advantages over the splitless technique for trace samples.[8] For the same purpose, cold on-column injection is also increasing in popularity as a technique for the analysis of the trace compounds, because of its higher precision and accuracy.

DIRECT AND ON-COLUMN INJECTION

Direct injection is often confused with on-column injection. Direct injection allows the injection of liquid samples into a heated injection port. After injection, the

sample is subsequently vaporized and then completely directed onto the column.[5,9] The evaporation of sample occurs in the inlet, which is heated independently from the column oven. The most commonly used inlet is a glass liner, and no sample splitting or venting occurs during or after injection. Direct injection is limited to widebore or megabore columns.[5] In on-column injection, the sample enters the column directly from the syringe and does not contact other surfaces. On-column injection generally indicates cold on-column injection for capillary columns.[5] The terms "hot on-column injection" and "on-column flash vaporization" are elsewhere introduced.[9] The hot on-column mode is different from the direct injection in the inlet that is used and in the termination point of the syringe needle during injection.[8] The technique is called direct injection when a glass inlet sleeve is used, and the evaporation of the injected sample occurs outside the column. With an on-column injection, a specially designed liner or a part of the column is used as inlet which allows the injection of the liquid sample inside the column and the evaporation of the sample also occurs on the column wall surface.[5,9] This simple technique is usually used for packed column GC. However, it has recently become popular because it can also be used with capillary columns (0.32 and 0.53 mm I.D.).

Specially designed injection port inlet sleeves have been available on the market for direct and hot on-column injection.[7,8] In the direct injection mode, 2–4 mm I.D. inlet sleeves are commonly used, which permit a sufficient space for sample evaporation; however, the on-column mode is usually performed by inserting a 26-gauge needle inside a 0.53 mm I.D. column. Direct injection is more favorable because it is less problematic than the hot on-column mode.[9] Because the liner can trap non-volatile residues before entering the column, this technique is suitable for dirty samples. Compared to the splitless mode, the direct injection is advantageous, involving less adsorption of the solutes and better sensitivity. However, with this technique, the adsorption of the sample may occur on the inlet sleeve during the evaporation process.[9] In this case, the hot on-column mode offers more benefits.

COLD ON-COLUMN INJECTION TECHNIQUE

As the name indicates, the cold on-column injector allows the injection of the sample directly as a liquid onto the column, of which the inlet and/or outlet section is maintained at a lower temperature than the oven. After the solutes are focused in the inlet section of column, the sample is then vaporized as the oven temperature is increased. In this way, all of the sample components are transferred into the column, so that the sample discrimination attributed to the syringe needle heating during injection is eliminated; it is also convenient for the analysis of thermally labile compounds.[1,10] The possibility of peak broadening is due only to band broadening in space.[5,11] This technique yields excellent quantitative precision and accuracy for samples that contain less volatile and highly volatile compounds.[12–14] Unlike the on-column flash vaporization injection, cold on-column is the true on-column technique, because both the injection of the sample and the evaporation occur inside the column.

An injector device for on-column work was first introduced by Schomburg in 1977.[15] In 1978, Grob and Grob[16] developed an excellent injector design which requires, principally, a syringe guide and a stop valve. A standard syringe with stainless steel needle of 0.23 mm I.D. (32-gauge) and 8 cm in length was used for the commonly used 0.32 mm I.D. glass capillary column. The needle is introduced through a conical aperture into the 0.3 mm inlet channel, close to the stop valve. By pushing down the syringe and guiding the needle into the capillary column, the sample is injected onto the column. After injection, the syringe is moved back, the valve is closed, and the syringe is finally withdrawn. The bottom of the body is cooled by a fan-driven air circulator to maintain the low temperature of the column inlet. This is called primary cooling. Complete construction of the design was described by Grob and Grob.[16] Further development of the cold on-column injection device included the use of secondary cooling, which is done by circulating air directed from a jacket surrounding the capillary inlet toward the injection area of the column.[17] The secondary cooling system is to cool the area of the column where the sample is actually injected. The use of secondary cooling can totally eliminate syringe discrimination and ensures that the temperature of the needle channel can be controlled to avoid solvent evaporation. The secondary cooling is advantageous, especially when the injector is combined with temperature programming.[1,18] Fig. 1 shows a typical on-column injector with provision for secondary cooling of the column inlet. The evolution of the cold on-column injection technique occurred because syringes with fused silica needles had been introduced to replace commonly employed metal needles; the injection onto a capillary column of 0.22 mm I.D. then became reality. The fused silica needles are inert and perfectly straight.[5,7] This innovative work makes the on-column injection technique gain more acceptance. The programmed-temperature on-column injector was then developed, in which the column inlet is housed in a separate injection oven, so that the column inlet temperature can be programmed from subambient to about 350°C and thermostated independently of the column oven.[1] For thermally labile compounds, it is suggested that the temperature is programmed at a low heating rate,

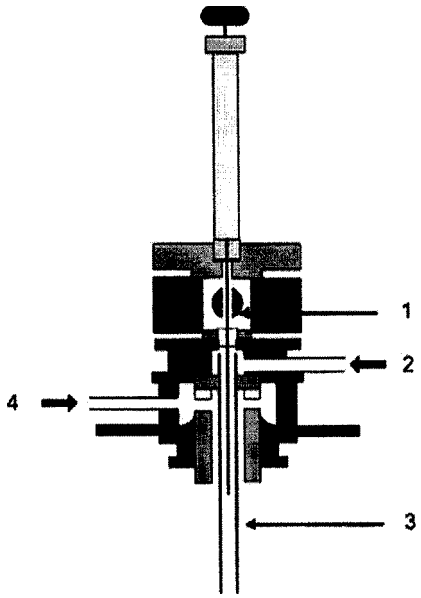

Fig. 1 Schematic diagram of a typical cold on-column injector with provision for secondary cooling of the column inlet. 1: Rotating valve, 2: carrier gas, 3: capillary column, 4: secondary cooling.

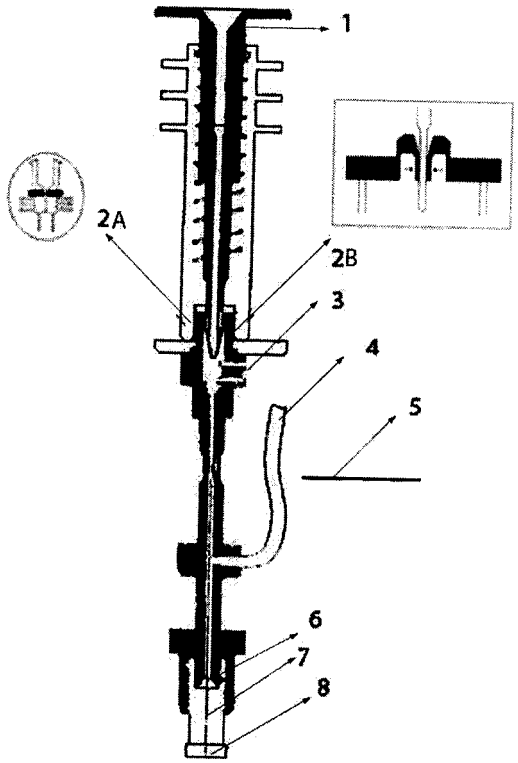

Fig. 2 Schematic diagram of a cross section of a cold on-column injector with a duck-bill valve. 1: Cool tower needle guide, 2A: disk septum for automated injections, 2B: isolation valve for manual injections, 3: frit, 4: carrier gas, 5: oven wall, 6: ferrule, 7: capillary column, 8: column nut.
Source: From Sample introduction, in *High Resolution Gas Chromatography*.[5]

whereas a rapid rise is favored for vaporization of samples containing highly different boiling point components.[6,7] A version of an on-column injector design that offers a low thermal mass, which facilitates cooling, has been developed. In this injector, a duck-bill valve constructed from a soft elastomer, such as in a flexible septum, is applied to form a gas-tight seal compressed by the column inlet pressure. When the needle guide is depressed, the isolation valve is parted and the metal guide is forced through the duck-bill valve.[5] This permits the syringe needle to pass the valve and enter the column. When the plunger is released, gas flow through the column is restored. The system can be performed for manual and automated injections. The duck-bill valve is modified with a disk septum when automated cool on-column injection is applied (Fig. 2). A movable on-column injector has also been introduced to facilitate the up-and-down movement of the column oven wall.[13] The cold on-column injection technique can now be operated in the constant-pressure, constant-flow, or pressure-programmed modes, allowing the reduction of analysis times. Moreover, electronic pressure programming offers the advantages that column pressure can be controlled accurately and precisely, resulting in very low relative standard deviations of retention time reproducibility.[5] The most suitably used carrier gas is hydrogen.[5,6]

The attractive features of cold on-column injection are that they allow analysis at a low temperature; thus it is the most convenient method for analysis for thermally unstable compounds. Compared with the flash vaporizing injection technique, it is also the method of choice for analysis of the samples with widely different boiling point components, because the cold on-column injection technique enables quantitative transfer of a sample and thereby provides a more accurate result. However, there are also difficulties with this method, such as peak splitting and peak spreading due to band broadening in space. These effects frequently result when large volume injections are performed. Because the sample enters the column inlet as a liquid plug, the injection of larger sample volumes forms several meters of a layer distributed on the column wall and they remain there until the column temperature increased. This is called a flooded zone situation, which is responsible for peak broadening and double peaks. The length of the flooded zone is related to the volume sample injected, the polarity difference between the solvent and the stationary phase, and the column temperature used. Injecting a small sample volume (<1 μl) can minimize the peak distortion and yield good results in terms of the peak shape and analytical precision. The speed of injecting the sample

into the column also has an effect on sample loss during on-column injection. It is suggested to inject the samples rapidly at the temperature of the column oven, but not higher than the boiling point of the solvent. Depressing the plunger at a slow rate causes a part of the sample to adhere to the needle, and the sample component is discriminated. As the detection level is restricted by the small injection volume, a large volume sampling method is frequently required to enhance the detectability, especially for trace analysis.[19] Using a technique called "retention gap," which allows the injection of a large volume of sample (>2 μl), can minimize the peak distortion. The retention gap is a length of fused silica tubing connected to the front of the analytical column by means of a suitable connector. It is actually a precolumn that does not contain any stationary phase, and the surface is deactivated to reduce solute interaction. Unlike the usual fused silica column, the retention gap has, consequently, a low or negligible retention character. To obtain a uniform sample film on the column wall, the solvent used should be selected in such a way that it wets the surface of the retention gap. Injection of the sample into the retention gap is followed by the evaporation of the solvent, leading to focusing of the sample components. When the solvent has completely evaporated, the solutes are sharply focused on the stationary phase. This approach has shown great success to improve peak shapes for many types of samples. As a general rule, typically used retention gaps are 25 to 50 cm in length, or about 25–30 cm for each microliter of solvent injected. A retention gap of 7 m × 0.32 μm I.D. enables injection of volumes up to about 50 μl; whereas 250 μl can be injected using a 10 m × 0.53 μm I.D. uncoated precolumn. The use of a retention gap offers some advantages; it allows the operation of an automated injection with regular syringe needles.[20,21] Moreover, the retention gap can act as guard column which reduces contamination when "dirty samples" are analyzed.[4,6] On-column injection with a retention gap technique performs better than PTV solvent splitting for the analysis of volatile, labile, and high-boiling components, but it is sensitive to contamination of the precolumns with non-evaporating sample by-products. Large-volume, cold on-column injections are increasing in popularity as methods for analysis of trace-level components and, especially, for environmental analysis.[22–25]

CONCLUSIONS

Cold on-column injection is an injection technique for GC which offers some advantages: elimination of sample discrimination, elimination of sample alteration, and high analytical precision and accuracy. Peak splitting or peak distortion, which may occur as a result of polarity mismatches of solvent, stationary phase, and solutes, can be reduced by means of a retention gap. Today, the cold on-column technique using a retention gap is one of the most commonly employed techniques for large-volume injections

ACKNOWLEDGMENTS

The authors thank DAAD (Deutscher Akademischer Austauschdienst), Bonn, Germany, for the financial support during our short visit at TU Braunschweig and at the University of Duesseldorf in 2002. We are also grateful to Miss Ivy Widjaja and Mr. Dedy Triono for their technical assistance.

REFERENCES

1. Schomburg, G. In *Gas Chromatography, A Practical Course*; VCH Verlagsgesellschaft: Weinheim, 1990.
2. Sandra, P. In *Sample Introduction in Capillary Gas Chromatography*; Hüthig: Heidelberg, 1985.
3. Grob, K. In *Split and Splitless Injection in Capillary GC*; Hüthig: Heidelberg, 1998.
4. Poole, C.F.; Poole, S.K. In *Chromatography Today*; Elsevier: Amsterdam, 1991.
5. Sandra, P. Sample introduction. In *High Resolution Gas Chromatography*; Hyver, K.J., Ed.; Hewlett-Packard Co. 1989.
6. Ravindranath, B. In *Principles and Practice of Chromatography*; Ellis Horwood Limited: Chichester, 1989.
7. Fowlis, I.A. In *Gas Chromatography: Analytical Chemistry by Open Learning*; John Wiley & Sons: New York, 1995.
8. http://www.chromtech.net.au/pdf/rtxflash.pdf (accessed January 2004).
9. Sandra, J.F. Gas chromatography. In *Ullmann's Encyclopedia of Industrial Chemistry*; Wiley-VCH Verlag GmbH: Weinheim, 2002.
10. Grob, R.L.; Barry, E.F.; Eds. In *Modern Practice of Gas Chromatography*; Wiley Interscience: New York, 1997
11. Adamovics, J.A.; Eschbach, J.C. In *Gas Chromatography in Chromatographic Analysis of Pharmaceutical*; Marcel Dekker, Inc.: New York, 1997.
12. Badings, H.T.; De Jong, C. Glass capillary gas chromatography of fatty acid methyl esters. A study of conditions for the quantitative analysis of short- and long-chain fatty acids in lipids. J. Chromatogr. **1983**, *279*, 493–506.
13. Geeraert, E.; Sandra, P.; De Schepper, D. On-column injection in the capillary gas chromatography analysis of fats and oils. J. Chromatogr. **1983**, *279*, 287–295.
14. Bonilla, M.; Enriquez, L.G.; McNair, H.M. Use of cold on-column injection for the analysis of putrescine and cadaverine by gas chromatography. J. Chromatogr. Sci. **1997**, *35* (2), 53–56.
15. Schomburg, G. Sampling technique in capillary gas chromatography. J. Chromatogr. **1977**, *142*, 87–102.
16. Grob, K.; Grob, K., Jr. On-column injection on to glass capillary columns. J. Chromatogr. **1978**, *151*, 311–320.

17. Galli, M.; Trestianu, S. Benefits of a special cooling system to improve precision and accuracy in non-vaporizing on-column injection procedures. J. Chromatogr. **1981**, *203*, 193–205.
18. http://www.gaschromatographs.com/sample.asp (accessed January 2004).
19. Hinshaw, J. Capillary inlet systems for gas chromatographic trace analysis. J. Chromatogr. Sci. **1988**, *26*, 49–55.
20. Grob, K. On-column injection of large volumes using the retention gap technique in capillary gas chromatography. J. Chromatogr. **1985**, *334*, 129–155.
21. David, F.; Sandra, P.; Stafford, S.S. Application of retention gaps for optimized capillary GC. In *Application Note 228–245, Publ. No 43*; Hewlett-Packard Co., March 1994; 5962E–7904E.
22. http://www.textronica.com/aplicate/struktur/an9142.pdf (accessed in January 2004).
23. http://www.jtbaker.com/techlib/documents/quest2.htm (accessed in January 2004).
24. http://www.chem.agilent.com/cpdocs/5890%20Series%20II%20Cool%20On%20Column%20Operating%20Manual.pdf (accessed in January 2004).
25. Wilson, B.; Nixon, D.; Klee, M. Large-volume injection for gas chromatography using COC-SVE. In *Application Note 228–377, Publication No. 23*; Agilent Technology, March 1997; 5965E–7923E.

BIBLIOGRAPHY

1. Grob, K. In *On Column Injection in Capillary Gas Chromatography*; Hüthig: Heidelberg, 1998

Open-Tubular and Micropacked Columns for SFC

Brian Jones
Selerity Technologies, Inc., Salt Lake City, Utah, U.S.A.

INTRODUCTION

Supercritical fluid chromatography (SFC) with opentubular columns was first demonstrated in 1981 by Novotny and coworkers.[1] This technique, known as capillary SFC, was made available to the analytical community through the introduction of several commercial instruments in 1986. Initially difficult to use, improvements in instrumentation and hardware, coupled with a wider array of columns and restrictor options designed specifically for the technique, becoming available, have led to a general acceptance of the method in many laboratories. Not only useful as a research tool, capillary SFC is firmly established as an essential analytical method for production support and quality control in many industries. Some of these include chemical and petroleum manufacturing, pharmaceuticals, polymers, and environmental monitoring.

Packed columns have also been used in SFC for many years, predating capillaries by nearly 20 years. Many columns originally developed for liquid chromatography (LC) have found utility in SFC and have varied in internal diameter from smaller than 50 μm to very large-preparative-scale sizes. Definitions vary, but for purposes here, micropacked columns are considered to have internal diameters less than 2 mm. These smaller diameter columns are also in wide use and offer significant benefits with regard to mobile-phase consumption and detector compatibility than their large-bore counterparts. The selectivity and performance of micropacked columns are complimentary to those of capillaries, and instrumentation is available that is compatible with both separation techniques, allowing for the separation of a wide range of analytes and rapid switchover between methods. Several reviews have been published.[2–4]

PRESSURE DROP EFFECTS

Elution of a particular compound in SFC is a function of its extent of interaction with the column stationary phase and the solvating strength of the mobile phase, with the latter being a direct function of density. The density is affected by temperature and pressure and, in the case of separations with capillary columns that are inherently open and exhibit little pressure drop across their length, it is essentially constant throughout. By contrast, packed columns exhibit much more resistance to mobile-phase flow and can experience a considerable density drop during SFC analysis, producing a potentially significant loss in separation efficiency. Commercial packed columns, tested only by high-performance liquid chromatography (HPLC), may not show these deficiencies in their test reports. The only reliable gauge of suitability of a column for SFC is a performance test in the SFC mode. Columns tested under SFC conditions and tested for suitability for a specific SFC method have been commercially available for some time.

The pressure drop effect limits the usable length of packed columns to approximately 25 cm, although micropacked columns prepared specifically for SFC can be used to longer lengths.[5] The particle size also plays a role, with packing materials smaller than 5 μm producing the highest pressure drops. Whereas short columns dominate in packed column SFC, typical parameters for capillary columns are 3–10 m in length, 50 μm in inner diameter, and a stationary-phase film thickness of 0.25 μm, which give the best compromise in loadability, analysis speed, and efficiency.

Calculated practical efficiencies for a compound with a capacity factor of 2 and a CO_2 mobile phase are shown for each type of column in Table 1. It is clear that capillary columns are capable of delivering high efficiency separations in SFC, but at the expense of analysis time when compared to packed columns.

ACTIVITY

Silica surfaces are the chief source of activity in columns for SFC and, even though many of the columns are well deactivated, the residual silanol sites can lead to tailing or adsorption of analytes. The low surface area of capillary columns is responsible for much higher levels of inertness than their packed counterparts based on silica particles. Capillary columns have been used successfully in the analysis of active compounds, including isocyanates, acid halides, organic acids, amines, peroxides, azo compounds, and many others. The low temperatures required for elution make analysis of active and labile compounds viable.

Silica particles have high surface areas and usually contain a large number of exposed residual silanol groups after derivatization. These groups impart a significant degree of polarity to packed columns and can be used to advantage, for example, in the determination of aromatics in fuels.[6] For more active solutes, modifiers are used to reduce tailing and improve quantitation.

Table 1 Calculated practical efficiencies for compound with a capacity factor of 2 and CO_2 mobile phase.

Column type	Particle diameter, internal diameter (μm)	Length (m)	Plates at low density (100 atm, 100°C)	Plates at high density (100 atm, 100°C)	Linear velocity (cm/sec) at low density	Linear velocity (cm/sec) at high density
Packed	5	0.1	5,200	9,100	0.6	2.1
Capillary	50	10	102,000	19,000	2.5	5.8

Source: From *Analytical Supercritical Fluid Chromatography and Extraction.*[2]

MODIFIERS

The addition of cosolvents to the mobile phase can be effective in adjusting selectivity and improving sample solubility. As the most dramatic effect with polar modifiers is seen in the interaction with the surface silanol groups, even small amounts of cosolvents change the elution characteristics of packed columns. With capillary columns, the effect is related more to solvent strength of the mobile phase than surface modification, and higher modifier levels are required to produce significant changes in retention.

One of the drawbacks of using modifiers is their response in some of the detectors. The flame ionization detector (FID) is very popular with capillary and micropacked columns in SFC because of its near-universal response and high sensitivity and the lack of response of CO_2 as the most popular mobile phase. The low mass flow rate of the mobile phase in small columns allows for a direct interfacing of the column to the FID and other detectors without flow splitting or back-pressure regulation.

SAMPLE INTRODUCTION

The small internal volume and low mobile-phase mass flow rates in capillary and micropacked column SFC place significant demands on the injection system and connections. The injector must deliver a small, narrow band of material onto the head of the column and must not contain any void volume or unswept area in the flow path. Several methods of injection are in common use, including the following:

1. Split, where the column is placed in the injector such that it intercepts a portion of the sample stream with the excess carried past and out of the system through a flow restrictor. This method gives the highest efficiencies, but it can produce some sample discrimination.
2. Timed-split, where the sample loop is placed in the flow stream for short periods, and the time in the inject position determines the amount on column. This is the most popular injection method and gives good efficiency and reproducibility. It requires fast actuation and an internal sample loop.
3. Split-splitless, which is performed with a split assembly and a split vent shutoff valve. This method enables larger volumes to be admitted onto the columns and the split activates to reduce tailing by sweeping residual amounts of material out of the system.

The use of a retention gap can allow for higher efficiencies and larger injection volumes on capillary columns.[7] The retention gap is a section of uncoated tubing placed between the column and the injector, which allows the analytes to refocus into a narrow band at the head of the column. This uncoated section can be built right into the capillary column such that no additional connections are required.

RESTRICTORS

Restrictors are required at the ends of SFC columns to maintain supercritical conditions throughout the column and to limit overall flow. Several options exist, with frit restrictors being the most popular, followed by integral and linear formats. The frit restrictor is made by casting a porous ceramic material inside fused-silica tubing with the flow rate dependent on length and pore size. These restrictors are robust and are easily tuned to the desired flow rate by trimming small sections off of the frit end. The multiple flow paths are also resistant to plugging. Frit restrictors are supplied in varied porosities in the end of deactivated 50 μm inner diameter tubing and are attached to the end of the column using low dead-volume connectors. Integral restrictors are made by heating fused-silica tubing to its melting point and allowing it to collapse to a single orifice of very small diameter.The end can be ground to form a larger opening, but this process requires considerable patience. This type of restrictor can be fabricated in the end of the column such that no connectors are required, but the single orifice is more susceptible to plugging with stray particles than are other types. Linear restrictors are made from short lengths of fused-silica tubing with narrow internal diameters. These are interfaced to the column with low-dead-volume connectors, but the long pressure drop across the tubing length can cause some analytes to precipitate prematurely and produce detector spiking.

STATIONARY PHASES

A wide variety of stationary phases and bonded-phase particles for SFC are available. Capillary columns are coated with substituted and cross-linked polysiloxanes, which exhibit good inertness, efficiency, and stability. There are three main classes of capillary column stationary phases for SFC: apolar, polarizable, and polar.

Apolar

Methyl silicone, 5% phenyl-substituted silicone, and 50% octyl-substituted silicone separate generally on the basis of solute volatility. The most significant interactions are inherently weak van der Waal's. These phases have the highest diffusion properties and give the highest efficiencies. Highly polar materials overload easily on these columns and produce wedge-shaped peaks.

Polarizable

The 50% phenyl-substituted silicone and 30% biphenyl-substituted silicone stationary phases are moderately polar and contain polarizable aromatic rings that exhibit induced dipoles in the presence of dipolar solutes such as alcohols, phenols, amines, nitriles, ketones, and so forth. They give selectivity without extended retention of polar solutes because the dipole-induced–dipole interaction is relatively weak. Temperature affects the extent of this polarization and can be used as a variable in optimizing separations.

Polar

The 25% and 50% cyanopropyl phases exhibit permanent dipoles that interact strongly with polar solutes. Because this translates into longer retention times for polar solutes, only lower-molecular-weight materials of this type can be eluted. Polarizable (aromatic and unsaturated hydrocarbons) and weakly dipolar solutes are good candidates for analysis with these phases. Aliphatic hydrocarbons overload easily but elute rapidly.

Micropacked columns are available with most of the bonded-phase packings used in HPLC. Porous and nonporous silica particles are optionally functionalized with covalently ound silanes or other strongly adsorbed materials. Alkyl-bonded silicas produce separations, generally based on solute volatility, but with the potential for selectivity differences based on interaction with silanol groups. Underivatized silica is popular for petroleum separations of aliphatic and aromatic hydrocarbons. Silver-ion-containing silica columns are selective for olefin separations. Fluoroalkyl-bonded silicas produce unique selectivities and show good sample capacities for fluorocarbons. Polybutadiene-derivatized zirconia particles have also been used in SFC as have particles based on cross-linked organic polymers. These latter types show different selectivities because of the absence of surface silanol groups. Chiral-bonded phases capable of resolving enantiomers are seeing wide use, particularly in the pharmaceutical market.

RECENT ADVANCES

Recent developments in capillary and micropacked column SFC have centered on making the technique easier and more reliable to use. Columns are available that are fitted with restrictors, performance tested by SFC, and are ready to install. Dead-volume issues have been resolved with low-mass couplers and auto-depth-adjusting fingertight fittings suitable for high-pressure use. Packed columns have been developed and optimized for SFC use that have low pressure drops and high stabilities. The future should see a continuation of this trend, with more column options and formats becoming available and additional methods utilizing them seeing wide acceptance.

REFERENCES

1. Novotny, M.; Springston, S.R.; Peaden, P.A.; Fjeldstead, J.C.; Lee, M.L. Capillary supercritical fluid chromatography. Anal. Chem. **1981**, *53*, 407A.
2. Lee, M.L., Markides, K.E., Eds.; *Analytical Supercritical Fluid Chromatography and Extraction*; Chromatography Conferences: Provo, UT, 1990.
3. Caude, M., Thiebaut, D., Eds.; *Analytical Supercritical Fluid Chromatography and Extraction*; Harwood: Amsterdam, 1999.
4. Blomberg, L.G.; Demirbueker, M.; Haegglund, I.; Andersson, P.E. Supercritical fluid chromatography: Open tubular vs. packed columns. Trends Anal. Chem. **1994**, *13* (3), 126–137.
5. Li, W.; Malik, A.; Lee, M.L. Fused silica packed capillary columns using carbon dioxide slurries. J. Microcol. Separ. **1994**, *6* (6), 557–563.
6. Li, W.; Malik, A.; Lee, M.L.; Jones, B.A.; Porter, N.L.; Richter, B.E. Group-type separation of diesel fuels using packed capillary column supercritical fluid chromatography. Anal. Chem. **1995**, *67* (3), 647–654.
7. Chester, T.L.; Innis, D.P. Quantitative open-tubular supercritical fluid chromatography using direct injection onto a retention gap. Anal. Chem. **1995**, *67* (17), 3057–3063.

Open-Tubular Capillary Columns

Raymond P.W. Scott
Scientific Detectors Ltd., Banbury, Oxfordshire, U.K.

INTRODUCTION

Open-tubular columns were discovered by Golay[1] in the late 1950s and the first commercial columns were introduced in the early 1960s. The first capillary columns were fabricated from copper tubing 0.01 in. I.D. but, due to their somewhat variable geometry, were quickly replaced with the more rigid cupronickel tubing and, subsequently, by stainless-steel tubing.

DISCUSSION

Metal capillary columns need to be cleaned to remove traces of extrusion lubricants by washing them with methylene dichloride, methanol, and then water. They should also be washed with dilute acid to remove any metal oxides or corrosion products that remain adhering to the walls. The acid is removed with water and the tubing is again washed with methanol and methylene dichloride and dried in a stream of hot nitrogen.

Metal columns provide the expected high efficiencies and were used successfully for the analysis of low-polarity materials such as petroleum and fuel oils and, today, they are still extensively used for the analysis of hydrocarbons. Metal columns, however, although easily coated with dispersive stationary phases (e.g., squalane, Apiezon grease, etc.), do not coat well with the more polar stationary phases such as Carbowax®. In addition, the hot metal surface can cause decomposition and molecular rearrangement of many thermally labile materials that are being separated (e.g., the terpenes in essential oils). Metal can also react directly with some solutes by chelation and, as a result of surface adsorption, produce asymmetric and tailing peaks. Nevertheless, metal columns are rugged, easy to handle, and easy to remove and replace in the chromatograph, so their use has persisted in many applications despite the introduction of fused-silica columns.

In an attempt to eliminate surface activity, Desty et al.[2] introduced the first silica-based columns and invented an extremely clever device for drawing soft glass capillary columns. Desty produced both rigid soft glass and rigid Pyrex capillary columns, although their permanent circular shape rendered them a little difficult to connect to the injector and detector. It was found that, with special surface treatment, the rigid glass tubes could be coated with polar stationary phases. The demand for special surface processing evoked a large number of proprietary methods for column treatment. Fortunately, the frenetic interest in the surface deactivation of soft glass capillary tubes was curtailed by the introduction of the flexible fused-silica capillary columns by Dandenau and Zenner.[3]

The quartz fiber drawing technique used in the manufacture of data transmission lines was used to produce flexible *fused-silica* tubing. Basically, the solid quartz rod used in quartz fiber drawing was replaced by a quartz tube. In a similar manner to that used in the quartz fiber production, the quartz tubes were coated with polyimide to prevent moisture from attacking the surface and producing stress corrosion. Soft glass capillaries can be produced by the same technique at much lower temperatures,[4] but the tubes are not as mechanically strong or as inert as quartz capillaries. Flexibility was the main advantage to quartz capillaries, as it greatly facilitated the installation of the columns in the chromatograph. However, surface treatment is still necessary with a fused-quartz column to reduce adsorption and catalytic activity and render the surface wettable for efficient coating. The treatment may involve washing with acid, silanization, and other types of chemical treatment, including the use of surfactants.

Deactivation procedures used for commercial columns also tend to be highly proprietary. Adeactivation program for silica and soft glass columns that is suitable for most applications would first entail an acid wash. The column is filled with 10% (w/w) hydrochloric acid, the ends sealed, and the column then heated to 100°C for 1 hr. The column is then washed free of acid with distilled water and dried. This procedure is believed to remove traces of heavy metal ions that can cause adsorption and peak tailing. The column is then filled with a solution of hexamethyldisilazane, sealed, and heated to the boiling point of the solvent for 1 hr. This procedure blocks any hydroxyl groups on the surface that were generated during the acid wash. A polar or semipolar silane reagent might be preferable to facilitate coating if a polar stationary phase is to be used. The column is then washed with the pure solvent, dried at an elevated temperature in a stream of pure nitrogen, and is ready for coating.

Open-tubular columns can be coated internally with a liquid stationary phase or with polymeric materials that are subsequently polymerized to form a relatively rigid polymer coating. The two methods of coating are the *dynamic method of coating* and the *static method of coating*. In the dynamic coating procedure, a plug of solvent containing

the stationary phase is placed at the beginning of the column. The strength of the solution, among other factors, determines the thickness of the stationary-phase film. In general, the film thickness of an open-tubular column ranges from 0.25 mm to about 1.5 mm. As an estimate, a 5% (w/w) solution of stationary phase will provide a stationary film thickness of about 0.5 mm. After the plug has been run into the front of the column (sufficient solution should be added to fill about 10% of the column length), a gas pressure is used to force the plug through the column at about 2–4 mm/sec. When the plug has passed through the column, the gas flow is continued for about 1 hr. The gas flow should not be increased too soon, as ripples of stationary phase solution will form on the walls of the tube, which produces a very uneven film. After 1 hr, the flow rate is increased and the column stripped of solvent. The last traces of the solvent are removed by heating the column above the boiling point of the solvent at an increased gas flow rate.

In static coating, the entire column is filled with a solution of the stationary phase and one end connected to a vacuum. As the solvent evaporates, it retreats back down the tube, leaving a coating on the walls. The optimum concentration will depend on the stationary phase, the solvent, the temperature, and the condition of the wall surface. This process is very time-consuming but can proceed without attention and is often carried out overnight. This procedure is more repeatable than the dynamic method of coating, but, in general, it produces columns having a similar performance to those dynamically coated.

However-well the column may be coated, the stability of the column depends on the stability of the stationary-phase film, and thus on the constant nature of the surface tension forces holding it to the column wall. These surface tension forces can change with temperature or be effected by the samples used for analysis. As a consequence, the surface tension can be suddenly reduced and the film break up. It follows that the stationary phase should be bonded in some way to the column walls or polymerized *in situ*. Such coatings are called immobilized stationary phases and cannot be removed by solvent washing.

Some stationary phases that are polymeric in nature can sometimes be formed by coating the monomers or dimers on the walls and then initiating polymerization either by heat or a suitable catalyst. This locks the stationary phase to the column wall and is thus completely immobilized. Polymer coatings can be formed in the same way using dynamic coating. Techniques used for immobilizing the stationary phases are highly proprietary and little is known of the methods used. In any event, most chromatographers do not want to go to the trouble of coating their own columns and are usually content to purchase proprietary columns.

POROUS-LAYER OPEN-TUBULAR COLUMNS

There are two basic disadvantages to the coated capillary column. First, the limited solute retention that results from the small quantity of stationary phase in the column. Second, if a thick film is coated on the column to compensate for this low retention, the film becomes unstable resulting in rapid column deterioration. Initially, attempts were made to increase the stationary phase loading by increasing the internal surface area of the column. Attempts were first made to etch the internal column surface, which produced very little increase in surface area and very scant improvement. Attempts were then made to coat the internal surface with diatomaceous earth, to form a hybrid between a packed column and coated capillary. None of the techniques were particularly successful and the work was suddenly eclipsed by the production of immobilize films firmly attached to the tube walls. This solved both the problem of loading, because thick films could be immobilized on the tube surface, and that of phase stability. As a consequence, porous-layer open-tubular (PLOT) columns are not extensively used. The PLOT column, however, has been found to be an attractive alternative to the packed column for gas–solid chromatography (GSC) and effective methods for depositing adsorbents on the tube surface have been developed.

The open-tubular column is, by far, the most popular type of GC column in use today. As a result of its small internal cross section, however, extracolumn dispersion can become a serious problem. This means that open-tubular columns must be used with special types of injector and reduced volume connectors, and certain detectors must have specially designed sensor cells to avoid impairing column performance.

REFERENCES

1. Golay, M.J.E. *Gas Chromatography. 1998*; Desty, D.H., Ed.; Butterworths: London, 1958; 36.
2. Desty, D.H.; Goldup, A.; Wyman, B.F. J. Inst. Petrol. **1959**, *45*, 287.
3. Dandenau, R.D.; Zenner, E.M. An investigation of glasses for capillary chromatography. J. High Resolut. Chromatogr. **1979**, *2* (6), 351.
4. Ogan, K.L.; Reese, C.; Scott, R.P.W. Strong, flexible soft-glass capillary columns—a practical alternative to fused-silica. J. Chromatogr. Sci. **1982**, *20* (9), 425–428.

BIBLIOGRAPHY

1. Scott, R.P.W. *Techniques and Practice of Chromatography*; Marcel Dekker, Inc.: New York, NY, 1996.
2. Scott, R.P.W. *Introduction to Analytical Gas Chromatography*; Marcel Dekker, Inc.: New York, 1998.

Open-Tubular CEC

Joseph J. Pesek
Maria T. Matyska
Department of Chemistry, San Jose State University, San Jose, California, U.S.A.

INTRODUCTION

In capillary electrochromatography (CEC), there are two general approaches to this hybrid technique that combine features of both high-performance liquid chromatography (HPLC) and capillary electrophoresis (CE): the packed column configuration that utilizes stationary phases similar to HPLC, and the open tubular format where the stationary phase is immobilized on the capillary wall. A smooth transition exists from μ-HPLC to packed capillary CEC by adjusting the ratio of pressure-driven flow to electrically-driven flow. This adjustment results in an infinite number of hybrid techniques that can be generated from pure μ-HPLC (no electric field component) to pure packed capillary CEC (no pressure component). The transition region between CE and packed capillary CEC is not so smooth. The bridge is provided by open tubular capillary electrochromatography (OTCEC). There are not, however, the infinite number of choices that can be generated as in the bridge between μ-HPLC and packed capillary CEC. In all forms of CEC, there are two major separation mechanisms: solute-bonded phase interactions (as measured by the capacity factor, k') and electrophoretic mobility (μ_{ep}).

DEVELOPMENT AND USE OF OTCEC

The first effective OTCEC separations indicating chromatographic interactions were demonstrated a number of years ago by Tsuda and coworkers[1] using an octadecyl modified 30 μm I.D. capillary. A more definitive way of proving that chromatographic effects are possible in the open tubular format can be obtained through the separation of optical isomers. A number of chiral selectors, such as cyclodextrin and several cellulose derivatives that were bonded to the inner wall of fused silica capillaries, resulted in the separation of enantiomers.[2,3] Since the two optical isomers have identical electrophoretic mobilities, separation can only be achieved through differences in solute/bonded phase interactions. It has also been demonstrated that molecularly imprinted polymers bonded to the inner wall of a fused silica capillary can be another approach for a stationary phase in OTCEC.[4] Another, more often tested, approach involves immobilizing a relatively thick polymeric film[5,6] on the inner surface of the capillary. In this case, the bonded material is extended from the wall so that analytes have a shorter distance to travel in order to produce solute/bonded phase interactions (i.e., a chromatographic separation mechanism). Each of these early studies showed that OTCEC was feasible, at least for the limited number of samples and experimental conditions tested.

The focus of OTCEC for improving separation capabilities is with column technology. In the simplest approach, stationary phases are bonded to the inner wall of a fused silica capillary using standard organosilanization reactions, because free silanol groups exist on the surface. In this format, the OTCEC technique is often hampered by two fundamental problems that seriously limit its potential as a viable separation method: the low capacity of the column due to the small area available for bonding a stationary phase, and the long distance that molecules would have to migrate to interact with the bonded moiety. The latter problem could be addressed by reducing the column I.D., but this is often an unsatisfactory solution because such a decrease further limits the sample size, as well as the detection path length, in absorbance measurements and, hence, the detection limit of the analyte. Small diameter capillaries generally necessitate the use of higher sensitivity fluorescence detection or mass spectroscopy.

Column technology in OTCEC utilizes coating or direct bonding of various organic moieties to the capillary wall, as well as a number of approaches that are designed to increase the amount of stationary phase in the capillary. The simplest approach involves the physical adsorption of molecules to the wall. One successful example of this approach involves coating the inner wall of the capillary with a polymeric surfactant, very often a polyelectrolyte multilayer (PEM).[7] Direct bonding of a stationary phase to the fused silica wall often involves the use of organic groups with a high specificity for certain analytes. Examples of such compounds are calixarenes[8] that function as a host phase, or aptamers[9] that also have a high degree of molecular recognition. One method for increasing the amount of stationary phase and reducing the distance that solutes must travel to interact with it is to create a thin film on the surface. Thin films (0.15–0.20 μm) of molecularly imprinted polymers have been successful for enantiomeric separations.[10]

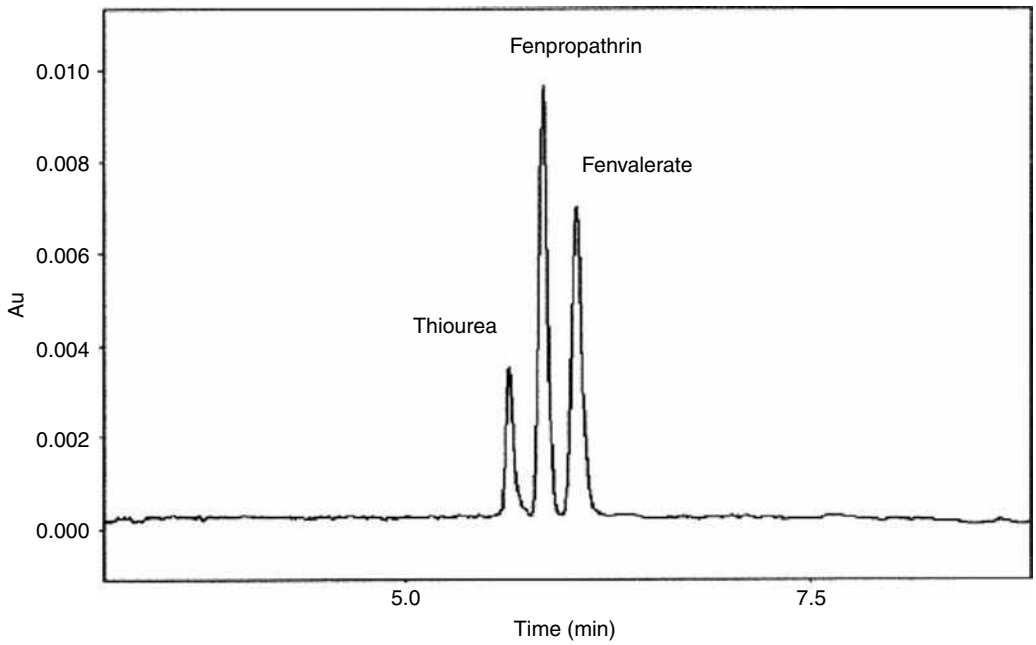

Fig. 1 Electrochromatogram of the separation of fenpropathrin and fenvalerate. Conditions: Au-APTMS coated capillary 30 cm × 20 μm I.D.; mobile phase: methanol–25 m*M* NaH_2PO_4 (75:25) pH 3.0; voltage: −25 kV; sample: thiourea, fenpropathrin, and fenvalerate in 100% methanol. Injection: −5 kV for 3 sec, UV detection: 200 nm.
Source: From Alkylthiol gold nanoparticles in open-tubular capillary electrochromatography, in J. Chromatogr.[15]

More extensive measures, beyond simple coatings, are necessary to expand OTCEC from a technique for a few specific applications to a more general method that can solve a broad range of analytical problems. One approach to accomplish this goal is to create a porous layer on the inner wall of the capillary. For example, a porous silica layer was deposited inside a narrow bore capillary (<10 μm I.D.) and then modified with a C_{18} stationary phase.[11] This column was able to separate a number of polycyclic aromatic hydrocarbons. A more widely used methodology for increasing the loadability and capacity factors in OTCEC utilizes sol–gel processes[12] that are based on the polymerization of alkoxides, such as tetramethoxysilane or tetraethoxysilane. This approach results in a porous silicate network on the surface of the capillary with variable chemical properties being produced as other substituted silanes are added to the sol–gel reaction process. The retention characteristics of the sol–gel phases are controlled by the amount of monomeric species in the initial solution.[13] Phases with hydrophilic, hydrophobic, and chiral properties have been fabricated.

Another approach for increasing the limited loading capacity for an ordinary fused silica capillary involves coating the wall with nanoparticles. Both latex[14] and gold[15] nanoparticles have been shown to be feasible. The latex materials, which are bound electrostatically to the wall, are composed of a quaternary ammonium ion exchange functionality and have been used for the separation of inorganic anions. The gold nanoparticles have the advantage of being covalently attached to the wall through an aminopropyl linkage. One reagent used was dodecanethiol, which leads to a relatively hydrophobic surface for reversed phase applications. An example of a separation done on a gold nanoparticle coated capillary is shown in Fig. 1.

A final capillary format utilizes both an increase in the surface area, as well as a different approach to the chemical modification of the surface for the stationary phase.[16] In this method, the surface is etched with ammonium bifluoride, a reagent that produces the same effects as HF but does not have the inherent safety risks. This etching process can increase the surface area of the capillary by a factor of 1000 or more and the etching agent becomes a part of the new wall matrix, making it more biocompatible and suitable for the analysis of basic compounds. After etching, the surface is modified by a silanization/hydrosilation reaction protocol to attach an organic moiety as the stationary phase, but it also converts virtually all of the silanols to hydride species. The high resolving power of this particular format is demonstrated in Fig. 2, which shows the analysis of PEGylated proteins.[17] These modified proteins can exist in a large number of similar chemical structures, making the separation of all species particularly difficult.

A possible new application for OTCEC exists in microfluidic chips, where open channels are the most common and easiest to fabricate configuration. Often, these devices utilize channels of just a few microns is diameter. These relatively small dimensions allow some separations to be

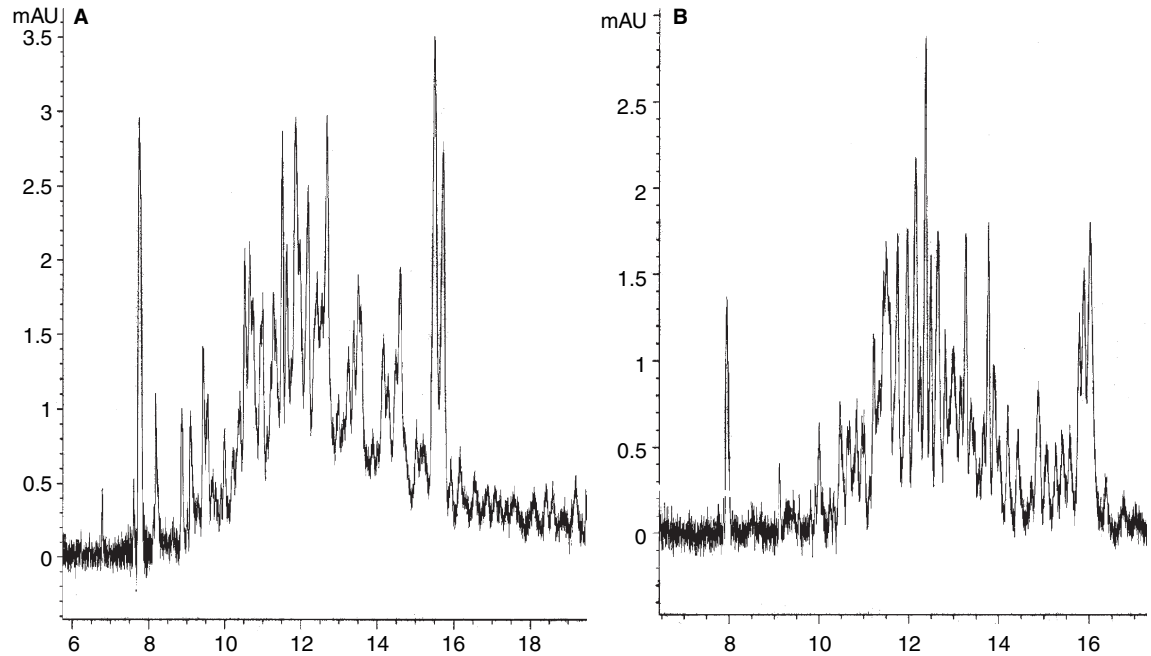

Fig. 2 Separation of PEGylated proteins on an etched cholesteryl modified capillary. A, PEG-catalase and B, PEG-protease. I.D = 50 μm, $L = 58$ cm, $l = 49.5$ cm, $V = 20$ kV, Buffer pH 2.14, injection 5 sec @ 50 mbar, detection at 210 nm.
Source: From Separation of PEGylated proteins by open tubular capillary electrochromatography, in J. Chromatogr.[17]

achieved in just a few seconds. However, these small channel dimensions make detection difficult, so that only the most sensitive methods, such as laser-induced fluorescence are practical. An example of a proteomic analysis for a trytpic digest of a protein is shown in Fig. 3.

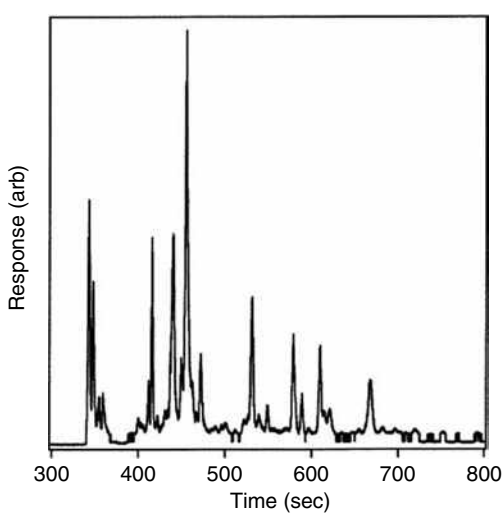

Fig. 3 Open tubular capillary electrochromatography separation on a chip of TRITC-labeled tryptic peptides of β-casein.
Source: From Two-dimensional electrochromatography/capillary electrophoresis on a microchip, in Anal. Chem.[18]

CONCLUSIONS

While OTCEC has been a known technique for a number of years, recent developments in column formats have advanced the technology so that it is a viable method for an increasing number of analyses. The dual mechanisms of electrophoretic mobility and chromatographic interactions offer a wide range of variables that can be used to optimize difficult separations. The development of miniaturized and microfluidic versions of OTCEC are likely to have significant impacts in pharmaceutical, forensic, and environmental analyses.

REFERENCES

1. Tsuda, T.; Nomura, K.; Nakagawa, G. Open-tubular microcapillary liquid chromatography with electro-osmosis flow using a UV detector. J. Chromatogr. **1982**, *248*, 241–271.
2. Armstrong, D.; Tang, Y.; Ward, T.; Nichols, M. Derivatized cyclodextrins immobilized on fused-silica capillaries for enantiomeric separations via capillary electrophoresis gas chromatography, or supercritical fluid chromatography. Anal. Chem. **1993**, *65*, 1114–1117.
3. Mayer, S.; Schurig, V. Enantiomer separation by electrochromatography in open tubular columns coated with chirasil-DEX. J. Liq. Chromatogr. **1993**, *16*, 915–917.
4. Bruggeman, O.; Freitag, R.; Whitcomb, M.J.; Vulfson, E.N. Comparison of polymer coatings of capillaries for capillary electrophoresis with respect to their applicability to

molecular imprinting and electrochromatography. J. Chromatogr. A, **1997**, *781*, 43–53.
5. Ruan, Y.; Kraak, J.C.; Poppe, H. Separation and evaluation of cross-linked polyacrylate stationary phases for open tubular liquid chromatography. Chromatographia **1993**, *35*, 597–606.
6. Swart, C.R.; Kraak, J.C.; Poppe, H. Preparation and evaluation of cross-linked polyacrylate-coated fused-silica capillaries for reversed-phase open-tubular liquid chromatography. J. Chromatogr. **1994**, *670*, 25–38.
7. Kapnissi, C.P.; Akbay, C.; Schlenoff, J.B.; Warner, I.M. Analytical separations using molecular micelles in open-tubular capillary electrochromatography. Anal. Chem. **2002**, *74*, 2328–2335.
8. Wu, X.; Liu, H.; Liu, H.; Haddad, P.R. Preparation and characterization of *p-tert*-butylcalix[8]arene bonded capillaries for open-tubular capillary electrochromatography. Anal. Chim. Acta **2003**, *478*, 191–197.
9. Clark, S.l; Remcho, V.T. Aptamers as analytical reagents. Electrophoresis **2002**, *23*, 1335–1340.
10. Schweitz, L. Molecularly imprinted polymer coatings for open-tubular capillary electrochromatography prepared by surface initiation. Anal. Chem. **2002**, *74*, 1192–1196.
11. Crego, A.L.; Martinez, J.; Marina, M.L. Influence of mobile phase composition on electroosmotic flow velocity, solute retention and column efficiency in open-tubular reversed-phase capillary electrochromatography. J. Chromatogr. A, **2000**, *869*, 329–337.
12. Quigley, C.; Marlin, N.D.; Melin, V.; Manz, A.; Smith, N.W. Advances in capillary electrochromatography and micro-high performance liquid chromatography monolithic columns for separation science. Electrophoresis **2003**, *24*, 917–944.
13. Guo, Y.; Colon, L.A. A stationary phase for open tubular liquid chromatography and electrochromatography using sol–gel technology. Anal. Chem. **1995**, *67*, 2511–2516.
14. Breadmore, M.C.; Macka, M.; Avdalovic, N.; Haddad, P.R. Open-tubular ion-exchange capillary electrochromatography of inorganic anions. Analyst **2000**, *125*, 1235–1241.
15. O'Mahony, T.; Owens, V.P.; Murrihy, J.P.; Guihen, E.; Holmes, J.D.; Glennon, J.D. Alkylthiol gold nanoparticles in open-tubular capillary electrochromatography. J. Chromatogr. A, **2003**, *1004*, 181–193.
16. Pesek, J.J.; Matyska, M.T. Electrochromatography in chemically modified etched fused silica capillaries. J. Chromatogr. **1996**, *736*, 255–264.
17. Pesek, J.J.; Matyska, M.T.; Krishnamoorthi, V. Separation of PEGylated proteins by open tubular capillary electrochromatography. J. Chromatogr. A, **2004**, *1044*, 317–322.
18. Gottschlich, N.; Jacobson, S.C.; Culbertson, C.T.; Ramsey, J.M. Two-dimensional electrochromatography/capillary electrophoresis on a microchip. Anal. Chem. **2001**, *73*, 2669–2674.

Open-Tubular Columns: Golay Dispersion Equation

Raymond P.W. Scott
Scientific Detectors Ltd., Banbury, Oxfordshire, U.K.

INTRODUCTION

The open-tubular column or capillary column is the one most commonly used in gas chromatography (GC) today. The equation that describes dispersion in open tubes was developed by Golay,[1] who employed a modified form of the rate theory, and is similar in form to that for packed columns. However, as there is no packing, there can be no multipath term and, thus, the equation only describes two types of dispersion. One function describes the longitudinal diffusion effect and two others describe the combined resistance to mass-transfer terms for the mobile and stationary phases.

DISCUSSION

The Golay equation takes the following form:

$$H = \frac{2D_m}{u} + \frac{f_1(k')r^2}{D_m}u + \frac{f_2(k')r^2}{K^2D_s}u \tag{1}$$

where H is the height of a theoretical plate or the variance/unit length, D_m is the diffusivity of the solute in the mobile phase, D_s is the diffusivity of the solute in the stationary phase, r is the column radius, k' is the capacity ratio of the solute, K is the distribution coefficient of the solute, and u is the mobile-phase linear velocity.

Open-tubular columns behave in exactly the same way as packed columns with respect to pressure. The same mathematical arguments can be reduced which results in the modified form of the equation shown in Eq. 2. As the column is geometrically simple, the respective functions of k' can also be explicitly developed.

$$H = \frac{2D_m}{u_0} + \frac{(1+6k'+11k'2)r^2}{24(1+k')^2D_{m(0)}}u_0 + \frac{2k'df^2}{3(1+k')^2D_s(\gamma+1)}u_0 \tag{2}$$

where u_0 is the exit velocity of the mobile phase and $D_{m(0)}$ is the diffusivity of the solute measured at the exit pressure. As the film is thin, $r \gg df$; then,

$$\frac{(1+6k'+11k'2)r^2}{24(1+k')^2D_{m(0)}} \gg \frac{2k'df^2}{3(1+k')^2D_s(\gamma+1)}$$

and, thus,

$$H = \frac{2D_{m(0)}}{u} + \frac{(1+6k'+11k'2)r^2}{24(1+k')^2D_{m(0)}}u_0 \tag{3}$$

By differentiating Eq. 3 and equating it to zero, expressions can be obtained for u_{opt} and $H_{\min}$ in a manner similar to the method used for a packed column:

$$u_{0(\text{opt})} = 2\frac{D_{m(0)}}{r}\left(\frac{12(1+k')^2}{1+6k'+11k'2}\right)^{1/2} \tag{4}$$

$$H_{\min} = \frac{r}{2}\left(\frac{1+6k'+11k'2}{3(1+k')^2}\right)^{1/2} \tag{5}$$

The approximate efficiency of a capillary column operated at its optimum velocity (assuming the inlet/outlet pressure ratio is small) can be simply calculated. If only the dead volume is considered (i.e., $k' = 0$), Eq. 3 reduces to

$$H = \frac{2D_m}{u} + \frac{1}{24}\frac{r^2}{D_m}u \tag{6}$$

Differentiating and equating to zero,

$$\frac{dH}{du} = -\frac{2D_m}{u^2} + \frac{1}{24}\frac{r^2}{D_m} = 0 \quad \text{or} \quad u = \frac{\sqrt{48}D_m}{r}$$

Substituting for u in Eq. 6 and simplifying,

$$H = \frac{2D_m r}{\sqrt{48}D_m} + \frac{1}{24}\frac{r^2}{D_m}\frac{\sqrt{48}D_m}{r} = 0.289r + 0.289r = 0.577r$$

Thus, the efficiency of a capillary column of length (l) can be assessed as

$$n = \frac{l}{0.6r} \tag{7}$$

The column efficiency will be inversely proportional to the column radius and the analysis time will directly proportional to the column radius and inversely proportional to the diffusivity of the solute in the mobile phase.

REFERENCES

1. Golay, M.J.E. *Gas Chromatography, 1958*; Desty, D.H., Ed.; Butterworths: London, 1958; 36.

BIBLIOGRAPHY

1. Scott, R.P.W. *Introduction to Analytical Gas Chromatography*; Marcel Dekker, Inc.: New York, 1998.
2. Scott, R.P.W. *Techniques and Practice of Chromatography*; Marcel Dekker, Inc.: New York, 1996.

Optical Activity Detectors

Hassan Y. Aboul-Enein
Pharmaceutical and Medicinal Chemistry Department, Pharmaceutical and Drug Industries Research Division, National Research Center, Dokki, Cairo, Egypt

Ibrahim A. Al-Duraibi
Pharmaceutical Analysis Laboratory, King Faisal Specialist Hospital and Research Center, Riyadh, Saudi Arabia

INTRODUCTION

Optical activity detectors are capable of specifically detecting chiral compounds, taking advantage of their unique interactions with polarized light. Much of the work on the development of prisms and other devices for the production of polarized light was done in the early part of the nineteenth century. However, the measurement of optical activity is often used for enantiomeric purity determination of chiral compounds, which by definition have either a center or plane of asymmetry. Enantiomers rotate the plane of polarized light in opposite directions, although in equal amounts. The isomer that rotates the plane to the left (counterclockwise) is called the levo isomer and is designated (−), whereas the one that rotates the plane to the right (clockwise) is called the dextro isomer and is designated (+). Questions of optical activity are of extreme importance in the field of asymmetric chemical synthesis and in the pharmaceutical industry.

DETECTION PRINCIPLE

Fig. 1 shows the basic optimal system of the optical rotation detector, which is based on the non-modulated polarized beam-splitting method. The light radiated from the light source is straightened by the plane polarizer, then to the lens for beam formation and concentration, and then to the flow cell.

The plane-polarized light which goes through the flow cell is rotated by optically active substances (chiral compounds) according to their specific optical rotations and concentrations. The light then enters the polarized beam splitter and is divided into two beams according to the polarized beam directions. These beams are detected by two photodiodes as shown.

The angle of the plane polarizer is adjusted so that the two photodiodes may receive the same beam intensity when no optically active substance is present in the flow cell.When optically active substances are present in the flow cell, the difference between the beam intensities received by the two photodiodes is not zero. Therefore, the difference has a linear relation with specific optical rotation and concentration of the optically active substance and can be expressed by where is the difference of beam intensities received by the two photodiodes (i.e., output of signal level), K is a constant determined by cell structure and light intensity of the light source, $[\alpha]$ is the specific optical rotation of the chiral compound, and C is the concentration of the chiral compound.

POLARIMETRY THEORY

Most forms of optical spectroscopy are usually concerned with the measurement of the absorption or emission of electromagnetic radiation. Ordinary, natural, unreflected light behaves as though it consists of a large number of electromagnetic waves vibrating in all possible orientations around the direction of propagation. If, by some means, we sort out from the natural conglomeration only those rays vibrating in one particular plane, we say that we have plane-polarized light. Of course, because a light wave consists of an electric and a magnetic component vibrating at right angles to each other, the term "plane" may not be quite descriptive, but the ray can be considered planar if we restrict ourselves to noting the direction of the electrical component. Circular polarized light represents a wave in which the electrical component (and, therefore, the magnetic component also) spirals around the direction of propagation of the ray, either clockwise ("right-handed" or dextrorotatory) or counterclockwise ("left-handed" or levorotatory). If, following the passage of the plane-polarized ray through some material, one of the circularly polarized components, say the left circularly polarized ray, has been slowed down, then the resultant would be a planepolarized ray rotated somewhat to the right from its original position. In addition, lasers have been incorporated into two optical rotation methods to date: polarimetry and circular dichroism.

OPTICAL ROTATION AND OPTICAL ROTATORY DISPERSION

A polarimeter measures the direction of rotation of plane-polarized light caused by an optically active substance. The

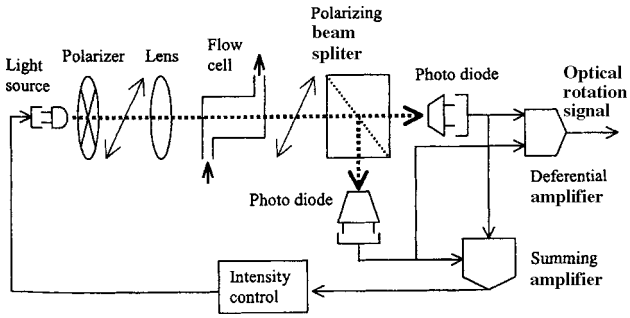

Fig. 1 Optical rotation detector.

specific optical activity of an asymmetrical molecule varies with the wavelength of the light used for its determination. This variation is called optical rotatory dispersion (ORD). In ORD, rotations are measured over a range of wavelengths rather than at a single wavelength, usually covering the ultraviolet (UV) as well as the visible region.

CIRCULAR DICHROISM

In this technique, the molecular extinction coefficients of a compound are measured with both left and right circularly polarized light, and the difference between these values is plotted against the wavelength of the light used. The phase angle between the projections of the two circularly polarized components is altered by passage through the chiral medium, but their amplitudes will be modified by the degree of absorption experienced by each component. This differential absorption of left- and right-circularly polarized light is termed circular dichroism (CD). So, circular dichroism measurements provide both absorbance and optical rotation information simultaneously.

CIRCULARLY POLARIZED LUMINESCENCE SPECTROSCOPY

Circularly polarized luminescence spectroscopy (CPLS) is a measure of the chirality of a luminescent excited state. The excitation source can be either a laser or an arc lamp, but it is important that the source of excitation be unpolarized to avoid possible photoselection artifacts. The CPLS experiment produces two measurable quantities, which are obtained in arbitrary units and related to the circular polarization condition of the luminescence. It is appropriate to consider CPLS spectroscopy as a technique that combines the selectivity of CD with the sensitivity of luminescence. The major limitation associated with CPLS spectroscopy is that it is confined to emissive molecules only.

VIBRATIONAL OPTICAL ACTIVITY

The optical activity of vibrational transitions has been conducted. The infrared (IR) bands of a small molecule can easily be assigned with the performance of a normal coordinate analysis, and these can usually be well resolved. One of the problems associated with vibrational optical activity is the weakness of the effect. Instrumental limitations of infrared sources and detectors create additional experimental constraints on the signal-to-noise ratios. Two methods suitable for the study of vibrational optical activity have been developed:

- *Vibrational Circular Dichroism*: Vibrational circular dichroism (VCD) could be measured at good signal-to-noise levels. Vibrational optical activity is observed in the classic method of Grosjean and Legrand.
- *Raman Optical Activity*: The Raman optical activity (ROA) effect is the differential scattering of leftor right-circularly polarized light by a chiral substrate where chirality is studied through Raman spectroscopy.

FLUORESCENCE-DETECTED CIRCULAR DICHROISM

Fluorescence-detected circular dichroism (FDCD) is a chiroptical technique in which the spectrum is obtained by measuring the difference in total luminescence obtained after the sample is excited by left- and right-circularly polarized light. For the FDCD spectrum of a given molecular species to match its CD spectrum, the luminescence excitation spectrum must be identical to the absorption spectrum.

FACTORS AFFECTING THE MEASUREMENT OF OPTICAL ROTATION

The rotation exhibited by an optically active substance depends on the thickness of the layer traversed by the light, the wavelength of the light used for the measurement, and the temperature of the system. In addition, if the substance being measured is a solution, then the concentration of the optically active material is also involved and the nature of the solvent may also be important. There are certain substances that change their rotation with time. Some are substances that change from one structure to another with a different rotatory power and are said to show mutarotation. Mutarotation is common among the sugars. Other substances, owing to enolization within the molecules, may rotate so as to become symmetrical and, thus, lose their rotatory power. These substances are said to show racemization. Mutarotation and racemization are influenced not only by time, but also by pH, temperature,

and other factors. Of course, rotations that determined for the same compound under the same conditions are identical. Therefore, in expressing the results of any polarimetric measurement, it is, therefore, very important to include all experimental conditions.

TEMPERATURE

Temperature changes have several effects on the rotation of a solution or liquid. An increase in temperature increases the length of the tube; it also decreases the density, thus reducing the number of molecules involved in the measurement. It causes changes in the rotatory power of the molecules themselves, due to association or dissociation and increased mobility of the atoms, and affects other properties. In addition, temperature changes cause expansion and contraction of the liquid and a consequent change in the number of active molecules in the path of the light.

The unique ability of the optical rotation detector to respond to the sign of rotation allows precise enantiomeric purity determination even if the enantiomers are only partially resolved. The sign of rotation is also useful in establishing enantiomer elution order.

Because the optical rotation detectors only respond to optically active compounds, enantiomeric purity determination to precisions of better than 0.5% can be achieved and is possible in even the complex mixtures. The detection can also be used as part of a flow injection analysis system to determine amount and enantiomeric purity of a drug in dosage form.

The applications using optical rotation detectors include the following:

1. Qualitative analysis of chiral compounds, including drugs, pesticides, carbohydrates, amino acids, liquid crystals, and other biochemicals
2. Determination of enantiomeric purity of chiral compounds
3. Monitoring an enzymatic reaction
4. Qualitative analysis of proteins
5. Use as a conventional polarimeter

However, the disadvantages of optical rotation detectors may be limited by shot or flicker noise, which are dependent on the optical and mechanical properties of the system or by noise in the detector electronics. Generally, the usefulness of this technique has been limited by the lack of sensitivity of commercially available instruments.

BIBLIOGRAPHY

1. Allenmark, S. *Techniques Used for Studies of Optically Active Compounds, in Chromatographic Enantioseparation: Methods and Application,* 2nd Ed.; Ellis Horwood Ltd: London, 1991.
2. Beesley, T.E.; Scott, R.P.W. An introduction to chiral chromatography. In *Chiral Chromatography*; Beesley, T.E., Scott, R.P.W., Eds.; John Wiley & Sons, Inc.: New York, 1998; 1–11.
3. Dodziuk, H. Physical methods as a source of information on the spatial structure of organic molecules. In *Modern Conformational Analysis, Elucidating Novel Exciting Molecular Structures*; Chanda, R., Ed.; VCH: New York, 1995; 48–54.
4. Edkins, T.J.; Shelly, D.C. Measurement concepts and laser-based detection in high-performance micro separation. In *HPLC Detection: Newer Methods*; Patonay, G., Ed.; VCH: New York, 1992; 1–15.
5. Goodall, M.D.; Lloyd, D.K. A note on an optical rotation detector for high-performance liquid chromatography. In *Chiral Separations*; Stevenson, D., Ed.; Plenum Press: New York, 1988; 131–133.
6. Sheldon, R.A. Introduction to optical isomersion. In *Chirotechnology: Industrial Synthesis of Optically Active Compounds*; Marcel Dekker, Inc.: New York, 1993; 25–27.
7. Weston, A.; Brown, P.R. *HPLC and CE Principles and Practice*; Academic Press: San Diego, CA, 1997.
8. Yeung, E.S. Polarimetric detectors, in detectors for liquid chromatography. In *Detectors for Liquid Chromatography*; Yeung, E.S., Ed.; John Wiley & Sons: New York, 1986; 204–228.

Optical Quantification or Densitometry in TLC

Joseph Sherma
Department of Chemistry, Lafayette College, Easton, Pennsylvania, U.S.A.

INTRODUCTION

Direct optical quantification in thin-layer chromatography (TLC) involves sample preparation, application of standard and sample zones, layer development, and in situ measurement of zones with a slit-scanning densitometer, diode array scanner, videodensitometer, or flatbed scanner. High-sample throughput (cost efficiency) and excellent accuracy, precision, sensitivity, linearity, robustness, and ruggedness are possible by use of high performance layers developed by capillary action or forced flow with optimized mobile phases; proper instrumental or manual application techniques; development of standards and multiple samples on the same plate under controlled conditions; uniform manual or semiautomated derivatization (detection) procedures; and computerized, automated scanning and data handling. The open-bed, simultaneous-development operation of TLC offers inherent advantages compared to single-sample quantitative column methods such as high-performance liquid chromatography (HPLC).

Densitometry was first used to directly measure the amount of light absorbed by radioactive spots on films or stained protein bands on electrophoresis gels in the transmission mode. TLC slit scanners were then developed to directly measure the diffuse reflectance of colored, ultraviolet (UV) absorbing, and fluorescent zones on a layer, followed by videodensitometers for documentation and quantification of layer images. Most recently, a commercial diode array scanner and office flatbed scanners (as purchased or modified) have been used for quantitative TLC.

Some non-densitometric methods that can be used for TLC quantification are described only briefly in this entry. The majority of the coverage is given to densitometry, which is the most widely used, highly sensitive [typical detection limits are in the medium picogram (fluorescence) to low nanogram (absorbance) range of analyte per zone], versatile, convenient, and reliable quantitative TLC method.

NON-DENSITOMETRIC QUANTIFICATION

Quantitative evaluation of thin-layer chromatograms can be performed by direct, in situ visual and indirect elution techniques. Visual evaluation involves comparison of the sizes and intensities of color or fluorescence between sample and standard zones spotted, developed, and detected on the same layer. The series of standards is chosen to have concentrations or weights that bracket those of the sample zones. After matching a sample with its closest standard, accuracy and precision are improved by respotting a more restricted series of bracketing standards with a separate sample spot between each of two standard zones. Accuracy no greater than 5–10% is possible for trained personnel using visual evaluation. The determination of ochratoxin A in coffee[1] and pharmaceutical dosage forms[2] are examples of practical applications of visual comparison of fluorescent zones and derivatized (colored) or UV-absorbing (fluorescence-quenched) zones, respectively.

The elution method involves scraping off the separated zones of sample aliquots and bracketing standards, and elution of the substances from the layer material with a strong, volatile solvent. The eluates are concentrated and analyzed by use of a sensitive spectrometry method (e.g., UV–Visible, infrared, or mass spectrometry), gas chromatography (GC), HPLC, immunoassay, electrophoresis, or electroanalysis. Scraping and elution must be performed manually because the only commercial automatic micropreparative elution instrument has been discontinued by its manufacturer. The scraping/elution method is tedious and time consuming and prone to errors caused by incorrect choice of the sizes of the areas to scrape, incomplete collection of sorbent, and incomplete or inconsistent elution recovery of the analyte from the sorbent. It is used today mostly as an off-line interface with spectrometric and other chromatographic methods for confirmation of the identity of sample zones (qualitative analysis) and seldom for quantitative analysis.

PRINCIPLES AND THEORY OF DENSITOMETRY

In order to achieve the optimum accuracy, precision, and sensitivity, most quantitative analyses are performed by using high-performance TLC (HPTLC) plates and direct quantification by means of a modern optical densitometric scanner with a fixed sample light beam in the form of a rectangular slit that is selectable in height (e.g., 0.4–10 mm) and width (20 μm–2 mm). Densitometers measure the difference in absorbance or fluorescence signal between a TLC zone (in the form of a peak) and the empty plate background (baseline) and relate the measured signals from a series of standards to those of unknown samples through a calibration plot. Modern computer-controlled densitometers can produce linear or polynomial calibration plots relating

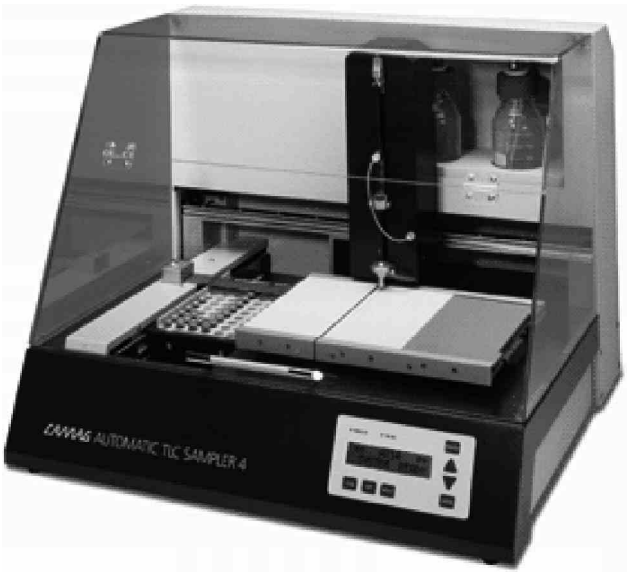

Fig. 1 Automatic TLC Sampler 4 used for fully automated application of precisely controlled volumes of samples and standards between 0.1 and 50 μl from a rack of vials as spots or bands to preselected origins on a plate.
Source: Photo courtesy of Camag Scientific Inc., Wilmington, North Carolina.

absorbance or fluorescence to weight of the standards and can determine bracketed unknowns by automatic interpolation from the plot. Samples and standards are usually applied manually onto plates with a preadsorbent (or preconcentrating zone) or using an automated or semiautomated instrument such as the one shown in Fig. 1. Zones in the form of bands usually produce better quantitative results than round spots.

The usual Lambert–Beer Law that is the basis of solution spectrometry is not valid for densitometry because both absorption and scattering of radiation occur during direct zone measurement on a layer. The Kubelka–Munk equation is usually used to relate signal intensity and zone concentration (weight per zone) for the reflectance (absorption) mode of densitometry:

$$(1-R)^2/2R = 2.303e(C/S)$$

where R is the light reflected from an infinitely thick opaque layer, e is the molar absorption coefficient of the analyte, C is the zone weight, and S is the layer scatter coefficient. Because layers are not infinitely thick, this equation is only an inexact model for TLC that leads to densitometry calibration plots (scan areas vs. zone weights for a series of standards) that are linear (pseudolinear) at lower weights and curve downward toward the weight (x) axis, and do not pass through the 0,0 point. For a wide weight range, better accuracy and precision are often obtained from a calibration plot based on second order polynomial regression. Samples are quantified by interpolation of sample weights from the calibration plot.

For fluorescence densitometry, the following equation describes emission at low-sample concentrations:

$$I = kI_0eaC$$

where I is the fluorescence intensity, k is a proportionality constant including the quantum yield, I_0 is the irradiation intensity of the excitation source, e is the molar absorption coefficient, a is layer thickness, and C is the analyte weight applied. The presence of the I_0 term in the equation means that more fluorescence is emitted with a more intense source, and lower amounts of analyte can be measured; this is why a xenon or mercury lamp, rather than deuterium, is used for fluorescence densitometry. Calibration plots are usually linear over two or three orders of magnitude for low analyte weights and pass through 0,0; for large weights, self-absorption causes the plot to curve towards the weight axis. Compared to absorbance, fluorescence measurements have greater selectivity because excitation and emission wavelengths can be chosen to "tune-out" interferences; sensitivity is 10–1000 times higher; and the emission signal is less dependent on zone shape or distribution. The advantages of fluorescence measurement may be realized for non-fluorescent compounds by pre- or post-chromatographic derivatization reactions with suitable fluorogenic reagents.

INSTRUMENTAL DESIGN AND SCANNING MODES

A commercial densitometer and a schematic diagram of the light path arrangement used in scanning are shown in Figs. 2 and 3, respectively.[3] The plate is mounted on a stage or platform that can be moved in the x- and y-directions, controlled by a stepping motor drive, to allow each chromatogram track to be scanned in, or opposite to, the direction of mobile phase development. A tungsten–halogen lamp is used as the source for scanning colored zones in the 400–800 nm range (visible absorption) and a deuterium lamp for scanning UV-absorbing zones directly or as quenched zones on phosphor-containing layers (F-layers) in the 190–450 nm range. The monochromator used with these continuous wavelength sources is a grating in modern instruments; some older instruments used a quartz prism, and low priced instruments designed for dedicated applications may have a monochromatic filter. The detector is a photomultiplier tube (PMT), photodiode, or photoresistor inclined above the layer at an angle (e.g., 30°) to measure diffusely reflected radiation. (Some scanners, e.g., Fig. 3, make use of a reference PMT in addition to the measuring PMT in the single beam mode. The reference PMT puts out a constant signal that is compared to the signal from the measuring PMT to produce a difference signal that is more accurate than a direct signal from a single measuring PMT because lamp aging and short-term fluctuations are

Fig. 2 TLC Scanner 3.
Source: Photo courtesy of Camag.

compensated for and warm-up time required for lamp stabilization is reduced.)

For normal fluorescence scanning, a high intensity xenon continuum source or a mercury vapor line source is used, and a cutoff or narrow-pass filter is placed between the plate and detector to block the exciting UV radiation and transmit the visible emitted fluorescence. For fluorescence measurement in the reversed beam mode, a monochromatic filter is placed between the source and plate and the monochromator between the plate and detector. In this mode, the monochromator selects the emission wavelength, rather than the excitation wavelength as in the normal mode.

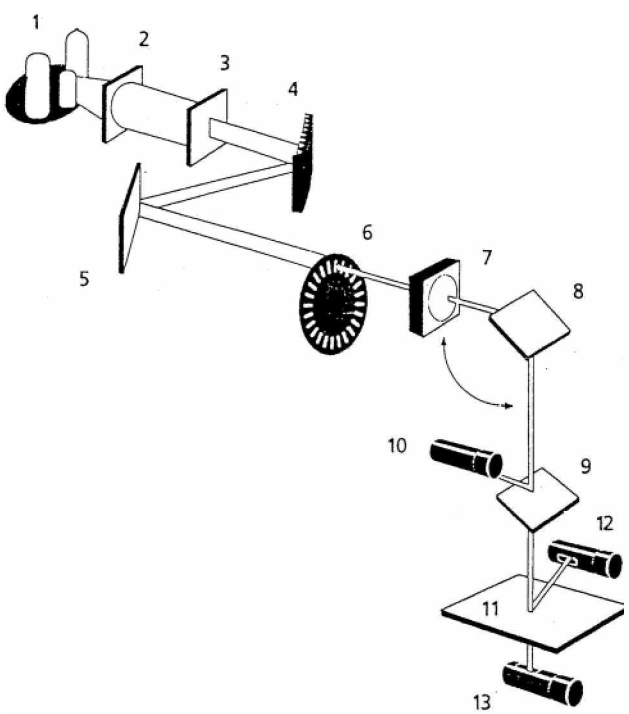

Fig. 3 Light path diagram of TLC Scanner 3. 1, Lamp selector; 2, entrance lens system; 3, entrance slit; 4, grating monochromator; 5, mirror; 6, 20 fixed-slit aperture disk; 7, lens system positioned in accordance with the slit size selected (choices are 0.5–12 mm length and 0.025–1.2 mm width); 8, mirror; 9, beam splitter; 10, reference PMT; 11, plate to be scanned; 12, measuring PMT; 13, photodiode (transmission).
Source: From Instrumental thin layer chromatography, in *Handbook of Thin Layer Chromatography*.[3]

Simultaneous measurement of reflection and transmission, or transmission alone, can be carried out by means of a detector positioned on the opposite side of the plate (Fig. 3). Ratio recording double beam densitometers, which can correct for background disturbances and drift caused by fluctuations in the source and detector, were designed earlier with two PMT detectors simultaneously recording the two beams (double beam in space), but later densitometers were equipped with a chopper and one detector (double beam in time). Dual wavelength, single beam scanning minimizes matrix interference and baseline problems if two similar wavelengths can be found, only one of which is absorbed by the analyte. For this method, a light beam is selected by a mirror and passes through two separate monochromators to isolate the two different wavelengths. The two beams are alternated by a chopper and recombined into a single beam representing a difference signal at the detector. Zigzag or meandering or flying-spot scanning with a small point or spot of light is possible with densitometers having two independent stepping motors to move the plate in the x- and y-axes (Shimadzu CS 9000 and Desaga CD 60). Computer algorithms integrate the maximum absorbance measurements from each swing to produce a distribution profile of zones having any shape (even distorted). The potential advantages of scanning zones with a moving light spot are offset by problems with lower spatial resolution and errors in data processing, and the method is not as widely used as conventional scanning of chromatographic tracks with a fixed slit. Some older densitometers had the ability to rotate the plate while scanning for measurement of circular and anticircular chromatograms.

Single-wavelength, single-beam, fixed-slit scanning is most often used and can produce excellent results when high quality plates and analytical techniques are employed. Positioning of the slit for scanning can be achieved manually or automatically. The slit length is chosen to be longer than the zone length (for bands) or zone diameter (for spots), or equal length (usually central) segments of homogeneous bands can be scanned (termed aliquot scanning). A small slit height improves the resolution of scan peaks for closely spaced zones.

SPECTRAL MEASUREMENT

Modern scanners have a computer-controlled, motor-driven monochromator that allows automatic recording of in situ absorption and fluorescence excitation spectra. Identification is aided by comparison of sample and standard zone spectra. Zone purity is determined by superimposition of spectra from different areas of a single

zone. The spectral maximum determined from the in situ spectrum is usually the optimal wavelength for scanning standard and sample areas for quantitative analysis. Because of possible sorbent effects, the in situ spectrum of a substance may not match its spectrum obtained in solution. For best results, comparison among spectra from different zones should be made for similar substance weights.

DATA HANDLING

The densitometer is connected to a recorder, integrator, or computer. A personal computer with software designed specifically for TLC is most common for data handling and automation of the scanning process in modern instruments. With a fully automated system, the computer can carry out the following functions: data acquisition by scanning a complete plate following a preselected geometric pattern with control of all scanning parameters; automated peak searching and optimization of scanning for each fraction located; multiple wavelength scanning to find, if possible, a common wavelength for all substances to be quantified, to optically resolve fractions incompletely separated by TLC, and to identify sample fractions by comparison using pattern recognition techniques of spectra with those of authentic standards cochromatographed on the same plate or stored in a spectrum library; baseline location and correction; setting of peak markers, computation of peak areas and/or heights of samples and codeveloped standards, and processing of the analog raw data to quantitative digital results, including calculation of calibration plots by linear or polynomial regression, interpolation of sample concentrations, statistical analysis of reproducibility, and presentation of a complete analysis report; and storage of raw data on disk for later reintegration, calibration, and evaluation with different parameters. For GMP and/or GLP applications, the report contains the date and time of the last change plus a unique system-generated identification number.

DIODE ARRAY SCANNER

The J&M TLC 2010 scanner (Fig. 4) contains a diode array detector rather than a PMT. Plates can be scanned rapidly with high spectral resolution and signal-to-noise ratio using tungsten (visible) and deuterium (UV) light sources. Each compound can be analyzed at its optimum wavelength for maximum sensitivity, and complete spectra of all substances on the plate can be acquired simultaneously in real time during the analysis to aid in zone identification and purity determination. Fiber-optics technology is used to separate the scanning and detection units, which allows performance similar to that found in HPLC diode array detectors. The solarization-free fiber

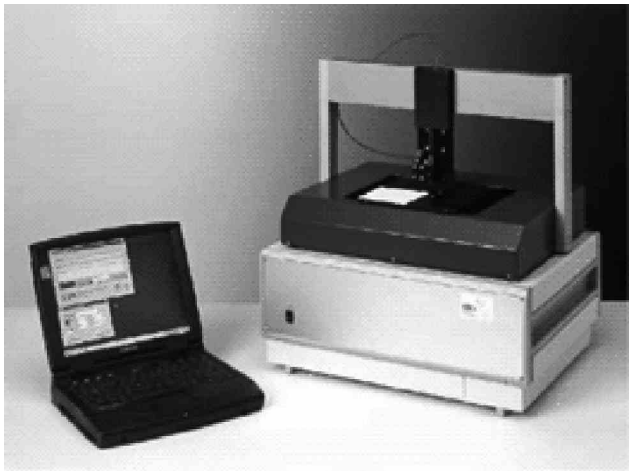

Fig. 4 J&M 2010 TLC Diode Array Scanner (TIDAS TLC 2010).
Source: Photo courtesy of SpectrAlliance, Inc., St. Louis, Missouri.

optics can operate from 1000 nm down to 190 nm without the use of a cutoff filter. A fiber-optic probe is used to scan plates containing up to 18 chromatograms at distances between 400 and 600 μm with an optical resolution of 160 μm. Software parameters are similar to those for HPLC diode array detection, including peak purity, resolution, identification by spectral library matching (Fig. 5), and quantification.

VIDEODENSITOMETRY

Video camera systems are available from several manufacturers for documentation and densitometric quantification of TLC plates. As an example, the Camag VideoScan (Fig. 6) consists of the VideoStore documentation system, which includes a lighting module with short- and long-wave UV and visible sources upon which the layer is placed, a CCD camera with zoom and long-time

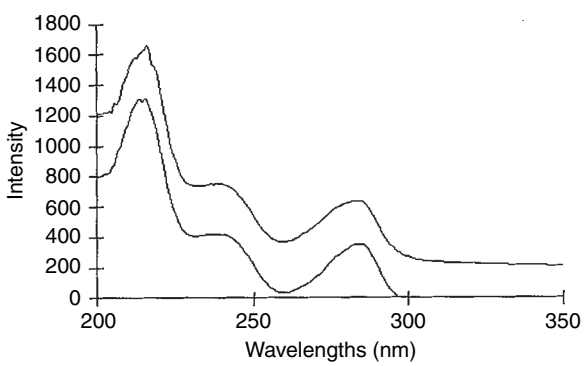

Fig. 5 Codeine identification in urine; sample zone spectrum (top) and library spectrum (bottom), with a computer-determined "hit-list" match of 98%.
Source: Figure courtesy of SpectrAlliance, Inc.

Fig. 6 VideoScan videodensitometer.
Source: Photo courtesy of Camag.

integration capability, plus a PC under MS-Windows control with software for evaluation of images captured with a frame grabber, a monitor, and a printer. An image of all zones on the entire layer is obtained by the VideoStore camera simultaneously. The VideoScan software for quantitative evaluation allows display of the chromatogram tracks of the layer image acquired with the video camera as analog curves and calculation of their peak properties (R_f, height, area, height percent, and area percent). Quantification can be performed via peak areas or heights, with single or multilevel calibration (linear or polynomial regression).

Current video scanners can measure spots in the visible absorption, UV absorption, fluorescence, transmittance, and reflectance modes. They have potential advantages, including rapid data collection, simple design with virtually no moving parts, and ability to quantify two-dimensional chromatograms,[4] but they cannot perform spectral analysis. Current commercial instruments have not yet been shown to have the required capabilities, such as sensitivity, resolution, wavelength range, or the ability to illuminate the plate uniformly with monochromatic light of selected wavelength, to match the performance of slit scanning densitometers. However, videodensitometric analyses can often be validated at acceptable levels for many quantitative applications.[5]

DIGITAL CAMERA DENSITOMETERS

Instead of being based on computer analysis of a digitized signal from a video camera, a densitometer featuring a 3.3 mega pixel color digital camera, 3 × optical zoom lens, and overhead (reflected) 254 and 366 nm light and transmitted white light is available from Analtech (Fig. 7). The

Fig. 7 ChromaDoc-It TLC imaging system.
Source: Photo courtesy of Analtech, Newark, Delaware.

image analysis software, with a large selection of image capture and effects settings, generates quantitative data of lanes and bands as well as detailed, user-configured reports. Camag manufactures the DigiStore documentation system, which also uses a digital camera; images captured with the DigiStore can be quantified with VideoScan software.

DENSITOMETRY USING FLATBED SCANNERS

Zones on TLC plates can also be measured with a flatbed scanner. As with a CCD camera, chromatogram images are stored in digital form, and tracks and zones are detected and quantified with specialized software.[6,7] Commercial office scanners can be used for naturally colored zones or colored zones produced by postchromatographic derivatization.[8] Modified flatbed scanners have been described for use in quantification of fluorescent[9,10] and fluorescence-quenched[11] zones. As CCD cameras, flatbed scanners, and associated specialized software improve, quantification by image analysis will become increasingly competitive with slit scanners in the future.

APPLICATIONS AND PRACTICAL ASPECTS OF DENSITOMETRY

Densitometric quantification has been applied to virtually every type of analyte and sample. The greatest number of applications is for the analysis of drug and pharmaceutical compounds, most of which have structures including chromophores that cause strong UV absorption. These compounds are readily quantified by measuring the decrease in reflectance as a result of absorbance of radiation from a short-wave UV source on an F-layer.[12] The dark zones of

UV-absorbing compounds quantified by scanning at 254 nm (or a nearby wavelength of maximum analyte absorption) on fluorescent F-layers are commonly called "fluorescence-quenched zones" and the process "fluorescence quenching," even though use of these terms may not be technically correct in relation to the true measurement process occurring with the usual densitometer configuration (i.e., no cutoff filter blocking the excitation radiation from reaching the detector).

Lipids are compounds that are not easily analyzed by GC or HPLC because they lack volatility and the presence of a chromophore leading to UV absorption. The most successful way to quantify lipids is by densitometry after separation and detection on the layer with a chromogenic reagent, most notably phosphomolybdic acid.[13] The quantification of amino acids in biological samples[14] and dietary supplements[15] after detection with ninhydrin is another example of densitometry in the visible absorption mode. Fluorescence densitometry has been applied to the determination of naturally fluorescent compounds such as pyrene[16] and compounds derivatized with a fluorogenic reagent pre- or post-TLC (e.g., fumonisin B-1 reacted with fluorescamine).[17] HPTLC/densitometry is very widely used in pharmaceutical analysis, and inherent advantages compared to HPLC and full validation of procedures in accordance with international guidelines have been described.[18,19]

The steps in a typical densitometric quantitative analysis, regardless of analyte type, are the following:

1. Prepare a standard reference solution.
2. Prepare a sample solution in which the analyte is completely dissolved and impurities have been reduced to a level at which they will not produce chromatographic zones that interfere with scanning of the analyte.
3. Choose a layer and mobile phase combination that will separate the analyte as a compact zone with an R_f value in the range of 0.2–0.8.
4. Apply the standard and sample aliquots to the layer using an instrument (Fig. 1), or manually with a micropipet onto preadsorbent, laned plates. Generally, three or four standard zones are applied in constant volumes from a series of standard solutions with increasing concentrations, or in a series of increasing volumes from a single standard solution. The sample volume applied must provide an amount of analyte zone with a weight that is bracketed by the standard amounts.
5. Develop the plate in an appropriate chamber, and dry the mobile phase under a fumehood or in an oven.
6. Apply a detection reagent, if necessary, by spraying or dipping. The reagent should produce a stable colored, UV-absorbing, or fluorescent zone having high contrast with the layer background.
7. Scan the natural or induced absorption or fluorescence of the standard and sample zones on the plate using a densitometer with optimized parameters.
8. Generate a calibration plot by linear or polynomial regression of the scan areas and weights of the standards and interpolate the weights in the sample zones from the curve.
9. Calculate the concentration of analyte in the sample from the original weight of the sample, the original total volume of the sample test solution, the aliquot volume of the test solution that is spotted, the interpolated analyte weight in that spotted volume from the calibration curve, and any numerical factor required because of dilution or concentration steps needed for the test solution to produce a bracketed scan area for the analyte zone in the sample chromatogram.
10. Validate the precision of the TLC analysis by replicated determination of the sample and accuracy by comparison of the results to those obtained from analysis of the same sample by an established independent method or calculation of recovery from analysis of a spiked preanalyzed sample or spiked blank sample. Other validation parameters include specificity, detection limit, quantification limit, linearity, and range.[20]

ADVANTAGES OF TLC/DENSITOMETRY COMPARED TO HPLC

The following are some advantages of TLC/densitometry compared to the other major LC method, HPLC:

1. A wide range of mobile and stationary phases combined with capillary flow and forced flow one- and two-dimensional and multiple and gradient development modes lead to high separation selectivity.
2. The simultaneous analysis of multiple samples on a single plate leads to higher sample throughput (lower analysis time) and less cost per sample. Up to 36 tracks are available for samples and standards on a 10 cm × 20 cm HPTLC plate.
3. The ability to generate a unique calibration plot using standards developed under the same conditions as samples on each plate (in-system calibration) leads to statistical improvement in data handling and better analytical precision and accuracy and eliminates the need for an internal standard for most analyses.
4. Detection is versatile and flexible because the mobile phase is removed prior to detection. Because the detection process is static (the zones are stored on the layer), multiple, complementary sensitive, selective, or universal detection methods can be used. As

an example, niacinamide and γ-aminobutyric acid in dietary supplement capsules were quantified by HPTLC on a single plate using densitometry in the fluorescence-quenching mode for the former and the visible mode after spraying with ninhydrin for the latter.[21]

5. Storage of the chromatogram also allows scanning to be repeated with different parameters without time constraints and assures that the entire sample is available for detection and scanning.
6. Less sample cleanup can be tolerated because plates are not reused. Every sample is analyzed on a fresh layer without sample carryover or cross-contamination. Crude, complex, or dirty samples can be more easily analyzed.
7. Solvent use is very low for TLC, both on an absolute and per-sample basis, leading to reduced purchase and disposal costs and safety concerns.

CONCLUSIONS

The principles, procedures, and instrumentation for densitometric quantification of zones on TLC or HPTLC plates have been described briefly. The reading list below provides sources of more detailed information on these topics, as well as on applications to virtually all sample and analyte types. The results of TLC/densitometry are complementary with those from other analytical techniques, and the method has unique advantages for many analyses.

REFERENCES

1. Pittet, A.; Royer, D. Rapid, low cost thin layer chromatographic screening method for the detection of ochratoxin A in green coffee at a control level of 10 $\mu g\ kg^{-1}$. J. Agric. Food Chem. **2002**, *50* (2), 243–247.
2. Kenyon, A.S.; Layloff, T.; Sherma, J. Rapid screening of tuberculosis drugs by thin layer chromatography. J. Liq. Chromatogr. Relat. Technol. **2001**, *24* (10), 1479–1490.
3. Reich, E. Instrumental thin layer chromatography. In *Handbook of Thin Layer Chromatography,* 3rd Ed.; Sherma, J., Fried, B., Eds.; Marcel Dekker, Inc.: New York, NY, 2003; 135–151.
4. Petrovic, M.; Kastelan-Macan, M.; Babic, S. Quantitative evaluation of 2D chromatograms with a CCD camera. J. Planar Chromatogr.-Mod. TLC **1998**, *11* (5), 353–356.
5. Petrovic, M.; Kastelan-Macan, M.; Lazaric, K.; Babic, S. Validation of thin layer chromatography quantitation determination with a CCD camera and slit scanning densitometer. J. AOAC Int. **1999**, *82* (1), 25–30.
6. Mustoe, S.P.; McCrossen, D. A comparison between slit densitometry and video (flatbed scanner) densitometry for quantitation in thin layer chromatography. Chromatographia **2001**, *53* (Part 2, Suppl. S 2001), S474–S477.
7. Gerasimov, A.V. Use of the software processing of scanned chromatogram images (flatbed scanner) in quantitative planar chromatography. J. Anal. Chem. **2004**, *59* (4), 348–353.
8. Johnson, M.E. Rapid, simple quantitation in thin layer chromatography using a flatbed scanner. J. Chem. Educ. **2000**, *77* (3), 368–372.
9. Stroka, J.; Peschel, T.; Tittlebach, G.; Weidner, G.; van Otterdijk, R.; Anklam, E. Modification of an office scanner for the determination of aflatoxins after TLC separation. J. Planar Chromatogr.-Mod. TLC **2001**, *14* (2), 109–112.
10. Mustoe, S.; McCrossen, S. TLC image capture and analysis by use of a prototype device for visualizing fluorescence. J. Planar Chromatogr.-Mod. TLC **2001**, *14* (4), 252–255.
11. Campbell, A.; Chejlava, M.; Sherma, J. Use of a modified flatbed scanner for documentation and quantification of thin layer chromatograms detected by fluorescence quenching. J. Planar Chromatogr.-Mod. TLC **2001**, *16* (3), 244–246.
12. Sullivan, C.; Sherma, J. Development and validation of an HPTLC–densitometry method for assay of caffeine and acetaminophen in multicomponent extra strength analgesic tablets. J. Liq. Chromatogr. Relat. Technol. **2003**, *26* (20), 3453–3462.
13. Schneck, J.L.; Fried, B.; Sherma, J. Effects of tonicity on the release of neutral lipids in *Echinostoma caproni* adults and observations on lipids in excysted metacercariae. Parasitol. Res. **2004**, *92* (4), 285–288.
14. Ponder, E.L.; Fried, B.; Sherma, J. Thin layer chromatographic analysis of free pool amino acids in cercariae, rediae, encysted metacercariae, and excysted metacercariae of *Echinostoma caproni*. J. Liq. Chromatogr. Relat. Technol. **2003**, *26* (16), 2697–2702.
15. Hess, B.; Sherma, J. Quantification of arginine in dietary supplement tablets and capsules by silica gel high performance thin layer chromatography with visible mode densitometry. Acta Chromatogr. **2004**, *14*, 60–69.
16. Spangenberg, B.; Lorenz, K.; Nasterlack, S. Fluorescent enhancement of pyrene measured by thin layer chromatography with diode array detection. J. Planar Chromatogr.-Mod. TLC **2003**, *16* (5), 331–337.
17. Preis, R.A.; Vargas, E.A. A method for determining fumonisin B-1 in corn using immunoaffinity column cleanup and thin layer chromatography–densitometry. Food Addit. Contam. **2000**, *16* (6), 463–468.
18. Renger, B. Quantitative planar chromatography as a tool in pharmaceutical analysis. J. AOAC Int. **1993**, *76* (1), 7–12.
19. Renger, B. Contemporary thin layer chromatography in pharmaceutical quality control. J. AOAC Int. **1998**, *81* (2), 333–339.
20. Ferenczi-Fodor, K.; Vegh, Z.; Nagy-Turak, Z. Validation and quality assurance of planar chromatographic

procedures in pharmaceutical analysis. J. AOAC Int. **2001**, *84* (4), 1265–1276.
21. Hess, B.; Sherma, J. Quantitative determination of GABA in nutritional supplement products by high performance thin later chromatography. Am. Lab. (Shelton, CT) **2005**, *37* (1), 28, 30–32, 34, 36–37.

BIBLIOGRAPHY

1. Dammertz, W.; Reich, E. Planar chromatography and densitometry. In *Planar Chromatography—A Retrospective View for the New Millennium*; Nyiredy, Sz., Ed.; Springer Scientific Publisher: Budapest, Hungary, 2001; 234–246.
2. Fried, B.; Sherma, J. *Thin Layer Chromatography—Techniques and Applications,* 4th Ed.; Marcel Dekker, Inc.: New York, NY, 1999; 197–222.
3. Pollak, V.A. Theoretical foundations of optical quantitation. In *Handbook of Thin Layer Chromatography,* 1st Ed.; Sherma, J., Fried, B., Eds.; Marcel Dekker, Inc.: New York, NY, 1991; 249–281.
4. Poole, C.F. *The Essence of Chromatography*; Elsevier Science B.V.: Amsterdam, Netherlands, 2003.
5. Prosek, M.; Pukl, M. Basic principles of optical quantitation in TLC. In *Handbook of Thin Layer Chromatography,* 2nd Ed.; Sherma, J., Fried, B., Eds.; Marcel Dekker, Inc.: New York, NY, 1996; 273–306.
6. Prosek, M.; Vovk, I. Basic principles of optical quantification in TLC. In *Handbook of Thin Layer Chromatography,* 3rd Ed.; Sherma, J., Fried, B., Eds.; Marcel Dekker, Inc.: New York, NY, 2003; 277–306.

Optimization of TLC

Teresa Kowalska
Institute of Chemistry, Silesian University, Katowice, Poland

Wojciech Prus
School of Technology and the Arts in Bielsko-Biała, Bielsko-Biała, Poland

INTRODUCTION

The principal task of chromatography is the separation of mixtures of substances. By "optimization" of the chromatographic process, we mean enhancement of the quality of the separation by changing one or more parameters of the chromatographic system. An ability to foresee, correctly, the direction and scope of these changes is the most important goal of each optimization procedure.

Use of chemometrics to devise procedures suitable for the most crucial stage of optimization, optimization of selectivity, is generally performed in three steps:

1. Selection of the experimental method which best suits the analytical problem considered. At this stage, a chromatographic technique is chosen that ensures that the best possible range of retention parameters is obtained for each individual component of the separated mixture.
2. Establishing the experimental conditions that enable quantification of the influence of the optimized parameters of a chromatographic system on solute retention.
3. Fixing the experimental conditions at values that provide the optimum separation selectivity.

Chemometric optimization of the chromatographic system consists, in fact, in predicting local maxima in multiparametric space and, then, in further deciding which of these parameters is global with regard to the overall efficiency of a given chromatographic system.

QUALITY OF CHROMATOGRAPHIC SEPARATIONS

Elementary Criteria

The simplest way of quantifying the separation of two chromatographic bands, 1 and 2, is to calculate the difference between their respective retention parameters; that is, the difference between their R_F values,

$$\Delta R_F = R_{F_2} - R_{F_1} \tag{1}$$

or between their R_M values,

$$\Delta R_M = R_{M_1} - R_{M_2} = \log \frac{k_1}{k_2} = \log \alpha \tag{2}$$

where k_1 and k_2 are the capacity (retention) factors of the chromatographic bands and α is the separation factor.

The terms most frequently used to characterize the separation of two chromatographic bands are the separation factor, α,

$$\alpha = \frac{k_1}{k_2} \tag{3}$$

where $k_1 > k_2$, and the resolution, R_S,[1]

$$R_S = \frac{2(z_2 - z_1)}{w_1 + w_2} = \frac{2l\Delta R_F}{w_1 + w_2} \tag{4}$$

where z_1 and z_2 are the distances of the geometric centers of two chromatographic bands, 1 and 2, from the origin, l is the distance from the origin to the mobile phase front, and w_1 and w_2 are the diameters of the two chromatographic bands, measured in the direction of eluent flow.

Other elementary criteria include the separation factor, S,[2]

$$S = \frac{k_2 - k_1}{k_1 + k_2 + 2} \tag{5}$$

the peak-to-valley ratio of the bands, P,[3]

$$P = \frac{f}{g} \tag{6}$$

(where f and g are, respectively, the average peak height and valley depth, characteristic of a given pair of neighboring solutes on a chromatogram), the fractional peak overlap, FO,[4]

$$\mathrm{FO} = \frac{A_n - A_{n,n-1} - A_{n,n+1}}{A_n} \tag{7}$$

(where A_n is the surface area of the part of the band originating from the pure single compound, $A_{n,n-1}$ is the surface area of the fractional overlap of the nth and $(n-1)$th bands, and $A_{n,n+1}$ is the surface area of the fractional overlap of the nth and $(n+1)$th bands), and the selectivity parameter, R_R,[5]

$$R_R = \frac{R_{F_1}}{R_{F_2}} \tag{8}$$

where $R_{F_1} > R_{F_2}$.

Criteria for the Quality of Chromatograms

One method which can be used to establish the optimum conditions for the separation of a complex mixture (i.e., not only a pair) of compounds consists in searching for the maximum of a function denoted the chromatogram quality criterion. The evaluation of separation selectivity can be conducted with the aid of different criteria of chromatogram quality such as the sum of resolution, $\sum R_S$,[6] the sum of separation factors, $\sum S$,[2] and other sums and products of elementary criteria, selected examples of which are the resolution product, ΠR_S,[7] (Fig. 1)

$$\prod R_S = \exp\left(\sum \ln R_S\right), \tag{9}$$

the product of the separation factors, ΠS,[8] the product of the fractional peak overlap, Π FO,[9] and the product of the peak-to-valley ratio of the bands, ΠP.[10]

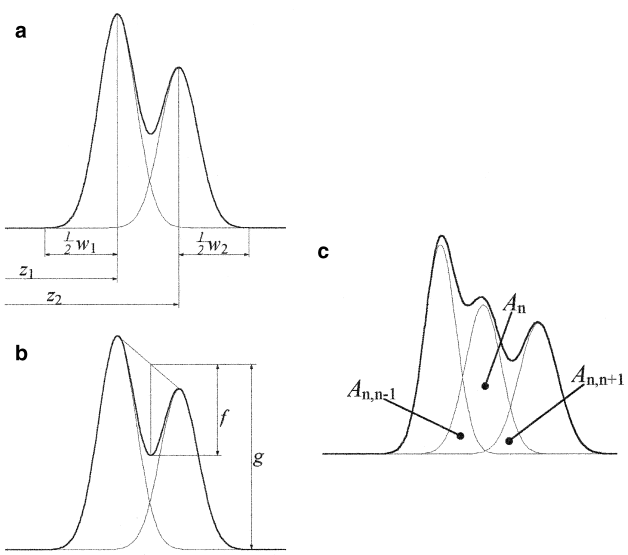

Fig. 1 Graphical interpretation of the selected elementary criteria: (a) resolution, R_s; (b) the peak-to-valley ratio, P; (c) the fractional peak overlap, FO.

There are also other, more complex criteria, including the normalized resolution product, r,[11]

$$r = \prod_{i=1}^{n-1} \frac{R_{S_{i,i+1}}}{R_S} = \prod_{i=1}^{n-1} \frac{S_{i,i+1}}{S} \tag{10}$$

where n is the number of the chromatographic bands,

$$\bar{R}_S = \frac{1}{n-1} \sum_{i=1}^{n-1} R_{S_{i,i+1}}$$

and

$$\bar{S} = \frac{1}{n-1} \sum_{i=1}^{n-1} S_{i,i+1}$$

and the minimum R_S,[8]

$$R_{S,\min} \geq x \text{ or } \max R_{S,\min} \tag{11}$$

The minimum of α is used as a criterion of the quality of chromatograms in liquid chromatography.[12]

Other criteria are the total peak overlap, φ,[13]

$$\varphi = \sum \exp(-2R_S), \tag{12}$$

the informing power, P_{inf},[14]

$$P_{\text{inf}} = \sum_{i=1}^{n} \log_2 S_i \tag{13}$$

and the chromatographic response function, CRF,[10]

$$\text{CRF} = \sum_{i=1}^{n} \ln P_i \tag{14}$$

(where P_i is the peak-to-valley ratio for the ith pair of chromatographic bands).

Performance of the Chromatographic System

One measure of the performance of a given chromatographic system is the number of the theoretical plates per chromatographic band (N). In its simplest form, this can be defined as

$$N = \frac{l}{H} \tag{15}$$

where l is the distance from the origin to the eluent front and H is the height equivalent to one theoretical plate (H is sometimes also denoted height equivalent to theoretical plate (HETP)).

The average height equivalent to one theoretical plate ($\bar{H}$) can be calculated from the relationship [15]

$$\bar{H} = \frac{(\sigma_i)^2}{(z_r - z_0)R_F} = \frac{(w_i)^2}{16 z_x} \tag{16}$$

where σ_i is the standard deviation, which characterizes the width of the chromatographic spot, or the band width on the densitogram, w_i is the spot width (or the width of the peak base on the densitogram), z_r–z_0 is the distance from the origin to the eluent front, and z_x is the distance from the origin to the geometric center of the chromatographic spot.

The relationship between the height equivalent to one theoretical plate (H) and the velocity of the mobile-phase flow is given by the simplified van Deemter equation [16]

$$H = A + \frac{B}{u} + Cu \tag{17}$$

where u is the linear velocity of the mobile phase, A is a constant characterizing eddy diffusion, B is a constant characterizing molecular diffusion, and C is a constant characterizing resistance to interphase mass transfer. This particular issue is of considerable significance in planar chromatographic separations, during the course of which the velocity of the mobile phase changes.

The concept of separation number (SN) in planar chromatography is a practical approach to the task of quantification of chromatographic system performance. According to this concept, such performance can simply be evaluated by calculating how many components of the separated mixture can be comfortably accommodated (i.e., without any overlap of adjacent components) along the direction of migration of the eluent. A convenient relationship proposed in Ref. [17] enables easy calculation of the numerical value of SN:

$$\mathrm{SN} = \left(\log\frac{b_0}{b_1}\right)\left(\log\frac{1 - b_1 + b_0}{1 + b_1 - b_0}\right)^{-1},$$

or, simplified,

$$\mathrm{SN} \approx \frac{1}{b_0 + b_1} \tag{18}$$

where b_0 is the width at half-height of a spot at the origin and b_1 is the width at half-height of a spot at R_F=1 (extrapolated) (b_0 and b_1 are in R_F units).

SEMIEMPIRICAL OPTIMIZATION STRATEGIES

Strategies used for optimization of selectivity can basically be divided into three separate groups: (a) the simultaneous strategy, (b) the sequential strategy, and (c) the interpretative strategy.

Simultaneous Strategy

In this strategy, one must accomplish all the experiments according to a plan devised earlier. All the results obtained must then be carefully evaluated, the optimum experimental conditions being chosen on this basis.

Sequential Strategy

In this strategy, the optimum experimental conditions are approached in a series of consecutive steps. The choice of any step results strictly from the outcome of all those accomplished previously. One example of a relevant algorithm is the simplex method[18]; the PRISMA[19] geometrical method is a suitable example of the overall optimization approach.

Interpretative Strategy

This method enables prediction of the quality of a separation on the basis of a relatively limited number of the experimental data, collected in previous experiments. According to this approach, the chromatographic results are interpreted in terms of the retention functions, valid for each individual solute separately. Some good examples of the interpretative strategy are the so-called "window diagrams" approach[20] and the search for the extremum of the multiparameter response function with the aid of the genetical algorithm.[21]

REFERENCES

1. Kowalska, T. Theory and mechanism of thin-layer chromatography. In *Handbook of Thin-Layer Chromatography*; Sherma, J., Fried, B., Eds.; Chromatographic Science, Series Marcel Dekker, Inc.: New York, 1991; Vol. 55, p.50.
2. Jones, P.; Wellington, C.A. Optimisation in chromatography: Theory and application to the separation of aromatic acids in reversed-phase liquid chromatography. J. Chromatogr. **1981**, *213*, 357–361.
3. Kaiser, R. *Gas-Chromatographie*; Geest und Portig: Leipzig, 1960.
4. Schoenmakers, P.J. *Optimization of Chromatographic Selectivity.A Guide to Method Development*; Journal of Chromatography Library Elsevier: Amsterdam, 1986; Vol. 35, 123–125.
5. Prus, W.; Kowalska, T. J. Planar Chromatogr.-Mod. TLC **1995**, *8*, 205–215.
6. Berridge, J.C. Unattended optimisation of reversed-phase high-performance liquid chromatographic separations using

the modified simplex algorithm. J. Chromatogr. **1982**, *244*, 1–14.
7. Glajch, J.L.; Kirkland, J.J.; Squire, K.M.; Minor, J.M. Optimization of solvent strength and selectivity for reversed-phase liquid chromatography using an interactive mixture-design statistical technique. J. Chromatogr. **1980**, *199*, 57–79.
8. Schoenmakers, P.J.; Drouen, A.C.J.H.; Billiet, H.A.H.; de Galan, L. A simple procedure for the rapid optimization of reversed-phase separations with ternary mobile phase mixtures. J. Chromatographia **1982**, *15* (11), 688–696.
9. Smits, R.; Vanroelen, C.; Massart, D.L. The optimisation of information obtained by multicomponent chromatographic separation using the simplex technique. Fresenius Z. Anal. Chem. **1975**, *273* (1), 1–5.
10. Morgan, S.L.; Deming, S.N. Optimization strategies for the development of gas-liquid chromatographic methods. J. Chromatogr. **1975**, *112*, 267–285.
11. Drouen, A.C.J.H.; Schoenmakers, P.J.; Billiet, H.A.H.; de Galan, L. An improved optimization procedure for the selection of mixed mobile phases in reversed phase liquid chromatography. L. Chromatographia **1982**, *16* (1), 48–52.
12. Deming, S.N.; Turoff, M.L.H. Optimization of reverse-phase liquid chromatographic separation of weak organic acids. Anal. Chem. **1978**, *50* (4), 546–548.
13. Giddings, J.C. Optimum conditions for separation in gas chromatography. Anal. Chem. **1960**, *32* (12), 1707–1711.
14. Massart, D.L.; Smits, R. Informing power of a chromatographic method and its use as a quality criterion. Anal. Chem. **1974**, *46* (2), 283–286.
15. Guiochon, G.; Siouffi, A.M. Study of the performance of thin-layer chromatography: Spot capacity in thin-layer chromatography. J. Chromatogr. **1982**, *245* (1), 1–20.
16. Van Deemter, J.J.; Zuiderweg, F.J.; Klinkenberg, A. Longitudinal diffusion and resistance to mass transfer as causes of nonideality in chromatography. Chem. Eng. Sci. **1965**, *5* (6), 271–289.
17. Geiss, F. *Fundamentals of TLC (Planar Chromatography)*; Hüthig: Heidelberg, 1987.
18. Spendley, W.; Hext, G.R.; Hinsworth, F.R. Sequential application of simplex design in optimisation and evolutionary optimisation. Technometrics **1962**, *4*, 441.
19. Nyiredy, Sz.; Meier, B.; Erdelmeier, C.A.J.; Sticher, O. "PRISMA": A geometrical design for solvent optimization in HPLC. J. High Resolut. Chrom. **1985**, *8* (4), 186–188.
20. Laub, R.J.; Purnell, J.H. Criteria for the use of mixed solvents in gas-liquid chromatography. J. Chromatogr. **1975**, *112*, 71–79.
21. Holland, J.H. *Adaptation in Natural and Artificial Systems*; University of Michigan Press: Ann Arbor, 1975.

Organic Acids: TLC Analysis

Natasa Brajenovic
Institute for Medical Research and Occupational Health, Zagreb, Croatia

INTRODUCTION

A very large number of papers report new research works on analyses of organic acids by thin-layer chromatography (TLC), paper chromatography, high-performance liquid chromatography (HPLC), and other analytical techniques. One of the most popular and widely used separation techniques for qualitative and quantitative analyses in the laboratory is TLC.

The reason for using TLC is its wide applicability to a great number of different types of samples, high sensitivity, and speed of separation with relatively low cost. This technique is very fast, and many separations can be accomplished in less than an hour.

The development of different methods of analysis in TLC is a very important area of organic chemistry and biochemistry. Analysis of organic acids by TLC is widely applied in different fields of environmental, pharmaceutical, industry, industrial foods, organic chemistry, cosmetics, clinical, and biochemical assays.

OVERVIEW

Here, we present scientific activity in the analysis of organic acids by TLC in a period from 1993 to 2004. The review is based on a search of *Current Contents and Science Citation Index*, using different combinations of key words relevant for TLC, organic acids, and different kinds of organic acids, such as amino acids, carboxylic acids, humic acids, aromatic carboxylic acids, and fatty acids. In addition, the journals publishing papers covering specific topics related to the analysis of organic acids by TLC were searched directly: *Analytica Chimica Acta*, *Analytical Chemistry*, *Journal of Microbiological Methods*, *Journal of LC and Related Technologies*, *Journal of Chromatography (Parts A and B)*, *Chromatographia*, and *Journal of Pharmaceutical and Biochemical Analysis*.

GENERAL CONSIDERATIONS

Stationary Phase

Typical thin-layer separations are performed on flat glass or plastic plates that are coated with a thin and adherent layer of particles, which constitute the stationary phase.[1] Commercial plates come in two categories: conventional [thick layers (200–250 μm) of particles having sizes of 20 μm or greater] and high-performance plates (film thickness of 100 μm and particles whose diameters are 5 μm or less).

Silica gel is the most extensively used adsorbent in TLC because it leads to excellent, uncomplicated separations. It can be successfully employed for both qualitative and quantitative TLC analyses. It is usually used as a stationary phase in separations and analysis of alkaloids, various organic acids (especially amino acids and their derivatives), steroids, lipids, vitamins, plant pigments, pesticides, drugs, carbohydrates, phenolic substances, etc.

Besides silica gel, cellulose, and aluminum oxide, various other impregnated plates are also frequently used as stationary phases.[1]

Mobile Phase

Many different solvents and mixtures of solvents are used as mobile phases for the analysis of organic acids by TLC, such as chloroform, ethyl acetate, methanol, benzene, etc.

Identification

For identification in qualitative TLC, a great number of visualization reagents are used.[1] If compounds are not colored, a UV lamp may be used to visualize the plates. The quantitative determination of sample components is performed according to the following:

1. Extracting the stained spot with solvent and analyzing it spectrophotometrically; or
2. Scanning the plate densitometrically.[1]

APPLICATIONS

Pharmaceutical Industry, Medicine, Biochemistry, and Biology

TLC is used for the analysis of free amino acids from sanguine plasma in different progression states in maladies: diabetes, renal syndrome, and hepatic cirrhosis.[2] Elution was performed on cellulose plates and the densitometry was achieved with a photodensitometer (Shimadzu CS-9000) at 575 nm. In the case of hepatic cirrhosis, a better resolution was obtained. A mixture of *n*-butanol–acetone–acetic

acid–water (35 : 35 : 7 : 23 vol/vol/vol/vol) was used as the mobile phase.

A simple and fast method for identification of bifidobacteria using TLC analysis of short chain fatty acids in a culture broth is proposed (Table 1).[3] This approach has many advantages: the total time required to analyze organic acids is approximately 50 min; and the identification protocol is simpler, quicker, and more economical than conventional identification methods.

Mycolic acids analysis by TLC has been employed by several laboratories worldwide as a method for fast identification of *Mycobacterium*.[4] *Mycobacterium tuberculosis* strains identified by classical methods were confirmed by their mycolic acid content.

Using aminopropyl-modified silica gel plates in a normal phase system, the retention behavior of 12 acidic drugs and biologically active aromatic acids was investigated by high-performance TLC.[5]

The metabolism of aromatic amino acids (phenylalanine and tyrosine) can be studied following the excretion of their characteristic phenolic acid metabolites in urine using chromatographic methods. These apply acids to the investigations of amino acids themselves in diagnostics. Thin layers of cellulose or silica gel on aluminum foil were used as stationary phases.[6] The retention factor (R_f) of clinically important compounds in the three solvent systems is presented in Table 2.

TLC is also used for direct enantiomeric resolution of D,L-arginine, D,L-histidine, D,L-lysine, D,L-valine, and D,L-leucine on silica gel plates impregnated with optically pure (1*R*, 3*R*, 5*R*)-2-azabicyclo[3,3,0]octan-3-carboxylic acid, which serves as a chiral selector in the pharmaceutical industry.[7] To successfully resolve D,L-amino acids, various combinations of acetonitrile–methanol–water were proposed. The spot was detected by ninhydrin (0.2% in acetone).

TLC is often applied as an industrial control procedure in the synthesis of 2-hydroxy-3-naphthalenecarboxylic acids, on silica gel plates with chloroform–methanol–acetic acid (50:20:1) as developer.[8] 2-Hydroxy-3-naphthalenecarboxylic acid is an important intermediate in the synthesis of dyestuffs and drugs.

Separation of amino acids and their identification in different mixtures are frequent tasks encountered in biochemistry. TLC is a fast, simple, and inexpensive approach to attain this goal. Because some of the components are UV-inactive, other methods, such as vibrational spectroscopy, should be applied for detection and identification. Comparative study based on Raman spectroscopy of TLC spots of some weak Raman scatterers (essential amino acids) was carried out using four different visible and near-infrared laser radiation wavelengths: 532, 633, 785, and 1064 nm.[9] The best results were obtained with simple silica gel plates.

Table 1 Retention time (R_f) and detection color of standard organic acids.

Organic acids	R_f value	Methyl red + bromophenol blue
Lactic acid	0.53 (Upper spot)	Red
	0.37 (Lower spot)	Red
Acetic acid	0.44	Blue
Propionic acid	0.54	Blue
Butyric acid	0.61	Blue
Succinic acid	0.12	Yellow
Citric acid	0.03	Dark yellow
	0.52	Red

Source: From Thin layer chromatographic determination of organic acids for rapid identification of bifidobacteria at genus level, in J. Microbiol. Methods.[3]

Table 2 R_f values (× 100) of urinary phenolic acids.

Compound	BzAc[a]		IprBuAm[b]		BuE[c]
	Cel[d]	SG[e]	Cel[d]	SG[e]	SG[e]
Phenyllactic acid	88	68	65	62	—
Phenylpyruvic acid	86	68	80	80	87
p-OH cinnamic acid	83	60	36	52	88
Hippuric acid	74	30	59	57	35
p-OH mandelic acid	11	6	28	40	34
p-OH phenylacetic acid	63	61	39	43	81
Vanillic acid	96	77	19	36	84

[a]BzAc = benzene–acetic acid (glacial)–water (70 : 29 : 1).
[b]IprBuAm = isopropanol–*n*-butanol–*t*-butanol–ammonia–water (40 : 20 : 20 : 10 : 20).
[c]BuE = *n*-butanol–ethanol–water (100 : 5 : 10).
[d]Cellulose.
[e]Silica gel.
Source: From Urinary phenolic acids by thin-layer chromatography, in Clin. Chim. Acta.[6]

Environmental, Water, Plant, and Soil Applications

The occurrence of chlorinated organic compounds in fish from polluted waters is rather frequent.[10] Chlorinated carboxylic acids of fatty acid character have also been shown to account for up to 90% of the extractable organically bound chloride (EOCl) in fish. Purification by TLC of methyl esters of dichlorotetradecanoic, dichlorohexadecanoic, and dichlorooctadecanoic acids was used. They were detected at 1200 ppm of EOCl in fish.

Organic acid complexes with metal ions significantly affect the mobility of metal ions in plants and soils. Toxic metals also react with organic acids and have a harmful influence on the environment.

Many plants contain a variety of free acids such as acetic acid, citric acid, fumaric acid, malic acid, succinic acid, oxalic acid, glycolic acid, etc.[11–13] They are components

Table 3 TLC procedures for separation of organic acids.

Standards/simple	Stationary phase	Mobile phase
Mixture, organic acids	Merck silica gel	*n*-Butylformate/90% formic acids/H_2O (7 : 2 : 1, vol/vol)
	Cellulose powder or silica gel	1-Propanol concentrated in ammonium hydroxide (7 : 3 or 3 : 2)
2-Hydroxybenzoic acid (salicylic acid)	Silica gel or Fe(III)-impregnated silica gel or aluminum oxide	Tap water
4-Hydroxybenzoic acid	Silica gel or Fe(III)-impregnated silica gel or aluminum oxide	Tap water
3,4,5-Trimethoxybenzoic acid	Silica gel or Fe(III)-impregnated silica gel or aluminum oxide	Tap water
3,4,5-Trihydroxybenzoic acid (gallic acid)	Silica gel or Fe(III)-impregnated silica gel or aluminum oxide	Tap water
4-Hydroxy-3,5-dimethoxybenzoic acid	Silica gel or Fe(III)-impregnated silica gel or aluminum oxide	Tap water
1,2-Benzenedicarboxylic acid	Silica gel or Fe(III)-impregnated silica gel or aluminum oxide	Tap water

Adapted from Dashek & Micales,[11] Iskrić, Hadžija, & Kveder,[14] and Kveder et al.[15]

of citric cycle, whereas the others are intermediates in the pathway from carbohydrates to aromatic compounds.[11] Following extraction, organic acids can be separated and detected with a variety of techniques. TLC methods have been also employed to separate certain organic acids,[11,14,15] as presented in Table 3.

TLC of some plant phenolics, which play an important role in plant metabolism, was carried out on cellulose.[12] The solvents were: 2% formic acid, 20% potassium chloride, isopropyl alcohol–ammonium hydroxide–water (8 : 1 : 1), and 10% acetic acid. The plates were examined under UV light after development. The results of the chromatographic analysis of some phenolic acids are shown in Table 4.

The composition of lignin (an important component of plant cell walls) is very complex.[13] *p*-Coumaric acid, cinnamic acid, ferulic acid, and others are among the products of lignin biodegradation (Fig. 1). TLC is a very rapid method for their separation and is usually completed in a very short time. Six different solvents were used as developer (Table 5), with silica gel being used as a stationary phase.

Humic acids are also products of lignin biodegradation. The characterization of humic acids by TLC on Fe(III)-impregnated silica gel with tap water as developer has been presented.[14] During the chromatographic process, complexes between Fe(III) from the support group and the active functional group from humic acid are formed, causing successive attaching and detaching of Fe(III) from the support of Fe(III) hydroxy/oxide. These results could partially answer how the process of metal migration in soils and sediments progresses.

Some carboxy and benzene derivatives related to humic materials were also examined by TLC.[15] Aluminum oxide, silica gel, and Fe(III)-impregnated silica gel plates were used as supports, whereas the mobile phase was

Table 4 Chromatographic behavior of some plant phenolic acids.

	R_f				Detection		
Compound	**A**	**B**	**C**	**D**	**UV**	**DSA**	**DNA**
o-Coumaric acid	0.34	0.39	0.29	0.51	F	Orange	Violet
m-Coumaric acid	0.43	0.26	0.33	0.52	F	Orange	Violet
p-Coumaric acid	0.34	0.33	0.28	0.47	Q	Red	Blue
o-Hydroxybenzoic acid (salicylic acid)	0.70	0.57	0.44	0.62	F	Yellow	Red
m-Hydroxybenzoic acid	0.37	0.63	0.58	0.70	F	Yellow	Rose
p-Hydroxybenzoic acid	0.27	0.59	0.52	0.70	Q	Yellow	Red
Gallic acid	0.09	0.33	0.31	0.46	F	Green-brown	Tan

F = fluorescence; Q = quenching; DSA = diazotized sulfanilic acid; DNA = diazotized *p*-nitroaniline.
Developers: A = 2% formic acid; B = 20% potassium chloride; C = isopropyl alcohol–ammonium hydroxide–water (8 : 1 : 1); D = 10% acetic acid.
Source: From Thin-layer chromatography of some plant phenolics, in J. Chromatogr.[12]

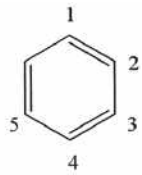

	1	2	3	4	5
Benzoic acid	-COOH	-H	-H	-H	-H
Salicylic acid	-COOH	-OH	-H	-H	-H
Gallic acid	-COOH	-H	-OH	-OH	-OH
Pyrogallol	-H	-H	-OH	-OH	-OH
Hydroquinone	-OH	-H	-H	-OH	-H
Resorcinol	-H	-H	-OH	-H	-OH
Cinnamic acid	-CH=CH-COOH	-H	-H	-H	-H
Ferulic acid	-CH=CH-COOH	-H	-O-CH_3	-OH	-H
p-Coumaric acid	-CH=CH-COOH	-H	-H	-OH	-H

Fig. 1 Chemical structure of simple phenolics and some components of lignin.
Adapted from Sharma, Bhat, & Singh[13] and Iskrić, Hadžija, & Kveder.[14]

water. The results are presented in Table 3. It was concluded that the hydroxy/oxide layer of iron and aluminum can affect the mobility of simple organic molecules in soil. On the other side, organic molecules having carboxy and hydroxy groups can improve the dissolution of hydroxy/oxides of iron or aluminum in soils and sediments.

Food Analysis, Agriculture, and Industry

There are several acids that are widely used in industries. For example, synthetic carboxylic acid esters are used in the perfume industry. Benzoic acids are used as sodium salts in the food industry as inhibitors of microorganism growth.[16]

Benzoic acid derivatives often contain amino, hydroxy, carboxy, and nitro groups. Analysis of substituted benzoic acids by TLC was performed on silica gel, polyamide, and cellulose containing UF_{254} fluorescent indicator.[17] For the mobile phase, different mixtures were used: hexane–acetic acid; hexane–ethyl acetate–formic acid; chloroform–methanol–phosphoric acid; cyclohexane–acetic acid; benzene–ethanol; etc. Because benzoic acid derivatives have similar retention parameters, their separation requires a thorough optimization of conditions (the nature of the stationary phase, the composition of the mobile phase, and the pH of the solutions).

For the separation of benzoic acids, planar electrochromatography was used.[18] In this approach, an electro-osmotic flow is used to drive the mobile phase in TLC. Planar electrochromatography has several advantages over classical TLC, especially substantially faster separation. For example, separation by planar electrochromatography can be 10 times faster than that using ordinary TLC.

TLC analysis of agricultural products, foods, beverages, and plant constituents is described by Sherma[19] in a review paper. In laboratories throughout the world, TLC is widely used for food analysis and qualitative control. Numerous applications of TLC have been reported in the area of food composition, involving determinations of compounds such as lipids, sugars, amines, vitamins, and organic acids such as amino acids and fatty acids.

Table 5 Different solvent systems used as developers for TLC separation for simple phenolic and related compounds such as cinnamic acid, *p*-coumaric acid, ferulic acid, and tannic acid.

1) Chloroform–methanol–acetic acid (90 : 10 : 1)
2) Petroleum ether (60–80°C)–ethyl acetate–formic acid (40 : 60 : 1)
3) Benzene–dioxane–acetic acid (85 : 15 : 1)
4) Chloroform–ethyl acetate–acetic acid (50 : 50 : 1)
5) Toluene–acetonitrile–formic acid (70 : 30 : 1)
6) Petroleum ether (60–80°C)–methanol–acetic acid (90 : 10 : 1)

Source: From Thin-layer chromatography of gallic acid, methyl gallate, pyrogallol, phloroglucinol, catechol, resorcinol, hydroquinone, catechin, epicatechin, cinnamic acid, *p*-coumaric acid, ferulic acid and tannic acid, in J. Chromatogr. A.[13]

VARIOUS ORGANIC COMPOUNDS

TLC analysis is also highly applicable to the determination of aromatic organic acids.[20] In human organisms, aromatic acids are synthesized as metabolites in intoxication by toluene, xylene, and ethyl benzene.[16] These

compounds are easily absorbed through the skin or respiratory system, and are oxidized to aromatic acids. The separation, identification, and quantitative analyses of aromatic acids are also necessary because they appear as semiproducts of the biosynthesis of aromatic amino acids in plants (phenolic acids), and metabolites of numerous toxic substances, drugs, and catecholamines. Polar adsorbents and polar-bonded stationary phases are also widely used in carboxylic separation by TLC, often coupled with densitometry.

Dansyl chloride (DNS-Cl; 5-dimethylaminonaphthalene-1-sulfonyl chloride) is used in analytical chemistry to fluorescently label substances. This process of dansylation creates fluorescent derivatives, which can be detected with great sensitivity. The method for the dansylation of hydroxyl (–OH) and carboxylic acid (–COOH) functional groups has been described.[21] Fluorescent labeling by dansyl chloride has applications in LC, HPLC, TLC, and MS. Fast TLC was accomplished using acetone as the resolving solvent, and resulted in good differentiation of analytes.

Many TLC systems for the separation of amino acids have been described.[22–24]

Copper sulphate and polyamide were tried as impregnants for improving the separation of 20 amino acids on silica gel layers. MeOH–BuOAc–AcOH–pyridine (20 : 20 : 10 : 5) was used as the solvent system.[22]

D-Enantiomers of amino acids have been frequently reported in various tissues of diverse organisms. A simple and rapid method of separating optical isomers of amino acids on a reverse-phase (RP) TLC plate is described.[23] Amino acids, derivatized with 1-fluoro-2,4-dinitrophenyl-5-L-alanine amide, were spotted onto a RP TLC plate. Acetonitrile in triethylamine–phosphate buffer was used as the developer.

For the evaluation of protein structure, identification of amino acids is extremely important. TLC is an appropriate method in this field. A variety of spray reagents are used, among which ninhydrin is the most popular one due to its high sensitivity.[24] Ninhydrin produces a purple/violet color with most amino acids. A typical experimental setup includes chromatographic plates prepared from silica gel; *n*-propanol–water (70 : 30) mixture was used as a mobile phase. For complex mixtures of substances, two-dimensional chromatography is preferred, using *n*-propanol–water (70 : 30) mixture and methanol–chloroform (3:1) mixture as the two developers.

CONCLUSIONS

TLC is a very widely used chromatographic technique in research activities of analytical chemists in many laboratories in the world. Many articles dealing with the development of new analytical methods for the analysis and separation of different organic acids in various fields have been published. There is a constant need for qualitative and quantitative analyses of organic acids in the pharmaceutical, cosmetic, and food industries; in medicine, biology, organic chemistry, and biochemical analysis; and in environmental studies. The important reasons for frequent applications of TLC in qualitative and quantitative analyses of organic acids are its high sensitivity, fast separation of components, and relatively low cost.

REFERENCES

1. Skoog, D.A.; Holler, J.F.; Nieman, T.A. High-performance liquid chromatography. In *Principles of Instrumental Analysis,* 5th Ed.; Vondeling, J. Sherman, M. Bortel, J. Messina, F., Pecuilis, V., Eds.; M. Brooks/Cole, Thomson Learning, Inc.: London, 1998; 725–766.
2. Gocan, S.; Ghizdavu, L.; Ghizdavu, L. TLC of some free amino acids from sanguine plasma. J. Pharm. Biomed. Anal. **2001**, *26*, 681–685.
3. Ki-Yong, L.; Jae-Seong, S.; Tae-Ryeon, H. Thin layer chromatographic determination of organic acids for rapid identification of bifidobacteria at genus level. J. Microbiol. Methods **2001**, *45*, 1–6.
4. Leite, C.Q.F.; Desouza, C.W.O.; Leite, S.R.D. Identification of mycobacteria by thin layer chromatographic analysis of mycolic acids and conventional biochemical method—four years of experience. Mem. Inst. Oswaldo Cruz **1998**, *93* (6), 801–805.
5. Bieganovska, M.L. Retention behaviour of some acids drugs and biologically active compounds on silica and aminopropyl silica layers. Chem. Anal. **1995**, *40* (6), 859–867.
6. Ersser, R.S.; Oakley, S.E.; Seakins, J.W.T. Urinary phenolic acids by thin-layer chromatography. Clin. Chim. Acta **1970**, *30*, 243–249.
7. Bhushan, R.; Martens, J.; Thuku Thiongo, G. Direct thin layer chromatography enantioresolution of some basic DL-amino acids using a pharmaceutical industry waste as chiral impregnating reagent. J. Pharm. Biomed. Anal. **2000**, *21*, 1143–1147.
8. Revilla, A.L.; Havel, J.; Borovcová, J.; Vrchlabsky, M. Capillary zone electrophoresis of hydroxynaphthalenecarboxylic acids. Purity monitoring of β-hydroxynaphthoic acid in industry. J. Chromatogr. A, **1997**, *772*, 397–402.
9. István, K.; Keresztury, G.; Szép, A. Normal Raman and surface enhanced Raman spectroscopic experiments with thin layer chromatography spots of essential amino acids using different laser excitation sources. Spectrochim. Acta, Part A: Mol. Biomol. Spectrosc. **2003**, *59*, 1709–1723.
10. Mu, H.; Wesén, C.; Novák, T.; Sundin, P.; Skramstad, J.; Odham, G. Enrichment of chlorinated fatty acids in fish lipids prior to analysis by capillary gas chromatography with electrolytic conductivity detection and mass spectrometry. J. Chromatogr. A, **1996**, *731*, 225–236.
11. Dashek, W.V.; Micales, J.A. Isolation, separation, and characterization of organic acids. In *Methods in Plant Biochemistry and Molecular Biology*; Dashek, W.V., Ed.; CRC Press: Boca Raton, FL, 1997; 107–113.

12. Jangaard, N.O. Thin-layer chromatography of some plant phenolics. J. Chromatogr. **1970**, *50*, 146–148.
13. Sharma, O.P.; Bhat, T.K.; Singh, B. Thin-layer chromatography of gallic acid, methyl gallate, pyrogallol, phloroglucinol, catechol, resorcinol, hydroquinone, catechin, epicatechin, cinnamic acid, *p*-coumaric acid, ferulic acid and tannic acid. J. Chromatogr. A, **1998**, *822*, 167–171.
14. Iskrić, S.; Hadžija, O.; Kveder, S. Behaviour of humic acids on Fe(III)-impregnated silica gel compared with model substances. J. Liq. Chromatogr. **1994**, *17* (7), 1653–1657.
15. Kveder, S.; Iskrć, S.; Zambeli, N.; Hadžija, O. The behaviour of some benzene derivatives on thin layers of aluminum oxide—comparison with plain and Fe(III) impregnated silica gel. J. Liq. Chromatogr. **1991**, *14* (18), 3277–3282.
16. Waksmundzka-Hajnos, M. Chromatographic separation of aromatic carboxylic acids. J. Chromatogr. B, **1998**, *717*, 93–118.
17. Sumina, E.G.; Shtykov, S.N.; Dorofeeva, S.V. Ion-pair reversed-phase thin-layer chromatography and high-performance liquid chromatography of benzoic acids. J. Anal. Chem. **2002**, *57* (3), 210–214.
18. Nurok, D.; Koers, J.M.; Carmichael, A. Role of buffer concentration and applied voltage in obtaining a good separation in planar electrochromatography. J. Chromatogr. A, **2003**, *983*, 247–253.
19. Sherma, J. Thin-layer chromatography in food and agricultural analysis. J. Chromatogr. A, **2000**, *880*, 129–147.
20. Sherma, J. Planar chromatography. Anal. Chem. **1992**, *64*, 134R–147R.
21. Bartzatt, R. Dansylation of hydroxyl and carboxylic acid functional groups. J. Biochem. Biophys. Methods **2001**, *47*, 189–195.
22. Srivastava, S.P.; Bhushan, R.; Chauhan, R.S. TLC separations of amino acids on silica gel impregnated layers. J. Liq. Chromatogr. **1984**, *7* (7), 1359–1365.
23. Nagata, Y.; Iida, T.; Sakai, M. Enantiomeric resolution of amino acids by thin-layer chromatography. J. Mol. Catal. B. Enzym. **2001**, *12*, 105–108.
24. Laskar, S.; Sinhababu, A.; Hazra, K.M. A modified spray reagent for the detection of amino acids on thin layer chromatography plates. Amino Acids **2001**, *21*, 201–204.

Organic Extractables from Packaging Materials: Identification and Quantification

Dennis R. Jenke
Technology Resources Division, Baxter Healthcare Corporation, Round Lake, Illinois, U.S.A.

INTRODUCTION

Plastic materials are widely used in medical items, such as solution containers, transfusion sets, transfer tubing, devices, and packaging systems. The physiochemical nature of these materials provides medical products with their necessary, desirable performance characteristics. While an important performance characteristic of plastics used in medical application is chemical inertness, interactions between a plastic material and a contacted pharmaceutical product are well documented. Such interactions may include sorption, the uptake of product components by the plastic material, or leaching, i.e., the release of plastic material components into the product. In the case of leaching, both the identities of the leached substances and their accumulation levels may impact the ultimate utility of the product.

A review, related to the chromatographic methods used to assess the accumulation of leachable substances from packaging materials used for pharmaceutical products, is provided. This considers methods used to identify and/or quantify such leachables in actual products or product-simulating solvent systems.

DISCUSSION

The assessment of the impact of the accumulation of leached substances in pharmaceutical products contacted by a plastic material during their manufacture, storage, and/or use is a multifaceted undertaking involving disciplines within the applied physical, chemical, and biological sciences. While numerous strategies can be envisioned, and have been utilized to perform such an assessment, considerations include the identification of the leached substances and the measurement of the actual or probable accumulation levels of the identified substances. The identification process is an extensive investigation that utilizes sensitive and information-rich scouting of analytical methods for the dual purposes of first revealing the leachables and then providing relevant information (e.g., formula and structure) that leads to their identification. In the worst-case scenario, such an analytical investigation is conducted blind; that is, the analytical team is faced with the unenviable challenge of finding an unknown number of unknown compounds, many of which accumulate in the product at levels much lower than its other constituents. These constituents may include both additives and non-material-related contaminants such as ingredient impurities and degradation products. This search for material-derived leachables in pharmaceutical products is greatly facilitated if it is conducted with information-rich analytical methodologies that exhibit a comprehensive ability to respond to a large population of analytes in both a universal, but very specific, manner. The dual performance requirements of universality and specificity are the primary reasons why chromatographic methods are almost exclusively used in investigations specifically associated with organic leachables.

Given the variety of packaging materials used in pharmaceutical applications, the population of potential primary and secondary organic leachables is large and compositionally diverse. While an analytical chemist has a multitude of chromatographic tools with which to perform a leachables assessment, some guidance in terms of successfully applied strategies and methods can greatly facilitate the assessment. Thus this entry contains a general compilation of published chromatographic methods and strategies that have been successfully applied to the identification and quantification of packaging material leachables. Examples are provided for each major separation strategy [e.g., high-performance liquid chromatograpy (HPLC), gas chromatography (GC), thin-layer chromatography (TLC), and supercritical fluid chromatography (SFC)] and for most commonly employed detection methods [e.g., ultraviolet (UV), mass spectrometry (MS), and flame ionization detection (FID)]. While the compilations in Tables 1–4 are by no means exhaustive, they are sufficiently broad in scope to provide the investigator with a general overview of the ways in which chromatography has been applied to meet the objectives of a leachables investigation.all

Tables 1–4 provide general method details, such as column type, elution and detection conditions, and other operating conditions. The materials investigated, as well as the specific leachables examined, are also indicated. General comments are provided in terms of sample preparation. Given the number of methods cited, it is not possible here to provide detailed chromatographic profiles, which are readily available in the cited references.

Table 1 Examples of HPLC methods used to identify and/or quantify packaging system extractables.

Material	Sample matrix	Sample preparation	Column	Mobile phase	λ (nm)	Other	Extractables	Refs.
PVC	Saline extracts	Extraction into hexane	Shandon ODS C_{18}, 200 × 4.6 mm, 200 × 2.1 mm	ACN/MeOH (9 : 1)	270	20 μl, 0.8 or 0.17 ml/min	Di-ethylhexyl-phthalate	[1][a]
PVC, PE, PS	Organic solvents	Direct injection	Spherisorb C_{18} ODS-2, 250 × 4.6 mm, 5 μm	MEOH/phosphate buffer, pH 5.5 (1 : 1)	225	20 μl, 1 ml/min	Monomers, caprolactam, aminocaproic acid	[2]
PVC, PE, PS	Organic solvents	Direct injection	Spherisorb C_{18} ODS-2, 250 × 4.6 mm, 5 μm	ACN/tetrahydrofuran (THF) (95 : 5)	280	20 μl, 1 ml/min	Antioxidants [Butylated hydroxy toluene (BHT), Irganox 1010, Irganox 1076]	[2]
PET	Oils	Solvent partitioning (ACN/hexane) with evaporative concentration	Microsorb C8, 250 × 4.6 mm, 5 μm	A = water/ACN (85 : 15), B = ACN/water (85 : 15)[b]	254	20 μl, 1.5 ml/min	PET oligomers (trimer-octamer), plasticizers (diethylene glycol dibenzoate)	[3]
PET	Oils	Solvent partitioning (ACN/hexane) with evaporative concentration	Microsorb C8, 250 × 4.6 mm, 5 μm	A = water/MEOH/AA (85 : 15 : 0.25), B = ACN/water (85 : 15)[c]	254	20 μl, 1.5 ml/min	PET oligomers, terephthalic acid, dimethylterephthalate, bis(2-hydroxyethyl) terephthalate	[4][a]
PP	Solvent extracts (hexane, ethyl acetate, diethyl ether)	Solvent evaporation, reconstituted in chloroform/MEOH	Spherisorb ODS-1, 50 × 4.6 mm, 5 μm	15–40% ethyl acetate gradient in 75 : 25 MEOH/water	271	35°C, 2 ml/min	Antioxidants (BHT, Irganox 1010, Irganox 1076, Irgafos 168)	[5][a]
HDPE	Dissolution with mobile phase	Direct injection	Spherisorb C_{18} ODS-2, 150 × 4.6 mm, 3 μm	MEOH/water/AA (66.5 : 32.5 : 1)	280	20 μl, 1 ml/min	Phenolic antioxidants[d]; propyl *p*-hydroxybenzoate	[6][a]
Laminated polyolefin	Drug product	SPE concentration, residue reconstituted in ethanol	LiChrosorb C18 ODS-2, 250 × 4.6 mm, 5 μm	MEOH/water (70 : 30)	280	20 μl	Caprolactam, butylhydroxytoluene, phthalic acid derivative	[7]

(Continued)

Table 1 Examples of HPLC methods used to identify and/or quantify packaging system extractables. *(Continued)*

Material	Sample matrix	Sample preparation	Column	Mobile phase	λ (nm)	Other	Extractables	Refs.
Filter cartridges	Water or ethanol extracts	Direct injection or after evaporative concentration	Nucleosil 100-5, RP18, 250 cm	MEOH/water (90 : 10), ACN/water (60 : 40)	220	20 μl, 1 ml/min	Phthalates, fatty acids, phenols, siloxanes, acrylates, aliphatics, amides[e]	[8][f]
PC	Methylene chloride extract	Direct injection after polymer ppt with methanol	Shandon Hypercarb S, 150 × 4.6 mm, 7 μm[g]	MEOH/water/ACN (25.0 : 26.2 : 48.8)	sec[h]	20 μl 0.5 ml/min	Bisphenol A	[9]
PET, PVC	Solvent extraction	Solvent evaporation reconstituted in IPA	Spherisorb ODS-2[g]	Various binary mixtures	254	Various flow rates	Erucamide, PET oligomers	[10]
Polyolefin	Pharmaceutical products	Extract with chloroform, reconstituted in 2-propanol	Spherisorb LC-SI, 250 × 4.6 mm, 5 μm	*n*-Hexane/2-propanol (9 : 1)	210	25 μl, 1.5 ml/min	Caprolactam	[11]
PVC	Pharmaceutical products	Direct injection	Nucleosil ODS, 200 × 4.6 mm, 5 μm	ACN/water (pH 2.7)[i]	sec[j]	1 ml	Phthalic acid, phenol Cyclohexanone Phthalide, benzoic acid Benzaldehyde, bispenol A Butyl hydroxyanisol Mono-(2-ethylhexyl) phthalate Dibutyl phthalate Di(2-ethylhexyl) phthalate	[12]
PVC	Leaching of administration sets	Direct injection	Econosphere C18, 150 × 4.6 mm, 5 μm	A = 1% acetic acid	254	1 ml/min, 50 μl, 35°C	Phthalide	[13][a]
				B = ACN 50% B for 3.5 min, change to 65% B			Monobutyl phthalate Mono-(ethylhexyl) phthalate	
Adhesives	Extraction with water, 50°C, 3 days	Direct injection	NovaPak C18, 150 × 2.1 mm	40-min gradient from 5–85% ACN in 0.1% acetic acid	220[k]	0.25 ml/min	1,3-Benzenedicarboxylic acid, mono(7,12-dioxo-3,6,13,16-tetraoxaoctadec-17-en-1-yl) ester Hexanedioic acid, 2-[2-[(5-carboxy-1-oxopentyl)oxy] ethoxy] ethyl 2-(ethenyloxy) ethyl ester	[14]

PP	Extraction with acetonitrile	Direct injection after filtration	Waters Symmetry C8, 150 × 3.9 mm	Start at 30 : 70 ACN/water, to 100% ACN at 10 min, to 30% ACN at 30 min, hold at 30% ACN for 10 min	MS EI Atmospheric pressure chemical ionization (APCI) UV	0.4 ml/min, 10 μl	1,3-Benzenecarboxylic acid, 2-[2-[(carboxy benzoyl)oxy]ethoxy] ethyl 2-(ethyloxy)ethyl ester Naugard XL, Irganox 1076 1-Octadecanol, NC-4 3-(3,5-Di-*tert*-butyl-4-hydroxyphenyl) propanoic acid 7,9-Di-*tert*-butyl-1-oxaspiro-[4,5deca-6,9-diene-2,8-dione	[15]

Solvent abbreviations include MeOH = methanol; ACN = acetonitrile; AA = acetic acid.
Material abbreviations include PP = polypropylene; PVC = poly(vinyl chloride); HDPE = high-density polyethylene; PC = polycarbonate; PS = polystyrene; PET = polyethylene terephthalate.
[a]Method performance data provided in this reference.
[b]Gradient was as follows: 0.0 min, 70% A; 18.0 min, 0% A; 22.0 min, 0% A; 23.0 min, 70% A.
[c]Gradient was as follows: 0.0 min, 95% A; 8.0 min, 40% A; 16.0 min, 30% A; 17.0 min, 0% A; 21.0 min, 0%A; 22.0 min, 95% A.
[d]Specific compounds detected included propyl-3,4,5 trihydroxy benzoate, 2-*tert*-butyl-4-methoxy phenol, 2-*tert*-butylphenol, 2-*tert*-butyl-4-methylphenol, and octyl-3,4,5-trihydroxybenzoate.
[e]This cited reference documents numerous compounds in these and other general compound classes.
[f]Fourier transform-infrared spectroscopy analysis of collected peaks used to confirm analyte identification.
[g]Various column sizes used.
[h]Fluorescence detection.
[i]Gradient was as follows: 5% ACN for 2 min; 5–50% ACN in 28 min; 50–98% ACN in 15 min.
[j]Multiple wavelengths are used.
[k]Compound identification performed via MS and MS/MS using both APCI and electrospray ionization (ESI) in the positive ion mode.

Table 2 Examples of GC methods used to identify and/or quantify packaging system extractables.

Material	Sample matrix	Sample preparation	Column	Oven program	Detection	Other	Extractables	Refs.
Rubber	Water extract, 121°C, 2 hr	Evaporative concentration	Cross-linked methyl silicone 25 m × 0.3 mm I.D.	30°C for 1 min, ramp at 8°C/min to 250°C	FID 325°C[a]	Splitless injection, $T = 250$°C	2-Butoxyethanol Cyclohexanone Diphenylamine 9,10-Dihydro-9,9-dimethyl-acridine	[16]
			DB-Wax-30N, 0.25 mm I.D.	34°C for 1 min, ramp at 6°C/min to 200°C			Dibutylformamide 1,1,2,2-Tetrachloroethane Acetophenone 2-Phenyl-2-propanol Benzothiazole 2,2,5,5-Tetramethyl-tetrahydrofuran	
PET	Solvent extracts, 40°C, 10 days	Evaporative concentration	HP1, 50 × 0.25 mm	200–280°C at 8°C/min	FID 280°C	Split injection $T = 250$°C	Isophthalic acid Terephthalic acid PET oligomers	[17]
PVC	Water extract	Evaporative concentration	J&W DB-5, 15 m × 0.53 mm, 15 μm film	32°C, 1.5 min; to 75 °C at 6°C/min; to 250°C at 30°C/min, hold for 2 min	FID 350°	3 μl (splitless), $T = 210$°C	Cyclohexanone	[18]
PVC	Products	Acidification, solvent extraction, evaporative concentration	J&W DB-5, 30 m × 0.32 mm, 0.25 μm film	30°C for 0.5 min, to 225°C at 6°C/min	FID 350°C	Cold on-column injection	Di(ethylhexyl) phthalate Dibutyl phthalate cyclohexanone, phthalide 2-Ethyl-1-hexanol 2,6-Di-*tert*-butyl-*p*-cresol	[19][b]
Filter cartridges	Water or ethanol extracts	Solid phase extraction (SPE) with evaporative concentration	J&W DB-5, 60 m	60°C for 2 min, to 280°C at 10°C/min, hold	MS	1 ml, split, $T = 250$°C	Phthalates, fatty acids, phenols, siloxanes, acrylates, aliphatics, amides[c]	[8]
PC	Methylene chloride extract	Direct injection after polymer ppt with methanol	Restek RTx-5 FSOT, 30 m × 0.25 mm, 1.0 μm film	100°C, to 280°C at 10°C/min, hold for 3 min	MS *m/z* 213, $T = 290$°C	2 μl, split, $T = 280$°C	Bisphenol A	[9]
PVC	Pharmaceutical products	Solvent extraction, evaporative concentration	3% QF-1 or 3% SE-30 on Supelcoport	120°C for 1 min, to 225°C at 4°C/min	MS EI +, $T = 230$°C	$T = 230$°C	9,10-Epoxystearate ester	[20]
Rubber stoppers	Methylene chloride extracts	Direct injection	J&W DB-5MS, 30 m × 0.25 mm, 0.25 μm film	50°C for 5 min, to 275°C at 10°C/min, hold for 20 min	MS EI +, $T = 200$°C, 50–650 amu	1 μl, splitless, 200°C	Tributoxyethylphosphate BHT, diphenylamine 4-(2,2,3,3-tetramethylbutyl) phenol 2,2′-Methylenebis[6,(1,1 dimethylethyl)-4-ethyl] phenol	[21]

Laminated polyolefin[d]	Soxhlet and *n*-heptane extracts	Evaporative concentration with and without silylation	J&W DB-5, 30 m × 0.32 mm, 0.25 μl film	From 100°C to 280°C at 10°C/min	MS[e]	$T = 220$°C	Penta- to octa-decane Phthalic acid esters Mono- to hepta-cosane 13-diocosenoic acid	[22,23][f]
PET	Soxhlet extraction	Evaporative concentration, with and without silylation	J&W DB-1, 15 m × 0.53 mm, 1-μm film	50°C, hold for 10 min, to 280°C at 10°C/min	MS SIM mode, also FID	$T = 280$°C	Alkyl esters of nonanoic acid Ethylene glycol, BHT Phthalic acid esters Plamitic, stearic, oleic acid Terephthalic acid Alkyl terephthalic acid esters 2,6-bis-(1,1-methylethyl)-4-ethyl phenol Pyrogallol	[24][f]
Polyolefin	Solvent extraction	Evaporative concentration	TRB-5, 60 m × 0.25 mm, 0.5 μm film	40°C for 1 min, to 300°C at 20°C/min, hold for 26 min	MS EI +	1 μl, splitless, $T = 300$°C	Aliphatic hydrocarbons, straight-chained, branched and cyclic[f,g]	[25][h]
PE[i]	Solvent extraction	Direct injection	DB-1, 30 m × 0.25 mm, 0.32 μm film	50°C for 2 min, to 340°C at 5°C/min, hold for 10 min	MS EI +, 40–700 Da, $T = 270$°C	Splitless, $T = 250$°C	1,3-Di-*tert*-butyl benzene Oligomers 2,4-Di-*tert*-butylphenol Oxidized antioxidants Butanoic acid vinylester	[26][f,j]
Rubber[k]	Water extraction	Evaporative concentration	3% OV17 on Cas-Chrom Q, 1.5 m × 2 mm	140–200°C at 10°C/min	MS EI +, $T = 250$°C	2 μl, $T = 250$°C	Benzothiazole derivatives[l]	[27]

See legend of Table 1 for a list of material abbreviations.

[a]MS was used in compound identification.

[b]Method performance data are provided in this reference.

[c]This reference documents numerous extracted compounds in these general categories.

[d]Laminated film consisting of glycol-modified polyethylene terephthalate (PETG), polyvinylidene chloride (PVDG), and polyethylene (PE) with a polyurethane adhesive.

[e]GC/infrared spectroscopy analysis was also used under differing operating parameters to aid in compound identification.

[f]These cited references document numerous compounds in these and other general compound classes.

[g]Straight chained = C_{12}–C_{25}; branched = C_{19}–C_{30}; cyclic = C_{24}–C_{35}.

[h]Similar methods were used to identify compounds from polystyrene (styrene, styrene derivatives, glycolic esters of C16–C25 fatty acids, *trans*-1,2-diphenylcyclobutane).

[i]Material was gamma-irradiated prior to analysis.

[j]A similar method was used to identify compounds from PP, PVC, PS, PET, and polyamide.

[k]Components of disposable syringes.

[l]Identified compounds include 2-hydroxybenzothiazole, 2-mercaptobenzothiazole, 2-(methylmercapto)benzothiazole, 2-(2-hydroxyethoxy)benzothiazole, and 2-(2-hydroxyethylmercapto)benzothiazole.

Table 3 Examples of GC methods used to identify and/or quantify volatile packaging system extractables.

Material	Sample matrix	Sample preparation	Column	Oven program	Detection	Other	Extractables	Refs.
Paper and board	Extracts in water, ethanol, or chloroform	2.5 g sample per vial; 70°C for 30–60 min	Chrompack CP-Sil 8 CB, 50 m × 0.32 mm, 1.2 μm film	70°C for 2 min, ramp at 5°C/min to 110°C	MS	Also used diffusion trapping	Butanal, pentanal, hexanal Heptanal, 2-heptanal Ethyl acetate, chloroform Methyl acetate, nonanal *o*- and *p*-xylene, benzene, benzaldehyde, others	[28]
PVC bags	Portions of bags from actual products	1–5 mg sample per vial, 120°C for 5–20 min	SE-54, 20m × 0.2 mm	30°C for 2 min, ramp at 10°C/min to 280°C	MS	Evolved gas trapped in a container cooled with liquid nitrogen	Ethanol, pentane Acetic and formic acids Cyclohexanal, xylene Cyclohexanone, pentanal Heptanal, nonanal Phthalates, BHT Tetradecanoic acid Hexadecanoic acid	[12]
Polyolefin packaging material	7 cm^2 portion of the material	Investigated effect of temperature from 30°C to 125°C with a 3 min desorption	2% OV-7 on Aue 2 m × 2 mm	Start at 0°C, ramp at 10°C/min to 150°C	FID and MS	Also used purge and trap	Methanol, 1-propanol *t*-Butanol, toluene 2-Methyl-2-propanol 1-Ethoxy-2-propanol Methyl ethyl ketone 2-(2-Hydroxypropoxy-1 propanol	[29]

Drinking water in plastic bottles	Water solution	1 L of water stripped with N_2 at 600/ml/min for 8 hr, trapped on activated carbon	HP Ultra 2, 30 m × 0.53 mm, 1.5 μm film	40°C for 2 min, ramp at 10°C/min to 120°C, hold for 3 min.	MS	Analyte desorbed with CS_2 from activated carbon	2-Ethyl-1-hexanol Di-2-ethylhexyl phthalate	[30]
Irradiated poly-ethylene film	Pieces of film	Gas evolved at 80°C, transferred through trap with 3 L of N_2 at 50 ml/min Trapped volatiles desorbed at 200°C into N_2	Porapak Q, 3.1 m × 3.2 mm[a] or Ucon Oil HB2000 LB550X, 80 m × 0.2 mm[b]	60°C for 8 min, ramp to 230°C at 4°C/min[a] or 60°C for 16 min, ramp to 140°C at 4°C/min[b]	FID and MS	Tenax-GC 18 cm × 5 mm (60/80 mesh) rap used	Acetic acid, butyric acid Ethanol, isopropanol *n*-Propanol, *n*-butane 2-Pentanaone, 2-hexanone 3-Hexanaone, 3-heptanaone Toluene, butanal Acetaldehyde, propane Propionic acid	[31]

[a]Used for low-boiling compounds.
[b]Used for high-boiling compounds.

Table 4 Examples of miscellaneous chromatographic methods used to identify or quantify material extractables.

Material	Test sample	Method description	Extractables	Refs.
Polypropylene	Aqueous food-simulating solvents	Capillary SFC. Column: 10 m × 50 mm I.D. SB-Biphenyl-30, 0.25 μm film. Mobile phase = CO_2, linear flow rate ≈ 3 cm/sec. Pressure program, 100–400 bar; temperature program, 55–100°C. 1 μl injection using solvent venting with gas purging. Retention gap was 1.8 m × 100 μm deactivated fused silica. Detection by FID and MS.	Pentaerythrityl-tetrakis((3-(3,5-di-*tert*-butyl-4-hydroxy-phenyl) propionate) (*N*,*N*′-bis(2-hydroxyethyl)-C12.C14-amine) Tris-2,4-di-*tert*-butylphenyl)phosphite	[32]
Polyolefins, polypropylene, polyethylene	Soxhlet extracts	Capillary SFC. Column: 10 m × 50 μm I.D. fused silica capillary coated with cross-linked 5% phenyl-methypolysiloxane (0.4 μm film). Mobile phase = CO_2. Various temperature and pressure gradients used. Detection = FID at 300°C	Stearic acid, Irganox 1010 Irganox PS802, Atmos 150 Mono- and di-glycerides Alkenes, cycloalkanes	[33]
Polypropylene	Soxhlet extracts	Capillary SFC. Column: 10 m × 50 μm I.D. fused silica capillary coated with cross-linked methylpolysiloxane (SB-Methyl-100) or 50% octyl-substituted methylpolysiloxane (SB-Octyl-50), 0.25 μm film. Mobile phase = CO_2. Pressure program, 129–350 atm at 3 atm/min; temperature = 110°C. Detection = FID.	Additives including Topanol, Irgafos 168, Irganox 1076, Irganox 1330, Irganox 1010, ethylbenzoate, ethyl stearate	[34]
Polyolefin laminate	Drug product stored in plastic bags, SPE preparation	HPTLC. Plate = 10 × 20 cm silica gel. Mobile phase: acetone–chloroform–concentrated sodium hydroxide (20:80:0.2). Photodensitometric detection, at 200 and 234 nm before derivitization, 388 nm after derivitization with ninhydrin and 580 nm after derivitization with Bratton/Marshall reagent.	ε-Caprolactam Irganox 1010 Butylhydroxytoluene 4,4′-methylene dianiline	[7]
Polyethylene	Organic and water extracts	HPTLC. Plate = 10 × 10 cm Fertigplatten Kiselgel 40. Mobile phase: chloroform/cyclohexane (12:1). Densitometric detection.	Irganox 1076 3,5-di-*tert*-butyl-4-hydroxy-phenyl propionic acid	[35]

Preinjection sample preparation is not a chromatographic issue per se. Nevertheless, it is an important consideration in the successful application of a complete analytical process. Nerin et al.[36] reviewed sample treatment techniques applicable to polymer extract analysis, including headspace methods, supercritical fluid extraction, and solid phase microextraction.

REFERENCES

1. Aignasse, M.F.; Prognon, P.; Stachowicz, M.; Gheyouche, R.; Pradeau, D. A simple and rapid HPLC method for determination of DEHP in PVC packaging and releasing studies. Int. J. Pharm. **1995**, *113*, 241–246.
2. Yagoubi, N.; Baillet, A.; Pellerin, F.; Ferrier, D. Physico-chemical behavior of β-irradiated plastic materials currently used as packages and medical products. Nucl. Instrum. Methods Phys. Res. **1995**, *105*, 340–344.
3. Begley, T.H.; Hollifield, H.C. Migration of dibenzoate plasticizers and polyethylene terephthalate cyclic oligomers from microwave susceptor packaging into food-simulating liquids and foods. J. Food Prot. **1990**, *53*, 1062–1066.
4. Begley, T.H.; Hollifield, H.C. Liquid chromatographic determination of residual reactants and reaction by-products in polyethylene terephthalate. J.A.O.A.C. **1989**, *72*, 468–470.
5. Rybak, K.E.; Sarzynski, W.; Dawidowicz, A.L. Migration of antioxidant additives from polypropylene investigated by means of reversed phase high performance liquid chromatography. Chem. Anal. **1992**, *37*, 149–159.
6. Yagoubi, N.; Baillet, A.; Mur, C.; Baylocq-Ferrier, D. Determination of phenolic antioxidants in pharmaceutical formulations by liquid chromatography and migration study on HDPE packagings. Chromatographia **1993**, *35*, 455–458.
7. Sarbach, C.; Yagoubi, N.; Sauzieres, J.; Renaux, C.; Ferrier, D.; Postaire, E. Migration of impurities from a multi-layer plastics container into a parenteral infusion solution. Int. J. Pharm. **1996**, *140*, 169–174.
8. Reif, O.W.; Solkner, P.; Rupp, J. Analysis and evaluation of filter cartridge extractables for validation in pharmaceutical

downstream processing. PDA J. Pharm. Sci. Technol. **1996**, *50*, 399–410.
9. Biles, J.E.; McNeal, T.P.; Begley, T.H.; Hollifield, H.C. Determination of bisphenol-A in reusable polycarbonate food-contact plastics and migration into food-simulating liquids. J. Agric. Food Chem. **1997**, *45*, 3541–3544.
10. Buiarelli, F.; Cartoni, G.; Coccioli, F. HPLC and GC-MS determination of compounds released to mineral waters stored in plastic bottles of PET and PVC. Annal. Chim. **1993**, *83*, 93–104.
11. Ulsaker, G.A.; Teien, G. Identification of caprolactam as a potential contaminant in parenteral solutions stored in overwrapped PVC bags. J. Pharm. Biomed. Anal. **1992**, *10*, 77–80.
12. Arbin, A.; Jacobsson, S.; Hanninen, K.; Hagman, A.; Ostelius, J. Studies on contamination of intravenous solutions from PVC-bags with dynamic headspace GC-MS and LC-diode array techniques. Int. J. Pharm. **1986**, *28*, 211–221.
13. Snell, R.P. Solid-phase extraction and liquid chromatographic determination of monophthalates and phthalide extracted from solution administration sets. J.A.O.A.C. **1993**, *76*, 531–534.
14. Tiller, P.R.; El Fallah, Z.; Wilson, V.; Huysman, J.; Patel, D. Qualitiative assessment of leachables using data-dependent liquid chromatography/mass spectrometry and liquid chromatography/tandem mass spectrometry. Rapid Commun. Mass Spectrom. **1997**, *11*, 1570–1574.
15. Yu, K.; Block, E.; Balogh, M. LC-MS analysis of polymer additives by electron and atmospheric-pressure ionization: Identification and quantification. LC GC **2000**, *18*, 162.164.166.168.170.172.174.176.178.
16. Danielson, J.W. Toxicity potential of compounds found in parenteral solutions with rubber stoppers. J. Parenter. Sci. Technol. **1992**, *46*, 43–47.
17. Dobias, J.; Voldrich, M.; Proks, M. Migration of polyethylene terephthalate oligomers from packaging into food simulant liquids. Potav. Vedy **1996**, *14*, 25–32.
18. Snell, R.P. Gas chromatographic determination of cyclohexanone leached from hemodialysis tubing. J.A.O.A.C. **1993**, *76*, 1127–1132.
19. Snell, R.P. Capillary GC analysis of compounds leached into parenteral solutions packaged in plastic bag. J. Chromatogr. Sci. **1989**, *27*, 524–528.
20. Ulsaker, G.A.; Teien, G. Determination of 9,10-epoxystearate ester in intravenous solutions stored in poly(vinyl chloride) bags, using gas chromatography–single-ion monitoring mass spectrometry. Analyst **1984**, *109*, 967–971.
21. Milano, C.J.; Bailey, L.C. Evaluation of current compendial physicochemical test procedures for pharmaceutical elastomeric closures and development of an improved HPLC procedure. PDA J. Pharm. Sci. Technol. **1999**, *53*, 202–210.
22. Kim-Kang, H.; Gilbert, S.G. Permeation characteristics of and extractables from gamma-irradiated and non-irradiated plastic laminates for a unit dosage injection device. Packag. Technol. Sci. **1991**, *4*, 35–48.
23. Kim-Kang, H.; Gilbert, S.G. Isolation and identification of potential migrants in gamma-irradiated plastic laminates by using GC/MS and GC/IR. Appl. Spectrosc. **1991**, *45*, 572–580.
24. Kim, H.; Gilbert, S.G.; Johnson, J.B. Determination of potential migrants from commercial amber polyethylene terephthalate bottle wall. Pharm. Res. **1990**, *7*, 176–179.
25. Veiga-Rial, M.; Sarria-Vidal, M.; de la Montana-Migueslez, J.; Simal-Gandura, J. Identification of residual constituents in plastic packaging for dairy products. Rec. Res. Devel. Agric. Food Chem. **1999**, *3*, 305–311.
26. Demertzis, P.G.; Franz, R.; Welle, F. The effects of γ-irradiation on compositional changes in plastic packaging films. Packag. Technol. Sci. **1999**, *12*, 119–130.
27. Salmona, G.; Assaf, A.; Gayte-Sorbier, A.; Airaudo, C.B. Mass spectral identification of benzothiazole derivatives leached into injections by disposable syringes. Biomed. Mass Spectrom. **1984**, *11*, 450–454.
28. Castle, L.; Offen, C.P.; Baxter, M.J.; Gilbert, J. Migration studies from paper and board food packaging materials. I. Compositional analysis. Food Addit. Contam. **1997**, *14*, 35–44.
29. Eiceman, G.A.; Karasek, F.W. Identification of residual organic compounds in food packages. J. Chromatogr. **1981**, *210*, 93–103.
30. Vitali, M.; Leoni, V.; Chiavarni, S.; Cremisini, C. Determination of 2-ethyl-1-hexanol as contaminant in drinking water. J.A.O.A.C. **1993**, *76*, 1133–1137.
31. Azuma, K.; Hirata, T.; Tsunoda, H.; Ishitani, T.; Tanaka, Y. Identification of volatiles from low density polyethylene film irradiated with an electron beam. Agric. Biol. Chem. **1983**, *47*, 855–860.
32. Berg, B.E.; Hegna, D.R.; Orlien, N.; Greibrokk, T. Determination of low levels of polymer additives migrating from polypropylene to food simulated liquids by capillary SFC and solvent venting injection. Chromatographia **1993**, *37*, 271–276.
33. Dilettato, D.; Arpino, P.J.; Nguyen, K.; Bruchet, A. Investigation of low mass oligomers and polymer additives from plastics. Part II: application to polyolefin soxhlet extracts. J. High Res. Chromatogr. **1991**, *14*, 335–342.
34. Moulder, R.; Kithinji, J.P.; Raynor, M.W.; Bartle, K.D.; Clifford, A.A. Analysis of chemical additives in polypropylene films using capillary supercritical fluid chromatography. J. High Res. Chromatogr. **1989**, *12*, 688–691.
35. Corti, P.; Murratzu, C.; Franchi, G.; Lencioni, E.; Pancini, R. Evaluation of chemical residues in food and drugs: Evaluation of an antioxidant given from high density polyethylene food containers. Acta Toxicol. Ther. **1988**, *9*, 205–221.
36. Nerin, C.; Rubio, C.; Salafranca, J.; Batlle, R. The simplest sample treatment techniques to assess the quality and safety of food packaging materials. Rev. Anal. Chem. **2000**, *19*, 435–465.

Organic Polymer Additives: Identification and Quantification

Dennis R. Jenke
Technology Resources Division, Baxter Healthcare Corporation, Round Lake, Illinois, U.S.A.

INTRODUCTION

Plastic materials are widely used in numerous industries. The physiochemical nature of these materials provides a multitude of diverse products with their necessary, desirable performance characteristics. Commercial plastics are very complex materials. In addition to the various base polymers, commercially viable plastics contain a number of compounding ingredients (additives) whose purpose is to give the material its desired physical and/or chemical properties. Table 1 provides a brief summary of the types of additives typically encountered in commercial polymer systems.

Polymers and polymer systems are characterized for many reasons including the development of new materials or material sources, the end-use applications, the life test studies, the manufacturing control and troubleshooting, and the material or vendor identification. As it is typically the additive package that establishes the performance and processing properties of the commercial polymer, characterization of a polymer system for its additive package is essential in terms of material development, manufacturing, use, reuse, and, ultimately, disposal. A complete polymer characterization includes both the identities of the additives and their levels in the product. The identification and the quantification of additives in compounded polymers is generally a difficult task for the following reasons:

1. There is a wide variety of chemically diverse additive types. Literally, thousands of additives are commercially available, ranging from pure compounds, with molecular weights that vary from approximately 100 up to a few thousand mass units, to oligomers with up to 50 (or more) components.
2. Many additives are labile; thus, they are difficult to analyze without decomposition.
3. Complex mixtures of additives will normally be present in a commercial formulation.
4. Separation of the base polymer and the fillers from the organic additives are often required prior to additive analysis.
5. The levels of the organic additives in a commercial polymer may be quite low (and variable) compared to the base polymer and its associated fillers.

It is for these reasons that chromatographic methods of analysis have been widely employed in polymer characterization. In this entry, a review related to the chromatographic methods used to assess the identity and level of additives in polymer systems is provided.

DISCUSSION

Given the variety of additives used in commercial polymers, the task of characterizing such multicomponent systems for their additive packages can be daunting. While an analytical chemist has a multitude of chromatographic tools with which to perform an additive characterization, some guidance in terms of successfully applied strategies and methods can greatly facilitate the assessment. Thus this manuscript contains a general compilation of published chromatographic methods and strategies that have been successfully applied to the identification and the quantification of a large number of the more commonly encountered packaging material additives (Table 2 shows a listing of additives considered in this work's cited references). Examples are provided for each major separation strategy [e.g., high-performance liquid chromatography (HPLC), gas chromatography (GC), thin-layer chromatography (TLC), supercritical fluid chromatography (SFC)] and for most commonly employed detection methods [e.g., ulraviolet (UV), mass spectrometry (MS), flame ionization detector (FID)]. While the compilations in Tables (3–10) are by no means exhaustive or comprehensive, they are sufficiently broad in scope to provide the investigator with a general overview of the ways in which chromatography has been applied to meet the objectives of a polymer's characterization.

Tables (3–10) provide general method details, such as separation medium, elution, and detection conditions, and other operating conditions. The level of detail associated with each citation reflects the level of detail provided by the citation's author(s). The

Table 1 Common additives and fillers.

Classification	Purpose	Examples
Antioxidants	Prevent thermal and/or oxidative degradation during processing, handling, and use. Typically are radical scavengers which interrupt the chain propagation steps of polymer autooxidation	Irganox 1010, Irgafos 168, BHT
Light stabilizers	Absorb UV light to prevent photooxidation	Tinuvin 327, 328, 384, 440, etc. (derivatives of 2-hydroxy-benzophenone)
Heat stabilizers	Protect polymers during thermal processing	Metallic salts, especially of weak fatty acids (e.g., zinc stearate)
Plasticizers	Increase the workability, flexibility or distensibility of polymer	Derivatives of organic acids such as adipic, azelic, citric, phosphoric, phthalic, trimellitic acids
Lubricants (slip agent)	Reduce polymer adhesion to metal surfaces during processing	Derivatives of fatty acids (esters, amides, metal salts, Erucamide, silicones)
Viscosity improvers	Control the flow and the sagging of prepolymers	Ethoxylated fatty acids
Accelerators, activators	Compounds that control the rate or the nature of cure of elastomers	Zinc oxide, stearic acid, 2-2′-dithiobis-benzothiazole, zinc dialkyldithio-carbamate
Mold release agents	Prevent adhesion between two surfaces (e.g., sticking of polymer and metal mold)	Derivatives of fatty acids, Montan wax, silicones, diethylene glycol monostearate, ethylene bis (stearamide)
Fillers (extenders)	Finely dissolved solids added to polymer systems to improve properties or to reduce cost	Calcium carbonate, kaolin, talc, alumina trihydrate
Flame retardants	Decrease flammability	Alumina trihydrate, mixtures of halogenated organics and antimony oxide
Antistatic agents	Dissipate electrostatic surface charge on polymer surfaces	Quaternary ammonium compounds, long-chain derivatives of glycols and polyhydric compounds, Atmos 150, *N*,*N*-bis-(2-hydroxy-ethyl) alkyl-amine
Colorants	Improve the appearance of polymers, mask discoloration due to processing	Carbon black, titanium dioxide, azo-type dyes
Antimicrobial agents (biocides)	Reduce growth of microbes on polymer surfaces	Copper 8-hydroxyquinolate, *n*-(trichloromethylthio) phthalate
Cross-linking agents	Molecules that have two or more groups capable of reacting with the functional groups of polymer chains, where such a reaction connects or links the chains	2-Mercaptobenzothiazole, benzoyl peroxide, dicumyl peroxide, sulfur, toluene diisocyanate
Blowing agents	Gas-forming agents that facilitate the expansion of the polymer during processing	Nitrogen, toluenesufonyl semicarbazide, 1,1′-azobisforamide, phenyltetrazole

materials investigated, as well as the specific additives examined, are also indicated. General comments are provided in terms of sample preparation. Given the number of methods cited, it is not possible to provide chromatographic profiles which are readily available in the cited references.

In generating this review, the author balanced two objectives. The first objective was to summarize the most current technologies that are utilized for the task of polymer characterization, thus providing the researcher with the most relevant and state-of-the-art tools for the task at hand. Thus emerging automated and hyphenated techniques, coupled with online sample preparation, high-efficiency separations, and selective and sensitive detection [e.g., supercritical fluid extraction (SFE)/HPLC/MS], have a prominent place in this review. However, this author also notes that more historically relevant methods, such as GC and HPLC with UV detection, remain capable of providing

Table 2 Chemical names for the additives cited in this manuscript.

Trade name	Chemical name	CAS RN
AcraWax C	*N*,*N*′-ethylenebistearamide	110-30-5
Adkstab PEP-24G	Cyclinepentan tetrail bis (2,4-di-*tert*-butylphenyl) phosphite	29741-53-7
AM340		
ATBC	*O*-Acetyl-tri-*n*-butyl citrate (see Citroflex A-4)	—
Atmos 150	A mixture of glycerol mono- and distearate	11099-07-3
BAC-E	2,6-bis-[(Azidophenyl) methylene]-4-ethylcyclohexanone	
BBP	Benzyl *n*-butyl phthalate	85-68-7
Benzoflex-2860	A mixture of 19% di (2-ethylhexyl) adipate, 57% diethyleneglycol dibenzoate, 24% triethyleneglycol dibenzoate	400609-45-2
BEHB	Butylated hydroxyethylbenzene	
Behenamide	Docosanoic acid amide	3061-75-4
BHA	2-*tert*-Butyl-4-hydroxyanisole	25013-16-5
BHT	2,6-Di-*tert*-butyl-*p*-cresol	128-37-0
BHET	bis-(2-Hydroxyethyl) terephthalate	
Bis-A-bis azide	1,1′-(1-Methylethylidene)-bis-[4-(4-axidophenoxybenzene]	
Bisphenol A	2,2′-bis-(4-Hydroxyphenyl) propane	80-05-7
Brominated bisphenol A		
Brominated phenol		
Butyl oleate	9-Octadecanoic acid, butyl ester	142-77-8
Butyl palmitate	Hexadecanoic acid, butyl ester	111-06-8
Butyl stearate	Octadecanoic acid, butyl ester	123-95-5
Calcium stearate	Stearic acid, calcium salt	1592-23-0
Caprolactam	2-Oxohexamethyleneimine	105-60-2
Chimasorb 81	2-Hydroxy-4-*n*-octyloxybenzophenone	1843-05-6
Chimassorb 119 FL		
Chimassorb 944	Poly-[[6-[1,1,3,3,-tetramethylbutyl) amino]-1,3,5-triazine-2,4-diyl] [2.2.6.6-tetramethyl-4-piperidinyl) imino]-1,6-hexanediyl [2,2,6,6-tetramethly-4-piperidinyl) imino]]	71878-19-8
Citroflex A-4	2-Acetoxy-1,2,3-propanetricarboxylic acid tributyl ester	77-90-7
Cyanox 425	2,2′-Methylene-bis-(6-*tert*-butyl-4-ethylphenol)	88-24-4
Cyanox 1790	1,3,5-tris-(4-*tert*-Butyl-3-hydroxy-2,6-dimethylbenzyl)-1,3,5-triazine-(1*H*,3*H*,5*H*) trione	40601-76-1
Cyanox 2246	See Irganox 2246	—
Cyasorb UV 9		
Cyasorb UV-24	2,2′-Dihydroxy-4-methoxybenzophenone	131-53-3
Cyasorb UV 531	2-Hydroxy-4-(octyloxy) benzophenone	1843-05-6
Cyasorb UV 1084	2,2′-Thiobis-(4-*tert*-octylphenoxy) (nibutylamine) nickel	14516-71-3
Cyasorb UV 1164	2,4-bis-(2,4-Dimethylphenyl)-6-(2-hydroxy-4-octyloxyphenyl)-1,3,5-triazine	2725-22-6
Cyasorb 2908	3,5-Di-*tert*-butyl-4-hydroxybenzoate	67845-93-6

(Continued)

Table 2 Chemical names for the additives cited in this manuscript. *(Continued)*

Trade name	Chemical name	CAS RN
Dechlorane Plus	1,2,3,4,7,8,9,10,13,13,14,14-Dodecachloro-1,4,4a,5,6,6a,7,10,10a,11,12,12a-dodecahydro-1,4,7,10-dimethanodibenzo [*a*,*e*] cyclooctene	13560-89-9
DEHA	Di-(2-ethylhexyl) adipate, dioctyl adipate	103-23-1
Di-Cup	Dicumyl peroxide	80-43-3
Dibutyl sebacate		109-43-3
DEG	Diethylene glycol	111-46-6
DBP	Di-*n*-butyl phthalate	84-74-2
DEHP, DOP	Di-(2-ethylhexyl) phthalate	117-81-7
Dinonyl phthalate	1,2-Benzenedicarboxylic acid, dinonyl ester	84-76-4
DMTDP	3,3′-Thiodipropionic acid di-*n*-tetradecyl ester	16545-54-3
DSTDP	Dioctadecyl 3,3′-thiodipropionate	693-36-7
DLTDP	Dilauryl 3,3′-thiodipropionate	123-28-4
Docosane		629-97-0
Eicosane		112-95-8
Epoxol 9.5	Epoxidized linseed oil	8016-11-3
EG	Ethylene glycol	107-21-1
Erucamide	*cis*-13-Docosenamide	112-84-5
Ethyl palmitate	Hexadecanoic acid ethyl ester	628-97-7
Ethyl linoleate	9,12-Octadecanoic acid ethyl ester	544-35-4
Ethyl oleate	9-Octadecanoic acid ethyl ester	111-62-6
Ethyl stearate	Octadecanoic acid ethyl ester	111-61-5
Ethanox 330	See Irganox 1330	—
Hexadecane		544-76-3
Hexacosane		630-01-3
Hostanox O3	bis-[3,3-bis-(4-Hydroxy-3-*tert*-butylphenyl) butanoic acid] ethylene glycol ester	32509-66-3
Hostavin TMN 20	2,2,4,4-Tetramethyl-21-oxo-7-oxa-3,20-diazadispiro [5.1.11.2] heneicosane	64338-16-5
Ionol 220	2,6-Di-(*tert*-butyl)-4-methylphenol (see Topanol OC)	—
Ionox 100	4-Hydroxymethyl-2,6-di-*tert*-butylphenol	88-26-6
Ionox 129	2,2′-Ethylidenebis-(4,6-di-*tert*-butylphenol)	35958-30-6
Ionox 220	4,4-Methylenebis-(2,6-di-*tert*-butylphenol)	118-82-2
Irgafos 168	tris-(2,4-Di-*tert*-butylphenyl) phosphite	31570-04-4
Irgafos P-EPQ	Tetrakis-(2,4-di-*tert*-butylphenyl)-4,4′-biphenylene diphosphonite	38613-77-3
Irganox 245	Triethylene glycol bis-3-(3-*tert*-butyl-4-hydroxy-5-methyl) propionate	36443-68-2
Irganox 259	1,6-bis-[3-(3,5-Di-*tert*-butyl-4-hydroxyphenyl) propionyloxy] hexane	35074-77-2
Irganox 565	2,4-bis-(Octylthio)-6-(3,5-di-*tert*-butyl-4-hydroxyanilino)-1,3,5-triazine	991-84-4
Irganox 1010	Tetrakis-methylene-(3,5-di-*tert*-butyl-4- hydroxyhydrocinnamate)-methane	6683-19-8
Irganox 1035	2,2′-Thiodiethylene-bis-[3-(3,5-di-*tert*-butyl-4- hydroxyphenyl) propionate]	41484-35-9
Irganox 1076	Octadecyl-3-(3′,5′-di-(*tert*-butyl)-4′-hydroxyphenyl) propionate	2082-79-3
Irganox 1098	*N*,*N*-bis-[3-(3,5-di-*tert*-butyl-4-hydroxyphenyl) propionyl] hexamethylene-diamine	23128-74-7

(Continued)

Table 2 Chemical names for the additives cited in this manuscript. *(Continued)*

Trade name	Chemical name	CAS RN
Irganox 1222	Diethyl-(3,5-di-*tert*-butyl-4-hydroxybenzyl) phosphonate	976-56-7
Irganox 1330	1,3,5-Trimethyl-2,4,6-tris-(3,5-di-*t*-butyl-4-hydroxy-benzyl)-benzene	1709-70-2
Irganox 1425	Calcium bis-(ethyl 3,5-di-*tert*-butyl-4-hydroxybenzylphosphonate)	65140-91-2
Irganox 2246	2,2′-Methylene-bis-(4-methyl-6-*tert*-butylphenol)	119-47-1
Irganox 3052 FF	2,2′-Methylenebis-(6-*tert*-butyl-4-methylphenol) monoacrylate	61167-58-6
Irganox 3114	1,3,5-tris-(3,5-Di-*t*-butyl-4-hydroxybenzyl)-*s*-triazine-2,4,6-(1*H*,3*H*,5*H*) trione	27676-62-6
Irganox MD1024	3,5-bis-(1,1-Dimethylethyl)-4-hydroxybenzenepropionic acid	32687-78-8
Irganox MD1025	*N*,*N*-bis-[1-oxo-3(3,5-di-*tert*-butyl-4-hydroxyphenyl) propane] hydrazine	
Irganox PS800	Di-lauryl thio-dipropionate	123-28-4
Irganox PS802	Di-stearyl thio-dipropionate	693-36-7
Isonox 129	2,2′-Ethylidenebis-[4,6-di-*tert*-butylphenol]	35958-30-6
Kemamide U	See Oleamide	—
Lauric acid	Dodecanoic acid	143-07-7
Lowinox 22M46	See Irganox 2246	—
MHET	Mono-(2-hydroxyethyl) terephthalate	155603-50-2
Myristic acid	Tetradecanoic acid	544-63-8
	N,*N*-bis-(2-hydroxyethyl) alkyl-amine	
Naugard SP		94765-89-6
Naugard XL-1	2,2′-Oxamidobis-[ethyl 3-(3,5-di-*tert*-butly-4- hydroxyphenyl) propionate]	70331-94-1
Naugawhite	2-2′-Methylenebis-(4-methyl-6-nonylphenol)	7786-17-6
NC-4	1-(2,6-Dimethylphenylimino) imidazolidine	4859-06-7
Nonflex CBP	2,2′-Methylenebis-(6-(1-methylcyclohexyl)-*p*-cresol)	77-62-3
Noclizer M-17	2,6-Di-*tert*-butyl-4-ethylphenol	4130-42-1
Octadecane		593-45-3
ODO	Octabromodiphenyl oxide	32536-52-0
Oleamide	9-Octadecenamide	301-02-0
Palmitic acid	Hexadecanoic acid	57-10-3
Palmitamide	Hexadecanoic acid amide	629-54-9
Permanax WSP	2,2′-Methylenebis-[4-methyl-6-(1-methylcyclohexyl) phenol]	77-62-3
Sanol LS744		
Sanol LS770		
Santonox	See Yoshinox SR	—
Santowhite	4,4′-Butylidenebis-(3-methyl-6-*tert*-butylphenol)	85-60-9
Seesorb 101	2-Hydroxy-4-methylbenzophenone	131-57-7
Seesorb 202	4-*tert*-Butylphenylsalicylate	87-18-3
Seenox DM	3,3′-Thio-dipropionic acid dimyristyl ester	16545-54-3
Sodium benzoate	Benzoic acid, sodium salt	532-32-1
Stearamide	Octadecanamide	124-26-5
Stearic acid	Octadecanoic acid	57-11-4
Synprolam	Quaternary ammonium compounds, di-C13—C15-alkylmethyl, chlorides	308074-61-5
Terephthalic acid		100-21-0
TETO	Glyceryl tri-epoxyoleate	

(Continued)

Table 2 Chemical names for the additives cited in this manuscript. *(Continued)*

Trade name	Chemical name	CAS RN
Tetradecane		629-59-4
Tetracosane		646-31-1
Tinuvin 120	2′,4′-Di-*tert*-butylphenyl-3,5-Di-*tert*-butyl-4-hydroxybenzoate	4221-80-1
Tinuvin 144	2-*tert*-Butyl-2-(4-hydroxy-3,5-di-*tert*-butylbenzyl) [bis (methyl,2,2,6,6-tetramethyl-4-piperidinyl)] dipropionate	63843-89-0
Tinuvin 234	2[2′-Hydroxy-3,5-di-91,1-dimethylbenzyl) phenyl]-2*H*-benzotriazole	70321-86-7
Tinuvin 292	bis (1-Methyl-2,2,6,6,tetramethylpiperidinyl) sebacate	41556-26-7
Tinuvin 312	*N*-(2-ethyoxyphenyl)-*N*′-(2-ethylphenyl)-ethanediamine	23949-66-8
Tinuvin 320	2-(2-Hydroxy-3,5-di-*tert*-butylphenyl)-2*H*-benzotriazole	3846-71-7
Tinuvin 326	2-(3-*tert*-Butyl-2-hydroxy-5-methylphenyl)-2*H*-5-chlorobenzotriazole	3896-11-5
Tinuvin 327	2-(2′-Hydroxy-3′,5′-di(tertbutyl) phenyl)-2*H*-5-chlorobenzotriazole	3864-99-1
Tinuvin 328	2-(2′-Hydroxy-3′,5′-di(tertbutyl) phenyl)-2*H*-chlorobenzotriazole	25973-55-1
Tinuvin 329	2-(2′-Hydroxy-5′-*tert*-octylphenyl) benzotriazole	3147-75-9
Tinuvin 350	2-(2*H*-benzotriazol-2-yl)-4-(1,1-dimethylethyl)-6-(2-methylpropyl) phenol	134440-54-3
Tinuvin 384	Octyl 3-[3-(2*H*-benzotriazol-2-yl)-5-*tert*- butyl-4-hydroxyphenyl] propionate	84268-23-5
Tinuvin 662		
Tinuvin 770	(2-(2-Hydroxy-3,5-bis (1-methyl-1-phenylether) phenyl) benzotriazole)	52829-07-9
Tinuvin 1130	α-[3-[2-(2*H*-benzotriazol-2-yl)-5-(1,1,-dimethylethyl)-4-hydroxyphenyl]-1-oxopropyl-hydroxy-poly (oxy-1,2-ethanediyl)	194810-48-2
Tinuvin P	2-(2-Hydroxy-5-methylphenyl)-2*H*-benzotriazole	2440-22-4
TNPP	tris (Nonylphenyl) phosphite	26523-78-4
Topanol CA	1,1,3-tri (3-*tert*-butyl-4-hydroxy-6-methylphenyl) butane	1843-03-4
Topanol OC	2,4,6-tri-*tert*-butylphenol	128-37-0
TPP	Triphenyl phosphate	115-86-6
Tributylacetylcitrate	See Citroflex A-4	—
Ultranox 626	bis (2,4-Di-*t*-butylphenyl)-pentaerythritol-diphosphite	26741-53-7
Uvitex OB	2,5-bis (5′-*tert*-Butyl-2′-benzoazolyl) thiophene	7128-64-5
Vulkanox CS		94766-18-4
Wingstay T		12674-05-4
Yoshinox 425	2,2′-Methylenebis (4-ethyl-6-*tert*-butylphenol)	88-24-4
Yoshinox BB	See Santowhite	—
Yoshinox SR	4,4′-Thiobis [3-methyl-6-*tert*-butylphenol]	96-69-5
Zinc stearate	Stearic acid, zinc salt	557-05-1

researchers with accurate, precise, and pertinent information. Thus this review attempts to maintain a historical perspective as well.

While it is not a chromatographic issue per se, pre-injection sample preparation, nevertheless, is an important consideration in the successful application of a complete analytical process. This fact is borne out in the observation that recent technological advances in polymer characterization focus not only on the analytical characterization of a test sample but also on the method of generation of that sample. Innovation in sample preparation is driven both by scientific considerations [the difficulty, but necessity, of isolating the analytes of interest (additives) from the sample matrix (bulk polymer) in such a way that the additives are not impacted by the process (e.g., Ref.[52])] and by practical considerations associated with all analytical chemistry (e.g., time and cost efficiency). While it is beyond the

Table 3 Examples of HPLC methods (UV detection) used to identify and/or quantify packaging system additives.

Material	Additive(s)	Sample preparation	Column	Mobile phase	λ (nm)	Other	Refs.
PE	Dicumyl peroxide, Santonox®	Extract with methanol, concentrate (evaporative)	Lichrosorb RP 18, 250 × 4.6 mm, 10 μm	Methanol/water, 80/20	254	1 ml/min	[1]
PVC	Di-(2-ethylhexyl) phthalate (DEHP), epoxidized linseed oil, tris (nonyphenyl) phosphite (TNPP)	Dissolve in tetrahydrofuran (THF), precipitate polymer with methanol, dry and dissolve residue	μPorasil C_{18}	Carbon tetrachloride-dicloromethane (65/35)	280	1 ml/min	[2]
LDPE, PP	BHT, Cyasorb 531, Tinuvin 327, Irganox 1076	Reflux with CCl_4 or THF, filter, concentrate	μBondapak C_{18}, 60 × 0.39 cm	Methanol/water/THF, 63/7/30	254	2 ml/min	[3]
LDPE, HDPE	Tinuvin P, BHT, BEHB, Oleamide, Cyasorb UV 531, Isonox 129, AM340, Irganox 1010, Irganox 3114, Erucamide	Soxhlet, ultrasonic or microwave extraction with various solvent systems	Nova-Pak C_{18}, 150 × 3.9 mm, 4 μm	A = water; B = acetonitrile; 3/2 initial, linear gradient to 100% B in 5 min	200	1.5 ml/min, $T = 50°C$	[4]
PP	Irgafos 168, Irganox 1076, Irganox 3114, Irganox 1010, Tinuvin P, Irgafos PEP-Q	Microwave extraction with 98/2 methylene chloride/2-propanol	Nova-Pak silica (150 × 3.9 mm, 4 μm) or resolve silica (150 × 3.9 mm, 5 μm)	70/30 *n*-butyl chloride/ methylene chloride	225	1.5 ml/min, $T = 30°C$	[4]
Polyolefin	Irganox (245, 259, 565, 1010, 1035, 3114); Tinuvin (P, 234, 320, 326, 327, 328)	N/A[a]	Capcell Pak C_{18}, 250 × 4.6 mm	Methanol/water mixtures (95/5, 90/10, 88/12, 85/15)	multiple	1 ml/min, $T = 45°C$, 20 μl	[5]
Polyolefin	BHT, BHA, Irganox 1010, Irganox 565, Tinuvin 327, Tinuvin P	N/A[a]	Licrosphere 100 RP 18, 250 × 4.6 mm, 5 μm	Various binary and tertiary mixtures of methanol, water, and acetonitrile	multiple	20 μl	[6]
General	BHT, Irganox antioxidants (245, 259, 565, 1010, 1035, 1076, 1098, 1222, 1330, etc.); UV absorbers (Tinuvin P, 312, 320, 327, 328, etc.)	N/A[a]	Ultrabase UB225, 250 × 4.6 mm, 5 μm; LiChrospher 100 RP 18e, 250 × 4.6 mm, 5 μm; Spheri 5-ODS, 250 × 4.6 mm, 5 μm	Quaternary gradient of THF, water, methanol, acetonitrile	Multiple wavelength UV and laser light-scattering[b]	1 ml/min, 20 μl, ambient temperature	[7][c]
General	BHT, BHA	N/A[a]	Whatman Partisil PXS 10/25 ODS-2	0.05 *M* $LiClO_4$ in 85% methanol	UV-electrochemical fluorescence	1 ml/min, 20 μl, $T = 40°C$	[8][d]

(Continued)

Table 3 Examples of HPLC methods (UV detection) used to identify and/or quantify packaging system additives. *(Continued)*

Material	Additive(s)	Sample preparation	Column	Mobile phase	λ (nm)	Other	Refs.
PP, ABS	Numerous[e]	Dissolve in $MeCl_2$, precipitate polymer with methanol	Spherisorb S30DS2, 150 × 4.6 mm, 3 μm	A = Acetonitrile; B = water; Initial = 40% A, ramped to 100% A in 15 min, maintained at 100% for 17 min	210, 280	1 ml/min (2 ml/min after 22 min); 10 μl	[9]
PE	Topanol OC; Cyasorb UV 531; Irganox 1010, 1076, 1330	SFE contrasted to Soxhlet extraction with dichloromethane	Kaseisorb ODS-5, 550 × 0.53 mm	Methanol	254 nm	Column pressure = 100 atm	[54]
PP	Irganox 1010, Irgafos 168	SFE	Licrosorb RP-18, 200 × 4.6 mm, 5 μm	Gradient from methanol/water (95/5) to 100% methanol in 17 min	280 nm	1.5 ml/min, 20 μl	[11]
Polyolefin	Irganox PS802, 1010, 1076, 1425; calcium stearate; sodium benzoate	Microwave-assisted solvent extraction	Various; e.g., Microsper C_{18}, 250 × 4.6 mm, 5 μm	Water/acetonitrile/*iso*-propanol; Start = 12/88/0; 0.1 min = 5/65/30; 10 min = 0/65/30; 18 min = 0/65/30	273 nm, light scattering	2 ml/min, 10 μl, $T = 50°C$	[12]
PMMA	Irganox 1010, 1076; Irgafos 168	SFE	Nova-Pak C_{18}, 5 μm	Acetonitrile/water gradient; start at 80/20, change to 100/0 in 5 min	254 nm	50 μl	[13]
Dielectric resins	BAC-E, bis-A-bis-azide	Dissolution in THF	Zorbax RX C8, 100 × 4.5 mm, 5 μm[f]	A = 50/50 acetonitrile/water; B = 90/10 mixture. Gradient was start ramp form 0% A to 100% B in 5 min, hold at 100% B for 5 min	254 nm (380 nm for internal standard)	3 ml/min	[14]

ABS = acrylonitrile–butadiene–styerene; HDPE = high-densitypolyethylene; LDPE = low-density polyethylene; PC = polycarbonate; PE = polyethylene; PMMA = polymethylmethacrylate; PP = polypropylene; PS = polystyrene; PVC = polyvinyl chloride.

[a]This reference examined the elution characteristics of the cited additives as a function of mobile phase and, thus, did not characterize actual polymers.

[b]These authors report that the UV response for the analytes is typically 5 to 50 times greater than the light-scattering response.

[c]Numerous other examples of separations provided.

[d]For BHA, the sensitivity was EC > UV (230 nm) > Fl. For BHT, the sensitivity was UV (280 nm) > EC > Fl.

[e]This study examined the elution characteristics, sensitivity, and analytical recoveries of over 25 additives.

[f]Preanalytical column sample cleanup was achieved online by SEC. This preanalytical processing was accomplished with a 25 cm × 250 μm I.D. fused silica capillary column (PL-Gel 50 Å, 5 μm) and a THF mobile phase at 1.3 μl/min.

Table 4 Examples of HPLC methods [infrared (IR) detection] used to identify and/or quantify packaging system additives.

Material	Additive(s)	Sample preparation	Column	Mobile phase	λ (nm)	Other	Refs.
Polyurethane	Irganox 1010	Extraction with *n*-hexane	μ-Porasil C_{18}	*n*-hexane/ dichloromethane, 80/20	254[a]	1 ml/min	[15]
PVC, PP, PE	Ionol 220, Irganox 1076, Tinuvin 327, Tinuvin 328, Cyasorb UV 531	Extraction with acetonitrile or methanol, evaporative concentration	RP: Spherisorb ODS-2, 100 × 1.0 mm, 3 μm; SEC: PL-Gel, 250 × 4.6 mm, 5 μm, 500 Å	RP = methanol/ water (95./5); SEC = Dicloromethane	280[b]	0.1–0.2 ml/min	[16]
PP	Irganox 1010, 3114; Tinuvin 326, 327	N/A[c]	Zorbax ODS, 250 × 4.6 mm		N/A[d]	0.5 ml/min, 20 μl	[17]
PP, PE	Irganox 245, 259, 1010, 1076, 1098, 3114; Irgafos 168; Tinuvin 234, 327, 328, 350; Sanowhite, Ethanox 330; Lowinox 22M46; Kemamide U; Naugard; BHT; Ultranox 626; Cyasorb 2908; Cyasorb UV 531	N/A[c]	Sperisorb ODS-2, 250 × 4.6 mm, 5 μm	Several cited[e]	280 nm and evaporative light scattering[f]	1 ml/min, 50 μl, ambient temperature	[18][g]

PE = polyethylene; PP = polypropylene; PVC = polyvinyl chloride.

[a]Peak collected on potassium bromide powder and an IR spectrum obtained off-line.

[b]Online Fourier transform infrared spectroscopy (FTIR) with spray-jet interface, deposition on a moving zinc selenide substrate. UV for quantitation, IR for identification.

[c]This reference examined the detection characteristics of the cited additives and, thus, did not characterize actual polymers.

[d]Used surface-enhanced infrared spectroscopy with effluent deposition on an Ag metal film (BaF_2 substrate). Reported a detection limit of 10 ng.

[e]Several separations are cited in this manuscript. A gradient using methanol and water was used for the separation of nine additives. Initial composition, 94/6 methanol/water for 7 min, change immediately to 100% methanol, hold for 14 min.

[f]Portion of column effluent deposited on a rotating germanium disk via drying nebulization.

[g]Detection limits by IR were generally near 0.2 μg, with quantities needed for accurate identification in the 0.5–1.0 μg range.

Table 5 Examples of HPLC methods (MS detection) used to identify and/or quantify packaging system additives.

Material	Additive(s)	Sample preparation	Column	Mobile phase	Detection	Other	Refs.
General(PP)	BHT, Irganox 1010, Irganox 1076, Irganox 1330, Santowhite	N/A[a]	ODS, 250 × 2.1 mm, 5 μm	A = 75/25 acetonitrile/water; B = 50/50 THF/ acetonitrile; 0 min = 100% A, 10 min = 60% A, 20 min = 100% B, 30 min = 100% B, 32 min = 100% A	UV, 280 nm. Moving belt MS interface, chemical ionization (CI) and electron input ionization (EI) spectra obtained	0.2 ml/ min, 10 μl	[19]
PVC	Mono-alkyl esters and di-alkyl phthalates	N/A[a]	Symmetry C-8, 150 × 3.9 mm, 5 μm	A = 0.1 *M* ammonium acetate in 10/90 methanol/ water; B = 0.1 *M* ammonium acetate in methanol 0% to 100% B over 25 min, hold for 5 min	UV, 277 nm. Thermospray MS, + ions	1 ml/ min	[20]
PP	NC-4, Naugard-XL, Irganox 1076	Extract with acetonitrile at 60°C for 72 hr	Symmetry C8, 150 × 3.9 mm, 3 μm	A = acetonitrile; B = water; 0 = 30% A, 10 min = 100% A, 30 min = 30% A, 40 min = 30% A	Multiple λ UV. MS = EI and atmospheric pressure chemical ionization (APCI) [positive ion, single ion monitoring (SIM)]		[21]
PP	Irganox 245, BHA, BHT, Bispenol A, Topanol CA	N/A	Hypersil H5ODS, 100 × 4.6 mm, 5 μm	80/20 deuterated acetonitile/water	UV, IR, MS, nuclear magnetic resonance (NMR)[b]	1 ml/ min	[21]

PP = polypropylene; PVC = polyvinyl chloride.

[a]This reference examined the elution characteristics of the cited additives as a function of mobile phase and thus did not characterize actual polymers.

[b]The column effluent was split after the column (95/5) between the FTIR flowcell [attenuated total reflection (ATR) used] and the MS detector (single quad, positive ions). The effluent from the FTIR cell was directed through the UV and ultimately nmR detectors.

Table 6 Examples of SFC methods used to identify and/or quantify packaging system additives.

Material	Additive(s)	Sample preparation	Column	Mobile phase	Detection	Other	Refs.
General (PE)	Numerous[a]	N/A[b]; SFE	C_{18}, 250 × 4.6 mm	CO_2 with methanol modifier; 2% methanol for 1 min, linear to 10% after 10 min, hold for 5 min	APCI-MS (+ and − ionization), UV	2 ml/min, 10 μl	[22][c]
PE	BHT, Tinuvin 326	SFE with various traps	Fused silica capillary (10 m × 0.1 mm I.D.) with octyl phase, 0.5 μm film	CO_2, pressure program (100 atm for 10 min, increased at 5 atm/min for 20 min)	FID	Column $T = 90°C$	[23]
Polyolefin (PP, PE)	BHT; Irganox PS800, PS802, 1010, 1076, 1330, 2246; Tinuvin P, 320, 326; Irgafos 168; Atmos 150	Soxhlet extraction with chloroform	Fused silica capillary (10 m × 0.05 mm I.D.) with 5% phenyl-polymethylsiloxane, 0.4 μm film	Various pressure and temperature programs with CO_2 were reported	MS, EI	1 μl injection	[5,24][d,e]
PP	Numerous[f]	Soxhlet extraction with diethyl ether for 15 hr, precipitate polymer with ethanol	Fused silica capillary (15 m × 0.1 mm I.D.) with 5% phenyl-polymethylsiloxane, 0.5 μm film	CO_2 at 140°C; pressure = 150 atm for 12 min, ramp to 350 atm at 3 atm/min	FID, FTIR microscope	2 μl split injection, $T = 150°C$	[26]
PE	BHT, Irganox 1010, Irgafos 168	SFE (contrasted to Soxhlet extraction)	Fused silica capillary (15 m × 0.1 mm I.D.) with SB-Biphenyl-30, 0.5 μm film	CO_2 at 140°C; pressure = 100 atm, ramp to 200 atm at 3 atm/min, ramp at 10 atm/min to 400 atm	IR (flow through cell)	—	[27]
General	Tinuvin P, 326, 234, 770; Chimasorb 81, Irganox 1010, 1076, 1330; Irgafos 168, Irgafos P-EPQ, *N*,*N*-bis (2-hydroxyethyl) alkyl-amine	N/A[b]	Fused silica capillary (20 m × 0.1 mm I.D.) with DB-5, 0.4 μm film	CO_2; pressure = 10.6 MPa for 10 min, ramp to 15 MPa in 3.5 min, hold for 5 min; ramp at 0.5 MPa/min to 35 MPa, hold for 10 min	FID and MS (EI, 70 eV)	2 ml/min, $T = 140°C$	[10]

(Continued)

Table 6 Examples of SFC methods used to identify and/or quantify packaging system additives. *(Continued)*

Material	Additive(s)	Sample preparation	Column	Mobile phase	Detection	Other	Refs.
LDPE	BHT, BHEB, Isonox 129, Irganox 1010, 1076	Online SFE	Deltabond cyano, 100 × 1.0 mm I.D., 5 μm	100 atm for 3 min, 100–330 atm for 7 min, 330–450 atm for 1.5 min	FID	Column $T = 100°C$	[28][g]
Polyurethane	BHT, Irganox 1010, Irganox 1076, dinonyl phthalate[h]	Online SFE	30% biphenyl polysiloxane, 10 m × 50 μm I.D., 0.25 μm film	CO_2; hold at 100 atm for 5 min, ramp at 5 atm/min to 300 atm, ramp at 20 atm/min to 400 atm	MS (EI)	Column $T = 100°C$	[29]
Nylon, polystyrene	Caprolactam and oligomers, stearic acid, Irganox 1076	Online SFE	Deltabond cyano, 100 cm × 1 mm, 5 μm	CO_2; hold at 100 atm for 2 min, ramp at 15 atm/min	FTIR	Column $T = 100°C$	[30]
PE, PP	BHT; Erucamide; Irgafos 168, Irganox 1010, 1076; Tinuvin 326, 770; Isonox 19; DLTDP	Online SFE	Deltabond 300 Octyl, 250 cm × 1 mm	CO_2; hold at 1500 psi for 6 min, ramp at 200 psi/min to 6000 psi	FID	FID $T = 350°C$; Column $T = 150°C$	[30]

LDPE = low-density polyethylene; PE = polyethylene; PP = polypropylene.
[a]Additives examined included: BHT; Irganox 245, 1010, 1035, 1076, 1330, 1425, PS802; Irgafos 168; Tinuvin 327, 328, 384 440, 622, 770, 1130; Topanol CA; Cyasorb UV1164; Oleamide; Erucamide; Synprolam; Chimassorb 944.
[b]This reference examined the elution characteristics of the cited additives as a function of mobile phase and, thus, did not characterize actual polymers.
[c]This reference provides elution characteristics and relative intensities for specific positive and negative ions.
[d]The performance of the SFC method was compared to that of an isocratic reversed-phase (RP)-HPLC method (UV detection).
[e]GC/MS was also used for compound identification.
[f]Additives included: Topanol OC; Tinuvin P, 292, 320, 326, 328, 770, 440, 144; Chimassorb 81; Erucamide; Irganox PS800, PS802, 245, 1010, 1035; MD1025, 1076, 1330, 3114.
[g]The SFE extraction was also coupled with HPLC separation and detection of the analytes.
[h]This method produced other additive peaks whose parent compound could not be identified.

Table 7 Examples of SEC/GPC methods used to identify and/or quantify packaging system additives.

Material	Additive(s)	Sample preparation	Column	Mobile phase	Detection	Other	Refs.
PP	General[a]	Extraction with THF	Porogel A-1 (slurry-packed)	THF	Refractive index (RI) (collected fraction tested via IR for identification)	2 ml/min, column $T = 30°C$	[32]
PS, PVC	Tinuvin P, TNPP, TETO	Solvent extraction	500, 100 and 50 Å PL-Gel (poly (styrene-divinylbenzene) 30 × 0.77 cm, 10 μm	THF	UV	2 ml/min, column $T = 30°C$	[33]
Polyolefin (PP, PE)	BHT; Cyasorb UV 9; Cyasorb UV 1084; Tinuvin 326, 327; Irganox 1076	General[b]	SEC (PL-Gel, 50 Å, 300 × 7.5 mm) coupled with normal phase (Nucleosil 100-7 OH, 250 × 4.6 mm, 7 μm)	*n*-hexane/ dichloromethane (73/27)	UV at 254 and 280 nm	0.9 ml/min, column $T = 35°C$	[34]
Polyolefin copolymers	Numerous[c]	Dissolution in THF	SEC (Uktrastyragel 10^4, 50 Å, 300 × 0.25 mm, 10 μm) coupled with GC (DB-1, 15 m × 0.32 mm I.D., 0.25 μm film)	SEC; THF mobile phase. GC; 100°C for 6 min, ramp at 16°C/min to 350°C	UV at 254 nm for SEC, MS (EI) for GC	For SEC: 3.0 μl/min, 0.2 ml injected	[35]

PE = polyethylene; PP = polypropylene; PS = polystyrene; PVC = polyvinyl chloride.

[a]This reference generated additive profiles for various test materials but did not specify the individual additives found.

[b]This reference examined the chromatographic characteristics of the cited additives as a function of mobile phase and, thus, did not characterize actual polymers.

[c]This reference documented chromatographic characteristics for many individual additives including plasticizers (phthalates, Citroflex A-4, TNPP); amides; Irganox and Irgafos antioxidants; UV absorbers (Tinuvin, Cyansorb); fatty acids (palmitic, stearic); Naugard XL-1; etc.

Table 8 Examples of TLC methods used to identify and/or quantify packaging system additives.

Material	Additive(s)	Sample preparation	Plate	Mobile phase	Detection	Other	Refs.
Rubber	Numerous[a]	N/A[b]	Silica gel G, thickness of 250–300 μm	Numerous solvent systems examined vs. compound class	Various UV and visible developing reagents	Sample size: 3–5 μl	[36]
Polyolefin	Tinuvin 144, 770; Hostavin TMN 20	Extraction with chloroform, polymer precipitation, evaporative concentration	Alumina F254, 20 × 20 cm plate, 0.25 mm thickness	88/12, *n*-hexane/ *iso*-propanol	Chlorination with chlorine gas, sprayed with potassium iodide starch solution	Sample size: 10 μl	[37]
Elastomers	BHT, Cyanox 2246, Cyanox 425, Permanax WSP, Naugawhite, Wingstay T, Naugard SP, Vulkanox CS	Soxhlet extraction with acetone, evaporative concentration	Merck 11845 silica gel	Benzene	Sprayed with 2.34% sodium tetraborate, 0.33% sodium hydroxide, and 0.1% methanolic solution of *N*-chlorodichloro-2,6-*p*-benzoquinone monoimine	Sample size: 20 μl	[38]
PP, PVC	Irganox 1010, Tinuvin 770, Chimassorb 119 FL, DEHP	N/A[b]	Silica gel 60 F254, 5 × 10 cm plate, 250 μm thickness	Toluene-diethyl ether (10/1) on first plate, acetone-formic acid (4/6) on second plate	UV for plate 1, plate 2 visualized by iodine vapor. Spots removed from plate 2 and analyzed by FTIR	Sample size: 2 μl	[39]

PP = polypropylene; PVC = polyvinyl chloride.
[a]This reference documents the chromatographic properties of over 100 rubber-related amine and phenolic antioxidants, antiozonants, guanidines, accelerators, and amine hydrochlorides.
[b]This reference examined the chromatographic characteristics of the cited additives and, thus, did not characterize actual polymers.

Table 9 Examples of GC methods used to identify and/or quantify packaging system additives.

Material	Additives	Sample preparation	Column	Oven program	Detection	Other	Refs.
PET	Diethylene glycol	High temperature and pressure extraction with water	Numerous[a]	Isothermal at 180°C	FID and thermal conductivity detector (TCD)	Injector $T = 260$°C; detector $T = 270$°C; He carrier at 50 ml/min	[40]
PET	BHET, EG, DEG, TA, MHET[b]	N/A;[c] samples TMS derivatized with BSFTA (80°C for 10 min)	3% OV101 on 80–100 mesh Chromosorb W, 6 ft, 0.125 in. o.d., 0.05 in. I.D.	80°C for 3 min, ramp at 15°C/min to 265°C	FID	Injector $T = 270$°C; detector $T = 280$°C; He carrier at 50 ml/min, 2 μl injection	[41]
Elastomers	Various antioxidants and additives	N/A[c]	3% SP2100 on 80–100 mesh Supelcoport	150°C for 2 min, ramp at 10°C/min to 250°C	MS	Injector $T = 270$°C; He carrier at 35 ml/min	[42]
Polyolefins	BHT; Irganox 1010, 1076, 2246; Irgafos 168, Santowhite	Refluxed in acetone for 2–3 hr, evaporated to dryness and dissolved in chloroform	PS264, 15 m × 0.32 mm I.D., 0.15 μm film	90°C to 280°C at 5°C/min	FID	Detector $T = 300$°C; He carrier at inlet pressure of 0.5 kg/cm^2	[43]
PVC	Benzoflex 2860, ATBC, DEHA[d]	SFE	SPB-5 fused silica capillary, 30 m × 0.25 mm I.D., 0.25 μm film	110°C to 260°C at 10°C/min	FID	Detector, injector $T = 300$°C; He carrier at 50 cm/sec, 1 μl splitless	[44]
Polyolefins	Numerous[e]	Reflux with chloroform, evaporative concentration	HR-1701 (14% cyanopropylphenylmethyl-siloxane) fused silica capillary, 15 m × 0.53 mm I.D., 1.0 μm film	100°C for 2 min, 20°C/min to 210°C, 1.5°C/min to 222°C 8°C/min to 350°C, hold for 10 min	FID	Injector and detector $T = 350$°C; He carrier at 5 ml/min, 1 μl splitless injection	[45]
Petroleum resin	Numerous[e]	Dissolve in *n*-hexane, cleanup with silica column	DB-1701 (14% cyanopropylphenylmethyl-siloxane) fused silica capillary, 15 m × 0.53 mm I.D., 1.0 μm film	150°C for 2 min, 20°C/min to 210°C, 1.5°C/min to 222°C, 8°C/min to 350°C, hold for 10 min	FID	Injector and detector $T = 300$°C; He carrier at 5 ml/min, 2 μl split injection (1:100 ratio)	[45]
PE	Numerous[f]	Dissolution	UA-1 HT (dimethylpolysiloxane) fused silica capillary, 30 m × 0.25 mm I.D., 0.1 μm film	Start at 50°C, ramp at 20°C/min to 300°C, hold for 10 min	MS, EI, 70 eV, 40–700 *m/z*	Injector $T = 250$°C; He carrier at 1 psi, 1 μl split injection (1/2 ratio)	[46]

PE = polyethylene; PET = polyethylene terephthalate; PVC = polyvinyl chloride.

[a]Columns used included: Carbowax 20M, Chromosorb W-HMDS, Aeropak Number 30, 10 ft × 1/8 in. × 0.055 in. I.D.

[b]BHET = bis (2-hydroxyethyl) terephthalate; EG = ethylene glycol; DEG = diethylene glycol; TA = terephthalic acid; MHET = mono-(2-hydroxyethyl)terephthalate.

[c]This reference examined the chromatographic characteristics of the cited additives and, thus, did not characterize actual polymers.

[d]ATBC = *O*-acetly-tri-*n*-butyl citrate; DEHA = di(ethylhexyl) adipate.

[e]Additives chromatographed included antioxidants (BHT; Irganox 1076, 1330; Yoshinow BB, SR, 2246 R; Irgafos 168; Ultranox 626; Topanol CA; DLTDP; DMTDP; DSTDP), light stabilizers (Sanol LS744, LS770; Tinuvin 120, 326, 327; UV 531), and slip agents (palmitic acid amide, oleic amide, stearic acid amide, erucic amide).

[f]This reference included the separation of 53 polymer additives including antioxidants, UV stabilizers, lubricants, and plasticizers. Performance details are provided.

Table 10 Examples of pyrolysis/GC methods used to identify and/or quantify packaging system additives.

Material	Additives	Pyrolysis conditions	Column	Oven program	Detection	Other	Refs.
Polyolefin, PMMA	Hostanox O3; Hostavin N 20; Irganox 3052 FF; Irganox 3114; Tinuvin 320, 329, 350	100 μg sample at 550°C	RTX-5 fused silica capillary, 60 m × 0.32 mm I.D., 0.5 μm film	60° to 300°C at 7°C/min	MS (EI, 45–700 mass range)	Injector $T = 260$°C; detector $T = 270$°C; He carrier at 50 ml/min	[47]
PVC Cellulose Copolymer[c] PS/PC blend PU	DEHP Dioctyl adipate Dibutyl sebacate, tributyl acetylcitrate TPP Mixture of didecyl phthalate esters	0.5 mg sample at 700°C	DB-5 fused silica capillary, 30 m × 0.25 mm I.D., 1.0 μm film	40°C for 4 min, ramp at 10°C/min to 320°C, hold for 18 min	MS (EI, 15–650 mass range)	Injector $T = 300$°C; detector $T = 300$°C; 30/1 injection split	[48][a,b]
Epoxy resin[d] Poly-(diallyl-phthalate) ABS	Brominated bisphenol A Dechlorane Plus Octabromodiphenyl oxide	0.5 mg sample at 950°C	DB-5 fused silica capillary, 30 m × 0.25 mm I.D., 1.0 μm film	40°C for 4 min, ramp at 10°C/min to 320°C, hold for 18 min	MS (EI, 15–650 mass range)	Injector $T = 300$°C; detector $T = 300$°C; 30/1 injection split	[49][a,e]
PC-ABS blend	Brominated phenol, triphenyl phosphate						
General	Various waxes, stearic acid, butyl stearate, zinc stearate, butyl oleate, butyl palmitate, stearamide, AcraWax C	0.5 mg sample at 950°C	DB-5 fused silica capillary, 30 m × 0.25 mm I.D., 1.0 μm film	40°C for 4 min, ramp at 10°C/min to 320°C, hold for 18 min	MS (EI, 15–650 mass range)	Injector $T = 300$°C; detector $T = 300$°C; 30/1 injection split	[50][a,f]
General	Irganox 565, 1010; MD1024, 1035, 1076, 1425, 3114; Irgafos 168	0.5 mg sample at 950°C	DB-5 fused silica capillary, 30 m × 0.25 mm I.D., 1.0 μm film	40°C for 4 min, ramp at 10°C/min to 320°C, hold for 18 min	MS (EI, 15–650 mass range)	Injector $T = 300$°C; detector $T = 300$°C; 30/1 injection split	[51][a,g]

ABS = acrylonitrile–butadiene–styerene; PC = polycarbonate; PMMA = polymethylmethacrylate; PS = polystyrene; PU = polyurethane; PVC = polyvinyl chloride.
[a]A more rapid oven program was also used to produce pyrograms via FID detection.
[b]This manuscript deals with plasticizers as a class of additives.
[c]Vinyl chloride–vinylidene chloride copolymer.
[d]Cross-linked epoxy resin (thermoset of bisphenol A diglycidyl ether).
[e]This manuscript deals with flame retardants as a class of additives.
[f]This manuscript deals with lubricants as a class of additives.
[g]This manuscript deals with antioxidants as a class of additives.

Table 11 Solubility of polymers.

Polymer	Soluble in
Alkyd resin	Chlorinated hydrocarbons, lower alcohols, esters
Acrylonitrile-butadiene-styrene terepolymer	Methylene chloride
Polyacrylamide	Water
Polyamides	Phenols, *m*-cresol, concentrated mineral acids, formic acid
Polycarbonate	Ethanolamine, dioxane, chlorinated hydrocarbons, cyclohexanone
Polyethylene	Dichlorobenzene, pentachloroethylene, dichloroethylene, tetralin
Poly (ethylene terephthalate)	Cresol, concentrated sulfuric acid, chlorophenol, trichloroacetic acid
Polyformaldehyde	Dichlorobenzene, DMF, chlorophenol, benzyl alcohol
Polystyrene	Aromatic and chlorinated hydrocarbons, pyridine, ethyl acetate, dioxane, chloroform, acetone
Polytetrafluoroethylene	Fluorocarbon oil
Polyurethanes	Dioxane, THF, DMF, dimethylsulfoxide (DMSO), *m*-cresol, formic acid, 60% sulfuric acid
Poly (vinyl chloride)	Cyclohexanone, THF, dimethylformamide (DMF), ethylene dichloride
Poly (vinylidene chloride)	THF, ketones, DMF, chlorobenzene
Vinyl chloride–vinyl acetate copolymers	Methylene chloride, THF, cyclohexanone

scope of this manuscript to exhaustively discuss sample preparation strategies for polymer characterization, this general information is provided to facilitate an important step of the overall analytical process. In terms of specific sample preparation methods, Nerin et al.[53] have recently provided a review of sample treatment techniques applicable to polymer extract analysis including headspace methods, supercritical fluid extraction, and solid-phase microextraction. In terms of general knowledge, Table 11 provides solubility information relevant to polymer dissolution.

REFERENCES

1. Duval, M.; Giguere, Y. Simultaneous determination of the antioxidant, the crosslinking-agent and decomposition products in polyethylene by reversed-phase HPLC. J. Liq. Chromatogr. **1982**, *5*, 1847–1854.
2. Sreenivasan, K. High-performance liquid chromatographic method for the simultaneous separation and determination of three additives in poly(vinyl chloride). J. Chromatogr. **1986**, *357*, 433–435.
3. Francis, V.C.; Sharma, Y.N.; Bhardwaj, I.S. Quantitative determination of antioxidants and ultraviolet stabilizers in polymer by high performance liquid chromatography. Angew. Makromol. Chem. **1983**, *113*, 219–225.
4. Nielson, R.C. Extraction and quantitation of polyolefin additives. J. Liq. Chromatogr. **1991**, *14*, 503–519.
5. Jinno, K.; Yokoyama, Y. Retention prediction for polymer additives in reversed-phase liquid chromatography. J. Chromatogr. **1991**, *550*, 325–334.
6. Lesellier, E.; Saint Martin, P.; Tchapla, A. Separation of six polymer additives using mobile-phase optimization software. LC GC Int. **1992**, *5*, 38–43.
7. Lesellier, E.; Tchapla, A. Sequential optimization of the separation of a complex mixture of plastic additives by HPLC with a quaternary gradient and a dual detection system. Chromatographia **1993**, *36*, 135–143.
8. Masoud, A.N.; Cha, Y.N. Simultaneous use of fluorescence, ultraviolet, and electrochemical detectors in high performance liquid chromatography-separation and identification of phenolic antioxidants and related compounds. J. HRC & GC **1982**, *5*, 299–305.
9. Skelly, N.E.; Graham, J.D.; Iskandarani, Z.; Priddy, D. Reversed-phase liquid chromatographic separation of polymer additives combined with photodiode-array detection and spectral sort software. Polym. Mater. Sci. Eng. **1988**, *59*, 23–27.
10. Bucherl, T.; Gruner, A.; Palibroda, N. Rapid analysis of polymer homologues and additives with SFE/SFC-MS coupling. Packag. Technol. Sci. **1994**, *7*, 139–154.
11. Thilen, M.; Shishoo, R. Optimization of experimental parameters for the quantification of polymer additives using SFE/HPLC. J. Appl. Polym. Sci. **2000**, *76*, 938–946.
12. Marcato, M.; Vianello, M. Microwave-assisted extraction by fast sample preparation for the systematic analysis of additives in polyolefins by high-performance liquid chromatography. J. Chromatogr. A, **2000**, *869*, 285–300.
13. Nasim, N.; Taylor, L.T. Polymer-additive extraction via pressurized fluids and organic solvents of variously cross-linked poly(methylmethacrylates). J. Chromatogr. Sci. **2002**, *40*, 181–186.
14. Patrick, D.W.; Strand, D.A.; Cortes, H.J. Automation and optimization of multidimensional microcolumn size exclusion chromatography-liquid chromatography

for the analysis of photocrosslinkers in Cyclotene 400 series advanced electronic resins. J. Sep. Sci. **2002**, *25*, 519–526.
15. Sreenivasan, K. A combined chromatographic and IR spectroscopic method to identify antioxidant in biomedical polyurethane. Chromatographia **1991**, *32*, 285–286.
16. Somsen, G.W.; Rozendom, E.J.E.; Gooijer, C.; Velthorst, N.H.; Brinkman, U.A.Th. Polymer analysis by column liquid chromatography coupled semi-on-line with Fourier transform infrared spectrometry. Analyst **1996**, *121*, 1069–1074.
17. Sudo, E.; Esaki, Y.; Sugiura, M. Analysis of additives in a polymer by LC/IR using surface-enhanced infrared absorption spectroscopy. Bunseki Kagaku **2001**, *50*, 703–707.
18. Jordan, S.L.; Taylor, L.T. HPLC separation with solvent elimination FTIR detection of polymer additives. J. Chromatogr. Sci. **1997**, *35*, 7–13.
19. Vargo, J.D.; Olson, K.L. Identification of antioxidant and ultraviolet light stabilizing additives in plastics by liquid chromatography/mass spectrometry. Anal. Chem. **1985**, *57*, 672–675.
20. Baker, J.K. Characterization of phthalate plasticizers by HPLC/thermospray mass spectrometry. J. Pharm. Biomed. Anal. **1996**, *15*, 145–148.
21. Yu, K.; Block, E.; Balogh, M. LC-MS analysis of polymer additives by electron and atmospheric-pressure ionization: Identification and quantification. LC-GC **2000**, *18*, 162–178.
22. Carrott, M.J.; Jones, D.C.; Davidson, G. Identification and analysis of polymer additives using packed-column supercritical fluid chromatography with APCI mass spectrometric detection. Analyst **1998**, *123*, 1827–1833.
23. Daimon, H.; Hirata, Y. Directly coupled supercritical-fluid extraction/capillary supercritical-fluid chromatography of polymer additives. Chromatographia **1991**, *32*, 549–554.
24. Arpino, P.J.; Dilettato, D.; Nguyen, K.; Bruchet, A. Investigation of antioxidants and UV stabilizers from plastics: Part I. Comparison of HPLC and SFC; Preliminary SFC/MS study. J. High Resolut. Chromatogr. **1990**, *13*, 5–12.
25. Arpino, P.J.; Dilettato, D.; Nguyen, K.; Bruchet, A. Investigation of antioxidants and UV stabilizers from plastics: Part II. Application to polyolefin soxhlet extracts. J. High Resolut. Chromatogr. **1991**, *14*, 335–342.
26. Raynor, M.W.; Bartle, K.D.; Davies, I.L.; Williams, A.; Clifford, A.A.; Chalmers, J.M.; Cook, B.W. Polymer additive characterization by capillary supercritical fluid chromatogaphy/Fourier transform infrared microspectrometry. Anal. Chem. **1988**, *60*, 427–433.
27. Wieboldt, R.C.; Kempfert, K.D.; Dalrymple, D.L. Analysis of antioxidants in polyethylene using supercritical fluid extraction/supercritical fluid chromatography and infrared detection. Appl. Spectrosc. **1990**, *44*, 1028–1034.
28. Zhou, L.Y.; Asharf-Khorassani, M.; Taylor, L.T. Comparison of methods for quantitative analysis of additives in low density polyethylene using supercritical fluid and enhanced solvent extraction. J. Chromatogr. A, **1999**, *858*, 209–218.
29. MacKay, G.A.; Smith, R.M. Supercritical fluid extraction-supercritical fluid chromatography-mass spectrometry for the analysis of additives in polyurethanes. J. Chromatogr. Sci. **1994**, *32*, 455–460.
30. Jordan, S.L.; Taylor, L.T.; Seemuth, P.D.; Miller, R.J. Analysis of additives and monomers in nylon and polystyrene. Text. Chem. Color. **1997**, *29*, 25–32.
31. Ryan, T.W.; Yocklovich, S.G.; Watkins, J.C.; Levy, E.J. Quantitative analysis of additives in polymers using coupled supercritical fluid extraction-supercritical fluid chromatography. J. Chromatogr. **1990**, *505*, 273–282.
32. Howard, J.M. Gel permeation chromatography and polymer additive systems. J. Chromatogr. **1971**, *55*, 15–24.
33. Shepherd, M.J.; Gilbert, J. Analysis of additives in plastics by high performance size exclusion chromatography. J. Chromatogr. **1981**, *218*, 703–713.
34. Nerfin, C.; Salafranca, J.; Cacho, J.; Rubio, C. Separation of polymer and on-line determination of several antioxidants and UV stabilizers by coupling size-exclusion and normal-phase high-performance liquid chromatography columns. J. Chromatogr. A, **1995**, *690*, 230–236.
35. Cortes, H.J.; Bell, B.M.; Pfeiffer, C.D.; Graham, J.D. Multidimensional chromatography using on-line coupled microcolumn size exclusion chromatography-capillary gas chromatography-mass spectrometry for determination of polymer additives. J. Microcolumn Sep. **1989**, *1*, 278–288.
36. Kreiner, J.G.; Warner, W.C. The identification of rubber compounding ingredients using thin-layer chromatography. J. Chromatogr. **1969**, *44*, 315–330.
37. Sevini, F.; Marcato, B. Chromatographic determination of some hindered amine light stabilizers in polyolefins. J. Chromatogr. **1983**, *260*, 507–512.
38. Airaudo, C.B.; Gayte-Sorbier, A.; Creusevau, R.; Dumont, R. Identification of phenolic antioxidants in elastomers for pharmaceutical and medical use. Pharm. Res. **1987**, *4*, 237–239.
39. He, W.; Shanks, R.; Amarasinghe, G. Analysis of additives in polymers by thin-layer chromatography coupled with Fourier transform-infrared microscopy. Vibr. Spectrosc. **2002**, *30*, 147–156.
40. Ponder, L.H. Gas chromatographic determination of diethylene glycol in poly(ethylene terephthalate). Anal. Chem. **1968**, *40*, 229–231.
41. Atkinson, E.R., Jr.; Calouche, S.L. Analysis of polyethylene terephthalate prepolymer by trimethylsilyation and gas chromatography. Anal. Chem. **1971**, *43*, 460–462.
42. Kiang, P.H. The application of gas chromatography/mass spectrometry to the analysis of pharmaceutical packaging materials. J. Parenter. Sci. Technol. **1981**, *35*, 152–161.
43. Pasquale, G.D.; Galli, M. Determination of additives in polyolefins by capillary gas chromatography. J. High Resolut. Chromatogr. Commun. **1984**, *7*, 484–486.
44. Guerra, R.M.; Marin, M.L.; Sanchez, A.; Jimenez, A. Analysis of citrates and benzoates used in poly(vinyl chloride) by supercritical fluid extraction and gas chromatography. J. Chromatogr. A, **2002**, *950*, 31–39.
45. Nagata, M.; Kishioka, Y. Determination of additives in polyolefins and petroleum resin by capillary GC. J. High Resolut. Chromtogr. **1991**, *14*, 639–642.
46. Kawamura, Y.; Watanabe, Z.; Sayama, K.; Takeda, Y.; Yamada, T. Simultaneous determination of polymer

additives in polyethylene by GC/MS. Shokuhin Eiseigaku Zasshi **1997**, *38*, 307–318.
47. Meyer-Dulheuer, T.; Pasch, H.; Geissler, M. Direct analysis of additives in polymeric materials by pyrolysis-gas chromatography-mass spectrometry. KSG Kautsch. Gummi Kunstst. **2000**, *53*, 574–581.
48. Wang, F.C. Polymer additive analysis by pyrolysis-gas chromatography. I. Plasticizers. J. Chromatogr. A, **2000**, *883*, 199–210.
49. Wang, F.C. Polymer additive analysis by pyrolysis-gas chromatography: II. Flame retardants. J. Chromatogr. A, **2000**, *886*, 225–235.
50. Wang, F.C.; Buzanowski, W.C. Polymer additive analysis by pyrolysis-gas chromatography: III. Lubricants. J. Chromatogr. A, **2000**, *891*, 313–324.
51. Wang, F.C. Polymer additive analysis by pyrolysis-gas chromatography: IV. Antioxidants. J. Chromatogr. A, **2000**, *891*, 325–336.
52. Gasslander, U.; Jaegfeldt, H. Stability and extraction features in the determination of Irganox-1330 in a polyalkane copolymer. Anal. Chim. Acta **1984**, *166*, 243–251.
53. Nerin, C.; Rubio, C.; Salafranca, J.; Batlle, R. The simplest sample treatment techniques to assess the quality and safety of food packaging materials. Rev. Anal. Chem. **2000**, *19*, 435–465.
54. Hirata, Y.; Okamoto, Y. Supercritical fluid extraction combined with microcolumn liquid chromatography for the analysis of polymer additives. J. Microcolumn Sep. **1989**, *1*, 46–50.
55. Louden, D.; Handley, A.; Lenz, E.; Sinclair, I.; Taylor, S.; Wilson, I.D. Reversed-phase HPLC of polymer additives with multiple on-line spectroscopic analysis (UV, IR, 1H nmR, and MS). Anal. Bioanal. Chem. **2002**, *373*, 508–515.

Organic Solvents: Classification for CE

Ernst Kenndler
Institute for Analytical Chemistry, University of Vienna, Vienna, Austria

INTRODUCTION

In capillary electrophoresis (CE), several criteria can be applied to classify solvents [e.g., for practical purposes based on the solution ability for analytes, on ultraviolet (UV) absorbance (for suitability to the UV detector), toxicity, etc.]. Another parameter could be the viscosity of the solvent, a property that influences the mobilities of analytes and that of the electro-osmotic flow (EOF) and restricts handling of the background electrolyte (BGE). For more fundamental reasons, the dielectric constant (the relative permittivity) is a well-recognized parameter for classification. It was initially considered to interpret the change of ionization constants of acids and bases according to Born's approach. This approach has lost importance in this respect because it is based on too simple assumptions limited to electrostatic interactions. Indeed, a more appropriate concept reflects solvation effects, the ability for H-bonding, or the acido-base property of the solvent.

CLASSIFICATION OF SOLVENTS

A first classification, according to the dielectric constant ϵ (with a somewhat arbitrary value about 20 or 30 to distinguish the two main classes), is still useful, because the dielectric constant reflects the extent of ion association and ion-pairing. In solvents with a high dielectric constant, called polar solvents, ion-pairing is nearly negligible in dilute solutions. Acid strength can be assigned by a numerical value, independent of the base with which it undergoes reaction. Non-polar solvents, on the other hand (i.e., those with low dielectric constant), support ion-pairing, and the acidity is dependent on the choice of the reference base. Further grouping of the solvents is based on their ability for H-bond formation. Note that this scheme disregards the solvents' own acidity or basicity (this criterion is taken for the latter scheme).This is shown in Table 1. A typical H-bonded solvent, termed protic solvents, is water or methanol. Aprotic solvents (although containing H atoms or being able to accept H bonds) lack the ability to donate hydrogen bonds. The lower alcohols (except methanol) are grouped in the class with low ε. They are protic as well (they are able to donate hydrogen bonds), in contrast to the fourth group, where, for example, dioxane and tetrahydrofurane are found.

The solvents can be grouped according to another classification scheme introduced by Brønsted. It has significance for the evaluation of acido-basic equilibria in the particular solvents, especially for the interpretation of the changes of the pK values of weakly acidic (or basic) analytes and their degree of protolysis. Obviously, it is also of main importance for the evaluation of the pH scales in the different solvents or solvent mixtures. It differentiates, mainly, three groups: amphiprotic, dipolar aprotic, and inert solvents. As the first scheme, it also relates to the "polarity" of the solvent (expressible by the dielectric constant, too). *Amphiprotic* solvents have acidic and basic properties as well. These solvents, HS, are able to form lyonium ions, H_2S^+ with the proton, and stable lyate ions, S^-. Examples for *amphiprotic neutral* solvents (with high ε) are water and methanol. In the classification given in Table 1, they belong to the H-bonded solvents.

Amphiprotic protogenic solvents have higher acidic properties, but lower basic ones (always in comparison to

Table 1 Classification of solvents for potential use in CE, according to their dielectric constant, ε, and their ability for H-bond formation.

High ε		Low ε	
H-bonded	**Non-H-bonded**	**H-bonded**	**Non-H-bonded**
Water	Acetonitrile	Ethanol	Acetone
Methanol	*N*,*N*-Dimethylformamide	*n*-Propanol	Dioxane
Ethylene glycol	*N*,*N*-Dimethylacetamide	*i*-Propanol	Tetrahydrofuran
Formamide	Dimethyl sulfoxide	*n*-Butanol	
Acetamide		*tert*-Butanol	
N-Methylformamide			
N-Methylacetamide			

water). Examples are formic and acetic acid. *Amphiprotic protophilic* solvents have lower acidity and higher basicity than water, with formamide or ethanolamine as examples. *Aprotic dipolar* solvents have low acidity and (occasionally) basicity as well, with *N*,*N*-dimethylformamide and dimethylsulfoxide as examples for protophilic dipolar solvents and acetonitrile for a protophobic dipolar solvent.

Solvents with low ε and without the ability to form H bonds are also classified as dipolar aprotic solvents in some cases. Examples are dioxane and tetrahydrofuran, which have e values smaller than 7. They have reduced applicability in CE; however, their aqueous mixtures might be of some interest.

Inert solvents (according to the second classification scheme) have insignificant applicability for CE, as dissociation into free ions is reduced (and solubility of electrolytes is very low). Charged analytes form stable ion pairs there. Examples are the halogenated or aliphatic and aromatic hydrocarbons (e.g., octane, benzene).

BIBLIOGRAPHY

1. Bates, R.G. Medium effect and pH in nonaqueous and mixed solvents. In *Determination of pH, Theory and Practice*; John Wiley & Sons: New York, 1973; 211–253.
2. Covington, A.K.; Dickinson, T. Introduction and solvent properties. In *Physical Chemistry of Organic Solvents Systems*; Covington, K., Dickinson, T., Eds.; Plenum Press: London, 1973; 1–23.
3. Kenndler, E. Organic solvents in capillary electrophoresis. In *Capillary Electrophoresis Technology*; Guzman, N.A., Ed.; Basel, Hong Kong: Marcel Dekker, Inc.: New York, 1993; 161–186.
4. King, E.J. Acid-base behaviour. In *Physical Chemistry of Organic Solvent Systems*; Covington, A.K., Dickinson, T., Eds.; Plenum Press: London, 1973; 331–403.
5. Kolthoff, I.M.; Chantooni, M.K.K. General introduction to acid-base equilibria in nonaqueous organic solvents. In *Treatise on Analytical Chemistry, Part I, Theory and Practice*; Kolthoff, I.M., Elving, P.J., Eds.; John Wiley & Sons: New York, 1979; 239–301.

Organic Solvents: Effect on Ion Mobility

Ernst Kenndler
Institute for Analytical Chemistry, University of Vienna, Vienna, Austria

INTRODUCTION

The ionic mobility, μ_i, of a species, i, is the velocity, v of a particle that moves under the influence of an electric field, E, of unit strength:

$$\mu_i = \frac{\nu_i}{E} \tag{1}$$

The dimension of the mobility is square meter per volt per second. The values of the mobilities range from more than 300 units for the proton in water to about 5 units for large organic ions in solvents with high viscosities. The mobility depends on the size and shape of the solvated ion, on its charge, and on the viscosity and temperature of the solution. Thus, it is clear that the mobility is a function of the solvent.

Three kinds of mobility can be distinguished: the absolute mobility, μ^0 in an infinitely diluted solution, the actual mobility of the fully charged ion at the ionic strength, I, of the solution, and the effective mobility, μ^{eff}, which depends on the degree of ionization, α.

IONIC MOBILITIES OF WEAK ELECTROLYTES

For higher ionic strengths, no quantitative theoretical description of the dependence of the mobility on the ionic strength exists. Even for lower ionic strengths, theory is directed, rather, to spherical ions of 1:1 electrolytes with low charge (Debye–Hückel–Onsager theory, see below) than to multiple charged ions with irregular geometry. An expression derived empirically relates the logarithm of the correction factor for the mobility on the square root of the ionic strength and the charge number of the analyte.

The degree of dissociation, on the other hand, depends, in a well-defined manner, on the pK of the analyte and the pH of the solution, according to the Henderson–Hasselbalch equation. α, is a function of pK_a and pH: for example, for monobasic neutral acids

$$\alpha = \frac{1}{1 + 10^{\text{p}K_a - \text{pH}}} \tag{2}$$

For this type of acid, the total mobility can be expressed as

$$\mu_i^{tot} = \mu_i^{eff} + \mu_{EOF} = \frac{\mu_i^0 f}{1 + 10^{\text{p}K_{a,i} - \text{pH}}} + \mu_{EOF} \tag{3}$$

Here, μ_i^0 is the absolute mobility, that of the ion at infinite dilution, f is the correction factor that takes into account the deviation from ideal behavior. It can be seen that an additional parameter occurs in this equation: the mobility of the electro-osmotic flow (EOF), μ_{EOF}, which occurs in many cases in the separation systems and leads to an additional velocity vector of the solutes.

INFLUENCE OF ORGANIC SOLVENTS

Eq. 3 is the key expression that enables understanding of the influence of the solvent on the mobility. From this expression, it follows that solvents may affect the following:

- the absolute mobility
- the correction factor, f
- the ionization constants, K_a, of the analytes and the buffering electrolytes
- the mobility of the EOF

Absolute Mobility

A first approach to take into account the solvent's effect on the absolute mobility of an ion was made by Walden. It is based on the Stokes' law of frictional resistance. Walden's rule states that the product of absolute mobility and solvent viscosity is constant. It is clear that the serious limitation of this model is that it does not consider specific solvation effects, because it is based on the *sphere-in-continuum* model. However, it delivers an appropriate explanation for the fact that, within a given solvent, the mobility depends on temperature to the same extent as the viscosity (in water, for example, the mobility increases by about 2.5% per degree Kelvin).The mobilities do not deviate too much from Walden's rule in some binary mixtures of water with organic solvents. This model is, on the other hand, not appropriate for forecasting or explaining the effect of the solvent on the mobility in a more general manner (see Table 1).

Table 1 Absolute mobilities and walden products of some anions in pure solvents.

	Water		Methanol		Acetonitrile	
Ion	μ_{abs}	$\eta\lambda^0$	μ_{abs}	$\eta\lambda^0$	μ_{abs}	$\eta\lambda^0$
Li^+	40.0	0.34	41.0	0.22	071.8	0.24
K^+	76.2	0.65	54.5	0.29	086.6	0.29
$(CH_3)_4N^+$	46.5	0.40	71.2	0.33	098.0	0.33
$(C_4H_9)_4N^+$	20.2	0.17	40.4	0.21	063.6	0.21
Cl^-	79.2	0.68	54.3	0.28	092.2	0.31
J^-	79.6	0.68	65.1	0.34	105.7	0.35
CH_3COO^-	42.4	0.36	40.8	0.21	110.9	0.37

Note: μ_{abs} is measured in 10^{-5} cm^2/Vs; $\eta\lambda^0$ is measured in $Pcm^2/\Omega mol$ where λ^0 is the single ion conductance at infinite dilution.

Taking specific solvation effects into account makes it clear that the hydrodynamic radius, r_h, of an ion depends on the solvent, due to the different solvation shell established:

$$r_{h,i} = \frac{z_i e_0}{6_{\pi\eta\mu_i}} \tag{4}$$

where e_0 is the electron charge and z_i is the charge number. This expression is valid for a spherical ion. It is obvious that by a simple geometrical argument, this radius changes for an ion with crystal radius, r_{cryst} according to solvation by n_h molecules of solvent, S, with radius, r_s, in the solvation shell:

$$r_h^3 = r_{cryst}^3 + n_h r_S^3 \tag{5}$$

Because n_h and r_S may change, the hydrodynamic radius and, therefore, the absolute mobility change as well.

Correction Factor

The correction factor, f, relates the actual mobility of a fully charged particle at the ionic strength under the experimental conditions to the absolute mobility. It takes ionic interactions into account and is derived for not-too-concentrated solutions by the theory of Debye–Hückel–Onsager using the model of an ionic cloud around a given central ion. It depends, in a complex way on the mean ionic activity coefficient. The resulting equation contains the solvent viscosity and dielectric constant in the denominator. In all cases, the factor is <1. The actual mobility is always smaller than the absolute mobility.

Ionization Constant

Organic solvents influence the ionization constants of weak acids or bases in several ways (note that they in-fluence the analytes and the buffer as well). Concerning ionization equilibria, an important solvent property is the basicity (in comparison to water), which reflects the interaction with the proton. From the most common solvents, the lower alcohols and acetonitrile are less basic than water. Dimethyl sulfoxide is clearly more basic. However, stabilization of all particles involved in the acido-basic equilibrium is decisive for the pK_a shift as well. For neutral acids of type HA, the particles are the free, molecular acid, and the anion, A^-. In the equilibrium of bases, B, stabilization of B and its conjugated acid, HB^+, takes place. As most solvents have a lower stabilization ability toward anions (compared to water), they shift the pK_a values of acids of type HA to higher values in general. No such clear direction of the change is found for the pK_a values of bases; however, they undergo less pronounced shifts.

Mobility of the EOF

According to the Smoluchowsky equation, the mobility of the EOF is

$$\mu_{EOF} = \frac{\varepsilon\varepsilon_o\zeta}{\eta} \tag{6}$$

where ε and ε_0 are the permittivity of the medium and the vacuum, respectively, η is the solvent viscosity, and ζ is the zeta potential of the electric double layer. Roughly, the mobility of the EOF should depend on the ratio of relative permittivity to viscosity of the solvent and on the conditions of the electric double layer of the surface of the capillary in capillary electrophoresis (CE). As in most cases, fused-silica capillaries are used in CE, and its ζ potential is a function of the buffer pH, because the silanol groups at the surface are weak acids, with pK values around 5–6. It follows that the solvent affects the pK of the silanol as well, in a manner similar to that for the ionization constants of the analytes and the buffers. Nearly all solvents shift the pK values of the silanol groups toward a higher, pure acetonitrile and to even to very high values.

BIBLIOGRAPHY

1. Conway, B.E. *Ion Hydration in Chemistry and Biophysics*; Elsevier: Amsterdam, 1981
2. Fernandez-Prini, R.; Spiro, M. Conductance and transference numbers. In *Physical Chemistry of Organic Solvent Systems*; Covington, A.K., Dickinson, T., Eds.; Plenum: London, 1973; 525–679.
3. Kenndler, E. Organic solvents in capillary electrophoresis. In *Capillary Electrophoresis Technology*; Guzman, N.A., Ed.; Marcel Dekker, Inc.: New York, 1993; 161–186.
4. Schwer, C.; Kenndler, E. Electrophoresis in fused silica capillaries: The influence of organic solvent on the electroosmotic velocity and the zeta potential. Anal. Chem. **1991**, *63*, 1801–1807.

Organic Solvents: Influence on pKa

Ernst Kenndler
Institute for Analytical Chemistry, University of Vienna, Vienna, Austria

INTRODUCTION

The influence of solvents on the ionization equilibrium is related to their electrostatic and their solvation properties. The value of the ionization constant of an analyte is closely determined, in practice, by the pH scale in the particular solvent. It is clear that it is most desirable to have a universal scale which is able to describe acidity (and basicity) in a way that is generally valid for all solvents. It is, in principle, not the definition of an acidity scale in theory which complicates the problem; it is the difficulty of approximating the measured values in practice to the specifications of the definition. The pH scale, as is common in water, is applicable only to some organic solvents (i.e., mainly those for which the solvated proton activity is compatible with the Brønsted theory of acidity). The applicability of an analog to the pH scale in water decreases with decreasing relative permittivity of the solvents and with their increasing aprotic character.

A scale that would enable us to compare the acidity in all solvents could be based on the transfer activity coefficient on the proton (see *CE in Nonaqueous Media*, p. 342). The effect of the solvent of any species can be expressed in the same way as for the proton by this concept and applied to all particles involved in the thermodynamic equilibrium.

MEDIUM EFFECT AND IONIZATION CONSTANTS OF WEAK ACIDS AND BASES

The ionization of a weak neutral acid, HA, is described according to

$$HA = H^+ + A^-$$

For the weak base, B, for formal reasons, it is favourably expressed for its conjugated cation acid:

$$HB^+, \text{by } HB^+ = H^+ + B$$

The corresponding changes of the ionization constants of these weak acids can be expressed by the particular transfer activity coefficients, ${}_m\gamma_i$, on the single species, i, according to

$$\Delta \mathrm{p}K_{a,\mathrm{HA}} = {}_{\mathrm{S}}\mathrm{p}K_{a,\mathrm{HA}} - {}_{\mathrm{W}}\mathrm{p}K_{a,\mathrm{HA}} = \log\left(\frac{{}_m\gamma_{\mathrm{H}^+}\,{}_m\gamma_{\mathrm{A}^-}}{{}_m\gamma_{\mathrm{HA}}}\right) \quad (1)$$

$$\Delta \mathrm{p}K_{a,\mathrm{HB}^+} = {}_{\mathrm{S}}\mathrm{p}K_{a,\mathrm{HB}^+} - {}_{\mathrm{W}}\mathrm{p}K_{a,\mathrm{HB}^+} = \log\left(\frac{{}_m\gamma_{\mathrm{H}^+}\,{}_m\gamma_{\mathrm{B}}}{{}_m\gamma_{\mathrm{HB}^-}}\right) \quad (2)$$

S and W indicate organic solvent and water, respectively. The transfer activity coefficients, ${}_m\gamma_i$, is the ratio of the activity coefficients in the particular solvents: ${}_m\gamma_i = {}_W\gamma_i / {}_S\gamma_i$.

Eqs. 1 and 2 enable the interpretation of the changes in pK_a values in the different organic solvents, compared to water. One must take into account not only the stabilization of the proton (this is given by the mutual basicity of the solvents) but also the different ability to stabilize the other individual particles. Besides the neutral particles HA and B, oppositely charged ions H^+ and A^- take part in the equilibrium in case of the neutral acids, and equally charged HB^+ and B^+ ions in case of the cation acid. This occurrence leads to a different change of the pK_a values for these two different types of weak electrolytes, depending on the ability of the solvent to stabilize anions or cations.

Nearly all organic solvents stabilize anions worse than water. For this reason, the pK_a values of neutral acids are larger in organic solvents (it is obvious that strongly basic solvents like amines may level out this effect). In lower alcohols, for example, the pK_a values increase by several units. In acetonitrile, which has generally even less cation stabilization ability in addition, the pK_a values may increase by 16 units. The effect of many solvents on weak bases (expressed by the pK_a of the corresponding cation acid) is much lower. pK_a values change only by few units. An exception is acetonitrile, due to the reason mentioned earlier.

It should be noted that traces of water have a great influence on the shift of pK_a values in all solvents, because there is a steep change of the pK_a with increasing water content of the organic solvent. It should be also pointed out that the pK_a of the silanol groups at the surface of the commonly used fused-silica material is affected by the choice of the solvent, too. It is also shifted to higher values (in water the pK_a is around 5–6).

Table 1 Ionization constants of neutral and cation acids of type HA and HB+, respectively, in water, amphiprotic, and dipolar aprotic solvents.

	pK_a						
Acid	**W**	**MeOH**	**EtOH**	***t*-BuOH**	**ACN**	**DMSO**	**DMF**
Acetic	4.73	9.7	10.3	14.2	22.3		13.3
Chloro acetic	2.81	7.8	8.3	12.2	18.8		10.1
Benzoic	4.21	9.4	10.1	15.1	20.7	11.0	12.3
3,4-Dimethyl benzoic	4.4	9.7		15.4	21.2	11.4	13.0
3-Bromo benzoic	3.81	8.8	9.4	13.5	20.3	9.7	11.3
4-Nitro benzoic	3.45	8.3	8.9	12.0	18.7	9.0	10.6
2,4,6-Trinitro phenol	0.3	3.7	4.1	4.8	11.0	—	—
Ammonium	9.2	—	—	—	16.5	10.5	—
Ethylammonium	10.6	—	—	—	18.4	11.0	—
Triethylammonium	10.7	10.9	—	—	18.5	9.0	—
Anilinium	4.6	—	5.7	—	10.6	3.6	—
Pyridinium	5.2	5.2	—	—	12.3	3.4	—

BIBLIOGRAPHY

1. Bates, R.G. Medium effect and pH in non-aqueous and mixed solvents. In *Determination of pH, Theory and Practice*; John Wiley & Sons: New York, 1973; 211–253.
2. Kenndler, E. Organic solvents in capillary electrophoresis. In *Capillary Electrophoresis Technology*; Guzman, N.A., Ed.; Marcel Dekker, Inc.: New York, 1993; 161–186.
3. Kolthoff, I.M.; Chantooni, M.K. General introduction to acid-base equilibria in nonaqueous organic solvents. In *Treatise on Analytical Chemistry*; Kolthoff, I.M., Elving, P.J., Eds.; John Wiley & Sons: New York, 1979; 239–301.
4. Sarmini, K.; Kenndler, E. Ionization constants of weak acids and bases in organic solvents. J. Biophys. Biochem. Methods **1999**, *38*, 123–137.

Organic Substances: Lipophilicity Determination by RP/TLC

Gabriela Cimpan
Sirius Analytical Instruments Ltd., East Sussex, U.K.

INTRODUCTION

Lipophilicity is an important physicochemical parameter for organic substances, related to their biological activity. According to 1993 International Union of Pure and Applied Chemistry (IUPAC) recommendations, the partition coefficient $P_{o/w}$ or $K_{o/w}$ is a "measure of lipophilicity by determination of the equilibrium distribution between octan-1-ol and water, as used in pharmacological studies and in the assessment of environmental fate and transport of organic chemicals":

$$P_{o/w} = \frac{C_o}{C_a} \quad (1)$$

where C_o and C_a are the equilibrium concentrations of the compound in the organic and the aqueous phase. The organic phase is usually *n*-octanol, alkane, or chloroform, and can be any other water-immiscible solvent. Qualitatively, the partition coefficient measures the preference of the compound for the non-polar phase, and from the thermodynamic perspective, it gives information about the intermolecular forces affecting a compound in solution.

DISCUSSION

The partition coefficient between *n*-octanol and water, $P_{o/w}$, can be measured experimentally using the "shake-flask" method, or can be calculated from structural fragments. The direct measurement of $P_{o/w}$ values by equilibration between *n*-octanol and water is difficult, time consuming, requires a fairly pure compound that must be available in an adequate quantity, and has a limited measurable lipophilicity range, not suitable for very lipophilic or very hydrophilic compounds. Measurable P (generic notation for the partition coefficient) values are usually in the range 10^{-2}–10^{7}. As these values extend over several orders of magnitude, they may be expressed logarithmically (as $\log_{10}$), and $\log P$ is often used instead of P for practical reasons.

Reversed-phase liquid chromatography (LC) has been widely used as an alternative method for $\log P_{o/w}$ determination, modeling the partition of a compound between the lipid layer and the biological membrane of a cell. The compound partitioning into a lipid layer rules the biological activity of substances, such as the absorption of drugs and their metabolites, the in vivo bioaccumulation of organic compounds, etc.

TLC was the first form of LC used for lipophilicity estimations. Reversed-phase TLC (RP-TLC) has distinct advantages compared to conventional methods for $\log P_{o/w}$ determination. It is a rapid and reliable method, having a good reproducibility, and it only needs a small amount of sample (μg/ml) that does not have to be pure. In an RP-TLC experiment, several samples can be run simultaneously, making the method an attractive option for high throughput screening of new organic compounds, especially in the pharmaceutical industry. In TLC, the retention parameter, R_F, is defined as the ratio between the migration distances of the compound and of the mobile phase, both measured from the sample application position (Eq. 2). The term R_M was introduced to facilitate a linear relationship with the $\log P$ values, and it is defined similar to the capacity factor, k, in HPLC (Eq. 3).

$$R_F = \frac{z_x}{z_f} \quad (2)$$

where z_x and z_f are the migration distances of the component and of the mobile phase between the start and the front line.

$$R_M = \log\left(\frac{1}{R_F} - 1\right) \quad (3)$$

The stationary phase in RP-TLC can be C8 or C18 chemically bonded silica gel, or a silica gel layer impregnated with paraffin or silicone oil. Better correlations are usually obtained for the R_M values vs. $\log P$ on C18 reversed phase, probably because the secondary interactions between the compound and the free silanol groups on the silica surface are stronger on C8 phases than on C18. The samples are usually detected by fluorescence quenching or by spraying the plate with specific derivatization reagents. The measurements of R_M values on silica layers impregnated with oils have lower reproducibility than those on silica C8 or C18 bonded phase.

The mobile phase used in the lipophilicity measurements by RP-TLC is usually a binary mixture of an organic solvent and water. The organic solvent can be methanol, acetonitrile, or acetone. The first two can also be used in reversed-phase high-performance liquid chromatography

(HPLC) (RP-HPLC) measurements, but acetone is restricted due to its absorption in low wavelength UV.

The correlations between log P and R_M are frequently linear for non-ionic and ionic compounds. When a compound contains one or more ionizable substituents, the pH and the ionic strength of the eluent modify the apparent lipophilicity according to the ratio of neutral and ionized species.

Extensive experimental results show the existence of a linear relationship between the retention parameter R_M and the concentration of organic modifier in the mobile phase, φ, in a similar way to the RP-HPLC experiments:

$$R_M = a_0 + a_1\varphi \tag{4}$$

where φ is the concentration of the organic modifier in the mobile phase, and a_0 and a_1 are the intercept and the slope of the linear relationship (4); a_0 corresponds to the R_{Mw} value obtained in the case when pure water (or aqueous buffer) is the mobile phase. Experimentally, the R_{Mw} value can be measured only for very hydrophilic compounds. Practically, the R_{Mw} value is extrapolated from the linear relationship (4) to 0% organic modifier in the mobile phase. The extrapolation method was confirmed by the good linear correlations obtained between the experimental and the extrapolated R_{Mw} values. In theory, the extrapolated R_{Mw} value should have the same value regardless of the nature of the organic modifier in the aqueous mobile phase. Practically, these values are slightly different, probably due to errors in the linear fit, and usually have little influence on the lipophilicity measurements. Sometimes, a positive or negative deviation of R_M values from the linear relationship (4) was observed, especially at low concentrations of organic modifier in the mobile phase (Fig. 1). In some cases, the deviation from the linearity can be significant; hence, the extrapolation method is not applicable.

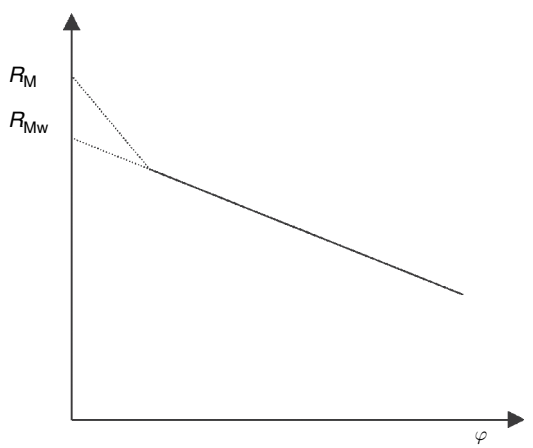

Fig. 1 The relationship between the R_M values and the organic modifier concentration (φ) in the aqueous mobile phase for RP-TLC lipophilicity measurements.

In practice, the R_{Mw} values correlate well with the log $P_{o/w}$ values, usually by a linear fit:

$$R_M = b_0 + b_1 \log P_{o/w} \tag{5}$$

where b_0 and b_1 are the coefficients, the intercept and the slope, respectively. Eq. 5 is similar to the linear relationships obtained in RP-HPLC between log k and log P values.

The extreme values for R_F are 0, obtained for very lipophilic compounds that remain at the start line, and 1, for very hydrophilic compounds that migrate to the mobile-phase front. As a consequence, the obtained R_M values can be situated between $-\infty$ and $+\infty$. Practically, the R_F values can be measured in the range 0.03–0.97, which means that R_M values can be measured in the range –1.5 to +1.5.

The R_{Mw} values for hydrophilic compounds can be obtained experimentally or by extrapolation. The relationship obtained between the experimental and the extrapolated R_{Mw} is linear, having an intercept value $m \cong 0$ and slope n approximately 1:

$$R_{Mw,experimental} = m + nR_{Mw,extrapolated} \tag{6}$$

Eq. 6 was verified experimentally for structurally different compounds and provided the validity of the extrapolation method for the R_{Mw} values, in the cases when direct measurement is not possible, e.g., for very lipophilic compounds.

Regardless of the nature of the organic modifier used in the aqueous mobile phase, a linear relationship can be obtained between the intercept and the slope of Eq. 4. This means that the intercept value, $a_0 = R_{Mw}$, is correlated with the slope a_1:

$$R_{Mw} = a + ba_1 \tag{7}$$

The linear correlation shown in Eq. 7 is not influenced by the value of the slope a_1. Considering a methanol–water mobile phase, an increase of methanol concentration will produce a more rapid decrease of R_M values for the lipophilic compounds than for the hydrophilic ones. This means that the lipophilic substances are more sensitive to variations in the mobile-phase composition.

The linear relationship between a_0 and a_1 values [Eq. 4] is an important relationship in the lipophilicity measurements. The intercept, $a_0 = R_{Mw}$, can be considered a measure of the partition of a compound between an aqueous, polar mobile phase and a non-polar stationary phase. The physicochemical significance of the slope, a_1, is not completely established. It was demonstrated experimentally that the slope shows the rate of increase in compound solubility in the mobile phase. The solubility increases as a consequence of the decrease of the mobile phase polarity.

The slope, a_1, depends on the non-polar surface of the organic compound; hence, it is the part of the compound that interacts with the non-polar stationary phase.

The correct measurement of the R_F values is very important because it affects the calculation of the R_{Mw} values and further correlations. Manual measurement of the R_F values includes an error of ± 1 mm, compared with the precision of a densitometer, which is ± 0.01 mm. The start and the front lines should also be exactly established, in order to reduce the measurement error. The "front line" in TLC is approximately equivalent with the "dead time/volume" concept in HPLC. The marker substance used in HPLC (such as inorganic salts) can be applied to estimate the exact front line in TLC. The measurement error for the front line is about 0.03 mm for a migration distance of 80 mm, for any concentration of the organic modifier in the aqueous mobile phase.

BIBLIOGRAPHY

1. Biagi, G.L.; Barbaro, A.M.; Recanatini, M. Determination of lipophilicity by means of reversed-phase thin-layer chromatography. III. Study of the TLC equations for a series of ionizable quinolone derivatives. J. Chromatogr. A, **1994**, *678*, 127–137.
2. Biagi, G.L.; Barbaro, A.M.; Sapone, A.; Recanatini, M. Determination of lipophilicity by means of reversed-phase thin-layer chromatography. I. Basic aspects and relationship between slope and intercept of TLC equations. J. Chromatogr. A, **1994**, *662*, 341–361.
3. Biagi, G.L.; Barbaro, A.M.; Sapone, A.; Recanatini, M. Determination of lipophilicity by means of reversed-phase thin-layer chromatography. II. Influence of the organic modifier on the slope of the thin-layer chromatographic equation. J. Chromatogr. A, **1994**, *669*, 246–253.
4. Cimpan, G.; Bota, C.; Coman, M.; Grinberg, N.; Gocan, S. A lipophilicity study for some 2-hydrazinothiazolic derivatives with antifungal activity by reversed phase thin layer chromatography. J. Liq. Chromatogr. Relat. Technol. **1999**, *22*, 29–40.
5. Cserháti, T.; Forgács, E. Effect of TLC support characteristics and coating on the lipophilicity determination of phenols and aniline derivatives. J. Chromatogr. Sci. **2002**, *40*, 564–568.
6. Kaliszan, R. *Quantitative Structure–Chromatographic Retention Relationships*; John Wiley & Sons: New York, 1987.
7. Lambert, W.J. Modeling oil–water partitioning and membrane permeation using reversed-phase chromatography. J. Chromatogr. A, **1993**, *656*, 469–484.
8. Leo, A.; Hansch, C.; Elkins, D. Partition coefficients and their uses. Chem. Rev. **1971**, *71*, 525–616.
9. Poole, S.K.; Poole, C.F. Separation methods for estimating octanol–water partition coefficients. J. Chromatogr. B, **2003**, *797*, 3–19.
10. Tomlinson, E. Chromatographic hydrophobic parameters in correlation analysis of structure-activity relationships. J. Chromatogr. **1975**, *113*, 1–45.

Overpressured Layer Chromatography

Jan K. Rozylo
Department of Adsorption Chromatography and Planar Chromatography, Marie Curie-Sklodowska University, Lublin, Poland

INTRODUCTION

Conventional thin-layer chromatography (TLC) in our experience, known under the name planar chromatography, uses horizontal or vertical glass or Teflon chambers for the development of chromatograms. As stationary phases, commonly known adsorbents or supports based on silica gel, aluminium oxide, magnesium silica, cellulose, and so forth are used; particle sizes are about 20 μm. The migration of the mobile phase is based on the phenomenon of capillary forces. This chromatographic method is described, in detail, in other sections of this volume.

This method is characterized by many limitations which either can cause unsatisfactory separation of a mixture of substances or lead to long development times (even up to several hours) or, sometimes, makes use of solvents of high viscosity impossible. The efficiencies of such chromatographic systems are also rather low.

DISCUSSION

In conventional TLC, the velocity of chromatogram development depends on the dimension of stationary-phase particles, viscosity of the mobile phase, distance from the start line of the mobile phase, and other parameters. Therefore, there is no possibility of regulation of resolution by change of migration velocity of mobile-phase flow; the distance between the solvent reservoir and the solvent front (z_f) varies with time (t) according to

$$z_f^2 = kt$$

where k is a constant that depends on the chromatographic system (mobile phase and adsorbent) and the size of sorbent particles constituting the layer and presents a parabolic relationship.

As the most popular planar liquid chromatographic technique, TLC uses a vapor phase of solvent above the sorbent layer, which has an important influence on the resolving power.

Many of the inconveniences of TLC are avoided in overpressured layer chromatography (OPLC), which is a logical extension of the theory and practice developed in HPLC which can now be used in the field of planar liquid chromatography. This extension offers some exceptional advantages to a chromatographer. OPLC is, in practical terms, a planar HPLC technique. OPLC integrates many of the benefits of TLC, high-performance TLC, and HPLC. This technique corresponds to an HPLC column having a relatively thin, wide cross section and using a pressurized ultramicrochamber with standard chromatoplates. Eluent is forced into the sorbent layer by the means of a pump which enables development of chromatograms with forced flow of the mobile phase (more precise penetration into micropores). The eluent migrates against the sorbent resistance imposed by external pressure on the sorbent surface, and the vapor phase is excluded. In the case of OPLC, there is a linear relationship between the distance (z_f) of the solvent front from the starting point and the migration time (t):

$$z_f = kt$$

where k is a constant that depends on the rate of solvent flow, on the externally applied pressure, and on the size of the particles constituting the layer. In principle, k is constant throughout the development and independent of the rate of solvent migration. In OPLC, R_F the parameter is also used to describe the position of the separated analyte and, in this case, the R_F values do not depend on the starting distance.

The parameters characterizing chromatographic systems in TLC, such as average plate height (H), reduced plate height (h), and theoretical plate number (N), are calculated in a similar way in OPLC, but, practically, they do not depend on either average particle diameter (d_p) or the start distance (s_0). In OPLC, the start distance has no influence on the efficiency of separation, and the average plate hight is nearly constant on a layer of exceptionally fine particles, even over a longer development distance. Thus, the major advantage of OPLC over other planar techniques lies in this fact. We can say that OPLC permits relatively large plate numbers to be obtained and can be applied more favorably in the case of smaller particles.

BASIC INSTRUMENTATION FOR OPLC

As far as OPLC is concerned, the method, in principle, differs from conventional TLC in the design of the

equipment that is used. The first attempts at construction of chromatographic pressure chambers were made in the beginnings of the 1960s. However, only at the end of the 1970s, Tyihák, Mincsovics, and Kalász were successful in construction of a well-operating OPLC chromatograph called Chrompress 10 (maximum pressure permitted in this chamber was 1.0 MPa) and, later, in the 1980s, Chrompress 25 (2.5 MPa) (Labor MIM, Hungary) and the most modern Personal OPLC BS-50 (OPLC-NIT, Budapest, Hungary) (5.0 MPa). In Poland, during 1980–1990, a pressure thin-layer chromatograph was constructed (Cobrabid, Warsaw); however, due to its narrow range of operating pressures (0.8 MPa), it was not widely used.

We will describe only the most up-to-date OPLC system. This fully automatic OPLC system allows separation of mixtures on an analytical and on a semipreparative scale. The fundamental separation process occurs on a chromatographic plate (constructed of glass or aluminum foil) with sorbent (Fig. 1) covered and compressed by a special polyethylene or Teflon foil, pressured by water. In this way, a flat, thin chromatographic column is created. This technique also requires a special chromatoplate which is sealed at the edges, which prevents the eluent from flowing off the chromatoplate in an unwanted direction. According to the technique of chromatogram development used (unidirectional, bidirectional, circular, online, off-line, parallel coupled multilayer, serial coupled multilayer), all four margins of a plate, three margins, two opposite margins can be impregnated, or they can be left uncoated.

In linear development of a chromatogram, unidirectional or bidirectional developments of the chromatogram are possible. Similarly, as in liquid column chromatography, there are possible, in this case, either online or off-line techniques of sample application, separation, and detection, as well as various modifications (e.g., partly offline method). Bidirectional development can also be vertical. Using vertical bidimensional development, applying different eluents, components of complex, difficult mixtures can be separated. The separation of such mixtures is also possible by means of this technique using multiple automatic development of chromatogram.

In OPLC, the changes in composition of the eluent give good possibilities for special separation techniques such as isocratic and gradient separation. The choice of mobile phase can be effectively and quickly determined using the optimization model Prisma according to Nyiredy. This is a three-dimensional model that correlates the solvent strength and the proportion of eluent constituent, which determines the selectivity of the mobile phases according to Snyder's solvent classification.

The newest apparatus for overpressured layer chromatography, "Personal OPLC BS-50" manufactured in Hungary, is shown in Fig. 2. Generally speaking, it consists

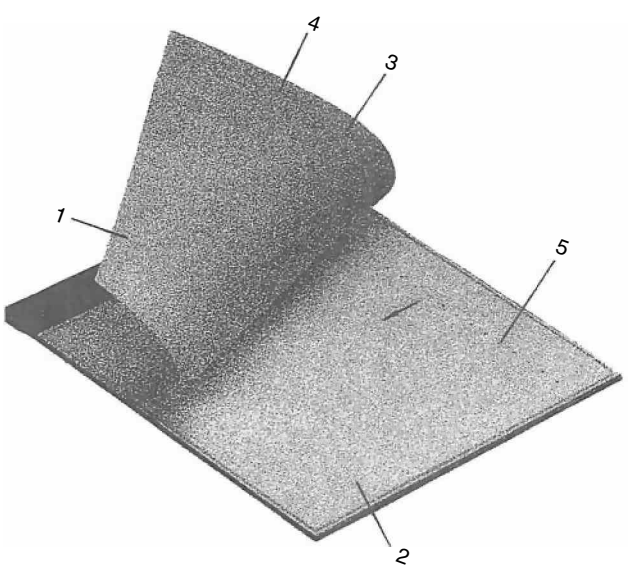

Fig. 1 Cassette of foil-backed layer for linear development: 1 = cover sheet, 2 = sorbent layer, 3 = eluent puncture, 4 = eluent trough, 5 = sample application site.

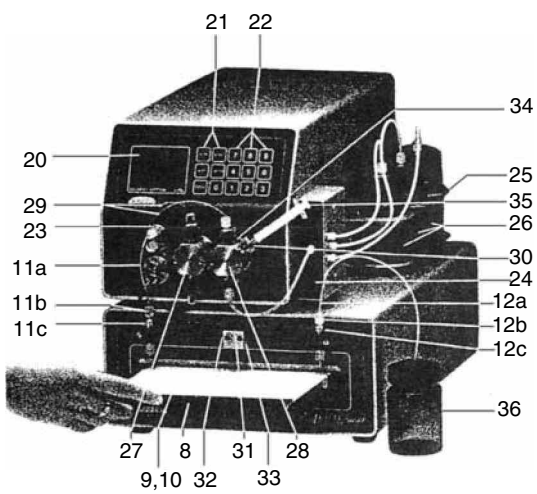

Fig. 2 Personal OPLC BS-50 apparatus: 9,10 = Teflon cover sheet of cassette, upper and lower, respectively; 11a = tube driving eluent from pressure gauge to chamber inlet connector; 11b = end connector for tube 11a; 11c = chamber–eluent– inlet connector; 12a = tube for eluent outlet of the chamber; 12b = end connector for tube 12a; 12c = chamber–eluent–outlet connector; 20 = display; 21 = function keys; 22 = numeric keys; 23 = pressure gauge for eluent; 24 = eluent switching valve; 25 = tank holder; 26 = eluent tanks A, B, and C; 27 = pump head for hydraulic liquid delivery; 28 = pump head foreluent delivery; 29 = hydraulic liquid and eluent connecting tubes; 30 = connecting stub for syringe to fill up eluent pump; 31 = middle hole of T distributor for fitting tubes in case of two-directional development; 32 = left hole of T distributor for fitting tubes in case of two-directional development; 33 = right hole of T distributor for fitting tubes in case of two-directional development; 34 = hole for piston rinsing against deposition; 35 = syringe.

of the separation chamber and a liquid delivery system. The separation chamber contains the following units: (a) holding unit, (b) hydraulic unit, (c) troy layer cassette, and (d) drain valve. The apparatus also has a pumping system for eluent delivery and for the hydraulic liquid delivery. The entire apparatus and the total chromatogram development process are controlled by a computer system. The apparatus and the method of chromatogram development is characterized by high reproducibility of results and chromatographic parameters. External pressure (5 MPa), eluent flow rate and its volume, and development time can be automatically programmed. The OPLC-BS-50 chamber works in off-line and online systems. Using this equipment, it is possible to separate 70–100 or even more samples at the same time, depending, of course, on the chosen technique of the OPLC process.

This OPLC method is charaterized by high precision for determination of retention parameters and reproducibility of results.

ADVANTAGES

- Separation of components which the former TLC techniques failed to achieve
- Smaller attainable plate height over longer migration distances
- Rapid separation and high resolution for industrial control
- Optimization of resolution as a function of solvent velocity, development distance, and temperature
- Possibility of using high-viscosity eluents and poorly wettable stationary phases
- Possibility of both quantitative evaluation and preparative applications
- Efficient separation of multicomponent samples
- Different development modes: unidirectional, bidimensional, continuous online, and off-line Long migration distances on fine-particle layers with short development times
- No air interactions
- Minute consumption of developing solvent
- Programmable operating system.

Some applications include analytical and preparative analyses in all types of biological, biochemical, pharmaceutical, clinical, forensic, food, and environmental laboratories.

BIBLIOGRAPHY

1. Kaiser, R.E. *Einfuerung in die HPLC*; Huethig: Heidelberg, 1987.
2. Kaiser, R.E.; Rieder, R.I. *Planar Chromatography*; Kaiser, R.E., Ed.; Huethig: Heidelberg, 1986; Vol. 1, 165.
3. Mincsovics, E.; Ferenczi-Fodor, K.; Tyihák, E. *Handbook Thin-Layer Chromatography*; Sherma, J., Fried, B., Eds.; Marcel Dekker, Inc.: New York, 1996; 173.
4. Nyiredy, Sz.; Erdelmeier, C.A.J.; Sticher, O. *Proc. Int. Symp. TLC with Special Emphasis on Overpressured Layer Chromatography (OPLC)*; Tyihak, E., Ed.; LABOR MIM: Budapest, 1986; 222.
5. Nyiredy, Sz.; Meszaros, S.Y.; Dallenbach-Toelke, K.; Nyiredy-Mikita, K.; Sticher, O. J. High Resolut. Chromatogr. Chromatogr. Commun. **1987**, *10*, 352.
6. Rózyło, T.K.; Siembida, R.; Tyihak, E. Measurement of formaldehyde as dimedone adduct and potential formaldehyde precursors in hard tissues of human teeth by overpressured layer chromatography. Biomed. Chromatogr. **1999**, *13* (8), 513.
7. Ruoff, A.D.; Giddings, J.C. Paper geometry and flow velocity in paper chromatography. J. Chromatogr. **1960**, *3*, 438.
8. Tyihák, E.; Mincsovics, E.; Kalász, H. New planar liquid chromatographic technique: Overpressured thin-layer chromatography. J. Chromatogr. **1979**, *174*, 75.
9. Tyihák, E.; Mincsovics, E.; Kalász, H.; Nagy, J. Optimization of operating parameters in overpressured thin-layer chromatography. J. Chromatogr. **1981**, *211*, 45.
10. Tyihák, E.; Mincsovics, E.; Tétényi, P.; Zámbó, I.; Kalász, H. Applicability of overpressured thin-layer chromatography in phytochemistry. Acta Horticult. **1980**, *96*, 113.

Oxolinic Acids: HPLC Analysis

Abdul Rahman
Assessment Service Unit, Airlangga University, Surabaya, Indonesia

Mochammad Yuwono
Gunawan Indrayanto
Faculty of Pharmacy, Airlangga University, Surabaya, Indonesia

INTRODUCTION

Oxolinic acid (OA) (5-ethyl-5,8-dihydro-8-oxo-1,3-dioxolo[4,5-*g*]quinoline-7-carboxylic acid) is an antibacterial agent that belongs to the class of quinolone derivatives (Fig. 1). Quinolone antibiotics are active against a variety of gram-positive and gram-negative bacteria; they act by inhibiting DNA gyrase (topoisomerase II), a bacterial enzyme involved in DNA replication, recombination, and repair, leading to bacterial cell damage.

Oxolinic acid is widely used in farming, including shrimp, fish, chicken, and swine farming.[1–4] Compared to other drugs, quinolone antibiotics have a rapid bactericidal effect against most susceptible organisms.[5] Another advantage of OA in farming is its shorter half-life, which means it can be eliminated faster from the animal tissues, hence minimizing its residual effects. Excessive use of these antibacterial agents may cause residual effects in the animal tissues intended for human consumption. Therefore, to ensure human food safety, the European Union has set maximum residue limits (MRL) for these compounds; for OA, the limit in fish muscle is 300 μg/kg.[6,7]

Various analytical methods have been developed for the analysis of OA in pharmaceutical preparations, plasma, urine, and animal tissues. Other authors also developed methods for analyzing OA as a pollutant in aquatic plants and sediments.[8–10] Methods commonly used for the analysis of OA are bioassay, thin-layer chromatography (TLC) fluorescence, high-performance liquid chromatography (HPLC) with ultraviolet or fluorescence detection, HPLC–mass spectrometry (HPLC–MS), HPLC-ES–MS, gas chromatography–mass spectrometry (GC–MS), and capillary electrophoresis.[4,11–13] Capitan-Vallvey et al.[14] developed a phosphorimetric sensor method for detecting OA in human urine and cow's milk. Among these methods, HPLC is preferred.

SAMPLE PREPARATION

Analysis of OA in biological matrices is quite complicated, owing to the very complex nature of the sample, which may lead to difficulties in extraction procedures. Furthermore, the very low concentration of these agents has become the second obstacle. Generally, two methods of extraction are being used, i.e., liquid–liquid extraction (LLE) and solid-phase extraction (SPE). In general, SPE is generally preferred, because of its simplicity.

Liquid–Liquid Extraction Methods

For LLE, the acid–base solubility property of OA (soluble in organic solvent in acidic condition and soluble in basic aqueous solution) was utilized.[8] The lower cost of chemicals used in liquid–liquid separation makes this method more cost effective. The only disadvantage is that it is time consuming and tedious. Some authors found that the recovery of OA by LLE was higher than that by SPE.[1,2,8] Solvents commonly used for LLE methods are summarized in Table 1.

Solid-Phase Extraction Methods

For solid-phase extraction, the offline procedure, based on sample pretreatment on disposable SPE cartridges, and a totally automated online procedure, based on column switching, have been developed. The column switching procedure involves the use of a polystyrene-divinylbenzene column for sample concentration and cleanup.[16]

The principle of SPE is based on selective retention of the analyte on a bonded silica material. Frequently used solid-phase materials include C_2-, C_8-, C_{18}-, CN-, and

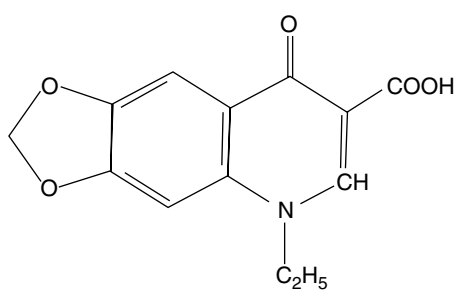

Fig. 1 Chemical structure of OA.

Table 1 Solvents frequently used for traditional liquid–liquid extraction methods for OA.

Matrices	Solvents	Recovery (%)	Refs.
Fish serum and muscles	ACN–THF (95 : 5)	95.1 (serum) 92.0 (muscle)	[15]
Fish tissues	NaOH–acetone; re-extracted by $CHCl_3$–H_3PO_4	97	[1]
Feces and urine of *Scophthalmus maximus*	Feces: aqueous $ZnSO_4$, NaOH 0.1 *M*, and ACN; Urine: NaOH, chlorhydric acid, and chloroform	102 (feces) 91.6 (urine)	[2]
Fish muscle	Buffer solution, pH 9, and acetonitrile; then washed with *n*-hexane	69	[6]
Aquatic plants	1 *M* NaOH aqueous solution then re-extracted with $CHCl_3$ in acidic condition	68.3	[8]
Meat	Na_2SO_4 and ACN; washed twice with *n*-hexane	85 ± 7	[13]

phenyl-bonded phases. An idealized SPE protocol involves trapping the analyte on a solid phase, washing off interferences that are less attracted to the sorbent, then eluting analyte(s) and leaving interferences with greater attraction bound to the sorbent.[17] For OA, C_2-, C_8-, and CN-bonded phases gave excellent recovery and, by using C_2-bonded phase, up to 100.1% recovery may be achieved.[16]

The SPE cartridge must be conditioned prior to use. Usually, the solvents used for preconditioning are MeOH and water;[18,19] MeOH, water, and 0.05 *M* phosphate buffer at pH 7;[7] MeOH and 5% MeOH in 0.001 *M* phosphoric acid;[1] MeOH, acetate buffer, pH 3–4, and 0.5 m*M* OCN;[11] and MeOH and 1.0 *M* orthophosphoric acid.[16] The common methods used for sample preparation using SPE are given in Table 2.

HPLC CONDITIONS

Among the methods for analyzing OA, HPLC combined with UV, fluorescence, or diode array detection is the most used. The applied HPLC conditions are summarized in Table 3, and a typical chromatogram and UV-spectrum of OA is presented in Fig. 2.

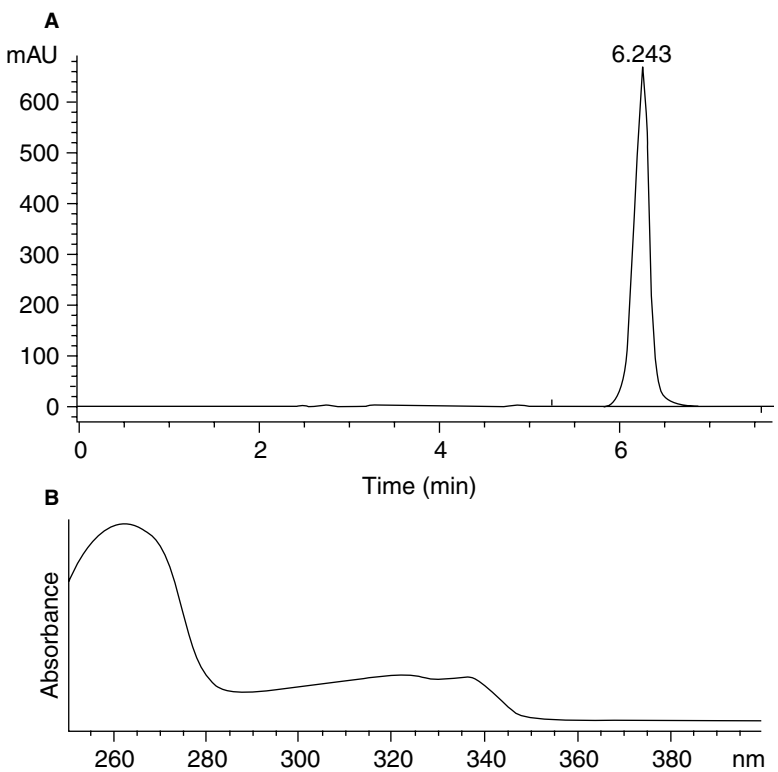

Fig. 2 A, HPLC chromatogram of standard OA at 261 nm (Sigma, Cat. No. 14698-29-4); column: Hypersil BDS C-18®; eluent: H_3PO_4 (pH 3): ACN (70 : 30 v/v); and B, UV-Spectrum of OA peak.

Table 2 Cartridge and solvents used for SPE methods for OA.

Matrices	Sample extraction	Cartridges	Solvents for cleaningup	Solvents for eluting OA	Recovery (%)	Refs.
Fish and pork tissues	0.05 *M* phosphate buffer pH 7.4	C_{18}	Water	MeOH : 30% NH_4OH (75 : 25; v/v)	92.8	[19]
Chicken tissue	CH_2Cl_2, re-extracted with 1 *M* NaOH; neutralized with phosphate buffer pH 7		Phosphate buffer, water, and ACN	4% TFA in water : ACN (25 : 75; v/v) followed by ACN	94	[7]
Feces and urine of *S. maximus*	10% $ZnSO_4$ solution : 0.1 *M* NaOH : ACN (2 : 20 : 60; v/v)	Various		MeOH, ACN, H_3PO_4 solution, and water	<35%	[2]
Salmon plasma	Plasma applied directly to cartridges	C_2-, C_8-, C_{18}-, CN-, and pH-bonded phases	Water and then 1 *M* H_3PO_4	ACN : MeOH : 1 *M* H_3PO_4 (80 : 10 : 10; v/v)	98.7	[16]
Animal feed	0.2% Metaphosphoric acid in water : ACN (1 : 3; v/v)	Gilson ASPEC XL®	0.025 *M* H_3PO_4 adjusted to pH 3 with NaOH, and then water is added	MeOH	73–90	[18]
Plasma	Plasma applied directly to cartridges	C_{18}	Acetate buffer pH 3–4 and water	MeOH : H_2O (70 : 30; v/v)	131	[11]
Plasma	Plasma applied directly to cartridges	C_{18}	Water and 0.05% H_3PO_4	ACN 6×	92.18	[20]
Fish	Phosphate buffer pH 7 adjusted to pH 3 before it is applied to cartridges	C_{18}	Water	Phosphate buffer pH 9 : MeOH (9 : 1; v/v)	97.92	[3]
Artemia nauplii: live fish feed	Dihydrogen phosphate buffer	C_{18}	*n*-Hexane	0.1 *M* phosphate buffer pH 3 : MeOH: (9 : 1; v/v).	100.8 ± 6.3%	[21]

Table 3 Chromatographic condition in analyzing OA.

Column	Mobile phase	Detector	Remarks	Refs.
ODS	MeOH : 0.1 *M* phosphate buffer pH 3, 45 : 55 (v/v)	UV detector: 254 nm	Sample: *A. nauplii*; capacity: 2.66 ± 0.12; asym. factor: 0.90. At pH > 3, peak tailing of OA occurred; at MeOH > 50% OA peak was coeluted with other substances. DL:[a] 0.012 μg/g QL:[b] 0.2 μg/g	[21]
PLRP-S® + RP18E® precolumn	Gradient ACN in 0.02 mol/L phosphoric acid pH 2.2	Fluorescence detector: 280–320 nm and 350–480 nm	Correlation coefficient: 0.990 DL:[a] 5 μg/kg sample QL:[b] 75 μg/kg sample	[6]
LiChroSpher 100 RP-18®	ACN 0.02 *M* : H_3PO_4 : DMF (10 : 60 : 30, v/v); flow rate: 0.8 ml/min	UV detector: 340 nm	Sample: plasma of *Dicentrarchus labrax* Rt: 5.91 min (R.S.D. = 0.40%); linearity (0.2–25 μg/ml): $y = 0.28x + 0.038$; $r = 0.985$; DL:[a] 0.014 μg/ml sample QL:[b] 0.2 μg/ml sample	[20]
PuroSpher-RP18E®	0.001 *M* H_3PO_4 : ACN : 67 : 33 (v/v) pH 3.4; flow rate: 0.6 ml/min	Fluorescence detector: 330/360 nm	Sample: feces and urine of *S. maximus* Rt: 5.6 min; DL:[a] 0.20 μg/g (feces); 0.02 μg/g (urine) QL:[b] 1.00 μg/g (feces); 0.06 μg/kg (urine)	[2]
LiChroSpher 100 RP-18E®	ACN : 0.02 *M* H_3PO_4 (24 : 76 v/v) pH 2.3; flow rate: 1.0 ml/min	UV detector: 262 nm	Sample: shell of blue mussel Rt: 6.3 min DL:[a] 0.012 μg/g QL:[b] 0.040 μg/g	[10]
RP18	Linear gradient, ACN in 0.02 *M* H_3PO_4 pH 2.2; 20–45% ACN (12 min); 45% ACN (5 min);	Fluorescence detector: 260/380 nm	Sensitivity: 0.5 ng/g DL:[a] n.a. QL:[b] 75 μg/kg	[6]

	45–20% ACN (2 min); and 20% ACN (3 min); flow rate 0.8 ml/min			
C_5 LUNA® 150 × 4.6 mm	Gradient, ACN : THF : KH_2PO_4 0.004 *M* pH 2.6 (50 : 1 : 49; v/v)ACN : THF : KH_2PO_4 0.012 *M* pH 2.6 (1 : 10 : 89; v/v); flow rate: 1 ml/min	Diode array detector: 278 nm Fluorescence detector: 324/366 nm	Sample: fish feed Rt: 22.9 min; Linear range: 0.10–25 μg/ml DL:[a] 0.4 mg/kg QL:[b] 5 mg/kg	[18]
Hisep® shielded hydrophobic phase (Supelco, Bellefonte, Pennsylvania, U.S.A.)	0.05 *M* citric acid : 0.2 *M* Na_2HPO_4 buffer, pH 2.5 in 10 m*M* tetra-*n*-butyl ammonium bromide acetonitrile (85 : 15; v/v); flow rate: 1 ml/min	UV detector 265 nm	Sample: fish muscle and serum Extraction: ACN : THF (95 : 5) (muscle) Rt: 14 min Linearity range: 0.25–50 μg/ml (correlation coefficient $\geq$ 0.999) DL:[a] 0.05 μg/ml (serum); 0.1 μg/g (muscle) QL:[b] n.a.	[15]
Symmetry® C18	ACN : 0.02 *M* phosphate buffer pH 3.0 (34 : 66; v/v); flow rate: 1 ml/min	Fluorescence detector: 312/366 nm	Sample: fish and pork tissues Extraction: SPE C_{18}DL:[a] 5 ng/g, QL:[b] 20 ng/g $r > 0.9993$ (0.4–12 ng)	[19]

n.a.: data not available.
[a]Detection limit.
[b]Quantitation limit.

CONCLUSIONS

Various HPLC methods have been developed and used to analyze oxolinic acid in various matrices. The suitable methods for sample preparation and extraction largely depend on the nature of samples. Extraction using SPE methods have not always given better results when compared to traditional liquid–liquid extraction methods. The most used HPLC column for analyzing OA is a C_{18} column combined with UV or fluorescence detectors.

REFERENCES

1. Rogstad, A.; Hormazabal, V.; Yndestad, M. Simultaneous extraction and determination of oxolinic acid and flumequine in fish tissues by high performance liquid chromatography. J. Liq. Chromatogr. **1989**, *12*, 3073–3086.
2. Pouliquen, H.; Armand, F. Determination of oxolinic acid in faeces and urine of turbot (*Scopothalamus maximus*) by high-performance liquid chromatography using flourescence detection. J. Chromatogr. B, **2000**, *749*, 127–133.
3. Saad, B.; Mohamad, R.; Mohamed, N.; Lawrence, G.D.; Jab, Md.S.; Saleh, M.I. Analytical, nutritional and clinical methods. Determination of oxolinic acid in feeds and cultured fish using capillary electrophoresis. Food Chem. **2002**, *78*, 383–388.
4. Su, S.-C.; Chang, M.-H.; Chang, C.-L.; Chang, P.-C.; Chou, S.-S. Simultaneous determination of quinolones in livestock and marine products by high performance liquid chromatography. J. Food Drug Anal. **2003**, *11*, 114–127.
5. Park, H.R.; Kim, T.H.; Bark, K.M. Physicochemical properties of quinolone antibiotics in various environments. Eur. J. Med. Chem. **2002**, *37*, 443–460.
6. Roudaut, B.; Yorke, J.C. High-performance liquid chromatographic method with fluorescence detection for the screening and quantification of oxolinic acid, flumequine and sarafloxacin in fish. J. Chromatogr. B, **2002**, *780*, 481–485.
7. Barrón, D.; Jiménez-Lozano, E.; Bailac, S.; Barbosa, J. Simultaneous determination of flumequine and oxolinic acid in chicken tissues by solid phase extraction and capillary electrophoresis. Anal. Chim. Acta **2003**, *477*, 21–27.
8. Delepee, R.; Pouliquen, H. Determination of oxolinic acid in the bryophyte Fontialis antipyretica by liquid chromatography with flourescent detection. J. Chromatogr. B, **2002**, *775*, 89–95.
9. O'Reilly, A.; Smith, P. Use of indirect conductimetry to establish predictive no effect concentrations of oxytetracycline and oxolinic acid in aquatic sediments. Aquaculture **2001**, *196*, 13–26.
10. Pouliquen, H.; Gouelo, D.; Larhantec, M.; Pilet, N.; Pinault, L. Rapid and simple determination of oxolinic acid and oxytetracycline in the shell of the blue mussel (*Mytilus edulis*) by high-performance liquid chromatography. J. Chromatogr. B, **1997**, *702*, 157–162.
11. Hernandez, M.; Borrull, F.; Calull, M. Determination of quinolones in plasma samples by capillary electrophoresis using solid-phase extraction. J. Chromatogr. B, **2000**, *742*, 255–265.
12. Fierens, C.; Hillaert, S.; Van den Bossche, W. The qualitative and quantitative determination of quinolones of first and second generation by capillary electrophoresis. J. Pharm. Biomed. Anal. **2000**, *22*, 763–772.
13. Fuh, M.-R.S.; Chan, S.-A.; Wang, H.-L.; Lin, C.-Y. Determination of antibacterial reagents by liquid chromatography-electrospray-mass spectrometry. Talanta **2000**, *52*, 141–151.
14. Capitan-Vallvey, L.F.; Al-Barbarawi, O.M.A.; Fernandez-Ramos, M.D.; Avidad, R. Determination of oxolinic acid in cow's milk and human urine by means of a single-use phosphorimetric sensor. Talanta **2003**, *60*, 247–255.
15. Ueno, R.; Aoki, T. High-performance liquid chromatographic method for the rapid and simultaneous determination of sulfamonomethoxine, miloxacin and oxolinic acid in serum and muscle of cultured fish. J. Chromatogr. B, **1996**, *682*, 179–181.
16. Rasmussen, K.E.; Tonnesen, F.; Thanh, H.H.; Rogstad, A.; Aanesrud, A. Solid-phase extraction and high performance liquid chromatographic determination of flumequine and oxolinic acid in salmon plasma. J. Chromatogr. **1989**, *496*, 355–364.
17. Stevenson, D. Immuno-affinity solid-phase extraction. J. Chromatogr. B, **2000**, *745*, 39–48.
18. Pecorelli, I.; Galarini, R.; Bibi, R.; Floridi, Al.; Casciarri, E.; Floridi, A. Simultaneous determination of 13 quinolones from feeds using accelerated solvent extraction and liquid chromatography. Anal. Chim. Acta **2003**, *483*, 81–89.
19. Ramos, M.; Aranda, A.; Garcia, E.; Reuvers, T.; Hooghuis, H. Simple and sensitive determination of five quinolones in food by liquid chromatography with fluorescence detection. J. Chromatogr. B, **2003**, *789*, 373–381.
20. Loussouarn, H.S.; Pouliquen, H.; Armand, F. High-performance liquid chromatographic determination of oxolinic acid in the plasma of seabass (*Dicentrarchus labrax*) anaesthetized with 2-phenoxyethanol. J. Chromatogr. B, **1997**, *698*, 251–259.
21. Touraki, M.; Ladoukakis, M.; Prokopiou, C. High performance liquid chromatographic determination of oxolinic acid and flumequine in the live fish feed *Artemia*. J. Chromatogr. B, **2001**, *751*, 247–256.

Packed Capillary LC

Fernando M. Lanças
Institute of Chemistry of São Carlos (USP), University of São Paulo, São Carlos, Brazil

INTRODUCTION

Liquid chromatography (LC) was the first chromatographic mode to be developed in the beginning of the twentieth century. For almost 70 years, it was employed without major modifications until the end of the 1960s when an instrumental version of LC was finally produced. Before this milestone, LC was performed mainly in large-bore glass tubing packed with large-diameter solid particles. To differentiate the instrumental version developed in the late 1960s from the non-instrumental, usually referred as the "classical" version, the former was named high pressure liquid chromatography and, later, high-performance liquid chromatography (HPLC). Because HPLC used smaller particles as the stationary phase, the columns had to be packed at higher pressures in order to obtain a more stable bed required by the higher pressures used in these techniques. Altogether, HPLC offered a much higher efficiency (number of plates) than "conventional LC" and, as a consequence, higher resolution (separation power) as well. The standard HPLC columns used in the 1970s consisted of particles of 5–10 μm packed in stainless-steel tubing of 4.0–4.6 mm inner diameter (I.D.) and 15–25 cm long. Typical flow rates under these conditions are ~1–2 ml/min. In a typical quality control laboratory (8 hr a day; 5 days a week, 20 days a month; 12 months a year), more than 100 L of chromatographic solvent are generated in a 1 year period. Most of these solvents are highly toxic to man and the environment, requiring special waste storage, transportation, and final disposal. As a consequence, a miniaturization of the HPLC techniques using less solvent became important immediately after its development.

A major step in the miniaturization of HPLC columns was done early in 1967 by Horváth and coworkers,[1,2] when investigating the parameters that influence the separation of nucleotides in a 1 mm I.D. column. These columns were then named microbore columns. A further step in the miniaturization process was done in 1973, by Ishii and coworkers, by separating polynuclear aromatic hydrocarbons (PAHs) in a 0.5 mm I.D. polytetrafluoroethylene (PTFE) column. The term micro-LC was then introduced to differentiate this technique from HPLC, which uses larger-bore columns.[3–5] Shortly after, Scott and Kucera published several articles dealing with microbore (1 mm I.D. columns) LC.[6,7] In spite of the fast development in its early days (late 1960s and early 1970s), the miniaturization of HPLC followed a slow progress until recently, with the development of LC/mass spectrometry (MS) using electrospray-type interfaces.

CAPILLARY LC

Capillary liquid chromatography (CLC) is a mode of HPLC that deals with columns having internal diameters equal to, or smaller than, 0.5 mm. This number is limited by the internal diameter of the fused-silica tubing commercially available, which is the most popular tubing used in this area. The CLC columns are usually 15–60 cm long, having internal diameters <0.5 mm and being either coated or packed with the stationary phase. Due to the small inner diameter of the CLC columns, this technique is more demanding in instrumentation than HPLC, particularly with respect to the solvent delivery, sample introduction, and detection systems.

Sample Introduction

Because the column inner diameter is small, the amount of stationary phase is also very small and, as a consequence, the amount of sample that can be introduced into the column without overloading is very small (typically a few nanoliters). In most cases, the preferred sample introduction system consists of an injection valve containing an internal loop smaller than 0.1 ml.

Pumping System

Because the eluent flow rate is relatively small (typically a few microliters per minute), the pump used to deliver it to the column is critical. There are two major approaches being used: pumps capable of delivering flow rates in the range of few microliters per minute (usually syringe-type pumps) or reciprocating pumps using a flow splitter. In both cases, reproducible flow rates are hard to obtain using commercially available pumps.

Detectors

Almost all detectors currently used in HPLC have been evaluated to be used in CLC. The major modification required, in most cases, is a decrease in the detector cell volume in order to accommodate the small sample volume without considerable peak broadening. Ultraviolet–visible

(UV–Vis), fluorescence, electrochemical, mass spectrometric, and several other detectors have been successfully used with CLC.

Columns

Capillary LC columns can be generally made in two different ways: wall-coated open tubular (WCOT) or packed columns. Coating the internal wall of the tubing (usually fused silica) with a thin film of a solvent-resistant polymer makes WCOT columns and is the same technology as used for capillary gas chromatography (GC) columns. Usually, cross-linked or immobilized phases are preferred in order to avoid stationary-phase removal by the eluent. The major drawback of these columns is that they have to be made with an internal diameter smaller than 20 mm in order to be highly efficient for complex separations, thus justifying their use instead of the packed capillary columns.[8] This places great demands on the instrumentation, the eluent quality, the sample preparation step, and so forth, thus making it impractical at this moment. As an alternative, the packed capillary columns using the technology already available to prepare HPLC columns is less instrument demanding and have been gaining more acceptance, every day becoming the preferred form of CLC.

ADVANTAGES OF CAPILLARY LC

The advantages of CLC are consequences of its miniaturization.[9] Due to its miniaturized size, it requires much less stationary phase than does ordinary HPLC and, as a consequence, more expensive phases can be used to prepare the columns. This includes chiral phases, experimental new materials, expensive biocompounds, and so forth. In the same way, the amount of mobile phase is very small, thus leading to a savings in buying, storing, and discarding the solvent, allowing the use of expensive eluents such as deuterated solvents and chiral modifiers such as cyclodextrins, transition metals, and so forth. In many cases, the total amount of mobile phase in one separation is just 10 ml (1 μml/min; 10 min run); this explains why this technique is sometimes referred to as "one-drop chromatography." The amount of sample injected is also very small, so it becomes an important technique when the sample size is critical, such as in biomedical studies (brain, spine liquid, newborn tests, etc.), forensic chemistry (fire debris, explosives, blood residues), environmental analysis, and several other application fields.

Other advantages of CLC, when compared to HPLC, includes its higher permeability,[10] chemical inertia, easier coupling to other separation and identification systems such as MS, GC, and nuclear magnetic resonance, and the possibility of making longer columns, thus achieving more plates (efficiency) and resolution.

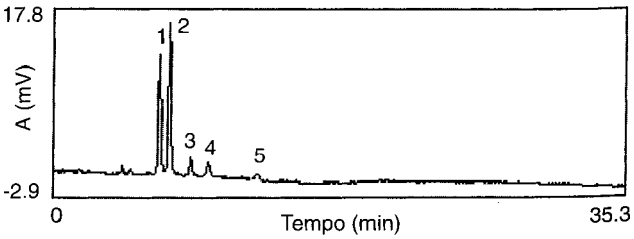

Fig. 1 Capillary LC chromatogram of a river water solidphase extract containing PAHs. Column: fused silica (20 cm × 0.25 mm) H2O home-packed with RP-18 (5 mm). Mobile phase: ACN/H2O (75 : 25), flow rate 4 ml/min, UVdetection at 254 nm. Compound identity: 1 = fenanthrene, 2 = anthracene, 3 = fluoranthene, 4 = pyrene, 5 = crysene.

Fig. 1 shows a chromatogram of a separation of PAHs using a packed capillary column. As can be verified, a good separation is obtained with minute amounts of stationary phase, mobile phase, and sample.

LIMITATIONS OF CAPILLARY LC

In spite of the several advantages over HPLC, CLC has not yet achieved its maturity as a separation technique to be used worldwide, particularly as a routine technique for quality control laboratories. Among the limitations still hindering the further development of CLC, one of the most critical ones is the very limited availability of commercial equipment dedicated to this technique. Even so, most systems are simple adaptations of parts already used for HPLC, by just decreasing their sizes and volumes without specifically having CLC in consideration. Therefore, in order to become a routine technique as its counterpart in GC, capillary LC still has to have a broader interest for the instrument manufacturing companies in the technique before it will spread out beyond the academic environment. Those who have worked with packed columns in GC in the 1960s have already seen this same history.

ACKNOWLEDGMENTS

Professor F. Lanças wishes to thank FAPESP (Fundação de Apoio à Pesquisa do Estado de São Paulo) and CNPq (Conselho Nacional de Desenvolvimento Científico e Tecnológico) for financial support to his laboratory.

REFERENCES

1. Horváth, C.G.; Preiss, B.A.; Lipsky, S.R. Fast liquid chromatography. Investigation of operating parameters and the separation of nucleotides on pellicular ion exchangers. Anal. Chem. **1967**, *39*, 1422.

2. Horváth, C.G.; Lipsky, S.R. Rapid analysis of ribonucleosides and bases at the picomole level using pellicular cation exchange resin in narrow bore columns. Anal. Chem. **1969**, *41* (10), 1227–1234.
3. Ishii, D.; Sakurai, K. 73 Abstract 1B05 Tokyo, Conference of Applied Spectrometry; 1973.
4. Ishii, D.; Asai, K.; Hibi, K.; Jonokuchi, T.; Nagaya, M. A study of micro-high-performance liquid chromatography: I. Development of technique for miniaturization of high-performance liquid chromatography. J. Chromatogr. **1977**, *144*, 157.
5. Ishii, D.; Asai, K.; Jonokuchi, T. Studies of micro high-performance liquid chromatography: II. Application to gel permeation chromatography of techniques developed for micro high-performance liquid chromatography. J. Chromatogr. **1978**, *151*, 147.
6. Scott, R.P.W.; Kucera, P. The exclusion properties of some commercially available silica gels. J. Chromatogr. **1976**, *125*, 251.
7. Scott, R.P.W.; Kucera, P. Mode of operation and performance characteristics of microbore columns for use in liquid chromatography. J. Chromatogr. **1979**, *169*, 51.
8. Menet, H.; Gareil, P.; Rosset, R. Dead-volume free termination for packed columns in microcapillary liquid chromatography. Anal. Chem. **1984**, *56*, 2990.
9. Verzele, M.; Dewaele, C. Liquid chromatography in packed fused silica capillaries or micro-LC: A repeat of the capillary gas chromatography story? J. High Resolut. Chromatogr. **1987**, *10* (5), 280–287.
10. Shelly, D.; Gluckman, J.; Novotny, M. Dead-volume free termination for packed columns in microcapillary liquid chromatography. Anal. Chem. **1984**, *56* (14), 2990–2992.

Particle Separation: Acoustic FFF

Niem Tri
Ronald Beckett
Water Studies Centre, Monash University, Melbourne, Victoria, Australia

INTRODUCTION

Field-flow fractionation (FFF) is a suite of elution methods suitable for the separation and sizing of macromolecules and particles.[1] It relies on the combined effects of an applied force interacting with sample components and the parabolic velocity profile of carrier fluid in the channel. For this to be effective, the channel is unpacked and the flow must be under laminar conditions. Field or gradients that are commonly used in generating the applied force are gravity, centrifugation, fluid flow, temperature gradient, and electrical and magnetic fields. Each field or gradient produces a different subtechnique of FFF, which separates samples on the basis of a particular property of the molecules or particles.

RESEARCH AND DEVELOPMENTS

The potential for using acoustic radiation forces generated by ultrasonic waves to extend the versatility of FFF seems very promising. Although only very preliminary experiments have been performed so far, the possibility of using such a gentle force would appear to have huge potential in biology, medicine, and environmental studies.

Acoustic radiation or ultrasonic waves are currently being exploited as a non-contact particle micromanipulation technique.[2] The main drive to develop such techniques comes from the desire to manipulate biological cells and blood constituents in biotechnology and fine powders in material engineering.

In a propagating wave, the acoustic force, F_{ac}, acting on a particle is a function of size given by[1]

$$F_{ac} = \pi r^2 E Y_p \tag{1}$$

where r is the particle radius, E is the sound energy density, and Y_p is a complicated function depending on the characteristics of the particle which approaches unity if the wavelength used is much smaller than the particle. Particles in a solution subjected to a propagating sound wave will be pushed in the direction of sound propagation. Therefore, sized-based separations may be possible if this force is applied to generate selective transport of different components in a mixture. In a FFF channel, it is likely that the receiving wall will reflect at least some of the emitted wave. If the channel thickness corresponds exactly to one-half wavelength, then a single standing wave will be created (see Fig. 1). For a single standing wave, it is interesting to note that three pressure (force) nodes are generated, one at each wall and one in the center of the channel.

Yasuda and Kamakura[3] and Mandralis and coworkers[4] have demonstrated that it is possible to generate standing-wave fields between a transducer and a reflecting wall, although of much larger dimensions (1–20 cm) than across a FFF channel. Sound travels at a velocity of 1500 m/sec through water, which translates to a wave of frequency of approximately 6 MHz for a 120 μm thick FFF channel.

The force experienced by a particle in a stationary acoustic wave was reported by Yosioka and Kawasima[5] to be

$$F_{ac} = 4\pi r^3 \kappa E_{ac} A \sin(2\kappa x) \tag{2}$$

where r is the particle radius, κ is the wave number, E_{ac} is the time-averaged acoustic energy density, and A is the acoustic contrast factor given by

$$A = \frac{1}{3}\left(\frac{5\rho_p - 2\rho_l}{\rho_l + 2\rho_p} - \frac{\gamma_p}{\gamma_l}\right) \tag{3}$$

where ρ_p and γ_p are the particle density and compressibility, respectively, and ρ_l and γ_l are the liquid density and compressibility, respectively. Thus, in a propagating wave, the force on a particle has a second-order dependence, and in a standing wave, the force is third order. This should give rise to increased selectivity for separations being carried out in a standing wave.[6]

Due to the nature of the acoustic fields, the distribution of the particles will depend on the particle size and the compressibility and density of the particle relative to the fluid medium. Closer examination of the acoustic contrast factor shows that is may be negative (usually applicable to biological cells which are more compressible and less dense relative to the surrounding medium) or positive (as is in many inorganic and polymer colloids). Therefore, acoustic FFF (AcFFF) has tremendous potential in very clean separations of cells from other particles. One

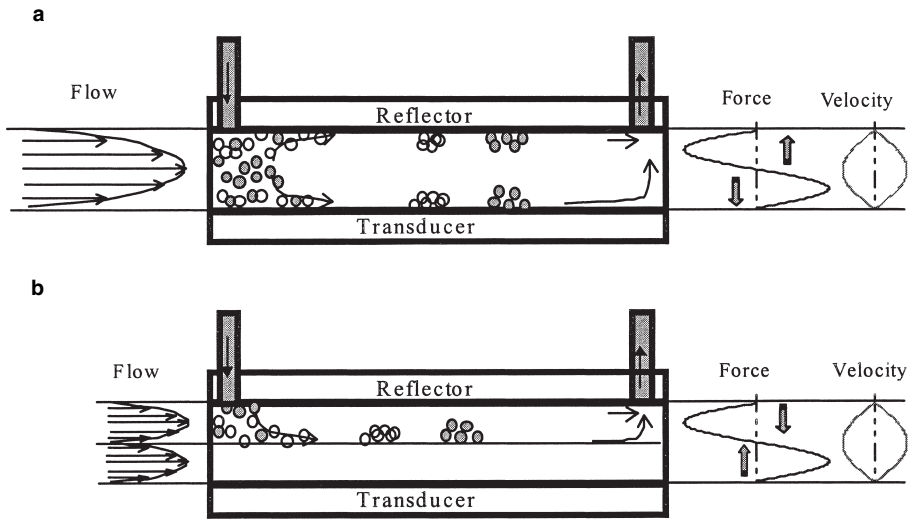

Fig. 1 Acoustic FFF channels suitable for particles with (a) A , 0 and (b) A . 0, utilizing a divided acoustic FFF channel.

important application may be for the separation of bacterial and algal cells in soils and sediments.

If the acoustic contrast factor A , 0, then a conventional FFF channel will enable normal and steric mode FFF separations to be carried out (Fig. 1a).

However, if A . 0, then the particles will migrate toward the center of the channel. In this case, a divided FFF cell could be used as shown in Fig. 1b. This ensures that particles are driven to an accumulation wall rather than the center of the channel where the velocity profile is quite flat and selectivity would be minimal.

Johnson and Feke[7] effectively demonstrated that latex spheres migrate to the nodes (center of the cell) and Hawkes and coworkers[8] showed that yeast cells migrate to the antinodes (walls of the cell). These authors used a method similar to split-flow thin-cell (SPLITT), which is another technique closely related to FFF, also originally developed by Giddings.[9] Semyonov and Maslow[10] demonstrated that acoustic fields in a FFF channel affected the retention time of a sphere of 3.8 μm diameter when subjected to varying acoustic fields. However, the high resolution inherent in FFF has not yet been exploited.

Naturally, with some design modifications to the FFF channel, SPLITT cells could be used for sample concentration or fluid clarification.

REFERENCES

1. Giddings, J.C. Nonequilibrium theory of field-flow fractionation. J. Chem. Phys. **1968**, *49*, 81.
2. Kozuka, T.; Tuziuti, T.; Mitome, H.; Fukuda, T. Noncontact micromanipulation using an ultrasonic standing wave field. Proc. IEEE **1996**, 435–440.
3. Yasuda, K.; Kamakura, T. Acoustic radiation force on micrometer-size particles. Appl. Phys. Lett. **1997**, *71* (13), 1771.
4. Mandralis, Z.; Bolek, W.; Burger, W.; Benes, E.; Feke, D.L. Enhanced synchronized ultrasonic and flow-field fractionation of suspensions. Ultrasonics **1994**, *32* (2), 113–122.
5. Yosioka, K.; Kawasima, Y. Particle separation with ultrasound radiation force. Acustica **1955**, 5, 167.
6. Berthod, A.; Armstrong, D.W. Theoretical study on the use of secondary equilibria for the separation of small solutes by field flow fractionation. Anal. Chem. **1987**, *59* (19), 2410–2413.
7. Johnson, D.A.; Feke, D.L. Separ. Technol. **1995**, 5, 251.
8. Hawkes, J.J.; Barrow, D.; Coakley, W.T. Microparticle manipulation in millimetre scale ultrasonic standing-wave at megahertz frequencies. Ultrasonics **1998**, 36 (9), 925–931.
9. Giddings, J.C. Optimized field-flow fractionation system based on dual stream splitters. Anal. Chem. **1985**, *57* (4), 945–947.
10. Semyonov, S.N.; Maslow, K.I. Acoustic field-flow fractionation. J. Chromatogr. **1998**, *446*, 151–156.

Particle Size: Gravitational FFF Determination

Pierluigi Reschiglian
Department of Chemistry "G. Ciamician", University of Bologna, Bologna, Italy

INTRODUCTION

Particle size distribution analysis was considered, in one of the latest Pittsburgh Conferences, as one of the most outstanding trends in analytical science. This is not an overstatement, as most of the real samples of analytical interest occur either in dispersed form or in dispersed matrices. Just for argument's sake, in industrial applications the characterization of the size of sample particles is routine and is an essential part of the overall quality control procedures. In the medical field, for particles used to carrier drugs, the size is a critical performance factor (e.g., liposomes). In the food industry, the alcoholic yield from fermentation of starch, and even the taste of chocolate, depends on the size of particles of which these samples are composed.

BACKGROUND

Before discussing our method for determining particle size, it is necessary to briefly review the definition of size distribution. If all particles of a given system were spherical in shape, the only size parameter would be the diameter. In most real cases of irregular particles, however, the size is usually expressed in terms of a sphere *equivalent* to the particle with regard to some property. Particles of a dispersed system are never of either perfectly identical size or shape: A spread around the mean (*distribution*) is found. Such a spread is often described in terms of standard deviation. However, a frequency function, or its integrated (cumulative) distribution function, more properly defines not only the spread but also the shape of such a spread around the mean value. This is commonly referred to as the *particle size distribution* (PSD) profile of the dispersed sample.

An examination of technical literature and trade publications indicates that a wide variety of instruments are commercially available for PSD analysis.[1] The classical methods are based on either electrical properties (e.g., the Coulter Counter® principle) or optical properties (e.g., laser scattering) of the analyte. However, none of these techniques are separation methods. Because particulate dispersions are often highly complex in terms of the polydispersity index, multimodal size distribution, and density, it is hardly possible, without the use of separative methods, to obtain an accurate determination of their size distribution. Among separative chromatography-like methods, one can consider hydrodynamic chromatography and field-flow fractionation (FFF). The application to PSD of a subset of the latter family of methods is the topic of this entry.

PSD by FFF

Field-flow fractionation is a broad family of liquid chromatographic-like techniques which have been shown, over more than 20 years, to be able to fractionate and characterize high-molecular-weight species in a size range spanning five orders of magnitude, from macromolecules to micron-size particles.[2] FFF has been demonstrated to be a rapid method for the determination of the mean diameters and polydispersities of particulate samples. When compared to standard methods for PSD analysis, the main advantage of FFF lies in the fact that FFF is a separation method which has some common features with liquid chromatography. The output from an FFF experiment is a function of the detector signal vs. the retention time of the analyte. Whereas, in liquid chromatography, such an analytical response is referred to as the *chromatogram*, in FFF it is commonly defined as the *fractogram*. However, when it is compared to classical liquid chromatography, the existence of a direct relationship between retention and some physical properties of the analyte, such as the size, is a fundamental feature of most FFF techniques. The theory of FFF retention has been fully explained elsewhere,[2] and references therein] as well as in other entries of this encyclopedia. What is important to focus on here is that, in FFF, particle size determination of the analyte can be obtained by means of a direct numerical conversion of the retention scale, whereas the relative amount of separated analyte is, as in the case of chromatograms, in some way proportional to the signal intensity. The basic procedures for the two conversions is the topic of this entry.

Gravitational FFF: An Economical Device for PSD Analysis of Micron-Size Dispersions

Here, we treat the case of PSD analysis of particulate systems of micron-size range (i.e., with a size distribution extending above 1 μm). Since 1994, in our laboratories, this topic has been dealt with by means of a low-costsubset of sedimentation FFF (SdFFF), the gravitational field-flow fractionation (GrFFF) technique.[3] GrFFF had already

been applied to the fractionation of a variety of micron-size dispersion, either inorganic as commercial chromatographic supports[4] or biological, as cells and parasites.[5] In no cases, however, had PSD been performed through GrFFF. As an SdFFF subset, GrFFF requires the application of a sedimentation field that, in this case, is simply Earth's gravity applied perpendicularly to a very thin, empty channel with a rectangular cross section. The big advantage of GrFFF, compared to other techniques for the characterization of particulate matter, lies in its very low cost (~$50 for a homemade channel) and easy implementation in a standard high-pressure liquid chromatography (HPLC) system (the channel can simply replace the standard HPLC column). The GrFFF channel employed here can be easily built as described elsewhere.[3–9] It is basically a ribbonlike capillary channel which consists of two mirror-polished plates, of either glass or plastic material (e.g., polycarbonate) which are clamped together over a thin sheet of either Teflon or Mylar from which the channel volume has been removed. Simplicity and economy of use make it possible for laboratories that are not specialized in PSD analysis to perform dimensional characterization of supermicron particles dispersions with limited effort and cost.

We shall show here that GrFFF is capable of performing reliable, quantitative PSD analysis of particulate matter. Some basics of the overall procedure will be overviewed and the relevant questions presented. In fact, in order to obtain a PSD by means of GrFFF, the conversion of the retention time axis into the analyte size axis is necessary. For the same reason, the detector signal axis must be converted into mass (or concentration) of the fractionated analyte.

PROCEDURE AND DISCUSSION

From a GrFFF Fractogram to a PSD

The diameter scale can be obtained from retention coordinates (i.e., the retention time axis) by applying to the fractogram the well-known, approximate expression that is valid for highly retained samples in GrFFF:[3]

$$d_i = \frac{wV_0}{3\gamma}\frac{1}{V_{r,i}} \tag{1}$$

where d_i (cm) is the diameter value corresponding to the ith data point of the fractogram, the retention volume of which is $V_{r,i}$ (cm^3). V_0 (cm^3) is the void volume of the GrFFF channel, w (cm) is the channel thickness and γ is the so-called hydrodynamic correction factor, the knowledge of which is, therefore, required for PSD analysis.

In practice, PSD curves can be obtained directly from the experimental, digitized peak (fractogram), $y_i(V_{r,i})$ once it is converted to a function of particle diameter with the use of Eq. 1. The frequency function of particle size is expressed as[3]

$$f_{m,i} = \frac{\delta m_i}{\delta d_i} = \frac{\delta m_i}{\delta V_{r,i}}\frac{\delta V_{r,i}}{\delta d_i} \tag{2}$$

where $\delta m_i / \delta V_{r,i}$ (g/cm^3) is the mass concentration of the analyte at the ith digitized point and $\delta V_{r,i}$ and δd_i are the differences in retention volume and particle diameter between the ith and the $(i-1)$th digitized points, respectively. The incremental quantity δd_i can be calculated for any given $\delta V_{r,i}$ by Eq. 1.

As far as the conversion of the analytical response y_i is concerned, the most used detectors in GrFFF have been, until now, conventional ultraviolet (UV) detectors commonly used for HPLC. With this type of detector, the amount of particles with diameter d_i is proportional to the detector response at the ith point. With particulate samples, in fact, because of UV detector optics, the response is a *turbidity* signal read within an angle between the incident light and the photosensor (i.e., usually smaller than ~10°) rather than the *absorbance*. This turbidity signal can be assumed to be directly proportional to the sum of all cross-sectional areas of the particulate sample components at any time. The validity of the above assumption, in the case of particles which are about 10-fold larger than the incident wavelength, is discussed elsewhere.[6] The mass frequency function can thus be expressed as[7]

$$f_{m,i} \propto (\text{UV signal})_i(d_i)\frac{\delta V_{r,i}}{\delta d_i} \tag{3}$$

For the reader's convenience, a scheme of the required conversion is represented in Fig. 1. It is evident that it is rather straightforward to derive a PSD from a GrFFF experiment.[3] An example of GrFFF–PSD analysis for a sample of silica particles commonly used as the stationary phase in HPLC (5 μm LiChrospher, Merck) is reported in Fig. 2a. For the sake of comparison, the PSD of the same

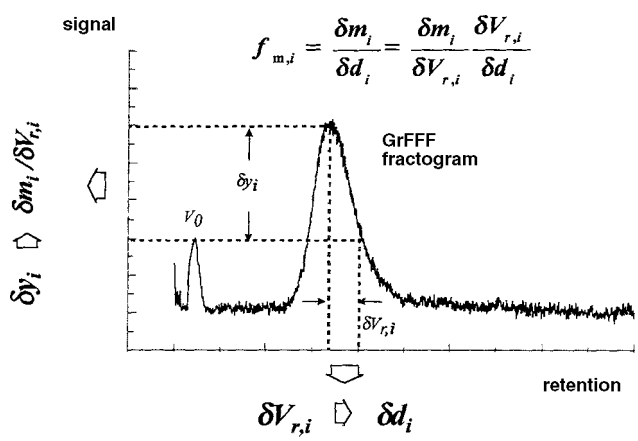

Fig. 1 Scheme for the conversion from a fractogram to a frequency function of particle size.

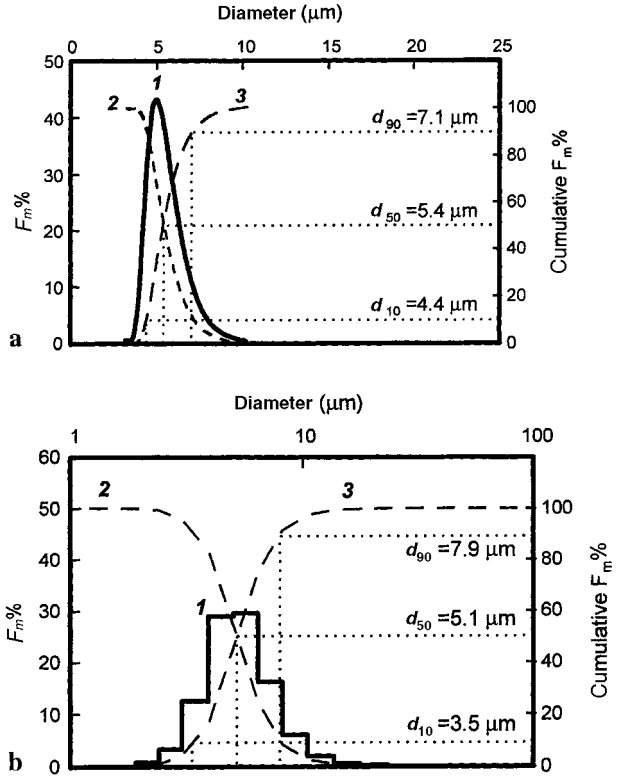

Fig. 2 Comparison between normalized, frequency functions of size (F_m %) of silica particles for HPLC packing (5 μm; Li-Chrospher, Merck, Darmstad); nominal distribution percentiles: $d_{10} = 3.7$ μm, $d_{50} = 5.0$ μm, $d_{90} = 6.8$ μm); curve 1 (full line): F_m %; curve 2 (dashed line): F_{cum} %; curve 3 (dashed line): $100 - F_{cum}$ %. (a) GrFFF/PSD: Sample load: 100 μg; channel: $90 \times 2 \times 0.020$ cm; mobile phase: Milli-Q water/Triton X-100, 0.1% (v/v)/NaN_3 0.02% (w/v); flow rate: 1.010 ± 0.004 cm^3/min; UV detection: 330 nm; experimental $\gamma = 0.70$. (b) Laser diffraction PSD (Malvern MASTERSIZER®, Malvern Instruments Ltd., UK).

sample obtained by laser diffraction is reported in Fig. 2b. We can observe that PSD resolution is higher in GrFFF than in laser diffraction, where just a histogram is obtained. On the other hand, accuracy is comparable when the experimental distribution moments (i.e., the percentiles indicated as d_{10}, d_{50}, d_{90}) are compared to the nominal values given by the manufacturer. We must point out that differences in distribution moment values as high as 10% are commonly reported when different, uncorrelated techniques for PSD studies are compared.[1]

Quantitative Particle Size and Sample Amount Distribution in GrFFF

We have derived an original method by which quantitative particle size and sample amount distribution (PSAD) in GrFFF can be obtained by applying to Eq. 2 a derivation of the Lambert–Beer law in flowthrough systems.[7] If compared to standard PSD, a PSAD thus represents a distribution of the *real* mass of the analyte as a function of size, rather than a functional expression only *proportional* to mass.

For particle dispersions in the micron-size interval, which is the typical application range of GrFFF, it has been demonstrated that the sample amount exiting the detector cell, N_0 (g), can be expressed as

$$\frac{AF}{Kb} = N_0 \tag{4}$$

where A (min) is the peak area, F (cm^3/min) is the flow rate, b (cm) is the cell thickness, and K (cm^2/g) is the total extinction coefficient of the particulate sample. If the extinction coefficient can be assumed to be approximately constant, as in the case of particles whose size is at least 10 times higher than the incident wavelength,[6] the detector reading, expressed as "absorbance" at the ith point is related to the real turbidity signal from the detector (τ_i) by the equation[7]

$$A_i = Kc_i b = \frac{\tau_i}{2.303} b \tag{5}$$

where c_i (g/cm^3) is the analyte concentration at the ith point of the fractogram; that is,

$$c_i = \frac{\delta m_i}{\delta V_{r,i}}$$

Therefore, the turbidity signal can be expressed as

$$\tau_i = 2.303K \frac{\delta m_i}{\delta V_{r,i}} \tag{6}$$

and the PSD expression for the frequency function, which is, in Eq. 3, just proportional to particle mass, can be transformed into a real function in mass directly from Eq. 6, thus giving[7]

$$f_{m,i} = \frac{\delta m_i}{\delta d_i} = \frac{\tau_i}{2.303K} \frac{\delta V_{r,i}}{\delta d_i} \tag{7}$$

Integration of Eq. 7 yields the cumulative distribution which gives, plotted as percent distribution, the size distribution percentiles (d_{10}, d_{50}, d_{90}). Moreover, once it is related to the injected sample amount, it gives the cumulative distribution of analyte mass as a function of size, with its asymptotic value giving the total sample recovery. Some examples of GrFFF/PSAD of silica samples used as HPLC column packing are reported in Ref.[7]

Direct Conversion of Retention to Size; Secondary Effects

As shown earlier, the direct conversion from retention time to particle diameter values (Eq. 1) requires that the correction factor γ is predicted or experimentally estimated. It is known that, in GrFFF, γ can be influenced by either hydrodynamic or other effects as those due to the mobile phase[8] and the channel walls' nature.[9] All of these effects can influence particle size determination by GrFFF.

We have been developing an approach to the evaluation of the second-order effects, which act on GrFFF retention, and to the prediction of the correction factor γ. Among these effects, prominent are those due to hydrodynamic forces which lift the analyte particles away from the accumulation wall during their elution. GrFFF really shows a significant dependence of retention (and, thus, of the parameter γ) on the flow rate: The higher the flow rate, the higher the lift and, therefore, the lower the retention. In order to evaluate particle lift and, thus, particle retention, the semiempirical model given by Williams et al. has been applied.[10–12] This model is known to predict particle elevation from the accumulation wall in sedimentation field-flow fractionation (SdFFF), of which GrFFF it is just a subset, as noted earlier. A description of the hydrodynamic and other secondary effects on GrFFF retention is far above the introductory nature of this entry. However, just to introduce the reader to the possibility of obtaining a direct conversion of retention to size by predicting γ, the above-mentioned model can be used for relating retention volume to particle mean elevation during elution as follows:[10]

$$V_{r,i} = V_0 \left[6f\left(\frac{2\delta}{d_i}\right)\frac{x_i}{w}\left(1-\frac{x_i}{w}\right)\right]^{-1} \tag{8}$$

where x_i (cm) is the distance of the center of the particles from the accumulation wall ($x_i = \delta + d_i/2$) and $f(2\delta/di)$ is an empirical function. It was shown that under optimized experimental conditions, in a properly designed GrFFF system, a balance between secondary effects of forces other than hydrodynamic forces can give negligible effects.[9] In this way, particle elevation is predictable. In this case, also, the value of γ can be estimated, thus allowing for the direct conversion of retention time to analyte size without previous calibrations (*standardless*). This possibility of calculating γ is a task still in progress and it will open more promising uses of GrFFF for dimensional analysis of suspended particulate matter, because PSD can be obtained in the "single-run" mode (i.e., without previous calibration). This could be a significant enhancement in the future evolution of GrFFF/PSD. In fact, in the GrFFF/PSD example in Fig. 2a, the conversion from retention to size was performed only by means of an experimental evaluation of the parameter γ, with a calibration plot formerly obtained with standards.[3]

ACKNOWLEDGMENTS

Giancarlo Torsi, Dora Melucci, Andrea Zattoni, and Gabriele Berardi of the Department of Chemistry "G. Ciamician," Bologna, Italy, are duly acknowledged.

REFERENCES

1. Barth, H.G., Ed.; *Modern Methods of Particle Size Analysis*; John Wiley & Sons: New York, 1984.
2. Giddings, J.C. Field-flow fractionation: Analysis of macromolecular, colloidal and particulate materials. Science **1993**, *260*, 1456.
3. Reschiglian, P.; Torsi, G. Determination of particle size distribution by gravitational field-flow fractionation: Dimensional characterization of silica particles. Chromatographia **1995**, *40*, 467.
4. Pazourek, J.; Chmelík, J. Characterization of chromatographic silica gel support particles by graviational field-flow fractionation. J. Microcol. Separ. **1997**, *9* (8), 611–617.
5. Bernard, A.; Paulet, B.; Colin, V.; Cardot, Ph.J.P. Red blood cell separation by gravitational field-flow-fractionation: Instrumentation and applications. Trends Anal. Chem. **1995**, *14* (6), 266–273.
6. Reschiglian, P.; Melucci, D.; Torsi, G. A quantitative approach to the analysis of particulate matter in field-flow fractionation with UV-Vis. detectors. The application of an absolute method. Chromatographia **1997**, *44*, 172.
7. Reschiglian, P.; Melucci, D.; Zattoni, A.; Torsi, G. Quantitative approach to field-flow fractionation for the characterization of supermicron particles. J. Microcol. Separ. **1997**, *9* (7), 545–556.
8. Reschiglian, P.; Melucci, D.; Torsi, G. Experimental study on the retention of silica particles in gravitational field-flow fractionation effects of the mobile phase composition. J. Chromatogr. A, **1996**, *740*, 245.
9. Melucci, D.; Gianni, G.; Torsi, A.; Zattoni, A.; Reschiglian, P. Experimental analysis of second-order effects on graviational field-flow fractionation retention of silica particles. J. Liq. Chromatogr.. Relat. Technol. **1997**, *20* (16–17), 2615.
10. Williams, P.S.; Koch, T.; Giddings, J.C. Characterization of near-wall hydrodynamic lift forces using sedimentation field-flow fractionation. Chem. Eng. Commun. **1992**, *111*, 121.
11. Williams, P.S.; Lee, S.; Giddings, J.C. Characterization of hydrodynamic lift forces by field-flow fractionation. Inertial and near-wall lift forces. Chem. Eng. Commun. **1994**, *130*, 143.
12. Williams, P.S.; Moon, M.H.; Xu, Y.; Giddings, J.C. Effect of viscosity on tetention time and hydrodynamic lift forces in sedimentation/steric field-flow fractionation. Chem. Eng. Sci. **1996**, *51*, 4477.

Particles and Macromolecules: Focusing FFF

Josef Janca
Department of Chemistry, University of La Rochelle, La Rochelle, France

INTRODUCTION

The original idea of focusing field-flow fractionation (focusing FFF)[1] was introduced in 1982. Giddings[2] proposed the same principle in 1983 under the name hyperlayer FFF. A more detailed methodology of focusing FFF was developed later by the exploitation of various separation mechanisms.[3] The emerging discipline of isoperichoric focusing FFF represents a generalization of the original concept.[4]

The principle of focusing FFF is different from that of the polarization FFF. The crucial difference between the focusing and polarization mechanisms is that the intensity and direction of the driving field force must be dependent on the position across the channel and converging in focusing FFF, whereas it is position independent in polarization FFF. The sample components are focused at different altitudes across the channel and, consequently, eluted at different velocities corresponding to their positions within the flow velocity profile in focusing FFF, as shown in Fig. 1A. Although focusing FFF is as yet in a stage of fundamental investigation, some applications concerning the fractionation of macromolecular and particulate species have been published.

METHODS AND TECHNIQUES

Focusing can take place only if a gradient of the effective forces exists and the magnitude of these converging forces is position dependent and is zero at the focusing point. Various combinations of fields and gradients determining the focusing FFF methods and techniques can be exploited, as demonstrated in the following subsections.

Effective Property Gradient of the Carrier Liquid Combined with a Field Action

The gradient of an effective property of the carrier liquid combined with the action of a field can lead to the focusing of macromolecules or particles. For example, a density gradient combined with a gravitational or centrifugal field leads to focusing of the species at their isopycnic positions, amphoteric species focus at their isoelectric points in a pH gradient combined with an electrical field, and so forth. All these phenomena are known under the general term *isoperichoric focusing*, introduced by Kolin.[5]

Usually, the same primary field forces as those that produce the effective property gradient, are used to generate the focusing. However, the use of secondary field forces of a different nature to generate the focusing phenomenon within the corresponding gradient established by the primary field is possible; for example, isopycnic focusing of large-sized uncharged particles due to a weak gravitational field force was found effective under dynamic focusing FFF conditions, where the density gradient was generated by an electrical field acting on small charged colloidal particles suspended in the carrier liquid.[6] The construction of the fractionation channel is extremely simple, as shown in Fig. 1B. This principle, applied under static or dynamic FFF conditions, is promising for high-performance analytical and micropreparative separations.

Although focusing under static conditions, without the action of perpendicularly (with respect to the focusing axis) applied bulk flow, can lead to good separation of the focused species, theoretical calculations, as well as experimental tests, have shown increase in resolution under the dynamic conditions of focusing FFF.

Cross-Flow Velocity Gradient Combined with a Field Action

The velocity gradient of the carrier liquid across the fractionation channel, generated by transversal flow through semipermeable walls, which opposes the action of an external field, can produce the focusing phenomenon. A longitudinal flow is applied simultaneously. This method is called elutriation focusing FFF and has been used to separate model mixtures of polystyrene latex particles and silica particles in a trapezoidal cross-section channel.[7] The principle of this fractionation channel is shown in Fig. 1c. A similar focusing FFF principle can be utilized in a rectangular cross-section channel with two opposite semipermeable walls if the flow rates through the walls are different.[8]

Lift Forces Combined with a Field Action

The hydrodynamic lift forces appearing at high flow rates of the carrier liquid, combined with field forces, are able to concentrate suspended particles into focused layers. While the field forces in polarization and steric FFF concentrate the retained species at the accumulation wall, the lift

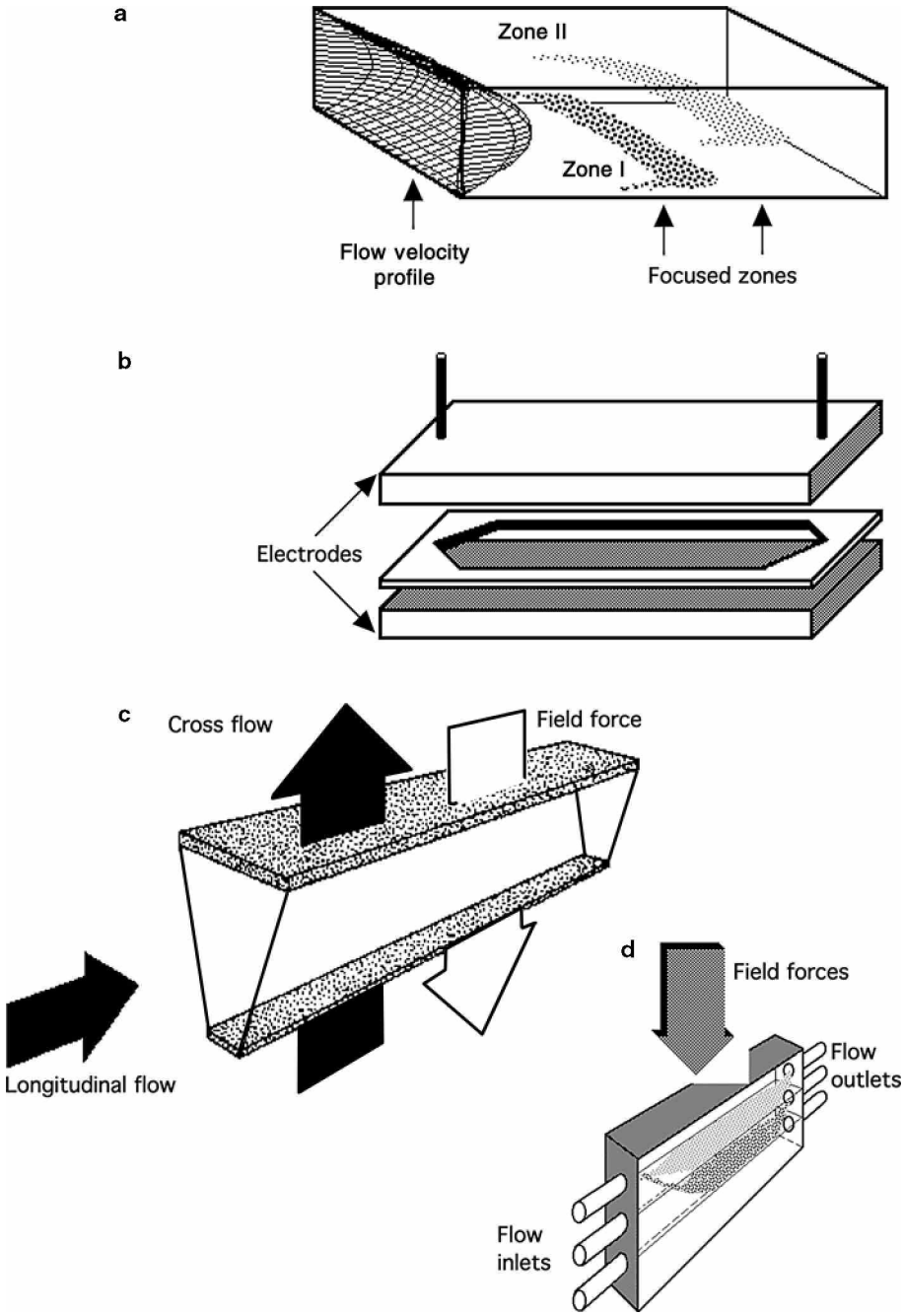

Fig. 1 Principle of focusing field-flow fractionation. a, Section of the channel demonstrating the principle of focusing FFF with two distinct zones focused at different positions and the parabolic flow velocity profile; b, Design of the channel for dynamic focusing FFF in coupled electrical and gravitational fields; c, Schematic representation of the trapezoidal cross-section channel for elutriation focusing FFF; and d, Separation channel for continuous preparative focusing FFF operating in natural gravitational field with three inlet capillaries allowing one to preform the step density gradient by pumping three liquids of different densities and with three outlet capillaries to collect the separated fractions.

forces, becoming operational at high flow rates, pull the particles away from this wall. As a result, the transition from polarization or steric to focusing FFF appears first, followed by the proper focusing effect. In most published works, the appearance of the lift forces generating the focusing effect has been observed in sedimentation and flow FFF. For example, Wahlund and Litzen[9] observed the interference of the lift forces in polarization flow FFF carried out in an asymmetrical channel with one semi-permeable wall. Such interference perturbs the separation. However, in some cases, the lift forces have been exploited under optimized operational conditions and, as a result, high-speed and high-performance separations have been achieved. Two examples of such spectacular separations have been published for sedimentation FFF[10] and very recently for microthermal focusing FFF.[11] Although this focusing FFF method is just beginning to be used in real applications, its main advantages, high speed and high performance, seem to make it very promising.

Shear Stress Combined with a Field Action

A high-shear gradient can lead to the deformation of macromolecular coils. The entropy gradient thus

generated produces the driving forces that displace the macromolecules into a low-shear zone. The reversed elution order of high-molecular-weight polystyrenes in thermal FFF at high flow rates could be attributed to this phenomenon,[12] but another possibility to explain the reversed elution order cannot be neglected.[13]

Gradient of a Non-homogeneous Field Action

The use of a high-gradient magnetic field has been proposed to separate paramagnetic and diamagnetic species by a mechanism of focusing FFF.[14] Various aspects of focusing FFF carried out under these conditions have been discussed, but no experimental results have been published until now.

Preparative Fractionation

No principal difference distinguishes the analytical and preparative uses of focusing FFF. Both types of fractionation can be carried out under conditions of continuous operation,[15] which represents the high-performance experimental arrangement for preparative FFF. The fractionation channel, equipped with several outlet capillaries at various positions (and occasionally with several inlets to preform a stepwise gradient in the direction of the focusing), allows one to fractionate the sample, which is introduced continuously into the channel, and to collect the focused layers eluted at the individual outlets. A schematic representation of such a fractionation channel is shown in Fig. 1.

The experimental implementation of this technique has been demonstrated by the fractionation of various samples of silica particles by applying natural gravitation and a counteracting cross-flow gradient. The silica particles were separated according to size. Isopycnic or isoelectric focusing FFF, already performed on an analytical scale, can easily be transformed into such continuous large-scale separation.

APPLICATIONS

Focusing FFF represents an important contribution to the science and technology of separation and analysis of macromolecules of synthetic or natural origin. The range of molar masses and sizes of particles in submicron and micron ranges, supramolecular structures, organized biological species such as the cells and microorganisms, and so forth that can be fractionated by focusing FFF is very large.

Molecules that do not interact sufficiently with the imposed fields, such as low-molar-mass species, and that, consequently, do not exhibit the focusing effect can still be separated. The condition is that an equilibrium between them and the effectively focused species should be established. As a result, species that originally do not undergo the separation processes can be transported and thus fractionated with the "carrier" focused species.

The most important field of potential applications of focusing FFF is in research and technologies related to the life sciences and macromolecular chemistry. Problems related to trace analysis, which have enormous importance in the protection of the environment and many other scientific and technological activities, have already stimulated the development of new analytical separation methods. Focusing FFF is one of them, representing an alternative choice whenever macromolecular or particulate species are concerned.

The newest achievements in focusing FFF clearly indicate that most of the experimental implementations have been with model systems. Practical applications for daily laboratory use, elaborated to the minutest details, have rarely been described. However, the most significant advantages of these methods, already mentioned earlier, are evident. Some of these advantages are inherently related to the separation principle of focusing FFF, such as the absence of a large surface area inside the separation channel, which is of crucial importance for sensitive biological materials, which can be denatured by contact with active surfaces.

The operational variables, such as the strength of the field, the flow rate, and so forth, can be manipulated continuously in a very wide range. Another advantage is that although specific FFF apparatuses are already in production, the instruments commercially available for liquid chromatography (LC) can easily be adapted for use with focusing FFF methodology. All specific components of the complete focusing FFF apparatuses are identical to those for LC, except the separation channel, which, in most cases, is not difficult to construct in the laboratory. Certainly, focusing FFF represents a large field of challenges, soliciting creativity and inventiveness in theory, methodology, and practical applications.

REFERENCES

1. Janča, J. Sedimentation–flotation focusing field-flow fractionation. Makromol. Chem. Rapid Commun. **1982**, *3*, 887.
2. Giddings, J.C. Hyperlayer field-flow fractionation. Sep. Sci. Technol. **1983**, *18*, 765.
3. Janča, J. *Field-Flow Fractionation: Analysis of Macromolecules and Particles*; Marcel Dekker, Inc.: New York, 1988.
4. Janča, J. Isoperichoric focusing field-flow fractionation for characterization of particles and molecules. J. Liq. Chromatogr. Relat. Technol. **1997**, *20*, 2555.

5. Kolin, A. *Electrofocusing and Isotachophoresis*; Radola, B.J., Graesslin, D., Eds.; de Gruyter: Berlin, 1977.
6. Janča, J.; Audebert, R. New concept in focusing field-flow fractionation and thin layer isopycnic focusing: coupling of primary electric field with secondary gravitational force. Mikrochim. Acta **1993**, *111*, 163.
7. Urbankova, E.; Janča, J. An attempt at experimental elutriation focusing field-flow fractionation. J. Liq. Chromatogr. **1990**, *13*, 1877.
8. Janča, J. Elutriation focusing field-flow fractionation. Makromol. Chem. Rapid Commun. **1987**, *8*, 233.
9. Wahlund, K.G.; Litzen, A. Application of an asymmetric flow field-flow fractionation channel to the separation and characterization of proteins, plasmids, plasmid fragments, polysaccharides, and unicellular algae. J. Chromatogr. **1989**, *461*, 73.
10. Koch, T.; Giddings, J.C. High speed separation of large (> 1 μm) particles by steric field-flow fractionation. Anal. Chem. **1986**, *58*, 994.
11. Janča, J.; Ananieva, I.A.; Menshikova, A.Yu.; Evseeva, T.G. Micro-thermal focusing field-flow fractionation. J. Chromatogr. B, **2004**, *800*, 33.
12. Giddings, J.C.; Li, S.; Williams, P.S.; Schimpf, M.E. High-speed separation of ultra-high molecular weight polymers by thermal/hyperlayer field-flow fractionation. Makromol. Chem. Rapid Commun. **1988**, *9*, 817.
13. Janča, J.; Martin, M. Influence of operational parameters on retention of ultra-high molecular weight polystyrenes in thermal field-flow fractionation. Chromatographia **1992**, *34*, 125.
14. Semyonov, S.N.; Kuznetsov, A.A.; Zolotaryov, P.P. Theoretical examination of focusing field-flow fractionation. J. Chromatogr. **1986**, *364*, 389.
15. Janča, J.; Chmelik, J. Focusing in field-flow fractionation. Anal. Chem. **1984**, *56*, 2481.

PCR Products: CE Analysis

Mark P. Richards
Livestock and Poultry Sciences Institute (LPSI), Agricultural Research Service, U.S. Department of Agriculture (USDA-ARS), Beltsville, Maryland, U.S.A.

INTRODUCTION

It is now possible to routinely analyze very small amounts of DNA using a procedure known as the polymerase chain reaction (PCR).[1] PCR involves repeatedly subjecting a buffered salt solution containing deoxyribonucleotide triphosphates (dNTPs), two strand-specific oligonucleotide primers, a thermalstable DNA polymerase enzyme (Taq), and a small amount of the DNA to be analyzed to a three-step temperature cycle. Using PCR, discrete regions of the source DNA molecules are copied and amplified by the repetitive cycling to readily detectable levels. It is also possible to analyze RNA sequences with PCR after an initial DNA strand (cDNA) and one complementary to it are produced from the original RNA template by the reverse transcription (RT) reaction.[2] The combined process, RT–PCR (also referred to as RNA–PCR), has been effectively used to study small amounts of RNA, such as individual messenger RNAs (mRNAs) or viral RNA, present in tissues and physiological fluids. Both PCR and RT–PCR produce double-stranded DNA (dsDNA) fragments of various sizes which are subsequently isolated and characterized by a number of qualitative and quantitative methodologies.

DISCUSSION

The most common method of analyzing PCR and RT–PCR products involves separating a portion of the reaction mixture by agarose slab gel electrophoresis with ethidium bromide staining to detect the presence of the amplified dsDNA fragments.[3] There are several disadvantages associated with slab-gel techniques, including the following:

1. Gel casting and handling are costly, labor intensive, and not readily automated.
2. A significant portion of the PCR or RT–PCR sample is typically consumed by this mode of analysis.
3. Buffer and reagent consumption, and hazardous waste generated from the use of radioactive probes and ethidium bromide stain, can be considerable.
4. Quantitation requires additional steps and instrumentation for gel imaging and analysis.

During the past decade, capillary electrophoresis (CE)-based techniques have been developed and refined for the analysis of dsDNA products of PCR and RT–PCR.[4–7] CE has several advantages over conventional slab-gel separation techniques, including the following:

1. Capillary electrophoresis instrumentation is fully automated with respect to sample injection, separation, on-capillary detection, and postrun data analysis.
2. Because the separation is conducted in a narrow-bore capillary that facilitates Joule heat dissipation, higher field strengths can be used, resulting in enhanced resolution and shorter run times.
3. Very small amounts (nl) of sample are required for the analysis, thus preserving more of the original sample for subsequent procedures, such as cloning or sequencing.

Considering the expanding base of CE applications, it is becoming clear that the majority, if not all, of conventional slab-gel separation techniques can be readily adapted to capillary format. Analysis of PCR products by CE is becoming more routine and it will likely become one of the primary applications of CE in the area of DNA separations.[6] This entry describes the use of CE-based techniques for the analysis of dsDNA products from PCR and RT–PCR.

Table 1 summarizes selected parameters that are important for establishing a robust and reproducible technique for the separation and quantification of dsDNA products of PCR and RT–PCR using CE. Important advances have been made in a number of areas, including capillary coatings, sieving gel matrices, and high-sensitivity detection methods. Because of a

Table 1 Analysis of PCR products by CE: selected technique parameters.

Capillaries
Untreated (bare-fused silica): not frequently used
Coated: polyacrylamide, polysiloxane (e.g., DB-1, DB-17), polyvinyl alcohol
Separation matrix
Buffer: 89–100 m*M* Tris-boric acid, 2 m*M* EDTA, pH 8.2–8.5 (1X TBE)
Sieving gel
Chemical (fixed) gels: cross-linked polyacrylamide, bonded to capillary wall
Replaceable Gels (entangled polymer networks): linear polyacrylamide, methyl cellulose, hydroxypropylmethyl cellulose, hydroxyethylcellulose, polyethylene oxide, polyvinyl alcohol, agarose
Intercalating dyes: 9-aminoacridine (non-fluorescent), ethidium bromide, TOTO, YOYO, YO-PRO-1, TO-PRO-1, TO-PRO-3, SYBR Green I, EnhanCE™
Sample injection
Hydrodynamic: high reproducibility; useful for quantitative analyses; direct injection of untreated samples possible
Electrokinetic: affected by sample salt concentration (i.e., prior dialysis or dilution of the sample required)
Detectors
Ultraviolet (UV): 254–260 nm, least sensitive
Laser-induced fluorescence (LIF): up to 1000 × more sensitive than ultraviolet
Data analysis
Qualitative: optimization of PCR conditions and product characterization
Quantitative:
Relative: ratio of product (target) to "housekeeping" gene or other heterologous dsDNA internal standard
Competitive: ratio of product (target) to homologous, modified internal standard (competitor); most accurate estimate
Applications
Clinical/diagnostic: screening for genetic abnormalities and diseases
Forensic: human identity testing
Biotechnology: genetic analysis, gene expression, genotyping

nearly identical linear negative charge density at neutral pH and above, dsDNA molecules exhibit an electrophoretic mobility in free solution that is independent of molecular size.[3] Therefore, a gel or sieving matrix is required to effect a separation based on molecular size and, for that reason, capillary gel electrophoresis (CGE) has become the specific separation mode most often used for PCR product analysis. Because of the negative charge on DNA molecules, uncoated (bare fused silica) capillaries, which above pH 7 exhibit a strong electro-osmotic flow (EOF) in the direction of the cathode, are rarely if ever used. Instead, capillaries treated with a specific interior surface coating to greatly reduce or completely eliminate EOF are routinely employed in the separation of DNA, a process that is conducted in reversed polarity mode (i.e., cathode at the capillary inlet side). Capillary surface coatings can either be covalently bound to the surface or dynamically adsorbed to the wall. Examples of typical surface coatings include polyacrylamide, polysiloxanes (dimethyl and phenyl–methyl), cellulose derivatives, and polyvinyl alcohol.[4–7]

Early CGE separations of dsDNA made use of capillaries in which a polyacrylamide gel was polymerized in and linked to the wall of the capillary, producing what has been referred to as a fixed or chemical gel.[4–7] Although such gels are capable of extremely high resolution due to a well-controlled pore size, they are not commonly used for PCR product analysis because of the problems related to air bubble formation and limited useful lifetime.[5] The development of replaceable sieving gels (also referred to as entangled polymer networks) that can be flushed from the capillary after the separation is complete has been one of the major factors in establishing CGE as a routine method for PCR product analysis. With this system of replaceable gels, a "new" gel is used for each separation. Some of the most widely used replaceable gel compounds include linear polyacrylamide, alkylcelluloses, polyethylene oxide, agarose, and polyvinyl alcohol.[4–7] These polymer compounds are employed to produce viscous buffered solutions that enable the separation of dsDNA in a capillary based on molecular size.[5] In general, the pore size and, hence, the resolving capacity for dsDNA molecules are controlled by simply manipulating the gel concentration.

One factor that initially hampered the direct analysis of PCR samples by CGE was the presence of high levels of salt, especially chloride ions, in the samples injected into the capillary. Electrokinetic injection, which is the requisite loading method when using fixed gels, is severely affected by the presence of high salt concentration because it impairs the loading of dsDNA into the capillary. Although PCR samples can be injected directly into capillaries using replaceable gels, the presence of salts adversely affects the quality of the results obtained. Also, the presence of other components in the PCR sample (dNTPs, primer oligonucleotides, etc.) not only affect the separation, but they can also obscure peaks when ultraviolet (UV) detection is employed. Fortunately, two relatively simple cleanup methods have been devised to counteract the effects of the PCR sample matrix. The two most common methods are sample microdialysis (float dialysis) and dilution of the sample (20–100-fold) with deionized water prior to CGE.[6] Both methods are effective in reducing the adverse effects of salts, but sample dilution necessitates the use of high-sensitivity detection to compensate for the reduction in the dsDNA concentration.

An important development in CE technology that has helped to promote the analysis of PCR products by CGE is the introduction of laser-induced fluorescence (LIF) detection.[4–7] Because LIF can increase the sensitivity of detection for dsDNA by more than 400-fold over UV detection, it has become the method of choice for the vast majority of dsDNA separations.[5] A practical illustration of the advantage of LIF detection is that typical separations of PCR products by slab-gel electrophoresis with ethidium bromide staining require approximately 5 ng of DNA per band for adequate detection, whereas, with CGE–LIF, subpicogram levels of DNA are readily detected.[6]

In order to employ LIF detection, it is necessary to label the dsDNA molecules with a fluorescent compound prior to and/or during their separation by CGE. Two approaches have been employed. The first, and most common, involves the incorporation of an intercalating dye into the separation gel buffer (and, in some cases, into the sample loading buffer), which is highly fluorescent only when bound to dsDNA. Table 1 lists a number of commonly used intercalating dyes. Both monomeric and dimeric dyes have been developed and used to detect PCR products.[8] They offer unique advantages in that they enhance detection sensitivity two to three orders of magnitude over UV detection, and separation resolution and selectivity are often improved with their inclusion.[4] A second approach involves labeling of the primers used in PCR with a fluorophore, such as fluorescein, to produce 5′-end-labeled dsDNA products that can be separated and detected by CGE–LIF. The former approach offers the highest sensitivity with the amount of intercalating dye bound proportional to the size of the dsDNA fragment (i.e., the larger the fragment, the more dye will be bound). Not only do intercalating dyes label the dsDNA for detection, but they also can enhance the selectivity and resolution of dsDNA fragments of similar size.[4,6] Intercalating dyes can also produce anomalous effects on peak shape, depending on such factors as their concentration in the separation or sample buffer and certain sequence-dependent properties of the dsDNA (e.g., %GC composition). These effects result from the binding and retention of differing amounts of dye molecules by the dsDNA fragments during CGE. Therefore, care must be taken to carefully evaluate the use of a specific intercalating dye with a particular PCR product in order to generate reproducible results.

Capillary gel electrophoresis–LIF analysis of PCR and RT–PCR products has been applied to the areas of clinical diagnostics, forensics, and biotechnology. Screening of patients for genetic and infectious diseases, human identity testing using PCR-amplified DNA fragments from specific polymorphic genomic regions (loci) defined by a variable number of tandem repeats (VNTRs) or short tandem repeats (STRs), analysis of mitochondrial DNA, genotyping, and gene expression studies are only a few examples of these applications.[4–7] The types of results that can be gained from CGE analysis of PCR products are twofold. First, CGE is useful in a qualitative evaluation of PCR by separating target DNA from non-specific products and demonstrating that a single dsDNA fragment resulted from the amplification. CGE is also a rapid method of evaluating various PCR parameters (e.g., cycle number, temperature, $[Mg^{2+}]$, [dNTPs], etc.) for optimizing the efficiency of the reaction. Another use for CGE is to accurately determine the size of the PCR products. This approach has been applied to DNA profiling in human subjects by an assessment of PCR amplified alleles resulting from VNTRs and STRs.[6]

The ability to do on-capillary detection and to calculate integrated peak areas from the collected data makes CGE–LIF very useful for the quantification of PCR- and RT–PCR-generated dsDNA products. The quantity of the amplified product can be indicative of the efficiency of PCR and this information can be used to optimize the reaction. Such information is also useful in determining the amount of a specific DNA or RNA present in the analyzed sample. Quantitation can be achieved by relative or absolute estimates. A ratio of target DNA peak area to the peak area of an added dsDNA internal standard gives an estimate of the relative amount of target DNA generated by PCR. Internal-standard dsDNAs can derive from genes that remain at constant levels in the sample (are unaffected by experimental treatments), such as the so-called "housekeeping" genes or they can be added amounts of a known quantity of a purified and well-characterized dsDNA, such as restriction enzyme digest fragments of genomic DNA. For example, the digestion of ϕX174 bacteriophage DNA with *Hae*III produces 11 distinct dsDNA

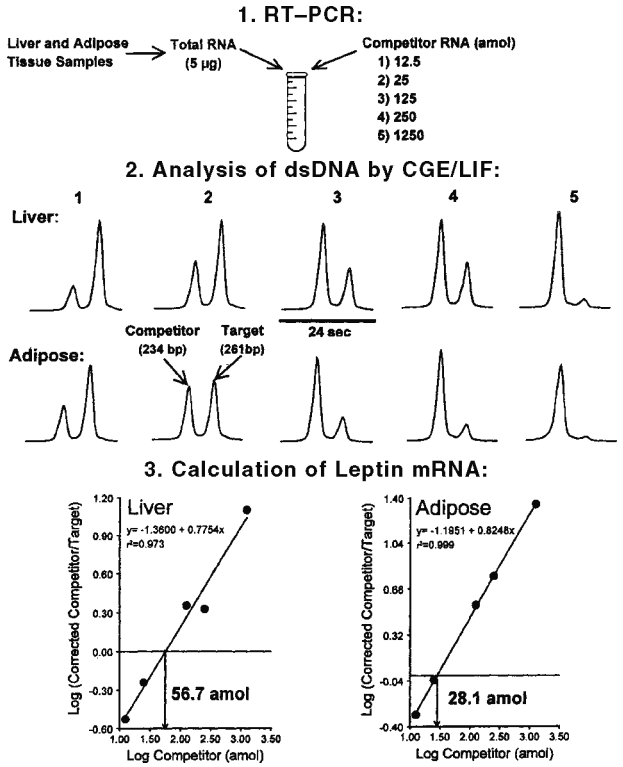

Fig. 1 Analysis of leptin gene expression in chicken liver and adipose tissue by QC–RT–PCR using capillary gel electrophoresis with laser-induced fluorescence detection (CGE–LIF). Target (261 bp) and competitor (234 bp) dsDNA amplicons were separated on a DB-1-coated capillary (27 cm × 100 mm inner diameter) at a field strength of 300 V/cm in a replaceable sieving matrix consisting of 0.5% HPMC in 1XTBE buffer with 0.5 µg/ml EnhanCE™ intercalating dye. RT–PCR samples (1–2 µl) were diluted 1:100 with deionized water and introduced into the capillary by electrokinetic injection. Separations were completed in under 5 min. A portion (4.4–4.8 min) of each separation shows the changes in the competitor and target peaks. CGE–LIF was more sensitive in detecting both amplicons than agarose slab gel electrophoresis with ethidium bromide staining. The integrated peak area ratio of competitor/target for a series of five individual samples (to which increasing amounts of a synthetic competitor RNA were added prior to RT–PCR) is used to calculate the amount of leptin mRNA (amol) in total RNA isolated from liver and adipose tissue by linear regression analysis.

fragments ranging in size from 72 to 1353 bp.[6] The latter type of standardization also affords the opportunity to accurately determine the size of the PCR product in addition to estimating its quantity when appropriate standards are chosen. Such standards can be obtained from commercial sources.

The most accurate means for quantitation of PCR products, especially those of low copy number, involves a method known as competitive PCR. In quantitative-competitive PCR (QC–PCR), known amounts of an internal standard (competitor) are co-amplified along with an unknown amount of target DNA. The competitor's sequence is chosen to be nearly identical to that of the target except for a small addition or deletion of sequence. The competitor is designed to use the same set of primers as the target so that a competition for them develops. Because the target and competitor are exposed to identical PCR conditions, the ratio of the two products should remain constant even after the reaction has reached its plateau phase. Thus, by plotting the different competitor/target peak area ratios against the amount of added competitor and extrapolating from the point at which the ratio is equal to 1, the amount of target DNA in the original sample can be determined in absolute terms. For RT–PCR, a competitor RNA is used to correct for variable conditions in both the RT and PCR steps.[9,10]

Fig. 1 depicts a scheme for the estimation of leptin mRNA (encoded by the obese gene, *ob*) contained in total RNA samples isolated from liver and adipose tissues of chickens. Using QC–RT–PCR with CGE–LIF, it was possible to derive absolute estimates (in attomoles) of leptin mRNA. Others have demonstrated a further extension of QC–RT–PCR with CGE–LIF called multiplexing, in which more than one competitor–target pair is subjected to co-amplification and subsequent analysis by CGE–LIF.[9,11] With multitarget QC–RT–PCR, it is possible to monitor PCR-amplified dsDNA corresponding to several genes simultaneously in a single sample assuming PCR conditions have been optimized for each product formed.[11]

Future applications of CE to PCR product analysis will arise from improvements in CE instrumentation. Advances in miniaturization of CE devices by producing glass chips with etched channels of <1 cm in length have already been demonstrated as a feasible method for ultrafast (<45 sec) separations of dsDNA.[4–7] The use of multiple capillaries or capillary arrays has proven to be useful in dedicated devices for DNA sequencing.[4–7] Recently, it has been possible to integrate PCR amplification and CE separation in a single device using an array of eight capillaries for high sample throughput.[12] This technology will undoubtedly produce dedicated CE instruments for PCR product analysis that will feature rapid run time and high throughput. New detection methods such as mass spectrometry offer the promise of increases in selectivity, detection sensitivity, and more accurate quantification of PCR products. It is now clear that, in the future, CEbased analyses of PCR products will continue to get faster and more reliable while achieving wider acceptance by biomedical and biotechnology laboratories.

REFERENCES

1. Mullis, K.B.; Faloona, F.A. Specific synthesis of DNA in vitro via a polymerase-catalyzed chain reaction. Methods Enzymol. **1987**, *155*, 335–350.

2. Chelly, J.; Kahn, A. RT–PCR and mRNA quantitation. In *The Polymerase Chain Reaction*; Mullis, K.B., Ferre, F., Gibbs, R.A., Eds.; Birkhauser: Boston, 1994; 97–109.
3. Barron, A.E.; Blanch, H.W. DNA seperations by slab gel, and capillary electrophoresis: Theory and practice. Separ. Purif. Methods **1995**, *24* (1), 1–118.
4. Guttman, A.; Schwartz, H.E. Separation of DNA. *Capillary Electrophoresis Theory and Practice,* 2nd Ed.; Camilleri, P., Ed.; CRC Press: Boca Raton, FL, 1998; 397–439.
5. Ulfelder, K.J.; McCord, B.R. Separation of DNA by capillary electrophoresis. In *Handbook of Capillary Electrophoresis,* 2nd Ed.; Landers, J.P., Ed.; CRC Press: Boca Raton, FL, 1997; 347–378.
6. Butler, J.M. Separation of DNA restriction fragments and PCR products. In *Analysis of Nucleic Acids by Capillary Electrophoresis*; Heller, C., Ed.; Verlag Vieweg: Wiesbaden, 1997; 195–217.
7. Righetti, P.G.; Gelfi, C. Capillary electrophoresis of DNA. In *Capillary Electrophoresis in Analytical Biotechnology*; Righetti, P.G., Ed.; CRC Press: Boca Raton, FL, 1996; 431–476.
8. Skeidsvoll, J.; Ueland, M. Analysis of double-stranded DNA by capillary electrophoresis with laser-induced fluorescence detection using the monomeric dye SYBR Green I. Anal. Biochem. **1995**, *231*, 359–365.
9. Fasco, M.; Treanor, C.P.; Spivack, S.; Figge, H.L.; Kaminsky, L.S. Quantitative RNA-polymerase chain reaction products by capillary electrophoresis using laser fluorescence. Anal. Biochem. **1995**, *224*, 140–147.
10. Borson, N.D.; Strausbauch, M.A.; Wettstein, P.J.; Oda, R.P.; Johnston, S.L.; Landers, J.P. Direct quantitation of RNA transcripts by competitive single-tube RT–PCR and capillary electrophoresis. Biotechniques **1998**, *25*, 130–137.
11. Lu, W.; Han, D.S.; Yuan, J.; Andrieu, J.M. Multi-target PCR analysis by capillary electrophoresis and laser-induced fluorescence. Nature **1994**, *368*, 269–271.
12. Zhang, N.; Tan, H.; Yeung, E.S. Automated and integrated system for high-throughput DNA genotyping directly from blood. Anal. Chem. **1999**, *71*, 1138–1145.

Peak Skimming for Overlapping Peaks

Wes Schafer
Merck Research Laboratories, Rahway, New Jersey, U.S.A.

INTRODUCTION

Any discussion of quantitating overlapped peaks should be prefaced by stating that baseline resolution of peaks is the only means of absolutely assuring the accuracy of their integration. All deconvolution methods involve assumptions that can affect accuracy. These methods are particularly inaccurate in cases of small peaks eluting on the tails of much larger peaks where percent errors are measured by two to three orders of magnitude.[1,2] In any case, the accuracy of all baseline methods generally increases with increasing resolution between the overlapping pair of peaks.

DISCUSSION

This discussion is confined to single-channel chromatographic analyses such as high-performance liquid chromatography (HPLC) with single-wavelength ultraviolet (UV) detection or gas chromatography with flame ionization or thermal conductivity detection. Three-dimensional (multichannel) techniques such as photodiode-array, multiwavelength detection may allow deconvolution based on component characteristics such as absorptivity at multiple wavelengths rather than peak shape. These techniques and/or the required information about the components are not always available, however, and many routine analyses are still conducted with single-channel detection because of their lower cost and relative simplicity.

In the overlap region between two unresolved chromatographic peaks, the detector response is a function of the response due to the first peak and the response due to the second peak. For a single-channel detector, this is mathematically equivalent to a single equation with two unknowns, which is impossible to solve. Detection and integration schemes, in such cases, must make assumptions regarding the shapes of the chromatographic peaks in order to attribute the response in the overlap region to one peak or the other. In some cases, the assumption is based on the ease of determining the baseline and, in other cases, on theoretical models of chromatographic peaks such as Gaussian or exponentially modified Gaussian (EMG) distributions.

Chromatographic data analysis systems generally employ three methods for determining baselines in overlapping peaks: *perpendicular drop*, *linear tangential skim*, and *exponential skim* (see Fig. 1). In order to choose the most appropriate method, the analyst must understand the assumptions and weaknesses of the three methods.

The perpendicular drop method produces accurate peak areas for symmetrical overlapped peaks of similar height and width. In this case, the portion of the second peak attributed to the first peak is offset by the portion of the first peak attributed to the second peak and vice versa. For overlapped peaks of significantly different size, the perpendicular drop method always overestimates the peak area of the smaller peak as the smaller peak gains more area from the larger peak than it "loses" to the larger peak. Quantitation errors are further exacerbated in the case of a smaller peak imposed on the tail of a much larger tailing peak. This method tends to show little injection-to-injection variability because of its simplicity.

Linear tangential skimming, on the other hand, consistently underestimates the area of the smaller peak by neglecting that portion of the peak area under the tangential baseline. As seen in Fig. 1, it is easy to visually underestimate the size of a peak that is unresolved from a significantly larger one, giving the appearance that the linear tangential skim method is much more accurate than it is. The relative simplicity of this method makes it rugged as well.

Many commercial software packages offer a non-linear exponential skimming method as well. As it has been estimated that 90% of all chromatographic peaks can be modeled by an exponentially modified Gaussian function,[3] this method should be the most accurate for tailing overlapped peaks. The algorithms for calculating such baselines are considerably more complicated, however, and the reproducibility of the technique may be problematic for some separations. The calculation of necessary parameters may limit its usefulness in extreme cases of tailing and peak width. In addition, the ability of exponential skimming to mimic symmetrical (Gaussian) peaks may also be an issue in some software. Examination of the constructed baselines is crucial in determining the proper use of this technique.

The peak area errors for the two most studied deconvolution methods (i.e., perpendicular drop and linear tangential skim) are dependent on a complex combination of resolution, relative peak width, relative peak height, and asymmetry ratio.[1] Exponential skimming assumes that the tailing of the first peak can be described by an exponential decay and that the peaks are sufficiently resolved to

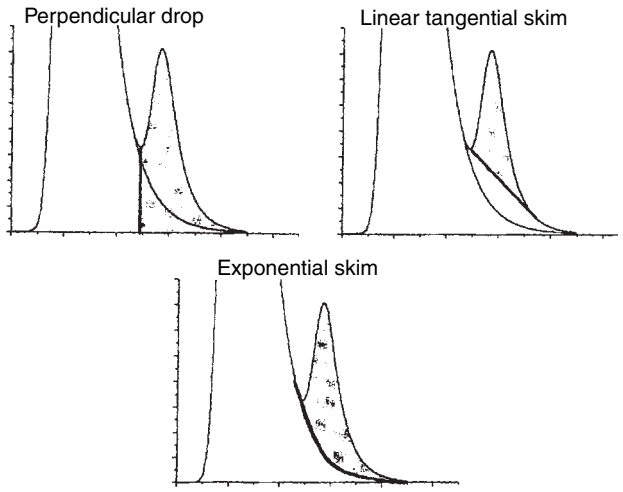

Fig. 1 Common methods for determining the baselines of overlapping peaks.

determine the decay parameters. Nonetheless, some broad generalizations can be made:

1. For symmetrical overlapped peaks of equal size and width, the perpendicular drop method provides accurate peak areas. Peak heights may still be overestimated.
2. In general, exponential skimming should be used when the first peak tails significantly or when the peak widths are significantly different. Care should be given that the area calculated by this method does not exceed the area by the perpendicular drop method, which already overestimates peak area.
3. For cases when exponential skimming is not possible or appropriate, due to extremely poor resolution or tailing, the tangential skim method should be used when the peak widths of the unresolved peaks vary significantly (>2:1).[2]
4. Quantitation by peak height should also be considered. It has been shown that peak height is more accurate in cases where the sizes of the overlapping peaks vary widely (>100:1). Quantitation is also generally more accurate for peak pairs of disparate size if the smaller peak elutes first.[1]

Although only doublets have been considered here, the arguments can be extended to multiplets by considering the effects on the front and tail of surrounded peaks.

REFERENCES

1. Meyer, V.R. Quantitation of chromatographic peaks in the 0.1 to 1.0% range. J. Chromatographia **1995**, *40* (1), 15–22.
2. Foley, J.P. Equations for chromatographic peak modeling and calculation of peak area. Anal. Chem. **1987**, *59*, 1984–1987.
3. Papas, A.N.; Tougas, T.P. Accuracy of peak deconvolution algorithms within chromatographic integrators. Anal. Chem. **1990**, *62*, 234–239.

Pellicular Supports for HPLC

Danilo Corradini
Institute of Chromatography, Rome, Italy

INTRODUCTION

In current practice, high-performance liquid chromatography (HPLC) supports consist of siliceous or polymer-based materials having pore sizes in the range of 80–120 Å for chromatography of small molecules and of 300–1000 Å for large biological molecules. Diffusional resistances in the stagnant mobile phase in the retentive material can have a significant influence on the efficiency of separation, particularly for large molecules of biological origin. Furthermore, pore size distribution of many mesoporous particles is rather wide and poor mass recovery is frequently encountered due to entrapment of macromolecules in the porous interior.

DISCUSSION

One approach to minimize mass-transfer resistance in a stagnant mobile phase employs specially designed particles with a bimodal network of pores. The larger pores (1000 Å) facilitate convective transport of the mobile phase inside the particles, whereas the small pores (500 Å) are explored by the sample components by diffusion only and provide the necessary surface area for adequate sorption capacity.

Another approach consists in eliminating the pore structure, using pellicular column packing materials. These HPLC supports are mechanically stable, fluidimpervious microspheres with a thin retentive layer on the surface.[1,2] Such a stationary-phase configuration facilitates the interactions of the analytes with the active moieties of the stationary phase, which are completely exposed to the mobile-phase steam in the interstitial space of the column packing material. Because the diffusional path length in the retentive surface layer of the pellicular stationary phase is very short, the plate height contribution to the *C* term in the van Deemter equation is relatively small. It should be recalled that the *C* term in the van Deemter equation estimates the contribution to the plate height of the resistance to mass transfer. As a result, the absence of intraparticulate diffusional resistance and the fast mass transfer between the stationary and the mobile phases due to the small particle size allows high column efficiency, even at relatively high flow rates. In addition, the lack of internal pore structure eliminates the undesirable steric effects encountered in HPLC of large biological molecules with mesoporous stationary phases, resulting in good sample recovery.

With porous materials, the largest contribution to the total surface area is due to the area contained within particles; it is related to the pore volume, surface area, and pore diameter. As a result, there is little variation in the total surface area of packing materials with different diameters, but identical pore size. On the other hand, with pellicular particles, the total surface area within a column is a function of particle size. Consequently, stationary phases having the pellicular configuration have an adsorption capacity lower than the conventional mesoporous particles. This appears to be particularly so with micropellicular materials in HPLC of small molecules. With large molecules such as proteins, the loading capacity of columns packed with traditional mesoporous particles may be only three or four times higher than that of columns packed with the micropellicular stationary phases.[3] However, this somewhat low loading capacity is still adequate in the analytical mode and is more than compensated for by the high analytical speed and efficiency obtained with pellicular stationary phases.

Conventionally, the phase ratio is the volume of the active moieties of the stationary phase divided by the volume of the mobile phase in the column. From the particular configuration of pellicular stationary phases described earlier, it follows that they have a relatively low phase ratio with respect to that of the conventional packing materials employed in HPLC.

A variety of micropellicular packing materials has been developed for the analysis of both small and large molecules by various HPLC modes, including ion exchange (IEC), metal interaction (MIC), reversed-phase (RPC),[4] and affinity chromatography (AC).[5] Besides analytical applications, other possible utilization of micropellicular stationary phases includes fundamental kinetic and thermodynamic studies of the retention mechanisms on a well-defined surface. Nevertheless, a relatively limited variety of micropellicular columns are commercially available. They are mainly restricted to ion-exchange and reversed-phase stationary phases. This may reflect certain practical disadvantages of micropellicular sorbents.

Columns packed with pellicular stationary phases of small particle size have low permeability and, therefore, cannot be operated at relatively high flow rates due to the pressure limitation of commercial HPLC instruments. However, due to the non-porous structure, micropellicular particles are generally more stable at higher temperature than conventional porous materials. Consequently, in the

absence of limitation due to the thermal stability of either the sample or the bonded stationary phase, a column packed with non-porous materials can be operated at elevated temperatures with practical advantages from column permeability and sorption kinetics. This appears to be particularly so with several micropellicular materials employed in reversed-phase HPLC. By increasing the column temperature, the viscosity of the mobile phase decreases with concomitant increases in column permeability, which allows operating the column at high flow rates. In addition, with increasing temperature, sample diffusivity also increases and, in many cases, the sorption kinetic improves.

The elevated mechanical and thermal stabilities of pellicular stationary phases having a solid, fluid-impervious core have favored the development of non-porous particles tailored for the rapid HPLC analysis of peptides, proteins, and other biopolymers. Most of these applications are in RPC.

Although governed by the same separation mechanism, RPC of proteins differs significantly from that of small molecules because of high molecular weight and complex tertiary structure of these macromolecules. A large molecular size is associated with low diffusivity and molecular complexity is associated with multipoint interactions of proteins with the hydrophobic stationary phase, which complicate the dynamics of the separation process. In addition, the elution of certain proteins may be further complicated by conformational changes associated with the retention mechanism. Hence, RPC of proteins and other complex macromolecules is generally performed under the gradient elution mode, which reduces analysis time and improves the performance of separation. In the reversed-phase gradient elution mode, proteins are believed to be retained at the column inlet until, at some point in the gradient, corresponding to the proper mobile-phase composition, they are desorbed completely. Proteins then move through the column without apparent further interaction with the hydrophobic stationary phase.

In most cases, RPC of peptides and proteins are performed under denaturing conditions using hydro-organic mobile phases containing acidic additives such as trifluoroacetic or phosphoric acid. Because the elution strength of the mobile phase increases by decreasing its polarity, the appropriate gradient is produced by increasing the concentration of the organic solvent in the hydro-organic mobile phase during the chromatographic run. The variation of the eluent composition as a function of time gives the gradient shape, which is steep in the case of fast analysis performed with micropellicular reversed phase (i.e., high rate of change of mobile-phase composition during gradient elution).

Steep gradients require high flow rates in order to maintain satisfactory differences in retention of the analytes. According to Snyder and Standalius,[6] the influence of the gradient parameters on retention is given by

$$k = \frac{t_g F}{1.15 \Delta\phi V_m S} \quad (1)$$

where k is the effective capacity factor for gradient elution, which is the value of the corresponding capacity factor under isocratic conditions (k') for the peak when it reaches the column midpoint, t_g is the gradient time (time from the beginning to the end of the gradient), F is the flow rate, $\Delta\phi$ is the variation of the fraction of organic solvent in the mobile phase during gradient, is the column void volume, and S is the slope of the plot of the logarithmic retention factor (k') against mobile-phase composition under isocratic conditions. The value of the parameter S is related to the magnitude of the hydrophobic contact area and the number of the interaction sites established between the solutes and the stationary phase during the separation process. In comparison to small molecules, biopolymers have a larger contact area with the stationaryphase surface and, as a result, the retention is very sensitive to the content of the organic solvent in the hydro-organic mobile phase (i.e., the value of the parameter S is relatively large).

Eq. 1 clearly shows that in order to maintain K constant while decreasing t_g, the flow rate must be proportionally increased. Because of the favorable mass-transfer properties of pellicular stationary phases, columns packed with such material can be employed at a high flow rate without loss in resolution. Moreover, pellicular column packings have a negligible intraparticulate void volume and, after the gradient, can be rapidly reequilibrated to the starting conditions. Finally, the thermal stability generally exhibited by these stationary phases allows running the gradient at relatively elevated temperature with the beneficial effect of reducing the viscosity of the mobile phase, which reflects on reducing the column inlet pressure. In addition, temperature influences the retention behavior of the analytes. Generally, the chromatographic retention decreases with increasing temperature, with concomitant improvement in column efficiency due to increased solute diffusivity and faster mass transfer. However, with proteins, the retention may increase and efficiency decrease when temperature promotes further unfolding of the protein.

Pellicular packings may also consist of a fully functionalized layer encapsulating solid particles, where there is no physical attachment of the active layer to the core particles[7] or as colloidal particles bearing charged moieties (latex) electrostatically bound to a solid core functionalized with groups of opposite charge (Fig. 1).[8] Most of the anion-exchange columns in use today for either carbohydrate or ion chromatography are packed with electrostatically latexcoated pellicular ion exchangers. These sorbents consist of three parts: (a) a highly cross-linked polymeric non-porous core, (b) a sulfonated layer at the outer surface of the solid core, and (c) a monolayer coating of anion-exchange latex particles functionalized with quaternary

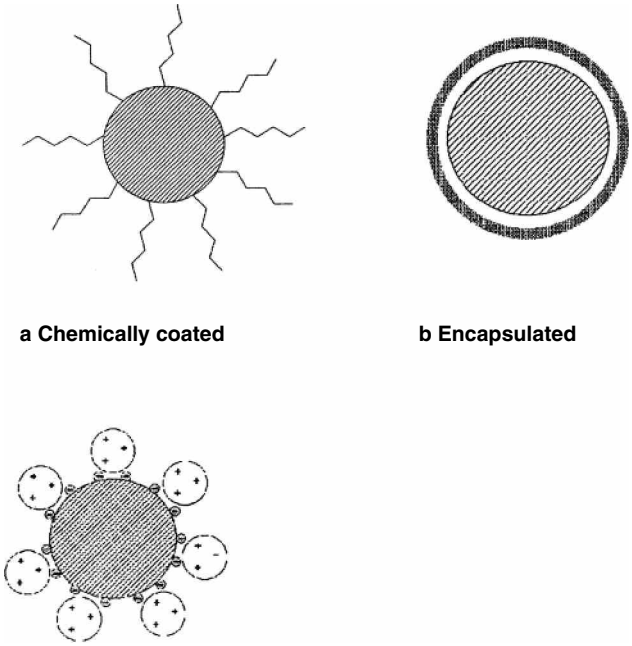

Fig. 1 Shematic representation of pellicular stationary phases consisting of covanlently bonded functional groups at the surface (a) funtionalized layer-encapsulating solid particles (b) and functionalized particles electrostatistically bound to a solid core groups of opposite charge (c).

ammonium compounds. The solid support and the latex particles are manufactured separately and brought together after independent quality control performed to remove particle agglomerates. This allows easy control of phase thickness, which results from the monodisperse latex particles, attached to the solid core by electrostatic forces. As a result, loading capacity increases with increasing the diameter of the latex particles, which generally ranges from 50 to 500 μm. For a 250 mm × 4 mm I.D. column, the corresponding loading capacity ranges from 5 to 150 μmEq/column.

The highly cross-linked polymeric non-porous core may consist of either a polystyrene-divinylbenzene or an ethylvinylbenzene-divinylbenzene substrate. The latex coatings are generally made from vinylbenzenylchloride polymer cross linked with divinylbenzene and fully functionalized with an appropriate quaternary amine for introducing anion-exchange properties.

Pellicular anion-exchange sorbents may also consist of quaternized latex hydrophobically coated onto the surface of an unsulfonated polystyrene solid core. However, using hydro-organic mobile phases can easily wash off the latex particles held onto the particle surface by hydrophobic interactions.

REFERENCES

1. Horváth, Cs.; Priess, B.A.; Lipsky, S.R. Fast liquid chromatography. Investigation of operating parameters and the separation of nucleotides on pellicular ion exchangers. Anal. Chem. **1967**, *39*, 1422–1428.
2. Unger, K.K.; Jilge, G.; Kinkel, J.K.; Hearn, M.T.W. Evaluation of advanced silica packings for the separation of biopolymers by high-performance liquid chromatography II. Performance of non-porous monodisperse 1.5-m silica beads in the separation of proteins by reversed-phase gradient elution high-performance liquid chromatography. J. Chromatogr. **1986**, *359*, 61–72.
3. Varady, L.; Kalghatgi, K.; Horváth, Cs. Rapid high-performance affinity chromatography on micropellicular sorbents. J. Chromatogr. **1988**, *458*, 207–215.
4. Kalghatgi, K. Micropellicular stationary phases for rapid protein analysis by high-performance liquid chromatography. J. Chromatogr. **1990**, *499*, 267–278.
5. Mao, Q.M.; Johnston, A.; Prince, I.G.; Hearn, M.T.W. High-performance liquid chromatography of amino acids, peptides and proteins *1: CXIII. Predicting the performance of non-porous particles in affinity chromatography of proteins. J. Chromatogr. **1991**, *548*, 147–163.
6. Snyder, L.R.; Standalius, M.A. *High-Performance Liquid Chromatography: Advances and Perspectives*; Horváth, Cs., Ed.; Academic Press: New York, 1984; 195–309.
7. Giddings, H . U.S. Patent 3,488,922, 1970.
8. Small, H.; Stevens, T.S.; Bauman, W.C. Novel ion exchange chromatographic method using conductimetric detection. Anal. Chem. **1975**, *47*, 1801–1809.

Peptides and Proteins: TLC Analysis

C. Marutoiu
Department of Chemistry, Lucian Blaga University of Sibiu, Sibiu, Romania

M.L. Soran
National Institute of Research and Development for Isotopic and Molecular Technology, Cluj-Napoca, Romania

INTRODUCTION

Thin-layer chromatography (TLC) and the more modern technique—high-performance thin-layer chromatography (HPTLC)—have numerous applications in proteins chemistry. These techniques are used for the quantitative determinations of peptides (nanograms), identification of peptides in partially hydrolyzed proteins, correlation of chromatographic properties for peptides and their constituent amino acids, as well as identification and characterization of proteins present in small quantities.

Various mixtures of peptides and proteins can be separated and identified using different stationary phases, such as silica gel, cellulose, mixtures of cellulose and silica gel, hydroxylapatite, ion exchangers, and other chemically modified stationary phases.

SEPARATION OF PEPTIDES

Various types of peptides can be separated on cellulose plates using various mobile phases, e.g.,

- *n*-butanol–acetic acid–pyridine–water (15:3:10:12, v/v);
- *n*-butanol–acetic acid–5% NH_4OH (11:6:3, v/v);
- chloroform–34% NH_4OH–ethanol (2:1:2, v/v);
- ethanol–pyridine–water–acetic acid (5:5:3:1, v/v);
- *n*-butanol–acetic anhydride–water (4:1:1, v/v);
- *n*-butanol–acetic acid–water (4:1:1, v/v);
- chloroform–methanol (3:1, v/v);
- chloroform–methanol–acetic acid (45:4:1, v/v);
- phenol–water (3:1, v/v);
- *n*-butanol–pyridine–water (15:10:3, v/v);
- *n*-butanol–pyridine–acetic acid–water (130:20:6:24, v/v);
- chloroform–methanol–water (68:25:4, v/v);
- chloroform–acetone (5:1, v/v; 8:2, v/v; 9:1, v/v);
- propanol–acetic acid–water (3:3:2, v/v);
- chloroform–methanol–17% NH_4OH (2:2:1, v/v);
- isoamyl alcohol–ethanol–acetic anhydride–pyridine–water (175:50:13:175:150, v/v);
- *iso*-propyl alcohol–ethanol–NH_3 (4:4:3, v/v);
- *iso*-propyl alcohol–1 N HCl (3:3, v/v);
- 0.1 N HCl–96% ethanol (1:1, v/v);
- 0.5 N HCl–ethanol–acetone (5:3:0.5, v/v);
- *iso*-butanol–pyridine–water (7:7:6, v/v);
- isoamyl alcohol–pyridine–water (7:7:6, v/v).

The following mobile phases have been used for separations on silica gel plates:

- *n*-butanol–acetone–water–pyridine (15:3:10:12 or 30:6:30:24 or 60:20:6:11, v/v);
- *n*-butanol–acetone–water (5:2:3, v/v);
- chloroform–methanol (7:3 or 9:1 or 1:9, v/v);
- *n*-butanol–acetic acid–water–ethyl acetate (1:1:1:1, v/v);
- *n*-butanol–pyridine–acetic acid–water (12:4:1:4 or 15:10:3:12 or 15:10:6:12, v/v);
- water–ethyl acetate–propanol (2:5:3, v/v);
- *n*-butanol–acetic acid–water (4:1:1, v/v);
- ethyl acetate–pyridine–acetic acid–water (56:20:6:11, v/v);
- dichloromethane–methanol–acetone (19:3:1 or 40:1:2 or 19:2:1 or 20:1:1 or 20:2:1, v/v);
- hexane–ethyl acetate–acetone (11:7:1, v/v);
- *n*-butanol–acetone–ethyl acetate–water (1:1:1:1, v/v);
- dichloromethane–methanol–10% NH_3 (10:1:0.1 or 10:3:0.1, v/v);
- *n*-butanol–dioxane–water (4:5:1, v/v).

Silica gel impregnated with 5% liquid paraffin in petroleum ether is another stationary phase, which is sometimes used for the separation of peptides. The separations are performed using the mixture methanol–water (1:4, v/v) as mobile phase.

The separation of this class of substances on silica gel C-18 is performed with dichloromethane–hexane (5:95, v/v) and methanol–water (1:1, v/v).

DETECTION OF PEPTIDES ON CHROMATOGRAPHIC PLATES

The detection of peptides is performed using various visualizing reagents. The hexa- and penta-peptides are visualized either in UV light after spraying with Pauly's reagent (4-sulfo-benzenediazonium hydroxide in 2 N Na_2CO_3), by the Reindel–Hoppe procedure, or by spraying with ninhydrin. The peptides of type Ac-Pro-Val-Val-Ser-Gly-NH_2,

Ac-Pro-Glu-Val-Ala-Gly-NH_2 can be visualized with chlorine–toluidine reagent. The cyclic peptides can be visualized by immersion of the developed chromatographic plates in 20% trichloracetic acid for 10 min and 5 min in 0.3% Serwa Blue W aqueous solution. In the case of peptides with a poly-[Lys(X_i-DL-Ala_m)] formula, the detection is performed with 0.3% ninhydrin solution in acetone and starch–KI reagent.

The tri- and tetra-peptides, in various mixtures, separated on silica gel plates, are identified in UV light or by spraying with ninhydrin, t-BuOCl/starch–KI, or Sakaguchi reagent.

The method of the iodine-starch reagent consists of the introduction of the developed plate into an iodine vapor atmosphere for 5 min, followed by spraying with 1% aqueous starch solution. The peptides produce blue spots.

Morin reagent is also used for the detection of peptides. The developed plates are dried and sprayed with 0.05% morin (3,5,7,2′,4′-pentahydroxyflavone) solution in methanol and activated for 2 min at 100°C. In this case, the peptides produce yellowish-green fluorescent spots on a green fluorescent background or dark absorption spots under UV light. The detection limit is just about 2 μg/spot. Detection of ^{32}P-labelled opioid peptides is done by autoradiography.

SEPARATION OF PROTEINS

A mixture of 14 proteins (cytochrome C, ribonuclease, lysozyme, myoglobin, α-chymotrypsin, trypsin, ovomucoid pepsin, ovalbumin, hemoglobin, bovine serum albumin, bovine γ-globulin, thyroglobulin, and macroglobulin) was separated on Sephadex G-100 and Sephadex G-200 plates, using 0.5 *M* NaCl solution as mobile phase.

The neoglycoproteins were separated on silica gel using dichloromethane–methanol (9:1, v/v), dichloromethane–acetone (8:2, v/v), or acetone–25% NH_3 (6:4, v/v) as mobile phase. Using DEAE-cellulose on chromatographic plates and a mobile phase containing 0.01 *M* sodium phosphate solution, bicine, or sodium chloride, proteins such as albumin, transferrine, lactoferrine, and lysozyme are separated as reference compounds. The optimum pH-value for the separation is 8.5.

The composition of protein and lipid in chemically modified keratin fibers was analyzed on silica with chloroform–methanol (80:2, v/v). A rapid immunochromatographic method for the analysis of protein antigens, based on a "sandwich" assay format, uses monoclonal antibodies of two distinct specificities, one covalently immobilized to a defined detection zone on a porous membrane, while the other serves as a label. The sample is mixed, and is then passed along the porous membrane by capillary action, giving a blue color with the antibodies in the detection zone. The detection limit can be below the nanomolar range for the antigen, as in the case of the human chorionic gonadotropin.

Two-dimensional TLC separations of 4-*N*,*N*-dimethylaminoazobenzene 4′-isothiocyanate protein derivatives were performed on polyamide using an acetic acid–water (1:2, v/v) mixture for development in one direction and toluene–hexane–acetic acid (2:1:1, v/v) mixture for the second direction.

TLC of HBsAG segments (HBsAG = hepatitis B-virus) was done on silica with solvent systems obtained by mixing ethyl acetate with a stock solution of pyridine–acetic acid–water (20:6:11, v/v). TLC separation of high-density lipoprotein and oxidized high-density lipoprotein were performed on silica gel with chloroform–NH_3–methanol–water (180:11:108:11, v/v) systems.

DETECTION OF PROTEINS

The neoglycoproteins were identified by spraying the plates with sulfuric acid. A series of proteins and lipids separated from the mixture were visualized by exposure to iodine vapors. HBsAG segments were visualized by spraying with tolidine–KI after chlorination.

The proteins separated on gel layers are transferred onto filter paper (Whatman 0.3 mm) and are visualized by the usual methods of paper chromatography, i.e., the dried paper is introduced, for 15 min, into Amido Black 10B (0.6 g) dissolved in methanol/ethanol (750 ml), water (450 ml) and glacial acetic acid (100 ml) mixture and treated three times with 1% acetic acid for 30 min each time. Alternatively, the paper is stained in a 1% solution of bromophenol blue saturated with mercuric chloride for 5 min and then treated five times with 0.5% acetic acid for 30 min each time.

CONCLUSION

Separation of peptides and proteins has been described with many examples being included. Effective visualization techniques are also discussed.

BIBLIOGRAPHY

1. Birnbaum, S.; Uden, C.; Magnusson, C.G.M.; Nielsson, S. Latex based thin-layer immunoaffinity chromatography for quantitation of protein analytes. Anal. Biochem. **1992**, *206*, 168.
2. Choli-Papadopoulou, T.; Kamp, R.M. *Protein Structure Analysis*; Kamp, R.M., Choli-Papadopoulou, T., Wittman-Liebold, B., Eds.; Springer-Verlag, 1997.
3. Luo, Q.; Andrade, J.D.; Caldwell, K.D. Thin layer Ion-Exchange chromatography of proteins. J. Chromatogr. **1998**, *816*, 97.
4. Bhushan, R.; Martens, J. *Handbook of Thin-Layer Chromatography*; Third Edition Revised and Expanded; Sherma, J., Fried, B., Eds.; Marcel. Dekker, Inc.: New York, 2003;
5. Schön, I.; Szirtes, T.; Rill, A. Synthesis of HBSAG segments in solution. Acta Chim. **1991**, *128*, 751.
6. Shellenberg, P. Dunnschicht-chromatographie non peptid-zwischenprodukten. Angew. Chem. **1962**, *74* (3), 118.
7. Szurmai, Z.; Szabo, L.; Liptak, A. Diethylene and triethylene glycol spacers for the preparation of neoglycoproteins. Acta Chim. **1989**, *126*, 259.

Peptides, Proteins, and Antibodies: Capillary Isoelectric Focusing

Anders Palm
Cell and Molecular Biology, Astra Zeneca, Lund, Sweden

INTRODUCTION

Capillary isoelectric focusing (CIEF) is a high-resolution technique for protein and peptide separation performed at academic sites and in the biotechnology and pharmaceutical industries for the analysis and characterization of, for example, recombinant antibodies and other recombinant proteins, isoforms of glycoproteins, point mutations in hemoglobin, and peptide mapping. Also, hyphenation to mass spectrometry and chipbased CIEF (microfabrication) have shown promise. CIEF kits and specific recipes/application notes are available from vendors of capillary electrophoresis (CE) equipment, as are a vast amount of publications and handbooks of CE published over recent years.

Capillary isoelectric focusing is a rapid analysis technique with typical run times of 5-30 in, fully automated with online detection and real-time data acquisition, and minute sample consumption (a few microliters is enough for repetitive injections). A linear dynamic range over one order of magnitude is achievable, and a detectability down to 5-10 μg/ml. A resolution of ΔpI-0.01 is possible under optimized conditions. Reproducibility of p*I* determination is typically $<0.5\%$ (RSD) using internal standards.

SAMPLE SALT CONTENT

For high-performance analysis, it is important that the sample applied has a low salt content.[1] Salt concentrations below 10 m*M* is preferable; concentrations above 40–50 m*M* should be desalted. The salt will compress the pH gradient so that it will occupy only some part of the capillary. Hereby, the resolution will decrease and the risk for protein precipitation will increase (see the section on Focusing, below). Also, focusing time will have to be increased as well as focusing/mobilization time being less reproducible.

AMPHOLYTES

Several commercial ampholytes are available covering broad-range (pH 3–10) and narrow-range pH gradients (e.g., pH 6–8). Broad-range gradients are suitable for analysis of proteins covering a wide spectrum of isolectric points, whereas narrow-range gradients are preferable for high-resolution separations where only minor differences in protein p*I*'s are expected.[2] Tailor-made gradients can easily be made by mixing ampholytes of different pH ranges or by adding ampholyte spacers.[3] It is preferable, also, to mix ampholytes (with a similar pH interval) from different suppliers so as to create a smoother gradient. Typical concentrations of ampholytes used are 1–5% (v/v); the concentration employed will affect, for example, the protein load, resolution, and focusing/mobilization voltage and time.

ADDITIVES

Additives are used in the sample-ampholyte solution either: (a) to suppress protein aggregation/precipitation or (b) to decrease the electro-osmotic flow (EOF) velocity and/or protein adsorption to the capillary surface. Protein precipitation is often a major problem in CIEF due to a highly concentrated protein band, and because electrostatic repulsion is minimal at the p*I*, proteins interact strongly by hydrophobic interactions (also hydrogen-bonding) causing irreproducible migration time and peak area quantification, and sometimes capillary clogging.[1,2] Precipitates are often seen as "spikes" in the electropherogram. Strategies to minimize precipitation include reducing the protein concentration and focusing time, applying a lower field strength, and/or using various additives. Because as high a resolution and detection sensitivity as possible are strived for, additives are often the first choice. Many such additives are used to enhance the solubility of proteins like (a) non-ionic detergents (e.g., reduced Triton X-100 and Brij-35), (b) zwitterions (e.g., CAPS and sulfobetain), (c) carbohydrates (e.g., sucrose, sorbitol, and cellulose derivatives), (d) urea, and (e) organic modifiers (e.g., ethylene glycol and glycerol). It is also common to mix different additives.[3] There seems to be no universal solubilization recipe covering all sorts of proteins. Instead, tailor-made recipes often must be worked out whenever precipitates are encountered. The commonly used mixture of 8 *M* urea and 2% detergents, as employed in the first dimension in two-dimensional gel electrophoresis, often performs well, although attention must be paid to protein modification causing artifacts in the electropherogram.[1]

Because urea also denatures proteins (in contrast to the other, more mildly, solubilizers), a shift in p*I* might be expected. See Ref.[3] for new types of solubilizers used in CIEF.

Additives used for decreasing the EOF and/or protein adsorption are often cellulose derivatives [e.g., hydroxypropylmethylcellulose (HPMC)]. The cellulose adsorbs to the capillary surface. Hereby, the viscosity will increase at the capillary surface (more than in bulk solution), causing a reduction in EOF as well as a decrease in protein adsorption to the capillary wall. The tendency for protein precipitation will also decrease by addition of cellulose derivatives.

FOCUSING

Focusing is the process where ampholytes and proteins migrate to their respective p*I* positions in the capillary. During focusing, current will decrease, as the current carrier ampholytes cease to migrate, and finally reach a constant value when the pH gradient is fully developed and the steady state has been attained (certain gradient drifts are often observed in CIEF whose presence will affect performance and reproducibility)[2] Normally, focusing is considered complete when current has decreased to 10% of its original value; a longer focusing time increases the risk for protein precipitation.

Resolution in CIEF is described by the following formula:

$$\Delta \mathrm{p}I = 3\left(\frac{D(d\mathrm{pH}/dx)}{E(d\mu/d\mathrm{pH})}\right)^{1/2}$$

where D is the diffusion coefficient, dpH/dx is the change of pH with distance x, E is the electric field strength, and $d\mu/d$pH is the change of mobility with pH.[2] The importance of the applied voltage is clearly seen, as a higher field strength gives a better resolution and shorter focusing time. Field strengths between 300 and 700 V/cm are normally used. The optimal voltage may be determined experimentally from a series of runs with different voltages. The formula also reveals that proteins attain a higher resolution than peptides because their D values are lower and $d\mu/d$pH is higher.

MOBILIZATION

Single-Step CIEF

In single-step (electro-osmotic displacement) CIEF, focusing and mobilization take place simultaneously.[1,2] Here, a dynamically coated (or static coated with reasonably high EOF) capillary is used where the EOF is fast enough to sweep all proteins by the detector in a reasonable time frame and slow enough to simultaneously allow the protein zones to focus. Additives are used to manipulate the velocity of the EOF as well as to decrease protein adsorption. The single-step method benefits from short analysis times and an extended capillary lifetime but suffers from lower detectability (due to lower protein load), compromised resolution, and non-linearity of the p*I* calibration curve.[4] A variant of the single-step CIEF is to use whole-column imaging detection where all the focused bands in the capillary are detected simultaneously without any need for mobilization.[5]

Two-Step CIEF

Two-step CIEF is used when EOF in the capillary is strongly reduced. After focusing is complete, a separate mobilization step is applied where the protein bands are transported past the fixed detector. Mobilization can be achieved either by chemical means [for cathodic (anodic) mobilization, the composition of the catholyte (anolyte) is changed; thereby the pH gradient will change], or by applying a positive/negative pressure, or by a mixture of both.[1,2] A pressure will induce zone broadening due to the parabolic flow profile; a modest pressure in combination with highvoltage will preserve the high-resolution pattern 4. Pressure mobilization offers good reproducibility (migration times and p*I* values) and a linear p*I* calibration curve. Chemical mobilization shows the same performance and also exhibits the highest resolution, at the expense of longer migration times. Anodic mobilization affords a better resolution of the acidic region, whereas cathodic mobilization is preferable for the basic region.[4]

DETECTION

Absorbance detection at 280 nm is mostly used. Below 220 nm is preferable for sensitive protein/peptide detection but is not possible because of background-absorbing ampholytes.[2] Proteins with chromophores (e.g., hemoglobins) can be detected at visual wavelengths. However, because CIEF is a concentrating technique (the protein bands will be concentrated about 100-fold during focusing), a fairly good sensitivity for most proteins is still attainable at 280 nm. For high-sensitivity analysis, laser-induced fluorescence detection might be an alternative, but it requires a labeling procedure.[5,6] By labeling, a change in intrinsic p*I* might occur and the same analyte might be subjected to multiple labeling sites showing several peaks in the electropherogram (especially proteins). This might, however, be the only choice for peptides lacking tyrosine and tryptophan. Whole-column imaging detection (no mobilization step needed) with different detection schemes is also possible for proteins and peptides.[5]

Capillary isoelectric focusing coupled to mass spectrometry has gained popularity in recent years (by analogy to two-dimensional gel electrophoresis). Additional information obtained from mass spectrometry includes not only precise molecular-weight determination but also the possiblity for peptide sequencing. Analysis of hemoglobin variants, recombinant proteins, and monoclonal antibodies have been demonstrated.[1,7,8]

APPLICATION OF CIEF TO PEPTIDES, PROTEINS, AND ANTIBODIES

Peptides

Peptides are not as commonly analyzed by CIEF as are proteins; one reason is their lower resolution, another their lower (or lack of) detectability at 280 nm (the wavelength mostly used). The separation of tryptic digests (peptide mapping) of proteins have been performed by using absorption detection at 280 nm and refractive index gradient imaging detection; no exact correlations were observed between measured and calculated p*I* values.[1,5] Refractive index detection is a universal detection method (i.e., independent of chromophores like tyrosine and tryptophan) but suffers from low sensitivity. Assays of trypsin activity have also been performed with laser-induced fluorescence detection for enhanced sensitivity, with detectability down to picomolal concentrations.[5,6]

Hemoglobins

Analysis of hemoglobin (Hb) variants are of major clinical importance. Many hematological disorders exist where the globin chains have been subjected to alterations (e.g., point mutations or deletion of gene sequence). Four hemoglobin, variants (A, F, S, and C) having very close p*I* values (from 7 to 7.40) are often employed as standards to demonstrate the high resolving power of CIEF.[2] Several other variants are possible to resolve (e.g., the separation of Hb A from its glycated form whose p*I*'s differ only by 0.01 or less).[1,3] Quantitative determination of is routinely used for assessing the degree of diabetes. To improve the resolution between Hb A and spacers, β-alanine and 6-aminocaproic acid were added to a mixture of pH 3–10 and pH 6–8 ampholytes in a coated capillary.[3] The spacers flatten the pH gradient in the p*I* region of the Hb's, thus allowing full separation.

Antibodies

Analysis of microheterogeneity in natural and recombinant monoclonal antibodies is a challenge where CIEF seems to be particularly well suited (see Fig. 1).[4] Minor modifications (e.g., deamidation, improper folding, and a change in glycosylation pattern) arising from protein synthesis or posttranslational modifications are often detected by CIEF.[1,2,9] The use of CIEF and comparison to flat-bed IEF for routine analysis of recombinant immunoglobins have been demonstrated with a coated capillary, methylcellulose, and a two-step mobilization procedure. The performance of the analysis and coating stability were constant for over 150 analyses with qualitatively and quantitatively equivalent immunoglobulin focusing profiles obtained via CIEF and IEF. Intra-assay reproducibility was less than 2% RSD for peak areas and 1% RSD for migration time. Interassay (72 hr) reproduciblity was less than 8% RSD for peak areas and 3% for migration time.[10]

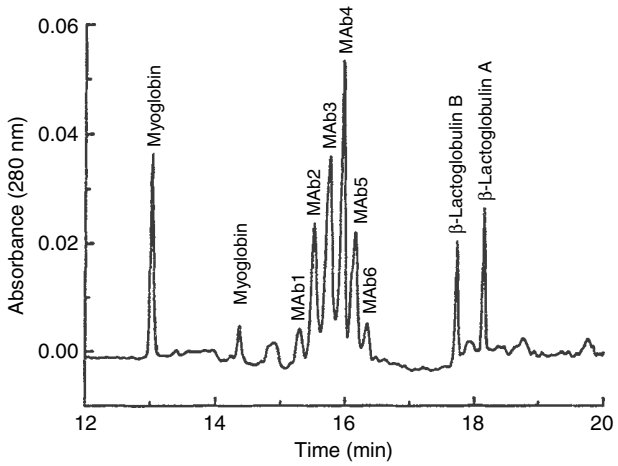

Fig. 1 CIEF of a mouse monoclonal antibody (MAb). Antibody concentration: 0.5 mg/ml; concentration of the marker proteins (myoglobin and β-lactoglobulin): 0.05 mg/ml; capillary: μ-SIL DB-1, 27 cm total length (20 cm to detector); carrier ampholytes: 4% Pharmalyte pH 3–10 including 1% TEMED and 0.8% methylcellulose (MC); anolyte: 10 m*M* H_3PO_4 in 0.4% MC; catholyte: 20 m*M* NaOH. Focusing for 2 min at 20 kV, followed by obilization at low pressure (0.5 psi) at 20 kV.
Source: From Capillary isoelectric focusing: A routine method for protein analysis?, in Electrophoresis.[4]

GLYCOPROTEINS

Applications of CIEF for the separation of isoforms of transferrin have been reported by several groups.[1,2,5] Transferrin contains different number of sialic acid residues, with an additional −1 charge added per residue. Also, transferrin bound to different amount of iron atoms has been separated by CIEF.[1,2,5] Glycoforms of recombinant tissue-type plasminogen activator (rtPA) is another sialic acid containing protein which has been the subject of analysis by CIEF.[1,2,11] A rapid (<10 min) one-step method was developed using a coated capillary, HPMC, and urea in a mixture of pH 3–10 and pH 5–8 ampholytes. Ten species could be detected. Intra-assay precision was less than 5% for peak migration times and 10% for normalized peak areas.[11]

REFERENCES

1. Rodriguez-Diaz, R.; Wehr, T.; Zhu, M. Capillary isoelectric focusing. Electrophoresis **1997**, *18* (12–13), 2134–2144.
2. Liu, X.; Sosic, Z.; Krull, I.S. Capillary isoelectric focusing as a tool in the examination of antibodies, peptides and proteins of pharmaceutical interest. J. Chromatogr. A, **1996**, *735*, 165.
3. Righetti, P.G.; Bossi, A.; Gelfi, C. Capillary isoelectric focusing and isoelectric buffers: An evolving scenario. J. Capillary Electrophoresis **1997**, *4* (2), 47–59.
4. Schwer, C. Capillary isoelectric focusing: A routine method for protein analysis? Electrophoresis **1995**, *16* (1), 2121–2126.
5. Fang, X.; Tragas, C.; Wu, J.; Mao, Q.; Pawliszyn, J. Recent developments in capillary isoelectric focusing with whole-column imaging detection. Electrophoresis **1998**, *19* (13), 2290.
6. Shimura, K.; Matsumoto, H.; Kasai, K. Assay of trypsin activity by capillary isoelectric focusing with laser-induced fluorescence detection. Electrophoresis **1998**, *19* (13), 2296–2300.
7. Wei, J.; Lee, C.S.; Lazar, I.M.; Lee, M.L. Capillary isoelectric focusing-electrospray ionization time-of-flight mass spectrometry for protein analysis. J. Microcol. Separ. **1999**, *11* (3), 193–197.
8. Hagmann, M.-L.; Kionka, C.; Schreiner, M.; Schwer, C. Characterization of the F(ab')2 fragment of a murine monoclonal antibody using capillary isoelectric focusing and electrospray ionization mass spectrometry. J. Chromatogr. A, **1998**, *816*, 49.
9. Krull, I.S.; Liu, X.; Dai, J.; Gendreau, C.; Li, G. HPCE methods for the identification and quantitation of antibodies, their conjugates and complexes. J. Pharm. Biomed. Anal. **1997**, *16*, 377.
10. Tang, S.; Nesta, D.P.; Maneri, L.R.; Anumula, K.R. A method for routine analysis of recombinant immunoglobulins (rIgGs) by capillary isoelectric focusing (cIEF). J. Pharm. Biomed. Anal. **1999**, *19*, 569.
11. Moorhouse, K.G.; Eusebio, C.A.; Hunt, G.; Chen, A.B. Rapid one-step capillary isoelectric focusing method to monitor charged glycoforms of recombinant human tissue-type plasminogen activator. J. Chromatogr. A, **1995**, *717*, 61.

Peptides: CCC Separation

Ying Ma
Yoichiro Ito
National Heart, Lung, and Blood Institute (NHLBI), National Institutes of Health (NIH), Bethesda, Maryland, U.S.A.

INTRODUCTION

Countercurrent chromatography (CCC),[1–4] because it uses no solid support in the separation column, is particularly suitable for the separation and purification of peptides which often present a problem of irreversible adsorption onto solid supports. Since the 1970s, the horizontal flow-through coil planet centrifuge (CPC) has been used for the separation of a variety of natural and synthetic peptides.[5] High-speed CCC,[6,7] which was developed in the 1980s, has improved partition efficiency in terms of resolution and separation times, yielding up to a few thousand theoretical plates in a few hours. During the last decade, a preparative scheme called pH-zone-refining CCC was developed. This method yields multigram quantities of pure fractions at an extremely high concentration.[8,9] More recently, a new column, called spiral disk assembly, was designed for high-speed CCC to separate peptides and proteins using polar two-phase solvent systems.[10]

The performance of these CCC instruments has been examined using butanol-based solvent systems and a set of dipeptide samples containing a tyrosine and/or a tryptophan moiety, which allows monitoring of the effluent at 280 nm.

HORIZONTAL FLOW-THROUGH CPC

Fig. 1A shows the original prototype of the horizontal flow-through CPC (HCPC), which can be operated without rotary seals.[5] A set of coiled tubes is arranged around the rotary shaft, which undergoes a specific planetary motion (type-J): The column assembly rotates about its own axis and revolves around the centrifuge axis at the same angular velocity, in the same direction. This planetary motion allows each helical turn of the column to retain the stationary phase of either the organic or the aqueous phase while vigorously mixing the two phases at each rotation cycle.

The system provides a stable retention for polar solvent systems up to 40% of the total column capacity. A typical separation of a set of dipeptides is illustrated in Fig. 1B. Using a two-phase solvent system composed of 1-butanol/acetic acid/water (4:1:5, vol/vol/vol), seven components were well resolved in 70 hr.

Before the advent of high-speed CCC, the method was utilized for the purification of various samples such as synthetic peptides, cholecystokinin analogs, and their fragments (HCPC; Table 1).

HIGH-SPEED CCC USING TYPE-J PLANETARY MOTION

High-speed CCC is considered to be the most advanced form of CCC in terms of partition efficiency and separation times. The design of the apparatus is similar to that of the HCPC, except that the coiled column is mounted coaxially onto the column holder. Since the early 1980s, the method has been widely used for the separation and purification of a variety of natural and synthetic products, including peptides and their derivatives.[6,7] Except for hydrophobic ring peptides such as gramicidin and bacitracin, most of the peptides are separated using polar butanol solvent systems, including 1-butanol/acetic acid/water (4:1:5), 1-butanol/aqueous trifluoroacetic acid (TFA; 1 : 1), and so on—typical examples of which are shown in Fig. 2A and B. Occasionally, one encounters a problem of carryover loss of the stationary phase from the multilayer coil separation column of the high-speed CCC centrifuge. To alleviate this problem, a new column, called spiral disk assembly, has recently been designed.[10] When mounted on the type-J high-speed CCC rotor, it enhances the retention of the stationary phase because of its radially acting centrifugal force gradient through the spiral channel. Thus the method enables the use of highly polar solvent systems with low interfacial tension, such as aqueous–aqueous polymer phase systems used for protein separation.

HIGH-SPEED CCC USING CROSS-AXIS CPC

This CCC scheme produces a unique pattern of planetary motion: The axes of the rotation and the revolution are perpendicular to each other. This planetary motion produces a centrifugal force vector acting across the diameter of the multilayer coil to enhance the retention of the

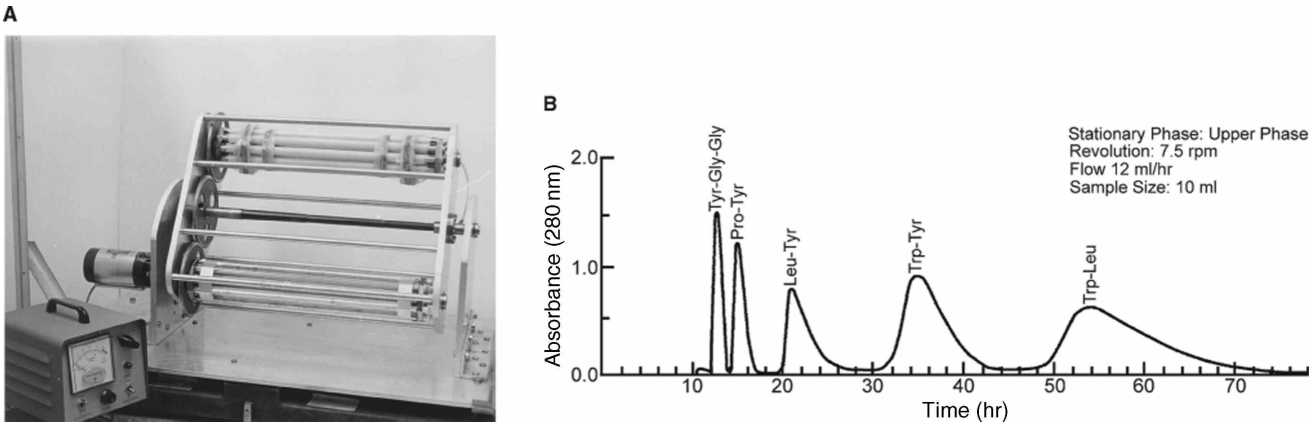

Fig. 1 Photograph of the horizontal flow-through coil planet centrifuge (A) and the chromatogram of dipeptide separation (B).

Table 1 Peptide samples and two-phase solvent systems for standard CCC techniques.

Peptide sample	Solvent system[a]	CCC instrument[b]
Dipeptides	1-BuOH/AcOH/H_2O (4 : 1 : 5)	TCC, HCPC, mLCPC ICPC, SDA
Dipeptides	1-BuOH/DCA/NH_4OAc (100 : 1 → 2 : 100)	ICPC, ACPC
Synthetic peptide	1-BuOH/AcOH/H_2O (4 : 1 : 5)	HCPC (6, 5, 9, and 15 mers)
Des-enkephalin γ-endorphin (12 mers)	1-BuOH/0.1% TFA (1 : 1)	HCPC
Cholecystokinin fragments (four to eight mers)	1-BuOH/AcOH/H_2O (4 : 1 : 5)	HCPC
	1-BuOH/0.2–0.5 *M* NH_4OAc (1 : 1)	HCPC
	1-BuOH/0.1% TFA (1 : 1)	HCPC
Cholecystokinin fragments sulfonated	1-BuOH/0.2–0.5 *M* NH_4OAc (1 : 1)	HCPC
	1-BuOH/EtOH/Hex/AcOH/H_2O (3 : 1 : 2 : 1 : 5)	HCPC
	1-BuOH/AcOH/H_2O (4 : 1 : 5)	HCPC
Cholecystokinin analog	$CHCl_3$/AcOH/H_2O (2 : 2 : 1)	MLCPC
Bacitracins	$CHCl_3$/95% EtOH/H_2O (4 : 3 : 2)	HCPC, MLCPC, XCPC
Gramicidins	$CHCl_3$/C_6H_6/MeOH/H_2O (15/15/23/7)	HCPC, MLCPC, XCPC DCCC
WAP-8294A	1-BuOH/EtOH/0.005 TFA (pH 2.5) (1 : 3 : 4)	MLCPC
Tyrocidines	$CHCl_3$/MeOH/0.1 m HCl (19 : 19 : 12)	DCCC
Colistins A and B	1-BuOH/0.04 m TFA (1 : 1)	MLCPC
Kangdisu/colistin E	1-BuOH/2% DCA + 5% NaCl (1 : 1)	MLCPC
Bombesin	1-BuOH/1% DCA (1 : 1) at 50°C	MLCPC
Bovine insulin	2-BuOH/3% DCA (1 : 1)	ICPC, ACPC
	1-BuOH/0.5% DCA (1 : 1) at 50°C	MLCPC

[a]ACN = acetonitrile; AcOH = acetic acid; BuOH = butanol; DCA = dichloroacetic acid; EtOH = ethanol; NH_4OAc = ammonium acetate; Hex = hexane; MeOH = methanol; TFA = trifluoroacetic acid.
[b]CPC = coil planet centrifuge; ACPC = type-I L-angle rotor CPC; DCCC = droplet CCC; HCPC = horizontal flow-through CPC; MLCPC = type-J multilayer CPC; SDA = spiral disk assembly; TCC = toroidal coil centrifuge; ICPC = type-I CPC; XCPC = cross-axis CPC.

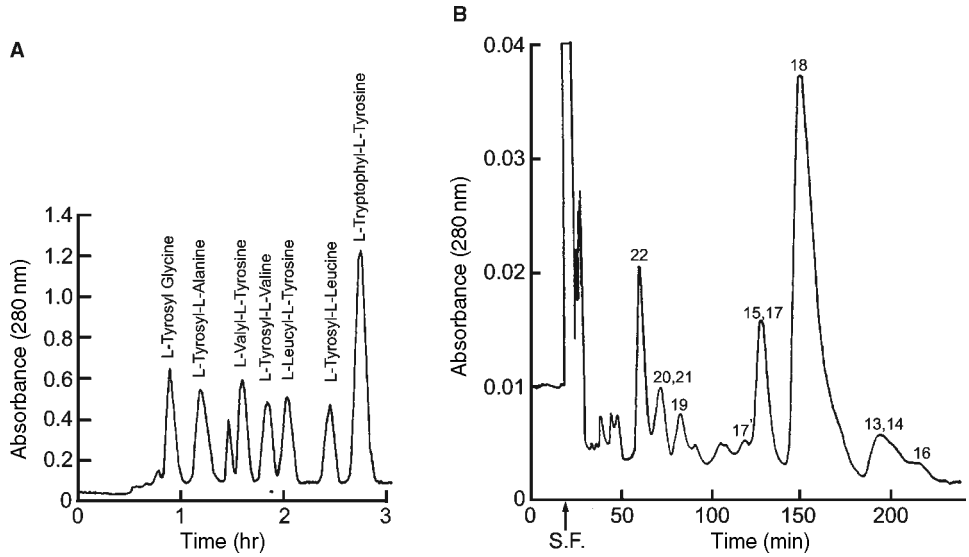

Fig. 2 Chromatograms obtained by high-speed CCC. (A) Separation of a set of dipeptides by gradient elution. Experimental conditions are as follows: apparatus: type-J multilayer CPC prototype with a 10 cm revolution radius; column: multilayer coil, 1.6 mm I.D., 130 m length, 285 ml total capacity; sample: dipeptide mixture 70 mg; solvent system: linear gradient between the starting medium of 1-butanol/dichloroacetic acid/0.1 *M* ammonium formate (1 : 0.01 : 1) and the ending medium of 1-butanol/0.1 *M* ammonium formate (1 : 1); mobile phase for 4 hr: lower aqueous phase; flow rate—214 ml/hr; revolution: 800 rpm; detection: 280 nm; retention of stationary phase: 55% of the total column capacity. (B) Separation of bacitracins by high-speed CCC. Bacitracins A and F are separated in peaks 18 and 22, respectively. Separation conditions are as follows: apparatus: Shimadzu type-J multilayer CPC (model HSCCC-1A; Shimadzu Corporation, Kyoto, Japan) with a 10 cm revolution radius; column: multilayer coil, 1.6 mm I.D., 325 ml capacity; sample: 50 mg; solvent system: chloroform/ethanol/methanol/water (5 : 3 : 3 : 4); mobile phase: lower organic phase; flow rate: 3 ml/min; detection: 254 nm.

Table 2 Peptide samples and solvent systems for pH-zone-refining CCC.

Peptide[a] (weight; g)	Solvent system[b]	Key reagents[c] Retainer	Eluter	Ligand
CBZ dipeptides (0.8 g)	MBE/ACN/H_2O (2 : 2 : 3)	TFA (16 m*M*/SP)	NH_3 (5.5 m*M*/MP)	—
CBZ dipeptides (3 g)	MBE/ACN/H_2O (2 : 2 : 3)	TFA (16 m*M*/SP)	NH_3 (5.5 m*M*/MP)	—
CBZ tripeptides (0.8 g)	1-BuOH/MBE/ACN/H_2O (2 : 2 : 1 : 5)	TFA (16 m*M*/SP)	NH_3 (2.7 m*M*/MP)	—
Dipeptide βNA (0.3 g)	MBE/ACN/H_2O (2 : 2 : 3)	TEA (5 m*M*/SP)	HCl (5 m*M*/MP)	—
Dipeptides (1 g)	MBE/ACN/50 m*M* HCl (4 : 1 : 5) (SP)	TEA (20 m*M*/SP)		DEHPA (30%/SP)
	MBE/1-BuOH/ACN/H_2O (2 : 2 : 5 : 1) (MP)		HCl (20 m*M*/MP)	
Bacitracins (5 g)	MBE/50 m*M* HCl (SP)	TEA (40 m*M*/SP)		DEHPA (10% SP)
	MBE/H_2O (MP)		HCl (20 m*M*/MP)	

[a]CBZ = carbobenzoyl; βNA = naphthyl amide.
[b]ACN = acetonitrile; BuOH = butanol; MBE = methyl *tert*-butyl ether; MP = mobile phase; SP = stationary phase.
[c]DEHPA = di-[2-ethylhexyl]phosphoric acid; TFA = trifluoroacetic acid; MP = mobile phase; SP = stationary phase.

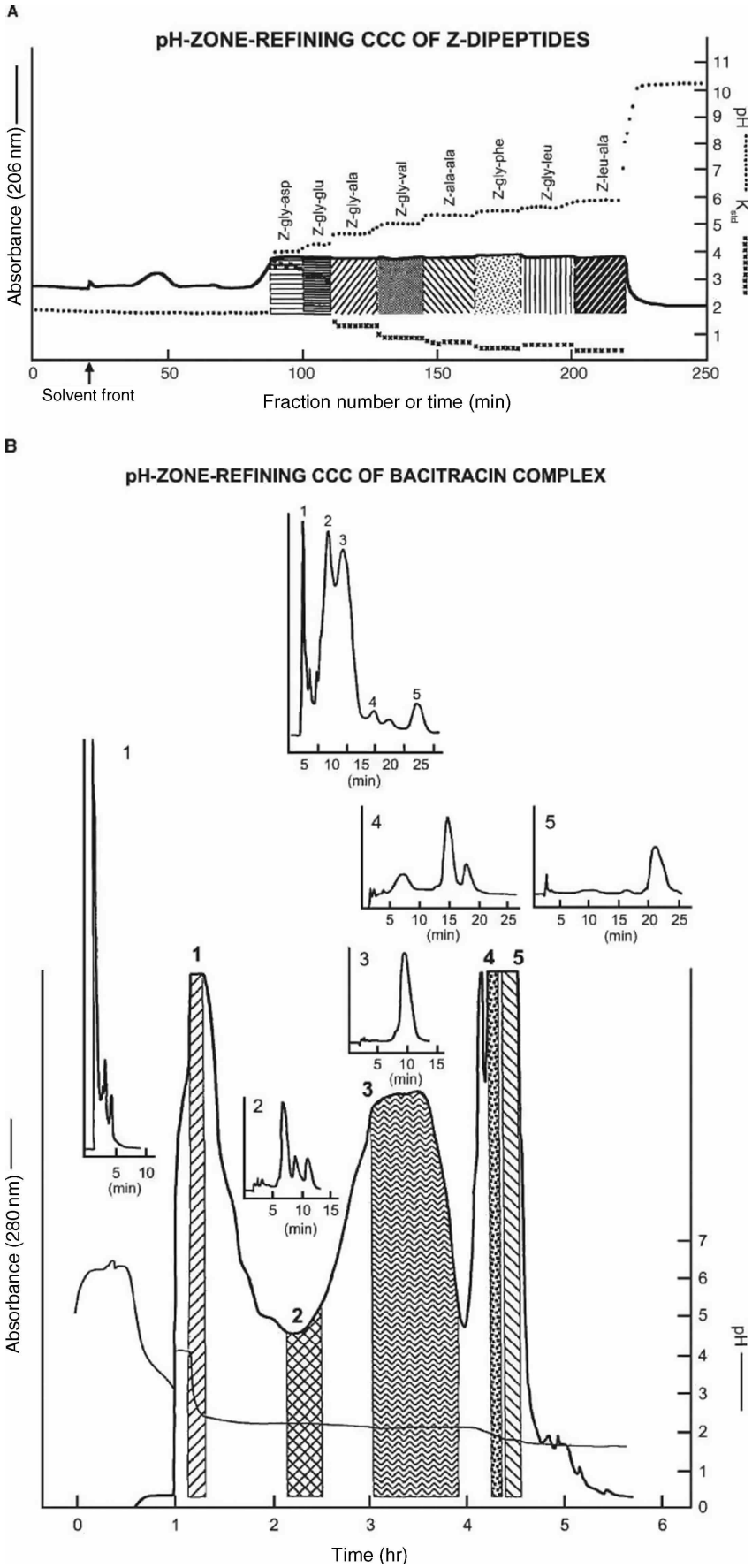

Fig. 3 Chromatograms obtained by pH zone-refining CCC. A, Separation of CBZ(Z) dipeptides. Experimental conditions are as follows: apparatus: type-J multilayer CPC (PC Inc., Potomac, Maryland, U.S.A.) with a 10 cm revolution radius; column: multilayer coil, 1.6 mm I.D., 325 ml capacity; solvent system: methyl *tert*-butyl ether/acetonitrile/water (2 : 2 : 3), 16 m*M* TFA in organic phase (pH 1.83), and 5.5 m*M* NH_3 in aqueous phase (pH 10.62); sample: eight CBZ(carbobenzyloxy) dipeptides as indicated in the chromatogram, each 100 mg in 50 ml of solvent (25 ml in each phase): flow rate: 3.3 ml/hr in head-to-tail elution mode; detection: 206 nm; revolution: 800 rpm; retention of stationary phase: 65.1%. (B) Separation of bacitracin complex. HPLC analysis indicated that two major components, bacitracins A and B, were isolated in peaks 3 and 5, respectively. Experimental conditions are as follows: apparatus and column: same as above; solvent system: methyl *tert*-butyl ether/acetonitrile/water (4 : 1 : 5), 40 m*M* triethylamine, 10% DEHPA in the organic stationary phase, and 20 m*M* HCl in aqueous mobile phase; flow rate: 3 ml/min; sample: 5 g of bacitracin dissolved in 40 ml of solvent (20 ml in each phase); revolution: 800 rpm; detection: 280 nm.

stationary phase, whereas the system yields less efficient resolution than the type-J high-speed CCC. Although the system was successfully utilized for the separation of bacitracin and gramicidin having a potential for a large-scale preparative separation of more polar peptides, the method is currently used almost exclusively for the separation of proteins with aqueous–aqueous polymer phase system.[11]

pH Zone-Refining CCC

In addition to the standard high-speed CCC technique described above, peptides can be purified by using a large-scale preparative method, called pH zone-refining CCC, in which analytes form a train of highly concentrated rectangular peaks with minimum overlapping.[8,9] The solvent system and the separation procedure of this technique are quite different from the standard high-speed CCC. The method requires a pair of special agents called "retainer" and "eluter." As suggested by their names, the retainer serves to retain the analyte in the stationary phase and the eluter serves to elute the analyte with the mobile phase. The separation of free peptides requires another agent, called an affinity ligand, such as di-[2-ethylhexyl]phosphoric acid (DEHPA), which is introduced into the stationary phase to enhance the retention of the analyte in the column. The typical retainers, eluters, and affinity ligands, together with the two-phase solvent systems, are listed in Table 2. Usually, the separation is performed with a two-phase solvent system containing *tert*-butyl methyl ether (MBE) as a major organic solvent (Table 2), which, because of its less viscous nature, gives higher stationary phase retention and partition efficiency than the butanol solvent systems.

Fig. 3A and B illustrates typical chromatograms. obtained by pH-zone-refining CCC (Table 2).

CONCLUSIONS

The CCC technique is well suited for the separation of peptides and related compounds because it eliminates sample loss and denaturation caused by the solid support used in conventional LC. The method separates multigram quantities of peptide samples using pH zone-refining CCC.

REFERENCES

1. Ito, Y.; Bowman, R.L. Countercurrent chromatography: Liquid–liquid partition chromatography without solid support. Science **1970**, *167*, 281–283.
2. Ito, Y. Principle and instrumentation of countercurrent chromatography. In *Countercurrent Chromatography: Theory and Practice*; Mandava, N.B., Ito, Y., Eds.; Marcel Dekker, Inc.: New York, 1988; 79–442 (Chapter 3).
3. Conway, W.D. *Countercurrent Chromatography: Apparatus, Theory and Applications*; VCH: New York, 1990.
4. Ito, Y. Countercurrent chromatography (minireview). J. Biochem. Biophys. Methods **1981**, *5* (2), 105–129.
5. Ito, Y. Countercurrent chromatography. In *Methods in Enzymology*; Enzyme Structure, Part I; Hirs, C.H.W., Timasheff, S.N., Eds.; Academic Press: New York, 1983; Vol. 91, 335–351.
6. Ito, Y. Apparatus and methodology of high-speed countercurrent chromatography. In *High-Speed Countercurrent Chromatography*; Chemical Analysis Series; Yoichiro, I., Conway, W.D., Eds.; Wiley Interscience: New York, 1996; Vol. 132, 3–43.
7. Ito, Y. High-speed countercurrent chromatography. CRC Crit. Rev. Anal. Chem. **1986**, *17* (1), 65–143.
8. Ito, Y.; Ma, Y. pH-Zone-refining countercurrent chromatography. J. Chromatogr. A, **1996**, *753*, 1–36.
9. Ma, Y.; Ito, Y. Peptide separation by pH-zone-refining countercurrent chromatography. J. Chromatogr. A, **1997**, *771*, 81–88.
10. Ito, Y.; Yang, F.-Q.; Fitze, P.E.; Sullivan, J.V. Spiral disk assembly for high-speed countercurrent chromatography. J. Liq. Chromatogr. Relat. Technol. **2003**, *26* (9 & 10), 1355–1372.
11. Ito, Y.; Menet, J.-M. Coil planet centrifuges for high-speed countercurrent chromatography. In *Countercurrent Chromatography*; Jean-Michel, M., Thiébaut, D., Eds.; Marcel Dekker: New York, 1999; 87–119 (Chapter 3).

Peptides: HPLC Analysis

Karen M.Gooding
Eli Lilly and Company, Indianapolis, Indiana, U.S.A.

INTRODUCTION

The rapid advancement in peptide research over the past 25 years must be attributed, in part, to the effectiveness of high-performance liquid chromatography (HPLC), particularly reversed-phase chromatography, in the separation and analysis of peptides. The resolution and selectivity of this technique allows peptides to be effectively isolated and purified from closely related substances. It also separates most or all of the components of complex biological mixtures such as tryptic digests of proteins.

MODES OF HPLC

Peptides, which are composed of amino acids linked by amide bonds, are often found in random coil to semi-defined conformations, depending on their lengths and structures. As such, most of the composite amino acids are available to interact with the bonded phase of an HPLC support. Although the variety of amino acid characteristics, such as charge, polarity, and hydrophobicity, would suggest that multiple modes of HPLC would be effective for separation, reversed-phase chromatography has shown the ultimate success in selectivity and resolution of peptides. Hydrophilic interaction chromatography (HICIC) is a good alternative for hydrophilic peptides or other mixtures that are not separated well by reversed-phase chromatography (RPC), whereas cation-exchange chromatography can be effective for highly cationic species. Size-exclusion chromatography (SEC) is a difficult technique for analysis of peptides, due to their varying solubilities and high degrees of hydrophobicity and charge; however, it is invaluable for resolution from dimers and aggregates.

REVERSED-PHASE CHROMATOGRAPHY

Reversed-phase chromatography is a method in which molecules are bound hydrophobically to non-polar ligands in the presence of a polar solvent. Solutes are generally bound in an acidic mobile phase with elution occurring during a gradient to an organic solvent. Molecules will tend to be unfolded due to the combination of acidic and organic mobile phases and the hydrophobic bonded phase. Consequently, binding involves most of the amino acids, depending on the conformation. RPC can differentiate peptides which vary in the positions of their amino acids, as well as in their identities, thus making it a powerful analysis tool. Very high selectivity is attained even for complex biological mixtures, such as the tryptic digest of human growth hormone shown in Fig. 1.[1]

There are many ligands used for RPC, but the most popular for peptide analysis are octadecyl (C_{18}) and octyl (C_8) chains. Little difference in selectivity for peptides is observed with ligand chain-length variation; however, mass recovery of very hydrophobic species may be enhanced on the shorter chains. Many RPC bonded phases are synthesized by silane bonding, with or without endcapping, which results in a hydrophobic layer on a silanol surface. Recently, more hydrophilic–hydrophobic phases have been developed whereby amide linkages are embedded in the non-polar layer to provide a wettable area which may be more compatible with some biological molecules. Due to their higher efficiencies, silica-based supports are generally used for peptide analysis; however, polymeric supports are effective for operation at high pH. The silica matrix is sometimes a factor in retention because silanols on reversed-phase supports are rarely totally eliminated. Most peptide analyses use supports with pore diameters of at least 300 Å to allow access to the bonded phase; non-porous supports offer a high-resolution option with significantly lower capacities. Dynamic loading capacities of peptides on porous analytical reversed-phase columns (250×4.6 mm I.D.) are usually 100–500 μg.

Due to the multiple functional groups found in peptides, selectivity can be vastly changed by operational factors. Variable mobile-phase parameters include organic modifiers, pH, ion-pair agents, and gradient rates. Acetonitrile is the most popular organic solvent for RPC of peptides due to its transparency at low wavelengths ($<$210 nm) and its tendency to yield narrow peak widths. The strength of the organic solvent which causes elution increases from methanol to acetonitrile to isopropanol. Acidic pH is generally utilized to minimize silanol interactions; however, distinct pH conditions yield different selectivities. Ion-pairing agents, such as trifluoroacetic acid, are often added to the mobile phase to change the ionic or hydrophobic properties of either or both of the solute and the bonded phase. Amounts of 0.1% added to both the aqueous and the organic mobile phases are usually adequate, but optimal concentrations can be determined experimentally. Trifluoroacetic acid (TFA) is the most popular ion-pairing agent for peptides, imparting some

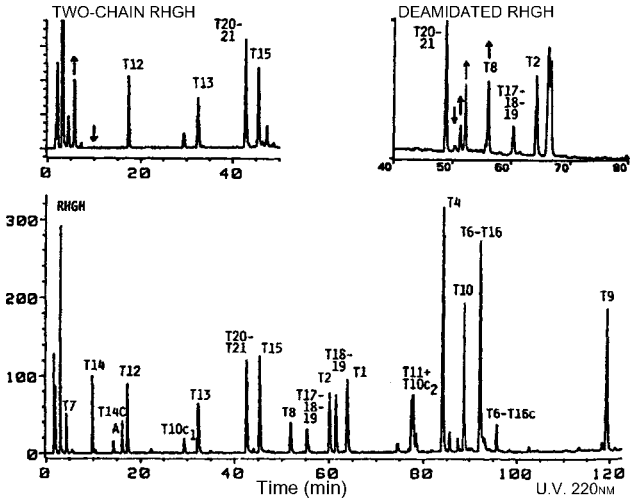

Fig. 1 Tryptic maps of the intact and (insets) degraded forms of recombinant human growth hormone (RHGH). The separation was achieved on a Nucleosil C-18 column (150 × 3.9 mm inner diameter) with a 120 min mobile-phase gradient from 10 m*M* potassium phosphate (pH 2.85) to 60% acetonitrile in the starting buffer. The flow rate was 1 ml/min and detection was at 214 nm.
Source: From *HPLC of Biolgical Macromolecules: Methods and Applications*.[1]

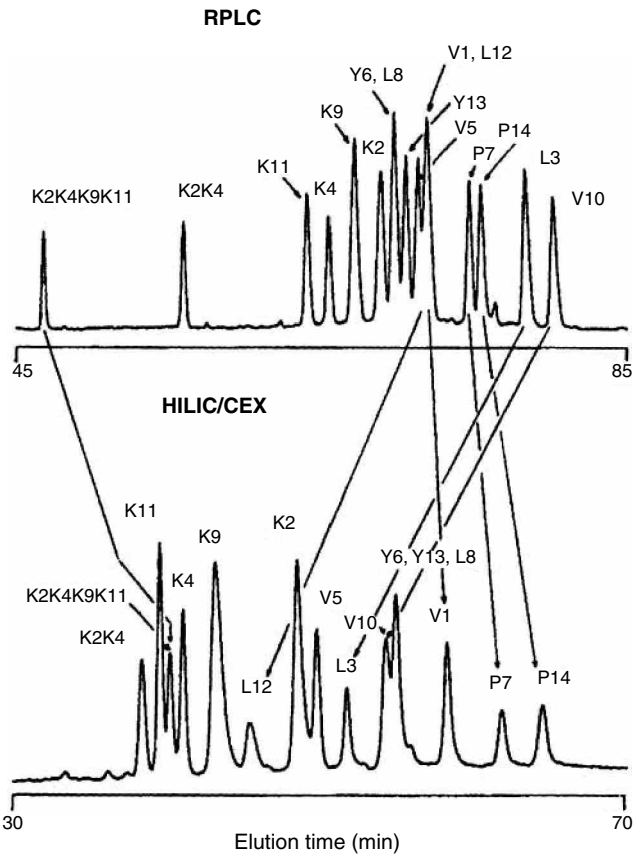

Fig. 2 Comparison of RPLC and HILIC/CEX elution profiles of cyclic peptides. RPC: Zorbax 300XDB-C_8 column; linear gradient (0.5% acetonitrile/min) from 0.05% aqueous trifluoroacetic acid (TFA) to 0.05% TFA in acetonitrile at 1 ml/min; at 70°C and detection at 210 nm. HILIC/CEX: Polysulfoethyl A column; 5 min isocratic elution with buffer A (20 m*M* aqueous triethylammonium phosphate with 90% acetonitrile), followed by linear gradient (2.5 m*M* sodium perchlorate/min) from buffer A to buffer B (buffer A containing 400 m*M* sodium perchlorate with 80% acetonitrile); at 30°C and detection at 210 nm.
Source: From Hydrophilic interaction/cation-exchange chromatography for separation of cyclic peptides, in J. chromatogr.[2] with permission of Elseivier Science.

additional hydrophobicity to amine groups and neutralizing cationic charges.

Most RPC peptide separations utilize gradient rather than isocratic conditions. Small peptides may be resolved well isocratically; however, due to multipoint interactions, larger ones yield broad peaks and tailing unless gradients are used. Shallow gradients generally improve resolution in an analytical mode or purity in preparative applications. For complex mixtures, 0.5–1% organic/min is usually a satisfactory rate. Increased temperatures can be implemented to reduce both retention times and the pressure generated by small-particle-diameter supports.

HYDROPHILIC INTERACTION CHROMATOGRAPHY

Hydrophilic interaction chromatography is a variation of normal-phase chromatography in which solutes are retained on a polar bonded phase under high concentrations (80–90%) of organic solvent and released during a gradient to a more aqueous solvent. If the polar bonded phase contains a charge, a salt gradient can also be implemented, yielding separation by both charge and polarity. HILIC is most effective for polar peptides which are often poorly retained by RPC. Fig. 2 compares the differences in selectivity and resolution of a cation-exchange (CEX) procedure on a HILIC column with that of RPC for a peptide mixture.

The HILIC - bonded phases are hydrophilic, consisting of amide and/or polyhydroxy functionalities. Pore diameters are at least 300 Å to allow penetration of peptides. Supports can be based on either silica or polymer because the matrix is not exposed to the solutes.

Mobile-phase manipulation causes variations in selectivity in HILIC. Although a buffer is used for pH control, it may also serve to change the hydrophobicity of the solutes by ion-pairing. More hydrophobic ions such as acetate will decrease retention. The pH is a less important factor than the identity of the salt in HILIC selectivity. The organic modifier and its initial concentration directly affect retention and resolution. At least 80–90% organic is usually required to achieve adequate retention of hydrophilic peptides. For HILIC/cation exchange (HILIC/CEX), a

salt gradient is implemented to separate the hydrophilic peptides by charge, as can be seen in Fig. 2.[2]

ION-EXCHANGE CHROMATOGRAPHY

Ion-exchange chromatography (IEC) separates peptides by ionic attraction of their composite amino acids to charges on the stationary phase. Selectivity is dependent on the number and the identity of the amino acids, as well as their spatial arrangement. A peptide with charges grouped together will bind differently than one whose charges are dispersed. IEC has been most successful for cationic peptides that cannot always be analyzed effectively by RPC.

Supports for IEC possess either anion- or cation-exchange functionalities which are positively or negatively charged, respectively. They are also classified as weak or strong to correspond to their titration curves, similar to acid and base designations. Generally, strong cation-exchange supports are used for peptide analysis. The pore diameter is important in that it must be large enough to allow access of the peptides so that they are effectively retained and have optimum loading capacities.

In IEC, solutes are bound in a low-ionic-strength buffer (0.02–0.05 *M*) at an appropriate pH (often 1–2 pH units from the p*I*). Elution occurs when the ionic strength is increased during a concentration gradient of a salt in the same buffer. Isocratic elution may successfully separate small peptides with one or two charged groups, but larger peptides with more charged groups will require gradients for good peak shapes, resolution, and reproducibility. The nature of the salt in IEC has a major effect on selectivity due to interaction of the composite ions with either the stationary phase or the solutes. The hydrophobicity of many peptides may necessitate the addition of 5–10% organic solvent to improve peak shape. This can usually be included in the mobile phase without deleterious effects on the separation.

SIZE-EXCLUSION CHROMATOGRAPHY

Size-exclusion chromatography is a method in which molecules are separated by size due to differential permeation into a porous support. It requires complete solubility of the analytes in the mobile phase and elimination of all interactions with the bonded phase. In these respects, SEC is not as useful for the separation of peptides as it is for proteins because peptides vary drastically in solubility, charge, and hydrophobicity. Peak capacity in SEC is fairly low compared to other HPLC methods because all separations must occur in the internal volume (V_i) of the support, which is generally less than half the volume of mobile phase in the column. Despite these deficiencies, SEC can be very effective for separating peptides from dimers, aggregates, small molecules, proteins, and other molecules which differ by size.

Supports for SEC of proteins are designed to be neutral and very hydrophilic to avoid interaction of the solutes with the support by ionic or hydrophobic mechanisms. The base matrix can be either silica or polymer; efforts are made to totally mask its properties with a carbohydrate-like stationary phase. The pore structure is critical to successful SEC. Not only must the total pore volume (V_i) be adequate for separation, the pore diameter must be consistent and nearly homogeneous for attainment of maximum resolution between molecules with relatively small differences in molecular size (radius of gyration or molecular weight). A twofold difference in size is usually required for separation by SEC. Retention in SEC is directly related to the logarithm of the radius of gyration or the molecular weight. Because peptides do not all have the same shapes, their molecular volumes may not correspond uniformly to their molecular weights unless they are in the presence of sodium dodecyl sulfate (SDS) or another denaturing agent.

The mobile phase is a critical factor in SEC because it must eliminate all solute–support interactions. This may require adjustment to low pH or to an ionic strength which eliminates ionic interactions (0.05–0.2 *M*) and/or the addition of 5–10% organic solvent to remove hydrophobic binding. Due to their variations in physical properties, it is sometimes difficult to eliminate all the ionic and hydrophobic interactions of a mixture of peptides using a single mobile phase.

DETECTION

The detectability of peptides varies greatly, depending on their amino acid composition. The aromatic amino acids (tyrosine, tryptophan, and phenylalanine) offer selective detection by ultraviolet (UV) light at 280 or 254 nm or by fluorescence detection. In the absence of these amino acids, low wavelengths (<220 nm), which also detect many other substances, including components of the mobile phase, must be used. TFA and acetonitrile are compatible with low wavelengths, making this system a popular one for peptide analysis by RPC. Alternatively, the amine functionalities of peptides can be derivatized using precolumn or postcolumn techniques with compounds such as fluorescamine. In this way, selective and sensitive detection methods like fluorescence can be implemented. Mass spectrometry also provides a viable, albeit, expensive means of detection of peptides.

CONCLUSIONS

High-performance liquid chromatography provides a rapid and effective means for the analysis and purification of peptides. RPC is the primary and most universally

successful mode, with HILIC and IEC offering alternative methods for hydrophilic peptides or others where RPC is ineffective. HILIC and IEC are also orthogonal modes to RPC for preparative or identification purposes. The ability to change selectivity using the mobile phase in HPLC methods makes them versatile techniques which can be rapidly optimized and implemented.

REFERENCES

1. Frenz, J.; Hancock, W.S.; Henzel, W.J.; Horvath, Cs. *HPLC of Biological Macromolecules: Methods and Applications*; Gooding, K.M., Regnier, F.E., Eds.; Marcel Dekker, Inc.: New York, 1990, p. 145.
2. Mant, C.T.; Kondejewski, L.H.; Hodges, R.S. Hydrophilic interaction/cation-exchange chromatography for separation of cyclic peptides. J. Chromatogr. **1998**, *816*, 79–88, 99.

BIBLIOGRAPHY

1. Cunico, R.L.; Gooding K.M.; Wehr T. *Basic HPLC and CE of Biomolecules*; Bay Bioanalytical Laboratories: Richmond, CA, 1998.
2. Gooding, K.M., Regnier, F.E., Eds.; *HPLC of Biological Macromolecules: Methods and Applications;* Marcel Dekker, Inc.: New York, 1990.
3. Hancock, W.S., Ed.; *High Performance Liquid Chromatography in Biotechnology*; John Wiley & Sons: New York, 1990.
4. Hearn, M.T.W., Ed.; *HPLC of Protiens, Peptides and Polynucleotides*; VCH: New York, 1991.
5. Katz, E.D., Ed,; *High Performance Liquid Chromatography: Principles and Methods in Biotechnology*; John Wiley & Sons: New York, 1996.
6. Mant, C.T. Hodges, R.S., Eds.; *High-Performance Liquid Chromatography of Peptides and Proteins*; CRC Press: Boca Raton, FL, 1991.

Peptides: Purification with Immobilized Enzymes

Jamel S. Hamada
Southern Regional Research Center, Agricultural Research Service, U.S. Department of Agriculture (USDA-ARS), New Orleans, Louisiana, U.S.A.

INTRODUCTION

Affinity chromatography is a powerful separation technique that exploits specific binding properties among biomolecules. For protein purification, the enrichment obtainable in single-step affinity chromatography sometimes exceeds 1000-fold. This high selectivity is due to the vast variety of specific interactions that characterize the functional properties of protein molecules. Like any other affinity chromatography technique, purification of peptides by immobilized enzymes captures the unique interactions between biomolecules (see Refs.[1–3]). For example, many enzymes reversibly bind to their organic cofactor molecules and inhibitors. The separation of such enzymes from other proteins can be easily achieved by using a chromatography column containing immobilized inhibitors. Inversely, the enzyme inhibitors can be isolated and purified to a high degree of purity by affinity chromatography using immobilized enzymes. Because affinity chromatography is a most selective technique, it may be used alone as a single chromatography step for peptide purification. However, as many input-material contaminants as possible must be removed prior to using affinity chromatography (e.g., before the affinity chromatography step). For instance, ultrafiltration or gel permeation chromatography (GPC) is sometimes used concurrently to separate the high- and low-molecular-weight forms while exchanging buffers. In this entry, the focus will be on the use of affinity chromatography to purify peptides when the immobilized ligand is an enzyme.

GENERAL PRINCIPLES OF PEPTIDE PURIFICATION BY IMMOBILIZED ENZYMES

The first step in this type of chromatography is the preparation of the column by enzyme immobilization on activated support. Enzymes are immobilized by covalent bonding to a packing of a chromatography column (i.e., a support solid matrix such as a cross-linked agarose bead). A mixture of components containing the peptide of interest is applied to the column. Peptides are bound with a high degree of specificity to the immobilized enzyme that functions as an ionic, hydrophobic, aromatic, or stoically active binding site, depending on the particular circumstances. The unbound contaminants, which have no affinity for the ligand, are washed through the column, leaving the desired peptide bound to the matrix. Bound peptides are released by manipulating the composition of the eluant buffers. Generally, the elution of the peptide is accomplished by changing the pH and/or salt concentration or by applying organic solvents or a molecule that competes for the bound ligand (Fig. 1).

EXAMPLES OF PURIFICATION OF PEPTIDES BY IMMOBILIZED ENZYMES

Purification of Protein Hydrolysates

Proteases possess special characters, including their ability to cleave at certain amino acid sites such as at the hydrophobic or neutral residues. This cleavage specificity produces protein hydrolysates that vary significantly in their molecular weights, charge characteristics, functional profiles, and, thus, their potential specific interactions. Using immobilized proteases for peptide purification is a typical application of this type of affinity chromatography. Trypsin is a serine protease; that is, it contains an essential serine at its active site and cleaves the peptide bond next to a basic amino acid residue. Anhydrotrypsin is an inert derivative of trypsin and, thus, has no catalytic activity. It contains dehydroalaninein in place of the active serine residue site. The modified enzyme has 20-fold more affinity for product peptides produced by tryptic cleavage than substrate peptides. C-Terminal arginine peptides adhere more tightly than COOH-terminal lysine peptides. Accordingly, immobilized anhydrotrypsin has been used as an affinity ligand for the purification of these peptides. Because of widely varied peptide structure, further specificity may be obtained during elution, which usually involves decreasing pH gradients.

Purification of Pawpaw Glutamine Cyclotransferase

Pawpaw glutamine cyclotransferase (PQC) was purified 279-fold to near homogeneity by a combination of ion-exchange chromatography on SP-Sepharose, hydrophobic interaction chromatography on Fractogel TSK Butyl-650, and affinity chromatography on immobilized trypsin.[4] Trypsin was immobilized on Affigel-10 (Bio

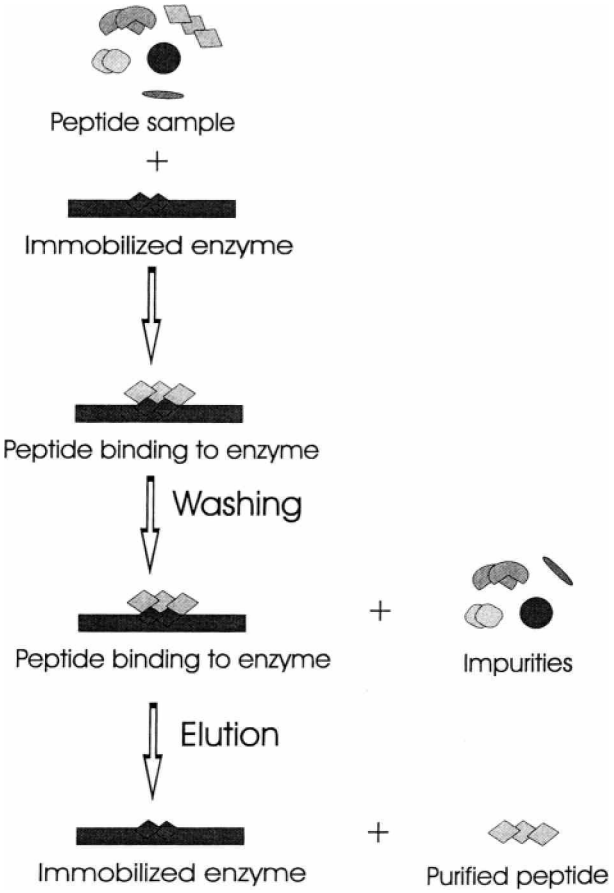

Fig. 1 Schematic illustration of purification of a peptide by affinity chromatography on an immobilized enzyme.

Rad Laboratories) according to procedures recommended by the manufacturer. After the concentration of pooled fractions from the last purification step (Fractogel column) by ultrafiltration, affinity chromatography was used. Partially purified PQC was injected into a 12.5 × 1.6 cm inner diamater column of immobilized trypsin gel preequilibrated in the eluting buffer (20 m*M* in 50 m*M* Tris-HCl buffer, pH 8.2). Affinity purification was accomplished because PQC contains a unique and highly basic polypeptide chain containing covalently attached phosphate groups without any disulfide bonds.

Purification of Enzyme Inhibitors

Enzyme inhibition may be reversible or irreversible with different inhibitors. Irreversible inhibitors usually form covalent bonds and, thus, are not useful for this type of affinity chromatography. Reversible inhibitors work by a variety of mechanisms, but usually competitive inhibitors structurally resemble the peptide substrates and bind the active center. *Trichosanthes kirilowii* trypsin inhibitor analog (Ala-6-TTI) is a trypsin inhibitor in which methionine at position 6 is replaced by alanine. Affinity chromatography was used to purify expressed fusion protein containing large proteins and (Ala-6)-TTI, with methionine as a connecting residue.[5] After cyanogen bromide cleavage and reduction of the fusion protein, followed by affinity chromatography separation on trypsin-Sepharose 4B as a matrix and on the immobilized trypsin, the fully active (Ala-6)-TTI was obtained in a high purity and high yield. The trypsin inhibitory activity and amino acid composition of the recombinant (Ala-6-TTI) were consistent with those of the natural one.

An essentially pure extracellular glycoprotein proteinase inhibitor was isolated from the latex of green fruits of papaya by a single affinity chromatography purification step.[6] An immobilized trypsin-Sepharose CL 4B column was prepared according to the manufacturer (Amersham Pharmacia Biotech), which provided elaborated bulletins for the preparation procedures and applications of these affinity gel columns. Latex extract was applied to the column after equilibration with 20 m*M* Tris-HCl, pH 8.0, containing 0.5 *M* NaCl and 0.05 *M* $CaCl_2$. The column was extensively washed with the same buffer until ultraviolet (UV) absorbance became undetectible. The bound trypsin inhibitor was eluted with 0.02 *M* HCl and recovered by lyophilization after dialysis against water.

Purification of Dipeptidyl Peptidase IV

Dipeptidyl peptidase IV (E.C. 3.4.14.5) cleaves off N-terminal dipeptides from peptides when a proline or alanine is at the penultimate position. The enzyme was purified from human seminal plasma and prostasomes by a two-step scheme of ion-exchange chromatography on DEAE–Sepharose, followed by affinity chromatography on adenosine deaminase (E.C. 3.5.4.4)–Sepharose.[7] This scheme resulted in a pure, native protein with an overall yield ranging from 35% to 55%. The preparation obtained was free of contaminating aminopeptidase activity.

Purification of Recombinant Proteins via Peptide Accession

Purification of peptides by immobilized enzymes is a relatively recent approach that may have a potential use in the purification of genetically engineered proteins. Purification of recombinant proteins is often difficult and involves many purification steps for a very low yield. Smith et al.[8] found that a specific metal-chelating peptide on the NH_2 terminus of a protein can be used to purify that protein with immobilized ion affinity chromatography. The nucleotide sequence that codes for the expressed protein is extended to include codons for the chelating peptide. This concept of amino acid addition to recombinant proteins can also be beneficial in protein purification by affinity chromatography with immobilized enzymes.

This will have an impact on the cloning, expression, and the purification of proteins.

CONCLUSIONS

Affinity purification of peptides by immobilized enzymes relies on the highly specific interaction of an ionic, hydrophobic, aromatic, or stoically active binding site on the desired peptide to the immobilized enzyme. The unbound contaminants are washed through and the desired peptide is released by buffer elution. This technique is beneficial in the purification of many peptides and can also be used for affinity chromatography of recombinant proteins after cloning and expression.

REFERENCES

1. Bell, J.E.; Bell, E.T. Protein purification: Affinity chromatography. In *Proteins and Enzymes*; Prentice-Hall: Englewood Cliffs, NJ, 1988; 45–63.
2. Carlsson, J.; Janson, J.-C.; Sparrma, M. Affinity chromatography. In *Protein Purification: Principles, High Resolution Methods, and Applications*; Janson, J.C., Ryden, L., Eds.; VCH: New York, 1989; 275–329.
3. Schott, H. *Affinity Chromatography*; Chromatographic Science Series; Marcel Dekker, Inc.: New York, 1984; Vol. 27.
4. Zerhouni, S.; Amrani, A.; Nijs, M.; Smolders, N.; Azarkan, M.; Vincentelli, J.; Looze, Y. Purification and characterization of papaya glutamine cyclotransferase, a plant enzyme highly resistant to chemical, acid and thermal denaturation. Biochem. Biophys. Acta **1998**, *1387*, 275–290.
5. Chen, X.M.; Qian, Y.W.; Chi, C.W.; Gan, K.D.; Zhang, M.F.; Chen, C.Q. Chemical synthesis, molecular cloning, and expression of the gene coding for the Trichosanthes trypsin inhibitor—A squash family inhibitor. J. Biochem. (Tokyo) **1992**, *112*, 45–51.
6. Odani, S.; Yokokawa, Y.; Takeda, H.; Abe, S.; Odani, S. The primary structure and characterization of carbohydrate chains of the extracellular glycoprotein proteinase inhibitor from latex of Carica papaya. Eur. J. Biochem. **1996**, *241*, 77–82.
7. De-Meester, I.; Vanhoof, G.; Lambeir, A.M.; Scharpe, S. Use of immobilized adenosine deaminase (EC 3.5.4.4) for the rapid purification of native human CD26/dipeptidyl peptidase IV (EC 3.4.14.5). J. Immunol. Methods **1996**, *189*, 99–105.
8. Smith, M.C.; Furman, T.C.; Ingolia, T.D.; Pidgeon, C. Chelating peptide-immobilized metal ion affinity chromatography. A new concept in affinity chromatography for recombinant proteins. J. Biol. Chem. **1988**, *263*, 7211–7215.

Pesticides: GC Analysis

Fernando M. Lanças
Institute of Chemistry of São Carlos (USP), University of São Paulo, São Carlos, Brazil

M.A. Barbirato
Chromatography Laboratory, University of São Paulo, São Carlos, Brazil

INTRODUCTION

In spite of the worldwide controversy which has surrounded the use of pesticides for many years, there can be little doubt that they provide one of the most effective contributions to increasing crop production and they have helped the farmer to improve the quality and variety of our foodstuffs. However, even when used correctly, these compounds can cause ecological consequences, public health problems, and the occurrence of toxic residues in foodstuffs. These problems make necessary the development of analytical methodologies that allow the appropriate monitoring of pesticides residues.

One of the most important analytical techniques used today is high-resolution gas chromatography (HRGC). The pesticide residues can be analyzed by specific or multiresidue methods. When crops are treated with several pesticides, the use of a multiresidue method is preferable due the reduced cost and time of analysis. The methods of pesticides residue analysis usually present an initial step of extraction with a solvent which is not miscible with water, followed by a cleanup step and the analyte determination by gas chromatography (GC).

EXTRACTION METHODS

Sample preparation represents a formidable challenge in the chemical analysis of the "real-world" samples. Not only is the majority of total analysis time spent in sample preparation, but also it is the most error-prone, least glamorous, and the most labor-intensive task in the laboratory. The components to be separated from the matrix are usually taken up with an auxiliary substance such as a carrier gas, an organic solvent, or an adsorbent. These separation processes can be regarded as extraction procedures [i.e., liquid–liquid extraction (LLE), liquid–solid extraction (LSE), Soxhlet extraction (SE), solid-phase extraction (SPE), supercritical fluid extraction (SFE), solid-phase microextraction (SPME), etc.].

Soxhlet extraction has been the standard extraction method of the analyst for nearly 90 years. The complete extraction produces a high-volume diluted solution that usually needs to be concentrated prior to analysis. The choice of solvent determines the solvating power as well as the temperature of the extraction. Perhaps the greatest disadvantage of using the Soxhlet method is the utilization of expensive, high-purity organic solvents such as acetone and methylene chloride.

Liquid–liquid extraction uses two immiscible liquids as the two phases. The sample is dissolved in one of the liquids (refinate) which comes in contact with the other liquid (extractant) into a separatory funnel, under agitation, to increase the contact area among the phases. Some mixing time is usually necessary for efficient phase exchange. Multiple extractions are also mandatory if quantitative extraction is desired. Sample transfer can become a problem, especially if phase emulsions are produced.

Solid–liquid extraction, normally performed at room temperature, is a simpler version of Soxhlet extraction (Fig. 1). The extraction of sample components is performed by blending the sample with a solvent. The choice of the extraction solvent can be determined by the analyst's experience, the equipment available in the laboratory, the type of sample to be analyzed, and the range of target analytes. Ethyl acetate is usually more powerful than acetone for extraction of more polar compounds. As regards selectivity, acetone is preferable because the amount of polar coextracted matrix interference will be less.

Solid-phase extraction is based on low-pressure LC, where a short column is filled with an adsorbent. The separation mechanisms are based on the intermolecular interactions among analyte molecules and functional groups of sorbent. The choice of eluent is made by the relationship between the eleutropic value (Σ°) and the analyte polarity. SPE is fast, selective, and economical if compared with the extraction methods described previously. It can be applicable to both non-polar and polar analytes, but both matrix and analyte must be in the liquid state.

Supercritical fluid extraction provides, for the first time, a viable alternative to other traditional sample preparation techniques which are slow, composed of several steps, and make use of organic solvents. A supercritical fluid can be defined as any substance that is above its critical temperature and critical pressure. A supercritical fluid exhibits physicochemical properties intermediate between those of liquids and gases. Specifically, its relatively high (liquid-like) density gives good solvating

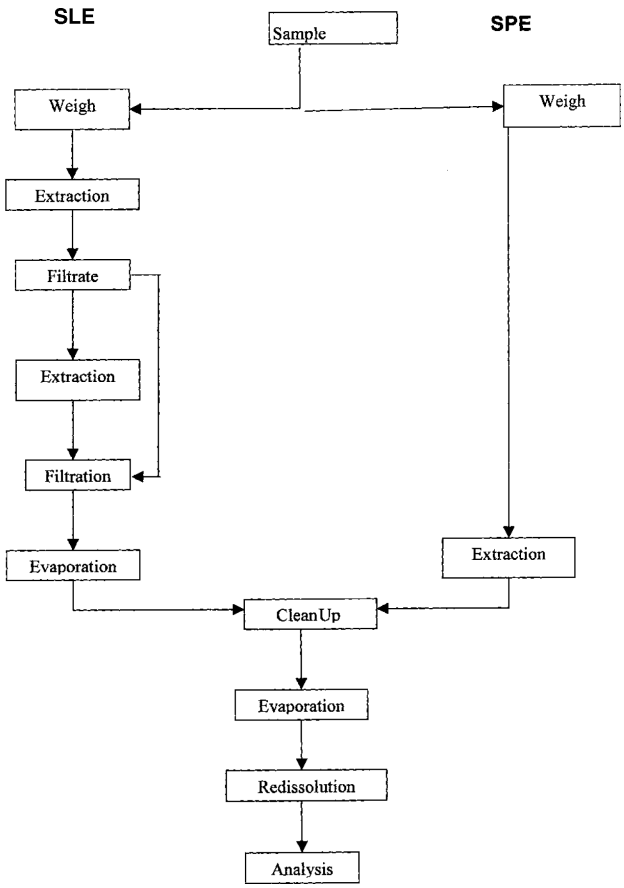

Fig. 1 Schematic diagram of the main steps of the solid–liquid extraction and supercritical fluid extraction methodologies for pesticide residue analysis.

power, whereas its relatively low viscosity and high diffusivity (gas-like) values provide appreciable penetrating power into the matrix. These latter two properties have been shown to give rise to higher rates of solute mass transfer into a supercritical fluid than into a liquid.

Supercritical CO_2 is the fluid with more applications at the present time, due to its readily amenable critical conditions ($T_c = 31.3°C$; $P_c = 72.9$ atm) and high volatility and diffusivity, and it also is inert, inexpensive, non-flammable, nontoxic, and miscible with most solvents. It has been used to extract compounds ranging from low polarity to moderate polarity. The extraction of polar compounds can be performed by supercritical CO_2 modified by the addition of a small volume of a polar liquid solvent.

The major parameters that influence the supercritical fluid extraction are temperature, pressure/density, fluid composition, particle size, matrix type, and extract collection system.

Solid-phase microextraction is based on the adsorption of an analyte in a fused-silica fiber externally coated with a stationary phase and following a thermal desorption in the injector of a GC. The fiber is introduced into the aqueous sample. In SPME, usually equilibrium among the aqueous samples and the stationary organic phase occurs instead of an exhaustive extraction. The pH, ionic strength, temperature, time, and agitation of the sample can exert an influence on the quality of the extract. The SPME process can integrate sampling, extraction, concentration, and sample introduction in just one step.

CLEANUP PROCEDURES

No single cleanup method is able to cover the entire matrix range. The need for a cleanup procedure prior to GC analysis is largely dependent on the complexity of the matrix and the range of analytes to be analyzed.

The most important cleanup procedures are liquid–liquid partition, LC in a column of silica, florisil, and/or alumina, gel permeation chromatography, and solid-phase extraction. Gel permeation chromatography (GPC) is the most universally applicable cleanup method for the removal of high-molecular-weight compounds. It is most favorable towards the multimatrix aspect and includes most pesticides. GPC has its limitations in the analyses of samples with a high load of coextractives and does not offer selectivity with respect to interference with low molecular weights. A selectivity gain can be obtained by the application of an additional cleanup using a small-scale chromatographic separation on silica, florisil, or alumina.

GC ANALYSIS

For the set up a GC-based multiresidue method for a specific pesticide–matrix combination, information is needed on GC retention and detectability of the analytes; also, the need for a cleanup procedure must be evaluated.

In general, the nature of the analyte determines the choice of stationary phase. For example, for the separation of organochlorine and pyrethroid pesticides, a non-polar stationary phase such as DB-1 (or OV-1) is recommended. For the separation of somewhat more polar compounds, such as organophosphorus compounds, OV-17 (or DB-1701) can be applied. In addition, for confirmation purposes, the use of two columns with distinct stationary-phase polarities (e.g., DB-1 and DB-1701) is certainly required. A polar stationary phase (e.g., DB-wax) is suitable for the more polar compounds such as methamidofos, but its application to some detection modes is limited due to stationaryphase bleeding.

Due its robustness, particularly toward uncleaned samples, on-column, splitless injection is the most widely applied technique for sample introduction.

The conventional sensitive and specific GC detection such as electron-capture detector (ECD) (see Fig. 2), flame thermionic detector (FTD), and flame photometric detector (FPD) are still widely used in pesticide residue analysis. In recent years, mass spectrometric detection is becoming

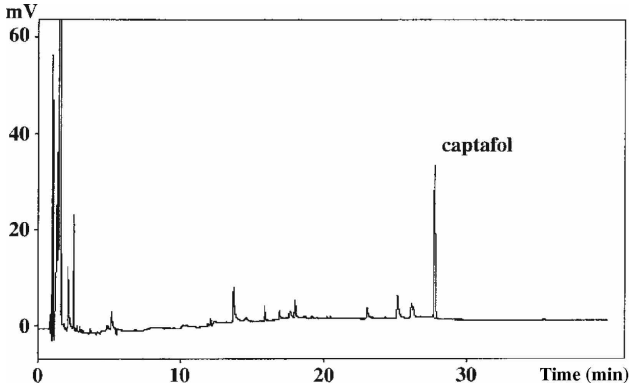

Fig. 2 Gas chromatogram (ECD) resultant from the analysis of captafol residues in tomato, after supercritical fluid extraction with neat CO_2 without further cleanup.

more and more important. Although other types of mass analyzers are commercially available, the equipment used in modern residue laboratories is based on two major types: the classical quadrupole mass analyzers and those based on the ion trap (also called tridimensional quadrupole).

For most compounds, the information on the *m/z* fragments were obtained with a quadrupole instrument. It should be mentioned, however, that the sensitivity of quadrupole detectors must be enhanced by means of limited mass range scanning or by selected ion monitoring, whereas ion-trap-based instruments offer a fair sensitivity with simultaneous monitoring of the complete *m/z* range.

ACKNOWLEDGMENTS

Professor Lanças wishes to express his appreciation to the Brazilian Agencies FAPESP (Fundação de Amparo à Pesquisa do Estado de São Paulo) and CNPq (Conselho Nacional de Desenvolvimento Científico e Tecnológico) for their financial support for our research programs.

BIBLIOGRAPHY

1. Font, G.; Mañes, J.; Moltó, J.C.; Picó, Y. Solid-phase extraction in multi-residue pesticides analysis of water. J. Chromatogr. **1993**, *642*, 135–161.
2. General Inspectorate for Health Protection; Ministery of Public Health, Welfare and Sport *Analytical Methods for Pesticides Residues in Foodstuffs,* 6th Ed.; The Netherlands, 1996.
3. Hedrick, J.L.; Mulcahey, L.J.; Taylor, L.T. Supercritical fluid extraction. Microchim. Acta **1992**, *108*, 115–132.
4. Hennion, M.C.; Call Dit-Coumes, C.; Pichon, V. Traces analysis of polar organic pollutants in aqueous samples: tools for the rapid prediction and optimisation of the SPE parameters. J. Chromatogr. A, **1998**, *823*, 147–161.
5. Ling, Y.C.; Teng, H.C.; Castwright, C. Supercritical fluid extraction and cleanup of organochlorine pesticides in chinese herbal medicine. J. Chromatogr. A, **1999**, *835* (1–2), 145–157.
6. Mol, H.G.J.; Janssen, H.G.M.; Cramers, C.A.; Vreuls, J.J.; Brinkman, U.A.T. Trace level analysis of micropollutants in aqueous samples using gas chromatography with on-line sample enrichment and large volume injection. J. Chromatogr. A, **1995**, *703*, 277–307.
7. Peñalver, A.; Pocurull, F.; Marcé, R.M. Trends in solid-phase microextraction for the determining organic pollutants in environmental samples. Trends. Anal. Chem. **1999**, *18* (8), 557–568.
8. van der Hoff, G.R.; van Zoonen, P. Traces analysis of pesticides by gas chromatography. J. Chromatogr. A, **1999**, *843*, 301–322.

Pesticides: TLC Analysis

Joseph Sherma
Department of Chemistry, Lafayette College, Easton, Pennsylvania, U.S.A.

INTRODUCTION

Thin-layer chromatography (TLC) is complementary to gas chromatography (GC), high-performance liquid chromatography (HPLC), capillary electrophoresis (CE), and immunochemical methods for the determination of single and multiple residues of many classes of pesticides (e.g., insecticides, herbicides, and fungicides) in a variety of food, feed, biological, and environmental samples. The increasing use of TLC for pesticide analysis is due to the wide variety of available stationary phases, optimization of mobile phases, and modern instruments for separation and quantification. The off-line development arrangement of TLC allows significant advantages in many pesticide analyses, including high sample throughput, because many samples can be chromatographed simultaneously on a single plate. This entry reviews the steps of pesticide analysis by TLC and offers selected examples of applications to a variety of pesticides and sample matrices.

MATERIALS AND TECHNIQUES

This section contains an overview of the materials and techniques most widely used in TLC pesticide analysis at the current time. Additional information on specific layers and mobile phases and methods for sample preparation, development, detection, and quantification for a number of particular pesticides and samples are given in the "Example Applications" at the end of this entry.

Sample Preparation

Trace pesticide analysis involves extraction and cleanup steps prior to TLC. Extraction is carried out with a solvent of appropriate polarity by Soxhlet, homogenization, or shaking, followed by liquid/liquid partitioning and/or column adsorption or GPC cleanup. Because each plate is used only once, another advantage of TLC is the possibility of analyzing cruder samples than could be injected into a GC or HPLC column without ruining the analysis, thereby reducing the number of sample preparation steps. These conventional procedures, which are slow and consume large volumes of solvents, have been largely superseded. Simple dissolving procedures are used for sample preparation in pesticide formulation analysis.

A number of modern methods for pesticide residue extraction and cleanup are being applied more frequently. Solid-phase extraction (SPE) using small, disposable cartridges, columns, or disks is employed for isolation and cleanup of pesticides from water and other samples prior to TLC analysis, especially using reversed-phase (RP) octadecyl (C-18) bonded silica gel phases. Microwave-assisted extraction (MAE) is a time- and solvent-saving method for removing residues from samples such as soils. Supercritical fluid extraction (SFE) has been used for sample preparation in the screening of pesticide-contaminated soil by conventional TLC and automated multiple development (AMD). Ultrasonic solvent extraction (USE) and videodensitometry have been combined for quantification of pesticides in soil. Matrix solid-phase dispersion (MSPD) with TLC and GC has been used to determine diazinon and ethion in nuts.

Stationary and Mobile Phases

Most pesticide analyses have been performed by normal- or straight-phase (NP) TLC using commercial plates precoated with silica gel. Lipophilic-bonded phase silica gel layers, mainly C-18, have been used for RPTLC. Other precoated layers used less often for pesticide analysis include aluminum oxide, magnesium silicate (Florisil), polyamide, inorganic ion exchangers, cellulose, acetylated cellulose (reversed phase), and polar modified silica gel layers containing bonded amino, cyano, diol, and thiol groups. Treatment with mixtures of sorbents or impregnation with various reagents has been used to prepare layers with special selectivity properties. High-performance TLC (HPTLC) plates with smaller particles of sorbent provide improved resolution, shorter analysis time, higher detection sensitivity, and more precise and accurate in situ quantification compared to conventional TLC plates. Plates with a preadsorbent or concentrating zone may provide cleanup by retaining some interfering substances from impure samples, and they allow application of larger sample amounts for quantification of very low pesticide concentrations without loss of zone resolution. Plates with a silica gel layer adjacent to a C-18 strip (Whatman Multi-K CS5) have been shown to separate complex mixtures of pesticides by two-dimensional (2-D) TLC with different separation mechanisms in each direction (Fig. 1). Soil TLC is a technique in which the studied soil serves as the stationary phase; it is used for investigation of pesticide mobility and adsorption in soils, which can have serious influence on the pollution of groundwater.

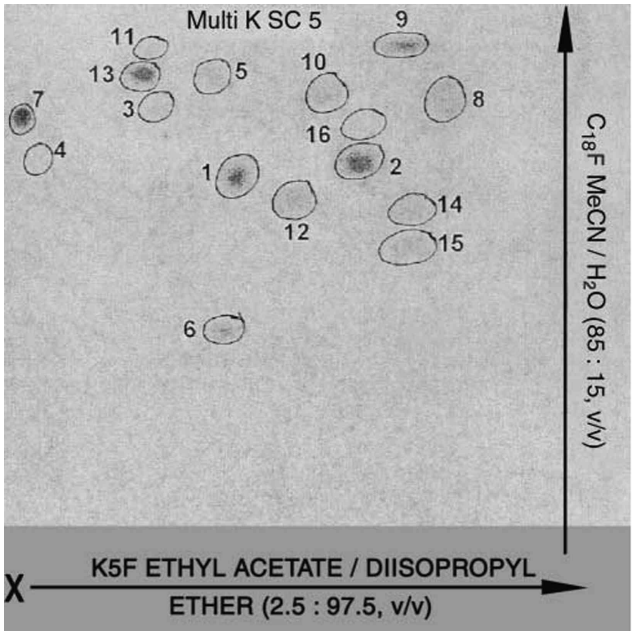

Fig. 1 Photograph taken with a videodensitometer of a Whatman Multi-K SC5 plate showing the 2-D separation of a 16-component mixture of pesticides. The fluorescence-quenched zones are outlined for clarity. Direction 1: ethyl acetate–diisopropyl ether (2.5 : 97.5) mobile phase on the 20 cm × 3 cm K5F silica gel strip (normal phase TLC); direction 2: acetonitrile–water (85 : 15) on the adjacent 20 cm × 17 cm C-18F bonded silica gel layer (RPTLC). X: Origin. Pesticides: 1, propaquizafop; 2, quizalofop-P; 3, triadimefon; 4, triadimenol; 5, fenoxycarb; 6, quinoxyfen; 7, cyromazine; 8, oxyfluorfen; 9, fluoroglycofen; 10, acetochlor; 11, metazachlor; 12, piperonyl butoxide; 13, furalaxyl; 14, pyriproxyfen; 15, buprofezin; 16, clofentezine.
Source: From Separation of a mixture of pesticides by 2D-TLC on two-adsorbentlayer Multi-K SC5 plate, in J. Liq. Chromatogr. Relat. Technol.[1] with permission of Marcel Dekker, Inc.

The mobile phase for a particular separation is usually selected empirically using prior personal experience and literature reports of similar separations as a guide. Typical mobile phases that have been used for separations of many classes of pesticides on silica gel have been mixtures of hexane–acetone, toluene–acetone, chloroform–diethyl ether, and toluene–methanol, while mobile phases for RPTLC analyses on C-18 layers are usually methanol–water and acetonitrile–water mixtures. Computer-assisted, systematic mobile-phase optimization schemes are being used more frequently, especially the PRISMA model.

Application of Samples and Standards

Initial zones in the form of round spots are applied manually to the origins of the layer using a glass micropipet such as a 10 or 25 μl digital microdispenser. In addition, partly or fully automated instruments are available for application of solutions as spots or bands in the microliter to nanoliter range. Compact bands are also produced when samples are applied manually with a micropipet as diffuse vertical streaks to plates containing a preadsorbent zone. Band application is advantageous for obtaining tighter zones, high resolution separations, and accurate and precise quantitative results by densitometry.

Chromatogram Development Techniques

Pesticide analyses have usually been carried out in paper-lined, vapor-saturated glass N-chambers using a single ascending development with the mobile phase. Increased resolution is obtained by 2-D development, overpressured layer chromatography (OPLC), and AMD with gradient elution. An AMD separation of a complex pesticide mixture, with multiple wavelength scanning to provide confirmation of identity, is shown in Fig. 2.

Zone Detection

Pesticides are detected after development as colored, ultraviolet (UV)-absorbing, or fluorescent zones after reaction with a more or less selective derivatization reagent applied to the layer by spraying or dipping. Silver nitrate with UV irradiation is an example of a chromogenic detection reagent used to visualize chlorinated pesticides, while arsenic trichloride–sulfuric acid has been used to detect various pesticide classes. Phenolic pesticides and metabolites are detected as fluorescent zones under 366 nm UV light by use of 7-chloronitrobenzo-2-oxa-1,3-diazole to produce fluorescent 4-nitrobenzofuran derivatives, or by means of Pauly's reagent (sulfanilic acid + KNO_2 + NaOH) for compounds that can form intensely colored azo dyes.

Pesticides that absorb shortwave (254 nm) UV light, particularly those with aromatic rings and/or conjugated double bonds, can be detected by fluorescence quenching on a layer containing a fluorescent indicator (phosphor).

Biological methods of detection have included enzyme inhibition for organophosphorus (OP) pesticides. After mobile-phase development, the layer is sprayed with esterase-1 (*Bacillus subtilis*), followed by 1-thionaphthyl acetate substrate, and finally [2,2′-azo(1-naphthol-8-chloro-3,6-disulfonic acid) 4,4′-diphenyl disulfide] indicator to produce pink zones on a blue background with 0.05–5 ng minimum detection limits. Herbicides have been detected by inhibition of the Hill photosynthesis reaction.

Another important advantage of the off-line operation of TLC is the versatility achieved by use of multiple detection methods. For example, the layer can be viewed under longwave (366 nm) and shortwave UV light, followed by one or more chromogenic, fluorogenic, or biological detection methods; if more than one derivatization reagent is used, only the final one can be destructive.

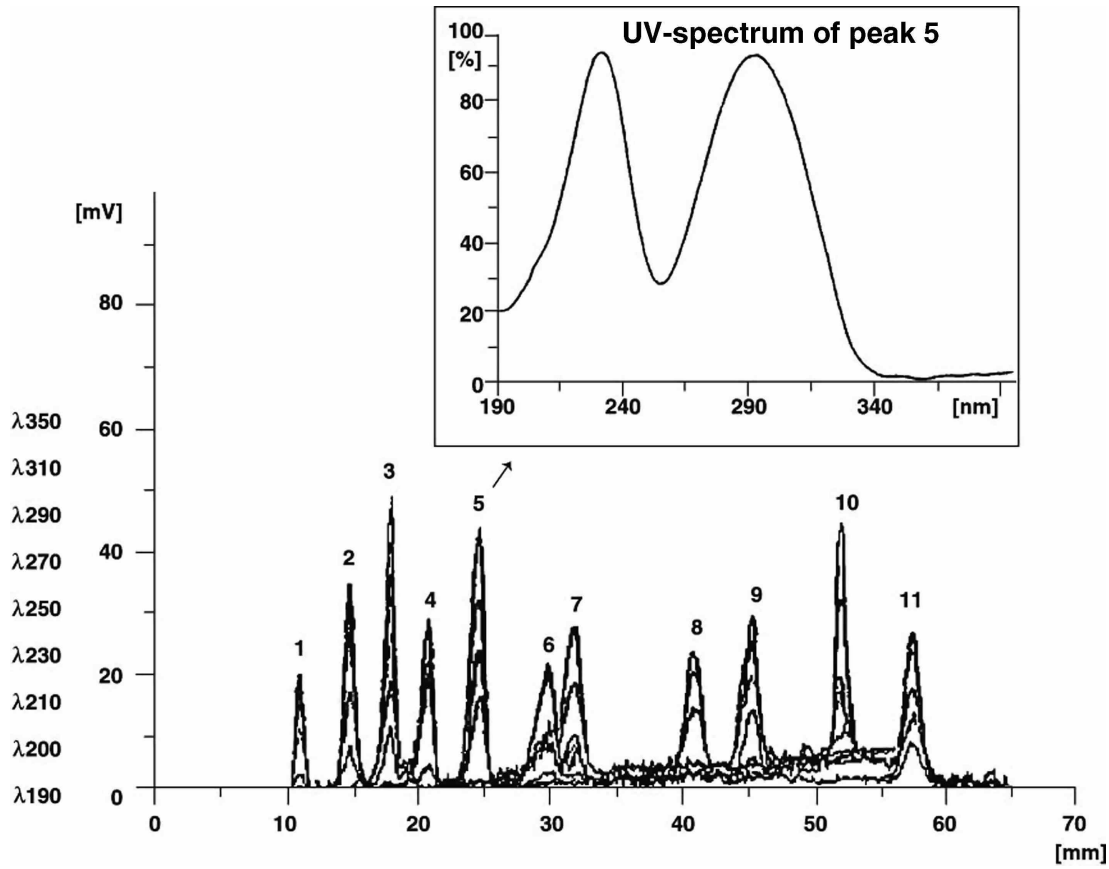

Fig. 2 Multiwave chromatogram of a mixture of 11 pesticides (50 ng/compound) and in situ UV spectrum of peak 5. Compounds represented by peaks: 1, clopyralid acid; 2, triclopyr acid; 3, bitertanol; 4, atraton; 5, chloridazon; 6, sethoxydim; 7, atrazine; 8, iprodione; 9, desmedipham; 10, ethofumesate; 11, pendimethalin.
Source: From Screening of 265 pesticides in water by thin layer chromatography with automated multiple development, in Anal. Chem.,[2] with permission of the American Chemical Society.

Quantitative Analysis

Quantitative pesticide analyses are performed by measuring the areas of sample and standard zones on an HPTLC plate using a slit-scanning densitometer or videodensitometer (CCD camera). Calibration plots are prepared for each analyte (scan areas vs. weights of a series of standards), and sample weights are interpolated from the plots. Validation protocols must be applied to evaluate factors such as linearity, detection limit, accuracy, precision, and ruggedness of the analysis. Excellent accuracy and precision can be obtained because samples and standards are chromatographed and measured in parallel under the same conditions on a single TLC plate.

When a videodensitometer (CCD camera) is used, the image of the layer is first recorded and stored (useful for qualitative documentation purposes), and quantitative software transforms the image into chromatographic data by measuring the pixels comprising the sample zones (unknown analyte weights) vs. corresponding standard zones (known weights) through calibration plots.

Identification and Confirmation of Zones: TLC Combined with Spectrometry

The identification of unknown pesticide zones is initially based on comparison of the migration of sample zones relative to standards developed on the same layer (R_f values) and colors obtained with selective chromogenic and fluorogenic detection reagents. Many densitometers can record in situ UV and visible absorption and fluorescence excitation spectra to confirm compound identification by comparison of unknown spectra with stored standard spectra obtained under identical conditions or spectra of standards measured on the same plate. Additional confirmation methods include off-line and online (coupled, hyphenated) combination of TLC with infrared, Raman, photoacoustic, or mass spectrometry (MS); MS/MS; GC; or HPLC. Identification of pesticides by multiwavelength UV scanning is demonstrated in Fig. 1.

Special Techniques

Thin-layer radiochromatography (radio-TLC) is widely applied for a variety of environmental studies involving

radiolabeled pesticides, such as plant uptake from soil; bioaccumulation in fish; dissipation from soil; metabolism in soil, plants, and fish; and environmental fate. Techniques employed for detection, identification, and quantification of radioactive zones include contact autoradiography, liquid scintillation counting, electronic autoradiography, and storage phosphor screen imaging.

The determination of the lipophilicity of pesticides is important because their bioaccumulation and tendency for degradation and biotransformation are related to lipid solubility. TLC has advantages for lipophilicity studies compared to traditional partition coefficient measurement in an octanol–water system.

EXAMPLES OF PESTICIDE TLC ANALYSIS APPLICATIONS

Separation of 16 Pesticide Standards

- Sample preparation: Standard mixture was applied as a 0.5% solution.
- Layer: Whatman Multi-K SC5 plate described in Fig. 1.
- Mobile phase: 2-D development with the mobile phases given in Fig. 1.
- Detection: Fluorescence quenching under 245 nm UV light.[1]

Screening of 265 Pesticides in Water

- Sample preparation: SPE on a C-18 column or liquid/liquid extraction with dichloromethane.
- Layer: HPTLC silica gel.
- Mobile phase: Universal gradient based on dichloromethane.
- Detection: UV absorption densitometry (see Fig. 2).[2]

Determination of Carbaryl and Propoxur in Water

- Sample preparation: Chloroform extraction; grain samples were also analyzed.
- Layer: Silica gel G.
- Mobile phase: Acetone–hexane (1 : 4) or butanol–acetic acid–water (3 : 1 : 6, butanol layer).
- Detection: Spray with diazotized *p*-nitroaniline followed by aqueous NaOH to produce blue and purple spots, respectively.
- Quantification: Colored sample and standard zones were scraped and eluted with 6 *M* NaOH and the solutions measured by spectrometry.
- Validation: Recovery of 25–100 ng of the pesticides added to water ranged from 98% to 100%.[3]

Determination of 24 Pesticides in Water

- Sample preparation: Samples (1000 ml) of ground, surface, and drinking water were extracted using a C-18 SPE cartridge; the cartridge was eluted with 3 ml of acetonitrile, and the eluate was used directly for TLC or cleaned up on a silica column eluted with acetonitrile.
- Layer: HPTLC silica gel 60F-254; samples applied by the spray-on technique using a Linomat IV.
- Mobile phase: AMD with 20-step universal gradients based on dichloromethane containing 0.1% acetic acid, methanol, and hexane (screening gradient) and *t*-butyl methyl ether containing 0.1% acetic acid, acetonitrile, and hexane (confirmatory gradient).
- Detection and identification: Comparison of sample and standard chromatograms scanned at six different wavelengths with a densitometer.[4]

Determination of Carbamate Insecticides in Water

- Sample preparation: Pesticides recovered from pond water by SPE on a C-18 column eluted with ethyl acetate.
- Layer: Channeled preadsorbent HPTLC silica gel.
- Mobile phase: Toluene–acetone (4 : 1) (carbaryl, carbofuran, methiocarb) or hexane–acetone–chloroform (75 : 15 : 10) (propoxur).
- Detection: Plate dipped into *p*-nitrobenzenediazonium fluoborate chromogenic reagent.
- Quantification: Densitometric scanning of sample and standard zones at 610 nm (carbaryl), 550 nm (carbofuran, propoxur), or 510 nm (methiocarb).
- Validation: Recovery averaged 97% for analysis of water spiked with pesticides at 0.5–5 ppm.[5]

Determination of Atrazine and Its Major Metabolites in Soils

- Sample preparation: Soil was extracted with methanol, the suspension was filtered, and the filtrate was concentrated by evaporation.
- Layer: HPTLC reversed phase plates; samples were applied with a Nanomat III.
- Mobile phase: Methanol–water (7 : 3); development in a horizontal chamber.
- Quantification: Zones were scanned at 222 nm with a dual-wavelength flying-spot densitometer; standard curves were prepared by quadratic regression analysis, which gave a higher correlation coefficient than linear regression.

– Validation: Recovery of atrazine from fortified samples ranged from 87% to 97%; the detection limit of the method was 20 ng.[6]

Determination of Cymiazole and Pentachlorophenol (PCP) in River Water and Honey

– Sample preparation: The pesticides were extracted from water and honey using C-18 SPE.
– Layer: Channeled preadsorbent high performance silica gel.
– Mobile phase: Toluene–methanol (9:1) for PCP; hexane–acetone–methanol–glacial acetic acid (35:10:5:0.1) for cymiazole; paper-lined twin trough chamber.
– Detection: Fluorescence quenching under 254 nm UV light; 200 ng sensitivity.
– Quantification: Scanning densitometry at 215 nm for PCP and 265 nm for cymiazole.
– Validation: Recoveries from water at concentrations of 0.25–5 ppm ranged from 97.7% to 100% for PCP and from 89.5% to 94.9% for cymiazole. Recoveries from honey at 10 and 50 ppm ranged from 94.0% to 96.1% for PCP and from 91.9% to 93.7% for cymiazole.[7]

Determination of Diflubenzuron in Water

– Sample preparation: Extraction on a C-18 SPE column eluted with acetonitrile.
– Layer: Channeled preadsorbent high performance silica gel.
– Mobile phase: Ethyl acetate–toluene (1:3); paper-lined glass HPTLC chamber.
– Detection: Spraying with 6 *M* HCl, heating for 10 min at 180 °C, and spraying with Bratton–Marshall reagent [sodium nitrite and *N*-(1-naphthyl) ethylenediamine dihydrochloride]; purple-blue band, 100 ng sensitivity.
– Quantification: Scanning densitometry at 550 nm.
– Validation: Sensitivity was 0.1 μg, recoveries at 50 μg/L 95–97% with relative standard deviations (RSDs) of 2–3%; semiquantitative limit of determination 125 ng/L.[8]

Determination of OP Insecticides in Water

– Sample preparation: C-18 SPE.
– Layer: Preadsorbent silica gel.
– Mobile phase: Hexane–acetone (4:1).
– Detection: 5% $MgCl_2$, 0.3% *N*,2,6-trichlorobenzoquinoneimine; 100 ng limit of detection (LOD).
– Quantification: Scanning densitometry.[9]

Separation of Organochlorine and OP Insecticides

– Sample preparation: Standard solutions (0.1%) in benzene; 5 μl applied.
– Layer: Silica gel 100F.
– Mobile phase: Heptane–acetone (4:1).
– Detection: Zones viewed under 254 and 366 nm UV light.[10]

Determination of Metribuzin and Its De-ethyl, Deisopropyl, and Hydroxy Metabolites in Soil and Water

– Sample preparation: Soil was extracted with methanol–0.01 *M* calcium chloride dihydrate (4:1), and the extract was filtered and cleaned up on a C-18 cartridge; water samples were eluted directly through the cartridge.
– Layer: Hydrocarbon-impregnated RPTLC plates; zones applied with a Nanomat III.
– Mobile phase: Methanol–water (45:55).
– Quantification: Scanning at 290 nm with a dual-wavelength flying-spot densitometer; standard curves produced by linear regression.
– Validation: Recoveries of metribuzin from water samples fortified at 10 and 100 μg/L ranged from 85% to 92%, and from 73% to 86% from soils fortified at 2 mg/kg; the LOD for metribuzin was 30 ng.[11]

Determination of Alachlor, Atrazine, and α-Cypermethrin in Water

– Sample preparation: SPE on Empore C-18 disks eluted with dichloromethane or hexane.
– Layer: RP-$18F_{254}$; samples applied as bands with a Linomat IV.
– Mobile phase: 2-Propanol–water mixtures optimized by the window diagrams method.
– Detection and quantification: Videodensitometry of fluorescence-quenched zones at 254 nm.
– Validation: Recoveries were 94.7–104.2% for 250–1000 ml water samples.[12]

Determination of Phenylurea Herbicides in Drinking Water

– Sample preparation: SPE on C-18 cartridges eluted with acetonitrile.
– Layer: (I) Bonded diol-F, (II) bonded amino-F, and (III) silica gel-F.
– Mobile phase: (I) Water–acetone–methanol (6:1:3), (II) chloroform–toluene (8:2), and (III) benzene–triethylamine–acetone (75:15:10).

- Detection: Viewing under 254 and 366 nm UV light.
- Quantification: UV absorption scanning densitometry; a fluorodensitometric screening method involving thermal hydrolysis and subsequent derivatization of the corresponding anilines with fluorescamine was also developed.
- Validation: Recoveries were 87–102% for 1 L of water spiked with 1 μg of pesticide; the LOD was improved 25-fold by derivatization.[13]

Analysis of Formulations of Pyrethrins

- Sample preparation: Formulations were dissolved in ethyl acetate, standard pyrethroids in cyclohexanone–Tween 80 (9:0.1 w/w).
- Layer: Aluminum-backed silica gel $60F_{254}$; solutions applied with a Linomat IV.
- Mobile phase: Hexane–toluene (1:1); development in a twin-trough chamber.
- Quantification: Scanning densitometry at 220 nm.
- Validation: Recoveries of laboratory-prepared test formulations ranged from 95% to 99%.[14]

Screening of Pesticides in Tomatoes

- Sample preparation: Atrazine, carbaryl, carbofuran, chloroxuron, diuron, dimethoate, imazalil, oxamyl, and methamidophos were extracted from tomatoes with ethyl acetate–$NaHCO_3$ and the extract cleaned up by semiautomatic GPC.
- Layer: Silica gel 60F.
- Mobile phase: Ethyl acetate or dichloromethane.
- Detection: *O*-Toluidine–potassium iodide (*O*-TKI) and *p*-nitrobenzenediazonium fluoborate (NBFB) chromogenic reagents. Minimum detection quantities were 12–125 ng for *O*-TKI and 60–70 ng for NBFB.[15]

Fate of ^{14}C-Diazinon in Compost, Soil, and Worms

- Sample preparation: Sequential acetone extraction.
- Layer: Silica gel $60F_{254}$ HPTLC and silica gel GF TLC.
- Mobile phase: Chloroform–acetone (8:1) or ethyl acetate–benzene–chloroform–propanol (2:2:1:1).
- Detection and quantification: Autoradiography.[16]

Chlorpyrifos Degradation in Soil

- Sample preparation: Surface and subsurface clay loam soils were incubated with radiolabeled chlorpyrifos, and samples were extracted with methanol by ambient shaking and SFE.
- Layer: Silica gel F.
- Mobile phase: Toluene–methanol–hexane (18:1:1).
- Detection: Chlorpyrifos and its metabolite 3,5,6 trichloropyridinol (TCP) were detected as fluorescence-quenched zones under 254 nm UV light. Bands were scraped and radioactivity measured by liquid scintillation counting.[17]

CONCLUSIONS

The determination of pesticides is important because of the serious and growing concerns about their possible detrimental effects on human and animal health, the food supply, and the environment. TLC, along with GC, HPLC, and immunoassay, are the major methods for analyzing water, soil, food, biological, and other sample types for pesticides and their residues having a great variety of structures and modes of action. The following lists of References and Bibliography contain sources of detailed information on the procedures and instrumentation of TLC and applications to pesticide analysis, which will augment the material presented in this entry.

REFERENCES

1. Tuzimski, T.; Wojtowicz, J. Separation of a mixture of pesticides by 2D-TLC on two-adsorbent-layer Multi-K SC5 plate. J. Liq. Chromatogr. Relat. Technol. **2005**, *28* (2), 277–287.
2. Butz, S.; Stan, H.J. Screening of 265 pesticides in water by thin layer chromatography with automated multiple development. Anal. Chem. **1995**, *67* (3), 620–630.
3. Bose, D.; Shivhare, P.; Gupta, V.K. Thin layer chromatographic separation and determination of carbaryl and propoxur. J. Planar Chromatogr.-Mod. TLC **1994**, *7* (5), 415–418.
4. de la Vigne, U.; Jaenchen, D. Determination of pesticides in water using automated multiple development (AMD). J. Planar Chromatogr.-Mod. TLC **1990**, *3* (1), 6–9.
5. McGinnis, S.C.; Sherma, J. Determination of carbamate insecticides in water by C-18 solid phase extraction and quantitative HPTLC. J. Liq. Chromatogr. **1994**, *17* (1), 151–156.
6. Johnson, R.M.; Halaweish, F.; Fuhrmann, J.J. Analysis of atrazine and associated metabolites by reverse-phase high performance thin layer chromatography. J. Liq. Chromatogr. **1992**, *15* (17), 2941–2957.
7. Sherma, J.; McGinnis, S.C. Determination of pentachlorophenol and cymiazole in water and honey by C-18 solid phase extraction and quantitative HPTLC. J. Liq. Chromatogr. **1994**, *18* (4), 755–761.
8. Sherma, J.; Rolfe, C. Determination of diflubenzuron residues by solid phase extraction and quantitative high performance thin layer chromatography. J. Chromatogr. **1993**, *643* (1–2), 337–339.
9. Sherma, J.; Bretschneider, W. Determination of organophosphorus insecticides in water by C-18 solid phase extraction

and quantitative TLC. J. Liq. Chromatogr. **1990**, *13* (10), 1983–1989.
10. Lekic, M.; Korac, F. Separation of organochlorine and organophosphorus insecticides by thin layer chromatography. J. Planar Chromatogr.-Mod. TLC **2000**, *13* (4), 314–316.
11. Johnson, R.M.; Pepperman, A.B. Analysis of metribuzin and associated metabolites in soil and water samples by solid phase extraction and reversed-phase thin layer chromatography. J. Liq. Chromatogr. **1995**, *18* (4), 739–753.
12. Babic, S.; Mutavdzic, D.; Kastelan-Macan, M. SPE preconcentration and TLC determination of alachlor, atrazine, and alpha-cypermethrin in water samples. J. Planar Chromatogr.-Mod. TLC **2003**, *16* (2), 160–164.
13. Hamada, M.; Wintersteiger, R. Determination of phenylurea herbicides in drinking water. J. Planar Chromatogr.-Mod. TLC **2002**, *15* (1), 11–18.
14. Sharma, K.K. Determination of active ingredient in synthetic pyrethroid formulations by high performance thin layer chromatography/densitometry. J. AOAC Int. **2002**, *85* (6), 1420–1424.
15. Moraes, S.L.; Rezende, M.O.O.; Nakagawa, L.E.; Luchini, L.C. Multiresidue screening methods for the determination of pesticides in tomatoes. J. Environ. Sci. Health B, **2003**, *B38* (5), 605–615.
16. Leland, J.E.; Mullins, D.E.; Berry, D.F. The fate of ^{14}C-diazinon in compost, compost-amended soil, and uptake by earthworms. J. Environ. Sci. Health B, **2003**, *B38* (6), 697–712.
17. Yucel, U.; Ylim, M.; Gozek, K.; Helling, C.S.; Sarykaya, Y. Chlorpyrifos degradation in Turkish soil. J. Environ. Sci. Health B, **1999**, *B34* (1), 75–95.

BIBLIOGRAPHY

1. Cserhati, T.; Forgacs, E. Hyphenated techniques in thin layer chromatography. J. AOAC Int. **1998**, *81* (2), 329–332.
2. Cserhati, T.; Forgacs, E. Effect of TLC support characteristics and coating on the lipophilicity determination of phenols and aniline derivatives. J. Chromatogr. Sci. **2002**, *40* (10), 564–568.
3. Fodor-Csorba, K.; Pesticides. In *Handbook of Thin Layer Chromatography,*1st Ed.; Sherma, J., Fried, B., Eds.; Marcel Dekker, Inc.: New York, NY, 1991; 663–715.
4. Fodor-Csorba, K. Pesticides. In *Handbook of Thin Layer Chromatography,* 2nd Ed.; Sherma, J., Fried, B., Eds.; Marcel Dekker, Inc.: New York, NY, 1996; 753–817.
5. Follweiler, J.; Sherma, J. *Handbook of Chromatography—Pesticides*; CRC Press: Boca Raton, FL, 1984.
6. Fried, B.; Sherma, J. *Practical Thin Layer Chromatography—A Multidisciplinary Approach*; CRC Press: Boca Raton, FL, 1996.
7. Fried, B.; Sherma, J. *Thin Layer Chromatography*, 4th Ed.; Marcel Dekker, Inc.: New York, NY, 1999.
8. Husain, S.W.; Kiarostami, V.; Morrovati, M.; Tagebakhsh, M.R. Multiresidue determination of diazinon and ethion in pistachio nuts by use of matrix solid phase dispersion with lanthanum silicate co-column and gas chromatography. Acta Chromatogr. **2003**, *13*, 208–214.
9. Johnson, R.M.; Sims, J.T. Sorption of atrazine and dicamba in Delaware coastal plain soils: A comparison of soil thin layer chromatography and batch equilibrium results. Pestic. Sci. **1998**, *54* (2), 91–98.
10. Kastelan-Macan, M.; Babic, S. Pesticides. In *Handbook of Thin Layer Chromatography,* 3rd Ed.; Sherma, J., Fried, B., Eds.; Marcel Dekker, Inc.: New York, NY, 2003; 767–805.
11. Koeber, R.; Niessner, R. Screening of pesticide contaminated soil by supercritical fluid extraction and high performance thin layer chromatography with automated multiple development. Fresenius J. Anal. Chem. **1996**, *354* (4), 464–469.
12. Mazaruk, M.; Witkiewicz, Z. The analysis of organophosphorus warfare agents in the presence of pesticides by overpressured thin layer chromatography. J. Planar Chromatogr.-Mod. TLC **1991**, *4* (5), 379–384. (Paper includes optimization of the mobile phase using the PRISMA model.)
13. Orinak, A.; Arlinghaus, H.F.; Vering, G.; Justinova, M.; Orinakova, R.; Turcaniova, L.; Halama, M. New interfaces for coupling TLC with TOF SIMS. J. Planar Chromatogr.-Mod. TLC **2003**, *16* (1), 23–27.
14. Petrovic, M.; Babic, S.; Kastelan-Macan, M. Quantitative determination of pesticides in soil by thin layer chromatography and videodensitometry. Croat. Chem. Acta **2000**, *73* (1), 197–207.
15. Petrovic, M.; Kastelan-Macan, M.; Lazaric, K.; Babic, S. Validation of thin layer chromatography determination with CCD camera and slit-scanning densitometer. J. AOAC Int. **1999**, *82* (1), 25–30.
16. Sherma, J. Pesticide analysis by thin layer chromatography. In *Analytical Methods for Pesticides and Plant Growth Regulators*; Zweig, G., Sherma, J., Eds.; Academic Press: San Diego, CA, 1973; Vol. VII 3–87.
17. Sherma, J. Pesticide analysis by thin layer chromatography. In *Analytical Methods for Pesticides and Plant Growth Regulators;* Zweig, G., Sherma, J., Eds.; Academic Press: San Diego, CA, 1980, Vol. XI, 79122.
18. Sherma, J. Pesticide analysis by thin layer chromatography. In *Analytical Methods for Pesticides and Plant Growth Regulators;* Zweig, G., Sherma, J., Eds.; Academic Press: San Diego, CA, 1986, Vol. XIV, 1–39.
19. Sherma, J. Thin layer chromatography of pesticides—A review of recent techniques and applications. J. Liq. Chromatogr. **1982**, *5* (6), 1013–1032.
20. Sherma, J. Thin layer chromatography of pesticides. J. Planar Chromatogr. Mod. TLC **1991**, *4* (1), 7–14.
21. Sherma, J. Determination of pesticides by thin layer chromatography. J. Planar Chromatogr.-Mod. TLC **1994**, *7* (4), 265–272.
22. Sherma, J. Thin layer chromatography in environmental analysis. Rev. Anal. Chem. **1995**, *XIV* (2), 75–120.
23. Sherma, J. Review: Determination of pesticides by thin layer chromatography. J. Planar Chromatogr.-Mod. TLC **1997**, *10* (2), 80–89.
24. Sherma, J. Recent advances in thin layer chromatography of pesticides. J. AOAC Int. **1999**, *82* (1), 48–53.

25. Sherma, J. Advances in techniques and applications of pesticide determination in foods and beverages. Food Test. Anal. **1999**, *5* (2), 25–26,34.
26. Sherma, J. Thin layer chromatography in food and agricultural analysis. J. Chromatogr. A, **2000**, *880* (1–2), 129–147.
27. Sherma, J. Thin layer chromatography in environmental analysis. In *Planar Chromatography*; Nyiredy, Sz., Ed.; Springer Scientific Publisher: Budapest, Hungary, 2001; 569–584.
28. Sherma, J. Recent advances in thin layer chromatography of pesticides. J. AOAC Int. **2001**, *84* (4), 993–999.
29. Sherma, J. Recent advances in thin layer chromatography of pesticides: A review. J. AOAC Int. **2003**, *86* (3), 602–611.
30. Sherma, J. Planar chromatography. Anal. Chem. **2004**, *76* (12), 3251–3262. (See also reviews of TLC each even-numbered year in this journal beginning in 1970.)
31. Sherma, J., Fried, B., Eds.; *Handbook of Thin Layer Chromatography*; 3rd Ed.; Marcel Dekker: New York, NY, 2003.
32. Singh, K.K.; Shekhawat, M.S. Thin layer chromatographic methods for analysis of pesticides residues in environmental samples. J. Planar Chromatogr.-Mod. TLC **1998**, *11* (3), 164–185.
33. Somsen, G.W.; Morden, W.; Wilson, I.D. Planar chromatography coupled with spectroscopic techniques. J. Chromatogr. A, **1995**, *703* (1–2), 613–665.
34. Vashkevich, O.V.; Gankina, E.S. Quantitative determination of organophosphorus pesticides by HPTLC with detection by enzyme inhibition. J. Planar Chromatogr.-Mod. TLC **1990**, *3* (4), 354–356.
35. Wang, Q.S.; Yan, B.W.; Zhang, L. Computer-assisted optimization of two-step development high performance TLC. J. Chromatogr. Sci. **1996**, *34* (4), 202–205.
36. Wilson, I.D. The state of the art in thin layer chromatography–mass spectrometry: A critical appraisal. J. Chromatogr. A, **1999**, *856* (1–2), 429–442.

pH: Effect on MEKC Separation

Koji Otsuka
Shigeru Terabe
Department of Material Science, Himeji Institute of Technology, Hyogo, Japan

INTRODUCTION

In micellar electrokinetic chromatography (MEKC), the effect of the constituents of the buffer is not significant, whereas the pH is critical, especially for ionizable analytes, as well as to the electrokinetic velocities. The change in the buffer pH, especially in the lower-pH region, causes a significant change in the velocity of the electro-osmotic flow (EOF).

ELECTROKINETIC VELOCITIES

When sodium dodecyl sulfate (SDS) is employed as an ionic micelle or pseudo-stationary-phase in MEKC, the relationship between the velocity of the EOF, v_{EOF}, and the migration velocity of the SDS micelle, v_{mc}, is given as

$$v_{mc} = v_{EOF} + v_{cp} \tag{1}$$

where v_{cp} is the electrophoretic velocity of the SDS micelle. The sign of each velocity is defined as plus when the migration is toward the cathode and as minus when toward the anode.

The dependence of these electrokinetic velocities on pH is shown in Fig. 1.[1] In the case of capillary zone electrophoresis (CZE), with a bare fused-silica capillary, the pH greatly affects the EOF velocity (i.e., significantly decreases with the decrease in pH from 8 to 3). In MEKC, however, the dependence on pH is different from that in CZE, especially under weakly acidic conditions (pH 7.0–5.5). In the range of pH between 7.0 and 5.5, v_{EOF} slightly decreases with the decrease in pH, due to the adsorption of the SDS molecule or monomer on the inside wall of the capillary. On the other hand, v_{EOF} rapidly decreases with the decrease in the pH below 5.5. The decrease of v_{EOF} is mainly caused by the decrease in the zeta-potential of the inside wall of the capillary, because the dissociation of silanol groups on the capillary wall is more suppressed as the solution becomes more acidic.

The electrophoretic velocity of the SDS micelle (v_{cp}) (i.e., $v_{mc} - v_{EOF}$) is almost constant over the pH range in Fig. 1; that is, the charge of the SDS micelle is almost constant in this pH range.

The migration velocity of the SDS micelle (v_{mc}) changes from positive to negative at a pH below 5.0, which means that the SDS micelle migrates toward the anode; thus, the migrating direction of the SDS micelle is opposite that of the EOF. One should note that the reproducibility of retention times was low in acidic solutions, especially below pH 5.0, compared with that in neutral SDS solutions.

MIGRATION TIME

The migration time, t_R of a neutral solute in MEKC is represented by

$$t_R = \left(\frac{1+k}{1+(t_0/t_{mc})k}\right)t_0 \tag{2}$$

where t_0 is the migration time of an unretained solute or insolubilized solute by the micelle at all, t_{mc} is that of the micelle, and k is the retention factor of the solute. Here, we define the sign of the migration time as positive when the solute migrates toward the cathode or the velocity of the solute, v_s is positive, and vice versa. When neutral SDS solutions are employed, the t_{mc} is positive and of any neutral solute is always positive and limited to between t_0 and t_{mc}. Under acidic condition, or typically pH below 5.0, the neutral solute totally solubilized by the SDS micelle, such as Sudan III, migrates toward the anode and, hence, t_{mc} becomes negative, whereas the solute insolubilized by the micelle (e.g., methanol) migrates toward the cathode. By considering Eq. 2, it is apparent that the migration time of the solute whose capacity factor is equal to $-(t_{mc}/t_0)$ becomes infinity when $t_{mc} < 0$ and the solute never migrates in the column, whereas the solute of $k > -(t_{mc}/t_0)$ migrates toward the same directions as the micelle.

RESOLUTION

In MEKC, the resolution, of two peaks of which the retention factors are and is described as (see *Retention Factor: MEKC Separation*, p. 2033):

$$R_s = \frac{N^{1/2}}{4}\left(\frac{\alpha-1}{\alpha}\right)\left(\frac{k_2}{1+k_2}\right)\left(\frac{1-t_0/t_{mc}}{1+(t_0/t_{mc})k_1}\right) \tag{3}$$

For the closely migrating peaks, we can assume that $k_1 = k_2 = k$. Then, the fourth term of the right-hand

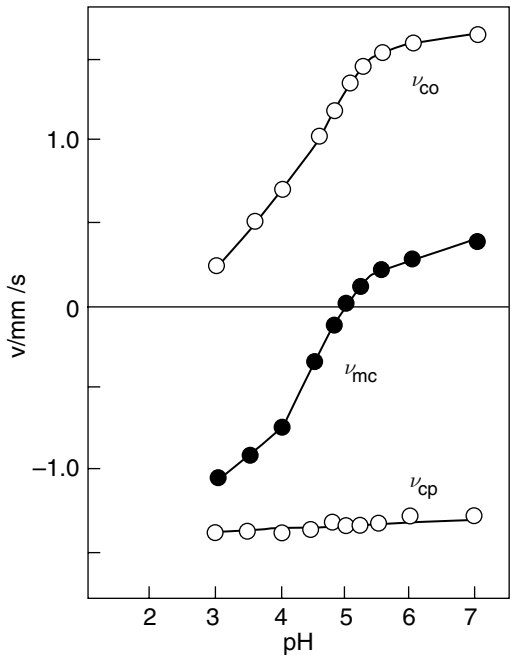

Fig. 1 Dependence of electrokinetic velocities on pH: v_{co} = velocity of the EOF, v_{mc} = migration velocity of the micelle, v_{cp} = electrophoretic velocity of the micelle.
Source: From Effects of pH on electrokinetic velocities in micellar electrokinetic chromatography, in J. Microcol. Separ.[1]

side of Eq. 3 will become infinity when k is equal to $-t_{mc}/t_0$ thus, the resolution will become maximum or infinity. The function $f(k)$, the product of the last two terms in Eq. 3, is written as

$$f(k) = \left(\frac{k_2}{1+k_2}\right)\left(\frac{1 - t_0/t_{mc}}{1 + (t_0/t_{mc})k_1}\right) \quad (4)$$

The value of $f(k)$ approaches infinity, as in the case of t_R as k becomes close to $-t_{mc}/t_0$ and, consequently, R_s becomes quite large. Hence, a considerably large R_s will be obtained for a solute having k close to $-t_{mc}/t_0$, although a quite long t_R is required for such a solute.

MIGRATION WINDOW

The parameter t_0/t_{mc} is related to the migration window. As long as t_{mc} is positive, a smaller value of t_0/t_{mc} gives a wider migration window. Some attempts to extend the migration window have been made by (a) the addition of organic modifiers (e.g., methanol, acetonitrile, and 2-propanol) to the micellar solution and (b) the use of capillaries of which the inside walls were chemically modified to reduce the silanol-group concentration. In each case, the extension was mainly achieved through decreasing the EOF owing to a decrease of the zeta-potential of capillaries. As mentioned earlier, the migration window is no longer limited when acidic micellar solutions (i.e., pH below 5.0) are employed. The value of zero for t_0/t_{mc} corresponds to the case of conventional chromatography, in which the elution range is infinity; in other words, the solute of $k = \infty$ (e.g., Sudan III) never comes out from the capillary. The case also causes the infinite migration window.

IONIZABLE SOLUTES

If the ionized form of the solute has the same charge as the micelle, it will be incorporated into the micelle less than with its neutral form. By contrast, the ionized form of the solute will be bound to the micelle more strongly than its neutral form if the ionized solute has the opposite charge to that of the micelle. The dependence of the apparent retention factor, on the buffer pH for chlorinated phenols has been investigated in an SDS/MEKC, where both the ionizable solutes or chlorinated phenols and SDS have negative charge. The apparent retention factor was calculated by the usual equation for the retention factor in MEKC:

$$k_{app} = \frac{t_R - t_0}{[1 - (t_R/t_{mc})]t_0} \quad (5)$$

regardless of whether the solutes were ionized or not. For acidic compounds, the increase in pH will promote ionization; then, the distribution coefficient to the SDS or an anionic micelle will be decreased. For example, the apparent retention factor for 2,3,4,5-tetrachlorophenol ($pK_a = 5.6$) was dramatically changed from ~100 at pH 6.0 to 4 at pH 9.0.

It is often essential to find the optimum pH for the separation of ionizable solutes, where closely spaced peaks are obtained.

BIBLIOGRAPHY

1. Foret, F.; Kriváková, L.; Bocek, P. *Capillary Zone Electrophoresis*; VCH: Weinheim, 1993; 67–74.
2. Lukacs, K.D.; Jorgenson, W. Capillary zone electrophoresis: Effect of physical parameters onseparation efficiency and quantitation. J. High Resolut. Chromatogr. Commun. **1985**, *8*, 405–411.
3. Otsuka, K.; Terabe, S. Micellar electrokinetic chromatography. Bull. Chem. Soc. Jpn. **1998**, *71*, 2465–2481.
4. Otsuka, K.; Terabe, S.; Ando, T. Electrokinetic chromatography with micellar solutions: Retention behaviour and separation of chlorinated phenols. J. Chromatogr. **1985**, *348*, 39–47.

REFERENCE

1. Otsuka, K.; Terabe, S. Effects of pH on electrokinetic velocities in micellar electrokinetic chromatography. J. Microcol. Separ. **1989**, *1*, 150–154.

Phenolic Acids in Natural Plants: HPLC Analysis

E. Brandsteterova
A. Ziakova-Caniova
Department of Analytical Chemistry, Slovak Technical University, Bratislava, Slovakia

INTRODUCTION

Many medicinal and food plants contain large amounts of antioxidants other than vitamin C, vitamin E, and carotenoids. The antioxidative effects are mainly due to phenolic compounds: phenolic acids, flavonoids, and phenolic diterpenes. These natural antioxidants can exert considerable protection, in humans, against aging and cancer caused by free radicals, and can replace synthetic antioxidants such as butylated hydroxyanisole (BHA) and butylated hydroxytoluene (BHT), which are suspected to have toxic and carcinogenic effects on humans.

Phenolic acids constitute a large group of naturally occurring organic compounds with a broad spectrum of pharmacological activities. It was found that they possess not only antioxidant but also antiviral and antibacterial properties. The antioxidant activity of phenolics is generally combined with hydroxyl groups on their molecules. Phenolic acids are widely distributed in natural plants, e.g., fruits, vegetables, various medicinal and other plants. Phenolic acids occur in plants in different concentrations and, of course, each plant sample could be specific enough for the presence of different phenolic acids and their derivatives in combination with the other groups of phenolic compounds. Very often, all important phenolics present in plant samples are analyzed simultaneously.

Phenolic acids include the benzoic acids (C_6–C_1), e.g., gallic, vanillic, syringic, protocatechuic, *p*-hydroxybenzoic acid, as well as cinnamic acids (C_6–C_3), e.g., caffeic, *p*-coumaric, ferulic, sinapic acids, and their depsides and derivates, e.g., rosmarinic acid and lithospermic acid (Fig. 1).[1] Phenolic acids and flavonoids in plants may occur in the free form, but they are often glycosylated with various sugars, especially glucose. Phenolic acids may also be present in the esterified as well as bound forms. Free phenolic acids are found especially in herbs and spices and, very often, in compounds responsible for antioxidant activity (benzoic and cinnamic acids and some of their derivatives). The bound forms are more common for the fruits, vegetables, and other plant materials. Therefore, in some cases, it is necessary to combine the analysis of their free and bound forms.

HPLC OF PHENOLIC ACIDS

The content of various phenolic acids in plants can be determined using various analytical instrumental methods gas chromatography, thin-layer chromatography, and capillary electrophoroesis (GC, TLC, CE), but high-performance liquid chromatography (HPLC), with a broad range of detection possibilities, is the best method of choice for routine analysis. HPLC techniques offer a real chance to separate simultaneously all analyzed components together with their possible derivatives or degradation products. In many cases, this method enables the determination of low concentrations of analytes in the presence of many other interfering and coeluting components. There are many advantages influencing the increased popularity of the HPLC technique in plant material analysis, such as the large choice of commercially available columns with very desirable properties; the application of all chromatographic separation principles, including the use of new generation sorbents; and the possibility of combining two or more columns in a switching mode.[2]

HPLC Columns

The columns used for the separation of phenolic acids are mainly reversed-phase (RP), other silica-based chemically bound phases, and non-silica polymers or mixed inorganic–organic phases. Special silica sorbents with reduced metallic residue contents and minimum residual silanol groups on the surface could positively influence peak symmetry without the strict demands for the successful separation of acidic analytes. Almost exclusively, RP C_{18} phases ranging from 100 to 250 mm in length and usually with an internal diameter of 3.9 to 4.6 mm are recommended. Particle sizes are in the range of 3–10 μm. Short 50–100 mm columns with 3 μm particles have also been tested for fast phenolic acid separations. Narrow bore columns (internal diameter 2 mm) are recommended especially for HPLC/MS applications.[3,4] Some problems could arise with the applications of narrow or microbore columns in the direct injections of plant extracts; there is the possibility of plugging the column after repeated injections. In these cases, an additional clean-up step has to be applied instead of just the simple extraction assay. Moreover, in the case when columns with lower diameters and particle sizes are used, the adaptation of HPLC equipment is often necessary, e.g., ultra violet (UV) detection cells with reduced

Benzonic acid derivates:

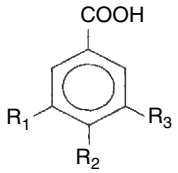

Gallic acid, $R_1 = R_2 = R_3 = OH$
p-Hydroxybenzoic acid, $R_1 = R_3 = H$, $R_2 = OH$
Protocatechuic acid, $R_1 = R_2 = OH$, $R_3 = H$
Vanillic acid, $R_1 = OMe$, $R_2 = OH$, $R_3 = H$
Syringic acid, $R_1 = R_3$, $OMe = R_2 = OH$

Cinnamic acid derivates:

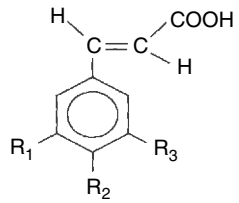

Caffeic acid, $R_1 = R_2 = R_3 = OH$
p-Coumaric acid, $R_1 = R_3 = H$, $R_2 = OH$
Ferulic acid, $R_1 = OMe$, $R_2 = OH$, $R_3 = H$
Sinapic acid, $R_1 = R_2$, $OMe = R_3 = OH$

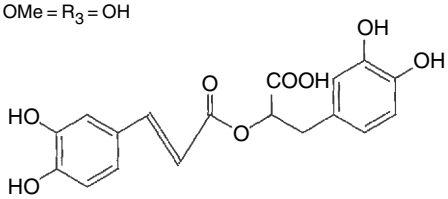

Rosmarinic acid

Fig. 1 Structures of phenolic acids.
Source: From HPLC analysis of phenolic compounds, in *Food Analysis by HPLC*.[1]

volume, low injection volumes, pumps with well-controlled low flow-rate, and low diameter capillary connections.[1]

Some published results have confirmed the fact that the quality of sorbent (purity, end-capping) and the particle size does not have a very significant influence on the peak symmetry of the analyzed phenolic acids,[5] but the chromatographic resolution and the efficiency of the column (number of theoretical plates) are better for columns with very good free silanol group covering, end-capping, or embedding. Maybe, it is the main reason for the use of good quality commercially available columns for most phenolic acid analyses in plant materials during the last years.[6] Especially, if a great number of analytes are required to be separated simultaneously, the column with the best separation properties is applied. The choice of columns depends also on the developed sample preparation technique, because the less clean extracts could decrease the lifetime of or cause damage to the column.

Most HPLC analyses of phenolic acids are performed at ambient column temperature, but moderately higher temperatures between 30° and 40°C have also been recommended in the analysis of fruits, vegetables, and other plants.

HPLC Mobile Phases

Both isocratic and gradient elution are applied for phenolic acid analyses. The choice depends on the number and type of analytes and the nature of plant matrix. Methanol, acetonitrile, and tetrahydrofurane are the most commonly used organic modifiers, as well as aqueous acidified solvents such aqueous acetic acid, formic acid, phosphoric acid, or perchloric acid. In some cases, acetonitrile leads to better resolution in a shorter analysis time than methanol and, generally, acetonitrile gives sharper peak shapes, resulting in a higher plate number. However, methanol is often preferable to acetonitrile because of its non-toxic properties and the possibility of using higher percentages in the mobile phase (lower solvent elution strength) which could protect the HPLC column. Also, tetrahydrofurane, with its high elution strength, could be applied to phenolic acid separations.[1] As most phenolic acids have p*K*s of about 4, the recommended pH range for the HPLC assay is pH = 2–4. It is important to avoid the ionization of analytes during analysis to improve the resolution and reproducibility of the retention characteristics. The most available columns allow the application of mobile phases with pH of about 2. The pH value is controlled by adding small amounts of acids to the water–organic mixture. Some authors also recommend the use of aqueous buffers (citrate buffer, phosphate buffer, ammonium acetate buffer) instead of the addition of acid. The buffer concentration can vary from 5 to 50 m*M*. The next alternative for controlling analyte retention may be the application of ion-pairing reagents, added to the aqueous mobile phases. However, the new generation of sorbents recommended for simultaneous separation of acids and bases can be applied without ion-pairing agents. An additional advantage of these new sorbents is the possibility of working with aqueous mobile phases with very low organic solvent content or without any organic modifier at all. The isocratic mode has been recommended for extracts containing components with very similar properties, especially with similar polarities in the purified extracts, with a small number of impurities or for coeluting compounds. Free phenolic acids (chlorogenic, protocatechuic, *p*-hydroxybenzoic, caffeic, vanillic, syringic, *p*-coumaric, and ferulic) could be isolated from some samples of medicinal plants or pharmaceutical preparations using a simple isocratic mobile phase (methanol–water–acetic acid).[7,8] Simple isocratic elutions have also been used for the analysis of phenolic acids in fruit products.[9] The same isocratic mobile phases were applied in the HPLC separations of simple phenolic acids using two columns of different properties. Chromatograms are illustrated in Fig. 2A and B. It is obvious from both chromatograms that the quality of the column, e.g., good end-capping of free silanol groups on the silica surface and low content of metal ions in silica material, can significantly influence the separation of analytes. Chromatographic resolution values are better

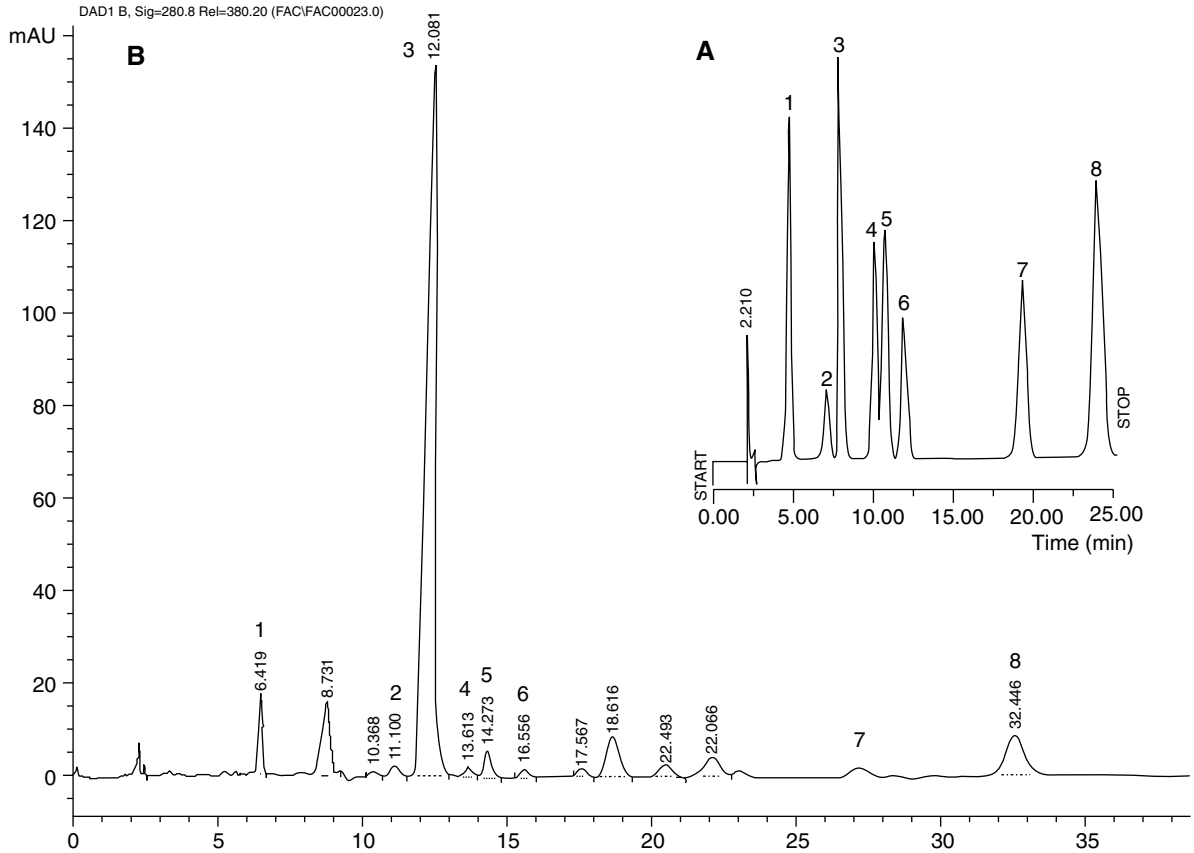

Fig. 2 HPLC chromatogram of phenolic acids using (A) ODS Hypersil column, (B) Symmetry C_{18} column and isocratic elution. Conditions: (A) column: ODS Hypersil (200 × 4.6 mm, 5 μm), mobile phase: methanol–water–acetic acid (25 : 75 : 1), flow-rate 1 ml/min; (B) column: Symmetry C_{18} (250 × 4.6 mm, 5 μm), mobile phase: methanol–0.001 *M* phosphoric acid (23 : 77), flow-rate 1 ml/min. Peaks: 1) protocatechuic acid; 2) chlorogenic acid; 3) *p*-hydroxybenzoic acid; 4) vanillic acid; 5) caffeic acid; 6) syringic acid; 7) *p*-coumaric acid; 8) ferulic acid.
Adapted from Glowniak, Zgorka, & Kozyra[7] and Zgorka & Kawka.[8]

for the Symmetry™ column, which makes quantitative analysis much simpler and reproducible. In the case when phenolic acids of different chemical structures and different polarities have to be analyzed simultaneously, gradient elution is necessary. Of course, in this case also, the choice of column is also a very important consideration. HPLC separation of phenolic acids of different polarities (e.g., protocatechic, caffeic, rosmarinic acids) using different quality columns often requires gradient elution.[5,10] This separation is illustrated in Fig. 3A and B. It can be seen from the chromatograms that there is no significant difference in the asymmetry values for all analytes, but the efficiencies of the two columns and the possibility of more compounds being separated at the same time are much higher for the Symmetry™ column. The same situation occurs if phenolic acids of different polarities, as well as other groups of phenolic compounds (flavonoids, diterpenes), have to be determined in a single analytical run. In this case, the separation of more analytes of different chemical structures has not been realized using a column without special properties. The simultaneous HPLC separation of different phenolic acids and flavonoids that could be present in some medicinal plants is demonstrated in Fig. 4.[10] The Symmetry C_{18} column and gradient elution were used. All analytes were separated in about 30 min, with the sufficient resolution. The same choice of mobile phase components is used for the gradient mode as was mentioned for the isocratic elution. This means using organic–water mixtures with controlled pH, or organic–buffer compositions. The binary linear or step gradients are mostly used. Concerning the elution order of separated phenolic acids, it is obvious that individual compound retention depends on their polarities and, of course, on the character of the stationary phase that is used. Generally, phenolic acids are eluted from RP columns according to decreasing polarities. Loss of polar hydroxy groups and the presence of the methoxy groups or ethylenic side chains could decrease the polarity and increase the retention time. Of course, the derivatives of common phenolic acids with two or more aromatic rings

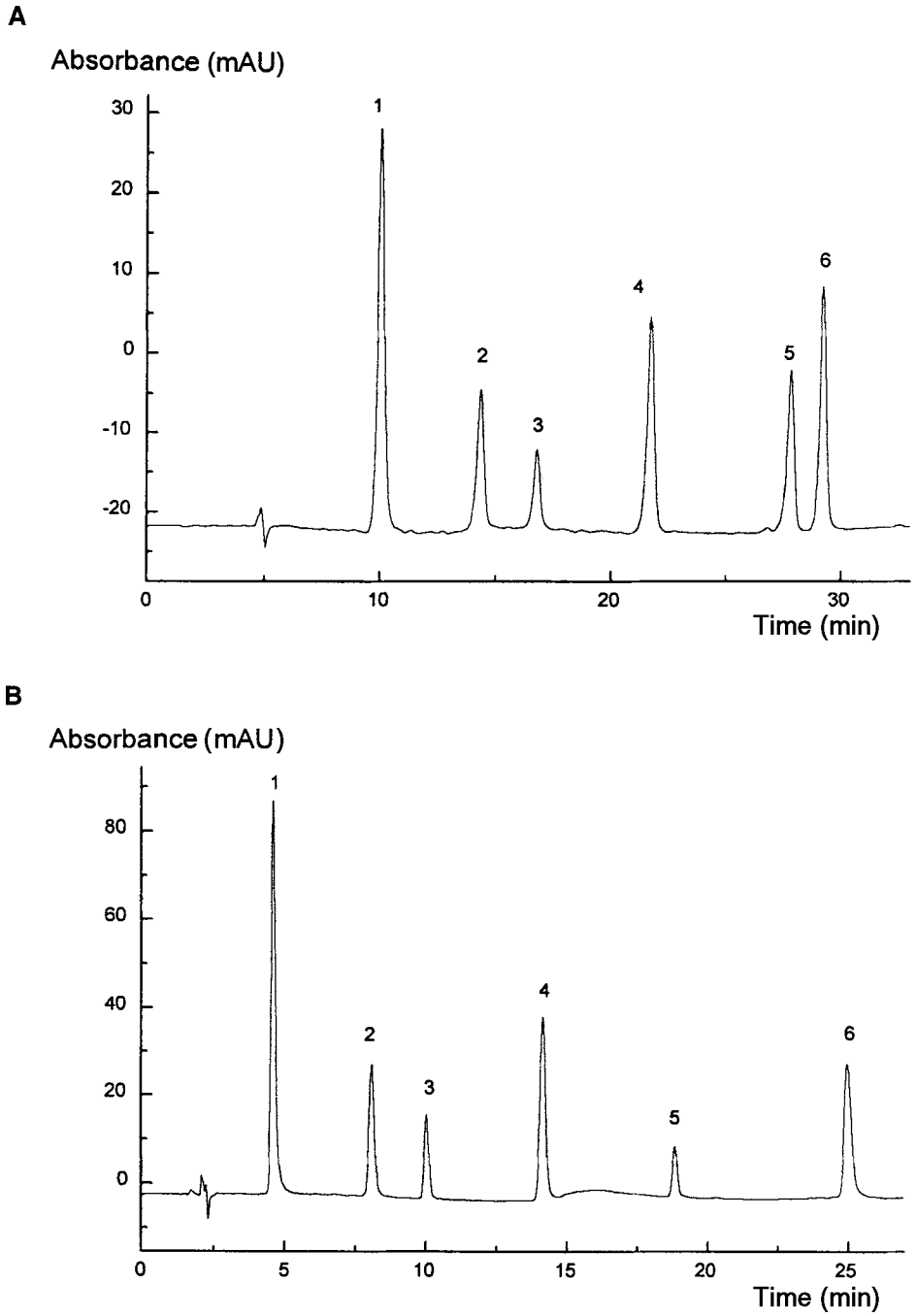

Fig. 3 HPLC analysis of phenolic acids using (a) Separon SGX C_{18} column and (b) Symmetry C_{18} column and gradient elution. Conditions: (A) column: Separon SGX C_{18} (250 × 4.6 mm, 7 μm), mobile phase: methanol–water (pH = 2.5, adjusted with formic acid), linear gradient from 15% methanol to 75% methanol in 40 min, flow-rate 0.5 ml/min; (B) column: Symmetry C_{18} (150 × 3.9 nm, 5 μm), mobile phase and flow-rate same as in (a). Peaks: 1) gallic acid, 2) protocatechuic acid, 3) catechin, 4) caffeic acid, 5) sinapic acid, 6) rosmarinic acid.

are less polar and are eluted much later than others. So, the gradient scheme has to be managed individually, according to the number and chemical properties of the analyzed compounds. Some phenolic acids could be present in natural plants as geometric isomers. Their simultaneous separation is usually possible using RP stationary phases. The greatest number of phenolic acids occurs in nature as *trans*-isomers, but on exposure to UV radiation or daylight they are gradually transformed to *cis*-isomers, which elute, usually, before *trans*-isomers.[1,5] For this reason, the stability studies of analyzed compounds are valuable and the results have to be taken into consideration during the sample preparation method development. UV radiation and elevated temperature could decrease the extraction recoveries and lower the reproducibility of the assay.

HPLC Detection

Phenolic acids absorb well in the UV range, but no single wavelength is sufficient for their simultaneous monitoring

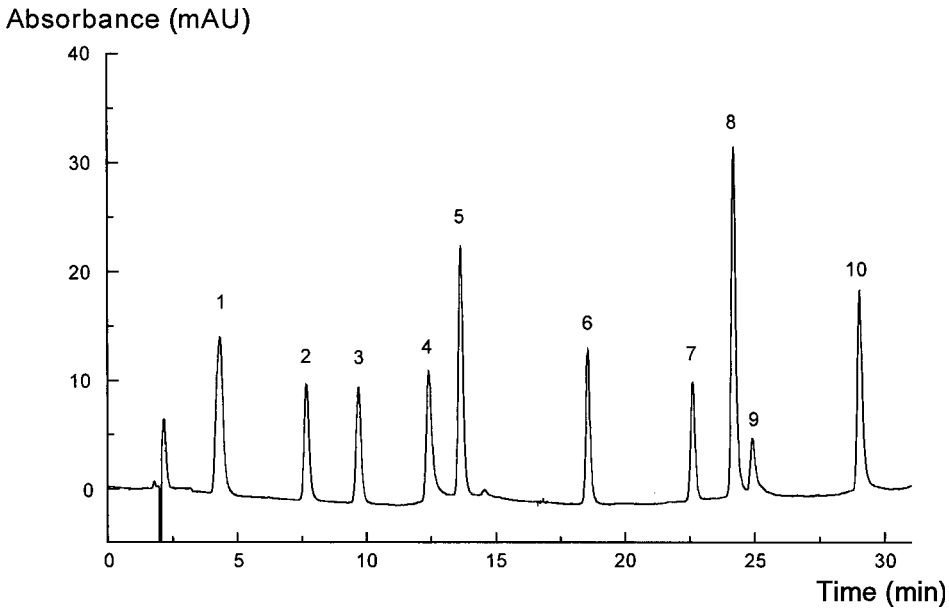

Fig. 4 HPLC analysis of phenolic acids and flavonoids using Symmetry C_{18} column and gradient elution. Conditions: column: Symmetry C_{18} (150 × 3.9 nm, 5 μm), mobile phase the same as in Fig. 3B, flow-rate 0.6 ml/min. Peaks: 1) gallic acid, 2) protocatechic acid, 3) catechin, 4) epigallocatechin gallate, 5) caffeic acid, 6) ferulic acid, 7) rutin, 8) rosmarinic acid, 9) myricetin, 10) quercetin.

in extracts of various natural plant extracts. Therefore, variable-wavelength UV or diode-array (DA) detectors are the most commonly used in the HPLC analyses of phenolic acids. Most of the benzoic acid derivatives have absorption maxima at 246–262 nm, with a shoulder at 290–315 nm, except for gallic and syringic acids with absorption maxima at 271 and 275 nm, respectively. The cinnamic acids absorb in two ranges: 225–235 and 290–330 nm. As was mentioned previously, the maxima of the UV spectra differ significantly for the individual phenolic acids; the range of wavelengths for their detection is wide (210–370 nm). Systematic studies of the absorbance spectra recommended for their simultaneous separation require the following single wavelengths: 254, 280, and 320 nm; for dual monitoring: 254 and 280 nm, or 280 and 320 nm. However, detection at 280 nm is the most generally used wavelength for the simultaneous separation of mixtures of phenolic acids.[1] Of course, DAD is the best detection choice, as it enables scanning of the UV spectra of all solutes passing through the detector; it could help in the identification of individual compounds in the extracts of complex mixtures, such as extracts of natural plants. Moreover, DAD also gives important information about the purities of all analytes.

Fluorescence detection is not very often used in phenolic acid analysis, but, in cases when very low concentrations of some analytes or many interfering compounds are present in extracts, the combination of UV and DAD with fluorescence detector could be valuable. However, the same problems could arise as in the UV detection, i.e., establishing the correct excitation and emission wavelengths, as large differences for several phenolic acids were observed. In this case, the rapid scanning fluorescence detector, in combination with DAD, is available for applying multiple excitation and emission wavelengths.[8]

Electrochemical detection is very sensitive for the compounds that can be oxidized or reduced at low-voltage potentials. Therefore, it could also be applied in the HPLC analysis of phenolic acids that are present in natural samples at very low concentrations. With the recent advances in electrochemical detection, multi-electrode array detection is becoming a powerful tool for detecting phenolic acids and flavonoids in a wide range of samples. The multi-channel coulometric detection system may serve as a highly sensitive way for the overall characterization of antioxidants; the coulometric efficiency of each element of the array allows a complete voltametric resolution of analytes as a function of their reaction (redox) potential. Some peaks may be resolved by the detector, even if they are unresolved when they leave the HPLC column.[11]

The detection and identification of phenolic compounds, including phenolic acids, have also been simplified using mass spectrometry (MS) techniques online, coupled to the HPLC equipment. The electrospray ionization (ESI) and atmospheric pressure chemical ionization (APCI) interfaces dominate the analysis of phenolics in herbs, fruits, vegetables, peels, seeds, and other plants. In some cases, HPLC, with different sensitivity detectors (UV, electrochemical, fluorescence), and HPLC/MS are simultaneously used for the identification and determination of phenolic acids in natural plants and related food products.[4,12,13] In some papers, other spectroscopic instrumental techniques (IR, ^{1}H NMR, and ^{13}C NMR) have also been applied for the identification of isolated phenolic compounds.[3]

SAMPLE PREPARATION

Sample handling is a very important part of the method development for HPLC determination of phenolic acids in

natural plants. Because of the great variability of phenolic acids (different polarity, acidity, number of hydroxyl groups, and aromatic rings), the various concentration levels of individual analytes, and the very complex natural matrix with many interfering components, the choice of the technique for their isolation and quantification differs from one described HPLC assay to the next. In some cases, only a one-step extraction and simple clean-up procedure are sufficient before the HPLC analysis, but the most often described HPLC assays include two or more steps of sample preparation, especially in the case of fruits and vegetable samples. It is obvious that each step contributes, on one hand, to the higher sensitivity and selectivity, but, on the other hand, it could increase the number of errors and decrease the recovery of the method. Therefore, it is very important to choose the optimal preparation of plant material according to the chemical structures and properties of analyzed compounds.

Liquid Extraction (LE)

Liquid extraction is the most commonly used procedure prior to HPLC analysis of phenolic acids in natural plants. Most of these samples are not of liquid consistency, and they cannot be injected directly into the HPLC column. Therefore, the analytes have to be isolated from the matrices in which they exist naturally before HPLC analysis. Of course, as the first steps of the preparation procedure, there are sample handling, milling, grinding, and homogenization. These steps can also influence the results of the complete HPLC assay. In many cases, the analyst has the possibility to control all preparation steps and to evaluate their influence on the analytical results. Commonly used extraction solvents are alcohols (methanol, ethanol), acetone, diethyl-ether, and ethyl acetate. However, very polar phenolic acids (benzoic, cinnamic acids) could not be extracted completely with pure organic solvents, and the mixtures of alcohol–water or acetone–water are recommended. On the other hand, the less polar analytes (phenolic acid derivatives) are not isolated quantitatively from plant matrices using only pure water as the extraction solvent. Less polar solvents (dichlormethane, chloroform, hexane, benzene) are suitable for the extraction of non-polar extraneous compounds (waxes, oils, sterols, chlorophyll) from the plant matrix. Of course, other factors (e.g., the choice of pH, temperature, sample-to-solvent volume ratio, and the number and time intervals of individual extraction steps) also play an important role in the extraction procedure. All these factors influence recovery values and, of course, the validation parameters of the complete assay. Therefore, it is necessary to optimize the extraction conditions.[5] The analysis of free phenolic acids, especially in fruits and vegetables, also often requires a hydrolysis step, as the phenolic acids could be found, in these sources, in the conjugated form and rarely in the free state. The assays could employ either acidic, alkaline, or enzymatic hydrolysis. An alkaline hydrolysis is used to break ester complexes (the most common form of phenolic acids) and acidic hydrolysis is used to disrupt glycoside linkages. Alkaline hydrolysis can be accomplished using 2N NaOH for some hours, at ambient or lower temperatures, often under nitrogen stream. Acidic hydrolysis is performed often at higher temperatures (100°C) with 2N HCl for some hours. But not all extracts are clean enough to be injected directly into the HPLC column. So, it is necessary sometimes to use additional clean-up step(s).

Extraction and clean-up procedures also apply column LC, solid-phase extraction (SPE), super critical fluid extraction (SFE), or matrix solid-phase dispersion (MSPD). The preferred approach is determined according to the nature of the plant matrix and the number and chemical properties of analyzed phenolic acids.

Solid-Phase Extraction

SPE is a good choice for the clean-up procedure for crude plant extracts. This technique, which applies all separation principles, has become very popular in the past decade. The advantage of SPE over LE is that SPE is faster and more reproducible, and fairly clean extracts are obtainable, emulsion creation is avoided, and smaller volumes are applied. From the environmental point of view, a lower consumption of toxic solvents is the reality of this technique. In some cases, more than one single-functional group SPE cartridge is used, or two or more SPE cartridges with different sorbents could be combined.[7–9] New generation sorbents are now also commercially available with hydrophilic–lipophilic properties which enable the simultaneous separation of both polar and less polar compounds. Very simple SPE assay is required for all acidic and basic analyte isolation from the "crude" plant extract and high recoveries are common for this simple procedure. The great advantage of SPE is the possibility of combining the SPE procedure, online, with the HPLC equipment and realizing the so-called direct sample analysis (DSA). This means that the "crude" extract of plant material is injected directly into this SPE/HPLC system.

Matrix Solid-Phase Dispersion

MSPD is the next alternative for sample preparation of fruits, vegetables, herbs, cereals, and other plants. It is convenient for liquid and semi-liquid samples. This technique is a multi-residual assay which consists of matrix homogenization with a solid silica phase placed into a short column, as in SPE. Analytes and matrix interferences are retained on the mixed solid-phase material with completely new separation characteristics. Specific elution allows one to obtain analytes after the elimination of matrix compounds via washing steps. This

technique combines homogenization, cellular disruption, extraction, fractionation, and purification in a single process. MSPD has many advantages: the sample is dispersed over a large surface area, the volumes of extraction solvents are low in comparison with liquid extraction, and so, as is the case with SPE, it can be automated. The application of MSPD as the preparation step before HPLC analysis of various analytes in plants, fruits, and vegetables has been reviewed.[14] This technique has also been tested for phenolic acids in herb materials.[10]

Supercritical Fluid Extraction

Supercritical fluids are attractive extraction agents, as the solvent power (density) can be manipulated over a wide range of temperatures and pressures. The solvating power of a supercritical fluid is varied by controlling the pressure or by adding organic modifiers such as methanol. SFE provides relatively clean extracts because the degradation of certain compounds by lengthy exposure to high temperatures and oxygen is avoided, and chlorophyll and other non-polar compounds are insoluble in supercritical CO_2. This technique is amenable to medicinal or other plant samples[15] and it can be combined also with other preparation techniques such as LE or SPE. Some problems could arise if SFE is used for some fruit and vegetable samples with high percentages of water. All samples are usually dried before the SFE assay. For some phenolic compounds, the extraction recoveries are not very high, as the content of organic modifier is, in many cases, not sufficient for their complete isolation, especially in the case of very polar phenolic acids.

APPLICATIONS

Herbs and Other Plants

Most papers dealing with phenolic acid HPLC analysis in herbs describe only simple liquid extraction without the hydrolysis step. Acetone, methanol, or alcoholic–water or acetone–water mixtures are applied.[16] Very rarely, pure water is used as the extraction solvent.[11] It was found that the extraction recoveries for water extracts are often lower in comparison to alcoholic–water mixtures, especially when the simultaneous separation of polar and less polar phenolic acids has been performed. Sometimes, the control of pH can improve the recovery.[5] If necessary, *n*-hexane, chloroform, diethyl ether, benzene–acetone, petroleum ether, or other less polar solvents are recommended for removing interfering compounds. The extraction is usually performed by refluxing the samples for a specific time in a Soxhlet apparatus, with simple mechanical or magnetic stirring of the sample with the extraction solvent, or by plant sample maceration. The application of an ultrasonic bath for the liquid extraction has also become popular in recent years. The hydrolysis steps have also been recommended for medicinal species preparation, especially when other phenolic compounds are also analyzed simultaneously with phenolic acids in herbs.[17]

Other plants (cereals, seeds, rye, nuts, barley, malt) can also be extracted with organic solvents or their mixtures with water, but, in many cases, less polar solvents are also used for the elimination of pigments, oils, non-polar and macromolecular compounds. Many of these assays have also included acidic and/or alkaline hydrolysis steps, column liquid clean-up procedures, or SPE. The simultaneous separation of phenolic acids and other phenolic compounds in these samples also complicates the preparation step. Very often, multi-step liquid extraction and sample clean-up assays are recommended. It is necessary to select extraction solvents according to the polarities of the analytes and the form of their bonding to the sample matrix. Very often, both free and bound phenolic acids are separated in plant samples, and hydrolyzed and non-hydrolyzed materials are analyzed separately. In some cases, two or more hydrolysis methods are applied for the analyses of cereals and nuts.[18,19]

Fruits and Vegetables

In the sample preparation step for fruits and vegetables, liquid extraction is performed combined with optimized hydrolysis before the HPLC analysis of phenolic acids.[20,21] A high quality column (e.g., Symmetry C_{18}) with simple gradient elution was used for the HPLC separation of phenolics expected to be present in vegetable samples before and after the hydrolysis steps.[21] In the cases when not only phenolic acids but also other phenolic compounds are determined in these samples, the extraction procedure consists, in many cases, of multi-step extractions and clean-up procedures. Column liquid chromatography or SPE is also recommended.[4] But sometimes the simple water extraction assay has been recommended for more fruits (strawberry, orange, grape, apple, banana, pear, etc.) and vegetable samples (carrot, potato, tomato, cucumber, leaf lettuce, eggplant, cauliflower, cabbage, garlic, onion, spinach).[11] It depends on the character of the sample matrix and the detection mode of the HPLC assay. The use of fluorescence, EC, or MS detectors also makes the sample preparation procedure much simpler by comparison with the common generally used detectors (e.g., UV), where more interfering components could be eluted simultaneously with phenolic acids and, for this reason, they have to be removed effectively in the preparation step.

More knowledge about the separation conditions for the HPLC analysis of phenolic acids in plant materials is available in the cited references. Some of them represent chapters in books with abundant additional information

about the above topic,[1,2] or review article,[6] with details from more than 60 papers published in the last 5 years, dealing with the choice of stationary phases, mobile phases, detection, sample preparation of plants prior to phenolic acid HPLC analyses, etc.

CONCLUSIONS

HPLC is a preferred technique for routine monitoring of phenolic acids in natural plants. With various detection possibilities, or their combinations, and completed with effective sample preparation procedures, HPLC enables the determination of phenolic acids occurring in herbs, fruits, vegetables, and other plants, in both free and bound forms; very often, phenolic acids are analyzed simultaneously with the other phenolics. Chromatographic conditions for these analyses are not complicated when efficient, commercially available, reversed-phase columns are applied. A new generation of sorbents can improve the separation parameters and, with their high separation power, can influence the number of analyzed compounds within a given relatively short separation time. The mobile phases used are also very simple (organic–water mixtures with controlled pH) and both isocratic and gradient modes are recommended. In the case of the simultaneous separation of many phenolic compounds, gradient elution is more suitable. Because of the complexity of some natural plant samples, the sample preparation procedure is the most important step of the entire assay. But today, many techniques offer the real possibility of preparing the sample before the HPLC analysis with sufficient specificity. Liquid extraction has to be, in many cases, the first step of the preparation stage. SFE or MSPD could also be suitable alternatives. Attention should be devoted to effective clean-up methods for plant extracts, such as simple column chromatography or SPE in off-line or online modes. The combined techniques, such as HPLC–MS, are very valuable for the possible identification of all analyzed compounds. The column-switching technique, with online connected columns (one as preparation and the second as the analytical column), enables the direct injection of the crude plant extract into the HPLC system, without special complicated clean-up procedures.[10] It is obvious that all these prospective methods, which today are commonly applied in the HPLC analyses of other analytes, will also find importance and practical use in the analysis of phenolic acids in plant materials.

REFERENCES

1. Lee, H.S. HPLC analysis of phenolic compounds. In *Food Analysis by HPLC,* 2nd Ed.; Nollet, L.M.L., Ed.; Marcel Dekker, Inc.: New York, 2000; 775–824.
2. Brandšteterova, E.; Kubalec, P.; Bovanova, L. HPLC determination of antimicrobial residues in edible animal products. In *Food Analysis by HPLC,* 2nd Ed.; Nollet, L.M.L., Ed.; Marcel Dekker, Inc.: New York, 2000; 621–691.
3. Nawwar, M.A.M.; Marzouk, M.S.; Nigge, W.; Linscheid, M. High-performance liquid chromatographic/electrospray ionization mass spectrometric screening for polyphenolic compounds of *Epilobium hirsutum*—The structure of the unique ellagitannin epilobamide. Mass Spectrom. **1997**, *32*, 645–654.
4. Ryan, D.; Robards, K.; Lavee, S. Determination of phenolic compounds in olives by reversed-phase chromatography and mass spectrometry. J. Chromatogr. A, **1999**, *832*, 87–96.
5. Caniova, A.; Brandsteterova, E. HPLC analysis of phenolic acids in *Melissa officinalis*. J. Liq. Chromatogr. Relat. Technol. **2001**, *24* (17), 2647–2659.
6. Caniova, A.; Brandsteterova, E. HPLC analysis of phenolic acids in plant material. Chem. Anal. (Warsaw) **2001**, *46*, 757–780.
7. Glowniak, K.; Zgorka, G.; Kozyra, M. Solid-phase extraction and reversed-phase high-performance liquid chromatography of free phenolic acids in some *Echinacea* species. J. Chromatogr. A, **1996**, *730*, 25–29.
8. Zgorka, G.; Kawka, S. Application of conventional UV, photodiode array (PDA) and fluorescence (FL) detection to analysis of phenolic acids in plant material and pharmaceutical preparations. J. Pharm. Biomed. Anal. **2001**, *24*, 1065–1072.
9. Amakura, Y.; Okada, M.; Tsuji, S.; Tonogai, Y. Determination of phenolic acids in fruit juices by isocratic column liquid chromatography. J. Chromatogr. A, **2000**, *891*, 183–188.
10. Brandsteterova, E.; Ziakova, A. unpublished results.
11. Guo, Ch.; Cao, G.; Sofic, E.; Prior, R.L. High-performance liquid chromatography coupled with coulometric array detection of electroactive components in fruits and vegetables: Relationship to oxygen radical absorbance capacity. J. Agric. Food Chem. **1997**, *45* (5), 1787–1796.
12. Mailard, M.N.; Giampaoli, P.; Cuvelier, M.E. Atmospheric pressure chemical ionization (APcI) liquid chromatography-mass spectrometry: Characterization of natural antioxidants. Talanta **1996**, *43*, 339–347.
13. Whittle, N.; Eldridge, H.; Bartley, J. Identification of the polyphenols in barley and beer by HPLC/MS and HPLC/electrochemical detection. J. Inst. Brew. **1998**, *105* (2), 89–99.
14. Barker, S.A. Matrix solid-phase dispersion. J. Chromatogr. A, **2000**, *885*, 115–127.
15. Palma, M.; Taylor, L.T. Extraction of polyphenolic compounds from grape seeds with near critical carbon dioxide. J. Chromatogr. A, **1999**, *849*, 117–124.
16. Yuan, J.P.; Chen, H.; Chen, F. Simultaneous determination of rosmarinic acid, lithospermic acid B and related phenolics in *Salvia miltiorrhiza* by HPLC. J. Agric. Food Chem. **1998**, *46*, 2651–2654.
17. Andrade, P.B.; Seabra, R.M.; Valentao, P.; Areias, F. Simultaneous determination of flavonoids, phenolic acids, and coumarins in seven medicinal species by HPLC/diode-array detector. J. Liq. Chromatogr. Relat. Technol. **1998**, *21* (18), 2813–2820.

18. Weidner, S.; Amarowicz, R.; Karamac, M.; Dabrowski, G. Phenolic acids in caryopses of two cultivars of wheat, rye and triticale that display different resistance to pre-harvest sprouting. Eur. Food Res. Technol. **1999**, *210*, 109–113.
19. Yurttas, H.C.; Schader, H.W.; Warthesen, J.J. Antioxidant activity of non-tocopherol hazelnut (*Corylus spp*.) phenolics. J. Food Sci. **2000**, *65* (2), 276–280.
20. Bocco, A.; Cuvelier, M.E.; Richard, H.; Berset, C. Antioxidant activity and phenolic composition of citrus peel and seed extracts. J. Agric. Food Chem. **1998**, *46*, 2123–2129.
21. Nuutila, A.A.; Kammiovirta, K.; Oksman-Caldentey, K.M. Comparison of methods for the hydrolysis of flavonoids and phenolic acids from onion and spinach for HPLC analysis. Food Chem. **2002**, *76*, 519–525.

Phenolic Compounds: HPLC Analysis

P.B. Andrade
D.M. Pereira
P. Valentão
Requimte, Department of Pharmacognosy, Faculty of Pharmacy, University of Porto, Porto, Portugal

Abstract
In this entry, the main parameters related to phenolics chemistry and analysis by chromatography are discussed. The most used extractive techniques, such as solid-phase extraction (SPE) and matrix solid-phase dispersion (MSPD), will be referred and compared. In addition, the most relevant analytical approaches, including high-performance liquid chromatography–diode-array detector (HPLC–DAD), LC–mass spectrometry (LC–MS), and LC–nuclear magnetic resonance (LC–NMR), will be presented, focusing on the advantages and disadvantages of each method.

INTRODUCTION

Phenolic compounds are secondary metabolites quite widespread in nature. They play several physiological roles in the plants where they occur, but many of them are also favorable to human health because of their biological activities. Recently, these compounds have been recognized as important in chemical fingerprints in metabolomic studies of several matrices.[1]

The characteristics of high-performance liquid chromatography (HPLC) make it the method of choice for the separation of these compounds. Many improvements have been achieved in this field; however, it was in the area of devices for detection and identification coupled to HPLC that more advances were made in recent years. In this entry, an overview of the chemistry of phenolics and their extraction, purification, and analysis procedures by HPLC is provided.

CHEMISTRY

According to Metcalf,[2] there are expected to be about 50,000–100,000 products resulting from secondary metabolism. It is estimated that about 20% of all carbon fixed by photosynthesis is channeled to the phenylpropanoid pathway, thus generating most of the phenolics found in nature.

Among phenolic compounds, flavonoids are of exceptional interest, as they represent one of the most ubiquitous and widely spread groups of natural products present in a majority of plants.

Flavonoids can be described as compounds that include carbon in an arrangement C_6–C_3–C_6 or, more accurately, that possess the phenylbenzopyran function. Therefore, according to the degree of oxidation and saturation of the heterocyclic ring, flavonoids can be classified into different classes (Fig. 1). Additionally, flavonoids may be modified by hydroxylation, methoxylation, or *O*-glycosylation of hydroxyl groups, as well as direct *C*-glycosylation of carbon atoms in the flavonoid skeleton. In *O*-glycosides sugar substituents are bound to a hydroxyl group of the aglycone, usually located at position 3 or 7, whereas *C*-glycosides have sugar groups bound to a carbon of the aglycone, usually C_6 or C_8. Flavonoid glycosides can also be acylated with aliphatic or acidic aromatic molecules.[3]

With a basic skeleton of C_6, there are simple phenols and benzoquinones; with C_6–C_1 structure, there are hydroxybenzoic acids such as gallic acid; C_6–C_2 corresponds to phenylacetic acids; and with C_6–C_3 skeleton there is a larger class including hydroxycinnamic acids, coumarines, and chromones. Sometimes these structures appear duplicated, giving rise to lignoids. Naphthoquinones have a C_6–C_4 structure, while xanthones exhibit a C_6–C_1–C_6 one. Stilbenes and anthraquinones are C_6–C_2–C_6 compounds.

EXTRACTION AND PURIFICATION

Sample preparation is fundamental for the analysis of phenolics in natural matrices, namely, medicinal plants, and is far more critical for quantification than for identification. The suitable procedure for extraction of phenolics from a plant material depends on the nature of the sample, particularly its physical state, and on the type of phenols to be extracted. The conditions employed should be as mild as possible to avoid chemical artifacts arising from hydrolysis, oxidation, and isomerization.[4]

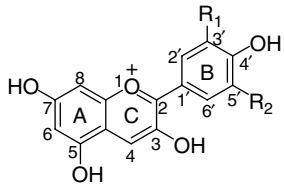

ANTHOCYANIDIN	R_1	R_2
Cyanidin	OH	H
Delphinidin	OH	OH
Malvidin	OCH_3	OCH_3
Pelargonidin	H	H
Peonidin		H
Petunidin	OCH_3	OH

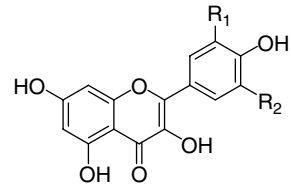

FLAVONOL	R_1	R_2
Quercetin	OH	H
Kaempferol	H	H
Myricetin	OH	OH
Isorhamnetin	OCH_3	H
Laricitrin	OH	OCH_3
Syringetin	OCH_3	OCH_3

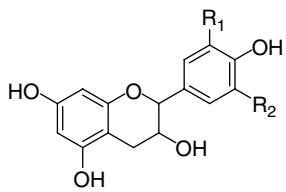

FLAVAN-3-OL	R_1	R_2
Catechin	OH	H
Gallocatechin	OH	OH

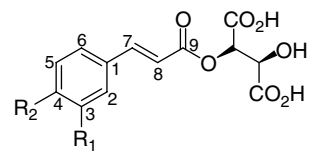

HYDROXYCINNAMIC ACID	R_1	R_2
Caftaric	OH	OH
Coutaric	H	OH
Fertaric	OCH_3	OH

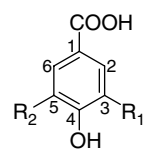

HYDROXYBENZOIC ACID	R_1	R_2
Protocatechuic	OH	H
Vanilic	OCH_3	H
Syringic	OCH_3	OCH_3
Gallic	OH	OH

Fig. 1 Main classes of phenolics found in nature.

This assumes that compounds are not covalently bound to the matrix, which is generally accurate in the case of flavonoids but not for phenolic acids. Some of these interferences may be avoided, at least partially, by the addition of an antioxidant, such as *tert*-butyl-4-hydroxyanisole, *tert*-butylhydroquinone, or sodium fluoride, which acts as a polyphenol oxidase inhibitor.

Depending on the aim of the work, hydrolysis of the extracts may be a useful approach, as this step decreases the number of compounds to be identified/quantified, thus

resulting in a better resolution and better characterization of the matrix. Acid hydrolysis is used to remove the sugar moiety, yielding the aglycones. Alkaline hydrolysis is applied when the objective is deacylation of sugars and the break of the covalent bond that phenolic acids may have with the matrix. For an example, please see the work by Ferreres et al.[5] However, when the aim of the work is profiling the endogenous phenolics in an extract, hydrolysis is usually not used, as it drastically changes the identity of compounds.

Although there are several extraction procedures at present, classical extraction with aqueous methanol and solid-phase extraction (SPE) are the most commonly used.[6] Some interfering compounds such as lipids, carotenoids, and chlorophylls can be removed from the water–alcohol extracts with hexane, chloroform, or petroleum ether. The defatted extracts may be analyzed directly or after partitioning of the phenolics with ethyl acetate. The suitable extraction conditions are dependent on the compound(s) and on the matrix of origin. For instance, extraction of flavonoids from biological fluids is one of the fastest tasks. This happens as a consequence of the simple manipulation of relatively small amounts of samples, in addition to good analytical characteristics, namely, limit of detection and relative standard deviation.[6]

Solid samples involve, in a general way, the most tedious and time-consuming procedures, particularly when isolating compounds in pure form and considerable amounts.

For some years, SPE, an adsorption–desorption technique, has been widely used in procedures of purification, trace enrichment, and class fractionation of phenolics. The SPE extraction of phenolics is usually performed using C_{18}-bonded silica reversed-phase (RP) sorbents, styrene–divinylbenzene copolymers, or graphitized carbon black, but other new polymeric sorbents such as RP105 and Oasis HLB are successfully used in the separation and preconcentration of phenolic acids.[7]

In C_{18}-bonded silica RP sorbents, the separation of phenolic acids is greatly affected by the number of free silanol groups. Silva et al.[8] showed that C_{18} non-end-capped columns are more suitable for the recovery of several phenolic acids and flavonoids than C_{18} end-capped ones. An enhanced recovery was obtained when 1% of methanol, serving as wetting agent, was added to the samples.

An alternative to official methods involving classical extraction and/or SPE techniques is matrix solid-phase dispersion (MSPD), a technique that has been widely used in the past years for the isolation of a range of drugs, pesticides, naturally occurring constituents, and other compounds from different complex plant and animal tissues, providing, in many cases, equivalent or superior results.[9,10] The main advantage of MSPD is the elimination of the several steps necessary for the analysis of solid, semisolid, and/or highly viscous biological samples, namely, preparation, extraction, and fractionation.[11] In this technique, all these steps are combined in just one, once the entire sample is homogeneously dispersed in a solid support, usually a C_{18}- or C_8-bonded silica, creating a unique chromatographic phase that is used as the stationary phase of a column. Extraction of analytes and cleanup are carried out simultaneously, with generally good analytical parameters such as recovery and precision.

In MSPD, sample is completely disrupted and dispersed into particles of very small size, which enhances a surface area required for subsequent extraction of the compounds, whereas in solid–liquid (SL)-SPE, sample disruption must be carried out separately and several compounds must be discarded before an extractive solution is found suitable for application on SPE column. While in SPE the extracted compounds are usually absorbed onto the top of the column packing material, in MSPD they are absorbed throughout the column. Physical and chemical interactions among the components of the system are greater in MSPD than those occurring in classical SPE or other forms of liquid chromatography (LC).

Despite the advantages present, namely, simplicity, speed, and requirement of much less solvent than in classical methods, MSPD is very rarely used in the extraction of phenolics. Only a few studies on MSPD can be referred to, such as the study of phenolic acids[12] or isoflavonoids.[13] Additionally, these studies do not show clearly that the complete extraction of phenolics can be accomplished by MSPD.

Xiao et al.[13] compared the efficiency of MSPD with ultrasonic and Soxhlet methods to extract isoflavonoids from radix astragali, the dried root of a Chinese medicinal plant. Four main isoflavonoids were identified, two aglycones and two glycosides, but while the amounts of the two aglycones were higher when using MSPD, the efficiency of extracting the glycosides was better if conventional techniques, ultrasonic or Soxhlet (especially the last one), were applied. Rijke et al.[14] used MSPD to extract and isolate isoflavone glucoside malonates from leaves of leguminous plants. However, when compared to solid–liquid extraction, the efficiency of extracting the glycosides was found to be lower. In the work of Ziaková et al.,[12] the extraction of phenolic acids from a medicinal plant (*Melissa officinalis*) was tried by MSPD, but the results obtained were not quantitatively compared with any other conventional techniques.

Dopico-García et al.[11] tested the ability of MSPD to extract phenolic compounds from white grapes in just one step, simplifying the SL-SPE analytical procedure. Phenolic compounds under study were determined using HPLC coupled to a diode-array detector (DAD). The recoveries obtained for phenolics were, in general, lower using MSPD than using SL-SPE. In some MSPD assays, only the recoveries obtained for the pair quercetin-3-*O*-glucoside/quercetin-3-*O*-rutinoside and for epicatechin were similar to those obtained using SL-SPE. So, for the pair quercetin-3-*O*-glucoside/quercetin-3-*O*-rutinoside, the

signal obtained with the assay 6-MSPD was similar to the one obtained with SL-SPE (101%), but a very high volume of solvent (150 ml of ethanol), not usual in MSPD, was required. The best results for epicatechin were obtained with the experiment 5-MSPD when a sorbent obtained by mixing 50% non-end-capped C_{18} and 50% end-capped C_{18} was used. The amount of epicatechin obtained corresponded to 90% of that found with SL-SPE. For the rest of the phenolics the recoveries obtained using MSPD were very poor in comparison to those obtained using SL-SPE. The pair kaempferol-3-*O*-glucoside/kaempferol-3-*O*-rutinoside was not recovered at all in the experiment 6-MSPD, even though the highest elution volumes were used. This indicates that probably these compounds were eluted with the first solvent [aqueous HCl (pH 2)] instead of ethanol. Recoveries of quercetin and kaempferol, in all the assays carried out by MSPD, were always much lower than those obtained using SL-SPE, with the best recoveries being around only 30%. So, comparing MSPD and SL-SPE for extracting phenolic compounds from white grapes, MSPD was found to be a simpler and faster technique, but a complete extraction of all compounds studied could not be achieved. Although MSPD could be a useful tool to identify the phenolic composition of white grapes, for this matrix SL-SPE was preferred to get quantitative recoveries of these compounds.

The main problem in the analysis of phenolics in plant-derived foods such as honey, fruit juices, and jam, is the high content of sugars and other polar compounds which cause interphasing when liquid–liquid partitions are chosen as a method of extraction.

The use of the non-ionic polymeric resin Amberlite XAD, by an adsorption–desorption technique, solved this problem. Tomás-Barbéran et al.[15] demonstrated that the polystyrene resins (XAD-2, XAD-4, and XAD-16) were more useful for the fractionation of flavonoids into aglycones and glycosides compared to the polyacrylic resins (XAD-7 and XAD-8). Amberlite XAD-2 was the more suitable non-ionic polymeric resin for the recovery and further fractionation of flavonoids from sugar-rich foods.

Apart from these techniques, supercritical fluids extraction (SFE) is the preferred technique in many areas of active compounds extraction. However, in what concerns to flavonoids, its utility is highly influenced by the matrix's composition. For example, in the case of isolation of non-polar flavonoid aglycones by SFE, when compared with classical techniques, SFE provided identical or sometimes better results. Nevertheless, when water-soluble glycosides are considered, the use of SFE results in considerably different yields.[16,17] Still, the use of aqueous methanol constitutes a useful and balanced extraction solvent that allows the extraction of both aglycones and flavonoid glycosides, depending on the conditions used, such as time and temperature, among others. Other reported solvents used for extraction are acetone, ethanol, and dimethyl sulfoxide (DMSO), with the water-to-solvent ratios being adjusted in accordance to the properties of the compounds to be extracted. Although DMSO presents properties that make it an excellent solvent, like the fact that it dissolves both polar and non-polar compounds and is miscible with a wide range of organic solvents as well as with water, one of the problems associated with the use of this solvent is due to its low volatility. Therefore, enhanced extraction can be achieved by using methanol or ethanol with 5–10% DMSO, which has a lower boiling point and allows an easier evaporation in subsequent stages of extraction.

DETECTION AND IDENTIFICATION

LC-UV/LC-DAD

All flavonoid aglycones contain at least one aromatic ring and therefore efficiently absorb UV light. The A-ring is responsible for the first maximum, found in the 240–285 nm range, and the second maximum, observed at 300–550 nm, is due to the substitution pattern and conjugation of the C-ring.[18]

When a UV detector works at a fixed wavelength, the obtained information is still very limited. In this case, to identify a compound using different experimental conditions, cochromatography is necessary with authentic reference compounds. DADs are much more useful, because they yield the full record of the UV–Vis spectrum of each compound. Because each class of phenolic compounds has a characteristic spectrum, identification is facilitated, although a safe characterization still requires a standard to compare retention time and UV spectra (see Fig. 2 for an example).

When two compounds with very close, or even superimposable, retention times and identical UV spectra are found in a chromatogram, it is necessary to use more sophisticated detectors that can yield much more structural information without requiring the isolation of the compounds. LC–mass spectrometry (LC–MS) and LC–nuclear magnetic resonance (LC–NMR) are often used, as it will be presented later.

HPLC-DAD is still the main technique used for phenolics quantification, a parameter not usually determined by other techniques such as LC–MS, given its poor sensibility.

Because of the great number of different flavonoid glycosides in nature, one cannot proceed with their quantification using authentic standards, as most of them are not commercially available. However, because sugar moieties are poor chromophores, their influence on UV absorption behavior of glycosides is smallest when compared with that of the aglycones. So, it is a common practice to quantify glycosides using standards of the corresponding aglycone, or a similar one.

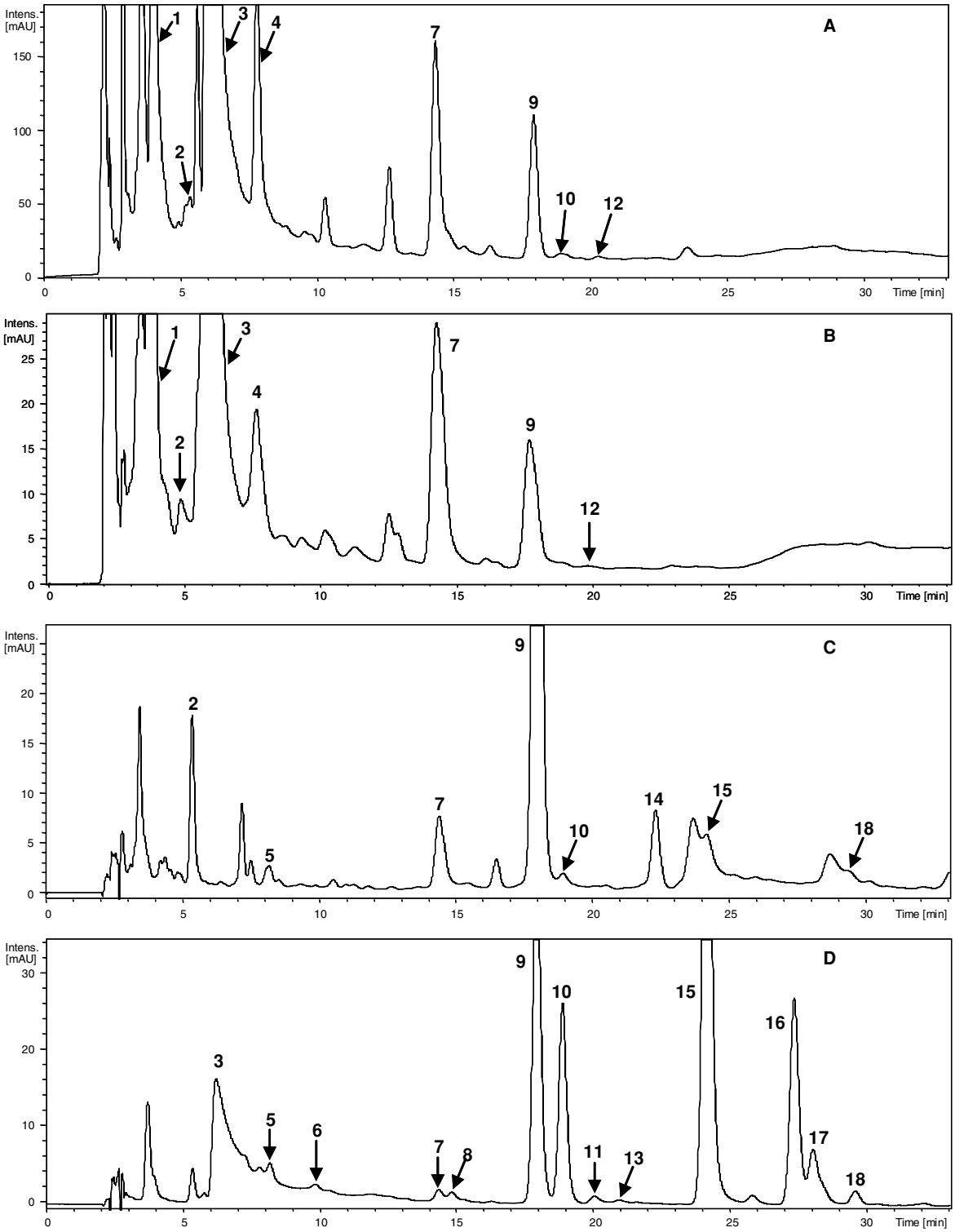

Fig. 2 HPLC-DAD chromatograms of *Catharanthus roseus* extracts: (A) stems, (B) leaves, (C) seeds, and (D) petals. Detection at 340 nm. (1) 3-*O*-caffeoylquinic acid; (2) kaempferol-3-*O*-(2,6-di-*O*-rhamnosyl-galactoside)-7-*O*-hexoside; (3) 4-*O*-caffeoylquinic acid; (4) 5-*O*-caffeoylquinic acid; (5) kaempferol-3-*O*-(6-*O*-rhamnosyl-galactoside)-7-*O*-galactoside; (6) kaempferol-3-*O*-(6-*O*-rhamnosyl-galactoside)-7-*O*-glucoside; (7) quercetin-3-*O*-(2,6-di-*O*-rhamnosyl-galactoside); (8) quercetin-3-*O*-(2,6-di-*O*-rhamnosyl-glucoside); (9) kaempferol-3-*O*-(2,6-di-*O*-rhamnosyl-galactoside); (10) kaempferol-3-*O*-(2,6-di-*O*-rhamnosyl-glucoside); (11) quercetin-3-*O*-(6-*O*-rhamnosyl-galactoside); (12) isorhamnetin-3-*O*-(2,6-di-*O*-rhamnosyl-galactoside); (13) quercetin-3-*O*-(6-*O*-rhamnosyl-glucoside); (14) isorhamnetin-3-*O*-(2,6-di-*O*-rhamnosyl-glucoside); (15) kaempferol-3-*O*-(6-*O*-rhamnosyl-galactoside); (16) kaempferol-3-*O*-(6-*O*-rhamnosyl-glucoside); (17) isorhamnetin-3-*O*-(6-*O*-rhamnosyl-galactoside); (18) isorhamnetin-3-*O*-(6-*O*-rhamnosyl-glucoside).
Adapted from New phenolic compounds and antioxidant potential of *Catharanthus roseus,* in J. Agric. Food Chem.[19]

In contrast to flavonoids, standards of most of the phenolic acids are commercially available and their positive identification can be performed by comparison of the retention time and characteristic UV absorbance with those of authentic reference compounds.

As regards hydroxycinnamic acids, they absorb at two regions of the UV spectrum, presenting a maximum at 225–235 nm and two other, very near of each other, by 290–330 nm. The double absorption in this region arises from the presence of *cis* and *trans* isomers, and the ratio between these two forms contributes to the final spectrum. In alkaline medium, all three maxima suffer a bathochromic shift. The different esters of the same acid present similar spectrum, regardless of the molecule presenting the alcohol function (quinic acid, sugar, or tartaric acid).[20]

In what concerns benzoic acids, the UV spectrum is more influenced by the hydroxylation degree of benzenic moieties than that of hydroxycinnamic acids. Methylation of hydroxyl groups has almost no effect on the UV spectrum. Only dihydroxylated benzoic acids present two maxima.[20]

LC–MS

MS has proved to be a very powerful technique in the analysis of flavonoids and phenolic acids mainly due to its high sensitivity and the possibility of coupling with different chromatographic techniques such as gas chromatography (GC–MS), capillary electrophoresis (CE–MS), and especially LC–MS. Nowadays, techniques such as LC-DAD–MS, and particularly LC-DAD–electrospray ionization (ESI)/MS, are regarded as necessary tools for the analysis of phenolics in natural matrices.[21,22]

The amount of information obtained by multisignal MS or MS–MS renders two levels for identification of compounds: positive and provisional. Positive identification can be achieved when reference compounds are available, thus allowing comparison of both retention time and UV spectra. However, when no standards are available, generally provisional identification takes place. In this case, although the identity of subunits such as aglycones, sugars, and acyl moieties is elucidated, the positions of glycosidic and acyl linkages remain unknown, with the exception of some fragmentation patterns that allow a positive identification of the glycosidic bonds (Fig. 3).[22] In many cases, a taxonomic approach may help in identification (e.g., most flavonoid glycosides present a 7-*O* linkage); however, NMR analysis is usually necessary. Nevertheless, the level of identification required in food and botanical analysis is a question worth postulating . For example, in the analysis of beverages (such as wines) and oils, most of the time, profile analysis yielding provisional identification is enough for quality control and detection of adulteration.

Spectroscopy by UV–Vis and MS, when in total ion count mode, yields comparable detection limits for flavonoids, in the range of 10 ng. When single ion monitoring (SIM) mode is used, MS analysis provides better detection limits, usually below 1 ng.[21] SIM mode, however, causes loss of valuable information concerning fragmentation pattern, which is very important for the identification of many compounds.

With the advent of atmospheric pressure ionization (API) sources, LC–MS coupling has become more efficient and accessible, causing this technique to be one of the most used for online flavonoid analysis nowadays.

Comparison of different API sources such as ESI, atmospheric pressure photoionization (APPI), and atmospheric pressure chemical ionization (APCI), is available in literature.[23] ESI is more frequently used in flavonoid analysis; however, APCI is gaining popularity and in some cases better responses are obtained in this mode.

The highest sensitivity can be obtained by the use of ESI in negative ion mode, usually involving an eluent consisting of an acidic ammonium acetate buffer. When using positive ion mode, the lowest detection limits involve the use of 0.5% formic acid. Also, negative ion mode results in limited fragmentation, which is particularly suited for molecular mass determination, especially when the concentration of compounds is low.[22]

In the formation of adducts, or even molecular complexes, with solvent or acid molecules, the peak at the highest *m/z* ratio may not correspond to the molecular ion species ($[M + H]^+$ in positive mode and $[M - H]^-$ in negative mode). Instead, $[2M + H]^+$ or $[2M - H]^-$ may be formed. This issue may be corrected by an increase in cone voltage, which diminishes formation of both adducts and complexes.[21]

While negative ion mode is very useful to identify known compounds, the first-order mass spectrum yielded by positive ion mode can provide more structural information. So, the combined use of both ionization modes can give additional accuracy to the molecular mass determination, which is particularly relevant when noise levels are high.[21]

Besides spectroscopic data, chromatographic retention times can also add further knowledge to the compounds' chemistry. In general, on C_{18}- or C_8-RP columns, more polar compounds are eluted first. Thus, increase in glycosylation results in decrease in retention times. In contrast, acylation, methylation, or prenylation have a distinct effect—rising retention time, although the position where this occurs may play a significant role in chromatographic behavior. In what concerns aglycones, flavanones precede flavonols, which in turn precede flavones, for compounds with an equivalent substitution pattern.[24]

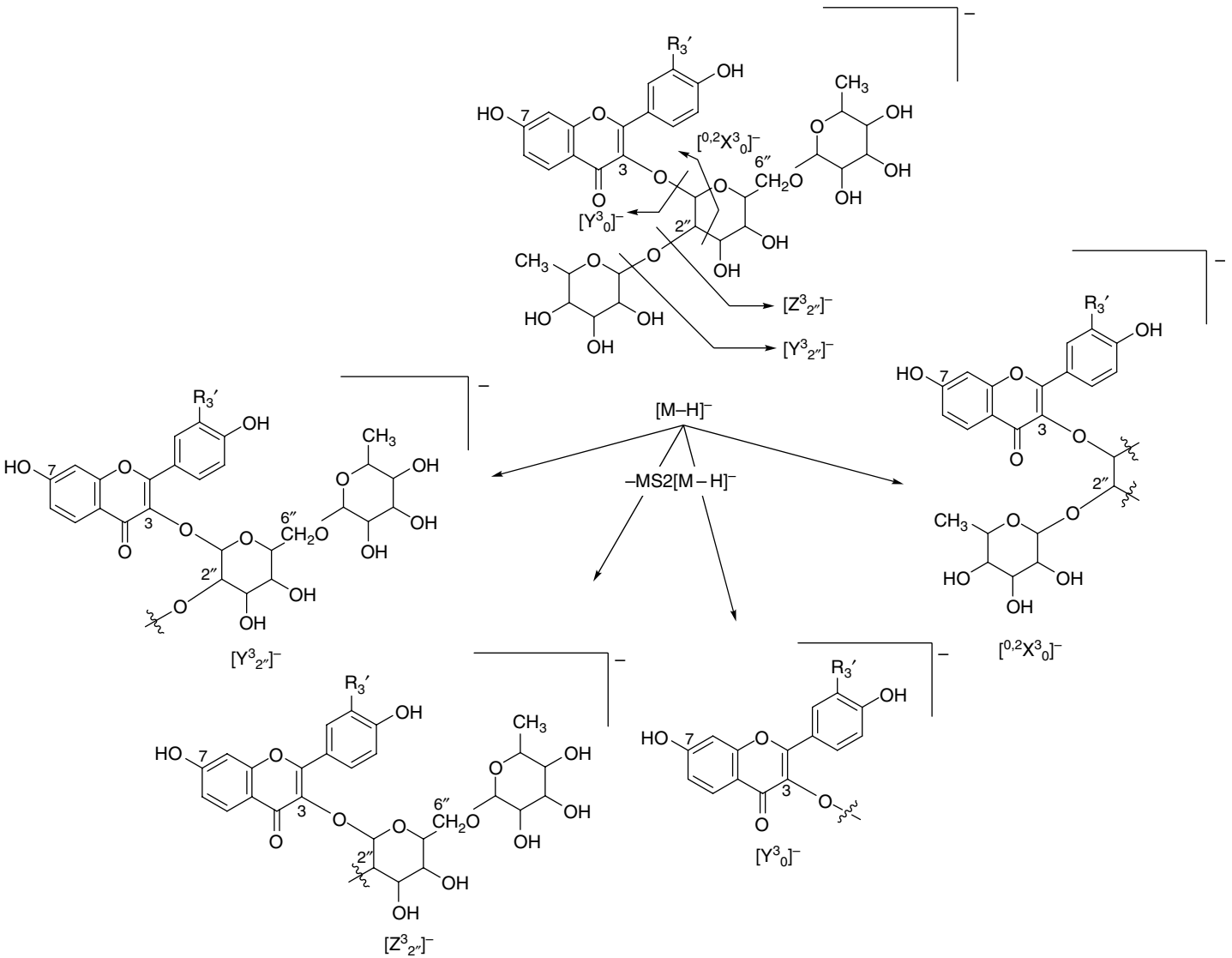

Fig. 3 —MS2[M–H]⁻ fragmentation of flavonol-3-*O*-(2,6-di-*O*-rhamnosyl-hexoside) from *Catharanthus roseus*. Adapted from New phenolic compounds and antioxidant potential of *Catharanthus roseus,* in J. Agric. Food Chem.[19]

LC–NMR

In recent years, LC–NMR has been attracting a lot of attention from the natural products area. Its main advantages include differentiation of isomers and information of substitution patterns on aromatic ring systems and sugar configurations. However, low sensitivity (consequence of small energy gap between the ground and excited nuclear spin rates), prohibitive prices (of both equipment and deuterated solvents), and long analysis time, sometimes reaching days, are the main disadvantages of this technique. The advantages and disadvantages of this analytical method have been carefully reviewed in many works.[24,25] Still, MS techniques have their place as they provide important information such as about functional groups and molecular mass. So, the ideal system would be LC–NMR–MS or LC–NMR–MS–MS.

When working with online flow NMR, the acquisition time is limited by the short presence of the sample in the detection coil as a consequence of the flow rates commonly used, thus resulting in poor signal-to-noise ratio. Also, when the flow rate is reduced by a factor of 3–10, better signal-to-noise ratio can be registered, followed by an increase in experimental acquisition time, which may lead to diffusion processes that can influence the separation of peaks eluting from the LC column. To surpass this problem, accumulation of peaks into storage loops for off-line NMR at a later stage has been proposed.[26]

As it has already been stated, one of the main disadvantages of LC–NMR is its low sensitivity (LC–NMR remains less sensitive than UV or MS detection). Some technical advances have successfully improved the analytical parameters such as cryogenic temperatures, making this technique even more attractive. The procedure consists of cooling the receiver coil to cryogenic temperatures, while the sample remains at ambient temperature. This limits the noise voltage associated with signal detection, and when compared with regular probes, signal-to-noise ratio is ameliorated by a factor of 3–4.

Alternatively, the application of SPE to concentrate the compounds of interest has been successfully developed as a way to counter the somewhat low sensitivity of LC–NMR. This method is a powerful technique for universal, quick, and selective sample preparation, which recently originated methods that combine LC–NMR with SPE.

CONCLUSIONS

Phenolic compounds are still the objects of numerous studies, mainly concerning their extraction, purification, and analytical methods. This is because these compounds, especially flavonoids, are responsible for an increasing number of beneficial biological activities in humans.

So, methods with higher sensitivity and lower detection limit are required as a tool to keep up with the recent developments in the knowledge of bioactivity of phenolics.

REFERENCES

1. Allwood, J.W.; Ellis, D.I.; Goodcare, R. Metabolomic technologies and their application to the study of plants and plant–host interaction. Physiol. Plantarum **2008**, *132*, 117–135.
2. Metcalf, R.L. Plant volatiles as insect attractants. CRC Crit. Rev. Plant Sci. **1987**, *5*, 251–301.
3. Macheix, J.J.; Fleuriet, A.; Billot, J. *Fruit Phenolics*; CRC Press: Boca Raton, FL, 1990.
4. Antolovich, M.; Prenzler, P.; Robards, K.; Ryan, D. Sample preparation in the determination of phenolic compounds in fruits. Analyst **2000**, *125*, 989–1009.
5. Ferreres, F.; Andrade, P.B.; Valentão, P.; Gil-Izquierdo, A. Further knowledge on barley *(Hordeum vulgare* L.) leaves *O*-glycosyl-*C*-glycosyl flavones by liquid chromatography-UV diode-array detection-electrospray ionisation mass spectrometry. J. Chromatogr. A **2008**, *1182* (1), 56–64.
6. Molnár-Perl, I.; Fuzfai, Z. Chromatographic, capillary electrophoretic and capillary electrochromatographic techniques in the analysis of flavonoids. J. Chromatogr. A, **2005**, *1073* (1–2), 201–227.
7. Kledjus, B.; Kubán, V. High performance liquid chromatographic determination of phenolic compounds in seed exudates of *Festuca arundinacea* and *F. pretense*. Phytochem. Anal. **2000**, *11* (6), 375–379.
8. Silva, B.M.; Andrade, P.B.; Seabra, R.; Ferreira, M.A. Determination of selected phenolic compounds in quince jams by solid-phase extraction and HPLC. J. Liq. Chromatogr. Relat. Technol. **2001**, *24* (18), 2861–2872.
9. Barker, S.A. Matrix solid-phase dispersion. J. Chromatogr. A, **2000**, *885* (1–2), 115–127.
10. Kristenson, E.M.; Ramos, L.; Brinkman, U.A.Th. Recent advances in matrix solid-phase dispersion. Trends Anal. Chem. **2006**, *25* (2), 96–111.
11. Dopico-García, M.S.; Valentão, P.; Jagodziñska, A.; Klepczyñska, J.; Guerra, L.; Andrade, P.B.; Seabra, R.M. Solid-phase extraction versus matrix solid-phase dispersion: Application to white grapes. Talanta **2007**, *74* (1), 20–31.
12. Ziaková, A.; Brandsteterová, E.; Blahová, E. Matrix solid-phase dispersion for the liquid chromatographic determination of phenolic acids in *Melissa officinalis*. J. Chromatogr. A, **2003**, *983* (1–2), 271–275.
13. Xiao, H.B.; Krucker, M.; Albert, K.; Liang, X.M. Determination and identification of isoflavonoids in radix astragali by matrix solid-phase dispersion extraction and high-performance liquid chromatography with photodiode array and mass spectrometric detection. J. Chromatogr. A, **2004**, *1032* (1–2), 117–124.
14. de Rijke, E; de Kanter, F.; Ariese, F.; Brinkman, U.A.Th.; Gooijer, C. Liquid chromatography coupled to nuclear magnetic resonance spectroscopy for the identification of

isoflavone glucoside malonates in *T. pratense* L. leaves. J. Sep. Sci. **2004**, *27* (13), 1061–1070.
15. Tomás-Barbéran, F.A.; Blásquez, M.A.; Garcia-Viguera, C.; Ferreres, F.; Tomás-Lorente, F. A comparative study of different Amberlite XAD resins in flavonoid analysis. Phytochem. Anal. **1992**, *3* (4), 178–181.
16. Lin, M.C.; Tsai, M.J.; Wen, K.C. Supercritical fluid extraction of flavonoids from Scutellariae Radix. J. Chromatogr. A, **1999**, *830* (2), 387–395.
17. Scalia, S.; Giuffreda, P.; Pallado, P. Analytical and preparative supercritical fluid extraction of chamomile flowers and its comparison with conventional methods. J. Pharm. Biomed. Anal. **1999**, *21* (3), 549–558.
18. Mabry, T.J.; Markham, K.R.; Thomas, M.B., Eds., *The Systematic Identification of Flavonoids*; Springer-Verlag: New York, 1970.
19. Ferreres, F.; Pereira, D.M.; Valentão, P.; Andrade, P.B.; Seabra, R.M.; Sottomayor, M. New phenolic compounds and antioxidant potential of *Catharanthus roseus*. J. Agric. Food Chem. **2008**, *56*, 9967–9974.
20. Riberéau-Gayon, P. *Les composes phénoliques des végétaux*; Dunod: Paris, 1968.
21. Cuyckens, F.; Claeys, M. Mass spectrometry in the structural analysis of flavonoids. J. Mass. Spectrom. **2004**, *39* (1), 1–15.
22. Rauha, J.P.; Vuorela, H.; Kostiainen, R. Effect of eluent on the ionization efficiency of flavonoids by ion spray, atmospheric pressure chemical ionization, and atmospheric pressure photoionization mass spectrometry. J. Mass Spectrom. **2001**, *36* (12), 1269–1280.
23. de Rijke, E.; Zappey, H.; Ariese, F.; Gooijer, C.; Brinkman, U.A.Th. Liquid chromatography with atmospheric pressure chemical ionization and electrospray ionization mass spectrometry of flavonoids with triple-quadrupole and ion-trap instruments. J. Chromatogr. A, **2003**, *984* (1), 45–58.
24. Wilson, I.D.; Brinkman, U.A.Th. Hyphenation and hypernation: The practice and prospects of multiple hyphenation. J. Chromatogr. A, **2003**, *1000* (1–2), 325–356.
25. Wolfender, J.-L.; Ndjoko, K.; Hostettmann, K. Liquid chromatography with ultraviolet absorbance–mass spectrometric detection and with nuclear magnetic resonance spectrometry: A powerful combination for the on-line structural investigation of plant metabolites. J. Chromatogr. A, **2003**, *1000* (1–2), 437–455.
26. Exarchou, V.; Godejohann, M.; van Beek, T.A.; Gerothanassis, I.P.; Vervoort, J. LC-UV-solid-phase extraction-NMR-MS combined with a cryogenic flow probe and its application to the identification of compounds present in Greek oregano. Anal. Chem. **2003**, *75*, 6288–6294.

Phenolic Drugs: TLC Detection

Alina Pyka
Department of Analytical Chemistry, Medical University of Silesia, Sosnowiec, Poland

Abstract
This entry describes applications of indicators as new visualizing reagents (alkaline blue, aniline blue, neutral red, brilliant green, bromophenol blue, bromothymol blue, brilliant cresyl blue, thymol blue, phenol red, bromocresol green, helasol green, spands, titan yellow, eosin yellow, erythrosin B, eriochrome black T, dimethyl yellow, and thymolphthalein), and various visualizing systems, always including a saturated aqueous solution of variamine blue hydrochloride and other reagent [e.g., 0.1% aqueous HCl, 1% aqueous $Ni(NO_3)_2$, 2% aqueous $CuSO_4$, 0.1% aqueous Na_2CO_3, 1% dithizone in methanol, and 1% aqueous ethylenediaminetetraacetic acid (EDTA)] for the detection of selected phenolic drugs (bamethane, ethamivan, hexachlorophene, salicylanilide, pyrocatechin, thymol, pentazocine, phloroglucinol, eugenol, niclosamide, terbutaline, methyldopa, norepinephrine, eugenol, α-naphthol, polybasic phenols, adrenaline, dopamine, phenylephrine, metaraminol, fenoterol, and bithionol) in thin-layer chromatography (TLC). Six dyes as new visualizing reagents, namely, gentian violet, methylene violet, methylene blue, methyl green, malachite green, and Janus blue, have been used to detect ibuprofen on silica gel $60F_{254}$ and to detect estradiol on neutral aluminum oxide $60F_{254}$ and on neutral aluminum oxide $150F_{254}$. Broadening index, detection index, characteristic of densitometric band, modified contrast index, limit of detection, densitometric visualizing index (DVI), and linearity range of detected compounds were used for the evaluation of visualizing effects of applied visualizing reagents. It was shown that visualizing effect depends on the chemical structure of the visualizing reagent, the structure of the substance detected, and the chromatographic adsorbent applied. The usefulness of densitometry to direct the detection of some phenolic drugs was also shown.

INTRODUCTION

The separated substances on thin layer can be detected by the following methods:

- Physical (individual color of substance or fluorescence of substance in UV light)
- Chemical (colored reactions of separated substances with visualizing reagents)
- Physicochemical (e.g., the application of isotopes as visualizing reagent)
- Biological (the application of biodetectors)

The visualizing reagents are of special significance for detecting separated compounds on thin layers. In view of the detection mechanism of the compound, the visualizing reagents can be sorted as follows:

- Conservative reagents, which do not destroy separated substances
- Destructive reagents, which destroy or change the structure of separated substances[1–3]

Currently, the most important field of application of thin-layer chromatography (TLC) is pharmacy. The number of publications in the field of pharmacy has steadily increased.[1,3] It results from the fact that contemporary TLC is a fully instrumentalized and automated technique. Many phenol derivatives have definite pharmacological and biological properties.[4] For example, the drugs that command special attention are the drugs acting on the peripheral nervous system (adrenaline, dopamine, phenylephrine, metaraminol, fenoterol, bamethane, terbutaline, methyldopa, norepinephrine), drugs acting on the central nervous system (ethamivan), drugs applied in taeniasis (bithionol, niclosamide), analgesic drugs (pentazocine), and fungicidal and bacteriostatic drugs (hexachlorophene, salicylanilide, pyrocatechin, arbutin, thymol, phloroglucinol, eugenol, and *o*-, *m*-, and *p*-cresol). However, α-naphthol is often applied as a component of some dermatological ointments. Moreover, phenolic compounds are present in numerous phytomedicines. Phenolic compounds are very widespread, particularly among floral plants. Free phenols often occur as components of essential oils. Phenolic compounds are also widespread as phenolic glycosides, phenolic acids, and polyphenols. Phenolic compounds as phenolic acids are solid components of plants (caffeic acid, chlorogenic acid). Also, some alkaloids have phenolic character (morphine).[2,5]

There are good analytical and physicochemical reasons for describing new visualizing reagents; these reasons and the most important reagents and techniques for different

types of organic compounds, including phenols, have been described elsewhere.[1,3,6–20] For example, Barton's reagent was used to detect dopamine; chloramine T–sodium hydroxide, sucrose–hydrochloric acid, and Pauly's reagents to detect phloroglucinol; Emerson reagent to detect thymol and eugenol; fast black salt K–sodium hydroxide reagent to detect terbutalina; potassium hexaiodoplatinate reagent to detect pentazocine; potassium hexacyanoferrate(III)–ethylenediamine reagent to detect dopamine, noradrenaline, and adrenaline;[1,3,6] aniline–diphenylamine–phosphoric acid, lead(IV) acetate–dichlorofluorescein, Gibb's and Millons reagents, and Berlin blue reaction to detect arbutin; natural products–polyethylene glycol reagent to detect chlorogenic acid; vanillin–sulfuric acid reagent to detect eugenol, thymol, and carvacrol; and anisaldehyde–sulfuric acid reagent to detect thymol.[5] This entry describes applications of indicators as new visualizing reagents for the detection of selected phenolic drugs in TLC.

NEW VISUALIZING REAGENTS

The phenolic drugs bamethane, ethamivan, hexachlorophene, salicylanilide, pyrocatechin, thymol, pentazocine, phloroglucinol, eugenol, niclosamide, terbutaline, methyldopa, and norepinephrine on silica gel 60 (E. Merck, #1.05721, glass plates) were detected by Pyka, Gurak, and Bober.[7] Plates with methyldopa, norepinephrine, terbutaline, bamethane, and ethamivan were developed with a mixture of glacial acetic acid–*n*-butanol–water (1:4:1, v/v) as the mobile phase. Plates with phloroglucinol, pentazocine, hexachlorophene, pyrocatechin, niclosamide, salicylanilide, and thymol were developed with a mixture of chloroform–methanol (9:1, v/v). The plate with eugenol was developed with benzene as the mobile phase. Thirteen new visualizing reagents were used to detect the above-mentioned phenolic drugs. Alkaline blue, aniline blue, neutral red, and brilliant green were used as 50 mg/100 ml aqueous solutions. Bromophenol blue, bromothymol blue, brilliant cresyl blue, thymol blue, phenol red, bromocresol green, and helasol green were used as 50 mg/100 ml solutions in 2% aqueous sodium hydroxide solution. Bromophenol blue solution was prepared directly before use. Additionally, brilliant cresyl blue and bromocresol green were used as 50 mg/100 ml aqueous solutions. Plates were evaluated 5 min after spraying (variant 1). They were then heated at 100°C for 15 min and re-examined (variant 2).

By means of these visualizing reagents—alkaline blue, aniline blue, bromophenol blue, bromothymol blue, alkaline solution of brilliant cresyl blue, bromocresol green, thymol blue, and an aqueous solution of brilliant cresyl blue—it is possible to detect all of the drugs investigated at the level of 100 μg. Using the remaining visualizing systems (neutral red, brilliant green, phenol red, and aqueous solution of bromocresol green), it is also possible to detect 100 μg of the drugs investigated except methyldopa, terbutaline, norepinephrine, and ethamivan. These could not be detected by means of neutral red; ethamivan could not be detected by means of helasol green, thymol blue, and aqueous solution of bromocresol green; bamethane and salicylanilide could not be detected with phenol red. Detection limit (detectability), detectability index, and broadening index were used to describe visualizing effects for phenolic drugs, which were detected by particular visualizing reagents. The definitions and equations for calculation of the broadening index and detectability index were given earlier.[7,8,9]

A good visualizing reagent has a relatively large numerical value of broadening index (evaluation after heating at 120°C for 30 min) for a particular detected substance (small spot area, which refers to 100 μg of substance detected). The broadening indices for the drugs investigated, with the best visualizing reagents (evaluation after heating at 120°C for 30 min), are equal to 67 $\mu g/mm^2$ for methyldopa with brilliant cresyl blue (brown spot), 99 $\mu g/mm^2$ for norepinephrine with alkaline blue (orange-red spot), 270 $\mu g/mm^2$ for terbutaline with aniline blue (yellow-green spot), 455 $\mu g/mm^2$ for bamethane with brilliant green (white spot), 345 $\mu g/mm^2$ for ethamivan with aniline blue (white-blue spot), 152 $\mu g/mm^2$ for phloroglucinol with bromocresol green (orange spot), 84 $\mu g/mm^2$ for pentazocine with bromophenol blue (light blue), 71 $\mu g/mm^2$ for hexachlorophene with brilliant green (green spot), 62 $\mu g/mm^2$ for pyrocatechin with bromocresol green (brown spot), 278 $\mu g/mm^2$ for niclosamide with bromothymol blue (light brown spot), 217 $\mu g/mm^2$ for salicylanilide with alkaline solution of bromocresol green (light blue spot), 135 $\mu g/mm^2$ for thymol with bromocresol green (white-blue with white border spot), and 68 $\mu g/mm^2$ for eugenol with bromothymol blue (light yellow spot).[7]

The detection limits of the investigated phenolic drugs with the tested visualizing reagents, directly after spraying (variant 1), or after 30 min heating at 120°C (variant 2), as well as the detection indices were determined. For the detection limits, the investigated drugs revealed that only in some cases is the detection better after the plates are heated. Levels of detection of the phenolic drugs are in the following ranges (in microgram): for pyrocatechin 0.3–5.0; for pentazocine 0.5–100; for norepinephrine 0.6–100; for niclosamide 0.8–50; for salicylanilide 0.8–100; for methyldopa 1.2–4.8; for terbutaline 2.0–30; for thymol 2.0–100; for hexachlorophene 3.0–25; for phloroglucinol 3.0–30; for bamethane 10.0–100; for eugenol 5.0–10; and for ethamivan 40.0–100. The most sensitive detections are obtained for pyrocatechin with alkaline blue, brilliant green, helasol green (300 ng); pentazocine with aniline blue (500 ng); norepinephrine with bromothymol blue (600 ng); niclosamide and salicylanilide with brilliant green (800 ng); methyldopa with aqueous solution of bromocresol green (1.2 μg). The best visualizing reagents for

the drugs investigated (being phenol derivatives) are brilliant green as well as aniline blue. These two visualizing reagents were used for densitometric research (on Shimadzu densitometer). Hexachlorophene, niclosamide, and salicylanilide as well as methyldopa, terbutaline, and bamethane were detected with brilliant green, and then the densitometric analysis of chromatograms was determined. Norepinephrine and terbutaline were detected with aniline blue. For hexachlorophene (10 μg), niclosamide (5.0 μg), and salicylanilide (15.0 μg), an optimum wavelength of incident light $\lambda = 617.9$ nm was detected. Densitogram of hexachlorophene, niclosamide, and salicylanilide after spraying with brilliant green is as shown in Fig. 1A. Methyldopa (50 μg), terbutaline (100 μg), and bamethane (100 μg) were detected by means of brilliant green as optimum wavelength $\lambda = 380.5$ nm was selected. Densitogram for these three drugs is presented in Fig. 1B. The peak, derived from methyldopa, has an irregular shape, suggesting that methyldopa contained impurities that (using the given mobile phase) could not be completely separated. For norepinephrine (5.0 μg) and terbutaline (15.0 μg), detected by means of aniline blue, an optimum wavelength for densitometric analysis, $\lambda = 371$ nm, was chosen. Densitogram obtained for norepinephrine and terbutaline is presented in Fig. 1C. The densitograms show that both aniline blue and brilliant green have good properties as visualizing reagents with respect to the substances detected. However, brilliant green, because of its properties, causes heterogeneity of adsorbent surface, observed as noise. This effect is not observed for aniline blue. Some of the visualizing reagents reported here can be used as new visualizing reagents for the qualitative determination of phenolic drugs. The colors of chromatographic spots, detection limits, and detectability indices of phenolic drugs investigated, obtained with selected reagents (including the best reagents aniline blue and brilliant green), were presented earlier.[7–10] These reagents can be used to identify compounds analyzed by TLC, based on R_F values and on the different colors of the chromatographic spots. Further investigations showed that guaiacol cannot be detected using the above-mentioned visualizing reagents.[11] The quantitative determinations of pyrocatechin and norepinephrine were carried on silica gel 60 (E. Merck, #1.05721). The conditions used for chromatography were identical to those described earlier.[7] The plates were sprayed with alkaline blue, bromothymol blue, and phenol red, and heated at 120°C for 30 min. Six replicate analyses were performed; the areas (square millimeter) of the spots obtained were measured planimetrically and the average areas were calculated. It was stated that the pyrocatechin detected with alkaline blue can be quantitatively determined in the range from 2.0 to 90 μg. However, norepinephrine detected with bromothymol blue or phenol red can be quantitatively determined in the range from 5.0 to 100 μg.[11]

Arbutin, without visualizing reagents, was densitometrically analyzed. Standard solutions of arbutin were spotted on aluminum foil-backed plates precoated with a 0.2 mm layer of silica gel $60F_{254}$ (#1.05554, E. Merck). Ethyl acetate–methanol–water in volume composition 100:13.5:10 was used as the mobile phase. The plate was developed at a distance of 14 cm. After drying the plate, arbutin was densitometrically investigated on Camag TLC Scanner 3. The absorption photometric scan in reflectance (remission) was carried out at $\lambda = 285$ nm. Spectrodensitogram and densitogram of arbutin (10 μg) are presented in Fig. 2.[11] Densitometry without visualizing reagent was also used for the quantitative determination of arbutin (*Vaccinium vitis idaeae*) in the leaves of cowberry collected from Suwalszczyzna, Poland.[12] Arbutin was extracted using methanol. Chromatography was performed on glass TLC plates with layers of silica gel (E. Merck, #1.05715) and using the above-mentioned mobile phase. The quantitative densitometric analysis on Camag TLC Scanner 3 was performed using internal standard solution method. On the basis of densitometric analysis, it was shown that band characterized by absorption maximum of arbutin is placed at $\lambda_{max} = 285$ nm. The second absorption band is at $\lambda = 225$ nm. 35 mg and 47 mg arbutin were determined in 1 g of herbs in cowberry leaves coming from collections in 2005 and 2006, respectively. The method presented is accurate, selective, and precise, and can be used for routine quality control analysis and quantitative determination of arbutin in cowberry leaves.[12]

Pyka et al.[13] also applied various visualizing systems, always including a saturated aqueous solution of variamine blue hydrochloride and other reagent, for example, 0.1% aqueous HCl, 1% aqueous $Ni(NO_3)_2$, 2% aqueous $CuSO_4$, 0.1% aqueous Na_2CO_3, 1% dithizone in methanol, and 1% aqueous ethylenediaminetetraacetic acid (EDTA) to detect selected essential oil components after their separation on silica gel 60 (E. Merck, #1.05744). These visualizing reagents can be used for the qualitative identification of eugenol and thymol. Yet, guaiacol cannot be detected by using these visualizing reagents.[13]

Wardas and Pyka[14] and Wardas, Lipska, and Lebek[15] investigated spands, titan yellow, eosin yellow, helasol green, phenol red, thymol blue, bromothymol blue, bromophenol blue, bromocresol green, erythrosin B, eriochrome black T, and brilliant cresyl blue in aqueous sodium hydroxide (50 mg/100 ml of 5% NaOH), and dimethyl yellow and thymolphthalein in methanolic solution (50 mg/100 ml) as well as aniline blue and alkaline blue in aqueous solutions (50 mg/100 ml) as visualizing reagents to detect cresol and naphthol isomers, which were separated on three adsorbents (aluminum foil-backed plates precoated with 0.2 mm layers of either silica gel 60 or a mixture of silica gel 60 with Kieselguhr F_{254}, as well as on glass plates precoated with 0.15 mm layer of Polyamide $11F_{254}$). The best visualizing reagents for the detection of α-naphthol on silica gel 60 are titan yellow, eosin, helasol green, and

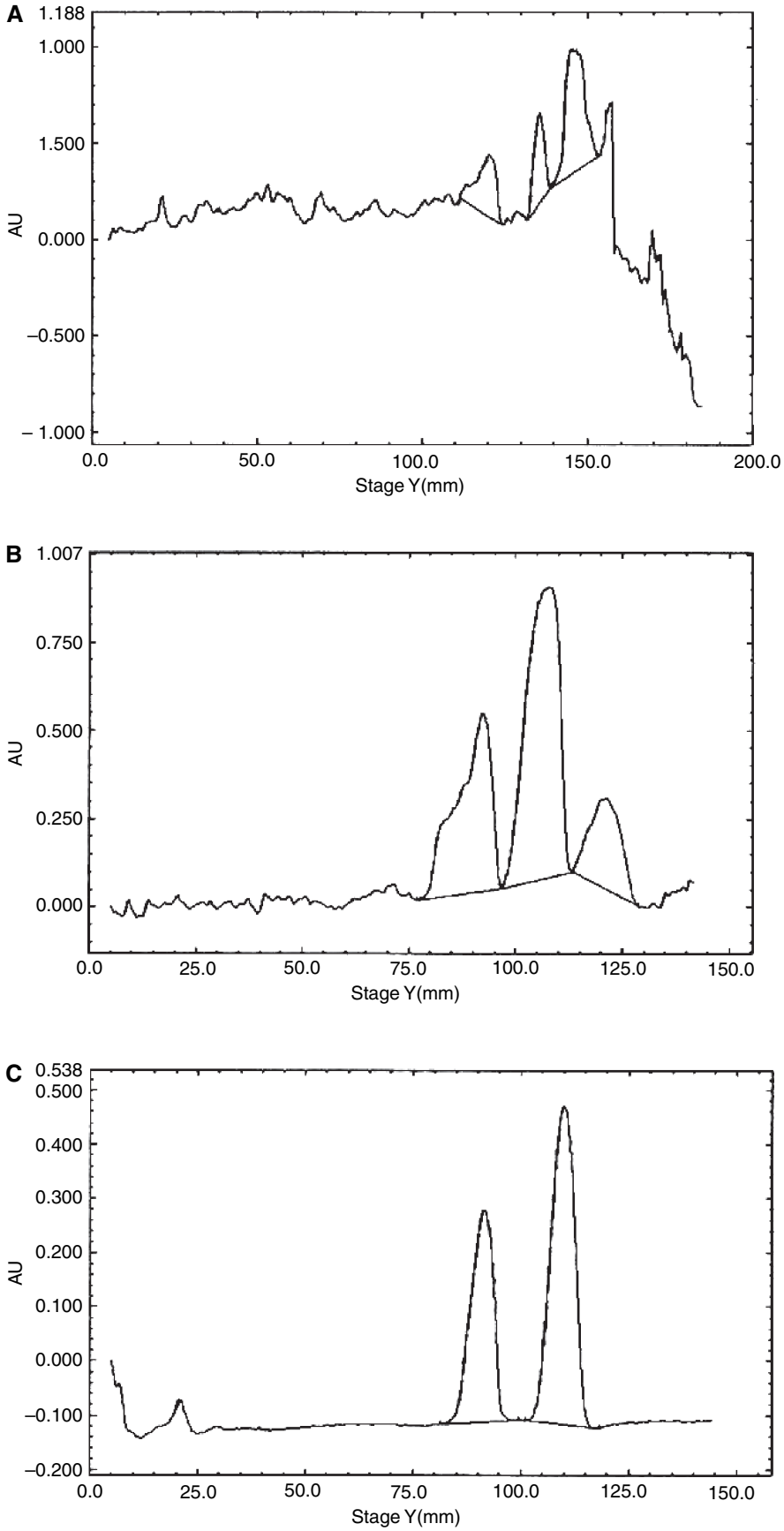

Fig. 1 Densitograms of: A, hexachlorophene (1), niclosamide (2), and salicylanilide (3) after spraying with brilliant green at $\lambda = 617.9$ nm; B, methyldopa (1), terbutaline (2), and bamethane (3) after spraying with brilliant green at $\lambda = 380.5$ nm; C, norepinephrine (1) and bamethane (2) after spraying with aniline blue at $\lambda = 371$ nm.

Source: From New visualizing reagents for selected phenolic drugs investigated by thin layer chromatography, in J. Liq. Chromatogr. Relat. Technol.[7]

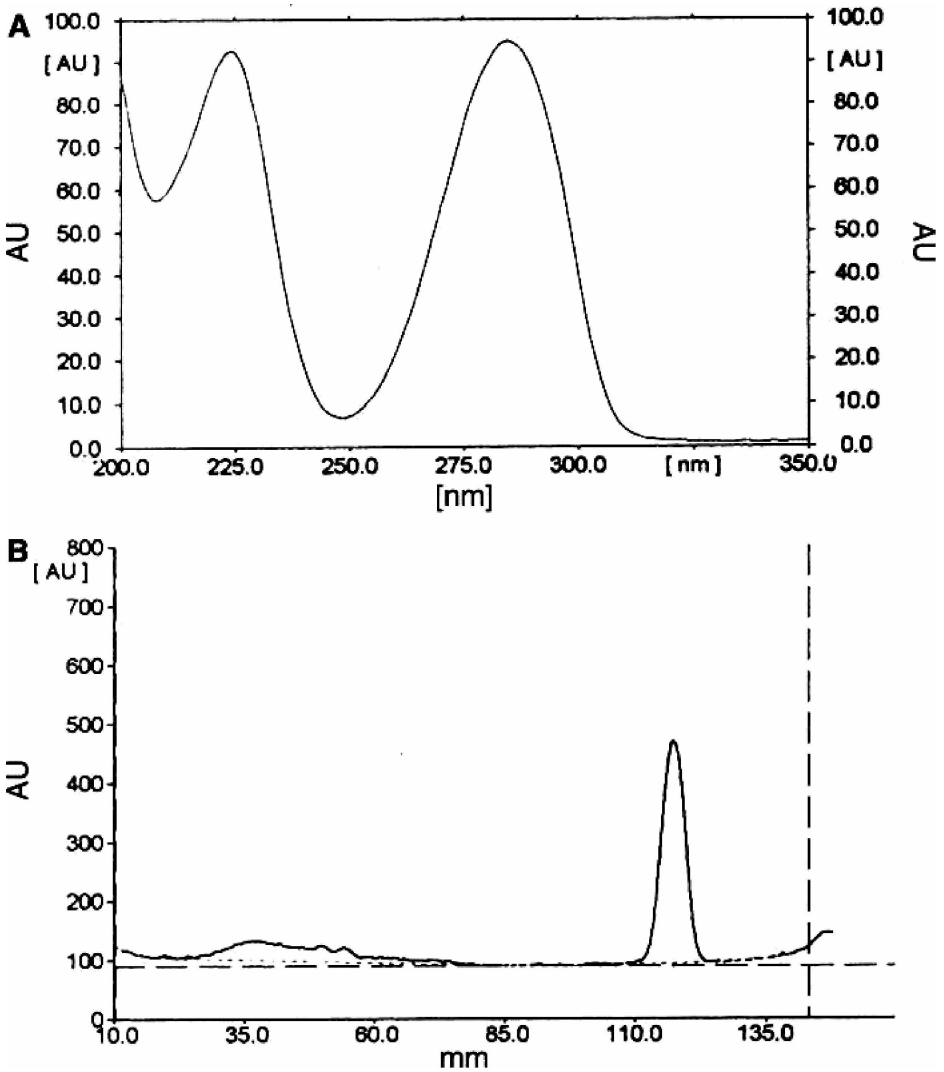

Fig. 2 Spectrodensitograms (A) and densitograms (B) of 10 mg arbutin (Camag TLC Scanner; slit dimensions: 6.00 × 0.30 mm, Micro; scanning speed: 20 mm/sec for detection and 20 nm/sec for spectrum scan; data resolution: 100 mm/step for detection and 1 nm/step for spectrum scan; λ = 285 nm; deuter lamp; measurement type: remission; measurement mode: absorption).
Source: From Pyka, A. Unpublished data.[11]

bromothymol blue (brown spots in each cases).[14,15] Detection limit of α-naphthol using these visualizing reagents is between 0.10 and 0.14 μg. Bromocresol green, titan yellow, and eosin yellow are the best visualizing reagents for the detection of α-naphthol chromatographed on a mixture of silica gel 60 and Kieselguhr F_{254} (detection limit: between 0.10 and 0.15 μg; brown, brown-gray, and green-gray spots, respectively).[14,15] However, for the detection of α-naphthol on Polyamide $11F_{254}$, bromocresol green (detection limit: 2.5 μg; brown spot) is best.[15] Titan yellow is the best visualizing reagent for the detection of *m*-cresol on silica gel 60 (detection limit: 1.08 μg; faint brown spot).[16]

Wardas, Lipska, and Lebek[17] also investigated the 16 new visualizing reagents (alkacymetric, complexometric, and redoxymetric indicators) to detect polybasic phenols. The best visualizing reagents for the detection of hydroquinone, pyrogallol, and phloroglucinol on silica gel 60 are brilliant cresyl blue to detect hydroquinone (detection limit: 500 ng; light brown spot); and alkaline blue to detect pyrogallol and phloroglucinol (detection limits: 500 ng and 100 ng, respectively; brown and orange spots, respectively). The best visualizing reagents for the detection of hydroquinone, pyrogallol, and phloroglucinol on a mixture of silica gel 60 and Kieselguhr F_{254} are erythrosin B to detect hydroquinone (detection limit: 500 ng; brown spot); thymolphthalein to detect pyrogallol (detection limit: 500 ng; light brown spot); and alkaline blue to detect phloroglucinol (detection limit: 500 ng; orange spot). The best visualizing reagents for the detection of hydroquinone, pyrogallol, and phloroglucinol on Polyamide $11F_{254}$ are bromocresol green to detect hydroquinone (detection limit: 500 ng; brown spot); brilliant cresyl blue to detect pyrogallol (detection limit: 100 ng; yellow spot); and brilliant green to detect phloroglucinol (detection limit: 100 ng; orange spot).[17]

Wardas, Lipska, and Bober[18] examined indicators for the detection of adrenaline, dopamine, phenylephrine, metaraminol, fenoterol, and bithionol after TLC

fractionation on silica gel $60F_{254}$, Polyamide $11F_{254}$, and mixture of silica gel 60 and Kieselguhr F_{254} using glacial acetic acid–*n*-butanol–water (1:4:1, v/v) as the mobile phase. They investigated the following indicators as visualizing reagents: phenol red, thymol blue, bromothymol blue, bromophenol blue, cresol green, erythrosin B, eriochrome black T, brilliant cresyl blue, eosin yellow, titan yellow, helasol green dissolved in 5% NaOH, as well as bromocresol green, aniline blue, alkaline blue, brilliant cresyl blue, and brilliant green dissolved in water. Additionally, dimethyl yellow and thymolphthalein dissolved in methanol were applied, but before being used, the chromatographic plate was sprayed with 5% NaOH. In each case, the concentration of the solutions was 0.5 mg/ml. Most reagents give positive visualizing effects on silica gel $60F_{254}$, a bit less on a mixture of silica gel 60 and Kieselguhr F_{254}, and the least on Polyamide $11F_{254}$. Detection levels of these phenolic drugs on silica gel $60F_{254}$ are in the following ranges (in microgram): for adrenaline 0.1–10.0; dopamine 0.1–10; for phenylephrine 0.25–20; for metaraminol 0.5–20; for fenoterol 0.1–15; and for bithionol 0.5–50. Detection levels of these phenolic drugs on a mixture of silica gel 60 and Kieselguhr F_{254} are in the following ranges (in microgram): for adrenaline 0.25–15.0; for dopamine 0.25–7.5; for phenylephrine 0.5–15; for metaraminol 0.5–15; for fenoterol 0.5–12.5; and for bithionol 2.5–10. Detection levels of these phenolic drugs on Polyamide $11F_{254}$ are in the following ranges (in microgram): for adrenaline 2.5–100; for dopamine 0.75–100; for metaraminol 50–100; and for fenoterol 5–100. The best detectability, equal to 100 ng, was obtained on silica gel $60F_{254}$, in the case of adrenaline with brilliant cresyl blue dissolved in water, as well as dopamine and fenoterol with bromocresol green and brilliant cresyl blue dissolved in 5% NaOH. The best detectability on mixture of silica gel 60 and Kieselguhr F_{254} is 250 ng for adrenaline and dopamine with bromocresol green in 5% NaOH, on the polyamide 750 ng for dopamine with eosin yellow. However, phenylephrine and bithionol are not detected on Polyamide $11F_{254}$ with the studied visualizing reagents. Characteristics of the visualizing effect for adrenaline, dopamine, phenylephrine, metaraminol, fenoterol, and bithionol with the best visualizing reagents investigated on Kieselgel $60F_{254}$, Kieselgel 60/Kieselguhr F_{254}, and Polyamide $11F_{254}$ were presented earlier.[8,9,10,18]

Recently, the modified broadening index, detection index, densitometric visualizing index (DVI), and modified contrast index were used for the evaluation of detectability effects of salicylanilide, estradiol, and ibuprofen.[19–21] Estradiol is a steroid compound, but it contains an aromatic ring with hydroxyl group about phenolic character. Salicylanilide was detected on glass plates precoated with a 0.50 mm layer of silica gel $60F_{254}$ (E. Merck, #1.05744) and with a 0.25 mm layer of silica gel $60F_{254}$ (E. Merck, #1.05715), as well as on aluminum plates precoated with a 0.20 mm layer of silica gel $60F_{254}$ (E. Merck, #1.05554), silica gel 60 (E. Merck, #1.05553), and a mixture of silica gel 60 and Kieselguhr F_{254} (E. Merck, #1.05567), with and without the use of brilliant green as a visualizing reagent. It was stated that salicylanilide bands without the use of a visualizing reagent are invisible on the chromatogram in a visible light. Dark green spots of salicylanilide on green background are visible on the chromatograms after an application of brilliant green as a visualizing reagent. The obtained chromatographic spots of the investigated salicylanilide on the applied chromatographic sorbents after the use of brilliant green were durable and visible for over 6 weeks. The R_F values of salicylanilide are in the range from 0.75 to 0.88 depending on the applied chromatographic plates. Spectrodensitometric evaluation of salicylanilide with and without the use of a visualizing reagent was performed. For example, spectrodensitograms of salicylanilide with and without the use of brilliant green as a visualizing reagent on the #1.05744, #1.05715, and #1.05567 plates are presented in Figs. 3–5, respectively. It was stated that salicylanilide without the use of a visualizing reagent has fundamental absorption band at the similar values of the wavelength equal to 307 or 308 nm on #1.05744, #1.05715, #1.05554, and #1.05553 plates. However, the absorption maximum of salicylanilide on a mixture of silica gel 60 and Kieselguhr F_{254} without the use of a visualizing reagent is somewhat shifted and it is equal to 312 nm, whereas the obtained spectrodensitograms of salicylanilide without the use of a visualizing reagent differ in the intensity of the additional absorption bands depending on the chromatographic sorbents. The resultant spectrodensitograms of salicylanilide after detection with brilliant green differ in the wavelength of absorption maximum. The absorption maximum of salicylanilide occurs at 268 nm on #1.05715, #1.05554, and #1.05553 plates; at 305 nm on #1.05567 plate, and at 597 nm on #1.05744 plate. Simultaneously, the resultant spectrodensitograms of salicylanilide after the use of brilliant green also differ in the number and intensity of the additional absorption bands on the particular chromatographic plates. The obtained spectrodensitograms of the studied salicylanilide with and without the use of brilliant green as a visualizing reagent indicate that applied sorbents have an influence on the wavelength of the obtained fundamental absorption band (λ_{max}) and the additional absorption bands, as well as on their intensity values (in astronomical units). This fact indicates the necessary standardization of the spectrodensitometric investigations regarding the applied chromatographic conditions. Therefore, the spectrodensitograms of salicylanilide can be correctly compared only on the same chromatographic plate. This fact has fundamental significance in identification analysis.

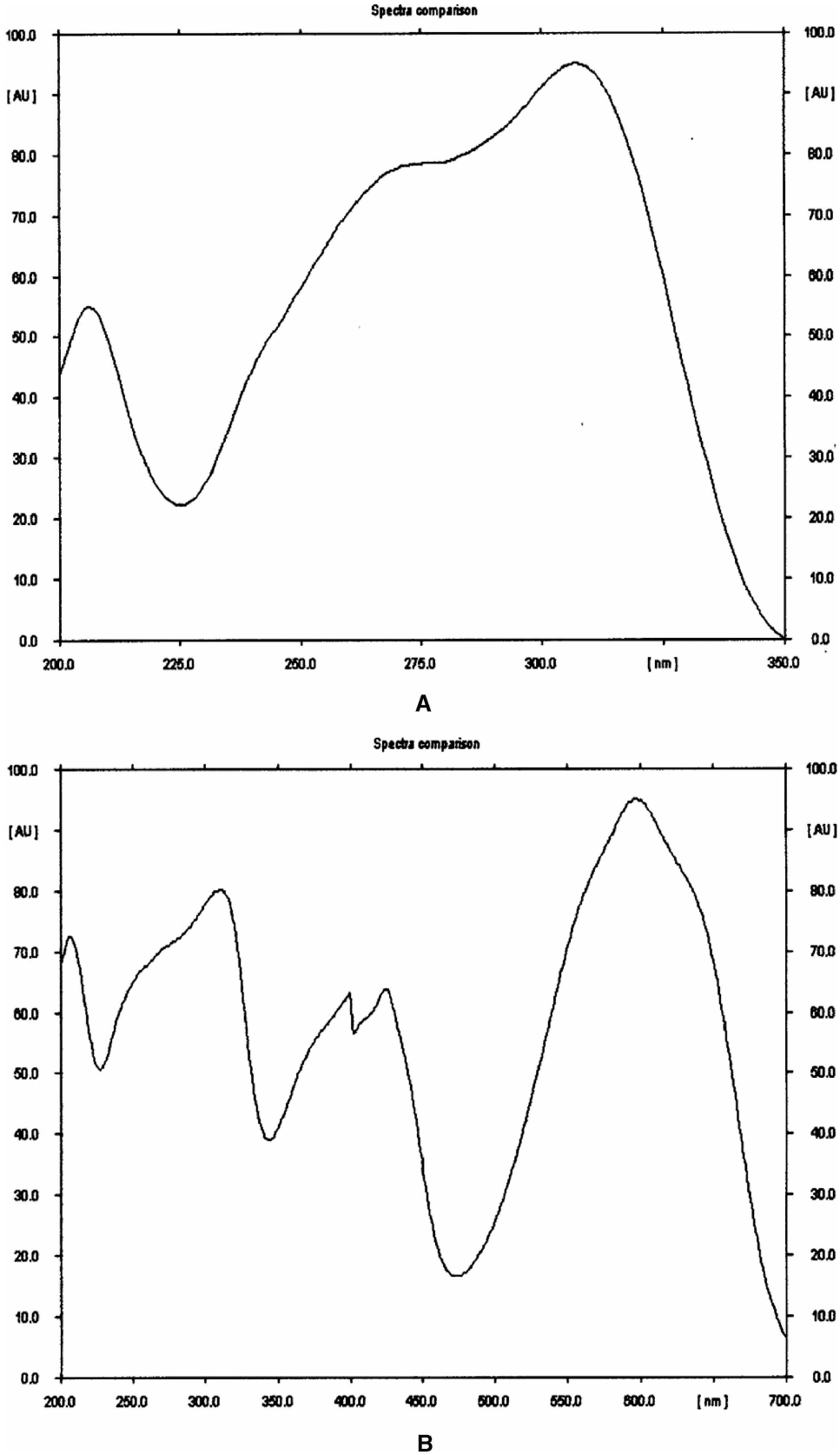

Fig. 3 Spectrodensitograms of salicylanilide on glass plates precoated with 0.50 mm layer of silica gel $60F_{254}$ (E. Merck, #1.05744): A, without the use of a visualizing reagent; B, with the use of brilliant green as a visualizing reagent.
Source: From The application of densitometry to evaluate the visualizing effects of salicylanilide using brilliant green, in J. Liq. Chromatogr. Relat. Technol.[19]

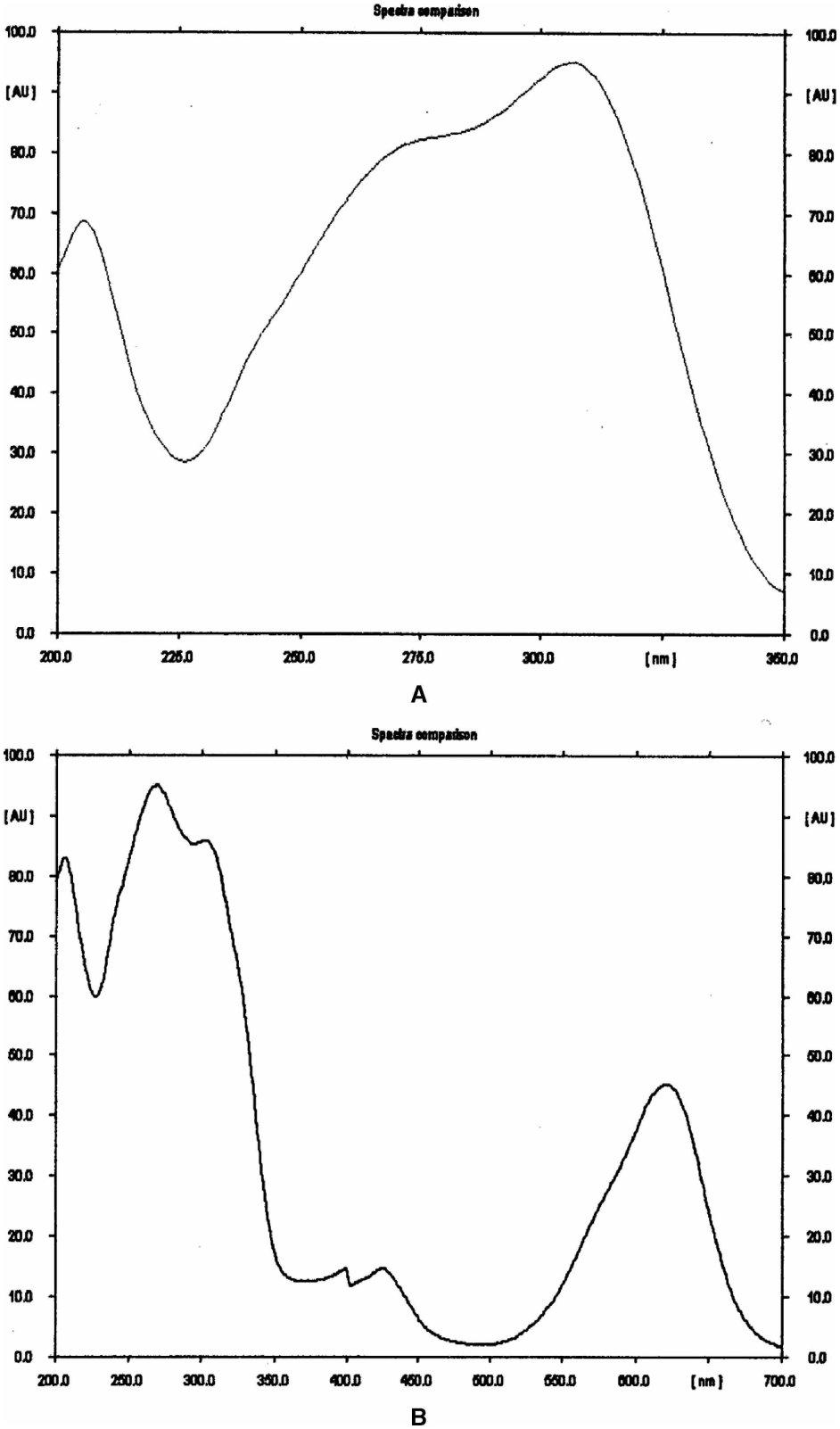

Fig. 4 Spectrodensitograms of salicylanilide on glass plates precoated with 0.25 mm layer of silica gel $60F_{254}$ (E. Merck, #1.05715): A, without the use of a visualizing reagent; B, with the use of brilliant green as a visualizing reagent.
Source: From The application of densitometry to evaluate the visualizing effects of salicylanilide using brilliant green, in J. Liq. Chromatogr. Relat. Technol.[19]

The absorption maximum, broadening index, detection index, characteristic of densitometric band, modified contrast index, limit of detection, DVI, and linearity range of salicylanilide on the particular chromatographic plates with and without the use of brilliant green are presented in Tables 1 and 2, respectively.

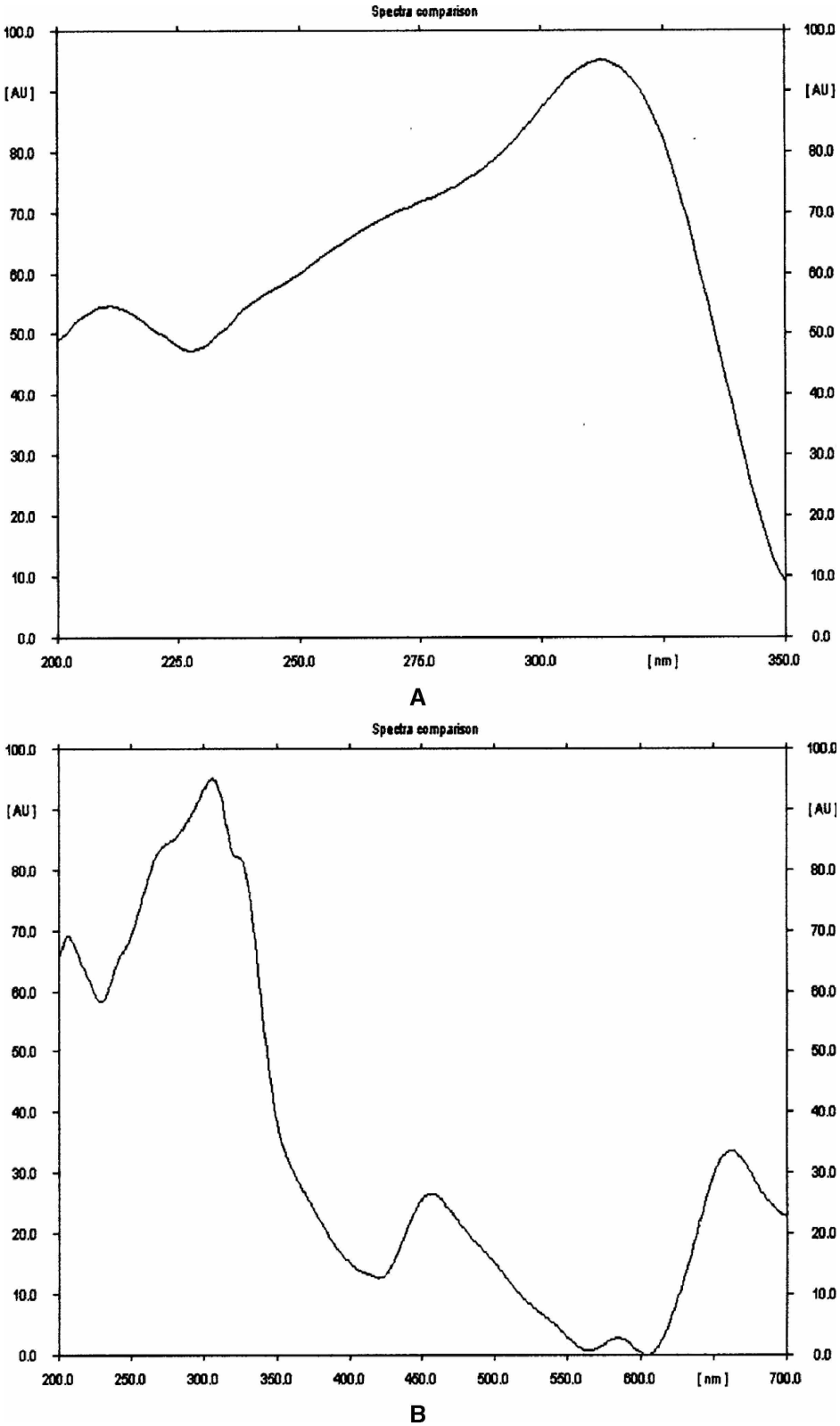

Fig. 5 Spectrodensitograms of salicylanilide on aluminum plates precoated with 0.20 mm layer of a mixture of silica gel 60 and Kieselguhr F_{254} (E. Merck, #1.05567): A, without the use of a visualizing reagent; B, with the use of brilliant green as a visualizing reagent.
Source: From The application of densitometry to evaluate the visualizing effects of salicylanilide using brilliant green, in J. Liq. Chromatogr. Relat. Technol.[19]

On the basis of values of DVI, it was stated that the best detection effects of salicylanilide were obtained without the use of a visualizing reagent. The worst detection effect of salicylanilide without the use of a visualizing reagent was obtained on a mixture of silica gel 60 and Kieselguhr F_{254}. However, on the remaining sorbents similar visualizing

Table 1 The absorption maximum, broadening index, detection index, characteristic of densitometric band, modified contrast index, limit of detection, densitometric visualizing index (DVI), and linearity range of salicylanilide on the particular chromatographic plates without the use of a visualizing reagent.

Chromatographic plates	λ_{max} (nm)	Broadening index (μg/AU)	Detection index (μg/AU)	Densitometric band characteristic of 50 μg salicylanilide			Modified contrast index (AU/deg)	Limit of detection (μg)	DVI [AU/(μg deg)]	Linearity range (μg/spot) (r, correlation coefficient)
				Area (AU)	Height (AU)	α				
#1.05744[a]	307	0.686	0.07/1590	72889	707	9	78.5	0.07	11.570	5.00 ÷ 30.00 ($r = 0.9802$)
#1.05715[b]	307	0.557	0.07/1155	89761	717	11	65.2	0.07	11.657	5.00 ÷ 50.00 ($r = 0.9904$)
#1.05554[c]	307	0.608	0.07/1199	82263	776	8	97.0	0.07	14.690	3.00 ÷ 20.00 ($r = 0.9832$)
#1.05553[d]	308	0.434	0.07/1813	115248	785	11	71.4	0.07	14.967	5.00 ÷ 25.00 ($r = 0.9917$)
#1.05567[e]	312	1.021	0.70/3190	48953	581	8	72.6	0.70	0.874	1.00 ÷ 30.00 ($r = 0.9902$)

[a]Glass plates precoated with 0.50 mm layer of silica gel $60F_{254}$.
[b]Glass plates precoated with 0.25 mm layer of silica gel $60F_{254}$.
[c]Aluminum plates precoated with 0.20 mm layers of silica gel $60F_{254}$.
[d]Aluminum plates precoated with 0.20 mm layer of silica gel 60.
[e]Aluminum plates precoated with 0.20 mm layer of a mixture of silica gel 60 and Kieselguhr F_{254}.
Source: From The application of densitometry to evaluate the visualizing effects of salicylanilide using brilliant green, in J. Liq. Chromatogr. Relat. Technol.[19]

Table 2 The absorption maximum, broadening index, detection index, characteristic of densitometric band, modified contrast index, limit of detection, densitometric visualizing index (DVI), and linearity range of salicylanilide on particular chromatographic plates with the use of brilliant green as a visualizing reagent.

Chromatographic plates	λ_{max} (nm)	Broadening index (μg/AU)	Detection index (μg/AU)	Densitometric band characteristic of 50 μg salicylanilide			Modified contrast index (AU/deg)	Limit of detection (μg)	DVI [AU/(μg deg)]	Linearity range (μg/spot) (r, correlation coefficient)
				Area (AU)	Height (AU)	α				
#1.05744[a]	597	0.544	0.70/11112	91842	704	8	88.0	0.70	1.640	3.00 ÷ 30.00 ($r = 0.9929$)
#1.05715[b]	268	0.544	1.00/20067	91765	592	16	37.0	1.00	0.574	3.00 ÷ 40.00 ($r = 0.9896$)
#1.05554[c]	268	0.977	0.70/4826	51183	463	9	51.4	0.70	0.812	1.00 ÷ 15.00 ($r = 0.9982$)
#1.05553[d]	268	0.595	1.00/14321	84087	583	13	44.8	1.00	0.647	3.00 ÷ 40.00 ($r = 0.9897$)
#1.05567[e]	305	0.800	1.00/26102	62492	566	9	62.9	1.00	0.694	3.00 ÷ 50.00 ($r = 0.9967$)

[a]Glass plates precoated with 0.50 mm layer of silica gel $60F_{254}$.
[b]Glass plates precoated with 0.25 mm layer of silica gel $60F_{254}$.
[c]Aluminum plates precoated with 0.20 mm layers of silica gel $60F_{254}$.
[d]Aluminum plates precoated with 0.20 mm layer of silica gel 60.
[e]Aluminum plates precoated with 0.20 mm layer of a mixture of silica gel 60 and Kieselguhr F_{254}.
Source: From The application of densitometry to evaluate the visualizing effects of salicylanilide using brilliant green, in J. Liq. Chromatogr. Relat. Technol.[19]

effects of salicylanilide were obtained, whereas the best visualizing effect of salicylanilide with the use of brilliant green as a visualizing reagent was obtained on glass plates precoated with 0.50 mm layer of silica gel $60F_{254}$ (E. Merck, #1.05744). It was stated that the DVI is the objective parameter describing the visualizing effect of detected salicylanilide.[19]

Five dyes, namely, gentian violet, methylene violet, methylene blue, malachite green, and Janus blue, have been used as new visualizing reagents to detect estradiol on neutral aluminum oxide $60F_{254}$ and on neutral aluminum oxide $150F_{254}$. Barton's reagent, rhodamine B, and sulfuric acid were used as the comparative visualizing reagents. Limit of detection (detectability), detection index, modified broadening index, modified contrast index, and linearity range were determined for estradiol following the use of these visualizing reagents. It was stated that the proposed modified contrast index is the objective parameter describing the applied visualizing reagents. The influence of a solid support on obtained visualizing effects was found. The angles (α) between the tangents at the inflection points and the curves of the densitometric peaks are more compact on neutral aluminum oxide $60F_{254}$ than on neutral aluminum oxide $150F_{254}$. This observation indicates that the utility of any particular visualizing reagent depends on the type of chromatographic support used. For the quantitative research of investigated estradiol, sulfuric acid (VI), Barton's reagent, gentian violet, and methylene violet were found to be relatively good.[20]

Six dyes, namely, gentian violet, methylene violet, methylene blue, methyl green, malachite green, and Janus blue, have been used as new visualizing reagents to detect ibuprofen on silica gel $60F_{254}$. Rhodamine B was used as the comparative visualizing reagents. The limit of detection (detectability), detection index, broadening index, modified contrast index, DVI, and linearity range were determined for ibuprofen following the use of these visualizing reagents. It was stated that the earlier proposed DVI is an objective parameter describing the applied visualizing reagents. The best way for detecting ibuprofen is the densitometric method without using a visualizing reagent. Among all the new visualizing reagents studied, methylene violet is the best to detect ibuprofen.[21]

The obtained visualizing effects and the non-destructive properties of applied visualizing reagents, in relation to investigated salicylanilide, estradiol, and ibuprofen, indicate that there has been progress in the range of analysis for these compounds on a thin layer. This fact has definite analytical, pharmaceutical, and physicochemical significance.[19–21]

CONCLUSIONS

- Indicators and dyes described as visualizing reagents in this entry should serve as a supplement to those used previously for the detection of phenolic drugs.
- Broadening index, detection index, characteristic of densitometric band, modified contrast index, limit of detection, DVI, and linearity range of detected compounds are important parameters for the evaluation of visualizing effects of used visualizing reagents.
- The visualizing effect depends on the chemical structure of the visualizing reagent, the structure of the substance detected, as well as the chromatographic sorbent applied.
- Particular application will have these visualizing reagents, which, with substances present in analyzed mixtures, will give diversified colors of chromatographic spots.
- The best and most universal visualizing reagents for the detection of bamethane, ethamivan, hexachlorophene, salicylanilide, pyrocatechin, thymol, pentazocine, phloroglucinol, eugenol, niclosamide, terbutaline, methyldopa, and norepinephrine investigated on silica gel 60 are aniline blue and brilliant green dissolved in water. These visualizing reagents have relatively good properties for quantitative research of investigated phenolic drugs.[7]
- Eugenol and thymol can also be qualitatively detected on silica gel by using visualizing reagents based on a saturated aqueous solution of variamine blue hydrochloride.[13]
- The best visualizing reagents for the detection of α-naphthol are the following: titan yellow, eosin, helasol green, and bromothymol blue in aqueous sodium hydroxide (50 mg/100 ml of 5% NaOH) on silica gel 60; bromocresol green, titan yellow, and eosin yellow on mixture of silica gel 60 and Kieselguhr F_{254}; and bromocresol, titan yellow, and thymolphthalein on Polyamide $11F_{254}$.[14,15]
- Titan yellow is the best visualizing reagent for the detection of *m*-cresol on silica gel 60 (detection limit: 1.08 μg).[16]
- The best visualizing reagents are brilliant cresyl blue, erythrosin B, and bromocresol blue for the detection of hydroquinone; alkaline blue, thymolphthalein, and brilliant cresyl blue for pyrogallol; and alkaline blue and brilliant green for phloroglucinol.[17]
- The most universal visualizing reagents for adrenaline, dopamine, phenylephrine, metaraminol, fenoterol, and bithionol are the following: bromocresol green and brilliant cresyl blue dissolved in 5% NaOH on silica gel $60F_{254}$; bromocresol green, brilliant cresyl blue, and eriochrome black T dissolved in 5% NaOH on a mixture of silica gel and Kieselguhr F_{254}; eosin yellow dissolved in 5% NaOH on Polyamide $11F_{254}$.[18]
- The usefulness of densitometry for detection of some phenolic drugs was shown.[7,11]
- Visualizing effects and non-destructive properties of applied visualizing reagents (brilliant green, gentian violet, methylene violet, methylene blue, methyl green, malachite green, and Janus blue), in relation to investigated salicylanilide, estradiol, and ibuprofen,

indicate that progress in the range of analysis of these compounds on thin layer has taken place. This fact has definite analytical, pharmaceutical, and physicochemical significance.[19–21]

ACKNOWLEDGMENT

This research was financed by the Ministry of Science and Information Society Technologies by resources reserved for science in the years 2005–2008 as research project No. 3 T09A 155 29.

REFERENCES

1. Jork, H.; Funk, W.; Fischer, W.; Wimmer, H. *Dünnschicht-Chromatographie, Reagenzien und Nachweismethoden, Physikalische und Chemische Nachweismethoden: Grundlagen, Reagenzien I*; VCH: Weinheim, Germany, 1989.
2. Sherma, J.; Fried, B. Eds. *Handbook of Thin-Layer Chromatography*; 3rd Ed.; Marcel Dekker, Inc.: New York, 2003; [Revised and Expanded].
3. Jork, H.; Funk, W.; Fischer, W.; Wimmer, H. *Thin-Layer Chromatography: Reagents and Detection Methods; Physical and Chemical Detection Methods: Activation Reactions, Reagents Sequences, Reagents II; Vol 1b*; VCH: Weinheim, Germany, 1994.
4. Pawelczyk, E. *Drug Chemistry (in Polish)*; PZWL: Warsaw, 1986.
5. Wagner, H.; Bladt S. *Plant Drug Analysis, A Thin Layer Chromatography Atlas*; Springer: Berlin, Germany, 1996.
6. Merck, E. *Firmenbroschüre Anfärbereagenzien für Dünnschicht- and Paper Chromatographie*; Darmstadt: Germany, 1980; 1–100.
7. Pyka, A.; Gurak, D.; Bober, K. New visualizing reagents for selected phenolic drugs investigated by thin layer chromatography. J. Liq. Chromatogr. Relat. Technol. **2002**, *25*, 1483–1495.
8. Pyka, A. Phenolic Drugs, new visualizing reagents for detection in TLC. In *On-line Supplement of Encyclopedia of Chromatography* (ISBN 0-8247-2153-5); Cazes, J., Ed.; Marcel Dekker, Inc.: New York, 2004; 1–8;
9. Pyka, A. Phenolic Drugs, new visualizing reagents for detection in TLC. In *Encyclopedia of Chromatography* (ISBN 0-8247-2785-1); 2nd Ed.; Cazes, J., Ed.; Taylor & Francis, Inc.: New York, 2005; 1267–1273.
10. Pyka, A. Phenolic Drugs, new visualizing reagents for detection in TLC. In *On-line Supplement of Encyclopedia of Chromatography*; 2nd Ed.; DOI:10.1081/E-ECHR-120043427; http://dx.doi.org/10.1081/E-ECHR-12004342; Cazes, J., Ed.; Taylor & Francis, Inc.: New York, 2007; 1:1, 1–9.
11. Pyka, A. Unpublished data.
12. Pyka, A.; Bober, K.; Stolarczyk, A. Densitometric determination of arbutin in cowberry leaves (*Vaccinium vitis idaeae)*. Acta Polon. Pharm. Drug. Res. **2007**, *63* (5), 395–400.
13. Pyka, A.; Gurak, D.; Bober, K.; Niestrój, A. Application of new visualizing agents for selected essential oil components in TLC. Chem. Anal. (Warsaw) **2002**, *47*, 691–699.
14. Wardas, W.; Pyka, A. Visualizing agents for phenols and naphthols in thin layer chromatography. J. Planar Chromatogr.-Mod. TLC **1992**, *5*, 471–474.
15. Wardas, W.; Lipska, I.; Lebek, J. Alkacymetric agents application to phenols visualizing in thin layer chromatography. Chem. Anal. (Warsaw) **1998**, *43*, 99–106.
16. Wardas, W.; Pyka, A. Visualizing agents for phenols in thin layer chromatography. J. Planar Chromatogr.-Mod. TLC **1991**, *4*, 334–336.
17. Wardas, W.; Lipska, I.; Lebek, J. New visualizing agents for selected polybasic phenols and chlorophenols in thin-layer chromatography. J. Planar Chromatogr.-Mod. TLC **2000**, *13*, 317–320.
18. Wardas, W.; Lipska, I.; Bober, K. TLC fractionation and visualization of selected phenolic compounds applied as drugs. Acta Polon. Pharm. Drug. Res. **2000**, *57*, 15–22.
19. Pyka, A. The application of densitometry to evaluate the visualizing effects of salicylanilide using brilliant green. J. Liq. Chromatogr. Relat. Technol. **2008**, *31*, 1943–1958.
20. Pyka, A.; Klimczok, W.; Gurak, D. Evaluation of visualizing reagents for estradiol on thin layer by densitometric method. J. Liq. Chromatogr. Relat. Technol. **2008**, *31*, 555–566.
21. Pyka, A. Analytical evaluation of visualizing reagents used to detect ibuprofen on thin layer. J. Liq. Chromatogr. Relat. Technol. **2009**, *32*, 578–588.

Phenols and Acids: TLC Analysis

Luciano Lepri
Alessandra Cincinelli
Department of Chemistry, University of Florence (UNIFI), Florence, Italy

Abstract
A wide variety of stationary phases have been used to separate substituted monocyclic phenols and phenolic acid compounds and their derivates by thin-layer chromatography (TLC). In particular, the composition of phenolic acids and flavonoids in leaves, roots, and fruits of several plants and in natural products has been extensively studied by the two-dimensional TLC by using cellulose or silica gel plates in one direction and silanized silica gel in the second direction. Quantitative determinations of flavonoids components of plant extracts were widely performed.

INTRODUCTION

Phenol is a weak acid (pK_a 9.98), and the effect of a ring substituent on the acid strength depends on whether the group is electron withdrawing or releasing, its position, and its ability to give resonating structures. Phenolic groups occur in a large number of natural and industrial products, ranging from phenolic resins, herbicides, fungicides, surfactants, alkaloids, steroids, aglycones, and glycosides to numerous other groups.

A comprehensive review of phenolic compounds in biochemical, environmental, industrial, and consumer products, as well as sample preparation prior to thin-layer chromatography (TLC), has been made by Tyman.[1]

CHROMATOGRAPHIC BEHAVIOR OF MONOCYCLIC PHENOLS

Substituted monocyclic phenols have been widely studied in several stationary phases (alumina, silica gel, cellulose, polyamide, chitin) and also on chemically modified adsorbents (silanized silica gel, cyano- and amino-silica plates), ion-exchange layers, and impregnated plates.

Phenols can be detected with Fast Blue Salt B, diazotized orthanilic acid or dianisidine, alkaline chloramine T reagent, by spraying an ammoniacal silver nitrate solution, followed by exposure to UV light, or with a modified potassium ferricyanide–ferric chloride reagent, and also by exposing the wet layer successively to nitrogen dioxide ($Cu + HNO_3$) and ammonia vapors.

Silica Gel, Alumina, Cellulose, and Polyamide

Layers of silica gel 60 and alumina have been employed for the separation and identification of 126 monocyclic phenols eluted with solvents of increasing polarity (benzene, di-isopropyl ether, and ethanol).[2] Alumina is more basic than silica gel and strongly retains phenolic compounds, particularly those with more acidic properties such as chloro- and nitrophenols, even when eluted with a medium-polarity solvent.

Table 1 reports the retention data relative to several substituted monocyclic phenols examined on silica gel 60 in benzene and di-isopropyl ether.

The presence of a 2-substituent or 2,6-substituent results in an increase in the R_f value with benzene as eluent. However, 2,6-dinitrophenol is retained more in benzene than are 2,4- and 2,5-isomers. The sequence of their R_f values ($R_{f2,6} = 0.04 < R_{f2,4} = 0.07 < R_{f2,5} = 0.38$) is in agreement with that of the corresponding pK_a values ($pK_{a2,6} = 3.71 < pK_{a2,4} = 4.09 < pK_{a2,5} = 5.22$); hence, these two facts can be closely bound up with one another.

Di-isopropyl ether allows the separation of nitrophenol isomers and of several nitroalkyl and nitrochlorophenols as well as of dihydroxy- and trihydroxybenzenes. Dimethyl and trimethylphenols are better resolved on alumina plates than on silica gel when eluting with the above-mentioned solvent:

Dimethylphenols

$$R_{f3,4} = 0.22 < R_{f3,5} = 0.26 < R_{f2,4} = 0.28 < R_{f2,3} = 0.39 < R_{f2,5} = 0.44 < R_{f2,6} = 0.52$$

Trimethylphenols

$$R_{f3,4,5} = 0.16 < R_{f2,4,5} = 0.23 < R_{f2,3,5} = 0.46 < R_{f2,4,6} = 0.51$$

Hydrogen bonding, steric effects, and acid–base properties of phenols are involved in their retention on silica gel and alumina with benzene and isopropyl ether as eluents.

Table 1 R_f values of substituted monocyclic phenols in different chromatographic conditions.

	Silica gel 60		Cellulose + ethyl oleate[a]	Silanized silica + 4% DBS[b]		RP-18 + 4% HDBS[c]		
Compound	**A**	**B**	**C**	**D**	**E**	**F**	**G**	**pK_a (25°C)**
Phenol	16	74	79	35	62	—	—	10.02
2-Methylphenol	24	78	62	20	35	—	—	10.32
3-Methylphenol	16	75	67	20	40	—	—	10.09
4-Methylphenol	15	74	66	19	36	—	—	10.27
2,3-Dimethylphenol	25	80	45	11	20	—	—	10.54
2,4-Dimethylphenol	28	83	42	11	19	—	—	10.60
2,5-Dimethylphenol	25	77	47	11	21	—	—	10.41
2,6-Dimethylphenol	40	76	40	12	20	—	—	10.63
3,4-Dimethylphenol	15	75	53	12	24	—	—	10.36
3,5-Dimethylphenol	1,573	51	12	25	—	—	10.19	—
2-Ethylphenol	27	77	40	10	21	—	—	10.2[d]
3-Ethylphenol	17	72	48	11	28	—	—	9.9[d]
4-Ethylphenol	15	69	45	11	24	—	—	10.0[d]
2-Chlorophenol	42	75	53	24	89	48	77	8.48
3-Chlorophenol	20	74	43	14	64	34	50	9.02
4-Chlorophenol	16	69	46	14	50	34	37	9.38
2,3-Dichlorophenol	38	63	28	22	85	35	78	7.45[e]
2,4-Dichlorophenol	38	65	22	16	78	27	69	7.75[e]
2,5-Dichlorophenol	41	77	20	28	85	41	81	7.35[e]
2,6-Dichlorophenol	56	83	31	55	88	59	86	6.79[e]
3,4-Dichlorophenol	15	63	21	7	57	18	48	8.39[e]
3,5-Dichlorophenol	—	—	14	9	64	16	55	7.93[e]
2,3,4-Trichlorophenol	—	—	—	18	68	29	66	7.59
2,3,5-Trichlorophenol	—	—	—	25	69	36	63	7.23
2,3,6-Trichlorophenol	49	76	—	45	82	52	74	6.12
2,4,5-Trichlorophenol	32	67	7	22	70	42	63	7.33
2,4,6-Trichlorophenol	49	76	15	37	73	43	63	6.42
3,4,5-Trichlorophenol	—	—	—	9	52	16	50	7.74
2,3,4,5-Tetrachlorophenol	—	—	—	14	46	35	44	6.96
2,3,4,6-Tetrachlorophenol	36	50	4	—	—	—	—	—
2,3,5,6-Tetrachlorophenol	—	—	—	25	50	38	43	5.44
Pentachlorophenol	20	21	2	13	33	—	—	5.26
2-Nitrophenol	69	79	—	61	92	—	—	7.23
3-Nitrophenol	7	62	—	29	92	—	—	8.40
4-Nitrophenol	4	46	—	66	92	—	—	7.15
Catechol (1,2)	2	49	—	—	—	—	—	—
Resorcinol (1,3)	0	39	—	56	87	—	—	9.81
Hydroquinone (1,4)	0	43	—	67	e.s.[f]	—	—	10.35

Eluents: A, benzene; B, isopropyl ether; C, 75% aqueous ethanol; D, 0.1 *M* NH_3 + 0.1 *M* NH_4Cl in 30% methanol (pH 9.02); E, 1 *M* NH_3 in 30% methanol (pH 1.30); F, 0.1 *M* NH_3 + 0.1 *M* NH_4Cl in 60% methanol; G, 1 *M* NH_3 in 40% methanol.

[a]Fifteen grams cellulose impregnated with a solution of ethyl oleate in ether (70 ml of a 0.75% solution).

[b]Twenty grams silanized silica gel 60 HF (C_2) mixed with a 4% triethanolamine dodecylbenzenesulfonate (DBS) solution in 95% ethanol.

[c]RP-18 ready-to-use plates dipped in a 4% dodecylbenzenesulfonic acid (HDBS) solution in 95% ethanol.

[d]pK_a values at 28°C.

[e]pK_a values at 29°C.

[f]Elongated spot.

Only a limited number of researches have focused on cellulose plates, microcrystalline cellulose being the most used stationary phase with solvents such as ethyl acetate–*n*-propanol–25% ammonia (3:5:2), water–formic acid (98:2), *n*-amyl alcohol–acetic acid–water (10:6:5), and benzene–propionic acid–water (4:9:3).

Polyamide is an especially useful adsorbent for the separation of phenols owing to the formation of hydrogen bonds between the phenolic compounds and the amide group of the polymer. Organic solvents of increasing polarity and aqueous–organic solutions have been used as eluents: benzene, chloroform, ethyl acetate, water–methanol, water–acetone, water–acetic acid, and cyclohexane–acetic acid (93:7) mixtures. Water–propanol–27% ammonia (1:8:1), *n*-butanol–5 *M* ammonia (100:33), and *n*-butanol–ethanol–ammonia (5:1:1) have been employed for nitrophenols.

Chemically Modified Sorbents, Ion-Exchange Resins, and Impregnated Plates

A wide study of the chromatographic behavior of alkyl, halogenated phenols, and phenols containing alkyl and halogen groups by reversed-phase TLC has been performed by Bark and Graham[3] on cellulose impregnated with ethyl oleate eluted with aqueous ethanol (Table 1).

The phenols can be removed by the stationary phase as a result of solvation of the phenolic group by the proton acceptor eluent (water or ethanol), which may be influenced by steric factors and by altering the polarity of the phenolic grouping. Under these chromatographic conditions, relationships between R_m values and structural descriptors of selected alkoxyphenols and also new methods of calculation of their partition coefficients were proposed by Pyka.[4]

Long-chain alkylphenols present in natural cashew nut shell liquid have been chromatographed on argentated silica gel G (10% w/w silver nitrate) with diethyl ether–light petroleum–formic acid (30:70:1) as eluent for the separation of unsaturated constituents.

Alkylphenols, nitrophenols, halogenophenols, and polyhydroxybenzenes have been extensively studied on thin layer of anion and cation exchangers with cellulose, paraffin, and polystyrene matrices and on silanized silica gel impregnated with anionic and cationic surfactants. The best results have been obtained by using cation exchangers and anionic surfactants as impregnating agents.[5,6]

The parameters that determine the retention of phenols on layers of silanized silica gel untreated and impregnated with anionic surfactants are the same that affect retention on cation exchangers (i.e., organic modifier percentage, ionic strength, and, particularly, pH of the eluent).

With regard to the influence of pH, the protonated form of the phenols exhibits a higher affinity toward the stationary phase than the deprotonated form.

In the relationship

$$K_d = \frac{[HA]_R + [A^-]_R}{[HA]_S + [A^-]_S} \frac{V}{W} \quad (1)$$

K_d represents the distribution coefficient, $[HA]_R$, $[A^-]_R$, $[HA]_S$, and $[A^-]_S$ are the concentrations of the protonated and deprotonated forms of the phenol in the resin and in the solution, V is the volume of the solution, and W is the weight of the resin. Introducing the K_a value in Eq. 1 and combining with the Martin–Synge equation for partition TLC, Lepri et al.[5] obtained the following relationship:

$$\left(\frac{1}{R_f} - 1\right) = \left(\frac{1}{R_{fac}} - 1\right) \frac{[H^+]}{K_a + [H^+]} + \left(\frac{1}{R_{falk}} - 1\right) \frac{K_a}{K_a + [H^+]} \quad (2)$$

where R_{fac} and R_{falk} are the R_f values of the protonated and deprotonated form of the phenol achieved by eluting with strong acidic and alkaline solutions, respectively.

Although the major change in $\left(\frac{1}{R_f} - 1\right)$ with pH occurs at pH = pK_a, by differentiating R_f twice with respect to log $[H^+]$ and equating to zero, the following relation is obtained:

$$[H^+] = K_a \frac{R_{fac}}{R_{falk}} \quad (3)$$

On the basis of Eq. 3, we can predict that the lower is the R_{fac}/R_{falk} ratio, the more will be the shift in the mean R_f value of R_{fac} and R_{falk} with respect to the pH = pK_a value.

Many nitrophenols, chlorophenols, and bromophenols can be easily separated by this technique by eluting with aqueous–organic solutions at different pH values (Table 1).

The mechanism of chromatographic separation of selected phenols on cyano-modified silica layers, eluted with nine non-aqueous and five aqueous solvents was studied, and it was concluded that both cyano and silanol groups participate in the interactions with solutes.

CHROMATOGRAPHIC BEHAVIOR OF PHENOLIC ACIDS AND THEIR DERIVATIVES

In general, silica gel has been more widely used than cellulose, polyamide, silanized silica gel, and aminopropylsilica for the separation of phenolic acids and their derivatives arising from clinical studies or extracted from plant material.

The selected eluents for silica gel are chloroform–ethyl acetate–formic acid (5:4:1), *n*-hexane–ethyl acetate–formic acid (15:9:2), chloroform–acetic acid–water (2:1:1), toluene–dichloromethane–formic acid (40:50:10), and dichloromethane–acetic acid–water (100:50:50, lower phase).

Table 2 hR_F of phenolic acids from the foliage of *P. tauricum* Bieb after acid hydrolysis on 10 × 10 cm cellulose plates (Merck) by 2-D TLC.

Phenolic acid	$hR_{F(1D)}$	$hR_{F(2D)}$	Color after derivatization with diazotized sulfanilic acid
Protocatechuic acid	14	51	Brown
Chlorogenic acid	6	56	Light brown
Gentisic acid	45	55	Gray
p-Hydroxybenzoic acid	47	57	Yellow
Vanillic acid	76	45	Orange
Caffeic acid	21	19	Brown
Syringic acid	76	39	Red
p-Coumaric acid (*trans*)	55	21	Red
p-Coumaric acid (*cis*)	55	70	Red
Ferulic acid (*trans*)	76	12	Violet
Ferulic acid (*cis*)	76	58	Violet

First direction: toluene–methanol–acetic acid–acetonitrile (75.5:10:5:7.5 v/v); second direction: sodium formate–formic acid–water (10:1:200 w/v/v).

Recently, two-dimensional TLC (2-D TLC) on cellulose plates had been used for the separation of phenolic acids extracted from plants (i.e., leaves, roots, and fruits of *Peucedanum verticillare* L. Koch ex DC; leaves, inflorescences, and rhizomes of *Silphium perfoliatum*[7]) by eluting with benzene–methanol–acetonitrile–acetic acid (80:10:5:5) in the first direction and sodium formate–formic acid–water (10:1:200 w/v/v) in the second direction. Table 2 shows the hR_f values obtained for phenolic acids from *Peucedanum tauricum* Bieb foliage by 2-D TLC on cellulose plates.

Detection was performed by UV light (366 nm), by spraying with 3% methanolic $FeCl_3$ or by derivatization of phenolic acids with diazotized sulfanilic acid.

Selected phenolic compounds (i.e., phenolic acids and flavnoids) were separated by normal-phase and reversed-phase 2-D chromatography on connected plates (diol or silica plates connected to RP-18W plates). Optimization of mobile phases was performed by plotting retention against eluent composition. Phenolic compounds present in extracts from *Verbacum* sp. and *Polygonum* sp. were separated by 2-D TLC.[8]

Three ellagitannins (corilagin, gernaiin, dehydrogeraniin) and two gallotannins (methyl gallate-3-*O*-glucoside, 3-*O*-galloylshikimic acid) were isolated from the aerial parts of *Erodium cicutarium* (Geraniaceae) and identified by TLC on cellulose, silica gel 60, and silanized silica gel (RP-18W plates) by eluting with water–acetic acid (94:6), di-isopropyl ether–acetone–98% formic acid (5:4:1), and water–methanol–98% formic acid (69:30:1), respectively.

Phenolic aldehydes and ketones have been chromatographed on silica gel G and cellulose plates as their phenylhydrazones formed in situ. Toluene–chloroform–acetone (5:3:2), chloroform–acetone (8:2), anisole–methanol (8:2), and anisole–chloroform–acetone (5:3:2) are the eluents used for silica gel while the layers of cellulose have been eluted with 2% formic acid, 20% potassium chloride, 10% acetic acid, or 2-propanol–ammonia–water (8:1:1).

Long-chain alkylphenolic acids and their derivatives have been separated on silica gel G by eluting with light petroleum (60–80°C)–ethyl ether–dimethylformamide–acetic acid (75:85:5:1).

Reversed-phase TLC on silanized silica gel layers (OPTI-UPC$_{12}$, SilC$_{18}$-50, and RP-18 plates), untreated and impregnated with anionic and cationic surfactants has been used for the separation of catecholamines, phenolic acids, and glycols excreted in the urine. Many interesting separations have been achieved on OPTI-UPC$_{12}$ plates by eluting with 1 *M* HCl + 3% KCl in water (biogenic amines) and with 1 *M* sodium acetate in water (urinary phenolic acids and glycols). Recently, biogenic amines and their derivatives were separated on RP-18 plates and NH_2-bonded silica gel with chloroform–methanol (9:1) or ethanol–5% aqueous diethylamine (95:5) as eluents, respectively. Finally, very good separations of norepinephrine, dopamine, epinephrine, normetanephrine, and metanephrine were obtained on plates of silanized silica gel eluted with phosphate buffer (pH 6.98)–methanol (1:1 v/v).

A paper investigated 18 phenolic acids on aminopropylsilica plates; the best separations were achieved by eluting with heptane-di-isopropyl ether–acetic acid (4:5:1 v/v) or petroleum ether-di-isopropyl ether–acetic acid (6:3:1 v/v).[9]

Determination of the hydrophobicity of phenolic acids and flavonoids from chromatographic data is an important non-analytical application of reversed-phase TLC since experimentally obtained R_{Mw} values (R_M extrapolated at 0% organic modifier, usually methanol in water) are related to selected ADME (*a*bsorption, *d*istribution, *m*etabolism, *e*limination) data.[10] In addition, TLC chromatogram

fingerprints are generally employed for evaluation and comparison of the composition of herbal drugs. For example, flavonoid content was used for effective and reliable quality control of the drugs from dog rose on silica gel 60 F_{254} plates by 1-D and 2-D chromatography.[11]

QUANTITATIVE DETERMINATIONS

Phenols occurring in water have been quantified by in situ densitometry after coupling with diazotized *p*-nitroaniline or by using vanadium pentoxide and dichlorofluorescein.

An interesting paper analyzed phenols included in the list of priority pollutants of Environmental Protection Agency (EPA) on silica gel G F_{254} high-performance TLC (HPTLC) plates and polyamide plates after solid-phase extraction from water.[12]

In situ quantitation has been performed by adsorption UV or Vis light measurements of the color developed with Würster's salts.

Planar chromatography has also been used to separate and quantify several common phenols in contaminated land leachates after derivatization with 3-methyl-2-benzothiazolinone hydrazone and extraction of the resulting azo dyes.

Recently, phenolic acids and flavonoid content of Croatian propolis samples were identified and determined by scanning densitometry at UV absorption maximum of each compound.

Chromatographic analysis was performed on 10×20 cm silica gel F_{254} high-performance TLC plates by eluting with chloroform–methanol–formic acid (44:3.5:2.5).[13]

REFERENCES

1. Tyman, J.H.P. Phenols, aromatic carboxylic acids, and indoles. In *Handbook of Thin-Layer Chromatography*; Sherma, J., Fried, B., Eds.; Marcel Dekker, Inc.: New York, 1996; 877–920.
2. Dietz, F.; Trandy, J.; Koppe, P.; Rubelt, C. Detection and photometric determination of 126 phenolic compounds in water using four group-specific reagents. Chromatographia **1976**, *9*, 380–396.
3. Bark, L.S.; Graham, J.T. Studies in the relationship between molecular structure and chromatographic behaviour. J. Chromatogr. **1966**, *23*, 417–442; J. Chromatogr. **1996**, *25*, 357–366.
4. Pyka, A. New method of calculation of the partition coefficients of selected alkoxyphenols, investigated by RPTLC. J. Planar Chromatogr.-Mod. TLC **2004**, *17*, 58–60; J. Planar Chromatogr.-Mod. TLC **2003**, *16*, 131–136.
5. Lepri, L.; Desideri, P.G.; Landini, M.; Tanturli, G. Chromatographic behaviour of phenols on thin-layers of cation and anion exchangers. J. Chromatogr. **1975**, *109*, 365–376; J. Chromatogr. **1976**, *129*, 239–248.
6. Lepri, L.; Desideri, P.G.; Heimler, D. Reversed-phase and soap thin-layer chromatography of phenols. J. Chromatogr. **1980**, *195*, 339–348.
7. Kowalski, R.; Wolski, T. TLC and HPLC analysis of the phenolic acids in *Silphium perfoliatum* L. leaves, inflorescences and rhizomes. J. Planar Chromatogr.-Mod. TLC **2003**, *16*, 230–236.
8. Hawryl, A.M.; Waksmundzka-Haynos, M. Separation of phenolic compounds by NP and RP two-dimensional thin-layer chromatography on connected plates. J. Planar Chromatogr.-Mod. TLC **2006**, *19*, 92–97.
9. Wójciak-Kosior, M.; Skalska, A. Thin-layer chromatography of phenolic acids on aminopropylsilica. J. Planar Chromatogr.-Mod. TLC **2006**, *19*, 200–203.
10. Mornar, A.; Medic-Saric, M.; Jasprica, I. ADME data for polyphenols characterized by reversed-phase thin layer chromatography. J. Planar Chromatogr.-Mod. TLC **2006**, *19*, 409–417.
11. Nowak, R. TLC fingerprints analysis of the European dog rose. J. Planar Chromatogr.-Mod. TLC **2007**, *20*, 43–48.
12. Bladek, J.; Rostkowshi, A.; Neffe, S. The application of TLC to the determination of phenol residues in water. J. Planar Chromatogr.-Mod. TLC **1998**, *11*, 330–335.
13. Cvek, I.; Medic-Saric, M.; Mornar, A. High performance thin-layer chromatographic analysis of the phenolic acid and flavonoid content of Croatian propolis samples. J. Planar Chromatogr.-Mod. TLC **2007**, *20*, 429–435.

Phospholipids and Glycolipids: Normal-Phase HPLC Analysis

Yiwen Yang
Department of Chemical and Biochemical Engineering, Zhejiang University, Hangzhou, China

INTRODUCTION

Analytical methods for phospholipid and glycolipid classes by normal-phase high-performance liquid chromatography (HPLC) have been incompletely reviewed. Silica columns with evaporative light scattering detection (ELSD) were mostly used. The poly(vinyl alcohol)-grafted silica column with ELSD could be used to separate them, simultaneously.

PHOSPHOLIPIDS AND GLYCOLIPIDS

Phospholipids are divided into two main groups:[1] glycerolphospholipids and sphingolipids. Glycerolphospholipids are derived from glycerol with a polar headgroup and fatty acid esterified at the *sn-1* and/or *sn-2* positions of the glycerol backbone. Sphingolipids are derived from sphingosine. Principal phospholipids classes are phosphatidylcholine (PC), phosphatidylethanolamine (PE), phosphatidylinositol (PI), phosphatidylglycerol (PG), phosphatidic acid (PA), phosphatidylserine (PS), lysophosphatidylcholine (LPC), and sphingomyelin (Sph or SM).[2,3]

Glycolipids are glycosylated derivatives of lipids, such as acylglycerols, ceramides, and prenols.[4] They are divided into three main groups: glycoglycerolipids, glycosphingolipids, and glycophosphatidylinositols. Glycoglycerolipids designate glycolipids containing one or more glycerol residues. Glycosphingolipid designates lipids containing at least one monosaccharide residue and either a sphingoid or a ceramide. The glycosphingolipids can be subdivided into two groups: neutral glycosphingolipids, e.g., mono-, oligo-, polyglycosylsphingoids and mono-, oligo-, polyglycosylceramides, and acidic glycosphingolipids, e.g., sialoglycosphingolipids, uronoglycosphingolipids, sulfoglycosphingolipids, phosphoglycosphingolipids, phosphonoglycosphingolipids, etc. Glycophosphatidylinositols designate glycolipids, which contain saccharides glycosidically linked to the inositol moiety of PIs.

Every class of phospholipids and glycolipids contains many molecular species, owing to the structural and/or positional difference in the fatty acid moiety. Therefore, they are complex mixture.

The main purpose of normal-phase HPLC analysis of phospholipids and glycolipids is to separate and quantify according to class, although a few molecular species can be elucidated when HPLC–tandem mass spectrometry (MS/MS) is used.[5]

SEPARATION OF PHOSPHOLIPIDS AND GLYCOLIPIDS

Phospholipids and glycolipids have been usually fractionated from total lipids by thin-layer chromatography (TLC) or column chromatography.[6] Then, they were later analyzed by HPLC separately.

For phospholipids separation, various HPLC columns, e.g., silica,[1,2,7–9] NH_2,[10] diol,[5,11,12] and polyvinyl alcohol[13] have been used. Silica columns were most often used. Both isocratic[7] and gradient[1,2,5,6,8,9,11–13] mobile phases have been used. The most often used mobile phases are chloroform-methanol-water and hexane-isopropanol-water systems. The phospholipid classes can be separated very well by carefully adjusting the composition and time schedule of mobile phases.

For glycolipids separation, a few HPLC columns, e.g., NH_2,[14] and silica,[15–17] have been used. Isocratic[16] or gradient[14,15,17] mobile phases are used.

A few articles are concerned with the simultaneous separation of phospholipids and glycolipids.[18,19] The poly(vinyl alcohol) column gave excellent results.[20] However, complex mobile phases were needed.

DETECTION AND QUANTIFICATION

As detection methods, ultraviolet (UV) detection,[6,7,14–16] refractive index (RI),[9] ELSD,[1,8,9,12,13,17–20] MS,[2,11] and tandem MS[5,11] have been used. To quantify the phospholipid and glycolipid classes, ELSD has been very successful. But, ELSD does not always result in a linear response.[1,9] It should be noted that, because of the absence of a specific absorption peak for lipids, and every peak in normal HPLC is, in fact, a mixed response, UV detection does not allow their quantitative estimation.[21,22]

CONCLUSIONS

Normal-phase HPLC is useful for the separation and quantification of phospholipid and glycolipid classes. Silica columns with ELSD are mostly used. A poly(vinyl

alcohol)-grafted silica column, with ELSD, can be used to separate them, simultaneously.

REFERENCES

1. Avalli, A.; Contarini, G. Determination of phospholipids in dairy products by SPE/HPLC/ELSD. J. Chromatogr. A, **2005**, *1071* (1–2), 185–190.
2. Hayakawa, J.; Okabayashi, Y. Simultaneous analysis of phospholipid in rabbit bronchoalveolar lavage fluid by liquid chromatography/mass spectrometry. J. Pharm. Biomed. Anal. **2004**, *35*, 583–592.
3. Fang, J.S.; Barcelona, M.J. Structural determination and quantitative analysis of bacterial phospholipids using liquid chromatography/electrospray ionization/mass spectrometry. J. Microbiol. Meth. **1998**, *33*, 23–25.
4. IUPAC-IUBMB Joint Commission, Nomenclature of glycolipids. Carbohydr. Res. **1998**, *312*, 167–175.
5. Uran, S.; Larsen, A.; Jacobsen, P.B.; Skotland, T. Analysis of phospholipid species in human blood using normal-phase liquid chromatography coupled with electrospray ionization ion-trap tandem mass spectrometry. J. Chromatogr. B, **2001**, *758* (2), 265–275.
6. Ramadan, M.F.; Morsel, J.T. Phospholipid composition of niger (Guizotia abyssinica Cass.) seed oil. Lebens. Wissenschaft Technol. Food Sci. Technol. **2003**, *36* (2), 273–276.
7. Helmerich, G.; Koehler, P. Comparison of methods for the quantitative determination of phospholipids in lecithins and flour improvers. J. Agric. Food Chem. **2003**, *51*, 6645–6651.
8. Bunger, H.; Pison, U. Quantitative-analysis of pulmonary surfactant phospholipids by high-performance liquid-chromatography and light-scattering detection. J. Chromatogr. B, Biomed. Applic. **1995**, *672* (1), 25–31.
9. Zhang, Y.Y.; Yang, Y.W.; Jiang, H.L.; Ren, Q.L. Quantification of soybean phospholipids in soybean degummed oil residue by HPLC with evaporative light scattering detection. J. Liq. Chromatogr. Relat. Technol. **2005**, *28* (9), 1333–1343.
10. Kiuchi, K.; Ohta, T.; Ebine, H. High-performance liquid-chromatographic separation and quantitative-analysis of synthetic phospholipids. J. Chromatogr. **1977**, *133* (1), 226–230.
11. Hvattum, E.; Larsen, A.; Uran, S.; Michelsen, P.M.; Skotland, T. Specific detection and quantification of palmitoyl-stearoyl-phosphatidylserine in human blood using normal-phase liquid chromatography coupled with electrospray mass spectrometry. J. Chromatogr. B, **1998**, *716* (1–2), 47–56.
12. Neron, S.; El Amrani, F.; Potus, J.; Nicolas, J. Separation and quantification by high-performance liquid chromatography with light scattering detection of the main wheat flour phospholipids during dough mixing in the presence of phospholipase. J. Chromatogr. A, **2004**, *1047* (1), 77–83.
13. Fagan, P.; Wijesundera, C. Liquid chromatographic analysis of milk phospholipids with on-line pre-concentration. J. Chromatogr. A, **2004**, *1054* (1–2), 241–249.
14. Antonopoulou, S.; Nomikos, T.; Oikonomou, A.; Kyriacou, A.; Andriotis, M.; Fragopoulou, E.; Pantazidou, A. Characterization of bioactive glycolipids from Scytonema julianum (cyanobacteria). Comp. Biochem. Physiol. Part B: Biochem. Mol. Biol. **2005**, *140* (2), 219–231.
15. Demopoulos, C.A.; Kyrili, M.; Antonopoulou, S.; Andrikopoulos, N.K. Separation of several main glycolipids into classes and partially into species by HPLC and UV-detection. J. Liq. Chromatogr. Relat. Technol. **1996**, *19* (5), 771–781.
16. Ramadan, M.F.; Morsel, J.T. Analysis of glycolipids from black cumin (*Nigella sativa* L.), coriander (*Coriandrum sativum* L.) and niger (Guizotia abyssinica Cass.) oilseeds. Food Chem. **2003**, *80* (2), 197–204.
17. Sugawara, T.; Miyazawa, T. Separation and determination of glycolipids from edible plant sources by high-performance liquid chromatography and evaporative light-scattering detection. Lipids **1999**, *34* (11), 1231–1237.
18. Christie, W.W.; Urwin, R.A. Separation of lipid classes from plant-tissues by high-performance liquid-chromatography on chemically bonded stationary phases. HRC-J. High Res. Chromatogr. **1995**, *18* (2), 97–100.
19. Picchioni, G.A.; Watada, A.E.; Whitaker, B.D. Quantitative high-performance liquid chromatography analysis of plant phospholipids and glycolipids using light-scattering detection. Lipids **1996**, *31* (2), 217–221.
20. Deschamps, F.S.; Chaminade, P.; Ferrier, D.; Baillet, A. Assessment of the retention properties of poly(vinyl alcohol) stationary phase for lipid class profiling in liquid chromatography. J. Chromatogr. A, **2001**, *928* (2), 127–137.
21. Yamagishi, T.; Akiyama, H.; Kimura, S.; Toyoda, M. Quantitative determination of phosphatidylcholine by an HPLC-RI system. J. Amer. Oil Chem. Soc. **1989**, *66* (12), 1801–1808.
22. Yang, Y.W.; Li, Y.; Wu, C.J.; Ren, Q.L.; Wu, P.D. Determination of soybean phosphatidylcholine by HPLC-RI. J. Instrum. Anal. **2004**, *23* (5), 118–121.

Photodiode-Array Detection

Hassan Y. Aboul-Enein
Pharmaceutical and Medicinal Chemistry Department, Pharmaceutical and Drug Industries Research Division, National Research Center, Dokki, Cairo, Egypt

Vince Serignese
Pharmaceutical Analysis Laboratory, King Faisal Specialist Hospital and Research Center, Riyadh, Saudi Arabia

INTRODUCTION

Analysis is an integral part of research, clinical, and industrial laboratory methodology. The determination of the components of a substance or the sample in question can be qualitative, quantitative, or both. Techniques that are available to the analyst for such determinations are abundant. In absorption spectroscopy, the molecular absorption properties of the analyte are measured with laboratory instruments that function as detectors. Those that provide absorbance readings over the ultraviolet–visible (UV–Vis) light spectrum are commonly used in high-performance liquid chromatography (HPLC). The above method is sufficiently sensitive for quantitative analysis and it has a broader application than other modes of detection.

DISCUSSION

The most advanced UV–Vis detector that is used in HPLC is the diode array. Compared to its predecessors, the diode array generates a large amount of spectral information without compromising sensitivity or wavelength resolution. In order to discuss the properties of the diode-array detector, a brief historical description of its technological development is presented.

HISTORICAL BACKGROUND AND SCHEMATICS

Early on, UV–Vis detectors produced data at one wavelength only fixed-wavelength detector (FWD). Because compounds of interest do not absorb light at a fixed wavelength with equal efficiencies, the next step was to develop a detector with an adjustable wavelength range. Modifications were required in the light source. The high-energy-emitting mercury lamp in the FWD was replaced with a deuterium and/or tungsten lamp. The latter light source gave detectable energies over a wider wavelength range. The addition of a wavelength selector (monochromator) provided accurate wavelength adjustments from 190 to 800 (UV–Vis) nm. Hence, the variable-wavelength detector (VWD) was established.

At this point, single-wavelength data acquisition remained a bottleneck, restricting the analyst to one basic characteristic tool to identify the analyte: the amount of time the analyte is retained on the chromatographic column (i.e., the retention time). If there are four compounds in the sample to be analyzed, this would require a minimum of four injections to identify them. Additional work would be needed for cross-identification and so on. The concept of multiple-wavelength detection was introduced.

The diode-array detector collects data with a maximum wavelength bandwidth of 190–800 nm. All wavelengths in that range are accounted for simultaneously. As shown in Fig. 1, the upper portion represents a single detector element with three components: the photodiode, a capacitor, and (FET) field effect transistor switch. Shining light onto a single detector element produces a signal which is processed and then expressed as a digital absorbance reading. This response is for one wavelength only. The FWDs and VWDs are equipped with a single detector element. The bottom portion of Fig. 1 displays the schematics of a linear diode-array detector. Many detector elements, all of the same composition as described above, are in a linear arrangement. Each detector element is dedicated to a particular wavelength bandwidth such that there are enough of them to cover the UV–Vis light spectrum. This unit produces signals that cover the entire UV–Vis light spectrum. Simultaneous wavelength detection was now possible with the diode array.

Fig. 2 displays the optical components of the diode-array detector. A deuterium lamp will emit light onto the flow cell, which has liquid continuously flowing through it. A shutter is provided between the light source and the flow cell, which can either be fully open or closed. The beam of light will then travel to the diffraction grating, where it will be separated into wavelengths ranging from 190 to 800 nm. The separated light will finally reach the diode array and a signal will be produced that is proportional to the amount of light received. For a detailed account of this topic, the reader is referred to the selected references cited.

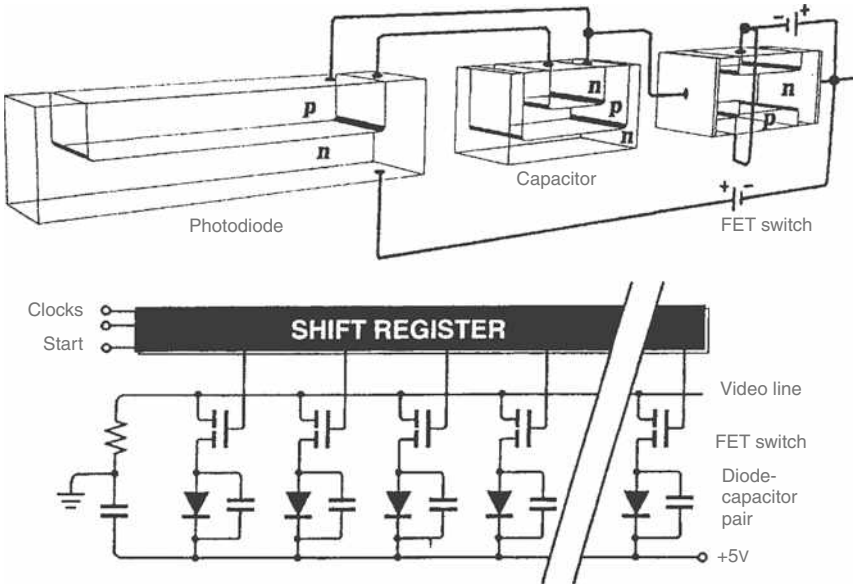

Fig. 1 Diagram of a single photodiode-capacitor switch (top) and an electronic schematic of the linear array (bottom).

APPLICATIONS

Thus far, we have given a brief account on the technological development of the diode-array detector. Its applications offer several advantages to the user, which have been made possible primarily by the current computer hardware and software that are available on the market. Data acquisition and analysis are computer driven. The information acquired from the diode array can be analyzed to tailor the user's preferences. This area represents an emerging field and further advancements in analytical software tools will ultimately determine the true potential of diode-array detection.

As stated previously, a major improvement achieved with the diode array is that fewer attempts are required to identify the components of a sample mixture. A single injection can be sufficient for sample identification when spectral information in addition to peak retention time is part of the collected data. Through software capabilities, spectra can be extracted from the chromatogram of each individual peak. The spectral information combined with the retention times can be used to identify the chromatographic peaks. Furthermore, the spectra can be compared to spectral libraries compiled from the literature for purposes of spectral matching. Many proprietary software programs have been developed for the diode-array instrument. It is up to the user's discretion to determine how he can best utilize these resources.

At first, one may show skepticism at the usefulness of diode-array detection because other analytical systems are more sensitive and offer similar features such as peak identification and purity checks. For these alternatives, one would have to refer to gas chromatography/mass spectroscopy (GC/MS), liquid chromatography/mass spectroscopy (LC/MS), and tandem mass spectrometry (MS-MS). However, one must keep in mind the significantly higher costs as a tradeoff for enhanced sensitivity.

When assessing the merits of the diode array, the user should consider the various steps that are involved in

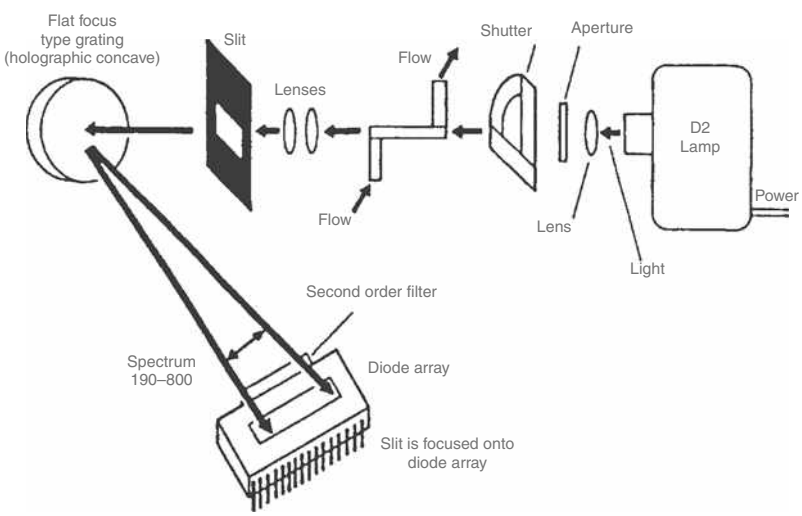

Fig. 2 Optics unit components.
Source: Reprinted from *Waters 990 + Photodiode Array Detector Operator's Manual 1989*; courtesy of Waters Corporation, Milford, MA.

methods development. It will become clear that for every hurdle one encounters, diode-array detection renders the task less laborious. It is most often than not that in developing new procedures you are confronted with drawbacks such as contaminants, peak overlap, artifacts, sample cleanup, and baseline noise. For instance, the presence of a shoulder on a major chromatographic peak raises questions as to its origin. With the aid of the diode array, a spectral profile of the shoulder peak will quickly determine its existence. A flat line of low absorbance throughout its spectra indicates that it is an artifact. The user can then go back to his procedure and ascertain if the root of the problem is systematic. The direction problem-solving takes is crucial and if gone astray, vast amounts of time are wasted. The same shoulder obtained with a FWD could have led the user to perform a time-dependent study. In this case, it was incorrectly assumed that the shoulder peak was a degradation product and additional injections at increased time intervals would show the shoulder peak increasing in size, indicating the compound of interest was degrading. Even though the analyst would eventually achieve the same result in the latter situation, the former approach is less time-consuming.

Diode-array detection has found its way into the pharmaceutical industry and the clinical laboratory. The widespread use of HPLC analysis in the product development cycle of pharmaceuticals provided an open door for the diode array. Throughout the different phases of drug development, the identification of a peak and its homogeneity must be established. The diode array confirms peak identity and compound purity by spectral analysis. Peak spectra are overlaid with spectra from standards (that are stored on the computer hard drive) for identification and spectra from the upslope, apex, and downslope of a chromatographic peak are overlaid to test for purity. Because the diode array performs continuous-flow spectral acquisition in the HPLC mode, the method can be automated to screen for thousands of compounds where only one will have the desired pharmacological action. Drug screening is common in drug development procedures, which goes hand-in-hand with drug metabolism and quantitative analysis. Diode-array detection is effective in all of these areas.

Peak purity is of utmost importance in the quality control of pharmaceutical products. The contents of the product must be known with great certainty before it is sold to the consumer. Adjunct laboratories test the stability of the product in order to determine its expiry date. All by-products are accounted for and the amount of active ingredient is referenced. The diode array in HPLC analysis is used to determine all of the above information.

In the clinical laboratory setting, methods of analysis are used to diagnose disease and for therapeutic drug monitoring. Diode array-HPLC techniques will determine the drug concentrations and its metabolite levels in biological matrices. From these results, dosing regimens can be outlined that are specifically tailored to patients with respect to therapeutic drug concentration and drug dose, thereby avoiding drug toxicity. These procedures will ensure the safety and efficacy of clinically administered drugs.

CONCLUSIONS

The photodiode-array detector is a powerful analytical instrument that has provided enhanced detection capabilities with the addition of detailed spectral information via its multisignal detection technology. Its applications are HPLC based and can be found in basic research, automated analysis, pharmaceutical product development, and the clinical laboratory environment. Through spectral acquisition and analysis, a wealth of information can be obtained about the identity and purity of a compound. Combined with high selectivity and sensitivity, this mode of detection is essential for qualitative and quantitative HPLC analysis.

BIBLIOGRAPHY

1. Green, R.B. Absorption detectors for high-performance liquid chromatography. In *Detectors for Liquid Chromatography*; Yeung, E.S., Ed.; John Wiley & Sons: New York, 1986; 42–46.
2. Huber, L., George, S.A., Eds.; *Diode Array Detection in HPLC*; Marcel Dekker, Inc.: New York, 1993.
3. Lloyd, D.K. Instrumentation: Detectors and integrators. In *High Performance Liquid Chromatography*; Lough, W.J., Wainer, I.W., Eds.; Blackie Academic & Professional/ Chapman & Hall: London, 1996; 120–125.
4. McMaster, M.C. Hardware specifics. In *HPLC: A Practical User's Guide*; VCH: Weinheim, 1994; 112–114.
5. Scott, R.P.W. Liquid chromatography detectors. In *Techniques and Practice of Chromatography*; Marcel Dekker, Inc.: New York, 1995; 284–287.

Photophoretic Effects in FFF of Particles

Vadim L. Kononenko
Institute of Biochemical Physics, Russian Academy of Sciences, Moscow, Russia

INTRODUCTION

The basic principle underlying the field-flow fractionation (FFF) method of particle separation is the combination of the transversely non-uniform velocity profile of a carrier fluid in a channel with the transverse force field acting on the particles to be separated. Due to the different magnitudes of transverse force applied to the various fractions in a particle mixture, these fractions tend to occupy different laminas of a non-uniform channel flow. As a result, they move along the channel with effectively different velocities and become separated eventually. This universal principle underlies the high versatility and remarkable instrumental power of the FFF subtechnique family, due to the wide variety of driving forces used. Accordingly, further development of FFF is primarily associated with the use of new types and combinations of physical and physicochemical agents influencing particle and molecule redistribution across the flow.

Among the possible new force agents, the interaction of light with particles leading to their motion (photophoresis) attracts special attention. It is due to the universal nature of this interaction, present for all kinds of particles and molecules, as well as to the numerous interaction mechanisms that exist. Thus, photophoretic FFF techniques, if developed, have the potential to separate particles according to their size, optical constants, and physicochemical properties relevant to photophoretic mechanisms. The present entry considers the basic theoretical principles underlying the photophoretic effects, and their possible use in FFF. Both direct and indirect mechanisms of particle photophoresis are discussed, followed by a brief overview of experimental data on the photophoresis of particles and liquid droplets in fluids. Feasibility studies aimed at photophoretic FFF are outlined, and some possible instrumental realizations are discussed.

MECHANISMS OF PHOTOPHORESIS

The idea of photophoretic FFF emerged many years ago,[1] but it still remains one of the less developed branches of the rich family of FFF techniques.[2] However, its potential advantages seem to ensure eventual practical realization. The known photophoretic mechanisms can be classified into two families. The direct-type mechanisms are associated with momentum transfer from an electromagnetic field to a particle or a molecule irradiated during the scattering, refraction, or absorption of light. The known indirect photophoretic mechanisms involve, as a primary light action, non-uniform heating of particles and/or the establishment of a temperature gradient across a channel due to light absorption in the carrier fluid. Such heating leads to conventional thermophoresis of particles due to tangential gradients of interfacial energy arising near the particle surface. The whole phenomenon can be referred to as photothermophoresis.

Direct Photophoretic Mechanisms

The direct photophoretic mechanisms include light pressure and the action of the so-called gradient force.[3–8] The gradient force[6–8] arises from the spatial non-homogeneity of the electromagnetic field, if any. It has the same nature as the force acting on electric dipoles in a static divergent field. It is characteristic of focused light beams, evanescent waves near refractive index boundaries, etc. In general, calculation of the direct photophoretic force requires the solution of the optical problem of light scattering by a particle. In this problem, a particle is characterized either by the complex dielectric permittivity $\varepsilon(\lambda_0) = \varepsilon'(\lambda_0) - i\varepsilon''(\lambda_0)$ relative to the permittivity ε_m of the surrounding medium, or by the complex refractive index relative to that of the surrounding medium, n_0, at the wavelength λ_0 of light, $m(\lambda_0) = n_r(\lambda_0) - i\kappa(\lambda_0)$. Here, λ_0 is the wavelength of light in vacuum, n_r is the relative refraction index, κ is the index of absorption, and $\varepsilon' = n_r^2 - \kappa^2$, $\varepsilon = 2n_r\kappa$. The solution of the scattering problem is obtained using either wave optics theory,[3–5] or the geometrical (ray) optics description,[7,8] depending on the particle size parameter $\rho = 2\pi a n_0/\lambda_0$, where $2a$ is the characteristic particle dimension (the diameter for spherical particles). The wave optics approach is based on Lorenz–Mie theory in the case of plane incident waves,[3,4] and on various generalizations of this theory in the case of focused laser beams (see Ref.[5] and the references therein). In practice, the ray optics description is valid (and more suitable) starting from $a \sim 10$ μm for visible light. In both approaches, the calculations result in the following general-type expression for photophoretic force acting on the particle:

$$\vec{F}_{ph} = \varepsilon_m \frac{\pi a^2}{c} \widehat{Q}_{pr}(\varepsilon, \rho, \vec{r})\vec{J}_0 \qquad (1)$$

Here, $|\vec{J}_0|$ is the incident light irradiance (or light intensity) at the beam axis measured in units of energy per unit time per unit area, $\vec{J}_0/J_0$ gives the light propagation direction, c is the velocity of light in vacuum, and $\widehat{Q}_{\rm pr}(\varepsilon,\rho)$ is the dimensionless efficiency factor of the radiation pressure.[3] In a general case of a spatially non-homogeneous light beam, the photophoretic force has both longitudinal and transverse components relative to $\vec{J}_0$. Hence, $\widehat{Q}_{\rm pr}(\varepsilon,\rho,\vec{r})$ is a tensor; its components depend on the particle's coordinate vector $\vec{r}$.

According to Eq. 1, a particular relation of the direct photophoretic force to the optical characteristics of a particle, as well as to the beam parameters, is described by the radiation pressure factor $\widehat{Q}_{\rm pr}(\varepsilon,\rho,\vec{r})$. In general, it can be obtained only numerically. However, the analytical results exist in some limiting cases, namely, for Rayleigh scattering, Rayleigh–Gans scattering, and the case of very large particles.[3,4] In the context of FFF applications, it is instructive to consider a spherical particle of radius a placed in a wide, slightly divergent gaussian light beam under Rayleigh–Gans scattering conditions, i.e., $|\varepsilon-1| \ll 1$, $2\rho|\varepsilon-1| \ll 1$.

A Rayleigh–Gans particle in a gaussian beam

The light intensity distribution in a gaussian beam is as follows:

$$J(r,z) = J_0 \frac{{w_0}^2}{w(z)^2}\exp\left[-\frac{r^2}{w(z)^2}\right]$$
$$w(z)^2 = {w_0}^2\left(1+\frac{z^2}{{R_0}^2}\right) \tag{2}$$

Here, r is the distance from the beam axis, z is the distance along this axis, w_0 is the effective beam radius, $R_0 = 2\pi n_0 {w_0}^2/\lambda_0$ is the diffraction length of the beam, and $\Delta\theta = \lambda/(2\pi n_0 w_0)$ is its angular divergence. Assume that the beam width is comparatively large, $w_0 \gg a$, and divergence is small, $\Delta\theta \ll 1$. In this case, according to Refs.[9,10] the direct photophoretic force $F_{\rm ph}$ for a Rayleigh–Gans particle can be written as the sum of the radiation pressure force $F_{\rm pr}$ and the gradient force F_∇:

$$\vec{F}_{\rm ph} = \vec{F}_{\rm pr} + \vec{F}_\nabla$$
$$\vec{F}_{\rm pr}(r,z) = \varepsilon_{\rm m}\frac{\pi a^2}{c}Q_{\rm pr}(\varepsilon,\rho)\vec{J}(r,z)$$
$$\vec{F}_\nabla(r,z) = \varepsilon_{\rm m}\frac{2\pi a^3}{c}\left(\frac{\varepsilon'-1}{\varepsilon'+2}\right)\vec{\nabla}J(r,z) \tag{3}$$

The analytical expression for $Q_{\rm pr}(\varepsilon,\ \rho)$ is presented in Ref.[10] Calculating $\vec{\nabla}J(r,z)$ using Eq. 2 and regarding $(\varepsilon'+2) \approx 3$ because $|\varepsilon-1| \ll 1$, we obtain the following from Eq. 3.

$$F_{\rm ph||}(r,z) \equiv F_{\rm pr} + F_{\nabla||} \approx \varepsilon_{\rm m}\frac{\lambda^2\rho^2}{4\pi c}\left\{\frac{1}{4}(\varepsilon'-1)^2 I_1(\rho) + \frac{4}{3}\varepsilon''\rho - \frac{2\lambda\rho {w_0}^2 z}{3\pi {R_0}^2 w(z)^2} \times\left[1-\frac{r^2}{w(z)^2}\right](\varepsilon'-1)\right\}J(r,z)$$
$$F_{\rm ph\perp}(r,z) \equiv F_{\nabla\perp} \approx -\varepsilon_{\rm m}\frac{\lambda^3\rho^3 r}{6\pi^2 c w(z)^2}(\varepsilon'-1)J(r,z) \tag{4}$$

The analytical expression for $I_1(\rho)$ obtained in Ref.[9] and its plot are presented in Ref.[10,11] $I_1(\rho)$ is an increasing function, with the small-amplitude oscillations superimposed. For small particles ($\rho \ll 1$), $I_1(\rho) \approx (32/27)\rho^4$, whereas for large ones ($\rho \gg 1$), $I_1(\rho) \approx 2[\ln(4\rho) + 0.5772] - 3$. In the whole range $2 \le \rho \le 20$, the global variation of $I_1(\rho)$ rather closely approximates $2.37\ \ln(\rho)$.

Eq. 4 demonstrates clearly the basic dependences of the photophoretic force, namely, its variation with the size and optical parameters of the particle, with the beam's parameters, and with the particle position relative to the symmetry point $r = 0$, $z = 0$ of the gaussian beam. The longitudinal component $F_{\rm ph||}$ includes the common light pressure (the first two terms in the braces) and the gradient force (the third term in the braces), both dependent on the particle position. The light pressure is always directed away from the light source. Its magnitude varies with $J(r, z)$ according to Eq. 2, mainly due to the variation of the beam radius $w(z)$. The longitudinal component of the gradient force, $F_{\nabla||}$ depends on the particle distance z from the beam's symmetry plane $z = 0$ (linearly for small z). However, the magnitude of $F_{\nabla||}$ is very small for slightly divergent beams due to $w_0 \gg \lambda$. The transverse component, $F_{\rm ph\perp}$, has the gradient term $F_{\nabla\perp}$ only, varying as $rJ(r)$. The magnitude of $F_{\rm ph\perp}$ is substantially greater, $F_{\rm ph\perp}/F_{\nabla||} \sim (R_0/w_0)^2$. The direction of gradient components $F_{\nabla||}$ and $F_{\rm ph\perp}$ depends on the sign of $(\varepsilon'-1)$. If $\varepsilon' > 1$, the gradient force is directed to the symmetry point $r = 0$, $z = 0$, where the light intensity is maximal. If $\varepsilon' < 1$, this force pulls the particle out of the beam.

Consider now variation of light pressure with the size and optical parameters of a particle.[9–11] Fig. 1 illustrates the size dependence of $F_{\rm pr}$ according to Eq. 4. Depending on the value of ratio $|(\varepsilon'-1)|/\varepsilon''$,non-absorbing, "low absorbing," and "highly absorbing" particles can be distinguished conventionally. For non-absorbing particles with $\varepsilon'' = 0$, Eq. 4 gives $F_{\rm pr} \propto (\varepsilon'-1)^2\rho^6 J(r, z)$ practically up to $\rho \sim 1$ (Fig. 1, curves 1, 2). For "low absorbing" particles with $\varepsilon'' \ll (\varepsilon'-1)^2$, it follows from Eq. 4 that $F_{\rm pr} \propto \varepsilon''\rho^3 J(r, z)$ at $\rho \ll 1$, changing to $F_{\rm pr} \propto (\varepsilon'-1)^2\rho^6 J(r, z)$ at higher ρ, and returning to the initial ρ^3 dependence at very large ρ, if the inequality $2\rho|\varepsilon-1| < 1$ still holds at such ρ (Fig. 1, curves 4, 5).

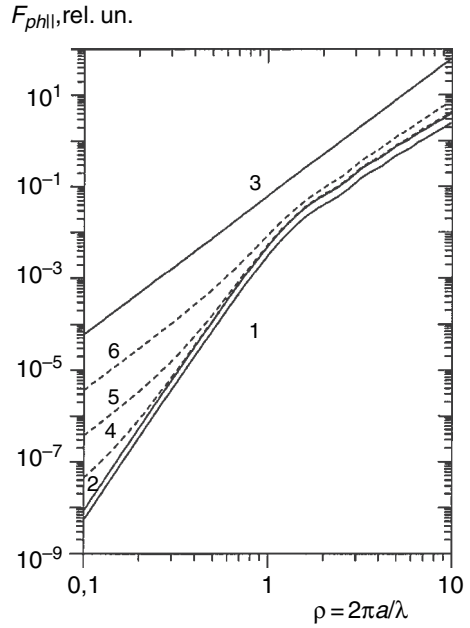

Fig. 1 Size dependence of photophoretic force, calculated for particles of various materials in water ($\varepsilon_m = 1.782$) according to Eq. 4. 1, Glass ($\varepsilon'\varepsilon_m = 2.28$, $\varepsilon'' \approx 0$ at $\lambda_0 = 589$ nm); 2, latex ($\varepsilon'\varepsilon_m = 2.53$, $\varepsilon'' \approx 0$ at $\lambda_0 = 589$ nm); 3, carbon black ($\varepsilon'\varepsilon_m = 2.4$, $\varepsilon'' = 2.38$ at $\lambda_0 = 489$ nm); 4–6, model substances with $\varepsilon'\varepsilon_m = 2.53$ and (4), $\varepsilon'' = 0.001$ (5), 0.01 (6), 0.1.

The transverse gradient force $F_{\nabla\perp}$ may exceed the radiation pressure F_{pr} for all $\rho < 1$ if the beam radius is as small as $w_0 < \lambda/|\varepsilon' - 1|$, while for the longitudinal gradient force $F_{\nabla\|}$, that requires $w_0 < \lambda\Delta\theta/|\varepsilon' - 1|$, i.e., high enough beam focusing. For the "highly absorbing" particles (Fig. 1, curves 3, 6), classified by condition $(\varepsilon' - 1)^2 \ll \varepsilon'' \ll |\varepsilon' - 1|$, the radiation pressure is due to the light absorption, mainly, and $F_{pr} \propto \varepsilon''\rho^3 J(r, z)$. Here, $F_{\nabla\perp} > F_{pr}$ if the beam radius $w_0 < \lambda|\varepsilon' - 1|/4\pi\varepsilon''$, and $F_{\nabla\|} > F_{pr}$ if $w_0 < \lambda\Delta\theta\,|\varepsilon' - 1|/4\pi\varepsilon''$.

In general, the analysis shows the pronounced and diverse character of the dependences of direct photophoretic forces on both the size and optical parameters of a particle. These features form the fundamental basis for FFF applications.

The analysis of the direct photophoretic mechanism presented above for Rayleigh–Gans scattering conditions gives a clear general insight into the problem. The range of quantitative validity of Eq. 4 is, in practice, $\rho < 2$–3. The results for higher ρ are summarized in Ref.[10] In the case of very large particles ($\rho \gg 1$ or $a > \sim 10$ μm for the visible range of light), the direct photophoretic force is better calculated using the geometrical optics approach. It considers the incident light as a multitude of elementary rays reflected and refracted at the particle boundary, including multiple reflections/refractions inside the particle. Each reflection/refraction is accompanied by a change of ray momentum, which results in light pressure on the particle surface at the ray incidence point. The total acting force is obtained by integrating this pressure over the particle surface.[7,8] In the framework of the ray approach, there is no computational difference between the radiation pressure and the gradient force.

Indirect Photophoretic Mechanisms

The indirect mechanisms of photophoresis considered so far are associated with heating due to light absorption. Consequently, the solution of the photothermophoretic problem consists of three consecutive steps: first, determination of the light intensity distribution inside and outside the irradiated particle; second, the calculation of the temperature field within the particle and in the surrounding medium generated by the light absorption; third, the calculation of thermophoretic mobility of a particle in this field using appropriate physicochemical models for the particle, the surrounding medium, and their interface. These three constituent problems are rather independent mutually. Thus, in principle, the results of various independent treatments can be combined to obtain the final solution. It is natural also to consider two complementary extremes: a light-absorbing particle surrounded by transparent liquid, and a transparent particle placed in a channel flow of light-absorbing fluid.

An absorbing particle in a transparent fluid

Here, the aim of the optical problem is the calculation of the light intensity distribution (heat source function) inside the particle, $B(x, z) = E_i^2(x, z)/E_0^2$, $E_i(x, z)$ being the internal electric field strength, E_0 the incident wave amplitude, x the radial distance from the main particle diameter parallel to the light propagation direction, and z the distance from the particle center along this diameter. There are three domains of the particle size parameter ρ where both the internal field patterns and their calculation procedures are essentially different. If $\rho \ll 1$ (Rayleigh scattering), the internal field can be considered as a plane wave, decaying along the main diameter due to absorption. For intermediate $\rho \sim$ 1–10, the particle behaves like a spherical cavity, and the internal field distribution is a complicated system of minima and maxima.[12–14] Here, the $B(x, z)$ distribution depends strongly on a particular combination of particle size parameter and optical constants, and can be found only using the rigorous Mie theory. Qualitatively, the general tendency of $B(x, z)$ transformation with the increase of ρ is the formation of two global maxima ("hot spots" in a case of moderate absorption) at the main particle diameter. This is an early stage of geometrical optics focusing of light rays entered the particle and undergoing the first and the second internal reflections. Another important feature is morphology-dependent resonances occurring in large ($\rho \sim$ 40–50) transparent particles.[13,14] The physical nature of such resonances is the formation of standing light

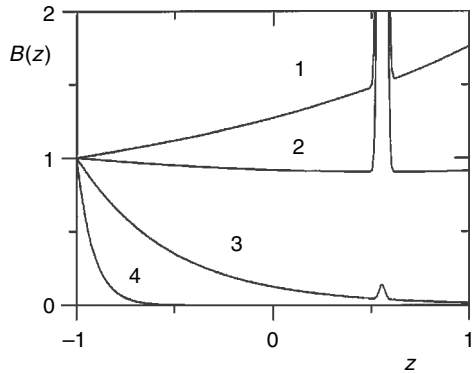

Fig. 2 Light intensity distribution along the main diameter inside a large particle, calculated using the geometrical optics approach and considering the first internal reflection of rays. (1), $\kappa\rho = 0.06$ (2), 0.23 (3), 1.22 (4), 6.1; $n_r = 1.2$, however, the picture is qualitatively valid for $1 < n_r < \sqrt{2}$.

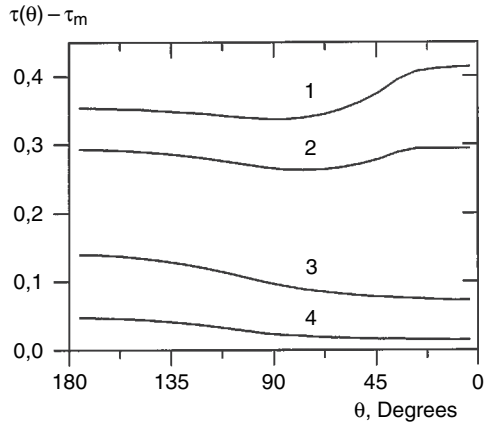

Fig. 3 Distributions of dimensionless surface temperature calculated for a large light-absorbing particle. $k_i = k_e$, $n_r = 1.2$, $\kappa\rho = 0.06$ (1), 0.23 (2), 1.22 (3), 6.1 (4). $\theta = 180°$ corresponds to illuminated pole.

waves near the particle surface from the traveling waves confined by almost total internal reflection. They accumulate the energy of the incident wave near the surface periodically in ρ. In the third domain, $\rho \gg 10$, the particle behaves like a tiny spherical lens, which focuses (if $n_r > 1$) or expands (if $n_r < 1$) the incident radiation. The focusing (expansion) process begins inside the particle due to refraction of the incident rays at the illuminated hemispherical boundary. Here, the $B(x, z)$ distribution is calculated using the geometrical optics approach,[10,15,16] and the general relations are obtained between the field distribution and particle parameters.[10]

Fig. 2 shows the distribution of $B(x, z)$, and hence the heat sources, along the main optical axis of a large particle calculated for various magnitudes of absorption.[10] When the absorption is small, the shadow hemisphere is heated preferentially due to internal focusing of light. With the increase of absorption, the light is attenuated considerably before it reaches the central plane $z = 0$, and so the illuminated hemisphere shows greater heat production. These features are illustrated by the distributions of the surface temperature of a particle, as shown at Fig. 3. They are obtained by solution of the thermal conductivity problem for a spherical particle in a medium, with the density of internal heat sources given by $B(x, z)$. The procedure is described in Refs.[10,16] The dimensionless temperature $\tau(r, \theta)$ is expressed in the units of characteristic temperature $T_0 = 2\kappa\rho n_r a J_0/n_0 k_i$ of particle heating due to light absorption. Here, k_i is the thermal conductivity of the particle material, $T_0\tau_m$ is the ambient temperature far from the particle, r is the distance from the particle center, and θ is the polar angle measured from the shadow pole of the particle. Hence, with the increase of absorption coefficient, not only does the particle temperature increase, but the mean temperature gradient across the particle surface $[T(180°) - T(0°)]/2a$ changes its sign. Fig. 4 illustrates such dependence calculated for a particle irradiated with a 1 W Ar^+-ion laser beam focused onto a spot of $\sim 2 \times 10^{-4}$ m diameter. As Fig. 4 shows, for $\kappa > (3–5) \times 10^{-3}$, the temperature gradient may exceed 5×10^5 K m^{-1}, which is a typical value of thermal FFF.[17]

In general, the analysis presented evidences a real possibility of strong non-homogeneous heating of particles by focused light. It is very important that internal heating by light generate a strong temperature gradient just along the particle surface (Fig. 4), which is rather difficult to achieve with an external temperature gradient because of the high thermal conductivity of the particles. Hence, this feature of heating with light should naturally lead to pronounced thermophoretic effects.

The final step in considering photothermophoresis is the calculation of thermophoretic mobility of a light-absorbing

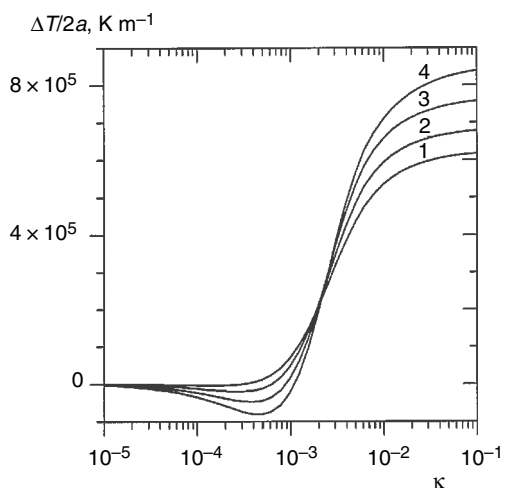

Fig. 4 Dependence of characteristic temperature gradient across the particle surface on the light absorption coefficient. $a = 25 \times 10^{-5}$ m, $\rho = 406$, $J_0 = 10^7$ W m^{-2}, $k_i = k_e = 1$ W m^{-1} K^{-1}, (1), $n_r = 1.1$ (2), 1.2 (3) 1.3 (4), 1.4.

particle in a temperature field generated due to absorption. To keep the connection with normal thermophoresis, it is natural to define the magnitude of photothermophoretic mobility of a particle b_{phth} by the relation[10]

$$u_{\text{phth}} = b_{\text{phth}} \frac{T_0}{a}, \qquad \frac{T_0}{a} = \frac{2\kappa\rho n_{\text{r}}}{n_0 k_{\text{i}}} J_0 \tag{5}$$

Here, T_0/a is the characteristic gradient of the temperature field, u_{ph} is particle velocity, and k_{i} is the thermal conductivity of the particle. The sign of b_{phth} is taken, usually, as positive when the directions of $\vec{u}_{\text{ph}}$ and $\vec{J}_0$ coincide. The calculations of u_{ph}, and hence b_{phth}, can be done on the basis of well-established approaches[18,19] developed for a constant external temperature gradient, with appropriate modifications accounting for a local non-homogeneity.[10] The results are essentially different for liquid droplets in immiscible fluid, and for solid particles in a liquid. In the former case, the motion of a droplet is induced by the gradient of the temperature-dependent surface tension. The whole phenomenon is usually referred to as "thermocapillary motion." It is directed parallel to the temperature gradient, i.e., to the heat source in the case of external heating, because the surface tension diminishes with the increase of temperature. The thermophoretic mobility of a droplet in external constant-gradient temperature field b_{th} is shown to be[20,21]

$$b_{\text{th}} = \frac{2k_{\text{e}}a}{(2\eta_{\text{e}} + 3\eta_{\text{i}})(2k_{\text{e}} + 3k_{\text{i}})} \left|\frac{\text{d}\sigma}{\text{d}T}\right| \tag{6}$$

Here, η_{i} and η_{e} are viscosity coefficients, k_{i} and k_{e} are thermal conductivities of a droplet and a fluid, σ is the surface tension, and T is the absolute temperature. A specific variation of the surface temperature $T_0\tau(r, \theta)$ of an irradiated particle (Fig. 3) formally results in certain weighted averaging of b_{th} over the polar angle θ. The exact solution has not been obtained yet, but arguments similar to those used in the case of a solid particle[10] suggest the following form for the final b_{phth} expression for a fluid droplet:

$$\begin{aligned} b_{\text{phth}} &= b_{\text{th}} g_{\text{an}}(n_{\text{r}}, \kappa\rho) \\ g_{\text{an}}(n_{\text{r}}, \kappa\rho) &= -A \int_0^{\pi} \frac{\text{d}\tau(a,\theta)}{\text{d}\theta} \sin^2\theta \, \text{d}\theta \end{aligned} \tag{7}$$

Here, A is a positive constant of the order of unity, and $\tau(a, \theta)$ is the dimensionless temperature of the particle surface in units of T_0.

The thermophoretic mobility of a solid particle in a liquid is considered in Ref.[10] The result has the form

$$\begin{aligned} b_{\text{phth}} &= b_{\text{th}} g_{\text{an}}(n_{\text{r}}, \kappa\rho) \\ g_{\text{an}}(n_{\text{r}}, \kappa\rho) &= -\frac{1}{4}\left(2 + \frac{k_{\text{i}}}{k_{\text{e}}}\right) \int_0^{\pi} \frac{\text{d}\tau(a,\theta)}{\text{d}\theta} \sin^2\theta \, \text{d}\theta \end{aligned} \tag{8}$$

Here, b_{th} is the conventional thermophoretic mobility of a particle, which corresponds to a constant temperature gradient in the fluid.[10]

The function $g_{\text{an}}(n_{\text{r}}, \kappa\rho)$ in Eqs. 7 and 8 accounts for the anisotropy of particle heating by light. Its behavior due to variation of particle size and optical parameters is considered in Refs.[10,16] For small $\kappa\rho \ll 1$, when the shadow hemisphere is heated preferentially due to internal focusing of light (Fig. 3), the temperature gradient $\text{d}\tau(a, \theta)/\text{d}\theta$ is negative, and so $g_{\text{an}}(n_{\text{r}}, \kappa\rho)$ is positive. With the increase of $\kappa\rho$, the surface temperature gradient changes its sign (Fig. 4), and $g_{\text{an}}(n_{\text{r}}, \kappa\rho)$ goes through zero in the range $\kappa\rho \sim 0.1$–0.3 and then stays positive. According to Eqs. 7 and 8, the product $b_{\text{th}} g_{\text{an}}(n_{\text{r}}, \kappa\rho)$ defines the magnitude and the sign of photothermophoretic velocity of a particle, while the product $g_{\text{an}}(n_{\text{r}}, \kappa\rho)\kappa\rho$ describes the variation of indirect photophoretic force with particle parameters, according to Eq. 5. For liquid droplets $b_{\text{th}} > 0$, according to Eq. 7. Therefore, for small values of $\kappa\rho$, the indirect photophoretic force acting on a droplet is positive, i.e., parallel to the light propagation vector. With the increase of $\kappa\rho$, it goes through zero and becomes negative (antiparallel to the light direction). The situation is just the opposite with solid particles in an electrolyte solution. Here, b_{th} is negative;[10] consequently, the indirect photophoretic force is negative for $\kappa\rho \ll 1$, goes through zero in the range $\kappa\rho \sim 0.1$–0.3, and then stays positive and increases monotonically for $\kappa\rho > 0.5$, saturating at very high $\kappa\rho$ values ~ 40.[10]

Thus, the analysis shows a pronounced dependence of indirect photophoretic force on the size, optical, and thermophysical properties of particles. It is essential that this force is always accompanied by direct light pressure and, for non-homogeneous light beams, by the gradient force. So, the question of their proportion arises. The estimates for large absorbing solid particles ($2a \sim 5 \times 10^{-5}$ m, $\kappa \sim 0.1$) show that the photothermophoretic force could be comparable to the light pressure.[10] What is more, experiments with various emulsions of oil/water or water/oil type containing resonantly absorbing additives to the dispersed phase demonstrated negative phoresis, i.e., the motion of liquid droplets toward the laser source.[21] The velocities measured were as high as 10 cm/s. This means that in the measuring conditions,[21] the indirect photophoretic force exceeded the light pressure substantially. These features of interrelation between direct and indirect photophoretic mechanisms further increase the potentialities of FFF applications, due to the variety of possible combinations.

A transparent particle in a strongly absorbing fluid

This limiting case is physically identical to common thermophoresis, however, with unusual temperature profile in the channel flow due to the specific way of heat production. According to FFF geometry, the light propagation

direction should be perpendicular to the transparent wall of a flat channel of width w_c. If the absorption coefficient of the carrier fluid, κ_f is high enough, $w_c\kappa_f > 1$, the heat source function $B(z)$, and hence the heat production, is localized mainly near the illuminated wall. The exact solution for the transverse temperature profile in the channel can be obtained numerically, using the equation of convective heat transfer with the source function $B(z)$ and the Navier–Stokes equation. In these equations, the temperature dependence of fluid viscosity should be taken into account. Qualitatively, for $w_c\kappa_f > 1$, the temperature profile has a small rise and the maximum near the illuminated wall, followed by a steep decay toward the rear wall. Thus, near the less heated ("cold") wall of a channel, where the particles are accumulated usually in conventional Thermal FFF, this profile is quite similar to the conventional one. However, in the photophoretic arrangement discussed, particles will be pressed additionally against the "cold" wall by the light pressure.

OBSERVATIONS AND USE OF PHOTOPHORETIC EFFECTS

Systematic experimental studies of direct and indirect photophoretic mechanisms of particle and droplet motion in fluids have not been conducted yet. However, some data are available on characteristic velocities and their dependence on the size, refractive index, and absorption coefficient of irradiated objects.[10,11,21–23] For fluid droplets, both negative (in the case of high absorption[21]) and positive (for transparent droplets[22]) photophoresis has been observed. This is in agreement with the theory of indirect photophoresis reviewed above. For nine oil-in-water emulsion systems with droplet size 1–5 μm studied in,[22] the positive photophoretic velocity of a droplet was found to be linearly proportional to the droplet radius, and almost linearly dependent on the refractive index of the droplet substance in the range $n_r n_0 = 1.42$–1.59. Typical velocities were 5–20 μm/s at a CW Nd:YAG ($\lambda_0 = 1064$ nm) laser power of 100–300 mW focused into the beam with $w_0 \sim 20$ μm.

For solid particles, both transparent and absorbing ones, in water, only positive photophoresis has been observed.[10,11,23] The relation between particle velocity u_{phth} (in μm/s) and laser beam intensity J_0 (in 10^7 W m^{-2}) was measured in Ref.[10] using an Ar^+-ion laser ($\lambda_0 = 514.5$ nm) power of 0.1–0.8 W focused into a beam with $w_0 \sim 40$ μm. The result was $u_{phth} \approx 1.1J_0$ for latex particles of 9.87 μm diameter with $m(589\text{ nm}) = 1.191$, and $u_{phth} \approx 4.8J_0$ for carbon black particles of ~ 12 μm diameter with $m(489\text{ nm}) = 1.27 - i \times 0.52$. The observed variation of velocity with particle size and optical constants[10] corresponded qualitatively to Eq. 4. The authors of Ref.[23] measured the size dependence of photophoretic velocity for polystyrene microparticles ($n_r n_0 = 1.59$) in water in the range $2a = 0.78$–2.84 μm, using a CW Nd:YAG ($\lambda_0 = 1064$ nm) laser power of 120 mW focused into a beam with $w_0 \sim 20$ μm. The size variation of $u_{phth} \sim 7$–37 μm/s was practically linear. It was also described rather well by Eq. 1, where the optical pressure efficiency $Q_{pr}(\varepsilon, \rho)$ was calculated using Mie theory.[23]

Therefore, both experimental observations and theoretical estimates of photophoretic effects show that particle velocities in the range 10–100 μm/s (depending on the particle material and the light intensity) can be easily achieved with focused laser radiation. These values are comparable with the flow velocities used in some FFF subtechniques,[2,17] and hence can be exploited for particle separation. Some initial studies have been done already, but, not in the classical FFF arrangement yet. In the experiments described in Ref.[10] the laser beam was focused onto the entrance glass window of a round metallic capillary in the direction of suspension flow inside the capillary. The elution curves for polydisperse carbon black particles were registered in the gravity-sedimentation FFF mode with the laser power switched on and off. Typical curves had a strong initial maximum corresponding to elution of small particle' fractions, and a considerably lower secondary maximum corresponding to large particles. The light action resulted in shape changes of elution curve, which evidenced the acceleration of the large particles along the flow.[10]

In another series of works (see Ref.[24] and the references therein), the laser beam was combined with a coaxial capillary flow in the opposite, i.e., counterflow, manner. That gave the possibility to balance the light pressure acting on the particle with the hydrodynamic drag force, and to nearly (or completely) arrest the particle movement along the axis. Another feature was that the gaussian beam waist ($z = 0$ in Eq. 2) was positioned at the capillary axis far from the entrance window. Due to the axial divergence of the gaussian beam Eq. 2, the light pressure F_{phll} acting on the particle depended on its axial position z (Eq. 4). As a result, the arresting points were different for particles of various sizes and/or optical properties, thus enabling particle separation. The separation process was monitored microscopically using a video system coupled with a CCD camera. A gradual reduction of laser power after achieving the separation permitted the elution of small to large particles. Particle size was calculated from the laser power corresponding to the fraction eluted. The authors called their technique "optical chromatography."[24]

POSSIBLE ARRANGEMENTS OF PHOTOPHORETIC FFF

The results[10,24] evidence that photophoretic effects can be used successfully for particle separation in the longitudinal field-flow geometry. The practical implementation of photophoretic FFF in the canonical transverse field-flow geometry requires high irradiance of a whole strip along a

transparent channel wall, instead of focusing light onto a spot. Estimates show that high enough levels of irradiance can be achieved for this purpose using some known arrangements for the optical pumping of lasers. Another way is to exploit the gradient photophoretic force generated in the carrier fluid by evanescent light waves at the boundary with the transparent channel wall, the latter acting as a waveguide for a pumping laser beam. Regardless of particular arrangement, photophoretic FFF techniques encounter another major problem: The transparency of the channel wall should not degrade substantially with time despite the permanent contact with the suspension flow and high irradiation levels. One of the most promising ways of practical implementation is the use of photophoretic force in combination with some counterbalancing force, primarily the gravitational force. That enables implementation of photophoretic FFF in the particle-focusing mode of operation. This mode is very efficient for particle separation.[1,2,17]

CONCLUSIONS

The use of photophoretic effects in FFF of particles is a very promising direction for the further development of this separation method, offering a broad field of practical applications. As the theoretical overview has demonstrated, these effects are influenced by the remarkable diversity of particles' material properties, including geometrical, optical, and thermophysical characteristics. The use of these effects offers a unique possibility of including the optical properties of particles and molecules in the nomenclature of separation parameters. It promises to exploit the high spectral selectivity, in particular the resonant character, of light pressure exerted upon some solid state and molecular structures, to separate species identical in their density and geometry parameters. Such selectivity can be achieved in several ways: first, by exploiting the intrinsic optical properties of the species, and second, using special preparative procedures, such as selective staining of species, or their chemical and immunological binding to special carrier particles (molecules), having appropriately designed optical characteristics and serving as a kind of photonic tug.

The overview of experimental investigations of photophoresis of particles and droplets in fluids shows that particle velocities large enough for separation purposes can be readily achieved with the modern techniques of light generation. Based on these theoretical and experimental fundamentals, the analysis of some possible arrangements of photophoretic FFF leads to the conclusion that the practical implementation of this novel FFF subtechnique is quite realistic. The implementation of photophoretic FFF may possibly have a general impact on the further development of this separation method. With the present instrumental realizations, FFF is accomplished mainly using macroscopically designed external fields, such as the acceleration field or external temperature gradient and, in this sense, separation channels with "macroscopic" dimensions. The new concepts of optical trapping and micromanipulation of particles,[25] together with modern optical technologies and technologies of channels microfabrication, offer quite novel approaches in FFF, based on microscopically designed optical fields. Such approaches, apart from new separation possibilities, may lead to substantial miniaturization of FFF instruments, and to operation with microscopic samples—in other words, to FFF implementation at the microscopic level.

REFERENCES

1. Giddings, J.C. Field-flow fractionation. Chem. Eng. News **1988**, *66*, 34–45.
2. Martin, M. Theory of field flow fractionation. In *Advances in Chromatography*; Brown, P.R., Grushka, E., Eds.; Marcel Dekker, Inc.: New York, 1998; Vol. 39, 1–138.
3. Van de Hulst, H.C. *Light Scattering by Small Particles*; Dover Publications, Inc.: New York, 1981.
4. Bohren, C.F.; Huffman, D.R. *Absorption and Scattering of Light by Small Particles*; Interscience: New York, 1983.
5. Gouesbet, G.; Maheu, B.; Grehan, G. Light scattering from a sphere arbitrarily located in a Gaussian Beam, using a Bromwich formulation. J. Opt. Soc. Am. A, **1988**, *5* (9), 1427–1443.
6. Ashkin, A. Applications of laser radiation pressure. Science **1980**, *210* (4474), 1081–1088.
7. Ashkin, A. Forces of a single-beam gradient laser trap on a dielectric sphere in the ray optics regime. Biophys. J. **1992**, *61* (2), 569–582.
8. Liebert, R.B.; Prieve, D.C. Forces exerted by a laser beam on a microscopic sphere in water: Designing for maximum axial force. Ind. Eng. Chem. Res. **1995**, *34* (10), 3542–3550.
9. Kats, A.V. The radiation force acting upon a particle in an electromagnetic field with an arbitrary ratio of particle size and field wavelength. Sov. Radiophys. J. **1975**, *18* (4), 566–576. (in Russian).
10. Kononenko, V.L.; Shimkus, J.K.; Giddings, J.C.; Myers, M.N. Feasibility studies on photophoretic effects in field-flow fractionation of particles. J. Liq. Chromatogr. Relat. Technol. **1997**, *20* (16 & 17), 2907–2929.
11. Kononenko, V.L.; Giddings, J.C.; Myers, M.N. On the possibility of photophoretic field-flow fractionation. J. Microcolumn Sep. **1997**, *9* (4), 321–327.
12. Dusel, P.W.; Kerker, M.; Cooke, D.D. Distribution of absorption centers within irradiated spheres. J. Opt. Soc. Am. **1979**, *69* (1), 55–59.
13. Chylek, P.; Pendleton, J.D.; Pinnick, R.G. Internal and near-surface scattered field of a spherical particle at resonant conditions. Appl. Opt. **1985**, *24* (23), 3940–3942.
14. Hill, S.C. Morphology-dependent resonances. In *Optical Effects Associated with Small Particles*; Barber, P.W., Chang, R.K., Eds.; World Scientific Publications: Singapore, 1988; 3–61.

15. Chowdhury, D.Q.; Barber, P.W.; Hill, S.C. Energy-density distribution inside large nonabsorbing spheres by using Mie theory and geometrical optics. Appl. Opt. **1992**, *31* (18), 3518–3523.
16. Kononenko, V.L.; Shimkus, J.K. Photophoresis of large absorbing particles in a transparent liquid. Colloid J. **1997**, *59* (5), 609–619.
17. Janča, J. *Field-Flow Fractionation*; Marcel Dekker, Inc.: New York, 1988.
18. Levich, V.G.; Krylov, V.S. Surface-tension-driven phenomena. Ann. Rev. Fluid Mech. **1969**, *1*, 293–316.
19. Anderson, J.L. Colloid transport by interfacial forces. Ann. Rev. Fluid Mech. **1989**, *21*, 61–99.
20. Yong, N.O.; Goldstein, J.S.; Block, M.J. The motion of bubbles in a vertical temperature gradient. J. Fluid Mech. **1959**, *6*, 350–356.
21. Sukhodol'skii, A. T. Light-capillary phenomena. Bull. Acad. Sci. USSR. Phys. Ser. **1986**, *50* (6), 51–57.
22. Hirai, A.; Monjushiro, H.; Watarai, H. Laser photophoresis of a single droplet in oil in water emulsions. Langmuir **1996**, *12* (23), 5570–5575.
23. Monjushiro, H.; Hirai, A.; Watarai, H. Size dependence of laser-photophoretic efficiency of polystyrene microparticles in water. Langmuir **2000**, *16* (22), 8539–8542.
24. Makihara, J.; Kaneta, T.; Imasaka, T. Optical chromatography. Size determination by eluting particles. Talanta **1999**, *48* (3), 551–557.
25. Dholakia, K., Spalding, G.C., Eds.; *Optical Trapping and Optical Micromanipulation, Proceedings of* SPIE SPIE; 2004; Vol. 5514.

pH-Peak-Focusing and pH-Zone-Refining CCC

Yoichiro Ito
National Heart, Lung, and Blood Institute (NHLBI), National Institutes of Health (NIH), Bethesda, Maryland, U.S.A.

Hisao Oka
Food-Related Chemistry, Laboratory of Chemistry, Aichi Prefectural Institute of Public Health, Nagoya, Japan

INTRODUCTION

These two countercurrent chromatography (CCC) techniques are mutually related: pH-peak-focusing CCC is for analytical-scale separations and pH-zone-refining CCC is for preparative-scale separations.

DISCUSSION

The pH-peak-focusing CCC technique was developed from an accidental finding that a thyroxine analog produced an unusually sharp elution peak.[1,2] The cause was found that an acid present in the sample solution affected the retention time of the analyte (Fig. 1A). The mechanism of this peak-sharpening effect is shown in Fig. 1B, where a portion of the separation column contains the organic stationary phase in the upper half and the aqueous mobile phase in the lower half. Because of its non-linear isotherm, the acid in the sample solution forms a sharp trailing border which traps the analyte in the following manner: When the analyte molecule is present in the mobile phase (position 1), it is protonated by low pH and transferred into the organic stationary phase (position 2). As the sharp acid border moves forward, the analyte molecule is exposed to high pH (position 3), deprotonated, and transferred back to the aqueous mobile phase (position 4), where it quickly migrates through the acid border to repeat the above cycle. Consequently, the analyte molecules are trapped with the sharp acid border and eluted as a sharp peak, together with the acid border. A similar effect can be produced by introducing an organic acid in the stationary phase.

Fig. 2A shows the separation of DNP-amino acids using three spacer acids (i.e., acetic acid, propionic acid, and *n*-butyric acid) in the stationary phase.[2] Hydrophilic DNP-glutamic acid is eluted between acetic and propionic acids; DNP-alanine between propionic and *n*-butyric acids, and hydrophobic DNP-leucine after *n*-butyric acid. The method can be effectively applied for the separation and concentration of a small amount of organic ions present in a large volume of the sample solution. However, the most useful application has been found in the preparative-scale separation. When the sample size of the above DNP-amino acids is increased each from 6 mg to 600 mg, a strange chromatogram was produced as shown in Fig. 2B, where all peaks became rectangular in shape, each associated with its own specific pH. The elimination of the spacer acids resulted in the fusion of

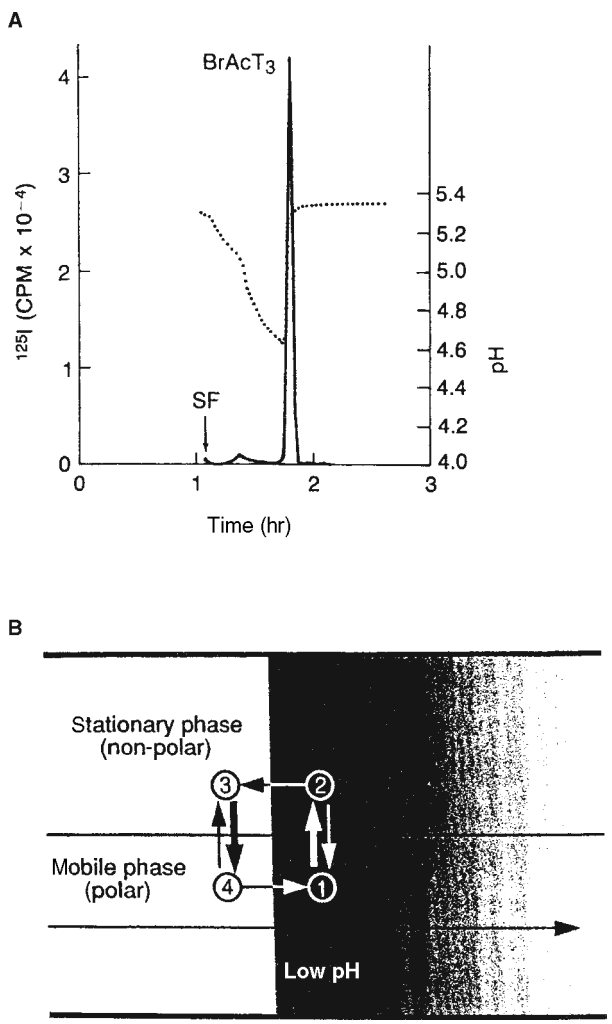

Fig. 1 A, Sharp analyte peak produced by an acid in the sample solution; and B, mechanism of sharp peak formation.

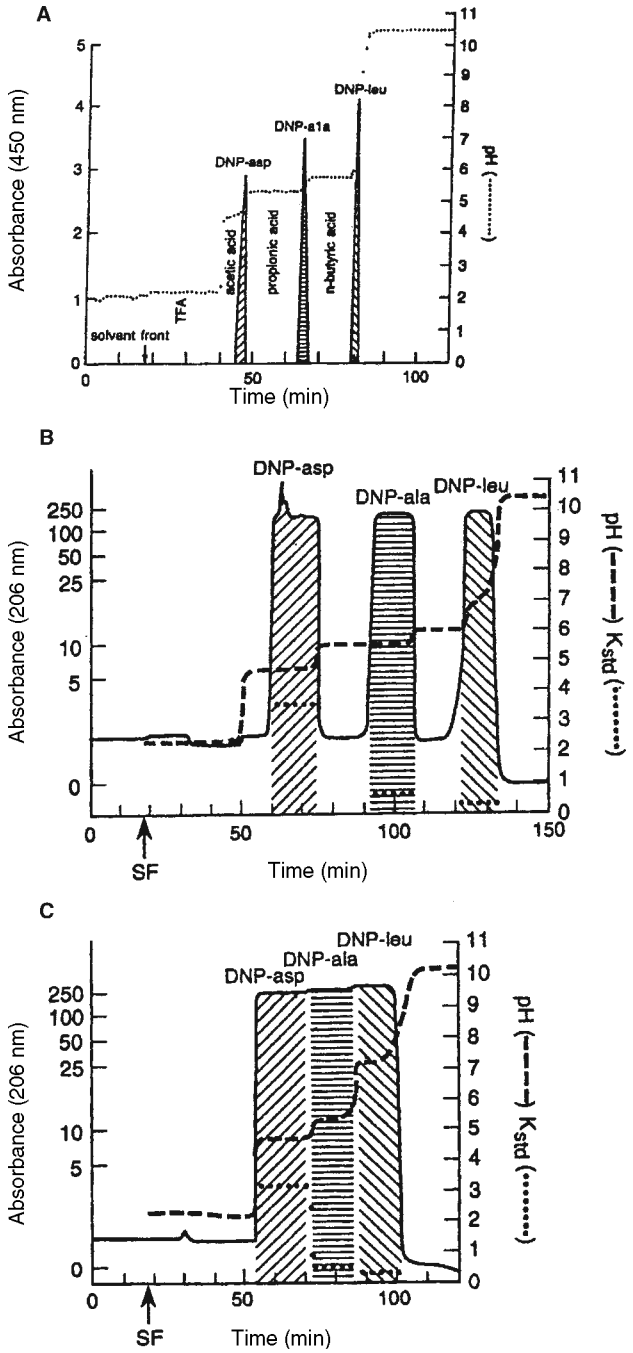

Fig. 2 Separation of three DNP-amino acids showing a transition from pH-peak-focusing CCC to pH-zone-refining CCC. A, Analytical separation by pH-peak-focusing CCC (6 mg each component); B, formation of rectangular peaks by increasing sample size (600 mg each component); and C, elimination of three spacer acids to form fused rectangular peaks.

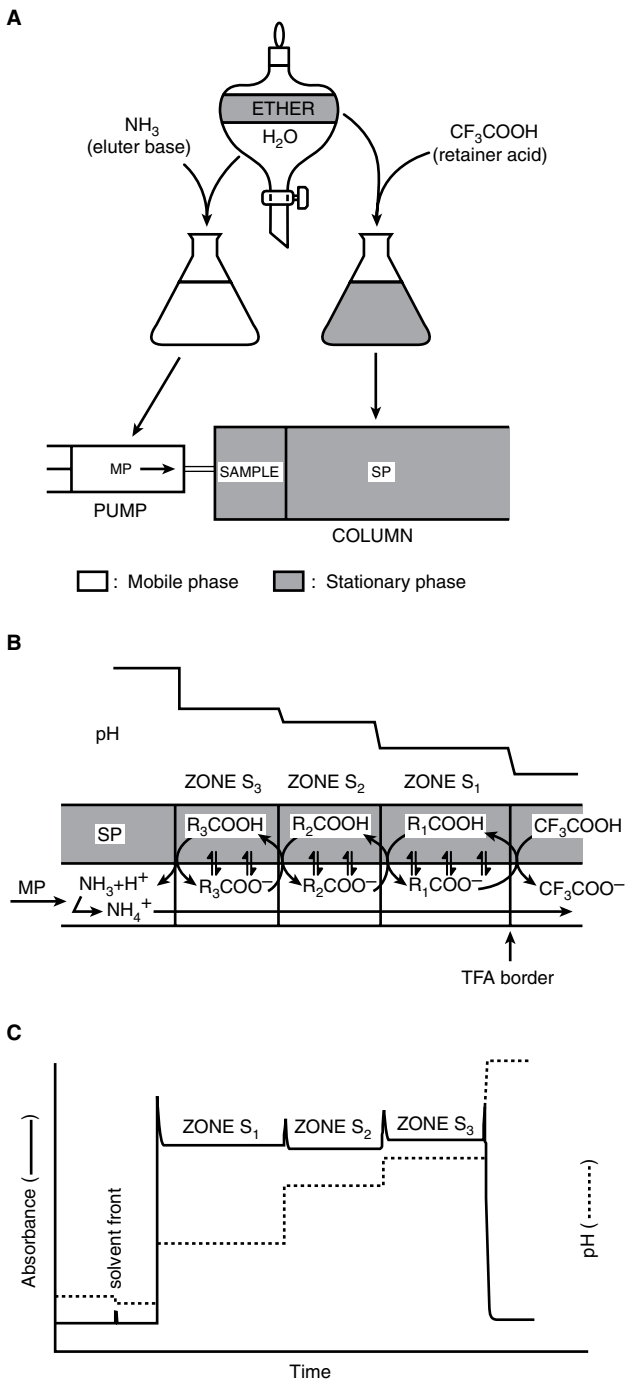

Fig. 3 Mechanism of pH-zone-refining CCC. A, Preparation for the model experiment; B, chemohydrodynamic equilibrium in the separation column; and C, elution profile of three major analytes.

these peaks while maintaining their own pH, suggesting that the rectangular shape of each peak is well preserved (Fig. 2C).[2–4]

The mechanism of this pH-zone-refining CCC (for the separation of acidic compounds) is illustrated by the following model experiment.[2,4,5] Fig. 3A shows the preparation of the solvent phases. Ether and water are equilibrated in a separatory funnel and separated. A suitable amount (usually 10–40 m*M*) of TFA (trifluoroacetic acid) ("retainer") is added to the lighter organic phase, which is then used as the stationary phase. Ammonia (10–40 m*M*) ("eluter") is added to the heavier aqueous phase, which is used as the mobile phase. The experiment

is initiated by filling the entire column with the stationary phase, followed by injection of a sample solution containing three major acidic analytes and then, the column is eluted with the mobile phase while the apparatus is rotated at a desired g-force. Fig. 3B shows steady-state chemohydrodynamic equilibrium established in the separation column. The retainer acid TFA forms a sharp trailing border which travels through the column at a constant rate substantially lower than that of the mobile phase.

Three analytes S_1, S_2, and S_3 each form a discrete pH zone behind the sharp retainer border in the order of their pK_a's and hydrophobicities. The proton transfer takes place at each zone boundary according to the difference in pH between the neighboring zones, causing solute exchange between the two phases, as indicated by curved arrows. Once the equilibrium is established, all solute zones move at a same rate determined by that of the sharp retainer border. Charged impurities present in each zone are eliminated either forward or backward according to their pK_a's and hydrophobicities, and accumulated at the zone boundaries. Consequently, the analytes are eluted as fused rectangular peaks with minimum pK_a overlap associated with sharp impurity peaks at their boundaries (Fig. 3C).

The relationship between the zone pH (pH_{zone}) and pK_a in the present method is given by the following equation:[2,4,5]

$$\mathrm{pH}_{\mathrm{zone}} = \mathrm{p}K_{\mathrm{a}} + \log\left(\frac{K_D}{K} - 1\right) \quad (1)$$

where K_D and K indicate the distribution coefficient (an indicator for hydrophobicity) and distribution ratio of the analytes, respectively. When the pK_a and K_D of the analyte are known, the zone pH can be computed from the K value.

Table 1 Samples and solvent systems applied to standard pH-zone-refining CCC.

Sample[a]	Solvent system[b] (vol. ratio)	Pair of acid–base reagents[c]	
		Retainer	Eluter
DNP-Amino acids	MBE/AcN/H_2O (4 : 1 : 5)	TFA (200 μl/SS)	NH_3 (0.1%/MP)
Proline (OBzl) (1 g)	MBE/H_2O	TEA (10 m*M*/SP)	HCl (10 m*M*/MP)
Amino acid (OBzl) (0.7 g)	MBE/H_2O	TEA (10 m*M*/SP)	HCl (10 m*M*/MP)
Amino acid (OBzl)) (10 g)	MBE/H_2O	TEA (5 m*M*/SP)	HCl (20 m*M*/MP)
CBZ dipeptides (0.8 g)	MBE/AcN/H_2O (2 : 2 : 3)	TFA (16 m*M*/SP)	NH_3 (5.5 m*M*/MP)
CBZ dipeptides (3 g)	MBE/AcN/H_2O (2 : 2 : 3)	TFA (16 m*M*/SP)	NH_3 (5.5 m*M*/MP)
CBZ tripeptides (0.8 g)	BuOH/MBE/AcN/H_2O (2 : 2 : 1 : 5)	TFA (16 m*M*/SP)	NH_3 (2.7 m*M*/MP)
Dipeptide-(0.3 g)	MBE/AcN/H_2O (2 : 2 : 3)	TEA (5 m*M*/SP)	HCl (5 m*M*/MP)
Indole auxins (1.6 g)	MBE/H_2O	TFA (0.04%/SP)	NH_3 (0.1%/MP)
TCF (0.01–1 g)	DEE/AcN/10 m*M* $AcONH_4$ (4 : 1 : 5)	TFA (200 μl/SS)	MP
Red #3 (0.5 g)	DEE/AcN/10 m*M* $AcONH_4$ (4 : 1 : 5)	TFA (200 μl/SS)	MP
Orange #5 (0.01–5 g)	DEE/AcN/10 m*M* $AcONH_4$ (4 : 1 : 5)	TFA (200 μl/SS)	MP
Orange #10 (0.35 g)	DEE/AcN/10 m*M* $AcONH_4$ (4 : 1 : 5)	TFA (200 μl/SS)	MP
Red #28 (0.1–6 g)	DEE/AcN/10 m*M* $AcONH_4$ (4 : 1 : 5)	TFA (200 μl/SS)	MP
Eosin YS (0.3 g)	DEE/AcN/10 m*M* $AcONH_4$ (4 : 1 : 5)	TFA (200 μl/SS)	MP
Amaryllis alkaloids (3 g)	MBE/H_2O MBEH_2O (DPCCC)	TEA (5 m*M*/SP) HCl (10 m*M*/SP)	HCl (5 m*M*/MP) TEA (10 m*M*/MP)
Vinca alkaloids (0.3 g)	MBE/H_2O (DPCCC)	HCl (5 m*M*/SP)	TEA (5 m*M*/MP)
Structural isomers (15 g)	MBE/AcN/H_2O (4 : 1 : 5)	TFA (0.32%/SP)	NH_3 (0.8%/MP)
Stereoisomers (0.4 g)	Hex/EtOAc/MeOH/H_2O (1 : 1 : 1 : 1)	TFA, octanoic acid	NH_3 (0.025%/MP)
Fish oil (0.5 g)	Hex/EtOAc/H_2O (4 : 1 : 5)	TFA (10 m*M*/SP)	NH_3 (0.1%/MP)
NDGA derivatives (10 g)	MBE/H_2O	TFA (25 m*M*/SP)	NaOH (100 m*M*/MP)

[a]DNP: dinitrophenyl; CBZ: carbobenzoxy; OBzl: benzylesters; bNA: naphthyl amide; TCF: tetrachlorofluorescein; amaryllis alkaloids: crinine, powelline, and crinamidine; vinca alkaloids: vincamine and vincine; structural isomers: 2- and 6-nitro-3-acetamido-4-chlorobenzoic acid; stereoisomers: 4-methoxymethyl-1-methyl-cyclohexane carboxylic acid; fish oil: mixture of docosahexaenoic acid and eicosapentaenoic acid; NDGA: nordihydroguaiaretic acid.

[b]The upper organic phase was used as the stationary phase (SP) and the lower aqueous phase as the mobile phase (MP), except in DPCCC, where the relationship is reversed MBE: methyl-*t*-butyl ether; AcN: acetonitrile; BuOH: *n*-butanol; Hex: hexane; EtOAc: ethyl acetate; MeOH: methanol; $AcONH_4$ ammonium acetate; DEE: diethyl ether; DPCCC: displacement mode.

[c]TFA: trifluoroacetic acid; AcOH: acetic acid; SP: in stationary phase; MP: in mobile phase; SS: in sample solution; TEA: triethylamine.

Table 2 Samples and solvent systems applied to affinity pH-zone-refining CCC.

Sample[a]	Solvent systems[b] (vol. ratio)	Set of key reagents[c]		
		Retainer	Eluter	Ligand
(±)-DNB-leucine (2 g)	MBE/H_2O	TFA (40 m*M*/SP)	NH_3 (20 m*M*/MP)	DPA (40 m*M*/SP)
(±)-DNB-valine (2 g)	MBE/H_2O	TFA (40 m*M*/SP)	NH_3 (20 m*M*/MP)	DPA (40 m*M*/SP)
Catecholamines (3 g)	MBE/H_2O	NH_4OAc (200 m*M*/SP)	HCl (50 m*M*/MP)	DEHPA (20%/SP)
Dipeptides (1 g) (hydrophobic)	MBE/AcN/50 m*M* HCl 4 : 1 : 5 (SP) MBE/AcN/H_2O (4 : 1 : 5) (MP)	TEA (20 m*M*/SP)	HCl (20 m*M*/MP)	DEHPA (10%/SP)
Dipeptides (1 g) (hydrophilic)	MBE/BuOH/AcN/50 m*M* HCl (2 : 2 : 1 : 5) (SP) MBE/BuOH/AcN/H_2O (2 : 2 : 1 : 5) (MP)	TEA (20 m*M*/SP)	HCl (20 m*M*/MP)	DEHPA (30%/SP)
Bacitracins (5 g)	MBE/50 m*M* HCl (1 : 1)(SP) MBE/H_2O (MP)	TEA (40 m*M*/SP)	HCl (20 m*M*/MP)	DEHPA (10%/SP)
FD&C Yellow #6 (2 g)	MBE/AcN/H_2O (2 : 2 : 3)	H_2SO_4 (0.2%/SP)	NH_3 (0.4%/MP)	TDA (5%/SP)

[a]DNB: dinitrobenzoyl.
[b]MBE: methyl *t*-butyl ether; AcN: acetonitrile; BuOH: *n*-butanol.
[c]TFA: trifluoroacetic acid; ammonium acetate; TEA: triethylamine; DPA: *N*-dodecanoyl-L-proline-3,5-dimethylanilide; DEHPA: di-(2-ethylhexyl) phosphoric acid; TDA: tridodecylamine; SP: organic stationary phase; MP: aqueous mobile phase.

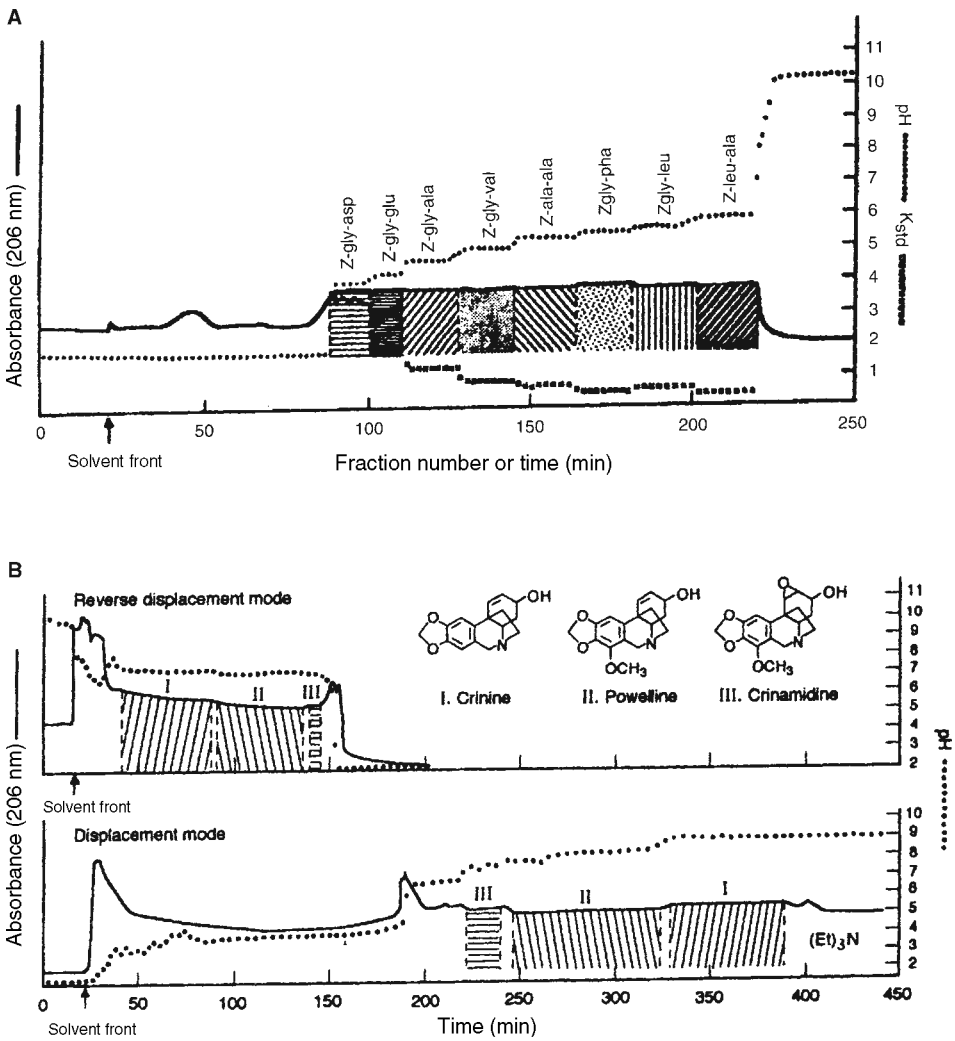

Fig. 4 Some applications of pH-zone-refining CCC. A, Separation of eight CBZ dipeptides (see Table 1);[4,8] B, separation of amaryllis alkaloids using both the lower phase (upper chromatogram) and upper phase (lower chromatogram) as the mobile phase (see Table 1);[4,9] C, separation of catecholamines using a ligand (see Table 2);[4,12] and D, separation of two groups of dipeptide each using an affinity ligand,[4,13] (see Table 2).

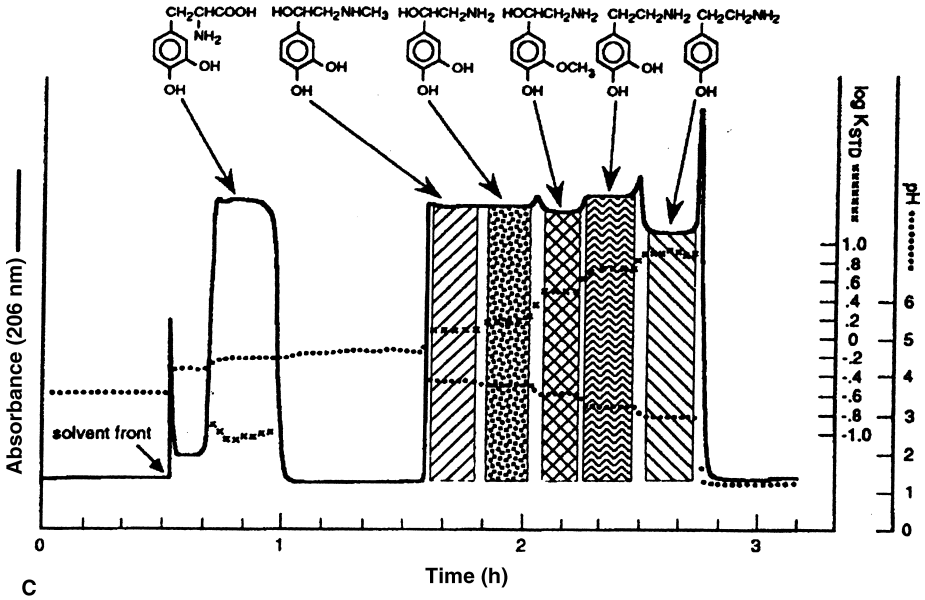

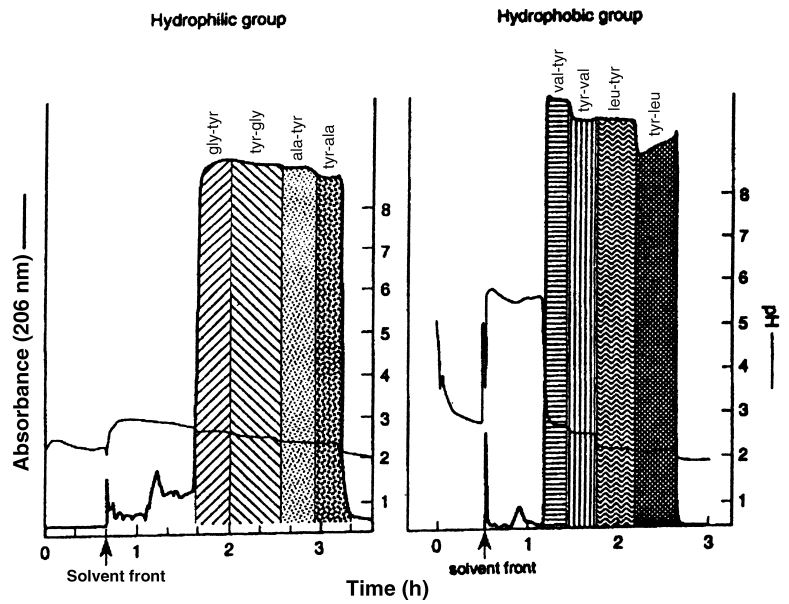

Fig. 4 (*Continued*)

The pH-zone-refining CCC technique shares many unique features with displacement chromatography[6] and has several important advantages over the standard CCC technique such as (a) large sample-loading capacity, (b) highly concentrated fractions, (c) concentration and detection of minor impurities, and (d) monitoring the effluent by pH. The method has been successfully applied to the separation of various organic acids and bases, including the derivatives of amino acids[4,7] and peptides,[8] alkaloids,[4,9] hydroxyxanthene dyes,[3,4,10] anti-human immunodeficiency virus lignans,[11] indole auxins,[4] structural and stereoisomers,[4] and so forth. (Table 1). By being analogous to affinity chromatography, the method allows the use of an affinity ligand dissolved in the liquid stationary phase for separations of special analytes, including highly polar compounds such as catecholamines,[4,12] and sulfonated dyes,[4] enantiomers,[4] and zwitterions such as free peptides,[4,13] (Table 2). Fig. 4A and B illustrates a few examples of these applications.

REFERENCES

1. Ito, Y.; Shibusawa, Y.; Fales, H.M.; Cahnmann, H.J. Studies on an abnormally sharpened elution peak observed in counter-current chromatography. J. Chromatogr. **1992**, *625*, 177–181.

2. Ito, Y. pH-peak-focusing and pH-zone-refining countercurrent chromatography. In *High-Speed Countercurrent Chromatography*; Ito, Y., Conway, W.D., Eds.; Chemical Analysis Series Wiley–Interscience: New York, 1996; Vol. 132, 121–175.
3. Weisz, A.; Scher, A.L.; Shinomiya, K.; Fales, H.M.; Ito, Y. A new preparative-scale purification technique: pH-zone-refining countercurrent chromatography. J. Am. Chem. Soc. **1994**, *116*, 704–708.
4. Ito, Y.; Ma, Y. pH-zone-refining countercurrent chromatography. J. Chromatogr. A, **1996**, *753*, 1–36.
5. Ito, Y.; Shinomiya, K.; Fales, H.M.; Weisz, A.; Scher, A.L. pH-zone-refining countercurrent chromatography: a new technique for preparative separation. In *ACS Monograph on Modern Countercurrent Chromatography*; Conway, W.D., Petroski, R.J., Eds.; 1995; 154–183.
6. Horvath, C.; Nahum, A.; Frens, J.H. High-performance displacement chromatography. J. Chromatogr. **1981**, *218*, 365.
7. Ma, Y.; Ito, Y. Separations of basic amino acid benzyl esters by pH-zone-refining counter-current chromatography. J. Chromatogr. A, **1994**, *678*, 233–240.
8. Ma, Y.; Ito, Y. Separation of peptide derivatives by pH-zone-refining counter-current chromatography. J. Chromatogr. A, **1995**, *702*, 197–206.
9. Ma, Y.; Ito, Y.; Sokoloski, E.; Fales, H.M. Separation of alkaloids by pH-zone-refining counter-current chromatography. J. Chromatogr. A, **1994**, *685*, 259–262.
10. Weisz, A. Separation and purification of dyes by conventional countercurrent chromatography and pH-zone-refining countercurrent chromatography. In *Countercurrent Chromatography*; Ito, Y., Conway, W.D., Eds.; Chemical Analysis Series Wiley–Interscience: New York, 1996; Vol. 132, 337–384.
11. Ma, Y.; Qi, L.; Gnabre, J.N.; Huang, R.C.C.; Chou, F.E.; Ito, Y. J. Liq. Chromatogr. **1998**, *21*, 171–181.
12. Ma, Y.; Socoloski, E.; Ito, Y. pH-zone refining countercurrent chromatography of polar catecholamines using di-(2-ethylhexyl)phosphoric acid as a ligand. J. Chromatogr. A, **1996**, *724*, 348–353.
13. Ma, Y.; Ito, Y. Peptide separation by pH-zone-refining countercurrent chromatography. J. Chromatogr. A, **1997**, *771*, 81–88.

Planar Chromatography: Automation and Robotics

Wojciech Markowski
Department of Inorganic and Analytical Chemistry, Medical University of Lublin, Lublin, Poland

INTRODUCTION

Automation involves the use of systems (instruments) in which an element of non-human decision has been interpolated. It is defined as the use of combinations of mechanical and instrumental devices to replace, refine, extend, or supplement human actions and faculties in the performance of a given process, in which at least one major operation is controlled, without human intervention, by a feedback system. A feedback system is defined as an instrumental device combining sensing and commanding elements that can modify the performance of a given act.[1]

Three approaches to the automation process can be distinguished, taking into account the criterion of flexibility of the automation device.[2,3] The first, denoted as flexible, is characterized by the possibility of adaptation of the instruments to new and varying demands required from the laboratory; examples of these instruments are robots. The second approach, denoted as semiflexible, involves some restrictions for the tasks executed by the instrument; the tasks are controlled by software via a keyboard. As examples, autosamplers or robots of limited capacity can be cited. In the third approach, the instruments can execute one or two tasks, without the possibility of adapting to new requirements; examples include supercritical fluid extractors and diluters. Automation of an analytical laboratory gives several benefits: better reproducibility, increase in the number of samples that can be analyzed, and freedom of personnel to do more creative tasks (e.g., method development and interpretation of results). Harmful conditions in the laboratory or other workplace can be avoided, and the equipment of the laboratory can be more effectively utilized. Automation improves worker safety and product quality. It provides exact timing and uniform sample handling, which ensure precision and accuracy. It allows for the transfer of methods from one laboratory to another, since the methods are saved on any medium (diskette, CD), and they can be executed by instruments that are identical wherever they are implemented. Before illustration of the possibility of automation in thin-layer chromatography (TLC), let us consider the ideal, fully automated analytical laboratory. In such a laboratory, the sample is processed from its entry into the laboratory hopper, through the many operations until the final report is printed out and the sample is stored for future analysis. To illustrate the feasibility of automation in TLC,[4] the fundamental operations in an analytical laboratory, including the chromatographic process, are given in Fig. 1. The first and basic stage of the process, not limited to TLC, but also occurring in other chromatographic techniques, is the preparation of samples. This is the most tedious, time-consuming, and error-generating process in the whole analytical cycle and can be fully automated, or the automated stations may be complementary to operations or tasks executed individually. For instance, in a station, a volume of liquid is transferred from the first to a second container, an internal standard is added, and the solution is diluted and mixed. Further actions may be executed manually. Another, more advanced solution consists in automated execution of the tasks by the station, and the sample is transferred from one station to the other by a robot or another transport device. In a limited version, only the most critical stages are automated by the use of robots with limited, strictly defined movements; examples are automated processes of solid-phase extraction (SPE), heating, and mixing. The robots are controlled by software and the operator chooses the suitable values of the parameters from given ranges (e.g., autosampler).

At the end of the procedures, with chromatographic methods as the last step, the raw data collected during chromatographic analysis are critically reviewed by specific software designed for this purpose. If the results are not as expected, samples will be available for repeated analysis.

PREPARATION OF PLATES

In most laboratories using planar chromatography, precoated plates are used in everyday practice. Self-coating plates should be considered when special layers are required and when suitable precoated plates are not available on the market. Another reason for the application of the self-coating procedure is the cost of precoated plates following from the very high throughput—number of analyzed samples—and the limited budget of most laboratories. Special layers contain silver nitrate, buffer components, or a mixture of adsorbents. A special case is when the binder used in a commercial precoated plate might interfere with detection. A self-prepared layer of good quality can be obtained by automatic coating. Fig. 2 presents an example of an automatic coating device.[5] The glass plates to be coated are conveyed underneath a hopper filled with the adsorbent suspension. The automatic TLC plate coater is supplied with a fixed gate for preset layers of 300 and 500 μm, an adjustable gate for layer

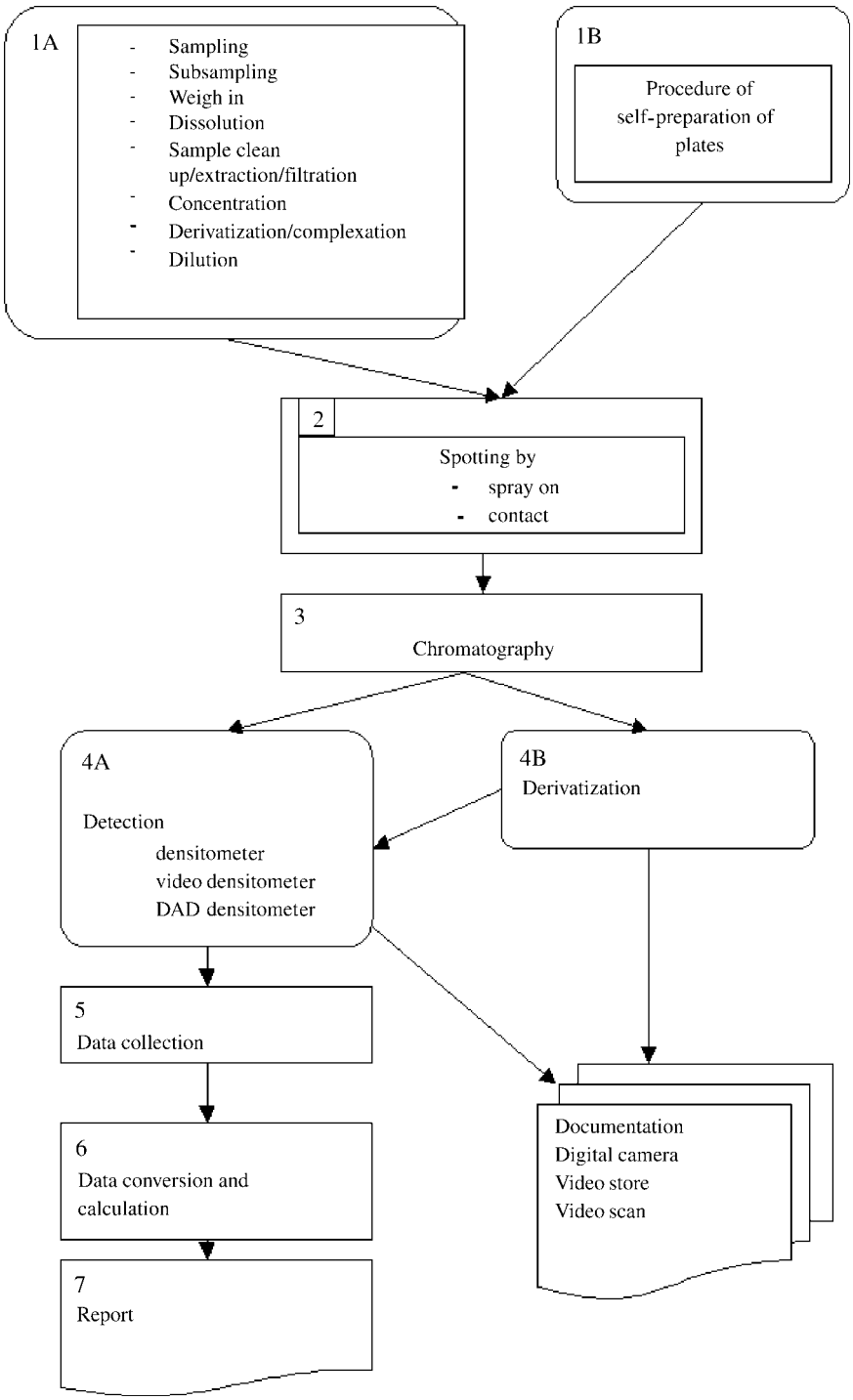

Fig. 1 Possible steps in an analytical laboratory for the process of automation.

thicknesses of 0–2 mm, and a plate holder for eight 20 × 20 cm plates. The plates are moved by a motorized conveying system at a uniform feed rate of 10 cm/sec to ensure a uniform layer.

SAMPLE APPLICATION

The selection of the sample application technique and the device to be used depends on sample volume, number of samples to be deposited, and precision and degree of automation required. During sample application, some minimum requirements must be fulfilled. The application of the sample onto the thin layer is a critical moment, owing to later localization by the scanner (densitometer) and the beginning of the chromatographic process at the moment of contact of the liquid sample with the chromatographic bed. There are two principal ways to deposit a sample onto the plate. They are contact spotting and spray-on application. Therefore, the applicator must

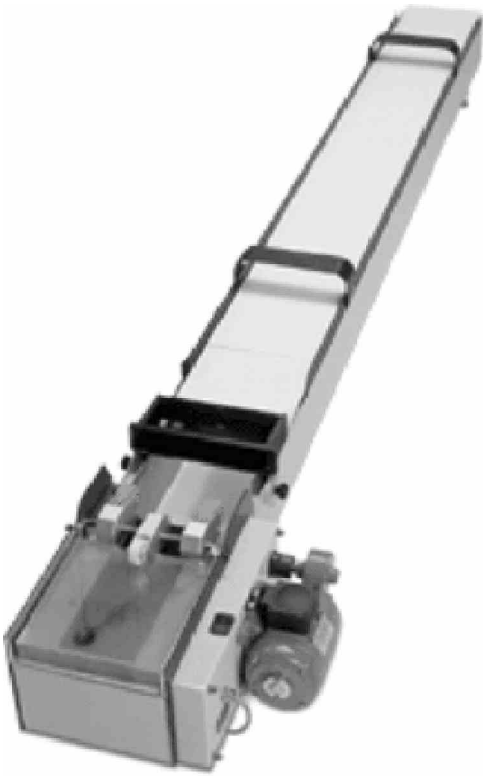

Fig. 2 Camag automatic TLC plate coater.
Source: Courtesy of Camag.[5]

guarantee the exact localization of the sample, particularly for quantitative analyses and uniform compact cross-section of the starting band. Typical values are from 1 to 4 mm for conventional layers (TLC), and for high-precision TLC (HPTLC) the upper limit is 1.5 mm. These demands limit the volume of sample applied to the layer. For TLC, the typical volume is from 0.5 to 5 μl but for HPTLC, typical volumes spotted can be from 0.1 to 1.0 μl. The above limitation is valid when samples are applied as spots. In the case when the spray-on technique (narrow bands) is used, there is possibility of the application of larger volumes. The simplest version of applicator is presented in Fig. 3 (Nanomat 4).[5] It serves for easy application of samples onto TLC and HPTLC plates or sheets, precisely positioned and without damage to the layer. The actual sample dosage is applied with disposable capillaries that are precisely guided by the universal capillary holder. Capillaries are loaded into the holder from dispenser magazines, then filled with sample solution and placed on the applicator head of the device. Capillary volumes of 0.5, 1, 2, and 5 μl are available. The volume precision is $R = \pm 0.25\%$, $CV = \pm 0.6\%$. The next stage with a more complicated degree of automation represents semiautomatic applicators. Semiautomatic applicators presently available have the volume range of 20 nl–10 μl (e.g., TLC—Spotter PS 01 Desaga). The sample is delivered from 0.5, 1.0, and 10 μl syringes. The piston stroke can be set in a continuous

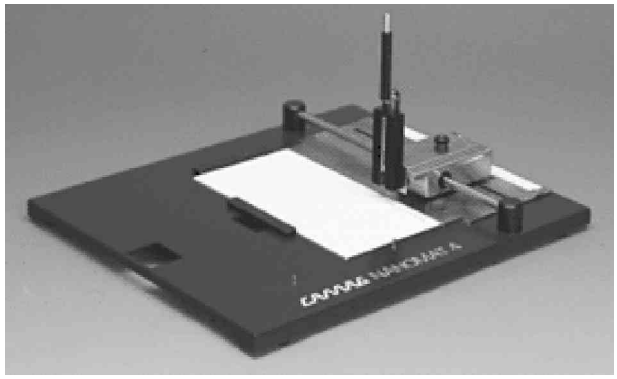

Fig. 3 Simplest automatic applicator (Nanomat 4).
Source: Courtesy of Camag.[5]

manner. To apply the sample, the piston is stopped and the solution is injected from the end of the capillary; the whole volume of the sample is displaced from the capillary. The position of the end of the capillary is adapted to the layer thickness; the spring-relieved syringe guide warrants that the capillary needle only lightly touches the adsorbent layer, avoiding damage to it. The change of position is automatic. The device permits application of spots or streaks at a distance of 5 mm from the edge of the plate; the syringe can be washed twice. The next step in automation is represented by Desaga TLC Applicator AS 30 or Camag Linomat 5. These automatic applicators can be operated in stand-alone mode or under the control of computer software. They are composed of an application module, interface, software, and an IBM PC-AT. The application module dispenses samples from a stainless-steel capillary that is connected to a dosage syringe operated by a stepping motor. Samples can be applied as spots or bands onto TLC plates or sheets up to 20×20 cm. Bandwise sample application uses the spray-on technique; for spotwise application, either contact transfer or spraying may be selected. The samples are contained in vials, which may be sealed with regular septa. The vials are arranged in racks with 16 positions; two racks may be inserted per application program. The application pattern can be selected for normal development, for development from both sides, and for circular and anticircular chromatography. Camag Automatic TLC Sampler 4 (ATS 4) meets all the requirements for fully automatic sample application (Fig. 4).[5] The device allows for both methods of application of samples and additionally for "overspotting," which can be used in prechromatographic derivatization, spiking, etc.

DEVELOPMENT OF THE CHROMATOGRAM

The next important stage is chromatogram development. Automatic developing chambers (Automatic Developing

Fig. 4 Full automatic applicator (ATS 4).
Source: Courtesy of Camag.[5]

Chamber, Camag), DC-MAT (Byron), and TLC-MAT (Desaga) are automatically operating development systems. They increase the reproducibility of the chromatographic results because the development is carried out under controlled conditions. The progress of the solvent front is monitored by a sensors. The development process is terminated as soon as the mobile phase has traveled the programmed distance. Preconditioning, tank or sandwich configuration, solvent migration distance, and the drying conditions are selectable. All relevant parameters are entered via a keypad. The AMD2 system (Automated Multiple Development, Camag)[5] is a fully automated version of multiple development and stepwise technique with a free choice of mobile-phase gradient (Fig. 5). Because the chromatogram is developed repeatedly in the same direction and each individual run is somewhat farther than the last, a focusing of the separated substance zones takes place in the direction of development. The chromatography is reproducible because the mobile phase is removed from the separation chamber after each step and the layer is completely freed from the mobile phase, in vacuum. Then, a fresh mobile phase is introduced for the next run. Provided all parameters, including solvent migration increments, are properly maintained, which is only possible with a fully automatic system, the densitogram of a chromatogram track can be superimposed with a matched-scale diagram of the gradient. Another device for automated development is the chamber constructed by Tyihak and Mincsovics,[6] in which the adsorbent layer is placed between two plates and the mobile phase flows under increased applied pressure. It can be operated in the linear or radial mode. Another automated device is the ultra-micro-rotation chromatograph (UMRC), where the eluent is delivered to the center of a rotating TLC plate.[7] A simple device was constructed by Delvordre, Reynault, and Postaire[8] in which the liquid is pumped out (by vacuum), which causes the flow of the mobile phase and decreases the vapor pressure.

DERIVATIZATION

Derivatization can be carried out both before and after development of the plate. In the latter case, it may be

Fig. 5 Device for automated multiple development (AMD2).
Source: Courtesy of Camag.[5]

Fig. 6 Chromatogram immersion device.
Source: Courtesy of Camag.[5]

applied before detection or after scanning densitometry. Derivatization may be carried out using the device constructed by Kreuzig (Anton Paar KG), where the sprayer moves along a vertical guide while the plate moves horizontally.[9] Another method of derivatization consists in immersion of the plate into a suitable reagent solution. For this purpose, devices available from Camag or Desaga can be used (Camag Chromatogram Immersion Device III, or Desaga TLC Dip-Fix), in which a low-velocity motor causes the immersion and removal of the plate from the reagent solution (Fig. 6).[5]

EVALUATION

Thin-film chromatographic detection, in contrast to other chromatographic techniques, requires stopping of development, drying of the layer, and scanning with an appropriate detector. There are basically two alternatives for the evaluation of thin-layer chromatograms: elution of the separated substance from the layer followed by photometric determination (indirect determination), and in situ evaluation (scanning) directly on the TLC plate. The in situ evaluation of the chromatogram is carried out using a high-resolution chromatogram spectrophotometer (densitometer) (Fig. 7) [5] to scan each chromatogram track, from start to solvent front in the direction of development, by means of a slit. The measurements are carried out either in the visible-light range for colored or fluorescent substances or in the ultraviolet (UV) range for UV-light-absorbing solutes. The wavelength of maximum absorption is generally selected as the measurement wavelength. The scanning process yields absorption or fluorescence scans (peaks), which are also used to assess the quality of chromatographic separation. TLC plates are generally scanned in the reflectance mode (diffuse reflectance), meaning that monochromatic light is directed by a mirror onto the layer surface at 90° and the diffuse reflectance is measured at 45° by means of a detector. The optical pathways used for absorption and fluorescence measurements are identical in commercially available scanners. The only difference is the light source : visible-light measurements are performed using tungsten lamps, whereas high-pressure mercury lamps are used for fluorescence measurements and deuterium lamps for absorption measurements in the UV range. In the case of fluorometric detection, it is also necessary to place a cutoff filter in front of the detector to prevent comeasurement of the short-wavelength excitation radiation. All functions of the scanner are controlled from a personal computer that is linked via an RS232 interface. The scanner transmits all measurement data, in digital form, to the computer for processing with the specific software. The final report is based on the following sequence: raw data acquisition, integration, calibration, and calculation. Integration is performed, post run, from the raw data gathered during scanning (i.e., after all tracks of a chromatogram plate have been measured). Integration results can be influenced by selecting appropriate integration parameters. As all measured raw data remain stored on a disk, reintegration with other parameters is possible at any time. The system automatically defines and corrects the baseline and sets fraction limits. The operator can accept these or override the automatic process by video integration. All steps can be followed on the screen. The option to get a "visual impression" of the chromatogram is one of the inherent advantages of planar chromatography over all other chromatographic techniques. White light is required for imaging colored chromatogram zones; long-wave UV light reveals fluorescing substances. Ultraviolet-absorbing substances can be visualized under short-wave UV light, provided the layer contains a UV indicator. The well-established lighting unit Camag Reprostar (Fig. 8) [5] provides all three types of light. Combined with a modern high-resolution digital camera, it forms an affordable documentation system for planar chromatograms and similar objects.

ROBOTS

Laboratory robots are adapted now for linking all of the steps between extraction and obtaining the analysis results. They are able to automate lengthy, routine, multistep analyses. They require electronic

Fig. 7 Densitometer linked with personal computer.
Source: Courtesy of Camag.[5]

communication in real time to know the operating time and possible breakdowns exactly. A robotics system allows space saving and easier integration of equipment in the laboratory. Today, a conventional robot has a movable arm. The purpose of the arm is to extend the capabilities of the human arm. There are five basic parts to every robotic arm: controller, arm, drive, end effector, and sensor. There are also five basic functions: base, shoulder, elbow, pitch, and roll. Most modern robots belong to one of four categories: Cartesian, spherical, and cylindrical robots, and revolute arms.[10] In 1989, Prosek et al.[4] developed a planar chromatography robot (Fig. 9). Its arm, supported by a rotating base, executed movements with four degrees of freedom. Its work envelope comprised four tanks: the first for cleaning, the second for development, and the last two for

Fig. 8 Video scanner.
Source: Courtesy of Camag.[5]

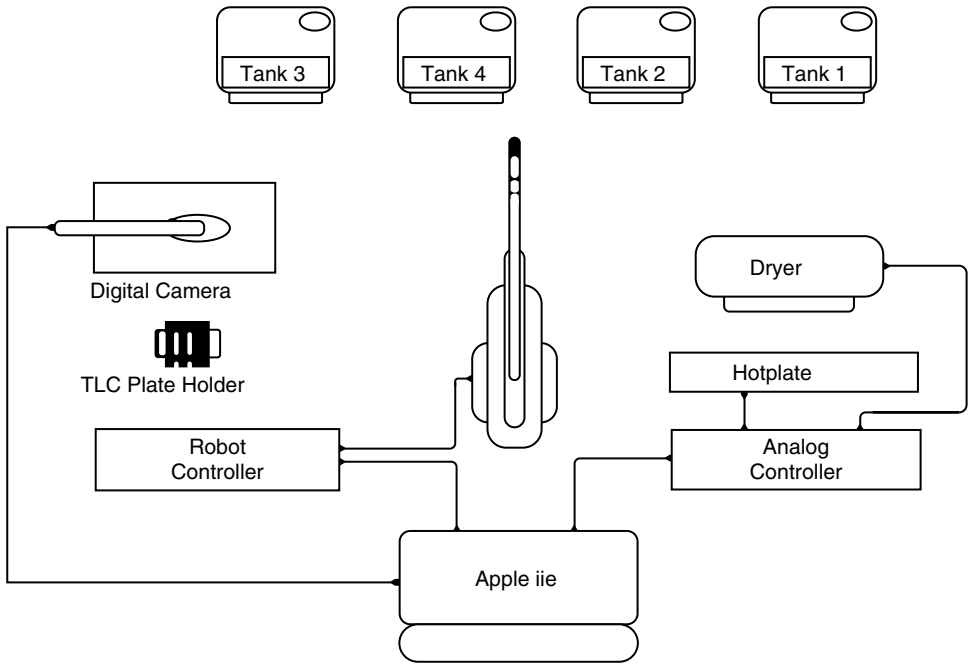

Fig. 9 Planar chromatography robot after Prosek.
Source: From Automation of thin layer chromatography with a laboratory robot, in J. Planar. Chromatogr.[4] Copyright Research Institute for Medicinal Plants, Hungary, 2004.

derivatization by dipping. Also required were a hot plate, a drying system, and a digital camera for evaluation of the derivatized plate. The system was controlled by an Apple IIe computer. The planar chromatography automaton was designed by Delvordre and Postaire with the objective of reducing the number of human movements required for the handling of precoated plates.[10] This device uses a conveyor-belt-like system to sustain all the chromatographic steps along with their own supply of reagents and tools. The procedure comprises six stages. Using this method, qualitative and quantitative data are obtained 50–150 min after starting the procedure.

CONCLUSIONS

Technological progress has enabled semi- and full automation of every stage of the planar chromatography technique. Coupling of automation of the sample preparation process and automation of TLC have strongly enhanced the advantages this separation method. Such improvements will now meet the requirements of the industrial sector (mainly pharmaceutical and plant industries) not only in terms of productivity, effectiveness, reduced cost, good laboratory practice (GLP), and environmental quality, but also on the technical side (validation, flexibility, evolution). Complete chromatographic automation will bring planar chromatography to the same level as other chromatographic methods.

REFERENCES

1. *IUPAC Compendium of Analytical Literature*; Pergamon Press: Oxford, 1978; 22–23.
2. Majors, R.E.; Holden, B.D. Laboratory robotics and its role in sample preparation. LC–GC Int. **1993**, *6* (9), 530.
3. Luquede Castro, M.D.; Velasco-Arjona, A. Towards the most rational use of robotics within the overall analytical process. Anal. Chim. Acta **1999**, *384*, 117–125.
4. Prosek, M.; Pukl, M.; Smidownik, A.; Medja, A. Automation of thin layer chromatography with a laboratory robot. J. Planar Chromatogr. **1989**, *2* (6), 244.
5. http://www.camag.com. **2004**.
6. Tyihak, E.; Mincsovics, E. Overpressured-layer chromatography (optimum performance laminar chromatography) (OPLC). In *Planar Chromatography. A Retrospective View for the Third Millennium*; 1st Ed.; Nyiredy, Sz, Springer: Budapest, 2001; 137–176.
7. Nyiredy, Sz. Rotation planar chromatography. In *Planar Chromatography. A Retrospective View for the Third Millennium*; 1st Ed.; Nyiredy, Sz, Springer: Budapest, 2001; 177–199.
8. Delvordre, P.; Reynault, C.; Postaire, E. Vacuum planar chromatography (VPC): A new versatile technique of forced flow planar chromatography. J. Liq. Chromatogr. Relat. Technol. **1992**, *15* (10), 1673–1679.
9. Kreuzig, F. Derivatization of substances, separated on thin-layer plates, by means of an automatic spreaying device. J. Chromatographia **1980**, *13* (4), 238.
10. Postaire, E.P.R.; Delvordre, P.; Sarbach, C. Automation and robotics in planar chromatography. In *Handbook of Thin-Layer Chromatography*; 2nd Ed.; Sherma, J., Fried, B., Eds.; Marcel Dekker, Inc.: New York, 373–385.

Plant Extracts: TLC Analysis

Gabriela Cimpan
Sirius Analytical Instruments Ltd., East Sussex, U.K.

INTRODUCTION

Thin-layer chromatography (TLC) is a powerful method for separating mixtures of compounds of very different polarity. Plant extracts are usually hydroalcoholic solutions, containing complex mixtures of compounds, many of them being still unidentified. Although plant extracts are widely used in homeopathic medicine for the treatment of different medical conditions the control of these drugs is often performed by qualitative analysis. TLC can provide a chromatographic "fingerprint" of a plant extract used for identification purposes, and usually a photograph is attached to the analysis certificate.[1] The colors of the separated spots and their position relative to standard substances are important characteristics for the plant extract identification. Quantitative analysis is usually performed by spectrophotometry or by chromatographic methods and spectrophotometric detection. Some methods are included in pharmacopeias.

DISCUSSION

TLC Analysis of Plant Extracts in Pharmacopeias

The TLC separation of plant extracts is described in different pharmacopeias,[2–5] and is usually performed on silica layers, and sometimes on silica hydrocarbon (C8, C18) bonded layers. Alumina and other stationary phases are not excluded.

The plant extract samples can be applied directly onto the plate, or a specific class of compounds is extracted in a suitable solvent before TLC. The polarity of the solvent used for extraction should be similar with that of the compound mixture to be separated and analyzed. The samples can be applied onto the plates manually by using calibrated micropipettes or by automated applicators. The samples are applied as spots or bands, and the mobile phase migration distances vary between 8 and 15 cm, depending on the sample complexity and/or the plate size.

Normal presaturated chambers are the most common chambers used for sample development. The mobile phases used for the TLC development are characteristic to different classes of compounds. The classification of medicinal plants takes into account the presence of different classes of compounds, which are separated by using the so-called TLC fingerprint method. The analyzed compounds can be: alkaloids, anthracene derivatives, bitter drugs, cardiac glycoside drugs, coumarin drugs, drugs containing essential oils, flavonoids, saponin drugs, drugs containing triterpenes, etc. For example, mixtures containing chloroform and diethylamine are used for the TLC separation of plant extracts containing alkaloids, and toluene–ethyl acetate for drugs containing essential oils.[1]

After development, the plates are dried in a gentle air stream, at room temperature, and are examined in ultraviolet (UV) or visible light, with or without derivatization, depending on the chemical nature of the separated compounds. The examination in UV light is performed at 254 nm by quenching the thin-layer fluorescence, or at 366 nm when the natural fluorescence of compounds is observed. Several alkaloids (quinine, quinidine, cinchonine, cinchonidine, noscapine, berberine), anthraglycosides, coumarin derivatives (scopoletin, aesculetin), or flavonoids (chlorogenic acid, rutin) have natural fluorescence and can be visualized at 366 nm. The natural fluorescence of compounds can be enhanced by spraying with different reagents, leading to low detection limits. Flavonoids show a yellow-green fluorescence after consecutively spraying with alcoholic solutions of diphenylboryloxyethylamine and polyethylene glycol 4000. The compounds that cannot be derivatized for fluorescence at 366 nm, are sprayed with specific reagents and examined in visible light. The derivatization reactions can take place at room temperature or the TLC plate should be heated on a thermostated plate, at a specific temperature, for approximately 10 min. In both situations, the chromatographic plate should be examined immediately, and eventually photographed. Ninhydrin is a good detecting reagent for amino acids and other biocompounds containing the primary amino group, and the compounds can be observed as blue-violet spots after heating at 100°C. Terpenoids, bitter principles, or saponins can be visualized as red-violet spots by spraying the plate with an acidic solution of anisaldehyde and heating at 100°C.

The pharmacopeias describe the quality control of the plant extracts by the succession of the separated spots obtained after TLC, including the color, order and position on the plate compared to the reference substances. The description should match the TLC separation of the plant extract. The correspondence of the spots is important for the qualitative analysis of the medicinal plant. The reference substances chosen and mentioned in pharmacopeias can also be present in the analyzed plant extract, or can be

used for a comparison with the R_F values of the separated compounds in the plant extract.

Trends in the TLC Analysis of Plant Extracts

The exact chemical composition of a plant extract is not always completely known. Many published papers have tried to identify the compound's structure by coupling chromatography with spectrometric methods. Modern densitometers are able to record the "in-situ" UV/Vis spectra of a separated substance on a TLC plate.[6] TLC can also be coupled with other methods in order to enhance the compound identification, e.g., mass spectrometry (MS) or nuclear magnetic resonance (NMR). There is instrumentation available to record the "in-situ" spectra on the TLC plate, or of the separated substance, removed from the plate together with the layer, and then extracted in a small volume of an adequate solvent.[6,7]

It is well known that the concentration of active substances in medicinal plants can vary widely in different parts of the plant, and it depends on the harvesting time. The quantitative determination of active substances is then very useful for a plant extract analysis. Densitometry is used for the evaluation of the separated substances on a TLC plate. The quantitative determination uses a calibration curve of a reference substance, or a standard method using internal or external standards. Fig. 1 shows the densitograms of two medicinal plant extracts, *Uva ursi* and *Vaccinium vitis-idaea*, both containing arbutin as one of the bioactive substances. The TLC plates are scanned in UV or Vis light, usually in the reflectance mode.

Automated Multiple Development (AMD) has been successfully applied for the separation of compounds from plant extracts. This is a technique using the concentration gradient to separate substances differing widely in polarity. Usually, the gradient starts from a polar composition decreasing in steps to a medium polar mobile phase, and ending with non-polar mixtures of solvents or to a single non-polar solvent. In this way, complex mixtures of compounds from a plant extract can be separated, from very polar to non-polar, between the start and the front solvent line. Usually, the migration distance is 8 cm, and the number of steps can be a maximum of 25 in order to achieve a reasonable development time. The development distances increase as the solvent polarity is decreased. As the total number of compounds in a plant extract is very difficult to estimate, the AMD technique always yields a greater number of separated spots than a monodimensional or a two-dimensional isocratic TLC development.[8] Most of the reference substances used in plant extract analysis have natural origin. As a consequence, they are not always very pure or can lead to decomposition compounds. The separation power of an AMD method can show a greater number of compounds in a reference substance than an isocratic TLC method.

Glycerinic plant extracts have various applications in traditional medicine, but they cannot be analyzed directly by TLC due to the presence of glycerin that should be removed first from the sample.[9] Solid-phase extraction (SPE) is a fast and convenient method for the separation of glycerin. The organic compounds from the analyzed plant extract are retained in the SPE cartridge on a non-polar stationary phase (usually silica-C18); the glycerin and the non-selectively retained compounds are eluted with a polar mobile phase (which can be a diluted solution of methanol in water). The retained compounds are eluted from the cartridge with a stronger mobile phase, usually acidified with a mineral acid, and the obtained solution can be analyzed by TLC directly or after concentration. The SPE recovery is very good, around 100%, and the method is successfully applied for the plant extract cleanup before TLC.

Planar chromatography is widely used in medicinal plant research for the identification of new active

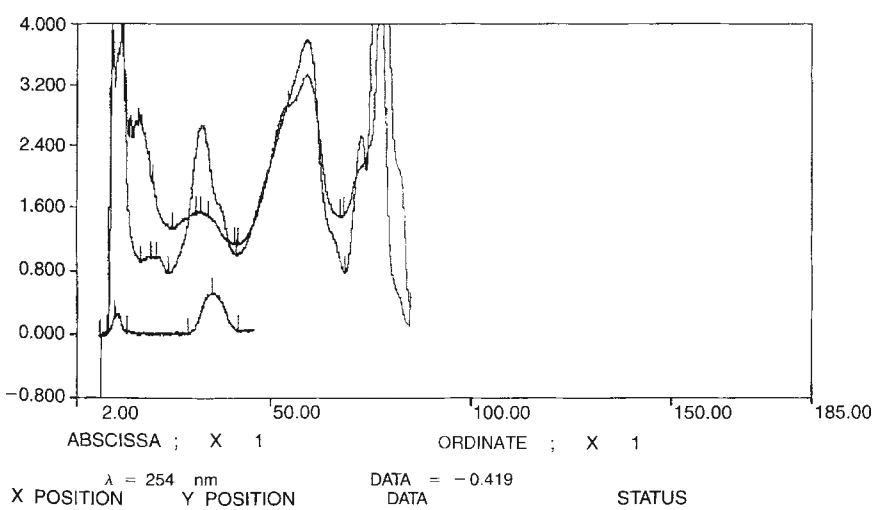

Fig. 1 The densitometry of *Uva ursi* and *Vaccinium vitis-idaea*, two alcoholic plant extracts containing arbutin. Arbutin (reference substance) is the last one, and *Vaccinium vitis-idaea* contains less arbutin than *Uva ursi*; silica gel plate, $\lambda = 254$ nm.

compounds, control of selective isolation procedures of active compounds (extraction, purification, fractionation, etc.), qualitative and quantitative analysis.[10]

REFERENCES

1. Wagner, H.; Bladt, S. *Plant Drug Analysis* 2nd Ed.; Springer Verlag: Berlin, 1996; (2nd printing 2001).
2. *Homöopathisches Arzneibuch (HAB 2003)*; Deutscher Apotheker Verlag: Stuttgart; Govi-Verlag GmbH: Frankfurt, 2003.
3. *La Pharmacopée Française*; Adrapharm: Paris, 1996;
4. *Deutsches Arzneibuch (DAB 2004)*; Deutscher Apotheker Verlag: Stuttgart, 2004.
5. The United States Pharmacopoeia, USP Quality Review, No. 65, Developing Standards Monographs, 1999.
6. Gocan, S.; Cimpan, G. Compound identification in thin-layer chromatography using spectrometric methods. Rev. Anal. Chem. **1997**, *16*, 1–24.
7. Ossipov, V.; Nurmi, K.; Loponen, J.; Haukioja, E.; Pihlaja, K. High-performance liquid chromatographic separation and identification of phenolic compounds from leaves of *Betula pubescens* and *Betula pendula*. J. Chromatogr. A, **1996**, *721*, 59–68.
8. Olah, N.-K.; Muresan, L.; Cimpan, G.; Gocan, S. NP-HPTLC and AMD of *Artemisia abrotanum, Artemisia absinthium, Artemisia vulgaris* and *Artemisia cina* hydroalcoholic extracts. J. Planar Chromatogr.-Mod. TLC **1998**, *11*, 361–364.
9. Cobzac, S.; Cimpan, G.; Olah, N.; Gocan, S. The quantitative determination of rutin from different glycerinic plant extracts by SPE/TLC/densitometry. J. Planar Chromatogr.-Mod. TLC **1999**, *12*, 26–29.
10. Nyiredy, Sz.; Głowniak, K. Planar chromatography in medicinal plant research (550–568). Cimpan, G. Pre- and post-chromatographic derivatisation (410–445). In *Planar Chromatography. A Retrospective for the Third Millennium*; Nyiredy, Sz., Ed.; Springer Scientific: Budapest, 2001.

Plant Toxins: TLC Analysis

Philippe J. Berny
Toxicology Unit, National Veterinary School of Lyon, Marcy L'Etoile, France

INTRODUCTION

Analysis of plants is a vast and complex field of analytical chemistry. There is a constant need for new compounds or active ingredients for pharmaceutical or other interesting properties. Plant chemistry is such that a wide variety of compounds may be produced within the different organs. Toxins usually represent only a small fraction of the total organic matter of the plant. It is important, however, to be able to analyze and detect those toxins, especially when poisoning cases are suspected. Although vegetal toxins are extremely diverse in nature, a common feature among them is that they are heatunstable. Consequently, standard GC or GC/MS procedures cannot be routinely used to detect them, and the use of LC appears of benefit.

Analysis of plant toxins is required in the following circumstances:

1. When plant poisoning is suspected in human beings or in animals: In this situation, the analyst must be able to separate the plant toxin from its plant matrix and/or from an animal tissue of fluid. The toxin is also diluted as compared with the plant product.
2. For research or development purposes: when a family of plants is under investigation and the presence of a toxin is suspected and not expected (therapeutic use).
3. When a family of toxins is well known, like the pyrrolizidine alkaloids,[1] it is highly interesting to screen suspected plants for their presence when poisoning is suspected in animals and there may be some residues in food, even in animals which did not present any disorder.

In this entry, we will review some examples of these three areas of plant chemistry and see how TLC or high-performance thin-layer chromatography (HPTLC) can fulfill the various requirements.

INVESTIGATION OF SUSPECTED POISONING CASES

Poisoning by plants can occur with various animal species, including human beings. It obviously occurs most frequently in herbivores like cattle or sheep and examples of analytical investigation are more common in these species. Unfortunately, it is generally necessary to screen rumen content for plant toxins and this matrix is extremely rich in organic constituents, including natural pigments. Careful and adapted cleaning steps are necessary. When alkaline or acidic substances are to be determined, pH-based liquid–liquid separation may be used.

Our first example is based on a very severe acute poisoning case with yew trees (*Taxus* sp.). These trees contain a highly toxic group of toxins known as taxins. Cattle or sheep usually do not eat the leaves or branches of yew trees because of their bitter taste. Unfortunately, bitterness tends to disappear when the leaves are dessicated, but toxicity remains and animals may eat enough to become deadly sick. One published example mentioned poisoning in 43 cattle, with 17 dead before any treatment or diagnosis could be attempted.[2] Diagnosis may rely on the epidemiological evidence of poisoning (cut branches) or on necropsy (branches in the rumen), but these elements may not necessary be conclusive and analytical techniques may represent the only way of confirming a tentative diagnosis. The published method for yew tree analysis in cattle relied on the analysis of rumen contents and identification of taxol. This alcohol is specific of the *Taxus* genus, although it may not be the toxic substance, but it is easily obtained from commercial dealers, whereas taxins have to be extracted and purified.

The development of scanners for HPTLC also offers better potential and we have further developed the method of Panter et al.[2] with ultraviolet (UV) scanning (at 238 nm) and quantification prior to derivatization (confirmatory analysis). Eventually, diagnosis relies on the determination of Taxins (primarily taxin B) in the rumen content. As an example, Fig. 1 provides a densitogram of a rumen content with identification of taxin peaks and the solid-phase UV spectrum of this compound in a case of confirmed yew tree poisoning. The same technique could be applied to determine the most toxic part of the plant, the effect of season on the toxin content, and so forth. For example, it was found that the leaves contained about 0.03% taxol, while the stem and twigs contained around 0.001% and 0.0006%, respectively.[2]

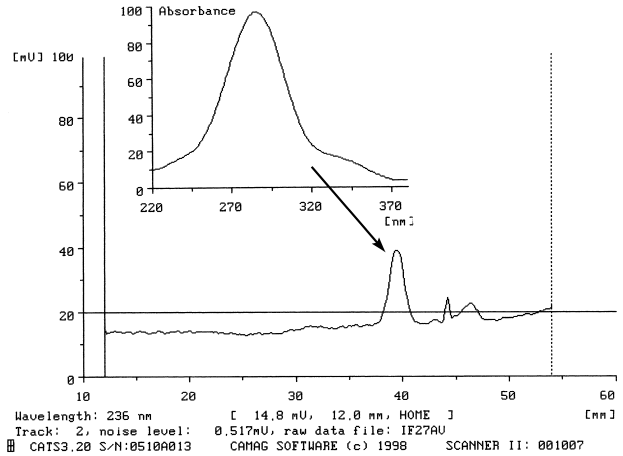

Fig. 1 Rumen content with taxin B (arrow) and its UV spectrum.

IDENTIFICATION OF TOXINS IN PLANT SCREENINGS FOR RESEARCH OR DEVELOPMENT PURPOSES

Some plants are famous for the presence of toxic substances. One major group of toxicants involved is the pyrrolizidine alkaloids. These substances induce severe poisoning manifested by emaciation, anemia, and skin lesions which may develop over months or years and may eventually result in the death of the poisoned animals. These compounds represent both a toxic and economic threat in some areas of the world, (e.g., in the Himalayans).[1] Screening of plants may be highly desirable to prevent these losses. Winter et al.[1] developed screening methods based either on HPLC or on TLC. They used silica gel plates with a mixture of ethylacetate, acetone, ethanol, and ammonia (5/3/1/1) and postchromatographic derivatization with *o*-chloranil and Erlich's reagent. This technique was only qualitative but gave results in accordance with reference HPLC techniques. With these two techniques, the authors analyzed over 350 samples (various plants, plant parts, and locations) to determine the presence and amount of alkaloids.

Another example of the use of TLC in research is given by Ma et al.,[3] who used TLC as a taxonomic tool to classify plants. Their example was based on the lycopodium alkaloids of plants from the Lycopodiacae family. The TLC technique used was qualitative and also relied on postchromatographic derivatization with Dragendorff's reagent.[3] It should be stated that plant toxins are usually recognized by means of qualitative TLC and visualization based on postchromatographic derivatization procedures. Common solutions rely on common reactions of alkaloids, and the use of Dragendorff's reagent is one of these solutions (combined mixture of tartaric acid, bismuth nitrate, and potassium iodide), and vanillin reagent enables the detection of amines and amino acids.

The Chinese pharmacopoea uses a wide range of plants and herbal medicines and Chinese scientists have been publishing methods and techniques for decades, identifying therapeutic substances or toxic ingredients of traditional remedies. The interested reader should refer preferentially to the *Journal of Chinese Herbal Medicine* to find analytical methods.

Identification of new compounds may start with TLC analysis of plant extracts. For instance, Jakupovic et al.[4] isolated and further identified several diterpenes from *Euphorbia segetalis*. Similarly, chamomile essential oil (*Chamomilla reticulata*) was analyzed with 11 different development systems and the authors discussed both the most efficient (separation power) and the ideal way they are to be used to identify an unknown component in such a complex mixture, using the minimum number of TLC systems.[5] This area of work still has to be investigated, considering the wide variety of the vegetal reign and of potential plant toxins.

DETECTION OF RESIDUES IN FOOD

This part is certainly the least developed, to our knowledge. It is important to remember, however, that an animal may ingest a toxic plant and may also survive. If this is the case, and provided this animal or its production are intended for human consumption, one should be able either to analyze tissues and fluids for toxin residues or to monitor fluids (plasma, milk, urine) to determine whether this animal or its productions can be considered safe for human consumption. There are very limited examples of such occurrences. In our laboratory, we analyzed muscular tissues after a confirmed yew tree poisoning case (*Taxus baccata*).

Three animals did not display any significant trouble except for a transient depression, which resolved itself after 12 h. These animals were butchered and muscle samples were analyzed for taxin residues, as they were known to be exposed to it. Our analytical technique (extraction in alkalinized methylene dichloride) followed by TLC development based on a modification of a published technique (9685), showed that the muscle samples contained between 0.012 and 0.015 μg/g taxin (wet weight). The presence of taxin in muscle tissues had never been previously reported in cattle after moderate poisoning. Based on this result, the meat was not considered edible. This example is, simply, to illustrate that residues of plant toxins in food-producing animals should be part of a research or development protocol whenever possible.

CONCLUSIONS

Plant toxins represent one of the most important areas of analytical development and the few techniques related herein

should only be considered as mere examples of the numerous possibilities of TLC in this field. With the development of densitometry and multiple development systems, the separation power of TLC and its quantitative potential are increasing as well. Considering the usual thermal instability of many plant toxins and their high polarity, HPTLC certainly offers one of the most powerful technologies for the detection, identification, and quantification of plant toxins.

REFERENCES

1. Winter, H.; Seawright, A.A.; Noltie, H.J.; Mattocks, A.R.; Jukes, R.; Wangdi, K.; Gurung, J.B. Pyrrolizidine alkaloid poisoning of yaks: Identification of the plants involved. Vet. Rec. **1994**, *134* (6), 135.
2. Panter, K.E.; Molyneux, R.J.; Smart, R.A.; Mitchell, L.; Hansen, S. English yew poisoning in 43 cattle. J. Amr. Vet. Med. Assoc. **1993**, *202* (9), 1476.
3. Ma, X.Q.; Jiang, S.H.; Zhu, D.Y. Alkaloid patterns in Huperzia and some related genera of Lycopodiaceae Sensu Lato occurring in China and their contribution to classification. Biochem. Syst. Ecol. **1998**, *26*, 723.
4. Jakupovic, J.; Jeske, F.; Morgenstern, T.; Marco, J.A.; Berendsohn, W. Diterpenes from *Euphorbia segetalis*. Phytochemistry **1998**, *47*, 1583.
5. Medic-Saric, M.; Stanic, G.; Males, Z.; Saric, S. Application of numerical methods to thin-layer chromatographic investigation of the main components of chamomile (*Chamomilla recutita* (L.) Rauschert) essential oil. J. Chromatogr. A, **1997**, *776*, 355.

Plate Number: Effective

Raymond P.W. Scott
Scientific Detectors Ltd. Banbury, Oxfordshire, U.K.

INTRODUCTION

The concept of the effective plate number was introduced in the late 1950s by Purnell and Bohemen[1] and Desty and Golup.[2] Its introduction arose directly as a result of the development of the capillary column. It was noted that the very high efficiencies were only realized from open-tubular columns for solutes eluted close to the column dead volume (i.e., for solutes eluted at very low k' values). In addition, the high efficiencies in no way reflected the increase in resolving power that would be expected from a packed column with much higher stationary-phase loading.

This poor performance, relative to the high efficiencies produced, results from the high phase ratio inherent with open-tubular columns. The high phase ratio is due to there being very little stationary phase in the capillary column (the film is very thin). The corrected retention volume of a solute is directly proportional to the amount of stationary phase in the column, and solutes, in general, are eluted from a capillary column at relatively low k' values relative to the magnitude of their distribution coefficient.

DISCUSSION

To compensate for what appeared to be very misleading efficiency values, the *effective plate number* was introduced. The effective plate number uses the *corrected retention distance*, as opposed to the *total retention distance* to calculate the efficiency. Thus, the effective plate number is significantly smaller than the true plate number for solutes eluted at low k' values. At high k' values, the two measures of efficiency converge. In this way, the effective plate number appears to more nearly correspond to the column resolving power. The efficiency of the column (n) in number of theoretical plates has been shown to be given by

$$n = 4\frac{y^2}{x^2}$$

where y is the retention distance, and x is the peak width.

Now, the number of "effective plates" (N), by definition, is given by

$$N = 4\frac{(y - y_0)^2}{x^2} \tag{1}$$

where y_0 is the retention distance of an unretained solute (the position of the dead point). Now, from the plate theory,

$$\frac{y}{x} = \frac{n(v_m + Kv_s)}{2\sqrt{n}(v_m + Kv_s)}$$

thus,

$$\frac{y - y_0}{x} = \frac{n(v_m + Kv_s) - nv_m}{2\sqrt{n}(v_m + Kv_s)}$$

By dividing through by v_m and noting that

$$\frac{Kv_s}{v_m} = k'$$

then,

$$\frac{y - y_0}{x} = \frac{\sqrt{n}k'}{2(1 + k')}$$

Consequently,

$$4\left(\frac{y - y_0}{x}\right)^2 = n\left(\frac{k'}{1 + k'}\right)^2 = N \tag{2}$$

Equation 2 describes the relationship between the efficiency of a column in theoretical plates and the efficiency given in "effective plates." It is also seen that the calculation of the number of "effective plates" in a column does not provide an arbitrary measure of the column performance, but is directly related to the number of theoretical plates in the column as defined by the plate theory. It should be noted that as k' becomes large, n and N converge to the same value.

The effective plate number has an interesting relationship to the function for the resolution of a column that was suggested by Giddings.[3] Giddings proposed that the function $k'\Delta k'$ could be a means of defining the resolving power R of a column. He employed this function in an analogous manner to the function used in spectroscopy to define resolution (i.e., $\lambda/\Delta\lambda$, where $\Delta\lambda$ is the minimum wavelength increment that can be differentiated at a wavelength λ). The value taken by Giddings for $\Delta k'$ was the bandwidth at the base of the eluted peak which is equivalent to twice the peak width or 4σ. Thus, from the plate theory,

$$R = \frac{k'}{\Delta k'} = \frac{nkv_s}{4\sqrt{n}(v_m + Kv_s)}$$

Again, dividing through by v_m and noting that

$$\frac{Kv_s}{v_m} = k'$$

then,

$$R = \frac{\sqrt{n}k'}{4(1 + k')} = \frac{\sqrt{N}}{4} \quad (3)$$

It is seen from Eq. 3 that the resolving power of the column, as defined by Giddings, will be directly proportional to the square root of the number of effective plates. As a consequence, R can be used by the chromatographer to directly compare the resolving power of columns of any size or type. However, the value of R will vary with the value of k' for the solute, and so comparison between columns must be made using solutes that have the same k' value.

REFERENCES

1. Purnell, J.H.; Bohemen, J. Diffusional band spreading in GC columns. J. Chem. Soc. **1961**, 2030.
2. Desty, D.H.; Goldup, A. *Gas Chromatography 1960*; Scott, R.P.W., Ed.; Butterworths: London, 1960; 162.
3. Giddings, J.C. *The Dynamics of Chromatography*; Marcel Dekker, Inc.: New York, 1965; 265.

BIBLIOGRAPHY

1. Scott, R.P.W. *Liquid Chromatography Column Theory*; John Wiley & Sons: Chichester, 1992; 19.
2. Scott, R.P.W. *Introduction to Analytical Gas Chromatography*; Marcel Dekker, Inc.: New York, 1998

Plate Theory

Raymond P.W. Scott
Scientific Detectors Ltd., Banbury, Oxfordshire, U.K.

INTRODUCTION

Originally derived by Martin and Synge[1] and extended by Said,[2] the plate theory provides an equation that describes the elution curve (the chromatogram) of a solute. By differentiating the elution curve equation and equating to zero, an expression for the retention volume of a solute can be obtained. By equating the second differential to zero, an equation for the variance and standard deviation (the peak width) can be obtained, and from these equations, methods for calculating the column efficiency can be derived, together with the numerous equations that describe resolution.

DISCUSSION

The plate theory assumes that the solute is in equilibrium with the mobile and stationary phases. Due to the continuous exchange of solute between the two phases as it progresses down the column, equilibrium between the phases can *never* actually be achieved. To accommodate this non-equilibrium condition, a technique originally introduced in distillation theory is adopted, where the column is considered to be divided into a number of cells or plates. Each cell is allotted a finite length and, thus, the solute spends a finite time in each cell. The size of the cell is such that the solute is considered to have sufficient residence time to achieve equilibrium with the two phases. Thus, the smaller the plate, the more efficient the solute exchange between the two phases and, consequently, the more plates there are in the column. As a result, the number of theoretical plates contained by a column has been termed the *column efficiency*. The *plate theory* shows that the peak width (the dispersion or peak spreading) is inversely proportional to the square root of the efficiency and, thus, the higher the efficiency, the narrower the peak. Consider the equilibrium that is assumed to exist in each plate; then

$$X_s = KX_m \tag{1}$$

where X_m is the concentration of solute in the mobile phase, X_s is the concentration of solute in the stationary phase, and K is the distribution coefficient of the solute between the two phases.

It should be noted that K is defined with reference to the stationary phase (i.e., $K = X_s/X_m$), thus the larger the distribution coefficient, the more the solute is distributed in the stationary phase. Differentiating Eq. 1,

$$dX_s = KdX_m \tag{2}$$

Consider three consecutive plates in a column, the $p-1$, the p, and the $p+1$ plates and let there be a total of n plates in the column. The three plates are depicted in Fig. 1.

Let the volumes of mobile phase and stationary phase in each plate be v_m and v_s, respectively, and the concentrations of solute in the mobile and stationary phase in each plate be $X_{m(p-1)}$, $X_{s(p-1)}$, $X_{m(p)}$, $X_{s(p)}$, $X_{m(p+1)}$, and $X_{s(p+1)}$, respectively. Let a volume of mobile phase, dV, pass from plate $p-1$ into plate p, at the same time, displacing the same volume of mobile phase from plate p to plate $p+1$. In doing so, there will be a change of mass (dm) of solute in plate p that will be equal to the difference in the mass entering plate p from plate $p-1$ and the mass of solute leaving plate p and entering plate $p+1$. A simple mass balance procedure can be applied to plate p. Thus, bearing in mind that mass is the product of concentration and volume, the change of mass of solute in plate p will be

$$dm = (X_{m(p-1)} - X_{m(p)})dV \tag{3}$$

Now, if equilibrium is to be maintained in the plate p, the mass (dm) will distribute itself between the two phases, which will result in a change of solute concentration in the mobile phase of $dX_{m(p)}$ and in the stationary phase of $dX_{s(p)}$. Then,

$$d_m = v_s dX_{s(p)} + v_m dX_{m(p)} \tag{4}$$

Substituting for $dX_{s(p)}$ from Eq. 2,

$$d_m = (v_m + Kv_s)dX_{m(p)} \tag{5}$$

Equating Eqs. 3 and 5 and rearranging,

$$\frac{dX_{m(p)}}{dV} = \frac{X_{m(p-1)} - X_{(p)}}{v_m + Kv_s} \tag{6}$$

The volume flow of the mobile phase will now be measured in units of $v_m + Kv_s$, instead of milliliters. Thus, the new variable (v) can be defined as

$$v = \frac{V}{v_m + Kv_s} \tag{7}$$

The function $v_m + Kv_s$ is termed the "plate volume" and, thus, the flow of mobile phase will be measured in "plate volumes" instead of milliliters. The "plate volume" can be defined as that volume of mobile phase that would

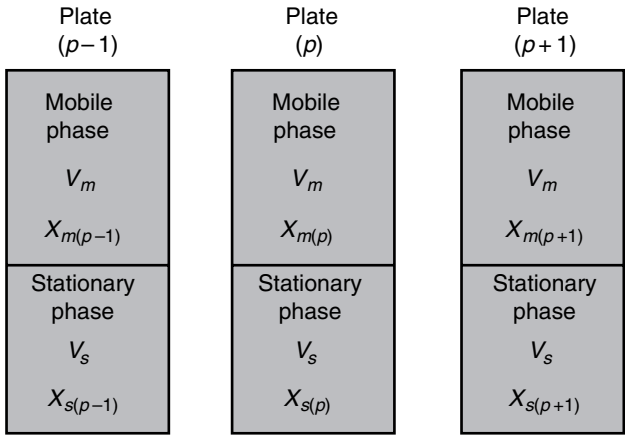

Fig. 1 The three consecutive plates in a column.

contain all the solute that is in the plate at the equilibrium concentration of the solute in the mobile phase.

Differentiating Eq. 7,

$$dv = \frac{dV}{v_m + Kv_s} \tag{8}$$

Substituting for dV from Eq. 8 in Eq. 6,

$$\frac{dX_{m(p)}}{dV} = X_{m(p-1)} - X_{(p)} \tag{9}$$

Eq. 9 is the basic differential equation that describes the rate of change of concentration of solute in the mobile phase in plate p with the volume flow of mobile phase through it. Thus, the integration of Eq. 9 will provide the equation for the elution curve of a solute eluted from any plate in the column. A simple algebraic solution to Eq. 9 is given in Ref.[3] and the resulting elution curve equation for plate n of a column of n plates is shown to be

$$X_{m(n)} = \frac{X_0 e^{-v} v^n}{n!} \tag{10}$$

Eq. 10 is the basic elution curve equation; it is a Poisson function, but when n is large, the function approximates to a normal error function or Gaussian function. In practical chromatography systems, n is always greater than 100 and, thus, all chromatographic peaks will be Gaussian or nearly Gaussian in shape.

THE RETENTION VOLUME OF A SOLUTE

The retention volume of a solute is that volume of mobile phase that passes through the column between the injection point and the peak maximum. It is, therefore, now possible to determine that volume by differentiating Eq. 10 and equating to zero and solving for v. Restating Eq. 10,

$$X_{m(n)} = X_0 \frac{e^{-v} v^n}{n!}$$

$$\frac{dX_{m(n)}}{dv} = X_0 \frac{-e^{-v} v^n + e^{-v} n v^{n-1}}{n!}$$

$$= X_0 \frac{-e^{-v} v^{n-1}}{n!} (n - v)$$

Equating to zero and solving for v,

$$n - v = 0 \quad \text{or} \quad v = n$$

Thus, n plate volumes of mobile phase have passed through the column (remembering that the volume flow is measured in "plate volumes" and not in milliliters). Thus, the volume passed through the column (in ml) will be

$$V_r = n(v_m + Kv_s)$$
$$= nv_m + nKV_s \tag{11}$$

Now, the total volume of mobile phase and stationary phase in the column (V_m and V_s, respectively) will be the volume of mobile phase and stationary phase per plate multiplied by the number of plates (i.e., nv_m and nv_s). Thus,

$$V_r = V_m + KV_s \tag{12}$$

Returning to Eq. 13, it is also possible to derive an equation for the adjusted retention volume, V_r'. Now,

$$V_r{}' = V_r - V_m \tag{13}$$

Thus, from Eqs. 11 and 13,

$$V_r{}' = V_m^+ KV_s - V_m = KV_s \tag{14}$$

For the use of the plate theory to determine peak widths and column efficiency, see *Columns: Resolving Power*, p. 491.

REFERENCES

1. Martin, A.J.P.; Synge, R.L.M. A new form of chromatogram employing two liquid phases. Biochem. J. **1941**, *35* (12), 1358.
2. Said, A.S. Theoretical-plate concept in chromatography. Am. Inst. Chem. Eng. J. **1956**, *2* (4), 477.
3. Scott, R.P.W. *Liquid Chromatography Column Theory*; John Wiley & Sons: Chichester, 1992; 19.

BIBLIOGRAPHY

1. Scott, R.P.W. *Techniques and Practice of Chromatography*; Marcel Dekker, Inc.: New York, 1996.
2. Scott, R.P.W. *Introduction to Analytical Gas Chromatography*; Marcel Dekker, Inc.: New York, 1998.

Pollutant–Colloid Association by FFF

Ronald Beckett
Water Studies Centre, Monash University, Melbourne, Victoria, Australia

Bailin Chen
Department of Chemistry, University of Kentucky, Lexington, Kentucky, U.S.A.

Niem Tri
Water Studies Centre, Monash University, Melbourne, Victoria, Australia

INTRODUCTION

The association of pollutants such as trace metals, nutrients, and toxic organic molecules to colloids is intimately connected to the health of natural waters. Colloids, with their large specific surface area, play a dominant role in the transportation and eventual deposition of these pollutants. Of particular interest is the size speciation data. It is important to know not only the total amount of pollutant present but also where it is distributed. It has been inherently difficult to study pollutant–colloid interactions because of the lack of methods for particle size determination and fractionation as well as the low concentrations of pollutants present in many systems.This entry outlines a new approach using field-flow fractionation (FFF).

DISCUSSION

Field-flow fractionation is a separation and elution technique similar to chromatography.[1] It is based on the application of a field perpendicular to the flow of the axis of a thin (100–500 μm) channel. An externally applied field drives unlike particles to different positions across the thin channel, where they are caught up in different flow velocities. For small particles, typically less than 1 μm, the elution time depends on the particle's interaction with the field and its diffusivity. Separations in this mode, termed the *normal* mode, have the smaller particles eluting ahead of the larger particles. Larger particles tend to stay near the channel wall and move through the channel with the lower flow velocities.An alternate mode, termed the *steric* or *hyperlayer* mode, is for particles greater than about 1 μm. A reversal of the elution order is observed because they necessarily protrude into the higher flow velocities (due to their physical size). Utilizing these two modes, it is possible to probe a mass range spanning 15 orders of magnitude, starting from molecules of 1000 Da molecular weight up to particles 50 μm in diameter.

Further, it is possible to utilize different fields to yield the various FFF subtechniques. The two most common fields are centrifugal and fluid cross-flow, which give rise to the sedimentation and flow FFF subtechniques. Other fields currently in use include thermal, electrical, and magnetic fields. In the normal mode, it is possible to extract physical parameters from retention data. For example, sedimentation FFF using a centrifugal force gives information about the buoyant mass, and flow FFF gives information about the sample's diffusivity or hydrodynamic diameter.

Environmental samples often have a broad size distribution and are often heterogenous in density and chemical composition, and to add to the complexity, natural particles often have an irregular shape.[2] Thus, it is easy to appreciate that FFF with its wide and flexible range of operating parameters is the ideal tool to divide these broad distributions into discrete, roughly monodisperse fractions for subsequent analysis. Sedimentation and flow FFF, in particular, have been used to measure the size distribution of environmental samples. Karaiskakis et al., first demonstrated that it is possible to correlate chemical content (major elements such as Al, Ca, Fe, Si, and S found in bulk minerals) with particle size using sedimentation FFF with energy dispersive X-ray analysis (EDXA).[3] However, due to the low sensitivity and long analysis time of FFF–EDXA,the technique was abandoned for the analysis of pollutants.

Much more sensitive and less time-consuming techniques such as mass spectrometry, atomic emission, and atomic absorption are needed for the analysis of pollutants. Detectors such as graphite furnace–atomic absorption spectrometer (GF–AAS), inductively coupled plasma–mass spectrometer (ICP–MS), or inductively coupled plasma–atomic emission spectrometer (ICP–AES) seem to be ideal candidates for the analysis of trace metals because of their very low detection limits. The high temperatures used avoid the need for tedious digestions in many samples. FFF–gas chromatography–mass spectrometry could perhaps be used in the analysis of particular organic molecules. Another extremely sensitive technique applied in the study of adsorption behavior of pollutants is to add radiolabeled adsorbates (such as $^{33}PO_4^{3-}$, ^{14}C-atrazine, and ^{14}C-glyphosate) to study the distribution of the pollutant as a function of size.

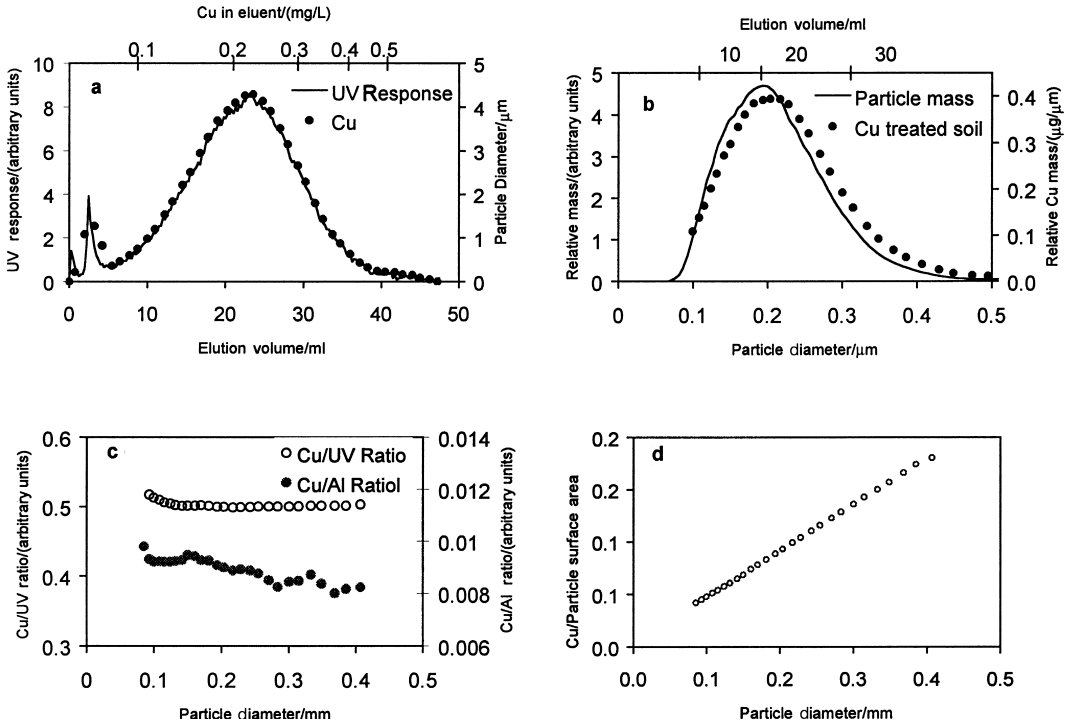

Fig. 1 Graphs showing (a) fractogram and copper concentration in eluent, (b) corresponding size distribution, (c) copper concentration distribution and element ratio distribution of copper in soil sample, and (d) copper per unit surface area distribution.

CONTAMINANT SPECIATION DATA

In recent years, the direct coupling of the FFF channel to GF–AAS, high-resolution ICP–MS, and ICP–AES has been implemented. It has enabled high resolution size-based speciation data for pollutants to be collected. In the first instance, the data acquired by these methods is a fractogram [an instrumental signal, usually but not necessarily from an ultraviolet (UV) detector, representing the mass of eluted sample as a function of the retention time]. The retention time is rigorously but not linearly related to the particle size (i.e., diameter) and may be easily calculated from FFF theory. Suitable algorithms can be used to generate a mass-based size distribution. Fig. 1a and b show an example of recent work conducted in our laboratory demonstrating the distribution of copper in contaminated soils represented as a fractogram and a size distribution.

Element concentrations in the eluent are also recorded if a suitable detector is used. This can be processed in a similar fashion to the UV signal to yield an eluent-based size distribution. If the element detector signal is divided by the mass detector signal, we obtain a quantity which is proportional to the concentration in the sample particles. When this quantity is plotted against particle diameter, we obtain the element concentration distribution for the sample (Fig. 1c). It is often useful to plot the element atomic ratio distributions for elements of interest.This graph is particularly useful for deducing size-based speciation data for trace elements.

The main feature of this experiment is that although the copper content in the soil roughly follows the fractogram (Fig. 1a) and the size distribution (Fig. 1b), the concentration of copper is higher for the smaller particles (Fig. 1c). However, a comparison of the copper/aluminium ratio shows that there is no change across the size distribution for this sample. Fig. 1d shows that the surface-coating density of copper is increasing with particle size, suggesting a denser or thicker coating of copper as the particle size increases.

Contado et al.,[4] coupled sedimentation FFF indirectly to GF–AAS as well as directly to ICP–MS to produce element composition data across the size distribution. The high levels of Cu, Pb, Cr, and Cd found were associated with colloidal particles taken from a river situated in a highly industrialized site. The two methods give comparable results, with online coupling of ICP–MS having a higher resolution, but ICP–AES yields data for some elements (such as potassium and calcium) where ICP–MS produces interferences.

ADSORPTION BEHAVIOR OF POLLUTANTS

The adsorption behavior of colloidal material onto river particles can play a vital role in the transport and fate of pollutants. FFF methods provide a means to evaluate the relative importance of different fractions in adsorption of contaminants in soils and sediments.

One particularly sensitive method employs the adsorption of radioactive material to natural particles.[5] Radiolabeled ^{32}P (as H_3PO_4) and ^{14}C (as glyphosate and atrazine) were adsorbed onto the river water colloid samples for several hours, then separated using sedimentation FFF and specific size fractions were collected. The

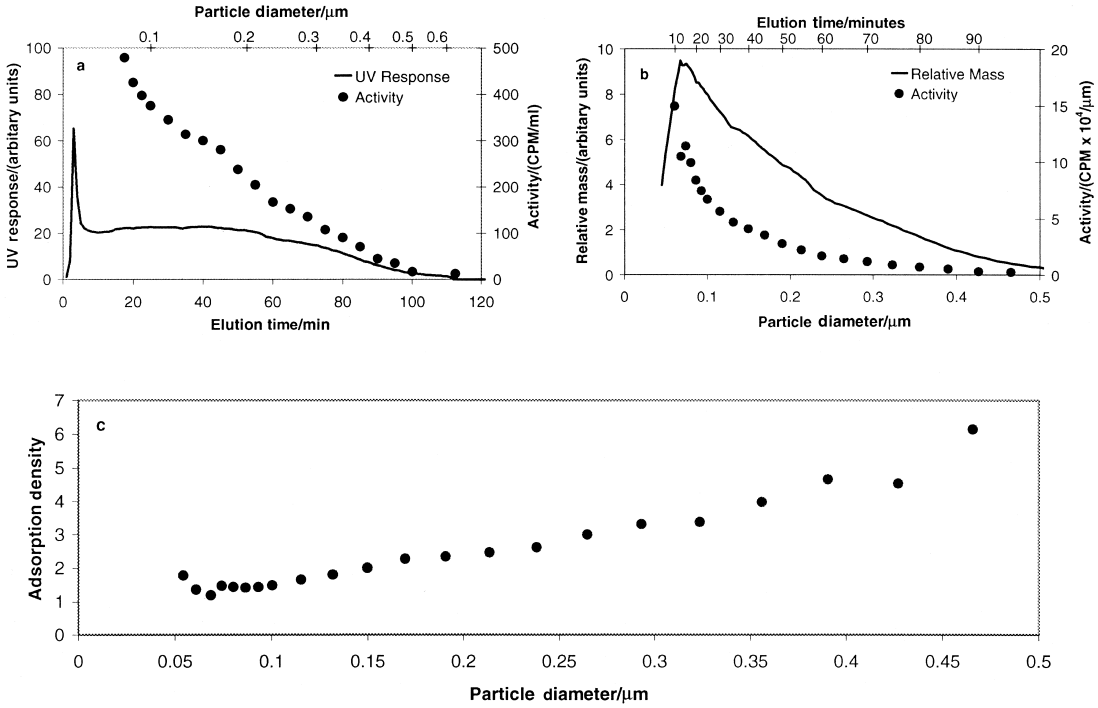

Fig. 2 Graphs showing ^{14}C-glyphosate on river suspended-particulate matter. (a) Particle mass and adsorbate fractograms; (b) particle size distribution and pollutant adsorption distribution; (c) surface-adsorption density distribution.

fractions were subsequently analyzed for their β-activity. These data yield adsorbate (activity)-based fractograms and size distribution (Fig. 2a and b).

Dividing the adsorbate size distribution by the mass size distribution gives an adsorbate concentration (i.e., the amount adsorbed per mass of particles) distribution as outlined previously. Fig. 2b shows that the smaller particles contain the highest pollution content. This is consistent with the concept that smaller particles have a higher specific surface area, but changes in geochemistry of the particle with size could also be involved.

If the adsorption were uniform, we would expect the adsorbate concentration to increase with decreasing size.This effect can be eliminated if the amount of adsorbate per unit area of particles is estimated. Assuming that the particles are spherical and have constant density, it is possible to calculate the relative amount adsorbed per unit surface area as a function of particle diameter. This plot is known as a surface adsorption density distribution (SADD). Fig. 2c shows the SADD plot for ^{14}C-glyphosate adsorbed onto a river suspended-colloid sample. This trend could be attributed to changes of particle size (as these calculations are based on a spherical particle), changes in mineralogy, and coating density across the size range.

The method outlined is also applicable to trace metal data collected by ICP–MS and ICP–AES. Recently, Hassellov et al., demonstrated that it is possible to measure major elements as well as a range of trace metals, including Cs, Cd, Cu, Pb, Zn, and La.[6] Further, they showed that it was possible to obtain speciation data across the size range.

Field-flow fractionation separations combined with other high-sensitivity analytical techniques are capable of yielding more detailed information than has been possible with existing methods. Although, at this stage, there are still many uncertainties to the interpretation of the trends observed, this method is certain to provide further insights into the nature of pollutant–colloid interactions in natural waters.

REFERENCES

1. Giddings, J.C.; Yang, F.J.; Myers, M.N. Flow-field-flow fractionation: A versatile new separation method. Science **1976**, *193* (4259), 1244–2145.
2. Beckett, R. The application of field-flow fractionation techniques to the characterization of complex environmental samples. Environ. Tech. Lett. **1987**, *8*, 339–354.
3. Karaiskakis, G.; Graff, K.A.; Caldwell, K.D.; Giddings, J.C. Sedimentation field-flow fractionation of colloidal particles in river water. Int. J. Environ. Anal. Chem. **1982**, *12*, 1–15.
4. Contado, C.; Blo, G.; Fagioli, F.; Dondi, F.; Beckett, R. Characterization of river po particles by sedimentation field-flow fractionation coupled to GFAAS and ICP-MS. Colloids Surf. A: Physicochem Eng. Aspects **1997**, *120* (1–3), 47–59.
5. Beckett, R.; Hotchin, D.M.; Hart, B.T. Use of field-flow fractionation to study pollutant—colloid interactions. J. Chromatogr. **1990**, *517*, 435–447.
6. Hassellov, M.; Lyven, B.; Beckett, R. Sedimentation field-flow fractionation coupled online to inductively coupled plasma mass spectrometry–new possibilities for studies of trace metal adsorption onto natural colloids. Environ. Sci. Technol. **1999**, *33* (24), 4528–4531.

Pollutants: Chiral CE Analysis

Imran Ali
Department of Chemistry, Jamia Millia Islamia (A Central University), New Delhi, India

Hassan Y. Aboul-Enein
Pharmaceutical and Medicinal Chemistry Department, Pharmaceutical and Drug Industries Research Division, National Research Center, Dokki, Cairo, Egypt

Tabrez A. Khan
Department of Chemistry, Jamia Millia Islamia (A Central University), New Delhi, India

Abstract
Analysis of chiral pollutants by capillary electrophoresis (CE) is a new trend in separation science. This entry describes separation and identification of chiral xenobiotics by using CE. Attempts have been made to describe types of chiral selectors, applications, optimization of separations, detection strategies, mechanisms of chiral separations, CE *vs* chromatography and sample preparation methods.

INTRODUCTION

More than 60,000 organic compounds are in use by human beings globally and, presumably, some of these are toxic and contaminating our environment. Some pesticides, phenols, plasticizers, and polynuclear aromatic hydrocarbons are chiral toxic pollutants. About 25% of agrochemicals are chiral and are sold as their mixtures. It is well known that one of the two enantiomers of the chiral pollutants/xenobiotics may be more toxic than the other enantiomer.[1] This is an important information to the environmental chemist when performing environmental analysis, as the data of simple analyses do not distinguish which enantiomeric structure of a certain pollutant is present and which is harmful. Biological transformation of the chiral pollutants can be stereoselective; thus uptake, metabolism, and excretion of enantiomers may be very different.[1] Therefore, the enantiomeric composition of the chiral pollutants may be changed in these processes. Metabolites of the chiral pollutants are often chiral. Thus to obtain information on the toxicity and biotransformation of the chiral pollutants, it is essential to develop a suitable method for the analysis of the chiral pollutants. Therefore, diverse groups of people ranging from the regulators to the materials industries, clinicians and nutritional experts, agricultural scientists, and environmentalists are asking data on the ratio of the enantiomers of the chiral pollutants. Chromatographic modalities, e.g., gas chromatography (GC) and high-performance liquid chromatography (HPLC), have been used for the chiral analysis of the pollutants. The high polarity, low vapor pressure, and the need for derivatization of some environmental pollutants make GC method complicated. The inherent limited resolving power, complex procedures involved in the optimization of the chiral resolution of the pollutant, and the use of large amounts of solvents and sample volumes are the main drawbacks of HPLC. Conversely, capillary electrophoresis (CE) is a versatile technique of high speed and sensitivity, which is a major trend in analytical science; some publications on the chiral analysis of pollutants have appeared in recent years. The high efficiency of CE is due to the flat flow profile originated and to a homogeneous partition of the chiral selector in the electrolyte which, in turn, minimizes the mass transfer. Some reviews have appeared in the literature on the chiral analysis of the environmental pollutants by CE.[2–5] These authors have discussed analytical chemistry, environmental occurrence, environmental fate of chiral pollutants, and chiral analyses. Therefore, in this entry, attempts have been made to explain the advancement in the art of enantiomeric resolution of the chiral pollutants by CE.

CHIRAL SELECTORS

As in the case of chromatography, a chiral selector is also required in CE for enantiomeric resolution. Generally, suitable chiral compounds are used in the background electrolyte (BGE) as additives and hence are called chiral selectors or chiral BGE additives. There are only a few publications available that deal with the chiral resolution on a capillary coated with the chiral selector in CE.[6] The analysis of the chiral pollutants discussed in this entry is restricted only to the use of chiral selectors in the BGE. The most commonly used chiral BGE additives are cyclodextrins (CDs), macrocyclic glycopeptide antibiotics, proteins, crown ethers, ligand exchangers, and alkaloids.[7,8] A list of these chiral BGE additives is presented in Table 1.

Table 1 Some of the most commonly used chiral selectors.

Chiral selectors (chiral BGE additives)	Refs.
Cyclodextrins	[8,9]
Macrocyclic glycopeptide antibiotics	[9]
Proteins	[9,10]
Crown ethers	[9,11]
Alkaloids	[9]
Polysaccharides	[9,12]
Calixarines	[9,12]
Imprinted polymers	[13]
Ligand exchangers	[13]

APPLICATIONS

CE has been used for the analysis of chiral pollutants, e.g., pesticides, polynuclear aromatic hydrocarbons, amines, carbonyl compounds, surfactants, dyes, and other toxic compounds. Moreover, CE has also been utilized to separate the structural isomers of various toxic pollutants such as phenols, polyaromatic hydrocarbons, and so on. Sarac, Chankvetadze, and Blaschke[14] resolved the enantiomers of 2-hydrazino-2-methyl-3-(3,4-dihydroxyphenyl)propanoic acid using CD as the BGE additive. The CDs used were native, neutral, and ionic in nature with phosphate buffer as BGE. Welseloh, Wolf, and Konig[15] investigated the CE method for the separation of biphenyls, using a phosphate buffer as BGE with CD as the chiral additive. Miura et al.,[16] used CE for the chiral resolution of seven phenoxy acid herbicides using methylated CDs as the BGE additives. Furthermore, the same group[17] resolved 2-(4-chlorophenoxy) propionic acid (MCPP), 2-(2,4-dichlorophenoxy) propionic acid (DCPP), (2,4-dichlorophenoxy) acetic acid (2,4-D), 2-(4-chlorophenoxy) propionic acid (2,4-CPPA), [(2,4,5-trichlorophenoxy) acetic acid (2,4,5-T)], 2-(3-chlorophenoxy) propionic acid (2,3-CPPA), 2-(2-chlorophenoxy) propionic acid (2,2-CPPA), 2-phenoxypropionic acid (2-PPA), and silvex pesticides using CDs, with negatively charged sulfonyl groups, as the chiral BGE additives. Gomez-Gomar et al.,[18] investigated the simultaneous enantioselective separation of (±)-cizolirtine and its impurities, (±)-*N*-desmethylcizolirtine, (±)-cizolirtine-*N*-oxide, and (±)-5-(hydroxybenzyl)-1-methylpyrazole by CE. Otsuka et al.,[19] described the latest advancement by coupling CE with mass spectrometry (MS); this setup was used for the chiral analysis of phenoxy acid herbicides. The authors also described an electrospray ionization (ESI) method for the CE–MS interface. Generally, non-volatile additives in sample solutions sometimes decrease the MS sensitivity and/or signal intensity. However, heptakis(2,3,6-tri-*O*-methyl)-β-CD (TM-β-CD) was used as a chiral selector; it migrated directly into the ESI interface. By using the negative-ionization mode, along with a methanol–water–formic acid solution as a sheath liquid and nitrogen as a sheath gas, stereoselective resolution and detection of three phenoxy acid herbicide enantiomers were successfully achieved with a 20 m*M* TM-β-CD in a 50 m*M* ammonium acetate buffer (pH 4.6).[20] Zerbinati et al.,[21] resolved the four enantiomers of the herbicides mecoprop and dichlorprop using an ethylcarbonate derivative of β-CD with three substituents per molecules of hydroxypropyl-β-CD and native β-CD. The performances of these chiral selectors have been quantified by means of two-level full-factorial designs and the inclusion constants were calculated from CE migration time data. Klein et al.,[22] reported the analysis of stereoisomers of metolachlor and its two polar metabolites [ethane sulfonic acid (ESA) and oxanilic acid (OXA)] by CE by taking γ-CD. Jarman et al.,[23] separated the enantiomers of metalaxyl, imazaquin, fonofos (dyfonate), ruelene (cruformate), and dichlorprop in CE with CD chiral selectors. Metalaxyl underwent enantioselective transformation; in one soil, the half-life for the *R*-(+)-enantiomer was 17 days while that for the *S*-enantiomer was 69 days. On the contrary, imazaquin and fonofos exhibited non-selective enantiomer loss over the three months of their incubation time. Furthermore, ruelene and dichlorprop were transformed selectively in a variety of soils. As per the authors, CE is supposed to be a simple, efficient, and inexpensive technique to study the transformation of chiral pesticides. Fig. 1 indicates electropherograms of metalaxyl enantiomers in a series of slurry samples revealing the change in enantioselective degradation pattern with the incubation time. Recently, Garrison, Schmitt-Kopplin, and Avants[24] described CE with CD as chiral selectors for the enantiomeric separation. For neutral analytes, sodium dodecyl sulfate was added. The pesticides in soils and sediment samples are extracted with methanol and analyzed by CE. The analysis of the chiral pollutants by CE is summarized in Table 2. To show the nature of the electropherograms, the chiral separation of dichlorprop enantiomers is shown in Fig. 2 with different concentrations of α-CD.[21]

OPTIMIZATION OF SEPARATIONS

The analysis of the chiral pollutants by CE is very sensitive and, hence, is controlled by a number of experimental parameters. The optimization parameters may be categorized into two classes, i.e., the independent and dependent parameters. The independent parameters are under the direct control of the operator. These parameters include the choice of the buffer, pH of the buffer, ionic strength of the buffer, type of chiral selectors, voltage applied, temperature of the capillary, dimension of the capillary, BGE additives, and various other parameters. Conversely, the dependent parameters are those directly affected by the independent parameters and are not under the direct control of the operator. These types of parameters are field strength (V/m), electro-osmotic flow (EOF), Joule heating, BGE viscosity, sample diffusion, sample mobility, sample charge, sample size and shape, sample interaction

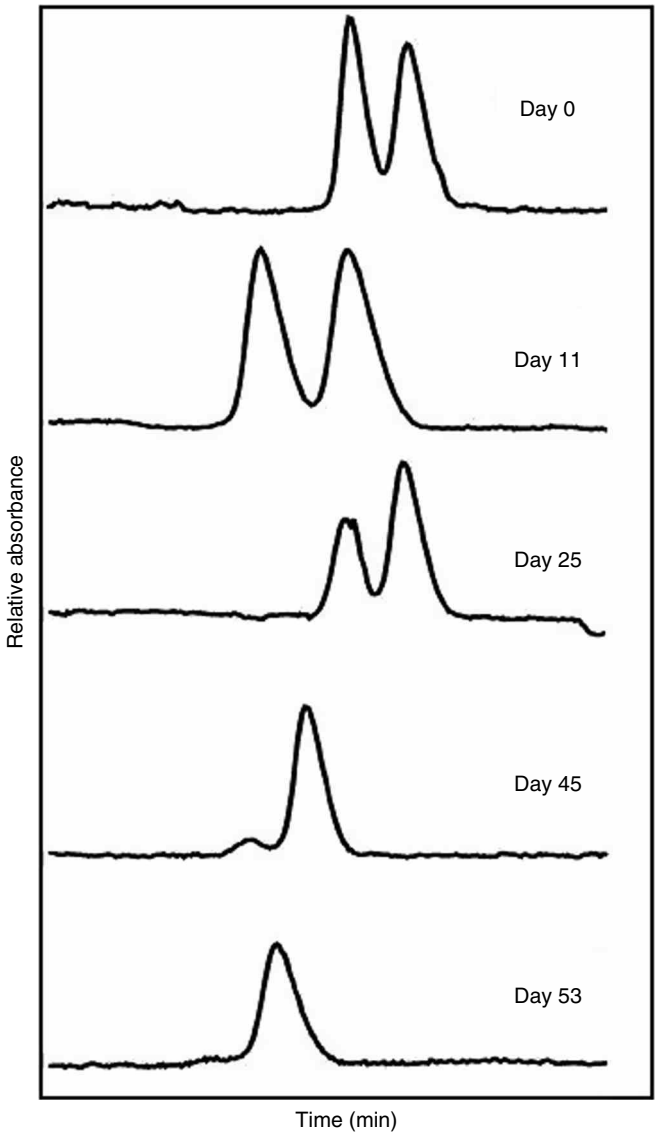

Fig. 1 Electropherograms of metalaxyl enantiomers in a series of slurry samples revealing the change in enantioselective degradation pattern with incubation time. The first peak is *R*-(+)-metalaxyl. Migration times vary with time due to changes in the CE column EOF. **Source:** From Application of capillary electrophoresis to study the enantioselective transformation of five chiral pesticides in aerobic soil slurries, in J. Agric. Food Chem.[23]

with capillary and BGE, molar absorptivity, and so on. Therefore, the optimization of chiral resolution can be controlled by varying all of the parameters mentioned above. For detailed information on the optimization of chiral analysis, one should consult our review.[2] Yi et al.,[27] reported a fast, simple, and sensitive CE method to study the separation and degradation of imazaquin enantiomers in field soils. The separations were optimized by pH, concentration of the buffer electrolyte, type and concentration of the chiral selectors, applied voltage, and temperature. The chiral selector used was hydroxypropyl-β-CD. However, a protocol for the optimization of the chiral analysis is given in Fig. 3.

DETECTION

Normally, the chiral pollutants in the environment occur at low concentrations and, therefore, a sensitive detection method is essential and is required in chiral CE. The most commonly used detectors in the chiral CE are UV, electrochemical, fluorescence, and MS. Mostly, the detection of the chiral resolution of drugs and pharmaceutical in CE has been achieved by a UV mode[16,34] and therefore the detection of the chiral pollutants may be achieved by the same method. The selection of the UV wavelength depends on the type of buffer, chiral selector, and the nature of the environmental pollutants. The concentration and sensitivity of UV detection are restricted insofar as the capillary diameter limits the optical path length. It has been observed that some pollutants, especially organochlorine pesticides, are transparent to UV radiation and, therefore, for such applications, electrochemical detection and MS are the best choices. Some chiral selectors, such as proteins and macrocyclic glycopeptide antibiotics, are UV-absorbing in nature and, hence, the detection of enantiomers becomes poor.

Table 2 Chiral analysis of some pollutants by capillary electrophoresis.

Chiral pollutants	Electrolytes	Detection	Refs.
Fenoprop, mecoprop, and dichloroprop	20 m*M* tributyl-β-CD in 50 m*M* ammonium acetate, pH 4.6	MS	[19]
Dichloroprop and 2-(2,4-dichlorophenoxy) propionic acid	100 m*M* acetic acid-sodium acetate buffer (pH 5.0) containing α-, β-, and γ-CDs	UV 206 nm	[21]
Metalaxyl, imazaquin, fonofos (dyfonate), ruelene (cruformate), and dichlorprop	30 m*M* Na-TB, pH 8.5, buffer with 100 m*M* SDS as the micelle, 15% AcN, and 40 m*M* γ-CD as the chiral selector	—	[23]
2-Phenoxypropionic and, dichloroprop, Fenoxaprop, fluaziprop, haloxyfop, and Diclofop enantiomers	75 m*M* Britton-Robinson buffer with 6 m*M* Vancomycine	—	[26]
Imazqaquin isomer	50 m*M* sodium acetate, 10 m*M* dimethyl-B-CD, pH 4.6	—	[27]
Imazaquin enantiomers	Sodium hydrogen phosphate (50 m*M*) at pH 10.1 containing 30 m*M* hydroxypropyl-β-CD (HP-β–CD)	—	[25]
Phenoxy acid herbicides	200 m*M* sodium phosphate, pH 6.5 with various Concentration of OG	—	[27]
Diclofop	50 m*M* sodium acetate, 10 m*M* trimethyl-β-CD, pH 3.6	—	[27]
Imazamethabenz isomers	50 m*M* sodium acetate, 10 m*M* trimethyl-β-CD, pH 4.6	—	[27]
2-(2-Methyl-4-chlorophenoxy) propionic acid	0.05 *M* lithium acetate containing α-CD	UV 200 nm	[28]
2-(2-Methyl-4-6-dichlorophenoxy) propionic acid	0.05 *M* lithium acetate containing β-CD	UV 200 nm	[28]
2-(2-4-Dichlorophenoxy) propionic acid	0.05 *M* lithium acetate containing Heptakis-(2,6-di-*O*-methyl)-β-CD	UV 200 nm	[28]
2-(2-Methyl chlorophenoxy) propionic acid and 2-(2-4-Dichlorophenoxy) propionic acid	0.05 *M* lithium acetate containing Heptakis-(2,6-di-*O*-methyl)-β-CD	UV 200 nm	[29]
2-(2-Methyl chlorophenoxy) propionic acid	0.05 *M* NaOAc, pH 4.5 with a-CD	UV230 nm	[30]
Phenoxy acid	0.1 *M* phosphate buffer, pH 6 with		
	Vancomycine	—	[31]
	Ristocetin	—	[31,32]
	Teicoplanin	—	[31,33]
	0.1 *M* phosphate and acetate buffer	—	[34]
	containing OM-OG	—	[35]
Phenoxy acid derivatives	β-CD and TM β-CD	—	[31,36]
Silvex	0.4 *M* borate, pH 10 containing *N,N-bis*-(D-gluconamidopropyl)-cholamide (Big CHAP) and deoxycholamide (Deoxy big CHAP)	—	[37]

Only few reports are available in the literature dealing with the limits of the detection for the chiral resolution of environmental pollutants by CE, indicating milligram per liter to microgram per liter as the limits of the detection. Tsunoi et al.,[17] carried out an extensive study on the determination of the limits of the detection for the chiral resolution of herbicides. The authors used a 230 nm wavelength for the detection and the minimum limit of the detection achieved was 4.7×10^{-3} *M* for 2,4-dichlorophenoxy acetic acid. On the contrary, Mechref and El Rassi[36] reported better detection limits for herbicides in the derivatized mode, in comparison to the underivatized mode. For example, the limit of the detection was enhanced by almost 1 order of magnitude from 1×10^{-4} *M* (10 pmol) to 3×10^{-5} *M* (0.36 pmol). In the same study, the authors reported 2.5×10^{-6} *M* and 1×10^{-9} *M* as the limits of the detection for the herbicides by fluorescence and laser-induced fluorescence detectors, respectively. Asami and Imura[38] described the trace enantiomeric compositions of glufosinate (D,L-GLUF); a phosphorus-containing amino acid-type herbicide; in a river. The chiral separation and detection (10^{-9} *M*) were achieved by solid-phase extraction and γ-CD-based CE.

SAMPLE PREPARATION

Many impurities are present in the samples of environmental or biological origin. Therefore, sample pretreatment is a

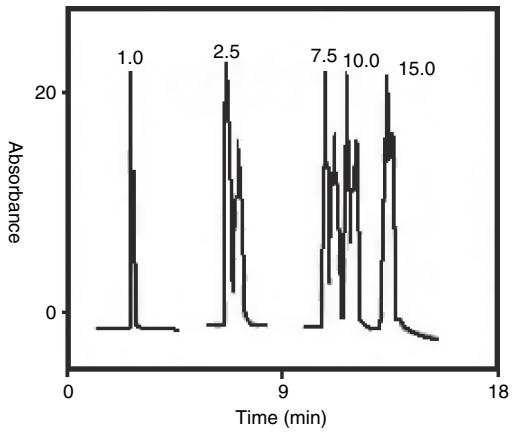

Fig. 2 Electropherograms of dichlorprop herbicide enantiomers with increasing concentrations of α-cyclodextrin (CD).
Source: From New derivatives of cyclodextrins as chiral selectors for the capillary electrophoretic separation of dichlorprop enantiomers, in J. Chromatogr. A.[21]

very important and necessary step for reproducible chiral resolution. Real samples often require the application of simple procedures, such as filtration, extraction, dilution, and so on. A search of the literature conducted and discussed herein (Table 2) indicates that all of the chiral resolution of the environmental pollutants was carried out by CE in laboratory synthesized samples only. Therefore, no report is published on the sample pretreatment before the chiral resolution of the environmental pollutants by CE. Some reviews have been published, however, on the pretreatment and sample preparation methodologies for the achiral analysis of pollutants.[39,40] Therefore, these approaches may be utilized for the preconcentration and sample preparation in the chiral CE of the environmental pollutants. Dabek-Zlotorzynska, Aranda-Rodriguez, and Keppel-Jones[40] reviewed the sample pretreatment methodologies for environmental analysis before CE. Moreover, some reviews have also been published in the

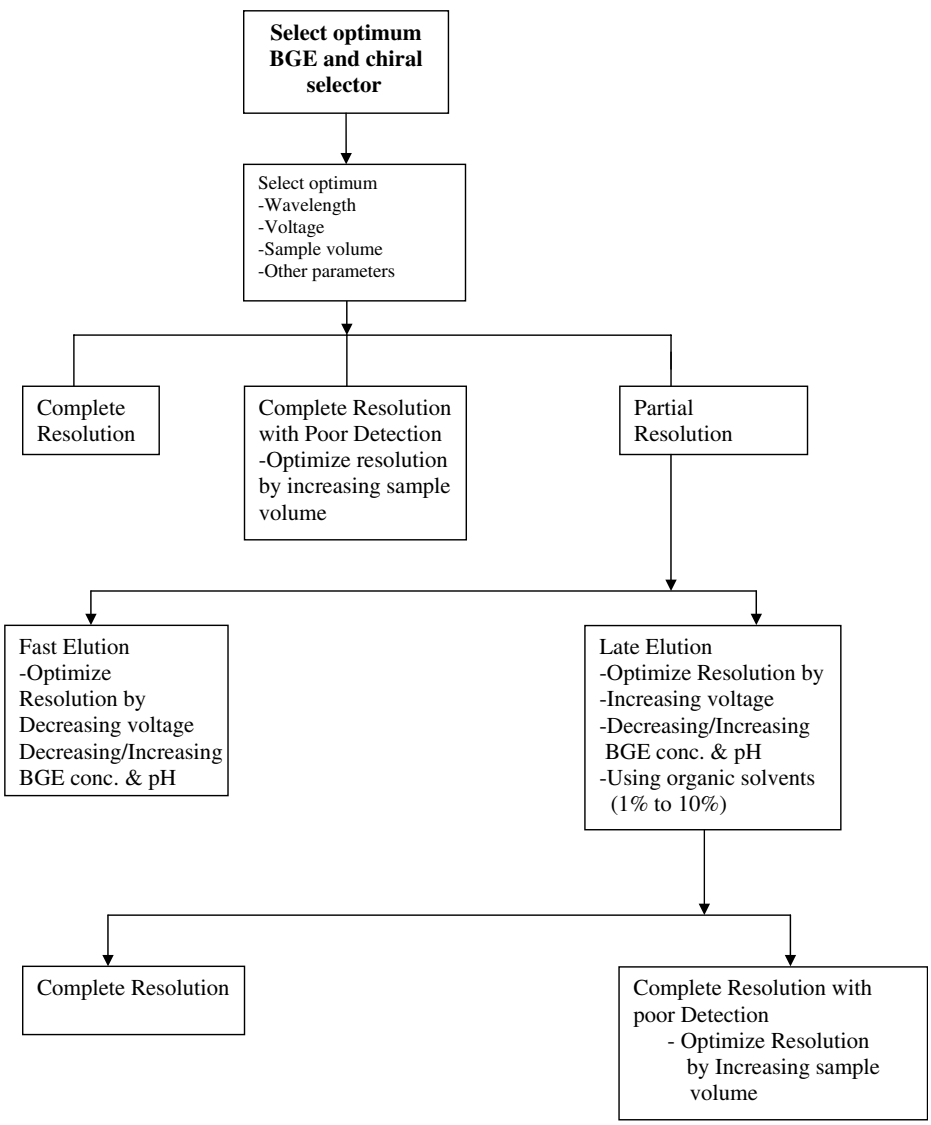

Fig. 3 The protocol for the development and optimization of CE conditions for the chiral separation.

last few years on this issue.[41–43] Whang and Pawliszyn[44] designed an interface that enables the solid-phase microextraction (SPME) fiber hyphenation to CE. They prepared a semi-custom-made polyacrylate fiber to reach the SPME–CE interface. The authors tested the developed interface to analyze phenols in water and, therefore, the same may be used for the chiral resolution of the pollutants.

MECHANISMS OF CHIRAL SEPARATIONS

It is well known that a chiral environment is essential for the enantiomeric resolution of the racemates. In CE, this situation is provided by the chiral compounds used in the BGE and is known as the chiral selector or chiral BGE additive. Basically, the chiral recognition mechanisms in CE are similar to those in chromatography using a chiral mobile-phase additive mode, except that the resolution occurred through different migration velocities of the diastereoisomeric complexes in CE. The chiral resolution occurred through diastereomeric complex formation between the enantiomers of the pollutants and the chiral selector. The formation of the diastereomeric complexes depends on the type and the nature of the chiral selectors used and the nature of the pollutants.

In the case of CDs, the inclusion complexes are formed and the formation of diastereomeric complexes is controlled by a number of interactions, such as π–π complexation, hydrogen bonding, dipole–dipole interaction, ionic bonding, and steric effects. Zerbinati, Trotta, and Giovannoli[20] used ethylcarbonate-β-CD and native α-CD for the chiral resolution of mecoprop and dichlorprop. The authors calculated the performance of these chiral selectors by means of a two-level full factorial design and calculated inclusion constants from the CE migration time data. Furthermore, they have proposed the possible structure of inclusion complexes on the basis of molecular mechanics simulations. Chankvetadze et al.,[45] explained the chiral recognition mechanisms in CD-based CE using UV, nuclear magnetic resonance (NMR), and ESI–MS methods. Furthermore, the authors determined the structures of the diastereomeric complexes by an X-ray crystallographic method.

The macrocylic antibiotics have some similarities and differences with the CDs. Most of the macrocyclic antibiotics contain ionizable groups and, consequently, their charge and possibly their three-dimensional conformation can vary with the pH of BGE. The complex structures of the antibiotics containing different chiral centers, inclusion cavities, aromatic rings, sugar moieties, and several hydrogen donor and acceptor sites are responsible for their surprising chiral selectivities. This allows for an excellent potential to resolve a greater variety of racemates. The possible interactions involved in the formation of diastereomeric complexes are π–π complexation, hydrogen bonding, inclusion complexation, dipole–dipole interactions, steric interactions, and anionic and cationic binding. Similarly, the diastereomeric complexes are formed with other chiral selectors involving specific interactions. In this way, the diastereomeric complexes possessing different physical and chemical properties are separated on the chiral path (achiral phase). The different migration times of these formed diastereomeric complexes depend on their sizes, charges, and their interactions with the capillary wall and, as a result, these complexes are eluted at different time intervals.

CAPILLARY ELECTROPHORESIS VS. CHROMATOGRAPHY

Today, chromatographic modalities are used frequently for the analysis of chiral pollutants. The wide application of HPLC is due to the development of various chiral stationary phases and excellent reproducibility. However, HPLC suffers from certain drawbacks, as the chiral selectors are fixed on the stationary phase and, hence, no variation in the concentrations of the chiral selectors can be carried out. Moreover, a large amount of the costly solvent is consumed to establish the chiral resolution procedure. Additionally, the poor efficiency in HPLC is due to the profile of the laminar flow, mass transfer term, and possible additional interactions of enantiomers with the residual silanol groups of the stationary phase. GC also suffers from certain drawbacks as discussed in the "Introduction."

On the contrary, the chiral resolution in CE is achieved using the chiral selectors in the BGE. The chiral separation in CE is very fast and sensitive, involving the use of inexpensive buffers. In addition, the high efficiency of CE is due to the flat profile created and to a homogeneous partition of the chiral selector in the electrolyte which, in turn, minimizes the mass transfer. Generally, the theoretical plate number in CE is much higher in comparison to chromatography and, thus, a good resolution is achieved in CE. In addition, more than one chiral selector can be used simultaneously for optimizing the chiral analysis. However, reproducibility is the major problem in CE and, therefore, the technique is not popular for the routine chiral analysis. The other drawbacks of CE include the waste of the chiral selector as it is used in the BGE. In addition, chiroptical detectors, such as polarimetric and circular dichroism, cannot be used as detection devices because of the presence of the chiral selector in the BGE. Moreover, some of the well-known chiral selectors may not be soluble in the BGE and, thus, a stationary bed of a chiral selector may allow the transfer of the advantages of a stationary bed inherent in HPLC to electrically driven technique, i.e., CE. This will allow CE to be coupled with the MS, polarimeter, circular dichroism, and UV detectors without any problem. Briefly, at present CE is not a very popular technique as is chromatography for the chiral analysis of pollutants, but it will gain momentum in the near future.

CONCLUSION

Monitoring of the chiral pollutants at trace levels is a very important and demanding field in the present scenario. CE has been gaining importance in the area of chiral analysis of various racemates. This entry indicates only few reports on the chiral resolution of environmental pollutants by CE. Moreover, it has not achieved a respectable place in the routine chiral analysis of these pollutants due to its poor reproducibility and to the limitations of detection. Therefore, many scientists have suggested various modifications to make CE a method of choice. To achieve good reproducibility, the selection of the capillary wall chemistry, pH and ionic strength of the BGE, chiral selectors, detectors, and optimization of BGE have been described and suggested for the analysis of organic and inorganic pollutants.[46–51] In addition, some other aspects should also be addressed so that CE can be used as a routine method in this field. The most important points related to this include the development of new and better chiral selectors, detector devices, and addition of a cooling device in the CE apparatus. In addition, chiral capillaries should be developed and the CE device should be coupled with sample preparation units, MS, polarimetric, and circular dichroism detectors, which may result in good reproducibility and improved limits of detection. The advancement of CE as a chiral analysis technique has not yet been fully explored and research in this direction is currently underway. In summary, the growth of CE is underway and will be developed fully in the near future. Let's hope for the best future and perspectives of CE in chiral pollutants analyses.

REFERENCES

1. Ariens, E.J.; van Rensen, J.J.S.; Welling, W., Eds.; *Stereoselectivity of Pesticides, Biological and Chemical Problems: Chemicals in Agriculture*; Elsevier: Amsterdam, 1988; Vol. 1.
2. Ali, I.; Gupta, V.K.; Aboul-Enein, H.Y. Chiral resolution of the environmental pollutants by capillary electrophoresis. Electrophoresis **2003**, *24*, 1360–1374.
3. Wong, C.S. Environmental fate processes and biochemical transformations of chiral emerging organic pollutants. Anal. Bioanal. Chem. **2006**, *386*, 544–558.
4. Chu, B.; Guo, B.; Wang, Z.; Lin, J.M. Recent advances in enantiomeric separation of chiral environmental pollutants by capillary electrophoresis. Se Pu **2007**, *25*, 657–663.
5. Hernandez-Borges, J.; Rodriguez-Delgado, M.A.; Garcia-Montelongo, F.J.; Cifuentes, A. Chiral analysis of pollutants and their metabolites by capillary electromigration methods. Electrophoresis **2005**, *26*, 3799–3813.
6. Jung, M.; Mayer, S.; Schurig, V. Enantiomer separations by GC, SFC and CE on immobilized polysiloxane bonded cyclodextrins. LC-GC **1994**, *7*, 340–347.
7. Blaschke, G.; Chankvetadze, B. Enantiomer separation of drugs by capillary electromigration techniques. J. Chromatogr. A, **2000**, *875*, 3–25.
8. Zaugg, S.; Thormann, W. Enantioselective determination of drugs in body fluids by capillary electrophoresis. J. Chromatogr. A, **2000**, *875*, 27–41.
9. Chankvetadze, B. *Capillary Electrophoresis in Chiral Analysis*; John Wiley & Sons: New York, 1997.
10. Raginaka, J. Enantiomer separation of drugs by capillary electrophoresis using proteins as chiral selectors. J. Chromatogr. A, **2000**, *875*, 235–254.
11. Tanaka, Y.; Otsuka, K.; Terabe, S. Separation of enantiomers by capillary electrophoresis-mass spectrometry employing a partial filling technique with a chiral crown ether. J. Chromatogr. A, **2000**, *875*, 323–330.
12. Aboul-Enein, H.Y.; Wainer, I.W.; Eds.; *The Impact of Stereochemistry on Drug Development and Use*; John Wiley & Sons: New York, 1997; Vol. 142.
13. Gtibitz, G.; Schmid, M.G. Chiral separation principles in capillary electrophoresis. J. Chromatogr. A, **1997**, *792*, 179–225.
14. Sarac, S.; Chankvetadze, B.; Blaschke, G. Enantioseparation of 3,4-dihydroxyphenylalanine and 2-hydrazino-2methyl-3-(3,4-dihydroxyphenyl)propanoic acid by capillary electrophoresis using cyclodextrins. J. Chromatogr. A, **2000**, *875*, 379–387.
15. Welseloh, G.; Wolf, C.; Konig, W.A. New technique for the determination of interconversion processes based on capillary zone electrophoresis: Studies with axially chiral biphenyls. Chirality **1996**, *8*, 441–445.
16. Miura, M.; Terashita, Y.; Funazo, K.; Tanaka, M. Separation of phenoxy acid herbicides and their enantiomers in the presence of selectively methylated cyclodextrin derivatives by capillary zone electrophoresis. J. Chromatogr. A, **1999**, *846*, 359–367.
17. Tsunoi, S.; Harino, R.; Miura, M.; Eguchi, M.; Tanaka, M. Separation of phenoxy acid herbicides by capillary electrophoresis using a mixture of hexakis(2,3-di-*O*-methyl)- and sulfopropylether-α-cyclodextrins. Anal. Sci. **2000**, *16*, 991–993.
18. Gomez-Gomar, A.; Ortega, E.; Calvet, C.; Merce, R.; Frigola, J. Simultaneous separation of the enantiomers of cizolirtine and its degradation products by capillary electrophoresis. J. Chromatogr. A, **2002**, *950*, 257–270.
19. Otsuka, K.; Smith, J.S.; Grainger, J.; Barr, J.R.; Patterson, D.G., Jr.; Tanaka, N.; Terabe, S. Stereoselective separation and detection of phenoxy acid herbicide enantiomers by cyclodextrin-modified capillary zone electrophoresis–electrospray ionization mass spectrometry. J. Chromatogr. A, **1998**, *817*, 75–81.
20. Zerbinati, O.; Trotta, F.; Giovannoli, C. Optimization of the cyclodextrin assisted capillary electrophoresis separation of the enantiomers of phenoxy acid herbicides. J. Chromatogr. A, **2000**, *875*, 423–430.
21. Zerbinati, O.; Trotta, F.; Giovannoli, C.; Baggiani, C.; Giraudi, G.; Vanni, A. New derivatives of cyclodextrins as chiral selectors for the capillary electrophoretic separation of dichlorprop enantiomers. J. Chromatogr. A, **1998**, *810*, 193–200.
22. Klein, C.; Schneider, R.J.; Meyer, M.T.; Aga, D.S. Enantiomeric separation of metolachlor and its metabolites using LC–MS and CZE. Chemosphere **2006**, *62*, 1591–1599.
23. Jarman, J.L.; Jones, W.J.; Howell, L.A.; Garrison, A.W. Application of capillary electrophoresis to study the

enantioselective transformation of five chiral pesticides in aerobic soil slurries. J. Agric. Food Chem. **2005**, *53*, 6175–6182.
24. Garrison, A.W.; Schmitt-Kopplin, P.; Avants, J.K. Analysis of the enantiomers of chiral pesticides and other pollutants in environmental samples by capillary electrophoresis. Methods Mol. Biol. **2008**, *384*, 157–170.
25. Desiderio, C.; Polcaro, C.M.; Padiglioni, P.; Fanali, S. Enantiomeric separation of acidic herbicides by capillary electrophoresis using vancomycin as chiral selector. J. Chromatogr. A, **1997**, *781*, 503–513.
26. Penmetsa, K.V.; Leidy, R.B.; Shea, D. Enantiomeric and isomeric separation of herbicides using cyclodextrin modified capillary zone electrophoresis. J. Chromatogr. A, **1997**, *790*, 225–234.
27. Yi, F.; Guo, B.; Peng, Z.; Li, H.; Marriott, P.; Lin, J.M. Study of the enantioseparation of imazaquin and enantioselective degradation in field soils by CZE. Electrophoresis **2007**, *28*, 2710–2716.
28. Nielen, M.W.F. Enantio-separation of phenoxy acid herbicides using capillary zone electrophoresis. J. Chromatogr. A, **1993**, *637*, 81–90.
29. Nielen, M.W.F. LIMS: A report on the 7th International LIMS Conference held at Egham, UK, 8–11 June, 1993. Trends Anal. Chem. **1993**, *12*, 345–356.
30. Garrison, A.W.; Schmitt, P.; Kettrup, A. Separation of phenoxy acid herbicides and their enantiomers by high-performance capillary electrophoresis. J. Chromatogr. A, **1994**, *688*, 317–327.
31. Gasper, M.P.; Berthod, A.; Nair, D.E.; Armstrong, D.W. Comparison and modeling of vancomycin, ristocetin A and teicoplanin for CE enantio-separations. Anal. Chem. **1996**, *68*, 2501–2514.
32. Armstrong, D.W.; Gasper, M.P.; Rundlet, K.L. Highly enantioselective capillary electrophoretic separations with dilute solutions of the macrocyclic antibiotic ristocetin A. J. Chromatogr. A, **1995**, *689*, 285–304.
33. Rundlet, K.L.; Gasper, M.P.; Zhou, E.Y.; Armstrong, D.W. Capillary electrophoretic enantiomeric separations using the glycopeptide antibiotic, teicoplanin. Chirality **1996**, *8*, 88–107.
34. Mechref, Y.; El Rassi, Z. Capillary electrophoresis of herbicides: Evaluation of octylmaltopyranoside chiral surfactant in the enantiomeric separation of phenoxy acid herbicides. Chirality **1996**, *8*, 518–524.
35. Mechref, Y.; El Rassi, Z. Capillary electrophoresis of herbicides: III. Evaluation of alkylglucoside chiral surfactants in the enantiomeric separation of phenoxy acid herbicides. J. Chromatogr. A, **1997**, *757*, 263–273.
36. Mechref, Y.; El Rassi, Z. Capillary electrophoresis of herbicides: I. Pre-column derivatization of chiral and achiral phenoxy acid herbicides with a fluorescent tag for electrophoretic separation in the presence of cyclodextrins and micellar phases. Anal. Chem. **1996**, *68*, 1771–1777.
37. Mechref, Y.; El Rassi, Z. Micellar electrokinetic capillary chromatography with insitu charged micelles: VI. Evaluation of novel chiral micelles consisting of steroidal-glycoside surfactant-borate complexes. J. Chromatogr. A, **1996**, *724*, 285–296.
38. Asami, T.; Imura, H. Absolute determination method for trace quantities of enantiomer of glufosinate by γ-cyclodextrin modified capillary zone electrophoresis combined with solid-phase extraction and on-capillary concentration. Anal. Sci. **2006**, *22*, 1489–1493.
39. Martinez, D.; Cugat, M.J.; Borrull, F.; Calull, M. Solid-phase extraction coupling to capillary electrophoresis with emphasis on environmental analysis. J. Chromatogr. A, **2000**, *902*, 65–89.
40. Dabek-Zlotorzynska, E.; Aranda-Rodriguez, R.; Keppel-Jones, K. Recent advances in capillary electrophoresis and capillary electro-chromatography of pollutants. Electrophoresis **2001**, *22*, 4262–4280.
41. Haddad, P.R.; Doble, P.; Macka, M. Developments in sample preparation and separation techniques for the determination of inorganic ions by ion chromatography and capillary electrophoresis. J. Chromatogr. A, **1999**, *856*, 145–177.
42. Fritz, J.S.; Macka, M. Solid-phase trapping of solutes for further chromatographic or electrophoretic analysis. J. Chromatogr. A, **2000**, *902*, 137–166.
43. Pedersen-Bjegaard, S.; Rasmussen, K.E.; Halvorsen, T.G. Liquid–liquid extraction procedures for sample enrichment in capillary zone electrophoresis. J. Chromatogr. A, **2000**, *902*, 91–105.
44. Whang, C.; Pawliszyn, J. Solid phase microextraction coupled to capillary electrophoresis. Anal. Commun. **1998**, *35*, 353–356.
45. Chankvetadze, B.; Burjanadze, N.; Pintore, G.; Bergenthal, D.; Bergander, K.; Mühlenbrock, C.; Breitkreuz, J.; Blaschke, G. Separation of brompheniramine enantiomers by capillary electrophoresis and study of chiral recognition mechanisms of cyclodextrins using NMR spectroscopy, UV spectrometry, electrospray ionization mass spectrometry and X-ray crystallography. J. Chromatogr. A, **2000**, *875*, 471–484.
46. Pacakova, V.; Coufal, P.; Stulik, K. Capillary electrophoresis of inorganic cations. J. Chromatogr. A, **1999**, *834*, 257–275.
47. Liu, B.F.; Liu, B.L.; Cheng, J.K. Analysis of inorganic cations as their complexes by capillary electrophoresis. J. Chromatogr. A, **1999**, *834*, 277–308.
48. Valsecchi, S.M.; Polesello, S. Analysis of inorganic species in environmental samples by capillary electrophoresis. J. Chromatogr. A, **1999**, *834*, 363–385.
49. Timerbaev, A.R.; Buchberger, W. Prospects for detection and sensitivity enhancement of inorganic ions in capillary electrophoresis. J. Chromatogr. A, **1999**, *834*, 117–132.
50. Horvath, J.; Dolnike, V. Polymer wall coatings for capillary electrophoresis. Electrophoresis **2001**, *22*, 644–655.
51. Mayer, B.X. How to increase precision in capillary electrophoresis. J. Chromatogr. A, **2001**, *907*, 21–37.

Pollutants: HPLC Analysis in Water

Silvia Lacorte
Department of Environmental Chemistry, Chemical and Environmental Research Institute of Barcelona (IIQAB), Barcelona, Spain

INTRODUCTION

Over the last decade, industry, agriculture, and human activities have led to the discharge of organic compounds to surface and coastal waters through accidental spills and waste discharges, resulting in waters of poor chemical quality. Among others, pesticides, detergents, halogenated aromatics, and pharmaceutical compounds are commonly found in continental waters at levels of ng/L or μg/L. To control the sources of pollution and spills, the Environmental Protection Agency of the United States (USEPA), Environment Canada, and the European Union have set quality indices and directives to protect the water quality, human salubrity, and guarantee the utilization of natural resources. Compounds of environmental interest are toxic and persistent organic pollutants, listed in the American and European Priority Lists, and emerging contaminants for which more analytical and toxicological information is needed to evaluate their potential impact upon the environment. Examples of emerging contaminants are surfactants, hormones, plasticizers, and pharmaceuticals. Some of those have endocrine disrupting properties and are capable of mimicking or antagonizing the actions of steroid hormones, affecting the health of humans and wildlife species by disrupting their normal endocrine function. Because pollutants of different physicochemical properties are present at extremely low concentrations in complex environmental water samples, the analytical procedure should provide both a sensitive and selective detection and should generate accurate and precise data.

DISCUSSION

Traditionally, gas chromatography (GC) was the preferred approach for the analysis of pollutants in water, due to the high sensitivity and selectivity of a variety of detectors such as the nitrogen–phosphorus detector (NPD), flame ionization detector (FID), or flame photometric detector (FPD), and the ease of coupling to mass spectrometry (MS). However, high-performance liquid chromatography (HPLC) or LC is the most powerful approach for the determination of polar, non-volatile, and thermolabile compounds (i.e., those which are not GC amenable). The purpose of this entry is to provide an overview of the main liquid chromatography (LC) techniques to determine priority and emerging organic pollutants in water.[1] The recent developments in detection techniques [including diode-array detection (DAD), fluorescence detection (FD), electrochemical detection (ECD)] and especially the ability to connect an LC to MS through atmospheric pressure ionization sources (API) have increased substantially the use of LC for water monitoring. The methods described here are group-specific and cover the analysis of 1) pesticides and herbicides, including metabolites, 2) polycyclic aromatic hydrocarbons (PAHs), 3) phenols, 4) surfactants, 5) phthalates, 6) steroid hormones, and 7) pharmaceutical and personal care products. The objective is to recommend suitable LC techniques for several chemical families and to provide information on quality parameters and applicability in water analysis. Table 1 classifies pollutants commonly found in water and summarizes the main LC techniques used for their determination. All methods proposed achieve limits of detection (LODs) at the low ppb–ppt level and reproducibilities below 10%, provided LC is combined with a preconcentration and adequate cleanup step.

PESTICIDES

Much concern is being given to the determination of pesticides in water due to their toxicological and neurotoxicological properties and to the severe rules imposed by the legislation that aims to protect natural resources. Many pesticides, including their degradation products, are water soluble, non-volatile, and polar, which leads to LC as the preferred approach. LC with ultraviolet (UV) or DAD are especially used for the analysis of organophosphorus and phenoxyacid pesticides, triazines and phenylurea herbicides, and quat herbicides and, in general, for compounds presenting a suitable chromophore (e.g., an aromatic moiety). The main advantages of LC/DAD are related to its robustness and ease of use and to the fact that it offers absorbance spectra that can be used to identify pesticides through spectral comparison. UV/DAD can be combined with acetonitrile–water mixtures because of their absorbance cutoff. Interferences caused by UV-absorbing compounds (e.g., humic and fulvic acids) can affect the quantification of target analytes.

LC/FD is more selective than LC/DAD and provides better sensitivity for naturally fluorescent compounds, as well as for many other compounds, such as glyphosate or

Table 1 Families of priority and emerging pollutants, principal method of analysis proposed, and main sources.

Compound class	Extraction	LC method	Main sources
Pesticides (organophosphorus phenoxyacid, phenylurea, triazines, carbamates, quats)	LLE, SPE, SPME, online SPE	UV, DAD, FD, MS	Agriculture, household, non-agricultural
Polycyclic aromatic hydrocarbons	SPE, LLE	FD, DAD, MS	Natural, anthropogenic
Chlorophenols	SPE, LLE	DAD, ED, CD, MS	Paper, pulp, plastic industry
Surfactants (alcohol ethoxylates, linear alkylbenzene sulfonates, nonylphenol ethoxylates)	LLE, SPE, online SPE, SPME	DAD, MS, MS/MS	Leather, textile, metal, food industry, household
Phthalates	LLE, SPE, SPME	DAD, MS	Plasticizers, additives
Steroid sex hormones (estrogens, progestrogens)	SPE, Online SPE	UV, DAD, MS/MS	Natural and synthetic sex hormones
Pharmaceuticals and personal care products	LLE, SPE	DAD, FD, MS, MS/MS, IT/MS, TOF/MS	Household, veterinary, pharmaceutical industry, not prescription drugs, diagnostic agents, fragrances
Antibiotics (tetracyclines, macrolide, penicillins, quinolones)			
Analgetics/antiinflammatory drugs (ibuprofen, diclofenac)			
Lipid regulators (fenofibric acid, gemfibrozil, clofibric acid)			
Antiseptic (triclosan) Musk compounds (galaxolide, tonalide, muskketone; muskxylene)			

SPE, solid-phase extraction; LLE, liquid–liquid extraction; SPME, solid-phase microextraction; DAD, diode-array detector; CD, coulometric detector; ED, electrochemical detector; FD, fluorescence detector; MS, mass spectrometry; IT, ion trap; TOF, time-of-flight.

carbamates, which are precolumn or postcolumn derivatized to yield fluorescent reaction products. An alternative to LC/FD for the analysis of aryl *N*-methylcarbamates and *N*-phenylcarbamates is LC with ED because these compounds can be easily oxidized at 1.1 V. However, complex water samples, such as wastewater or industrial effluents, might 1) increase the detection limits, 2) inhibit analyte detectability, or 3) interfere or coelute with the analytes.

Matrix effects can be avoided by using MS. Mass spectrometry is characterized by being highly selective and sensitive and, in addition, it offers spectral information that permits the unequivocal identification of target compounds. LC/MS with atmospheric pressure chemical ionization (APCI) and electrospray ionization (ESI) interfaces have been applied to monitor pesticides and produce chemical ionization mass spectra with molecular information, depending on set-up conditions. Limits of detection at ng/L and the linear response range over two orders of magnitude have been reported.[2]

POLYCYCLIC AROMATIC HYDROCARBONS

Polycyclic aromatic hydrocarbons are considered as priority pollutants due to their mutagenic and carcinogenic properties. They are introduced in the environment from natural sources [e.g., incomplete combustion of organic matter from natural processes (volcanic eruptions, fires)] or anthropogenic, such as burning of fossil fuels, waste incineration, and traffic. The concentration of PAHs in water is generally low due to the hydrophobicity of some compounds, and hence, very sensitive methods are needed to detect ng/L levels. GC with FID or MS are commonly used for their determination. However, because PAHs have natural fluorescent properties, LC/FD is advantageous over GC/MS because of its ability to measure the different PAH isomers, and comparable detection limits are obtained. LC/DAD and LC/APCI/MS can also be applied and have the advantage that hydroxylated PAH transformation products can be identified.[3]

PHENOLIC COMPOUNDS

Phenol and its derivatives are generated in a wide variety of industrial processes (e.g., manufacture of plastics, dyes, drugs, glues) and in the pulp and paper industry, and can also be formed as degradation products of some pesticides. Chlorophenols are toxic to aquatic organisms and to man, and even at low concentrations in water, they can be the cause of unpleasant taste and odor.

Current official analytical methods include GC with FID or MS and involve a derivatization step. However, there is a general trend to switch to LC procedures to avoid sample manipulation and because derivatization of phenols is not straightforward. Common detection techniques are

UV detection at 280 and 310 nm for nitrophenols and pentachlorophenol. LC/DAD is recommended because spectral libraries can be used for confirmation purposes. In terms of sensitivity, LC with ED or coulometric detectors (CD) produces better response than UV or DAD. However, electrochemical detection for LC has never become so popular as its inherent sensitivity and selectivity is affected by electrode fouling and poor reproducibility. Moreover, electroactive matrix components can increase the background current and make ED less robust for water monitoring. Therefore, this technique can only be recommended for monitoring clean water samples such as groundwater. LC with direct or indirect FD for phenols provided acceptable detection limits, but problems related to the derivatization step made the technique less attractive. Similar to other organic pollutants, phenolic compounds can be detected by LC/APCI/MS and LC/ESI/MS in negative ion mode and produce, in general, the deprotonated molecule as base peak. The advantage of APCI and ESI is that an increase of the extraction voltage enhances fragmentation via collision-induced dissociation (CID) and provide structural information, useful for confirmation and identification purposes.[4] Moreover, phenols are good candidates for capillary electrophoresis (CE) and capillary zone electrophoresis (CZE) because they permit a fast separation of polar and ionic compounds, have a high resolution, and are compatible with most LC detectors, including MS. In addition, trace enrichment can be performed in the capillary using isotachophoresis, making the technique suitable for water analysis.

SURFACTANTS

Linear alkylbenzenesulfonates (LAS), alcohol ethoxylates (AEO), and nonylphenol ethoxylates (NPEO) are synthetic surfactants used in the formulation of detergents and other cleaning products and are widely applied in the dye and leather industry and other industrial processes. These compounds have aroused considerable interest due to the large quantities produced globally and to the potential estrogenic effect of some of their degradation products. Their low volatility and anionic form of some make LC-based methods the preferred approach.[5] Due to the presence of different positional isomers and the biodegradation intermediates, LC/MS, and in particular with ESI, is the only technique that enables their identification and quantification in environmental waters. In addition, nonylphenol and octylphenol, are the main persistent metabolites of alkylphenol ethoxylates (APEs), which are both GC and LC amenable.

PHTHALATES

Phthalate esters (PAEs) are plasticizers used in the manufacturing of polyvinyl chloride (PVC) epoxy resins, adhesives, and lacquers for coating the inside of food containers. Minor applications are in cosmetics, insect repellents, insecticide carriers, and propellants. They are considered ubiquitous pollutants but show slight endocrine disrupting properties. The main problem of analyzing phthalate ethers still remains as regards the external contamination coming either from the extraction procedure or from the injection port. Provided an efficient extraction method is used (employing LLE, SPE with glass cartridges or SPME), phthalates can be detected at ppb levels using LC/DAD or at somewhat lower levels using LC/MS with either ESI or APCI interfaces.[6] One of the main problems is the difficulty to provide 100% recoveries using those techniques due to blank interferences. It is thus important to work with appropriate surrogate standards, e.g., deuterated compounds.

STEROID SEX HORMONES

Natural and anthropogenic steroid sex hormones are released to the environment in the proximity of large urban areas. Synthetic hormones can mimic the 17-β-estradiol and can produce estrogenic or feminizing effects at concentrations as low as 1 ng/L. Since many hormones are thermally unstable, ionic, or polar, LC combined with a highly efficient preconcentrating technique is the method of choice for their analysis. Detection can be performed by UV and DAD, although in many instances a more selective and sensitive detector is needed. As a result, MS is commonly used since it permits the identification, quantification, and confirmation in one single analysis. Among the LC/MS interfaces, both ESI and APCI can be used. ESI is well suited for the analysis of polar compounds, whereas APCI is more effective for medium polarity substances.[1] In most applications, ESI is operated in negative ion mode ionization, which offers better sensitivity than positive ion mode. In general, the $[M - H]^-$ and $[M + H]^+$ modes are formed under negative and positive modes. Since high sensitivity and selectivity is needed and not always met by single quadrupole mass analyzers, ion trap, time-of-flight analyzers or tandem MS are generally used to determine these compounds. Mode of operation includes selected ion monitoring (SIM) or selected reaction monitoring (SRM). Identification is performed by retention time match against a standard and by identification of target compounds at three ions or by monitoring the MS/MS transitions. In such cases, selectivity is enhanced and the problem of false positives is minimized.

PHARMACEUTICALS AND PERSONAL CARE PRODUCTS

The extensive use of pharmaceutical compounds and active ingredients in personal care products (PPCPs) has generated concern due to their ubiquity, persistence, and

bioaccumulation. Pharmaceuticals are continuously released to the environment via wastewaters from manufacturing industries, hospital effluents, and disposal of expired products. Most relevant pharmaceuticals in water are antibiotics, anti-inflammatory drugs, lipid regulators, and musk compounds. Their risk is often associated to imperceptible effects that can accumulate over time to yield serious changes. One clear example is the development of resistant bacteria due to the release of antibiotics in the environment. Concentrations found in wastewaters are generally of 1–100 μg/L, whereas in surface waters they are found at ng/L concentration. One of the main issues in the analysis of pharmaceuticals is to provide unequivocal identification. For such purposes, LC/MS based methods are used. Due to the lack of fragmentation of some compounds using a single quadrupole, ion trap or tandem MS are the preferred options. Among the interfaces used, both APCI and ESI provide good sensitivity although ESI gives lower LODs. A review of the methods used for several families of pharmaceuticals is given by Sacher et al.,[7] who indicate LC/ESI/MS/MS method performance and quality parameters (limits of detection, limits of determination, and limits of identification) for several families of pharmaceuticals.

CONCLUSIONS

Many organic pollutants in water can be analyzed with LC techniques at trace levels. From the different LC methods discussed in this entry, several remarks can be made: 1) For routine water monitoring, LC/DAD is the most common detection device used to analyze polar, thermolabile, and non-volatile compounds due to its robustness, high sample throughput, and the possibility of obtaining a UV spectrum that can be used for analyte confirmation; 2) LC/FD and ECD are more selective and sensitive than DAD and are especially useful for the monitoring of PAHs, carbamates, and phenols; 3) LC/MS with API sources and different combinations of mass analyzers have become highly robust techniques and the preferred option for the identification, confirmation, and quantification of organic pollutants in water. In addition, all LC techniques described can be coupled, on line, with solid-phase extraction, so that LODs can be decreased and their total automation permits to achieve high-sample throughput.

REFERENCES

1. Lopez de Alda, M.J.; Diaz-Cruz, S.; Petrovic, M.; Barceló, D. Liquid chromatography–(tandem) mass spectrometry of selected emerging pollutants (steroid sex hormones, drugs and alkylphenolic surfactants) in the aquatic environment. J. Chromatogr. A, **2003**, *1000*, 503–526.
2. Lacorte, S.; Barceló, D. Determination of parts per trillion levels of organophosphorus pesticides in groundwater by automated on-line liquid-solid extraction followed by liquid chromatography/atmospheric pressure chemical ionization mass spectrometry using positive and negative ion modes of operation. Anal. Chem. **1996**, *68* (15), 2464–2470.
3. Koeber, R.; Niessner, R.; Bayona, J.M. Comparison of liquid chromatography–mass spectrometry interfaces for the analysis of polar metabolites of benz[a]pyrene. Fresenius J. Anal. Chem. **1997**, *359*, 267–273.
4. Puig, D.; Barceló, D. Determination of phenolic compounds in water and wastewater. Trends Anal. Chem. **1996**, *15* (8), 362–376.
5. Jahnke, A.; Gandrass, J.; Ruck, W. Simultaneous determination of alkylphenol ethoxylates and their biotransformation products by liquid chromatography/electrospray ionisation tandem mass spectrometry. J. Chromatogr. A, **2004**, *1035* (1), 115–122.
6. Céspedes, R.; Petrovic, M.; Raldúa, D.; Saura, U.; Piña, P.; Lacorte, S.; Viana, P.; Barceló, D. Integrated procedure for determination of endocrine-disrupting activity in surface waters and sediments by use of the biological technique recombinant yeast assay and chemical analysis by LC–ESI–MS. Anal. Bioanal. Chem. **2004**, *378*, 697–708.
7. Sacher, F.; Lange, F.T.; Braunch, H.J.; Blankenhorn, I. Pharmaceuticals in groundwaters: Analytical methods and results of a monitoring program in Baden-Württemberg, Germany. J. Chromatogr. A, **2003**, *938*, 199–210.

Polyamides: GPC/SEC Analysis

Tuan Q. Nguyen
Department of Materials Science, Polymer Laboratory, Swiss Federal Institute of Technology, Lanne, Switzerland

INTRODUCTION

Synthetic polyamides (PA) are among the mostly widely used engineering thermoplastics, owing to their high strength and toughness, stiffness, abrasion resistance, and retention of physical and mechanical properties over wide temperature ranges. The material's outstanding properties are, to a large extent, due to their semicrystalline morphology and the cooperative intermolecular hydrogen-bonding of the amide groups. The strength of these dipolar interactions are reflected in the melting points, which are much higher in polyamides than in polyesters having comparable structures.

Proteins, including wool and silk fibers, are made up by the linkage of α-amino acids and constitute the most widespread source of natural polyamides.

Synthetic PAs are produced by polycondensation of bifunctional monomers or by cationic and anionic ringopening polymerization of lactams. Polymers obtained with the first technique are linear, whereas chain branching may occur with anionic polymerization. Based on their chemical structure, synthetic polyamides may be classified into two categories:[1]

1. Aliphatic polyamides, also known under the generic name nylon. Industrial nylons with the general structure $[\text{-RNHCO-}]_n$, such as PA-6, PA-11, and PA-12, are called monadic; those with the general structure $[\text{-NHR}_1\text{NHCOR}_2\text{CO-}]_n$ are called dyadic (PA-4,6, PA-6,6, PA-6,9, PA-6,10, and PA-6,12).
2. Aromatic polyamides or aramids. The best known in the specialty fiber market are Nomex™ (poly-*m*-phenyleneisophthalamide) and Kevlar™ (poly-*p*-phenyleneterephthalamide).

A number of polymers with structures related to those of polyamides have been developed, some of which have achieved commercial importance, such as

CONHNH (polyhydrazide), OOCNR (polyurethane), and CONRCO (polyimide).

SEC ELUANTS FOR POLYAMIDES

High cohesive strength confers an exceptional solvent resistance to PAs, which can be dissolved only under rather drastic conditions (i.e., in highly corrosive solvents at temperatures close to the polymer melting point). This limited solubility leads to serious difficulties in the solution characterization of these polymers, such as in the determination of molecular-weight distribution (MWD). Selection of a solvent medium which is good for the polymer, chemically inert, and compatible with the stationary phase is crucial to a successful size-exclusion chromatographic (SEC) analysis.[2] These criteria are particularly demanding for many aramids, which are also rigid-rod polymers. Poly-*p*-phenyleneterephthalamide, for instance, has been analyzed in 97% sulfuric acid on silica columns.

Recently, a less corrosive room-temperature eluant consisting of methane sulfonic acid + 5% methane sulfonic anhydride + 0.1 *M* sodium methane sulfonate has been reported for Kevlar and Technora fibers. Separation was performed on Hastelloy C columns packed with 4000 Å SAX 10 μm particles (Polymer Laboratories), using ultraviolet (UV) detection and poly(benzoxazole) for calibration.[3] Work on the SEC characterization of aramids is extremely limited and generally lacks details of molecular-weight (MW) accuracy. In the following section, we will focus exclusively on aliphatic polyamides.

HIGH-TEMPERATURE SOLVENTS

The first mention of SEC analysis of PA-6 and PA-6,6 is by Goebel (1967), using *m*-cresol at 135°C with Styragel® columns. It was soon realized, however, that PA degrades extensively within a few hours under the above experimental conditions; alternative solvents have been proposed, most of which can be used only at elevated temperatures, due to solubility or viscosity problems:[4]

- *O*-Chlorophenol at 100°C
- Hexamethylphosphoramide (85°C)
- Dimethylacetamide + 2.5% LiCl (100–130°C)
- Benzyl alcohol (130°C).

In addition to the necessity for high-temperature SEC, each of the above solvents has its own drawbacks, such as adsorptive effects with phenol derivatives, column blocking, and carcinogenicity with hexamethylphosphoramide and corrosion of stainless steel by the dimethylacetamide–LiCl mixture.

Benzyl alcohol has been tested at 100°C on silica columns. To prevent potential solute interactions with silica stationary phase, it is recommended to prefer cross-linked PS columns with benzyl alcohol at 130°C and polytetrahydrofurans as calibration standards (polystyrene and polyethylene oxide standards interact with the stationary phase under the analytical conditions).[5]

LOW-TEMPERATURE ELUANTS

Fluorinated Alcohols

Most solvents which dissolve nylon at room temperature are either too toxic (nitrobenzene) or too corrosive [strong acids: sulfuric, formic, dichloroacetic; concentrated alcoholic salt solutions (e.g., methanol + $CaCl_2$)] to be safely used as an SEC eluant. Fluorinated alcohols constitute an exception: It has been known for a long time that trifluoroethanol (TFE), tetrafluoropropanol (TFP), or hexafluoroisopropanol (HFIP), owing to the presence of strong electron-withdrawal groups ($-CF_2-$ and $-CF_3$), have the propensity to dissolve a large number of polymeric materials which possess receptive sites for H-bonding formation (proteins, stereoregular polyesters, and, more recently, polyaniline).

The application of fluoroalcohols for dissolving polyethylene terephthalate (PET) and polyamides dates back from the early 1960s. Dissolution tests show that the solubility of polyamides improves with the acidity of the fluoroalcohol and decreases with increasing steric hindrance of substituents adjacent to the hydroxyl group. The use of HFIP for the SEC of PA-6,6 and PET on porous glass and μ-Styragel columns was described by Drott in 1971. TFE was tested in the following year for the SEC separation of Nylon 6, using fractionated PMMA for calibration. Fluoroalcohols are hygroscopic and should be dried before use to avoid formation of corrosive products. Polymer adsorption was observed when the water content in the eluent is $>0.03\%$. Moisture in TFE and HFIP can induce the formation of carboxylate end groups in nylon. Electrostatic repulsion between these groups and residual carboxyl ions present in cross-linked PS packings will lead to ion exclusion, which can be suppressed with the addition of a salt (sodium acetate, sodium trifluoroacetate, or tetraethyl ammonium chloride) in the 10^{-2} M concentration range. At present, HFIP is the preferred room-temperature eluant for the SEC characterization of nylons and polyesters. TFE, although four times less expensive than HFIP, is more toxic and has limited dissolution capability for polyesters and for nylons with long alkyl sequences. In addition to high cost, the use of HFIP entails a number of difficulties, such as high volatility, health hazards, incompatibility with a PS–DVB-based stationary phase (particularly with columns of pore sizes <1000 Å), insolubility of PS standards, and the presence of non-steric exclusion effects. Most of these problems have now been largely solved: Calibration can be done with commercially available anionic poly(methyl methacrylate) (PMMA) standards or with "absolute" detection, incompatibility with the stationary phase is minimized with columns specially designed for HFIP (Polymer Laboratories, Shodex, Waters), and closed-loop distillation and the use of narrow-bore columns substantially reduces solvent consumption.

Despite this progress, SEC with HFIP remains an expensive procedure due to extra investment in fluorinated solvent and special columns. Finally, it should be noted that HFIP with a pK_a of 9.3 is sufficiently acidic to react with the nitrogen in aromatic polyimides, resulting in ring-opening solvolysis.

Mixed Eluants

In search of less expensive, less toxic, and lower viscosity eluants, a few authors have proposed diluting the active ingredient with a common SEC eluant such as toluene, dichloromethane, or chloroform. To lower the operating temperature and minimize polymer degradation, mixtures of *m*-cresol with chlorobenzene (50 : 50, v/v, 43°C), dichloromethane (50 : 50, room temperature), and chloroform have been used, with 0.25 wt% benzoic acid added to prevent adsorption. In the same vein, *o*-chlorophenol has been diluted with chloroform (25 : 75) and used at 20°C. The main disadvantage in this latter solvent was a small *dn/dc* for the polymer, which rendered refractive index measurements difficult. In addition, careful purification of the phenol is required to obtain a detection signal. Dichloroacetic acid diluted to 20 vol% with dichloromethane has been proposed as the mobile phase. However, even at this concentration, PA tends to degrade at room temperature.

Among the different solvent combinations, it appears that mixtures based on fluorinated alcohols give the best results in terms of stability of the polymer and compatibility with the stationary phase (conventional silica or PS–DVB columns can both be used). As with pure fluoroalcohols, a salt should be added to suppress polyelectrolyte effects. Toluene, with 20 vol% HFIP, has been used for the SEC fractionation of PA-12 (Fig. 1). However, based on thermodynamic excess properties, this solvent combination should be less efficient in terms of solvation power than mixtures of HFIP with chloroalkanes.

Mixtures of HFIP or TFE with $CHCl_3$ and CH_2Cl_2 have been successfully tested as SEC eluants. HFIP–CH_2Cl_2 mixtures have the advantage of being more stable, of low toxicity, and UV transparent up to 200 nm (an assess for UV-absorption detection) and are better solvents for PA than the other mixtures.[6] On the negative side, HFIP–CH_2Cl_2 forms a 30 : 70 (v/v) azeotrope at 30°C, thus limiting its use to room temperature. HFIP–$CHCl_3$ does not have an azeotrope, whereas TFE–$CHCl_3$ possesses a lower azeotrope at 55°C.

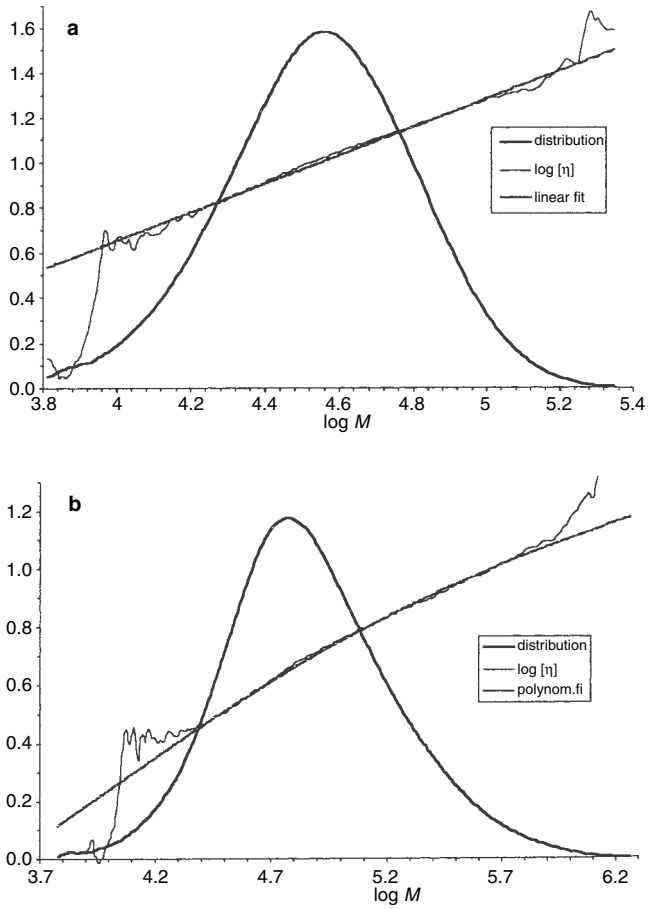

Fig. 1 SEC-viscometry characterization of a linear (a) and a branched (b) PA-12 synthesized by anionic polymerization, with different activators. Analysis conditions: mixed eluant 5:95 v/v; HFIP/CH_2Cl_2 at 30°C; Styragel-HR2/3/4/5 columns.

Problems Associated with Mixed Eluants

The use of mixed eluants in SEC analysis was proposed long ago to take advantage of the desirable properties of both solvent systems. Possible consequences of preferential solvation of the stationary phase and the polymer by one of the eluant components must, however, be critically evaluated: changes in mixture composition with polymer hydrodynamic volume, differences in composition of the mobile phase and of the solvent in the pores, dependence of the refractive index signal on elution volume, and the possibility of interference of the system peak with the oligomer signal in refractive index detection. Solvent recycling is more difficult and the original composition must be readjusted after distillation.

N-TRIFLUOROACETYLATION

N-Trifluoroacetylation remains a common technique to solubilize aliphatic PA for SEC analysis:[7]

$$\text{CONH}- + (\text{CF}_3\text{CO})_2\text{O} \rightarrow -\text{CON}(\text{COCF}_3)- + \text{CF}_3\text{COOH} \quad (1)$$

With a twofold to threefold excess in trifluoroacetic anhydride, reaction 1 is quantitative within 1 day at room temperature. The *N*-trifluoroacetylated polyamides (NTFA–PA) are soluble in many ordinary organic solvents, such as acetone, methylene chloride, chloroform, and tetrahydrofuran. In addition to the change in solubility, another remarkable feature of *N*-trifluoroacetylation is a near-two-orders-of-magnitude increase in the UV-absorption coefficient of the amide band, accompanied by a large bathochromic shift. Trifluoroacetylated polyamides have a rather small *dn/dc* in CH_2Cl_2 and detection was better achieved by UV absorption. Once prepared, the NTFA–PA solutions are unstable in the presence of atmospheric humidity and should be used immediately to avoid reverse hydrolysis, which converts the fluorinated polymer back into the original polyamide. It has been reported that SEC separation of NTFA–PA does not follow the universal calibration in dichloromethane, whereas better agreement was obtained in tetrahydrofuran. Comparative SEC analyses of NTFA–PA in both solvents on Styragel columns show, nevertheless, identical results.[6]

CONCLUSIONS

Size-exclusion chromatography analysis of PAs remains a difficult enterprise in comparison to other amorphous thermoplastics which can be readily dissolved in common solvents at room temperature. To improve MW accuracy, calibration should be performed with absolute detection (online viscometer, light scattering) or with a broad MWD polymer standard of identical chemical composition to the analyzed sample. Among the high-temperature eluants, benzyl alcohol is the less corrosive and seems to give the most reliable results. In low-temperature SEC, HFIP remains the best eluant, provided the necessary extra investment is not a problem. A mixed-eluant based on HFIP is a reasonable alternative to pure HFIP for long alkyl nylons (PA-12, PA-11). For shorter alkyl sequences, the high percentage of HFIP (>10 vol%) required for dissolution of the polymer may interfere with the size-exclusion mechanism of separation.[6] *N*-Trifluoroacetylation of the PA remains an interesting alternative, provided due care is given to prevent contact of the derivatized compound with reagents (water, alcohols, etc.) able to cause scission of the -N-$COCF_3$ bond.

REFERENCES

1. Alger, M.S.M. *Polymer Science Dictionary*; Elsevier Applied Science: London, 1989; 288.

2. Wang, P.J. *Handbook of Size Exclusion Chromatography*; Chromatography Science Series; Wu, C.S., Ed.; Marcel Dekker, Inc.: New York, 1995; Vol. 69, 161.
3. Nelson, R.M.; Warren, M.W. *International GPC Symposium '96*; Waters Corporation: Milford, MA, 1996; 453.
4. Goedhart, D.J.; Hussem, J.B.; Smeets, B.P.M. *Liquid Chromatography of Polymers and Related Materials II*; Delamare, X., Ed.; Chromatography Science Series 13; Cazes, J. Marcel Dekker, Inc.: New York, 1980; 203.
5. Marot, G.; Lesec, J. Size exclusion chromatography of polyamides. J. Liq. Chromatogr. Relat. Technol. **1988**, *11* (16), 3305.
6. Nguyen, T.Q. *International GPC Symposium '98*; Waters Corporation: Milford, MA, 1998; 135.
7. Jacobi, E.; Schuttenberg, H.; Schulz, R.C. A new method for gel permeation chromatography of polyamides. Makromol. Chem. Rapid Commun. **1980**, *1* (6), 397.

Polycarbonates: GPC/SEC Analysis

Nikolay Vladimirov
Research Center, Hercules Inc., Wilmington, Delaware, U.S.A.

INTRODUCTION

Polycarbonate (PC) polymers are amorphous thermoplastics with excellent toughness, clarity, and high heatdeflection temperatures. They are one of the better thermoplastics where strength and elastic moduli are concerned, offering both excellent impact strength and rigidity. In general, PCs are linear aromatic polyesters of carbonic acid. Polycarbonates can be described as polymeric combinations of bifunctional phenols, or bisphenols, linked together through carbonate linkages.

DISCUSSION

Robertson et al. used gel permeation chromatography (GPC) to examine PCs produced by different synthetic routes. They concluded that this method is superior to end-group analysis. Hoore and Hillman carried out fractionations of PCs by GPC to procure narrow molecular-weight-distribution (MWD) fractions which were used to calibrate the columns of a GPC system and an experimental "*Q* factor" of 23.8 was found. The calibration was further confirmed by membrane osmometry and light-scattering measurements.[1] The "*Q* factor" method is the simplest conversion method for molecular-weight calculations that provides data closer to the real molecular weights while still using polystyrene (PS) standards, but it lacks accuracy because it assumes the extended chain length of the polymer in solution. Most flexible polymers are not extended, but, rather, they are randomly coiled in solution. The more reliable method is to use the concept of the "hydrodynamic volume".[2] A comprehensive listing of Mark–Houwink coefficients *K* and *a* for different solvents and temperatures are published in the *Polymer Handbook*.[3] PC standards for calibration have been commercially available for the past several years from Polymer Standard Service Co. (Mainz, Germany) and American Polymer Standards Co. (Mentor, Ohio, U.S.A.).

The polymerization of trimethylene carbonate (1,3-dioxan-2-one) with a complexation catalyst was studied by Kriecheldorf et al.[4] On the basis of GPC measurements employing a universal calibration, weightaverage molecular weights up to approximately 22,000 were found. A combination of four Ultrastyragel columns was used, with nominal pore sizes of 100, 500, 1000, and 10,000 Å. The detector was a Waters M410 differential refractometer. The molecular weights were estimated from GPC results by means of intrinsic viscosities determined in dichloromethane at 25°C and an universal calibration curve, based on commercial PS standards.

Wang and Gonsalves[5] investigated the enzymecatalyzed synthesis of poly(ethyl phenol) (PEP), which was modified by copolymerization with PCs. GPC was carried out on a system equipped with a differential refractive index detector (DRI) and four Ultrastyragel columns in tetrahydrofuran (THF) with a flow rate of 1 ml/min. A calibration plot, constructed with PS standards, was used to determine the molecular weights. Based on the results, a slight difference between the high- and low-temperature products was observed for the pristine PC. The copolymers PC-*co*-PEP had higher molecular weights when compared to the pristine material, due to the linkage between PC and PEP, which effectively doubled the molecular weights.

GPC was used for the analysis of fullerene-functionalized polycarbonates, achieved by direct reaction of PC and fullerenes with aluminum chloride as a catalyst. THF was used as the eluent and the system was calibrated with PS standards. The working wavelength for the ultraviolet (UV) detector was 340 nm, where the starting PC was hardly detectable, but the reaction product gave two UV peaks, a strong peak in the "normal" molecular weight (MW) region and a weak peak in the very high MW region. Because THF is a non-solvent for fullerenes, the solubility of the polymers in THF and the GPC data served as evidence for the existence of a covalent bonding between the fullerene and PC.[6]

The influence of molecular structure on the degradation mechanism of degradable polymers of poly (trimethylene carbonate), poly(trimethylene carbonate*co*- caprolactone), and poly(adipic anhydride) was explored by Albertsson and Eklund.[7] Measuring the change of the mass and the molecular weight for the 104, 103 polymeric samples during degradation is a good indication of the degradation rate and an initial measure of material deterioration. The value of the molecular weight is not absolute, but, rather, it is relative to PS standards. This is sufficient for this study, which is simply concerned with the change in molecular weight relative to the starting value in order to evaluate the degradation. While the molecular weight decreased, an increase in the polydispersity was observed for some of the samples.

Studies of the thermal decomposition of the products under a nitrogen atmosphere were carried out by combining

LC under critical conditions of adsorption (LACCC) and SEC methods with matrix-assisted laser desorption/ionization–time-of-flight spectrometry (MALDI-TOF) and post-column derivatization. The critical conditions of polymer adsorption in the LC and an optimal matrix system for MALDI-TOF are reported. The changes of molar mass distribution and chemical heterogeneity are said to be due to the simultaneous processes of degradation and recombination.[8]

Branching by reactive end groups, syntheses, and thermal branching of 4-hydroxybenzocyclobutene (BCB-OH)/*p-tert*-butylphenol coterminated bisphenol PC was investigated by Marks et al.[9] Reactive end groups on bisphenol A (BA) PCs allow for significant structural changes in this condensation polymer that are not accessible by direct synthetic routes. Commercially offered branched PCs have improved melt rheological properties, compared to their linear analogues; they are manufactured by incorporation of a trifunctional comonomer in the PC polycondensation process. A GPC system, equipped with a UV detector (GPC-UV), and LC were used for the analyses. A Hewlett-Packard 1047 DRI detector and a LALLS (CMX-100) (low-angle light scattering) photometer were connected in series. Values of *dn*/*dc* were estimated from the DRI responses and sample concentrations. Five TSK MicroPak H-series (3 GMH6, 1 G500H6, and 1 G400H8) columns were used at 30°C with THF as the eluent at 1 ml/min. Heating to 300°C for 20 min causes the BCB-OH/PTBT BA PCs to branch or cross-link. The molecular weight and polydispersity of the branched polymers increase to a value at which the onset of the gel formation is observed. GPC–LALLS (M_w 135,100 and 310,700) was performed on two of the branched samples; it shows, as expected, a significantly higher molecular weight, particularly M_w, than indicated by GPC-UV (M_w 70,600 and 64,600, respectively).

The M_w by GPC-UV of each series of BCB-OH/PTBT BA PCs increases exponentially up to the gel point. The apparent decrease in M_w after the gel point reflects the values of the soluble fraction only, which are, therefore, not representative of the entire sample. LC was applied to investigate the types and distribution of BCB reaction products formed.

Unfortunately, none of the hyperbranched polymers studied to date has demonstrated good mechanical properties. A hyperbranched PC is also expected to be a brittle material, but such a structure may prove interesting as a highly functionalized prepolymer for composites, coatings, and other applications. Hyperbranched PCs were synthesized and characterized by Bolton and Wooley.[10] The products were prepared by the polymerization of an A_2B monomer derived from 1,1,1-*tris*(4′-hydroxyphenyl)-ethane. Silylation of the phenol terminated material with *tert*-butyldimethylsilyl chloride, followed by degradation of the carbonate linkages by reaction with lithium aluminum hydride and analysis of the products by HPLC allowed for the determination of the degree of branching, which was found to be 53%. The molecular weights of the carbonyl imidazolide-, phenol-, and *tert*-butyldimethylsilyl ether-terminated hyperbranched polycarbonates were 16,000, 77,000, and 82,000, respectively, from GPC, based on polystyrene standards, 23,000, 180,000, and 83,000, respectively, from GPC with LALLS, and 24,000, 160,000, and 88,000, respectively, from GPC with SEC software. SEC was conducted on a Hewlett-Packard series 1050 HPLC with a Hewlett-Packard 1047A refractive index detector, a Wyatt MiniDawn laser-light-scattering detector, and a Viscotek Model 110 differential viscometer. Two 5 μm Polymer Laboratories PL gel columns (300 × 7.7 mm), connected in series, were used with THF as an eluent.

Bailly et al. investigated the separation of polycarbonate oligomers by SEC and reversed-phase LC.[11] The separation of PC oligomers was achieved by SEC with styrene–divinylbenzene microparticle gel as a stationary phase and dichloromethane as a mobile phase. Oligomers were separated up to 10 repeating monomer units. SEC is useful for the analyses of the low-molecular- weight content of commercial PC samples. Retention times are significantly influenced by the nature of end groups (O– or OH–O–) (O-phenyl), indicating that adsorption occurs with hydroxy-terminated oligomers. Also, SEC results were compared with reversed- phase HPLC data.

Although the molecular weight of the bisphenol A polycarbonate repeat unit is relatively high, the separation of PC oligomers by SEC is difficult and has, thus, received little attention up to now. The problem is complicated by the existence of three oligomer families resulting from the addition of chain modifiers (monofunctional phenols) during the synthesis of the polymer by the usual interfacial method. The SEC results are compared with those obtained by reversed-phase HPLC for the same systems. Adsorption of phenolic compounds is known to occur on the surface of PS-DVB gels. When several types of oligomers are simultaneously present, interpretation of chromatograms becomes difficult and should be done with caution. This is particularly true when analyzing the oligomer content of commercial PC samples. The resolution obtained by reversed-phase HPLC remains superior, but, in most cases, quantitative result cannot be obtained by this technique because of solubility problems. In contrast with previous claims, the nature of the end groups was observed to significantly influence the retention time of PC oligomers by SEC. The presence of the hydroxy terminal groups induces a reversible adsorption of the compounds onto the columns. This effect is very important for oligomers having two hydroxy end groups.

As a consequence, the precise determination of the number-average molecular weights of PC samples by SEC is possible only if the nature of the oligomers present is taken into account.

REFERENCES

1. Crompton, T.R. *The Analysis of Plastics*; Pergamon Press: New York, 1984; 354.
2. Mori, S. HPLC application to polymer analysis. In *Handbook of HPLC*; Katz, E. Eksteen, R. Schooenmakers, P., Miller, N., Eds.; Marcel Dekker, Inc: New York, 1998; 836.
3. Brandrup, J., Immergut, E.H., Eds.; *Polymer Handbook, 3rd Ed.*; John Wiley & Sons: New York, 1989; VII/23.
4. Kricheldorf, H.R.; Jensen, J.; Kreiser-Saunders, I. Makromol. Chem. **1991**, *192*, 2391–2399.
5. Wang, J.; Gonsalves, K.E. Synthesis and film formation of polycarbonate-co-poly(p-theylphenol). J. Polym. Sci. Part A: Polym Chem. **1999**, *37* (2), 169–178.
6. Tnag, B.Z.; Peng, H.; Leung, M.; Song, Ch.; Takashi, M.; Kai Su; et al. Synthesis and optical properties of fullerene-functionalized polycarbonates. Macromolecules **1998**, *31*, 103–108.
7. Albertsson, A.-C.; Eklund, M. Influence of molecular structure on the degradation mechanism of degradable polymers: In vitro degradation of poly(trimethylene carbonate), poly (trimethylene carbonate-co-caprolactone), and poly(adipic anhydride). J. Appl. Polym. Sci. **1995**, *57* (1), 87–103.
8. Wachen, O.; Reichert, K.H.; Kruger, R.P.; Much, H.; Schulz, G. Thermal decomposition of biodegradable polyesters-III. Studies on the mechanisms of thermal degradation of oligo-1.-lactide using SEC, LACCC and MALDI-TOF-MS. Polym. Degrad. Stabil. **1997**, *55* (2), 225–231.
9. Marks, M.J.; Newton, J.; Scott, D.C.; Bales, S.E. Branching by reactive end groups, synthesis and thermal branching of 4-hydroxybenzocyclobutene/*p*-tert-butylphen coterminated bisphenol A polycarbonates. Macromolecules **1998**, *31* (25), 8781–8788.
10. Bolton, D.H.; Wooley, K.L. Synthesis and characterization of hyperbranched polycarbonates. Macromolecules **1997**, *30* (7), 1890–1896.
11. Bailly, Ch.; Daoust, D.; Legras, R.; Mercier, J.P. Chemical nucleation, a new concept applied to the mechanism of action of organic acid salts on the crystallization of polyethylene terephthalate and bisphenol–A polycarbonate. Polymer **1986**, *27* (5), 776–782.

Polyesters: GPC/SEC Analysis

Sam J. Ferrito
Analytical Services Department, Cooper Power Systems, Franksville, Wisconsin, U.S.A.

INTRODUCTION

Gel permeation chromatography (GPC), also known as size-exclusion chromatography (SEC), has proved to be an extremely useful analytical technique for characterizing the molecular-weight distribution (MWD) of polyesters. The MWD of a polymer can provide valuable information regarding the molecular composition. For example, along with relative molecular-weight averages, polydispersity, intrinsic viscosity, and branching information can be obtained.

DISCUSSION

Thermoplastic polyesters are popular engineering polymers because they offer excellent chemical and heat resistance, along with desirable electrical properties. When reinforced with glass or mineral fillers, they can be used to replace materials such as metals, ceramics, composites, and other less suitable plastics. In addition, thermoplastic polyesters offer excellent mechanical properties while retaining good processability.[1] Unfortunately, the polyester molecule is readily susceptible to hydrolysis. Hydrolytic degradation of the polymer causes random chain scissions to occur, normally at the ester linkages (R–CO–O–R′), which cause a reduction in molecular weight and, in turn, a reduction in mechanical integrity.[2,3] GPC can be used to monitor the hydrolytic process and predict product performance.[4]

Aromatic polyesters, because of their crystalline structure and polar nature, require the use of aggressive solvents and/or elevated temperatures to dissolve the polymer.[5] Various solvent blends can also be incorporated to aid in the dissolution process.[6,7]

Early work involving high-temperature GPC of polyesters utilized solvents such as meta-cresol and ortho-chlorophenol as mobile-phase solvents. These solvents are very viscous and require system temperatures of between 140°C and 150°C. Both solvents are also very dangerous and difficult to handle.[8,9]

More recently, hexafluoroisopropanol (HFIP) has been used successfully as a mobile phase for both polyesters and polyamides.[4,9,10] Unfortunately, HFIP is very expensive and dangerous to handle. HFIP requires special care and attention due to its extreme corrosiveness to eyes and skin. *Handling should be conducted only by trained professionals equipped with proper splash goggles and face shields for eye/face protection, and appropriate impervious gloves, aprons, and other protective equipments, as noted on the Material Safety Data Sheet for HFIP*. Mobile-phase distillation is necessary due to the extreme cost of the solvent. Some laboratories have reported using blends of HFIP and methylene chloride or HFIP and chloroform successfully in an effort to reduce solvent costs.[7,10–13]

Hexafluoroisopropanol is able to dissolve most polyesters and polyamides (nylons) at room temperature in about 4–8 hr. Sodium trifluoroacetate (NATFAT) is typically added to suppress any polyelectrolyte effects that could occur in HFIP.[9] GPC columns made from cross-linked polystyrene-divinylbenzene are typically used to perform the separation.[14] Calibration is generally performed using poly(methyl methacrylate) standards instead of polystyrene standards, due to solubility constraint.[5,15]

Typical polyesters characterized by GPC include polyethylene terephthalate (PET), polybutylene terephthalate (PBT), and polycyclohexylenedimethylene terephthalate (PCT). Polyphthalamides (PPA) and polyamides are also commonly analyzed.

Polyester detection is normally accomplished by using refractive index detection in conjunction with either viscometry or low-angle laser light scattering (LALLS).

The viscosity data are a quantitative gauge for monitoring the loss of high-molecular-weight chains within the polymer. Because the viscometer detector operates by measuring the pressure drop across a capillary tube, the intrinsic viscosity at a constant flow rate can be measured as follows[11,16]:

$$P = \left(\frac{8}{\pi}\right)\left(\frac{L}{r^4}\right)\eta F$$

where P is the pressure drop across the capillary, L is the capillary length, r is the internal radius of the capillary, η is the viscosity of fluid (GPC column effluent), and F is the flow rate.

Universal calibration incorporates intrinsic viscosity data with molecular-weight information provided by polymer standards of differing composition. Absolute molecular-weight determinations have proved to be inaccurate in HFIP due to non-size-exclusion interactions occurring within the process.[6,17] Typically, *relative* molecular-weight comparisons are reported when using the procedure. However, if *absolute* molecular-weight values are required, light-scattering techniques have been utilized with greater success.[18–20]

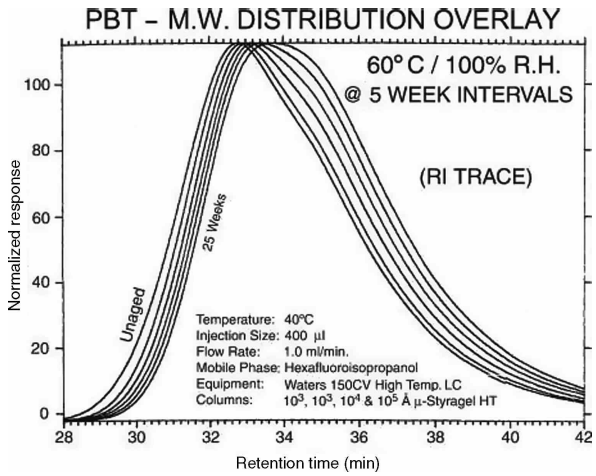

Fig. 1 Degradation of PBT at 60°C and 100% relative humidity; samples for analysis were taken at 5 week intervals.

Data derived from GPC analysis are commonly used to monitor the hydrolytic stability of various thermoplastic polyesters used under conditions requiring exposure to elevated temperatures and humidity. Polyester hydrolysis results in shifts in MWD toward lower molecular weight with a corresponding lowering of the intrinsic viscosity. A reduction in mechanical properties also is evident when hydrolysis occurs. Changes in mechanical properties can also be caused by moisture absorption and by weakening of the glass–fiber bond. GPC can distinguish between the chemical and physical changes occurring in the material.

Fig. 1 compares the changes that occur to PBT due to aging of the polymer at 60°C and 100% relative humidity for a total of 25 weeks. Samples were removed at 5 week intervals, and the molecular-weight distributions were compared. Polymer hydrolysis was evident by regular shifts in molecular-weight distribution toward lower molecular weight.[4]

CONCLUSIONS

Gel permeation chromatographic analysis will serve as a valuable technique for evaluating the newly developed hydrolysis-resistant polyesters and for monitoring the weatherability of polyesters in outdoor applications.

REFERENCES

1. Yokley, E. Thermoplastics for electrical applications. Electrical Manuf. November **1991**, 11–13.
2. Kellenher, P.G.; Bebbington, G.H.; Falcone, D.R.; Ryan, J.T.; Wentz, R.P. Thermal and hydrolytic stability of poly(butylene terephthalate). *37th Antec SPE, 1979; 527–531.*
3. Gardner, R.J.; Martin, J.R. Effective of relative humidity on the mechanical properties of thermoplastic polyesters. *37th Antec SPE, 1979; 831–834.*
4. Ferrito, S.J. An analytical approach toward monitoring degradation in engineering thermoplastic materials used for electrical applications. International GPC Symposium Proceedings; 1994; 675–684.
5. Mori, S. Size exclusion chromatography of poly(ethylene terephthalate) using hexafluoro-2-propanol as the mobile phase. Anal. Chem. **1989**, *61*, 1321–1325.
6. Moroni, A.; Havard, T. Characterizations of polyesters and polyamides through SEC and light scattering using 1,1,1,3,3,3-hexafluoro-2-propanol as eluent. In *International GPC Symposium '96*, 1996; 229–238.
7. Wu, C.-S., Ed.; In *Handbook of Size Exclusion Chromatography*; Chromatographic Science Series; Marcel Dekker: New York, 2003; Vol. 69, 169–172.
8. Water Division of Millipore: Solubilizing polyester (PET) for high temperature GPC analysis. Polym. Notes. April, **1998**, *3* (1).
9. Yau, W.W.; Kirkland, J.J.; Bly, D.D. Modern Size-Exclusion Liquid Chromatography; John Wiley & Sons: New York, 1979; 390–394.
10. Nguyen, Q. GPC-viscometry characterization of polyamides and polyethylene terephthalate in HFIP/CH_2CL_2 mixtures. In *International GPC Symposium '98*; 1998; 135–153.
11. Miller, R.L.; Seymour, R.W.; Branscome, L.W. The application of size-exclusion chromatography to study molecular-weight changes of flame-retardant fiber-reinforced polyesters. Polym. Eng. Sci. **1991**, *592*, 31–38.
12. Milana, M.R.; Denaro, M.; Arrivabene, L.; Maggio, A. Gel permeation chromatography (GPC) of repeatedly extruded polyethylene terephthalate (PET). Food Addit. Contamin. **1998**, *15* (3), 355–361.
13. Weidner, S.; Kuehn, G.; Werthmann, B.; Schroeder, H.; Just, U.; Borowski, R.; Decker, R.; Schwarz, B.; Schumuecking, I.; Seifert, I. In *A New Approach of Characterizing the Hydrolytic Degradation of Poly(ethylene terephthalate) by MALDI-MS*; John Wiley & Sons: New York, 1997; 2183–2192.
14. Meehan, E.; Oakley, S.; Warner, F. *The Application of a Novel Particle Technology for GPC Using HFIP as Eluent*; Polymer Laboratories Ltd.: Shropshire, UK; 353–356.
15. The Gel Permeation Chromatography of Poly(tetramethylene terephthalate); John Wiley & Sons: New York, 1977; 2293–2295.
16. Ekmanis, J.L. GPC analysis of polymers with an on-line viscometer detector. International GPC Symposium Proceeding; 1991;
17. Szesztay, M.; Laszlo-Hedvig, Z.S.; Tudos, F. Gel permeation chromatography identification of polyester oligomers with different endgroups. J. Appl. Polym. **1991**, *48*, 227.
18. Sibilia, J.P., Ed.; In *A Guide to Materials Characterization and Chemical Analaysis* 2nd Ed.; VCH Publishers: New York, 1996.
19. Pavlov, A.V.; Gur'yanova, V.V.; Karan'yan, O.M.; Morozov, A.G.; Prudskova, T.N. Modern methods for studying the molecular characteristics of polymers. Int. Polym. Sci. Technol. **1993**, *20* (12), T/41–T/44.
20. Berkowitz, S. Viscosity-molecular weight relationships for poly(ethylene terephthalate) in hexafluoroisopropanol-pentafluorophenol using SEC-LALLS. J. Appl. Polym. Sci. **1984**, *29*, 4353–4361.

Polymer Characterization and Degradation: Pyrolysis–GC/MS Techniques

Alfonso Jiménez
Department of Analytical Chemistry, Nutrition and Food Sciences, University of Alicante, Alicante, Spain

Roxana A. Ruseckaite
Research Institute of Material Science and Technology (INTEMA), University of Mar del Plata, Mar del Plata, Argentina

Abstract
This entry examines several recent advances in pyrolysis gas chromatography–mass spectrometry (Py–GC/MS). The use of analytical pyrolysis coupled to GC/MS in polymer studies has greatly increased in the past few years because of the hyphenation between a technique permitting a fast thermal program to yield volatile fragments with a powerful tool for their identification. The classical application of Py–GC/MS to thermoplastics has been extended recently to thermosets and even to biopolymers and biocomposites. The use of these techniques to study alternative methods for waste treatment has also been considered as an important and recent feature, showing possibilities for further improvement in the amount of its applications. A brief overview on the identification of polymer additives by Py–GC/MS has also been carried out.

INTRODUCTION

Gas chromatography (GC) is one of the most important instrumental techniques in analytical science. It is fast, sensitive, and allows combination with a wide range of detection methods with good selectivity. However, the application area of GC is limited because the molecules to be analyzed have to be thermally stable and sufficiently volatile. Numerous molecules, in particular macromolecules, do not meet these requirements. Polymers are not volatile; some of them have low solubility in most solvents and/or decompose easily during heating. Therefore, the direct application of powerful analytical tools, such as gas chromatography–mass spectrometry (GC/MS), is difficult on most polymers and composite materials. In such cases, some pretreatment to break polymer macromolecules are necessary to get the adequate chromatographic separation. The strategies exploited include conversion of macromolecules into smaller species and approaches to reduce the polarity of molecules.

Pyrolysis (Py) involves the thermal degradation of organic matter in an oxygen-free environment. There are many applications of analytical pyrolysis, and a large number of them are focused on polymers. From the fingerprints of the pyrolysis products of such macromolecules, valuable information can be obtained about the initial samples. Nowadays pyrolysis in combination with GC/MS is commonly used for the characterization of a wide range of polymeric materials, ranging from synthetic polymers to complex environmental mixtures and biomacromolecules. Some monographs[1,2] and entries[3–7] on this subject have been published in the last few years.

During pyrolysis the polymer sample is subjected to a fast thermal program to yield volatile fragments. Once formed, the highly reactive compounds are rapidly flushed out of the pyrolyzer to avoid secondary reactions. Therefore, the obtained degradation products are characteristic of the polymer and can be used to determine structural parameters of the original material. In addition, pyrolysis of plastics mainly generates oil and gases, which are useful products for energy generation or chemicals. In summary, pyrolysis techniques combined with GC (Py–GC) and GC/MS (Py–GC/MS) have extended the application of GC to materials of low volatility.

Depending on the heating mechanism, pyrolysis systems have been classified into two groups: continuous-mode pyrolyzers (e.g., furnace pyrolyzer) and pulse-mode pyrolyzers (e.g., heated filament, Curie point, and laser pyrolysis). All of them are extensively used in polymer characterization and degradation studies.

Pulse-mode pyrolyzers are the fastest, and they are mostly used in Py–GC/MS devices. The filament type pyrolyzer uses a pulse of a high electric current sent through a resistive piece of metal (frequently platinum). The Curie point pyrolyzer uses a ferromagnetic

metal coil and a high-frequency generator for extremely rapid heating of the samples to a fixed final temperature (it normally takes less than 1 sec to complete a program from room temperature to around 1000°C). The laser pyrolysis or micropyrolysis system consists of the laser and the associated optical devices; the sample chamber and cold trap; and a GC/MS for separation and detailed molecular characterization of the pyrolysis products.

Py–GC/MS techniques have been used in general for thermoplastics and some examples are presented here, but some recent studies on pyrolysis and thermal degradation of thermosets were carried out.[8–10] These resins lose their properties and become brittle solids after curing, and consequently they are neither fusible nor soluble in any solvent. Therefore direct chromatographic analysis of cured resins is not possible, unless Py–GC/MS is used.

POLYMER CHARACTERIZATION

In addition to composition determination, in particular for the gases produced after burning, the polymer microstructure can be explored based on the monomers/oligomers and/or their related fragments.[11] Recently a lot of work has been published in this field, covering fundamental studies as well as advanced applied developments.[12–15] Several copolymers were studied to demonstrate the power of Py–GC in microstructure determination.[16,17] In some circumstances, it was necessary to use a prepyrolysis derivatization technique to alter the sample degradation pathway. This technique can be used in any type of Py–GC method and can be combined with other derivatization procedures to get unique fragments for each polymer analyzed.

One particular and interesting application of the characterization of polymer structures after recycling process in polyesters was developed with the use of Py–GC/MS and Py–GC coupled to Fourier transform infrared spectroscopy (Py–GC/FTIR) techniques in the presence of tetramethylammonium hydroxide.[15] Authors suggested that biphenyl-type cross-linking structures would be considerably formed during the material recycling process of poly(butyleneterphthalate) (PBT) and poly(ethyleneterphthalate) (PET), which might in turn be attributed to the deteriorated properties of the recycled materials of the wasted polyester.

The recent introduction of biopolymer formulations as potential replacements of commodities in some applications has led to a rising interest in the structural studies of such materials. Py–GC/MS has become a very useful technique, as the information obtained can aid in structure elucidation of biopolymers as well as in providing detailed compositional information that can be used to differentiate structurally similar biopolymers. Some studies have recently been published in this area.[16–18]

There are many different approaches to measure the molar mass of polymeric materials. Nevertheless, for most of the traditional methods, such as gel permeation chromatography (GPC), the measurement is performed using dilute solutions of the polymer. Many polymers are not easily diluted in common solvents. In many circumstances, there is a need for a molar mass determination method that could operate under a solid-phase condition. Py–GC has been used to determine the number-average molar mass (M_n) via end-group analysis (EGA). The M_n of several polymers, such as poly(methyl methacrylate) (PMMA),[19] polycarbonate (PC),[20] and phenyl group-terminated polybutadienes (PBDs),[21] has been investigated. More recently, hyphenated systems based on size exclusion chromatography (SEC-Py–GC/MS) have been adapted to allow the use of aqueous solvents as applied in the characterization of water-soluble polymers.[22] The main advantage of these techniques is that no sample preparation is required. The success of these developments elevates the role of Py–GC as an important technique for the determination of number-average molar mass in polymers.

Other polymer properties, such as tacticity, can be studied by Py–GC. One example was the characterization of methyl methacrylate (MMA) sequences in the copolymers of MMA and various acrylates and their cross-linked polymers.[23] Tacticity was determined by Py–GC based on the relative peak intensities of the diastereomeric MMA tetramers in the pyrograms.

Py–GC/MS detection is routinely used to identify intractable polymers including cross-linked rubbers. The presence of characteristic degradation products in the pyrolysate is sufficient to positively identify poly(butadiene-acrylonitrile) rubbers.[24] The method is based on the identification of compounds in the pyrolysate that can be attributed to areas of the copolymer rubber where acrylonitrile and butadiene molecules adjoin.

Another interesting possibility for rapid characterization of synthetic polymers is the combination of laser-based pyrolysis systems (i.e., not linked to a thermal activation but to a photochemical activation) with fast gas chromatography–time-of-flight mass spectrometry (GC/TOF-MS). A combined instrument that was recently developed[25,26] joins the advantages of sampling by the laser, reconcentration of the volatile products, and sample introduction to the GC/TOF-MS. This method uses a UV laser as a fragmentation source, which can create pyrolysis fragments without prior sample pretreatment and with reduced analysis time. The potential for using lasers as a highly directional thermal source in analytical pyrolysis studies of natural biopolymers was further investigated by the laser micropyrolysis GC/MS analysis.[27] It was observed that laser micropyrolysis GC/MS can be used to measure the molecular composition of small ($\geq$50 μm) lignin quantities within complex matrices such as soils and coals by in situ analysis.

Some interesting methods have recently been developed for the very fast identification of compounds in particular samples. For example, direct temperature-resolved mass spectrometry (DTMS) is a fast fingerprinting method suited for the recognition of many classes of compounds, permitting the physical separation of low molar mass compounds by evaporation and polymer cross-linked fractions by a gradual rising of the temperature of the filament probe.[28] The analytical process at high temperature under DTMS conditions is equivalent to in-source pyrolysis mass spectrometry where analytes are analyzed collectively and not as separate fractions. This method has been applied to characterize asphalt samples from painting materials.[29]

PYROLYSIS OF POLYMER WASTES

Pyrolysis techniques have also shown a great potential for the study of thermal degradation of polymer wastes, which are common in urban and industrial residues. Commodity polymers in general are not biodegradable when buried in landfills. They can be the source of undesirable emissions [e.g., HCl in poly(vinyl chloride) (PVC) incineration]. An attractive solution to this problem is recycling by pyrolysis.[15,30–32] For example, some research was carried out to obtain the separation of PVC and PET.[33] This method permitted an easy separation of both materials at high temperatures, avoiding the formation of large amounts of HCl inherent to the PVC thermal degradation. A vacuum pyrolysis technology, known as the Pyrocycling™ process, which produces pyrolysis under vacuum conditions and reduces the incidence of secondary reactions in comparison to slow pyrolysis at atmospheric pressure, has been proposed.[34] GC/MS has been used to detect and determine all volatiles generated in this process.

Significant effort has recently been put in for the elimination of polymer wastes from electric and electronic equipment (WEEE) by pyrolysis. WEEE includes mainly epoxy resins and styrene polymers. They often contain brominated aromatics, which are highly contaminant. However, their elimination by simple thermal treatments is no longer possible as one of the most important drawbacks in dealing with thermal treatment of WEEE is the likely production of supertoxic halogenated dibenzodioxins and dibenzofurans. A pyrolysis method at low temperature range was developed, which limited the formation of such toxic by-products and reduced pyrolysis costs, even at relatively long residence times in the reactor.[30,35]

Copyrolysis of municipal solid waste (MSW) has led to a good separation when coupled to GC/MS. MSW is usually mainly composed of plastic residues (e.g., from packaging) and organic matter. During incineration of MSW each component may have a positive or negative influence on the thermal behavior of the others. Therefore, pyrolysis can also be envisaged as a tool for analyzing these effects. Some studies have approached this process, e.g., with the use of blends based on carbon and polymeric residues.[36] Another possibility is the study of the thermal decomposition of polystyrene as a way to separate this polymer from others during MSW treatment.[37]

Some effort has recently been made to study copyrolysis of wood biomass and polyolefins.[38] The effects of reaction temperature, wood–polymers mixture composition, and catalysts on the mixture's conversion into liquids and gases were established and discussed. The optimum temperature of wood–plastic mixture conversion, which corresponded to the maximum total liquid products yield, was close to 400°C. In the cohydropyrolysis processes the non-additive increase of the wood–plastic mixture conversion degree and of the distillable fractions yields took place as a result of the chemical interaction between radical fragments of wood and the thermal decomposition of polyethylene.

More work was carried out to study the effect of wood, cellulose, lignin, and activated charcoal on the thermal decomposition of polystyrene (PS) and polyethylene (PE) occurring in municipal waste.[39] Py–GC/MS revealed that these materials had a similar influence on PS and PE thermal decomposition under slow and fast heating conditions. The effect is related to the char-forming capability of the wood-derived additives; thus cellulose had the least and pure charcoal had the greatest influence on the decomposition of the polymers studied. The yield of monomers, dimers, and trimers decreased, and the formation of other products (e.g., toluene, ethyl benzene, and α-methyl styrene) was detected in the obtained pyrograms.

Chromatographic techniques can also be used to evaluate the performance of pyrolysis of waste products and the possibilities for recycling to give residues such as tires, automobile shredder residues, or commingled plastics an added value for further use. Some studies have considered the potential of Py–GC/MS as a tool for investigating the possibilities and limitations of pyrolysis as a means of recycling of polymers.[40,41] Through monitoring by GC, the kinetics of formation of hydrocarbon products can be determined. These products are interesting as raw materials for the petrochemical industry (mainly light olefins and aromatics) and for the synthesis of basic materials in tire manufacturing (isoprene and 1,3-butadiene). Some of the results obtained in these studies were used to determine the composition by GC/MS analysis of the composite derived oils, to establish the possibilities of reusing or treating and reusing.

Many studies were carried out for the pyrolysis treatment of residues obtained from particular sectors, such as automotive[42] and electronic industries.[43] Because pyrolysis involves the thermal degradation of plastic materials in the absence of air, it could yield valuable hydrocarbon products, while at the same time facilitating the recovery of the metal components. Pyrolysis would facilitate the recovery of both chemical hydrocarbons and metals embedded or mixed with

the plastic waste stream. The fractionation and identification of each component is easily carried out by GC/MS. Special attention has recently been given to the recovery of paint residues from automotive industry wastes.[44,45] It was shown that using Py–GC/MS it was possible to distinguish between members of a series of modified alkyl resins used in paint manufacture including those that were indistinguishable by FTIR. The identification of paint pyrolysis products enables easy discrimination of samples on the basis of their composition.

Another important application of Py–GC/MS techniques is the evaluation of contamination caused by industrial wastes consisting of usual polymers such as PVC, PS, poly(vinyl acetate) (PVA), polybutadiene (PB), poly(acrylonitrile-*co*-styrene-*co*-butadiene) (ABS), styrene-butadiene random (SBR) and styrene-butadiene-styrene block (SBS) copolymers. The presence of synthetic polymers in environmental samples is indicated by anomalously high levels of styrene and benzene in the pyrograms, and by the detection of selected markers (e.g., chlorobenzene for PVC, acetic acid for PVA, benzenebutanenitrile for ABS, cyclohexenylbenzene for styrene-butadiene rubbers), which are useful for better identification of individual polymers. This method was applied to a particular case of contamination in an Italian lake near an industrial area.[46,47]

THERMAL DEGRADATION OF BIODEGRADABLE POLYMERS AND BIOCOMPOSITES

Eco-friendly biodegradable polymers and biocomposites are relatively novel materials that can contribute to reduce the dependence on fossil sources. Because of their renewable nature and biodegradability, environmentally benign composite materials with properties comparable to those of some widely used commodities can be produced. Py–GC/MS has developed as a useful tool for the study of thermal degradation of such polymers and composites, and many studies have recently been published for biodegradable polymers, such as polycaprolactone (PCL),[48,49] polyhydroxyalcanoates (PHAs) and their copolymers,[50–52] poly(lactic acid) (PLA),[53,54] and carbohydrates, including starch and cellulose.[55,56]

In all cases Py–GC/MS proved to be a rapid and highly sensitive method to determine thermal degradation of biodegradable polymers by determining the evolved reaction products without using any time-consuming pretreatment. Py–GC/MS elucidates the microstructure of polymers, and in life time studies of polymers it was shown to be a versatile tool to study the extent of degradation. In addition and because this technique requires only trace amounts (about 0.1 mg or less) of the sample, the small difference in the composition of the residual polymer film recovered during a biodegradation test can be analyzed.

IDENTIFICATION OF POLYMER ADDITIVES BY PY–GC/MS

Polymer additives are essential in polymer processing and they determine end-use properties. A polymer additive is supposed to give some particular characteristics to the polymer. There are a large variety of additives depending on the desired properties, and their chemical structure can be very complex. Sometimes the identification and/or determination of such additives is difficult to be carried out by a single technique, and to establish the feasibility of environmentally and economically interesting plastic components it is necessary to determine their additive content. Some work was carried out to get a fast method for the identification of plastic additives by Py–GC/MS.[57,58]

Analytical determination of polymer additives is sometimes complicated, as evaporation of volatile fractions and degradation can occur simultaneously. Py–GC/MS has shown the potential to separate and finally identify volatiles in liquid polymers or oils, which are usually charged with additives. The onset temperature of thermal degradation of a liquid polymer and the characteristics of the pyrolysis at higher temperatures can be assessed by studying the volatiles produced. However, this approach requires that the true thermal degradation products be identified and not just any components that are simply evaporated from the sample. An innovative method, called the temperature-sequence GC method, was proposed.[59,60] In this method the same sample is subjected to a sequence of 10 sec pyrolyses at increasing temperatures, and for each temperature the complete chromatogram of the volatile products is recorded. This method has the potential to provide good characterization of the volatile products, but its disadvantage is that not enough temperature steps can be taken to allow the onset temperature of degradation.

Many studies on the identification of polymer additives by Py–GC/MS have been published recently; for example, an innovative method based on direct analysis of polymers containing polymeric hindered amine light stabilizers (HALS) by using pyrolysis coupled to GC/MS was applied successfully for fast and straightforward identification of these additives.[61] Each of the HALS showed different pyrolysis gas chromatograms containing characteristic pyrolysis products. As a result, HALS additives with very similar chemical structures, e.g., Chimassorb® 944 and Chimassorb® 2020, could be distinguished.

REFERENCES

1. Liebman, S.A.; Levy, E.J.; Eds. *Pyrolysis and GC in Polymer Analysis*; Marcel Dekker Inc.: New York, U.S.A., 1985.
2. Moldoveanu, S.C. *Analytical Pyrolysis of Natural Organic Polymers*; Elsevier: Amsterdam, 1998.

3. Wang, F.C.Y. Polymer analysis by pyrolysis gas chromatography. J. Chromatogr. A, **1999**, *843*, 413–423.
4. Moldoveanu, S.C. Pyrolysis GC/MS, present and future (recent past and present needs). J. Micro. Sep. **2001**, *13*, 102–125.
5. Jiménez, A.; Ruseckaite, R.A. Pyrolysis–GC/MS Techniques for Polymer Characterization and Degradation. In *Encyclopedia of Chromatography*, 2nd Ed.; Cazes, J., Ed.; Taylor & Francis: New York, 2005, 1396–1400.
6. Kaal, E.; Janssen, H.G. Extending the molecular application range of gas chromatography. J. Chromatogr. A, **2008**, *1184*, 43–60.
7. Sobeih, K.L.; Baron, M.; González-Rodríguez, J. Recent trends and developments in pyrolysis–gas chromatography. J. Chromatogr. A, **2008**, *1186*, 51–66.
8. Sobera, M.; Hetper, J. Pyrolysis–gas chromatography–mass spectrometry of cured phenolic resins. J. Chromatogr. A, **2003**, *993*, 131–135.
9. Vasile, C.; Brebu, M.A.; Karayildirim, T.; Yanik, J.; Darie, H. Feedstock recycling from plastics and thermosets fractions of used computers. II. Pyrolysis oil upgrading. Fuel **2007**, *86*, 477–485.
10. Valkama, S.; Nykänen, A.; Kosonen, R.; Ramani, R.; Tuomisto, F.; Engelhart, P.; ten Brinke, G.; Ikkala, O.; Ruokolainen, J. Hierarchical porosity in self-assembled polymers: Post-modification of block copolymer–phenolic resin complexes by pyrolysis allows the control of micro- and mesoporosity. Adv. Funct. Mater. **2007**, *17*, 183–190.
11. Wang, F.C.Y. The microstructure exploration of thermoplastic copolymers by pyrolysis–gas chromatography. J. Anal. Appl. Pyrol. **2004**, *71*, 83–106.
12. Gozet, T.; Hacaloglu, J. Pyrolysis mass spectrometry analyses of poly(3-methylthiophene). J. Anal. Appl. Pyrol. **2005**, *73*, 257–262.
13. Causin, V.; Marega, C.; Schiavone, S.; Della Guardia, V.; Marigo, A. Forensic analysis of acrylic fibers by pyrolysis–gas chromatography/mass spectrometry. J. Anal. Appl. Pyrol. **2006**, *75*, 43–48.
14. Lizarraga, L.; Verdejo, T.; Molina, F.V.; González-Vila, F.J. Pyrolysis–gas chromatography/mass spectrometry applied to the identification of different states of polyaniline. J. Anal. Appl. Pyrol. **2007**, *80*, 485–488.
15. Kawai, K.; Kondo, H.; Ohtani, H. Characterization of crosslinking structure in terephthalate polyesters formed through material recycling process by pyrolysis-gas chromatography in the presence of organic alkali. Polym. Degrad. Stabil. **2008**, *93*, 1781–1785.
16. Kaal, E.; de Koning, S.; Brudin, S.; Janssen, H.G. Fully automated system for the gas chromatographic characterization of polar biopolymers based on thermally assisted hydrolysis and methylation. J. Chromatogr. A, **2008**, *1201*, 169–175.
17. Dieckow, J.; Mileniczuk, J.; González-Vila, F.J.; Knicker, H.; Bayer, C. No-till cropping systems and N fertilisation influences on organic matter composition of physical fractions of a subtropical Acrisol as assessed by analytical pyrolysis (Py–GC/MS). Geoderma **2006**, *135*, 260–268.
18. Oudia, A.; Mészáros, E.; Jakab, E.; Simoes, R.; Queiroz, J.; Ragauskas, A.; Novák, L. Analytical pyrolysis study of biodelignification of cloned *Eucalyptus globulus* (EG) clone and *Pinus pinaster* Aiton kraft pulp and residual lignins. J. Anal. Appl. Pyrol. **2009**, *85*, 19–29.
19. Ito, Y.; Tsuge, S.; Ohtani, H.; Wakabayashi, S.; Atarashi, J.; Kawamura, T. Characterization of branched alkyl end groups off poly(methyl methacrylate) by pyrolysis–gas chromatography. Macromolecules **1996**, *29*, 4516–4519.
20. Ishida, Y.; Kawaguchi, S.; Ito, Y.; Tsuge, S.; Ohtani, H. Characterization of copolymer type polycarbonates by reactive pyrolysis-gas chromatography in the presence of organic alkali. J. Anal. Appl. Pyrol. **1997**, *40–41*, 321–328.
21. Wang, F.C.-Y.; Meunier, D.M. Number-average molecular mass determination of polymeric material by pyrolysis–gas chromatography. J. Chromatogr. A, **2000**, *888*, 209–217.
22. Kaal, E.R.; Kurano, M.; Geissler, M.; Janssen, H.G. Hyphenation of aqueous liquid chromatography to pyrolysis-gas chromatography and mass spectrometry for the comprehensive characterization of water-soluble polymers. J. Chromatogr. A, **2008**, *1186*, 222–227.
23. Kiura, M.; Atarashi, J.I.; Ichimura, K.; Ito, H.; Ohtani, H.; Tsuge, S. Tacticity of methacrylic copolymers and their crosslinked polymers studied by pyrolysis-gas chromatography. J. Appl. Polym. Sci. **2000**, *78*, 2140–2144.
24. Hiltz, J.A. Pyrolysis gas chromatography–mass spectrometry identification of poly (butadiene-acrylonitrile) rubbers. J. Anal. Appl. Pyrol. **2000**, *55*, 135–150.
25. Meruva, N.K.; Metz, L.A.; Goode, S.R.; Morgan, S.L. UV laser pyrolysis fast gas chromatography/time-of-flight mass spectrometry for rapid characterization of synthetic polymers: Instrument development. J. Anal. Appl. Pyrol. **2004**, *71*, 313–325.
26. Metz, L.A; Meruva, N.K.; Morgan, S.L.; Goode, S.R. UV laser pyrolysis fast gas chromatography/time-of-flight mass spectrometry for rapid characterization of synthetic polymer: Optimization of instrumental parameters. J. Anal. Appl. Pyrol. **2004**, *71*, 327–341.
27. Greenwood, P.F.; van Heemst, J.D.H.; Guthrie, E.A.; Hatcher, P.G. Laser micropyrolysis GC–MS of lignin. J. Anal. Appl. Pyrol. **2002**, *62*, 365–373.
28. Van den Berg, K.J.; Boon, J.J.; Pastorova, I.; Spetter, L.F.M. Mass spectrometric methodology for the analysis of highly oxidized diterpenoid acids in old master paintings. J. Mass Spectrom. **2000**, *35*, 512–533.
29. Languri, G.M.; Van der Horst, J.; Boon, J.J. Characterisation of a unique asphalt sample from the early 19th century Hafkenscheid painting materials collection by analytical pyrolysis MS and GC/MS. J. Anal. Appl. Pyrol. **2002**, *63*, 171–196.
30. Luda, M.P.; Euringer, N.; Moratti, U.; Zanetti, M. WEEE recycling: Pyrolysis of fire retardant model polymers. Waste Manag. **2005**, *25*, 203–208.
31. Dignac, M.F.; Houot, S.; Francou, C.; Derenne, S. Pyrolytic study of compost and waste organic matter. Org. Geochem. **2005**, *36*, 1054–1071.
32. Parres, F.; Sánchez, L.; Balart, R.; López, J. Determination of the photo-degradation level of high-impact polystyrene (HIPS) using pyrolysis–gas chromatography–mass spectrometry. J. Anal. Appl. Pyrol. **2007**, *78*, 250–256.
33. Kulesza, K.; German, K. Chlorinated pyrolysis products of co-pyrolysis of poly(vinyl chloride) and poly(ethylene terphthalate). J. Anal. Appl. Pyrol. **2003**, *67*, 123–134.

34. Miranda, R.; Pakdel, H.; Roy, C.; Vasile, C. Vacuum pyrolysis of commingled plastics containing PVC. II. Product analysis. Polym. Degrad. Stabil. **2001**, *73*, 47–67.
35. de Marco, I.; Caballero, B.M.; Chomón, M.J.; Laresgoiti, M.F.; Torres, A.; Fernández, G.; Arnaiz, S. Pyrolysis of electrical and electronic wastes. J. Anal. Appl. Pyrol. **2008**, *82*, 179–183.
36. Straka, P.; Nahunkova, J.; Brokova, Z. Kinetic pyrolysis of coal with polyamide-6. J. Anal. Appl. Pyrol. **2004**, *71*, 213–219.
37. Chauhan, R.S.; Gopinath, S.; Razdan, P.; Delattre, C.; Nirmala, G.S.; Natarajan, R. Thermal decomposition of expanded polystyrene in a pebble bed reactor to get higher liquid fraction yield at low temperatures. Waste Manag. **2008**, *28*, 2140–2145.
38. Sharypov, V.I.; Beregovtsova, N.G.; Kuznetsov, B.N.; Baryshnikov, S.V.; Cebolla, V.L.; Weber, J.L.; Collura, S.; Finqueneisel, G.; Zimmy, T. Co-pyrolysis of wood biomass and synthetic polymers mixtures: Part IV: Catalytic pyrolysis of pine wood and polyolefinic polymers mixtures in hydrogen atmosphere. J. Anal. Appl. Pyrol. **2006**, *76*, 265–270.
39. Jakab, E.; Blaszó, M.; Faix, O. Thermal decomposition of mixtures of vinyl polymers and lignocellulosic materials. J. Anal. Appl. Pyrol. **2001**, *58–59*, 49–62.
40. Aguado, R.; Olazar, M.; Vélez, D.; Arabiourrutia, M.; Bilbao, J. Kinetics of scrap tyre pyrolysis under fast heating conditions. J. Anal. Appl. Pyrol. **2005**, *73*, 290–298.
41. Miskolczi, N.; Bartha, L. Investigation of hydrocarbon fractions from waste plastic recycling by FTIR, GC, EDXRFS and SEC techniques. J. Biochem. Biophys. Methods **2008**, *270*, 1247–1253.
42. Day, M.; Cooney, J.D.; Mackinnon, M. Degradation of contaminated plastics: A kinetic study. Polym. Degrad. Stabil. **1995**, *48*, 341–349.
43. Day, M.; Cooney, J.D.; Touchette-Barrette, C.; Sheenan, S.E. Pyrolysis of mixed plastics used in the electronics industry. J. Anal. Appl. Pyrol. **1999**, *52*, 199–224.
44. Thorburn Burns, D.; Doolan, K.P. The discrimination of automotive clear coat paints indistinguishable by Fourier transform infrared spectroscopy via pyrolysis–gas chromatography–mass spectrometry. Anal. Chim. Acta **2005**, *539*, 157–164.
45. Zieba-Palus, J.; Zadora, G.; Milczarek, J.M.; Kóscielniak, P. Pyrolysis–gas chromatography/mass spectrometry analysis as a useful tool in forensic examination of automotive paint traces. J. Chromatogr. A, **2008**, *1179*, 41–46.
46. Fabbri, D.; Tartari, D.; Trombini, C. Analysis of poly(vinyl chloride) and other polymers in sediments and suspended matter of a coastal lagoon by pyrolysis-gas chromatography–mass spectrometry. Anal. Chim. Acta **2000**, *413*, 3–11.
47. Fabbri, D. Use of pyrolysis-gas chromatography/mass spectrometry to study environmental pollution caused by synthetic polymers: A case study: The Ravenna lagoon. J. Anal. Appl. Pyrol. **2001**, *58–59*, 361–370.
48. Draye, A.C.; Persenaire, O.; Brozek, J.; Roda, J.; Kosek, T.; Dubois, Ph. Thermogravimetric analysis of poly(ε-caprolactam) and poly[(ε-caprolactam)-*co*-(ε-caprolactone)] polymers. Polymer **2001**, *42*, 8325–8332.
49. Ruseckaite, R.A.; Jiménez, A. Binary mixtures based on polycaprolactone and cellulose derivatives: Thermal degradation and pyrolysis. J. Therm. Anal. Cal. **2007**, *88*, 851–856.
50. Fraga, A.; Ruseckaite, R.A.; Jiménez, A. Thermal degradation and pyrolysis of mixtures based on poly(3-hydroxybutyrate-8%-3-hydroxyvalerate) and cellulose derivatives. Polym. Test. **2005**, *24*, 526–534.
51. González, A.; Irusta, L.; Fernández-Berridi, M.J.; Iriarte, M.; Iruin, J.J. Application of pyrolysis/gas chromatography/Fourier transform infrared spectroscopy and TGA techniques in the study of thermal degradation of poly (3-hydroxybutyrate). Polym. Degrad. Stabil. **2005**, *87*, 347–354.
52. Sato, H.; Hoshino, M.; Aoi, H.; Ishida, Y.; Aoi, K.; Ohtani, H. Compositional analysis of poly(3-hydroxybutyrate-*co*-3-hydroxyvalerate) by pyrolysis-gas chromatography in the presence of organic alkali. J. Anal. Appl. Pyrol. **2005**, *74*, 193–199.
53. Westphal, C.; Perrot, C.; Karlsson, S. Py–GC/MS as a means to predict degree of degradation by giving microstructural changes modelled on LDPE and PLA. Polym. Degrad. Stabil. **2001**, *73*, 281–287.
54. Cornelissen, T.; Yperman, J.; Reggers, G.; Scheurs, S.; Carleer, R. Flash co-pyrolysis of biomass with polylactic acid. Part 1: Influence on bio-oil yield and heating value. Fuel **2008**, *87*, 1031–1041.
55. Aries, M.E.; Polvillo, O.; Rodríguez, J.; Hernández, M.; González-Pérez, J.A.; González-Villa, F.J. Thermal transformations of pine wood components under pyrolysis/gas chromatography/mass spectrometry conditions. J. Anal. Appl. Pyrol. **2006**, *77*, 63–67.
56. Torri, C.; Lesci, I.G.; Fabbri, D. Analytical study on the production of a hydroxylactone from catalytic pyrolysis of carbohydrates with nanopowder aluminium titanate. J. Anal. Appl. Pyrol. **2009**, *84*, 25–30.
57. Bart, J.C.J. Polymer/additive analysis by flash pyrolysis techniques. J. Anal. Appl. Pyrol. **2001**, *58–59*, 3–28.
58. Herrera, M.; Matuschek, G.; Kettrup, A. Fast identification of polymer additives by pyrolysis-gas chromatography/mass spectrometry. J. Anal. Appl. Pyrol. **2003**, *70*, 35–42.
59. Lehrle, R.S.; Pattenden, C.S. The quantitative measurement of the thermal stabilities of low-MW oils. Polym. Degrad. Stabil. **1999**, *63*, 89–94.
60. Lehrle, R.S.; Duncan, R.; Liu, Y.; Parsons, I.W.; Rollinson, M.; Lamb, G.; Barr, D. Mass spectrometric methods for assessing the thermal stability of liquid polymers and oils: Study of some liquid polyisobutylenes used in the production of crankcase oil additives. J. Anal. Appl. Pyrol. **2002**, *64*, 207–227.
61. Coulier, L.; Kaal, E.R.; Tienstra, M.; Hankemeier, Th. Identification and quantification of (polymeric) hindered-amine light stabilizers in polymers using pyrolysis–gas chromatography–mass spectrometry and liquid chromatography–ultraviolet absorbance detection–evaporative light scattering detection. J. Chromatogr. A, **2005**, *1062*, 227–238.

Polymer Formulations: Additives

Roxana A. Ruseckaite
Research Institute of Material Science and Technology (INTEMA), University of Mar del Plata, Mar del Plata, Argentina

Alfonso Jiménez
Department of Analytical Chemistry, Nutrition and Food Sciences, University of Alicante, Alicante, Spain

Abstract
Polymer additives fulfill several functions, both in processing the material and in improving the properties of the product, and can act, for example, as antioxidants, light stabilizers, antistatic agents, flame retardants, or plasticizers. There are hundreds of chemical compounds that are currently used as additives in polymer formulations. However, some of them are currently under discussion because of toxicological and environmental issues. Identification and eventual determination of polymer additives is an important issue in many fields, mainly in the area of packaging materials where additive migration from food contact materials may have potential toxic effects in humans. International regulations require that pharmaceutical, biomedical, cosmetic, and packaging materials do not interact physically or chemically with their contents or environments. Direct analysis of additives in the polymer matrix is difficult due to the small amounts usually added. Chromatographic techniques, either on their own or hyphenated to powerful analytical detection techniques, have shown a great potential to determine and eventually identify many of these compounds. This entry analyzes the recent advances in extraction, sampling, separation, as well as detection methods for the identification and analysis of a variety of typical polymer and biopolymer additives.

INTRODUCTION

During the past 50 years polymers have essentially changed human life, and the plastic industry has developed materials increasingly adapted to specific uses.[1] Processing, durability, and end-use response of plastic items result from an adequate and precise combination of the desired polymer and additives. Both technically and economically, additives form a large and increasingly significant part of the polymer industry. Additives such as lubricants, plasticizers, antioxidants, light stabilizers, colorants and dyestuffs, antistatic agents, surfactants, and preservatives are all commonly encountered in various polymer formulations, including synthetic polymers, biopolymers, composites, and biocomposites.[2–11]

There are hundreds of chemical compounds that are currently used as additives in polymer formulations. However, some of them are currently under discussion because of toxicological and environmental issues.[12,13] The increasing use of biopolymers and biodegradable polymers in commercial applications has encouraged the search for compatible and safe additives. A major portion of additive research is nowadays focused on compounds that are on the Food and Drugs Administration's (FDA's) Generally Regarded as Safe (GRAS) list.[14] Table 1 summarizes some of the most common and new additives used in polymer and biopolymer formulations.

For some decades plasticizers have gained industrial importance because their primary role is to improve flexibility and processability of polymeric materials. In general, plasticizers are low-molar-mass compounds (LMMC) that can disrupt polymer chain interactions by forming secondary bonds with polymer chains.[2,9] Lubricants increase the overall rate of processing or improve the release properties during processing and molding operations.[10]

Antioxidants are one of the main families of additives where much work has been carried out during the past few years. They preserve chemical and physical-mechanical properties of polymers both during processing and under in-use conditions.[11] In particular, natural antioxidants, mostly hindered phenols, are chosen to replace synthetic ones mainly in biopolymer and biocomposites formulations to render them completely compatible with different biologically active environments (e.g., natural environments and human body). Side effects of some synthetic antioxidants, such as butyl hydroxytoluene (BHT) and butyl hydroxyanisole (BHA), have been documented, and this has stimulated the substitution of synthetic antioxidants by natural ones.[15,16] Among them, tocopherol,[17] ferulic acid,[18] sorbic acid,[19] ascorbic acid,[20] and vegetable oil with essential fatty acids[21] are those most commonly found in biopolymer formulations.

Light stabilizers are able to reduce photo-oxidation and protect polymers from UV radiation damage. In general,

Table 1 Some common polymer and biopolymer additives.

Additive	Chemical name	Acronym/commercial name
Lubricants	Stearic acid	SA
	Stearamide	STA
	N,N′-ethylene-*bis*-stearamide	EBS
Plasticizers	Di(2-ethylhexyl) phthalate	DEHP; DOP
	Dibutyl phthalate	DBP
	Di(2-ethylhexyl) adipate	DOA
	Trioctyl trimellitate	TOTM
	Triethyl citrate, tributyl citrate, acetyl butyl citrate	TeC, TbC, ATBC
	di(propylene)(glycol)dibenzoate	Benzoflex 9–88
	Polyadipates	PAD
	Triethyleneglycol	TEG[a]
	Poly(ethyleneglycol)s	PEGs
	Poly(propyleneglycol)s	PPGs
	Sorbitol	SOR[a]
	Glycerol	GLY[a]
	Diethanol amine, triethanolamine	DETA, TEA
Antioxidants	Di-*t*-butyl-*p*-cresol	Bisphenol A
	Dioctadecyl (3,5-di-*t*-butyl-4-hydroxy benzyl) phosphate	Irganox 1093
	2,2′-methylene bis-(4-methyl-6-tert- butylphenol)	Irganox 2246
	Tris(2-methyl-4-hydroxy-5-*t*-butylphenyl)-butane	Irganox 1076
	α-tocopherol	Vitamin E[a]
	Ascorbic acid	AA[a]
	Sorbic acid	SA[a]
	Butylhydroxytoluene	BHT
	O-butylhydroxyanisole	BHA
	Ferulic acid	FA
	Essential oils and plant extracts	Rosemary extract
		Oregano extract
		Aloe vera
Light stabilizers	2-(2′-hydroxy-3,3,5-di-tert-amylphenyl) benzotriazole	Tinuvin 328 (Ciba)Tinuvin 928
	2-Hydroxy-4-*n*-octoxybenzophenone	Chimassorb (Ciba)Chimassorb 81
	Poly-{[6-[(1,1,3,3-tetramethylbutyl)-imino]-1,3,5-triazine-2,4-diyl] [2-(2,2,6,6-tetramethylpiperidyl)-amino]-hexamethylene-[4-(2,2,6,6-tetramethyl piperidyl)-imino]}	Chimassorb 944
	Benzophenone-type ultraviolet absorbers1,3-*bis*-[(2′-cyano-3′,3′-diphenylacryloyl)oxy]-2,2-*bis*-{[(2′-cyano-3′,3′-diphenylacryloyl)oxy]methyl}-propane-*N,N′-bis*-formyl-*N,N′-bis*-(2,2,6,6-tetramethyl-4-piperidinyl)-hexamethylenediamine	Univul (BASF); Uvinul 3030[a]; Uvinul 4050 H[a]
	Titanium dioxide (Rutilo)	TiO_2[a]
Organic flame retardant	Tetrabromobisphenol A	TBBA
	Hexabromocyclododecane	HBCD
	1,2,3,4,7,8,9,10,13,13,14,14-dodecahydro-1,4,4α,5,6,6α,7,10,10α,11,12,12a-dodecahydro-1,4,7,10-dimethanodibenzo[αε] cyclooctene	Dechlorane Plus

[a]Generally recognized as safe—a term used by the FDA.
Source: From http://www.foodsafety.gov/~rdb/opa-gras.html.[14]

they respond to the structure of the hindered amine and are known as hindered-amine light stabilizers (HALS).[5] Owing to their high molar mass, these additives have the advantage of limited mobility, and therefore their loss during processing or use is negligible.

Food preservation requires the use of integral solutions where the packaging plays a more active role. In this context, active packaging strategies aimed at the integration and/or controlled release of active molecules in conventional or renewable packaging systems, giving them an added value, are being developed. Evidences in the literature widely support the incorporation of antimicrobial food components and additives into packaging materials to reinforce the hurdle concept in the food production chain.[22] These compounds have proven to have an antimicrobial or bacteriostatic effect on spoilage of foods by pathogenic microorganisms, yeasts, and fungi. Several strategies intended to incorporate low-molecular-weight antimicrobial food components and bacteriocines to different films used for food packaging applications are described in the literature.[22–27] In this framework, the formulation of active packaging systems with controlled migration of natural antioxidants to foodstuff may result in prolonged shelf life and preservation of quality of the product.[27] Active substances like plant extracts and essential oils are being added to biopolymer formulations to produce biodegradable active films with antimicrobial and/or antioxidant properties.[28,29] On the contrary, aromatic ketones are being used to modify stable polymers commonly used in the manufacture of packaging materials such as polystyrene (PS) and poly(vinyl chloride) (PVC), in an attempt to make them degradable in natural environments.[30]

Flame retardants are a class of materials that are compounded into plastics to have certain defined reactions during combustion.[31] Brominated flame retardants (BFR) (Table 1) are widely used in many applications because of their low cost and high efficiency. However, the effect of such compounds on health has been studied and some of them such as octabromodiphenyl ether (octa-BDE), a type of BFR, are highly toxic, and its production has therefore been banned by the European Union. Therefore, there is a desire in the general flame retardant market to replace halogenated flame retardants with halogen-free alternatives. New phosphorus-based flame retardants seek to solve drawbacks of these more traditional non-halogens.[32] Nanoclays and carbon nanotubes are beginning to find use as antidripping agents in flame retardant packages.[33]

Identification and eventual determination of polymer additives is an important issue in many fields, mainly in the area of packaging materials where additive migration from food contact materials may have potential toxic effects in humans.[3,34–37] In biomedical applications, plasticizers present in the polymer [e.g., Di(2-ethylhexyl) phthalate (DEHP) in PVC] will readily leach into the liquids passing through it, particularly for lipid-containing fluids, e.g., blood. There is a great concern about the toxicity of DEHP, especially for risk groups such as patients in hemodialysis.[38] International regulations require that pharmaceutical, biomedical, cosmetic, and packaging materials do not interact physically or chemically with their contents or environments. Therefore, the possible release of polymer additives by plastic containers should be monitored, controlled, and minimized. Chromatographic techniques, either on their own or hyphenated to powerful analytical detection techniques, have shown a great potential to determine and eventually identify many of these compounds.

As was pointed out above, it is evident that the new reliable and rapid analysis method for polymer additives is a challenging task for several reasons: quality control, additive depletion/stability during processing and lifetime, litigation, migration studies, contamination, government regulations, and the development of new materials.

EXTRACTION AND SAMPLING METHODS

Techniques currently in use for the analysis of polymer additives have been extensively reviewed.[9,34–36] The most common analytical procedures on solid materials usually involve sample preparation and discontinuous and continuous extraction procedures[37,39] prior to the determination step, which is usually carried out by chromatographic techniques coupled to a variety of detection systems. Some innovative approaches have recently been proposed as alternatives to conventional extraction methods such as liquid–liquid extraction, liquid–solid extraction, and sonication. One example is the use of dispersive liquid–liquid microextraction (DLLME), which uses microliter volumes of extraction solvents along with a few milliliters of dispersive solvents such as methanol, acetonitrile, acetone, or tetrahydrofurane. This strategy was applied for preconcentration of organophosphorus pesticides from aqueous samples.[40] This method was very efficient and repeatable when applying for the concentration of three commercially available polymer additives, Irganox® 1076, Irganox® 1010, and Irgafos® 168, from aqueous solutions.[41]

For environmental reasons, direct examination of polymers by spectroscopy and/or by non-destructive methods is preferred over solvent-consuming techniques.[35] Poleunis et al.[42] reported the use of time-of-flight secondary ion mass spectrometry (ToF-SIMS) to analyze additive migration toward polymer surface in thin films of amorphous polyester containing variable quantities of an antioxidant (Irgafos® 168) and a UV stabilizer (Hostavin® N30). The results obtained were promising, but authors stated that ToF-SIMS data can be compared quantitatively only if the surfaces have undergone identical treatments.

Other analytical procedures, such as supercritical fluid extraction (SFE) and microwave-assisted extraction (MAE), are gaining significant attention. SFE is commonly applied to many analyses that require extraction from solid matrices and has found important applications in the

extraction of aromatic amines, organotin stabilizers, light stabilizers, and antioxidants from different polymers.[43–45] In general, compared with Soxhlet extraction, SFE ensures higher extraction efficiencies. New and improved SFE-based methods are being developed nowadays. SFE coupled to supercritical fluid chromatography (SFE–SFC) is a promising method and is believed to have a great potential in determining polymer additives.[46] In MAE, sample and solvent (or a mixture of solvents) are allocated in a vessel and microwave radiation is applied at adequate temperature. Samples are then recovered, filtered, and analyzed, generally, by a chromatographic technique. This method was successfully applied to extract commercial antioxidants (present in concentrations varying from 0.05 to 0.35 wt%) from pharmaceutical and cosmetic polyolefinic-based packaging materials.[47] For insoluble or highly cross-linked polymers, these approaches are difficult to apply; thermo-analytical extraction techniques that consist of liberating the additive by heating are required in these instances. Some thermo-analytical techniques, such as thermo-gravimetric analysis (TGA) or temperature programed pyrolysis (TPPy), specifically take advantage of relatively slow heating, in particular in combination with appropriate detection modes such as mass spectrometry (MS) (e.g., TG–MS, TG–FTIR, TPPy–MS). In such volatile removal techniques, the additives are usually detected at temperatures below the decomposition temperature of the polymer.

Other emerging environmentally-friendly extraction technique is liquid-phase microextraction assisted by porous membranes, especially hollow fiber liquid-phase microextraction (HFLPME).[48] This method is versatile and can be adapted to many analytical instruments. Dynamic HFLPME coupled with gas chromatography (GC) was applied for determining essential oils (ginger, oregano, and cinnamon) as migrants from several active films [ethylene-vinyl alcohol copolymers (EVOH)] with potential antioxidant and antimicrobial activity. Results indicate that active films containing ginger can be directly marketed without problems. Authors stated that the proposed method opens new perspectives to a technique limited until now to biomedical and environmental applications.

SEPARATION AND DETECTION

Among all chromatographic techniques that can be applied for the separation and identification of polymer additives after the extraction step, high-temperature capillary gas chromatography (CGC),[49,50] high-performance liquid chromatography (HPLC),[45,51–54] supercritical fluid chromatography (SFC),[26] size-exclusion chromatography (SEC),[55] capillary electrophoresis (CE),[56] and thin-layer chromatography (TLC),[57] are the most frequently used. In general, these techniques are coupled to different detection systems such as mass spectrometry (MS), matrix-assisted laser desorption ionization (MALDI) in combination with ToF mass spectrometry (MALDI-ToF), and Fourier transform infrared (FTIR) spectroscopy and microscopy.[57]

The separation and determination of antioxidants in polymers showed the potential use of LC for the separation and isolation of tocopherols in polymers and biopolymers.[17] It was shown that, although a large number of LC peaks were formed, they mainly corresponded to different stereoisomeric forms of only a small number of oxidative coupling products of tocopherol. Compared to classical LC, nano-LC[51] is advantageous because it is more efficient and less volume of the mobile phase is required, which in turn increases the sensitivity and reduces waste. On the contrary, this technique requires extraction procedures prior to analysis and currently the instrumentation and packed columns used are very expensive. SFE commercial system with the addition of a single six-portion valve and coupled to a reversed-phase LC system to perform online SFE–LC analysis was used for the quantitative determination of Irganox® 1010, Irganox® 1076, and Irgafos® 168 in poly(methylmethacrylate) (PMMA).[45] This SFE–LC online method was demonstrated to be more accurate because the analytes could be extracted at relatively low temperatures in the absence of light and under anaerobic conditions.

Flame retardants in polymer electronic waste were also identified by HPLC–UV/MS, and a comparison with GPC–HPLC–UV was carried out.[52] Brominated and phosphate-based flame retardants were determined. Pressurized liquid extraction followed by HPLC–UV/MS proved to be a powerful tool and covered all the compounds studied. GPC–HPLC–UV could be part of a routine quality control as reproducibility and limit of quantification are sufficient to give accurate results at levels around 0.1% dry mass.

HPLC–MS with atmospheric pressure chemical ionization (APCI) was recently used to evaluate the potential for the analysis of radiolysis products in polyethylene terephthalate (PET) irradiated with ^{60}Co gamma rays in order to evaluate the effect of such radiation on this polymer.[53] Results indicate that highly radiation-resistant polymers, such as PET, form measurable amounts of low-molar-mass degradation compounds, with their yield depending on the radiation conditions (presence or absence of air).

A new method for determining *N,N′*-ethylene-*bis*-stearamide (EBS), which is used as a high melting point lubricant for a variety of polymers, was developed by using normal-phase HPLC with evaporation-light scattering detection (ELSD).[54] First, EBS structure was characterized by GC–MS. EBS was identified, but two other molecular species (C16/C18 and C16/C16) were also present in large amounts. EBS in ethylene-vinyl acetate (EVA) was determined by dissolution/precipitation extraction method prior to HPLC procedure. Gel permeation chromatography (GPC) was envisaged in order to separate low-molar-mass compounds, despite the poor resolution. NP-HPLC with apolar solvent was used and EBS was quantified as the

unique peak as different molecular species could not be separated by NP-HPLC. This method turned out to be rapid and efficient for quantitative determination of EBS.

A food/antimicrobial coating system with sorbic acid as active compound, agar gel as model food, and wheat gluten or beeswax film as edible coating was studied by Guillard and coworkers.[14] The change in sorbic acid concentration with time, in the film and in the model food, was determined by measuring its concentration in agar gel after extraction with water by HPLC–UV. HPLC was also used recently to evaluate the kinetics of thymol (biopreservative) release from zein films.[23] Samples were immersed in water and the release of thymol was evaluated by measuring the concentration of the surrounding solution until an equilibrium value was reached. HPLC was used with a C18 reverse-phase column and detection at a wavelength of 277 nm. In all these applications, the separation step is one of the most critical during the whole analytical process.

GC combined with different extraction and detection techniques, such as Py–GC, Py–GC/MS, SFE–GC, thermodesorption cooled injection system (TD-CIS)–GC/MS among others, has been widely applied to the analysis of many additives. The use of Py–GC and Py–GC/MS in the determination of lubricants, antioxidants, plasticizers, and flame retardants was discussed in depth by Wang and coworkers.[9–11] In the case of antioxidants, Py–GC seems to provide an approach that minimizes sample preparation and follows it with a one-step effective separation and identification. A fast identification of low-molecular-weight antioxidants, which desorbed better before the polymer chain underwent decomposition, was achieved using MS detection.[49] Lubricants, which can be classified into fatty acids, their esters and amide derivatives, and waxes with a high number of carbon atoms, can be identified by Py–GC.[10] The most important advantage of Py–GC in plasticizer analysis is the elimination of sample preparation and the fact that all information can be obtained in a single experiment. The analysis of organic flame retardants requires the use of MS detection owing to the presence of halogen atoms in their structure. Off-line SFE–GC/MS was used to determine phenol, citrates, and phthalates in PVC with efficiencies of around 100%.[43,44]

Quite recently Bonini et al.[37] reported an easy method to control the migration of common plasticizers used in polymeric films for food contact packaging. The method they proposed is the result of the adaptation and optimization of the method used for determining phthalates in soft plastics for toys. The procedure comprises a Soxhlet extraction followed by a multiresidue gas chromatography analysis with flame ionization detector (FID) to evaluate the real content of plasticizers and their migration into food simulants. The procedure was applied to commercially available films for food packaging (not identified in the study). The average extraction yield was about 95%, and the chromatographic analysis was able to determine and clearly separate 16 compounds with detection limits ranging from 0.07 to 0.7 wt%. However, it is not clear whether the application of this method for the determination of these additives in biopolymers would be easy, because of the potential problems in the extraction of analytes prior to GC analysis. Therefore, the potential application of this sensitive method to biopolymers is a matter of research.

Despite its high resolution, conventional GC/MS encounters problems in solving all components in samples such as elastomers, particularly when they contain large amounts of multicomponent species. The use of two consecutive GC columns could be the solution. The method uses a non-polar column that concentrates the retained compounds for a short time and then sends them to a second shorter and narrower polar column situated in its own compartment within the main oven. The mass spectrometer is located at the end of the second column. The result of having two columns coupled in this way is that compounds can be separated by their volatility in the first column and by polarity in the second one. This strategy has been demonstrated to provide good results for additives in elastomers with a considerable increase in resolving power.[50]

SEC is usually applied to characterize complex mixtures of low-molecular-weight additives with molar masses between 150 and 1000 Da. This technique allows the classification of individual components in complex mixtures based on molar mass or hydrodynamic volume, and not on boiling point (like in GC) or polarity (in HPLC). This technique provided a reasonable separation for methylene-bridged hindered phenols and alkylated diphenylamines.[58] Compared with HPLC, SEC shows high reproducibility and simplicity in the chromatogram, which makes identification easier.

TLC remains one of the most widely used techniques for a simple and rapid qualitative separation.[57] The combination of TLC with spectroscopic detection techniques, such as FTIR or nuclear magnetic resonance (NMR), is a very attractive approach to analyze polymer additives. Infrared microscopy is a powerful technique that combines the imaging capabilities of optical microscopy with the chemical analysis abilities of infrared spectroscopy. FTIR microscopy allows obtaining of infrared spectra from microsized samples. Off-line TLC–FTIR microscopy was used to analyze a variety of commercial antioxidants and light stabilizers.[57] Transferring operation and identification procedure by FTIR takes about 20 min. However, the main drawbacks of TLC–FTIR are that TLC is a time-consuming technique and usually needs solvent mixtures, which makes TLC environmentally unsound, analytes must be transferred for FTIR analysis, and TLC–FTIR cannot be used for quantifying purposes.

Microemulsion electrokinetic chromatography (MEEKC) is an electrophoretic method that can be classified as an extension of micellar electrokinetic chromatography (MEKC) where the micelles are substituted by oil droplets. The high solubilizing ability of MEEKC allows the analysis of highly hydrophobic and aromatic polymer additives, such

as antioxidants. This technique was applied in the separation of commercial antioxidants from polypropylene (PP).[56] Two different approaches were investigated. When an acidic buffer and a negative separation voltage were used, incomplete separation of the analytes resulted. However, by using an alkaline buffer joined to a positive separation voltage the baseline separation of all analytes was achieved in less than 25 min. MEEKC is a superior separation method for these analytes, with respect to separation time, selectivity, and efficiency.

Finally, it is important to mention that huge efforts are being carried out for the development of more powerful extraction/chromatographic techniques/detection systems combinations. In this sense, highly specific stationary phases are being designed by molecular imprinting (MI).[59] MI is known as a technique that allows the fabrication of artificial receptors with recognition properties. Compounds of similar structure, like a group of β-lactam antibiotics, can be separated based on the application of molecularly imprinted polymers (MIP) as highly specific stationary phases in HPLC or capillary electrochromatography. Synthetic antioxidants, such as BHA and BHT, have been selected as templates for generating an MIP (BHA–MIT and BHT–MIT), as well as a control polymer (CP) in the absence of any template. BHA-MIT was successfully applied as the stationary phase in liquid chromatography and showed a higher affinity as compared to its CP.

CONCLUSION

The improvement in the number of published works in this area during the last years is a clear sign of the importance of the methods based on chromatography for the qualitative and quantitative analysis of polymer and biopolymer additives. This trend is expected to continue in the coming years as a response to the more stringent international regulations about additives for plastic materials and the need for more specific properties of polymer materials.

REFERENCES

1. Vert, M., In *Biodegradable Polymers and Plastics*, Vert, M.; Feijen, J.; Albertsson, A.C.; Scott, G.; Chiellini, E., Eds.; Royal Society of Chemistry: Cambridge, UK, 1992.
2. Rahaman, M.; Brazel, C.S. The plasticizer market: An assessment of traditional plasticizers and research trends to meet new challenges. Prog. Polym. Sci. **2004**, *29*, 1223–1248.
3. Lau, O.W.; Wong, S.K. Contamination in food from packaging material. J. Chromatogr. A, **2000**, *882*, 225–270.
4. Jana, T.; Roy, B.C.; Maiti, S. Biodegradable film 7. Modification of the biodegradable film for fire retardancy. Polym. Degrad. Stabil. **2000**, *69*, 79–82.
5. Coulier, L.; Kaal, E.R.; Tienstra, M.; Hankemeier, Th. Identification and quantification of (polymeric) hindered-amine light stabilizers in polymers using pyrolysis–gas chromatography–mass spectrometry and liquid chromatography–ultraviolet absorbance detection–evaporative light scattering detection. J. Chromatogr. A, **2005**, *1062*, 227–238.
6. Choi, J.S.; Park, W.H. Effect of biodegradable plasticizers on thermal and mechanical properties of poly(3-hydroxybutyrate). Polym. Testing, **2003**, *23*, 455–460.
7. Lucena, M.C.C.; de Alencar, A.E.V.; Mazzeto, S.E.; Da Soares, S. The effect of additives on the thermal degradation of cellulose acetate. Polym. Degrad. Stabil. **2003**, *80*, 149–155.
8. Harper, D.; Wolcott, M. Interaction between coupling agent and lubricants in wood–polypropylene composites. Compos. Part A, **2004**, *35*, 385–394.
9. Wang, F.C.Y. Polymer additive analysis by pyrolysis–gas chromatography I. plasticizers. J. Chromatogr. A, **2000**, *883*, 199–210.
10. Wang, F.C.Y.; Buzanowski, W.C. Polymer additive analysis by pyrolysis–gas chromatography III. Lubricants. J. Chromatogr. A, **2000**, *891*, 313–324.
11. Wang, F.C.Y. Polymer additive analysis by pyrolysis–gas chromatography IV. antioxidants. J. Chromtogr. A, **2000**, *891*, 325–336.
12. Heudorf, U.; Mersch-Sundermann, V.; Angerer, J. Phthalates: Toxicology and exposure. Int. J. Hyg. Environ. Health, **2007**, *210*, 623–634.
13. Williams, G.M.; Iatropoulos, M.J. Evaluation of potential human carcinogenicity of the synthetic monomer ethyl acrylate, Regul. Toxicol. Pharmacol. **2009**, *53*(1), 6–15.
14. http://www.foodsafety.gov/~rdb/opa-gras.html (accessed December 2008).
15. Perez-Bonilla, M.; Salida, S.A; van Beek, T.; Linares-Palomino, P.J.; Altarejos, J.; Nogueras, M.; Sánchez, A. Isolation and identification of radical scavengers in olive tree (Olea europaea) wood. J. Chromatogr. A, **2007**, *1112*, 311–318.
16. Cruz, J.M.; Sanchez-Silva, A.; Sendón-García, R.; Franz, R.; Paseiro-Losada, P. Studies of mass transport of model chemicals from packaging into and within cheeses. J. Food Eng. **2008**, *87* (1), 107–115.
17. Al-Malaika, S.; Issenhuth, S.; Burdick, D. The antioxidant role of vitamin E in polymers. V. Separation of stereoisomers and characterisation of other oxidation products of DL-α-tocopherol formed in polyolefins during melt processing. J. Anal. Appl. Pyrolysis **2001**, *73*, 491–503.
18. Nuthong, P.; Benjakul, S.; Prodpran, T. Effect of phenolic compounds on the properties of porcine plasma protein-based film. Food Hydrocolloids **2009**, *23*, 736–741.
19. Guillard, V.; Issoupov, V.; Redl, A.; Gontard, N. Food preservative content reduction by controlling sorbic acid release from a superficial coating. Innovat. Food Sci. Emerg. Tech. **2009**, *10* (1), 108–115.
20. Seacheol-Min, J.; Krochta, J.M. Ascorbic acid-containing whey protein film coatings for control of oxidation. J. Agric. Food Chem. **2007**, *55*, 2964–2969.
21. Oms-Oliu, G.; Soliva-Fortuny, R.; Martín-Belloso, O. Using polysaccharide-based edible coatings to enhance quality and antioxidant properties of fresh-cut melon. WLT **2008**, *41*, 1862–1870.
22. Active Packaging Research and Developments. In *Innovations in Food Packaging*, Han J.H., Ed., Elsevier: Amsterdam, 2001, 61

23. Gutiérrez, L.; Sánchez, C.; Batlle, R.; Nerin, C. New antimicrobial active package for bakery products. Trend Food Sci. Tech. **2009**, *20* (2), 92–99.
24. Gómez-Guillén, M.C.; Pérez-Mateos, M.; Gómez-Estaca, J.; López-Caballero, E.; Giménez, B.; Montero, P. Fish gelatin: A renewable material for developing active biodegradable films. Trend Food Sci. **2009**, *20* (1), 3–16.
25. Gemli, S.; Yemenicioğlu, A.; Altınkaya, S.A. Development of cellulose acetate based antimicrobial food packaging materials for controlled release of lysozyme. J. Food Eng. **2009**, *4*, 453–462.
26. Gómez-Estaca, J., Bravo, L., Gómez-Guillén, M.C., Alemán, A., Montero, P. Antioxidant properties of tuna-skin and bovine-hide gelatin films induced by the addition of oregano and rosemary extracts. Food Chem. **2008**, *112*, 18–25.
27. Ben Arfa, A.; Combes, S.; Preziosi-Belloy, L.N.; Gontard, N. Antimicrobial activity of carvacrol related to its chemical structure. Lett. Appl. Microbiol. **2006**, *43* (2), 149–154.
28. Mastromatteo, M.; Barbuzzi, G.; Conte, A.; Del Nobile, M.A. Controlled release of thymol from zein based film. Innovat. Food Sci. Emerg. Tech. **2009**, *10* (2), 222–227.
29. US Registration Brings Global Status for Avecias's New Plastic Antimicrobial. Plastic Additives & Compounding **2003**, *5* (4), 8.
30. Kaczmarek, H.; Swicatek, M.; Kaminska, A. Modification of polystyrene and poly(vinyl chloride) for the purpose of obtaining packaging materials degradable in the natural environment. Polym. Degrad. Stabil. **2004**, *83*, 35–45.
31. Wang, F.C.Y. Polymer additive analysis by pyrolysis–gas chromatography II. Flame retardants. J. Chromatogr. A, **2000**, *886*, 225–235.
32. Quintana, JB.; Rodil, R.; Reemtsma, T.; García-López, M.; Rodríguez, I. Organophosphorus flame retardants and plasticizers in water and air II. Analytical methodology, Trends Analyt. Chem. **2008**, *27*, 904–915.
33. Laoutid, F.; Bonnaud, L.; Alexandre, M.; López-Cuesta, J.M.; Dubois, Ph. New prospects in flame retardant polymer materials: From fundamentals to nanocomposites, Materials Sci. Eng. **2009**, *63* (3), 100–125.
34. Bart, J.C.J. Polymer/additive analysis at the limits. Polym. Degrad. Stabil. **2003**, *82*, 197–205.
35. Bart, J.C.J. Direct solid sampling methods for gas chromatographic analysis of polymer/additive formulations. Polym. Testing **2001**, 20, 729–740.
36. Bart, J.C.J. Polymer additive analysis by flash pyrolysis techniques. J. Anal. Appl. Pyrolysis **2001**, *58–59*, 3–28.
37. Bonini, M.; Errani, E.; Zerbinati, G.; Ferri, E.; Girotti, S. Extraction and gas chromatography evaluation of plasticizers in food packaging films. Microchem. J. **2008**, *90*, 31–36.
38. Matsumoto, M.; Hirata-Koizumi, M.; Ema, M. Potential adverse effects of phthalic acid esters on human health: A review of recent studies on reproduction. Regul. Toxic. Pharm. **2008**, *50*, 37–49.
39. Sendón García, R.; Sánchez Silva, A.; Cooper, I.; Franz, R.; Paseiro Losada, P. Revision of analytical strategies to evaluate different migrants from food packaging materials, Trends Food Sci. Tech. **2006**, *17*, 354–366.
40. Berijni, S.; Assadi, Y.; Anbia, M.; Milani-Hosseini, M.R.; Aghaee, E. Dispersive liquid–liquid microextraction combined with gas chromatography-flame photometric detection: Very simple, rapid and sensitive method for the determination of organophosphorus pesticides in water. J. Chromatogr. A, **2006**, *1123*, 1–9.
41. Farajzadeh, M.A.; Bahram, M.; Jönsson, J.A. Dispersive liquid-liquid microextraction followed by high-performance liquid chromatography–diode array detection as an efficient and sensitive technique for determination of antioxidants. Anal. Chim. Acta **2007**, *591*, 69–79.
42. Poleunis, C.; Médard, N.; Bertrand, P. Additive quantification on polymer thin films by ToF-SIMS: Aging sample effects. Appl. Surf. Sci. **2004**, *231–232*, 269–273.
43. Garrigós, M.C.; Reche, F.; Pernías, K.; Jiménez, A. Optimization of parameters for the analysis of aromatic amines in finger-paints. J. Chromatogr. A, **2000**, *896*, 291–298.
44. Guerra, R.M.; Marín, M.L.; Sánchez, A.; Jiménez, A. Analysis of citrates and benzoates used in poly(vinyl chloride) by supercritical fluid extraction and gas chromatography. J. Chromatogr. A, **2002**, *950*, 31–39.
45. Ashraf-Khorassani, M.; Nazem, N.; Taylor, L.T. Feasibility of supercritical fluid extraction with on-line coupling reverse-phase liquid chromatography for quantitative analysis of polymer additives. J. Chromatogr. A, **2003**, *995*, 227–232.
46. Möller, J.; Strömberg, E.; Karlsson, S. Comparison of extraction methods for sampling of low molecular compounds in polymers degraded during recycling. Eur. Polym. J. **2008**, *44*, 1583–1593.
47. Marcato, B.; Guerra, S.; Vianello, M.; Scalia, S. Migration of antioxidant additives from various polyolefinic plastics into oleaginous vehicles. Int. J. Pharm. **2003**, *257*, 217–225.
48. Pezo, D.; Salafranca, J.; Nerín, C. Development of an automatic multiple dynamic hollow fibre liquid-phase microextraction procedure for specific migration analysis of new active food packaging containing essential oils. J. Chromatogr. A, **2007**, *1174*, 85–94.
49. Herrera, M.; Matuschek, G.;, Kettrup, A. Fast identification of polymer additives by pyrolysis–gas chromatography/mass spectrometry. J. Anal. Appl. Pyrolysis. **2003**, *70*, 35–42.
50. Forrest, M.; Holding, S.; Howells, D. The use of two-dimensional GC–MS for the identification and quantification of low molecular weight compounds from high performance elastomers. Polym. Testing **2006**, *25*, 61–74.
51. Fanali, S.; Camera, E.; Chankvetadze, B.; D'Orazio, G.; Quaglia, M.G. Separation of tocopherols by nano-liquid chromatography. J. Pharm. Biomed. **2004**, *35*, 331–337.
52. Schlummer, M.; Brandl, F.; Mäurer, A.; van Eldik, R. Analysis of flame retardant additives in polymer fractions of waste of electric and electronic equipment by means of HPLC–UV/MS And GPC–HPLC-UV. J. Chromatogr. A, **2005**, *1064*, 39–51.
53. Buchalla, R.; Begley, T.H.; Characterization of gamma-irradiated polyethylene terephthalate by liquid-chromatography–mass-spectrometry (LC–MS) with atmospheric pressure chemical ionization (APCI). Radiat. Phys. Chem. **2006**, *75*, 129–137.
54. Gaudin, K.; Ho-Sung, H.; Bleton, J.; Joseph-Charles, J.; Dallet, Ph.; Puig, P.; Dubost, J.P. Determination of N,N′-Ethylenebisstearamide (EBS) additive in polymer by normal phase liquid chromatography with evaporative light scattering detector. J. Chromatogr. A, **2007**, *1167*, 27–34.
55. Kaal, E.R.; Alkema, G.; Kurano, M.; Geissler, M.; Janssen, H.G. On-line size exclusion chromatography–pyrolysis-gas

chromatography–mass spectrometry for copolymer characterization and additive analysis, J. Chromatogr. A, **2007**, *1143*, 182–189.
56. Hilder, E.F.; Klampfl, C.W.; Buchberger, W.; Haddad, P.R. Separation of hydrophobic polymer additives by microemulsion electrokinetic chromatography. J. Chromatogr. A, **2001**, *922*, 293–302.
57. He, W.; Shanks, R.; Amarasinghe, G. Analysis of additives in polymers by thin-layer chromatography coupled with Fourier transform–infrared microscopy. Vibrational Spectroscopy, **2002**, *30*, 147–156.
58. Greene, S.V.; Gatto, V.J. Size-exclusion chromatography method for characterizing low molecular mass antioxidant lubricant additives. J. Chromatogr. A, **1999**, *841*, 45–54.
59. Brüggemanna O.; Visnjevski A.; Burch R.; Patel, P. Selective extraction of antioxidants with molecularly imprinted polymers. Anal. Chim. Acta **2004**, *504*, 81–88.

Polymers and Particles: ThFFF

Martin E. Schimpf
Chemistry Department, Boise State University, Boise, Idaho, U.S.A.

Abstract
Thermal field-flow fractionation (ThFFF) can be applied to the analysis of virtually any polymer or copolymer that can be dissolved in an organic solvent, subject to low-molecular-weight limitations discussed in this entry. Water-soluble polymers are more difficult to separate because thermal diffusion, and therefore retention, is weak in water and other protic solvents. Still, certain non-ionic polymers can be separated, and with the use of mobile phase additives, even charged materials have been retained. Proteins, on the other hand, have not been successfully separated by ThFFF.

POLYMERS

For a detailed discussion of the application of ThFFF to the analysis of various polymers see Ref. 1. Although ThFFF is mostly applied to lypophilic polymers due to their strong thermal diffusion (hence, high level of retention), other significant applications exist. For example, polyethylene oxide and polyethylene glycol show strong retention in a range of aqueous solvents, including deionized water, while polystyrene sulfonate is moderately retained in 5 mM tris-Na_2SO_4 buffer.[2] Other hydrophilic polymers that could not be retained in water have been separated in aprotic solvents. For example, a variety of polysaccharides, including pullulans, dextrans, various starches, and Ficoll™, have been separated in dimethyl sulfoxide (DMSO).[3] Ficoll is a highly branched copolymer of sucrose and epichlorohydrin. Dextrans have been separated in mixtures of water and DMSO.

ThFFF can also be combined with instrumentation that yields information on molecular weight directly, such as multiangle light scattering[4] and mass spectrometry.[5,6] Such combinations are powerful because ThFFF can greatly enhance the precision of the molecular weight information by separating the analyte into more monodisperse fractions prior to molecular weight analysis.

The major limitation of ThFFF occurs in the separation of low-molecular-weight materials. Thus, the technique is not widely applicable to molecular weights below about 10^4 g/mol. This limit can be somewhat reduced by the use of solvent mixtures.[7,8] For example, polystyrene components as small as 2500 g/mol were resolved in a mixture of tetrahydrofuran and dodecane.[4] Even lower molecular weights than 2500 g/mol have been retained, but only through the use of special channels, which were highly pressurized to increase the temperature gradient without boiling the solvent.

ThFFF has virtually no upper limit to the molecular weights that can be resolved. The channel is not packed with a stationary phase, and the flow of carrier liquid through the channel is laminar. As a result, large materials can be eluted without plugging the channel, and fragile materials are eluted without being damaged. In a comparison of ThFFF and size exclusion chromatography (SEC),[9] for example, it was found that SEC consistently underestimates the molecular weight of ultra-high-molecular-weight polymers, even when extremely low flow rates are employed and a multiangle light scattering detector is used to directly measure the molecular weight of the eluting components.[4] In addition to the problem of shear-induced damage, SEC suffers from anomalous retention effects due to adsorptive interactions between the high-molecular-weight polymers and the stationary phase. Although not completely absent, surface interactions are minimized in ThFFF because there is no packing material. Finally, the resolution of ThFFF for ultra-high-molecular-weight polymers is vastly superior to that of SEC. As a result, ThFFF enjoys a unique niche in the separation of these materials.

Another application in which ThFFF enjoys an advantage over SEC is the analysis of high-temperature polymers. The operating temperature is limited only by the degradation temperature of the spacer used to form the channel, which for polyimides can be as high as 600 K. In the analysis of high-molecular-weight polyethylene,[10] for example, temperatures in excess of 400 K are required for the samples to be soluble. Under these conditions, column stability and separation efficiency limit the application of SEC. In contrast, such samples can be routinely analyzed with commercially available ThFFF channels.

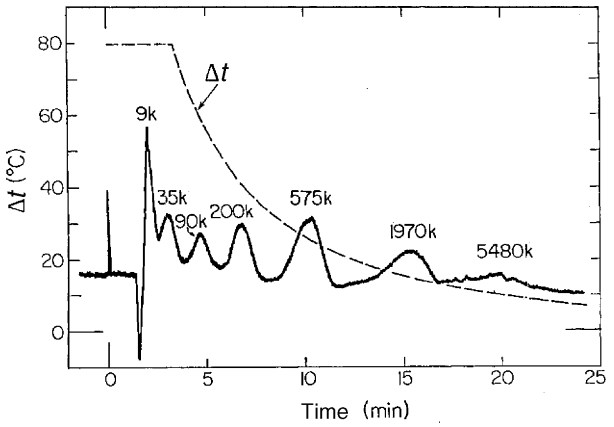

Fig. 1 Separation of seven polymers of indicated molecular weights by programed ThFFF.
Source: Reproduced with permission from Polymer separation by ThFFF: High-speed power programming, Chapter 1, in *Polymer Characterization by Interdisciplinary Methods.*[11]

Retention times in FFF are affected by the magnitude of the applied field, which can therefore be optimized for a particular molecular weight range. For extremely broad-molecular-weight distributions, the field can be programed. Fig. 1 illustrates the separation of polystyrene standards ranging in molecular weight from 9000 to 5.5 million g/mol in a single run.[11] Note that the elution order is from low- to high-molecular weight. The field, which is expressed in Fig. 1 by the temperature difference (ΔT) between the hot and the cold walls, was programed to exponentially decay from 80 to 10 K over the course of the 25 min separation.

POLYMER GELS

ThFFF is also unique in its ability to handle gel-containing polymers. To analyze such materials by SEC, the sample solution must first be filtered to prevent damage in the form of contamination or even blockage in the column. With ThFFF, such samples can be directly injected into the channel, and the gel content can even be characterized. The advantage of ThFFF for analyzing samples in which the gel contains information that is critical to the analysis has been demonstrated with acrylate elastomers.[9] ThFFF was used to correlate the gel content of such elastomers to mechanical properties after SEC combined with viscometry and light scattering failed to elucidate any difference among the samples. In a related application, ThFFF also proved superior in the analysis of natural rubber,[4,12] where the ability to analyze unfiltered samples was a clear advantage.

POLYMER BLENDS AND COPOLYMERS

The driving force for polymer retention in ThFFF is thermal diffusion, which varies with polymer composition. As a result, polymer blends and copolymers can be separated even when the molecular weights or diffusion coefficients of the components are identical. Furthermore, as thermal diffusion can be measured quantitatively by ThFFF through the thermal diffusion coefficient (D_T), the compositional distribution can, in principle, be directly obtained from elution profiles, provided the dependence of D_T on composition is known. In practice, however, there are several complications. First, retention does not yield D_T directly, but rather the Soret coefficient, which is the ratio of D_T to the ordinary diffusion coefficient (D). As compositional information is contained in D_T alone, an independent measure of D must be available. Second, a general model for the dependence of D_T on composition has not been established; therefore the dependence must be empirically determined for each polymer–solvent system. Fortunately, D_T is independent of molecular weight,[13] and for certain copolymers, the dependence of D_T on chemical composition has been established. With random copolymers, for example, D_T is a weighted average of the D_T values for the corresponding homopolymers, where the weighting factors are the mole fractions of each component in the copolymer.[14] For block copolymers, solvent mixtures can be used to obtain a linear dependence of D_T on composition.[15] As a result, the composition of random copolymers can be determined by combining ThFFF with methods either for calculating or measuring D. For example, dynamic light scattering can be directly used to measure D, while SEC can be used to measure D through calibration curves that relate log$D$ to the retention volume.[13] Mark–Houwink coefficients can also be used to calculate D.[16] Once the value of D is obtained for a separated component, the D_T value of that component can be calculated from its ThFFF retention and used to obtain compositional information.[17–19] The method was first demonstrated in the determination of both molecular weight and composition of styrene–isoprene copolymers, where an online viscometer was used to obtain both D and viscosity-average molecular weight of the components separated by ThFFF.[19] Even more powerful is the combination of ThFFF and SEC in producing 2-D separations. Here, the components are first separated by SEC; fractions from the SEC elution profile, which have similar D values, are further separated according to chemical composition by ThFFF.[15,20]

COLLOIDS AND PARTICLES

Historically, the application of FFF to colloids and particles has been limited to flow and sedimentation FFF. However, the ThFFF channel is not only capable of separating these materials, it is also simpler in design and can be used with both aqueous and organic solvents. Furthermore, the dependence of retention on chemical composition

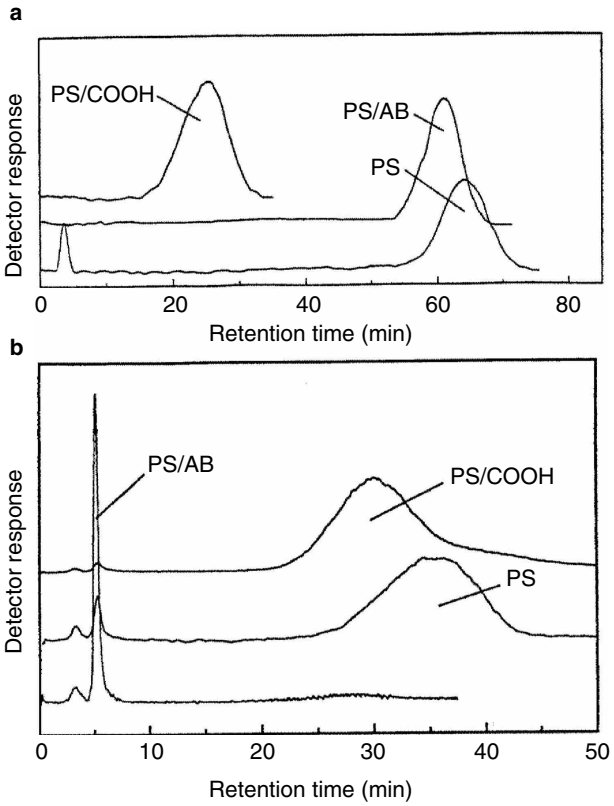

Fig. 2 A comparison of ThFFF elution profiles for 0.2 μm particles of polystyrene (PS), carboxylated PS (PS/COOH), and (aminated PS (PS/AB): a) in an aqueous solution containing 9 m*M* NaN_3 and 0.05 wt% FL-70 surfactant (pH 8.5); b) in 10 m*M* phosphate buffer (pH 4.7). Differences in retention are due to differences in thermal diffusion, which is governed by the composition and energy of the particle surface.

presents unique opportunities for the separation of such materials.

The application of ThFFF to a variety of colloids and particles has been demonstrated in both aqueous and organic carrier liquids.[21–25] Fig. 2 illustrates the dependence of retention on the surface composition of polystyrene particles. The three particles are similar in size, but the surface of one of the samples has been carboxylated, while that of another has been aminated. The relative order of elution of the three particles can be changed by modifying the carrier liquid.[21] Increasing the strength of the carrier liquid generally leads to an increase in retention up to a certain point, beyond which a plateau value is reached.[21–23]

Finally, in the separation of micron-sized particles the elution order is reversed, with larger particles eluting ahead of smaller ones due to negligible diffusion. In this case, particles are "lifted" into the faster-moving flowstreams by hydrodynamic forces that increase with particle size. In this so-called hyperlayer mode, particle retention tends to decrease with the flow rate of the carrier liquid, as well as with particle size.[25]

EXPERIMENTAL CONSIDERATIONS

One of the most common mistakes made in the analysis of polymers by ThFFF and SEC is the injection of too much sample; this is often referred to as overloading. It is important to understand that *D*, and therefore retention volume (V_r), varies strongly with polymer concentration above the so-called critical concentration (c^*), where polymer solutions undergo an abrupt transition from "dilute to semidilute" behavior. In the semidilute regime, polymer coils tangle with one another and the magnitude of *D* dramatically drops. Therefore, it is important to keep the polymer concentration below c^* to avoid overloading effects, which manifest as peak "fronting" and an increase in V_r. With excessive overloading, additional peaks appear in ThFFF due to the formation and separation of aggregates.

Although experienced users of SEC are aware of overloading effects, they are not always aware that overloading occurs with a smaller sample load in ThFFF. First, the channel has a relatively small volume (1–2 ml); therefore, injection volumes are smaller (3–30 μl) as compared to those in SEC. More importantly, the sample is initially concentrated against one wall by the field. The extent of concentration varies with the sample and the magnitude of the applied field. A general rule that should be used to avoid overloading when a new method is being developed is to prepare the sample with a concentration that is one-tenth of the expected critical concentration. Of course, the critical concentration varies with molecular weight and other factors. In general, it is typical to use a sample concentration that is between one-fourth and one-tenth of that used in SEC. Sample concentrations between 0.01 and 1 mg/ml are typical. When one is uncertain of the critical concentration, the injected concentration should be varied and the elution profiles examined for indications of sample overloading. Otherwise peak shape and reproducibility will be compromised. With recent advances in the sensitivity of detectors used for polymer analysis, sample overloading is less of a problem because even highly dilute samples can be analyzed, but overloading can still occur if the user is not aware of the potential.

CONCLUSION

ThFFF is a separation technique that complements SEC in two primary ways. First, its resolving power increases with the molecular weight of the sample, and it virtually has no upper-molecular-weight limit. Second, it separates polymers depending on their chemical composition and their molecular weight. ThFFF can also be used to separate colloids and particles by size and surface composition. Because the shear forces in the FFF channel are less,

ThFFF has found a unique niche in the separation of ultra-high-molecular-weight polymers and other fragile materials, as well as polymer gels and particles that tend to clog chromatography columns.

Universal calibration of ThFFF channels can be achieved, but one additional piece of information is required for each polymer–solvent system under consideration, which is the thermal diffusion coefficient. Fortunately, this coefficient is independent of molecular weight, so only one such coefficient is required for each system. Such coefficients are available in the literature for many systems, or they can be measured using ThFFF. Once the thermal diffusion coefficients are obtained, universal calibration plots are based on the same principles as those used in SEC, and utilize intrinsic viscosity measurements. A thorough discussion of ThFFF and its applications can be found in the *Field-Flow Fractionation Handbook.*[1]

REFERENCES

1. Schimpf, M.E.; Caldwell, K.D.; Giddings, J.C., Eds. *Field-Flow Fractionation Handbook*; Wiley Interscience: New York, 2000.
2. Kirkland, J.J.; Yau, W.W. Thermal field-flow fractionation of water-soluble macromolecules. J. Chromatogr. **1986**, *353*, 95.
3. Lou, J.; Myers, M.N.; Giddings, J.C. Separation of polysaccharides by thermal field-flow fractionation. J. Liq. Chromatogr. **1994**, *17*, 3239.
4. Lee, S.; Molnar, A. Determination of molecular weight and gel content of natural rubber using thermal field-flow fractionation. Macromolecules **1995**, *28*, 6354.
5. Kassalainen, G.E.; Williams, S.K.R. Coupling thermal field-flow fractionation with matrix-assisted laser desorption/ionization time-of-flight mass spectrometry for the analysis of synthetic polymers. Anal. Chem. **2003**, *75*, 1887–1894.
6. Basile, F.; Kassalainen, G.E.; Williams, S.K.R. Interface for direct and continuous sample-matrix deposition onto a MALDI probe for polymer analysis by thermal field flow fractionation and off-line MALDI-MS. Anal. Chem. **2005**, *77*, 3008–3012.
7. Rue, C.A.; Schimpf, M.E. Thermal diffusion in liquid mixtures and its effect on polymer retention in thermal field-flow fractionation. Anal. Chem. **1994**, *66*, 4054–4062.
8. Kassalainen, G.E.; Williams, S.K.R. Lowering the molecular mass limit of thermal field-flow fractionation for polymer separations. J. Chromatogr. A, **2003**, *988*, 285–295.
9. Lee, A. Gel content determination of polymer using thermal field flow fractionation, Chapter 6. In *Chromatography of Polymers: Characterization by SEC and FFF*; Provder, T., Ed.; ACS Publications: Washington, DC, 1993; 77–88.
10. Pasti, L.; Roccasalvo, S.; Dondi, F.; Reschiglian, P. High temperature thermal field flow fractionation of polyethylene and polystyrene. J. Polym. Sci. B, **1995**, *33*, 1225.
11. Giddings, J.C.; Kumar, V.; Williams, P.S.; Myers, M.N. Polymer separation by thermal FFF: High-speed power programming, Chapter 1. In *Polymer Characterization by Interdisciplinary Methods*; Craver, C.D., Provder, T., Eds.; ACS Publications: Washington, DC, 1990, 1–10.
12. Kim, W.-S.; Elum, C.H.; Molnar, A.; Yu, J.-S.; Lee, S. Repeatability and reproducibility of thermal field flow fractionation in Molecular weight determination of processed natural rubber. Analyst **2006**, *131* (3), 429–433.
13. Schimpf, M.E.; Giddings, J.C. Characterization of thermal diffusion of copolymers in solution by thermal field flow fractionation. J. Polym. Sci., Polym. Phys. Ed. **1989**, *27*, 1317–1332.
14. Schimpf, M.E.; Wheeler, L.M.; Romeo, P.F. Copolymer retention in thermal field-flow fractionation. In *Chromatography of Polymers: Characterization by SEC and FFF*; Provder, T., Ed.; ACS Publications: Washington, DC, 1993, 63–76.
15. Jeon, S.J.; Schimpf, M.E. Cross-fractionation of copolymers using SEC and thermal field-flow fractionation for determination of molecular weight and composition. In *Chromatography of Polymers: Hyphenated and Multidimensional Techniques*, Provder, T., Ed.; ACS Symposium Series No. 731, Chapter 10; ACS Publications: Washington, DC, 1999; 141–161.
16. Gao, Y.; Chen, X.J. Universal calibration for thermal field-flow fractionation. Appl. Polym. Sci. **1992**, *45*, 887–892.
17. Nguyen, M.; Beckett, R. Determination of thermal diffusion coefficients using thermal field-flow fractionation and Mark-Houwink constants. Anal. Chem. **2004**, *76*, 2382–2386.
18. Schimpf, M.E.; Giddings, J.C. Characterization of thermal diffusion of copolymers in solution by using thermal field-flow fractionation. J. Polym. Sci., Polym. Phys. Ed. **1990**, *28*, 2673–2680.
19. Schimpf, M.E. Determination of molecular weight and composition in copolymers using thermal FFF combined with viscometry. In *Chromatographic Characterization of Polymers*, Provder, T., Barth, H.G., Urban, W., Eds.; Advances in Chemistry Series 247, Chapter 14; ACS Publications: Washington, DC, 1995; 183–196.
20. van Asten, A.C.; van Dam, R.J.; Kok, W.Th.; Tijssen, R.; Poppe, H. Determination of the compositional heterogeneity of polydisperse polymer samples by the coupling of size-exclusion chromatography and thermal field-flow fractionation. J. Chromatogr. A, **1995**, *703*, 245.
21. Jeon, S.J.; Nyborg, A.; Schimpf, M.E. Compositional effects in the retention of colloids by thermal field-flow Fractionation. Anal. Chem. **1997**, *67*, 3442–3450.
22. Shiundu, P.M.; Mungut, S.M.; Williams, S.K.R. Practical implications of ionic strength effects on particle retention field-flow Fractionation. J. Chromatogr. A, **2003**, *984*, 67–79.
23. Pasti, L.; Agnolet, S.; Dondi, F. Thermal field-flow fractionation of charged submicrometer particles in Aqueous Media. Anal. Chem. **2007**, *79*, 5284–5296.
24. Shiundu, P.M.; Williams, P.S.; Giddings, J.C. Magnitude and direction of thermal diffusion of colloidal particles measured by thermal field-flow fractionation. J. Coll. Interf. Sci. **2003**, *266*, 366–376.
25. Regazzetti, A.; Hoyos, M.; Martin, M. Influence of operating parameters on the retention of chromatographic particles by thermal field-flow fractionation. Anal. Chem. **2004**, *76*, 5787–5798.

Polymers: Additives

M.L. Marín
Alfonso Jiménez
Department of Analytical Chemistry, Nutrition and Food Sciences, University of Alicante, Alicante, Spain

INTRODUCTION

The need for developing methods of analysis for additives in plastics materials is increasing day by day because of several aspects. First, as toxicological studies are developed, there is the presence of some substances which have been banned in specific products. Second, in production, it is necessary to carry out a quality control for additive levels. It is also necessary to determine the stability of the additives when the polymer is processed. In this case, some additional compounds, often undesirable, can be generated and their control becomes necessary. Finally, the analysis will let us know the composition of a plastic product.

It is possible to use techniques in which the additives can be determined by direct analysis of the sample, such as nuclear magnetic resonance (NMR) spectrometry, ultraviolet (UV) spectrometry, and UV desorption–mass spectrometry (MS). These techniques are very useful when the concentrations of additives in the polymer are high. However, when additives are present in trace levels, it is necessary to carry out a preliminary extraction/concentration step before analysis. Some of the most common additives used in plastics materials are presented in Table 1.

SAMPLE PREPARATION

As was previously mentioned, a preliminary extraction step is necessary for samples in which a low level of organic compounds of interest must be determined. The extraction presents advantages when compared to the direct plastics analysis solution. In this case, the polymer is dissolved directly in an organic solvent and then precipitated. This procedure is not selective and the polymer residues can affect the analysis of the additives. When an extraction is carried out, higher selectivities can be obtained when the appropriate extraction conditions are used.

Traditional methods of extraction, such as Soxhlet, have been replaced by modern techniques as supercritical fluid extraction (SFE), microwave-assisted extraction (MAE), ultrasonic extraction, and accelerated solvent extraction (ASE) during recent years. The application of specific methods to these kinds of samples has permitted the development of a great number of other extraction methods. In the following list, a brief description is given:

- SFE: This method uses pressure and temperature for fluids above their critical points. Under these conditions, the density and diffusivity of a supercritical fluid are between those of liquids and gases, resulting in an increase of the solvent power.
- MAE: In this case, the sample and solvent are placed in a vessel and microwave radiation is applied. The solvent is heated under pressure above its normal boiling point so it remains in the liquid state.
- ASE: Common solvents are used, at elevated temperatures and pressures, to increase the speed and efficiency of the extraction process.

In general, each of these procedures presents advantages: They are faster, an extract concentration step is not necessary, a minimal amount of solvents is used, so they are environmentally friendly, and cleaner extracts are obtained. Thus, when the extract is obtained, a separation technique such as chromatography, can be applied in order to analyze the sample qualitatively and quantitatively.

There are many publications showing the applications of SFE to the determination of polymer additives. Antioxidants such as Irganox 2246, BHT and others, as well as UV stabilizers such as Tinuvin P, have been effectively extracted with supercritical CO_2. Extraction conditions varied from 15 to 25 MPa at 60°C and with a total time of 30 min.[1] If microwaves are applied to extract these compounds, a mixture of solvents can be used (acetone–heptane, for example) and time is considerably reduced (from 3 to 6 min).

Phthalate plasticizers are extracted with the same supercritical fluid at a pressure of 48 MPa at 95°C for the same amount of time.[2] Other phthalate plasticizers, such as TOP and TOTM are extracted from poly(vinyl chloride) (PVC) by ASE with ether at 100°C for 20 min.

CHARACTERIZATION OF POLYMER ADDITIVES WITH CHROMATOGRAPHIC TECHNIQUES

There are several techniques that can be used for the determination of polymer additives after extraction;

Table 1 Common additives used in plastic products.

Additive type	Chemical name	Commercial name
Antioxidants	Di-*t*-butyl-*p*-cresol	Bisphenol A
	Dioctadecyl (3,5-di-*t*-butyl-4-hydroxybenzyl)phosphate	Irganox 1093
	2,2′-Methylene bis (4-methyl-6-*t*-butylphenol)	Irganox 2246
	Tris(2-methyl-4-hydroxy-5-*t*-butylphenyl)-butane	Topanol CA
	4,4′-Thio-bis (6-*t*-butyl-*m*-cresol)	Santonox
Light stabilizers	2-(2′-hydroxy-3,3,5-di-*t*-amylphenyl)benzotriazole	Tinuvin 328
	Bis(2,2,6,6-tetramethylpiperidin-4-yl)sebacate	Tinuvin 770
	2-(2-Hydroxy-5-methylphenyl)-2*H*-benzotriazole	Tinuvin P
	2-Hydroxy-4-*n*-octoxybenzophenone	Chimassorb 81
Plasticizers	Di(2-ethylhexyl) phthalate	DEHP
	Disononyl phthalate	DINP
	Di(2-ethylhexyl) adipate	DOA
	Dipropylene glycol dibenzoate	Benzoflex 9–88
	Tributyl-*O*-acetylcitrate	Citroflex A
	Tris(2-ethylhexyl) phosphate	TOP
	Trioctyl trimellitate	TOTM
Colorants	Monoazo benzimidazole pigment	
	Pigment Red 176	
	Solvent Blue 97	
Flame retardants	Tetrabromobisphenol A	TBBA
	Hexabromocyclododecane	HBCD

for example, high-performance liquid chromatography (HPLC), supercritical fluid chromatography (SFC), and high-temperature capillary gas chromatography (GC) are the most widely used. Capillary gas chromatography is especially useful because it combines high resolution with the possibility of coupling the instrument with some sophisticated detection techniques, such as mass spectrometry (MS), Fourier transform infrared (FTIR), or atomic emission detection (AED). MS is the most suitable detector for GC; it is very easy to prepare a personal spectral library for identification of separated species. There are also commercially available spectral libraries. Apart from the fact that the versatility of GC is due to its detectors, the injection systems provide a higher number of applications; for instance: on-column, split/splitless, and headspace techniques, among others. Today, almost every organic substance can be analyzed by gas chromatography, because of the development of high-temperature injectors. The combination of SFC with MS is also useful. In some cases, an online extraction is used, such as SFE–SFC.[3]

The case of HPLC is quite different, because of the peak broadening or, sometimes, when the additives cannot be eluted from the stationary phase. However, it is a very useful technique when analyzing high-molecular-weight additives and, in combination with diode-array detection, provides an important tool for qualitative analysis. An important application is the determination of organic colorants in cosmetics.[4] HPLC is also applicable for the determination of linear and cyclic derivatives from poly(ethylene terephthalate), extracts of which were obtained using supercritical CO_2.[5]

OTHER DETECTION SYSTEMS

The analysis of extracts is also possible by using other techniques, such as infrared spectrometry. This kind of detector is very useful because it provides a total spectrum for the analyte. For example, a method for analyzing poly(dimethylsiloxane) oil from polymer samples was developed by Kirschner et al. [6] In this case, the extractor is directly coupled to the spectrometer. However, it is also possible to carry out offline analyses with high recoveries. This combination was also used by Raynor et al.[7] in order to analyze some UV stabilizers such as Tinuvin 770, Irganox 1010, and Topanol OC. In this case, a preliminary separation was carried out by supercritical fluid chromatography.

REFERENCES

1. Arpino, P.J.; Dilettato, D.; Nguyen, K.; Bruchet, A. Investigation of antioxidants and UV stabilizers from plastics. Part I: Comparison of HPLC and SFC; preliminary SFC/MS study. J. High-Resol. Chromatogr. **1990**, *13*, 5–12.
2. Marín, M.L.; Jiménez, A.; Berenguer, V.; López, J. Optimization of variables on the supercritical fluid

extraction of phthalate plasticizers. J. Supercrit. Fluids **1998**, *12*, 271–277.
3. Daimon, H.; Hirata, Y. Directly coupled supercritical fluid extraction/capillary supercritical-fluid chromatography of polymer additives. Chromatographia **1991**, *32*, 549–554.
4. Rastogi, S.C.; Barwick, V.J.; Carter, S.V. Identification of organic colorants in cosmetics by HPLC–diode array detection. Chromatographia **1997**, *45*, 215–228.
5. Küppers, St. The use of temperature variation in supercritical fluid extraction of polymers for the selective extraction of low molecular weight components from poly(ethylene terephthalate). Chromatographia **1992**, *33*, 434–440.
6. Kirschner, C.H.; Jordan, S.L.; Taylor, L.T.; Seemuth, P.D. Feasibility of extraction and quantification of fiber finishes via on-line SFE/FT-IR. Anal. Chem. **1994**, *66*, 882–887.
7. Raynor, M.W.; Bartle, K.D.; Davies, I.L.; Williams, A.; Clifford, A.A.; Chalmers, J.M.; Cook, B.W. Polymer additive characterization by capillary supercritical fluid chromatography/Fourier transform infrared microspectrometry. Anal. Chem. **1988**, *60*, 427–433.

Polymers: Concentration Effects on ThFFF Separation and Characterization

Wenjie Cao
Mohan Gownder
Huntsman Polymers Corp., Odessa, Texas, U.S.A.

INTRODUCTION

The understanding of the effects of sample concentration (sample mass) in field-flow fractionation (FFF) has being obtained gradually with the improvement of the sensitivity (detection limit) of high-performance liquid chromatography (HPLC) detectors. Overloading, which was used in earlier publications, emphasizes that there is an upper limit of sample amount (or concentration) below which sample retention will not be dependent on sample mass injected into the FFF channels.[1] Recent studies show that such limits may not exist for thermal FFF (ThFFF) (may be true for all the FFF techniques in polymer separation), although some of the most sensitive detectors on the market were used.[2]

Experimental results indicate that the effects of sample mass include, but not exclusively, the following aspects.

Increased Polymer Retention

Fig. 1 shows the fractograms of ThFFF to show the concentration effects for poly(methyl methacrylate) (PMMA) in tetrahydrofuran (THF), where M_p is the peak average molecular weight, m is the sample mass in micrograms injected into the ThFFF channel, and t^0 is the retention time of a nonretained species such as toluene. When the molecular weight (MW) of a polymer is moderate or higher, say above 300×10^3 g/mol for PMMA in THF, a moderate increase in concentration will result in longer retention. As reported in Ref.,[2] the detector limits for the study was 0.09 μg of sample mass for 1000×10^3 g/mol polystyrene using an ultraviolet (UV) detector and 1 μg for 570×10^3 g/mol PMMA with an evaporative light-scattering detector. The retention was measured for sample masses ranging from these limits to more than 20 μg and was consistently found to increase with the increase in sample mass. The high limit, below which polymer retention is not dependent on concentration, was not found.

Broader Polymer Peaks

Increased concentration will increase band broadening in all chromatographic techniques, but it seems that the effect of concentration on band broadening is more serious in FFF, due to its concentration enhancement as shown by Fig. 1, and by Fig. 5 of Ref.[1] More details will be discussed in the next section.

Distorted Peaks and Double-Topped Peaks (Ghost Peaks)

When the amount of sample mass injected into the ThFFF channel is moderate, say 1–10 μg for a typical channel, the peaks are pretty symmetrical and not much distortion may be observed for small polymers, as shown by Fig. 1. Increased retention may be observed for high-MW polymers.[2] When sample mass is further increased, say more than 20 μg, distorted peaks, even double-topped peaks or ghost peaks, may be observed for high-MW polymers as shown by Fig. 1, Fig. 6 of Ref.,[1] and Fig. 3 of Ref.[2] The detailed report and discussion of double-topped peaks can be found in both Refs.[1,2]

ENHANCED VISCOSITY IS BLAMED FOR THE SAMPLE CONCENTRATION EFFECTS

The viscosity of a polymer solution is highly dependent on concentration, temperature, and MW, as discussed below.

Concentration and Viscosity Enhancement in FFF

The amount of sample injected into the FFF channels can affect the retention time, primarily by influencing the viscosity of the solute–solvent mixture in the sample zone.[1,2] Unlike other chromatographic polymer separation methods [e.g., gel permeation chromatography–size-exclusion chromatography (GPC–SEC) and temperature rising elution fractionation (TREF), etc.], the viscosity of the fluid is not homogeneous at a given channel (column) cross section. In order for the samples to be retained by FFF, the concentration must be larger near the accumulation wall than that near the depletion wall.[3,4] In chromatography, sample concentration changes only along one dimension (i.e., the flow axis) whereas in FFF, sample concentration varies along two dimensions, one being the flow axis and the other one is across the channel thickness, which is

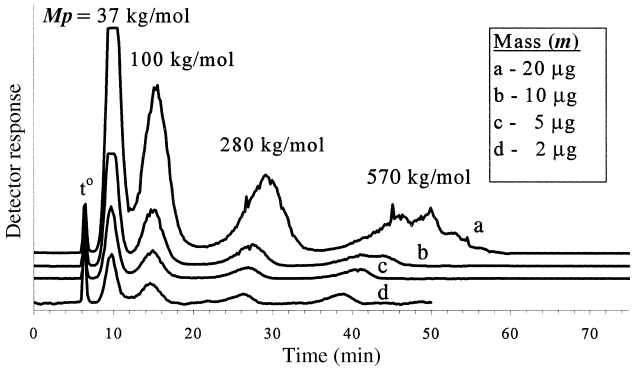

Fig. 1 Fractograms of PMMA in THF showing the effect of sample concentration on retention. Experimental conditions: cold-wall temperature, 25°C, *T*, 50°C; flow rate, 0.1 ml/min.

perpendicular to the flow axis. The concentration across the channel thickness varies due to the migration of the molecules under the influence of the temperature gradient across the ThFFF channel.[3] The concentration distribution is approximately exponential as given by

$$c(x) = c_0 \exp\left(\frac{-x}{\lambda w}\right) \tag{1}$$

where $c(x)$ is the concentration at distance x across the channel thickness measured from the accumulation wall, c_0 is the concentration at the accumulation wall, w is the channel thickness, and λ is the retention parameter or reduced mean thickness of the sample zone. Shortly after injection, the sample zone is assumed to broaden into a Gaussian distribution along the z axis, corresponding to the direction of flow down the channel. The two-dimensional concentration becomes[5]

$$c(x,z) = c_{00} \exp\left(\frac{-(z-Z)^2}{2\sigma^2}\right) \exp\left(\frac{-x}{\lambda w}\right) \tag{2}$$

where Z is the distance traveled by the center of the zone down the channel. The concentration at the accumulation wall at the center of the zone, c_{00}, is found from[6]

$$c_{00} \simeq \frac{V_{\text{inj}} c_{\text{inj}} L}{(2\pi\sigma^2)^{1/2} V^0 \lambda} \tag{3}$$

where V_{inj} is the volume of sample injected, V^0 is the void volume (channel volume), c_{inj} is the concentration of the injected sample, L is the length of the channel, and σ is the sum of the variances contributing to the zone breadth.

A rough calculation using Eq. 3 indicates that the concentration of c_{00} can be as high as 20 times the concentration of the original polymer solution. The concentration of the sample zone, therefore, can be enhanced dramatically in FFF.

The relationship between viscosity and concentration of polymer solution is very complex. Several empirical equations are necessary to describe the viscosity behavior of a polymer solution's dependence upon concentration. As an example, the following equation can be used for dilute solutions:[7]

$$\eta = 0.54 + 1.3374C + 1.1593C^2 \tag{4}$$

where η is viscosity in centipoise and C is the concentration in grams per deciliter.

For the concentration where a microgel may be formed, the following equation is proposed:[8]

$$\eta = BM^3C^{3.7} \tag{5}$$

where B is a constant and M is the polymer's molecular weight.

Although various empirical equations can be found in the literature, the common aspect is that the viscosity of a polymer solution is highly dependent on concentration and molecular weight.

Temperature Dependence of Viscosity

The effect of temperature on the viscosity of the carrier can be expressed as[5]

$$\frac{1}{\eta} = a_0 + a_1T + a_2T^2 + a_3T^3 \tag{6}$$

where a_0, a_1, a_2, and a_3, are empirically obtained coefficients.

As Eq. 6 shows, the viscosity of a polymer solution is highly dependent on temperature. The sample zone of a high-MW polymer is pressed much closer to the cold wall in ThFFF. Its viscosity is more enhanced than with a low-MW polymer. The concentration effect, therefore, is more serious for high-MW polymers in ThFFF.

Molecular-Weight Dependence of Viscosity

If the temperature and concentration are kept the same, the viscosity of higher-MW polymer solution is higher, as shown by Eq. 2; thus, more distortion of its peak is expected, as shown by Fig. 1.

Unlike most of the elution separation methods, such as HPLC, GPC/SEC, gas chromatography (GC), and so forth, where the concentration of the sample zone will never be higher than the stock solution before injection, FFF will concentrate the samples, that is to say that sample concentration will be enhanced near the accumulative wall of FFF and the cold wall in ThFFF. The higher the MW of the polymer, the more the concentration will be enhanced and the lower the temperature of the sample zone will be. All three factors, concentration, temperature, and MW, contribute

simultaneously to enhance the viscosity of the sample zone of the polymers in ThFFF. The viscosity of the sample zone can reach such extension that there is a tendency for the carrier fluid to flow over the top of the zone, with increased velocity in the region above the sample zone. The moving fluid will go over the sample zone, thus resulting in a longer retention for the sample zone; this is like a sticky slump going slowly on the floor of a river. A longer retention will be observed even if the flow rate of the carrier is constant.

When the MW of the polymer is so large that its zone is compressed close to the cold wall, the temperature of the sample zone becomes, essentially, the temperature of the cold wall, 25°C in many experiments. The viscosity is enhanced so much that the flow velocity of the carrier fluid is further distorted, so that deformed or double-topped peaks will be produced.

For the double-topped peaks, pseudo-gel, formed near the cold wall, is also proposed due to the low temperature and high concentration of the sample zone in ThFFF.[2,9] The behavior of a pseudo-gel solution is quite different from the polymer solution from which it is formed. The diffusion coefficient of a pseudo-gel is much smaller than that of the original polymer, and the viscosity of the pseudo-gel solution will be much larger than that of the original polymer solution. The pseudo-gel, in theory, will be compressed closer to the cold wall and will elute out of the channel later than the parent molecules. However, as the size of the pseudo-gel cluster increases, hydrodynamic effects will result in an earlier emergence from the channel.[3] If either of these scenarios occurs in the ThFFF channel, double peaks might be observed for a sample of a single peak without "overloading."[10]

CONCLUSIONS

Any attempts to obtain the parameters of the chromatograms and the physicochemical constants which are measurable in theory, by FFF, will be affected by the sample mass injected into the FFF channel. All of the concentration effects on the chromatograms discussed in the previous sections will be transferred, in turn, to those measured parameters and the physicochemical constants, such as the mass selectivity (S_m), the common diffusion coefficient (D), the thermal diffusion coefficient (D_T) and so forth. The increased retention of large polymers will result in enhanced mass selectivity in ThFFF. For a long time, this enhanced selectivity, in turn, the enhanced ThFFF universal calibration constant n, has led to confusion concerning the accuracy and repeatability of FFF, because different research groups have reported different data for selectivity and physicochemical constants measured by FFF for a given polymer–solvent combination.[2,11] Recent studies show that the enhanced selectivity and the different values of the physicochemical constants reported by different laboratories, measured by ThFFF, may be caused by different concentrations (sample mass) used by different laboratories.

REFERENCES

1. Caldwell, K.D.; Brimhall, S.L.; Gao, Y.; Giddings, J.C. Sample overloading effects in polymer characterization by field-flow fractionation. J. Appl. Polym. Sci. **1988**, *36* (3), 703–719.
2. Cao, W.J.; Marcus, M.N.; Williams, P.S.; Giddings, J.C. Sample mass effects on thermal field-flow fractionation retention and universal calibration. Int. J. Polym. Anal. Charact. **1998**, *4*, 407.
3. Giddings, J.C. Field-flow fractionation: Analysis of macromolecular, colloidal and particulate materials. Science **1993**, *260*, 1456.
4. Giddings, J.C. Universal calibration in size exclusion chromatography and thermal field-flow fractionation. Anal. Chem. **1994**, *66*, 2783–2787.
5. Giddings, J.C.; Yang, F.J.F.; Myers, M.N. Sedimentation field-flow fractionation. Anal. Chem. **1974**, *46*, 1917–1924.
6. Caldwell, K.D.; Brimhall, S.L.; Gao, Y.; Giddings, J.C. Sample overloading effects in polymer characterization by field-flow fractionation. J. Appl. Polym. Sci. **1988**, *36*, 703.
7. Tanford, C. *Physical Chemistry of Macromolecules*; John Wiley & Sons: New York, 1961; Chap. 6.
8. DeGennes, P.G. Dynamics of entangled polymer solutions. II. Inclusion of hydrodynamic interactions. Macromolecules **1976**, *9*, 594.
9. Tan, H.; Moet, A.; Hiltner, A.; Baer, E. Thermoreversible gelation of atactic polystyrene solutions. Macromolecules **1983**, *16* (1), 28–34.
10. Hoyos, M.; Martin, M. Retention theory of sedimentation field-flow fractionation at finite concentration. Anal. Chem. **1994**, *66*, 1718–1730.
11. Sisson, R.M.; Giddings, J.C. Effects of solvent composition on polymer retention in TFFF. Anal. Chem. **1994**, *66*, 4043.

Polymers: Degradation in GPC/SEC Columns

Raniero Mendichi
Institute of Macromolecular Chemistry, National Research Council (CNR), Milan, Italy

INTRODUCTION

Size-exclusion chromatography (SEC) is a well-established method for the determination of the molar mass distribution (MMD) of polymers. However, the determination of the MMD by SEC substantially excludes ultrahigh-molar-mass (UHMM) polymers. Actually, it is well accepted that UHMM polymeric samples degrade, by shearing or elongational forces, in the SEC columns. The upper limit of the molar mass for a successful SEC fractionation without degradation of the sample depends on the broadness of the MMD of the sample from the SEC columns used and, obviously, from the experimental conditions. Successful SEC fractionations of narrow MMD standards up to 1×10^7 g/mol of molar mass have been reported. Instead, when the MMD of the sample is broad, rarely does the molar mass of the polymeric samples exceed the upper limit of 1×10^6 g/mol.

DISCUSSION

Whenever SEC fractionation has been applied to UHMM polymers, severe problems, strongly interrelated, have been invariably reported. The degradation of UHMM polystyrene during SEC fractionation in a good solvent has been often reported. The degradation of some other UHMM synthetic polymers [polyethylene, polyisoprene, polyacrylamide, polyisobutylene, poly(methyl methacrylate), etc.] has been reported. Besides, the degradation of some natural polysaccharides such as hyaluronic acid has been reported. The possible degradation of the polymeric sample is not the only problem of the SEC fractionation of UHMM polymers. The degradation of the UHMM sample in the SEC columns is often accompanied by some other important problems, such as (a) concentration effects, (b) anomalous flow, (c) poor column resolution (band broadening), and (d) very poor reproducibility.

Generally, the practical difficulties in the SEC fractionation exponentially increase with the polymer molecule's dimension, hydrodynamic volume, hence with the molar mass and the conformation, stiffness, of the polymer. For many years, SEC has been considered inadequate for the fractionation of UHMM polymers. In the past, there have been many theoretical and experimental studies[1,2] to elucidate a better knowledge of the degradation of UHMM polymers. Furthermore, there have been notable improvements in the SEC column's performance. At this time, there are commercially available SEC columns specifically designed for the fractionation of UHMM polymers.

Evidence of the degradation of the polymeric sample may be found by using qualitative and quantitative methods. From a qualitative point of view, an accurate analysis of the chromatogram of a series of narrow MMD standards with increasing molar mass, under identical analytical conditions, would be self-evident. The resolution of the SEC columns, almost in the low-molar-mass range, generally is very good. In the high-molar-mass range, $M > 1 \times 10^6$ g/mol, the resolution of the SEC columns quickly decreases. In the presence of the degradation of the sample, the resolution of the SEC columns is poor or absent. Furthermore, the peak shapes of degraded UHMM narrow standards is abnormally broad with a severe tailing. Obviously, we assume the absence of non-steric fractionation. To find evidence of the degradation of broad MMD samples is more difficult. The analysis of the peak shape of a broad MMD sample requires experience. Generally speaking, a chromatogram that presents too steep slopes, shoulders, excessive tailing, or multipeaks is suspect from the point of view of the degradation of the sample. Obviously, the origin of these anomalous shapes of the chromatogram could be different. Concentration effects and anomalous flow often accompany the degradation of the sample. The qualitative analysis is used only to identify the problem.

A quantitative analysis of the degradation of the sample substantially requires the use of an online absolute detector such as light scattering (SEC-LS). In this case, the online LS detector directly measures, without calibration, the molar mass of the sample. The characterization of a series of narrow MMD standards with increasing and known molar mass evidences the degradation of the sample. The simple direct comparison of the known molar mass of the standards and the molar mass value obtained from the LS detector provides an estimate of the extent of the degradation under the experimental conditions used. Furthermore, if the dispersity D of the standards is very narrow (i.e., $D \leq 1.05$), the central part of the $M = f(V)$ plot, where M is the molar mass and V the elution volume, of each standard from the LS detector could be substantially flat. In fact, the central part of the peaks of the standards could be considered homogeneous in molar mass and the residual broadness of the peak is substantially due to the band broadening of the system. In the presence of degradation of the sample, the $M = f(V)$ plot of a narrow

standards is not flat (M = constant) but steep. The method could be used to set up the experimental condition (columns set, flow rate, sample concentration) to avoid the degradation of the sample.

Fig. 1 shows the experimental $M = f(V)$ plot of a narrow MMD polystyrene (PS) standard ($M = 1.15 \times 10^7$ g/mol, $D = 1.03$) from an online LS detector. The experimental conditions were as follows: one column, packed with 16 μm spherical particles of porous silica; tetrahydrofuran as the mobile phase; 0.8 ml/min flow rate; 0.1 mg/ml of sample concentration; 100 μl injection volume. Fig. 1 evidences the quick decrease of the molar mass of the sample due to the degradation of the UHMM PS sample in the column. A fractionation with the identical experimental conditions, column, and concentration and a 0.2 ml/min flow rate shows a constant $M = f(V)$ plot (i.e., the absence of degradation).

The origin of the degradation of the sample could be in the SEC columns and, for UHMM polymers, also in some other critical part (detector cell, long narrow capillary tube, injector, etc.) of the fluidic system. The extent of degradation also depends on the experimental conditions, particularly the flow rate and the concentrations of the polymeric solutions. In an SEC column, there are three parameters that have to be optimized for a successful fractionation of UHMM polymers. Two parameters are related to the packing of the column: particle size and pore size. The last parameter, often incorrectly ignored, is the dimension of the pores of the inlet and outlet frits of the column. It is well accepted that for a successful fractionation of UHMM polymers, one must use SEC columns with the diameter of the particles larger than 10 μm. In organic solvents, 20 μm particle columns are customarily used. However, in aqueous solvent, there are commercially available 15 μm nominal, maximum 17 μm particle columns. Obviously, the efficiency of the column quickly decreases with the increase of particle size. As usual, one needs to find a reasonable compromise between discordant effects.

The influence of the pore size on the degradation of the sample is not generally accepted. However, to obtain a meaningful fractionation on the basis of the dimension of the macromolecules, it is necessary that the pore size be higher than the dimensions of the molecules. The maximum dimension of UHMM macromolecules could be of several hundreds of nanometers. Polymer degradation strongly decreases with the large pore size of the frits of the columns. The commercially available 20 μm-particle SEC columns commonly use 10 μm inlet and outlet frits. Finally, it is very important to remember that partially obstructed frits could cause strong polymer degradation.

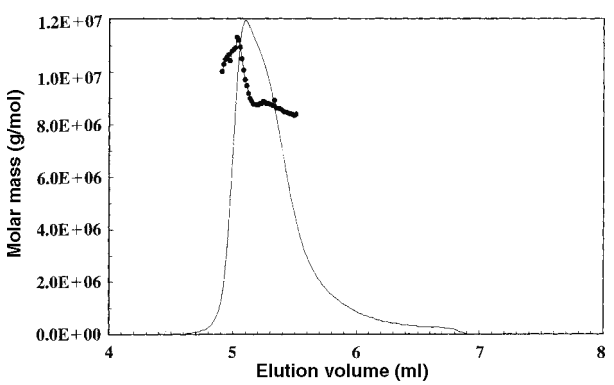

Fig. 1 Experimental $M = f(V)$ plot from an online LS detector.

Also, the experimental conditions have to be optimized to avoid the degradation of UHMM samples. Particularly, the flow rate and concentration of the sample are two critical parameters. Polymer degradation strongly increases with the increase of the flow rate. For a successful fractionation of UHMM macromolecules, it is necessary to use a very low flow rate. With UHMM macromolecules, it is not unusual to use a flow rate of 0.2 ml/min or less.

The influence of the polymer concentration is well known in SEC. Theoretically, SEC assumes independence of the elution volume with regard to the concentration of the molecular species. Practically, it is well known that a high concentration of the sample solution leads to distortion of the polymer peak and dependence of the elution volume on the concentration of the sample. The "concentration effect"[3] depends on the difference in molecular mobility between the pure solvent and the viscous polymeric solution. This difference causes nonuniform flow, often called "viscous fingering," and, as a result, multiple peaks. In addition, it is well known that a high sample concentration decreases the hydrodynamic volume of the macromolecules. SEC fractionation is based on the hydrodynamic volume of the macromolecules; hence, this effect causes the dependence of the elution volume on the concentration, at least for high-molar-mass polymers.

The concentration, with UHMM macromolecules, also influences the degradation of the sample. Hence, in the fractionation of UHMM polymers, the concentration is very critical and has to be as low as possible. A sample concentration of 0.1 mg/ml or less is not unusual with UHMM polymers. In this case, it is necessary to use the minimal sample concentration that is consistent with the sensitivity of the concentration detector.

To avoid the degradation of the sample, some authors suggest the use of an ideal "theta" solvent as the mobile phase.[4] It is well known that the dimension of the macromolecules depends on the expansion factor α (excluded volume). For an ideal theta solvent, $\alpha = 1$ and the dimension of the macromolecules is minimal. For many polymers, an ideal theta solvent is known. For example, cyclohexane at 34.0°C is an ideal solvent for polystyrene polymers. For a polyelectrolyte polymer, ideal solvent means infinite ionic strength. Obviously, this condition is impracticable. Nevertheless, for example, the dimension of the macromolecules of an hyaluronic acid, anionic polymer, sample ($M = 7.4 \times 10^6$ g/mol) approximately

decreases 20% when the solvent is changed from 0.15 *M* to 0.5 *M* NaCl. The use of ideal solvents to avoid the degradation of the sample is not generally accepted. In fact, using ideal solvents as the mobile phase could cause absorption of the polymer onto the column's packing. Also, some authors hypothesize that the degradation of the sample could also increase with ideal solvents.

At equilibrium conditions, at very low concentration, the elution volume of a macromolecule should be independent of the flow rate. However, with increasing molar mass in the UHMM range, in the absence of degradation, the elution volume strongly depends on the molar mass of the sample. This result does not depend on the concentration of the sample. This "retardation" effect occurs also at very low concentrations below the overlapping concentration c^*. The "retardation" of UHMM macromolecules has been studied by several workers;[5,6] it is a very complex effect and substantially still not well understood. The "retardation" effect is particularly meaningful in proximity to the exclusion limit of the columns and when the pore size approximately equals or is lower than the sizes of the macromolecules. A trivial conclusion is that for a successful fractionation of UHMM macromolecules without "retardation" effects, one must use SEC columns with ultralarge pore sizes.

Degradation of the sample and related problems, such as the "concentration effect" and anomalous flow, are the more important problems in the fractionation of UHMM polymers. The critical point in the characterization of the UHMM polymers is the fractionation in the SEC columns. For a successful fractionation of UHMM macromolecules, one must use specifically designed SEC columns with large particle sizes and ultralarge pore sizes. Furthermore, many aspects of the experimental protocol, such as flow rate and sample concentration, which is not critical in the usual molar mass range, become determining with UHMM polymers. A successful characterization of UHMM polymers requires optimization of the experimental protocol. Each step of the experimental protocol should be performed methodically to achieve the absence of sample degradation and reliable results.

REFERENCES

1. Bueche, F.J. Mechanical degradation of high polymers. J. Appl. Polym. Sci. **1960**, *4* (10), 101–106.
2. Giddings, J.C. J. Adv. Chromatogr. **1982**, *20*, 217.
3. Rudin, A.; Wagner, R.A. Solvent and concentration dependence of hydrodynamic volumes and GPC elution volumes. J. Appl. Polym. Sci. **1976**, *20* (6), 1483–1490.
4. Soltes, L.; Berek, D.; Mikulasova, D. Characterization of the extremely high molecular mass polystyrene by gel permeation chromatography. Colloid & Polym. Sci. **1980**, *258* (6), 702.
5. Chubarova, E.V.; Nesterov, V.V. Behavior of macromolecules in nonhomogenous hydrodynamic fields: Degradation mechanism of macromolecules. ACS Symp. Ser. **1996**, *635*, 127.
6. Cheng, W.; Hollis, D.J. Flow-rate effect on elution volume in size-exclusion chromatography. J. Chromatogr. **1987**, *408*, 9–19.

Polymers: GPC Determination of Intrinsic Viscosity

Yefim Brun
Waters Corporation, Milford, Massachusetts, U.S.A.

INTRODUCTION

The intrinsic viscosity is a widely used measure of molecular weight, M, and size (dimensions) of macromolecules in dilute solution. Important information about macromolecular architecture and conformations can be obtained from the molecular-weight dependence of intrinsic viscosity for a homologous series of polymers. Size exclusion chromatography (SEC) provides a unique opportunity to measure this dependence in a single chromatographic run. Another striking coincidence is that the dimensions of a macromolecule associated with its frictional properties in dilute solution (i.e., with the intrinsic viscosity) determine the elution time (volume) in size-exclusion separation. This allows one to use the intrinsic viscosity measurement as a crucial intermediate step in the determination of molecular weights and molecular-weight distributions of polymers. From the above, it might be assumed that online intrinsic viscosity measurements represent an important aspect of contemporary gel permeation chromatography (GPC).

SOLUTION VISCOSITY

There are several dilute solution viscosity quantities used in the determination of the intrinsic viscosity. The size of macromolecules in solution is associated with an increase in viscosity of the solvent brought about by the presence of these molecules. Relative viscosity is a dimensionless quantity representing a solution/solvent viscosity ratio, $\eta_r = \eta/\eta_0$, where η and η_0 are the solution and solvent viscosities, respectively. The specific viscosity $\eta_{sp} = \eta_r - 1$ is the fractional increase in viscosity between the solution and solvent. The effect of the concentration can be normalized by division of η_{sp} by the concentration C, expressed in grams per deciliter (g/dl). This concentration-normalized viscosity is termed the reduced specific viscosity or η_{sp}/C (the International Union of Pure and Applied Chemistry (IUPAC) preferred term is viscosity number). Another related term, the inherent viscosity, is expressed as $\eta_{inh} = (\ln \eta_r)/C$ (the IUPAC preferred term is logarithmic viscosity number).

In order to relate viscosity to molecular weight, the value of reduced (or inherent) viscosity is extrapolated to zero concentration. This parameter is called the intrinsic viscosity $[\eta]$, and is usually expressed in deciliters per gram (dl/g) (the IUPAC preferred term is limiting viscosity number, ml/g):

$$[\eta] = \lim(\eta_{sp}/C) = \lim \eta_{inh}(C \to 0) \quad (1)$$

Practically, the limit in Eq. 1 is achieved when the concentration is so low that the frictional interactions between an individual macromolecule and a solvent are not affected by the presence of other macromolecules in the same solution. Under these conditions, which are typical for the GPC/SEC experiments, the difference between the reduced and intrinsic viscosities is negligible.

CALCULATION OF INTRINSIC VISCOSITY IN GPC

The opportunity to measure the dilute polymer solution viscosity in GPC came with the continuous capillary-type viscometers (single capillary or differential multicapillary detectors) coupled to the traditional chromatographic system before or after a concentration detector in series (see *Viscometric Detection in GPC/SEC*, p. 2411). Because liquid continuously flows through the capillary tube, the detected pressure drop across the capillary provides the measure for the fluid viscosity according to the Poiseuille's equation for laminar flow of incompressible liquids.[1] Most commercial online viscometers provide either relative or specific viscosities measured continuously across the entire polymer peak. These measurements produce a viscometry elution profile (chromatogram). Combined with a concentration-detector chromatogram (the concentration versus retention volume elution curve), this profile allows one to calculate the instantaneous intrinsic viscosity $[\eta]_i$ of a polymer solution at each data point i (time slice) of a polymer distribution. Thus, if the differential refractometer is used as a concentration detector, then for each sample slice i,

$$[\eta]_i \approx \frac{\eta_{sp,i}}{C_i} = \frac{\nu \eta_{sp,i}}{n_i} \quad (2)$$

where Δn is the refractive index change due to the polymer in solution, detected by the refractometer and $\nu = dn/dc$ is the refractive index increment of the polymer. The quantity calculated from Eq. 2 is often designated as "observed" intrinsic viscosity, $[\eta]_{obs}$.

As can be seen from Eq. 2, the observed intrinsic viscosity for each slice is proportional to the ratio of two detectors' responses. It follows that detector noise,

which is an irreducible component of the measurement process, introduces noise in the intrinsic viscosity that depends on this ratio. However, two detectors have different sensitivities at the tails of polymer distribution: the concentration detector is less sensitive to the high-molecular-weight end and the viscometer is less sensitive to the opposite end. Thus, the noise increases dramatically on both tails of the distribution, where the ratio (2) does not produce physically meaningful values. For example, the logarithm of intrinsic viscosity computed from the slice ratios (2) sometimes does not increase monotonically with molecular weight (i.e., with decreasing elution volume V) even for the flexible coillike polymers (curves 2 in Fig. 1).

Fitting a smooth, multivariate model to a time series of noisy data is an effective way to produce a more precise estimate of the measured quantity at each sample time. Typically, the logarithm of intrinsic viscosity is modeled as a low-order polynomial in elution volume V using a least-squares fitting to the experimental data.[2–4] The intrinsic viscosity calibration curve ($\log[\eta]_{\text{fit}}$ vs. V) obtained this way depends on properties of the polymer as well as that of the chromatographic system (e.g., columns). It can be used for diagnostic information concerning the GPC–viscometry system[5] and also to refine such system parameters as interdetector volume and band broadening (see *Band Broadening in GPC/SEC*, p. 147).

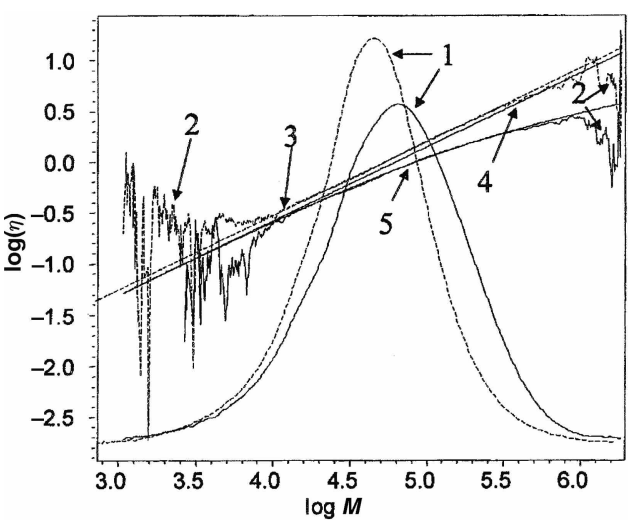

Fig. 1 Molecular-weight-distribution (MWD) and viscosity-law plots for NIST PE1475 high-density polyethylene (dashed lines) and NIST PE1476 low-density polyethylene (solid lines). The curves are (1) MWD, (2) observed viscosity, (3) fitted viscosity for linear polyethylene, (4) extrapolated fitted viscosity for polyethylene with short-chain branches only, and (5) fitted viscosity for branched polyethylene.

APPLICATION OF INTRINSIC VISCOSITY IN GPC TO POLYMER CHARACTERIZATION

Molecular Weight and Molecular-Weight Distribution Determination

The most important feature that has been added to conventional GPC by the viscometer detector through the intrinsic viscosity calculation is the ability to determine the "absolute" molecular weight distribution (MWD) without any additional assumptions about the polymer chemical structure. This goal is accomplished by applying the universal calibration concept, which establishes the hydrodynamic volume $H = [\eta]M$ as a universal parameter governing the size-exclusion separation. The MWD can be determined in three steps. First, the set of narrow polydispersity polymers with known molecular weights (narrow standards) covering the entire region of column size-exclusion separation is selected to construct the universal (or hydrodynamic volume) calibration curve, $\log H$ vs. elution volume V (see *GPC/SEC: Calibration with Universal Calibration Techniques*, p. 1006). This curve is then used to calculate the molecular-weight calibration curve via the relationship $\log M = \log H - \log[\eta]_{\text{fit}}$, where these quantities are obtained from the (smooth) hydrodynamic and intrinsic viscosity calibration curves. Finally, the MWD is constructed by plotting the concentration C as a function of $\log M$ across the polymer distribution (curves 1 in Fig. 1). Different statistical moments of this distribution (i.e., average molecular weights, including viscosity-average molecular weight M_v) can be calculated by appropriate summation over the slice data and compared with the values obtained by bulk measurements.[6]

Intrinsic Viscosity Distribution

The intrinsic viscosity is a fundamental property of the polymer sample in solution, and thus the intrinsic viscosity distribution (IVD) (C vs. $\log[\eta]$) with associated statistical moments may be used to characterize polymers without converting this distribution into a MWD.[7] The IVD can be determined in GPC–viscometry directly, without resorting to universal calibration. This distribution depends not only on the polymer sample itself but also on the solvent and the temperature, and hence does not possess the versatility of the MWD. Nevertheless, the IVD measurement in GPC–viscometry is much less sensitive to experimental conditions than any calibration curve and, hence, can be successfully used in industry (e.g., for quality control of polymers in production).

Size and Molecular Structure of Polymers

The GPC–viscometry with universal calibration provides the unique opportunity to measure the intrinsic viscosity as a function of molecular weight (viscosity law, $\log[\eta]_{\text{fit}}$

versus log M) across the polymer distribution (curves 3 and 4 in Fig. 1). This dependence is an important source of information about the macromolecule architecture and conformations in a dilute solution. Thus, the Mark–Houwink equation usually describes this law for linear polymers: $\log[\eta] = \log K + \alpha \log M$ (see *Mark–Houwink Relationship*, p. 1429). The value of the exponent α is affected by the macromolecule conformations: Flexible coils have the values between 0.5 and 0.8, the higher values are typical for stiff anisotropic ("rod"-like) molecules, and much lower (even negative) values are associated with dense spherical conformations.

The determination of the viscosity law in GPC–viscometry is even more important for branched polymers. Branches reduce the sizes of a macromolecule, including its hydrodynamic volume H. This size reduction is reflected by the changes in the shape and position of the viscosity law plot for a branched polymer. Short-chain branches usually do not change the linearity and slope of the Mark–Houwink plot and just decrease the value of parameter K, whereas the long-chain branches cause bending of the corresponding plot.

These features of the viscosity-law plots for branched polymers are demonstrated in Fig. 1 with two NIST (National Institute of Standards and Technology, U.S.A.) polyethylene standards as examples: high-density linear polyethylene PE1475 and low-density branched polyethylene PE1476. This last one contains both short- and long-chain branches. Dashed straight line 3 represents the Mark–Houwink plot for linear polyethylene, parallel solid line 4 takes into account the short-chain branches, and polyethylene with both types of branches (PE1476) is described by solid curve 5.

For further information on the intrinsic viscosity determination in GPC, including the use of the light-scattering detector, see Ref.[8] and *GPC/SEC Viscometry from Multiangle Light Scattering*.

REFERENCES

1. Mays, J.W.; Hadjichristidis, N. Polymer characterization using dilute solution viscometry. In *Modern Methods of Polymer Characterization*; Barth, H.G., Mays, J.W., Eds.; John Wiley & Sons: New York, 1991; 227–269.
2. Kuo, C.-Y.; Provder, T.; Koehler, M.E.; Kah, A.F. Use of a viscometric detector for size exclusion chromatography. In *Detection and Data Analysis in Size Exclusion Chromatography*; Provder, T., Ed.; American Chemical Society: Washington, D.C., 1987; 130–154.
3. Lew, R.; Cheung, P.; Balke, S.T.; Mourey, T.H. SEC–viscomter detector systems. I. Calibration and determination of Mark-Houwink constants. J. Appl. Polym. Sci. **1993**, *47*, 1685–1700.
4. Brun, Y.; Nielson, R.; Gorenstein, M.; Hay, N. New results in polymer characterization using multidetector GPC. In *Proceedings, International GPC Symposium*; 1998; 48–67.
5. Balke, S.T.; Cheung, P.; Lew, R.; Mourey, T.H. Single-capillary viscometer used for accurate determination of molecular-weights and Mark-Houwink constants. J. Liquid Chromatogr. **1990**, *13*, 2929–2955.
6. Lesec, J. Problems encountered in the determination of average molecular weights by GPC viscometry. In *Liquid Chromatography of Polymers and Related Materials II*; Cazes, J., Delamare, X., Eds.; Chromatographic Science Series Marcel Dekker, Inc.: New York, 1980; Vol. 13, 1–17.
7. Yau, W.W.; Rementer, S.W. Polymer characterization by SEC Viscometry: Molecular Weight (MW), Size (Rg) and Intrinsic Viscosity (IV) Distribution. J. Liq. Chromatogr. **1990**, *13* (4), 627.
8. Jackson, C.; Barth, H.G. Molecular weight-sensitive detectors for size exclusion chromatography. In *Handbook of Size Exclusion Chromatography*; Wu, C., Ed.; Chromatographic Science Series Marcel Dekker, Inc.: New York, 1995; Vol. 69, 103–145.

Polymers: Solvent Effects in ThFFF Separation

Wenjie Cao
Mohan Gownder
Huntsman Polymers Corp., Odessa, Texas, U.S.A.

INTRODUCTION

The early research of Myers et al.[1,2] shows that polymer thermal field-flow fractionation (ThFFF) retention and thermal diffusion are solvent dependent. Recently, Sisson and Giddings[3] indicated that polymer ThFFF retention could be increased by mixing solvents. Rue and Schimpf[4] extended the molecular-weight range that can be retained by ThFFF to much lower molecular weights (<10 kDa) by using solvent mixtures without using extreme experimental conditions. There are several other reports on the effect of solvents on polymer retention, selectivity, and the universal calibration in FFF in last few years.[5]

DISCUSSION

The dissolving of a polymer into a solvent is governed by the free energy of mixing,[6]

$$\Delta G_m = \Delta H_m - T\Delta S_m \tag{1}$$

where ΔG_m is the free-energy change of the solution, ΔH_m is the enthalpy change of the solution, and ΔS_m is the entropy change of the solution.

The enthalpy change is given by

$$\Delta H_m = V\left(\left(\frac{\Delta {E_1}^v}{V_1}\right)^{1/2} - \left(\frac{\Delta {E_2}^v}{V_2}\right)^{1/2}\right)^2 \phi_1\phi_2 \tag{2}$$

where V is the volume of the mixture, ΔE_i^v is the energy of vaporization for species i, V_i is the molar volume of species i, and ϕ_i is the volume fraction i in the solution.

The solubility parameter, δ_i, has been defined[6] as the square root of the cohesive energy density (CED), $\Delta E_i^e/V_i$, and describes the strength of attraction between molecules:

$$\delta_i = \left(\frac{\Delta {E_i}^v}{V_i}\right)^{1/2} \tag{3}$$

Eq. 1 may be rewritten as

$$\Delta G_m = V(\delta_1 - \delta_2)^2\phi_1\phi_2 - T\Delta S_m \tag{4}$$

Because the second term, the entropy term, is always positive for the process of polymer dissolution, the deciding factor in determining the sign of the Gibbs energy change in Eq. 4 is the first term, which contains the solubility parameters of the polymer and the solvent. In general, $(\delta_1 - \delta_2)^2$ must be small for the polymer and the solvent to be miscible. A polymer dissolves most easily in a solvent whose solubility parameter matches it or is close to its own. This is consistent with the "like dissolves like" rule.

If a polymer is easily soluble in a solvent, by convention, the solvent is called a good solvent, and the converse, it is a poor solvent.[6] Therefore, a solvent whose δ value is close to the δ value of a polymer family is a good solvent for this polymer family. As examples, the δ value of polystyrene (PS) is about 18, which is closer to the δ value of 18.6 of tetrahydrofuran (THF) than the d value of 16.8 of cyclohexane (CH). Therefore, THF is expected to be a better solvent for PS than CH. For polyisoprene (PIP), the situation is reversed; CH is a better solvent than THF.

Polymer molecules tend to spread out to a larger hydrodynamic size in a good solvent than they do in a poor solvent, which results in a reduced diffusion coefficient D as the Stoke–Einstein equation shows:

$$D = \frac{kT}{6\pi\eta R_h} \tag{5}$$

where k is the Boltzmann constant, T is the absolute temperature, η is the solvent viscosity, and R_h is the hydrodynamic radius of the polymer molecules in a solvent.

The retention of polymer molecules in ThFFF is determined by the diffusion coefficient and the thermal diffusion coefficient D_T illustrated approximately by[8]

$$\frac{t_r}{t^0} \approx \frac{1}{6\lambda} = \frac{\Delta T}{6}\frac{D_T}{D} \tag{6}$$

where λ is the reduced mean layer thickness of a sample zone in the ThFFF channel, is the polymer retention time, t^0 is the elution time of the non-retained species, and ΔT is the temperature difference across the channel thickness.

From the point of view of diffusion, the reduced D, obtained by replacing a poor solvent with a good solvent, will result in smaller λ if ΔT and other experimental conditions are kept unchanged. The reduced λ (sample zone is closer to the accumulation wall) will cause the polymer molecules to elute out of the ThFFF channel later because of the parabolic flow inside a ThFFF channel.[8] Higher retention, therefore, should be expected for polymers eluted by good solvents in ThFFF.

D_T for the polymer solution is not well understood. There are several theories of polymer thermal diffusion in liquids. Extensive reviews have been done by Schimpf and colleagues in several publications.[4,9] As an example, the radiation pressure theory of Gaeta and Scala shows that D_T is proportional to the cross-sectional area of the solute molecules:[10]

$$D_T = Z_A\left(\frac{\kappa_s}{U_s} - \frac{\kappa_p}{U_p}\right)\frac{\sigma}{f} \tag{7}$$

where Z_A is the acoustical impedance, a quantity related to the density and velocity of sound waves in the polymer and solvent, κ_p and κ_s are the thermal conductivity of the polymer and solvent, respectively, U_p and U_s are the corresponding velocities of sound in the two media, f ($f \propto \eta R_h$) is the frictional coefficient, and σ ($\sigma = \pi R_h^2$) is the cross-sectional area of the polymer molecules.

As discussed earlier, the sizes, or cross-sectional areas, of polymer molecules dissolved in a good solvent are larger than that in a poor solvent. Therefore, the D_T of a polymer in a good solvent is predicted to be larger than that in a poor solvent according to Eq. 7.

From the point of view of both diffusion and thermal diffusion (assuming Gaeta's theory is correct in this case), ThFFF retention of a polymer should be larger in a good solvent than in a poor solvent.

The study of Sisson and Giddings[3] shows that polymer retention in some binary solvents can be enhanced while retention is relatively unaffected or even diminished in other cases. In the case of a mixture of 30% dodecane and 70% THF, polymer retention was enhanced by 35% relative to pure THF. The low end of the molecular-weight range, which can be analyzed by ThFFF, therefore, can be expanded further down by using binary carriers.

Rue and Schimpf[4] investigated component partition of a solvent mixture under thermal gradient. It is indicated that when one solvent is a significantly better solvent for a polymer, then the gradient of this solvent will cause the polymer to migrate in the same direction as the thermophoretic motion of this solvent. This is called solubility-based migration as a partitioning effect. When the better solvent partitions to the cold wall of the ThFFF channel, polymer retention is enhanced; when the better solvent partitions to the hot wall, retention is diminished. Five polystyrene samples, ranging in molecular weight from 2500 to 179,000, were separated in a mixture carrier containing 45 vol% THF in *n*-dodecane. This separation was the first time that polymers of molecular weight below 2500 become separated from the void peak without using extreme experimental conditions such as channel pressurization, ultrahigh ΔT, and so forth.

If the solvent effect is the same for both small and large polymer homologs, the selectivity will not be changed by switching solvents. This might not be the case, because small polymer molecules tend to be spread out to the maximum length of the flexible chain, even in a relatively poor solvent, whereas larger polymer molecules may need better solvents to spread out to their maximum. A different solvent effect might, therefore, be expected when a poor solvent is replaced by a good solvent for a homologous polymer series, and vice versa. It is possible, therefore, to manipulate the selectivity of polymer separation by ThFFF through solvent selection. Any dependence of D_T on molecular weight may be different for different solvents, and this may also contribute to changes in selectivity. Better retention and,

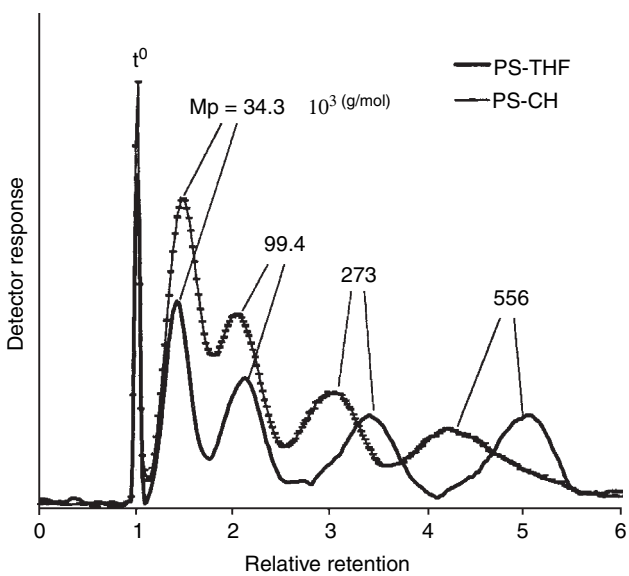

Fig. 1 Fractograms of PS in THF and CH. $\Delta T = 50°C$; $T_c = 25°C$. Flow rate is 0.1 ml/min and sample mass is 1 μg.

probably, better selectivity are expected for PS in THF and PIP in CH among the possible four polymer–solvent pairs, as an example.

Fig. 1 shows the overlaid fractograms of PS eluted by THF and CH under the same experimental conditions of cold-wall temperature, temperature drop, flow rate, and sample mass (1 μg).[5] The fractograms show that a small PS of molecular weight 34,300 is retained approximately the same in both THF and CH, whereas the retentions of larger polymers show significant differences in the two solvents, with the larger PS retained longer in THF. This indicates that using better solvents may enhance both retention and selectivity.

REFERENCES

1. Myers, M.N.; Caldwell, K.D.; Giddings, J.C. A study of retention in thermal field-flow fractionation. Separ. Sci. Technol. **1974**, *9* (1), 47–70.
2. Kirkland, J.J.; Boone, L.S.; Yau, W.W. Retention effects in thermal field-flow fractionation. J. Chromatogr. **1990**, *517*, 377–393.
3. Sisson, R.M.; Giddings, J.C. Effects of solvent composition on polymer retention in thermal field-flow fractionation: Retention enhancement in binary solvent mixtures. Anal. Chem. **1994**, *66*, 4043–4053.
4. Rue, C.A.; Schimpf, M.E. Thermal diffusion in liquid mixtures and its effect on polymer retention in thermal field-flow fractionation. Anal. Chem. **1994**, *66*, 4054–4062.
5. Cao, W.J.; Williams, P.S.; Myers, M.N. Solvent effects on polymer retention and universal calibration in ThFFF in preparation.
6. Brandrup, J.; Immergut, E.H. *Polymer Handbook,* 3rd Ed.; John Wiley and Sons: New York, 1989.
7. de Gennes, P.G. *Scaling Concepts in Polymer Physics*; Cornell University Press: Ithaca, NY, 1979.
8. Giddings, J.C. Field-flow fractionation: Analysis of macromolecular, colloidal and particulate materials. Science **1993**, *260*, 1456–1465.
9. Schimpf, M.E.; Giddings, J.C. Characterization of thermal diffusion in polymer solutions by thermal field-flow fractionation: Dependence on polymer and solvent parameters. J. Polym. Sci. Part B: Polym. Phys. **1989**, *27* (6), 1317–1332.
10. Gaeta, F.S.; Scala, G.; Brescia, G.; Di Chiara, A. Characterization of macromolecules in liquid solutions by thermal diffusion. I. Dependence of the soret coefficient on the nature of the dispersing medium. J. Polym. Sci.: Polym. Phys. Ed. **1975**, *13* (1), 177–202.

Polystyrene: ThFFF

Seungho Lee
Department of Chemistry, Hannam University, Taejon, Korea

INTRODUCTION

Thermal field-flow fractionation (FFF) is an elution-type separation technique applicable to the characterization of various synthetic organic polymers with molecular weights higher than about 10^4.[1] In thermal FFF, a dilute solution of polymer sample is injected into a thin ribbon-shaped flow channel across which an external "field" (in the form of a temperature gradient) is applied. Under the influence of the temperature gradient, different components of the sample are carried down the channel at different velocities, leading to the elution of different components at different times—separation is obtained.

MOLECULAR WEIGHT-BASED SEPARATION

In thermal FFF, retention time t_r is given by[2]

$$t_r = \frac{t^0 \Delta T}{6}\left(\frac{D_T}{D}\right) \tag{1}$$

for well-retained components. Here, t^0 is the channel void time (a constant for a given channel dimension), ΔT the temperature drop across the channel, D_T the thermal diffusion coefficient, and D the mass diffusion coefficient. For most polymeric materials, D is related to the molecular weight M by

$$D = \frac{A}{M^b} \tag{2}$$

Combining Eqs. 1 and 2 yields

$$t_r = \frac{t^0 \Delta T D_T}{6A} M^b \tag{3}$$

It has been shown that D_T is independent of branching configuration and molecular weight for homopolymers (such as polystyrene) in a given solvent.[3] Thus, under fixed experimental conditions, the retention time of polystyrene depends only on the molecular weight, resulting in a molecular weight-based separation: The retention time increases as the molecular weight increases.

EFFECT OF ΔT IN POLYSTYRENE SEPARATION

It is seen from Eq. 3 that dt_r/dM (the difference in retention time for the same molecular weight difference) increases with ΔT, indicating that the separation (and thus the resolution) between two polystyrene components increases with ΔT. However, the gain in resolution comes at the cost of time, as the use of higher ΔT requires longer analysis time. An optimum condition for ΔT must be determined for each sample by observing the time and the elution profile at various ΔT. Finding the optimum ΔT is relatively easy for samples having narrow molecular weight distributions. However, for samples having broad distributions, finding the optimum ΔT may not be trivial. Field programming may be required for samples having broad molecular weight distributions to prevent excess retention of late-eluting high-molecular-weight components.[4] In a field-programmed thermal FFF, ΔT generally starts at high and is gradually decreased during a run. Fig. 1 shows a separation of four polystyrene standards having nominal molecular weights ranging from 47,000 to about 1 million daltons.

DETERMINATION OF PHYSICOCHEMICAL PROPERTIES

The simplicity of both retention mechanism and the channel geometry of thermal FFF allows one to theoretically predict the degree of retention of a sample, provided certain physicochemical properties of the sample are known. Conversely, one may determine the physicochemical properties of a sample by measuring its retention time (or volume).

Determination of Diffusion Coefficients

As seen in Eq. 1, retention time in thermal FFF is a function of the ratio of two diffusion coefficients, D_T/D. If one of the two diffusion coefficients is known, the other

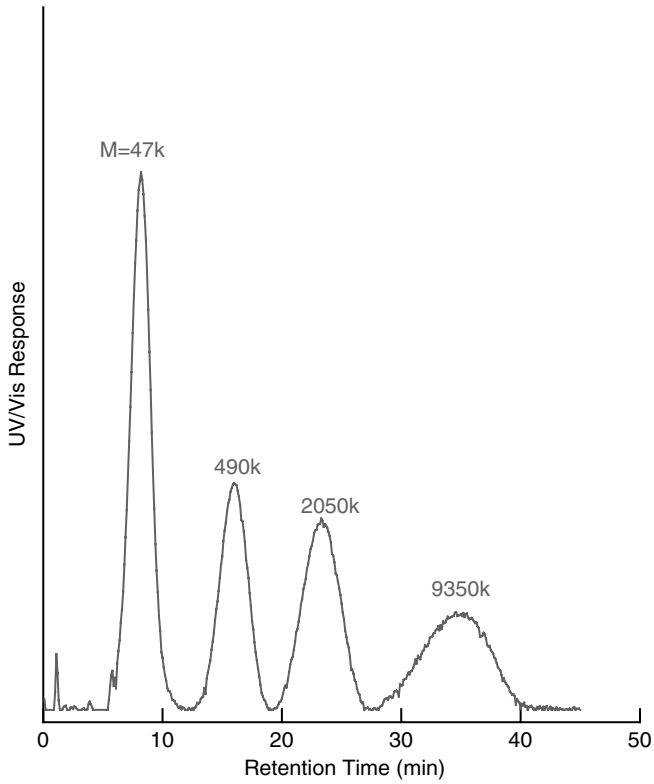

Fig. 1 Thermal FFF separation of polystyrene standards having nominal molecular weights as indicated. Power programming was used with initial $\Delta T = 80°C$, predecay time $t_1 = 3$, $t_a = -6$, and hold $\Delta T = 10°C$. The solvent/carrier was tetrahydrofuran and the flow rate was fixed at 0.2 ml/min.

can be determined directly from the retention time using Eq. 1. It is noted that the values of the diffusion coefficients may vary in various solvents.

Determination of Molecular Weight

If the values of A, b, and D_T are available, the molecular weight of a polymer can be directly determined from its retention time using Eq. 3. If D_T is not available, one may use a calibration curve [$\log(D/D_T)$ vs. $\log M$] constructed with a series of narrow polystyrene standards of known molecular weights. For the molecular weight analysis of an unknown, the D/D_T value of the sample is first calculated from its measured retention time, and then the molecular weight is determined from the calibration curve.

Use of molecular weight-sensitive detectors (e.g., differential viscometer or light-scattering detector) eliminates the need for calibration. With a differential viscometer used as a detector for thermal FFF, the intrinsic viscosity is first measured for each retention time and then converted to molecular weight using Mark–Houwink constants.[5] The use of accurate values of Mark–Houwink constants is essential in this method. Unlike the viscometer, the light-scattering detector measures the absolute molecular weight of the polymers directly. In multiangle light scattering, the scattered light intensity is measured over a broad range of scattering angles, allowing the determination of molecular size (radius of gyration) as well as molecular weight.[6]

ANALYSIS OF HIGH-MOLECULAR-WEIGHT POLYSTYRENE

Thermal FFF is often compared with size-exclusion chromatography (SEC) as both can be used for the same application, that is, the molecular weight determination of polymers. In SEC, the elution volume of the sample in a column (or in a column set) is limited to values between the interstitial volume of the column ("total exclusion limit") and the total liquid volume ("total permeation limit"). The resolving power of SEC quickly drops as the elution volume approaches these limits. By contrast, there is no theoretical limit in thermal FFF, and the applicable molecular weight is virtually unlimited in the high molecular weight range. Also, the openness of the channel minimizes the shear degradation and adsorption of polymers. Thermal FFF is thus useful for characterizing high-molecular-weight polymers, including samples containing microgel, that are difficult to analyze using SEC.[7]

It is noted, however, that for polymers of molecular weight below about 10,000 Da, SEC may be more useful than thermal FFF. Analysis of such low-molecular-weight samples using thermal FFF requires the application of very high ΔT, which may require the use of a pressurized system to avoid boiling of the solvent.

REFERENCES

1. Giddings, J.C. Field-flow fractionation: separation and characterization of macromolecular–colloidal–particulate materials. Science **1993**, *260*, 1456.
2. Shiundu, P.M.; Remsen, E.E.; Giddings, J.C. Isolation and characterization of polymeric and particulate components of acrylonitrile–butadiene–styrene (ABS) plastics by thermal field-flow fractionation. J. Appl. Polym. Sci. **1996**, *60*, 1695.
3. Schimpf, M.E.; Giddings, J.C. Characterization of thermal diffusion in polymer solutions by thermal field-flow fractionation: dependence on polymer and solvent parameters. Polym. Sci. B. Polym. Phys. **1989**, *27*, 1317.
4. Williams, P.S.; Giddings, J.C. Power programmed field-flow fractionation: a new program form for improved uniformity of fractionating power. Anal. Chem. **1987**, *59*, 2038.
5. Kirkland, J.J.; Rementer, S.W. Polymer molecular weight distributions by thermal field flow fractionation using Mark–Houwink constants. Anal. Chem. **1992**, *64*, 904.
6. Lee, S.; Kwon, O.-S. Characterization of ultrahigh molecular weight intraocular lens material using thermal field-flow fractionation coupled with multi angle laser light scattering. Polym. Mater. Sci. Eng. **1993**, *65*, 408.
7. Lee, S.; Molnar, A. Determination of molecular weight and gel content of natural rubber using thermal field-flow fractionation. Macromolecules **1995**, *28* (18), 6354–6356.

Porous Graphitized Carbon Columns in LC

Irene Panderi
School of Pharmacy, Division of Pharmaceutical Chemistry, University of Athens, Athens, Greece

INTRODUCTION

Liquid chromatography (LC) is a separation technique which is used widely in many different areas of analytical chemistry and provides a powerful tool for the separation and quantification of substances in various matrices. Nowadays, the majority of the high-performance liquid chromatography (HPLC) methods are carried out in reversed-phase mode using a non-polar stationary phase and a polar-mobile phase.

The most popular reversed-phase columns are manufactured from silica-based bonded phases, and, among those, the C_{18}-type bonded phase is most frequently used. These bonded phases are prepared by reacting silica with a reactive silane that carries the hydrophobic ligand after which the phase is named. However, the poor stability of silica at extreme pH values, along with the presence of underivatized silanol groups that most frequently cause secondary interactions, limits the application of silica-based supports in LC.

POROUS GRAPHITIZED COLUMNS

Over the years, serious efforts have been devoted to the development of new reversed-phase packing materials in attempts to overcome the drawbacks of silica-based bonded phases. Thus reversed-phase separations can also be performed on polymeric columns. The great majority of these columns consist of styrene-divinylbenzene-, methacrylate-, or polyvinylalcohol-based phases and appear to be more stable over a wide pH range. Divinylbenzene packings are stable over the whole pH range, while the other two substrates (methacrylate and polyvinylalcohol) are hydrolytically stable between pH 2 and 12. Thus these polymer-based packings can be used at extreme pH values where silica-based columns degrade rapidly. However, silica-based columns are still more efficient and provide a much greater choice of different silica-based packings than polymeric columns.

The expectation that graphitized carbon-packing material would show high chemical stability over the entire pH range (pH = 0–14), and ultimate hydrophobic properties, led to a number of investigations in this area.[1] There have been many attempts to manufacture reversed-phase carbon-based packings by the use of carbon black[2] and led to the development of graphitized carbon black (GTCB) supports. Unfortunately, these supports were unsuitable for routine chromatographic analyses because of their extremely poor mechanical stability. Several trials have been made to overcome this limitation until the successful preparation of porous graphitized carbon (PGC) packing material.[3]

Porous graphitized carbon packing material was developed by Knox et al.[4–6] to provide a reversed-phase support that could have sufficient hardness to withstand high pressures, such as those encountered in HPLC, and would not suffer from the disadvantages of silica-based bonded supports. This packing material was produced by the templation method using silica gel as template. Actually, a 7 μm spherical porous silica gel template was impregnated with a phenol hexamine mixture and then heated to 150°C to form phenol-formaldehyde resin within the pores of silica gel. This polymer was further heated slowly to 900°C under a stream of oxygen-free nitrogen. The silica–carbon particles were then treated with potassium hydroxide to dissolve the silica template, and the remaining porous carbon was heated to a high temperature in the range of 2000–2800°C to anneal the surface, remove micropores, and, depending upon the temperature, produce some degree of graphitization. The particle size, shape, porosity, and pore size are determined by the choice of template material. It is thus possible to produce porous graphitized carbons with a range of pore and surface properties.[7]

The surface characteristics of the porous graphitized carbon have been extensively investigated.[8] X-ray diffraction provides useful information about the degree of graphitization. The Bernal structure of perfect three-dimensional graphite is one of the forms of carbon atoms to which the term graphitization can be applied and is clearly presented in Fig. 1a. However, perfect graphite is rarely formed synthetically from amorphous solid carbon because the bonding between the carbon atoms within the graphitic layers is extremely strong, while the interlayer bonding is weak. Graphitization tends to develop by the formation of graphitic layers, which are initially randomly oriented. The reorganization of these layers into ordered three-dimensional graphite requires high activation energy (above 3000°C). Thus most synthetic carbons, when heated to about 3000°C, lead to a two-dimensional graphite structures. The atomic-molecular structure of PGC is clearly presented in Fig. 1b; it is a two-dimensional graphite molecular structure (Warren structure), otherwise termed turbo static carbon structure, in which graphitic

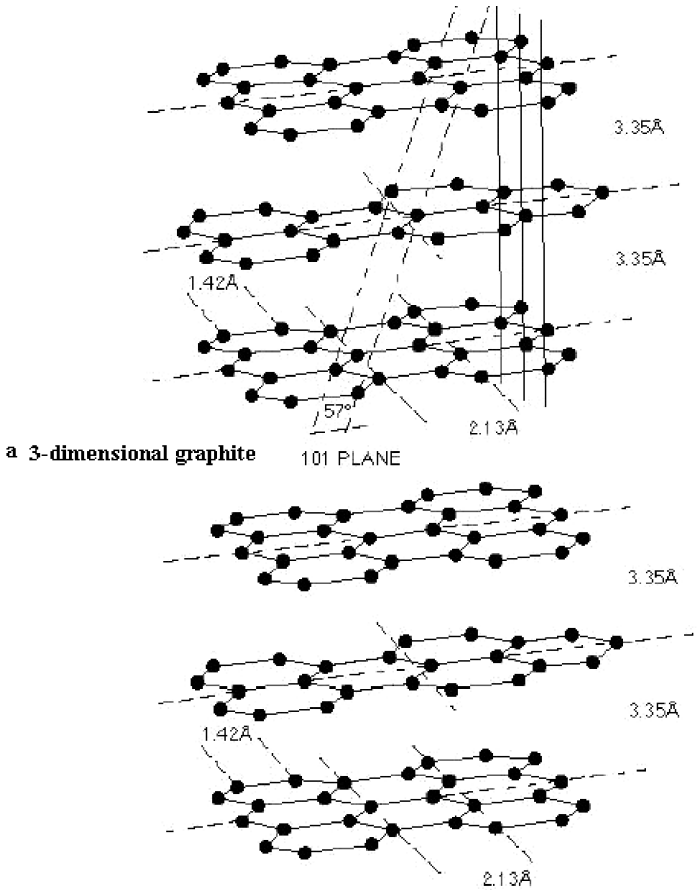

Fig. 1 Atomic structures of graphites. a, Bernal structure of perfect three-dimensional graphite; and b, Warren structure of two-dimensional turbostatic graphite with no layer registration.
Source: Reproduced by kind permission of Thermo-Hypersil-Keystone.

layers are randomly oriented and, unlike three-dimensional graphite, there is no ordering of the atoms between layers. The high-resolution electron micrograph of PGC supports is presented in Fig. 2 and reveals a structure that is composed entirely of flat graphitic layers of hexagonally arranged carbon atoms showing sp^2 hybridization. The graphitic layers are randomly twisted and interleaved in a complex way, and, unlike silica gel, there are no surface functional groups.

It is important to mention that attempts have been made to construct porous carbon supports using entirely different carbonization procedures.[9,10] One involved the carbonization of hydrocarbons on porous zirconia microplates.[11] The type of chromatographic support that is obtained by this procedure is highly dependent upon the type of hydrocarbons used. In particular, when saturated hydrocarbons are used as the carbon source, the loading capacity and efficiency of the carbon supports are much greater than those obtained by unsaturated hydrocarbons. In other carbonization attempts, the three-dimensional channels of zeolites were used as templates to prepare porous carbon.[12] The nanospaces in zeolites are packed with carbon and then the carbon is extracted from the zeolite framework. The resultant carbons are highly porous with surface areas greater than 2000 m^2/g.

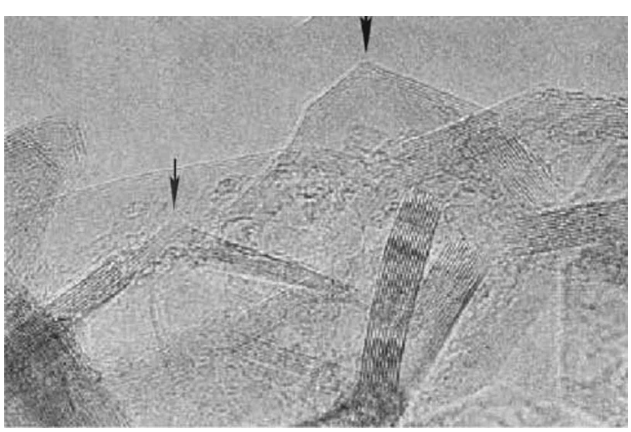

Fig. 2 High-resolution electron micrographs of porous graphitized carbon.
Source: Reproduced by kind permission of Thermo-Hypersil-Keystone.

Nowadays, PGC are one of the most new reversed-phase packing materials with a homogenous hydrophobic surface, but they can also be used in the normal-phase mode.[13] At the end of the 1980s, PGC packing materials were made available, the most common one under the trade name Hypercarb. This packing material exhibits a well-defined pore structure, allowing a good mass transfer of a large number of solutes and a specific surface area in the range 150–200 m^2/g that gives improved retention possibilities of solutes and maintains a linear sample capacity over a large concentration range. It is totally unaffected by aggressive eluents as it exhibits high chemical stability, probably because of the lack of ordering between the graphitic layers, and can withstand high temperature. Moreover, it does not suffer from swelling or shrinking and it is hydrolytically stable across the entire pH range 0–14. Its retention and selectivity behavior is quite different from that of reversed-phase bonded phases. Porous graphitized carbon is recommended for the separation of highly polar and ionized compounds, and it gives an unrivaled stereoselective surface with unique ability to resolve isomeric and closely related compounds.[14,15] It is thus suitable for large, fairly rigid molecules with a multitude of polar groups, such as many natural compounds and new drugs.[16]

CHROMATOGRAPHIC CHARACTERISTICS AND RETENTION BEHAVIOR OF POROUS GRAPHITIZED CARBON COLUMNS

The chromatographic retention on PGC columns has been extensively investigated.[17] Results indicate that PGC offers a unique retention mechanism that could be explained by a combination of various kinds of selective interactions between solutes, mobile phases, and PGC packing material.[18] These supports are not only strongly hydrophobic in comparison to the other traditional reversed-phase packing materials such as silica-based packings, but they also retain solutes through electronic (π–π) interactions. The delocalization of the π-electrons in the large graphitic layers and the high polarizability of the carbon are responsible for strong dispersion interactions. In addition, charge-induced interaction between the graphite surface and the polar substituents of the solutes, steric effects, along with hydrophobic interactions, affect the mechanism of retention onto PGC.

It was observed that, where purely hydrophobic surface–solute interactions are present, it will require higher concentrations of organic modifier to elute such solutes.[8] Several efforts have been made to categorize solvent strength data for PGC supports into an eluotropic series using various types of solutes. Although the choice of organic modifier offers a route to modify the retention of solutes on PGC columns, the results indicated that organic modifiers did not show common eluotropic behavior and that their effects on retention are mainly dependent on the type of solutes.[19] Thus it is possible to arrange solvents in an order of eluotropic strength for particular types of solutes. Solvent strength data for aniline, naphthalene, ethyl benzene, and phenol are presented in Fig. 3; they indicate that methanol and acetonitrile show low eluotropic strengths for aniline, naphthalene, and ethyl benzene, while for phenol, the same solvents have higher values of eluotropic strength. On the other hand, dioxane and tetrahydrofuran have higher eluotropic strengths for the majority of solutes.

A study of the retention characteristics of several aromatic hydrocarbons on PGC, using methanol as the mobile phase, showed that this graphite packing is an extremely strong adsorbent in comparison to other silica-based packing materials.[20] Studies on the effect of eluent pH on the retention of isomers of ionizable substituted benzene compounds, including isomers with electron-donating and electron-withdrawing substituents, on PGC and ODS packings, provided valuable information on how the surface structure of the stationary phase can affect solute retention and selectivity.[21] The retention factors of unionized solutes were generally greater on PGC than those on ODS, confirming previous observations that neutral compounds are more strongly retained on the PGC packing material. The fact that ionic interactions with ionized solutes were essentially absent on the surface of PGC implies that the retention order is probably governed by a solute molecular orientation effect induced by competing interactions of solute between the stationary phase and the mobile phase. Fig. 4 shows the effect of eluent pH and hence ionization on the retention of the zwitterionic aminobenzoic acid isomers. The greater retention is achieved where neither acid nor basic substituent is ionized. In particular, as the mobile phase pH increased, the retention factor rose initially to a peak value and then began to fall again.[22] The homogeneous and flat crystalline surface of PGC packing is thought to be responsible for its unique selectivity toward the discrimination of ionizable aromatic isomers compared with an ODS packing material. Thus adsorption onto a graphite surface depends on how well many of its atoms can fit onto the flat surface. Thus planar molecules and straight chain hydrocarbons can fit onto the graphite surface, whereas, as the planarity of such molecules is destroyed by the presence of non-planar rings, the adsorption is deteriorated and a parallel decrease in retention is observed. An excellent example that reflects the unique surface properties of the graphitic carbon is the reversal of the elution order of isomeric xylenes when separated on PGC columns in comparison to the elution order of these isomers on reversed-phase silica-based packing.[8] The methyl groups are sufficiently large that adjacent carbon atoms in the ring are just above the graphite surface and so are not as strongly retained as they would be in a totally planar molecule such as benzene. In the case of *o*-xylene and *p*-xylene, four carbon atoms

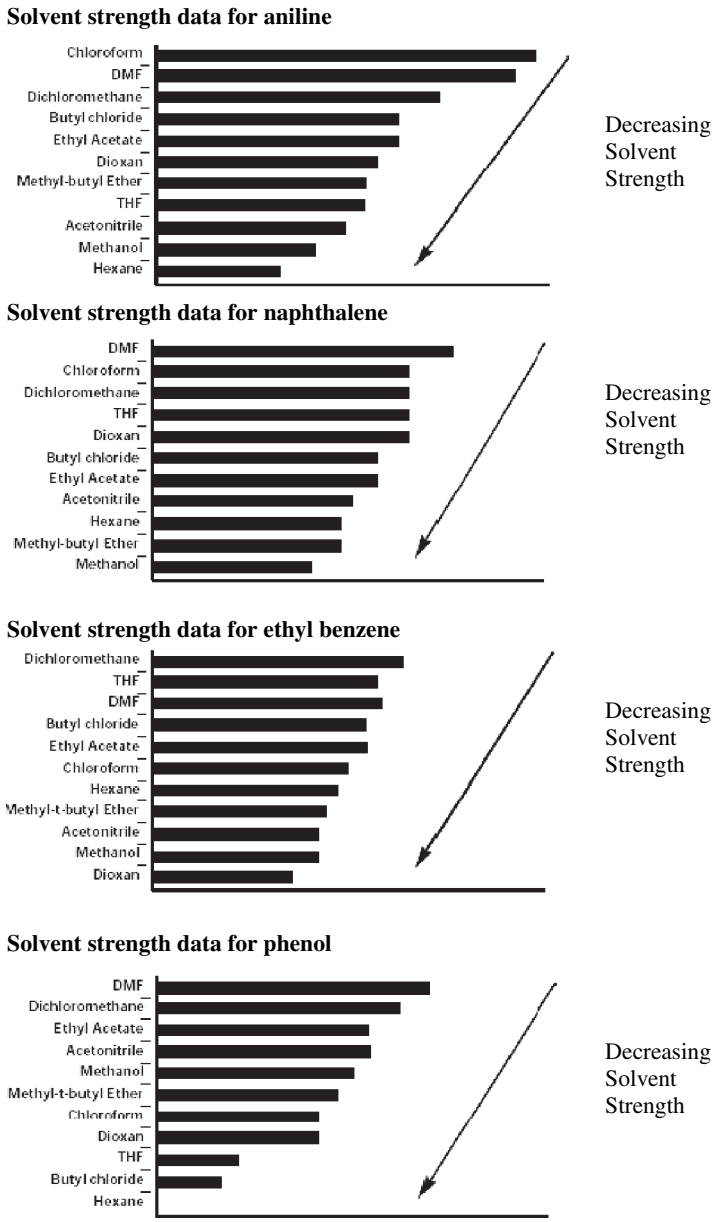

Fig. 3 Solvent strength data on porous graphitized carbon columns for the retention of aniline, naphthalene, ethyl benzene, and phenol.
Source: Reproduced by kind permission of Thermo-Hypersil-Keystone.

contact the graphite surface (two from methyl groups and two from the ring), whereas, in the case of *m*-xylene, only three carbon atoms contact the surface (two from methyl groups and one from the ring). Therefore *m*-xylene elutes first on PGC supports, while the isomers elute later.

The retention of polar compounds (mono-, di-, and tri-substituted benzenes) on PGC, silica-based, and apolar copolymer supports[14] was performed using unbuffered methanol water as eluent. The relationship between log k and the volume fraction of methanol was calculated separately for each solute. It was found that porous graphitic carbon retains polar compounds fairly well under reversed-phase conditions, while the retention factor increased with an increase in the number of polar substituents. In particular, the retention behavior of polar solutes on PGC supports is mainly governed by several polarity parameters (Hammett's constant, proton-donor capacity, and steric effects of substituents) and is quite different from that observed with other reversed-phase supports. Thus it was concluded that charge-induced interactions between the graphite surface as well as steric effects force the polar groups close to the graphite surface. This type of interaction is called "polar retention effect on graphite," (PREG),[23] and proved to be more important than hydrophobic interactions in the retention mechanism of polar compounds.

Separation of various cationic and anionic compounds on PGC columns with a mobile phase containing an electronic modifier (e.g., trifluoroacetic acid) and an organic modifier (e.g., acetonitrile) in the eluent has also been demonstrated.[24] In the same study, positively and negatively charged ions were well separated in the same

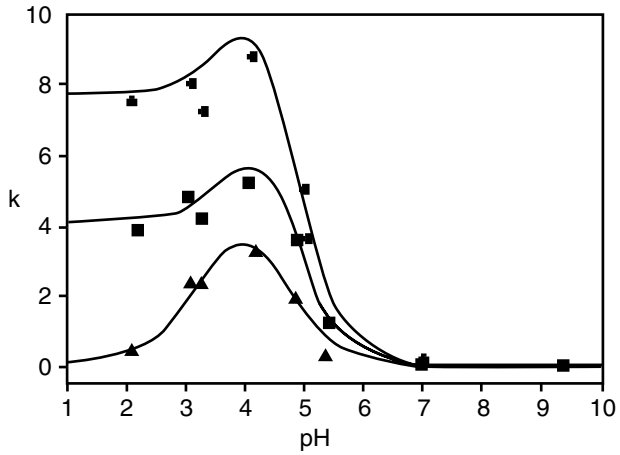

Fig. 4 Effect of the pH of the mobile phase on the retention of aminobenzoic acid isomers. (●): *o*-isomer, (▲): *m*-isomer, and (■): *p*-isomer.
Source: Reproduced by kind permission of Thermo-Hypersil-Keystone.

chromatogram. Thus PGC seems to behave equally as an electron donor and electron acceptor and proved to be an important stationary phase for the separation of ionized solutes by a mechanism other than ion exchange. It was concluded that the retention of anionic compounds is mainly dominated by electronic interaction between the solute and the delocalized electron clouds on the graphitized carbon surface, while cationic compounds are mainly retained by ion suppression or ion pairing consistent with a reversed-phase interaction with the hydrophobic carbon surface.

Another example of electronic interaction between the graphite and ionic solutes is the retention of metal ions on PGC supports.[25,26] Such electronic interaction, either electron donation or acceptance, is presumably between the available orbitals of metal ions and the electronic cloud of the flat graphite surface. The addition of a small concentration of oxalic acid into aqueous mobile phase tends to modify the graphite surface and to increase, through complexation, the range of metal ions retained.

It is extremely important to understand the interactions that govern retention on the graphite surface to better utilize this material and begin to predict how changes in the system will influence carbon-based separation processes.[27] A qualitative insight into the chemical interaction that is involved in the retention process on graphite has been recently achieved through solvatochromic linear solvation energy relationships (LSERs).[28] A variety of solute descriptors were used to correlate retention on graphite. Multiple linear regression of log k' values of 26 solutes against the LSER solute parameters indicated that all parameters were significant. Data of the fitting coefficients indicate that a combination of three solute parameters, size, dipolarity/polarizability, and hydrogen bond basicity, dictates a solute's retention. A spectral mapping technique (SPM) was also employed[29] for the evaluation of the retention mechanism of solutes on PGC; barbiturates were chosen as probe solutes in this study, while mixtures of dioxane-water were used as eluents.[30] Spectral mapping technique proved to be a valuable tool to separate retention strength and the selectivity of solutes and organic modifiers and thus promote a better understanding of the separation process. In particular, through SPM, it was concluded that the retention strength of organic modifiers depends on the electronic parameter characterizing the resonance effect, suggesting that electronic interaction exerts a considerable impact on the elution strength of organic modifiers on PGC. The fact that the calculated lipophilicity of the drugs had no significant role in the chromatographic characteristics indicates, again, that the retention mechanism differs from that of octadecylsilica phase where lipophilicity is the most important parameter influencing the retention. The interaction between the graphite surface and the planar ring of the solute molecules contributes to the retention.

APPLICATION AREAS

Porous graphitized carbon columns have successfully been applied for the analysis of various compounds by HPLC. As already mentioned, PGC shows a highly ordered crystalline structure with large bands of delocalized electrons, so that the retention mechanism is a mixture of hydrophobic and electronic interactions and is very different from that observed with silica-based bonded phases and apolar copolymers.[31] Thus the following criteria must be taken into consideration during the development of a chromatographic separation on PGC columns: 1) strength of organic modifier for particular type of analytes; 2) ionization of the analytes and pH dependence as well as the effect of organic modifiers on control of ionization and pH dependence; 3) effect of the electronic modifier on analytes retention; and 4) effect of analyte shape.

Pharmaceuticals

HPLC has become the most popular chromatographic technique in drug analysis. A literature survey reveals a number of papers that take advantage of the benefits of porous graphitized carbon columns for the separation and determination of several compounds of pharmaceutical interest.[32] In particular, this material possesses several advantages, most notably its physical and chemical stability, as well as a highly stereoselective surface able to resolve diastereomers and geometric isomers; also, it is most applicable to the separation of small ionizable molecules that are not retained with octadecylsiloxane (ODS) columns.

Two different LC systems, equipped with porous graphitized carbon and silica-based RP-8 columns, respectively, were used for the assay of alprenolol and its related substances in quality control.[33] The ability of the PGC system to separate metoprolol and closely related substances was also tested; baseline separations with high column efficiencies were obtained. The robustness of the proposed methods was investigated using experimental design and evaluation with multivariate calculations. The results indicated that the PGC column, with its unique selectivity, excellent stability against alkaline mobile phases, and high column efficiency, is a proper complement to the traditional silica-based reversed-phase supports. Another method describes the simultaneous determination of paracetamol and its related compounds, 4-aminophenol and 4-chloroacetanilide, in pharmaceutical preparations, using PGC column.[34] The chromatographic behavior of the three compounds under variable mobile phase compositions was thoroughly investigated, and the results indicated that retentions were dependent upon organic phase nature, concentration, and pH. Stronger eluents with dipolar properties, such as tetrahydrofuran, could be used with PGC to avoid long retention times for late eluting compounds. The retention selectivities of these compounds on PGC were compared with those on octadecylsilica (ODS) packing materials in reversed-phase liquid chromatography. Porous graphitized carbon columns showed high retention selectivity, rapid equilibrium, and a high stability during the analysis than commercially used ODS columns.

Several amines of pharmaceutical interest (e.g., alprenolol, sotalol, terbutaline, promethazine, and trimipramine) have been well separated with high enantioselectivity using, mainly, *N*-benzyloxycarbonylglycyl-L-proline (L-ZGP) and also *N*-benzyloxycarbonylglyclglycl-L-proline (L-ZGGP) as chiral selectors on PGC column with methanol containing bases as mobile phase.[35] The retention of the enantiomeric amines was found to increase with increasing concentration of the anionic form of L-ZGP. Previous investigation[36] showed an improvement in peak symmetry in the presence of a mobile phase amine. Hence the addition of an alkylamine in the mobile phase in excess of L-ZGP was also investigated and led to a decrease in retention and enantioselectivity. The unique adsorption properties of porous graphitic carbon were also used for separation of racemic amines using chiral counterions dissolved in mobile phases; it was found that a column temperature below 0°C improved the enantioselective resolution.[37] Recently, two newly synthesized chiral di-anionic ions were tested as additives for enantiomeric resolution of a set of amino alcohols on a Hypercarb porous graphitized carbon column.[38] Z-L-Aspartyl-L-proline was used as a di-anionic counterion and resolved 9 of 12 tested racemates. One of its diastereoisomers, Z-L-Aspartyl-D-proline, was also tested, but resulted in low separation factors. The study showed the necessity to titrate the counterion with sodium hydroxide to its di-anionic form to optimize the resolution. Increased retention and enantioselectivity were observed with decreased column temperature.

Stepwise regression analysis and principal component analysis were used to examine the effect of various physicochemical parameters on the retention of 16 monoamine oxidase inhibitory drugs (proparlgylamine derivates) on a PGC column, using ethanol–water mixtures as eluents.[39] Both steric and electronic parameters were found to affect the retention of monoamine oxidase drugs on the graphite surface. An investigation was also carried out on the retention characteristics of 11 steroidal drugs on PGC using water–tetrahydrofuran mixtures as eluents.[40] The logarithm of the capacity factor of each compound was linearly related to the percentage of tetrahydrofuran in the eluent. Principal component analysis was also used to correlate the retention characteristics and the physicochemical parameters of the steroidals. Steric conditions and electrostatic interactions were also found to be responsible for the retention of these compounds onto PGC packings. The porous graphitized carbon column proved to be suitable for the separation of the anticancer drug, taxol, a highly functionalized taxane diterpene amine, in bark and foliage of different Taxus species using water dioxane as eluent.[41,42]

Bio-organic Substances

Because of the considerable importance of the analysis of bio-organic compounds in biochemical and biophysical research, many LC methods have been developed and applied for their separation and purity control. There is now growing evidence that PGC columns can contribute considerably to this application area. The flat graphite surface is able to differentiate between closely related compounds such as the structures of several carbohydrates found in nature.

The chromatographic behavior of oligosaccharide alditols containing two to five monosaccharides has been reported on a Hypercarb porous graphitized carbon column using gradient elution from water to acetonitrile in the presence of 0.05% trifluoroacetic acid.[43] Elution patterns were based on size, charge, and linkage such that isomeric compounds could be separated from each other. In particular, the nature of the linkage appeared to play an important role with (1,3)-linked compounds eluting before the (1–4) linkage.

The chromatographic characteristics of 14 peptides have been determined on a PGC column, using acetonitrile–water mixtures as eluents.[44] The majority of peptides showed irregular retention behavior; their retention decreased with increasing concentration of acetonitrile, reached a minimum, and increased again with increasing concentration of acetonitrile. For the elucidation of the relationship between the various physicochemical parameters and retention characteristics, principal component

analysis (PCA) was employed. Calculations indicated that the impact hydrophobicity, steric, and electronic parameters on the retention of peptides on a PGC column are similar, yet the steric parameters of substituents exert the highest impact on retention.

Porous graphitized carbon has also been explored for HPLC of monosaccharides and disaccharides released from proteoglycans and fluorescently labeled oligosaccharide derivatives for fluorescence detection.[45] Sulfated oligosaccharides show good retention and separation behavior on PGC columns. Gradient elution using mixtures of water with acetonitrile containing trifluoroacetic acid was used to perform the separation on a PGC column. The disadvantage of the anion exchange and reversed-phase ion-pair chromatography is that they require high salt concentrations that are not readily removed when compared with PGC which employs low concentrations of trifluoroacetic acid. Therefore PGC-based chromatography may be useful for two-dimensional sugar mapping and preparation of pure oligosaccharides, including the monitoring of derivatization efficiency with 2-aminobenzamide labels for reagent array analysis method sequencing, mass spectrometry (MS), and NMR. In particular, LC/electrospray MS was used as a tool for the analysis of sulfated oligosaccharides from mucin glycoproteins prepared from pig stomach and colon.[46] A PGC column, along with an amino-bonded column, were used and oligosaccharides were eluted with linear gradients of acetonitrile and water containing 5 m*M* ammonium hydrogen carbonate or formate buffers at basic pH values. Results indicated the benefits of both the amino-bonded and PGC-type chromatography in LC/electrospray ionization–mass spectrometry (ESI–MS) to achieve separations of mixtures of sulfated oligosaccharide alditols. Compounds co-eluting on one column could be separated on the other, indicated by the differing number of isomers separated in each system. The elution order of sulfated oligosaccharides does not appear to be pH-dependent on the PGC column. Various linear and branched oligosaccharides were labeled with 9-aminofluorene and further analyzed on a porous graphitized carbon column using acetonitrile water in 0.05% trifluoroacetic acid as eluent with MS detection.[47]

Ten guanidino compounds were analyzed in the serum of nephritic patients using a porous graphitized carbon column in combination with ion-pair LC and a postcolumn derivatization procedure using ninhydrin as a reagent.[48] The retention mechanism of guanidino compounds on PGC was thoroughly investigated by computational chemical calculation using molecular mechanism (MM2). The retention mechanism of cationic compounds on PGC proved to be electrostatic interaction for cationic guanidino compounds and hydrophobic interaction for molecular-form compounds. It was found that the micelle formation of hydrophobic ion-pair reagents reduces the retention of guanidine compounds. The successful separation of guanidino compounds was achieved by the addition of octanesulfonate in citric buffer. The authors suggest the use of a small precolumn packed with octadecyl-bonded silica to eliminate small particles and hydrophobic compounds from the analyzed samples.

Residue Analysis

The development of methods for the chromatographic separation and quantitation of trace levels of environmental pollutants is always in demand. However, these polar analytes cannot be easily retained on the most commonly used silica-based columns. It has been shown that, for some polar compounds, the retention in water can be very high using PGC columns.[31]

An online technique coupling preconcentration via a precolumn packed with PGC and LC with a PGC analytical column has been applied to the trace-level determination of some polar and water-soluble organic pollutants from environmental waters.[49] As these analytes are much more retained by the graphite surface than by silica C_{18}, preconcentration on the PGC precolumn cannot be coupled online with a widely used and more efficient C_{18} silica analytical columns. In this study, applications were presented for the trace-level determination of 2-chloro-4-aminophenol, chloroanilines, aminophenols, and cyanuric acid; these organic compounds are included in the EC environmental priority pollutant list. The influence of the sample matrix was investigated with drinking and river water samples.

The environmental pollutants 3,4-dimethoxybenzaldehyde (DMB) and 3,4-dimethoxyphenylacetone (DMPA) were separated and quantitated in treated and untreated industrial wastewaters on PGC columns using HPLC and diode array detection.[50] The effect of aerobic and anaerobic treatments on the decomposition rate of DMB and DMPA was also investigated; both techniques were found to be suitable for the decomposition of these pollutants in wastewaters. Furthermore, the chromatographic behavior of 16 environmental pollutants has been investigated on alumina and porous graphitic carbon columns using *n*-hexane as eluent.[51] The fact that solutes were not retained on PGC surface using *n*-hexane as mobile phase indicates the greater polarity of the alumina stationary phase compared with that of PGC.

A further example for the analysis of trace levels of pollutants is the determination of polychlorinated dibenzodioxins and polychlorinated dibenzofurans in milk.[52] The method includes gel permeation chromatography, alumina cleanup, and porous graphitized carbon chromatography, followed by analysis by GC/high-resolution MS. Moreover, the potential of porous graphitic carbon as an HPLC adsorbent for the isolation of halogenated aromatic compounds has been demonstrated by the fractionation of polychlorinated biphenyls (PCBs), chlorinated pesticides, polychlorinated dibenzo-*p*-dioxins (PCDDs), and

polychlorinated dibenzofurans (PCDFs).[53,54] The proposed procedures can be used in routine bases for the determination of PCDDs and PCDFs in soil extracts because of the reproducible behavior of PGC compared with activated carbons and the convenience of a single solvent elution method.

CONCLUSIONS

Porous graphitized carbon as a packing material meets all the requirements necessary for selective and effective stationary phases, such as rigidity of microparticles, adequate surface area, and uniformity of the surface. The development of this highly pH-stable column was motivated by the fact that the use of silica-based supports in HPLC is limited by the low stability of silica at extreme pH values and by the undesirable electrostatic interactions that occur in silica-based columns between the polar substructures of solutes and the free silanol groups not covered by the hydrophobic ligand. Porous graphitic carbon is extremely hydrophobic, and the retention of ordinary compounds is quite long compared with that of the commonly used silica-based columns. Thus the high adsorption properties for polar compounds make PGC a most interesting complement to traditional silica supports. Moreover, the unique surface makes the PGC material suitable for separation of closely related structures, e.g., positional isomers and diastereomers. It has also been used to separate enantiomers using chiral mobile-phase additives.

ACKNOWLEDGMENT

The author gratefully acknowledges Dr. Rachel Phillips, Product Manager of Thermo-Hypersil-Keystone, for the illustrations.

REFERENCES

1. Chiantore, O.; Novak, I.; Berek, D. Characterization of porous carbon for liquid chromatography. Anal. Chem. **1988**, *60*, 638–642.
2. Unger, K.K. Porous carbon packings for liquid chromatography. Anal. Chem. **1983**, *55*, 361A–375A.
3. Gilbert, M.T.; Knox, J.H.; Kaur, B. Porous glassy carbon, a new column packing material for gas chromatography and high-performance liquid chromatography. Chromatographia **1982**, *16*, 138–146.
4. Knox, J.H.; Gilbert, M.T. U.K. Patent 7939449, 1982.
5. Knox, J.H.; Gilbert, M.T. Preparation of porous carbon. U.S. Patent 4263268, 1982.
6. Knox, J.H.; Gilbert, M.T.W. German Patent P 2946688-4, 1982.
7. Matisova, E.; Skrabakova, S. Carbon sorbents and their utilization for the preconcentration of organic pollutants in environmental samples. J. Chromatogr. A, **1995**, *707*, 145–179.
8. Knox, J.H.; Kaur, B.; Millward, G.R. Structure and performance of porous graphitic carbon in liquid chromatography. J. Chromatogr. **1986**, *352*, 3–25.
9. Obayashi, T.; Ozawa, M.; Kawase, T.; Tonen Corporation. Eur. Pat. 0458548A, 1990.
10. Yokoyama, A.; Kawai, T.; Moriya, H.; Komiya, K.; Kato, Y.; Nippon Carbon Co. Ltd.; Tosoh Corporation. Eur. Pat. 0484176A, 1990.
11. Forgacs, E.; Cserhati, T.; Bordas, B. Application of multivariate mathematical–statistical methods for the comparison of the retention behaviour of porous graphitized carbon and octadecylsilica columns. Anal. Chim. Acta **1993**, *279* (1), 115–122.
12. Kyotashi, T.; Nagai, T.; Inoue, S.; Tomita, A. Formation of new type of porous carbon by fcarbonization in zeolite nanochannels. Chem. Mater. **1997**, *9*, 609–615.
13. Tanaka, N.; Tanigawa, T.; Kimata, K.; Hosoya, K.; Araki, T. Selectivity of carbon packing material in comparison with octadecylsilyl- and pyrenylethylsilylsilica gels in reversed-phase liquid chromatography. J. Chromatogr. **1991**, *549*, 29–41.
14. Hennion, M.C.; Coquart, V.; Guenu, S.; Sella, C. Retention behaviour of polar compounds using porous graphitic carbon with water-rich mobile phases. J. Chromatogr. A, **1995**, *712*, 287–301.
15. Forgacs, E.; Cserhati, T. Retention strength and selectivity of porous graphitized carbon columns. Theoretical aspects and practical applications. Trends Anal. Chem. **1995**, *14* (1), 23–29.
16. Ross, P.; Knox, J.H. *Advances in Chromatography*; Brown, P., Grushca, E., Eds.; Marcel Dekker Inc.: New York, 1997; Vol. 37, 121–162.
17. Forgacs, E. Retention characteristics and practical application of carbon sorbents. J. Chromatogr. A, **2002**, *975*, 229–243.
18. Weber, T.P.; Jackson, P.T.; Carr, P.W. Chromatographic evaluation of porous-carbon-clad zirconia microplates. Anal. Chem. **1995**, *67*, 3042–3050.
19. Knox, J.H.; Kaur, B. Carbon in liquid chromatography. In *High Performance Liquid Chromatography*; Brown, P., Hartwick, R.A., Eds.; John Wiley and Sons: New York, 1989; 189–222.
20. Kriz, J.; Adamcova, E.; Knox, J.H.; Hora, J. Characterization of adsorbents by high-performance liquid chromatography using aromatic hydrocarbons. Porous graphite and itscomparison with silica gel, alumina, octadecylsilica and phenylsilica. J. Chromatogr. A, **1994**, *663*, 151–161.
21. Wan, Q.H.; Shaw, P.N.; Davies, M.C.; Barrett, D.A. Chromatographic behaviour of positional isomers on porous graphitic carbon. J. Chromatogr. **1995**, *697*, 219–227.
22. Wan, Q.H.; Davies, M.C.; Shaw, P.N.; Barrett, D.A. Retention behaviour of ionisable isomers in reversed-phase liquid chromatography: A comparative study of porous graphitic carbon and octadecyl bonded silica. Anal. Chem. **1996**, *68*, 437–446.
23. Hennion, M.C.; Coquat, V. Comparison of reversed-phase extraction sorbents for the on-line trace enrichments of polar organic compounds in environmental aqueous samples. J. Chromatogr. **1993**, *642* (1–2), 211–224.
24. Gu, G.; Lim, C.K. Separation of anionic and cationic compounds of biomedical interest by high-performance liquid

chromatography on porous graphitic carbon. J. Chromatogr. **1990**, *515*, 183–192.
25. Merly, C.; Lynch, B.; Ross, P.; Glennon, J.D. Selective ion chromatography of metals on porous graphitic carbon. J. Chromatogr. A, **1998**, *804* (1–2), 187–192.
26. Elfakir, C.; Chaimbault, P.; Dreux, M. Determination of inorganic anions on porous graphitic carbon using evaporative light scattering detection—Use of carboxylic acids as electronic competitors. J. Chromatogr. A, **1998**, *829* (1–2), 193–199.
27. Kaliszan, R.; Osmialowski, K.; Bassler, B.J.; Hartwick, R.A. Mechanism of retention in high-performance liquid chromatography on porous graphitized carbon as revealed by principal component analysis of structural descriptor of solutes. J. Chromatogr. **1990**, *499*, 333–344.
28. Jackson, P.T.; Schure, M.R.; Weber, T.P.; Carr, P.W. Intermolecular interactions involved in solute retention on carbon media in reversed-phase high-performance liquid chromatography. Anal. Chem. **1997**, *69*, 416–425.
29. Forgacs, E.; Cserghati, T. Solvent strength and selectivity on porous graphitised carbon column separated by a spectral mapping technique using barbiturates as solutes. Anal. Sci. **2001**, *17*, 307–312.
30. Forgacs, E.; Csethati, T. Relationship between retention characteristics and physicochemical parameters of solutes on porous graphitized carbon column. J. Pharm. Biomed. Anal. **1998**, *18*, 505–510.
31. Coquart, V.; Hennion, M.C. Trace level determination of polar phenolic compounds in aqueous samples by high-performance liquid chromatography and on-line preconcentration on porous graphitic carbon. J. Chromatogr. A, **1992**, *600* (2), 195–201.
32. Kaur, B. The use of porous graphitic carbon in high performance liquid chromatography. LC-GC **1990**, *8*, 468–474.
33. Karlsson, A.; Berglin, M.; Charron, C. Robustness of the chromatographic separation of alprenolol and related substances using silica-based stationary phase and selective retention of metoprolol and related substances on a porous graphitic carbon stationary phase. J. Chromatogr. A, **1998**, *797*, 75–82.
34. Monser, L.; Darghouth, F. Simultaneous LC determination of paracetamol and related compounds in pharmaceutical formulations using a carbon-based column. J. Pharm. Biomed. Anal. **2002**, *27*, 851–860.
35. Huynh, N.H.; Karlsson, A.; Pettersson, C. Enantiomeric separation of basic drugs using *N*-benzyloxycarbonylglycyl-L-proline as counter ion in methanol. J. Chromatogr. A, **1995**, *705*, 275–287.
36. Karlsson, A.; Pettersson, C. Enantiomeric separation of amines using *N*-benzoxycarbonyl-glycyl-L-proline as chiral additive and porous graphitic carbon as solid phase. J. Chromatogr. A, **1991**, *543*, 287–297.
37. Karlsson, A.; Charron, C. Reversed-phase chiral ion-pair chromatography at a column temperature below 0°C using three generations of Hypercarb as solid-phase. J. Chromatogr. A, **1996**, *732*, 245–253.
38. Karlsson, A.; Karlsson, O. Chiral ion-pair chromatography on porous graphitized carbon using N-blocked dipeptides as counter ions. J. Chromatogr. A, **2001**, *905*, 329–335.
39. Forgacs, E.; Cserhati, T. Effect of physicochemical parameters on the retention of some monoamine oxidase inhibitory drugs on a porous graphitized carbon column. J. Chromatogr. B, **1996**, *681*, 197–204.
40. Forgacs, E.; Csarhati, T. Separation of steroidal drugs on porous graphitized carbon column. J. Pharm. Biomed. Anal. **1998**, *18*, 15–20.
41. Nemeth-Kiss, V.; Forgacs, E.; Cserhati, T.; Schmidt, G. Determination of taxol in Taxus species grown in Hungary by high-performance liquid chromatography-diode array detection. Effect of vegetative period. J. Chromatogr. A, **1996**, *750*, 253–256.
42. Nemeth-Kiss, V.; Forgacs, E.; Cserhati, T.; Schmidt, G. Taxol content of various Taxus species in Hungary. J. Pharm. Biomed. Anal. **1996**, *14*, 997–1001.
43. Davies, M.; Smith, K.D.; Harbin, A.M.; Hounsell, E.F. High-performance liquid chromatography of oligosaccharide alditols and glycopeptides on a graphitized carbon column. J. Chromatogr. A, **1992**, *609* (1,2), 125–131.
44. Nemeth-Kiss, V.; Forgacs, E.; Cserhati, T. Anomalous retention behaviour of peptides on porous graphitized carbon column. J. Chromatogr. A, **1997**, *776*, 147–152.
45. Davies, M.J.; Hounsell, E.F. Comparison of separation models of high-performance liquid chromatography for the analysis of glycoprotein- and proteoglycan-derived oligosaccharides. J. Chromatogr. A, **1996**, *720*, 227–233.
46. Thomsson, K.A.; Karlsson, N.G.; Hansson, G.C. Liquid chromatography–electrospray mass spectrometry as a tool for the analysis of sulfated oligosaccharides from mucin glycoproteins. J. Chromatogr. A, **1999**, *854*, 131–139.
47. Franz, A.H.; Molinski, T.F.; Lebrilla, C.B. MALDI-FTMS Characterization of oligosaccharides labelled with 9-aminofluorene. J. Am. Soc. Mass Spectrom. **2001**, *12*, 1254–1261.
48. Inamoto, Y.; Inamoto, S.; Hanai, T.; Tokuda, M.; Hatase, O.; Yoshii, K.; Sugiyama, N.; Kinoshita, T. Liquid chromatography of guanidine compounds using a porous graphite carbon column and application to their analysis in serum. J. Chromatogr. B, **1998**, *707*, 111–120.
49. Guenu, S.; Hennion, M.C. On-line sample handling of water-soluble organic pollutants in aqueous samples using porous graphitic carbon. J. Chromatogr. A, **1994**, *665* (2), 243–251.
50. Cserhati, T.; Forgacs, E. Simultaneous determination of 3,4-dimethoxybenzaldehyde and 3,4-dimethoxyphenylacetone in industrial waste waters by high-performance liquid chromatography-diode array detection. J. Chromatogr. A, **1996**, *750*, 257–261.
51. Cserhati, T.; Forgacs, E. Relationship between the retention characteristics on an alumina column and physico-chemical parameters of some environmental pollutants. J. Chromatogr. A, **2000**, *869*, 41–48.
52. Van Rhijn, J.A.; Traag, W.A.; Kulik, W.; Tuinstra, L.G. Automated clean-up procedure for the gas chromatographic-high-resolution mass spectrometric determination of polychlorinated dibenzo-*p*-dioxins and dibenzofurans in milk. J. Chromatogr. **1992**, *595* (1–2), 289–299.
53. Creaser, C.S.; Al-Haddad, A. Fractionation of polychlorinated biphenyls, polychlorinated dibenzo-*p*-dioxins, and polychlorinated debenzofurans on porous graphitic carbon. Anal. Chem. **1989**, *61* (11), 1300–1302.
54. Chiantore, O.; Novac, I.; Berek, D. Characterization of porous carbon for liquid chromatography. Anal. Chem. **1988**, *60*, 638–642.

Potential Barrier FFF

George Karaiskakis
Physical Chemistry Laboratory, Department of Chemistry, University of Patras, Patras, Greece

INTRODUCTION

Potential barrier field-flow fractionation (PBFFF), developed by Karaiskakis, is a combination of potential barrier chromatography and field-flow fractionation (FFF). It can be applied to separate colloidal particles and is based on differences in size or in any physicochemical parameters involved in the potential energy of interaction between the particles and the material of the FFF channel wall. Of the various quantities which affect the total potential energy (surface potential, Hamaker constant, and Debye–Huckel reciprocal distance), none is as accessible to empirical adjustment as the ionic strength of the suspending medium. This quantity depends on both the concentration and the cationic or anionic charge of the indifferent electrolyte added to the carrier solution. In its simplest form, the PBFFF technique consists in changing the ionic strength of the carrier solution from a high value, where only one of the colloidal components of the mixture subject to separation is totally adhered at the beginning of the FFF channel wall, to a lower value, where the total number of adhered particles is released.

The method has been applied to the separation of hematite and titanium dioxide submicron spherical particles, to the separation of submicron hematite spherical particles with different sizes, to the separation of various mixed sulfides with supramicron polydisperse irregular particles, and to the concentration of dilute colloidal samples, in both the normal and the steric modes of operation of sedimentation FFF.

PRINCIPLE OF PBFFF

Field-flow fractionation is a family of high-resolution techniques capable of separating and characterizing colloids and macromolecules. In normal FFF, the particles form a Brownian-motion cloud that extends a short distance into the channel. Separation is possible because the solvent flows at different velocities at various points within the channel. The smaller particles, whose cloud protrudes out into the faster laminae, are transported more rapidly than the larger particles, so that the two populations are soon separated. In the steric mode of operation, which happens when the protrusion of particles into the flow stream is determined by their physical bulk instead of by diffusion, the larger particles are elute earlier than the smaller ones.

In normal sedimentation FFF (SdFFF) the retention volume, of a spherical particle is immediately related to its diameter, d, via

$$V_r = \frac{\pi G w \Delta\rho V_0}{36kT} d^3 \tag{1}$$

where G is the sedimentation field strength expressed in acceleration, w is the channel thickness, $\Delta\rho = | \rho_s - \rho |$ is the density difference between the particle (ρ_s) and the carrier liquid (ρ), V_0 is the void volume of the channel, k is Boltzmann's constant, and T is the absolute temperature.

In the sedimentation steric FFF (Sd/StFFF), the retention volume of a spherical particle is immediately related to the diameter via

$$V_r = \frac{wV_0}{3\gamma}\frac{1}{d} \tag{2}$$

where γ is a dimensionless factor that accounts for the drag-induced reduction in velocity, as well as for the increase in velocity due to the activity of lift forces. To find γ, it is necessary to have a linear calibration curve of log V_r vs. log d for standard particles of known size and nature (e.g., polystyrene latex beads). The easier way of working in the steric mode of FFF is that using the Earth's gravity as the external field (gravitational FFF = GFFF).

In the normal mode of the SdFFF operation, the potential energy, $\varphi(x)$, of a spherical particle is given by

$$\varphi(x) = \frac{\pi d^3}{6} \Delta\rho G x \tag{3}$$

where x is the coordinate position of the center of particle mass.

When the colloidal particles interact with the SdFFF channel wall, the potential energy given by Eq. 3 must be corrected, so as to include the potential energy of interaction, $\varphi(h)$. The latter can be estimated by the sum of the contributions of the van der Waals, $\varphi_6(h)$, and double-layer, $\varphi_{DL}(h)$, forces, and the total potential energy, φ_{tot}, of a spherical particle in PBSdFFF is given by the relation

$$\begin{aligned}\varphi_{\text{tot}} &= \varphi(x) + \varphi(h) \\ &= \varphi(x) + \varphi_6(h) + \varphi_{\text{DL}}(h) \\ &= \frac{4}{3}\pi a^3 \Delta\rho G x + \frac{A_{132}}{6}\left[\ln\left(\frac{h+2a}{h}\right) - \frac{2a(h+a)}{h(h+a)}\right] \\ &\quad + 16\varepsilon a\left(\frac{kT}{e}\right)^2 \tan h\left(\frac{e\psi_1}{4kT}\right)\tan h\left(\frac{e\psi_2}{4kT}\right)e^{-\kappa h}\end{aligned} \tag{4}$$

where h is the separation distance between the sphere and the channel wall, a is the particle radius, A is the effective Hamaker constant, ε is the dielectric constant of the liquid phase, e is the electronic charge, ψ_1 and ψ_2 are the surface potentials of the particle and the wall, respectively, and κ is the reciprocal Debye length.

The last equation shows that the energy in PBSdFFF is a function of the size and of the surface potential of the particle, of the Hamaker constant, and of the ionic strength of the carrier solution, as the reciprocal double-layer thickness is immediately related to the ionic strength of the suspending medium. Thus, selectivity in PBSdFFF results from differences in particle size or chemical composition of the particles and of the suspending medium, where the latter will affect the surface potential and the Hamaker constant of the particle, as well as the medium's ionic strength.

APPLICATIONS OF PBFFF

As model samples for the verification of the PBFFF as a separation technique, colloidal samples of hematite and titanium dioxide with submicron monodisperse spherical particles were used. In the first example, the fractionation of titanium dioxide [TiO_2 with the nominal diameter obtained by a transmission electron microscope (TEM) of 0.298 μm] and hematite-I [α-Fe_2O_3(I) with nominal diameter obtained by TEM of 0.148 μm] spherical particles was succeeded by the PBSdFFF technique. Fig. 1a shows the fractionation of the TiO_2 and α-Fe_2O_3(I) particles by the normal SdFFF mode of operation, and Fig. 1b shows the fractionation of the same particles by the potential barrier mode of SdFFF. The latter is based on the difference of the total potential energy of interaction between the colloidal particles and the channel wall due to the variation of the ionic strength of the suspending medium.

In the PBSdFFF technique, the mixture was introduced into the channel with a carrier solution containing 0.5% (v/v) detergent FL-70, 0.02% (w/w) NaN_3 and 3×10^{-2} M KNO_3. At this high electrolyte concentration, all of the TiO_2 colloidal particles adhered at the beginning of the SdFFF Hastelloy-C channel wall, whereas all of the α-Fe_2O_3(I) particles were eluted from the channel. The average diameter of the eluted α-Fe_2O_3(I) particles determined by Eq. 1 was found to be 0.143 μm, in good agreement with that obtained

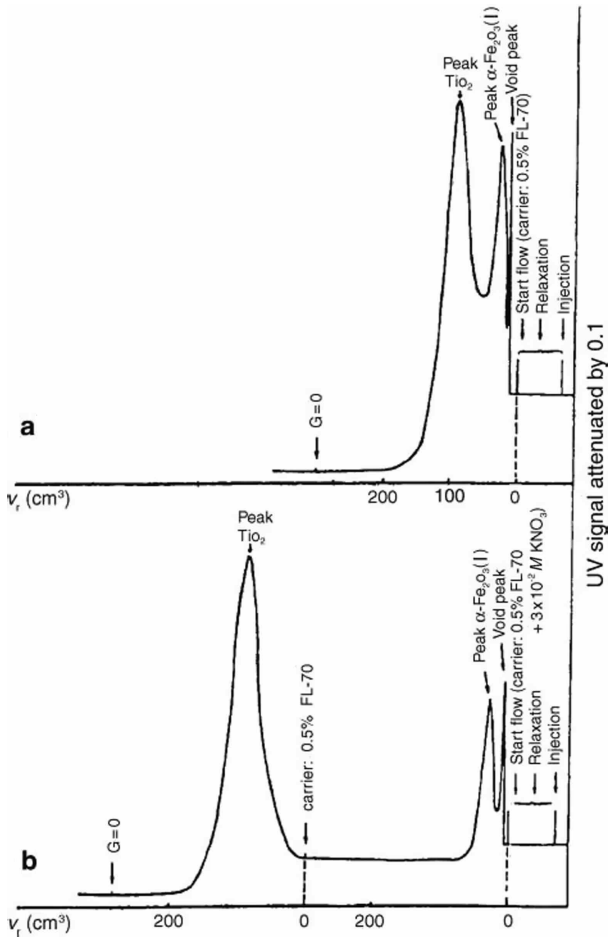

Fig. 1 Fractionation of α-Fe_2O_3(I) (with nominal diameter 0.148 μm) and TiO_2 (with nominal diameter 0.298 μm) colloidal particles by (a) the normal SdFFF and (b) the PBSdFFF technique. The experimental conditions, except for those given in the scheme, were as follows: field strength = 15.5 g, flow rate = 150 cm^3/hr, void volume of the channel = 2.06 cm^3.
Source: Reproduced with permission from G. Karaiskakis et al. (1990) *J. Chromatogr. 517*: 345; copyright Elsevier Science Publishers B.V.

by TEM (0.148 μm) or determined by normal SdFFF (0.150 μm). Changing the carrier solution to one containing only 0.5% (v/v) detergent FL-70, whose ionic strength is 1×10^{-3} M, released all the adhered TiO_2 particles and gave a particle diameter (0.302 μm) in good agreement with that obtained by TEM (0.298 μm).

In order to show whether the size of the particles and not their nature is responsible for the variation of the total interaction energy between the colloids and the channel wall, a second example of fractionation was performed by using two samples of hematite with different particle diameters [α-Fe_2O_3(I) with nominal diameter 0.148 μm and α-Fe_2O_3(II) with nominal diameter 0.248 μm]. In the present case, the separation is based only on the particle size difference, as the Hamaker constants and the surface potentials of the two samples are identical. That obtained by the PBFFF

technique fractogram had the same form as that of Fig. 1b, except for the fact that the peak of α -Fe_2O_3(II) was in the position of TiO_2. The critical electrolyte (KNO_3) concentration for the adhesion of α-Fe_2O_3(II) particles at the beginning of the SdFFF channel wall was found to be 3×10^{-2} *M*, whereas at this high concentration of KNO_3, the whole number of α-Fe_2O_3(I) particles are eluted from the channel. Variation of the carrier solution to one containing only 0.5% (v/v) detergent FL-70 and 0.02% (w/w) NaN_3 without any amount of KNO_3 released the total number of adherent α-Fe_2O_3(II) particles. The particle diameters obtained by the PBFFF technique [0.151 μm for α-Fe_2O_3(I) and 0.244 μm for α-Fe_2O_3(II)] are in excellent agreement with those found by normal SdFFF [0.145 μm for α-Fe_2O_3(I) and 0.237 μm for α-Fe_2O_3(II)] or determined by TEM [0.148 μm for α-Fe_2O_3(I) and 0.248 μm for α-Fe_2O_3(II)].

In PBFFF, the variation of the potential energy of interaction between the colloidal particles and the channel wall can be succeeded, except for the variation of the ionic strength, by changing also the pH and the nature of the suspending medium. Polydisperse, irregular supramicron colloidal particles of the mixed sulfides $Cu_xZn_{1-x}S$ ($0 < x < 1$) were used as model samples to verify the applicability of the potential barrier gravitational field-flow fractionation (PBGFFF), based on the variation of the above parameters, to fractionate colloidal particles.

A general methodology for the analysis of a colloidal mixture by PBSdFFF consists in injecting into the column the mixture with a carrier solution in which the ionic strength is too high to assure total adhesion of all the components of the mixture, except for the one with the lower attractive force with the channel wall. Then, a programmed decrease of the ionic strength of the carrier solution is applied to release, *in time*, the adherent particles according to their size and/or surface characteristics. As the PBSdFFF technique is based on particle–wall interactions, its applications can be extended by using different from Hastelloy-C materials, such as stainless steel, Teflon, and polyimide. PBSdFFF is also a convenient and accurate method for the *concentration* and analysis of *dilute* colloidal samples. The major advantage of the proposed concentration procedure is that the method can concentrate particles even of the same size but with different surface potentials and/or Hamaker constants. The method has considerable promise for the separation and characterization, in terms of particle size, of dilute complex colloidal materials, such as those of natural water, where particles are present in low concentration.

FUTURE DEVELOPMENTS

Looking to the future, it is reasonable to expect continuous efforts to improve the theoretical predictions and to expand the applications of the potential barrier methodology of FFF to more complex and dilute colloidal samples. The latter can be easily succeeded by constructing FFF channels from various materials of well-defined composition.

BIBLIOGRAPHY

1. Athanasopoulou, A.; Karaiskakis, G. Potential barrier gravitational field-flow fractionation for the analysis of polydisperse colloidal samples. Chromatographia **1995**, *40*, 734.
2. Athanasopoulou, A.; Karaiskakis, G. Potential barrier gravitational field-flow fractionation based on the variation of the pH solution for the analysis of colloidal materials. Chromatographia **1996**, *43*, 369.
3. Giddings, J.C. Separ. Sci. **1966**, *1*, 123.
4. Hansen, M.E.; Giddings, J.C. Retention perturbations due to particle-wall interactions in sedimentation field-flow fractionation. Anal. Chem. **1989**, *61*, 811.
5. Hansen, M.E.; Giddings, J.C.; Beckett, R. Colloid characterization by sedimentation field-flow fractionation: VI. Perturbations due to overloading and electrostatic repulsion. J. Colloid. Interf. Sci. **1989**, *132* (2), 300.
6. Karaiskakis, G., Cazes J., Eds.; In J. Liquid Chromatogr. Relat. Technol.1997; *20* (16 & 17), (special issue)
7. Karaiskakis, G.; Koliadima, A. Potential barrier field-flow fractionation for the separation and characterization of colloidal particles. Chromatographia **1989**, *28*, 31.
8. Koliadima, A.; Karaiskakis, G. Potential-barrier field-flow fractionation, a versatile new separation method. J. Chromatogr. **1990**, *517*, 345.
9. Koliadima, A.; Karaiskakis, G. Concentration and characterization of dilute colloidal samples by potential-barrier field-flow fractionation. Chromatographia **1994**, *39*, 74.
10. Koliadima, A.; Gavril, D.; Karaiskakis, G. Investigation of the coagulation and adhesion phenomena in colloids by field-flow fractionation. J. Liq. Chromatogr. Relat. Technol. **1999**, *22* (18), 2779.

Preparative HPLC Optimization

Michael Breslav
Johnson & Johnson Pharmaceutical Research and Development, LLC, Spring House, Pennsylvania, U.S.A.

Vera Leshchinskaya
Bristol-Myers Squibb Co., Princeton, New Jersey, U.S.A.

INTRODUCTION

Preparative high-performance liquid chromatography (PHPLC) has assumed an increasingly important role in chemical and pharmaceutical research and development. Earlier, in the 1980s (and even the mid-1990s), this technique was avoided in the industry. However, nowadays preparative chromatography has become an essential part of common practice at both laboratory and production scale. This tendency is favored by the considerable progress achieved recently in developing selective and stable stationary phases for a large variety of separation problems, as well as new techniques and instrumentation.

General comparison of the goals and targets of analytical and preparative chromatography demonstrates some similarities, but also major differences. In analytical HPLC, the ultimate goal is to extract information, while preparative applications are designed to isolate pure compounds. Analytical methods often target resolution of all compounds in the mixture, whereas preparative separations are planned for isolation of one or only a few compounds present in a mixture. In analytical chromatography, the emphasis is on resolution, while the critical parameters in preparative chromatography are the amount of compound produced per unit of time, product purity, recovery, and separation cost.[1] Optimization of all these parameters is always a compromise (Fig. 1).

The approach used for PHPLC optimization depends on the scale of a particular laboratory or industrial chromatographic separation. Large-scale PHPLC optimization goals that ultimately lead to a product with a given minimum purity may include targeting for a maximum amount of the purified material per weight unit of stationary phase per time unit (g/kg/day), maximum amount of the purified material per mobile phase unit per time unit (g/L/day), maximum production rate (g/day), lowest cost ($/kg), and/or maximum recovery (%). Separation expenses (cost of solvents, stationary phase, labor, and equipment usage) should be compared to the value of the product being purified. Overall production cost is a function of purification expenses and production rate. Rapid development of continuous processes, such as simulated moving bed (SMB)[2] and Varicol,[3] has led a growing body of theoretical work to describe and predict separation parameters for a large scale of PHPLC. These techniques are designed to improve the production rate and cost by continuous feed injection and product collection, thus decreasing solvent consumption compared to conventional batch PHPLC. As a result, the solvent usage is greatly reduced, production rate increases, and products are obtained in higher concentrations. However, development of the continuous processes is longer and requires special hardware.

When dealing with large-quantity production of a selected material, it is worthwhile to invest a substantial effort in mathematical modeling of the non-linear chromatographic process.[4] In contrast, when preparing small amounts of material, optimization principles can be applied qualitatively since time becomes the most crucial parameter for the delivery of the pure compounds for the initial testing. Economic aspects are less critical for laboratory scale PHPLC compare to production scale purifications.

This entry focuses mainly on practical aspects of PHPLC optimization for the most common bench scale chromatography.

SPECIFIC ASPECTS OF PHPLC OPTIMIZATION PROCESS

The success of preparative chromatography is strongly related to the way the analytical separation is optimized. As for analytical applications, a resolution of about 1.5–2 is considered to be satisfactory; however, optimization of preparative separations is more difficult due to non-linear effects under overloading conditions and some specific aspects that are discussed below.

Unlike analytical separations, preparative methods may have a number of specific constraints related to the stability of the compound in solution, cost and handling of the large volumes of mobile phase, bulk stationary phase, and special hardware. Preparative chromatography also has the added complication of demanding maximum solubility of the sample in the mobile phase as well as buffer limitations. Lack of solubility causes problems in achieving desired load and also raises concerns about the possibility of

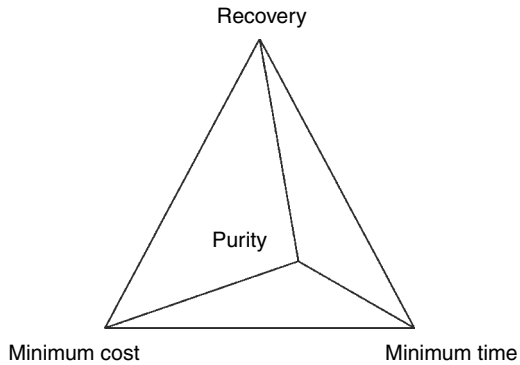

Fig. 1 Purity, recovery, time, and cost of purification can be optimized, but not maximized simultaneously.

sample precipitation inside the injector, solvent lines, and column. Since the ultimate goal of any preparative run is the isolation of a certain amount of pure material, the mobile phase as well as its additives should be easily removable at the end of purification. Therefore, the solvent and modifiers (buffers, acids, and bases) used in the process should be volatile. Factors such as safety hazards associated with large-volume solvent usage, non-specific adsorption on a column, and potential contamination of the product through the leaching of the stationary phase need to be considered as well. Most of these concerns should be addressed during the optimization process prior to scale-up.

Regardless of differences in scale and application, a number of variables are critical in PHPLC optimization strategy and have a pronounced effect on the purity and recovery of the product as well as the time and cost required for the separation. Some of these parameters are discussed below.

RETENTION

It is advantageous to use the minimum retention factor (k) necessary for isolating the product and providing the desired purity, since cycle time is decreased and the production rate is increased. In both normal phase and reversed-phase modes, the concentration of the product in collected fractions decreases when retention increases. In displacement chromatography, longer sample retention provides a more concentrated product fraction. As retention increases, column efficiency increases, but the cycle time and solvent consumption are increased as well. The optimum retention is in the range of $k = 1.2$–2.0 for isocratic separations and $k = 3$–4 for gradient separations. If the difference in retention of impurities and the desired material is large enough, the separation should be optimized, e.g., weakly retained impurities eluted from the column in the void volume. Impurities that are retained significantly longer than the product need to be washed off from the column at the end of the run cycle using a step gradient with a strong eluent; this step may include flow reversal.

SELECTIVITY

Separation of the material of interest and closely retained impurities is greatly affected by changes in selectivity (α, separation factor). Selectivity is described as $\alpha = k_2/k_1$, where k_1 and k_2 are the retention factors for adjacent peaks. Whether a touching band or an overlapping band strategy is adopted, the production rate that can be achieved with a given column is proportional to at least the square of $(\alpha - 1)/\alpha$ and sometimes to the cube of this ratio.[5] Therefore, selectivity is among the factors that have a great effect on the throughput and overall cost of purification. Optimization of the analytical separation for further scale-up should be targeted for a selectivity value at least 1.2 or greater to maintain reasonable cost of preparative purification process. Increasing the selectivity value up to 2 or 3 significantly improves the throughput of separation. Selectivity can be optimized by changing the solvent composition as well as pH and nature of buffer added to the mobile phase.[6] It is also dependent on the chemistry of the stationary phase being used. Therefore, a careful screening of mobile and stationary phase combinations is necessary to select the best method for scale-up.

MOBILE PHASE

When choosing an optimum mobile phase composition, along with the search for the best selectivity value, a number of considerations should be kept in mind. These include parameters such as solvent viscosity, sample solubility in the mobile phase, pH, volatility of solvents/buffers, solvents cost, and safety hazards.

The viscosity of the mobile phase influences the backpressure and efficiency of the separation. The higher the backpressure, the lower the flow rate that can be used, and consequently the longer the run time. Lowering the viscosity increases mass transfer, and hence the efficiency of the separation is improved (the peaks are narrower).

The solubility of the product in the mobile phase is an important parameter. Low solubility of the crude material in a mobile phase may require alterations in the method to prevent on-column precipitation of the material. If a number of different mobile phase mixtures provides similar selectivity, the one in which the product is most soluble should be selected.

Peak shape and preparative loadability are improved for neutral or non-ionized forms of purified compounds. Thus, loading of acidic compounds is improved with low-pH mobile phases, and loadability of basic compounds is higher with basic-pH mobile phases.[7]

Isolation of the product after separation is easier if the solvents and additives to the mobile phase are volatile. Concentration of the product in reversed-phase PHPLC fractions requires evaporation, lyophilization, or dialysis of water-containing mobile phase. Acetonitrile/water but not methanol-containing solutions can be lyophilized. Another approach is to concentrate the fraction by diluting it with water and injecting and concentrating the product on a separate column followed by elution using a pure organic solvent. This method provides a concentrated solution of the product in an organic phase. In normal phase PHPLC, non-aqueous solvents are easily removed from the product by evaporation and are less expensive to dispose of than water-containing mobile phases. At the same time, the use of high volumes of low-boiling flammable organic solvents may represent a safety concern. Accordingly, a less volatile solvent, heptane, for example, rather than hexane, should be used.

Usage of low-boiling organic acids as mobile phase modifiers simplifies workup due to their high volatility. It is common to add trifluoroacetic acid (TFA) to water/organic mobile phases as an ion-pairing reagent in reversed-phase PHPLC. It is important, however, to maintain a sufficient concentration of TFA, especially during loading of the sample, in order to insure adequate concentration of the counter-ion. Any residual TFA can be effectively removed by freeze–drying and/or anion-exchange chromatography. Neutral and basic pH are achieved using ammonium acetate, ammonium, and ammonium bicarbonate additives. These buffers are easily removable at the end of purification as well.

Since the cost of the mobile phase often represents more than half of the total cost of the separation (except the lower cost of carbon dioxide in supercritical fluid chromatography, SFC), it is worthwhile to minimize the solvent consumption and also to increase the concentration of the product in the eluted fractions. Regeneration of the mobile phase is an economical choice at high solvent consumption rates. Regeneration may include distillation of the used mobile phase followed by adjustment of the mobile phase composition if necessary.

STATIONARY PHASE

A number of factors should be considered when choosing a stationary phase for a particular separation task. The chemistry of the stationary phase controls selectivity and therefore production rate. Packing efficiency and loading capacity have a great impact on the throughput, i.e., the amount of mixture injected into the chromatograph per unit time. Mechanical stability of the stationary phase under packing conditions is also an important consideration.

Chemistry of the Stationary Phase

Depending on a particular separation task and combining the knowledge of the analyte's physicochemical properties with that of the phase's characteristics, it should be feasible to weigh the column selection accordingly. Reversed-phase types of stationary phases are widely used in PHPLC due to availability in bulk quantities, easy regeneration, and reliability when scaled up from analytical to preparative conditions. In reversed-phase PHPLC, the choice between stationary phases with longer or shorter alkyl chains (C_3, C_8, and C_{18}) depends mainly on the lipophilicity of the compounds to be separated. In order to assure that retention times are not too long for highly lipophilic compounds, a shorter alkyl chain length is preferred. This allows for faster separation and consequently less organic solvent in the mobile phase, thereby cutting down on solvent costs. However, if evaporation of the collected fractions is critical, then using a longer alkyl chain length stationary phase with a more volatile mobile phase may be advantageous.

A number of novel stationary phases are commercially available now in bulk quantities for in-house packing or in prepacked preparative size columns. These media can be used to meet different separation needs, such as separation of compounds with polar functional groups, highly hydrophilic compounds, basic analytes, etc. The newest additions to the selective packing materials include custom-tailored molecular imprinted polymers.[8]

While regeneration is a regular procedure in reversed-phase chromatography, normal phase chromatography has disadvantages associated with strong binding of polar impurities to the silica surface. However, because of the low price of the bare silica, the stationary phase is often discarded after one or several runs. Normal phase separations are widely used in flash chromatography due to the low price of disposable silica-gel-containing cartridges and easy scale-up from thin-layer chromatography (TLC). Improvements in selectivity and production rate in this case can be achieved by increasing the difference in a number of column volumes eluted between the product and a closely retained impurity (ΔC_v).

$$\Delta C_v = 1/R_{f1} - 1/R_{f2}$$

where R_{f1} and R_{f2} are mobility coefficients of the separated compounds obtained using TLC.

Efficiency of the Packing Material

Efficiency of the packing material is an important consideration in the PHPLC optimization process. When the load is kept sufficiently small, not exceeding the value corresponding to the touching band, it is obvious that the higher efficiency allows injection of more feed. Scale-up of "better than baseline" analytical separation often benefits from increased production rate of the target material. However,

under overloading conditions, pure products may still be recovered with a "less than baseline" separation, although with a lower yield. When a pure compound is injected at a sufficiently high load, there is no effect of the column efficiency on the peak profile. When a mixture is injected, the region where the band interferes is strongly dependent on the column efficiency due to the displacement effect. Therefore, it is preferable to work with highly efficient columns in PHPLC. Using stationary phases with smaller particle size can increase efficiency. Another factor that influences efficiency is flow rate.

Particle size

Decrease in particle size results in increased column efficiency. In preparative chromatography, in practice it is not possible to increase the column efficiency indefinitely, for both practical and economical reasons. Pressure drop is inversely proportional to the square of the particle diameter. Ease of packing of columns decreases with decreasing particle size. Current average particle sizes for reversed-phase PHPLC are in the range of 7–20 μm. In preparative liquid carbondioxide-based SFC, smaller particles in the 5–10 μm range are used due to the low viscosity of the mobile phase.

If the stationary phase contains particles of different sizes, the fraction of larger particles controls the efficiency and the fraction of smaller particles controls the backpressure. The use of high-quality packing with a narrow particle size distribution allows for increased production rates with less backpressure and higher flow rates.

Column length

Production rate (g/day) in batch chromatography increases with increased size of the column. However, backpressure also increases with longer column length. Columns of different lengths, packed with particles of different sizes of the same material, may have a similar production rate provided that the ratio of d_p^2/L is the same, where d_p is the diameter of the particles and L is the length of the column.

Flow rate

Production rate increases at higher flow rates; however, some decrease in separation efficiency occurs. The upper limit of the flow rate depends on the ability of the stationary phase and hardware of the PHPLC system to withstand the higher backpressure. Many non-covalently bonded large-pore fragile enantioselective stationary phases may not be able to withstand higher flow rates and pressure.

Loading Capacity

The total capacity of the column may be found using frontal analysis.[9] A loading factor that represents the percentage of the loaded amount vs. total capacity of the column is one of the major parameters of optimization. The loadability of the stationary phase, and hence the throughput and production rate, is proportional to a specific surface area of a stationary phase. Most of the specific area is located within the pores and therefore can be controlled by the pore size and the pore volume. The pore size of the particles should be large enough to allow the molecules to readily diffuse into and out of the pores. The choice of optimum pore size is dictated by the size of the analyte molecules. Pore sizes usually vary from 60 to 80 Å for small molecules to 150 Å for proteinlike molecules. Larger pores (>150 Å) may give fragile particles that cannot be compressed.

Mechanical Stability

Small particle size material requires a high-pressure slurry packing procedure. It is preferable to work with spherical particles since they have better mechanical stability and thus longer life than irregular ones. Axial compression columns allow for efficient in-house packing of columns with bulk stationary phases. Systems utilizing radially compressed, preloaded disposable cartridges are commercially available.

TEMPERATURE

Increase in temperature usually improves resolution and solubility and decreases the viscosity of the mobile phase. Consequently, the production rate increases, provided that the selectivity of separation or stability of the separated compounds and stationary phases is not compromised. In contrast, resolution in chiral chromatography often improves at lower temperatures.

GRADIENT PROGRAM

Gradient elution provides a better production rate and higher recovery than using isocratic conditions. The gradient profile decreases peak tailing compared to isocratic elution. After sample injection in reversed-phase PHPLC, gradient elution starts with a slightly weaker mobile phase (lower percentage of organic) than required to elute the product with a desired retention and then increases slowly in order to decrease the tailing. The gradient used is shallower when the target compound is the late-retained peak of the two peaks separated. The slope of the gradient should be steep enough to avoid dilution of the product fraction. Too shallow a gradient decreases production rate and complicates isolation of the product. After most of the product has eluted, the gradient is raised stepwise in order to elute all late-retained impurities from the column. The

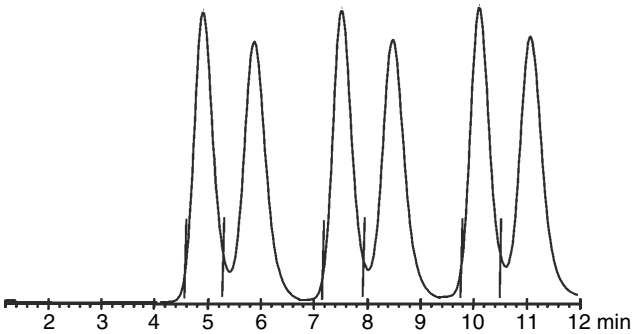

Fig. 2 Stacked injections.

column is equilibrated again with at least one column volume before the cycle is repeated.

Isocratic elution is preferable in batch mode for the separation of closely related analytes to enhance selectivity and allow automation and short injection cycle. Automated injections provide an opportunity for repetitive unattended operation. In isocratic separations, sample injection is often done before the previously injected product elutes from the column, thus reducing cycle time and solvent consumption (Fig. 2). This technique is especially useful in chiral chromatography, where automated processes are used to decrease the required amount of expensive stationary phases, lowering the overall separation expenses.

ELUTION ORDER

If a compound is the major component in a mixture, the production rate increases if the impurities are eluted first. However, it is preferable for the product to be eluted prior to any closely retained impurity if a compound is not the main component in the mixture.[4] Under self-displacement conditions, the product can actually be separated in a more concentrated solution than in touching-band separation, especially if a later-retained impurity is in high concentration. The production rate in this case can be improved by an increase in loading despite some decrease in recovery.

SAMPLE-LOADING PROCEDURE

Unlike conventional small volume injections in analytical HPLC, preparative chromatography often requires loading larger sample quantities in larger volumes and/or strong solvents in order to increase separation throughput, which, in turn, may compromise resolution. Obviously, the narrower the zone of the sample during and after loading, the better the separation results. This is particularly difficult to achieve for low-soluble samples, and, in normal phase chromatography, the problem is usually overcome by using the column impregnation (dry injection) technique. In this case, a suspension of silica in the sample solution is concentrated to dryness and placed in a separate sample injection module before the actual column.

Recently, the at-column dilution technique has been designed in reversed PHPLC to decrease the size of the loading zone by concentrating the sample on the top of the column before separation starts.[10,11] This is achieved by mixing the sample solution stream with a "weak" mobile phase flow at the top of the chromatographic column so that the resulting composition of the mobile phase provides adsorption of the sample on the top of the column. During at-column dilution loading, the sample is first absorbed on the top of the column while the sample solvent is separated and completely eluted from the column. Separation then continues using selected gradient or isocratic methods. Variations in loading design may include injection of the sample solution in the stream of the strong mobile phase component or separate injection pump.[a] The resulting composition of the mobile phase and sample solution combined flow during at-column dilution loading (percentage organic in water/organic mixture) depends on the composition of the mobile phase, composition of the sample solution, and flow rates of the mobile phase and sample solution:

$$\%\,\text{organic} = A * B/(B + C) + C * D/(B + C)$$

where A is the % organic in a sample feed solution at loading, B the feed flow rate at loading, C the mobile phase flow rate at loading, and D the % organic in mobile phase at loading.

At-column dilution allows for processing of low-soluble samples often in large volumes of strong or aggressive solvents and reprocessing of the chromatographic fractions enriched with the target material.

SCALE-UP ISSUES

Direct scale-up of an analytical HPLC method at touching-band conditions is feasible only when there is a need for small (mg) amounts of the isolated material or repetitive automated injections are used to isolate larger quantities of the desired compound. When using a touching-band optimization technique, the amount of material loaded may be increased until visible peak broadening occurs and the first sign of overlapping between the product peak and closely retained impurities is observed. The amount of product that may be loaded onto a column under touching-band conditions can be estimated as[12]

$$w \approx 1/9 w_s[(\alpha - 1)/\alpha]^2$$

[a]Breslav, M. Author's laboratory practice.

where w_s is the column capacity, which may be experimentally found by frontal analysis or less accurately estimated as w_s (mg) ≈ 0.4 (column surface area, m^2).

Overloading of the column provides a better production rate than the touching-band technique. In general, Gaussian peak shape and base-line resolution are not a requirement in PHPLC. Overloading causes interaction between the compounds during chromatography, which creates a sample self-displacement effect. This reduces peak tailing of the earlier eluting peak of the product and leads to increased purity and concentration of the eluted band. In contrast, if the concentration of the closely retained earlier eluted compound is higher than that of the product, the tag-along effect compromises separation.

FRACTION COLLECTION

Automated fraction collection with optimized cut points can contribute significantly to the overall efficiency of preparative separation. Until recently, ultraviolet (UV) directed fraction collection has been commonly used. However, with the necessity to purify a large number of combinatorial libraries consisting of thousands of crude reaction mixtures, the amounts of fractions that need to be collected, analyzed, combined, and tracked is enormous. To address the above issues, a number of commercial high-throughput PHPLCs coupled to tandem mass spectrometry have been developed recently. These automated HPLC/MS systems allow purification of combinatorial libraries at a 50–100 mg scale with a throughput of 250–500 samples/instrument/day.[13] Along with UV detection, the method uses real-time ion signals to trigger fraction collection, and only the masses of the compounds of interest are collected. This format avoids the problem of large fraction collector arrays and eliminates the need for post-purification analysis or pooling of fractions collected. Along with the preparative-scale purifications of combinatorial libraries, preparative liquid chromatography/mass spectrometry (LC/MS) is successfully used in drug discovery to isolate minor compounds from complex mixtures for further structure elucidation or to prepare reference standards.

DESIGN OF THE OPTIMIZATION EXPERIMENT

Nonlinearity of the Langmuir adsorption isotherms is observed even in non-competitive chromatographic processes. Individual adsorption isotherms can be found experimentally using frontal analysis at overload conditions; however, the adsorption isotherms in the separation of mixtures are different because of the interference with other compounds. In PHPLC method development efforts to optimize preparative chromatography using software that allows computer simulated modeling of non-linear effects in preparative chromatography are under way.[14]

Experimental optimization of preparative separation conditions and loading study are usually done on analytical scale. Primary evaluation and selection of the stationary and mobile phases, column efficiency, and product retention experiments under over load conditions are usually done on analytical 0.46×25 cm columns filled with the stationary phase available in bulk quantities for PHPLC. A particular set of chromatographic conditions also includes column dimensions, gradient conditions, sample diluent, and collection points. These conditions are evaluated to obtain maximum recovery of the desired material with required purity, or the maximum available purity for the required yield based on the HPLC analysis of collected fractions. Not all of the separation parameters can be improved simultaneously, and the optimization process often requires multiple experiments. In addition, separation problems, such as sample "bleeding" through the column during loading, or the product not completely eluting from the column, should be identified and corrected. Steps of a carefully designed HPLC optimization experiment include: 1) preliminary recording of the peak area/concentration plot for a pure product standard; 2) calculation of the amount of the target material in the solution prepared for separation; 3) running the designed separation and collecting all fractions by time, starting after the eluted void volume and ending after the column is washed with the strong mobile phase for regeneration (*note*: During the time in which the product and closely retained impurities elute, samples have to be taken more frequently); 4) analysis of all collected fractions to determine the purity (A) and the recovery (C) of the product in each fraction; and 5) measurement of the material balance of the product amount before and after separation.

The calculated product recovery $C_{\Sigma i}$ (%) if i fractions are combined is

$$C_{\Sigma i} = C_1 + C_2 + \cdots + C_i$$

The calculated product purity $A_{\Sigma i}$ (%) if i fractions are combined is

$$A_{\Sigma i} = (A_1 \times C_1 + A_2 \times C_2 + \cdots + A_i \times C_i)/ (C_1 + C_2 + \cdots + C_i)$$

where $C_1, C_2, \ldots, C_i$ = product recovery (%) in fractions 1, 2,..., i is calculated as a part of the total desired product presented in the injected crude material; A_1, A_2,..., A_i = product purity (%) in fractions 1, 2,..., i.

Comparison of the optimization results on recovery and purity assists in the selection of the optimized PHPLC conditions for scale-up. After optimum conditions are determined, a scale-up factor (Y) can be calculated, based

on the results obtained on an analytical column, using the following equation:

$$Y = L_1 \times (D_1)^2 / L_2 \times (D_2)^2$$

where L_1 and L_2 specify column lengths for the scale-up column and analytical column, respectively, and D_1 and D_2 are the respective internal column diameters.

PREPARATIVE CHROMATOGRAPHY IN DRUG DEVELOPMENT PROCESS

Preparative HPLC is routinely and successfully used in drug discovery for the isolation of biologically active compounds from synthetic combinatorial libraries for initial screening. In process chemistry, it is used for the preparation of pure standards and for the purification of sufficient amounts of the synthetic intermediates to help in the optimization of synthetic routes. Preparative chromatography is also used as an effective tool for the isolation of minor impurities (sometimes present at the less than 0.1% level) for consequent structural elucidation. Use of PHPLC in the preparation of the final batches of the drug substance still remains an ultimate dilemma for pharmaceutical companies because of the high, scale-dependent cost of this technique. However, with the rapid development of continuous processes, preparative chromatography is attracting considerable interest for industrial separations in the pharmaceutical industry, particularly for the resolution of enantiomers. At a drug evaluation level, PHPLC provides a definitive way to speed up synthesis and testing of prospective drug candidates, followed by elimination of the less successful compounds, and to subsequently redirect resources in search for new efficient and safe drugs.

REFERENCES

1. Ganetsos, G.; Barker, P.E. Preparative and production scale chromatography. In *Chromatographic Science*; Marcel Dekker, Inc.: New York, 1993; Vol. 61, 786.
2. Zhong, G.; Guiochon, G. Fundamentals of simulated moving bed chromatography under linear conditions. Adv. Chromatogr. **1998**, *39*, 351–400.
3. Toumi, A.; Engell, S.; Ludemann-Hombourger, O.; Nicoud, R.M.; Bailly, M. Optimization of simulated moving bed and Varicol processes. J. Chromatogr. A, **2003**, *1006* (1), 15–31.
4. Guiochon, G. *Fundamentals of Preparative and Nonlinear Chromatography*; Academic Press: Boston, 1994; 701.
5. Golshan-Shirazi, S.; Guiochon, G. Dependence of the production rate on the relative retention of two components in preparative chromatography. J. Chromatogr. A, **1990**, *523* (1–2), 1–10.
6. Snyder, L.R.; Kirkland, J.J.; Glajch, J.L. *Practical HPLC Method Development,* 2nd Ed.; John Wiley & Sons: New York, 1997; 765.
7. Neue, U.D.; Wheat, T.E.; Mazzeo, J.R.; Mazza, C.B.; Cavanaugh, J.Y.; Xia, F.; Diehl, D.M. Differences in preparative loadability between the charged and uncharged forms of ionizable compounds. J. Chromatogr. A, **2004**, *1030* (1–2), 123–134.
8. Shea, K.J. Recent developments in molecular imprinting. Polymer Preprints **2003**, *44* (1), 653.
9. Lisec, O.; Hugo, P.; Seidel-Morgenstern, A. Frontal analysis method to determine competitive adsorption isotherms. J. Chromatogr. A, **2001**, *908* (1–2), 19–34.
10. Blom, K.F. Two-pump at-column-dilution configuration for preparative liquid chromatography-mass spectrometry. J. Comb. Chem. **2002**, *4* (4), 295–301.
11. Neue, U.D.; Mazza, C.B.; Cavanaugh, J.Y.; Lu, Z.; Wheat, T.E. At-column dilution for improved loading in preparative chromatography. Chromatographia **2003**, *57* (Suppl.), 121–127.
12. Jandera, P.; Komers, D.; Guiochon, G. Effects of the composition of the mobile phase on the production rate in reversed-phase overloaded chromatography. J. Chromatogr. A, **1997**, *787* (1–2), 13–25.
13. Rosentreter, U.; Huber, U. Optimal fraction collecting in preparative LC/MS. J. Comb. Chem. **2004**, *6* (2), 159–164.
14. Boysen, H.; Wozny, G.; Laiblin, T.; Arlt, W. CFD simulation of preparative HPLC columns with consideration of nonlinear isotherms. Chem. Eng. Technol. **2003**, *26* (6), 651–655.

Preparative TLC

Edward Soczewinski
Teresa Wawrzynowicz
Department of Inorganic and Analytical Chemistry, Medical University of Lublin, Lublin, Poland

INTRODUCTION

Thin-layer chromatography (TLC) is mostly used as a separation technique combined with qualitative (identification) and quantitative analytical methods; the lower limit of the sample size depends on the sensitivity of detection. For ultraviolet (UV) and chemical detection, it is usually in the microgram or nanogram range. The separated spots can also be isolated for further investigations (chemical derivatization, mass spectrometry, or as chromatographic standards). To increase the scale, the dimensions and thickness of the layer are increased so that it is no longer "thin"; Nyiredy[1] proposed denoting preparative planar chromatography with the abbreviation PLC (preparative layer chromatography) (1 mg to 1 g). The flow of mobile phase during development may be due to capillary forces, pressure [forced-flow planar chromatography (FFPLC), overpressured layer chromatography (OPLC)], or centrifugal force (rotation planar chromatography, RPC).

DISCUSSION

In analytical TLC, linear adsorption isotherms and compact spots are obtained for the loading of sample below 10^{-3} g mixture/1 g adsorbent. To increase throughput, PLC is operated under overloaded conditions, at 1 mg/1 g adsorbent or more. The overloading can be of concentration or volume type; the former is more advantageous.[2]

The main goal of PLC is not the maximal peak (spot) capacity, but the maximal yield of separation.

The increased sample size is obtained by multiple spotting along the start line; when larger volumes are spotted, a series of microcircular chromatograms is obtained as the starting band; streaking from a syringe moving along the start line (e.g., as aerosol—using a programed applicator); especially in OPLC, online zonal application across the plate is possible: The sample is injected into the continuous stream of eluent, distributed across the plate in a narrow channel parallel to the edge, and collected at the farther end of the layer so that the layer acts as a flat column.[1] Similar online injection and collection is possible in centrifugal RPC.

The online application of sample, even of large volumes, is possible with certain horizontal chambers provided with distributors (Camag linear chamber, DS-chamber[3,4]). When the mixture contains few components and the selectivity of the system is high, even large volumes of sample can be introduced from the edge of the layer so that the components are partly separated already in the application stage (frontal chromatography) and, because of mutual displacement effects, may become fully separated during development (Fig. 1), with high yield. To form a compressed starting band, the sample should be dissolved in a solvent weaker than the eluent.

Wide starting bands can also be formed by putting the edge of the plate in the sample solution. To avoid contamination of the eluent in the chamber during development, its bottom is covered by a strip of paper wetted with the eluent; more eluent is introduced when the starting band leaves the edge of the plate.

For thicker layers, the attainment of equilibrium in the gas–mobile phase–adsorbent system to avoid complicating effects (solvent demixing, preadsorption) is more difficult. The solutes migrate in a non-equilibrated layer with differentiated velocity—more rapidly in the surface layer (because of the evaporation of solvent) and less rapidly closer to the carrier plate.

Two stages of PLC determine the success of separation: application of the sample and development. In the former stage, three different situations are possible: (a) sample dissolved in the eluent; (b) sample dissolved in diluted eluent; (c) sample dissolved in a solvent of different quantitative and qualitative compositions.

In case (a), minimal disturbances can be expected at the start of development; however, a wide starting band may be obtained. To obtain a narrow starting band, it is advantageous to dissolve the sample in a weaker solvent, {i.e., of lower content of modifier [case (b)]}.The solubility of the sample is the limiting factor here; the rule is to dissolve a large sample in a small volume of solvent. A good solvent of low eluent strength is chloroform or dichloromethane (e.g., for alkaloids), toluene, or ethers. The application of sample solvent different from the eluent [case (c)] may lead to precipitation of the solutes at the beginning of development; the gradual dissolution of the precipitate in the mobile phase is reflected by comblike tailing of the starting band. It should also be taken into account that, in TLC, the ratio of volumes of the sample solvent (e.g., 0.5 ml) and eluent is greater than in analytical and

preparative column chromatography and may have a more significant effect on the variation of eluent strength of the mobile phase. Evaporation of the sample solvent before development may cause precipitation of the solutes; their delayed dissolution in the mobile phase leads to tailing, which is detrimental to separation. Therefore, online application of the sample is advantageous.

The choice of mobile phase in PLC is also determined by the subsequent recovery of the separated solutes. Less volatile components (water, acetic acid, butanol) should be avoided, as well as non-volatile components—buffer solutions and ion association reagents. Normal-phase chromatography and non-aqueous eluents should, therefore, be preferred. The rules of choice of eluents are otherwise similar to those for analytical chromatography (i.e., basing on eluotropic and isoeluotropic series) depending on the properties of the separated solutes. Usually, eluents giving R_F values in the lower range (0.1–0.5) are chosen, because the application of larger sample volumes leads to wide starting zones and increase of R_F values. For polar adsorbents, ethyl acetate belongs to the recommended modifiers, because of the good solubility of many non-polar and moderately polar solutes, rapid equilibrium, and easy evaporation of the separated fractions.

In PLC, sorbents applied in TLC are usually used: silica, alumina, Florisil, cellulose, and silanized silica. Binding agents such as gypsum and somewhat lower amounts of water are recommended (e.g., for 1 mm silica layers, the weight ratio of water and adsorbent is 1:1.5 or 1:2). Plates with thicker layers should be dried in air in a horizontal position for a longer time (e.g., for 1 mm layers, ~1 hr; for 2 mm layers, 2–4 hr) and then dried and activated in an oven in gradually increasing temperatures. Equilibration in the chamber should also be prolonged. Because chemically bonded adsorbents are relatively expensive and, moreover, reversed-phase (RP) sorbents are poorly wettable by aqueous eluents, polar adsorbents and non-aqueous eluents of low viscosity are usually applied in PLC. Special precoated plates of 0.5–2 mm layers are commercially available (e.g., silica gel 60 $F_{254+366}$). Such plates can be applied directly without activation; however, drying at 80°C for 2 hr is recommended. Although the capacities of layers increase with their thickness, the separation efficiency decreases for thickness above 1.5 mm, so that optimal for PLC are layers of 0.5–1 mm thickness.

The development distance in PLC should not exceed 20 cm, because of the decreasing flow rate for longer distances and increasing diffusion of zones. A suitable system should have a resolution $R_s \geq 1.5$ in the analytical scale.

Marked improvement of separation efficiency in the separation of complex samples may be obtained by stepwise gradient elution[5] because of enhanced mutual displacement of the components in the concentrated starting band. A simple stepwise gradient of four to five steps is frequently sufficient; the generation of stepwise gradients is possible in some types of horizontal chambers[6] by consecutive delivery of eluent fractions of increasing concentrations of modifier.

Preparative layer chromatography can also be used as a pilot technique for column preparative chromatography in the same solvent–adsorbent system.

REFERENCES

1. Nyiredy, S. *Handbook of TLC,* 2nd Ed.; Sherma, J., Fried, B., Eds.; Marcel Dekker, Inc.: New York, 1996.
2. Snyder, L.R.; Dolan, J.W. In *Advances in Chromatography*, Brown, P.R., Ed. CRC Press: Boca Raton, 1998, Vol. 38, 115.
3. Soczewinski, E. *Planar Chromatography*; Kaiser, R.E., Ed.; Hüthig: Heidelberg, 1986; Vol. 1, 79–117.
4. Dzido, T.H.; Matysik, G.; Soczewinski, E. J. Planar Chromatogr.-Mod. TLC **1991**, *4*, 161.
5. Soczewinski, E.; Matysik, G.; Polak, B. Improvement of separation in zonal preparative thin-layer chromtography by gradient elution. Chromatographia **1994**, *39* (7–8), 497.
6. Soczewinski, E.; Czapinska, K.; Wawrzynowicz, T. Migration off zones off test dyes in preparative thin-layer chromatography: Stepwise gradient elution. Sep. Sci. Technol. **1987**, *22* (8), 2101–2110.

Procyanidins: CCC Separation with Hydrophilic Solvent Systems

Akio Yanagida
Yoichi Shibusawa
Division of Pharmaceutical and Biomedical Analysis, School of Pharmacy, Tokyo University of Pharmacy and Life Science, Tokyo, Japan

Yoichiro Ito
National Heart, Lung, and Blood Institute (NHLBI), National Institutes of Health (NIH), Bethesda, Maryland, U.S.A.

Abstract
An efficient separation of apple procyanidins (oligomeric catechins) was performed by high-speed countercurrent chromatography (HSCCC) in a one-step operation from an apple condensed tannins fraction using a hydrophilic two-phase solvent system composed of methylacetate-water (1:1, v/v). In further matrix-assisted laser desorption initiation–time-of-flight mass spectrometry (MALDI–TOF-MS) analyses of the solute oligomers, the elution order of the procyanidins in the HSCCC was coincident with their degree of polymerization.

INTRODUCTION

Unripe apple contains polyphenols (including dihydrocalcons, phenolic acids, and others), constituting up to 50% of the total mass of solids; beside consisting of monomers, dimers, trimers, and oligomers of catechin and/or epicatechin, which are called apple procyanidins or apple condensed tannins (ACTS). Highly polymerized procyanidins have attracted attention in the fields of pharmacology and food chemistry because of their physiologic activities, such as hair growth promotion, antiallergic, antibiotic, and inhibitory activities against enzymes and receptors. These properties of procyanidins depend on the degree of polymerization of catechin and/or epicatechin.

In order to correlate these pharmaceutical activities with their degree of polymerization, it is necessary to establish an efficient, reliable separation method. However, the application of liquid chromatography (LC) to the separation of these procyanidin oligomers is difficult because the oligomers above hexamers tend to cause irreversible adsorption onto the column packing materials.

Countercurrent chromatography (CCC)[1] is a liquid–liquid partition technique that eliminates various complications arising from the use of solid supports. The high-speed CCC (HSCCC), the most advanced form in terms of partition efficiency and separation time, has been used for the separation and purification of a wide variety of natural products. The recent model of HSCCC, which facilitates the stationary phase retention for polar solvent systems, is particularly useful for the separation of hydrophilic, highly polymerized procyanidins.[2,3]

APPARATUS

The CCC separation of procyanidin oligomers from apple condensed tannin was performed using a type-J HSCCC centrifuge (Fig. 1). The apparatus holds a multilayer coiled separation column and counterweight symmetrically at a distance of 10 cm from the central axis of the centrifuge. The separation column is fabricated by winding a single piece of 2.0 mm I.D. and 21 m long polytetrafluoroethylene (PTFE) tubing directly onto the holder hub, making four coiled layers between a pair of flanges. The total capacity of the column is about 72 ml. The speed of the apparatus is regulated at 1000 rpm with a speed controller. The coil rotates around its axis as it simultaneously revolves around a central axis, producing an efficient mixing of the two phases while retaining a sufficient amount of the stationary phase in the column.

Fig. 1 Photograph of the type-J multilayer coil planet centrifuge.

PREPARATION OF ACTS FOR CCC SAMPLE

The unripe apples were homogenized in potassium pyrosulfite solution, and the mixture was allowed to stand for 1 day. The supernatant was centrifuged and filtered with a glass filter funnel. The filtrate was applied to adsorption chromatography, and the ACT fraction was evaporated and lyophilized. Purified ACTs were a mixture of monomers (catechin and/or epicatechin) and oligomers from dimers to pentadecamers, as shown in Fig. 2.

MEASUREMENT OF PARTITION COEFFICIENT OF CATECHIN AND/OR EPICATECHIN AND ACTS

CCC utilizes a pair of immiscible solvent phases that have been pre-equilibrated in a separatory funnel: One phase is used as the stationary phase and the other as the mobile phase. In order to achieve efficient separation of higher polymerized, large oligomers from ACTs, the partition coefficient values (K_D) of catechin and/or epicatechin and ACTs were determined in the following four hydrophilic solvent systems:

1. *n*-Butanol/water (1:1)
2. *n*-Butanol/acetic acid/water (4:1:5)
3. Methyl *tert*-butyl ether/acetonitrile/water (2:2:3)
4. Methyl acetate/water (1:1)

As the chromatographic process in CCC is based on the partition of a solute between the mobile and stationary phases, the K_D value is the most important parameter in CCC. A K_D value of around 1.0 is most desirable in CCC, wherein a solute with $K_D = 1.0$ elutes with its retention volume equivalent to the total column capacity. In the above two-phase solvent systems, the K_D values of monomers (catechin and/or epicatechin) were greater than 1.0, and those of the ACTs are always smaller than 1.0, suggesting that monomers are more hydrophobic than their oligomers present in ACTs. Among these four solvent systems, we selected a simple binary system of methyl acetate/water for the separation of procyanidin oligomers from ACTs by CCC.

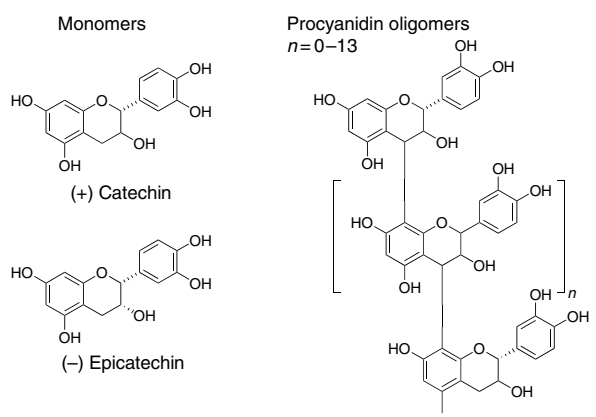

Fig. 2 Chemical structures of catechin, epicatechin, and procyanidin oligomers.

CCC SEPARATION OF ACTS BY HYDROPHILIC SOLVENT SYSTEM

Fig. 3 shows a chromatogram obtained from ACTs using the two-phase solvent system composed of methyl acetate/water (1:1). After filling the multilayer coil with the lower aqueous stationary phase, 2 ml of the sample solution, containing 100 mg of ACTs, was injected into the column. The separation was performed by pumping the upper phase into the column at a flow rate of 1.0 ml/min at 1000 rpm rotational speed. The effluent was monitored at 280 nm and fractions were collected at 3 ml per tube. The masses of the fractionated oligomers were determined by matrix-assisted laser desorption initiation/time-of-flight mass spectrometry (MALDI–TOF-MS) analysis.

After the elution of the trimers, the lower aqueous phase was eluted through the column to facilitate a rapid elution of the oligomers still remaining in the column. The tetramers and pentamers fraction, the pentamers, hexamers, and heptamers fraction, and higher polymerized oligomers over the hexamers fraction were subsequently eluted from the column in this order. Interestingly, the elution order is also coincident with the degree of polymerization of catechin and/or epicatechin. With the exception of the solutes in last large peak (highly polymerized catechins), the degrees of polymerization of solute oligomers in all CCC fractions in Fig. 3 were clearly determined by MALDI–TOF-MS analyses. The lower stationary phase retained in the column was

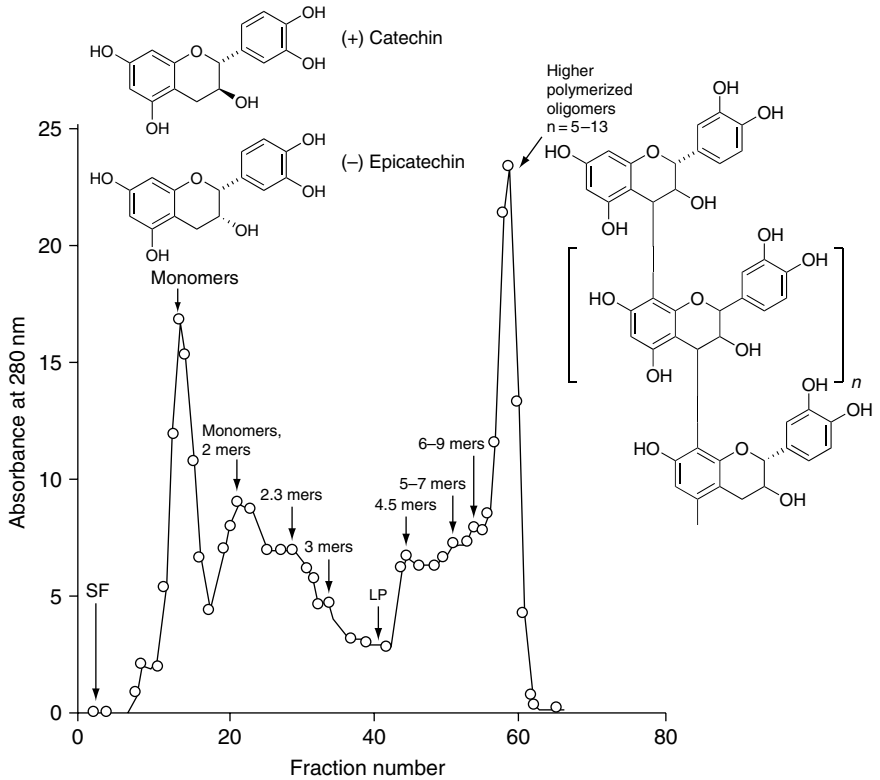

Fig. 3 Separation of procyanidins in the order of their degree of polymerization by countercurrent chromatography.

estimated as 82% of the total column capacity (72 ml) prior to the application of the elution with lower phase. The separation was completed within 3 hr.

The chromatogram shown in Fig. 3 was the first separation profile of oligomeric procyanidins by HSCCC using a two-phase solvent system. In recent times, other hydrophilic solvent systems, such as hexane/methyl acetate/acetonitrile/water three-phase system,[4,5] methyl *tert*-butyl ether/1-butanol/acetonitrile/water two-phase systems,[6,7] and ethyl acetate/1-butanol (or 2-propanol)/water two-phase systems,[8,9] were also applied to HSCCC separations of other proanthocyanidins and/or related polyphenolic oligomers.

CONCLUSIONS

The results indicate that the present method is capable of fractionating the apple procyanidin oligomers from ACTs according to the degree of polymerization. The highly polymerized, very hydrophilic oligomers, which tend to be adsorbed on the column packing materials by high-performance liquid chromatography (HPLC), were all recovered from the CCC column.

REFERENCES

1. Conway, W.D. *Countercurrent Chromatography: Apparatus and Applications*; Wiley-VCH: New York, 1990.
2. Shibusawa, Y.; Yanagida, A.; Ito, A.; Ichihashi, K.; Shindo, H.; Ito, Y. High-speed counter-current chromatography of apple procyanidins. J. Chromatogr. A, **2000**, *886*, 65–73.
3. Shibusawa, Y.; Yanagida, A.; Isozaki, M.; Shindo, H.; Ito, Y. Separation of apple procyanidins into different degree of polymerization by high-speed counter-current chromatography. J. Chromatogr. A, **2001**, *915*, 253–257.
4. Shibusawa, Y.; Yanagida, A.; Shindo, H.; Ito, Y. Separation of apple catechin oligomers by CCC. J. Liq. Chromatogr. Rel. Technol. **2003**, *26* (9 & 10), 1609–1621.
5. Shibusawa, Y.; Yamakawa, Y.; Noji, R.; Yanagida, A.; Shindo, H.; Ito, Y. Three-phase solvent systems for comprehensive separation of a wide variety of compounds by high-speed counter-current chromatography. J. Chromatogr. A, **2006**, *1133*, 119–125.
6. Salas, E.; Fulcrand, H.; Poncet-LeGrand, C.; Meudec, E.; Köhler, N.; Winterhalter, P.; Cheynier, V. Isolation of flavanol-anthocyanin adducts by countercurrent chromatography. J. Chromatogr. Sci. **2005**, *43*, 488–493.
7. Yanagida, A.; Shoji, A.; Shibusawa, Y.; Shindo, H.; Tagashira, M.; Ikeda, M.; Ito, Y. Analytical separation of tea catechins and food-related polyphenols by high-speed counter-current chromatography. J. Chromatogr. A, **2006**, *1112*, 195–201.
8. Köhler, N.; Wray, V.; Winterhalter, P. Preparative isolation of procyanidins from grape seed extracts by high-speed counter-current chromatography. J. Chromatogr. A, **2008**, *1177*, 114–125.
9. Köhler, N.; Wray, V.; Winterhalter, P. New approach for the synthesis and isolation of dimeric procyanidins. J. Agric. Food Chem. **2008**, *56*, 5374–5385.

Programmed Flow GC

Raymond P.W. Scott
Scientific Detectors Ltd., Banbury, Oxfordshire, U.K.

INTRODUCTION

There are three methods that can be used to accelerate the elution of strongly retained peaks during chromatographic development. Flow programing, where the flow of mobile phase is continuously increased during the development of the separation, temperature programing, and gradient elution, the latter being exclusively used in liquid chromatography. We reserve our discussion here to flow programing.

DISCUSSION

Flow programing is not as effective in reducing the elution time of well-retained components and tends to cause increased band dispersion; it is, however, more gentle than temperature programing and would be chosen when separating thermally labile materials. The complexity of the theoretical treatment depends on whether the mobile phase is compressible or not. In gas chromatography, the mobile phase is compressible, and this must be taken into account in the first theoretical treatment.

We shall assume that under flow programing conditions, the mass flow rate will be increased linearly with time (i.e., $Q_{0(t)} = (Q_0' + \alpha t)$ where Q_0' is the *initial exit flow rate*, $Q_{0(t)}$ is the exit flow rate after time t and α is the program rate. These conditions are usual for modern gas flow programing devices that utilize mass flow controllers which are computer operated. Now, if ΔV_0 is an increment of exit flow, measured at atmospheric pressure, then employing the usual pressure correction factor, the corrected gas flow (ΔV_r) will be

$$\Delta V_r = \frac{3}{2}\Delta V_{r(0)}\left(\frac{\gamma^2 - 1}{\gamma^3 - 1}\right)$$

where γ is the inlet/outlet pressure ratio of the column. Then, under the above-defined programing conditions,

$$\Delta V_{r(t)} = \frac{3}{2}\left(\frac{\gamma_t{}^2 - 1}{\gamma_t{}^3 - 1}\right)(Q_0 + \alpha t)\Delta t \qquad (1)$$

where (γ_t) is the inlet/outlet pressure ratio at time t and $\Delta V_{r(t)}$ is the increment of volume flow at time t.

Now, as the flow is increased, the inlet pressure will also increase and, thus, the inlet/outlet pressure ratio (γ) will change progressively during the program; the *mean* flow rate will be reduced according to the pressure correction function and the decrease in elution rate will not be that which would be expected. Consider an open-tubular column; from Poiseuille's equation,

$$P_0 Q_{(0)t} = \frac{(P_t{}^2 - P_0{}^2)\pi a^4}{16\eta l}$$

or

$$P_0(Q_0 + \alpha t) = \frac{(P_t{}^2 - P_0{}^2)\pi a^4}{16\eta l} \qquad (2)$$

where P_t is the inlet pressure at time t, P_0 is the outlet pressure (atmospheric), η is the viscosity of the gas at the column temperature, l is the length of the open-tubular column, and a is the radius of the open-tubular column.

A similar equation would be used for a packed column, except the constant (π/16) would be replaced by the D'Arcy constant for a packed bed. Rearranging,

$$\frac{P_0(Q_0 + \alpha t)16\eta l}{\pi a^4} + P_0{}^2 = P_t{}^2$$

thus,

$$\gamma_t = \frac{P_t}{P_0} = \left(\frac{(Q_0 + \alpha t)16\eta l}{P_0 \pi a^4} + 1\right)^{0.5} \qquad (3)$$

Assuming the column dimensions are 320 μm in inner diameter (radius $a = 0.0160$ cm) and 30 m in length, and it is operated at 120°C using nitrogen as the carrier gas which, at that temperature, has a viscosity of 129×10^{-6} P, then, by using Eq. 3, the change (γ)

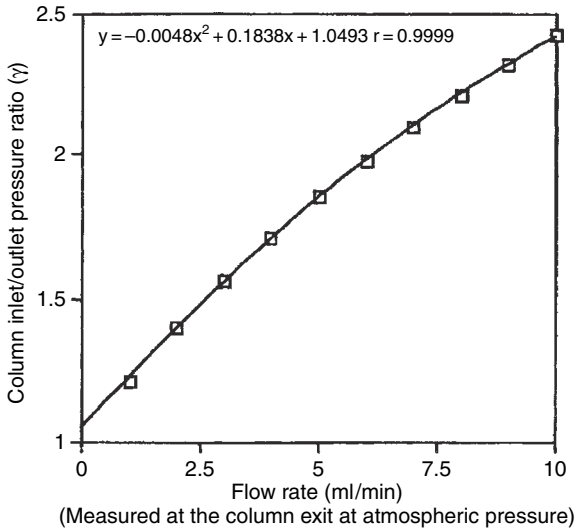

Fig. 1 The relationship between the inlet/outlet pressure ratio and exit flow rate for an open-tubular column.

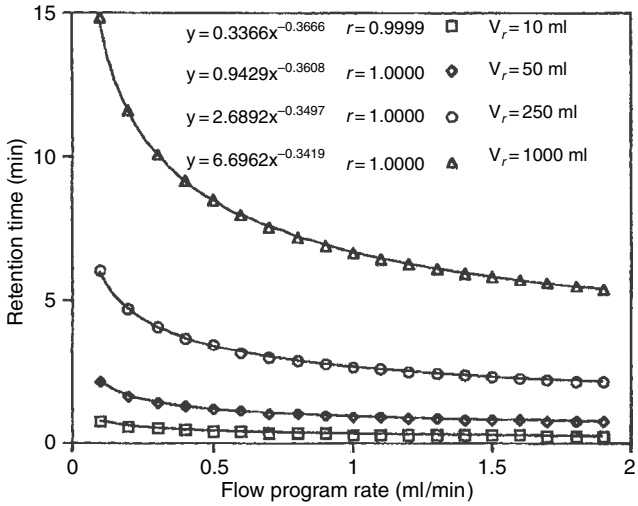

Fig. 2 Curves relating elution time to flow program rate for solutes having different retention volumes.
Source: From *Gas Chromatography 1964*.[1]

can be calculated for different flow rates. The relationship between flow rate (as measured at the column exit and at atmospheric pressure) and the column inlet/outlet pressure ratio is shown in Fig. 1. The inlet/outlet pressure ratio changes significantly during a mass flow rate program, which will attenuate the elution rate as shown by the pressure correction factor. It is seen that the curve is a close fit to a second-order polynomial function, but this relationship is fortuitous, although it might be used empirically to predict inlet/outlet pressure ratios.

It is now possible to use the values for γ_t to calculate when the solute is eluted at the retention time t_r for different flow program rates. Employing Eq. 1, when the sum of all the increments of ΔV_r is equal to the retention volume V_r, then t will be t_r, the retention time:

$$V_r = \sum_{t=0}^{t=t_r} \frac{3}{2}\left(\frac{{\gamma_t}^2 - 1}{{\gamma_t}^3 - 1}\right)(Q_0 + \alpha t)$$

With a simple computer program, the retention time t_r can be calculated for a range of different program rates (α) and for solutes having retention times of 10, 50, and 250 ml, respectively. The column was again assumed to be 320 mm in inner diameter and 30 in length and operated at 120°C using nitrogen as the carrier gas which, at that temperature, has a viscosity of 129×10^{-6} P. The results are shown in Fig. 2.

The effect of program rate on retention time is much as would be expected. For any individual solute, the retention time is related to some power of the solute retention volume, but the indices vary significantly with the retention volume of the solute. This relationship does not have a theoretical explanation at this time but

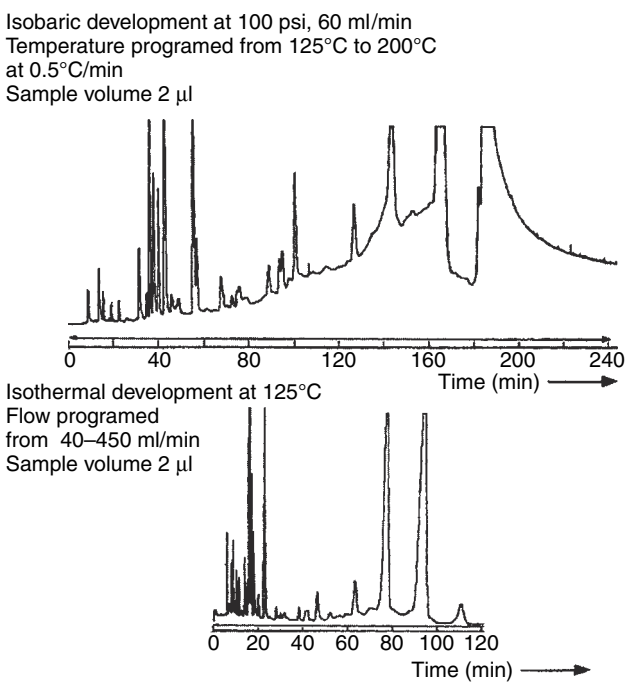

Fig. 3 The separation of lemon grass oil by temperature programing and by flow programing.

might be useful for predicting retention times from experimental data. Despite the attenuating effect of the pressure correction factor, the use of flow programing is effective in reducing the retention time of strongly retained solutes. However, unless the diffusivities of the solutes in the mobile phase are high (i.e., mobile phases such as hydrogen or helium are employed), there will be significant peak dispersion at the higher velocities, the column efficiency will be reduced, and resolution will be lost.

An excellent example of the use of flow programing was given in a very early article describing the technique.[1] Lemon grass oil contains two substances that are very thermally labile, and these are eluted very late in the chromatogram. If temperature programing is employed, the substances decompose at the higher temperatures, producing a sloping baseline as shown in the upper chromatogram in Fig. 3. The baseline does not return to its normal level until the thermally unstable compounds have been completely eluted. If the separation is carried out isothermally at a temperature where the decomposition is minimal, and the mixture is developed by flow programing, all the solutes are eluted on a relatively stable baseline. The elution times are high, due to long packed columns being employed, as opposed to capillary columns.

REFERENCE

1. Scott, R.P.W. *Gas Chromatography 1964*; Goldup, A., Ed.; The Institute of Petroleum, 1964; 25.

BIBLIOGRAPHY

1. Scott, R.P.W. *Introduction to Analytical Gas Chromatography*; Marcel Dekker, Inc.: New York, 1998.
2. Scott, R.P.W. *Techniques of Chromatography*; Marcel Dekker, Inc.: New York, 1995.

Programmed Temperature GC

Raymond P.W. Scott
Scientific Detectors Ltd., Banbury, Oxfordshire, U.K.

INTRODUCTION

Temperature programing becomes necessary when the sample contains components that have polarities and/or molecular weights that extend over a wide range. Such samples, if separated isothermally, may well result in the less retained solutes being adequately resolved and eluted in a reasonable time. However, the more polar or higher-molecular-weight solutes may be held on the column for an inordinately long period, and the solute peaks, when they are eluted, are likely to be wide and flat and difficult to evaluate quantitatively. To avoid this situation, the column temperature can be progressively increased during development so that the late eluting peaks are accelerated through the column and are still sharp and eluted in a reasonable time. This procedure is called temperature programing.

APPLICATION

The corrected retention volume of a solute (V_r') is given by (see *Rate Theory in GC*, p. 2000)

$$V_r' = KV_s$$

where K is the distribution coefficient of the solute with respect to the stationary phase and V_s is the volume of stationary phase in the column.

The value of K varies with temperature in the following manner (see *Thermodynamics of Retention in GC*, p. 2307)

$$\ln(K) = -\left(\frac{\Delta H}{RT} - \frac{\Delta S}{R}\right)$$

$$\text{or} \quad K = \exp\left[-\left(\frac{\Delta H}{RT} - \frac{\Delta S}{R}\right)\right]$$

where ΔH is the standard enthalpy of distribution, ΔS is the standard entropy of distribution, R is the gas constant, and T is the absolute temperature. Thus,

$$V_r' = \exp\left[-\left(\frac{\Delta H}{RT} - \frac{\Delta S}{R}\right)\right]V_s$$

It is seen that as T increases, K decreases. It follows that K and, consequently, the retention volume can be progressively decreased by increasing the column temperature. In practice, this is usually achieved by situating the column in an oven, the temperature of which is controlled by appropriate electronic circuitry. Theoretically, the temperature of the oven can be increased as any function of time, but almost all program profiles are linear in form.

Consequently, programing the column from temperatures T_1 for a period of t, using a linear program (i.e., $T = T_1 + \alpha t$, where t is the elapsed time), the mean value of K will be given by the following function:

$$K = t_1^{-1}\sum_{t=0}^{t=t_1}\exp\left[-\left(\frac{H}{R(T_1+\alpha t)} - \frac{S}{R}\right)\right]$$

where t_1 is the time period of the program. [Preferably t_1 for maximum accuracy, should be defined in small units (e.g., seconds and not minutes).] Similarly, the program rate α must be defined in degrees Celcius per second.

Now, when the solute is eluted, V_r' will equal the product of the mean flow rate Q_m and t_1, which will be the retention time; that is,

$$V_r' = Q_m t_1$$

The mean flow rate through a GC column is given by[1]

$$Q_m = Q_0\frac{3(\gamma^2-1)}{2(\gamma^3-1)}$$

where γ is the and/or pressure ratio and Q_0 is the exit flow rate.

Thus, when the solute elutes,

$$V_r' = V_s K\sum_{t=0}^{t=t_1}\exp\left[-\left(\frac{H}{R(T_1+\alpha t)} - \frac{S}{R}\right)t_1\right]$$
$$= Q_0\frac{3(\gamma^2-1)}{2(\gamma^3-1)}t_1$$

where V_s is the volume of stationary phase in the column.

Solving for t in the classical manner is a cumbersome mathematical procedure and it is easier to employ a numerical method to calculate t. To demonstrate the effect of temperature programing on solute elution, a computer program was used to calculate the retention time of a given solute eluted at different programing rates. The data used

were that of Liao and Martire[1] for 3-methyl hexane chromatographed on *n*-octadecane at temperatures of 30°C, 40°C, 50°C, and 60°C.

By curve-fitting the retention data to the reciprocal of the absolute temperature, the numeric form of the distribution coefficient was found to be

$$K = \exp\left(\frac{1737.777}{T} - 2.75115\right)$$

A simple computer program provided values for the retention time, calculated for different linear program rates, and the results are shown as curves relating retention time to program rate in Fig. 1. The and/or pressure ratio (γ) was assumed to be 2 and the flow rate at the column exit was 20 ml/min (0.3333 ml/s). The logic of the program was based on a search for that value of t where the value (V_r') of equaled the product of t and the mean column flow rate. It should be noted that the data were reported as the corrected retention volume per gram of stationary phase; thus, for simplicity, the curves are calculated on the assumption that the column contains 1 g of stationary phase. Retention times for columns containing more stationary phase would be appropriately longer. Due to the change in both the density and viscosity of a gas with temperature, the mean flow rate will change slightly during the program, but the error will be small, provided that a *mass flow controller* is employed and not a pressure controller. For the calculations, the inlet pressure was assumed to remain constant throughout the program.

This procedure is a general method for calculating the effect of the program rate on retention time. Basically, the corrected retention volume must be measured for each solute of interest at two different temperatures to provide the thermodynamic constants. The above equations will then allow the effect of different linear temperature programs on the corrected retention volume to be calculated for each solute. The effect of program rate on resolution can also be observed if some solutes elute close together. In fact, the equation can be used for program functions other than linear, but these are rarely employed. The relationship between retention time and program rate is approximately linear and can be assumed so for most practical purposes. For more accurate work, a second-order polynomial should be used to describe the retention time as a function of the program rate, which can give very accurate values.

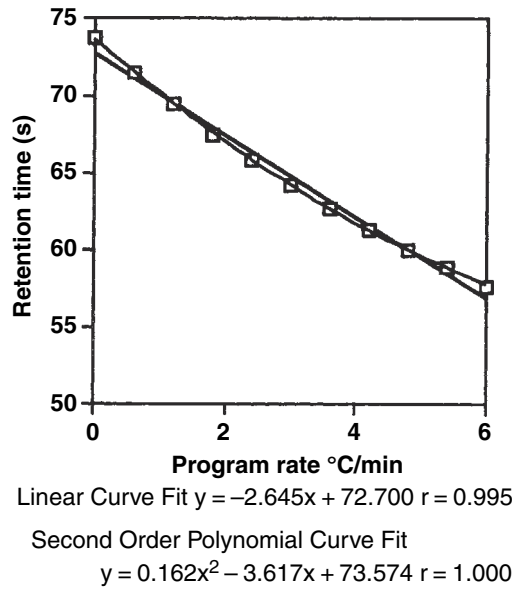

Fig. 1 Graph of retention time versus program rate.

REFERENCE

1. Liao, H.L.; Martire, D.E. Thermodynamics of molecular association by gas-liquid chromatography. VII. Hydrogen bonding of aliphatic alcohols to di-n-octyl ether, di-n-octyl thioether, and di-n-octylmethylamine. J. Am. Chem. Soc. **1972**, *94* (10), 2058–2062.

BIBLIOGRAPHY

1. Scott, R.P.W. *Introduction to Analytical Gas Chromatography*; Marcel Dekker, Inc.: New York, 1998.
2. Scott, R.P.W. *Techniques of Chromatography*; Marcel Dekker, Inc.: New York, 1995.

Prostaglandins, Isoprostanes, and Synthetic Prostanoid Drugs: Analysis by HPLC

Harald John
Bundeswehr Institute of Pharmacology and Toxicology, Munich, Germany

Abstract
Prostaglandins (PGs), isoprostanes (IPs), as well as thromboxanes are unsaturated oxidized derivatives of naturally occurring ubiquitous arachidonic acid and similar fatty acid precursors exhibiting very weak UV absorptivity. Whereas PGs are produced enzymatically via the cyclooxygenase(COX)-complex, iPs are generated following a non-enzymatic free-radical mechanism. These compounds are multifunctional physiological regulators and act as chemical messengers in mammalian cellular behavior, thus affecting, e.g., platelet aggregation or contraction and dilation of muscles and vessels. Due to this widespread biological activity synthetic structural analogs (prostanoids) are administered as drugs characterized by optimized efficacy and stability for therapeutic intervention of, e.g., pulmonary arterial hypertension, glaucoma, and induction of abortion.

To elaborate physiological mechanisms of action and investigate pharmacokinetic characteristics, bioanalytical procedures that allow selective trace level quantification are required. The more or less lipophilic and acidic compounds are typically extracted from biological fluids after acidification by liquid–liquid extraction (LLE), solid-phase extraction (SPE), or by the more sophisticated novel approaches of online techniques making use of on-column hydrophilic–lipophilic interactions. To achieve sufficient lower limits of quantification, PGs are often converted into highly UV-absorbing or fluorescent derivatives. Chromatographic separations by reversed-phase (RP) high-performance liquid chromatography (HPLC) coupled to sensitive and selective mass spectrometric (MS) or fluorescence detection are well-established tools that overcome the drawbacks of the more classical and conventional gas chromatographic techniques. The use of modern LC–MS techniques by electrospray ionization (ESI) and collision-induced dissociation (CID) for analyte fragmentation realize an optimum of selectivity as well as sensitivity. In addition time-consuming sample preparation steps as well as derivatization can be avoided, making LC–MS/MS the most promising chromatographic technique for PG analysis.

INTRODUCTION: PHYSIOLOGY AND CHEMISTRY[1–3]

Prostaglandins (PGs) are a class of substances representing natural metabolites of three 20-carbon fatty acids differing in their number of double bonds: arachidonic acid (AA, 5,8,11,14-eicosatetraenoic acid); 8,11,14-eicosatrienoic acid; and 5,8,11,14,17-eicosapentaenoic acid. In the following discussion, only the bisenoic PGs (produced from AA), which dominate most biological systems, will be discussed. Free AA acts as a substrate for the cyclooxygenase (COX) enzyme complex and consecutively several specific enzymes including isomerases, reductases, and synthases produce thromboxanes (TXs) and further PGs as demonstrated in Fig. 1. Furthermore, in recent years, four groups (type III–VI) of the AA-derived isoprostanes (iPs) were investigated extensively. These iPs are isomeric to PGs that are physiologically produced as racemic mixtures by non-enzymatic reactions based on free-radical mechanisms initiated by reactive oxygen species implicated in membrane damage (Fig. 2). Their weak ultraviolet (UV) absorption maxima are found at 192 nm and at 217 nm for PGA_2, 228 nm for 15-oxo-PGE_2, and 278 nm for PGB_2, arising from delocalized electron systems of conjugated double bonds and oxo groups. Prostanoids are known for their high and widespread physiological potency in acting as chemical messengers capable of regulating cellular behavior in mammalian tissues. The influences on platelet aggregation, contractory or dilatory effects on muscles and vessels, mediating inflammatory diseases, and pain are only a few examples that make these compounds of great interest for diagnostic and therapeutic purposes. Therefore, numerous additional synthetic prostanoid drugs, which possess chemical structures similar to naturally occurring PGs but exhibit improved pharmacological properties like prolonged stability and enhanced biological potency, are approved and used in therapy.

Currently, prostanoids are administered for various therapeutic interventions: e.g., 1) treprostinil, beraprost, and iloprost (Fig. 3) are analogs of PGI_2 (prostacyclin) which are used to treat pulmonary arterial hypertension (PAH) to overcome the drawback of short circulation

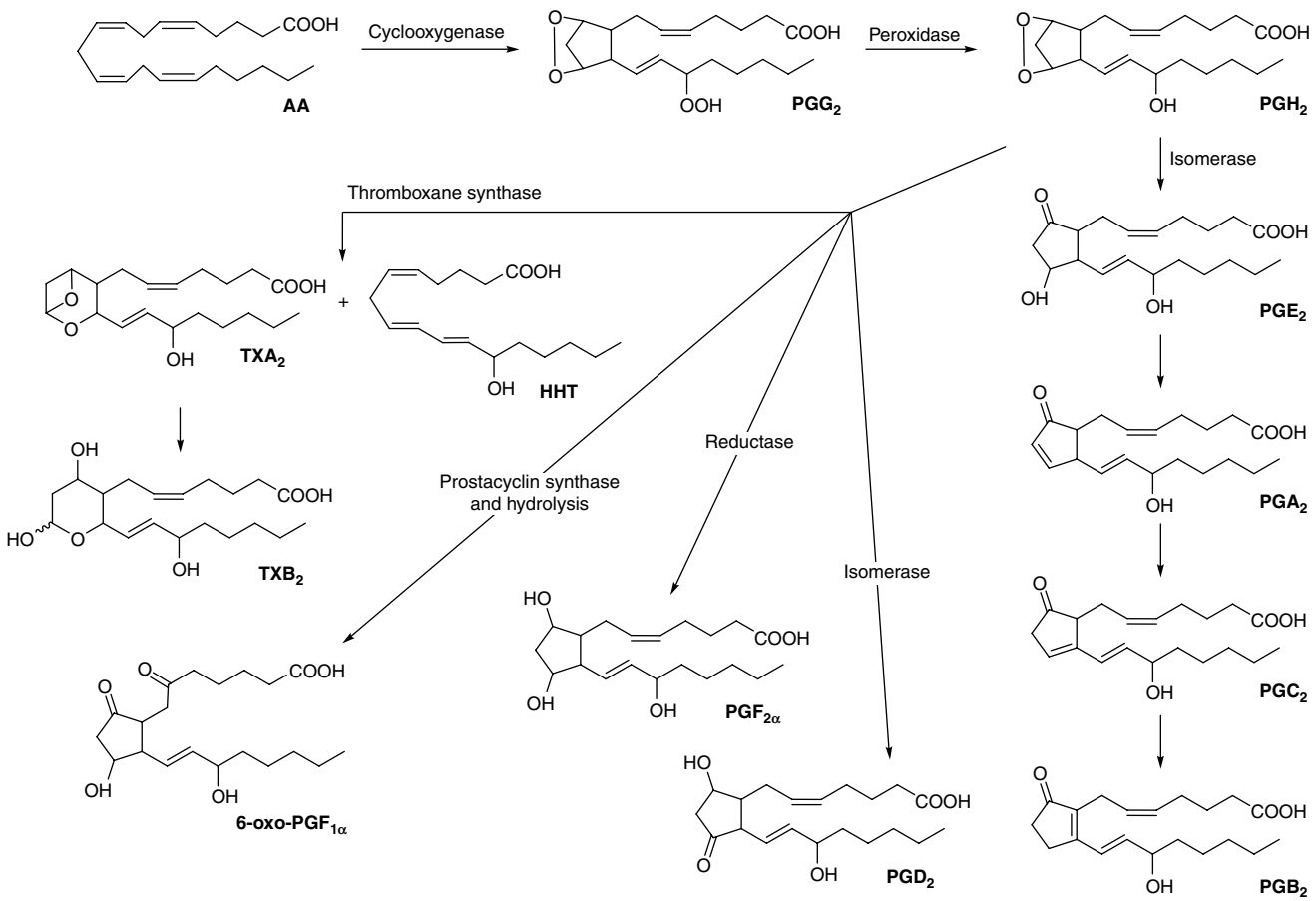

Fig. 1 Cyclooxygenase-initiated metabolization of arachidonic acid (AA) to prostaglandins (PGs) and thromboxanes (TXs).

half-life of epoprostenol (sodium salt of PGI_2) applied as a potent vasodilator and antithrombotic agent; 2) synthetic analogs of $PGF_{2\alpha}$ (Fig. 1) act as potent and selective agonists on the $PGF_{2\alpha}$ receptor and are therefore used for the treatment of glaucoma to reduce intraocular pressure (travoprost and latanoprost, Fig. 3), or to induce estrus in mares in veterinary medicine (fluprostenol, Fig. 3); cloprostenol (Fig. 3) is an additional $PGF_{2\alpha}$ analog that is 200 times more potent than $PGF_{2\alpha}$ itself to terminate pregnancy and elicits luteolysis and uterine contraction; 3) structural analogs of PGE_2 (Fig. 1) are clinically used for, e.g., postoperative cervical dilatation and induction of abortion (sulprostone, Fig. 3); 4) analogs of PGE_1 can be clinically beneficial by decreasing the frequency of gastric mucosal lesions (ulceration) occurring in patients receiving nonsteroidal anti-inflammatory drugs (misoprostol, Fig. 3) and by their strong vasodilatory and antiplatelet activities (limaprost, Fig. 3). An additional large number of prostanoid compounds are known for therapeutic intervention and physiological regulation but a more detailed introduction would go beyond the scope of this entry.

In contrast to endogenous PGs, several prostanoid drugs contain esterified or amidated carboxyl groups, thus acting as prodrugs that need to be converted into their free acids for optimum activity (e.g., bimatoprost, latanoprost, travoprost; Fig. 3). Following in vivo administration, liberated drugs exhibit improved biological activity for which reason the corresponding drug concentrations are adjusted to be much smaller than those known for endogenous PGs. Therefore, analytical methods that allow the trace-level determination of PGs, iPs, and prostanoid drugs from different complex biological sources like serum, plasma, seminal fluid, urine, or culture medium are needed.

In many cases, endogenous PGs are measured by highly specific immunoassays, although they do not enable the simultaneous determination of multiple components in a single experiment. Besides high-performance liquid chromatography (HPLC) techniques, gas chromatography (GC) methods are often used in combination with mass spectrometry (MS), flame ionization detector (FID), or electron capture detectors (ECD). However, HPLC is still a very useful, versatile, and widespread tool for analytical or preparative separation and detection under mild conditions, allowing qualitative and quantitative measurement of oxygen-sensitive prostanoids. In addition, the development of prostanoid drugs is also supported by highly efficient HPLC techniques used in preclinical and clinical trials for selective pharmacokinetic studies toward drug approval.

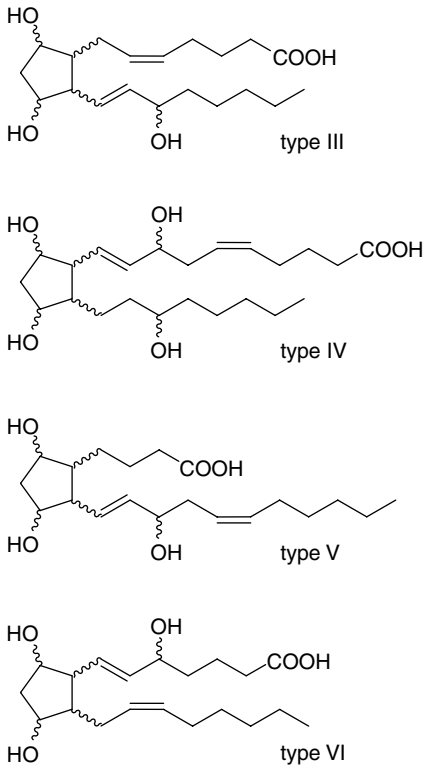

Fig. 2 Arachidonic acid derived groups of isoprostanes (types III–VI).

SAMPLE PREPARATION[4–6]

Endogenous prostanoids only occur in trace levels in complex biological samples. Therefore, the removal of substances impairing chromatographic resolution and detection, and concentration of the analytes are required. Most of the samples are extracted using liquid–liquid extraction (LLE) or solid-phase extraction (SPE) methods without longer time of storage, thus avoiding the non-enzymatic production of iPs by autoxidation of AA.[7] Owing to the free carboxylic groups of prostanoids, samples are acidified to pH 3–4 usually by acetic (HOAc), formic, citric, or hydrochloric acid. Acidification to lower pH values has to be avoided owing to the chemical instability and degradation of some PGs: PGE_2 dehydrates irreversibly to PGA_2, isomerizing to PGB_2; PGD_2 might be dehydrated to an inverted version of PGA_2. Epimerization at C15 and *cis–trans* isomerization may occur, as demonstrated for the TX synthase product 12-*S*-hydroxyheptadecatrienoic acid (HHT).[8] LLE is carried out by the addition of a onefold to fivefold volume of non-polar solvents like diethyl ether, chloroform, or ethyl acetate, followed by shaking or stirring for a few minutes. Consecutive centrifuging enables efficient phase separation and pellets the particulate matter resulting in recoveries of 80–98%. Repetition of this procedure is seldom done and does not improve the recovery significantly. The organic layers are evaporated to dryness under reduced pressure or a gentle stream of nitrogen, to concentrate the prostanoids prior to further preparations or chromatography. Extraction of biological samples using petrol ether or hexane at neutral pH values prior to extraction of acidified matrix removes non-polar fatty acids and lipids, preventing their possible negative interferences.

Using SPE methods, adsorption of prostanoids is routinely and efficiently done by a straight-phase material like silic acid or by a reversed-phase C_{18} material. Clean up and washing steps using eluents of rising polarity for silica-based columns (e.g., increasing content of methanol in an ether–hexane–toluene mixture) or decreasing polarity for octadecyl columns [e.g., increasing content of acetonitrile (ACN), ethanol, or ethyl acetate in an aqueous mixture] enable sufficient extraction. These stepwise and fractionating procedures allow consecutive elution of different substance classes like polar compounds (polar lipids), fatty acids and their monohydroxy derivatives, PGs and TXs, and hydrophilic components. Recoveries for all prostanoids are in the range 90–98%. Recent applications—especially for synthetic drugs—make use of the macroporous OASIS HLB material, which allows combined hydrophilic–lipophilic interactions with the analyte. This adsorbent is a copolymer of divinylbenzene (lipophilic) and *N*-vinylpyrrolidone (hydrophilic) applicable in cartridges or 96-well plate formats.[9] Extracts are evaporated to dryness prior to further processing.

For avoiding these manual and time-consuming extraction methods, the use of packed precolumns coupled to reversed-phase (RP)-HPLC equipped with a conventional six-port injector is a suitable alternative, especially for small sample volumes. Techniques for online sample preparation combined with two-dimensional (2-D) HPLC allow PG extraction on a strong cation exchange material directly transferable onto RP-separation columns as recently described for the analysis of cell culture supernatants with tandem MS (MS/MS) detection.[10]

DERIVATIZATION[11–14]

Owing to the low physiological concentrations in the femtomolar to picomolar range and the very weak UV absorptivity of prostanoids, derivatization is often required when analyzing by HPLC procedures. Many methods that improve detection sensitivity and selectivity have been developed allowing the quantitative and qualitative determination of these eicosanoids. Most of these techniques represent a selective and rapid precolumn derivatization of the extracted sample. Many procedures, especially for esterification of the carboxylic function, have been established. In the following discussion, the stationary phases used for the separation of derivatized PGs are indicated in parentheses. Fluorescent derivatives with exceedingly high UV absorptivities can be obtained in almost quantitative yields by *p*-(9-anthroyloxy)-phenacyl bromide, also known as panacylbromide

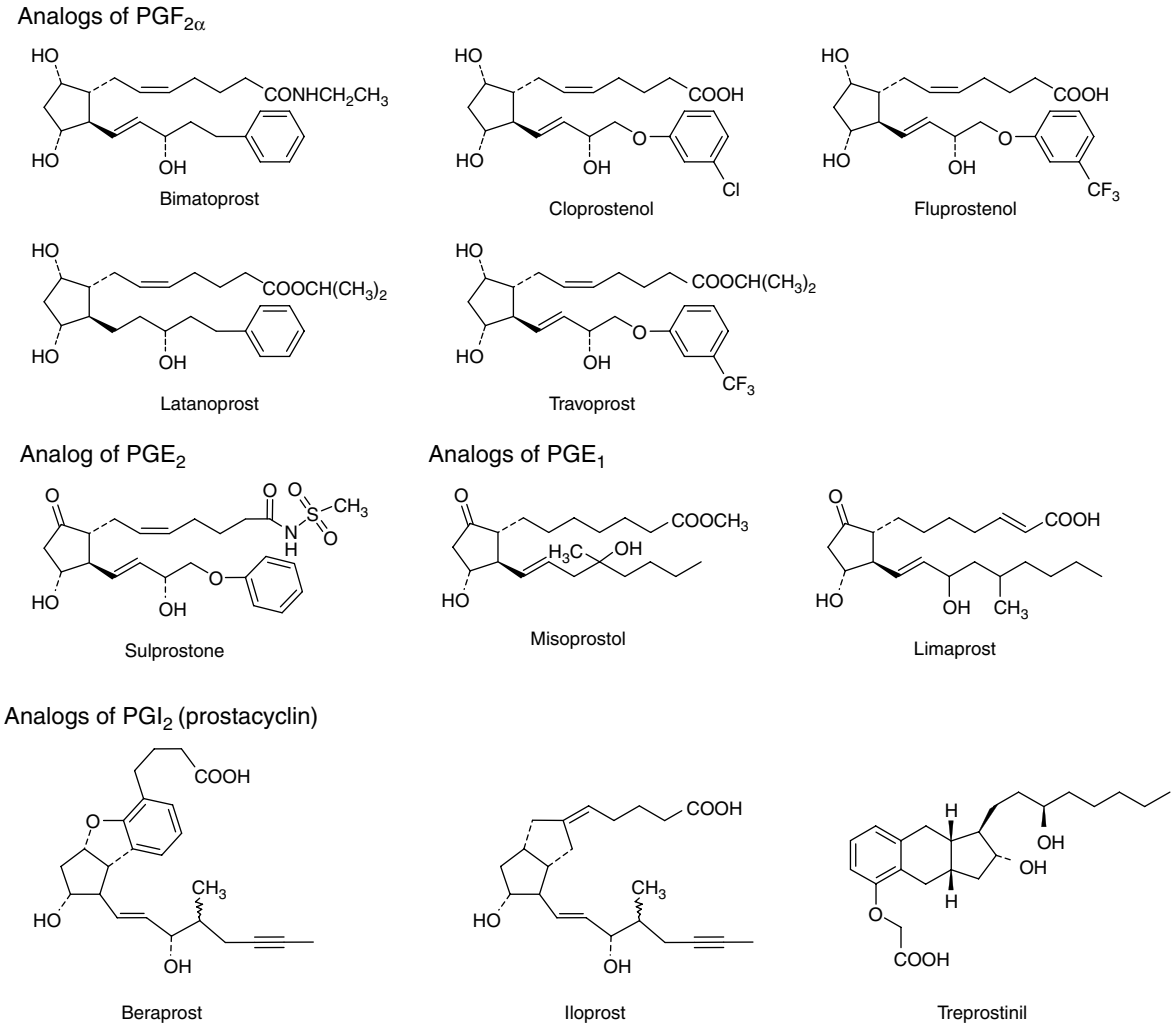

Fig. 3 Chemical structures of common synthetic prostanoid drugs.

(LiChrosorb 100 Diol, or μ-Bondapak C18, or Radial Pak B). Panacyl esters are produced within 0.5–2 hr under mild reaction temperatures between 20°C and 45°C. This reaction requires alkaline reagents like KOH or K_2CO_3 as catalysts in an organic solvent and, additionally, crown ethers as phase-transfer agents. Ultraviolet detection is possible at 254 nm combined with fluorescence detection at about 450 nm after excitation at about 360 nm. Interferences of native fluorescent compounds are weak owing to their emission wavelength range of 300–400 nm.

Comparable phenacyl esters are synthesized with *p*-bromophenacyl bromide or *p*-nitrophenacyl bromide with a similar spectroscopic behavior (both μ-Bondapak C18). Useful derivatization by tagging the COOH group can also be done with α-bromo-2′-acetonaphthone resulting in well-soluble and strongly UV-absorbing (254 nm) naphthanyl esters after a reaction time of only 10 min at ambient temperature (LiChrosorb Si-100). Furthermore, coumarin derivatives (substituted at position 7 for higher fluorescence quantum yields) are predestinated to fluorescent ester preparation (λ_{ex} ~330–390 nm and λ_{em} ~410–470 nm) using 4-bromomethyl-7-methoxycoumarin (LiChrosorb 100 Diol or Varian CN-10 Micropak) or 4-bromomethyl-7-acetoxycoumarin (BrMAC) (LiChrosorb RP18). In addition, 2-(2,3-naphthalimino)ethyl trifluoromethanesulfonate (NE-OTf) was introduced to derivatize the carboxyl groups of eicosanoids, enabling analyte fluorescence detection at 396 nm after excitation at 260 nm (Symmetry C18). These derivatives are also very well-detectable in the positive-selected ion mode by electrospray ionization (ESI)–MS (Fig. 4). Luminarin-4 (a labeling reagent with a quinolizinocoumarin structure) in combination with peroxyoxalate (Ultraspher ODS-2 or Spherisorb ODS-2) enables chemiluminescence detection. These reactions requiring catalysis and phase-transfer agents are carried out under more drastic conditions at about 70°C in aprotic solvents. When using BrMAC, postcolumn hydrolysis of separated PG esters, which results in detection limits of about 10 fmol, is neccessary for online detection of the fluorophore. Hydrazone or amide derivatives

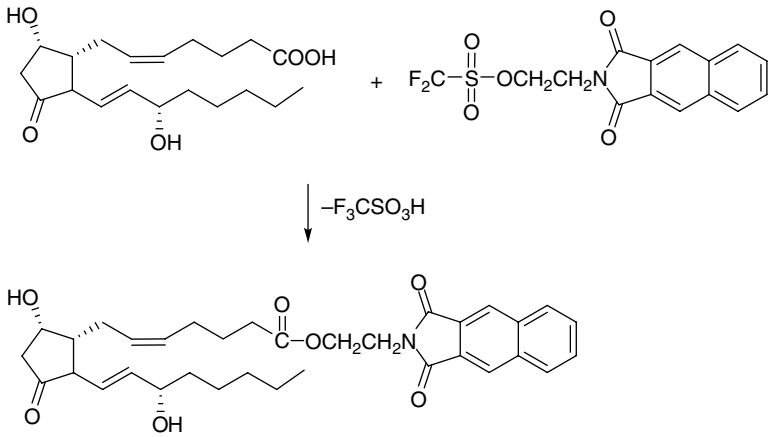

Fig. 4 Derivatization of PGD_2 with 2-(2,3--naphthalimino)ethyl trifluoromethanesulfonate (NE-OTf) for fluorescence and mass spectrometric detection.
Source: From Fast and simple online sample preparation coupled with capillary LC–MS/MS for determination of prostaglandins in cell culture supernatants, in J. Sep. Sci.[10]

are also suitable for fluorescence detection as well as 3-bromomethyl-6,7-dimethoxy-1-methyl-2(1H) quinoxalinone (YMC Pack C8) and 4-(*N,N*-dimethylaminosulfonyl)-7-(1-piperazinyl)-2,1,3-benzoxadiazole (DBD-PZ, $\lambda_{ex} = 440$ nm, $\lambda_{em} = 569$ nm), for converting the COOH group of numerous natural PGs within 30 min at room temperature, or 9-anthroyldiazomethane (ADAM) characterized by its low stability (Nucleosil ODS-silica). Electrochemical detection of readily reduced active compounds can be carried out with low applied potential owing to low background current and noise level in the oxidative mode after COOH derivatization using compounds with aromatic structures like 2,4-dimethoxyaniline (Nucleosil C18), 2-bromo-2′-nitroacetophenone, *p*-nitrobenzyloxyamine, or 2,4-dinitrophenylhydrazine. Thermospray (TSP)–MS detection has been used after esterification with diazomethane followed by oxime synthesis using trimethylanilinium hydroxide (TMAH) and separation on Zorbax ODS.

In addition to the derivatization of the COOH function, PGs can also be modified using their hydroxyl functions. Oxidation with pyridinium dichromate to 15-oxo-PGs enables UV detection at 230 nm on account of the conjugated oxo and C13=C14 double bonds (Microbore C18). Analysis using TSP–MS in the positive-ion mode is possible after overnight reaction at 5°C with acetic anhydride in pyridine to form acetyl derivatives capable of better chemical ionization. About 20 PGs have been determined in the range of 0.5–10 pmol using the selected ion monitoring (SIM) method without a gradient system (Nucleosil 100-5C18).[15] Combined derivatization to panacyl esters prior to methoximation using methoxamine hydrochloride enables good chromatographic separations, especially for the hemiacetalic TXB_2 and $PGF_{2\alpha}$ (Ultraspher ODS C18 or LiChrocart Superspher 100-RP-18). Furthermore, oxo functions present in most PGs can be modified to *p*-nitrobenzyloximes at 40°C within 2 hr, after methyl ester formation by diazomethane, allowing UV detection at 254 nm (μ-Bondapak C18).

In general, quantitative analyses are carried out as usual, using internal or external standards and calibration curves. Detection limits in the lower picogram range can be achieved depending on the selected derivatization procedure.

MOBILE AND STATIONARY PHASES[6,11,16]

In most cases, PGs or their derivatives are separated by partition chromatography on reversed-phase columns using gradients of organic solvents and water with increasing organic content during elution. ACN enables better separation than MeOH when combined with aqueous media acidified using HOAc, trifluoric acid, or phosphoric acid. Separated by rising hydrophobicity, pure PGs are eluted typically in the following order of retention times: 6-oxo-$PGF_{1\alpha}$ < TXB_2 < $PGF_{2\alpha}$ < PGE_2 < PGD_2 < 13,14- dihydro-15-oxo-$PGF_{2\alpha}$ < 13,14-dihydro-15-oxo-PGE_2 < PGA_2 < PGB_2. Monohydroxy metabolites of AA and other fatty acids often present in PG-containing samples are eluted at much higher content of organic solvents, demanding a wide-range gradient.

Early PG analysis using HPLC techniques was carried out as adsorption chromatography on normal-phase (NP) columns packed with silica or alumina. A non-polar mobile phase consisting of organic solvents (hexane, toluene, ethyl acetate, and HOAc) allows separation of PGs that are unstable in aqueous media (e.g., PGH_2 on cyano- or phenyl-bonded phases). Usually, the injection medium must be fairly polar to dissolve the PGs. This is achieved by the addition of small volumes of isopropanol resulting in much poorer resolution of monohydroxy acids simultaneously analyzed. Furthermore, NP chromatography enables excellent separation of geometrical isomers like PGE_2 and PGD_2. The lock–key type steric fitting of solute molecules with the discrete adsorption sites of the silica surface is responsible for this effect. However, adsorption chromatography requires a strict control of

temperature, as it influences retention time and, therefore, reproducibility and ruggedness.

Besides the dominating NP and RP techniques, silver-ion-loaded cation- and strong-anion-exchange chromatographies have been introduced as well. The silver-ion method, based on interactions between Ag^+ and double bonds and polar–polar attractive forces between the stationary phase and the solute, is carried out using polar solvents containing low concentrations of ACN. The separation of *cis–trans* isomers can be achieved by this chromatographic modification. Anion-exchange chromatography has been described for underivatized PGs using tromethamine acetate–ACN mixtures at neutral pH as mobile phase and a pellicular strong anion-exchange column as stationary phase.

However, NP or RP methods represent the most powerful and common chromatographic techniques allowing PG analysis with very good reproducibility, sensitivity, wide linear ranges for quantitative analysis, and a broad spectrum of detectors.

RADIO- AND UV DETECTION[3,6,11,15,17]

For investigating metabolization or stability of prostanoids, radiolabeled precursors or analytes are often used. The tritiated or ^{14}C-labeled compounds can easily be detected without any further derivatization using online or off-line liquid scintillation, which is not impaired by any interferences from matrix components. Efficient, though less sensitive, PG analysis is possible by UV detection (190–210 nm) of underivatized substances, which demands the removal of interfering contaminants or simple sample matrices like buffers or some cell supernatants.

LC–MS ANALYSIS[9,10,18–24]

During the last few years, the reliability and sensitivity of modern mass spectrometric equipment has improved, and interface technologies for online detection of HPLC eluates that have a broad applicability have been introduced. ESI and atmospheric pressure chemical ionization (APCI) sources were designed to operate with high aqueous chromatographic flow rates (>1 ml/min) allowing the selective detection of cationic analytes in the positive-ion mode or anionic analytes in the negative-ion mode. Owing to technical advancement LC–MS today represents a reliable alternative to the traditionally used GC–MS methods applied in a constantly rising number of studies. The soft ESI conditions prevent fragmentation of prostanoids during the ionization process, enabling the detection of intact molecules in the full-scan mode. Subsequent optional fragmentation by collision-induced dissociation (CID) in the mass analyzer during MS/MS generates specific fragments (product ions) which are of highest value for the identification of compounds. Furthermore, LC–MS allows the quantification of PGs and related compounds without derivatization and long chromatographic separation times, and at the same time characterized by lower limits of detection and quantification of approximately 10 pg/ml of sample fluid. Highly selective detection in the negative selected reaction monitoring (SRM) mode enables simultaneous measurement of multiple analytes even if they coelute. These outstanding features are highly important for the investigation of iPs, which naturally appear in various endogenous isoforms of identical molecular weights. Usually, LC–ESI–MS/MS measurements are performed on triple quadrupole mass spectrometers to detect the underivatized singly charged quasi-molecular ion $[M–H]^-$ resulting from the loss of a proton. Negative ionization is supported by the use of ammonium acetate buffer at a basic pH (about 7.4–9). The corresponding MS/MS fragmentation pattern often shows a typical loss of 44 amu owing to the cleavage of the carboxylate anion, as well as further signals allowing the unambiguous assignment to individual molecular structures. Characteristic transitions from parent ions to product ions increase method selectivity and the signal-to-noise ratio, which are important for low limits of quantification. Quantitative analyses of PGs and iPs from cell culture medium, urine, or organ extracts are often performed using related tetradeuterated compounds as internal standards resulting in excellent precision and accuracy. On account of these obvious advantages, LC–MS/MS procedures are highly valuable for quantitative screening approaches of eicosanoids in biological fluids including not only prostanoids but also leukotrienes as recently demonstrated in the investigation of 23 analytes in rat kidney tissue.[25]

Nowadays, especially pharmaceutical applications make use of the highly selective and sensitive LC–MS/MS methods for both qualitative and quantitative analysis. Depending on the structure of the synthetic prostanoids, product ions of highest intensity generated by CID may be derived from larger non-natural substituents, e.g., 3-trifluoromethylphenolate (from travoprost or fluprostenol, Fig. 3).[22]

Reliable hardware and software tools for coupling techniques and system control have enabled the establishment of more complex two- or multidimensional HPLC systems, which allow consecutive chromatographic steps performed online on different stationary phases also including steps of analyte trapping or sample preparation.[9,26,27]

In contrast to the commonly applied ESI negative-ion mode, a sophisticated method has been described using postcolumn addition of a $AgBF_4$ solution in isopropanol as a cationization reagent for neutral lipids. The resulting adducts of the analyte and silver cations allow the MS detection in the positive mode. This technique has been successfully applied to the discovery of PGE_2 methyl ester 15-acetate isolated from gorgonian corals.[28] Although derivatization procedures are unusual for LC–MS analyses of PGs and iPs, pentafluorobenzyl (PFB) bromide has been

used to modify the COOH group for subsequent LC–APCI–MS/MS investigations. The resulting PFB derivatives dissociate during electron capture ionization liberating a free PFB radical and an anionic analyte detectable by the negative-ion mode MS.[29] Despite the anionic properties of dissociated prostanoids, unusual detection in the positive ESI mode was also reported targeting ammoniated molecules produced during chromatographic separation in the presence of ammonium acetate.[30]

SPECIAL FEATURES OF HPLC IN PROSTAGLANDIN ANALYSIS

Besides quantitative determinations of endogenous PGs, HPLC techniques have been used for some special features in clinical, chemical, and pharmaceutical research, including investigations of stability, metabolization and enantiomeric purity, thermodynamic characterizations of chemical equilibria, validation of immunological methods by matrix separations, and preparative purifications.[5,6,8,11,16,31,32]

CONCLUSIONS

Methods based on HPLC for the quantitative or qualitative analysis of PGs, iPs, and prostanoid drugs are widely used as reliable and sensitive procedures. As UV detection of unlabeled analytes is often of insufficient selectivity and sensitivity, especially for complex biological samples, derivatization protocols have been introduced for transforming the lipid analytes into strongly fluorescent or UV-absorbing compounds. Modern MS detection overcomes the drawbacks of time-consuming derivatization steps, thus allowing direct measurement of natural compounds by LC–ESI–MS/MS technologies. Formation of the quasi-molecular ion $[M–H]^-$ enables straightforward, comfortable, and rapid analysis in the negative-ion mode. Subsequent collision-induced fragmentation in MS/MS experiments provides additional information for structure elucidation and confirmation. Thus, HPLC techniques are highly important tools of instrumental analysis in prostaglandin research used for quantification, identification, and elaboration of thermodynamic equilibria and chemical or physiological reactions.

REFERENCES

1. Hamberg, M.; Samuelsson, B. Prostaglandin endoperoxides. Novel transformations of arachidonic acid in human platelets. Proc. Natl. Acad. Sci. U.S.A. **1974**, *71* (9), 3400–3404.
2. Rokach, J.; Kim, S.; Bellone, S.; Lawson, J.A.; Pratico, D.; Powell, W.S.; FitzGerald, G.A. Total synthesis of isoprostanes: Discovery and quantitation in biological systems. Chem. Phys. Lipids **2004**, *128* (1–2), 35–56.
3. Gao, L.; Zackert, W.E.; Hasford, J.J.; Danekis, M.E.; Milne, G.L.; Remmert, C.; Reese, J.; Yin, H.; Tai, H.H.; Dey, S.K.; Porter, N.A.; Morrow, J.D. Formation of prostaglandins E_2 and D_2 via the isoprostane pathway. J. Biol. Chem. **2003**, *278* (31), 28479–28489.
4. Powell, W.S. Rapid extraction of arachidonic acid metabolites from biological samples using octadecylsilyl silica. Methods Enzymol. **1982**, *86*, 467–477.
5. Powell, W.S.; Colin, D.F. Metabolism of arachidonic acid and other polyunsaturated fatty acids by blood vessels. Prog. Lipid Res. **1987**, *26* (3), 183–210.
6. Green, K.; Hamberg, M.; Samuelsson, B.; Frölich, J.C. Extraction and chromatographic procedures for purification of prostaglandins, thromboxanes, prostacyclin, and their metabolites. In *Advances in Prostaglandin and Thromboxane Research*; Frölich, J.C. Ed.; Raven Press: New York, 1978; Vol. 5, 15–38.
7. Lawson, J.A.; Li, H.; Rokach, J.; Adiyaman, M.; Hwang, S.W.; Khanapures, S.P.; FitzGerald, G.A. Identification of two major F_2 isoprostanes, 8,12-iso- and 5-epi-8,12-iso-isoprostane $F_{2\alpha}$-VI, in human urine. J. Biol. Chem. **1998**, *273* (45), 29295–29301.
8. John, H.; Schlegel, W. Thermodynamic and structural characterization of *cis–trans* isomerization of 12-*S*-hydroxy-(5*Z*,8*E*,10*E*)-heptadecatrienoic acid by high-performance liquid chromatography and gas chromatograpy–mass spectrometry. Chem. Phys. Lipids **1999**, *95* (2), 181–188 and *97* (2), 195–196.
9. Lee, J; Kim, H.; Jeong, J.C.; Park, E.S.; Hwang, K.W.; Yang, S.J.; Jeong, J.H. Determination of beraprost in human plasma by high-performance liquid chromatography–tandem mass spectrometry. J. Chromatogr. B, **2007**, *859*, 229–233.
10. Rinne, S.; Ramstad Kleiveland, C.; Kassem, M.; Lea, T.; Lundanes, E.; Greibrokk, T. Fast and simple online sample preparation coupled with capillary LC–MS/MS for determination of prostaglandins in cell culture supernatants. J. Sep. Sci. **2007**, *30*, 1860–1869.
11. Toyóoka, T. Use of derivatization to improve the chromatographic properties and detection selectivity of physiologically important carboxylic acids. J. Chromatogr. B, **1995**, *671* (1–2), 91–112.
12. Blau, K.; Halket, J. *Handbook of Derivatives for Chromatography*; 2nd Ed.; John Wiley & Sons: Chichester, New York, Brisbane, Toronto, Singapore, 1993.
13. Yue, H.; Strauss, K.I.; Borenstein, M.R.; Barbe, M.F.; Rossi, L.J.; Jansen, S.A. Determination of bioactive eicosanoids in brain tissue by sensitive reversed-phase liquid chromatographic method with fluorescence detection. J. Chromatogr. B, **2004**, *803* (2), 267–277.
14. Toyoòka, T.; Ishibashi, M.; Terao, T.; Imai, K. Sensitive fluorometric detection of prostaglandins by high performance liquid chromatography after precolumn labeling with 4-(*N*,*N*-dimethylaminosulphonyl)-7-(1-piperazinyl)-2,1,3-benzoxadiazole (DBD-PZ). Biomed. Chromatogr. **1992**, *6*, 143–148.
15. Yamane, M.; Abe, A. High-performance liquid chromatography–thermospray mass spectrometry of prostaglandin

and thromboxane acetyl derivatives. J. Chromatogr. **1991**, *568* (1), 11–24.
16. Hamilton, J.G.; Karol, R.J. High performance liquid chromatography (HPLC) of arachidonic acid metabolites. Prog. Lipid Res. **1982**, *21* (3), 155–170.
17. Alix, E.; Schmitt, C.; Strazielle, N.; Ghersi-Egea, J.F. Prostaglandin E_2 metabolism in rat brain: Role of the blood–brain interfaces. Cerebrospinal Fluid Res. **2008**, *5* (5) (doi:10.1186/1743-8454-5-5).
18. Takabatake, M.; Hishinuma, T.; Suzuki, N.; Chiba, S.; Tsukamoto, H.; Nakamura, H.; Saga, T.; Tomioka, Y.; Kurose, A.; Sawai, T.; Mizugaki, M. Simultaneous quantification of prostaglandins in human synovial cell-cultured medium using liquid-chromatography/tandem mass spectrometry. Prostaglandins Leukot. Essent. Fatty Acids **2002**, *67* (1), 51–56.
19. Li, H.; Lawson, J.A.; Reilly, M.; Adiyaman, M.; Hwang, S.W.; Rokach, J.; FitzGerald, G.A. Quantitative high performance liquid chromatography/tandem mass spectrometric analysis of the four classes of F_2-isoprostanes in human urine. Proc. Natl. Acad. Sci. U.S.A. **1999**, *96* (23), 13381–13386.
20. Murai, Y.; Hishinuma, T.; Suzuki, N.; Satoh, J.; Toyota, T.; Mizugaki, M. Determination of urinary 8-epi-prostaglandin $F_{2\alpha}$ using liquid chromatography–tandem mass spectrometry: Increased excretion in diabetics. Prostaglandins Other Lipid Mediat. **2000**, *62* (2), 173–181.
21. Kempen, E.C.; Yang, P.; Felix, E.; Madden, T.; Newman, R.A. Simultaneous quantification of arachidonic acid metabolites in cultured tumor cells using high-performance liquid chromatography/electrospray ionization tandem mass spectrometry. Anal. Biochem. **2001**, *297* (2), 183–190.
22. McCue, B.A.; Cason, M.M.; Curtis, M.A.; Faulkner, R.D.; Dahlin, D.C. Determination of travoprost and travoprost free acid in human plasma by electrospray HPLC/MS/MS. J. Pharm. Biomed. Anal. **2002**, *28*, 199–208.
23. Cao, H.; Xiao, L.; Park, G.; Wang, X.; Azim, A.C.; Christman, J.W.; van Breemen, R.B. An improved LC–MS/MS method for the quantification of prostaglandins E_2 and D_2 production in biological fluids. Anal. Biochem. **2008**, *372*, 41–51.
24. Haschke, M.; Zhang, Y.L.; Kahle, C.; Klawitter, J.; Korecka, M.; Shaw, L.M.; Christians, U. HPLC–atmospheric pressure chemical ionization MS/MS for quantification of 15-F_{2t}-isoprostane in human urine and plasma. Clin. Chem. **2007**, *53* (3), 489–497.
25. Blewett, A.J.; Varma, D.; Gilles, T.; Libonati, J.R.; Jansen, S.A. Development and validation of high-performance liquid chromatography–electrospray mass spectrometry method for the simultaneous determination of 23 eicosanoids. J. Pharm. Biomed. Anal. **2008**, *46*, 653–662.
26. Komaba, J.; Masuda, Y.; Hashimoto, Y.; Nago, S.; Takamoto, M.; Shibakawa, K.; Nakade, S.; Miyata, Y. Ultra sensitive determination of limaprost, a prostaglandin E1 analogue, in human plasma using on-line two-dimensional reversed-phase liquid chromatography–tandem mass spectrometry. J. Chromatogr. B, **2007**, *852*, 590–597.
27. Roston, D.A.; Wijayaratne, R. Two-dimensional liquid chromatographic method for resolution of prostaglandin enantiomers. Anal. Chem. **1988**, *60*, 950–958.
28. Schneider, C.; Manier, M.L.; Hachey, D.L.; Brash, A.R. Detection of the 15-acetate of prostaglandin E_2 methyl ester as a prominent component of the prostaglandins in the gorgonian coral plexaura homomalla. Lipids **2002**, *37* (2), 217–221.
29. Lee, H.S.; Williams, M.V.; DuBois, R.N.; Blair, I.A. Targeted lipidomics using electron capture atmospheric pressure chemical ionization mass spectrometry. Rapid Commun. Mass Spectrom. **2003**, *17* (19), 2168–2176.
30. Eichold, T.H.; Kuhlenbeck, D.L.; Baker, T.R.; Stella, M.E.; Amburgey, J.S.; deLong, M.A.; Hartke, J.R.; Cruze, C.A.; Pierce, S.A.; Wehmeyer, K.R. Use of short high-performance liquid chromatography columns and tandem-mass spectrometry for the rapid analysis of a prostaglandin analog, fluprostenol, in rat plasma. J. Chromatogr. B, **2000**, *741*, 213–220.
31. John, H.; Schlegel, W. Reversed-phase high-performance liquid chromatographic method for the determination of the 11-hydroxythromboxane B_2 anomers equilibrium. J. Chromatogr. B, **1997**, *698* (1–2), 9–15.
32. John, H.; Schlegel, W. Structural and thermodynamic investigations of metabolites of the thromboxane synthase pathway. Anal. Chim. Acta **2002**, *465* (1–2), 441–450.

Protein Immobilization

Jamel S. Hamada
Southern Regional Research Center, Agricultural Research Service, U.S. Department of Agriculture (USDA-ARS), New Orleans, Louisiana, U.S.A.

INTRODUCTION

Affinity chromatography is a powerful high-resolution separation technique for biomolecules. It is based on a highly specific and unique stereochemical interactions between biomolecules. Examples of these interactions are the binding of enzymes to coenzymes and inhibitors and the interactions between antigens (e.g., protein A) and antibodies. In affinity chromatography, a ligand is covalently bound to a solid matrix which is packed into a chromatography column. A mixture of components is then applied to the column. The unbound contaminants, which have no affinity for the ligand, are washed through the column, leaving the desired component (protein, peptide, etc.) bound to the matrix. Elution is accomplished by changing the pH and/or salt concentration or by applying organic solvents or a molecule which competes for the bound ligand. The purpose of this entry is to review methods for immobilization of protein ligands for affinity chromatography.

MATRIX MATERIAL (CARRIER)

Immobilized ligand is prepared by covalently attaching the biospecific ligand to a chromatographic bed support material, the matrix. A variety of insoluble support materials are used as matrices in affinity chromatography. These include agarose, cellulose, crosslinked dextran, polystyrene, polyacrylamide gels, and porous silica gels. The majority of matrices used in affinity chromatography are either agarose based or polyacrylamide based. The available reactive groups on these matrices are hydroxyl and amide nitrogen groups, respectively. By far the most popular support materials in use are beaded derivatives of agarose due to their ideal physical and chemical characteristics that are necessary for ligand immobilization. For instance, Sepharose, a bead-formed agarose gel manufactured by Amersham Pharmacia Biotech, has virtually all the features required of a successful matrix for immobilizing biologically active molecules. The hydroxyl groups on the sugar residues can easily be used to covalently attach a ligand. Sepharose 4B (Amersham Pharmacia Biotech) is the most popular and widely used matrix. Its advantages include open-pore structure, molecular exclusion limit of 20×10^6 Da, easy and good binding capacities, and low non-specific attachment. A spacer arm, which is interposed between the matrix and ligand, is sometimes needed to facilitate the binding particularly when coupling small molecules (e.g., enzyme cofactors). Spacer arms are also useful for coupling ligands containing free carboxyl or amine groups and for further chemical reactions to permit the attachment of phenolic groups and diazonium derivatives to agarose matrix.

PROTEIN LIGANDS

Protein ligands most commonly used in affinity chromatography are as follows: (a) protein with very high specific affinity for moieties on the desired protein; a wide range of plant lectins with a variety of sugar specificities are used as ligands to purify glycoproteins and enzymes having sugar moieties in their structures; (2) immobilized antibodies, which represent the ideal affinity separation because of the precise specificity of many antibodies, particularly monoclonial antibodies, to their specific antigens; (3) proteins or enzymes with unique affinity for other proteins or peptides, which are used as affinity ligands for the particular proteins or peptides.

PREPARATION OF IMMOBILIZED PROTEINS

The immobilization of proteins and enzymes through covalent bond formation between the protein or enzyme and an activated insoluble carrier entails two processes of activation and coupling. These procedures are classified on the basis of the type of reaction that facilitates the bonding between the protein and the insoluble carrier. Mostly, with matrices containing readily available hydroxyl groups such as agarose derivatives, a variety of activation procedures are used, after which the amino groups of protein ligands are readily incorporated into the matrix (coupling reaction). After coupling of the protein ligands to the matrix, unreacted activated coupling groups are usually hydrolyzed to inactive derivatives during washing of the coupling resin at lower pH. Alternatively, these groups can be blocked by adding an excess of an inert blocking reagent. The following methods are most commonly used for activation and coupling of protein ligands to agaraose and other matrices.

Cyanogen Bromide Activation Method

The aim of the reaction of cyanogine bromide with hydroxyl groups on agarose matrix is to produce reactive carrier to which proteins can be coupled through amino groups. Cyanogen bromide activation method is the most used method for the preparation of affinity gels because of its simplicity and its mild reaction conditions, particularly for immobilizing sensitive proteins such as enzymes and antibodies. Cyanogen bromide reacts with these hydroxyl groups and converts them to imidocarbonate groups, as shown in Fig. 1. Agarose activated with cyanogen bromide have been used to bind a variety of proteins and enzymes. The activated groups react with primary amino groups of a protein ligand to form isourea linkages according to the reactions in Fig. 1.

Acylation Reactions

In this type of protein immobilization, reactions involve the acylation of an NH_2 group on a protein or an enzyme by pendent groups of the carrier such as azide, acid anhydride, carbodiimide, sulfonyl chloride, and hydroxysuccinimide esters. Copolymers of acrylamide and maleic anhydride have been useful for enzyme immobilization through the acid anhydride reaction with the enzyme. This system of

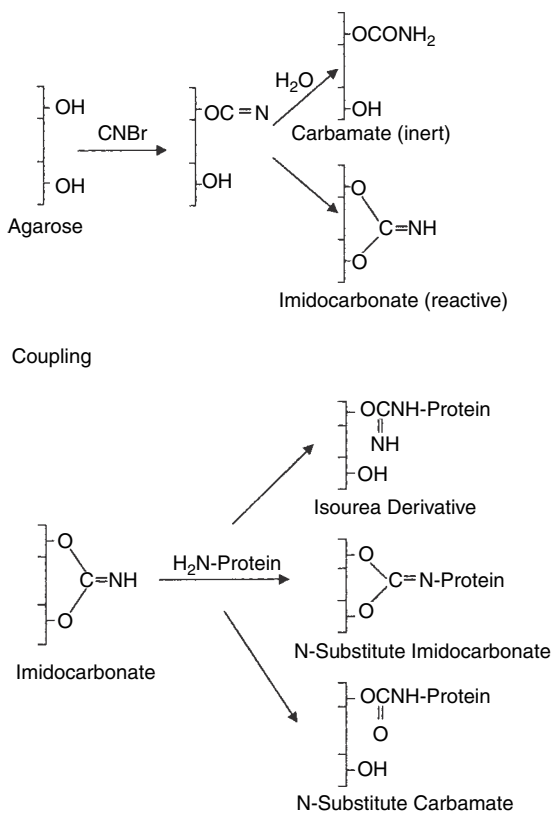

Fig. 1 Immobilization of protein ligands on agarose (activation and coupling) by cyanogen bromide.

protein immobilization involves the use of a reagent that contains an acylating or alkylating agent and a group which can form a covalent link with a carrier polymer. For instance, few protein immobilization methods are based on condensation by carbodimides (e.g., dicyclohexylcarbodimide). Mixing the carbodiimide reagent with the matrix and a protein ligand, stable amide bonds can be formed between an amino group on the ligand and a carboxyl group of matrix (or vise versa) in a one-step procedure of activation and coupling as follows:

$$R{-}COOH + R_1N{=}C{=}NR_2 \rightarrow R{-}C(NHR_1){-}O{-}C{=}NR_2$$

Soluble protein — Carbomiide — Immobilized protein

Arylation Reactions

Arylation or alkylation are used for activation of support and linking of a protein ligand. In such reactions, the functional group on the carrier combines with an NH_2 group of the protein (e.g., by 3-fluoro-4,6-dinitrophenyl group or 2–4 dichloro-*S*-triazine). In this approach, a chloro-*S*-triazine is coupled to an arylazide. The azide is converted to a nitrene, which upon activation by light reacts with a polymer carrier to form a covalent bond. The chlorotriazine then couples with the protein.

Alkylation Reactions by Bisepoxirane, Epichlorohydrin, and Divinylsulfone

Bisepoxirans activations allows the coupling of ligands containing —OH, —NH_2, and —SH groups with agarose matrix. Here, the ligands are provided automatically with a hydrophilic spacer arm.

Organic Sulfonyl Chlorides, Tosyl and Tresylchloride Methods

These methods enable the activation and the coupling of ligands containing —NH_2 and —SH groups with matrices such as agarose, cellulose, or silica derivatives.

Methods for Polyacrylamide Matrices

The glutaraldehyde and hydrazine reactions are used for matrices having amide groups such as polyacrylamide. Glutaraldehyde and hydrazine react with the polymer, and the enzyme or protein is readily bound to the treated polymer. The mechanism of the reactions involved in the activation and coupling are not well understood. In general, insoluble supports such as polyacrylamide, which tend to swell in water, form immobilized proteins or enzymes when mixed with a solution and treated with

Table 1 Activated affinity matrices marketed by two major soft-gel chromatography suppliers for coupling of protein ligands.

Matrix	Ligand specificity	Activator and functional groups	Manufacturer
CNBr-activated Sepharose 4B (or Fast Flow)	—NH_2	CNBr	Amersham Pharmacia Biotech
EAH Sepharose 4B	—COOH	Carbodiimide coupling via 6-carbon spacer arm	Amersham Pharmacia Biotech
ECH Sepharose 4B	—NH_2	Carbodiimide coupling via 6-carbon spacer arm	Amersham Pharmacia Biotech
Epoxy-activated Sepharose 6B	—NH_2, —OH, —SH	1,4-bis (2, 3-epoxypropoxy-butane)	Amersham Pharmacia Biotech
Activated Thiol Sepharose 4B	—SH, —C ═O, —CNH	Glutathione-2-pyridyl disulfide	Amersham Pharmacia Biotech
Affi-Gel 10 gel (or Affi-Prep 10, pressure stable)	—NH_2	*N*-Hydroxysuccinimide ester via 10-atom spacer arm	Bio-Rad Laboratories
Affi-Gel 15 gel	—NH_2	*N*-Hydroxysuccinimide ester via 15-atom spacer arm	Bio-Rad Laboratories
Affi-Gel 102 gel	—COOH	Carbodiimide coupling	Bio-Rad Laboratories
CM Bio Gel A	—NH_2	Carboxymethyl, carbodiimide coupling	Bio-Rad Laboratories

glutaraldehyde. Polyacrylamide support is activated by treatment with hydrazine (heated) followed by sodium nitrite in hydrochloric acid. The amino groups of protein ligands can then be coupled to the activated matrix via stable amide bonds.

AFFINITY SUPPORTS: ACTIVATED AND READY-TO-USE MEDIA

Chromatography suppliers offer affinity gels for a wide range of biomolecular applications. Availability of activated supports allows the users to make their own affinity matrix of choice by coupling a ligand such as an antibody, enzyme, antigen, or receptor. Ready-activated supports or matrices are less expensive than the ready-to-use matrices usually offered by the same manufacturer. These activated matrices are dependable and provide flexibility and convenience in affinity chromatography. With this particular option, the chromatographer has the choice of preparing affinity matrix by activating a support, then coupling or only coupling using ready-to-use activated affinity supports. Table 1 shows the activated supports marketed by two major soft-gel chromatography suppliers that are suitable for coupling of affinity protein ligands.

On the other hand, ready-to-use matrices have a specific ligand already coupled to an affinity support. Amersham Pharmacia Biotech has developed a wide range of ready-to-use affinity gels with specific protein ligands coupled to the matrix. In specified bulletins, Amersham Pharmacia Biotech details the preparation procedures of these affinity gel columns containing immobilized proteins. Applications include monoclonal and polyclonal antibodies, fusion proteins, glycoproteins, enzymes, cells, and other proteins such as fibronectin, and membrane proteins. Likewise, Bio-Rad Laboratories offer two types of supports. One type such as Affi-Gel supports, based on agarose or polyacrylamide, are available as lowpressure gels suitable for most laboratory-scale affinity purification with a peristaltic pump or gravity flow elution. Affi-Prep supports, based on a pressurestable macroporous polymer, are suitable for preparative and process scale applications. The immobilized protein ligands in these ready-prepared matrices include lectins, protein A, gelatin, avidin, and calmodulin. Affi-Gel and Affi-Prep protein A supports are used to produce highly purified immunoglobulins (IgG), to selectively remove IgG prior to analysis of other immunoglobulin classes, or to adsorb immune complexes to purify antigens. Protein A from *Staphylococcus aureus* binds to the F_c region of immunoglobulins, especially IgG from mammalian species. Affi-Prep supports offer linear flow rates up to 2000 cm/hr, pressure stability up to 1000 psi (70 bar), and high chemical stability, according to the manufacturer.

CONCLUSIONS

In affinity chromatography, a ligand is covalently bound to a solid matrix by matrix activation and ligand coupling. In protein immobilization, a covalent bond is formed between

the protein ligand and an insoluble solid matrix or carrier. Most of protein immobilization steps entail the formation of the insoluble immobilized proteins on crosslinked agarose gels. Most common reactions used in making immobilized proteins and enzymes are discussed. These processes are classified on the basis of the type of reaction which forms the covalent bond between the protein and the insoluble carrier. Also, a wide range of commercial ready-to-use supports with specific protein ligands already coupled to a base matrix are discussed.

BIBLIOGRAPHY

1. Bell, J.E.; Bell, E.T. Protein purification: affinity chromatography. In *Proteins and Enzymes*; Prentice-Hall: Englewood Cliffs, NJ, 1988; 45–63.
2. Carlsson, J.; Janson, J.-C.; Sparrma, M. Affinity chromatography. In *Protein Purification: Principles, High Resolution Methods, and Applications*; Janson, J.C., Ryden, L., Eds.; VCH: New York, 1989; 275–329.
3. Dunlab, R.B. *Immobilized Biochemicals and Affinity Chromatography*; Plenum Press: New York, 1974.
4. Ganttsos, G.; Barker, P.E. *Preparative and Production Scale Chromatography*; Cazes, J., Ed.; Chromatographic Science Series; Marcel Dekker, Inc.: New York, 1993.
5. Kennedy, J.F.; White, C.A. Principle of immobilization of enzymes. In *Handbook of Enzyme Biotechnology*; Wiseman, A., Ed.; Ellis Horwood: Chichester, 1986; 147–207.
6. Low, C.R.L. *Affinity Chromatography*; John Wiley International: London, 1974.
7. Pharmacia Fine Chemicals. *Affinity Chromatography: Principles & Methods*; Pharmacia Fine Chemicals: Uppsala, 1978.
8. Schott, H. *Affinity Chromatography*; Chromatographic Science Series; Marcel Dekker, Inc.: New York, 1984; Vol. 27.
9. Scouten, W.H. *Affinity Chromatography*; John Wiley & Sons: New York, 1981.
10. Sofer, G.K. Current applications of chromatography in biotechnology. Bio/Technol. **1986**, *4* (8), 712–715.

Proteins: Affinity Ligands

Ji-Feng Zhang
Massachusetts Institute of Technology, Cambridge, Massachusetts, U.S.A.

INTRODUCTION

Affinity chromatography using proteins as ligands explores the three-dimensional complementary molecular interactions between the ligand and its target. This non-covalent and reversible binding are the results of ionic interaction, hydrophobic interaction, hydrogen-bonding, and van der Waals–London forces. The binding constant between the immobilized ligand and the target molecule ranges from $10^4/M$ to $10^8/M$. The multiplicity of the interaction forces offers the superior specificity to protein-based affinity chromatography for biomolecule separation among all the chromatographic techniques.

DISCUSSION

After the protein ligand is immobilized on a matrix support, a crude sample mixture, including the desired substance, is loaded into the affinity column under appropriate conditions. If the desired molecule forms a stable and reversible complex with the protein ligand, it will be retained and all the other contaminants are washed away. Then, the eluting buffer disrupts the binding between the desired substance and the protein ligand to recover the substance. When the interaction between the desired molecule and the ligand is too weak to form a stable complex with the ligand, it is eluted later than all the other substances in the crude sample and an eluting buffer is not required.

Protein-based affinity chromatography has found wide applications in both academic and industrial settings. The affinity chromatography using proteins as the ligand is an indispensable technique for recombinant protein purification. This review will touch the general aspects of matrix, immobilization of protein ligands, and the application of protein-based affinity chromatography. It is by no means an exhaustive review of the current technologies in protein-based affinity chromatography and only serves as an introduction to this topic. Interested readers should explore those articles listed in Bibliography for more information.

MATRIX

One of the key elements for protein-based affinity chromatography is the matrix, on which the protein ligand is immobilized. The ideal matrix material should have the following characteristics (Porath, 1974): insolubility, sufficient permeability, large surface area, strong mechanical strength, zero adsorption capacity, resistance to microbial and enzyme attack, chemical reactivity for coupling protein ligand, and stability under the operating conditions. Based on their physical strength, the matrices can be divided into two categories: low pressure and high pressure. For example, agarose, dextran, polyacrlyamide, and methacrylate are typical low-pressure matrices and silica and polystyrene–divinylbenzene are high-pressure matrices.

When a matrix is chosen in affinity chromatography applications, its advantages and disadvantages should be taken into account to assess its potentials and limitations. Agarose is hydrophilic and, therefore, its matrix surface has low non-specific binding. The presence of the hydroxyl group from agarose provides a convenient way for immobilizing the protein ligand. The drawbacks of agarose are its solubility in hot water and non-aqueous solutions and its susceptibility to microbial degradation. The lack of mechanical strength for agarose limits its application only in low-pressure operation and the separation process is slow. Silica and synthetic polymers are the alternative choices of matrix support. The major advantages for those matrix supports over agarose are their rigidity, reduced diffusion rate, and well-defined pore size (i.e., 5–20 μm in diameter). The above factors decide that those matrices can be operated in fast linear flow rate under high pressure to achieve rapid separation. Non-specific binding in silica-based matrices is a concern because of the negative-charged silanol groups and because also silica has increased solubility at alkaline pH.

IMMOBILIZATION

The unique specificity of affinity chromatography is the result of the complementary interaction between the protein ligand and the target in the separation

process. It is therefore essential to maintain the structure integrity of the protein ligand during immobilization of protein ligand. It is critical to consider the following in the immobilization step: (a) The binding site in the protein ligand should be accessible after the immobilization; (b) the amino acids located at the binding site should not be modified during the immobilization step; (c) the three-dimensional structure of the binding site should be maintained after the coupling step.

Usually, the immobilization of protein ligand is a two-step process: (1) activation and functionalization of the matrix and (2) coupling of the protein ligand to the modified matrix. To avoid the possible reactions between the rest of the activated sites and the protein components from the sample, a third step is often required to quench those activated sites after the protein ligand is coupled. The most exploited function groups for coupling from the protein ligand are the C-terminal carboxyl group, the carboxyl groups of glutamic and aspartic acids, the N-terminal α-amino group, and the ϵ-amino group of lysine. Sometimes, phenolic hydroxyl groups of tyrosine, imidazole anion of histidine, or the –SH group of cysteine residues may be the candidates for coupling. The ideal linkage between the matrix and the protein ligand from Step 1 should be fairly hydrophilic and neutral to avoid the introduction of a non-specific interaction. Carbonyldiimidazole and 2-fluoro-1-methylpyridinium toluene-4-sulfonate are two of the popular reagents for activation of the hydroxyl-containing matrix and coupling with an aminecontaining protein ligand.

Because there are many options of immobilization chemistries, different immobilization strategies should be evaluated for a particular protein ligand. After immobilization, the binding site should be affected in a minimal way so that the binding function is maintained. The protein ligand could have multiple sites for coupling with the activated matrix surface. The immobilization could be a random process if those sites are located in a similar steric environment. Another undesired scenario is immobilization by multiple-site attachment, which could destroy the native structure of the protein ligand and loss of its binding ability. If feasible, site-specific immobilization is preferred because it would give better reproducibility in both surface chemistry and column performance. Carbohydrate moieties from glycoproteins (i.e., antibodies and enzymes) are often particularly taken advantage of as the coupling sites because, generally, the complementary binding site in the protein ligand is away from the oligosaccharide chains. Immunoglobins (IgG) is often immobilized through the carbohydrates on the F_c region, and, as a result, the binding sites are readily available located on the F_{ab} region of IgG.

The leaching of the protein ligand presents a significant problem for introducing contaminants into the purified product. The solvolysis of the bonds between either the matrix–activator or activator–protein is the major source of leaching. It is the reason that an extra chromatography step is often required to remove protein ligand contaminant after affinity chromatography purification.

APPLICATIONS

Adsorption and desorption are involved in the operation of affinity chromatography utilizing proteins as affinity ligands. One of the major differences for protein-based affinity chromatography from other modes of chromatographic techniques (i.e., ion-exchange chromatography, reversed-phase (RP) chromatography, and hydrophobic interaction chromatography) is that the protein ligand could be denatured or attacked in other ways and lose its affinity consequently. Extreme pH, heat, and organic solvents are worrisome for protein-based affinity chromatography. If any one of them is employed, its effect on the column life should be evaluated.

For method development in protein-based affinity chromatography, the theme is to promote the specific interaction between the protein ligand and its counterpart and minimize the non-specific interaction between the matrix and the sample components. Because ionic and hydrophobic interactions contribute to the specific binding between the ligand and its counterparts, ionic strength and pH are probably the two simple and convenient parameters to be evaluated for separation method development. The variation of pH can affect the charge distribution on both the protein ligand and its target, leading to a different binding constant between them. Changing the ionic strength of the solution could modulate the hydrophobic interaction. Another very important parameter is the binding kinetics between the immobilized protein ligand and its target. The flow rate study could provide some clue on how fast the binding reaches the equilibrium. The strategy for minimizing the non-specific interaction depends on the surface chemistry of the matrix. For example, a running buffer of high ionic strength (0.2 *M*) can suppress the non-specific ionic interaction between the sample components and the negative-charged silanol group on the silica matrix.

Many proteins have been utilized as affinity ligands and there are literally thousands of references using this technique. The following are a few samples of proteins used as affinity ligands. Antibodies or antigens are used as immunoaffinity ligand to separate the complementary counterparts. Often, only a single purification step is needed because of the superior selectivity of

immunoaffinity column. Protein A and protein G are the perfect ligands for antibody purification because of their specificities and robustness.

In summary, affinity chromatography using proteins as affinity ligands provides a unique scheme for purification. Currently, a great number of matrices are available and the chemistries for immobilization of protein ligands are significantly improved. The specific three-dimensional interaction between the protein ligand and its counterpart distinguishes this technique from other chromatography methods. The key issue is maintaining the structure integrity of the binding site in the protein ligand throughout the immobilization and column operation.

BIBLIOGRAPHY

1. Dorsey, J.G.; Cooper, W.T.; Siles, B.A.; Foley, J.P.; Barth, H.G. Liquid chromatography: Theory and methodology. Anal. Chem. **1998**, *70*, 591R–644R.
2. Lowe, C.R. Adv. Mol. Cell Biol. **1996**, *15B*, 513–522.
3. Ohlson, S.; Bergstorm, M.; Pahlsson, P.; Lundblad, A. Use of monoclonal antibodies for weak affinity chromatography. J. Chromatogr. **1997**, *758*, 199.
4. Pommerening. *Affinity Chromatography: Practical and Theoretical Aspects*; Marcel Dekker, Inc.: New York, 1985.
5. Porath, J. General methods and coupling procedures. Methods Enzymol. **1974**, *34*, 13–30.
6. Turkova, J. *Bioaffinity Chromatography*; Elsevier: Amsterdam, 1993.

Proteins: Cross-Axis Coil Planet Centrifuge Separation

Yoichi Shibusawa
Division of Pharmaceutical and Biomedical Analysis, School of Pharmacy, Tokyo University of Pharmacy and Life Science, Tokyo, Japan

Yoichiro Ito
National Heart, Lung, and Blood Institute (NHLBI), National Institutes of Health (NIH), Bethesda, Maryland, U.S.A.

Abstract
The different types of cross-axis coil planet centrifuges (cross-axis CPCs) were tested for the retention of the stationary phase of aqueous–aqueous polymer-phase systems such as poly(ethylene glycol) (PEG) 1000–potassium phosphate and PEG 8000–dextran T500. The XL and XLL CPC are suitable for the PEG 1000–potassium phosphate, which has a relatively large difference in density between the two phases. On the other hand, the XLLL and L CPC are required to acheive satisfactory phase retention phase retention of the PEG–dextran system. These cross-axis CPCs were utilized for the separation of several proteins.

INTRODUCTION

Countercurrent chromatography (CCC) is a form of support-free liquid–liquid partition chromatography in which the stationary phase is retained in the column with the aid of the Earth's gravity or a centrifugal force.[1] Partition of biological samples such as proteins, nucleic acids, and cells has been carried out using various aqueous polymer-phase systems.[2] Among many existing polymer-phase systems, poly(ethylene glycol)–dextran (PEG–dextran) and PEG–phosphate systems have been most commonly used for the partition of biological samples. Whereas these polymer-phase systems provide an ideal environment for biopolymers and live cells, high viscosity and low interfacial tension between the two phases tend to cause a detrimental loss of stationary phase from the column in the standard high-speed CCC centrifuge system (known as type J).

The cross-axis coil planet centrifuge (cross-axis CPC), with column holders at the off-center position on the rotary shaft, enables retention of the stationary phase of aqueous–aqueous polymer-phase systems such as PEG 1000–potassium phosphate and PEG 8000–dextran T500. Since the last decade, various types of cross-axis CPC (types XL, XLL, XLLL, and L) have been developed for performing CCC with highly viscous aqueous polymer-phase systems.[3,4] The separation and purification of protein samples, including lactic acid dehydrogenase (LDH) from bovine heart crude extract,[5] single-stranded DNA binding protein (SSB) from *Escherichia coli* cell lysate,[6] glucosyltransferase from *Streptococcus mutans* cell lysate[7] and *Streptococcus sobrinus* cell culture medium,[8] maltose-binding protein-tagged histone deacetylase from *E. coli* cell lysate,[9] and so on, were achieved using these cross-axis CPCs.[10]

APPARATUS

The cross-axis CPCs, which include types X and L and their hybrids, are mainly used for protein separations. These modified versions of the high-speed CCC centrifuge have a unique feature among the CPC systems in that the system provides reliable retention of the stationary phase for viscous polymer-phase systems. Fig. 1 presents a photograph of the latest type XL CPC unit and schematically illustrates the orientation and motion of the coil holder in the cross-axis CPC system, where R is the radius of revolution. There are five types of cross-axis CPC, in which the degree of lateral shift of the coil holder is conventionally expressed by L/R. This parameter for types X, XL, XLL, XLLL, and L CPCs is 0, 1, 2, 3.5, and ∞, respectively. Our studies have shown that the stationary-phase retention is enhanced by laterally shifting the position of the coil holder along the rotary shaft, apparently due to the enhancement of a laterally acting force field across the diameter of the tubing.

The polymer-phase system composed of PEG and potassium phosphate has a relatively large difference in density between the two phases, so that it can be retained well in both XL and XLL column positions, which provide efficient mixing of the two phases. On the other hand, the viscous PEG–dextran system, with an extremely low interfacial tension and a small density difference between the two phases, has a high tendency of emulsification under vigorous mixing. Therefore, the use of either the XLLL or L column position, which produces less

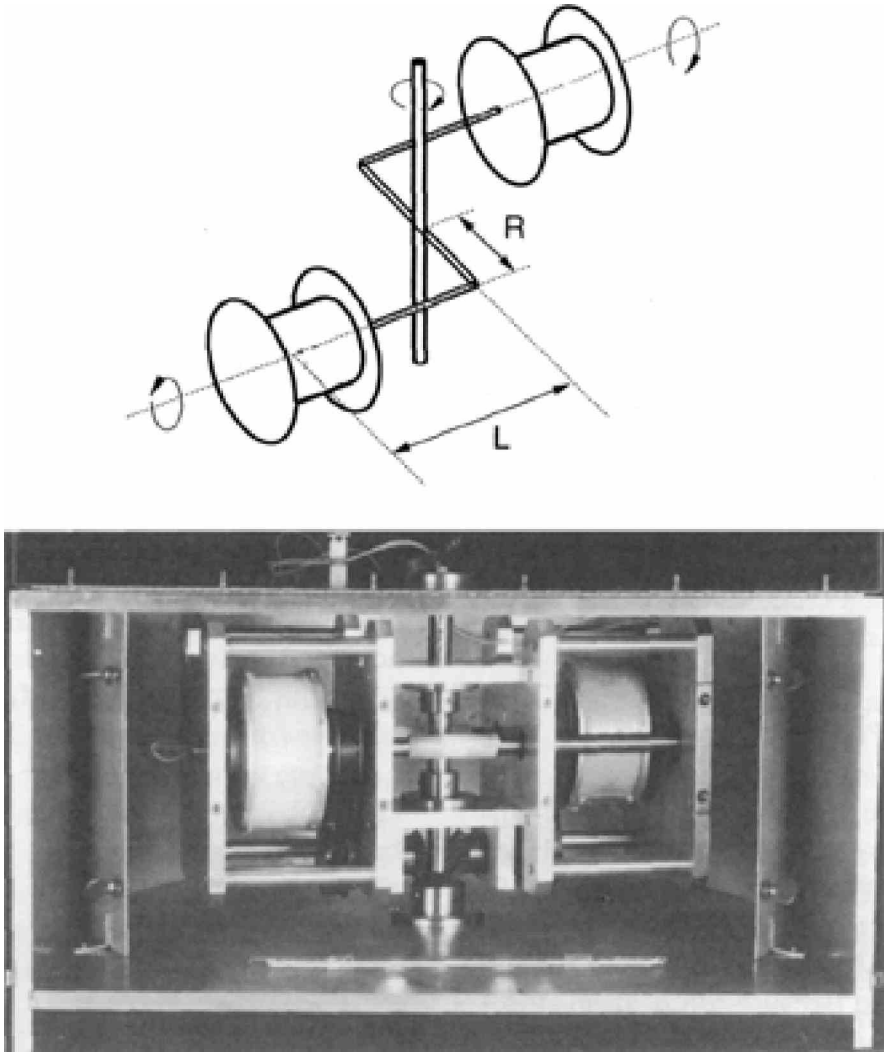

Fig. 1 Photograph of the latest type XL cross-axis coil planet centrifuge (cross-axis CPC).

violent mixing and an enhanced lateral force field, is required to achieve satisfactory phase retention of the PEG–dextran system.

The photograph of the XL cross-axis CPC ($L/R = 1.0$) equipped with a pair of multilayer coil separation columns is shown in Fig. 1. The multilayer coil separation column was prepared from a 2.6 mm inner diameter (I.D.) polytetrafluoroethylene (PTFE) tubing by winding it onto the coil holder hub, forming multiple layers.

POLYMER-PHASE SYSTEMS FOR PROTEIN SEPARATION

CCC utilizes a pair of immiscible solvent phases that have been pre-equilibrated in a separating funnel: One phase is used as the stationary phase and the other as the mobile phase. A solvent system composed of 12.5% or 16.0% (w/w)PEG 1000 and 12.5% (w/w) potassium phosphate is usually used for the type XL and XLL cross-axis CPCs. These solutions form two layers: The upper layer is rich in PEG and the other layer is rich in potassium phosphate. The ratio of monobasic to dibasic potassium phosphates determines the pH of the solvent system. This effect can be used for optimizing the partition coefficient of proteins.

A solvent system composed of 4.4% (w/w) PEG 8000, 7.0% (w/w) dextran T500, and 10 m*M* potassium phosphate is used with the type XLLL and L cross-axis CPCs for the separation of proteins that are not soluble in the PEG–phosphate system. This two-phase solvent system consists of the PEG-rich upper phase and the dextran-rich lower phase. The cross-axis CPC may be operated in four different elution modes: P_IHO, P_{II}TO, P_ITI, and P_{II}HI. The parameters P_I and P_{II} indicate the direction of planetary motion, where P_I indicates counterclockwise and P_{II} clockwise when observed from the top of the centrifuge. H and T indicate the head–tail elution mode, and I and O the inward–outward elution mode along the holder axis. In mode I (inward), the mobile phase is eluted against the laterally acting centrifugal force, and in mode O (outward), this flow direction is reversed. These three parameters

yield a total of four combinations for the left-handed coils. Among these elution modes, the inward–outward elution mode plays the most important role in the stationary-phase retention for the polymer-phase systems. To obtain a satisfactory retention of the stationary phase, the lower phase should be eluted outwardly along the direction of the lateral force field (P_IHO and P_{II}TO) or the upper phase in the opposite direction (P_ITI or P_{II}HI).

APPLICATION OF CROSS-AXIS CPC FOR PROTEINS

Type XL Cross-Axis CPC

The performance of the XL cross-axis CPC, equipped with a pair of columns with a 165 ml capacity, was evaluated for purification of LDH from a crude bovine heart filtrate. Successful separation of the LDH fraction was achieved with 16% (w/w) PEG 1000–12.5% (w/w) potassium phosphate at pH 7.3. The separation was performed at 500 rpm at a flow rate of 1.0 ml/min using the potassium phosphate-rich lower phase as the mobile phase. The sodium dodecyl sulfate–polyacrylamide gel electrophoresis (SDS–PAGE) analysis of the LDH fractions showed no detectable contamination by other proteins. The enzymatic activity was also preserved in these fractions.

The purification of SSB from an *E. coli* lysate was also performed by CCC using the XL cross-axis CPC. About 5 ml of *E. coli* lysate was separated by CCC using a polymer-phase system composed of a 16% (w/w) PEG 1000 and 17% (w/w) ammonium sulfate aqueous polymer two-phase solvent system. The precipitation of proteins in the lysate took place in the CCC column, and the SSB protein was eluted in the fractions. Many other impurities were eluted immediately after the solvent front or precipitated in the column. The identities of the proteins in the fractions and the precipitate were confirmed by SDS–PAGE.

Type XLL Cross-Axis CPC

The XLL cross-axis CPC, with a 250 ml capacity column, was used for the purification of recombinant enzymes such as purine nucleoside phosphorylase (PNP) and uridine phosphorylase (UrdPase) from a crude *E. coli* lysate. The polymer-phase system used in this separation was 16% (w/w) PEG 1000–12.5% (w/w) potassium phosphate at pH 6.8. The separation was performed at 750 rpm at a flow rate of 0.5 ml/min using the upper phase as the mobile phase. About 1.0 ml of crude lysate, containing PNP in 10 ml of the above solvent system, was loaded into the multilayer coil. Purified PNP was harvested in 45 ml fractions. The SDS–PAGE analysis clearly demonstrated that PNP was highly purified in a one-step elution with the XLL cross-axis CPC.

The capability of the XLL cross-axis CPC was further examined in the purification of a recombinant UrdPase from a crude *E. coli* lysate under the same experimental conditions as described earlier. The majority of the protein mass was eluted immediately after the solvent front (between 105 and 165 ml elution volume), whereas the enzyme activity of UrdPase coincided with the fourth protein peak (between 225 and 265 ml elution volume). The result indicates that the recombinant UrdPase can be highly purified from a crude *E. coli* lysate within 10 hr using the XLL cross-axis CPC.

Type XLLL Cross-Axis CPC

Although PEG–phosphate systems yield a high efficiency separation, some proteins show low solubility due to a high salt concentration in the solvent system. In this case, the PEG–dextran polymer-phase system with a low salt concentration can be alternatively used for the separation of such proteins. Because the dextran–PEG system has high viscosity and extremely low interfacial tension, it tends to cause emulsification and loss of the stationary phase in the XLL or XL cross-axis CPCs. This problem is minimized using the XLLL cross-axis CPC, which provides a strong lateral centrifugal force to provide a more stable retention of the stationary phase.

Type L Cross-Axis CPC

Cross-axis CPC provides for the universal application of protein samples with a dextran–PEG polymer-phase system. Using a prototype of the L cross-axis CPC with a 130 ml column capacity, a profilin–actin complex was purified directly from a crude extract of *Acanthamoeba* with the same solvent system as used for the serum protein separation earlier. The sample solution was prepared by adding the proper amounts of PEG 8000 and dextran T500 to 2.5 g of the *Acanthamoeba* crude extract to adjust the two-phase composition similar to that of the solvent system used for the separation. The experiment was performed by eluting the upper phase at 0.5 ml/min under a high revolution rate of 1000 rpm. The profilin–actin complex was eluted between 60 and 84 ml fractions and well separated from other compounds. The retention of the stationary phase was 69.0% of the total column capacity.

CONCLUSIONS

The overall results of our studies indicate that the retention of the stationary phase of polymer-phase systems in the cross-axis CPCs is increased by shifting the column holder laterally along the rotary shaft. Separation of proteins with high solubility in the PEG–phosphate system can be performed with the XL or XLL cross-axis CPC at a high

partition efficiency. Proteins with low solubility in PEG–phosphate systems may be separated with a dextran–PEG system using the XLLL or L cross-axis CPC, which provides more stable retention of the stationary phase.

REFERENCES

1. Conway, W.D. *Countercurrent Chromatogaphy: Apparatus and Applications*; VCH: New York, 1990.
2. Albertsson, P.-A. *Partition of Cell Particles and Macromolecules*; 3rd Ed.; Wiley-Interscience: New York, 1986.
3. Shibusawa, Y.; Ito, Y. Protein separation with aqueous–aqueous polymer systems by two types of counter-current chromatographs. J. Chromatogr. **1991**, *559*, 695.
4. Shibusawa, Y.; Ito, Y. Countercurrent chromatography of proteins with polyethylene glycol–dextran polymer phase systems using type-XLLL cross axis coil planet centrifuge. J. Liq. Chromatogr. **1992**, *15*(15 & 16), 2787.
5. Shibusawa, Y.; Eriguchi, Y.; Ito, Y. Purification of lactic acid dehydrogenase from bovine heart crude extract by counter-current chromatography. J. Chromatogr. B, **1997**, *696*, 25.
6. Shibusawa, Y.; Ino, Y.; Kinebuchi, T.; Shimizu, M.; Shindo, H.; Ito, Y. Purification of single-strand DNA binding protein from an *Escherichia coli* lysate using counter-current chromatography, partition and precipitation. J. Chromatogr. B, **2003**, *793*, 275.
7. Yanagida, A.; Isozaki, M.; Shibusawa, Y.; Shindo, H.; Ito, Y. Purification of glucosyltransferase from cell-lysate of *Streptococcus mutans* by counter-current chromatography using aqueous polymer two-phase system. J. Chromatogr. B, **2004**, *805*, 155.
8. Shibusawa, Y.; Isozaki, M.; Yanagida, A.; Shindo, H.; Ito, Y. Purification of glucosyltransferase from *Streptococcus sobrinus* cell culture medium by combined use of batch extraction and countercurrent chromatography with a polymer phase system. J. Liq. Chromatog. & Rel. Technol. **2004**, *27*(14), 1.
9. Shibusawa, Y.; Takeuchi, N.; Tsutsumi, K.; Nakano, S.; Yanagida, A.; Shindo, H.; Ito, Y. One-step purification of histone deacetylase from Escherichia coli cell-lysate by counter-current chromatography using aqueous two-phase system. J. Chromatogr. A, **2007**, *1151*, 158.
10. Shibusawa, Y. *High-Speed Countercurrent Chromatography*; Ito, Y.; Conway, W.D., Eds.; Chemical Analysis Series. Wiley-Interscience, 1996; Vol. 132, 121.

Proteins: Flow FFF Separation

Galina Kassalainen
S. Kim Ratanathanawong Williams
Department of Chemistry and Geochemistry, Colorado School of Mines, Golden, Colorado, U.S.A.

INTRODUCTION

Flow field-flow fractionation (flow FFF) is a separation method that is applicable to macromolecules and particles.[1] Sample species possessing hydrodynamic diameters from several nanometers to tens of microns can be analyzed using the same FFF channel, albeit by different separation mechanisms. For macromolecules and submicron particles, the normal-mode mechanism dominates and separation occurs according to differences in diffusion coefficients. Flow FFF's wide range of applicability has made it the most extensively used technique of the FFF family.

DISCUSSION

The characteristic feature of flow FFF is the superimposition of a second stream of liquid perpendicular to the axis of separation. This cross-flow drives the injected sample plug toward a semipermeable membrane that acts as the accumulation wall. The cross-flow liquid permeates across the membrane and exits the channel, whereas the sample is retained inside the channel in the vicinity of the membrane surface. Sample displacement by the cross-flow is countered by diffusion away from the membrane wall. At equilibrium, the net flux is zero and sample clouds of various thicknesses are formed for different sample species. As with other FFF techniques, a larger diffusion coefficient D leads to a thicker equilibrium sample cloud that, on average, occupies a faster streamline of the parabolic flow profile and subsequently elutes at a shorter retention time t_r. For well-retained samples analyzed by flow FFF, t_r can be related to D and the hydrodynamic diameter d by

$$\frac{t^0}{t_r} = \frac{6D}{Uw} = \frac{2kTV^0}{\dot{V}_c w^2 \pi \eta d} \tag{1}$$

where t^0 is the void time, U is the field-induced velocity, w is the channel thickness, k is the Boltzmann constant, T is the temperature, V^0 is the channel void volume, $\dot{V}_c$ is the cross-flow rate, and η is the viscosity of the carrier liquid. Eq. 1 pertains to normal-mode separations.

It is apparent, from Eq. 1, that the primary sample property measured by flow FFF is the diffusion coefficient. Secondary information includes the hydrodynamic diameter which can be obtained via the Stokes–Einstein equation and the molecular weight if the molecule shape factor is constant. Unlike other FFF techniques, the retention time in flow FFF is determined solely by the diffusion coefficient rather than a combination of sample properties. As a consequence, flow FFF is well suited for analyses of complex sample mixtures and the transformation of the fractogram to a diffusion or size distribution is straight forward. In addition, flow FFF is applicable to a wide range of samples regardless of their charge, size, density, and so forth.

Flow FFF was first introduced as a method for protein separation and characterization by Giddings et al. in 1977.[2] This first publication discusses the advantages of flow FFF over other protein separation methods that were used at the time (e.g., polyacrylamide gel electrophoresis and size-exclusion chromatography [SEC]). Flow FFF permits the calculation of diffusion coefficients and hydrodynamic diameter of proteins in different solution environments directly from retention data using straightforward analytical relationships. No other technique provides simultaneous separation and measurement of D and d for each sample component without the need for additional information such as charge and density. Moreover, the protein molecular weights (MWs) calculated from FFF diffusion coefficient data are on a sounder theoretical basis than that derived from electrophoretic mobility in gels or chromatographic retention data. The absence of packing material in a channel makes flow FFF suitable for the analysis of fragile high-MW proteins and protein complexes in comparison with SEC where shear forces and interfacial interactions can cause changes in the structure and activity of molecules. Flow FFF can be used to separate and characterize mixtures of proteins, protein aggregates, and protein complexes with a single FFF analysis covering a 500–1000-fold size difference. A series of SEC columns with different exclusion limits would be needed to span a similar size range. The cross-flow rate is programmed (i.e., decreased with respect to time) to maintain separation times of 5–20 min. The open FFF channel structure permits the analysis of protein samples suspected of containing precipitated material without special pretreatment. This is not possible by SEC and gel electrophoresis.

The main disadvantage of flow FFF is the lack of commercially available membranes with flat non-adsorbing surfaces, uniform permeability, and batch-to-batch reproducibility. These features may affect retention time, separation efficiency, and sample recovery. Numerous studies and technical improvements have been done to ensure optimum performance.

The traditional flow-FFF method, also called symmetrical flow FFF, utilizes a channel with permeable depletion and accumulation walls. The cross-flow liquid enters the channel through a microfiltration frit that acts as the depletion wall and exits through an ultrafiltration membrane that acts as the accumulation wall.[1–3] Membranes with nominal MW cutoffs in the range of 5000–30,000 Da are used to ensure that the protein sample remains in the FFF channel. Hydrophilic ultrafiltration membranes made from regenerated cellulose, cellulose acetate, and modified polyethersulfone have been used.

The sample capacity in a flow FFF channel with standard dimensions is several hundred micrograms. Sample overloading causes band broadening and a shift in retention time. The experimental procedure involves sample injection followed by a stop-flow period when the axial or channel flow is stopped and the sample is transported to equilibrium positions at the accumulation wall under action of the cross-flow. At the end of the stop-flow period, channel flow is resumed and the sample is fractionated while being swept toward the outlet. The elution of proteins is monitored with an ultraviolet (UV) spectrophotometric detector set at 280 or 210 nm wavelength. Other online detectors that are being used or evaluated include multiangle light scattering (MALS) which yields MW and photon correlation spectroscopy (PCS), which yields D. Flow FFF provides the narrow polydispersity sample fractions required for accurate MW and D determinations by the light-scattering detectors. These detectors provide a second independent measure of MW and D for comparison with values calculated from FFF retention times. In addition, MALS can be used to distinguish the polydispersity of the sample from band broadening. The main disadvantages of MALS detection for protein flow-FFF applications are the low sensitivity and particulate-free solvent requirement.

Symmetrical flow FFF has been successfully used to analyze numerous purified proteins and their dimers, protein conjugates, sodium dodecyl sulfate (SDS)–protein complexes, including precipitate[1–3] and other biological samples, as summarized in Table 1. In these applications, sample pretreatment was not required even when the proteins of interest were present in complex matrices such as plasma, dairy products, and wheat flour (in contrast to SEC and electrophoresis). Ultracentrifugation, which is commonly used to fractionate these samples, requires over 24 hr in comparison with the 5–40 min for flow FFF. The short analysis time gives flow FFF an advantage in analyzing the large number of samples encountered in the medical diagnostics, pharmaceutical, and food industries. Separation efficiencies are usually of the order of several hundred theoretical plates for a typical channel length of 25–30 cm.

A later modification of flow FFF, called asymmetrical flow FFF, has generated up to 2600 theoretical plates in the separation of viruses.[4] In the asymmetrical channel, the permeable frit or depletion wall is replaced with an impermeable glass plate. The flow of carrier liquid entering the inlet of the channel is the source of both the cross-flow and channel flow. The sample is injected through an additional port located about 2–3 cm downstream from the channel inlet. For asymmetrical flow FFF, the retention mechanism is the same as for the traditional symmetrical mode. The observed higher efficiency may be based on the different relaxation procedures. In the asymmetrical channel, a so-called focusing procedure is used. The injected sample is focused to a narrow zone at the accumulation wall under action of two opposing flows (introduced simultaneously through the inlet and outlet of the channel). However, this focusing procedure has some potential drawbacks. It may promote chain entanglement of high-MW macromolecules and increase adsorption on the membrane. Lower sample capacity (several micrograms) and recovery have been observed in comparison with the symmetrical flow FFF.

Asymmetrical flow FFF has been successfully applied to several practical problems, such as the separation of monoclonal antibodies and their aggregates in downstream processing, ribosomes, and plasma protein studies (see Table 1). For example, flow FFF separations of ribosomes and their subunits have led to an alternative method of optimizing the fermentation process without having to measure protein yields.[12] Flow FFF is the technique uniquely suited for separating highly glycosylated proteins such as 10^6 Da acid phosphatase (Apase) in cultivation media.[13] Buffers commonly used in chromatographic methods cause changes in the enzymatic activity of APase.

A second variant to the traditional symmetrical flow FFF channel utilizes a hollow-fiber membrane. Even though its feasibility in separating proteins has been demonstrated,[14] its development has been hindered by the lack of membranes suitable for use as an FFF channel.

Several studies involving FFF channel modifications and new experimental procedures have been aimed at increasing detectability. For example, frit–outlet flow FFF utilizes a section of the frit depletion wall near the channel outlet to remove sample-free carrier and, thus, concentrate the separated sample just prior to its reaching the detector. A 10-fold increase in the detector

Table 1 Examples of flow FFF protein analyses.

Application	Flow FFF type	Summary
Ribosomes from *Escherichia coli*	Asymmetrical	Separation of ribosomes, their subunits, and t-RNA/low-MW protein mixture in samples collected at different protein production phases and in the presence of antibiotics, specific genes, and proteins; calculation of a ribosome number per cell and a ribosome fraction using peak area.[13]
Yeast acid phosphatase (APase)	Asymmetrical	Separation of APase in cultivation medium; identification of APase peak by enzymatic activity measurements.[14]
Proteins from wheat flour	Asymmetrical	Fractionation of wheat proteins in the size range from 5 to 45 nm; separation of gliadins from glutenin.[5]
Wheat protein fractions	Symmetrical	Size distribution of wheat protein fractions (albumins and globulins, gliadins, glutenins) prepared by extraction; influence of oxidation on size distribution of high-MW glutenin.[6]
Monoclonal antibodies (Mab) from hybridoma cell culture	Asymmetrical	Separation of five Mab aggregates (immunoglobulins) in half the time needed for GPC; only three partially resolved peaks were obtained by GPC; separation of samples containing precipitated material.[7]
Proteins in homogenized dairy products	Symmetrical	Separation of whey proteins from fat globules; fractionation of whey proteins and casein micelles; effect of carrier ionic strength, cross-flow rate, pH, and membrane type on retention and size distribution of micelles.[8]
Reconstituted skim milk casein	Symmetrical	Fractionation of colloidal Ca^{2+}-caseinate complexes in milk samples in size range 10–50 nm after the preliminary fractionation of 10–600-nm colloids with sedimentation FFF.[9]
Plasma protein interactions with polymer colloids	Symmetrical	Measurement of changes in particle (PS latex) size due to aggregation and adsorption of proteins; effect of Pluronic™ surfactants on aggregation and protein adsorption.[10]
Lipoproteins in human plasma	Symmetrical	Separation of low-MW proteins, HDL, LDL, and VLDL. Determination of subspecies in the lipoprotein fractions with linear programmed cross-flow rate; observation of lipoprotein profiles for different individuals.[17]
Drug/plasma protein interactions	Asymmetrical	Separation of albumin, HDL, α-macroglobulin, and LDL. Determination of drug distribution in FFF fractions using a fluorimetric detector.[11]
Viruses (purified)	Asymmetrical	Separation of five aggregates of the Satellite tobacco necrosis virus; isolation of the Cow pea mosaic virus.[12]

response of purified proteins was achieved without any effect on retention time or resolution.[15] Frit–inlet flow FFF involves a modification at the channel inlet that enables the transport of sample to the accumulation wall without using stop-flow relaxation.[15,16] As a result, the experimental operation is simpler and the detector signal is free of fluctuations caused by stopping and resuming axial flow through the channel. Enhanced detectability can also be realized by programming the cross-flow rate during the run to accelerate elution of highly retained components.[16] Another experimental approach involves using the ultrafiltration membrane that serves as the accumulation wall to remove low-MW interferences. A nominal 30,000 Da MW cutoff membrane was used to selectively remove low-MW proteins from a blood plasma sample to allow determinations of high-, low-, and very low-density lipoproteins (HDL, LDL, and VLDL, respectively).

A fundamental study was performed to demonstrate that flow FFF is a good alternative technique for the rapid measurement of protein diffusion coefficients.[17] The results obtained for 15 proteins were in good agreement (within 4%) with the literature data based on classical methods and a group of modern methods such as photon correlation spectrometry (PCS), laminar flow analysis, a chromatographic relaxation method, and analytical split-flow thin-cell (SPLITT) fractionation. The advantages of flow FFF are the high-speed separations and the calculation of D values directly from retention data.

ACKNOWLEDGMENTS

G. Kassalainen was supported by a grant from ACTR/ACCELS with funds provided by the U.S. Information Agency and S. K. R. Williams by a Colorado School of Mines start-up grant.

REFERENCES

1. Giddings, J.C. Field-flow fractionation: Analysis of macromolecular, colloidal, and particulate materials. Science **1993**, *260* (5113), 1456–1465.
2. Giddings, J.C.; Yang, F.J.; Myers, M.N. Flow field-flow fractionation as a methodology for protein separation and characterization. Anal. Biochem. **1977**, *81*, 395–407.
3. Giddings, J.C.; Benincasa, M.A.; Liu, M.-K.; Li, P.J. Separation of water soluble synthetic and biological macromolecules by flow field-flow fractionation. J. Liq. Chromatogr. Relat. Technol. **1992**, *15* (10), 1729–1747.
4. Litzen, A.; Wahlund, K.-G. Zone broadening and dilution in rectangular and trapezoidal asymmetrical flow field-flow fractionation channels. Anal. Chem. **1991**, *63*, 1001–1007.
5. Wahlund, K.-G.; Gustavson, M.; MacRitchie, F.; Nylander, T.; Wannerberger, L. J. Cereal Sci. **1996**, *23*, 113–119.
6. Stevenson, S.G.; Ueno, T.; Preston, K.R. Anal. Chem. **1999**, *71*, 8–14.
7. Litzen, A.; Walter, J.K.; Krischollek, H.; Wahlund, K.-G. Anal. Biochem. **1993**, *212*, 469–480.
8. Jussila, M.A.; Yohannes, G.; Riekkola, M.-L. J. Microcol. Separ. **1997**, *9*, 601–609.
9. Udabage, P.; Sharma, R.; Murphy, D.; McKinnon, I.; Beckett, R. J. Microbiol. Separ. **1997**, *9*, 557–563.
10. Li, J.-T.; Caldwell, K.D. Colloids Surf. B: Biointerfaces. **1996**, *7*, 9–22.
11. Madorin, M.; van Hoogevest, P.; Hilfiker, R.; Langwost, B.; Kresbach, G.M.; Ehrat, M.; Leuenberger, H. Pharm. Res. **1997**, *14*, 1706–1712.
12. Nilsson, M.; Bulow, L.; Wahlund, K.-G. Use of flow field-flow fractionation for the rapid quantitation of ribosome and ribosomal subunits in Escherichia coli at different protein production conditions. Biotechnol. Bioeng. **1997**, *54*, 461–467.
13. Litzen, A.; Garn, M.B.; Widmer, H.M. Determination of acid phosphatase in cultivation medium using asymmetrical flow field-flow fractionation. J. Biotechnol. **1994**, *37*, 291–295.
14. Wijnhoven, J.E.G.J.; Koorn, J.-P.; Poppe, H.; Th. Kok, W. Influence of injected mass and ionic strength on retention of water-soluble polymers and proteins in hollow-fibre flow field-flow fractionation. J. Chromatogr. A, **1996**, *732*, 307–315.
15. Li, P.; Hansen, M.; Giddings, J.C. Advances in frit-inlet and frit-outlet flow field-flow fractionation. J. Microcol. Separ. **1997**, *10* (1), 7–18.
16. Li, P.; Hansen, M.; Giddings, J.C. Separations of lipoproteins from human plasma by flow field-flow fractionation. J. Liq. Chromatogr. Relat. Technol. **1997**, *20* (16–17), 2777–2802.
17. Liu, M.-K.; Li, P.; Giddings, J.C. Rapid protein separation and diffusion coefficient measurement by frit inlet flow field-flow fractionation. Protein Sci. **1993**, *2*, 1520–1531.

Proteins: HPLC Analysis

Karen M. Gooding
Eli Lilly and Company, Indianapolis, Indiana, U.S.A.

INTRODUCTION

Proteins were first separated chromatographically in the 1950s when carbohydrate gels were found to be effective as matrices for liquid chromatography (LC). When high-performance liquid chromatography (HPLC) gained popularity, it was assumed that its higher flow rates and concomitantly higher pressures would destroy the biological activity of proteins by disrupting their three-dimensional (tertiary) structures. This was proven incorrect in the mid-1970s, when several groups, including those of Fred Regnier at Purdue university and Jiri Coupek of Czecho slovakia, demonstrated that high recoveries accompanied the high resolution of HPLC methods for protein analysis.

MODES OF HPLC

The importance of tertiary structure on the biological activity of proteins implies that the most successful HPLC methods are those employing mobile and stationary phases, which cause minimal disruption of these features. Size-exclusion chromatography (SEC) and ion-exchange chromatography (IEC) are the gentlest methods in this regard and are generally compatible with any additives needed to enhance stability. Hydrophobic interaction and affinity chromatography have somewhat higher risk of denaturation due to either their mobile phase [high salt for hydrophobic interaction chromatography (HIC)] or stationary phase (affinity). Reversed-phase and hydrophilic interaction chromatography cause greater disruption of tertiary structure due to the presence of organic solvents, acidic pH, and/or hydrophobic stationary phases. Nonetheless, reversed-phase chromatography has shown great utility in the separation of many proteins.

SIZE-EXCLUSION CHROMATOGRAPHY

Size-exclusion chromatography is a method in which molecules are separated by size due to differential permeation into a porous support. This technique is especially useful for the separation of proteins because they are macromolecules frequently found in the presence of smaller and larger species. The peak capacity in SEC is fairly low compared to other HPLC methods because all separation must occur in the internal volume of the support, which is generally less than half the volume of the mobile phase in the column. Despite this deficiency, SEC is very effective for separating proteins from small molecules, polymeric forms, and other molecules which differ by size.

Supports for SEC of proteins are designed to be neutral and very hydrophilic to avoid disruption of protein structure and interaction of the solutes with the support by ionic or hydrophobic mechanisms. The base matrix can be either silica or polymer; efforts are made to totally mask its properties with a carbohydrate like stationary phase. The pore structure is critical to successful SEC. Not only must the total pore volume (V_i) be adequate for separation, the pore diameter must be consistent and nearly homogeneous for attainment of maximum resolution between molecules with relatively small differences in molecular size (radius of gyration or molecular weight). A twofold difference in size is usually required for separation by SEC. Pore homogeneity can be assessed from the slope of the calibration curve of the logarithm of the molecular weight vs. the retention time or the partition coefficient (K_D): $K_D = (V_R - V_0)V_i$, where V_R is the retention volume and V_0 is the void or excluded volume. A less steep slope results in the separation of more closely related molecular weights. Fig. 1 shows both an analysis of a protein mixture on an SEC column and its calibration curve. The second calibration curve is for a column with a smaller pore diameter, showing its effectiveness for separating smaller solutes.

The mobile phase is a critical factor in SEC because it must eliminate all solute–support interactions. This is effected by adjustment of pH (usually to neutrality), ionic strength (0.05–0.2 *M*), and/or addition of 5–10% organic solvent or stabilizing agents. The ionic and hydrophobic properties of proteins and their attraction to the stationary phase must be totally removed.

ION-EXCHANGE CHROMATOGRAPHY

Ion-exchange chromatography separates proteins by ionic interaction of their surface amino acids with charges on the stationary phase. Selectivity is dependent on the number and the identity of the amino acids, as well as their spatial arrangement. A protein with charges grouped in a patch on its surface will bind differently than one whose charges are dispersed throughout the surface. IEC is so selective that it can resolve isoforms and variants differing by only one

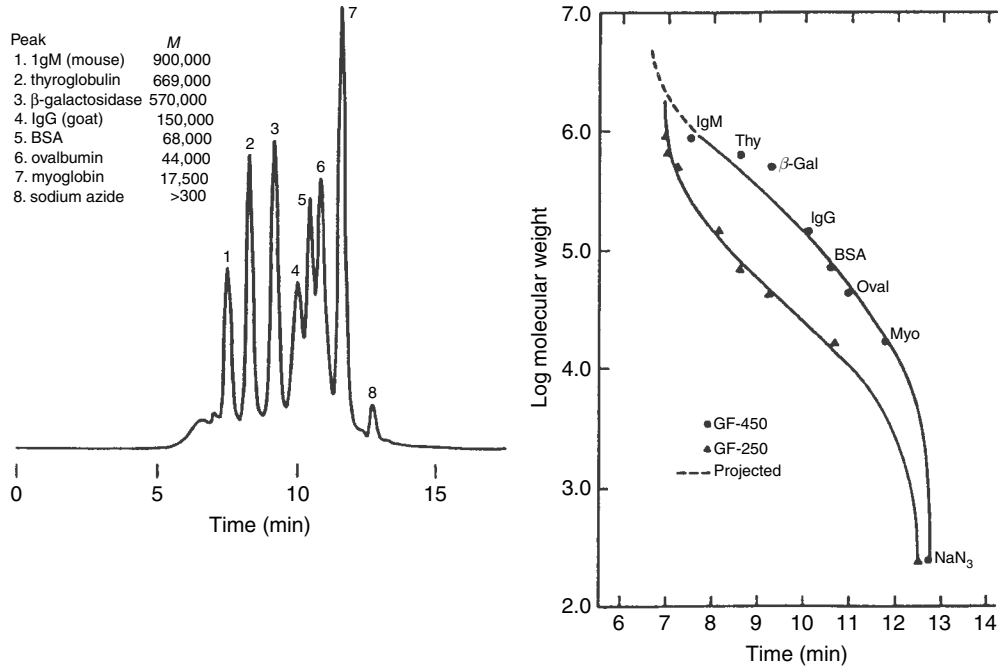

Fig. 1 Analysis of a mixture of proteins on ZORBAX® GF450. Calibration curves of proteins on ZORBAX GF250 and GF450 columns. Mobile phase: 0.2 *M* sodium phosphate, pH 7.5; UV detection at 280 nm.
Source: Reprinted with permission of Hewlett-Packard.

amino acid. Loading on porous IEC supports is high (100 mg/g), making IEC invaluable in purification techniques.

Supports for IEC possess either anion- or cation-exchange functionalities which are positively or negatively charged, respectively. They are also classified as weak or strong to correspond to their titration curves, similar to acid and base designations. The stationary phase totally covers the silica or polymer support matrix. The pore diameter is important in that it must be large enough to allow access of the protein. This affects not only retention but also loading capacity.

In IEC, proteins are bound in a low-ionic-strength buffer (0.02–0.05 *M*) at an appropriate pH (often 1–2 pH units from the p*I*). Elution occurs when the ionic strength is increased during a concentration gradient of a salt in the same buffer. Because proteins bind via multipoint interactions, gradients are necessary for good peak shapes, resolution, and reproducibility. The pH gradients are less commonly used but can also be effective. The nature of the salt in IEC has a major effect on selectivity due to interaction of the composite ions with either the stationary phase or the solutes. Fig. 2 illustrates the differences in retention of several proteins when various salts are used as the mobile phase for anion-exchange and cation-exchange chromatography. Additives which increase protein stability or improve peak shape can usually be included in the mobile phase without deleterious effects on the separation. Lower temperatures can be used to preserve biological activity, but they also result in higher retention.

HYDROPHOBIC INTERACTION CHROMATOGRAPHY

HIC is a method in which proteins in a high salt environment interact hydrophobically with non-polar ligands. Effective salts are antichaotropic, meaning that they promote the ordering of water molecules at surfaces. Selectivity is based on the hydrophobic amino acids and patches on the surface of the proteins. Many proteins, which generally remain in their native states in this technique, retain their biological activities when separated by HIC.

Supports for HIC have short alkyl chains or phenyl functionalities, the length of which is related to retention. The matrix can be either silica or polymer, as it is totally covered by the bonded phase and, thus, not exposed to the solute. Pore diameters are at least 300 Å to allow access by proteins. Loading capacities are high and similar to those of ion-exchange supports.

In HIC, molecules are bound with a high concentration of salt, usually ammonium or sodium sulfate (1–2 *M*) in a buffer (0.02–0.05 *M*). Elution is attained by a gradient to a lower concentration of salt in the buffer. The pH is controlled and is usually in the range of 6–8, but it is not a critical factor in selectivity. Additives to enhance protein stability are generally compatible with the process. Contrary to its effect on other modes of chromatography, reducing the temperature decreases the retention in HIC due to its being an entropy-driven technique.

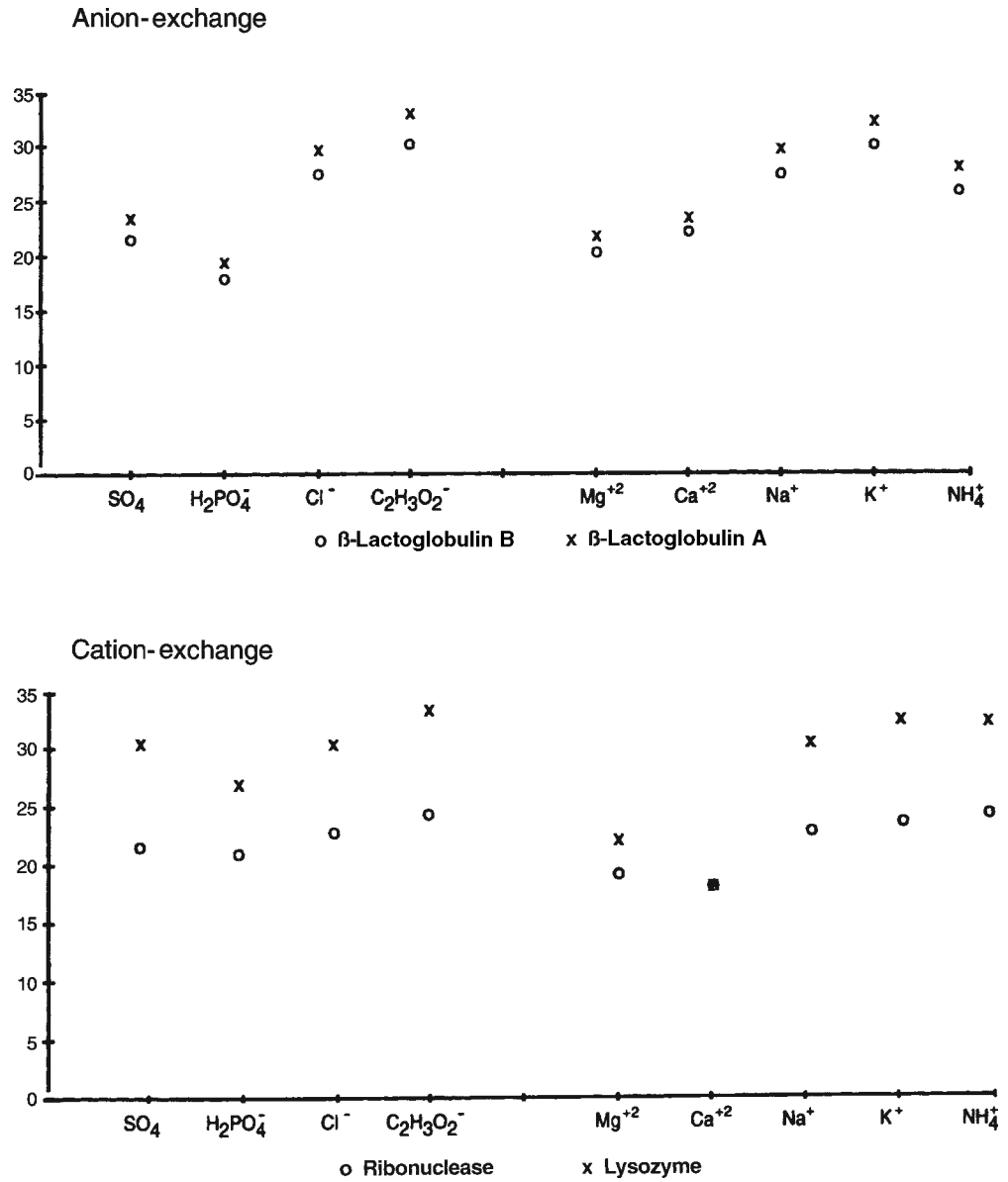

Fig. 2 Effect of salt on protein retention. Columns: SynChropak AX300 and SynChropak CM300; 30 min gradient from 0–1 *N* salt in 0.02 *M* Tris, pH 7.
Source: Reprinted with permission from *Basic HPLC and CE of Biomolecules*, Bay Bioanalytical Laboratories, Richmond, VA, 1998.

AFFINITY CHROMATOGRAPHY

Affinity chromatography (AFC) is a method in which biomolecules are attracted to ligands due to biospecificity. AFC is a very specific and selective technique in the aspect that many ligands are used, being customized to the analyte of interest. It is generally unlike other HPLC processes because particle diameters are larger and retention tends to be bind-release rather than partitioning, thus separating one protein or class of proteins from everything else in a mixture. Recoveries of biological activity are often high.

The variety of ligands for AFC includes proteins, cofactors, and any other molecules for which a solute has special affinity. Some common ligands are protein A, antibodies, and concanavalin A. Elution is attained by either a change in pH or ionic strength conditions or the addition of a competitor for the binding. Conditions are as varied as the number of ligands.

REVERSED-PHASE CHROMATOGRAPHY

Reversed-phase chromatography (RPC) is a method in which molecules are bound hydrophobically to non-polar ligands in the presence of a polar solvent. Solutes are generally bound in an acidic mobile phase with elution

occurring during a gradient to an organic solvent. The combination of acidic and organic mobile phases and a hydrophobic bonded phase usually results in tertiary structure disruption, which may or may not be reversible. Binding involves internal as well as surface amino acids depending on the extent of unfolding. The utility of RPC for protein analysis is limited by its generally denaturing characteristics; however, it can be a good method for non-preparative techniques where preservation of biological activity is unimportant. Some enzymes, such as trypsin and chymotrypsin, can be renatured after RPC, regaining biological activity.

There are many ligands used for RPC, but the most popular for protein analysis are butyl (C_4) and octyl (C_8). Little difference in selectivity for proteins is observed with ligand-chain-length variation, but mass recovery is often enhanced on the shorter chains. Due to their higher efficiencies and wettability, silica-based supports are generally used for protein analysis. The silica matrix is sometimes a factor in retention because reversed-phase bonded phases often do not totally eliminate silanols on the support. Pore diameters used for proteins are at least 300 Å; non-porous supports offer a high-resolution option with lower capacities. Loading capacities of RPC are at least 50% lower than those of IEC or HIC.

Many operational factors can change selectivity in RPC. The strength of the organic solvent which causes elution increases from methanol to acetonitrile to isopropanol. Acetonitrile is the most popular solvent due to its transparency at low wavelengths (<210 nm) and its tendency to yield narrow peak widths. The transparency is not critical for proteins, which can usually be detected at 254 or 280 nm. Ion-pairing agents, such as trifluoroacetic acid, can be added to the mobile phase to change the ionic or hydrophobic properties of either or both of the bonded phase or the solute. Generally, acidic pH is utilized to minimize silanol interactions; however, distinct pH conditions yield different selectivities. Increased temperatures result in shorter retention times and are especially effective in reducing the pressure generated by small-particle-diameter supports.

HYDROPHILIC INTERACTION CHROMATOGRAPHY

Hydrophilic interaction chromatography (HILIC) is a variation of normal-phase chromatography in which solutes are retained on a polar bonded phase under high concentrations (80–90%) of organic solvent and released during a gradient to a more aqueous solvent. The organic mobile phase usually causes at least partial denaturation of proteins.

The HILIC bonded phases are hydrophilic, including amide and/or polyhydroxy functionalities. Pore diameters are at least 300 Å to allow penetration of proteins. Supports can be based on either silica or polymer because the matrix is not exposed to the solutes.

The mobile phase can offer some differences in selectivity in HILIC. A buffer is usually used to control pH. It may also serve to change the hydrophobicity of the solutes by ion-pairing; thus, it may greatly effect retention. For this reason, the pH is less important than the identity of the salt. The denaturing aspects of HILIC diminish its utility in protein analyses, particularly for preparative purification.

CONCLUSIONS

High-performance liquid chromatography provides a number of rapid and effective methods for analysis and purification of proteins and enzymes. In modes such as SEC and IEC, quantitative yields are often obtained with full preservation of biological activity. The ability to change selectivity using the mobile phase has resulted in versatile techniques which can be rapidly optimized and implemented.

BIBLIOGRAPHY

1. Cunico, R.L.; Gooding, K.M.; Wehr, T. *Basic HPLC and CE of Biomolecules*; Bay Bioanalytical Laboratories: Richmond, CA, 1998.
2. Gooding, K.M., Regnier, F.E., Eds.; *HPLC of Biological Macromolecules: Methods and Applications*; Marcel Dekker, Inc.: New York, 1990.
3. Hancock, W.S., Ed.; *High Performance Liquid Chromatography in Biotechnology*; John Wiley & Sons: New York, 1990.
4. Hearn, M.T.W., Ed.; *HPLC of Proteins, Peptides and Polynucleotides*; VCH: New York, 1991.
5. Horvath, Cs., Nikelly, J.G., Eds.; *Analytical Biotechnology: Capillary Electrophoresis and Chromatography*; American Chemical Society: Washington, DC, 1990.
6. Katz, E.D., Ed.; *High Performance Liquid Chromatography: Principles and Methods in Biotechnology*; JohnWiley & Sons: New York, 1996.
7. Mant, C.T., Hodges, R.S., Eds.; *High-Performance Liquid Chromatography of Peptides and Proteins*; CRC Press: Boca Raton, FL, 1991.

Pump/Solvent Delivery System Design for HPLC

Andrei Medvedovici
Victor David
Department of Analytical Chemistry, University of Bucharest, Bucharest, Romania

Abstract
Constructive and functional principles of solvent delivery systems used in high-pressure liquid chromatography (HPLC) as well as in ultra-high-pressure liquid chromatography (UHPLC) are discussed. The main building parts such as solvent degassers, HPLC and UHPLC pumps, proportioning valves, inlet and outlet valves, mass flow sensors, pressure sensors, mixers, and dampers are described. The different technical setups for solvent gradient formation are highlighted together with micro/nano flow creating principles. Some aspects related to maintenance and troubleshooting of solvent delivery systems are also discussed. Basic operational qualifications principles are reviewed.

INTRODUCTION

The solvent delivery system (SDS) is an integral part of the structure of a liquid chromatograph that has the following functions:

1. Conditioning the components of the mobile phase (filtering and degassing).
2. Mixing the components to obtain the required composition of the mobile phase.
3. Pumping the mobile phase through the chromatographic system at a controlled flow rate, without any variations (pulses), if possible. Accurately measuring the flow rate and regulating it through feedback of the column flow against the primary pump flow (optional characteristic of pumping systems at micro- or nano-level flow rates).
4. Measuring the pressure within the chromatographic system.
5. Preserving the chromatographic column from any possible damage brought about by the mobile phase (optional).

GENERAL CONSIDERATIONS

The SDS belonging to a liquid chromatograph represents a multimodular system. It incorporates a solvent container (having storage and conditioning roles), a high-pressure pump (includes the functions of proportioning and mixing of components and pressure measurement), a damper (to attenuate flow pulses), and a precolumn to act on the mobile phase so as to preserve the integrity of the stationary phase (e.g., elimination of residual water from mobile phases designated for normal-phase separation mechanism or saturation of $[Si(OH)_6]^{2-}$ ions in the case of alkaline mobile phases in contact with silica gel-based stationary phases). Integration of the SDS in a liquid chromatograph is schematically represented in Fig. 1.

Development of liquid chromatography over the last decade refers to the following evolution directions: 1) increase in the pressure regime sustained by the pumps at very high or ultrahigh levels; 2) capability of delivering micro or nano flow rates. The very high-pressure chromatography, or ultra-pressure liquid chromatography (UPLC), deals with a relatively moderate extension of the pressure regime sustained by the SDS up to 600–1400 bar. This can normally be achieved using commercially available instrumentation with improvements in terms of materials and production technologies of the different active constructive elements. Ultra-high-pressure liquid chromatography (UHPLC) deals with pressure regimes between 1400 and 9000 bar and requires special constructive modifications of the pumping systems. Very high and ultra-high-pressure LC applications involve separations carried out on columns packed with sub-two-micrometers particle size stationary phases, low internal diameters (below 1 mm), and increased lengths (up to 60 cm). The major achievements of such separations are increased resolution, very high separation speed, and improved sensitivity.

The ongoing tendency to reduce particle size and column internal diameter leads also to a reduction of the required optimal flow rates. Micro-LC applications consist of columns with internal diameters less than 1 mm and require flow rates between 1 and 100 μl/min. Nano-LC applications require flow rates in the 100–1000 nl/min range. For a micro- or nano-LC setup, the flow is controlled by means of a flow sensor (FS) situated after the purge valve. The FS works in a feedback loop with the electronically controlled

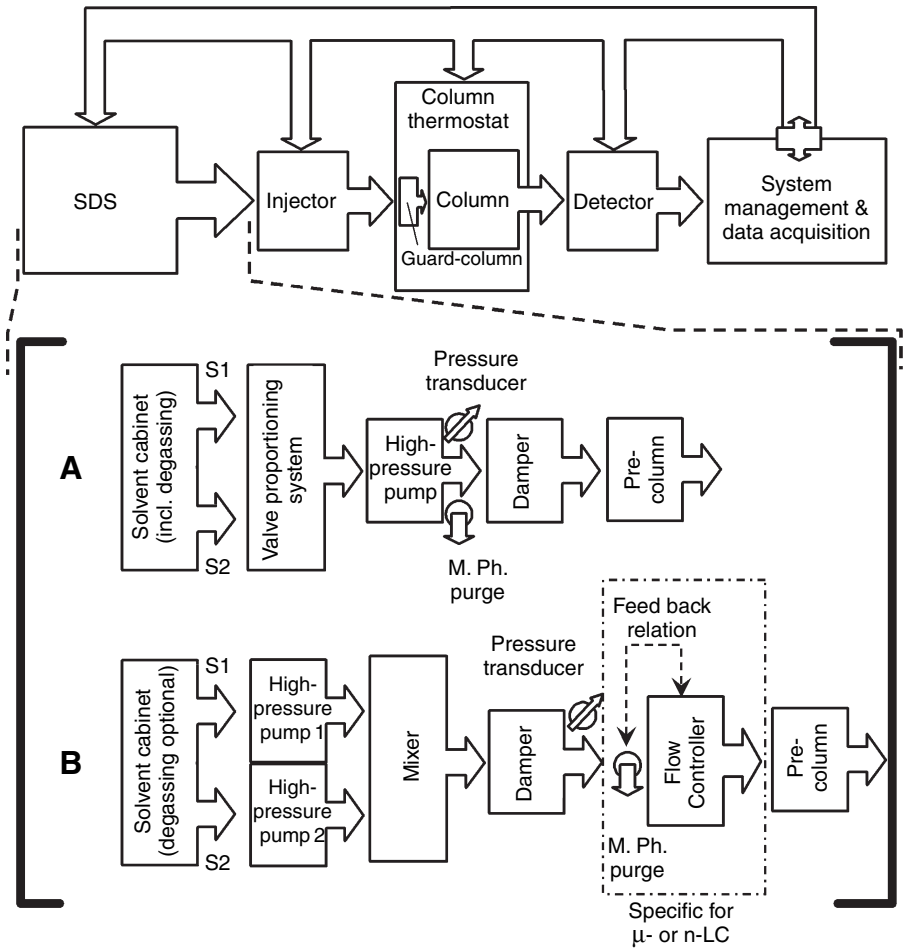

Fig. 1 General diagram of an SDS within the structure of a liquid chromatograph. A, Low-pressure solvent mixing design; B, High-pressure solvent mixing design.

purge valve, allowing the maintenance of precise and accurate flow rate values in the micro- or nanoliters per minute range.

The use of ultra-high-pressure regimes and/or flow rates in the micro- or nanoliters per minute range imposes unique requirements on LC system hardware, such as pumps, valves, injectors, connecting tubing, column construction, stationary phases, column heating systems, detection flow cells, and the detector's data collecting speed.

CLASSIFICATION

Isocratic SDS is used when the mobile phase contains a unique component or the components are premixed. It is obvious that such an SDS is designated only for isocratic elution. The structure of the SDS depicted in Fig. 1A is known as the low-pressure mixing setup. It uses a single high-pressure pump, and the components of the mobile phase (generally not more than four) are proportioned before entering the pump, at low pressure. Such a setup strongly requires a solvent degassing module. More often, air solubility in individual solvents is higher, compared to the case of mixed solvents. Mixing components under a low-pressure regime, before entering the pump, will produce degassing within the pump body, thereby resulting in a cavitation phenomenon and significant variations of the flow rate and pressure. Precision and accuracy in the formation of the mobile-phase composition are poorer, compared to those in the setup presented in Fig. 1B. This model uses a high-pressure pump for each solvent component (usually two components). Components are mixed under a high-pressure regime, after their controlled delivery. Because a high-pressure regime increases gas solubility in liquids, degassing of the individual components should be considered as optional. Both low-pressure and high-pressure solvent mixing configurations are used for the gradient elution mode in LC. However, isocratic elution is also possible, by automated mixing of the components of the mobile phase in definite volumetric proportion by the SDS itself.

CONSTRUCTIONAL ASPECTS

Solvent Containers

Solvent containers are generally used for storage, online filtering, and, eventually, degassing of the constituents of

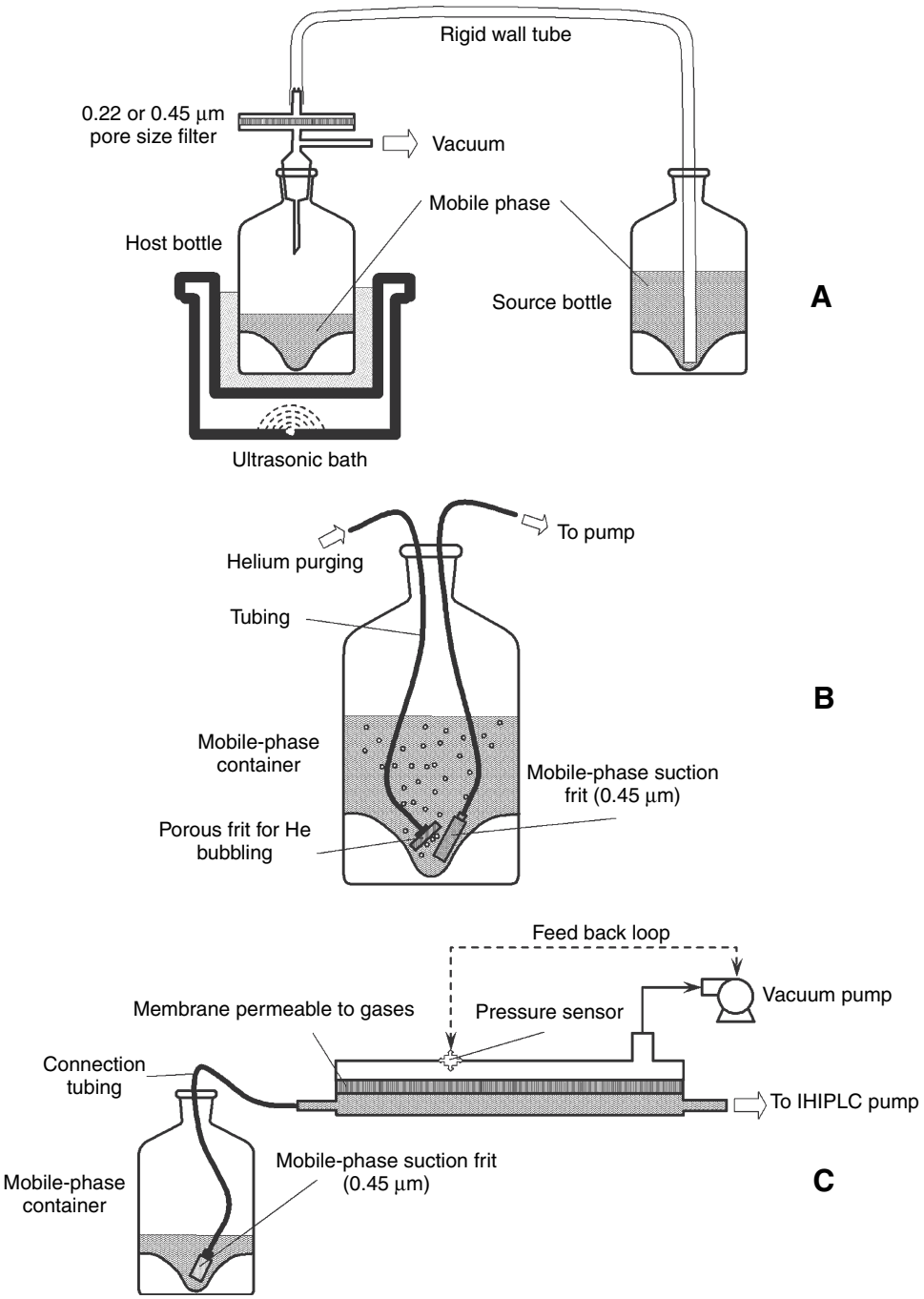

Fig. 2 Different modes for degassing solvents: A, off-line vacuum filtration and ultrasound; B, online helium purging; and C, online vacuum degassing system.

the mobile phase. Liquids are stored in glass bottles of appropriate volume and geometry. If solvent or solvent mixtures stored in containers are subject to photo- or biodegradation under the effect of sunlight, the use of amber glass bottles is strongly recommended. Addition of preservatives to the constituents of the mobile phase may be possible if such compounds are tolerated by the chromatographic separation and/or the detection system (e.g., sodium azide is usually added to mobile phases containing sodium acetate buffers and for size exclusion separation mechanism on saccharidic stationary phases to preserve the integrity of both mobile and stationary phases). Solvents are suctioned from reservoirs by means of 0.45 μm pore size frits (metal- or ceramic-based materials are used). Appropriate geometry of the reservoir bottom may facilitate the use of the solvent until the last droplet (Fig. 2).

When metal frits are used, the possible corrosive effects of solvents and/or additives on the material should be duly considered (e.g., hydrochloric acid produced in chloroform during storage reacts with stainless-steel frits). Bacterial growth within the constituents of the mobile phase may also block the pores. Technical solutions for solvent degassing are extremely variable. The first attempts were oriented toward heating the solvent in its reservoir just below the boiling point (dissolved air is eliminated on account of its decreased solubility in the liquid phase). Despite its efficacy, such an approach became obsolete, owing to some major drawbacks: 1) necessity of cooling the solvents back to the ambient temperature before pumping and 2) safety concerns related to the inflammability of the solvents. An off-line solution for solvent degassing is given in Fig. 2A. The mobile-phase component is transferred from one bottle to another under vacuum and filtration over 0.22 μm pore size membrane with simultaneous application of ultrasound. Degassing may be effective over a period of time depending on the nature of the mobile-phase constituents. Another approach (Fig. 2B) relies on a continuous helium purge through the solvent. As helium has the lowest solubility in liquids, it readily removes dissolved gases. The process is continuous, online, simple, and effective, but expensive (because of the use of large volumes of highly purified helium). The technical solution illustrated in Fig. 2C is based on the component transfer through a bicompartmental evacuated chamber having an inner separation membrane that is permeable to gases. The low-pressure regime is kept under control by means of a sensor working in a feedback loop with the vacuum pump. Good degassing yield is obtained, and the process runs online, but it requires more expensive equipment. Moreover, salt deposition (from buffers) strongly affects membrane efficiency, while malfunctioning of the vacuum system and/or excessive flows may result in membrane breakout and serious leakages.

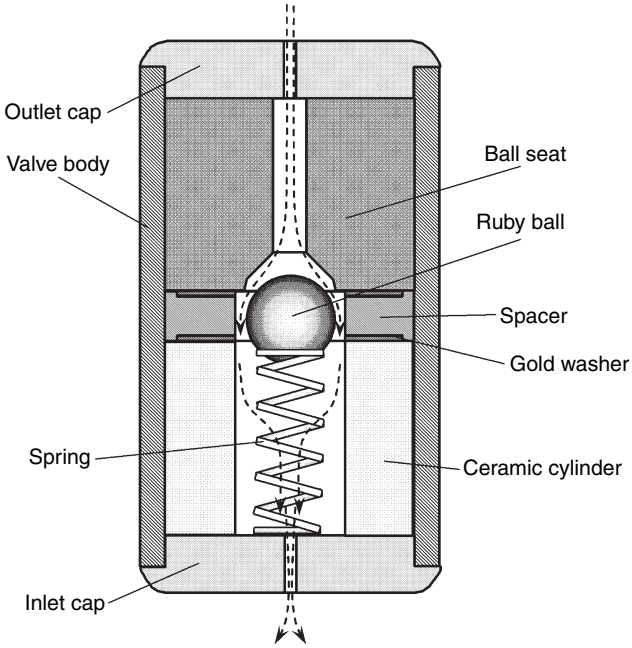

Fig. 4 Construction of a ball valve (inlet or outlet) for high-pressure pumps.

High-Pressure Pumps

The high-pressure pump design is most often based on the operational principle of the piston pump (Fig. 3).

The reciprocating movement of the piston within the pump body (cylinder) causes solvent delivery. Owing to the direct contact of piston and inner pump body surfaces with the carried liquids, high chemical inertness is required. Pistons are usually made of ceramics, synthetic sapphire, or zirconia, while the pump body may be produced from titanium, stainless steel, or even polymeric materials (e.g., PEEK^{TM}). Prevention of back flush of liquid from the pump body to the solvent reservoir when the piston moves forward is achieved by means of an inlet

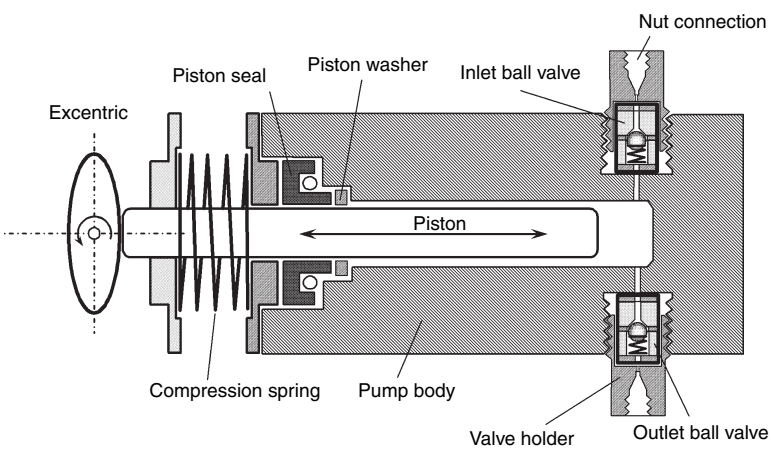

Fig. 3 Scheme of a single-piston high-pressure pump.

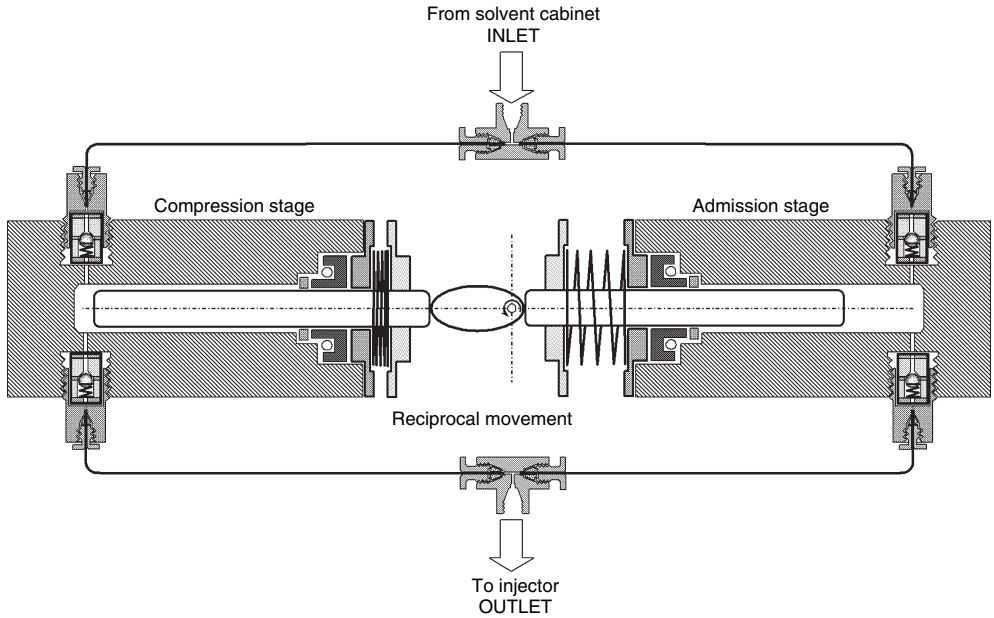

Fig. 5 Construction of a reciprocal high-pressure pump for HPLC.

ball check valve. The back flush from the connection tubing to the pump body when the piston moves backward is prevented by the outlet ball check valve. Ball check valves allow unidirectional passage of the liquid by means of a ruby ball moving out or into a specially designed seat according to the liquid flow direction (Fig. 4). Perfect fitting of the ruby ball against the seat could optionally be enhanced by means of a spring.

The single-piston pump delivers a pulsed flow (flow occurs when the piston is moving forward and flow stops when the piston is moving backward). To reduce flow pulses, the solvent admission into the pump body can be realized by means of a fast backward movement of the piston. Under such conditions, liquid compressibility and viscosity should be taken into consideration.

One of the easiest solutions to generate constant flows uses two piston pumps operating at 180° out of phase (meaning that one of the pumps is in admission, while the other is in the compression stage). This design is called the reciprocal mode and is illustrated in Fig. 5.

Increased flow control can be achieved by replacing the piston with an elastic membrane. The membrane is periodically flexed by means of a viscous liquid (e.g., mineral oil) contained in a closed cavity in which a piston moves forth and back at a high frequency (~10 Hz). Oil is recirculated in the cavity through a unidirectional valve. A second cavity, containing the mobile phase, fits to the elastic membrane. The flow through this cavity is determined by the inlet and outlet ball check valves. Such a design represents the membrane (or diaphragm) pump, a basic scheme of which is given in Fig. 6. The membrane pump has two major drawbacks: 1) if the membrane fails, the mineral oil gets mixed with the mobile phase, which may irreversibly damage the column and 2) liquid admission through the inlet valve must be achieved at a positive pressure regime (meaning that a low-pressure pump is required).

The only possibility to deliver a pulse-free mobile-phase flow through the chromatographic system is the syringe pump design (Fig. 7). Frequently used in the past for micro-LC applications (flow rates below 10 μl/min), the syringe pump suffers from limitation of the delivered

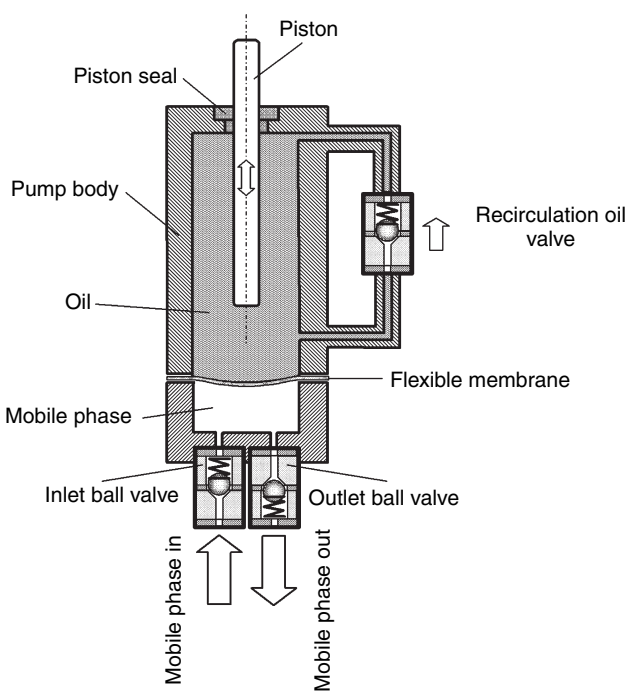

Fig. 6 Construction of a membrane (diaphragm) pump.

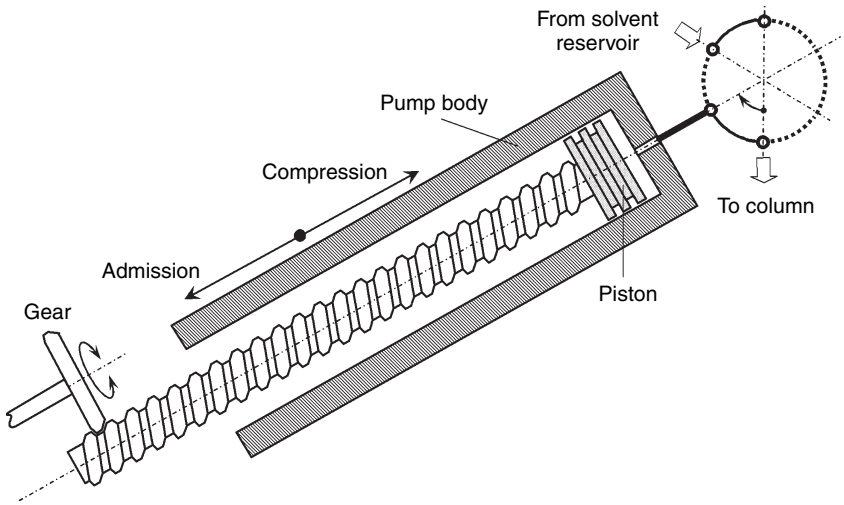

Fig. 7 Syringe pump.

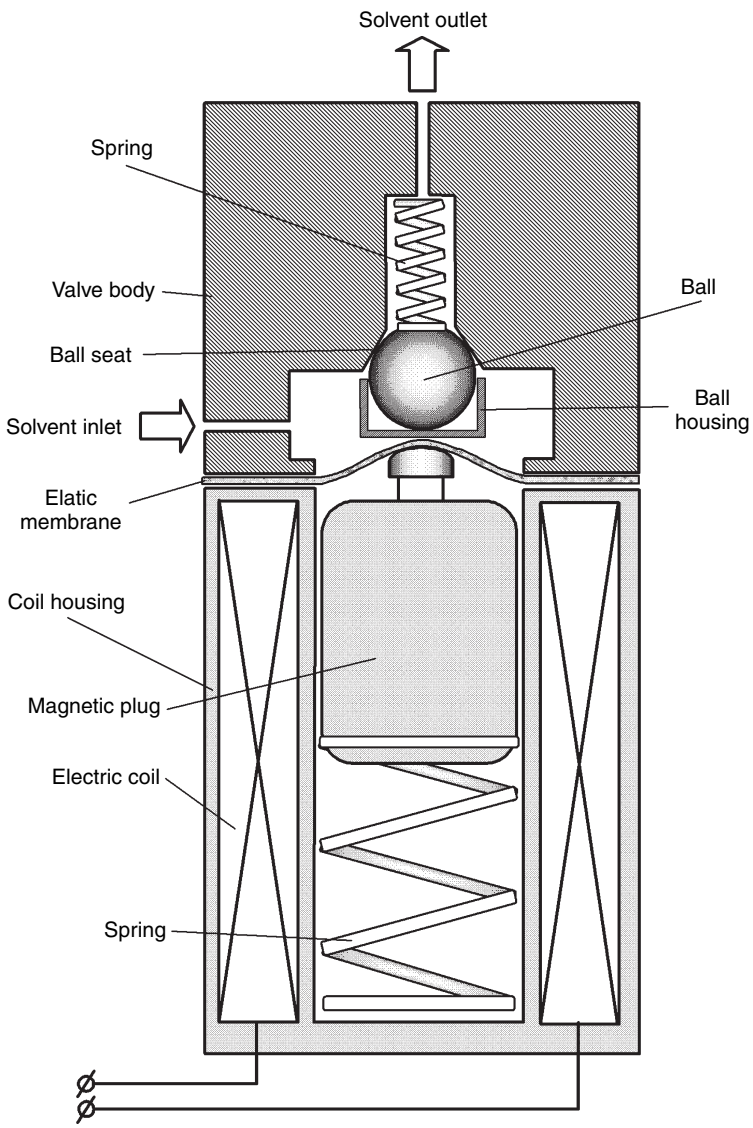

Fig. 8 Electrically driven proportioning valve for low-pressure mixing in HPLC configurations.

volume of the mobile phase (resulting in the limitation of the chromatographic run time) and from some major technical difficulties in creating composition gradients.

Generally, high-pressure pumps may work in two different modes: constant flow and constant pressure. Usually, the constant-flow mode characterizes LC, while the constant-pressure mode is often used in capillary supercritical fluid chromatography (SFC).

Mobile-phase composition control is achievable in the low-pressure solvent mixing setup by means of electrically driven proportioning valves placed between the solvent containers and the high-pressure pump. Proportioning valves' working principle is similar to that of the ball valves fitted to the high-pressure pump (Fig. 8). Pushing the ball into and out of the seat is controlled by means of a magnet plunger operated within a coil (activated when electric current passes through it and deactivated when the flow is cut). Proportioning valves work on time-based cycles. For instance, if the time cycle is 1 sec and it is necessary to create a mobile phase by mixing solvents A, B, and C in the volumetric ratio of 1:1:2, the proportioning valves corresponding to A and B remain open for 0.25 sec, while that corresponding to C is kept open for 0.5 sec.

Ultra-High Pressure Pumps

The earliest and still the most commonly used pumps for UHPLC are air-driven liquid pumps, or pneumatic amplifier pumps. The piston area on the air-driven side is much larger than that on the liquid side, so that very high liquid pressures are obtained via relatively low air pressures. The major advantages of pneumatic amplifier pumps refer to high pressure levels (9000 bars) obtained, commercial availability, and relatively low costs. Disadvantages are mainly related to the fact that pneumatic amplifier pumps are controlled by pressure instead of volume, which makes difficult the generation of elution gradients, and their large sizes.

Another approach to generate ultra-high pressures is to use a conventional HPLC pump with a hydraulic amplifier (see Fig. 9). The differential area provided by the difference in the diameters of the pistons creates a pressure amplification that is proportional to the ratio of the areas. Specifically, the pressure amplification can be calculated as follows:

$$P_2 = P_1 \times \frac{D^2}{d^2}$$

where P_2 and P_1 are the pressures acting on the secondary and the primary pistons, and D and d are the diameters of the primary and the secondary pistons, respectively. As an example, if the diameter of the primary piston is 3 cm and the diameter of the secondary one is 0.5 cm then the pressure will be amplified 36 times; if the HPLC pump delivers the hydraulic fluid at 300 bar, then the pressure in the UHPLC part will be 10,800 bar. In addition to pressure amplification, the hydraulic amplifier also creates a flow reduction. As the primary and the secondary pistons have substantially identical linear velocities, the difference in cross-sectional areas results in a reduction in flow rate, computed according to the following relationship:

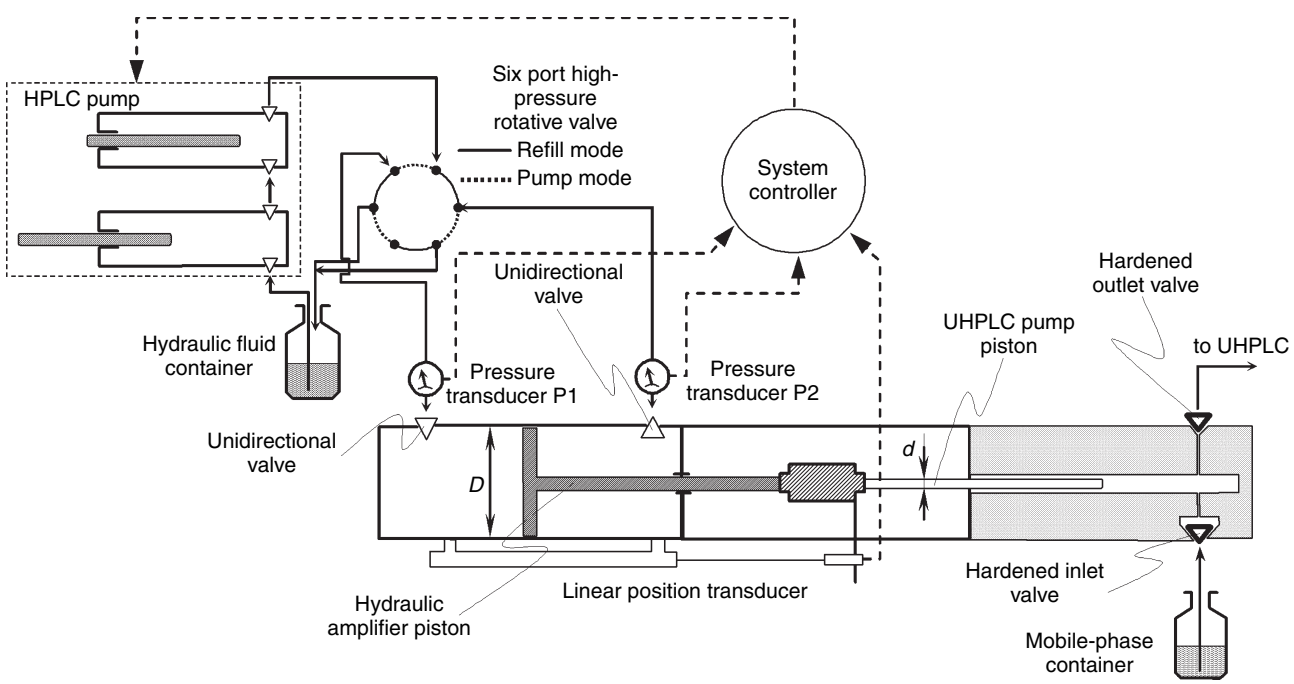

Fig. 9 Hydraulic amplification principle for ultra-high-pressure liquid chromatography applications.

$$F_2 = F_1 \times \frac{d^2}{D^2}$$

where F_1 and F_2 are the flow rates in the primary and secondary stages, and d and D are the diameters of the secondary and the primary pistons, respectively. Considering the piston diameters from the previous example and a flow rate of the HPLC pump of 2 ml/min, the UHPLC flow will drop to 0.056 ml/min.

In UHPLC conditions, solvents become compressible. Consequently, a significant portion of the piston stroke is used for compressing the solvent. Owing to this fact, it is advantageous to run the primary HPLC pump at high flow rates until the desired secondary operating pressure is achieved. As well, both compression and decompression

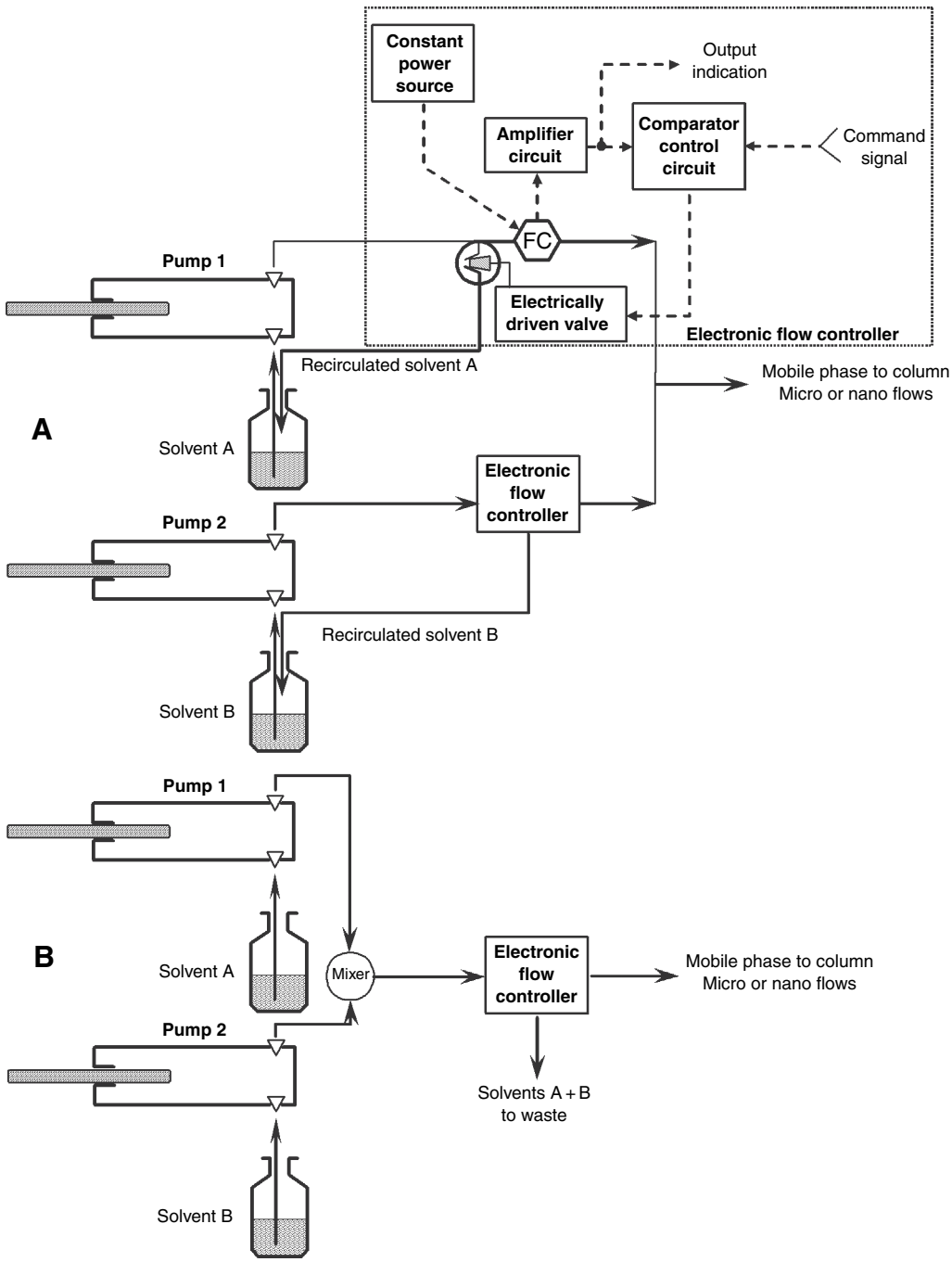

Fig. 10 Micro/nano pump functioning principle: A, flow control and solvent recirculation for each pump and B, flow control and purging of mobile-phase excess after mixing.

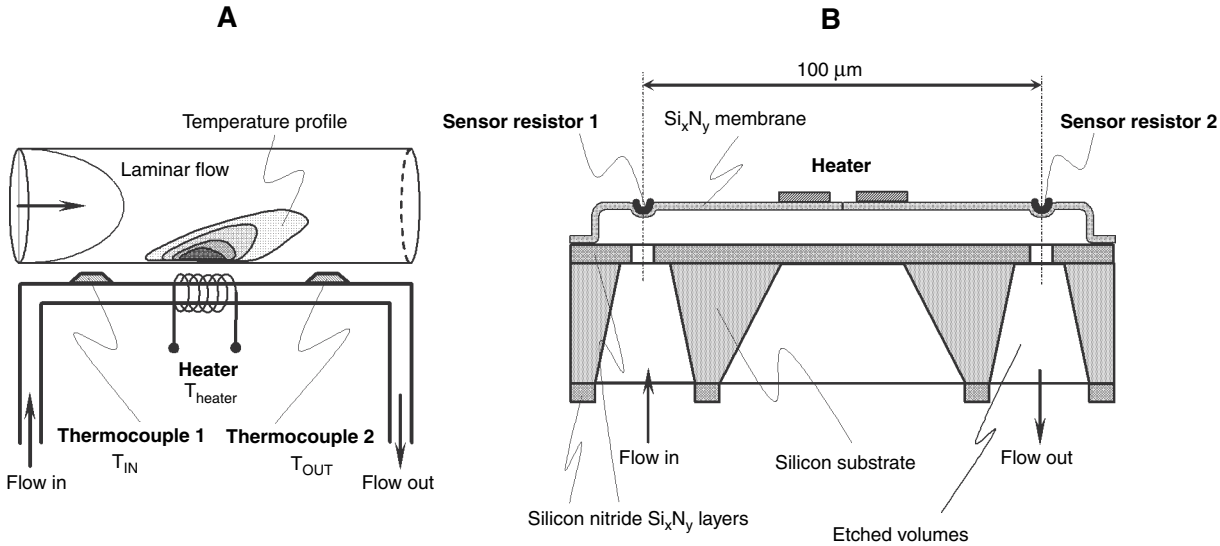

Fig. 11 Thermal mass flow sensing principle (A) for normal flows and (B) for micro and nano flows (MEMS).

stages of the eluent must be considered in terms of heating and changes in the solvent's structure.

Micro- and Nano-HPLC Pumps

Operation of HPLC pumps for delivering micro- to nanoliters per minute flow rates is based on the capability to make precise flow measurements and the feedback control through an electronically driven purge valve situated before the flow sensing area. Such an electronic flow control system may be placed after formation of the required mobile-phase composition (from two or more high-pressure pumps) or may be used for each specific pump. In the first case, the mobile-phase flow exceeding the threshold is purged as a waste, while in the second case the solvent may be recirculated back to the reservoir. The two setups are depicted in Fig. 10A and B.

The measuring principle of a thermal mass FS is as follows: the flow is led through a U-shaped tube where two temperature sensor elements (or a configuration of constantan–copper thermopiles) are placed with a heater in the middle. When there is no flow through the pipe, the temperature profile is symmetric around the heater (see Fig. 11A). When the fluid is flowing through the pipe, from left to right, the temperature profile will shift to the right side. The temperature shift is obtained as the difference ΔT between the upstream and downstream sensor measurements. The signal output of the sensor is proportional to the mass flow according to the relationship

$$\text{Output} \propto \Phi_m = \frac{P}{\Delta T \times c_p \times K}$$

where Φ_m is the mass flow, P is the power feed to the heater, ΔT is the temperature shift, c_p is the heat capacity of the fluid, and K is the sensor's constant.

The construction of a FS having nanoliters per minute measuring capability is based upon micromachining technology (see Fig. 11B). The flow sensing process takes place in a silicon nitride microchannel created by etching of a poly-Si sacrificial layer. Inlet and outlet of the channel are obtained by KOH etching of the backside of the substrate. The platinum resistors deposited on the top of the microchannel perform liquid flow sensing by monitoring the temperature profiles of the heater placed in the middle position. Such devices are called "micro-electrical-mechanical systems" (MEMS), which are micromachined systems containing both electrical and mechanical components with characteristic sizes ranging from nanometers to millimeters. MEMS based on resonant Coriolis mass flow sensing are also commercially available.

Damper

The main role of the damping unit is to reduce flow fluctuations. The functioning principle is based upon the attenuation of the mobile-phase flow fluctuations by means of an elastic membrane separating two cavities. In the first cavity, a liquid with a low compressibility coefficient is introduced. The mobile phase runs through the other cavity. Usually, the damper also incorporates the pressure transducer. The liquid filling the first cavity pushes back the plunger placed on the opposite side of the elastic membrane. Outside the cavity, the plunger is placed in direct contact with a sensor monitoring the pressure within the chromatographic system (Fig. 12).

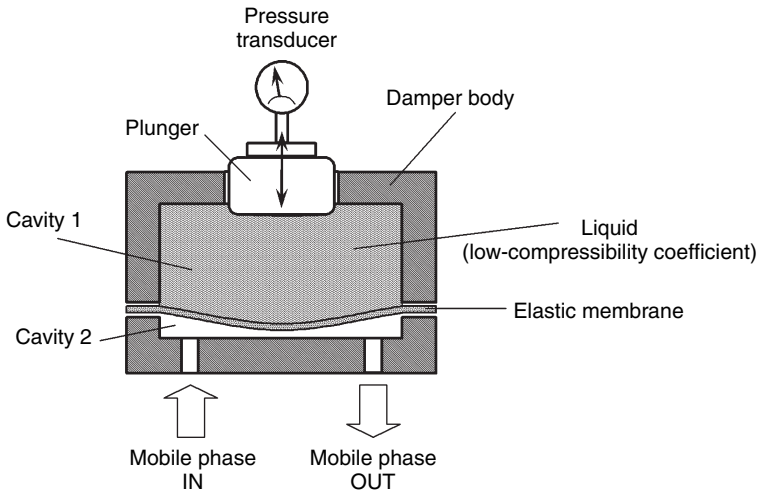

Fig. 12 Scheme of a damper incorporating the pressure transducer.

Mixer

Mixers are designed to ensure homogeneity of the mobile phase, whose composition is determined by means of the pumping system from two or more solvents. Mixing of the mobile-phase constituents is achieved in dynamic or static mode. The dynamic mixer is based on the principle of a magnetic stirrer, as shown in Fig. 13A. The static mixer may be a simple column packed with stainless-steel spheres; tortuosity of the flow through the packing induces mixing of the components (Fig. 13B). It is essential that the internal volume of the mixing unit be as small as possible. This feature will reduce the delay between gradient formation in the pumping system and in the chromatographic column (same observation is valid also for dampers).

Precolumn

The precolumn acts on the mobile phase. Its role is to reduce unwanted interactions between mobile and stationary phases within the chromatographic column. It is well-known that traces of water contained in organic solvents accumulate on the silica gel surface. Water bound to silanol sites is strongly retained by means of hydrogen bonds and will shift the phase retention mechanism from adsorption to partition, resulting in serious disturbances in the chromatographic behavior. A precolumn packed with a desiccant material will solve this problem related to the normal-phase retention mechanism. An alkaline-buffered mobile phase strongly influences the characteristics of silica gel-based stationary phases, owing to its dissolution as complex anions. If such a problem is expected, a precolumn packed with silica gel will saturate the mobile phase and will consequently preserve the stationary phase from deterioration.

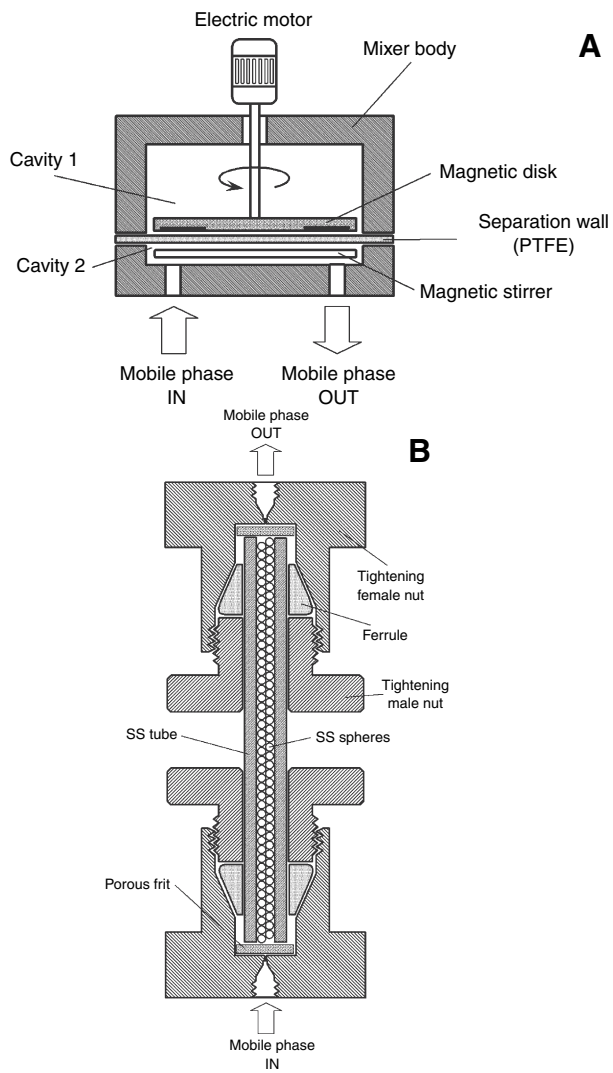

Fig. 13 Mixers: A, dynamic mixer and B, static mixer.

Table 1 Some problems related to the functioning of HPLC pumps.

Problems	Observable symptoms	Solution
	Solvent cabinet	
Blocked frit	No accurate mixing proportioning; serious shifts in retention pressure remains constant, but at a level different from the usual	Change frit or clean the blocked one with 60% nitric acid and ultrasounds
Air bubbles within solvent connecting tubes	Pressure and flow fluctuations	Degas the solvents off-line; purge the pumping system
Membrane permeable to gases broken in the vacuum-based degasser	Large flow and pressure variations; significant leaks in the online degasser	Replace degassing chamber
Defective vacuum pump in the degasser	Pressure and flow fluctuation; unstable baseline in chromatogram	Replace vacuum pump
	Pump	
Defective seal	Leak behind pump head; pressure and flow variations	Replace seal
Scratched piston surface	Leak behind pump head; pressure and flow variations	Replace piston
Defective inlet or outlet ball valve	Pulsed flow; very low flow; large "shark tooth" pressure variation; sinusoidal baseline	Clean ball valve in methanol–water mixture and ultrasound; change ball valve
Defective proportioning valve	Inaccurate composition of the mobile phase; irreproducible retention; large shifts in retention time within the chromatogram	Replace proportioning valve
Broken piston	No flow; visual observation	Replace piston and piston seal
Air entrapment within the pump body	Large flow and pressure variations	Purge pump
Seal incompatibility with one or more of the solvents	Excessive baseline noise, short column life time	Replace the seal with another seal compatible with the solvents used
	Mixers and damper	
Blocked frits (static mixers)	High-pressure regime within the system	Replace or clean frits
Burned electrical motor (dynamic mixer)	Erratic retention in chromatogram; small and random pressure variations	Replace electric motor
Broken membrane in the damper	Fluctuations in flow; large variations in pressure readouts (if pressure transducer is incorporated in the damper); mobile-phase contamination	Replace membrane

Troubleshooting SDS

Problems related to the functioning of SDS are highly varied, and they induce serious disturbances in a chromatographic system. A summary of commonly arising malfunctions is illustrated in Table 1.

Maintenance of SDS

To keep the SDS properly functioning, some actions are mandatory to be carried out during daily activity. Maintenance operations should be carried out with rigorous frequency, and interventions should be noted in a log.

The following actions are advisable:

1. When using mobile phases containing inorganic buffers, flush the system with water at the end of the working sessions, starting with the solvent container.
2. When the mobile phase contains concentrated inorganic buffer solutions, use an online piston/seal-washing accessory.
3. Replace piston seals at least once a year and pistons every two years.
4. Do not use hydrochloric acid solution as an aqueous component of the mobile phase.
5. Periodically inspect and wash the suction frits within the solvent container.
6. When inorganic buffers are used, filter the solvent through a 0.45 μm membrane before use.
7. Repeat SDS operational qualification after each mechanical intervention in the pump.
8. When changing from reversed-phase to normal-phase separation mechanism, flush the SDS intermediately with *i*-propanol.
9. If the pump is opened, replace the piston seal.

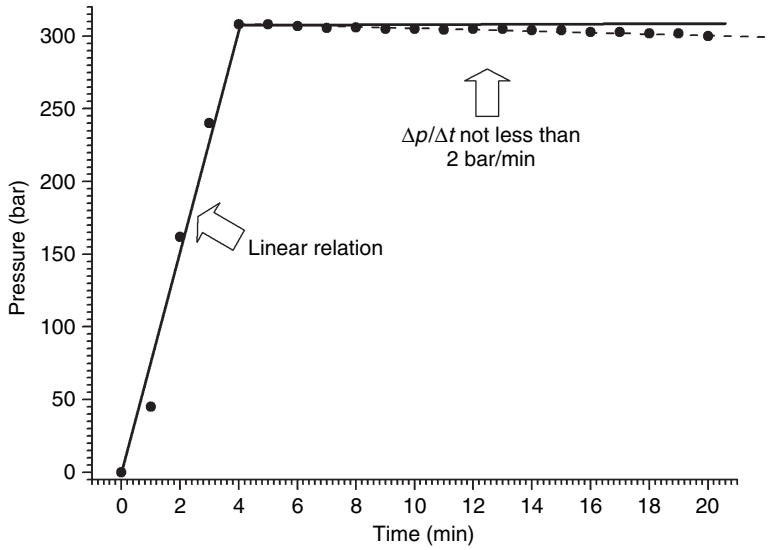

Fig. 14 Plot illustrating the tightness test for HPLC pumps.

OPERATIONAL QUALIFICATION OF AN SDS

Operational qualification of the SDS refers to the following aspects:

1. Pressure readout accuracy test
2. Tightness or leak test
3. Accuracy of the delivered flow rate
4. Gradient formation test
5. Dwell time test

Pressure Readout Accuracy Test

This test should be considered optional, as long as pressure indications are precise and accurate. Verification of the pressure accuracy relates to a null indication when the sensor is isolated from the system (usually the damper incorporating the pressure transducer is removed from the LC configuration) and the indication of a true value when a restriction is placed within the system instead of the column, generating a known pressure drop for a specified flow rate and a given density of the mobile phase.

Leak Test

The leak test formally checks for loss of tightness within the SDS. More specifically, it focuses on possible leaks at the piston seal level. To carry out the test, the SDS is isolated from the chromatographic system and is fed and flushed with degassed i-propanol. After an appropriate equilibration period, the flow rate is set to a low value (i.e., 0.1 ml/min) and the outlet of the SDS is blocked. Pressure readouts are monitored. On reaching a pressure regime of above 300 bar, the flow rate is set to zero and monitoring of pressure indications is continued for at least 5 min. Plotting the pressure readouts against time should generate a result analogous to the dependence in Fig. 14. There are two mandatory criteria to be fulfilled. The first relates to a linear pressure ramp observed during the first stage of the test (corresponding to the low flow rate). The second imposes a pressure variation on the plateau corresponding to the null flow rate with a slope ranging from –2 to 0 bar/min.

Accuracy of the Delivered Flow

This test requires additional equipment, such as certified analytical balance, certified thermometer, certified chronograph, and certified class A volumetric flask and a piece of stainless-steel tubing having 0.12 mm I.D. and 2 m length. The SDS is fed and flushed with degassed HPLC-grade water until full equilibration is achieved. The chromatographic column is replaced with a piece of stainless-steel tubing, acting as a restrictor, and the detector is taken out of the configuration. A flow rate value is set on the SDS controller, and the mobile phase is collected over a period of time at the other end of the restrictor, into a previously weighed volumetric flask. Collected effluent is checked for volume by weighing with an analytical balance. Density correction for water should be made if the measured temperature is outside the $25 \pm 1^{\circ}C$ interval. Alternatively, it is possible to check the time period needed to fill up the volumetric flask up to a specified mark, measured with a chronograph. Deviations higher than $\pm 1\%$ with respect to the set flow rate values should be considered as out of the acceptable limits. An ideal flow rate accuracy test should be run three times consecutively for at least three values covering the assumed operational interval of flow rates.

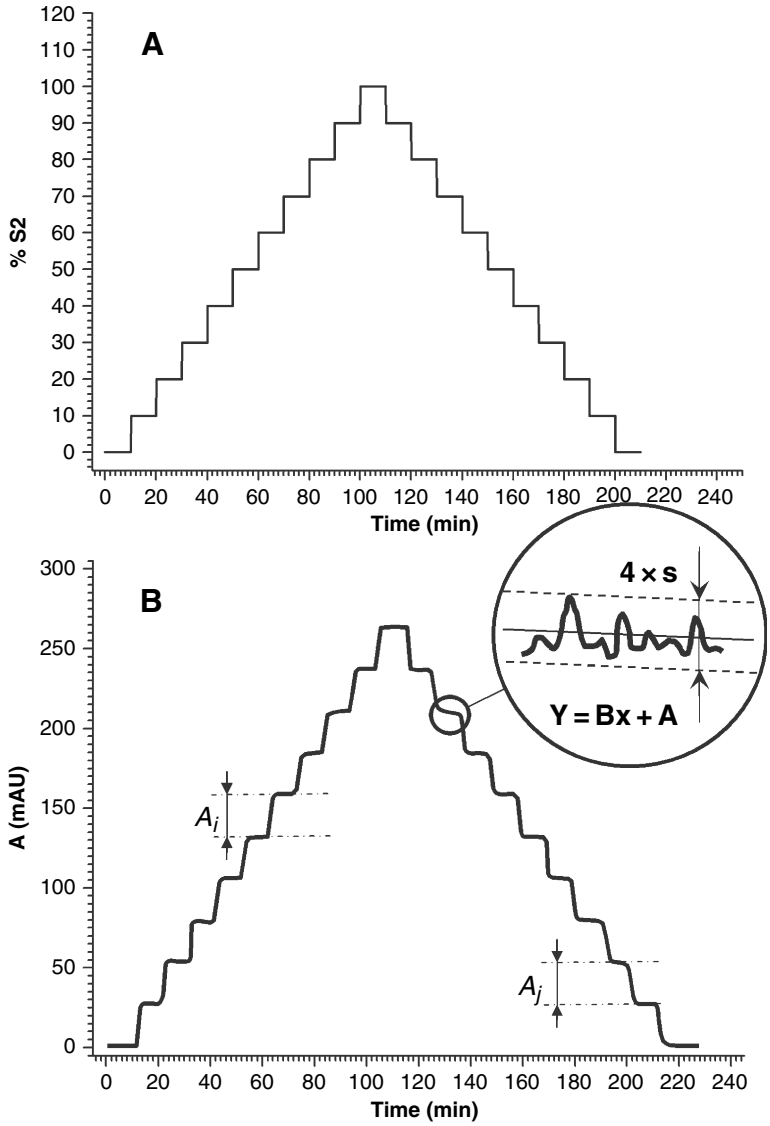

Fig. 15 The gradient test for operational qualification of high-pressure pumps in LC: A, typical gradient profile for checking the accuracy of gradient formation and B, result of the gradient formation test to be evaluated for documenting pump status.

Gradient Formation Test

The test uses two channels of the SDS. The first channel (S1) is fed with HPLC-grade water, while the second one (S2) carries aqueous 5% acetone solution (acetone acts as a UV-active tracer). Configuration of the chromatographic system is complete, including a UV-qualified detector monitoring at 254 nm wavelength. The chromatographic column is replaced by a restrictor. A gradient program is built up on the SDS controller, as illustrated in Fig. 15A. The gradient program consists of successive 10% stepwise increases of S2 volumetric proportion in the mobile phase, followed by at least 10 min of isocratic plateaus. After changing the mobile-phase composition from 100% S1 to 100% S2, the same procedure is used to go back to 100% S1. Baseline shift has to be recorded. The result is depicted in Fig. 15B.

In the data sheet, we need to measure A_i and A_j jumps. Relative standard deviations for A_i and A_j values should be lower than 0.5%. Accuracy of gradient formation is evaluated by calculating the mean optical absorbance value corresponding to each plateau. Conversion of the mean absorbance values into %S2 is carried out by applying the following relationship:

$$\%S2_{(Plateau)} = (\overline{A}_{(Plateau)} - \overline{A}_{(\%S2=0)}) \times \frac{100}{(\overline{A}_{(\%S2=100)} - \overline{A}_{(\%S2=0)})}$$

Biases against set values obtained for each plateau should not be higher than 0.5% for binary pumps (solvents

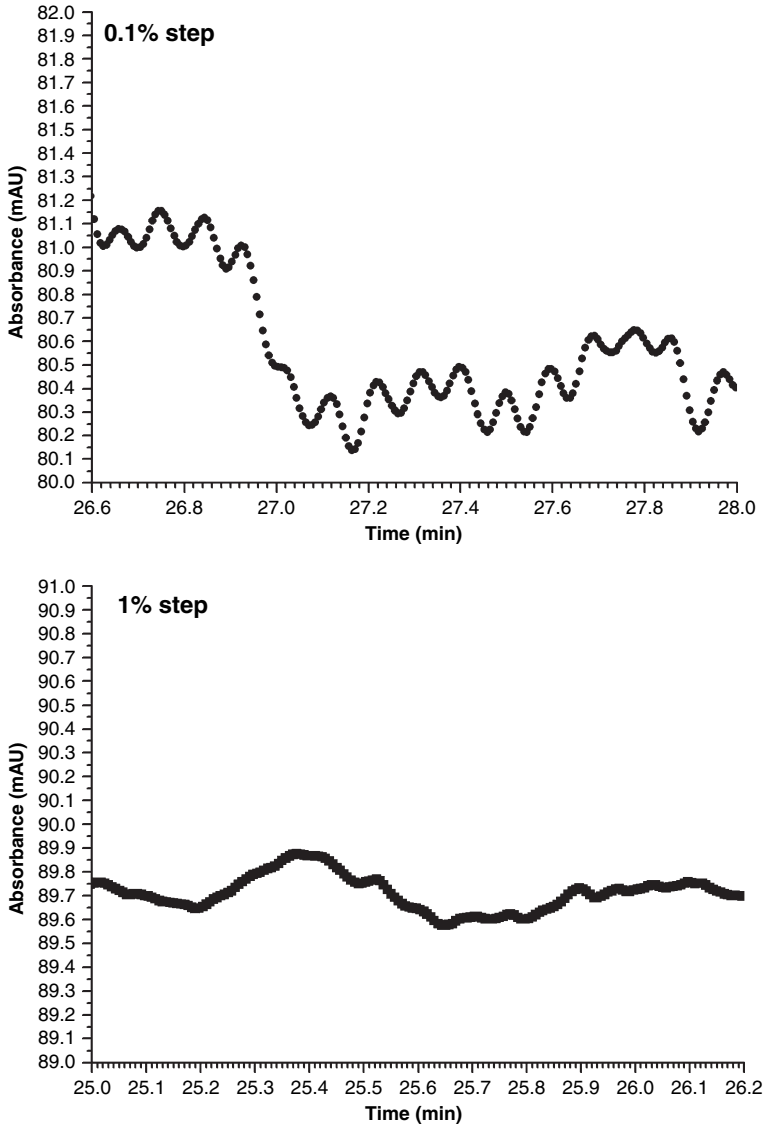

Fig. 16 Ripple of the HPLC pump on a constant-composition plateau during gradient formation test for 0.1% and 1% modification steps.

mixed at a high-pressure regime) and 0.7% for quaternary pumps (solvents mixed via proportioning valves at a low-pressure regime).

The linear regression applied to the data sets obtained over each plateau should be characterized by a slope as close as possible to 0. The normal dispersion (four times the standard deviation) of experimental data acquired over each plateau should correspond to a maximum 0.5% variation of the %S2 (such acceptance criteria is known as ripple). For SDS especially featured for sensitive applications (including micro or nano ones), the same algorithm may be applied for 1% or even 0.1% modification steps for the S2 channel. Reducing the amplitude of the step gradient should be compensated by a proportional increase of the UV tracer in the S2 channel. Some differences in ripple for 0.1% and 1% gradient steps are illustrated in Fig. 16 (note that the extension of the ordinate is the same and corresponds to 2 mAU).

Dwell Time Test

The dwell time test calculates the delay in gradient formation between the pump and the detection area (transit duration of a modification in mobile-phase composition over the chromatographic system). Chromatographic system characteristics are identical to those used during the gradient formation test. The only difference is in the application of the gradient profile. The stepwise gradient profile is replaced by a linear gradient of the S2 solvent (i.e., 5%/min). The time corresponding to the median of the height jump of the monitored baseline is determined (Fig. 17). The

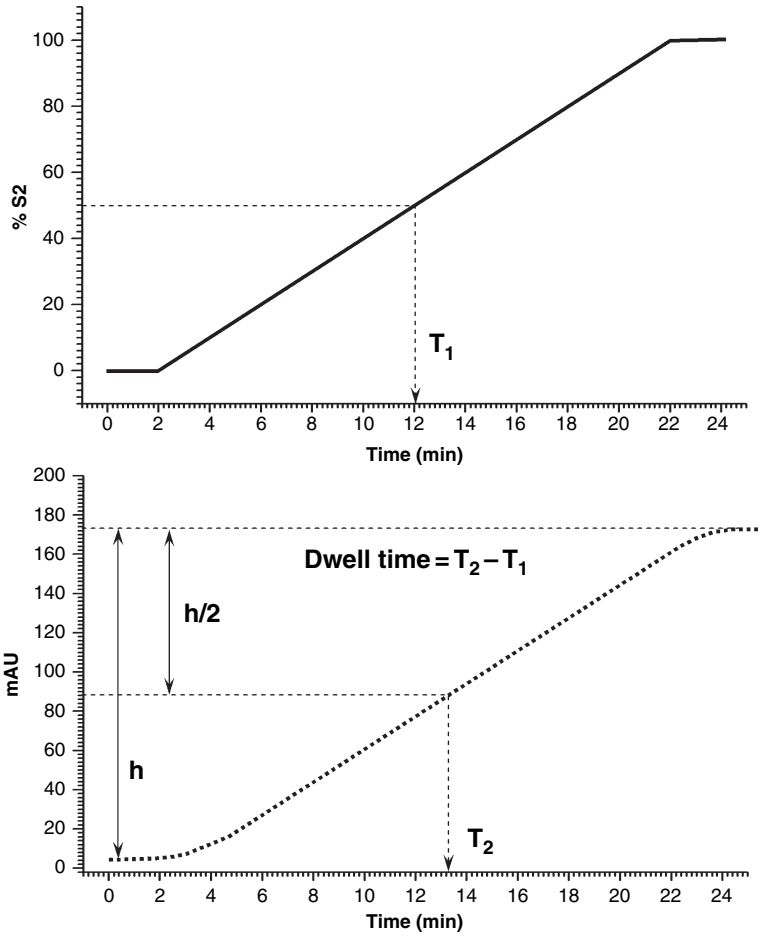

Fig. 17 Determination of the dwell time for HPLC systems: A, applied gradient and B, resulting data plot.

difference between the experimentally determined value and the theoretical time moment corresponding to the middle of the set gradient profile is called the dwell time. Dwell time should be as low as possible.

Operational qualification of an SDS should be repeated yearly. Each maintenance operation carried out during this period comprises the requalification of the SDS. Acceptance limits presented above should be considered as recommendations only. Other specific intervals may be imposed depending on the intrinsic quality of the tested systems and the characteristics of the applications running on these systems.

System suitability tests should be considered to certify that an SDS system operates accurately during each specific application. The system suitability test(s) are more often analyzed before the standard/sample sequences. Adequate acceptance criteria should be imposed. SDS functionality may be expressed in terms of absolute retention, chromatographic resolution between a critical pair, and noise amplitude. Generally, such criteria also include the column quality characteristics.

CONCLUSIONS

The desirable characteristics of an SDS for chromatographic applications have been presented. Design features of isocratic, low-pressure gradient, and high-pressure gradient SDSs as well as ultra-high-pressure hydraulic amplifiers are described, together with test protocols for ensuring their proper operation. An annual maintenance/validation program is recommended.

BIBLIOGRAPHY

1. Dolan, J.W.; Snyder, L.R. *Troubleshooting HPLC Systems: A Comprehensive Approach to Troubleshooting LC Equipment and Separations*; Humana Press: Totowa (U.S.A.), 1989; 165–200.
2. Snyder, L.R.; Kirkland, J.J. Chapter 3: Equipment. In *Introduction to Modern Liquid Chromatography*, 2nd Ed.; Wiley-Interscience: New York, 1979; 83–124.

3. Hanai, T. Chapter 2. Instrumentation. In *HPLC: A Practical Guide, RSC Chromatography Monographs*; Smith, R.M., Ed.; The Royal Society of Chemistry: Cambridge, 1999; 11–30.
4. *Agilent 1100 Series Quaternary Pump*, Reference Manual, Agilent Technologies: Waldbronn, Germany, 1999.
5. Sadek, P.C. *Troubleshooting HPLC Systems: A Bench Manual*; Wiley-Interscience: New York, 1999.
6. Schwartz, H.E.; Karger, B.L.; Kucera, P. Gradient elution chromatography with microbore columns. Anal. Chem. **1983**, *55* (11), 1752–1760.
7. Gilroy, J.J.; Dolan, J.W. Gradient performance checks. *LCGC North America*, **2004**, *22* (10), 982–988.
8. Ventura, D.A.; Nikelly, J.G. Pulse dampening system for high pressure liquid chromatography. Anal. Chem. **1978**, *50* (7), 1017–1018.
9. Van Lenten, F.J.; Rothman, D. Pressure control of a liquid chromatograph pump. Anal. Chem. **1976**, *48* (9), 1430–1432.
10. Nikelly, J.G.; Ventura, D.A. Pulse dampener for high pressure liquid chromatography. Anal. Chem. **1979**, *51* (9), 1585–1588.
11. Del'Ova, V.E.; Denton, M.B.; Burke, M.F. Ultrasonic degasser for use in liquid chromatography. Anal. Chem. **1974**, *46* (9), 1365–1366.
12. Gerhardt, G.C.; Compton, B.J. Hydraulic amplifier pumps for use in ultrahigh pressure liquid chromatography. U.S. Patent 6,712, 587 B2, April 30, 2004.
13. Eschelbach, J.W.; Jorgenson, J.W. Improved protein recovery in RPLC by the use of ultrahigh pressures. Anal. Chem. **2006**, *78* (5), 1697–1706.
14. Colón, L.A.; Cintrón, J.M.; Anspach, J.A.; Fermier, A.M.; Swinney, K.A. Very high pressure HPLC with 1 mm I.D. columns. Analyst **2004**, *129* (6), 503–504.
15. Wu, S.; Lin, Q.; Yuen, Y.; Tai, Y.C. MEMS flow sensors for nano-fluidic applications. Sens. Actuators A, **2001**, *89* (1–2), 152–158.
16. Lambert, D.K. Mass flow sensing with heat waves: The effect of gas pressure. Int. J. Heat Mass Tran. **1993**, *36* (10), 2623–2634.
17. Enoksson, P.; Stemme, G.; Stemme, E. A silicon resonant sensor structure for Coriolis mass flow measurement. J. MEMS **1997**, *6* (2), 119–125.

Purge-Backflushing Techniques in GC

Silvia Lacorte
Department of Environmental Chemistry, Chemical and Environmental Research Institute of Barcelona (IIQAB), Barcelona, Spain

Anna Rigol
Department of Analytical Chemistry, University of Barcelona, Barcelona, Spain

INTRODUCTION

Monitoring of volatile organic compounds (VOCs) in the environment has become a subject of concern because many of these compounds are toxic and persistent[1] and, in addition, are responsible for odor and taste problems in various types of water.[2] Their presence in water is mainly associated with industrial and urban discharges, chlorination of municipal wastewater, or on-land application of pesticides.[3] Analysis of VOCs has been performed using various techniques involving purge and trap (P&T), headspace, liquid–liquid extraction, solid-phase microextraction (SPME), or closed loop stripping analysis (CLSA).[4] However, P&T is the most commonly used technique because it permits the extraction of a wide range of analytes of different chemistries.

The present work is an overview of purge–trap, coupled to GC (P&T–GC) for the analysis of a wide range of VOCs. This technique has been applied to the determination, in water and solid matrices, of compounds that have sufficiently high volatility and low water solubility to be removed from water, e.g., aromatic hydrocarbons, alcohols, aldehydes, ketones, chloroaliphatic compounds, halogenated compounds, etc. In this technique, VOCs are sparged (purged) from the sample by bubbling inert gas for a fixed period of time. Purged sample components are trapped in a solid sorbent trap, generally containing Tenax®. Afterwards, the trap is rapidly heated and backflushed with helium to desorb the trapped sample components and introduce them directly into the GC. Desorption can be performed with cryofocusing, which lead to better peak shapes. Chromatographic techniques are then used to identify and quantify target compounds. This entry reports the optimization parameters of P&T–GC, such as sample volume, type of trap and analytical column, most widely used detectors for VOCs, and precautions that have to be taken with the sample handling and analysis of VOCs, in order to have a reliable result. Finally, the last section will be devoted to the monitoring of VOCs in environmental waters, comprising surface, groundwater, and industrial effluents.

OPTIMIZATION OF THE PURGING CONDITIONS

VOCs represent a group of contaminants of low reactivity, characterized for having low water solubility (from 0.05 to 19 g/L at 25°C), vapor pressures of 0.13–25 kPa (184 kPa for bromomethane), boiling points (bp) ranging from −13.9 to 180°C, and Henry's law constants varying, in general, from 0.1 to 3 kPa m^3/mol. The Henry's law constant is used to predict the movement of VOCs in the environment, but it is also a key factor to determine the stripping process during P&T analysis. Purgable compounds must have a sufficiently high Henry's law constant to enable extraction from water or solid matrix.

P&T is a standardized method dictated by the U.S. Environmental Protection Agency (US EPA), Series 500 and 600, and is extensively used due to its wide application range, good precision, absence of solvents, ease of coupling with GC, and the possibility of automation. When a MS detector is used, as described in US EPA Method 524.2,[5] more than 60 compounds can be analyzed in a single run. In this method, 5–25 ml of water is purged with He at a flow rate of 30–40 ml/min for 11 min at ambient temperature. Compounds are retained in a trap which is, thereafter, heated to 180–230°C to desorb the compounds either with or without cryofocusing. Fig. 1 shows a general scheme of a P&T device. The stripping efficiency depends on the partition coefficients of the compounds, while the efficiency in trapping the stripped VOCs depends on the type of compounds and on the retention characteristics of the trap. Several purge parameters can be optimized to afford higher sensitivity and selectivity. The most relevant are:

(i) Type of trap column.
(ii) Purged sample volume.
(iii) Gas flow rate and purging time.
(iv) Desorption conditions.

Typical values are indicated in Table 1.

The type of trap should be selected so that target analytes can be easily trapped and efficiently removed. It should provide good recoveries and good chromatograhic resolution so that VOCs can be precisely

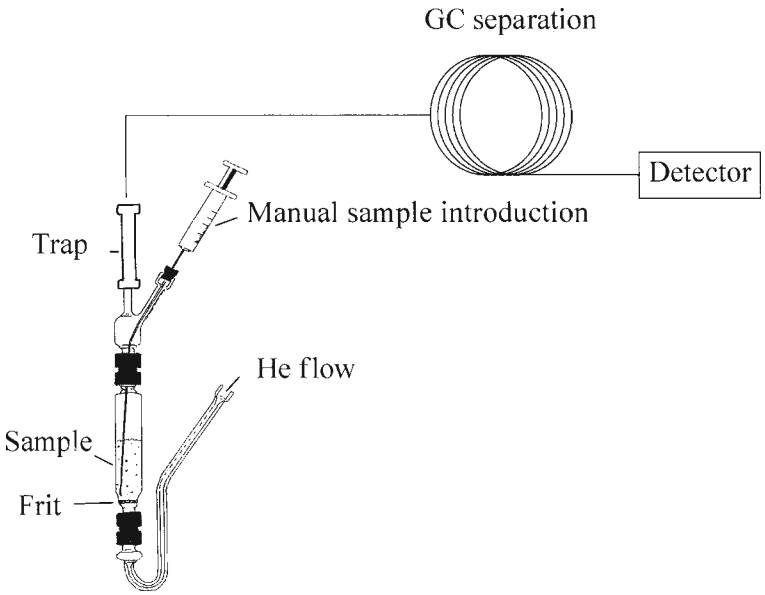

Fig. 1 Schematic of manual purge and trap GC for the analysis of volatile organic compounds in water.

quantified. Different types of trap sorbents are generally available in the market. Tenax® was widely adopted in 1970; it provided reliable results with high precision and detection limits at the μg/L levels.[5] It is stable at temperatures of 180°C, and, if properly cleaned, no background contamination is observed. The main drawback is that it may lead to losses of the more volatile compounds such as vinyl chloride. This problem can be overcome by the use of mixed sorbents with Tenax®-SilicaGel-Charcoal or Tenax®-activated charcoal (Spherocarb/Carvosieve). These sorbents permit trapping of compounds with higher molecular weights and support higher desorption temperatures, thereby enabling faster transfer of the analytes and better chromatographic separations. These combined phases also provide more reliable recoveries and allow the retention of a broader range of chemicals. The use of activated carbon and Tenax® is especially suitable to trap the lightest VOCs. Because the analytes are desorbed by backflushing the trap, compounds with high molecular weights are never in contact with the strong sorbent; thus, they are easily eluted. Baking of the trap is necessary to avoid memory effects between different samples. The baking temperature and time depends on the type of trap used. In general, the system is set at 230°C for 10 min, and, with these conditions, no carryover is generally observed.

Table 1 Parameters that can be optimized during P&T–GC/MS and common values used for the determination of a wide range of VOCs in waters.

P&T conditions		GC/MS conditions	
Type of trap	Tenax	Interface temperature	250°C
	Combined phases	Injector	Split/splitless ratio, 20:1
Sample volume	5–20 ml	Column	DB-624
Purge temperature	35°C	Temperature program	35°C (5 min) to 160°C at 7°C/min (1 min) and to 210°C at 5°C/min
Purge flow rate	20–50 ml/min		
Desorption temperature	180–250°C	Carrier	He, 1 ml/min (max. 1.2)
Desorption flow rate	3–4 ml/min	MS source temperature	200°C
Desorption time	1–5 min	Emmission current	100 μ;A
Bake time	10–15 min	Detector voltage	380 V
Bake temperature	230–280°C	Scan range	35–300 amu

The sample volume that can be purged depends on the system configuration and the type of sample to be analyzed. Foaming is one of the problems that arises when purging samples with high organic content. In such cases, the sample should be diluted, or a small sample volume should be sparged. In order to have a reproducible result, a 25 ml vessel should be filled with at least 5 ml and up to 15 ml. Lower volumes may lead to high intraday variations. Higher volumes often produce problems of clogging and contamination of the trap, and, often, this may lead to long cleaning requirements for achieving stable baselines. The sample volume is also strongly related to the type of matrix involved. For "clean" water samples, such as ground or drinking water, the established purged volume is 11–13 ml, according to the EPA methods. This permits the achievement of detection limits below 0.1 μg/L for most compounds. For industrial

effluents and charged waters, it is advisable to dilute the samples, e.g., to ~5–10%. This still permits detection of the analytes of interest and, at the same time, avoids interference. For soil and sediment samples, Kester[6] has described a protocol in which 4 g of sample is dispersed in methanol. After sonication for 1 min, followed by centrifugation, an aliquot of, generally, 100 μl is added to HPLC water which is purged as indicated above. This protocol is easy to perform, but suffers from low sensitivity, because only a small aliquot of the sample is analyzed. Increasing the volume of the extract results in a methanol peak that may overlap with some of the analytes of interest. More suitable are the specific configurations especially designed to purge solid samples, such as soils and sediments, which are provided with large bore tubes and orifices to prevent clogging and can be adapted for homogenizing the samples to provide precise extraction and delivery of analytes.

The gas flow rate and purging time must be optimized to achieve maximum sensitivity. According to EPA Method 524.2, a pre-fixed value is purged with He at 40 ml/min for 11 min. Higher purging time or flow may lead occasionally to lower limits of detection. However, precaution has to be exercised so as not to exceed the breakthrough volume, which would lead to poor recoveries.

Desorption of the analytes is accomplished by heating the trap to 180–200°C and simultaneously backflushing with an inert gas at 3–4 ml/min for around 4–5 min. If P&T is coupled to an MS system, the desorption time must be optimized to a minimum value so that it ensures the total desorption of the analytes from the trap without affecting the vacuum requirements of MS. The use of a cryogenic interface or cryofocusing is recommended to improve peak shapes. In this case, desorbed analytes are transferred to a cool trap set at −150°C. Desorption from the cool trap is performed by heating at 250–300°C; analytes are transferred into a capillary column. At this time, the temperature program of the GC starts. The injector is then programmed in a split ratio of 20:1.

Instrumentation is available from various suppliers, and sample loading can be performed either manually or by using automated systems. Automation implies no sample manipulation and the sources of errors are minimized. Being, therefore, a highly robust technique. The automated system permits a high sample throughput and is especially indicated in routine monitoring programs.[3] Recent work related to the use of P&T for survey of VOCs in surface waters indicates the suitability and robustness of the technique for long-term monitoring studies.[7]

SEPARATION USING VARIOUS COLUMNS

Typical columns for the analysis of VOCs are 60–75 m, 1–3 μm film thickness and high internal diameter (0.32, 0.53, or even 0.75 mm), which copes with the high flow rates often necessary to transfer the analytes from the purging device to the GC. When a wide bore column is used, chromatography can start with the onset of thermal desorption. For narrow bore columns, cryofocusing is advisable for better peak separation. GC/MS conditions are shown in Table 1. The injector is programmed in splitless mode for 2 min, and the column flow rate is maintained constant throughout acquisition. If MS is used, the flow rate should be adjusted to 1 ml/min.

For the analysis of VOCs, the most common column is a 75 m × 0.53 mm I.D. DB-624 fused silica capillary with 3 μm film thickness. A typical DB-624 permits detection from vinyl chloride (bp = −13.9°C and solubility = 2700 g/L) up to 2-chloronaphthalene (bp = 256°C), being therefore suitable to determine a wide range of compounds of different volatilities and polarities. For specific applications, e.g., control of trihalomethanes in drinking water, a short column of 30 m can be used, and the analysis time is, of course, reduced.

DETECTION TECHNIQUES

Depending on target analytes to be determined, different detectors can be used, e.g., electron capture detector which offers high sensitivity and selectivity for halogenated compounds,[8] MS which permits the analysis of a large number of compounds,[9] and atomic emission detector[10] which has been used for the analysis of environmental samples. Increasingly, however, P&T is coupled to GC with MS detection. This technique, described and validated in the EPA method 524.2,[5] permits the analysis of a large number of analytes within a single run, gives confirmatory data according to the acquisition technique (scan mode or selected ion monitoring, registering three ions per compound for confirmatory purposes), and, finally, gives limits of detection at the 0.1 or 0.01 μg/L level, ideal for the analysis of VOCs in environmental matrices. For these reasons, it is the sole technique that avoids false positives/negatives by unequivocally assuring the presence of analytes using a single column.

Irrespective of the detection method used, the analysis of VOCs often involves the presence of interferences in the chromatogram. This is normally due to VOCs present in the atmosphere, such as normal laboratory solvents (acetone, dichloromethane, chloroform, acetonitrile, or methanol) which can be detected, especially when using a universal detector such as a mass spectrometer which operates under vacuum. This problem is eliminated when the laboratory of analysis is free of solvents and is isolated, especially from urban areas.

QUALITY CONTROL OF THE PROCESS

Due to their high volatility, the analysis of VOCs is complex and needs extreme precautions, both with the samples

and with the preparation of standard solutions. The growing need to provide reliable results leads to quality control charts for a long-term guarantee of the data generated in each laboratory. Test samples and standard solutions should be kept at 4°C, but not for more than 15 days, in order to avoid sample degradation. In addition, samples should be gathered and kept without any headspace volume in order to avoid losses of the more volatile compounds. The analytical control charts involve both the analysis of reagent blanks and spiked blanks and demonstration of laboratory accuracy and precision. The analysis of reference and certified materials is highly recommended for method validation as indicated in a recent publication.[11]

On a routine basis, the use of internal standard and surrogate is necessary to ensure an accurate measurement of all VOCs throughout an analytical experiment. In optimizing the analytical method, it is essential to use one or more surrogates that will cover the whole range of compounds studied. Depending on the equipment used, the surrogate can be automatically pumped into the purging vessel. Otherwise, the surrogate mixture can be added directly to the sample with the minimum amount of solvent possible. If an internal standard is used, a split/splitless injector is needed for direct injection. However, this option is not advisable for quantification purposes as response factors of different test compounds may vary considerably. The most common compounds used as surrogates (or internal standard, depending on the application) are fluorbenzene, 1,2-dichlorobenzene d_4, bromochloromethane, difluorobenzene, chlorobenzene d_6, 4-bromofluorobenzene, and 1,4-dichlorobutane, among others, which elute at different intervals throughout the chromatogram. The surrogate will serve not only for method control but for analyte quantification, if properly selected.

Calibration curves should be prepared by spiking HPLC or groundwater samples with the test mixture at concentrations that permit a wide linear range. Normally, VOCs are found in environmental waters at 0.1–10 μg/L. Therefore, typical linear ranges are from 0.01 to 2–3 μg/L, with higher concentrations leading to poor linearity. "Charged" samples may have levels up to 200 μg/L and should be diluted prior to purging. In addition, a sample sequence should always include a blank sample, calibration standards or quality control standards, and samples. Blank analysis with HPLC water should be performed often (every four to five samples, depending on the matrix) to avoid carryover effects. It is crucial to have blanks which are void of interferences. Therefore, precautions must be taken in cleaning the glass material, which must be performed in an ultrasonic bath, followed by rinsing with acetone and, afterward, with distilled water. All sample preparation has to be done in a laboratory atmosphere that is free of solvents.

Quantification should be done using response factors or calibration curves. Using internal standards, variability with automated systems should not exceed 5–10%. In contrast, manual purging equipment connected to an MS can have up to 10–20% variation, depending on the compounds studied. External calibration is not recommended because a response variation of up to 50% can be detected. Limits of detection and recoveries of test compounds should be calculated in order to verify the suitability of the method for specific applications. Quality parameters of selected VOCs are indicated in Table 2. According to the US EPA, recoveries higher than 70% are acceptable. If using an internal standard for quantification, results should not be corrected by recovery. However, if external calibration is used, the percentage recovery should be indicated and used for quantification.

ENVIRONMENTAL APPLICATION

Large amounts of VOCs are generated in industrialized areas and eventually are discharged into surface waters or transported by the atmosphere. Once in the environment, VOCs can be absorbed into biota and soil, and, depending on soil characteristics, they can eventually migrate to groundwater by leaching.[1,7] Compounds detected depend on the type of waters analyzed. Several directives indicate the need to regulate the use and discharge of VOCs into the environment. Some widely used and toxic VOCs are included in priority pollutant lists, and stringent regulatory requirements have resulted in routine monitoring of these compounds in different types of waters. Solvents, such as chloroform, toluene, benzene, dichloromethane, and chlorethenes, are widely used in industrial manufacturing and organic synthesis. Others, chlorobenzenes or chloropropenes, are used as solvents in the formulation of fats and in dye manufacturing. The final fate and ecotoxicological impact that they may cause depends on the type of water and their concentrations.

Surface Waters

Extensive monitoring, carried out to determine halogenated VOCs in surface water from Portugal, revealed the presence of chloroform, tetrachloroethylene, trichloroethylene, and carbon tetrachloride in 13–50% of the samples analyzed, with a median of 0.1–0.3 μg/L, except for punctual contaminated areas close to big cities where these compounds were detected up to 18 μg/L. Also, high concentrations were found in agricultural areas, where solvents are used in many pesticide formulations.[8]

Table 2 Compounds studied, retention time (min), molecular weight (MW) and other two most abundant ions monitored (in bold, ion used for quantification), and calibration data obtained for spiked groundwater samples at 1 μg/L using automated P&T coupled to GC/MS.

		Monitored ions							
Compound	**RT (min)**	**MW**	**Ion1**	**Ion2**	**Linearity (μg/L)**	R^2	**%R**	**STD**	**LD (μg/L)**
Vinyl chloride	2.57	**62**	64	—	0.04–2.20	0.9846	65	10.8	0.300
Dichloromethane	5.40	84	**49**	86	0.04–2.20	0.8192	105	10.2	0.062
1,1-Dichloroethane	7.58	98	**63**	83	0.04–2.20	0.9899	99	2.9	0.017
Chloroform	10.79	118	**83**	85	0.04–2.20	0.9524	93	4.2	0.002
1,1,1-Trichloroethane	11.29	132	**97**	61	0.04–2.20	0.9842	95	9.7	0.021
Carbon tetrachloride	11.81	152	**117**	119	0.04–2.20	0.9974	90	4.9	0.002
Benzene	12.45	**78**	77	52	0.04–2.20	0.9901	98	9.5	0.002
1,2-Dichloroethane	12.54	98	**62**	—	0.04–2.20	0.9813	97	7.4	0.002
Trichloroethylene	14.40	**130**	95	60	0.04–2.20	0.9752	97	10.5	0.010
1,2-Dichloropropane	15.02	112	**63**	76	0.04–2.20	0.9804	99	5.7	0.011
Dibromomethane	15.34	172	**174**	93	0.04–2.20	0.9964	91	3.2	0.022
1,3-Dichloropropane	17.11	110	**75**	—	0.04–2.20	0.9910	90	3.6	0.042
Toluene	18.01	92	**91**	65	0.04–2.20	0.9876	93	8.4	0.007
1,1,2-Trichloroethane	19.17	132	**97**	83	0.04–2.20	0.9825	92	7.5	0.023
Tetrachloroethylene	19.55	**164**	129	94	0.04–2.20	0.9867	91	3.5	0.014
Ethylbenzene	22.27	106	**91**	77	0.04–2.20	0.9901	90	5.3	0.014
1,1,1,2-Tetrachloroethane	22.28	166	**83**	131	0.04–2.20	0.9919	91	4.7	0.029
m + *p*-Xylene	22.62	106	**91**	77	0.04–2.20	0.9924	91	2.1	0.036
O-Xylene	23.73	106	**91**	77	0.04–2.20	0.9947	99	2.3	0.015
Bromoform	24.26	250	**173**	91	0.04–2.20	0.9939	98	2.1	0.027
Isopropylbenzene	24.80	120	**105**	77	0.04–2.20	0.9874	94	2.4	0.058
1,1,2,2-Tetrachloroethane	25.67	166	**83**	131	0.04–2.20	0.9388	98	2.1	0.020
1,2,3-Trichloropropane	25.76	146	**75**	110	0.04–2.20	0.9910	95	1.7	0.035
1,3-Dichlorobenzene	28.38	**146**	148	111	0.04–2.20	0.9820	96	2.3	0.014
1,4-Dichlorobenzene	28.67	**146**	148	111	0.04–2.20	0.9812	97	5.3	0.017
1,2-Dichlorobenzene	29.73	**146**	148	111	0.04–2.20	0.9802	96	4.0	0.016
Hexachloroethane	30.48	234	**117**	201	0.04–2.20	0.9834	97	4.3	0.115
1,2,4-Trichlorobenzene	34.84	**180**	145	—	0.04–2.20	0.9792	99	3.4	0.009
Hexachlorobutadiene	35.41	258	**225**	190	0.04–2.20	0.9916	97	4.2	0.061
1,2,4,5-Tetrachlorobenzene	39.79	216	—	—	0.04–2.20	0.9895	98	2.9	0.009
1-Chloronaphthalene	41.91	**162**	127	—	0.04–2.20	0.9678	74	2.6	0.014

—: No formation of additional fragment ions at 70 eV.
RT = retention time; %R = percentage of recovery; STD = standard deviation; LD = limit of detection.

In another study,[3] in which 41 compounds of different families were studied, 37 were detected at least once at levels between 0.01 and 28 μg/L, same with that which was found in a monitoring survey carried out in surface waters from Greece.[12]

Drinking Water

Other applications of P&T are related to the control of trihalomethanes in finished drinking water. Fig. 2 shows a typical profile where chloroform, bromodichloromethane, dibromochloromethane, and bromoform were detected at 80–100 μg/L. The technique, when coupled to MS, can also be applied to identify compounds responsible for taste and odor problems in water.[13]

Groundwater Samples

Groundwater is a stable reservoir of organic pollutants. An extensive monitoring study carried out in the United States revealed that 7% of the ambient

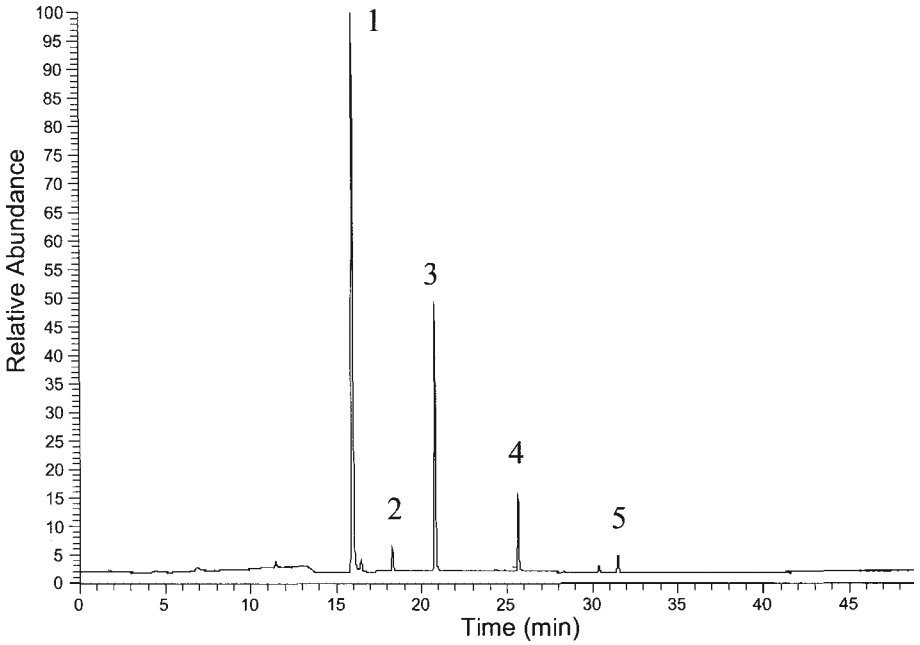

Fig. 2 P&T–GC/MS of drinking water containing: 1) chroroform; 2) 1,1,2,2-tetrachloroethene; 3) bromodichloromethane; 4) dibromochloromethane; and 5) bromoform.

groundwater resources of the United States contain at least one VOC at levels of 0.2 μg/L and, in urban areas, 47% of the sampled wells were positive.[7] A compound now of interest is methyl *tert*-butyl ether (MTBE), which is the most widely used ether oxygenate added to gasoline as an octane booster.[14] MTBE enters the environment during all phases of the petroleum fuel cycle. Due to its high solubility (25–50 g/L), low K_{ow} (0.94–1.43), and Henry's law constant (55.3 Pa m^3/mol), MTBE remains dissolved in surface water, where it can volatilize into the atmosphere. A small fraction can partition into soil and eventually reach groundwater where it can persist for more than 200 days, causing odor problems at low concentrations.

Industrial Effluents

A recent study indicated that more than 50 VOCs were found in effluents from high-tech industries, leading to pollution of surrounding river waters and inducing bad atmospheric odor. Benzene, toluene, chloroform, and dichloromethane were the major contributors of industrial discharges and were detected in 30% or more of the analyzed samples.[15]

CONCLUSIONS

The analysiss of VOCs in water and solid samples is complex due to the large number of compounds to be analyzed and because precaution has to be taken to provide accurate and reliable results. The use of P&T–GC/MS is the most adequate for trace analysis of VOCs because limits of detection at the ng/L levels can be achieved and confirmatory analysis can be performed. Although P&T is a well-established technique, several analytical parameters can be optimized to obtain high sensitivity and selectivity. For the specific target analytes, method optimization and quality assurance are necessary. The main drawbacks of this technique result from the fact that high purity gases are required and that the system can be easily polluted when charged samples are analyzed, producing carry over effects. These problems can be eliminated if precautions are taken in optimizing the analytical conditions prior to analysis.

REFERENCES

1. Heinrich-Ramm, M.; Jakubowski, B.; Heinzow, J.M.; Christensen, E.; Olson, O.; Hertel, E. Biological monitoring for exposure of volatile organic compounds. IUPAC Recommendations 2000. Pure Appl. Chem. **2000**, *72*, 385–436.
2. Ventura, F.; Matia, L.; Romero, J.; Boleda, R.M.; Marti, I.; Martín, J. Taste and odor events in Barcelona's water supply. Water Sci. Technol. **1995**, *31* (11), 63–68.
3. Martinez, E.; Llobet, I.; Lacorte, S.; Viana, P.; Barcelo, D. Fully automated purge and trap coupled to GC–MS for the low level determination of volatile organic compounds in water. J. Chromatogr. A, **2002**, *959*, 181–190.

4. Dewulf, J.; Van Langenhoven, H. Anthropogenic volatile organic compounds in ambient air and natural waters: a review of recent developments of analytical methodology, performance and interpretation of field measurements. J. Chromatogr. A, **1999**, *843*, 163–177.
5. Eichelberger, J.W.; Munch, J.W.; Bellar, T.A. *Measurement of Purgable Organic Compounds in Water by Capillary Column Gas Chromatography/Mass Spectrometry, Revision 4.0, EPA Method 524.2*; Environmental Monitoring Systems Laboratory, Office of Research and Development, US Environmental Protection Agency: Cincinnati, OH, 45268, 1992; 5–50.
6. Kester, P.E. *Analysis of Volatile Organic Compounds in Soils by Purge and Trap Gas Chromatography*; Tekmar Company: Cincinnati, OH, 1987.
7. Squillace, P.J.; Morgan, M.J.; Lapham, W.W.; Price, C.V.; Clawges, R.M.; Zogorski, J.S. Volatile organic compounds in untreated ambient groundwater of the United States, 1985–1995. Environ. Sci. Technol. **1999**, *33*, 4176–4187.
8. Martinez, E.; Llobet, I.; Lacorte, S.; Viana, P.; Barcelo, D. Patterns and levels of halogenated volatile compounds in Portuguese surface waters. J. Environ. Monit. **2002**, *4*, 1–7.
9. Lee, M.R.; Lee, J.S.; Hsiang, W.S.; Chen, C.M. Purge and trap gas chromatography–mass spectrometry in the analysis of volatile organochlorine compounds in water. J. Chromatogr. A, **1997**, *775*, 267–274.
10. Silgonier, I.; Rosenberg, E.; Grassenbauer, M.J. Determination of volatile organic compounds in water by purge and trap gas chromatography coupled to atomic emission detector. J. Chromatogr. A, **1997**, *768*, 259–270.
11. Huybrechts, T.; Dewulf, J.; Moerman, O.; van Langenhove, H.J. Evaluation of purge and trap–high resolution gas chromatography–mass spectrometry for the determination of 27 volatile organic compounds in marine water at ng L^{-1} concentration level. J. Chromatogr. A, **2000**, *893*, 367–382.
12. Kostopoulou, M.N.; Golfinopoulos, S.K.; Nikolau, A.D.; Xilourgidis, N.K.; Lekkas, T.D. Volatile organic compounds in the surface waters of Northern Greece. Chemosphere **2000**, *40*, 527–532.
13. Ventura, F.; Romero, J.; Pares, J. Determination of dicyclopentadiene and its derivatives as compounds causing odors in groundwater supplies. Environ. Sci. Technol. **1997**, *31*, 2368–2374.
14. Schmidt, T.C.; Duong, H.A.; Berg, M.; Haderlein, B. Analysis of fuel oxygenates in the environment. Analyst **2001**, *126*, 405–413.
15. Wu, C.H.; Lu, T.; Lo, J.G. Analysis of volatile organic compounds in wastewater during various stages of treatment for high-tech industries. Chromatographia **2002**, *56*, 91–98.

Quantitation by External Standard

Tao Wang
Merck Research Laboratories, Rahway, New Jersey, U.S.A.

INTRODUCTION

An important feature of modern high-performance liquid chromatography (HPLC) is its excellent quantitation capability. HPLC can be used to quantify the major components in a purified sample, the components of a reaction mixture, and trace impurities in a complex sample matrix. The quantitation is based on the detector response with respect to the concentration or mass of the analyte. In order to perform the quantitation, a standard is usually needed to calibrate the instrument. The calibration techniques include an *external standard method*, an internal standard method, and a standard addition method. For cases in which a standard is not available, a method using normalized peak area can be used to estimate the relative amounts of small impurities in a purified sample.

In this entry, only the external standard method is discussed. Detailed discussions of other quantitation methods can be found in other entries of this encyclopedia or in Ref.[1]

DISCUSSION

The external standard method is the most general method for determination of the concentration of an analyte in an unknown sample. It involves the construction of a calibration plot using external standards of the analyte, as shown in Fig. 1. A fixed volume of each standard solution of known concentration is injected into the HPLC and the peak response of each injection is plotted versus the concentration of the standard solution. The standards used are called "external standards" because they are prepared and analyzed separately from the unknown sample(s). After constructing the calibration plot, the unknown sample is prepared, injected, and analyzed in exactly the same manner. The concentration of the analyte in the unknown sample is then determined from the calibration plot or from the response factor of the unknown sample versus that of the standard.

If the calibration plot is linear, the concentration of the analyte in the unknown sample can be determined based on the linear equation of the calibration plot:

$$Y = a + bX \tag{1}$$

where Y is the peak response of the analyte, X is the concentration of the analyte, a is the intercept, and b is the slope. The concentration X is

$$X = \frac{Y - a}{b} \tag{2}$$

In the example shown in Fig. 1, where $a = 0$ and $b = 2 \times 10^6$ the concentration (X) of the unknown sample (U), which shows a peak response of $Y = 500{,}000$, is determined to be 0.25 mg/ml using Eq. 2.

Alternatively, after the linear calibration range has been established, the concentration of an unknown sample can be determined using the *response factor*. A response factor (RF), sometimes called a *sensitivity factor*, is determined from a standard within the linear calibration range as:

$$RF = \frac{\text{Standard peak response}}{\text{Standard concentration}} \tag{3}$$

If two or more standards of different concentrations within the linear range are measured, the RF value can be taken as the average value of the response factors for all these standards to minimize the uncertainty in determining the RF. In the example shown in Fig. 1, the RF is the slope of the calibration plot and equals 2×10^6 for all three standards because the plot is linear with a zero intercept.The concentration (X) of the analyte in the unknown sample (U) can be calculated as

$$X = \frac{\text{Sample peak response}}{RF} \tag{4}$$

which is $500{,}000/(2 \times 10^6)$ 0.25 mg/ml. When RF is used for quantitation, the concentration(s) of the standard(s) selected should be similar to the expected concentration of the unknown sample.

In the aforementioned techniques, it is important that the calibration plot be linear over certain concentration range and the concentration of the sample fall within this linear range (as shown in Fig. 1) so that an interpolation can provide accurate measurement of the sample concentration. If the concentration of the sample falls outside the established linear range, extrapolation of the calibration plot should be used with caution. To ensure accuracy, it is recommended that dilution be carried out to bring the concentration of the sample into the linear range prior to the analysis.

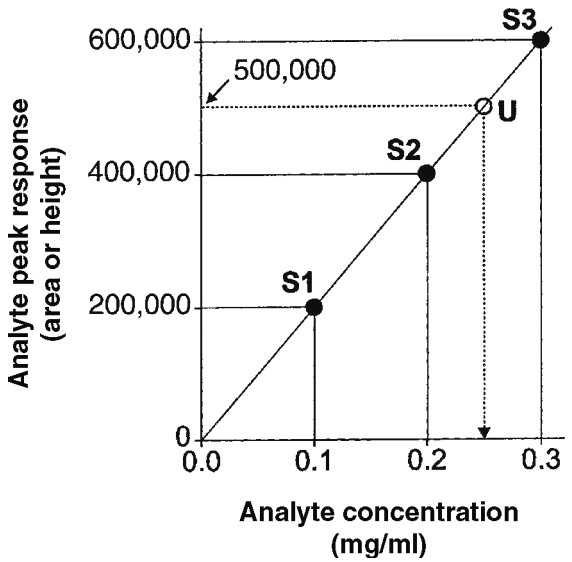

Fig. 1 Linear calibration plot for external standard method. S1, S2, and S3: external standards for calibration; U: unknown sample.

In unusual cases, where the calibration plot is not linear, the concentration of an unknown sample can be determined by interpolation of results between standards or by fitting the results of the standards into a non-linear equation and using the non-linear equation to calculate the concentration of the unknown sample. When interpolation is used, the concentrations of the two standards used to bracket the sample should be as close to the concentration of the sample as possible to enhance the accuracy of the result. When a non-linear equation is used, a large enough number of standards is needed in order to more accurately determine the non-linear equation. Obviously, quantitation in a non-linear range involves more labor and presents a higher potential of error. Therefore, this approach is used only when there are no other alternatives.

In the external standard method,it is critical that the injections are precise. With modern instruments which employ autosamplers, adequate precision (typically $\leq$0.5%) can be achieved using full-loop injection. Poorer injection precision is normally associated with manual injections or with partial-loop injections by autosamplers.

It is also critical to keep the chromatographic conditions (such as flow rate and column temperature) constant during the analysis of all standards and samples. Fluctuations of the chromatographic conditions during the analysis can cause inconsistent peak responses, which, in turn, will cause quantitation error. It is common that the HPLC system is tested using standards to ensure that the system is performing properly and reliably prior to the analysis of samples. This procedure of validating system performance is referred to as "system suitability test."

Detailed discussions on sources of error related to the external standard method, including sampling and sample preparation, chromatographic effects, and data system effects, can be found in Ref.[1] Ref.[2] presented detailed discussions on the precision in HPLC.

The peak response used for quantitation can be either peak height or peak area. Peak height is usually used when incomplete resolution of the analyte peak is encountered, because the peak height measurement is subject to less interference from the adjacent overlapping peaks. On the other hand, peak area is less influenced by changes in instrumental or chromatographic parameters. The choice of peak height or peak area for quantitation requires the understanding of the effects of chromatographic parameters on the precision of each approach. The influence of certain chromatographic parameters on the precision of peak height and peak area methods, as well as the preferred method among the two when various chromatographic parameters are subject to change, are discussed in detail in Refs.[1,3]

More thorough discussions on external standard method can be found in Refs.[1,3,4]

REFERENCES

1. Snyder, L.R.; Kirkland, J.J.; Glajch, J.L. *Practical HPLC Method Development,* 2nd Ed.; John Wiley & Sons: New York, 1997; 643–684.
2. Grushka, E.; Zamir, I. *Chemical Analysis*; High Performance Liquid Chromatography; Brown, P.R., Hartwick, R.A., Eds.; John Wiley & Sons: New York, 1989; Vol. 98, 529–561.
3. Snyder, L.R.; Kirkland, J.J. *Introduction to Modern Liquid Chromatography,* 2nd Ed.; John Wiley & Sons: NewYork, 1979; 541–574.
4. Scott, R.P.W. *Quantitative Analysis using Chromatographic Techniques*; Katz, E., Ed.; John Wiley & Sons: New York, 1987; 63–98.

Quantitation by Internal Standard

J. Vial
A. Jardy
Analytical Chemistry Department, City of Paris Industrial Physics and Chemistry Higher Educational Institution (ESPCI), Paris, France

INTRODUCTION

The principle involved is the addition of a known quantity of a foreign substance (internal standard) to the analyzed sample, the response coefficient of which is known or arbitrarily fixed. Quantitation by the internal standard method enables one to compensate for errors in the injected volume.[1]

The same quantity of constituent I (internal standard) is added both to the reference solution and to the solution to be analyzed. I is supposed to interfere with none of the constituents present in the sample. This methodology is based on the constancy of the ratios between the proportionality coefficient observed on both chromatograms (determination and calibration).

ASSAY CHROMATOGRAM

The assay solution includes precisely and accurately known weights of the product to be determined and of the internal standard. An injection of an approximately known volume of this solution is made. From the resulting chromatogram, areas of peaks corresponding to the internal standard and to the product(s) to be analyzed are measured. Let M_E be the weight of the sample including solute D, the assay of which τ_D is to be determined, M_I be the weight of the internal standard I, A_D be the peak area of solute D, A_I be the peak area of the internal standard, K_D be the response coefficient of the product D, and K_I be the response coefficient of the internal standard. It is possible to establish the following relationships:

$$M_E\tau_D = K_D A_D \tag{1}$$

$$M_I = K_I A_I \tag{2}$$

and

$$\tau_D = \frac{K_D}{K_I}\frac{A_D}{A_I}\frac{M_I}{M_E} \tag{3}$$

CALIBRATION CHROMATOGRAM

The protocol is similar to the calibration solution, including accurately and precisely known weights of reference and internal standard (dilutions must be analogous to those of the assay chromatogram). An injection of an approximately known volume of this calibration solution is made. From the resulting chromatogram, areas of peaks corresponding to the internal standard and to the reference material are measured. Let M_R be the weight of the reference material, the assay of which τ_R is known, M_I' be the weight of the internal standard I, A_R be the peak area of the reference material, and A_I' be the peak area of the internal standard. Thus, it is possible to establish the following relations:

$$M_R\tau_R = K_D A_R \tag{4}$$

$$M_I' = K_I A_I' \tag{5}$$

and

$$\frac{K_D}{K_I} = \frac{M_R}{M_I'}\tau_R\frac{A_I'}{A_R} \tag{6}$$

CALCULATION OF τ_D, THE ASSAY OF PRODUCT D IN THE SAMPLE

Combining relation 3 and relation 6, it is possible to determine τ_D, the purity of the product D, by

$$\tau_D = \frac{A_D}{A_I}\frac{A_I'}{A_R}\frac{M_I}{M_E}\frac{M_R}{M_I'}\tau_R \tag{7}$$

Some conditions are required for Eq. 7 to be valid: Areas and weights must be expressed in the same unit system both for analysis and calibration; because precision and accuracy of this method only depend on the precision and accuracy of weighings, they depend neither on the precision and accuracy of the dilutions nor on the injected volume (unlike the external standard method). It requires no preliminary determination of the proportionality coefficients. However, if some points of the sample handling are fully corrected by the use of an internal standard, other difficulties still remain.[2]

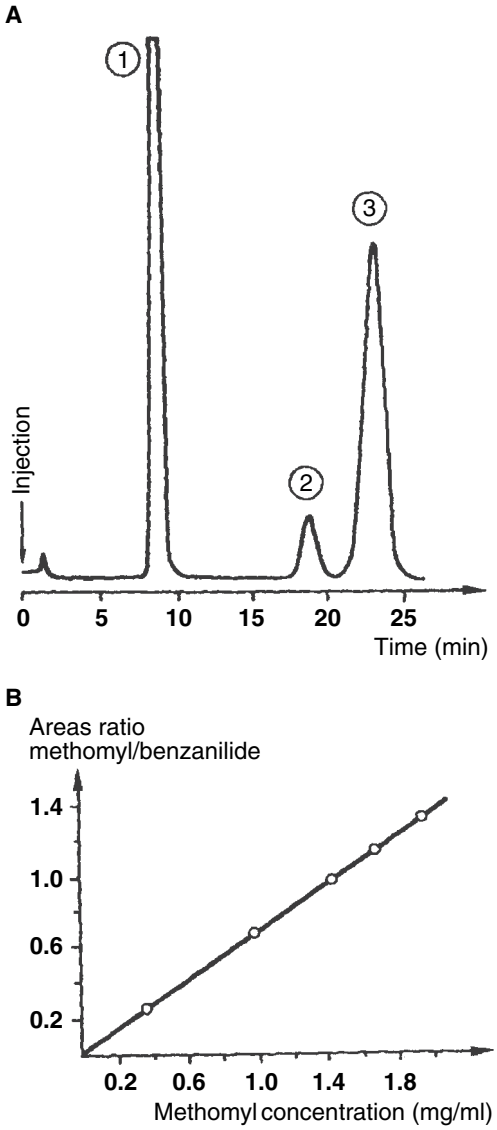

Fig. 1 Insecticide analysis by the internal standard method: (A) chromatogram; (B) calibration curve. 1: Benzanilide (internal standard); 2: methyl-*N*-hydroxythioacetimidate; 3: methomyl.
Source: From Precise quantitative analysis with a stable, high-speed liquid-liquid chromatography column. J. Chromatogr. Sci.[5]

Moreover, this method can quickly become laborious because an internal standard elution which is compatible with the analysis conditions must be found. Conditions that must be fulfilled by the internal standard are its purity must be known and it must be chemically inert toward solutes and mobile phase; on the one hand, its retention time must be different from those of all the constituents present in the sample and, on the other hand, it should be as close as possible as the retention time(s) of the product(s) to be determined. It has also been demonstrated that a necessary correlation was required between chromatographic behaviors of the internal standard and the product to quantify.[3] Otherwise, the use of an internal standard can even degrade the precision of the results. A comparison of the precision of internal and external standard has also been carried out through a liquid chromatography (LC) collaborative study.[4]

The internal standard's coefficient of response for the detector used must be of the same order of magnitude as the one of the product to be determined; in no way can it be present as an impurity in the sample; it must be added at a concentration level that gives a peak area more or less equivalent to the one of the product to be determined. Homologues of the product to be analyzed may be used as internal standards.

The chromatogram given Fig. 1 illustrates the internal standard methodology. Here, methomyl was quantified using benzanilide as the internal standard. Using the calibration curve, the unknown methomyl assay in insecticides is deduced from the area ratio, after the addition to the sample of the same quantity of internal standard as in the calibration steps.

The internal standard method is less often used in LC than in gas chromatography (GC) because injection of repeatable volumes has been made easier by the use of precise and reliable injection systems (loop valves). More generally, gradually, the internal standard method is being abandoned. The external standard method is, nowadays, the most common method and the use of an internal standard seems to be restricted to very specific applications; for example, when preliminary to the chromatographic analysis, the solute of interest must be extracted by means of a complex protocol.

REFERENCES

1. Rosset, R.; Caude, M.; Jardy, A. *Chromatographies en phases liquide et supercritique*; Masson: Paris, 1991; 731–733.
2. Snyder, L.R.; Van der Wal, S. Precision of assays based on liquid chromatography with prior solvent-extraction of the sample. Anal. Chem. **1981**, *53*, 877.
3. Haefelfinger, P. Limits of the internal standard technique in chromatography. J. Chromatogr. **1981**, *218*, 73.
4. Pauls, R.E.; McCoy, R.W. Comparison of the precision of internal and external standard calibration in an interlaboratory liquid chromatographic study. J. High-Resolut. Chromatogr. **1986**, *9* (10), 600–601.
5. Leitch, R.E. Precise quantitative analysis with a stable, high-speed liquid-liquid chromatography column. J. Chromatogr. Sci. **1971**, *9* (9), 531.

BIBLIOGRAPHY

1. Snyder, L.R.; Kirkland, J.J. *Introduction to Modern Liquid Chromatography,* 2nd Ed.; John Wiley & Sons: New York, 1974; 552–556.
2. Snyder, L.R.; Kirkland, J.J.; Glajch, J.L. *Practical HPLC Method Development,* 2nd Ed.; John Wiley & Sons: New York, 1997; 657–660.

Quantitation by Normalization

J. Vial
A. Jardy
Analytical Chemistry Department, City of Paris Industrial Physics and Chemistry Higher Educational Institution (ESPCI), Paris, France

INTRODUCTION

The principle of this method is quite simple. Provided that for each solute, i, the analytical signal lies within the linearity range, the peak area is proportional to the weight of solute having passed through the detector cell, thus, that was present in the injected volume,

$$m_i = K_i A_i \tag{1}$$

where A_i is the peak area of solute i and K_i is the response coefficient. Therefore, the percentage in weight of each analyte is given by

$$\%_i \frac{K_i A_i}{\sum_i K_i A_i} \times 100 \tag{2}$$

DISCUSSION

To apply this method in high-performance liquid chromatography (HPLC), several conditions have to be fullfilled: All the analytes present in the sample to be analyzed must elute from the column (no irreversible retention), with enough resolution and, furthermore, have to be detected. All the response coefficients have to be known, or at least attainable experimentally, which, in turn, implies that all the solutes are available separately in a high degree of purity. This method is unable to determine the percentage of any constituent of the mixture if a response coefficient is missing.

On the other hand, an advantage lies in the fact that there is no need to accurately know the amount of sample injected.

Practically, quantitation by the normalization method is not in as common use in HPLC as it is in gas chromatography (GC). It is highly recommended to avoid its implementation in the case of samples for which the qualitative composition is not known exactly. It is only convenient in routine analysis, as in quality control, when the qualitative composition does not vary.

Moreover, note that, except in very particular cases, the approximation to consider all the K_i equal (Eq. 3) is highly hazardous in HPLC, unlike in GC:

$$\%_i \frac{A_i}{\sum_i A_i} \times 100 \tag{3}$$

A few examples of where it is possible are the following: Use of a refractive index detector, trace analysis of related substances (impurities) in pharmaceutical products, with UV detection at very low wavelength, when the accuracy of the result is of little interest[1] (e.g., when chromatography is used to monitor a chemical reaction), and when a relative value is enough. In this situation, the simplified relationship 3 is sufficient, but the analyst must not forget that the proportions found in this way are not the true proportions.

In conclusion, its efficiency and simplicity make quantitation by normalization a very attractive method that generally requires few injections. Nonetheless, it must be kept in mind that it requires the knowledge of the response coefficients for all the constituents in the mixture. The a priori hypothesis of equality for all response coefficients seldom corresponds to reality and can lead to hazardous results.

REFERENCE

1. Tranchant, J. *Manuel pratique de chromatographie en phase gazeuse*; Masson: Paris, 1995; 620–623.

BIBLIOGRAPHY

1. Parris, N.A. *Instrumental Liquid Chromatography*; Elsevier: Amsterdam, 1976; 243.
2. Rosset, R.; Caude, M.; Jardy, A. *Chromatographies en phases liquide et supercritique*; Masson: Paris, 1991; 729–730.
3. Snyder, L.R.; Kirkland, J.J.; Glajch, J.L. *Practical HPLC Method Development,* 2nd Ed.; John Wiley & Sons: New York, 1997; 654–655.

Quantitation by Standard Addition

J. Vial
A. Jardy
Analytical Chemistry Department, City of Paris Industrial Physics and Chemistry Higher Educational Institution (ESPCI), Paris, France

INTRODUCTION

The principle involved is that, provided the analytical signal is proportional to concentration, the initial analyte content is determined through measurement of this signal before and after the addition of a known amount of the analyte to the analyzed sample. The method of standard addition, also denoted as "spiking," is used when an analyte is to be quantified inside a matrix, the effects of which are likely to affect the chromatographic peak behavior. In this case, the sample itself is used as the calibration matrix.

DISCUSSION

Commonly, the unknown concentration is deduced from the increase in the peak height or the peak area resulting from the addition of known amounts of pure analyte to the sample (at least one or two additions). A comparison of peak height versus peak area for quantitation is given in Ref.[1] A more convenient protocol, which gives information both on the precision and the accuracy of the results, is the following. After each addition, the area of the chromatographic peak is measured. Then, the parameters of the regression line are computed using a least-squares regression method. The analyte quantity in the sample corresponds to the intercept-to-slope ratio, denoted x_0. When the dilution produced by additions cannot be neglected, it is necessary to take it into account. Let A_0 be the peak area of the analyte to be determined on the chromatogram obtained with the unknown sample, A_i be the peak area of the same analyte on the chromatogram obtained after the ith addition, x_i be total quantity of analyte added after the ith addition, and f_i be the dilution factor after the ith addition. Then, a line of the areas corrected by the dilution factor versus the amount of analyte added is plotted (Fig. 1). The expression of the corrected area A_i* is

$$A_i^* = A_0 + (A_i - f_i A_0) \tag{1}$$

If, on the chromatogram, there is another peak other than that of the analyte, well resolved, but close enough, it can be used as a tracer to evaluate f_i. Let A_t be the peak area of the tracer on the chromatogram obtained with the unknown sample and A_{ti} the peak area of tracer on the chromatogram obtained after the ith addition of pure analyte:

$$f_i = \frac{A_{ti}}{A_t} \tag{2}$$

Otherwise, the dilution factor f_i must be evaluated in another way.

Then, the parameters of the calibration curve are computed by mean of a linear least-squares regression:

$$A_i^* = a + bx \tag{3}$$

The result is given by

$$x_0 = \left(\frac{a}{b}\right) \tag{4}$$

The method of standard additions would give the true result if there were no experimental errors. Practically, this is never the case and, so, a weakness of the method appears concerning the reliability of the provided result (unknown concentration). Effectively, the use of extrapolation of a calibration curve is always less conformable and reliable than interpolation, especially concerning the errors on predicted values.[2–4] The problem is even more explicit when the result is expressed along with its confidence interval. Confidence curves of the regression line must, thus, be used. Their expression is

$$A_i^* = a + bx \pm \hat{\sigma}_{y/x} t_{\alpha,(n-2)} \times \left(\frac{1}{n} + \frac{(x-\bar{x})^2}{\sum_i (x_i - \bar{x})^2}\right)^{1/2} \tag{5}$$

In Eq. 5, $\hat{\sigma}_{y/x}$ represents the estimated residual variance of the regression, $t_{\alpha,(n-2)}$ is the limit value that a Student's variable with $n-2$ degrees of freedom has α chances out of 100 not to exceed in module, and n is the number of points used. Confidence limits of the result correspond to the zero of Eq. 5. No exact analytical solutions are available, but either it is possible to solve it numerically or approximate solutions can be

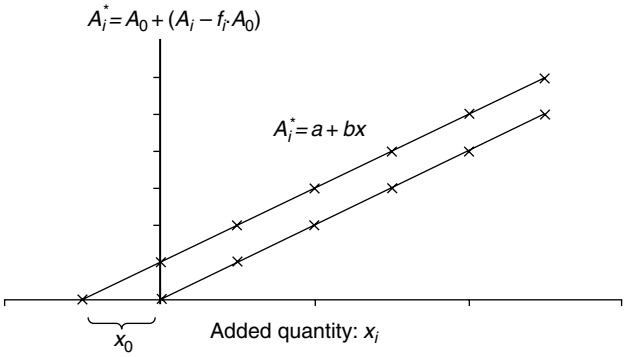

Fig. 1 Visualization of the standard addition methodology. The dotted line represents the calibration line obtained when the analyte of interest is not present in the matrix.

used. An approximate expression of the standard deviation of the result is

$$\hat{\sigma}_{x_0} \simeq \frac{\hat{\sigma}_{y/x}}{b}\left(\frac{1}{n} + \frac{\bar{y}^2}{b^2 \sum_i (x_i - \bar{x})^2}\right)^{1/2} \quad (6)$$

This leads to the following confidence interval (CI) for the unknown concentration:

$$\hat{\sigma}_{x_0} \simeq \frac{\hat{\sigma}_{y/x}}{b}\left(\frac{1}{n} + \frac{\bar{y}^2}{b^2 \sum_i (x_i - \bar{x})^2}\right)^{1/2} \quad (7)$$

To avoid having an excessively large interval, it is strongly advised to take enough points in a relatively widespread range. A compromise must be found for the spacing out of the points. It must be maximum to decrease the error on predicted values, but all the points must, nevertheless, belong to the linear range. An example of an application describing the analysis of 5-hydroxyindolacetic acid in human cerebrospinal fluid is given in Ref.[1]

However, the method of standard addition is not only useful to quantify an analyte present in a matrix, it can also be employed to check if the matrix introduces any proportional error. Similar additions of analyte are made to a blank matrix (the dotted line in Fig. 1) and if there is no proportional error, then the slopes of both regression lines are equal. Therefore, the slope equality has to be tested through a convenient statistical test. To conclude, the method of standard additions is a powerful method that enables to quantify an analyte present in a matrix susceptible to modify its behavior. Nevertheless, this method is somewhat tedious, because it requires many preparations and injections to obtain enough points for a sufficient reliability.

REFERENCES

1. Snyder, L.R.; Kirkland, J.J.; Glajch, J.L. *Practical HPLC Method Development,* 2nd Ed.; John Wiley & Sons: New York, 1997; Chap. 14.
2. Commissariat à l'énergie atomique. In *Statistique appliquée à l'exploitation des mesures, Tome I & Tome II*; Masson: Paris, 1978; 139–141.
3. Massart, D.L.; Vandeginste, B.G.M.; Deming, S.N.; Michotte, Y.; Kaufman, L. *Chemometrics, a Textbook*; Elsevier: Amsterdam, 1988; 34, 117, 119.
4. Miller, J.C.; Miller, J.N. *Statistics for Analytical Chemistry,* 2nd Ed.; Ellis Horwood: Chichester, 1988; 103, 117–120.

BIBLIOGRAPHY

1. Snyder, L.R.; Kirkland, J.J. *Introduction to Modern Liquid Chromatography,* 2nd Ed.; John Wiley & Sons: New York, 1974; 571.

Quantitative Structure-Retention Relationship by TLC

N. Dimov
Chemical Pharmaceutical Research Institute (NIHFI), Bulgarian Pharmaceutical Group Ltd., Sofia, Bulgaria

INTRODUCTION

The retention behavior of a compound in a chromatographic system is governed by three global factors: stationary phase–mobile phase combination, experimental conditions, and the compound's structure. In thin-layer chromatography (TLC), there is a huge choice of combinations: between stationary phases, a much greater choice of mobile-phase components, and less complex experimental conditions. It follows that an optimization strategy is necessary in order to come closer to the wanted separation. Keeping in mind that, for example, with an experimental design, 2^n experiments are necessary, where n is the number of factors, and one has to accept several factors a priori before starting the optimization. Depending on the result achieved, the separation is accepted as satisfactory or the optimization efforts continue. Once the analytical method is established (validated), it is available for application. The new problem became the reference substances necessary for system suitability verification and for identification. Although two difficult-to-separate compounds are enough for the verification, many reference materials are necessary for the identification of all compounds of interest. One of the steps helping to overcome this problem is the so-called quantitative structure–retention relationship (QSRR). It is assumed, in QSRR, that the first two global factors (stationary phase–mobile phase combination and experimental conditions) are already established and the obtained retention depends only on the compound's structure.

DISCUSSION

There is a great number of publications on QSRR in TLC (e.g., Refs.[1–3]). The protocol to be followed in QSRR calculations has, in general, the following steps: (1) composition of the experimental data set, (2) molecular structure entry, (3) structure descriptor calculation, (4) regression between experimental data and descriptors.

The compound's structure is entered using, typically, computer graphics. Each structure is optimized by molecular mechanics, which is followed by molecular orbital calculations. Topological indices, electronic parameters, physicochemical properties, indicator variables, and so forth are used as molecular structure descriptors.

The existing QSRR calculation methods are limited to the ideal case of an isolated molecule; that is, in all cases, the descriptor values are calculated at minimum molecular energy. Thus, it is accepted a priori that the structure of the analyte molecule is rigid enough to maintain its three-dimensional (3D) structure after contacts with the stationary phase. Although such assumption is disputable, this practice continues, because of the lack of knowledge of how the solute molecule is located on the stationary phase, lack of identity of chromatographic contact regions, and the impossibility of calculating the interaction forces developed between them.

To move aside from this impediment, the following have been realized:

- The interaction forces between the solute molecule and chromatographic phases during the chromatographic process release energy higher than the rotational barrier of solute bonds.
- Due to this excess of energy, the solute 3D structure undergoes changes that allow its better location on stationary phase.
- Predicting the exact 3D structure, as it is sorbed on the surface of the stationary phase, is impossible, but presuming several energetically possible structures for one and the same structure allows us to enter into Step 2 several descriptor values for one and the same analyte and use them further in Step 3. It is assumed that one of the calculated descriptor's values could give the "searched best fit" between the experimental and calculated retention values.

If the descriptors used in the most accurate predictive equation are calculated at the minimum heat of formation (CHF), then the analyte has been sorbed as a rigid molecule. If greater accuracy is achieved at higher CHF,

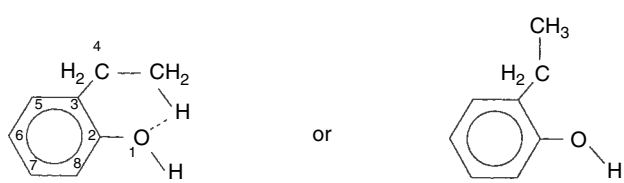

Rotamer "a" Rotamer "b"

Fig. 1 Rotamer structures.

Table 1 Comparison of experimentally obtained data with two different mobile phases R_M with R_M values calculated according to Eqs. 1 or 2, respectively.

No.	Compound	R_M exp. I[1a]	R_M calc. Eq. 1 phase I	R_M exp. phase II[2b]	R_M calc. Eq. 2 phase II	R_M calc. Eq. 3 phase III
1	*o*-Ethylphenol rotamer a	–0.31	–0.31	–0.50	–0.50	–0.48
2	*o*-Ethylphenol rotamer b	–0.31	–0.33	–0.50	–0.52	–0.47
3	*m*-Ethylphenol	–0.16	–0.18	–0.35	–0.40	–0.38
4	*p*-Ethylphenol	–0.14	–0.13	–0.31	–0.31	–0.30
5	*o*-Chlorophenol rotamer a	–0.23	–0.23	–0.43	–0.41	–0.44
6	*o*-Chlorophenol rotamer b	–0.23	–0.21	–0.43	–0.40	–0.46
7	*m*-Chlorophenol	–0.12	–0.11	–0.37	–0.32	–0.35
8	*p*-Chlorophenol	–0.07	–0.07	–0.25	–0.25	–0.25
9	*o*-Toluidine	0.07	0.07	–0.03	–0.03	–0.03
10	*m*-Toluidine	0.16	0.16	0.05	0.04	–0.05
11	*p*-Toluidine	0.27	0.26	0.16	0.17	–0.16

[a]Silica gel plates 60 F_{254} with *n*-C_7H_{16}–C_6H_6–diethylether = 1 : 1 : 1.
[b]Same plate with *n*-C_7H_{16}–C_6H_6–diethylether = 1 : 2 : 2.

the starting 3D structure has been changed during the chromatographic process.

This assumption will be tested first with the retention data for R_m of 9 benzene derivatives (predominantly rigid structures) and, next, for the R_f of 15 benzodiazepines (versatile structures with many s bonds) separated on silica gel. The data for benzene derivatives were taken from the literature,[4] where several mobile phases had been used. Two mobile phases with different polarities have been chosen.

In the first case, only two from all nine studied benzene derivatives have rotamers (see Fig. 1). From all tested combinations among the calculated descriptors, only one answers both to the accuracy and statistical requirements:

$$R_M = -5.50 \pm 0.22 + (24.57 \pm 0.88)\mathrm{DD}[1] + (4.19 \pm 0.19)Q[6] + (1.26 \pm 0.19)Q[5] \quad (1)$$

for mobile phase I with correlation coefficient $r = 0.9966$, variance $v = 1.96 \times 10^{-4}$, and $F = 483$, and

$$R_M = -7.04 \pm 0.52 + (29.84 \pm 2.08)\mathrm{DD}[1] + (4.51 \pm 0.45)Q[6] + (1.88 \pm 0.44)Q[5] \quad (2)$$

for mobile phase II with correlation coefficient $r = 0.9870$, variance $v = 1.1 \times 10^{-3}$, and $F = 127$. DD[1] stands for the donor delocalization energy of the –O– atom, and $Q[5]$ and $Q[6]$ stand for the charges of the fifth and sixth atoms, respectively. The increased influence of the –O– atom with the most polar mobile phase suggests checking another quantum-chemical local descriptor for the –O– atom. Eq. 3 gives a statistically better prediction of the experimental values of R_M:

$$R_M = -0.93 \pm 0.09 + (10.73 \pm 0.55)\mathrm{AD}[1] + (3.00 \pm 0.31)Q[6] + (1.65 \pm 0.29)Q[5] \quad (3)$$

with $r = 0.9913$, variance $v = 6.4 \times 10^{-4}$, and $F = 267$. AD[1] stands for the acceptor delocalization energy of the –O– atom. The better-fitted rotamers from *o*-ethylphenol and *o*-chlorophenol are with the higher heat of formation. In the above-given final regression, only these rotamers have been included.

The calculated retention is compared with the experimental value in Table 1. From a statistical point of view, the improvement when using the rotamer with better fit is insignificant ($F_{9,9} = 1.26$ and 1.07) and the assumption could be considered as disputable. This can be explained by the small number of compounds that are able to rotate around the s-bond in the total matrix. Independent of the reliability of the assumption, a beneficial conclusion can be drawn from Eqs. ([1–3]). They demonstrate that the

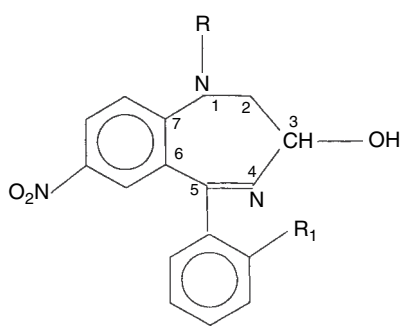

Fig. 2 Diazepine structures.

Table 2 Experimental and calculated R_f values obtained with two mobile phases: cyclohexane–toluene–diethylamine (m.ph. I) and chloroform–methanol (m.ph. II).

		m.ph. I		m.ph. II			
No. (1)	**-azepam (2)**	$R_{f\text{exp}}$ **(3)**	$R_{f\text{calc}}$ **(4)**	$R_{f\text{exp}}$ **(5)**	$R_{f\text{calc}}$ **(6)**	R_f **m.ph. I (7)**	CHF_{min} **m.ph. II (8)**
1	Nitra-	0	0.1	36	39.5	0.1	41.9
2	Oxa-	0	–0.7	40	40.0	–2.8	43.4
3	Lor-	1	–0.7	36	34.5	–2.7	37.8
4	Nord-	4	10.4	55	51.8	14.0	63.8
5	Lormet-	6	6.6	67	64.3	11.2	75.7
6	Tem-	8	6.2	59	63.2	13.4	67.0
7	Flunitra-	10	11.5	72	66.0	11.7	66.0
8	Nimet-	12	12.7	77	73.4	12.9	61.7
9	Cam-	13	13.2	79	80.3	10.3	74.8
10	Hal-	18	17.9	76	79.2	17.3	79.6
11	Flur-	30	34.0	48	49.8	34.6	46.2
12	Pin-	31	27.5	79	79.3	24.4	72.3
13	Tetra-	34	33.5	75	73.8	32.7	66.3
14	Pra-	36	28.5	74	69.4	26.8	79.3
15	Med-	40	42.4	74	79.1	42.8	79.1

retentions of the studied benzene derivatives are governed in the studied cases only by local descriptors and predominately by the local descriptors for the –O– atom in the hydroxyl group. The connectivity index used in many studies (e.g., Ref.[5]) showed, in the studied case, a correlation coefficient of only 0.285.

The assumption is undoubtedly verified with the retention data for R_f of 15 benzodiazepines separated on silica. The data were taken from the literature[6] because the authors had corrected, graphically, the R_f values to those obtained with reference materials and, hence, more exact values can be expected.

Three statistically equivalent equations have been obtained. One is presented as follows:

$$R_f = -234.9 \pm 43.2 + (47.27 \pm 4.50)\text{EN} + (2918 \pm 350)\text{DD}[5] + (10.7 \pm 1.8)\text{InVNH} \quad (4)$$

with correlation coefficient $r = 0.949$, variance $v = 13$, and $F = 69$. EN represents the electronegativity, DD[5] is the donor delocalization energy of atom 5 (see Fig. 2), and InVNH is an arbitrarily chosen indicator variable, accounting for the presence (value 1) or absence (value 0) of a substituent at the azepine *N* atom. All parameters have statistically insignificant interrelations, r_i. The R_f values calculated with Eq. 4 are given in column 4 of Table 2 and can be compared with the experimental results given in column 3. Although some of the chosen rotamers are identical to the conformers at the lowest molecular energy, the variance obtained when the descriptors were calculated for all molecules at their minimum calculated heats of formation (CHF_{min}) are statistically higher (32.7). Their values are given in column 7 of Table 2. Taking into account the criterion relevant to acceptance of the hypothesis, it is apparent that the accuracy, if a flexible structure approach is assumed, is higher.

Another conclusion from Eq. 4 is that benzodiazepine's retention, again, is governed by local descriptors (about 65% contribution of DD[5]) rather than by global molecular properties (about 35% from EN). The general conclusion is that it seems possible to increase the accuracy of QSRR calculations in TLC, assuming that flexible 3D analyte structures undergo some changes during the process of adsorption onto silica gel. As a result, a better fit between the calculated and experimental retention data can be achieved if several energetically possible structures for one and the same analyte are presumed.

REFERENCES

1. Kier, L.B.; Hall, L.H.; Murrey, M.J.; Randic, M. Molecular connectivity I: Relationship to nonspecific local anesthesia. J. Pharm. Sci. **1975**, *64* (12), 1971–1974.
2. Sherma, J.; Fried, B. *Handbook of Thin-Layer Chromatography*; Marcel Dekker, Inc.: New York, 1989.
3. Kiridena, W. Structure-driven retention model for solvent selection and optimization in reversed-phase thin-layer chromatography. J. Chromatogr. **1998**, *802*, 335–347.
4. Wardas, W.; Pyka, A. J. Planar Chromatogr.-Mod. TLC **1990**, *3*, 425–428.
5. Pyka, A. J. Planar Chromatogr.-Mod. TLC **1996**, *9*, 181–184.
6. Japp, M.; Garthwaite, K.; Geeson, A.; Osselton, M. Collection of analytical data for benzodiazepines and benzophenones. J. Chromatogr. **1988**, *439*, 317–324.

Quantitative Structure-Retention Relationships: TLC Analysis

L. Zhang
Qin-Sun Wang
National Key Laboratory of Elemento-Organic Chemistry, Nankai University, Tianjin, China

INTRODUCTION

The study of quantitative structure–retention relationships (QSRRs) is one of the most important theoretical fields of chromatography; it has become a new investigation branch of chromatographic science.

QSRR studies are widely investigated in high-performance liquid chromatography (HPLC), gas chromatography (GC), and thin-layer chromatography (TLC). Recently, QSRR studies in TLC have attracted more and more researchers.[1] It is known that TLC has some advantages: It is rapid, relatively simple, low cost, and easy to operate, there is a wide choice of adsorbents and solvents, and very small amounts of substance are needed. In this entry, the establishment and application of QSRR studies are reviewed.

ESTABLISHMENT OF QSRR EQUATIONS

Non-specific parameters, physicochemical parameters, and topological indices are the main parameters used in QSRR studies in TLC. The establishment of QSRR equations in TLC are reviewed according to these parameters.

BASED ON NON-SPECIFIC PARAMETERS

Non-specific parameters include the number of carbon atoms in a molecule, molecular volume, solvent-accessible surface, and so forth. This is relatively simple, and the most commonly used non-specific parameter is the number of carbon atoms in the compound.

There is a relationship between the number of carbon atoms and the retention data in HPLC and GC; a similar relationship was also found in TLC. Boyce and Milborrow[2] found that there was a linear relationship between the R_m values and the number of carbon atoms in the R group of *N*-*n*-alkyltritylamines (ph_3 CNHR). Janjic et al.[3] carried out a series of studies on the relationship between transition metal complexes and the number of carbon atoms in the complexes.

Because of their simplicity, non-specific parameters can be obtained relatively conveniently, but it is not very well correlated for complex molecules.

BASED ON PHYSICOCHEMICAL PARAMETERS

Physicochemical parameters are widely used in QSRR studies. Among the many physicochemical parameters, lipophilicity is one of the most widely used parameters in TLC-QSRR studies. As is well known, there is a linear relationship between the R_m [$R_m = \log(1/R_f - 1)$] values and the connection of organic modifier in mobile phase:

$$R_m = R_{m0} + bc$$

where c is the concentration of organic modifier in mobile phase and b is the slope, which is the decrease of R_m values when the concentration of organic modifier in the mobile phase increases 1%. R_m is the intercept of the TLC equation which represents the extrapolated value (i.e., the theoretical value at 0% organic solvent). This linear relationship has been verified by many workers.[2,4]

Pliska and Schmidt[5] first described the theoretical relationship between R_f and P values and presented the details of the computational procedure. At the same time, the relationship between the intercept R_{m0} and the slope b in the TLC equation was also studied by many other researchers. Biagi et al.[4] performed extensive work in this field. They found that R_{m0} values were not dependent on the nature of the organic solvent and that it does not make much difference whether the organic solvent is acetone, methanol, or acetonitrile. In addition, there is a linear relationship between the intercept (R_{m0}) and the slope (b). Biagi et al. considered that the existence of the linear relationship is a reason why the chromatographic method can be used to determine lipophilicity. The intercept of the TLC equation can be considered as a measure of the partitioning of the compounds between a polar mobile phase and a non-polar stationary phase (i.e., as the result of the balance between the interactions with the non-polar phase and the interactions with the polar phase), whereas the slope of the TLC equation indicates the rate at which the solubility of the compound increases in the mobile phase.[4] There are many studies dealing with this aspect.

BASED ON TOPOLOGICAL INDICES

Based on the plot of the suppressed hydrogens of the molecular under study, the calculation methods of molecular connectivity indices was developed. It has been used in many fields, such as the studies of correlation between structure and physicochemical and pharmacological properties, especially the relationship between structure and retention behavior, and the evaluation of the hydrophobicities of organic compounds by chromatographic methods.

The relationship between the retention behavior of benzodiazepine, sulfamides, substituted anilines, barbiturates, a group of natural phenolic derivatives, diethanolamine isomers, amino acids, sulfoether, thioalcohol, 2,4-dinitrophenylhydrazones, and their molecular connectivity indices were studied. All of the results indicate that the R_f or R_m values are highly correlated with molecular connectivity indices.

Pyka[6–8] performed a series of experiments applying topological indices to QSRR studies in TLC. Topological indices, such as Gutman, Randic, and Wiener indices as well as other indices were used. A new optical index (I_{opt}) was proposed,[6] which enables distinction between isomers of D- and L-configuration. Pyka also established a new stereoisomeric topological index (I_{STI}), which enables distinction between stereoisomers with hydroxyl groups in axial and equatorial positions. Using this index, the retention behavior of stereoisomeric menthols and thiol have been studied.

Introducing topological indices to QSRR studies widens the possibility of correlation analysis. Molecular connectivity indices are calculated according to molecular structure; it is relatively objective. Topological indices can be calculated without synthesizing the compound. In addition, using topological indices, the molecular structure can be described by some parameters which have physicochemical significance. However, there is also a limitation in the range of application of topological indices. They can be applied as the sole parameter only when they have been correlated with other features of molecular structure, such as volume, ring size, carbon chain length, and so forth. Generally, they are combined with other parameters that characterize other properties of the compounds of interest.

COMBINATION OF SEVERAL KINDS OF PARAMETERS

As we can see, every kind of parameters have limitations; thus, the combination of several kinds of parameters is advantageous. The combination of several kinds of parameters can often completely reflect the properties of compounds. Wang et al.[9] conducted some studies in this field. They introduced several structural parameters to study the correlation between the molecular structures of *O*-ethyl-*O*-aryl-*N*-isopropyl phosphoroamidothioates, *O*-ethyl, *O*-isopropylphosphoro(thioureido) thioates, and their retention factors in high-performance TLC (HPTLC), respectively.

APPLICATION OF QSRR STUDIES IN TLC

Prediction of Retention and Separation

From the discussion earlier, it can be seen that all the QSRR equations established in the previous part can be used to predict R_f or R_m values of compounds. This goal of QSRR is very easy to comprehend.

Determination of Lipophilicity

Many works[5] have illustrated that there is a linear relationship between R_m values and log P. R_{m0} values also can be used to measure the lipophilicities of chemical substances. In general, the chromatographic method is an excellent alternative to the traditional flask-shaking method for lipophilicity determination. It avoids the difficulties that one may encounter in the flask-shaking method. It is simple and rapid and requires only minute amounts of substances (which need not necessarily be very pure); it does not need quantitative analysis; the nature of the organic modifier does not affect the measurement of the lipophilic character, as the value is not affected by the organic modifier.

Evaluation of Some Physicochemical Parameters of Chemicals

The research on the evaluation physicochemical parameters using the TLC-QSRR equation is very limited. Until now, only the log $E_{T(30)}$ values of some organic solvents[10] and the pK_a values of some substituted phenols[8] have been predicted using this method. In addition, topological indices are introduced to evaluate the pK_a values.

Evaluation of Biological Activities of Compounds

Although, as early as 1965, Boyce and Milborrow[2] studied the relationship between R_m values of *N*-*n*-alkyltritylamines (ph_3 CNHR) and their LD_{50} values, the research on this aspect is limited. When only the R_m values is considered, the activity [log(1/C) or LD_{50}] is correlated with the square of R_m.

Topological indices were also introduced to study the biological activities of compounds. Pyka[7] studied the relationship among R_m values, topological indices, and biological activity [log(1/C)]. All of the equations he obtained show good correlation. There is a good agreement between predicted log(1/C) values and experimental log(1/C) values.

EXPLANATION OF SEPARATION MECHANISM

Theoretically speaking, a good QSRR equation can reflect the most characteristic parameters that influence the retention behavior of compounds. Thus, it can explain the retention mechanism quantitatively and qualitatively, but research on this aspect has made only poor progress until now.

Cserhāti and Forgacs[11,12] did some work on this field which illustrates the high impact of steric interactions on retention. However, until now, some of his hypotheses[12] need further experimental verification to support them.

PROSPECTS

Quantitative structure–retention relationships play a vital role in chromatographic research. The research and application fields of QSRR studies are becoming increasingly broad. Up to now, compounds used in QSRR studied are homologous series. How to establish QSRR equations that fit different kinds of compounds requires much more experimental effort.

From the viewpoint of application, QSRR equations in TLC are mainly used for retention prediction. The explanation of the separation mechanism awaits further investigation. With the application of various statistical methods, it is possible to select the primary retention-effect factors from many solute related factors which will offer explanations of separation mechanisms.

In conclusion, QSRR studies are making excellent progress in recent years, due to increased interest in this field of study. We can anticipate that QSRR studies will become more and more important in the future.

REFERENCES

1. Wang, Q.S.; Zhang, L. Review of research on quantitative structure-retention relationships in thin-layer chromatography. J. Liq. Chromatogr. Relat. Technol. **1999**, *22* (1), 1.
2. Boyce, C.B.; Milborrow, B.V. A simple assessment of partition data for correlating structure and biological activity using thin-layer chromatography. Nature **1965**, *208* (5010), 537.
3. Janic, T.J.; Vuckovic, G.; Celap, M.B. Linear interdependence of R_m pair values of substances in salting-out planar chromatography. Chromatographia **1996**, *42* (12), 675.
4. Biagi, G.L.; Barbaro, A.M.; Sapone, A.; Recanatini, M. Determination of lipophilicity by means of reversed-phase thin-layer chromatography: I. Basic aspects and relationship between slope and intercept of TLC equations. J. Chromatogr. A, **1994**, *662*, 341.
5. Pliska, V.; Schmidt, M.; Fauchere, J.-L. Partition coefficients of amino acids and hydrophobic parameters of their side-chains as measured by thin-layer chromatography. J. Chromatogr. **1981**, *216*, 79.
6. Pyka, A. J. Planar Chromatogr.-Mod. TLC **1991**, *4*, 316.
7. Pyka, A. J. Planar Chromatogr.-Mod. TLC **1994**, *7*, 108.
8. Pyka, A. J. Planar Chromatogr.-Mod. TLC **1996**, *9*, 52.
9. Wang, Q.S.; Yan, B.-W.; Yang, H.-Z. J. Planar Chromatogr.-Mod. TLC **1997**, *10*, 118.
10. Ahmad, A.; Muzaffar, Q.S.; Andrabi, A.; Qureshi, P.M. Solvent polarity as a function of R_f in thin-layer chromatography of selected nitro functions. J. Chromatogr. Sci. **1996**, *34* (8), 376.
11. Cserhāti, T.; Forgacs, E. Influence of the physicochemical parameters of propargylamine derivatives on their retention on α-cyclodextrin polymer-coated support. J. Liq. Chromatogr. Relat. Technol. **1995**, *18* (14), 2783.
12. Cserhāti, T. Relationship between the physicochemical parameters of 3,5-dinitrobenzoic acid esters and their retention behaviour on β-cyclodextrin polymer support. Anal. Chim. Acta **1994**, *292*, 17.

Radiochemical Detection

Eileen Kennedy
Novartis Crop Protection, Inc., Greensboro, North Carolina, U.S.A.

INTRODUCTION

Radiochemical detectors are devices that allow the measurement of low-energy γ-rays or β-particles emitted by radioisotopes. Substances called scintillators absorb the energy that is produced by the radioactive decay and transform it into light. The light from the scintillator, the intensity of which is directly proportional to the energy of the radioisotope emission, can be detected by a photomultiplier to provide an electrically countable pulse. Radiochemical detectors have been developed for various chromatographic techniques, the most common of which is high-performance liquid chromatography (HPLC). In HPLC, the detection of radioisotopes in a column eluate has allowed quantitation of discrete radiolabeled peaks in real time and in a generally non-destructively manner.

DISCUSSION

Gamma-emitters, such as iodine-125, which give off energy in the form of photons rather than particles, are more strongly penetrating than β-emitters. A radiochemical detector for γ-rays is generally composed of a cylindrical block of specially activated sodium iodide enclosed in a thin aluminum shell. One face of the block is optically coupled to a single photomultiplier. The eluate from the HPLC column passes through a coil or U-tube, which is placed in the well of the block. As the eluate passes through the coil, g-radiation is stopped by the very dense sodium iodide, producing light that can be measured by the photomultiplier.

Beta-emitters such as tritium (H-3) or carbon-14 (C-14) are the most commonly used radioisotopes in drug metabolism, agricultural metabolism, and toxicology studies. In HPLC, the radiochemical detector can be off-line or online. Off-line detection requires coupling the chromatograph to a fraction collector. The collected fractions are combined with a suitable liquid scintillation cocktail and then counted by a liquid scintillation counter. This method allows for the control of parameters such as counting time to improve sensitivity, but it suffers from being labor and time intensive. Online or flow-through radiochemical detectors can be homogeneous or heterogeneous. In homogeneous flow through detectors, a scintillation cocktail is added to the column eluate prior to detection in a liquid flow cell. The energy of decay from the b radionuclide is transferred to the scintillation cocktail via a solvent molecule. The liquid flow cell offers the highest sensitivity in online detectors but precludes recovery of the entire sample and requires an additional pump for delivery of the scintillation cocktail. In heterogeneous counting, the column eluate passes directly through a flow cell packed with a suitable solid scintillator such as yttrium silicate, calcium fluoride, or lithium glass. Use of the solid flow cell involves no additional costs for the scintillation cocktail and simplifies waste disposal. However, the solid cells have a lower counting efficiency, particularly with tritium, and can suffer from high backgrounds due to contamination. In both homogeneous and heterogeneous counting, light energy is detected by a pair of photomultiplier tubes located on either side of the flow cell, which is most often composed of a flat coil of thin-wall tubing situated in a transparent case. The photomultiplier tubes are located in fairly close proximity to each other (typically less than in. apart). Most commercially available radiochemical HPLC detectors use coincidence electronics in order to reduce noise pulses. With a coincidence counter, events are only recorded when both photomultiplier tubes are stimulated by light to give a pulse output within 20–50 ns of each other. A multichannel pulse-height analyzer sorts the outputs from the coincidence counter. A computer is then generally used to process data from the radiochemical detector as well as other online detectors and the results are presented either on a monitor or printer.

Unlike other chromatographic measurements such as ultraviolet (UV) absorption, the measurement and quantitation of radioactivity are based on time. Although a known percentage of a radioisotope will decay over a relatively long time, within that time period, the instantaneous rate of decay is not known. Because radioactive decay is a statistical process, the quality of a radioactivity measurement improves as a function of time. In other words, the longer the sample is counted, the more accurate (or statistically relevant) the measurement of the radioactivity. With off-line radiochemical detection, even very small peaks can be counted for a sufficiently long time to allow for a statistically relevant measurement. With online detection, the total flow rate and the cell volume fix the counting time. Online detection of low-level peaks can be improved by either a slower flow rate or by a larger flow cell. For solid flow cells, the total flow rate is equal to the mobile-phase flow rate. For liquid flow cells, the total flow rate is equal

to the mobile-phase flow rate plus the flow rate of the liquid scintillator. The latter is frequently expressed as a ratio of scintillator to mobile phase. As compared to other HPLC detectors, the volume of the flow cell is relatively large in the radiochemical detector. Flow cells typically range from 250 to 500 μl for solid cells and from 1000 to 2000 μl for liquid cells. Upward limits on the size of the flow cell are governed by the possibility of more than one peak being present in the cell at any one given time. However, assuming sufficient resolution, a larger flow cell should allow for a longer counting time and, hence, a more accurate measurement of radioactivity in a given peak. The actual amount of time that the column eluate will remain in the vicinity of the photomultiplier tubes is defined as the residence time. The residence time (R), in seconds, can be calculated as follows:

$$R\frac{V}{F} \times 60$$

where V is the cell volume in microliters and F is the total flow rate in milliliters per minute.

The counts per minute (cpm) can then be calculated for each peak in the sample as follows:

$$\text{cpm} = \frac{N}{R}$$

where N is the total net counts observed in the peak after background subtraction and R is the residence time in minutes.

Disintegrations per minute (dpm) are equal to cpm in the rare cases where the counting efficiency is 100%. Otherwise, dpm can be calculated as follows:

$$\text{dpm} = \frac{\text{cpm}}{E}$$

where E is the counting efficiency expressed as a percentage.

The efficiency of a radiochemical detector can be defined as the number of counts that are detected in the peak after background subtraction divided by the total number of radioactive events that actually occurred in the sample during the counting period. The approximate counting efficiencies that can be achieved with solid flow cells are fairly low for tritium (up to 10%) and significantly better for C-14 (up to 90%). With liquid flow cells, the counting efficiencies are greater than 55% for tritium and greater than 95% for C-14. Under isocratic conditions, the counting efficiency remains constant and can be readily determined by injecting a known amount of activity into an HPLC system, collecting the resultant peak as a single entity and counting it in a liquid scintillation counter. The number of disintegrations in the recovered peak is then compared to the calibrated activity of the standard. With gradient elution, the counting efficiency will generally change as the mobile-phase composition changes. In this situation, an efficiency calibration or quench curve can be obtained by injecting a constant known level of radioactivity during an otherwise blank gradient run. The calibration curve is then used to correct subsequent HPLC runs.

The minimum amount of radioactivity that can be detected by a flow-through radiochemical detector is a subject of continuing debate. It is generally accepted that a fairly sharp peak that contains counts that are at least twice background can be detected. One formula for calculating the minimum detectable activity (MDA) is given by

$$\text{MDA} = \frac{BW}{RE}$$

where B is the background count in cpm, W is the base width of the peak in minutes, R is the residence time in minutes, and E is the counting efficiency expressed as a percentage.

In practical terms, for a 500 dpm peak with a base width of 20 sec, a counting efficiency of 70% and a residence time of 12 sec, we would observe 70 counts, which would be spread out over the peak width, plus the residence time (a total of 32 sec). For a detector that has a 10 cpm background, we would observe 5.3 counts over the same time period of 32 sec. The ratio of the observed peak counts to background would be 13:1 and the peak should be clearly visible. However, under the same conditions, a 50 dpm peak would have a count to background ratio of only 1.3:1 and it is doubtful that this peak could be observed in online counting. In the latter situation, off-line radiochemical detection may be used to clarify the presence or absence of such a low-level peak.

BIBLIOGRAPHY

1. INUS Home Page http://www.inus.com (accessed August 1999).
2. Parvez, H., Reich, R., Lucas-Reich, S., Parvez, S., Eds.; *Progress in HPLC Volume 3: Flow Through Radioactivity Detection in HPLC*; VSP: Ultrecht, 1988.
3. Scott, R.P.W. *Chromatographic Detectors*; Marcel Dekker, Inc.: New York, 1996; 315–327.

Radiolytic Degradation Products: Monitoring Priority Pollutants

S. Bilal Butt
Rashid Nazir Qureshi
Central Analytical Facility Division, Pakistan Institute of Nuclear Science and Technology, Islamabad, Pakistan

INTRODUCTION

Speedy industrialization has provided much comfort to human beings; however, its adverse effects have emerged in the shape of environmental deterioration.[1] Untreated industrial wastewater has become a great health-risk. It has been found that treated wastewater that is discharged into the water carrying bodies is not free of toxic contaminants, particularly the so-called emerging pollutants.[2] The situation is critical in underdeveloped countries where pollution monitoring systems are not well established. Additionally, the indiscriminate domestic use of synthetic compounds generally known as products of personal care (PPC) has also introduced toxic compounds into the environment.[3] Many of these pollutants from industrial and municipal waste are toxic, persistent, and not readily biodegradable. Also, the current trend of urbanization and increased anthropogenic activity have further deteriorated the already endangered environmental situation. Public health is at risk because of the presence of these toxic pollutants in the environment, particularly in terms of the quality of potable (drinking) water. Industries discharging pollutants into the environment include oil refineries, tanneries, textile plants, and the food, pharmaceutical, paint, and coal processing industries. This entry will focus attention on the contamination of surface, ground, and potable water by industrial and municipal wastewater. The role of chromatography will be highlighted.

MONITORING OF POLLUTION IN POTABLE WATER

Monitoring the concentrations of various pollutants in industrial wastewater, as well as surface and ground water, with precision and accuracy is a difficult task. Wastewater is a complex matrix that normally contains organic pollutants of non-polar to polar nature in addition to bulk inorganic contaminants. Additionally, interferences are likely when handling complex mixtures of compounds. Under these circumstances, chromatography has played an important role and has provided solutions to complex analytical problems. It is extremely important to have an excellent analytical technique that can accurately and precisely monitor the concentrations of pollutants before and after the appropriate treatment process. The strength of chromatography is the fact that it can analyze diverse types of pollutants in water such as PAHs,[4] NO_2–PAHs,[5] and chlorophenols.[6] Emerging contaminants present in potable water are also of great health concern.[3] The elimination of such organic contaminants is key in the production of drinking water and the reuse of water resources. The emerging contaminants most commonly found in raw and wastewater are surfactants,[7] antiseptics,[8] acidic pharmaceuticals/PPC,[2] and polar pesticides.[9] The removal efficiency of these toxic compounds in wastewater treatment plants was found to be low.[10] Therefore, in addition to the untreated wastewater, these sewage effluents are also among the sources of these pollutants and their metabolites in water.

ROLE OF CHROMATOGRAPHY IN MONITORING WATER PURIFICATION EFFICIENCY

Currently, a variety of technologies is incorporated into the processing of industrial and municipal wastewater treatments. The most commonly employed are:

1. Activated Sludge Treatments (AST);
2. Membrane Bioreactors (MBRs);
3. Advanced Oxidation Processes (AOP);
4. Radiolytic Degradation of Contaminants.

The pollutant removal efficiencies of these processes, at different processing stages, are frequently performed by incorporating a variety of chromatographic techniques. For comparison only, AST and radiolytic processes will be considered. AST is a state of the art wastewater treatment process (WWTP) that is preceded by conventional physicochemical pretreatment steps. The level of acidic pharmaceuticals such as carbamazapine, diclofenac, and naproxen in the influent and effluent of an AST facility was monitored by chromatography and the removal efficiency was found to be low.[11]

Chlorinated phenoxy acids are used extensively as herbicides in agriculture, as algaecides in paints, and as coating agents. These are the main sources of their introduction in to the aquatic system. Their removal efficiency using

AST, as monitored by chromatography, is also not satisfactory.[12] Alkylphenol surfactants remain the most widely used non-polar surfactants. The formation of treatment resistance-metabolites out of parent surfactants has been noticed using chromatographic techniques.[13]

Moreover, irrespective of degradation technique chromatography has been used as an effective monitoring tool in the biodegradation of hexachlorocyclohexane (HCH). The potential biodegradation of HCH isomers was evaluated using gas chromatography–mass spectrometry (GC–MS).[14]

IONIZING RADIATION FOR PURIFICATION OF WATER AND WASTEWATER

Ionizing radiation, gamma radiation source or electron beam, is an excellent tool for the purification of polluted water and wastewater.[15] It involves the reaction of primary radiolytic water products, i.e., ($^{\cdot}$OH, e^{-}_{aq}, H) with the pollutants and the formation of secondary short-lived species from the pollutants. The secondary process causes the formation of precipitates that absorb pollutants. The general principal is that radiolytic treatment, in combination with traditional methods such as flotation, coagulations, adsorption, and aeration, is employed for the purification of water and wastewater. Irradiation is used as a facilitating step for the removal of pollutants. In the development of these technologies, chromatography has played a key role in evaluating the efficiency of any process. In this reference, selective wastewater and drinking water treatment processes will be outlined in the context of the important role of chromatography in water purification.

RADIOLYTIC DEGRADATION OF WASTE PETROLEUM PRODUCTS

A process has been studied for the removal of petroleum products, i.e., motor oil, diesel fuels, and residual fuel oil, from wastewater by gamma irradiation. In this regard, the prominent and decisive role of chromatography in this process will be highlighted.

The ^{60}Co γ-source was utilized for studies of water polluted with petroleum products. For this purpose, a heterogeneous system of water–petroleum products was studied. The total concentration of all petroleum products was 150 mg dm^{-3} in the form of an emulsion in bulk water or as a film on the water surface. The removal of petroleum products was studied by monitoring chemical oxygen demand, optical absorbance in the UV–Visible and IR regions, and by

Table 1 Coefficients $K(10)$, $K(15)$, and $K(25)$ for γ-irradiated heterogeneous system (t retention time, X and M mean characteristic and molecular, respectively).

No.	Component	X ion (m/z)	t (min)	M ion (m/z)	$K(10)$	$K(15)$	$K(25)$
1	Toluene	91	7.77	92	—	2.5	>1000
2	Ethylbenzene	91	10.84	106	1.7	1.9	>1000
3	*m*-Xylene	91	11.11	106	4.5	4.8	>1000
4	*O*,*p*-Xylenes	91	11.93	106	4.5	4.3	>1000
5	*n*-Propylbenzene	105	13.98	120	6.3	8.4	>1000
6	1-Methyl-3-ethylbenzene	105	14.29	120	6.5	9.1	>1000
7	1-Methyl-4-ethylbenzene	105	14.89	120	7.5	9.8	>1000
8	1,2, 3-Trimethylbenzene	105	15.35	120	6.4	8.7	>1000
9	1-Methyl-2-propylbenzene	105	17.22	134	15.4	35.1	>1000
10	1-Methyl-3-propylbenzene	105	17.79	134	15.3	47.6	>1000
11	Dimethylethylbenzene	119	18.37	134	17.5	49.9	>1000
12	1,2,4,5-Tetramethylbenzene	119	20.63	134	6.5	30.0	>1000
13	Tetralin	104	21.02	132	6.6	10.6	>1000
14	Naphthalene	128	21.80	128	2.3	3.1	>1000
15	1-Methylnaphthalene	142	25.18	142	3.3	12.1	>1000
16	2-Methylnaphthalene	142	25.71	142	4.3	12.2	>1000
17	*n*-Alkane C14	57	27.41	226	4.3	24.4	339
18	*n*-Alkane C15	57	30.02	240	4.4	21.5	334
19	*n*-Alkane C16	57	32.47	254	4.6	21.6	254
20	*n*-Alkane C17	57	34.73	268	4.7	21.8	225
21	*n*-Alkane C18	57	36.83	282	4.8	26.3	194

gravimetry and gas chromatography with mass spectrometry.[16] Precipitation was observed when the heterogeneous system was irradiated with γ-rays. After the separation of the precipitate, the remaining petroleum products were extracted in CCl_4 and analysed by GC–MS. The gravimetric analysis showed that 96% of the petroleum products were precipitated at a 25 kGy dose. GC–MS gave in-depth information on the remaining individual components of the petroleum products in the range of 40–500 mAU. The measurements were conducted in the dichloromethane extract from the initial systems (150 mg dm^{-3}) and irradiated once after the precipitate separated. Detailed information about the main compounds, their retention times, characteristic and molecular ions in initial and irradiated systems, and coefficients of the decrease in their concentration upon γ-irradiation to doses of 10, 15, and 25 kGy are given in Table 1.

The data in this table are evidence that chromatography provided information about the removal efficiency of individual compounds and, with that information, it will be easier to assess, decide, and select the type of wastewater purification technology.

DEGRADATION OF ENDOCRINE-DISRUPTING COMPOUNDS

Some chemicals belong to the so-called endocrine disrupting family and their presence in water is of great concern because of their adverse effects on living things. One such compound is *p*-nonylphenol (NPs), which is a by-product of the non-polar surfactant alkylphenoxy polyethoxylate (APE) and has the highest estrogenic activity among synthetic chemicals.[17] This surfactant is mainly used in the textile and paint industries and they are the main sources of its release into the aquatic system.[18] Annual production of NPs and APE is approximately 17,000 and 47,000 tons, respectively, in Japan alone. Around 40,000 tons per year are released into the water environment.[19] NPs degradation with gamma irradiation has been investigated. The concentration of degraded NPs and formation of degradation products have been identified by LC–UV, fluorescence, and LC–MS with atmospheric pressure chemical ionization (APCI) in the negative mode. The concentration of organic acids such as formic and oxalic acid, as final degradation products, was measured by ion chromatography. It is assumed that OH adducts of the NPs are produced during irradiation. LC–MS was used to monitor peak area at a mass to charge ratio of 235 mAU as irradiation products of NPs, at an initial concentration of 1 μg dm^{-3} as a function of dose. Two main irradiation products were detected at 6.3 and 8.5 min retention times. Keeping in view the oxidation of *p*-cresol and 4-ethylphenol, it was proposed that OH adducts of mass 235 are produced from NPs. These masses were assigned to the proposed OH adducts 4-nonylcatechols and 1-(*p*-hydroxyphenyl)-1-non-anols as the degradation products.

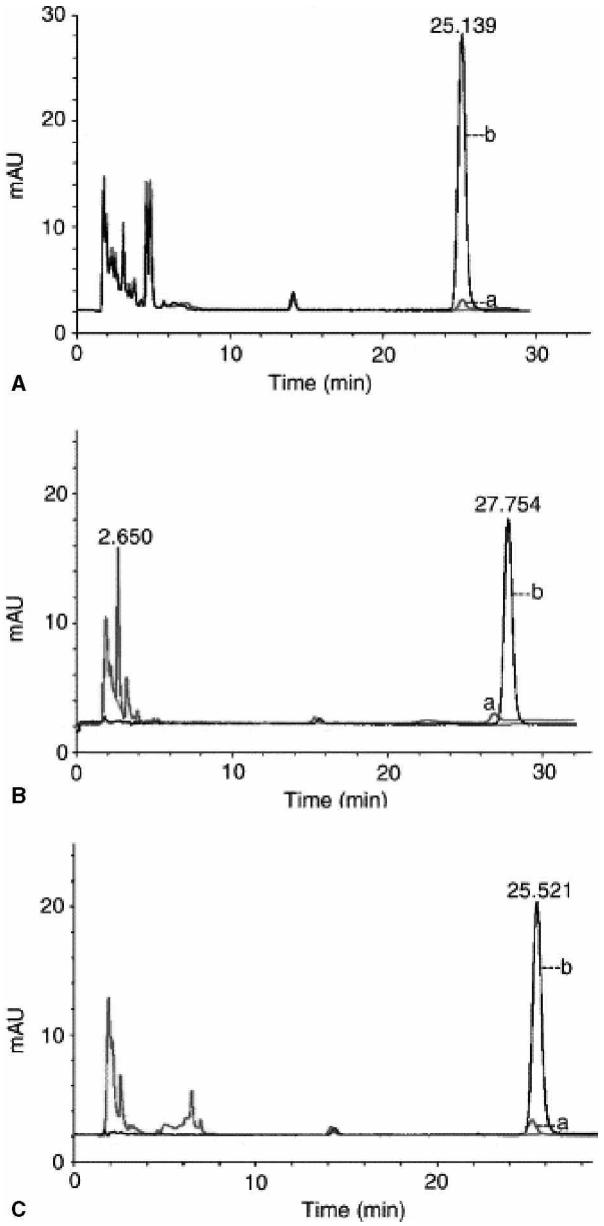

Fig. 1 Chromatographic monitoring of degraded B(*a*)P by 10 kGy γ-irradiation. Column: Discovery C18; mobile phase: methanol: water (80:20); flow rate: 1 ml/min; λ max: 280 nm. [A]: (a) 5 mg dm^{-3} B(*a*)P in methanol, [B]: (a) 2 mg dm^{-3} B(*a*)P in methanol–water [C]: (a) 2 mg dm^{-3} B(*a*)P in methanol–water + surfactant. (b) Doping of each irradiated solution with 1 mg dm^{-3} B(*a*)P.

DEGRADATION OF POLYCYCLIC AROMATIC HYDROCARBONS

The combustion process of fossil fuels and the coal processing industry introduce significant quantities of polycyclic aromatic hydrocarbons (PAHs) into the environment. Sixteen PAHs are known as priority pollutants and are persistent, carcinogenic, and very toxic. The permissible

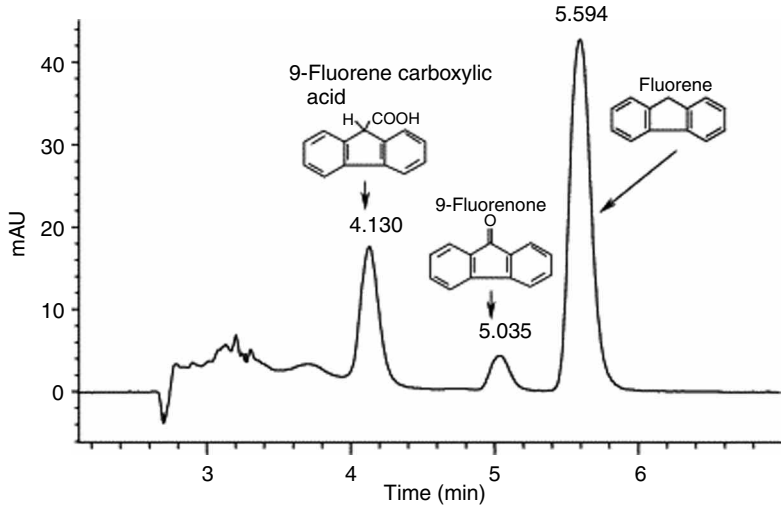

Fig. 2 HPLC chromatogram (column: Zorbax SB-phenyl 4.6 × 250 mm; solvent: 20 vol% H_2O + 80 vol% CH_3OH) of degradation products resulting from 5×10^{-5} mol/L FLU in aerated aqueous solution (pH = 9.6), after γ-rays treatment (0.35 kGy, dose rate: 71 Gy/min). Injection volume: 30 μl. Indication: 2.8–3.95 min mixture of aldehyde and carboxylic acids; 4.13 min 9-FCA; 5.035 min 9-FLE; 5.594 FLU, registered at λ = 260 nm.

limit of two of these PAHs, i.e., benzo(*a*)pyrene [B(*a*)P] and fluorine, in air is 10^{-6} and 2×10^{-3} mg m^{-3}, respectively.[20] The main sources of B(*a*)P are automobile exhaust[21] and the coke oven industry.[4] Its alarming concentration in potable water[22] and urine[23] has been reported. The toxic nature of PAHs, their degradation, and that of B(*a*)P in particular has been investigated using ionizing radiation. The efficiency of the degradation process has been evaluated by various chromatographic techniques. The selected concentrations of B(*a*)P were irradiated in a 50% methanol–water medium with varied doses of γ-rays. The reduction in B(*a*)P concentration was monitored using HPLC–UV, as shown in Fig. 1.[24] It was proposed that degradation products that appear early in the elution order on a reversed phase column are likely to be polar in nature and could be due to the formation of compounds bearing ketonic and carboxylic functional groups. In another study, fluorene degradation was carried out in an aqueous medium as a function of an absorbed radiation dose.[20] The major identified degradation products were 9-fluorenone and 9-fluorene carboxylic acid, in addition to a mixture of aldehydes and carboxylic acids, using HPLC–UV, florescence, and electrochemical detection. The elution behavior of fluorene's degraded products is depicted in Fig. 2.

CONCLUSION

The monitoring of environmental pollutants' degradation and their remediation has emerged as a key issue. In particular, the issue of potable water quality is a great public health concern. The main sources of its pollution are industrial wastewater, municipal waste, and the effluents of wastewater treatment facilities. A number of technologies have been introduced for the purification of polluted water. The efficiency and effectiveness of these processes, i.e., the removal of pollutants, is monitored by incorporating a variety of chromatographic techniques, namely, LC–UV, fluorescence, electrochemical analysis, and gas chromatography with FID and ECD. LC–MS is being used extensively for polar compounds to avoid a derivatization step as exists in gas chromatography.

REFERENCES

1. Petrovi, M.; Gonzalez, S.; Barceló, D. Analysis and removal of emerging contaminants in wastewater and drinking water. Trends Anal. Chem. **2003**, *22* (10), 685–696.
2. Ternes, T.A.; Meisenheimer, M.; McDowell, D.; Sacher, F.; Brauch, H.-J.; Haist-Gulde, B.; Preuss, G.; Wilme, U.; Zulei-Seibert, N. Removal of pharmaceuticals during drinking water treatment. Environ. Sci. Technol. **2002**, *36* (17), 3855.
3. Richardson, S.D. Environmental mass spectrometry: Emerging contaminants and current issues. Anal. Chem. **2004**, *76*, 3337–3364.
4. Lim, B.-R.; Hu, H.-Y.; Fujie, K. Biological degradation and chemical oxidation characteristics of coke-oven wastewater. Water Air Soil Pollut. **2003**, *146* (1–4), 23–33.
5. Kuo, C.-T.; Chen, H.-W.; Lin, S.-T. Trace determination of nitrated polycyclic aromatic hydrocarbons using liquid chromatography with on-line electrochemical reduction and fluorescence detection. Anal. Chim. Acta **2003**, *482* (2), 219–228.
6. Liu, J.-F.; Liang, X.; Chi, Y.-G.; Jiang, G.-B.; Cai, Y.-Q.; Zhou, Q.-X.; Liu, G.-G. High performance liquid chromatography determination of chlorophenols in water samples after preconcentration by continuous flow liquid membrane extraction on-line coupled with a precolumn. Anal. Chim. Acta **2003**, *487* (2), 129–135.
7. Jonkers, N.; Knepper, T.P.; de Voogt, P. Aerobic biodegradation studies of nonylphenol ethoxylates in river water using liquid chromatography–electrospray tandem mass spectrometry. Environ. Sci. Technol. **2001**, *35* (2), 335–340.
8. Graovac, M.; Todorović, M.; Trtanj, M.I.; Kopečni, M.M.; Čomor, J.J. Gas chromatographic determination of 5-chloro-2-(2, 4-dichlorophenoxy)-phenol in the

wastewater of a slaughterhouse. J. Chromatogr. A, **1995**, *705* (2), 313–317.
9. Ding, W.-H.; Liu, C.-H.; Yeh, S.P. Analysis of chlorophenoxy acid herbicides in water by large-volume on-line derivatization and gas chromatography–mass spectrometry. J. Chromatogr. A, **2000**, *896* (1–2), 111–116.
10. Ternes, T.A. Occurrence of drugs in German sewage treatment plants and rivers. Water Res. **1998**, *32* (11), 3245–3260.
11. Tixier, C.; Singer, H.P.; Oellers, S.; Müller, S.R. Occurrence and fate of carbamazepine, clofibric acid, diclofenac, ibuprofen, ketoprofen, and naproxen in surface waters. Environ. Sci. Technol. **2003**, *37* (6), 1061–1068.
12. Gerecke, A.C.; Schärer, M.; Singer, H.P.; Müller, S.R.; Schwarzenbach, R.P.; Sägesser, M.; Ochsenbein, U.; Popow, G. Sources of pesticides in surface waters in Switzerland: Pesticide load through wastewater treatment plants—current situation and reduction potential. Chemosphere **2002**, *48* (3), 307–315.
13. Petrovic, M.; Barcelo, D. Concentration of surfactants in wastewater treatment plants. In *Analysis and Fate of Surfactants in the Aquatic Environment*; Knepper, T., de Vooght, P., Barcelo, D., Eds.; Elsevier: Amsterdam, The Netherlands, 2003; 655–673.
14. Quiltero, J.C.; Moreira, M.T.; Feijoo, G.; Lema, J.M. Effect of surfactant on the soil desorption of hexachlorohexane (HCH) isomers and their anaerobic biodegradation. J. Chem. Technol. Biotechnol. **2005**, *80*, 1005–1015.
15. Pikaev, A.K. New data on electron beam purification of wastewater. Radiat. Phys. Chem. **2002**, *65*, 515–526.
16. Podzorova, E.A.; Pikaev, A.A.; Buryak, A.K.; Ul'yanov, W.; Pikaev, A.K. Chromato-mass-spectrometric study of radiation-chemical purification of water from petroleum products. Khim. Vys. Energ. **2001**, *35* (2), 83–90.
17. Kimura, A.; Taguchi, M.; Ohtani, Y.; Takigami, M.; Shimada, Y.; Kojima, T.; Hiratsuka, H.; Nam, H. Decomposition of *p*-nonylphenols in water and elimination of their estrogen activities by ^{60}Co γ-ray irradiation. Radiat. Phys. Chem. **2006**, *75*, 61–69.
18. Uguz, C.; Iscan, M.; Ergüven, A.; Isgor, B.; Togan, N. The bioaccumulation of nonyphenol and its adverse effect on the liver of rainbow trout (Onchorynchus mykiss). Environ. Res. **2003**, *92* (3), 262–270.
19. Ministry of the Environment, Japan. Report on screening test for endocrine disrupting property of *p*-nonylphenols to fishes, Ministry of the Environment: Tokyo, Japan, August 2001 (in Japanese).
20. Popov, P.; Getoff, N. Decomposition of aqueous fluorene by γ-rays and product analysis. Radiat. Phys. Chem. **2004**, *69* (5), 387–393.
21. Erustes, J.A.; Andrade-Eior, A.; Cladrea, A.; Forteza, R.; Cerda, V. Fast sequential injection determination of benzo(*a*)pyrene using variable angle fluorescence with on-line solid-phase extraction. Analyst 2001, *126* (4), 451.
22. Grifoll, M.; Solanas, A.M.; Bayona, J.M. Bioassay-directed chemical characterization of genotoxic agents in the dissolved and particulate water phases of Besos and Llobregat rivers, Barcelona, Spain. Arch. Environ. Contam. Toxicol. 1992, *23* (1), 19–25.
23. Ulrica, C.; Ke, Y.; Jan-Olof, L.; Conny, O.; Thor, N.; Kari, H.; Lars, H. Genotoxic exposure of pot room workers. Scand. J. Work Environ. Health 1999, *25* (1), 24–32.
24. Bilal Butt, S.; Qureshi, R.N.; Ahmed, S. Monitoring of radiolytic degradation of benzo(*a*)pyrene using γ-rays in aqueous media by HPLC. Radiat. Phys. Chem. 2005, *74* (2), 92–95.

Radius of Gyration Measurement by GPC/SEC

Raniero Mendichi
Institute of Macromolecular Chemistry, National Research Council (CNR), Milan, Italy

INTRODUCTION

Fundamental properties of macromolecules, such as viscoelasticity and flow behavior, primarily depend on the dimensions and the conformations of macromolecules. Primary biological functions substantially depend on the dimensions of natural macromolecules such as proteins and enzymes. Hence, a primary method to understand the physical properties of macromolecules, synthetic and natural, involves determination of the dimension as a function of the molar mass. A convenient method to fractionate macromolecules is the size-exclusion chromatography (SEC) technique. SEC fractionation is rapid and efficient and requires small amounts of the polymeric sample. A method to measure the dimension of the macromolecules as a function of the molar mass is an online technique to a SEC system.

DISCUSSION

The simplest parameter to quantify the dimension of a macromolecule is the end-to-end distance. The end-to-end distance is the spatial distance between the end groups of a linear chain. Unfortunately, there are no experimental direct methods to measure the end-to-end distance of a macromolecule. Furthermore, the end-to-end distance has no meaning for a chain without end groups (ring) and with many end groups (branched). Instead, the dimension of every type of macromolecule can be always quantified by the gyration radius $\langle s^2 \rangle^{1/2}$.

There are several experimental methods to measure $\langle s^2 \rangle^{1/2}$. Macromolecules can be represented as N segments (monomers, groups) of mass m_i and distance r_i from the center of gravity. The gyration radius $\langle s^2 \rangle^{1/2}$ is defined as the mass average of r_i:

$$\langle s^2 \rangle^{1/2} = \left(\frac{\langle \Sigma m_i r_i^2 \rangle}{\Sigma m_i} \right)^{1/2} \quad (1)$$

Actually, the term "gyration radius" is a misnomer; it originates from the kinematics, but is very popular. More correctly, it should be called "root mean square radius." Non-rigid macromolecules possess conformational mobility; hence, their dimension requires an additional average, $\langle \rangle$, over all the conformations. The dimension of a macromolecule also depends on its long-range interactions, excluded volume, and the polymer-solvent interactions. Therefore, $\langle s_0^2 \rangle^{1/2}$ denotes the dimension of the macromolecules in the unperturbed ideal state and $\langle s^2 \rangle^{1/2}$ denotes the expanse dimension as a consequence of the excluded volume. Finally, macromolecules are generally polydisperse and, by analogy to the molar mass, $\langle s^2 \rangle_n^{1/2}$ denotes the numeric average, $\langle s^2 \rangle_w^{1/2}$ denotes the weight average, and $\langle s^2 \rangle_z^{1/2}$ denotes the z average.[1]

Size-exclusion chromatography fractionation is steric, that is, dimensional. In theory, a SEC system could be calibrated by means of some appropriate standards of known dimensions and, in this way, to measure. SEC fractionation depends on the hydrodynamic radius R_H of the macromolecules: $R_H \propto M[\eta]$ where $[\eta]$ is the intrinsic viscosity. $\langle s^2 \rangle^{1/2}$ and R_H are two different parameters. $\langle s^2 \rangle^{1/2}$ and match is an equilibrium parameter; R_H is a dynamic parameter and depends on the method by which it is obtained. R_H becomes the Stokes radius R_D in diffusion measurements and the Einstein radius R_η in viscosity measurements. Because SEC fractionation depends on R_H, the method is not appropriate for a direct measure of $\langle s^2 \rangle^{1/2}$. Convenient experimental methods to measure $\langle s^2 \rangle^{1/2}$ are scattering techniques.

The $\langle s^2 \rangle^{1/2}$ value of macromolecules usually ranges from 2 to 3 nm (globular proteins) to several hundred nanometers (particles). The range of $\langle s^2 \rangle^{1/2}$ values determines the more appropriate scattering technique. Smaller dimensions of the molecules require shorter wavelengths of the radiation. Light-scattering (LS) wavelengths range from approximately 400 to 700 nm. The minimum $\langle s^2 \rangle^{1/2}$ value that could be measured by LS is 8–10 nm and 5–6 nm in the more favorable case (shorter wavelength). If the dimension of the molecules is small, we need to use other scattering techniques such as x-ray or neutrons.

A modern LS photometer uses coherent light (i.e., laser) with vertical polarization. In our specific case, LS concerns the interaction of the light with matter with a solution of macromolecules. In an LS experiment, we measure the intensity of the scattering. Furthermore, to measure the $\langle s^2 \rangle^{1/2}$ value, we need the angular variation of the scattering. Because we want to measure online to a SEC system, after the fractionation in the columns, we need to measure the angular variation of the scattering instantaneously (i.e., simultaneously) over a wide range of angles. In this case, we need an online multiangle light-scattering (MALS) detector.

Following Zimm,[2,3] the intensity of the scatteringof a solution of macromolecules is in relation to themolar mass of the sample by

$$\frac{Kc}{\Delta R(\theta)} = \frac{1}{MP(\theta)} + 2A_2C + \ldots \quad (2)$$

where $\Delta R(\theta)$ is the scattering excess (Rayleigh factor) at angle θ of the solution with regard to the pure solvent, θ is the angle between the incident light and the detector, M is the molar mass, c is the concentration, A_2 is the second virial coefficient, and K is an optical constant [$K = (4\pi^2 n_0{}^2(dn/dc)^2)/(N_a\lambda_0{}^4)$, where n_0 is the refractive index of the solvent, dn/dc is the refractive index increment of the polymer, λ_0 is the wavelength of the light *in vacuo*, and is Avogadro's number].

The parameter of interest for the measurement of $\langle s^2\rangle^{1/2}$ is the form factor $P(\theta)$. A macromolecule may not be considered as a single point of scattering. In this case, the light scattered from two different points of the same macromolecule will not be in phase: destructive interference. The intensity of the scattering in the presence of the destructive interference is lower for large molecules. The interference depends on the angle of measure of the intensity of the scattering. The interference is absent at 0° angle and highest at 180°. The interference depends on the shape and on the dimension of the molecules. Therefore, there has been introduced a form factor $P(\theta)$ which quantifies the interference. $P(\theta)$ is defined as the ratio between the Rayleigh factor in the presence of interference ($\theta > 0°$) and the Rayleigh factor in the absence of interference ($\theta > 0°$). Thus, by definition,

$$P(\theta) \equiv \frac{R(\theta)}{R(\theta = 0°)} \quad (3)$$

Eq. 3 states that $P(\theta) = 1$ for $\theta = 0°$, independent of the dimension of the molecules, and $P(\theta) < 1$ for $\theta > 0°$ when the dimension of the molecules is comparable with the wavelength l. Fortunately, $P(\theta)$ is a useful method for measuring the dimension of the molecules $\langle s^2\rangle^{1/2}$. Debye[4] showed that the $P(\theta)$ could be expressed independently of the shape and conformation of the macromolecules. Considering the reciprocal of $P(\theta)$ [$P(\theta)^{-1}$], Debye obtained the following equation:

$$P(\theta)^{-1} = 1 + \frac{1}{3}\mu^2\langle s^2\rangle \quad (4)$$

where $\mu = 4\pi/\lambda \sin(\theta/2)$, $\lambda = \lambda_0/n_0$ is the wavelength of the light in the medium. Eq. 4 is valid in the limit $\mu^2\langle s^2\rangle/3 \ll 1$. From the initial slope of the $P(\theta)$ versus $\sin^2(\theta/2)$ plot, we can estimate the gyration radius value $\langle s^2\rangle^{1/2}$.

To estimate M and $\langle s^2\rangle^{1/2}$ values, Eqs. 2 and 4, we need to extrapolate to infinite dilution: $c = 0$. When the MALS detector is used as an online detector in a SEC system to estimate the $\langle s^2\rangle^{1/2}$ of the molecules, we have only a concentration. In a SEC fractionation, it is generally assumed that each instant, slice, contains molecules homogeneous in molar mass and in dimension. In this case, considering the very low concentrations of the macromolecules that elute from the SEC columns, the term ${}_2A_2c$ of Eq. 2 is ignored. However, the exact concentration of each slice has to be known. Thus, the measure of M and $\langle s^2\rangle^{1/2}$ values by a MALS detector requires a concentration detector also, usually a differential refractometer or an ultraviolet (UV) photometer. Combining Eq. 2, deprived of the $2A_2c$ term, with Eq. 4, we obtain

$$\frac{Kc}{\Delta R(\theta)} = \frac{1}{M} + \frac{16\pi^2\langle s^2\rangle}{3\lambda^2 \mathrm{M}}\sin^2\left(\frac{\theta}{2}\right) \quad (5)$$

Using an online dual-detector SEC system, MALS, and concentration from a linear regression of $Kc/\Delta R(\theta)$ on $\sin^2(\theta/2)$, we obtain the molar mass M from the intercept and the dimension of the molecules $\langle s^2\rangle^{1/2}$ from the slope. If the macromolecules are polydisperse, we obtain[3] the averages M_w and $\langle s^2\rangle_z{}^{1/2}$. Fig. 1 shows the $Kc/\Delta R(\theta)$ versus $\sin^2(\theta/2)$ plot of a single slice from a polysaccharide, hyaluronic acid, sample. Fig. 1 shows the classical three parameters that could be obtained at each elution volume: c_i from the concentration detector, M_i and $\langle s^2\rangle_i{}^{1/2}$ from the MALS detector. An accurate measure of $\langle s^2\rangle_i{}^{1/2}$ is not simple. The measurement requires a good signal to-noise ratio, especially at low angles. In addition, if the dimension of the macromolecules is small, the measure of the slope of the $Kc/\Delta R(\theta)$ versus $\sin^2(\theta/2)$ plot is inaccurate. Conversely, if the dimension of the macromolecules is too large, the angular variation of the intensity of the scattering could be not linear. In this case, it is quite difficult to estimate an accurate value of the initial slope of the plot.

Because, for each fraction of the sample, the online MALS detector measures both M_i and $\langle s^2\rangle_i{}^{1/2}$ from a single sample, it is possible to obtain the $\langle s^2\rangle^{1/2} = f(M)$ power law of the polymer. The power law $\langle s^2\rangle^{1/2} = f(M)$ is a very

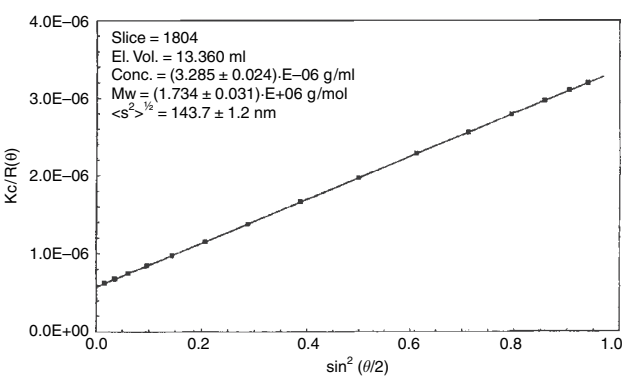

Fig. 1 $Kc/\Delta R(\theta)$ versus $\sin^2(\theta/2)$ plot of a single slice from a hyaluronic acid sample.

important function for understanding the conformation (flexible coils, compact spheres, rigid rods) of the macromolecules. In fact, if the molar mass distribution of the sample is adequately broad, it is possible, from a linear regression of $\log(\langle s^2\rangle^{1/2})$ on $\log(M)$, to estimate the constants K and α of the power law $\langle s^2\rangle^{1/2} = KM^{\alpha}$. Specifically, the slope α of the power law contains fundamental information of the conformation of the macromolecule in solution.

There are several commercially available online MALS detectors. Wyatt Instruments (Santa Barbara, California, U.S.A.) commercializes two MALS detectors: Dawn-DSP (18 angles) and mini-Dawn (3 angles: 45°, 90°, and 135°). Precision Detectors (Franklin, Massachusetts, U.S.A.) commercializes a double-angle LS:15° and 90°. SEC online measurement of $\langle s^2\rangle^{1/2}$ could be performed by other techniques. Viscotek Co. (Houston, Texas, U.S.A.) commercializes an alternative three-detector SEC system, the SEC^3. The SEC^3 system consists of (1) an online viscometer (VISC), (2) an online rightangle LS detector (RALS), and (3) a concentration detector. This three-detector SEC system also measures $\langle s^2\rangle^{1/2}$. More exactly, $\langle s^2\rangle^{1/2}$ is calculated, using an iterative algorithm, from the intrinsic viscosity, by VISC, and the molar mass obtained by the RALS detector. For each instant i, the algorithm is divided into three steps:

- $[\eta]_i$ is measured from VISC; the molar mass is M_i is calculated by RALS using Eq. 2 and $P(\theta) = 1$. In this first step, M is generally underestimated as a consequence of the destructive interference.
- $\langle s^2\rangle^{1/2}$ is calculated by the Flory–Fox equation (Eq. 6). The Ptitsyn–Eizner equation (Eq. 7) considers the expansion of the macromolecules due to the excluded volume. In Eq. 6 and 7, $\phi_0 = 2.86 \times 10^{23}$ and $\varepsilon = (2a - 1)/3$, where a is the slope of the Mark-Houwink–Sakurada equation.

Finally, $P(\theta)$ is calculated by the Debye equation (Eq. 4):

$$\langle s^2\rangle^{1/2} = \frac{1}{\sqrt{6}}\left(\frac{M[\eta]}{\phi(\varepsilon)}\right)^{1/3} \tag{6}$$

$$\phi(\varepsilon) = \phi_0(1 - 2.63\varepsilon + 2.86\varepsilon^2) \tag{7}$$

At this point, the algorithm restarts the first step, with $P(\theta)$ equal to the new calculated value from the previous iteration. The algorithm converges very quickly. A detailed description of the SEC^3 algorithm can be found in Ref. [5]

To measure the dimension of macromolecules is a very delicate task. However, the dimension is a primary parameter needed to understand the physical properties of a macromolecule. We have described two experimental methods, MALS and SEC^3 to measure $\langle s^2\rangle^{1/2}$ online to a SEC system.

REFERENCES

1. Wyatt, P.J. Light scattering and the absolute characterization of macromolecules. Anal. Chim. Acta **1993**, *272*, 1.
2. Zimm, B.H. The scattering of light and the radial distribution function of high polymer solutions. J. Chem. Phys. **1948**, *16* (12), 1093.
3. Kratochvil, P. *Classical Light Scattering from Polymer Solutions*; Elsevier: Amsterdam, 1987.
4. Debye, P. J. Phys. Colloid Chem. **1947**, *51*, 18.
5. Yau, W.W.; Rementer, S.W. Polymer characterization by SEC viscometry: molecular weight (MW), size (Rg) and intrinsic viscosity (IV) distribution. J. Liq. Chromatogr. Relat. Technol. **1990**, *13* (4), 627.

Rate Constants: Determination from On-Column Chemical Reactions

Richard Thede
Institute of Chemistry and Biochemistry, University of Greifswald, Greifswald, Germany

INTRODUCTION

The determination of rate constants from chemical reactions occurring simultaneously with the separation process has been studied since the early 1960s. Apparently, the first paper in this field was published by Kallen and Heilbronner,[1] covering the first-order reaction of the dehydrogenation of cyclopropane to cyclopropene on a molecular sieve.

The work done until the early 1970s was summarized by Langer and Patton,[2] who put it under the framework of the ideal chromatographic reactor (ICR) model. The correspondence of the rate constants from first-order irreversible reactions was demonstrated by them as well as by Gil-Av and Herzberg-Minzly.[3]

During the 1980s, the liquid chromatographic reactor[4] got into focus as well as studies on chromatographic reactors with void zones,[5,6] enabling a separate determination of the rate constants in the mobile and the stationary phase.

In the field of determining rate constants through on-column chromatographic reactions, the investigation of reversible first-order reactions got an outstanding position because of their pharmaceutical applications with respect to enantiomers. After the early work of Keller and Giddings,[7] and Cremer and Kramer,[8,9] the methodology was developed mainly by the groups of Trapp, Schoetz, and Schurig,[10] Mannschreck and Kiessl,[11] and Hochmuth and Koenig.[12]

The aforementioned contributions are based on linear partition equilibrium of educts and products. Linear non-equilibrium reactors as well as non-linear reactors—the latter for preparative chromatography—have also been studied largely, but not primarily in the determination of rate constants. There are also methods using stopped or reversed flow of the mobile phase, especially in gas chromatography.[13]

The model of ideal linear non-equilibrium chromatography is sufficient to cover all cases of practical importance, in which rate constants were determined.

In general, the following assumptions were made: isothermal separation column, no radial concentration gradients, constant plug flow of the mobile phase, and linear sorption isotherm.

The mass balance equations for any reactant and product can be written as follows:

$$\frac{\partial c_\mathrm{i}}{\partial t} = -u\frac{\partial c_\mathrm{i}}{\partial x} + \sum \nu_{\mathrm{ij M}} r_\mathrm{jM} - k_\mathrm{fi} q_\mathrm{i} c_\mathrm{i} + k_\mathrm{fi} a_\mathrm{i}$$

$$\frac{\partial a_\mathrm{i}}{\partial t} = \sum \nu_\mathrm{ijs} \frac{v_\mathrm{s}}{v_\mathrm{M}} r_\mathrm{js} + k_\mathrm{fi} q_\mathrm{i} c_\mathrm{i} - k_\mathrm{fi} a_\mathrm{i}$$

Additional simplifications are mostly made:

1. The reactions are not limited by the mass transfer, i.e., $\frac{a_\mathrm{i}}{c_\mathrm{i}} \approx q_\mathrm{i}$ at any x.
2. The chromatographic process produces a certain peak shape, i.e., $c_\mathrm{i} = m_\mathrm{i}(x)\ \Psi_\mathrm{i}(x,t)$ (in the simplest case, $\Psi_\mathrm{i}(x,t)$ represents a Gaussian).
3. Retention times and peak broadening depend linearly on the spatial coordinate.

Assumption (1) permits the development of methods for the determination of first-order irreversible and—with restrictions—also for first-order reversible reactions. It is characteristic for the ICR model.

Assumptions (2) and (3) are required for a realistic modeling of non-first-order irreversible reactions, as well as for the approximation of chromatogram shapes by mathematical–analytical equations. Together with assumption (1) they form the Extended ICR (EICR) model.

RATE CONSTANTS FROM SIMPLE REACTIONS USING PEAK AREAS AND MOMENTS

R → P

The model equations take the form

$$\frac{\partial c_\mathrm{R}}{\partial t} = -u\frac{\partial c_\mathrm{R}}{\partial x} - k_\mathrm{M} c_\mathrm{R} - k_\mathrm{fR} q_\mathrm{R} c_\mathrm{R} + k_\mathrm{fR} a_\mathrm{R}$$

$$\frac{\partial a_\mathrm{R}}{\partial t} = -k_\mathrm{S} a_\mathrm{R} + k_\mathrm{fR} q_\mathrm{R} c_\mathrm{R} - k_\mathrm{fR} a_\mathrm{R}$$

$$\frac{\partial c_\mathrm{P}}{\partial t} = -u\frac{\partial c_\mathrm{P}}{\partial x} + k_\mathrm{M} c_\mathrm{R} - k_\mathrm{fP} q_\mathrm{P} c_\mathrm{P} + k_\mathrm{fP} a_\mathrm{P}$$

$$\frac{\partial a_P}{\partial t} = k_S a_R + k_{fP} q_P c_P - k_{fP} a_P$$

which by the ICR condition (1) can be reduced to

$$\frac{\partial c_R}{\partial t}(1 + q_R) = -u\frac{\partial c_R}{\partial x} - k_a c_R$$

$$\frac{\partial c_P}{\partial t}(1 + q_P) = -u\frac{\partial c_P}{\partial x} + k_a c_R$$

$$k_a = k_M + q_R k_s$$

To get expressions for the peak areas and reaction duration, the following operations are carried out

$$\int_0^\infty \frac{\partial c_R}{\partial t}(1 + q_R)\mathrm{d}t = 0 = \int_0^\infty \left(-u\frac{\partial c_R}{\partial x} - k_a c_R\right)\mathrm{d}t$$
$$= -u\frac{\mathrm{d}m_{R0}}{\mathrm{d}x} - k_a m_{R0}$$

$$\int_0^\infty \frac{\partial c_R}{\partial t}(1 + q_R)t\mathrm{d}t = -(1 + q_R)m_{R0}$$
$$= \int_0^\infty \left(-u\frac{\partial c_R}{\partial x} - k_a c_R\right)t\mathrm{d}t = -u\frac{\mathrm{d}m_{R1}}{\mathrm{d}x} - k_a m_{R1}$$

$$\int_0^\infty \frac{\partial c_P}{\partial t}(1 + q_P)\mathrm{d}t = 0$$
$$= \int_0^\infty \left(-u\frac{\partial c_P}{\partial x} + k_a c_R\right)\mathrm{d}t = -u\frac{\mathrm{d}m_{P0}}{\mathrm{d}x} + k_a m_{R0}$$

The solutions are easily found

$$m_{R0} = m_{R00}\exp(-k_a t_0)$$

$$m_{P0} = m_{R00}[(1 - \exp(-k_a t_0)]$$

$$\mu_{R1} = t_{rR} = \frac{m_{R1}}{m_{R0}} = t_0(1 + q_R)$$

Transforming the solutions for the zeroth moments into expressions for peak areas yields

$$A_R = A_{R0}\exp(-k_a t_0)$$

$$A_P = f_P A_{R0}[1 - \exp(-k_a t_0)]$$

forming the basis of the practical methods[14] to determine the rate constant:

Internal standard method

The inlet peak area is expressed by an internal standard being completely separated from the reaction chromatogram and inert with respect to the reaction. Then $f_S A_S = A_{R0}$, and

$$\ln\frac{A_R}{A_S} = \ln f_S - k_a t_0$$

from which k_a can be evaluated by linear regression from peak areas for varied linear flow rate.

Product–reactant method

Sometimes, the sensitivity factor f_p approaches 1 (i.e., in gas chromatography using the flame ionization detector for reactions in which the number of carbon atoms is not changed or in liquid chromatography using ultraviolet detection for reactions in which the absorption center is not involved).

Then $A_R + A_P = A_{R0}$, and

$$\ln\frac{A_R}{(A_R + A_P)} = -k_a t_0$$

As reactant and product cannot be separated completely—the reaction occurs until the very end of the column—the coelution of product and reactant must be corrected for by diminishing the apparent reactant peak area (v_{int} is the "speed of the recorder")

$$\Delta A_R = v_{int}\int_{t_B}^{t_{min}} h_{min}\int_{t_B}^{t}\frac{1}{\sqrt{2\pi\sigma_R^2}}\exp\left[-\frac{(t-\tau)^2}{2\sigma_R^2}\right]\mathrm{d}\tau\mathrm{d}t$$

This expression can be solved analytically, but the result is quite voluminous and not given here. A typical chromatogram is shown in Fig. 1. The dissociation of dicyclopentadiene is a worked example.[14]

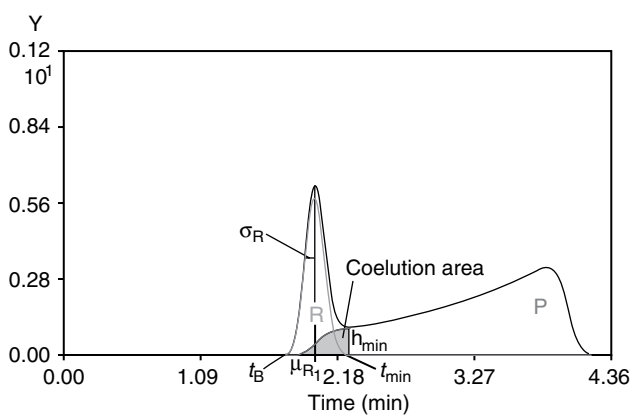

Fig. 1 Typical chromatogram from a first-order reaction with the parameters necessary for the determination of the rate constant. The areas from product and reactant are split at t_{min}.

The correction can be circumvented in case of $f_p \neq 1$ using the total area method

$$\frac{A_{tot}}{A_S} = \frac{(A_{R0} - A_{R0}f_p)}{A_S}\exp\left(-k_a\frac{l}{u}\right) + \frac{A_{R0}f_p}{A_S}$$
$$= C_1\exp(-k_a t_0) + C_2$$

and in case of $f_p \approx 1$ using the total moment method[15,16]

$$\mu_{1tot} = \frac{\int_0^\infty (y_R + y_P)t\mathrm{d}t}{\int_0^\infty (y_R + y_P)\mathrm{d}t}$$
$$= (1 + q_P)t_0 + \frac{(q_R - q_P)}{k_a}[1 - \exp(-k_a t_0)]$$

from which k_a can be obtained by non-linear regression

2R → P

The model equations take the form

$$\frac{\partial c_R}{\partial t} = -u\frac{\partial c_R}{\partial x} - 2k_M c_R^2 - k_{fR}q_R c_R + k_{fR}a_R$$

$$\frac{\partial a_R}{\partial t} = -2k_S a_R c_{sR} + k_{fR}q_R c_R - k_{fR}a_R$$

$$\frac{\partial c_P}{\partial t} = -u\frac{\partial c_P}{\partial x} + k_M c_R^2 - k_{fP}q_P c_P + k_{fP}a_P$$

$$\frac{\partial a_P}{\partial t} = k_S a_R c_{sR} + k_{fP}q_P c_P - k_{fP}a_P$$

Using simplification (1) as well as $K_R = c_{sR}/c_R$ yields

$$\frac{\partial c_R}{\partial t}(1 + q_R) = -u\frac{\partial c_R}{\partial x} - 2k_a c_R^2$$
$$\frac{\partial c_P}{\partial t}(1 + q_P) = -u\frac{\partial c_P}{\partial x} + k_a c_R^2$$

$$k_a = k_M + k_S q_R K_R$$

Using simplification (2) and carrying out the same operations as in the first-order case

$$\int_0^\infty \frac{\partial c_R}{\partial t}(1 + q_R)\mathrm{d}t = 0$$
$$= \int_0^\infty \left(-u\frac{\partial c_R}{\partial x} - 2k_a c_R^2\right)\mathrm{d}t$$
$$= -u\frac{\mathrm{d}m_{R0}}{\mathrm{d}x} - 2k_a m_{R0}^2\int_0^\infty \Psi^2(x,t)\mathrm{d}t$$

$$\int_0^\infty \frac{\partial c_R}{\partial t}(1 + q_R)t\mathrm{d}t = -(1 + q_R)m_{R0}$$
$$= \int_0^\infty \left(-u\frac{\partial c_R}{\partial x} - 2k_a c_R^2\right)t\mathrm{d}t$$
$$= -u\frac{\mathrm{d}m_{R1}}{\mathrm{d}x} - 2k_a m_{R0}^2\int_0^\infty t\Psi^2(x,t)\mathrm{d}t$$
$$= -u\mu_{R1}\frac{\mathrm{d}m_{R0}}{\mathrm{d}x} - um_{R0}\frac{\mathrm{d}\mu_{R1}}{\mathrm{d}x} - 2k_a m_{R0}^2$$
$$\times\int_0^\infty \Psi^2(x,t)\mathrm{d}t\frac{\int_0^\infty t\Psi^2(x,t)\mathrm{d}t}{\int_0^\infty \Psi^2(x,t)\mathrm{d}t}$$

$$\int_0^\infty \frac{\partial c_P}{\partial t}(1 + q_P)\mathrm{d}t = 0$$
$$= \int_0^\infty \left(-u\frac{\partial c_P}{\partial x} + k_a c_R^2\right)\mathrm{d}t$$
$$= -u\frac{\mathrm{d}m_{P0}}{\mathrm{d}x} + k_a m_{R0}^2\int_0^\infty \Psi^2(x,t)\mathrm{d}t$$

From the equations, it follows directly that

$$2m_{P0} + m_{R0} = m_{R00}$$

For *any* symmetric function for the reactant peak shape Ψ

$$\mu_{R1} = t_r = \frac{l}{u}(1 + q_R)$$

For a *Gaussian* reactant peak shape

$$-u\frac{\mathrm{d}m_{R0}}{\mathrm{d}x} = k_a\frac{m_{R0}^2}{\sqrt{\pi}\sigma_R(x)}$$

which can be solved assuming

$$\sigma_R(x) \approx \sigma_R\sqrt{x}$$

(This approximation can be concluded from "numerical experiments.")

The result is[17]

$$\frac{m_{R00}}{m_{R0}} = 1 + \frac{2k_a m_{R00}}{\sqrt{\pi}\sigma_R}t_0$$

The m_{R00} on the right side of the equation must be evaluated from the inlet amount n_{R0} and the volume flow $\dot{v}$

$$m_{R00} = \frac{n_{R0}}{\dot{v}}$$

Methods similar to first order can be used:

Internal standard method

$$\frac{A_S}{A_R} = f_s + f_s \frac{2k_a m_{R00}}{\sqrt{\pi}\sigma_R} t_0$$

Product–reactant method with sensitivity factor $f_p = 2$

$$\frac{A_P + A_R}{A_R} = 1 + \frac{2k_a m_{R00}}{\sqrt{\pi}\sigma_R} t_0$$

The area correction diminishing A_R (v_{int} is the "speed of the recorder")

$$\Delta A_R = v_{int} \int_{t_B}^{t_{min}} h_{min} \int_{t_B}^{t} \frac{1}{\sqrt{\pi\sigma_R^2}} \exp\left[-\frac{(t-\tau)^2}{\sigma_R^2}\right] d\tau dt$$

The characteristic chromatogram can be seen in Fig. 2. A worked example is the aldol-condensation of propanol.[17] The construction of a total area and a total moment method, respectively, are also possible; however, because the reactants' standard deviation must be obtained anyhow, these methods have never been used.

$R_1 + R_2 \rightarrow P$

This reaction can only be carried out under defined conditions, if the faster reactant overtakes the slower reactant. If the faster reactant overtakes the slower one *completely* within the column, the peak areas of the single reactants (without reaction) and the reactants after a reaction can be compared directly (Fig. 3).

Calculations similar to those carried out for the dimerization type lead to the following result

$$\ln\left(\frac{A_{R1}}{A_{R01}}\right) - \ln\left(\frac{A_{R2}}{A_{R02}}\right) = k_a t_0 \frac{(m_{R01} - m_{R02})}{|tr_{R1} - tr_{R2}|}$$

k_a can be found by linear regression, and as in the dimerization type, the zeroth moments in the right side of the equation must be evaluated from the inlet amounts. The addition of tetrachloroterephthaloyl chloride to pyridine has been investigated.[18]

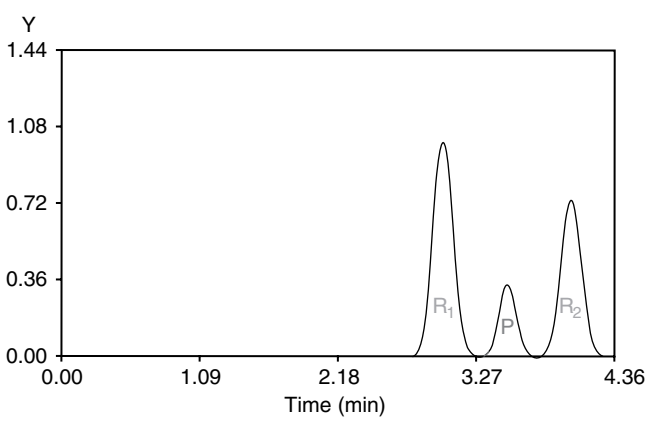

Fig. 3 Typical chromatogram from a second-order reaction (pulse overlay) with complete separation.

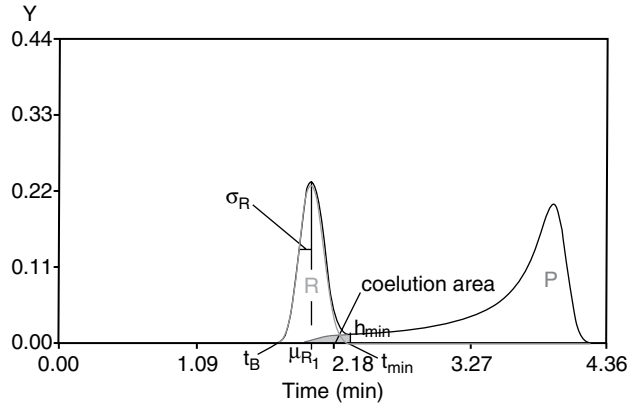

Fig. 2 Typical chromatogram from a second-order reaction (dimerization type).

$R_1 \rightleftarrows R_2$

The area-based determination of rate constants from first-order reversible reactions is possible owing to the fact that molecules of R_1 produced by R_2 do not return under the primary peak of R_1, and vice versa. This means that the area of the primary peaks diminishes like in a simple irreversible reaction. The internal standard method together with the peak area correction gives appropriate results for these reactions too in case of small conversions.[19]

RATE CONSTANTS FROM COMPLEX REACTIONS USING CHROMATOGRAM SHAPES

As can be seen from the chromatograms given for consecutive (Fig. 4)[20] and reversible reactions (Fig. 5), the coelution problem is much more serious than in simple reactions. Moreover, in reversible reactions starting from samples with equilibrium composition, the peak areas are

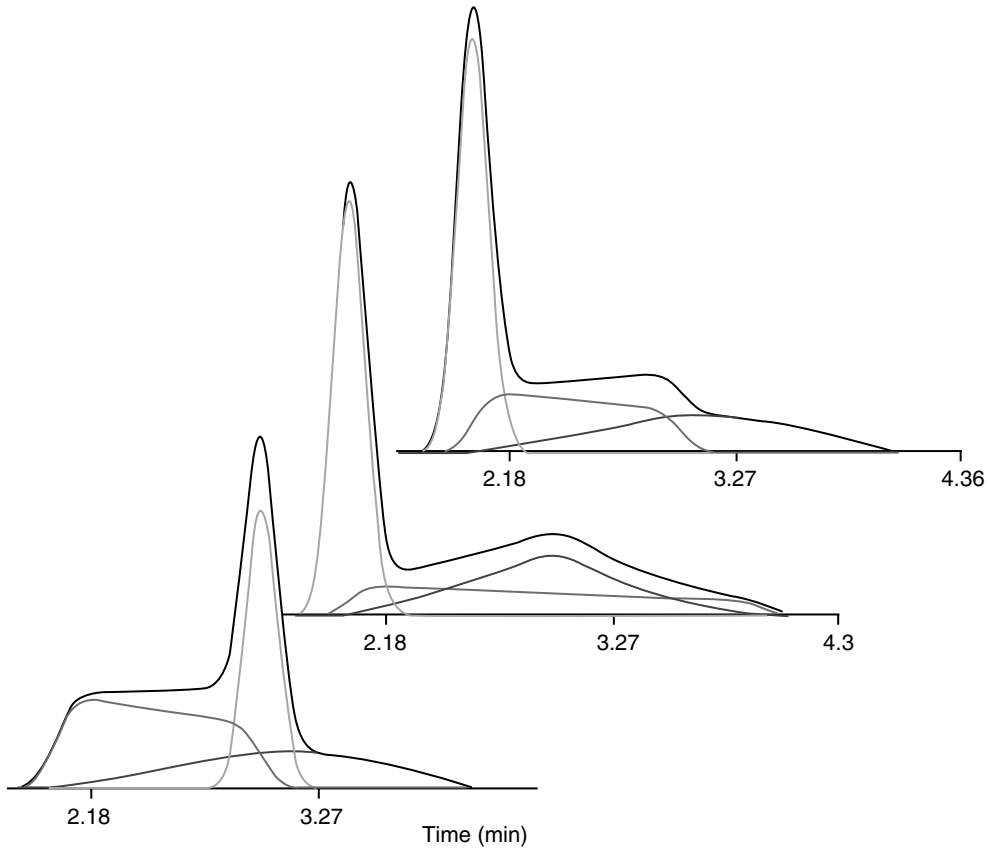

Fig. 4 Chromatograms for the consecutive reaction R → I → P and the elutions orders R, I, P; R, P, I, and I, R, P, respectively.

not changed by the chromatographic reactor owing to the principle of microkinetic reversibility.[21] However, the chromatogram is characteristically shaped by the reaction kinetic processes.

Therefore, fitting of computed chromatograms to the experimental chromatogram is a method of choice in these cases. Such chromatograms were evaluated basing on the discontinuous model (plate model) or on a numerical solution of the balance equations by the finite difference method.[22] Such purely numerical procedures are still quite time consuming, and therefore for rapid calculations mathematical–analytical approximations have been developed on the basis of the Keller–Giddings equation covering the meaningful field of reversible reactions, especially enantiomerizations,[23] and on the basis of the EICR assumptions for differentially small components of the product peaks leading to analytical approximations for all types of the aforementioned reactions.[24]

Recently, Trapp and Schurig[25] published a simplified analytical function for reversible reactions, by the help of which the apparent rate constant of an enantiomerization can be found from the retention times, standard deviations, and maximum heights of the educts, and the maximum height of the interconversion plateau between the educt peaks.

SEPARATE DETERMINATION OF RATE CONSTANTS FOR STATIONARY AND MOBILE PHASE BY SIMULATED RECYCLING VIA VOID ZONES

In general, the rate constants determined by on-column chromatographic methods are a weighed sum of the rate constants within the stationary and the mobile phase, the retention capacity (and in non-first-order reactions also the partition coefficient) being the weighing factor. Certainly, for some catalyzed reactions occurring only within the mobile or the stationary phase, the decomposition is possible, if the dead time is known.

Griffith, Chu, and Langer[5] suggested the application of a simulated recycling of the internal chromatogram, i.e., the substances pass through a chromatographic column, then through an empty capillary, the length of which is sufficient for a residence time similar to that in the mobile phase of the column, and finally through another column of the same type like the first. Then, extra peak(s) is formed, which is only owing to the reaction in the mobile phase.

For irreversible first-order reactions (Fig. 6), the peak area of the extra peaks is sufficient for the separate determination of the mobile phase rate constant, but for complex reactions, the fitting method via numerical or approximate

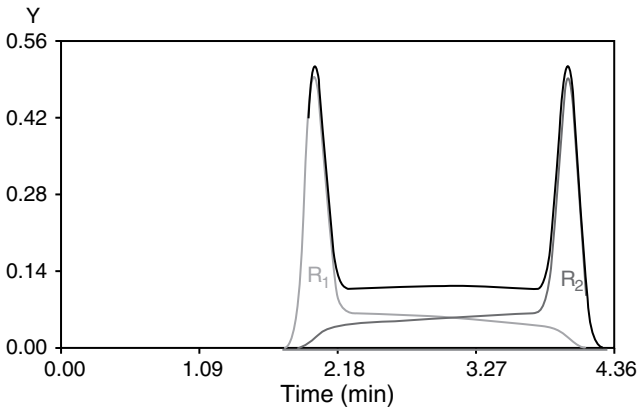

Fig. 5 Chromatogram from a reversible first-order reaction with comparable forward and backward rate constants starting from an equilibrated mixture (i.e., enantiomerizations).

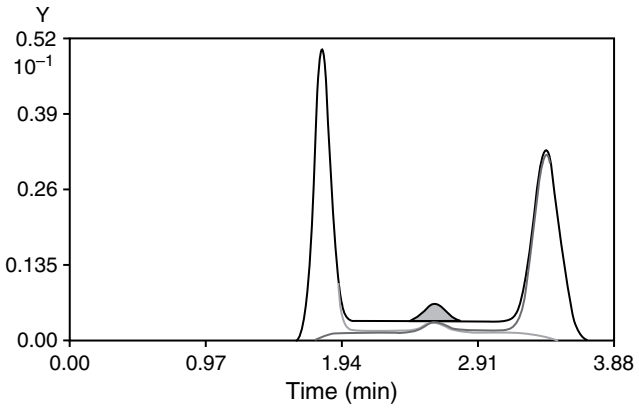

Fig. 7 Extra peak in a chromatogram from a reversible first-order reaction occurring on a system consisting of two identical columns connected by a void capillary (simulated recycling).

analytical computations has to be applied, the latter of which was tested for enantiomerizations (Fig. 7) as well as for isomerizations.[26]

SYMBOLS

A:	Peak area
a:	Stationary phase concentration (including phase ratio)
c:	Mobile phase concentration
f:	Sensitivity factor ($f_P = A_P/A_R$; $f_S = A_S/A_R$ for the *same* inlet amounts)
k:	Rate constants
k_a:	Apparent rate constant (as to be specified for reaction type and order)
k_f:	Mass transfer coefficient
l:	Column length
m_0:	Zeroth moment, concentration-time area
q:	Retention capacity
r:	Rate of reaction
t:	Time
t_0:	Dead time
u:	Linear flow rate
v:	Volume
x:	Spatial coordinate
t_r:	Retention time
Ψ:	Peak shape function
ν:	Stoichiometric coefficient

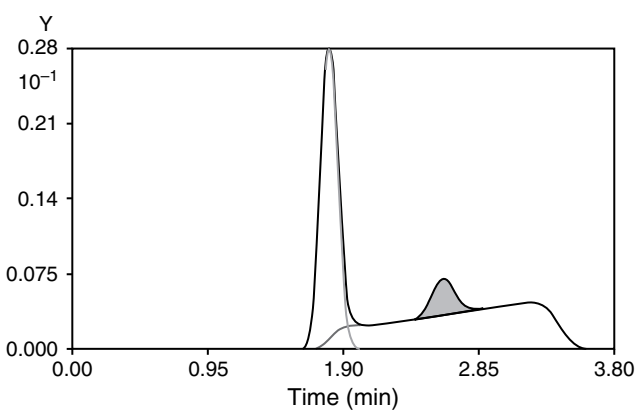

Fig. 6 Extra peak in a chromatogram from a first-order reaction occurring on a system consisting of two identical columns connected by a void capillary (simulated recycling).

INDICES

i:	Substance index
j:	Reaction index
M:	Mobile phase
P:	Product
R:	Reactant
s:	Stationary phase
S:	(Internal) standard
0:	Column inlet

CONCLUSIONS

The determination of rate constants from reactions occurring simultaneously on-column with the separation process has been demonstrated for a variety of first-order reaction types as well as for simple second-order reactions. Assuming retentions times from minutes to hours, sample amounts in the microliter range and conversions in the middle range, first-order rate constants from 10^0–10^{-3}/min and second-order rate constants from 10^4–10^{-1} dm^3/mol/min are accessible, which, however, are in general apparent rate constants, a weighed average of the rate constant in the mobile and the rate constants in the stationary phase. That the latter problem can be solved generally by use of chromatographic reactors

with void zones (simulated recycling) must be proven by further investigations.

REFERENCES

1. Kallen, J.; Heilbronner, E. The vapor-chromatograph of a labile compound. Helvet. Chim. Acta **1960**, *43*, 489–500.
2. Langer, S.H.; Patton, J.E. Chemical reactor applications of the gas chromatographic column. In *New Developments in Gas Chromatography*; Purnell, J.H., Ed.; Wiley: New York, 1973; Vol. 11, 293–373.
3. Gil-Av, E.; Herzberg-Minzly, Y. Gas-chromatographic study of the rate of Diels-Alder addition. Proc. Chem. Soc. **1961**, *8*, 316.
4. Jeng, C.Y.; Langer, S.H. Reaction kinetics and kinetic processes in modern liquid chromatographic reactors. J. Chromatogr. **1992**, *589* (1–2), 1–30.
5. Griffith, T.D.; Chu, A.H.T.; Langer, S.H. Multicolumn gas chromatographic reactor studies of the dissociation reactions of dicyclopentadiene and its methyl derivatives. Chem. Engn. J. **1987**, *36* (2), 73–91.
6. Chu, A.H.T.; Langer, S.H. Void-column liquid chromatographic reactor studies to determine reaction rates in mobile and stationary phases. J. Chromatogr. **1987**, *384*, 231–248.
7. Keller, R.A.; Giddings, J.C. Multiple zones and spots in chromatography. J. Chromatogr. **1960**, *3*, 205–220.
8. Kramer, R. Simultaneous reaction gas chromatography with a reversible first order reaction I. J. Chromatogr. **1975**, *107* (2), 241–252.
9. Cremer, E.; Kramer, R. Simultaneous reaction gas chromatography with a reversible first order reaction II. J. Chromatogr. **1975**, *107* (2), 253–263.
10. Trapp, O.; Schoetz, G.; Schurig, V. Determination of enantiomerization barriers by dynamic and stopped-flow chromatographic methods. Chirality **2001**, *13* (8), 403–414.
11. Mannschreck, A.; Kiessl, L. Enantiomerization during HPLC on an optically active sorbent. Deconvolution of experimental chromatograms. Chromatographia **1989**, *28* (5–6), 263–266.
12. Hochmuth, D.H.; Koenig, W.A. Determination of the rotational energy barrier of planar-chiral cyclophanes using dynamic enantioselective gas chromatography and computer simulation. Liebigs Ann. **1996**, *6*, 947–951.
13. Katsanos, N.A.; Thede, R.; Roubani-Kalantzopoulou, F. Diffusion, adsorption and catalytic studies by gas chromatography. J. Chromatogr. A, **1998**, *795* (2), 133–184.
14. Langer, S.H.; Patton, J.E. Gas-chromatographic reactor study of the kinetics of dicyclopentadiene dissociation. J. Phys. Chem. **1972**, *76* (15), 2159–2170.
15. Thede, R.; Pscheidl, H.; Haberland, D. Analysis of the first absolute statistical total moment of reaction chromatograms for determining the rate constants of first-order irreversible reactions. Z. Phys. Chem. **1985**, *266* (6), 1089–1105.
16. Jeng, C.Y.; Langer, S.H. Rate process analysis in the liquid chromatographic reactor: An application of the first statistical moment. Ind. Engn. Chem. Res. **1991**, *30* (7), 1489–1499.
17. Thede, R.; Moeller, E.; Pscheidl, H.; Haberland, D. On the determination of rate constants of irreversible non-first-order reactions by means of reaction gas chromatography. II. Simple irreversible second-order reactions of the type $2A \rightarrow B$. Z. Phys. Chem. **1990**, *271* (5), 891–895.
18. Thede, R.; Haberland, D.; Deng, Z.; Langer, S.H. Second-order kinetics in the liquid chromatographic reactor. J. Chromatogr. A, **1994**, *683* (2), 279–291.
19. Lebl, M.; Gut, V. Calculation of the rate constant of a reversible reaction from the chromatographic peaks for muramyldipeptide anomers. J. Chromatogr. **1983**, *260* (2), 478–482.
20. Thede, R.; Haberland, D.; Below, E.; Joensson, J.A. Determination of rate constants of consecutive first order reactions occurring on chromatographic columns. J. Liq. Chromatogr. **1995**, *18* (6), 1137–1156.
21. Bürkle, W.; Karfunkel, H.; Schurig, V. Dynamic phenomena during enantiomer resolution by complexation gas chromatography. J. Chromatogr. **1984**, *288*, 1–14.
22. Jung, M.; Schurig, V. Determination of enantiomerization barriers by computer simulation of interconversion profiles: Enantiomerization of diaziridines during chiral inclusion gas chromatography. JACS **1992**, *114* (2), 529–534.
23. Veciana, J.; Crespo, M.I. Dynamic HPLC, a method for determining rate constants, energy barriers, and equilibrium constants for dynamic molecular processes. Angew. Chem. Int. Ed. Engl. **1991**, *30* (1), 74–76.
24. Thede, R.; Haberland, D.; Fischer, C.; Below, E.; Langer, S.H. Parametric studies on the determination of enantiomerization rate constants from liquid chromatographic data by empirical peak shape equations for multi-step consecutive reactions. J. Liq. Chromatogr. **1998**, *21*, 2089–2102.
25. Trapp, O.; Schurig, V. Novel direct access to enantiomerization barriers from peak profiles in enantioselective dynamic chromatography: Enantiomerization of dialkyl-1,3-allenedicarboxylates. Chirality **2002**, *14* (6), 465–470.
26. Lange, J.; Haberland, D.; Thede, R. Separate determination of rate constants from reversible reactions in chromatographic column and eluent using empirical peak shape equations. J. Liquid Chromatogr. Relat. Techol. **2003**, *26*, 285–296.

Rate Theory in GC

Raymond P.W. Scott
Scientific Detectors Ltd., Banbury, Oxfordshire, U.K.

INTRODUCTION

The rate theory examines the kinetics of exchange that takes place in a chromatographic system and identifies the factors that control band dispersion. The first explicit height equivalent to a theoretical plate (HETP) equation was developed by Van Deemter et al. in 1956[1] for a packed GC column. Van Deemter et al. considered that four spreading processes were responsible for peak dispersion, namely *multi-path dispersion*, *longitudinal diffusion*, *resistance to mass transfer in the mobile phase*, and *resistance to mass transfer in the stationary phase*.

THE MULTIPATH EFFECT

In a packed column, the individual solute molecules will describe a tortuous path through the interstices between the particles, and some will randomly travel shorter routes than the average and some will travel longer routes. Consequently, those molecules taking the shorter paths will move ahead of the mean and those that take the longer paths lag behind the mean which will result in band dispersion. Van Deemter et al. derived the following function for the multipath variance contribution ($\sigma_M{}^2$) to the overall variance per unit length of the column (σ^2):

$$\sigma_M{}^2 = 2\lambda d_p \tag{1}$$

where d_p is the particle diameter of the packing and λ is a constant that depends on the quality of the packing.

LONGITUDINAL DIFFUSION

Driven by the concentration gradient, solutes naturally diffuse when contained in a fluid. Thus, a discrete solute band will diffuse in a gas or liquid, and because the diffusion process is random, it will produce a concentration curve that is Gaussian in form. This diffusion effect occurs in the mobile phase of both packed gas chromatography (GC) and liquid chromatography (LC) columns. The longer the solute band remains in the column, the greater will be the extent of diffusion. Because the residence time of the solute in the column is inversely proportional to the mobile-phase velocity, the dispersion will also do the same. Van Deemter et al. derived the following expression for the variance contribution by longitudinal diffusion ($\sigma_L{}^2$) to the overall variance per unit length of the column (σ^2):

$$\sigma_L{}^2 = \frac{2\gamma D_m}{u} \tag{2}$$

where D_m is the diffusivity of the solute in the mobile phase, u is the linear velocity of the mobile phase, and γ is a constant that depends on the quality of the packing.

RESISTANCE TO MASS TRANSFER IN THE MOBILE PHASE

During migration through the column, the solute molecules are continually transferring from the mobile phase to the stationary phase and back again. This transfer process is not instantaneous; a finite time is required for the molecules to traverse (by diffusion) through the mobile phase in order to reach the interface and enter the stationary phase. Thus, those molecules close to the stationary phase enter it immediately, whereas those molecules some distance away will find their way to it some time later. However, because the mobile phase is moving, during this time interval, those molecules that remain in the mobile phase will be swept along the column and dispersed away from those molecules that were close and entered the stationary phase immediately. This dispersion is called the resistance to mass transfer in the mobile phase.

Van Deemter derived the following expression for the variance contribution by the resistance to mass transfer in the mobile phase ($\sigma_{\mathrm{RM}}{}^2$) to the overall variance per unit length of the column (σ^2):

$$\sigma_{\mathrm{RM}}{}^2 = \frac{f_1(k')d_p{}^2}{D_m}u \tag{3}$$

where k' is the capacity ratio of the solute and the other symbols have the meaning previously ascribed to them.

RESISTANCE TO MASS TRANSFER IN THE STATIONARY PHASE

Dispersion caused by the resistance to mass transfer in the stationary phase is exactly analogous to that in the mobile phase. Solute molecules close to the surface will leave the

stationary phase and enter the mobile phase before those that have diffused further into the stationary phase and have a longer distance to diffuse back to the surface. Thus, as those molecules that were close to the surface will be swept along in the moving phase, they will be dispersed from those molecules still diffusing to the surface.

Van Deemter derived an expression for the variance from the resistance to mass transfer in the stationary phase ($\sigma_{\mathrm{RS}}{}^2$) which is as follows:

$$\sigma_{\mathrm{RS}}{}^2 = \frac{f_2(k')d_f{}^2}{D_S}u \tag{4}$$

where k' is the capacity ratio of the solute, d_f is the effective film thickness of the stationary phase, D_S is the diffusivity of the solute in the stationary phase, and the other symbols have the meaning previously ascribed to them.

As all the dispersion processes are random, the individual variances can be added to arrive at the total variance of the peak leaving the column:

$$\sigma^2 = \sigma_{\mathrm{M}}{}^2 + \sigma_{\mathrm{L}}{}^2 + \sigma_{\mathrm{RM}}{}^2 + \sigma_{\mathrm{RS}}{}^2 \tag{5}$$

where σ^2 is the total variance/unit length of the column.

Thus, substituting for and from $\sigma_{\mathrm{M}}{}^2$, $\sigma_{\mathrm{L}}{}^2$, $\sigma_{\mathrm{RM}}{}^2$, and $\sigma_{\mathrm{RS}}{}^2$ from Eqs. 1–4, respectively,

$$\sigma^2 = 2\lambda d_p + \frac{2\gamma D_m}{u} + \frac{f_1(k')d_p{}^2}{D_m}u + \frac{f_2(k')d_f{}^2}{D_S}u \tag{6}$$

Now, the variance per unit length of a column is numerically equivalent to ratio of the column length to the column efficiency[2] [i.e., the height of the theoretical plate (H)]; thus,

$$H = 2\gamma d_p + \frac{2\gamma D_m}{u} + \frac{f_1(k')d_p{}^2}{D_m}u + \frac{f_2(k')d_f{}^2}{D_S}u \tag{7}$$

hence the term "HETP equation" for the equation for the variance per unit length of a column. Unfortunately, due to the compressibility of the gaseous mobile phase, neither the linear velocity nor the pressure is constant along the column, and as the diffusivity (D_m) is a function of pressure, the above form of the equation is only approximate. The Van Deemter equation was modified to take into account the compressibility of the carrier gas by Ogan and Scott.[3] The complete HETP equation for a GC column that takes into account the compressibility of the carrier gas will be

$$H = 2\lambda d_p + \frac{2\gamma D_m(o)}{u_o} + \frac{f_1(k')d_p{}^2}{D_{m(o)}}u_o + 2\frac{f_2(k')d_f{}^2}{D_S(\gamma+1)}u_o \tag{8}$$

where u_o is the linear gas velocity at the column outlet, D_m is the diffusivity of the solute measured at the column outlet pressure, and γ is the inlet/outlet column ratio.

It is seen that Eq. 8 is very similar to Eq. 7 except that the velocity used is the *outlet* velocity, *not* the *average* velocity, and that the diffusivity of the solute in the gas phase is taken as that measured at the column outlet pressure (i.e., atmospheric). The shape of the H vs. u curve is hyperbolic; it has a minimum value of $H_{\min}$ at the optimum velocity u_{opt} (i.e., at the optimum velocity, the column will have a maximum efficiency). Expressions for $H_{\min}$ and u_{opt} can be obtained by differentiating Eq. 8 with respect to u and equating to zero, solving for u_{opt} and substituting u_{opt} for u in Eq. 8 to obtain $H_{\min}$.

REFERENCES

1. Van Deemter, J.J.; Zuiderweg, F.J.; Klinkenberg, A. Longitudinal diffusion and resistance to mass transfer as causes of nonideality in chromatography. Chem. Eng. Sci. **1956**, *5* (6), 271–289.
2. Scott, R.P.W. *Liquid Chromatography Column Theory*; John Wiley & Sons: Chichester, 1992; 97.
3. Ogan, K.; Scott, R.P.W. Optimization of capillary parameters for gas chromatography. J. High Resolut. Chromr. July, **1984**, *7* (7), 382–388.

BIBLIOGRAPHY

1. Scott, R.P.W. *Techniques of Chromatography*; Marcel Dekker, Inc.: New York, 1995.
2. Scott, R.P.W. *Introduction to Analytical Gas Chromatography*; Marcel Dekker, Inc.: New York, 1998.

Refractive Index Detector

Raymond P.W. Scott
Scientific Detectors Ltd., Banbury, Oxfordshire, U.K.

INTRODUCTION

The first practical refractive index detector was described by Tiselius and Claesson[1] in 1942 and, despite its limited sensitivity and its use being restricted to separations that are isocratically developed, it is still probably the fifth most popular detector in use today. Its survival has depended on its response, as it can be used to detect any substance that has a refractive index that differs from that of the mobile phase. It follows that it has value for monitoring the separation of such substances as aliphatic alcohols, acids, carbohydrates, and the many substances of biological origin that do not have ultraviolet (UV) chromophores, do not fluoresce, and are non-ionic.

DISCUSSION

When a monochromatic ray of light passes from one isotropic medium (A) to another (B), it changes its wave velocity and direction. The change in direction is called refraction and the relationship between the angle of incidence and the angle of refraction is given by Snell's law of refraction, namely

$$n_B{}' = \frac{n_B}{n_A} = \frac{\sin(i)}{\sin(r)}$$

where i is the angle of incident light in medium A, r is the angle of refractive light in medium B, is the refractive index of medium A, is the refractive index of medium B, and is the refractive index of medium B relative to that of medium A.

The refractive index of a substance is a dimensionless constant that normally decreases with increasing temperature; values are taken at 20°C or 25°C using the mean value taken for the two sodium lines of the spectrum. The optical systems that are used to exploit the refractive index for detection purposes are many and varied. One procedure is to construct a cell in the form of a hollow prism through which the mobile phase can flow. A ray of light is passed through the prism, which will be deviated from its original path, and is then focused onto a photocell. As the refractive index of the mobile phase changes, due to the presence of a solute, the angle of deviation of the transmitted light will also alter and the amount of light falling on the photocell will change. This method of refractive index monitoring is used by many manufacturers in their refractive index detector designs.

Another method evolved from the work of Fresnel. The relationship between the reflectance from an interface between two transparent media and their respective refractive indices is given by Fresnel's equation:

$$R = \frac{1}{2}\left(\frac{\sin^2(i-r)}{\sin^2(i+r)} + \frac{\tan^2(i-r)}{\tan^2(i+r)}\right)$$

where R is the ratio of the intensity of the reflected light to that of the incident light and the other symbols have the meanings previously assigned to them.

Now,

$$\frac{\sin(i)}{\sin(r)} = \frac{n_1}{n_2}$$

where is the refractive index of medium 1, and is the refractive index of medium 2.

Consequently, if medium 2 represents the liquid eluted from the column, then any change in n_2 will result in a change in R, and, thus, the measurement of R could determine changes in n_2 resulting from the presence of a solute. An example of a refractive index detector that functions on the Fresnel principle is shown in Fig. 1. Light from a tungsten lamp is directed through an infrared (IR) filter (to prevent heating the cell) to a magnifying assembly that splits the beam into two beams. The two beams are focused through the sample and reference cells, respectively. Light refracted from the mobile-phase/prism surface passes through the prism assembly and is then focused on two photocells. The prism assembly also reflects light to a user port where the surface of the prism can be observed. The output from the two photocells is electronically processed and either passed to a potentiometric recorder or to a computer data acquisition system. The range of refractive index covered by the instrument for a given prism is limited and, consequently, three different prisms are usually made available to cover the refractive index ranges of 1.35–1.4, 1.31–1.44, and 1.40–1.55, respectively.

Another variant on the refractive index detector arose from the work of Christiansen on crystal filters.[2] If a cell is packed with particulate material having the same refractive index as the mobile phase passing through it, light will pass through the cell with little or no refraction or scattering. If, however, the refractive index of the mobile phase

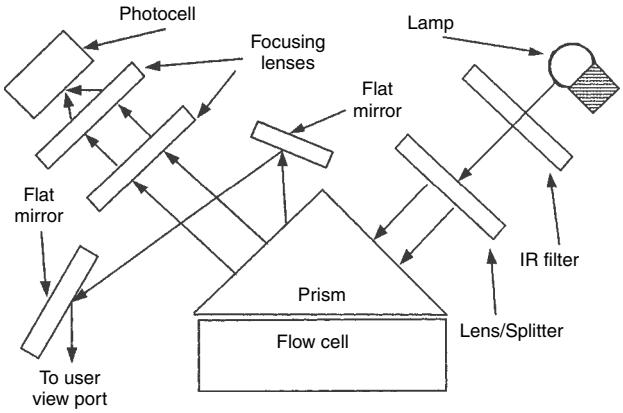

Fig. 1 A diagram of the optical system of a refractive index detector operating on the Fresnel method.
Source: Courtesy of the Perkin Elmer Corporation.

changes, there will be a refractive index difference between the mobile phase and that of the packing. This difference results in light being refracted away from the incident beam, reducing the intensity of the transmitted light. If the transmitted light is focused onto a photocell and the refractive index of the packing and mobile phase initially matched, then any change in refractive index resulting from the elution of a peak will cause light scattering and a reduction in light falling on the sample photocell and, thus, provide a differential output.

In practice, because the optical dispersions of the media are likely to differ, the refractive index will only match at one particular wavelength and, thus, the fully transmitted light will be largely monochromatic. Light of other wavelengths will be proportionally dispersed depending on the their difference from the wavelength at which the two media have the same optical dispersion. It follows that a change in refractive index of the mobile phase will change both the intensity of the transmitted light and its wavelength. This device has been manufactured but was not a commercial success due to its limited sensitivity and the need for different packing for different applications.

Another detector that functions on the change in refractive index of the column eluent is the interferometer detector, which was first developed by Bakken and Stenberg[3] in 1971. The detector responds to the change in the effective path length of a beam of light passing through a cell when the refractive index of its contents changes due to the presence of an eluted solute. If the light transmitted through the cell is focused on a photocell coincident with a reference beam of light from the same source, interference fringes will be produced; the fringes will change as the path length of one light beam changes with reference to the other, and, consequently, as the concentration of solute increases in the sensor cell, a series of electrical pulses will be generated as each fringe passes the photocell. The effective optical path length (d) depends on the change in refractive index (Δn) and the path length (l) of the sensor cell as follows:

$$d = \Delta n l$$

Further, it is possible to calculate the number of fringes (N) (sensitivity) which move past a given point (or the number of cyclic changes of the central portion of the fringe pattern) in relation to the change in refractive index by the equation

$$N = \frac{2\Delta n l}{\lambda}$$

where l is the wavelength of the light employed.

The larger the value of N for a given n, the more sensitive the detector will be. Therefore, l needs to be made as large as possible but will be limited by the dead volume of the column and the dispersion that can be tolerated before chromatographic resolution is impaired. The smallest cell (1.4 μl) (a cell volume that would be suitable for use with microbore columns) is reported to give a sensitivity of about 2×10^{-7} RI units at a signal-to-noise ratio of 2. Consequently, for benzene (RI = 1.501) sensed as a solute in *n*-heptane (RI = 1.388), this sensitivity would represent a minimum detectable concentration of 5.6×10^{-5} g/ml. The alternative 7 μl cell would decrease the minimum detectable concentration to about 1×10^{-6} g/ml, similar to that obtained for other refractive index detectors. However, the cell volume is a little large for modern high-efficiency columns. This type of RI detector has also been made commercially available but is somewhat more expensive with little gain in sensitivity over that obtained from simpler devices.

Another detector based on refractive index change is the thermal lens detector. When a laser is focused on an absorbing substance, the refractive index may be affected in such a way that the medium behaves as a lens. This effect was first reported by Gorden et al.[4] Thermal lens formation results from the absorption of laser light, which may be extremely weak. The excited-state molecules subsequently decay back to ground state and, as a result, localized temperature increases occur in the sample. Because the refractive index of the medium depends on the temperature, the resulting spatial variation of refractive index produces an effect which appears equivalent to the formation of a lens within the medium. The temperature coefficient of refractive index is, for most liquids, negative; consequently, the insertion of a liquid in the laser beam produces a concave lens that results in beam divergence.

The thermal lens effect has been used for LC detection with a small-volume sensor cell. Basically, it consists of a *heating* laser, the light from which is passed directly through the sample, and another laser which passes light through the cell in the opposite direction. When an absorbing solute arrives in the cell, a thermal lens is produced that

causes the probe light to diverge and, consequently, the intensity of the light falling on a photocell is reduced. The cell can be made a few microliters in volume and would thus be suitable for use with microbore columns. A sensitivity of 10^{-6} AU is claimed with a linear dynamic range of about three orders of magnitude. The use of two lasers adds significantly to the cost of the device. Basically, as the thermal lens detector is a special form of the refractive index detector, it can be considered as a type of universal detector. However, like other RI detectors, it cannot be used with gradient elution or flow programing and its sensitivity is no better than, if as good as, other refractive index detectors.

The refractive index detectors are very versatile in that they can detect all substances that have a different refractive index than that of the mobile phase. However, they are also one of the least sensitive detectors ($\sim 1 \times 10^{-6}$ g/ml); they have a linear dynamic range of about two to three orders of magnitude. They are extremely sensitive to flow rate, temperature, and pressure changes and cannot be used with gradient elution. Nevertheless, they are very popular for the detection of certain classes of compounds.

REFERENCES

1. Tiselius, A.; Claesson, D. Adsorption analysis by interferometric observation. Ark. Kem. Mineral. Geol. **1942**, *15B* (18).
2. Christiansen, C. Untersuchungen über die optischen Eigenschaften von fein verteilten Körpern. Ann. Phys. Chem. **1884**, *3*, 298.
3. Bakken, M.; Stenberg, V.J. Interferometer as a detector for liquid chromatography. J. Chromatogr. Sci. **1971**, *9* (10), 603.
4. Gorden, J.P.; Leite, R.C.C.; Moore, R.S.; Posto, S.P.S. Long-transient effects in lasers with inserted liquid samples. Bull. Am. Phys. Soc. **1964**, *9* (2), 501.

BIBLIOGRAPHY

1. Scott, R.P.W. *Liquid Chromatography for the Analyst*; Marcel Dekker, Inc.: New York, 1994.
2. Scott, R.P.W. *Chromatographic Detectors*; Marcel Dekker, Inc.: New York, 1996.

Relaxation Effects in FFF

Athanasia Koliadima
Physical Chemical Laboratory, Department of Chemistry, University of Patras, Patras, Greece

INTRODUCTION

Field-flow fractionation (FFF) is a reliable technique for separation and characterization of colloids and polymers. It is a dynamic separation technique based on the differential elution of the sample constituents by a laminar flow, in a flat ribbon-like channel, according to their sensitivity to an external field applied in the perpendicular direction to that of the flow. Resolution in the FFF system is a function of the time allowed to equilibrate (or relax) the sample within the channel under the force field, with the mobile phase not flowing prior to fractionation.

RELAXATION EFFECTS IN FFF

Field flow fractionation is an elution method wherein solutes are separated as they are washed through a column. The FFF channel is empty and an external applied force is solely responsible for the fractionation phenomenon. As soon as a solute species enters the FFF channel, the external field begins to force it toward the far wall of the channel. As it begins to concentrate at the wall, however, diffusion counteracts additional concentration. Soon, a thin, steady-state layer is established next to the wall. The distribution of the solute species in this layer is exponential and can be expressed as[1]

$$c = c_0 e^{-x/l} \tag{1}$$

where c is the concentration of solute at distance x (which is the coordinate position above the accumulation wall of the channel) from the lower wall, c_0 the analyte concentration at the accumulation wall, and l the approximate mean thickness of the solute layer (cloud thickness). A finite time is required for the formation of exponential layer under the influence of the field.[2] Until this equilibrium layer is formed, any downstream migration will be accompanied by a decrease in the retention, an increase in the retention parameter, and an increase in the plate height, H. This distortion can be removed by a stop-flow method in which flow is halted after injection for a period adequate to establish the exponential distribution. So the relaxation or equilibrium time, t_r, is the average time of travel under the influence of the field, from the center of the channel, $x = w/2$ to the quasiequilibrium center of gravity, x_{cg}. The latter obeys the equation:[1,2]

$$t_r = \frac{\left[\frac{w}{2} - x_{cg}\right]}{U} \tag{2}$$

where w is the channel thickness and U is the velocity induced by the field on the particles. The velocity U is linked to the field force on each particle as

$$U = \frac{F}{f} \tag{3}$$

where F is the field force to each particle and f is the friction coefficient of an analyte particle.

The x_{cg} is given by the equation:[1]

$$x_{cg} = w\left[\lambda - (e^{1/\lambda} - t)^{-1}\right] \tag{4}$$

where λ is equal to l/w.

So, substitution of this into Eq. 2 yields an equivalent expression of the t_r in terms of the FFF retention parameter, λ:[1,2]

$$t_r = \frac{w^2 \lambda}{D}\left[\frac{1}{2} - \lambda + (e^{1/\lambda} - 1)^{-1}\right] \tag{5}$$

where D is the analyte diffusion coefficient.

The diagrams in Fig. 1 illustrate how the particle concentration profile relaxes in the FFF channel under the influence of a sedimentation force field.[3] Initially, at time zero, particles are homogeneously distributed across the channel. Under the force field (as time progresses), the particle concentration profile is as predicted by the kinetic theory developed by Yau and Kirkland,[3] and the particles are compacted toward the bottom wall. After 5 min relaxation, or longer (in typical operating conditions), as shown in Fig. 1, particle concentration approaches the steady-state or equilibrium condition and will no longer vary with increasing relaxation time.

On the other hand, the velocity of the particles after 5 min relaxation reaches a level that is predicted by the equilibrium theory, after which the unrelaxed particles travel half the length of the channel in higher than predicted velocity streams before they are relaxed to their equilibrium l values. All the above are shown in Fig. 2. As a result of the above, a better resolution can be achieved. Fig. 3 is a composite of fractograms obtained with relaxation times varying from 0 to 20 min and shows

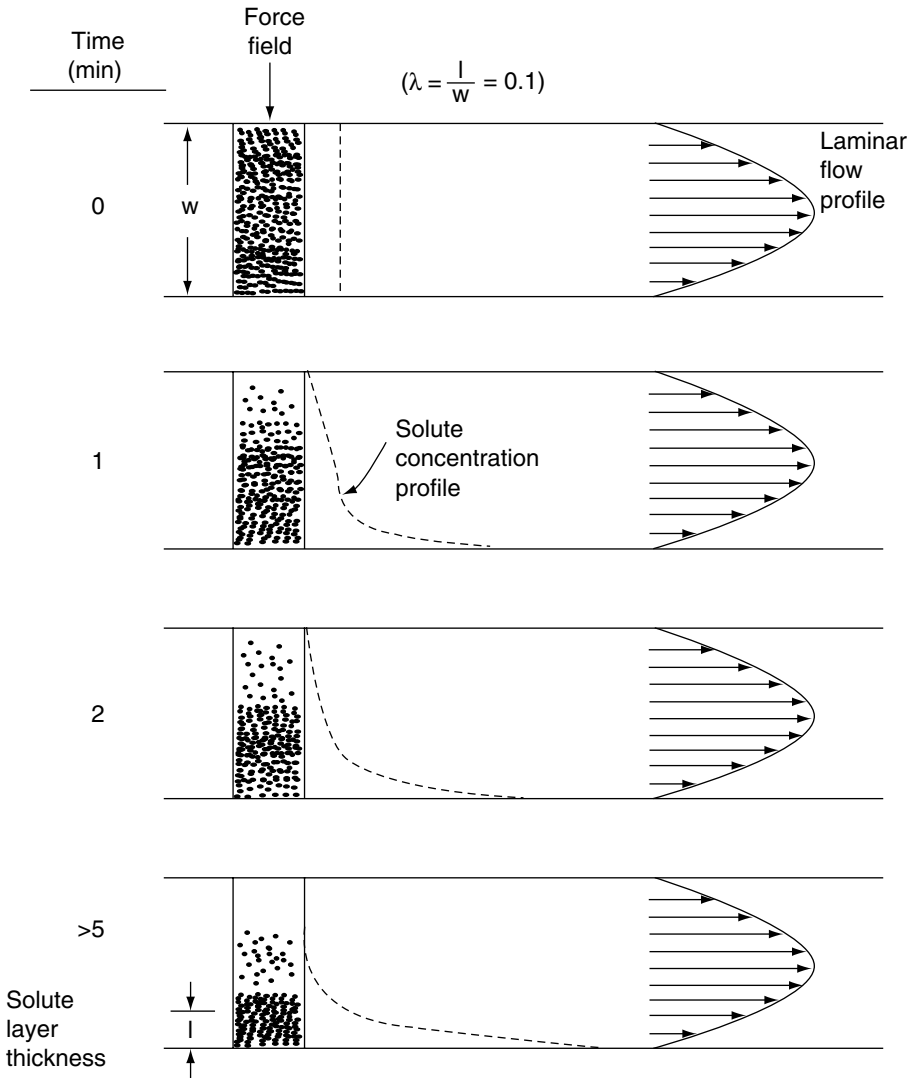

Fig. 1 Relaxation of solute concentration profile under sedimentation force field.
Source: From Nonequilibrium effects in sedimentation field flow fractionation, in Anal. Chem.[3]

how the relaxation time affects resolution.[4] Note that, although there is an optimum relaxation time for better resolution according to the experimental conditions, the resolution volume increases slightly with increasing relaxation time (Fig. 3, dotted line).

Relaxation time is one of the most important contributions to the plate height. The variance of the distribution of the distances traveled by the particles when they all have reached the accumulation wall is calculated by the equation:[2,5]

$$H_r = \frac{17}{140}\frac{w^2\langle v\rangle^2}{L|v|^2} = \frac{17}{140}\frac{1}{L}\left(\frac{\lambda w^2\langle v\rangle}{D}\right)^2 \quad (6)$$

where $\langle v\rangle$ is the mean carrier velocity and L is the column length.

This contribution to H can be relatively important, especially when operating at high-flow rates and for slowly diffusing species, as it is proportional to $(\langle v\rangle/D)$.[2] However, there are some experimental possibilities for considerably reducing this relaxation contribution to H. So, the time, t_p, needed to generate one theoretical plate is given by the equation:[6]

$$t_p = 4\frac{l^2}{D} \quad (7)$$

A separation requiring N plates for resolution requires a time of Nt_p, which is equal to

$$t = 4\frac{N l^2}{D} \quad (8)$$

Eqs. 5 and 8 show that relaxation time can be manipulated by changing the w and l parameters. So, to minimize the relaxation time and, consequently, the total analysis time, we need to reduce the above-mentioned parameters.

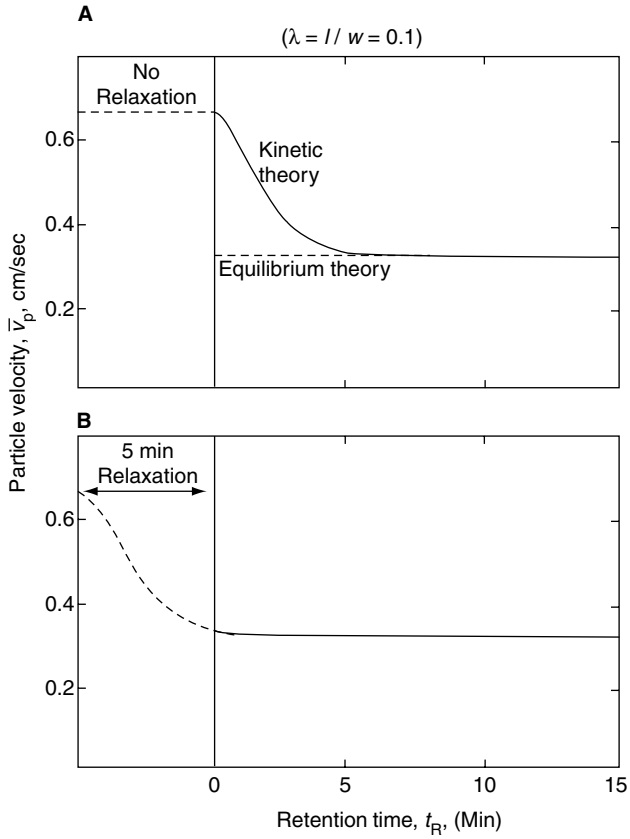

Fig. 2 Effect of relaxation on solute migration velocity in constant-field SFFF.
Source: From Nonequilibrium effects in sedimentation field flow fractionation, in Anal. Chem.[3]

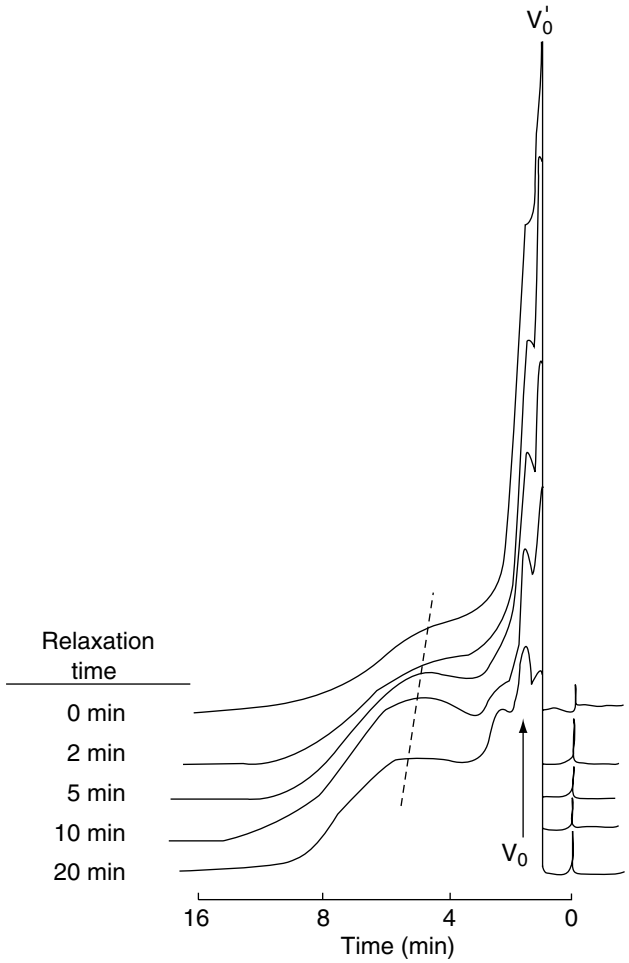

Fig. 3 Effect on relaxation time on the resolution peak of 0.2% polystyrene latex 0.091 μm.
Source: From Sedimentation field flow fractionation of macromolecules and colloids, in Anal. Chem.[4]

Several techniques have been developed to minimize the *l* parameter.[6,7] Various programing methods have been proposed. In the field programing technique, the field force increases and the analyzed particles come into the optimal range, each size effectively taking its turn at optimal migration. One problem with field programing is that, in the course of each particle's wait, during which it has a suboptimal *l*, it may migrate anomalously owing to steric effects or possibly absorb onto the wall. Another problem is that, when the field strength is changed rapidly to get quickly through the particle size range, particles are unable to diffuse enough to steady-state values of *l*. In this technique, the steady-state conditions depend on the secondary relaxation process. Corresponding to each specific value of the field strength, there is an equilibrium or steady-state distribution of particles near the accumulation wall for any type of particle. When the field strength changes from one value to another, a corresponding change occurs in a steady-state distribution. So, the particle cloud requires a finite time to adjust from one steady-state condition to another (secondary relaxation). Although corrections for this secondary relaxation have been developed, this programing technique cannot be applied to complex samples having particles of various densities and shapes.[7,8]

Another programing method alternative to field programing is flow programing,[6] in which the field is held constant while the flow is increased. According to this method, the *l* parameter takes higher values for small particles and, thus, takes a long time, t_p, to generate a plate Eq. 7 and is displaced through the channel slowly to gain adequate plates. Larger particles give small *l*; however, if the largest particles have *l* too small for normal migration, anomalous results will be found. So, flow programing promises to work well over a given range of *l* values, but the practical magnitude of that range is probably limited.

Another way to reduce the *l* parameter could be owing to the increase of the total potential energy of interaction.[9] This could succeed with the variation of the ionic strength of the carrier solution. The increase of the ionic strength decreases the repulsive forces between the particles and the accumulation wall making the van der Waals attractive forces more significant.

The above methods have a main disadvantage that the extreme decrease of the l values leads to several complications, including increasing particle wall interactions and steric effects as the l approaches the particle diameter. Instead of minimizing the l parameter, the channel thickness, w, can be reduced. A common method is to use a thin flow splitter in the inlet region separating two flow ports located at the two walls.[5,6] The sample is introduced into the port near the accumulation wall, while the carrier is introduced into the other one. The effective thickness of the sample stream is controlled by the ratio of these two inlet flows; with this streamlined convergence, the sample would be held in a thin layer near the accumulation wall, requiring little time for relaxation.

CONCLUSIONS

Relaxation in FFF is the main factor for the exponential layer to form under the influence of the external field. The minimizing of relaxation time could lead to reduction of the total analysis time for the separation and characterization of colloidal samples by field flow fractionation. Looking into the future, it is reasonable to expect more experimental and theoretical work for further investigation.

REFERENCES

1. Hovingh, M.E.; Thomson, G.H.; Giddings, J.C. Column parameters in thermal field flow fractionation. Anal. Chem. **1970**, *42*, 195–203.
2. Giddings, J.C.; Yang, F.J.F.; Myers, M.N. Sedimentation field flow fractionation. Anal. Chem. **1974**, *46*, 1917–1924.
3. Yau, W.W.; Kirkland, J.J. Nonequilibrium effects in sedimentation field flow fractionation. Anal. Chem. **1984**, *56*, 1461–1466.
4. Kirkland, J.J.; Yau, W.W.; Doerner, W.A. Sedimentation field flow fractionation of macromolecules and colloids. Anal. Chem. **1980**, *52*, 1944–1954.
5. Martin, M.; Williams, P.S. NATO ASI Series C: Mathematical and Physical Sciences. In *Theoretical Advancement in Chromatography and Related Separation Techniques*; Dondi, F., Guiochon, G., Eds.; Kluwer: Dordrecht, The Netherlands, , 1992; Vol. 383, 513–580.
6. Giddings, J.C. Optimized field flow fractionation system based on dual stream splitters. Anal. Chem. **1985**, *57*, 947–949.
7. Giddings, J.C. Simplified nonequilibrium theory of secondary relaxation effects in programmed field flow fractionation. Anal. Chem. **1986**, *58*, 735–740.
8. Giddings, J.C.; Caldwell, K.D. Field flow fractionation: Choices in programmed and nonprogrammed operation. Anal. Chem. **1984**, *56*, 2093–2094.
9. Hansen, M.; Giddings, J.C. Retention perturbations due to particle–wall interactions in sedimentation field flow fractionation. Anal. Chem. **1989**, *61*, 811–819.

Resin Microspheres as Stationary Phase for Liquid Ligand Exchange Chromatography

Zhikuan Chai
Research Center for Eco-Environmental Sciences, Chinese Academy of Sciences, Beijing, China

INTRODUCTION

Among the separation modes of liquid chromatography (LC), ligand exchange chromatography (LEC) is a particularly useful technique in many applications:

1. Chiral separation of optical isomers in chiral ligand exchange chromatography (CLEC).[1] In this method, complexes of transition metal ions and enantiomeric molecules are formed. Chiral separation is a result of the differences between the free energies of the intermediate diastereomeric complexes formed. For the separation to be successful, the sample molecule must have two polar functional groups with the correct spacing, which can simultaneously act as ligand for the divalent transition metal ion. For this reason, the underivatized racemic amino acids with their amino and carboxyl groups and other similar compounds, such as amino alcohols, hydroxy acids, and diamines, can be resolved with CLEC.

   Chiral separation of racemic drugs is required by the pharmaceutical industry because different optical forms of the drugs often play different roles in their pharmacological action, metabolism, and toxicity. Chiral ligand exchange chromatography plays an important role in this respect.[2]
2. Affinity separation of proteins in immobilized metal ion affinity chromatography (IMAC).[3] The method is based on the fact that some protein molecules, having specific residues on the surface, can form complexes with metal ions immobilized on the sorbent matrix. Retention is determined by the coordination interactions forming the complexes. Immobilized metal ion affinity chromatography can be performed under very mild, non-denaturing conditions with extremely high selectivity; it is particularly suitable for preparative group fractionation of complex extracts and bio-fluids.
3. Separation of organic compounds capable of complexing with transition metal ions through N, S, O, and π-electrons in the molecule. The separation mechanism is similar to IMAC. With its high selectivity, the sample concentration can be low, from 10^{-7} g/ml (amino acids) to 10^{-9} g/ml (fluorides). Ligand exchange is now routinely applied to anion chromatography by using the coordination-unsaturated complex, because such a charged complex is an anion exchange group as well. The corresponding sorbent has specific anion exchange selectivity, originating from their dual capabilities: the normal anion exchange and the ligand exchange capability.[4]

This entry discusses resin microspheres as the stationary phases for LEC. As a detailed review article on the LEC stationary phases was written in 1990,[5] attention is given here to the publications thereafter.

STATIONARY PHASES

Chiral ligand exchange chromatography can be performed either on an achiral stationary phase with a chiral mobile phase or on a chiral stationary phase; IMAC is performed on the metal ion immobilized stationary phase. The latter two stationary phases may be symbolized by the same formula as

M–S–L–Me

where M is the matrix; S, the spacer; L, the ligand; and Me, the metal ion.

The base matrices are divided into two groups. The inorganic matrices are based on silica or zirconia, on which the transition metal ion is complexed with the ligand bonded on the matrix. The inorganic sorbents have high column efficiency but low capacity and low chemical stability. The ligand can also be coated prior to, or during, the experiment, on the octadecylated silica (ODS) reversed phase (RP), which presents the most inexpensive but efficient and selective sorbent for CLEC.

The organic matrices are based on natural or synthetic polymers. This group of stationary phases has high capacity, high chemical stability, but low column efficiency; it is promising for preparative applications.

The spacer connects the matrix with the ligand, which plays a significant role in affinity chromatography, including IMAC. The active site of a biological substance is often located deep within the molecule and the adsorbent prepared by coupling the small ligand directly to the matrix can exhibit low capacities because of the steric interference

between the matrix and the substances binding to the ligand. In these circumstances, a spacer is interposed between the matrix and the ligand to facilitate effective binding. The length of the spacer is critical. If it is too short, the spacer is ineffective and the ligand fails to bind substances in the sample. If it is too long, non-specific effects become pronounced and reduce the selectivity of the separation. $-CH_2CH(OH)CH_2-$ and $-CH_2CH(OH)CH_2-O(CH_2)_4O-CH_2CH(OH)CH_2-$ are the commonly used spacers in IMAC; they are obtained from reactions with epichlorohydrin and butanediol bis(glycidyl) ether, respectively. In CLEC, introducing flexible spacers improves the column efficiency by minimizing the steric constraints for the ligand exchange reactions; introducing long hydrocarbon spacers would increase the retentions of heavy amino acids. $-CH_2-$ and $-CH_2CH(OH)CH_2-$ are the commonly used spacers in CLEC. Methylene groups are introduced by chloromethylation of polystyrene or by the reaction of formaldehyde with an amide. For polyacrylamide, the short spacer of methylene is not stable under acidic and basic conditions, causing significant ligand leakage. The epoxy spacer may influence the elution order of the enantiomers by complexing of the hydroxyl group in the N-substituent of the ligand amino acid with the central metal ion in CLEC.

In CLEC, the ligand is a chiral selector. Out of 35 amino acids tested, the bidentate ligands L-proline and L-hydroxyproline were shown to be the best chiral chelating ligands: Almost all racemic amino acids could be easily and completely resolved into enantiomers on the L-hydroxyproline-modified polystyrene resin with aqueous ammonia solutions as the eluent. The tridentate ligand iminodiacetic acid (IDA) is most widely used in IMAC. The others are aminosalicylic acid, 8-hydroxyquilonine (8HQ), carboxymethylated amino acids, and ethylenediaminetetraacetic acid (EDTA). The ligand content ranges from 10^{-5} to 10^{-3} mol/g of sorbent. It was found that monomeric ligands bonded onto the matrix were less stable, while the polymeric ligands, such as L-proline grafted polystyrene, were stable, even at elevated temperatures.

Depending on the analytes, a variety of transition metal ions are adopted for LEC. For instance, Cu(II), Ni(II), Zn(II), Cd(II), Ag(I), and Hg(II) are chosen for N- and S-containing analytes, Ca(II), Mg(II), Mn(II), Fe(III), Al(III), Ti(IV), and Zr(IV) for O-containing analytes, and Ag(I) and Hg(II) for π-electron-containing analytes. For this reason, Cu(II) is commonly used in CLEC of racemic amino acids, while Cu(II), Zn(II), and Fe(III) are used in IMAC for histidine and tryptophan residues and phosphate residues containing proteins, respectively.

RESIN MICROSPHERE STATIONARY PHASES

Polystyrene

Polystyrene (PS) is of primary importance to LEC. The first LEC experiments were performed with PS beads. In 1961, the Cu(II) form of Chelex 100, a PS resin containing the strongly complexing IDA groupings, was used to selectively isolate the whole range of amino acids from sea water. In 1971, a PS resin modified with L-proline and complexed with Cu(II) was used to separate amino acid racemates. The experimental conditions (pH, ionic strength of the mobile phase, organic modifier, temperature), elution order of enantiomers, and ligands for CLEC were studied with the PS column. It was found that, on the PS–CH_2–L-proline or L-hydroxyproline–Cu(II) column, almost all the L-amino acids eluted ahead of the D-acids, except for the tridentate amino acids histidine, allo-hydroxyproline, aspartic acid, and glutamic acid. Recently, the PS–IDA–Cu(II) particles were used for the separation of aromatic amines with methanol/ammonia as the eluent.[6]

Macronet isoporous PS is a polymer in which pores are formed as a result of homogeneously crosslinking by rigid bridges among linear macromolecules. High ligand loading and high exchange rate are the characteristics of the sorbent. For instance, the matrix containing 11 mol% of crosslinks of diphenylmethane could have a ligand loading capacity of 2.78 mmol/g of dry resin and, as shown in Fig. 1, a glass microcolumn (100 mm × 1 mm I.D.) filled with 5–10 μm microparticles of the polymer with ligand (*R*)-*N*,*N*′-dibenzyl-1,2-propanediamine could have a column efficiency of 3500 theoretical plates, enabling

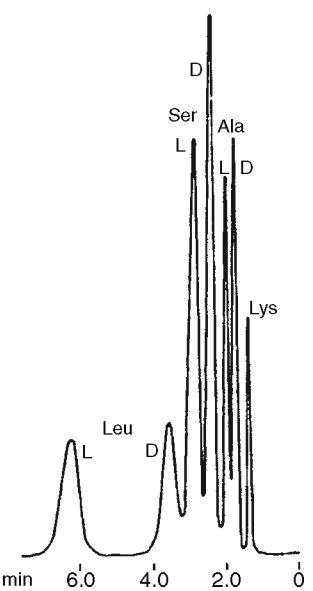

Fig. 1 Chromatogram of a mixture of racemic lysine (Lys), alanine (Ala), serine (Ser), and leucine (Leu) on a glass microcolumn (100 mm × 1 mm I.D.) packed with the chiral diamine resin. Eluent: 0.25 *M* sodium acetate + 1.5×10^{-3} *M* copper (II) acetate, pH 5.2, flow rate 1 ml/hr, room temperature. Attention: The elution time runs from right to left and lysine is not resolved.
Source: From High-performance ligand chromatography of α-amino acids on a polystyrene resin with fixed ligands of the type (*R*)-*N*′,*N*′-dibenzyl-1,2-propanediamine, in Chromatographia.[7]

complete resolution of a mixture of three racemic amino acids into six components under isocratic conditions.[7]

If PS is grafted onto the benzene ring with hydrophobic groups such as *n*- or *tert*-butyl, cyclohexyl, cyclohexylpropyl at the ortho-position of the chiral ligand, the hydrophobic interaction between the group and the enantiomeric molecule influences the stability of the intermediate diastereomeric complex. An increased enantioselectivity with respect to most amino acids was observed for the modified sorbent containing the cyclohexylpropyl group. Thus, modification of polymer skeletons may increase the enantioselectivity in racemate chromatography, as in the case with amino acids containing hydrophobic α-radicals.

The LEC experiment can be performed on ion exchange resins. Sulfonated PS beads were used to absorb the transition metal cation ions. The beads of low-cross-linking (4–8% divinylbenzene) gave narrow and more symmetric chromatographic peaks. A variety of cations, from +1 to +4 valency, were loaded onto the resin; numerous compounds such as phenols, alcohols, sugars, nucleic acids, aromatic acids, sulfur-containing compounds, β-diketones, amine bases, aromatic amines, pyridine derivatives, ethanolamines, aziridines, alkylhydrozines, aliphatic diamines, and unsaturated esters were separated. For instance, the Pb(II) form of Aminex HPX-87P, the Bio-Rad sulfonated PS gel, was used for qualitative and quantitative carbohydrate analysis of fermentation substrates and broths at 85°C with water as the mobile phase; glucose, xylose, galactose, arabinose, and mannose were separated.[8] Phosphorylated PS was used in place of sulfonated PS in LEC because the cation ion exchanger gave similar results but retained metal ions more strongly.

An optically active and electroconductive polymeric sorbent was prepared by coating the PS–L-proline–Cu(II) beads with conducting polymer polypyrrole. Applying a potential difference of ±1.5 V to the column, racemic lysine and aspartic acid were separated according to their charge characteristics and were simultaneously resolved with respect to their optical isomerism.[9]

Polyacrylamide

Contrary to PS, polyacrylamide is a hydrophilic polymer. This may increase the ligand exchange rate, i.e., the column efficiency. Thus on the polyacrylamide–CH_2–L-proline–Cu(II) macroporous microspheres, the enantiomers of valine, threonine, isoleucine, serine, phenylalanine, tyrosine, tryptophan, and asparagine were completely resolved in less than 1 hr with water as the eluent. The efficiency was markedly improved. However, the methylene bridge between the ligand and the matrix was not stable under acidic and basic conditions. The same sorbent, but with a long spacer, $–CH_2CH_2OCH_2CH(OH)CH_2–$, was prepared with L-proline content 1.76 mmol/g of dry polymer.[10] When the polymer was soaked in 0.1 *M* HCl, 0.1 *M* NaOH or 1 *M* NH_3, aqueous solutions, respectively, at room temperature for 1 week, the nitrogen content and Cu(II) capacity of the polymer did not change, indicating that the polymer was stable under moderately acidic and basic conditions. The new sorbent had high enantioselectivity for racemic amino acids.

Polyarylamide beads were also used for IMAC. The Biogel P200–glut–thio–Pt(II) beads were used for separation of biotin-labeled bovine serum albumin (BSA) from their unlabeled counterpart,[11] where Biogel P200 is a commercial product of polyacrylamide, glut—glutaraldehyde, thio—thiourea. At pH 4.8, 73% of BSA–biotin was bound. A 1.0 *M* imidazole–HCl solution, at pH 7, was successfully used to elute the bound BSA–biotin, indicating that binding to immobilized Pt(II) was reversible.

Acrylic Polymer

Separon is a commercial product of poly(hydroxyethyl methacrylate) (PHEMA) resin microspheres. The glycidyl Separon was reacted with L-proline to obtain the chiral sorbent Separon–epoxy–L-proline–Cu(II). The copper content of the resin was 0.3 mmol/g, which probably corresponded to the content of L-proline fixed ligand. The CLEC results showed high enantioselectivities for amino acids with aqueous ammonium carbonate as the eluent and were in good qualitative agreement with the result obtained on a silica gel sorbent having similar chiral ligands. All the sorbents retained the L-enantiomers of amino acids more strongly, the only exception being proline, for which the elution of the L-isomer preceded that of the D-isomer.

Recently, PHEMA microspheres have been more and more extensively used for IMAC. Separon–IDA–Fe(III) or Cu(II) was prepared. It was found that Cu(II) interacted preferentially with histidine and tryptophan residues, while Fe(III) preferred phosphate residues, as demonstrated by the separation of lysozyme, ribonuclease A, myoglobin, and transferrin on the Cu(II) column and ovalbumin on the Fe(III) column, respectively.[12] The PHEMA–Congo Red–Cu(II) and PHEMA–Cibacron Blue F3GA–Zn(II) microspheres were applied for adsorption of BSA.[13] Without incorporating the metal ions, the dyed sorbents were already good stationary phases for affinity chromatography. As shown in Fig. 2, the additional adsorption was attributed to metal–protein complexion, while the nonspecific BSA adsorption on the pure polymer was almost zero.

The weak cation exchange resin can also be used for LEC. Poly(acrylic-methacrylic acid)-type of carboxylic cation exchanger was loaded with blue-green Ni(II)–ammonia complex cations. A diamine, 1,3-diamino-2-hydroxypropane, in a dilute aqueous solution (0.001 *M*) which also contained a 100-fold excess of ammonia, was absorbed on the column and recovered as a sharp effluent band of high concentration (up to 40% w/v) by passing concentrated aqueous ammonia through the column. The weak ion exchanger retained the transition metals stronger

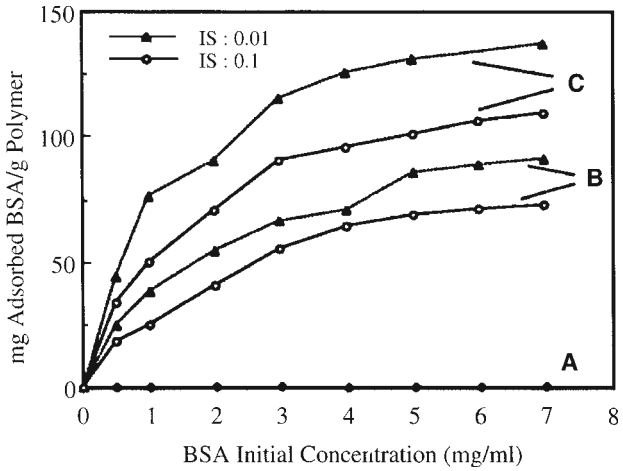

Fig. 2 Bovine serum albumin adsorption on microbeads at two different ionic strength (IS): (A) plain poly(hydroxyethyl methacrylate) (PHEMA); (B) Congo Red-derivatized PHEMA; (C) Congo Red-Cu(II)-derivatized PHEMA.
Source: From Congo red and Cu(II) carrying poly(ethylene glycol dimethacrylate-hydroxyethyl methacrylate) microbeads as specific sorbents. Albumin adsorption/desorption, in J. Chromatogr. A.[13]

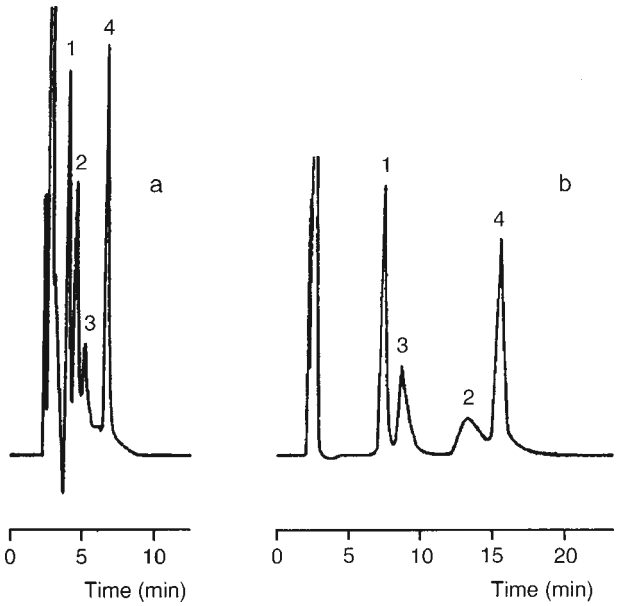

Fig. 3 Typical chromatograms of mixed sample containing (1) chloride, (2) bromide, (3) nitrate, and (4) sulfate. Anion-exchange groups (a) $H(bpa\text{-}ODP)^{+}$ and (b) $Cd(bpa\text{-}ODP)^{2+}$ are from the bpa-ODP, protonated, and complexed with Cd(II), respectively. Bpa-ODP is *N*,*N*-bis(2-pyridylmethyl)octadecylamine-coated octadecylated poly(vinyl alcohol). Eluent: 5 mmol/L benzenesulfonate (pH 5.0).
Source: From Ion chromatography using a charged complex anion-exchange group, in Anal. Chim. Acta.[4]

Pump – Reverse

and showed higher efficiency in chromatography of aromatic solutes than the sulfonated PS-type sorbent.

Hydroxylated Polyether

TSK PW is a hydrophilic polymer gel containing the group $–CH_2CH(OH)CH_2O–$ as the main constituent component, which can be readily activated and chemically modified. Other features are high porosity, low specificity in adsorption, high mechanical strength, and chemical stability at pH 2–12. L-Phenylalanine, L-tryptophan, and L-histidine were grafted through epichlorohydrin onto the gel; the Cu(II) form resin was used to resolve neutral, acidic, and aromatic amino acids with fairly good column efficiency.

TSK 5PW–IDA–Cu(II) microspheres (maximum copper loading 18.5 μmol/ml of packed gel) were used for equilibrium binding of histidine-containing cytochrome *c* in IMAC.[14] TSK 5PW–IDA–Zr(IV) microspheres (IDA content 20 μmol/ml of packed gel) were used for the separation of phenols and carboxylic acids. The sorbent was studied as a model to obtain some insight into the retentions on zirconia.[15]

Hydrophilic Vinyl Polymer

TSK Toyopearl is a spherical porous hydrophilic vinyl polymer; it is generally thought that the polymer is poly(vinyl alcohol). TSK Toyopearl–IDA–Zr(IV) microspheres (IDA content 33 μmol/ml gel) were prepared for the separation and preconcentration of fluoride at ng/ml level in a flow system.[16]

The amino-functionalized TSK Toyopearl was further modified as bis(2-pyridylmethyl)-aminated polymer (bpa-P, bpa content 0.43 mmol/g). As the bis(2-pyridylmethyl) amino (bpa) group is a tridentate ligand, and the preferable coordination number of Cu(II) is 4, the formed complex is a charged complex anion exchange group and acts not only as a simple ion exchange group but also as a ligand exchange group originating from its Lewis acidity. The sorbent, thus, showed a special anion exchange property in ion chromatography. Asahipak ODP is an octadecylated poly(vinyl alcohol) porous beads for RP chromatography. When *N*,*N*-bis(2-pyridylmethyl)octadecylamine was coated onto the polymer (bpa-ODP, bpa content 15.2 μmol/ml) for anion chromatography, the column efficiency was greatly improved, as shown in Fig. 3.[4]

Polyvinylamine

L-Proline was grafted onto the hydrophilic polymer via epichlorohydrin; the Cu(II) form resin was used for the CLEC separation of racemic phenylalanine, histidine, and tryptophan.[17]

Table 1 LEC on resin microspheres since 1990.

Polymer matrix	Ligand	Metal ion	Analyte	Refs.
1. CLEC				
Polypyrrole-coated PS	L-proline	Cu(II)	Amino acids	[9]
Polyacrylamide with a long spacer	L-proline	Cu(II)	Amino acids	[10]
Polyvinylamine	L-proline	Cu(II)	Amino acids	[17]
UF	(+)L-2-amino-5-ureidopentanioc acid	Cu(II)	Amino acids	[18]
UF	L-proline	Cu(II)	Amino acids	[19]
Guaran	Borate		Mandelic acid	[22]
2. IMAC				
Polyacrylamide (Biogel P200)	Glut-thio	Pt(II)	Biotin labeled BSA	[11]
PHEMA (Separon)	IDA	Cu(II)	Lysozyme, ribonuclease A, myoglobin, transferrin	[12]
PHEMA (Separon)	IDA	Fe(III)	Ovalbumin	[12]
PHEMA	Congo red	Cu(II)	BSA	[13]
PHEMA	Cibacron blue F3GA	Zn(II)	BSA	[13]
Hydroxylated polyether (TSK PW)	IDA	Cu(II)	Cytochrome *c*	[14]
Sepharose	IDA	Cu(II)	Ovalbumin, lysozyme, LDH	[20]
Sepharose	OPS or 8HQ	Fe(III)	Cytochrome *c*, myoglobin	[21]
3. Other LEC				
PS	IDA	Cu(II)	Aromatic amines	[6]
Sulfonated PS		Pb(II)	Carbohydrate	[8]
Hydroxylated polyether (TSK PW)	IDA	Zr(IV)	Phenols, carboxylic acids	[15]
Hydrophilic vinyl polymer (TSK Toyopearl)	IDA	Zr(IV)	Fluoride	[16]
Hydrophilic vinyl polymer (TSK Toyopearl)	Bpa	Cu(II)	Anion	[4]
Bpa-coated octadecylated poly(vinyl alcohol) (Asahipak ODP-50)	Bpa	Cu (II)	Anion	[4]

PS—polystyrene; UF—urea–formaldehyde resin; glut—glutaraldehyde; thio—thiourea; BSA—bovine serum albumin; PHEMA—poly(hydroxyethyl methacrylate); IDA—iminodiacetic acid; LDH—lactate dehydrogenase; OPS—*O*-phosphoserine; 8HQ—8-hydroxyquinoline; Bpa—bis(2-pyridylmethyl)amine.

Urea–Formaldehyde Resin

Urea–formaldehyde resin (UF) is a hydrophilic condensation polymer. The UF monosized non-porous microspheres were prepared with (+) L-2-amino-5-ureidopentanoic acid as the chiral ligand. The microspheres exhibited exceptional mechanical strength, chemical stability in the pH range 1–13, and low tendency toward swelling in solvents; they were used for the CLEC separation of amino acids.[18] Later, the porous UF microspheres were also prepared and L-proline was grafted via epichlorohydrin onto the polymer (L-proline content 0.28 mmol/g). Eighteen D,L-amino acids were resolved on the sorbent with aqueous ammonia containing 30% acetonitrile; all the D-acids eluted first, except for proline.[19]

Polysaccharides

Polysaccharides are natural polymers including agarose, dextran, cellulose, and guaran.

Sepharose, a commercial product of agarose, is widely used as a good sorbent for IMAC. This is because agarose has a high permeability to large protein molecules and there are no hydrophobic or electrostatically charged groups in the chemical structure. Sepharose–epoxy–IDA–transition metal ion is the standard structure as the sorbent for IMAC. Recently, ovalbumin, lysozyme, and lactate dehydrogenase (LDH) were purified using the Cu(II) form column. The experiments were run in displacement mode with a synthetic copolymer of vinyl imidazole and vinyl caprolactam as the displacer. Vinyl caprolactam renders the copolymer with thermo-sensitivity, i.e., a property

of the copolymer to precipitate nearly quantitatively from aqueous solution on increase of the temperature to 48°C. For the first time, it was clearly demonstrated that a polymer displacer was more efficient than a monomeric displacer (imidazole) of the same chemical nature, probably because of the multipoint interaction of imidazole groups within the same macromolecule with one Cu(II) ion.[20] Besides, Sepharose-*O*-phosphoserine (OPS, OPS content 0.40 mmol/g of dry gel) or 8-hydroxyquinoline (8HQ, 8HQ content 0.52 mmol/g) resins were prepared. The 8HQ–Fe(III) resin had a higher capacity for tuna heart cytochrome *c* than the 8HQ–Al(III) or –Yb(III) resins, while the 8HQ–Cu(II) and 8HQ–Ca(II) resins did not bind this protein. The equivalent IDA chelates showed no binding either. The OPS–Fe(III) resin bound tuna heart cytochrome *c* and horse myoglobin but did not bind hen egg white lysozyme.[21]

Sephadex is a commercial product of dextran. The polymer in Cu(II) form was employed for group separation of amino acids and proteins. Carboxymethylated dextran gel was found useful as a sorbent for LEC of enzymes.

Carboxymethyl-, diethylaminoethyl (DEAE)-, *p*-aminobenzyl-, and phosphate-cellulose, in combination with antimony, cobalt, mercury, and silver ions, were employed in LEC for separation of amines in organic solvents.

Guaran is a polygalactomannan containing *cis*-OH groups. It is well known that the tetrahedral borate ions readily form tetrahedral complexes with the *cis*-OH groups. Thus the borate immobilized polymer (boron content 0.7 mmol/g) was used for enantioseparation of racemates such as 1,2- or 1,3-dihydroxy compounds or α-hydroxy acids.[22] This appears to be the first example of the use of boron as a complexing ion in CLEC.

Glucosamine Polymer

Chitosan is a natural glucosamine polymer obtained from crab shells. The polymer retains Cu(II) more strongly than does cellulose. It was used in LEC of amino acids, peptides, and enzymes.

CONCLUSIONS

Table 1 summarizes the LEC studies since 1990. As a stationary phases for CLEC, the weakness of resin microspheres is in their low column efficiencies. The study of polypyrrole-coated polystyrene microspheres presented an effort to overcome the weakness, where a second electrokinetic interaction was added in addition to the coordination interaction. A high protein adsorption is always needed as a stationary phase for IMAC. The study of PHEMA microspheres modified with dye plus metal ion was interesting, where the protein adsorption was greatly increased by metal complexion plus dye affinity.

ACKNOWLEDGMENT

The author is grateful to NSFC for the grant 29635010.

REFERENCES

1. Davankov, V.A. 30 years of chiral ligand exchange. Enantiomer **2000**, *5*, 209–223.
2. Subert, J. Progress in the separation of enantiomers of chiral drugs by high performance liquid chromatography without their prior derivatization. Pharmazie **1994**, *49*, 3–13.
3. Porath, J. Immobilized metal ion affinity chromatography. Protein Expr. Purif. **1992**, *3*, 263–281.
4. Hiroyama, N.; Umehara, W.; Makizawa, H.; Honjo, T. Ion chromatography using a charged complex anion-exchange group. Anal. Chim. Acta **2000**, *409*, 17–26.
5. Davankov, V.A. Packings in ligand exchange chromatography. In *Packings and Stationary Phases in Chromatographic Techniques*; Unger, K.K., Ed.; Marcel Dekker: New York, 1990, Chapter 9.
6. Liu, Y.; Yu, S. Copper(II)-iminodiacetic acid chelating resin as a stationary phase in the immobilized metal ion affinity chromatography of some aromatic amines. J. Chromatogr. **1990**, *515*, 169–173.
7. Davankov, V.A.; Kurganov, A.A. High-performance ligand chromatography of α-amino acids on a polystyrene resin with fixed ligands of the type (*R*)-*N*′,*N*′-dibenzyl-1,2-propanediamine. Chromatographia **1980**, *13*, 339–341.
8. Marko-Varga, G.; Buttler, T.; Gorton, L.; Olsson, L.; Durand, G.; Barcelo, D. Qualitative and quantitative carbohydrate analysis of fermentation substrates and broths by ligand chromatographic techniques. J. Chromatogr. A, **1994**, *665*, 317–332.
9. Lee, H.S.; Hong, J. Chiral and electrokinetic separation of amino acids using polypyrrole-coated adsorbents. J. Chromatogr. A, **2000**, *868*, 189–196.
10. Yan, H.; Cheng, X.; Ni, A.; He, B. Resolution of amino acid enantiomers by ligand exchange chromatography on a new chiral packing. J. Liq. Chromatogr. **1993**, *16*, 1045–1055.
11. Miles, D.; Garcia, A.A. Separation of biotin labeled proteins from their counterparts using immobilized platinum(II) affinity chromatography. J. Chromatogr. A, **1995**, *702*, 173–189.
12. Coupek, J.; Vins, I. Hydroxyethyl methacrylate-based sorbents for high performance liquid chromatography of proteins. J. Chromatogr. A, **1994**, *658*, 391–398.
13. Denizli, A.; Salin, B.; Piskin, E. Congo red and Cu(II) carrying poly(ethylene glycol dimethacrylate-hydroxyethyl methacrylate) microbeads as specific sorbents. Albumin adsorption/desorption. J. Chromatogr. A, **1996**, *731*, 57–63.

14. Todd, R.J.; Johnson, R.D.; Arnold, F.H. Multiple-site binding interactions in metal-affinity chromatography: I. Equilibrium binding of engineered histidine-containing cytochrome-*c*. J. Chromatogr. A, **1994**, *662*, 13–26.
15. Yuchi, A.; Mizuno, Y.; Yonemoto, T. Ligand-exchange chromatography at zirconium(IV) immobilized on iminodiacetic acid-type chelating polymer gel. Anal. Chem. **2000**, *72*, 3642–3646.
16. Yuchi, A.; Matsunaga, K.; Niwa, T.; Terao, H.; Wada, H. Separation and preconcentration of fluoride at ng/ml level with a polymer complex of zirconium (IV) followed by potentiometric determination in a flow system. Anal. Chim. Acta **1999**, *388*, 201–208.
17. Yuan, Z.; He, B. Preparation of polyvinylamine ligand exchange resin grafted with L-proline. Chin. Sci. Bull. **1991**, *36*, 903–906.
18. Sinibaldi, M.; Castellani, L.; Federivi, F.; Messina, A.; Girrell, A.M.; Lentini, A.; Tesarova, E. New organic monosized microspheres for use in enantiomer separations by high performance liquid chromatography. J. Liq. Chromatogr. **1995**, *18*, 3187–3203.
19. Chai, Z.; Zheng, X.; Sun, X. Urea–formaldehyde resin microspheres as a new packing material for liquid chromatography: Ligand exchange. J. Liq. Chromatogr. & Relat. Technol. **2002**, *25*, 69–81.
20. Arvidsson, P.; Ivanov, A.E.; Galaev, I.Y.; Mattiasson, B. Polymer versus monomer as displacer in immobilized metal ion affinity chromatography. J. Chromatogr. B, **2001**, *753*, 279–285.
21. Zacharion, M.; Traverso, I.; Hearn, M.T.W. High-performance liquid chromatography of amino acids, peptides and proteins: CXXXI. *O*-Phosphoserine as a new chelating ligand for use with hard Lewis metal ions in the immobilized-metal affinity chromatography of proteins. J. Chromatogr. **1993**, *646*, 107–120.
22. Mathur, R.; Bohra, S.; Mathur, V.; Narang, C.K.; Mathur, N.K. Chiral ligand exchange chromatography on polyglactomannan (guaran). Chromatographia **1992**, *33*, 336–338.

Resolution in HPLC: Selectivity, Efficiency, and Capacity

J.E. Haky
Department of Chemistry and Biochemistry, Florida Atlantic University, Boca Raton, Florida, U.S.A.

INTRODUCTION

Liquid chromatography (LC) involves the analysis of mixtures. The goal of such an analysis is to achieve the greatest possible separation of the components in the mixture in the least amount of time. If performed successfully, the resulting chromatogram can be employed to obtain precise and accurate data describing the concentrations of the components in the mixture being analyzed.

DISCUSSION

The degree of separation of components of a mixture by a liquid chromatographic method is reflected in the resulting chromatogram. For best analytical results, peaks in the chromatogram must be completely resolved from each other, with little or no overlap. The degree of separation of between adjacent chromatographic peaks is a function of the distance between peak maxima and their corresponding peak widths. For Gaussian peaks, this is adequately described by the peak resolution, R_s, defined as the ratio between the difference in the retention times t_1 and t_2 of two peaks and the average of the widths, W_1 and W_2 of the two peaks at their baselines, as shown by

$$R_s = \frac{t_2 - t_1}{0.5(W_1 + W_2)} \tag{1}$$

A resolution of $R_s = 1$ corresponds to about a 4% overlap of two adjacent peaks and is adequate for many chromatographic analyses. Baseline resolution occurs at R_s values of 1.5 or higher.[1]

As shown by Eq. 1 the resolution of components in a liquid chromatographic separation is dependent on: (1) their relative retention on a particular chromatographic system, and (2) their peak widths. To optimize these parameters for maximum resolution, a clear understanding of their nature and the factors that affect them is necessary. Although the retention time of a component adequately describes the amount of time a particular solute takes to elute from a chromatographic system, a more useful parameter describing chromatographic retention is the capacity factor k. This parameter is defined as the ratio of time spent by a solute in the stationary phase to the time it spends in the mobile phase. It can be calculated by Eq. 2, where t_R is the retention time of the peak of interest and t_0 (the "dead-volume time") is the retention time of a solute that is known not to interact with the stationary phase:

$$k = \frac{t_R - t_0}{t_0} \tag{2}$$

Additionally, the relative retention of two peaks in a chromatogram may be defined by the selectivity factor, α, defined by Eq. 3, where k_1 and k_2 are capacity factors of the early- and late-eluting peaks, respectively:

$$\alpha = \frac{k_2}{k_1} \tag{3}$$

The widths of chromatographic peaks are dependent on the degree to which a band of solute molecules spreads out, over the time it spends passing through a chromatographic system. This band spreading is best defined in terms of theoretical plates, N, which can be calculated from Eq. 4, where t_R and W are the retention time and width of the peak of interest, respectively:

$$N = 16\left(\frac{t_R}{W}\right)^2 \tag{4}$$

Higher values of N correspond to lower degrees of band broadening and narrower peaks. On this basis, theoretical plates can be described as a measure of the efficiency of a given chromatographic system.[2]

Chromatographic resolution of any two components in a mixture is dependent on three factors: (1) the overall efficiency of the chromatographic system, as described by the number of theoretical plates N, (2) the inherent selectivity of the system, described by the selectivity factor α, and (3) the degree of retention of each of the components, described by their capacity factors k. For two peaks having approximately equal widths, capacity factors of k_1 and k_2, and a mean theoretical plate number N, the following quantitative relationship can be derived between chromatographic resolution and these parameters[3]:

$$R_s = \left(\frac{N^{1/2}}{4}\right)\left(\frac{\alpha - 1}{\alpha}\right)\left(\frac{k_2}{1 + k_2}\right) \tag{5}$$

To a first approximation, each of the terms in Eq. 5 can be treated as independent of each other. Therefore, in the

development of a liquid chromatographic method for analysis or isolation of the components of any mixture, experimental conditions can be varied to modify each of these three terms to maximize resolution.

Analysis of Eq. 5 indicates that resolution increases with the square root of the number of theoretical plates in the chromatographic system. Thus, a fourfold increase in N is required to increase the resolution by a factor of 2. Experimentally, N may be increased most directly by (1) increasing the length of the column, (2) reducing the size of the particles of the stationary phase, or (3) using a mobile phase of lower viscosity. However, in modern analytical LC, most of these options are impractical for the following reasons: (1) Increasing the length of the column can increase system back-pressures and the time required to complete the separation to unworkably high levels. (2) Stationary phases with particle sizes below 3 μm are not generally available, owing to excessively high system back-pressures they can cause and their short lifetimes. (3) Because most recommended mobile phases for liquid chromatographic separations are those with low viscosity, there are few alternative mobile phases with lower viscosity available.

For these reasons, attempting to improve resolution by increasing the number of theoretical plates in the chromatographic system is not generally recommended as a first choice in liquid chromatographic method development. Nevertheless, the effect of theoretical plates on overall resolution is important to consider in certain situations, such as in the scaling up of an analytical method to a preparative method, when stationary phases of larger particle sizes are often employed, resulting in lower values of N and poorer resolutions.[1]

Adjusting the selectivity of the chromatographic system, as measured by α, is often a useful technique in improving separations in LC. Such adjustments need to be made with consideration of the second term in Eq. 5, which is $(\alpha - 1)/\alpha$. When $\alpha = 1$, the term is equal to zero, resulting in no resolution. This indicates that the chromatographic system must exhibit some selectivity toward the components of the mixture before any separation is possible. The term rapidly increases as a increases up to about $\alpha = 2$, beyond which only small increases are exhibited.[2] Thus, varying chromatographic conditions to obtain a selectivity factor equal or greater than 2 will often give the best resolutions.

In LC, system selectivity can be modified by a number of techniques, including (1) changing the composition or pH of the mobile phase, (2) changing the column temperature, and (3) changing the type of stationary phase that is employed. Of these, the first method is the easiest to accomplish and is most often the first to be utilized in method development for improving selectivity.

Resolution can often be improved in liquid chromatographic separations simply by changing the retention of the components, which corresponds to changing the capacity factor k of the components to be separated. Rapid increases in the third term in Eq. 5, $k_2/(1 + k_2)$ occur as the capacity factor increases, up to $k_2 = 5$. The term increases only slowly beyond this value.[2] Therefore, in most separations by LC, optimal resolution of mixtures occurs when each component has capacity factor values between 2 and about 10. Increasing k values to higher values results in longer analysis times with minimal improvements in resolution.[2]

The effect of the capacity factor on resolution can be further exhibited by manipulation of Eq. 5 to predict the number of required theoretical plates N_{req} for a given resolution. Eq. 6 enables such predictions:

$$N_{req} = 16R_S^2\left(\frac{\alpha}{\alpha - 1}\right)^2\left(\frac{k_2 + 1}{k_2}\right)^2 \quad (6)$$

Assuming a difficult separation of two components with $\alpha = 1.05$ and a reasonable goal of obtaining a resolution R_s of 1.0, the number of theoretical plates required at various capacity factor values can be calculated. For a capacity factor of 1.0, a minimum of 28,200 plates is required. For a capacity factor of 2.0, the required number of plates drops to 15,880. Because many liquid chromatographic systems usually do not exhibit efficiencies greater than 25,000 theoretical plates, it is evident from these calculations that developing methods for difficult separations should be performed when the capacity factors of the components to be separated are adjusted so they are all greater than 2.

In LC, adjusting capacity factors is most often accomplished by changing the composition of the mobile phase. In reversed-phase chromatography, for example, decreasing the amount of organic component in the mobile phase (e.g., from 80% methanol, 20% water to 50% methanol, 50% water) will generally result in lower capacity factors for all components of the mixture. Empirical models and computer software have been developed which allow the user to predict mobile-phase compositions, which will result in capacity factors of all components in a mixture to be in the optimal range of 2–10. Such programs utilize data obtained from an analysis performed using gradient elution (i.e., continuously varying mobile-phase composition throughout the separation process).[3] In many cases, however, experimental variation of mobile-phase compositions through a trial-and-error process can be equally effective in obtaining a composition giving an optimal capacity factor range for all components.

In summary, resolution in LC is dependent on three factors: (1) the efficiency of the chromatographic system, measured by the theoretical plate value N; (2) the selectivity of the chromatographic system, measured by the selectivity factor α; and (3) the degree of retention of the

components on the chromatographic system, measured by the capacity factor *k*. Although each of these can be independently varied to obtain acceptable separations, most method development in LC is successfully performed through the initial choosing of the proper LC technique (e.g., normal phase, reversed phase, ion exchange) followed by optimizing capacity factors and system selectivity by varying the composition of the mobile phase.

REFERENCES

1. Snyder, L.R.; Kirkland, J.J. *Introduction to Modern Liquid Chromatography*, 2nd Ed.; John Wiley & Sons: New York, 1979.
2. Poole, C.F.; Poole, S.K. *Chromatography Today*; Elsevier: New York, 1991; 1–50.
3. Snyder, L.R.; Kirkland, J.J.; Glajch, J.L. *Practical HPLC Method Development*, 2nd Ed.; John Wiley & Sons: New York, 1997.

Response Spectrum

Dennis R. Jenke
Technology Resources Division, Baxter Healthcare Corporation, Round Lake, Illinois, U.S.A.

INTRODUCTION

Chromatographic methods are used for a variety of purposes in real-world applications. Chromatography, in its multitude of manifestations, can be used for the purpose of scouting and discovery (i.e., to "uncover" the presence of compounds or entities in samples of unknown composition). In fact, the unique versatility of chromatography as a scouting and discovery tool is based on the almost limitless (or so it seems) combination of separation and detection strategies that can be coupled and brought to bear in investigative situations.

Once an entity has been observed to produce a chromatographic response, chromatographic procedures can be used to either characterize or identify the entity. The characterization/identification processes are facilitated by the chromatographic process, wherein both the elution and the detection properties of the entity provide information that can be useful for these purposes. The chromatographic methods may produce information that can be used to characterize the entity, which ultimately may lead to a proposal for its identity, and/or it may be used to confirm the accuracy of a proposed entity.

Although chromatography is generally considered to be an analytical tool, it also has an important role in process chemistry as a means of isolating and/or purifying substances from complex or dilute mixtures. Preparative chromatographic methods for the generation of laboratory-scale to commercial-scale quantities of pure substances are well documented in the chemical and patent literature.

OVERVIEW

As important as are the three previously mentioned applications of chromatography (Table 1), it is accurate to observe that the primary use of chromatography is for the purpose of establishing the concentration of a known entity (analyte) in a specific sample. As few chromatographic detection strategies are absolute (i.e., their response function can be derived from first scientific principles), the quantitation process includes the characterization of the response function, where the response function is the mathematical relationship that exists between the concentration of an analyte in a standard and the response that is produced by the chromatographic system when such a standard is processed by the chromatographic method.

As shown in Fig. 1, the entire domain or spectrum of a chromatographic method's response extends from the lowest analyte concentration that can be confirmed to reliably produce a chromatographic response (limit of detection, or LOD) to the highest analyte concentration for which an increase in concentration produces an increase in response (limit of range, or LOR). Although the nature of the response function is chromatographic method-specific (although most methods have a response function similar to that shown in Fig. 2), all share, to one degree or another, the spectral characteristics shown in Fig. 1.

It is an interesting aspect of the current state of affairs in chromatographic science that although there is nearly universal agreement among practitioners with respect to the members of the chromatographic response spectrum (e.g., the concept of all methods having a LOD is universally accepted), there is significant discussion among practitioners as to the definition of, and correct method for determining, the various response spectrum members (e.g., how do you determine LOD?). Although various scientific organizations [e.g., International Union of Pure and Applied Chemistry (IUPAC), American Chemical Society (ACS), United States Environmental Protection Agency (USEPA), and International Conference on Harmonization (ICH)] have proposed standard definitions and determination procedures for some of the members of the response spectrum, it is interesting to note that the procedures are not the same, and it is fair to say that not all investigators accept such methods as being scientifically the most valid or rigorous.

The purpose of this entry is to provide an overview of the chromatographic response spectrum and its various members. As a general review, it will not be complete but will strive to be comprehensive and non-judgmental.

THE CHROMATOGRAPHIC RESPONSE SPECTRUM

The chromatographic response spectrum, illustrated in Fig. 1, establishes the boundaries of the response function and breaks the response domain into appropriate categories and regions. The spectrum begins at the lowest analyte concentration that reproducibly produces a discernible analyte response (LOD) and ends at the highest analyte concentration that produces a response that is discernibly different from the response produced at a

Table 1 Application of chromatographic methods.

Nature	Purpose	Desirable response characteristics
Scouting/discovery	"Find" substances present in a sample of unknown composition	Sensitive, specific, with broad scope and range, "universal" response
Identification or characterization	Identify or characterize substance(s) that produce chromatographic responses	Sensitive, specific, "information-rich"
Isolation/purification	Separate a substance from all others in a complex mixture	Sufficient selectivity and specificity
Quantification	Determine the concentration at which a substance is present in a sample	Accurate, precise, specific, sensitive, "universal" response, known response function

lower analyte concentration (LOR). Between the LOD and the LOR are the limit of identification (LOI; the lowest analyte concentration at which the identity of an analyte can be confirmed), the limit of quantitation (LOQ; the lowest analyte concentration at which assay performance meets various standards of accuracy and precision), and the limit of linear range (LOLR; the highest concentration at which the response function is best described by a linear model). Between these limits are various regions of the response spectrum, including the following:

- *Not detected*: Either no response or a response less than that of the LOD.
- *Detected, not identified*: Response between the LOD and the LOI.
- *Detected, identified*: Response between the LOI and the LOQ.
- *Linear dynamic range*: Range of analyte concentrations over which the relationship between the analyte concentration and the method response can be described by a linear model of the form

$$\text{Response} = \text{Slope}\ (\text{concentration}) + \text{Intercept}$$

- *Dynamic range*: Range of analyte concentrations over which the relationship between the analyte concentration and the method response can be described by a mathematical model of the form:

$$\text{Response} = \text{Function}\ (\text{concentration})$$

- *Out of range*: Response is not related to the concentration of the analyte.

THE LIMIT OF DETECTION

Definition

As with many concepts in the analytical sciences, the concept of LOD suffers from the curse of intuition. That is to say that although the concept is, on an intuitive level, clear to all practitioners of the analytical sciences, if one were to ask the practitioners to define the term and describe its determination, one would end up with nearly as many definitions and determination methods as there are practitioners. This is borne out in the scientific literature, which contains literally hundreds of references with the more or less general content of "my (our) definition of the LOD and how I (we) recommend you determine it" (e.g., Table 2). It is borne out by the fact that although several organizations have attempted to unify, or harmonize, the individual definitions, their own results, in fact, are not the same.

Part of the problem is that although the concept is intuitively obvious, it is sufficiently multifaceted that a concise but truly complete and rigorous definition (i.e., one that leaves all questions answered) is difficult to

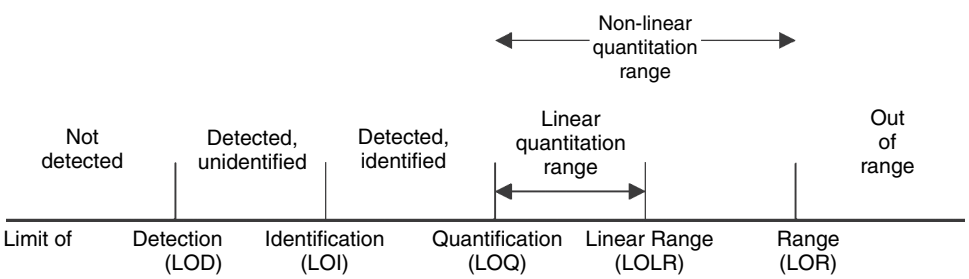

Fig. 1 The response spectrum for chromatographic analysis. The complete response spectrum extends from that analyte concentration at which a chromatographic response can be reliably confirmed to have occurred (LOD) to that concentration above which an increase in concentration no longer produces an increase in chromatographic response (LOR).

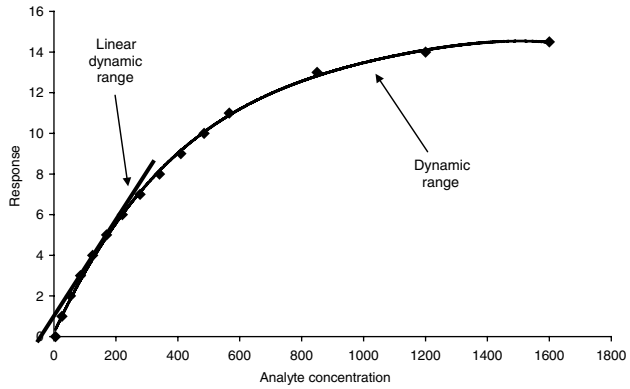

Fig. 2 Typical response function for a chromatographic method. The linear dynamic range and the dynamic range of the method are illustrated.

craft. Another part of the problem is that many definitions seek to define the term in a way that predisposes it to a certain method of determination. It is a simple statement of fact that there is a diversity of opinion on the answers to questions related to the "issues" associated with the subtle aspects of the LOD and that there are numerous mathematical methods that have been devised, which "get at" the essence of the LOD. The challenge is to draft a definition that acknowledges that these differences exist and then handles these differences not by specifying which of literally tens of candidate methods and approaches are correct but rather by requiring that the methods and approaches used be specified as part of reporting the LOD. Such a definition follows:

> The LOD is the lowest concentration of a specified analyte in a sample of specified composition, determined and calculated by specified analytical and mathematical processes, that produces, with a specified consistency, a response for a specified method implemented on a specified instrument system, which one can verify, with a specified level of confidence, is different from the response produced by a sample blank that is known not to contain the analyte.

Whether this definition is the "best" one or not, there is something "troubling" about this definition. The "problem" is that, now, it is "too complicated" to report the LOD. By this definition, it is not enough to just report a number—one must also report the context in which the number is valid. Details about the LOD required by the definition include the following:

1. The analyte's identity.
2. Description of the test sample.
3. Description of the test method (e.g., mobile phase, column, flow rate, injection size, and so on).
4. Description of the instrumentation used.
5. Description of the analytical procedure used to generate the data from which the LOD was determined.
6. Description of the mathematical process by which the LOD was determined.

Methods of Determination

Signal to noise (graphical)

A useful characteristic of a chromatographic analysis is that it results in a pictorial record of the analysis (a chromatogram). This pictorial record can be examined and used to quantify the performance characteristics of the method (and instrument system) used. Performance characteristics useful to a determination of LOD include the magnitude of the analytical signal S for the analyte (e.g., the height of the analyte peak) and the magnitude of the variation in system response when the analyte is not eluting from the system (referred to as the system noise N). These characteristics are illustrated in Fig. 3. It is clear that a comparison of S and N provides a means of establishing detectability. Specifically, a relationship between LOD, S, N, and the analyte concentration that produced the chromatogram being examined (C) can be proposed as follows:

$$\text{LOD} = C[F(N/S)]$$

In this equation, F is a factor that literally can be interpreted as: "How much higher must the peak be than the noise in order for you to be confident that what you are calling a peak is in fact a peak and not just a manifestation of the noise?" Although several values have been proposed for F, it is generally accepted that $F = 3$ is the appropriate choice. However, in the interest of clarity, LOD values obtained by the signal-to-noise method must be footnoted with the value of F used.

Although the signal-to-noise method for determining LOD is conceptually straightforward, its simplicity may lead to issues. Three practical issues of importance are: 1) the analyte level in the sample used to produce the chromatogram from which S and N are obtained; 2) the means of obtaining N; and 3) the number of injections that must be used to obtain the LOD.

Considering these details in somewhat greater detail, it is clear that the calculation of LOD requires that both the signal-to-noise and the peak response be measured effectively. This can be effectively accomplished only over a relatively small range of analyte levels, which themselves are near the LOD. As a general rule of thumb, LOD should be determined from a chromatogram derived from a sample containing an amount of analyte that is from 5–15 times the LOD.

Although the concept of the noise is simple enough, its effective measurement can be quite complicated. As it is desired that the noise measured be representative of the

Table 2 Various definitions for the LOD.

Quantity	Definition	Calculation	Refs.
MDL	MDL = minimum concentration of a substance that can be identified.	$MDL = t_{(n-1,\ 1-\alpha=0.99)} \times S_i$[a]	[1]
Detection limit (C_L)	C_L = lowest concentration of the analyte that can be distinguished with reasonable confidence from a field blank.[b]	$C_L = k \times s_B/S$[c]	[2]
Detection limit (c_L)	c_L = concentration equivalent to the smallest measure that can be detected with reasonable certainty for a given analytical procedure.	$c_L = (x_L - \mu_{b1})/S$[d]	[3]
Detection limit (c_L)	c_L = the number, expressed in units of concentration or amount, that an analyst can determine to be statistically different from an analytical blank.	$c_L = (x - \mu_{b1})/S$[e,f]	[4]
LOD	LOD = lowest concentration of an analyte that the analytical process can reliably detect.	$LOD = k \times s_B/S$[c]	[5]
Detection limit (c_L)	c_L = lowest concentration of an analyte that can be distinguished from a field blank with reasonable statistical confidence.	$c_L = k \times s_B/S$[c,g]	[6]
LOD	LOD = concentration of an analyte that produces a signal that exceeds the signal observed from a blank by an amount equal to three times the standard deviation for replicate measurements on the blank.	—	[7]
LOD	LOD = lowest concentration of an analyte in a sample that can be detected but not necessarily quantitated.[h]	$LOD = 3.3 \times s_B/S$ or $LOD = (F \times C \times N)/S$[i]	[8]
LOD	LOD = lowest analyte concentration that can be detected but not quantified under the stated experimental conditions; LOD = lowest concentration that can be distinguished from the background noise with a certain degree of confidence.	$LOD = (F \times C \times \times \times N)/S$[i,j] or $LOD = F \times s_B$ or $LOD = F \times s_B/S$[k]	[9]
LOD	LOD = concentration derived from the smallest measure that can be detected with a reasonable certainty for a given analytical procedure; LOD = lowest concentration of an analyte that the analytical process can reliably detect.	[l]	[10]

[a] S_i = standard deviation of responses obtained from seven portions of a sample (containing less than 10 × the MDL of the analyte) taken through the entire analytical method.

[b] A field blank is a hypothetical sample that contains zero concentration of the analyte.

[c] k = *A factor that should have at least a value of 3;* s_B = standard deviation of the blank response (based on a minimum of 10 determinations); and S = method's sensitivity.

[d] x_L = Minimum detectable response = $\mu_{b1} + (ks_{b1})$, where μ_{b1} = mean of replicate analyses of a blank (a minimum of 20 is recommended), k = a numerical factor chosen according to the confidence level desired (a value of 3 is strongly recommended); and s_{b1} = the standard deviation of the blank responses. S is the sensitivity of the method.

[e] Use of a value of $k = 3$ is recommended as it allows for a 99.86% level of confidence for a blank signal that follows a normal distribution and an 89% level of confidence for a non-normal distribution.

[f] A more reliable value for c_L is obtained if S (typically determined as the slope of a plot of response vs. concentration) is replaced with a confidence interval $[S \pm (ts_S)]$ reflecting the uncertainty of the slope.

[g] The key features of the LOD analysis are: 1) 16 replicate blank determinations; 2) a blank is devoid of the analyte; and 3) the calibration curve must be generated to calculate the sensitivity (slope).

[h] This definition is attributed to USP, section $< 1225 >$.

[i] C = *Analyte concentration in an analyzed sample,* N = peak-to-peak noise in the sample chromatogram, S = magnitude of analyte signal in the sample chromatogram (peak height), and F = statistical factor (typically 2 or 3).

[j] These authors note that F can vary from 2 to 5.

[k] These authors note that k can have a value of 3.0 or 3.3.

[l] These authors expand the basic relationship $LOD = ks_B/S$ to include: 1) the use of population statistics (vs. sample set statistics); 2) the use of the pooled standard deviation (vs. the blank standard deviation); 3) a consideration of situations where the intercept of the calibration curve is non-zero; and 4) a consideration of the errors in calibration parameters (slope and intercept).

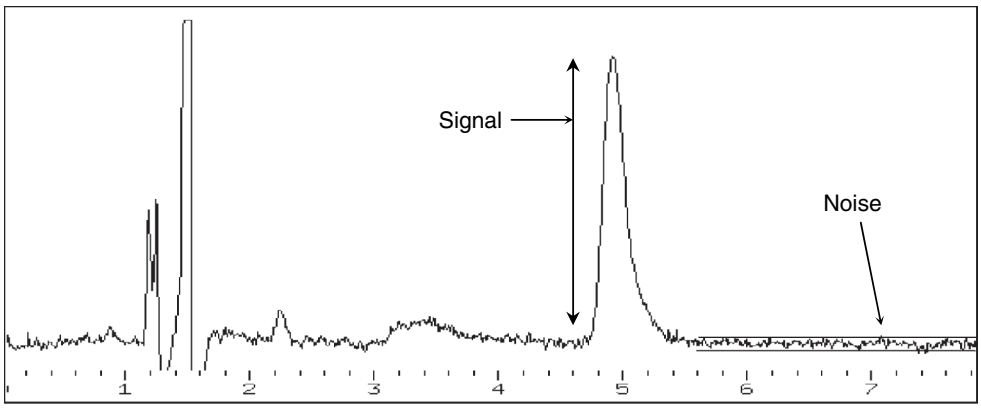

Fig. 3 Signal and noise measurements illustrated. The signal is measured from the apex of the peak to the middle of a straight-line peak base. The noise is measured as the distance between straight lines constructed from the tops and bottoms of the baseline variation. The noise should be measured in a clean portion of the chromatogram and should include a fair representation of the inherent baseline variation.

analytical method and instrumental system, it is anticipated that *N* must be measured over a relatively wide portion of the chromatogram; typical recommendations suggest that a portion equal to 10–20 times the width of the analyte peak be used to measure the signal *S*. It is clear that the portion of the chromatogram used to measure *N* must be clear from analytical responses (such as those produced by other analytes, internal standards, and sample matrix components). Practically speaking, it may be difficult to "find" a chromatographic region that is sufficiently "wide" and "undisturbed" to produce an appropriately representative *N*.

The LOD can be calculated from *S* and *N* obtained from a single chromatogram. However, this may not be an appropriate approach given the large variation in analytical signal that occurs at analyte levels near the LOD. As analytical signals can vary by 20% (or more) from injection to injection at analyte levels near the LOD, it is suggested that LOD be calculated from a minimum of three sample chromatograms and that the reported LOD be the mean of the individual results.

Although the previous discussion implies that the signal and noise are determined from the same chromatogram, other investigators have suggested that it is appropriate to measure the magnitude of the noise in the elution region of the analyte on a chromatogram derived from a sample blank.

Recently, Coleman et al.[11] have observed that although *S*/*N* is a height-based determination, it is most typically the case that peak area is used for analyte quantitation. Thus these authors have proposed a procedure for setting a meaningful lower limit on peak area *S*/*N*.

One of the most common criticisms of the *S*/*N* approach is the subjective nature of the noise measurement. Although it is certainly the case that estimates for the noise may vary from one investigator to the next, such differences tend to be small, certainly well within a factor of 2.

Variation in the method blank (IUPAC/ACS)

In response to the confusion that existed regarding numerous and conflicting data on detection limits, the IUPAC adopted a model for LOD calculations in the 1970s.[3] This standard was reaffirmed by the ACS Subcommittee on Environmental Analytical Chemistry in the early 1980s.[5,12] The IUPAC/ACS procedure is based on two method characteristics: 1) the variation (standard deviation) of multiple blank measurements; and 2) the relationship between the response and the analyte concentration (at concentrations near the LOD). If R_B is the mean blank responses and s_B is the standard deviation of the blank, then the LOD is calculated as:

$$\text{LOD} = R_B + ks_B$$

where k is a numerical constant whose value is chosen in accordance with the confidence level desired. As this calculation of LOD produces a result in response units, the concentration LOD is obtained using the slope S of the method's calibration curve:

$$\text{LOD} = (R_B + ks_B)/S$$

This process is illustrated in Fig. 4.

The analytical procedure used to produce the data from which the LOD is calculated is as follows:

1. A statistically significant number of blank measurements are made. Although at least 10 and as many as 20 replicates have been recommended, 16 measurements are generally selected.
2. The standard deviation of the blank measurements is calculated (in units of response, not concentration).
3. Five standard solutions of varying analyte concentrations (prepared in the blank matrix) are analyzed and a calibration curve of response vs. concentration is

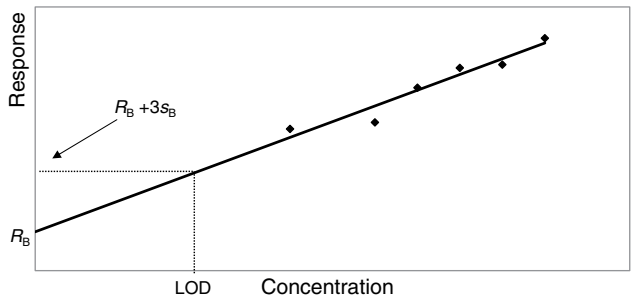

Fig. 4 Calibration graph showing the LOD. This graph illustrates the IUPAC method for determining the LOD. R_B = response of the blank; s_B = standard deviation of multiple determinations of the blank responses.

constructed. If the range of the standard concentrations is appropriately chosen, then the calibration curve is typically linear and its slope can be determined.

4. The LOD is calculated with the generated data per LOD equation. A value of $k = 3$ is strongly recommended.

Numerous authors have proposed modifications of the IUPAC/ACS approach, typically based on a more rigorous statistical analysis of method variation and its contributing factors. Although such approaches are undoubtedly scientifically more rigorous, they typically require more complex computations and their practical significance is open to question.

One significant practical problem with the IUPAC methodology occurs in the situation wherein the blank produces no analytical signal—a circumstance that is commonly encountered in chromatographic analyses. In such circumstances, it may be possible to estimate the "virtual" standard deviation at zero concentration.[13] In this graphical technique (Fig. 5), the standard deviation (in response units) of replicate analyses of successively more dilute samples is plotted vs. the analyte concentration. The *y*-intercept of this plot (S_0) represents the virtual standard deviation at zero concentration. The LOD is calculated by substituting S_0 for s_B in the IUPAC LOD equation.

Another, more practical problem associated with the IUPAC methodology is the time-consuming requirement of 16 replicate analyses (injections for chromatographic analysis) of the blank. To address this issue, the ICH has devised a methodology for the calculation of LOD that is similar in concept to the IUPAC method but is different in its application.[14] By the ICH definition, the LOD is expressed as:

$$\text{LOD} = 3.3(\sigma/S)$$

where σ is the standard deviation of the response and S is the slope of a method's calibration curve. In the ICH

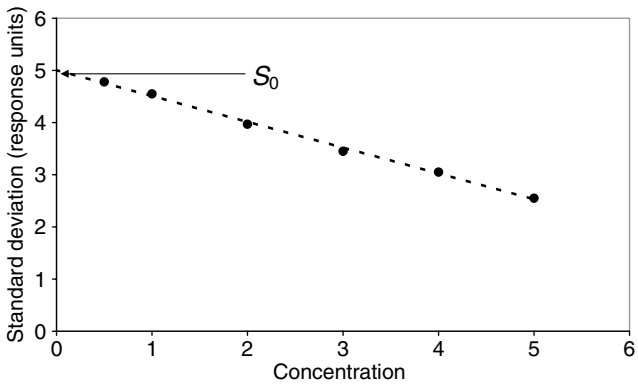

Fig. 5 Determination of LOD based on the projected standard deviation at zero concentration (S_0). The LOD is calculated as the concentration that corresponds to a response three times the value of S_0. Although the relationship between concentration and standard deviation shown here is linear, non-linear relationships between these two variables are likely.

computation, σ can be determined based on one of three data: 1) the standard deviation of the blank; 2) the residual standard deviation of the regression line; or 3) the standard deviation of the *y*-intercepts of regression lines.

95% Confidence intervals around the best-fit line

This graphical method, illustrated in Fig. 6, is a variation of the standard deviation-based approaches discussed previously. In this approach, the 95% confidence bounds are obtained for the best-fit, regression-based, calibration line. The upper 95% confidence bound, extrapolated to zero analyte concentration, reflects the statistical "limit" as it relates to calibration bias and imprecision, and establishes the LOD in terms of response. Mathematically, this response LOD is converted to a concentration LOD by

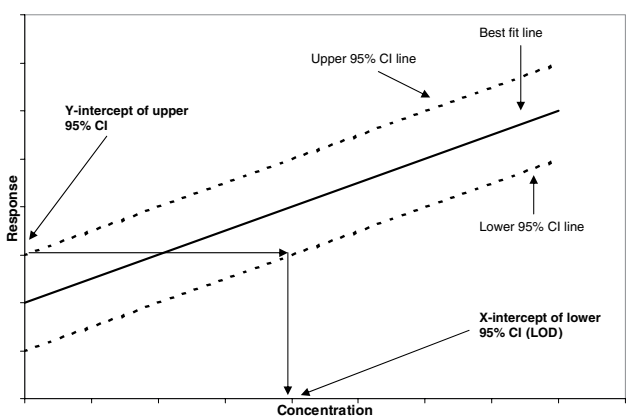

Fig. 6 Graphical determination of the LOD based on the 95% CI lines surrounding the best-fit regression model.
Source: From Determination of LOD and LOQ of an HPLC method using four different techniques, in Pharm. Technol.[13]

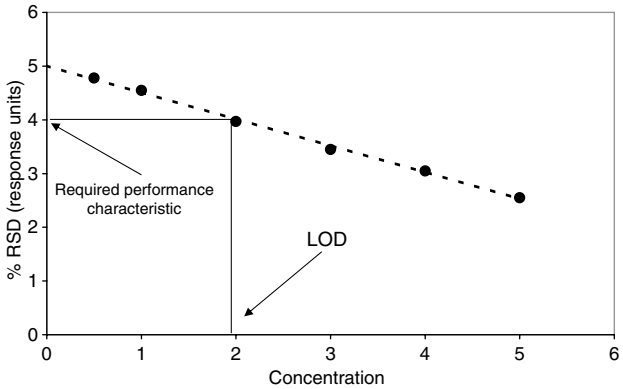

Fig. 7 Determination of LOD based on a specified performance requirement. In this example, the LOD is defined as the lowest analyte concentration with a percent relative standard deviation of not more than 4%. The interpolated value of LOD is approximately two concentration units. Although the relationship between concentration and percent relative standard deviation shown here is linear, non-linear relationships between these two variables are likely.

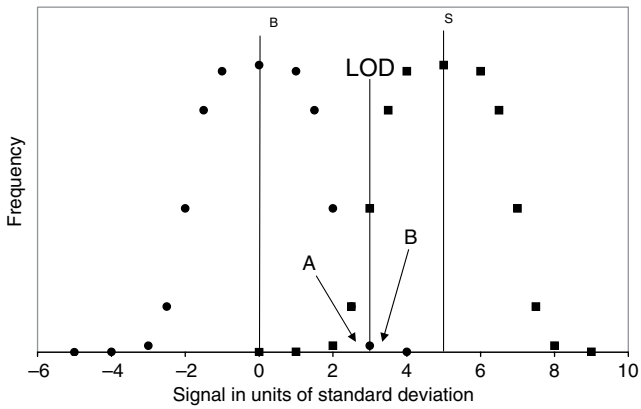

Fig. 8 Normal distribution of responses for the field blank (mean response = μ_B; •) and for the sample (mean response = μ_S; ■). Although the sample has a mean analyte value above the LOD, the potential for a false-negative response (sample analyzed with signal less than the LOD obtained, therefore concluding that the analyte is not present in the sample) exists and its probability is defined by region A in the sample's response distribution. As the sample's mean signal increases, the probability of a false negative decreases. The probability for a false positive (blank producing a signal greater than the LOD, thus concluding that the blank contains the analyte) is defined by region B in the blank's response distribution.

inputting the response LOD into the lower 95% confidence bound and by solving for concentration. Graphically, this can be accomplished as shown in Fig. 6.

Lowest concentration exhibiting required performance

As an alternative to the methodologies based on standard deviation, one can define the LOD (or LOQ) to be the lowest concentration that produces an analytical response that meets predefined quality requirements. For example, one might define the LOD as the lowest analyte concentration that produces a percent relative standard deviation (%RSD) of 10%. The LOD can be determined by performing replicate analyses of successively more dilute samples. The LOD could be estimated if one plots percent relative standard deviation vs. the analyte concentration (Fig. 7).

Minimization of false conclusions

In the context of LOD, false positive and false-negative responses can be defined as follows: false positive—a response for a blank that contains no analyte that falls above the LOD (i.e., a blank that is concluded to contain the analyte); false negative—a response for a sample that contains the analyte that falls below the LOD (therefore it is concluded that the sample does not contain the analyte at detectable levels). False-positive and false-negative responses are possible due to the assay variation (responses for a given sample are represented by a frequency distribution and not a single result). This scenario is illustrated in Fig. 8. To a certain extent, the definition and value for LOD depend on whether it is acceptable to have a false-positive or false-negative response.

Elimination of false positives is accomplished by having the LOD defined and calculated by the IUPAC procedure. With a k value of 3, the possibility of a false positive is less than 0.2% if the data are normally distributed, and less than 11% if hey are not. If greater confidence is required that false positives will not occur, a larger value of k may be necessary in the LOD calculation.

Consideration of false negatives requires that one take into account two response distributions: the response distribution for the blank, and the response distribution for the sample. A false negative will occur in the region where sample and blank response distributions overlap. If the detection limit is defined as that sample concentration for which the response distributions would not overlap (i.e., the LOD is that sample concentration for which a false-negative response cannot be obtained), then clearly the LOD depends on both the standard deviation of the blank and the standard deviation of the sample. Although it is beyond the scope of this manuscript to assess this scenario in a statistically rigorous manner, the following example may serve to illustrate the relationship between LOD and a false negative. In this example, the response populations of the blank and the sample are normally distributed and the standard deviation of both populations is the same. If the means of the blank and the sample populations differ by six times the standard deviation, there is less than a 1% chance that a response within the sample's distribution will also fall in the blank's

distribution (thereby creating a false negative). In such an example, one would be justified in calculating LOD as:

$$\mathrm{LOD} = R_B + 6s_B$$

where R_B and s_B have been defined previously as the mean and standard deviation of the blank response respectively.

Method detection limit

Methods for determining the LOD that are based on the analysis of a field blank that does not contain the analyte of interest are problematic in many real-world applications because either such samples do not exist, or would be impossibly difficult to create. As such a circumstance is frequently encountered in environmental analysis, the USEPA adopted a detection limit procedure, termed the method detection limit (MDL), which focuses on an operational definition of detection limit.[15] Specifically, the MDL is defined as the minimum concentration of a substance that can be measured and reported with 99% confidence that the analyte concentration is greater than zero. The MDL is determined from a replicate analysis of a sample of a specified matrix. Specifically, at least seven aliquots of sample, spiked to contain a concentration of from one to five times the method's estimated MDL, are analyzed. The MDL calculated from these results is statistically tested to determine its "reasonableness." If the result fails the testing, this iterative process begins again with a new estimate of the MDL.

Other methods

The analytical literature abounds with additional methods for the calculation of LOD. Most of these additional methods are variations on the procedures discussed herein, where the variation involves a more rigorous statistical assessment of the various aspects of a method's response function and variation. Although such derivations are mathematically and statistically rigorous, from a practical perspective, it is open to debate whether use of such derivations: 1) clarifies the meaning of the LOD; 2) improves the utility of the LOD; or 3) has the potential to become universally accepted.

Sensitivity vs. Detectability

A frequent error encountered in evaluating the performance of an analytical system is to confuse the concepts of sensitivity and detectability. Although both concepts address facets of a system's response, they are not identical, but rather complementary. Sensitivity relates to the ability of the system to respond to changes in analyte concentration and is most typically reflected as the slope of the method's response function. Detectability, as has been noted previously, is the ability of the method to distinguish between two responses (those responses that arise in the presence and absence of the analyte in the sample matrix of interest). It is possible to have a very sensitive method that has a relatively poor detection limit, especially if the method is very unselective or prone to high blanks. However, an insensitive method is very unlikely to exhibit a low LOD. Thus sensitivity is a necessary—but not sufficient—condition for the achievement of a low LOD.

General Comments

The following observations, relevant to LOD and its determination, are summarized from the various cited references.

A detection limit must be viewed as a temporary limit to current methodology.[1]

The LOD is governed by both instrumental factors (e.g., capability of the analytical instrument and column) and procedural factors (e.g., recovery of the analyte from the sample). It varies with the type of sample, different batches of blank, and type and condition of instrumentation.[16] Factors other than the analytical method itself that can influence the detection limit include the following:[2]

1. The analyst.
2. The analytical environment.
3. The brand of instrumentation used.
4. The quality of reagents.
5. The nature of the samples.
6. The calibration protocol.
7. The use of blank correction.

Column efficiency can affect *S/N* measurements; therefore analysts should account for both the type and the age of the column when determining the LOD. The maintenance status of chromatographic components (e.g., detectors and injectors) will also affect the ability to measure limits.[8] In trace analysis, the LOD is greatly influenced by the recovery of the compound; adsorption to glassware, instability or volatility, incomplete reaction (during derivatization), and poor laboratory technique are some of the causes of sample loss during analysis.[16]

Most paradigms for the calculation of LOD are based on the following simple models of an analytical system:[2]

1. The random error is normally distributed.
2. The population parameters are known.
3. The analytical method is unbiased.
4. The "field blank" is effectively a sample with zero analyte concentration.
5. The variance in the field blank measurement is essentially equal to the variance for samples with very low analyte levels.
6. The matrices of the field blank and samples are effectively identical, so that no unique interference effects are present.

Inherent in the model are the principles that the measured signal consists of an analytical signal (response to the analyte) and a blank signal (background, noise, or measured signal for a blank), and that both the analytical and blank signals fluctuate.[17] Additionally, it is generally assumed that the process has a linear response function.[18]

The calculated LOD can easily vary by an order of magnitude through the use of different statistical approaches.[4]

A value of $k = 3$ is considered minimal because it implies definite risks of 7% for false-positive (concluding that the analyte is present when it is absent) and false-negative (the reverse) decisions.[5]

To a certain extent, the correct calculation of LOD depends on whether greater harm is likely to be caused by false positives or false negatives.[7]

The entire sequence of operations, from procurement of the sample through the final measurement step, ultimately determines the LOD.[7]

Random error, reported as the coefficient of variation, ranges from about 25% to 100% at the LOD.[18]

Numerical values that have been proposed for k in the determination of LOD are summarized in Ref.[17] and range from 1.00 to 20.

It is better to regard the LOD as a useful but approximate guide to an analytical procedure. The value of LOD should be stated with one significant figure only, and duplicate results differing by a factor of less than 2 should not normally be regarded as significantly different.[16]

THE LIMIT OF IDENTIFICATION

As noted in the discussion of LOD, a false negative occurs when a response for a sample that is known to contain the analyte falls below the LOD. In such a case, it would be concluded (falsely) that the sample does not contain the analyte at detectable levels. At some point on the method's response spectrum between the LOD and the LOQ, there is an analyte concentration above which there is a very small chance that a false negative could occur. At this concentration, the vast majority of the responses that make up the sample's response population would fall above the LOD. This concentration is termed the LOI. Thus the LOI is defined as follows:

> The LOI is that analyte concentration at which the probability of obtaining a false-negative response (i.e., a response that is below the LOD) for a sample known to contain the analyte is below a specified value defined by the required level of confidence.

If the response populations of the sample and its associated blank are both normally distributed and if the standard deviations of the populations are similar, the LOI can be calculated as:

$$\mathrm{LOI} = R_B + 6s_B$$

where R_B and s_B have been defined previously as the mean and standard deviation of the blank response, respectively. In such as case, the probability of a false-negative response is 0.13% at the 95% level of confidence. Lack of normality in either response distribution, a greater variation in the response distribution of either the sample or the blank, or a higher required level of confidence would require that the LOI calculation have a multiplier larger than six in the s_B term.

THE LIMIT OF QUANTIFICATION

Definition

If it is an accurate observation that the LOD is a difficult concept to effectively define, the opposite is true for the LOQ. It is generally accepted that the LOQ is linked to method performance expectations including accuracy and precision. Thus a common definition of LOQ is as follows:

> The LOQ is the lowest concentration of the analyte that can be measured with acceptable accuracy and precision under the stated experimental conditions.

Methods of Determination

As LOQ and LOD are related concepts, it is not surprising that the methods suitable for determining LOD are, in most cases, also suited for the determination of LOQ, at least from a conceptual standpoint. Several of the more commonly cited means of determining the LOQ are described as follows.

As a multiple of the LOD

Once a method's LOD has been determined (by any of several methods as noted earlier), the LOQ can be calculated as a simple multiple of the LOD. Although a multiple of 3.3 is commonly cited (where 3.3 is the ratio of 10 : 3), LOQs are routinely calculated as three to five times the LOD.

Signal to noise (graphical)

As was the case with LOD, the LOQ can be calculated from a signal-to-noise evaluation of a chromatogram arising from a field sample known to contain the analyte at a concentration approximately equal to the LOQ. The LOQ is typically calculated as the analyte concentration required

to produce a signal that is 10 times larger than the peak-to-peak noise.

Based on analysis of spiked samples

This approach represents a literal interpretation of the LOQ definition. The LOQ is assessed by analyzing replicates of a field blank spiked with a low level of the analyte (near the LOQ), along with calibration standards. The accuracy (spike recovery) and precision of the replicate analyzes are compared to prespecified performance expectations. If the expectations are met, then the spiked concentration is an estimate of the LOQ. A more accurate determination of the LOQ would involve an iterative process whereby samples containing different levels of the analyte are all repetitively analyzed. The LOQ would fall somewhere between the lowest concentration that meets the performance expectations and the highest concentration that fails to meet the expectations.

Based on standard deviation of the noise

A representative (field) blank is repetitively analyzed and the LOQ is calculated as a multiple (typically 10) of the standard deviation of the blank's responses (divided by the slope of the calibration curve). This is equivalent to the IUPAC/ACS method for determining LOD.

Based on calculated confidence intervals around the calibration curve

Calibration data, obtained at analyte concentrations near the LOQ, are fitted (by an unweighted linear regression) and the confidence intervals (CIs) are calculated. The LOQ is determined as the concentration for which the interval (at a specified level of confidence) does not overlap the CI of the matrix blank (used as a standard).

Based on background interferences and the reproducibility of the response

Responses are obtained from replicate analyses ($n = 4$) of a field blank and the field blank spiked to contain a level of analyte that is close to the LOQ. The means of the obtained responses are tested statistically (with the *t*-test) to determine whether they are statistically different. If the difference is significant, the variability of the response in the spiked sample is evaluated by taking the ratio of its mean response to the response standard deviation. If the ratio is greater than or equal to 3, then the spiked concentration is taken as the LOQ.

Based on confidence intervals

Once again, field blanks and spiked field blanks are repetitively analyzed. The LOQ is determined as the concentration at which the lower confidence level of the mean of the spiked sample responses is at least four times greater than the upper confidence level for the mean blank response.

GENERAL DISCUSSION

It is clear from both the definition of LOQ and several of its methods of determination that a key aspect of establishing an LOQ is defining appropriate performance expectations. Although appropriate performance expectations may vary from method to method and especially from application to application, some general guidance in terms of what level of performance is reasonable to expect at the LOQ is given as follows:

- For bioanalytical LC methods, the accuracy criterion is ± 20% (80–120% of the "known" value) and the RSD should be less than 20%.[9]
- The LOQ is the lowest concentration for which RSD is less than 5%.[13]
- An *S/N* of 10 or less than 10% RSD is a good value as a rule of thumb.[8]
- A recovery of 70–130% and a precision of 10% RSD are required at the LOQ.[19]

A survey of validation data in trace level analyses reported that the following criteria for accuracy, obtained from various references, are pertinent:[20]

1. Below 100 ppb, 60–110% recovery is acceptable; above 100 ppb, 80–100% recovery is acceptable.
2. Below 1 ppm, 70–120% recovery is acceptable.
3. Impurities present at 0.1–10% should produce data within ± 5% of actual.

The linkage of the LOQ to performance expectations clearly differentiates LOQ from LOD. LOD is a calculated result. LOQ is a calculated result compared to a performance expectation. It is the aspect of the performance expectation that makes the link between LOQ and the application more obvious than the link between LOD and the application. Although it is possible for the same method to have two different LOQ values, depending on the needs of different applications, the method will have only one LOD.

It has been previously noted that it has historically been possible to obtain widely different values for LOD and LOQ, depending on the approach used and the statistical "multiplier" applied. As the LOD and LOQ concepts have evolved and have become more standardized and harmonized, obtaining such widely varying results is no longer commonplace. A recent study[13] examined LOD and LOQ values obtained for a multianalyte, gradient, UV-based high-performance liquid chromatography (HPLC) method by four different techniques, including: 1) a performance

Table 3 LOD and LOQ estimated for a gradient LC/UV assay with three analytes.

Analyte	Method 1[a]	Method 2[b]	Method 3[c]	Method 4[d]
LOD (mg/ml)				
A	0.06	0.05	0.02	0.04
B	0.04	0.04	0.02	0.04
C	0.04	0.10	0.05	0.10
LOQ (mg/ml)				
A	0.21	0.09	0.07	0.08
B	0.13	0.09	0.05	0.06
C	0.14	0.13	0.16	0.15

[a]LOQ is the lowest concentration that produces an injection to injection precision of NMT 5%. LOD = 0.3LOQ.
[b]Based on the graphical extrapolation of the plot of standard deviation of replicate injections vs. analyte concentration to zero concentration (to produce S_0, the standard deviation at zero concentration). LOD = concentration that corresponds to $3S_0$, LOQ = concentration that corresponds to $10S_0$. This is the ICH convention (Fig. 4).
[c]The 95% confidence lines are drawn around the best-fit regression plot of peak response vs. analyte concentration. A horizontal line is drawn from the *y*-intercept of the upper 95% CI line to the lower 95% CI line. A vertical line is drawn from the intersection point on the lower 95% CI line to the *x*-axis, yielding the *x*-intercept. The *x*-intercept is the LOD whereas the LOQ is 3.3LOD (Fig. 5).
[d]Based on the chromatographic signal to noise. LOD = $3N/S$; LOQ = $10N/S$ (Fig. 3).
Source: From Determination of LOD and LOQ of an HPLC method using four different techniques, in Pharm. Technol.[13]

expectation of percent relative standard deviation less than 5%; 2) a plot of standard deviation vs. concentration (ICH approach); 3) use of the 95% CI of the best-fit regression line; and 4) signal to noise (graphical). The results of this study are summarized in Table 3. In general, the results obtained via the four methods all agreed to within a factor of 2–3, and the differences between results were distributed randomly (i.e., no method gave consistently lower or higher results). Thus the authors of this study concluded that the four techniques were essentially equivalent and all were suitable for satisfying USP or ICH requirements.

Finally, the following discussion, obtained from Ref.[18] may be a useful and practical means of highlighting the meaning of, and differences between, LOD and LOQ.

Think of the LOQ as a "Beware of Dog" sign posted on the fence around a property, and the LOD as a "Beware of Dog" sign posted in the middle of the fenced yard. One may walk up and touch the first sign fairly safely. However, stay away from that second sign. Do not go into the yard.

A second example is as follows:

> A driver finds himself on an apparently deserted road that extends all the way to the horizon. As a good driver should, he periodically looks to the horizon to check for oncoming traffic. For the longest time, he sees nothing. Then, suddenly, he catches a glimpse (he thinks) of something out there. As he keeps on checking, he is not quite sure; does he see something or not? Is it really something or just a glint off the windshield? At this point, the object is below the driver's LOD. However, as time goes on, the object appears to be there every time he looks up. He is now reasonably confident that there is an object out there. The object has reached its LOD. As the driver and the object continue to move closer, the object grows in size and is more distinguishable from the background. Finally, the driver is virtually 100% confident that the object is out there and, in fact, it appears to be a car (as opposed to a truck or motorcycle). The object has reached its LOI. As time continues and the objects move still closer (with the net result that the car gets bigger and bigger), eventually the driver is able to ascertain that the car is, in fact, a Porsche 914 roadster, containing a driver and her passenger. At this point, the LOQ has been reached.

REPORTING LOW-LEVEL RESULTS

Once the various detectability limits have been defined and established for an analytical method, the question as to the proper format for reporting low-level results arises. To address this question, it is pertinent to observe that the three detectability limits (LOD, LOI, and LOQ) clearly divide the lower end of the response spectrum into finite regions (Figs. 1 and 9). Thus the question of how to report a low-level result boils down to what region of the response spectrum does the result fall in, and what is the appropriate reporting convention for that region.

The lowest response region in the spectrum is that which has the LOD as the upper bound. It is clear that if a response that is smaller than the response associated with the LOD is observed, the analytical result should be reported as "less than the LOD" or "not detected." In either case, the method's LOD must be reported [e.g., "< LOD (= 2 ppm)." It is also appropriate to report the method by which the LOD was determined, although this is done only infrequently.

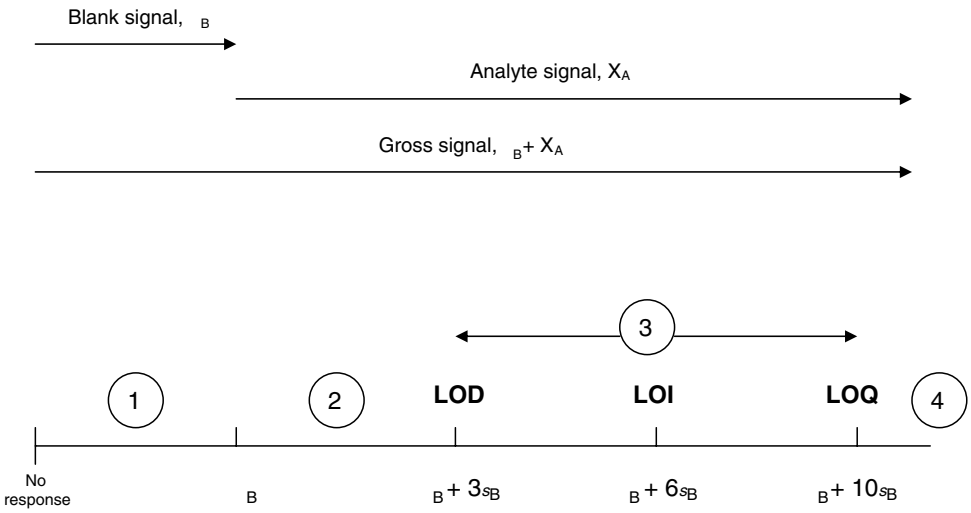

Fig. 9 Diagrammatic representation of various limits and their relationship to the mean blank response (μ_B) and the standard deviation of the blank response (s_B). The numbered regions include: 1) the region of the blank signal (reported as "not detected" and reporting the LOD); (2) the region of the blank variation (reported as "not detected" and reporting the LOD); 3) the region of detection and identification (reported as less than the LOQ and reporting the LOQ); and 4) the region of quantification (reporting the result).

Although the above discussion appears to be straightforward, the circumstance in which no response is observed is a bit more complex. Although there is a temptation to report such a result as a zero concentration, doing so is not correct except in the circumstance that the method's LOD is a single molecule. In all other circumstances, a non-observed response can be produced by an analyte that is either truly not present or an analyte whose level is well below the LOD. Thus as was the case of the response below the LOD, a sample that produces no analytical response is reported as "< LOD" or "not detected," with the LOD and its method of determination being cited.

Moving to higher analyte levels in the sample, the next region in the response spectrum is that region defined by the LOD at the low end and the LOI at the high end. Responses in this region are clearly above the LOD; thus one is confident that the response is "real" (i.e., the response arises from the elution of an analyte from the chromatographic column and into the detector). However, the amount of analyte present is insufficient to allow for its accurate identification. In this case, it is appropriate to report the result as "detected, unidentified" and to cite the method's LOI and its method of generation. Although it is appropriate to note that the analyte concentration in a sample producing a response that falls between the LOD and the LOI is greater than the LOD, this information may or may not be relevant to the interpretation of the result.

The next region one encounters as the response continues to increase is that region which falls between the LOI and the LOQ. As the response is above the LOI, the identity of the compound responsible for the response can be (and presumably is) identified. Thus the compound's identity is noted and the measurement status of the analyte peak is reported as "detected, identified." It is also appropriate to report the concentration of the analyte in such a sample as "< LOQ" and to cite the value of the LOQ and its means of determination. Although it may be tempting to "estimate" the analyte concentration in a sample whose response falls between the LOI and the LOQ, doing so is of limited value as the response function is typically poorly defined in this response region and the response is prone to a high degree of variability.

Although the above directions are clear-cut, there are circumstances where reporting a number is highly desirable (e.g., when the result is part of a data population that is undergoing statistical analysis). In such cases, it may be appropriate to report the analyte's calculated concentration, but care must be taken to ensure that the method's response function in the region of the analyte response is known. Such a result should be termed a concentration estimate and should be reported along with the qualifying notation "< LOQ" and the LOQ should be reported.

It goes without saying that it is appropriate to report the calculated concentration of an analyte whose response is above the LOQ. However, the reader is cautioned to remember that the response region near the LOQ is characterized by a high degree of imprecision and inaccuracy, and that good sense should be exercised in the use of significant figures in the reported value.

THE DYNAMIC RANGE

Because the primary use of chromatography is to establish the concentration of a known entity (analyte) in a specific sample and because few chromatographic detection strategies are absolute (i.e., their response function can be derived from first scientific principles), a useful chromatographic

method must have an analyte concentration region over which a response function can be established. This response function (or calibration curve) is the mathematical relationship that exists between the concentration of an analyte in a standard and the response that is produced when such a standard is processed by the chromatographic method. The dynamic range of a method is that concentration region for which a useful response function can be established. In this context, the term "useful" has three aspects. The first aspect is that the response function must be such that the sensitivity of the method is sufficient for the method's intended application. Although a flat line response function (no change in response produced by a change in analyte concentration) can readily be described mathematically, such a response function would be useless from a quantitative perspective. The second aspect is that the response function must be unique in the sense that every response is produced by a sample containing a single amount of the analyte. Although many chromatographic detectors reach a "flat line" state at high concentration (i.e., no change in response occurs as analyte concentration changes), there are some detectors (e.g., mass spectrometers) whose response actually "bends backward" (i.e., response decreases as concentration both increases and decreases). In such a circumstance, a sample may produce a response that is linked (via the response function) to two analyte concentrations. Inputting a sample's response into a calibration curve and obtaining multiple concentrations is clearly an outcome of limited value. The final aspect is that the response function must adequately "fit" or represent the analytical data from which it is derived. If the fit is poor (i.e., if there is a large difference between the measured response at a specific concentration vs. the response calculated from the regression model), then clearly the response function is not representative of its source data and any calculation based on the response function will be inaccurate.

The terms range and dynamic range are frequently encountered and occasionally incorrectly used interchangeably. The dynamic range is method specific and reflects the largest concentration difference for which a suitable response function can be obtained. The range of a method is application specific and does not necessarily represent the full capability of the method. Thus, for example, the range of an assay used for the purpose of quantifying an active ingredient in a finished pharmaceutical product need be only for 80–120% of the ingredient's nominal concentration in the actual test sample.[21] In many cases, such an application-driven range is just a small portion of the method's true dynamic range.

A subset of the dynamic range is the linear dynamic range. The linear dynamic range is that portion of the range for which the appropriate response function is a linear one. Historically, obtaining a linear calibration model has been the desired outcome of an analytical method development activity and most guidance for analytical method validations include an assessment of linearity (along with the subtle expectation that the desired response function is, in fact, a linear one). As numerous other calibration models exist and can readily be judged in terms of their appropriateness of fit, the desire for a linear response function is truly a throwback to the days when the only regression analysis tools were a pencil and straightedge. In modern chromatographic analysis, there is no underlying need for the response function to be linear and, in fact, there are many fundamental reasons to anticipate that certain detection methods are, by their very nature, non-linear in their response over every practically useful concentration range. It is noted in passing that the entire dynamic range may be made up of numerous smaller concentration regions whose response function is a linear one.

As a general rule of thumb, the LOQ is typically the low point of a method's dynamic range. The concentration at the high end is usually dictated by a lack of sensitivity, which leads to increased uncertainty, and is clearly method-dependent.

It is noted that the apparent dynamic range can be expanded at the high-concentration end via sample dilution provided that the dilution itself does not materially impact the response (e.g., via sample matrix effects). Additionally, a sample preparation process that accomplishes the concentration of the analyte may decrease a method's limit of detectability.

THE LIMIT OF RANGE

The LOR is that analyte concentration at which the method's response function is either no longer useful or no longer determinable. As noted previously, the LOR may reflect that concentration for which:

1. No response function that adequately fits the analytical data can be found.
2. The method exhibits inadequate sensitivity.
3. The method exhibits insufficient accuracy or precision.
4. The response function produces multiple values for a single input quantity.

Although it is typically the case that the LOR is defined by limitations in the detection portion of the analytical system, this is not necessarily the case in chromatographic analysis. Clearly chromatographic performance (such as loss of resolution or poor peak shape) at high analyte concentrations can be the limiting factor in terms of establishing a method's LOR, Additionally, other factors, such as injection-to-injection carryover at high concentration and analyte stability issues in high concentration standard or sample solutions, may represent practical method limitations that ultimately define a method's LOR.

CONCLUSIONS

The response spectrum in chromatographic analysis extends from the lowest analyte concentration that consistently produces a recognizable response to the highest analyte concentration that produces a response that is uniquely different from the response produced at a different analyte concentration. In this manuscript, the response spectrum has been partitioned into several appropriately concise regions via the use of concentration limits that correspond to the functions or purposes of chromatographic analysis (detection, identification, and quantitation). Methods for calculating, using and reporting the various limits were discussed. The position at which a particular response falls on the response spectrum dictates the utility and reliability of the analyte concentration assigned to that response.

REFERENCES

1. Glaser, J.A.; Foerst, D.L.; McKee, G.D.; Quave, S.A.; Budde, W.L. Trace analyses for wastewaters. ES&T **1981**, *15*, 1426–1435.
2. Analytical methods committee recommendations for the definition, estimation and use of the detection limit. Analyst **1987**, *112*, 199–204.
3. Analytical chemistry division, international union of pure and applied chemistry nomenclature, symbols, units and their usage in spectrochemical analysis: II. Data interpretation. Spectrochim. Acta **1978**, *33*, 241–245.
4. Long, G.L.; Winefordner, J.D. Limit of detection, a closer look at the IUPAC definition. Anal. Chem. **1983**, *55*, 712A–720A.
5. ACS committee on environmental improvement, subcommittee on environmental analytical chemistry guidelines for data acquisition and data quality evaluation in environmental chemistry. Anal. Chem. **1980**, *52*, 2242–2249.
6. Lindstedt, J. Limit of detection methodologies. Plating Surf. Finish. **1993**, *80*, 81–86.
7. Wehry, E. Quantitative measurements. In *Handbook of Instrumental Techniques for Analytical Chemistry*; Prentice Hall: Upper Saddle River, NJ, 1997; 73–80, Chap. 4.
8. Krull, I.; Swartz, M. Determining limits of detection and quantitation. LC/GC **1998**, *16*, 922–923.
9. Rosing, H.; Man, W.Y.; Doyle, E.; Bult, A.; Beijnen, J.H. Bioanalytical liquid chromatographic method validation. A review of current practices and procedures. J. Liq. Chromatogr. Relat. Technol. **2000**, *23*, 329–354.
10. Mocak, J.; Bond, A.M.; Mitchell, S.; Scollary, G. A statistical overview of standard (IUPAC and ACS) and new procedures for determining the limits of detection and quantification: Applied to voltammetric and stripping techniques. Pure Appl. Chem. **1997**, *69*, 297–328.
11. Coleman, J.; Wrzosek, T.; Roman, R.; Peterson, J.; McAllister, P. Setting system suitability criteria for detectability in high-performance liquid chromatography methods using signal-to-noise ratio statistical tolerance intervals. J. Chromatogr. A, **2001**, *917*, 23–27.
12. American chemical society committee report Principles of environmental measurement. Anal. Chem. **1983**, *55*, 2210–2218.
13. Paino, T.C.; Moore, A.D. Determination of LOD and LOQ of an HPLC method using four different techniques. Pharm. Technol. **1999**, *23*, 86–88.
14. Validation of analytical procedures: Methodology. International Conference on Harmonization of Technical Requirements for Registration of Pharmaceuticals for Human Use, Geneva, Switzerland, November, 1996 ICH-2QB.
15. *Definition and Procedure for the Determination of the Method Detection Limit, Revision 1.12*; U.S. Environmental Protection Agency, Environmental Monitoring and Support Laboratory: Cincinnati, 1981.
16. Mehta, A.C. Trace measurement. Lab. Pract. **1989**, *38*, 29–30.
17. Oresic, L.S.; Grdinic, V. Kaiser's 3-sigma criterion: A review of the limit of detection. Acta Pharm. Jugosl. **1990**, *40*, 21–61.
18. Clark, M.J.R.; Whitfield, P.H. Conflicting perspectives about detection limits and about the censoring of environmental data. Water Resour. Bull. **1994**, *30*, 1063–1079.
19. Jenke, D.R.; Poss, M.; Story, J.; Odufu, A.; Zietlow, D.; Tsilpetros, T. Development and validation of liquid chromatographic methods for the identification and quantification of organic compounds leached from a laminated polyolefin material. J. Chromatogr. Sci. **2004**, *42* (7), 388–395.
20. Jenke, D.R. Chromatographic method validation: A review of current practices and procedures: Part II. Guidelines for primary validation parameters. Instrum. Sci. Technol. **1998**, *26*, 1–18.
21. ⟨1225⟩ Validation of compendial methods. In *The United States Pharmacopeia, USP 26*; United Sates Pharmacopeial Convention, Inc.: Rockville, MD, 2002; 2239–2242.

Retention Factor: MEKC Separation

Koji Otsuka
Shigeru Terabe
Department of Material Science, Himeji Institute of Technology, Hyogo, Japan

INTRODUCTION

In micellar electrokinetic chromatography (MEKC), an ionic surfactant micelle, such as sodium dodecyl sulfate (SDS), is used as a pseudo-stationary phase that corresponds to the stationary phase in liquid chromatography (LC). Here, the separation principle of MEKC with an anionic micelle (e.g., SDS) under a neutral condition is briefly considered. When high voltage is applied across the whole capillary, the entire solution migrates toward the cathode by electroosmotic flow (EOF) while the SDS micelle is forced toward the anode by electrophoresis. The EOF is stronger than the electrophoretic migration of the SDS micelle and, hence, the micelle migrates toward the cathode at a more retarded velocity than the EOF.

When a neutral analyte is injected into the micellar solution at the anodic end of the capillary, it will be distributed between the micelle and the surrounding aqueous phase. The analyte, which is not incorporated into the micelle at all, migrates toward the cathode at the same velocity as the EOF. The analyte totally incorporated into the micelle migrates at the lowest velocity, or at the same velocity as the micelle, toward the cathode. The more the analyte is incorporated into the micelle, the slower the analyte will migrate. A neutral analyte always migrates at a velocity between the two extremes (i.e., the velocities of the EOF and micelle). The analytes are detected in an increasing order of the distribution coefficients by a detector located at the cathodic end of the capillary. The migration time of the electrically neutral analyte is limited between the two extremes: the migration time of a solute that is not incorporated into the micelle at all, t_0, and that of the micelle, t_{mc}.

Under an acidic condition, however, the absolute value of the velocity of the EOF becomes lower than that of the electrophoretic velocity of the SDS micelle and, therefore, the micelle migrates toward the anode. By contrast, when a cationic surfactant is employed instead of SDS, the direction of the EOF will be reversed or toward the anode, due to the adsorption of the surfactant molecule on the inside wall of the capillary and changing the surface charges.

RETENTION FACTOR

In MEKC, the retention factor, k, for a neutral compound can be defined as n_{mc}/n_{aq} where n_{mc} and n_{aq} are the number of the analyte incorporated into the micelle and in the surrounding aqueous solution, respectively. The retention factor can be related to the migration time of the solute, t_R as

$$k = \frac{t_R - t_0}{t_0(1 - t_R/t_{mc})} \tag{1}$$

or

$$t_R = \left(\frac{1 + k}{1 + (t_0/t_{mc})k}\right)t_0 \tag{2}$$

The reciprocal of t_0/t_{mc} or t_{mc}/t_0 is a parameter representing the migration time window. One should note that when the migration time of the micelle is infinite or the micelle does not migrate in the capillary at all, the value t_0/t_{mc} will be zero; then, Eqs. 1 and 2 become identical to those for conventional LC.

In MEKC, $k = \infty$ means that t_R becomes equal to t_{mc} and the solute migrates at the same velocity as the micelle.

When $t_0 = 0$ or the EOF is completely suppressed, Eq. 2 becomes

$$t_R = \left(1 + \frac{1}{k}\right)t_{mc} \tag{3}$$

Here, the surrounding aqueous phase does not move at all in the capillary and only the micelle migrates toward the anode if an anionic micelle is employed. Note that the EOF is not essential in MEKC.

When the solute has an electrophoretic mobility Eq. 1 will be more complicated, that is, the migration of the ionic solute includes a portion generated by the micelle when the solute is incorporated into the micelle and also the other portion generated by the electrophoresis of the solute itself.

RESOLUTION

Resolution, R_s in MEKC is given as

$$R_s = \left(\frac{N^{1/2}}{4}\right)\left(\frac{\alpha - 1}{\alpha}\right)\left(\frac{k_2}{1 + k_2}\right)\left(\frac{1 - (t_0/t_{mc})}{1 - (t_0/t_{mc})k_1}\right) \tag{4}$$

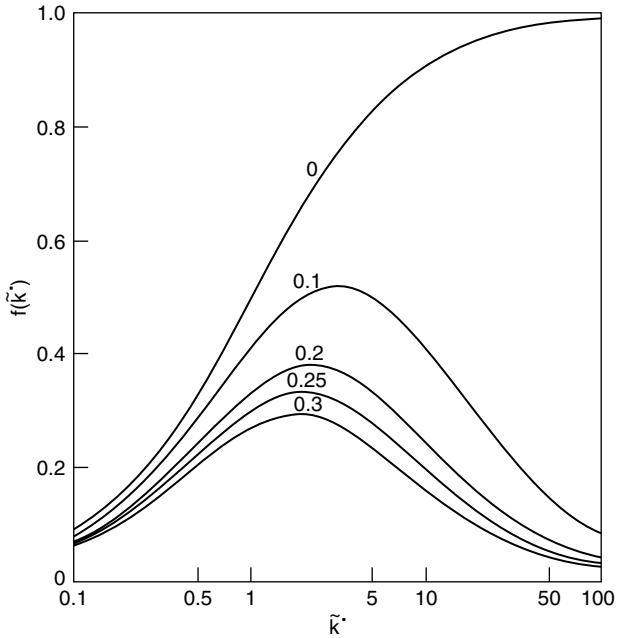

Fig. 1 Dependence of $f(k)$on capacity factor k. The values of are given on each line.
Source: From Electrokinetic chromatography with micellar solution and open-tubular capillary, in Anal. Chem.[4] with permission from the American Chemical Society.

where N is the theoretical plate number, α is the separation factor equal to k_2/k_1 and k_1 and k_2 are the retention factors of analytes 1 and 2, respectively. When $t_0/t_{mc} = 0$, Eq. 4 will be identical to that for conventional LC.

The separation factor α is altered by the combination of the structure of the micelle as the pseudo-stationary phase and the aqueous phase as a solvent of the micelle. Because k is included in the last term of the right-hand side of Eq. 4, the effect of k on R_s in MEKC is different from that in conventional chromatography. The last two terms in Eq. 4 are defined by the function as

$$f(k) = \left(\frac{k_2}{1+k_2}\right)\left(\frac{1-(t_0/t_{mc})}{1-(t_0/t_{mc})k_1}\right) \tag{5}$$

Then, we can calculate the optimum value of the retention factor, k_{opt}, for accomplishing the maximum R_s by differentiating Eq. 5, that is,

$$k_{opt} = \left(\frac{t_{mc}}{t_0}\right)^{1/2} \tag{6}$$

Under a neutral condition, k_{opt} is close to 2 for SDS micelles as the pseudo-stationary phase, as shown in Fig. 1. Practically, the recommended range of k is between 0.5 and 10.

RETENTION FACTOR AND DISTRIBUTION COEFFICIENT

The retention factor can be related to the distribution coefficient, K, between the micelle and aqueous phase by

$$k = K\left(\frac{V_{mc}}{V_{aq}}\right) \tag{7}$$

where V_{mc} and V_{aq} are the volumes of the micelle and aqueous phase, respectively. The value V_{mc}/V_{aq} or the phase ratio, can be written as

$$\frac{V_{mc}}{V_{aq}} = \frac{\bar{\nu}(C_{sf} - CMC)}{1 - \bar{\nu}(C_{sf} - CMC)} \tag{8}$$

where C_{sf}, $\bar{\nu}$, CMC are the concentration of the surfactant, partial specific volume of the micelle, and critical micelle concentration, respectively. At a low micellar concentration, we can arrange Eq. 8 as

$$k \simeq K\bar{\nu}(C_{sf} - CMC) \tag{9}$$

Thus, k can be adjusted by manipulating C_{sf}. Eq. 9 shows that k increases linearly with C_{sf}, and we can calculate K from the slope of this relationship. Also, K remains constant regardless of C_{sf}. The applicability of Eq. 9 under various conditions and for various surfactants has been examined in a number of reports.

BIBLIOGRAPHY

1. Otsuka, K.; Terabe, S. Micellar electrokinetic chromatography. Bull. Chem. Soc. Jpn. **1998**, *71*, 2465–2481.
2. Quirino, J.P.; Terabe, S. Electrokinetic chromatography. J. Chromatogr. A, **1999**, *856*, 465–482.
3. Terabe, S.; Deyl, Z. Micelles as separation media in chromatography and electrophoresis. J. Chromatogr. A, **1997**, *780.*
4. Terabe, S.; Otsuka, K.; Ando, T. Electrokinetic chromatography with micellar solution and open-tubular capillary. Anal. Chem. **1985**, *57*, 834–841.
5. Vindevogel, J.; Sandra, P. *Introduction to Micellar Electrokinetic Chromatography*; Hüthig: Heidelberg, 1992.

Retention Gap Injection Method

Raymond P.W. Scott
Scientific Detectors Ltd., Banbury, Oxfordshire, U.K.

INTRODUCTION

In GC analysis employing capillary columns, split injections are usually necessary to ensure that a very small sharp sample is placed on the column. This is important for maintaining column efficiency by not overloading the column. However, split injections generally result in an unrepresentative sample being placed on a capillary column (see *Split/Splitless Injector*, p. 2227), and because of this, on-column injection is usually preferred for accurate quantitative analysis. On-column injection requires a relatively large-diameter capillary column to be used to permit the penetration of the injection syringe needle into the column. However, although this procedure ensures that a representative sample is placed onto the column, other problems can arise. On injection, the sample readily separates into droplets that act as separate, individual injections. These separate sample sources can cause widely dispersed peaks and serious loss of resolution and, in the extreme, double or multiple peaks. Grob[1] suggested a solution to this problem which he termed the *retention gap method of injection*.

DISCUSSION

This procedure (Fig. 1) involves removing the internal coating of stationary phase from the first few centimeters of the column. This can be done by heating and volatilizing or burning off the phase. Alternatively, if the stationary phase is sufficiently soluble, it can be removed by a suitable solvent. The sample is then injected into the uncoated section of the column, and although the sample will probably split into droplets, the solvent will still vaporize in the normal way. As there is no stationary phase present, all the components of the mixture will travel at the speed of the mobile phase down the uncoated length of column until they reach a coated section. At this point, they will be absorbed into the stationary phase and all the components of the mixture will accumulate and form a compact sample at the start of the coated portion of the column. This technique is usually practiced in conjunction with temperature programming, the program being started at a fairly low temperature. The relatively low temperature facilitates the accumulation of all the solutes at one point in the column (i.e., where the stationary-phase coating begins). The temperature program is then started, and the solutes are eluted through the column in the normal way. The success of this method depends on there being a significant difference between the boiling points of the sample solvent and those of the components of the sample. In general, however, this procedure does significantly improve the quality of the separation and allows accurate quantitative results to be obtained.

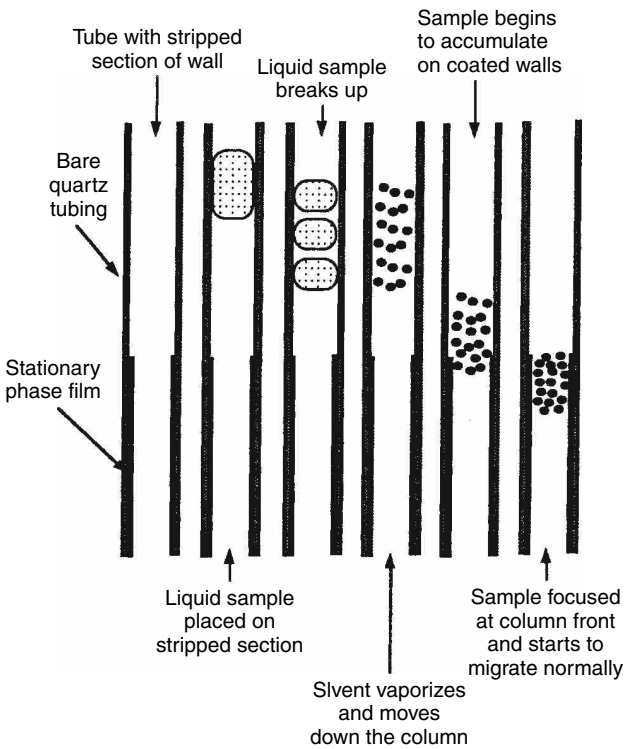

Fig. 1 The retention gap method of injection.

REFERENCES

1. Grob, K. *Classical Split and Splitless Injection in Capillary Gas Chromatography*; Huethig: Heidelburg, 1987.

BIBLIOGRAPHY

1. Grant, D.W. *Capillary Gas Chromatography*; John Wiley & Sons: Chichester, 1995.
2. Scott, R.P.W. *Techniques and Practice of Chromatography*; Marcel Dekker, Inc.: New York, 1996.
3. Scott, R.P.W. *Introduction to Analytical Gas Chromatography*; Marcel Dekker, Inc.: New York, 1998.

Retention Time and Retention Volume

Raymond P.W. Scott
Scientific Detectors Ltd., Banbury, Oxfordshire, U.K.

INTRODUCTION

The *retention time* of a solute is the elapsed time between the *injection point* and the peak maximum of the solute. The different properties of the chromatogram are shown in Fig. 1. The *volume of mobile phase* that passes through the column between the injection point and the peak maximum is called the *retention volume*. If the mobile phase is incompressible, as in liquid chromatography (LC), the retention volume (as so far defined) will be the simple product of the *exit flow rate* and the *retention time*.

APPLICATION

If the mobile phase is compressible, the simple product of retention time and flow rate will be incorrect, and the *retention volume* must be taken as the product of the *retention time* and the *mean flow rate*. The true *retention volume* has been shown to be given by[1]

$$V_r = V_{r'}\frac{3}{2}\left(\frac{\gamma^2-1}{\gamma^3-1}\right) = Q_0 t_r \frac{3}{2}\left(\frac{\gamma^2-1}{\gamma^3-1}\right)$$

where the symbols have the meanings defined in Fig. 1, and $V_{r'}$ is the retention volume measured at the column exit and γ is the inlet/outlet pressure ratio.

The retention volume V_r will include the dead volume V_0, which, in turn, will include the actual dead volume V_m and the extracolumn volume V_E.

Thus,

$$V_r = V_E + V_m + V_{r'}$$

The retention time can be taken as the product of the distance on the chart between the injection point and the peak maximum and the chart speed, using appropriate units. More accurately, it can be measured with a stopwatch. The most accurate method of measuring V_r for a non-compressible mobile phase, although considered antiquated, is to attach an accurate burette to the detector exit and measure the retention volume in volume units. This is an absolute method of measurement and does not depend on the accurate calibration of the pump, chart speed, or computer acquisition level and processing.

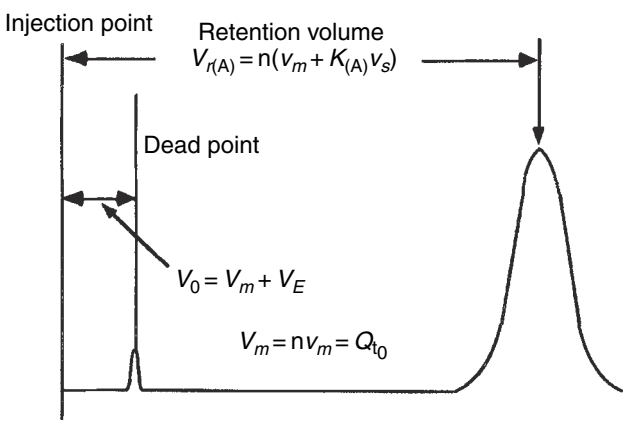

Fig. 1 Diagram depicting the dead point, dead volume, and dead time and retention volume of a chromatogram. V_0 is the total volume passed through the column between the point of injection and the peak maximum of a completely unretained peak, V_m is the total volume of mobile phase in the column, $V_{r(A)}$ is the retention volume of solute A, V_E is the extra column volume of mobile phase, v_m is the volume of the mobile phase per theoretical plate, v_s is the volume of the stationary phase per theoretical plate, K_A is the distribution coefficient of the solute between the two phases, n is the number of theoretical plates in the column, and Q is the column flow rate measured at the exit.

REFERENCE

1. Scott, R.P.W. *Introduction to Analytical Gas Chromatography*; Marcel Dekker, Inc.: New York, 1998; 77.

BIBLIOGRAPHY

1. Scott, R.P.W. *Liquid Chromatography Column Theory*; John Wiley & Sons: Chichester, 1992; 19.
2. Scott, R.P.W. *Techniques and Practice of Chromatography*; Marcel Dekker, Inc.: New York, 1996.

Reversed-Flow GC

Athanasia Koliadima
Physical Chemistry Laboratory, Department of Chemistry, University of Patras, Patras, Greece

INTRODUCTION

During the last 25 years, a gas flow perturbation technique has been used for physicochemical measurements in homogeneous and heterogeneous systems. This technique is reversed-flow gas chromatography (RF-GC). In this entry, the basic theoretical principles, the experimental setup, and the applications of this technique are reviewed.

REVERSED-FLOW GAS CHROMATOGRAPHY

Reversed Flow Gas Chromatography was introduced in its preliminary form in 1980 by Professor N. A. Katsanos and his colleagues at the University of Patras.[1] Until now, more than on 100 original articles, five reviews, and two books have been published referring to this technique and its applications.

Before dealing with the basic theoretical principals of RF-GC, we have to describe the experimental setup of this technique.

Instrumentation

For applying the RF-GC, a commercial gas chromatograph, slightly modified, is necessary. The modification consists of a T-shaped cell constructed from a glass or stainless steel chromatographic tube inside the chromatographic oven and a four- or six-port gas valve, inside or outside of the oven (Fig. 1).

This cell contains the sampling column which has two branches $l + l'$ and the diffusion column L_1. The diffusion column (20–80 cm × 3–5 mm inner diameter), connected perpendicularly to the sampling column (0.6–2.0 m × 3–5 mm inner diameter) at its midpoint, contains only a stagnant column of the carrier gas, which also flows through the empty sampling column, either from D_1 to D_2 or vice versa. Depending on the system under study, the diffusion column has some differences:

a. An injection port is added at the closed end of the diffusion column when diffusion coefficients in binary gas mixtures are measured.
b. A small glass vessel containing liquid is connected at the end of the diffusion column when physicochemical parameters for the interaction between gases and liquids are calculated.
c. Near the closed end, a small length of the diffusion column is filled with particles of solid when interaction phenomena between gases and solids are investigated.

The sampling column is devoid of any solid or liquid material; for separation purposes, an additional separation column is placed before the detector.

The connection to an appropriate detector flame ionization detector, thermal conductivity detector, flame photometric detector, nitrogen phosphorous detector (FID, TCD, FPD, NPD, etc.) is achieved via the four- or six-port valve being operated manually or electronically. The carrier gas (helium, nitrogen, argon, artificial air, etc.) flows via the valve only through the sampling column, at low flow rates (e.g., 25 cm^3/min) held constant during the experiments.

Procedure

The RF-GC, being a flow perturbation technique, is the change in the direction of flow of the carrier gas and this is done by using the four- or six-port valve. The carrier gas turns to flow in the opposite direction for a short time period t' (10–60 sec), smaller than the gas hold up time in the sections l and l' of the sampling column. Then, it is restored to its original direction of flow. Two questions arise now: why we change the direction of flow of carrier gas and what would we observe by this change?

If a solute is diffused slowly into the stagnant gas column of the carrier gas in the diffusion column, an asymmetric chromatographic signal is obtained, rising rather steeply and falling slowly with time after the maximum. The height of the chromatographic curve, which is obviously proportional to the concentration of the solute at the junction point, $z = 0$ and $x = l'$ of the sampling column; thus, it describes this concentration as a function of time.

This is expected in all of the above three cases (a)–(c) but, in the last two, the asymmetric chromatographic bands are distorted by different physicochemical phenomena, such as adsorption/desorption, possible reaction, etc. occurring between solute and liquid or solid material. The gaseous diffusion still transfers solute to the junction $x = l'$, where it is taken up by the passing carrier gas through the sampling column, but the diffusion rate is now different than before and the chromatographic band looks different. This distortion of the chromatographic band can be used for studying the phenomena mentioned

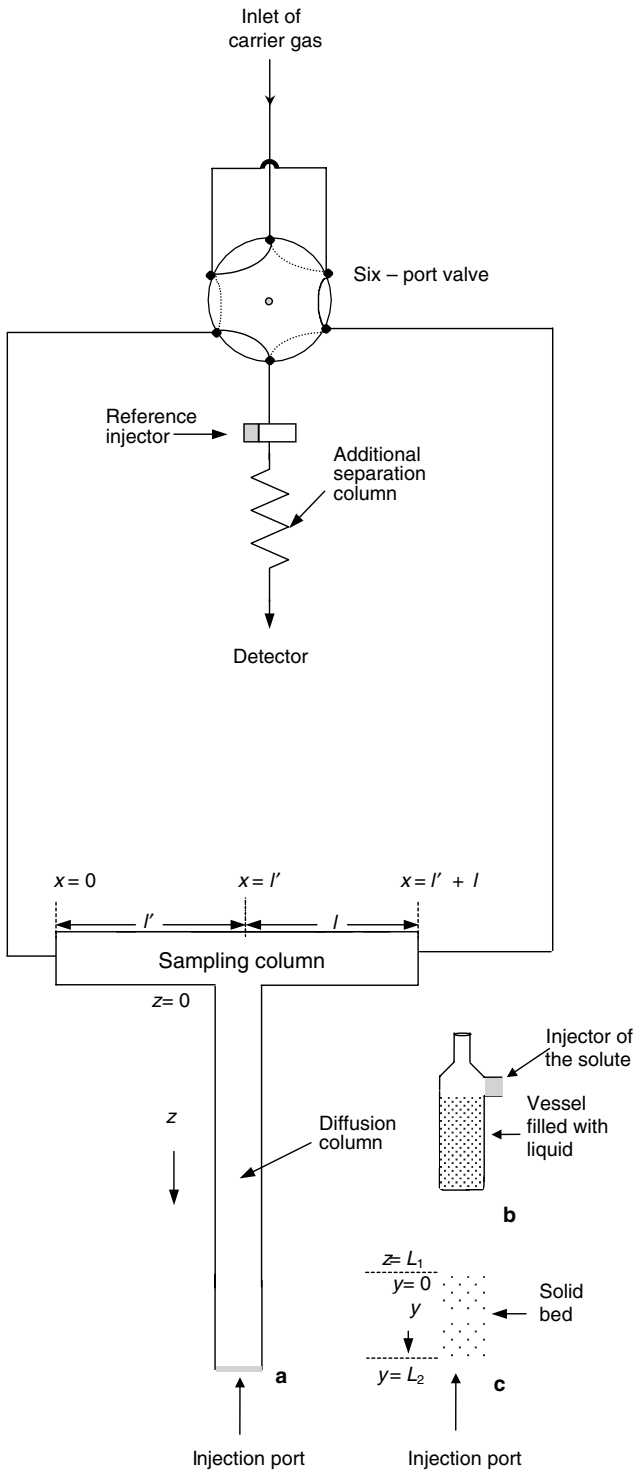

Fig. 1 Schematic representation of columns and gas connections for studying (a) diffusion coefficients in binary gas mixtures, (b) interaction between gases and liquids, and (c) interaction between gases and solids.

above, but many corrections have to be made before use and undesirable difficulties are introduced.

We can overcome the difficulties by applying the flow reversal of the carrier gas. This reversal produces a narrow

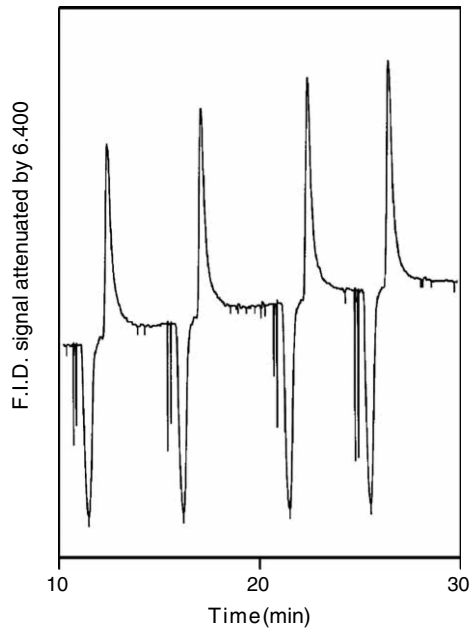

Fig. 2 A reversed-flow chromatogram showing sample peaks for the diffusion of 1-butene into nitrogen (corrected volume flow rate $\dot{V} = 0.33\,\mathrm{cm}^3/\mathrm{sec}$) at 343.2 K and 1 atm.

fairly symmetrical extra chromatographic peak (*sample peak*), which is superimposed on the continuous chromatographic band, and records the concentration of the solute at the junction $x = l'$, at time t when the flow reversal is made. An example of sample peaks is given in Fig. 2.

The sample peak can be made as narrow as we want, since the width at its half-height is equal to the duration t' of the backward flow of the carrier gas through the empty sampling column. The procedure can be repeated many times, giving a long series of sample peaks at various times t.

The sample peak is predicted theoretically by the so-called chromatographic sampling equation[2]:

$$\begin{aligned} c = {} & c_1(l', t_0 + t' + \tau)u(\tau) + c_2(l', t_0 + t' - \tau) \\ & [1 - u(\tau - t')] \times [u(\tau) - u(\tau - t'_M)] + c_3(l', t_0 - t' \\ & + \tau)u(t_0 + \tau - t')\{u(t_0 - t')[1 - u(\tau - t'_M)] \\ & - u(\tau - t')[u(\tau) - u(\tau - t'_M)]\} \end{aligned} \tag{1}$$

where c is the concentration of the solute at the detector, $c_1(l', \ldots)$, $c_2(l', \ldots)$, and $c_3(l', \ldots)$ are concentrations at the point $x = l'$ (cf. Fig. 1), t_0 is the total time from injecting the solute into the system to the last backward flow, t' is the time interval of backward flow, $\tau = t - t_M$, t being the time from the last restoration of the carrier gas, t_M and t'_M are the gas hold times in the sections l and l', respectively and, finally, the various u's are unit step functions for the arguments shown in parentheses.

Eq. 1 describes the concentration-time curve of the sample peaks created by flow reversals, and it has been derived analytically[2,3] using mass balances, rates of

change, etc. and integrating the resulting partial differential equations under given initial and boundary conditions. The concentration of the solute is usually given as the sum of three terms, c_1, c_2, and c_3, all referring to the junction of the sampling and the diffusion column (Fig. 1), but to different values of the time variable. Although Eq. 1 predicts that sample peaks are square, those actually obtained are not square, owing, most probably, to non-ideality.

The area under the curve or the height H from the continuous signal of the sample peak, measured as a function of time, is proportional to the concentration of the substance under study at the junction $x = l'$ of the sampling cell.

Although the experimental arrangement differs a little in the cases mentioned above (a–c), the relationship between the heights of the sample peaks H and the concentration $c(l', t_0)$ in all cases is given by the following equation[2,4]:

$$H^{1/M} = gc(l', t) \tag{2}$$

where M (dimensionless) is the response factor for the detector ($M = 1$ for the linear FID) and g a proportionality constant, having units of cm per mol cm^{-3}.

Diffusion Coefficients in Binary Gas Mixtures

If a small amount of solute A (usually 0.5–10 cm^3 of gas at atmospheric pressure) is injected into the cell through the injection port and, after a certain time during which no signal is noted, an asymmetric concentration-time curve of A is recorded, usually decaying slowly. At a certain known time (from the moment of injection), the flow reversal is started and repeated at various times, t, producing the known sample peaks. By using suitable mathematical analysis, the following equations describing the variation of H with t are derived[2,5,6]:

$$ln(H^{1/M}t^{3/2}) = ln(gN_1) - \frac{L^2}{4D_{AB}}\frac{1}{t} \tag{3}$$

$$ln(H^{1/M}) = ln(gN_2) - \frac{3D_{AB}}{L^2}t \tag{4}$$

where

$$N_1 = \frac{mL}{\dot{V}(\pi D_{AB})^{1/2}} \tag{5}$$

$$N_2 = \frac{\pi m D_{AB}}{\dot{V}L^2} \tag{6}$$

m is the injected amount of solute in moles, D_{AB} the diffusion coefficient of solute A into the carrier gas B, L the length of the diffusion column (cf. Fig. 1), and $\dot{V}$ the volumetric flow-rate in cm^3/sec.

The diffusion coefficient value, D_{AB}, can be calculated by using Eq. 3 or Eq. 4. For short-duration experiments and for long diffusion columns, Eq. 3 is more accurate, while Eq. 4 is more accurate for short diffusion column lengths and for experiments of long duration. Also, the selection of the equation giving the more accurate gaseous diffusion coefficient by RF-GC can be based on the comparison of the two experimental values found from Eqs. 3 and 4 with those given in the literature or calculated from known empirical equations.[7,8]

The same equations can be used for calculating, simultaneously, diffusion coefficients for each substance in multicomponent gas mixtures. This is achieved by using a separation column before the detector (cf. Fig. 1), which can effect the separation of all components of the gas mixture.

Diffusion coefficients of various hydrocarbons into the carrier gases N_2, H_2, and He, determined by RF-GC, can be found in the literature.[3,5,9]

Finally, the dependence of D_{AB} on temperature T is given by the relationship

$$D = AT^n \tag{7}$$

to which all theoretical and semiempirical equations lead. By plotting ln D vs. ln T, one calculates the exponent n of Eq. 7. The various values of n, calculated from diffusion coefficient values obtained by RF-GC, vary between 1.59 and 1.77.[3] These lie between 1.5 and 1.81, values predicted from the literature.[8,10,11]

Physicochemical Parameters for Gas–Liquid Interaction

For calculating physicochemical parameters for the interaction between gas and liquid, a small glass vessel is connected at the end of the diffusion column containing the liquid. A small amount of the solute A is injected at the carrier gas–liquid interface (Fig. 1b). As before, an asymmetric concentration-time curve of A is recorded, but now, it is distorted because of the various phenomena occurring between gas and liquid. Again, the flow reversals at certain times produce sample peaks, the heights of which are proportional to the concentration of solute A at the junction $x = l'$. Using suitable mathematical analysis,[12] the equation which describes the concentration as a function of the time was derived:

$$H/2 = c(l',t) = A_1\exp(B_1t) + A_2\exp(B_2t) + A_3\exp(B_3t) \tag{8}$$

where the pre-exponential coefficients, A_1, A_2, and A_3, can be written as explicit functions of B_1, B_2, and B_3, the geometrical characteristics of the cell and other experimental quantities, but this is not needed for the calculation of the above mentioned physicochemical quantities. The

exponential coefficients of time B_1, B_2, and B_3 are used first for the calculation of the diffusion coefficient of the solute A into the liquid (D_L, cm^2/sec), the partition coefficient of the solute A between the liquid at the interface, and the carrier gas (K, dimensionless) and Henry's law constant for the dissolution of the solute into the liquid (H^+, atm) according to the following equations[12]:

$$X = \frac{9AD_z}{KL_1L_2} + \frac{6D_z}{L_1^2} + \frac{6D_L}{L_2^2} = -(B_1 + B_2 + B_3) \tag{9}$$

$$Y = \frac{18AD_z^2}{KL_1^3L_2} + \frac{18AD_zD_L}{KL_1L_2^3} + \frac{36D_zD_L}{L_1^2L_2^2} = B_1B_2 + B_1B_3 + B_2B_3 \tag{10}$$

$$Z = \frac{36AD_z^2D_L}{KL_1^2L_2^3} = -B_1B_2B_3 \tag{11}$$

$$H^+ = \frac{R_gTd}{KM_L} \tag{12}$$

where X, Y, and Z are auxiliary parameters, A is the ratio of cross-sectional areas in z and y regions, a_z and a_L, respectively (cm^2), L_1 and L_2 are lengths in z and y regions, respectively (cm), d is the density of the liquid, M_L is the molar mass of the liquid, and D_z is the diffusion coefficient of the solute A into carrier gas, which can be determined as previously described.

For the calculation of the other parameters, such as overall mass transfer coefficients of the solute A into the carrier gas (K_G, cm/sec) and in the liquid (K_L, cm/sec) and, from them, gas (k_G, cm/sec) and liquid (k_L, cm/sec) film transfer coefficients, gas (r_G, sec/cm) and liquid (r_L, sec/cm) phase resistances for the transfer of the solute into the liquid, thickness of the stagnant film in the liquid phase (z_L, cm), partition coefficient of the solute between the liquid bulk and the carrier gas (K', dimensionless), and partition coefficient of the solute between the liquid at the interface and the bulk (K'', dimensionless), the following equations are adopted[12]:

$$X_1 = \frac{12D_z/L^2 + 4k/L + k'}{1 + kL/5D_z} = (-B_1 + B_2 + B_3) \tag{13}$$

$$Y_1 = \frac{24D_z^2/L^4 + 24kD_z/L^3 + 12k'D_z/L^2}{1 + kL/5D_z} = B_1B_2 + B_1B_3 + B_2B_3 \tag{14}$$

$$Z_1 = \frac{24k'D_z^2/L^4}{1 + kL/5D_z} = -B_1B_2B_3 \tag{15}$$

$$K_L = k'V_L/a_L; \quad K_G = ka_z/a_L; \quad \frac{1}{K_L} = \frac{1}{k_L} + \frac{K'}{k_G}; \quad z_L = \frac{D_L}{k_L}; \quad K'' = \frac{K}{K'} \tag{16}$$

where X_1, Y_1, and Z_1 have different physicochemical meaning than above X, Y, and Z, $L = L_1$ (gas phase), $k = K_Ga_L/a_z$ and $k' = K_La_L/V_L$ (liquid volume).

All the above calculations can be made by the means of a non-linear regression PC program in GW-BASIC.[12] The only measurable quantities needed for the calculations of all physicochemical quantities are the height H of the extra chromatographic peaks, the time t when these peaks are produced, and the geometrical characteristics of the experimental cell.

The same experimental arrangement, but different mathematical analysis, has been applied for studying homogeneous catalytic reactions in the liquid phase[13] and for calculating mass transfer coefficients for the evaporation of liquids, and diffusion coefficients of vapors by RF-GC.[14]

Physicochemical Parameters for Gas–Solid Interaction

Reversed Flow Gas Chromatography has been used to study the kinetics of various surface-catalyzed reactions, as well as for other physicochemical measurements. The experimental setup is given in Fig. 1c where, near the closed end of the diffusion column, a small amount of solid is placed and the length of this section is denoted as L_2, while the solute A is injected by means of an injection port.

The mathematical analysis for calculating all of the above parameters is described in detail in a recent published book[15] and a review article.[16] Here, only the necessary equations are summarized.

The concentration of the solute at the junction $x = l'$, as a function of time, is given by the following equation:

$$c(l',t) = G\left[A_1^0\exp(B_1t) + A_2^0\exp(B_2t) + A_3^0\exp(B_3t)\right] \tag{17}$$

where

$$A_1^0 = \frac{B_1^2 + kB_1}{(B_1 - B_2)(B_1 - B_3)}; \quad A_2^0 = \frac{B_2^2 + kB_2}{(B_2 - B_1)(B_2 - B_3)}; \quad A_3^0 = \frac{B_2^2 + kB_2}{(B_3 - B_1)(B_3 - B_2)} \tag{18}$$

$$G = \frac{n_Aa_1a_2}{\dot{V}(a_1 + a_2 + a_2Q)}; \quad a_1 = \frac{2D_z}{L_1^2}; \quad a_2 = \frac{2D_y}{L_2^2}; \quad Q = \frac{2a_yL_2}{a_zL_1}; \quad k = k_2 + k_R \tag{19}$$

L_1 and L_2 are the lengths of the sections z and y, respectively (Fig. 1c), a_Z and a_y are the cross sectional areas of the regions z and y, respectively, $\dot{V}$ is the volumetric flow rate

of the carrier gas, n_A is the amount (mol) of the solute introduced as a pulse at $y = L_2$, D_z, and D_y are the diffusion coefficients of the solute into the carrier gas and in the region of the solid bed, respectively, k_R is the rate constant for adsorption/desorption of the solute on the bulk solid, and k_2 is the rate constant of a possible first-order or pseudo-first-order surface reaction of the adsorbed substance.

The height H of the extra chromatographic peaks, obtained by the repeated flow reversals, is again proportional to the gaseous concentration (Eq. 2). This can be combined with Eq. 17, the result being

$$H^{1/M} = gG\sum_{i=1}^{3} A_i^0 \exp(B_i t) = \sum_{i=1}^{3} A_i \exp(B_i t) \tag{20}$$

where $A_i = gGA_i^0$ in cm.

Using a non-linear regression analysis PC program in GW-BASIC,[4] one can calculate the exponential and pre-exponential coefficients from the measured pairs H, t. From these, k_R, k_2, D_y, and the isotherm proportionality constant k_1 of the solute on the solid is carried out. The following—Eqs. 21–23 and Eq. 18—are used:

$$X = \frac{a_1 a_2}{a_1 + a_2 + a_2 Q} + k = -(B_1 + B_2 + B_3) \tag{21}$$

$$Y = \frac{a_1 a_2 k + (a_1 + a_2 Q) k_1 k_R}{a_1 + a_2 + a_2 Q} = B_1 B_2 + B_1 B_3 + B_2 B_3 \tag{22}$$

$$Z = \frac{a_1 + a_2 Q}{a_1 + a_2 + a_2 Q} k_1 k_2 k_R = -B_1 B_2 B_3 \tag{23}$$

where X, Y, and Z are auxiliary parameters.

From the above calculated parameters, through the following Eqs. 24 and 25, the overall deposition velocity (V_d), which is equivalent to an overall mass transfer coefficient of the gaseous solute to the solid surface, corrected for the activated adsorpion/desorption and surface reaction, and the reaction probability γ of the solute with the surface under study, are found:

$$V_d = \frac{k_1 V'_G(\text{empty})\epsilon}{A_S} \cdot \frac{k_2}{k_R + k_2} \tag{24}$$

$$1\gamma = \left(\frac{R_g T}{2\pi M_B}\right)^{1/2} \cdot \frac{1}{V_d} + \frac{1}{2} \tag{25}$$

where A_S is the total surface area of solid, cm^2, V'_G the gaseous volume of the section y of the experimental cell (cf. Fig. 1c), cm^3, R_g the ideal gas constant, J/K/mol, M_B the molar mass of analyte, kg/mol and T the absolute temperature, K.

For calculating adsorption energies, local monolayer capacities, local adsorption isotherms, and probability density functions for the deposition of the injected solute on the solid surface, the height H of the reversed-flow peaks and the physicochemical parameters B_i and A_i are used. The necessary relations are as follows:

The adsorption energy ε is expressed by the next relationship

$$\epsilon = RT \ln\left(\frac{K}{K^0}\right) \tag{26}$$

where K is the Langmuir constant[17] and K^0 is described by statistical mechanics.[18]

The local isotherm θ_t is calculated by the relationship

$$\vartheta_t = \frac{c_s^*}{c_{max}^*} = 1 - \exp(-KR_g T c_y) \tag{27}$$

where is the local adsorbed concentration of the injecting gas in equilibrium with that in the gaseous state, given by Eq. 29 of Ref. 16 c_y is the gaseous concentration of the solute in the gas phase above the solid, obtained by Eq. 28 of Ref. 16, and c^*_{max} is the local with respect to time monolayer capacity.

This capacity c^*_{max} is obtained by the equation:

$$c^*_{max} = \frac{c_s^*}{\vartheta_t} \tag{28}$$

Finally, the probability density function over time for the adsorption energy is given as follows:

$$f(\varepsilon;\ t) = \frac{1}{RT}\left[\frac{KRT(\partial c_s^*/\partial t) + (\partial^2 c_s^*/\partial c_y \partial t)}{\partial(KR_g T)/\partial t} - \frac{\partial c_s^*/\partial c_y}{KR_g T}\right] \tag{29}$$

The expressions for all derivatives, with respect to time in the above relationship, have been given in detail elsewhere.[15]

For studying lateral molecular interactions, the following equation is used:

$$K' = K^0 \exp\left(\frac{\varepsilon}{RT} + \beta\theta_t\right) = K \exp(\beta\theta_t) \tag{30}$$

where $\beta = z\omega/RT$, ω denoting the lateral interaction energy and z the number of neighbors for each adsorption site. Thus, $z\omega\theta_t$ is the added to ε deferential energy of adsorption due to lateral interactions. The $\beta\theta_t$ is the lateral molecular interaction energy and, for its calculation, the height H of sample peaks and the time t, together with some auxiliary physical quantities, are needed, while β is given by the relationship

$$\beta = \frac{1}{c_y}\left[\frac{\exp(KRTc_y) - 1}{KRT} - \frac{c_s^*}{\partial c_s^*/\partial c_y}\right] \quad (31)$$

The surface diffusion coefficient D_s of adsorbate molecules is obtained by the relationship

$$D_s = \frac{D_z\varepsilon_M^2 - D_y}{\partial\vartheta/\partial p} = \frac{D_z\varepsilon_M^2 - D_y}{K^0(1-\vartheta)}\exp\left(-\frac{\varepsilon}{RT}\right) \quad (32)$$

where D_z is the diffusion coefficient of the adsorbate in the carrier gas in the absence of solid, ε_M is the macro void fraction of the bed, D_y is experimentally calculated as described above in Eq. 19 and, finally, θ is given by the Jovanovic isotherm Eq. 22,[16] and the partial derivative of θ with respect to p by Eq. 38 of [16] From the above, it is obvious that only the height H and the time t are necessary for calculating surface diffusion coefficients.

The same data (height and time) used, so far, can be employed to calculate the net adsorption rate as a function of time with lateral molecular interactions, together with the rate constants of adsorption k_α (min^{-1}) and desorption k_d (min^{-1}).

Differentiating Eq. 27 with respect to time, one obtains the rate of θ_t, i.e., the net adsorption rate:

$$\frac{\partial\theta_t}{\partial t} = \left[KRT\frac{\partial c_y}{\partial t + c_y}\frac{\partial(KRT)}{\partial t}\right]\exp(-KRTc_y) \quad (33)$$

The various functions and the derivatives on the right-hand side have already been defined, while $\partial c_y/\partial t$ is given by Eq. 42.[16] If the $\partial\theta_t/\partial t$ calculated by Eq. 3 represents the local net adsorption rate, it can be written in a way analogous to Eqs. 5–22 of Jaroniec and Madey[19]

$$\frac{\partial\theta_t}{\partial t} = k_\alpha c_y RT(1-\theta_t) - k_d\theta_t\ exp(-\beta\theta_t) \quad (34)$$

Setting $K = k_\alpha/k_d$ according to microscopic reversibility, K being calculated from KRT value, and all the other quantities being known, only k_α is unknown in Eq. 34, and both rate constants k_α and k_d, can be found as functions of time and of θ_t.

All above calculations are carried out simultaneously by means of a GW-BASIC program. Also, RF-GC has been applied for measured chemical kinetic properties and surface energies of catalysts.[20]

With the exception of the three cases (a)–(c), which are described in detail, the RF-GC has been applied to determine physicochemical parameters in denuder tubes.[21] This is a special case of the gas–solid interaction where the wall of the diffusion column is covered with a thin layer of the adsorbent, forming a so-called denuder tube. The mathematical analysis in this case assumes a non-steady state condition and a non-zero longitudinal diffusion. The mathematical analysis is given in detail[21] and the same physicochemical quantities as previously can be calculated.

CONCLUSION

As described in detail, RF-GC is a technique which can be applied for studying homogeneous and heterogeneous systems by calculating various physicochemical parameters. The experimental arrangement is quite simple and quantities determined only difficultly by other techniques are easily carried out. These parameters are diffusion coefficients of gases into gases and liquids, rate constants for the adsorption and adsorption/desorption of gases, on and from solid surfaces, deposition velocities and reaction probabilities for the adsorption of gases onto solid surfaces, overall and time-dependent fractional conversions of various reactants into products, under steady- or non-steady-state conditions, activation parameters (energy and entropy) for various physical and chemical processes (adsorption, desorption, heterogeneous reaction, etc.), mass transfer and partition coefficients across gas–solid boundaries, local adsorption isotherms, local adsorbed concentrations, local maximum monolayer capacities, local adsorption energies, lateral molecular interactions of the adsorbed molecules, surface diffusion coefficients of the reactants and products on heterogeneous catalytic surfaces, standard free energies of adsorption, and geometric means of the London surface free energies for adsorption of gases on solid surfaces, adsorption rates on heterogeneous surfaces, effectiveness factors and Thiele-type modulus for catalytic materials.

REFERENCES

1. Katsanos, N.A.; Georgiadou, I. Reversed—flow gas chromatography for studying heterogeneous catalysis. J. Chem. Soc. Chem. Commun. **1980**, *5*, 242–243.
2. Katsanos, N.A. *Flow Perturbation Gas Chromatography*; Marcel Dekker Inc.: New York, 1988; 102, 108, 121.
3. Katsanos, N.A.; Karaiskakis, G. Temperature variation of gas diffusion coefficients measured by the reversed-flow sampling technique. J. Chromatogr. **1983**, *254*, 15–25.
4. Sotiropoulou, V.; Vassilev, G.P.; Katsanos, N.A.; Metaxa, H.; Roubani-Kalantzopoulou, F. Simple determinations of experimental isotherms using diffusion denuder tubes. J. Chem. Soc. Faraday Trans. **1995**, *91* (3), 485–492.
5. Katsanos, N.A.; Karaiskakis, G. Measurement of diffusion coefficients by reversed-flow gas chromatography instrumentation. J. Chromatogr. **1982**, *237*, 1–14.
6. Karaiskakis, G.; Katsanos, N.A.; Niotis, A. Measurement of diffusion coefficients in multicomponent gas mixtures by the reversed-flow gas chromatography. Chromatographia **1983**, *17*, 310–312.
7. Bird, R.B.; Stewart, W.E.; Lightfoot, E.N. *Transport Phenomena*; Wiley: New York, 1960; 744–746.

8. Fuller, E.N.; Schettler, P.D.; Giddings, J.C. A new method for prediction of binary gas-phase diffusion coefficients. Ind. Eng. Chem. **1966**, *58*, 19–27.
9. Karaiskakis, G.; Gavril, D. Determination of diffusion coefficients by gas chromatography. J. Chromatogr. **2004**, *1037*, 147–189.
10. Giddings, J.C. *Dynamic of Chromatography*; Marcel Dekker: New York, 1965; 269.
11. Huang, T.C.; Huang, C.H.; Yang, F.J.F.; Kuo, C.H. Measurements of diffusion coefficients by method of gas-chromatography. J. Chromatogr. **1972**, *70*, 13–24.
12. Rashid, K.A.; Gavril, D.; Katsanos, N.A.; Karaiskakis, G. Flux of gases across the air-water interface studied by reversed-flow gas chromatography. J. Chromatogr. A, **2001**, *934*, 31–49.
13. Stolyarov, B.V.; Katsanos, N.A.; Agathonos, P.; Kapolos, J. Homogeneous catalysis studied by reversed-flow gas chromatography. J. Chromatogr. **1991**, *550*, 181–192.
14. Karaiskakis, G.; Katsanos, N.A. Rate coefficients for evaporation of pure liquids and diffusion coefficients of vapors. J. Phys. Chem. **1984**, *88*, 3674–3678.
15. Katsanos, N.A.; Karaiskakis, G. *Time-Resolved Inverse Gas Chromatography and Its Applications*; HNB Publishing: New York, 2004; 72–143.
16. Katsanos, N.A. Determination of chemical kinetic properties of heterogeneous catalysts. J. Chromatogr. **2004**, *1037*, 125–145.
17. Heuchel, M.; Jaroniec, M.; Gilpin, R.K. Application of a new numerical—method for characterizing heterogeneous solids by using gas solid chromatographic data. J. Chromatogr. **1993**, *628*, 59–67.
18. Fowler, R.H. *Statistical Mechanics*; 2nd Ed.; Cambridge University Press: Cambridge, U.K., 1936; 829.
19. Jaroniec, M.; Madey, R. *Physical Adsorption on Heterogeneous Solids*; Elsevier: Amsterdam, 1988.
20. Katsanos, N.A.; Gavril, D.; Kapolos, J.; Karaiskakis, G. Surface energy of solid catalysts measured by inverse gas chromatography. J. Colloid Interf. Sci. **2004**, *270*, 455–461.
21. Topalova, I.; Katsanos, N.A.; Kapolos, J.; Vasilakos, Ch. Simple measurement of deposition velocities and wall reaction probabilities in denuder tubes. Atm. Environ. **1994**, *28*, 1791–1802.

Reverse-Phase Chromatography

Joseph J. Pesek
Maria T. Matyska
Department of Chemistry, San Jose State University, San Jose, California, U.S.A.

INTRODUCTION

Classical liquid chromatography (LC) is typically practiced in what is referred to as the normal-phase mode; that is, the stationary phase is usually a polar sorbent such as silica and alumina and the mobile phase consists of a non-polar constituent such as hexane modified with a somewhat more polar solvent such as chloroform or ethyl acetate. In this mode, the more polar compounds are preferentially retained. The reversed-phase (RP) mode utilizes the opposite approach for the separation of non-polar analytes or compounds that have some hydrophobic character. In this case, the stationary phase must consist of sorbent that is non-polar in nature and the mobile phase is composed of a primary polar solvent, usually water, that is modified by a more non-polar constituent such as methanol, acetonitrile, or tetrahydrofuran.

DISCUSSION

In order to make RP chromatography a rapid and efficient method, it is necessary to force the mobile phase through the stationary phase using high pressure. Therefore, the stationary phase must be a mechanically stable entity possessing the desired non-polar properties for RP operation. This result is accomplished typically by using particulate silica, which is stable under high pressure, and modifying the surface with a non-polar organic moiety. The modification takes place by reacting the silanol (Si–OH) groups on the silica surface with a suitable reagent, most often an organosilane compound ($X_3Si–R$ or $XR'R'Si–R$, where X is a reactive group such as Cl or methoxy, R' is a small organic group such as methyl, and R is another organic moiety, most often octyl (C_8) or octadecyl (C_{18}), in the RP mode. These silica modifications result in a primarily hydrophobic surface that can preferentially retain the more non-polar compounds in a mixture. The degree of hydrophobicity is controlled by both the length of the alkyl chain and the density of bonded groups on the surface, usually expressed in terms of micromoles per square meter. Due to the fact that original silica material has a high surface area (typically 100–300 m^2/g), the amount of hydrophobic material in the chromatographic column is considerable (from a few to as much as 20% by weight), leading to substantial interactions between solutes and the stationary phase. RP stationary phases are available with a variety of hydrophobic groups on the surface and bonding densities on silica particles of different diameters, surface areas, and pore sizes. In addition to the RP separation materials consisting of silica, some commercial products are also fabricated on other oxides such as alumina or zirconia or consist of polymeric matrices.

The second major component in modern high-performance liquid chromatography (HPLC) is the mobile phase. Since the stationary phase is a non-polar entity, the mobile phase must be more polar to allow retention of the analytes. The most polar solvent for RP-HPLC is water, but the overall polarity of the mobile phase can be adjusted by introducing variable amounts of any of a number of organic solvents. In LC, retention of solutes is a result of its relative affinity for the stationary and mobile phases. This can be described mathematically by the equation

$$k' = \frac{(\text{Amount of analyte})_{\text{SP}}}{(\text{Amount of analyte})_{\text{MP}}}$$

where k' is the equilibrium constant referred to as the capacity factor that relates the amounts of the analyte in the stationary phase (SP) and the mobile phase (MP). Therefore, the mobile phase exerts considerable influence on the retention and, hence, the separation of solutes. This factor makes HPLC a very powerful separation technique in that the mobile phase can be adjusted to accommodate a wide variety of solutes (from large biomolecules to small organic and inorganic compounds) having a range of chemical properties. Simultaneously, the selection of the mobile-phase composition will determine the degree of interaction between the solute and the stationary phase.

Most RP-HPLC separations are done in the isocratic mode (i.e., where the composition of the mobile phase is held constant during the analysis). This approach is suitable when the sample consists of analytes having similar properties or where their hydrophobicities encompass a small or moderate range. Under these conditions, all solutes in the sample will be eluted over a reasonable time span (i.e., not too short to prevent resolution of individual analytes and not too long to result in an inconvenient analysis period). Therefore, proper selection of the mobile-phase composition is essential in the development of any RP separation method. Fortunately, due to the decades of

long practice of RP-HPLC, there exists in the literature and from commercial sources, a wealth of information on suitable mobile-phase compositions for particular types of sample, especially for the C_{18} stationary phase. In addition, the retention of solutes on hydrophobic phases has been modeled mathematically and there exist computer programs for assisting in the optimization of mobile-phase composition in the solution of various separation problems.

A single mobile composition is often not suitable for samples that contain a wide range of chemical properties or hydrophobicities. Under these conditions, an isocratic method may leave the early eluting components unresolved and the analytes having strong retention with inconveniently long elution times. The solution to this problem is to change the mobile-phase composition in a systematic way during the course of the separation. This approach is referred to as gradient elution. In gradient elution, the mobile-phase composition initially is weak (with a large percentage of the most polar component) and becomes increasingly stronger (containing greater amounts of the less polar modifier) as the separation process continues. With this approach, the retention of the less hydrophobic compounds is increased at the beginning of the separation, whereas the retention of the more hydrophobic compounds is diminished at the end of the elution period. The simplest approach to gradient elution is to vary the mobile-phase composition linearly from the beginning to the end of the analysis period. In addition to the rate of change of the mobile-phase composition, the initial and final amounts of the two solvents are also variables that can be changed to improve resolution within the shortest analysis times. Besides linear gradients, other formats have been developed to optimize separations. These gradient methods include a constant composition at the beginning and/or the end of the analysis as C18 well as concave, convex, or step profiles. The main disadvantage of the gradient method is the time required for the column to reequilibrate to the initial mobilephase conditions. This reequilibration time can be from several minutes up to a half-hour or longer. However, modern instrumentation (pumps and pump controllers) has made reproducible gradients relatively easy to achieve.

Another means of controlling eluent strength is the use of ternary or quaternary solvent mixtures instead of the more common binary approach. Each solvent has its own unique properties that can be used to improve the separation of difficult-to-resolve analytes or to shorten the analysis time without sacrificing resolution. Although gradients and more complex solvent matrices are more difficult to model than binary isocratic systems, software exists for such purposes and can assist in method development.

The basic equipment for the RP mode is similar to most other types of HPLC. It consists of solvent reservoirs (one to four), a high-pressure pump, a mixing device that can create any combination of binary solvents or higher order as well as gradients (optional), an injection device, the column, and a detector connected to a data processing device. Ultraviolet (UV) detection is most often used in the RP mode, but fluorescence, refractive index, and electrochemical properties, as well as coupling to a mass spectrometer are also possible. Qualitative information is obtained by comparing the retention times of unknown compounds to those of known standards, whereas quantitative information comes from calibration curves of the peak area vs. concentration. The coupling of LC to mass spectrometers and nuclear magnetic resonance (NMR) spectrometers is becoming more common, which makes positive identification of unknown compounds in a mixture much easier.

APPLICATIONS

One of the primary factors responsible for the development of HPLC was the need to separate mixtures containing hydrophobic compounds that were not sufficiently volatile for analyzing by GC or were thermally unstable after volatilization. Although some compounds that are normally non-volatile can be made volatile by derivatization, this process adds an extra step to the analytical method. However, under any circumstances, a large majority of chemical species, perhaps as much as 70%, cannot be analyzed by GC. Among the most significant of these compounds are ionic species, both organic and inorganic, as well as most biomolecules. With greater demand for the analysis of biologically related samples for medical, pharmaceutical, and biotechnological purposes, the need for reliable RP-HPLC methods continues to increase. Although it is impossible to review all types of sample amenable to RP-HPLC analysis, a few examples will be given to illustrate the breadth of applications possible by this technique.

Because the mechanism of separation is primarily based on differences in hydrophobicity, a simple mixture of aromatic hydrocarbons can be used to illustrate the operation of the RP method. A chromatogram of such a separation is shown in Fig. 1, where the elution times are benzene < toluene < ethylbenzene < isopropylbenzene < *t*-butylbenzene < anthracene. When the RP mechanism is functioning, compounds are eluted in order of increasing hydrophobicity, as illustrated in Fig. 1. By increasing the degree of hydrophobicity either through longer alkyl chains [more saturated or unsaturated (aromatic) hydrocarbon groups] or more alkyl chains (higher bonding density), retention times (larger k' values) become longer under constant mobile-phase conditions. This principle applies to a wide variety of organic compounds. The organic molecules can also have a polar functional group such as an alcohol, ether, amine, or cyano, for example, but the RP method can still be used. In this case, the polar groups may diminish the overall hydrophobicity of the compound, but

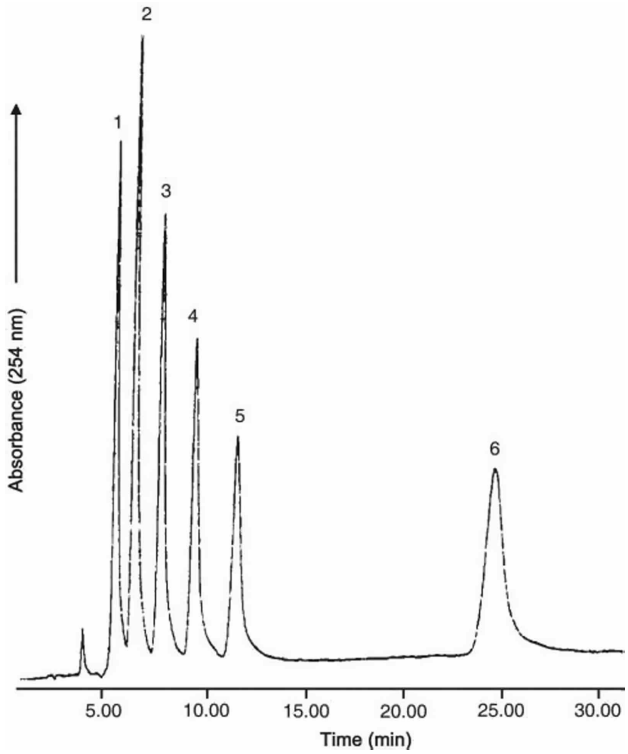

Fig. 1 Separation of RP test mixture on a C_{22} bonded phase. Mobile phase: 50 : 50 acetonitrile–water. Solutes: 1 = benzene; 2 = toluene; 3 = ethylbenzene; 4 = isopropylbenzene; 5 = *t*-butylbenzene; 6 = anthracene.

there will still be some retention on a typical RP stationary phase such as octadecyl (C_{18}). A simple example is benzene and phenol. The addition of a hydroxyl group makes phenol less hydrophobic than benzene, so it will be eluted first.

The above example illustrates the principle of relative retention (i.e., that benzene is retained more strongly than phenol). In order to determine absolute retention, the k' values of each compound must be measured as follows:

$$k' = \frac{t_R - t_0}{t_0}$$

where t_R = the retention time of compound and t_0 is the time to elute an unretained compound. In HPLC, the t_0 is equivalent to measuring the elution time for air in GC. Therefore, selection of a suitable compound that will not be retained is crucial to accurate measurement of k' values. Because retention is based on hydrophobicity, the t_0 marker should be very hydrophilic (i.e., very polar or ionic). Two compounds often selected for this determination are KNO_3 and uracil. They both fulfill the requirement for hydrophilic properties and also have absorbance in the UV, which facilitates detection.

Whereas the overall hydrophobic nature of the stationary phase is the most important factor in determining retention, bonded-phase structure can also influence k' values. This effect can be observed in the separation of polycyclic aromatic hydrocarbons (PAHs). For stationary phases with a high bonding density and/or a high degree of association between adjacent bonded organic moieties, molecules that are more planar are preferentially retained. The National Institute of Standards and Technology (NIST) has developed reference mixtures to measure this effect.

In addition to a wide range of polar and non-polar hydrocarbons that can be analyzed by RP-HPLC, it is also possible to separate ionic species. Because water is used as part of almost all mobile phases, those species which are acids and bases can be neutralized by control of pH. In cases where neutralization is not possible, then the addition of a counterion into the mobile phase so that the analyte will form a neutral complex can be used to enhance RP retention. The same principle can be applied to inorganic species by forming a neutral complex that results in RP retention.

Large biomolecules, while being charged under most aqueous mobile-phase conditions, still have significant hydrophobic portions that interact with the stationary phase. In many complex mixtures of proteins and peptides, the degrees of interaction with the stationary phase (k' values) vary over a broad range. Therefore, gradient elution methods are often required. An example of such a gradient method for the separation of a biochemical mixture is shown in Fig. 2. Finally, although water is used almost exclusively as the weak solvent in RP methods, a few types of sample require the use of other mobile-phase components. For

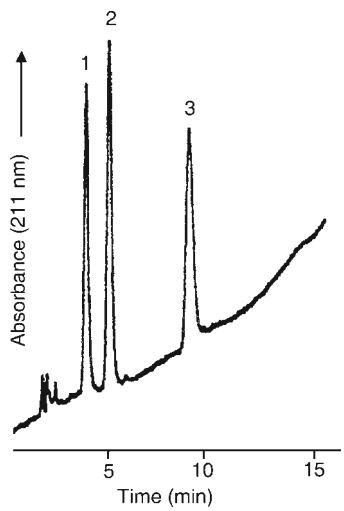

Fig. 2 Gradient separation of peptide mixture on a C_{30} bonded phase. Mobile phase, linear gradient from 25% to 45% A in 15 min. A = 0.1% trifluoroacetic acid (TFA) in 75 : 25 acetonitrile–water and B = 0.1% TFA in water. Solutes: 1 = bradykinin; 2 TFA angiotensin III; 3 = angiotensin I.

example, the separation of triglycerides and fatty acids often utilize acetone as the weak solvent in the RP mode.

BIBLIOGRAPHY

1. Cunico, R.L.; Gooding, K.M.; Wehr, T. *Basics HPLC and CE of Biomolecules*; Bay Bioanalytical Laboratory: Richmond, CA, 1998.
2. Kirkland, J.J. The use of porous silica-based column packings in HPLC method development. Curr. Issues HPLC Technol. (LC–GC Suppl.). **1997**, 546–555.
3. Mant, C.T., Hodges, R.S., Eds.; *High Performance Liquid Chromatography of Peptides and Proteins*; CRC Press: Boca Raton, FL, 1991.
4. Poppe, H. Column liquid chromatography. In *Chromatography,* 5th Ed.; Heftmann, E., Ed.; Elsevier: Amsterdam, 1992.
5. Snyder, L.R. Theory of chromatography. In *Chromatography,* 5th Ed.; Heftmann, E., Ed.; Elsevier: Amsterdam, 1992.
6. Vansant, E.F.; Van Der Voort, P.; Vrancken, K.C. *Characterization and Chemical Modification of Silica*; Elsevier: Amsterdam, 1995.

Rf

Luciano Lepri
Alessandra Cincinelli
Department of Chemistry, University of Florence (UNIFI), Florence, Italy

Abstract
The R_f value is the fundamental parameter in planar chromatography to describe the position of a spot on a developed chromatogram. R_f values in linear, circular, and anticircular chromatography were defined. Correlations between these types of R_f were evidenced for conversion of linear R_f values in circular and anticircular and unidimensional multiple development. Definition of thermodynamic and relative R_f values were also reported and discussed. In addition, the importance of R_M value, which has a linear relationship with structural elements of the solute and can be used to characterize molecular hydrophobicity in reversed planar chromatography, was evidenced.

INTRODUCTION

The R_f value is the fundamental parameter in planar chromatography and describes, numerically, the position of a spot on a developed chromatogram.

THE R_F VALUE IN LINEAR DEVELOPMENT

The method for determining R_f values is based on the measurement of two lengths in a thin-layer chromatogram and the calculation of their ratio:

$$R_f = \frac{\text{Distance of spot center from start}}{\text{Distance of solvent front from start}}$$

where "start" is the sample application point.

R_f values are between 0 and 1 (solute remains at start or runs with the solvent front, respectively), and the maximum number of significant figures after the decimal point is currently two. R_f values are often multiplied by a factor of 100 (hR_f).

R_f values can be disturbed by side effects or demixing of the multicomponent solvent used. In order to obtain reproducible R_f values, much attention must be paid to the reproducibility of the system.

THE R_F VALUE IN CIRCULAR AND ANTICIRCULAR DEVELOPMENT

Linear R_f values can be transferred to the circular (centrifugal) technique with the equation

$$R_{f\,\text{lin}} = R_f\,\text{circ}^2$$

This equation holds only if the starting line is close to the center of the layer and identical to the solvent entry position. Migration of the mobile phase is radial toward the periphery. Circular R_f values are higher than the linear ones with the exception of $R_f = 0$ and $R_f = 1$. The increase in the circular R_f values is greater in the lower range, and solutes are better resolved in this range with respect to linear development.

In anticircular (centripetal) development, the samples are applied in a circle close to the edges of the plate and the development proceeds from the circle toward the center.

The equation for conversion of linear R_f values is

$$R_{f\,\text{lin}} = 1 - \left(1 - R_{f\,\text{anticirc}}\right)^2$$

and the resolution of the anticircular mode is better in the upper R_f range.[1]

THE R_F VALUE IN UNIDIMENSIONAL MULTIPLE DEVELOPMENT

Unidimensional multiple development is the repeated development of a plate over the same distance with an eluent of constant composition after careful drying between development steps.

The R_f after n identical development steps is

$$R_{f\,n} = 1 - \left(1 - R_f\right)^n$$

where R_f is the retention factor of the solute after a single development.[2]

Since in the second and in all consecutive runs the lower spot migrates before the upper one does, thus reducing ΔR_f with respect to the resolution achieved in the previous run, the resolution-lessening effect is stronger the higher the R_f values are.

DEFINITION OF THERMODYNAMIC R_F VALUE

According to the Martin–Synge model of partition chromatography,[3,4] the thermodynamic R_f value (R_f'), based on the chromatographic equilibrium process of solute distribution between the mobile and stationary phase, can be expressed as the fraction of the relative time spent by a solute molecule in the mobile phase (A) or fraction of solute molecules in the mobile phase (B)

$$R_f' = \underset{\text{(A)}}{\frac{t_m}{t_m + t_s}} = \underset{\text{(B)}}{\frac{n_m}{n_m + n_s}}$$

where the subscripts m and s refer to mobile and stationary phase, respectively.

Because the fractions of solute molecules and respective mole numbers are identical, it is possible to achieve the fundamental relation (1) connecting R_f' value with the distribution coefficient $K_d = C_s/C_m$ and the phase ratio V_s/V_m:

$$R_f' = \frac{m_m}{m_m + m_s} = \frac{C_m V_m}{C_m V_m + C_s V_s} = \frac{1}{1 + K_d\left(\frac{V_s}{V_m}\right)}$$

In the Martin–Synge relationship (1), C_m and C_s are molar concentration of solute in the mobile and stationary phase, while V_s and V_m are the volumes of these two phases. V_s/V_m is numerically equal to A_s/A_m, the ratio of the phase cross-section normal to the direction of the solvent flow, which better describes the local conditions in thin-layer chromatography (TLC). The validity of the equation is limited, since the amount of solvent on the layer decreases toward the solvent front and, therefore, the phase ratio changes.

R_f' values are generally higher than R_f values and can be related to each other by the following experimental relation:

$$R_f' = \xi R_f$$

where ξ is the disturbing factor ($1 \leq \xi \leq 1.6$).[1] Eq. 1 usually holds in the R_f region up to 0.7 since the greatest changes of the solvent front are observed at the end of the chromatogram.

THE R_{ST} NUMBER

Relative R_f values, generally called R_{st} or R_x values, can also be used but are inadequate to render R_f values independent of uncontrolled parameters, since they are dependent on the phase ratio.

$$R_{st} = \frac{(R_f)_i}{(R_f)_{st}} = \frac{\text{Migration distance of substance, i}}{\text{Migration distance of reference substance, st}}$$

These values can be higher than 1.

THE R_M VALUE

Since the R_f value has no linear relationship with structural elements of the solute, R_M values [log $(1 - R_f)/R_f$] of members of a homologous series can be used to show quantitative relations with the number of "homologous structural elements."

In addition R_M value can be used to characterize molecular hydrophobicity in reversed-phase planar chromatography by elution with water–organic solvent mixtures according to the Soczewiński–Wachtmeister equation:[5]

$$R_M = R_{Mo} - S\Phi$$

where R_{Mo} is the R_M factor extrapolated at zero percentage of organic solvent and is usually accepted as a measure of lipophilicity, S is related to the specific surface area of the solute and Φ is the volume fraction of the organic modifier (usually methanol). Lipophilicity is widely used in quantitative structure activity relationship (QSAR) for prediction of the biological activity of substances.[6,7]

REFERENCES

1. Geiss, F. *Fundamentals of Thin-Layer Chromatography (Planar Chromatography)*; Alfred Hüthig Verlag: Heidelberg, Germany, 1987, 87–114.
2. Szabady, B. The different modes of development. In *Planar Chromatography. A Retrospective View for the Third Millennium*; Nyiredy Sz., Ed.; Springer Scientific Publisher: Budapest, 2001, 88–99.
3. Martin, A.J.; Synge, R.L.M. A new form of chromatogram employing two liquid phases. Biochem. J. **1941**, *35*, 1358.
4. James A.T.; Martin A.J. Gas–liquid partition chromatography; the separation and micro-estimation of volatile fatty acids from formic acid to dodecanoic acid. Biochem. J. **1952**, *50*, 679.
5. Soczewiński, E.; Wachtmeister, C.A. The relation between the composition of certain ternary two-phase solvent systems and R_M values. J. Chromatogr. **1962**, *7*, 311.
6. Flieger, J.; Tatarczak, M. Effect of inorganic salts as mobile-phase additives on lipophilicity values determined by reversed-phase thin layer chromatography for new 1,2,4-triazole derivatives. J. Planar Chromatogr. -Mod. TLC **2006**, *19*, 386.
7. Djaković-Sekulić, T.; Perišić-Janjić, N.; Sârbu, C.; Lozanov-Crvenković, Z. Partial Least-Squares Study of the effects of organic modifier and physicochemical properties on the retention of some thiazoles. J. Planar Chromatogr. -Mod. TLC **2007**, *20* (4), 251.

Rotation Locular CCC

Kazufusa Shinomiya
College of Pharmacy, Nihon University, Chiba, Japan

INTRODUCTION

Rotation locular countercurrent chromatography (RLCCC) was introduced in the early 1970s[1,2] as a preparative CCC system. In general, the existing CCC systems may be classified into two groups according to the mode of solute partitioning. One is called the hydrostatic equilibrium system (HSES) and the other is called the hydrodynamic equilibrium system (HDES). RLCCC belongs to HSES as does droplet CCC, whereas the high-speed CCC is the most advanced form of HDES, which has been widely used for the separation and purification of natural products.

Although RLCCC is less efficient than high-speed CCC, in terms of resolution and separation times, it has advantages of a large-sample loading capacity and universal application of two-phase solvent systems. Retention of the stationary phase is accomplished simply by adjusting the column rotation speed and flow rate according to physical properties of the solvent system. In addition, RLCCC can be effectively performed with a short column by alternatingly eluting the column with the two solvent phases. This "alternating CCC" method[3,4,5,6] is described later in some detail.

Rotation locular countercurrent chromatography is particularly suitable for the preparative separation of natural products, and the apparatus is commercially available through Tokyo Rikakikai Co., Ltd., Tokyo, Japan.

APPARATUS

Rotation locular countercurrent chromatography uses a separation column containing a series of cylindrical partition units called "locules." This locular column is made by inserting multiple centrally perforated disks into a PTFE (polytetrafluoroethylene) or glass tubing at regular intervals. Multiple column units are connected in series with PTFE tubing and mounted in parallel around the rotary shaft of the apparatus. The column assembly is held at a constant angle from the horizontal plane and rotated at a moderate rate (60–80 rpm). Fig. 1 schematically illustrates the RLCCC apparatus. In each locule, the two phases form a horizontal interface and efficient stirring of each phase is produced by rotation of the column assembly. The system provides the choice of the mobile phase, where the upper phase is eluted in an ascending mode and the lower phase in a descending mode through the inclined column. The solutes present in the sample solution are subjected to an efficient partition process between the two phases, in each locule, and, finally, eluted according to their partition coefficients.

In the early prototype instrument,[1] the columns were fabricated from relatively large-bore PTFE tubing of 4.6 mm inner diameter (I.D.) with PTFE disk inserts having 0.8 mm-diameter holes. These disks were spaced in 3 mm intervals to form 47 locules in each unit. A number of column units were connected in series to provide 5000 locules with a total capacity of 100 ml. The capability of the system was demonstrated with the separation of DNP (dinitrophenyl)–amino acids using a two-phase solvent system composed of chloroform–acetic acid–0.1 *M* HCl at a 2:2:1 volume ratio. In this system, nine DNP–amino acids were resolved within 70 hr at about 3000 theoretical plates.

A commercial RLCCC instrument is equipped with a set of 16 locular column units of 16 mm I.D. and 61 cm in length, containing 37 locules in each unit. The column assembly consists of 592 locules with an 800 ml capacity. At a flow rate of 15–25 ml/hr, the system can yield 250–400 theoretical plates, which corresponds to 2.3–1.5 locules/plate.[7]

SEPARATION PROCEDURE

Each separation is initiated by filling the column with either the upper or lower phase of an equilibrated two-phase solvent system. In order to avoid trapping air bubbles in the column, the solvent should be introduced through the bottom of each column, which is kept in a vertical position. Then, the column assembly is tilted at a desired angle (25–30°) from the horizontal plane. After the sample solution is introduced into the column, the mobile phase is eluted from the column while the apparatus is rotated at a desired rate (60–80 rpm). In order to retain a large volume of the stationary phase, the lower phase is eluted downward from the upper terminus and the upper phase upward from the lower terminus of the column assembly. The effluent from the outlet of the column is continuously monitored with an ultraviolet (UV) monitor and collected into test tubes using a fraction collector.

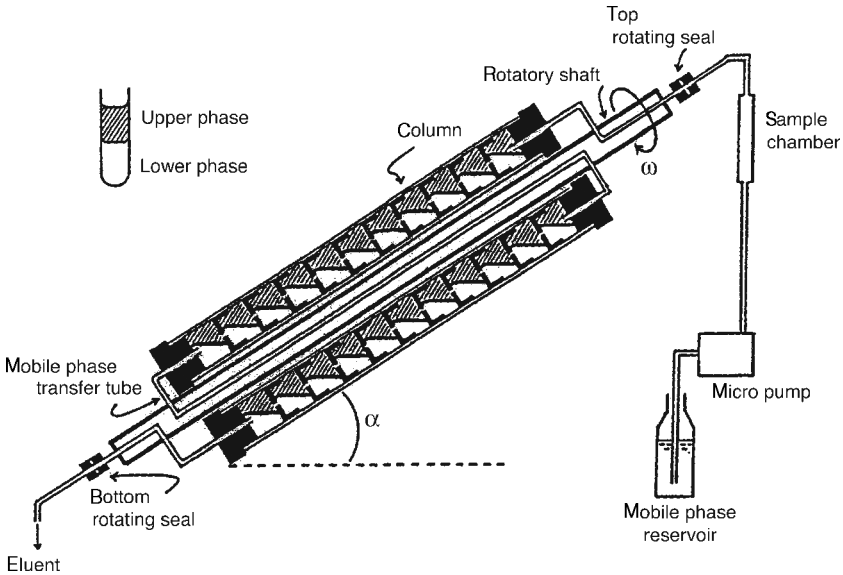

Fig. 1 Rotation locular countercurrent chromatography apparatus.

APPLICATIONS

Because the apparatus became commercially available in the late 1970s, RLCCC has been applied mainly to the preparative separation of natural products, due to its large sample loading capacity. As with other CCC systems, the partition efficiency of the RLCCC system highly depends on the choice of the suitable two-phase solvent system which gives a partition coefficient close to unity ($K \approx 1$) for the targeted compound. The K value can be obtained from a simple spectrophotometric measurement, thin layer chromatography (TLC), or high performance liquid chromatography (HPLC), whichever is appropriate.

SEPARATION OF NATURAL PRODUCTS

Two-phase solvent systems composed of chloroform–methanol–water at various volume ratios are frequently used for the separation of moderately hydrophobic compounds, including flavone aglycones, phenylpropanoids, iridoid glycosides, and so forth.[8]

The separation of more polar compounds, such as glycosides, can be achieved using a polar solvent system composed of ethyl acetate–water with a suitable modifier. Flavonoid glycosides were separated with ethyl acetate–1-propanol–water (2:1:2) and saponins with ethyl acetate–ethanol–water (2:1:2).

CHIRAL SEPARATION

The separation of (±)-norephedrine was first performed by RLCCC using a solvent system composed of 1,2-dichloroethane and 0.5 *M* aqueous sodium hexafluorophosphate (pH 4) containing chiral tartaric acid ester (dinon-5-yl tartrate).[9] This method produced an efficient resolution of enantiomers at purities of over 95% from 200 mg of racemate.

Rotation locular countercurrent chromatography can be applied to the chiral separation with an aqueous–aqueous polymer phase system using bovine serum albumin (BSA) as a chiral selector. In our laboratory, the RLCCC separation of D- and L-enantiomers of kynurenine was achieved from 200 mg of D,L-kynurenine using a solvent system composed of 10% (w/w) polyethylene glycol 8000 and 5% (w/w) disodium hydrogen phosphate containing 6% (w/w) BSA.[10] Because of a long settling time of the polymer phase system under unit gravity, the method required a discontinuous operation as used in the conventional countercurrent distribution apparatus, which consisted of 3 min for mixing, 10 min for settling, and 1 min for transfer of the mobile phase to the next locule at a flow rate of 1.0 ml/min. Using the lower mobile phase, L-kynurenine was eluted first, followed by D-kynurenine, and the separation was completed in 60 h.

ALTERNATING CCC METHOD

In this modified method, upper and lower phases are alternatingly used as the mobile phase by eluting the lower phase in the descending mode and the upper phase in the ascending mode through the respective terminus of a short locular column assembly.

Each separation is initiated by filling the entire column with the upper phase of the equilibrated two phase solvent system. Following the injection of the sample solution, the column is eluted with the lower phase while the apparatus is rotated at 60–70 rpm. After a desired period of elution, when the target compound is about to elute, the mobile phase is switched to the upper phase, which is eluted at the

same flow rate but in an ascending mode in the opposite direction. This alternating elution process with the upper and the lower phases is repeated until the desired component is well resolved.

In our laboratory, this method was applied to the purification of food mono-azo dyes.[3] Amaranth, New Coccine, and Sunset Yellow FCF were purified at 99.7%, 99.5%, and 99.3%, respectively, from 1–2.5 g of commercial dyes. Continued research has led to the purification of impurities present in commercial Sunset Yellow FCF that include RS-SA (trisodium salt of 3-hydroxy-4-[sulfophenyl] azo-2,7-naphthalene disulfonic acid), GS-SA (1-[4-sulfophenyl]azo)-2-naphthol-6,8-disulfonic acid), DONS (disodium salt of 6,6′-oxybis-2-naphthalene sulfonic acid), and 2N-SA (sodium salt of 4-[(2-hydroxy-1-naphthalenyl)azo]benzenesulfonic acid). The method successfully isolated GS-SA from Sunset Yellow FCF.[4,5,6]

REFERENCES

1. Ito, Y.; Bowman, R.L. Countercurrent chromatography – liquid-liquid partition chromatography without solid support. J. Chromatogr. Sci. **1970**, *8* (6), 315.
2. Ito, Y.; Bowman, R.L. Countercurrect chromatography. Anal. Chem. **1971**, *43* (13), 69A–75A.
3. Kabasawa, Y.; Tanimura, T.; Nakazawa, H.; Shinomiya, K. Application of counter alternative current chromatography to purification of food mono-azo dyes. Anal. Sci. **1992**, *8*, 351–353.
4. Ogura, N.; Nakamura, Y.; Shinomiya, K.; Kabasawa, Y. Separation of impurities in commercial food yellow no. 5 by counter alternative current chromatography and structural analyses. Anal. Sci. **1995**, *11*, 759–763.
5. Snyder, J.K.; Nakanishi, K.; Hostettmann, K.; Hostettmann, M. Applications of rotation locular countercurrent chromatography in natural products isolation. J. Liq. Chromatogr. **1984**, *7*, 243–256.
6. Kubo, I.; Marshall, G.T.; Hanke, F.J. *Countercurrent Chromatography: Theory and Practice*; Mandava, N.B., Ito, Y., Eds.; Marcel Dekker, Inc.: New York, 1988; 493–507.
7. Conway, W.D. *Countercurrent Chromatography: Apparatus, Theory, and Applications*; VCH: New York, 1990.
8. Hostettmann, K.; Hostettmann, M.; Marston, A. *Preparative Chromatography Techniques: Applications in Natural Product Isolation*; Springer-Verlag: Berlin, 1986.
9. Domon, B.; Hostettmann, K.; Kovacevic, K.; Prelog, V. Separation of the enantiomers of (±)-norephedrine by rotation locular counter-current chromatography. J. Chromatogr. **1982**, *250*, 149–151.
10. Sato, Y.; Shinomiya, K.; Kabasawa, Y. Aqueous two-phase partitioning method by using rotation locular countercurrent chromatograph-an application to enantiomeric separation. J. Chem. Soc. Japan **1994**, 1067–1071.

Sample Application in TLC

Joseph Sherma
Department of Chemistry, Lafayette College, Easton, Pennsylvania, U.S.A.

INTRODUCTION

This entry describes the general considerations, procedures, and instruments that are important for the correct application of sample and standard zones in thin-layer chromatography (TLC) and high-performance TLC (HPTLC). The application of spots and bands manually and by semiautomated and completely automated instrumental techniques is covered.

GENERAL ASPECTS

Application of small, homogeneous, exactly positioned initial zones of sample and standard solutions having accurate and precise volumes, without damaging the layer surface, is critical for achieving maximum resolution and reliable qualitative and quantitative analysis in TLC and HPTLC. The volumes applied and the method of application depend on the type of analysis to be performed (qualitative or quantitative), the kind of layer used, and the detection limit.

Choice of the Application Solvent

The choice of the solvent for applying standard and sample zones depends mainly on its ability to completely dissolve the analyte(s). Another factor in the choice of the solvent is safety; for example, benzene and chlorinated hydrocarbons should be avoided, if possible. After considering solubility and safety, the chosen solvent should have low viscosity and sufficient volatility to allow complete evaporation from the layer before mobile phase development; it should be as low in chromatographic solvent strength as possible to retard the possibility of "prechromatography" during application, that will increase the developed zone size, and it should wet the layer to provide adequate penetration of the layer by the sample (a problem mostly for non-polar chemically bonded layers and aqueous sample solutions). Weak strength is provided by non-polar solvents for normal phase layers such as silica gel and polar solvents for reversed phase layers such as C_{18} chemically bonded silica gel.

Pretreatment of Samples Prior to Application

Cleanup of samples is not as critical for TLC as it is for column chromatography because plates are not reused. Simple dissolving or liquid–liquid extraction with immiscible solvents and pH control is often sufficient. For more complex samples, cleanup of extracts by column adsorption chromatography or a more modern method such as solid phase extraction, supercritical fluid extraction, or solid phase microextraction is usually applied. Cleanup is not as important in TLC because strongly sorbed matrix components that could irreversibly destroy a high-performance liquid chromatography column or carryover and be detected in later samples can be applied onto the plate if the subsequent development and detection of the analyte are not adversely affected.

Characteristics and Placement of Initial Zones

For high efficiency and resolution of analytes during mobile phase development, initial zone size in the direction of development for round spots should be no greater than 2–6 mm for TLC and 1–2 mm for HPTLC. Volumes leading to these sizes are typically 0.5–5 μl for TLC and 0.1–1 μl for HPTLC; larger volumes of low concentration standards or analytes can be used when applying bands manually using a plate with a preadsorbent zone. The origin line is usually located 1.5–2.5 cm from the bottom of TLC plates, or 1.0 cm for HPTLC plates. The location of the starting point can be marked with a soft pencil on the right and left edges of the plate to aid lineup of the initial zones; more helpful is the use of a commercial application template to guide initial zone positioning in a straight horizontal line, with correct spacing between samples (usually 15 mm for TLC or 5 mm for HPTLC).

In most TLC and HPTLC analyses reported in the literature, no special sequence is stated for location of the initial zones of the standards and unknown samples along the origin line. For example, methods for semiquantitative TLC estimation of drug impurities are contained in various pharmacopeias; it is typically stated that visual comparison should be made of simultaneously chromatographed sample and standard spot intensities, but no special initial zone application locations are suggested.

For quantitative analysis, a special positioning scheme for manual or automatic application called the "data pair method" has often been recommended for reducing systematic errors owing to chromatographic parameters and obtaining the best densitometric results. In this method, all solutions are applied twice, with

duplicates not placed next to each other, but separated by one-half the width of the plate.

Application of Standard Solutions for Quantitative Analysis

It is often stated that it is best to apply samples and standards in the same volume and same solvent to form identical initial zones. This would require applying a fixed volume of a series of standard solutions with increasing concentrations to prepare a calibration graph for quantitative analysis. It is more convenient to apply variable volumes from a single standard solution for calibration, and appropriate volumes of samples to obtain scan areas bracketed within the calibration graph. Accurate and precise results can be obtained with this latter approach by use of the spray-on band application instruments (see the following) or manual application to preadsorbent plates.

Drying the Applied Samples Before Plate Development

The solvent used in sample application must be completely removed before the development stage. This step is carried out with or without heating, depending on the volatility of the sample solvent and the volatilities and thermal stabilities of the analytes. Plates are often dried at room temperature in a horizontal position inside fume hood; a stream of air or nitrogen may be passed over the layer to hasten evaporation. If heat is required, a hair dryer or other type of blower, laboratory oven, or plate heater (Camag Scientific, Inc., Wilmington, Delaware, U.S.A.) is used.

MANUAL INITIAL ZONE APPLICATION

Fully manual application of samples as spots is carried out using disposable fixed volume glass microcapillary pipets, or adjustable volume microdispensers with disposable glass capillaries. Respective examples of these are Drummond (Broomall, Pennsylvania, U.S.A.), Microcaps, which empty by capillary action when touched gently to the layer surface, and Digital Microdispensers, which empty when the plunger is pushed. It is best to keep the capillary tip at a 90° angle to the plate during use. Manual application is used to apply spots directly to the layer or for applying solution aliquots to a preadsorbent for formation of bands. Microcaps are handled in a simple rubber holder similar to the top of an eyedropper; volumes applied are usually 0.5–10 μl, and accuracy of better than 1% can be obtained. Spot size for larger volumes is minimized by applying the sample in small increments on top of each other with complete drying of the solvent after each application, e.g., 20 μl applied in four 5 μl portions; this technique improves resolution, but requires additional time and increases the chances for layer damage. The glass capillaries can be reused without fear of cross-contamination if thorough washing with solvent and next solution is carried out; disposal of the capillaries between different samples is most convenient. Capillaries tend not to fill reproducibly when dipped into certain types of sample solutions [i.e., solvents with high density (e.g., chloroform) or low capillary forces (e.g., hexane); surfactant solutions or viscous liquids] and, in these cases, the use of a syringe type applicator is preferable.

TLC and HPTLC plates with a preadsorbent zone on the bottom simplify and improve manual sample application, especially for larger volumes and crude samples (e.g., biological fluids). Solutions are applied quickly and diffusely to the preadsorbent and are automatically focused into narrow band-shaped initially at the preadsorbent–separation sorbent interface during mobile phase development; this interface serves as the starting point (origin) for calculation of the R_f values of developed zones. The preadsorbent, which is composed of diatomaceous earth or large pore volume silica gel, does not retain or resolve the analytes in samples, but may retain some matrix components to simplify sample pretreatment. Use of preadsorbent plates with lanes or channels facilitates proper positioning of the initial zones and lineup of the measuring slit of a densitometer when scanning chromatograms on the developed plate. Samples are applied as a streak or series of spots down the middle of the preadsorbent area, starting 2 mm below the layer interface, about 5 mm up from the bottom of the plate so that the origin line does not extend into the mobile phase pool in the development chamber, which is normally about 3 mm deep. Large-pore volume silica gel concentrating zones (e.g., on plates from EMD Chemicals, an affiliate of Merck KGaA, Darmstadt, Germany) are thinner and will not tolerate as much applied sample (i.e., they have less sample capacity) compared to diatomaceous earth preadsorbent zones on plates from, e.g., Whatman Inc. (Clifton, New Jersey, U.S.A.) and Analtech Inc. (Newark, Delaware, U.S.A.).

In addition to the use of disposable pipets for manual application, some workers apply samples for HPTLC quantitative determinations by hand in 50–200 nl volumes, using either an adjustable microliter syringe (>50 μl) or fixed-volume platinum–iridium capillary (200 nl) fused into a glass tube. Because these devices are reused, they must be fully rinsed between solutions to eliminate any possible "memory effect" from previous solutions.

INSTRUMENTAL INITIAL ZONE APPLICATION

This section describes a limited selection of available sample application instruments having different degrees of automation. These instruments are representative of others that are commercially available.

Fig. 1 Camag Nanomat 4. The applicator head with attached capillary pipet is lowered onto the layer at the selected position. The capillary touches the layer with constant pressure, which is determined solely by the friction of rest against a permanent magnet. **Source:** Courtesy of Camag.

Camag Nanomat

For TLC or HPTLC, initial zones in the form of spots can be applied from a disposable 0.5, 1, 2, or 5 μl fixed-volume, self-loading glass capillary pipet held in a rocker-type spotting device (the Nanomat 4, Camag) (Fig. 1) that mechanically controls its positioning and brings the capillary tip in gentle and uniform contact with the layer to discharge the solution without damage to the layer. This instrument is relatively of low cost and requires manual filling of the selected capillary held in a holder, placement of the holder on the applicator head, movement to the correct layer positions using a click-stop grid mechanism, and lowering and lifting of the head via a spring mechanism to apply the sample.

Analtech AutoSpotter

The Analtech TLC AutoSpotter (Fig. 2) is a semiautomated device with which up to 18 samples can be applied at one time in the form of spots as the drive bar moves to depress the syringe plungers and dispel the sample solutions. The unit has custom-made syringes with blunt Teflon-tipped needles that minimize sample "creep back" and increase reproducibility. Teflon plunger tips eliminate possible metal-to-glass contamination. Syringes are available in 10, 25, 50, 100, and 250 μl volumes. Samples can be applied at variable rates ranging from 3–30 min, depending on the chosen drive bar speed. An integral heater strip runs beneath the TLC plate at the point of delivery to aid solvent evaporation. The strip temperature and delivery rate are adjustable to give the smallest possible sample zone sizes. Features include digital temperature readout, adjustable needle guide, and alternative syringe templates for use with scored and channeled plates.

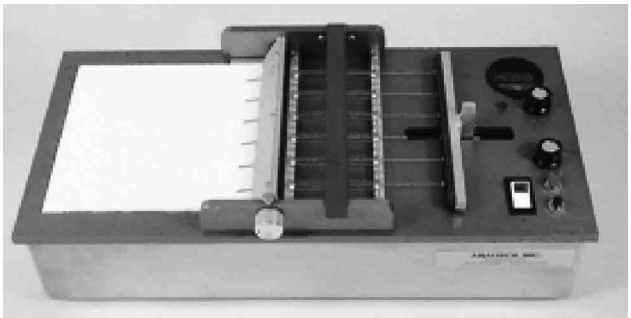

Fig. 2 TLC autospotter.
Source: Courtesy of Analtech.

Desaga TLC Spotter PS 01

The semiautomatic PS 01 from Desaga GmbH (Wiesloch, Germany) applies 10 nl to 10 μl samples to TLC and HPTLC plates as spots for quantitative analysis. Positions of application can be 5, 6, 10, 12, or 15 mm apart and 15 mm from the bottom of TLC plates or 5 mm with HPTLC plates. Solution discharge rate is 100 nl/sec for the 1 μl syringe, or 15 nl/sec using the "L" function. Filling, emptying, and rinsing of the syringe are performed by pressing the appropriate keys on the control panel.

Camag Linomat

Sample application in the form of bands is advantageous for high-resolution separations of complex or multicomponent samples, improved detection limits, and accurate and precise quantitative scanning densitometry. However, fewer samples can be applied per plate in the form of bands, compared to spots. Scanning of bands is done using the aliquot technique, in which the light source measuring slit is set to cover the center 50–75% length of the applied band, or a slit length that covers the entire sample band length can be used; samples applied as spots must be scanned with a slit covering the entire zone.

Narrow, homogeneous sample bands of controlled length [1 mm (spot) to 195 mm] can be applied by use of a semiautomatic spray-on device (the Camag Linomat 5, Fig. 3), in which the plate is mechanically moved right to left in the X-direction beneath a fixed syringe from which 0.1–2000 μl of sample is sprayed by an atomizer operating with a controlled nitrogen gas pressure. The optimum distance of the syringe needle from the precoated layer is usually 1 mm. The rate of application is adjustable to accommodate sample solutions with different volatilities and viscosities. Typical band lengths are 4–10 mm for analytical work and longer bands for preparative-scale separations.

The user fills the syringe with the sample, places the syringe into the instrument, and selects the sample volumes and Y-position via a keypad or by downloading a method from a personal computer (PC). The instrument exactly

Fig. 3 Linomat 5.
Source: Courtesy of Camag.

positions the initial zones, which facilitates automated scanning after chromatogram development. Operation can be in a stand-alone mode or under the control of winCATS software. In the stand-alone mode, up to 10 application methods can be downloaded and stored locally. With the correct choice of application parameters, less volatile and higher strength sample solvents can be tolerated without forming broadened initial zones. The ability to apply larger volumes to an HPTLC plate without loss of resolution lowers the determination limits with respect to the concentration of the solution, which aids in trace analysis. Complex, impure samples can often be successfully quantified only if bands are applied rather than spots.

Camag Automatic TLC Sampler 4

The Camag Automatic TLC Sampler 4 (ATS 4) is an advanced, fully automated, PC-controlled device for sequential application of up to 66 samples from a rack of 2 ml septum-covered vials or 96 samples from well plates (15 05 45 mm height) as spots by contact transfer (0.1–5 μl) or as bands by the spray-on technique (0.5–>50 μl); a motor driven dosing syringe sucks up the sample volume and feeds a steel capillary connected to a capillary atomizer. The speed, volume, and X- and Y-position pattern of application are controllable, and a programmable rinse cycle between the applications can eliminate cross-contamination.

Spraying in the form of rectangles enables application of larger volumes of low concentration samples, or use of higher delivery speeds, without washing away the layer. The spray jet moves back and forth in the Y-direction over the plate, which moves left to right in the X-direction; the sample is applied in a zigzag pattern within a rectangle. Before chromatography, the rectangles are focused into narrow bands by predevelopment with a strong mobile phase. An optional heated spray nozzle allows increased application speed, which is important for aqueous solutions.

Overspotting can be performed (also with the Linomat), in which more than one sample can be applied to a single initial zone position. These samples can include multiple standard reference compounds from different vials to prepare an in situ mixture, sample plus spiking solution, for validation of quantitative analysis by the standard addition method, or sample plus reagent, for in situ prechromatographic derivatization.

Samples applied with the ATS 4 can be positioned for normal, double-sided, or circular chromatographic development. Analyses performed with this applicator, combined with densitometric chromatogram evaluation controlled by the same PC with Windows-based WinCats software, comply with good manufacturing practices/good lab practices (GMP/GLP), installation qualification (IQ)/operational qualification (OQ), and 21 Code of Federal Regulations (CFR) Part 11 (drug analysis) requirements.

Desaga AS30

The AS30 (Desaga) is another software controlled, fully automated band or spot applicator that also works according to a spray-on technique, in which a stream of gas carries the sample from the cannula tip onto the plate. The syringe does not have to be manually filled by the user, as with the Linomat. During the filling process, the dosing syringe is positioned over the tray, which collects rinsing and flushing solvent and excess sample. The sample is injected into the body of the syringe through a lateral opening. After the syringe has been filled, a stepping motor moves the piston downwards to dose the fillport. A second stepping motor moves the tower sideways across the plate. The microprocessor controls both the motors and the gas valve for accurate and precise application in the form of spots or bands, both without layer contact. All parameters for application of up to 30 samples are entered via the keyboard. The user is guided through the clearly structured menu by the two-line LCD display.

Analtech Sample Streaker

The TLC Sample Streaker from Analtech (Fig. 4) is a manual device used to apply large volumes of solution to preparative-layer chromatography (PLC) plates. For PLC, large-volume initial zones are applied in the form of a continuous band across the layer, and this is accomplished with the sample streaker by the mechanical action of

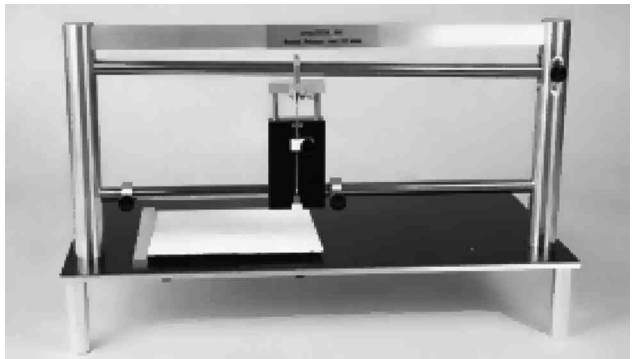

Fig. 4 TLC sample streaker.
Source: Courtesy of Analtech.

pushing the syringe (optional 250 or 500 μl volume) downward as it moves across the sloping stainless steel bar. A 1 mm wide band of sample can be applied to a PLC plate up to 40 cm wide. The device is faster and will apply the sample in a straighter, more homogeneous band than is possible with hand spotting, and the adsorbent will not be scratched during operation.

CONCLUSIONS

The principles, procedures, and instrumentation for application of sample and standard zones in TLC and HPTLC have been described briefly. A reading list is included, which contains references from which more details can be obtained. By using these techniques, the highest quality results possible for qualitative, semiquantitative, and quantitative results will be obtained.

BIBLIOGRAPHY

1. Bethke, H.; Santi, W.; Frei, R.W. Data-pair technique, a new approach to quantitative thin layer chromatography. J. Chromatogr. Sci. **1974**, *12* (7), 392–397.
2. Fried, B.; Sherma, J. *Thin Layer Chromatography-Techniques and Applications*, 4th Ed.; Marcel Dekker, Inc.: New York, NY, 1999; 77–87.
3. Hahn-Deinstrop, E. *Applied Thin Layer Chromatography*; Wiley-VCH: New York, 2000; 48–66.
4. Omori, T. Modern sample application methods. In *Planar Chromatography*; Nyiredy, Sz., Ed.; Springer Scientific Publisher: Budapest, Hungary, 2001; 120–136.
5. Poole, C.F. *The Essence of Chromatography*; Elsevier Science B.V.: Amsterdam, The Netherlands, 2003; 499–567.
6. Reich, E. Instrumental thin layer chromatography (planar chromatography). In *Handbook of Thin Layer Chromatography*, 3rd Ed.; Sherma, J., Fried, B., Eds.; Marcel Dekker, Inc.: New York, 2003; 135–151.

Sample Injectors with Mobile Parts for GC

Piotr Słomkiewicz
Zygfryd Witkiewicz
Institute of Chemistry, Jan Kochanowski University, Kielce, Poland

INTRODUCTION

Regardless of the state of matter of the separated mixture, a technique used for introduction of samples into the gas chromatograph has to meet certain criteria, mostly mutually excluding ones. A sample of the possibly lowest volume should be introduced into the chromatographic column to ensure preservation of the internal state of equilibrium. Small sample volume requires application of a high-sensitivity detector and can make interpretation of the chromatographic results difficult, owing to a high level of detector noise. Those contradictory requirements are especially clear in case of chromatographic analyses of environmental samples obtained by extraction with a solvent. In this kind of samples, the substances assayed, also solid ones, can be dissolved in a relatively large amount of a solvent, presenting certain troubles for the analysis, especially using capillary columns. There are methods of dosing of this kind of samples. The methods allow evaporation of excess solvent from the sample. Among others, injectors with mobile parts are designed for this purpose. Possibility of sample concentration through solvent evaporation realized before the sample being introduced into the column is a characteristic feature of those injectors. Principle of those injectors consists of application of diluted sample onto a mobile part of the injector and evaporation of solvent in proper temperature. The solvent is then evacuated with a carrier gas, the mobile element with concentrated sample is transferred to the inlet of a chromatographic column and finally the analytes are introduced into the column.

INJECTOR WITH A MOBILE NEEDLE

Injector with a mobile needle[1,2] is usually utilized for analysis of not highly volatile, mostly solid substances (Fig. 1). It has a form of a glass tube 1 with a glass (or other, e.g., quartz) needle 2 tipped with a steel core 3 placed inside. The needle can be moved with a magnet 4 located on an external wall of the tube. Carrier gas is fed through the inlet 5 into the injector. The gas is either directed into the capillary column, or can be released to the atmosphere through the valve 6 located in the upper part of the tube. Introduction of a sample into the capillary column is realized in the following way: sample-containing needle of a micro-syringe is pierced through a membrane 9 located on the side of the injector and applies the sample of analyzed substances onto the tip of the elevated needle of the injector. The valve 6 is opened and solvent evaporates from the tip of the needle. Solvent vapors and the carrier gas are released through the outlet 7. After the solvent is completely evaporated, the valve 6 is closed, needle 2 lowered into the heated inlet of the column, and sample components are evaporated into the column.

There are some drawbacks connected with the glass injector with mobile needle. They are: complicated service requiring several manipulations while injecting the sample, and difficult application of the sample with a micro-syringe onto the tip of the injector needle; small mechanical resistance of the glass structure, and application of a single stream of carrier gas for feeding the capillary column and for removal of solvent vapors from the injector. Application of a single stream causes that the carrier gas does not flow through the column when vapors are being evacuated, or the flow becomes very limited. This changes column work conditions and interferes with operation of the detector.

TWIN-CHAMBER NEEDLE INJECTOR

Drawbacks of the glass injector with a mobile needle were removed with the twin-chamber needle injector.[3] A set of improvements has been made in this injector. They are easier application of samples with a micro-syringe onto the tip of the injector needle, two independent gas paths utilized: carrier gas for feeding the capillary column and carrier gas for removal of solvent vapors from the needle. Time required for evaporation of solvent from the sample applied onto the needle and the time of analytes evaporation are reduced by usage of two heated chambers.

Fig. 2 shows a scheme of a twin-chamber injector with a needle, during the sample introduction. In this injector, the needle is tipped with sintered quartz 1 in the bottom, and with a steel core 2 in the top. The needle can be moved with a magnet 3 in a quartz tube 4. The tube is fixed with two housings: lower 5 and upper 6, made of acid-resistant steel.

The needle can be introduced into the quartz tube of the injector through a ball valve 7 located in the upper housing. When the needle is lifted, its tip remains in the

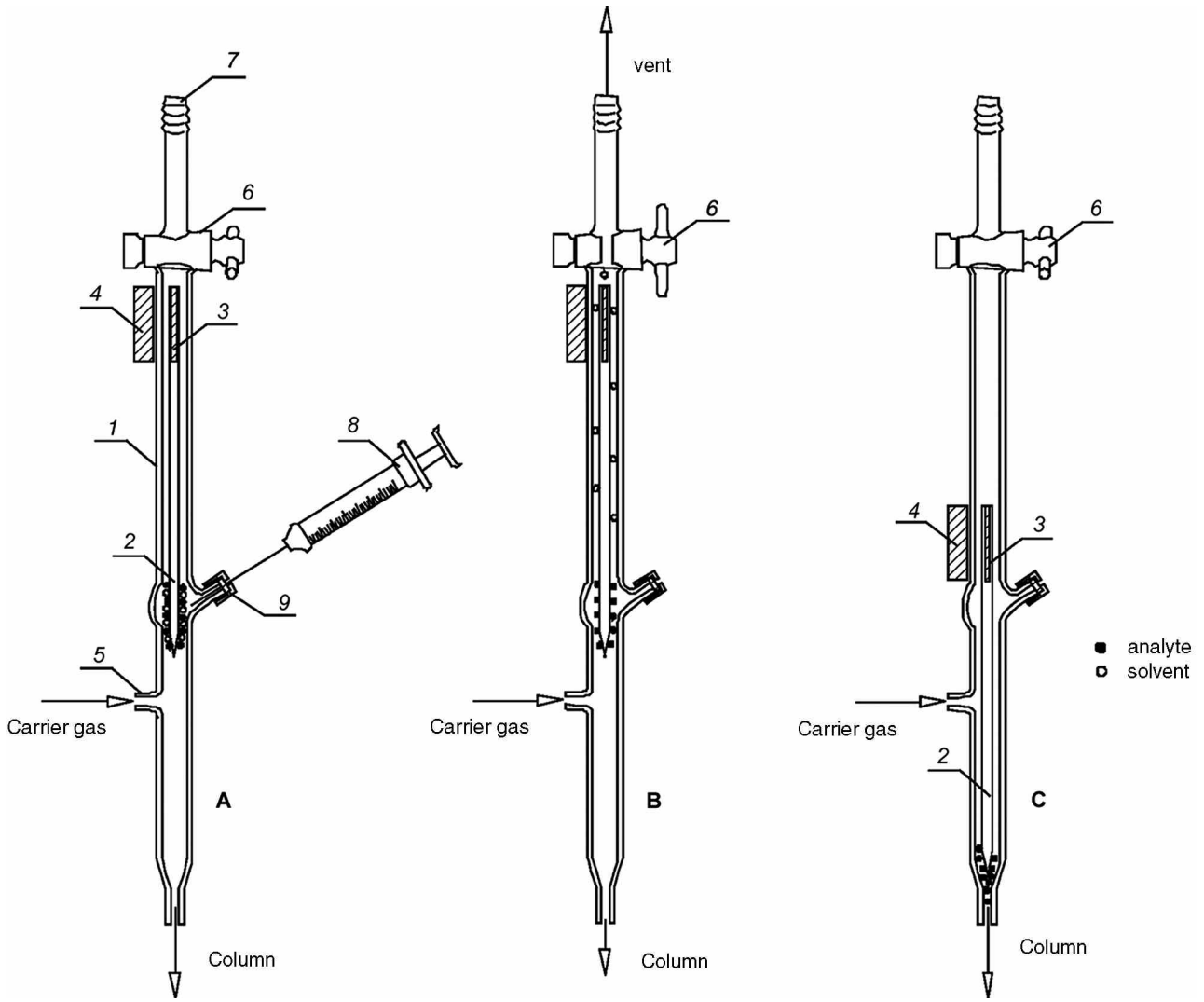

Fig. 1 Diagram of the injector with a mobile needle. 1 – glass tube, 2 – needle, 3 – steel core, 4 – magnet, 5 – carrier gas inlet, 6 – valve, 7 – carrier gas outlet, 8 – micro-syringe, 9 – membrane. Position: A, sample injecting; B, solvent evaporation; and C, analyte injecting into the chromatographic column.

injecting cylinder 8 within the lower housing. The injecting cylinder 8 has glass windows through which application of sample with a micro-syringe onto the sintered tip of the needle can be watched. To make this operation easier, there is an eyepiece with magnifying lens located in front of the front window, and a matt plate is located behind the back window. Below the injecting cylinder 8, there is a heated chamber 9, connected with the injecting cylinder 8 with a ball valve 10. The lower part of the injector is the heated chamber 11, separated from the chamber 9 by a ball valve 12. Chambers 9 and 11 are heated with electric heaters 13 and 14. Constant or variable temperature can be maintained inside the chambers. This is especially true for the chamber 11, in which analytes can be gradually evaporated from the sintered tip of the needle, in order to achieve better separation. Radiators 15, 16, and 17 protect the lower part of the injector and the ball valves 10 and 12 against excessive heat.

The needle with deposited sample is introduced into the heated chamber 9, where solvent evaporates. Then, the needle is transferred into the chamber 11, where temperature is higher, and where the sample becomes evaporated. The sample is thus introduced into the chromatographic column.

Carrier gas and auxiliary gas is supplied to the injector. Carrier gas is separated into two streams. The first stream feeds the chromatographic column. Flow of this stream is turned on with a solenoid valve 19 and the gas flows through the inlet 20 and the chamber 11 to the port 21 of the chromatographic column.

The other stream of carrier gas serves for feeding the chromatographic column when the ball valve 12 is open. In this case, the flow of carrier gas is turned on by the solenoid

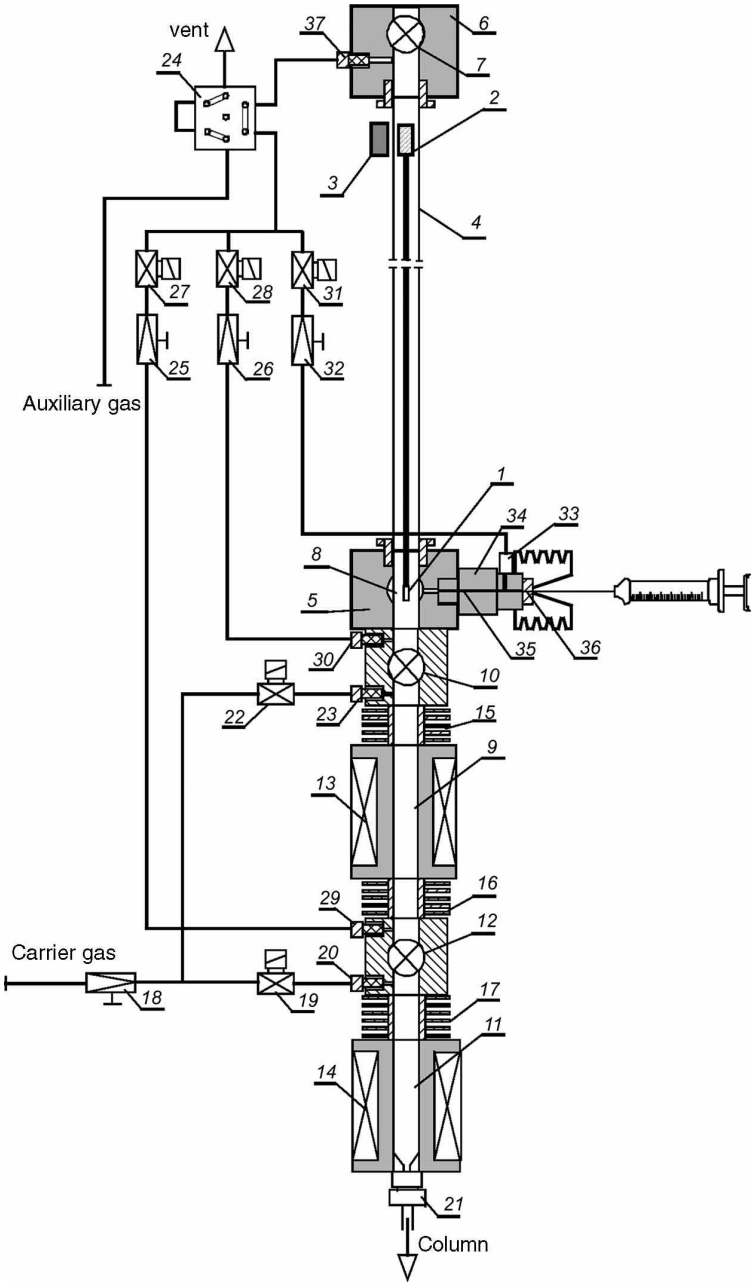

Fig. 2 Diagram of the twin-chamber injector with a needle in position of sample application. 1 – quartz sinter, 2 – steel core, 3 – magnet, 4 – quartz tube, 5, 6 – lower and upper housing, 7, 10, 12 – ball valve, 8 – injecting cylinder, 9 – solvent evaporating chamber, 11 – analyte evaporating chamber, 13, 14 – electric heater, 15, 16, 17 – radiator, 18, 25, 26, 32 – needle valve, 19, 27, 28, 31 – solenoid valve, 20, 23 – carrier gas inlet, 21 – chromatographic column port, 24 – six-way valve, 29, 30, 33 – auxiliary gas inlet, 34 – connector pipe for sample introduction, 35 – micro-syringe needle channel, 36 – membrane, 37 – auxiliary gas outlet.

valve 22 and the gas flows through the inlet 23, chamber 9 and chamber 11 to the port 21 of the chromatographic column.

An auxiliary gas stream is used for evaporation of solvent from the sample applied onto the sintered tip of the needle. The gas flows through the six-way valve 24 to two needle valves 25 and 26, operated by solenoid valves 27 and 28. Part of the auxiliary stream flows through the inlet 29 into the chamber 9.

To evaporate solvent from the sample applied onto the sintered tip of the needle (Fig. 3), flow of the auxiliary gas through the injector is opened by the solenoid valve 27. The stream of gas flows through the inlet 29 into the chamber 9. After the ball valve 10 is opened, the needle of the injector is descended into the chamber 9, where solvent evaporates fast from the sample. Simultaneously, carrier gas flows through the solenoid valve 22 (the solenoid valve 19 is closed).

It is also possible to evaporate solvent from the sample applied onto the needle in the injecting cylinder 8 without descending the needle of the injector into the chamber 9 (Fig. 2). This procedure is possible in the case of solvents characterized with low heat of vaporization. In this case, auxiliary gas flows through the inlet 30 over the ball valve

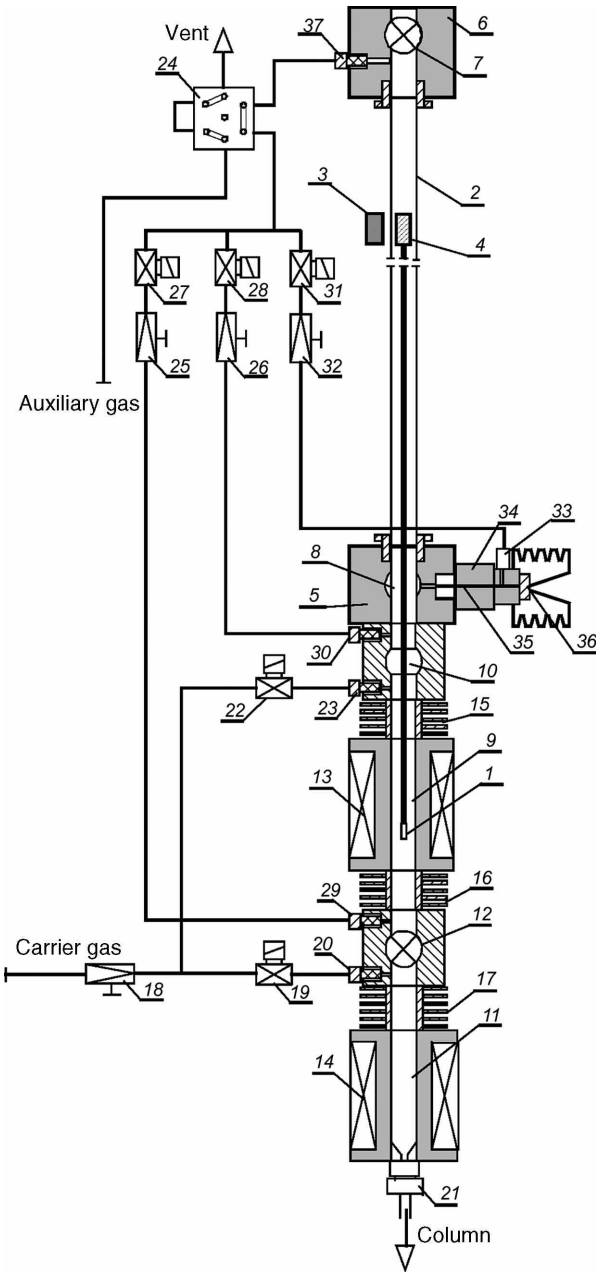

Fig. 3 Diagram of the twin-chamber injector with a needle in position of sample evaporation from the needle inside the first chamber (denotation, as for Fig. 2).

10. Part of the stream, through the solenoid valve 31 and the needle valve 32 is carried to the outlet 33 of the sample connector pipe 34, to wash the channel inside the microsyringe needle 35 and remove possible trace residues of the sample.

Both parts of the auxiliary gas stream unite in the injecting cylinder 8, from which, through the quartz tube 3, they are carried away to the outside of the injector, along with the solvent vapors, through the outlet 37 and the six-way valve 24.

After solvent becomes evaporated, the sample is introduced into the column. The ball valve 12 separates the path of carrier gas introduced into the column from the path of auxiliary gas, and simultaneously protects inlet of the capillary column against accidental drip of the applied sample from the sintered tip of the needle, which could potentially overload the column and would result in necessity of its time-consuming cleaning. After the ball valve 12 is opened, the needle can be descended (Fig. 4) into the chamber 11 and evaporate analytes from the sintered tip, introducing

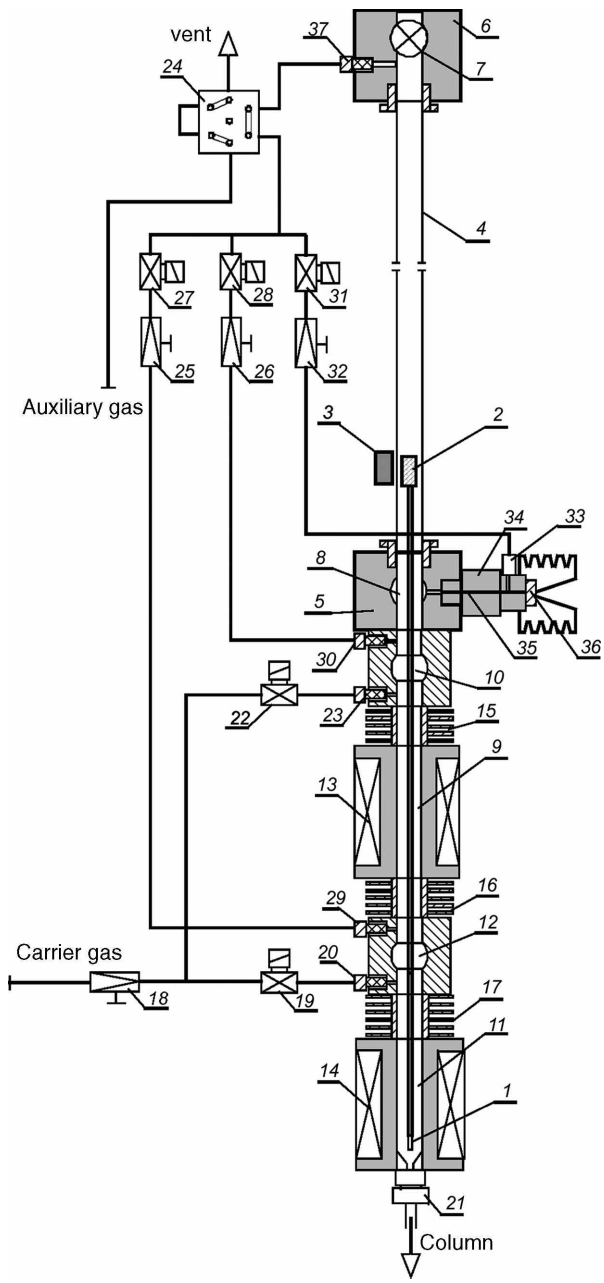

Fig. 4 Diagram of the twin-chamber injector with a needle in position of sample evaporation from the needle inside the second chamber (denotation, as for Fig. 2).

Table 1 Diagram of the needle and valve arrangements during various work positions of the twin-chamber injector, Figs. 2–4.

						Solenoid valve position (valve no.)				
			Ball valve position (valve no.)			Path of carrier gas		Path of auxiliary gas		
No.	Function	Needle position	10	12	Auxiliary gas	19	22	27	28	31
1	Sample application onto a needle	Injecting cylinder	C	C	Connected	O	C	C	O	O
2	Removal of a low-evaporation heat solvent from the needle	Injecting cylinder	C	C	Connected	O	C	C	O	O
3	Removal of a high-evaporation heat solvent from the needle	Chamber 9	O	C	Connected	O	C	C	C	O
4	Introduction of a sample part	Chamber 11	O	O	Disconnected	O	C	C	C	C

(O – open, C – closed).

them into the chromatographic column. After the injection is over, the needle is elevated, the ball valve 12 is closed, and solenoid valve 19 is opened (the solenoid valve 22 is closed). A list of valve positions during various injector work arrangements is presented in Table 1.

CHROMATOGRAPHIC INJECTOR WITH A MOBILE CONTAINER

An injector with a mobile needle can be improved by replacing the needle with a mobile container for the sample.[4] Compared with the previously described injectors equipped with needles, larger volumes of sample can be introduced into the container. After introducing the sample, the container can be placed in the stream of carrier gas inside a heated chamber. When solvent is evaporated, components of the sample can be transferred from the container into the chromatographic column.

Injector container (Fig. 5) is a quartz tube 1 with a quartz sinter 2 placed inside. There is a packing 3 (glass wool or glass granules) inside the tube. Sample is applied onto that packing. Using the micro-syringe, the sample can be introduced into the container through the openings 4 in its wall. A magnet 5 is located on top of the container.

The container can be moved in the injector tube 7 with a magnet (Fig. 6). For this purpose, a mobile mandrel 6 tipped with steel cores on both ends is used. The tube 7 is fixed in two housings: lower 9 and upper 10, made of acid-resistant steel. The container 1 and the mobile mandrel 6 can be placed inside the quartz tube of the injector after opening the ball valve 11 located within the upper housing 10.

When the injector container is lifted, its side openings 4 (Fig. 5) remain in the injecting cylinder 12 within the lower housing. The cylinder has glass windows through which application of sample with a micro-syringe onto the filling of the container can be watched. To make this

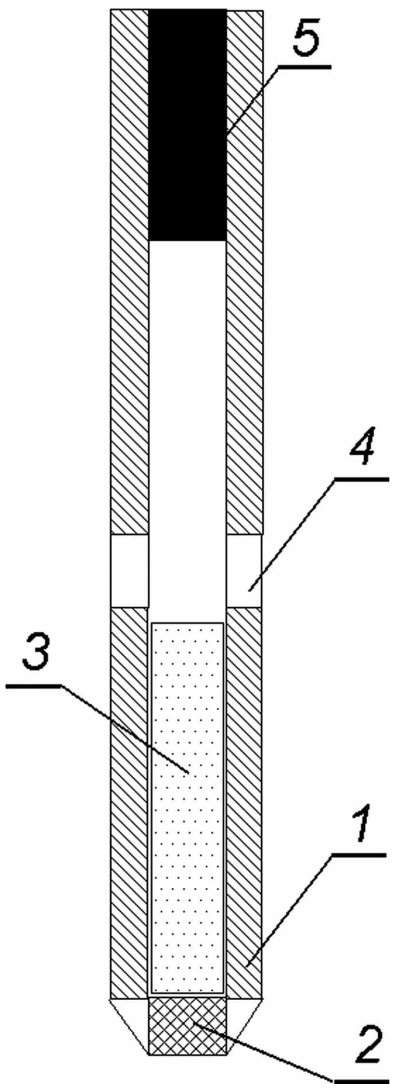

Fig. 5 Diagram of the longitudinal section of the container: 1 – quartz tube, 2 – quartz sinter, 3 – filling, 4 – openings, 5 – fixed magnet.

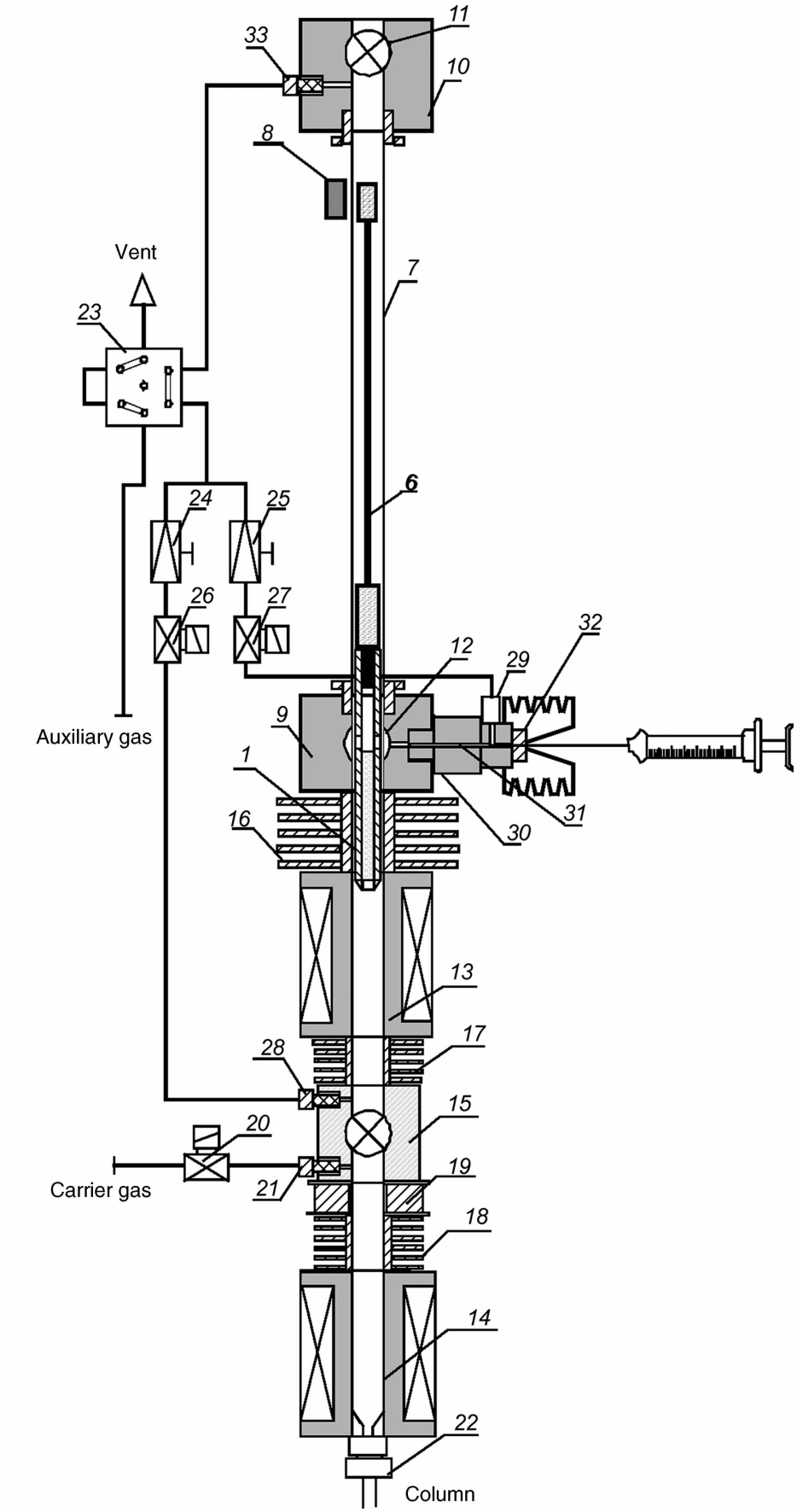

Fig. 6 Diagram of the injector with a mobile container in position for application of a sample with a micro-syringe. 1 – container, 6 – mandrel, 7 – quartz tube, 8 – magnet, 9 – lower housing, 10 – upper housing, 11, 15 – ball valve, 12 – injecting chamber, 13, 14 – electrically heated chamber, 16, 17, 18 – radiator, 19 – solenoid, 20, 26, 27 – solenoid valve, 21 – carrier gas inlet, 22 – chromatographic column port, 23 – six-way valve, 24, 25 – needle valve, 28, 29 – auxiliary gas inlet, 30 – connecting pipe for sample introduction, 31 – micro-syringe needle channel, 32 – membrane, 33 – auxiliary gas outlet.

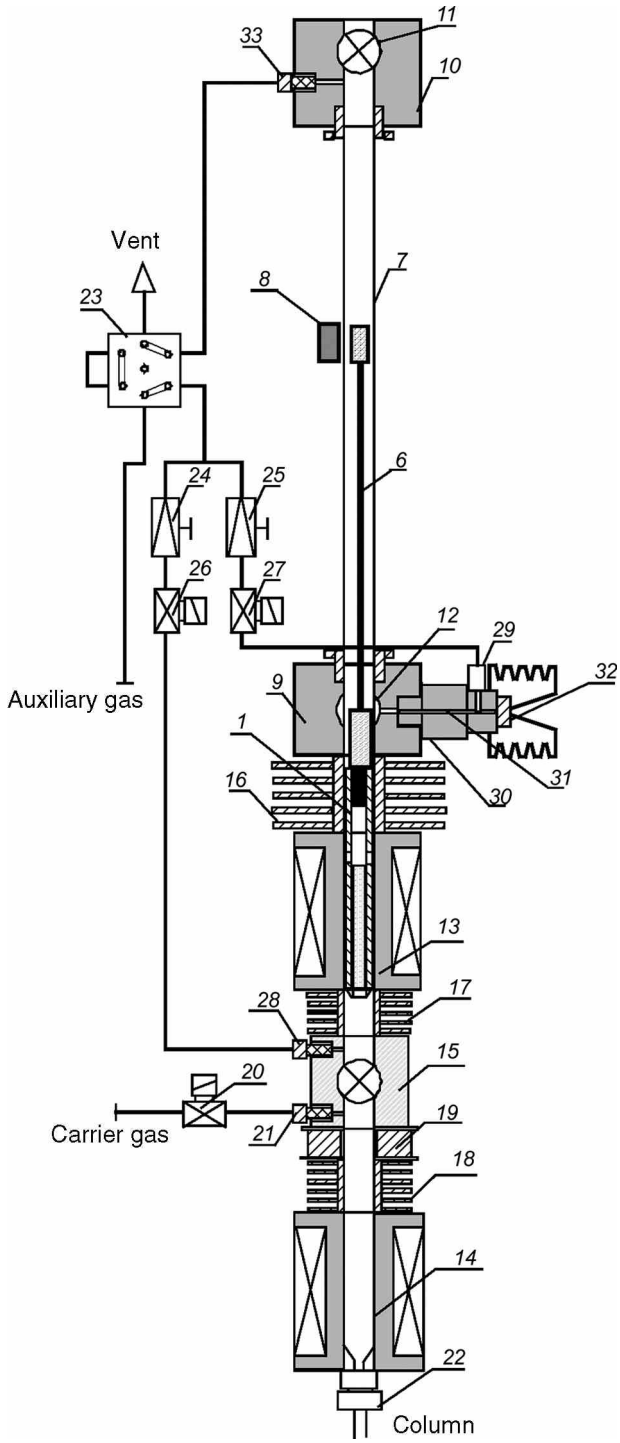

Fig. 7 Diagram of the injector with a mobile container in the position for solvent evaporation (denotation, as for Fig. 6).

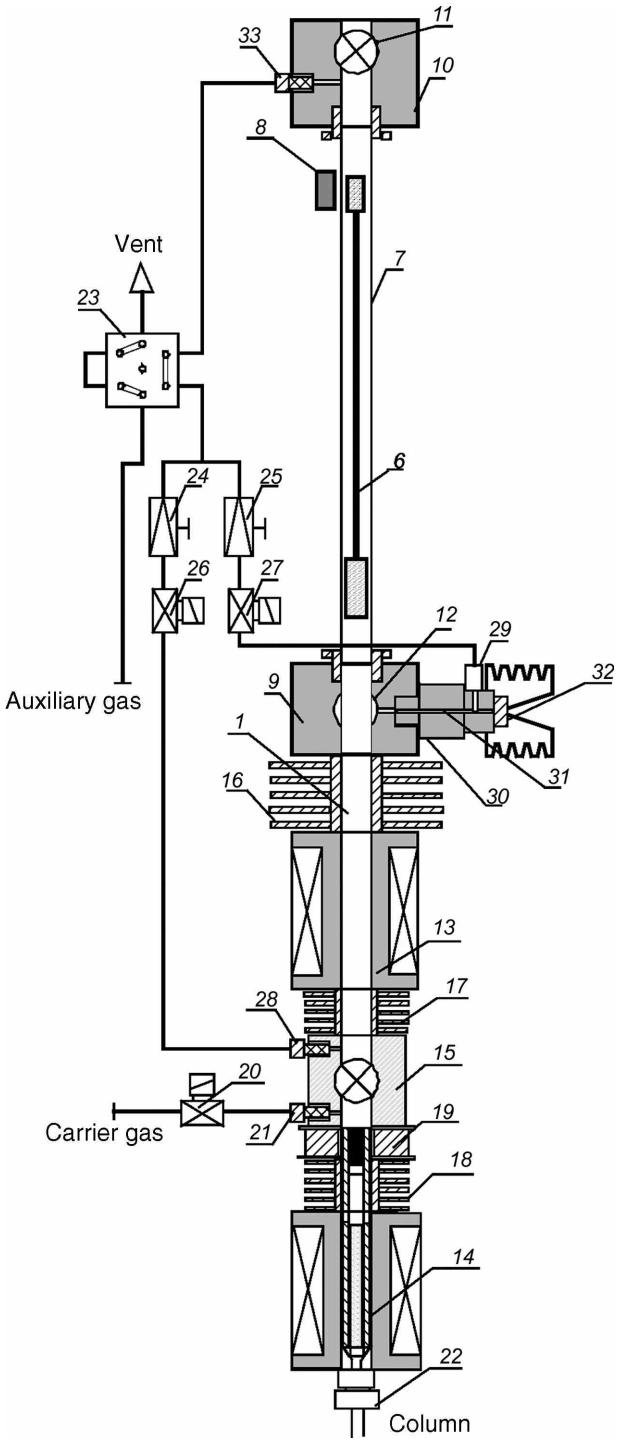

Fig. 8 Diagram of the injector with a mobile container in position for introduction of a sample into the chromatographic chamber (denotation, as for Fig. 6).

operation easier, there is an eyepiece with magnifying lens located in front of the front window, and a matt plate is located behind the back window. The first electrically heated chamber 13 is connected to the injecting cylinder 12. The second heated chamber 14 is separated from the first one by a ball valve 15. The chambers (13 and 14) can be heated to a constant temperature, or their temperature can be programmed to achieve a preliminary separation of components of the sample applied onto the packing of the container. Radiators 16, 17, and 18 protect the lower part of the injector, the ball valve 15, and the solenoid valve 19 against excessive heat.

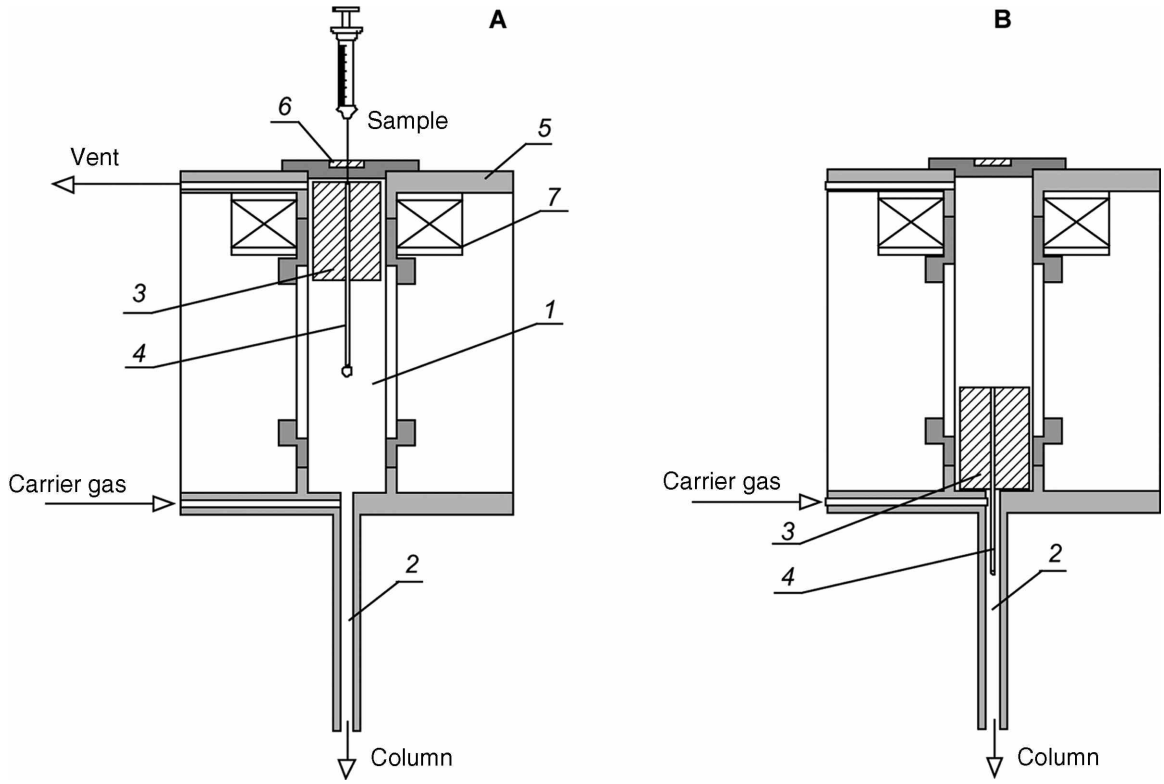

Fig. 9 Automatic injector (A) position of sample application (B) sample injecting position. 1 – evaporating chamber, 2 – injecting chamber, 3 – mobile unit, 4 – wire, 5 – injector body, 6 – membrane, 7 – solenoid.

The injector is supplied with carrier gas and auxiliary gas. Carrier gas is supplied through the solenoid valve 20, inlet 21, chamber 14, and port 22 into the chromatographic column.

After the sample is applied onto the packing of the container, solvent can be evaporated before analytes are transferred into the chromatographic chamber. The procedure consists of lowering the injector container into the heated chamber 13 where solvent is rapidly evaporated from the sample: the ball valve 15 is closed (Fig. 7). Auxiliary gas is used in the container for evaporation of solvent from the sample. The gas flows through the six-way valve 23 into two needle valves 24 and 25 with solenoid valves 26 and 27. Part of the auxiliary gas stream flows through the needle valve 24, through the inlet 28, heated container 1 in the chamber 13, and carrying vapors of solvent flows into the injecting cylinder 12. The other part of the gas stream is supplied through the needle valve 25 into the inlet 29 of the connecting pipe for sample introduction 30, to wash channel of the micro-syringe needle 31 and remove possible remains of the sample. Both parts of the auxiliary gas stream unite in the injecting cylinder 12, from which, through the quartz tube 7, they are carried away to the outside of the injector along with the solvent vapors, through the outlet 33 and the six-way valve 23.

After the solvent is evaporated, the sample can be transferred from the container into the chromatographic column. The procedure (Fig. 8) consists of closing the flow of auxiliary gas through the chamber 13 using the six-way valve 23 (and closing the solenoid valves 26 and 27). Then, the ball valve 15 is opened and the mandrel 6 with the magnet-connected container is lowered into the heated chamber 14. Upon turning the solenoid 19 on, the container becomes immobilized and it is possible to disconnect the mandrel from the container.

After lifting the mandrel 6 up, it is possible to close the ball valve 15 and the sample from the container is introduced into the chromatographic column. An electromagnetic field produced by the solenoid pushes the conical part of the container against the cone-shaped socket in the bottom of chamber 14. This forces the carrier gas to flow through the packing of the container.

After injection is completed, the solenoid is turned off, the ball valve 15 is opened, and the container is taken out from the chamber 14 using the mandrel; the container is moved to the position presented in Fig. 6. The ball valve 15 is closed.

AUTOMATIC SOLID-PHASE INJECTOR

An automatic solid-phase injector[5] is manufactured as a device that can be fitted to the heated block of virtually any gas chromatographic injector available in the market. A diagram of the injector is presented in Fig. 9. The injector

is composed of three principal parts: the evaporation chamber 1, the injection chamber 2 located inside the heated block, and the mobile unit 3 with tungsten wire 4. With a micro-syringe, a sample is applied over the tungsten wire (Fig. 9A). Carrier gas is supplied from the bottom of the injector body 5 and part of it flows through the injecting chamber 2 into the chromatographic column, and the remaining part flows through the evaporation chamber to the outlet located in the upper part of the injector body. Solvent vapors are carried away from the sample placed on the tungsten wire along with the carrier gas flowing through the injecting chamber. After the solvent is removed, the mobile unit 3 is descended with a solenoid 7 to the bottom of the injector body and the tungsten wire 4 is placed in the heated injecting chamber 2 (Fig. 9B). Then, the sample is evaporated and carried by the carrier gas; it is introduced into the chromatographic column. After the injection is over, the mobile unit 3 is moved with a solenoid 7 to the top of the injector body.

The mobile unit of the injector can be equipped with a small crucible or a sorption tube instead of the tungsten wire, depending on the sample matrix.

REFERENCES

1. Cramers, C.A.; Vermeer, E.A. Direct sample introduction of high boiling compounds onto glass capillary columns. Comparison of manual and automatic sampling. Chromatographia **1975**, *8* (9), 479–481.
2. Witkiewicz, Z. *Podstawy chromatografii*; WNT: Warszawa, 2005.
3. Słomkiewicz, P.M. Nowe konstrukcje dozowników z ruchomą igłą. Aparatura Badawcza i Dydaktyczna **2000**, *5* (3), 135–146.
4. Słomkiewicz, P.M. Dozownik chromatograficzny z ruchomą kolumną wstępną. Patent P-192935.
5. http://www.brechbuehler.com/

Sample Introduction Techniques for HPLC

Victor David
Andrei Medvedovici
Department of Analytical Chemistry, University of Bucharest, Bucharest, Romania

Abstract
The content of this entry deals with the first step of the chromatographic process, namely the sample transfer between operator and chromatographic column. The functioning principles, construction and operation of switching valves, automated injection, and selective injectors are widely discussed. Separation efficiency is also influenced by the connecting tubing, and the general relationship between its geometry and chromatographic parameters is analyzed. Some known examples of focusing effects occurring after large volume injection of samples in solvents other than the mobile phase are given. Finally, the main problems related to the malfunction of injectors and their origins are explained, and the qualification of injectors is described.

INTRODUCTION

The injector is an interface that achieves reproducible and accurate transfer of a sample volume between the system operator and the chromatographic column in a front (band) as narrow as possible. Usually, for analysis by high-performance liquid chromatography (HPLC), samples are prepared in a liquid state (as a solution in an appropriate solvent or mixture of solvents, obtained as a result of sample preparation of solid or liquid samples). For practical reasons (avoiding column overloading), even for analytes in a liquid state under ambient conditions, dilution in appropriate solvents is more often used.

The vector transferring a sample from the injector to the head of the chromatographic column is the mobile phase. Thus, injector should be positioned between the mobile-phase delivery system and the chromatographic column (or guard column, if one is used). The requirement that sample transfer takes place as a thin front at the head of the chromatographic column is necessary to minimize, as much as possible, extra-column loss of efficiency. The volume of the connection between the injector and the column should be considered as critical. The lower the injected sample volume and the flow rate, the lower should be the connection volume between the injector and the column. In HPLC, separations are usually driven at a pressure regime higher than ambient and, generally, limited to 400 bar. Pressure limitations are more often imposed by column and/or stationary-phase characteristics (e.g., organic copolymers, or swelled or synthesized stationary phases are used at reduced pressure regime). Therefore, the injectors work under pressurized conditions, and sample transfer has to be realized at ambient pressure without any loss in terms of liquid tightness or serious interruption of the mobile flow in the system.

Usually, injectors are designated for a quantitative transfer of the sample into the column, without any other selective action. However, owing to the increased complexity of the samples, specific injectors have been designed for selective transfer of specific sample constituents. The requirement for continuously decreasing detection limits in chromatographic separations has also led to the development of injectors that enable sample concentration. Insertion of a guard column between the injector and the chromatographic column represents a common approach for acting on the sample matrix to avoid stationary-phase contamination. When the declared aim of the chromatographic process is the assay of some compounds from a sample, the volume accuracy for the injection stage need not be assumed as critical, unless the quantitation limit of the process is affected.

FUNCTIONING PRINCIPLE, CONSTRUCTION, AND OPERATION

Injectors for HPLC are usually called "switching valves" and comprise a stator and a rotor. The stator is used for making connection to the other components of the HPLC system, by means of tubing and the corresponding tightening elements (generally, ferrules and nuts). The rotor is a movable piece that achieves connection between the different ports on the stator. The movement of the rotor from one position to another effects a different set of connections between the ports and, consequently, different liquid flows through the injector. One position of the rotor allows direct connection between the mobile-phase delivery system and the chromatographic column, and a simultaneous connection between the syringe insertion port, the sample loop, and the waste line. This position is known as the LOAD position. The complementary position of the rotor with respect to the LOAD position achieves connection of the mobile-phase delivery system, sample loop, and chromatographic column

on the one hand and the connection of the syringe needle port to the waste line, on the other. This position is generally named the INJECT position. Sample can be loaded into a tubing loop of known and precise internal volume connected to two diametral ports of the stator or directly to the channel from the rotor surface making connection between two vicinal ports on the stator side. The former setup is known as the "external sample loop," while the latter is known as the "internal sample loop" design. The external sample loop design requires six ports on the stator and a 60° rotation of the rotor, while the internal loop device requires only four ports on the stator and a 120° rotation of the rotor. Contact between the rotor and the stator should be tight enough to conserve the pressure regime within the HPLC system but should allow an easy switching movement. The functioning principle is illustrated in Fig. 1. Different constructions of the external and internal sample loop injectors are given in Figs. 2 and 3, respectively.

For external loop injectors, three operation modes are used. First, one supposes that the volume of the sample withdrawn into the syringe is higher than the loop volume, the excess being eliminated via the waste line. This technique is known as the "full loop" mode, which does not require accuracy in the functioning of the sampling syringe as long as the sample volume is larger than that of the loop. The "partial loop" mode imposes the withdrawal of an accurate volume of the sample by means of the syringe. The sample volume is lower compared to the volume of the external loop and, consequently, the sample only partially fills the loop. The "all volume injection" mode requires that the sample (having a considerably lower volume compared to the volume of the external loop) is withdrawn into the syringe needle between two air gaps and a solvent. During the loading operation, the whole sample band is brought within the external loop.

Some examples of commercially available valve supplies are Beckman/Altex, Rheodyne, SSI, Valco, and Waters.

Classification Criteria

Classification criteria applied for injectors used in liquid chromatographic systems are listed in Table 1:

For liquid chromatography (LC) systems micromachined by means of etching of silicon wafers, injection of sample volumes in the range of picoliters up to a few nanoliters is feasible. For such applications, injection is not based on valve switching, but rather on intersection of micromachined channels.

Automated Injection and Selective Injection

Automated injection refers to both automated sample loading and valve switching. Sample volume is user settable and can normally range from 1 to 900 μl. Sample is withdrawn into an external loop having a volume at least equal to the upper limit of the interval, connected between a syringe or stepper pump and a needle. Sample transfer to the column is achieved by means of a six-port rotating valve, often electronically switched, after bringing the needle into the needle seat. Two designs are available. The first setup allows an up and down movement of the needle in the needle seat. Vials are brought from a specific rack by means of a 2-D or 3-D (robotic arm) movement under the needle for sample withdrawal and then put back to their original location. The second technical solution is based on a 3-D movement of the needle from the needle seat to a vial positioned in a fixed rack, followed by sample withdrawal and return to the needle seat. A basic scheme is given in Fig. 4.

Selective injection involves discrimination during the transfer of the analytes to the analytical column, based on some of their physical or chemical properties. In HPLC, selective injection should be considered as being directly related to solid-phase extraction (SPE) or solid-phase microextraction (SPME) processes. However, modules allowing automated off-line SPE or SPME should not be considered as selective injection. An online setup between SPE/SPME

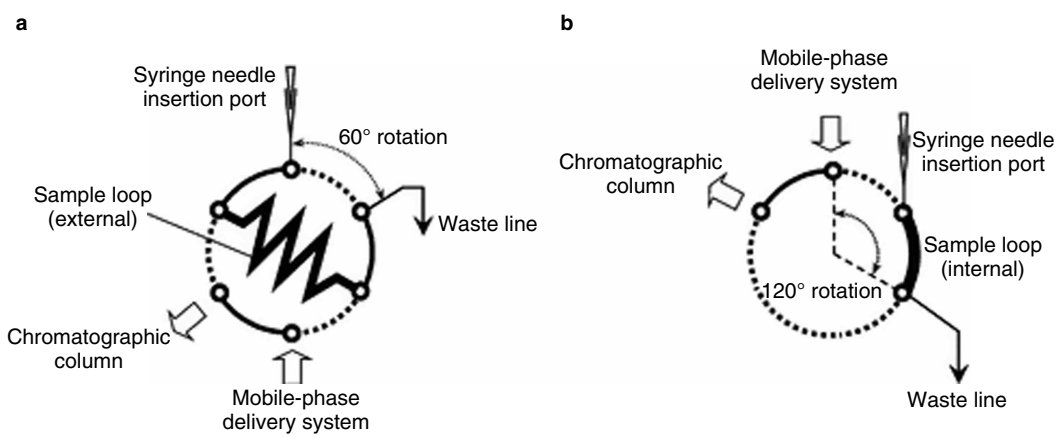

Fig. 1 Injectors for HPLC (a) External sample loop (b) Internal sample loop.

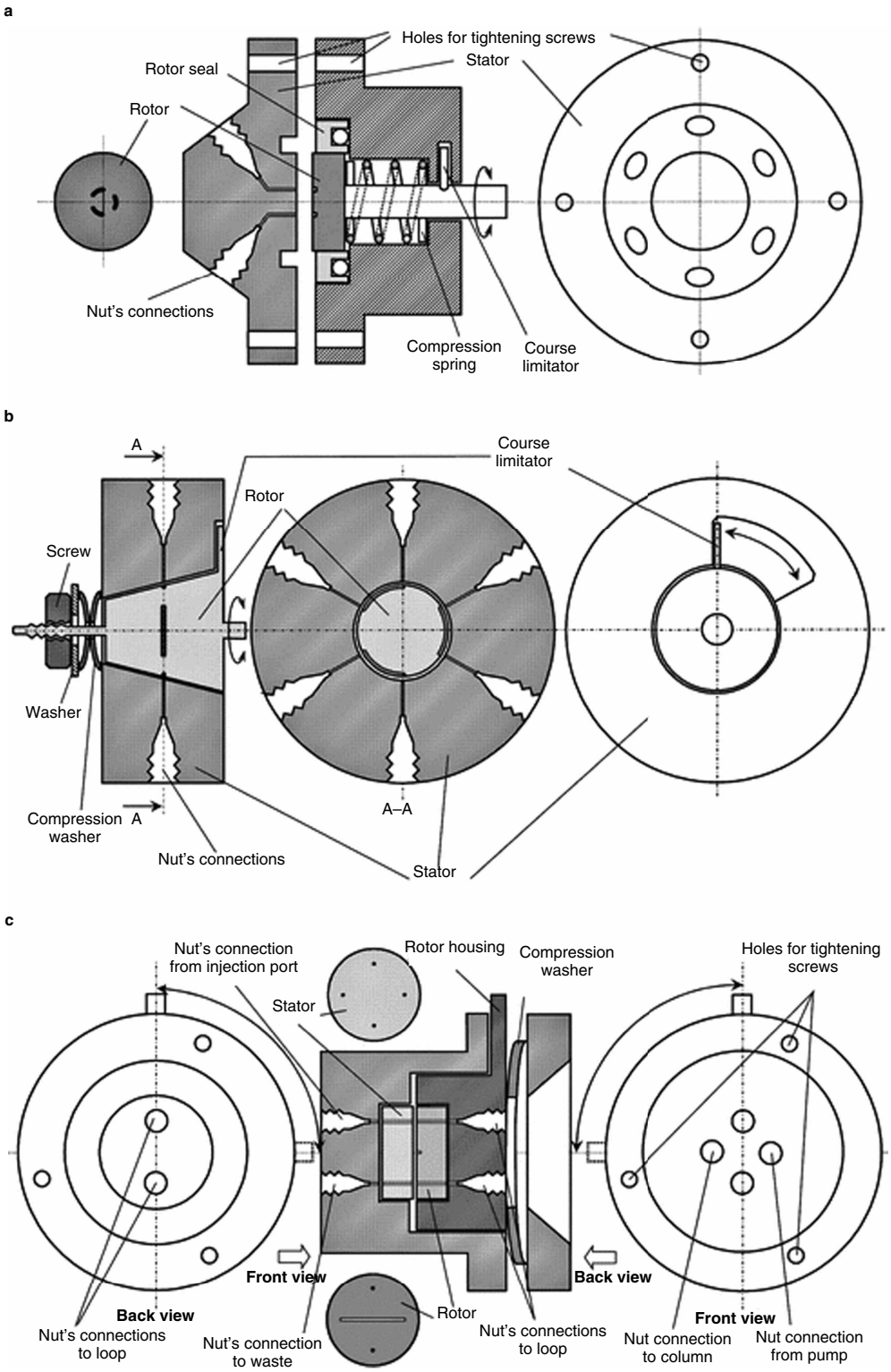

Fig. 2 Different construction types of external sample loop valves: a, Rheodyne; b, Valco; c, Beckman.

and the HPLC system represents a selective injection system. Basically, desorption of the isolated analytes is achieved by means of the mobile phase, usually oriented in a back-flush direction through the extraction cartridge. This basic principle demands a special care on the mobile-phase composition during injection, allowing fast desorption kinetics. A slow release of the analyte from the adsorbent will tremendously affect the efficiency of the separation process (broad band transfer to the column). Basic stages of the SPE process (adsorbent wash, accommodation with the sample solvent,

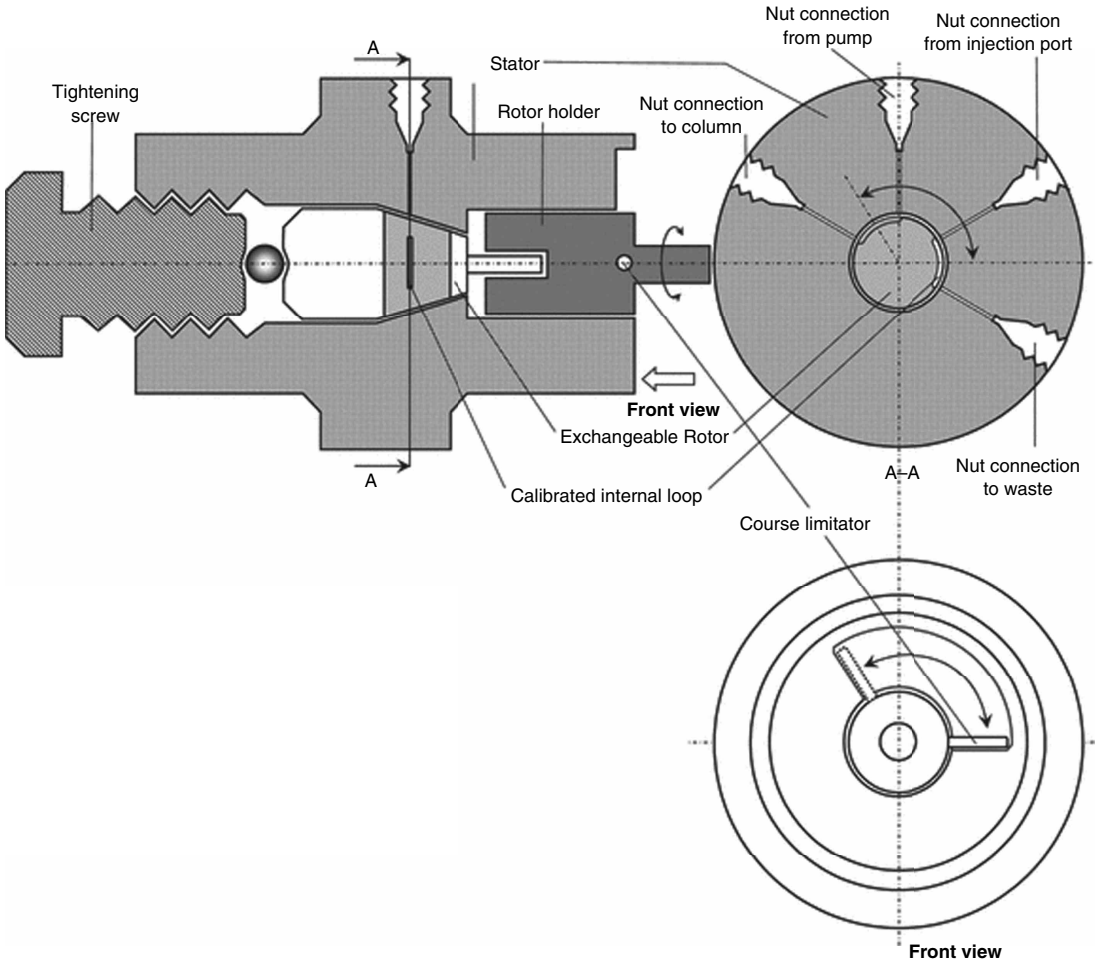

Fig. 3 Construction of an internal sample loop injector.

sample loading, elimination of the remaining matrix, drying the adsorbent and sample desorption) are fulfilled by coupling two six-port rotating valves and a programmable liquid handler (Fig. 5).

Adsorbent wash, accommodation with the sample solvent, sample loading, and elimination of the remaining matrix are processes related to the INJECT position of the valve A and the LOAD position of the valve B.

Table 1 Classification criteria for LC injection systems.

#	Criteria	Type of injection
1	Transferred sample volume	for micro LC applications (injected volumes ranging from 20 to 500 nl) for analytical LC applications (injected volumes ranging from 0.5 to 900 μl) for preparative LC applications (injected volumes ranging from 1 to 10 ml)
2	Sample loop position	internal loop (associated to nano volumes transfer) external loop (associated to analytical and preparative purposes)
3	Way of achieving injection	manual sample loading, manual valve switching manual sample loading, automated valve switching automated sample loading, automated valve switching (autosamplers)
4	Selectivity of injection	unselective selective (associated to sample preparation methods such as derivatization, solid-phase extraction or microextraction, realized off-line or online)
5	Object of the transfer	the sample a fraction resulting from a previous chromatographic separation (multi-dimensional LC interfacing)

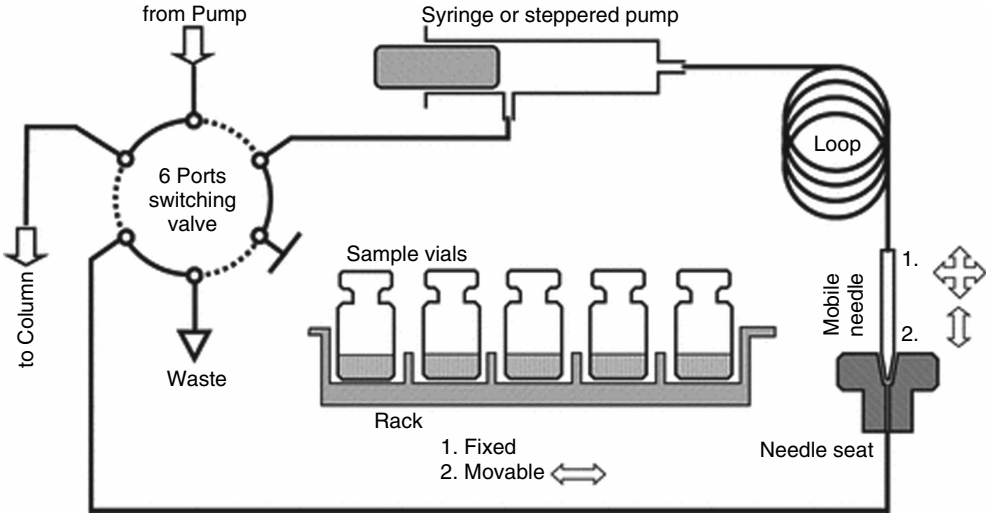

Fig. 4 General setup for an autosampler.

Drying the adsorbent (extremely important when the solvent used for remaining matrix elimination is not fully miscible with the mobile phase) requires the switching of valve A to the LOAD position. Sample desorption is achieved by switching the valve B to the INJECT position.

The SPME hyphenation to HPLC is even simpler. The external loop of a classic injection valve is replaced by a T-adapter, allowing insertion of the SPME needle and pushing out the fiber (Fig. 6). For desorption of the analytes, the valve is moved to the INJECT position. The return to the

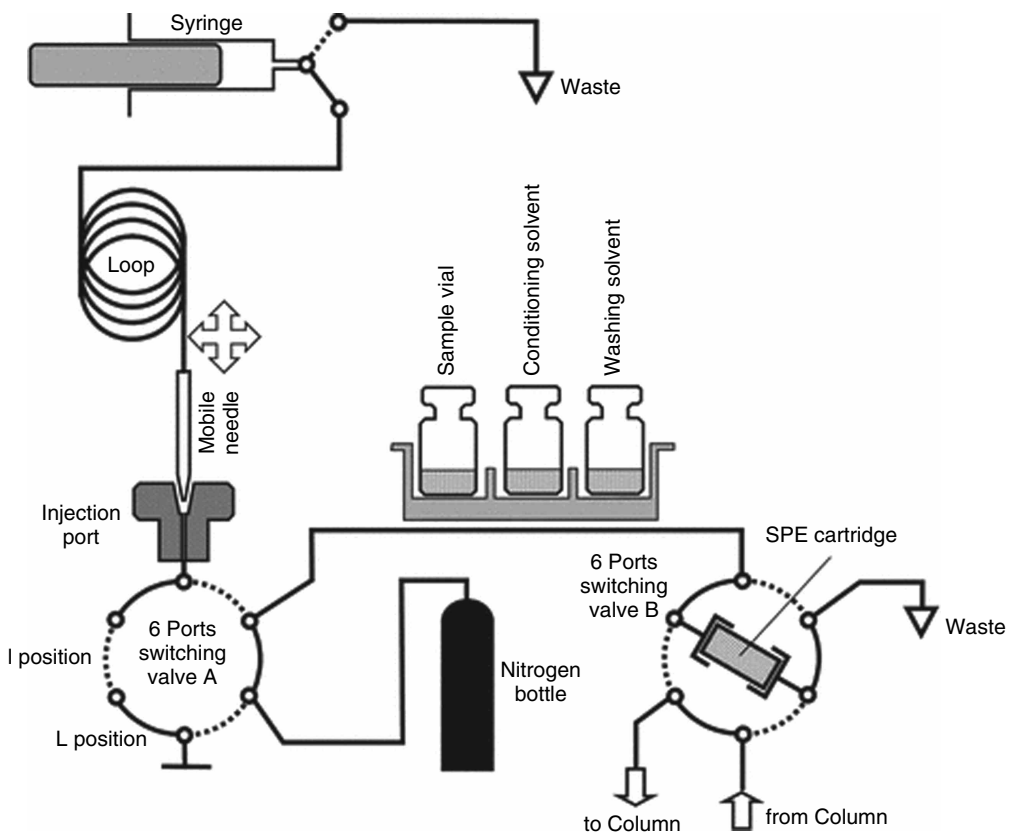

Fig. 5 Online coupling between SPE and liquid chromatography resulting in a selective injection configuration.

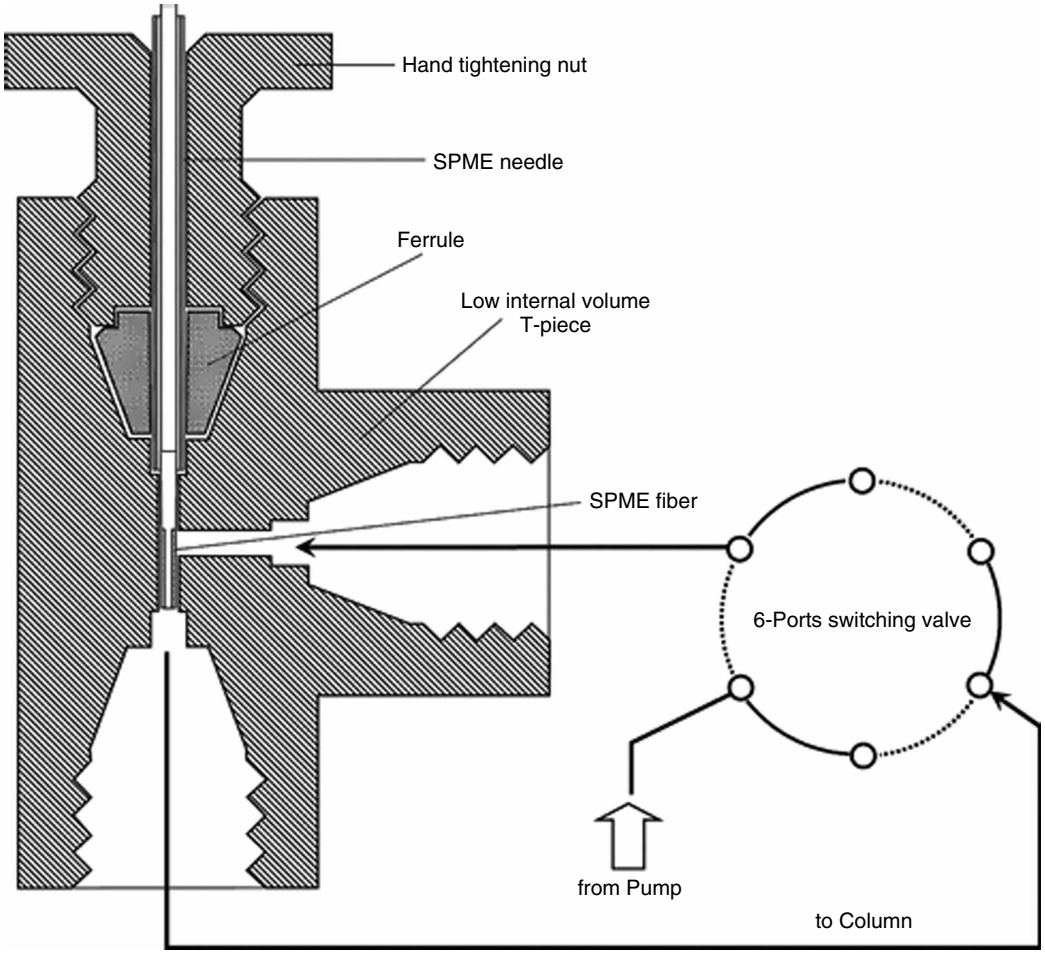

Fig. 6 Selective injection in LC by adapting SPME technique to the online desorption.

LOAD position of the valve isolates, again, the T-adapter and allows retraction of the fiber and withdrawal of the SPME needle. Special attention should be given to the compatibility of the fiber with the mobile phase, to eliminate risks associated with fiber material swelling.

A separate discussion relates to the automated off-line precolumn derivatization of the analytes, achievable by means of an autosampler. Derivatization brings a selective character to the injection process. Sample, reagents, and buffers can be transferred from vials to the loop or to an empty vial. Operations such as mixing of the reaction media, repetitive dilutions, and even sample concentration are possible.

Phenomena Related to Injection

Once the valve is switched for injection, the sample front is transferred to the column via the connecting tubing. Immediately after injection, the sample occupies a cylindrical zone in the transfer tubing. The length of the cylindrical zone depends upon the relative compressibility coefficients of the mobile phase and the sample solvent. When the injected zone moves toward the column, two phenomena occur simultaneously: the first relates to frictional forces to the tubing walls, resulting in a hyperbolic profile of the laminar flow, while the second relates to longitudinal diffusion of the analytes and the sample solvent within the mobile phase. Frictional forces are directly related to flow rate, viscosity of the sample solvent, and smoothness of the inner tubing walls, and are inversely related to the internal diameter of the tubing. Longitudinal diffusion is directly related to diffusivity of the analytes and sample solvent within the mobile phase and is inversely related to flow rate, tubing cross section (contact surfaces between zones), volume of the sample (initial cylinder length), and concentration of analytes. This is illustrated qualitatively in the Fig. 7.

The contribution of connecting tubing to extra-column effects has been already discussed in the literature. All parameters have been studied experimentally to obtain a mathematical relationship describing their mutual dependence. Such an equation is given below, where the band broadening in a chromatographic system is considered to be inversely affected by the flow rate

$$L = \frac{40 \times V_R^2 \times D_M}{\pi \times F \times \mathrm{id}^4 \times N} \quad (1)$$

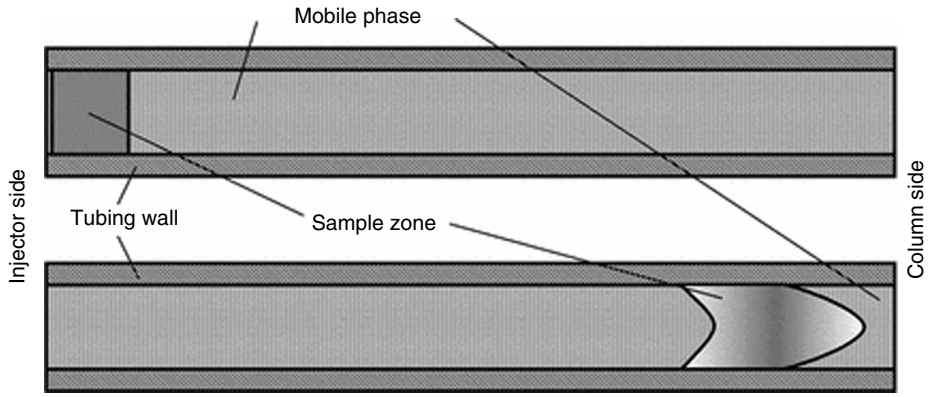

Fig. 7 Sample front during transfer from the injector to the chromatographic column.

where L is the column length (cm), V_R is the retention volume (ml), I.D. is the column internal diameter (cm), F is the flow rate (ml/sec), D_M is the diffusivity of the solute in the mobile phase (cm^2/sec), and N is the peak efficiency (theoretical plates).

Eq. 1 can be rewritten if we consider the following relationships:

$$N = \frac{L}{H} \tag{2}$$

$$V_R = t_R \times F \tag{3}$$

$$t_R = t_0 \times (1 + k') \tag{4}$$

$$V_0 = t_0 \times F \tag{5}$$

where H is the height equivalent to the theoretical plate (cm), t_R is the retention time of the solute (sec), t_0 is the column dead time (sec), k' is the capacity factor of the solute, and V_0 is the volume of the mobile phase within the column, or void volume (ml).

Eq. 6 results after making the above substitutions:

$$H = \frac{\pi \times \mathrm{id}^4 \times L^2 \times F}{40 \times V_0^2 \times D_M \times (1 + k')^2} \tag{6}$$

As the band broadening associated with the injector (H_{inj}) may be considered as the ratio between the length of the connection tubing between the injector and the column (L_{tub}) and the corresponding equivalent efficiency loss N_{tub}, i.e.,

$$H_{inj} = \frac{L_{tub}}{N_{tub}} \tag{7}$$

it clearly follows that

$$L_{tub} = \frac{\pi \times L^2 \times \mathrm{id}^4 \times F \times N_{tub}}{40 \times V_0^2 \times (1 + k')^2 \times D_M} \tag{8}$$

According to Eq. 8, it is possible to calculate the length of the connection tubing having an internal diameter of 0.127 mm (red lines), 0.178 mm (green lines), or 0.254 mm (blue lines), generating 5% loss in efficiency for a solute characterized by a capacity factor of 1 and a diffusion coefficient of 10^{-5} cm^2/sec, separated under a flow rate of 1 ml/min (Fig. 8).

Briefly discussing the results from Fig. 8, it can be inferred that connection tubing between the injector and the column having an internal diameter of 0.127 or 0.178 mm and a length below 50 cm should induce no major loss in terms of peak broadening for chromatographic columns having their void volumes below 2 ml. However, it is important to note that tubing with low internal diameter and significant length will generate a significant pressure drop in the LC system, especially for applications based on higher flow rates.

The effect of injection in the resulting chromatogram can usually be observed as a negative peak, owing to valve switching, which generates a short interruption in the mobile-phase flow through the chromatographic system. If the sample solvent is different from the mobile phase and is

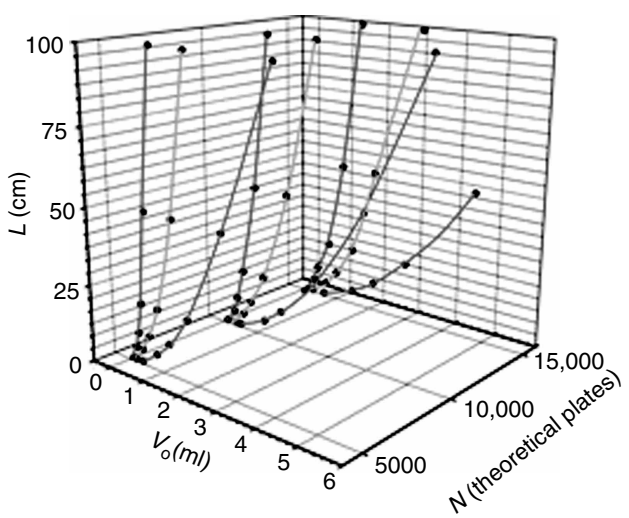

Fig. 8 The approximate length of connection tubing that causes a 5% loss of observed efficiency. Particular conditions are given in the text.

detectable, then the corresponding peak may get overlaid onto the injection pattern. This effect can be used as an indicator of the dead time (t_0) of the chromatographic process.

Focusing Effects on Injection

It is generally accepted that injection volumes less than 5 μl do not induce observable effects on the overall efficiency, retention, and shape of the chromatographic peaks owing to the influence of sample solvent. It is also assumed that, on using the mobile phase as the sample solvent, injection volume does not represent a critical parameter (no influence on efficiency, retention, and peak shape is observed) for the separation process. However, if an analyte is consistently more soluble in the sample solvent than in the mobile phase, and the injection volume exceeds a given limit, focusing of the analyte in the sample solvent occurs on injection, drastically affecting peak shape, retention, and efficiency. This may be explained as follows: the analyte remains dissolved in the plug created by the front of the injected sample volume in the mobile-phase flow. In this case, the distribution constant (K) between the stationary phase and the sample solvent is significantly lower than that corresponding to the partition between the stationary phase and the mobile phase. Obviously, the molecules of the analyte will be carried on by the sample solvent plug along the chromatographic column. Simultaneously, the longitudinal diffusion at the interface between sample solvent front and the mobile phase will give rise to a population of the analyte molecules transferred to the mobile phase, which will obey the "correct" partition mechanism. Therefore, the retention is drastically reduced for a significant number of analyte molecules, whereas for the diffusing molecules the retention will have the true value. Peak

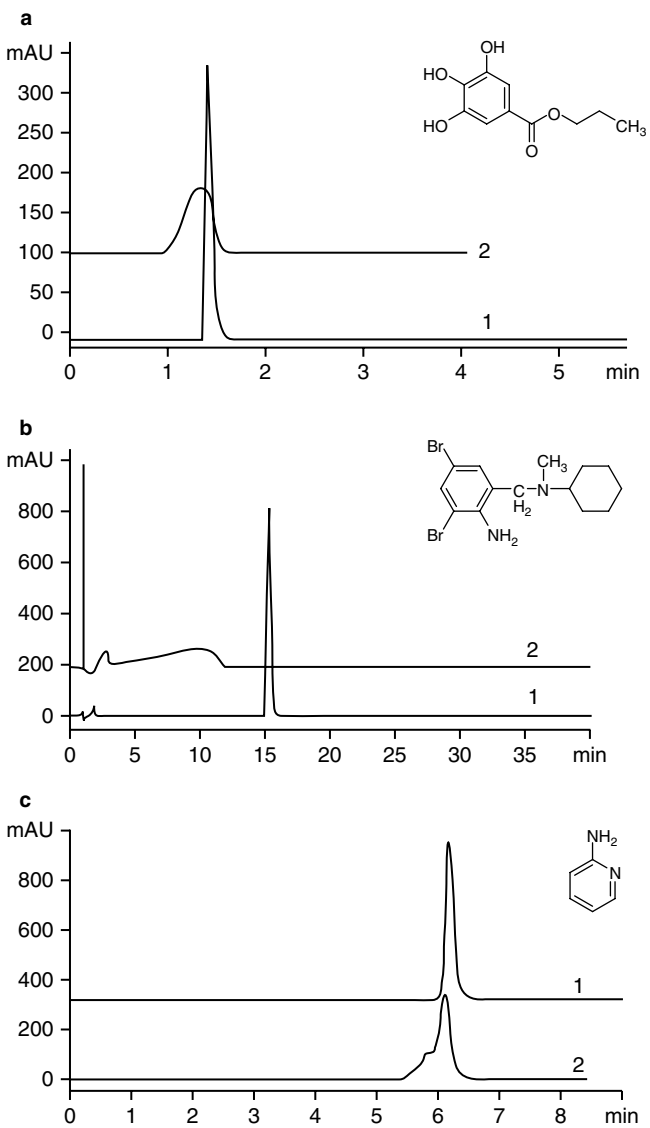

Fig. 9 Focusing of the analyte in the sample solvent on injection **a**, Assay of propyl gallate. Chromatographic column: Chromolith Performance RP-18e, 10 cm × 4.6 mm I.D. × 5 μm d.p., Temperature: 25°C, Flow rate: 2 ml/min, Mobile phase: MeOH/ACN/aq. 0.1% H_3PO_4 = 12/24/64 v/v/v, λ = 273 nm, Injection volume: 100 μl, Sample concentration: 10 mg/L [1] sample solvent is the mobile phase, [2] sample solvent is MeOH/ACN/aq. 0.1% H_3PO_4 = 20/40/40 v/v/v; b, Assay of bromehexine. Chromatographic column: Hypersil BDS 3–C18, 10 cm × 4.6 mm I.D. × 3 μm d.p., Temperature: 25°C, Flow rate: 1 ml/min, Mobile phase: ACN/aq. 0.1% H_3PO_4 brought to a pH of 7 with triethylamine = 75/25 v/v, Detection wavelength λ: 240 nm, Injection volume: 5 μl, Sample concentration: 5 g/L [1] sample solvent is the mobile phase, [2] sample solvent is ACN/aq. 3% HCl = 75/25 v/v; **c**, Assay of 2-aminopyridine. Chromatographic column: Purosphere Star—C18, 12.5 cm × 4 mm I.D. × 5 μm d.p., Temperature: 25°C, Flow rate: 0.7 ml/min, Mobile phase: ACN/aq. 80 mM sodium octane sulfonate brought to a pH of 2.8 with H_3PO_4 = 20/80 v/v, Detection wavelength λ: 290 nm, Injection volume: 50 μl, Sample concentration: 28 mg/L [1] sample solvent is the mobile phase, [2] sample solvent is ACN/water brought to a pH of 2.8 with H_3PO_4 = 20/80 v/v.

shape is, thus, seriously affected, resulting in splitting of bands for the same analyte (as can be seen in Fig. 9a).

Conversely, if the solubility of the analyte in the sample solvent is much lower than that in the mobile phase, large-volume injection may be allowed without any risk in terms of peak shape alteration, erratic retention, and efficiency loss. In this case, soon after coming into contact with the stationary phase in the head of the chromatographic column, the molecules of the analyte are readily distributed to it. The plug of the sample solvent runs through the column, but the molecules of the analyte are free to participate in the correct partition process between the stationary phase and the mobile phase. The focusing of the analyte in stationary phase now comes into effect, resulting in the preservation of the elution properties. Among chromatographers, the following rule sums up the above-mentioned circumstances: high volume injection is allowed in LC without any risk of affecting the elution results, if the elutropic strength of the sample solvent is lower than that of the mobile phase at the beginning of separation.

Focusing of analytes in the sample solvent can get extended by "subtle" effects. As illustrated in Fig. 9b, such phenomena affecting retention, efficiency, and peak shape may occur when the pH of the sample front is widely different from the pH of the mobile phase and the buffering capacity of the mobile phase is exceeded. In the given example, the analyte is forced into a protonated form within the injection front of the sample, while the separation process assumes a non-protonated form. Fig. 9c illustrates almost the same effect appearing in ion-pairing separation mechanism. Injection of high volumes of the sample in solvents which do not contain the ion-pairing agent, keeps the analyte in unassociated form, strongly reducing partition toward the stationary phase and focusing the molecules in the injection front. The retention, peak shape, and efficiency are again strongly affected.

Recently, it has been proved in some applications that large volume injection of samples in hydrophobic solvents (*n*-hexane, *n*-pentane, *i*-octane) is possible, with a gradual reduction of retention and a relatively small loss in terms of peak efficiency. Two conditions are, however, necessary to apply such an injection approach: the solutes must be soluble in hydrophobic solvents and, meanwhile, they have to be less hydrophobic than the sample solvent to avoid competition with solvent molecules in partitioning between the mobile phase and the stationary phase.

Troubleshooting

The main problems related to the malfunctioning of the injectors in LC are summarized in Table 2. More often, defective injection will introduce major problems related to precision of the analytical method and will tremendously affect quantitation. Malfunctions generally originate from inadequate tightness between stator and rotor surfaces in the switching valve or needle and needle seat, respectively (for auto samplers). Accuracy problems are related to the syringe or defective stepping pump operation and/or tightness.

Qualification of LC Injectors

Manual injectors are operationally qualified for repeatability and carryover. Autosamplers are additionally checked for accuracy. Injection systems are qualified after the solvent delivery system and the detector. To eliminate "subjective" effects, the chromatographic column is excluded from the setup for qualifying injectors. The column is replaced by a low internal diameter, significant length stainless steel tubing, generating a pressure drop similar to that in a packed column (about 100 bar).

Table 2 Troubleshooting injectors (major malfunctions events).

Observed malfunctions	Origin / Location
Overpressure in the LC system	Blocked channels on the rotor face or blocked loop; Blocked needle or needle seat; Incomplete switching of the valve.
Leakage, pressure drop	Lack of tightness between rotor and stator surface; Lack of tightness between needle and needle seat; Lack of tightness located to the piston of the syringe/steppering pump; Inadequate connections with fittings on the stator.
Low precision on injection	Accidental scratches made between channels on the rotor surface (usually generated by the use of improper needles tips of the injection syringe); Specific adsorption of the analytes on the rotor surface or within the loop (should be considered in relation to mobile-phase composition and/or sample solvent); Lack of tightness within injection port on the syringe needle walls.
Ghost peaks generated within chromatogram	Lack of inertness of some parts of the injector in direct contact with the mobile phase and/or sample solvents; Contamination of the needle from a previous injection process.
Peak broadening effect	High void volume of the connection tubing between injector and column; Improper connection of the ferrule on the tubing resulting in a void volume generated in the stator port.
Erratic sample injection	Defective movement of the needle or the vials in the autosampler.

Repeatability

A solution of a standard reference compound is obtained in a suitable solvent. This solution is repeatedly injected into the system, recording the chromatograms. After peak area integration, the mean value, standard deviation, and relative standard deviation (RSD) are estimated. Acceptance criteria refer, generally, to an RSD% value below 1%, if the injection volume is lower than 10 μl and 0.5% for higher injection volumes. Usually, for statistical computation, a series of 10 determinations are required. Plotting the integrated peak areas against the serial number of the injection process may represent an efficient way for evaluating a trend. A random distribution of the integrated peak area around the mean value should be observed. Continuously increasing or decreasing peak area values reflects a trend and should be investigated as an abnormal phenomenon.

Carryover

The carryover test checks for residual memory effects. Basically, it measures the residual peak area of the target compound in the chromatogram of a blank sample injected immediately after injection of a concentrated solution of the compound (e.g., 1000 mg/L). The carryover effect is evaluated as the percentage of the residual peak area in the blank chromatogram with respect to the peak area of the analyte after the injection of the concentrated solution. Limits of 0.1–0.2% could be considered as acceptable.

Accuracy

The accuracy test should be conducted especially for autosamplers. It consists of systematically increasing the injection volume from a solution of a reference standard compound. Set volumes should cover the whole working volume interval of the given autosampler module. The plot of the integrated peak areas against the nominal value of the injection volume must be linear and characterized by a correlation coefficient higher than 0.99. The correlation coefficient may be calculated according to the following relationship:

$$r_{xy} = \frac{\sum x_i y_i - \frac{1}{n}\sum x_i \sum y_i}{\sqrt{\sum x_i^2 - \frac{1}{n}\left(\sum x_i\right)^2} \times \sqrt{\sum y_i^2 - \frac{1}{n}\left(\sum y_i\right)^2}} \quad (9)$$

where x_i are set injection volumes, y_i are the integrated peak areas, $i = 1, \ldots, n$ is the serial number of the injections carried out for different volumes.

For the accuracy test it is important that the absolute amount of the target analyte for the lower injected volume is at least equal to the limit of quantitation (LOQ) and the corresponding amount of the compound at the higher injected volume does not exceed the linearity domain.

CONCLUSIONS

This entry deals with modern approaches used for introducing samples from the operator to the chromatographic column.

BIBLIOGRAPHY

1. Dolan, J.W. Attacking carryover problems. LCGC **2001**, *19* (10), 1050–1054.
2. Dolan, J.W. Autosampler carryover. LCGC **2001**, *19* (2), 164–168.
3. Dolan, J.W. Autosamplers, Part I— Design features. LCGC **2001**, *19* (4), 386–391.
4. Dolan, J.W. Autosamplers, Part II—Problems and solutions. LCGC **2001**, *19* (5), 478–482.
5. Dolan, J.W.; Snyder, L.R. *Troubleshooting HPLC Systems: A Comprehensive Approach to Troubleshooting LC Equipment and Separations*; Humana Press, Totowa (USA), 1989; 235–285.
6. http://www.chromtech.com/Valves/
7. http://www.idex_hs.com/
8. Layne, J.; Farcas, T.; Rustamov, I.; Ahmed, F. Volume-load capacity in fast-gradient liquid chromatography: Effect of sample solvent composition and injection volume on chromatographic performance. J. Chromatogr. A, **2001**, *913* (1–2), 233–242.
9. Martin, M.; Eon, C.; Guiochon, G. Study of the pertinency of pressure in liquid chromatography. II. Problems in equipment design. J. Chromatogr. A, **1975**, *108* (2), 229–241.
10. McEnery, M.; Tan, A.; Alderman, J.; Patterson, J.; O'Mathuna, S.C.; Glennon, J.D. Liquid chromatography on-chip; progression towards a μ-total analysis system. Analyst, **2000**, *125* (1), 25–27.
11. Medvedovici, A.; David, V.; David, V.; Georgita, C. Retention phenomena induced by large volume injection of solvents non-miscible with the mobile phase in reversed-phase liquid chromatography. J. Liq. Chromatogr. Relat. Technol. **2007**, *30* (2), 199–213.
12. O'Neill, A.P.; O'Brien, P.; Alderman, J.; Hoffman, D.; McEnery, M.; Murrihy J.; Glennon, J.D. On-chip definition of picolitre sample injection plugs for miniaturised liquid chromatography. J. Chromatogr. A, **2001**, *924* (1–2), 259–263.
13. Rezai, M.A.; Famiglini, G.; Cappiello, A. Enhanced detection sensitivity by large volume injection in reversed-phase micro-high-performance liquid chromatography. J. Chromatogr. A, **1996**, *742* (1–2), 69–78.
14. Udrescu, S.; Medvedovici, A.; David, V. Effect of large volume injection of hydrophobic solvents on the retention of less hydrophobic pharmaceutical solutes in RP-LC. J. Sep. Sci. **2008**, *31* (16–17), 2939–2945.
15. Vallano, P.T.; Shugarts, S.B.; Woolf, E.J.; Matuszewski, B.K. Elimination of autosampler carryover in a biological HPLC-MS/MS method: A case study. J. Pharm. Biomed. Anal. **2005**, *36*, 1073–1078.

Sample Preparation

W. Jeffrey Hurst
Hershey Foods Technical Center, Hershey, Pennsylvania, U.S.A.

INTRODUCTION

Before any sample can be subjected to chromatography, some type of sample preparation is required, which can be as simple as filtration or an involved solid-phase extraction protocol. Sample preparation is that activity or those activities necessary to prepare a sample for analysis. The ultimate goal of sample preparation is to provide the component of interest in solution, free from interferences, and at a concentration appropriate for detection. Sample preparation can be divided into a number of classes of activities: solvent extraction, sorbent extraction and compound isolation, headspace, and membrane separations, with each of these areas further divided into techniques that apply to the category of activities.

SAMPLE EXTRACTION

Should the sample be solid, the first step would involve the extraction of the sample with an appropriate solution that would solubilize the compound of interest and remove as few interfering compounds as possible. This operation is sometimes conducted using a blender or other mixer to provide as homogeneous extract an as possible. Alternatively, one could use a Soxhlet or similar apparatus to extract the sample.

The standard methods that one would use in sample preparation for chromatography include filtration, sedimentation, centrifugation, liquid–liquid extraction (LLE), open-column chromatography, and concentration/evaporation. Filtration for sample preparation may be performed on numerous occasions in a sample preparation protocol, with the first filtration being used to separate large-particulate matter from solvent. The final filtration before chromatography likely uses a 0.45 μm or smaller disposable filter unit to prevent small-particulate matter from contaminating the chromatographic system. Other methods to prepare a sample for analysis through extraction include supercritical fluid extraction (SFE), pressurized fluid extraction (PFE), and microwave-assisted solvent extraction (MASE). There will continue to be additions to this list, as techniques evolve and modifications of the more standard techniques are made.

When SFE was initially introduced, it was thought that it might be the panacea for sample extraction because it used a very innocuous solvent, CO_2. The operator varied pressure, temperature, flow rate, and extraction time, with some extraction protocols requiring the use of small amounts of polar modifiers. All of these variables affected the solvating power of the carbon dioxide. In addition to the carbon dioxide, other supercritical fluids have been used to vary the extraction selectivity.

In MASE, the sample and solvent are heated directly, in contrast to more conventional schemes, where the vessel is heated to extract the sample. The MASE technique uses a combination of microwave energy and a pressurized environment to enhance the extraction efficiency of some species. The energy adsorbed in a microwave is based on two complementary phenomena: molecular dipole rotation and ionic conductance. The sample solvents are placed in a closed vessel that absorbs microwaves. This facilitates the extraction of the samples of interest and has been applied to a variety of sample types and matrixes, with one of the most notable successes being its use in the automation of sample preparation of environmental samples. Conversely, open vessel microwave heating can be used to reduce solvent volumes and concentrate samples for subsequent analysis.

PFE uses standard solvents at elevated temperatures and pressures to increase extraction efficiency. The technique uses standard laboratory solvents that would be used to extract the compound of interest, but PFE techniques use solvent near supercritical temperatures. The high pressure does not allow the solvent to boil, hence increasing its penetration, while the high temperature increases solvent viscosity. Samples are placed in stainless-steel extraction vessels that are loaded into the device, which has been programmed for the extraction protocol. Instruments are available from a variety of manufacturers who allow extraction of either a single or multiple samples. In a variant of the technique, sometimes different solid-phase sorbents are placed in the extraction vessel to allow for a more selective extraction using PFE.

SORBENT EXTRACTION AND COMPOUND ISOLATION

One of the techniques that is increasingly used and has replaced more of the traditional methods of sample preparation is solid-phase extraction (SPE). SPE, introduced in the early 1970s, offers the possibility of, if not eliminating, at least reducing the tedium in sample

preparation. SPE has been called "digital chromatography," where samples can be introduced onto a device, interferences removed, and the analyte of interest eluted in a small amount of solvent. Conversely, the SPE device can be used as a flow-through cleanup device. The method can be used on many occasions as a substitute for LLE.

There is a wide diversity in not only SPE packing types but also SPE formats. The packing types parallel those used in open-column chromatography and HPLC. Second-generation-type supports such as Water's OASIS and the Varian NEXUS are seen as universal supports for many sample types, with other similar supports unique for SPE in continual development. Although the early SPE devices were cartridge or syringe barrel based, the formats have evolved to support the growing demands in drug discovery through the development of microtiter plate formats to support high-throughput screening (HTS) activities. In addition to columns, there has also been a growth in disk-based SPE devices, with exciting developments in the application of molecular imprinted polymers (MIPs), where imprints of molecules are formed on plastic supports. The initial success in the application of these devices has been in drug discovery and development. In addition to the large number of general supports, there are an increasing number of special purpose supports for specific applications such as dinitrophenylhydrazine (DNPH) columns for the determination of aldehydes and ketones, columns for explosive analysis, and columns for the analysis of samples for proteomic studies. Finally, there are a number of solid-phase devices that incorporate some sort of filter material into the unit. One can also purchase filter devices that work in conjunction with microtiter plate devices or as standalone units for applications such as protein precipitation.

Solid-phase microextraction (SPME) was developed as an alternative to many other sample preparation methods because it uses virtually no solvents or complicated equipment. It is an adsorption/desorption method where the compounds of interest are adsorbed onto a coated fused silica fiber. After a given time, the fiber is placed in a gas chromatography (GC), where the compounds are thermally desorbed. SPME has recently been adapted for use in HPLC, where compounds that are adsorbed are desorbed using an appropriate solvent.

A related technique that has come into use in recent years and is similar to SPME is stir-bar sorptive extraction (SBSE). Like SPME, it is a solventless technique allowing not only extraction but also concentration of the analyte of interest. In this technique, a stir bar is coated with a relatively thick layer of polydimethylsiloxane film that is placed in the solution containing the compound of interest, where the compound is adsorbed onto the film. The technique initially has been applied to the extraction and isolation of organic compounds from aqueous systems. An additional advantage is that the thicker film used with SBSE allows for the extraction and isolation of larger masses of analytes, thereby allowing an increased concentration of material to be available for analysis. The analytes can be desorbed thermally or by the use of an appropriate solvent.

Matrix solid-phase dispersion (MSPD) is an SPE variant where samples are ground and mixed with a support. In the initial application, samples were placed in a disposable column previously packed with Florisil, which trapped the fat from the sample and allowed the compounds of interest to be eluted. This has successfully been applied to the determination of lipophilic pesticides from both fatty and non-fatty matrixes. Recently, an orthogonal technique, dispersive solid-phase extraction, for the isolation and analysis of a variety of pesticides on numerous food matrixes has been introduced. The technique is called QuEChERS, which stands for quick, easy, cheap, effective, rugged, and safe. The technique offers advantages in time and solvent usage since it uses approximately 10 ml of solvent per sample when compared to the potentially hundreds of milliliters of solvent used for more standard extraction and isolation protocols. It uses a combination of $MgSO_4$ and primary secondary amine (PSA) sorbent not only to remove water and non-target compounds, but also isolate the compounds of interest.

HEADSPACE

This term can be applied to a number of techniques including static headspace, purge and trap, and thermal desorption. All of these techniques involve the extraction of a gaseous component from a solid or liquid sample. Static headspace is usually a one step technique where the component of interest is extracted from the sample held in a closed vessel usually at elevated temperatures and then injected onto the GC. Purge and trap is a multistep technique where the compound of interest is extracted into a matrix and then thermally desorbed onto the GC for analysis. SPME used in conjunction with GC analysis could be considered a purge and trap technique. In thermal desorption, the sample is heated rapidly and isolated using a cryogenic trap with the compounds isolated thermally desorbed.

MEMBRANE SEPARATION

Two additional techniques that are used in sample preparation protocols are ultrafiltration and microdialysis. In ultrafiltration, pressure is applied to a membrane and those molecules smaller than the molecular-weight cutoff can pass through while molecules larger are retained. This technique can be used as a way of sample concentration or as a way to eliminate higher-molecular-weight compounds from an analytical scheme. Membranes are available with cutoffs ranging from 300 to 300,000 daltons. Microdialysis differs from the other techniques because it is in vivo sampling and has been applied to the

determination of drugs and other biomolecules from tissues, organs, and biological fluids. In microdialysis, molecules can diffuse across a membrane, resulting in either direct or reverse dialysis.

AUTOMATION

Finally, no discussion of this topic would be complete without mention of the place of automation in sample preparation and its impact on this activity. Laboratory robotics' initial focus was on the automation of sample preparation and it is used in that way in many laboratories, but "islands of automation" have developed within certain organizations where certain portions of sample preparation such as SPE are automated. This initial automation used cartridge-based sorbents, but current applications involved the use of microtiter-based formats.

CONCLUSIONS

As sample preparation evolves, there is going to be not only growth in the variety of techniques, but also the use of a combination of techniques, such as the SPE/PFE example mentioned earlier. Sample preparation is an extremely broad subject, because there are techniques that are more likely used by those in different industry segments. This entry has provided an overview of some of the methods of sample preparation that are widely used. The reader is referred to the Bibliography for in-depth discussion on these topics.

BIBLIOGRAPHY

1. Anastassades, M.; Lehotay, S.; Stanbaher, D.; Schenck, F.J. Fast and easy multiresidue method employing acetonitrile extraction/partitioning with "dispersive solid phase extraction" for the determination of pesticide residues in produce. J. AOAC Int. **2003**, *86*, 412.
2. Applied Separations Inc. Applications of supercritical fluid extraction. CD-based application base. www.appliedseparations.com
3. Baker, S.A. Preparation of milk samples for immunoassay and liquid chromatographic screening using matrix solid-phase dispersion. J. AOAC Int. **1994**, *77*, 848.
4. Current Trends and Developments in Sample Preparation. LC-GC **1999** (Suppl.).
5. Current Trends and Developments in Sample Preparation. LC-GC **1998** (Suppl.).
6. David, F.; Tienpont, B.; Sandra, P. Stir-bar sorptive extraction of trace organic compounds from aqueous matrices. LC-GC Europe **2003**, *21* (2).
7. Henion, J.; Brewer, E.; Rule, G. Sample preparation for LC/MS/MS. Anal. Chem. **1998**, *70*, 650A–656A.
8. Kingston, H.M.; Haswell, S.J. *Microwave-Enhanced Chemistry. Fundamentals, Sample Preparation, and Applications*; Oxford University Press, 1997.
9. Kolb, B. Headspace sampling with capillary columns. J. Chromatogr. A, **1999**, *842*, 163.
10. Snyder, L.R.; Kirkland, J.J.; Glajch, J.L. *Practical HPLC Method Development*; 2nd Ed.; John Wiley & Sons: New York, 1997.
11. Van Horne, K.C. *Handbook of Sorbent Extraction Technology*; Varian Sample Preparation Products: Harbor City, CA, 1994.
12. Zang, Z.; Pawliszyn, J. Headspace solid phase microextraction. Anal. Chem. **1993**, *65*, 1843.

Sample Preparation and Stacking for CE

Zak K. Shihabi
Department of Pathology, Wake Forest University, Winston-Salem, North Carolina, U.S.A.

Abstract
The sample matrix affects the separation in capillary electrophoresis (CE) much more than it does in high-performance liquid chromatography (HPLC). It affects the resolution, quantification, and precision through effects on the current conductance and through effects on the capillary walls. Proteins tend to bind to the capillary wall and change the analysis unpredictably. Samples of biological or industrial origin and those with low concentration require special preparation and thoughtful planning for separation in order to avoid the deleterious effects of the sample. Emphasis on simple stacking and concentration methods is presented to overcome the poor detection limits of CE and to bring it closer to HPLC.

INTRODUCTION

Unlike in high-performance liquid chromatography (HPLC), the composition (matrix) of the sample itself greatly affects several aspects of the separation in capillary electrophoresis (CE): migration, resolution, quantification, sensitivity, detection, and precision. Although the sample, in most instances, constitutes a very small portion of the overall volume in the capillary once injected (0.5–5%), the matrix of the sample has profound effects on the migration of analytes in CE. This is due to two main factors: the contribution of the sample to the total current conductance and its interaction with the capillary walls (especially proteins). The conductance is related to the voltages, the current, and the field strength, all of which affect the migration (velocity) of the analytes and also the peak shape obtained for the analytes.

As CE has a relatively low sensitivity, owing to the short light pathway of the capillary, there is a tendency to inject large volumes of sample to enhance detection. However, as the sample size or its ionic strength increases, the matrix effects and the contribution to the current conductance become much more significant. Also, as the ionic strength of the separation buffer is decreased to speed up the analysis, the matrix effects become more significant.

It is not well appreciated that in CE there is a relationship, or an interaction, between the sample matrix, the buffer, and the capillary wash between the samples. Because of the large surface area to the capillary volume, the sample matrix affects the charges on the capillary wall. Samples obtained from clean sources, or pure standards, generally do not require much or any preparation, while those from biological fluids, foods, and industrial sources often have a complex matrix (excess of ions and proteins), which necessitates special or clever manipulation not just of the sample but also of the separation buffer and the degree of capillary wash. This depends on the concentration of the analytes relative to the contaminants. For example, we routinely analyze cryoglobulins for diagnosis of vasculitis.[1] These proteins being cationic in nature precipitate and bind easily to the capillary walls, ruining the separation. Capillary wash between samples with the traditional sodium hydroxide of 0.2 mol/L is not sufficient. In order to deal with such a problem, a special wash between samples with high concentration (10%) of phosphoric acid was critical. This explains why a method described in the literature based on pure standards needs further modification for its successful use in routine analysis.

Sample preparation in CE requires careful thinking and strategy to obtain a good analysis. There is also a relationship between the sample matrix and the separation buffer. Based on how the sample is prepared and how the separation buffer is selected, sample matrix effects can be either favorable or detrimental to the analysis. In other words, it can lead to improved separation, with concentration of the analytes on the capillary (stacking) or to poor separation with band broadening. Matrix effects in capillary zone electrophoresis (CZE) are different from those observed in micellar electrokinetic chromatography (MEKC). Also, the matrix effects are different in electroinjection compared to hydrodynamic injection. These facts can be highly discouraging for a researcher new to this technique. However, understanding the basics of matrix effects is very important for avoiding poor separation or poor peak shape.[2] The two most common techniques in CE are CZE and MEKC. Other techniques such as size separation, nonaqueous CE, and isoelectric focusing are less utilized, and furthermore, they are quite specialized techniques. Hence, we focus here on sample preparation for CZE and MEKC. The aim of this entry is to offer the reader both basic and practical information on how to overcome deleterious sample matrix effects and how to turn them around to be favorable for the overall analysis.

EFFECT OF SAMPLE MATRIX IN CAPILLARY ZONE ELECTROPHORESIS

The most important elements encountered as matrix in the sample affecting the CE are the different ions, proteins, pH, and diluents. These constituent factors can vary widely between different samples, which can affect greatly the separation in CE. Often, when the sample matrix is different from that of the standards, erroneous quantification resulting from changes in the peak shape (especially for peak height) and, consequently, poor recovery is observed. If there is an interaction between the sample and the capillary walls or changes in the charge on the surface of the capillary, precision suffers greatly due to changes in electro-osmotic flow (EOF).

Sample Ionic Strength

Ions are very important in electrophoresis. They carry, or conduct, current. A sufficient ionic strength is important for the solubility of some compounds such as proteins. However, there is an inverse relationship between electrophoretic mobility and ionic concentration. In the hydrodynamic injection mode, when some of the analyte ions migrate from a high-conductivity region in the sample to a low-conductivity area in the buffer, they accelerate, resulting in non-symmetrical multiple peaks, or band spreading. In the electrokinetic injection mode, the excess ions in the sample decrease the migration or transfer of the analytes into the capillary, leading to a diminished detector signal. Pure standards prepared in water compared to those added to serum or diluted in saline solutions show differences in peak shape and a large difference in the detector signal, causing the quantification to be difficult. In other words, an excess of ions in the sample, especially with large sample volumes, ruins both the separation and the quantification in CE, with the effects being more pronounced in electroinjection.

Proteins

At low concentrations and under appropriate conditions, proteins have little effect on separation in CE. However, at high concentrations in the sample together with low ionic strength in the buffer, many proteins, especially the cationic ones, tend to be adsorbed preferentially onto the inlet side of untreated capillary walls, changing the zeta potential, which in turn affects the EOF. Even the slightest variation in the EOF along the capillary length causes an increase in band spreading and a decrease in peak symmetry, leading to very poor reproducibility. An excess of proteins in the samples causes poor reproducibility, especially of migration time; thus, the capillary requires a more thorough wash between injections. In our experience, even small amounts of some types of paraproteins present in serum ruin the capillary after a single injection unless a thorough wash is employed. Fortunately, untreated capillaries are not that expensive to replace.

pH

The ionization and net charge of the sample components are affected significantly by changes in the pH of the sample. As a result, the migration rate, the solubility, the theoretical plate number, and the peak height could all get affected. Proper dilution of the sample with an appropriate buffer is the first step in separation. Usually, the sample is diluted with the same solvent used as the electrophoresis buffer; however, in some instances, a pH of the sample different from that of the buffer is selected to concentrate the sample on the capillary (stacking).

Diluent Type

In most cases, the sample is dissolved in aqueous buffers similar to the electrophoresis buffer, but at a higher dilution. However, as discussed later, using some organic solvents (especially acetonitrile and acetone) as sample

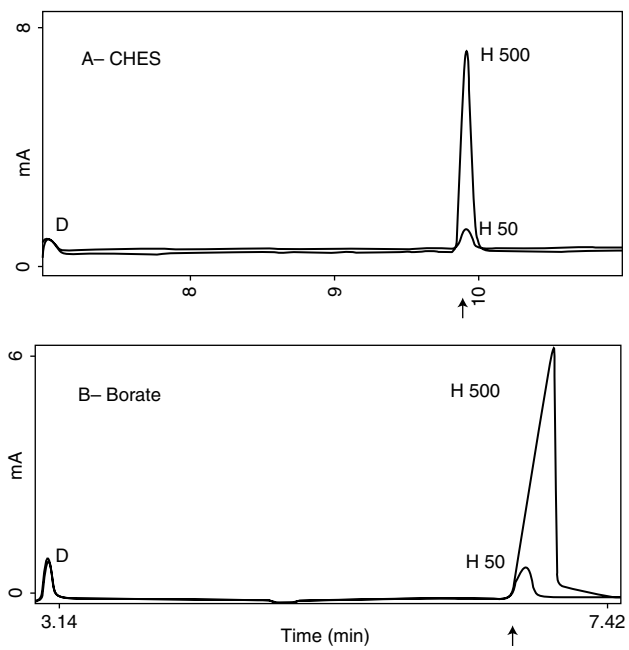

Fig. 1 Effect of both sample concentration and buffer type on migration time for hippuric acid (H): A, Symmetrical peak shape with separation buffer CHES 150 mmol/L, pH 9.0, 214 nm; hippuric acid 500 mg/L (top peak) and 50 mg/L(lower peak) and B, Distorted peak shape using separation buffer borate 150 mmol/L, pH 9.0, 214 nm; hippuric acid 500 mg/L (top peak) and 50 mg/L (lower peak) (D = DMSO; arrow indicates common or constant migration time).
Source: With permission from Effect of sample composition on electrophoretic migration: Application to hemoglobin analysis by capillary electrophoresis and agarose electrophoresis, in J. Chromatogr. A.[2]

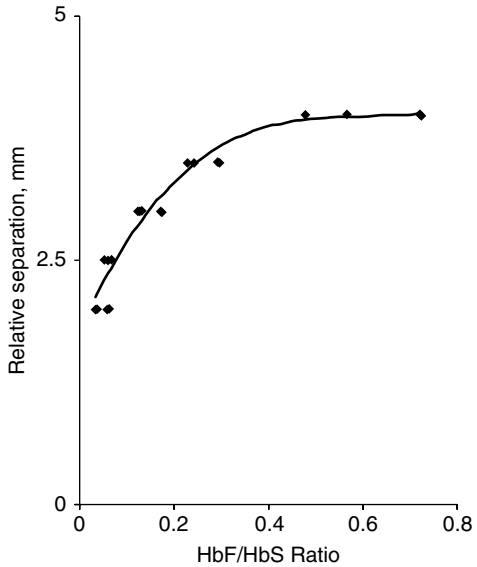

Fig. 2 Ratio of HbF/HbS and the relative distance between the two variants (in mm) by agarose electrophoresis (Sebia).
Source: With permission from Effect of sample composition on electrophoretic migration: Application to hemoglobin analysis by capillary electrophoresis and agarose electrophoresis, in J. Chromatogr. A.[2]

diluent can yield much better separation due to the stacking effect.

Analyte Concentration in the Sample

Some unexpected factors can affect the peak shape and migration in CE. For example, concentration of the analyte itself in the sample can have an effect on the peak shape, which can be remedied by dilution or by using a different buffer as illustrated in Fig. 1.[2] In this figure, hippuric acid at low concentrations shows a good peak shape in CE using borate or *N*-cyclohexyl-2-aminoethanesulfonic acid (CHES) buffer. However, when the concentration is increased tenfold, the peak shape deteriorates in the borate but not in the CHES buffer.

Migration can also get affected by the concentration of the analyte in the sample. This is much better observed in gel electrophoresis where multiple samples are applied to the gel and the same analytes align exactly with respect to each other. However, this does not happen all the time. For example, hemoglobin (Hb)F in the presence of large amounts of HbS changes its migration depending on its concentration. As the ratio HbF:HbS decreases, the migration time of HbF decreases too (see Fig. 2).[2]

MATRIX EFFECTS IN MEKC

MEKC is often used for separating neutral and hydrophobic molecules. The effect of sample matrix in MEKC is less dramatic than in CZE. The surfactants in MEKC offer a great advantage for samples with high protein content. They solubilize the proteins and decrease wall interactions, thereby eliminating the need for extraction or deproteinization, and allow direct sample injection, provided the proteins do not interfere with the detection of the analytes of interest.

Surfactants in the Sample

Surfactants are sometimes added to the sample to solubilize the analytes. In general, a low concentration of the surfactant in the sample favors peak height. A surfactant in the sample different from that in the running buffer can give a slightly better peak height.

Surfactant in the Buffer

A high sodium dodecyl sulfate (SDS) concentration in the running buffer causes an increase in peak height. However, at the same time, high SDS concentrations result in excessive current generation and long migration times. Peaks with higher capacity factors (k') are more affected by the surfactants in the buffer.

Organic Solvents in the Sample

MEKC is often employed in the separation of non-polar compounds. The addition of an organic solvent to the sample to solubilize the analyte, especially with large sample injection, decreases peak height as well as resolution. Thus, the concentration of these solvents needs to be kept to the minimum.

SAMPLE VOLUME AND STACKING

Concentrating the sample in the capillary is called stacking. It is a very simple method to perform in routine analysis. Because of the relatively low sensitivity of detection in CE, a high sample volume is very desirable to improve the signal-to-noise ratio. Unfortunately, a simple increase in the sample volume, under continuous buffer separation (the same buffer in the sample, capillary, anode, and cathode), leads to sample overloading. The theoretical plate number in CE drops considerably with an increase in the sample (volume). For example, the theoretical plate number dropped from 800,000 to less than 10,000 when the injection time was increased from 0.2 to 15 sec.[3] Low sample volume offers very high theoretical plate numbers, but at the same time yields very small detector signals. The rule of thumb is to keep the sample plug, under non-stacking conditions, at less than 1% of the capillary length.[4]

The general idea behind most of the stacking methods is to inject a very large sample and induce the same

molecules in different regions of the injection plug to migrate with different velocities, so that the two edges of the sample come closer to each other before the electrophoresis step. Discontinuity in the capillary buffer with regard to concentration, pH, ions, or conductivity is the key to induce differences in molecular migration. This discontinuity can be introduced in the capillary simply by dissolving the sample in a buffer or diluent different from the electrophoresis buffer. Some of the stacking methods are applicable for the majority of the analytes, while others are limited to a very few or certain compounds.

Stacking in CZE

A large sample volume is injected and the two edges of the sample are induced to migrate toward each other. This mechanism leads to enhanced sensitivity, higher plate numbers, and better separations. Stacking in CZE can be brought about by various manipulations of the sample. Further, a combination of two different methods can give a higher concentration factor.

Low Ionic Strength in the Sample

Most often CE analyses employ this simple method. Here, the sample is dissolved in the same solvent used as the electrophoresis buffer but at a 10 times lower concentration. This causes the sample resistance and the field strength in the sample plug to increase. In turn, this causes the ions to migrate rapidly until they are slowed at the interface of the separation buffer. They stack as a sharp band at the boundary between the sample plug and the separation buffer with the positive ions lining up in front of the negative ions before entering the separation buffer. As a result of this simple manipulation, the sample can be concentrated up to 10 times.[5] This stacking effect can be utilized with both pressure and electrokinetic injections (field amplification injection). A similar stacking can also be accomplished by injecting a very short plug of water into the capillary before injecting the sample.

pH Adjustment

Stacking based on adjusting the pH for samples with multiple charges has been described. Peptides can be concentrated by dissolving the sample in buffer 2 pH units above the net p*I*, so that they are negatively charged. As the potential is turned on, the peptides initially migrate toward the anode until they are stopped by the interface of the separation buffer, where they concentrate. After the short pH gradient of the sample dissipates in the separation buffer, the peptides become positively charged. Thus, they migrate toward the cathode as a sharp zone. Catecholamines were concentrated based on the same principle at acidic conditions in the sample.

Transient Isotachophoresis

One of the earliest methods for ion separation (later used for sample concentration on the capillary) is isotachophoresis (ITP) based on the work of Kohlrausch. This method concentrates dilute samples using buffers that are discontinuous with respect to the ions, all of which have to migrate at the same velocity, regardless of their mobility, during the electrophoresis. A fast-mobility ion at a high concentration is used as a leading ion while a slow-mobility ion is used as a terminating ion. The sample ions have intermediate mobility. At equilibrium, samples of low concentration and intermediate ion mobility change their field strength, by adjusting their concentration, to keep pace with the velocity of the leading ion. The electric field strength is inversely proportional to the ion mobility in that region. If a few sample ions accidentally enter the leading zone, they encounter lower field strength, so that they slow down. However, if some sample ions slow down in the terminating ion region, they are exposed to higher field strength and speed up, catching up with their own segment. Thus, the difference in field strength between terminating and leading zones dictates the stacking. ITP is often considered a concentration and purification method. It can concentrate a sample ten- to thousandfold. The concentrated segments can be coupled to CZE by several methods using a single capillary or separate capillaries for further separation and quantification.

As the velocities of the ions are affected by factors such as the charge, pH, concentration, and coions, successful ITP requires careful attention to all these details, which makes it difficult to use in practice. A simpler form of ITP is transient ITP (t-ITP), which is easier to couple to CZE (in the same capillary).[6–8] Under appropriate conditions, a concentration step due to a brief ITP can occur before the sample enters the separation buffer. In many instances, the t-ITP step occurs accidentally in samples containing high concentrations of salts (self-stacking) or it can be induced by the addition of an appropriate leading/terminating ion to samples with a complex matrix. The method can concentrate both small and large molecules.

Karger et al.[9,10] have described two strategies for coupling ITP to CZE. The first method uses on-column t-ITP. After the sample is injected, a leading or terminating electrolyte is chosen based on the mobility of both the analyte and the coion of the background electrolyte. This method gives an approximate fiftyfold increase in sensitivity. In the second method, a second CZE column is coupled to the ITP column. This involves a more complicated system, but it yields up to a thousandfold increase in sensitivity.[10] Karger et al. have also shown the advantages of coupling t-ITP with CZE for concentration of several model proteins such as cytochrome *c*, lactoglobulin, ribonuclease, and lysozyme for both UV and mass spectrometric detection.[10]

Transient Pseudo-isotachophoresis (Acetonitrile Stacking)

Many biological samples such as serum contain close to 70,000 mg/L of proteins that can adsorb, denature on the inlet, and clog the small pores of the column in HPLC or bind to the walls of the capillary. To analyze drugs and endogenous small molecules present in serum, these compounds have to be extracted either by liquid or by solid phase. Both extraction methods avoid the proteins, concentrate the analytes, and yield clean chromatograms, but they are laborious procedures especially for routine analysis. A more common procedure for drug analysis in serum involves removal of proteins by the addition of 2 volumes of acetonitrile and occasionally by the addition of acids or heavy metal salts.[4] Acetonitrile is a common reagent for deproteinization in both HPLC and CE. It requires 2 volumes of acetonitrile to 1 volume of serum to completely remove serum proteins.[4,11] The advantages here are the simplicity and speed of deproteinization by acetonitrile. However there is an opposite effect of acetonitrile in HPLC vs. that in CE.

Effect of acetonitrile in HPLC: When the recovery of small molecules analyzed in serum is calculated based on the peak height of aqueous standards also treated by acetonitrile similar to serum, a high recovery is obtained. However, when the calculation is based on aqueous standards diluted in the mobile phase (pump solvent) a low recovery is obtained. In analyses of drugs in serum, acetonitrile in the sample decreases the peak height and limits the amount of sample to be injected on the column due to the formation of a short gradient leading to a nonsymmetrical peak shape with a decrease in the plate number.[12] Alternative deproteinizing mixtures for acetonitrile in HPLC have been proposed.[12]

Effect of acetonitrile in CE: When acetonitrile is present in the sample at a concentration of ~60–80% together with a low concentration of ~1% of sodium chloride (normally present in serum), stacking occurs. In practice, the biological samples (1 volume) are deproteinated by mixing with 2 volumes of acetonitrile and injecting the supernatant after centrifugation directly into the CE apparatus. Acetonitrile can be used to remove the excess of proteins; however, it has several additional advantages in CE. It reverses the harmful effects of ions present in serum, allows larger volumes of sample (about a third of the capillary volume) to be injected, and solubilizes many analytes better. The overall effect is an approximate twentyfold increase in sensitivity (Fig. 3). This is a general stacking method applicable for many compounds. Anionic compounds are easy to stack by this method. Cationic compounds stack better in acetonitrile using a high concentration of zwitterionic buffers (Fig. 4). Two different mechanisms are behind this stacking. Acetonitrile in the absence of salts has low conductivity and hence causes stacking by high field strength. However, acetonitrile in the presence of salts causes stacking by another

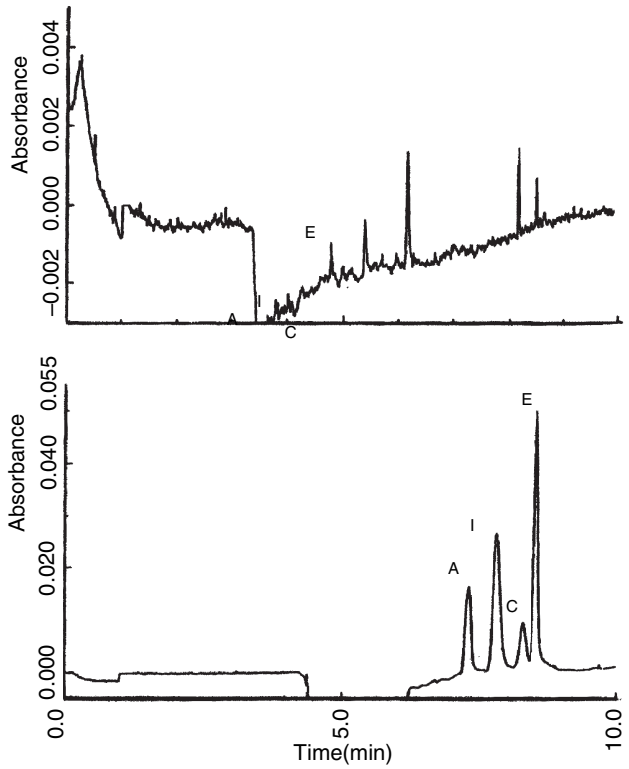

Fig. 3 Separation and stacking of some natural peptides (A = angiotensin, I = insulin B chain, C = impurity in the insulin B chain, and E = Leu-enkephalin). Top: at 1.5% loading of the capillary; bottom: at 30% loading of the capillary.
Source: With permission from Peptide stacking by acetonitrile-salt mixtures for capillary zone electrophoresis, in J. Chromatogr. A.[26]

mechanism, transient pseudo-ITP.[13–16] The salts act as leading ions, while acetonitrile acts as a pseudoterminating ion (i.e., it provides the high field strength for stacking). Short-chain alcohols and acetone can also accomplish the same effect.[13] Optimum conditions for stacking by this method have been described.[15] Further, this method has been extended for the stacking of enantiomers.[16]

Stacking in MEKC

Stacking in MEKC is more difficult than in CZE. It requires controlling of several parameters, and it works for certain compounds better than it does for others, e.g., a higher efficiency of stacking is achieved with highly retained analytes. Also, polarity reversal, which is required in some procedures, is not easily accomplished on some CE instruments.

Several strategies have been devised by Quirino and Terabe for stacking in MEKC.[17,18] The main principles involved are low conductivity in the sample, removing the bulk of the sample buffer, reversed micelle migration, and sweeping (or interaction of) the analytes into the micelles. In the normal stacking mode, the neutral molecules are

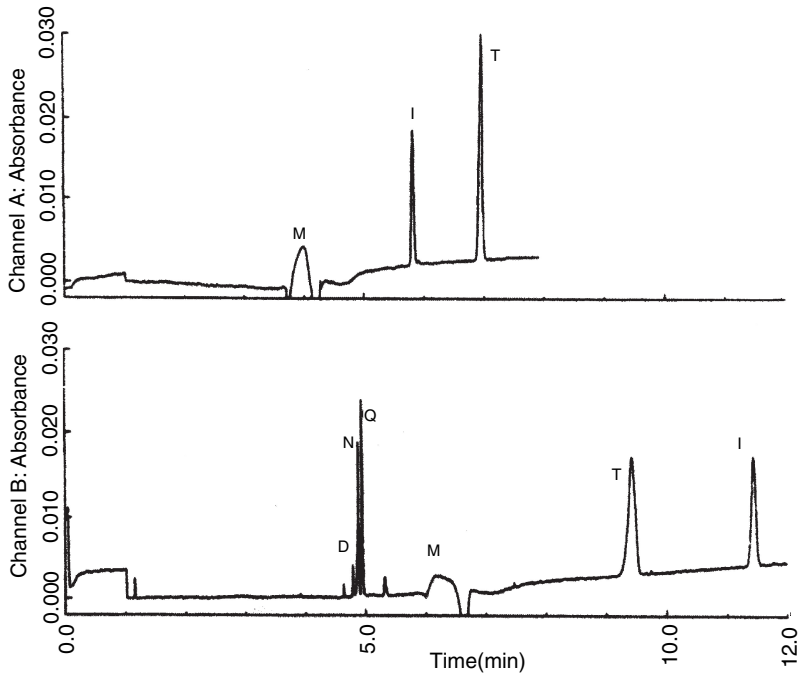

Fig. 4 Effect of the separation buffer type on stacking at a sample loading of 12% of the capillary volume. Top: Borate buffer 210 m*M*, pH 8.6; bottom: triethanolamine 160 m*M*, tricine 50 m*M*, pH 8.6 containing 10% acetonitrile. Separation of a mixture of weakly cationic and weakly anionic compounds in the same run: doxepin (D, 50 mg/L), *N*-acetylprocainamide (N, 50 mg/L), quinine (Q, 20 mg/L), theophylline (T, 50 mg/L) and iothalamic acid (I, 20 mg/L) at 14 kV, 254 nm; (M = Electro-osmotic flow).
Source: With permission from Stacking of weakly cationic compounds by acetonitrile for capillary electrophoresis, in J. Chromatogr. A.[27]

solubilized in a low-conductivity medium, e.g., in water or a very low concentration of micelles, to accelerate their migration. Another approach is to use reversed-migration micelles for stacking. Samples are prepared in low-conductivity matrices and injected as long plugs into the capillary. The polarity of the applied voltage is initially negative to facilitate stacking of the analytes and also the removal of the bulk of the sample matrix. Samples therefore stack as concentrated zones in the boundary between the sample and the separation zones. Once the current reaches 97–99% of the predetermined value, the polarity is switched to positive to enable the separation and detection of the stacked zones.[17] To avoid changes in polarity, the micelles can be prepared in acidic buffer with negative polarity, so that the micelles have a higher electrophoretic velocity than the EOF. The micelles from the cathodic vessel enter the neutral sample zone and cause the stacking, followed by the separation step.[18] Stacking here is mainly dependent on analyte retention factors and the nature of the pseudostationary phases.

Quirino and Terabe have also devised the "sweeping" concept, in which the sample itself has no additives or complexation reagents. These additives are added to the separation buffer. The analyte, the pseudostationary phase, or both should have electrophoretic velocities when an electric field is applied. The extent of preconcentration is dictated by the strength of the interaction between the analyte and the pseudophase.[19] A mixed mode for further stacking is one in which the sample is concentrated first by field-amplified injection under non-micellar conditions. The buffers are changed and the polarity is reversed to induce sweeping of the analytes into a micellar SDS solution, giving a great increase in sensitivity for some cations.

A different approach for stacking introduced by Palmer et al.[20] involves a high-conductivity sample matrix invoked to transfer field amplification from the sample zone to the separation buffer. This causes the micellar carrier in the separation buffer to stack before it enters the sample zone. Micelle stacking is induced by simply adding a salt to the sample matrix to achieve a two- to threefold increase in conductivity as compared to that of the separation buffer. Neutral analytes moving out of the sample zone with EOF are efficiently concentrated at the micelle front.[20] Stacking of neutral analytes based on electrokinetic injection of high-salt sample matrixes by EOF, occurring simultaneously with the injection procedure, has also been described.[20]

SAMPLE BAND BROADENING AND DESTACKING

Band broadening can occur due to many factors in CE. Often it occurs when the sample size is increased greatly in the continuous buffer mode or when the conductivity of the sample increases over that of the separation buffer. It can occur due to thermal effects or band spreading in the connection assemblies. Higher conductivity can accidentally arise from extra salts in the sample or just from a very high concentration of the sample. These effects can lead to non-symmetrical peaks too. Non-symmetrical peaks can appear as migration times (in CE) or migration distances (in agarose electrophoresis), not matching well with those of the standards (Figs. 1 and 2).[2]

METHODS OF SAMPLE PREPARATION FOR CE

Sample extraction and purification yield clean samples suitable for separation by CE. Unfortunately, they require time and extra steps. In the previous section, different simple maneuvers that avoid these extra steps were discussed. However, if the sample analytes are too low in concentration and are present in an unusually complex matrix, sample extraction and purification become necessary as the last resort. Here, several methods used for sample preparation suitable for CE are described. Some of the described methods are applicable to different or several kinds of analytes, while others are more suited for specific ones.

Dilution and Direct Sample Injection

One of the main advantages of CE for routine analysis in industrial and clinical settings is the simplicity of sample introduction. If the compound of interest has a strong absorbance and/or is present in a high concentration relative to that of the interfering compounds, it can be injected directly without any sample preparation or with simple dilution with an appropriate solvent.

To tolerate extra ions in the sample, the ionic strength of the buffer should be as high as possible. Many separations of pure standards utilize very low-ionic-strength buffers so as to apply high voltages and thus accomplish the separation in a short period of time. However, this approach does not work well for biological and industrial samples, where the samples have many components and contain high salts and proteins. In these cases, high-ionic-strength buffers are needed for the separation, which dictate low voltages and thus result in slow separations. High-ionic-strength buffers also favor stacking.

MEKC has the advantage of tolerating small concentrations of proteins without ruining the capillary. The surfactants used for the micelles solubilize the proteins and release the bound drugs (or small molecules). However, the wavelength and the separation conditions have to be chosen in such a way that the proteins do not interfere with or mask the compounds of interest. Several drugs have been successfully analyzed with direct serum or urine injection, especially by MEKC, where the micelles solubilize the proteins.[21]

Extraction with Direct Injection from Organic Solvent

Some analytes can be extracted with organic solvents nonmiscible in water, such as chloroform or methylene dichloride, and injected directly as illustrated in Fig. 5. The advantages include eliminating both the matrix effects and the tedious step of evaporation. However, this will be restricted to compounds highly soluble in the organic solvents and/or present in relatively high concentration.[22]

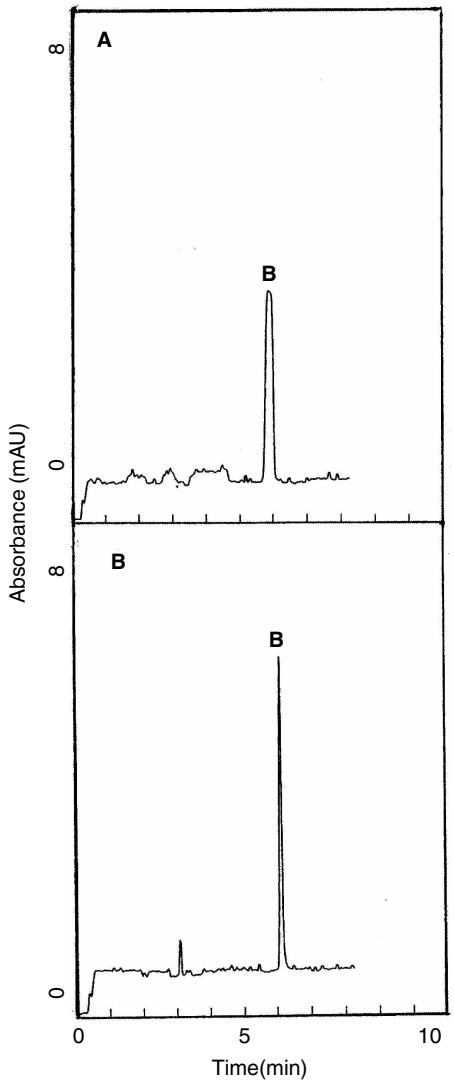

Fig. 5 Extraction of analytes with organic solvents (A) Benzoic acid standard 30 mg/L in the electrophoresis buffer (separation under non-stacking) and (B) Benzoic acid 30 mg/L in 10 mmol/L HCl extracted with chloroform (containing 10% methanol) with direct chloroform injection for 40 sec on a capillary 50 μm × 40 cm, 214 nm, and 12 kV. Separation buffer: boric acid 400 mg, sodium carbonate 200 mg, polyethylene glycol 200 mg in 100 ml water. (B = benzoic acid.)

Extraction and Precipitation

If the analyte is present at very low concentrations in the presence of overwhelming interfering compounds, cleanup and concentration steps become necessary. Solvent extraction procedures similar to those of chromatographic techniques are often used for sample

preparation for drugs and many other small molecules. Solid-phase methods are very popular because of the wide choice of packing material. Sample extraction methods offer two other main advantages in CE, namely, sample concentration and elimination of both sample ions and proteins. Double solvent extraction is very useful for electrokinetic injection, especially for basic compounds. It eliminates the variability resulting from matrix effects in electrokinetic injection. Some compounds such as proteins can be precipitated preferentially with organic solvents and reconstituted.

In the last few years, there has been an interest in new microextraction methods, which are more suitable for CE, especially because this technique does not require large volumes of the sample.[23]

1. *Solid-phase microextraction* (SPME) is a solvent-free sample preparation technique commercially available using a thin coating, such as of polymethylsiloxane, polyacrylate, or carbowax, of varying thicknesses attached to the surface of a fused fiber (e.g., silica) as the extraction medium. The fiber is dipped first into the sample for a certain period of time, then into the eluting solvent, e.g., organic solvent, and injected directly. Initially, this technique was applied for the analysis of organic compounds by gas chromatography (GC) in the field of environmental sciences; however, it has been successfully extended to the analysis of a wide variety of compounds such as naproxen and tricyclic drugs by CE and liquid chromatography (LC). Extraction yield depends on optimizing the pH, salt, temperature, and time.
2. *Molecular imprints*: A template is prepared in such a way that certain selected compounds interact with it, based on steric and chemical memory. They are analogous to antibodies in immunoassays, where they can also be used in competitive assays. Molecular imprints have been used in LC and CE.
3. *Membranes*: In this technique, different membrane types such as microporous, homogenous, ion exchange, and asymmetric have been employed for sample preparation for GC, HPLC, and CE. The extraction in this technique can be further automated.
4. *Immunoaffinity solid-phase extraction*: An antibody attached to a solid material is used to bind the compounds of interest. Optimization of the binding and elution and miniaturization of this type of sample cleaning have been applied for CE and LC.
5. *Homogeneous liquid–liquid extraction*: This uses the phase separation phenomenon from homogeneous solutions as salting effect or cloud point extraction, with the target solute being extracted into a small volume of a separate phase. This method can give high concentration and is suited for CE.

Sometimes extraction does not yield a sufficiently concentrated sample for the desired sensitivity. In such cases, dissolving the sample in an appropriate solvent can give a further concentration based on stacking especially if used in a long and a wide capillary.[24] The importance of sample extraction and concentration together with stacking for CE has been emphasized by dedicating a special issue of *Journal of Chromatography A* to this subject.[23]

Dialysis

Dialysis is one of the simplest techniques for the desalting and purification of proteins; however, it is a slow process. Large molecules can be separated from small ones through special dialysis membranes, which are available with different molecular weight cutoff points. However, the use of small commercial dialysis cells or blocks is more suitable for CE than the use of traditional bags.

Filtration and Ultrafiltration

Small volumes can also be filtered rapidly through special filtration devices in a microfuge at 15,000 × *g*. As in dialysis, the filtration membranes come with different cutoff pores for different molecular weights. Both sides of the filtration chambers can be used for CE analysis based on whether the compound of interest has a high or low molecular weight.

Organic Solvent Deproteinization

In HPLC, alcohols and especially acetonitrile are often added to the biological samples to remove (serum) proteins. In CE, in addition to the removal of proteins, the presence of acetonitrile and small-chain alcohols in the sample leads to stacking, as discussed earlier. Protein removal can also be accomplished by alcohols such as ethanol and by acids such as trichloroacetic acid. In CE, precipitation with acids is less desirable than the precipitation with organic solvents, as it increases the salt load. Following precipitation, proteins can also be dissolved in the appropriate buffers and assayed by CE.

Desalting

Desalting is a difficult procedure to perform in routine assays. There are several methods for desalting, such as: 1) dialysis, as described earlier; 2) using ion exchangers, e.g., Chelax 100 and AG 50X2; and 3) reversing the polarity during CE. Organic solvent extraction is another simple method for eliminating ions. In general, the use of high-ionic-strength running buffers enables the direct analysis of samples containing relatively high salt concentration, eliminating in many instances the need for desalting.

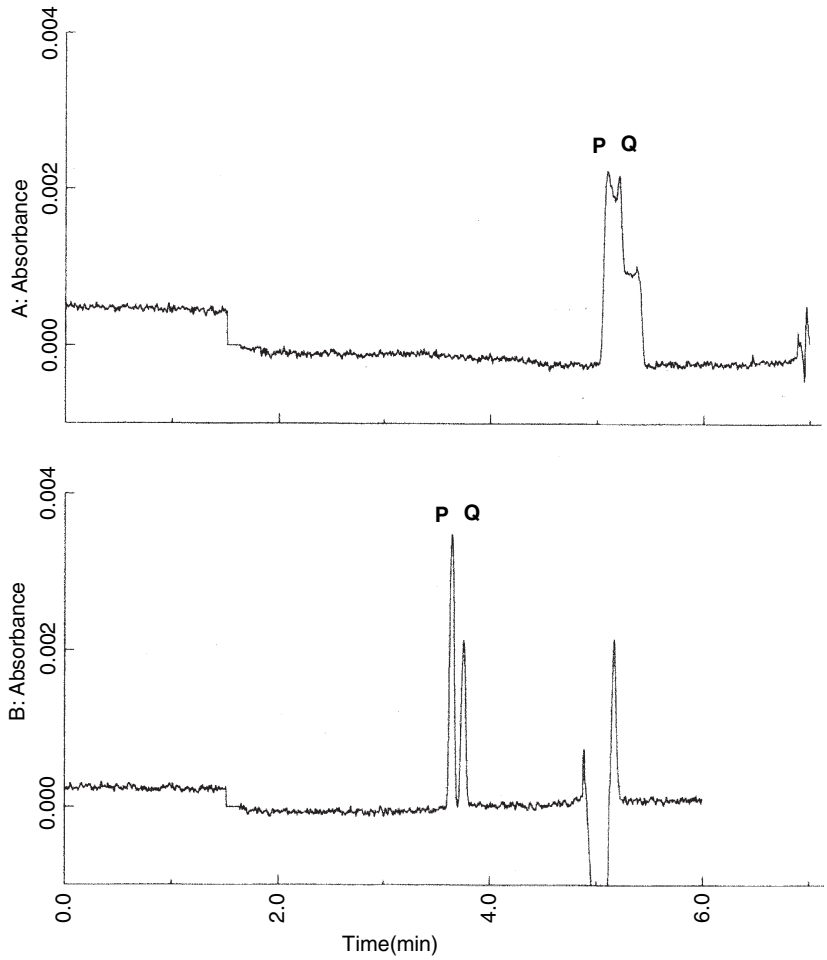

Fig. 6 Comparison of pressure injection vs. electroinjection. Propranolol (P, 10 mg/L) and quinine (Q, 10 mg/L) in serum deproteinated with 2 volumes of acetonitrile. Top: Pressure injection 30 sec; bottom: Electromigration injection at 2 kV for 30 sec. Electrophoresis buffer: 90 mmol/L phosphate buffer, pH 6.2.

Gel Filtration

This technique can be used to purify proteins of different sizes and also for desalting.

Solid-phase ligands binding/antibodies bound to inert beads: The recent interest in proteomics placed great emphasis on analyzing proteins and peptides from biological fluids that are present in very low concentration among numerous different proteins (~10,000), some with very high concentration (such as albumin, globulins, and transferrin). If the abundant proteins are not removed first, they make the analysis very difficult by overloading the capillary. Several methods can be used to remove these proteins and enrich those of interest; some are commercially available as kits. In general, several separation or binding steps are used to remove or enrich these proteins e.g., size exclusion, anion exchange chromatography, hydrophobic chromatography, and especially antibodies bound to inert beads or solid-phase ligands. Several of the purification methods discussed above have been compared for protein purification and analysis by CE.[25]

MATRIX EFFECTS IN ELECTROINJECTION VS. HYDRODYNAMIC INJECTION

The common mode of sample introduction on the capillary is hydrodynamic injection making use of low pressure, vacuum, or height. Electrokinetic injection (or electromigration) is less frequently used. The latter method shows bias in the peaks when multiple components are present in the sample. Early peaks tend to be taller because the more positive components migrate faster. This method is also more susceptible to matrix effects. Small ions, including H^+ present in the sample, decrease the peak height of the analytes, i.e., decrease transfer of the sample to the capillary through a decrease in field strength in the sample. Thus, this method is excellent when dealing with pure samples prepared in water or pure standards.

On the other hand, under appropriate conditions, electroinjection can yield better stacking and better separation than hydrodynamic injection. It has been observed that just by dissolving the sample in acetonitrile, in place of water or an aqueous buffer, 2 to 10 times better stacking can be obtained by electroinjection (due to the high field

amplified injection) as compared to pressure injection (Fig. 6), or as compared to samples prepared in water. As the analytes concentrate at the inlet of the capillary, the whole capillary is left for better separation action. Other organic solvents enhance the sensitivity of electroinjection to different degrees. These solvents offer the added advantage of removing proteins from the sample.

CONCLUSIONS

Unlike in HPLC, the sample matrix is very important in CE. The sample matrix affects resolution, quantification, and precision through its influence on the current conductance and effects on the capillary walls. The sample matrix tends to ruin the separation; however, under appropriate conditions, it can improve separation. Samples with a clean matrix can be injected directly without treatment on the capillary. However, samples from biological or industrial origin and those with low concentration require special preparation or thoughtful planning for separation to avoid the deleterious effects of the sample matrix. In addition, these samples also require special buffers with specific ionic strength, special washing solutions, and steps for the capillary between samples. Different strategies to improve the separation for both hydrodynamic and electroinjection in CE through different methods of sample preparation and buffer manipulation have been presented.

REFERENCES

1. Shihabi, Z.K. Analysis and general classification of serum cryoglobulins by capillary zone electrophoresis. Electrophoresis **1996**, *17*,1607–1612.
2. Shihabi, Z. Effect of sample composition on electrophoretic migration: Application to hemoglobin analysis by capillary electrophoresis and agarose electrophoresis. J. Chromatogr. A, **2004**, *1027*, 179–184.
3. Vinther, A.; Soeberg, H. Mathematical model describing dispersion in free solution capillary electrophoresis under stacking conditions. J. Chromatogr. **1991**, *559*, 3–26.
4. Shihabi, Z.K. Effect of sample matrix on capillary electrophoresis. In *Handbook of Electrophoresis*; Landers, J.P., Ed.; 2nd Ed., CRC Press: Boca Raton, FL, 1997; 457–477.
5. Burgi, D.S.; Chien, R.-L. Optimization in sample stacking for high-performance capillary electrophoresis. Anal. Chem. **1991**, *63*, 2042–2047.
6. Gebauer, P.; Bocek, P. Recent application and developments of capillary isotachophoresis. Electrophoresis **1997**, *18*, 2154–2161.
7. Krivankova, L.; Bocek, P. Synergism of capillary isotachophoresis and capillary zone electrophoresis. J. Chromatogr. B, **1997,** *689*,13–34.
8. Krivankova, L.; Pantukova, P.; Bocek, P. Isotachophoresis in zone electrophoresis. J. Chromatogr. A, **1999**, *838*, 55–70.
9. Foret, F.; Szoko, E.; Karger, B.L. On-column transient and coupled column isotachophoretic preconcentration of protein samples in capillary zone electrophoresis. J. Chromatogr. **1992**, *608*, 3–12.
10. Thompson, T.J.; Foret, F.; Vouros, P.; Karger, B.L. Capillary electrophoresis/electrospray ionization mass spectrometry: Improvement of protein detection limits using on-column transient isotachophoretic sample preconcentration. Anal. Chem. **1993**, *65*, 900–906.
11. Shihabi, Z.K. Stacking in capillary zone electrophoresis. J. Chromatogr. A, **2000**, *902*, 107–117.
12. Shihabi, Z.K. Analytes Recovery from deproteinized serum for HPLC. J. Liq. Chromatogr. & Relat. Tech. **2008**, *31*, 3159–3168.
13. Shihabi, Z.K. Transient pseudo-isotachophoresis for sample concentration in capillary electrophoresis. Electrophoresis **2002**, *23*, 1612–1617.
14. Shihabi, Z.K. Therapeutic drug monitoring by capillary electrophoresis (review). J. Chromatogr. A, **1998**, *807*, 27–36.
15. Kong, Y.; Zheng, N.; Zhang, Z.; Gao, R. Optimization stacking by transient pseudo-isotachophoresis for capillary electrophoresis: Example: Analysis of plasma glutathione. J. Chromatogr. B, **2003**, *795*, 9–15.
16. Choy, T.M.; Chan, W.-H.; Lee, A.M.; Huie, C.W. Stacking and separation of enantiomers by acetonitrile–salt mixtures in micellar electrokinetic chromatography. Electrophoresis **2003**, *24*, 3116–3123.
17. Quirino, J.P.; Terabe, S. Online concentration of neutral analytes for micellar electrokinetic chromatography: II. Reversed electrode polarity stacking mode. J. Chromatogr. A, **1997**, *791*, 255–267.
18. Quirino, J.P.; Terabe, S. On-line concentration of neutral analytes for micellar electrokinetic chromatography. 3. Stacking with reverse migration micelles. Anal. Chem. **1998**, *70*, 149–157.
19. Quirino, J.-P.; Kim, J.-B.; Terabe, S. Sweeping: concentration mechanism and applications to high-sensitivity analysis in capillary electrophoresis. J. Chromatogr. A, **2002**, *965*, 357–373.
20. Palmer, J.; Munro, N.J.; Landers, J.P. A universal concept for stacking neutral analytes in micellar capillary electrophoresis. Anal. Chem. **1999**, *71*, 1679–1687.
21. Shihabi, Z.K.; Hinsdale, M.E. Serum iohexol analysis by micellar electrokinetic capillary chromatography. Electrophoresis **2006**, *27*, 2458–2463.
22. Shihabi, Z.K. Direct injection of organic solvent extracts for capillary electrophoresis. Electrophoresis **2008**, *29*, 1672–1675.
23. Shihabi, Z.; Deyl, Z. Preconcentration and sample enrichment techniques. J. Chromatogr. A, **2000**, *902*, 1–309.
24. Shihabi, Z.K. Enhanced detection in capillary electrophoresis: Example determination of serum mycophenolic acid. Electrophoresis **2009**, *30*, 1516–1521.
25. Blanco, D.; Junco, S.; Expósito, Y.; Gutiérrez, D. Study of various treatments to isolate low levels of cider proteins to be analyzed by capillary sieving electrophoresis. J. Liq. Chromatogr. **2004**, *27*, 1523–1539.
26. Shihabi, Z.K. Peptide stacking by acetonitrile-salt mixtures for capillary zone electrophoresis. J. Chromatogr. A, **1996**, *744*, 231–240.
27. Shihabi, Z.K. Stacking of weakly cationic compounds by acetonitrile for capillary electrophoresis. J. Chromatogr. A, **1998**, *817*, 25–30.

Sample Preparation for HPLC

Ioannis N. Papadoyannis
Victoria F. Samanidou
Laboratory of Analytical Chemistry, Chemistry Department, Aristotle University of Thessaloniki, Thessaloniki, Greece

INTRODUCTION

Among the various steps of a sample analysis, from sample collection to the final report of the results, the most tedious and time-consuming one is the *sample preparation*, which requires almost two-thirds of the total analysis time. It is also the most error-prone part of the process, as it contributes about 30% in the sources of errors, impacting on the precision and the accuracy of the overall analysis.

An effective sample preparation helps the analytical chemists to cope with today's increasing demands in the laboratory. No matter how sophisticated the available analytical equipment is, the limits of the analytes' detectability in any analytical procedure eventually depend on the effectiveness of the sample preparation.

OVERVIEW

The main objectives of sample preparation are as follows:

1. Matrix modification in order to:
   a. Prepare the sample for introduction (injection) onto chromatographic column.
   b. Render the solvent suitable for the analytical technique to be used.
   c. Prolong the instrument's lifetime (e.g., column lifetime).
2. Clean-up purification in order to:
   a. Remove impurities and obtain the required analytical performance and selectivity.
   b. Reduce matrix interference.
3. Analyte enrichment (preconcentration) in order to improve the method sensitivity (reduction of the limits of detection and quantification).

The sample, prior to high-performance liquid chromatography (HPLC) analysis, has to be in a liquid state. By contacting the sample with a solvent, the analytes are extracted. Then, the solvent is separated from solid residue by means of decantation, filtration, or centrifugation. Furthermore, it can be concentrated by evaporation.

Typical traditional and modern approaches of sample preparation techniques for liquid and solid samples are summarized in Table 1. These techniques are further discussed under the respective paragraphs.

SELECTION OF THE SUITABLE SAMPLE PREPARATION TECHNIQUE

The term sample preparation may refer to the various stages of the analysis procedure, as shown in Fig. 1. An ideal sample pretreatment technique should have the following characteristics:

1. Simplicity and rapidity.
2. High extraction efficiency with quantitative and reproducible analyte recoveries.
3. Specificity for the analytes.
4. High sample throughput.
5. Fewer manipulation steps to minimize the analyte losses.
6. Amenability to automation.
7. Use of the minimum amount of solvent, compatible with many analytical techniques.
8. Low cost regarding reagents and equipment.

As no ideal sample preparation technique exists, each technique has to be considered according to its own advantages and disadvantages. The analyst may choose the most suitable one when developing a method, depending on several parameters such as sample matrix, nature, physical and chemical properties of analytes, concentration, and analytical technique that is to be applied.

Automation is one issue of paramount importance, as the biggest problem with sample preparation is time. The benefits of automation, apart from the obvious economic one, include the reduced manual operations and laboratory materials required, the increased sample throughput and productivity per instrument, and the higher precision with minimal risk regarding the handling of contagious or radioactive samples.

Table 1 Typical sample preparation techniques for liquid and solid samples.

Liquid samples	Solid samples
Dilution	Solid–liquid extraction (shake filter)
Evaporation	Forced-flow leaching
Distillation	Soxhlet extraction and automated Soxhlet extraction
Microdialysis	Homogenization
Lyophilization	Sonication
Liquid–liquid extraction (LLE)	Dissolution
Automated LLE	
Solid-phase extraction (SPE)	Matrix solid-phase dispersion
Automated SPE	
SPE disk technology	Accelerated solvent extraction
SPME	Supercritical fluid extraction (SFE)
Direct analysis by column-switching techniques (online techniques)	Microwave-assisted extraction
Stir bar sorptive extraction	Gas-phase extraction Thermal desorption

Source: From Sample preparation perspectives, in LC GC Int. [1]

PRELIMINARY SAMPLE PREPARATION PROCEDURES

Frequently, intermediate stages may be required prior to the extraction techniques for sample preparation. These are to minimize the analyte solubility in the matrix and to maximize the selective isolation for a quantitative, rapid extraction of the analyte of interest (e.g., changing of pH or ionic strength). Proteins must be removed prior to extraction by denaturation with organic solvents or chaotropic agents, precipitation with acid (pH modification), addition of a compound that competes for binding sites, or use of restricted-access media. Conjugated components may need to be hydrolyzed to release the free compound. Lipids may be extracted into a non-polar organic solvent.

Once transferred into a liquid phase, the sample can either be directly injected or treated further using the steps outlined in Table 2.

TRADITIONAL LIQUID SAMPLE PREPARATION TECHNIQUES

Liquid–Liquid Extraction

Sample dilution can occasionally be applied if the analyte is present in such a high concentration that the analyte is still detectable, although this is rarely efficient. For the major part of the analyses, the analyte has to be isolated from the sample by using an extraction technique.

For many years, liquid–liquid extraction (LLE) was the classical technique for the preparation of liquid samples. In spite of several drawbacks, it was widely used in all fields of analysis. It usually involves mixing of an aqueous sample solution with an equal volume of immiscible organic solvent for a period of time, and then allowing these two liquid phases to interact so that the analytes of interest are extracted from the aqueous layer into the organic layer, as the organic solvent has a larger affinity for them. The selectivity and efficiency of the extraction process are governed by the choice of the two immiscible liquids. The more hydrophilic compounds prefer the aqueous phase, and the more hydrophobic compounds will be found in the organic solvent, as

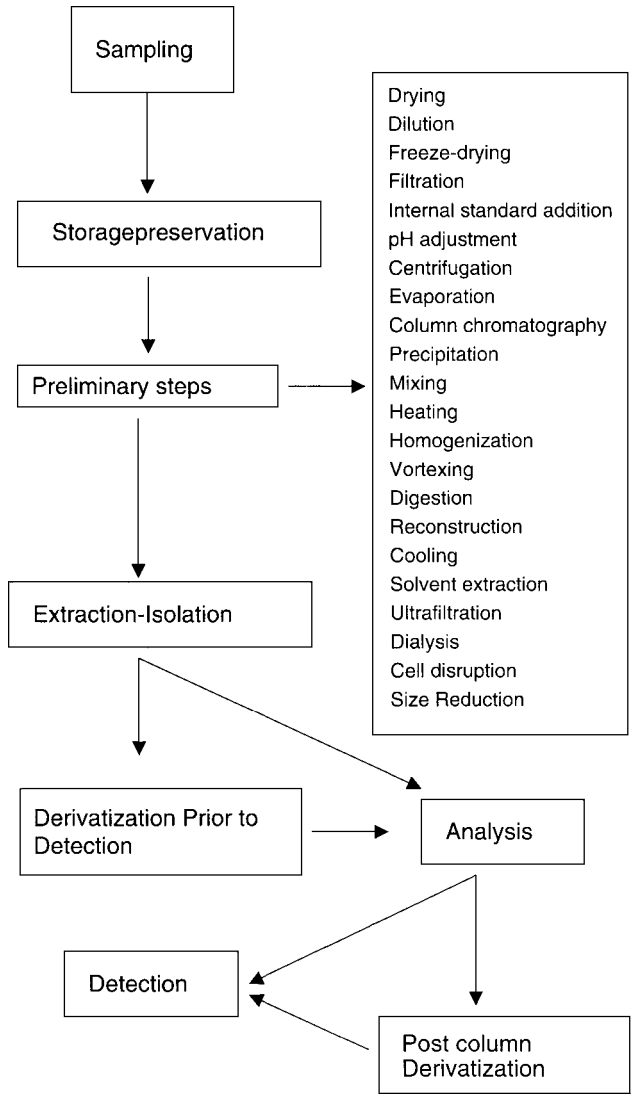

Fig. 1 Stages of sample preparation.

Table 2 Further treatment requirements for a sample in liquid phase before analysis.

- Dilution to the appropriate concentration ranges with a compatible solvent in case it is too concentrated.
- Concentration by LLE, SPE, evaporation, or lyophilization.
- Derivatization to stabilize, freeze-drying, and storage at 4°C, far from light or air exposition, in case it is reactive or thermally or hydrolytically unstable.
- Removal of unwanted high-molecular-weight substances by size exclusion chromatography, dialysis, ultrafiltration, precipitation, and use of supported liquid membrane.
- Removal of particulate matter by filtration, centrifugation, or sedimentation.
- Solvent exchange if the solvent is not compatible with the analytical method.
- Solvent can be removed by evaporation, lyophilization, or distillation, and the analytes can be reconstituted in a solvent and at a concentration suitable for the technique that will be used for analysis.
- Addition of internal standard.

"like" dissolves "like." Organic solvents such as methylene chloride, chloroform, ethyl acetate, and diethyl ethers are preferred as they can be easily removed by evaporation. Chelating and other complexing agents, ion pairing, and chiral reagents may also be used. After the immiscible liquids are separated, the layer containing the extracted analytes is removed, concentrated to dryness, and reconstituted in an appropriate solvent that is compatible with the analytical system (e.g., the HPLC mobile phase).

A limitation of this technique is that polar, water-miscible solvents cannot be used for the extraction. Other drawbacks of this technique are:

1. The use of large quantities of organic solvents, leading to a considerable cost for their acquisition and disposal.
2. The formation of emulsions during the mixing procedure.
3. Evaporation of the solvent is time-consuming.
4. The coextraction of other matrix-interfering components with similar properties.
5. It is difficult to be automated in its classical form (using a separation funnel or similar apparatus), although a number of flow-system LLE approaches have been presented, applying the principle of flow injection analysis.

In the latter approach, a chemical reaction or complexation takes place in a mixing-reaction coil, resulting in an extractable component segmented with an organic immiscible solvent steam at the phase segmenter, where small reproducible droplets of one phase are formed in the other. The phase containing the analytes of interest can be monitored by a flow-through detector, and the unwanted phase is directed to waste.

Automation in LLE has been also introduced using an instrumentation that can automate all or part of the extraction and concentration process. A number of autosamplers and workstations for HPLC and gas chromatography (GC) can perform LLE. Robotic systems can be used to handle larger-volume LLE.

Column Extraction–Liquid–Liquid Extraction

Column extraction based on the theory of LLE is a widely used technique in biochemistry, toxicology, pharmaceutical analysis, and other fields. Extrelut by Merck (Darmstadt, Germany) and Extube by Varian (Harbor City, California, USA) are commercially available prepacked columns used in these applications (Fig. 2A). Extraction is performed by fixing an aqueous solution or suspension to a supporting material (stationary phase) and allowing the other immiscible solvents (mobile phase) to pass over it. The two phases are in contact, thus permitting a continuous and multistep extraction to occur. This technique can replace the conventional LLE in a separating funnel, and thus it becomes more efficient and practical as no emulsions can be formed, less solvent volumes are used, and preparation time is reduced. Body fluids (e.g., urine) are the best example for the application of in-column LLE.

MODERN LIQUID SAMPLE PREPARATION TECHNIQUES

Solid-Phase Extraction

Solid-phase extraction (SPE) is a particularly attractive, fast, and effective technique for the isolation and preconcentration of target analytes that avoids or eliminates the disadvantages of LLE, tending to replace it in many applications.

The principle of SPE involves a partitioning of analytes to be extracted between two phases: a solid phase, the sorbent, and a liquid phase, the matrix, which contains possible interferences. Analytes must have a greater affinity for the solid phase than for the sample matrix (retention or adsorption step), and they are subsequently removed by eluting with a solvent that has a greater affinity for the analytes (elution or desorption step). The different mechanisms of retention or elution are a result of intermolecular forces among three components: the analyte, the active sites on the surface of the sorbent, and the liquid phase or matrix.

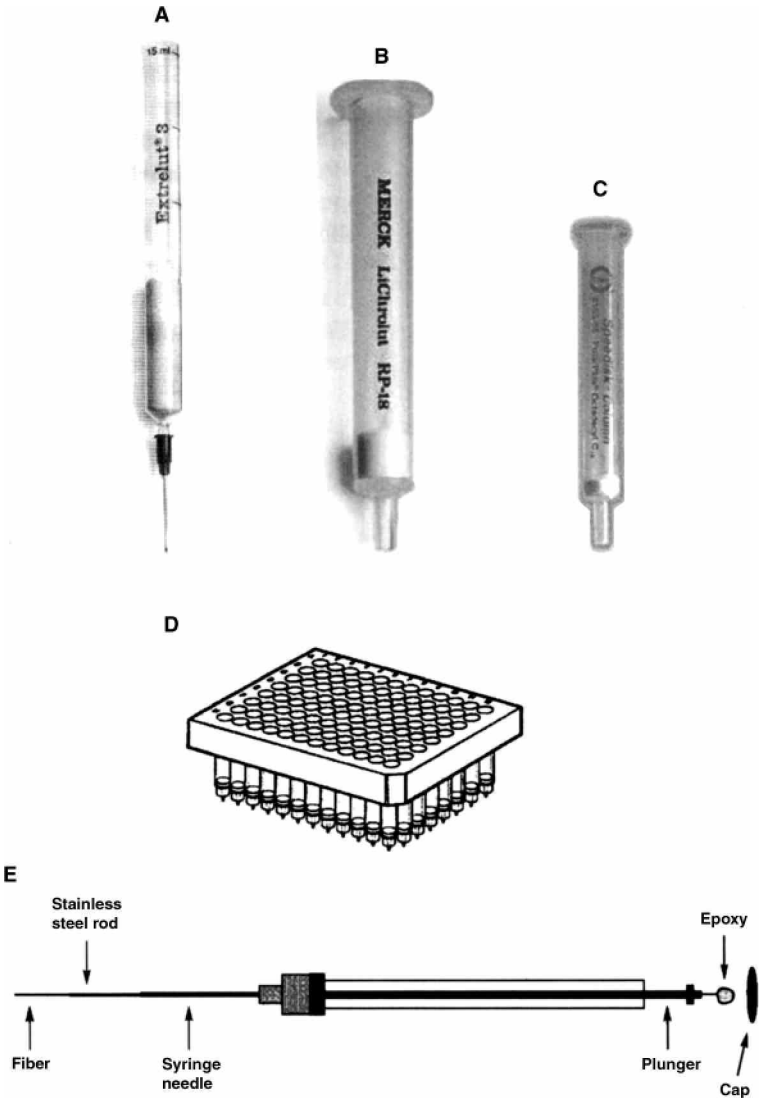

Fig. 2 (A) Extrelut column for LLE; (B) SPE cartridge; (C) SPE cartridge, disk format; (D) 96-well extraction plate; and (E) SPME device.

Solid-phase extraction objectives, apart from the removal of interfering compounds and the preconcentration of the sample, include:

1. The fractionation of the sample into different compounds or groups of compounds as in classical column chromatography.
2. The storage of analytes that are unstable in a liquid medium or with relatively high volatility.
3. The derivatization by reactions between the reactive groups of the analyte(s) and those on the adsorbent surface.

The major types of commercially available SPE product configurations are:

1. Syringe barrel columns.
2. Cartridges.
3. 96-Well plates.
4. Disk membranes.
5. Solid-phase extraction vacuum manifolds for simultaneous processing of 10, 12, 20, and 24 SPE tubes.

Fig. 2 illustrates the typical commercially available SPE formats.

Solid-phase extraction cartridges are available in a wide variety of sizes, with packing capacities ranging from 20 mg to 10 g and with reservoir volumes as large as 30 ml. In this configuration, extraction is carried out by a disposable cartridge of polypropylene, in a shape similar to an injection syringe without plunger and without injection needle. The column is filled with the sorbent (particle size of 40 μm) fixed between two frits (pore size of 20 μm) of polypropylene. The upper part of the barrel serves as a sample reservoir. The column can be connected to extraction systems by Luer fittings.

Although gravity can facilitate the flow of most organic solvents through the columns, samples and more viscous

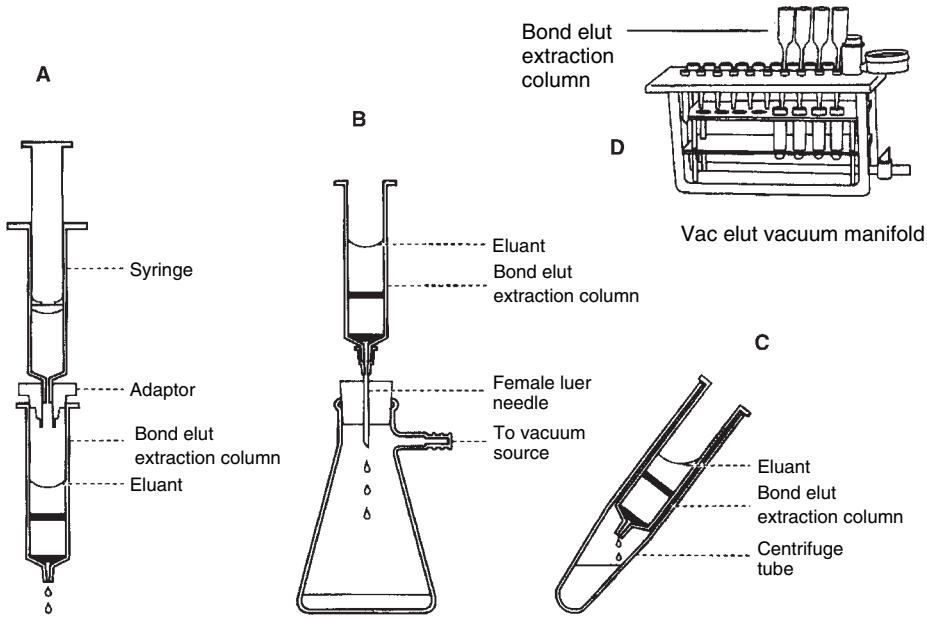

Fig. 3 Different ways of SPE process. (A) Positive pressure; (B) vacuum; (C) centrifugation; and (D) vacuum manifold.

solvents must be drawn by vacuum applied to the column outlet, by positive pressure applied to the column inlet (gas pressure from a syringe), or by centrifugation (Fig. 3). The typical flow rate ranges between 0.2 and 1.5 ml/sec.

All sample types are amenable to SPE with suitable handling: solids, liquids, semisolids, etc. Solid-phase extraction is extensively used in sample preparation, as it offers a fast, safe, and convenient means for subsequent analysis by chromatographic techniques [HPLC, thin-layer chromatography (TLC), GC, etc.]. The major benefit is that it requires less solvent than conventional LLE methods. Impurities are removed and the analytes are concentrated, leading to a higher sensitivity in subsequent analysis. The SPE process can be carried out either online or off-line.

Solid-phase extraction is performed according to the following steps:

1. Conditioning of the sorbent (i.e., solvation; activation of functional groups) and preparation of the sorbent to interact with the sample.
2. Sample loading. The sample, optionally containing the internal standard, is forced through the sorbent of the cartridge. The component of interest and some undesired compounds are adsorbed by the sorbent. In this step, the interaction between the analyte and the sorbent should be predominant. The most effective sorbent facilitates the interaction between the functional groups and the analyte. To enhance the retention of the analyte, the sample can be diluted with water, so that the polarity of the environment of the analyte is increased.
3. Washing to remove the undesired polar matrix constituents. A solvent of low elution strength is chosen as a washing solvent (water or a buffer) so that the analyte is not eluted from the sorbent. Only after the completion of this step may some air pass through the column.
4. Sorbent drying. This may be necessary to remove water if the elution solvent is immiscible with it. Drying can be performed by vacuum aspiration, nitrogen flow, or centrifugation. Analytes in a purified form are now present on the column.
5. Elution or extraction process. This aims for the quantitative recovery of the analyte that is achieved by selective desorption of the compounds of interest from the sorbent with a suitable solvent and collects the cartridge effluent. The interaction between the analyte and the elution solvent should be so strong that the interaction between analyte and sorbent will be overcome.
6. Solvent evaporation. The extract is directly injected or evaporated under a gentle stream of nitrogen and reconstituted in the mobile phase or after the addition of internal standard.

The optimization of SPE must be executed in each of these steps for best performance. Two different approaches can be chosen:

1. The analyte is retained on the sorbent while components pass through to waste. The analyte will be eluted later from the sorbent, with a suitable solvent, to be analyzed.
2. The matrix components are adsorbed while the analyte is evacuated.

The first approach is generally preferred as less sorbent is required and isolate preconcentration is possible. The

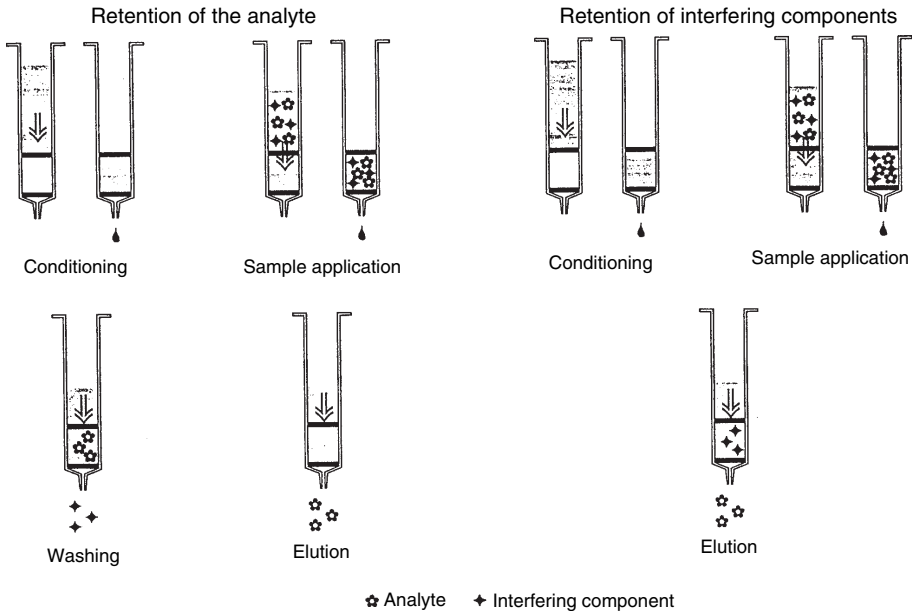

Fig. 4 The steps of solid-phase extraction technique.

second approach is selected when interferences are present but the concentration of analytes is not required (Fig. 4).

Solid-Phase Extraction Sorbents

Several SPE sorbents have been developed. These can be classified according to the primary interaction possibilities of the functional groups of the sorbents, mostly non-polar, polar, or ionic. Ionic groups consist of cation exchange and anion exchange sorbents and contain functional moieties that can act as ion exchangers. Silica-based sorbents include the following: reversed phase (RP)—highly hydrophobic octadecyl (C_{18}), octadecyl (C_{18}), octyl (C_8), ethyl (C_2), cyclohexyl, and phenyl; wide-pore RP—butyl (C_4); normal phase—silica modified by cyano (–CN), amino ($–NH_2$), and diols; adsorption, silica gel, fluorisil, and alumina; and ion exchangers, amino ($–NH_2$), quaternary amine (N^+), carboxylic acid (–COOH), and aromatic sulfonic acid ($ArSO_2OH$). Other sorbents with a wide variety of specifications are also introduced in SPE: polymeric sorbents are polystyrene–divinylbenzene (PS–DVB) resins that overcome many of the limitations of the silica-based phases. The broader range of pH stability increases the range of method development and flexibility, providing greater analyte retention of polar compounds than C_{18} sorbents. However, a conditioning step with a wetting solvent is still required.

Hydrophilic–lipophilic polymeric sorbents have been recently introduced, claiming that no conditioning step is required as the sorbent preserves analyte retention, even if the bed dries out. Commercially available products include Oasis by Waters and Abselut by Varian. These are copolymers of polyvinyl pyrrolidone (a hydrogen acceptor, which increases the water wettability of the polymer) and a cross-linked PS–DVB resin that provides the RP retention necessary to retain analytes. These are designed to extract an extensive spectrum of analytes: lipophilic, hydrophilic, acidic, basic, and neutral. They exhibit greater pH stability and enhanced retention over C_{18}-bonded silica.

Mixed-mode sorbents contain both non-polar and strong ion (cation and/or anion) exchange functional groups, targeted for the extraction of basic drugs.

Affinity sorbents such as the *restricted-access matrix* sorbents, *immunosorbents*, or *molecularly imprinted polymers* (MIPs) have been introduced as well. These are based upon molecular recognition using antibodies with a high degree of selectivity or with molecularly imprinted polymer.

Graphitized carbon: Porous graphitic carbon, similar to the liquid chromatography (LC)-grade Hypercarb, is available in SPE cartridges. This is characterized by a highly homogenous and ordered structure, made of large graphitic sheets with a specific area approximately 120 m^2/g. Compounds are retained by both hydrophobic and electronic interactions so that non-polar analytes, and also very polar analytes, can be retained from aqueous matrices. Owing to the different retention mechanism, acetonitrile and methanol can be inefficient, and it is preferable to use methylene chloride or tetrahydrofuran.

Column selection is based on the nature of the analytes, the nature of the sample matrix, the degree of purity required, the nature of the major contaminants, and the analytical technique applied.

Sorbent–Isolate Interaction

The most common chemical interactions between sorbent and isolates are non-polar (van der Waals forces or

dispersion forces), polar (hydrogen bonding, dipole–dipole, and induced dipole–dipole), ion exchange (ionic), and covalent interactions.

Non-polar interactions are the weakest interactions, which are exerted between the CH bonds of the analyte and those of the sorbent, usually C_{18}. Because these are facilitated by a polar solvent environment, they play a crucial role in the bioanalysis of blood, plasma, serum, and urine.

Isolated compounds include alkyl, aromatic, alicyclic, or functional groups with significant hydrocarbon structure. All isolates have a potential for non-polar interaction (except inorganic ions and compounds with polar groups, e.g., carbohydrates). Because of this fact, the non-polar interactions are non-selective and allow the extraction of groups of compounds with different structures. Retention is facilitated by a polar solvent, while elution is facilitated by an organic solvent with sufficient non-polar character (MeOH, ACN, etc.). A wash solvent should be more polar than that used for elution.

Polar interactions occur between a polar group of the sorbent and a polar group of the isolate. Silica is the typical adsorbent. Examples of groups that exhibit polar interactions are carbonyl, carboxyl, hydroxyl, sulfhydryl, and amine groups; rings with hetero atoms and with unequal electron distributions; as well as groups with π-electrons, such as aromatic rings and double or triple bonds. Hydrogen bonding is one of the most significant polar interactions. Polar interactions are stronger than non-polar ones. Although they provide greater selectivity, they have the disadvantage of being facilitated by a non-polar environment. Highly polar solvent facilitates elution, while wash solvent should be less polar than those used for elution.

Ionic interactions are exhibited between two groups (of analyte and sorbent) with opposite charge. These are the strongest interactions that can be seen between an analyte and a sorbent. Because few compounds possess either a cationic or an anionic group, the selectivity is high. Ionic interactions can only be effected in a polar environment. For an actual ionic interaction, it is necessary that the respective functional groups of sorbent and analyte are both ionized. Analytes can be eluted in two ways:

1. By using an elution solvent of such a pH that the respective functional groups of either the sorbent or the analyte are neutralized.
2. By using an elution buffer with a high concentration of a counterion (an ion of a charge opposite to that of the functional group of the sorbent), which will compete for the active sites of the sorbent with the analyte. Evidently, a combination of both elution ways is possible.

Applications of SPE include clinical analysis, pharmaceuticals, food analysis, environmental analysis, agrochemicals, forensic samples, etc.

Solid-Phase Extraction Disk Technology

Solid-phase extraction in disk format has been designed to overcome the limitations of the conventional packed-bed SPE columns. Disks exhibit minimal channeling, have small void volumes, do not require frits, have low capacity for interference (cleaner extracts are provided), and capture analytes of interest very effectively. They require lower solvent volumes, providing a faster sample processing and an increased throughput. Disk products include rigid disk, flexible disk, and thin packed beds of small particles between two retained screens.

A typical extraction sequence is similar to the traditional SPE, although 500 μl of the appropriate solvent is sufficient for disk conditioning and extraction of the analytes. Several types of disk extraction media are commercially available in different dimensions depending on the application and sample volume. The most prevalent are paper-based, membrane-based, glass fiber-based, and polytetrafluoroethylene (PTFE)-based products. Commercially available products are Speediscs by Baker, Empore by 3M, Novo Clean by Alltech, and SPEC by Ansys Technol.

AUTOMATED SOLID-PHASE EXTRACTION SYSTEMS

Solid-phase extraction automation is accomplished off-line and online. In off-line automation, SPE cartridges are not directly connected to the high-pressure flow stream of the analytical instrument. In online SPE, the solid-phase device is inserted into, and becomes part of, the liquid or gas flow stream. Obviously, the hardware interfacing requirements for the two approaches differ. In the manual mode, a simple vacuum is used to pull the liquids through the cartridge. However, in the automated mode, positive gas or liquid pressure is more commonly used to push liquids through the cartridge. Off-line automated SPE usually involves some form of robotic manipulation using flexible robotic arms and semiflexible modified *x–y–z* liquid handling devices. Most of these systems are controlled by dedicated personal computers.

The benefits of the automated solid-phase extraction are:

1. Analysts can redirect their time to other tasks.
2. Automated systems can provide a higher sample throughput with higher accuracy and precision because of minimized systematic errors than do manual systems.

Early automated systems processed individual samples *in series*. The next sample in the series was not started until

the preceding sample had been completed or was on its way. However, this approach was slower than manual systems. Automated *parallel processing* SPE, where numerous samples are extracted simultaneously with significantly improved throughput, seems to be more practical. Such automated systems can achieve treatment of up to 400 samples per hour.

Autosamplers offer at some level sample preparation functions such as dilution, internal standard addition, and calibration standard preparation. In addition, some automated liquid handling devices have built-in heating, cooling, SPE, and other functions for performing automated sample preparation. These operations are controlled by a computer system.

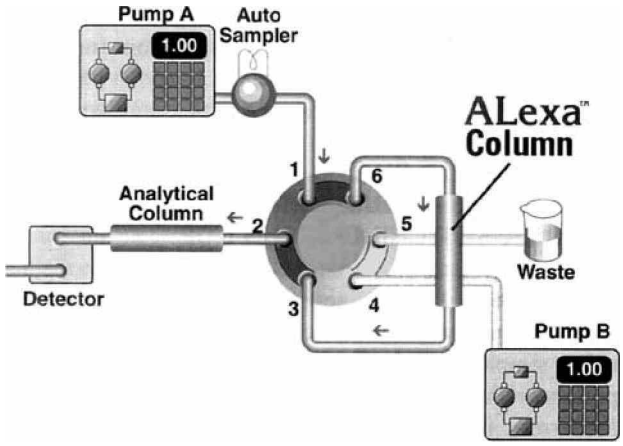

Fig. 5 Online SPE–LC column-switching technique.

ONLINE SOLID-PHASE EXTRACTION–LIQUID CHROMATOGRAPHY COLUMN-SWITCHING TECHNIQUE

Online SPE–LC utilizes the principle of *column switching*. A typical online arrangement is performed using simple electrically or pneumatically driven (six-port) switching valves and commercial precolumns and holders. A fresh disposable precolumn is used for every sample, and extraction is carried out in a way similar to the off-line sequence. A solvent delivery unit provides the solvent necessary to purge, wash, and activate the precolumn, and to apply the required volume of sample. High-pressure switching valves are used to couple two or more columns that trap either defined volumes or the collected samples, usually in a loop, and direct them to a second, usually the analytical, column. Valve configuration can be used for conventional HPLC analysis, and it can perform more advanced functions such as diverting the mobile phase containing the desired solutes from the first column to the second column for defined periods of time, a process called *heart-cutting* or *on-column concentration* (trace enrichment). Additionally, it can perform "backflushing" of specific sample components from one column to waste, which leaves only the peak of interest on the second column and front-cutting and end-cutting when needed. Selecting the appropriate valve and actuating it at the correct time cause different fractions of the sample to follow different paths through the column network.

In the most common case, the pretreated biofluid is injected onto the cartridge or precolumn, which retains the target molecules. Interfering sample constituents are flushed into waste. The analytes retained on the bonded phase of the cartridge or precolumn are eluted, online, via the switching valve onto the analytical column. Simultaneously to the analytical separation, an exchange of the cartridge or reconditioning of the precolumn takes place (Fig. 5).

The separation of the sample occurs not only by chromatographic means, but also by physical means that are under the control of the analyst and unrelated to the chemical properties of the analyte, thus resulting in very efficient separations.

Column-switching techniques have been used to analyze a sample directly, without any pretreatment stages, with the advantage of easy automation. The increase in safety and the improved analytical speed and accuracy often make up for the initial cost of the additional equipment that is required. Automating the column-switching systems can usually be accomplished using the timed-event tables included with HPLC instrument-control software; this enables a simpler and a more accurate control of complex column networks with minimal contamination and loss.

The limitation of column switching includes restricted sample enrichment. Another limitation is that the sample throughput using this approach probably will not be as high as for the other methods. Finally, it is considered too complicated to be practical, although modern instruments make these procedures relatively straightforward.

SOLID-PHASE MICROEXTRACTION

Solvent-free sample preparation techniques attract widespread attention to reduce the use of toxic organic solvents. Solid-phase microextraction (SPME) is a *solvent-free* technique for sample preparation that can integrate sampling, extraction, concentration, and sample introduction into single step, resulting in high sample throughput.

Generally, the term *microextraction* refers to an extraction technique where the volume of the extracting phase is very small in relation to the volume of the sample, and the extraction of the analytes is not exhaustive. The fraction of the initial analyte extracted depends on the partitioning of the analyte between the sample matrix and the extraction phase. The higher the affinity of the analyte for the extraction phase, the greater the amount of analyte is extracted.

Once sufficient extraction time has been reached and equilibrium has been established, further increases in extraction time do not affect the amount of analyte extracted.

Solid-phase microextraction is an adsorption/desorption technique used to analyze the volatile and non-volatile compounds in both liquid and gaseous samples used as an alternative to the headspace, purge-and-trap, solid-phase extraction, or simultaneous distillation/extraction techniques. Analytes are thermally desorbed and directly introduced into any gas chromatograph or GC/mass spectrometry (MS) system. When coupled to HPLC with the proper interface, the analytes are washed out of the fiber by the mobile phase.

The SPME device, shown in Fig. 2E, consists of a 1 cm length of narrow diameter fused silica optical fiber, coated on the outer surface with a thin film of stationary phase and bonded to a stainless steel plunger, and a holder such as a modified microsyringe. The fused silica fiber can be drawn into a hollow needle by using the plunger on the fiber holder. The fiber assembly consists of an outer protective septum-piercing needle and an inner fiber attachment needle to which the fiber is epoxied. The septum flange prevents GC or HPLC mobile phase from escaping when injecting. When not in use or during transfer, the fiber retracts into the needle. The SPME processing steps include:

1. Penetration of the syringe through the septum of the sample vial.
2. Extension of the fiber into the sample or in the headspace. Organic analytes partition into the stationary phase of the fiber until equilibrium is reached.
3. Retraction of the fiber into the syringe needle and, once the equilibrium is reached, withdrawal of the syringe from the sample vial.
4. Insertion/introduction of the needle into the GC port, depression of the plunger, and thermal desorption of the analytes. Alternatively, the analytes are washed out of the fiber by the HPLC mobile phase via a modified HPLC six-port injection valve and a desorption chamber that replaces the injection loop in the HPLC system. The SPME fiber is introduced into the desorption chamber, under ambient pressure, when the injection valve is in the load position. The SPME/HPLC interface enables mobile phase to contact the SPME fiber, remove the adsorbed analytes, and deliver them to the separation column. Analytes can be removed via a stream of mobile phase (dynamic desorption) or, when the analytes are more strongly adsorbed to the fiber, the fiber can be soaked in mobile phase or another stronger solvent for a specific period of time (e.g., 1 min) before the material is injected onto the column (static desorption) (Fig. 6).
5. Removal of the syringe from the injection port. It is now ready for resampling. The thermal or solvent treatment of the coated fiber in the injection port ensures that the fiber is free from interferences or residual compounds.

With solid or dirty matrices, such as sludge and biological fluids, the technique can be operated in the headspace mode as the fiber is exposed to the gas phase above the sample. Agitation by stirring or sonication of the sample matrix improves the transport of analytes from the bulk sample phase to the vicinity of the fiber. Other parameters that influence the partition equilibrium are the sample matrix, temperature, and properties of the coating and analyte (e.g., the thickness of the coating and the distribution constant for the analyte). An equilibrium time of 30–60 min is usually enough for direct immersion SPME. Full equilibrium is not necessary for high accuracy and precision from SPME, but consistent sampling time and other sampling parameters are essential. The vial size, the sample volume, and, when using liquid samples, the depth that the fiber is immersed into the sample should be consistent. The desorption of an analyte from an SPME fiber depends on the boiling point of the analyte, the thickness of the coating on the fiber, and the temperature of the injection port. As with any other extraction/concentration technique, it is best to use multiple internal standards, and to treat the standards and the analytes in an identical manner.

The equilibrium conditions can be described as:

$$n = K_{fs}V_fV_sC_0/K_{fs}V_f + V_s \quad (1)$$

where n is the number of moles extracted by the coating, K_{fs} is a fiber coating/sample matrix distribution constant, V_f is the fiber coating volume, V_s is the sample volume, and C_0 is the initial concentration of a given analyte in the sample.

As indicated by Eq. 1, after equilibrium has been reached, there is a direct proportional relationship between the sample concentration and the amount of analyte extracted.

Complete extraction can be achieved for small sample volumes when distribution constants are reasonably high. When the sample volume is very large, Eq. 1 can be simplified to:

$$n = K_{fs}V_fC_0 \quad (2)$$

In this equation, the amount of extracted analyte is independent of the volume of the sample. In practice, there is no need to collect a defined sample prior to analysis, as the fiber can be exposed directly to the ambient air, water, production steam, etc.

The commercially available fibers include polydimethylsiloxane (PDMS; 100, 30, and 7 μm), PDMS–divinylbenzene (PDMS–DVB; 65 μm), polyacrylate (PA; 85 μm), carboxen–PDMS (CAR–PDMS; 75 and

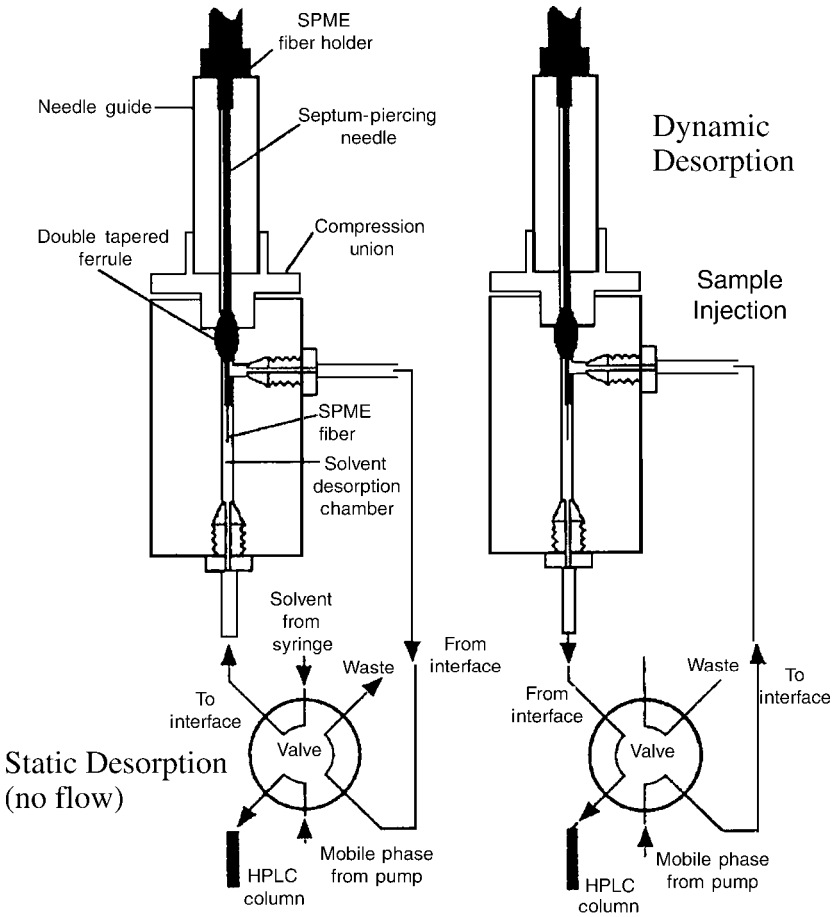

Fig. 6 SPME/HPLC interface.

85thinsp;μm), Carbowax–DVB (CW–DVB; 65 and 75 μm), Carbowax-templated resin (CW-TPR; 50 μm), and DVB–CAR–PDMS (50/30 μm). The type of fiber used affects the selectivity of extraction. In general, polar fibers are used for polar analytes, and non-polar types are used for non-polar analytes. Selectivity toward target analytes and interferences can be enhanced by surfaces common to affinity chromatography. Fibers can be reused up to 100 analyses or more depending on the sample matrix, on the care of the analyst, and on the applications for which used.

MEMBRANE-BASED SEPARATIONS

There are a number of different membrane techniques which have been suggested as alternatives to the SPE and LLE techniques. It is necessary to distinguish between porous and non-porous membranes, as they have different characteristics and fields of application. In porous membrane techniques, the liquids on each side of the membrane are physically connected through the pores. These membranes are used in Donnan dialysis to separate low-molecular-mass analytes from high-molecular-mass matrix components, leading to an efficient cleanup, but no discrimination between different small molecules. No enrichment of the small molecules is possible; instead, the mass transfer process is a simple concentration difference over the membrane. Non-porous membranes are used for extraction techniques.

The introduction of membranes in the field of sample preparation contributes to minimal organic solvent use, minimal contamination and exposure to toxic or dangerous samples, automation, and effective cleanup and analyte isolation.

Membranes in Sample Filtration

Membrane filters are used to remove particulates from samples and solvents prior to HPLC analysis and also for the preparation of liquid samples, where no solvent is used. Typical materials of construction for membrane filters are usually synthetic polymeric materials, although natural substances, such as cellulose, and inorganic materials, such as glass fibers, are also used: acrylic copolymer, aluminum oxide, cellulose acetate, glass fiber, mixed cellulose esters, nitrocellulose, nylon, polycarbonate, polyester, polyether sulfone, polypropylene polysulfone, PTFE, PVC, etc. The compatibility of the polymeric material with the solvents used must be a great concern of their different chemical properties.

Membranes are available in sheet, roll, disk, capsule, cartridge, and hollow-fiber formats. For sample filtration, disk-format membranes are the most popular devices. Disks are sold in loose form or packed in disposable syringe filters or cartridges; common diameters commercially available are 3, 7, 13, 25, 47, and 96 mm, or even larger. Samples are filtered by manually applying a positive pressure or in a vacuum manifold.

DIALYSIS AND MICRODIALYSIS

Dialysis is a membrane barrier separation process in which differential concentration forces one or more sample analytes to transfer from one fluid to another through a membrane. In dialysis, the solution containing the analyte of interest (whose concentration is depleted) is called the "feed" and the fluid receiving the analyte is called the "dialysate." Dialysis is used to remove salts and low-molecular-weight substances from solutions or to remove high-molecular-weight interferences (e.g., proteins) and to allow the measurement of small molecules.

Other variations of the porous membrane techniques include microdialysis and electrodialysis, where a membrane promotes selective transport of charged compounds.

Microdialysis is a technique for in vivo sampling of living tissues or animals, where sampling is performed by means of a probe containing the semipermeable membrane. It is used for medical applications and for online monitoring of extracellular chemical events in living tissues. The membrane is placed at the end of a small piece of a small-diameter, fused silica tubing that is inserted into the tissue of an animal, being in direct contact with the interstitial space. A flowing fluid that can be void of substances of interest, or include physiologically or pharmacologically active substances, is used on the other side of the membrane. The concentration gradient across the membrane enables the diffusion of substances from the interstitial space into the dialysis probe. Usually, the probe is held in place mechanically so the animal can move freely. The outlet of the probe is connected to a collection vial or, in some cases, an HPLC microvalve that enables online analysis using a microbore column. Microdialysis has the advantages of easy operation, rapid isolation of components of interest from complicated and dirty matrices, and lower consumption of organic solvents. Pharmacokinetic studies can also be executed.

Dialysis can also be used as an online sample preparation technique for the deproteinization of biological samples prior to HPLC. Selecting the appropriate semipermeable membrane for the dialyzer can prevent interference from large macromolecules. Samples are introduced into the feed (or donor) chamber, and solvent is pumped through the lower acceptor (or recipient) chamber. The smaller molecules diffuse through the membrane to the acceptor chamber and are directed to an HPLC valve for injection. In case of low concentrations of compounds of interest, a trace enrichment step may be required; this is accomplished with a column placed downstream of the dialyzer that will retain the analyte until the concentration is sufficient for detection. After this step, the analyte can be backflushed into the HPLC system. The technique is useful for blood studies as sampling can be achieved continuously without blood withdrawal. A commercial online system, such as Asted from Gilson, used for both cleanup and enrichment by a combination of dialysis with SPE, is shown in Fig. 7.

Membranes in Extraction

Non-porous membranes are used, as already mentioned, in membrane extraction techniques. A non-porous membrane is a liquid or a solid (e.g., polymeric) phase that is placed between the two phases, usually liquid but sometimes gaseous. This arrangement permits the versatile chemistry of LLE to be used and extended, thus providing a highly effective cleanup as well as a high enrichment factor, and technical realizations can easily be automated. In most cases, there is no, or insignificant, use of organic solvents. The technique is known as *supported liquid membrane*. An advantage of the membrane techniques is that they are amenable to automation and connection to chromatographic instruments.

AFFINITY TECHNIQUES—IMMUNOAFFINITY EXTRACTION

A high degree of molecular selectivity can be achieved with affinity chromatography and affinity extractions. These techniques are based on *molecular recognition* (antigen–antibody interactions). Because the antibodies are highly selective toward the analyte used to initiate the immune response, the corresponding immunosorbent may extract and isolate this analyte from complex matrices in a single step, thus eliminating matrix interference.

Immunosorbents are used in medical and biological fields because they are available for large molecules and are easily obtained, while obtaining selective antibodies for small-size molecules is more difficult. The first step in making an immunosorbent is to develop antibodies with the ability to recognize the desired analytes. Then immunosorbents are obtained by immobilizing the antibodies on solid supports by covalent bonding, adsorption, or encapsulation. The sorbent must be chemically and biologically inert, easily activated, and hydrophilic to avoid non-specific interactions. The common choices are activated silica, Sepharose, agarose gel, etc.

The immunoextraction procedure may be "off-line" or "on-line." In the off-line approach, the immunosorbent is

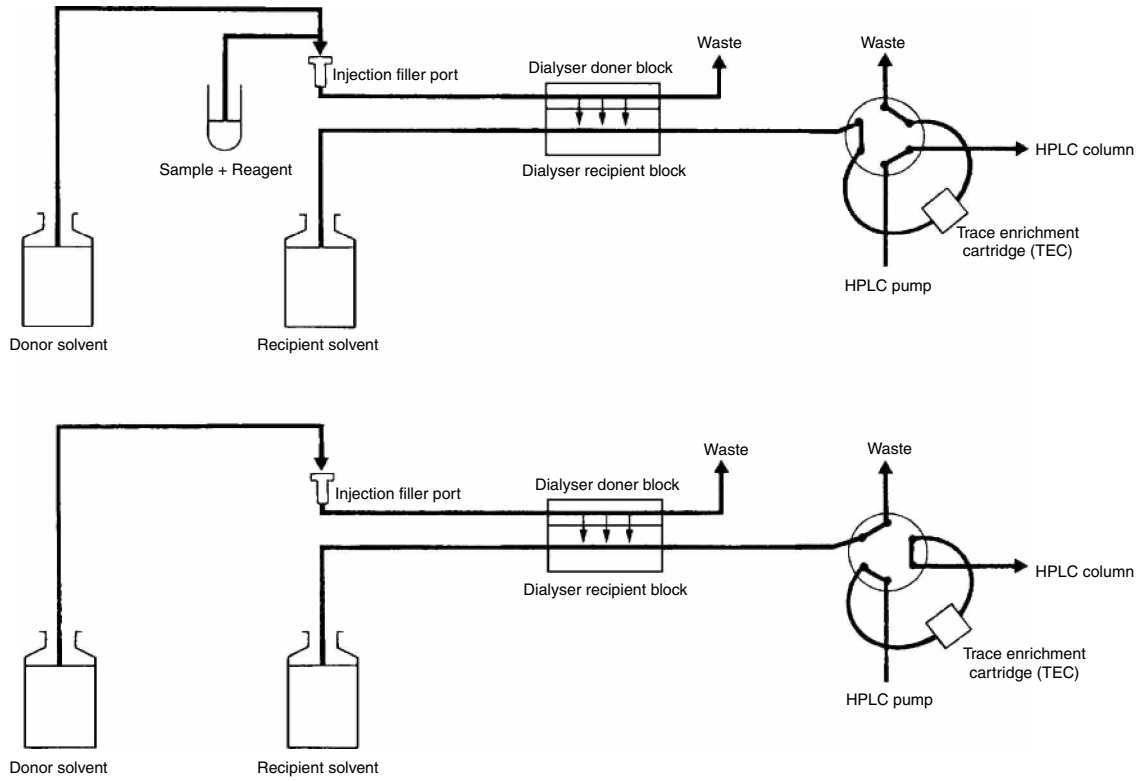

Fig. 7 Online sample preparation by dialysis.

packed into a disposable cartridge. A typical SPE sequence is followed. The sorbent is first conditioned, then the sample is applied, washed to eliminate interference, and analytes of interest are desorbed by the appropriate eluent system, which may be a displacer agent, a chaotropic agent, an aqueous–organic solvent mixture, or a solution that alters pH. With the online approach, the immunosorbent is packed into a precolumn incorporated in a six-port switching valve, where the immunoextraction is performed at the load position, while desorption is achieved at the inject position.

MOLECULARLY IMPRINTED POLYMERS

One approach to synthesize the antibody mimics has been the development of MIP. These involve the preparation of polymers with specific recognition sites for certain molecules. The desired affinity can be introduced by adding an amount of the compound of interest to the polymerization reaction. This "pattern" (template) chemical may be removed after polymerization, leaving vacant sites of a specific size and shape, suitable for binding the same chemical again, from an unknown sample. Like immunosorbent, the recognition is a result of shape and a mixture of hydrogen, hydrophobic, and electronic interactions. Molecularly imprinted polymers have the advantage to be prepared more rapidly and easily, using well-defined methods, and to be stable at high temperatures over a large pH range and in organic solvents. They have found applications in LC, as normal and chiral stationary phases, and in areas where they can be substitutes of natural antibodies (i.e., immunoassays, sensors, and SPE). Noncovalent imprinting protocols are the most commonly used for preparing MIPs using acrylic or methacrylic monomers—often, with methacrylic acid and ethylene glycol dimethylacrylate as cross-linkers. A problem related to the use of MIPs in SPE is the difficulty in removing all the template analytes, even after extensive washing, and the difficulty in establishing a quantitative and rapid desorption as a result of the high greed of the MIP for the analytes.

RESTRICTED-ACCESS MATERIALS

Special sorbents possessing restricted-access properties have been developed to allow the direct injection of biological matrices into the online SPE–LC systems. These sorbents, the so-called *restricted-access materials*, combine the size exclusion of proteins and other high-molecular-mass matrix components that are prohibited from entering the pores of the packing, and they are not well retained by the column. Therapeutic drugs and other small molecules permeate the pores of the column packing material where they partition and are retained by

conventional retention mechanics, such as hydrophobic, ionic, or affinity interactions at the inner pore surface. They are suitable for handling biological samples because they prevent the access of proteins, thus allowing online cleanup and trace enrichment for the determination of several drugs and their metabolites in various biological fluids in the same step.

TRADITIONAL APPROACHES OF SOLID SAMPLE PREPARATION

Solid samples such as biological tissues may be prepared for extraction by a stepwise process that begins with the disruption of the gross architecture of the sample. This modifies the physical state of the sample and provides the extracting medium with a greater surface area per unit mass. Methods reducing the sample particle size include homogenizing, cutting, milling, mincing, blending, macerating, pulverizing, chopping, grinding, sieving, and crushing. Additionally, samples may be frozen in liquid nitrogen or by exposure to dry ice, or they may be freeze-dried to produce a material that can be mechanically pulverized. The finely divided powder that is produced may then be extracted.

Dissolution is the predominant process that takes place before solid samples are injected into HPLC in order to be converted into a liquid state. This is accomplished either by dissolving the entire sample matrix, or by leaching the analytes from the solid matrix using a suitable solvent.

For many years, the *traditional sample preparation* methods, such as the Soxhlet extraction, were applied. Most of these methods have been used for more than 100 years, and they mostly require large amounts of organic solvents. These methods were tested during those times, and the analysts were familiar with the processes and protocols required. However, the trends in recent years are automation, short extraction times, and reduced organic solvent consumption. Modern approaches in solid sample preparation include microwave-assisted solvent extraction (MASE), pressurized liquid extraction, accelerated solvent extraction (ASE), matrix solid-phase dispersion (MSPD), automated Soxhlet extraction, supercritical fluid extraction (SFE), gas-phase extraction, etc.

Solid–liquid extraction (SLE) refers to the classic extraction technology that is achieved by using the appropriate solvent that selectively dissolves the analyte of interest. The most common form of SLE is the "shake-filter" method that involves the addition of an organic solvent for organic compounds or dilute acid or base for inorganic compounds to the sample, and also agitation to allow the analytes to dissolve into the surrounding liquid until they have completely migrated. Heating or refluxing the sample in hot solvent may speed up the extraction process. The insoluble substances are subsequently removed by filtration or centrifugation. A faster and more complete extraction is achieved by *sonication*, where the sample is immersed into a solvent within a vessel that is placed in an ultrasonication bath. The ultrasonic agitation allows more intimate solid–liquid contact, and the gentle heating generated during sonication can aid the extraction process. The extract can either be directly injected, or treated further according to the procedures described under "Preliminary Sample Preparation Procedures."

SOXHLET EXTRACTION

In this technique, the solid sample is placed in a "thimble" that is a disposable, porous container made of stiffened filter paper or Pyrex glass. The thimble is placed in the Soxhlet apparatus designed to repeatedly siphon the solvent with the extracted components, after the inner chamber that holds the thimble is filled to a specific volume with solution. The siphoned solution containing the dissolved analytes is returned to the boiling flask, and the process is repeated until the analyte is successfully removed from the solid matrix. Soxhlet extractions are usually slow, often requiring 24 hr or more. However, it requires little operator involvement after the sample is loaded, and refluxing proceeds until the termination of the extraction. Rows of Soxhlet extractors may be used usually under fume hoods, when the technique is integrated into routine analysis. In relation to modern extraction techniques, it is a low-cost method. The Soxhlet extraction glassware is rather inexpensive; however, the cost is elevated by the large solvent volumes required. Small-volume Soxhlet extractors and thimbles can accommodate sample amounts of a few milligrams. Method development involves the choice of the suitable solvent or solvent mixture (azeotrope) of high volatility, so that it is easily removed and has a high affinity for the analyte but a low affinity toward the solid sample matrix.

A fully automated Soxhlet extraction has been patented as Soxtec by Foss Tecator (Sweden) based on a four-step solvent extraction technique. The sample is rapidly dissolved during the first step in boiling solvent. The remaining soluble matter is efficiently removed at the second step, while distilled solvent is collected at the third step. In the fourth step, the sample cup lifts off the hot plate, utilizing residual heat to predry while eliminating boil-dry risk.

FORCED-FLOW LEACHING

Forced-flow leaching is an extraction technique that can provide a nearly quantitative recovery of many organic compounds. In this technique, the sample of interest is packed into a 20 cm × 4 mm stainless steel column. An extraction solvent is pumped under a gas pressure of 2.5 kg/cm^2 through the column, which is heated close to

the solvent's boiling point. The results are comparable to Soxhlet extraction, but the extraction time is reduced from 24 to 0.5 hr using the forced-flow technique. An advantage of this method is that the sample is subjected continuously to fresh, hot solvent, and the effluent from the column can be collected easily for further treatment.

MODERN APPROACHES OF SOLID SAMPLE PREPARATION

Supercritical Fluid Extraction

Supercritical fluid extraction is a modern sample preparation technique of great interest and utility for complex matrices, primarily considered as an alternative for Soxhlet and sonication extraction for solid and semisolid matrices.

A *supercritical fluid* is defined as a substance above its critical temperature and pressure, which means that it does not condense or evaporate to form a liquid or a gas, but is a fluid with intermediate properties. These properties change from gas-like to liquid-like as the pressure is increased.

A typical supercritical fluid extractor includes a supercritical fluid (most often CO_2 or CO_2 with an organic modifier) source, a means of pressurizing the fluid, a pumping system (for the liquid CO_2), an extraction thimble, a device to depressurize the supercritical fluid (flow restrictor), an analyte collection device, temperature-control systems for several zones, and an overall system controller.

The CO_2 remains a liquid throughout the pumping or compression zones and passes through small-diameter metal tubing as it approaches the extraction thimble itself. The fluid then passes through the extraction thimble at a flow rate and a time period predetermined at the method development stage. The supercritical fluid containing extracted analytes flows through additional capillary tubings until it reaches the restrictor zone.

Applications of SFE include the extraction of salts, proteins, carbohydrates, peptides, amino acids, and other interfering polar compounds in a biological matrix. It shows its best advantage for extracting the analytes from solids and semisolids, rather than from liquids and fluids, mainly because of the extraction thimble's design. The extraction thimbles and associated pieces are made of porous materials such as nickel, chlorofluorocarbon compounds, and stainless steel materials that are very similar to the frits used in HPLC columns. To extract a liquid sample by SFE successfully, it has to be first mixed with a solid material such as diatomaceous earth or alumina, so that the sample is no longer in a liquid state. An SPE filter bed medium may also be used while passing a liquid sample through this first.

A drawback of this technique is a clear need for SFE to be carried out on reference materials of known composition determined by an alternative technique. The advantages of SFE in comparison to LLE are:

1. Less organic solvent is used in reduced time (extraction times can be less than 0.5 hr).
2. Carbon dioxide as an extraction solvent has the advantage of low critical temperature; additionally, it is cheap, non-toxic, and non-explosive. It is classified as a non-polar solvent that can be modified to more polar solvent by the addition of organic solvents (modifiers) such as lower alcohols (e.g., methanol).
3. Online and off-line analytical scale SFE can be applied. In the former, the coupling step (i.e., the transfer and collection of extracted analytes from the SFE to the chromatographic system) is of great importance.

PRESSURIZED SOLVENT EXTRACTION–ACCELERATED SOLVENT EXTRACTION

As an alternative to SFE with carbon dioxide or other supercritical fluids, it was proposed that heating the organic solvents under pressure above their boiling point, but below their supercritical point, would enhance the speed of reaction and solvent strength. This technique, known as the *pressurized solvent extraction* (PSE), provides an easy method for extraction, reducing the amount of solvent required and speeding up the process. The system is marketed as ASE by Dionex Corporation (Sunnyvale, California, U.S.A.). Because PSE represented an extension of existing methods, it attracted attention and is often adopted by official organizations.

MATRIX SOLID-PHASE DISPERSION

Matrix solid-phase dispersion handles viscous solid, solid, or semisolid samples directly by blending with a solid-phase support, such as silica or bonded silica, similar to those used in SPE columns. This is performed by placing a small quantity ($\sim$ 0.5 g) of the sample into a glass mortar and blending it with a glass or agate pestle. The bonded phase acts as a lipophilic binding solvent that assists in sample factorization. The best ratio of sample-to-solid support-bonded phase is 1:4 (or other, depending on the application). The isolation of polar analytes from biological samples is assisted by the use of polar solid support phases and less polar analytes by the less polar phase. The sample components dissolve and disperse into the bound organic phase on the surface of the particle, leading to the complete disruption of the sample and its dispersion over the surface.

The conditioning of the material to be used for MSPD can greatly enhance the analyte recovery. Once the MSPD blending process is completed, the material is transferred to a column constructed from a syringe barrel or other appropriate device containing a frit that retains the entire sample, which is compressed to form column packing by using a modified syringe plunger. A second frit is placed on top of the material, which is compressed so that no channels are formed. The addition of eluting solvent to the column may be preceded by the use of some or all of the solvent to backwash the mortar and pestle. Approximately 8–10 ml of solvent is used to perform the elution. However, most target analytes are eluted in the first 4 ml.

Because the entire sample is present in the column, it is possible to perform multiple or sequential elutions, which can be conducted by gravity flow, by application of pressure to the head of the column, or by placing the columns on a vacuum manifold and applying suction.

If the eluate from an MSPD column is not adequately clean for direct injection, additional steps may be necessary to remove the coeluted matrix components, either by using other solid-phase material packed at the bottom of the MSPD column, or by eluting the analytes from the MSPD column directly onto a second SPE column for sample cleanup and analyte concentration. Sorbents similar to SPE can be used. The ionic state of the sample components is sometimes necessary to be modified to assure that certain interactions occur between the solid support and the eluting solvent. This may be accomplished by adding acids, bases, salts, chelating or dechelating agents, antioxidants, etc. at the time of the sample blending and/or as an additive to the eluting solvent.

Matrix solid-phase dispersion provides results equivalent to older official methods. However, it generally requires 95% less solvent and 90% less time than classical methods. Matrix solid-phase dispersion has been applied to the isolation of drugs, herbicides, patricides, and other pollutants from animal tissue.

DERIVATIZATION IN HPLC

In some cases, the enhancement of detectability is required in trace analysis, when the analytes do not possess a UV-absorbing, fluorescent, or electroactive functionality; therefore derivatization is necessary. A reaction with a fluorotag will produce a highly fluorescing derivative of the compound of interest; thus very low concentrations are detectable. An improvement of UV detectability can also be obtained by a reaction with a chromotag.

The derivatization for HPLC is performed either "off-line" (pre-column) before injection into the column, or "on-line" (post-column) by mixing the reagent with the column effluent.

Precolumn derivatization offers some advantages vs. postcolumn derivatization, as it involves less reaction restrictions, simpler equipment, and no time limitation regarding kinetics, provided that all species are stable. It can be performed either manually or automated. However, there are several drawbacks such as the introduction of contaminants, a possible loss of analyte as a result of side reactions, adsorption, degradation, and incomplete reactions.

By postcolumn derivatization, the analyte is derivatized after the separation and before the detection by using a reaction detector. The simplest way is to add a reagent solution to the column effluent with an extra pump. After the mixing T-piece, a reactor with a suitable holdup volume is inserted to allow reaction to take place. The benefits of this approach are that chromatographic separation is not affected and reaction is not required to be complete.

The most common *fluorotags* (fluorescent reagents) are dansyl chloride and *o*-phthalaldehyde (OPA). *Chromotags* include *p*-bromophenacyl bromide (PBPB) for derivatization of carboxylic acids (K-salts) with a crown ether catalyst, ninhydrin for primary amines forming complexes that have their adsorption maxima at about 570 nm, and dansyl chloride for primary and secondary amines, including amino acids, thiols, imidazoles, phenols, and aliphatic alcohols.

Chiral derivatization can be applied to improve the separation of enantiomers.

CONCLUSIONS

The analytical process typically consists of several discrete stages, such as sampling, preparation, instrumental analysis, quantification, data reporting, and interpretation; each step is critical in obtaining accurate and reproducible results.

A sample preparation step is often necessary to isolate the components of interest from a sample matrix, as well as to purify and to concentrate the analytes. The quality of sample preparation is pivotal in the overall quality of the analysis. Despite the advances in instrumentation and computer technology, many sample preparation practices are based on the 19th century technologies (e.g., the commonly used Soxhlet extraction that was developed more than 100 years ago).

An ideal sample preparation technique should be solvent-free, simple, inexpensive, efficient, selective, amenable to automation, and compatible with a wide range of separation methods and applications. It should also allow for the simultaneous separation and concentration of the components.

There is no universal sample preparation method, as sample preparation depends strongly on the analytical demands, as well as the size and nature of the sample. What is beyond any doubt is the continuously increasing

demand for improved selectivity, sensitivity, reliability, and rapidity in the process of sample preparation.

Among the previously discussed sample preparation techniques, SPE offers a fast, safe, and convenient means for subsequent analysis by chromatographic techniques (HPLC, TLC, GC, etc.). The major benefit is that it requires less solvent than conventional LLE methods. Impurities are removed and the analytes are concentrated, leading to a higher sensitivity in subsequent analysis.

Modern techniques are currently driving out conventional approaches because of their many advantages, including speed, use of less environmentally hazardous solvents, better facilitation for the control of the extraction, as well as automation and online combination of the extraction with other analytical techniques. A major concern when developing techniques for sample preparation is the possibility for automating the entire analytical process, which might lead to increased sample throughput and reduced manual operations with obvious economic benefits, as well as higher accuracy and precision.

Miniaturization has become a dominant trend in analytical chemistry. The development of techniques such as micro-LLE (in-vial extraction), ambient static headspace, disk cartridge SPE, SPME, MSPD, and MASE, which use smaller sample size, minimize solvent use, and are amenable to automation, is a positive sign for analytical science. The combination of modern sample preparation techniques may result in more cost-effective and faster analysis, higher sample throughput, lower solvent consumption, and less manpower, while maintaining, or even improving, sensitivity. Speed in sample preparation is a prerequisite in any analytical method. The future in sample preparation depends on new sorbents and new formats developed for SPE or SPME that exhibit higher selectivity and greater convenience for method development.

REFERENCE

1. Majors, R.E. Sample preparation perspectives. LC GC Int. **1991**, *5* (2), 12–20.

BIBLIOGRAPHY

1. Arthur, C.; Potter, D.; Buchholz, K.; Motlagh, S.; Pawliszyn, J. Solid phase microextraction for the direct analysis of water: Theory and practice. LC GC **1992**, *10* (9), 656–661.
2. Barker, S.A. Matrix solid-phase dispersion. J. Chromatogr. A, **2000**, *885*, 115–127.
3. Blevins, D.D.; Hall, D.O. Recent advances in disk format solid-phase extraction. LC GC **1998**, *13* (5), S16–S21.
4. Eskilsson, C.S.; Bjorklund, E. Analytical-scale microwave-assisted extraction. J. Chromatogr. A, **2000**, *902*, 227–250.
5. Georga, K.A.; Samanidou, V.F.; Papadoyannis, I.N. The use of novel solid phase extraction sorbent materials for HPLC quantitation of caffeine metabolism products methylxanthines and methyluric acids in samples of biological origin. J. Chromatogr. B, **2001**, *759*, 209–218.
6. Hennion, M.-C. Solid-phase extraction: Method development, sorbent, and coupling with liquid chromatography. J. Chromatogr. A, **1996**, *856*, 3–54.
7. Huck, W.; Bonn, G.K. Recent developments in polymer-based sorbents for solid-phase extraction. J. Chromatogr. A, **2000**, *885*, 51–72.
8. Johnsson, J.A.; Mathiasson, L. Membrane based techniques for sample enrichment. J. Chromatogr. A, **2000**, *902*, 205–225.
9. Jönsson, J.A.; Mathiasson, L. Membrane-based techniques for sample enrichment. J. Chromatogr. A, **2000**, *902*, 205–225.
10. Lord, H.; Pawliszyn, J. Microextraction of drugs. J. Chromatogr. A, **2000**, *902*, 17–63.
11. Lord, H.; Pawliszyn, J. Review. Evolution of solid-phase microextraction technology. J. Chromatogr. A, **2000**, *885*, 153–193.
12. Majors, R.E. New approaches to sample preparation. LC GC Int. **1995**, *8* (3), 128–133.
13. Majors, R.E. The changing role of extraction in preparation of solid samples. LC GC Int. **1996**, *9* (10), 638–648.
14. Papadoyannis, I.N.; Tsioni, G.K.; Samanidou, V.F. Simultaneous determination of nine water and fat soluble vitamins after SPE separation and RP-HPLC analysis in pharmaceutical preparations and biological fluids. J. Liquid Chromatogr. **1997**, *20* (19), 3203–3231.
15. Rossi, D.T.; Zhang, N. Automating solid-phase extraction: Current aspects and future prospects. J. Chromatogr. A, **2000**, *885*, 97–113.
16. Samanidou, V.F.; Imamidou, I.P.; Papadoyannis, I.N. Evaluation of solid phase extraction protocols for isolation of analgesic compounds from biological fluids prior to HPLC determination. J. Liq. Chromatogr. Relat. Technol. **2001**, *25* (2), 185–204.
17. Smith, R.M. Supercritical fluids in separation science—The dreams, the reality and the future. J. Chromatogr. A, **1999**, *856*, 83–115.
18. Ulrich, S. Solid-phase microextraction in biomedical analysis. J. Chromatogr. A, **2000**, *902*, 167–194.
19. van de Merbel, N.C. Membrane-based preparation coupled on-line to chromatography or electrophoresis. J. Chromatogr. A, **1999**, *856*, 55–82.
20. Wells, D.A. 96-Well plate products for solid-phase extraction. LC GC Eur. **1999**, *12* (11), 704–715.
21. Westwood, S.A., Ed.; *Supercritical Fluid Extraction and Its Use in Chromatographic Sample Preparation*; Blackie Academic and Professional (an imprint of Chapman and Hall): Glasgow, UK, 1993.

Sample Preparation for Ion Chromatography

Rajmund Michalski
Institute of Environmental Engineering, Polish Academy of Science, Zabrze, Poland

INTRODUCTION

Separation methods, such as gas and liquid chromatography, can provide high resolution of complex mixtures of almost every matrix, from gases to biological macromolecules, and detection limits down to femtograms or even lower. Sample preparation is often a neglected area, which over the years has received much less attention and research than the chromatographic separation or detection stages.

The entire advanced analytical process can be invalidated if any unsuitable sample preparation method has been employed before the sample reaches the chromatograph.[1] In general, sample preparation methods are based on converting a real, complex matrix into a sample in a format that is suitable for analysis by a specific analytical technique. They have a common aim, such as the following:

- Removal of potential interferences from the sample, thus increasing the selectivity of the method
- Increasing the concentration of the analyte(s) and, thus, the sensitivity of the determination
- Converting the analyte into a more suitable form, if necessary
- Providing a robust and reproducible method that is independent of variations in the sample matrix

In modern analytical chemistry and, particularly, in trace analysis, sample preparation is usually more important than the determination method itself for the accuracy and reproducibility of the results.[2] Adequate sample preparation is becoming more important because it allows full exploitation of all of the potential chromatographic methods, including ion chromatography.

SAMPLE PREPARATION METHODS FOR ION CHROMATOGRAPHY

Ion chromatography is well established as a regulatory method for the analysis of anions and cations in environmental samples, as there are few alternative methods that can determine multiple ions in a single analysis. Ion chromatography offers an enormous range of possibilities for the selection of stationary and mobile phases and, in combination with different detection techniques, usually is able to solve even difficult separation problems.

The most important fields of ion chromatography applications are for water and waste water analysis, in the food and beverages industry, and for the semiconductor, clinical, and pharmaceutical sectors.[3–5]

Ion chromatography has reached a high stage of development; the only deficits remaining to be found are in the sample preparation area, which is necessary when an analytical method cannot provide good separation and quantification due to interferences from sample matrix components. Sample matrix effects can include shortened retention times, poor peak efficiency, poor resolution, poor reproducibility, and irregular baseline.

Sample treatment before analysis is necessary to protect expensive analytical columns and increase their lifetimes. Columns used for ion chromatography require absolutely particle-free sample solutions. Unfiltered solutions can cause increased column back pressures and, therefore, in some cases, results in vastly reduced column life.

In practice, real samples whose compositions may vary significantly, can only be analyzed after a more or less complicated sample preparation procedures. The most important practical reasons when and why sample preparation is necessary include:

- Analyte concentration is too high or too low
- Analyte concentrations differ essentially
- The presence of components that may cause interference by peak overlapping
- Samples containing particles
- Solid samples
- Gaseous samples

Sample preparation methods for the wide range of problems to be solved with ion chromatography methods are very numerous and the apparatus and time required for sample preparation vary considerably. The choice of the sample preparation method depends on the physical state and the composition of the sample. The crucial criteria are the choice of the separation mode and analytical conditions, as well as availability of apparatus configurations.[6]

The performance of the separation column, with regard to its resolution, capacity, pH, stability, and compatibility with organic solvents can also be decisive for the basic need for sample preparation or for type of sample pretreatment that is finally chosen.

The most important sample preparation methods for chromatographic analyses (including ion chromatography), taking into consideration the sample form (liquid, solid or gaseous) are:[7]

1. Liquid samples (filtration, dilution, pH adjustment, standard addition, derivatisation, liquid–liquid extraction, solid-phase extraction, distillation, microdiffusion, and membrane separation)
2. Solid samples (drying, homogenization, dissolution, extraction/leaching, digestion, ashing, and combustion)
3. Gaseous samples (absorption in liquids, adsorption on solid phases, membrane sampling, and chemical conversion)

Water samples for analysis by ion chromatography should be collected in plastic containers, such as polytetrafluoroethylene (PTFE), polypropylene (PP), polystyrene (PS), or high-density polyethylene (HDPE). Glass bottles can contribute ionic contamination when performing trace analysis. Polyvinylchloride (PVC) should absolutely be avoided.

The majority of water samples collected for ion chromatography analysis require little or no sample pretreatment. Drinking water samples usually require no pretreatment other than filtration through a 0.45 μm filter to remove particulates. Most waste water often requires only dilution and filtration to bring the analytes of interest into the working range of the method.

Filtration using membrane filters with a pore size of 0.45 μm is the most common sample pretreatment procedure for ion chromatography. For biologically active samples, the use of sterile filters with a pore size of 0.2 μm is strongly advisable. Filters are made either from PTFE, polyvinyldienedifluoride (PVDF), or similar material. Cellulose filters are generally unsuitable. Filter materials differ in pore size, porosity, filtration speed, compatibility with acids, abuse, and organic solvents, as well as in their adsorption properties and blank values.

Recently, membrane separation techniques have achieved great importance in technical applications for separating substances. The variety of available membranes allows one to take advantage of very different separation mechanisms.[8]

Classical filtration and microfiltration are not normally regarded as being membrane techniques, but are directly linked to ultrafiltration with regard to their aims and their procedures. Ultrafiltration is a filtration technique in which the membranes have pore sizes that are much smaller than those used in membrane filtration.

The combination of dialysis with ion chromatography was first published by Nordmayer and Hansen.[9] However, its commercialization by Metrohm has established it as a very versatile, efficient, user-friendly, and automated sample preparation technique.[10]

The term "dialysis" covers separation methods that are based on the transport of molecules or ions through a semipermeable membrane. A differentiation is made between various types of dialysis (passive dialysis, Donnan dialysis, and electrodialysis), according to the driving force and the type of separation membrane that is used.[11]

Active Donnan dialysis is employed most commonly with ion chromatography and is useful for clean-up of sample solutions at extreme pHs.[12] Electrodialysis can be used with ion chromatography for the off-line analysis of strongly alkaline samples containing trace amounts of common inorganic anions.[13]

Liquid–liquid extraction is of little importance in the context of ion chromatographic analysis.[14] Separation via the gas phase is a method with a comparatively high degree of selectivity, as only a few of the analytes that can be determined by ion chromatography can be converted to a volatile form.

For the isolation and preconcentration of analyte ions, as well as separation of interfering matrix components, the various versions of solid-phase extraction are suitable. This involves passing the sample solution through a small column (solid-phase cartridge) that is filled with a suitable sorbent material which either retains the analyte ions or the interfering matrix components. The versatility of solid-phase extraction allows this technique to be used for purification, preconcentration, solvent exchange, desalting, derivatisation, as well as, for sample fractionation.

For the practical performance of solid-phase extraction, many manufactures offer ready-to-use cartridges filled with sorbent materials, as well as devices for passing the sample solution through the sorbent bed, either manually, semi-automatically, or fully automatically.[15]

Solid-phase systems are available commercially, both in column and cartridge form, and also in the format of extraction discs.[16]

Depending on the properties of the components to be preconcentrated or purified, and of the matrix, there is a large number of sorbent available, such as:[17]

- Nonpolar, reversed phase (e.g., octadecyl C_{18}, octyl C_8, ethyl, phenyl, graphite carbon, styrene/divinylbenzene copolymers)
- Polar, normal phases (e.g., cyano, amino, diol, silica gel, florisil, alumina)
- Ion exchangers (e.g., quaternary amine, carboxylic acid, sulfonic acid, cation exchanger, anion exchanger)

Polyvinylpyrrolidine has been shown to be very suitable as the sorbent for the separation of humic materials, tannins, lignins, as well as organic dye compounds, phenolic materials, aldehydes, and aromatic acids.[18] Non-polar solid-phase extraction can be used for the preconcentration of heavy metals as complex compounds and their subsequent determination by cation-exchange chromatography.

Many environmental samples (e.g., sea water, waste water, and brines) contain high concentrations of chloride, sulfate, and sodium ions. Matrix removal of chloride and sulfate is based on the precipitation of these anions with counterions from sulfonated resins. Fully sulfonated cation exchange resins are available with a variety of counterions. The most commonly used counterions are: Ag^+, Ba^{2+}, and H^+, for matrix elimination of chloride, sulfate and general cations, respectively.

Many of the sample preparation techniques for ion chromatography can also be performed using online instrumentation, which can be easily automated and is less time-consuming than off-line techniques.[19]

Automated matrix elimination can also be performed using "heart-cut" techniques.[20]

A novel solution to the problem of performing ion chromatography separation on high ionic strength samples has been the usage of the dominant matrix ion as eluent ("matrix elimination ion chromatography").

In the field of ion chromatography, solid-phase extraction is frequently used for the preconcentration of analytes from samples with an organic matrix, e.g., solvents, fruit juices, body fluids, or for the determination of nitrate and nitrite in meat products.[21]

Solid Sample Treatment for Ion Chromatography

The determination of ionic substances, or substances that can be converted into ionic form from solid samples, is an important field of application of ion chromatography. This includes the analysis of soils, sediments, dusts, geological materials, various industrial products, as well as biological samples and all types of foodstuffs. The sample preparation methods for solid substances can be classified according to whether treatment with a liquid, fusion, ashing, or combustion of the dry sample is necessary.

The analysis of solids by ion chromatography requires either the transfer of the whole sample, or at least the ions of interest, into an aqueous phase. This can be carried out in different ways, depending on the solubility of the analyzed substance and the ionic content to be determined.[22] Dissolution of the sample or extraction of the ions to be determined is normally carried out at room temperature, but can also be accelerated by gentle warming or by heating the solvent up to the boiling point. Solvent extraction which employs, basically, the principles of traditional solvent extraction, but with a higher temperature and pressure, shows better extraction properties.

The choice of extracting solution is dependent on both the sample matrix and upon the nature of the determined ions. Water is preferred, in order to avoid introducing extraneous peaks into the final chromatogram. Sometimes, water combined with a miscible solvent such as methanol, solutions of dilute acid or base, dilute salt solutions, or even the eluent, can be used.

If an aqueous extraction is not sufficient, it may be necessary to consider a wet chemical digestion. Open digestions can be carried out relatively simply in heat resistant vessels on a hotplate. Digestions under pressure require special vessels and the necessary safety precautions must be observed.

Acid digestion with concentrated mineral acids is basically inappropriate for ion chromatography because the excess of the acid coanion can lead to the appearance of a large, interfering peak in the final chromatogram and can also cause column overloading. If mineral acids such as HCl, H_2SO_4, or HNO_3 have to be used, the difference in retention times between the sample anions and the solvent anion should be as large as possible.

For acid extraction followed by the determination of the standard anions (Cl^-, NO_2^-, NO_3^-, PO_4^{3-}, SO_4^{2-}) by ion chromatography with direct conductivity measurement, tartaric acid, perchloric acid, and/or formic acid can be used. For chemical suppression ion chromatography, acetic acid, or formic acid can be used for determining the standard anions.

In general, acid digestion is better suited to preparing samples which are to be analyzed for cations (e.g., transition metals and rare earth elements) using ion chromatography with post column reaction detection.[23]

An alternative to the acid digestion of solid samples is fusion under alkaline conditions. The procedure is usually very labor intensive, takes a long time, and involves a high risk of errors from contamination and loss of analyte. This method can be used for the determination of fluoride and chloride in geological materials after fusion with sodium carbonate and subsequent injection into an ion chromatography column.

Other possible ways of solid sample preparation for ion chromatographic analysis are dry ashing using air as the oxidizing agent or combustion in an atmosphere of pure oxygen. With ashing, the dry and homogenized sample is mineralized in a combustion boat by heating it in a muffle furnace for several hours at temperatures of, typically, 300–800°C. Then, the ashes are dissolved in water or, if necessary, in a dilute mineral acid.

Combustion techniques are very useful for preparation of samples in which heteroatoms can be converted to ionic species suitable for determination by ion chromatography. Combustion is, therefore, used frequently for the analysis of biological samples, pharmaceutical preparations, polymerized substances, coal and other fuels, as well as foodstuffs and other samples with a very high organic matrix content.[24] Generally, conventional ion chromatographic methods for solid samples are:

1. Fusion methods
   - Alkaline with NaOH, KOH, Na_2CO_3, K_2CO_3
   - Acidic with $KHSO_4$, $K_2S_2O_7$
   - Fluorination, chlorination, sulfurization

2. Combustion methods

   – Burning the sample in air/oxygen
   – Oxygen bomb, calorimeter bomb
   – Combustion in a stream of oxygen
   – Combustion in an oxyhydrogen flame

3. Wet chemical digestions

   – Open acid digestion with reflux
   – Pressure digestion
   – UV pyrolysis

The determination of substances present in gaseous form by ion chromatography is usually preceded by preconcentration through absorption into a suitable liquid or absorption of the component on a solid sorbent material or on a reagent impregnated filter. The composition of the absorption solution plays an important role with the regard to the completeness of the gas separation and conversion. Only in very few cases can the separation of several gaseous substances take place simultaneously. Gases such as HF, NO_x, SO_2, SO_3, or NH_3 are absorbed in ultrapure water (possible with addition of H_2O_2 to oxidize sulfite to sulfate), dilute bases, or sodium carbonate solutions. Gases, such as NH_3, are absorbed in acidic solutions, e.g., sulfuric acid.

Diffusion denuders are a possible future example of diffusion-controlled gas sampling. All these methods are batch methods involving many manual work steps and offer a relatively poor temporal resolution. By the use of membrane-supported gas sampling (permeation denuders, wet-effluent scrubbers), continuous sampling and determination can be realized; it is also easy to automate.[25]

CONCLUSIONS

Sample preparation is a growing and developing area of ion chromatography in recent years. The variety of sample preparation methods is great, yet it is not always easy to find a suitable method for the specific problem to be solved. For a single problem, there are often several potential versions; the user has to make a selection based on various criteria.

Future development in ion chromatography might include the development of new stationary phases offering different separation selectivities and detection modes to those that are currently available; the increased usage of ion chromatography in hyphenated techniques and further advances in sample treatment which allow extension of the application of ion chromatography to more complex samples.

REFERENCES

1. Smith, R. Before the injection—modern methods of sample preparation for separation techniques. J. Chromatogr. **2003**, *1000*, 3–27.
2. Namiesnik, J. Trace analysis-challenges and problems. Crit. Rev. Anal. Chem. **2002**, *32* (4), 271–300.
3. Jackson, P.E. Ion chromatography in environmental analysis. In *Encyclopedia of Analytical Chemistry*; Meyers, R.A., Ed.; Wiley: Chichester, UK, 2000; 2779–2801.
4. Vanatta, L.E. Application of ion chromatography in the semiconductor industry. Trends Anal. Chem. **2001**, *20* (6–7), 336–345.
5. Buldini, P.L.; Cavalli, S.; Trifirò, A. State-of-the-art ion chromatographic determination of inorganic ions in food. J. Chromatogr. **1997**, *789* (1–2), 529–548.
6. Slingby, R.; Kaiser, R. Sample treatment techniques and methodologies for ion chromatography. Trends Anal. Chem. **2001**, *20*, 288–295.
7. Haddad, P.R.; Jackson, P.E. Sample handling in ion chromatography. In *Ion Chormatography—Principles and Applications*; Journal of Chromatography Library Series; 1990. 409–462.
8. Miro, M.; Frenzel, W. The potential of microdialysis as an automatic sample-processing technique for environmental research. Trends Anal. Chem. **2005**, *24* (4), 324–333.
9. Nordmeyer, F.R.; Hansen, L.D. Automatic dialyzing-injection system for liquid chromatography of ions and small molecules. Anal. Chem. **1982**, *54*, 2605–2609.
10. Saubert, A.; Frenzel, W.; Schafer, H.; Bogenschutz, G.; Schafer, J. *Sample Preparation Techniques for Ion Chromatography*; Metrohm: Herisau, Switzerland, 2004.
11. Borba, B.M.; Brewer, J.M.; Camarda, J. On-line dialysis as a sample preparation technique for ion chromatography. J. Chromatogr. **2001**, *919* (1), 59–65.
12. Haddad, P.R. Sample clean-up methods for ion chromatography. J. Chromatogr. **1989**, *482*, 267–278.
13. Haddad, P.R.; Laksana, S. On-line analysis of alkaline sample with a flow-through electrodialysis device coupled to an ion chromatography. J. Chromatogr. **1994**, *671*, 131–139.
14. Ko, Y.W.; Gremm, T.J.; Abbt-Braun, G.; Frimmel, F.H.; Chiang, P.C. Determination of dichloroacetic acid and trichloroacetic acid by liquid–liquid extraction and ion chromatography. Fresenius J. Anal. Chem. **2000**, *366* (3), 244–248.
15. Simpson, N.J.K. *Solid-Phase Extraction. Principles, Techniques and Applications*; Marcel Dekker, Inc.: New York, 2000.
16. Saari-Nordhaus, R.; Nair, L.M.; Anderson, J.M. Elimination of matrix interferences in ion chromatography by the use of solid phase extraction discs. J. Chromatogr. **1994**, *671*, 159–163.
17. Fritz, J.S. *Analytical Solid-Phase Extraction*; Wiley-VCH: New York, 1999.
18. Thurman, E.M.; Millls, M.S. *Solid-Phase Extraction: Principles and Practice*; Wiley: New York, 1998.
19. Montgomery, R.M.; Saari-Nordhaus, R.; Nair, L.M.; Anderson, J.M. On-line sample preparation techniques for ion chromatography. J. Chromatogr. **1998**, *804* (1–2), 55–62.

20. Villasenor, S.R. Matrix elimination in ion chromatography by heart-cut column switching techniques. J. Chromatogr. **1992**, *602*, 155–161.
21. Siu, D.C.; Henshall, A. Ion chromatographic determination of nitrate and nitrite in meat products. J. Chromatogr. **1998**, *804*, 157–160.
22. Haddad, P.R.; Doble, P.; Macka, M. Developments in sample preparation and separation techniques for the determination of inorganic ions by ion chromatography and capillary electrophoresis. J. Chromatogr. **1999**, *856* (1–2), 145–177.
23. Bruzzoniti, M.C.; Mentasti, E.; Sarzanini, C.; Braglia, M.; Cocito, G.; Kraus, J. Determination of rare earth elements by ion chromatography. Separation procedure optimization. Anal. Chim. Acta **1996**, *322* (1–2), 49–54.
24. Oleksy-Frenzel, J.; Wischnack, S.; Jekel, M. Application of ion-chromatography for the determination of the organic-group parameters AOCl, AOBr, and AOI in water. Fresenius J. Anal. Chem. **2000**, *366* (1), 89–94.
25. Komazaki, Y.; Hamada, Y.; Hashimoto, S.; Fujita, T.; Tanaka, S. Development of an automated, simultaneous and continuous measurement system by using a diffusion scrubber coupled to ion chromatography for monitoring trace acidic and basic gases (HCl, HNO_3, SO_2 and NH_3) in the atmosphere. Analyst **1999**, *124* (8), 1151–1157.

Sample Preparation for TLC

Joseph Sherma
Department of Chemistry, Lafayette College, Easton, Pennsylvania, U.S.A.

INTRODUCTION

This entry describes the classical and modern sample preparation methods that have been used prior to qualitative and quantitative analysis by thin-layer chromatography (TLC) and high-performance (HP) TLC. Extraction and cleanup methods that are covered include classical methods such as liquid–liquid extraction (LLE) and Soxhlet extraction, as well as modern methods such as solid-phase extraction (SPE), pressurized liquid extraction (PLE), and supercritical fluid extraction (SFE). Modern methods have not been as widely applied in TLC as for other modes of chromatography, e.g., column high-performance liquid chromatography (HPLC).

OVERVIEW

After collection of a representative sample, sample preparation is the first step in a TLC analysis, followed by application of initial zones of samples and corresponding standards to the layer (plate); development of the layer with the mobile phase to achieve the separation; detection of the zones by their color, ultraviolet (UV) absorbance, or fluorescence, either natural or induced by postchromatographic derivatization with a detection reagent; documentation of the chromatograms using a system with a CCD (charged couple device) camera (videodensitometer), digital camera, or flatbed scanner; identification of unknown zones in sample chromatograms; quantification of the analyte by densitometry; and validation of the results. The later steps will not provide a correct result unless sample preparation is carried out properly.

Extraction procedures should recover essentially all of the analyte from the sample and leave behind as many of the impurities as possible. Cleanup procedures are designed to reduce matrix interferences while not losing any of the analyte and increasing its concentration as much as possible. General, practical aspects of modern sample preparation methods have been described in earlier articles,[1,2] but not their use in TLC. The purpose of this entry is to review the procedures used prior to TLC analysis and illustrate analytes and samples for which each has been applied successfully; details of the TLC methods after sample preparation will not be given but can be found in the cited references.

Sample preparation requirements are not as strict for TLC because the layer is used only once, instead of repeated injection of samples onto an HPLC column. The presence of strongly-sorbed impurities, even solid particles, in samples is of no concern if the subsequent development and zone detection are not adversely affected. These materials can build up on an HPLC column and destroy its performance. In TLC, every sample is separated on fresh stationary phase, without carryover or cross-contamination. Therefore, TLC can require fewer cleanup steps during sample preparation, saving effort, time, and expense. This advantage allows many kinds of liquid samples to be applied directly to a plate with no sample preparation except to remove any carbonation, e.g., beverages analyzed for Sucralose,[3] caffeine,[4] or aspartame[5] content using TLC-densitometry. Direct application is facilitated by use of plates with a preadsorbent zone, which may retain certain impurities at the origin during mobile-phase development.

TRADITIONAL LIQUID EXTRACTION

As stated above, cleanup of samples is not as critical for TLC as it is for column chromatography because plates are not reused. Simple dissolving or LLE with immiscible solvents and pH control is often sufficient. For more complex samples, cleanup of extracts by column adsorption chromatography, or a more modern method, such as SPE, is usually applied.

As an example of liquid sample extraction with an immiscible solvent in which the analyte is highly soluble, phenolic compounds in Croatian red wine were determined by LLE with diethyl ether at pH 2.0.[6]

One of the most used solvent partitioning methods involves chloroform–methanol (2:1) extraction followed by washing the organic phase with 0.88% KCl and filtering out and solid residue by passing through glass wool (the Folch procedure). This method has been especially successful with biological samples, e.g., for the recovery of lipids and phospholipids from snail tissue, hemolymph, and shells and from medicinal leeches.[7] A modified Folch procedure, with reextraction of the upper phase with water-saturated butanol, was described for recovering lipids from human normal and pathological tissues.[8]

When extract cleanup is needed, an adsorbent column can be used. For example, sample preparation for

determination of polycyclic aromatic hydrocarbons in sugar beet included saponification of the sample, several LLEs, and a silica gel column cleanup.[9]

SOXHLET EXTRACTION

This is a reflux-type extraction technique in which a solid sample is put in a thick, stiff paper thimble, in which solvent repeatedly fills and siphons. The analyte is exhaustively extracted, usually over a period of hours, without operator intervention. Soxhlet extraction was used in the TLC determination of the main alkaloid, tetrandrine, of *Stephania tetrandra* (methanol-5% conc. ammonia solvent);[10] lipids from grain sorghum DDG (*n*-hexane solvent);[11] and secondary amines from some Nigerian foodstuffs (petroleum ether, 60–90°C, solvent).[12]

ULTRASONIC EXTRACTION

Ultrasonic extraction of the pesticides atrazine, propham, chlorpropham, diflubenzuron, alpha-cypermethrin, and tetramethrin from soil was optimized in terms of the solvent (acetone), duration of sonication, and number of extraction steps. Comparisons with shake-flask and Soxhlet extractions made using reversed-phase (RP) TLC on C-18 plates showed advantages in extraction efficiencies, simplicity of use, and low-solvent consumption for ultrasonic extraction.[13]

EXTRELUT COLUMN LIQUID EXTRACTION

Extrelut columns (Merck, Darmstadt, Germany) can be used to perform LLE in place of a separatory funnel. The tube is packed with diatomaceous earth, and an aqueous sample is poured in. When a suitable organic solvent is then passed through, the analyte is eluted, while water and polar compounds in the sample are retained on the column. Applications are illustrated by the use of Extrelut extraction prior to TLC for the determination of nicotine and its metabolite cotinine in urine samples of children of smoking parents[14] and of caffeine in coffee.[15]

DIALYSIS

Dialysis is a cleanup method in which the analyte passes from one solution to another through a membrane while impurities do not transfer. The process can be set up to remove either low-molecular-weight or high-molecular-weight interferences. As examples, dialysis was used to extract the mycotoxin patulin from apple juice using ethyl acetate in a diphasic system,[16] and to remove low-molecular-weight constituents from bark extracts prior to carbohydrate and phenol analysis.[17]

SPE

SPE cleanup is carried out by passing sample extracts through a conditioned cartridge packed with a sorbent. A series of solvents is passed through to elute various analytes in different fractions prior to TLC. Impurities are eluted in separate fractions and discarded or remain on the column after elution of the analytes. SPE is also carried out in disks, but cartridges have been mostly used for TLC applications. In many analyses, cleanup by both LLE and SPE are carried out.

The following SPE sorbents have been reported for sample preparation prior to TLC analyses: C_8 chemically bonded silica gel in the TLC profiling of impurities in MDMA synthesis from piperonal;[18] amino-bonded silica for fractionation of lipid classes[19] and recovery of lipids from Gaucher and Krabbe's disease patient tissue;[8] C_{18} silica gel for drugs in river water,[20] resveratrol and piceid in wine,[21] and evolved alachlor collected in ethylene glycol;[22] $AgNO_3$-modified silica gel for determination of docosahexaenoic acid in bovine milk;[23] SBD-1 (styrene divinyl benzene) for organophosphorus pesticides in water;[24] and Florisil for two oxycholesterols in raw and cooked meat.[25]

SPE was coupled online between HPLC and TLC for the quantitative determination of 4(5)-methylimidazole in caramel.[26]

MICROWAVE-ASSISTED EXTRACTION

A prototype extractor based on conventional Soxhlet principles, but assisted in the cartridge zone by focused microwaves, was shown to accelerate the extraction of lipids from sausage products.[27]

PLE

In PLE, solvent is pumped into an extraction vessel containing the sample and is heated (e.g., 60–200°C) and pressurized (3.5–20.0 MPa). The method is also termed pressurized solvent extraction (PSE) and accelerated solvent extraction (ASE). Solvent consumption and extraction time are reduced by increasing the solubility of the analyte in the solvent and increasing the kinetic rate of desorption of the analyte from the sample matrix.

An extract containing caretenoids, phenolic compounds, and degradation products of chlorophylls was obtained from microalga using an optimized PLE procedure with ethanol at 115°C for 15 min, followed by silica gel TLC analysis of the extract.[28] PLE extracts

from a selection of herbs were compared using TLC analysis with extracts obtained according to Pharmacopoeia monographs; PLE was found to give equivalent or higher extraction yields and was faster and required less solvent.[29] The fat content of homogenized poultry meat samples was analyzed using PLE, TLC, and capillary gas chromatography (CGC); two different solvent mixtures (chloroform–methanol and *n*-hexane–isopropanol) were tested at various temperatures and pressures for PLC.[30] Lipids were extracted with pentane–hexane or dichloromethane and determined by Iatroscan rod TLC with a flame ionization detector (TLC–FID) in the analysis of a wide array of marine biota tissues.[31] PLE of yew twigs with methanol at 100°C was found to give the best yield of taxoids when compared with methanol maceration and methanol ultrasonic extraction; the crude extracts were purified by alumina column SPE followed by zonal micropreparative silica gel TLC, and quantification was by C-18 column HPLC.[32]

SFE

SFE involves extraction of the analyte from a sample using a supercritical fluid, a substance above its critical temperature and pressure. The extractant used most often is CO_2 plus an organic modifier such as 1–10% methanol. Solvating power can be adjusted by changing the fluid and/or its modifier, temperature, or pressure. SFE increases the recovery rate in many cases compared to liquid extraction and eliminates the cost of purchase and problems of storage and disposal of organic solvents.

The following are examples of TLC analyses in which SFE was the method used for sample preparation: lipids in wool (analysis by TLC–FID);[33,34] lipids in fish feed (TLC–FID);[35] the pesticide chlorpyrifos and its degradation products in soil;[36] hydrocarbons in heavy petroleum products (TLC–FID);[37] aromatic and aliphatic hydroperoxides in solid matrices (online sample transfer to TLC plates);[38] colored fractions from a Mediterranean brown alga;[39] essential oil in foods;[40] and cyanazine from soil (silica gel TLC-densitometry at 220 nm).[41]

IMMUNOAFFINITY EXTRACTION AND CLEANUP

Immunoaffinity (IA) methods are based on the principle of molecular recognition via very selective antigen–antibody interactions. Their use for sample preparation prior to TLC has been mostly for determination of toxins. The following are selected examples: the steroid animal drug trenbolone and its metabolite in bovine urine;[42] fumonisin B1 in corn with methanol–water (80:20) extraction followed by IA column cleanup;[43] aflatoxins B1, B2, G1, and G2 in foods regulated within the European Community using methanol extraction, IA column cleanup, and densitometric quantification;[44] deoxynivalenol (vomatoxin) in wheat flour and malt by extraction with water and polyethylene glycol, IA column cleanup, and HPTLC-fluorescence densitometry;[45] and ochratoxin A in green coffee using extraction with methanol-aq. $NaHCO_3$, IA column cleanup, and normal or RP TLC-densitometry.[46]

PRE–TLC DERIVATIZATION

The major method of zone detection for compounds that are not naturally colored, UV-absorbing, or fluorescent is to apply a postchromatographic dip or spray reagent, often followed by heating the layer to complete the reaction. However, samples are sometimes derivatized prechromatography[47] if the derivative is more readily separated and/or detected by TLC. Derivatives can be formed in solution and then applied to the layer, or the reaction can be carried out in situ at the origin by overspotting the reagent after applying the underivatized sample.

Reagents for the pre-TLC formation of sensitively detected fluorescent derivatives have been most successfully used, usually with fluorodensitometric quantification after separation. The following are examples of reagents used in this approach: monodansylpiperazine and monodansylcadaverine for fatty acids (automated gradient multiple development);[48] monodansylcadaverine for carboxylic acids (densitometric quantification at 10–210 pmol/zone);[49] monodansylcadaverine and *N*,*N*′-dicyclohexylcarboimide for C_{20} fatty acids in rat placenta (C_{18} silica gel layers);[50] dansyl chloride and sodium carbonate for putrescine, spermidine, spermine, and histamine on alumina plates;[51] dansyl chloride for morphine and 6-monoacetyl morphine as its marker in urine (200–400 pg/zone);[52] dansyl chloride for 20 beta-blockers (0.2 ng detection limit);[53] and 6% mercuric acetate solution for dipalmitoylphosphatidylcholine and 1-palmitoyl-2-oleylphosphatidylcholine, with visualization by dipping into cupric sulfate solution and densitometry at 365 nm.[54]

CONCLUSION

The methods used for sample preparation prior to TLC and HPTLC analysis are described. Included are traditional and modern procedures for extraction, cleanup, and derivatization. The references cited contain details of the sample preparation, as well as the following chromatographic methods. Only by use of optimized techniques, such as those given, can high quality results be obtained for qualitative and quantitative analysis.

REFERENCES

1. Sherma, J. Modern sample preparation technology. I. Automated SPE. Inside Lab. Manag. **2001**, *5* (5), 14–19.
2. Sherma, J. Modern sample preparation technology. II. Automated SPME, ASE, SFE, MAE, automated Soxhlet extraction. Inside Lab. Manag. **2001**, *5* (6), 33–38.
3. Spangenberg, B.; Stroka, J.; Arranz, I.; Anklam, E. A simple and reliable HPTLC method for the quantification of the intense sweetener Sucralose. J. Liq. Chromatogr. Relat. Technol. **2003**, *26* (16), 2729–2739.
4. Sherma, J.; Miller, R.L., Jr. Quantification of caffeine in beverages by densitometry on preadsorbent HPTLC plates. Am. Lab. (Shelton, CT) **1984**, *16*, 126–127.
5. Sherma, J.; Chapin, S.; Follweiler, J.M. Quantitative TLC determination of aspartame in beverages. Am. Lab. (Shelton, CT) **1985**, *17* (3), 131–133.
6. Rastija, V.; Mornar, A.; Jasprica, L.; Srecnik, G.; Medic-Saric, M. Analysis of phenolic compounds in Croatian red wines by thin layer chromatography. J. Planar Chromatogr. Mod. TLC **2004**, *17* (1), 26–31.
7. Sherma, J.; Fried, B. Thin layer chromatographic analysis of biological samples. A review. J. Liq. Chromatogr. Relat. Technol. **2005**, *28* (15), 2297–2314.
8. Bodennec, J.; Pelled, D.; Futerman, A.H. Aminopropyl solid phase extraction and 2D TLC of neutral glycosphingolipids and neutral lysoglycosphingolipids. J. Lipid Res. **2003**, *44* (1), 218–226.
9. Loncar, E.S.; Kolarov, L.A.; Malbasa, R.V.; Skrbic, B.D. J. Serbian Chem. Soc. **2005**, *70* (10), 1237–1242.
10. Blatter, A.; Reich, E. Qualitative and quantitative HPTLC methods for quality control of *Stephania tetrandra*. J. Liq. Chromatogr. Relat. Technol. **2004**, *27* (13), 2087–2100.
11. Wang, L.; Weller, C.L.; Hwang, K.T. Extraction of lipids from grain sorghum DDG. Trans. ASAE **2005**, *48* (5), 1883–1888.
12. Uhegbu, F.O. Dietary secondary amines and liver hepatoma in Port Harcourt, Nigeria. Plant Foods Hum. Nutr. **1997**, *51* (3), 257–263.
13. Babic, S.; Petrovic, M.; Kastelan-Macan, M. Ultrasonic extraction of pesticides from soil. J. Chromatogr. A, **1998**, *823* (1–2), 3–9.
14. Diab, A.M.; Abdul-Kawy, A.; Abdel-Rahman, M.; Abou-Amer, A. Nicotine and cotinine in urine of passively smoking children. Bull. Nat. Res. Cent. (Egypt) **1997**, *22* (1), 43–50.
15. Sommer, K.; Venke, S.C. An experiment on the isolation of natural products. Naturwissenschaften im Unterricht Chemie **2004**, *15* (4), 18–21.
16. Prieta, J.; Moreno, M.A.; Blanco, J.L.; Suarez, G.; Dominguez, L. Determination of patulin by diphasic dialysis extraction and thin layer chromatography. J. Food Prot. **1992**, *55* (12), 1001–1002.
17. Churms, S.C.; Stephen, A.M. Chromatographic separation and examination of carbohydrate and phenolic components of the non-tannin fraction of black wattle bark extract. J. Chromatogr. **1991**, *550* (1–2), 519–537.
18. Kochana, J.; Wilamowska, J.; Parczewski, A. TLC profiling of impurities of 1-(3, 4-methylenedioxyphenyl)-2-nitropropene, an intermediate in MDMA synthesis. J. Liq. Chromatogr. Relat. Technol. **2004**, *27* (15), 2297–2314.
19. Flurkey, W.H. Use of solid phase extraction in the biochemistry laboratory to separate different lipids. Biochem. Mol. Biol. Edu. **2005**, *33* (5), 357–360.
20. Sajewicz, M. Use of densitometric TLC for detection of selected drugs in river water in south Poland. J. Planar Chromatogr.-Mod. TLC **2005**, *18* (102), 108–111.
21. Chen, M.; Shu, Y.Q.; He, J.G.; Dai, Y.Q. Determination of resveratrol and piceid in wine by thin layer chromatography-fluorescence scanning. Chinese J. Anal. Chem. **2005**, *33* (5), 635–638.
22. Dailey, O.D. Volatilization of alachlor from polymeric formulations analyzed by reversed phase HPTLC with densitometry. J. Agric. Food Chem. **2004**, *52* (22), 6742–6746.
23. Kozutsumi, D.; Kawashima, A.; Adachi, M.; Takami, M.; Takemoto, N.; Yonekubo, A. Determination of docosahexaenoic acid in milk using affinity solid phase purification with argentous ions and modified thin layer chromatography. Intl. Dairy J. **2003**, *13* (12), 937–943.
24. Hamada, M.; Wintersteiger, R. Fluorescence screening of organophosphorus pesticides in water by an enzyme inhibition procedure on TLC plates. J. Planar Chromatogr.-Mod. TLC **2003**, *16* (1), 4–10.
25. Janoszka, B.; Warzecha, L.; Dobosz, C.; Bodzek, D. Determination of 7-ketocholesterol and 7-hydroxycholesterol in meat samples by TLC with densitometric detection. J. Planar Chromatogr.-Mod. TLC **2003**, *16* (3), 186–191.
26. Mueller, E.; Jork, H. Online coupling of HPLC, solid phase extraction, and TLC (HPLC–OSP–TLC). J. Planar Chromatogr.-Mod TLC **1993**, *6* (1), 21–28.
27. Priego-Lopez, E.; Velasco, J.; Dobarganes, M.C.; Ramis-Ramos, G.; de Castro, M.D.L. Focused microwave-assisted Soxhlet extraction: an expeditive approach for the isolation of lipids from sausage products. Food Chem. **2003**, *83* (1), 143–149.
28. Jaime, L.; Mendiola, J.A.; Herrero, M.; Separation and characterization of antioxidants from *Spirulina platensis* microalga combining pressurized liquid extraction, TLC, and HPLC–DAD. J. Sep. Sci. **2005**, *28* (16), 2111–2119.
29. Benthin, B.; Danz, H.; Hamburger, M. Pressurized liquid extraction of medicinal plants. J. Chromatogr. A, **1999**, *837*, 211–219.
30. Toschi, T.G.; Bendini, A.; Ricci, A.; Lercker, G. Pressurized solvent extraction of total lipids in poultry meat. Food Chem. **2003**, *83* (4), 551–555.
31. Ylitalo, G.M.; Yanagida, G.K.; Hufnagle, L., Jr; Krahn, M.M. Determination of lipid classes and lipid content in tissues of aquatic organisms using a thin layer chromatography-flame ionization detection (TLC–FID) microlipid method. In *Techniques in Aquatic Toxicology*; Ostrander, G.K., Ed.; CRC Press LLC: Boca Raton, FL, 2005; 227–237.
32. Hajnos, M.L.; Waksmundzka-Hajnos, M.; Gawdzik, J.; Dawidowicz, A.L.; Glowniak, K. Influence of the extraction mode on the yield of taxoids from yew tissues – preliminary experiments. Chemia Analit. (Warsaw, Poland) **2001**, *46* (6), 831–838.
33. Dominguez, C.; Jover, E.; Bayona, J.M.; Erra, P. Effects of carbon dioxide modifier on the lipid composition of wool wax extracted from raw wool. Anal. Chim. Acta **2003**, *477* (2), 233–242.

34. Coderch, L.; Fonollosa, J.; Marti, M.; Garde, F.; de la Maza, A.; Parra, J.L. Extraction and analysis of ceramides from internal wool lipids J. Am. Oil Chem. Soc. **2002**, *79* (12), 1215–1220.
35. Johnson, R.B.; Barnett, H.J. Determination of the fat content in fish feed by supercritical extraction and subsequent lipid classification of the extract by thin layer chromatography-flame ionization detection. Aquaculture **2003**, *216* (1–4), 263–282.
36. Yucel, U.; Ylim, M.; Gozek, K.; Helling, C.S.; Sarykaya, Y. Chlorpyrifos degradation in Turkish soil. J. Environ. Sci. Health, B. **1999**, *34* (1), 75–95.
37. Oschmann, H.J.; Prahl, U.; Severin, D. Separation of paraffin from crude oil by supercritical fluid extraction. Petrol. Sci. Technol. **1998**, *16* (1–2), 133–143.
38. Esser, G.; Klockow, D. Detection of hydroperoxides in combustion aerosols by supercritical fluid extraction coupled to thin layer chromatography. Mikrochim. Acta **1994**, *113* (3–6), 373–379.
39. Subra, P.; Boissinot, P. Supercritical fluid extraction from a brown alga by stepwise pressure increase. J. Chromatogr. **1991**, *543* (2), 413–424.
40. Guo, Zh.; Zhang, X.; Zhang, J. Study of the composition of ginger essential oil prepared by supercritical carbon dioxide. Chinese J. Chromatogr. (Sepu) **1995**, *13*, 156–160.
41. Goli, D.M.; Locke, M.A.; Zahlatowicz, R.M. Supercritical fluid extraction from soil and HPLC analysis of cyanazine herbicides. J. Agric. Food Chem. **1997**, *45*, 1244–1250.
42. van Ginkel, L.A.; van Blitterswijk, H.; Zoontjes, D.; van den Bosch, R.W.S. Assay of trenbolone and its metabolite 17 alpha-trenbolone in urine based on immunoaffinity chromatographic cleanup and off-line high performance liquid chromatography-thin layer chromatography. J. Chromatogr. **1988**, *445*, 385–392.
43. Preis, R.A.; Vargas, E.A. A method for determining fumonisin B1 in corn using immunoaffinity column cleanup and thin layer chromatography–densitometry. Food Addit. Contam. **2000**, *17* (6), 463–468.
44. Stroka, J.; van Otterdijk, R.; Anklam, E. Immunoaffinity column cleanup prior to thin layer chromatography for the determination of aflatoxins in various food matrices. J. Chromatogr. A **2000**, *904* (2), 251–256.
45. Ostry, V.; Skarkova, J. Development of an HPTLC method for the determination of deoxynivalenol in cereal products. J. Planar Chromatogr.-Mod. TLC **2000**, *13* (6), 443–446.
46. Santos, E.A.; Vargas, E.A. Immunoaffinity column cleanup and thin layer chromatography for determination of ochratoxin A in green coffee. Food Addit. Contam. **2002**, *19* (5), 447–458.
47. Funk, W.; Kerler, R.; Schiller, J.T.; Dammann, V.; Arndt, F. Prechromatographic derivatization of samples for HPTLC. HRC&CC, High Resolut. Chromatogr. Commun. **1982**, *5* (10), 534–538.
48. Junker-Burcheit, A.; Jork, H. Prechromatographic in-situ derivatization of fatty acids in the picomole range. Part 1: HPTLC of fluorescent monodansylpiperazine and monodansylcadaverine derivatives. Fresenius' Z. Anal. Chem. **1988**, *331* (3–4), 387–393.
49. Junker-Burcheit, A.; Jork, H. Monodansylcadaverine as a fluorescent marker for carboxylic acids. In situ prechromatographic derivatization. J. Planar Chromatogr.-Mod. TLC **1989**, *2* (1), 65–70.
50. Frank, H.G.; Graf, R. Determination of unsaturated C_{20} fatty acids in rat placenta by high performance TLC. Proceedings of 6th International Symposium Instrumentation Planar Chromatography (Interlaken 1991), Institute of Chromatography, Bad Duerkheim, FRG, 1991, 91–95.
51. Surgova, T.M.; Sidorenko, M.V.; Kofman, I.S.; Vinnitsky, V.B. Determination of histamine in the presence of polyamines by spectrodensitometric TLC. J. Planar Chromatogr. Mod. TLC **1990**, *3* (1–2), 81–82.
52. Schuetz, H.; Erdmannn, F. Quantitative HPTLC in toxicology. GIT Fachz. Lab. **1993**, *37*, 18–22.
53. Schuetz, H.; Meister, T. Thin layer chromatographic screening program for commonly used beta-blockers. Arzneim.-Forsch. **1989**, *40*, 651–653.
54. Renger, B. Quantitative planar chromatography as a tool in pharmaceutical analysis. J. AOAC Int. **1993**, *76*, 7–13.

BIBLIOGRAPHY

1. Hurst, W.J. Sample Preparation. In *Encyclopedia of Chromatography*, 3rd Ed.; Cazes, J., Ed.; Taylor & Francis: New York, 2010; 2077.
2. Papadoyannis, I.N.; Samanidou, V.F. Sample preparation for HPLC. In *Encyclopedia of Chromatography*, 3rd Ed.; Cazes, J., Ed.; Taylor & Francis: New York, 2010; 2090.

Scale-Up of CCC

Ian A. Sutherland
Brunel Institute for Bioengineering, Brunel University, Uxbridge, Middlesex, U.K.

INTRODUCTION

There are few processes that can be predictably scaled up from laboratory to production scale without difficulties. Preparative high-performance liquid chromatography (HPLC), for example, is not a linear scale up; it is expensive and uses large volumes of solvents. The product can become hydrolyzed by or react with the column, which can induce chemical/steric/chiral conformation changes and often requires significant prepurification with further risk of degradation.

Countercurrent chromatography (CCC)[1,2] is a process that avoids these difficulties. It is a form of liquid–liquid chromatography without a solid support, which separates soluble natural product substances on their partition, or differential solubility, between two immiscible solvents. The principle of separation (partition) is the same in both the laboratory and the production plant and is generic in that it can be applied to an extremely broad range of purification problems in many industries. Furthermore, because there is no solid support, there is 100% sample recovery and no need for any prepurification.

BACKGROUND INFORMATION

A recent review on CCC as a preparative tool[3] described an extremely useful comparison of four different CCC approaches and concluded that "the real future belongs to the new generation of centrifugal instruments." They concluded that more reliable designs were required, that there was a need to accommodate higher loads on the 100 g to 1 kg scale, and that truly preparative instruments needed to be developed. They called for a better understanding of the mechanisms of separation in order to achieve this.

Ito's work[4] on pH zone refining makes a valuable contribution to the scale-up scenario. It offers a method of operating existing instruments preparatively when purifying ionizable compounds with the ability of achieving sample loadings two orders of magnitude higher than normal. Sutherland et al.[5] demonstrate that preparative gram-quantity separations of crude plant extracts use one-tenth the volume of solvents compared to the equivalent prep-HPLC. Sandlin and Ito[6] have shown that CCC is feasible using a "J"-type coil planet centrifuge with tubing bore up to 5.5 mm internal diameter and have successfully demonstrated fractionations in 750 ml coils, but at relatively low flow, speed, and β value. They have also investigated the effect on resolution of increasing sample volume and sample concentration.[7] Ito and colleagues[7–9] have described unit-gravity (non-centrifugal) slowly rotating coil devices, which would be suitable for large-scale CCC separations.

PARAMETERS AFFECTING SCALE-UP

The main parameters affecting scale-up have been analyzed in detail by Sutherland et al.[10] For scale-up of CCC to be successful, they recommended that two measures or responses had to be maintained as the process was scaled up: retention of the stationary phase and resolution of the sample components. It was emphasized that even if it was possible to retain phases as the tubing bore increased, it was possible that the hydrodynamics of the mixing and settling zones may not work as well, as the bulk volume to surface area ratio increased.

They studied three "J"-type coil planet centrifuges with different coil sizes: analytical ($d = 0.76$ mm), lab prep ($d = 1.6$ mm),and process ($d = 3.68$ mm). By constructing the coils from stainless steel, they were able to increase flow considerably without risk of bursting the tubing or causing the tubing to work loose under the action of high cyclic forces, which can be a common problem (see later). They first showed that there was no difference in retention between coils made with stainless steel or polytetrafluoroethylene (PTFE). This was an important experiment that showed that retention was a hydrodynamic process and not governed by the surface properties of the tubing-wall material.

THE EFFECT OF THESE SCALE-UP PARAMETERS ON RETENTION

Fig. 1 shows Sutherland et al.'s plot of retention against flow for the three CCC units with different bore sizes. It clearly shows how increasing the tubing bore not only allows higher throughput but also shows that retention with larger bores is far more tolerant or stable when flow is increased, a very important discovery for industrial scale-up. They went on to demonstrate that increasing speed allowed even higher retention and linear flows of the mobile phase and that the mean Reynold's

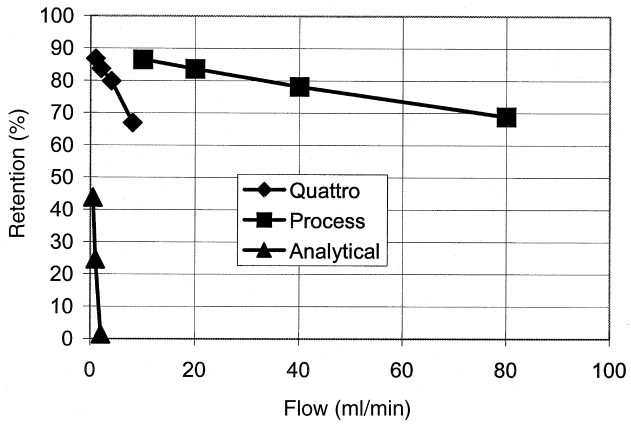

Fig. 1 Variation of retention with flow for different tubing bores: an analytical CCC (0.76 mm), a Bunel CCC (1.6 mm), and a process CCC (3.68 mm).

numbers of the mobile-phase flow were still well within the laminar flow region.

They concluded that increasing two of the three major variables affecting scale-up, speed and tubing bore, actually improved retention. The third, flow, decreased retention as flow increased but less so as the bore increased. Tubing material and retention of the stationary phase therefore are no barrier to the industrial scale-up of CCC.

THE RETENTION BEHAVIOR OF DIFFERENT PHASE SYSTEMS

Du et al.[11] have shown that there is a linear relationship between retention and the square root of flow. The negative gradient of this line gives an indication of the stability of the retention process for a given phase system: The shallower the negative gradient, the more stable the process and the higher the flow possible for a given retention. Tables 1 and 2 give the linear regressions for the phase systems tested on the process-scale CCC[10] at 800 and 1200 rpm, respectively. In all cases, the lower phase is the mobile phase pumping from head (center) to tail (periphery). Retention was measured at four different flow rates: 10, 20, 40, and 80 ml/min, except for the butyl alcohol–acetic acid–water (4:1:5) phase system where only flows of 10 and 20 ml/min were tested before retention dropped below 50%. A range of two-phase solvent systems are listed across the polarity range. In the case of hydrophilic low interfacial tension phase systems like butyl alcohol–acetic acid–water (4:1:5), a high speed of rotation was required to achieve a reasonably high retention.

THE EFFECT OF THESE SCALE-UP PARAMETERS ON RESOLUTION

There has not been any significant change in resolution detected[10] as the bore size increases, provided the sample volume injected maintains the same ratio of coil volume. This is a significant finding, as in most chromatography processes, resolution reduces as the process is scaled up. Resolution was found to increase with increasing speed of rotation as would be expected due to the increased number of mixing and settling cycles per unit time.

The effect of flow on resolution is shown in Fig. 2 for the process CCC[10] running at 1200 rpm. The resolution is between benzyl alcohol and phenyl ethanol resolved using the heptane–ethyl acetate–methanol–water (1.4:0.1:0.5:1.0) phase system. Resolution drops off with increasing flow as would be expected, as the sample will have experienced fewer mixing and settling steps before it elutes and the retention is lower. However, the increased flow appears to improve mixing, as it can be seen that this drop off is only gradual. Doubling flow does not halve resolution and so it would appear advantageous to increase flow as much as possible in the scale-up process.

ENGINEERING CHALLENGES OF SCALE-UP

Sutherland et al.[10] and, earlier, Sandlin and Ito[6] have shown that scale-up is feasible. It can be seen that over 60% retention has been achieved for a broad range of phase systems with flows of 0.1 L/min in a 1 L capacity coil. This leads to the solvent front ($k = 0$) eluting in 4 min and the $k = 1$ point in 10 min with sample volumes of at least 0.1 L possible. All this adds up to sample process

Table 1 Regression analysis between retention (S_f) ($\sqrt{F}$) and the square root of flow for phase systems tested on the process CCC at 800 rpm.

Solvent system	Linear regression	Correlation
Heptane–ethyl acetate–methanol–water (1.4:0.1:0.5:1.0)	$S_f = 97.27 - 3.1341\sqrt{F}$	0.9936
Heptane–ethyl acetate–methanol–water (1.4:0.6:1.0:1.0)	$S_f = 95.73 - 3.3658\sqrt{F}$	0.9988
Heptane–ethyl acetate–methanol–water (1.4:2.0:2.0:1.0)	$S_f = 102.02 - 6.0416\sqrt{F}$	0.9950
Iso–hexane–acetonitrile (1:1)	$S_f = 106.74 - 6.9389\sqrt{F}$	0.9994

Table 2 Regression analysis between retention (S_f) and the square root of flow ($\sqrt{F}$) for phase systems tested on the process CCC at 1200 rpm.

Solvent system	Linear regression	Correlation
Heptane–ethyl acetate–methanol–water (1.4:0.1:0.5:1.0)	$S_f = 97.724 - 2.3506\sqrt{F}$	0.9991
Heptane–ethyl acetate–methanol–water (1.4:0.6:1.0:1.0)	$S_f = 100.41 - 3.107\sqrt{F}$	0.9877
Heptane–ethyl acetate–methanol–water (1.4:2.0:2.0:1.0)	$S_f = 103.63 - 5.2379\sqrt{F}$	0.9996
Iso–hexane–acetonitrile (1:1)	$S_f = 105.84 - 5.2228\sqrt{F}$	0.9996
Butyl alcohol–acetic acid–water (4:1:5)	$S_f = 100.65 - 11.484\sqrt{F}$	1.0

throughputs of up to 1 L/hr or in weight terms as much as 1 kg/day.

However, before this can be realized, the engineering of the coil planet centrifuge will have to be made more reliable. The cyclical forces that produce the unique mixing and settling zones within the coiled tubes can cause them to shake apart and loosen. Janaway et al.[12] have solved this problem by developing new techniques for winding coils. As the scale increases, the volumes of samples being pumped through become extremely high; therefore, designing flying leads that can be guaranteed to not leak becomes paramount. The coil planet centrifuge is a rotating piece of equipment and bearings can wear out. With such high cyclical forces, the reliable engineering of larger CCC units will not be trivial.

So far, Sutherland et al.[10] have only been working with 110 mm radius coil planet centrifuge (CPC) rotors with a capacity of 1 L, which can be operated in a conventional laboratory. Sandlin and Ito[6] have gone as high as 150 mm with capacities of 0.75 L but with a lower speed and b value. The engineering challenge will be to build the next generation of process units at larger rotor radius with capacities of tens or hundreds of liters, but they would need to be installed in hazards plants using intrinsically safe manufacturing practices.

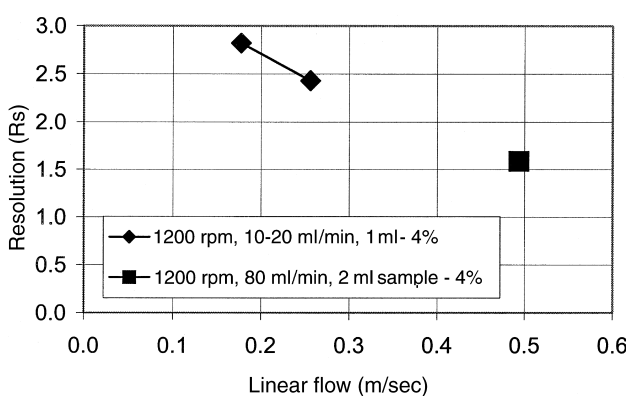

Fig. 2 Variation of resolution with flow for benzyl alcohol and phenyl ethanol in a heptane–ethyl acetate–methanol–water (1.4:0.1:0.5:1.0) phase system.

CONCLUSIONS

The chromatographic scale-up of countercurrent chromatography appears feasible, but there are engineering challenges ahead which will need to be solved before this promising new technology can be realized.

ACKNOWLEDGMENTS

Some of the work presented was undertaken as part of a BBSRC/DTI LINK Consortium study on the "Industrial Scale up of Countercurrent Chromatography." The author would like thank both the BBSRC and the DTI for their financial support and the members of the consortium[10] who have also contributed toward progressing the scale-up of countercurrent chromatography near to reality.

REFERENCES

1. Conway, W.D. *Countercurrent Chromatography: Apparatus, Theory and Applications*; VCH: New York, 1990;
2. Ito, Y. Principle, apparatus, and methodology of highspeed countercurrent chromatography. In *High Speed Countercurrent Chromatography*; Ito, Y., Conway, W.D., Eds.;Chemical Analysis Series John Wiley & Sons: New York, 1996; Vol. 132, 3–44.
3. Marston, A.; Hostettmann, K. Countercurrent chromatography as a preparative tool—Applications and perspectives. J. Chromatogr. **1994**, *658*, 315–341.
4. Ito, Y. pH-Peak-focusing and pH-zone-refining countercurrent chromatography. In *High Speed Countercurrent Chromatography*; Ito, Y., Conway, W.D., Eds.; Chemical Analysis Series John Wiley & Sons: New York, 1996; Vol. 132, 121–175.
5. Sutherland, I.A.; Brown, L.; Forbes, S.; Games, D.; Hawes, D.; Hostettmann, K.; McKerrell, E.H.; Marston, A.; Wheatley, D.; Wood, P. Countercurrent chromatography (CCC) and its versatile application as an industrial

purification & production process. J. Liquid Chromatogr. **1998**, *21* (3), 279–298.
6. Sandlin, J.L.; Ito, Y. Gram quantity separation of DNP (dinitrophenyl) amino acids with multi-layer coil counter-current chromatography (CCC). J. Liquid Chromatogr. **1984**, *7* (2), 323–340.
7. Sandlin, J.L.; Ito, Y. Large-scale preparative countercurrent chromatography with a coil planet centrifuge. J. Liquid Chromatogr. **1985**, *8* (12), 2153–2171.
8. Ito, Y.; Bhatnagar, R. Improved scheme for preparative CCC with a rotating coil assembly. J. Chromatogr. **1981**, *207*, 171–180.
9. Du, Q.; Wu, P.; Ito, Y. Low-speed rotary countercurrent chromatography using a convoluted multilayer helical tube for industrial separation. Anal. Chem. **2000**, *72*, 3363–3365.
10. Sutherland, I.A.; Booth, A.; Brown, L.; Kemp, B.; Games, D.E.; Graham, A.S.; Guillon, G.G.; Hawes, D.; Hayes, M.A.; Janaway, L.; Lye, G.J.; Massey, P.; Preston, C.; Shering, P.; Shoulder, T.; Strawson, C.; Wood, P. Industrial scale-up of countercurrent chromatography. J. Liq. Chromatogr. Relat. Technol. **2001**, *24* (11), 1523–1532.
11. Du, Q.; Wu, C.; Qian, G.; Wu, P.; Ito, Y. Relationship between the flow-rate of the mobile phase and retention of the stationary phase in counter-current chromatography. J. Chromatogr. A, **1999**, *835*, 231–235.
12. Janaway, L.; Hawes, D.; Sutherland, I.A.; Wood, P. Chromatography Apparatus (coil winding process and winding tubing into a coil) UK Patent Application No 0015486.4, 23 June 2000.

SEC with On-Line Triple Detection: Light Scattering, Viscometry, and Refractive Index

Susan V. Greene
Ethyl Petroleum Additives Corp., Richmond, Virginia, U.S.A.

INTRODUCTION

During the 1980s, accurate molecular weights (M) and molecular-weight distributions (MWDs) could be obtained by size-exclusion chromatography (SEC) in conjunction with multiangle light scattering (LS), SEC using conventional calibration, or SEC in combination with viscometry (VISC) using universal calibration (UC). In addition to generating M and MWD, the viscometer with UC yields conformational and branching information. The impetus to combine the two advanced detector technologies of LS and VISC into a single, efficient, and accurate SEC method has been fueled by a growing interest to characterize both natural polymers and the increasing array of synthetic polymers.[1,2]

New electronics and improved computer data acquisition capabilities have permitted the development of SEC with online triple detection using LS, VISC, and refractometry. Online triple detection is known as size-exclusion chromatography cubed (SEC^3) with the three dimensions being defined by the three detectors.[3] The use of eliminates the requirement for column calibration, unlike conventional and universal calibration, where a premium is put on control of variables such as flow rate, temperature, and column resolution. SEC^3 can offer advantages in polymer production quality control as well as in research and development of new polymers.

THEORY

The schematic for one possible configuration of SEC^3 hardware is shown in Fig. 1. When polymer molecules exit from the SEC column(s), they are simultaneously monitored in real time by three online detectors: right-angle laser LS,[4] VISC, and refractive index (RI). The following simplified equations illustrate the variables that relate to the responses of the three detectors:

$$(M)\left(\frac{dn}{dc}\right)^2(C) \rightarrow \text{LS} \tag{1}$$

$$([\eta])(C) \rightarrow \text{VISC} \tag{2}$$

$$\left(\frac{dn}{dc}\right)(C) \rightarrow \text{RI} \tag{3}$$

The term dn/dc refers to the change in RI of a polymer relative to its concentration. The LS detector responds to M, the VISC detector responds to the intrinsic viscosity ($[\eta]$), which is inversely proportional to molecular density, and the RI detector monitors concentration (C). A single narrow standard is used to determine the offset constants related to the interdetector volume for a given three-detector system.[5] Either C or dn/dc of a polymer sample must be known a priori in order to calculate the other variable using the RI detector (Eq. 3). Once both dn/dc and C are known, the LS and VISC (Eqs. 1 and 2) can be solved to determine M and $[\eta]$, respectively, for a polymer sample.[3] Structural information, such as chain flexibility, branching, and intramolecular interactions are all related to $[\eta]$. Several key polymer properties related to $[\eta]$ are as follows:

- *Chain Length*. As the chain length increases, $[\eta]$ increases and the density decreases. This behavior can be fitted to the well-known Mark–Houwink (M-H) equation (Eq. 4) relating M (approximate chain length) to $[\eta]$. The M-H constant a is the slope of the double-logarithmic plot of $[\eta]$ vs. M, and log K is its intercept.

$$[\eta] = KM^a \tag{4}$$

- *Conformation*. If a polymer molecule is folded onto itself, instead of keeping the fully extended chain, the density will be higher resulting in a lower $[\eta]$. This can be induced either by strong intramolecular attractions (e.g., hydrogen-bonding) or by a poor solvent. The Flory–Fox equation[3] calculates $[\eta]$ for a linear flexible coil molecule in solution, relating $[\eta]$ to radius of gyration, R_g. Eq. 5 shows this linear flexible coil example, where ϕ is the Flory-Fox constant.

$$[\eta]M = 6^{2/3}\phi {R_g}^3 \tag{5}$$

- *Chain Flexibility*. If two polymers have the same M, the stiff chain one will produce a coil of lesser density and greater $[\eta]$, compared with its flexible coil counterpart.

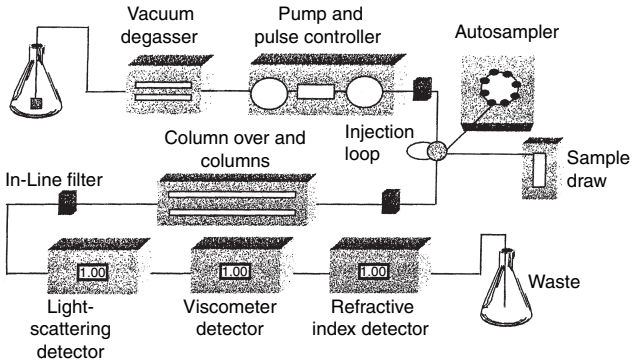

Fig. 1 Hardware schematic for a typical SEC^3 triple online detector configuration.

- *Chain Branching*. A branched molecule is more compact, having greater density and lower $[\eta]$ than its linear counterpart. The Zimm–Stockmayer theory defines the g factor for a polymer as the ratio of $[\eta]$ for the branched polymer to $[\eta]$ of the linear polymer, at the same molecular weight, with ε being the shape factor ($\sim$0.75).

$$g = \left(\frac{[\eta]_{\text{branched}}}{[\eta]_{\text{linear}}} \right)^{1/\varepsilon} \tag{6}$$

  Once g is determined, the branching number B_n (number of branches per molecule), the branching frequency λ (number of branches per arbitrarily selected repeat unit of molecular weight), and f (number of arms for a star) can be calculated. Determinations of B_n, λ and f require equations specific to the type of branching for that polymer.[6]
- *Aggregation*. Colloidal suspension particles are aggregates, which are formed due to poorly dissolved molecules. Aggregates are more dense and have a lower $[\eta]$ than their non-aggregated counterparts. The LS detector responds strongly to such aggregates. When a low VISC response is coupled with a high LS response, the presence of an aggregate is confirmed.

Thus, the SEC^3 data obtained from its LS detector determine the MWD, whereas the VISC detector characterizes conformation and branching. The efficiency of SEC^3 is a consequence of no column calibration requirement for the determination of M and MWD. The precision of the system is limited only by the signal-to-noise ratios of the LS and RI detectors, not by chromatographic variables such as flow rate and column retention. Sophisticated software is required to display the SEC^3 picture of molecular structure.

APPLICATIONS

Four examples of polymer characterization by SEC^3 will be discussed: a dextran sample with branching transitions, a pair of brominated polystyrene (PS) samples, aggregation in chitosan, and a PS star polymer. SEC^3 numerical results for dextran, chitosan, and star-branced PS are listed in the corresponding figure captions.

Dextran is a randomly branched polysaccharide with both long- and short-chain branching. The overlay of the traces generated by the three detectors in Fig. 2 shows a large shift toward a higher M for the LS detector, compared to the other two detectors. This indicates polydispersity within the sample, especially in the high-molecular-weight region of the MWD. Because long-chain branching decreases $[\eta]$ more than short-chain branching, the M-H plot indicates a transition from short- to long-chain

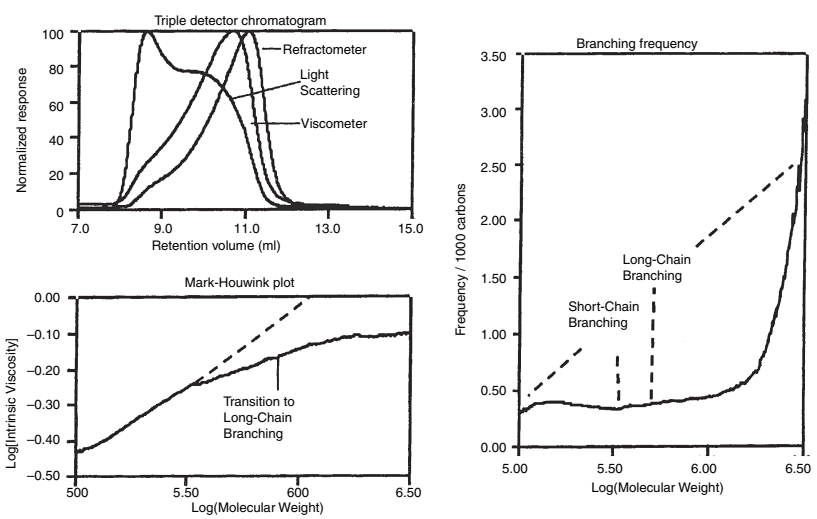

Fig. 2 In the triple-detector overlay of dextran, the shift of the LS detector toward a higher M indicates polydispersity. Both the M-H and branching frequency plots show a randomly branched polysaccharide, with both short- and long-chain branching. $M_n = 230{,}000$, $M_w = 540{,}000$, $M_z = 1{,}160{,}000$, $[\eta] = 0.54$ dl/g, $B_n = 26.6$, $\lambda = 0.43$, $dn/dc = 0.142$, $a = 0.287$, $\log K = -1.852$.

branching at $\log(M) = 5.5$, where the plot deviates from linearity. The branching frequency plot is another visual presentation of the transition from short- to long-chain branching within dextran's MWD. Again, the slope of the curve change indicates a branching transition.

An overlay of the MWDs of two samples of brominated PS is shown in Fig. 3. From the MWD overlay, it is not clear if the MWD difference is a result of two PS samples of the same M_w brominated at different levels, or two PS samples with different M_w brominated at the same level. The M-H plot, which also includes linear PS without bromination, shows that the plots of the two samples in question lie on top of each other. The superposition of the two graphs shows that two PS samples of different were brominated to the same level. The M-H plots of these two samples would be parallel to each other if PS samples of the same M_w were brominated at different levels.

Chitosan is a stiff-chain polysaccharide that has a tendency to aggregate in aqueous solution. Aggregation is indicated when a low VISC response is coupled with a high response from the LS detector. Examples of chitosan with and without aggregation are shown in Fig. 4. Note the close similarity between the non-aggregated chromatograms of the VISC and LS detectors' responses,

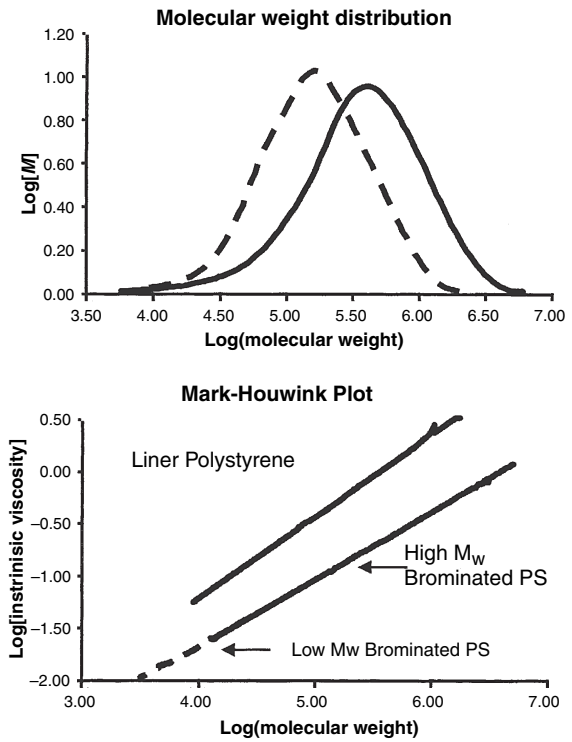

Fig. 3 Two polystyrene (PS) samples with different MWDs are compared in the upper chromatogram. In the lower graph, M-H plots of these same two samples lie on top of each other, indicating they have the same $[\eta]$ across their MWDs. It can be concluded that two PS samples of different M_w were brominated at the same level. A linear PS sample is included in the M-H plot for the purpose of comparison.

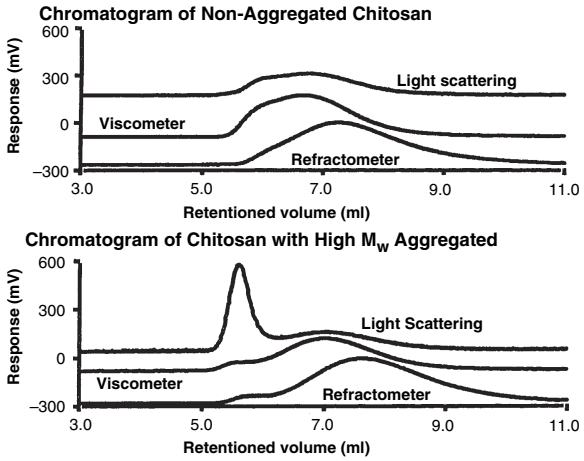

Fig. 4 Triple-detector chromatograms of non-aggregated and aggregated chitosan are compared. For the non-aggregated sample, both the LS and VISC detectors respond similarly. Aggregation in chitosan is indicated in the lower chromatogram, where the VISC response is low and the LS response is high. Non-aggregated chitosan: $M_n = 75{,}000$, $M_w = 260{,}000$, $M_z = 1{,}100{,}000$, $[\eta] = 7.9$ dl/g. Aggregated chitosan: $M_n = 90{,}000$, $M_w = 780{,}000$, $M_z = 3{,}000{,}000$, $[\eta] = 6.8$ dl/g.

respectively. For the aggregated sample, the LS response is much greater than that for the viscometer.

Star polymers are created when long-polymer chains are grouped covalently to a center core. The resulting polymer

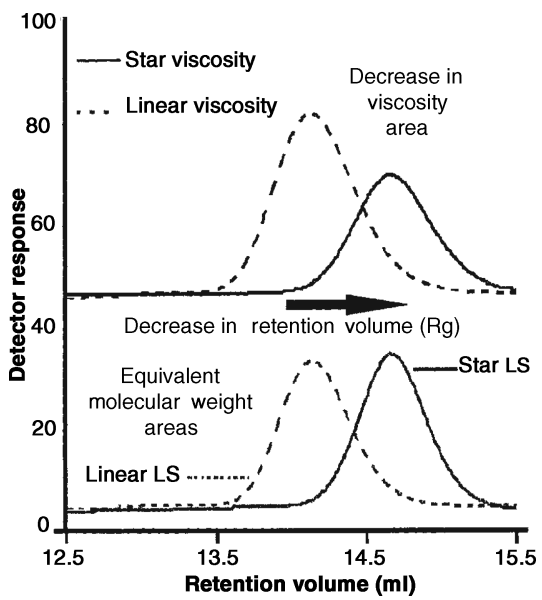

Fig. 5 The VISC traces (upper chromatogram) and the LS traces (lower chromatogram) are overlayed for a linear and a star-branched polymer with the same M. Star-branching creates a denser polymer with lower $[\eta]$ and a smaller R_g. Linear PS: $M_w = 100{,}000$, $[\eta] = 0.495$ dl/g, $R_g = 14$ nm. PS-star: $M_w = 100{,}000$, $[\eta] = 0.318$ dl/g, $R_g = 10$ nm, $f = 5$.

is denser with decreased [η], compared with a linear polymer of the same *M*. Fig. 5 compares VISC and LS detector chromatograms obtained for linear and star-branched PS, both with the same *M*. The difference in [η] is demonstrated by the area difference between the viscometer peaks of the two samples. The areas of the LS detector response are the same for both samples, but the delay elution of the star polymer confirms the star's increased density and smaller in accordance with Eq. 5.

CONCLUSIONS

Three capture its ability to reveal qualitative structural information in a visual format. The applications discussed show how peak displacement of the triple-detector chromatograms reflects polymer polydispersity (dextran), how detector response can relate to aggregation (chitosan), and how peak area differences can indicate a change in polymer chemical composition (PS vs. PS-star). The M-H plots (dextran, brominated PS) give information about polymer conformational changes, structural differences, and branching distributions.[7]

The SEC^3 technique has been in existence for 10 years. It is a relative newcomer to the analytical arena. The amount of information (molecular weight, conformational, and branching) produced, given the ease with which it can be generated, makes SEC^3 a very attractive technique. Recently, the triple detector system has been used in conjunction with temperature rising elution fractionation (TREF) to expand fundamental understanding of polymer structure–property relationships.[8]

ACKNOWLEDGMENTS

The author thanks Dr. Max A. Haney (Viscotek Corp.) and Dr. Tze-Chi Jao (Ethyl Petroleum Additives, Inc.) for reviewing the manuscript, Dr. Wei Sen Wong (Viscotek Corp.) for contributing figures and related information, and Dr. André M. Striegel (Solutia Inc.) for helpful discussions of SEC theory.

REFERENCES

1. Yau, W.W. New polymer characterization capabilities using SEC with on-line MW-specific detectors. Chemtracts–Macromol. Chem. **1990**, *1*, 1–36.
2. Jackson, C.; Barth, H.G.; Yau, W.W. Polymer characterization by SEC with simultaneous viscometry and laser light scattering measurements. In *Waters International GPC Symposium Proceedings*; 1991; 751–764.
3. Haney, M.A.; Gillespie, T.; Yau, W.W. Viewing polymer structures through the triple "Lens" of SEC^3. Today's Chemist Work, **1994**, *3* (11), 39–43.
4. Haney, M.A.; Jackson, C.; Yau, W.W. SEC–viscometry–right angle light scattering. In *Waters International GPC Symposium Proceedings*; 1991; 49–63.
5. Cheung, P.; Balke, S.T.; Mourey, T.H. Data interpretation for coupled molecular weight sensitive detectors in SEC: Interdetector transport time. J. Liquid Chromatogr. **1992**, *15* (1), 39–69.
6. Gillespie, D.T.; Hammons, H.K.; Bryan, S.R. Branching and polymer modification analysis through SEC^3. In *MolMass International Conference Proceedings*; 1996, www.chem.leeds.ac.uk/molmass 99
7. Rose, L.J.; Beer, F. Characterization of long chain branching in LDPE's using SEC with on-line viscosity and light scattering detectors. In *MolMass International Conference Proceedings*; 1999, www.chem.leeds.ac.uk/molmass 99.
8. Yau, W.W.; Gillespie, D.T. Triple-detector TREF instrument for polyolefin research. In *Waters International GPC Symposium Proceedings*; 1998; 252–256.

BIBLIOGRAPHY

1. Brandrup, J., Immergut, E.H., Eds.; *Polymer Handbook,* 4th Ed.; John Wiley & Sons: New York, 1999.
2. Burchard, W. Solution properties of branched macromolecules. Adv. Polym. Sci. **1999**, *143*, 113–194.
3. Lovell, P.A. Dilute solution viscometry. In *Comprehensive Polymer Science*; Booth, C., Price, C., Eds.; Pergamon Press: New York, 1989; 173–197.

SEC: High Speed Methods

Peter Kilz
Polymer Standards Service GmbH, Mainz, Germany

INTRODUCTION

Size-exclusion chromatography (SEC) is the established method to determine macromolecular properties in solution. It is the only technique that allows efficient measurement of property distributions for a wide range of applications. Recent trends in industrial laboratories and research institutes have been focused on increasing the analytical throughput in order to increase productivity. Quality control and combinatorial chemistry demand the optimization of high-throughput methods. Increased analytical throughput can also save time and resources (e.g., instrumentation) in production-related fields. In combinatorial research, high-throughput analytical techniques are a bare necessity, because of the huge numbers of samples being synthesized;[1,2] and references therein. In either situation, the slowest step in the process will determine the overall turnaround time. The importance of high-speed analytical techniques becomes obvious when research companies synthesize over 500 targets per day, but only about 100 samples can be analyzed. The potential of new synthetic methods and in-line production control cannot be fully utilized until the typical SEC run times of 40 min are substantially reduced.

METHODS FOR FAST SEC ANALYSES

There have been several approaches to overcome the traditionally slow SEC separations, which are caused by the diffusion processes in SEC columns. Most of them are column-related (see the sections "High-Speed SEC Columns," "Small Particle Technology," and "Smaller SEC Column Dimensions" below); one utilizes the column void volume (see the section "Overlaid Injections"), while another replaces separation with simplified sample preparation (see the section "Flow Injection Analysis"). Cloning existing methods and instrumentation is also reviewed with respect to the potential time gain (see the section "Cloning of SEC Systems"). Benefits and limitations of each method are summarized in Table 1.

High-Speed SEC Columns

The pore volume of the column packing has been shown to be one of the major factors influencing peak resolution in SEC. True high-speed separations, with good resolution, requires special high-speed columns, which allow fast flow rates, possess high separation volumes, and allow solutes to easily access the pores.[3] PSS GmbH is currently the only vendor of high-speed columns for SEC. Their high-speed columns replace conventional columns one to one, which allows for a trouble-free method transfer from an existing conventional application to a high-speed application. High-speed SEC can be performed in about 1 min, cutting down analysis time by about 10%, with similar resolution on existing instrumentation.[4] Fig. 1 shows a comparison of an SEC separation of polystyrene standards in THF on a conventional column and on a high-speed column, analyzed on the same instrument.

Precision and accuracy of high-speed separations have been investigated for various applications. Both the accuracy of molar mass results and the reproducibility have been comparable to results from conventional columns.[3]

Fig. 2 shows the overlay of 10 out of 60 repeats of a commercial polycarbonate sample analyzed in tetrahydrofurane (THF). They overlap almost perfectly. Each run took about 2.5 min, and the total run time for 60 repeats was about 2 hr.

The overall time savings can even be larger when taking the complete analytical process into account. The total run time of an instrument consists of the preparation and equilibration time, the time needed for running the calibration standards, and the run times for the unknown samples. If 10 individual standards are used for calibration and 10 samples are run, the total run time on a conventional system will be about 2 days. The same work carried out on a high-speed system will only require about 3 hr, and can be easily performed in a single day.[4]

The cost-saving aspects of high-throughput SEC techniques can be substantial and have been evaluated for different scenarios.[5]

Polyolefins, other synthetic polymers, and water-soluble macromolecules have been investigated in high-speed SEC systems. High-speed SEC can be a major time saver in two-dimensional chromatography applications, which require about 10 hr analysis time for cross-fractionation.[6] This can be reduced by a factor of 10, to about 1 hr, which makes it much more interesting for many laboratories. Details on these and additional high-speed applications can be found in Ref.[4]

Small Particle Technology

Reducing particle size of the SEC column packings reduces the time requirements in SEC because of the increased mass transfer and resultant separation efficiency.

Table 1 Synopsis of methods for increased SEC throughput.

Approach	Advantages	Disadvantages	Beneficial for...
Instrument cloning	No method change Easy to implement No additional training	High investment cost High maintenance Higher operating cost More people More space Limited throughput gain	Sample increase of up to 3 ×
High-speed column	No method change Uses existing equipment 1 : 1 application transfer No additional training Minimizes investment (column only) SEC separations in 1 min Time gain ~10 × No additional shear High efficiency Runs with conventional software	No eluent savings	QC/QA Increased throughput (10 ×) Use with exiting methods
FIA	Uses existing equipment Saves eluent	No separation Limited time gain Not applicable for copolymers/blends Requires molar mass sensitive detectors Only primary information (conc., Mw, IV) Needs method change Needs special software	Samples difficult to separate Utilize existing instruments
Overlaid injections	No method change Uses existing equipment No additional training Low cost	Needs overlaid injection-ready software	QC/QA known samples
Small columns	Uses existing equipment Minimizes investment Saves eluent Runs with current software	Limited time savings Needs method adaption Optimization of: injection volumes detection systems Shear degradation Low efficiency	Low-resolution applications Low-time-saving requirements Single detector applications
Needs training			
Limited throughput increase			

Hence, columns can become smaller in dimensions while maintaining resolution. This approach has been used for many years. Column bank lengths dropped from several meters to now typically 60 cm with current SEC column particle sizes of 5 μm as compared with about 100 μm in the early 1960s. During the same period, time requirements dropped from about 6 hr to less than 1 hr.

Unfortunately, this approach is very limited now because of the high shear rates in columns packed with small particles (less than 5 μm), which can cause polymer degradation.

Smaller SEC Column Dimensions

The reduction of column dimensions can, in theory, substantially reduce the time requirements of the separation. However, several limitations predicted by chromatographic theory have to be considered.[7,8] A study of the influence of column dimensions on fast SEC separations has been published in Ref.[4] It has been found difficult to optimize and transfer existing methods and, in many cases, new equipment had to be purchased.

Overlaid Injections

This approach has also been used when SEC separations required hours; it can cut down analysis time by a factor of 2. It utilizes the fact that about 50% of the SEC elution time is needed to transport the solutes through the interstitial volume of the columns. This allows us to inject another sample before the current one is already totally eluted. The

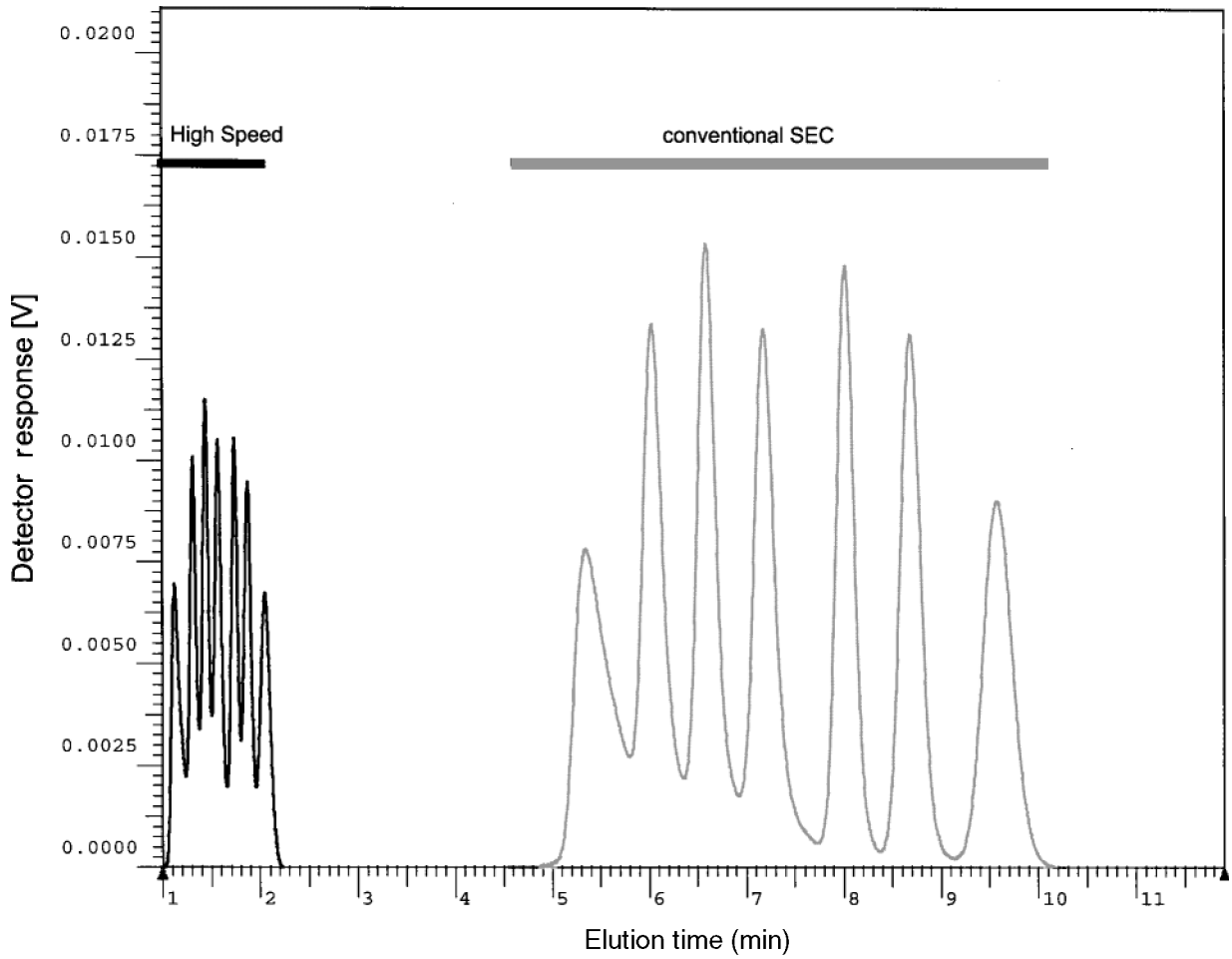

Fig. 1 Chromatogram of conventional SEC column (right part) compared to high-speed SEC column (left part); tested on identical instrument with polystyrene standards, in THF.

optimum injection interval, Δt_{min}, can be calculated from the separation properties of the instrument:

$$t_{min} = (V_t - V_0)/F$$

where V_t is the total penetration volume of column(s), V_0 is the total exclusion volume of column(s), and F is the volumetric flow rate.

The required parameters are easily determined from a molar mass calibration curve.

Today, this method can be combined with appropriate software to automate data acquisition and data processing. It is easy to use, requires no additional investment, and no method modifications are necessary.

Flow Injection Analysis (FIA)

Another approach to cut down on analysis time is to avoid separation and inject samples directly into detector cells. FIA has received some attention recently and is, therefore, mentioned in this review. Because it does not rely on any separation, advantages and limitations will be summarized only.

This method uses the HPLC equipment for sample handling and requires molar mass sensitive detectors (such as light scattering and/or viscometry) to obtain a mean property values from each detector (Mw and/or IV, respectively). The FIA result from a concentration detector yields polymer content in a sample, which can also be determined with other well-established methods. The FIA approach requires expensive and well-maintained equipment, and will not save much time or solvent; furthermore, no distribution information is available.

Cloning of SEC Systems

The number of processed samples can be increased proportionally by increasing the number identical systems. The time and analytical requirements for each sample are not changed, but the number of samples per hour can be increased. Because no change in analytical methods is necessary, cloning SEC instruments and methods is straightforward and can be carried out in most environments.

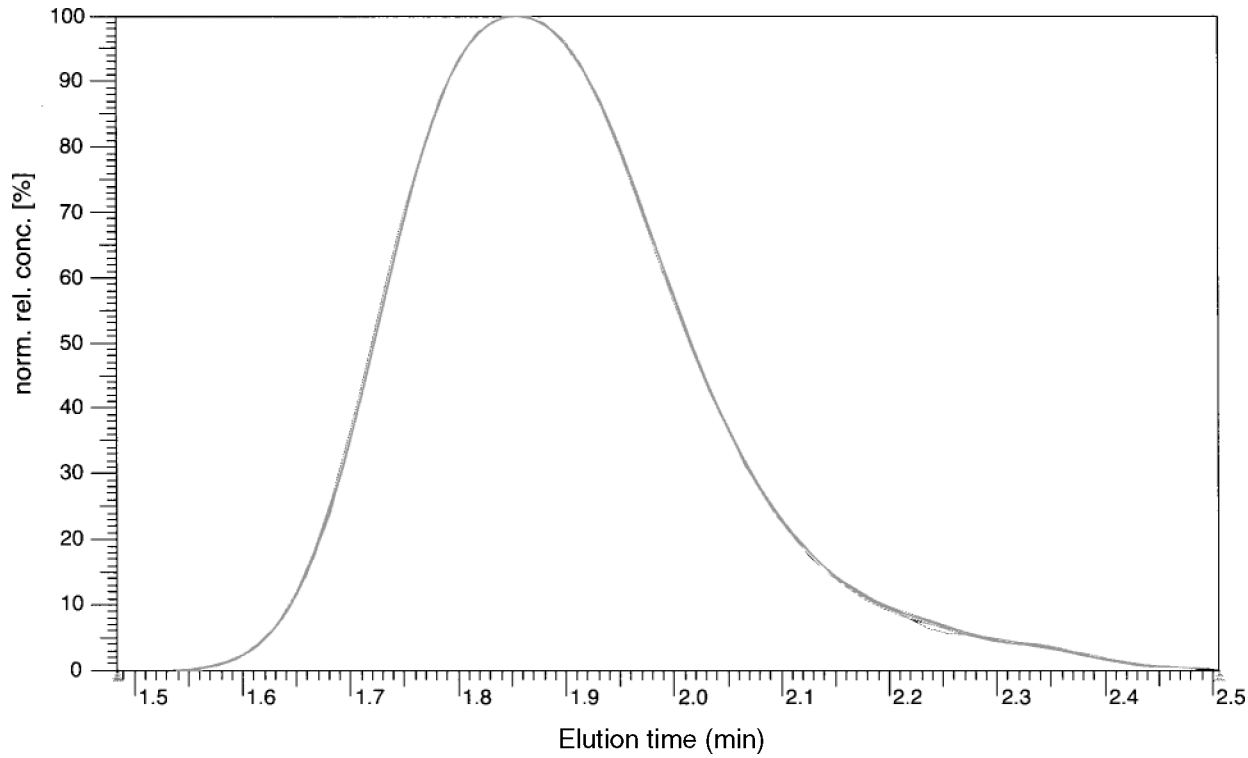

Fig. 2 Overlay of 10 out of 60 repeats of a commercial polycarbonate analysis, in THF, on PSS SDV 5 μm high speed 10^3, 10^5 Å column; measured Mw = (29,610 ± 150) g/mol (nominal sample molar mass by producer: 30,000 g/mol).

This approach, however, is clearly limited by the availability of important resources such as laboratory space, operators, instrumentation, and software licenses. Cloning systems can become very costly; time and effort for instrument maintenance and operation increases proportionally.

True parallelization of analytical processes has, so far, not been very successful. In such set-ups, only the separation module (in general the column) is set up in parallel, while solvent delivery, injection, detection, and data processing are multiplexed. These systems will no longer be as simple in operation and maintenance as the cloned systems.

CONCLUSIONS

Time requirements of SEC experiments can be reduced substantially by using high-speed SEC columns. The availability of high-speed columns allows an increase in SEC separations by a factor of 10 and run times of 1 min are possible. Precision and accuracy of results are comparable with existing methods. Existing methods and instrumentation can still be used with high-speed columns.

The time gain of high-speed columns can open up SEC methodology for

a. Monitoring and controlling processes online;
b. Using SEC methods routinely in QC labs;
c. Allowing high-throughput screening for new materials design;
d. Being a useful tool in combinatorial chemistry; and
e. Studying monitoring time-critical processes.

REFERENCES

1. Nielson, R.B.; Safir, A.L.; Petro, M.; Lee, T.S.; Huefner, P. Polym. Mater. Sci. Eng. **1999**, *80*, 92.
2. Brocchini, S.; James, K.; Tangpasuthadol, V.; Kohn, J. A combinatorial approach for polymer design. J. Am. Chem. Soc. **1997**, *119*, 4553.
3. Kilz, P.; Reinhold, G.; Dauwe, C. *Proceedings of the International GPC Symposium 2000; Las Vegas, NV*; Waters Corp.: Milford, MA, 2001; (CD-ROM).
4. Kilz, P. Methods and columns for high speed SEC separations. In *Handbook for Size Exclusion Chromatography and Related Techniques*; Wu, C.-S., Ed.; Marcel Dekker: New York, 2002, *in press.*
5. Reinhold, G.; Hofe, T. GIT Fachz. Lab. **2000**, *44*, 556.
6. Kilz, P.; Pasch, H. Coupled LC techniques in molecular characterization. In *Encyclopedia of Analytical Chemistry*; Meyers, R.A., Ed.; John Wiley & Sons: New York, 2000; Vol. 9, 7495–7543.
7. Giddings, J.C.; Kucera, E.; Russell, C.P.; Myers, M.N. Statistical theory for the equilibrium distribution of rigid molecules in inert porous networks. Exclusion chromatography. J. Phys. Chem. **1968**, *72*, 4397.
8. Glockner, G. *Liquid Chromatography of Polymers*; Hüthig: Heidelberg, 1982.

Sedimentation FFF: Surface Phenomena

George Karaiskakis
Physical Chemistry Laboratory, Department of Chemistry, University of Patras, Patras, Greece

INTRODUCTION

The study of the interfacial phenomena between the channel wall and the colloidal suspension under study in sedimentation field-flow fractionation (SdFFF) is of great significance in investigating the resolution of the SdFFF separation method and its accuracy in determining particles' physicochemical quantities. The particle–wall interactions in SdFFF affect the exponential transversal distribution of the analyte and the parabolic flow profile, leading to deviations from the classical retention theory, thus influencing the accuracy of analyte quantities measured by SdFFF. Among the various particle–wall interactions, our discussion focuses on the van der Waals' attractive and electrostatic repulsion forces, which play dominant roles in SdFFF surface phenomena.

SEDIMENTATION FIELD-FLOW FRACTIONATION

By the expression "surface phenomena" in SdFFF, we mean all the forces that are active when a particle approaches the channel wall. These include the van der Waals attractive and electrostatic repulsive forces, as well as the Born repulsive and solvent restructuring forces. Additionally, hydrodynamic forces due to shear near the SdFFF wall will be important for larger particles, especially at high-flow rates. Our discussion focuses on the first two forces (van der Waals' attractive and electrostatic repulsive), which exert a dominating effect on retention behavior in SdFFF.

When the colloidal particles under study do not interact with the sedimentation FFF channel wall, the potential energy of a spherical particle, $\varphi(x)$, is given by the relation:[1,2]

$$\varphi(x) = \frac{1}{6}\pi d^3 \Delta\rho G x \tag{1}$$

where d is the particle diameter, $\Delta\rho$ the density difference between the particle and the carrier liquid, G the sedimentation field expressed in acceleration, and x the coordinate position of the center of particle mass.

In the case when surface phenomena are present in SdFFF, which means that the colloidal particles interact with the channel wall, the potential energy given by Eq. 1 must be corrected so as to include the potential energy of interaction, which can be estimated by the classical DLVO theory. It involves estimations of the repulsive energy, φ_R, due to overlap of electric double layers and the London–van der Waals' attractive energy, φ_A, in terms of the particle–wall distance h and their summation to give the total interaction energy, φ_{tot}, in terms of the distance h.

The φ_R particle–wall repulsive energy can be represented in terms of the distance $h = x - d/2$, the gap width between the wall and the particle's closest surface, by the following relation:[1–6]

$$\varphi_R = 8\varepsilon d\left(\frac{kT}{e}\right)^2 \tanh\left(\frac{e\psi_1}{4kT}\right)\tanh\left(\frac{e\psi_2}{4kT}\right) e^{-\kappa h} \tag{2}$$

where ε is the dielectric constant of the medium, e is the electronic charge, ψ_1 and ψ_2 are the surface potentials of the particles and the wall plane, respectively, and κ is the reciprocal double-layer thickness given by the expression:

$$\kappa = \left(\frac{2e^2 I}{\varepsilon kT}\right)^{1/2} = \left(\frac{8\pi e^2 N_A I}{1000 ekT}\right)^{1/2} \tag{3}$$

where I is the ionic strength of the suspending medium. In order for Eq. 2 to be valid, the distance $1/\kappa$ must be small enough compared to d and h, so $\kappa d \gg 1$ and $\kappa x \gg 1$.

The van der Waals' attractive potential energy between the particles and the channel wall, φ_A, is given by the elation:[1–6]

$$\varphi_A = +\frac{A_{132}}{6}\left[\ln\left(\frac{x + d/2}{x - d/2}\right) - \frac{dx}{(x + d/2)(x - d/2)}\right] \tag{4}$$

where A_{132} is the effective Hamaker constant, which depends not only on the molecular properties of the particles and the wall material, but also on the suspending medium. Subscripts 1 and 3 refer to the particle and the wall material, respectively, while subscript 2 represents the medium.

Eq. 4, when $h \ll d/2$, approaches:

$$\varphi_A = -\frac{A_{132} d}{12(x - d/2)} \tag{5}$$

When the van der Waals' force is dominated by the dispersion interactions, A_{132} can be approximated by:[1,4]

$$A_{132} \approx \pm\sqrt{A_{131}A_{232}} \approx \left(\sqrt{A_{11}} - \sqrt{A_{33}}\right) \times\left(\sqrt{A_{22}} - \sqrt{A_{33}}\right) \quad (6)$$

where A_{ii} and A_{iji} are Hamaker constants for two bodies of material i interacting in vacuum and in suspending medium j, respectively.

Hamaker constants, which for some materials are given in the literature,[4] can be calculated on the basis of the Lifshitz theory as presented in Eq. 7 below,where n_1, n_2, and n_3 are the refractive indices of the three media, ε_1, ε_2, and ε_3 are the corresponding static dielectric constants, and v_e is the mean value of the absorption frequency of the three media.

The Hamaker constants A_{ii} can also be determined experimentally by measuring the corresponding surface tensions, since:[1,7]

$$A_{ii} \approx 2.1 \times 10^{-21}\gamma_{ii} \quad (8)$$

where γ_{ii} is in mJ m^{-2} and A_{ii} in J.

From Eqs. 2–4 and 8, and the potential curves, which express the variation of φ_R, φ_A, and φ_{tot} with the distance h, the following conclusions can be drawn:

1. The particle–wall repulsive energy (φ_R) is a function of the surface potentials of the particle (ψ_1) and the wall (ψ_2), the dielectric constant of the medium (ε), the electronic charge (e), the particle diameter (d), and the ionic strength of the suspending medium (I), as the reciprocal double-layer thickness is immediately related to I. φ_R decreases by a decrease in the particle diameter, surface potential of the particle and the wall, and the dielectric constant of the medium, as well as by an increase in the ionic strength of the dispersing medium and the temperature. Of all of the above quantities that affect φ_R, none is as accessible to empirical adjustment as κ. This quantity depends on both the concentration and valence of the indifferent electrolyte. Another way of decreasing φ_R is the variation of the surface potential of the particles by changing the suspension's pH.
2. The particle–wall attractive energy (φ_A) is a function of the effective Hamaker constant (A_{132}), of the particle diameter, and the separation distance between the particle and the channel wall. The Hamaker constant can be easily varied by adding, to the suspending medium, various amounts of detergent to change the medium's surface tension, which, as Eq. 8 shows, affects A.
3. The net potential energy of interaction between the colloidal particles and the SdFFF channel wall, $\varphi_{tot} = \varphi_R + \varphi_A$, which is the resultant of the repulsive and the attractive components, vs. their separation distance, h, shows a maximum and two minima, although some of these features may be masked if one contribution greatly exceeds the other [cf. Fig. 12.12 of Ref.[7]]. The height of the maximum above $\varphi_{tot} = 0$ is the energy barrier, while the deeper minimum is the primary minimum, and the more shallow one the secondary minimum. If no barrier is present, or if the height of the barrier is negligible compared to thermal energy, then the net potential energy of attraction will pull the particles close to the channel surface into the primary minimum, after which partial or total adhesion of the particles on the channel wall occurs, which may be reversible or not. In case the potential energy barrier is appreciable compared to thermal energy, the colloidal particles under investigation are prevented from adhering in the primary minimum. If the depth of the secondary minimum is small enough compared to thermal energy, then the particles will simply diffuse away from the channel wall, the system will be stable, and no surface phenomena are present in SdFFF. It must also be pointed out that adhesion of the particles on the channel wall may occur in the secondary minimum but, in that case, the adsorption may be reversible.

General Comments

1. The larger the Hamaker constant, the larger is the attraction between the particles and the channel wall.
2. The higher the surface potential of the particles, the larger will be the repulsion between the particles and the SdFFF wall.
3. The lower the concentration of the electrolyte, the longer is the distance of the particle from the SdFFF channel wall before the repulsion drops significantly.

Perturbations in Retention Ratio

The retention ratio with particle–wall interaction, R_p, may be smaller or larger than that of the classical theory, depending on whether the attractive or the repulsive force

$$A_{132} \approx \frac{3hv_e}{8\sqrt{2}} \cdot \frac{\left(n_1^2 - n_3^2\right)\left(n_2^2 - n_3^2\right)}{\left(n_1^2 + n_3^2\right)^{1/2}\left(n_2^2 + n_3^2\right)^{1/2}\left[\left(n_1^2 + n_3^2\right)^{1/2} + \left(n_2^2 + n_3^2\right)^{1/2}\right]} + \frac{3}{4}kT\left(\frac{\varepsilon_1 - \varepsilon_3}{\varepsilon_1 + \varepsilon_3}\right)\left(\frac{\varepsilon_2 - \varepsilon_3}{\varepsilon_2 + \varepsilon_3}\right) \quad (7)$$

dominates in the total interaction energy between particles and the SdFFF channel wall.

When $\varphi_A = \varphi_R$, the surface phenomena do not influence the retention ratio and the resultant solute's quantities do not need any correction.

When $\varphi_A > \varphi_R$, the larger is the retention volume, and the smaller will be the experimental retention ratio, R_p. The latter leads to a particle size higher than that expected, making necessary its correction.

In the case when $\varphi_A < \varphi_R$, the larger is the R_p value and the smaller will be the particle size, also making necessary the relative correction.

When $\varphi_A \gg \varphi_R$, the particle–wall interaction leads to partial or total adhesion of particles on the SdFFF channel wall.

Correction of Particle Size in SdFFF Due to Particle–Wall Interaction

Perturbations to retention ratios due to particle–wall interactions may be described in terms of the semiempirical parameter δ_w having units of length.[8,9] A measure of δ_w, which is independent of field strength, may be obtained with the aid of a simple plot of determined experimental retention data, over a range of field strength, via the equation:[8]

$$\frac{R_p - 6\alpha}{6\lambda} = 1 + \frac{\delta_w}{l} \tag{9}$$

where R_p represents the perturbed retention ratio due to interactive forces between particles and the accumulation wall, $\lambda = l/w$ (l is the thickness of the particle cloud and w the thickness of the channel) and $a = d/2w$.

Eq. 9 shows that a plot of $(R_p - 6a)/6\lambda$ vs. $1/l$ should be a straight line with intercept 1 and slope δ_w. The δ_w value so determined can be used in the modified steric retention equation:[8]

$$R_p = 6(a - a^2) + 6\lambda(1 - 2\alpha - 2\lambda)\left(1 + \frac{\delta_w}{\lambda w}\right) \tag{10}$$

from which the corrected particle radius can be calculated. δ_w is a universal constant for a given carrier liquid, channel wall material, and particle material system.[8,9]

In the case of a positive δ_w, the repulsive particle–wall interaction predominates and the experimental particle diameter is smaller than the real one while, when δ_w is negative, the attractive component of interaction predominates, leading to particle diameters larger than those expected.

Partial Adhesion of Particles on the SdFFF Channel Wall

Partial adhesion on the SdFFF channel wall was achieved by using monodisperse spherical particles of polymethyl methacrylate (PMMA) with nominal diameter 0.358 μm.[10] The extent of the PMMA particles' adhesion and detachment on and from the channel wall depends on the concentration of the indifferent electrolyte $Ba(NO_3)_2$ added to the suspending medium to influence the total potential energy of interaction between the PMMA particles and the channel wall. When the concentration of the electrolyte exceeds a given value, which is called critical electrolyte concentration (*CEC*), total adhesion of the colloidal particles occurs at the beginning of the SdFFF channel wall.

While the addition of indifferent electrolytes to the carrier solution at concentrations lower than the CEC value does not influence the retention volume and, hence, the Stokes diameter of the particles under study in SdFFF, the same addition strongly influences the recovery of the colloidal particles, as it is dependent on the interaction energy between the particles and the channel wall.

At concentrations higher than the CEC, in which total adhesion of the colloidal particles occurs at the beginning of the SdFFF channel wall, the recovery is zero. At intermediate electrolyte concentrations, partial adhesion of the particles occurs and the recovery values vary between 0 and 100. It must be pointed out that the total recovery of the particles injected into the column after their detachment was verified by the fact that the area under the curve of the eluted peak, after the detachment of the adhered particles, was exactly the same as that obtained by SdFFF using a carrier solution in which the particles are not adhering to the channel wall.

Total Adhesion of Particles on the SdFFF Channel Wall

Total adhesion of particles on the SdFFF channel wall was achieved[11] with the following model samples:

Table 1 Debye's lengths for the adhesion ($\lambda^{adh.}$) and detachment ($\lambda^{det.}$) of the particles as a function of the corresponding ionic strengths $I^{adh.}$ and $I^{det.}$ of the suspending medium.

Sample	d (μm)	$I^{adh.}$	$I^{det.}$	$\lambda^{adh.}$ (nm)	$\lambda^{det.}$ (nm)
a-Fe_2O_3(I)	0.146	8.1×10^{-2}	—	1.08	—
		—	2.0×10^{-3}	—	6.87
a-Fe_2O_3(II)	0.258	3.1×10^{-2}	—	1.74	—
		—	2.0×10^{-3}	—	6.87
TiO_2	0.310	3.1×10^{-2}		1.74	—
		—	2.0×10^{-3}	—	6.87

Table 2 Collection of parameters used in the calculation of particle–wall interaction energies in SdFFF.

Material	Hamaker constant ($10^{20} \times A$/J)	Surface potential (mV)	Refs.
a-Fe_2O_3(I)	$A_{22} = 6.2$	−15.6	[1,12]
a-Fe_2O_3(II)	$A_{22} = 6.2$	−15.6	[1,12]
TiO_2	$A_{22} = 6.2$	−45.7	[1,12]
H_2O	$A_{33} = 4.4$	—	[1,12]
Stainless steel (SS)	$A_{22} = 22.0$	−24.0	[15,12]
SS-H_2O-I.O.[a]	$A_{132} = 1.02$	—	[1,12]

[a]I.O. = inorganic oxide [a-Fe_2O_3(I), a-Fe_2O_3(II), TiO_2].

1) hematite monodisperse spherical particles of two sizes [a-Fe_2O_3(I) with $d = 0.146$ μm and a-Fe_2O_3(II) with $d = 0.258$ μm], and 2) titanium dioxide (TiO_2) monodisperse spherical particles with $d = 0.310$ μm. Variation of the suspension ionic strength and, consequently, variation of Debye's length, by adding to the suspending medium [triply distilled water containing 0.5% (v/v) of detergent FL-70 and 0.02% (w/w) sodium azide as bacteriocide] various amounts of KNO_3, leads to total adhesion and/or to complete release of the particles under study.[11]

The critical ionic strengths of the dispersing medium with the corresponding Debye's lengths for the adhesion and detachment processes for the samples under study are compiled in Table 1. In all cases, the adhesion Debye's length is much smaller than the detachment one. Furthermore, there is a critical value of the λ parameter where the profile of the potential of the particle–wall interaction changes form, and the particles are totally adhered at the SdFFF channel wall. As λ is immediately related to the closest distance of separation of the particles from the substrate, h, the calculation of the φ_{tot} as a function of h, at various ionic strengths, I, of the suspension medium for the samples under study is of great significance. The necessary quantities for these calculations are summarized in Table 2, while the resultant maximum, φ_{max}, and secondary minimum, φ_{mn1}, energies for the adhesion and detachment of the particles used on and from the SdFFF channel wall, are compiled in Table 3, from which the following conclusions can be drawn:

1. The height of the barrier is enormous ($\sim 10^9$ kT), but independent of the ionic strength, as is the same for both conditions of adhesion and detachment. It is also dependent on the size and the chemical nature of the colloidal particles.
2. The depth of the secondary minimum is dependent on the suspension's ionic strength, as it is different for the conditions under which adhesion and detachment take place. The secondary minimum of the interaction profile becomes more prominent as the ionic strength and particle size increases. Thus, particle adhesion in the secondary minimum explains their reversible adsorption in SdFFF, even though the energy barrier is sufficient to prevent attachment in the primary minimum of the interaction energy curve.

Potential-Barrier Field-Flow Fractionation

The presence of surface phenomena in SdFFF, except for being a main source of error in calculating physicochemical quantities, could also be a basis for a new separation method called *Potential-Barrier Field-Flow Fractionation*, which can separate colloidal particles of different size or of any physicochemical parameter involved in the potential energy of interaction between the particles and the FFF channel wall.[1,2,10,11] The same method can be also used for the *concentration* and analysis of *dilute* colloidal samples, such as those of natural water, where particles are present in low concentration.[13]

CONCLUSIONS

The surface phenomena in SdFFF are the main factors influencing the accuracy of colloidal properties measured by field-flow fractionation. It is, therefore, important to point out the interactions between the colloidal particles and the SdFFF channel wall in order to correct the separation resolution and/or the analyte characterization.

Table 3 Maximum, φ_{max}, and secondary minimum, φ_{mn1}, energies for the adhesion and detachment of the particles used on and from the SdFFF channel wall.

Sample	d (μm)	Adhesion		Detachment	
		φ_{max} (kT)	φ_{mn1} (kT)	φ_{max} (kT)	φ_{mn1} (kT)
a-Fe_2O_3(I)	0.146	4.58×10^9	−3.23	4.58×10^9	−0.08
a-Fe_2O_3(II)	0.258	8.09×10^9	−3.58	8.09×10^9	−0.28
TiO_2	0.310	9.72×10^9	−4.70	9.72×10^9	−0.40

ACKNOWLEDGMENT

The author thanks Ms. M. Barkoula for her kind assistance.

REFERENCES

1. Koliadima, A.; Karaiskakis, G. Potential-barrier field-flow fractionation, a versatile new separation method. J. Chromatogr. A, **1990**, *517*, 345–359.
2. Karaiskakis, G. Potential barrier FFF. In *Encyclopedia of Chromatography,* 3rd Ed., Cazes, J., Ed.; Taylor & Francis: New York, 2010; 1900–1902.
3. Hiemenz, P.C. In *Principles of Colloid and Surface Chemistry*; Marcel Dekker, Inc.: New York, 1977; 457–647.
4. Shaw, D.J. In *Introduction to Colloid and Surface Chemistry,* 4th Ed.; Butterworths: Oxford, 1992; 210–232.
5. Hansen, M.; Giddings, J.C. Retention perturbations due to particle–wall interactions in sedimentation field-flow fractionation. Anal. Chem. **1989**, *61*, 811–819.
6. Mori, Y.; Kimura, K.; Tanigaki, M. Influence of particle–wall and particle–particle interactions on retention behavior in sedimentation field-flow fractionation. Anal. Chem. **1990**, *62*, 2668–2672.
7. Israelachvili, J. In *Intermolecular and Surface Forces,* 2nd Ed.; Academic Press: London, 1992; 176–259.
8. Williams, P.S.; Xu, Y.; Reschiglian, P.; Giddings, J.C. Colloid characterization by sedimentation field-flow fractionation: correction for particle–wall interaction. Anal. Chem. **1997**, *69*, 349–360.
9. Martin, M. Deviations to classical retention theory of field-flow fractionation. J. Chromatogr. A, **1999**, *831*, 73–87.
10. Karaiskakis, G.; Douma, M.; Katsipou, I.; Koliadima, A.; Farmakis, L. Study of the recovery of colloidal particles in potential-barrier field-flow fractionation. J. Liq. Chromatogr. Relat. Technol. **2000**, *23*, 1953–1959.
11. Karaiskakis, G.; Koliadima, A.; Farmakis, L.; Gavril, D. Potential-barrier field-flow fractionation: Potential curves and interactive forces. J. Liq. Chromatogr. Relat. Technol. **2002**, *25*, 2153–2172.
12. Kuo, R.J.; Matijevic, E. Particle adhesion and removal in model systems. III. Monodisperse ferric oxide in steel. J. Colloid Interface Sci. **1980**, *78*, 407–420.
13. Koliadima, A.; Karaiskakis, G. Concentration and characterization of dilute colloidal samples by potential-barrier field-flow fractionation. Chromatographia **1994**, *39*, 74–78.

Selectivity

Hassan Y. Aboul-Enein
Pharmaceutical and Medicinal Chemistry Department, Pharmaceutical and Drug Industries Research Division, National Research Center, Dokki, Cairo, Egypt

Ibrahim A. Al-Duraibi
Pharmaceutical Analysis Laboratory, King Faisal Specialist Hospital and Research Center, Riyadh, Saudi Arabia

INTRODUCTION

The selectivity *a*, also known as the relative retention, the separation factor, or chemistry factor, of a chromatographic column is a function of thermodynamic of the mass-transfer process and can be measured in terms of the relative separation of the peaks:

$$\alpha = \frac{t_{R2} - t_0}{t_{R1} - t_0} = \frac{k_2'}{k_1'} = \frac{K_2}{K_1}$$

where t_{R2} and t_{R1} are the retention times of compounds 2 and 1, respectively, t_0 is the retention time of unretained compounds, k_2' and k_1' are the capacity factors of compounds 2 and 1, respectively, and K_2 and K_1 correspond to the distribution coefficients of compounds 2 and 1, respectively.

So, the selectivity of the chromatographic system is a measure of the difference in retention times (or volume) between two given peaks and describes how effectively a chromatographic system can separate two compounds with slight variations in structure or molecular weight. For compounds with the same molecular weight, the structure difference may involve no more than compounds that are mirror images (i.e., optical isomers resulting from the presence of one or more asymmetric atoms). Therefore, when components interact with a column and are retained, they will be separated if their degrees of retention are not identical. Two components with identical retentions would have $\alpha = 1$, or no separation. For effective separation, an $\alpha = 1.5$ is desired.

OPTIMIZING THE SELECTIVITY

Separation problems become substantially more difficult as the number of components increases much above 10. Such complexity is often characteristic of environmental and biological samples. Different chromatographic modes offer potentially unlimited selectivity, but the conditions for optimal selectivity are correspondingly more difficult to find. A systematic basis for the combining of independent selectivity mechanism can provide a major boost to the overall selectivity. The overall effect is multiplicative, based on the separating power, or peak capacity, of each of the steps. The serial implementation of multiple origins of selectivity is the most practical approach at present.

The net retention of a particular solute depends on all the solute–solute, solute–mobile phase, solute–stationary phase, and stationary phase–mobile-phase interactions that contribute to the retention, which, consequently, affect the selectivity.

The selectivity is dependent on the temperature and the chemistry of the components that make up the chromatographic system (i.e., column, solvent, and the sample). So, it is necessary to understand the physicochemical basis of retention and the retention mechanism involved in high-performance liquid chromatography (HPLC) separation.

THE SAMPLE OR SOLUTE

The basic structure and number of functional groups in the solute molecule largely determine chromatographic retention. The functional group must be able to interact with the stationary-phase surface. Moreover, the strength of the retention is increased by the introduction of a second functional group. In addition, the type of functional group determines the elution order. Therefore, changing the chemical nature of the sample compounds or altering the functional group by chemical derivatization of an analyte should lead to compounds that can be will separated with higher α, because it will alter the chromatographic properties and the solubility of the analytes. Furthermore, the quantity of injected sample could affect k' values and column efficiency.

STATIONARY PHASE

Selectivity enhancement through choice of stationary phase can be a simplifying approach for difficult

separations, where interest is in certain critical pairs and where practical capacity is deemed important.

The nature of the stationary phase plays an important role in the improvement of the selectivity of a chromatographic system. Therefore, changing the chemical composition of the column from very non-polar to a higher polarity will cause the non-polar compounds to elute faster. Also, some phases have an affinity toward some compounds; therefore, selecting the ideal phase will improve the selectivity. For instance, the chromatographic selectivity in electron-acceptor and electron-donor stationary phase depends on the ability of the stationary phase to form complexes with solutes. The selectivity depends not only on the number and mutual position of electron-accepting substituents attached to aromatic skeleton but also on the nature of the spacer connecting the ligand with the silica surface. Also, in liquid–solid chromatography (LSQ), the sample retention is governed by adsorption to the stationary phase. For retention to occur, a sample molecule must displace one or more solvents from the stationary phase. In addition to this displacement effect, polar solvent or sample molecules can exhibit very strong interactions with particular sites on the stationary phase. The separation of enantiomers using a chiral mobile phase is possible only if transient diastereomeric complexes are formed in the stationary phase. For this to happen, the stationary phase must be chiral.

Another way to improve selectivity is by using column switching, which is, in its simplest form, the use of a number, *N*, of different chromatographic mechanisms in sequence, which will expand the overall selectivity of a liquid chromatography system by the *N*th power of that obtained from a single selectivity mechanism. Column switching can create tremendous separating power, but it is a requirement that each one in the sequence of selectivity mechanism not be redundant.

TEMPERATURE

Temperature is the first of the variables affecting selectivity. Increased temperature decreases retention time on the column, sharpens peaks, and produces a change in selectivity. However, temperature is generally limited, by solvent vapor pressures, to an effective range of 20–60°C; also important is the effect temperature has on the column packing.

Temperature affects sample solubility, solute diffusion, and mobile-phase viscosity in liquid chromatography (LC). With increasing temperature, the solute diffusion coefficient tends to increase while the mobile phase viscosity decreases, producing a favorable influence on the selectivity. The change in selectivity with temperature appears more pronounced in ion-pair chromatography than other HPLC methods. Therefore, temperature may be an important variable for optimizing selectivity in certain applications of ion-pair chromatography.

MOBILE PHASE

The most powerful approach to increase a is to change the composition of the mobile phase. If changing the concentration of the components in the mobile phase provides insufficient change, altering the chemical nature of one of the components will often be sufficient. Also, we can produce other a changes by adding mobile-phase modifiers to the mobile phase. The shifts in selectivity under certain circumstances have been attributed to the change in mobile-phase composition rather than to the stationary phase. Also, selectivity arises from the combined action of mobile phase and stationary phase. Change in mobile phase can result in significant differences in selectivity for various sample analytes which can be obtained when the relative importance of the various intermolecular interactions between solvent and solute molecules is markedly changed. It is frequently preferable to use mixtures of solvents, rather than a single, pure solvent, as the mobile phase. However, in many cases, selecting a mobile phase is still a trial-and-error procedure. Moreover, pH has a prominence as a tool to affect the separation of some compound solutes. Likewise, an impressive separation of optically active compounds has been demonstrated through the use of chiral reagents that induce a ligand-exchange mechanism. Therefore, it should be recognized that the harnessing of liquid-phase composition to control HPLC selectivity provides a major corridor for achieving separation in an increasingly systematic manner.

The difficulty in eliminating the silanol groups from the silica substrate make it necessary to neutralize them using additives in the mobile phase. Also, solvent strength generally increases with the volume percent of organic modifier. Its effect is most important when hydrophobic mechanisms contribute significantly to retention. In this case, changing the organic modifier can be used to adjust solvent selectivity, as normally practiced in reversed-phase chromatography. Mobile-phase additives (in normal phase), which are very polar, influence the adsorption of substances strikingly, even in the very low concentration range, because they are adsorbed preferentially. On the other hand, the stationary-phase selectivity can be altered for some phases by the addition of some compounds or metallic complexes to the mobile phase.

HPLC offers options to control selectivity through the mobile phase. Therefore, it is important to improve the practical understanding of liquid-phase compositions needed to achieve chemical selectivity.

BIBLIOGRAPHY

1. Ahuja, S. *Selectivity and Detectability Optimization in HPLC*; John Wiley & Sons: New York, 1989.

2. Freeman, D. Advances in liquid chromatographic selectivity. In *Ultrahigh Resolution Chromatography*; Ahuja, S., Ed.; American Chemical Society: Washington, DC, 1984.
3. Lochmiller, C.H. Approaches to ultrahigh resolution chromatography: Interaction between relative peak (N), relative retention (a), and absolute retention (k'). In *Ultrahigh Resolution Chromatography*; Ahuja, S., Ed.; American Chemical Society: Washington, DC, 194.
4. Meyer, V.R. *Practical High-Performance Liquid Chromatography,* 2nd Ed.; John Wiley & Sons: New York, 1993.
5. Poole, C.F.; Poole, S.K. *Chromatography Today*; Elsevier Science: Amsterdam, 1991.
6. Riley, C.M. Efficiency, retention, selectivity and resolution in chromatography. In *High Performance Liquid Chromatography, Fundamental Principles and Practice*; Laugh, W.J., Wainer, I.W., Eds.; Blackie Academic and Professional: Glasgow, 1996; 29–35.
7. Snyder, L.R.; Glajch, J.L.; Kirkland, J.J. *Practical HPLC Method Development*; John Wiley & Sons: New York, 1988.
8. Weston, A.; Brown, P.R. *HPLC and CE Principles and Practice*; Academic Press: San Diego, CA, 1997.

Selectivity Tuning

Ján Krupcik
Eva Benicka
Institute of Analytical Chemistry, Slovak University of Technology, Bratislava, Slovakia

INTRODUCTION

A very important quality criterion of an analytical method is its capability to deliver signals that are free from interferences. The ability to discriminate between the analyte and interfering components has, for many years, been expressed as the "selectivity" of a method and/or measurement system. This leads to a definition: *Selectivity of a method refers to the extent to which it can determine particular analyte(s) in a complex mixture without interference from other components in the mixture*.[1] In current analytical chemistry, selectivities based on multistage separation and detection principles are frequently used. In all these methods, the analytical tools are chosen in relation to the analytes in such a selective way that the tools give preference for the target analyte to be appropriately analyzed, either qualitatively or quantitatively. Techniques such as chromatography, electrophoresis, and membrane separations for all types of species tend to rely on selectivity in a separation process, exhibit *separation selectivity*. Hyphenated techniques like column gas or liquid chromatography–mass spectrometry (LC–MS), in which *separation and detection selectivities* are combined, are often required in legal situations when positive and non-biased identification is needed. In analytical methods, various kinds of interactions are utilized in discrimination processes. They can be based on, for example, chemical reactions, associate formation, adsorption to surfaces, inclusion phenomena, absorption of radiation, and biochemical (immunochemical or enzymatic) or electrochemical (redox) principles. To cope with overlap in responses to the useful interactions, modern methods usually rely on several *selectivity* generating steps (stages) to reduce the effects of interfering interactions. In the current analytical chemical literature, *selectivity* is very often expressed in combination with words such as *adjustment*, *tuning*, and *optimization*. In the separation methods, various terms are used to clarify the selectivity as, for example, *stereoselectivity*, *enantioselectivity*, and *shape selectivity*.[1]

RETENTION AND SELECTIVITY IN COLUMN CHROMATOGRAPHY

A separation is achieved in a chromatographic system by moving the solute zones apart and constraining their dispersion so that peaks are eluted discretely. To move the zones apart, each solute must be retained to a different (*selective*) extent, which means that their distribution coefficients must differ or they must interact with different volumes of stationary phase. Regulating the magnitude of the apparent distribution coefficients or modifying the quantity of stationary phase available to each solute, therefore, controls retention. The former is employed in interaction chromatography and the latter in exclusion chromatography. In practice, it is rare that either procedure is exclusive in any given separation, as both retentive processes are usually present to some extent. Interaction and exclusion processes, when they do occur together, act independently.[2]

Retention in chromatography can be, for an analyte i, expressed, e.g., by retention factor, k_i, using the following equation:

$$k_i = K_{\mathrm{D},i}\frac{V_\mathrm{s}}{V_\mathrm{m}} \tag{1}$$

where $K_{\mathrm{D},i}$ is a distribution coefficient, V_s and V_m are volumes of stationary, s, and mobile, m, phases in the column, respectively.

Distribution coefficient, $K_{\mathrm{D},i}$, can be calculated from an equation:

$$K_{\mathrm{D},i} = \frac{\bar{c}_{i,\mathrm{s}}}{\bar{c}_{i,\mathrm{m}}} \tag{2}$$

where average concentrations, $\bar{c}_i$, of a solute, i, in the mobile and stationary phases can be found from equations:

$$\bar{c}_{i,\mathrm{m}} = n_{i,\mathrm{m}}/V_\mathrm{m} \tag{3a}$$

$$\bar{c}_{i,\mathrm{s}} = n_{i,\mathrm{s}}/V_\mathrm{s} \tag{3b}$$

where $n_{i,\mathrm{m}}$ and $n_{i,\mathrm{s}}$ represents number of moles present in the mobile and stationary phases, respectively.

Distribution coefficient, $K_{\mathrm{D},i}$, can be used to calculate the Gibbs free energy difference, ($\Delta G_i^{\#}$), which characterizes overall interactions of the solute in the stationary and mobile phases as follows from equation:

$$\left(\Delta G_i^{\#}\right) = -RT \ln K_{D,i} \tag{4}$$

Evaluation of interactions of a solute with stationary and mobile phase may, however, be too complex for organic molecules containing various functional groups differing in polarity and interactive characteristics. This problem has been solved assuming that each group, *j*, of the molecule is associated with its own unique change in interaction energy, $\Delta G_{i,j}^{\#}$, independently, when transferred between phases. Thus, the overall interaction energy, $\Delta G_i^{\#}$, for an analyte *i*, can be approximated as the sum of its parts:

$$\Delta G_i^{\#} = \sum \Delta G_{i,j}^{\#} \tag{5}$$

Thus, the *separation selectivity* of the chromatographic system can be tuned by any parameter, which influences the interaction of an analyte with stationary and mobile phase.[3]

The *separation selectivity* may be tuned by the modification of both enthalpic and entropic terms:

$$\Delta G^{\#} = \Delta H^{\#} - T\Delta S^{\#} \tag{6}$$

SEPARATION SELECTIVITY CRITERIA IN COLUMN CHROMATOGRAPHY

In column chromatography, *the separation selectivity* is often expressed by *selectivity factor*, α, of a critical pair of sample components:

$$\alpha = \frac{k_j}{k_i} \tag{7}$$

where *k* is retention factor of compounds *i* and *j* and usually $k_j > k_i$ (see Fig. 1).

The number of adjacent peaks, *m*, in which *selectivity factor* is higher than a threshold value, $\alpha > \alpha_{thres}$, may be used to express overall *separation selectivity* of the chromatographic system for multicomponent sample separation:

$$m = 1 + \sum_{1}^{n-1} k_q \tag{8}$$

where $k_q = 1$ for those adjacent peaks for which $k_j/k_i \geq \alpha_{thres}$ otherwise $k_i = 0$.[4]

Selectivity coefficient in ion-exchange chromatography $k_{A/B}$ characterizes the ability of an ion-exchanger to select one of two ions present in the same solution.[5] *Selectivity coefficient* describing exchange of cations:

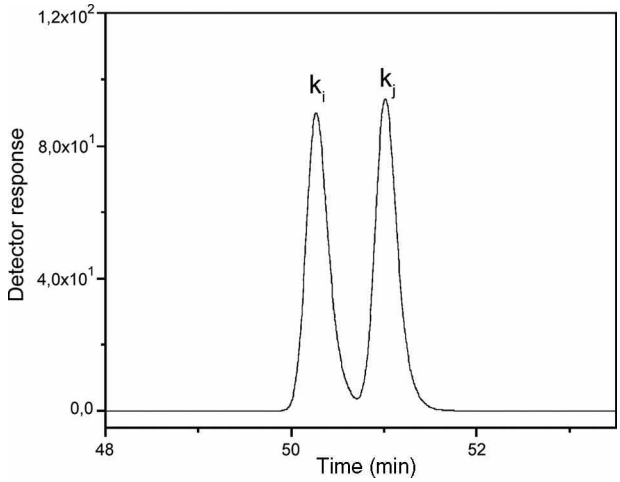

Fig. 1 Column chromatographic separation of two components.

$$Mg_S^{2+} + Ca_M^{2+} = Mg_M^{2+} + Ca_S^{2+}$$

is calculated from the equation:

$$k_{Mg/Ca} = \frac{[Mg^{2+}]_M \cdot [Ca^{2+}]_S}{[Mg^{2+}]_S \cdot [Ca^{2+}]_M} \tag{9}$$

and anions:

$$Cl_S^- + OH_M^- = Cl_M^- + OH_S^-$$

is calculated from the similar equation:

$$k_{Cl/OH} = \frac{[Cl^-]_M \cdot [OH^-]_S}{[Cl^-]_S \cdot [OH^-]_M} \tag{10}$$

where $[Mg^{2+}]$, $[Ca^{2+}]$, $[Cl^-]$, and $[OH^-]$ are equilibrium concentrations. Subscript S refers to the ion-exchanger ("stationary phase") and M to the external solution ("mobile phase"). Ions involved in the exchange are specified as subscripts. For exchanges of ions differing in charges, the numerical value of $k_{A/B}$ depends on the choice of the concentration scales of the ion-exchanger and the external solution. Concentration units must be, therefore, clearly stated for an exchange of ions differing in charges. The *corrected selectivity coefficient* ($k_{a,\ A/B}$) is calculated in a way identical to the calculation of *selectivity coefficient*, except that the concentrations are replaced by activities.[5]

SEPARATION SELECTIVITY TUNING IN COLUMN CHROMATOGRAPHY

Separation *selectivity* in column chromatography can be tuned in: (i) one column, and (ii) two or more columns coupled in series.

Single Column Separation Selectivity Tuning

For a given sample and separation mechanism, the *separation selectivity* of the chromatographic system depends on the nature of both mobile as well as stationary phase. Interactions of solute with mobile and stationary phases may include a mixture of non-polar dispersive and various polar forces. The terms "polar" and "non-polar" have been commonly used to describe a property of both the solute, as well as mobile and stationary phases. These terms, however, should not be confused with *selectivity*. The *separation selectivity* of a stationary phase can be changed discontinuously by selection of a proper column packing (by its polarity or other parameters), or tuned continuously, synthesizing tailor-made phases or mixing stationary phases differing in polarity.[6]

Tailor-made stationary phases

Tailor-made phases are specially synthesized materials to perform required *separation selectivity*. Thus, for example, in gas chromatography (GC), polyethylene glycol (PEG) may be acid-terminated to form a free fatty acid phase (FFAP) for the separation of non-esterified fatty acids. Tailor-made stationary phases are often used for the separation of isomers. This was instructively shown by synthesis of four tailored high-performance liquid chromatography (HPLC) stationary phases containing different functional groups, such as: C_{18}, C_{30}, alkylamide, and cholesterolic, for simultaneous HPLC separation of β- and γ-isomers of tocopherol.[7] It was pointed out that *separation selectivity* of each stationary phase has been a result of modulation in the mass transfer and set of unspecific interactions in the tertiary system comprising analyte, stationary, and mobile-phase interactions. Differences in observed retention and selectivity of tocopherols, together with the stationary-phase structure investigations, indicated that a spatial organization changing chemically bonded ligands as predominantly a solvation consequence. Molecular modeling studies were used to explain some of these complicated supramolecular phenomena, which caused cholesterolic stationary phase to offer beneficial performance in screening of tocopherols by HPLC and biomimetic studies of not completely recognized interactions of tocopherol isomers and biological membranes.[7]

Mixed stationary phases

Specialty columns are prepared to optimize *separation selectivity* for specified or standard analyses by mixing relative amounts of two or more distinct stationary phases.

Solute partition coefficient of an analyte, *i*, in a column consisting of two stationary phases differing in polarities, $K_{Di,AB}$, may be described by equation:

$$K_{Di,AB} = \Phi_A K_{Di,A} + \Phi_B K_{Di,B} \quad (11)$$

where $K_{Di,A}$ and $K_{Di,B}$ are corresponding partition coefficients in pure stationary phase *A* and *B* columns, respectively, and Φ_A and Φ_B are their volume fractions. This equation and its consequences also establish criteria for the analytical usefulness of mixed phases in column chromatography. For solutes and stationary phases for which the above equation is valid, it is also possible to predict an optimum composition at which the required separation selectivity is obtained.[8–10]

Main factors influencing separation selectivity in single column chromatography

Separation selectivity, in principle, may be tuned by thermodynamic parameters (temperature and pressure) and/or by polarity of stationary and mobile phase. The *separation selectivity* for a given sample is usually "optimized" by a trial-and-error approach on a column chosen by chromatographer.

The change of temperature under the isocratic, as well as programing, conditions is often used to *tune separation selectivity* in gas chromatographic separations. Temperature has not been very actively utilized in HPLC, mainly because of reported stability problems of the most commonly used stationary phases. However, more interest in the application of temperature for retention control has come nowadays because of the trend of miniaturization in chromatography and the availability of temperature-stable stationary phases.[11]

The column pressure practically does not influence the *separation selectivity* in gas and liquid chromatography. It, however, substantially influences the *separation selectivity* in supercritical fluid chromatography (SFC).[12]

Usually, the simplest *separation selectivity* tuning in HPLC is performed by tuning the composition of mobile phase polarity, mixing two or more solvents (under isocratic or gradient conditions), adding the concentration of the organic modifier and setting a proper pH for separation of given sample on a selected column at the laboratory temperature. The most effective way is to vary several parameters simultaneously.[13–15]

Separation Selectivity Tuning in Column Series

Columns of different polarities may be coupled in series under the conditions of dual column chromatography, two-dimensional chromatography, or comprehensive two-dimensional chromatography. In this part, only the *separation selectivity tuning* in dual column chromatography will be illustrated with some examples.

The *separation selectivity* of dual column HPLC, GC, and SFC coupled in series may be tuned by changing thermodynamic parameters and/or contribution of individual column polarities.[16–21] In analytical praxis, it is convenient to keep constant the entire column parameters

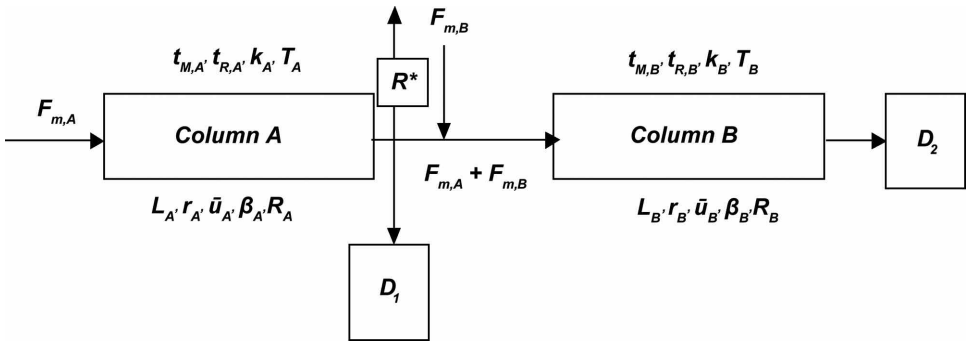

Fig. 2 Schematic of two chromatographic columns coupled in series. F_m – mobile-phase flow, t_M – mobile-phase hold-up time, t_R – retention time, k – retention factor, T – temperature, L – column length, r – column inner diameter, u – mobile-phase-flow rate, β – column phase ratio, R – column pneumatic resistance, R^* – pneumatic resistance, D – detector.

depicted in Fig. 2, except for mobile-phase flows ($F_{m,A}$, $F_{m,B}$) and/or temperatures (T_A, T_B) in individual columns. The selectivity factor of compounds i and j in a column series can then be calculated from the formula:

$$\alpha = \frac{k_{AB,j}\left(T_A, T_B, F_{m,A}, F_{m,B}\right)}{k_{AB,i}\left(T_A, T_B, F_{m,A}, F_{m,B}\right)} \tag{12}$$

where $k_{i,AB}(T_A, T_B, F_{m,A}, F_{m,B})$ is the retention factor of a compound, i, in the column AB series, T is the temperature, and F_m is the mobile-phase flow in individual A, B columns.

The retention factor of a solute in a coupled column series, $k_{i,AB}$, can, for equal column temperatures ($T_A = T_B$), be calculated from the following equation:

$$k_{i,AB} = x_A \cdot k_{i,A} + x_B \cdot k_{i,B} \tag{13}$$

where x_A and x_B are weight (retentivity) factor, calculated from the following equations:

$$x_A = \frac{t_{M,A}}{t_{M,AB}} = \frac{L_A \cdot F_{m,B}}{L_A \cdot F_{m,B} + L_B \cdot F_{m,A}} \tag{14}$$

$$x_B = \frac{t_{M,B}}{t_{M,AB}} = \frac{L_B \cdot F_{m,A}}{L_A \cdot F_{m,B} + L_B \cdot F_{m,A}} \tag{15}$$

where t_M is the mobile-phase hold-up time and L is column length.

From Eqs. (12–15), it follows that the *separation selectivity* of a column series can, for example, be tuned by changing the mobile-phase flows in individual columns.

Modification of Eq. 13 leads to a linear relationship of overall selectivity factor, $k_{i,AB}$, on weight (retentivity) factor, x_B:

$$k_{i,AB} = k_{i,A} + x_B\left(k_{i,B} - k_{i,A}\right) \tag{16}$$

The *separation selectivity tuning* in dual column chromatography may be illustrated by HPLC separation of the enantiomers of *N*-3,5-dinitrobenzoyl derivatives of some amino acids in two chiral β-cyclodextrin columns of opposite separation selectivity coupled in series. Fig. 3 shows

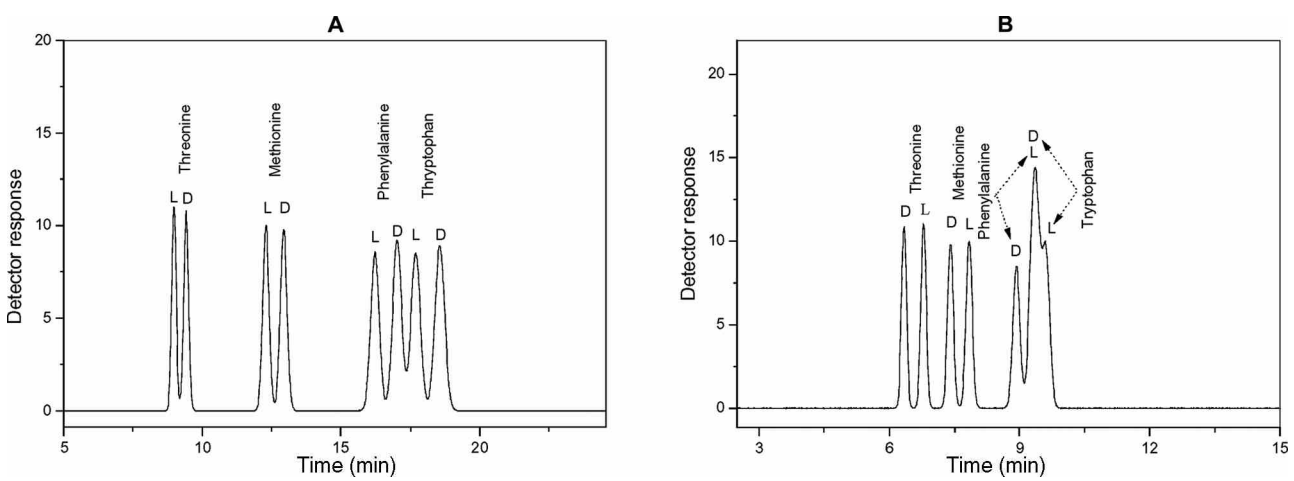

Fig. 3 HPLC separation of enantiomers of *N*-3,5-dinitrobenzoyl derivatives of threonine, methionine, phenylalanine, and tryptophan on individual Cyclobond 2000 SN (A) and 2000 RN (B) columns. Mobile phase consisted of 50% ACN and 50% water solution of TEAA-buffer at pH 2.

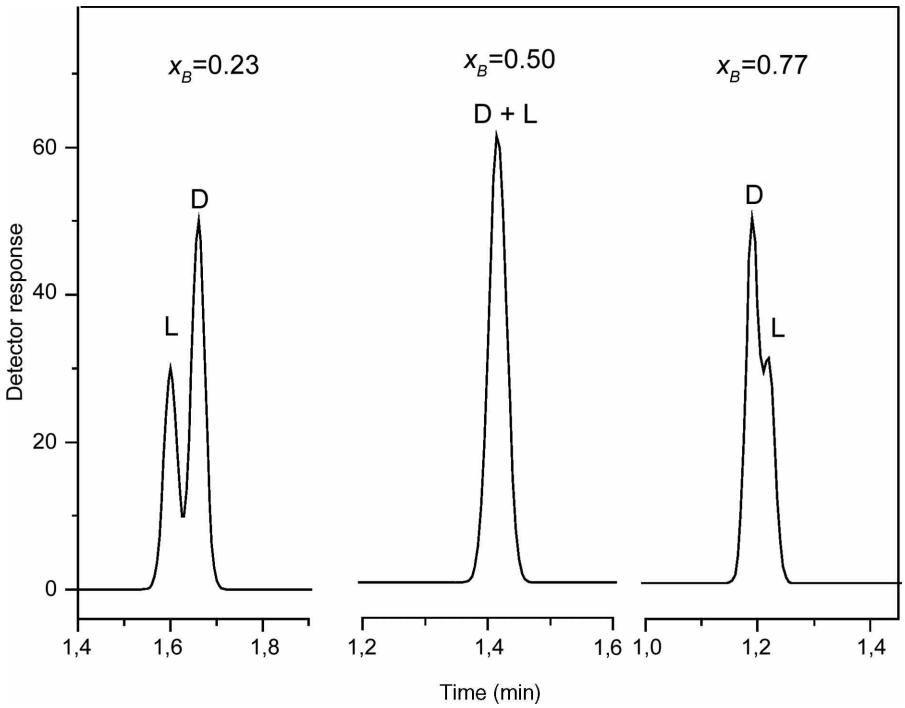

Fig. 4 Dependence of retention order of *N*-3,5-dinitrobenzoyl threonine enantiomers on retentivity factor, X_B.

the separation of enantiomers of the *N*-3,5-dinitrobenzoyl derivatives of tryptophan, phenylalanine, methionine, and threonine on individual columns. The flows of mobile phase in individual columns ($F_{m,A}$, $F_{m,B}$) were selected as variables in the column series. Fig. 4 depicts the dependence of the retention order of *N*-3,5-dinitrobenzoyl threonine enantiomers on retentivity factor, x_{RN}. Retention (k) and *separation selectivity* ($\alpha = k_L/k_D$) factors of enantiomers found by HPLC on individual Cyclobond 2000 SN (A) and 2000 RN (B) columns for *N*-3,5-dinitrobenzoyl derivatives of the studied amino acids listed in Table 1 were used to construct the dependence depicted in Fig. 5. This figure shows, in correspondence with Eq. 16, that the *separation selectivity* of two columns coupled in series may be used for optimization separation selectivity purposes.

COMPUTER-ASSISTED OPTIMIZATION OF SEPARATION SELECTIVITY IN COLUMN CHROMATOGRAPHY

After selecting a stationary phase and the mobile-phase components, several isocratic experiments are required to build a retention model. A computer-assisted multivariate procedure is often used to find the best combination of the working parameters.[22] *Separation selectivity* is often monitored by maximum resolvable components in the shortest time at separation of multicomponent samples.[4]

Various computer-assisted chromatographic optimization methods have been developed to optimize *separation selectivity*.[23–28] It should be pointed out that most of the method development strategies, as well as many types of chromatography softwares, have been focused on

Table 1 Retention (k) and selectivity ($\alpha = k_L/k_D$) factors found by HPLC on Cyclobond 2000 SN and 2000 RN columns* for *N*-3,5-dinitrobenzoyl derivatives of listed amino acids.

No.	*N*-3,5-dinitrobenzoyl derivative of	k_{SN}	α	k_{RN}	α
2	L-Tryptophan	4.29	0.97	2.09	1.09
1	D-	4.42		1.92	
4	L-Phenylalanine	3.82	0.92	1.89	1.05
3	D-	4.17		1.80	
6	L-Methionine	2.77	0.95	1.40	1.06
5	D-	2.91		1.32	
8	L-Threonine	1.77	0.95	1.06	1.07
7	D-	1.86		0.99	

*Cyclobond columns were purchased from ASTEC (http://www.astecusa.com/index.htm).

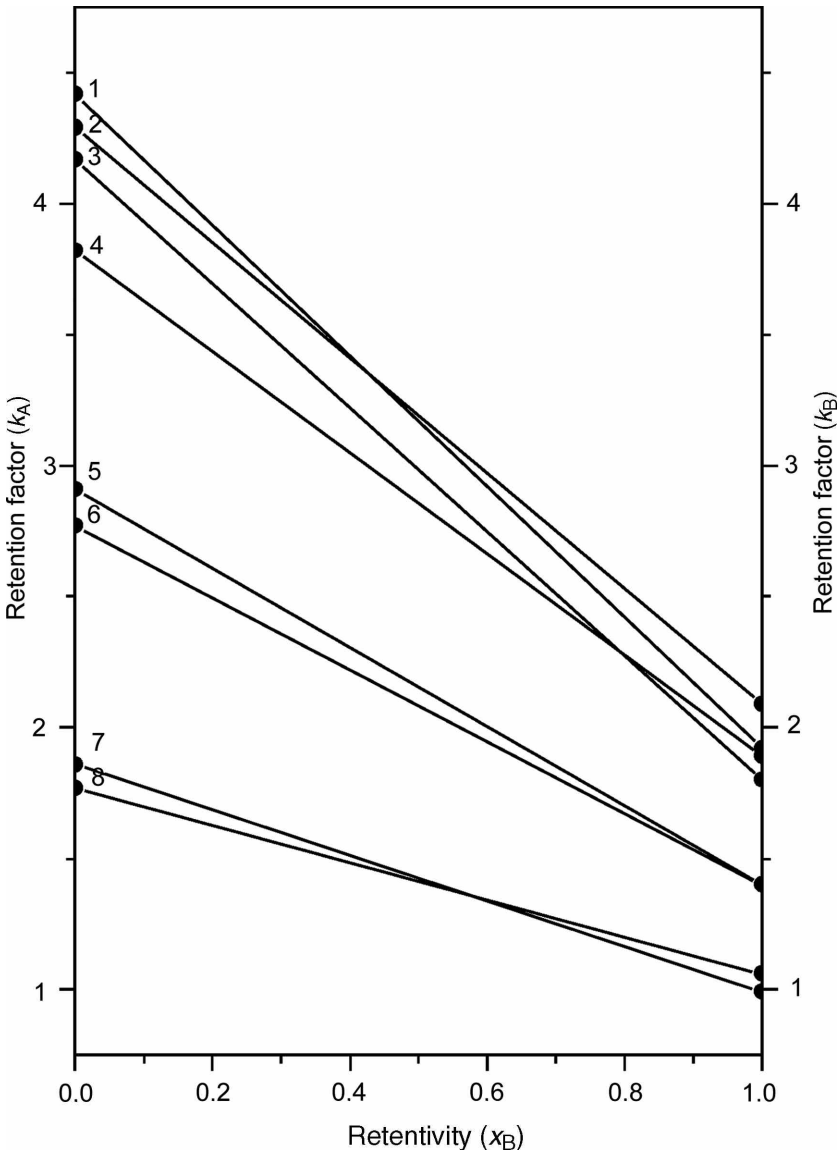

Fig. 5 Dependence of retention factor $k_{i,AB}$ of enantiomers of *N*-3,5-dinitrobenzoyl derivatives of studied amino acids on retentivity factor, X_B. For the identification of lines, compare numbers of lines with that listed in Table 1.

achieving the optimized *separation selectivity* of a complex mixture. This is an important milestone in the development of chromatographic method but, in addition to *separation selectivity*, there are many other method parameters that need to be optimized, as well.[29]

CONCLUSION

The selectivity tuning in chromatography, in general, encompasses all the discrete or continuous adjustments of separation procedure, materials, and conditions, leading to distinguishing of target compound, or group of similar compounds, from all other compounds present in a sample. The strategies utilized for selectivity tuning in particular case emerge from comprehension of chromatographic separation processes and their consequences for analysis of a compound in a sample. The optimization of separation selectivity, together with optimization of separation efficiency, may lead to resulting effect of full resolution of compounds subjected to chromatographic analysis.

REFERENCES

1. Vessman, J.; Stefan, R.I.; van Staden, J.F.; Danzer, K.; Lindner, W.; Thorburn Burns, D.; Fajgelj, A.; Müller, H. Selectivity in analytical chemistry. Pure Appl. Chem. **2001**, *73* (8), 1381–1386.
2. Poole, C.F. *The Essence of Chromatography*; Elsevier: Amsterdam, 2003; 1–72.
3. Giddings, J.C. *Unified Separation Science*; John Wiley & Sons, Inc.: New York, 1991; 24 pp.
4. Benicka, E.; Krupcik, J.; Repka, D.; Kuljovský, P.; Kaiser, R.E. Threshold criteria used for the optimization of

selectivity by tuning intermediate pressure for series-coupled columns in a dual-oven system. Anal. Chem. **1990**, *62*, 985–990.
5. McNaught, A.D., Wilkinson, A., Eds.; *IUPAC Compendium of Chemical Terminology,* 2nd Ed.; Blackwell Scientific Publications: Oxford, GB, 1997.
6. Sandra, P.; David, F.; Proot, M.; Diricks, G.; Verstappe, M.; Verzele, M. Selectivity and selectivity tuning in capillary gas chromatography. HRC&CC **1985**, *8*, 782–798.
7. Buszewski, B.; Krupczynska, K.; Bazylak, G. Effect of stationary phase structure on retention and selectivity tuning in the high-throughput separation of tocopherol isomers by HPLC. Comb. Chem. High Throughput Scr. **2004**, *7*, 381–389.
8. Laub, R.J.; Purnell, J.H. Criteria for the use of mixed solvents in gas-liquid chromatography. J. Chromatogr. A, **1975**, *112*, 71–79.
9. Laub, R.J.; Purnell, J.H.; Williams, P.S. Computer-assisted prediction of gas chromatographic separations. J. Chromatogr. A, **1977**, *134*, 249–261.
10. SEPSERV, Berlin, Helmholtzstr., D-10587 Berlin, Germany.
11. Lundanes, E.; Greibrokk, T. Temperature effects in liquid chromatography. In *Advances in Chromatography*; Grushka, E., Grinberg, N., Eds.; CRC Press: New York, 2006; Vol. 44, 45–77.
12. Lee, M.L., Markides, K.E., Eds.; *Analytical Supercritical Fluid Chromatography and Extraction*; Chromatography Conferences Inc.: Provo, UT, 1990, Chapter 2.
13. Wolcott, R.G.; Dolan, J.W.; Snyder, L.R. Computer simulation for the convenient optimization of isocratic reversed-phase liquid chromatography separations by varying temperature and mobile phase strength. J. Chromatogr. A, **2000**, *869*, 3–25.
14. Haber, P.; Baczek, T.; Kaliszan, R.; Snyder, L.R.; Dolan, J.W.; Wehr, C.T. Computer simulation for the simultaneous optimization of any two variables and any chromatographic procedure. J. Chromatogr. Sci. **2000**, *38* (9), 386–392.
15. Jupille, T.H.; Dolan, J.W.; Snyder, L.R.; Molnar, I. Two-dimensional optimization using different pairs of variables for the reversed-phase high-performance liquid chromatographic separation of a mixture of acidic compounds. J. Chromatogr. A, **2002**, *948*, 35–41.
16. Welsch, T.; Dornberger, U.; Lerche, D. Selectivity tuning of serially coupled columns in high performance liquid chromatography. HRC&CC **1993**, *16*, 18–26.
17. Kaiser, R.E.; Rieder, R.I. Polarity change in capillary GC by serial-column temperature optimization (SECAT-mode in Capillary GC). HRC & CC **1979**, *2*, 416–422.
18. Hirata, Y.; Tsuda, K.; Imamura, E. Serially coupled capillary columns supercritical fluid chromatography with midpoint pressure control. J. Chromatogr. A, **2005**, *1062*, 269–273.
19. Benicka, E.; Krupcik, J.; Lehotay, J.; Sandra, P.; Armstrong, D.W. Selectivity tuning in a HPLC multicomponent separation. J. Liquid Chromatogr. Relat. Technol. **2005**, *28* (10), 1453–1471.
20. Krupcik, J.; Spanik, I.; Benicka, E.; Zabka, M.; Welsch, T.; Armstrong, D.W. Selectivity tuning in chiral dual column gas chromatography. J. Chrom. Sci. **2002**, *40*, 483–488.
21. Dungelova, J.; Lehotay, J.; Krupcik, J. Selectivity tuning of serially coupled (S,S) Whelk-O 1 and (R,R) Whelk-O 1 columns in HPLC. J. Chrom. Sci. **2004**, *42* (3), 135–139.
22. Schoenmakers, P.J. *Optimization of Chromatographic Selectivity—A Guide to Method Development*; Elsevier: Amsterdam, 1986.
23. Snyder, L.R.; Dolan, J.W. HPLC computer-simulation—optimizing column conditions. Amer. Lab. **1986**, *18*, 37–40.
24. Dolan, J.W.; Snyder, L.R.; Djordjevic, N.M.; Hill, D.W.; Saunders, D.L.; Van Heukelem, L.; Waeghe, T.J. Simultaneous variation of temperature and gradient steepness for reversed-phase high-performance liquid chromatography method development. I. Application to 14 different samples using computer simulation. J. Chromatogr. A, **1998**, *803*, 1–31.
25. Fekete, J.; Morovjan, G.; Csizmadia, F.; Darvas, F. Methods development by an expert-system—advantages and limitations. J. Chromatogr. A, **1994**, *660*, 33–46.
26. Galushko, S.V.; Kamenchuk, A.A.; Pit, G.L. Software for method development in reversed-phase liquid-chromatography. Amer. Lab. **1995**, *27*, G33–J33.
27. Li, W.; Rasmussen, H.T. Strategy for developing and optimizing liquid chromatography methods in pharmaceutical development using computer-assisted screening and Plackett–Burman experimental design. J. Chromatogr. A, **2003**, *1016*, 165–180.
28. Dear, G.J.; Mallett, D.N.; Higton, D.M.; Roberts, A.D.; Bird, S.A.; Young, H.; Plumb, R.S.; Ismail, I.M. The potential of serially coupled alkyl-bonded silica monolithic columns for high resolution separations of pharmaceutical compounds in biological fluids. Chromatographia **2002**, *55*, 177–184.
29. Chester, T.L. Business-objective-directed, constraint-based multivariate optimization of high-performance liquid chromatography operational parameters. J. Chromatogr. A, **2003**, *1016*, 181–193.

Selectivity: Factors Affecting, in SFC

Kenneth G. Furton
Department of Chemistry, International Forensic Research Institute (IFRI), Miami, Florida, U.S.A.

INTRODUCTION

Retention and selectivity in supercritical fluid chromatography (SFC) are a complex function of many experimental variables and are not as easily rationalized as in the case of gas and liquid chromatography. Retention in SFC is dependent on temperature, density (and pressure drop), stationary-phase composition, and the mobile-phase composition. Many of these variables are interactive and do not change in a simple or easily predicted manner.[1]

EFFECT OF TEMPERATURE

Changes in retention at constant density are predictable from van't Hoff plots.The logarithm of the capacity factors is a linear function of the reciprocal of the column temperature, even down to subcritical conditions.[1] Analysis of the thermodynamics of the temperature-driven selectivity shifts in capillary SFC, at a constant mobile-phase fluid density, demonstrates the importance of stationary-phase polymer swelling. The other thermodynamic derivative contributing to temperature-driven selectivity shifts is the thermal pressure coefficient of the mobile-phase fluid.[2] Usually, temperature programing in SFC is done by increasing the temperature during a pressure, density, or eluent program, although negative temperature programs can also be employed to increase density. Although density conditions are the same either by decreasing temperature at constant pressure or by increasing pressure at constant temperature, the latter is preferable, as the higher diffusion coefficients at the higher constant temperature provide more favorable mass-transport properties.

EFFECT OF PRESSURE DROP (DENSITY DROP)

Selectivity is almost independent of pressure in high-performance liquid chromatography (HPLC) and gas chromatography (GC), whereas pressure (and corresponding density) is a very important parameter controlling selectivity in SFC, particularly if a significant pressure or density drop occurs along the column. In general, pressure drops are low when open-tubular columns are used, but they are significantly higher with packed columns and, therefore, have a significant effect on chromatographic resolution with packed column systems.[3] The observed selectivity, can be described by $\alpha_{obs}=e^{(B-mD)} \times (e^{bwL}-1)/mwL$, where the values for the constants B, m, and b will vary depending on the compound types being separated, the mobile phase, the stationary phase, and the temperature. D is the density of the mobile phase at the head of the column, w is the rate at which the density changes along the column, and L is the total column length. Because wL is simply the density change, $\Delta\rho$, across the column, the net result is that observed SFC selectivity changes caused by a linear density change along a column are only dependent on the total density drop which occurs. Therefore, in order to maintain constant selectivity as the density drop is increased, the density at the head of the column must be increased. Alternatively, if the density at the head of the column is kept constant while $\Delta\rho$ is increased, both selectivity and retention will increase.[4] Figure 1 demonstrates the effects of the density drop across a column for *n*-alkanes in carbon dioxide (data from Ref.[4]). Some general conclusions include that, on average, α_{obs} changes by 0.001 per 10% density drop up to a 30% density drop. Also, selectivity decreases more rapidly as density drops become larger and that selectivity increases at larger k' values where the mobile-phase density is lower.

EFFECT OF OVERALL DENSITY (PRESSURE AT CONSTANT TEMPERATURE)

The overall density of the mobile phase is one of the most important parameters used to optimize separations in SFC with density programing as common in SFC as temperature programing in GC and eluent composition in HPLC.[5] Capacity ratios, k', decrease roughly linearly at higher densities with different slopes for different classes of compounds, thereby affording changes in selectivity.[5] A similar effect is seen for the supercritical fluid elution of analytes from octadecylsilica sorbents, as seen in Fig. 2.[6]

Effect of Stationary Phase

In SFC, both packed and capillary columns are used, each with their specific advantages and disadvantages. Packed columns in SFC are very similar to those used in HPLC, with the most often used stationary phases being modified silicas. Column selectivity follows the same rules as it does in HPLC with aromatic hydrocarbons (e.g., more retained on octadecyl silica column than on bare silica).[5] A great variety

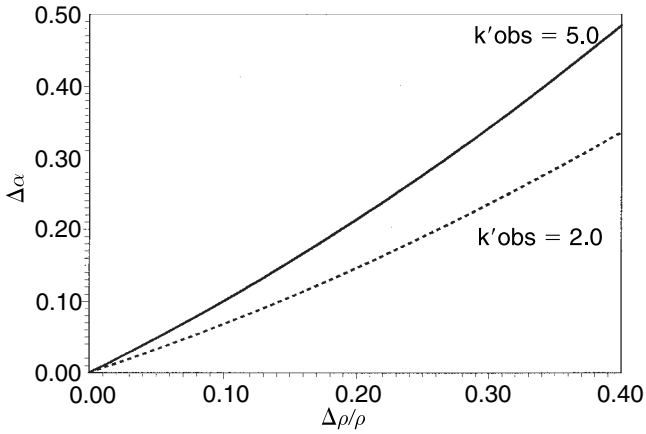

Fig. 1 Density drop effects on α at different k's for *n*-alkanes in carbon dioxide.

of different selective stationary phases have been used in packed column SFC. For example, racemic *N*-acetylamino acid *t*-butyl esters have been resolved on chiral (*N*-formyl-L-valylamino)propylsilica using methanol-modified carbon dioxide.[5] The most often used stationary phases for open-tubular SFC are immobilized films of polymeric materials—most commonly, polysiloxanes common to GC. Selecting a suitable stationary phase follows the same rules as in GC or HPLC, bearing in mind the frequently used carbon dioxide is a relatively non-polar eluent. For example, non-polar substrates such as hydrocarbons are strongly retained on a dimethyl column, whereas free carboxylic acids are more retained on a cyanopropyl column.

EFFECT OF MOBILE-PHASE COMPOSITION (POLARITY MODIFIERS)

Carbon dioxide is the most commonly used mobile phase in SFC, due to its low cost, low expense, low toxicity, and low-critical temperature and pressure. However, using the classification scheme of eluents by Snyder, carbon dioxide shows a polarity similar to that of hexane.[5] Therefore, the solvent power of eluents used in SFC is generally enhanced by adding small amounts of a second eluent modifier. Selection of the optimum solvents can be achieved in much the same way that selections are made for HPLC solvents, namely utilizing a solvent polarity/selectivity scheme. To be useful, a solvent characterization scheme must efficiently determine the solvent strength or polarity and the solvent selectivity. The polarity of non-electolytes is the capacity of the solvent for all intermolecular interactions (primarily dispersion, induction, orientation, and proton donor–acceptor interactions). Solvent selectivity is a measure of the relative capacity to enter into each specific interaction. The three primary specific interactions evaluated in all solvent characterization schemes are orientation (dipolar interaction), proton-donor (acidity), and proton-acceptor (basicity) interactions. One of the most widely used schemes is the solvent triangle introduced by Snyder and reevaluated over the years.[7] In Snyder's approach, solvent selectivity factors (using nitromethane), (using ethanol), and (using dioxane) are used to characterize the relative importance of orientation, proton acceptor (basicity) and proton donor (acidity), respectively. When these three terms are graphed against one another for the common solvents, a so-called selectivity triangle is generated where solvents with similar selectivities are clustered into eight major selectivity "groups." Additionally, a solvent polarity index, P', is calculated to provide a measure of the relative polarity of each solvent. Values for the various polarity/selectivity terms and critical constants are summarized in Table 1 for some common polarity/selectivity modifier solvents.[7,8] The most recent data for Snyder's terms from Ref.[3] have been included where available. Popular alternative schemes have utilized solvatochromic parameters based on the concept of linear solvation energy relationships to quantitatively probe-specific chemical interactions such as polarizability, hydrophobicity, and hydrogen-bonding interactions.

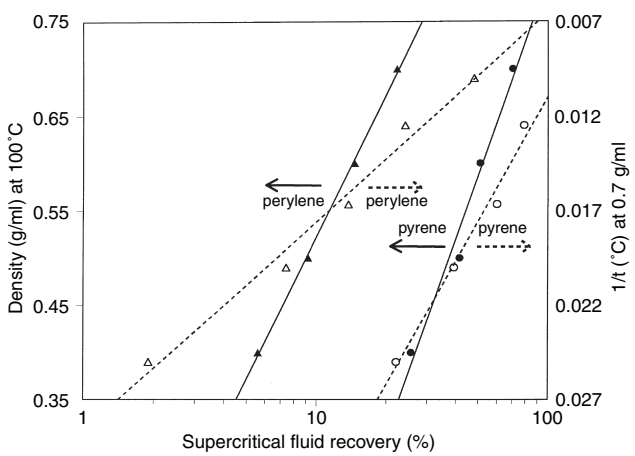

Fig. 2 Supercritical fluid recoveries of polycyclic aromatic hydrocarbons as a function of density and temperature.
Source: From *Supercritical Fluids Technology: Theoretical and Applied Approaches in Analytical Chemistry*.[6]

Table 1 Critical constants and polarity and selectivity parameters for common organic modifiers.

Solvent	P_c (psi)	T_c (°C)	P'	χ_d	χ_e	χ_n	Group	$\sum\alpha_2^H$	$\sum\beta_2^H$	$\sum\pi_2^H$
Carbon dioxide	1070.4	31.1						0.00	0.10	0.42
n-Hexane	436.6	234.4						0.00	0.00	0.00
Triethylamine	439.5	262.0	2.19	0.08	0.66	0.26		0.00	0.79	0.15
Diethyl ether	527.9	193.7	3.15	0.13	0.53	0.34	I	0.00	0.45	0.25
Ethylene chloride	735.3	250.0	3.5	0.21	0.30	0.49	V	0.10	0.11	0.64
Isopropanol	690.4	235.3	3.92	0.17	0.57	0.26	II	0.33	0.56	0.36
Ethyl acetate	555.5	250.2	4.24	0.22	0.36	0.42	VIa	0.00	0.45	0.62
Tetrahydrofuran	752.7	267.1	4.28	0.19	0.41	0.40	III	0.00	0.48	0.52
Methylene chloride	913.7	237.0	4.29	0.33	0.27	0.40	VII	0.10	0.05	0.57
Chloroform	778.9	263.4	4.31	0.35	0.31	0.34	VIII	0.15	0.02	0.49
Acetone	681.7	235.1	5.40	0.24	0.36	0.40	VIa	0.04	0.49	0.70
Pyridine	816.6	347.0	5.53	0.22	0.42	0.36	III	0.00	0.52	0.84
Acetonitrile	700.5	272.5	5.64	0.25	0.33	0.42	VIb	0.07	0.32	0.90
Acetic acid	839.8	319.7	6.13	0.30	0.41	0.30	IV	0.61	0.44	0.65
Methanol	1173.4	239.6	6.60	0.19	0.51	0.30	II	0.43	0.47	0.44
Water	3208.2	374.3	10.2	0.37	0.37	0.25	VIII	0.82	0.35	0.45

Solvatochromic descriptors described by Abraham are summarized in Table 1 , including the overall or summation hydrogen-bond acidity scale ($\sum\alpha_2^H$) basicity scale ($\sum\beta_2^H$) and dipolarity/polarizability descriptor ($\sum\pi_2^H$).[9] It has been shown that olvatochromic parameters may be successfully used to predict retention near the critical point in packed column SFC and may be useful in controlling selectivity of chiral separations.[10] Supercritical fluid selectivities are comparable to subcritical selectivities with minor differences attributable to the physical nature of modifier behavior under near-critical conditions where binary mobile phases may exhibit gross compositional hererogeneity at interfaces.[10] When organic modifiers are increasingly added to the mobile phase at constant pressure (density) and temperature, the retention of analytes increases or decreases, depending on whether the supercritical analytes are more or less soluble in the modifier compared to the supercritical fluid, provided that the column activity remains the same.[1]

MISCELLANEOUS AND COMBINED EFFECTS

Temperature, pressure, and density may also influence SFC selectivity in other ways. For example, water solubility in supercritical fluids generally increases with temperature, causing a shift the equilibrium of the number of water-deactivated silanol groups to carbon-dioxide-deactivated groups.[1] Therefore, the solubility of analytes in the mobile phases increases but so does retention for polar analytes due to increased stationary-phase activity.

REFERENCES

1. Poole, C.F.; Poole, S.K. *Chromatography Today*; Elsevier: Amsterdam, 1991; 601–643.
2. Roth, M. Thermodynamic background of selectivity shifts in temperature-programmed, constant-density supercritical fluid chromatography. J. Chromatogr. **1995**, *718* (1), 147–152.
3. Lou, X.; Janssen, H.-G.; Snijder, H.; Cramers, C.A. J. Chromatogr. **1995**, *718*, 147.
4. Peaden, P.A.; Lee, M.L. Theoretical treatment of resolving power in open tubular column supercritical fluid chromatography. J. Chromatogr. **1983**, *259*, 1.
5. Smith, R.M., Ed.; *Supercritical Fluid Chromatography*; Royal Society of Chemistry: London, 1988.
6. Furton, K.G.; Rein, J. *Supercritical Fluids Technology: Theoretical and Applied Approaches in Analytical Chemistry*; Bright, F.V., McNally, M.E.P., Eds.; ACS Symposium Series American Chemical Society: Washington, DC, 1992; Vol. 488, 237–250.
7. Rutan, S.C.; Carr, P.W.; Cheong, W.J.; Park, J.H.; Snyder, L.R. Re-evaluation of the solvent triangle and comparison to solvatochromic based scales of solvent strength and selectivity. J. Chromatogr. **1989**, *463*, 21–37.
8. Isco Tables, 9th Ed.; Isco, Inc., 1987; p. 10.
9. Abraham, M.H.; Whiting, G.S.; Doherty, R.M.; Shuely, W.J. Hydrogen bonding: XVI. A new solute salvation parameter, π2H, from gas chromatographic data. J. Chromatogr. **1991**, *587* (2), 213–228.
10. Cantrell, G.O.; Stringham, R.W.; Blackwell, J.A.; Weckwerth, J.D.; Carr, P.W. Effect of various modifiers on selectivity in packed-column subcritical and supercritical fluid chromatography. Anal. Chem. **1996**, *68* (20), 3645–3650.

Self-Assembled Organic Phase for RP/HPLC

Abul K. Mallik
M. Mizanur Rahman
Makoto Takafuji
Department of Applied Chemistry and Biochemistry, Kumamoto University, Kumamoto, Japan

Shoji Nagaoka
Kumamoto Industrial Research Institute, Kumamoto, Japan

Hirotaka Ihara
Department of Applied Chemistry and Biochemistry, Kumamoto University, Kumamoto, Japan

Abstract
Molecular ordering through self-assembling of organic stationary phase is very useful for increasing selectivity in high-performance liquid chromatography (HPLC). Herein, we introduce comb-shaped polymers as self-assembled organic stationary phase for HPLC so that the selectivity can be robustly enhanced by increasing polymer chain rigidity as well as grafting density. For example, comb-shaped poly(octadecyl acrylate)-grafted silica (prepared by *grafting-to* and *grafting-from* methods) columns showed very high selectivity toward polycyclic aromatic hydrocarbon (PAH) solutes with regard to grafting technique onto silica. A comparison of the results obtained with synthetic columns and with commercial octadecylsilylated silica (ODS) revealed the effectiveness of tailor-made columns. Potential application of polypeptide lipid-grafted type stationary phases for molecular recognition has also been described.

INTRODUCTION

Liquid chromatography has become an indispensable tool for both routine analysis and research in the pharmaceutical, biomedical, and biotechnology industries. On an analytical level reversed-phase high-performance liquid chromatography (RP-HPLC) is the most widespread technique, probably owing to the broad applicability of that mode of separation to a wide range of compounds and sample matrices. The majority of bonded phases employed in RP-HPLC are still of the reversed-phase *n*-alkyl type, mostly octadecylsilylated silica (ODS) or C18 and C8. The development of new chemically bonded stationary phases for reversed-phase liquid chromatography (RPLC), engineered for solving specific separation problems, has led to improved analyses of a broad range of compounds. Refinements in approaches used to characterize chemically modified surfaces have resulted in increased understanding of stationary-phase morphology, which in turn has permitted development of novel stationary phases with properties tailored for specific applications. Usually, retention and selectivity of solutes increases with increasing grafting density of the organic phase on silica.[1,2] Molecular ordering of the organic phase also increases the selectivity.[3,4] On the basis of these viewpoints, polymeric phases are reasonable tools as organic stationary phases, and polymer immobilization process can also play an important role in increasing the grafting density as well as improving molecular ordering. Generally, the surfaces of inorganic materials are functionalized with polymer chains by using either the *grafting-to* or the *grafting-from* method. *Grafting-to* method has some limitations while there are distinct advantages in the control of polymerization degree; a polymer with a terminal reactive group can be obtained by one-step telomerization, and usual spectroscopy is applicable for determination of the chemical structure before immobilization onto silica. The main disadvantage of this method is low grafting densities resulting from steric crowding of the reactive sites.[5] On the other hand, the *grafting-from* technique results in significantly higher grafting density because the steric barrier to incoming polymers imposed by the in situ grafted chains does not limit the access of smaller monomer molecules to the active initiation sites.[6–8] Though *grafting-to* is still a good method for the preparation of HPLC stationary phases, increasing attention has been devoted to *grafting-from* techniques, especially for high retentivity and selectivity.[9–11] One of the most extensively used *grafting-from* method is atom transfer radical polymerization (ATRP)[12,13] from initiator-grafted inorganic particle surface. In this entry, we introduce high-density polymeric organic phases with π-electron-containing moieties as stationary phases for selectivity enhancement using surface-initiated ATRP *(grafting-from*) technique. Further, it is also described how the concentration of carbonyl π-electrons, through peptide-derived low

molecular compounds and polymers, brings about extremely high selectivity enhancement in HPLC.

SELF-ASSEMBLED PHASES FOR MOLECULAR RECOGNITION

Biological organisms are constructed by molecular building blocks, and these molecules are assembled spontaneously through various intermolecular interactions.[14,15] Self-assembling systems provide supramolecular functions further than those of unit segment molecules in a solution state such as lipid membranes, proteins, and nucleic acids. For instance, self-assembled systems such as lipid membrane aggregates can provide a highly ordered microenvironment leading to a unique host–guest chemistry exceeding the functions of the original lipid. Thus, there are many reports on biomimetic approaches to reproduce lipid membrane functions with totally synthetic lipids.[16–18] One of the successful results is seen in L-glutamide-derived amphiphiles. For example, dialkyl L-glutamide-derived amphiphilic lipids form nanotubes,[19] nanohelices,[20] and nanofibers[21] based on bilayer structures in water and on the fact that intermolecular hydrogen bonding among the amide moieties not only contributes self-assembly[20] but also shows a very unique secondary chirality with extremely strong circular dichroism (CD) signals.[20] Another unique self-organization has been realized by lipophilic derivatives of L-glutamide even in organic solvents.[22] These low-molecular compounds can form nanofibrillar aggregates in organic solvents to make a gel through a three-dimensional (3-D) network formation. Hence, this phenomenon is often called as "molecular gelation," but the functions are rather more similar to those of lipid bilayer membranes than to those of conventional polymer gels.

This knowledge encourages us to apply biomimetic membranes for molecular recognition systems such as HPLC. However, lipid membrane systems suffer from a serious problem owing to their instability in organic solvents. To overcome this problem, we have reported the use of poly(octadecyl acrylate)-grafted silica (Sil-ODA$_n$) as a lipid membrane analogue for stationary phases in RP-HPLC.[23] Poly(octadecyl acrylate) cannot form bilayer structures in water but forms "*nanogels*" which undergo temperature-responsive phase transition between ordered and disordered structures like lipid membrane systems. Sil-ODA$_n$ showed unique separation behaviors with ordered-to-disordered phase transitions of long alkyl chains. In particular, very high selectivity toward polycyclic aromatic hydrocarbons (PAHs) was observed in the ordered (crystalline) state.[24,25] Detailed investigations showed that the highly ordered structure in Sil-ODA$_n$ induced the orientation of carbonyl groups that work as a π–π interaction source with solute molecules. We have also found that the aligned carbonyl groups are effective for recognition of length and planarity of PAHs through multiple π–π interactions.[26,27]

GRAFTING OF COMB-SHAPED POLYMER AS AN ORDERED ORGANIC PHASE

Polymer grafting onto a silica surface is a very useful approach to introduce highly ordered organic phases. Three main routes are usually reported for chemically attaching a polymer to a surface: 1) the *grafting-to* method, where end functionalized polymers react with appropriate surface sites; 2) the *grafting-from* method, where chains grow in situ from preformed surface-grafted initiators; and 3) surface copolymerization through a covalently linked monomer.

Polymer *Grafting-to* Method

Single-anchor grafting

A comb-shaped polymer as a lipid membrane analogue is readily prepared by radical telomerization of octadecyl acrylate. By using 3-mercaptopropyl trimethoxysilane (MPS) as a telogen, not only the degree of polymerization (n) can be controlled by adjusting the initial molar ratio of the monomer to telogen, but also the reactive terminal group can be introduced at one end of the polymer main chain. Thus, poly(octadecyl acrylate)-grafted silica (Sil-ODA$_n$) is prepared by mixing the polymer with appropriate porous silica gels (Fig. 1).[27]

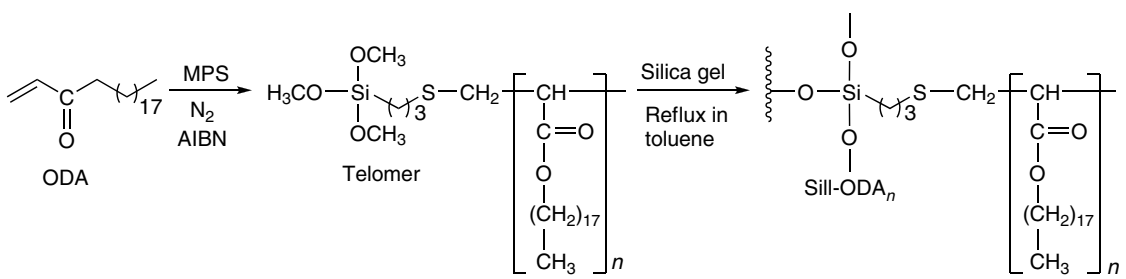

Fig. 1 Synthesis process for polymeric organic phase by one-step telomerization followed by immobilization onto silica through the terminal methoxysilyl group (grafting-to method).

The average degree of polymerization (n) is estimated by the proton ratio, based on the terminal methoxy group using proton nuclear magnetic resonance (H-NMR) spectroscopy. Immobilization of ODA_n is usually carried out by mixing with silica at reflux temperature for 72 hr in toluene. Silica gels with different pore sizes and diameters can be employed for the grafting process. Usually, silica gels with an average diameter of 5 μm, a pore size of 120 Å, and a specific surface area of 300 m^2/g are considered to be suitable for HPLC. The resultant polymer-grafted silicas indicate a distinct phase transition that can be assigned to a crystal-to-isotropic transition (Fig. 2a). This phase transition temperature is observed even in methanol, ethanol, and acetonitrile, and in their aqueous mixtures acting as usual mobile phases in RP-HPLC, although the peak-top temperature (T_c) somewhat decreases owing to solvation.[28]

The column packed with Sil-ODA_n shows very unique separation in RP-HPLC. Especially the uniqueness is emphasized when the solutes are PAHs. An extremely high separation factor, as compared with conventional ODS columns, is observed at temperatures below T_c: e.g., the separation factor $\alpha_{pentacene/chrysene}$ is 17.6 and 1.6 for Sil-ODA_n and conventional ODS columns respectively. To explain this unusual selectivity, we have proposed the multiple π–π interaction mechanism between PAHs and carbonyl groups of acrylate moieties in the ordered state.[27] This interaction is quite possible according to our previous calculations and experiments: 1) Fig. 3a shows the temperature dependencies of the separation factor α for geometrical isomers of stilbene. The poly(methyl acrylate) phase is less hydrophobic than Sil-ODA_n and ODS, as well as in a disordered state because of the absence of any long-chain alkyl groups, but the selectivity is distinctly higher than that in ODS. 2) A carbonyl-π–benzene-π interaction was simulated by the ab initio study.

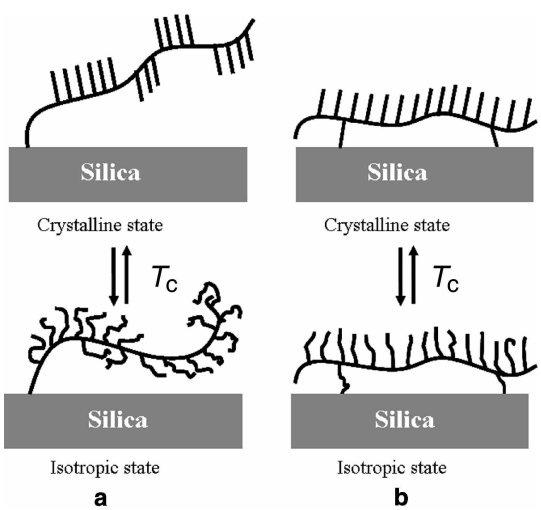

Fig. 2 Schematic illustrations of the phase transition behavior of silica-supported organic phases (a) Sil-ODA_n (single-anchor) (b) Sil-co-ODA_n (multianchor).

When HCHO and benzene was chosen as a model complex, the potential-energy curves indicated that the binding energy in HCHO–benzene was much larger (1.87 kcal/mol)[28–30] than that in benzene–benzene (0.49 kcal/mol) in plane-to-plane stacking.[31] 3) The selectivity with geometrical isomers from various substituted azobenzene compounds was investigated.[26] As a result, it was found that the separation factor between the *trans*- and *cis*-isomers was remarkably dependent on the electron-donating property of the substituent group. This strongly suggests that bonded ODA_n works as an electron-acceptor and a π–π interaction is brought about by a carbonyl-π moiety in ODA_n. This estimation was confirmed by the observation that addition of acetone as a carbonyl group-containing solvent to a mobile phase reduced the selectivity remarkably, whereas the presence of 2-propanol had almost no effect. Acetone works as a sort of an inhibitor for ODA_n–PAHs interactions.

These observations prompt us to propose multiple π–π interactions between carbonyl groups and PAHs. ODA_n, which is in an ordered state, interacts better with planar and slender PAHs such as *trans*-stilbene,[32] naphthacene, and pentacene[27] than with non-planar and bulky substances such as *cis*-stilbene[32] and *o*-terphenyl,[23] and less slender substances such as triphenylene[23] and coronene.[33] However, these unique selectivities distinctly decrease when ODA_n is in a disordered state, but rather similar to that of ODS. As shown in Fig. 3b, it is highly probable that multiple π–π interactions are more effective both in an ordered state and for planar and slender substances, but not in a disordered state.

Multianchor grafting

A reduction in the molecular mobility of a polymer chain as an organic stationary phase would lead to an increase in the selectivity in HPLC. Porphyrin derivative-bonded phases show a unique shape selectivity by retaining planar PAHs.[34] Similar molecular-planarity selectivity is also observed in cholesteryl-10-undecenoate-[35] and 4,4′-dipentyldiphenyl-bonded phases.[36] These phases contain rigid structures, and hence the limited mobility in their organic phases contributes to the shape selectivity. Similar phenomenon of selectivity increase can be observed in the comparison of the retention behaviors of polymeric and monomeric ODSs.[37]

From this viewpoint, poly(octadecyl acrylate) having the plural reactive groups in the side chain has been synthesized and immobilized onto silica (Fig. 2b). The polymer is obtained by a one-step cotelomerization with ODA and methacryloxypropyl trimethoxysilane (MAPTS). The monomer composition of the resultant copolymer is readily adjusted by the initial molar ratio and then estimated by ^{1}H-NMR spectroscopy. Sil-co-ODA_n prepared by multi-anchoring showed remarkably higher selectivity for PAHs with different molecular planarity (thickness) than for the corresponding Sil-ODA_n prepared by single anchoring although no significant difference was detected for planar

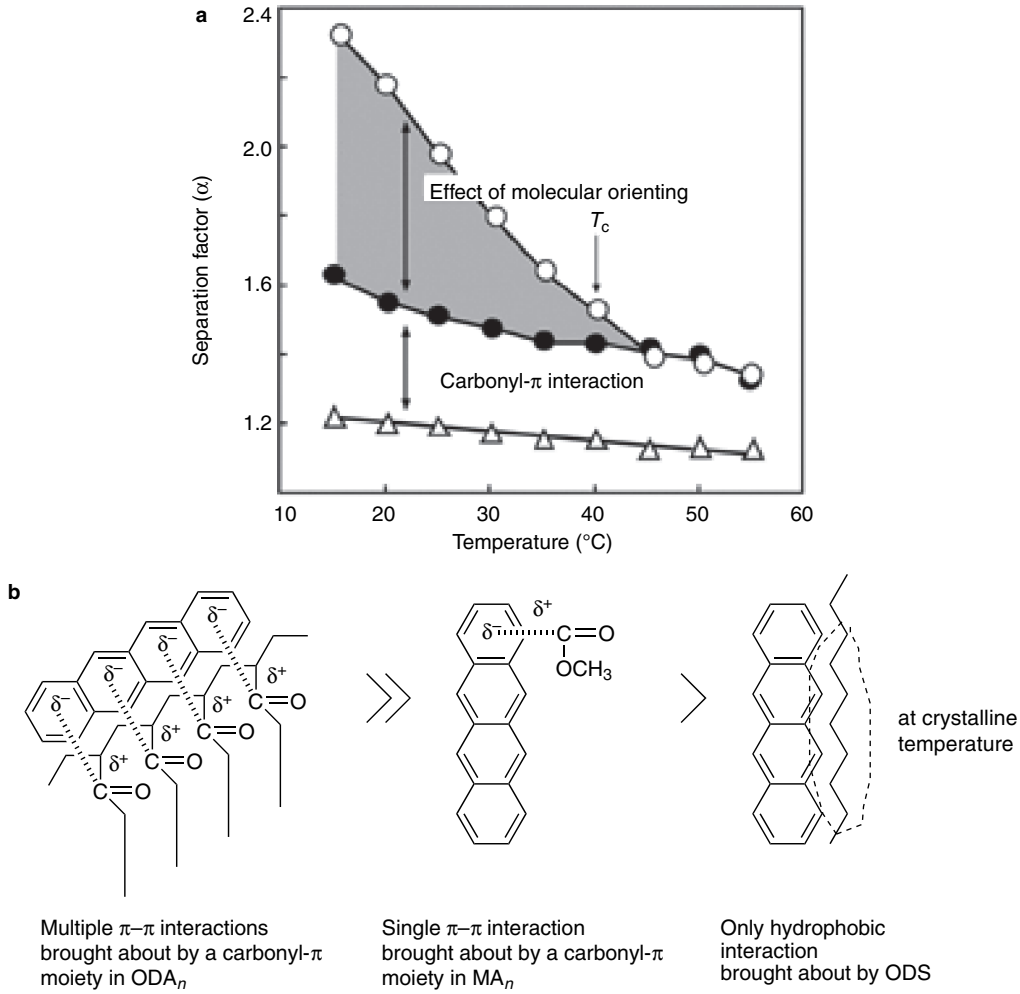

Fig. 3 (a) Temperature dependencies of the separation factors of *cis*- and *trans*-stilbene with columns: Sil-ODA$_n$ (open circles), Sil-MA$_n$ (solid circles), and ODS (open triangles). Mobile phase: methanol:water (70:30). Sil-MA$_n$: poly(methyl acrylate)-grafted silica. (b) Schematic illustrations of interaction mechanism between solutes and stationary phases.

PAHs.[32] This cannot be explained only by the increase of side-chain ordering, because it seems that there is no significant difference in the phase transition behavior between Sil-ODA$_n$ and Sil-co-ODA$_n$ in the mobile phase, as detected by differential scanning calorimetry (DSC) and suspension-state ^{1}H-NMR.[32] Therefore, we focus on the rigidity of the polymer main chain in Sil-co-ODA$_n$. It is certain that the mobility of the polymer main chain is relatively restricted by multianchoring effect in co-ODA$_n$ (Fig. 2b). This must be accompanied also by suppression of the mobility around the carbonyl groups for main interaction sites with PAHs. Therefore, it is estimated that the higher selectivity of Sil-co-ODA$_n$ can be attributed to the carbonyl groups on the rigid main chain, which are immobilized by both molecular ordering of the long-chain alkyl groups and multianchoring effect. Especially, the rigidity in Sil-co-ODA$_n$ reduces the interaction with bulky PAHs such as *cis*-stilbene and *o*-terphenyl. Based on these facts it is concluded that the molecular-shape selectivity observed with Sil-ODA$_n$ is derived from multiple carbonyl-π interactions, which is promoted by the ordering of the octadecyl groups in ODA$_n$ at temperatures below the phase transition temperature (T_c). In the same way, this interaction would be included as a main driving force in the shape selectivity observed with Sil-co-ODA$_n$.

Grafting-from Method for High-Density Polymeric Phase

The grafting-from technique involves the immobilization of initiators onto the substrate followed by in situ surface-initiated polymerization to generate a tethered polymeric phase. This approach has generally become the most attractive way to prepare thick, covalently tethered polymer brushes with a high grafting density. A variety of synthesis methods such as radical chain transfer reaction,[38] reverse ATRP,[39] living anionic surface-initiated polymerization,[40] ATRP,[41,42] dispersion polymerization,[43] and

reversible addition fragmentation chain transfer (RAFT) polymerization have been proposed for the preparation of polymer brushes. ATRP is one of the well-developed controlled living radical polymerization, and has been attracting much attention as a new route to well-defined polymers with low polydispersities and high grafting density.

As we have mentioned, the main limitation of telomerization followed by grafting, or the grafting-to method, is the low grafting densities owing to steric crowding of reactive sites during grafting process.[5] To overcome the limitations of the grafting-to technique, it is reasonable to use the grafting-from method to prepare poly(octadecyl acrylate)-grafted silica (Sil-gf-ODA$_n$) for HPLC packing material.[10] In the surface-initiated ATRP process (grafting-from) the polymer chains grow from the initiators that have been previously anchored onto the inorganic particle surface. Consequently, the grafted chains do not hinder the diffusion of the small monomers to the reaction sites, so that well-defined polymer chains with higher graft density can be obtained.[6,7,44]

The synthesis procedure for Sil-gf-ODA$_n$ is as follows: the ATRP initiator is synthesized from 2-bromo-2-methyl propionic acid undecyl ester by hydrosilation with trichlorosilane and then immobilized onto porous silica gel. The reaction between a trichlorosilane anchoring group and a surface OH group of silica results in the formation of a self-assembled monolayer on silica surface. The surface-initiated polymerization of ODA is carried out from the initiator-grafted silica using copper(I)bromide and *N*,*N*,*N*′,*N*″*N*‴-pentamethyldiethylenetriamine (PMDETA) as catalyst precursors (Fig. 4). The polymer-grafted stationary phase was characterized by diffuse reflectance infrared Fourier transform (DRIFT), elemental analysis, suspension-state ^{1}H-NMR, solid-state ^{13}C cross-polarization/magic angle spinning-nuclear magnetic resonance (CP/MAS-NMR), and DSC measurements. The surface coverage of ATRP polymerized ODA, Sil-gf-ODA$_n$, was calculated on the basis of elemental analysis results according to our previously reported method.[45] The grafting density of polymer chains on Sil-gf-ODA$_n$ is 3.75 μmol/m^2 which is significantly higher than that obtained from Sil-ODA$_n$ prepared by the grafting-to method (2.63 μmol/m^2).[10]

Characteristic features of high-density polymeric phase

The DSC thermogram of polymeric ODA (ODA$_n$) shows a sharp endothermic peak (T_c) in both the heating and the cooling processes. ODA$_n$ provided an endothermic peak at 47°C (T_{c2}, peak-top temperature) with a shoulder at around 42°C (T_{c1}) in the heating process (Fig. 5). By polarization microscopic analysis T_{c1} and T_{c2} can be assigned as crystalline-to-liquid crystalline and liquid crystalline-to-isotropic phase transitions, respectively, as mentioned above. Similar phase transitions were also observed even after immobilization on silica (Sil-ODA$_n$), as in methanol where the peak-top temperature (phase transition temperature) decreased from 47°C to 38°C,[45] which indicated that silica perturbs the molecular ordering. However, high-density Sil-gf-ODA$_n$ yields less reduction in peak-top temperature which is in the range from 47°C to 43°C (Fig. 5). These results indicate that the polymer side chains in high-density Sil-gf-ODA$_n$ remain ordered structures at higher temperatures, as compared to those in Sil-ODA$_n$.

Solid-state ^{13}C CP/MAS-NMR spectroscopy is a powerful tool for evaluation of the chemical composition and conformational properties of chemically modified surfaces. It is reported that the ^{13}C signal for $(CH_2)_n$ groups are observed at two resonances: One is at 32.6 ppm

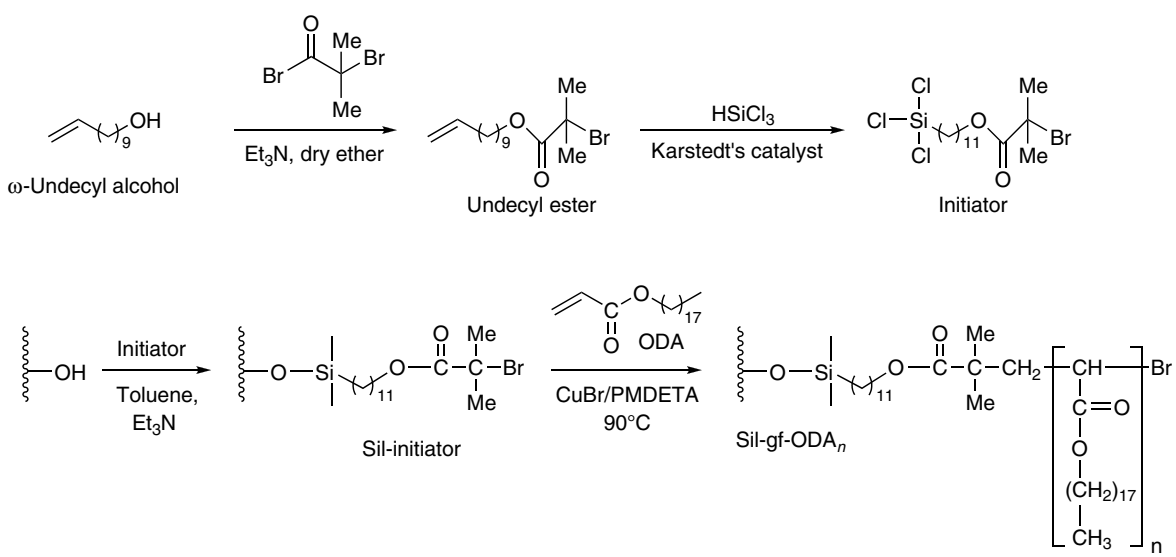

Fig. 4 Synthesis process of preparing polymeric organic phase by surface-initiated atom transfer radical polymerization (grafting-from method).

attributed to a *trans* conformation, indicating a crystalline and rigid state, and the other is at 30.0 ppm attributed to a *gauche* conformation, indicating disordered and mobile state.[46,47] Solid-state ^{13}C CP/MAS-NMR measurements were carried out at different temperatures from 25°C to 50°C for Sil-gf-ODA$_n$ and Sil-ODA$_n$ (Fig. 5). Fig. 6 shows transformation of $(CH_2)_n$ chains from ordered to disordered states (*trans* to *gauche*) as the temperature is increased. However, comparing the two approaches, Sil-gf-ODA$_n$ is more dominated by *trans* conformation than Sil-ODA$_n$ immobilized by the grafting-to method (Fig. 6A). The above result of improved order and rigidity of alkyl chains in Sil-gf-ODA$_n$ than in Sil-ODA$_n$ agrees with the DSC observation, and it is an important characteristic to understand the separation behavior of organic layers grafted onto the silica surface.

Retention mechanism

As discussed in the section "Single-anchor grafting," in high-density ODA$_n$ prepared by the grafting-from method, a main interaction source for molecular recognition is derived from a carbonyl-π moiety and not from molecular hydrophobicity. Fig. 7 shows the correlation between log *k* and log *P* for Sil-gf-ODA$_n$, Sil-ODA$_n$, and polymeric ODS (ODS-p) phases. These results indicate that Sil-gf-ODA$_n$ and Sil-ODA$_n$ have a retention mode in RP-HPLC similar to that of an ODS-p phase. Plots of log *k* vs. log *P* for alkylbenzenes and PAHs almost superimpose each other for ODS-p; however, a significant deviation is observed for PAHs and alkylbenzenes for Sil-ODA$_n$ and Sil-gf-ODA$_n$ demonstrating the existence of other possible interaction sites besides molecular hydrophobicity, which can be attributed to π–π interaction between a solute and a stationary phase. This is the most important feature of ODA$_n$-grafted silica. Furthermore, it is observed that Sil-gf-ODA$_n$ showed higher retention for PAHs as compared to alkylbenzenes. For example, log *P* of naphthacene (5.71) is smaller than that of octylbenzene (6.30), while log *k* of naphthacene (1.53) is higher than that of octylbenzene (0.93). The increase of log *k* for PAHs is accompanied by selectivity enhancement which provides specific interactive sites for PAHs that can recognize aromaticity besides molecular hydrophobicity. For instance, $\alpha_{naphthacene/benzene} = 33.0$ for Sil-gf-ODA$_n$, whereas Sil-ODA$_n$ and ODS-p yielded values of 26.8 and 10.8, respectively (Fig. 8).

Molecular-shape selectivity

Table 1 shows selectivity results for a series of PAHs on ODA$_n$-grafted silicas prepared from two different grafting

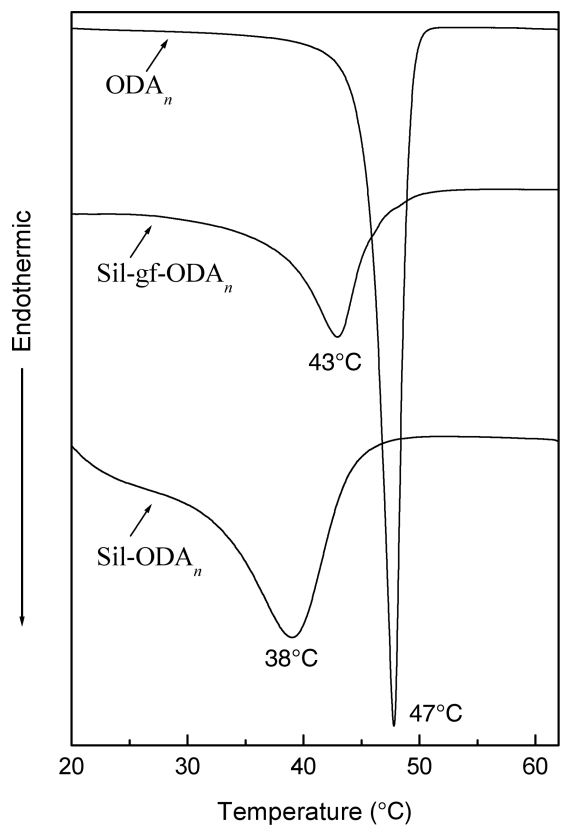

Fig. 5 Differential scanning calorimetry (DSC) thermograms of polymeric ODA (ODA$_n$), Sil-gf-ODA$_n$ (grafting-from), and Sil-ODA$_n$ (grafting-to).

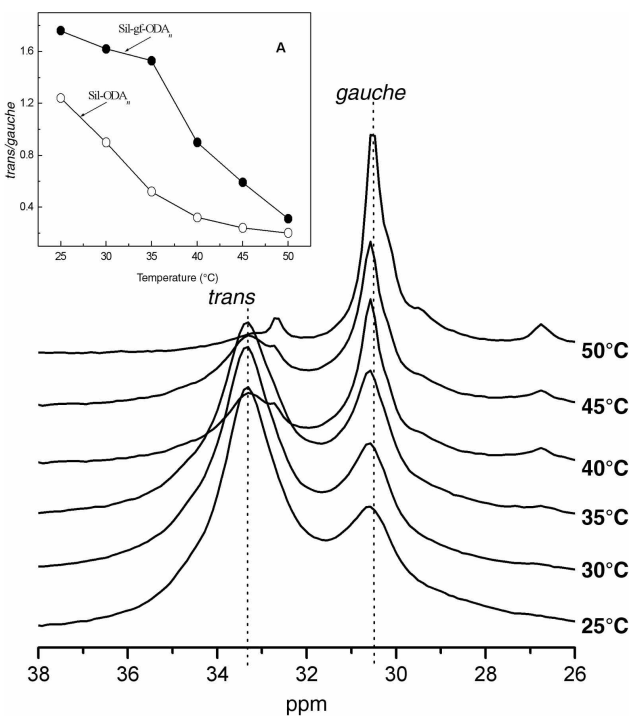

Fig. 6 Transformation of *trans* to *gauche* conformation of octadecyl moieties in solid-state ^{13}C CP/MAS-NMR of Sil-gf-ODA$_n$ with temperature. (A) Comparison of the ratio of *trans* to *gauche* conformation in solid-state ^{13}C CP/MAS-NMR of Sil-gf-ODA$_n$ and Sil-ODA$_n$.

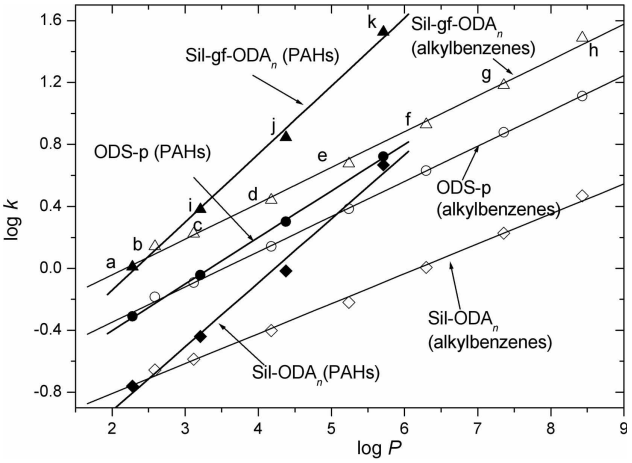

Fig. 7 log k vs. log P for ODS-p, Sil-ODA$_n$, and Sil-gf-ODA$_n$ stationary phases. Eluates: a, benzene; b, toluene; c, ethylbenzene; d, butylbenzene; e, hexylbenzene; f, octylbenzene; g, decylbenzene; h, dodecylbenzene; i, naphthalene; j, anthracene; k, naphthacene. Mobile phase: methanol:water (90:10); Column temperature: 30°C; Flow rate: 1.00 ml/min.

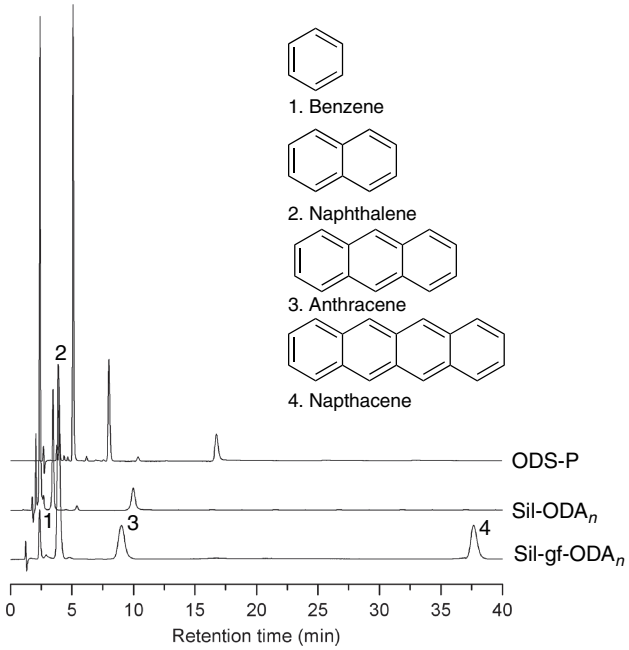

Fig. 8 Chromatograms for a mixture of benzene, naphthalene, anthracene, and naphthacene with Sil-gf-ODA$_n$, Sil-ODA$_n$, and ODS-p. Mobile phase: methanol:water (90:10); Column temperature: 30°C; Flow rate: 1.00 ml/min.

approaches, as well as for ODS-p. The selectivity in ODA$_n$ is discussed focusing on molecular planarity and length in PAHs.

Cis- and *trans*-stilbenes as geometrical isomers are good candidates for the evaluation of molecular-shape selectivity in HPLC. They have the same carbon number per molecule, and, thus, their molecular hydrophobicities are similar but the molecular planarities are absolutely different. The selectivity at 15°C is 1.33, 2.41, and 4.32 for ODS-p, Sil-ODA$_n$, and Sil-gf-ODA$_n$, respectively, clearly indicating higher selectivity by ODA$_n$-grafted silica prepared by *grafting-from* method; however, *grafting-to* approach also yielded a higher selectivity than that of ODS-p.

Another good example is the isomers of *o*-, *m*- and *p*-terphenyls. *o*-Terphenyl is bulky, and *p*-isomer is nearly planar. As summarized in Table 1, Sil-ODA$_n$ shows a better selectivity than that of ODS-p, and the selectivity is further enhanced in a high-density type, Sil-gf-ODA$_n$, although its

Table 1 Retention and separation factors of PAHs for Sil-gf-ODA$_n$, Sil-ODA$_n$, and ODS-p stationary phases at 15°C.

Solute	C_nH_n	Sil-gf-ODA$_n$		Sil-ODA$_n$		ODS-p	
		k	α	k	α	k	α
Benzene	C_6H_6	0.64		0.23		0.59	
			2.2		**1.9**		**2.1**
Naphthalene	$C_{10}H_8$	1.39		0.45		1.21	
			7.1		**6.3**		**5.4**
Anthracene	$C_{14}H_{10}$	4.60		1.44		3.22	
Triphenylene	$C_{18}H_{12}$	9.67		3.60		6.78	
			1.5		**1.4**		**1.2**
Benz[a]anthracene	$C_{18}H_{12}$	14.8		4.98		7.84	
			1.7		**1.5**		**1.2**
Chrysene	$C_{18}H_{12}$	16.5		5.48		8.07	
			4.3		**3.0**		**1.7**
Naphthacene	$C_{18}H_{12}$	41.4		10.7		11.4	
O-Terphenyl	$C_{18}H_{14}$	1.19		0.72		2.46	
			4.0		**1.9**		**1.7**
m-Terphenyl	$C_{18}H_{14}$	4.49		1.36		4.24	
			7.7		**3.9**		**2.2**
p-Terphenyl	$C_{18}H_{14}$	8.82		2.82		5.53	

Mobile phase: methanol:water (90:10); Column temperature: 15°C; Flow rate: 1.0 ml/min.

selectivity decreases remarkably at higher temperatures such as 60°C to be similar to those of ODS-p. These results indicate that the ODA$_n$ phase in a highly ordered state recognizes molecular planarity much better than ODS-p does; it should be noted that the organic phase in polymeric ODS has higher density than in conventional ODS.

To evaluate the planarity recognition capability of ODS phases, Tanaka et al.[48] has introduced the separation for a special mixture composed of two homologous alkylbenzenes and non-planar and planar PAHs. As shown in Fig. 9, it is observed that all compounds are resolved better for Sil-gf-ODA$_n$ than for ODS-p.

In addition, the ODA$_n$ phase shows better selectivity for molecular slenderness (length). In Table 1, this is distinctly seen in the selectivity of a mixture of benz[a]anthracene, chrysene, and naphthacene, which are completely planar compounds but different in their molecular lengths. The selectivity is much higher in Sil-gf-ODA$_n$, ($\alpha_{\text{naphthacene/chrysene}} = 3.32$) than in ODS-p ($\alpha_{\text{naphthacene/chrysene}} = 1.60$).

As mentioned above, the ODA$_n$ phase has a temperature-dependent ordered-to-disordered phase transition. Fig. 10 shows the selectivity for a planar triphenylene and a non-planar *o*-terphenyl in Sil-gf-ODA$_n$, Sil-ODA$_n$, and ODS-p. It shows that the effect of temperature is very low for ODS-p, while Sil-gf-ODA$_n$ and Sil-ODA$_n$ both showed remarkable temperature dependence with distinctly higher selectivity in Sil-gf-ODA$_n$ than in Sil-ODA$_n$ below the phase transition temperature, which is attributed to the ordered/disordered state of the ODA$_n$ moiety.

PEPTIDE LIPID-GRAFTED TYPES

In recent years, there has been renewed attention in synthetic polypeptides because of their potential application as biodegradable and biomedical polymers, as well as their ability to form highly ordered hierarchical structures through non-covalent forces such as hydrogen bonding. Incorporation of a high degree of amino acid functionality and chirality in the polymer chains can enhance the potential to form secondary structures (α-helix and β-sheet) and higher ordered structures. On the other hand, it is known that special kinds of peptide-derived lipids can form highly ordered structures such as lipid bilayer membranes.[21] In these cases, mostly hydrogen bonding interactions with peptide (amide) bonds play an important role in molecular assembling. One of the successful examples is an L-glutamic acid-derived lipid which can produce not only nanofibrillar aggregates such as helical and tubular structures but also show supramolecular functions on the base of chirally-ordered structures.[21] Therefore, the application of these self-assembling system is of great interest to scientists dealing with the preparation of new packing materials for HPLC.

With this background, we have done direct immobilization of a dialkyl L-glutamide-derived lipid (Glu-1) onto porous silica (Fig. 11).[33] Extremely enhanced selectivity was obtained for shape-constrained solutes, e.g., PAHs, aromatic positional isomers, and nucleic acid constituents. This finding encouraged us to develop polymeric peptide lipid type stationary phases.

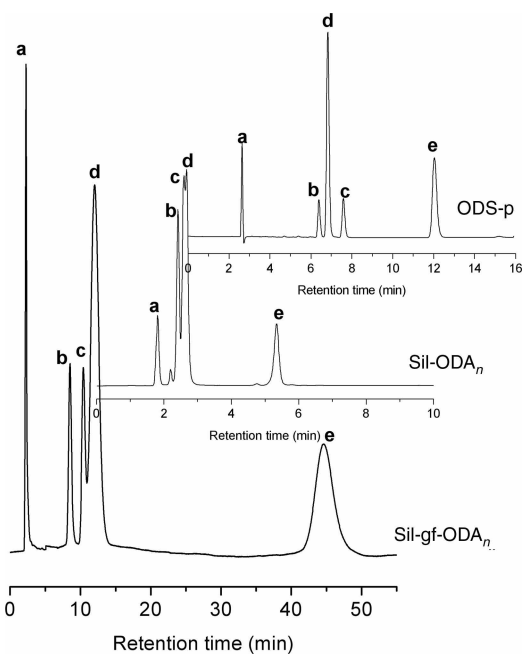

Fig. 9 Chromatograms for the Tanaka test mixture with Sil-gf-ODA$_n$, Sil-ODA$_n$, and ODS-p. Eluates: a, uracil; b, butylbenzene; c, pentylbenzene; d, *o*-terphenyl; e, triphenylene. Mobile phase: methanol:water (90:10); Column temperature: 30°C; Flow rate: 1.0 ml/min.

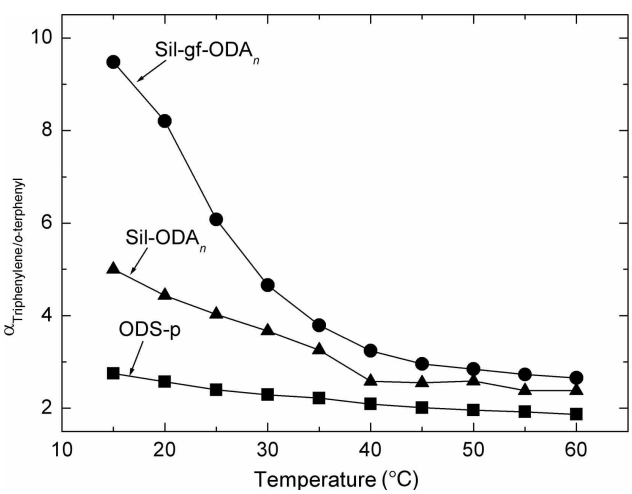

Fig. 10 Temperature dependencies of the separation factors between triphenylene and *o*-terphenyl with Sil-gf-ODA$_n$, Sil-ODA$_n$, and ODS-p. Mobile phase: methanol:water (90:10); Flow rate: 1.0 ml/min.

Silica-supported polymeric type stationary phases (Sil-Phe-1 and Sil-Phe-2) have also been synthesized from polymerizable group-introduced L-alanine lipids such as *N*′-octadecyl-N^{α}-[(*N*-acryloyl)-β-alanyl]- L-phenylalanine amide (Phe-1) and *N*′-octadecyl-N^{α}-(4-vinyl)benzoyl- L-phenylalanine amide (Phe-2) (Fig. 11). Telomerizations of Phe-1 and Phe-2 with silane coupling agent MPS were carried out, followed by immobilization onto silica.[49,50] These polymeric stationary phases showed remarkably enhanced molecular-shape selectivity as compared to ODS-p. Our detailed investigations showed that multiple π–π interactions played a key role in the recognition of molecular-shape of guest molecules. On the other hand, molecular-recognition ability of these polymeric-type peptide lipids are lower than those of monomeric type lipids.[33,49,50] In Glu-1, as compared to the L-phenylalanine–derivative lipid type, carbonyl groups (π–π interaction source) are more highly concentrated on a molecular unit. More functionality is one of the driving forces for multiple π–π interaction as well as molecular recognition in HPLC system.

CONCLUSIONS

In this entry, several kinds of comb-shaped polymers with highly ordered side chains have been introduced as attractive organic phases for RP-HPLC. Poly(octadecyl acrylate), ODA_n, is one of the simplest comb-shaped polymers, and its grafting for introduction onto silica surface is done by a one-step telomerization with 3-mercaptopropyl trimethoxysilane followed by immobilization with the terminal trimethoxysilyl group (*grafting-to* method). The chromatographic results are summarized as follows:

1. Extremely high separation ability is observed in π-electron substances such as PAHs. This is owing to the facts that carbonyl groups of ODA work as π–π interaction sources and that highly ordered state of the side chains promotes multiple π–π interaction with π-electron–containing solutes. Therefore, this selectivity is emphasized for molecular shapes such as planarity, bulkiness, and slenderness.
2. The immobilization of a polymer on a support material influences the resultant molecular-shape selectivity. For example, poly(octadecyl acrylate) having plural trimethoxysilyl groups in the side chain (co-ODA_n) was rigidly immobilized onto silica to observe the multianchoring effect of Sil-co-ODA_n. Compared with Sil-ODA_n, which is immobilized through a single terminal group at one end of the polymer main chain, Sil-co-ODA_n showed better selectivity: e.g., 1.4 times higher selectivity for the separation of triphenylene and *o*-terphenyl.
3. The *grafting-from* method is applicable for the immobilization of ODA_n onto silica. The advantage with this method is that it increases the density of polymeric phase on silica. An initiator-modified silica is prepared in advance, and then, surface-initiated ATRP is carried out with ODA. The resultant polymer-grafted silica (Sil-gf-ODA_n) shows higher surface coverage as well as molecular ordering. Consequently significant increase in the retention time and selectivity for PAHs are observed as compared to those in Sil-ODA_n prepared by the *grafting-to* method.

The use of peptide-derived lipids (Glu-1, Phe-1, and Phe-2) as organic stationary phases also has been described in this entry. These lipids not only have high potential ability as a self-assembling system but also are attractive as a carbonyl π-electron source. As a result, double-alkylated L-glutamide-derived stationary phase has been developed and extremely high selectivity is detected in HPLC as predicted. Polymeric types of peptide-derived lipids were also considered and developed, but their selectivity could not exceed that of the monomeric type lipids. This is probably due to the fact that radical polymerization of peptide-derived monomers disturb the stereoregularity of the resultant polymer main chain, and thus, sufficient molecular ordering is not obtained to increase the selectivity (multiple π–π interaction). Finally, it is concluded that subsidiary weak interactions, such as π–π interaction, can

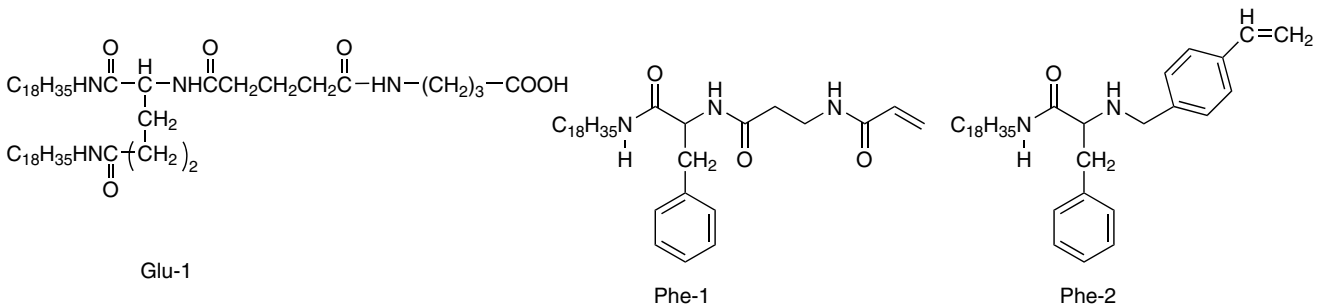

Fig. 11 Chemical structures of peptide lipids.

be remarkably enhanced by molecular ordering, and this concept leads us to highly selective HPLC.

REFERENCES

1. Dorsey, J.G.; Dill, K.A. The molecular mechanism of retention in reversed-phase liquid chromatography. Chem. Rev. **1989**, *89*, 331.
2. Sander, L.C.; Pursch, M.; Wise, S.A. Shape selectivity for constrained solutes in reversed-phase liquid chromatography. Anal. Chem. **1999**, *71*, 4821.
3. Wegmann, J.; Albert, K.; Pursch, M.; Sander, L.C. Poly(ethylene-co-acrylic acid) stationary phases for the separation of shape-constrained isomers. Anal. Chem. **2001**, *73*, 1814.
4. Meyer, C.; Skogsberg, U.; Welsch, N.; Albert, K. Nuclear magnetic resonance and high-performance liquid chromatographic evaluation of polymer-based stationary phases immobilized on silica. Anal. Bioanal. Chem. **2005**, *382*, 679.
5. Lyatskaya, Y.; Balazs, A.C. Modeling the phase behavior of polymer–clay composites. Macromolecules **1998**, *31*, 6676.
6. Ejaz, M.; Yamamoto, S.; Ohno, K.; Tsujii, Y.; Fukuda, T. Controlled graft polymerization of methyl methacrylate on silicon substrate by the combined use of the Langmuir–Blodgett and atom transfer radical polymerization techniques. Macromolecules **1998**, *31*, 5934.
7. Matyjaszewski, K.; Miller, P.J.; Shukla, N.; Immaraporn, B.; Gelman, A.; Luokola, B.B.; Siclovan, T.M.; Kickelbick, G.; Vallant, T.; Hoffmann, H.; Pakula, T. Polymers at interfaces: Using atom transfer radical polymerization in the controlled growth of homopolymers and block copolymers from silicon surfaces in the absence of untethered sacrificial initiator. Macromolecules **1999**, *32*, 8716.
8. Edmondson, S.; Osborne, V.L.; Huck, W.T.S. Polymer brushes via surface-initiated polymerizations. Chem. Soc. Rev. **2004**, *33*, 14.
9. Rahman, M.M.; Czaun, M.; Takafuji, M.; Ihara, H. Synthesis, self-assembling properties, and atom transfer radical polymerization of an alkylated L-phenylalanine-derived monomeric organogel from silica: A new approach to prepare packing materials for high-performance liquid chromatography. Chem. Eur. J. **2008**, *14*, 1312.
10. Mallik, A.K.; Rahman, M.M.; Czaun, M.; Takafuji, M.; Ihara, H. Facile synthesis of high-density poly(octadecyl acrylate)-grafted silica for reversed-phase high-performance liquid chromatography by surface-initiated atom transfer radical polymerization. J. Chromatogr. A, **2008**, *1187*, 119.
11. Hemström, P.; Szumski, M.; Irgum, K. Atom transfer radical graft polymerization initiated directly from silica applied to functionalization of stationary phases for high-performance liquid chromatography in the hydrophilic interaction chromatography mode. Anal. Chem. **2006**, *78*, 7098.
12. Wang, J.S.; Matyjaszewski, K. Controlled/"living" radical polymerization. Atom transfer radical polymerization in the presence of transition-metal complexes. J. Am. Chem. Soc. **1995**, *117*, 5614.
13. Kamigaito, M.; Ando, T.; Sawamoto, M. Metal-catalyzed living radical polymerization. Chem. Rev. **2001**, *101*, 3689.
14. Inglese, J.; Glickman, J.F.; Lorenz, W.; Caron, M.G.; Lefkowitz, R.J. Isoprenylation of a protein kinase. Requirement of farnesylation/alpha-carboxyl methylation for full enzymatic activity of rhodopsin kinase. J. Biol. Chem. **1992**, *267*, 1422.
15. O'Tousa, J.E.; Baehr, W.; Martin, R.L.; Hirsh, J.; Pak, W.L.; Applebury, M.L. The Drosophila ninaE gene encodes an opsin. Cell **1985**, *40*, 839.
16. Kunitake, T.; Okahata, Y.; Shimomura, S.; Yasunami, S.; Takarabe, K. Formation of stable bilayer assemblies in water from single-chain amphiphiles: Relationship between the amphiphile structure and the aggregate morphology. J. Am. Chem. Soc. **1981**, *103*, 5401.
17. Fuhrhop, J.-H.; Schnieder, P.; Boekema, E.; Helfrich, W. Lipid bilayer fibers from diastereomeric and enantiomeric *N*-octylaldonamides. J. Am. Chem. Soc. **1988**, *110*, 2861.
18. Yanagawa, H.; Ogawa, Y.; Furuta, H.; Tsuno, K. Spontaneous formation of superhelical strands. J. Am. Chem. Soc. **1989**, *111*, 4567.
19. Yamada, K.; Ihara, H.; Ide, T.; Fukumoto, T.; Hirayama, C. Formation of helical superstructure from single-walled bilayers by amphiphiles with oligo-L-glutamic acid-head group. Chem. Lett. **1984**, *10*, 1713.
20. Ihara, H.; Takafuji, M.; Hirayama, C.; O'Brien, D.F. Effect of photopolymerization on the morphology of helical supramolecular assemblies. Langmuir **1992**, *8*, 1548.
21. Ihara, H.; Takafuji, M.; Sakurai, T. Self-assembled nanofibers. In *Encyclopedia of Nanoscience and Nanotechnology*, Nalwa, H.S. Ed.; American Science Publishers: Stevenson Ranch, CA, 2004; Vol. 9, 473.
22. Ihara, H.; Hachisako, H.; Hirayama, C.; Yamada, K. Lipid membrane analogues: Formation of highly-oriented structures and their phase separation behavior in benzene. J. Chem. Soc. Chem. Commun. **1992**, *17*, 1244.
23. Hirayam, C.; Ihara, H.; Mukai, T. Lipid membrane analogs. Specific retention behavior in comb-shaped telomer-immobilized porous silica gels. Macromolecules **1992**, *25*, 6375.
24. Fukumoto, T.; Ihara, H.; Sakaki, S.; Shosenji, H.; Hirayama, C. Chromatographic separation of geometrical isomers using highly oriented polymer-immobilized silica gels. J. Chromatogr. A, **1994**, *672*, 237.
25. Chowdhury, M.A.J.; Boysen, R.I.; Ihara, H.; Hearn, M.T.W. Binding behavior of crystalline and non-crystalline phases: Evaluation of enthalpic and entropic contribution to the separation selectivity of non-polar solutes with a novel chromatographic sorbent. J. Phys. Chem. B, **2002**, *106*, 11936.
26. Ihara, H.; Sagawa, T.; Goto, Y.; Nagaoka, S. Crystalline polymer on silica. Geometrical selectivity for azobenzenes through highly-oriented structure. Polymer **1999**, *40*, 2555.
27. Ihara, H.; Goto, Y.; Sakurai, T.; Takafuji, M.; Sagawa, T.; Nagaoka, S. Enhanced molecular-shape selectivity for polyaromatic hydrocarbons through isotropic-to-crystalline phase transition of poly(octadecyl acrylate). Chem. Lett. **2001**, *12*, 1252.
28. Goto, Y.; Nakashima, K.; Mitsuishi, K.; Takafuji, M.; Sakaki, S.; Ihara, H. Selectivity enhancement of

diastereomer separation in RPLC using crystalline-organic phase-bonded silica. Chromatographia **2002**, *56*, 19.
29. Ihara, H.; Sagawa, T.; Nakashima, K.; Mitsuishi, K.; Goto, Y.; Chowdhury, J. Enhancement of diastereomer selectivity using highly-oriented polymer stationary phase. Chem. Lett. **2000**, *2*, 128.
30. Ihara, H.; Takafuji, M.; Sakurai, T.; Sagawa, T.; Nagaoka, S. Self-assembled organic phase for reversed-phase HPLC. In *Enclyclopedia of Chromatography*; Cazes, J., Ed.; Marcel Dekker: New York, 2005; 1528–1535.
31. Sakaki, S.; Kato, K.; Miyazaki, T.; Musashi, Y.; Ohkubo, K.; Ihara, H.; Hirayama, C. Structures and binding energies of benzene–methane and benzene–benzene complexes: An ab initio SCF/MP2 studies. J. Chem. Soc., Faraday Trans. **1993**, *9*, 659.
32. Shundo, A.; Nakashima, R.; Fukui, M.; Takafuji, M.; Nagaoka, S.; Ihara, H. Enhancement of molecular-shape selectivity in high-performance liquid chromatography through multi-anchoring of comb-shaped polymer on silica. J. Chromatogr. A, **2006**, *1119*, 115.
33. Rahman, M.M.; Takafuji, M.; Ansarian, H.R.; Ihara, H. Molecular shape selectivity through multiple carbonyl–π interactions with non-crystalline solid phase for RP-HPLC. Anal. Chem. **2005**, *77*, 671.
34. Chen, S.; Meyerhoff, M.E. Shape-selective retention of polycyclic aromatic hydrocarbons on metalloprotoporphyrin-silica phases: Effect of metal ion center and porphyrin coverage. Anal. Chem. **1998**, *70*, 2523.
35. Catabay, A.; Okumura, C.; Jinno, K.; Pesek, J.J.; Williamsen, E.; Fetzer, J.C.; Biggs, W.R. Retention behavior of large polycyclic aromatic hydrocarbons on cholesteryl 10-undecenoate bonded phase in microcolumn liquid chromatography. Chromatographia **1998**, *47*, 13.
36. Lochmüller, C.H.; Hunnicutt, M.L.; Mullaney, J.F. Effect of bonded-chain rigidity on selectivity in reversed-phase liquid chromatography. J. Phys. Chem. **1985**, *89*, 5770.
37. Wise, S.A.; Sander, L.C. Factors affecting the reversed phase liquid chromatographic separation of polycyclic aromatic hydrocarbon isomers. J. High Resolut. Chromatogr. Chromatogr. Commun. **1985**, *8*, 248.
38. Gautam, U.G.; Gautam, M.P.; Sawada, T.; Takafuji, M.; Ihara, H. Enhancement of retentivity and selectivity for PAHs in NP-HPLC by high-density immobilization of poly(4-vinylpyridine) as an organic phase on silica. Anal. Sci. **2008**, *24*, 615.
39. Wang, Y.; Pei, X.; He, X.; Lei, Z. Synthesis and characterization of surface-initiated polymer brush prepared by reverse atom transfer radical polymerization. Eur. Polym. J. **2005**, *41*, 737.
40. Advincula, R.; Zhou, Q.; Park, M.; Wang, S.; Mays, J.; Sakellariou, G.; Pispas, U.; Hadjichristidis, N. Polymer brushes by living anionic surface initiated polymerization on flat silicon (SiOx) and gold surfaces: Homopolymers and block copolymers. Langmuir **2002**, *18*, 8672.
41. Boyes, S.G.; Akgun, B.; Brittain, W.J.; Foster, M.D. Synthesis, characterization, and properties of polyelectrolyte block copolymer brushes prepared by atom transfer radical polymerization and their use in the synthesis of metal nanoparticles. Macromolecules **2003**, *36*, 9539.
42. Neugebauer, D.; Zhang, Y.; Pakula, T.; Matyjaszewski, K. Heterografted PEO-Pn BA brush copolymers. Polymer **2003**, *44*, 6863.
43. Jayachandran, K.N.; Chatterji, P.R. Synthesis of dense brush polymers with cleavable grafts. Eur. Polym. J. **2000**, *36*, 743.
44. Kim, J.-B, Bruening, M.L.; Baker, G.L. Surface-initiated atom transfer radical polymerization on gold at ambient temperature. J. Am. Chem. Soc. **2000**, *122*, 7616.
45. Ansarian, H.R.; Derakhshan, M.; Rahman, M.M.; Sakurai, T.; Takafuji, M.; Ihara, H. Evaluation of microstructural features of a new polymeric organic stationary phase grafted on silica surface: A paradigm of characterization of HPLC-stationary phases by a combination of suspension state ^{1}H NMR and solid-state ^{13}C-CP/MAS-NMR. Anal. Chim. Acta **2005**, *547*, 179.
46. Pursch, M.; Strohschein, S.; Handel, H.; Albert, K. Temperature-dependent behavior of C30 interphases. A solid-state NMR and LC-NMR study. Anal. Chem. **1996**, *68*, 386.
47. Tonelli, A.E.; Schiling, F.C.; Bovey, F.A. Conformational origin of the non-equivalent ^{13}C NMR chemical shifts observed for the isopropyl methyl carbons in branched alkanes. J. Am. Chem. Soc. **1984**, *106*, 1157.
48. Tanaka, N.; Tokuda, Y.; Iwaguchi, K.; Araki, J. Effect of stationary phase structure on retention and selectivity in reversed-phase liquid chromatography. J. Chromatogr. **1982**, *239*, 761.
49. Rahman, M.M.; Takafuji, M.; Ihara, H. Synthesis and assessment of molecular recognizability by RP-HPLC of an *N*-alkyl-β-Ala-L-Phe-derived organic phase with self-assembling ability. Anal. Bioanal. Chem. **2008**, *392*, 1197.
50. Rahman, M.M.; Takafuji, M.; Ihara, H. Preparation, telomerization and application of *N*-alkyl L-phenylalanine-derived polymerizable organogelator for reversed-phase high-performance liquid chromatography. J. Chromatogr. A, **2008**, *1203*, 59.

Separation Ratio

Raymond P.W. Scott
Scientific Detectors Ltd., Banbury, Oxfordshire, U.K.

INTRODUCTION

The *separation ratio* between two solutes has two uses. The first is to help identify a solute or confirm its identity. The second is to help calculate the minimum efficiency required to achieve a given separation (this aspect of the separation ratio will be discussed under resolution). The first chromatographic parameter to be used for solute identification, other than the corrected retention volume, is the capacity ratio of the solute.

DISCUSSION

The capacity ratio of a solute (k') was defined as the ratio of the distribution coefficient (K) of the solute to the phase ratio (a) of the column. In turn, the phase ratio of the column was defined as the ratio of the volume of mobile phase in the column (V_m) to the volume of stationary phase in the column (V_s); that is,

$$a = \frac{V_m}{V_s}$$

and, as

$$V_r' = KV_s$$

Thus,

$$k' = \frac{K}{a} = \frac{KV_s}{V_m} \quad \text{and} \quad k' = \frac{V_r'}{V_m}$$

where V_r' is the corrected retention volume of the solute.

As the measurement of k' does not depend on flow rate, it is unaffected by flow changes and is, thus, a more reliable measurement than corrected retention volume for solute identification.

Unfortunately, both V_m and V_s will vary between different columns and, due to the partial exclusion that can occur with porous supports and stationary phases, may vary between different solutes. For this reason, the separation ratio (a) was introduced as an identification parameter. For two solutes, (A and B), the separation ratio is defined as

$$\alpha_{A/B} = \frac{V'_{r(A)}}{V'_{r(B)}} = \frac{K_A V_s}{K_B V_s} = \frac{K_A}{K_B}$$

It is seen that the separation ratio is independent of all column parameters and depends only on the nature of the two phases and the temperature. Thus, comparing data from two different columns, providing that the same phase system is used in each, and the columns operated at the same temperature, then any two solutes will have the same separation ratio on both systems. Thus, the separation ratio will be *independent of the phase ratios* of the two columns and the *flow rates*. It follows that the separation ratio of a solute can be used more reliably as a means of solute identification.

In practice, a standard substance is often added to a mixture and the separation ratio of the substance of interest to the standard is used for identification purposes. The separation ratio is taken as the ratio of the distances in centimeters between the dead point and the maximum of each peak, or if data processing is employed and the flow rate is constant, chart distances can be replaced by the corresponding retention times.

BIBLIOGRAPHY

1. Scott, R.P.W. *Liquid Chromatography Column Theory*; John Wiley & Sons: Chichester, 1992; 26.
2. Scott, R.P.W. *Chromatographic Detectors*; Marcel Dekker, Inc.: New York, 1996.
3. Scott, R.P.W. *Introduction to Analytical Gas Chromatography*; Marcel Dekker, Inc.: New York, 1998.

Sequential Injections: HPLC Analysis

Raluca-Ioana Stefan
Jacobus F. van Staden
Chemistry Department, University of Pretoria, Pretoria, South Africa

Hassan Y. Aboul-Enein
Pharmaceutical and Medicinal Chemistry Department, Pharmaceutical and Drug Industries Research Division, National Research Center, Dokki, Cairo, Egypt

INTRODUCTION

All of the samples analyzed using a chromatographic technique need special preparation before they are introduced into the column. This process is laborious, not reliable enough, and often expensive. There are several steps involved in sample preparation: dialysis, dilution, extraction (selective extraction or concentration), and derivatization. Sometimes, the derivatization step is part of the extraction process. The expenses refer to the reagents and solvents of chromatographic purity grade. The sample preparation will become easier and not so expensive by automation.

Sequential injection analysis (SIA), introduced in 1990,[1,2] is a technique with a high potential for online process measurements. It is simple and convenient because sample manipulation can be automated. Furthermore, it consumes low volumes of reagents and solvents. Up to now, all the necessary steps done manually before introduction of the sample into the high-performance liquid chromatography (HPLC) were separately introduced in SIA systems. By including SIA in sample preparation, it became faster, more accurate, and precise. Contamination is reduced substantially and the objectivity of the analysis increased. The main advantages of the coupling of SIA with HPLC are high precision of sample injection into the column, low contamination, low consumption of sample, reagents, and solvents, and the short time of preparation that decreases the time of analysis.

DIALYSIS

For online measurements, the dialysis step is very important because, through dialysis, the solid particles can be retained, the solution can be purified, and also some of the interference can be eliminated. The main disadvantages of dialysis are the slow speed involved and the low recovery of analyte. These parameters can be improved by introducing the dialyser into the conduits of a SIA system.[3]

With the incorporation of a passive, neutral, semipermeable dialysis membrane into the conduits of the sequential injection system, the contact time of the sample zone with the membrane had much influence on the quantity of analyte that dialyzed through the membrane. It is necessary to determine, first, the time necessary to propel the entire sample zone over the membrane. After the propelling of the sample zone over the membrane, the flow direction is reversed and the sample zone is drawn back into the holding coil for fixed periods of time; usually these periods of time can vary from 2 to 60 sec. By increasing of the dialysis time, the sensitivity of dialysis and, finally, the sensitivity of the analytical information are increased. A long dialysis time is also not good to consider, because this increases the dispersion of the dialyzed sample (situated below the membrane) due to a longer time delay before it is drawn in the specific holding coil for analysis.

To increase the percentage of dialysis, as well as the dialysis time, multiple flow reversals with a time of 20 sec between each flow reversal is selected. Similar results are obtained by using a sequential injection system with the stopped-flow period around 150 sec. The advantage of utilizing the stopped-flow mode over multiple flow reversals in the sequential injection analysis systems is that it needs less programming and, also, it reduces the strain on the pump.

DILUTION

It is well known that HPLC techniques are performed at low concentration ranges. Sometimes, the sample is too concentrated in the analyte to be determined, and a dilution step is absolutely necessary. When a SIA system containing a dialyzer is utilized for sampling before a HPLC, the sample is already diluted. If the dilution is still not enough, a special step must be adopted in the program of the SIA system. The next step, when the analyte is extracted into a solvent, can also be considered a dilution.

There are two methods that can be adopted for a dilution in SIA: by using a dilution coil and by using a dilution step.[4,5] The easier dilution technique in SIA is by using a dilution step which can also be accomplished in a shorter time. There are three types of volumes that can control the dilution: the sample volume (the volume of sample or standard that is drawn into the holding coil via the sample

port), the transfer volume (the volume of sample plus accompanying wash in the holding coil and tubing that is transferred into the dilution conduit from the holding coil), and the analysis volume (the volume taken from the dilution conduit to the holding coil).[4]

CONCENTRATION

The concentration step is very easy to implement in sequential injection analysis. The system is very simple and the results are reproducible. Most of the time, this step is not necessary for HPLC. When it is necessary, it can easily be done in the same time with the extraction step.

EXTRACTION

There are two types of extraction that can be used in sampling. The first one involves a chemical reaction before the extraction, and the other one is just a simple extraction of analyte(s) from the solution. When a chemical reaction is involved, the derivatization step that may be necessary is included in the extraction step.

Extraction techniques that involve a chemical reaction can be classified as non-selective extraction or concentration, when more than one analyte is extracted from the solution by using the organic collectors (e.g., 8-hydroxyquinoline and dithizone derivatives) and selective extraction or separation. The first step in such an extraction technique is the formation of the complex by adding the reagent(s) to the solution of analyte, and after the extraction of the complex in an organic solvent. The problem that can arise in a SIA system with these types of extraction is the precipitate that is formed, and this can contaminate the other sample and also can block the tubing. To avoid these problems, it is necessary either to dilute the sample in such a way that the precipitation equilibria will not be reached and that all the complex will remain dissolved in the solution, or by derivatization of the ligands to make the complexes soluble in the aqueous olution by introducing hydrophilic groups into their structures (e.g., in the place of 8-hydroxyquinoline, the 7-iodo, 8-hydroxyquinoline, 5-sulfonic acid can be used).

Three types of SIA system were proposed in coupling with the extraction technique: The first one is based on the introduction of bubbles into the system,[6] the second system is based on wetting film that is formed on a Teflon tube wall,[7] and the third one is based on solid-phase extraction.[8] The most utilized system is the one based on bubbles. The most reliable is the one based on a Teflon tube wall, and the principle of functioning of this system is as follows. The aqueous sample is propelled through the segment of organic solvent whose flow is impeded due to hydrophobic interactions with the walls of Teflon extraction coil. This wall drag allows the faster moving aqueous sample to penetrate through and ultimately separate from the organic solvent. These steps are repeated with a reextraction into a second aqueous segment that is collected and which is going to the analyzer.[9]

DERIVATIZATION

This step can be included in the extraction techniques because, in most of the cases of extraction, the analytes are being transformed. This step is only necessary for analytes that cannot be determined directly in the form that they already exist in solution. In the SIA system, the derivatization process can be assimilated with a reaction between analyte(s) and reagent with the optimum parameters for both the reaction and SIA system;[8,10] the difference is that the product of the reaction is not channeled to the detector, but is channeled to the chromatograph.

SIA/HPLC SYSTEMS

Sequential injection is the perfect vehicle for HPLC, which, in turn, enhances sequential injection by eliminating the problem of dialysis, dilution, or concentration, extraction, and mixing reactants during the loading process. HPLC can be carried out in different modes: affinity chromatography, ion chromatography, extraction chromatography, and so forth.

Most of the SIA/HPLC systems have been applied for the separation and assay of radionuclides. The reason for selecting such a system is the potential radiation and contamination of an operator during the sampling process. By using SIA/HPLC systems, all steps are automated and the contact of the operator with them is minimal. Grate and Egorov[11] reviewed the 2 Sequential Injection Analysis in HPLC radiometric separation and gave to SIA/HPLC systems the main place between automatic analytical separation in radiochemistry. They found that the type of chromatography suitable for coupling with SIA is extraction chromatography. For radiochemical separation, a wide-bore holding coil, in combination with air segmentation and sequential loading and delivery of solutions, instead of zone stacking in the holding coil, is proposed.

Enzymes and antibody–antigen systems have been used to measure a large number of analytes in relation to SIA/HPLC systems.[12] A very interesting application of these systems is given when the HPLC is carried out in the bead injection (BI) form.[13] As BI is presently restricted to relatively short columns, it is focused on separations based on mobile-phase changes, rather than relying on the separating power provided by a large number of theoretical plates. The SIA/BI system has also been

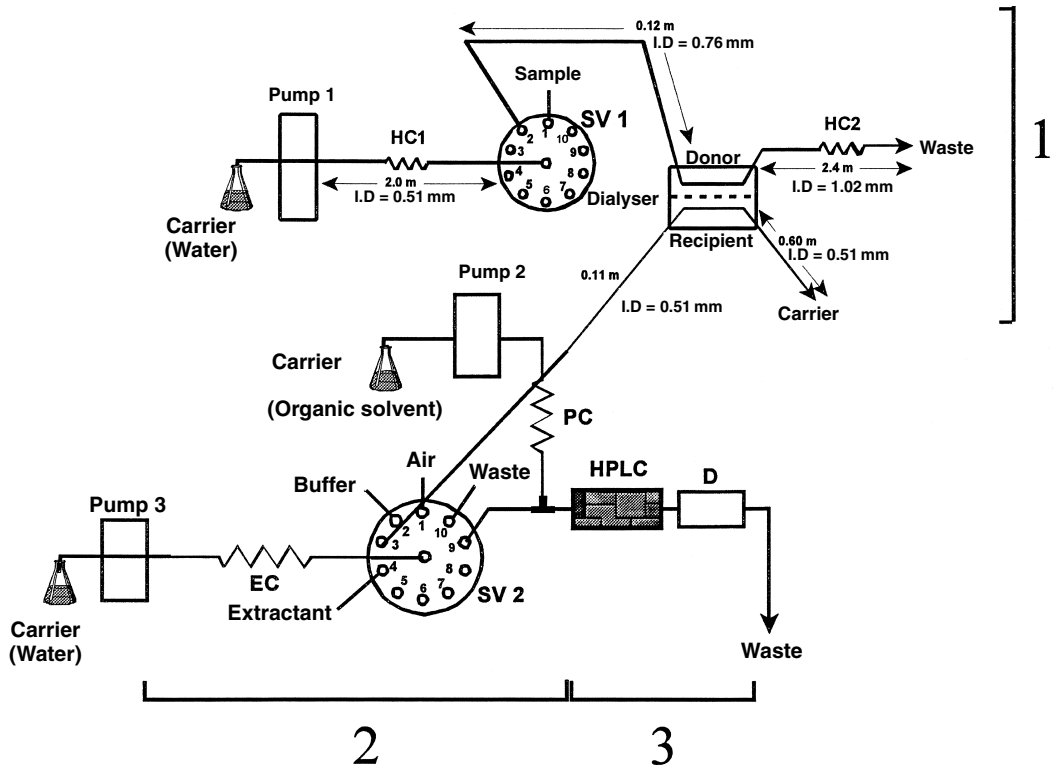

Fig. 1 Schematic representation of SIA/HPLC–detector system: 1: the dialysis unit; 2: the extraction (dilution, concentration, derivatization) unit; 3: the HPLC–D unit. SV is the selection valve; EC is the extraction coil; D is the detector.

applied with very good results for the separation of radionuclides.

An automated sequential trace enrichment dialyzer and gradient HPLC system is proposed for pharmacokinetic studies of drugs and their metabolites.[14] The dialyzer is essential in the determination of pharmaceutical compounds from tablets and biological fluids (e.g., blood). By its incorporation into the conduits of a SIA system and coupling with the HPLC, the objectivity and reproducibility of the measurements were increased.

FEATURES FOR SIA/HPLC SYSTEMS

The ideal system for sample preparation in a chromatographic method is that the operation of all the steps between sample dissolution and chromatography is done through a SIA technique (Fig. 1).The first part of the system will consist of a sample dialysis (unit 1) and the outlet will be channeled into the second unit consisting of concentration or dilution steps and extraction of the analyte. It is always assumed that the concentration, dilution, and derivatization steps can be done by extraction—in most cases, it is absolutely necessary.

The proposed SIA/HPLC (Fig. 1) system operates by a well-programmed computer which will be able to analyze all types of sample: from environment, from the food industry, from the pharmaceutical industry, and also biological samples.

CONCLUSIONS

The utilization of sequential injection analysis coupled with HPLC systems increases the reliability of an HPLC analysis considerably because the primary factor that contributes to the increasing uncertainty is the sample preparation. It is always necessary to look to the most reliable methods for sample preparation, because only these methods will give the best results after the automation by using sequential injection analysis. The best coupling must be concerned with the selectivity and sensitivity assured by a sequential analysis system and by the selectivity and sensitivity of the HPLC technique. The introduction of bead injection considerably improves the reliability of the discussed system.

REFERENCES

1. Rüzicka, J.; Marshall, G.D. Sequential injection: A new concept for chemical sensors, process analysis and laboratory assays. Anal. Chim. Acta **1990**, *237*, 329.

2. Rüzicka, J.; Marshall, G.D.; Christian, G.D. Variable flow rates and a sinusoidal flow pump for flow injection analysis. Anal. Chem. **1990**, *62*, 1861.
3. van Staden, J.F.; du Plessis, H.; Taljaard, R.E. Determination of iron(III) in pharmaceutical samples using dialysis in a sequential injection analysis system. Anal. Chim. Acta **1997**, *357*, 141.
4. Boron, M.; Guzman, J.; Rüzicka, J.; Christian, G.D. Novel single standard calibration and dilution method performed by the sequential injection technique. Analyst **1992**, *117* (12), 1839.
5. van Staden, J.F.; Taljard, R.E. On-line dilution with sequential injection analysis: A system for monitoring sulphate in industrial effluents. Fresenius J. Anal. Chem. **1997**, *357*, 577.
6. Luo, Y.; Al-Othman, R.; Rüzicka, J.; Christian, G.D. Solvent extraction–sequential injection without segmentation and phase separation based on the wetting film formed on a Teflon tube wall. Analyst **1996**, *121* (5), 601.
7. Grate, J.W.; Taylor, R.H. Sequential injection method with on-line soil extraction for determination of Cr(VI). Field Anal. Chem. Technol. **1996**, *1* (1), 39–48.
8. van Staden, J.F.; Taljard, R.E. Determination of ammonia in water and industrial effluent streams with the indophenol blue method using sequential injection analysis. Anal. Chim. Acta **1997**, *344*, 281.
9. Taljaard, R.E.; van Staden, J.F. S. Afr. J. Chem. **1999**, *52*, 36.
10. van Staden, J.F.; Taljard, R.E. Determination of sulphate in natural waters and industrial effluents by sequential injection analysis. Anal. Chim. Acta **1996**, *331*, 271.
11. Grate, J.W.; Egorov, O.B. Automating analytical separations in radiochemistry. Anal. Chem. **1998**, *70*, 779A.
12. Emneus, J.; Marko-Varga, G. Biospecific detection in liquid chromatography. J. Chromatogr. A, **1995**, *703*, 191.
13. Rüzicka, J.; Scampavia, L. From flow injection to bead Injection. Anal. Chem. **1999**, *71*, 257A.
14. Cooper, J.D.H.; Shearsby, N.J.; Taylor, J.E.; Fook-Sheung, C.T.C. Simultaneous determination of lamotrigine and its glucuronide and methylated metabolites in human plasma by automated sequential trace enrichment of dialysates and gradient high-performance liquid chromatography. J. Chromatogr. B, Biomed. Appl. **1997**, *702*, 227.

SFC

Fernando M. Lanças
Institute of Chemistry of São Carlos (USP), University of São Paulo, São Carlos, Brazil

M.C.H. Tavares
Chromatography Laboratory, University of São Paulo, São Carlos, Brazil

INTRODUCTION

A phase diagram, as shown in Fig. 1, can describe the physical stage of a substance of fixed composition. In this pressure–temperature diagram for CO_2, there are three lines describing the sublimation, melting, and boiling processes. These lines also define the regions corresponding to the gas, liquid, and solid states. Points along the lines (between the phases) define the equilibrium between two of the phases. The vapor pressure (boiling) starts at the triple point (Tp) and ends at the critical point (Cp). The critical region has its origin at the Cp. At this point, we can define a supercritical fluid (SF) as any substance that is above its critical temperature (T_c) and critical pressure (P_c). The T_c is, therefore, the highest temperature at which a gas can be converted to a liquid by an increase in pressure. The P_c is the highest pressure at which a liquid can be converted to a traditional gas by an increase in the liquid temperature. In the so-called critical region, there is only one phase and it possesses some of the properties of both a gas and liquid. Subcritical (liquid) CO_2 is found in the triangular region formed by the melting curve, the boiling curve, and the line that defines the P_c.[1]

DISCUSSION

Supercritical fluids begin to exhibit significant solvent strength when they are compressed to liquidlike densities. This makes physical sense intuitively because it is known that gases are not considered as good solvents.

The density of a pure solvent changes in the region of its Cp. For a reduced temperature ($T_r = T/T_c$) in the range 0.9–1.2°C, the reduced solvent density ($\rho_r = \rho/\rho_c$) can increase from gaslike values of 0.1 to liquidlike values of 2.5 as the reduced pressure ($P_r = P/P_c$) is increased to values higher than ~1.0 atm. However, as T_r is increased to 1.55, the SF becomes more expanded and reduced pressures greater than 10 are needed to obtain liquidlike densities. By operating in the critical region, the pressure and the temperature can be used to regulate density, which regulates the solvent power of a SF.[2]

The viscosity changes rapidly in the critical region; even at the high-pressure levels of 300–400 bar, it is only about 0.09 Cp, an order of magnitude below typical viscosities of liquid organic solvents.

The properties of gaslike diffusivity and viscosity, zero surface tension, coupled with liquidlike density, combined with the pressure-dependent solvating power of SF have provided the impetus for applying SF technology to analytical separation problems.

SUPERCRITICAL FLUID CHROMATOGRAPHY (SFC): AN INTRODUCTION

The first reported observation of the occurrence of a supercritical phase was made by Baron Cagniard de la Tour in 1822.[3] He noted visually that the gas/liquid boundary disappeared when heating each of them in a closed glass container increased the temperature of certain materials. From these early experiments, the critical point of a substance was first discovered. The first workers to demonstrate the solvating power of supercritical fluids for solids were Hannay and Hogarth in 1879.[4] They studied the solubility of cobalt(II) chloride, iron(III) chloride, potassium bromide, and potassium iodide in supercritical ethanol ($T_c = 243$°C, $P_c = 63$ atm).

Klesper et al. first demonstrated, in 1962, SFC by the separation of nickel porphyrins using supercritical chlorofluoromethanes as mobile phases.[5] Sie and Rijnders[6] and Giddings,[7] in 1966, developed the technique further, both practically and theoretically, as well as many applications. A few years later, Gouw and Jentof reviewed the general aspects of SFC, including different mobile phases, solute retention, selectivity, and applications.[8]

Until the beginning of the 1980s, SFC was characterized by the utilization of packed columns, in the so-called "LC-like SFC".[9] The introduction in 1981 of capillary open columns with small internal diameters and immobilized stationary phases has opened perspectives to the "GC-like SFC," or c-SFC (capillary supercritical fluid chromatography), with the great advantage of the high-resolution power of capillary columns. The combination of these columns with detectors traditionally utilized in gas chromatography (GC) allows the analysis of compounds with lower volatility and/or higher molecular weight than those in GC.[10]

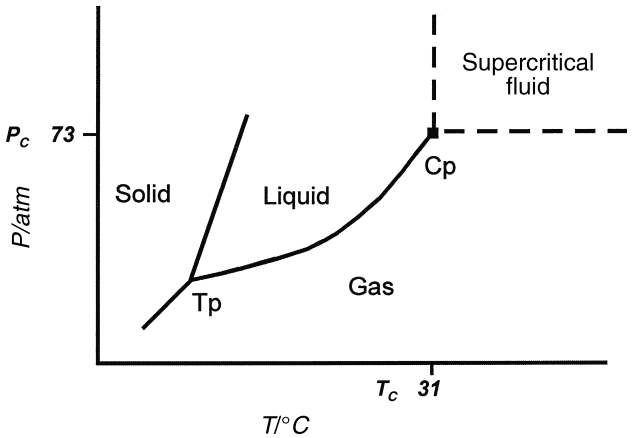

Fig. 1 Phase diagram for CO_2. P_c = critical pressure; T_c = critical temperature; Cp = critical point; Tp = triple point.

INSTRUMENTATION IN SFC

A schematic drawing of the main parts of the SFC system is shown in Fig. 2. It consists of a high-pressure pump for pressurizing and delivering the solvent, usually CO_2 connected to an oven, generally a modified gas chromatography used as the temperature controller for the SFC column. The injector should introduce small sample volumes into the column and a restrictor is placed between the end of the column and the detector to maintain the mobile phase in the supercritical state. A detailed description of each part of the system follows.

Mobile Phase

Pure CO_2 has been the preferred solvent due to its favorable properties. The CO_2 is used in siphoned cylinders to assist the transference of the solvent to the pump. CO_2 passes through a cooling system to increase its density before being inserted in the heating system. When required, a vessel containing a modifier can be added to the system in a way similar to that already well known in supercritical fluid extraction (SFE).

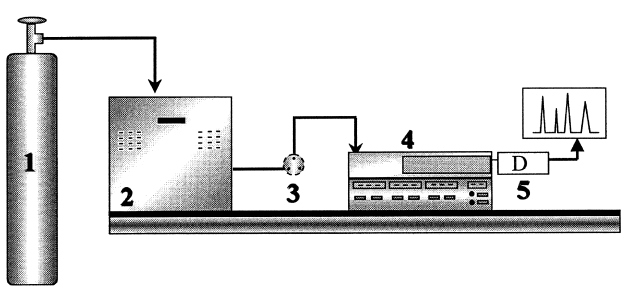

Fig. 2 Schematic drawing of a SFC apparatus. 1: CO_2 tank, 2: high-pressure pump, 3: injection valve, 4: oven (containing the column and restrictor), 5: detector (D).

Pump

Although several high-pressure pumps have been used in SFC, the syringe-type pump has been the preferred to deliver CO_2 into the system. This choice is made due to the absence of pulses of syringe pumps and the possibility of flow rate and pressure control.

Sample Introduction

Samples are usually injected through a high-pressure injection valve fitted with a small internal loop.

Temperature Control

To control and maintain the critical temperature of the mobile phase (CO_2), the column is installed in an oven, similar to those used for GC or high-performance liquid chromatography (HPLC), depending on the type of column used (Fig. 2).

Columns

Two types of columns are used in SFC: packed columns containing solid particles of small inner diameter or wall-coated open-tubular columns (WCOT), usually called just capillary columns. Packed columns have been preferred when capacity is the most relevant issue; capillary columns are selected when efficiency is the goal.

Restrictor

In order to maintain the desired SF mobile-phase conditions, the end of the column is connected to a restrictor. Although several types of restrictor are available,[11] the most popular is the linear restrictor, which consists of a small piece (~10 cm) of a fused silica or metal tube of small inner diameter (50 μm or less).

Detectors

One of the attractions of SFC is that it can use both GC- and LC-like detectors, including the almost universal flame ionization detector (FID) for non-volatile and volatile analytes after separation on either capillary or packed columns. Selective responses could be also obtained from a number of detectors as NPD, ECD, FPD, ultraviolet, Fourier transform infrared, nuclear magnetic resonance, and mass spectrometry (MS).

APPLICATION

An important field of application of analytical chemistry involves the isolation, identification, and quantification of

components in complex samples. Chromatography is one of the most used techniques, because modern chromatographic methods have an excellent separation power, are versatile, and can be used with several detection techniques.

During the last 15 years, the applications of supercritical fluids (SFC and SFE) have shown a fast advance; among others, from a historical perspective, SFC was developed after GC was well established and when HPLC was starting. The interest for SFC has grown with the GC and HPLC development and technological innovations that had occurred independently of SFC research, but surely allowed that commercial SFC instruments could be introduced in the 1980s.

SFC has been applied to environmental analyses, chemical foods, polymers, pharmaceutical, and agro-industry research. This process generates quite complex products, which has been analyzed by different chromatographic approaches, including SFC. Considering the complexity of these samples, a high-resolution technique is required. Even considering that packed column SFC has some advantages in certain cases, capillary columns coated with polymeric phases presents more efficiency (N) per column, being more adequate for complex samples.

As an example, in natural product analysis, SFC offers perspectives in the analysis of several classes of compounds that present difficulties in either conventional liquid chromatography (LC) or GC. In this area, it is very common that the analytes do not have chromophore groups, thus making difficult the detection through UV–Vis, the most popular HPLC detector. At the same time, several of them are not volatile enough to be analyzed by GC. In this case, the use of SFC with capillary columns and FID detection is a valuable tool. Fig. 3 shows a chromatogram of a mixture of triterpenes containing–COOH a functional group (betulinic acid, oleanolic acid, ursolic acid, and polpunonic acid).[12] These compounds are a good example of a class of compounds that presents biological activities and are difficult to be analyzed by either GC or HPLC without an additional derivatization step.

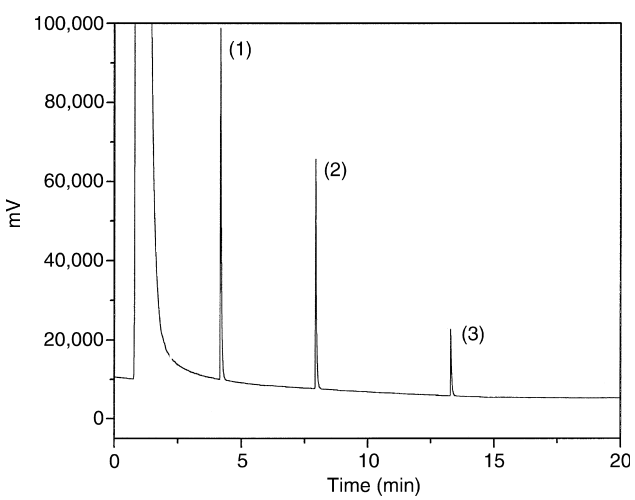

Fig. 3 c-SFC chromatogram of a mixture of triterpenic acids: (1) oleanolic acid, (2) ursolic acid, (3) polpulnonic acid. Column: 20 m × 100 μm × 0.20 μm (5% phenyl, 95% methyl polysiloxane cross-linked); $T = 80°C$; $P = 120$ atm.

CONCLUSIONS

SFC is a very important chromatographic technique still underestimated and underutilized. It presents characteristics similar to both GC and HPLC, although having its own characteristics. Whereas the column temperature control is the way to achieve a good separation in GC and the solvating power of the mobile phase is controlling factor in HPLC, in SFC the density of the fluid is the major factor to be optimized. Both packed (LC-like) and capillary (GC-like) columns have been used in this technique, which has found applications in practically all areas in which GC or HPLC has shown to be the selected separation technique.

REFERENCES

1. Taylor, L.T. *Supercritical Fluid Extraction*; John Wiley & Sons: New York, 1996; 1–30.
2. McHugh, M.A.; Kruponis, V.J. *Supercritical Fluid Extraction. Principles and Practice,* 2nd Ed.; Butterworth-Heinemann: Boston, 1994; 1–26.
3. Cagniard de la Tour, C. Ann. Chim. Phys. **1822**, *21* (2), 127, 178.
4. Hannay, J.B.; Hogarth, J. On the solubility of solids in gases. Proc. Roy. Soc. (London) **1879**, *29*, 324–326.
5. Klesper, E.; Corwin, A.H.; Turner, D.A. High pressure gas chromatography above critical temperatures (Communications to the Editor). J. Org. Chem. **1962**, *27* (2), 700–701.
6. Sie, S.T.; Rijnders, G.W.A. Separ. Sci. **1966**, *1*, 459–490, *2*, 699–727, 729–753, 755–777 (1967).
7. Giddings, J.C. Some aspects of pressure-induced equilibrium shifts in chromatography. Separ. Sci. **1966**, *13*, 73–80.
8. Gouw, T.H.; Jentoft, R.E. Supercritical fluid chromatography. J. Chromatogr. **1972**, *68*, 303–323.
9. Gere, D.R.; Board, R.; McManigill, D. Supercritical fluid chromatography with small particle diameter packed columns. Anal. Chem. **1982**, *54*, 736–740.
10. Novotny, M.; Springston, S.R.; Peaden, P.A.; Fjeldted, J.C.; Lee, M.L. Capillary supercritical fluid chromatography. Anal. Chem. **1981**, *53*, 407A–414A.
11. Smith, R.D.; Fulton, J.L.; Petersen, R.C.; Kopriva, A.J.; Wright, B.W. Performance of capillary restrictors in supercritical fluid chromatography. Anal. Chem. **1986**, *58*, 2057–2064.
12. Tavares, M.C.H.; Vilegas, J.H.Y.; Lanças, F.M. Separation of underivatised tritepene acids by capillary supercritical fluid chromatography. Phytochem. Anal. **2001**, *12* (2), 134–137.

SFC: MS Detection

Manuel C. Ventura
Pfizer Global Research and Development, Pfizer Inc., La Jolla, California, U.S.A.

INTRODUCTION

In recent years, supercritical fluid chromatography (SFC) has been exploited as an alternative to high-performance liquid chromatography (HPLC) because of its superior speed and enhanced selectivity for a wide range of organic compounds, with the exception of highly polar species. The higher diffusion coefficient and lower viscosity of the SFC mobile phase, primarily consisting of condensed CO_2, permit faster run times than HPLC with longer columns and thus higher plate counts. These properties combined with the advantages of mass spectrometry (MS) instrumentation used as chromatographic detectors gave rise to interest in coupling SFC with MS. When one considers chromatographic and mass spectrometric advantages available with this interface, SFC/MS is an attractive alternative to liquid chromatography (LC/MS) for many applications. The coupling of SFC with an increasing variety of MS sources and analyzers in recent years has enabled many new applications and enhancements to existing applications.

HISTORICAL DEVELOPMENT

Vacuum ionization sources such as electron impact (EI) or chemical ionization (CI), commonly used for GC/MS, were initially used when the first SFC/MS interfaces were assembled. In either EI or CI, more than a minimal gas load on the source is not tolerable. For SFC/MS with EI or CI, low source pressure is maintained using a low flow rate or split-flow direct fluid introduction (DFI), sometimes termed direct liquid introduction (DLI).[1] Alternatively, differential pumping of the effluent from a restrictive nozzle is feasible as used with the molecular beam interface employed in some early SFC/MS experiments.[2] Performance of such systems is compromised by adverse effects of gradient conditions on ionization and ion transmission. Increased pressure in the ion source resulting from high flow rates reduces ionization efficiency by EI and CI, thus limiting such experiments to low polarity species, which do not require high levels of polar organic modifier to elute by SFC.

Complex interfaces were also designed to eliminate the gas load on the mass spectrometer from the SFC effluent. Particle beam[3] and moving-belt[4] interfaces originally used for LC/MS were employed with some success, due to their capacity to limit the effect of the mobile phase on the MS analysis. In both cases, sensitivity is compromised due to inefficient mass transport and thermal degradation.

Thermospray interfaces, originally designed for constant vapor pressure conditions, have nonetheless been utilized for SFC/MS by several researchers.[5] Column effluent is vaporized in a heated fixed restrictor probe in which solutes are ionized by mobile-phase-mediated CI (e.g., with ammonium acetate) producing CI-like spectra (prevalent in MH^+ or MH^- ions). The popularity of simple atmospheric pressure ionization (API) sources has slowed further improvements to the thermospray interface.

RECENT DEVELOPMENTS

The recent success of SFC/MS using API sources has contributed to an overall decline in the use of many interface designs described earlier. API sources include electrospray ionization (ESI), atmospheric pressure chemical ionization (APCI), and atmospheric pressure photoionization (APPI). Along with providing usually unambiguous mass spectral identification (MH^+ or MH^- signals predominate), API sources for SFC/MS provide attractive advantages for the analytical chemist. Many commercially available interfaces originally designed for LC/MS require minimal modification to effectively couple an SFC to API-MS systems. Another advantage of API interfaces in SFC is the "self-volatilizing effect" of CO_2 in nebulization of the mobile-phase solutes.

Electrospray ionization occurs in the solution phase prior to vaporization at atmospheric pressure in the mass spectrometer source. Ions are desolvated in the strong electric potential gradient from the needle tip to the inlet of the mass analyzer. In the early period of SFC/ESI-MS development, Sadoun, Virelizier, and Arpino[6] constructed an interface using a 25–30 cm long fused silica restrictor (25 or 60 μm I.D.) with one end attached to the outlet of a packed column and the other end to the source (Fig. 1A). The last 10 cm of silica was coated with a layer of conductive nickel paint to simulate an electrospray needle. Employing a gradient with methanol/water as the polar modifier, detection limits in the low picogram range were reported; however, ionization efficiency was significantly affected by the mobile-phase composition, and severe tailing for low volatility compounds was observed. Some of these deficiencies were addressed by Pinkston and Baker[7]

using a sheath liquid of methanol/water/ammonium acetate with an ionspray (or pneumatically assisted electrospray) interface for open tubular or packed column SFC/MS. In the latter application, a syringe pump supplied methanol through a tee between the mobile-phase outlet and the transfer line to provide backpressure regulation without a variable restrictor valve (Fig. 1A). Advantages of this interface included reduced tailing and lowered modifier composition requirements in the gradient, allowing for higher flow rates and shorter retention times. Sjöberg and Markides described a similar sheath liquid-type ESI interface also convertible to an APCI interface.[8]

Atmospheric pressure chemical ionization is similar to ESI in that both ionization processes occur at atmospheric pressure. Ionization by APCI is fundamentally different, however, in that nebulized solute molecules encounter a plasma of protons, ions, and electrons generated by the corona discharge ionization of background N_2, H_2O, or methanol, and ionize either by proton transfer or charge exchange. The proton transfer agents, usually water or methanol, are supplied by saturating the N_2 nebulizing gas or using the SFC mobile-phase polar modifier, again usually methanol. The first report of packed column SFC with APCI by Huang, Henion, and Covey[9] described an interface in which the backpressure regulator was bypassed and the restrictor was a 20 μm I.D. stainless steel pinhole diaphragm. The effectiveness of this interface was limited by inadequate heating in the nebulization region resulting in chromatographic tailing for more involatile substances. This problem was addressed by the interface designed by Tyrefors, Moulder, and Markides.[10] This interface was constructed to maintain the temperature of the mobile phase in the column up to the tip of the restrictor and provide consistent intense vaporization conditions somewhat independent of flow rate. The outer tube was actively insulated with a heating coil, while a coaxial nebulizing gas flowed around the restrictor tube into which a fine heating wire was inserted. Other interface styles more popular in recent years include those reported by Morgan, Harbol, and Kitrinos[11] and Ventura et al.[12] In the former, the mobile phase exits the backpressure regulator through transfer tubing directly into the nebulizer of the APCI source. In the latter, a split from the compressed mobile-phase region through an ~1 m length of 50 μm capillary upstream of the backpressure regulator is directly adapted to the source (Fig. 1B).

Another API technique gaining popularity of late is APPI. This recently developed ionization mode[13,14] utilizes photons emitted from a lamp beam directed into the aerosol emitted from the nebulizer, typically of the same construction as an APCI nebulizer, to ionize solute molecules. Krypton lamps have been most commonly applied in LC/MS APPI research, as its photons' energies (10.0 and 10.6 eV) exceed the ionization potential (IP) of the majority of organic analytes while they are insufficiently energetic to ionize most mobile-phase solvents. Conveniently for SFC, CO_2 and methanol have higher IP than krypton photons, producing higher signal-to-noise than other API techniques for various types of ionizable solutes. This high signal-to-noise benefit, particularly in the non-polar range, is seeing increased utility especially in pharmaceutical applications.[15,16]

An unmodified APCI source can be further employed for the ionization technique coordination ion spray (CIS), which

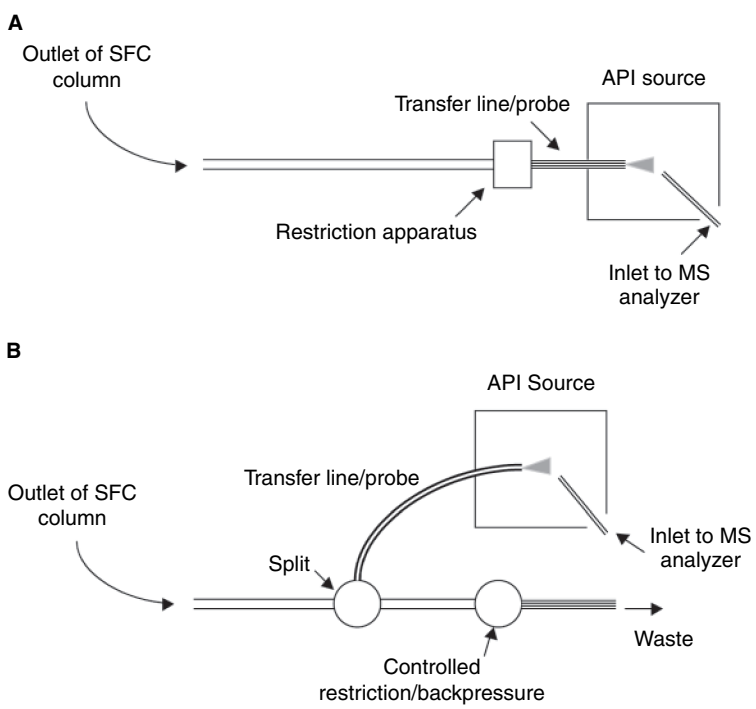

Fig. 1 Two general styles for interfacing SFC to API sources are depicted. In (A), the SFC column effluent is directed entirely into the API source. In some systems, the restriction apparatus is a simple transfer tube restriction used for low flow experiments. In others, a variable restrictor or backpressure regulator is used between the outlet and the source. In the configuration used by Pinkston and Baker,[7] the restriction apparatus is a series of tees to add a coaxial flow of nebulizing gas, an electrospray buffer sheath flow, and another to introduce liquid from a syringe pump to regulate mobile phase pressure. In (B), a direct interface is shown in which a split directs a fraction of the mobile phase flow toward the API source, while the remainder is sent to waste through a backpressure regulator or some controlled restriction to maintain system pressure.

is beneficial for detection of species that are difficult to ionize by standard API methods.[17,18] This technique, which relies on the introduction of a metal cation (such as Ag^+) solution upstream of the ESI or APCI nebulizer, was used with SI-SFC (silver ion SFC) as described by Sandra et al.[19] for the analysis of triglycerides in vegetable oil that are otherwise very difficult to ionize. The researchers showed that CIS-ESI-MS was able to produce intense molecular ion signals (as $[M + Ag^+]$) relative to APCI-MS for saturated triglycerides in SI-SFC separated oil samples.

Though SFC interfacing in an online fashion with an matrix assisted laser desorption ionization (MALDI) source has not yet been reported, the analysis of fractions from an SFC separation has been facilitated by the recent design of an online sample desorption device for MALDI.[20] In this device, the end of the column is connected to an integral restrictor positioned over a spot of C18 sorbent saturated with an appropriate sample matrix such as α-cyano-4-hydroxycinnamic acid. The technique was applied to the separation of a silicone oil. MALDI-MS elucidated the polymer distributions corresponding to fractions deposited over a range of SFC retention times.

Recent advances in MS technologies are being exploited by scientists simultaneously utilizing the separation characteristics offered by SFC. Accurate mass measurements afforded by high resolution time-of-flight (TOF) analyzers permit identification of unknown metabolites and new chemical species.[21] The TOF analyzer's fast spectral acquisition rate is beneficial for chromatographic integrity when coupled with SFC that can generate very narrow peaks.[22] SFC with tandem mass spectrometry (SFC-MS/MS) has also been shown useful for the enantioselective detection of trace level drugs in biological matrices.[23]

The inherent lower viscosity of the SFC mobile phase relative to HPLC yields significant advantages for chiral separation applications.[24] Indeed, preparative SFC is experiencing an increase in utilization in the pharmaceutical industry for chiral purification for a wide range of scales. Now, mass-directed purification technology has been incorporated with SFC for both chiral and achiral purification applications,[25] and commercial prep-SFC/MS systems are currently in development.

CONCLUSIONS

SFC/MS is now entering a more mature phase of development due to scientists' increasing experience with the technology. As system robustness and the well-known utilities of SFC/MS for many applications increase, the user base will continue to see growth. The community utilizing SFC and SFC/MS has driven the vendor market to produce ever more robust and fully integrated systems. Going forward, these technologies will not be avoided as before for such reasons as user unfamiliarity, hardware unavailability, or fragility. SFC/MS technology has now reached a rightful scientific position wherein the principal of the system will dictate that it be used in the many situations in which it is advantageous.

REFERENCES

1. Randall, L.G.; Wahrhaftig, A.L. Dense gas chromatograph/mass spectrometer interface. Anal. Chem. **1978**, *50*, 1703–1705.
2. Randall, L.G.; Wahrhaftig, A.L. Direct coupling of a dense (supercritical) gas chromatograph to a mass spectrometer using a supersonic molecular beam interface. Rev. Sci. Intr. **1981**, *52*, 1283–1295.
3. Edlund, P.O.; Henion, J.D. Packed-column supercritical fluid chromatography/mass spectrometry via a two-stage momentum separator. J. Chromatogr. Sci. **1989**, *27*, 274–282.
4. Berry, A.J.; Games, D.E.; Perkins, J.R. Supercritical fluid chromatographic and supercritical fluid chromatographic–mass spectrometric studies of some polar compounds. J. Chromatogr. **1986**, *363*, 147–158.
5. Via, J.; Taylor, L.T. Packed-column supercritical fluid chromatography/chemical ionization mass spectrometry of energetic material extracts using a thermospray interface. Anal. Chem. **1994**, *66*, 1385–1395.
6. Sadoun, F.; Virelizier, H.; Arpino, P.J. Packed-column supercritical fluid chromatography coupled with electrospray ionization mass spectrometry. J. Chromatogr. **1993**, *647*, 351–359.
7. Pinkston, J.D.; Baker, T.R. Development and application of packed-column supercritical fluid chromatography/pneumatically assisted electrospray mass spectrometry. J. Am. Soc. Mass Spectrom. **1998**, *9*, 498–509.
8. Sjöberg, P.J.R.; Markides, K.E. New supercritical fluid chromatography interface probe for electrospray and atmospheric pressure chemical ionization mass spectrometry. J. Chromatogr. **1997**, *A 785*, 101–110.
9. Huang, E.; Henion, J.D.; Covey, T.R. Packed-column supercritical fluid chromatography–mass spectrometry and supercritical fluid chromatography–tandem mass spectrometry with ionization at atmospheric pressure. J. Chromatogr. **1990**, *511*, 257–270.
10. Tyrefors, L.N.; Moulder, R.X.; Markides, K.E. Interface for open tubular column supercritical fluid chromatography/atmospheric pressure chemical ionization mass spectrometry. Anal. Chem. **1993**, *65*, 2835–2840.
11. Morgan, D.G.; Harbol, K.L.; Kitrinos, N.P., Jr. Optimization of a supercritical fluid chromatograph–atmospheric pressure chemical ionization mass spectrometer interface using an ion trap and two quadrupole mass spectrometers. J. Chromatogr. **1998**, *A 800*, 39–49.
12. Ventura, M.C.; Farrell, W.P.; Aurigemma, C.M.; Greig, M.J. Packed column supercritical fluid chromatography/mass spectrometry for high-throughput analysis. Part II. Anal. Chem. **1999**, *71*, 4223–4231.
13. Robb, D.B.; Covey, T.R.; Bruins, A.P. Atmospheric pressure photoionization: An ionization method for liquid chromatography–mass spectrometry. Anal. Chem. **2000**, *72*, 3653–3659.

14. Syage, J.A.; Evans, M.D.; Hanold, K.A. Photoionization mass spectrometry. Am. Lab. **2000**, *32*, 24–29.
15. Bolanos, B.; Greig, M.; Ventura, M.; Farrell, W.; Aurigemma, C.M.; Li, H.; Quenzer, T.L.; Tivel, K.; Bylund, J.M.R.; Tran, P.; Pham, C.; Phillipson, D. SFC/MS in drug discovery at Pfizer-La Jolla. Int. J. Mass Spectrom. **2004**, *238* (2), 85–97.
16. Quenzer, T.L.; Greig, M.J.; Robinson, J.M.; Bolanos, B.; Pham, C. Atmospheric pressure photoionization mass spectrometry: High throughput applications. In *Lab Automation 2003*; Palm Springs: CA, 2003; 104.
17. Rentel, C.; Gfrörer, P.; Bayer, E. Coupling of capillary electrochromatography to coordination ion spray mass spectrometry, a novel detection method. Electrophoresis **1999**, *20* (12), 2329–2336.
18. Bayer, E.; Gfrörer, P.; Rentel, C. Coordination-ionspray-MS (CIS-MS), a universal detection and characterization method for direct coupling with separation techniques. Angew. Chem. Int. Ed. **1999**, *38* (7), 992–995.
19. Sandra, P.; Medvedovici, A.; Zhao, Y.; David, F. Characterization of triglycerides in vegetable oils by silver-ion packed-column supercritical fluid chromatography coupled to mass spectroscopy with atmospheric pressure chemical ionization and coordination ion spray. J. Chromatogr. **2000**, *A 974*, 231–241.
20. Planeta, J.; Rehulka, P.; Chmelik, J. Sample deposition device for off-line combination of supercritical fluid chromatography and matrix-assisted laser desorption/ionization time-of-flight mass spectrometry. Anal. Chem. **2002**, *74*, 3911–3914.
21. Garzotti, M.; Rovatti, L.; Hamdan, M. Coupling of a supercritical fluid chromatography system to a hybrid (Q-TOF 2) mass spectrometer: On-line accurate mass measurements. Rapid Comm. Mass Spectrom. **2001**, *15*, 1187–1190.
22. Bolanos, B.J.; Ventura, M.C.; Greig, M.J. Preserving the chromatographic integrity of high-speed supercritical fluid chromatography separations using time-of-flight mass spectrometry. J. Comb. Chem. **2003**, *5*, 451–455.
23. Hoke, S.H.; Pinkston, J.D.; Bailey, R.E.; Tanguay, S.L.; Eichhold, T.H. Comparison of packed-column supercritical fluid chromatography-tandem mass spectrometry with liquid chromatography-tandem mass spectrometry for bioanalytical determination of (*R*)- and (*S*)-ketoprofen in human plasma following automated 96-well solid-phase extraction. Anal. Chem. **2000**, *72*, 4235–4241.
24. Berger, T.A. Chiral analysis of drugs. In *Packed Column SFC*; Smith, R.M., Ed.; The Royal Society of Chemistry: Cambridge, 1995; 176–191.
25. Wang, T.; Barber, M.; Hardt, I.; Kassel, D.B. Mass-directed fractionation and isolation of pharmaceutical compounds by packed-column supercritical fluid chromatography/mass spectrometry. Rapid Comm. Mass Spectrom. **2001**, *15*, 2067–2075.

Silica Capillaries: Chemical Derivatization

Joseph J. Pesek
Maria T. Matyska
Department of Chemistry, San Jose State University, San Jose, California, U.S.A.

INTRODUCTION

Capillaries for capillary electrophoresis (CE) are made of fused silica that has been drawn to precise internal and external diameters. Virtually all fused-silica capillaries used in CE, whether for home-made instruments or for commercial systems, have an external diameter of approximately 375 mm. Internal diameters vary over a wider range but generally lie between 50 and 100 mm. Smaller-diameter capillaries generally lead to detection problems, especially if spectroscopic methods are used, because the optical path length becomes too short. Larger-diameter capillaries dissipate heat inefficiently and can lead to band-broadening at higher applied voltages. All capillaries are covered externally with a polyimide coating for protection against breakage and to provide flexibility in fitting the typical column (50–100 cm) into the instrument.

BACKGROUND INFORMATION

Fused silica has surface properties that are similar to the porous particulate matter used as a support material in high-performance liquid chromatography (HPLC) packings. The most important features are the presence of silanol (Si—OH) groups that are polar and ionizable and siloxane linkages (Si—O—Si) that have a hydrophobic character. It is generally recognized that the silanols are the most influential in determining the surface properties of silica. For CE, the Si—OH moieties contribute in at least three ways to the overall performance of the electrophoretic experiment. The presence of silanols on silica surfaces can be considered as a result of the formation of a polymer during condensation of silicic acid. When the polymer cross-links, all four bond sites on each silicon atom do not form siloxane linkages, leaving a hydroxyl group in one position. Because the silanols are acidic groups, they can dissociate in the presence of aqueous solution and behave as any weak acid. The of this moiety is near 5 but can vary depending on the purity of the silica material. Therefore, when the pH of the solution in contact with the inner wall of the capillary is approximately 3 or less, the sites will be fully protonated and the surface will be polar. If the pH is 7 or greater, then the silanols will be fully ionized. The acidic nature of the silanols leads to two of the salient features of the fused-silica surface with respect to electrophoretic experiments. Upon ionization of at least some of the silanols, a double layer is created at the surface when a voltage is applied to a capillary filled with aqueous buffer. This double layer is responsible for electro-osmotic flow (EOF), the movement of solvent toward the cathode. Because of the acidic nature of the silanols, there also is a strong tendency to adsorb basic compounds when these groups are ionized. Finally, the silanol moiety can be considered a reactive group on the surface and it functions as the site for chemical modification of the inner wall. This property will be discussed in more detail later.

Because the first two properties of the silanol, creation of EOF and strong affinity for bases, can often be regarded as undesirable, the third property, the possibility of chemical modification, is used to eliminate these unwanted effects. The presence of EOF diminishes the ability of the CE experiment to separate solutes with very similar electrophoretic mobilities. For basic solutes, the acidic nature of the silanol can result in irreversible adsorption on the surface, which leads to either a complete loss of or greatly reduced detectability. When the silanol group has been modified with an organic moiety, the EOF is greatly diminished and the strong affinity for bases is significantly reduced or eliminated. In addition to chemical derivatization of the surface through a reaction at the silanol, it is also possible to modify the inner wall by adsorption of various compounds that masks the effect of the Si—OH group.

WALL COATING THROUGH CHEMICAL MODIFICATION

Chemical modification of the inner wall of fused-silica capillaries and the surfaces of porous silica supports for HPLC utilize the same reactions. The most common method is based on organosilanization. Within this general reaction scheme, there are two possible approaches, as shown in Table 1. The first possibility involves the use of an organosilane reagent ($RR'R'SiX$) with only a single reactive group (X). The substituents on the

Table 1 Types of reactions for modifying capillary walls.

Reaction type	Reaction	Surface linkages
Organosilane	a) $Si-OH + X-SiR'_2R \rightarrow Si-O-SiR'_2R + HX$ or b) 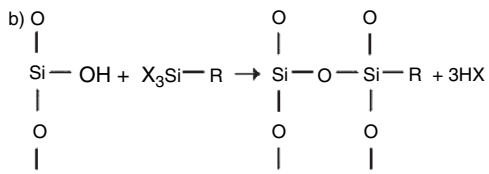	Si — O — Si — C
Chlorination followed by reaction of Grignard regents or organolithium compounds	$Si-OH + SOCl_2 \xrightarrow{\text{Toluene}} Si-Cl + SO_2 + HCl$ a) $Si-Cl + BrMgR \rightarrow Si-R + MgClBr$ or b) $Si-Cl + Li-R \rightarrow Si-R + LiCl$	Si — C
TES silanization	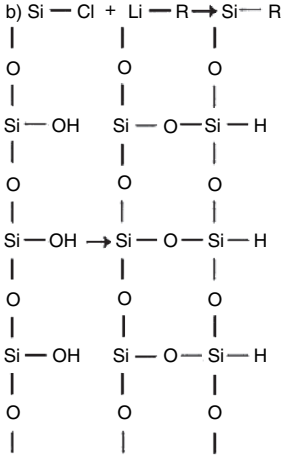	Si — H monolayer
Hydrosilation	$Si-H + CH_2=CH-R \xrightarrow{\text{Catalyst}} Si-CH_2-CH_2-R$	Si — C

silicon atom are as follows: X = halide most often Cl; R = the organic moiety giving the surface the desired properties (i.e., hydrophobic, hydrophilic, ionic, etc.); R′ = a small organic group typically methyl. This reaction leads to a single siloxane bond between the reagent and the surface. Because of the single point of attachment of the reagent, the resulting bonded material is referred to as a monomeric phase. The second approach to organosilanization involves a reagent with the general formula The substituents on the silicon atom in this reagent are defined earlier. The basic difference between the approaches as shown in Table 1 is that the reagent with three reactive groups results in bonding to the surface as well as cross-linking among adjacent bonded moieties and is referred to as a polymeric phase. This cross-linking effect provides extra stability to the bonded moiety but is less reproducible than the monomeric method. The one-step organosilanization procedure is relatively easy and the modification of the surface can be done by forcing the reagent continuously through the capillary or simply filling the capillary with the organosilane solution. The capillary is heated for about 1–2 hr and then rinsed with a solvent such as toluene to remove the excess reagent. As is the case with the production of stationary phases for HPLC, organosilanization accounts for virtually all of the commercially available chemically modified capillaries.

A second modification scheme that has been reported for the modification of capillaries is based on a chlorination/organometalation two-step reaction sequence. This process is also depicted in Table 1. In the first step, the silanols on the surface are converted to chlorides via a reaction with thionyl chloride. This step must be done under extremely dry conditions because the presence of any water results in the reversal of the reaction with hydroxyl replacing the chloride (Si—Cl), resulting in the regeneration of silanols (Si—OH). If the chlorinated surface can be preserved, then an organic group can be attached to the surface via a Grignard reaction or an organolithium reaction. The main advantage of this process is that it results in a very stable

silicon–carbon linkage at the surface. However, the stringent reaction conditions for the first step and the possibility of forming salts as by-products in the second reaction have resulted in relatively little commercial use of this process.

The third method reported for the modification of capillary inner walls involves first silanization of the silica surface followed by attachment of the organic group through a hydrosilation reaction. The process is also depicted in Table 1. In the first step, the use of triethoxysilane under controlled conditions results in a monolayer of the cross-linked reagent being deposited on the surface. This reaction results in the replacement of hydroxides by hydrides. In the second step, an organic moiety is attached to the surface via the hydride moiety in a catalyzed hydrosilation reaction. The catalyst is usually hexachloroplatinic acid (Speier's catalyst) but can be other transition metal complexes or a free-radical initiator. This process also results in a silicon–carbon bond at the surface, does not required dry conditions (water is required as a catalyst in the first step), and is applicable to a variety of unsaturated functional groups in the hydrosilation reaction, although terminal olefins are the most common. The silanization/hydrosilation method also has seen limited commercial utilization to date.

The result of all three of the chemical modification schemes described here is to eliminate or drastically reduce EOF. In some cases, the EOF can be reversed by the attachment of a positively charged group, such as $R—NH_3^+$ to the surface. Whether the EOF is diminished, eliminated, or reversed, separation is improved because electrophoretic mobility differences are enhanced. The replacement of silanols by various organic moieties also has beneficial effects with respect to the separation of basic compounds. An example of the difference in peak shapes seen for bare and modified capillaries is shown in Fig. 1. In some cases, the tailing observed for highly basic compounds is more severe than shown in the figure and in the worst cases irreversible adsorption results in the complete absence of a peak in the electropherogram.

Once a reaction scheme has been selected, then a choice must be made as to the type of surface that is suitable for a particular separation. The surface properties are controlled by the "R" group of the reactions shown in Table 1. Hydrophobic coatings can be achieved by using organic moieties that are common in reversed-phase (RP) HPLC. The most common would be either octadecyl (C_{18}) or (C_8) octyl In general, hydrophobic coatings are used for small molecule separations where the main concern is the suppression of EOF and the elimination of possible adsorption at the silanol sites. However, for the separation of proteins, peptides and DNA related species that have considerable hydrophobic character, it is more desirable to

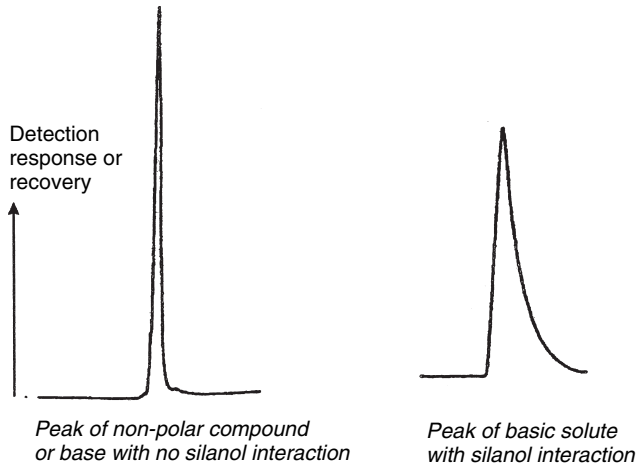

Fig. 1 Comparison of peak shapes for modified and bare capillaries.

have a hydrophilic coating. The presence of any neutral bonded group will reduce or eliminate the EOF and a hydrophilic species will prevent strong interactions with the surface that would occur if the coating was hydrophobic. Because of the importance of CE in the separation of biomolecules, considerable effort has been devoted to the development of hydrophilic wall coatings. By far, the most extensively used hydrophilic coating is polyacrylamide. The surface is first modified with a linker such as 3-methacryloxypropyltriethoxysilane having a double bond available as a site for acrylamide to attach and polymerize. Derivatives of polyacrylamide have also been bonded which result in increased stability at high pH. Other polymers such as polyethylene glycol, cellulose, and poly(vinyl alcohol) have also been used in order to achieve a hydrophilic surface. The presence of any polymer on the capillary usually results in a reasonably thick layer that shields the surface and drastically lowers or eliminates EOF. Polymers containing cationic or anionic species can also be useful in preventing adsorption of hydrophobic compounds on the surface as well as controlling EOF. The type charge on the polymer controls the direction of the EOF. For negatively charged groups (sulfonic acid), the direction is cathodic, and for positively charged groups (quaternary amine), the direction is anodic.

WALL COATING THROUGH BUFFER ADDITIVES

Another approach to reducing the EOF as well as wall adsorption is to add a compound to the running buffer that will compete with the solute for the silanol sites on the surface. These materials must have some affinity for the charged or polar sites on the inner wall and so they must, themselves, be hydrophilic or charged. Non-ionic

surfactants are hydrophilic to prevent solute adsorption on the wall and block the silanols in order to reduce the EOF. The use of cationic polymers in the buffer results in a reversal of EOF to the anodic direction, whereas the use of anionic polymers preserves the cationic direction but tends to stabilize the flow in comparison to a bare capillary. Other additives such as diaminoalkanes and polyvinylalcohol result in reduced EOF and less solute adsorption on the wall.

Column technology is one of the most rapidly developing areas of CE. The capillary is the key to separation, so it is likely that numerous column formats will be established to meet specific separation needs similar to stationary-phase development in HPLC.

BIBLIOGRAPHY

1. Altria, K.D. *Capillary Electrophoresis Guidebook: Principles, Operation and Applications*; Humana Press: Totowa, NJ, 1996.
2. Camilleri, P. *Capillary Electrophoresis*; CRC Press: Boca Raton, FL, 1998.
3. Landers, J.P. *Handbook of Capillary Electrophoresis*, 2nd Ed.; CRC Press: Boca Raton, FL, 1997.
4. Pesek, J.J.; Matyska, M.T. Column technology in capillary electrophoresis and capillary electrochromatography. Electrophoresis **1997**, *18*, 2228.
5. Vansant, E.F.; VanDerVoort, P.; Vrancken, K.C. *Characterization and Chemical Modification of the Silica Surface*; Elsevier: Amsterdam, 1995.

Silica Capillaries: Epoxy Coating

James J. Bao
Advanced Medicine Inc., San Francisco, California, U.S.A.

INTRODUCTION

Capillary electrophoresis (CE) has proven to be one of the best possible techniques available for the separation of proteins. However, CE separation of proteins is often complicated by the interaction between the analytes and the silanol groups on the inner surface of the capillary. This interaction often results in broad asymmetrical peaks, poor efficiency, altered electro-osmotic flow (EOF), reduced protein recovery, and poor reproducibility. Attempts have been made to reduce this interaction by chemically modifying the surface with a layer of chemical coating. Capillary coating has the advantage of allowing analysts to freely modify the composition of the buffer to optimize the separation. Different coatings have been made and each of them has unique characteristics. For protein separations, the most commonly used capillary coatings are hydrophilic coatings.[1–6] For example, epoxy coating is one of these hydrophilic coatings; various protein samples have been separated successfully on this coating.

PREPARATION OF EPOXY COATING

A typical procedure for preparing epoxy coating can be found in the literature.[7,8] Basically, a fused-silica capillary is activated with 1.0 *M* NaOH solution for 10–20 min and then washed with dilute HCl and water for another 20 min each. The washed capillary is then heated in an oven for 3 hr at 120°C with N_2 slowly passing through. A γ-glycidoxypropyltrimethoxysilane (GOX) in CH_2Cl_2 is pushed into the pretreated capillary and heated for 3 hr. Next, a solution of ethyleneglycol diglycidyl ether (EGDE) and 1,4-diazabicyclo-[2.2.2]-octane (DABCO) is forced through the column and allowed to react at 120°C for at least 3 hr. Finally, the capillary is washed with methanol at room temperature.

SEPARATION OF PROTEINS ON THE EPOXY COATING

Epoxy coating is a hydrophilic coating due to the high content of ether and hydroxyl groups. It is expected that this hydrophilic surface will reduce protein adsorption and, thus, is suited for protein separations.

SEPARATION OF MODEL PROTEINS AT NEUTRAL pH

The usefulness of this epoxy coating for protein separation can be demonstrated with the separation of various model proteins using 10–50 m*M* phosphate buffer near pH 7. The model proteins are lysozyme (p*I* 11), cytochrome-*c* (p*I* 10.2), ribonuclease-A (p*I* 9.3), α-chymotrypsinogen (p*I* 8.8), trypsinogen (p*I* 8.7), α-chymotrypsin (p*I* 8.4, 8.8), and myoglobin (horse heart, p*I* 7.3). They are all positively charged at pH 7 and have high tendency to adsorb onto the negatively charged walls of uncoated capillaries. Therefore, very poor separation is seen with an uncoated capillary. However, a good separation of these proteins can be achieved on the epoxytreated surface. Fig. 1 shows that all five proteins are baseline resolved with a high separation efficiency.

Coating the inner surface of capillary reduces the amount of surface silanol groups and, thus, the EOF in the capillary. The epoxy coating retains about one-third of the EOF of an uncoated capillary at pH 7. This EOF is critical for the separation and detection of samples containing neutral to slightly negatively charged proteins. For example, α-chymotrypsin, myoglobin (whale, p*I* 6.9), conalbumin (p*I* 6.3), carbonic anhydrase (p*I* 6.1), and α-amylase (p*I* 5.9) can also be separated at pH 7.

SEPARATION OF MODEL PROTEINS AT OTHER pHs

One of the major advantages of coating the inner surface of the capillary is that it allows the buffer pH to be freely adjustable to achieve the best separation. Coating reduces the effect of pH on EOF, electrophoretic mobility, and protein separation. For example, the EOF in the coated capillary has less than half (from 0 to 3×10^{-4} cm^2/VS) the variation as seen in the uncoated capillary (from 1×10^{-4} to 8×10^{-4} cm^2/VS) between pH 3 and 11.

The five positive model proteins as shown in Fig. 1 can also be separated at various other pHs (pH 4–10).[7] However, the migration times of these individual proteins vary with pH change differently. Although the electrophoretic mobility of these proteins changes accordingly with pH, the overall effect of pH on both EOF and electrophoretic mobility varies at different pH values. This

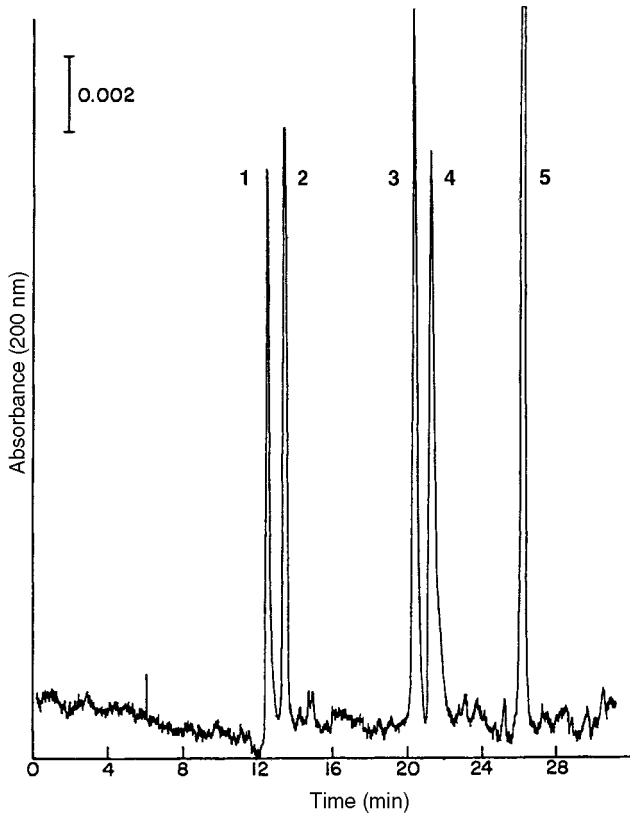

Fig. 1 CE separation of five basic model proteins in an epoxy-coated capillary. Experimental condition: 65 cm separation length, inner diameter/outer diameter 50/363 μm, 0.01 *M* phosphate buffer, pH 7, 300 V/cm, 17 μA. Peaks: (1) lysozyme, (2) cytochrome-*c*, (3) ribonuclease A, (4) α-chymotrypsonagen, and (5) myoglobin (horse heart).

variation provides a basis for optimizing pH for the separation of these proteins.

The theoretical plate number for the separation of these model proteins has a maximal value at pH 7. However, the peak capacity increases with pH because the separation window between lysozyme and myoglobin increases with pH, whereas the peak width does not change significantly. The resolution between the two pairs of proteins, ribonuclease A and α-chymotrypsinogen, and α-chymotrypsinogen and myoglobin, increases with the pH. However, the resolution between lysozyme and cytochrome-*c* increases slightly from pH 5 to 7, drops to zero at pH 8 (no separation at all), and then increases again as the pH is increased.

PROTEIN RECOVERIES

In general, the efficiency of protein separation in CE should be directly proportional to the separation length (i.e., $N = L/H$), where N is the theoretical plate number, L is the separation length, and H is the height-equivalent theoretical plate. Results obtained by locating two detectors at 20 and 65 cm from the injection end show that longer separation length gave much better separation. Much higher than expected separation efficiency is obtained from the 65 cm separation length segment than that from the 20 cm separation length. Therefore, a long capillary should be used when better resolution and higher efficiency are desired. However, no significant improvement in separation efficiency can be achieved when the capillary length exceeds 1 m. On the other hand, a short capillary is preferred when separation time is of major concern.

The adsorption of positive proteins onto the epoxy capillary surface can be quantitatively evaluated by using the two online detector design. From the responses of the two detectors, it is possible to determine the adsorption of proteins on the surface between the two detectors. Zero-percent recoveries have been reported on an uncoated capillary at pH 7 for lysozyme, cytochrome-*c*, ribonuclease A, and α-chymotrypsinogen. However, most of these proteins had recoveries between 84.4% and 95%, except for lysozyme (55.5%), on an epoxy-coated capillary. Therefore, coating does reduce protein adsorption significantly.

REPRODUCIBILITY AND STABILITY

The reproducibility of protein separation from run to run, day to day, segment to segment, column to column, and chemist to chemist is very high. From run to run, the % relative standard deviation (RSD) ($n = 5$) of migration times for neutral marker (MO) and lysozyme are 0.94 and 0.71, respectively. The % RSD in EOF for day to day ($n = 5$) and segment to segment ($n = 6$) are 2% and 3.5%, respectively. For column to column, the EOF at pH 7 varied from 0.5×10^{-4} to 2×10^{-4} with an average of 1.14×10^{-4} for nine columns coated over a 3-month period.

The major challenge to capillary coatings, especially hydrophilic coatings, is the stability. Adding a hydrophobic moiety into the coating may increase coating stability but interfere with protein separations. Epoxy coating provides a balance between hydrophilicity and stability. Epoxy is well known for its chemical and mechanical stability. The epoxy is covalently bound to the silica surface and is cross-linked to generate a stable surface. This coating has shown to be suitable for protein separations at pH 4–10. When stored at room temperature, this column is stable for at least several months.

SEPARATION OF CYTOCHROME-*c* VARIANTS

The separation of cytochrome-*c* variants was challenging because of their similarity in structure. Each of them differs

by only a few amino acids in their sequences. When five cytochrome-*c* variants were injected, only four peaks were obtained, with the horse and dog variants migrating together. Varying the experimental conditions still did not help the separation of the horse and dog variants. Very reproducible separations were obtained at pH 6–8.[8]

SEPARATION OF RECOMBINANT PROTEINS

BMP-2 is a recombinant protein which has the potential to develop into a biotech drug. Previous experiments with an uncoated capillary and a commercially available hydrophilic-coated column (Celect P150) failed to separate the BMP-2 components with reproducible results. By using the epoxy coating, the various BMP-2 components were separated. IL-11 is another recombinant protein under investigation. Using this epoxy coating, a CE method was developed to monitor the stability of IL-11 at different storage conditions. The results showed that there were some significant differences in the CE profiles of the three IL-11 samples stored at different temperatures for different periods of time.[8]

CONCLUSIONS

Epoxy coating is well suited for the separation of proteins in CE. This coating is easy to prepare and can be used for a broad range of pHs. High recoveries of proteins prove that this epoxy modified surface has reduced the protein adsorption significantly.

REFERENCES

1. Hjerten, S. High-performance electrophoresis: Elimination of electroendosmosis and solute adsorption. J. Chromatogr. **1985**, *347*, 191.
2. McCormick, R.M. Capillary zone electrophoretic separation of peptides and proteins using low pH buffers in modified silica capillaries. Anal. Chem. **1988**, *60*, 2322.
3. Bruin, M.; Huisden, R.; Kraak, J.C.; Poppe, H. Performance of carbohydrate-modified fused-silica capillaries for the separation of proteins by zone electrophoresis. J. Chromatogr. **1989**, *480*, 339.
4. Nashabeh, W.; El Rassi, Z. Capillary zone electrophoresis of proteins with hydrophilic fused-silica capillaries. J. Chromatogr. **1991**, *559*, 367.
5. Smith, J.T.; El Rassi, Z. Capillary zone electrophoresis of biological substances with surface-modified fused silica capillaries with switchable electroosmotic flow. J. High Resolut. Chrom. **1992**, *15* (9), 573–578.
6. Ren, X.; Shen, Y.; Lee, M.L. Poly(ethylene-propylene glycol)-modified fused-silica columns for capillary electrophoresis using epoxy resin as intermediate coating. J. Chromatogr. A, **1996**, *741*, 115.
7. Towns, J.K.; Bao, J.; Regnier, F.E. Synthesis and evaluation of epoxy polymer coatings for the analysis of proteins by capillary zone electrophoresis. J. Chromatogr. **1992**, *599*, 227.
8. Bao, J.J. Separation of proteins by capillary electrophoresis using an epoxy based hydrophilic coating. J. Liq. Chromatogr. Relat. Technol. **2000**, *23* (1), 61.

Silica Capillaries: Polymeric Coating for CE

Xi-Chun Zhou
Department of Chemistry, Cambridge University, Cambridge, U.K.

Lifeng Zhang
Environmental Technology Institute, Innovation Centre (NTU), Singapore

INTRODUCTION

The performance of capillary electrophoresis (CE) with an unmodified fused-silica capillary is dependent on the chemical properties of the silica surface. The residuals Si–OH groups on the surface lead to *electro-osmotic flow* (EOF), which contributes to solute migration. For cationic solutes moving toward the negative electrode, the EOF will diminish the resolution, because it contributes toward migration in this direction and reduces the overall migration time. For anionic solutes, EOF is necessary for migration toward the negative electrode or it retards the movement toward the positive electrode and enhances resolution. Therefore, when cationic solutes are the analytes, it is often desirable to diminish the EOF in order to enhance resolution and, therefore, a bare capillary may not be the best choice for a column in this situation.

Another drawback of the unmodified capillary is that the silanols are potential sites for adsorption of certain solutes, especially high-molecular-weight proteins, which leads to poor recovery of the analyte and variable migration times due to the decrease in EOF.

POLYMERIC COATINGS

Capillary columns modified with polymeric coatings are a desirable approach for controlling EOF and adsorption of solutes on the wall. In general, for a coating to be successful in CE, the polymers should be able to: (a) modify or suppress the EOF, (b) be stable for a long period (many injections) in the presence of aqueous buffer solutions so that migration times remain constant and good quantitative determinations are possible, and (c) suppress strong, or even irreversible, adsorption of analyte molecules (e.g., proteins).

According to the way polymers are attached to the column surfaces, the polymeric coatings can be differentiated between those substances that are covalently attached to the capillary surface and those coatings that are not covalently attached but are adsorbed to the surface by physical or ionic forces. Comparatively, adsorbed coatings are simpler to prepare, whereas covalent bonded coatings require elaborate chemical reactions. With regard to the mechanism by which prevention of adsorption of proteins occurs and the properties that they render to the coated surfaces, the compounds currently used as adsorbed coatings belong mainly to two categories: aminated or cationic polymers and hydroxylic or neutral polymers. Aminated polymers, such as polybrene, are adsorbed to the silica wall by Coulombic attraction.

The mechanism for which wall interactions are minimized is primarily due to the ionic repulsion of proteins and peptides at a pH below their p*I*. These polymers generate a positively charged layer at the surface of the silica wall and, therefore, lead to an anodal EOF. These polymer coatings are very stable and are useful over a wide pH range. Hydroxylic or neutral polymers are attached onto the silica wall by weaker interactions such as hydrogen-bonding. The mechanism for which wall interactions are minimized is described as a shielding of the silanol groups. Because these polymers are not charged, the EOF is, in most cases, suppressed. The working pH range is narrower and is limited to the acidic pH regime. Coating procedures may be varied to generate the coating thickness and homogeneity. Most commonly, the reagent is simply passed through the capillary in a suitable buffer. In the case of hydroxylic polymers, thermal immobilization is usually required. Prior to electrophoresis, the unbonded reagent is flushed from the capillary. The main limitation of adsorbed coatings is their instability under basic conditions.

A polymeric coating which is covalently bonded to the surface of capillary wall is the most significant approach among the surface deactivation methods. This method provides a more flexible approach in preventing adsorption of analytes and, at the same time, permits manipulation of separation parameters to optimize selectivity and efficiency. The silanization of the silica surface is an elegant method which enables the production of a large variety of polymer coatings that are chemically bonded to the capillary column surface. In general, polymers are attached to the silica surface by an Si–O–Si linkage or Si–C linkage. Many different mono-, di-, or tri-functional silanization reagents are commercially available or can be easily synthesized. The capillary coated with polymers via Si–C linkage show better stability under alkaline conditions and improved reproducibility of the separation than that of the Si–O–Si linkage.

Among the bonded materials described in the literature, polyacrylamide is one of the most popular and successful for achieving good protein separations. Initial studies were based on the bonding of the linker 3-methacryloxyptopyltriethoxysilane between the surface and the polymerized,

and in some cases cross-linked, acrylamide. The main drawback of this type of wall coating is its long-term stability. In order to overcome this effect, the surface silanization agent was replaced with 7-oct-1-enyltrimethoxysilane. Improvement in stability, as well as efficiency and reproducibility of migration times, in comparison to the columns with linear polyacrylamide bonded by the conventional method, was achieved. However, at the high pH range, the amido bonds in polyacrylamide are possibly hydrolyzed, leading to degradation of the attached polymer and a loss of column performance. In order to overcome this effect, N-substituted acrylamide monomers can be used which provide steric protection to the amido bond. Poly-(acryoylaminoethoxyethanol) was shown to have dramatically improved stability over polyacrylamide at a high pH. Poly-(*N*-(acroylaminoethoxy) ethyl-β-D-glucopyranose was demonstrated to be even more stable. In addition to the improved stability of the amido bond, the linkage of polymer to the capillary surface via a Si–C bond made through a silanization/hydrosilation process contributed greatly toward the length of coating's service.

Various types of polyethers and diol moieties are also effective hydrophilic coating, which often function in a manner similar to polyacrylamide. Different combinations of polyether with triethoxysilane groups or anchored poly(ethylene glycol)s have resulted in low EOF and low adsorptive coatings. It has also been possible to combine the characteristics of the two most common hydrophilic coatings by linking a polyvinylmethylsiloxanediol to linear polyacrylamide. As combining cellulose, functionalized polyethyleneimine and polyether in various proportions thus allows the control of EOF that is independent of pH. The mixed phase from ethylene glycol diglycidyl ether and glycidol also exhibits low EOF and protein adsorption. Polysiloxanes are another type of capillary coating used in the formation of mixed materials to produce surfaces more conducive to electrophoretic conditions.

Other types of polymers have also been attached to the inner walls of fused-silica capillaries through different linking agents. A common approach involves the bonding of a methacryl group via standard organosilane chemistry. Then, bonding of another species to the linker takes place by a double-bond reaction and polymerization. For example, in the case of a cellulose coating, the species attached to the linker can be allyl methylcellulose. Other polymers include cross-linked dextrin, triblock poly(ethylene oxide)–poly(propylene oxide) and poly(vinyl alcohol).

Charged polymeric coatings are also bonded to the column surface to control the adsorption and EOF, especially in the analysis of oppositely charged species in a single run, or for fast separation of analytes with sufficient differences in electromobilities. One effective approach is the cryptand-containing polymer coating, which generates a switchable EOF depending on the pH of the running buffer. Other charged coatings can be synthesized with sulfonic acid or quaternary ammonia groups that provide more stable EOF over a fixed buffer pH range.

Capillaries with chiral polymer coatings have been applied in CE for resolution of enantiomers. Possibly because of its inclusive effect, cyclodextrin seems to be an effective chiral selective agent when bonded to a fused-silica capillary surface. In this case, the purpose of the modification is to induce interactions with the chiral material on the surface. Certainly, the cyclodextrin moiety lowers EOF like other wall modifications because it diminishes the number of silanols. The lower EOF allows for slower migration of the solute through the column and, hence, more time for interaction with the chiral selector. The diminished number of silanols also results in less nonspecific interactions with the fused-silica surface, which would tend to degrade the enantiomeric separation.

Capillaries bonded with polymeric coatings are also applied to capillary electrochromatography (CEC) for separation of neutral molecules. In this case, the polymeric coating participate to solute–bonded phases interaction in a manner similar to open-tubular LC. Most polymeric coating preparations have followed the procedures typically used in open-tubular LC and GC.

Polymer-coated columns offer advantages in the respect that the surface is generally well shielded from the solutes as they migrate through the system. Most polymer procedures involve a multistep process that can often be time-consuming and/or experimentally difficult. Recently, it has been demonstrated that polymer coatings can be produced in a single step by mixing the polymer, a surface-derivatizing agent, and a cross-linking agent in a solvent that is then placed in the capillary. The coated capillary is then heat-treated, which removes the solvent and immobilizes the polymer film on the surface. A number of polymers were tested and higher efficiencies obtained for basic protein separation. The formation of organic–inorganic polymeric coatings by the sol–gel technique has also been reported to be a simpler way.

Further development in the preparation of polymeric coatings with more reproducible reaction conditions and better reagents will make the CE a more challenging separation technique.

BIBLIOGRAPHY

1. Chiari, M.; Neri, M.; Righetti, P.G. *Capillary Electrophoresis in Analytical Biotechnology*; Righetti, P.G., Ed.; CRC Series in Analytical Biotechnology CRC Press: Boca Raton, FL, 1996.
2. Heiger, D.N.; Majors, R.E. LC/GC **1995**, *13*, 13–23.
3. Li, S.F.Y. Capillary electrophoresis, principles practice and applications. J. Chromatogr. Lib. **1993**.
4. Schomburg, G. Polymer coating of surfaces in column liquid chromatography and capillary electrophoresis. Trends Anal. Chem. **1991**, *10*, 163–169.

Size Separations by CE

Robert Weinberger
CE Technologies, Inc., Chappaqua, New York, U.S.A.

Abstract
Size separations by capillary electrophoresis (CE) are performed using low viscosity and replaceable linear polymer solutions. The technique was employed for DNA sequencing during the Human Genome Project, which was completed in 2000. Current applications involve many modes of DNA separation as well as those involving sodium dodecyl sulfate (SDS) proteins. The purity of recombinant monoclonal antibodies is often determined using CE.

INTRODUCTION

Electrophoretic separation based on molecular size is the predominant technique for the separation of large biomolecules.[1] When using the traditional slab-gel, a rigid anticonvective gel is required to provide mechanical stability for the separation. These gels are designed for a single use at relatively low electric field strengths.

During the early days of high-performance capillary electrophoresis (HPCE), rigid gels were polymerized in situ within the capillary. These gel-filled capillaries were used for multiple runs at high field strengths. The capillaries were prone to failure and proved too unreliable for routine use. It was soon discovered that low-viscosity pumpable media was capable of defining molecular pores required for size separation. In the capillary format, the walls of the tube provide the requisite mechanical stability, so high-viscosity gels are unnecessary. These solutions are known as polymer networks, entangled polymers, or physical gels. When polymer networks are used for size separations, a fresh matrix is employed for each run. Through the use of high-pressure pumping systems, polymer networks suitable for DNA sequencing can be pumped in and out of the capillary.

This technology has facilitated the development of instruments containing arrays of 96 capillaries for high-throughput applications such as DNA sequencing. Other high-throughput DNA applications that will eventually incorporate this technique include genetic analysis and human identification. Ultimately, microfabricated devices may be used for many of these applications.

SEPARATION MECHANISM

Several mechanisms for the migration of macromolecules through polymer networks have been described. The Ogston model considers the molecule as a non-deformable sphere. The speed of migration is based on the mobility of the solute in free solution modified by the probability of an encounter with a restricting pore. This mechanism is operative when the radius of gyration of the macromolecule is less than or equal to the average pore size of the polymer network. Separation of sodium dodecyl sulfate (SDS) proteins is believed to occur following this mechanism.

Large biopolymers, such as DNA and oligosaccharides, do not follow the Ogston model. These molecules can deform during transit through the porous network. Instead, a strand of DNA can move through the polymer matrix in a snake-like manner known as reptation. It is also known that fragment resolution decreases as the length of the macromolecule increases. The molecules align with the electric field in a size-dependent manner. This process is known as biased reptation. This effect limits the size of DNA molecules that can be separated using conventional slab-gel techniques. The high electric field strength used in capillary electrophoresis (CE) further limits the separation. Beyond 20,000 base pairs (bp), separations become poor and pulsed-field techniques must be employed.[2] Equipment based on this technique is not available for commercial CE instrumentation.

Further masking a full understanding of the separation mechanism is the interaction of the macromolecule with the polymer network reagents. Separations have been reported in polymer concentrations far below what is required to define pores.[3]

DENATURATION OF MACROMOLECULES

Because separations occur based on molecular size, the macromolecule must be denatured to ensure that all solutes have the same charge-to-mass ratio. DNA and RNA are denatured by heating in formamide at 90°C for a few

minutes. This improves both the separation and the sizing accuracy.

To denature proteins, the disulfide bonds must be reduced and the molecule must be unfolded. Heating to 90–95°C for a few minutes in a solution composed of 0.1% SDS and a reducing agent, β-mercaptoethanol or dithiothreitol (DTT), is sufficient to denature most proteins. When the molecular weight of a protein is less than 10 kDa, the SDS binding stoichiometry may change, resulting in errors in the calculation of molecular weight.[4]

MATERIALS FOR POLYMER NETWORKS

A wide variety of polymeric materials can be employed for size separations. It appears that the molecular weight and concentration of the polymer is more important than the polymer type itself. Once the polymer concentration is greater than the overlap threshold, the porous matrix is defined and reproducible. Best results are obtained if the polymer does not interact with the macromolecules being separated.

Among the materials used as polymer network reagents are linear polyacrylamide (LPA), dimethylpolacrylamide, methylcellulose derivatives, poly(ethylene oxide), and others. The appropriate molecular weight of the polymer is important. Sometimes, blends of different molecular weight are used. For example, the mixture of 2% LPA (MW = 9 mDa) and 0.5% LPA (MW = 50 kDa) is used to separate DNA sequencing reaction products of up to 1000 bases in less than 1 hr, as shown in Fig. 1.[5] The viscosity of this polymer is 30,000 cps. The solution exhibits non-Newtonian properties as the viscosity drops upon the initiation of flow. The use of 2% LPA (MW = 16 mDa) and 0.5% LPA (MW = 250 kDa) at 125 V/cm extends the read length to 1300 bases in 2 hr.[6]

INJECTION

Electrokinetic injection provides the highest efficiency separations. If the salt concentration of the sample is greater than 50 m*M*, hydrodynamic injection gives better results. It is better to desalt the sample by dialysis, precipitation, or ultracentrifugation.

DETECTION

For SDS proteins, low-ultraviolet (UV) detection at 200 or 220 nm is used depending on the UV transparency of the polymer network. For oligonucleotides, UV detection at 260 nm is employed. When performing DNA sequencing, short tandem repeat or genetic analysis, laser-induced fluorescence (LIF) is the method of choice. Intercalating dyes such as YOYO or YO-PRO fluorescence when complexed in between the DNA strands are sometimes added to the background electrolyte when monitoring polymerase chain reaction (PCR) products and restriction digests and for genetic analysis. For DNA sequencing, the fluorescent tag is incorporated in the chain-terminating dideoxynucleotide reagent. When separating short tandem repeats for human identification, the PCR primers can incorporate the fluorescent tag.

APPLICATIONS

DNA applications, in particular DNA sequencing, human identification, and genetic analysis, dominate the field. Other DNA applications including oligonucleotides, antisense DNA, restriction fragments, plasmids, PCR products, hydridization (DNA probe), and RNA have also been demonstrated.[7,8]

DNA testing is rapidly becoming the predominant technique for human identification. The restriction fragment length polymorphism (RFLP) method requires large amounts of DNA (20–100 ng) and is extremely time-consuming and labor-intensive.

A PCR method employing short tandem repeats (STR) is now the method of choice. STRs are sequences where two to seven nucleotides of DNA are constantly repeated. Unlike the DNA of a gene, STRs are prone to DNA replication errors. The lengths of these fragments vary from one person to the next, thereby providing the potential for DNA fingerprinting. The use of PCR and LIF detection provides high sensitivity, so very little DNA is required. The need for higher specificity is addressed with multiplex PCR, where several dye-labeled primers simultaneously amplify multiple locations throughout the genome.

The most widely used genetic screening technique, PCR–RFLP, detects a mutation at a specific restriction endonuclease cleavage site at the mutation locus.[9] The products from other techniques such as amplification refractory mutation system (ARMS), single-strand conformational polymorphism (SSCP), heteroduplex polymorphism (HPA), constant denaturant capillary electrophoresis (CDCE), and PCR are usually separable using polymer networks.

PCR is particularly useful for genetic analysis because both amplification and primer-specific isolation of gene fragments occur simultaneously. Allele-specific amplification can be employed to detect a single-base-pair mutation through the use of a specially designed primer that is complementary to the mutated DNA.[10] PCR amplification takes place only if mutation is present. Fig. 2 illustrates the separation of multiplex PCR fragments in this case,

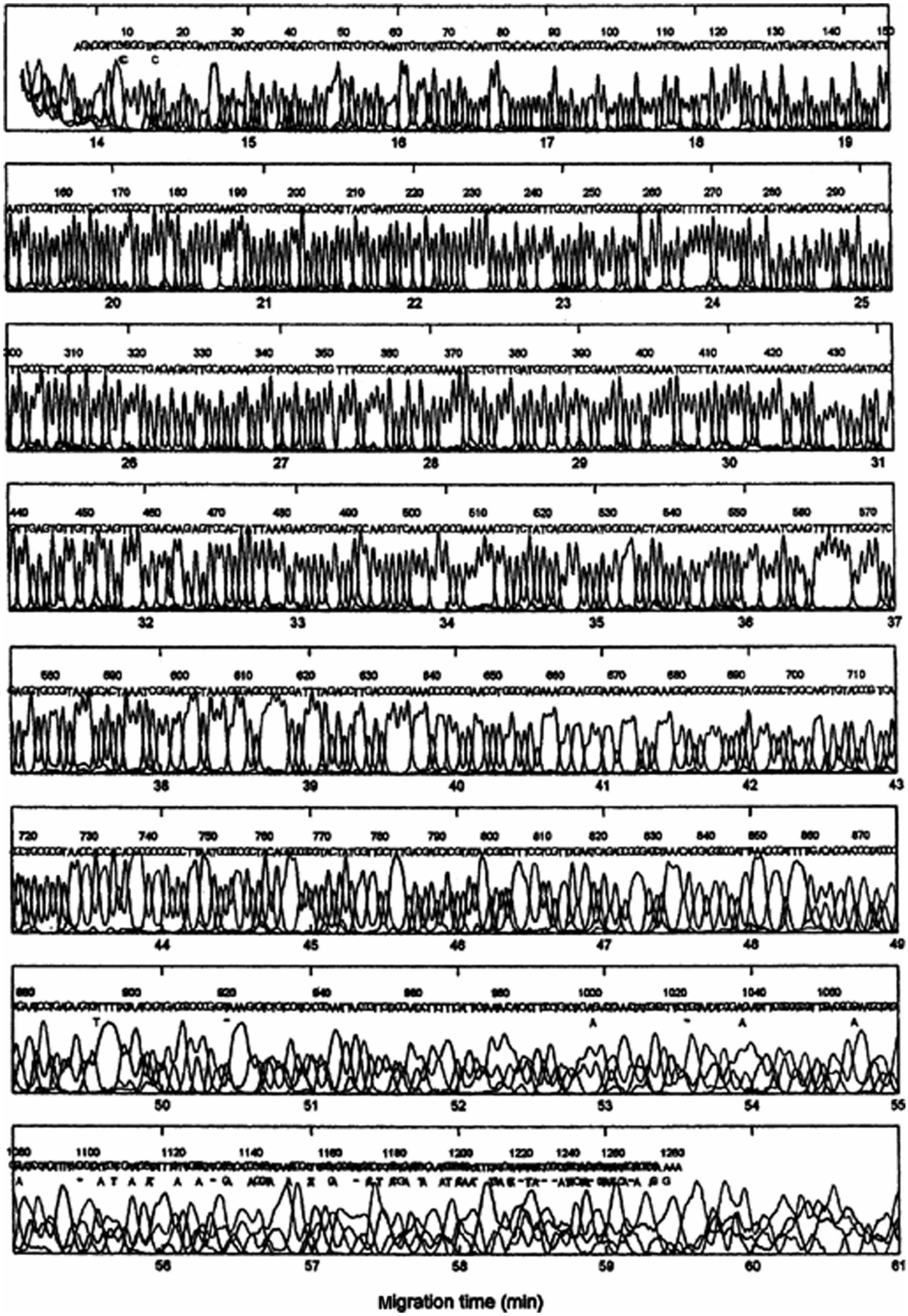

Fig. 1 Separation of DNA sequencing fragments. Conditions: capillary, 30 cm (45 cm total length) × 75 μm I.D., coated with poly(vinyl alcohol); background electrolyte, 2% linear polyacrylamide (LPA), 9 mDa and 0.5% LPA, 50 kDa in 7 *M* urea and 500 m*M* Tris/500 m*M* TAPS/20 m*M* EDTA; buffer, 50 m*M* Tris/50 m*M* TAPS/2 m*M* EDTA with urea in catholyte; injection, 25 V/cm for 10 sec; field strength, 200 V/cm; temperature, 60°C; detection, laser-induced fluorescence.

Source: From Routine DNA sequencing of 1000 bases in less than one hour by capillary electrophoresis with replaceable linear polyacrylamide solutions, in Anal. Chem.[5]

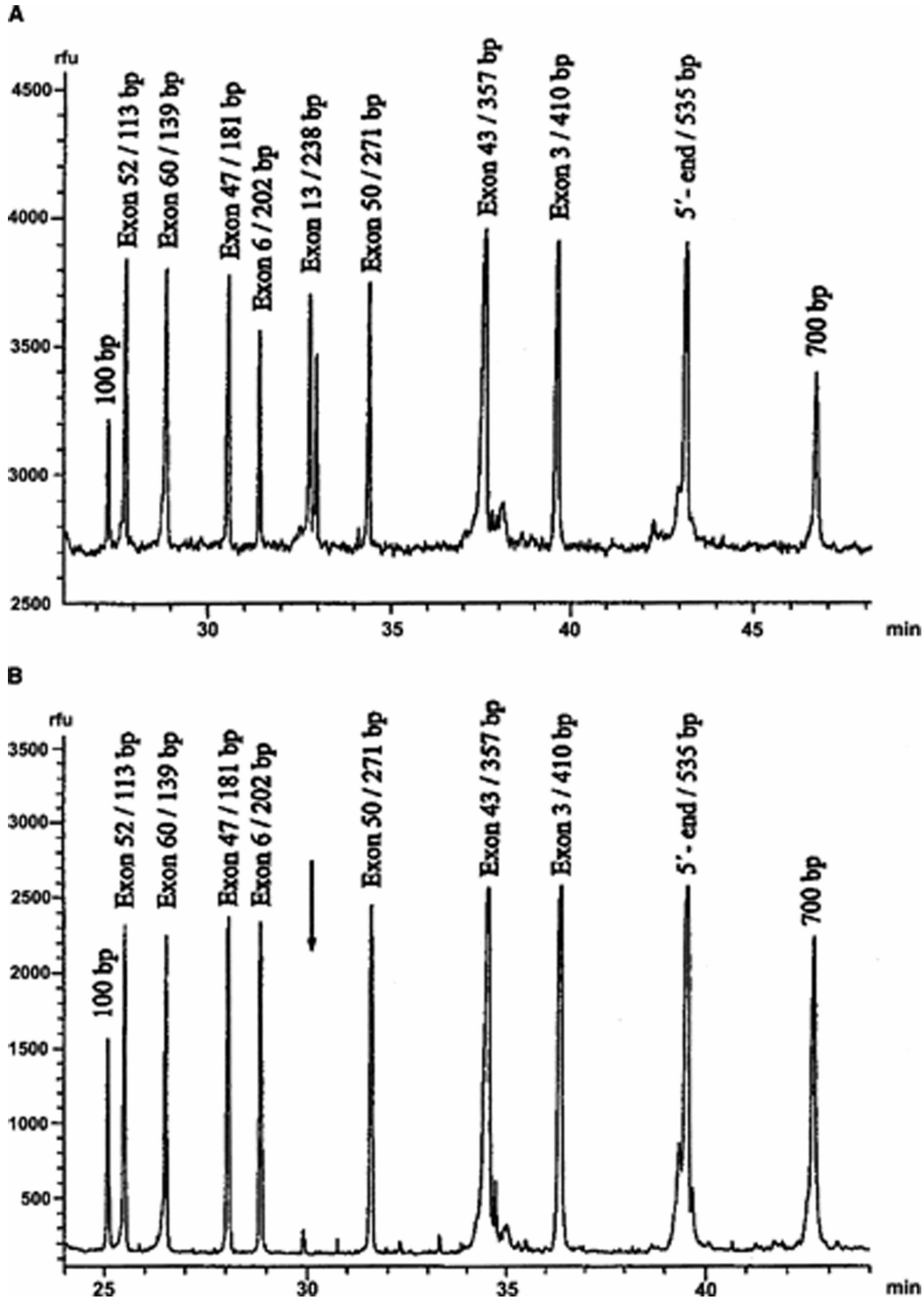

Fig. 2 Multiplex PCR profile of exons in Duchenne or Becker muscular dystrophy genes combined with (A) two flanking standards and (B) without standards. Capillary, 40 cm (65 cm total length) × 75 μm I.D., coated with polyacrylamide; background electrolyte, 0.5% poly(ethylene oxide), 1 mDa in 1 × Tris–borate–EDTA, 10 μ*M* aminoacridine, 2 n*M* Vistra Green; field strength, 108 V/cm; detection, LIF, 488 nm.
Source: From Rapid sizing of polymorphic microsatellite markers by capillary array elctrophoresis, in J. Chromatogr. A. Copyright 1997, Elsevier Science Publishers.[12]

searching for specific deletions in the dystrophin gene believed to result in Duchenne muscular dystrophy. The deletion is indicated by the arrow. Size separations for SDS proteins have become important in the biopharmaceutical industry, particularly for the separation of impurities in reduced and non-reduced monoclonal antibodies.

MICROCHIP ELECTROPHORESIS SYSTEMS

Instrumentation based on microfabricated chips is now widely available from multiple sources. Advances in many forms of DNA separations continue to appear in the literature. Sequencing of 600 bases in 6.5 min is the modern speed record for electrophoretic separations.[11] It is likely that alternative sequencing technology will displace electrophoretic sequencing. Microfabricated capillary array electrophoresis has been studied for human identification via STRs.[13] Genetic analysis by PCR has been reported for prenatal diagnosis of beta-thalassemia.[14] Microchip devices can automate the complete DNA analytical process, including DNA extraction, cleanup, PCR, and size separation.[15]

CONCLUSIONS

The sequencing of the human genome is one of the most complex analytical projects ever accomplished. While DNA sequencing may move to other technologies such as pyrosequencing, the fields of human identification and genetic analysis will continue to be performed in capillaries and ultimately in microfabricated systems. SDS proteins will continue to be separated using capillaries until the resolution of the microfabricated systems is improved.

REFERENCES

1. Westheimer, R.; Barnes, N.; Gronau-Czybalka; Habeck, C. *Electrophoresis in Practice: A Guide to Methods and Applications of DNA and Protein Separations*, 2nd Ed. John Wiley & Sons: New York, 1997.
2. Kim, Y.; Morris, M.D. Pulsed-field capillary electrophoresis of multikilobase length nucleic acids in dilute methyl cellulose solutions. Anal. Chem. **1994**, *66*, 3081.
3. Barron, A.E.; Blanch, H.W.; Soane, D.S. A transient entanglement coupling mechanism for DNA separation by capillary electrophoresis in ultra-dilute polymer solutions. Electrophoresis **1994**, *15*, 597.
4. Takagi, T. Capillary electrophoresis in presence of sodium dodecyl sulfate and a sieving medium. Electrophoresis **1997**, *18*, 2239.
5. Salas-Solano, O. et al. Routine DNA sequencing of 1000 bases in less than one hour by capillary electrophoresis with replaceable linear polyacrylamide solutions. Anal. Chem. **1998**, *70*, 3996.
6. Miller, A.W.; Sosic, Z.; Buckholz, B.; Barron, A.E.; Kotler, L.; Karger, B.L. DNA sequencing up to 1300 bases in two hours by capillary electrophoresis with mixed replaceable linear polyacrylamide solutions. Anal. Chem. **2000**, *72*, 1045.
7. Righetti, P.G., Ed.; *Capillary Electrophoresis in Analytical Biotechnology*; CRC Press: Boca Raton, FL, 1996.
8. Heller, C., Ed.; *Analysis of Nucleic Acids by Capillary Electrophoresis*; Vieweg: Weinheim, 1997.
9. Mitchelson, K.R.; Cheng, J. Point mutation screening by high-performance capillary electrophoresis. J. Capillary Electrophoresis **1995**, *2*, 137.
10. Barta, C.; Sasvari-Szekely, M.; Guttman, A. Simultaneous analysis of various mutations on the 21-hydroxylase gene by multi-allele specific amplification and capillary gel electrophoresis. J. Chromatogr. A, **1998**, *817*, 281.
11. Fredlake, C.P.; Hert, D.G.; Kan, C.W.; Chiesl, T.N.; Root, B.E.; Forster, R.E.; Barron, A.E. Ultrafast DNA sequencing on a microchip by a hybrid separation mechanism that gives 600 bases in 6.5 minutes. Proc Natl Acad Sci. **2008**, *105*, 467.
12. Mansfield, E.S.; Vainer, M.; Harris, D.W.; Gasparini, P.; Estivill, X.; Surrey, S.; Fortina, P. Rapid sizing of polymorphic microsatellite markers by capillary array electrophoresis. J. Chromatogr. A, **1997**, *781* (1–2), 295–305.
13. Greenspoon, S.A.; Yeung, S.H.; Johnson, K.R.; Chu, W.K.; Rhee, H.N.; McGuckian, A.B.; Crouse, C.A.; Chiesl, T.N.; Barron, A.E.; Scherer, J.R.; Ban, J.D.; Mathies, R.A. A forensic laboratory tests the Berkeley microfabricated capillary array electrophoresis device. J. Forensic Sci. **2008**, *53*, 828.
14. Hu, H.; Li, C.; Xiong, Q.; Gao, H.; Li, Y.; Chang, Q.; Liang, Z. Prenatal diagnosis of beta-thalassemia by chip-based capillary electrophoresis. Prenat. Diagn. **2008**, *28*, 222.
15. Easley, C.J., et al. A fully integrated microfluidic genetic analysis system with sample-in-answer-out capability. Proc. Natl. Acad. Sci. USA, **2006**, *103*, 19272.

Slow Rotary CCC

Qizhen Du
Institute of Food and Biological Engineering, Zhejiang Gongshang University, Hangzhou, China

INTRODUCTION

When the mobile phase of a two-phase solvent system is pumped into a rotating coil column around its horizontal axis, filled with the stationary phase, a satisfactory retention of the stationary phase can be obtained at three rotating speed ranges: below 10 rpm, from 20 to 150 rpm, and over 300 rpm. But only at a speed in the range of 20–150 rpm the two phases in the coil column can thoroughly mix to meet the requirement of partition chromatography.[1,2] Ito and Bowman[3] initially reported separations of a series of dinitrophenyl (DNP) derivatives of amino acids and peptides with this mode. Later, Ito and Bhatnagar[4,5] developed an apparatus equipped with an assembled column composed of ten small columns of 90 ml capacity. Further, Ito studied the hydrodynamic distribution of the two immiscible solvent phases in the slowly rotating column.[6] But this countercurrent mode was neglected because high-speed countercurrent chromatography (HSCCC), which adopted a planetary centrifugal mode, had been popularised since the 1980s. However, the utilization of HSCCC for industrial separations is limited because the apparatus possesses some disadvantages due to the planetary rotational mode, which causes three problems: (i) the operation should be attended carefully because of the high-speed rotation column; (ii) balancing is difficult due to the diversification of two phase solvents in the column; and (iii) inlet and outlet tubes are easily broken while the column rotates under high speed. In recent years, Du and Ito have developed a separation method using a slow rotary mode.[7,8] In contrast to HSCCC, this method is called slow rotary countercurrent chromatography (SRCCC).

APPARATUS

Fig. 1 shows a simplified cross-sectional view through the central axis of the apparatus equipped with an assembling column. The motor drives a rotary frame that consists of three aluminium arms rigidly bridged together with links. The frame holds two rotary elements: the countershaft and the centrally located column holder assembly. The countershaft is equipped with a toothed pulley at one end and a gear at the other end. The pulley of the countershaft is coupled with a toothed belt to an identical stationary pulley mounted on the stationary wall member of the apparatus. The coupling causes a counter-rotation of the countershaft on the rotary frame. This motion is further conveyed to the central column holder assembly by a 1:1 gear coupling. As a result, the column holder assembly rotates around its own axis at a rate twice that of the rotary frame, in the same direction. This particular design offers a great advantage in that the scheme allows flows in and out of the rotary column without the use of rotary seals. The assembling column provides an eccentric motion of each coil and allows the column to comprise more coils. But this mode does not show better retention of stationary phase than a single column with a larger coil diameter rotating around the axis itself. The later apparatus design for SRCCC introduced the design shown in Fig. 2. The apparatus horizontally holds a cylindrical column holder that can rotate around its axis, and the frame is similar to that shown in Fig. 1. Polytetrafluoroethylene (PTFE) tubing is directly wound around the holder hub, forming either a single-layer or a multilayer coil separation column. The coil column, made of tubes with larger inner diameters, permits a higher flow rate with satisfactory retention of the stationary phase, and the convoluted tube column gives higher retention of the stationary phase than standard wall tubes.[9]

To scale up the column for industrial separations, the chromatographic parameters using a convoluted PTFE tubing with an average I.D. (inner diameter) of 15 mm for developing a large chromatographic column were tested. The results showed that 1.5 cm I.D. convoluted PTFE tubing provides the following advantages: (i) it provides excellent retention of the stationary phase for many solvent systems, even at a high-flow rate of the mobile phase; (ii) it produces good mixing of the two phases, thus enabling efficient partitioning; (iii) increased sample size yields relatively low peak broadening; and (iv) increase in peak width and resolution using longer columns is predictable.[9] Therefore, a long holder with larger inner tubes can be used to make a column of up to 100 L in volume. In this case, a pair of rotary seals can be used as inlet and outlet (Fig. 3). Suitable rotary seals may be obtained commercially from Johnson-Fluiten, Milano, Italy.

SOLVENT SYSTEMS AND OPTIMUM ROTATIONAL SPEEDS

A suitable solvent system is the key to successful separation with countercurrent chromatography. But for some solvent systems, the retention of stationary phase would become insufficient, possibly caused by low interfacial

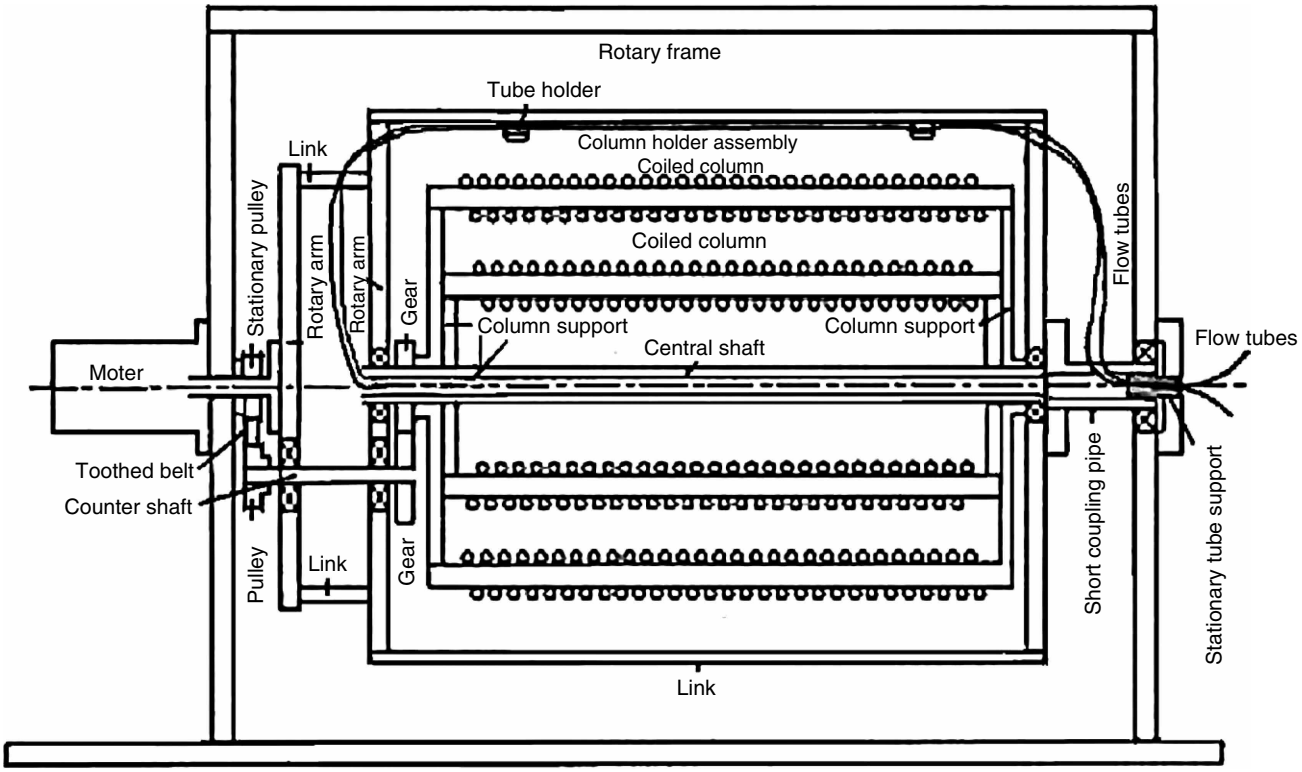

Fig. 1 Illustration of a seal-free flow-through rotary device.
Source: From Preparative counter-current chromatography with a rotating coil assembly, in J. Chromatogr.[4]

tension. Also, every solvent system possesses a critical rotational speed that gives optimum retention of the stationary phase. Therefore, more and more feasible solvent systems are expected to be reported for practical separations. Table 1 lists the optimum rotational speeds and retention rates of stationary phases of the reported solvent systems.

APPLICATION

One gram of DNP amino acids, composed of 500 mg DNP-glu and 500 mg DNP-ala, was separated with the solvent system composed of chloroform, acetic acid, and water (2:2:1). The apparatus was equipped with a 900 ml separation column consisting of ten units of glass coiled tube (0.5 cm I.D., 2.5 cm core diameter), connected in series with PTFE tubing. The separation yielded a peak resolution of about 1.7.[3]

Thirty grams of prepurified extract from the root of *P. lobata*, containing puerarin at a level of 60%, was separated using an apparatus equipped with a 10 L column with a two-phase solvent system composed of *n*-hexane, ethyl acetate, *n*-butanol, water, and acetic acid (1:1:2:6:0.2, v/v) at a flow rate of 5 ml/min at 21 rpm. The 10 L capacity column was prepared by winding 200 m, 8.5 mm I.D.

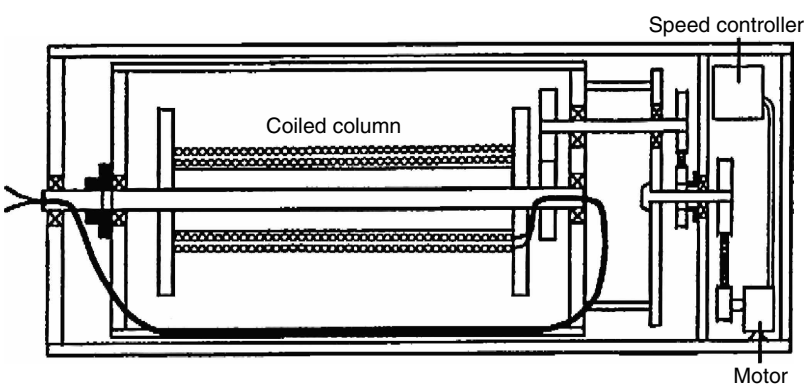

Fig. 2 Cross-sectional view of seal-free slow rotary countercurrent chromatography (SRCCC) instrument equipped with a large convoluted multilayer coil.

Source: From Low-speed rotary countercurrent chromatography using converted multilayer helical tube for industrial separation, in Anal. Chem.[7]

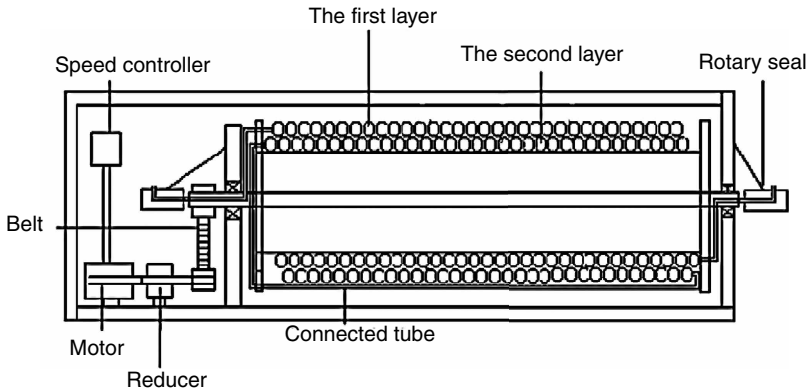

Fig. 3 Sketch of a slow rotary countercurrent chromatograph equipped with a pair of rotary seals.

convoluted tubing onto a 9 cm O.D. (outer diameter) column holder hub, making seven layers each consisting of 60 loops. The total elution time was 43 hr, and 38% of the stationary phase was retained when measured at the end of the run. Two major components, puerarin and 3′-methoxypuerarin, were resolved with a minimal overlapping zone. This separation yielded 16.7 g of puerarin at 91.2% purity, which corresponds to a recovery rate of 84.6%. Also, 150 g of dried extract of tea leaves containing epigallocatechin gallate (EGCG) at 30% was separated using the same apparatus with a two-phase solvent system composed of *n*-hexane, ethyl acetate, *n*-butanol, water, and acetic acid (0.5:1:2:6:0.2, v/v) at a flow rate of 5 ml/min at 21 rpm. The separation ran 72 hr, and retention of the stationary phase was 33%. In this separation, 40.05 g of EGCG was obtained at 92.8% purity, which corresponds to an 82.6% recovery rate.[7]

Nearly a kilogram (0.9 kg) of tea polyphenols containing 60% EGCG was separated using an apparatus equipped with a 40 L column. The 40 L column was made of 185 m of 17 mm average I.D. convoluted PTFE tubing wound onto a 2.4 m wide and 15 cm O.D. coil holder. The separation was performed at a 40 ml/min flow rate of the mobile phase to give a satisfactory result.[10] The apparatus was further used for isolation of salicin from the bark extract of *S. alba* and amygdalin from the fruit extract of *Semen armeniacae*. A 500 g amount of crude extract containing salicin at 13.5% was separated to yield 63.5 g of salicin at 95.3% purity in 20 hr using methyl *tert*-butyl ether–1-butanol (1:3) saturated by methanol–water (1:5) as a stationary phase and methanol–water (1:5) saturated by methyl *tert*-butyl ether–1-butanol (1:3) as a mobile phase. A 400 g amount of crude extract containing amygdalin at 55.3% was separated to yield 221.2 g of amygdalin at

Table 1 The optimum rotation speeds and retention rates of stationary phases of the reported solvent systems.

Solvent system	Optimum rotary speed (rpm)	Percent retention of stationary
n-BuOH–*n*-hexane–EtOAc–H_2O (2:2:1:6)	22	39.2
n-BuOH–*n*-hexane–EtOAc–H_2O–AcOH (2:1:0.5:6:0.2)	21	35.2
n-BuOH–*t*BME–CH_3CN–H_2O (2:2:1:5)	12	63.3
EtOAc–H_2O (1:1)	40	25.9
EtOAc–*n*-BuOH–H_2O (1:1:2)	20	51.4
EtOAc–AcOH–H_2O (3:1:3)	20	56.8
EtOAc–*n*-hexane–AcOH–H_2O (3:1:1:3)	20	60.0
n-Hexane–H_2O (1:1)	30	22.7
n-Hexane–MeOH (1:1)	30	50.0
n-Hexane–MeOH–H_2O (6:5:3)	60	75.5
n-Hexane–MeOH–EtOAc–H_2O (1:1:1:1)	40	60.0
$CHCl_3$–H_2O (1:1)	100	83.0
$CHCl_3$–MeOH–H_2O (4:3:2)	10	60.5
$CHCl_3$–MeOH–AcOH–H_2O (5:3:4:1)	100	85.0
$CHCl_3$–AcOH–H_2O (2:2:1)	100	79.5

Source: From Retention of stationary phase and partition efficiency of multilayer helical column rotated around its horizontal axis, in J. Liquid Chromatogr. Relat Technol.[2]

94.1% purity in 12 hr using ethyl acetate–1-butanol (1:2) saturated by water as a stationary phase and water saturated by ethyl acetate–1-butanol (1:2) as a mobile phase. The flow rate of the mobile phase was 50 ml/min.[11]

CONCLUSION

Slow rotary countercurrent chromatography possesses excellent separation efficiency, which is demonstrated by the above separations. The simplicity of the SRCCC system provides ease of scale-up, and its slow rotation column permits the system to be left unattended during the separation. Therefore, SRCCC is a promising CCC technology in the utilization of industrial separations.

REFERENCES

1. Ito, Y., Conway, W.D., Eds.; *High-Speed Countercurrent Chromatography*; Wiley-Interscience: New York, 1996; 3–43.
2. Wu, C.; Du, Q.; Ito, Y. Retention of stationary phase and partition efficiency of multilayer helical column rotated around its horizontal axis. J. Liquid Chromatogr. Relat Technol. **2000**, *23*, 2219–2224.
3. Ito, Y.; Bowman, R.L. Preparative countercurrent chromatography with a slowly rotating helical tube. J. Chromatogr. **1977**, *136* (2), 189–198.
4. Ito, Y.; Bhatnagar, R. Preparative counter-current chromatography with a rotating coil assembly. J. Chromatogr. **1981**, *207*, 171–180.
5. Ito, Y.; Bhatnagar, R. Improved scheme for preparative countercurrent chromatography (CCC) with a rotating coil assembly. J. Liquid Chromatogr. **1984**, *7*, 257–273.
6. Ito, Y. Studies on hydrodynamic distribution of two immiscible solvent phases in rotating coils. J. Liquid Chromatogr. **1988**, *11*, 1–19.
7. Du, Q.; Wu, P.; Ito, Y. Low-speed rotary countercurrent chromatography using converted multilayer helical tube for industrial separation. Anal. Chem. **2000**, *72*, 3363–3365.
8. Du, Q.; Ito, Y. Slow rotary countercurrent chromatography. J. Liq. Chromatogr. Related Technol. **2003**, *26*, 1827–1838.
9. Du, Q.; Winterhalter, P.; Ito, Y. Large inner diameter convoluted tubing for scale-up of slow rotary countercurrent chromatography. J. Liquid Chromatogr. Relat. Technol. **2003**, *26*, 1981–1991.
10. Du, Q.; Ito, Y. Review on scale-up of coil column countercurrent chromatographs. Curr. Pharm. Anal. **2005**, *1* (3), 309–318.
11. Du, Q.; Jerz, G.; He, Y.; et al. Semi-industrial isolation of salicin and amygdalin from plant extracts using slow rotary counter-current chromatography. J. Chromatogr. A, **2005**, *1074*, 43–46.

Solute Focusing Injection Method

Raymond P.W. Scott
Scientific Detectors Ltd., Banbury, Oxfordshire, U.K.

INTRODUCTION

In capillary-column gas chromatography (GC), split injections are necessary to ensure that a very small, compact sample is placed on the column. However, split injections generally result in an unrepresentative sample being placed on a capillary column; thus, on-column injection is usually preferred for accurate quantitative analysis.

DISCUSSION

On-column injection demands the use of large-diameter tubes to permit the penetration of the injection syringe needle into the column. However, this procedure also causes other problems to arise. On injection, the sample readily separates into droplets which act as separate, and individual, injections that cause widely dispensed peaks and serious loss of resolution. In the extreme, double or multiple peaks are formed. Grob[1] suggested two solutions to this problem: the retention gap method of injection and the solute focusing method.

The solute focusing method is claimed to be more effective than the retention gap method, but the technique requires more complicated equipment. In the solute focusing method, the injector is designed so that there are two consecutive, independently heated and cooled column zones, located at the beginning of the column. A diagram of the solute focusing system and its mode of action is shown in Fig. 1. Initially, both zones are cooled and the sample is injected onto the first zone, where immediate sample splitting almost inevitably occurs. The carrier gas is then allowed to preferentially remove the solvent by eluting it through the column, leaving the contents of the sample dispersed along the cooled section of the tube. The selective removal of the solvent occurs because the solvent components are significantly more volatile than the components of the sample, even at the reduced temperature. The first zone is then heated and the second zone is continued to be kept cool. The solutes in the first zone progressively elute through the zone at the higher temperature until they meet the cooled zone. The movement of all the components is now significantly slowed down and they begin to accumulate at the beginning of the cooled second zone. The net effect is that the entire sample is now focused at the beginning of the cooled portion of the column. The temperature of the second zone is now programmed to the appropriate rate and the separation developed in the usual manner. This technique has more flexibility than the retention gap method, but the apparatus and the procedure is more complex and expensive. It should be pointed out that sample splitting does not occur in packed columns. It follows that if the sample is amenable to separation on such columns, then the packed column may be the column of choice if high accuracy and precision are required.

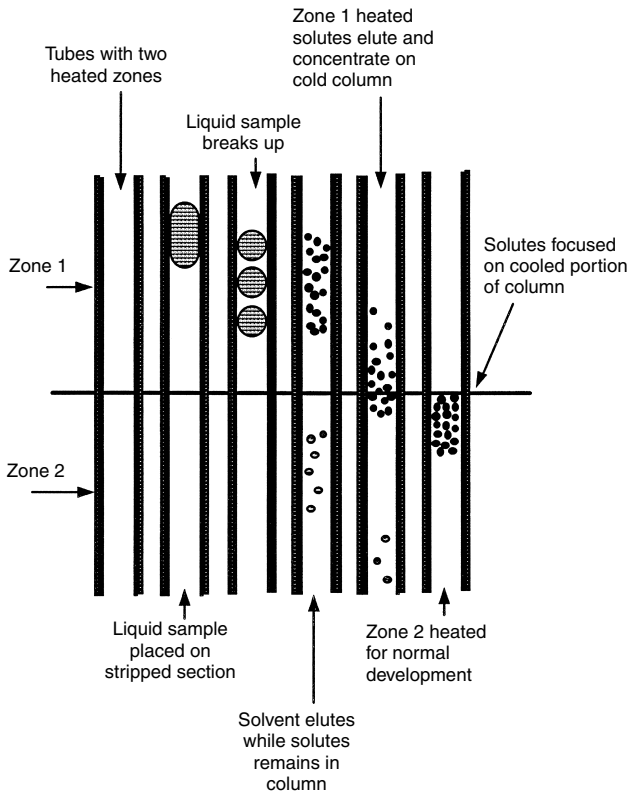

Fig. 1 The solute focusing method.

REFERENCE

1. Grob, K. *Classical Split and Splitless Injection in Capillary Gas Chromatography*; Huethig: Heidlburg, 1987.

BIBLIOGRAPHY

1. Grant, D.W. *Capillary Gas Chromatography*; John Wiley & Sons: Chichester, 1995.
2. Scott, R.P.W. *Techniques and Practice of Chromatography*; Marcel Dekker, Inc.: New York, 1996.
3. Scott, R.P.W. *Introduction to Analytical Gas Chromatography*; Marcel Dekker, Inc.: New York, 1998.

Solute Identification in TLC

Gabriela Cimpan
Sirius Analytical Instruments Ltd., East Sussex, U.K.

INTRODUCTION

Solute identification means qualitative analysis. Various methods are used today to identify a separated substance on a thin-layer chromatography (TLC) plate. Of all chromatographic methods, TLC provides a unique simultaneous separation of up to 70 samples on the same plate; therefore the reproducibility of the experimental conditions is not an issue because the experimental conditions are the same for all samples. This, together with the advantage of separating compounds with very different polarity and the possibility of using different detection methods for the same spot or for adjacent spots on the same plate, is the power of TLC.

UV–VIS DETECTION

Observing a substance in UV or visible light is the simplest way of detection and identification of the substance in TLC. If the substance is fluorescent, the identification is most reliable. However, many substances show similar behavior in UV light or have similar colors in visible light. Therefore a more accurate way of identification is required.

Often, the R_f value of the separated substances is compared with the R_f values of references. Not a long time ago, this information, together with the similar color, was usually enough to identify a substance. Today, modern densitometers are capable of measuring, more accurately, migration distances (therefore the R_f value) and to scan the in situ UV–Vis spectrum of the spot.

The majority of substances do not provide enough information based on their UV–Vis spectra; therefore a derivatization reaction should be applied to enhance the identification range. The derivatization is a chemical reaction designed to selectively improve the spectral characteristics of the separated substances and can be performed before or after the chromatographic separation. The prechromatographic derivatization can be performed during sample preparation or directly at the starting zone on the TLC plate. A preconcentration zone is recommended for the in situ prechromatographic derivatization reaction because all the formed substances will be concentrated at the starting point before the chromatographic separation. Postchromatographic derivatization can be non-destructive or destructive, and it is performed by covering the TLC plate with a homogenous layer of reagent, either by spraying or dipping. Sometimes, heating the plate is necessary for reaction completion.

If the substance is colored, the visible spectrum of the separated substance is recorded and compared with the reference spectrum. If the substance is not colored, but is active in UV light, there are two ways of identifying it, i.e., by fluorescence quenching, when the substance quenches the layer fluorescence, or by measuring the native fluorescence of the substance (before and/or after derivatization). UV–Vis fluorescence covers more than a third of the total methods of identification used in TLC, while the derivatization technique represents a similar percentage. All derivatization reactions are specific for chemical groups. The rest of about 20% consist of other methods of identification used in TLC: infra red (IR), mass spectrometry (MS), etc.

INFRARED DETECTION

The online technique for coupling high-performance thin--layer chromatography (HPTLC) with Fourier transform infrared spectroscopy (FTIR) has provided a powerful tool of using IR spectra and the rich information for the compound identification in TLC. The information contained in a UV–Vis spectrum is poor compared with IR, and only the chromophores can be identified by the former method. TLC was first coupled with FTIR in 1989, thereby providing a powerful tool for in situ measurement of separated compounds, with applications in the pharmaceutical, biological, environmental, and related sciences. Even the substances which do not absorb in UV have an IR spectrum; thus the method is universal. However, the strong IR absorption of the conventional stationary phases used in planar chromatography is a serious drawback of online coupling of HPTLC/FTIR.

The FTIR spectrometer is connected to the external unit by an interface mirror which diverts the beam to the spot on the plate. The reflected beam is then collected by using another set of mirrors and directed to a mercury cadmium telluride (MCT) narrow-band detector. This instrument can be used even with the strong absorbing layers used in TLC.

Various classes of drugs can be identified from complex mixtures by this method. UV–Vis spectra can help to recognize different structural groups; then, FTIR can further identify the compounds. All the spectra can be included in UV–Vis or IR spectral libraries and can be used as references for further assays.

The HPTLC/FTIR online coupling has been used for analyzing compounds from complex biological matrices where the number of compounds can be very high and the polarities very different; gradient development often has to be applied to obtain a separation.

Further development in obtaining and interpreting the data in this method will allow the identification and quantitation of separated unknown compounds.

RAMAN SPECTROSCOPY

Raman spectroscopy is the measurement of the wavelength and intensity of inelastically scattered light from molecules. The Raman scattered light occurs at wavelengths that are shifted from the incident light by the energies of molecular vibrations. The mechanism of Raman scattering is different from that of infrared absorption, and Raman and IR spectra provide complementary information. Typical applications are in structure determination, multicomponent qualitative analysis, and quantitative analysis. The most common light source in Raman spectroscopy is an Ar-ion laser. Because Raman scattering is a weak process, a key requirement to obtain Raman spectra is that the spectrometer should provide a high rejection of scattered laser light. New methods, such as very narrow rejection filters and Fourier-transform techniques, are becoming more widespread.

Special HPTLC plates allow direct Raman spectroscopy to be run after the separation without removal from the plate. They are made of a special 3–5 μm spherical silica gel on a 10 × 10 cm plate. The thickness is 0.1 mm to allow more of the compound to reside on the surface for this analysis.

Modern Raman spectrometers allow scanning of a surface up to A4 size, with XY translation stage and fine spatial adjustment to allow the operator to align the laser probe onto samples as small as 5 μm in diameter. Sample selection is assisted by the use of an integral video microscope with a rotating turret that can be fitted with up to four objective lenses to provide on-screen magnification of up to 500×.

Surface-enhanced resonance Raman scattering (SERRS) is a very sensitive technique with many applications, especially in forensic analysis. SERRS was successful in differentiating the majority of the 26 inks examined in an experiment designed to show that the method is less invasive than TLC and can be used coupled with an HPTLC plate.

MS DETECTION

The online coupling between TLC and MS provides a powerful combination for the detection and identification of substances separated by a planar chromatographic method. The online coupling between these two methods has to overcome the problem of vaporizing and introducing the sample into the mass spectrometer. Different methods are reported in the literature, but the analytical principle is the same: the sample is ionized from the layer surface by means of a laser beam, under vacuum, and in the presence of an energy-buffering matrix. Once the ions are transferred into the mass spectrometer, more sophisticated methods can be applied for data analysis and interpretation, e.g., MS/MS.

In planar chromatography, the sample is fixed on the layer and can be found in three-dimensional space. The interface between the layer and MS must separate the compound molecules from the layer molecules and must present a way to transport them into the MS, either via a liquid or a gaseous phase. The main difference between MS and the spectroscopic methods is that MS is a destructive method, consuming the sample, while the others are non-destructive.

The samples can be removed from the layer-by-laser desorption or matrix-assisted laser-desorption ionization (MALDI) which can be coupled with a time-of-flight (TOF), ion trap, or Fourier-transform mass spectrometer. MS/MS can also be an option for further analysis. The electron or chemical ionization methods are most commonly used to break the sample molecules into fragments (ions) in the gaseous phase. The obtained spectra can be used for sample identification by comparison with a spectral library. The laser desorption ionization assisted by a matrix (MALDI and SALDI techniques) uses the ionization of the sample at the surface of the thin layer, and the matrix plays a role of energy buffer. Electrospray ionization is another method of transferring the sample to the MS by spraying organic solvents containing the molecules of the sample.

The presence of the layer material, together with the sample, raises many problems in designing an appropriate interface for TLC/MS. More details can be found in the bibliographic references.

The instrumentation for TLC/MS is not as widespread as for other chromatographic methods (e.g., GC/MS and LC/MS) mainly because of the complexity of the interface involved.

IMAGE ANALYSIS

Image analysis has brought new possibilities to compound detection, identification, and quantitation in TLC; it takes advantage of the main benefit of planar chromatography, i.e., the possibility of separating and analyzing up to 70 samples on a single plate. The image can be obtained by charge-coupled device (CCD) cameras, digital camcorders, or flatbed scanners and can be further processed with a computer. The power of image-analysis systems relies on good resolution and contrast and the capacity to minimize the distortion and the perspective errors from a lens. The

settings of the factors for obtaining a good image can be different from sample to sample. Although the colored image is more similar to the real chromatographic plate, the black and white image, with shades of gray, can be interpreted better by the human eye, as it is more sensitive to small changes in black and white than are colors.

Charge-coupled devices have been used as detectors in planar chromatography, although more applications have been found in quantitative analysis. Videodensitometers have been used to measure the absorption or the fluorescence of a separated spot on a TLC plate.

The miniaturization of the TLC technique will be a challenge for image analysis, but, probably, this will be the technique for creating image libraries for compounds or for complex mixtures such as plant extracts.

PHOTOACOUSTIC DETECTION

Non-uniformity of the layer or of the sample distribution in the layer and light scattering are some of the difficulties that an online spectroscopic detection method has to overcome.

Photoacoustic detection measures the pressure variation caused by the heating of a gas in the vicinity of the sample. If the sample is enclosed in a photoacoustic cell equipped with a microphone, the modulated signal can be interpreted as a function of temperature, pressure, and the quantity of the sample.

Since photoacoustic spectroscopy (PAS) was first reported in 1975, the method was gradually improved, and now, nanograms to picograms of substances can be successfully detected and quantified on TLC plates. When the method was first developed, the separated spot had to be scratched from the plate and introduced into the PAS cell for the measurements; but now, the PAS cell can be fixed directly onto the layer surface. Other instruments can be laser-based densitometers with signal enhancement at a resonant frequency of the cell. The detection limit is very low in this case, and the linearity of the quantitative determination is over 3 orders of magnitude. Moreover, FTIR can be used in combination with the PAS technique for in situ measurements. The presence of helium might be necessary to prevent high background noise, which is mainly produced by the silica-based layer.

FLAME IONIZATION DETECTION

TLC coupled with online flame ionization detection (TLC/FID) has been developed for the analysis of organic substances which show no UV absorption and no fluorescence and which present difficulties by GC analysis.

Planar chromatography is usually performed on a quartz rod (Chromarod®) coated with a thin layer of silica or alumina onto which the sample is developed and separated. The rod is advanced at a constant speed through the flame of the FID, and the substances are ionized through energy obtained from the hydrogen flame. Influenced by the electric field applied to the poles of the FID, the ions generate electric current with an intensity proportional to the amount of each organic substance entering the flame. Spotting of the sample is performed with a specially designed application system; the rods are further developed in special development tanks, then the rods are scanned through the hydrogen flame.

Applications have been reported in many areas including analysis of lipids, oils, fatty acids, polymers, asphalt, and surfactants. The advantages of this method are high throughput, low cost per sample, easy quantitation using standard chromatography software, and simple method development analogous to standard TLC.

The quantitation of samples using Chromarods is not very linear, as the rods are not uniform, but nevertheless, the method remains a very useful tool for difficult samples.

DIGITAL AUTORADIOGRAPHY

Digital autoradiography (DAR) can be used in combination with TLC for the analysis of radiolabeled compounds, most frequently ^{3}H and ^{14}C. The method is simple and requires reasonably priced instrumentation; therefore it is widely used for biochemical and pharmacological applications. The instrumentation for TLC–DAR can scan a 20×20 cm area, the radioactivity bands are visualized with a digital radiograph, and the digital data are processed with a high-capacity computer.

The analysis of samples in biological matrices is extremely powerful compared with drawbacks such as narrow concentration range for quantitative measurements and long time required for spot detection. Digital autoradiography can be used in hyphenated off-line and online methods. A powerful example is TLC/DAR/FABMS/MS with applications in in vitro and in vivo metabolism studies.

BIOAUTOGRAPHY

Bioautography is a method developed for the study and analysis of biologically active substances from simple samples to complex biological matrices. Antimicrobial activity is the monitored parameter, and it can be either growth-inhibiting or growth-promoting.

The screening of biological activity can be performed by diffusion method, dilution method, and bioautography.

The diffusion method uses an agar layer impregnated with the organism being tested; a filter paper disk containing the sample is placed on top. After an appropriate incubation time, the paper disk is removed and the average diameter of each zone of growth inhibition is measured.

In the dilution method, the sample is mixed with a suitable medium which has been previously impregnated with the organism being tested. After the incubation time, the growth of microorganisms can be determined by comparing the test culture with a control culture.

Bioautographic methods involve a chromatographic layer containing the biologically active compound which migrates, by diffusion, to an inoculated agar plate. The inhibition zones can be easily visualized by specific reagents. In direct bioautography, the microorganisms grow directly on the TLC plate and further analysis steps are performed on the plate. Silica gel and cellulose plates produce good results, while polyamide and aluminum oxide are not recommended for this type of assay. Bioautography is an additional method for the screening of biologically active compounds and provides good selective postchromatographic detection.

BIBLIOGRAPHY

1. Barman, B.N. Hydrocarbon-type analysis of base oils and other heavy distillates by thin-layer chromatography with flame-ionization detection and by the clay–gel method. J. Chromatogr. Sci. **1996**, *34* (5), 219–225.
2. Bhullar, A.G.; Karlsen, D.A.; Backer-Owe, J.; Le Tran, K.; Skalnes, E.; Berchelmann, H.H.; Kittelsen, J.E. Reservoir characterization by a combined micro-extraction—Micro thin-layer chromatography(iatroscan) method: A calibration study with examples from the Norwegian North Sea. J. Pet. Geol. **2000**, *23* (2), 221–244.
3. Filthuth, H. J. Planar Chromatogr.-Mod. TLC **1989**, *2*, 198–202.
4. Filthuth, H. *Planar Chromatography in the Life Sciences*; Touchstone, J.C., Ed.; John Wiley & Sons: New York, 1990; 167–183.
5. Imaging techniques in Planar Chromatography. Proceedings of the 1st International Meeting, Vovk, I., Prošek, M., Medja, A., Ed.; Jezersko, Slovenia, 1999.
6. Kawazumi, H.; Yeung, E.S. Resonant cell laser-based photoacoustic densitometer for thin-layer chromatography. Appl. Spectrosc. **1988**, *42* (7), 1228–1231.
7. Kovar, K.A.; Enßlin, H.K.; Frey, O.R.; Rienas, S.; Wolff, S.C. J. Planar Chromatogr.-Mod. TLC **1991**, *4*, 246–250.
8. Nyiredy, Sz., Ed.; *Planar Chromatography, A Retrospective View for the Third Millennium*; Springer Scientific Publisher: Budapest, 2001.
9. Pfeifer, A.; Tolimann, G.; Ammon, H.P.T.; Kovar, K.A. J. Planar Chromatogr.-Mod. TLC **1996**, *9*, 31–34.
10. Rosencwaig, A.; Hall, S.S. Thin-layer chromatography and photoacoustic spectrometry. Anal. Chem. **1975**, *47*, 548–549.
11. Sweedler, J.V., Ratzlaff, K.L., Denton, M.B., Eds.; *Charge-Transfer Devices in Spectroscopy*; VCH: New York, 1994.
12. Viger, A.J.; Robert, J.K.; Selitrennikof, C.P. Mol. Plant-Microb. Interact. **1991**, *4*, 315–323.
13. Wilson, I.D. The state of the art in thin-layer chromatography-mass spectrometry: A critical appraisal. J. Chromatogr. A, **1999**, *856*, 429–442.
14. Wilson, I.D.; Morden, W. LC/GC Int. **1999**, *12*, 72–80.

Solvent Systems: Systematic Selection for HSCCC

Hisao Oka
Food-Related Chemistry, Laboratory of Chemistry, Aichi Prefectural Institute of Public Health, Nagoya, Japan

Yoichiro Ito
National Heart, Lung, and Blood Institute (NHLBI), National Institutes of Health (NIH), Bethesda, Maryland, U.S.A.

INTRODUCTION

High-speed countercurrent chromatography (HSCCC) produces highly efficient chromatographic separations of solutes without the use of solid supports.[1–3] Thus the method eliminates all complications caused by the solid support, such as adsorptive loss and deactivation of samples, tailing of solute peaks, contamination, etc. As with other CCC schemes, HSCCC utilizes two immiscible solvent phases, one as a stationary phase and the other as a mobile phase, and the separation is highly dependent on the partition coefficient values of the solutes, i.e., the ratio of the solute concentration between the mobile and stationary phases. Therefore the successful separation necessitates a careful search for the suitable two-phase solvent system that provides an ideal range of the partition coefficient values for the applied sample.

In the past, the search for suitable two-phase solvent systems entirely relied on a laborious and time-consuming trial-and-error method that has often discouraged the users of HSCCC, while the method for systematic solvent search has not been reported. In this entry, we introduce a method for the systematic selection of suitable two-phase solvent systems for HSCCC and its application to the separation of antibiotics and dyes.

HOW TO SELECT SUITABLE SOLVENT SYSTEM

In addition to the basic requirements of stability and solubility of the sample, the two-phase solvent system should satisfy the following.

1. For ensuring the satisfactory retention of the stationary phase, the settling time of the solvent system should be considerably shorter than 30 sec.

   Using the equilibrated two-phase solvent system, the settling time is measured as follows: A 2 ml volume of each phase (the total volume is 4 ml) is delivered into a 5 ml-capacity graduated glass cylinder, which is then sealed with a glass stopper. The solvent in the cylinder is gently mixed by inverting the cylinder five times and the cylinder is immediately placed on a flat table in an upright position. Then, the time required for the solvent mixture to settle into two clear layers is measured. The experiment is repeated several times to obtain the mean value.
2. For efficient separation, the partition coefficient (K) of the target compound(s) should be close to 1, and the separation factor (α) between the components should be greater than 1.5. If $K < 1$, the solutes are eluted close together near the solvent front, resulting in a loss of peak resolution, and, if $K > 1$, the solutes are eluted in excessively broad peaks and require a long elution time. The minimum α value of 1.5 is required for the baseline separation in a semipreparative CCC equipment providing a moderate partition efficiency of around 800 theoretical plates.

   The K value is determined simply by measuring the ultraviolet (UV) absorbance of the solute in each of the two phases after partitioning in the equilibrated two-phase solvent system and dividing the solute concentration in the upper phase by that in the lower phase. However, when the sample is a mixture of various components, the precise K values of each component cannot be determined by this method. In such a case, a mixture is partitioned with a two-phase solvent system as described above and the resulting upper and lower phases are analyzed by HPLC. Each K value is determined by dividing the corresponding peak area of the upper phase by that of the lower phase.
3. In addition to the above two major requirements, it is desirable that the solvent system provides nearly equal volumes of each phase to avoid excessive waste of the solvent.
4. It is also convenient to use a volatile solvent system: The pure compound is obtained simply by evaporating the collected fractions.

By keeping the above in mind, the following three series of solvent systems can provide an ideal range of the K values for a variety of samples: *n*-hexane/ethyl acetate/*n*-butanol/methanol/water,

Table 1 *n*-Hexane/ethyl acetate/*n*-butanol/methanol/water system.

n-Hexane	Ethyl acetate	*n*-Butanol	Methanol	Water
10	0	0	5	5 (hydrophobic)
9	1	0	5	5
8	2	0	5	5
7	3	0	5	5
6	4	0	5	5
5	5	0	5	5
4	5	0	4	5
3	5	0	3	5
2	5	0	2	5
1	5	0	1	5
0	5	0	0	5
0	4	1	0	5
0	3	2	0	5
0	2	3	0	5
0	1	4	0	5
0	0	5	0	5 (hydrophilic)

chloroform/methanol/water, and *tert*-butyl methyl ether/butanol/acetonitorile/water.

In each solvent series,[4] the partition coefficient of the sample can be finely adjusted by modifying the volume ratio of the components. The first series covers a broad range in both hydrophobicity and polarity continuously from *n*-hexane/methanol/water to *n*-butanol/water. The second series of chloroform/methanol/water provides moderate hydrophobicity and the third series of *tert*-butyl methyl ether/*n*-butanol/acetonitorile/water is suitable for hydrophilic compounds. Most of these two-phase solvent systems provide near 1 : 1 volume ratios of the upper/lower phases, together with the reasonable range of settling times in 30 sec or less, so that they can be efficiently applied to HSCCC and other centrifugal CCC schemes.

For the sample mixture with an unknown composition, the search for the suitable two-phase solvent system may be initiated with the partition coefficient measurement with *n*-hexane/ethyl acetate/*n*-butanol/methanol/water (5 : 5 : 0 : 5 : 5) (Table 1), chloroform/methanol/water (10 : 3 : 7) (Table 2) or *tert*-butyl methyl ether/butanol/acetonitorile/water (6 : 0 : 3 : 8) (Table 3). If the $K_{(org/aq)}$ value is too large, the search should be directed toward the more hydrophobic solvent systems and, if the K value is too small, the search should be directed toward the more hydrophilic solvent systems until the proper K values are obtained.

Table 2 Chloroform/methanol/water system.

Chloroform	Methanol	Water
10	0	10 (hydrophobic)
10	1	9
10	2	8
10	3	7
10	4	6
10	5	5
10	6	4
10	7	3 (hydrophilic)

Table 3 *tert*-Butyl methyl ether/*n*-butanol/acetonitrile/water system.

tert-Butyl methyl ether	*n*-Butanol	Acetonitrile	Water
1	0	0	1 (hydrophobic)
4	0	1	5
6	0	3	8
2	0	2	3
4	2	3	8
2	2	1	5 (hydrophilic)

If the above solvent search reaches the solvent system of *n*-hexane/methanol/water (2 : 1 : 1), which is suitable for the most hydrophobic compounds, and a more hydrophobic solvent system is required, one may reduce the amount of water from the above solvent system and/or replace methanol with ethanol. Some useful solvent systems for the extremely hydrophobic compounds are *n*-hexane/ethanol/water (6 : 5 : 2) and *n*-hexane/methanol (2 : 1). On the other hand, if the solvent search reaches the solvent systems of *n*-butanol/water or *tert*-butyl methyl ether/butanol/acetonitorile/water (2 : 2 : 1 : 5), which are suitable for the most hydrophilic compounds, and a still more hydrophilic solvent system is required, the above solvent system may be modified by the addition of acid or salt; trifluoroacetic acid (TFA) or ammonium acetate has been successfully used.

APPLICATION TO THE SEPARATION OF ANTIBIOTICS AND DYES

Separation of Bacitracin Components

Bacitracins (BCs) are peptide antibiotics produced by *Bacillus subtilis* and *Bacillus licheniformis*.[5] They exhibit an inhibitory activity against Gram-positive bacteria and are most commonly used as animal feed additives for domestic animals, such as calf and swine, for preventing bacterial infection and/or improving feed conversion efficiency. Over

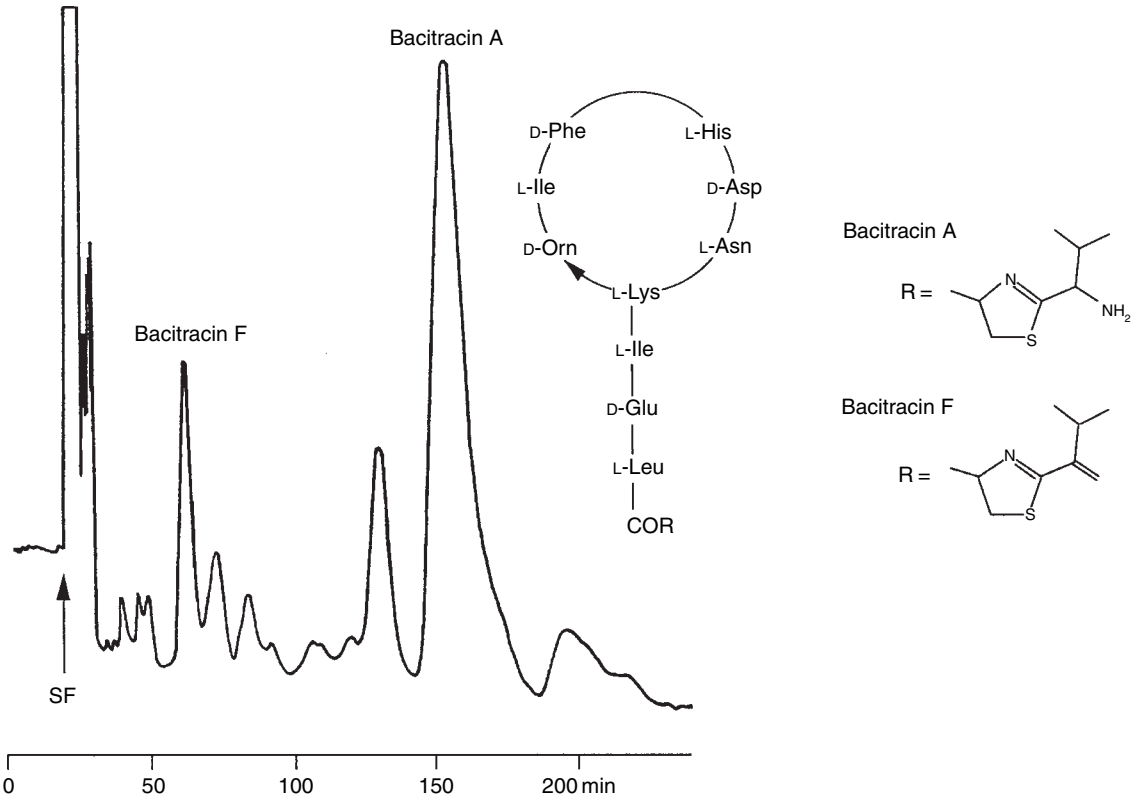

Fig. 1 HSCCC separation of bacitracin components. Solvent system: chloroform/ethanol/methanol/water (5 : 3 : 3 : 4); mobile phase: lower phase; flow rate: 3 ml/min; detection: 254 nm.

20 components are contained in the bacitracin complex, among which BC-A is the major antimicrobial component and BC-F is a degradation product having nephrotoxicity.

We tested three groups of two-phase solvent systems containing *n*-butanol, ethyl acetate, or chloroform as a major organic solvent, and ethanol and/or methanol as a modifier against water in each group. The most promising *K* values were obtained from the chloroform, ethanol, and/or methanol, water system. Among all combinations for the solvent volume ratio, chloroform/ethanol/methanol/water (5 : 3 : 3 : 4) yielded the most desirable *K* values, and the α values between the adjacent components are all greater than 1.5.

Fig. 1 shows a countercurrent chromatogram of bacitracin components using the chloroform/ethanol/methanol/water (5 : 3 : 3 : 4) system. A 50 mg amount of the bacitracin complex was loaded into the HSCCC column. The retention of the stationary phase was 72.7% and the elution time was about 3 hr. All components were eluted in an increasing order of their partition coefficients, yielding 5.5 mg of pure BC-A and 1.5 mg of pure BC-F.

Separation of Colistin Components

Colistin (CL) is a peptide antibiotic produced by *Bacillus polimyxa* var. *Colistinus*; it inhibits the growth of Gram-negative organisms. Colistin is a mixture of many components, among which the two main components are colistin A (CL-A) and colistin B (CL-B).[6] As in the case of bacitracin, CL is used as a feed additive.

CL is soluble in water, slightly soluble in alcohols, but insoluble in non-polar solvents such as hexane and chloroform. Based on these properties, we selected *n*-butanol and water as a basic solvent system. However, this combination was not suitable by itself, because the CL components were entirely partitioned into the lower aqueous phase. In order to partition the CL components partly into the *n*-butanol phase, various salts (sodium chloride and sodium sulfate) or acids (hydrochloric acid, sulfuric acid and TFA) were added as a modifier. A desirable effect was obtained by the addition of TFA, where the partition coefficients of CL components rose as the concentration of TFA in the solvent system was increased. As TFA forms an ion pair with amino groups in the molecule of CL, the hydrophobicity of CL components increases with the concentration of TFA, resulting in the partition of components toward the organic phase. In order to determine the optimal concentration of TFA in the solvent system, *K* values were measured at various TFA concentrations. The *K* value of each component increases with the TFA concentration and, at 40 m*M* TFA concentration, the *K* values of CL-A and CL-B reach 1.5 and 0.6, respectively. At this TFA concentration, the α values between the adjacent peaks are all greater than 1.5,

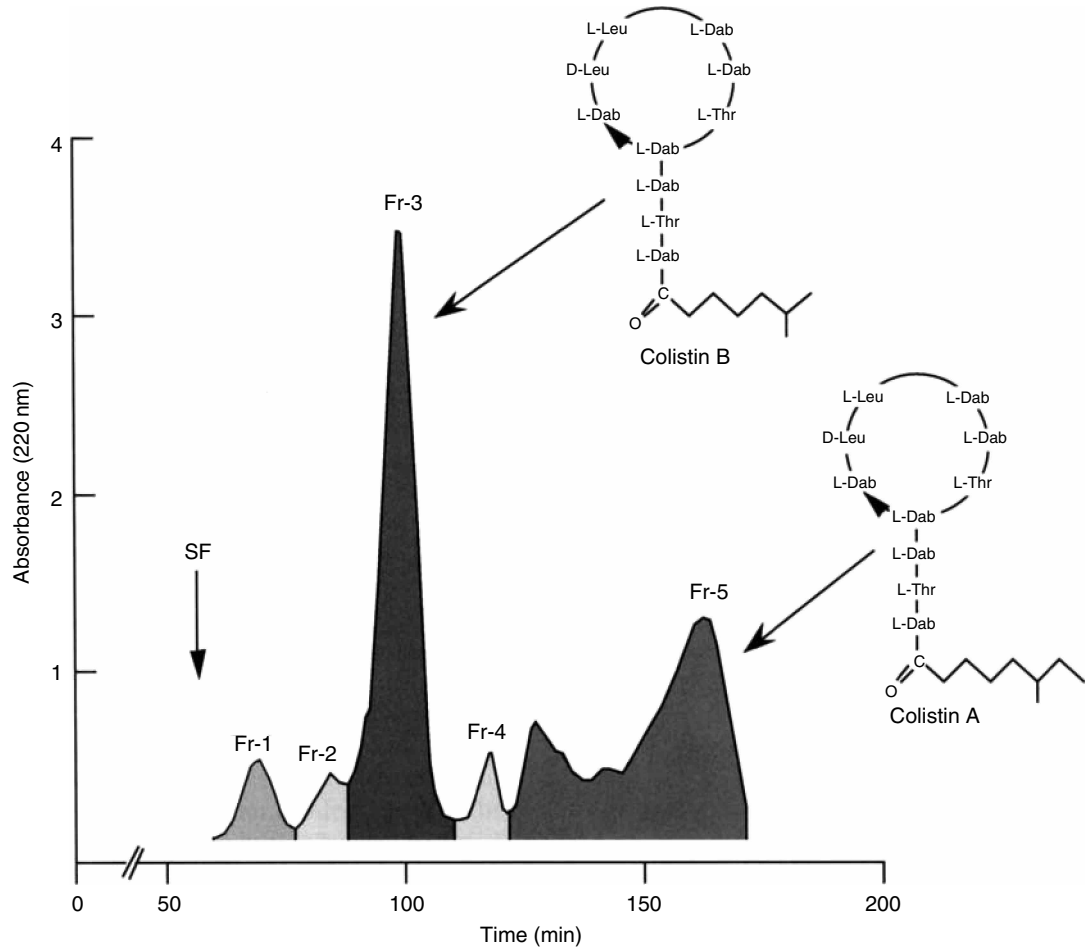

Fig. 2 HSCCC separation of colistin components. Solvent system: *n*-butanol/0.04 *M* trifluoroacetic acid (1 : 1); mobile phase: lower phase; flow rate: 2 ml/min; detection: 220 nm.

promising a good separation for all components. The settling time of the solvent system was 28 sec, which is within an acceptable range. Therefore we selected a solvent system of *n*-butanol/40 m*M* TFA aqueous solution (1 : 1) for the HSCCC separation of CL components.

Using the above solvent system, a 20 mg portion of commercial CL was separated by HSCCC. The retention of the stationary phase was 45%. The elution curve, monitored at 220 nm, is shown in Fig. 2. The yields of CL-A and CL-B were 9 mg each, and those of the other minor components were 0.5–1.0 mg. From HPLC analysis, the fractions of CL-A and CL-B each produced almost a single peak with a high purity of over 90%.

Separation of Ivermectin Components

Ivermectins B1 are broad-spectrum antiparasitic agents widely used for food-producing animals such as cattle, swine, and horse.[7] They are derived from avermectins B1, the natural fermentation products of *Streptomyces avermitilis*.

We have selected a two-phase solvent system composed of *n*-hexane, ethyl acetate, methanol, and water. As described above, this solvent system is conveniently used for the separation of components with a broad range of hydrophobicity by modifying the volume ratio between the four solvents. In the *n*-hexane/ethyl acetate/methanol/water (8 : 2 : 5 : 5) system first examined, the *K* values of the components were 0, 0.46, 0.61 (avermectin B1a); ∞, 1.86 (ivermectin B1b); 3.06 (ivermectin B1a); and 4.38, respectively. This indicates that the component corresponding to ivermectin B1a is mostly partitioned in the upper organic phase. Although the *n*-hexane/ethyl acetate/methanol/water (9 : 1 : 5 : 5) system somewhat improved the *K* value of ivermectin B1b to 2.31, it was still too large. Finally, a slightly less polar solvent mixture at the volume ratio of 19 : 1 : 10 : 10 yielded the best *K* values: 0, 0, 0.18 (avermectin B1a); 0.48, 0.79 (ivermectin B1b); 1.36 (ivermectin B1a); and 2.83, with desirable α values of over 1.5 for all components. The settling time of this solvent system was 7 sec, promising excellent retention of the stationary phase. In addition, the volume ratio between the two phases is nearly 1, indicating that either phase can be used as the mobile phase without wasting the solvents. Therefore the above solvent system was selected for the separation of ivermectin components.

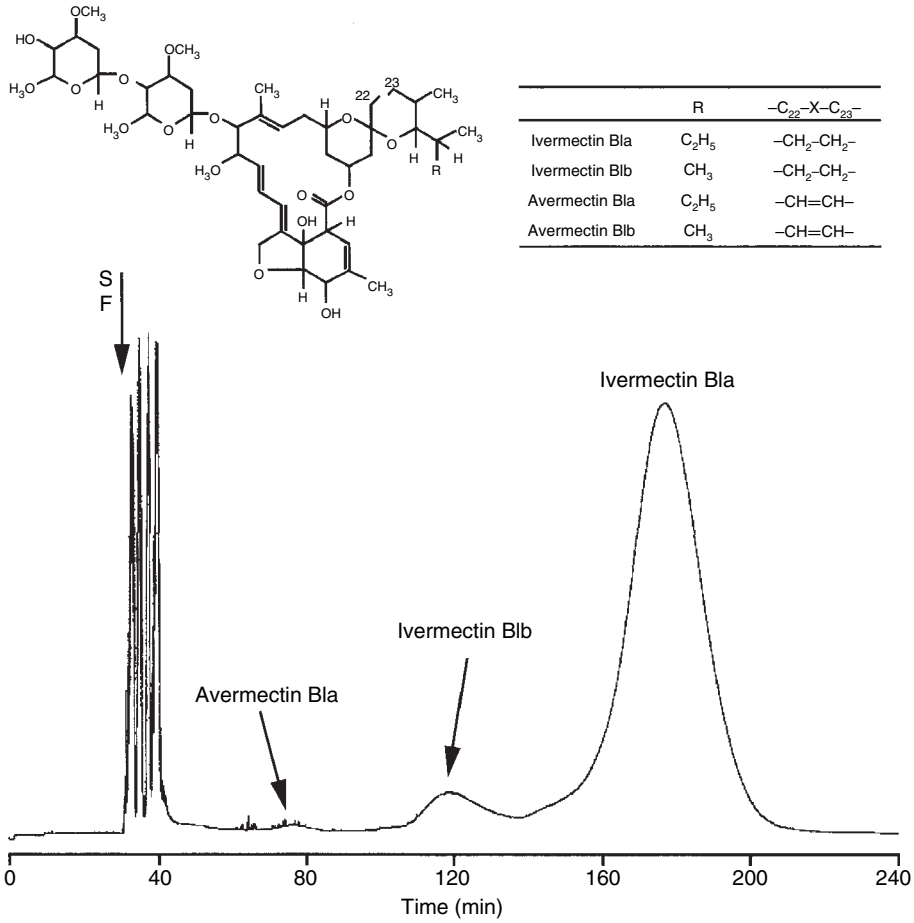

	R	–C_{22}–X–C_{23}–
Ivermectin Bla	C_2H_5	–CH_2–CH_2–
Ivermectin Blb	CH_3	–CH_2–CH_2–
Avermectin Bla	C_2H_5	–CH=CH–
Avermectin Blb	CH_3	–CH=CH–

Fig. 3 HSCCC separation of ivermectin components. Solvent system: *n*-hexane/ethyl acetate/methanol/water (19 : 1 : 10 : 10); mobile phase: lower phase; flow rate: 2 ml/min; detection: 245 nm.

A 25 mg quantity of crude ivermectin was separated using the above solvent system at a flow rate of 2 ml/min. The retention of the stationary phase was 67.6% and the total separation time was 4.0 hr. The HSCCC elution curve of the ivermectin components, monitored at 245 nm, is shown in Fig. 3, where all components are separated into three peaks. This separation yielded 18.7 mg of 99.0% pure ivermectin B1a (Fig. 3), 1.0 mg of 96.0% pure ivermectin B1b (Fig. 3), and 0.3 mg of 98.0% pure avermectin B1a.

Separation of Lac Dye Components

Lac dye is a natural food additive extracted from a stick lac, which is a secretion of the insect Coccus laccae (*Laccifer lacca* Kerr), and is widely used for coloring food.[8] It is known that its red color is derived from water-soluble pigments including laccaic acids A, B, C, and E.

Laccaic acids have two or three carboxyl groups, five or six hydroxyl groups, and/or one amino group, and are freely soluble in water, but only slightly soluble in organic solvents such as chloroform and ethyl acetate. Based on these physicochemical properties of laccaic acids, we selected a two-phase solvent system composed of *tert*-butyl methyl ether/*n*-butanol/acetonitrile/water, which has been frequently used as the solvent system for the separation of hydrophilic compounds as described earlier. In the *tert*-butyl methyl ether/*n*-butanol/acetonitrile/water (4 : 2 : 3 : 8) system first examined, the *K* values of the components were 0.08, 0.10 (laccaic acid C), 0.19, 2.00, 0.84 (laccaic acid B), and 0.60 (laccaic acid A), respectively. This indicates that the first component (*K* value: 0.08) and laccaic acid C (*K* value: 0.10) would be eluted together near the solvent front because of their small *K* values. A more polar solvent composition of *tert*-butyl methyl ether/*n*-butanol/acetonitrile/water (2 : 2 : 1 : 5) yielded the best *K* values, with desirable α values of over 1.5 for all components. The settling time of this solvent system is less than 30 sec, which ensures a satisfactory retention of the stationary phase in HSCCC as described before. Therefore we selected this solvent system for the separation of the lac dye components.

A 25 mg quantity of lac dye was separated using the above solvent system at a flow rate of 1 ml/min. The retention of the stationary phase was 83.6%. The total separation time was 8.3 hr. The absorbance of effluents in every tube was measured at 495 nm to draw the elution curve (Fig. 4). In the HPLC analysis of the original sample, laccaic acids A, B, and C constituted about 37.1%, 18.0%, and 35.5% of the total peak area at 280 nm, respectively. After only one-step operation by HSCCC, the purities of the above three components were increased to 98.1% (laccaic acid A), 98.2% (laccaic acid

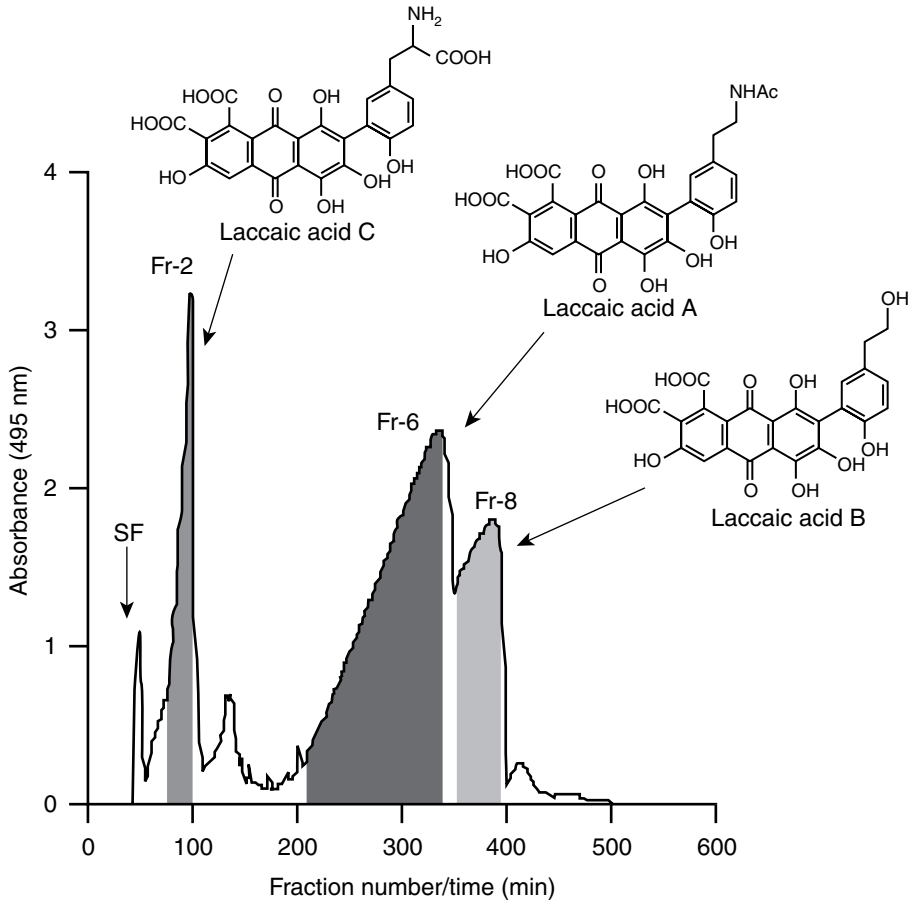

Fig. 4 HSCCC separation of lac dye components. Solvent system: *tert*-butyl methyl ether/*n*-butanol/acetonitrile/water (2 : 2 : 1 : 5); mobile phase: lower phase; flow rate: 1 ml/min; detection: 495 nm.

B), and 97.2% (laccaic acid C), respectively. These results demonstrate the high resolving power of HSCCC achieved by the careful selection of the proper solvent system.

CONCLUSIONS

Because of a support-free partition system, HSCCC provides an important advantage over other chromatographic methods by eliminating various complications, such as adsorptive loss and deactivation of samples, as well as contamination from the solid support. As shown by our examples, HSCCC can isolate various components from a complex mixture of natural products by carefully selecting the two-phase solvent system to optimize the partition coefficient (K) of the target component(s). The HSCCC system can also be applied to microanalytical-scale separations without excessive dilution of samples. We believe that HSCCC is an ideal method for the separation and purification of natural products.

REFERENCES

1. Mandava, N.B.; Ito, Y. *Countercurrent Chromatography—Theory and Practice*; Chromatographic Science Series Marcel Dekker Inc.: New York, 1988; Vol. 44.
2. Conway, W.D. *Countercurrent Chromatography—Apparatus, Theory, and Applications*; VCH: New York, 1990.
3. Ito, Y.; Conway, W.D. *High Speed Countercurrent Chromatography*; John Wiley & Interscience: New York, 1996.
4. Oka, F.; Oka, H.; Ito, Y. Systematic search for suitable two-phase solvent systems for high-speed counter-current chromatography. J. Chromatogr. **1991**, *538*, 99–108.
5. Harada, K.-I.; Ikai, Y.; Yamazaki, Y.; Oka, H.; Suzuki, M.; Nakazawa, H.; Ito, Y. Isolation of bacitracins A and F by high-speed counter-current chromatography. J. Chromatogr. **1991**, *538*, 203–212.
6. Ikai, Y.; Oka, H.; Harada, K.-I.; Suzuki, M.; Hayakawa, J.; Kawamura, N.; Nakazawa, H.; Ito, Y. Isolation of colistin A and B using high-speed countercurrent chromatography. J. Liq. Chromatogr. **1998**, *21*, 143–155.
7. Oka, H.; Ikai, Y.; Hayakawa, J.; Shimizu, A.; Hayashi, T.; Harada, K.-I.; Suzuki, M.; Takeba, K.; Nakazawa, H.; Ito, Y. Separation of invermectin components by high-speed counter-current chromatography. J. Chromatogr. A, **1996**, *723*, 61–68.
8. Oka, H.; Ito, Y.; Yamada, S.; Kagami, T.; Hayakawa, J.; Harada, K.-I.; Atsumi, E.; Suzuki, M.; Odani, H.; Akahori, S.; Maeda, K.; Nakazawa, H.; Ito, Y. Separation of lac dye components by high-speed countercurrent chromatography. J. Chromatogr. A, **1998**, *813*, 71–77.

Sorbents in TLC

Luciano Lepri
Alessandra Cincinelli
Department of Chemistry, University of Florence (UNIFI), Florence, Italy

Abstract
A review of all sorbents used as stationary phases in thin-layer chromatography (TLC) is reported. The specific application field of all sorbents is described according to their relative chemical–physical properties. New materials have been developed for the high-performance thin-layer chromatography (HPTLC) technique to offer both high-efficiency separations and high-sensibility analysis. In particular, silanized silica gel has been extensively used as stationary phase in reversed-phase (RP) chromatography for its hydrophobic properties.

INTRODUCTION

Since the introduction of commercial precoated plates in the mid-1960s, continual developments with regard to the increase of selectivity and the improvement of separation efficiency have been pursued [e.g., ready-to-use layers suitable for high-performance thin-layer chromatography (HPTLC) and overpressured layer chromatography (OPLC), polar and hydrophobic bonded phases, impregnated layers, and plates with concentrating zones]. A wide variety of thin-layer chromatography (TLC) and HPTLC precoated plates, which give reproducible results, are commercially available today, even if it is possible to prepare these plates in the laboratory. Homemade plates can allow access to stationary phases that are not otherwise available.

The average particle size and the range of particle sizes are smaller on HPTLC layers than on TLC layers (i.e., 2–10 and 5–17 μm, respectively, for Macherey-Nagel HPTLC and TLC silica plates), and a marked fall in theoretical plate heights is observed (about one order of magnitude smaller than on standard silica layers). Consequently, smaller plate sizes (from 20 × 20 to 10 × 10 cm) and sample volumes (from 1–3 to 0.1–0.2 μl) and shorter migration distances (from 10–16 to 3–8 cm) can be used. A rational classification system of commonly used sorbents in TLC is shown in Table 1.

HYDROPHILIC UNMODIFIED SORBENTS

Silica, Silica Gel, or Silicic Acid

These products are by far the most frequently used sorbents in TLC and are prepared by the dehydration of aqueous silicic acid generated by the addition of a strong acid to a silicate solution. Chemically, each silicon atom is surrounded by four oxygen atoms in the form of a tetrahedron. The surface of silica contains: 1) siloxane groups (Si–O–Si); 2) silanol groups (Si–OH); 3) water hydrogen bonded to the silanol groups; and 4) also non-sorbed "capillary" or bulk water. The silanol groups (about 8 μmol/m^2) represent adsorption-active surface centers that are able to interact with solvent and solute molecules during the separation process. The silanol active centers can differ slightly depending on whether they occur as isolated, vicinal, or geminal silanols.

Surface energy and surface extension together characterize the activity of silica ("activity" is the surface property of the adsorbent), and the size of the surface is reduced when covered with molecules such as water and glycol, which deactivate the surface of the sorbent. An increase in the surface activity results in lower R_f values, which, therefore, depend on silica porosity and humidity changes. The water content of the layer can be checked by measuring the absorption values of Reichardt's dye at 500 nm; the color of the dye changes from violet to pink with increasing silica gel humidity.[1] The surface pore diameter can vary over a wide range; TLC sorbents have pores of 40, 60, 80, and 100 Å. Pores of about 40 Å are termed "small," those major of 100 Å "large," and those of 60–80 Å "medium." Most sorbents for TLC have medium and large pores. The specific surface area of silica gel ranges from 200 to more than 800 m^2/g.

Activation by heating at 150–200°C removes the physically bound water. Water content of silica can be controlled by storing TLC plates at known humidity. The assumption that one silica is most suitable for adsorption and another for liquid–liquid partition chromatography is questionable and, moreover, irrelevant, because pure adsorption or partition retention mechanisms generally do not occur. Thin-layer

Table 1 Classification of the most used TLC sorbents.

General class	Sorbents
Polar inorganics (hydrophilic)	Silica gel, alumina, diatomaceous earth (kieselguhr), magnesium silicate (Florisil®)
Polar organics	Cellulose, starch, chitin, polyamide 6 or 11
Polar bonded phases	3-Aminopropyl, 3-cyanopropyl, and diol-modified silica
Hydrophobic bonded phases	C_2, C_8, C_{18}, C_{30}, and phenyl-modified silica; C_8-modified alumina; cellulose triacetate
Ion exchangers	
Inorganic	Zirconium(IV) phosphate, tungstate, and molybdate; titanium(IV) silicate; ammonium molybdophosphate and tungstophosphate; hydrous oxides
Organic	Polystyrene-based anion and cation exchangers, polymethacrylic acid; cellulose-based anion and cation exchangers; substance-specific complexing ligands
Impregnated layers	Silica impregnated with saturated and unsaturated hydrocarbons (squalene, paraffin oil); silicone and plant oils; complexing agents (silver ions, boric acid, and borates; carbohydrates; unsaturated and aromatic compounds); chelating compounds [ethylene diamine tetra-acetic acid (EDTA), digitonin]; transition metal salt; synthetic peptides; 18-crown-6 and ammonium sulfate; silanized silica gel impregnated with anionic and cationic surfactants
Gel filtration media	Cross-linked, polymeric dextran gels (Sephadex)
Chiral phases	Cellulose, cellulose triacetate, tribenzoate, and triphenylcarbamate; silanized silica gel impregnated with the copper(II) complex of (2*S*,4*R*,2′*RS*)-*N*-(2′-hydroxydodecyl)-4-hydroxyproline (CHIRALPLATE, HPTLC CHIR); molecular imprinting polymers (MIPs)

chromatographic silica gels have specific pore volumes ranging from 0.5 to 2.0 ml/g, and sorbents with the highest values are preferred for partition chromatography. Typical applications of silica gel in TLC separation of classes of organic compounds are listed in Table 2.

Alumina

The sorbents for TLC are obtained by thermal removal of water from hydrated aluminum hydroxide preparations at 200–600°C; the specific surface area of these aluminas ranges from 50 to 350 m^2/g. The aluminas for TLC have mean pore diameters of 60, 90, or 150 Å and specific pore volumes between 0.1 and 0.4 ml/g. The most frequently used crystalline form is γ-Al_2O_3 (specific surface 100–200 m^2/g). Aluminum cations, hydroxyl groups, and oxide ions are present on the surface, and the oxide ions are responsible for the basic properties of the sorbent. The use of gypsum (calcium sulfate hemihydrate) as a binder neutralizes the alumina surface. Aluminas with pH values of 9–10, 7–8, and 4–4.5 are designated basic, neutral, and acidic in character, respectively. Owing to the high density of hydroxyl groups (about 13 μmol/m^2), alumina tends to adsorb water and becomes deactivated. For this reason, the activation of aluminum oxide-precoated layers, before use, by heating for 10 min at 120°C is recommended.

Aluminas are of notable selectivity in adsorption chromatography of aromatic hydrocarbons; examples of separations of organic and inorganic compounds by adsorption and partition chromatography on layers of alumina are presented in Table 2.

Cellulose

Cellulose is formed by long chains of β-glucopyranose units connected one to another at the 1–4 positions. TLC sorbents are native fibrous cellulose and microcrystalline cellulose AVICEL. The polymerization degree of native cellulose ranges from 400 to 500 glucose units, and the fibers are shorter (2–20 μm) than those in paper chromatography, preventing the instantaneous spreading of solutes. The specific surface area is about 2 m^2/g. High-purity fibrous cellulose, obtained by washing under very mild acidic conditions and, successively, with organic solvents, is also used in TLC. AVICEL is formed by dissolving the amorphous part of native cellulose by hydrolysis with hydrochloric acid.

Partition chromatographic mechanisms operate on cellulose thin layers even if adsorption effects cannot be excluded (for separation of substance classes, see Table 2). Celluloses are naturally occurring chiral adsorbents and can be used for chiral separation of optically active amino acids and dipeptides.

Polyamides

Synthetic organic resins used in TLC are polyamide 6 (nylon 6) and polyamide 11, which consist of polymeric caprolactam and undecanamide, respectively. Therefore, polyamide 6 is more hydrophilic than polyamide 11, owing to the shorter hydrophobic chain of its monomeric unit.

Polyamide-precoated plates are currently used for the separation of phenols and phenolic compounds (i.e., anthocyanins, anthoxanthins, anthraquinone derivatives, and

Table 2 Application in normal and RP-TLC.

Sorbent	Substance class
Silica gel	Aflatoxins, alkaloids, anabolic compounds, barbiturates, benzodiazepines, bile acids, carbohydrates, etheric oil components, fatty acids, flavanoids, glycosides, lipids, mycotoxins, natural pigments, synthetic dyes, nitroanilines, nucleotides, peptides, pesticides, steroids, sulfonamides, surfactants, sweeteners, tetracyclines, vitamins
Alumina	Aromatic hydrocarbons, carbonyl compounds (DNPH derivatives), herbicides, hydrazines, insecticides, metal ions, fat-soluble vitamins, lipids, lipophilic dyes, polycyclic aromatic hydrocarbons (PAHs)
Cellulose	Amines, amino acids, antibiotics, artificial sweeteners, carbohydrates, catechols, chiral amino acids and dipeptides, flavanoids, PAHs, peptides
Alkyl- and aryl-bonded phases	Alkaloids, amides, amines, amino acids, amino phenols, antibiotics, antioxidants, barbiturates, fatty acids, indole derivatives, nucleobases, oligopeptides, optical brighteners, PAHs, peptides, phenols phthalates, porphyrins, preservatives, steroids, surfactants, tetracyclines
Amino-modified silica gel	Barbiturates, monosaccharides, nucleosides, nucleotides, pesticides, phenols, purine derivatives, steroids, vitamins
Cyano-modified silica gel	Alkaloids, amino acid derivatives, analgesics, antibiotics, benzodiazepines, carboxylic acids, carotenoids, pesticides, phenols, preservatives, steroids
Diol-modified silica gel	Digital glycosides, nucleosides, pesticides, pharmaceuticals, phospholipids, steroids
Cellulose-based ion exchangers	DNA adducts, DNA and RNA fragments, dyes for food, inorganic ions, steroids
Polystyrene-based ion exchangers	Amines, amino acids, inorganic ions, peptides, purine and pyrimidine derivatives
Ammonium tungstophosphate	Amines, amino acids, indole derivatives, oligopeptides, polyamines, sulfonamides
Silica gel impregnated with paraffin, silicon, and plant oils	Barbiturates, carboxylic acid esters, fatty acid derivatives, nitrophenols, polychlorobiphenyls (PCBs), peptides, pesticides, phenols, steroids, surfactants, triazines
Silanized silica gel impregnated with anionic and cationic surfactants	Aliphatic and aromatic amines, alkaloids, amino acids, amino sugars, carboxylic and sulfanilic acids, indole derivatives, nucleobases, nucleosides, nucleotides, peptides, dipeptides, polypeptides, phenols, phenothiazine bases, steroids, sulfonamides, water-soluble food dyes
Silver-impregnated silica gel	*cis*-Monoenoic esters, *cis*/*trans*- and *trans*/*trans*-dienoic esters, fatty acid cholesteryl esters, positional and geometric isomers of fatty acid methyl esters, terpenoids, prostaglandins
Polyamides	Amino acids and their derivatives, phenolic compounds, preservatives
Silanized silica gel impregnated with *N*-(2′-hydroxydodecyl)-4-hydroxyproline	Chiral α-amino acids, α-methyl amino acids and aliphatic or aromatic α-hydroxycarboxylic acids, chiral *N*-alkyl, *N*-carbamyl, and *N*-formyl amino acids, dipeptides and heterocyclic compounds

phenolic acids) using solvents of different elution strength [*N*,*N*-dimethyl formamide (DMF) > formamide > acetone > methanol > water]. Such eluents and solutes compete with the peptide groups of the polyamide for the hydrogen bonds.

Owing to the medium polarity of polyamide 6, the sorbent can be made more or less hydrophobic than the mobile phase by selecting appropriate polar and non-polar eluents; therefore, normal- and reversed-phase (RP) chromatography and also two-dimensional techniques can be developed.

POLAR AND HYDROPHOBIC BONDED PHASES

A variation of chromatographic selectivity in TLC has been obtained using surface-modified silica gel or cellulose.

ALKYL- AND ARYL-BONDED SILICA PLATES

These materials are suitable for RP-TLC owing to their lipophilic properties. The commonly used RP layers consist of dimethyl-(RP-2), octyl-(RP-8), octadecyl-(RP-18), and phenyl-bonded silica gel, type 60, with different mean particle sizes and particle size distributions. Recently, C_{30}-modified silica gel was proposed for the separation of tocopherol homologues.

The lipophilic character of the sorbent increases from RP-2 to RP-18, but it is also determined by the surface density of hydrophobic residues. Consequently, silicas are reacted to a different degree, either totally (100%) or partially (i.e., 50% of the reactive silanol groups), in order to obtain materials of various hydrophobicity and wettability.

Because aqueous–organic mixtures are commonly used as eluents, it should be noted that RP-18 plates can be developed with solvents containing a maximum water content of approximately 60% (v/v), whereas on 50% modified

silica layers, water percentages as high as 80% can be used. Wettable RP-18W plates for normal-phase and RP chromatography can be eluted with purely organic and aqueous–organic solvents as well as with purely aqueous eluents.

Hydrolytic cleavage of alkyl ligands from the silica surface depends on: 1) the pH of the mobile phase (although these phases are stable in the pH range from 3 to 9 only, hydrolytic cleavage usually occurs far more readily in an acidic rather than basic environment); and 2) the length of the chemical bonded ligands (long aliphatic chains prevent access of the mobile phase to the bonds, which anchor them to the silica matrix, more than short chains).[2]

Typical applications of RP chromatography are shown in Table 2. Beyond analytical applications, RP-TLC on bonded phases is also a tool for physicochemical measurements, particularly for molecular lipophilicity determination of biologically active compounds.

AMINO-, CYANO-, AND DIOL-MODIFIED PRECOATED SILICA LAYERS

These sorbents possess as functional groups cyano, amino, and diol residues bonded by short-chain hydrophobic spacers to the silica matrix. With regard to polarity, hydrophilic modified silicas range between unmodified silica and the non-polar alkyl- or aryl-bonded phases:

Silica > diol – silica > amino – silica > cyano – silica > RP material

In the case of NH_2 and CN plates, the functional groups are bonded through a trimethylene chain to the silica gel. The hydrophilic modified layers are wetted by all solvents, including water, and are useful for the separation of polar substances, which can cause problems with silica or alumina (see Table 2). The NH_2 ready-to-use plates can act as weak basic ion exchangers.

CELLULOSE- AND POLYSTYRENE-BASED ION EXCHANGERS

Several functional groups have been used to obtain cellulose anion exchangers [aminoethyl (AE), diethylaminoethyl (DEAE)] or cation exchangers [carboxymethyl (CM), phosphate (P)] for TLC. Polyethyleneimine (PEI) cellulose is not a chemically modified cellulose, but a complex of cellulose with PEI. These cellulose exchangers are particularly useful for the separation of proteins, amino acids, enzymes, nucleobases, nucleosides, nucleotides, and nucleic acids (Table 2).

Plates coated with a mixture of silica and cation- or anion-exchange resin are commercially available. These polystyrene-based ion exchangers are suited for separation of inorganic ions and organic compounds with ionic groups (Table 2).

The large surface area of cellulose exchangers causes a large number of functional groups to be close to the surface. The distances of the active groups are longer than on exchange resins (about 50 and 10 Å, respectively), but cellulose ion exchangers, despite their smaller exchange capacity compared with polystyrene-based exchangers, can be easily penetrated by large hydrophilic molecules, such as proteins, enzymes, and nucleic acids, which, therefore, interact with all the active groups. In contrast, the majority of ionic substituents of exchange resins do not participate in the reaction because they are located inside the synthetic resin matrix, which hydrophilic molecules cannot penetrate.

IMPREGNATED LAYERS

The selectivity of sorbents can be easily improved by their impregnation with suitable organic and inorganic substances. The impregnating agent can be added to the sorbent suspension before plate preparation or, alternatively, the precoated layers may be dipped into an appropriate solution containing the impregnating agent.

Ready-to-use impregnated plates are also commercially available [e.g., caffeine- or ammonium sulfate-impregnated silica for the separation of polycyclic aromatic hydrocarbons (PAHs) and surfactants, respectively]. A large number of impregnating agents have been tested, the ones most frequently used in TLC being silver nitrate, metal ions, cationic and anionic surfactants, silicone, and paraffin oil. Boric acid-impregnated silica gel layers are suitable for the resolution of carbohydrates and lipids (see Table 2).

Argentation chromatography, in which silver is used as a π complexing metal on a silica gel support, is usually employed for the separation of organic compounds with electron-donor properties because of the presence of unsaturated groups in the molecule of the analytes. TLC is particularly appropriate for applying silver complexation techniques because the instability of silver causes severe limitations to column lifetime and, therefore, to HPLC methods.

The first investigation on alkyl-bonded silica layers impregnated with anionic and cationic surfactants was carried out by Lepri, Desideri, and Heimler.[3] The optimal concentration of the alcoholic solution of the impregnating agent was found to be 4%. With regard to the layers, ready-to-use alkyl-bonded silica plates were found to have many advantages over the previously used homemade plates. An appropriate term proposed for this chromatographic technique is surely “dynamic ion-exchange chromatography.” The method can be applied to separation of a wide variety of ionic compounds and classes of compounds (see Table 2).

DEXTRAN GELS

Polymeric, cross-linked dextran gels, called Sephadex®, are used in size-exclusion TLC. Sephadex gels, which are available in coarse (100–300 μm), medium (50–150 μm), fine (20–80 μm), and superfine (10–40 μm) particle size distributions, must be applied in a total swollen condition as chromatographic sorbents and eluted with the aid of continuous development techniques. A typical application in TLC is the determination of molecular weights of proteins.[4]

LAYERS FOR CHIRAL CHROMATOGRAPHY

Only cellulose, modified cellulose (cellulose triacetate, tribenzoate, and triphenylcarbamate), and silanized silica gel impregnated with the copper(II) salt of derivatized L-hydroxyproline have been used as chiral stationary phases for the separation of enantiomeric solutes.

REFERENCES

1. Spangeberg, B.; Kaiser, R.E. The water content of stationary phases. J. Planar Chromatogr. Mod. TLC, **2007**, *20*, 307.
2. Kowalik, G.; Kowalska, T. Study of the hydrolytic cleavage of alkyl ligands from the surface of chemically bonded stationary phases by means of selected analytical techniques. J. Planar Chromatogr. Mod. TLC, **2001**, *14*, 224.
3. Lepri, L.; Desideri, P.G.; Heimler, D. Soap thin layer chromatography of some primary aliphatic amines. J. Chromatogr. **1978**, *153*, 77–82.
4. Fasella, P.; Giartosio, A.; Turano, C. Applications of thin-layer chromatography on Sephadex to the study of proteins. In *Thin-Layer Chromatography*. Marini-Bettòlo, G.B., Eds.; Elsevier: Amsterdam, **1964**; 205–211.

BIBLIOGRAPHY

1. Geiss, F. *Fundamentals of Thin Layer Chromatography* (*Planar Chromatography*); Alfred Hüthing Verlag: Heidelberg, Germany, **1987**; 225–246.
2. Grassini-Strazza, G.; Carunchio, V.; Girelli, A.M. Flat-bed chromatography on impregnated layers. J. Chromatogr. **1989**, *466*, 1–35.
3. Hauck, H.E.; Mark, M. Sorbents and precoated layers in thin layer chromatography. In *Handbook of Thin Layer Chromatography*; Sherma, J.; Fried, B., Eds.; Marcel Dekker, Inc: New York, **1996**; 101–128.
4. Kowalska, T. Adsorbents in thin-layer chromatography. In *Planar Chromatography: A Retrospective View for the Third Millennium*. Nyiredy, Sz., Ed.; Springer Scientific Publisher: Budapest, **2001**; 33–46.

Spiral Column Assembly for HSCCC

Yoichiro Ito
National Heart, Lung, and Blood Institute (NHLBI), National Institutes of Health (NIH), Bethesda, Maryland, U.S.A.

Abstract
Retention of the stationary phase in the standard multilayer coil for high-speed countercurrent chromatography (HSCCC) entirely depends on the Archimedean screw effect. However, it fails to retain a satisfactory amount of the stationary phase for the highly polar solvent systems such as polymer phase systems which are useful for separation of proteins and other macromolecules and cell particles. In order to improve the retention of the stationary phase, spiral column assemblies have been introduced, which can additionally utilize the radially acting centrifugal force to retain the heavier phase in the periphery and the lighter phase in the proximal portion of the spiral channel. Two different types of spiral columns were devised: the spiral disk assembly consists of a stack of multiple disks each having a spiral groove and the spiral tube assembly, which is made by inserting plastic tubing along the spiral groove of spiral tube support and forms multiple spiral layers. Performance of each system was examined using two different types of polar solvent systems, 1-butanol–acetic acid–water (4:1:5, v/v) and 12.5% (w/w) of polyethylene glycol (PEG)-1000 and 12.5% (w/w) of dibasic potassium phosphate in water each with suitable test samples. The results clearly demonstrate the useful application of spiral column countercurrent chromatography (CCC) for separation of polar compounds.

INTRODUCTION

The high-speed countercurrent chromatography (HSCCC) centrifuge uses a multilayer coil as a separation column, which produces high-efficiency separation with good retention of the stationary phase with a variety of two-phase solvent systems.[1,2] However, the method often fails to retain a satisfactory amount of the stationary phase for highly viscous, low interfacial solvent systems such as polymer phase systems, which are useful for the separation of macromolecules and particulates. Retention of the stationary phase in the conventional multilayer coiled column in the HSCCC system totally relies on the Archimedean screw force generated by the planetary motion of the column. However, this force is often too weak to retain the stationary phase for some polar solvent systems, such as aqueous–aqueous polymer phase systems, resulting in carryover of the stationary phase from the column.

The new spiral column designs described below improve the retention of the stationary phase by modifying the configuration of the column from a coil to a spiral, so that the centrifugal force gradient produced by the spiral pitch helps to distribute the heavier phase in the periphery and the lighter phase in the proximal portion of the column. This effect can be enhanced by increasing the pitch of the spiral. Although a spiral column can be prepared simply by winding the tubing into a flat spiral configuration,[3,4] it can provide a limited spiral pitch [outer diameter (O.D.) of the tubing]; additionally, the connection between the neighboring spiral columns is rather difficult. Two new column designs termed "spiral disk assembly"[5–10] and "spiral tube assembly,"[11,12] described below, solve these problems and provide a universal application of two-phase solvent systems including the polymer phase systems for HSCCC.

SPIRAL DISK ASSEMBLY

In this design, the separation column consists of a set of solid disks each with a single or plural spiral channel(s). In the first model, a single spiral channel is engraved in a plastic disk, which can be serially connected by stacking multiple disks sandwiched with Teflon sheet septa. In the second model, four spiral channels are incorporated in a single disk, symmetrically around the center, so that the spiral pitch increases four times that of the single spiral channel without losing column space. Connection between the neighboring spiral channels is formed by a short straight channel situated radially on the other side of the disk. A set of these disks can be serially connected by spacing a Teflon sheet between the neighboring disks, so that the column provides a large capacity that is somewhat comparable to that of the multilayer coil. The separation disk with a single spiral will serve as a control to evaluate the effect of pitch on partition efficiency.

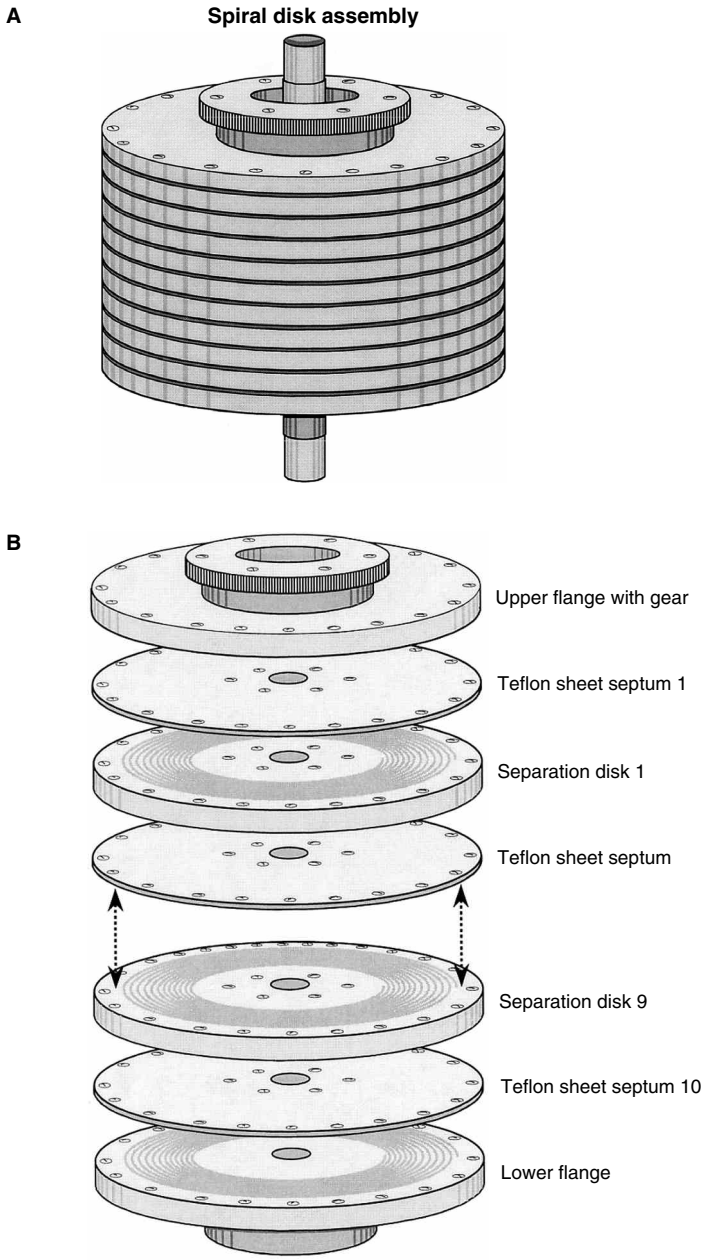

Fig. 1 Schematic illustration of the spiral disk assembly. A, Whole view and B, exploded view showing each component.

The design of the spiral column assembly is shown in Fig. 1. Fig. 1A shows a full view of the column assembly, which can be mounted on a type-J multilayer coil planet centrifuge (P.C., Inc., Potomac, Maryland, U.S.A.). The column components are illustrated in Fig. 1B. The column consists of a pair of flanges (one equipped with a gear), nine disks with spiral grooves, and 10 Teflon sheet septa. The design and dimensions of each component are illustrated in Fig. 2A–E.

The design of the individual separation disk with one spiral channel (diameter of 17.5 cm, thickness of 3 mm, with a 1.9 cm diameter center hole) is shown in Fig. 2A. The channel is 2.6 mm wide, 2 mm deep, with 1 mm ridge width, which gives a spiral pitch of 4 mm. The total channel length is about 4 m, comprising 12 spiral turns, with a total capacity of about 23 ml. The channel starts at the internal inlet (23 mm from the center) and extends to the external outlet (75 mm from the center), which is connected to the radial channel on the other side through a hole about 1 mm diameter. The performance of this single spiral column may be compared to that of the following four-channel spiral column, by using a polar butanol solvent system and polymer phase systems.

Design of the individual separation disk with four separate spiral channels is shown in Fig. 2B. A plastic

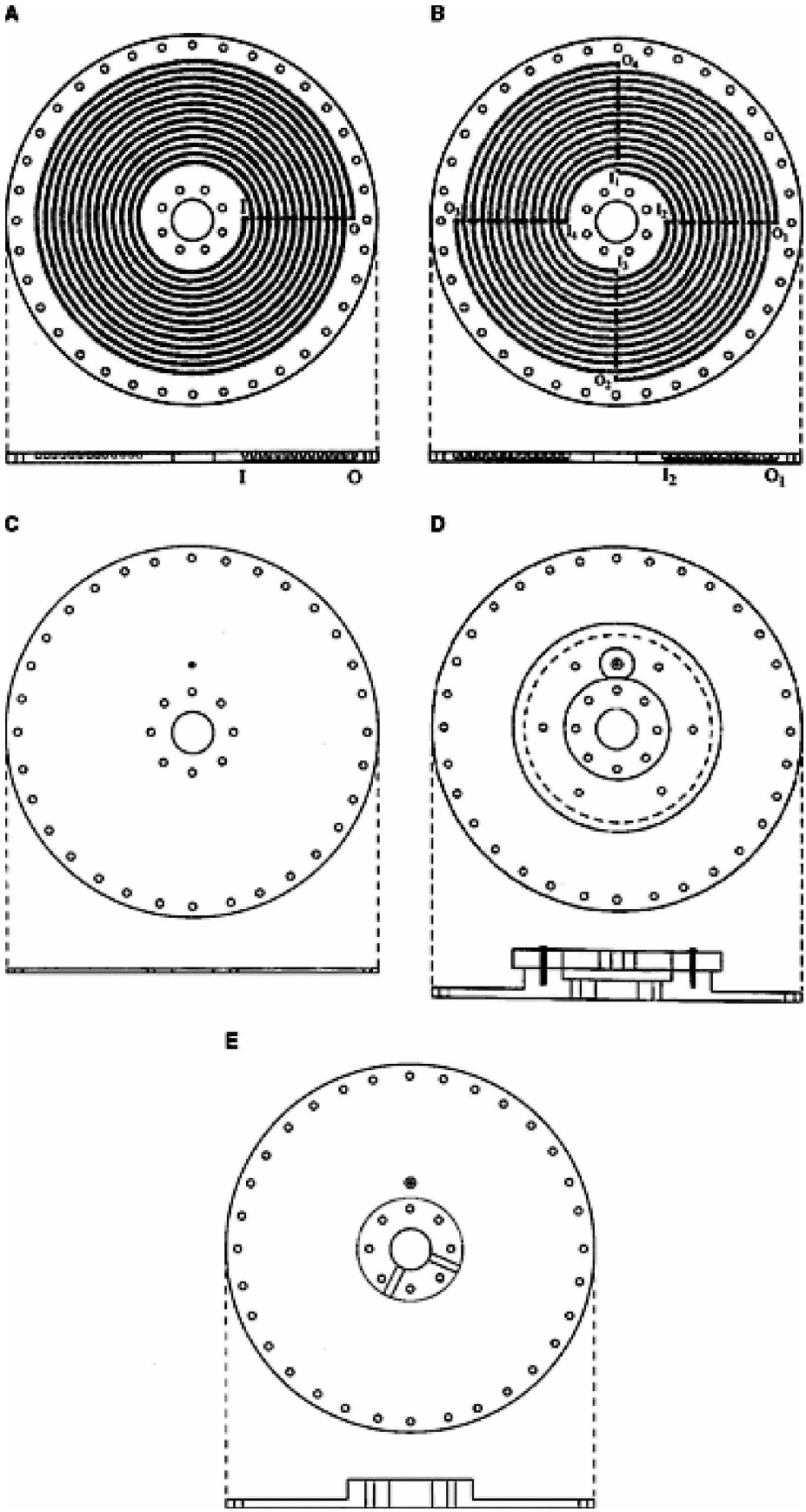

Fig. 2 Drawing of each component of the spiral disk assembly. A, Disk with a single spiral; B, disk with four spirals; C, Teflon sheet septum; D, upper flange equipped with a plastic gear; and E, lower flange.

disk (17.5 cm diameter and 4 mm thick, high-density polyethylene or polymonochlorotrifluoroethylene) has four spiral channels (grooves), each 2.6 mm wide, 2 mm deep, and about 1 m long, with a capacity of about 6 ml. The ridge between each groove is 1 mm and, therefore, the pitch of each spiral becomes as large as 16 mm (four times that of the single spiral channel). Each channel starts at the inner end (I_1, I_2, I_3, and I_4) to reach the outer end (O_1, O_2, O_3, and O_4, respectively). As shown in the diagram, each channel forms 3.25 spiral turns so that the outer end of channel 1 (O_1) radially coincides with the inner end of channel 2 (I_2), and those of channels 2, 3, and 4 (O_2, O_3, and O_4) similarly coincide with the inner ends of channels 3, 4, and 1 (I_3, I_4, and I_1), respectively. Each end of the channel (except for O_1) has a hole (about 1 mm diameter) through the disk to reach the other side, where a radial channel (dotted line) leads to the next spiral channel through another hole. The outer end of channel 4 (O_4) is connected to a similar radial channel that leads to channel 1 (I_1) of the next disk, or the column outlet, through an opening in the Teflon septum (Fig. 2C).

All disks have screw holes (clearing an 8–32 screw) at both inner and outer edges, at regular intervals (10° for the outer edge and 45° for the inner edge). Similar holes are also made in both the Teflon sheets and the flanges.

The design of the flanges is shown in Fig. 2D and E. The upper flange (Fig. 2D) is equipped with a plastic gear (9 mm thick, 10 cm pitch diameter), which engages with an identical stationary gear on the HSCCC centrifuge. Fig. 2E shows the lower flange, which has two screw holes (90° apart) for tightly fixing the column assembly against the column holder shaft (1.9 cm O.D.). The upper and lower flanges each have an inlet hole, which fits into an adapter with a 1/4–28 screw thread. They also have a set of screw holes (clearing an 8–32 screw) around the outer and inner edges as in the separation disks and the Teflon septa. The column assembly is mounted on the rotary frame of a multilayer coil centrifuge and counterbalanced with brass blocks. A pair of flow tubes from the column assembly is led downward through the center hole of the column holder shaft and passed through the hollow central pipe to exit the centrifuge at the center hole of the top plate, where it is tightly fixed with a pair of clamps. These tubes are protected with a sheath of Tygon tubing to prevent direct contact with metal parts.

EXPERIMENTAL PROCEDURE

Each two-phase solvent system is thoroughly equilibrated in a separatory funnel at room temperature, and the two phases are separated before use. The sample solution is prepared by dissolving the sample in an appropriate volume (1–5 ml) of the upper and/or lower phase of the solvent system. In each experiment, first the column is entirely filled with the stationary phase (upper or lower phase), followed by sample injection through the sample port. Next, the apparatus is rotated at 800 rpm, while the mobile phase is eluted through the column at the desired flow rate. The separation may be repeated by changing the direction of the revolution and/or the elution mode (head to tail and tail to head), although it is expected that the best result would be obtained by eluting either the lower phase from the internal terminal toward the external terminal of the spiral channel, in a tail-to-head elution mode, or the upper phase in the opposite direction in a head-to-tail mode. The effluent from the outlet of the column is continuously monitored through an ultraviolet (UV) detector.

BASIC STUDIES WITH SINGLE DISKS

Using a single disk with each channel design, a series of experiments were performed to evaluate the performance of the disk in terms of partition efficiency and retention of the stationary phase, by using three different types of two-phase solvent systems: 1-butanol–acetic acid–water (4:1:5, v/v/v) for separation of dipeptides; 12.5% (w/w) polyethylene glycol (PEG)-1000, 12.5% (w/w) dibasic potassium phosphate in water for protein separations; and 4% (w/w) PEG-8000, 5% (w/w) dextran T500 in water for measuring the retention of the stationary phase. The experiments were performed at various flow rates of the mobile phase, using four different elution modes: L–I–T (lower phase eluted from the inner terminal at the tail); L–I–H (lower phase eluted from the inter terminal at the head); U–O–T (upper phase eluted from the outer terminal at the tail); U–O–H (upper phase eluted from the outer terminal at the head). Four other reversed elution modes, including L–O–T, L–O–H, U–I–T, and U–I–H, showed considerably less retention of the stationary phase, compared with their counterparts, because of the adverse effect of the radial centrifugal force gradient. The dimensions of these four spiral channels are given in Table 1.

1-BUTANOL–ACETIC ACID–WATER (4:1:5) SYSTEM

Fig. 3A–D shows the separation of a standard sample mixture of trp–tyr (0.5 mg) and val–tyr (2 mg) with a two-phase solvent system composed of 1-butanol–acetic acid–water (4:1:5), by using a set of four different spiral columns (columns I–IV in Table 1).

Table 1 Dimensions of the four spiral channels used in the present studies.

Disk no.	Number of spirals	Width[a] (mm)	Depth[a] (mm)	Pitch (mm)	Capacity (ml)
Column I	1	2.6	2.0	4	23
Column II	1	1.5	3.7	4	21
Column III	4	2.6	2.0	16	23
Column IV	4	1.5	3.7	16	21

[a]The width of the spiral groove becomes the depth of the channel and the depth becomes the width of the channel when assembled.

In each chromatogram, the UV absorbance (280 nm) was plotted against the elution time together with the percent retention volume of the stationary phase relative to the total column capacity. In each group, a set of chromatograms is arranged according to the four different elution modes, i.e., L–I–T, L–I–H, U–O–T, and U–O–H, where L and U indicate the lower phase mobile and upper phase mobile, I and O denote eluting from internal terminal and external terminal of the spiral, and T and H represent "tail-to-head" and "head-to-tail" elution mode, each under various flow rates of the mobile phase.

In column I (Fig. 3A), the elution with upper phase from the head of the spiral (U–O–H) produces the best peak resolution and the highest percent retention of the stationary phase. The elution with the lower phase from the head of the spiral (L–I–T) also shows a good peak resolution up to a flow rate of 5 ml/min, in spite of low retention of the stationary phase. Elution of the lower phase from the head (L–I–H) retains a satisfactory amount of the stationary phase at the flow rate of 0.5–2 ml/min, while the peak resolution is much lower than that of its counterpart (L–I–T). The elution of the upper phase from the tail (U–O–T) shows no retention of the stationary phase, even at a low flow rate of 0.5 ml/min. These elution trends are also observed in column II (Fig. 3B), except that the peak resolution is much reduced in the elution of the lower phase from the tail (L–I–T), for a similar retention level of the stationary phase.

Fig. 3C and D shows the chromatograms obtained from the four-spiral disks under otherwise identical experimental conditions. It clearly indicates that the retention of the stationary phase is much improved in all elution modes. Although the peak resolution of the two dipeptides was substantially reduced, the flow rate could be increased up to 10 ml/min to yield a moderate degree of peak resolution, as emphasized by column IV (Fig. 3D). This suggests that if one uses a multichannel spiral disk with a large pitch, the separation of peptides might be achieved in a very short elution time.

PEG-1000–DIBASIC POTASSIUM PHOSPHATE POLYMER PHASE SYSTEM

Fig. 4A–D similarly illustrates the peak resolution between two protein samples (lysozyme and myoglobin, 10 mg each) in the PEG–phosphate system obtained from the four different spiral disks. In the single-spiral disks (Fig. 4A and B), the best results were obtained by eluting the upper PEG-rich mobile phase from the head end of the outer terminal (U–O–H); other modes resulted in low resolution. Except for L–I–T and I–O–T in column II, all groups show a satisfactory level of stationary phase retention with a flow rate of 0.5 ml/min, indicating that mixing of two phases in the spiral column is inefficient. This tendency is more pronounced in the four-spiral disks (Fig. 4C and D), which show much higher retention of the stationary phase (over 60%), but without any peak resolution. Corresponding columns in Fig. 4A and B show the latter to yield somewhat higher peak resolution, which is probably the result of the shallow channel with respect to the centrifugal force that facilitates mass transfer between the two phases. This suggests that the separation might be further improved by reducing the width of the spiral groove.

PEG-8000–DEXTRAN T500 POLYMER PHASE SYSTEM

A series of experiments was performed to examine the retention of the PEG–dextran polymer phase system without samples. Results are shown in Table 2, where percent retention of the stationary phase is indicated at the flow rates of 0.5–1 or 2 ml/min for each spiral column. The results indicate that, among the single-spiral disks (I and II), column I with a deep channel retained over 60% of the lower dextran-rich stationary phase (U–O–H and U–O–T) at a low flow rate of 0.5 ml/min while, under other conditions, the retention was substantially less than 50% of the total column capacity. In contrast, the four-spiral disks (columns III and IV) attained remarkably improved retention of over 50% for all elution modes, at 0.5 ml/min flow rate. Again, the results indicate the effect of the greater spiral pitch, which favors the retention of the stationary phase.

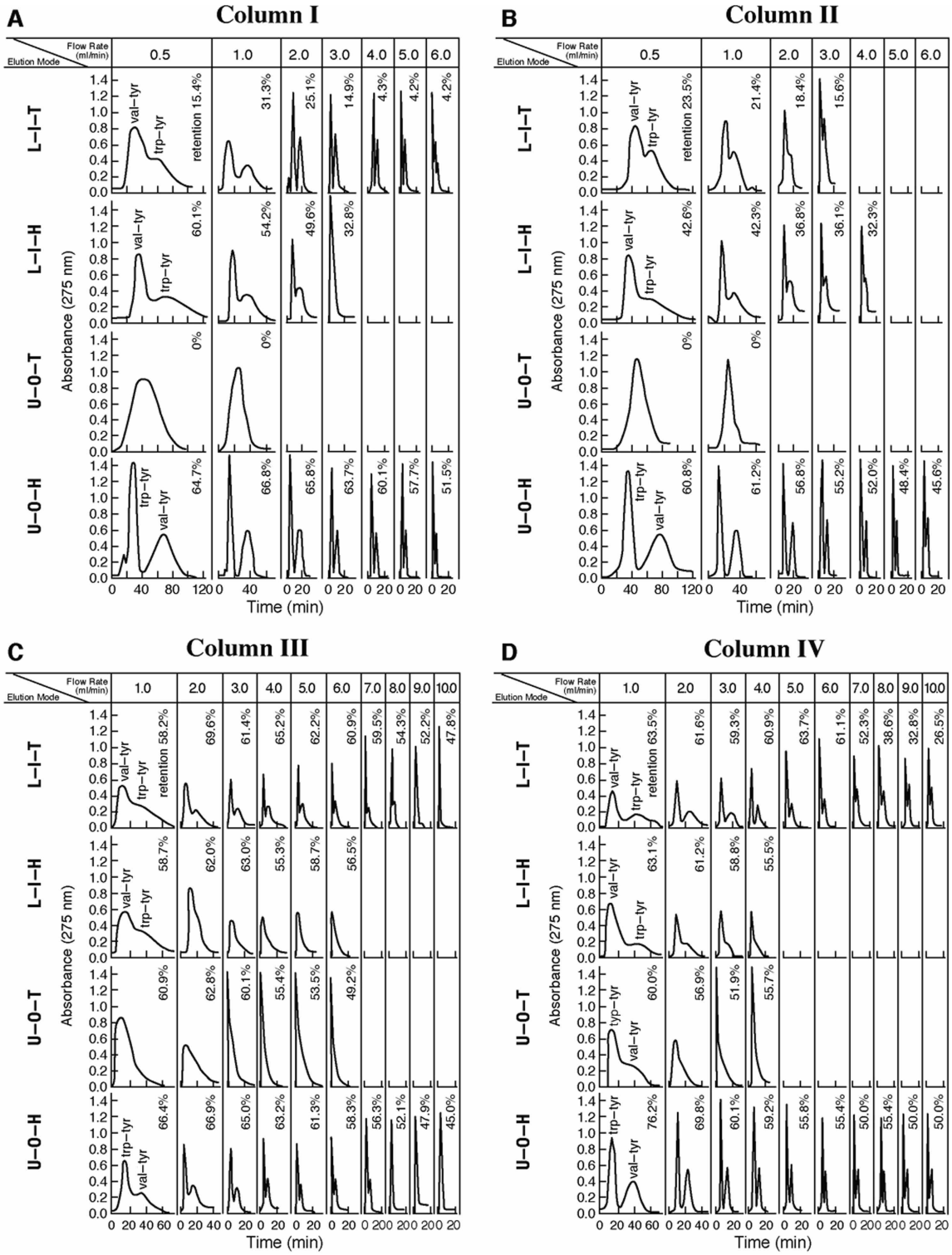

Fig. 3 Separation of peptides with a set of four single disks. A) Column I, B) column II, C) column III, and D) column IV (dimensions of the channels are listed in Table 1). Experimental conditions are as follows: apparatus: a type-J coil planet centrifuge with 10 cm revolution radius; sample: trp–tyr (0.5 mg), val–tyr (2 mg) in 1 ml of upper phase; solvent system: 1-butanol–acetic acid–water (4:1:5); elution modes: L–I–T, lower phase from the inner terminal at tail, L–I–H, lower phase from the inner terminal at head, U–O–T, upper phase from the outer terminal at tail, and U–O–H, upper phase from the outer terminal at head; flow rate: 0.5–10 ml/min as indicated; rpm: 800; stationary phase retention as indicated in the figure.

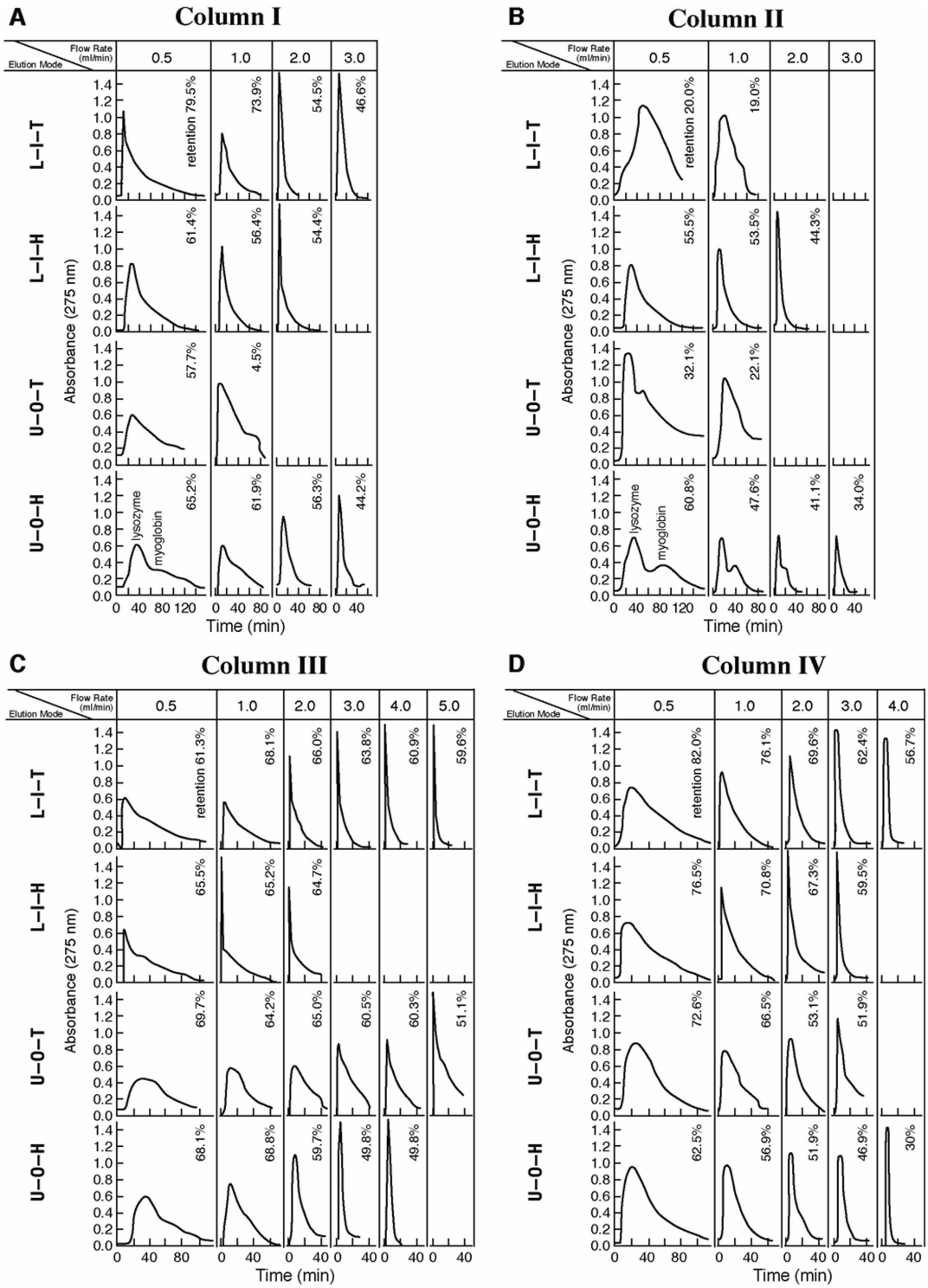

Fig. 4 Separation of proteins with a set of four single disks. A) Column I, B) Column II, C) Column III, and D) Column IV (dimensions of the channels are listed in Table 1). Experimental conditions are as follows: apparatus: type-J coil planet centrifuge with 10 cm revolution radius; sample: lysozyme and myoglobin each 5 mg in 1 ml of upper phase; solvent system: 12.5% (w/w) PEG-1000 and 12.5% (w/w) potassium diphosphate in water; elution modes: L–I–T, lower phase from the inner terminal at tail, L–I–H, lower phase from the inner terminal at head, U–O–T, upper phase from the outer terminal at tail, and U–O–H, upper phase from the outer terminal at head; flow rate: 0.5–5 ml/min as indicated; rpm: 800; stationary phase retention as indicated in the figure.

Table 2 Percent retention of 4% PEG-8000–5% Dextran T500 in 10 m*M* Na_2HPO_4 system.

Column	I	II	III	IV
Flow rate (ml/min)	0.5–1.0	0.5–1.0	0.5–1.0–2.0	0.5–1.0–2.0
L–I–T	40.0–14.8	14.3–3.3	61.1–50.0–14.3	55.6–33.3–4.0
L–I–H	37.1–2.0	10.9–6.5	53.9–47.8–17.4	52.0–33.3–9.6
U–O–T	71.8–32.3	31.0–17.4	67.8–65.7–50.0	64.4–56.0–42.7
U–O–H	61.9–28.0	15.1–10.1	59.8–46.8–45.1	58.5–54.5–44.0

PRELIMINARY SEPARATION WITH A MULTILAYER SPIRAL DISK ASSEMBLY

The performance of the present column design was examined by using a spiral disk assembly consisting of eight units of column I, with a total capacity of 165 ml. Results are shown in Fig. 5A and B. In Fig. 5A, a mixture of five dipeptides was well resolved and was completely eluted in 2 hr. The upper organic phase of the 1-butanol solvent system was eluted at a flow rate of 4 ml/min. Similar separations were shown with the standard multilayer coils in HSCCC, but only with more stable butanol solvent systems.[1]

Fig. 5B shows the separation of two stable proteins (lysozyme and myoglobin) by using a PEG-1000/K_2HPO_4 polymer phase system at a flow rate of 1 ml/min, where they were well resolved in slightly over 5 hr. As suggested by basic studies, the separation may be substantially improved by using the column II disk assembly, which provides a shallower channel to facilitate mass transfer in viscous polymer phases.

MIXER-SETTLER SYSTEM

The present system allows modification of the channel configuration and/or placing suitable inserts into the channel to improve the partition efficiency. Fig. 6 shows two spiral disks, each with a modified channel. In the locular disk (Fig. 6A) the spiral channels consist of multiple compartments called locules connected with a narrow duct and in the barricaded disk (Fig. 6B) barricades are made at the middle of the channel at regular intervals to divide the channel into multiple sections. Each system allows performing mixer-settler partitioning by placing a glass bead

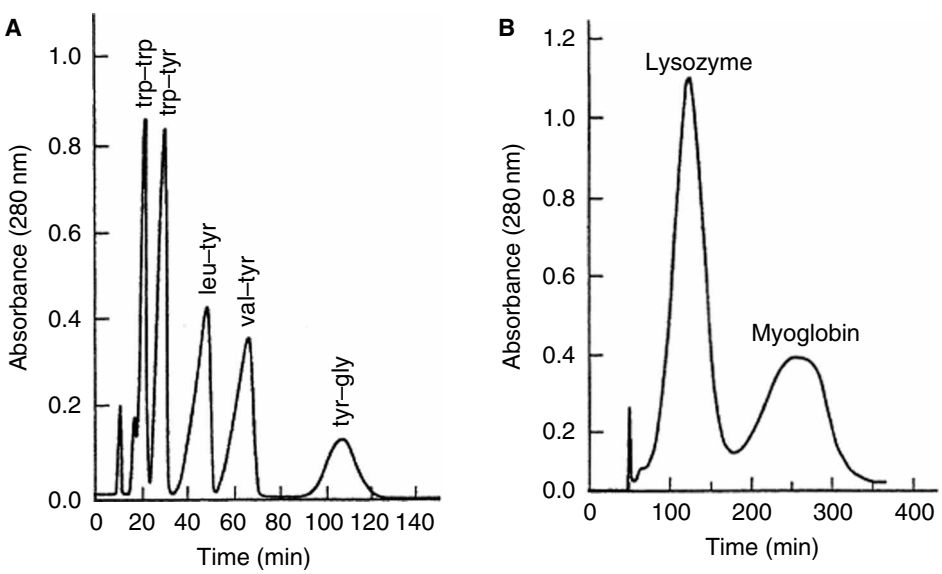

Fig. 5 Preliminary separation of peptides and proteins by a spiral disk assembly. A, Separation of a set of dipeptides and B, separation of lysozyme and myoglobin. Experimental conditions are as follows: apparatus: type-J coil planet centrifuge with 10 cm revolution radius; column: spiral disk assembly consisting of 8 disks (column I) with a total capacity of about 165 ml; sample: A, trp–trp (1.25 mg), trp–tyr (2.5 mg), leu–tyr (l0 mg), val–tyr (l0 mg), tyr–gly (10 mg) in 5 ml upper phase; B, lysozyme and myoglobin each 50 mg in 5 ml lower phase; solvent system: A, 1-butanol–acetic acid–water (4:5:1) B, 12.5% (w/w) PEG-1000, 12.5% (w/w) K_2HPO_4 in water; mobile phase: A, upper organic phase; B, upper PEG-rich phase; flow rate: A, 4 ml/min, B, 0.5 ml/min; elution mode: A, U–O–H; B, U–O–H; rpm: 800; retention of stationary phase: A) 60% and B) 77.4%.

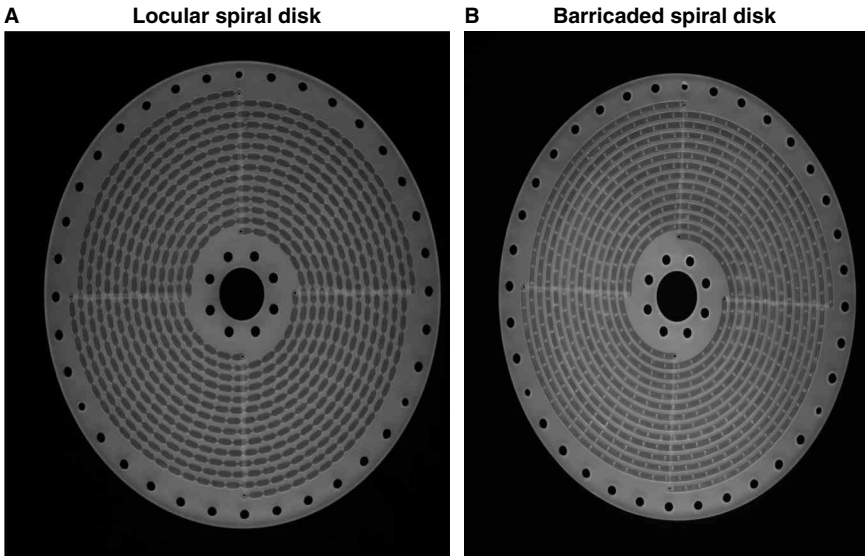

Fig. 6 Photograph of the four-spiral disks with modified channel configuration. A, locular spiral disk and B, barricaded spiral disk.

in every other compartment. The mechanism of this mixer-settler system is illustrated in Fig. 7. In the upper figure, under a fluctuating centrifugal force field the two phases are vigorously mixed by a vibrating glass bead in the mixing locule and they are separated in the next empty settling locule. Although this system gives excellent peak resolution of proteins, it tends to gradually lose the stationary phase from the mixing locule. This problem is solved by a barricaded spiral disk where two phases can freely countercurrent through the opening on the top and bottom of the barricade to maintain the stationary phase retention in the channel.

Fig. 8 illustrates comparison in protein separation between four different spiral disks at 800 rpm. The left panel shows the original spiral disk, which gives poor peak resolution. In the locular disk, the separation is improved, but the best separation was obtained from the mixer-settler spiral disks on the right. The chromatogram in Fig. 9 shows separation of five proteins obtained by mixer-settler countercurrent chromatography (CCC) using a barricaded spiral disk assembly consisting of eight disks. In Fig. 9A four proteins were well resolved while the fifth was still retained in the column. This may be the best protein separation ever achieved with the polymer phase system. However, this mixer-settler system is only useful for separation with polymer phase systems.

SPIRAL TUBE ASSEMBLY

This new column design uses the spiral tube support to make multiple spiral tube layers from a single piece of

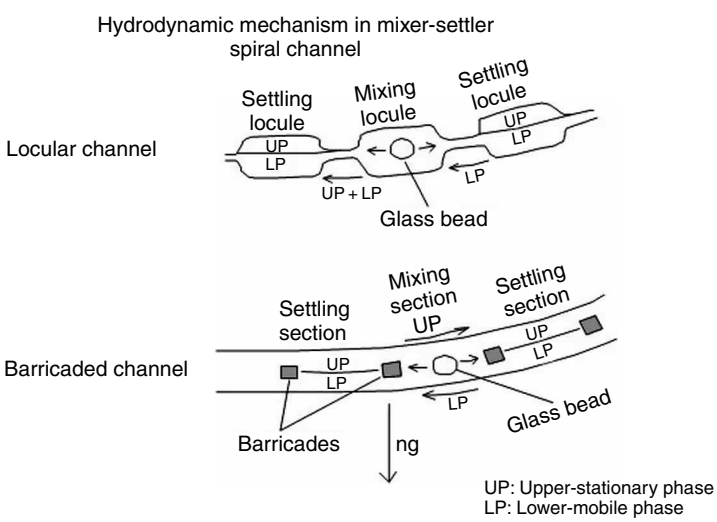

Fig. 7 Mechanism of mixer-settler HSCCC. In the locular channel disk (upper diagram), mixing locule receives the lower mobile phase, which it releases as a mixture of two phases through a narrow opening, resulting in a gradual loss of the stationary phase in the mixing locule. In the barricaded-channel disk (lower diagram), the two phases freely countercurrent through the opening at the top and bottom of the barricade to maintain the stationary phase retention in the channel.

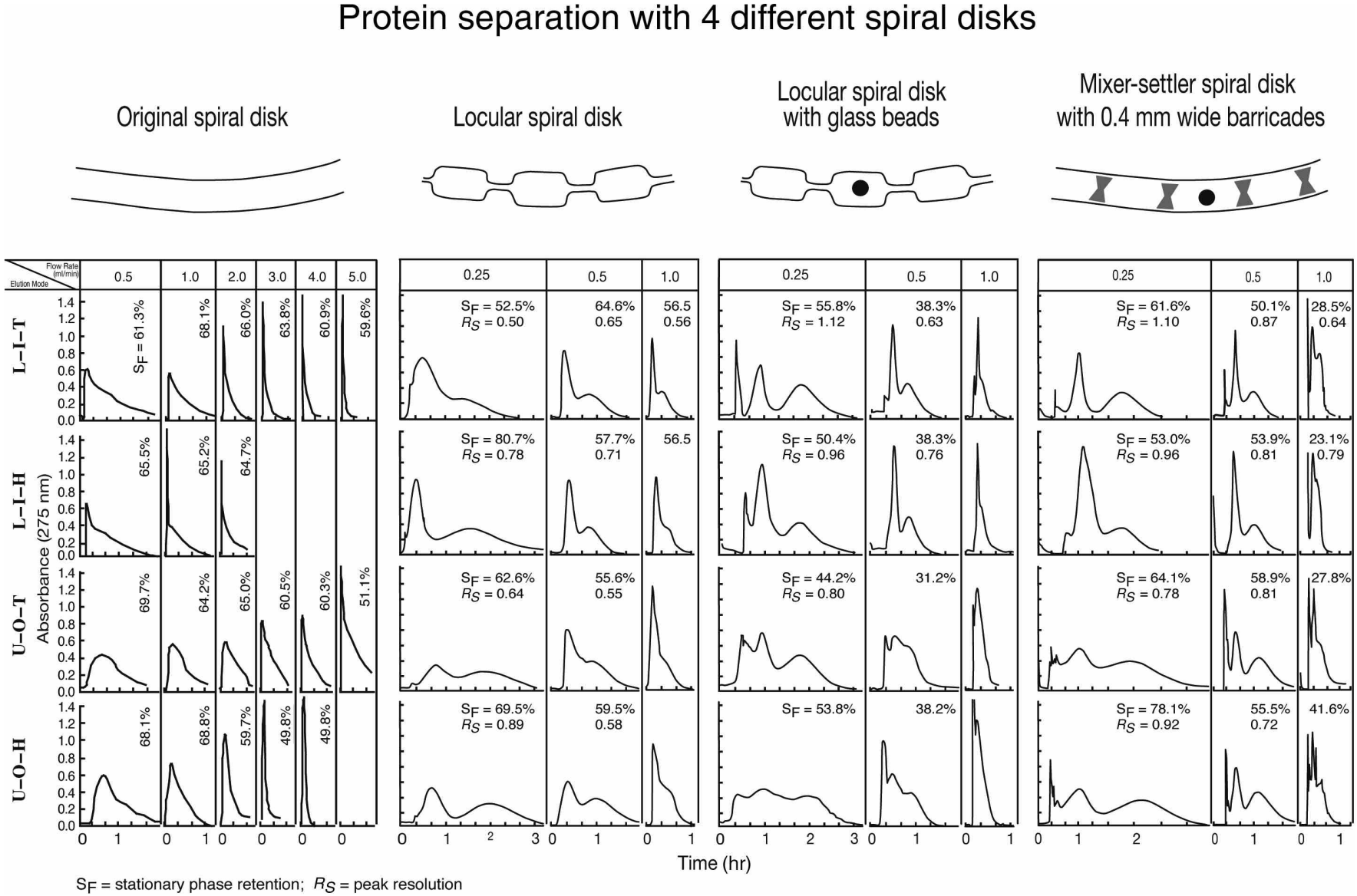

Fig. 8 Comparison of protein separation between four different spiral disks. Experimental conditions are as follows: apparatus: type-J coil planet centrifuge with 10 cm revolution radius; sample: lysozyme and myoglobin each 50 mg in 5 ml of upper phase; solvent system: 12.5% (w/w) PEG-1000 and 12.5% (w/w) K_2HPO_4 in water; rpm: 800.

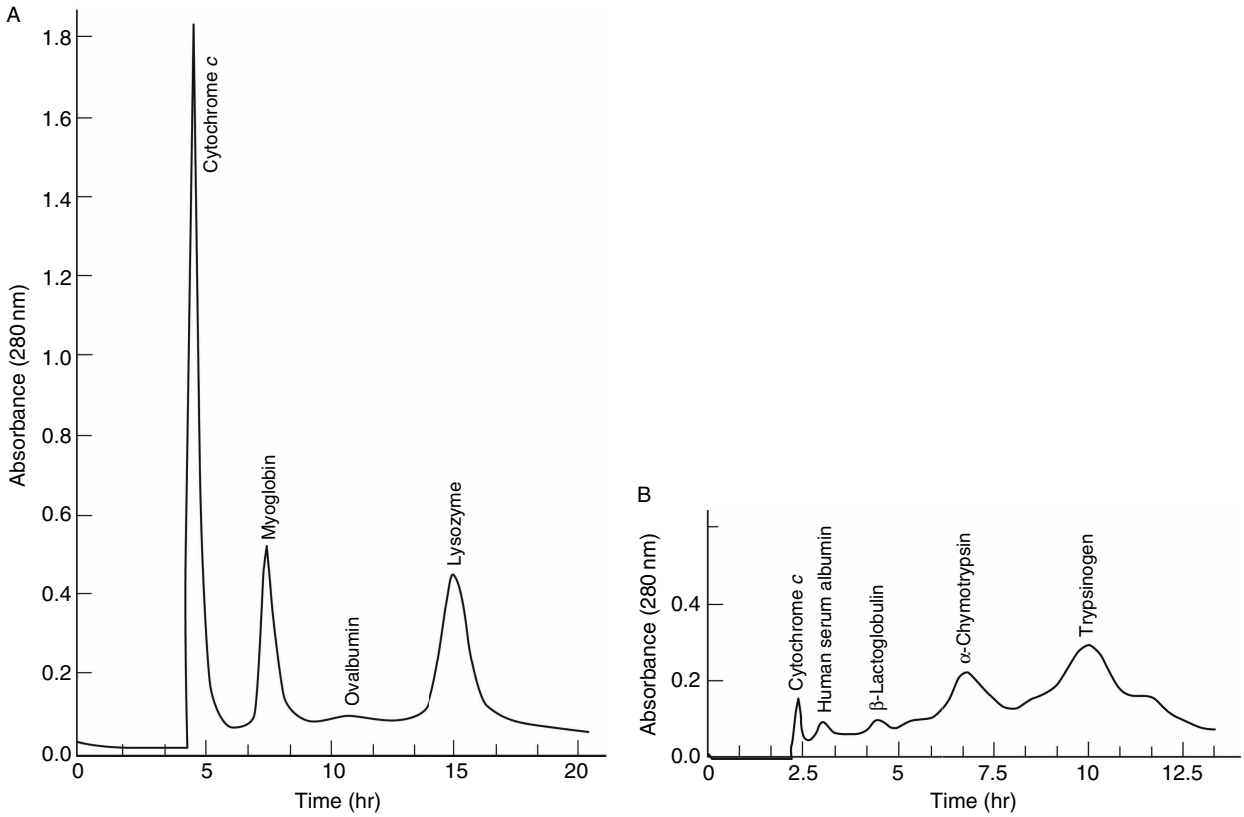

Fig. 9 Separations of five standard protein samples by mixer-settler HSCCC. Experimental conditions are as follows: apparatus: type-J coil planet centrifuge with 10 cm revolution radius; column: a mixer-settler spiral disk assembly consisting of eight barricaded disks with a 160 ml capacity; A, solvent system: 12.5% (w/w) PEG-1000 and 12.5% (w/w) K_2HPO_4; mobile phase: lower phase; sample: five proteins each 5–6 mg in 1 ml of each phase, cytochrome *c* ($K = 0.02$), myoglobin ($K = 0.59$), ovalbumin ($K = 1.26$), lysozyme ($K = 1.69$), and bovine serum albumin ($K = 1.95$); flow rate: 0.25 ml/min; rpm: 800; detection: 280 nm; stationary phase retention: 52%; B, solvent system: PEG1000/K_2HPO_4/KH_2PO_4/H_2O (16:8.3:4.2:71.5, w/w); sample: cytochrome *c* (5 mg, $K = 0.035$), human serum albumin (20 mg, $K = 0.4$), β-lactoglobulin (20 mg, $K = 0.69$), α-chymotrypsin (20 mg, $K = 1.2$), and trypsinogen (20 mg, $K = 2.1$) in 2 ml of each phase; flow rate: 0.5 ml/min; rpm: 1000; stationary phase retention: 53.6%.

tubing so that there is no risk of leakage of solvent through the junction. Fig. 10 shows two different designs for the spiral tube support. The first design shown on the left has an open slot at each terminal of the deep spiral grooves through which the tube is led to the other side of the disk and run along the radial groove toward the center, and finally returned to the upper side through the central hole to start the next spiral. One problem of this design is that a long tube must be passed through the central hole of the disk for winding each spiral. Another problem is that, as the number of spiral layers is increased, the length of the transfer tube and the dead space also increase.

These problems are solved in the second system shown on the right. The major improvement in the design is achieved by making the radial transfer grooves on the upper side of the disk. This avoids the necessity of passing the tube through the central hole, and the length of the transfer tube is kept minimum. In this system the transfer tubes are sandwiched between the spiral layers, limiting the column capacity. However, this problem is largely eliminated by a special process described later, and this system has been chosen for developing the spiral tube HSCCC.

Fig. 11 shows a photograph of the spiral tube support (aluminum) made at the NIH Machine Shop. It has four spiral grooves. The diameter of the support is about 16 cm and the depth of the spiral groove is about 5 cm. Later, the sharp bend at each end of the radial transfer grooves is rounded to prevent kinking of the tube. It accommodates about 40 m of 1.6 mm I.D. tube in nine spiral layers with a total capacity of about 100 ml.

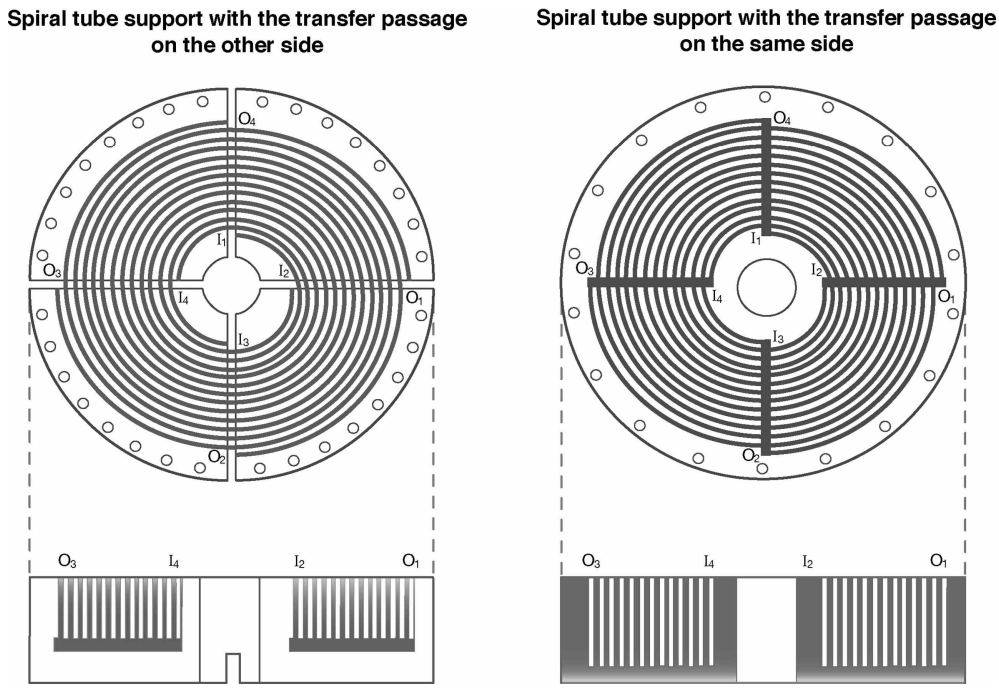

Fig. 10 Two different designs for spiral tube support.

The performance of this spiral tube assembly was tested for separating dipeptide samples, tryptophyl–tyrosine and valyl–tyrosine, with a two-phase solvent system composed of 1-butanol–acetic acid–water at a volume ratio of 4:1:5 at 800 rpm (Fig. 12). The best results were obtained by L–I–T and U–O–H elution modes where the two peptides were resolved within 30 min at a high flow rate of 5 ml/min (Fig. 12).

However, the separation of proteins is inefficient as expected from the results obtained from the spiral disk assembly described earlier. Improvement in protein separation in the present system can be achieved by changing the shape of the tube. When the tube is perpendicularly pressed at 1 cm intervals with a pair of pliers, the peak resolution in protein separation was improved remarkably from 0.68 to 1.10, as shown in Fig. 13. The separation of the dipeptides was also improved in spite of the reduced column capacity from 103 to 95 ml.

Fig. 14 shows protein separations with this cross-pressed spiral tube assembly consisting of nine spiral layers of a 1.6 mm I.D. tube with a total capacity of 95 ml at 800 rpm. The protein peaks were resolved even at a relatively high flow rate of 2 ml/min.

As mentioned earlier, the column capacity of this spiral tube assembly is limited by the transfer tubes

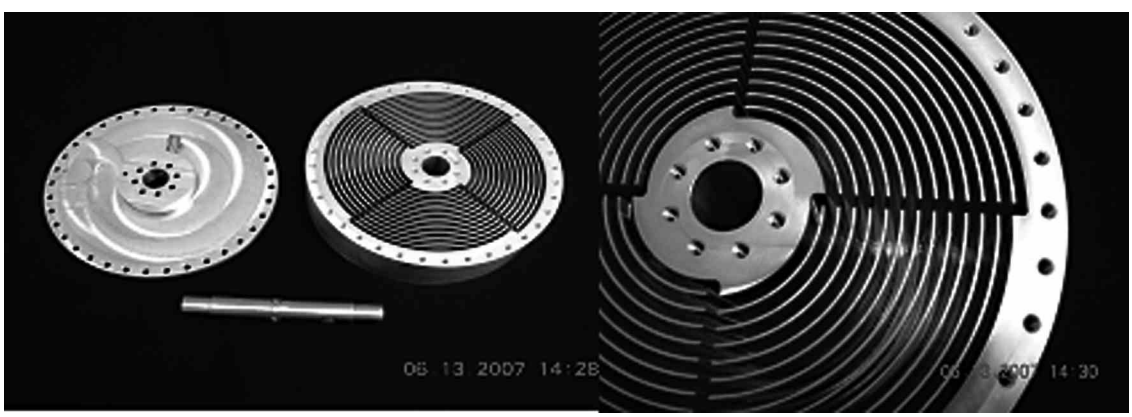

Fig. 11 Photograph of spiral tube support.

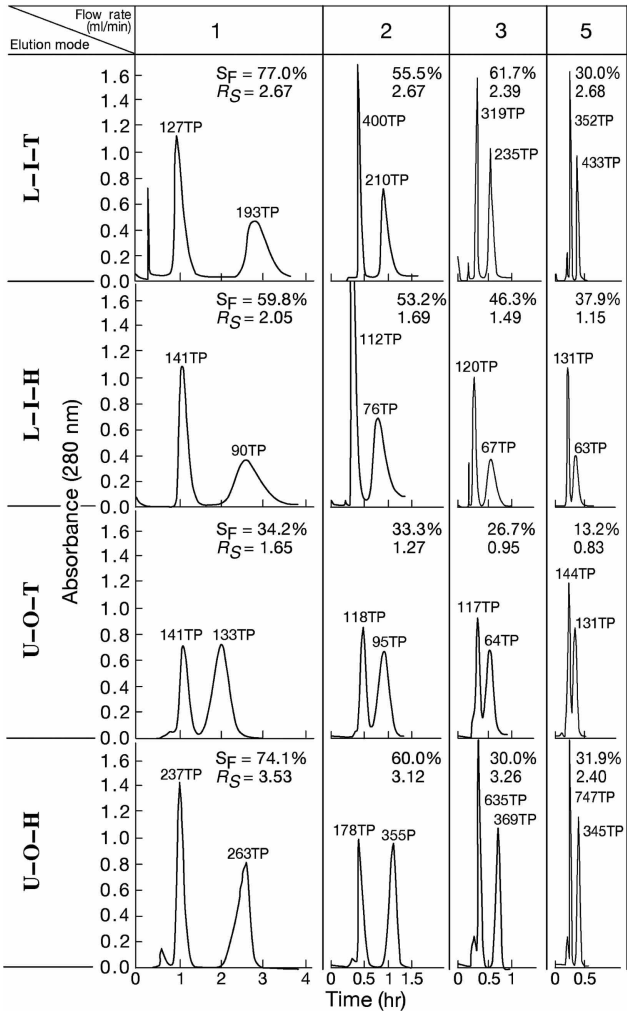

Fig. 12 Separation of dipeptides by spiral tube assembly at 800 rpm. Experimental conditions are as follows: apparatus: spiral tube with 1.6 mm I.D. and about 36 m long forming nine spiral layers with a total capacity of about 100 ml; solvent system: 1-butanol–acetic acid–water (4:1:5, v/v/v); Sample: trp–tyr (1.25 mg) and val–tyr (5 mg) in 0.5 ml of upper phase; monitoring system: Uvicord IIS at 280 nm; elution mode: L–I–T, lower phase pumped from the inner tail terminal of the spiral tube, L–I–H, lower phase pumped from the inner head terminal of the spiral tube, U–O–T, upper phase pumped from the outer tail terminal of the spiral tube, U–O–H, upper phase pumped from the outer head terminal of the spiral tube.

sandwiched between the spiral layers. This problem may be largely alleviated by compressing the four radial grooves using a specially made tool with rectangular teeth that fit to the radial grooves. This process gives three major advantages for the separation: first, the number of spiral layers is increased; second, the dead space in the transfer tubes is reduced; and, third, laminar flow of the two phases is interrupted as in the cross-pressed spiral tube.

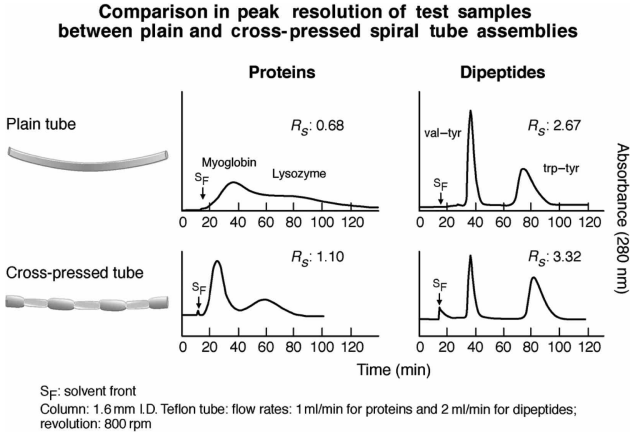

Fig. 13 Separation of proteins and dipeptides by plain spiral tube and cross-pressed tube assemblies. Experimental conditions are as follows: apparatus: type-J coil planet centrifuge with 10 cm revolution radius; separation column: plain spiral tube assembly: nine spiral layers about 40 m long, 1.6 mm I.D. FEP tube with a total capacity of 103 ml; cross-pressed spiral tube assembly: nine spiral layers about 40 m long, 1.6 mm I.D. FEP tubing cross-pressed at 1 cm interval with 95 ml capacity; solvent system: 12.5% (w/w) PEG-1000 and 12.5% (w/w) dibasic potassium phosphate in water (for protein separation); sample: lysozyme and myoglobin, each 5 mg in 1 ml of upper phase (for protein seperation), trp–tyr (1.25 mg) and val–tyr (5 mg) in 0.5 ml of upper phase (for dipeptide separation); elution mode: L–I–T; flow rate: 1 ml/min (for protein separation), 2 ml/min (for dipeptide separation); detection: 280 nm; rpm: 800.

Fig. 15 shows protein separation obtained by the spiral tube assembly with these two tube modifications of cross-pressing and radial groove compression. The column is made from a slightly smaller tube of 1.35 mm I.D. making 15 spiral layers with a total capacity of about 85 ml. The protein separation was performed in the L–I–T elution mode under various revolution speeds ranging from 600 to 1200 rpm. As the revolution speed is increased, the separation of the two peaks steadily improves and at 1200 rpm two protein peaks are well resolved. The separation is completed in 90 min at a high flow rate of 2 ml/min.

The spiral tube assembly can be successfully applied to the separation of dipeptides and proteins using highly polar solvent systems with sufficient stationary phase retention. Although a plain spiral tube assembly can be used for the separation of peptides, the partition efficiency is remarkably increased by modifying the tube configuration in two steps: cross-pressing and radial groove compression especially for protein separation with a polymer phase system. As the present system allows a high flow rate with high retention of the stationary phase, good peak resolution is obtained in a short elution time. This improved spiral tube assembly can be efficiently applied to all two-phase solvent systems for HSCCC.

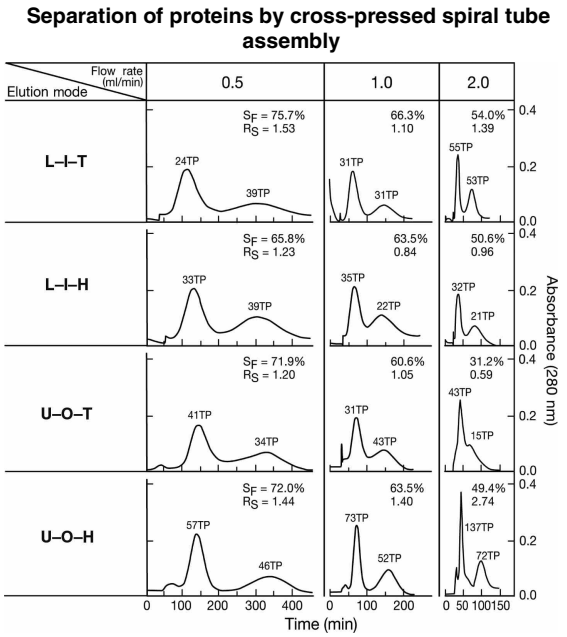

Fig. 14 Protein separation by cross-pressed spiral tube assembly at 800 rpm. Experimental conditions are as follows: apparatus: type-J coil planet centrifuge with 10 cm revolution radius; separation column: nine spiral layers about 40 m long, 1.6 mm I.D. polytetrafluoroethylene (PTFE) tubing cross-pressed at 1 cm interval with a 95 ml capacity; solvent system: 1.25% (w/w) dibasic PEG-1000 and 1.25% (w/w) potassium phosphate in water; sample: lysozyme and myoglobin, each 5 mg in 1 ml of upper phase; detection: 280 nm; rpm: 800.

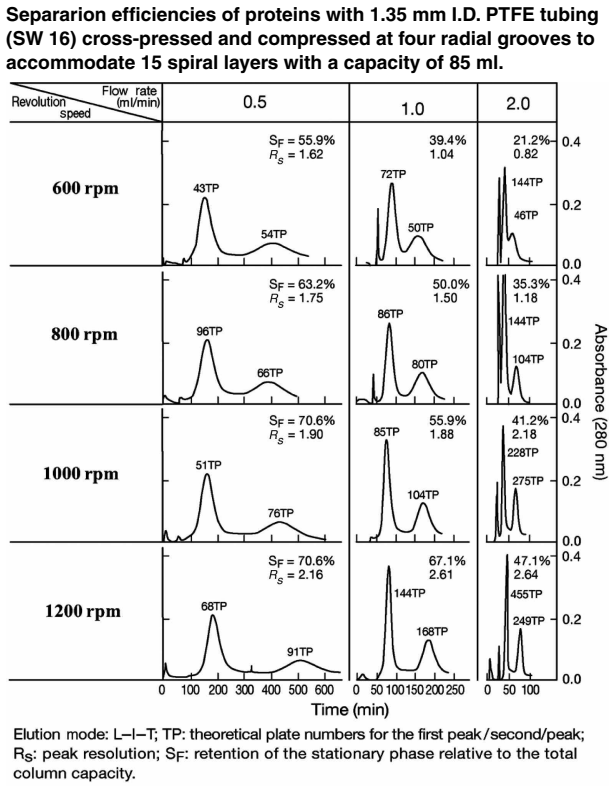

Fig. 15 Protein separation by cross-pressed and radial groove-compressed spiral tube assembly at various revolution speeds and flow rates. Experimental conditions are as follows: apparatus: type-J coil planet centrifuge with a 10 cm revolution radius; solvent system: 12.5% (w/w) PEG-1000 and 12.5% (w/w) dibasic potassium phosphate in water; sample: lysozyme and myoglobin, each 5 mg in 1 ml of upper phase; elution mode: L–I–T; detection: 280 nm.

REFERENCES

1. Ito,Y. *High-speed Countercurrent Chromatography*; Ito, Y., Conway, W.D., Eds.; Wiley-Interscience: New York, 1996.
2. Ito, Y. High-speed countercurrent chromatography. CRC Crit. Rev. Anal. Chem. **1986**, *17*, 65–143.
3. Berthod, A.; Billardello, B. Test to evaluate countercurrent chromatographs: Liquid stationary phase retention and chromatographic resolution. J. Chromatogr. A, **2000**, *902*, 323–335.
4. Shinomiya, K.; Kabasawa, Y.; Ito, Y. Protein separation by cross-axis coil planet centrifuge with spiral coil assemblies. J. Liq. Chromatogr. Relat. Technol. **2002**, *25* (17), 2665–2678.
5. Ito, Y.; Yang, F.-Q.; Fitze, P.E.; Sullivan, J.V. Spiral disk assembly for high-speed countercurrent chromatography. J. Liq. Chromatogr. Relat. Technol. **2003**, *26* (9–10), 1355–1372.
6. Ito, Y.; Yang, F.-Q.; Fitze, P.E.; Powell, J.; Ide, D. Improved spiral disk assembly for high-speed countercurrent chromatography. J. Chromatogr. A, **2003**, *1017*, 71–81.
7. Ito, Y.; Clary, R.; Sharpnack, F.; Metger, H.; Powell, J. Mixer-settler counter-current chromatography with multiple spiral disk assembly. J. Chromatogr. A, **2007**, *1172*, 151–159.
8. Ito, Y.; Qi, L.; Powell, J.; Sharpnack, F.; Metger, H.; Yost, J.; Cao, X.-L.; Dong, Y.-M.; Huo, L.-S.; Zhu, X.; Li, T. Mixer-settler countercurrent chromatography with a barricaded spiral disk assembly with glass beads. J. Chromatogr. A, **2007**, *1151*, 108–114.
9. Knight, M.; Ito, Y.; Finn, T.M. Separation of peptides by spiral countercurrent chromatography. J. Liq. Chromatogr. Relat. Technol. **2008**, *31*, 471–481.
10. Cao, X.-L.; Hu, G.-H.; Huo, L.-S.; Zhu, X.-P.; Li, T.; Ito, Y.; Powell, J. Stationary phase retention and preliminary application of a spiral disk assembly designed for high-speed counter-current chromatography. J. Chromatogr. A, **2008**, *1188*, 164–170.
11. Ito, Y.; Clary, R.; Powell, J.; Knight, M.; Finn, T.M. Spiral tube support for high-speed countercurrent chromatography. J. Liq. Chromatogr. Relat. Technol. **2008**, *31* (9), 1346–1357.
12. Ito, Y.; Clary, R.; Powel, J.; Knight, M.; Finn, T.M. Improved spiral tube assembly for high-speed counter-current chromatography. J. Chromatogr. A, **2009**, *1216*, 4193–4200.

Spiral Disk Assembly: Column Design for HSCCC

Yoichiro Ito
Fuquan Yang
National Heart, Lung, and Blood Institute (NHLBI), National Institutes of Health (NIH), Bethesda, Maryland, U.S.A.

INTRODUCTION

The high-speed countercurrent chromatography (HSCCC) centrifuge uses a multilayer coil as a separation column which produces high-efficiency separation with good retention of the stationary phase with a variety of two-phase solvent systems.[1,2] However, the method often fails to retain a satisfactory amount of the stationary phase for highly viscous, low interfacial solvent systems such as polymer phase systems, which are useful for the separation of macromolecules and particulates. A new column design called "spiral disk assembly," described below, provides a universal application of solvent systems, including the polymer phase systems for HSCCC.

PRINCIPLE

Retention of the stationary phase in the coiled column of the HSCCC system totally relies on the Archimedean screw force generated by the planetary motion of the column. However, this force is often too weak to retain the stationary phase for some polar solvent systems, such as aqueous–aqueous polymer phase systems, resulting in carryover of the stationary phase from the column.

The new spiral column design improves the retention of the stationary phase by modifying the configuration of the column from a coil to a spiral, so that the centrifugal force gradient produced by the spiral pitch helps to distribute the heavier phase in the periphery and the lighter phase in the proximal portion of the column. This effect can be enhanced by increasing the pitch of the spiral. Although a spiral column can be prepared simply by winding the tubing into a flat spiral configuration,[3,4] it can provide a limited spiral pitch [outer diameter (O.D.) of the tubing] and, additionally, the connection between the neighboring spiral columns is rather difficult.

These problems can be solved by making a single or plural spiral channel(s) in a solid disk. In the first model, a single spiral channel is made in a plastic disk, which can be serially connected by stacking multiple disks sandwiched with Teflon sheet septa. In the second model, four spiral channels are incorporated in a single disk, symmetrically around the center, so that the spiral pitch is increased by four times that of the above single spiral channel without losing the column sptace. Connection between the neighboring spiral channels is formed by a short straight channel situated radially on the other side of the disk. A set of these disks can be serially connected by spacing a Teflon sheet between the neighboring disks, so that the column provides a large capacity that is somewhat comparable to that of the multilayer coil. The separation disk with a single spiral will serve as a control to evaluate the effect of the pitch on the partition efficiency.

DESIGN OF THE SPIRAL DISK

The design of the spiral column assembly is shown in Fig. 1. Fig. 1a shows a full view of the column assembly, which can be mounted on the type-J multilayer coil planet centrifuge (P.C., Inc., Potomac, Maryland, U.S.A.). The column components are illustrated in Fig. 1b. The column consists of a pair of flanges (one equipped with a gear), nine disks with spiral grooves, and ten Teflon sheet septa. The drawing, and dimensions for each component are illustrated in Fig. 2a–e.

The design of the individual separation disk with one spiral channel (diameter: 17.5 cm, thickness: 3 mm, with a 1.25 cm diameter center hole) is shown in Fig. 2a. The dimensions of the channel are 2.6 mm wide, 2 mm deep, with 1 mm ridge width, which gives a spiral pitch of 4 mm. The total channel length is about 4 m, comprising 12 spiral turns, with a total capacity of ~23 ml. The channel starts at the internal inlet (23 mm from the center) and extends to the external outlet (75 mm from the center), which is connected to the radial channel on the other side through a hole of ~1 mm diameter. The performance of this single spiral column may be compared to that of the following four-channel spiral column, by using a polar butanol solvent system and polymer phase systems.

Design of the individual separation disk for four separate spiral channels is shown in Fig. 2b. A plastic disk (17.5 cm diameter and 4 mm thick, high-density polyethylene) has four spiral channels (grooves), each 2.6 mm wide, 2 mm deep, and ~1 m long, with a capacity of about 6 ml. The ridge between each groove is 1 mm and, therefore, the pitch of each spiral becomes as large as 16 mm (four times that of

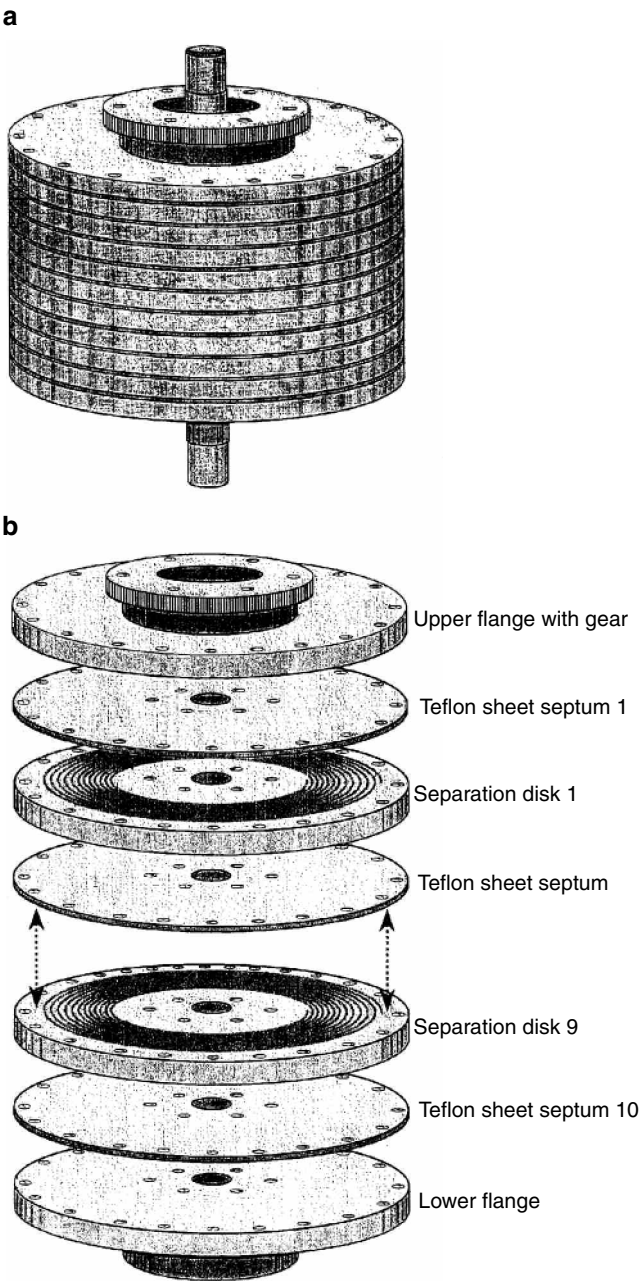

Fig. 1 Schematic illustration of the spiral disk assembly. a, Whole view. b, Exploded view showing each component.

the single spiral channel). Each channel starts at the inner end (I_1, I_2, I_3, and I_4) to reach the outer end (O_1, O_2, O_3, and O_4, respectively). As shown in the diagram, each channel forms 3.25 spiral turns so that the outer end of channel 1 (O_1) radially coincides with the inner end of channel 2 (I_2), and those of channels 2, 3, and 4 ($O_{2,3,4}$) similarly coincide with the inner ends of channels 3, 4, and 1 ($I_{3,4,1}$), respectively. Each end of the channel (except for O_1) has a hole (~1 mm diameter) through the disk to reach the other side, where a radial channel (dotted line) leads to the next spiral channel through another hole. The outer end of channel 4 (O_4) is connected to a similar radial channel which leads to channel 1 (I_1) of the next disk, or the column outlet, through an opening in the Teflon septum (Fig. 2c).

All disks have screw holes (clearing an 8–32 screw) at both inner and outer edges, at regular intervals (10° for the outer edge and 45° for the inner edge). Similar holes are also made in both the Teflon sheets and the flanges.

The design of the flanges is shown in Fig. 2d and e. The upper flange (Fig. 2d) is equipped with a plastic gear (9 mm thick, 10 cm pitch diameter), which engages with an identical stationary gear on the high-speed CCC centrifuge. Fig. 2e shows the lower flange, which has two screw holes (90° apart), for tightly fixing the column assembly against the column holder shaft (0.9 in. diameter). Both upper and lower flanges each have an inlet hole which fits into an adapter with a 1/4–28 screw thread. They also have a set of screw holes (clearing an 8–32 screw) around the outer and inner edges as in the separation disks and Teflon septa. The column assembly is mounted on the rotary frame of the multilayer coil centrifuge and counterbalanced with brass blocks. A pair of flow tubes from the column assembly is led downward through the center hole of the column holder shaft and passed through the hollow central pipe to exit the centrifuge at the center hole of the top plate, where it is tightly fixed with a pair of clamps. These tubes are protected with a sheath of Tygon tubing to prevent direct contact with metal parts.

EXPERIMENTAL PROCEDURE

Each two-phase solvent system is thoroughly equilibrated in a separatory funnel at room temperature and the two phases are separated before use. The sample solution is prepared by dissolving the sample in an appropriate volume (1–5 ml) of the upper and/or lower phase of the solvent system. In each experiment, the column is first entirely filled with the stationary phase (upper or lower phase), followed by sample injection through the sample port. Next, the apparatus is rotated at 800 rpm, while the mobile phase is eluted through the column at the desired flow rate. The separation may be repeated by changing the direction of the revolutions and/or elution mode (head to tail and tail to head), although it is expected that the best result would be obtained by eluting either the lower phase from the internal terminal toward the external terminal of the spiral channel, in a tail-to-head elution mode, or the upper phase in the opposite direction in a head-to-tail mode. The effluent from the outlet of the column is continuously monitored through an ultraviolet (UV) detector.

BASIC STUDIES WITH SINGLE DISKS

Using a single disk with each channel design, a series of experiments was performed to evaluate the performance of

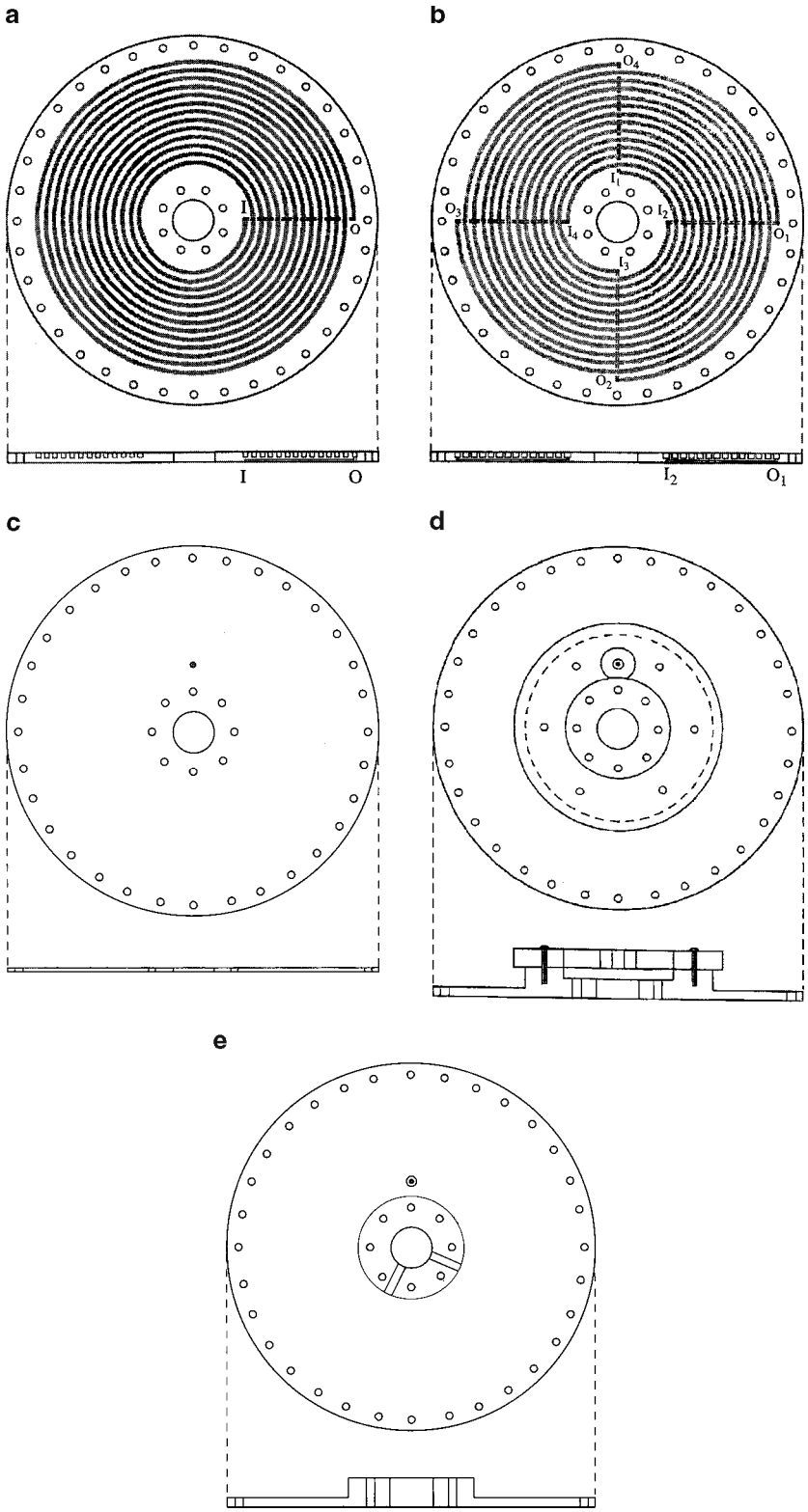

Fig. 2 Drawing of each component of the spiral disk assembly. a, Disk with a single spiral; b, Disk with four spirals; c, Teflon sheet septum; d, Upper flange equipped with a plastic gear; e, Lower flange.

the disk in terms of partition efficiency and retention of the stationary phase, by using three different types of two-phase solvent systems: 1-butanol/acetic acid/water (4 : 1 : 5, v/v/v) for separation of dipeptides; 12.5% (w/w) polyethylene glycol (PEG)-1000, 12.5% (w/w) dibasic potassium phosphate in water for protein separations; and 4% (w/w) PEG-8000, 5% (w/w) dextran T500 in water for measuring the retention of the stationary phase. The experiments were performed at various flow rates of the mobile phase, using four different elution modes, i.e., L–I–T (lower phase eluted from the inner

Table 1 Dimensions of four spiral channels used in the present studies.

Disk no.	Number of spiral	Width[a] (mm)	Depth[a] (mm)	Pitch (mm)	Capacity (ml)
Column I	1	2.6	2.0	4	23
Column II	1	1.5	3.7	4	21
Column III	4	2.6	2.0	16	23
Column IV	4	1.5	3.7	16	21

[a]The width of the spiral groove becomes the depth of the channel and the depth becomes the width of the channel when assembled.

terminal at the tail); L–I–H (lower phase eluted from the inter terminal at the head); U–O–T (upper phase eluted from the outer terminal at the tail); U–O–H (upper phase eluted from the outer terminal at the head). Four other reversed elution modes, including L–O–T, L–O–H, U–I–T, and U–I–H, showed considerably less retention of the stationary phase, compared with their counterparts, because of the adverse effect of the radial centrifugal force gradient. The dimensions of these four spiral channels are given in Table 1.

1-Butanol/Acetic Acid/Water (4 : 1 : 5) System

Fig. 3a–d shows the separation of a standard sample mixture of trp–tyr (0.5 mg) and val–tyr (2 mg) with a

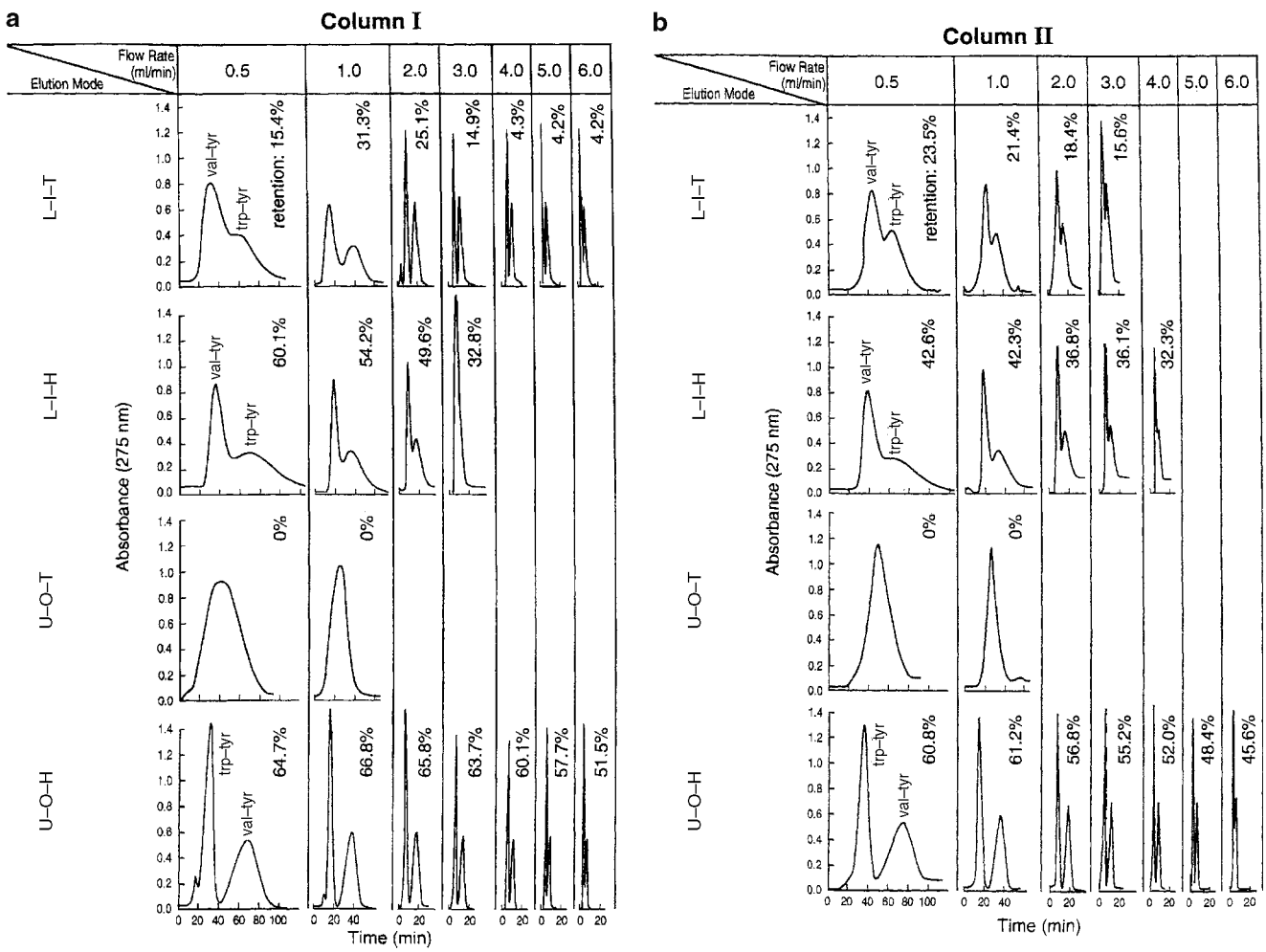

Fig. 3 Separation of peptides with a set of four single disks. Experimental conditions: apparatus, type-J coil planet centrifuge with 10 cm revolution radius; a, Column I. b, Column II. c, Column III. d, Column IV (dimensions of channels are listed in Table 1). Sample: trp–tyr (0.5 mg) + val–tyr (2 mg) in 1 ml of upper phase; solvent system: 1-butanol-acetic acid/water (4 : 1 : 5); elution modes: L–I–T, lower phase from the inner terminal at tail, L–I–H, lower phase from the inner terminal at head, U–O–T, upper phase from the outer terminal at tail, and U–O–H, upper phase from the outer terminal at head; flow rate: 0.5–10 ml/min as indicated; rpm: 800, stationary phase retention: indicated in the figure.

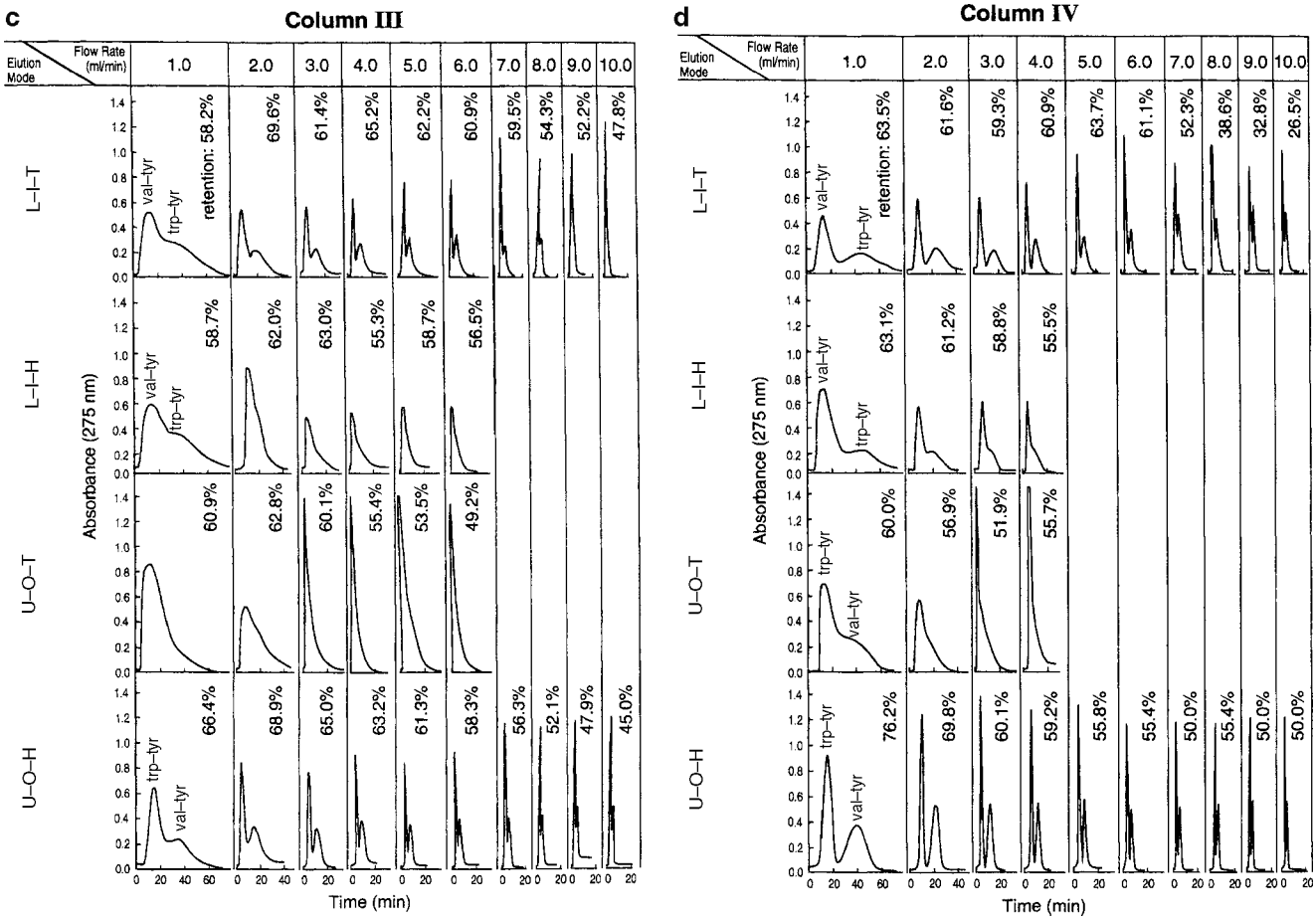

Fig. 3 (*Continued*)

two-phase solvent system composed of 1-butanol/acetic acid/water (4 : 1 : 5), by using a set of four different spiral columns (columns I–IV in Table 1).

In each chromatogram, the UV absorbance (280 nm) was plotted against the elution time, together with the % retention volume of the stationary phase relative to the total column capacity. In each group, a set of chromatograms is arranged according to the four different elution modes, i.e., L–I–T, L–I–H, U–O–T, and U–O–H, where L and U indicate the lower phase mobile and upper phase mobile; I and O denote eluting from internal terminal and external terminal of the spiral; and T and H represent "tail-to-head" and "head-to-tail" elution mode, each under various flow rates of the mobile phase.

In column I (Fig. 3a), the elution with upper phase from the head of the spiral (U–O–H) produces the best peak resolution and the highest % retention of the stationary phase. The elution with the lower phase from the head of the spiral (L–I–T) also shows a good peak resolution up to the flow rate of 6 ml/min, in spite of its low retention of the stationary phase. Elution of the lower phase from the head (L–I–H) retains a satisfactory amount of the stationary phase under the flow rate of 0.5–2 ml/min, while the peak resolution is much lower than those of its counterpart (L–I–T). The elution of the upper phase from the tail (U–O–T) shows no retention of the stationary phase, even at a low flow rate of 0.5 ml/min. These elution trends are also found in column II (Fig. 3b), except that the peak resolution is much reduced in the elution of the lower phase from the tail (L–I–T), under a similar retention level of the stationary phase.

Fig. 3c and d shows the chromatograms obtained from the four-spiral disks under otherwise identical experimental conditions. It clearly indicates that the retention of the stationary phase is much improved in all elution modes. Although the peak resolution of the two dipeptides was substantially reduced, the flow rate could be increased up to 10 ml/min to yield a moderate degree of peak resolution as emphasized by column IV (Fig. 3d).

This suggests that, if one used a multichannel spiral disk with a large pitch, the separation of peptides might be achieved in a very short elution time.

PEG 1000-Dibasic Potassium Phosphate Polymer Phase System

Fig. 4a–d similarly illustrates the peak resolution between two protein samples (lysozyme and myoglobin, 10 mg each) in the PEG–phosphate system obtained from the four

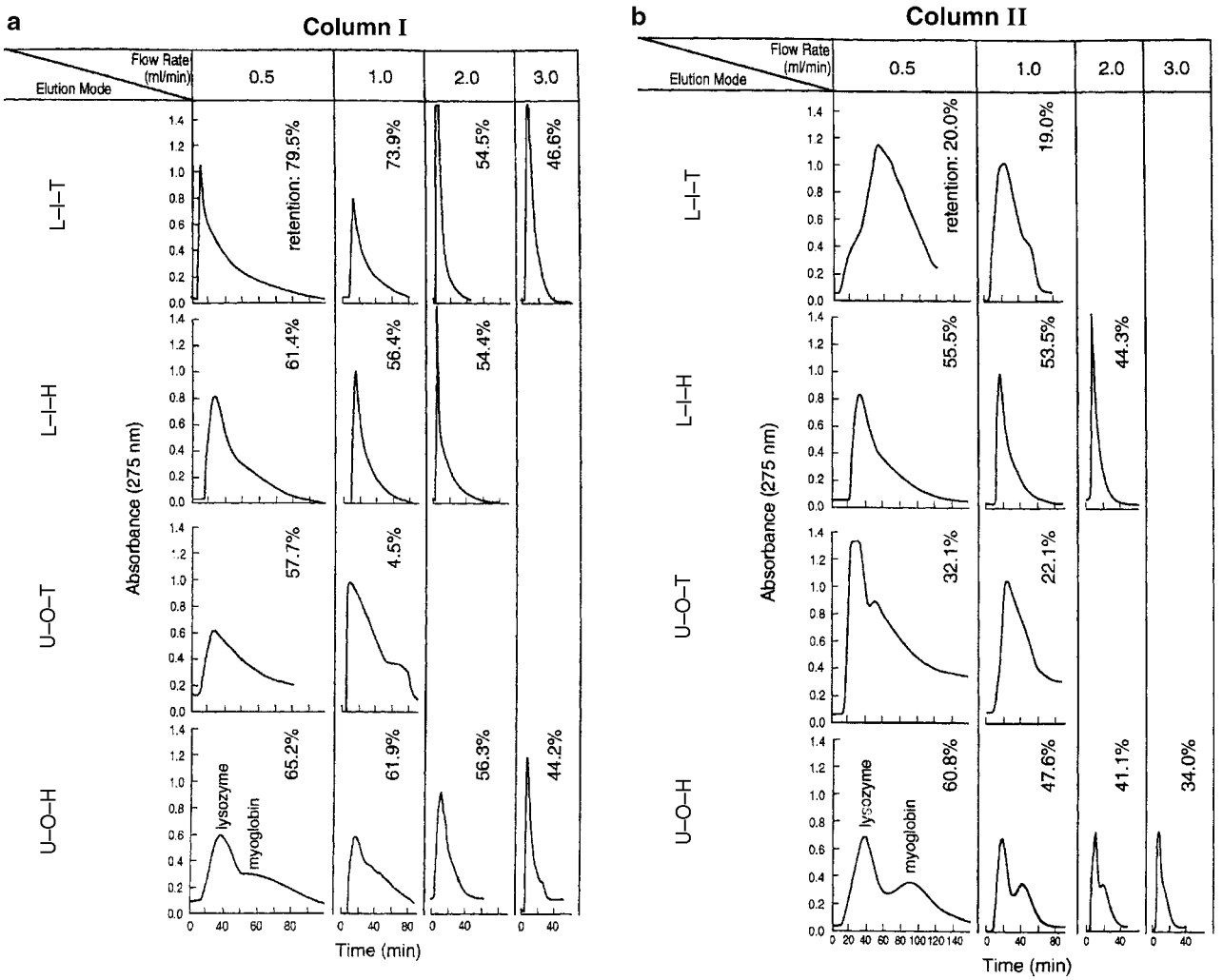

Fig. 4 Separation of proteins with a set of four single disks. Experimental conditions: apparatus, type-J coil planet centrifuge with 10-cm revolution radius; a, Column I. b, Column II. c, Column III. d, Column IV (dimensions of channels are listed in Table 1). Sample: lysozyme and myoglobin each 5 mg in 1 ml of upper phase; solvent system: 12.5% (w/w) PEG1000 and 12.5% (w/w) potassium diphosphate in water; elution modes: L–I–T, lower phase from the inner terminal at tail, L–I–H, lower phase from the inner terminal at head, U–O–T, upper phase from the outer terminal at tail, and U–O–H, upper phase from the outer terminal at head; flow rate: 0.5–5 ml/min as indicated; rpm: 800, stationary phase retention: indicated in the figure.

different spiral disks. In the single-spiral disks (Fig. 4a and b), the best results were obtained by eluting the upper PEG-rich mobile phase from the head end of the outer terminal (U–O–H); other modes resulted in low resolution. Except for L–I–T and I–O–T in column II, all groups show a satisfactory level of stationary phase retention with a flow rate of 0.5 ml/min, indicating that mixing of two phases in the spiral column is inefficient. This tendency is more pronounced in the four-spiral disks (Fig. 4c and d), which show much higher retention of the stationary phase (over 60%), but without any peak resolution. Comparing columns in Fig. 4a and b shows the latter to yield somewhat higher peak resolution, which is probably a result of the shallow channel which facilitates mass transfer between the two phases. This suggests that the separation might be further improved by reducing the width of the spiral groove.

PEG 8000–Dextran 500 Polymer Phase System

A series of experiments was performed to examine the retention of the PEG–dextran polymer phase system without samples. Results are shown in Table 2, where % retention of the stationary phase is indicated at the flow rates of 0.5–1 or 2 ml/min for each spiral column. The results indicate that, among the single-spiral disks (I and II), column I with a deep channel retained over 60% of the lower dextran-rich stationary phase (U–O–H and U–O–T), at a low flow rate of 0.5 ml/min while, under other conditions, the retention was substantially less than 50% of the total column capacity. In contrast, the four-spiral disks (columns III and IV) attained remarkably improved retention of over 50% for all elution modes, at 0.5 ml/min flow rate. Again, the results

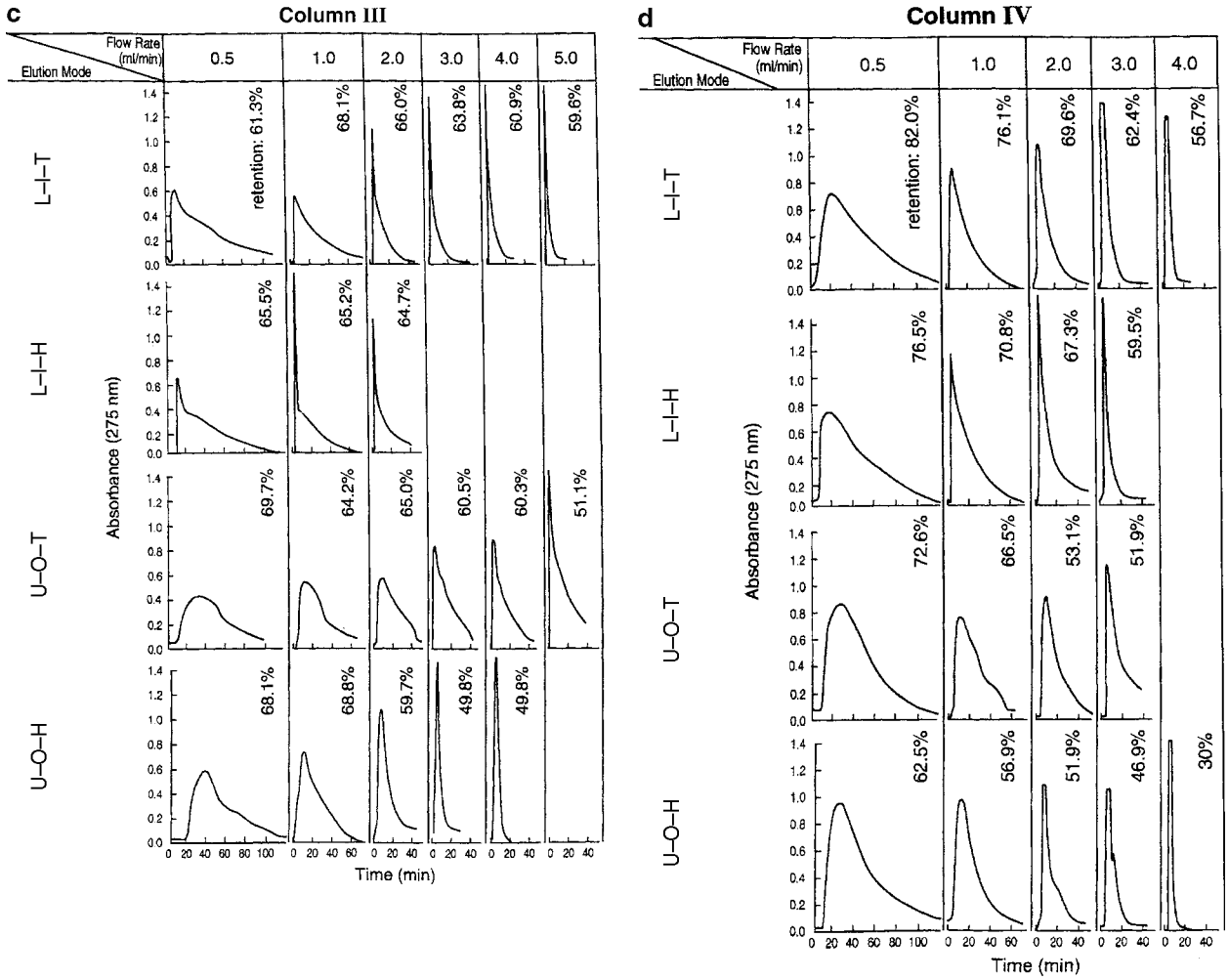

Fig. 4 (*Continued*)

indicate the effect of the greater spiral pitch, which favors the retention of the stationary phase.

PRELIMINARY SEPARATION WITH A SPIRAL DISK ASSEMBLY

The performance of the present column design was examined by using a spiral disk assembly consisting of eight units of column I, with a total capacity of 165 ml. Results are shown in Fig. 5a and b. In Fig. 5a, a mixture of five dipeptides was well resolved and was completely eluted in 2 hr. The upper organic phase of the 1-butanol solvent system was eluted at a flow rate of 4 ml/min. Similar separations were shown with the standard multilayer coils in HSCCC, but only with more stable butanol solvent systems.[1]

Fig. 5b shows the separation of two stable proteins (lysozyme and myoglobin) by using a PEG 1000/

Table 2 % Retention of 4% PEG8000–5% Dextran T 500 in 10 m*M* Na_2HPO_4 system.

	Column			
	I	**II**	**III**	**IV**
Flow rate (ml/min)	0.5 – 1	0.5 – 1	0.5 – 1 – 2	0.5 – 1.0 – 2.0
L–I–T	40.0 – 14.8	14.3 – 3.3	61.1 – 50.0 – 14.3	55.6 – 33.3 – 4.0
L–I–H	37.1 – 2.0	10.9 – 6.5	53.9 – 47.8 – 17.4	52.0 – 33.3 – 9.6
U–O–T	71.8 – 32.3	31.0 – 17.4	67.8 – 65.7 – 50.0	64.4 – 56.0 – 42.7
U–O–H	61.9 – 28.0	15.1 – 10.1	59.8 – 46.8 – 45.1	58.5 – 54.5 – 44.0

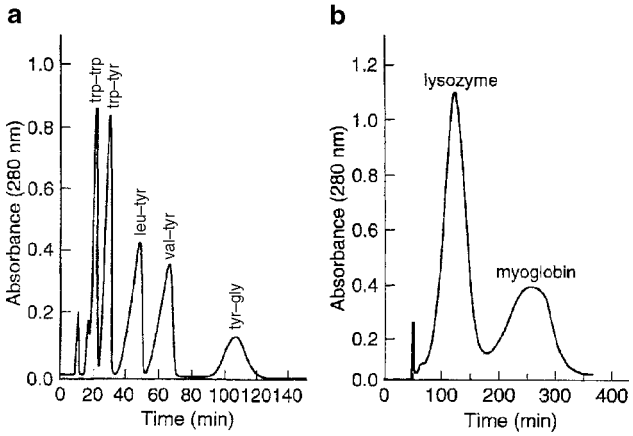

Fig. 5 Preliminary separation of peptides and proteins by a spiral disk assembly. a. Separation of a set of dipeptides. b. Lysozyme and myoglobin. Experimental conditions are as follows: apparatus: type-J coil planet centrifuge with 10 cm revolution radius; column: spiral disk assembly consisting of eight disks (column I) with a total capacity of about 200 ml; sample: a. trp–trp (1.25 mg), trp–tyr (2.5 mg), leu–tyr (l0 mg), val–tyr (l0 mg), tyr–gly (10 mg) in 5 ml upper phase. b. lysozyme and myoglobin each 50 mg in 5 ml lower phase; solvent system: a. 1-Butanol/acetic acid/water (4 : 5 : 1). b. 12.5% (w/w) PEG1000, 12.5% (w/w) K_2HPO_4 in water; mobile phase: a. Upper organic phase. b. Upper PEG-rich phase; flow rate: a. 4 ml/min. b. 0.5 ml/min, elution mode: a. U–O–H. b. U–O–H, revolution: 800 rpm, retention of stationary phase: a. 60%. b. 77.4%.

K_2HPO_4 polymer phase system at a flow rate of 1 ml/min, where they were well resolved in slightly over 5 hr. As suggested by the basic studies, the separation may be substantially improved by using the column II disk assembly, which provides a shallower channel to facilitate mass transfer in viscous polymer phases.

CONSIDERATION OF VARIOUS PARAMETERS GOVERNING PERFORMANCE OF THE SPIRAL COLUMN

Depth and Width of the Spiral Channel

Differing from the ordinary coiled column prepared from Teflon tubing, the channel of the spiral column has a rectangular cross-section. Because the centrifugal force acts along the radius of the disk, the width of the groove on the disk becomes the depth of the channel, and the depth of the groove becomes the width of the channel. Here it is reasonable to consider that a greater depth of the channel favors the retention of the stationary phase, while it provides a less efficient mass transfer rate. In the present studies, we used two different dimensions of the spiral channel: columns I and III are 2.6 mm in depth (or width of the groove) and 2.0 mm in width (or depth of the groove), while columns II and IV are 1.5 mm in depth and 3.7 mm in width. The experimental data clearly indicate that, with few exceptions, the deeper column (columns I and III) produces a better retention of the stationary phase. This trend is most clearly observed in the viscous PEG–dextran system in the single-channel spiral disks (columns I and II).

The effects of channel geometry on partition efficiency in terms of peak resolution gives a more complex picture: in the dipeptide separation with the butanol solvent system, the deeper channel of the single spiral disk (column I) produced a substantially better peak resolution, especially in the lower phase mobile mode (L–I–T), whereas the shallower channel in the four-spiral disks (column IV) produced a somewhat better separation than its counterpart. We do not understand the reason why higher peak resolution is obtained in the deeper channel of column I in L–I–T, despite the low retention of the stationary phase. In protein separation, with the PEG–phosphate system, the shallower spiral channel of the single-spiral disk displayed the best separation in the upper PEG-rich mobile phase, whereas both four-spiral disks (columns III and IV) showed less efficient separations.

The overall results suggest that the shallower channel shows better separation of proteins by using the PEG–phosphate polymer phase system and the deeper channel favors the retention of viscous PEG–dextran solvent systems.

Spiral Pitch

The effects of the spiral pitch on the present studies are observed by comparing the chromatograms between columns I and III for the deep channel and between columns II and IV for the shallow channel. It is clearly observed that, in the dipeptide separation with the 1-butanol solvent system, the greater pitch results in lower peak resolution at a given flow rate, while it provides higher retention of the stationary phase, thereby allowing a higher flow rate of the mobile phase to reduce the separation time. Similar effects are also observed in the protein separation with the PEG–potassium phosphate solvent system. In the PEG–dextran system, a greater pitch provides a substantial increase in retention of the stationary phase, some exceeding 50% retention at a flow rate of 1 ml/min.

Flow Rate of the Mobile Phase

The flow rate of the mobile phase is an important parameter which determines the elution time. In the dipeptide separation, the optimum flow rate producing the best peak resolution is present in all spiral disks. In the four-spiral disk systems (columns III and IV), which retain a large volume of the stationary phase, the application of a high flow rate of up to 10 ml/min is possible to reduce the separation time, without substantial loss of peak resolution. In the separation of proteins with PEG–phosphate, the low

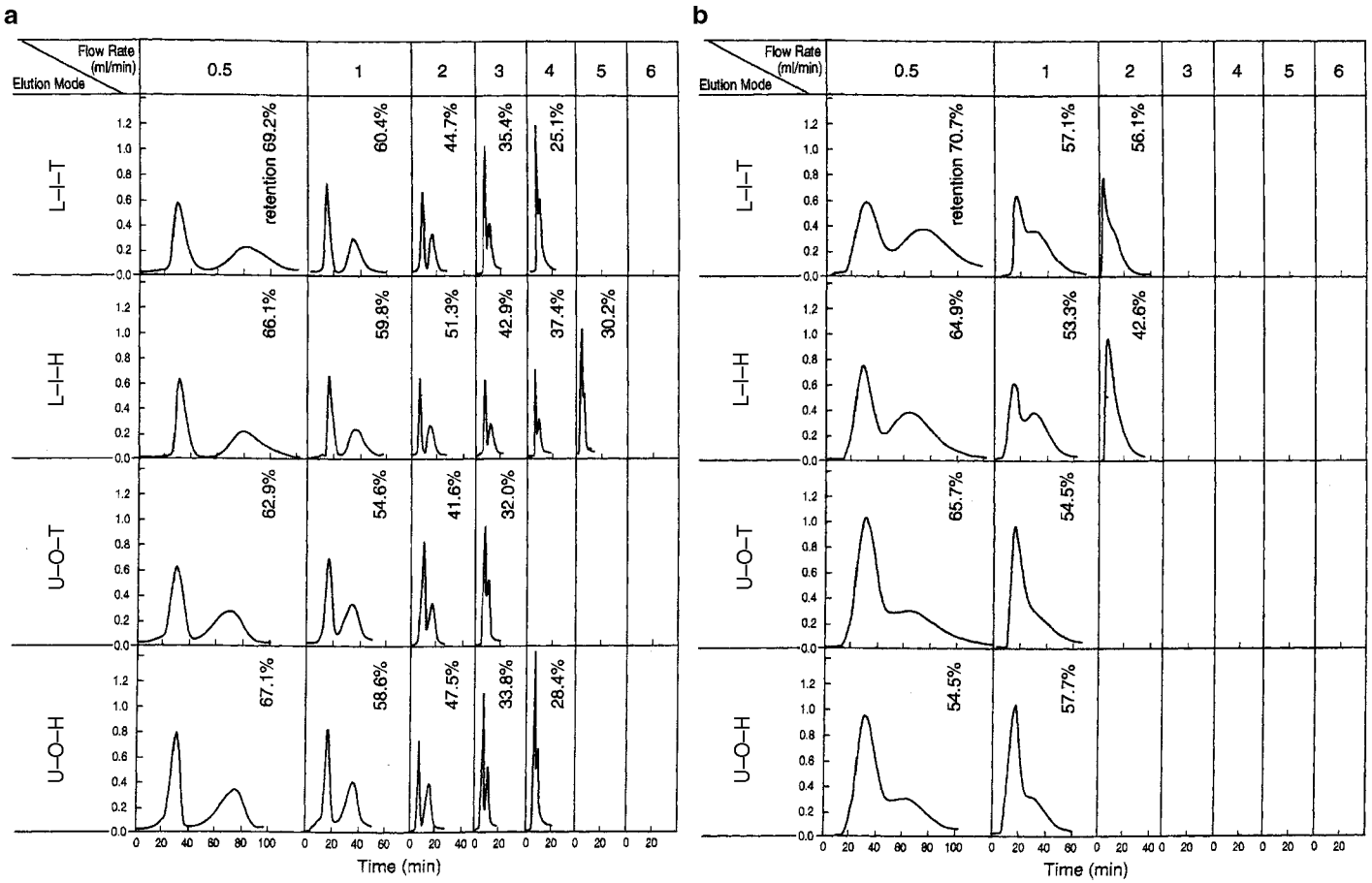

Fig. 6 Locular column IV. Four spiral channels: 1.5 mm (width) × 3.7 mm (depth), each 1 m long, locule: 1 cm × 310. a, 1-Butanol/acetic acid/water (4 : 1 : 5); and b, (PEG 1000-dibasic potassium phosphate (each 12.5%, w/w).

flow rate produced the best peak resolution with higher retention of the stationary phase.

EFFECTS OF VARIOUS INSERTS PLACED INTO THE CHANNEL SPACE

One of the advantages of the spiral disk over the spiral tubing is that the spiral channel can be modified in various ways to improve the partition efficiency. Early trials to place fine Teflon tubing (end closed) or small glass beads (less than 1.5 mm diameter) into the channel resulted in continuous carryover of the stationary phase, apparently a result of vigorous mixing (turbulence) caused by the rotating centrifugal force field. However, inserting short segments of Teflon tubing (~2 mm O.D., 2–3 mm in length) into the channel at regular intervals (1 cm) produced substantial improvement of the peak resolution, especially in column IV with high-pitch four spiral channels (Table 1). These findings suggest that the shape of the spiral groove can be modified into a locular configuration to improve the partition efficiency (Fig. 6).

CONCLUSIONS

The rectangular spiral channel embedded in a solid plastic disk, applied to the J-type HSCCC centrifuge, enhances the retention of stationary phase for viscous, low interfacial tension, two-phase solvent systems. Its main advantages are as follows:

1. Use of polymer phase systems for separation of biopolymers [proteins, deoxyribonucleic acid (DNA) and ribonucleic acid (RNA), and polysaccharides].
2. Reliable retention of the stationary phase for polar or low interfacial tension solvent systems (e.g., 1-butanol/water), which are useful for separation of bioactive compounds such as peptides.
3. Improved stationary phase retention against emulsification.
4. Application of the large column for industrial-scale separations by mounting the column assembly on the slowly rotating horizontal shaft.
5. The system allows further modification of the shape of spiral channels to improve the partition efficiency.

REFERENCES

1. Ito, Y. *High-Speed Countercurrent Chromatography*; Ito, Y., Conway, W.D., Eds.; Wiley-Interscience: New York, 1996.
2. Ito, Y. Test to evaluate countercurrent chromatographs. Liquid stationary phase retention and chromatographic resolution. CRC Crit. Rev. Anal. Chem. **1986**, *17*, 65–143.
3. Berthod, A.; Billardello, B. Protein separation by cross-axis coil planet centrifuge with spiral coil assemblies. J. Chromatogr. A, **2000**, *902*, 323–335.
4. Shinomiya, K.; Kabasawa, Y.; Ito, Y. Protein separation by cross-axis coil planet centrifuge with spiral coil assemblies. J. Liq. Chromatogr. Relat. Technol. **2002**, *25* (17), 2665–2678.

Split/Splitless Injector

Raymond P.W. Scott
Scientific Detectors Ltd., Banbury, Oxfordshire, U.K.

INTRODUCTION

The split/splitless detector has been designed for use with open-tubular columns or solid-coated open-tubular (SCOT) columns. Due to the small dimensions of such columns, they have very limited sample load capacity and, thus, for their effective use, require sample sizes that are practically impossible to inject directly. The split injector allows a relatively large sample (a sample size that is practical to inject with modern injection syringes) to be volatilized, and by means of a split-flow arrangement, a proportion of the sample is passed to the column while the remainder is passed to waste. A diagram of a split/splitless injector is shown in Fig. 1.

DISCUSSION

The body of the injector is heated to ensure the sample is volatilized and inside is an inert glass liner. This glass liner helps minimize any sample decomposition that might occur when thermally labile materials come in contact with hot-metal surfaces. The carrier gas enters behind the glass liner and is thus preheated. The sample is injected into the stream of carrier gas that passes down the center of the tube, a portion passes down the capillary column, and the remainder passes out of the system through a needle valve. The needle valve is used to adjust the relative flow rates to the column and to waste and, thus, controls the amount of sample that is placed on the column.

This process of sample injection has certain disadvantages. Due to the range of solute types present in most mixtures for analysis, the components will have different volatilities and their vapors will have different diffusivities in the carrier gas. Differential volatilization and diffusion rates will result in the sample that enters the capillary tube, being unrepresentative of the original mixture. For example, the more rapidly diffusing solutes will be more dispersed and, consequently, more diluted in the carrier gas than those of lesser diffusivity. This results in the slower-diffusing substances having a higher concentration in the sample entering the column than those of higher diffusivity. As a consequence, the sample will be proportionally unrepresentative of the original mixture. The differential sampling that results from split injection systems can become a serious problem in quantitative analysis with capillary columns.

An alternative approach is to use a splitless injection system. If the valve in Fig. 1 is closed, then all the sample passes into the column and there is no split; *ipso facto*, the device is a *splitless* injector. When used in the splitless mode, however, it is usual to employ a somewhat wider capillary column, which will allow the penetration of a small-diameter injection syringe and thus permit *on-column* injection. Under these circumstances, there can be no differential sampling of the form described. This procedure, however, introduces other injection problems that can affect both resolution and quantitative accuracy that need to be addressed (see *Retention Gap Injection Method*, p. 2035 and *Solute Focusing Injection Method*, p. 2187).

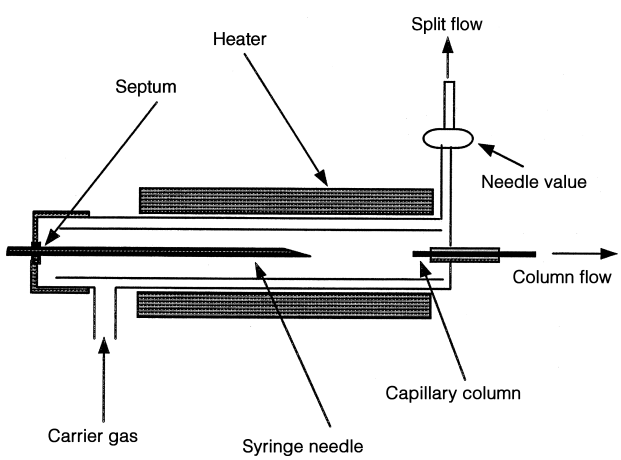

Fig. 1 Split/splitless injector.

BIBLIOGRAPHY

1. Grant, D.W. *Capillary Gas Chromatography*; John Wiley & Sons: Chichester, 1995.
2. Scott, R.P.W. *Techniques and Practice of Chromatography*; Marcel Dekker, Inc.: New York, 1996.
3. Scott, R.P.W. *Introduction to Analytical Gas Chromatography*; Marcel Dekker, Inc.: New York, 1998.

Stationary Phase Retention in CCC

Jean-Michel Menet
Aventis Pharma, Vitry-sur-Seine, France

INTRODUCTION

The retention of the stationary phase is a key parameter for countercurrent chromatography (CCC), as it influences all the chromatographic parameters describing a separation. First, it is important to closely monitor its value, commonly named SF; we give the reader three methods to determine this value. Then, the best conditions for obtaining the highest SF value are described for the three main CCC devices, which include: (a) a Sanki centrifugal partition chromatography, (b) a type J high-speed countercurrent chromatography, and (c) a cross-axis countercurrent chromatography. Finally, some theoretical approaches are introduced in order to estimate the value before any experimental work is performed.

HOW TO MEASURE SF

Fig. 1 indicates the principle of use of any CCC device for the equilibrium of two liquid, non-miscible phases. In this case, the stationary phase which is chosen is the lighter phase of the solvent system (dark gray in Fig. 1), whereas the mobile phase is indicated in white. For simplification, the coil is considered as an empty cylinder and the phenomena which occur inside the column are highly schematized as a stack of disks of mobile and stationary phases. This allows us to visualize the progression of the mobile phase inside the column. After the solvent system has reached equilibrium (complete settling of the two phases), the phase chosen as the stationary phase is pumped into the apparatus. The latter is considered as filled as soon as droplets of this stationary phase are expelled out of the column; this is Step 1 of Fig. 1.

The apparatus is then started, and when the desired rotational speed is reached, the mobile phase is pumped into the apparatus. A graduated cylinder is then put at the outlet of the apparatus. The two phases undergo a hydrodynamic or hydrostatic equilibrium inside the column while the mobile phase progresses toward the outlet of the column; this is Step 2. After a certain time, the mobile phase has reached the end of the column and then the first droplet of the mobile phase falls into the graduated cylinder; this Step 3. The experimenter then reads the volume, V_1, of the stationary phase which has been expelled from the column. The experiment is continued until the desired total volume is reached in the graduated cylinder. The experimenter can read the respective volumes of the stationary phase, named V_2, and the mobile one; this is, Step 4. Finally, the apparatus can be emptied (for instance, by pushing with nitrogen gas) and the liquids collected in another graduated cylinder; the volume of the stationary phase is V_3. For simplification purposes, the extracolumn volumes are neglected. Three measurements of the stationary phase retention are available:

- One just after the equilibrium inside the column: $SF_1 = (V_{column} - V_1)/V_{column}$
- One after a certain amount of time: $SF_2 = (V_{column} - V_2)/V_{column}$
- One by emptying the apparatus: $SF_3 = V_3/V_{column}$

If the equilibrium of the two phases was stable and not disturbed by any external event (change in rotational speed, flow rate, etc.), the three values of SF should be similar by a few percent of precision.

BEST CONDITIONS FOR SF FOR THE THREE MAIN CCC DEVICES

The best combinations of experimental parameters (e.g., choice of lighter or heavier phase, choice of the inlet to pump the mobile phase into, etc.) in order to retain the maximum amount of stationary phase inside the column are related to complex hydrodynamic phenomena which are based on the behavior of the solvent system inside the column of a given CCC apparatus. Many experiments have been carried out on the three main types of CCC devices by varying the experimental parameters and the solvent systems, in order to gather solvent systems by groups characterized by a combination of experimental parameters.

Sanki-Type Apparatus

The principle of this instrument has been precisely described in the entry (see *Centrifugal Precipitation Chromatography*, p. 378) devoted to this topic in this encyclopedia. The apparatus is a centrifuge, in which cartridges or plates are installed. Two rotating seals are required to allow the flow of the liquid phase: One stays at the top of the centrifuge, the other one at the bottom (solvent inlet and outlet).

Whatever the solvent system may be, the optimization for the best retention of the stationary phase is quite simple. Among the four possibilities, only two of them lead to a good retention of the stationary phase inside the cartridges

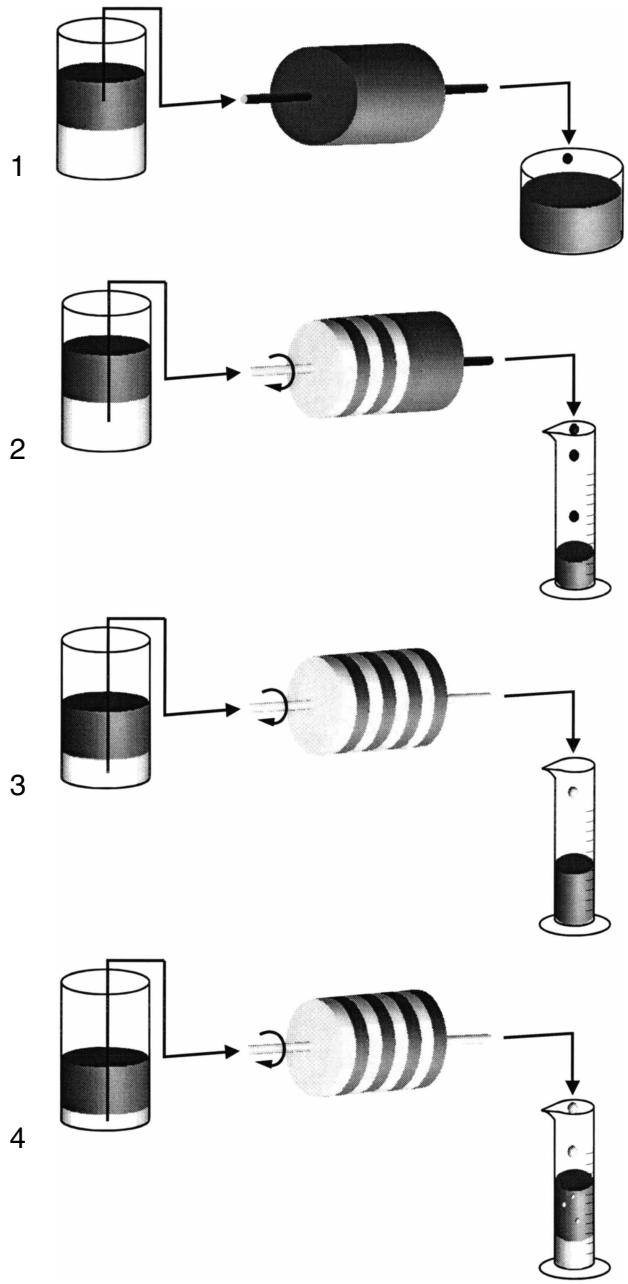

Fig. 1 Principle of the two-phase equilibrium inside a CCC column.

or the plates; they are based on the combination of the lighter mobile phase pumped from the bottom to the top seal, also called the "ascending" mode, and the heavier mobile phase pumped from the top to the bottom seal, also called the "descending" mode.

Type J Apparatus

The principle of this apparatus has been precisely described in an entry (see *Dual CCC*, p. 679) devoted to this topic in this encyclopedia. Two main parameters for using a two-phase solvent system with this apparatus are the choice of the heavier or the lighter mobile phase and the pumping mode [i.e., from the tail to the head or the head to the tail of the column (as a rotating coil defines a tail and a head, carrying, for instance, a small solid from the tail to the head)].

The designer of this type of device [Dr. Yoichiro Ito (National Institutes of Health, Washington, DC)], has tried various solvent systems in order to ascertain the best combinations of the two main parameters.[1] He observed that, among the four possibilities, only two led to the best retention of the stationary phase. However, the two optimal conditions were dependent on the nature of the solvent system and, for some solvent systems, on the geometrical dimension of the apparatus.

Ito has, consequently, decided to carry out a systematic study with 15 solvents.[1] His first conclusion was that only one condition was optimal among the two pumping modes for a given phase (i.e., lighter or heavier phase). The second conclusion was that the pumping modes to be used are reversed if the liquid phase is chosen as lighter instead of heavier, or vice versa.

Two groups of solvent systems have, consequently, been defined. One gathers solvent systems for which the two best combinations are the pumping of the lighter phase from the tail to the head of the column and the pumping of the heavier phase from the head to the tail of the column. The organic phases of such solvent systems are hydrophobic; thus, this group is called "hydrophobic" (e.g., hexane–water). The other group gathers solvent systems for which the two best combinations are the pumping of the lighter phase from the head to the tail of the column and of the heavier phase from the tail to the head of the column. The organic phases of such solvent systems are quite hydrophilic; thus, this group is called "hydrophilic" (e.g., butanol-2–water). The best combinations are reversed between the two groups.

However, there was a need to define a third group to take into account the behaviors of some solvent systems for which optimal combinations depend on the geometric dimensions of the apparatus. The discriminating parameter was found to be the β ratio of the coil radius on the distance between the two axis of rotation. For β values smaller than 0.3, solvent systems belonging to this third group behave like the solvent systems of the "hydrophilic" group. Conversely, for β values greater than 0.3, they behave like solvent systems of the "hydrophobic" group. The group was named "intermediate," which was also consistent with the mild hydrophobic (or hydrophilic) character of the organic phase (e.g., chloroform–methanol–water).

The main drawback of this classification comes from the experimental determination of the three groups. For a solvent system not previously studied, either by Ito or cited in the literature, the experimenter has to carry out four experiments in order to determine the two best combinations and, consequently, the group to which it belongs.

CROSS-AXIS-TYPE APPARATUS

The general principle of this type of apparatus is described in the corresponding entry (see *Proteins: Cross-Axis Coil Planet Centrifuge Separation*, p. 1935) of this encyclopedia. Contrary to the two previous CCC devices, four main parameters have to be considered here. Two of them are common to the other types of CCC units (i.e., choice of a lighter or a heavier phase and pumping mode from tail to head or from head to tail). Two additional parameters intervene: the pumping direction, from the inside to the outside of the core or reverse, and the rotation direction, clockwise or counterclockwise.

The same designer of this type of apparatus as for type J device, Ito, has applied the same procedure to classify various solvent systems by varying the main running parameters.[2,3] However, it has proven difficult to draw clear and precise conclusions from the results, because of the number of operating parameters. The methodology of experimental design has, consequently, emerged as the rational method to use for this purpose; it is easy to use and it elucidates the effects of the parameters and their interactions. A thorough, but global, analysis based on the experimental design methodology applied to the cross-axis-type device, was reported by Goupy et al.[4] The overall analysis carried out by the use of experimental design with a coil mounted in the L position simplifies the operation of the cross-axis apparatus, as the best combination does not depend on the solvent system. Indeed, the retention of the stationary phase is mainly related to the choice of the mobile phase and of the elution direction. A heavier mobile phase requires the outward elution direction, whereas a lighter mobile phase requires an inward elution direction.

Consequently, no classification among solvent systems may be built from their behaviors inside a cross-axis device.

THEORETICAL APPROACHES TO CORRELATE PHYSICAL PARAMETERS AND OBSERVED BEHAVIOR INSIDE A CCC COLUMN

The capillary wavelength and settling velocities have been retained as interesting parameters to step forward the description of the behavior of solvent system inside a CCC column. Moreover, they have also enabled a simple prediction of the effect of the temperature on the behavior of solvent systems, thus, on "Ito's classification."

The "theoretical" parameter capillary wavelength, λ_{cap}, has been precisely described by Menet et al.[4,5] The capillary wavelength is a means of describing the microscopic behavior at the interface between two immiscible liquids. It stands for the wavelength of the deformations which may occur at the interface of the two liquids or represents the mean diameter of drops of a liquid in another one. For common liquids, its average value is 1 cm in the Earth's gravitational field. For CCC devices, it is in the order of 1 mm, because of the generated centrifugal force field.

As the capillary wavelength only enables the description of the formation of droplets of one liquid in another one, it seemed interesting to introduce other "theoretical" parameters to better describe the dynamic phenomena occurring inside a CCC column. Two of these are presented here, namely V_{low} for the fall of a droplet of the heavier liquid phase (lower) in the continuous lighter one (upper) and V_{up} for the rise of a droplet of the lighter liquid phase in the continuous heavier one.

In order to determine if a correlation exists between "Ito's classification" and the values of the previous "theoretical" parameters, the 15 solvent systems used for the design of the classification have been studied. The values of interfacial tension, of densities, and of dynamic viscosities of the solvent systems were used to compute the values of the capillary wavelength and the settling velocities. The values of the three theoretical parameters have allowed to set ranges within which a solvent system is named "hydrophobic," "intermediate," or "hydrophilic." The main interest is that the knowledge of some physical parameters of the solvent systems allows one to know, before any experiments, the best combinations for the greatest stationary-phase retenion.

The values of the capillary wavelengths are smaller for "hydrophilic" solvent systems than those for "hydrophobic" ones: The first family of solvent systems tends to form small droplets of one phase in the other one, hence leading to a more stable emulsion. Their stationary phase is consequently less retained in the CCC column than the one of "hydrophobic" solvent systems; this phenomenon is well known in CCC.[1]

From additional studies of six new solvent systems and by studying the influence of the temperature, Menet et al. have shown the best classification is that based on V_{up}.[4]

REFERENCES

1. Mandava, N.B.; Ito, Y. *Countercurrent Chromatography—Theory and Practice*; Marcel Dekker, Inc.: New York, 1988.
2. Ito, Y.; Zhang, T.-Y. Cross-axis synchronous flow-through coil planet centrifuge for large-scale preparative counter-current chromatography: I. Apparatus and studies on stationary phase retention in short coils. J. Chromatogr. **1988**, *449*, 135–151.
3. Ito, Y. Cross-axis synchronous flow-through coil planet centrifuge (type XLL) *1: II. Speculation on the hydrodynamic mechanism in stationary phase retention. J. Chromatogr. **1991**, *538*, 67.
4. Goupy, J.; Menet, J.M.; Thiébaut, D. Experimental designs applied to countercurrent chromatography: definitions, concepts and applications. In *Countercurrent Chromatography*; Menet, J.M., Thiébaut, D., Eds.; Marcel Dekker, Inc.: New York, 1999.
5. Menet, J.M.; Thiébaut, D.; Rosset, R.; Wesfreid, J.-E.; Martin, M. Classification of countercurrent chromatography solvent systems on the basis of the capillary wavelength. Anal. Chem. **1994**, *66*, 168–176.

Stationary Phase Retention versus Peak Elution in CCC

Philip Wood
Brunel Institute for Bioengineering, Brunel University, Uxbridge, Middlesex, U.K.

INTRODUCTION

Walter Conway[1] adapted the countercurrent distribution (CCD) formula for predicting peak elution times for countercurrent chromatography (CCC). The equation for peak elution time is

$$t_D = \frac{V_C}{F}[S_f(D-1)+1] \quad (1)$$

where V_C is the column (coil) volume, F the mobile phase flow rate, S_f the stationary phase retention (expressed as a fraction), and D the distribution ratio. D is defined as the ratio of the total analytical concentration of a solute in the liquid stationary phase, regardless of its chemical form, to its total analytical concentration in the mobile phase.[2] This basic equation is the same regardless of the type of CCC equipment used. However, this equation does not take into account the extra-coil volumes or the sample volume. Originally, the influence of these volumes was not noticed because the extra-coil volumes were a small fraction of the column volume, sample volumes were small, less than 1% of the column volume, and elution times were measured in hours. However elution times can now be measured in minutes, sample volumes have increased to as much as 33% of coil volume[3] and extra-coil volumes are a much larger proportion of the column volume. These factors combined with the mobile phase flow rates now possible, 850 ml/min,[3] indicate that the accuracy of retention measurements should be improved to allow accurate predictions of the times between sample injection and peak detection to be made.

Shorter elution times mean that the time interval between peaks is also reducing. This interval is now measured in minutes, hence to collect the peak of interest requires precise knowledge of when it will elute.

To date, CCC has mainly been conducted with the aim of achieving baseline separations. However, CCC devices, both J-type high-speed countercurrent chromatography (HSCCC) centrifuges and centrifugal partition chromatography (CPC) machines, are now beginning to be used to manufacture pharmaceutical products where the sample loading is increased to the point where peaks are not fully resolved.[3–5] The higher the sample loading, the more asymmetric the peaks of a separation become, causing a loss of resolution and the merging of peaks. In case of the peaks that are not fully resolved peak shaving (precise fraction collection) is used to obtain the desired purity of a target solute. Peak shaving works efficiently if the asymmetric nature of peak elution is acknowledged.

PEAK ELUTION TIME

Put simply, peak elution time is the period between a sample entering the column and a peak eluting from the downstream end of the column. However, this definition is a little imprecise because the sample will take time to load into the coil and the peak will also take time to leave the column and reach the detector. In the past, injection times have been short compared with elution times; however, as separation times have become much shorter and injection volumes have increased, the injection time must be considered to accurately predict elution times. In Fig. 1,[6] it is demonstrated how peaks elute later as the sample volume was increased from 0.005 to 2 ml at a flow rate of 1 ml/min. The 0.005 ml sample took 0.3 sec while the 2 ml sample took 2 min to inject. Compared with the 25 min separation time, 0.3 sec is insignificant whilst 2 min represent 8% of the separation time.

The results presented in Fig. 1 were produced using the heptane : ethyle acetate : methanol : water (1.4 : 0.2 : 1 : 1 v/v) phase system in two 12.5 ml, 0.8 mm bore helical coils connected in series. These coils had a β-value of 0.88 at a rotor radius of 110 mm and were rotated at 1400 rpm in a J-type centrifuge. The concentration of each component was 10.5 mg/ml.

In Fig. 2,[6] the same separation modeled on the eluting CCD software developed by Sutherland, De Folter and Wood[7] is shown. In this model, each 5 μl of sample volume is represented by one injection step. This modeling reinforces the experimental observation that sample size needs to be taken into account.

A more precise definition is that the peak elution time is measured from the point when half the sample has entered the column[8] to the time of maximum peak height (the highest concentration of the sample component) elutes from the column. The time taken for half of the sample volume to enter the coil is ($t_{S/2}$),

$$t_{S/2} = \frac{V_{Sa}}{2F} \quad (2)$$

where V_{Sa} is the sample volume.

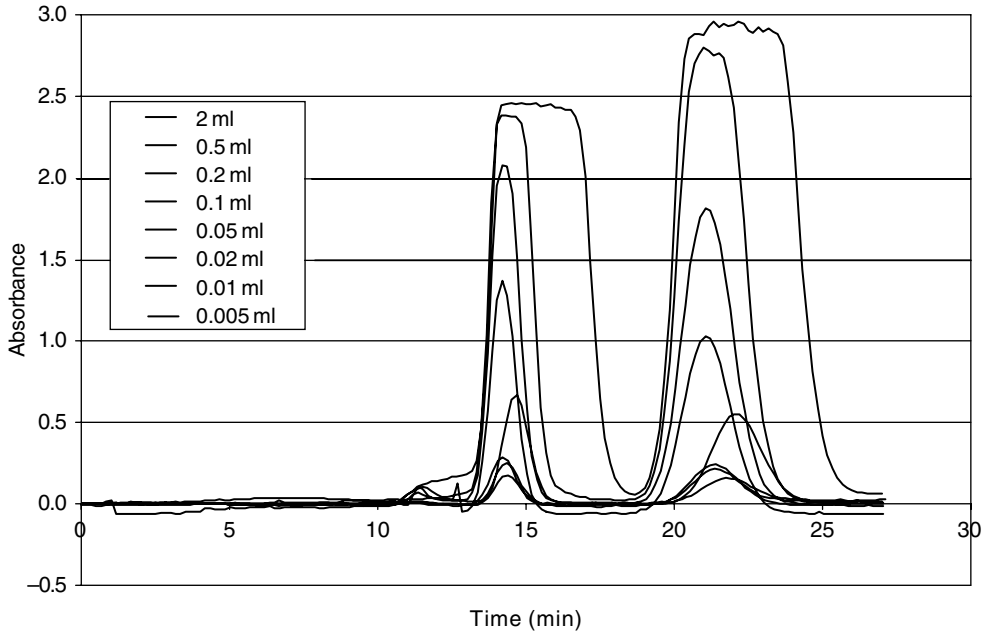

Fig. 1 The influence of sample volume on peak elution times for a benzyl alcohol and *p*-cresol separation.
Source: From Sample volume and resolution in analytical countercurrent chromatography, in Proceedings of the Pittsburgh Conference.[6]

Usually, when a separation is performed, the recording of the trace is started when the injector valve is triggered to insert the sample into the flow of mobile phase. However, the sample will not start to separate until it reaches the column after passing through tubing linking the injector valve to the column, see V_3 in Fig. 3. There is also a second period of time between the peak eluting from the column and arriving at the detector's cell, see V_4 in Fig. 3. The sum

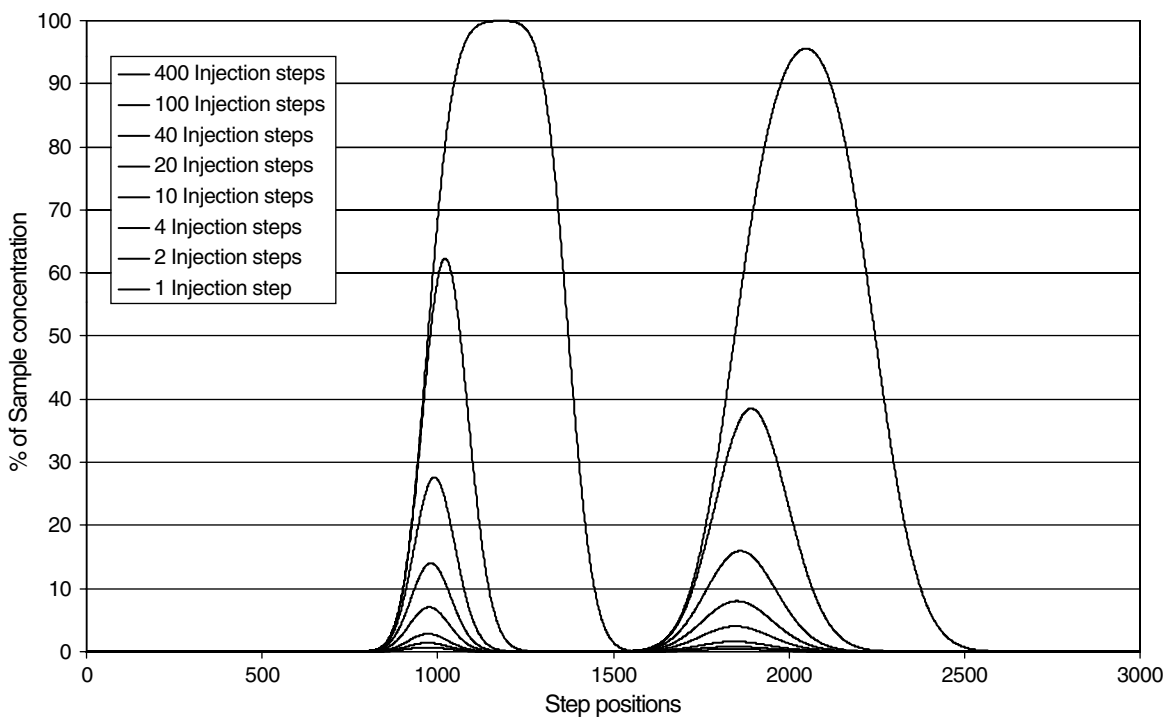

Fig. 2 A mathematical prediction of the benzyl alcohol and *p*-cresol separation shown in Fig. 1.
Source: From Modelling CCC using an eluting countercurrent distribution model, in J. Liq. Chromatogr. Relat. Technol.[7]

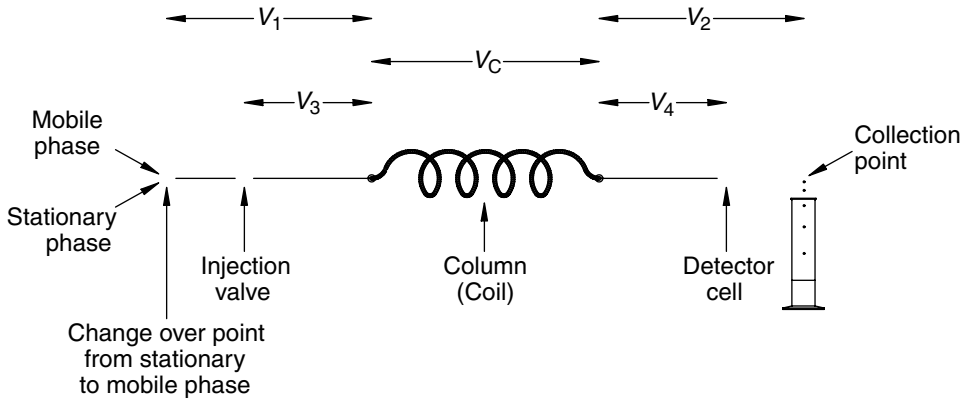

Fig. 3 Schematic diagram of a CCC system.

of these two extra volumes ($V_3 + V_4$) provides the chromatographic extra-coil volume (V_{Cext}). The time for the peak to pass through this volume is

$$t_{Cext} = \frac{V_{Cext}}{F} \tag{3}$$

Fig. 4 is a typical chromatogram for the separation of two components from a binary sample. It shows that the peak elution time (t_D) is determined by subtracting both the time (t_{Cext}) spent in the chromatographic extra-coil volume (V_{Cext}) and half the sample injection time ($t_{S/2}$) from the trace time (t_{tD}):

$$t_D = t_{tD} - t_{Cext} - t_{S/2} \tag{4}$$

Hence,

$$t_D = t_{tD} - \frac{V_{Cext}}{F} - \frac{V_{Sa}}{2F} \tag{5}$$

For peak b in Fig. 4, Eq. 5 can be rewritten as

$$t_b = t_{tb} - \frac{V_{Cext}}{F} - \frac{V_{Sa}}{2F} \tag{6}$$

A similar equation for peak a, from Fig. 4, can also be written. Therefore, it is necessary to know the chromatographic extra-coil volume (V_{Cext}) of a CCC system to accurately determine the elution time of a peak.

EXTRA-COIL VOLUMES

The extra-coil volumes are usually determined by calculation from the various volumes of the associated plumbing.

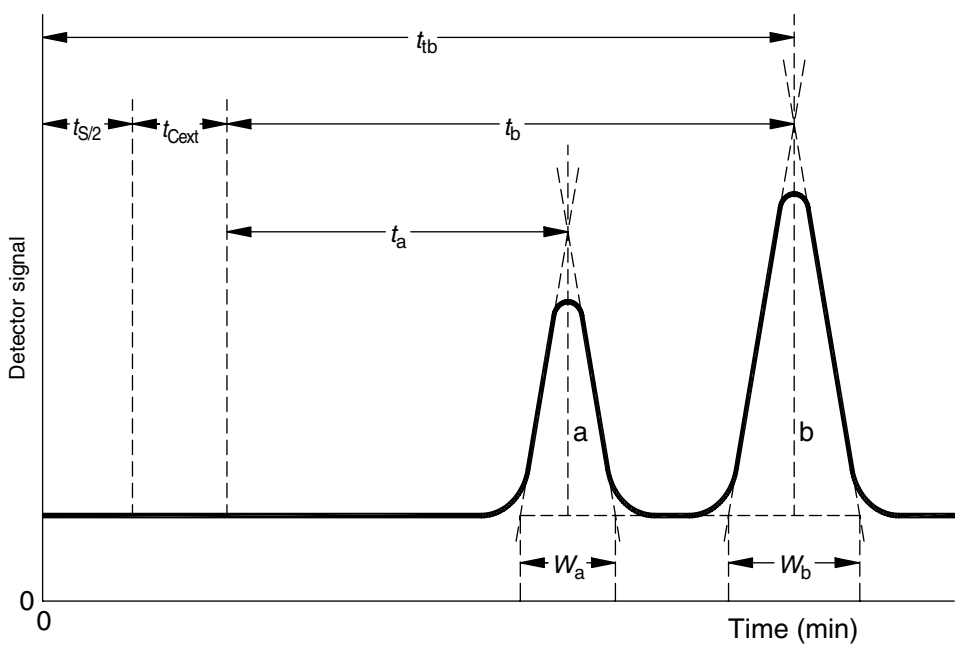

Fig. 4 Simplified chromatogram of a two-peak separation.

The components of the associated plumbing include flying leads, switching valves, injectors, detectors, and fraction collectors. There are two extra-coil volumes for any CCC device. The first is the chromatographic extra-coil volume (V_{Cext}) described earlier. The second one, the retention extra-coil volume (V_{ext}), is the volume between the point where the flow is switched from stationary to mobile phase and the column, V_1 in Fig. 3, plus the volume between the column and the collection point of the stationary and mobile phases, V_2 in Fig. 3. V_{ext} is usually larger than V_{Cext} because the switching point between the stationary and mobile phases is upstream of the injector valve and the collection point (fraction collector) is downstream of the detector's cell, where

$$V_{ext} = V_1 + V_2 \tag{7}$$

and

$$V_{Cext} = V_3 + V_4 \tag{8}$$

Using the wrong extra column volume can lead to common errors in determining stationary phase retention or calculating elution times. V_{ext} is used to determine the stationary phase retention and V_{Cext} is used to calculate elution times.

ACCURATE MEASUREMENT OF STATIONARY PHASE RETENTION

Precise prediction of the elution times relies upon knowing the accurate stationary phase retention (S_f). This can be measured in three different ways:

1. To determine how retention varies with the mobile phase flow rate for a given rotational speed. This method also confirms the retention extra-coil volume (V_{ext}), and will be discussed next.
2. To determine how retention varies with rotational speed for a given mobile phase flow rate.
3. Measuring the retention while performing an isocratic separation when the rotational speed and flow rate are constant.

The first two methods give information as to how a stationary phase will retain in a CCC system. It is recommended that the rotational speed and one flow rate from the first method forms one of the data points in the second method. The third method is used to ensure that the sample concentration and volume is not reducing the retention. Du, Ke and Ito[9] demonstrated how high-sample concentrations and large injection volumes could reduce retention.

The Theory of Measuring Retention

Stationary phase retention cannot be measured directly and, hence, its determination relies upon the measurement of displaced volumes of stationary phase (V_E) from a CCC system and a number of assumptions. The basic equations for the measurement of retention are:

By definition:

$$S_f = \frac{V_S}{V_C}$$

and because $V_S = V_C - V_m$ giving

$$S_f = \frac{V_C - V_m}{V_C}$$

Therefore

$$S_f = 1 - \frac{V_m}{V_C} \tag{9}$$

The volume of stationary phase (V_E) displaced from a CCC system by the mobile phase is equal to the sum of entire retention extra-coil volume V_{ext} and a proportion of the column volume. The latter is equal to the volume of mobile phase in the column (V_m), hence

$$V_E = V_m + V_{ext} \tag{10}$$

Rearranging Eq. 10 gives:

$$V_m = V_E - V_{ext} \tag{11}$$

Substituting for V_m from Eq. 11 into Eq. 9 gives:

$$S_f = 1 - \frac{V_E - V_{ext}}{V_C} \tag{12}$$

These equations are underpinned by the following list of assumptions, and errors are inevitable if any of these are not met. These are

1. The coil volume (V_C) is accurately known.
2. The volume of the retention extra-coil volume (V_{ext}) is accurately known.
3. The system was initially completely filled with only stationary phase, i.e., no mobile phase and no air bubbles.
4. No air is introduced while retention of stationary phase is being measured.
5. The amount of stationary phase displaced from a column by the mobile phase is equal to the volume of mobile phase in the column (V_m).

6. The mobile phase displaces all of the stationary phase from the retention extra-coil volume (V_{ext}), i.e., V_1 and V_2 (Fig. 3), only contain mobile phase.
7. The set flow rates are accurate and consistent throughout an experiment.
8. The flow of the mobile phase is steady, i.e., free from flow pulses and pressure irregularities.

Measuring the retention a number of times under the same conditions does not guarantee accuracy, as systematic errors may be present. Systematic errors may be caused if a number of the above assumptions are not met. However, measurement techniques that reduce these errors are now available and are explained in the following sections.

Measuring Retention at Constant Rotational Speed

First of all, the CCC system is completely filled with stationary phase. The column is rotated at a set speed and the mobile phase is pumped through the system at the lowest intended flow rate. This causes stationary phase to be displaced from the entire extra-coil volume (V_{ext}) and a proportion of the column volume. Once stationary phase stops being displaced, dynamic equilibrium is reached, and the minimum value of V_E is obtained. The mobile-phase flow rate is then increased, causing more stationary phase to be displaced from only the column. When dynamic equilibrium has been reached again, the next value of V_E is acquired. This process is repeated until five or six sets of readings have been taken. Eq. 12 is then used to calculate the retention S_f, and the value of V_{ext} can be determined as described below in the section titled "Measuring the Retention Extra-Coil Volume." In the case of a J-type centrifuge, retention (S_f) is plotted against the square root of the mobile phase flow rate. Once this test is complete, the CCC system can be emptied and the accuracy of the retention measurements can then be checked, see section titled "Checking the Accuracy of Retention Measurements."

Measuring Retention at Constant Mobile Phase Flow Rate

The procedure is the same as the one given in the previous section, except that the flow rate is constant and the centrifuge is first rotated at its highest speed. After reaching dynamic equilibrium, a value of V_E is obtained. The rotational speed is then decreased, causing a larger value of V_E to be acquired when dynamic equilibrium is achieved. Retention S_f is plotted against rotational speed, see Fig. 4 of Ref.[10]

Measuring Retention During an Isocratic Separation

After filling with stationary phase, the column is rotated at the desired speed and the mobile phase is pumped through the system at the required flow rate. When dynamic equilibrium has been achieved, V_E can be measured as described above. The nature of some samples can reduce the retention and therefore increase the value of V_E after sample injection. If this occurs, the followings approaches can be applied:

1. Simply reject the sample and look for any further reductions in retention.
2. Reduce the sample volume and/or concentration.
3. Increase rotational speed and/or reduce the mobile phase flow rate.

Measuring the Retention Extra-Coil Volume

There are two approaches to determine the retention extra-coil volume. The first is to calculate the volumes V_1 and V_2 from Fig. 3, as previously discussed. The second approach is to use data from measuring retention at a constant rotational speed and different flow rates. For a J-type centrifuge, V_E is plotted against the square root of the mobile phase flow rate. V_{ext} is the intercept on the vertical axis[11] (Fig. 5). The values determined by both methods are compared to ensure that an accurate volume of V_{ext} has been determined. This volume can then be used for the accurate prediction of retention. This value of V_{ext} will be constant until the set up is modified. This technique can be adapted for other CCC devices provided that the mathematical relationship between retention and mobile phase flow rate is known.

Checking the Accuracy of Retention Measurements

After measuring the retention, or performing a separation, the CCC system is emptied. The sum of the volume of the stationary phase (V_S) and mobile phase (V_{mp} not V_m) should be compared with the total volume of the system (V_{SYS}). The latter is the sum of the column volume (V_C) and the retention extra-coil volume (V_{ext}). If the sum of V_S and V_{mp} is less than V_{SYS}, then the system has not been completely emptied. If the sum of V_S and V_{mp} is greater than V_{SYS}, then the volumes V_C and V_{ext} should be checked. Alternatively, additional volumes of mobile and/or stationary phase have been collected for some reason. If the sum of V_S and V_{mp} is approximately equal to V_{SYS}, then the following check should be conducted.

The volume of mobile phase emptied from a CCC system (V_{mp}) should be equal to the volume of mobile

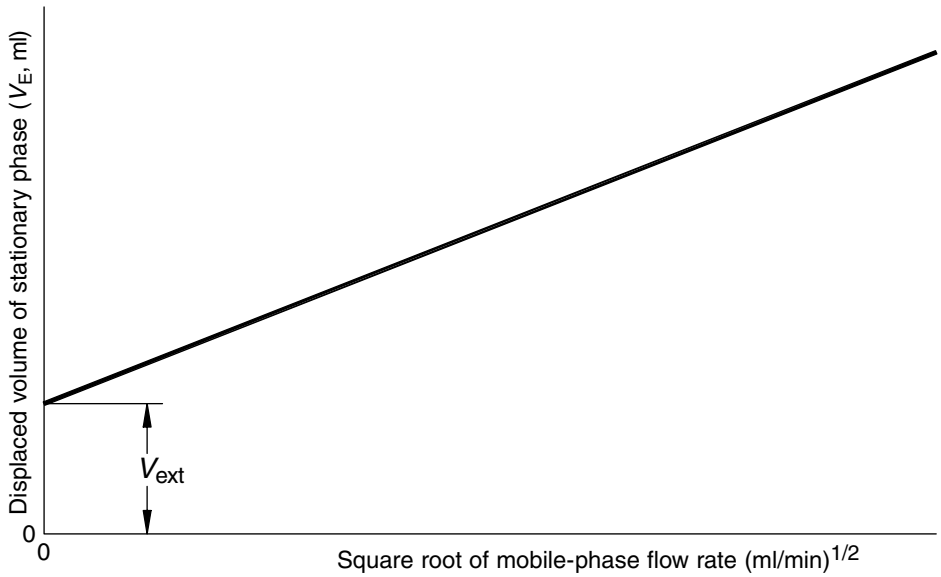

Fig. 5 The method of determining V_{ext} for a J-type centrifuge.
Source: From Determination of J-type centrifuge extra-coil volume using stationary phase retentions at differing flow rates, in J. Liq. Chromatogr. Relat. Technol.[11]

phase in the column (V_m) and the volume of mobile phase retained in the extra-coil volume (V_{ext}):

$$V_{mp} = V_m + V_{ext} \quad (13)$$

This can be rearranged to give

$$V_m = V_{mp} - V_{ext} \quad (14)$$

Substituting Eq. 14 for V_m into Eq. 10 gives:

$$V_E = V_{mp} - V_{ext} + V_{ext}$$

$$V_E = V_{mp} \quad (15)$$

The difference between these volumes determines the accuracy of the retention measurements.

COMMON ERRORS WHEN MEASURING RETENTION

The following is a list of possible errors in measuring retention and the effect on the measurement is explained:

1. Incorrect column volume (V_C). This error is because of the supplier or manufacturer not measuring this volume accurately. The process of winding a column can make the inner bore slightly oval, reducing the volume below that calculated using the original internal diameter.
2. Incorrect estimation of extra-coil volumes. In the section "Measuring the Retention Extra-coil Volume," it is shown how the calculations to estimate V_{ext} can be checked. Once this check has been conducted, it is quite simple to correct the calculated volume of V_{Cext}, if necessary.
3. If the errors in V_C and V_{ext} do not cancel out, the system volume will be incorrect. If this figure is too low, the system may not be completely emptied after a test, possibly leaving mobile phase in the column, see the next point.
4. If, at the start of a test, the column is not completely empty of mobile phase and this phase is not then completely displaced by filling with stationary phase, the readings of V_E will be too low, causing the value of S_f to be higher than it should be. This error is detected when the measured volume of V_{ext} is lower than previous measurements; see the section titled "Measuring the Retention Extra-coil Volume."
5. When a number of measuring cylinders are used to collect the displaced stationary phase. The error in determining the value of V_E will be the sum of reading errors from each measuring cylinder. Collecting the stationary phase in one large measuring cylinder with a suitably fine scale can reduce this error. Alternatively, when the lighter phase is used as the mobile phase, a measuring cylinder or burette can be fitted with a spout, see Fig. 1 of Ref.[12] This enables the lighter mobile phase to flow out of the spout and the denser stationary phase (V_E) is collected at the bottom.

6. Fluctuations in rotational speed of a CCC centrifuge will cause the retention to change, thereby causing errors. To reduce, and perhaps remove, this source of error, the manufacturers of CCC equipment should provide a better control of the set rotational speed.
7. Single head HPLC pumps create an unsteady flow with regular pulses, which, at best, reduces the retention achievable but, at worst, is a source of errors. Twin headed pumps that create a pulse free steady flow should be used.
8. The mobile phase flow rate should be checked to ensure that the set flow is being accurately delivered. Errors in the flow can be attributed to siphoning, incorrect operation of the one-way check valves in the pump heads or worn seals. Fitting a backpressure regulator downstream of the column stops siphoning and will force the one-way check valves to operate correctly.
9. At the higher mobile phase flow rates now being used to perform retention tests[12] and separations,[13] the mobile phase appears cloudy because of the stationary phase still being suspended in the mobile phase. There is often enough suspended stationary phase to cause errors in determining the retention.
10. The formation of small gas bubbles within the CCC system causes errors, even when a backpressure regulator is applied. Using degassed solvents reduces this error.

INCREASING RETENTION TO INCREASE RESOLUTION

Resolution is a measure of how well two adjacent peaks are separated from each other. For symmetrical peaks, the resolution is the difference in the elution times between the peaks divided by half of the sum of the peak widths. For the example shown in Fig. 4, the resolution is

$$R_S = \frac{2(t_b - t_a)}{W_a + W_b} \tag{16}$$

Either reducing the mobile phase flow rate or increasing rotational speed will provide a higher retention. The higher the retention, the longer the periods of time between the elution of successive peaks. This increases the value of the numerator of Eq. 16, thereby increasing the resolution. This can be further demonstrated by adapting Eq. 1 for three components with distribution ratios of 0, 1, and 2 to give:

Table 1 The elution times for all three peaks in all three separations.

	Elution times (min)		
Distribution ratio	$F = 1$ ml/min, $S_f = 0.5$	$F = 1$ ml/min, $S_f = 0.64$	$F = 0.5$ ml/min, $S_f = 0.64$
$D = 0$	5	3.5	7.1
$D = 1$	10	10	20
$D = 2$	15	16.5	32.9

when $D = 0$, then

$$t_0 = \frac{V_C(1 - S_f)}{F} \tag{17}$$

when $D = 1$, then

$$t_1 = \frac{V_C}{F} \tag{18}$$

when $D = 2$, then

$$t_2 = \frac{V_C(S_f + 1)}{F} \tag{19}$$

Consider a CCC device with a 10 ml column volume (V_C) used to separate these three components. This separation is repeated three times: the first with the rotational speed set to give a retention (S_f) of 0.5 and a mobile flow rate (F) of 1 ml/min, the second at a higher rotational speed where the retention has increased to 0.64 and a 1 ml/min flow rate and, finally, at the original rotational speed, but with a 0.5 ml/min flow rate to give a retention of 0.64.

As can be seen from Table 1, the elution times and the interval between peak elution have changed, in turn varying the resolution. However, the resolution cannot yet be predicted owing to the effects of flow rate and rotational speed on peak widths, which are not fully understood. Currently, an empirical approach is required when aiming to improve resolution using the approaches described above.

PEAK BROADENING WHEN ELUTING

Asymmetric peaks, similar to those in Fig. 6, are often observed in separations performed using CCC devices. The main reason for this is the higher retention of stationary phase in comparison to HPLC columns. The

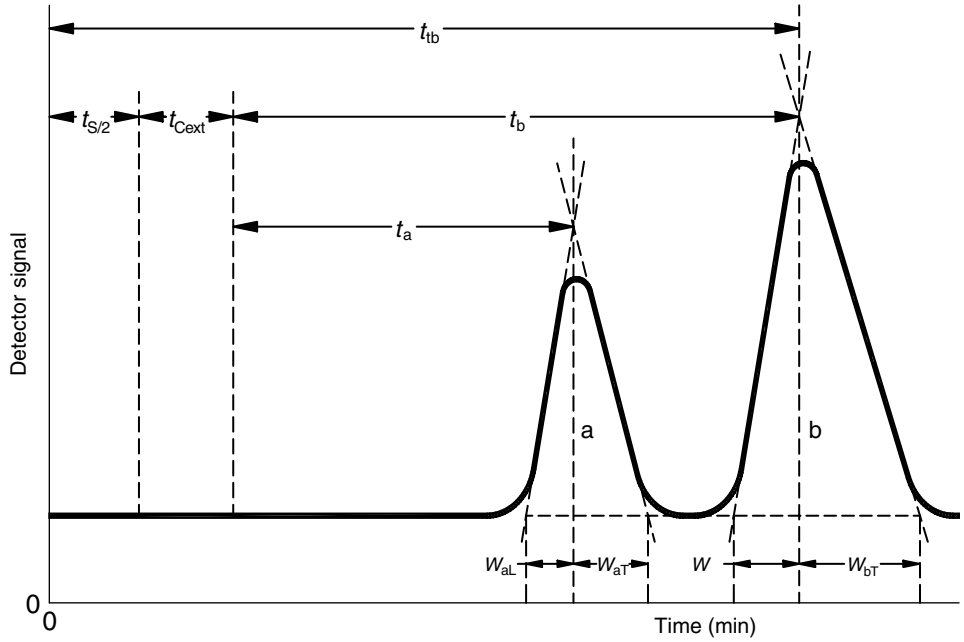

Fig. 6 Asymmetric peaks caused by a combination of high retention, sample volume, and sample concentration.

software developed by Sutherland, De Folter, and Wood[7] demonstrates the formation of asymmetric peaks. High concentration of samples, larger sample volumes, and higher distribution ratio (D) also increase the asymmetry of peaks. The leading edge of a peak elutes from the column, as a symmetrical peak would do. However, the tailing edge takes much longer to elute because most of the material is still dissolved in the stationary phase.[14] In Figs. 1 and 2, only a limited amount of asymmetry is shown, even though the S_f was 86%,[6] because the D values of benzyl alcohol and *p*-cresol were 0.4 and 0.7, respectively, in the phase system used and the sample concentration was too low.

Taking into account the asymmetry of peaks the formula for resolution (Eq. 16) needs to be modified. Let an L denote leading edges and a T denote tailing edges in Fig. 6. Therefore, the modified equation for resolution is

$$R_S = \frac{t_b - t_b}{W_{aT} + W_{bL}} \tag{20}$$

CONCLUSIONS

The theory and results presented herein have shown how the knowledge of both stationary phase retention and peak elution has been recently developed. The challenge still facing CCC is to understand the controlling influences on mass transfer and peak width. Such knowledge will allow the user to predict resolution and control a separation to match requirements.

REFERENCES

1. Conway, W.D. *Countercurrent Chromatography Apparatus, Theory and Applications*; VCH Publishers Ltd.: U.K., 1990; ISBN 0-89573-331-5.
2. Berthod, A.; Maryutina, T.; Shpigun, O.A.; Spivakov, B.; Ya, Y.; Sutherland, I.A. IUPAC recommendations for countercurrent chromatography. Proceedings of the Third International CCC Conference. Tokyo, Japan, Aug. 28–31, 2004.
3. Wood, P.; Garrard, I.; Hawes, D.; Ignatova, S.; Janaway, L.; Sutherland, I.A. CCC separations performed in minutes at both the analytical and industrial scales. Proceedings of the Third International CCC Conference, Tokyo, Japan, Aug. 28–31, 2004.
4. Sutherland, I.A.; Hawes, D.; Ignatova, S.; Janaway, L.; Wood, P.; Foucault, A.; Legrand, J.; Marchel, L.; Couillard, F. Review of progress toward the Industrial scale-up of CCC. Proceedings of the Third International CCC Conference, Tokyo, Japan, Aug. 28–31, 2004.
5. Margraff, R.; Intes, O.; Renault, J.H.; Garret, P. Partitron 25 a multi-purpose industrial centrifugal partition chromatograph: Rotor design and preliminary results on efficiency and stationary phase retention. Proceedings of the Third International CCC Conference, Tokyo, Japan, Aug. 28–31, 2004.

6. Wood, P.; Jones, J.; Kidwell, H.; Sutherland, I.A. Sample volume and resolution in analytical countercurrent chromatography. Proceedings of the Pittsburgh Conference, Abstract 720, New Orleans, U.S.A., Mar. 4–9, 2001.
7. Sutherland, I.A.; De Folter, J.; Wood, P. Modelling CCC using an eluting countercurrent distribution model. J. Liq. Chromatogr. Relat. Technol. **2003**, *26* (9–10), 1449–1474.
8. Conway, W.D. Extra-column dead volume in countercurrent chromatography. Proceedings of the Third International CCC Conference, Tokyo, Japan, Aug. 28–31, 2004.
9. Du, Q.Z.; Ke, C.Q.; Ito, Y. Separation of epigallocatechin gallate and gallocatechin gallate using multiple instruments connected in series. J. Liq. Chromatogr. Relat. Technol. **1998**, *21* (1–2), 203–208.
10. Ignatova, S.N.; Sutherland, I.A. A fast, effective method of characterizing new phase systems in CCC. J. Liq. Chromatogr. Relat. Technol. **2003**, *26* (9–10), 1551–1564.
11. Wood, P.; Janaway, L.; Hawes, D.; Sutherland, I.A. Determination of J-type centrifuge extra-coil volume using stationary phase retentions at differing flow rates. J. Liq. Chromatogr. Relat. Technol. **2003**, *26* (9–10), 1417–1430.
12. Wood, P.; Janaway, L.; Hawes, D.; Sutherland, I.A. Stationary phase retention in countercurrent chromatography: Modelling the J-type centrifuge as a constant pressure drop pump. J. Liq. Chromatogr. Relat. Technol. **2003**, *26* (9–10), 1373–1396.
13. Sutherland, I.A.; Hawes, D.; van den Heuvel, R.; Janaway, L.; Tinnion, E. Resolution in CCC: the effect of operating conditions and the phase system properties on scale-up. J. Liq. Chromatogr. Relat. Technol. **2003**, *26* (9–10), 1475–1491.
14. Berthod, A.; Hassoun, M.; Harris, G.H. The use of the liquid nature of the stationary phase in CCC: The elution-extrusion method. Proceedings of the Third International CCC Conference, Tokyo, Japan, Aug. 28–31, 2004.

Stationary Phases for Packed Column SFC

Stephen L. Secreast
Pharmaceutical Sciences, Pharmacia Corporation, Kalamazoo, Michigan, U.S.A.

INTRODUCTION

The name, packed column supercritical fluid chromatography (pSFC), has been applied to separations performed on particulate stationary phases, using mobile phases pressurized to supercritical, near-critical, or subcritical conditions.[1,2] Typically, the stationary phases used for pSFC are commercially available high-performance liquid chromatography (HPLC) columns, consisting of a porous solid support, usually with a covalently linked bonded phase to provide desired chromatographic interactions. Various column configurations have been used. Separate consideration of supercritical, near-critical, and subcritical pSFC applications provides a convenient, although arbitrary, means of subgrouping a discussion of the types of stationary phase used. More specific information on the stationary phases discussed in this overview can be found in Refs.[1–4]

SUPERCRITICAL APPLICATIONS

Supercritical pSFC applications can be defined as those in which the mobile phase is a single substance heated and pressurized above its critical point. Carbon dioxide has overwhelmingly been the compound of choice for these mobile phases. Stationary phases typically used for these applications have been polymeric materials or polymer-coated porous silica. Chromatography on uncoated silica-based stationary phases with CO_2 has, in general, been unsuccessful.

Polystyrene–divinyl benzene beads are the most common polymer material phases reported. The successful use of these phases has been mainly limited, however, to relatively hydrophobic compounds. Also, problems associated with bead physical instability, such as shrinking and swelling, affecting chromatographic reproducibility, have also been encountered. Stationary phases consisting of porous silica coated with a covalently bonded polysiloxane layer, containing cyano, phenyl, or alkyl functional groups, have been used with more success. The polymer coating is applied to the silica to mask excessive analyte–stationary phase polar interactions that generate poor peak shapes and yield incomplete analyte recovery with the neat CO_2 mobile phase. As with the polymer materials, these phases work best for hydrophobic compounds such as petroleum-based compounds, lipids, and plastics additives. The apparent degree of silica deactivation obtained with the polymer coating is insufficient to provide quality CO_2 chromatography for polar compounds. An example of plastic additives chromatography obtained with CO_2 on a polymer-coated stationary phase is shown in Fig. 1.[5]

Recently, interest in polymer-coated silica phases has been renewed, with investigators (Chen and Lee[2]) exploring the use of more efficient deactivation techniques and more polar polymers to coat silica particles for neat CO_2 chromatography. Polyethyleneimine-coated silica and amino-terminated polyethylene oxide-coated silica appear promising for pSFC of moderately polar basic compounds. Similarly, hydroxy-terminated polyethylene-oxide-coated silica has been used successfully for pSFC of alcohols and acids. Optimization and commercial production of these stationary phases could significantly extend the polarity range of compounds that can be chromatographed with neat supercritical CO_2.

NEAR-CRITICAL APPLICATIONS

Near-critical pSFC applications can be described as those where the mobile phase is solvent-modified CO_2, pressurized only enough to maintain a single phase, with temperatures near (typically less than) the critical temperature. Many commercially available HPLC bonded silica phases have been used with modified-CO_2 mobile phases to achieve normal-phase separations, the choice of stationary phase being dictated by sample polarity. The modifiers added to CO_2 acceptably overcome the unwanted analyte–silica interactions observed with neat CO_2 mobile phases. For structural separation of polar compounds such as pharmaceuticals [typically weak acids or bases of molecular weight (MW) < 1000], polar phases such as diol-, amino-, and cyano-bonded silica (or bare silica) are used. Numerous applications for pharmaceutical, natural product, environmental and other compound classes have been reported in the recent literature (reviewed in Refs.[1,2]). For structural separation of higher-molecular-weight, less polar compounds, octyl- or octadecyl silane (ODS)-bonded phases are used (Berger[1] and Lesellier and Tchapla[2]). The reported applications include stationary-phase columns obtained from many different commercial manufacturers, covering almost the complete range of packing particle size and pore size.

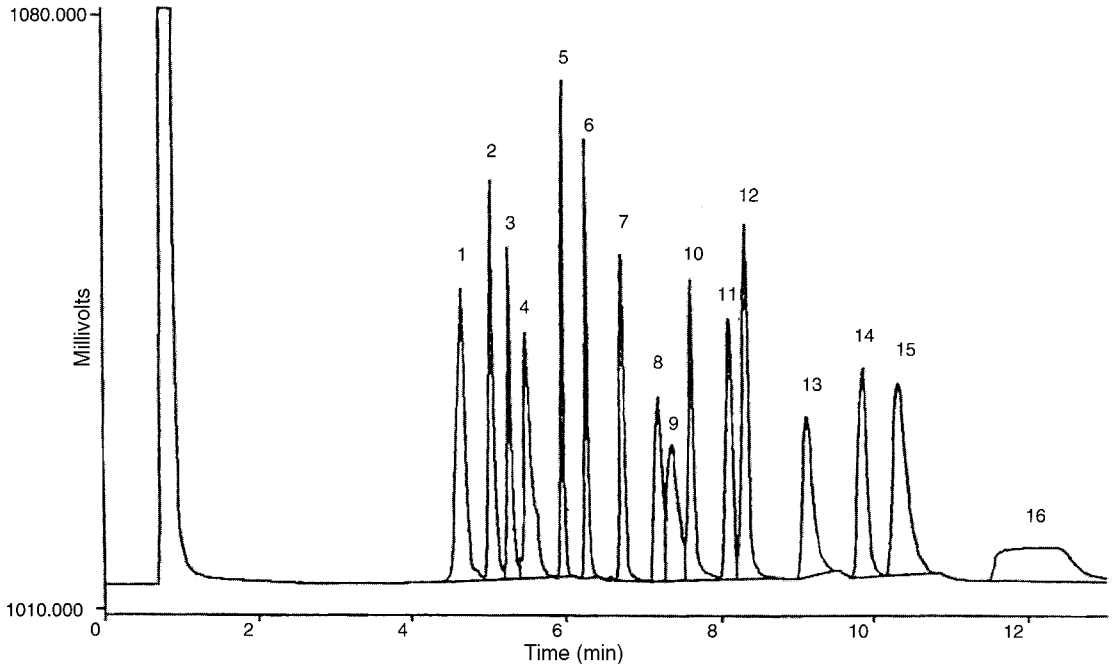

Fig. 1 Use of polymer-coated silica stationary phase with a neat carbon dioxide mobile phase. Column: Deltabond SFC Methyl (150 × 2.0 mm); mobile phase: CO_2; pressure gradient: 75 bar initial for 2 min, then 50 bar/min ramp to 180 bar, then 15 bar/min ramp to 300 bar; flow: 0.5 ml/min; temperature: 100°C; injection: 5 μl; detection: flame ionization detector; sample solvent: methylene chloride. Peak key: 1, BHT; 2, dimethyl azelate; 3, triethyl citrate; 4, tributyl phosphate; 5, methyl palmitate; 6, methyl stearate; 7, diethylhexyl phthalate; 8, Tinuvin 327; 9, Spectra-Sorb UV531; 10, tri(2-ethylhexyl) trimellitate; 11, dilauryl thiodipropionate; 12, Irganox 1076; 13, 1,3-diolein; 14, distearyl thiodipropionate; 15, Ionox 330; 16, Irganox 1010.

Modified-CO_2 mobile phases excel at stereochemical separations, more often than not outperforming traditional HPLC mobile phases. For the separation of diastereomers, silica, diol-bonded silica, graphitic carbon, and chiral stationary phases have all been successfully employed. For enantiomer separations, the derivatized polysaccharide, silica-based Chiralcel and Chiralpak chiral stationary phases (CSPs) have been most used, with many applications, particularly in pharmaceutical analysis, readily found in the recent literature (reviewed in Refs.[1,2]). To a lesser extent, applications employing Pirkle brush-type, cyclodextrin and antibiotic CSPs have also been described. In addition, the use of silica and graphitic carbon stationary phases with chiral modifiers added to the CO_2 mobile phase has been reported.

A major advantage of modified-CO_2 pSFC is that due to the low pressure and similarity of the mobile phases used for structural and stereochemical separations, multiple stationary-phase columns can be connected in series, generating separations not achievable by other chromatographic methods. Multiple columns of the same phase have been serially connected to provide significantly amplified chromatographic efficiencies.[1] A recent example chromatogram obtained by connecting four 250 × 4.6 mm Chiralpak AD columns in series is shown in Fig. 2.[6] With the four columns in series, concurrent separation of the four stereoisomers of each of two structurally different compounds was achieved.

Serial connection of different stationary phases provides some very interesting separations. The combination of different CSPs provides systems capable of resolving a wide range of enantiomers (Sandra et al.,[2] Gyllenhaal[2]). Recent applications combining normal-phase bonded-silica (diol, cyano, amino) columns with CSPs in series, to provide concurrent structural and stereochemical separations, have been described (Phinney,[4] Kline and Matuszewski,[4] and Williams et al.[4]). An example of chromatography obtained for a pharmaceutical compound and its degradants by connecting a Zorbax SB cyano column and three Chiralpak AD columns in series is shown in Fig. 3.[7] The cyano column provides the structural separation of the parent compound and the two degradants, and the Chiralpak columns provide concurrent enantiomer separations for the two degradants. The ability to combine different or multiple traditional HPLC stationary phases to generate unique separations is a hallmark of modified-CO_2 pSFC.

SUBCRITICAL APPLICATIONS

Recent work describing the use of subcritical water as a chromatographic mobile phase has been reported. Water heated to 100–200°C, pressurized to 20–50 bar, can be used as a reversed-phase chromatography eluant. This application exists somewhere in the boundary region

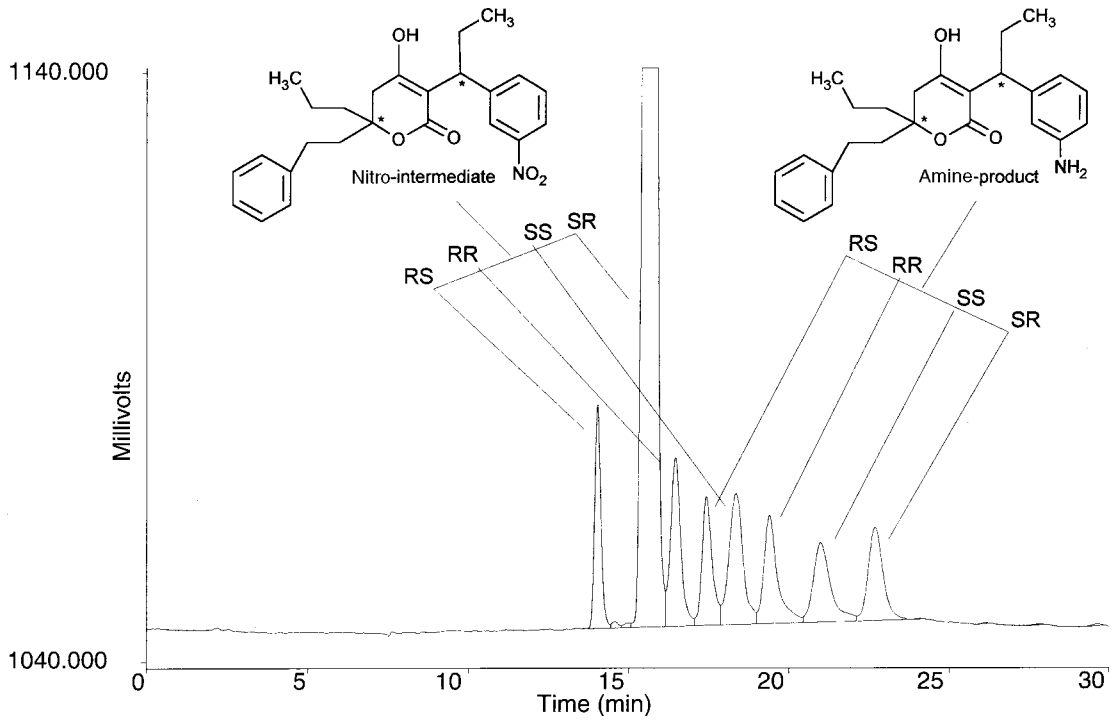

Fig. 2 Use of multiple columns (same stationary phase) in series to improve chromatographic efficiency. Columns: four Chiralpak AD (5 μm, 250 × 4.6 mm) in series; mobile phase: CO_2 with modifier gradient; modifier: ethanol–methanol–isopropylamine (50:50:0.5); gradient: 20% modifier for 2 min, then 1%/min ramp to 35%; flow: 2.0 ml/min; pressure: 150 bar; temperature: 35°C; injection: 5 μl; detection: UV 210 nm; sample solvent: methanol.

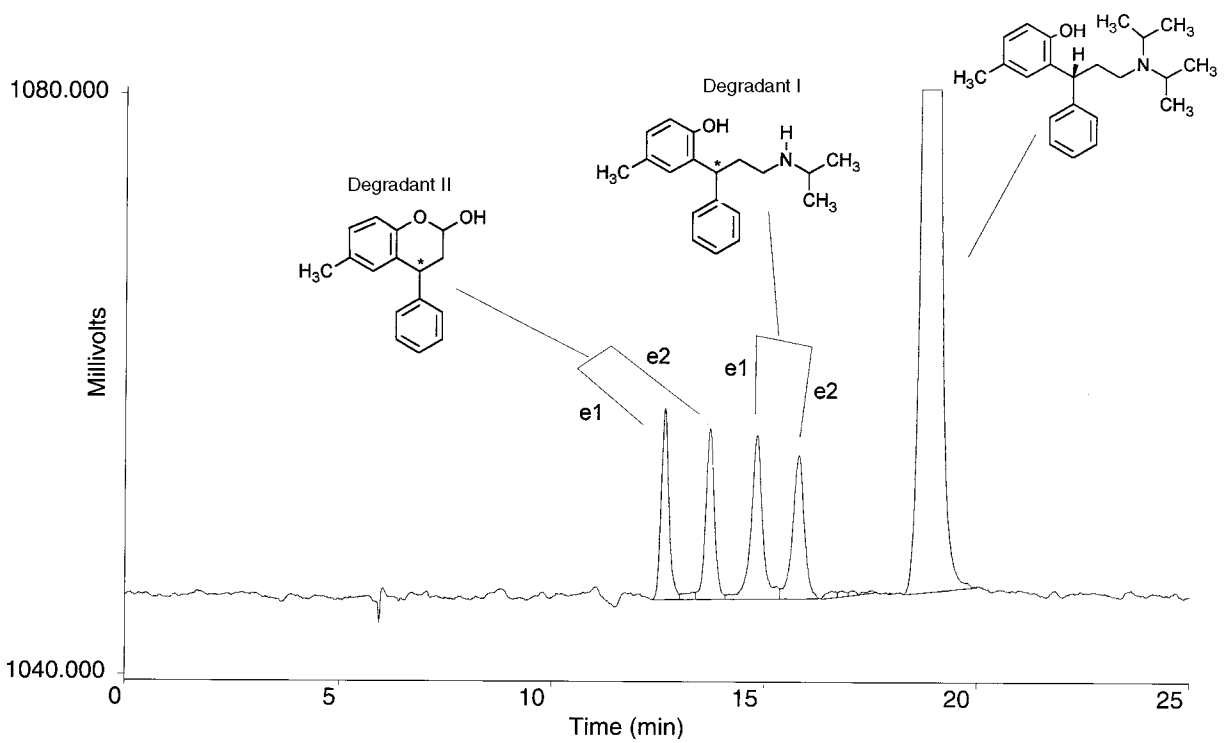

Fig. 3 Use of multiple columns in series (achiral and chiral stationary phases) to provide mixed-mode selectivity. Columns: Zorbax SB CN (5 μm, 250 × 4.6 mm) plus three Chiralpak AD (5 μm, 250 × 4.6 mm) in series; mobile phase: CO_2–methanol (containing 0.5% isopropylamine) (85:15); flow: 2.0 ml/min; pressure: 150 bar; temperature: 35°C; injection: 5 μl; detection: UV 220 nm; sample solvent: methanol.

between pSFC and HPLC. Stationary phases that have been used successfully for subcritical (or superheated) water chromatography include polystyrene–divinyl benzene beads,[8,9] ODS silica,[8,10] porous graphitic carbon,[11] and polybutadienecoated zirconia.[11] Of these phases, relatively rapid performance deterioration was reported for the ODS silica materials,[11] presumably due to silica solubility. As research in this area increases, undoubtedly so will the number of identified suitable stationary phases.

CONCLUSIONS

Packed column SFC stationary phases are very similar or identical to those used for HPLC. With neat CO_2 mobile phases, polymer or polymer-coated silica stationary phases have typically been used. With modified-CO_2 mobile phases, bonded-phase silica columns are typically used. For structural separations, diol, amino, or cyano stationary phases are most often used. For stereochemical separations, derivatized polysaccharide-bonded silica columns are most often the stationary phases of choice. A powerful feature of modified-CO_2 pSFC is the ability to serially connect different stationary phases to obtain enhanced or multiple mechanism separations. With subcritical (super heated) water mobile phases, the use of polymer, porous graphitic carbon, and polymer-coated zirconia stationary phases has been described.

REFERENCES

1. Berger, T.A. *Packed Column SFC*; Royal Society of Chemistry: Cambridge, 1995.
2. Anton, K., Berger, C., Eds.; *Supercritical Fluid Chromatography with Packed Columns*; Marcel Dekker, Inc.: New York, 1998.
3. 7th International Symposium on Supercritical Fluid Chromatography and Extraction, 1996.
4. 8th International Symposium on Supercritical Fluid Chromatography and Extraction, 1998.
5. Secreast, S.L. unpublished application. Packed-column supercritical fluid chromatography of plastics additives. *Pharmacia Study Report*; 1996.
6. Secreast, S.L.; Wade, L.K. 8th International Symposium on Supercritical Fluid Chromatography and Extraction, 1998.
7. Secreast, S.L. *American Association of Pharmaceutical Scientists Annual Meeting*; 1999.
8. Smith, R.M.; Burgess, R.J. Superheated water as an eluent for reversed-phase high-performance liquid chromatography. J. Chromatogr. A, **1997**, *785*, 49–55.
9. Miller, D.J.; Hawthorne, S.B. Subcritical water chromatography with flame ionization detection. Anal. Chem. **1997**, *69*, 623–627.
10. Yang, Y.; Belghazi, M.; Lagadec, A.; Miller, D.J.; Hawthorne, S.B. Elution of organic solutes from different polarity sorbents using subcritical water. J. Chromatogr. **1998**, *810*, 149–159.
11. Smith, R.M.; Burgess, R.J.; Chienthavorn, O.; Rose, J. Superheated water: A new look at chromatographic eluents for reversed-phase liquid chromatography. LC-GC **1999**, *17* (10), 938–945.

Stationary Phases: Reverse-Phase

Joseph J. Pesek
Maria T. Matyska
Department of Chemistry, San Jose State University, San Jose, California, U.S.A.

INTRODUCTION

The primary purpose for the developement of chemically modified stationary phases was to provide a separation medium that was suited to the type(s) of solute present in the mixture to be analyzed. Historically, silica gel was the most common material used in the early development of column liquid chromatography (LC). However, silica is a polar material that contains hydroxyl groups (silanols) that are both acidic and strongly hydrogen-bonding in character. These properties make it unsuitable as a stationary phase for many typical organic molecules that are predominantly hydrophobic compounds. In addition, the silanols interact strongly with basic compounds leading to poor chromatographic results.

DISCUSSION

In order to overcome these undesirable effects of silica and to have a medium more suitable for the separation of a large variety of organic compounds, modification of the surface is necessary to provide a more non-polar (hydrophobic) material. It is advantageous to retain silica as the primary material in the column because it possess physical and mechanical properties that make it particularly useful for modern liquid chromatography [i.e., the use of high-pressure liquid chromatography (HPLC) to force the mobile phase and sample through the system at a reasonable flow rate].

The desirable characteristics of silica are as follows: high mechanical strength, a narrow range of particle diameters, a variety of pore sizes, a broad range of surface areas, and the ability to be modified either chemically or physically by adsorption. It is the latter property (i.e., the ability for modification) that makes silica particularly useful as a separation medium in chromatography. Although physical adsorption has been used occasionally to modify silica surfaces for chromatographic purposes, its usefulness is limited because of the nature of modern HPLC. The use of high pressure creates shear forces at the stationary phase–mobile phase interface so that the absorbed moiety is removed from the silica surface even though the coating may be insoluble in the liquid being pumped through the column. Therefore, chemical modification is the only practical approach to modifying the silica surface in order to create a stationary phase that is compatible with the types of solutes to be separated. The most common method for modifying silica in order to produce a hydrophobic surface is organosilanization. Two types of reaction are available by this method. The first alternative is referred to as a monomeric approach:

$$\equiv Si - OH + X - SiR'_2R \rightarrow \equiv Si - O - SiR'_2 + HX$$

Here, the organosilane reagent is composed of a reactive group, X, which can be a halide, usually chloride, methoxy, or ethoxy; R′ is one of two small organic groüps usually methyl, and R is the main group that gives the surface its hydrophobic properties. The end result is a single point of attachment between the organosilane reagent and the surface. The second alternative shown in the following reaction is referred to as the polymeric approach for bonding

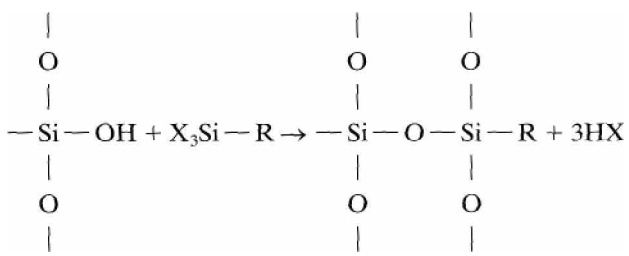

In this case, the organosilane reagent is composed of three reactive groups; X is as described earlier and R is the main organic group that provides the hydrophobic properties to the surface. Here, the end result is that the bonded phase is attached to the surface at one point and cross-linked to neighboring bonded organosilanes through a siloxane linkage. Both of these synthetic routes are used in the production of commercially available stationary phases for HPLC. The monomeric approach generally is more reproducible from batch to batch, whereas the polymeric approach leads to higher bonding densities (more R groups per unit surface area) and some additional stability due to the multiple sites of attachment.

In both types of reactions, it is the R group that determines the overall characteristics of the surface if there is a resonable bonding denisity as measured in terms of micromoles per square meter. There must be a significant number of organic moieties per unit surface area so that most of the silica is covered by the R groups and relatively few of

the siloxane and silanols are accessible. Under these conditions, when the organic moiety is hydrophobic, non-polar solutes will be selectively retained by the stationary phase. Even in the case where the bonding density is reasonably high, there is still the possibility that some silanols may be accessible to solutes. This is mainly a problem when the analytes are strongly basic compounds. In order to diminish the effect of unreacted silanols on the surface or those that can be created in the polymeric reaction process when complete cross-linking does not take place, a secondary reaction involving a small reactive organosilane can be used. Typically, this reagent is trimethylchlorosilane, a compound with one reactive group and three small organic moieties. This compound is small enough to fit into the larger spaces between bonded hydrophobic groups so that access to the surface will be even more limited for typical solutes. The process of bonding a small moiety to diminish the number of accessible silanols is referred to as "endcapping." Many commercial sources will often designate whether or not a particular bonded phase has been endcapped. The presence or absence of endcapping will determine the nature of the stationary phase surface and, hence, its retention characteristics.

However, it is still the main R group that controls the overall degree of hydrophobicity of the surface. Within this context, the predominant factors in determining the hydophobicity are the length of the alkyl chain or the total number of carbon atoms as well as the bonding density. Some examples of various alkyl groups that have been used as reversed-phase (RP) materials are shown in Table 1. The most common types of these phases are designated by where n is the number of carbon atoms for bonded linear alkyl hydrocarbon moieties. The simplest case is where $n = 1$ for the methylbonded phase (C_1). This material has the lowest degree of hydrophobicity and provides limited retention for most small organic molecules. However, for large biomolecules such as proteins and peptides that can have extensive hydrophobic regions as part of their three-dimensional structure, these phases can prove useful in limiting the strong interactions, leading to excessively long retention times for these compounds. As the degree of hydrophobicity decreases for these large species (i.e., the macromolecule has larger hydrophilic regions or the hydrophobic areas are buried within the three-dimensional structure), the stationary phase will have to become more non-polar. This is accomplished by extending the chain length of the bonded alkyl group. Hence, the C_2 and C_4 phases have been developed to accomplish this purpose. In general, the bonded phases C_1, C_2, and have been used for separations of large molecules. In order to develop more hydrophobic interactions, the next most common phase utilizes the octyl-bonded moiety (C_8). At relatively high bonding densities (3–4 $\mu mol/m^2$), a wide range of compounds can be separated in the reversed-phase mode with this bonded moiety. Although applications involving large molecules are readily found in the literature, the predominant use involves the separation of typical small [molecular weight (MW) < 500] organic compounds. The most common reversed-phased material contains the octadecyl moiety ($n = 18$) as the bonded group. Although there are reports of phases in the literature with n values between 8 and 18, these are relatively uncommon and have not found widespread use or commercial development. The C_{18}-bonded phase was the separation material used in most of the early development of HPLC; therefore, there are several decades of applications documented in the literature. It is still by far the most often used bonded material in reversed-phase HPLC and is available in a wide variety of forms (type of silica, pore size, surface area, monomeric, polymeric, endcapped, non-endcapped, etc.) from more than 100 commercial sources. Although small organic molecules account for the majority of applications, its early commercial availability and its role in the development of HPLC has lead to examples of separations involving a broad range of compounds, including ionic species, polar compounds, biomolecules, fatty acids, and diastereomers. Because most laboratories with HPLC equipment will have a C_{18} column available, and sometimes the only one on hand, it is the first choice for initial experiments. In addition, with the broad range of applications accessilble in the literature or from commercial sources, it is often easy to find a separation that is similar, allowing for selection of mobile-phase conditions that are likely to be suitable for solving a particular analytical problem.

As shown in Table 1, a number of other bonded groups have also found use in reversed-phase HPLC. Theoretically, there is no limit to the value of n for bonded alkyl groups. However, until recently, there has been little interest in phases longer than 18 carbons. Some recent studies have demonstrated interesting applications for the C_{30} phase so that its use as well as materials with alkyl chain lengths between 18 and 30 might become more common. phenyl-bonded group (with alkyl chains attaching it to the surface of various lengths) can also function in the reversed-phase mode. The possibility of utilizing $\pi - \pi$ interactions or charge-transfer effects with the phenyl phase leads to a different selectivity than the solely hydrophobic intereactions that are available from the common alkyl-bonded materials. A similar reasoning can be applied

Table 1 Bonded hydrophobic groups.

Methyl	$-CH_3$
Ethyl	$-CH_2CH_3$
Butyl	$-CH_2-(CH_2)_2-CH_3$
Octyl	$CH_2-(CH_2)_6-CH_3$
Octadecyl	$-CH_2-(CH_2)_{16}-CH_3$
Triacontyl	$-CH_2-(CH_2)_{28}-CH_3$
Phenyl	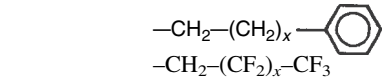
Perfluoro	$-CH_2-(CF_2)_x-CF_3$

for the phases where F is substituted for H in the bonded organic group.

Although the vast majority of stationary phases for RP/HPLC are based on chemically modified silica, there are a few other supports that have been investigated and some which are available commercially. Although silica has many advantages, its main limitation is the pH range over which it is stable. Depending on the type of silica, bonding method, and surface coverage, most chemically modified silicas are useful from pH 2 to 8. Outside of this range, most materials will experience some type of accelerated degradation. One solution to this problem is to substitute an oxide with a greater pH stability than silica. Some possibilities include alumina, zirconia, and titania, which can all be fabricated in particles with properties similar to those of silica (size, porosity, and surface area) as well as having hydroxide groups on the surface that can be used for chemical modification. Another approach is to use polymeric materials as supports in RP/HPLC. Polymers can be formed into beads similar to oxide particles, can be chemically modified to contain various organic functional groups to control their chromatographic properties, and can possess pH stability in strong acids and bases. If such modification or the basic structure of the polymer is hydrophobic, then these materials can be used in the reversed-phase mode. The main disadvantage to many polymeric materials is that they often expand or contract in various mobile-phase compositions, leading to non-reproducible chromatographic performance. Despite the potential pH advantages of these alternative supports, they have not been extensively exploited because of the long-term use of silica in the development of chemically bonded stationary phases and the limited number of applications where either very acidic or basic eluents are an absolute necessity.

The structure of the alkyl-bonded moiety on the support surface has been the subject of many investigations. A variety of spectroscopic and chromatographic methods have been employed to determine the configuration of various bonded organic groups (although the vast majority of studies have been on) in order to understand the mechanism of separation for typical solutes. There are many variables to be considered in these investigations, which include type of bonded group, bonding density, and the nature of the support surface. Some studies involve the presence of solvents to mimic the mobile phase, whereas others utilize the bonded material in the absence of any liquids. Despite these differences, some generalizations can be made about the structure of typical bonded phases in the presence of water–organic solvents, as illustrated in Fig. 1. At low concentrations of an organic constituent (A), the environment around the bonded moiety is polar and the hydrophobic chains tend to collapse on each other in order to minimize their exposure to the surronding solvent. As the percent of organic in the liquid around the bonded group increases (B → C), the medium is less polar and the groups are no longer strongly associated with each other. Although reversed-phase bonded materials have been availabe for many years, there is continued development to improve their chromatographic performance and to develop new phases for specialized applications.

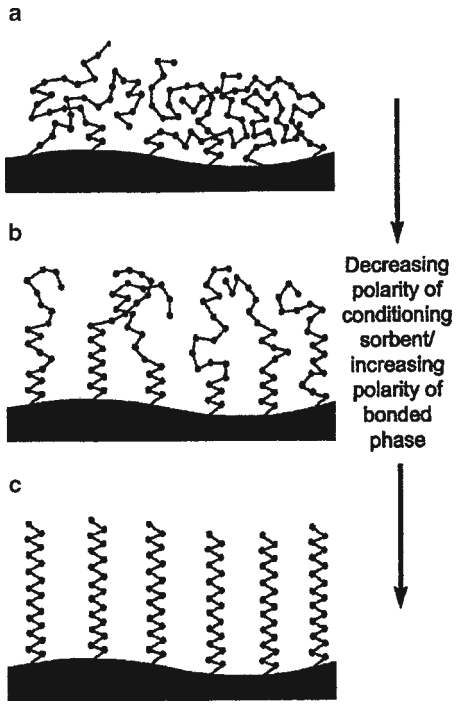

Fig. 1 Structure of a bonded phase as a function of polarity of a mobile phase: (a) highly polar mobile phase; (b) intermediate polarity mobile phase; (c) low-polarity mobile phase.

BIBLIOGRAPHY

1. Iler, R.K. *The Chemistry of Silica*; John Wiley & Sons: New York, 1979.
2. Marciniec, B. *Comprehensive Handbook on Hydrosilylation*; Pergamon Press: Oxford, 1992.
3. Nawrocki, Silica surface controversies, strong adsorption sites, their blockage and removal. Part I. J. Chromatographia **1991**, *31* (3–4), 177.
4. Nawrocki, Silica surface controversies, strong adsorption sites, their blockage and removal. Part II. J. Chromatographia **1991**, *31* (3–4), 193.
5. Pesek, J.J.; Matyska, M.T. Methods for the modification and characterization of oxide surfaces. Interf. Sci. **1997**, *5* (2–3), 103.
6. Pesek, J.J.; Matyska, M.T.; Sandoval, J.E.; Williamsen, E.J. Synthesis, characterization and applications of hydride-based surface materials for HPLC, HPCE and electrochromatography. J. Liquid Chromatogr. Relat. Technol. **1996**, *19*, 2843.
7. Unger, K.K. *Porous Silica*; Elsevier: Amsterdam, 1979.
8. Vansant, E.F.; Van Der Voort, P.; Vrancken, K.C. *Characterization and Chemical Modification of Silica*; Elsevier: Amsterdam, 1995.

Steroidal Alkaloid Glycosides: TLC Immunostaining

Waraporn Putalun
Hiroyuki Tanaka
Yukihiro Shoyama
Graduate School of Pharmaceutical Sciences, Kyushu University, Fukuoka, Japan

INTRODUCTION

The immunoassay system using monoclonal antibodies (MAbs) is indispensable to biological investigations. However, because this was rare for naturally occurring bioactive compounds having small molecular weights, we have prepared the MAbs and established assay systems using enzyme-linked immunosorbent assay (ELISA) for forskolin,[1] marijuana compound,[2] opium alkaloids,[3] solamargine,[4] ginsenoside Rbl,[5] crocin,[6] and glycyrrhizin.[7] Furthermore, the Western blotting method against ginseng saponins[8] and glycyrrhizin[9] have been established for the search of natural resources and for the breeding project of medicinal plants.

The natural resources of adrenocortical and sex hormones, which have been mainly supplied by diosgenin, are becoming rare in the world. The most important feature of solasodine is that it can be converted to dehydropregnenolone. Therefore, the steroidal alkaloid glycosides of solasodine type, such as solamargine, have become important as a starting material for the production of steroidal hormones. Rapid, simple, highly sensitive and reproducible assay systems are required for a large number of plants and a limited, small amount of samples, in order to select the strain of higher yielding steroidal alkaloid glycosides.

We present, here, a simple determination method for solasodine glycosides by using thin-layer chromatography (TLC)–immunostaining.

MATERIALS AND METHODS

Chemicals and Immunochemicals

Bovine serum albumin (BSA) and human serum albumin (HSA) were provided by Pierce (Rockford, Illinois, U.S.A.). Peroxidase-labeled anti-mouse IgG was provided from Organon Teknika Cappel Pruducts (West Chester, Pennsylvania, U.S.A.). Polyvinylidene difluoride (PVDF) membranes (Immobilon-N) were purchased from Millipore Corporation (Bedford, Massachusetts, U.S.A.). A glass microfiber filter sheet (GF/A) was purchased from Whatman International Ltd. (Maidstone, U.K.). All other chemicals were standard commercial products of analytical grade.

Solamargine and solasonine were isolated from fresh fruits of *S. khasianum* as previously described.[10] Solasodine was obtained from solamargine by acid hydrolysis as previously described.[10] Solamargine (1 mg) was dissolved in MeOH containing 1*M* HCl (1 ml). The mixture was heated at 70°C for 10, 20, 30, 60, and 90 min, respectively. Individual hydrolysates were evaporated *in vacuo* and applied to TLC. Spots developed on TLC were determined by and Dragendorff reagent.

TLC

Solasodine glycosides were applied to TLC plates and developed with chloroform–methanol–ammonia solution (7 : 2.5 : 1). A developed TLC plate was dried and then sprayed with blotting solution mixture of isopropanol–methanol–water (5 : 20 : 40, by volume). It was placed on a stainless-steel plate, then covered with a PVDF membrane sheet. After covering with a glass microfiber filter sheet, the whole plate was pressed evenly for 45 sec with a 130°C iron, as previously described,[11] but with a modification. The PVDF membrane was separated from the plate and dried.

Immunostaining of Solasodine Glycosides on PVDF Membrane

The blotted PVDF membrane was dipped in water containing $NaIO_4$ (10 mg/ml) under stirring at room temperature for 1 h. After washing with water, 50 m*M* carbonate buffer solution (pH 9.6) containing BSA (1%) was added and stirred at room temperature for 3 hr. The PVDF membrane was washed twice with phosphate buffer solution containing 0.05% of Tween 20 for 5 min, and then washed with water. The PVDF membrane was immersed in anti-solamargine MAb and stirred at room temperature for 1 hr. After washing the PVDF membrane twice with TPBS and water, a 1000 times dilution of peroxidase-labeled goat antimouse IgG in phosphate buffer solution containing 0.2% gelatin (GPBS) was added and stirred at room temperature for 1 hr. The PVDF membrane was washed twice with TPBS and water, then exposed to 1 mg/ml 4-chloro-l-naphthol–0.03% H_2O_2 in PBS solution which was freshly prepared before use for 10 min at room

temperature, and the reaction was stopped by washing with water. The immunostained PVDF membrane was allowed to dry.

RESULTS AND DISCUSSION

After solasodine glycosides were transfered to the PVDF membrane sheet from the TLC plate by heating as previously reported,[11] the PVDF membrane was treated with $NaIO_4$ solution, followed by conjugation with BSA, because solasodine glycosides on PVDF membrane are washed out by buffer solution or water without the formation of conjugate with carrier protein. The PVDF membrane was immersed in antisolamargine MAb and then peroxidase-labeled secondary MAb. When the substrate and were added, clear blue spots appeared.

Fig. 1 shows the immunostaining of acid hydrolysis products of solamargine hydrolyzed by 1*M* HCI for 10, 20, 30, and 60 min, respectively. Individual hydrolysates were applied to three TLC plates, then developed with a $CHCl_3$–MeOH–NH_4OH solvent system. Two plates were sprayed and colored with H_2SO_4. Fig. 1 shows the immunostaining (a) and stainings by H_2SO_4 (b) and Dragendorff reagent (c). When the staining sensitivities of the three methods were compared, the immunostaining was the highest, followed by the H_2SO_4, then Dragendorff reagent. It is easily suggested that product 1 may be aglycone of solamargine, solasodine and products 2–4 might be solasodine monoglycosides and diglycosides. Therefore, products 1–4 were identified as solasodine, 3-*O*-β-D-glucopyranosyl-solasodine, *O*-α-L-rhamnosyl-(1 → 4)-3-*O*-β-D-glucopyranosyl-solasodine and *O*-α-L-rhamnosyl-(1 → 2)-3-*O*-β-D-glucopyranosyl-solasodine,respectively, by direct comparison with authentic samples. Compared with two stainings between immunostaining (Fig. 1a) and staining (Fig. 1b), solasodine was not detected by immunostaining despite 44% of cross-reactivity;[4] the sugar moiety was necessary in this staining process. Thus, we separated two functions, the sugar moiety of solasodine glycosides conjugates to the membrane via Schiff base and an aglycone part which is stained by MAb.

Fig. 2 shows the immunostaining and H_2SO_4 staining of the crude extracts of *Solanum* species fruits which contain the higher solasodine glycosides.[10] Although the H_2SO_4 staining (Fig. 2b) detected many spots, including, probably, sugars and different types of saponins in various *Solanum* species, the immunostaining (Fig. 2a) detected only limited solasodine glycosides. Bands 1, 2, and 3 were identified to be khasianine, solamargine, and solasonine, respectively, by comparison with authentic samples. Different sensitivities between solamargine and solasonine were observed, and the sensitivity of solasonine was somewhat higher compared to that of solamargine. The detectable limit was 1.6 ng of solasonine, as previously reported.

This is the first report in which the TLC–immunostaining for solasodine glycosides is described. This assay method can be routinely used for survey of natural resources of solasodine glycosides as a simple and rapid analysis. Moreover, this methodology may be available for the assay in vitro *Solanum* plantlets; therefore, it makes it possible to study a large number of cultured plantlets, and a limited small amount of sample in vitro for the breeding of *Solanum* species containing a higher amounts of steroidal alkaloids. Furthermore, this system may be useful for the analysis of animal plasma samples of glycoside or glucronide not limited to solasodine glycosides and/or distributions in organs or tissues, because very low concentrations are expected. Although it is difficult to detect a low-molecular-weight compound by the Western blotting method, the approach described here will be particularly attractive in a wide variety of comparable situations as indicated in the distribution of solasodine glycosides in the fruit of *S. khasianum*. In the expanding studies of this result, naturally occurring pharmacologically active glycosides such as ginsenosides Rb_1,[8] and glycyrrhizin[9] have been investigated.

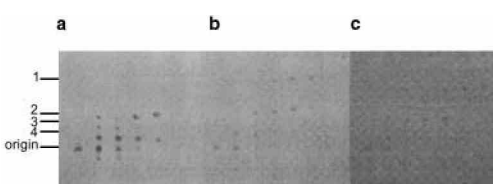

Fig. 1 Hydrolyzed products of solamargine by HCl. a, b, and c, show TLC–immunostaining and the stainings with sulfuric acid and with Dragendorff reagent, respectively. Solamargine was hydrolyzed by 1*M* HCl for 10, 20, 30, 60, and 90 min, respectively. Spots 1–4 were identified with solasodine, 3-*O*-β-D-glucopyranosyl solasodine, L-rhamnosyl-(1 → 4)-*O*-3-β-D-glucopyranosyl solasodine, L-rhamnosyl-(1 → 2)-3-β-*O*-D-glucopyranosyl solasodine, respectively.

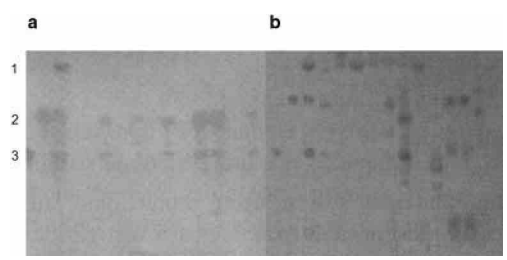

Fig. 2 TLC–immunostainings of steroidal alkaloid glycosides in the crude extracts of *Solanum* species fruits. Crude extracts were developed by a $CHCl_3$–MeOH–NH_4OH solvent system on silica gel TLC plate. After being transferred to a PVDF membrane, the membrane was treated with $NaIO_4$ and stained by MAb. Spots 1–3 were identified with khasianine, solamargine, and solasonine, respectively.

REFERENCES

1. Sakata, R.; Shoyama, Y.; Murakami, H. Production of monoclonal antibodies and enzyme immunoassay for typical adenylate cyclase activator, Forskolin. Cytotechnology **1994**, *16*, 101.
2. Tanaka, H.; Goto, Y.; Shoyama, Y. Monoclonal antibody based enzyme immunoassay for marihuana (cannabinoid) compounds. J. Immunoassay **1996**, *17*, 321.
3. Shoyama, Y.; Fukada, T.; Murakami, H. Production of monoclonal antibodies and ELISA for the baine and codeine. Cytotechnology **1996**, *19*, 55.
4. Ishiyama, M.; Shoyama, Y.; Murakami, H.; Shinohara, H. Production of monoclonal antibodies and development of an ELISA for solamargine. Cytotechnology **1996**, *18*, 153.
5. Tanaka, H.; Fukuda, N.; Shoyama, Y. Formation of monoclonal antibody against a major ginseng component, ginsenoside Rb1 and its characterization. Cytotechnology **1999**, *29*, 115.
6. Xuan, L.; Tanaka, H.; Xu, Y.; Shoyama, Y. Preparation of monoclonal antibody against crocin and its characterization. Cytotechnology **1999**, *29*, 65.
7. Tanaka, H.; Shoyama, Y. Formation of a monoclonal antibody against glycyrrhizin and development of an ELISA. Biol. Pharm. Bull. **1998**, *21*, 1391.
8. Fukuda, N.; Tanaka, H.; Shoyama, Y. Western blotting for ginseng saponins, ginsenosides using anti-ginsenoside Rb1 monoclonal antibody. Biol. Pharm. Bull. **1999**, *22*, 219.
9. Shan, S.J.; Tanaka, H.; Shoyama, Y. Western blotting method for the immunostaining detection of glucuronides of glycyrrhetic acid using anti-glycyrrhizin monoclonal antibody. Biol. Pharm. Bull. **1999**, *22*, 221.
10. Mahato, S.B.; Sahu, N.P.; Ganguly, A.X.; Kasai, R.; Tanaka, O. Steroidal alkaloids from Solanum khasian um: Application of 13C NMR spectroscopy to their structural elucidation. Phytochernistry **1980**, *19*, 2018.
11. Tanaka, H.; Putalun, W.; Tsuzaki, C.; Shoyama, Y. A simple determination of steroidal alkaloid glycosides by thin-layer chromatography immunostaining using monoclonal antibody against solamargine. FEBS Lett. **1997**, *404*, 279.

Steroids: Derivatization for GC Analysis

Raymond P.W. Scott
Scientific Detectors Ltd., Banbury, Oxfordshire, U.K.

INTRODUCTION

Steroids, bile acids, and similar compounds pose certain problems when they require to be derivatized for separation by gas chromatography (GC). The hydroxyl groups in the respective structures differ greatly in their reaction rate, which will depend on their nature (whether they are primary, secondary, or tertiary) and also, to a certain extent, on their steric environment.

DISCUSSION

After considerable research, which examined a wide variety of different derivatives, trimethylsilylation has emerged as the procedure of popular choice for steroid and steroidlike compounds. Pure compounds or biological extracts containing 3β-hydroxyl groups can be readily silylated by treatment with *N*,*O*-bis-trimethylsilyltrifluoroacetamide containing 1% trimethylchlorosilane at 60°C for 30 min, with or without added pyridine. *N*,*O*-bis-trimethylsilyltrifluoroacetamide, under some circumstances, can also be used alone or with a mixture of hexamethyldisilazane and trimethylchlorosilane (10:10:5 v/v/v) at 60°C for 30–60 min. The trimethylsilyl derivatives separate well on capillary columns carrying apolar stationary phases. The derivatives also provide excellent electron-impact mass spectra.

In addition, *N*,*O*-bis-trimethylsilyltrifluoroacetamide has been used very effectively for the silylation of estradiol and catechol estrogens. Employing *N*,*O*-bis-trimethylsilyltrifluoroacetamide : pyridine : trimethylchlorosilane (5:5:1 v/v/v) at 40°C for 8–10 hr, tetrahydroaldosterone (11β,18-epoxy-3α,16,21-trihydroxy-5β-pregnene-20-one) and aldosterone (11β,21-dihydroxy3,20-dio-exopregn4-en-18-al) have been derivatized. Employing stable isotope dilution, cortisol has been determined in human plasma by GC/MS after reacting the dimethoxime cortisol derivative with 50 μl of *N*,*O*-bis-trimethylsilyltrifluoroacetamide at 100°C for 2 hr.

More sterically hindered steroids and, in particular, the polyhydroxylated compounds were more efficiently derivatized with trimethylsilylimidazole. The ease of silylation of the ecdysteroids (polyhydroxylated anthrapod moulting hormones) tracked the following order: 2, 3, 22, 25 > 20 ≫ 14. Those substances containing a 14α-hydroxyl group require very strong reaction conditions. For example, 20-hydroxyecdysone could only be silylated using neat trimethylsilylimidazole at 100°C over a reaction period of 15 hr. It has also been established that the addition of 1% trimethylchlorosilane to the trimethylsilylimidazole catalyzed the reaction of the reagent with the 14α-hydroxyl group, reducing the reaction time to 4 hr at 100°C. The use of larger quantities of trimethylchlorosilane caused confusing side reactions to occur and should be avoided. However, the addition of potassium acetate also appeared to increase the reaction rate, allowing the reaction time to be reduced to 2–3 hr.

The conversion of the enol form of keto steroids to a silyl derivative is somewhat fraught with difficulties, as mixtures of silylated substances can be easily formed. Nevertheless, the quantitative conversion of keto steroids to their trimethylsilyl-enol ethers has been optimized. Silylation of dexamethasone (9α-fluor-11β, 17α,21-trihydroxy-16α-methyl-pregna-1,4-diene-3,20-dione) using *N*,*O*-bis-trimethylsilyltrifluoroacetamide in the presence of sodium acetate yielded the pure tetra-trimethylsilyl derivative. In this case, the trimethylsilyl-enol ether of the 20-one moiety was produced, leaving the 3-one group unreacted. An unusual reaction associated with the enolization of keto steroids is the aromatization of the (A) ring of norethynodrel (a 3-keto-5,10-ene-nor-19-methyl steroid) during trimethylsilylation. It has been suggested that, under routine silylation conditions, aromatic derivatives are very likely to form from 3-keto-4,5-epoxides of nor-19-methyl steroids. The yield of aromatic silylated products were greater when the more basic reagents were employed and at higher temperatures.

Formyl derivatives are also popular in situations where several groups have to be blocked, as in steroid analysis, because the formyl group adds little to the molecular weight. To prevent the formation of artifacts, the strength of the formic acid should be kept at 95% and reaction allowed to take place for 30 min at 40°C. Alternatively, sodium formate can be used, an example of which is in the preparation of the enol *tert*-butyldimethylsilyl derivatives of steroids and bile acids. Sodium formate solution (1 mg in 100 μl) is dried under a stream of nitrogen in a 1 ml reaction tube fitted with a Teflon-lined screw cap. The tube is then heated to 270°C for 30 min, cooled, and 10 μg of the steroid in 100 μl of methanol added. The solvent is evaporated under a stream

of nitrogen and 20 μl of *t*-butyldimethylsilylimidazole added. The tube is then filled with nitrogen, sealed, and heated at 100°C for 4 hr. Twenty microliters of 2-propanol are then added to remove excess reagent, the tube sealed, and then heated again to 100°C for 10 min. One-half milliliter of water is then added to the reaction mixture and then extracted three times with 0.5 ml of hexane. The hexane solution is concentrated under a stream of nitrogen and the concentrated solution is used for analysis.

The literature indicates that *t*-butyldimethylsilylimidazole is probably the most popular reagent for derivatizing steroids, and it is often used in conjunction with *t*-butyldimethylchlorosilane. These reagents form derivatives under relatively mild conditions (room temperature, reaction time, 1 hr), reaction goes close to completion, and relatively few side products are generated.

BIBLIOGRAPHY

1. Blau, K., Halket, J., Eds.; *Handbook of Derivatives for Chromatography*; John Wiley & Sons: New York, 1993.
2. Grant, D.W. *Capillary Gas Chromatography*; John Wiley & Sons: New York, 1996.
3. Scott, R.P.W. *Techniques of Chromatography*; Marcel Dekker, Inc.: New York, 1995.
4. Scott, R.P.W. *Introduction to Analytical Gas Chromatography*; Marcel Dekker, Inc.: New York, 1998.

Steroids: GC Analysis

Gunawan Indrayanto
Mochammad Yuwono
Suciati
Faculty of Pharmacy, Airlangga University, Surabaya, Indonesia

Abstract
Insufficient volatility and thermal stability are the biggest challenges in the application of gas chromatography for the analysis of steroids. The development of gas chromatography (GC) methods for steroids analysis should take in consideration thermal stability, the derivatization step to increase volatility, the stationary phase, and the detector. Several GC methods have been summarized for the analysis of various steroids including anabolic steroids, brassinosteroids, corticoids, estrogen, endocrine-disrupting chemicals, neurosteroids, sterols, steroid saponins, and steroid alkaloids.

INTRODUCTION

Steroids are a class of compounds that have a cyclopentanoperhydrophenanthrene skeleton, which occur in nature and in synthetic products, and which can be classified into six groups according to the number of C atoms: gonane (C-17), estrane (C-18), androstane (C-19), pregnane (C-21), cholane (C-24), and cholestane (C-27). These compounds, except for cholane, are natural hormones or hormone precursors. In the naturally occurring steroids, the fusion of rings B and C is always *trans* and of the rings C and D usually *trans* (*cis* in cardenolides and bufadienolides). Rings A and B are fused in *cis* and *trans* configurations with about equal frequency. Natural steroids possess either one or, more usually, two methyl groups at angular positions at which two rings meet. According to their function, steroid hormones can be divided into estrogens, androgens, gestagens, and corticoids.

The other steroids such as bile acids (cholane), vitamin D, saponin steroids, steroid alkaloids, cardiac glycosides, and brassinosteroids also have biologically important activities. Owing to the metabolic versatility of steroid molecules, extremely complex mixtures are often encountered, necessitating the use of chromatographic methods like high-performance liquid chromatography (HPLC), thin-layer chromatography (TLC), and gas chromatography (GC) for their analyses.

The application of GC to steroid analysis seems to face many difficulties owing to the insufficient volatility and thermolability of the steroids. The development of high-resolution gas chromatography (HRGC) and various derivatization procedures enables the efficient separation of complex steroid mixtures for application in clinical- and forensic toxicology and natural product analysis. The development of low-cost mass spectrometry (MS) detectors in recent years has also promoted the application of GC/MS systems for the analysis of complex mixtures.

THERMAL STABILITY OF STEROIDS

According to their thermal stability, steroids can be divided into three groups.[1] The first group of steroids can be analyzed by GC without any difficulties. This includes steroids that possess Δ^5-3-hydroxy, Δ^4-3-keto, $\Delta^{1,4}$-3-keto, 11-hydroxy, 17-hydroxy groups, and the phenolic ring A in free, ether, or ester form. The steroids of the second group possess tertiary hydroxyl groups (e.g., 17α-methyl-17-hydroxy steriods) and involve de-ethynlation of 17α-ethynyl-17-hydroxy steroids to 17-ketone. These steroids undergo a certain decomposition at high temperatures, but this decomposition could be suppressed by a careful selection of te GC experimental procedures. The third group of steroids decomposes during analysis by GC; hence, their direct chromatographic determination by GC cannot be carried out. The steroids belonging to this group are corticosteroids and Δ^4-3-hydroxy or acyloxy derivatives. Another source of instability is the possible decomposition of steroids and their derivatives by metals; so, using all-glass systems, including glass-line vaporizer of the GC equipment, is essential.[2]

DERIVATIZATION OF STEROIDS FOR GC ANALYSIS

The main objectives for the derivatization of steroids are to decrease heat sensitivity; avoid irreversible adsorption onto the stationary phase; increase volatility; increase the separation efficiency; achieve enhanced selectivity of separations,

and improve the sensitivity of the detectors.[2] Segura, Ventura, and Jurado[3] described some important general requirements for derivatization reactions: a single derivative should be formed for each analyte; the reaction should be simple and rapid, and they should occur under mild conditions; the derivate should be stable, reproducible, and produced with high yield; in quantitative analyses, the calibration curve should be linear. Different derivatization reagents in combination with catalyzers or antioxidants have been reported in literature.[4,5] In most cases, trimethylsilylation (TMS) derivatization is preferred using *N*-methyl-*N*-(trimethylsilyl)-trifluoroacetamide (MSTFA) as the derivatization reagent.[4,5] A mixture of MSTFA and trimethyliodosilane (TMIS), which is usually called MSTFA^{++}, can also be used as the derivatization reagent before GC–MS/MS analysis.[4] Other derivatization reagents, e.g., acetic acid anhydride, trifluoroacetic anhydride (TFA), pentafluoropropionic acid (PFPA), or heptafluorobutyric acid (HFBA) anhydride, can also be used.[3,6] For anabolic steroids and metabolites containing nitrogen, the use of acyl derivatives is also interesting.[3] The primary factor upon which the choice of a suitable derivative will be dependent is the type of detector used. For the application of the highly sensitive electron capture detector (ECD), it is quite favorable to prepare derivatives that show a high affinity for electrons; so, in such cases, chloroacetate and heptafluorobutirate derivatives are mostly used. For analysis of steroids using isotope dilution GC/MS (GC–ID/MS), silylation is not recommended on account of the fairly high abundance of ^{29}Si and ^{30}Si in natural silicon,[6] so derivatization using TFA, PFPA, or HFBA is preferred. Enzymatic hydrolysis is required before performing derivatization of glucono- or sulfoconjugated steroids in urine.[7,8] Derivatization of steroids using solid-phase microextraction (SPME) and head space methods was also described previously.[9] Conventional derivatization procedures used conventional heating process in an oven, sand bath or water bath, which is very time-consuming. Recently Zuo, Zhang, and Lin[10] reported the use of microwave in the formation of trimethylsilyl derivatives of estrogen steroids for GC–MS analysis. The advantage of this method is the minimization of the time needed for the derivatization process of estrogenic steroids. Also, the derivatives produced using microwave acceleration were identical and comparable to those produced by the conventional heating method. Detailed discussions of the derivatization methods for steroids are provided in an earlier entry in this encyclopedia[11] and in Refs. 3, 10.

STATIONARY PHASES

In the analysis of steroids by GC, silicone oils (SE-30, OV-1, OV-101) are most often used. These phases are suitable for the analysis of steroids on the basis of their molecular weight or the shape of the molecules. These silicone phases are considered as non-selective stationary phases. For separating stereoisomers or structural isomers, saturated or unsaturated derivatives, selective stationary phases such as methyltrifluoropropyl (QF-1, OV-210), methylphenylcyanopropyl (OV-225), and methyl-β-cyanoethyl (XE-60, AN-600) can be used.[2] For packed-column applications, solid supports such as Gas-Chrom Q, Gas-Chrom S, Chromosorb AW or DMCS, and Chromosorb W HP DMCS, with 3% concentration of the stationary phase, have been generally used.[1,12] For separating complex steroid mixtures, application of a glass or a fused-silica column is recommended. The length of the column is in the range between 17 and 30 m, diameter of 0.2–32 mm, and film thickness of 0.1–0.33 μm. The stationary phase consists mostly of polydimethylsiloxane, with 0–50% diphenyl groups.[6]

DETECTORS

The flame ionization detector (FID) is the detector most often used in steroid analyses. For very low concentrations of steroids, the application of ECD is needed. Thermal conductivity detectors (TCDs) cannot be used in the analysis of steroids because of their very low sensitivity.[1,2] For steroidal alkaloids, a nitrogen-specific detector (NPD) has also been used. By the use of dual detector systems (e.g., FID and NPD), closely related nitrogen-containing and non-nitrogen-containing steroids can be easily differentiated. The application of MS as detector was already discussed in a previous entry in this encyclopedia.[13] By using a GC/MS system, the identity of the peak(s) can be determined in an undisputed manner.[3]

GC PARAMETERS FOR STEROID IDENTIFICATION

The identification of steroids in an unknown sample can be based on GC or GC/MS parameters, such as relative retention times, retention indices, steroid number, mass spectra, and/or important ion fragments.

Relative retention time (RR_t) is defined as the ratio of the analyte's and the reference compound's retentions. The RR_t of sterols relative to cholesterol and cholestane, stearyl acetates to cholesteryl acetate, estrogen derivatives to cholestane, and estrogen TMS ether to cholestane, on various packed columns, was reported by Heftmann.[12] The RR_t of some estrane, androstane, and pregnane derivatives was also reported.[2]

The concept of retention index (RI) was first published by E. Kovats in 1961. Detailed discussion on RI is included in a previous entry in this encyclopedia.[14] Van Gelder[15] described the RI of various steroid alkaloids and saponins.

Steroid number (SN) is the sum of quantities characteristic of the skeleton and the functional groups in a molecule.[1,9]

$$SN = S + F_1 + F_2 + \ldots + F_N$$

where S is the number of C atoms, and $F_1, F_2, \ldots, F_N$ are values that are characteristic of the functional groups. The values of SN and F of some steroids, determined in packed columns, were already described in previous works.[1,12]

GC/MS parameters for anabolic steroid metabolites,[7,16,17] steroid alkaloids, and saponins,[15] and their MS data have been published previously.

SELECTED APPLICATIONS

Anabolic Steroids

Anabolic steroids, which are related in structure and activity to testosterone, are used to improve muscle mass and to accelerate recovery times from exercises. The use of anabolic steroids by athletes during competition and training was forbidden by the International Olympic Committee (IOC). Anabolic steroids have been abused not only by humans, but also for sporting purposes such as horse racing.[18,19,20] For doping control in sports, urine samples are mostly tested. The most often used anabolic steroids are androgens, such as testosterone.[4] It is not easy to detect parent compounds except for oxandrolone and testosterone, because the steroids are extensively metabolized.[21] Before derivatization, urine samples are passed through a Pasteur pipette containing Serdolit AD-2 slurry[21,22] or extracted using solid-phase extraction (SPE).[7,8] For conjugated steroids, hydrolysis is performed (at pH 8.5) before derivatization.[8] For analysis of anabolic steroids, Choi et al.[21] used an Ultra-2 cross-linked capillary column of 5% phenylmethylpolysiloxane (30 m × 0.2 mm, film thickness 0.33 μm) with an oven temperature of 150°C (2 min) to 300°C (2 min) with a step rate of 20°C/min; injection temperature of 300°C; and detection using MS (negative chemical ionization using methane) and tandem MS (MS/MS with collision energy for a collision-induced dissociation of 1.0). Yoon and Lee[8] used a glass capillary column (17 m × 2 mm) with an oven temperature of 180°C (6 min), then increased to 224°C (4°C/min), and finally to 300°C (15°C/min), and detection using MS (negative chemical ionization using methane). Ho et al.[19,20] reported the analysis of turinabol and mesterolone in horse urine using an HP1-MS column (~30 m × 0.25 mm, 0.25 μm film thickness) with constant helium flow at 1.2 ml/min. For the analysis of turinabol the oven temperature was set at 60°C (1 min), then increased to 220°C (60°C/min) and, finally, to 300°C (3°C/min), which was held for 5 min, while for mesterolone the column was initially set at a higher temperature of 120°C (0.5 min), then increased to 180°C (30°C/min), followed by an increase to 230°C (4°C/min), and finally to 300°C (30°C/min), which was held for 5 min. The MS analysis was performed on electron impact (EI) mode. The analysis of residual anabolic steroids in meat was reported by Fuh, Huang, and Lin.[23] The isolation was conducted by SPE. To derivatize the isolated steroids, $MSTFA^{++}$ was used. The enzymatic hydrolysis was not conducted, as previous studies have discovered that there was no significant hormone liberation involved in muscle, fatty tissue, and meat. The derivatization products were then subjected to GC–MS/MS analysis. For this purpose, a DB-5 GC column (30 m × 0.25 mm, with 0.25 μm film thickness) was used, with a flow rate of 1.0 ml/min. The oven temperature was initially set at 180°C (1 min), increased to 240°C (6°C/min, for 2 min), and finally increased to 290°C (6°C/min, held for 10 min). The MS analysis was performed on EI mode. Impens et al.[24] used a non-polar 5% phenyl-polysilphenylene-siloxane BPX-5 GC column to analyze anabolic steroids in bovine urine. The sample was derivatized with $MSTFA^{++}$ before being injected for the GC–MS/MS and GC–MS/MS/MS analyses. The oven temperature was initially set to 100°C (1 min), then increased to 250°C (30°C/min), followed by an increase to 290°C (2.5°C/min), and finally to 300°C (10°C/min), which was held for 1.5 min. Interested readers can consult Refs. 3, 8, and 18–25 for details.

Brassinosteroids

Brassinosteroids are steroidal plant hormones that are required for normal growth and development. Brassinosteroids are distributed in both aerial and underground parts of plants; however, the concentration is higher in the aerial parts.[26] About 40 brassinosteroids have been identified from the plant kingdom.[27] The use of brassinosteroids as an anticancer agent has been investigated by Malíková et al.[28] For the analysis of brassinosteroids, Park, Kim, and Kim,[27] Kim et al.,[29] and Kim, Kim, and Kim[26] used an HP-5 fused-silica column (30 m × 0.25 mm, film thickness 0.25 μm) with an oven temperature of 175°C (2 min), then elevated to 280°C (40°C/min). Prior to injection, the samples were treated with methaneboronic acid in pyridine (70°C for 30 min) to produce bismethaneboronate. For analyzing typhasterol, testosterone, 6-deoxytyphasterol, and 6-deoxoteasterone, Nomura et al.[30] silylated the methaneboronate to MB-TMS derivatives before injecting into the GC (capillary DB-1 column 25 m × 0.25 mm, 0.25 μm film thickness; oven temperature 170°C for 1.5 min, then increased to 280°C in steps of 37°C/min).

Corticoids

Corticoids or corticosteroids are divided into mineralocorticoids that act in the regulation of blood volume and metabolism of electrolytes, and glucocorticoids that act in saccharometabolism.[4,25] On account of the instability of

their dihydroxy acetone side chain at C-17, direct analysis using GC is impossible. Methoximation followed by TMS derivatization is the most widely used approach.[3] For the analysis of glucocorticoids, Mozzarino et al.[31] used an HP-1 fused-silica cross-linked methyl silicone capillary column (17 m × 0.20 mm, film thickness 0.11 μm) at a flow rate of 1 ml/min. The temperature was set at 180°C (4.5 min), increased to 230°C (3°C/min), followed by an increase to 290°C (20°C/min), and finally to 320°C (30°C/min). The derivatization with MSTFA/NH_4I/dithioerythrytol (1000:2:4, v/w/w) at 70°C for 20 min was conducted before GC–MS analysis. Shakerdi et al.[32] investigated a GC–MS method to analyze the excretion rate of 18-hydroxytetrahydro-11-dehydrocorticosterone using the non-homologous reference standard β-cortol. After derivatization the sample was injected to a DB-1 column (30 m × 0.322 mm, film thickness 0.25 μm). The oven temperature program was as follows: starting from 100°C (3 min) increased to 190°C at a rate of 20°C/min, then to 285°C at a rate of 2°C/min, which was held for 10 min. The analysis was performed on positive EI ionization mode. Interested readers should consult previous publications.[6,25,31,32]

Estrogens

Estrogens (C18) are regarded as typical female hormones owing to their importance in the estrous cycle. These hormones have been used in animal fattening because of their anabolic effects. These C18 steroids differ from all other steroids in a way characterized by the presence of an aromatic A ring and the lack of a methyl group at C-10. Fritsche[33] analyzed 17β-estradiol and estrone and the estrogenic metabolites estriol and 17β-estradiol in foodstuffs using a DB-5 fused-silica column (30 m × 0.25 mm, film thickness 0.25 μm) and detection using MS (EI, electron energy: 60 eV, ion source temperature: 180°C). The steroids were previously derivatized with *N*-methyl-*N*-trimethylsilyltrifluoroacetamide/TMIS/dithioerythrytol (1000:2:2) at 60°C for 15 min. Roy, Hachey, and Liehr[34] developed a GC method with a ^{53}Ni-pulsed ECD for measuring the rate of formation of 2-hydroxyestradiol and 4-hydroxyestradiol from estradiol in microsomal preparations. The steroids were converted to heptafluorobutyryl esters and separated with a DB-5 fused-silica capillary column (30 m × 0.25 mm). The GC conditions were splitless injection, 280°C injection temperature, and a temperature gradient of 30°C/min from 100°C to 245°C followed by a 5 min isothermal period at 245°C and a second temperature gradient of 1°C/min from 245°C to 265°C. GC analysis of the pentafluorobenzyl derivatives of estrogen in river water and effluents was also developed by Xiao, McCalley, and McEvoy.[35] Impens et al.[36] have undertaken a study on the residues of estrogens in kidney fat and meat. For this purpose the sample was derivatized with MSTFA, which was then subjected to GC–MS analysis. For this purpose, a non-polar 5% phenyl-polysilphenylene-siloxane SGE BPX-5 column (25 m × 0.22 mm, film thickness 0.25 μm) was used. The initial oven temperature was keep at 100°C for 1 min, then increased to 250°C at a rate of 30°C/min, then to 290°C (2.5°C/min), and finally to 300°C (10°C/min), which was held for 1.5 min. For further confirmation of the steroids a GC–MS/MS analysis was performed.

ENDOCRINE-DISRUPTING CHEMICALS

Endocrine-disrupting chemicals (EDCs) are exogenous substances that cause alterations of normal hormone function and physiological status in wildlife and in humans.[37,38] There are two major types of compounds classified as EDCs: phenolic and estrogenic. These dangerous chemicals can be released directly or indirectly from domestic or industrial waste as pollutants in aquatic environment. Analysis of EDCs in sludge and waste water samples have been described by Jeannot et al.[38] The samples were extracted by SPE with C18 cartridges and SPE with polymeric cartridges. Before GC–MS and GC–MS/MS analyses, the sample was derivatized with bis(trimethylsilyl)trifluoroacetamide (BSTFA). A CP-Sil 8 CB column (95% dimethyl-5% phenyl polysiloxane, 30 m × 0.25 mm, film thickness 0.25 μm) was used. The oven temperature was programmed at 85°C (3 min), then increased to 130°C (10°C/min), and then slowly to 300°C (3°C/min). Liu, Zhou, and Wilding[37] have developed a simultaneous analysis of EDCs in water samples using SPE–GC–MS method. For this purpose nine types of SPE cartridges were employed. The sample derivatization was carried out with BSTFA at 60–70°C for 30 min same as Jeannot et al.[38] The GC–MS analysis was conducted on a ZB5 (5% diphenyl-95% dimethyl polysiloxane) capillary column (30 m × 0.25 mm, film thickness 0.25 μm). The column temperature was initially set at 100°C (1 min), which was then increased to 200°C (10°C/min), followed at a rate of 15°C/min until it reached 260°C, and finally slowly increased at a rate of 3°C/min to 300°C, which was held for 2 min. Interested readers should consult Refs. 37 and 38.

Neurosteroids

Neurosteroids are steroids that are synthesized de novo in the central nervous system (androsterone, dihydrotestosterone, testosterone, allopregnanolone, isopregnanolone, and pregnanole). These steroids are synthesized from cholesterol or from a blood-borne precursor.[39] After the extraction of plasma and cerebrospinal fluids using SPE and derivatization with carboxymethoxime, pentafluorobenzyl, and trimethylsilyl, the derivatized samples were injected into a GC/MS system for quantitative evaluation with a selected-ion monitoring (SIM) method, which was used to maximize sensitivity as only a selected *m/z* is monitored. Details of the method have been described in Refs. 40 and 41. To analyze neurosteroids in the rat brain, Liere et al.[42,43] used a BPX5 column (5% phenyl-95% dimethyl polysiloxane, 25 m × 0.22 mm, film thickness

0.25 μm) and a BPX35 column (35% phenyl-65% dimethyl polysiloxane, 30 m × 0.25 mm, film thickness 0.25 μm). The oven temperature was set as follows: starting at 50°C (1 min), increased to 140°C (30°C/min), followed by an increase to 300°C (10°C/min) for the first column; and starting at 50°C (1 min), increased to 175°C at the rate of 30°C/min, and finally to 320°C at the rate of 10°C/min for the second column. The MS was performed in the EI mode. Before being injected to GC–MS, samples were derivatized with HFBA anhydride or triethylamine (TEA)/HFBA. A review article on the analysis of neurosterols and neurosteroids by MS has been published by Wang, Karu, and Griffiths.[41]

Sterols

Various TMS derivatives of sterols in tuna olive oil could be separated using CP-Sil 8 CB fused-silica column (15 m × 0.22 mm; 240°C isothermal; FID). Plant sterols (brassicasterol, campesterol, stigmasterol, and sitosterol) were analyzed using a fused-silica column (15 m × 0.25 mm, 260°C isothermal; FID).[44] The analysis of campesterol, sitosterol, and diosgenin using a glass-packed column (6 ft × 0.125 in.; 3% SE-30 on Gas Chrom Q, 220–270°C, 4°C/min; FID) was described.[45] The separation of plant sterols (cholesterol, campesterol, stigmasterol, and sitosterol), squalene, and some lupane triterpenes using a glass-packed column (2 m × 2 mm; 3% OV-1 on Gas Chrom Q; 200–280°C, 4°C/min; FID) was reported.[46] The analysis of sterols (β-sitosterol, stigmasterol, campesterol, and cholesterol) in sugarcane waxes was undertaken in a fused-silica capillary column, CP Sil 5 (25 m × 0.25 mm, film thickness 0.25 μm). The temperature was programmed from 150°C to 320°C at the rate of 6°C/min. The MS was recorded in EI mode. TMSi derivatives of sterols were prepared using HMDS/TMSiCl (NF ISO 6799).[47] Seo et al.[48] reported the analysis of squalene and phytosterol (β-sitosterol and stigmasterol) in *Eleutherococcus senticosus* using an HP-1 (25 m × 0.25 mm, film thickness 0.33 μm) methyl polysiloxane cross-linked capillary column. The temperature was programmed from 100°C to 250°C at the rate of 20°C/min. The amount of squalene and phytosterol was calculated from the ratio of the peak area of the relevant compound to that of the standard. To analyze the constituents (alkanes, esters, aldehydes, ketones, fatty acids, and sterols) of cuticular waxes from potato, GC–MS analysis was performed in a RTX-1 WCOT capillary column (30 m × 0.25 mm, film thickness 0.25 μm). The oven temperature was initially set to 200°C and then increased to 320°C (4°C/min), which was held for 15 min.[49] The analysis of phytosterol in fungus *Mortierella alpine* was conducted in a DB-5 column (30 m × 25 mm, film thickness 0.25 μm).[50] Analysis of plant sterols in food and vegetable oils has been reviewed by Abidi.[51] Kalo and Kuranne[52] described the GC analysis and electrospray tandem MS of free sterols in fats and oils.

Steroid Saponins and Steroid Alkaloids

Steroidal saponins are steroids coupled to sugar units. Before GC analysis, steroid saponins need to be derivatized to their acetyl, methyl, or trimethylsilyl ether derivatives. There are two methods that can be used to analyze steroidal saponins using GC. First, GC analysis was conducted on the steroidal saponins after the separation of aglycone and sugar moiety through hydrolysis. Second, the analysis was undertaken in steroidal saponins without hydrolysis of the sugar units. The latter method can be used if the sugar units are not attached to the steroids through ester linkage; otherwise, the deglycosylation of the steroidal saponins can occur in the injection port of the GC.[53]

The separation of diosgenin and solasodine was reported using a glass-packed column (6 ft × 0.125 in.; 3% SE-30 on Gas Chrom Q, 220–270°C, 4°C/min; FID). Diosgenin and its 5-α-derivative (tigogenin) can be separated well after derivatization using TFA, and analyzed using a glass-packed column (10 ft × 0.125 in.; 3% QF-1 on Gas Chrom Q; 220°C isothermal; FID).[45] Solanidine, demissidine (5-α-derivative of solanidine), and solasodiene, which could not be separated using a glass-packed column (1 m × 2 mm; 10% SE-30 on Chromosorb W-HP, 260–300°C, 5°C/min, FID), were separated well using a fused-silica column (50 m × 0.22 mm; CP-Sil 5, film thickness 0.12 μm; 290°C isothermal; FID).[13] Using a fused-silica column (50 m × 0.22 mm; CP-Sil 5 CB, film thickness 0.12 μm; 270°C isothermal; FID), various steroids, 5-α-cholestane, solanthrene, cholesterol, solanidine, demissidine, solasodiene, stigmasterol, diosgenin, tigogenin, solasodine, and tomatidine, could be separated without derivatization.[15] Some methods of analysis of solasodine using GC were described in a previous publication.[54]

Li et al.[55] has developed a method to analyze isosteroidal alkaloids (ebeiedine, ebeiedinone, ebeienine, hupehenine, isoverticine, verticine, verticinone, and imperialine) in *Fritillaria* species through direct injection of these alkaloids without precolumn derivatization. Two GC columns, namely Supelco SAC-5 (30 m × 0.25 mm, film thickness 0.25 μm) and HP-1 (12.5 m × 0.22 mm, film thickness 0.33 μm) were compared. The result has shown that in Supelco SAC-5 six out of the eight alkaloids tested were resolved better.

REFERENCES

1. Görög, S.; Szász, G. *Analysis of Steroid Hormone Drugs*; Elsevier Scientific Publishing Company: Amsterdam, 1985; 137–169.
2. Görög, S. *Steroid Analysis in the Pharmaceutical Industry*; Ellis Horwood Limited: Chichester, 1989; 114–125.
3. Segura, J.; Ventura, R.; Jurado, C. Derivatization procedure for gas chromatography–mass spectrometric determination

of xenobiotics in biological samples, with special attention to drug abuse and doping agents. J. Chromatogr. B, **1998**, *713*, 61–90.
4. Noppe, H.; Le Bizec, B.; Verheyden, K.; De Brabander, H.F. Novel analytical methods for the determination of steroid hormones in edible matrices. Anal. Chim. Acta **2008**, *611*, 1–16.
5. Quintana, J.B.; Carpinteiro, J.; Rodríguez, I.; Lorenzo, R.A.; Carro, A.M.; Cela, R. Determination of natural and synthetic estrogens in water by gas chromatography with mass spectrometric detection. J. Chromatogr. A, **2004**, *1024*, 177–185.
6. Wolthers, B.G.; Kraan, G.P.B. Clinical application of gas chromatography–mass spectrometry of steroids. J. Chromatogr. A, **1999**, *843*, 247–274.
7. Ayotte, C.; Goudreault, A.; Charlebois, A. Testing for natural and synthetic anabolic agents in human urine. J. Chromatogr. B, **1996**, *687*, 3–25.
8. Yoon, J.M.; Lee, H.K. Gas chromatography and mass spectrometric analysis of conjugated steroids in urine. J. Biosci. **2001**, *26*, 627–634.
9. Okeyo, P.; Rentz, S.M.; Snow, N.H. Analysis of steroids for human serum by SPME with head space derivatization. J. High Resolut. Chromatogr. **1999**, *20*, 171.
10. Zuo, Y.; Zhang, K.; Lin, Y. Microwave-accelerated derivatization for the simultaneous gas chromatography–mass spectrometric analysis of natural and synthetic estrogenic steroids. J. Chromatogr. A, **2007**, *1148*, 211–218.
11. Scott, R.P.W. Steroids: Derivatization for GC Analysis. In *Encyclopedia of Chromatography*, 3rd Ed.; Cazes, J., Ed.; Taylor & Francis: New York, 2010; 562–566.
12. Heftmann, E. *Chromatography of Steroids*; Elsevier Scientific Publishing Company: Amsterdam, 1976.
13. Scott, R.P.W. GC/MS systems. In *Encyclopedia of Chromatography*, 3rd Ed.; Cazes, J., Ed.; Taylor & Francis: New York, 2010; 976–981.
14. Zenkevic, I.G. Kováts, retention index system. In *Encyclopedia of Chromatography*, 3rd Ed.; Cazes, J., Ed.; Taylor & Francis: New York, 2010; 1304–1310.
15. Van Gelder, W.M.J. Steroidal glycoalkaloid in Solanum species: Consequences for potatoes breeding and food safety, Ph.D. Thesis; University of Wageningen: Holland, 1989.
16. Bowers, L.D.; Borts, D.J. Separation and confirmation of anabolic steroids with quadrupole ion trap tandem mass spectrometry. J. Chromatogr. B, **1996**, *687*, 69.
17. Schänzer, W.; Delahaut, P.; Geyer, H.; Machnik, M.; Horning, S. Long-term detection and identification of methandienone and stanozolol abuse in athletes by GC–high resolution mass spectrometry. J. Chromatogr. B, **1996**, *687*, 93–108.
18. Poelmans, S.; De Wasch, K.; De Brabander, H.F.; Van De Wiele, M.; Courtheyn, D.; Van Ginkel, L.A.; Sterk, S.S.; Delahaut Ph. Dubois, M.; Schilt, R.; Nielen, M.; Vercammen, J.; Impens, S.; Stephany, R.; Hamoir, T.; Pottie, G.; Van Poucke, C.; Van Peteghem, C. Analytical possibilities for the detection of stanozolol and its metabolites. Anal. Chim. Acta **2002**, *473*, 39–47.
19. Ho, E.N.M.; Kwok, W.H.; Leung, D.K.K.; Wong, A.S.Y. Metabolic studies of turinabol in horses. Anal. Chim. Acta **2007**, *586*, 208–216.
20. Ho, E.N.M.; Leung, D.K.K.; Leung, G.N.W.; Wan, T.S.M.; Wong, H.N.C.; Xu, X.; Yeung, J.H.K. Metabolic studies of mesterolone in horses. Anal. Chim. Acta **2007**, *596*, 149–155.
21. Choi, M.H.; Chung, B.C.; Kim, M.; Choi, J.; Kim, Y. Determination of 4 anabolic steroid metabolites by gas chromatography/mass spectrometry with negative ion chemical ionization and tandem mass spectrometry. Rapid Commun. Mass. Spectrom. **1998**, *12*, 1749–1755.
22. Choi, M.H.; Chung, B.C.; Lee, W.; Lee, U.C.; Kim, Y. Determination of anabolic steroid metabolites by gas chromatography/mass spectrometry with negative ion chemical ionization and tandem mass spectrometry. Rapid Commun. Mass. Spectrom. **1999**, *13*, 376–380.
23. Fuh, M.-R.; Huang, S.-Y.; Lin, T.-Y. Determination of residual anabolic steroid in meat by gas chromatography–ion trap-mass spectrometer. Talanta **2004**, *64*, 408–414.
24. Impens, S.; Van Loco, J.; Degroodt, J.M.; De Brabander, H. A downscaled multi-residue strategy for detection of anabolic steroids in bovine urine using gas chromatography–tandem mass spectrometry (GC–MS^3). Anal. Chim. Acta **2007**, *586*, 43–48.
25. Shimada, K.; Mitamura, K.; Higashi, T. Gas chromatography and high performance liquid chromatography of natural steroids. J. Chromatogr. A, **2001**, *935*, 141–172.
26. Kim, Y.-S.; Kim, T.-W.; Kim, S.-K. Brassinosteroids are inherently biosynthesized in the primary roots of maize, *Zea mays* L. Phytochemistry **2005**, *66*, 1000–1006.
27. Park, S.C.; Kim, T.W.; Kim, S.K. Identification of brassinosteroids with 24-*R*-methyl in immature seeds of *Phaseolus vulgaris*. Bull. Korean Chem. Soc. **2000**, *21*, 1274–1276.
28. Malíková, J.; Swaczynová, J.; Kolář, Z.; Strnad, M. Anticancer and antiproliferative activity of natural brassinosteroids. Phytochemistry **2008**, *69*, 418–426.
29. Kim, T.S.; Park, S.H.; Joo, S.H.; Kim, Y.S.; Choo, J.; Kim, S.K. Metabolism of typhasterol in suspension cultured cells of *Marchantia polymorpha*. Bull. Korean Chem. Soc. **2001**, *22*, 651–654.
30. Nomura, T.; Kitasaka, Y.; Tokatsuto, S.; Reid, J.B.; Fukami, M.; Yoko, T. Brassinosteroid/sterol synthesis and plant growth affected by lka and lkb mutation of pea. Plant Physiol. **1999**, *119*, 1517–1526.
31. Mozzarino, M.; Rossi, F.; Giacomelli, L.; Botrè, F. Effect of the systemic versus inhalatory administration of synthetic glucocorticoids on the urinary steroid profile as studied by gas chromatography–mass spectrometry. Anal. Chim. Acta **2006**, *559*, 30–36.
32. Shakerdi, L.A.; Connell, J.M.C.; Fraser, R.; Wallace, A.M. Analysis of biological samples by gas chromatography–mass spectrometry without a reference standard: Measurement of urinary 18-hydroxytetrahydro-11-dehydrocorticosterone excretion rate in human subjects. J. Chromatogr. B, **2003**, *784*, 367–373.
33. Fritsche, S. Steriod hormone in food: Analysis, occurrences, dietary intake and correlation with meat characteristics, Ph.D. Thesis; University of Hamburg: Germany, 1998.
34. Roy, D.; Hachey, D.L.; Liehr, J.G. Determination of estradiol 2- and 4-hydroxylase activities by gas chromatography with electron-capture detection. J. Chromatogr. **1991**, *567*, 309–318.

35. Xiao, X.-Y.; McCalley, D.V.; McEvoy, J. Analysis of estrogen in river water and effluents using solid-phase extraction and gas chromatography–negative chemical ionisation mass spectrometry of the pentafluorobenzyl derivatives. J. Chromatogr. A, **2001**, *923*, 195–204.
36. Impens, S.; De Wasch, K.; Cornelis, M.; De Brabander, H.F. Analysis on residues of estrogens, gestagens and androgens in kidney fat and meat with gas chromatography–tandem mass spectrometry. J. Chromatogr. A, **2002**, *970*, 235–247.
37. Liu, R.; Zhou, J.L.; Wilding, A. Simultaneous determination of endocrine disrupting phenolic compounds and steroids in water by solid-phase extraction gas chromatography–mass spectrometry. J. Chromatogr. A, **2004**, *1022*, 179–189.
38. Jeannot, R.; Sabik, H.; Sauvard, E.; Dagnac, T.; Dohrendorf, K. Determination of endocrine-disrupting compounds in environmental samples using gas and liquid chromatography with mass spectrometry. J. Chromatogr. A, **2002**, *974*, 143–159.
39. Baulieu, E.- E.; Robel, P.; Schumacher, M. Neurosteroids: Beginning of the story. Int. Rev. Neurobiol. **2001**, *46*, 1–32.
40. Kim, Y.S.; Zhang, H.; Kim, H.Y. Profiling neurosteroids in cerebrospinal fluids and plasma by gas chromatography/electron capture negative chemical ionization mass spectrometry. Anal. Biochem. **2000**, *277*, 187–195.
41. Wang, Y.; Karu, K.; Griffiths, W.J. Analysis of neurosterols and neurosteroids by mass spectrometry. Biochimie **2007**, *89*, 182–191.
42. Liere, P.; Akwa, Y.; Weill-Engerer, S.; Eychenne, B.; Pianos, A.; Robel, P.; Sjövall, J.; Schumacher, M.; Baulieu, E.-E. Validation of an analytical procedure to measure trace amounts of neurosteroids in brain tissue by gas chromatography–mass spectrometry. J. Chromatogr. B, **2000**, *739*, 301–312.
43. Liere, P.; Pianos, A.; Eychenne, B.; Cambourg, A.; Liu, S.; Griffiths, W.; Schumacher, M.; Sjövall, J.; Baulieu, E.-E. Novel lipoidal derivatives of pregnenolone and dehydroepiandrosterone and absence of their sulfated counterparts in rodent brain. J. Lipid. Res. **2004**, *45*, 2287–2302.
44. *Chromatography Illustrated*, Chromatograms: Gas Chromatography, Liquid Chromatography, Supercritical Fluid Chromatography, from the Editors of Journal Chromatography, 33–34.
45. Carle, R. Untersuchungen zur Stertoidalalkaloid-und Sapogeninfuehrung in Pflanzen und Zellkulturen der Gatung Solanum L. Ph.D. Thesis; University of Tubingen: Germany, 1979.
46. Indrayanto, G. Steroide und Triterpene in Zellkulturen, Ph.D. Thesis; University of Tubingen: Germany, 1983.
47. Nuissier, G.; Bourgeois, P.; Grignon-Dubois, M.; Pardon, P. Composition of sugarcane waxes in rum factory wastes. Phytochemistry **2002**, *61*, 721–726.
48. Seo, J.-W.; Jeong, J.-H.; Shin, C.-G.; Lo, S.-C.; Han, S.-S.; Yu, K.-W.; Harada, E.; Han, J.-Y.; Choi, Y.-E. Overexpression of squalene synthase in *Eleutherococcus senticosus* increases phytosterol and triterpene accumulation. Phytochemistry **2005**, *66*, 869–877.
49. Szafranek, B.M.; Synak, E.E. Cuticular waxes from potato (*Solanum tuberosum*). Phytochemistry **2006**, *67*, 80–90.
50. Nes, W.D.; Nichols, S. D. Phytosterol biosynthesis pathway in *Mortierella alpina*. Phytochemistry **2006**, *67*, 1716–1721.
51. Abidi, S. Chromatographic analysis of plant sterols in food and vegetable oils. J. Chromatogr. A, **2001**, *935*, 173–201.
52. Kalo, P.; Kuranne, T. Analysis of free sterols in fats and oils by flash chromatography, gas chromatography and electrospray tandem mass spectrometry. J. Chromatogr. A, **2001**, *935*, 237–248.
53. Oleszek, W.A. Chromatographic determination of plant saponins. J. Chromatogr. A, **2002**, *967*, 147–162.
54. Indrayanto, G.; Sondakh, R.; Syahrani, A.; Utami, W. Solasodine. In *Analytical Profile of Drugs and Excipients*; Brittain, G., Ed; Academic Press: San Diego, 1996, Vol. 24, 487–522.
55. Li, S.-L.; Li, P.; Lin, G.; Chan, S.-W.; Ho, Y.-P. Simultaneous determination of seven major isosteroidal alkaloids in bulbs of *Fritillaria* by gas chromatography. J. Chromatogr. A, **2000**, *873*, 221–228.

Steroids: TLC Analysis

Muhammad Mulja
GunawanIndrayanto
Faculty of Pharmacy, Airlangga University, Surabaya, Indonesia

INTRODUCTION

Steroids, which are a class of compounds that occur in nature and in synthetic products, have a cyclopentanoperhydrophenanthrene skeleton. The carbon atoms and rings are labeled according to the schemes shown in Fig. 1. The following classes of compounds belongs to sterioids: sterols, bile acids, cardenolides, androgens, estrogens, corticosteroids, steroid sapogenins, steroid alkaloids, ecdysteroids, and vitamin D.

In the naturally occuring steroids, the fusion of ring B and C is always trans and that of the ring C and D is usually *trans* (*cis* in the cardenolides and bufadienolides). Rings A and B are fused in cis and trans configurations with about equal frequency. The configuration of the substituents is referred to that of the 19-methyl group on C_{10}. Every substituent that is in a configuration identical to the methyl group i indicated by the β-position; substituents of opposite configuration are termed α-substituents (dotted lines). If the substituents lie in the planes of the rings, they are termed equatorial (e), and if perpendicular to the rings, they are called axial (a). Thus, for example, in an A/B *cis*-steroid, a 3β-hydroxy group is axial and equatorial in an A/B *trans*-steroid (see Fig. 1). In general, equatorial substituents are more stable than axial substituents. In various reactions, the formation of the former is favored.

In the field of steroid analysis, thin-layer chromatography (TLC) is still the method of choice, especially when many simultaneous analyses have to be carried out; hundreds of analyses can be performed in a short time and with small demands on equipment and space. Samples can be analyzed with minimal cleanup, and analyzing a sample by the use of multiple separation steps and static postchromatographic detection procedure is also possible because all sample components are stored on the layer without the chance of loss. The time required in TLC analysis is about 10–60 min. As little as 0.001 μg of steroids/spot can be can be detected by TLC. Using a TLC plate with thicker adsorbent layers (0.5–2 min), several grams of substance can be isolated (preparative TLC).

SORBENTS

The TLC of steroids has been tried on a great variety of sorbents, but various forms of silica gels are most frequently used. In order to achieve adequate stability, adhesion, and resistance to abrasion of the (pre-coated) layers, the sorbents usually contain a binder. Either they do not contain any additive at all, designated by "H" in the article designation, or gypsum ("G") as binder. The sorbents designated by "P" designates the addition of flourescent indicators and, if applicable, the number that follows gives the excitation wavelength and an "s" following this indicates the acid stability of the indicators. A number placed immediately after the name of the sorbent indicates the pore diameter of the sorbents (in Å). In high-performance thin-layer chromatography (HPTLC), the particle diameter is about 3–10 μg, whereas in TLC, it is about 4–25 μm. The plates can be easily prepared in the laboratory or readily purchased from commercial sources as precoated plates or sheets, but it is recommended to use ready-made (pre-coated) plates or sheets because they are more convenient and more uniform than those manually prepared in the laboratory.

An addition of 3–10% of silver nitrate to silica gel or kieselguhr is considerable helpful in the separation of sterols and steroids that differ only through an unconjugated double bond. For C_{27} steroid sapogenins and alkaloids, it was recommended to use a higher concentration of silver nitrate (15%). Precoated TLC/HPLTC plates can be dipped in a 20% silver nitrate solution for 15–20 min, then in the absence of light, drying the plate in air. Finally, it is activated in a drying oven. Impregnating silica gel with 10–25% formamide in acetone can be used for separating digitals glycosides, estrogens, and equilin. Impregnation with boric acid could be used, also, for the delicate separation of cardiac glycosides on silica gel layers. The silica gel can also be modified into non-polar reversed phases (RP) such as C_{18} (octadecyl function), C_8 (octyl function), CN (cyanopropyl function), NH_2 (aminopropyl function), and diol (vicnal hydroxyl function on C chains). Progesterone sterioids can be well separated using CN F_{254} and RP plates. Reversed phases C_{18}, C_8, and C_2 could be used for analyzing the ecdysone steroids and RP C_{18} for estrogen conjugates.

Other sorbents that have also been used for separating steroids in TLC are cellulose, kieselguhr, alumina, polyamide, magnesium oxide, and celite. Androstanes can be analyzed using cellulose layers impregnated with 1,2, propanediol. Layers consisting of alumina and magnesium oxide can be used to separate some sterols and sterol acetates.

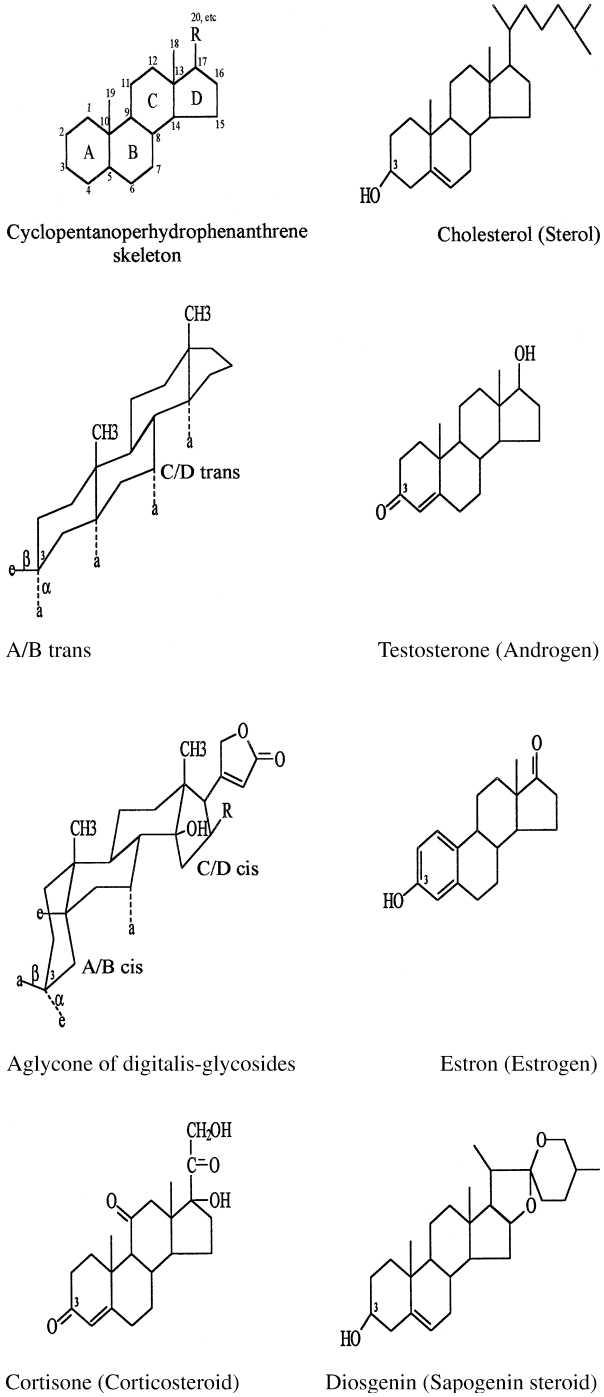

Fig. 1 The structure of some important steroids.

Layers of alumina that are deactivated with 2.5% acetic acid could be employed for separating some corticosteroids. An advantage of using alumina rather than silica gel in TLC of Δ^4-3-ketosteroids is that they form fluorescent oxidation products when the plate is heated to 150–180°C. As little as a nanogram of steroids can be detected by this method. By using a layer that consist of a mixture of $MgO\text{-}Al_2O_3\text{-}CaSo_4$ (15 : 5 : 1), complex mixtures of sterols their 3, 5 dinitrobenzoate derivatives can be resolved using hexane-ethyl acetate (9 : 1, v/v) as the mobile phase.

Although most steroids are stable on the silica gel layers, some steroids (e.g., estrogens and vitamin D) can be decomposed readily. To avoid the decomposition, a preliminary treatment of the sorbent with a solution of ascorbic acid (antioxidants) in ethanol is recommended.

DEVELOPMENT

Simple development will usually be enough for the TLC of steroids. In some cases, multidevelopment in the same or different solvent system or a two-dimensional technique is required to achieve better separation. For ensuring reproducibility of the R_f value, Neher[1] recommended the use of the same number of plates and always using fresh solvent for each run. A system containing a similar volatility maintains a more stable composition and, thus, has more reproducible R_f values during several runs. Our experiences shown that, by weighing the solvent components, the R_f values of testosterone (0.37) and estradiol (0.52) on silica gel plates were unchanged after four runs by using cyclohexane-ethyl acetate (1 : 1, w/w) as the mobile phase.

DETECTION

Destructive Detection Methods

Most of the reagents used for detecting steroid spots by *in situ* reactions (destructive reagents) contain sulfuric acid. Sulfuric acid, without any additive, can also produce characteristic colors and fluorescence response, as well as permanent black zones after heating. The initial color, the color after heating for 10 min, and the color in ultraviolet (UV) (366 nm) of various classes of steroids (141 compounds) were presented by Heftmann.[2] Other destructive reagents that are most generally applicable are antimony trichloride (Carr-Price's reaction; for vitamin D, cardenolides, bufadienolides, triterpenoids), aromatic aldehyde–acids (for sapogenin steroids, steroid alkaloids, ketosteroids), molybdophosphoric acid (reducing and unsaturated steroids, cholestrol ester, bile acids; blue on yellow background), chlorosulphonic acid–acetic acid (cardenolides, green, blue violet fluorescence), and phosphoric acid (color similar to sulfuric acid).

For the detection of ketosteroids, an *m*-dinitrobenzene solution can be used (17-keto-steroids, violet; 3-keto-Δ^4 groups, blue). Δ^4-3-Oxo steroids and $\Delta^{4,6}$-3-oxo steroids can be distinguished using a phthalic acid-*p*-phenylenediamine reagent, which gives yellow and orange-brown colors, respectively. Detailed discussion of the

destructive detection methods of steroid spots is described in the books of Mecek[3] and Touchstone.[4] Thus, by spraying and heating the plates, various class compounds of steroids can be deduced; to confirm this, cochromatography with authentic standards is needed. If the standard is unavailable, isolating the substance and then identification by spectroscopic analysis is recommended.

Non-destructive Detection Methods

Steroids containing an α,β-unsaturated structure, such as Δ^4-3-oxo, Δ^7-6-oxo, Δ^5-7-oxo and Δ^{16}-20-oxo groups, can be visualized under UV light (254 nm). For this purpose, the samples should be spotted on plates that contain a fluorescent indicator (GF_{254} or F_{254}). The steroids spots will appear as dark zones on the layer. Sorbent layers with out the indicator must be sprayed with a dilute solution of fluorescein or morin before exposure to UV light. This method has a great advantage over the destructive methods because the unchanged steroids can be eluted or isolated from the sorbents for further analysis.

Other non-destructive detection methods use iodine vapors or iodine–potassium iodide reagents (Mylius's reaction). Yellow, orange, or brown zones will appear on the layer. The zones will have to be marked, because the iodine will eventually evaporate. The sensitivity of the iodine test can be greatly increased by the use of layers containing rhodamine 6G. Most of the steroids are recovered unchanged after exposure for 30 min with iodine vapor, except for estrogen and Vitamin D.

FORMATION OF DERIVATIVES (MICROREACTION)

It is well known that steroid derivatives such as acetates, benzoates, propionates, and trifluoracetates can be better separated in TLC/HPTLC than the free substances themselves. These derivatization reactions can be performed directly on the TLC layers. Acetylation can be accomplished by treating 10–100 μg of steroids with 0.1 ml acetic anhydride and 0.1 ml pyridine for 8–16 hr at room temperature. Following the reaction, blowing with nitrogen at 60°C can remove the reagent. Benzoylation is carried out in the same way, but by using 0.1 ml benzoyl chloride. Propionylation is performed by dissolving the steroids in 0.3 ml of warm propionyl chloride and allowing the mixture to stand 10 min at 20°C. Extraction with hexane and washing with water and sodium carbonate solution can purify the ester. Trifluoroacetylation is performed by mixing the steroids with a small excess of trifluoroacetic anhydride in hexane.

QUANTITATIVE ANALYSIS

Spot Elution Technique

After elution from the chromatoplates, the separated steroids can be analyzed by using various methods such as UV–Vis spectroscopy or fluorometry. Although this method is very simple, at the present time its application is significantly diminished due to some disadvantages (e.g., it is difficult to locate the spot position accurately, nearly quantitative elution of the spots is required, the loss originating from irreversible adsorption during chromatography must be minimized, etc.). When the UV method is used, special care should be taken because the eluate of silica gel with some semipolar solvents (e.g., ethanol, methanol) exhibit absorption in the UV region. It is recommended to use a blank containing the same amount of adsorbents from an empty part of the plate.

In Situ TLC Technique (Densitometry)

In situ quantification of steroids on the chromatoplate can be performed by using UV (for UV-active steroids), Vis (usually using destructive reagents), and fluorometric methods. Fro UV-active steroids, such as corticosteroids, it is common to scan the steroid spots on the basis of fluorescence quenching at 254 nm using F_{254} precoated layers. Fro steroids that use destructive reagents for their visualization, a reflectance-absorbance method in the Vis range (370–700 nm) is used. The steroid sapogenins (diosgenin, hecogenin, manogenin, etc.), steroid alkaloids (solasodine, tomatidine), and total sterols may be assayed using an absorbance-reflectance densitometry method (in the Vis region) after treatment of the steroid spots with anisaldhyde-sulfuric acid reagent. It was found that this densitometric method was faster, simpler, and less expensive when compared to HPLC or gas liquid chromatography (GLC). Three methods are available for *in situ* fluorometric measurement. The first is to produce active derivatives on the layer by spraying with a suitable reagent. The second is to induce fluorescent derivatives prior to the analysis. The DL (detection limit) of the fluorometric method is much lower compared to the UV and Vis evaluation methods.

Validation of the Method

Before the assay methods can be used for routine application (e.g., in a quality control laboratory), it must first be validated. The parameters for the validation methods are specificity, linearity, accuracy, precision (repeatability and intermediate precision), DL, quantitation limit (QL), and applicable range. A detailed discussion is provided in Ref.[5]

APPLICATIONS

Many publications dealing with TLC/HPTLC steroid analysis have appeared every year. The publications can be summarized into categories as follows: analytical control of steroid formulations (drug preparations), determination of steroids in biological media and natural resources, and analytical control of the production of steroids (including raw material, synthesis, and biotransformation). A cumulative database of thousands of TLC methods (including steroids) is provided in compact-disk (CD) format by Camag.[6]

REFERENCES

1. Neher, R. TLC of steroids and related compounds. In *Thin Layer Chromatography*; Springer International Student Edition; Stahl, E., Ed.; Springer-Verlag: Berlin, 1969; 311–357.
2. Heftmann, E. *Chromatography of Steroids*; Journal of Chromatography Library; Elsevier Scientific: Amsterdam, 1976; 8, 14–27.
3. Macek, K. *Pharmaceutical Application of Thin-Layer and Paper Chromatography*; Elsevier: Amsterdam, 1972; 275–348.
4. Touchstone, J.C. *CRC Handbook of Chromatography of Steroids*; CRC Press: Boca Raton, FL, 1986; 27–40.
5. Renger, B.; Jehle, H.; Fisher, M.; Funk, W. Validation of analytical procedures in pharmaceutical analytical chemistry: HPTLC assay of theophylline in an effervescent tablet. J. Planar Chromatogr. **1995**, *8*, 269–278.
6. Camag bibilography service. In *Thin-Layer Chromatography Cummulative CD version 1.00*; Camag: Muttenz, 1997.

BIBLIOGRAPHY

1. Görög, S.; Szasz, G. *Analysis of Steroid Hormone Drugs*; Elsevier Scientific: Amsterdam, 1978.
2. Görög, S. *Analysis in the Pharmaceutical Industry*; Ellis Horwood: Chichester, 1989.

Supercritical Fluid Extraction

Christopher E. Bunker
Propulsion Directorate, Air Force Research Laboratory, Wright-Patterson Air Force Base, Ohio, U.S.A.

INTRODUCTION

Supercritical fluid extraction (SFE) was originally proposed as a process for compound separation or purification as early as 1879 by Hannay and Hogarth.[1,2] A rebirth of the field in the 1940s, and again in the 1970s, was brought about by significant advances in technology and a drive toward more energy-efficient and environmentally friendly processes.[1,2] Today, SFE is widely applied in various industries for purification of high-value chemicals or materials, for environmental remediation, and for incorporation into larger green processes that employ supercritical fluids as reaction solvents. Currently, its most widely known application is associated with the decaffeination process used in the treatment of coffee beans. Within the petroleum field, the application of SFE technology varies widely from cleanup procedures to high-value materials production.[3–5] In this entry, first we will discuss the properties of a supercritical fluid that make SFE an attractive alternative to normal liquid–solvent processes; next, we will describe the equipment and function of a typical SFE process; and, finally, current areas of interest in petroleum research will be reviewed briefly.

SUPERCRITICAL FLUID PROPERTIES

To understand the properties of a supercritical fluid, one must first understand what is meant by the term "supercritical." In this case, "supercritical" refers to that region of the phase diagram (Fig. 1) defined by temperatures greater than the critical temperature ($T > T_c$) and pressures greater than the critical pressure ($P > P_c$). In this region, the substance exists as a single phase, regardless of temperature or pressure. In most industrial applications, supercritical fluids are used in this region; however, it is important to note that a single phase exists for a substance at any pressure when the system is above T_c. Researchers investigating the properties of supercritical fluids have found it necessary to include the pressure region below P_c to obtain a full understanding of the nature of a supercritical fluid.[6–8] For this reason, the loose definition of a supercritical fluid is: any substance at a temperature greater than its critical temperature.

The most important properties of a supercritical fluid are the low densities between those of a gas and those of a liquid, which are easily tunable with a change in pressure at constant temperature, and the local density effects. The latter are termed solute–solvent and solute–solute clustering and are best understood as local concentrations of a solvent or solute, respectively, that are greater than the bulk concentration. These phenomena are attributed to the unique nature of a supercritical fluid (i.e., a supercritical fluid is macroscopically homogeneous but microscopically inhomogeneous, consisting of solvent clusters and free volumes). An experimentally observable effect related to this unique structure is critical opalescence, where a fluid viewed through an optical port is observed to become opaque as it transitions through the critical region. This phenomenon is attributed to the efficient scattering of light by the unique structure of a supercritical fluid in the near-critical region.

In SFE processing, the low and tunable fluid densities are of the greatest importance. For a constant temperature greater than T_c, low pressures yield gaslike densities, and high pressures yield liquidlike densities (Fig. 1). Increasing the pressure from low to high moves the fluid density through the near-critical region, where small changes in pressure result in large changes in fluid density (see Fig. 4 of Ref.[2] for an idealized density-vs.-pressure diagram). Because solubility is, to a first approximation, proportional to fluid density, the solubility of an analyte can be dramatically affected by small changes in pressure in the near-critical density region.

For many supercritical fluids, the solubilities of the compounds of interest, even in the high-density region, may be too low for practical application. This limitation can be overcome through the use of a cosolvent. Early on, researchers discovered that the addition of small amounts of a cosolvent could dramatically enhance the solubility of various analytes.[6–8] In many cases, the enhancement exceeded that predicted based on the bulk concentration of the cosolvent in the supercritical fluid. The results suggested an enhancement of solvent strength under supercritical conditions. The phenomenon, termed the entrainer effect, is related to solute–solute clustering; the entrainer effect served as preliminary evidence of unusual behaviors and pointed researchers toward solute–solute clustering.

Thus, taken as a whole, the tunable densities and tunable solubilities, the availability of cosolvents as property modifiers, the ability to utilize fluids that are gases under ambient conditions, and the possibility of employing fluids

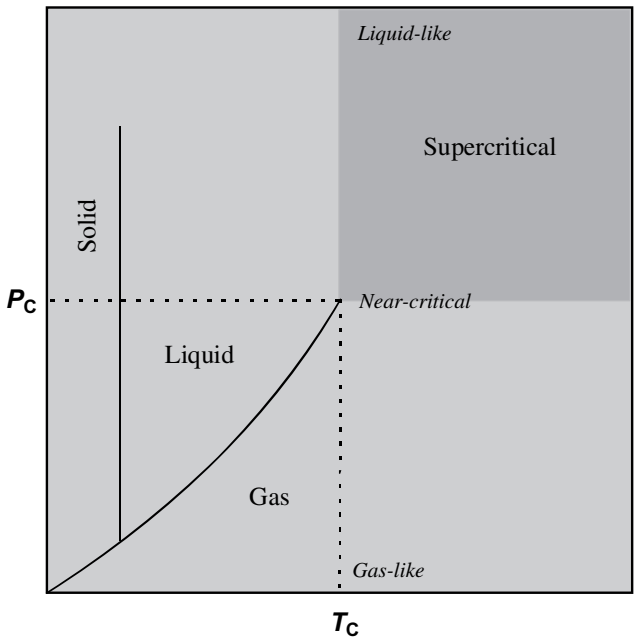

Fig. 1 Idealized phase diagram depicting the supercritical region. T_c and P_c are the critical temperature and pressure, respectively.

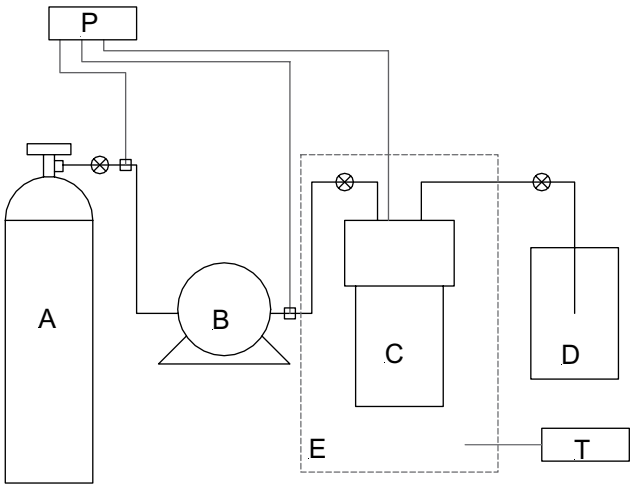

Fig. 2 Schematic for a typical laboratory-scale supercritical fluid extraction system: (A) fluid supply; (B) pump/delivery device; (C) extraction vessel; (D) collection vessel; (E) heated zone; (P) pressure measurement device; (T) temperature controller.

that are environmentally friendly (e.g., CO_2 or water) (the unique properties of supercritical fluids) make SFE a valuable alternative to normal liquid extraction processes.

SFE SYSTEM

The design of any SFE system will be a function of the application, and the details will vary depending on the size and the mode of the process (batch or continuous), the nature of the extracted material and the substrate (corrosive, toxic, and benign), and the fluid employed. The only guaranteed commonality with all such systems is the necessity to ensure safe operation. Proper safety precautions must be observed in the handling and maintenance of the required high-pressure equipment; the consequences of a failure can be severe.

A simple laboratory-scale SFE system is shown in Fig. 2. The system consists of a fluid supply, a pump/delivery device, an extraction vessel, a temperature-controlled zone, a collection vessel (including restrictor), and numerous valves, pressure gauges, and temperature sensors (although not shown, pressure-relief valves are highly recommended). Such systems embodying these components and offering many variations in operation (e.g., programmable control, recirculation, and multistage extraction) are readily available. In a typical extraction, the extraction vessel is loaded with the substrate to be extracted. In the configuration shown in Fig. 2, this would involve disassembly of the extraction vessel and manual loading of the material. In many industrial processes, this step is automated. Once loaded, the extraction vessel is equilibrated at the desired temperature ($T > T_c$), and fluid is introduced. For a static process, the system is brought to the desired pressure and sealed; for a continuous process, backpressure regulators or restrictors are used to maintain the pressure while the fluid is continuously flowed. In the recovery of the extracted material, it is important to recall that small changes in pressure in the vicinity of the critical region result in large changes in density and solubility. To avoid precipitation of the extracted material within the extraction system, additional fluid must flow to maintain the system pressure. Several collection vessel designs facilitate collection of the extracted material. The simplest ones involve expansion of the fluid into a low-pressure region, thus inducing nucleation and precipitation of the extracted material [rapid expansion of a supercritical solution (RESS)], expansion of the fluid into a collection liquid where the extracted material has good solubility (applicable to somewhat volatile species), or expansion of the fluid onto a solid absorbent. Other possibilities include recovery and recirculation of the supercritical fluid, secondary extraction with modification of the fluid, and reaction of the extracted material using the fluid as an alternative reaction solvent. The reader is referred to Refs.[1,2] for additional information.

CURRENT AREAS OF INTEREST IN PETROLEUM RESEARCH

With respect to the petroleum industry, research into supercritical fluids and SFE can be roughly divided into product-oriented research, property investigations, and environmental remediation efforts.[3–5] In a recent review, Rudzinski and Aminabhavi[3] noted that researchers have

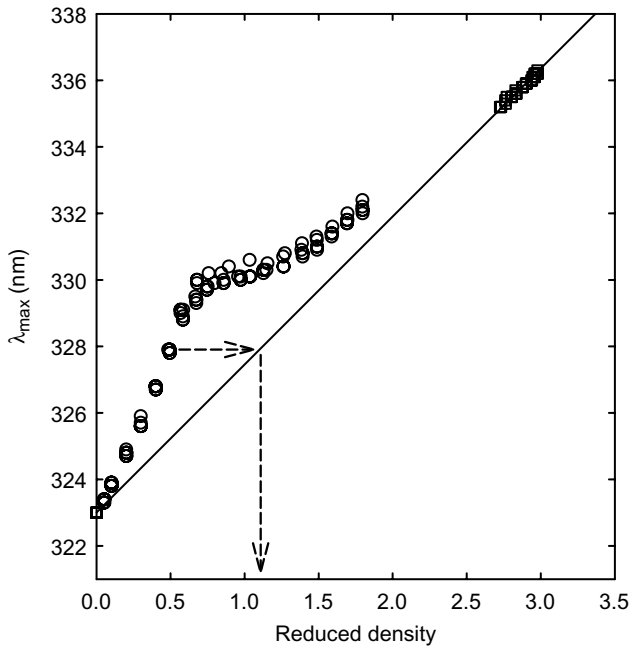

Fig. 3 Experimental data obtained for the spectral maximum of the pyrene excitation spectrum in supercritical toluene at 335°C as a function of reduced density: (—) normal liquid behavior; (ö) supercritical fluid data; (θ) liquid data.
Source: From Fundamental properties of supercritical fluids, in *Supercritical Fluid Technology in Materials Science and Engineering*.[7]

been investigating the application of SFE technology to the processing of coal, bitumen, oil shale, crude oil, and coal tar pitch. The fluids utilized included pure CO_2, modified CO_2, organic fluids such as propane and toluene, and water. Concerning property investigations, research is ongoing to understand the fundamental properties of high-temperature supercritical fluids because these fluids can serve as models for supercritical aviation fuel.[7] Fig. 3 demonstrates the unusual nature of supercritical toluene. Reduced density (density divided by the critical density) is plotted as a function of the solvation strength of toluene (λ_{max} is the solvatochromic shift of the excitation spectrum of the molecular probe, pyrene). The solid line represents the normal liquid behavior of toluene—a trend that is proportional to fluid density. The data obtained in supercritical toluene (circles) clearly deviate from that line. The dashed arrows demonstrate that, at any given point, the observed density is greater than the measured bulk density—a direct result of solute–solvent clustering—the implication being possible discrepancies between predicted properties based on bulk densities and observed properties influenced by local densities (the properties being solubility, viscosity, polarity, heat transfer characteristics, etc.). The goal of such research is to develop quantitative models capable of determining the local (as opposed the bulk) properties of a supercritical fluid. The significance of the discrepancies shown in Fig. 3 will be determined in future efforts to design and operate supercritical fluid fuel systems.

REFERENCES

1. McHugh, M.; Krukonis, V. *Supercritical Fluid Extraction,* 2nd Ed.; Butterworth-Heinemann: Newton, MA, 1994.
2. Taylor, L.T. *Supercritical Fluid Extraction; Techniques in Analytical Chemistry*; John Wiley and Sons: New York, 1996.
3. Rudzinski, W.E.; Aminabhavi, T.M. A review on extraction and identification of crude oil and related products using supercritical fluid technology. Energy Fuels **2000**, *14*, 464–475.
4. Levy, J.M. Fossil fuel application of SFC and SFE: A review. J. High Resolut. Chromatogr. **1994**, *17* (4), 212–216.
5. Kershaw, J.R.J. Supercritical fluids in coal processing. J. Supercrit. Fluids **1989**, *2*, 35–45.
6. Johnston, K.P., Penninger, J.M.L., Eds.; *Supercritical Fluid Science and Technology*; ACS Symposium Series; American Chemical Society: Washington, DC, 1989; Vol. 406.
7. Bunker, C.E.; Rollins, H.W.; Sun, Y.-P. Fundamental properties of supercritical fluids. In *Supercritical Fluid Technology in Materials Science and Engineering*; Sun, Y.-P., Ed.; Marcel Dekker: New York, 2002; 1–57.
8. Bruno, T.J., Ely, J.F., Eds.; *Supercritical Fluid Technology. Reviews in Modern Theory and Applications*; CRC Press: Boca Raton, FL, 1991.

Synthetic Dyes: HSCCC Separation

Adrian Weisz
Office of Cosmetics and Colors, Center for Food Safety and Applied Nutrition, U.S. Food and Drug Administration (USFDA), Washington, District of Columbia, U.S.A.

Abstract
This entry succinctly presents the application of high-speed countercurrent chromatography (HSCCC) in its various forms to the separation and purification of synthetic dyes used in food, drugs, and cosmetics.

INTRODUCTION

Countercurrent chromatography (CCC) is a liquid–liquid partition technique that does not involve use of a solid support. In high-speed countercurrent chromatography (HSCCC), one of the two immiscible liquid phases (the stationary phase) is retained in an Ito multilayered coil column by centrifugal force while the other liquid phase (the mobile phase) is pumped through the rotating column. A variation of HSCCC, known as pH-zone-refining CCC, was developed in the early 1990s. Both conventional HSCCC and pH-zone-refining CCC have been applied to the separation of synthetic dyes. The principles of these techniques, the instrumentation involved, the basis for selecting the two-phase solvent systems, and the separation procedure itself have all been discussed by Ito in the earlier literature[1–4] and in the countercurrent chromatography entries of the present volume. A general approach to the separation of synthetic dyes using HSCCC is shown in Fig. 1.

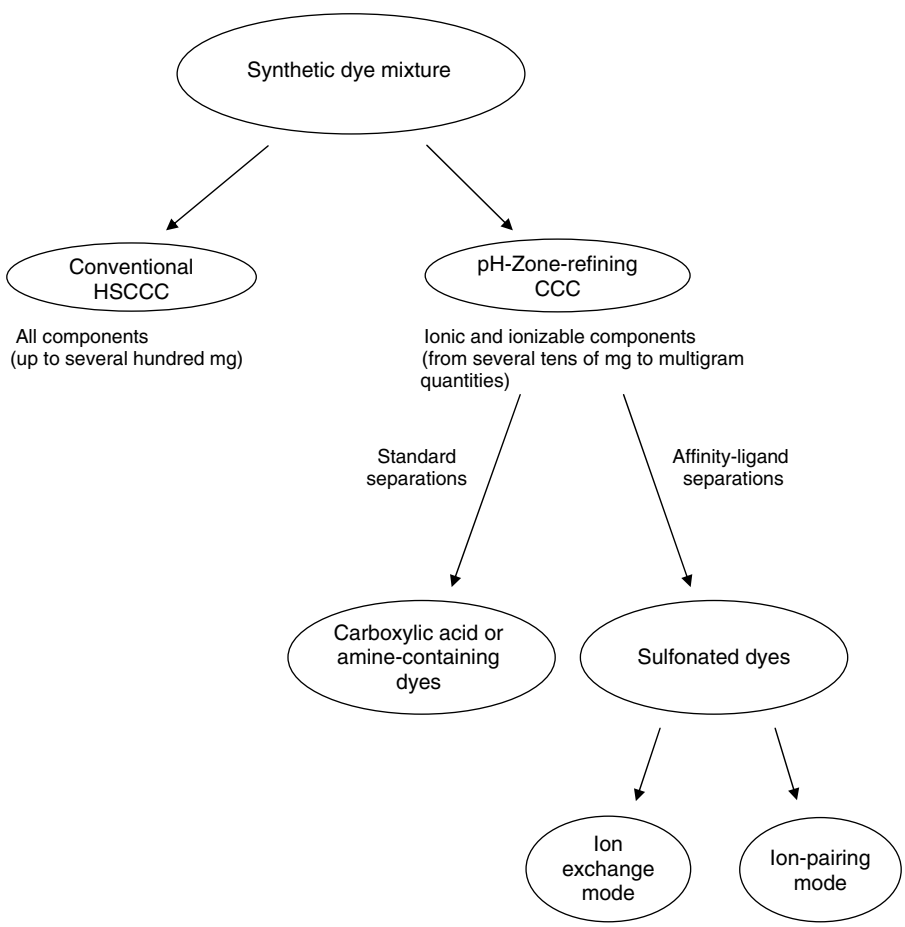

Fig. 1 General approach to the preparative separation of synthetic dyes using HSCCC.

CONVENTIONAL HSCCC

Conventional HSCCC has been used for synthetic dye separations since the mid-1980s. At that time, Fales et al.[5] separated various methylated homologues and contaminants from a 6 mg portion of the triphenylmethane dye Methyl Violet 2B (CI 42535), and Freeman and Willard[6] purified up to 520 mg of azo textile and ink dyes. Later applications have been documented for Sulforhodamine B (CI 45100)[7] and Phloxine B (CI 45410).[8]

There are two notable advantages of using this technique for the separation of synthetic dyes. First, it is applicable to the separation of both ionic and non-ionic components of a dye mixture. Second, it has been shown to be one of the best methods for successfully separating small quantities (20 mg or less) of dye mixtures. On the contrary, several hundred milligrams is the upper limit beyond which conventional HSCCC cannot be used for separating dye mixtures. Two examples of the application of this technique are shown in Figs. 2 and 3. Fig. 2 shows

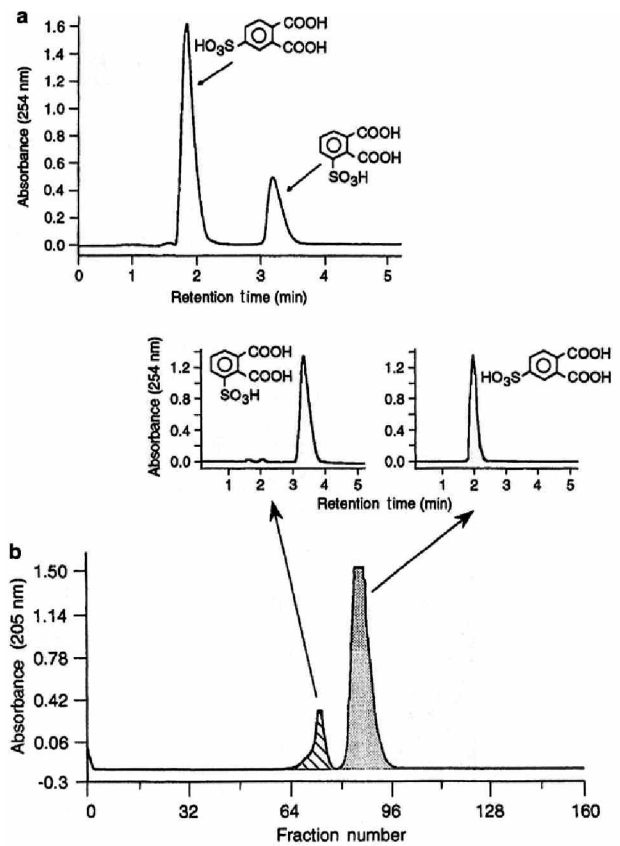

Fig. 2 Separation of 230 mg of a commercial mixture of two isomeric sulfophthalic acids by conventional HSCCC. a) HPLC analysis of the original mixture; b) HSCCC elution profile of the separation and HPLC analyses of the separated components.
Source: From Preparative separation of isomeric sulfophthalic acids by conventional and pH-zone-refining counter-current chromatography, in J. Chromatogr. A.[9]

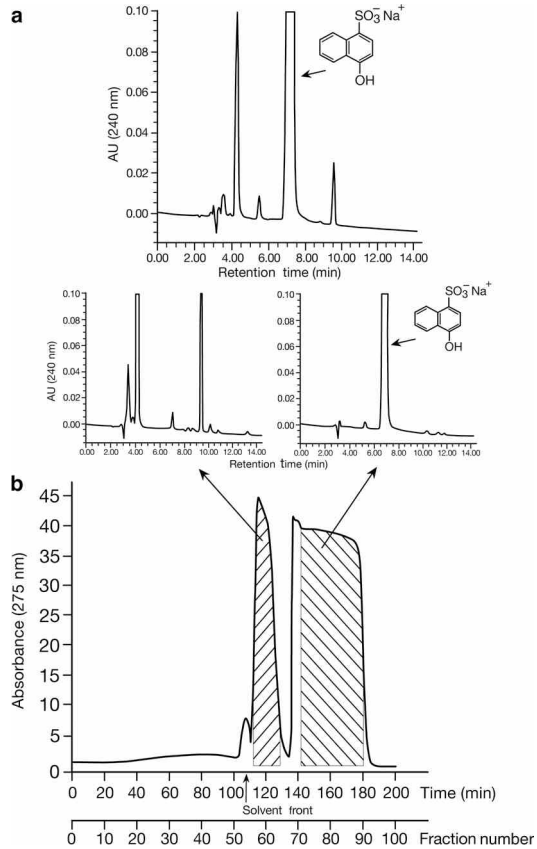

Fig. 3 Purification of 550 mg of "practical" grade 4-hydroxy-1-naphthalenesulfonic acid by conventional HSCCC. a) HPLC analysis of the original material; b) HSCCC elution profile of the separation and HPLC analyses of the separated components.
Source: From Preparative purification of 4-hydroxy-1-naphthalenesulfonic acid sodium salt by high-speed counter-current chromatography, in J. Chromatogr. A.[10]

the separation of 230 mg of a commercial mixture of two isomeric sulfophthalic acids,[9] and Fig. 3 shows the purification of 550 mg of commercially obtained "practical" grade 4-hydroxy-1-naphthalenesulfonic acid.[10] In both cases, the U.S. Food and Drug Administration (FDA) used the separated materials as standards in the development of analytical methods for batch certification of color additives.

pH-ZONE-REFINING CCC

pH-Zone-refining CCC is a relatively new preparative method of separation[3,4,11] that allows the separation of organic acids and bases according to their pK_a values and hydrophobicities. In contrast to conventional HSCCC, it permits the separation or purification of multigram quantities of dye mixtures, as long as those mixtures contain

ionic or ionizable components. The technique has been applied to the separation of synthetic dyes containing various functional groups, such as –COOH, –OH, $–NH_2$, and $– SO_3H$. Details on its application to dye separation were described.[12] Briefly, pH-zone-refining CCC of dyes can be divided into two categories:

1. Standard separations, for carboxylic acid- or amine-containing dyes
2. Affinity-ligand separations, for sulfonated dyes

STANDARD pH-ZONE-REFINING CCC

For separation by standard pH-zone-refining CCC, the sample components should be stable over a pH range of 1–10 during the separation period, and the minimum quantity of each targeted component should be no less than 0.1 mmol and preferably over 1 mmol. The requirements for the selection of a solvent system are different from those for conventional HSCCC separations. Carboxylic acid-containing dyes (e.g., xanthene dyes or their lactone analogues, fluoran dyes) may be separated by using an organic acid (e.g., trifluoroacetic acid) as a retainer in the organic stationary phase and a base (e.g., ammonia) as an eluter in the aqueous mobile phase. Dyes containing amino groups may be separated by using an organic base as a retainer (e.g., triethylamine) and an inorganic acid (e.g., HCl) as an eluter. The recommended steps in selecting an appropriate solvent system for the separation of dyes and the separation procedure have been described in detail elsewhere.[12]

Standard pH-zone-refining CCC was applied to the separation of pure components, sometimes multigram quantities, from the various types of halogenated fluoran and xanthene dyes shown in Table 1.

These dyes are used as biological stains and, except for Rose Bengal, as color additives permitted for coloring food (FD&C Red No. 3), drugs, and cosmetics in the United States. Standard pH-zone-refining CCC was also applied to the separation of contaminants from these colors and their intermediates. The purified contaminants were then used as reference materials in the development of analytical methods [high-performance liquid chromatography

Table 1 Fluoran and xanthene synthetic dyes separated by standard pH-zone-refining CCC.

U.S. listed name[a]	Common names[b]	CI no.[c]	CAS no.[d]	R_1	R_2	R_3
Fluoran structure			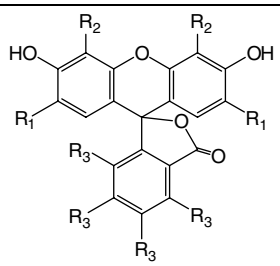			
D&C Orange No. 5	CI Solvent Red 72 Dibromofluorescein	45370:1	596-03-2	–H	–Br	–H
D&C Orange No. 10	CI Solvent Red 73 Diiodofluorescein	45425:1	38577-97-8	–H	–I	–H
	Tetrachlorofluorescein		6262-21-1	–H	–H	–Cl
Xanthene structure			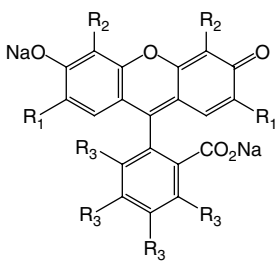			
D&C Red No. 22	CI Acid Red 87 Eosin Y	45380	17372-87-1	–Br	–Br	–H
D&C Red No. 28	CI Acid Red 92 Phloxine B Cyanosine	45410	18472-87-2	–Br	–Br	–Cl
FD&C Red No. 3	CI Acid Red 51 Erythrosine	45430	16423-68-0	–I	–I	–H
	CI Acid Red 94 Rose Bengal	45440	632-69-9	–I	–I	–Cl

[a]Names assigned by FDA after certification.
[b]Not used in the United States for the names of certified color additives.
[c]Color Index (CI) number. Not used in the United States for certified color additives.
[d]Chemical Abstracts Service (CAS) number.

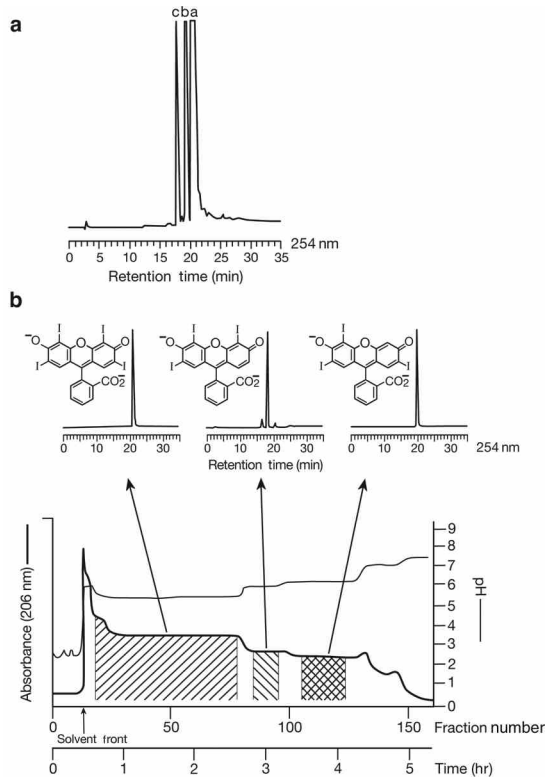

Fig. 4 Separation of a 3 g test portion of color additive FD&C Red No. 3 (Erythrosine, CI 45430) by standard pH-zone-refining CCC. a) HPLC analysis of the original dye; b) pH-zone-refining CCC elution profile of the separation and HPLC analyses of the separated components.
Source: From Preparative separation of components of the color additive FD&C Red No. 3 (erythrosine) by pH-zone-refining counter-current chromatography, in J. Chromatogr. A.[13]

(HPLC), thin-layer chromatography (TLC), etc.] for batch certification of the color additives. Fig. 4 shows the separation of components from a 3 g test portion of FD&C Red No. 3 (Erythrosine, CI 45430) using standard pH-zone-refining CCC.[13] More details of the separation of the dyes shown in Table 1 by standard pH-zone-refining CCC have been described.[14]

AFFINITY-LIGAND pH-ZONE-REFINING CCC

Sulfonated dyes have not been amenable to separation by standard pH-zone-refining CCC because of their very low pK_a values, which prevent their partitioning into the organic phase of a conventional two-phase solvent system. The addition of a ligand, either an ion-exchange reagent (e.g., dodecylamine) or an ion-pairing reagent (tetrabutylammonium hydroxide), and a retainer acid (e.g., HCl, H_2SO_4) facilitate the partitioning of the sulfonated dye components into the organic stationary phase, thus enabling their separation by pH-zone-refining CCC. The more stringent conditions require that the components of a sulfonated dye mixture be stable over a pH range of 0.5–13.5 during the time of the experiment. The details and conditions required for the separation of sulfonated dyes by affinity-ligand pH-zone-refining CCC in the ion-exchange mode and in the ion-pairing mode can be found elsewhere.[12] Fig. 5 shows the separation by affinity-ligand pH-zone-refining CCC in the ion-exchange mode of the main components from a 1.8 g portion of the color additive D&C Yellow No. 10 (Quinoline Yellow, CI 47005).[15] The two-phase solvent system used consisted of iso-amyl alcohol:methyl *tert*-butyl ether:acetonitrile:water (3:1:1:5). The ligand (dodecylamine), at a concentration of 5% (w/v), and sulfuric acid used as the retainer were added to the organic stationary phase. The separation obtained for the two monosulfonated positional isomers, 6SA (0.6 g) and 8SA (0.18 g),

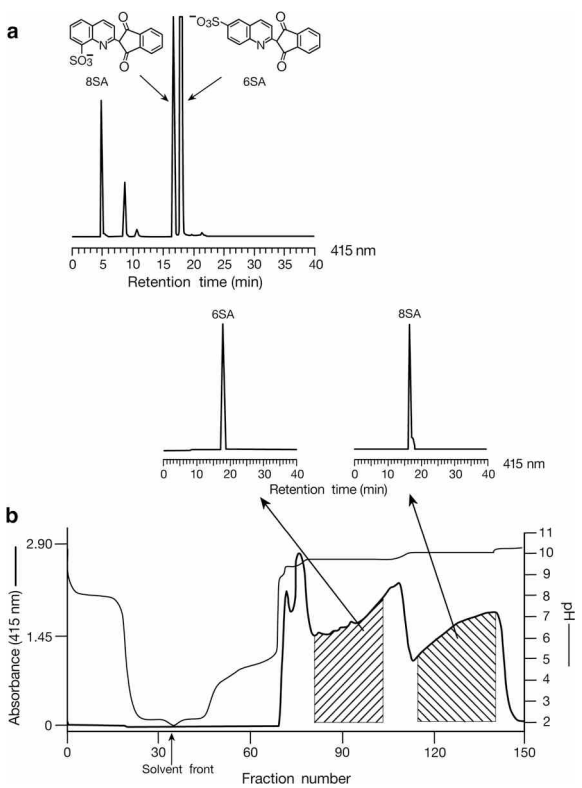

Fig. 5 Separation of a 1.8 g test portion of color additive D&C Yellow No. 10 (Quinoline Yellow, CI 47005) by affinity-ligand pH-zone-refining CCC in the ion-exchange mode. a) HPLC analysis of the original dye; b) pH-zone-refining CCC elution profile of the separation and HPLC analyses of the separated components.
Source: From Preparative separation of isomeric 2-(2-quinolinyl)-1H-indene-1,3(2H)-dione monosulfonic acids of the color additive D&C Yellow No. 10 (Quinoline Yellow) by pH-zone-refining counter-current chromatography, in J. Chromatogr. A.[15]

both at over 99% purity, is shown by the associated HPLC chromatograms in Fig. 5.

Using a modified procedure, the applications of this technique have been extended to the separation of the highly polar disulfonated and trisulfonated components of D&C Yellow No. 10 and Yellow No. 203 (the Japanese Quinoline Yellow, CI 47005).[16] Other sulfonated dyes such as the azo dyes FD&C Yellow No. 6 (Sunset Yellow, CI 15985)[4] and FD&C Red No. 40 (Allura Red, CI 16035) have also been separated by this method.

CONCLUSION

HSCCC in its conventional and pH-zone-refining modes is an effective method for the separation and/or purification of synthetic dyes. Conventional HSCCC is useful for separating both the ionic and non-ionic components of a dye mixture in quantities of up to several hundred milligrams. On the contrary, pH-zone-refining CCC is the method of choice if ionic or ionizable dye components are to be separated at the multigram level. The latter application is particularly noteworthy since there is no evidence in the literature of preparative-scale separation of multigram quantities of these dyes by any other chromatographic method. Furthermore, it is likely that with modifications of current HSCCC instrumentation, the technique could be scaled up for successful separation of kilogram quantities of dyes. Among the benefits of obtaining large quantities of highly purified dyes is the potential for standardization of biological stains, which in turn would enable reliable comparisons of data across medical laboratories.

REFERENCES

1. Ito, Y. Principle, apparatus, and methodology of high-speed countercurrent chromatography. In *High-Speed Countercurrent Chromatography*; Ito, Y., Conway, W.D., Eds.; John Wiley & Sons: New York, 1996; 3–44.
2. Ito, Y. Review: Golden rules and pitfalls in selecting optimum conditions for high-speed counter-current chromatography. J. Chromatogr. A, **2005**, *1065*, 145–168.
3. Ito, Y.; Shinomiya, K.; Fales, H.M.; Weisz, A.; Scher, A.L. pH-Zone-refining countercurrent chromatography—A new technique for preparative separation. In *Modern Countercurrent Chromatography*; Conway, W.D., Petroski, R.J., Eds.; American Chemical Society: Washington, DC, ACS Symposium Series, 1995; Vol. 593, 156–183.
4. Ito, Y.; Ma, Y. Review: pH-Zone-refining countercurrent chromatography. J. Chromatogr. A, **1996**, *753*, 1–36.
5. Fales, H.M.; Pannell, L.K.; Sokoloski, E.A.; Carmeci, P. Separation of methyl violet 2B by high-speed countercurrent chromatography and identification by Californium-252 plasma desorption mass spectrometry. Anal. Chem. **1985**, *57*, 376–378.
6. Freeman, H.S.; Williard, C.S. Purification procedures for synthetic dyes: 2. Countercurrent chromatography. Dyes and Pigments **1986**, *7*, 407–417.
7. Oka, H.; Ikai, Y.; Kawamura, N.; Hayakawa, J.; Yamada, M.; Harada, K.-I.; Murata, H.; Suzuki, M.; Nakazawa, H.; Suzuki, S.; Sakita, T.; Fujita, M.; Maeda, Y.; Ito, Y. Purification of food color Red No. 106 (Acid Red) using high-speed counter-current chromatography. J. Chromatogr. **1991**, *538*, 149–156.
8. Weisz, A.; Langowski, A.L.; Meyers, M.B.; Thieken, M.A.; Ito, Y. Preparative purification of tetrabromotetrachlorofluorescein and Phlorine B by centrifugal counter-current chromatography. J. Chromatogr. **1991**, *538*, 157–164.
9. Weisz, A.; Mazzola, E.P.; Murphy, C.M.; Ito, Y. Preparative separation of isomeric sulfophthalic acids by conventional and pH-zone-refining counter-current chromatography. J. Chromatogr. A, **2002**, *966*, 111–118.
10. Weisz, A.; Ito, Y. Preparative purification of 4-hydroxy-1-naphthalenesulfonic acid sodium salt by high-speed counter-current chromatography. J. Chromatogr. A, **2008**, *1198–1199*, 232–234.
11. Weisz, A.; Scher, A.L.; Shinomiya, K.; Fales, H.M.; Ito, Y. A new preparative-scale purification technique: pH-Zone-refining countercurrent chromatography. J. Am. Chem. Soc. **1994**, *116*, 704–708.
12. Weisz, A.; Ito, Y. High-speed countercurrent chromatography. Dyes. In *Encyclopedia of Separation Science*; Wilson, I.D., Adlar, E.R., Cooke, M., Poole, C.F., Eds.; Academic Press; London, 2000; Vol. 6, 2588–2602.
13. Weisz, A.; Andrzejewski, D.; Highet, R.J.; Ito, Y. Preparative separation of components of the color additive FD&C Red No. 3 (erythrosine) by pH-zone-refining counter-current chromatography. J. Chromatogr. A, **1994**, *658*, 505–510.
14. Weisz, A. Separation and purification of dyes by conventional high-speed countercurrent chromatography and pH-zone-refining countercurrent chromatography. In *High-Speed Countercurrent Chromatography*; Ito, Y., Conway, W.D., Eds.; John Wiley & Sons: New York, 1996; 337–384.
15. Weisz, A.; Mazzola, E.P.; Matusik, E.J.; Ito, Y. Preparative separation of isomeric 2-(2-quinolinyl)-1H-indene-1,3(2H)-dione monosulfonic acids of the color additive D&C Yellow No. 10 (Quinoline Yellow) by pH-zone-refining counter-current chromatography. J. Chromatogr. A, **2001**, *923*, 87–96.
16. Weisz, A.; Mazzola, E.P.; Ito, Y. Preparative separation of di- and trisulfonated components of Quinoline Yellow using pH-zone-refining counter-current chromatography. J. Chromatogr. A, **2009,** *1216,* 4161–4168.

Synthetic Dyes: TLC

Tibor Cserháti
Esther Forgács
Institute of Chemistry, Chemical Research Center, Hungarian Academy of Sciences, Budapest, Hungary

INTRODUCTION

Synthetic dyes are extensively used in many up-to-date industrial processes and research, mainly in the preparation of textile, food, and leather products, as well as in cosmetics and medicine. The widespread application of synthetic dyes has resulted in serious environmental pollution: Their occurrence in ground water and wastewater and the accumulation in sediment, soil, and various biological tissues has often been observed and reported. Dyes and intermediates can cause abnormal reproductive function in males and show marked toxic effects toward bacteria. The rate of biodegradation of the majority of synthetic dyes is very low, enhancing the toxicological hazard and environmental impact.

DISCUSSION

Commercial synthetic dyes generally contain more than one color product. As the knowledge of the exact composition of dye mixtures is prerequisite for their successful application in many fields of industry and research, many efforts have been devoted for the development of various chromatographic techniques suitable for their separation and quantitative determination. Moreover, the exact determination of the composition and quantity of synthetic dye is required in the control of industrial processes, in the following of efficacy of wastewater treatment, in environmental protection studies, and in forensic science.

The chemical structures of synthetic dyes show considerable variety. They generally contain more than one aromatic group, condensed aromatic substructures or heterocyclic rings (pyrazolone, thiazole, acridine, thiazine, oxazine) which are mainly hydrophobic, and, frequently, a polar basic or cationic group which is strongly hydrophilic. Due to these structural characteristics, they readily bind both to polar adsorptive and apolar reversed-phase (RP) chromatographic supports, making their successful separation difficult. As the synthetic dyes are not volatile and volatile derivatives are not known, gas chromatography (GC) methods cannot be employed for their analysis. Thin-layer chromatography (TLC), high-performance liquid chromatography (HPLC) and, to a lesser extent, capillary zone electrophoresis (CZE) have been equally applied for this purpose. Due to its inherent advantages (simplicity, low cost, rapidity, etc.), a large number of TLC methods have been developed and successfully applied for the analysis of synthetic dyes. Previous results obtained in the application of TLC for the separation of synthetic dyes were reviewed earlier.[1] The planar chromatography of dyes used in the leather[2] and cosmetic industries[3] was reviewed separately. The majority of TLC separations have been performed on the traditional silica layers using many solvents and solvent mixtures (chloroform, various alcohols, pyridine, *n*-hexane, toluene, ethyl acetate, etc.). The polar character of some substructures in the dyes frequently made necessary the addition of acidic (formic and acetic acid) or basic additives (ammonia, diethylamine) to the mobile phase to suppress the dissociation of these hydrophilic groups in order to increase, in this manner, the efficiency of separation and to improve spot shape. However, other than silica layers, various eluent additives have also been employed for the enhancement of the efficacy of TLC. Thus, microcrystalline cellulose thin layers were employed for the study of the retention behavior of some synthetic dyes such as methyl orange (4-[4-(dimethylamino)phenyl]azo]benzene acid sodium salt), methyl red (2-[4-(dimethylamino)phenyl]azo]benzoicacid), methyl yellow (*N*,*N*-dimethyl-4-(phenylazo)benzeneamine), ethyl orange (4-[4-(diethylamino) phenyl]azo]benzene acid sodium salt), ethyl red (2-[4-(diethylamino)phenyl]azo]benzoic acid), alizarin yellow R (2-hydroxy-5-[(4-nitrophenyl)azo]benzoic acid) and alizarin yellow 2G (2-hydroxy-5-[(3-nitrophenyl)azo]benzoic acid monosodium salt).[4] The R_f values of dyes obtained in the presence of various eluent additives are compiled in Table 1. The data clearly show that eluent additives can be successfully used for the modification of the retention behavior of azo dyes, improving the separation capacity of TLC.

Table 1 Values of azo dyes on microcrystalline cellulose thin layers (merck 557) with various eluent additives at room temperature (CD = cyclodextrin).

	0.5 *M* HCl		1 *M* Na_2CO_3			1 *M* NaCl		
Azo dye	α-CD polymer 1%	α-CD 1%	α-CD polymer 1%	α-CD 1%	Control	α-CD polymer 0.5%	β-CD polymer 0.5%	τ-CD polymer 0.5%
Methyl orange	1.00	0.77	0.89	0.72	0.10	1.00	0.80	0.79
Methyl red	0.38	0.17	0.30	0.14	0.08	0.13	0.24	0.23
Methyl yellow	0.92	0.73	0.69	0.40	0.00	0.88	0.55	0.54
Ethyl orange	1.00	0.97	0.91	0.73	0.44	1.00	0.97	1.00
Ethyl red	0.66	0.35	0.68	0.23	0.12	0.28	0.50	0.48
Alizarin yellow R	0.71	0.22	0.70	0.43	0.00	0.52	0.43	0.41
Alizarin yellow 2G	0.80	0.00	0.70	0.51	0.03	0.55	0.48	0.61

Source: From Adsorption chromatography on cellulose XIV. Some results using aqueous solutions of soluble cyclodextrin polymers as eluents, in J. Chromatogr. A.[4]

The separation characteristics of a considerable variety of other TLC supports were also tested using different dye mixtures (magnesia, polyamide, silylated silica, octadecyl-bonded silica, carboxymethyl cellulose, zeolite, etc.); however, these supports have not been frequently applied in practical TLC of this class of compounds. Optimization procedures such as the prisma and the simplex methods have also found application in the TLC analysis of synthetic dyes.[5] It was established that six red synthetic dyes (C.I. 15580; C.I. 15585; C.I. 15630; C.I. 15800; C.I. 15880; C.I. 15865) can be fully separated on silica high-performance TLC (HPTLC) layers in a three-solvent system calculated by the optimization models. The theoretical plate number and the consequent separation capacity of traditional TLC can be considerably enhanced by using supports of lower particle size (about 5 μm) and a narrower particle size distribution. The application of these HPTLC layers for the analysis of basic and cationic synthetic dyes has also been reviewed.[6] The advantages of overpressured (or forced flow) TLC include improved separation efficiency, lower detection limit, and lower solvent consumption, and they have also been exploited in the analysis of synthetic dyes.

The detection of synthetic dyes on any type of TLC or HPTLC support is very easy; they contain chromophore groups and can be seen without using an ultraviolet (UV) lamp or detection reagents.

The quantitative evaluation of the amount of dyes in a spot can be carried by the traditional method of scrapping the spot from the plate, dissolving the dyes in a solvent and measure the extinction of the solution. This method is time-consuming and the reproducibility is fairly poor. To date, quantitative evaluation methods such as videodensitometry and scanning densitometry have also found application in the TLC analysis of dyes. The reproducibility of these evaluation methods is higher and commensurate with those obtained by HPLC; the time consumption is signifacantly lower than that of the traditional "scraping-dissolving" method. The separation and quantitative determination of the impurities of the dye Phloxim B (2′,4′,5′,7′-tetrabromo-4,5,6,7-tetrachloro-3′,6′-dihydroxyspiro[isobenzofuran-1(3*H*),9′-[9*H*]xanthen-3-one-sodium salt) was performed on silica HPTLC layers.[7] A lower-halogenated impurity (2′,4′,5′-tribromo derivative) was separated by the mobile-phase acetone-chloroform-*n*-butylamine (66 : 24 : 4.5 v/v). Ethyl ester impurity was separated from the main fraction of Phloxim B with chloroform–glacial acetic acid (4 : 1 v/v). The concentration of impurities was determined *in situ* by videodensitometry. It was established that HPTLC–videodensitometry is rapid and reliable and can be successfully used for the measurement of impurities in Phloxim B. Although the TLC analysis of synthetic dyes is well established, the number of theoretical articles dealing with the quantitative relationship between retention characterisitcs, molecular structure, and physicochemical parameters of solutes is surprisingly low. The retention behavior of seven monotetrazolium and nine ditetrazolium salts on alumina and RP alumina was recently studied and the relationship between retention and physicochemical parameters of this class of synthetic dyes was elucidated by canonical correlation analysis.[8]

Calculations indicated that the retention on both TLC supports is of mixed character, including hydrophobic, electronic and steric parameters.

It can be concluded from the present state of the art of TLC analysis of synthetic dyes that the methods are mainly limited to the application of traditional TLC technique. Due to the rapidly developing instrumentation and

automation of the various steps of TLC analysis and the introduction of coupled methods (TLC/MS, TLC–Fourier transfer infrared spectrometry, etc.), their acceptance and successful application in the analysis of synthetic dyes can be expected in the near future. The use of new TLC techniques not only increases the separation capacity of the method but also considerably decreases the detection limit of solutes and may contribute to their identification.

REFERENCES

1. Gupta, V.K. *Handbook of Thin-Layer Chromatography*; Sherma, J., Fried, B., Eds.; Marcel Dekker, Inc.: New York, 1996; 1001–1032.
2. Muralidharan, D.; Sundara, Vss. Planar chromatographic analysis of leather dyes—A review. J. Soc. Leather Technol. Chem. **1995**, *79* (6), 178–180.
3. Gagliardi, L.; De Orsi, D.; Cozzoli, O. Cosmet. Toiletries Ed. Ital. **1995**, *16*, 34.
4. Lederer, M.; Nguyen, H.K.H. Adsorption chromatography on cellulose XIV. Some results using aqueous solutions of soluble cyclodextrin polymers as eluents. J. Chromatogr. A, **1996**, *723*, 405.
5. Morita, K.; Koike, S.; Aishima, T. Optimization of the mobile phase by the prisma and simplex methods for the HPTLC of synthetic red pigments. J. Planar Chromatogr. -Mod. TLC **1998**, *11*, 94.
6. Gharpure, A.B. Manufacture, analyses and evaluation of pesticides and plant protectants - A boon or a curse to the green revolution in India. Chemical Weekly **1997**, *42* (26), 169–172.
7. Wright, P.; Richfield-Fratz, N.; Rasooly, A.; Weisz, A. J. Planar Chromatogr. -Mod. TLC **1997**, *10*, 157.
8. Cserháti, T.; Kósa, A.; Balogh, S. Comparison of partial least-square method and canonical correlation analysis in a quantitative structure-retention relationship study. J. Biochem. Biophys. Methods **1998**, *36*, 131.

Taxanes: HPLC Analysis

Georgios A. Theodoridis
Laboratory of Analytical Chemistry, Chemistry Department, Aristotle University of Thessaloniki, Thessaloniki, Greece

INTRODUCTION

Taxanes have gained wide interest due to the pharmacological properties of paclitaxel (Taxol™), the most well-known member of this large family of natural products. Paclitaxel is a complex diterpene amide originally derived from the pacific yew tree. The drug has been characterized by the National Cancer Institute (NCI) as "the most important anticancer agent for the past 15 years." The interest in paclitaxel dates back to 1962, when crude extracts of *Taxus brevifolia* bark were tested in a large-scale exploratory plant-screening program of the NCI. Paclitaxel was identified as the active constituent of the bark extracts by Wani et al.[1] However, the clinical development of paclitaxel was delayed due to high toxicity, difficulties in formulation, and mainly its scarcity, which hampered a reliable supply for clinical use.

PACLITAXEL AND TAXANES

Awareness about paclitaxel increased dramatically in the late 1970s, when scientists at Albert Einstein Medical College (New York) described the unique mechanism of its cytotoxic action as a promoter of microtubule assembly. In contrast to most of the conventional anticancer drugs, paclitaxel inhibits mitosis through the enhancement of tubulin's polymerization and the consequent stabilization of microtubules. In 1983, the NCI commenced Phase I clinical trials. Six years later, the John Hopkins Oncology Center (Baltimore) reported exceptional clinical results for the treatment of ovarian cancer. The same year, Bristol-Myers Squibb was selected by the NCI as its partner to commercialize the drug under the trademark Taxol™. Since then, numerous other pharmaceutical companies focused on the development of novel anticancer agents of *Taxus* origin. Hence, a number of taxane pharmaceuticals were launched: Yewtaxan® (paclitaxel from Yew Tree Pharmaceuticals), paclitaxel (Napro; Australia). Researchers at the French CNRS, in cooperation with Rhone Poulenc (now Aventis), developed a semisynthetic derivative, starting from 10-deacetylbaccatin III (Fig. 1). The drug was called Taxotere and it exhibited attractive features compared to paclitaxel itself: better water solubility, potency, and the particular way of its production from a renewable source. Taxotere has received Food and Drug Administration (FDA) approval for the treatment of locally advanced or metastatic breast cancer and non-small cell lung cancer (NSCLC). Taxanes, in general, are used as a second-line cytostatic agent, meaning that they are often administered in cases where cancer recurs after chemotherapy with platinum drugs.

Paclitaxel is one of the best performers in the pharmaceutical market, with sales increasing by 62% in 1995 and reaching $941 million in 1997. Paclitaxel and taxotere have shown promising results in patients with advanced squamous cell carcinoma of the head and the neck, malignant melanoma, advanced NSCLC, small cell lung cancer (SCLC), germ cell cancer, urothelial cancer, esophageal cancer, non-Hodgkins lymphoma, and multiple myeloma. Furthermore, they have been tested in HIV and multiple sclerosis patients. Taxanes were also successfully combined with cisplatin, carboplatin, and/or etoposide in the treatment of patients with NSCLC, SCLC, or advanced squamous cell carcinoma of the head and neck.

The drugs are now considered a prototype for a new class of chemotherapeutic agents and research has been proceeding at record pace for years. The publication of five books on the chemistry, pharmacology, and medical therapy stands as a witness of the excitement that the compound has raised.[2–6]

Despite its low content (100 mg/kg of dry bark) and its notoriously slow growth, *T. brevifolia* was, until recently, the sole source of paclitaxel. Supply shortage and increasing demands for clinical use necessitated the investigation for alternative sources. Hence, plant species, tree parts, cell culture, fungi, and (semi)synthesis have been sought to solve the tremendous supply crisis in the mid-1990s. Nowadays, remaining problems include the compound's inherent toxicity, poor solubility in water, and difficulty encountered during formulation. Hence, optimization of the drug delivery, improvement of its molecular properties, and production of paclitaxel analogues (more potent, less toxic, and easier to formulate) are still a matter of considerable research and development efforts.

ANALYTICAL CHALLENGES AND METHODS

In general, the analysis of taxanes is driven by the following:

1. The need for the determination of paclitaxel (or docetaxel to a lesser extent) and their metabolites in biological samples.

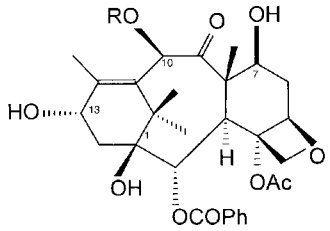

(1) 10-DAB III: R=H
(2) Baccatin III: R=Ac

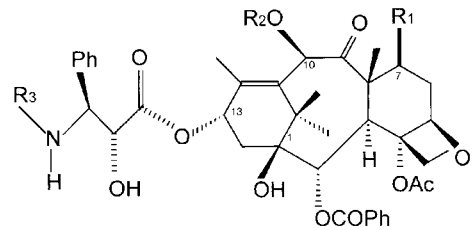

(3)	7-xylosyl-10-deacetylpaclitaxel B:	R1=xylose (β);	R2=H;	R3=tigloyl =
(5)	7-xylosyl-10-deacetylpaclitaxel:	R1=xylose (β);	R2=H;	R3 =Benzoyl
(6)	7-xylosyl-10-deacetylpaclitaxel C:	R1=xylose (β);	R2=H;	R3=*n*-Hexanoyl
(7)	10-deacetylpaclitaxel:	R1=OH (β);	R2=H;	R3=Benzoyl
(8)	7-xylosyl-paclitaxel:	R1=xylose (β);	R2=Ac;	R3=Benzoyl
(9)	Cephalomannine (Taxol B) :	R1=OH (β);	R2=Ac;	R3=tigloyl
(10)	7-epi-10-deacetylpaclitaxel:	R1=OH (α);	R2=H;	R3=Benzoyl
(11)	Paclitaxel :	R1=OH (β);	R2=Ac;	R3=Benzoyl
(12)	Paclitaxel C :	R1=OH (β);	R2=Ac;	R3=*n*-Hexanoyl
(13)	7-epi-paclitaxel :	R1=OH (α);	R2=Ac;	R3=Benzoyl
(14)	Docetaxel	R1=OH (α);	R2=Ac;	R3=butoxy carbonyl

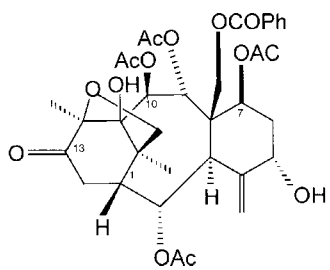

(4) Taxinine M

Fig. 1 Molecular structures of the most common taxanes.

2. The need for the purification or/and determination of taxanes in plant material, cell culture, or synthetic mixtures.

The starting point presides over the choice of the final analytical protocol. Analysis in biological samples for pharmacokinetic purposes poses limited difficulties because the determination of paclitaxel in human blood is rather straightforward. In contrast, analysis of plant samples deals with samples containing lesser quantities of a complex mixture of several taxanes. Separation and identification is thus a real challenge for the chromatographer.

Analysis of taxanes is performed almost exclusively by high-performance liquid chromatography (HPLC). Immunological techniques [enzyme-linked immunosorbent assay (ELISA), radioimmunoassay (RIA)] have found minimal use in screening human plasma and plant extracts. Such biological methods suffer from cross reactivity of several taxanes with paclitaxel and their use is thus limited in semiquantitative aspects.

MS, employing most of the ionization techniques, has been used either independently, or in combination with HPLC, for the determination of the dissociation scheme of paclitaxel or for the identification of taxanes and paclitaxel metabolites. Tandem MS has enhanced identification and structure elucidation capabilities in the analysis of either biological or plant samples.

A few research groups utilized other chromatographic techniques for the purification of taxanes from natural

sources or synthetic organic mixtures. Techniques such as TLC, flash chromatography, high-speed countercurrent chromatography (HSCCC), micellar electrokinetic chromatography (MEKC), and supercritical fluid chromatography (SFC) and extraction (SFE) have been used for either sample purification and/or analysis. TLC on silica gel has been used for the isolation and, together with NMR and MS, for the identification of new taxanes from several *Taxus* species. Visualization was accomplished by spraying the plates with anisaldehyde solution and heating. HSCCC provides an elegant method for fast and efficient processing of large sample quantities, a parameter of great importance for scale-up purposes. HSCCC is not based in adsorption chromatographic mechanisms, in contrast to the established taxane purification methods (including the FDA-approved official method), which employ column chromatography. A two-phase system of light petroleum–ethyl acetate–methanol–water purified plant samples of up to 400 mg, achieving purity of up to 97% for paclitaxel. MEKC performed on uncoated fused silica capillaries proved suitable for the analysis of paclitaxel, cephalomannine, and baccatin III in needle extracts. Finally, SFC has been carried out in both capillary and packed C_{18} or cyano columns. The packed cyano column gave the best performance for the analysis of taxanes after SFE of *Taxus baccata* clippings.

HPLC OF TAXANES

HPLC analysis of taxanes is achieved almost exclusively in reversed-phase (RP) mode on various stationary phases. The normal-phase HPLC mode has been applied in very limited cases and resulted in broad peaks and long analysis times (retention times of 45 min for paclitaxel and 38 min for cephalomannine). The nature of the sample is the main criterion for the choice of the stationary phase. Analysis of plant material is performed mostly on phenyl, biphenyl, and pentafluorophenyl materials, but silica-based cyano, C_{18}, and C_8 materials have been used as well. C_{18} phases are the most common material utilized in pharmacokinetic studies. Mobile phases typically consist of mixtures of methanol, acetonitrile, and water or buffer (mostly ammonium acetate). Detection is performed by UV, mostly in the low region of 225–230 nm. Taxanes give similar UV spectra with a minimum at 210–215 nm and a maximum at 225–232 nm. Therefore, detection is performed, preferably at 227–228 nm. Dual/multiple UV detection is performed in both low and upper regions, e.g., 227 and 273 nm; 230 and 280 nm; 227, 254, and 270 nm, etc. (Fig. 2).

In the reported LC-MS schemes, both positive and negative ionization modes have been used; however, positive ionization is the dominant mode. Thermospray and

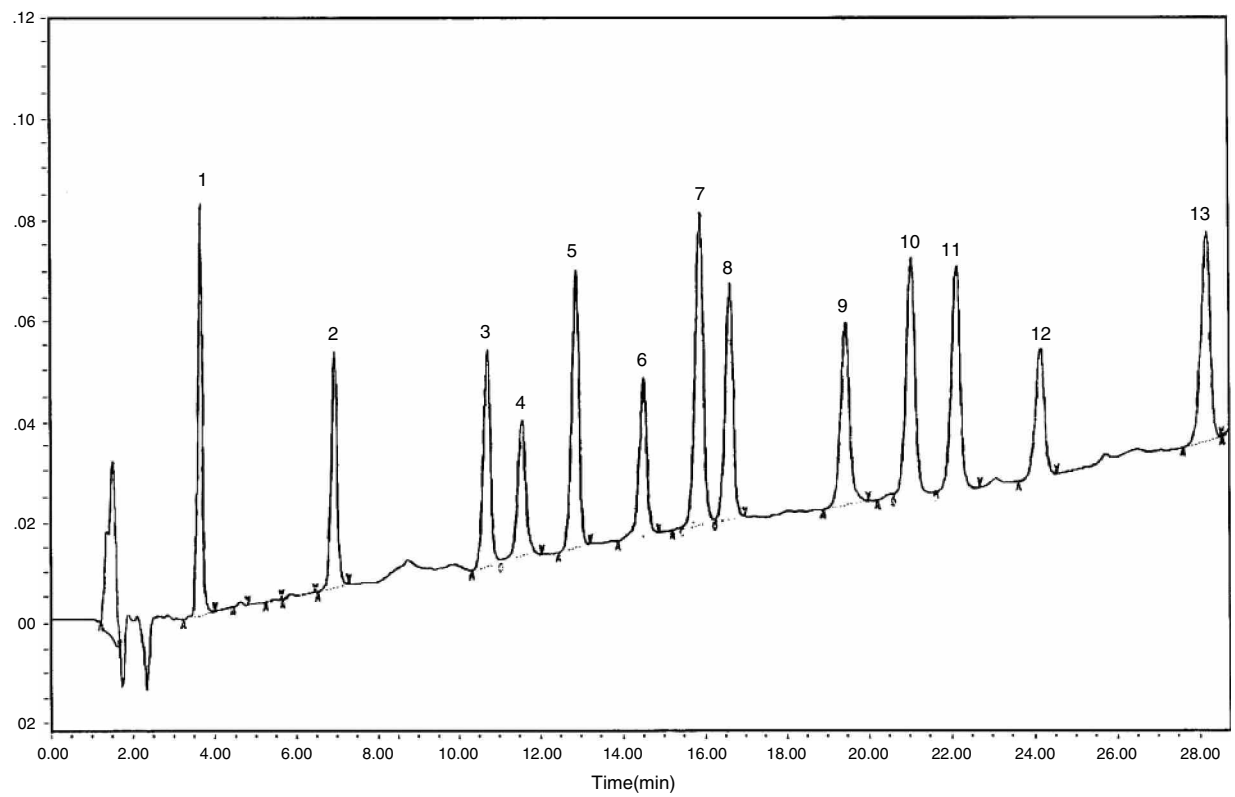

Fig. 2 UV spectra obtained by HPLC analysis of a *Taxus* cell culture extract. Detection with a photodiode array detector. **1** = Paclitaxel, **2** = cephalomannine, **3**, **4**, and **5** correspond to unknown interferences from the sample.

electrospray interfaces have been utilized for the coupling of RP mobile phases to the MS. In tandem MS, fragments are obtained from the taxane ring (ions with *m/z* 268 and 286) and the C-13 side ester chain (ions with *m/z* 569, 551, and 509).

Detailed description of the analytical separation systems for the analysis of paclitaxel by HPLC (stationary and mobile phases, sample type, sample pretreatment) can be found in a review that appeared recently.[7]

HPLC Analysis of Plant Material and Cell Culture

Analysis of paclitaxel in plant material bids a challenge for the separation scientist for many reasons:

1. The taxanes are present in low quantities in the original samples (either plant or cell culture).
2. The differences between the molecular structure of different taxanes are small (Fig. 1).
3. Plant extracts encompass a diversifying range of endogenous compounds.

These problems can be easily perceived in the reported chromatograms: broad peaks, long analysis times, and poor resolution from endogenous interferences.

Initially, researchers focused on the separation of paclitaxel from cephalomannine, a paclitaxel analogue that shares the C-13 ester side-chain and, therefore, exhibits cytotoxic activity. Cephalomannine was found to elute close to paclitaxel and caused interferences for determination and purification purposes. Lately, the main taxane targets are baccatin III and 10-deacetylbaccatin III (10-DAB III). Both compounds lack the C-13 side-chain (Fig. 1); thus, they do not show antitumour activity. Both baccatins, especially 10-DAB III, serve as synthons for the synthesis of paclitaxel or analogues. 7-Epi-paclitaxel differs from paclitaxel only in the stereochemistry of the hydroxy group in the C-7 position. 7-Epi-paclitaxel, a product of paclitaxel epimerization, shows cytotoxic activity and difficulty in separation from paclitaxel. The deacetyl derivatives of paclitaxel, 7-epi-paclitaxel, baccatin III, and cephalomannine, are also quite often the subject of analysis. The problems mentioned above designated a market for HPLC column manufacturers, which did not take long to fill with "tailor made" or "specialty" columns. Taxanes are probably the sole group of compounds that labeled so many HPLC columns: Phenomenex has produced three Curosil™ columns (silica-based RP packing material), Metachem Technologies also manufactured three Taxil™ columns, Zorbax made the SW-Taxane column (bonded silica), and Whatman the TAC 1 column. It should be pointed out that such columns are usually developed in order to solve special problems. According to their manufacturers, the chemical and physical properties of the packing material (which are often proprietary) are designed with appropriate characteristics for a specific analyte or group of analytes. However, it is often observed by many researchers (the author included) that the best results are actually obtained by utilizing a low-cost conventional material.[9] An example is illustrated in Fig. 3, which shows a UV chromatogram of a reference taxane mixture obtained by gradient elution on a generic phenyl column. The same chromatographic analysis performed on electrospray MS provided mass spectral data that were used for the identification of unknown peaks in *Taxus* bark extracts. Results are depicted in Table 1.

Sample Pretreatment of Plant Material and Cell Culture

Optimization of the extraction and purification of taxanes from plant material, tissue culture, or biological fluids has been the subject of extensive research. As mentioned already, taxanes are present in small quantities in a very complex matrix, thus making extraction and purification complicated. Simple extraction schemes do not cope with straightforward HPLC analysis because they are subject to column plugging and deterioration, low recovery, and poor chromatographic resolution. On the other hand, tedious and complex procedures that have been developed to overcome such problems require large amounts of solvent and long extraction times (surpassing even 48 hr).

A typical strategy takes advantage of the limited water solubility of taxanes to partition the compounds between water, and an apolar organic solvent (often a chloromethane). Hence, a plant material in the form of a crude methanolic plant extract is partitioned between water and dichloromethane; the dichloromethane fraction is evaporated to dryness, reconstituted in methanol, and analyzed by HPLC. Initially, such simple extraction procedures were used for the determination of taxanes in plant extracts, but they resulted in high back pressure and the need for frequent column flushing. Furthermore, as *Taxus* phytochemistry consolidated, analytical methods of higher resolving power became necessary. Additional extraction steps for the removal of non-polar components (especially from samples such as needles) utilized hexane or similar apolar solvents. The plant material is first extracted with hexane for the removal of waxes and other lipophilic substances. Alternative protocols employed techniques such as column chromatography, HSCCC, SFE, and semipreparative HPLC.

Recently, solid phase extraction (SPE) on several stationary phases has been extensively used in the pretreatment of both plant and biological samples. Typically, crude extracts are mixed with appropriate solvents (methanol or ethanol) and the resulting solutions are applied onto the SPE cartridges. The cartridges are next washed with appropriate solvents to take out impurities and, finally, the taxanes are eluted in an optimized "recovery solvent." The obtained taxane fraction is evaporated to dryness and, after reconstitution to solution, an aliquot is analyzed by HPLC.

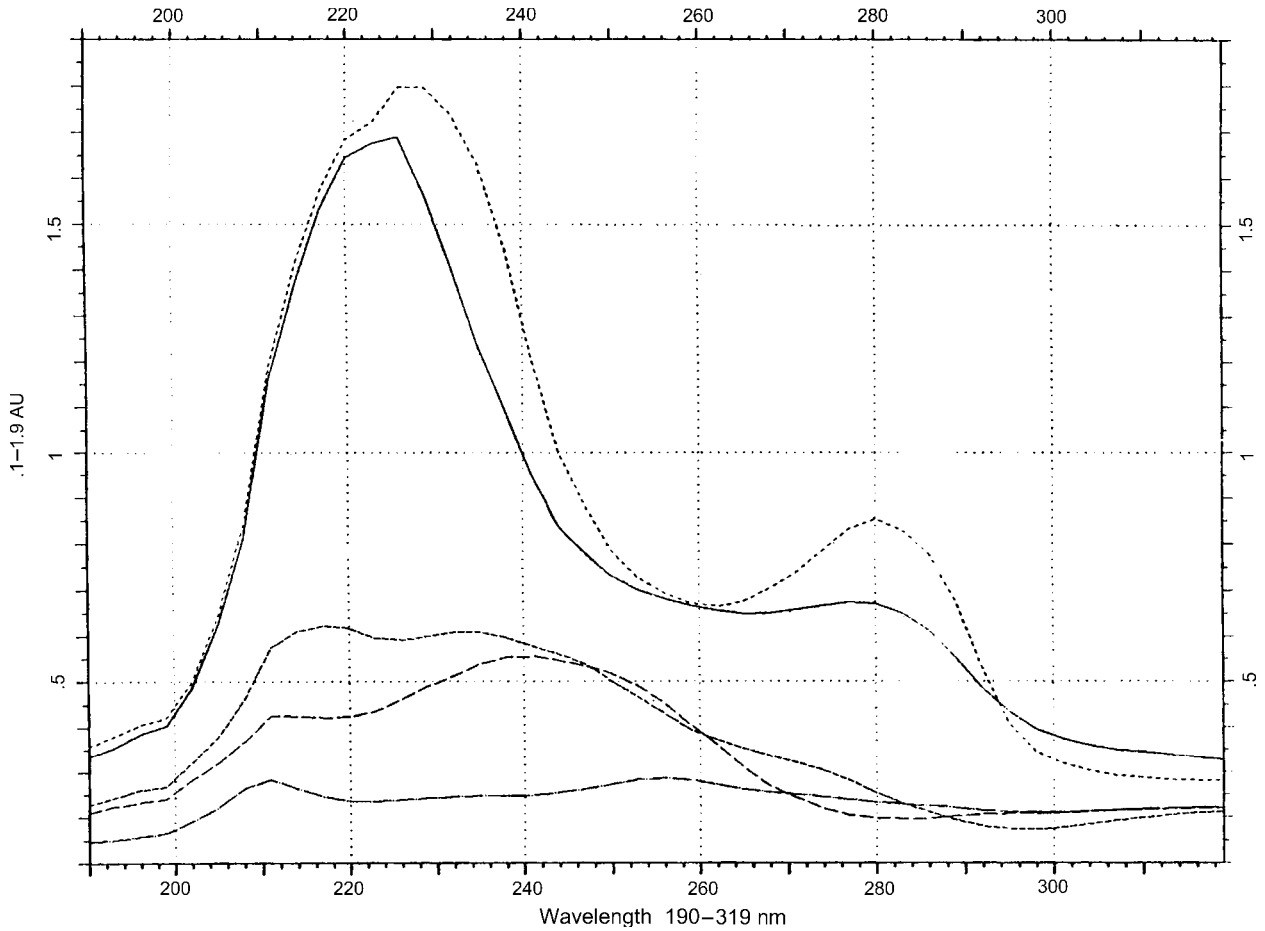

Fig. 3 Analysis of a taxane standard mixture. Chromatographic conditions: Column Novapak Phenyl column (Waters); eluted with the gradient program: Initially 100% A–0% B, linearly 56% A–34% B at 30 min and then back to 100% A–0% B at 32 min. A = 0.05 *M* CH_3COONH_4:CH_3CN 7:3 v/v, B = 0.05 *M* CH_3COONH_4:CH_3CN 1:9 v/v. Flow rate 0.8 ml/min and detection at 227 nm. Peak identities as in Fig. 1.

Source: From Determination of paclitaxel and related diterpenoids in plant extracts by high performance liquid chromatography with UV detection in high performance liquid chromatography-mass spectrometry, in J. Chromatogr. A.[9]

The author has studied the SPE of taxanes at length.[10] SPE offers an attractive alternative to the long and tedious liquid–liquid extraction schemes. The author's work on HPLC determination of taxanes[9] and SPE for the pretreatment of *Taxus* plant and cell culture samples[10] resulted in fast and robust schemes for either screening or accurate determination of taxanes in plant and cell cultures. In this work, problems were observed in liquid–liquid extraction of the cell suspension medium as a result of the formation of emulsions. Such formations are difficult to break and require time-consuming and laborious centrifugation. Therefore, the major goal of the developed SPE protocols was the straightforward application of aqueous medium on the SPE column. As a result, consumption of time and organic solvents was lowered significantly. Washing the cartridge with water and aqueous MeOH (up to 50% in water) facilitated the removal of many interfering matrix constituents. Taxanes were recovered from the SPE cartridge with the elution fraction of 80% MeOH.[10]

HPLC Analysis of Biological Material

Interest for the analysis of taxanes in biological fluids deals, in most cases, with the determination of the two pharmaceuticals, paclitaxel, and docetaxel, and their metabolites in blood plasma. The complexity of this matrix and the interference of endogenous compounds are, in principle, decreased, compared to plant material; therefore, extensive sample pretreatment and high chromatographic resolution are not essential. Thus, fast and simple separation systems with the use of a C_8 or a C_{18} column are often preferred. SPE is extensively used for sample pretreatment (especially in recent reports) because of its advantages over liquid extraction: limited organic solvent consumption, higher reproducibility and extraction efficiency, and cleaner extracts. Furthermore, sophisticated online SPE schemes that employ column switching or automated SPE increase sample throughput.

Paclitaxel and docetaxel are very lipophilic pharmaceuticals; thus, they bind to plasma proteins rapidly and to a

Table 1 Results of the LC/MS analysis of a taxane standard mixture and a *T. baccata* bark extract.

Compound	*m/z*	Peak	MW	t_R (min)	Bark
(**1**) 10-DAB III	562	$[M + NH_4]^+$	544	3.95	+
(**2**) Baccatin III	604	$[M + NH_4]^+$	586	6.88	+
(**3**) 7-Xylosyl-10-deacetyltaxol B	922	$[M + H]^+$	921	10.78	+
(**4**) Taxinine M	704	$[M + H]^+$	703	11.50	+
(**5**) 7-Xylosyl-10-deacetyltaxol	944	$[M + H]^+$	943	13.10	–
(**6**) 7-Xylosyl-10-deacetyltaxol C	938	$[M + H]^+$	937	14.60	+
(**7**) 10-Deacetyltaxol	812	$[M + H]^+$	811	15.65	+
(**8**) 7-Xylosyl-taxol	986	$[M + H]^+$	985	16.40	+
(**9**) Cephalomannine	832	$[M + H]^+$	831	19.65	+
(**10**) 7-Epi-10-deacetyltaxol	812	$[M + H]^+$	811	21.20	–
(**11**) Paclitaxel	854	$[M + H]^+$	853	22.15	+
(**12**) Taxol C	848	$[M + H]^+$	847	24.20	+
(**13**) 7-Epi-taxol	854	$[M + H]^+$	853	28.15	–

Chromatographic conditions are as in Fig. 2. t_R = retention time; (+) = detection of the compound; (–) = no detection.
Source: From Determination of paclitaxel and related diterpenoids in plant extracts by high performance liquid chromatography with UV detection in high performance liquid chromatography-mass spectrometry, in J. Chromatogr. A.[9]

great extent (>95%). Small quantities are excreted in urine because most of the drug is removed from the plasma metabolized in the liver and subsequently excreted into the bile.[2] Paclitaxel pharmacokinetics follow a bimodal distribution. Usually, such studies are modeled with a two-compartment system: a central administration compartment (plasma-liver) and a second peripheral compartment (tissue where the drug is transported by secondary mechanisms). It should be pointed out that the lipophilicity of taxane pharmaceuticals causes tremendous problems in formulation and clinical administration. Paclitaxel's vesicle is a mixture of 50% polyethoxylated castor oil (a surfactant labeled Cremophor EL), and 50% ethanol. This mixture causes serious adverse effects to patients. Cremophor is also subject to interferences in chemical analysis of pharmaceutical preparations of the drug. The drug is infused intravenously for varying time periods. Depending on the length of infusion, the concentration maximum in plasma varies from 3–4 μM (short infusion of 6 hr) to 0.7–0.9 μM (long infusion of 24 hr). Following HPLC, detection of paclitaxel by UV (227 nm) is sufficient; however, MS offers much higher sensitivity and identification capabilities.

Separation systems are rather simple and they employ solvents such as methanol or acetonitrile and buffers such as sodium acetate, ammonium acetate, or phosphate buffers. Isocratic elution suffices in most cases because the polarity of the drug is far different than most endogenous compounds, thereby enabling an easy chromatographic separation.

The sample that draws the greatest interest is human plasma, but other physiological human fluids, such as urine and bile, have also been the subject of analysis. To cover the needs of in vivo preclinical studies, many researchers developed methods for the determination of paclitaxel/docetaxel and their metabolites in samples from animal models such as rat and mouse.

Coupling of HPLC analysis to MS (either online or off-line) provided the means for structure elucidation and identification of taxane metabolites. Utilizing tandem MS (MS/MS), both aspects were significantly enhanced. Hydroxylation, epimerization, and hydrolysis are considered to be the main routes of metabolism of taxane pharmaceuticals.[3] The principal metabolites of both paclitaxel and docetaxel result from hydroxylation. Hydroxylation of paclitaxel was initially observed in rat and mouse, but the finding was later extended to human subjects. Nine metabolites of paclitaxel (mono or dihydro derivatives) have been identified in rat by HPLC, NMR, and LC/MS. With regard to docetaxel, 18 derivatives have been identified in the rat bile. Hydrolytic derivatives result from cleavage of the side C-13 chain, and include baccatin III and 10-DAB III. Epimerization of taxanes is mainly focused on the C-7 and C-10 atoms, and occurs in solution. Epimerization has also been detected in cell culture in both the medium and inside the cell. It should be stressed that epimers are not naturally occurring taxanes; thus, they are not found in plants.[2–3,8–9]

A detailed tabulated list of HPLC methods (columns, mobile phases, applications, and detection modes) can be found in Ref.[8]

CONCLUSIONS

Analysis of taxanes in biological samples and plant extracts is performed, mainly by RP-HPLC. Separation of paclitaxel from cephalomannine, baccatin III, and other taxanes is often performed with phenyl columns (especially for plant material analysis). For less complex biological samples, C_{18} columns are preferred because they give shorter analysis times. Extraction of plant material or cell cultures is often performed by water–

dichloromethane partitioning, but lately, the application of SPE has become a basic step in order to obtain cleaner samples, higher extraction recovery, better chromatographic resolution, and longer column lifetime. Detection of taxanes is performed, in most cases, at 227–228 nm.

REFERENCES

1. Wani, M.C.; Taylor, H.L.; Wall, M.E.; Coggon, P.; McPhail, A.T. Plant antitumor agents: VI. The isolation, and structure of taxol, a novel antileukemic and antitumor agent from *Taxus brevifolia* trees. J. Am. Chem. Soc. **1971**, *93*, 2325–2327.
2. Suffnes, M. *Taxol Science and Applications*; CRC Press: Boca Raton, 1995.
3. Farina, V. *The Chemistry and Pharmacology of Taxol*; Elsevier: Amsterdam, 1995.
4. McGuire, W.P.; Rowinski, E.K. *Paclitaxel in Cancer Treatment*; Marcel Dekker, Inc.: New York, 1995.
5. Georg, G. *Taxane Anticancer Agents*; Developed from a Symposium Sponsored by the Divisions of Chemical Health, and Safety, American Chemical Society: Washington, 1995.
6. Goodman, J.; Walsh, V. *The Story of Taxol: Nature, and Politics in the Pursuit of an Anti Cancer Drug*; Cambridge Univ. Press: Cambridge, 2001.
7. VanHaelen-Fastre, R.; Diallo, B.; Jaziri, M.; Faes, M.-L.; Homes VanHaelen, M. High-speed countercurrent chromatography separation of taxol and related diterpenoids from *Taxus baccata*. J. Liq. Chromatogr. **1992**, *15*, 697–706.
8. Theodoridis, G.; Verpoorte, R. Taxol analysis by HPLC. A review. Phytochem. Anal. **1996**, *7*, 169–184.
9. Theodoridis, G.; Laskaris, G.; de Jong, C.; Hofte, A.J.P.; Verpoorte, R. Determination of paclitaxel and related diterpenoids in plant extracts by high performance liquid chromatography with UV detection in high performance liquid chromatography-mass spectrometry. J. Chromatogr. A, **1998**, *802*, 297–305.
10. Theodoridis, G.; de Jong, C.; Laskaris, G.; Verpoorte, R. Application of SPE for the HPLC analysis of taxanes from *Taxus* cell cultures. Chromatographia **1998**, *47*, 25–34.

BIBLIOGRAPHY

1. Fang, W.; Wu, Y.; Zhou, J.; Chen, W.; Fang, Q. Qualitative, and quantitative determination of taxol and related taxanes in *Taxus cuspidata* Sied et Zucc. Phytochem. Anal. **1993**, *4*, 115–119.
2. Monsarrat, B.; Mariel, E.; Cros, S.; Gares, M.; Guenard, D.; Gueritte, V.; Wright, M. Taxol metabolism. Isolation and identification of three major metabolites of taxol in rat bile. Drug Metab. Dispos. **1990**, *18*, 895–901.
3. Rosing, H.; Lustig, V.; Koopman, F.P.; ten Bokkel Huinink, W.W.; Beijnen, J.H. Bio-analysis of docetaxel and hydroxylated metabolites in human plasma by high-performance liquid chromatography and automated solid-phase extraction. J. Chromatogr. B. Biomed. Sci. Appl. **1997**, *696*, 89–98.
4. Theodoridis, G.; Laskaris, G.; Verpoorte, R. HPLC analysis of taxoids in plant and plant cell tissue culture. Am. Biotechnol. Lab. **1999**, *17*, 40–44.
5. Vergniol, J.C.; Bruno, R.; Montay, G.; Frydman, A. Determination of taxotere in human plasma by a semi-automated high-performance liquid chromatographic method. J. Chromatogr. **1992**, *582*, 273–278.

Taxines: HPLC Analysis

Georgios A. Theodoridis
Laboratory of Analytical Chemistry, Chemistry Department, Aristotle University of Thessaloniki, Thessaloniki, Greece

INTRODUCTION

The toxicity of *Taxus* plants has been known for a long time (reports date as far back as the time of Julius Caesar).[1] In the 19th century, phytochemical work attributed *Taxus* toxicity to an alkaloid that was called taxine. This alkaloid was a complex mixture, isolated from leaves. Taxine was later shown to be a mixture of more than seven alkaloids, with taxine A and taxine B as main constituents. Taxines are very strong cardiotoxic agents; they cause convulsions, fall in blood pressure, and stopping of the heart in diastole. Phytochemical work on *Taxus* during the 1940s and 1950s was focused on taxines and their cinnamate analogues, taxinines. The discovery of the potent cytostatic agent paclitaxel in *Taxus* bark in the late 1960s overshadowed any interest in taxines. Paclitaxel and the semisynthetic derivative docetaxel attracted unprecedented interest and remained the major research topic for scientists on diverse areas as follows: phytochemistry, pharmacognosy, molecular pharmacology, synthetic chemistry, analytical chemistry, and, most of all, clinical medicine.

TAXINES

A chief problem in the early development of taxane pharmaceuticals was the establishment of a steady and dependable supply. Taxanes are present in low quantities in plants. In contrast, taxines are relatively abundant in plants (especially in *Taxus baccata* and *Taxus cuspidate*); they can serve as an alternative starting material for semisynthetic production of paclitaxel derivatives. The major taxines are taxine A and taxine B.[2,3] There is a significant structural resemblance between taxine B and taxanes (Fig. 1). Both groups share the main taxane ring; moreover, the C-5 side chain of the taxines has a close spatial position to the C-13 side chain of the taxanes (the latter is essential for antitumor activity). A biosynthetic hypothesis involved the intermediacy of a C-5 to a C-13 ester transfer; it was also demonstrated that taxine B can be converted into a baccatin V derivative. Taxines do not show antitumor activity, whereas the cardiotoxicity of taxol is lower compared to taxines but is undesirable for clinical administration. Hence, it was assumed that the structural features necessary for cardiotoxicity are different from the features necessary for antitumor activity. Understanding the factors responsible for the toxicity of taxines could lead to the design of taxol analogues with diminished cardiotoxicity. However, taxines do not show intrinsic antitumor activity, whereas the cardiotoxicity of paclitaxel is lower compared to taxines but is undesirable for clinical administration. Hence, it was assumed that the structural features necessary for cardiotoxicity are different from the features necessary for antitumor activity. Understanding the factors responsible for the toxicity of taxines could lead to the design of paclitaxel analogues with diminished cardiotoxicity. Sophisticated analytical methods are therefore necessary for their analysis and determination in plant or biological samples.

Unfortunately, research work on taxines was hampered by their instability and the loss of activity upon storage because of the loss of dimethylamino moiety from the C-3′ atom (Fig. 1) and the formation of corresponding cinnamates. Isolation of taxines is accomplished by alkaline/base extraction but it is difficult to obtain them in a purified form because of rapid acetate isomerization and/or decomposition to taxinines. To the author's knowledge, there are no taxine/taxinine reference compounds commercially available. It is no surprise therefore that there are limited works that report on the high-performance liquid chromatography (HPLC) of taxines. Taxines were found in plant extracts interfering in extraction, isolation, and analysis of paclitaxel from plant material.[2–6]

HPLC ANALYSIS OF TAXINES

Workers of the phytochemical group at the University of Wageningen identified and isolated six taxine alkaloids from the needles of *T. baccata*. Acidic extraction with 0.5% (v/v) H_2SO_4 was followed by an extraction with Et_2O and basic extraction with 25% aq. NH_3. Taxines were recovered with $CHCl_3$ with a yield of 0.5–1% for the total crude taxine fraction. This report comprises the first analytical methodology for the determination of taxines. HPLC analysis employed a C_{18} column, eluted by a linear gradient of acetonitrile over methanol and 0.05 *M* sodium dihydrogen phosphate buffer.[7]

The research group of P. Potier, a group that has long been engaged in research activity on *Taxus*, studied the analysis of four taxines and 10-DAB III in *Taxus* needles in investigations for highly productive plants. The authors developed a normal phase separation system (silica eluted with chlorofom/methanol/triethylamine, 99.4 : 0.5 : 0.1)

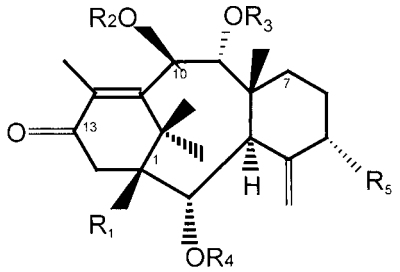

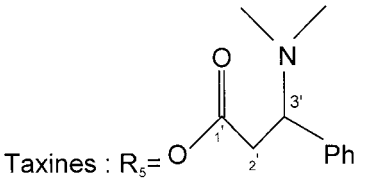

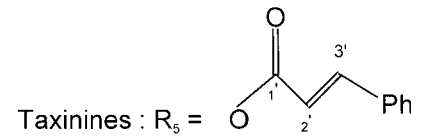

(1) R_1= OH, R_2 = R_3= R_4= H
(2) R_1= H, R_2= Ac, R_3= R_4= H
(3) R_1= OH, R_3= H, R_2= R_4= Ac
(4) R_1= OH, R_2= Ac, R_3= R_4= H
(5) R_1= OH, R_3= Ac, R_2= R_4= H
(6) R_1= H, R_3= Ac, R_2= R_4= H
(7) R_1= OH, R_2= H, R_3= R_4= Ac
(8) R_1= OH, R_2= R_3 = R_4= Ac
(9) R_1=H, R_2=R_3=R_4=Ac

(10) R_1= OH, R_2= R_3 = R_4= H
R_1= R_2= R_3 = R_4= H
R_1= OH, R_2= R_3 = R_4= Ac
R_1= H, R_2= R_3 = R_4= Ac

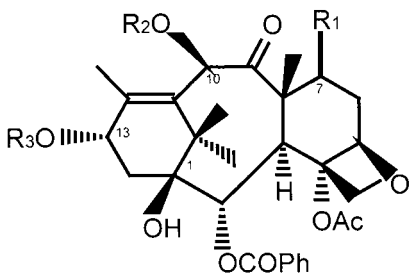

Paclitaxel: R_1= OH (β), R_2= Ac, R_3= Ph

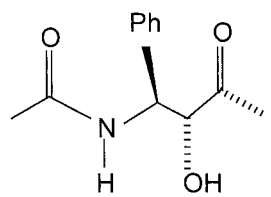

Cephalomannine: R_1= OH (β), R_2= Ac, R_3=

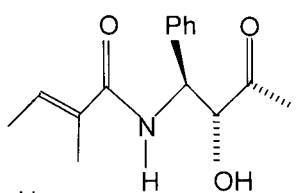

Baccatin III: R_1= OH (β), R_2= Ac, R_3= H

10-Deacetylbaccatin III: R_1= OH (β), R_2= H, R_3= H

Fig. 1 Molecular structures of taxines, taxinines, and taxanes.

for the evaluation of the total taxine content in *Taxus* needles. To separate the taxines, they used reversed phase (C_{18} eluted with acetonitrile/water/tetrahydrofuran, 23 : 77 : 0.5). The method, although it suffered from peak asymmetry and tailing, was useful for preparative objectives because it avoids the use of buffers.[8] Taxines have also been determined by gas chromatography/mass spectrometry (GC/MS) in a search of *Taxus* poisoning in cattle and horses. Even though taxines are molecules that are too large to be analyzed by GC, the authors actually measured an ion at 134 m/z^+, which was attributed to a specific fragment at the 2′ atom of the taxine side chain (Fig. 1).

The author's work on the HPLC analysis of taxines was a follow-up of previous research work on the HPLC of taxanes.[9,10] Unknown peaks present in the analysis of plant and cell culture extracts were suspected to be taxines. In previous works, several other researchers have reported the detection of impurity peaks in the extracts of *Taxus* × *media* (Hicksii) needles during the determination of taxanes. These uncharacterized impurities showed a UV maximum at 280 nm, with a A_{280}/A_{228} ratio of approximately 3.5. Using absorbance ratio with these two or similar wavelengths, the researchers managed to overcome quantitation problems.[11] Taxines and taxinines were also reported to cause problems in the HPLC analysis of taxanes, coeluting with the peak of paclitaxel.

In our work at Leiden University, apart from HPLC-photodiode array (PDA) detection, HPLC-electrospray mass spectrometry was used as characterization and identification tools. A semipurified taxine extract obtained with acid/base extraction of *T. baccata* needles was analyzed in reversed phase; nine taxines, one taxinine, and six taxanes were found present in the sample. Furthermore, 10-deacetylbaccatin III (paclitaxel's main precursor) and other taxanes were also found in the extract. Identification of the peaks was made with online liquid chromatography/mass spectrometry (LC/MS) and off-line nuclear magnetic resonance (NMR) following fraction collection at the end of the HPLC. Retention and spectral data of the identified peaks were used as tool to screen for taxines and taxinines in plant and cell culture extracts. Several

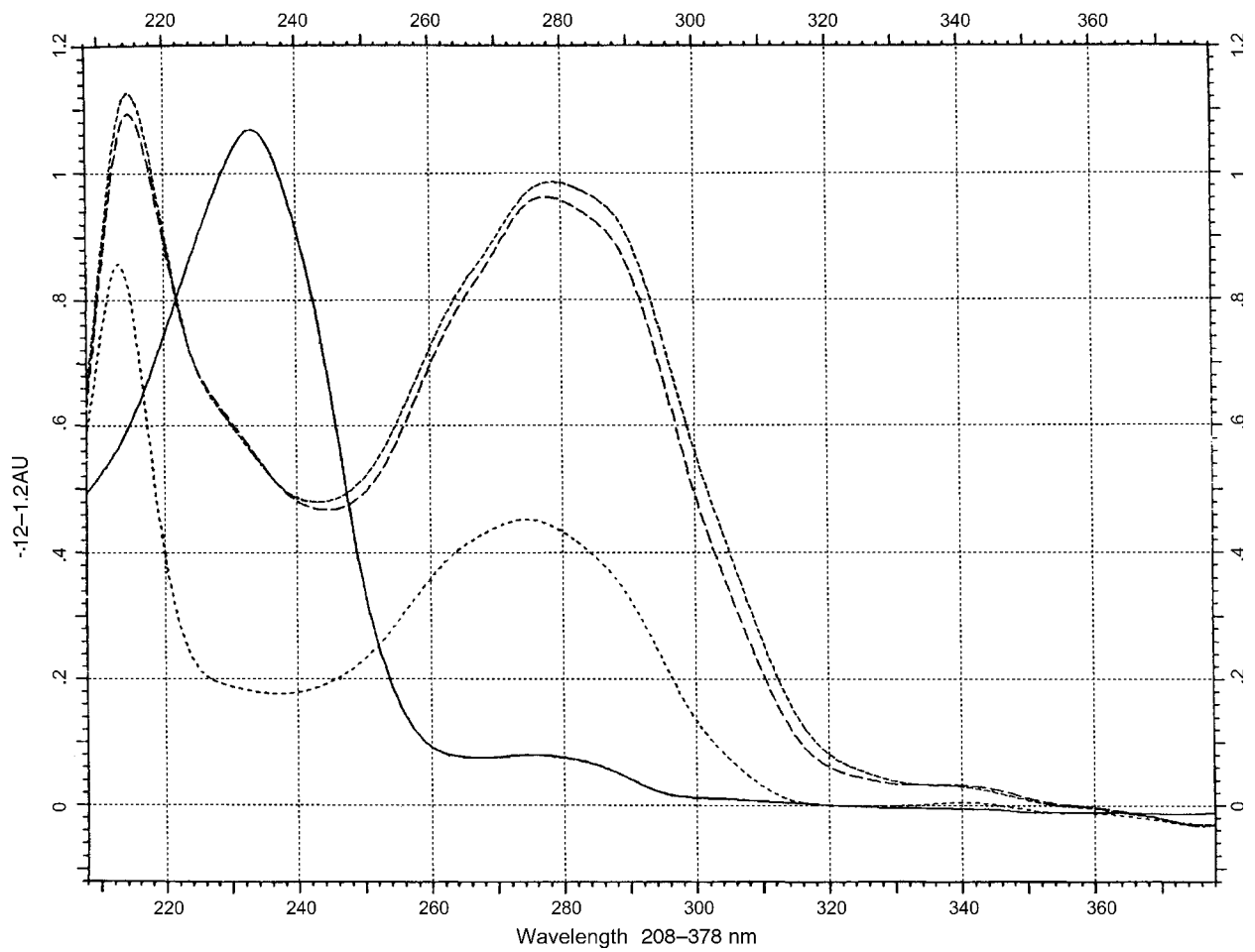

Fig. 2 UV spectra of a taxane (1), a taxine (2), and two taxinines (3).
Source: From Analysis of taxines in *Taxus* seeds, needles and cell culture by HPLC-PDA and HPLC-ESI-MS, in J. Liq. Chromatogr.[12]

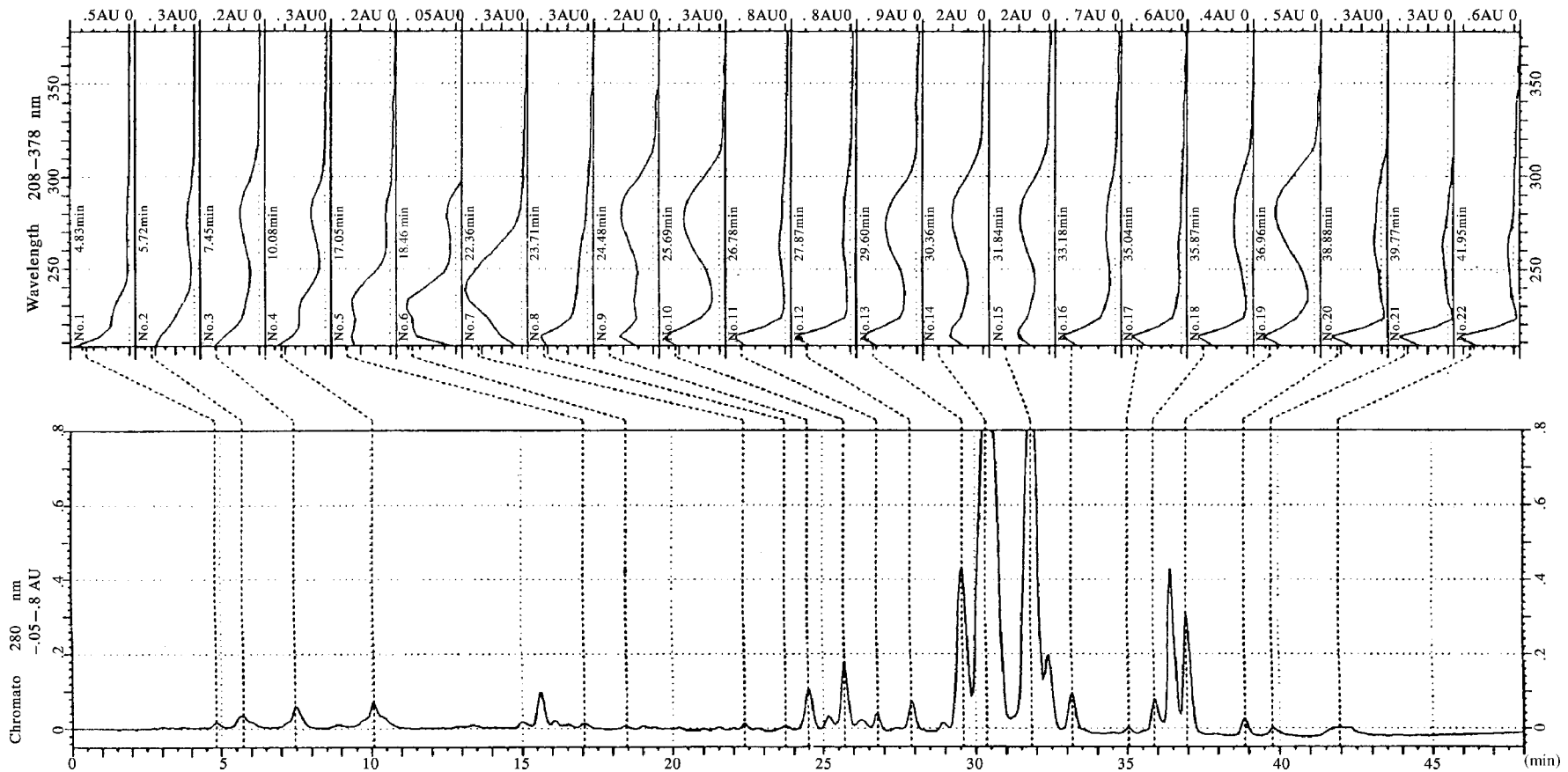

Fig. 3 HPLC analysis of the semipurified taxine extract. Conditions: Luna C_{18} Column (Phenomenex) eluted with a gradient program of methanol (B) over 0.05 *M* CH_3COONH_4 (A). Initially A : B 65 : 35 v/v, linearly to A : B 25 : 75 v/v (38 min), then to A : B 0 : 100 v/v (38.1 min), stable at A : B 0 : 100 v/v till 44.5 min, then back to A : B 65 : 35 v/v at 45 min. Flow rate: 0.8 ml/min. Peak identities in Table 1.

Source: From Analysis of taxines in *Taxus* seeds, needles and cell culture by HPLC-PDA and HPLC-ESI-MS, in J. Liq. Chromatogr.[12]

Table 1 Chromatographic data obtained after the LC-PDA and LC/MS analysis of the purified taxine mixture on the luna column.

Compound	t_R (min)	A_{227}/A_{249}	A_{227}/A_{280}	A_{249}/A_{280}	*m/z*
Taxane	13.5	3.57	10.66	2.96	N/Dt
10-DAB III	15.5	2.53	10.44	4.12	545
Taxane	17	3.8	10.12	2.78	N/Dt
Taxane	18.5	4.17	24.2	5.8	N/Dt
Ut	18.8	N/Dn	N/Dn	N/Dn	612
U	19.2	3.26	N/Dn	N/Dn	604
Taxane	20.3	3.22	15.1	4.72	584
U	22.4	1.16	13.1	11.36	584
2	24.5	2.03	0.93	0.46	568
1	25.4	1.62	1.08	0.66	542
3	25.8	1.21	1.10	0.92	626
Ut	25.8	N/Dn	N/Dn	N/Dn	642
5	26.8	1.60	1.12	0.66	568
Ut	27.4	N/Dn	N/Dn	N/Dn	628
Ut	27.7	1.97	0.94	0.48	584
Ut	29.6	1.30	2.25	1.73	628
4	30.4	1.16	1.13	0.98	584
5	31.8	1.28	1.23	0.96	584
7	32	1.85	0.93	0.47	626
Ut	32.3	3.83	N/Dn	N/Dn	610
U	32.6	5.63	3.25	0.57	784
8	33.1	1.75	0.88	0.51	668
Ut	33.6	1.75	0.90	0.50	612
Ut	36.5	1.44	0.32	0.45	668
Ut	37	1.90	0.45	0.32	610
Ut	38.9	3.77	1.19	0.31	654
Ut	39.5	2.18	1.02	0.47	610
9	41.4	1.88	1.50	0.80	652
Ut	41.9	N/Dn	N/Dn	N/Dn	668

Conditions as in Fig. 3.
U = unknown; Ut = unknown "taxine"; N/Dt = not detected; N/Dn = not determined.
Source: From Analysis of taxines in *Taxus* seeds, needles and cell culture by HPLC-PDA and HPLC-ESI-MS, in J. Liq. Chromatogr.[12]

members of both groups of compounds were found in samples of various origin. LC/MS verified the presence of some of the known taxines and taxinines in extracts of *Taxus* needles, pollen, and seeds.[9,10]

HPLC-PDA detection offers an alternative for the cost-effective separation of taxanes and taxines in complex plant extracts. The spectrum index plots in Fig. 2 depict the chromatographic analysis of the taxine-purified extract on a C_{18} column with gradient elution. The UV spectra of the detected peaks are illustrated in the upper part of the chromatogram. A clearer prospect of the corresponding spectra is given in Fig. 3. It can be seen that 227 nm represents the maximum for the UV spectrum of taxanes, whereas 280 nm is the λ_{max} of taxinines and taxines. Hence, 280 nm can be used as a "selective" wavelength for the detection of taxines and taxinines. Use of absorbance ratios between three (or more) wavelengths can also provide a means of identification.[13] The absorbance ratios obtained after the analysis of reference mixtures were as follows:

- For 10-DAB III: $A_{227}/A_{215} = 1.67$, $A_{227}/A_{249} = 2.99$, $A_{215}/A_{249} = 1.78$.
- For taxol: $A_{227}/A_{215} = 1.35$, $A_{227}/A_{249} = 3.51$, $A_{215}/A_{249} = 2.55$.

Comparison of these values with the ones calculated from peaks eluting at similar retention times in the analysis of extracts could be a fast way to verify the identity and to check the peak purity. Analysis of the semipurified taxine mixture by gradient HPLC-DAD revealed the presence of seven taxanes with 10-deacetylbaccatin III (10-DAB III) among them. All the nine expected taxines were positively identified (Table 1).

CONCLUSIONS

Taxines were the subject of very few reported works over the last two decades although, until the 1960s, they were in the heart of phytochemical work on *Taxus*. The major reason for this is the instability of taxines and the unavailability of reference compounds. It can be concluded that HPLC seems to be the best method for the analysis of taxines because all the publications reporting on the analysis of taxines employ HPLC. Since taxines are abundant in plants, they could offer an attractive alternative for the supply of high-value taxanes by semisynthesis.

REFERENCES

1. Wilson, C.R.; Sauer, J.-M.; Hooser, S.B. Taxines: A review of the mechanism and toxicity of yew (*Taxus* spp.) alkaloids. Toxicon **2001**, *39*, 175–185.
2. Kingston, D.G.I. Natural taxoids: Structure and chemistry. In *Paclitaxel Science and Application*; Suffness, M., Ed.; CRC Press: Boca Raton, 1995; 287–315.
3. Appendino, G. Naturally occurring taxanes. In *The Chemistry and Pharmacology of Paclitaxel and Its Derivatives*; Farina, V., Ed.; Elsevier: Amsterdam, 1995; 7–53.

4. Baxter, J.N.; Lythgoe, B.; Scales, B.; Scrowston, R.M.; Trippet, S. Taxine: part I. isolation studies and the functional group of *O*-cinnamoytaxicin-I. J. Chem. Soc. **1962**, 2964–2971.
5. Ettouati, L.; Ahond, A.; Poupat, C.; Potier, P. Revision structurale de la taxine B, alcaloide majortitaire des feulilies de l if Europe, *Taxus baccata*. J. Nat. Prod. **1991**, *54*, 1455–1458.
6. VanHaelen-Fastre, R.; Diallo, B.; Jaziri, M.; Faes, M.-L.; Homes VanHaelen, M. High speed countercurrent chromatography separation of taxol and related diterpenoids from *Taxus baccata*. J. Liq. Chromatogr. **1992**, *15*, 697–706.
7. Jenniskens, L.H.D.; van Rozendaal, E.L.M.; van Beek, T.A.; Wiegerinck, P.H.G.; Scheeren, H.W. Identification of six taxine alkaloids from *Taxus baccata* needles. J. Nat. Prod. **1996**, *59*, 117–123.
8. Adeline, M.T.; Wang, X.P.; Poupat, C.; Ahod, A.; Potier, P. Evaluation of taxoids from *Taxus* sp. crude extracts by high performance liquid chromatography. J. Liq. Chromatogr. Relat. Technol. **1997**, *20*, 3135–3145.
9. Theodoridis, G.; Laskaris, G.; Verpoorte, R. HPLC analysis of taxoids in plant and plant cell tissue culture. Am. Biotechnol. Lab. **1999**, *17*, 40–44.
10. Theodoridis, G.; Laskaris, G.; de Jong, C.; Hofte, A.J.P.; Verpoorte, R. Determination of paclitaxel and related diterpenoids in plant extracts by high performance liquid chromatography with UV detection in high performance liquid chromatography-mass spectrometry. J. Chromatogr. A, **1998**, *802*, 297–305.
11. Theodoridis, G.; Verpoorte, R. Taxol analysis by HPLC. A review. Phytochem. Anal. **1996**, *7*, 169–184.
12. Theodoridis, G.; Laskaris, G.; van Rozendaal, E.L.M.; Verpoorte, R. Analysis of taxines in *Taxus* seeds, needles and cell culture by HPLC-PDA and HPLC-ESI-MS. J. Liq. Chromatogr. **2001**, *24*, 2267–2282.
13. Castor, T.P.; Tyler, T.A. Determination of taxol in *Taxus* × *media* needles in the presence of interfering components. J. Liq. Chromatogr. **1993**, *16*, 723–731.

Taxoids: TLC Analysis

Tomasz Mroczek
Kazimierz Glowniak
Department of Pharmacognosy, Medical University of Lublin, Lublin, Poland

INTRODUCTION

Taxoids (Fig. 1) are diterpenoid compounds isolated from different yew species and possessing strong anticancer activity. They are applied usually in the treatment of cancers resistant to other antineoplastic drugs such as cisplatin or in conjunction with them. There are different chemical groups of natural taxoids, but among the most important is a group derived from 10-deacetylbaccatin III (10-DAB III), a diterpenoid compound occurring in high concentration in European yew, *Taxus baccata* L. It possesses a skeleton of four rings (6/8/6/4-membered), named taxan, and is a derivative of hexahydroxy-11-taxen-9-one. Baccatin III, which is another compound in this group, has in addition an acetyl group esterified with a β-OH group at position C-10. Paclitaxel and cephalomannine are less polar taxoids because they possess amide-acid side chains at position C-13. In case of paclitaxel, this is (2*R*,3*S*)-*N*-benzoyl-3-phenylisoserine, and in cephalomannine, (2*R*,3*S*)-*N*-tigloyl-3-phenylisoserine. There are also compounds in this group that have an epimer OH group at position C-7, and other substituents are also met. Thus, there are many compounds, usually with similar polarity and small differences in structure, that are difficult to separate.[1]

DESCRIPTION OF METHOD

Thin-layer chromatography (TLC) is mainly applied in micropreparative taxoid separation.[2–4] Silica gel $60F_{254}$ preparative plates are usually employed for this purpose. The problem of taxoid separation involves not only their similar chemical structure (e.g., paclitaxel vs. cephalomannine) but also the different coextracted compounds usually encountered in crude yew extracts (polar compounds such as phenolics and non-polar ones such as chlorophylls and biflavones); the separation is therefore very difficult. The common band of paclitaxel and cephalomannine was satisfactorily resolved from the extraneous fraction in isocratic elution with ethylacetate as polar modifier[4] and *n*-heptane–dichloromethane as solvent mixture, and was of suitable purity for high-performance liquid chromatography (HPLC) quantitative determination. The combination of micropreparative TLC separation of callus extract of *T. baccata* with *n*-hexane–ethylacetate (2:3) mobile phase and preparative HPLC on Lichrosorb RP-18 column enabled 10-DAB III isolation.[3]

Systematic studies on selection of the best mobile phases to ensure the best micropreparative separation of analyzed taxoids—especially of 10-DAB III as well as its less polar derivatives, baccatin III, paclitaxel, and cephalomannine, obtained from the extracts of fresh and dried needles and stems of *T. baccata*—have been undertaken by Mroczek and Głowniak.[2] The TLC investigation on silica gel included solvent systems with one and two polar modifiers and multicomponent mobile phases, as well as some multiple development techniques and gradient elutions. As polar modifiers, methanol, acetone, dioxane, ethylacetate and ethylmethylketone as well as their mixtures were reinvestigated; dichloromethane, chloroform, benzene, toluene, heptane, and their mixtures were used as solvents.

Using binary mobile phases containing 25–30% of one polar electron-donor modifier (acetone, dioxane) in dichloromethane or chloroform, high values of separation factor α (10-DAB III/paclitaxel) are observed as well as low elution of polar ballast compounds. Such chromatographic systems can be applied in separation by column chromatography (CC) of polar from less polar taxoids and their polar coextracted compounds in preliminary CC investigations on taxoids before further detailed studies. The addition (even just 15%) of a small amount of π-electron solvents such as benzene improves the separation of the band of less polar taxoids (paclitaxel, cephalomannine) and closely eluted chlorophylls. Mobile phases with two polar modifiers (acetone–methanol, ethylmethylketone–methanol) ensure relatively high values of α factor and the separation in the area of less polar taxoids is better in comparison with the separation obtained by single electron-donor mobile phases.

Because of the complexity of composition of yew extracts, different gradient elutions can be considered as further steps of detailed CC or TLC separations of different taxoids on silica gel.

The multicomponent solvent system consisted of benzene–chloroform–acetone–methanol (20:92.5:15:7.5) developed over a distance of 15 cm (2×; in some cases, a third development was necessary), which enabled very good separation of coextracted compounds with both 10-DAB III

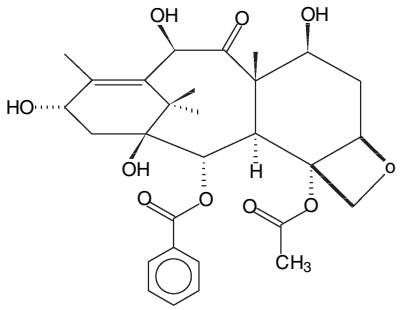

10-Deacetylbaccatin III (10-DAB III)

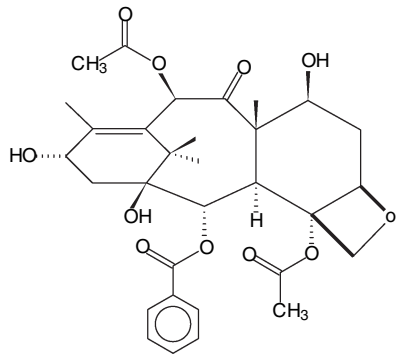

Baccatin III

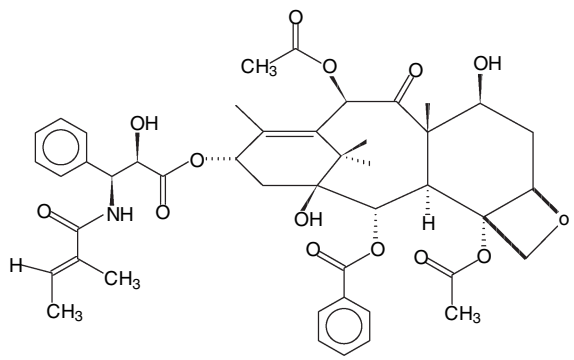

Cephalomannine

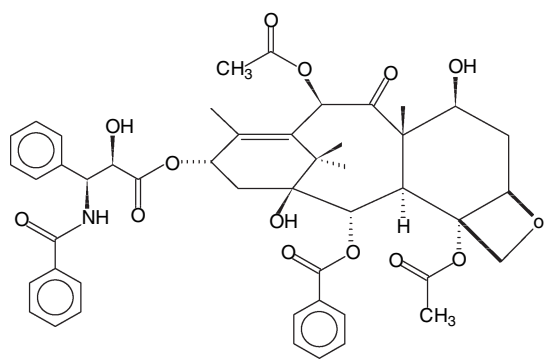

Paclitaxel

Fig. 1 Chemical structures of taxoids.

and paclitaxel; the separation of whole yew extracts (*T. baccata*) was also very good. The separation of taxoids was better in extracts obtained from fresh needles and stems than from dried plant material. The extracts from the dried needles contained the highest concentrations of ballast compounds interfering with the bands of analyzed taxoids. The common band of paclitaxel, cephalomannine, and baccatin III was satisfactory purified from coextractives; the 10-DAB III band could be easily isolated and further HPLC determination in two isocratic mobile phases was applied. The investigated taxoids eluted in the following order: paclitaxel + cephalomannine, baccatin III, and 10-DAB III. An interesting observation was the considerable slope of baccatin III retention on silica gel in comparison with that of its 10-deacetyl derivative (10-DAB III) (α 10-DAB III/baccatin III amounted to 2.8).[2] This indicates the more hydrophobic properties of baccatin III. This chromatographic behavior of baccatin III can be explained first by lack of a free OH group at position C-10 capable of competing with free OH groups on the surface of silica gel (hydrogen-bonding interactions). On the other hand, the presence of an acetyl (ester) group at position C-10 can impede adsorption of baccatin III on silica gel due to hydrogen-bonding interactions between the carbonyl group at position C-9 and OH groups on the surface of silica gel (a

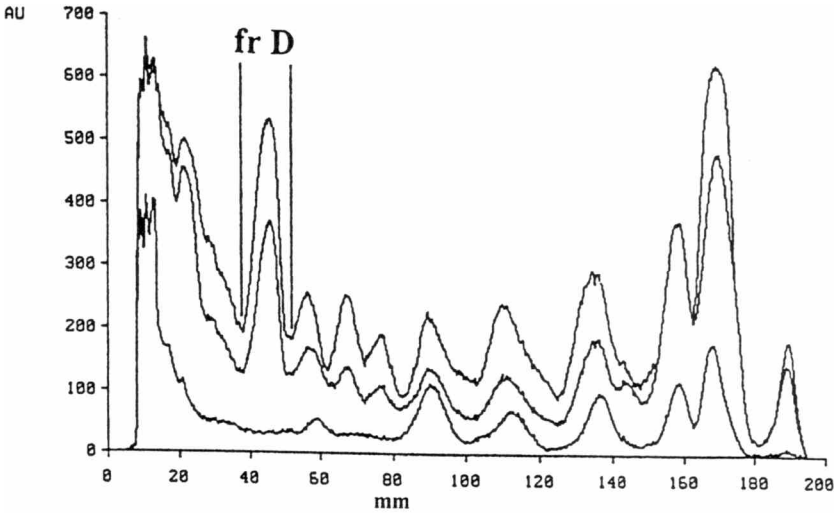

Fig. 2 Densitogram obtained from a preparative thin-layer chromatogram of the 10-DAB III fraction from the preparative column. TLC was performed on a 200 mm × 200 mm plate coated with a 0.5 mm layer of silica (E. Merck); the mobile phase was dichloromethane–dioxane–acetone–methanol, 84:10:5:1 (v/v). The chromatogram was scanned at three wavelengths—366, 254, and 230 nm (down to up) —by means of a Camag 3 scanner. The fraction isolated is indicated as "fr D".
Source: From Application of pseudo-reversed-phase systems to the purification and isolation of biologically active taxoids from plant materials, in chromatographia[7] © Vieweg Verlag/ *Chromatographia*, 2002.

kind of spherical hindrance, observed in computer modeling of spatial structure of taxoids by HYPERCHEM). The role of this carbonyl group in the polar properties of taxoids was confirmed by analysis of ^{1}H-NMR spectra. This can be responsible for the decrease of baccatin III retention on silica gel, which is similar to the retention of paclitaxel and cephalomannine, both of which possess an acetyl group at position C-10 and a low-polar side chain at position C-13. Because of the very slight difference in the structure of the amide substituent of the acyl side chain at position C-13 (*N*-benzoyl vs. *N*-tigloyl) and low polarities, these two compounds have the same retention on silica gel.

Similar solvent systems can be applied for analytical TLC of taxoids in screening of, for example, callus cultures for taxoid presence.[5]

Another approach in taxoid preparative separation included solid-phase extraction (alumina, silica, or RP-8 cartridges) followed by preparative TLC on silica gel plates with quaternary mobile phase consisting of dichloromethane–dioxane–acetone–methanol (83:5:10:2, v/v).[6,7] In this way, 10-DAB III, paclitaxel, and cephalomannine as well as two further taxoids could be easily isolated with relatively high efficiencies from yew materials (Fig. 2). Multiple development technique or further separation of the isolated taxoid fractions (especially less polar ones) on RP-2 silica bond stationary phase with methanol–water mixtures as mobile phases was applied for purification of the compounds isolated. 10-DAB III isolated in this way was relatively pure, as was shown in reversed-phase (RP)-HPLC analysis (Fig. 3).

An RP-TLC system with tertiary mobile phase [stationary phase: RP-18 F254s; mobile phase: water–methanol–tetrahydrofuran (5:2:3, v/v/v) applied twice] was used in the analysis of taxoid fractions obtained after high-speed countercurrent chromatography (HSCCC) isolation and was suitable for paclitaxel and cephalomannine qualitative determination.[8]

High-performance TLC/densitometric paclitaxel quantitative determination in different yew samples with two-stage gradient development has also been attempted[9] but, due to the high concentration of coextractives, it is difficult to estimate the precision of this method.

Stasko et al.[10] elaborated two interesting procedures of multimodal TLC for the separation of paclitaxel and related compounds from *T. brevifolia*. In the first procedure, a cyano-modified silica gel plate was developed, in the first dimension, in dichloromethane–hexane–acetic acid (9:10:1) and, in the second dimension, in water–acetonitrile–methanol–tetrahydrofuran (8:5:7:0.1). In the second procedure, a diphenyl-modified silica gel plate was developed, in the first dimension, in hexane–isopropanol–acetone (15:2:3) and, in the second dimension, in methanol–water (7:3). These two methods enabled paclitaxel resolution from both cephalomannine, which is impossible on silica gel plates, and at least 20 other compounds.

Fujino et al.[11] described an interesting radio-TLC method for the analysis of paclitaxel and its 3-OH and 6-OH metabolites. After incubation of ^{14}C-paclitaxel with human liver microsomes, the supernatants were developed using a solvent system consisting of toluene–acetone–formic acid (60:39:1, v/v) and quantified with a bioimaging analyzer. The results obtained correlated well with those from RP-HPLC.

Besides typical UV detection on plates with a fluorescent agent (F_{254}), different visualization methods can be applied:

1. Anisaldehyde spray reagent[10] (76% methanol, 19% *O*-phosphoric acid, and 5% *p*-anisaldehyde) followed by heating at 110°C for 5 min. Paclitaxel appears as a gray-brown spot.
2. A 3% sulfuric acid methanolic solution followed by heating at 115°C for 5 min (visualization: UV at 366 nm and VIS).[8]

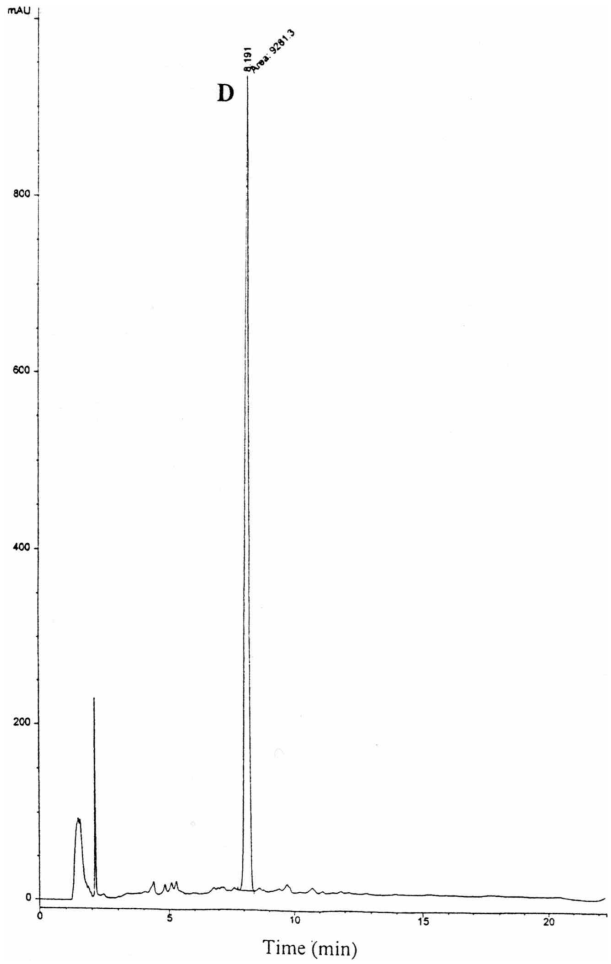

Fig. 3 HPLC chromatogram obtained from the TLC fraction containing 10-DAB III (D) as shown in Fig. 1. A 5 μm Waters Symmetry Shield C_{18} column, 150 mm × 4.6 mm I.D. was used and eluted with the gradient of acetonitrile in double distilled water.

Source: From Application of pseudo-reversed-phase systems to the purification and isolation of biologically active taxoids from plant materials, in Chromatographia.[7] © Vieweg Verlag/ *Chromatographia*, 2002.

3. A 3% sulfuric acid ethanolic solution, then a 1.5% solution of vanillin in ethanol, followed by heating at 105°C for 10 min.[5] DAB III appears as a gray spot.

CONCLUSIONS

Summing up this review, it should be emphasized that because of differences in composition of taxoids and other compounds in different yew and yew-derived materials, a suitable approach for TLC taxoid separation ought to include problems involving both taxoid separation and appropriate separation of coextracted compounds from taxoids, which usually are in higher concentration. The separation method should also be elaborated precisely for each type of extract. A combination of various solid-phase extraction and chromatographic techniques seems to be the most relevant approach to efficient preparative separation of taxoids.

REFERENCES

1. Suffness, M.; Cordell, G.A. *Taxus* alkaloids. In *The Alkaloids (Chemistry and Pharmacology)*; Brossi, A., Ed.; Academic Press: New York, 1985; Vol. 25, 6–18.
2. Głowniak, K.; Mroczek, T. Investigations of preparative thin-layer chromatographic separation of taxoids from *Taxus baccata* L. J. Liq. Chromatogr. **1999**, *22* (16), 2483–2502.
3. Zhiri, M.; Jaziri, Y.; Guo, R.; Vanhaelen-Fastre, M.; Vanhaelen, J.; Homes, K.; Yoshimatsu, K.; Shimomura, K. Tissue cultures of *Taxus baccata* as a source of 10-deacetylbaccatin III, precursor for the hemisynthesis of taxol. Biol. Chem. Hoppe-Seyler **1995**, *376*, 583–586.
4. Głowniak, K.; Zgórka, G.; Józefczyk, A.; Furmanowa, M. Sample preparation for taxol and cephalomannine determination in various organs of *Taxus* sp. J. Pharm. Biomed. Anal. **1996**, *14*, 1215–1220.
5. Gou, Y.; Jaziri, M.; Diallo, B.; Vanhaelen-Fastre, R.; Zhiri, A.; Vanhaelen, M.; Homes, J.; Bombardelli, E. Immunological detection and quantitation of 10-deacetylbaccatin III in *Taxus* sp. Biol. Chem. Hoppe-Seyler **1994**, *375*, 281–287.
6. Hajnos, M.L.; Głowniak, K.; Waksmundzka-Hajnos, M.; Kogut, P. Optimization of the isolation of some taxoids from yew tissues. J. Planar Chromatogr. **2001**, *14*, 119–125.
7. Hajnos, M.L.; Głowniak, K.; Waksmundzka-Hajnos, M.; Piasecka, S. Application of pseudo-reversed-phase systems to the purification and isolation of biologically active taxoids from plant materials. Chromatographia **2002**, *56* (Suppl.), S91–94.
8. Vanhaelen-Fastre, R.; Diallo, B.; Jaziri, M.; Faes, M.L.; Homes, J.; Vanhaelen, M. High-speed countercurrent chromatographic separation of taxol and related diterpenoids from *Taxus baccata*. J. Liq. Chromatogr. **1992**, *15* (4), 697–706.
9. Matysik, G.; Głowniak, K.; Józefczyk, A.; Furmanowa, M. Stepwise gradient thin-layer chromatography and densitometric determination of taxol in extracts from various species of *Taxus*. Chromatographia **1995**, *78* (41), 485–487.
10. Stasko, M.W.; Witherup, K.M.; Ghiorzi, T.J.; Mc Cloud, T.G.; Look, S.; Muschik, G.M.; Issaq, H.J. Multimodal thin-layer chromatographic separation of taxol and related compounds from *Taxus brevifolia*. J. Liq. Chromatogr. **1989**, *12* (11), 2133–2143.
11. Fujino, H.; Yamada, I.; Shimada, S.; Yoneda, M. Simultaneous determination of taxol and its metabolites in microsomal samples by a simple thin-layer chromatography radioactivity assay—inhibitory effect of NK-104, a new inhibitor of HMG-CoA reductase. J. Chromatogr. A, **2001**, *757*, 143–150.

Temperature Program: Anatomy

Raymond P.W. Scott
Scientific Detectors Ltd., Banbury, Oxfordshire, U.K.

INTRODUCTION

The principle of temperature programing in gas chromatography (GC) is based on the thermodynamic explanation of retention and is employed for samples that have components that cover a wide range of polarities and/or molecular weights. Its purpose is to accelerate the late eluting peaks through the column to reduce the analysis time and, at the same time, to maintain symmetrical elution profiles that are amenable to accurate quantitative assessment. As the temperature is increased, the magnitude of the distribution coefficient with respect to the stationary phase is reduced and, as a consequence, the retention volume and retention time is reduced. The programing rate must be chosen such that the integrity of the separation is maintained and the peak shapes are not distorted.

DISCUSSION

The programing procedure usually involves three stages. An initial isocratic period is introduced to efficiently separate the early eluting peaks with adequate resolution. The isocratic period is followed by a linear increase in column temperature with time, which accelerates the well-retained peaks so that they also elute in a reasonable time and are adequately resolved. The effect of linear programing can be calculated employing appropriate equations and the retention times of each solute predicted for different flow rates (see *Programmed Temperature GC*, p. 1918). To do this, some basic retention data must be measured at two temperatures and the results are then employed in the retention calculations. The temperature program often ends with a final isothermal period. This is usually introduced either because the upper temperature limit of the stationary phase has been reached and so a higher temperature will damage the column, or to purge any remaining, strongly retained solutes from the column. The upper temperature limit of the stationary phase should not be exceeded, as not only will the column be spoiled but the performance of the detector is often impaired and deposits are formed that can permanently increase the detector noise. Temperature programing is employed in most GC separations and the optimum programing conditions are usually easy to identify from a few preliminary separations using different gradients. If, however, there is a pair of solutes that elute close together (e.g., a pair of enantiomers) and there is a temperature of coelution, then some considerable effort may be necessary to identify the optimum temperature program[1] to achieve a satisfactory separation in a reasonable time.

Such situations, however, are not common, unless the applications involves complex samples such as multicomponent chiral mixtures.

REFERENCE

1. Beesley, T.E.; Scott, R.P.W. *Chiral Chromatography*; John Wiley & Sons: Chichester, 1998; 39.

BIBLIOGRAPHY

1. Scott, R.P.W. *Techniques of Chromatography*; Marcel Dekker, Inc.: New York, 1995.
2. Scott, R.P.W. *Introduction to Analytical Gas Chromatography*; Marcel Dekker, Inc.: New York, 1998.

Temperature: Effect on MEKC Separation

Koji Otsuka
Shigeru Terabe
Department of Material Science, Himeji Institute of Technology, Hyogo, Japan

INTRODUCTION

The distribution coefficient, K, of a solute for an equilibrium between the aqueous phase and micelle, or the micellar solubilization, depends on temperature; generally, the distribution coefficient decreases with an increase in temperature. This means that the migration time of a solute, t_R, will be reduced when the temperature is elevated under typical micellar electrokinetic chromatogaphy (MEKC) conditions, where, for example, sodium dodecyl sulfate (SDS) is employed as a pseudo-stationary phase at a neutral condition (i.e., pH 7). Also, the velocity of the electro-osmotic flow (EOF), u_{EOF} and the electrophoretic velocity of the micelle, u_{cp} (mc), will be increased by an increase in temperature because of a reduced viscosity of the micellar solution employed in a MEKC system.

DISCUSSION

The increase in temperature during a separation is observed to be due to Joule heating: Ideally, the retention factor, k, should be independent of the applied voltage or current, but, actually, k does depend on the applied voltage. Although the temperature of the separation capillary is controlled with a liquid coolant or a circulating airstream in most commercially available capillary electrophoresis (CE) instruments, the retention factor usually decreases, almost linearly, with an increase in the velocity of the EOF or an increase in the current. However, the dependence is much less than that observed in a CE system without forced-cooling apparatus.

The critical micelle concentration (CMC) and the partial specific volume, $\bar{v}$ depend on the temperature. The relationship between k and K is represented as

$$k = K\left(\frac{V_{mc}}{V_{aq}}\right) \tag{1}$$

where V_{mc} and V_{aq} are the volumes of the micelle and the remaining aqueous phase, respectively. The phase ratio, V_{mc}/V_{aq} is described as

$$\frac{V_{mc}}{V_{aq}} = \frac{\bar{v}(C_{sf} - \mathrm{CMC})}{1 - \bar{v}(C_{sf} - \mathrm{CMC})} \tag{2}$$

where C_{sf} is the surfactant concentration. Approximately, the volume of the micelle is negligible and, hence, Eq. 1 can be rewritten as

$$k = K\bar{v}(C_{sf} - \mathrm{CMC}) \tag{3}$$

For example, the CMC of SDS and $\bar{v}$ of the SDS micelle depend on temperature as presented in Table 1, where a 100 m*M* borate–50 m*M* phosphate buffer (pH 7.0) was used to prepare SDS solutions. It should be noted that the CMC value observed in a buffer solution or electrolyte solution is smaller than that in pure water (e.g., 8.1 m*M* at 20°C).

In MEKC, an ionic surfactant is used as a pseudo-stationary phase, and the Krafft point is also an important temperature. At a temperatures lower than the Krafft point, C_{sf} does not exceed the CMC, due to reduced solubility and, therefore, no micelle is formed. At the Krafft point, C_{sf} reaches the CMC and then the formation of the micelle is begun. The Krafft point of SDS is ~16°C in a pure water, whereas it is ~31°C for potassium dodecyl sulfate in pure water. Thus, a

Table 1 CMC of SDS and $\bar{v}$ of SDS micelle dependence on temperature.

Temp. (°C)	CMC (m*M*)	$\bar{v}$ (ml/g)
20	—	0.8562
22	2.8	—
25	2.9	0.8610
30	2.5	0.8686
35	2.6	0.8710
40	3.0	0.8758

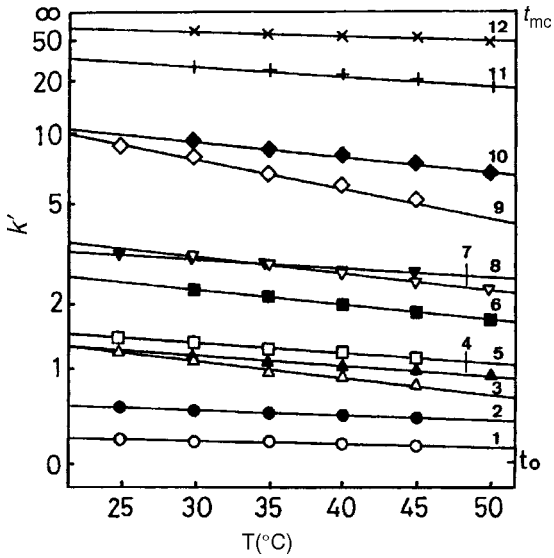

Fig. 1 Dependence of the retention factor, k', on temperature, T. The solutes are (1) resorcinol, (2) phenol, (3) *p*-nitroaniline, (4) *o*-cresol, (5) nitrobenzene, (6) 2,6-xylenol, (7) 2,4-xylenol, (8) toluene, (9) 2-naphthol, (10) *p*-propylphenol, (11) *p*-butylphenol, and (12) *p*-amylphenol. Capillary: 50 μm I.D. × 570 mm (effective length, 500 mm); separation solution: 50 m*M* SDS in 100 m*M* borate–50 m*M* phosphate buffer (pH 7.0); applied voltage: 15 kV; detection wavelength: 214 nm.
Source: From Micellar electrokinetic chromatography, in *Capillary Electrophoresis Technology*.[3]

potassium salt is not an adequate buffer component for the SDS/MEKC system.

Fig. 1 shows the dependence of the distribution coefficients on temperature for several solutes in MEKC, where SDS is employed as a pseudo-stationary phase. Different dependencies are observed among the solutes; that is, temperature affects the selectivity.

As mentioned, temperature seriously affects the migration time, whereas its effect on selectivity is not remarkable. It is important to maintain temperature precisely to obtain reproducible results.

REFERENCES

1. Terabe, S.; Otsuka, K.; Ando, T. Electrokinetic chromatography with micellar solution and open-tubular capillary. Anal. Chem. **1985**, *57*, 834.
2. Terabe, S.; Katsura, T.; Okada, Y.; Ishihama, Y.; Otsuka, K. Measurement of thermodynamic quantities of micellar solubilization by micellar electrokinetic chromatography with sodium dodecyl sulfate. J. Microcol. Separ. **1993**, *5*, 23.
3. Terabe, S. Micellar electrokinetic chromatography. In *Capillary Electrophoresis Technology*; Guzman, N.A., Ed.; Marcel Dekker, Inc.: New York, 1993; Vol. 64, Chap. 2.
4. Otsuka, K.; Terabe, S. Micellar electrokinetic chromatography. Bull. Chem. Soc. Jpn. **1998**, *71*, 2465.

Temperature: Mobility, Selectivity, and Resolution in CE

Jetse C. Reijenga
Department of Chemical Engineering and Chemistry, Eindhoven University of Technology, Eindhoven, The Netherlands

INTRODUCTION

Although not a major separation parameter, as in gas chromatography, the operating temperature clearly affects migration behavior in capillary electrophoresis (CE). This alone should be reason to work under uniform, well-thermostated conditions. The temperature affects bulk viscosity, electro-osmotic flow (EOF), ionic mobilities, even pK values and buffer pH.

BUFFER BEHAVIOR

A buffer for electrophoresis is usually prepared at room temperature by adding ingredients and measuring the final pH. When this buffer is used for CE at a different temperature, a different pH might result. For example, when a buffer consists of Tris-acetate at pH 5, Tris is fully charged and the temperature dependence of pK of acetic acid is the one involved. This value is small so that the pH of the buffer is virtually independent of temperature. This is not the case if the same buffer ingredients are used to prepare a buffer around pH 8; in that case, acetate is fully ionized and the pK of Tris is involved. This pK has a temperature coefficient of − 0.031 per degree; a 10°C increase leads to a 0.31 decrease in buffer pH (Table 1).

Table 1 pK Values and their temperature dependence of some buffer components.

Name	pK (20°C)	dpK/dT
Phosphoric acid, pK_1	2.12	*M*
Citric acid, pK_1	3.13	*M*
Formic acid	3.75	–0.000
Glycine, pK_1	3.75	–0.000
Acetic acid	4.76	–0.000
Histidine	6.12	–0.045
MES	6.15	–0.011
ACES	6.90	–0.020
Imidazole	6.95	–0.018
MOPS	7.20	–0.006
HEPES	7.55	–0.014
Tris	8.30	–0.031
Boric acid	9.24	–0.007
CHES	9.50	–0.009
Glycine, pK_2	9.77	*M*
CAPS	10.40	–0.009

In case of single-buffering background electrolyte solutions, the temperature coefficient of the buffer pH equals the temperature coefficient of the pK of the buffering ion. In case of a double-buffering system, pK's of both buffer anion and buffer cation are involved, which obviously makes the situation potentially more complicated.

In some situations, the pH of the buffer can be very critical. An example of such a critical pair of components is given in Fig. 1; a mixture of benzoic and 2,3-dimethoxy benzoic acid, analyzed around pH 4.67. A pH change of as little as 0.04 pH units will change the migration order.

Another aspect involved is buffer conductivity; on average, ionic conductivities have a temperature coefficient of around 2.5%/degree. A higher temperature, therefore (at constant voltage), leads to a higher current. This can have a significant effect on power dissipation and, through the corresponding plate-height terms, on separation efficiency (see *Band Broadening in CE*, p. 144).

SAMPLE ION BEHAVIOR

Ionic mobilities generally have a temperature coefficient of around +2.5%/degree, but it is not exactly the same for all ions. Incidentally, water viscosity has a temperature coefficient of approximately –2.5%/degree. This sometimes leads to the erroneous conclusion that ionic mobility is, by definition, inversely proportional to liquid viscosity, which is an oversimplification, originating also from the following relationship:

$$\mu = \frac{q}{6\pi\eta r}$$

in which q is the effective charge, η is the liquid viscosity, and r is the radius. The misunderstanding is that, in reality, the above relationship is valid only for rigid spherical particles, not necessarily for individual solvated ions.

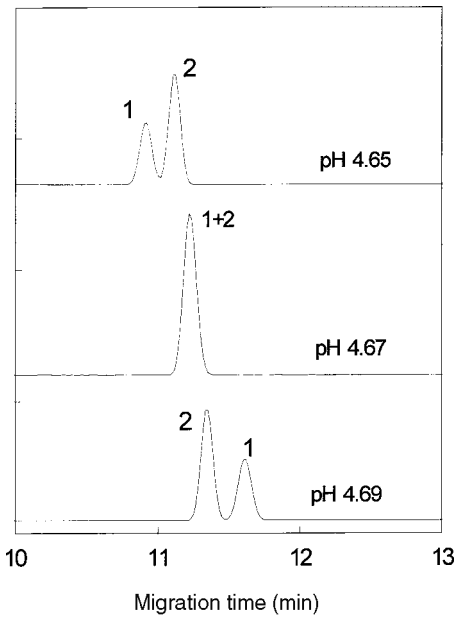

Fig. 1 Separation of benzoic acid (1) and 2,3-methoxy benzoic acid in 10 m*M* Tris-acetic acid buffer of three different pH values.

For the electro-osmotic flow, temperature-induced viscosity change at the plane of shear for the electric double layer is more straightforward. Analysis times will generally shorten with increasing temperature.

BIBLIOGRAPHY

1. Boček, P.; Deml, M.; Gebauer, P.; Dolník, V. *Analytical Isotachophoresis*; VCH: Weinheim, 1988.
2. Everaerts, F.M.; Beckers, J.L.; Verheggen, Th.P.E.M. *Isotachophoresis: Theory, Instrumentation and Applications*; Elsevier: Amsterdam, 1976.
3. Friedl, W.; Reijenga, J.C.; Kenndler, E. Ionic strength and charge number correction for mobilities of multivalent organic anions in capillary electrophoresis. J. Chromatogr. A, **1995**, *709*, 163.
4. Mohan, C. Buffers. *A Guide for the Preparation and Use of Buffers in Biological Systems*; Calbiochem: San Diego, CA, 1997.
5. Reijenga, J.C.; Kenndler, E. Computational simulation of migration and dispersion in free capillary zone electrophoresis: I. Description of the theoretical model. J. Chromatogr. A, **1994**, *659*, 403.
6. Reijenga, J.C.; Kenndler, E. Computational simulation of migration and dispersion in free capillary zone electrophories: II. Results of simulation and comparison with measurements. J. Chromatogr. A, **1994**, *659*, 417.
7. Reijenga, J.C.; Verheggen, Th.P.E.M.; Martens, J.H.P.A.; Everaerts, F.M. Buffer capacity, ionic strength and heat dissipation in capillary electrophoresis. J. Chromatogr. A, **1996**, *744*, 147.

Terpenoids: HPLC Separation

Gabriela Cimpan
Sirius Analytical Instruments Ltd., East Sussex, U.K.

INTRODUCTION

Terpenoids are C_{10} and C_{15}, usually volatile, organic compounds derived from plants; they are generally associated with characteristic fragrances. Some terpenes are alcohols (e.g., menthol from peppermint oil), and some terpenes are aldehydes (e.g., citronellal). Terpenes are made up of isoprene (C_5) units. Because terpenoids occur in complex mixtures in natural products or in plants, chromatography is a powerful method for their separation and further analysis. Gas chromatography (GC) provides good separations and low detection limits for the volatile compounds. This was the reason for the delay in the development of high-performance liquid chromatography (HPLC) methods for terpenoids and has become the method of choice for the non-volatile, thermolabile, or polar compounds.

OVERVIEW

High-performance liquid chromatography can be used as a separation method of volatile compounds, followed by GC or GC/MS for further separation and analysis. The most common assay is performed by reversed-phase HPLC, usually on C_{18}, when the separation of the compounds is according to their hydrophobicity, i.e., according to chain length and polar groups.

Sonication and liquid chromatography are a rapid pair of techniques for extraction and fractionation of plant material. The method combines extraction by sonication with a mixture of non-miscible solvents, rapid preseparation of the crude extract by vacuum-liquid chromatography (silica gel 60H), and separation by preparative, reversed-phase HPLC or classical liquid chromatography with polyvinylpyrrolidone.

HPLC can be also used as an analytical method for the separation, identification, and quantification of terpenoids.

TERPENOID ANALYSIS

The use of diode-array detection is limited because many of the terpenoids do not have chromophores for the UV region. Refractive index, evaporative light scattering detectors (ELSD), or low-UV detectors can overcome, to a certain extent, this problem. However, the refractive index detector has a lower sensitivity compared with the spectrophotometric detectors, and it will not be useful for trace analysis. The organic solvents used for the mobile-phase composition absorb the low-UV radiation, and this is another problem for the terpenoids analysis by HPLC.

Temperature influences dramatically the separations; in the literature, assays can be found performed at −15°C, with pentane as mobile phase on LiChrosorb Si60.

The stationary phase is usually C_8 or C_{18}, but the use of Spherisorb CN or Nucleosil columns was also reported. The mobile phase for reversed-phase chromatography is aqueous, while, for normal-phase chromatography, it generally contains pentane or hexane. The elution can be isocratic or with a gradient. The detection is usually UV in the range 116–254 nm.

One of the most studied plants is *Ginkgo biloba* because of its medical applications. *Ginkolides* are a group of unique terpene lactones with properties of improving cardiovascular and cerebrovascular activities. Ginko terpene lactones have very weak absorption below 220 nm; therefore HPLC cannot be coupled with UV detection methods. Infrared was proposed as an alternative, but HPLC/MS and HPLC/NMR have produced the best results in terms of simplicity, sensitivity, and selectivity. High-performance liquid chromatography-evaporative light-scattering detection (HPLC/ELSD) is an economic option for this type of measurements.

Ginkgolide A, B, C, and bilobalide in *G. biloba* leaves were determined simultaneously by RP/HPLC/ELSD. Methanolic extracts (10%) of the leaves were cleaned up by solid-phase extraction (SPE) via polyamide cartridge and silica gel cartridge, successively. RP/HPLC was carried out on a C_{18} column with MeOH–H_2O as mobile phase, eluted in gradient mode, and detected by ELSD. The poor linear response of ELSD could be compensated by multilevel calibration and logarithmic calculation. Methanol–water–orthophosphoric acid mobile phase was used in conjunction with refractive index (RI) detection.

Terpenes in *G. biloba* L. extracts were analyzed on a column packed with C_8 Nucleosil 300, and PrOH–THF–H_2O was used as the mobile phase with detection at 220 nm.

High-performance liquid chromatography was the first method of choice for the non-volatile terpenes as terpene trilactones. The analysis is performed by RP/HPLC on C_{18} with isocratic development either in methanol–water or methanol–water–THF. Detection can be carried out by

UV (taking into consideration poor UV absorption of the compounds), RI, ELSD, or MS.

Sesquiterpenes

Sesquiterpenes are C-15 terpenoids which can be found in natural products as hydrocarbons, oxygenated forms (aldehydes, ketones, etc.), or lactones. Sesquiterpene lactones can be found in a limited number of plant species and often have therapeutic properties.

The major constituents of the plant *Ambrosia maritima* L. were isolated using thin-layer chromatography (TLC) and identified by IR and GC/MS. From HPLC screening, ambrosin and damsin were detected at high levels in the leaves and flowers, while stems and seeds contained only traces. Sesquiterpenes from *Aucklandia lappa* (Decne.) were determined by HPLC. A Shim-pack CLC-ODS column (6.0×150 mm) was used as separation column, MeOH–H_2O (65:35) as mobile phase, and the detection wavelength was 225 nm.

The GC/MS and HPLC analyses of oils from *Salvia sclarea* provided a comparative analysis profile of different plant materials. Sesquiterpene hydrocarbons (e.g., germacrene D and β-caryophyllene), monoterpene alcohols (e.g., α-terpineol), diterpenoids (mainly sclareol), monoterpene hydrocarbons (e.g., myrcene, limonene, and the two ocimene isomers), and the principal components (linalyl acetate and linalool) were analyzed.

Two comparable procedures of reverse-phase HPLC with spectrophotometric detection at 254 nm, with mobile phases of MeOH–0.05 *M* acetate buffer (70 : 30) or THF–0.01 *M* phosphate buffer (55 : 45), were used to resolve leukomisin, matricarin, austricin, anhydroaustricin, and potential antiarteriosclerotic sesquiterpene lactones from aerial parts of *Artemisia leucodes*.

A new HPLC technique has been developed for the rapid analysis of sesquiterpene phytoalexins such as capsidiol, rishitin, luminin, and phytuberol. This method employs a cyanopropyl-bonded-phase column with an isocratic mixture of hexane and isopropanol. Flame ionization and UV detection were used for the analysis of capsidiol, rishitin, lubimin, phytuberol, and debneyol. Although both detectors proved to be useful, the signal response with the flame ionization detector was proportional to the mass of each of the phytoalexins, while the signal with the UV detector was proportional to the number of carbon–carbon bonds in each of the compounds.

The antifungal sesquiterpene dialdehydes polygodial and warburganal, from *Polygonum hydropiper*, were determined by HPLC on an ODS column using methanol–H_2O as a mobile phase. These sesquiterpene dialdehydes were accumulated in young leaves and shoots and possessed antifungal activity.

Fourteen sesquiterpenes of *Petasites hybridus* (L.) G.M. et Sch. were separated on a normal-phase Nucleosil 100-3 column with hexane-diisopropyl ether-acetonitrile mixtures as eluents and photodiode array detection.

Sesquiterpenes were also separated by chiral chromatography on a Chiracel OD column.

Sometimes, the analyzed compounds absorb significantly only below 220 nm. In this case, postcolumn derivatization was used for a better UV detection.

Terpenes

A liquid chromatography-tandem mass spectrometry (LC/MS/MS) method was developed to detect tumor-promoting diterpene esters of the tigliane and ingenane types within plant extracts. Fractionation on a C_{18} HPLC column was followed by MS/MS-multiple reaction monitoring (MRM).

Liquid chromatographic-thermospray mass spectrometry (LC/TSP/MS) was used for the analysis of crude plant extracts containing phenolic and terpene glycosides. In crude plant extracts, constituents of biological or pharmaceutical interest often exist in the form of glycosides. Mass spectral investigations of these metabolites require soft ionization techniques such as desorption chemical ionization (D/CI) or fast atom bombardment if information on molecular mass or sugar sequence is desired. Thermospray provides mass spectra similar to those obtained with positive-ion D/CI/MS using NH_3 and thus is potentially applicable to online analyses for these compounds and can be applied to plant extract analysis. Extracts of Gentianaceae, Polygalaceae, and Leguminosae species have been screened by LC/TSP/MS. High-performance liquid chromatography was performed on reversed-phase columns using methanol–water or acetonitrile–water gradients. Good optimization of the temperature of the source and the vaporizer was crucial for the observation of pseudomolecular ions of glycosides.

Triterpenes

Bisdesmosidic triterpene saponins were isolated from the aquatic plant *Ranunculus fluitans* L. (Ranunculaceae) in the Rhine river. The saponin structures were established by the identification of the aglycon and sugar moieties by HPLC and chiral capillary zone electrophoresis (CZE), ion-spray LC/MS, and extensive 1-D and 2-D homonuclear and heteronuclear NMR spectroscopy.

Many triterpene derivatives (some of them being new compounds) were isolated from the AcOEt fraction of Brazilian medicinal plant Carucaa, *Cordia multispicata* (Boraginaceae). The separation was performed on silica gel and reversed-phase HPLC columns, and the structures were elucidated by means of spectral methods, especially with 2-D NMR.

Several ginsenosides, previously obtained from *Panax ginseng* and *Panax notoginseng*, were analyzed by HPLC.

A new HPLC method permitted the separation of 13 triterpene glycosides isolated from different Astragalus species within 40 min. A water/acetonitrile gradient was used as eluent, RP-18 was used as stationary phase, and evaporative light scattering detection was used. The method facilitated differentiation of different Astragalus species.

Preparative HPLC

Successful preparative separations were obtained for pure compounds by RP/HPLC. When normal-phase chromatography was used, better results were obtained if the silica-based stationary phase was treated with silver ions.

Preparative HPLC was used to separate sterols and triterpene alcohols from the unsaponifiable matter in plant oils from *Camellia weiningensis* L., *Brassica juncea* L., and *Microula sikkimensis*. The isolated compounds were acetylated and further purified by $AgNO_3$-impregnated silica gel preparative TLC. The identification was done by IR and MS.

Oryzanols are mixtures of ferulic acid esters of triterpene alcohols and plant sterols. Oryzanols were extracted from crude rice by column chromatography on a silica gel column using different volumes and ratios of hexane and di-Et ether. The fraction containing 18% oryzanol was further enriched by rechromatography, then 98% pure oryzanol was crystallized.

Coupled Methods with HPLC

High-performance liquid chromatography can be coupled, online, with high-resolution gas chromatography (HRGC) and MS. Gas chromatography allows the separation of chemically similar compounds from the previous separation provided by HPLC between the compounds with different polarities.

When thermolabile compounds are present, GC cannot be used, so MS can be coupled directly with HPLC. Care should be taken when using ionization methods, as MS does not provide a characteristic fragment pattern and the molecule cannot be identified precisely.

Natural products are often sources for drugs. When screening a natural compound extract, many of the analyzed compounds have been analyzed previously; therefore a method capable of selecting the new compounds such as HPLC/NMR/MS is very useful. Many plant extracts were analyzed by this method. Alternatively, HPLC/UV/MS can be used to obtain rich spectral information [application on *Tanacetum parthenium* (L.) Schultz Bip., Asteraceae].

BIBLIOGRAPHY

1. Li, W.; Fitzloff, J.F. Simultaneous determination of terpene lactones and flavonoid aglycones in ginkgo biloba by high-performance liquid chromatography with evaporative light scattering detection. J. Pharm. Biomed. Anal. **2002**, *30*, 67–75.
2. Merfort, I. Review on the analytical techniques of sesquiterpenes and sesquiterpene lactones. J. Chromatogr. A, **2002**, *967*, 115–130.
3. Nishii, Y.; Yoshida, T.; Tanabe, Y. Enantiomeric resolution of a germacrene. D derivative by chiral high-performance liquid chromatography. Biosci. Biotechnol. Biochem. **1997**, *61* (3), 547.
4. van Beek, T.A. Chemical analysis of ginkgo *biloba* leaves and extracts. J. Chromatogr. A, **2002**, *967*, 21–55.
5. Vogg, G.; Achatz, A.; Kettrup, A.; Sandermann, A., Jr. Fast, sensitive and selective liquid chromatographic-tandem mass spectrometric determination of tumor-promoting diterpene esters. J. Chromatogr. A, **1999**, *855*, 563–573.
6. Wilson, I.D. Multiple hyphenation of liquid chromatography with nuclear magnetic resonance spectroscopy, mass spectrometry and beyond. J. Chromatogr. A, **2000**, *892*, 315–327.

Terpenoids: TLC Analysis

Simion Gocan
Department of Analytical Chemistry, Babes-Bolyai University, Cluj-Napoca, Romania

INTRODUCTION

Terpenes are among the most widespread and chemically diverse groups of natural products. Fortunately, despite their structural diversity, they have a simple unifying feature by which they are defined and by which they may be easily classified. Terpenes are a unique group of hydrocarbons, based on isoprene or an isopentane structure.

Terpenes can be classified by the number of five-carbon units they contain: hemiterpene (C_5), monoterpene (C_{10}), sesquiterpene (C_{15}), diterpene (C_{20}), triterpene (C_{30}), and tetraterpene (C_{40}). Like the monoterpenes, most of the sesquiterpenes are considered to be essential oils because they belong to the steam distillable fraction. Diterpenes have higher boiling points; they are considered to be resins. Triterpenes include common triterpenes, steroids, saponins, sterolins, and cardiac glycosides. The most common tetraterpenoids are the carotenoids. Sesquiterpenes exist in a variety of forms, including linear, bicyclic, and tricyclic frameworks. The type of cyclization can be with open chain, mono-, bi-cyclic, etc. Also, the number and positions of the double bonds, the asymmetric centers, and the type and number of functional groups distinguish numerous components of each group.

Terpenoids can be classified also into hydrocarbons, alcohols, carbonyl compounds, phenols, acids, esters, oxides, and peroxides.

CHROMATOGRAPHIC SEPARATION

Hydrocarbons

Generally speaking, thin-layer chromatography (TLC) has a large number of applications. The first problem with which the analyst is confronted concerns gathering information regarding the mixture to be separated, in terms of mixture polarity and the range of molecular masses. In the case of hydrocarbons that have one no-polar character, an adsorption separation technique is recommended. Terpene hydrocarbons (mono- and sesquiterpene) can be conveniently separated on layers of silica gel or alumina. Moreover, highly active layers are necessary. After the usual drying, they have to be stored in a vacuum desiccator at 30 mm Hg, containing potassium hydroxide as a desiccant. Because of the weak polar nature of the compounds, solvents of low polarity must be used as mobile phases for the separation. The most frequently used solvents as the mobile phase are as follows: petroleum ether, hexane, isopentane, dimethylbutane, cyclohexane, methylcyclohexane, benzene, chloroform, benzene-acetone (95:5, v/v), benzene-ethyl acetate (2:1, v/v), and toluene. The choice of solvent depends upon the polarities of the components of the terpene hydrocarbon mixtures on the desired separation. For the detection (visualization) of the compounds after separation, the solvent will be evaporated from the plate and various zones will be indicated by spraying with suitable reagents. On spraying with a fluorescein solution and exposing to bromine vapor, compounds that absorb bromine faster than the fluorescein show up as yellow spots on a pink background. Other reagents can be used for detection with good results; they include iodine vapor, vanilin/H_2SO_4, or $KMnO_4/H_2SO_4$, and a chloroform solution of antimony pentachloride. Very unreactive compounds can be located by spraying with a concentrated sulfuric–nitric acid mixture and heating to cause charring of the compounds.[1,2] Table 1 gives the R_f values of some terpenes on silica gel and alumina in various solvents used as mobile phases.

A good separation of sesquiterpene hydrocarbons has been performed on alumina in combination with a perfloroalkane (70°C to 80°C) mobile phase.[3]

To increase the resolution in TLC separation of some monoterpenes, silver nitrate-impregnated silica gel, with benzene as the mobile phase, was used. Three conclusions were drawn from these studies:[7] 1) cyclic terpenes with a single internal double bond did not readily form a π-complex; 2) cyclic or acyclic terpenes with two non-terminal double bonds do not readily form π-complexes unless the double bonds are *cis* conjugated; and 3) cyclic or acyclic terpenes with exocyclic or terminal double bonds do form π-complexes.

The silver nitrate-impregnated silica gel (25%) was applied to the separation of some sesquiterpenes. It was found that a mixture of β-selinene and caryophyllene could be separated satisfactorily by development with *n*-hexane and benzene–acetone (95:5, v/v) as mobile phases.[8] After the development, the plates are dried in air and then sprayed with a solution of chlorosulfonic acid in acetic acid (1:2) and heated at 130°C. Usually, different colored spots are observed, e.g., humulene, brown; caryophyllene, blue; longifolene, pink.

Oxygenated Terpenes

The problem of identifying individual compounds from essential oils is often complicated by the similarities in

Table 1 hR_f values of terpenes and color reaction with vanillin/H_2SO_4 reagent.

	Silica gel					Alumina			Silica gel impregnated $AgNO_3$		
									25%	3.125%	Vanillin/H_2SO_4 color
Compound	S_1	S_2	S_3	S_4	S_5	S_1	S_6	S_7	S_8		after 30 min
Monoterpenes											
Camphene	83	84	79	94	79	95			53		Light orange
p-Cymene	67	38	62	95	60	89					None
Limonene	41	54	96	66					35	62.5	Bluish green
d-Limonene	76					93					Bluish green
β-Myrcene	74					92					Blue
Mircene									20	50.5	Blue
α-Ocimene	71					91					Blue
t-β-Ocimene	71					91					Blue
Ocimene									35	52.0	Blue
α-Phellandrene									41	63.0	Blue
β-Phellandrene	79					93			50		Blue
α-Pinene	90	83	84	96	83	96			67		Blue
β-Pinene	88	80	75			95			46		Blue
α-Pyronene	80					90					Blue
β-Pyronene	80					90					Blue
Sabinene	75					93			29		Blue
Terpinolene	75	64	60			92			62		Bluish green
α-Terpinene	76					93			49	70.5	Bluish green
γ-Terpinene	76					93			59		Bluish green
α-Thujene	80					95					Blue
Verbenene	81					95					Blue
Sesquiterpenes											
		F	G								
γ-Bisabolene	71	10	8			93	50	33			Brownish green
δ-Cadinene	72	20	12			93	71	35			Dark blue
β-Caryophyllene	74	30	16			94	65	44			Purple
α-Cedrene	89	44	36			96	73	56			Purple
α-Humulene	65	12	8			90	35	30			Lavender
β-Santalene	78	20	15			94	64	48			Dark blue
β-Selenene	78	17	13			94	41	33			Dark green
Valencene	76	21	17			93	51	32			Maroon
Yalangene	88	40	32			96	87	64			Lavender
β-Zingaberene	75	18	13			94	57	30			Dark green

S_1 = Skellysolve B (hexanes);[3] S_2 = hexane;[4] S_3 = cyclohexane;[4] S_4 = benzene;[5] S_5 = 15% ethyl acetate in hexane;[5] S_6 = perfluoroalkene, b.p. 70–80°C;[3] S_7 = low boiling perfluokerosene;[3] S_8 = benzene, 25% $AgNO_3$,[6] and 3.125% $AgNO_3$.[7] Vanillin/H_2SO_4.[3]

molecular structures and physical properties. In a very important instance, the R_f values serve as a means of distinguishing two classes of material-hydrocarbons from non-hydrocarbons. Hydrocarbons have an appreciable R_f value with hexane as the mobile phase, whereas non-hydrocarbons have an R_f equal to zero (Table 2). By use of this property, it is possible to separate hydrocarbons from oxygenated compounds for the preparation of terpene oils. Table 2 contains the hR_f values of oxygenated terpenes on a silica gel thin-layer plate in different solvents that have been found useful for characterizing these types of materials.

Terpene Alcohols

The alcohols were chromatographed on silica gel using various eluent systems. The compounds were detected with the fluorescein–bromine reagent. The phosphomolybdenic acid reagent is very sensitive but non-specific. The anisaldehyde-sulfuric acid reagent is of higher sensitivity and specificity.

It is possible to achieve a separation of the stereoisomeric menthols on silica gel G layers using chloroform and a series of solvents that are nearly isoeluotropic with chloroform.[2] The following hR_f values were obtained: menthol, 32; isomenthol, 29; neomenthol, 40; and neoisomenthol, 36. With anisaldehide-sulfuric acid, a blue violet color is obtained. Another example is the stereoisomeric separation of *trans*, *trans*-farnesol, and *cis*, *trans*-farnesol on silica gel using ethyl acetate–benzene (5:95, v/v) as the mobile phase, giving hR_f values of 27 and 36, respectively. For the detection of these substances, the vanillin/H_2SO_4 reagent proved suitable.[10] This system, slightly modified, which used benzene-ethyl acetate (80:20, v/v), gives a good separation of all the

Table 2 hR_f values of some oxygenated terpenes and other essential oil constituents on silica gel in various eluent systems.

	Eluent system							
Compound	**S_1**	**S_2**	**S_3**	**S_4**	**S_5**	**S_6**	**S_7**	**Reagent**
Alcohols								
Citronellol	0	19	27	39	41	14		Yellow brown[a]
Nerol	0	14	26	38	42	16		Yellow brown[a]
Geraniol	0	12	20	40	43	15		Yellow brown[a]
Linalool	0	15	36	47	45	25		Yellow brown[a]
α-Terpineol	0	8	29	34	36	16		Yellow brown[a]
Menthol						21		
d-Neomentol						29		Yellow brown[a]
Borneol						17		
Aldehydes								
Citral	0	15	45	64	57		10	Yellow brown[b]
Lauric aldehyde	4	50	58	72	67			
Cinnamaldehyde	0	9	31	70	68			Orange brown[b]
Vanillin						5		Yellow orange[b]
Asarylaldehyde						6		Orange[b]
Furfural	0	6	21	44	41	10		Violet[b]
Anisaldehyde						13		Yellow[b]
Cuminic aldehyde						25		Yellow[b]
Benzaldehyde						25		
Ketones								
Carvone	0	37	45	72	62		10	Gray brown[b]
Methyl heptenone	0	35	48	74	62		13	Gray brown[b]
Pulegone	0	60	58	65	76			
Camphor	0	28	56	39	55			
Fenchone							9	Gray brown[b]
Piperitone							8	Gray brown[b]
Menthone							20	Gray brown[b]
Methyl nonyl ketone							16	Gray brown[b]
Esters								
Geranyl acetate	0	27	69	66	52			Gray blue[c]
Neryl acetate	0	39	69	56	50			Gray blue[c]
Citronellyl acetate	0	35	68	66	57			
Octyl acetate	0	50	98	98	82			
Terpinyl acetate	0	42	66	61	55			Gray blue[c]
Methyl anthranilate	0	26	52	65	53			
Ethyl anthranilate	0	25	58	70	46			
Carvyl acetate	0	64	69	79	67			
Oxides								
1,8-Cineol	0	12	48	68	68			
Linalool monoxide	0	3	21	20	20			

S_1 = hexane;[4] S_2 = chloroform (alcohol-free);[4] S_3 = ethyl acetate–hexane (15:85, v/v);[4] S_4 = ethyl acetate–chloroform (alcohol-free) (10:90, v/v);[4] S_5 = ethyl acetate–benzene (15:85, v/v);[4] S_6 = ethyl acetate–benzene (5:95, v/v);[9] S_7 = benzene.[2]
[a]Antimony pentachloride.
[b]*o*-Dianisidine.
[c]Vanillin/H_2SO_4.

stereoisomers of farnesol present in a commercial mixture, as well as other terpene alcohols.[11]

The silver nitrate-impregnated silica gel G was used to obtain a separation with a group of tetracyclic triterpene alcohols, which could not be separated on untreated silica gel. However, on silica gel G (Ag impregnated), the R_f values were sufficiently different so as to enable the substances to be identified separately. Chloroform was used as the mobile phase. The tetracyclic triterpenes were detected by spraying with one of the three reagents: 50% sulfuric acid in water or 10% phosphomolibdic acid in ethanol or chlorosulfonic and acetic acids (1:2) followed by heating in an oven at 150°C.[12]

Besides normal-phase TLC, reversed-phase TLC was used by impregnating the silica gel layer with paraffin or silicone oil and using hydrophilic solvents as mobile phases. By this method, it is possible to achieve a good separation of alcohols belonging to groups with the same number of carbon atoms.

Acids and Esters

Essential oils often contain esters of terpene alcohols; the most common are the acetates, formates, propionates, etc. The separation of different esters was performed on silica gel layers, using benzene, chloroform, and other similar solvents as mobile phases. All of the color reactions for terpene alcohols can be used for the detection of their esters. No differences have been observed in the color esters function as a result of their acid nature.

A group of triterpenic acids were found in *Bredemeyera floribunda*, *Alphitonia excelsa*, and *Crataegus oxyacantha*.[13] The separation was carried out on silica gel layers using diisopropyl ether–acetone (5:2, v/v). In this case, oleanic, oleanonic, ursolic, and betulinic acids showed the same hR_f value, i.e., 68. As cochalic, bredemolic, and machaerinic acids gave tailings in this eluent, addition of 5% pyridine to the same solvent gave the following R_f values: 15, 62, and 27, respectively. The compounds were detected with chlorosulfonic acid.

Another example of applications concerning separation of piperonylic, 5-, 2-, and 6-methoxypiperonylic acids was performed on silica gel layers using ethyl acetate–hexane–acetic acid (50:50:0.5, v/v) as the mobile phase. Detection was performed by spraying with a chromotropic–sulfuric acid reagent. With these conditions the following hR_f values of 64, 54, 47, and 37 were obtained, respectively.[14]

Aldehydes and Ketones

These compounds appear in various essential oils and are distinguished by characteristic odors. Some of them are easily produced by synthesis and are frequently used in the perfume industry. Aldehydes and ketones can be separated on silica gel thin-layer plates with solvents such as hexane, chloroform, and benzene in different proportions with ethyl acetate, or only in chloroform or benzene. The detection of the aldehydes can be performed by spraying with a solution of *o*-dianisidine in glacial acetic acid. Some ketones can be detected with the fluorescein–bromine spray, but compounds such as camphor, which are very unreactive, could be detected only by spraying with concentrated sulfuric acid containing nitric acid, followed by heat. A 5% solution of $AlCl_3$ in ethanol is specific for sesquiterpene lactones. Other terpenes, steroids, antrachinones, glycosides, and alkaloids do not interfere, nor do other types of lactones such as coumarins, cardenolides, and saturated or unsaturated γ-lactones. The reaction gives a violet or brown color on the layer, or yellow, brown, or green fluorescence under UV radiation at 366 nm, after spraying a plate with reagent solution and heating at 120°C for 10 to 15 min.[15]

The 2,4-dinitrophenylhydrazones have also been used as a means of separating terpene carbonyl compounds. The oxo-terpene was separated by means of these derivatives using silica gel with chloroform-carbon tetrachloride in various proportions (1:19, 1:9, 1:5.6 v/v) as well as petroleum ether-benzene (3:7, v/v). No spraying agent was used, as the spots themselves were distinctly colored.[16]

The ionone derivatives and pseudoionones were separated on silica gel layers with benzene as the mobile phase. The compounds, after development, were detected by spraying with either 2,4-dinitrophenylhydrazine or a vanillin-sulfuric acid mixture. The following mean R_f values were obtained: pseudoionone, 0.384; α-ionone, 0.580; β-ionone, 0.505; α-methylionone, 0.756; and β-methylionone, 0.699.[17] For improved separation, 14 terpenoids, e.g., α- and β-ionone, were subjected to TLC on silica gel impregnated with 15% $AgIO_3$, with benzene-ethyl acetate (4:1, v/v) as the mobile phase. The spots were detected by spraying the dried plate with methanol-sulfuric acid and heated at 110°C. The R_f values obtained were approximately equal to or considerably higher than those obtained on $AgNO_3$-impregnated plates.[18]

Oxides and Peroxides

Oxides and peroxides can occur in many essential oils by a photochemical reaction. 1,8-Cineol and linalool monoxide can be readily separated on silica gel thin layers with 1-nitropropane-hexane (1:1, v/v), as the mobile phase.[4] In this case, they have exhibited R_f values of 73 and 8, respectively.[4] Another pair of compounds, ascaridole and 1,8-cineol, can be easily separated on a silica gel layer, obtaining a value for chloroform as the mobile phase of 63 and 54, respectively.[2] The antimony chloride reagent gives a gray color. The potassium iodide-acetic acid-starch test is usually better than ferrous thiocyanate.

Phenylpropane and Phenol Derivatives

The separation of the hydroxyphenylpropane derivatives used in medicine and the perfume industry is of particular interest. Today, many useful drugs can be obtained from plants. TLC is one of the most rapid methods for the identification of the active substances in medicinal plant extracts containing hydroxyphenyl propane derivatives. Using silica gel plates with benzene solvent as the mobile phase could separate a series of these compounds. Besides silica gel thin layers, alumina and polyamide layers were used in combination with different solvents as mobile phases, for instance, chloroform, petroleum ether–acetic acid (95:5, v/v), or petroleum ether–pyridine (95:5, v/v). There are many different color reagents that can be used for the detection of the spots. A blue coloration is obtained after spraying with the phosphomolybdic acid reagent. The clearest color distinction is obtained by spraying a mixture of antimony tri- and penta-chloride (1:1), or anisaldehyde-sulfuric acid. Antimony trichloride solution makes the colors intense, but the spots do not show fluorescence immediately in long-wave UV light; but it does appear in about 1 day. Besides the R_f values, the colors of fluorescence can contribute to the identification of some compounds. For instance, eugenol methyl ether gives a greenish-yellow

fluorescence, and isoeugenol methyl ether (*cis–trans* mixture) shows up reddish brown.[1,2]

The following rules were obtained from the R_f values of a large group of phenylpropane and phenol derivatives under the conditions described above: 1) The polarity of the compound increases with increasing number of free phenol groups (OH). 2) Methylation of the hydroxyl group (OCH_3) decreases the polarity. The R_f values decrease with increasing of the methoxy number. For silica gel with benzene as the mobile phase in a saturation chamber: anethol, 1 OCH_3, h$R_f = 56$; eugenolmethyl ether, 2 OCH_3, h$R_f = 15$; and asarone, 3 OCH_3, h$R_f = 10$. 3) The effect of hydrogen bond formation between two adjacent phenolic groups and the consequent decrease in the polarity: *ortho*-compound < *p*-compound (safrol, h$R_f = 57$, and catechol, h$R_f = 0$). 4) Increase in the size of the alkylating group decreases the polarity: propenyl guaetol < benzyleugenol < methyleugenol. 5) When functional groups are situated closely together, the adsorption affinity of each is decreased and the R_f value of the compound increases. 6) The introduction of an aliphatic side chain on the nucleus has a negligible effect on the R_f values.[1,2]

Phenylpropane derivatives (feluric, caffeic, and chlorogenic acids) and flavonoids were identified in a methanolic extract from flowers of *Sambuci nigra* by using TLC on silica gel 60 F_{254}. The efficiency of 10 TLC eluent systems was investigated by three mathematical techniques. It has been established that the favorable mobile phases for TLC of compounds investigated are ethyl acetate–methanol–water (100:13.5:2.5:10, v/v) and ethyl acetate–formic acid–water (8:1:1, v/v).[19] In the same manner, there were selected optional solvent systems for the separation of caffeic acid, chlorogenic acid, and some flavonoids from methanolic extracts from *Lavandula flos*. It has been shown that the best eluent systems are ethyl acetate–formic acid acetic acid–water (100:11:11:27, v/v) and ethyl acetate formic acid–water (8:1:1, v/v).[20] Also, for TLC separation of the methanolic extract from *Rosmarinus officinalis* L. the system ethyl acetate–formic acid–acetic acid–water (100:11:11:27, v/v) has been found.[21] Detection of the phenolic acids and flavonoids was achieved by spraying the plates with 1% methanolic diphenylboryloxyethylamine, then 5% ethanolic polyethylene glycol 4000. The chromatograms were evaluated in UV light at 366 nm (phenolic acids appeared as blue spots and flavonoids as orange-yellow fluorescent spots).[22]

REFERENCES

1. Kirchner, J.G. *Thin-Layer Chromatography,* 2nd Ed.; John Wiley & Sons: New York, 1978; 897–923.
2. Stahl, E. *Thin-Layer Chromatography, A Laboratory Handbook*; Springer-Verlag: Berlin, 1965; 187–210.
3. Attaway, J.A.; Barabas, L.J.; Wolford, R.W. Analysis of terpene hydrocarbons by thin layer chromatography. Anal. Chem. **1965**, *37*, 1289–1290.
4. Miller, J.M.; Kirchner, J.K. Chromatostrips for identifying constituents of essential oils. Anal. Chem. **1953**, *25*, 1107–1108.
5. Kirchner, J.G.; Miller, J.M.; Keller, G.J. Separation and identification of some terpenes by new chromatographic technique. Anal. Chem. **1951**, *23*, 420–425.
6. Schantz, M.V.; Juvonen, S.; Hemming, R. Trennung von monoterpenen mittels silbernitrat-kieselgeldünnschichten. J. Chromatogr. **1965**, *20*, 618–620.
7. Lawrence, B.M. The use of silver nitrate impregnated silica gel layers in the separation of monoterpene hydrocarbons. J. Chromatogr. **1968**, *38*, 535–537.
8. Gupta, A.S.; Dev, S. Chromatography of organic compounds: I. thin-layer chromatography of olefins. J. Chromatogr. **1963**, *12*, 189–195.
9. Schantz, M.V.; Juvonen, S.; Oksanen, A.; Hakamaa, I. Abtrennung von terpenalkoholen aus terpengemischen als 3,5-dinitrobenzoate auf kieselgel-dünnschichtenSeparation of terpene alcohols from terpene mixtures as their 3,5-dinitrobenzoates on Kieselgel thin layers. J. Chromatogr. **1968**, *38*, 364–372.
10. Tyihák, E.; Vágujfalvi, D.V.; Hágony, P.L. Die gas- und dünnschichtchromatographische trennung der stereoisomeren farnesole und ihrer derivate I. Mitteilung. trans-trans und cis-trans-farnesol und derivate. J. Chromatogr. **1963**, *11*, 45–49.
11. McSweeney, G.P. Two methods for the thin-layer chromatographic separation of terpene alcohols and identification by a colour reaction. J. Chromatogr. **1965**, *17*, 183–185.
12. Ikan, R. Thin-layer chromatography of tetracyclic triterpenes on silica impregnated with silver nitrate. J. Chromatogr. **1965**, *17*, 591–593.
13. Tschesche, R.; Lampert, F.; Santzke, G. Über triterpene: VII. Dünnschicht- und ionenaustauscherpapierchromatographie von triterpenoiden. J. Chromatogr. **1961**, *5*, 217–224.
14. Beroza, M.; Jones, W.A. Silicic acid chromatography of methoxypiperonylic acids. Anal. Chem. **1962**, *34*, 1029–1030.
15. Villar, A.; Rios, J.L.; Simeon, S.; Zafra-Polo, M.C. New reagent for the detection of sesquiterpene lactones by thin-layer chromatography. J. Chromatogr. **1984**, *303*, 306–308.
16. Vashist, V.N.; Handa, K.L. Separation of 2.4-dinitrophenylhydrazones of oxo-terpenes by thin-layer chromatography. J. Chromatogr. **1965**, *18*, 412–413.
17. Dhont, J.H.; Dijkman, G.J. Separation of some isomeric ionones and methylionones by multiple thin-layer chromatography. Analyst **1964**, *89* (1063), 681–682.
18. Kohli, J.C.; Badaisha, K.K. Improved procedure for the thin-layer chromatography of terpenoids on silver ion-silica gel layers. J. Chromatogr. **1985**, *320*, 455–456.
19. Males, Z.; Medić-Šarić, M. J. Planar Chromatogr.-Mod. TLC **1999**, *12*, 345–349.
20. Medic-Saric, M.; Males, Z. Selection of an optimal set of solvents in thin-layer chromatography of flavonoids and phenolic acids of Lavandulae flos. Pharmazie **1999**, *54* (5), 362–364.
21. Medić-Šarić, M.; Males, Z. J. Planar Chromatogr. -Mod. TLC **1997**, *10*, 182–187.
22. Wagner, H.; Bladt, S.; Zainski, E.M. *Drogenanalyse*; Springer-Verlag: Berlin, 1983.

Thermodynamics of GPC/SEC Separation

Iwao Teraoka
Department of Chemistry, Polytechnic University, Brooklyn, New York, U.S.A.

INTRODUCTION

As with most other chromatographic separation methods, gel permeation chromatography–size-exclusion chromatography (GPC–SEC) is based on partitioning of analyte polymer molecules between the stationary phase (which, in the case of GPC–SEC, is contained within the pores of a porous stationary-phase support) and the mobile phase. Ideally, the mobile phase establishes a concentration equilibrium with the stationary phase at each plate in the column before being transferred to the next plate. The concentration equilibrium is dictated by an equal chemical potential of the polymer chain between the two phases.[1,2] In normal conditions of GPC–SEC, the polymer concentration c_M in the mobile phase is sufficiently low, and the solution behaves ideally dilute. Its chemical potential μ_M per molecule in the mobile phase is then given as

$$\mu_M = \mu^0 + k_B T \ln\left(\frac{c_M}{c^0}\right) \tag{1}$$

where μ^0 and c^0 are the chemical potential and the concentration, respectively, at an appropriate reference state, k_B is the Boltzmann constant, and T is the temperature. In the stationary phase, the chemical potential μ_S has additional terms due to changes in the entropy and the enthalpy upon bringing the polymer chain into the stationary phase:

$$\mu_S = \mu_0 + k_B T \ln\left(\frac{c_S}{c^0}\right) - T\Delta S + \Delta H \tag{2}$$

where c_S is the polymer concentration in the stationary phase, and ΔS and ΔH refer to the changes per chain. The partition coefficient K, defined as the ratio of the two concentrations, is then given as

$$K \equiv \frac{c_S}{c_M} = \exp\left(\frac{\Delta S}{k_B} - \frac{\Delta H}{k_B T}\right) \tag{3}$$

The primary purpose of GPC–SEC is to obtain a retention curve that represents the molecular weight (MW) distribution of the analyte. Because the retention volume is a linear function of the partition coefficient, the coefficient must be a monotonically decreasing or increasing function of MW.

In GPC–SEC, porous beads of various pore sizes are used as separating media. The solution in the pore channels is the stationary phase, and the volume of liquid between the beads constitutes the mobile phase. A linear polymer chain can take different conformations in the unrestricted mobile phase. The number of conformations, W, increases in a power law of N, with N being the degree of polymerization. In the stationary phase, however, all of the monomers on a single chain have to reside within the pore space. Thus, W does not increase as rapidly with N as in the mobile phase. Because the conformational entropy of the polymer chain is calculated as $k_B \ln W$, the geometrical confinement of the pore makes $\Delta S < 0$. The way $|\Delta S|$ increases with N is determined by the geometry of the polymer chain (whether the chain is linear or branched, whether the chain is swollen or not, whether the chain is stiff or not, etc.) and the pore geometry, but $|\Delta S|$ is roughly a function of the chain dimension to the pore size, as shown below. The detailed atomic sequence in each polymer is rather of second importance. This feature is responsible for the universality of GPC–SEC.

Columns used in GPC–SEC are supposed to provide negligible ΔH regardless of MW for a given polymer. Otherwise, the dependence of ΔH on MW, different from that of ΔS, will complicate the analysis of the retention curve. Furthermore, ΔH would exhibit widely different characteristics determined by the interactions among the polymer, the pore surface, and the solvent, and thus negate the universality of GPC–SEC. With negligible ΔH, the partition coefficient is determined solely by the decrease in the conformational entropy:

$$K = \exp\left(\frac{\Delta S}{k_B}\right) \tag{4}$$

Equivalently, K is the ratio of the probability to place the polymer chain in the pore without touching the pore walls, averaged over different conformations.

As MW increases, K decreases from 1 to 0. To have a high resolution in GPC–SEC, the dependence of K on MW needs to be sharp. Users of GPC–SEC also want the range of MW analysis in a single run to be as broad as possible, typically three to five decades. The finite range of K, however, makes the two requirements mutually exclusive, a severe restriction on the resolution. The resolution can be improved by increasing the number of theoretical plates, typically employing smaller porous beads and connecting a multiple columns in series. In normal-phase and reversed-phase high-performance liquid chromatography (RPHPLC), by contrast, a stationary phase that gives a large value of K,

in excess of unity, offers high resolution and a broad range of analyte composition in a relatively short column.

PARTITION COEFFICIENT

Examples for the plots of the partition coefficient as a function of the chain dimension are shown for some of the geometries of polymer molecules in a cylindrical pore of radius R_P. The simplest geometry is a sphere. The center of a spherical molecule of radius R_S is not allowed to get closer to the pore wall beyond the distance equal to the sphere radius. The ratio of the volume accessible to the sphere center to the total pore volume gives the partition coefficient. In Fig. 1, the two volumes are indicated by the interior and the exterior cylinders, respectively. Then,

$$K = \left(1 - \frac{R_S}{R_P}\right)^2 \tag{5}$$

The partition coefficient of a Gaussian chain of radius of gyration R_g was calculated by Casassa[3] and the partition coefficient of a rodlike molecule was obtained by Giddings et al.[4] The results are compared in Fig. 2. When plotted as a function of R_g/R_P, the three polymer geometries show only a small difference, except that, at large R_g/R_P, the rodlike molecule has a larger K than the other two geometries of the molecule. The plots were converted to functions of N, in Fig. 3, for the monomer size a equal to $R_P/100$. The partition coefficient of a star-branched polymer, in which each arm takes a Gaussian conformation, was calculated by Casassa and Tagami.[5]

The partition coefficient for a real chain (excluded volume chain) has not been obtained except by the scaling theory.[6] The theory gives only a qualitative relationship between K and N for chains sufficiently longer than the pore size ($R_g \gg R_P$):

$$\frac{\Delta S}{k_B} \equiv -N\left(\frac{a}{R_P}\right)^{1/\nu} \approx -\left(\frac{R_g}{R_P}\right)^{1/\nu} \tag{6}$$

where $\nu \approx 0.588$. A computer simulation result shows that, compared at the same R_g, the real chain has a slightly larger K than the ideal chain that allows monomer overlap.[7] It is

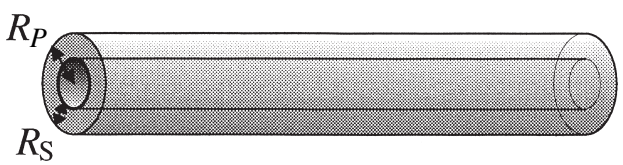

Fig. 1 The volume accessible to the center of a spherical molecule of radius R_S within a cylindrical pore of radius R_P is the interior cylinder of radius $R_S - R_P$.

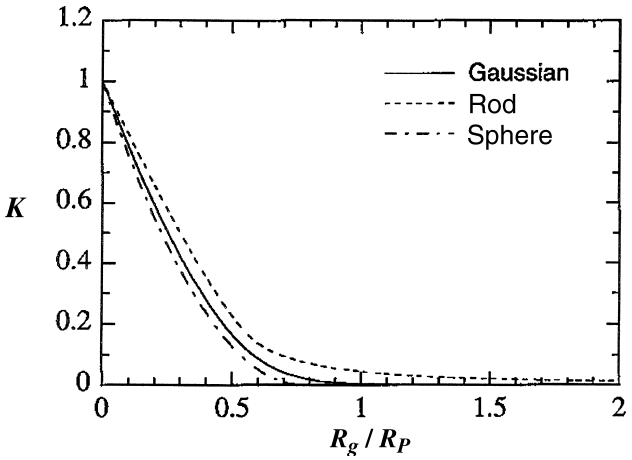

Fig. 2 Partition coefficient K plotted as a function of the radius of gyration R_g relative to the pore radius R_P for a spherical molecule, Gaussian chain, and a rodlike molecule.

common to both models for sufficiently long chains that $K \sim \exp(-\beta M)$, where β is a numerical coefficient and M is the molecular weight.

All of the currently used porous packing materials have a three-dimensional network structure, effectively giving rise to a pore size distribution. In these separating media, the dependence of K on N will be less sharp compared with the one in Fig. 3. It is desired by chromatographers that the retention time is a linear function of log M. Because the retention time is a linear function of K, the plot of K needs to be a linear function of log M in as broad a range of MWs as possible. A naturally occurring pore size distribution is not sufficient to cause the desired linearity. Therefore, mixed-bed columns, packed with porous materials of different pore-size-distribution ranges, have been developed and used broadly as "linear" columns.

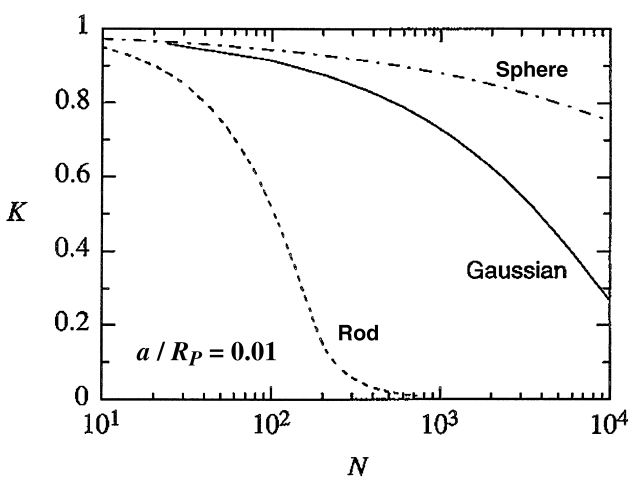

Fig. 3 Partition coefficient K plotted as a function of degree of polymerization, N, for a spherical molecule, Gaussian chain, and a rodlike molecule. The monomer size a is set to be $R_P/100$.

EFFECT OF INTERMOLECULAR INTERACTIONS

It is often observed that, as the concentration of the polymer solution injected increases at a constant injection volume, the retention curve shifts toward a longer time.[8] This effect, called "overloading," is manifested universally when the mobile phase is a good solvent for the polymer being analyzed and is more significant for a polymer of a higher MW. Simple thermodynamics explains this effect[2]: As c_M increases, the solution starts to deviate from the ideally dilute solution, and it becomes difficult to neglect the second virial coefficient A_2. For a solution in a good solvent, a positive A_2 makes μ_M larger than the one in the ideally dilute solution of the same concentration, as given by Eq. 1. The same change applies to μ_S. Since $c_S < c_M$, the increase in μ_M is greater than the increase in μ_S, resulting in an increase in K. At higher concentrations, the analyte polymer is retained longer, thereby delaying the retention curve. The concentration at which the effect of A_2 becomes not negligible is around the overlap concentration c^* which can be defined as $c^*[\eta] = 1$, where $[\eta]$ is the intrinsic viscosity. The actual concentration of c^* is low, especially for high-MW polymer. This is why a concentration as low as 0.1 wt% sometimes exhibits a concentration-dependent chromatogram.

Another mechanism that causes a change in the retention curve with concentration is intermolecular association. In a solution in which is negative, such as a solution in a poor solvent, a polymer chain tends to associate with other chains at higher concentrations. In effect, the pore in the GPC–SEC column senses the presence of suspensions of a larger dimension, causing the retention curve to shift to a shorter time.

REFERENCES

1. Giddings, J.C. *Unified Separation Science*; John Wiley & Sons: New York, 1991.
2. Teraoka, I. Polymer solutions in confining geometries. Progr. Polym. Sci. **1996**, *21* (1), 89–149.
3. Casassa, E.F. Equilibrium distribution of flexible polymer chains between a macroscopic solution phase and small voids. J. Polym. Sci. Polym. Lett. Ed. **1967**, *59* (9), 773–778.
4. Giddings, J.C.; Kucera, E.; Russell, C.P.; Myers, M.N. Statistical theory for the equilibrium distribution of rigid molecules in inert porous networks. Exclusion chromatography. J. Phys. Chem. **1968**, *72* (13), 4397–4408.
5. Casassa, E.F.; Tagami, Y. An equilibrium theory for exclusion chromatography of branched and linear polymer chains. Macromolecules **1969**, *2* (1), 14–26.
6. de Gennes, P.G. *Scaling Concepts in Polymer Physics*; Cornell University Press: Ithaca, NY, 1979.
7. Wang, Y.; Teraoka, I. Computer simulation of semidilute polymer solutions in confined geometry: Pore as a microscopic probe. Macromolecules **1997**, *30* (26), 8473–8477.
8. Roehm, R.E.; Martire, D.E.; Armstrong, D.W.; Bui, K.H. Theory of homopolymer retention in semidilute solutions using liquid chromatography. Macromolecules **1984**, *17* (3), 400–407.

Thermodynamics of Retention in GC

Raymond P.W. Scott
Scientific Detectors Ltd., Banbury, Oxfordshire, U.K.

INTRODUCTION

The Plate theory shows that retention volume of a solute is directly proportional to its distribution coefficient between the two phases. Classical thermodynamics provides an expression that relates the *equilibrium constant* which, in the case of chromatographic retention, will be the distribution coefficient to the change in *standard free energy* of the solute, when transferring from one phase to the other.

APPLICATION

The expression is

$$RT \ln K = -\Delta G_0$$

where R is the gas constant, T is the absolute temperature, and ΔG_0 is the standard free-energy change.

Now,

$$\Delta G_0 = \Delta H_0 - T\Delta S_0$$

where (ΔH_0) is the standard enthalpy change and ΔS_0 is the standard entropy change.

Thus,

$$\ln K = -\left(\frac{\Delta H_0}{RT} - \frac{\Delta S_0}{R}\right)$$

or

$$K = \exp\left[-\left(\frac{\Delta H_0}{RT} - \frac{\Delta S_0}{R}\right)\right] \quad (1)$$

Eq. 1 can also be used to identify the type of retention mechanism that is taking place in a particular separation by measuring the retention volume of the solute over a range of temperatures. Rearranging Eq. 1,

$$\log K = -\frac{\Delta H_0}{RT} + \frac{\Delta S_0}{R}$$

Bearing in mind that

$$V' = KV_S$$

$$\log V' = -\frac{\Delta H_0}{RT} + \frac{\Delta S_0}{R} - \log V_S$$

It is seen that a curve relating $\log(V')$ to $1/T$ should give a straight line, the slope of which will be proportional to the *enthalpy* change during solute transfer. In a similar way, the intercept will be related to the *entropy* change and, thus, the dominant effects in any distribution system can be identified from such curves. Curves relating to $1/T$ are called van't Hoff curves, which can be used to identify the mechanism of retention and elucidate the role played by temperature in a separation (see *van't Hoff Curves*, p. 2406 and *Chiral Separations by GC*, p. 425).

In the majority of distribution systems encountered in gas chromatography (GC), the slopes of the van't Hoff curves are positive and the intercept negative. The negative value of the intercept means that the standard entropy change of the solute has resulted from the production of a less random and more orderly system during the process of distribution. More important, this entropy change *reduces* the magnitude of the distribution coefficient. This means that the greater the forces between the molecules, the greater the energy (enthalpy) contribution, the larger the distribution coefficient, and the greater the retention. In contrast, any reduction in the random nature of the molecules or an increased amount of order in the system reduces the distribution coefficient and *attenuates* the retention. Thus, in the majority of distribution systems in chromatography, the enthalpy and entropy changes oppose one another in their effect on solute retention, although one will generally dominate over the other.

BIBLIOGRAPHY

1. Scott, R.P.W. *Techniques of Chromatography*; Marcel Dekker, Inc.: New York, 1995.
2. Scott, R.P.W. *Introduction to Analytical Gas Chromatography*; Marcel Dekker, Inc.: New York, 1998.

ThFFF

Martin E. Schimpf
Chemistry Department, Boise State University, Boise, Idaho, U.S.A.

Abstract
This entry provides an overview of thermal field-flow fractionation (ThFFF) and its application to polymer and particle analysis. The separation mechanism is described and contrasted with that in size exclusion chromatography (SEC). The two techniques are somewhat complementary. Thus, SEC typically provides superior resolution of low molecular weight (M) polymers (M <100,000 Da), while ThFFF excels in the separation of high-molecular weight polymers (M >100,000 Da), gels, and particles.

INTRODUCTION

Thermal field-flow fractionation (ThFFF) is a subtechnique of the FFF family that employs a temperature gradient as the applied field. This subtechnique is applied primarily to the analysis of industrial polymers that are soluble in organic liquids where the molecular weight range complements that of size exclusion chromatography (SEC). Thus, oligomers and polymers with molecular weights below about 10^4 g/mol are not generally separated well by ThFFF unless extraordinary measures are taken. On the other hand, the resolving power of ThFFF for polymers with molecular weights above 10^5 g/mol is generally several times that of SEC. For molecular weights above 10^6 g/mol, SEC is limited by shear-induced fragmentation of the chains as they travel through the packed bed under high pressure. In contrast, shear forces in the FFF channel are extremely low; therefore, ultra-high molecular-weight polymers, gels, and particles can be separated without degradation and without sample pretreatment.

ThFFF RETENTION

Like in other FFF subtechniques, materials are retained in ThFFF as a result of their field-induced concentration at one wall of the channel.[1] In ThFFF, this field is a temperature gradient. Several terms, including thermal diffusion, thermophoresis, and the Soret effect, are used to express the movement of materials in response to a temperature gradient.

Like other transport processes, thermal diffusion is typically quantified by a phenomenological coefficient that defines the dependence of a mass or energy movement on a potential-energy gradient. Thus, the thermal diffusion coefficient (D_T) relates the velocity (U_x) induced in a material by a temperature gradient: $U_x = D_T\,(dT/dx)$, where T is temperature and x represents the dimension in which the gradient is applied. This definition of thermal diffusion coefficient can be substituted into the general model of FFF retention to yield the following equation, which approximates the retention volume (V_r) of an analyte component in a ThFFF channel under the "normal" mode of operation:

$$\frac{V_r}{V^o} \cong \frac{\Delta T}{6}\frac{D_T}{D} \tag{1}$$

Here, ΔT is the temperature drop across the channel, which is set by the user, D is the ordinary (mass) diffusion coefficient, and the ratio D_T/D is the Soret coefficient. Parameter V^o is the geometric volume of the channel, which is constant for a given instrument. Note that V_r is the same parameter used to define retention in SEC, and that the ratio on the left side of Eq. 1 is the number of channel volumes required to flush a sample component through the ThFFF channel. Although Eq. 1 is an approximation, it becomes accurate to within 3% when $V_r/V^o > 10$. More important for this discussion, Eq. 1 characterizes the influence of analyte parameters D and D_T on retention in the normal mode of ThFFF.

The "normal" mode of ThFFF, as in all FFF subtechniques, refers to the situation in which analyte is freely diffusing away from the accumulation wall. However, if the field (ΔT) is high enough or the analyte is large enough, then the field-induced compression of sample is so great that the sample does not freely diffuse away from the wall, but is rather lifted away by hydrodynamic forces which increase with the analyte size. In this so-called hyperlayer mode, the elution order is reversed, with larger-molecular-weight components eluting ahead of their lower-molecular-weight counterparts of the same chemical composition. The particle size at which the elution order reverses is dependent on the channel thickness and the flow rate of the carrier liquid; under typical operating conditions the reversal occurs at a particle diameter of 1–2 μm. Thus, the hyperlayer mode is typically in operation for micron sized particles.[2] However, high-molecular-weight

polymers can also be separated efficiently in the hyperlayer mode by the use of elevated flow rates.[3]

According to Eq. 1, the retention of an analyte component in the normal mode is governed by the two transport coefficients D and D_T. Coefficient D scales directly with hydrodynamic volume and is the same parameter that differentiates retention in SEC. Thus, ThFFF, like SEC, separates materials according to differences in their hydrodynamic volume, which is related to molecular weight (M). However, V_r increases with D in SEC and decreases with D in ThFFF, so the elution orders are opposite in the two techniques; low-molecular-weight components elute ahead of higher-molecular-weight components in ThFFF.

While V_r scales with log D in SEC, it scales directly with D in ThFFF. As a result, the molecular weights of components are distributed across a wider range of retention volumes in ThFFF, as compared to SEC. Although resolving power benefits from this spread in molecular weight over V_r, ThFFF has fewer theoretical plates than SEC. As a result, the resolving power of ThFFF exceeds that of SEC only for molecular weights above about 10^5 g/mol, where the increasing compression of a greater range of M within a given range of V_r leads to a rapid decline in the resolving power of SEC.[4]

The dependence of retention on thermal diffusion imparts an additional dimension to the ThFFF separation that is not present in SEC. Although our understanding of thermal diffusion in solids and liquids is incomplete, certain aspects are clear. For example, thermal diffusion is very sensitive to the chemical composition of the polymer. As a result, ThFFF is capable of separating components that differ in composition, even when they have the same molecular weight or diffusion coefficient. An example[5] is the separation of polystyrene and poly(methyl methacrylate) standards by ThFFF as illustrated in Fig. 1. This separation cannot be accomplished with SEC because the diffusion coefficients (or hydrodynamic volumes) of the two materials are virtually identical. The ability of ThFFF to separate materials by chemical composition has spurred additional research designed to increase our understanding of thermal diffusion,[6] which in turn has led to the application of ThFFF to polymer blends and copolymers.[7]

Although D_T varies with the polymer–solvent system, it is independent of molecular weight in a given system, at least for random-coil homopolymers. The separation of differing-molecular-weight components is therefore based solely on differences in D, which means that the principles of universal calibration that are relevant to SEC are also applicable to ThFFF. Thus, a calibration curve made with one polymer–solvent system can be applied to other systems, provided the values of the thermal diffusion coefficient associated with each polymer–solvent system are available. Fortunately, accurate values of D_T can be obtained from the combination of ThFFF with any technique that measures D, such as dynamic light scattering[8]

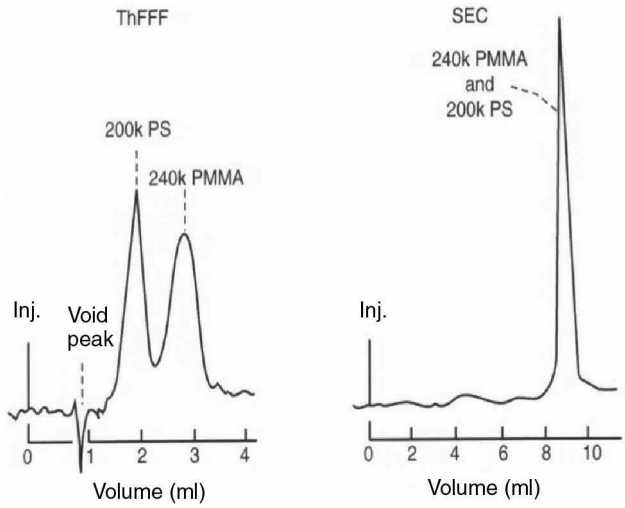

Fig. 1 Elution of similarly sized polystyrene (PS) and poly(methyl methacrylate) (PMMA) polymers by ThFFF and SEC, illustrating the dependence of ThFFF retention on polymer composition.
Source: From Field-flow fractionation, in *Comprehensive Polymer Science, Vol. I, Polymer Characterizations.*[5]

or even SEC; the latter is a secondary method that relies on calibration curves.[9] Values of D_T for many polymer–solvent systems are available in the ThFFF literature.

Compared to SEC, a broader concept of universal calibration is possible with ThFFF because ThFFF channels do not contain the inherent variability associated with SEC packing materials. As a result, relatively simple calibration curves can be employed, which are universal to all ThFFF channels that use the same cold-wall temperature. A common cold-wall temperature is important because both D and D_T vary with temperature. More complex calibration curves incorporate variations in cold-wall temperature.[10]

Retention in ThFFF is directly proportional to the temperature drop (ΔT) across the channel (see Eq. 1). The linear relationship between V_r and ΔT holds even for moderate levels of retention ($V_r/V^o > 3$). Having a predictable dependence of retention on ΔT means that ΔT can be efficiently tuned to optimize the trade-off between resolution and analysis time for each application. ΔT can also be varied over the course of a separation to resolve samples of extreme polydispersity in the most efficient manner. Decreasing ΔT over the course of a separation is analogous to temperature programing in gas chromatography or solvent programing in reversed-phase HPLC.

APPLICATIONS OF ThFFF

Historically, ThFFF has been applied primarily to the analysis of lipophilic polymers. The technique has not found

wide applicability to hydrophilic polymers because thermal diffusion, and therefore retention, is very weak in water.[11] Although a few hydrophilic polymers have been separated by ThFFF, they generally must have a high-molecular weight ($>10^5$ g/mol) to be adequately retained for characterization by ThFFF. Alternatively, an aprotic solvent such as dimethyl sulfoxide can be used to separate hydrophilic polymers with lower-molecular weights. However, flow FFF is more suited to the characterization of hydrophilic polymers.

The open FFF channel is especially suited to fragile materials, and ThFFF has found a definite niche in its application to ultra-high-molecular-weight polymers. Furthermore, as samples need not be filtered, ThFFF is the technique of choice for analyzing gels, rubbers, and other materials that tend to plug SEC columns.[12] Although other FFF subtechniques are more commonly used to separate particles, namely flow FFF and sedimentation FFF, ThFFF has the unique ability to separate particles by composition,[13,14] as well as by size.

Advances in our understanding of thermal diffusion in polymer solutions have led to increased application of ThFFF to copolymers. With random copolymers, for example, the dependence of D_T on chemical composition is now predictable,[7] so that compositional information can be obtained from retention measurements. With block copolymers, ThFFF can still be used to separate components according to molecular weight, branching, and composition, but independent measurements on the separated fractions must be made to get quantitative information, except when "special" solvents are used. Special solvents yield a predictable dependence of D_T on composition even for block copolymers.[7] Different solvents are "special" for different copolymer systems.

Like SEC, ThFFF with information-rich detectors makes a powerful combination. Detectors that yield information on the intrinsic viscosity, molecular weight, or chemical composition of eluting fractions provide detailed information on the distribution of such parameters in a complex sample. ThFFF can also be combined with SEC or hydrodynamic chromatography to achieve 2-D separations. The combination of SEC and ThFFF is a particularly powerful one and has been used to characterize variations in chemical composition of copolymers with molecular weight.[15]

MINIATURIZATION

Although not yet commercially viable, two groups are working on the miniaturization of ThFFF channels. When Giddings first addressed scaling effect in FFF,[16] he concluded that miniaturization has limited potential. However, Gale, Caldwell, and Frazer[17] showed that ThFFF can, in principle, benefit from it in certain ways. Early attempts at miniaturization have yielded mixed results,[18–20] owing in large part to difficulties with microscale injection and detection of the analyte, and it remains to be seen whether such channels will enjoy any significant market share in the future.

THE PRICE OF VERSATILITY

The ability of a single ThFFF channel to be used for the separation of lipophilic polymers, gels, rubbers, and particles makes it a very useful tool for polymer and colloid analysis. The versatility, however, comes at a price. As all of the various applications cannot be implemented with a single field strength or carrier liquid, the user must have more than just a basic familiarity with the technique. To use ThFFF efficiently, while taking advantage of its versatility, the user must understand the fundamentals behind the separation mechanism, and assimilate a certain amount of experience.

Perhaps the most common difficulty encountered by new users arises from their tendency to use high field strengths and high sample concentrations. Unlike in SEC, the elution volume is, in principle, without limit, and the application of a high field can easily lead to an elution time of hours. Thus, in the development of a new application, it is best to begin with a small temperature gradient (ΔT = 10–20 K), and then increase it as necessary to achieve the desired resolution.

For a detailed discussion of appropriate sample concentrations, see *Polymers and Particles: ThFFF*, p. 1869. In general, much lower sample concentrations are used in ThFFF as compared to SEC because the sample is initially concentrated at one wall by the field. Owing to the viscous nature of flow in the thin FFF channel, sample concentrations that are too high lead to poor resolution and reproducibility. On the other hand, although samples are initially concentrated by the field, extremely polydisperse samples eventually get diluted over a wide range of retention volumes owing to the high resolving power of the technique. As a result, such samples require highly sensitive detectors. Although this requirement once posed a significant problem, the availability of highly sensitive and universal detectors, such as the evaporative mass detector, has virtually eliminated the issue of sensitivity in ThFFF.

CONCLUSIONS

ThFFF is a technique that relies on an open channel and an applied temperature gradient to separate materials that respond to a temperature gradient. When employed in the "normal" mode of operation, the elution order of materials is generally opposite to that in SEC, with smaller molecules and particles eluting ahead of larger ones. The technique is applied primarily to lipophilic polymers, copolymers, and gels. Some hydrophilic polymers can also be separated; however, they must not

be charged and generally their molecular weight must be above 10^5 g/mol, and often higher. For hydrophilic polymers, an alternate FFF subtechnique, namely flow FFF is a much more powerful technique (see *FFF Fundamentals*, p. 849). ThFFF separates materials according to their chemical composition, making it applicable to polymer blends and copolymers. For a more detailed discussion of the application of ThFFF to polymers and particles, see *Polymers and Particles: ThFFF*, p. 1869 and the *Field-Flow Fractionation Handbook*.[1]

REFERENCES

1. Schimpf, M.E.; Caldwell, K.D.; Giddings, J.C.; Eds. *Field-Flow Fractionation Handbook*; Wiley Interscience: New York, 2000.
2. Regazzetti, A.; Hoyos, M.; Martin, M. Influence of operating parameters on the retention of chromatographic particles by thermal field-flow fractionation. Anal. Chem. **2004**, *76*, 5787–5798.
3. Giddings, J.C.; Li, S.; Schimpf, M.E. High-speed separations of ultra-high molecular weight polymer fractions by thermal/hyperlayer field-flow fractionation. Makromol. Chem. Rapid Commun. **1988**, *9*, 817–823.
4. Gunderson, J.J.; Giddings, J.C. Comparison of polymer resolution in thermal field-flow fractionation and size-exclusion chromatography. Anal. Chim. Acta **1986**, *189*, 1.
5. Gunderson, J.J.; Giddings, J.C. Field-flow fractionation. In *Comprehensive Polymer Science, Vol. I, Polymer Characterizations*; Booth, C.; Price, C.; Eds.; Pergamon Press: Oxford, 1989, 279–291.
6. Schimpf, M.E. Studies in thermodiffusion by thermal field-flow fractionation. Entropie **1999**, *217*, 67–71.
7. Schimpf, M.E.; Wheeler, L.M.; Romeo, P.F. copolymer retention in thermal field-flow fractionation. In *chromatography of Polymers* (ACS Symposium Series 521); Provder, T.; Ed.; ACS Publications: Washington, DC, 1993, 63–76.
8. Schimpf, M.E.; Giddings, J.C. Characterization of thermal diffusion in polymer solutions: Effect of molecular weight and branching. Macromolecules **1987**, *20*, 1561–1563.
9. Schimpf, M.E.; Giddings, J.C. Characterization of thermal diffusion in polymer solutions: Dependence on polymer and solvent parameters. J. Polym. Sci.; Polym. Phys. Ed. **1989**, *27*, 1317–1322.
10. Pasti, L.; Bedani, F.; Contado, C.; Mingozzi, I.; Dondi, F. Programmed field decay thermal field flow fractionation of polymers: A calibration method. Anal. Chem. **2004**, *76*, 6665–6680.
11. Semenov, S.N.; Schimpf, M.E. Thermophoresis of dissolved molecules and polymers: Consideration of the temperature-induced macroscopic pressure gradient. Phys. Rev. E **2004**, *69*, 011201.
12. Lee, S. Repeatability and reproducibility of thermal field-flow fractionation in molecular weight determination of processed natural rubber. Analyst **1997**, *131* (3), 429–433.
13. Shiundu, P.M.; Giddings, J.C. Separation of particles in nonaqueous suspension by thermal field-flow fractionation. Anal. Chem. **1995**, *67*, 2705.
14. Jeon, S.J.; Nyborg, A.; Schimpf, M.E. Compositional effects in the retention of colloids by thermal field-flow fractionation. Anal. Chem. **1997**, *69*, 3442.
15. van Asten, A.; van Dam, R.J.; Kok, W.T.; Tijssen, R.; Poppe, H. Determination of the compositional heterogeneity of polydisperse polymer samples by the coupling of size-exclusion chromatography and thermal field-flow fractionation. J. Chromatogr. **1995**, *703*, 245.
16. Giddings, J.C. Micro-FFF: Theoretical and practical aspects of reducing the dimension of FFF channels. J. Microcolumn Sep. **1993**, *5*, 407.
17. Gale, B.K.; Caldwell, K.D.; Frazer, A.B. Geometric scaling effects in electrical field flow fractionation. 1 theoretical analysis. Anal. Chem. **2001**, *73*, 2345.
18. Edwards, T.L.; Gale, B.K.; Frazer, A.B. A microfabricated thermal field-flow fractionation system. Anal. Chem. **2002**, *74*, 1211.
19. Janca, J. Micro-thermal field-flow fractionation in the analysis of polymers and particles: A review Int. J. Polym. Anal. Charact. **2006**, *11*, 57–70.
20. Bargiel, S.; Górecka-Drzazga, A.; Dziuban, J.A. A micromachined system for the separation of molecules using thermal field-flow fractionation method. Sens. Actuators A, **2007**, *110*, 328–335.

ThFFF: Cold Wall Effects

Martin E. Schimpf
Chemistry Department, Boise State University, Boise, Idaho, U.S.A.

Abstract
Controlling the temperature of the cold wall is important for obtaining the greatest possible precision in thermal field-flow fractionation (ThFFF). This entry describes the effect of temperature on the transport process, which underlies separation by ThFFF, as well as the practical implications of temperature when ThFFF is applied to polymer analysis.

INTRODUCTION

In field-flow fractionation (FFF), like chromatography, retention and resolution are affected by temperature. For calibration curves to be as precise as possible, or in the case of ThFFF, to universally apply a calibration curve to channels in different laboratories, it is important to closely control the temperature. In ThFFF, the analyte is typically compressed into a layer very close to the cold wall. Therefore, the temperature of the analyte is usually within a few degrees of the cold wall temperature. Consequently, the retention of a given component from one run to the next, or from one instrument to another, will be identical only if the cold wall temperatures are identical.

Fluctuations in the cold wall temperature (T_c) of a couple degrees are generally not a problem. For example, the retention of polystyrene in ethylbenzene decreases 1% for each 2°C increase in T_c when the temperature gradient (ΔT) is held constant.[1] This variation is typical of most polymer–solvent systems. Fluctuations in T_c greater than a couple of degrees, however, will affect both the accuracy and precision of molecular weight distributions that rely on calibration. Such fluctuations can be critical, for example, when retention is used to monitor small batch-to-batch variations in a quality control situation.

TEMPERATURE CONTROL AND ThFFF

The temperature of the cold wall depends on several factors. Heat transferred from the hot wall to the cold wall is typically removed by heat exchange with water. The cooling efficiency is affected by the temperature of the incoming water, which can vary by several degrees among different laboratories. The temperature of the incoming water may also vary by several degrees over time in a given laboratory. The effect of variations in the incoming water temperature can be attenuated with the use of a flow-control valve, since T_c also varies with the flow rate of the water. For example, a lower coolant flow rate can be used in the winter to offset the effect on T_c of the lower water temperature. An alternative to varying the flow rate is to maintain a constant water temperature by running it through a thermostated heater/chiller.

For a given polymer–solvent system, variations in T_c can be incorporated into the calibration equation.[2–4] However, applying T_c into the calibration requires the systematic accumulation of large amounts of data. Furthermore, the temperature dependence of the transport coefficients that govern retention vary with the polymer–solvent system. Consequently, calibration curves that incorporate temperature variations are not necessarily transferable from one polymer–solvent system to another.

Because there are well-defined equations that relate retention to the underlying transport coefficients, ThFFF retention can be used to measure those transport coefficients. In fact, the measurement of thermal diffusion coefficients by ThFFF can be used to obtain compositional information on polymer blends and copolymers (see *Polymers and Particles: ThFFF*, p. 1869). ThFFF is also used in fundamental studies of thermal diffusion because it is a relatively fast and accurate method for obtaining the transport coefficient that quantifies the concentration of material in a temperature gradient, namely the Soret coefficient. However, the accuracy of Soret coefficients obtained from ThFFF experiments depends on appropriate accounting for several factors that involve temperature. To understand the effect of temperature on transport coefficients, as well as the effect on ThFFF calibration equations, a brief outline of retention theory is provided in the following section.

THEORY OF ThFFF RETENTION

In all FFF subtechniques, retention depends on a balance of two opposing motions. The first motion is induced by the applied field and results in the concentration of material at

the accumulation wall (typically the cold wall in ThFFF). The buildup in concentration induces the opposing motion of diffusion. Both motions are accounted for in the retention parameter λ, which is defined for all FFF subtechniques as:

$$\lambda = \frac{D}{Uw} \tag{1}$$

where D is the (mass) diffusion coefficient, U is the field-induced velocity of the sample, and w is the channel thickness. In ThFFF, U is governed by the thermal diffusion coefficient (D_T) and the temperature gradient (dT/dx), which is applied in the same dimension (x) as the channel thickness (x varies in value from 0 at the cold wall to w at the hot wall). Using the dependence of U on D_T and dT/dx, the retention parameter in ThFFF can be expressed as:

$$\lambda = \frac{D}{D_T(dT/dx)w} \cong \frac{D}{D_T \Delta T} \tag{2}$$

where ΔT is the difference in temperature between the hot and the cold walls. Since x and w are in the same dimension, dT/dx can be approximated by $\Delta T/w$, therefore $w(dT/dx)$ is approximated by ΔT on the right-hand side of Eq. 2.

When the parameters in Eq. 1 are constant throughout the channel, the volume V_r of the fluid required to flush a sample component through the channel is related to λ by the following equation:

$$V_r = \frac{V^o}{6\lambda}\left[\coth\left(\frac{1}{2\lambda} - 2\lambda\right)\right]^{-1} \tag{3}$$

Here V^o is the volume of the fluid required to flush a sample that is not affected by the field ($U = 0$). In most FFF subtechniques, the parameters in Eq. 1 are in fact constant throughout the channel. In ThFFF, however, these parameters vary across the channel because they depend on temperature, which varies between the hot and the cold walls. As a result, Eq. 3 is only an approximation in ThFFF. Fortunately, the approximations associated with Eq. 3 are inconsequential for the determination of molecular weight distributions, so that the only concern is variations in T_c, as discussed above. For measuring transport coefficients, on the contrary, the approximations can lead to significant errors.

When calculating transport coefficients from the measured values of V_r, the retention parameter λ is first calculated using Eq. 3. Then, the Soret coefficient D_T/D is calculated from λ using Eq. 2. From the Soret coefficient, the value of D_T can be calculated if an independent measure of D is available. The accuracy of the resulting value is adjusted by the approximations involved in deriving Eq. 3. First, a parabolic velocity profile is assumed. In reality, the velocity profile is skewed toward the hot wall by a carrier-liquid viscosity (η) that varies across the channel as a result of the temperature gradient.[5] Variations in thermal conductivity (κ) with temperature across the channel must also be considered. Finally, the accuracy of Eq. 3 is compromised by an assumption that the analyte forms an exponential concentration profile, whereas in reality the profile is more complicated due to the temperature dependence of the transport coefficients.

The consequences of the temperature dependence of η, κ, D, and D_T have been discussed in several papers.[6–9] Ko, Richards, and Schimpf[6] demonstrated that the temperature dependence of the Soret coefficient actually increases the resolution of different molecular weight components. In a theoretical study by van Asten et al.,[7] it was shown that the consequence of ignoring the temperature dependence of κ has a nearly negligible effect on the accuracy of D/D_T values calculated using Eqs. 2 and 3. Ignoring the temperature dependence of η and D/D_T, on the contrary, can lead to significant errors when D/D_T values are calculated from the retention data. Several refinements to Eq. 3 have been made over the years. When these refinements are used, they yield accurate values for the transport coefficients. Although the resulting equations are quite complex, they are not required for the routine analysis of polymers by ThFFF.

CONCLUSION

Like most analytical techniques, the measurements employed in ThFFF are sensitive to temperature. The most critical temperature to control in ThFFF is the cold wall temperature. By controlling that temperature, the preparation of universal calibration plots is simple and straightforward. Once such plots are obtained, they can be applied to all ThFFF instruments with adequate control of the cold wall temperature. Without precise temperature control, universal calibration plots can still be obtained, but this involves a tedious procedure for each polymer–solvent system under consideration. The incorporation of cold wall temperature in ThFFF calibrations for polymer analysis is well described in the entry *ThFFF: Molecular Weight and Molecular Weight Distributions*.

REFERENCES

1. Brimhall, S.L.; Myers, M.N.; Caldwell, K.D.; Giddings, J.C. Study of temperature dependence of thermal diffusion in polystyrene/ethylbenzene by thermal field-flow fractionation. J. Polym. Sci., Polym. Phys. Ed., **1985**, *23*, 2443.
2. Cao, W.-J.; Williams, P. S.; Myers, M. N.; Giddings, J.C. Thermal field-flow fractionation universal calibration: Extension for consideration of variation of cold wall temperature. Anal. Chem. **1999**, *71*, 1597–1609.

3. Pasti, L.; Bedani, P.; Cantado, C.; Mingozzi, I.; Dondi, F. Programmed field decay thermal field-flow fractionation of polymers: A calibration method. Anal. Chem. **2004**, *76*, 6665–6680.
4. Pasti, L.; Ventosa, E.A.; Mingozzi, I.; Dondi, F. Determination of calibration function in thermal field-flow fractionation under thermal field programming. J. Sep. Sci. **2006**, *29*, 1088–1101.
5. Gunderson, J.J.; Caldwell, K.D.; Giddings, J.C. Influence of temperature gradient on velocity profiles and separation parameters in thermal field-flow fractionation. Sep. Sci. Technol. **1984**, *19*, 667.
6. Ko, G.-H.; Richards, R.; Schimpf, M.E. Enhanced mass selectivity in thermal field-flow fractionation due to the temperature dependence of the transport coefficients. Sep. Sci. Technol. **1996**, *31*, 1035.
7. van Asten, A.C.; Boelens, H.F.M.; Kok, W.Th.; Poppe, H.; Williams, P.S.; Giddings, J.C. Temperature dependence of solvent viscosity, solvent thermal conductivity, and Soret coefficient in thermal field-flow fractionation. Sep. Sci. Technol. **1994**, *29*, 513.
8. Martin, M.; Giddings, J.C. Retention and nonequilibrium peak broadening for a generalized flow profile in field-flow fractionation. J. Phys. Chem. **1981**, *85*, 727.
9. Martin, M.; van Batten, C.; Hoyos, M. Retention in field-flow fractionation with a moderate nonuniformity in the field force. Anal. Chem. **1997**, *69*, 1339.

ThFFF: Molecular Weight and Molecular Weight Distributions

Martin E. Schimpf
Chemistry Department, Boise State University, Boise, Idaho, U.S.A.

Abstract
In field flow fractionation (FFF), retention can be related to the applied field through a well-defined equation governing physicochemical parameters of the analyte. Therefore, in principle, FFF is a primary measurement technique that does not require calibration, but only if the governing physiochemical parameters are the analyte parameters of interest, or their relationship to the parameter of interest (such a molecular weight) is well defined. This entry outlines the procedures for obtaining molecular weights and molecular weight distributions (MWDs) from ThFFF elution profiles in various experimental situations.

METHODOLOGY

In thermal field-flow fractionation (ThFFF), the applied field is a temperature drop (ΔT) across the channel, and the physicochemical parameter that governs retention is the Soret coefficient, which is the ratio of the thermal diffusion coefficient (D_T) to the ordinary (mass) diffusion coefficient (D). Because ΔT is set by the user, retention in a ThFFF channel can be used to calculate the Soret coefficient of a polymer–solvent system. However, to calculate the molecular weight (M) or molecular weight distribution (MWD) of the polymer, the dependence of the Soret coefficient on M must be known. Because D_T is virtually independent of M, at least for solvated homopolymers, the dependence of retention on M reduces to the dependence of D on M. The separation of molecular weight components by D (or hydrodynamic volume, which scales directly with D) is a feature that ThFFF shares with size exclusion chromatograpy (SEC). In the latter technique, the dependence of retention on D forms the basis for universal calibration, as D scales directly with the product $[\eta]M$, where $[\eta]$ is the intrinsic viscosity. Thus, a single calibration plot prepared in terms of log ($[\eta]M$) vs. retention volume (V_r) can be used to measure M for different polymer compositions, provided an independent measure of $[\eta]$ is available. In ThFFF, a single calibration plot can be used for multiple polymers only when the values of D_T for each polymer–solvent system of interest are known. However, a single calibration plot, once established for a given polymer–solvent system, can be used with any ThFFF channel. In summary, calibration plots in SEC are specific to each column but can be made universal with respect to their application to a variety of different polymer compositions. Calibration plots in ThFFF are specific to each polymer–solvent system but universal with respect to different ThFFF channels. The following discussion outlines the various forms that can be used to calibrate a ThFFF channel and how they are used to obtain average values of M and MWDs.

The simplest calibration plot takes the following form:

$$\log V_r = a + S_m \log M \tag{1}$$

where a and S_m are calibration constants. The parameter S_m is referred to as the mass-based selectivity in the FFF literature and is very close but not identical in value to the exponent (b) which defines the dependence of D on M:

$$D = AM^b \tag{2}$$

The difference between S_m and b can be explained by the fact that components of different M experience different temperatures as they separate in the ThFFF channel (see *ThFFF: Cold Wall Effects*, p. 2312).[1]

Eq. 1 fails for very low levels of retention, which can occur with components of low-molecular weight. For such components, where V_r approaches the geometric (void) volume of the channel V^o, calibration plots in the form of Eq. 1 exhibit curvature. An alternate form of Eq. 1, which works over a wider range of retention levels, including low levels of retention, is:[2]

$$\log(V_r - V^o) = a + S_m \log M \tag{3}$$

Because ΔT can be varied to optimize the separation of different samples, it is convenient to incorporate the dependence of retention on ΔT into the calibration plot:

$$\log(\lambda \Delta T) = \phi + n \log M \tag{4}$$

Here, n and ϕ are calibration constants, and λ is the FFF retention parameter, which is calculated from V_r using the following equation:

$$V_r = \frac{V^o}{6\lambda[\coth(2\lambda)^{-1} - 2\lambda]} \quad (5)$$

When ΔT is incorporated into the calibration plot, retention parameter λ is used in place of $(V_r - V^o)$ in order to maintain linearity in the plot over a wide range of applied fields and retention levels.

Once the calibration constants ϕ and n have been determined for a given polymer–solvent system, Eq. 4 can be used for all ThFFF channels, provided the temperature of the cold wall (T_c) is held constant. The cold wall temperature affects the calibration plot because the Soret coefficient (D_T/D) and therefore ϕ varies with T_c. For a detailed discussion of temperature effects (see *ThFFF: Cold Wall Effects*, p. 2312). In a thorough study of temperature effects, Myers and coworkers[3] demonstrated that the dependence of the Soret coefficient on T_c can be accurately modeled by the following equation:

$$\frac{D}{D_T} = \lambda\Delta T = a' T_c^m \quad (6)$$

The validity of this model is illustrated in Fig. 1 by the linearity in plots of log $(\lambda\Delta T)$ vs. log $(T_c/298)$. Based on Eq. 6, the following universal calibration equation has been proposed:

$$\log(\lambda\Delta T) = \phi + m\log\left(\frac{T_c}{298}\right) - n\log\left(\frac{M}{10^6}\right) \quad (7)$$

In order to utilize Eq. 7, a set of linear plots of log $(\lambda\Delta T)$ vs. log $(M/10^6)$ is established for a given polymer–solvent system, with one plot being generated for each of several cold wall temperatures. Such plots run parallel to one another with slopes equal to n and with intercepts that equal $[\phi + m \log (T_c/298)]$. To obtain the values of ϕ and m, linear regression is performed on the intercept values as a function of $T_c/298$. In Eq. 7, the values of T_c and M are divided by 298 and 10^6, respectively, to avoid large extrapolations in obtaining the various intercept values by regression.

Although Eqs. 4 and 7 are applicable over a range of field strengths (ΔT values), the field must be held constant during any given analysis. A more complex calibration method is required when the field is programed, in order to more efficiently separate very broad polymer distributions.[4]

When a mass-sensitive detector such as a refractometer or photometer is used, the weight-average molecular weight (M_w) of a polymer sample is calculated from the calibration equation using the value of V_r that corresponds to the center of gravity of the elution profile. The center of gravity is defined by placing a vertical line through the

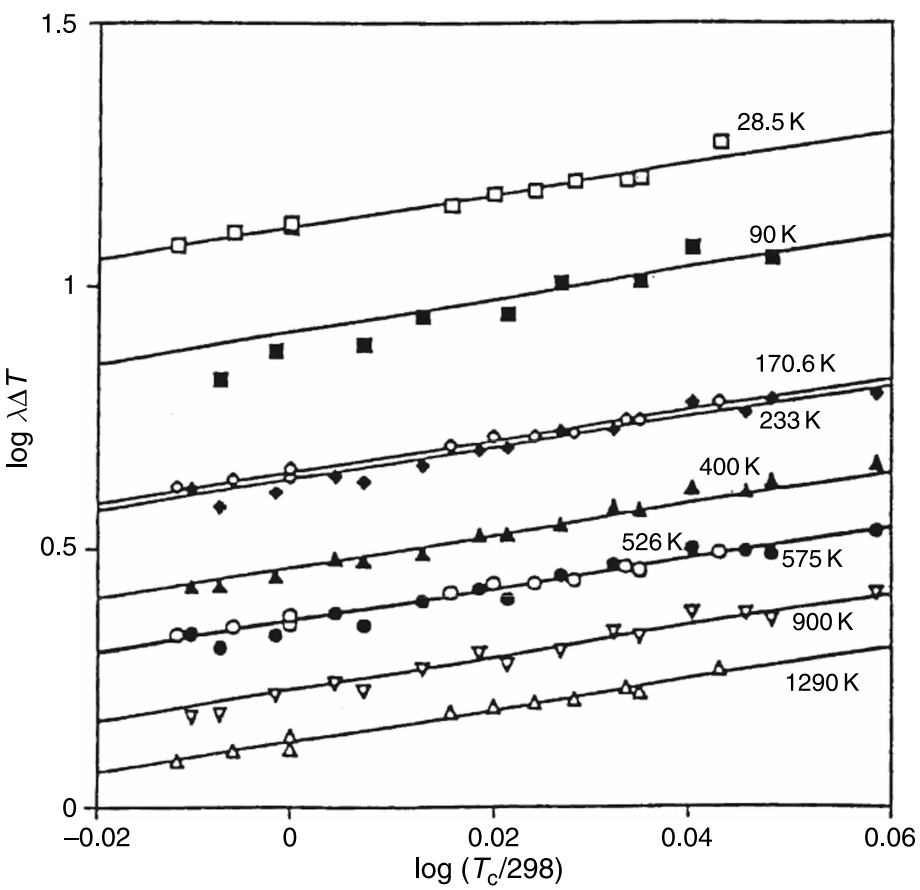

Fig. 1 Plots of log $\lambda\Delta T$ vs. log $T_c/298$ for polystyrene in tetrahydrofuran. The data were gathered using a variety of different ThFFF channels. Values of ΔT ranged from 30 to 70 K. **Source:** Reproduced with permission from Thermal field-flow fractionation universal calibration: Extension for consideration of variation of cold wall temperature, in Anal. Chem.[3]

elution profile such that the line bisects the profile into two halves of equal area. The intersection of this line with the elution–volume axis defines the weight-average V_r, which is converted to M_w through the calibration equation. If the elution profile has a Gaussian shape, then the weight-average V_r is the value of V_r that corresponds to the peak of the elution profile.

In ThFFF, the shape of the elution profile is not significantly affected by band broadening for polydisperse ($\mu > 1.2$) polymers, provided that low flow rates (<0.2 ml/min) are used. In that case, accurate information on the MWD can be obtained directly from the elution profile. For example, if a mass-sensitive detector is used, the signal (s) is linearly related to the mass of polymer in the eluting stream, and the number-average molecular weight (M_n) of the sample is calculated as:[2,5]

$$M_n = \frac{\sum s_i}{\sum \frac{s_i}{M_i}} \tag{8}$$

Here, the summation extends over small equal elements of elution volume from the beginning to the end of the elution profile. Thus, s_i is the detector signal of the ith digitized increment, and M_i is calculated from the associated value of V_r using the calibration equation. The weight-average molecular weight (M_w) is calculated as:

$$M_w = \frac{\sum s_i M_i}{\sum s_i} \tag{9}$$

Polydispersity μ, defined as the ratio M_w/M_n, thus becomes

$$\mu = \frac{\left(\sum s_i M_i\right)\left(\sum \frac{s_i}{M_i}\right)}{\left(\sum s_i\right)^2} \tag{10}$$

ThFFF elution profiles can also be converted into a detailed MWD. With a mass-sensitive detector, the elution profile is essentially a plot of the polymer concentration c (with units of mass/volume) in the eluting stream vs. V_r. In order to obtain the mass-based MWD, $m(M)$, we need to transform this profile using the following equation:

$$m(M) = c(V_r)\frac{dV_r}{dM} \tag{11}$$

The normalized and digitized form of this equation is

$$m_i = \frac{s_i}{\sum s_i}\frac{\Delta V_r}{\Delta M_i} \tag{12}$$

where ΔV_r is the fixed elution volume element corresponding to one digitized interval. In the case of linear calibrations, as defined by Eqs. 1 and 3, $d(\log V_r)/d(\log M)$ is a constant equal to S_m, and Eq. 12 is more conveniently expressed in the following form:

$$m_i = \frac{s_i}{\sum s_i}\frac{M_i}{V_{r,i}}S_m \tag{13}$$

If needed, the differential number MWD can be obtained by dividing $m(M)$ by M:

$$n(M) = \frac{m(M)}{M} \tag{14}$$

For polymers with low polydispersity ($\mu < 1.2$), a detailed MWD is not generally required, and simply calculating M_n and M_w from Eqs. 8 and 9 is generally adequate. However, the elution profile of such a narrow MWD is affected significantly by band broadening, which must be accounted for in order to obtain the most accurate possible values of M_n and μ.[6] Even the elution profile of more polydisperse samples ($\mu > 1.2$) can be affected by band broadening if high flow rates (>0.2 ml/min) are used. Fortunately, band broadening is well defined in ThFFF and can be removed by one of two methods. For samples of low polydispersity, μ is well approximated by[6]

$$\mu = 1 + \frac{H_P}{LS_m{}^2} \tag{15}$$

where L is the channel length and H_P is the polydispersity contribution to plate height (H). H_P is obtained by plotting the experimental H as a function of flow rate. With the appropriate technique,[6,7] such plots are linear and the y-intercept is equivalent to H_P. Alternatively, H_P can be obtained by subtracting the non-equilibrium band-broadening contribution to H (H-sub-N) from the experimentally measured value. Methods for calculating H_N from well-established models of band broadening in ThFFF can be found in the literature.[2] Since the elution profile of samples with low polydispersity are generally symmetrical, M_w is calculated using the peak value of V_r in the calibration equation, and then Eq. 15 is used to calculate μ. Finally, M_n is calculated from $\mu = M_w/M_n$.

Samples with higher polydispersity do not generally yield symmetrical elution profiles. Moreover, a detailed MWD [either $m(M)$ or $n(M)$] is often desired. As mentioned above, band broadening does not significantly affect the elution profile when low flow rates are used. Therefore, the elution profile can be directly converted into a MWD by the procedures outlined above. If, on the contrary, fast flow rates are used to shorten analysis time, the observed elution profile must be adjusted to account for the effects of band broadening. A deconvolution algorithm that filters out the band-broadening contribution to the elution profile is described in the literature.[2] Fig. 2 illustrates that the elution profiles

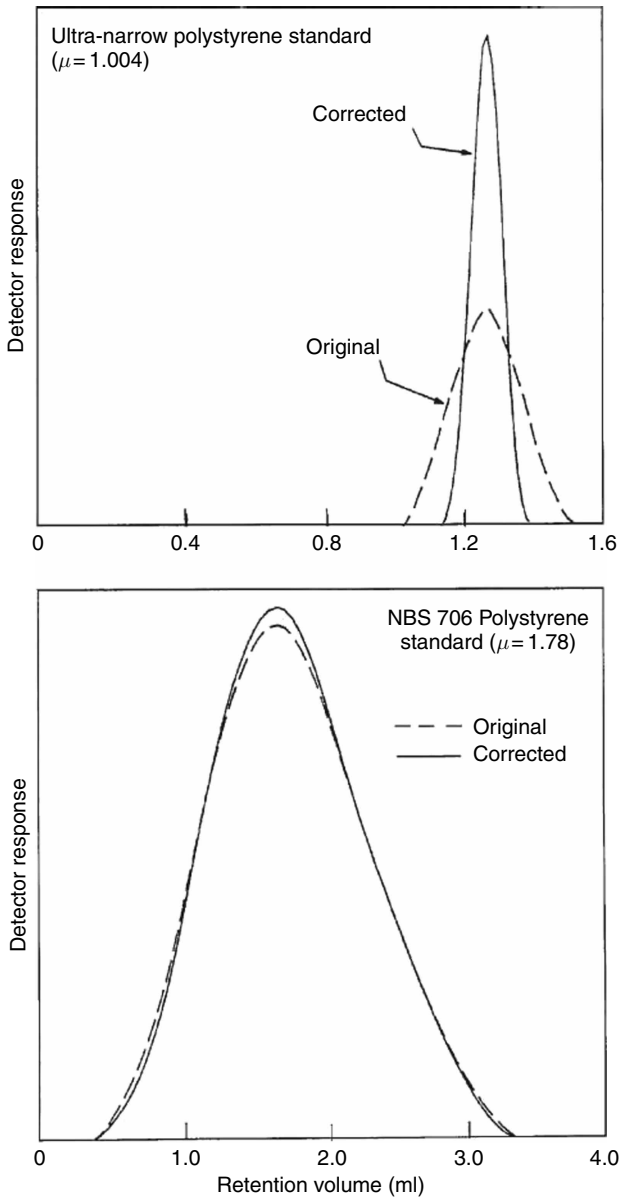

Fig. 2 ThFFF elution profiles before (original) and after (corrected) removing the effects of band broadening. With the polydisperse sample (NBS 706), which was analyzed at a flow rate of 0.4 ml/min, the effect of band broadening on the elution profile is minimal. The polydispersity values listed were determined using ThFFF.

before and after the effects of band broadening are removed for samples of both low and high polydispersity.

CONCLUSION

A variety of calibration procedures have been developed for characterizing the molecular weight and MWD of polymers by ThFFF. The procedures range in complexity depending on the desired flexibility. One of the unique features of ThFFF compared to SEC is the ability to tune the external field, in order to optimize the method for a given sample and/or molecular weight range. It is a simple matter to incorporate the field strength into the calibration plots, so that a single plot can be applied for a given polymer–solvent system under a range of applied temperature gradients. When the thermal diffusion coefficient is known for each polymer–solvent system under consideration, such coefficients can also be incorporated so that a single calibration plot can be applied to multiple polymer types.

For determining MWDs, the resolving power of ThFFF is high enough that band-broadening effects are generally negligible, except for nearly monodisperse materials or when high flow rates are used for rapid analysis. For cases in which band broadening is not negligible, the open ThFFF channel has a distinct advantage over SEC because band broadening is well understood and can be accurately modeled and precisely removed from the elution profile. As a result, techniques have been established that accurately account for the effect of band broadening on MWDs derived from ThFFF elution profiles. For more detailed information on the determination of molecular weight and MWDs by ThFFF, see *the Field-Flow Fractionation Handbook*.[7]

REFERENCES

1. Ko, G.H.; Richards, R.; Schimpf, M.E. Enhanced mass selectivity in thermal field-flow fractionation due to the temperature dependence of the transport coefficients. Sep. Sci. Technol. **1996**, *31*, 1035–1044.
2. Schimpf, M.E.; Williams, P.S.; Giddings, J.C. Accurate molecular weight distributions of polymers using deconvolution to remove system dispersion. J. Appl. Polym. Sci. **1989**, *37*, 2059–2076.
3. Cao, W.-J.; Williams, P.S.; Meyers, M.N.; Giddings, J.C. Thermal field-flow fractionation universal calibration: Extension for consideration of variation of cold wall temperature. Anal. Chem. **1999**, *71*, 1597–1609.
4. Pasti, L.; Bedani, F.; Contado, C.; Mingozzi, I.; Dondi, F. Programmed field decay thermal field-flow fractionation of polymers: A calibration method. Anal. Chem. **2004**, *76*, 6665–6680.
5. Tung, L.H. *Polymer Fractionation*; Cantow, M.J.R. Ed.; Academic: New York, 1967.
6. Schimpf, M.E.; Myers, M.N.; Giddings, J.C. Determination of polydispersity of ultra-narrow polymer fractions by thermal field-flow fractionation. J. Appl. Polym. Sci. **1987**, *33*, 117–135.
7. Schimpf, M.E., Caldwell, K.D., Giddings, J.C., Eds. *Field-Flow Fractionation Handbook*; Wiley Interscience: New York, 2000.

Thin Layer Radiochromatography

Joseph Sherma
Department of Chemistry, Lafayette College, Easton, Pennsylvania, U.S.A.

Abstract
The techniques and instruments for the detection and quantification of radiolabeled zones in thin layer chromatograms are described. Included are film autoradiography, liquid scintillation counting (LSC), storage phosphor imaging, and in situ radioactivity scanning. These methods are widely applied in radiopharmaceutical purity determination, metabolism studies, and many other chemical, biochemical, and biological investigations.

INTRODUCTION

Thin layer chromatography (TLC) is often used for the separation, detection, and qualitative and quantitative determination of radiolabeled substances. The method is termed thin layer radiochromatography (TLRC) or radio-TLC. Applications include following the course of chemical and biochemical reactions and determining the distribution of radiolabeled substances in a reaction mixture; metabolism studies of drugs, pesticides, pollutants, and natural substances in human, animal, and plant tissues or soil; assessing the purity of radiopharmaceuticals and isotopes; and for biochemical studies such as elucidation of biochemical pathways, radiotracer binding, and assessment of enzyme activity. TLRC is often the best method for carrying out such studies because of its low detection limits (often better sensitivity than radio high-performance liquid chromatography, HPLC); variety of methods for detecting and quantifying tagged compounds; capability for fast method development and serial analysis; and no sample loss due to sorption on a column (the entire sample is detected), and it can provide information complementary to that from radio-HPLC.

It is important to use proper safety precautions in TLRC experiments, such as working in a well-ventilated area (preferably a fume hood) and frequent monitoring of analysts for exposure. Both the half lives and energies of the isotopes used should be considered in designing safety protocols for sample handling and analytical procedures.

TLC PROCEDURES

The chromatographic analyses are normally carried out using precoated commercial TLC and high performance TLC (HPTLC) plates with one-dimensional (1-D) isocratic ascending development. Glass-backed plates are flat and uniform and best to use for direct scanning detection in TLRC. Plates with plastic or aluminum backing can be cut into sections, thereby facilitating liquid scintillation counting (LSC) or preparative isolation of separated compounds.[1] Normal-phase silica gel is the most widely used layer by far, but reversed-phase and ion-exchange layers have been reported in TLRC analyses. In many cases layers with a preadsorbent or concentrating zone are used because smaller, better-resolved zones can be obtained when large volumes of dilute solutions are applied.

Samples should be applied manually or with an automated instrument[2] as small spots or narrow bands sufficiently far apart to avoid measurement of radioactivity from adjacent lanes. Highest-resolution separations are obtained on HPTLC plates with optimized mobile phases and small-volume samples, if the level of activity allows. The layer should be dried after development under conditions that completely remove the mobile-phase constituents but do not volatilize sample components. Compound degradation on the plate can be checked by two-dimensional (2-D) development of a mixture with the same mobile phase; all of the zones will lie on a diagonal straight line if no decomposition occurs during development. Higher resolution for complex samples can be obtained by 1-D automated gradient elution multiple development (AMD) or forced flow development overpressured layer chromatography (OPLC), or by 2-D development at right angles with complementary mobile phases having different separation mechanisms.

Earlier sources[3–5] described methods and instruments (many now outdated and not commercially available) for detection and quantification of radioactivity in TLC and HPTLC. However, no book or journal article published since 2003 has included an updated description of the field, which is provided in this entry.

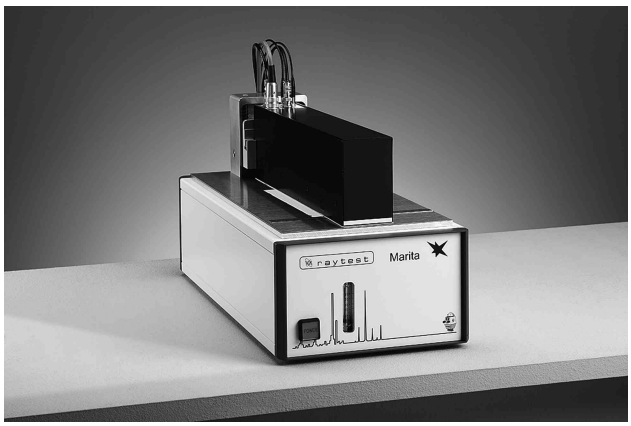

Fig. 1 MARITA Star beta radiation scanner.
Source: Raytest USA, Wilmington, North Carolina, U.S.A.

FILM AUTORADIOGRAPHY

In the classical autoradiography method, the thoroughly dried layer containing the separated radioactive zones (spots or bands) is put in direct contact with a photographic (X-ray) film or emulsion, which shows the image of the chromatogram as darkened zones after film development. The process involves detection of beta-particles based on reduction of silver ions to silver atoms within the film. Film development is carried out by standard photography processing methods in a darkroom.

When properly exposed, the resolution of the zones in autoradiography can be comparable to that on the original chromatogram and as high as any other radioactivity detection method. The major disadvantage is that exposure times can vary from a few hours to several weeks, depending on the amount of radioactivity in the TLC zones. Various commercial films are used, one of the newest and most sensitive being Biomax MR from Kodak (Rochester, New York, U.S.A.).

Enhancement of detection sensitivity in the range of 1–16 fold has been obtained by using an inorganic phosphor-coated intensifying screen placed behind the film. The phosphor emits light when beta-particles pass through the film, increasing film exposure.[4]

Fluorography is another sensitivity enhancement method in which a scintillator such as 2,5-diphenyloxazole (PPO) is added to the layer postchromatography using a commercial spray reagent. The energy of the disintegrating radionuclides is converted to light, which is detected by the film to produce a "fluorogam." In one study, Kodak X-OMAT R film treated with EN^{3}HANCE spray (New England Nuclear; PerkinElmer Life and Analytical Sciences, Shelton, Connecticut, U.S.A.) and exposed at dry ice temperature for 24 hr produced a 100–200 fold enhancement of the sensitivity of ^{3}H and ^{14}C detection compared to autoradiography.[4]

Qualitative assessment of chromatograms is made by visual inspection of the film and quantitative analysis by optical density measurement of the zones with a slit-scanning, video, digital camera, or flatbed scanner densitometer; these types of light-based densitometers, which are also used for quantification of colored, ultraviolet (UV) absorbing, and fluorescent TLC zones, have been described in previous articles.[6–9] Optical density is related to the amount of radioactivity through a calibration curve prepared using a set of radioactive standards during each exposure. The curve corrects for the variables related to the film type, exposure period, and film development procedure. Further details on film autoradiography are presented in Refs. 3 and 4.

LIQUID SCINTILLATION COUNTING

For LSC, radioactive zones are scraped from a glass-backed layer or cut from a layer with flexible backing (plastic or aluminum) and transferred into a vial, mixed with a scintillation solution (commercial "cocktails" are available), and indirectly quantified based on measurement of the light energy produced in a scintillator counter with a photomultiplier tube (PMT). As an alternative, scraped or cut zones can be eluted with solvent into a vial to isolate the radiolabeled sample and then counted. The number of counts for each zone can be plotted as a histogram profile of the radioactivity in the chromatogram along the lane of a TLC plate.

Because high resolution depends on small widths of adsorbent zones being scraped, LSC can be very labor intensive and time consuming. Scraping must be done manually with a commercial device such as a sharp, flat spatula because there are no commercial automatic scrapers available. Great care is needed to minimize loss of sorbent during scraping and transfer to vials.

Quenching effects of solvents, layer sorbents, and sample constituents are taken into account by modern LSC instruments. Samples with low levels of radioactivity are counted for a longer period and background correction is performed using a blank layer section taken from an area adjacent to the zone of radiolabeled compound.

In general, LSC is among the most sensitive and quantitative TLRC methods, but resolution is limited and great care is needed to obtain accurate and precise quantitative results. LSC is described further in Refs. 3 and 4.

PHOSPHOR IMAGING

Storage phosphor screen imaging is often termed filmless autoradiography. The phosphor screens are sensitive to any source of ionizing radiation, e.g., ^{14}C, ^{3}H, ^{35}S, ^{125}I, ^{32}P, ^{33}P, ^{18}F, and ^{99m}Tc. They contain small crystals of a

photostimulable phosphor coated on a support in which luminescence is produced and stored when exposed to radioactive TLC zones. The luminescence is evaluated by scanning with a laser in a reading device, and quantification is carried out by use of a calibration curve to exclude the effects of the phosphor screen type and exposure period. The screens can be reused after being erased by exposure to visible light.

The BAS-5000 bioimaging analyzer from Fujifilm Life Science USA (Stamford, Connecticut, U.S.A.) is an example of a phosphor screen imaging system. The imaging plate (IP) consists of 5 μm crystals of barium fluorobromide containing a trace amount of bivalent europium ($BaFBr:Eu^{+2}$) as a bioluminescence center coated on a polyester support film. When the crystal is exposed to a radiolabeled zone, the energy of the radioisotope ionizes the Eu^{+2} to Eu^{+3}, liberating electrons to the conduction band of the phosphor crystals. The electrons are trapped in the bromine vacancies introduced during the manufacturing process. The exposed IP is scanned with a laser beam of red light (633 nm) focused by a mirror while being moved in the reader; the photostimulated phosphorescence (PSL) released by the laser as photons of blue light (390 nm) is collected onto a PMT through a light collection guide and is converted to electrical signals. A 20 × 25 cm IP with the images of chromatograms from a 20 × 20 cm TLC plate can be scanned at 50 μm in as little as 5 min. Compared to X-ray film, sensitivity is about 100 times higher, processing is 10–100 times faster, and quantitative accuracy is greater.

The benchtop Cyclone Plus quantitative radiometric phosphor imager (PerkinElmer Life and Analytical Sciences) operates with the same storage phosphor and scanning process except that a helical scanning mechanism is used with the flexible phosphor screen loaded into a cylindrical carousel that spins at 360 rpm. This allows the instrument to be more compact and lower in cost than the BAS-5000, in which the phosphor screen is kept on a flat plane during scanning.

The following TLC applications cited by PerkinElmer for the Cyclone Plus are typical of other phosphor imaging systems: imaging of ^{3}H, ^{125}I, ^{14}C, ^{32}P, ^{33}P, ^{18}F, ^{90}Y, ^{99m}Tc, ^{111}In, and ^{177}Lu; nucleotide metabolism studies with ^{32}P- and ^{33}P-labeled adenosine triphosphate (ATP) or guanosine triphosphate (GTP); ^{14}C-UDPGA glucuronidation assay; quality control (QC) of ^{177}Lu- and ^{90}Y-DOTA-TOC; ^{18}F silica gel TLC for analysis of position emission tomography (PET) radiochemicals; QC of ^{99m}Tc; and radiochemical purity of ^{90}Y Zevalin.

RADIOSCANNERS FOR DIRECT MEASUREMENT ON TLC PLATES

Scanners with a position-sensitive proportional gas flow counter detector are used primarily for detection of beta radiation. The process involves ionization of the counting gas by interaction with radioactive TLC zones, producing a pulse of electrons that is proportional to the amount of radioactivity.

An example of this type of detector is the MARITA Star from Raytest USA (Wilmington, North Carolina U.S.A.; Fig. 1), an automatic single trace instrument for measurement of one 5 × 20 cm TLC plate. The Raytest RITA Star beta radiation layer analyzer can measure two 20 × 20 cm plates at once. The detector for each has an active length of 200 mm and active width of 20, 15, 10, 3, or 1 mm controllable by exchange of the diaphragm. The sensing element is gold plated for easy cleaning and long life. For measurement of low energy betas from ^{3}H, the counting tube is used without any window and is placed as close as possible to the radioactive TLC zone. Therefore, the detector rests on the surface of the layer in order to close the counting chamber and reduce gas leakage, and the gold-plated tungsten counting wire can be accurately aligned for optimum results. In the RITA Star, the counting tube is automatically moved to measure traces of multiple chromatograms on a layer. 2-D thin layer chromatograms are measured by assembling individual 1-D traces. Data collection, analysis, and documentation meet good laboratory practice (GLP) requirements. Both instruments are designed for maximum sensitivity for low-energy beta- emitting nuclides such as ^{3}H, ^{14}C, ^{35}S, ^{33}P, and ^{32}P; gamma- and positron-emitting nuclides such as ^{125}I, ^{99m}Tc, and ^{18}F can be detected more sensitively with the Raytest GITA or miniGITA Star (below).

The AR-2000 imaging scanner (Bioscan Inc., Washington, District of Columbia, U.S.A.) is another instrument that has a windowless gas-filled proportional detector and can detect gamma, beta, and positron emitters. Sensitivity for a 10 min analysis is 1000 dpm for ^{3}H and ^{125}I and 100 dpm for ^{14}C, ^{32}P, and most other isotopes, and resolution is 0.5–1 mm for ^{3}H, 1–2 mm for ^{14}C, and 3 mm for ^{32}P and most gamma emitters. An entire TLC lane can be imaged in under 1 min, and multiple lanes can be measured in a single automated run without operator intervention. Models are available that hold one, two, or three 20 × 20 cm TLC plates. Single-lane or 2-D color imaging and automated quantification can be performed with WinScan software, or with Bio-Chrom software for compliance with 21 CFR Part 11 U.S. Food and Drug Administration and GLP standards. Applications for which the AR-2000 have been used include PET or single photon emission computed tomography (SPECT) radiopharmaceutical QC and synthesis process control (compounds labeled with ^{18}F, ^{11}C, ^{99m}Tc, ^{111}In, etc.); pharmaceutical metabolite analysis for beta-, gamma-, or positron-labeled products; radiotracer toxicology studies with ^{14}C labeled organic compounds and agrochemicals; biosynthesis studies involving complex lipids, phospholipids, and glycolipids; radiochemical purity quality

assurance (QA) analyses for tracer or metabolism studies; radiolabeled reporter gene or enzyme assays; and quantitative radiolabeled biochemical separations (programmable scanning and quick-change magnetic collimators can be used for optimization of resolution and sensitivity).

The GITA gamma isotope TLC analyzer is an X–Y scanner controlled by a personal computer (PC) for automatic measurement, data evaluation, and report printing. It has a V-shaped bismuth germanate (BGO-V) crystal scintillation probe detector mounted in tungsten shielding, can be automatically energy-calibrated using a ^{137}Cs standard, and many energy windows can be preprogrammed for various nuclides. Up to 80 sample traces can be programmed in terms of location, scan speed, etc. in both directions on two 20 × 20 cm plates. Beta/positron detection can be made using an optional Geiger-Mueller (GM) detector (^{3}H is not detected). Collimators of 3 mm (stainless steel) and 5–20 mm (tungsten) size are available to optimize resolution and sensitivity for gamma detection of different nuclides. The miniGITA Star from Raytest is a scanner for gamma and beta/positron radiation from TLC zones that is similar to the GITA Star. The major differences are that the scan area is 5 × 20 cm and only one trace can be made at a time in the X direction.

CONCLUSION

TLRC can be used for animal, human, and plant metabolism analysis; radiochemical purity and stability assessment; toxicology and biochemical studies; and separation, detection, and quantification of separated radioactive zones of all compound classes. Traditional film autoradiography and LSC continue to be widely used, but phosphor imaging and layer scanners are being increasingly applied. The instruments for these methods are highly automated and can have significant advantages in terms of simplicity, speed, accuracy, precision, and sensitivity. The in situ scanner methods are direct analyses that minimize technician radiation exposure and do not require disposal of contaminated screens or liquid waste.

REFERENCES

1. Kowalska, T.; Sherma, J., Eds.; *Preparative Layer Chromatography*; CRC/Taylor and Francis: 2006.
2. Sherma, J. Sample application in TLC. In *Encyclopedia of Chromatography*, 3rd Ed.; Cazes, J., Ed.; Taylor & Francis: New York, 2010; 2053–2057.
3. Hazai, I.; Klebovich, I. Thin layer radiochromatography. In *Handbook of Thin Layer Chromatography*, 3rd Ed.; Sherma, J., Fried, B. Eds.; Marcel Dekker, Inc.: New York, 2003, 339–360.
4. Fried, B.; Sherma, J. *Thin Layer Chromatography*, 4th Ed., Marcel Dekker, Inc.: New York, 1999, Chapter 12, 235–267.
5. Klebovich, I. Application of planar chromatography and digital autoradiography in metabolism research. In *Planar Chromatography*, Nyiredy, Sz., Ed.; Springer Scientific Publisher: Budapest, Hungary, Chapter 16, 293–311.
6. Sherma, J. Optical quantification (densitometry) in TLC. In *Encyclopedia of Chromatography*, 2nd Ed.; Cazes, J., Ed.; Taylor & Francis: New York, 2005, 1150–1157.
7. Sherma, J. Optical quantification or densitometry in TLC. In *Encyclopedia of Chromatography*, 3rd Ed.; Cazes, J., Ed.; Taylor & Francis: New York, 2010, 1640–1647.
8. Sherma, J. A field guide to instrumentation: Quantitative thin layer chromatography densitometers. Inside Lab. Manag. **2000**, *4* (10), 5–9.
9. Sherma, J. A field guide to instrumentation: Instrumentation for modern thin layer chromatography. J. AOAC Int. **2008**, *91*, 51A–58A.

Three-Dimensional Effects in FFF: Theory

Victor P. Andreev
Institute for Analytical Instrumentation, Russian Academy of Sciences, St. Petersburg, Russia

INTRODUCTION

A field-flow fractionation (FFF) channel is normally ribbonlike. The ratio of its breadth b to width w is usually larger than 40. This was the reason to consider the two-dimensional (2D) models adequate for the description of hydrodynamic and mass-transfer processes in FFF channels. The longitudinal flow was approximated by the equation for the flow between infinite parallel plates, and the influence of the side walls on mass-transfer of solute was neglected in the most of FFF models, starting with standard theory of Giddings and more complicated models based on the generalized dispersion theory.[1] The authors of Ref.[1] were probably the first to assume that the difference in the experimental peak widths and predictions of the theory may be due to the influence of the side walls.

DISCUSSION

The essence of the side walls effect follows. The flow velocity turns to zero at the side walls as well as at the main (accumulation and depletion) walls of the FFF channel. Therefore, the flow profile is non-uniform, not only along the width of the channel but also along its breadth. The size of the regions near the side walls where the flow is substantially non-uniform is of the same order as w. The non-uniformity of the flow in both directions, combined with diffusion of solute particles, leads to Taylor dispersion and peak broadening that could be different from the one predicted by the 2D models.

The first 3D model of FFF was developed in Ref.[2] The 3D diffusion–convection equation was solved with the help of generalized dispersion theory, resulting in the equations for the cross-sectional average concentration of the solute and dispersion coefficients K_1 and K_2, representing the normalized solute zone velocity and the velocity of the corresponding peak width growth, respectively. Unfortunately, only the steadystate asymptotic values of dispersion coefficients $K_1(\infty)$ and $K_2(\infty)$ were determined in Ref.,[2] leading to the prediction of the solute peaks much wider than the experimental ones.

The incorrectness of the steady-state approach was noted by the authors of Ref.[3] and can be explained as follows. There are two characteristic diffusion times in an FFF channel: $t_{D1} = w^2/4\mathrm{D}$ and $t_{D2} = b^2/4\mathrm{D}$, where D is the diffusion coefficient of solute molecules. As the ratio b/w 40, then $t_{D1}/t_{D2} > 1600$. Experimental values of retention time are usually equal to several t_{D1}, but are never as large as $1600t_{D1}$. Thus, the steady-state values of K_1 and K_2 corresponding to $t > t_{D2}$ are never reached during the experiment. (For the channel with $w = 200$ μm, $b = 1$ cm, and solute with $D = 10^{-6}$ cm^2/sec, $t_{D1} = 100$ sec and $t_{D2} = 2.5 \times 10^5$ sec.)

In Ref.[3] the non-stationary solution was produced for $K_1(\tau)$ and $K_2(\tau)$ where $\tau = t/t_{D1}$, leading to much better correspondence with experimental peak widths. Similar to Ref.[2] not the exact equation for the flow profile in the rectangular channel but its approximation was used:

$$V_x(y,z) = V_{\max}\left(1 - \frac{4y^2}{w^2}\right)\left(1 - \frac{\cos h\left(2\sqrt{3}z/w\right)}{\cos h\left(\sqrt{3}b/w\right)}\right) \quad (1)$$

Only the case of uniform initial distribution of solute in the channel cross section was studied in Ref.[3]

A more general case was studied in Refs.[4,5] where different initial solute distributions were examined, including the distributions describing the syringe inlet with and without the stop-flow relaxation. The 3D generalized dispersion theory was used to solve the 3D diffusion–convection equation. Unlike Refs.[2,3] the exact equation for flow profile in the rectangular channel was used:

$$V_x(y,z) = 4V_{\max}\sum_{n=0}^{\infty}(-1)^n\left(1 - \frac{\cosh(2\varphi_n z/w)}{\cosh(\varphi_n b/w)}\right) \times \frac{\cos(2\varphi_n y/w)}{\varphi_n^3} \quad (2)$$

where $\varphi_n = (2n + 1)\pi/2$, $|z| \le b/2$, and $|y| \le w/2$, transversal coordinates (the zero of coordinates being at the axis of FFF channel).

The exact equation for the flow profile was chosen because, although approximation (1) gives very similar results for $K_1(\tau)$, the deviation for $K_2(\tau)$ could be very significant. Fig. 1 presents dependences of $K_2(\tau)$ for different values of the FFF parameter λ, calculated with the help of 3D[4] and 2D[1] models. It can be seen that the difference between 2D and 3D results is growing with time τ and is larger for smaller values of λ. The growth of $K_2(\tau)$ with time leads to the non-linear growth of the peak variance with time:

$$\sigma^2(t) = 2Dt + \frac{V_{\max}^2 w^4}{8D^2} \int_0^{4Dt/w^2} K_2(\gamma) d\gamma \quad (3)$$

If K_2 is constant for the typical experimental values of retention time, as predicted by the 2D theory, then $\sigma^2 \sim t$ and resolution $R_s \sim \sqrt{t}$, where $R_s = \Delta X/4\sigma$ and ΔX is the distance between peak maximums for two types of solute molecule. According to the 3D model, $K_2(\tau)$ grows with time, so $\sigma^2 \sim \alpha t + \beta t^2 + \ldots$, and there exists some value of retention time for each λ, when resolution stops growing with time.

This effect is even more pronounced for the case of a syringe inlet. At the beginning of the process, the solute is distributed in the region close to $z = 0$, so it does not feel the influence of the side walls and, only after the period of time commensurate with the second diffusion time t_{D2}, the solute particles diffuse to the side walls. That is why, at the beginning of the process, the value of K_2 is close to the 2D value of K_2 and is growing toward its asymptotic 3D value slower than for the case of the solute initially distributed uniformly in the channel's cross section (presented in Fig. 1).

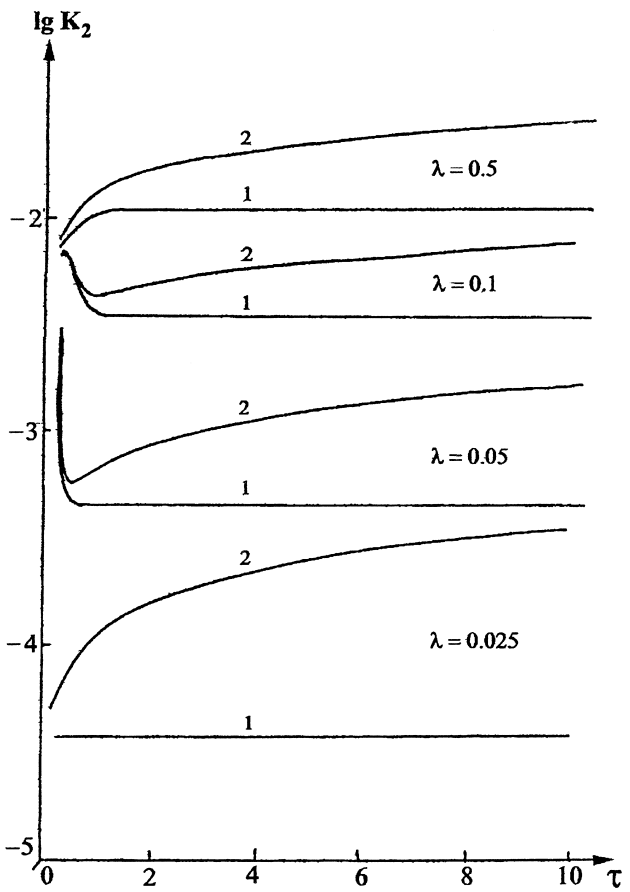

Fig. 1 Time dependences of the dispersion coefficient $K_2(\tau)$. Curve 1 : 2D model; curve 2 : 3D model. The solute was initially uniformly distributed in the channel cross section.

In Ref.[5] the time needed to separate two types of solute molecule with resolution $R_s = 1$ was studied for the cases of different initial solute distributions. It was shown, for example, that for solute molecules with $\lambda = 0.1$ and $\lambda = 0.125$, the time needed to separate them, predicted by the 3D model for uniform initial solute distribution, is 5% larger than predicted by the 2D theory, whereas, for the case of the syringe inlet, the value predicted by the 3D model is much closer to the 2D value (only 0.5% difference). The difference in 2D and 3D predictions can be more significant for closer values of λ, when the retention time needed to fractionate the solute is larger.

More complicated 3D effects were studied in Refs.[6,7] with the help of 3D Monte Carlo digital simulation performed with a rather powerful computer (RISK System/6000). Sedimentation FFF with different breadth-to-width channel ratios and both codirected and counterdirected rotation and flow were studied. Secondary flow forming vortexes in the y–z plane is generated in the sedimentation FFF channel, both due to its curvature, and the Coriolis force caused by the centrifuge rotation. The exact structure of the secondary flow was calculated by the numerical solution of the Navier–Stokes equations and was used in the Monte Carlo simulation of the movement of solute molecules.

It was shown that when rotation and flow are codirected, there is a considerable amount of molecules eluted prematurely before the main peak, because they are caught by the vortex of the secondary flow. This effect is practically negligible when the flow and rotation are counterdirected. So, the counterdirected mode is always preferable in sedimentation FFF. Note that this important practical finding of Ref.[7] is of pure 3D nature and cannot be done with the 2D theory.

The contribution of the channel endpieces to the peak broadening is certainly a 3D effect and should be mentioned here, although the theory used in Ref.[8] to analyze this effect was a 2D, not a 3D, one. In FFF instruments, the inlet and outlet tubes are connected with the rectangular FFF channel by triangular end-pieces. So, if the solute is introduced to the channel with the flow, then "the fanning out process between the inlet and the main rectangular section of the FFF channel leads to crescent-shaped bands, a type of distortion that persists down the channel and is responsible for some incremental band broadening".[8] The 2D (in the x–z plane) model was developed. The flow was considered to be ideal and described by the stream function, satisfying the Laplace equation. The streamlines calculated were used to simulate the solute band profile and to estimate the contribution of the endpieces effect to the theoretical plate height:

$$H_e = \frac{b^2 \beta^2 \tan^2(\theta/2)}{4L} \quad (4)$$

where L is the total FFF channel length, θ is the angle of the triangular endpiece, and β is a function of θ, determined from the calculated band profiles. It was shown that $\beta^2\tan^2(\theta/2)$ grows dramatically with θ, and is equal to 0.0226 for $\theta = 30^\circ$ and to 0.389 for $\theta = 120^\circ$. The role of the end effects must not be overestimated, as even for the channel with unusually large breadth $b = 6$ cm ($\theta = 75^\circ$), the absolute value of H_e was 0.0586 cm, much smaller than the typical FFF HETP values ($\sim$1 cm). Naturally, this type of contribution to peak width is absent if the solute is introduced by the syringe into the main rectangular section of the channel.

Finally, it must be said that in most of the practical cases, retention ratio and peak width are satisfactorily predicted by the 2D models. The role of the 3D models was to estimate the contributions of the 3D effects and to determine the optimal conditions when these contributions are negligible. As it was shown, to minimize the 3D effects, one must use FFF channels with a larger breadth-to-width ratio, use the syringe inlet, and/or use the longer endpieces with the sharper angle; in the case of sedimentation FFF, one is to avoid codirected flow and rotation mode.

REFERENCES

1. Krishnamurthy, S.; Subramanian, R.S. Exact analysis of FFF. Separat. Sci. Technol. **1977**, *12*, 347.
2. Takahashi, T.; Gill, W.N. Hydrodynamic chromatography: Three dimensional laminar dispersion in rectangular conduits with transverse flow. Chem. Eng. Sci. **1980**, *5*, 367.
3. Kim, E.K.; Chung, I.J. Transient convective mass transfer in rectangular FFF channels. Chem. Eng. Commun. **1986**, *42*, 349.
4. Andreev, V.P.; Khidekel, M.I. Field-flow fractionation in a rectangular channel. Three dimensional model. Nauchn. Apparat. **1989**, *4*, 123 (in Russian).
5. Andreev, V.P.; Khidekel, M.I. On the influence of the channel side walls on the resolution time in FFF. Zh. Phys. Chim. **1991**, *65*, 2619.
6. Shure, M.R. Digital simulation of sedimentation FFF. Anal. Chem. **1988**, *60*, 1109.
7. Shure, M.R.; Weeratunga, S.K. Coriolis-induced secondary flow in sedimentation FFF. Anal. Chem. **1991**, *63*, 2614.
8. Williams, P.S.; Giddings, S.B.; Giddings, J.C. Calculation of flow properties and end effects in FFF channels by a conformal mapping procedure. Anal. Chem. **1986**, *58*, 2397.

TLC/MS

Jan K. Rozylo
Department of Adsorption Chromatography and Planar Chromatography, Marie Curie-Sklodowska University, Lublin, Poland

INTRODUCTION

There are many methods of detection of substances following separation of mixtures by thin-layer chromatography (TLC) or, in wider aspect, planar chromatography (PC). Some of the methods have been used continuously since the beginnings of TLC. These are described in other sections of this volume. The newest method in this field is mass spectrometry (MS) coupled with planar chromatography. The concept of using MS as a detection method for samples separated by TLC is not new; it dates almost to the beginning of organic MS itself. It was Kaiser who suggested the possibility of using a coupled TLC/MS method in his review 30 years ago. Despite a long and successful history of application as a detector in gas chromatography (GC) and liquid–liquid chromatography (LLC), MS has been under-utilized as a detector for TLC. The need for application of this combined analytical method (i.e., mass spectrometric detection with separation by TLC) was evident by the late 1980s. The success of the method depended, above all, on the elaboration of suitable experimental means, devices, and solutions to the challenge of transfer of substances from TLC plates to the mass spectrometer.

BASIC PRINCIPLE OF MS AND ITS APPLICATION TO TLC

In a mass spectrometer, instead of an optical spectrum we have a mass spectrum of matter radiation. The necessary condition for using MS detection is ionization of components of the analyzed sample. Thus, we can say that MS is a destructive method of analysis. There are many techniques and systems for MS, but they all have the same three elements: source of ions, ion analyzer, and ion detector (Fig. 1).

SOURCE OF IONS

Positive ions can appear by simple removal of one electron. This process can be demonstrated by means of the equation

$$M \rightarrow M^+ + e$$

The M^+ ion is called a *molecular ion*. It is characterized by means of mass (m) and charge (z). In order to produce a molecular ion, there must be supplied energy at least equal to the energetic potential of the molecule. The first ionization potential for most organic molecules is between 8 and 15 eV. The studied sample is transferred to a vessel under vacuum in which there is an anode and a cathode. The potential difference between the anode and cathode is over 20 kV. With such a large potential difference and small distance between anode and cathode, there appear electrical discharges which cause the ionization of sample molecules. The positive ions are pushed away by repellent electrodes and directed toward an *acceleration gap*. Of course, it is possible that the electron would be captured by the analyzed molecule and produce a negative ion, but the probability of such a process is small. However, fragmentation of a negatively charged molecule is much easier than fragmentation of a positively charged molecule. The higher the ionization energy used, the greater will be the probability of fragmentation of a molecule.

ANALYSIS OF IONS

Magnetic fields affect charged molecules if these molecules are in motion. The direction of this action is perpendicular to the direction of the field and perpendicular to the direction of movement of the investigated ion. The strength of the force acting on an ion in a magnetic field depends on the ion charge and its velocity. The effects of the action of this force depend on mass and velocity. Finally, the ions move along arcs of circles and the deviation from their original direction of movement depends on their m/z ratio.

The most popular mass spectrometers used in chromatography are sector magnetic spectrometers. They are large, expensive, and relatively slow spectrometers. Their primary advantage is their high resolution. A constant, strong electrical field within the acceleration gap speeds the ions up to their terminal velocities. The ion beam goes into the analyzer, *in vacuum* (10^{-7} – 10^{-8} Tr), and is placed in the magnetic field. In order to obtain a spectrum, either the magnetic field in which the analyzer is located or the accelerating voltage between the electrodes in the acceleration gap is changed. The ion beam leads into a collector, where the signal is amplified by means of an electron multiplier.

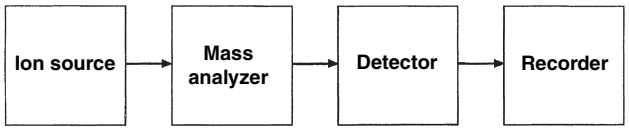

Fig. 1 Scheme of the mass spectrometry procedure.

QUADRUPOLE SPECTROMETER

The resolution of this spectrometer is not high, but the spectrometer is of relatively low cost and fast; it collects a full spectrum of the investigated substance in about 0.3 sec. In the spectrometer (also called *quadrupole filter*), there appears an electromagnetic field that causes the oscillation of ions. At given voltages, the oscillation amplitude of ions under a certain mass is larger than the distance between one of the pairs of electrodes; such ions are thrown out of the filter. Only the ions of a determined mass pass through the filter to the detector.

ION TRAP

In an ion trap, in contrast to other mass spectrometers, ionization and analysis occur in the same location but at different times. A chromatographic sample is introduced directly into the space between the electrodes where ionization takes place. An appropriate voltage across the electrodes causes the appearance of an electrical field within the trap. This field keeps the ions produced during ionization inside the trap and does not allow them to leave. When ionization is completed, the voltage of the electrodes is constantly changed so that the ions leave the trap in the order of increasing m/z ratio.

Soon after the advent of fast-atom bombardment (FAB) ionization, it was realized that there is an ionization technique ideally suited for analyzing compounds resolved on a TLC plate. There are several early examples of the direct analysis of spots from TLC plates (without prior extraction of the adsorbed material). Detection limits of these TLC-FAB-MS measurements depend on the sample, but they are typically in the 0.1–10-μg range.

The coupled TLC-FAB-MS, without the prior recovery of analyte from the TLC plate, provides a powerful tool for the unambiguous identification of sample components. The use of tandem MS/MS represents a further refinement of this approach, enabling identification to be performed even when the separated components are incompletely resolved from each other or are subject to background interference.

GENERAL APPROACHES TO SAMPLE PREPARATION FOR THE COUPLED TLC/MS

The following are combinations to these approaches:

1. The compound is eluted from the chromatographic plate, collected, and introduced into the MS as a discrete sample. In this method, samples collected from a TLC spot, identified with an independent method of visualization, must be sufficiently volatile to evaporate into the source of the MS.
2. The sample and support are not separated, but both are introduced simultaneously into the source of the MS. The spot is scraped from the support and placed on the direct insertion probe of the MS. As the probe is heated, the more volatile sample is evaporated into the source, whereas the fairly non-volatile chromatographic matrix remains in the probe.
3. The entire intact chromatogram is placed within the source of the mass spectrometer and analyzed.

For the last two methods, there is the assumption that extraneous material from the chromatogram does not unduly and adversely affect the quality of the mass spectrum recorded. The chromatogram is placed, intact, within a source housing and a spatially resolved map of organic or bio-organic compounds distributed across the surface is measured.

At the present time, the most up-to-date methods of ionization in TLC/MS are FAB and secondary ionization mass spectrometry (SIMS) in which organic molecules are sputtered from the surface by impact of a stream of high-energy molecules, and laser desorption (LD) in which sputtering of organic molecules from the surface of a support is due to the influence of high thermal energy produced by a laser beam onto a plate surface. The ions produced this way are usually even-electron $(M^+ + H)^+$ and appear by means of chemical ionization. The interpretation of the spectrum follows the same lines.

Bush designed an excellent instrument that can be used for analyses of TLC chromatograms by FAB-MS; it provides spatially discrete mass spectra directly from the surface layer.

SOME PRACTICAL PROBLEMS

The use of MS as a detector for TLC involves identification of substances in a mixture, as well their separation. A necessary condition in this approach is the purity of a sample within a spot on the chromatogram. A special problem is the large quantity of support and, sometimes, a binding material and mobile-phase residues. Some other factors that might potentially hinder TLC/MS are water, which is physically bound to the support, as well as, in some cases, the organic modifier of the support. A factor which complicates the detection process in TLC/MS may also be the presence of derivatives in a sample peak displayed on a chromatogram. That is why the analyzed sample should be as free of contamination with other additives as possible and the support matrix should be carefully removed before MS analysis. These indications refer, to a lesser degree, to other methods of detection that are performed after total extraction of sample molecules from a sample matrix. It is a widely known fact that most of the

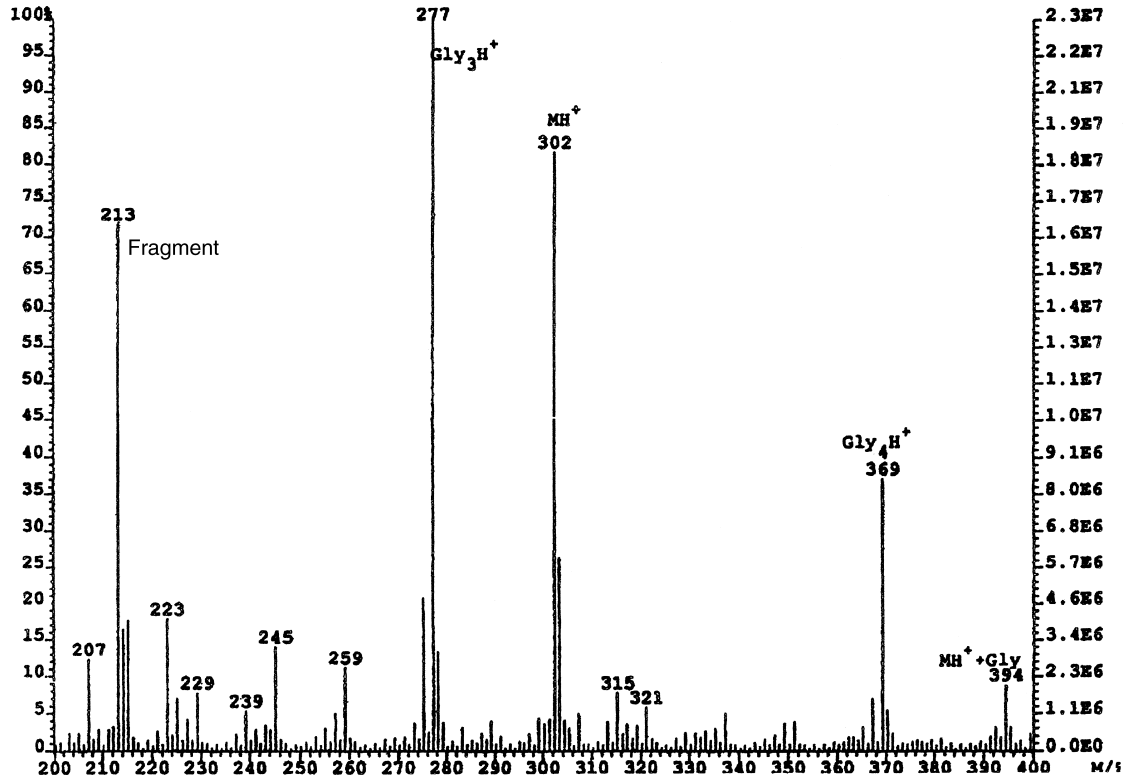

Fig. 2 TLC-FAB-MS spectrum obtained after of 1 μg deramciclane standard with an acidic mobile phase. Gly indicates glycerol clusters. **Source:** From J. Planar Chromatogr.-Mod. TLC **1997**, *10*, 90–96.

analyses using a TLC/MS method are performed after exhaustive extraction of the sample from the matrix.

There are also some practical problems connected with the instrumental issues of MS. Most of the sources used in mass spectrometers are so small that it is possible to also have, for example, a very small inlet for the gas or liquid. In this case, such TLC/MS methods may only be used if they are based on the introduction of samples via a stream of gas. The matrix, together with sample material, may be introduced directly into the MS source. Some types of instruments even allow for the insertion of a whole chromatographic plate into the MS source.

APPLICATIONS

Expansion in the field of analytical mass spectrometry has taken place in recent years; in particular, the applicability of TLC/MS in the field of chemical and biochemical science has been significantly broadened. This technique can now be used for the analysis of macromolecules such as peptides, proteins, oligosaccharides, and oligonucleotides, etc. (Fig. 2).

The combination of TLC and MS is well established and may be used for on- and off-line analyses. The increase in popularity of this combined technology also resulted from the improvements in the separating power of TLC and the widespread availability of suitable MS techniques for difficult-to-analyze molecules. The TLC/MS is, at present, a simple and readily implemented means of combining a separation with mass spectrometric identification of substances. With the development of MS suited to direct TLC analysis, it seems clear that the application of TLC/MS will grow in the next decade.

BIBLIOGRAPHY

1. Brown, S.M.; Bush, K.L. J. Planar Chromatogr.-Mod. TLC **1991**, *4*, 198.
2. Bush, K.L. *Handbook of Thin-Layer Chromatography*; Sherma, J., Fried, B., Eds.; Marcel Dekker, Inc.: New York, 1966; 183.
3. Bush, K.L.; Cooks, R.G.Z. Mass-spectrometry of large, fragile, and involatile molecules. Science **1982**, *218*, 247.
4. Bush, K.L.; Mullis, J.O.; Chakel, J.A. High-resolution imaging of samples in thin layer chromatograms using a time-of-flight secondary ion mass spectrometer. J. Planar Chromatogr.-Mod. TLC **1992**, *5*, 9–15.
5. Day, R.J.; Unger, S.E.; Cooks, R.G. Molecular secondary ion mass spectrometry. Anal. Chem. **1980**, *52*, 557A.
6. Kaiser, R.E. Thin-layer chromatography in direct coupling with gas chromatography and mass spectrometry. Chem. Britain **1969**, *5*, 54.
7. Martin, P.; Morden, W.; Wall, P.; Wilson, I. TLC combined with tandem mass spectrometry: Application to the analysis for antipyrine and its metabolites in extracts of human urine. J. Planar Chromatogr.-Mod. TLC **1992**, *5*, 255–258.
8. Nakagowa, Y. Iyo Masu Kenkuyukai Koensku **1984**, *9*, 39.

TLC: Sandwich Chambers

Simion Gocan
Department of Analytical Chemistry, Babes-Bolyai University, Cluj-Napoca, Romania

INTRODUCTION

In column chromatography, the stationary phase exists in a closed column that is adequately packed with a suitable sorbent. The stationary phase is preequilibrated with the mobile phase before the first sample is introduced. In this case, the stationary phase cannot be in contact with vapors of the mobile phase during the chromatographic process.

Column chromatography is different from thin-layer chromatography (TLC) because, in planar chromatography, and, therefore, in TLC, development generally starts with a dry stationary phase. Therefore, the mobile-phase front moves forward in the dry stationary phase. This process takes place in the limited, confined volume of the chromatographic chamber.

The kinetics of eluent migration will depend on the degree of saturation of the chamber. The eluent front runs faster in a saturated chamber than in an unsaturated one. The problem of the reproducibility R_f of values can be seriously affected by an unsaturated chamber.

The chromatographic chamber commonly used in TLC can be divided into two categories. A normal chamber (N chamber) is a chromatographic chamber of a large volume with a distance of gas phase in front of a thin-layer greater than about 3 mm. Conversely, a sandwich chamber (S chamber) is a small chromatographic chamber having a small volume and a distance of gas space in front of the thin layer plate less than 3 mm.

The equilibration of the sorbent thin layer with the vapor phase is easily achieved in the compact S chamber. A threefold larger variation of the R_f values for experiments in unsaturated atmosphere has been observed. Also, it has been proved that, in an unsaturated chamber, the so-called "edge effect" appears, owing to the more intense evaporation at the edge of the plate. This effect may be avoided by complete saturation of an N chamber with eluent vapor or by using an S chamber.

There are two methods for development, taking into account the position of the thin-layer plate (i.e., ascending, or vertical, and horizontal).

S CHAMBER

The S chamber (Fig. 1a) is limited to a small volume by using a thin-layer plate as a near wall (1) to the tank. The opposite wall is a cover plate (2) of small size. This is a frame plate, which has glass strips (5 mm wide and 3 mm thick) sintered along three edges. The two plates are held together by two clamps fixed at the vertical edges of the S chamber (3). This S chamber is placed in a trough which consists of a double jacket (4) of stainless steel filled with solvent (5). The other jacket can be turned to obtain slits at varying distances, which enables plates of different widths to be introduced and ensures a tight seal for the S chamber. The S chamber has a support (6) which permits a vertical position. Only 15 ml of mobile phase are needed for the thinlayer plate (20 × 20 cm). Before application, a 10 mm strip of adsorbent should be removed from three sides of the TLC plate.

There is another type of S chamber which permits prior saturation of the chamber atmosphere, simultaneously with the preconditioning of the adsorbent, before starting the chromatographic process (Fig. 1b). For this purpose, the adsorbent is removed (a 1 cm width) from all the sides of the plate (1). The opposite frame plate (2) contains, on all of its surface, a thin layer of sorbent. The two plates are fixed by two clamps (3). The chamber is introduced into the trough (4) through a slit. At the beginning, the level of the eluent (5) does not touch the bottom of adsorbent on the thinlayer plate (1). When saturation of the atmosphere is achieved, a volume of eluent is added to the eluent in the trough until the adsorbent is wetted. At this moment, the separation can be started.

Method of Operation

A template is indispensable for ensuring proper spacing of the starting spots during manual sample application. The sample is applied to the layer using a glass capillary or a micropipette of appropriate size (1–10 ml). Sample may be applied as bands to the TLC plates using a band applicator such as the Camag automatic TLC sampler. The automatic TLC sampler works by mechanically moving the plate. This applies the sample automatically by a controlled nitrogen spray from the syringe, forming narrow bands or spots on the plate surface. Programming, operation, and documentation are performed under a Windows-programmed environment.

When the samples have been applied, the frame plate is placed on the top of the TLC plate and fastened by two wide clamps at the right and left edges. In this way, the S chamber is ready to be placed into the trough filled with eluent. The S chamber is kept upright by a fork-shaped holding arm fixed to the trough. Then, the trough slit is sealed by gentle rotation of the outer jacket.

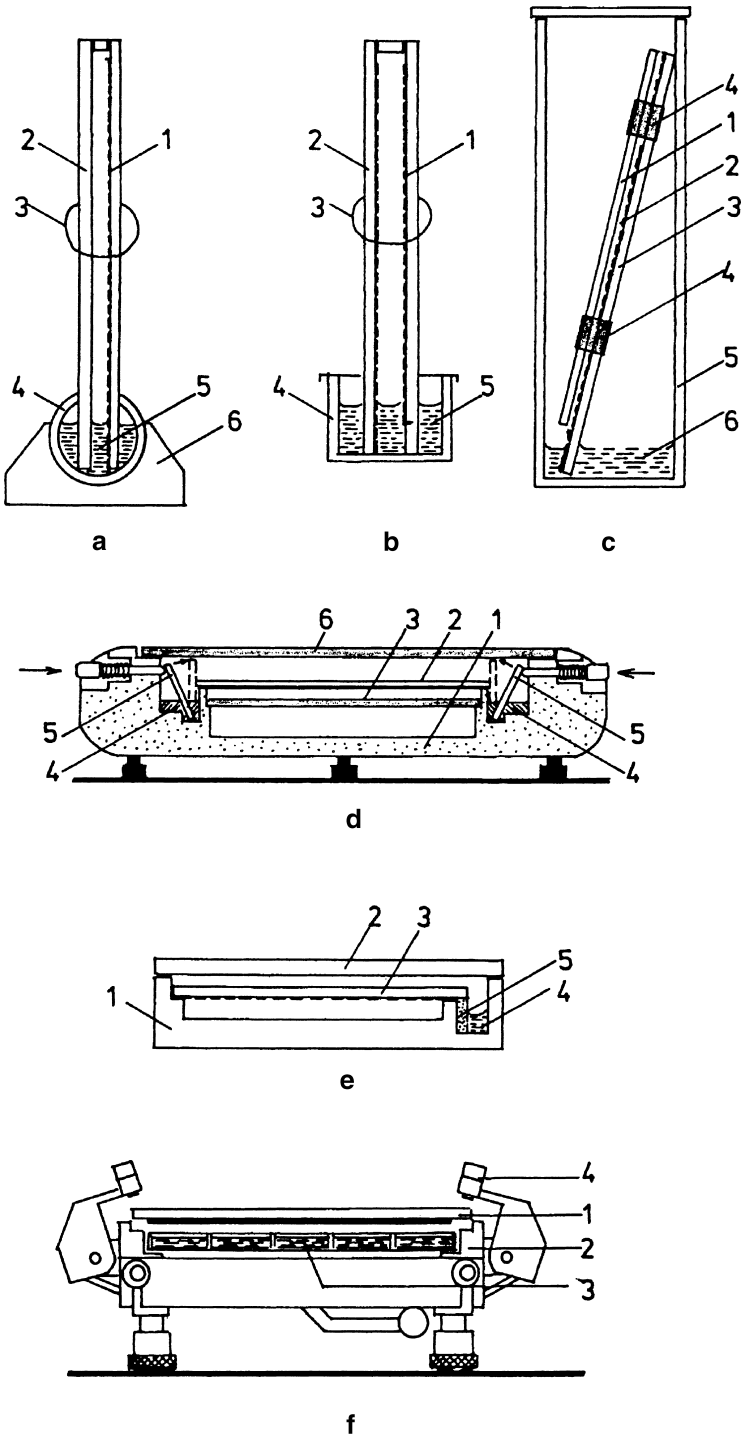

Fig. 1 Different TLC sandwich chambers: a, diagram of the S chamber; b, diagram of the saturation S chamber; c, diagram of the Camag sandwich cover plate; d, diagram of the Camag horizontal developing S chamber; e, diagram of the Desaga H-separation chamber; f, diagram of the Camag Vario-KS chamber.

The separation process can be considered finished when the eluent front touches the upper edge of the thin-layer plate.

CAMAG SANDWICH COVER PLATE

This type of S chamber has the purpose of reducing the volume of the gas phase, which is in front of the thin layer by a counterplate placed at a small distance (Fig. 1c). The cover glass (1) has two fixed glass spacers (2) located on two sides. The cover plate (1) is 2 cm shorter than the TLC plate (3) and is fixed so that it does not sit deeply into the eluent. The thin-layer plate and cover plate are held together by four stainless-steel clamps (4). The S chamber is not closed at the top edge. In this configuration, there is no need to scrape off the sorbent layer at the edges. With the Camag sandwich cover plate, the TLC plate can be developed into an N chamber (5) which contains, on the

flat bottom, the eluent (6). The N chamber is used only as eluent holder. This system permits simultaneous development of two plates.

HORIZONTAL S CHAMBER

The horizontal developing chamber is a sandwich-type chamber (Fig. 1d). The horizontal S chamber for TLC consists of a flat body of the chamber made from polytetrafluoroethylene (PTFE) (1) so that it is resistant to all liquids. The TLC or high-performance TLC (HPTLC) plate (2) lies on the supports with the thin layer facing downward. The glass plate (3) is used for development in the sandwich configuration (not presented with saturation configuration). A narrow trough (4) holds the eluent. Development is started by shifting the glass strips (5) to the chromatographic plate. In this way, a capillary slit is formed between glass strip and the trough wall, so that a vertical meniscus of the eluent is formed and rises instantaneously. It enters the layer evenly from its front. The glass strip (5) is tilted inward by pushing the rods (arrows). The chamber is kept covered with the glass plate (6) during both preequilibration and development.

Method of Operation

In the horizontal chamber, the HPTLC plate is developed from both opposing sides toward the middle. This permits the number of samples to be doubled, as compared with development in an N chamber. The horizontal S chamber is available for plate sizes 10 × 10 cm and 20 × 10 cm. The optimum separation distance for HPTLC silica gel, 45 mm, is still available.

The mobile phase is transported from the trough to the sorbent layer by surface tension and capillary forces and will continue to travel through the sorbent layer by capillary action. When a plate is developed from both edges simultaneously, the chamber must be kept in a perfectly horizontal position to allow the two solvent fronts the same rate of migration and to meet precisely in the middle. At this point, the capillary forces balance out and the chromatographic development ceases.

The chromatographic process takes less than 10 min per plate and the amount of solvent used is much smaller than in an N chamber. On a 20 × 20 cm HPTLC plate, it is possible to simultaneously develop, from both ends to the centers, up to 70 samples, or 35 samples in a single direction, from one end to the other.

The horizontal S chamber can be used in saturation configuration (N type) when the counter glass plate (3) is not inserted. In this way, the horizontal S chamber permits the conditioning of the adsorbent layer with the different solvent vapors by introducing several drops of the eluent or another solvent on the bottom of the chamber before placing the chromatographic plate face down.

H-SEPARATION CHAMBER

The H-separation chamber (DESAGA), a mini horizontal development chamber (Fig. 1e), is made of solvent resistant PTFE (1) covered with a sheet of glass (2) 4 mm thick. The HPTLC plate (5 × 5 cm) is laid down for development with the thin layer underneath (3). The mobile phase from the trough (4) is led by a glass frit rod (5) to the thin layer of sorbent. The groove in which the frit rod sits ensures even distribution. The maximum eluent consumption is 2 ml on the plates.

Method of Operation

The sample is applied to the starting line on the layer using a capillary of appropriate size. The applied spots have to be dried completely before the plate is introduced into the separation chamber. The effective migration distance on a plate of 5 × 5 cm is only 3 cm and the migration time is 3 min.

VARIO-KS CHAMBER

The Vario-KS chamber (Camag, Fig. 1f) is used for optimization of developing conditions for 10 × 10 cm plates by simultaneously testing of up to six different mobile phases and vapor equilibration conditions with N or S chamber conditions. Also, the Vario-KS chamber may be used for optimization of developing conditions for 20 × 20 cm TLC plates. The thin-layer plate (1) is laid down on the support (2). The eluent in the reservoir is connected to the thin layer of adsorbent by means of a filter paper strip. Under the thin-layer plate, there are many troughs (3) filled with solvents for preconditioning of the adsorbent layer. The chamber is tightly sealed by two clamps (4).

BIBLIOGRAPHY

1. Geiss, F. *Fundamental of Thin-Layer Chromatography*; Hüthig: Heidelberg, 1987.
2. Griberg, N., Ed.; *Modern Thin-Layer Chromatography;* 4th Ed.; Marcel Dekker, Inc: New York, 1990.
3. Kirchner, J.G. *Thin-Layer Chromatography,* 2nd Ed.; John Wiley & Sons: New York, 1978.
4. Sherma, J., Fried, B., Eds.; *Handbook of Thin-Layer Chromatography*; 4th Ed.; Marcel Dekker, Inc: New York, 1999.
5. Stahl, E., Ed.; *Thin-Layer Chromatography*; Springer-Verlag: New York, 1969.
6. Touchstone, J.C. *Practice of Thin-Layer Chromatography,* 3rd Ed.; John Wiley & Sons: New York, 1992.
7. Zalatkis, A., Kaiser, R.E., Eds.; *HPTLC: High Performance Thin-Layer Chromatography*; Elsevier: Amsterdam, 1977.

TLC: Theory and Mechanism

Teresa Kowalska
Institute of Chemistry, Silesian University, Katowice, Poland

Wojciech Prus
School of Technology and the Arts in Bielsko-Biała, Bielsko-Biała, Poland

INTRODUCTION

General classification of the modes of thin-layer chromatography (TLC) is based on the chemical nature of the stationary and mobile phases. Three types of TLC are widely recognized as different modes: adsorption TLC, normal-phase TLC, and reversed-phase (RP)/TLC.

ADSORPTION TLC

In this mode, active inorganic adsorbents (e.g., silica, alumina, or Florisil) are usually employed as stationary phases and, hence, the overall mechanism of retention is governed predominantly by the specific intermolecular interactions between the functionalities of the solutes, on the one hand, and active sites on the adsorbent surface, on the other. In adsorption TLC, aqueous mobile phases are never used, and stationary-phase activity prevails over the polarity of the mobile phase employed.

NORMAL-PHASE TLC

This mode of chromatography usually involves organic chemically bonded stationary phases with polar (e.g., 3-cyanopropyl) ligands. This particular mode is characterized by a mixed mechanism of solute retention: Solute molecules interact specifically with the polar functionalities of the organic ligand and with the residual active sites of the silica matrix, whereas their interactions with the hydrocarbon moiety of the organic ligands are entirely non-specific in nature. Again, aqueous mobile phases are never employed in normal-phase (NP) TLC, and stationary phase activity prevails over the polarity of the mobile phase employed.

RP TLC

This chromatographic mode usually involves aliphatic chemically bonded stationary phases with, for example, octyl, octadecyl, or phenyl ligands. The mode of chromatography also is characterized by a mixed mechanism of solute retention: Solute molecules interact specifically with the residual active sites of the silica matrix, whereas their interactions with the aliphatic ligands are non-specific (and predominantly hydrophobic) in nature. Reversed-phase (RP) TLC is usually performed with aqueous mobile phases containing organic modifiers [such as, e.g., methanol, acetonitrile (ACN), tetrahydrofuran (THF), etc.], and in this case, the activity of the stationary phase—as an exception—is less than that of the high-polarity mobile phase employed.

TLC PARAMETERS OF SOLUTE RETENTION

The parameter R_f is the quantity most commonly used to express the position of a solute in the developed chromatogram. It is calculated as a ratio:

$$R_f = \frac{\text{Distance of chromatographic spot center from origin}}{\text{Distance of solvent front from origin}} \quad (1)$$

Using symbols from Fig. 1, R_f can be given as

$$R_f = \frac{z}{l} \quad (2)$$

R_f values vary between 0 (solute remains at the origin) and 0.999 (solute migrates with the mobile-phase front). From a practical standpoint, the most reliable analytical results are achieved when the parameter R_f ranges from 0.20 to 0.80.

In the theory and practice of chromatography, another parameter of solute retention is also employed, the so-called R_M value. This quantity was defined by Bate-Smith and Westall[1] as

$$R_M = \log\left(\frac{1 - R_f}{R_f}\right) \quad (3)$$

SELECTED MODELS OF THE CHROMATOGRAPHIC PROCESS

The adsorption and partition mechanisms of solute retention are the two most universal mechanisms of

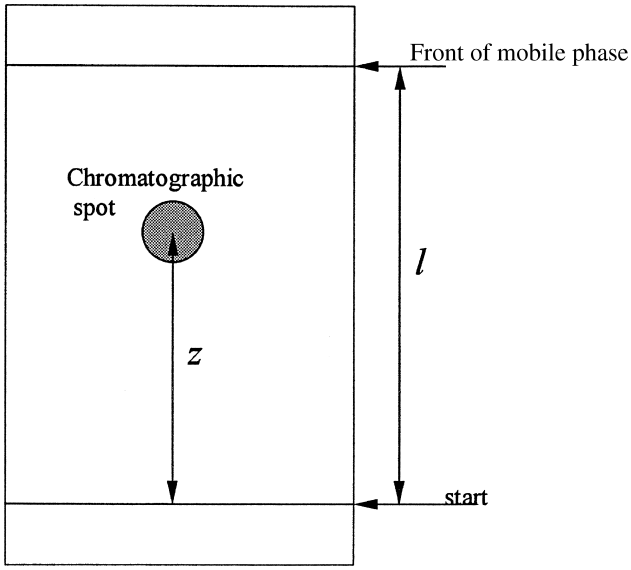

Fig. 1 The thin-layer parameters used to calculate the retention parameter R_f.

chromatographic separation, both operating on a physical principle. In fact, almost all solutes can be adsorbed on a microporous solid surface or be partitioned between two immiscible liquids. It is the main aim of semiempirical chromatographic models to couple the empirical parameters of retention with the established thermodynamic quantities generally used in physical chemistry. The validity of these models in chromatographic practice can hardly be overestimated, because when incorporated in separation selectivity-oriented optimization strategies, they often successfully help overcome the old trial-and-error approach used to optimize analyses. In the forthcoming sections, we will discuss a selection of the most popular and best-performing models and concepts of solute retention.

MARTIN AND SYNGE MODEL OF PARTITION CHROMATOGRAPHY

Partition chromatography was the first chromatographic technique to be given a thermodynamic foundation, by the pioneering work of Martin and Synge,[2] the 1952 Nobel Prize winners for chemistry. The Martin and Synge model describes the idealized parameter R_f (i.e., the parameter R_f') as

$$R_f' = \underset{\text{(I)}}{\frac{t_m}{t_m + t_s}} = \underset{\text{(II)}}{\frac{n_m}{n_m + n_s}} \underset{\text{(III)}}{\frac{m_m}{m_m + m_s}} \tag{4}$$

where t_m and t_s denote the time spent by a solute molecule in the mobile and stationary phases, respectively, n_m and n_s are numbers of solute molecules present in the mobile and stationary phases at equilibrium, and m_m and m_s are the respective numbers of moles.

Eq. 4 can be further transformed as follows:

$$R_f' = \frac{m_m}{m_m + m_s} = \frac{c_m V_m}{c_m V_m + c_s V_s} = \frac{1}{1 + c_s V_s / c_m V_m} \tag{5}$$

where c_m and c_s are the molar concentrations of the solute in the mobile and stationary phases, respectively, and V_m and V_s are volumes of these phases, respectively.

Assuming that

$$K = \frac{c_s}{c_m} \tag{6}$$

where K is the thermodynamic equilibrium constant for solute partitioning, we obtain

$$R_f = \frac{1}{1 + K\Phi} \tag{7}$$

where Φ is the so-called phase ratio (i.e., $\Phi = V_s/V_m$).

Eq. 7 unites the empirical retention parameter of the solute, R_f', with the established thermodynamic (i.e., theoretical) quantity K, expressed as

$$\ln K = \frac{\Delta {\mu_p}^0}{RT} \tag{8}$$

where $\Delta {\mu_p}^0$ is the standard chemical potential for partition. Hence, the retention model given by Eq. 8 can rightfully be called semiempirical.

SNYDER AND SOCZEWINSKI MODEL OF ADSORPTION CHROMATOGRAPHY

The semiempirical model of adsorption chromatography, analogous to that of Martin and Synge, was established only in the late 1960s by Snyder[3] and Soczewinski[4] independently, and it is often referred to as the displacement model of solute retention. The crucial assumption of this model is that the mechanism of retention consists in competition among the solute and solvent molecules for the active sites of the adsorbent and, hence, in a virtually endless process of the solvent molecules displacing those of the solute from the solid surface (and vice versa). Further, the authors assumed that some of the mobile phase remains adsorbed and stagnant on an adsorbent surface. This adsorbed mobile phase formally resembles the liquid stationary phase in partition chromatography. Thus—utilizing with imagination the main concept of the Martin and Synge model of partition chromatography—Snyder and Soczewinski

managed to define the R_f' parameter valid for adsorption chromatography as

$$R_f = \frac{t_m}{t_m + t_a} \equiv \frac{n_m}{n_m + n_a} = \frac{m_m}{m_m + m_a} = \frac{c_m(V_m - V_a W_a)}{c_m(V_m - V_a W_a) + c_a V_a W_a} \quad (9)$$

where t_m and t_a denote the time spent by a solute molecule in the mobile phase and on the adsorbent surface, respectively, n_m and n_a are numbers of solute molecules contained in the mobile phase and on the adsorbent surface at equilibrium, respectively, m_m and m_a are the numbers of moles of solute molecules contained in the non-adsorbed and adsorbed moieties of the mobile phase, respectively, c_m and c_a are molar concentrations of solute in the non-adsorbed and the adsorbed moieties of mobile phase, respectively, V_m is the total volume of mobile phase, V_a is the volume of the adsorbed mobile phase per unit mass of adsorbent, and W_a is the mass of adsorbent considered.

Transformation of Eq. 9 results in the relationship

$$R_f = \frac{1}{1 + K_{\text{th}}[V_a W_a/(V_m - V_a W_a)]} \quad (10)$$

where $K_{\text{th}} = c_a/c_m$, K_{th} being the thermodynamic equilibrium constant of adsorption, and $\Phi = V_a W_a/(V_m - V_a W_a)$.

SIMPLIFIED RELATIONSHIPS DERIVED FROM THE SNYDER AND SOCZEWINSKI MODEL

Two very simple relationships have been derived from the general framework of the Snyder and Soczewinski model of adsorption chromatography; these have proved useful for rapid prediction of solute retention in chromatographic systems employing binary mobile phases. One (known as the Soczewinski equation) proved successful for adsorption and normal-phase TLC; the other (known as the Snyder equation) proved similarly successful in RP TLC.

Soczewinski Equation

The Soczewinski equation[5] (Eq. 11) is a simple linear relationship with respect to $\log X_s$, linking the retention parameter (i.e., R_M) of a given solute with the quantitative composition of the binary mobile phase used:

$$R_M = C - n \log X_s \quad (11)$$

where C is, in the first instance, the equation constant (although with clear physicochemical significance), X_s is the molar fraction of the stronger solvent in the non-aqueous mobile phase, and n is the number of active sites on the surface of the adsorbent.

Apart from enabling rapid prediction of solute retention, the Soczewinski equation enables molecularlevel scrutiny of solute–stationary phase interactions. Thus, a numeric value of the parameter n of Eq. 11 of approximately unity ($n \approx 1$) implies one-point attachment of the solute molecule to the stationary-phase surface. Numerical values of n higher than unity indicate that in a given chromatographic system, solute molecules interact with the stationary phase at more than one point (so-called multipoint attachment).

Snyder Equation

The Snyder equation[6] (Eq. 12) is another simple linear relationship with respect to φ, which links the retention parameter (i.e., $\ln k$) of a given solute with the volume fraction of the organic modifier in the aqueous binary mobile phase (φ):

$$\ln k = \ln k_w - S_\varphi \quad (12)$$

where k is the retention coefficient of the solute [$k = (1 - R_f)/R_f$], k_w is the retention coefficient extrapolated for pure water as the mobile phase, and S is a constant characteristic of a given stationary phase.

CHROMATOGRAPHIC ACTIVITY OF ADSORBENTS AND ELUTION STRENGTH OF SOLVENTS[7–9]

Consequences of the Snyder and Soczewinski model are manifold, and they are of significant practical importance. The most spectacular conclusions of this model are: (a) the possibility of quantifying the activity of an adsorbent, and (b) the possibility of defining and quantifying the "chromatographic polarity" of solvents (known as their elution strength). These two conclusions could be drawn only upon the assumption of the displacement mechanism of solute retention. An obvious necessity in this model was to quantify the effect of displacement, which resulted in the relationship given by Eq. 13 for the thermodynamic equilibrium constant of adsorption, K_{th}, for an active chromatographic adsorbent and a monocomponent mobile phase:

$$\log K_{\text{th}} = \log V_a + \alpha(S^0 - A_{S^0}) \quad (13)$$

where α is a function of the adsorbent surface energy and is independent of the properties of the solute (it is known as the activity coefficient of the adsorbent; practical determination of its numerical values can be regarded as quantification of adsorbent activity), S^0 is the adsorption energy of a solute chromatographed on an active adsorbent with n-pentane as the monocomponent mobile phase, A_s is the surface area of the adsorbent occupied by an adsorbed

solute molecule, and ε^0 is the parameter usually referred to as the solvent elution strength, or simply solvent strength (it is the energy of adsorption of solvent per unit surface area of adsorbent).

Assuming that the adsorbent surface occupied by an adsorbed solute molecule (A_S) and that occupied by a stronger solvent (n_B) are equal, the eluent strength of a binary mobile phase, ε_{AB} has the following dependence on its quantitative composition:

$$\varepsilon_{AB} = \varepsilon_A + \frac{\log(x_B \times 10^{\alpha n_B(\varepsilon_B - \varepsilon_A)} + 1 - x_B)}{\alpha n_B} \quad (14)$$

where ε_A is the eluent strength of the weaker component (A) of a given binarymobile phase, ε_B is the eluent strength of the stronger component (B) of the same mobile phase, and x_B is the molar volume of the component B.

Combining Eqs. 13 and 14 gives the following relationship, which expresses the dependence of the retention parameter of a solute, R_M (= log k), on the quantitative composition of a given binary mobile phase:

$$\log k = \log V_a + \alpha[S^0 - A_{S^\varepsilon A}] - \frac{A_S \log(x_B \times 10^{\alpha n_B(\varepsilon_B - \varepsilon_A)} + 1 - x_B)}{n_B} \quad (15)$$

SCHOENMAKERS MODEL OF RP CHROMATOGRAPHY

In this particular model, it is assumed that Hildebrand's concept of the solubility parameter (δ), originally formulated for liquid non-ideal solutions, can also be applied to the solute and to the stationary and mobile phases of chromatographic systems.

The solubility parameter of any given substance (δ) is defined as

$$\delta = \sqrt{\frac{-E}{V}} \quad (16)$$

where E denotes its heat of vaporization at zero pressure, $-E$ is the energy of cohesion needed for transportation of one mole of an ideal gas phase to liquid phase, and V is the molar volume of the liquid.

One of the basic retention parameters (i.e., the solute's retention coefficient k) can be expressed as a function of the solubility parameters, δ:

$$\ln k_i = \frac{v_i}{RT}(\delta_m + \delta_s - 2\delta_i)(\delta_m - \delta_s) + \ln\left(\frac{n_s}{n_m}\right) \quad (17)$$

where v_i is the molar volume of the ith solute, δ_i, δ_s, and δ_m are respectively the solubility parameters of this solute and of the stationary and mobile phases employed, and n_s and n_m are respectively the numbers of moles of the stationary and mobile phases.

Finally, the principal equation of the Schoenmakers model[10] of solute retention in RP chromatography employing a binary aqueous mobile phase takes the parabolic form

$$\ln k = A\varphi^2 + B\varphi + C \quad (18)$$

where the equation constants A, B, and C have a clear physicochemical significance:

$$A = \frac{v_i}{RT}(\delta_a - \delta_w)^2 \quad (19)$$

$$B = 2\frac{v_i}{RT}(\delta_a - \delta_w)(\delta_a - \delta_i) \quad (20)$$

$$C = \frac{v_i}{RT}(\delta_w + \delta_s - 2\delta_i)(\delta_w - \delta_s) + \ln\left(\frac{n_s}{n_m}\right) \quad (21)$$

where δ_w and δ_a denote respectively the solubility parameters of water and of the organic modifier as the constituents of a given aqueous mobile phase.

REFERENCES

1. Bate-Smith, E.C.; Westall, R.G. Chromatographic behaviour and chemical structure I. Some naturally occuring phenolic substances. Biochim. Biophys. Acta **1950**, *4*, 427.
2. Martin, A.J.P.; Synge, R.L.M. A new form of chromatogram involving two liquid phases. Biochem. J. **1941**, *35*, 1358.
3. Snyder, L.R. *Principles of Adsorption Chromatography*; Marcel Dekker, Inc.: New York, 1968.
4. Soczewinski, E. Solvent composition effects in thin-layer chromatography systems of the type silica gel-electron donor solvent. Anal. Chem. **1969**, *41*, 179.
5. Snyder, L.R. Role of the solvent in liquid-solid chromatography. Review. Anal. Chem. **1974**, *46*, 1384.
6. Snyder, L.R.; Dolan, J.W.; Gant, J.R. Gradient elution in high-performance liquid chromatography: I. Theoretical basis for reversed-phase systems. J. Chromatogr. **1979**, *165*, 3.
7. Snyder, L.R.; Glajch, J.L. Solvent strength of multicomponent mobile phases in liquid–solid chromatography: Binary-solvent mixtures and solvent localization. J. Chromatogr. **1981**, *214*, 1.
8. Glajch, J.L.; Snyder, L.R. Solvent strength of multicomponent mobile phases in liquid–solid chromatography: Binary-solvent mixtures and solvent localization. J. Chromatogr. **1981**, *214*, 21.
9. Snyder, L.R.; Kirkland, J.J. *Introduction to Modern Liquid Chromatography,* 2nd Ed.; John Wiley & Sons: New York, 1979.
10. Schoenmakers, P.J.; Billiet, H.A.H.; De Galan, L. Influence of organic modifiers on the rentention behaviour in reversed-phase liquid chromatography and its consequences for gradient elution. J. Chromatogr. **1979**, *185*, 179.

TLC: Validation of Analyses

Gunawan Indrayanto
Mochammad Yuwono
Suciati
Faculty of Pharmacy, Airlangga University, Surabaya, Indonesia

Abstract
For obtaining reliable analysis results, the (high-performance) thin-layer chromatographic (TLC) method should be validated before using it as a quality control tool. The validation parameters that should be evaluated are stability of the analyte, specificity/selectivity, linearity, accuracy, precision, range, detection limit, quantification limit, and robustness/ruggedness.

INTRODUCTION

According to USP 30–NF 25,[1] validation of an analytical method is the process by which it is established, by laboratories studies, that the performance characteristics of the method meet the requirements for the intended analytical applications. Therefore, validation is an important step in determining the reliability and reproducibility of the method because it could confirm that the method is suitable to be conducted on a particular system. The performance parameters that should be determined in validation studies include specificity/selectivity, linearity, accuracy, precision, detection limit (DL), quantitation limit (QL), range, ruggedness, and robustness.[1,2] The parameters that are required to be validated depend on the type of the analyses; thus, different test methods require different validation schemes. The most common types of analyses are identification, quantitative determination of impurities, limit value determination of impurities, and quantitative determination of active ingredients.[3] Besides the general validation parameters mentioned above, the software and hardware of the thin-layer chromatographic (TLC) scanner should be validated first.[3,4] The validation of the instrument is categorized into design qualification (DQ), installation qualification (IQ), operation qualification (OQ), and performance qualification (PQ).[3]

STABILITY TESTING

A very important prevalidation method requirement is to test the stability of standards and samples. The analyte should be stable during sample preparations (at least 30 min) on the sorbent surface before development (at least 30 min) and during development (at least 1 hr).[5] The acceptance criteria are within 2%. The age mobile phase should also give the same value of R_f, T (tailing factor), and N (theoretical plate). The stability of the analyte should also be tested in biological matrices during storage. Reconstituted samples must remain stable in the solvents at the working temperature until spotted.[6] For fingerprint of herbal drugs, Reich, Schibli, and DeBatt[7] recommended to test the stability of analytes in solution and on the plate over 3 hr. Stability during chromatography should be tested using 2-dimensional development. If visualization requires a derivatization step, the stability must also be evaluated. Reich, Schibli, and DeBatt[7] suggested taking one image immediately after 5, 10, 20, 30 min, and 1 hr of derivatization, then the images are compared visually and by using video densitometry.

SPECIFICITY/SELECTIVITY

The terms specificity and selectivity are often used interchangeably. A method is said to be specific if it provides a response for only a single analyte. If the response in question is distinguished from all other responses, the method is said to be selective.[8] The International Conference on Harmonization (ICH)-2 does not differentiate both terms and defines specificity or selectivity as "the ability to unambiguously determine the analyte in the presence of other components whose presence is to be expected." This includes typical impurities, decomposition products, and matrix components.[3] The specificity of the method for TLC or high-performance TLC (HPTLC) analyses was proved by identification and purity checks of the analyte spots. This can be done by measuring in situ the ultraviolet and visible spectroscopy (UV–Vis) spectra of the analyte(s) and the authentic reference standard(s), those eluted on the same plate, and then by calculating their correlations (the r value should be ≥ 0.999). This correlation should be calculated on the upslope, the apex, and the downslope of the peaks. In a quality control laboratory, the selectivity

can be proven easily by spotting the standard, blank sample, possible impurities, or degradation products in the proposed system, analyte spot must not be interfered by other spots, which can be proven by calculating the resolution. If sources for impurities and degradation products are not available, the samples should be exposed to stress condition such as heat, UV light, acid, and base.[6] Other parameters should ideally be in the following range: R_f ($0.1 \leq R_f \leq 0.9$); tailing factor, T ($0.9 \leq T \leq 1.1$); resolution, R_s (≥ 1.0).[9] For proving the selectivity for analysis of botanical drugs, the availability of botanical reference material (BRM) is essential. It would be very nice if at least three authenticated BRM of each species from different origins can be used. This can be used to illustrate natural variability. A method is specific if during validation a sample representing target species showed identical fingerprint to that of BRM and samples representing other species give different fingerprints.[7]

LINEARITY

The linearity of a method is its ability to provide measurement results that are directly proportional to the concentration of the analyte or are directly proportional after mathematical transformation. The linearity is usually documented as the linear regression curve of the measured responses as a function of increasing analyte concentrations.[3] To perform linearity testing, it is recommended to use 5–10 concentrations with range equivalent to 80–120%,[9] 25–200%,[10] or 50–150%[11] of the expected content of the analyte. For the determination of degradant and preservative in the stability study, ranges of 0–40% and 50–110%, respectively, were recommended.[2] For dissolution testing ±20% over the specified concentration is tested, while for content uniformity a minimum of 70–130% of concentration is tested.[1] It is also essential that the basic calibration be performed by using independent samples and not by using samples that have been prepared by dilution and spotted on one TLC or HPTLC plate. For the evaluation of basic calibration line, several parameters can be used, for example, correlation coefficient (r), the relative process standard deviation value (V_{xo}), the Mandel's test, the X_p value,[12] the plot of response factor vs. concentration, the residual test, the analysis of variance (ANOVA), and so on. The lowest concentration used for the calibration curve must not be less than the value of X_p.[12] Camag (Muttents) calculated by using its CATS software the value of *sdv* [relative standard deviation (RSD) of the calibration curve] for expressing the linearity. If the reader is working with CATS software, the smallest value of *sdv* should be selected to determine the most suitable regression model that will be used for calibration. It is recommended that the correlation coefficient (r) alone not be used anymore. The correlation coefficient does not indicate the linearity or the lack thereof.[13] Readers should refer to previous works for further discussion.[12,14] The variance homogeneity over the whole range of the basic calibration line should also be proved using the F test.[9,12] If working range (WR) is defined as the ratio of the highest and lowest concentration of standards of the calibration or linear curve, it is recommended that a WR of not more than 10 be used; if WR is more than 10, a weighting regression should be used.[15] For quantitative analysis using TLC or HPTLC, the calibration curve must be performed on each plate; each plate should contain standards and unknown samples.

ACCURACY

Accuracy or trueness of an analytical method is given by the extent to which the value obtained deviates from the true value.[3] In the first approach, accuracy can be determined by analyzing a sample with known concentration and then by comparing the results between the measured and the true value. The second approach is by comparing the test results obtained from the new method to the results from the existing method that is known to be accurate. The third and fourth approaches are based on the percent recovery of known analyte spiked into blank matrices or products. The last technique is known as the standard addition method.[11] For spiking analyte into blank matrices, it is recommended to prepare the sample (laboratory-made preparation) in five different concentrations at the level of 80–120% of the target concentration. Experiences from our laboratory have shown that by using at least five levels of concentrations in duplicate (i.e., 80%, 90%, 100%, 110%, and 120% of target concentration), an accurate result can be achieved. On the contrary, for the standard addition method, the spiking concentrations are 30–60% of the label-claimed value. For dissolution studies, the accuracy should be tested at 40%, 75%, and 110% of the theoretical release.[6] To prove whether systematic errors do not occur, a linear regression of recovery curve of X_f (concentration of the analyte measured by the propose method) against X_c (nominal concentration of the analyte) should be constructed, and the confidence range of the intercept {VB(a_f)} and slope {VB(b_f)} from the recovery curves should be calculated for $p = 0.05$.[12]

PRECISION

The realistic standard deviations in TLC or HPTLC analyses are ~0.2% on multiple scanning of one spot, 0.8–1.5% on multiple spotting and analysis of the same sample solution, and 1.5–2.0% on multiple analysis of the same sample.[9] As a general rule, the standard deviation of a method should be lower than 1/6 of the specification range,[16] or the RSD value should not be more than 2%.[10] For validation purposes, precision is determined

by multiple application of the complete analytical procedure on one homogenous real sample. According to ICH, both repeatability and intermediate precision should be tested.[6] Repeatability is defined as precision under the same conditions, that is, same analyst, equipment, reagents, time, and TLC plate. Intermediate precision was performed by repeatability testing on the different combinations of analyst, equipment, reagents, and time within one laboratory. It is recommended to do 6–10 measurements on each repeatability studies.[9,10] A detailed discussion on the maximum of standard deviation for assay determination was published.[16] Other parameters that should be tested in the precision study are the David, Dixon or Grubbs, and Neumann test. Detailed discussion has been provided by Kromidas.[17] Reich, Schibli, and DeBatt[7] reported a detailed method to evaluate precision for qualitative analysis, in this case for HPTLC fingerprint of herbal drugs. They recommended to use at least three portions of the BRM and spotted onto three different plates. The fingerprint must be identical; the variability of R_f values of three markers should not exceed 0.01 across each plate, 0.02 for repeatability, 0.05 for intermediate, and 0.07 for reproducibility.

RANGE

The range of measurement is the interval for which linearity, accuracy, and precision have been tested. Analysis outside the range is not permitted.[1,3] For quality control purposes in a pharmaceutical industry, it is recommended to use a range from 80% to 120% of the target concentration, and for dissolution ±20% from upper and lower limit, respectively. For pharmacokinetic study, a wide range should be tested, the maximum value should exceed the highest expected concentration, and the minimum value is the QL.

DETECTION LIMIT AND QUANTITATION LIMIT

DL is defined as the lowest concentration of an analyte that can be detected under the analytical condition to be used. However, it cannot be quantitatively measured. QL is the lowest concentration that can be determined with acceptable accuracy and precision under the analytical conditions.[3] Generally, QL can be estimated as three times of DL.[2,14] DL and QL for instrumental (chromatographic) analytical methods can be defined in terms of the signal-to-noise ratio (2:1 to 3:1 for DL and 10:1 for QL[9] or in terms of the ratio of the standard deviation of blank response, the residual standard deviation of the calibration line, or the standard deviation of intercept (σ) and slope (S) (DL = $3.3\sigma/S$ and QL = $10\sigma/S$).[16] By constructing a linear regression of relatively low concentrations of analyte, accurate values of DL can be calculated, in this case, DL = X_p.[12] The authors recommend using 5–10 relatively low concentrations of analyte spotted on a TLC plate. DL can be increased by using pre- or postchromatographic derivatization.[3] For clinical application, QL should be at least 10% of the minimum effective concentration, and it should be within the linear WR.[6] For ensuring the safety of agricultural products, herbal medicines, and foods from the contamination of certain heavy metals, antibiotics, pesticides, and drugs by chemical analysis, DL of the method must be determined. DL should be less than the maximum permitted level of the toxic substances.

ROBUSTNESS/RUGGEDNESS

Robustness can be defined as a measure of the capability of the method to remain unaffected by small, but deliberate, variations in method parameters. It provides an indication of its reliability during normal usage.[1,18] Ruggedness of a method is the degree of reproducibility of test results obtained by the analysis of same samples under a variety of conditions such as different laboratories, analysts, and instruments; different lot of reagents; different days.[1] Some important parameters for the testing of TLC or HPTLC methods are the following: the stability of analyte in the solution being analyzed and on the plate before and after development; the influence of temperature and humidity; the method of application, scanning, and evaluation; the spot shape and size, eluent composition, and pH; the batch and sources of TLC plate; the sample volume; different chamber type; and the drying conditions of the plate.[3,18] In our laboratory, the design and analysis of effect of the robustness data were performed and calculated by using a multivariate statistical software. As an example, we studied the effect of small variation in the composition of mobile phase on R_f, T, and recovery of the active ingredient.[19] A detailed guidance for robustness/ruggedness testing has been published.[16] For robustness evaluation of botanical drugs, the R_f values of all markers should lie within the acceptance criteria of the intermediate precision.[7]

REPORTING RESULTS OF ANALYSIS

For reporting routine analytical results, it is recommended that its confidence interval[12] or uncertainty[17] or standard certainty[20] be included in the results of analysis; so the result is reported as:

$$\text{Mean} \pm \frac{t.\text{SD}}{\sqrt{N}}$$

where N is the number of replicates, SD is the standard deviation, and t is the value from the t table; if N is more than 10, the equation can be simplified as:[17]

$$\text{Mean} \pm 2 \times \text{SD} \ (\text{for } p = 0.05)$$

$$\text{Mean} \pm 3 \times \text{SD} \ (\text{for } p = 0.01)$$

Kaiser[20] suggested four replicates for analyzing samples, and in this case standard certainty can be estimated as three times the standard deviation.

CONCLUDING REMARKS

Important performance characteristics for TLC or HPTLC validation procedures have been described in brief in this entry to provide guidance to the analytical chemists. For obtaining reliable and reproducible analysis results, it is essential to validate the TLC or HPTLC method first, before using it for routine works in a quality control laboratory.

REFERENCES

1. *The United States Pharmacopoeia 30—The National Formulary 25*, The United States Pharmacopeial Convention, Inc.: Rockville, MD, 2007; 680–683.
2. Carr, G.P.; Wahlich, J.C. A Practical approach to method validation in pharmaceutical analysis. J. Pharm. Biomed. Anal. **1990**, *8* (8), 613–618.
3. Hahn-Deinstrop, E. *Applied Thin-Layer Chromatography*; Wiley-VCH Verlag GmbH: Weinheim, 2000, 201–205.
4. Prosek, M.; Puki, M.; Miksa, L.; Golc-Wondra, A. Quantitative thin-layer chromatography: Part 12. Quality assessment in QTLC. J. Planar Chromatogr. **1993**, *6* (1), 62–65.
5. Ferenczi-Fodor, K.; Vegh, Z.; Nagi-Turak, A.; Renger, B.; Zeller, M. Validation and quality assurance of planar chromatographic procedures in pharmaceutical analysis. J. AOAC Inter. **2001**, *84* (4), 1265–1276.
6. Yuwono, M.; Indrayanto, G. *Validation of Chromatographic Methods of Analysis*. In Brittain, G.; Eds.; Profiles of Drugs Substances, Excipients and Related Methodology Volume 32, Academic Press Elsevier Inc.: San Diego, 2005; 243–259.
7. Reich, E.; Schibli, A.; DeBatt, A. Validation of High-Performance Thin Layer Chromatographic Methods for the Identification of Botanical in a cGMP Environment. J. AOAC Inter. **2008**, *91* (1), 13–20.
8. Karnes, H.T.; Shiu, G.; Shah, V.P. Validation of bioanalytical methods. Pharm. Res. **1991**, *8* (4), 421–426.
9. Renger, B.; Jehle, H.; Fischer, M.; Funk, W. Validation of analytical procedure in pharmaceutical analytical chemistry; HPTLC assay of theophylline in an effervescent tablet. J. Planar Chromatogr. **1995**, *8* (4), 269–278.
10. Edwardson, P.A.D.; Bhaskar, G.; Fairbrother, J.E. Method validation in pharmaceutical analysis. J. Pharm. Biomed. Anal. **1990**, *8* (8), 929–933.
11. Green, J.M. A practical guide to analytical validation. Anal. Chem. **1996**, *68*, 305A–309A.
12. Funk, W.; Dammann, V.; Donnevert, G. *Qualitätssicherung in der Analytischen Chemie*. VCH Verlagsgesellschaft mbH: Weinheim. 1992; 10–44.
13. Analytical method committee. Uses (proper and improper) of correlation coefficient. Analyst **1998**, *113* (9), 1469–1471.
14. Ebel, S. Validerung in der DC/HPTLC. *WSA Würzburger Skripten zur Analytik. Reihe Validerung, Teil 6.3*. Bayerische Julius-Maximillians Universität, Institut für Pharmazie und Lebensmittelchemie: Würzburg, 1992; 41–58.
15. Kuss, H.-J. *Optimization of the Evaluation in Chromatography*. In Kromidas, S., Eds; HPLC Made to Measure. Wiley-VCH: Weinheim, 2006; 105–147.
16. Ermer, J. Validation in pharmaceutical analysis: Part 1. An integrated approach. J. Pharm. Biomed. Anal. **2001**, *24*, 755–767.
17. Kromidas, S. *Validerung in der Analytik*. Wiley-VCH: Weinheim, 1999; 52–171.
18. Van der Hyden, Y.; Nijhuis, A.; Smayers-Verbeke, J.; Vandeginste, B.M.G.; Massart, D.L. Guidance for robustness/ruggedness test in method validation. J. Pharm. Biomed. Anal. **2001**, *24*, 723–753.
19. Cholifah, S.; Noviansari, A.; Kartinasari, W.F.; Indrayanto, G. Densitometric determination of fenbendazole in veterinarian suspension: Validation of the method. J. Chromatogr R & T. **2007**, *30* (4), 489–498.
20. Kaiser, R.E. Methods for detecting and reducing systematic errors in quantitative planar chromatography. Part 1. Fundamentals of systematic quantitative errors. J. Planar Chromatogr. -Mod. TLC, **2005**, *18* (1), 51–56.

BIBLIOGRAPHY

1. Eurachem, *The Fitness for Purpose of Analytical Methods: A Laboratory Guide to Method Validation and Related Topics*. LGC (Teddington) Ltd., Middlesex, 1998.
2. Ermer, J.; McB. Miller, J. *Method Validation in Pharmaceutical Analysis*. Wiley-VCH: Weinheim, 2005.

Topological Indices: TLC

Alina Pyka
Department of Analytical Chemistry, Medical University of Silesia, Sosnowiec, Poland

Abstract
This entry covers the use of structural descriptors, namely, topological indices based on the adjacency, distance matrix, and information theory, as well as the electrotopological states to predict the R_F and R_M values, and the lipophilicity properties, of a variety groups of organic compounds investigated by thin-layer chromatography (TLC). This entry indicates that further investigations on the application of the topological indices in TLC are justifiable.

INTRODUCTION

Numerous activities and properties of organic compounds depend on the presence of specific atoms and/or functional groups in their structure. These features can be used for deriving QSAR (quantitative structure–activity relationship), QSPR (quantitative structure–property relationship), and QSRR (quantitative structure–retention relationship) models. Last, numerous valuable QSAR, QSPR, and QSRR models have been derived from topological indices and related descriptors, among other things the electrotopological states.[1] The range and fields of application of the topological indices are limited. The topological indices can be applied as a descriptor only when the correlated property is primarily dependent on the structure of a molecule. The compounds investigated were homologous series or mixtures of compounds from the different classes of organic compounds. The topological indices have been applied in chromatographic investigations, usually in gas chromatography (GC) and high-performance liquid chromatography (HPLC) techniques. The short distance traveled by a solute on a chromatographic plate is the reason for limited application of topological indices in thin-layer chromatography (TLC). The application of topological indices is an important field of theoretical chromatography. The topological indices open a new field of investigation in chromatographic science. Many scientists have reported the application of topological indices for prediction of the retention data for different groups of organic compounds. The extent of this application has been unexpectedly large in recent years and includes the application of the topological indices in TLC also.

In our previous entry we have summarized the applications of topological indices that were described in manuscripts published up to 2000.[2] Data presented in scientific literature up to 2000 indicate that the topological indices and electrotopological states can be used to predict and describe several properties and other phenomena: chromatographic separation, the partition coefficient in *n*-octanol–water system, and chromatographic lipophilicity, dipole moment, dissociation constant, biological activity, and water solubility for the different classes of organic compounds investigated.[2]

The objectives of this entry are the presentation and discussion of the significance of topological indices in TLC investigations that were described in the manuscripts from 2001. Scientific literature from 2001 described the applications of the structural descriptors, including the topological indices, to predict and describe: 1) the relative position of separated compounds on a chromatogram; 2) the retention parameters of the separated compounds on a thin layer; 3) the chromatographic lipophilicity and partition coefficients of investigated compounds; and 4) water solubility.

APPLICATION OF THE TOPOLOGICAL INDICES AND THE ELECTROTOPOLOGICAL STATES TO PREDICT THE RELATIVE SITUATION OF SEPARATED COMPOUNDS ON A CHROMATOGRAM

Pyka et al.[3] separated the selected essential oil components (menthol, (+)borneol, geraniol, linalool, carvone, camphor, (1R)-(−)fenchone) by adsorption thin-layer chromatography using benzene as the mobile phase. Investigated terpenes were characterized by selected topological indices based on connectivity: Randić ($^0\chi$, $^1\chi$, $^2\chi$, $^0\chi^\nu$, $^1\chi^\nu$, $^2\chi^\nu$, $^4\chi_c$, $^4\chi_c^\nu$), Gutman [(M, M^ν)], on distance matrix: Wiener (W), Rouvray (R), and Pyka (A, ^0B, ^1B) indices, and the S_i index. From among all the topological indices counted only the $S_{i(O)}$ index (the sum of the distance between the oxygen atom and all the remaining atoms in graph) and cluster Randić indices ($^4\chi_c$ and $^4\chi_c^\nu$) allow for estimation of the chromatograms obtained. The topological indices $S_{i(O)}$ are directly whereas the cluster

Table 1 R_M values (average of 10 measurements) and selected topological indices for the compounds investigated.

Compound	$R_{M(1)}$[a]	$R_{M(2)}$[b]	$R_{M(3)}$[c]	Topological indices		
				$^4\chi_c$	$^4\chi_c^v$	$S_{i(O)}$
Menthol	0.891	0.482	0.257	0	0	27.750
(+) Borneol	0.861	0.430	0.214	0.2464	0.2464	26.750
Geraniol	1.067	0.679	0.496	0	0	33.864
Linalool	0.707	0.276	0.080	0.2041	0.0913	29.750
(*R*)(−) carvone	0.510	−0.057	−0.187	0	0	24.500
Camphor	0.292	−0.187	−0.339	0.2327	0.2327	23.000
(1*R*)(−) Fenchone	0.214	−0.385	−0.498	0.2693	0.2693	21.000

[a]After single development in benzene.
[b]After double developments in benzene.
[c]After triple developments in benzene.
Source: From Application of topological indexes for evaluation of the TLC separation of selected essential oil components, in Acta Pol. Pharm. Drug Res. [3]

Randic indices $^4\chi_c$ and $^4\chi_c^v$ are inversely proportional to the R_M values of the terpenes investigated (Table 1). From the experimental data presented, it is apparent that the compounds can be ranked in accordance with increasing adsorption on silica gel in the order:

(+)borneol < menthol;
linalool < geraniol; and
(1*R*)-(−) fenchone < camphor < (*R*)(−)carvone

The S_i index is equal to the sum of a row in the distance matrix. This index measures the connection of atom i to the rest of the molecule. Low values of the S_i index indicate strongly connected positions (atom i strongly connected with the rest of the molecule), whereas high values of S_i are characteristic of weakly connected positions (atom i weakly connected with the rest of the molecule). The hydroxyl group determines the adsorption properties of terpenes investigated. For example, the $S_{i(O)}$ index for oxygen atom is greater for menthol than for (+)borneol. Similarly, the $S_{i(O)}$ for geraniol is greater than for linalool. Adsorption of menthol and geraniol is therefore greater than of (+)borneol and linalool, respectively. For the remaining terpenes investigated, the $S_{i(O)}$ index increases in the order: (1*R*)-(−)fenchone < camphor < (*R*)(−) carvone. The adsorption of these three terpenes increases in the same order. With the fact mentioned above, there exists the possibility of prediction of relative situation on the chromatogram of the terpenes investigated. For the rest of topological indices that possibility was not stated.[3]

Pyka and Bober[4] separated α- and γ-terpinene as well as α- and β-pinene on silica gel and on silica gel impregnated with various percentages of silver nitrate. It was stated that argentation thin-layer chromatography is an efficient technique for separation of isomeric α- and γ-terpinene as well as α- and β-pinene. The topological indices based on connectivity ($^0\chi$, $^1\chi$, $^2\chi$, M, χ_{012}), on distance matrix (W, I_B, A, ^0B, ^1B, ^2B, ^2B_q, C, D), S_i indices, and the electrotopological states for each atom in a molecule of the terpines investigated were calculated. The γ-terpinene has higher R_F values from α-terpinene in all chromatographic separations obtained. Likewise, α-pinene has higher R_F values as compared to β-pinene. The qualitative correlations between R_F values and topological indices $^2\chi$, D, and χ_{012} values of the investigated terpenes were stated. It was also stated that S_i index cannot explain the separation terpenes investigated in argentation thin-layer chromatography. The E-state values calculated for atoms of terpenes investigated are presented in Fig. 1. The E-state index is a structural descriptor for an atom within a covalently bonding molecule. The E-state index is formulated to encode information about the electronegativity, pi and lone-pair electron content, the topological status and the environment of an atom within a molecule. In argentation TLC the interactions between Ag^+ ions and double bonds of substances separated determine separation. For that the reason the electrotopological states of carbon atoms forming double bonds were analyzed. It was stated that the sum of electrotopological states of all carbon atoms forming double bonds is lower for γ-terpinene than for α-terpinene (Fig. 1). This sum is also lower for α-pinene than for β-pinene (Fig. 1). For that reason, γ-terpinene should form weak complexes with Ag^+ ions (higher R_F values) in relation to α-terpinene (lower R_F values). The α-pinene also should form weak complexes with Ag^+ ions (higher R_F values) in relation to β-pinene (lower R_F values). The above observations help in formulating the definite rules concerning relationships between chromatographic separation sequences and topological indices of the investigated terpenes. These rules with qualitative importance can be applied for estimation sequence during the preparative separation of isomers, which can be the subject of further physical, chemical, physicochemical, and pharmaceutical investigations.[4]

Pyka and Sliwiok[5] separated α-, β-, γ-, and δ-tocopherols by reversed-phase high-performance thin-layer

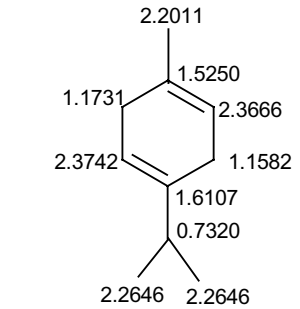

γ-Terpinene

$\sum E_{C=C}$ is equal **7.8765**

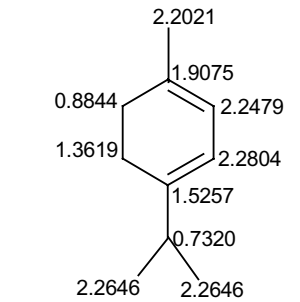

α-Terpinene

7.9615

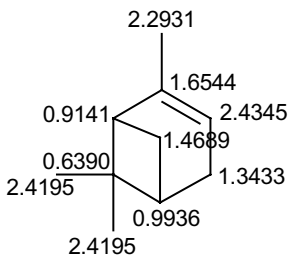

α-Pinene

4.0889

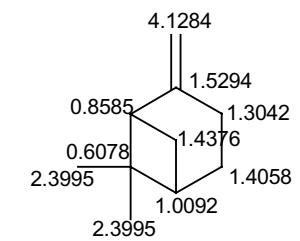

β-Pinene

5.6578

Fig. 1 The E-state values calculated for atoms of terpenes investigated and sum of electrotopological states ($\Sigma E_{C=C}$) for all carbon atoms forming double bonds.
Source: From On the importance of topological indices in research of α- and β-terpinene as well as α- and β-pinene separated by TLC, in J. Liq. Chromatogr. Relat. Technol.[4]

chromatography (RP-HPTLC). The selected topological indices based on connectivity (M, $^1\chi^\nu$), on distance matrix (W, ^0B, MTI), and on information theory (I_{AC}, $\overline{I}_{AC}$) were calculated for these tocopherols. As positional isomers, β- and γ-tocopherols possess the same numerical values of topological indices M, $^1\chi^\nu$, I_{AC}, and $\overline{I}_{AC}$. Only the numerical values of the topological indices ^0B and R_M values become smaller (decrease) in the following order: α-, β-, γ-, and δ-tocopherol.[5]

APPLICATION OF TOPOLOGICAL INDICES AND ELECTROTOPOLOGICAL STATES TO PREDICT THE RETENTION PARAMETERS OF SEPARATED COMPOUNDS ON THIN LAYER

The use of the structural descriptors to predict the retention parameters of the organic compounds, including drugs, is defined as QSRR.

Pyka and Dolowy[6] and Dolowy[7] applied some structural descriptors (M^ν, $^0\chi^\nu$, $^1\chi^\nu$, $^2\chi^\nu$, χ_{012}, W, A, ^0B, ^1B, C, $SdO_{(kw)}$, $SsOH_{(kw)}$, $SsOH_{(alif)}$ $SdO_{(amid)}$, and SsNH) to predict chromatographic separations of selected bile acids such as cholic acid (C), glycocholic acid (GC), glycodeoxycholic acid (GDC), chenodeoxycholic (CDC), deoxycholic acid (DC), lithocholic acid (LC), and glycolithocholic acid (GLC) on unmodified and modified silica gel plates and by using the mixture of *n*-hexane–ethyl acetate–acetic acid in various volume compositions as mobile phases. It was found that among all descriptors only the values of topological index C change inversely proportional to the R_F values and directly proportional to the R_M values of examined bile acids. Thus, only the topological index C was used for determining the correlation equations that allowed the calculation of R_F and R_M values of studied bile acids. The topological index C allowed obtaining linear equations with R_M values or quadratic equations with R_F values. Generally, they have found that the correlation equations that describe the relationships $R_F = f(C)$ have higher values of correlation coefficients than the relationship $R_M = f(C)$. The regression equations between R_F and R_M values and the topological index C for studied bile acids separated on unmodified silica gel (#1.05715, E. Merck) using the above-mentioned mobile phase in volume composition 22+22+5 are:

$$R_F = 164.577(\pm 32.978) - 11.007(\pm 2.289) \times C + 0.184(\pm 0.040) \times C^2 \quad n = 7 ; \quad (1)$$
$$R^2 = 98.47\%; \; F = 227.6; \; s = 0.058; \; p < 0.0003$$

$$R_M = -33.818(\pm 2.446) + 1.190(\pm 0.085) \times C$$
$$n = 7; \; R^2 = 97.49\%; \; F = 194.1;$$
$$s = 0.193; \; p < 0.004 \quad (2)$$

Selected *meta*- and *para*-alkoxyphenols have been separated by RP-HPTLC on cellulose impregnated with ethyl oleate, with ethanol–water, 25 + 75 and 40 + 60 (%, v/v), as mobile phases.[8] The R_M values of the alkoxyphenols have been correlated with the

structural descriptors based on the adjacency matrix ($^2\chi^\nu$, $^3\chi^\nu$, χ_{012}), on the distance matrix (W, A, ^0B, ^1B, D, C, ^2B, ^2B_q, ^3B, ^3B_q, I_B), and on electrotopological states (SssO, $ScCH_3$, SaaCH, SaasC, SsOH). Most accurate prediction of the R_M values of all the alkoxyphenols has been achieved by use of second- or third-degree polynomial correlation equations with structural descriptors from among the topological indices W, A, ^0B, ^1B, ^2B, ^2B_q, D, $^3\chi^\nu$, and I_B. The obtained regression equations can be used to calculate the R_M values of the alkoxyphenols studied. After recalculation these equations can also be used to predict the R_M values of the alkoxyphenols for which data were omitted when calculating the equations. For example, R_M data for *p*-butoxyphenol and *m*-pentoxyphenol separated using the mobile phase ethanol–water, 40 + 60 (%, v/v), were omitted and new correlation was obtained for separations:

$$\begin{aligned} R_{M(40+60)} &= 10.503(\pm 0.382) \times {}^0B - 4.670(\pm 0.168) \\ n &= 12;\ R_2 = 98.72\%;\ s = 0.080; \\ F &= 768;\ p < 0.001 \end{aligned} \quad (3)$$

The $R_{M(40+60)}$ values of *p*-butoxyphenol and *m*-pentoxyphenol were predicted by use of Eq. 3 and they are equal to 0.061 and 0.269, respectively, whereas the experimental $R_{M(40+60)}$ values for *p*-butoxyphenol and *m*-pentoxyphenol are equal to 0.035 and 0.269, respectively.

However, topological indices $^2\chi^\nu$, χ_{012}, C, SssCH, SassC, and SsOH can be used to calculate the R_M values of alkoxyphenols, but separately for the two homologous series, i.e., separately for *meta*-alkoxyphenols and *para*-alkoxyphenols.[8]

The R_M values of homologous series of higher alcohols and of methyl esters of higher fatty acids separated by RP-HPTLC can be calculated by use of monoparametric equations containing index based on the adjacency.[9] However, the R_M values of homologous series of fatty acids from pentanoic to tricosanoic separated by RP-HPTLC can be predicted on the basis of linear or quadratic equations using topological indices based on the distance matrix, the adjacency matrix, information theory, and electrotopological states.[10]

Luhua et al.[11] separated by normal-phase thin-layer chromatography (NP-TLC) (−)-ephedrine and (+)-pseudoephedrine. The topological indices based on connectivity and distance matrix A, W, and $^h\chi^\nu$ were calculated. The structures in particular of (−)-ephedrine and (+)-pseudoephedrine were described by topological indices $^h\chi^\nu$ that were applied to interpret the chromatographic separations.

Beteringe et al.[12] synthesized and separated by TLC the *Z* and *E* diasteroisomers of the *O*-methyloximes of testosterone and 17α-methyltestosterone. These compounds were characterized by the Pyka index I_{STI}, the Pogliani index $X_{cp}(p)$, the Schultz indices S and PRS, and the geometrical index J_{geom}. It was stated that R_F values were best correlated with the Schultz index S:

$$\begin{aligned} R_F &= 0.3554 \times S + 1.5309 \times 10^{-5} \\ n &= 6;\ r = 0.9895;\ s = 0.0277;\ F = 189.2 \end{aligned} \quad (4)$$

Pyka[13] separated phenol and its methyl derivatives by RP-HPTLC on RP-2 plates with three mobile phases: $R_{M(1)}$, 0.1 *M* CH_3COOH and 0.1 *M* CH_3COONa in 30% methanol (at pH = 5.00); $R_{M(2)}$, 0.1 *M* KH_2PO_4 in 30% methanol (at pH = 7.00); $R_{M(3)}$, 1 *M* ammonia in 30% methanol (at pH = 11.30)). It was affirmed that SaasC and SaaCH describe well the R_M values. For example:

$$\begin{aligned} R_{M(1)} &= 1.738(\pm 0.044) - 0.177(\pm 0.008) \times \text{SaaCH} \\ n &= 7;\ r = -0.995;\ s = 0.030,\ p < 0.0001 \end{aligned} \quad (5)$$

$$\begin{aligned} R_{M(2)} &= 1.650(\pm 0.027) - 0.168(\pm 0.005) \times \text{SaaCH} \\ n &= 7;\ r = -0.998;\ s = 0.019,\ p < 0.0001 \end{aligned} \quad (6)$$

$$\begin{aligned} R_{M(3)} &= 1.717(\pm 0.150) - 0.251(\pm 0.026) \times \text{SaaCH} \\ n &= 7;\ r = -0.974;\ s = 0.102,\ p < 0.0001 \end{aligned} \quad (7)$$

The steroids corticosterone acetate, 11-dehydrocortisone acetate, corticosterone, 11-dehydrocorticosterone, hydrocortisone, and cortisone have been separated by RP-HPTLC. The chromatographic data (R_M) and partition coefficient (log*P*) values of the compounds have been correlated with the numerical values of topological indices. The most accurate predictions of the R_M and log*P* values of the selected steroids were achieved by the use of monoparametric equations employing the topological index ^0B.[14]

Pyka and Sliwiok[15] separated six esters of nicotinic acids—methyl nicotinate, ethyl nicotinate, isopropyl nicotinate, butyl nicotinate, hexyl nicotinate, and benzyl nicotinate—by adsorption TLC on silica gel and a mixture of silica gel and kieselguhr. The mixtures containing *n*-hexane and acetone in the volume proportions (2 + 8, 3 + 7, 4 + 6, 5 + 5, 6:4, 7 + 3, 8 + 2) were used as the mobile phases. The R_M values of esters investigated have been correlated with the dipole moments (μ_{mph}) of the mobile phases applied, with numerical values of one topological index from among those based on the distance matrix (A, W, ^0B, ^1B, ^2B) or on the adjacency matrix ($^0\chi^\nu$, $^1\chi^\nu$, $^2\chi^\nu$), with electrotopological states: SaaCH, aaN, aasC, do, ssO, and dssC, and structural descriptors based on information theory (I_{SA} and $\overline{I}_{SA}$). Dipole moments were used to characterize mobile phases. All the equations obtained, which enable calculation of R_M on silica gel ($R_{M(1)}$) and on mixture of silica gel and kieselguhr ($R_{M(2)}$), had determination coefficients $R^2 > 92\%$. The best equations, which had determination coefficients $R^2 > 96\%$, were obtained with indices based on the

distance matrix Pyka (^0B, ^1B), with electrotopological state dssC and with index based on information theory I_{SA}, $\overline{I}_{SA}$ (only for $R_{M(1)}$ values obtained on silica gel). For example, the best equations of relationships between R_M values ($R_{M(1)}$ from silica gel and $R_{M(2)}$ from mixture of silica gel and kieselguhr) and structural descriptors of esters and dipole moments of mobile phases are given below:

$$\begin{aligned} R_{M(1)} &= -0.108(\pm 0.288) - 1.097(\pm 0.030) \times \mu_{mph} \\ &\quad + 0.806(\pm 0.121) \times {}^0B \\ n &= 42;\ R^2 = 97.20\%;\ F = 676.9; \\ s &= 0.076;\ p < 0.0001 \end{aligned} \tag{8}$$

$$\begin{aligned} R_{M(2)} &= -0.081(\pm 0.163) - 1.081(\pm 0.032) \times \mu_{mph} \\ &\quad - 4.108(0.484) \times \text{dssC} \\ n &= 36;\ R^2 = 97.35\%;\ F = 605.2; \\ s &= 0.081;\ p < 0.0001 \end{aligned} \tag{9}$$

The correlation Eqs. 8 and 9 can be used to calculate $R_{M(1)}$ and $R_{M(2)}$ values of investigated esters on silica gel and on mixture of silica gel and kieselguhr, respectively. For example, the relationship between R_M values measured experimentally on silica gel and values calculated by use of Eq. 8 is presented in Fig. 2.

Eqs. 8 and 9 can also be used to predict the R_M values of the esters of nicotinic acid, the measurement points of which have not been taken into consideration in the equation. A test was performed on Eqs. 8 and 9 to determine how well they predict R_M values of points not included in the training set. Two values were removed from the training sets (Eqs. 8 and 9). Butyl nicotinate separated in *n*-hexane:acetone, 6 + 4, v/v, and ethyl nicotinate separated in *n*-hexane:acetone, 3 + 7, v/v, were removed from Eq. 8. Hexyl nicotinate separated in *n*-hexane:acetone, 4 + 6, v/v, and butyl nicotinate separated in *n*-hexane:acetone, 6 + 4, v/v, were removed from Eq. 9. These subsets of two-parametric equations were recalculated as:

$$\begin{aligned} R_{M(1)} &= -0.110(\pm 0.300) - 1.097(\pm 0.032) \times \mu_{mph} \\ &\quad + 0.807(\pm 0.125) \times {}^0B \\ n &= 40;\ R^2 = 97.15\%;\ F = 630.0; \\ s &= 0.078;\ p < 0.0001 \end{aligned} \tag{10}$$

$$\begin{aligned} R_{M(2)} &= -0.078(\pm 0.174) - 1.081(\pm 0.034) \times \mu_{mph} \\ &\quad - 4.097(\pm 0.525) \times \text{dssC} \\ n &= 34;\ R^2 = 97.10\%;\ F = 518.8; \\ s &= 0.084;\ p < 0.0001 \end{aligned} \tag{11}$$

The $R_{M(1)}$ and $R_{M(2)}$ values for esters of nicotinic acids, omitted during the derivation of Eqs. 10 and 11 and subsequently predicted by use of these equations, are listed in Table 2.

Similarly, the dipole moments (or permittivity) of mobile phases and the topological indices have also been used to predict the R_M values of α-, β-, γ-, and δ-tocopherols separated on RP18 HPTLC plates using methanol, ethanol, *n*-propanol, and mixtures containing ethanol and water and *n*-propanol and water in the volume proportions 9.5 + 0.5 and 9 + 1 as mobile phases. The best regression equations were obtained using one topological index from among the topological indices $^2\chi^\nu$, ^0B, or C.[16]

Thirteen barbiturates have been separated by RP-HPTLC with 13 mobile phases (methanol–water in different volume compositions). The R_M values of barbiturates investigated have been correlated with the selected traditional structural descriptors, with the partition coefficients of the compounds, and with the dipole moments (μ_{mph}) or with the permittivities (ε_{mph}) of the mobile phases applied. The most accurate prediction of the R_M values of the

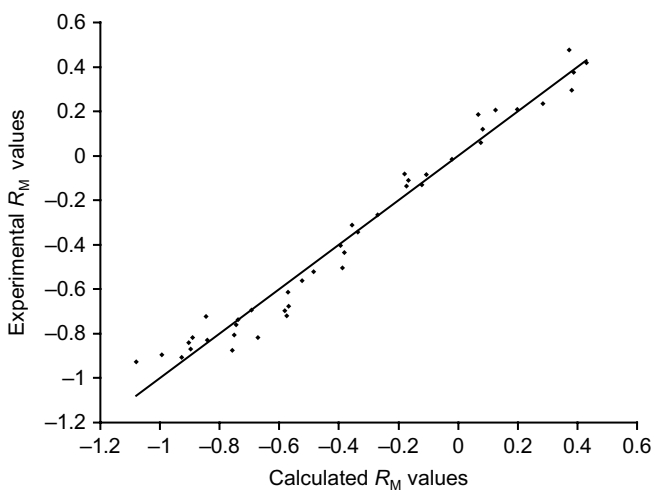

Fig. 2 Relationship between the experimental R_M values of nicotinic acid esters on silica gel and the R_M values calculated by use of Eq. 8.
Source: From use of traditional structural descriptors in QSRR analysis of nicotinic acid esters, in J. Liq. Chromatogr. Relat. Technol. [15]

Table 2 $R_{M(1)}$ and $R_{M(2)}$ values of compounds omitted from Eqs. 10 and 11 and predicted by these equations.

Silica gel (#1.05715)				Silica gel/kieselguhr (#1.05567)			
Omitted point	Experimental $R_{M(1)}$	Predicted $R_{M(1)}$ by Eq. 10	$\lvert\Delta R_{M(1)}\rvert$	Omitted point	Experimental $R_{M(2)}$	Predicted $R_{M(2)}$by Eq. 11	$\lvert\Delta R_{M(2)}\rvert$
Butyl nicotinate (*n*-hexane: acetone, 6 + 4, v/v)	–0.265	–0.270	0.005	Hexyl nicotinate (*n*-hexane: acetone, 4 + 6, v/v)	–1.288	–1.284	0.004
Ethyl nicotinate (*n*-hexane: acetone, 3 + 7, v/v)	–0.737	0.738	0.001	Butyl nicotinate(*n*-hexane: acetone, 6 + 4, v/v)	–0.849	–0.841	0.008

Source: From Use of traditional structural descriptors in QSRR analysis of nicotinic acid esters, in J. Liq. Chromatogr. Relat. Technol.[15]

barbiturates in all the mobile phases investigated were achieved by use of two-parametric equations employing the dipole moments (or the permittivities) of the mobile phases, one topological index from among the topological indices ${}^0\chi$, ${}^1\chi$, ${}^0\chi^\nu$, ${}^1\chi^\nu$, R, W, A, ${}^1B$, and three-parametric equations employing the dipole moments (or the permittivities) of the mobile phases, and two topological indices (I_B and ${}^1\chi$ as well as I_B and ${}^1\chi^\nu$), or one electrotopological descriptor (SdssC or SssssC) or Gutman index (M or M^ν), and selected partition coefficient.[17]

Niestroj, Pyka, and Sliwiok[18] separated higher fatty acids, hydroxy fatty acids, and their esters by RP-HPTLC using methanol and methanol–water (9.5 + 5 and 9 + 1) as mobile phases. The R_M values of the compounds have been correlated with the numerical values of the topological indices, with electrotopological states of the atoms attached to the carboxyl group of investigated compounds, with the number of hydrogen bond donors (#HD), with the molecular weights (M_w), and the dipole moments (μ_{mph}) of the mobile phases. The most accurate prediction of the R_M values of the acids and esters, for all the mobile phases investigated, was achieved by use of four-parametric equations relating the dipole moments of the mobile phases and three other parameters. For example:

$$\begin{aligned} R_M = & -52.5342(\pm 3.3486) + 31.9676(\pm 1.9528) \times \mu_{mph} \\ & - 4.1128(\pm 1.6669) \times {}^1B \\ & - 0.006111(\pm 0.000851) \times M^v \\ & - 0.2108(\pm 0.0250) \times \#HD \\ n = & \ 36;\ R^2 = 94.26\%;\ s = 0.086; \\ F = & \ 127.26;\ p < 0.0001 \end{aligned} \quad (12)$$

Pyka and Bober[19] separated methyl laureate, methyl myristate, methyl palmitate, methyl isostearate, methyl stearate, and methyl arachidate by RP-HPTLC on kieselguhr F_{254} with different amounts of paraffin oil (10% and 15%), using two different mobile phases (methanol + water and ethanol + water in volume composition 9 + 1, v/v). The R_M values of these compounds for all the stationary phases and mobile phases investigated could be correlated with the dipole moments of the mobile phases (μ_{mph}), with the percentage impregnation of the stationary phases (imp%), and with numerical values of one topological index from among those based on the distance matrix (W, A, ${}^0B$, ${}^1B$) or on the adjacency matrix (${}^1\chi$, ${}^1\chi^\nu$). For example:

$$\begin{aligned} R_M = & -12.7715(\pm 1.2059) + 6.8712(\pm 0.7082) \times \mu_{mph} \\ & + 4.0967(\pm 0.6232) \times \text{imp}\% \\ & + 0.00235(\pm 0.00008) \times A \\ n = & \ 24;\ R^2 = 97.91\%;\ s = 0.076; \\ F = & \ 312.6;\ p < 0.0001 \end{aligned} \quad (13)$$

The R_M values of *cis*- and *trans*-9-octadecenoic and 11-octadecenoic acids in all the applied stationary phases and mobile phases could also be correlated with dipole moments (or permittivities) of mobile phases, with the impregnation percentages of stationary phases, and with numerical values of one topological index (W, A, ${}^0B$, ${}^1B$, ${}^2B$, I_B) or electrotopological state of oxygen atoms.[20]

APPLICATION OF THE TOPOLOGICAL INDICES AND THE ELECTROTOPOLOGICAL STATES TO PREDICT CHROMATOGRAPHIC LIPOPHILICITY AND THE PARTITION COEFFICIENTS OF INVESTIGATED COMPOUNDS

The lipophilicity of any substance, including drugs, is a property that affects its biological activity. *n*-Octanol–water partition coefficients, usually expressed as log*P* values, which

can be computed or determined experimentally, are used as a measure of lipophilicity. Log*P* can be determined experimentally by the classical method of the measuring partition of an organic compound between a non-polar phase and water. Measurement of partition coefficients is not as easy as might be expected from their simple definition. Measurement by use of equilibration methods is frequently made difficult, or even impossible, by impurities in or the instabilities of a compound, by strong preference of a compound for one of the two phases of the system, or by the formation of stable emulsions after shaking. Practical problems arise for polar and highly lipophilic compounds (log $P > 4$). For this reason the suitability of experimental and theoretical approaches for determination of the lipophilicity of organic compounds, including drugs, remains a focus of scientific interest. Different partition chromatographic techniques and theoretical methods have been widely used as reliable alternatives to classical determination of log*P*.

The use of the structural descriptors to predict lipophilicity of the organic compounds, including drugs, is defined as quantitative structure–activity relationships (QSAR). Lipophilicity parameters obtained using RP-HPTLC for many groups of organic compounds were correlated with the different structural descriptors.[6,16,21–27]

Pyka et al.[6,21] determined the chromatographic lipophilicities of seven bile acids by RP-HPTLC on different sorbent using organic modifier–water in different volume compositions as mobile phases. It was found that lipophilicity determined chromatographically (R_{M0} and ϕ_0), theoretical values ($A\log P_s$, $IA\log P$, $C\log P$, $\log P_{Kowwin}$, $x\log P$, and $\log P_{Rekker}$), and experimental *n*-octanol–water values determined by the classical method ($\log P_{exp}$) correlated the best with topological indices M^{ν} and *C*.

Pyka and Niestrój[16] and Kepczynska, Bojarski, and Pyka[22] correlated the R_{M0} values obtained on RP18 TLC plates using methanol–water in different volume compositions as mobile phases and the theoretical partition coefficients ($IA\log P$, $C\log P$, $\log P_{Kowwin}$, $\log P_{Rek}$) of 13 barbituric acid derivatives with the different structural descriptors. It was stated that linear dependences exist between R_{M0} values, partition coefficients, and some topological indices. The R_{M0} values were best correlated with topological indices based on an adjacency matrix ${}^0\chi$, ${}^1\chi$, χ_{012}, ${}^0\chi^{\nu}$, ${}^1\chi^{\nu}$, and χ^{ν}_{012}, as well as distance matrix *R*, *W*, *A*, ${}^1B$, and *D* ($r \geq 0.96$). For example:

$$R_{M0} = -3.941(\pm 0.305) + 0.608(\pm 0.031) \times {}^0\chi^{v}$$
$$n = 13;\ r = 0.9862;\ s = 0.131;$$
$$F = 391;\ p < 0.0001 \quad (14)$$

It was also affirmed that ${}^0\chi$, ${}^1\chi$, ${}^0\chi^{\nu}$, and ${}^1\chi^{\nu}$ indices are the best for calculation of the particular partition coefficients ($r > 0.95$). For example:

$$IA\log P = -5.370(\pm 0.659) + 0.652(\pm 0.059) \times {}^0\chi$$
$$n = 13;\ r = 0.9582;$$
$$F = 123.2;\ s = 0.251;\ p < 0.0001 \quad (15)$$

$$C\log P = -6.154(\pm 0.570) + 0.730(\pm 0.051) \times {}^0\chi$$
$$n = 13;\ r = 0.9744;\ F = 206.3;$$
$$s = 0.217;\ p < 0.0001 \quad (16)$$

$$\log P_{Kowwin} = -4.394(\pm 0.409) + 0.878(\pm 0.055) \times \chi_{012}$$
$$n = 13;\ r = 0.9788;\ F = 251.0;$$
$$s = 0.177;\ p < 0.0001 \quad (17)$$

$$\log P_{Rek} = -6.167(\pm 0.461) + 0.755(\pm 0.041) \times {}^0\chi$$
$$n = 13;\ r = 0.9841;\ F = 337.4;$$
$$s = 0.176;\ p < 0.0001 \quad (18)$$

The satisfactory correlations between partition coefficients and some topological indices based on distance matrix: *R*, *W*, *A*, ${}^1B$, and *D* ($r > 0.93$) were also obtained.[16,22]

The selected pesticides monolinuron, chlortoluron, diuron, isoproturon, linuron, dimefuron, diflubenzuron, teflubenzuron, and lufenuron were separated by RP-HPTLC on $RP18WF_{254}$ plates, using methanol and water as the mobile phases, in which proportional content of methanol was from 35% to 85%. The topological indices based on connectivity—*Gutman* (M, M^{ν}) and *Randić* (${}^0\chi$, ${}^1\chi$, ${}^2\chi$, ${}^0\chi^{\nu}$, ${}^1\chi^{\nu}$, ${}^2\chi^{\nu}$)—were calculated for the investigated compounds. Obtained parameters of lipophilicity R_{M0} and ϕ_0 were correlated with topological indices. Only Gutman index M^{ν}, from among all topological indices, was useful in QSAR analysis of studied urea pesticides:[23]

$$R_{M0} = 0.6957(\pm 0.2187) + 0.004639(\pm 0.000498) \times M^{v}$$
$$n = 9;\ r = 0.9619;\ s = 0.308;$$
$$F = 86.57;\ p < 0.0001 \quad (19)$$

Nicotinic acid, esters of nicotinic acid (methyl nicotinate, ethyl nicotinate, isopropyl nicotinate, butyl nicotinate, hexyl nicotinate, benzyl nicotinate), nicotinamide, and *N*-methylnicotinamide were separated on RP18 and $RP18WF_{254}$ plates using methanol–water in different volume proportions as the mobile phases. Satisfactory linear regression equations were obtained between chromatographic lipophilicity R_{M0} or partition coefficients ($\log P_{exp}$, $A\log P_s$, $IA\log P$, $C\log P$, $\log P_{Kowwin}$, $x\log P$) and some topological indices (${}^0\chi^{\nu}$, ${}^1\chi^{\nu}$, ${}^2\chi^{\nu}$, A, ${}^1B$, ${}^2B$, I_{SA}, and $\overline{I}_{SA}$), and between lipophilicity ϕ_0 and electrotopological states SaaN and SdO.[24,25] However, for the above-mentioned compounds and *N*,*N*-diethylnicotinamide,

3-pyridinecarboaldehyde, 3-pyridinecarbonitrile, 3-pyridylmethanol, and methyl 3-pyridyl ketone, the chromatographic lipophilicity parameters (R_{M0} and ϕ_0) and the theoretical *n*-octanol–water partition coefficients correlated the best with the topological index *A*.[26]

The topological indices were also used to predict lipophilic properties of the examined steroids: androsterone, epi-androsterone, dehydro-epi-androsterone, testosterone, stigmasterol, β-sitosterol, estradiol, hydrocortisone, and cholesterol. The lipophilicity parameters R_{M0} and φ_0 were obtained by using RP-HPTLC on RP18W plates, with the use of methanol–water as a mobile phase. It was stated that the regression equations with the greatest correlation coefficients were found with the following structural descriptors: for lipophilicity parameter R_{M0}, with indices based on the distance matrix *R*, *W*, and *A*; and for lipophilicity parameter φ_o and theoretical *n*-octanol–water partition coefficient *x*log*P*, with index based on information theory $\overline{I}_{SA}$.[27]

Niestroj[28] proposed new methods for the calculation of partition coefficient (log*P*) for α-, β-, γ-, and δ-tocopherols separated by RP-HPTLC on RP18 HPTLC plates using ethanol and mixture of ethanol and water in the volume proportion 9.5 + 0.5 as mobile phases. The selected topological indices ($^0\chi^\nu$, $^1\chi^\nu$, $^2\chi^\nu$, and ^0B) and the theoretical partition coefficient (*A*logP_s, *IA*log*P*, *mi*log*P*, KOWWIN, *x*log*P*, and logP_{Rekker}) were calculated for studied tocopherols. It was stated that the numerical values of topological indices $^2\chi^\nu$ and ^0B as well as the R_F values of tocopherols investigated decreased in the order α-tocopherol > β-tocopherol > γ-tocopherol > δ-tocopherol. However, the values of the theoretical partition coefficients for the tocopherols investigated decreased in the order α-tocopherol > β-tocopherol = γ-tocopherol > δ-tocopherol. New methods for log*P* calculation were based on the following equations:

$$\log P_1 = \frac{^0B \log P_{Rek}}{2(R_{F1} + R_{F2})} \tag{20}$$

$$\log P_2 = \frac{\log P_{Rek}}{(R_{F1} + R_{F2})} \tag{21}$$

$$\log P_3 = \frac{10 \log P_{Rek}}{^1\chi^\nu (R_{F1} + R_{F2})} \tag{22}$$

$$\log P_4 = \frac{10 \log P_{Rek}}{^2\chi^\nu (R_{F1} + R_{F2})} \tag{23}$$

$$\log P_5 = \frac{4(^0B)}{(R_{F1} + R_{F2})} \tag{24}$$

$$\log P_6 = \frac{2(^2\chi^\nu)}{^0B(R_{F1} + R_{F2})} \tag{25}$$

$$\log P_7 = \frac{^0\chi^\nu}{2(R_{F1} + R_{F2})} \tag{26}$$

Next, $\log \overline{P}$ was calculated as average value from all theoretical partition coefficients (logP_1, logP_2, logP_3, logP_4, logP_5, logP_6, and logP_7). The log $\overline{P}$ values were equal to 11.87, 10.18, 9.35, and 8.02 for α-, β-, γ-, and δ-tocopherols, respectively. It was stated that the applied above-mentioned topological indices ($^0\chi^\nu$, $^1\chi^\nu$, $^2\chi^\nu$, and ^0B) with the R_F values enable calculation of the partition coefficient, which depends on the relative retention of the tocopherols.[28]

Podgorna[29] proposed the new lipophilic parameter (*W*) for porphyrin and alkyloxy porphyrin derivatives separated by RP-HPTLC on RP18 plates using CH_2Cl_2:MeOH 6 + 4 (v/v) as the mobile phase. The lipophilic parameter *W* was calculated on the basis of the R_F values and the topological index *A* using Eq. 27:

$$W = A \cdot \frac{R_{F1} + R_{F2}}{R_{F1} \cdot 1000} \tag{27}$$

where, $R_{F1} > R_{F2}$ and *A* is the topological index of Pyka.

The R_F values, numerical values of topological index *A*, the theoretical *n*-octanol-water partition cofficients *A*logP_s, *IA*log*P*, *C*log*P*, KOWWIN, *x*log*P*, logP_{Rekker}, and new lipophilicity parameter *W* are presented in Table 3. The calculated lipophilicity parameter *W* correlates rather well with log*P* according to Rekker.

APPLICATION OF THE TOPOLOGICAL INDICES AND THE ELECTROTOPOLOGICAL STATES TO PREDICT THE WATER SOLUBILITY OF INVESTIGATED COMPOUNDS

Niestroj[30] separated long-chain acids and hydroxyl fatty acids and its esters by RP-HPTLC using three mobile phases, and she proposed a new method for the calculation of water solubility from experimental R_M values and other physiochemical data. It was stated that the most accurate prediction of log*W* values of studied compounds was achieved by using four-parameter equations relating the R_M values of the compounds, the numerical values of the Pyka topological index ^0B, the electrotopological states of oxygen atoms of the carbonyl groups or of oxygen atoms of the hydroxyl groups, and the dipole moments (μ_{mph}) of the applied mobile phases.

Table 3 R_F values and topological index A values, the log$P$ values calculated by the computer programs, and by the Rekker equation, appointed experimentally and the lipophilicity parameter W of investigated porphyrins.

Compound	R_F stationary phase:RP18 mobile phase: CH_2Cl_2:MeOH 6 + 4(v/v)	Topological index A	$A\log P_s$	$IA\log P$	$C\log P$	KOWWIN	$x\log P$	$\log P_{Rekker}$	$\log P_{exp.}$	W
P1	0.76	324	3.04	0.33	6.47	6.01	2.04	0.83	1.58	0.62
P2	0.70	2,230	7.50	3.12	14.18	13.75	9.13	2.64	3.50	4.14
P3	0.60	4,682	10.29	7.33	22.65	21.60	16.80	10.95	9.00	8.43
P4	0.48	9,930	11.03	9.60	33.23	31.43	25.23	21.33	20.01	16.34
P5	0.31	19,908	10.64	—	45.92	43.21	—	33.78	—	32.77

P1 refers to porphine; **P2** to 5,10,15,20-tetra-(4-methoxyphenyl)porphyrin; **P3** to 5,10,15,20-tetra-(4-pentyloxyphenyl)porphyrin; **P4** to 5,10,15,20-tetra-(4-decyloxyphenyl)porphyrin; **P5** to 5,10,15,20-tetra-(4-hexadecyloxyphenyl)porphyrin.

Source: From Application of topological index and the R_F parameter to the estimation of lipophilic properties of selected porphyrins, in J. Liq. Chromatogr. Relat. Technol.[29]

CONCLUSIONS

This work is an assessment of the possibility of using topological indices including electrotopological states in TLC. Every work quoted is a new aspect of the use of topological indices and electrotopological states. Data from the scientific literature indicate that the topological indices discussed can be used to predict and describe retention, lipophilic parameters obtained by TLC, and water solubility for the different classes of organic compounds investigated.

The results of the studies presented indicate that the topological indices and electrotopological states discussed have significance in analytical and physicochemical investigations of organic compounds. Theoretical determination of the R_M or R_F values and lipophilic parameters of organic compounds has special significance if standards are not available. This entry indicates that further investigations on the application of the topological indices in TLC are justifiable.

ACKNOWLEDGMENT

This research was financed by the Ministry of Science and Information Society Technologies by resources reserved for science in the years 2005–2008 as research project No. 3 T09A 155 29.

REFERENCES

1. Devillers, J.; Balaban A.T. Topological Indices and Related Descriptors in QSAR and QSPR. Gordon and Breach Science Publishers: The Netherlands, 1999.
2. Pyka, A. The application of topological indexes in TLC, J. Planar Chromatogr. Mod. TLC **2001**, *14* (3), 152–159.
3. Pyka, A.; Bober, K.; Gurak, D.; Niestroj, A. Application of topological indexes for evaluation of the TLC separation of selected essential oil components. Acta Pol. Pharm. Drug Res. **2002**, *59* (2), 87–91.
4. Pyka, A.; Bober, K. On the importance of topological indices in research of α- and β-terpinene as well as α- and β-pinene separated by TLC. J. Liq. Chromatogr. Relat. Technol. **2002**, *25* (9), 1301–1315.
5. Pyka, A.; Sliwiok, J. Chromatographic separation of tocopherols. J. Chromatogr. A, **2001**, *935*, 71–76.
6. Pyka, A.; Dolowy, M. Application of structural descriptors for evaluation of some physicochemical properties of selected bile acids. Acta Pol. Pharm. Drug Res. **2004**, *61* (6), 407–413.
7. Dolowy, M. Application of selected topological indices to predict retention parameters of selected bile acids separated on modified TLC plates. Acta Pol. Pharm. Drug Res. **2008**, *65* (1), 51–57.
8. Pyka, A. Use of structural descriptors to predict the R_M values of *m*- and *p*-alkoxyphenols in RP TLC. J. Planar Chromatogr. Mod. TLC **2003**, *16* (2), 131–136.
9. Pyka, A. Investigation of the correlation between R_M values and selected topological indexes for higher alcohols, higher fatty acids and their methyl esters in RPTLC. J. Planar Chromatogr. Mod. TLC **2001**, *14* (6), 439–444.
10. Pyka, A.; Bober, K. Investigation of homologous series of fatty acids by TLC. Part I. Comparison of separations of fatty acids on RP-18 plates with and without a concentrating zone. J. Planar Chromatogr. Mod. TLC **2002**, *15* (4), 332–340.
11. Luhua, Z.; Fang, Y.; Lili, Y.; Bingren, X. Chromatographic separation of (−)-ephedrine and (+)-pseudoephedrine in the traditional Chinese medicinal preparation jiketing granule. Chem. Pharm. Bull. **2005**, *53* (11), 1494–1497.
12. Beteringe, A.; Baciu, I.; Caproiu, M.T.; Constatantinescu, T.; Balaban, A.T. *O*-Methyloximes of testosterone and of 17α-methylsterone: TLC and QSRR study of R_F values. J. Planar Chromatogr. Mod. TLC **2003**, *16* (4), 268–270.
13. Pyka, A. Application of electrotopological states in QSRR and QSAR analysis of isomeric methylphenols separated by RP-TLC. J. Planar Chromatogr. Mod. TLC **2008**, *21* (3), 205–208.
14. Pyka, A. Chromatographic data-topological index dependence for selected steroids. J. Liq. Chromatogr. Relat. Technol. **2001**, *24* (4), 453–460.
15. Pyka, A.; Sliwiok, J. Use of traditional structural descriptors in QSRR analysis of nicotinic acid esters. J. Liq. Chromatogr. Relat. Technol. **2004**, *27* (5), 785–798.
16. Pyka, A.; Niestrój, A. The application of topological indexes for prediction of the R_M values for tocopherols in RP-TLC. J. Liq. Chromatogr. Relat. Technol. **2001**, *24* (16), 2399–2413.
17. Pyka, A.; Kępczyńska, E.; Bojarski, J. Application of selected traditional structural descriptors to QSRR and QSAR analysis of barbiturates. Indian J. Chem. A, **2003**, *42A*, 1405–1413.
18. Niestroj, A.; Pyka, A.; Sliwiok, J. The use of topological indexes to predict the R_M values of higher fatty acids, hydroxyl fatty acids, and their esters in RPTLC. J. Planar Chromatogr. Mod. TLC **2002**, *15* (3), 177–182.
19. Pyka, A.; Bober, K. Prediction of the R_M values of selected methyl esters of higher fatty acids in RPTLC. J. Planar Chromatogr. Mod. TLC **2002**, *15* (1), 59–66.
20. Pyka, A.; Bober, K. Prediction of the R_M values of selected isomers of higher fatty acids of *cis* and *trans* configuration. Riv. Ital. Sost. Grasse **2001**, *78*, 477–482.
21. Pyka, A.; Dolowy, M.; Gurak, D. Use of selected structural descriptors for evaluation of the lipophilicity of bile acids investigated by RP HPTLC. J. Planar Chromatogr. Mod. TLC **2005**, *18* (6), 465–470.
22. Kepczynska, E.; Bojarski, J.; Pyka, A. Lipophilicity of barbiturates determined by TLC. J. Liq. Chromatogr. Relat. Technol. **2003**, *26* (19), 3277–3287.
23. Pyka, A.; Miszczyk, M. Chromatographic evaluation of the lipophilic properties of selected pesticides. Chromatographia **2005**, *61* (1/2), 37–42.
24. Pyka, A. Study of lipophilicity and application of selected topological indexes in QSAR analysis of nicotinic acid

derivatives. Part I. J. Planar Chromatogr. Mod. TLC **2004**, *17* (4), 275–279.
25. Pyka, A.; Klimczok, W. Study of lipophilicity and application of selected topological indexes in QSAR analysis of nicotinic acid derivatives. Investigations on RP18WF254 Plates. Part II. J. Planar Chromatogr. Mod. TLC **2005**, *18* (4), 300–304.
26. Pyka, A.; Klimczok, W. Significance of selected structural descriptors to estimate the lipophilic properties of vitamin PP and its derivatives. In *Chemometrics, Methods and Applications*; Zuba, D., Parczewski, A., Eds.; Institute of Forensic Research Publishers: Krakow, 2006, 335–340.
27. Pyka, A.; Babuska, M. Application of some topological indexes to evaluation of the physicochemical properties of selected steroid compounds. In *Chemometrics, Methods and Applications*; Zuba, D., Parczewski, A., Eds.; Institute of Forensic Research Publishers: Krakow, 2006, 329–334.
28. Niestroj, A. Comparison of methods for calculation of the partition coefficients of selected tocopherols. J. Planar Chromatogr. Mod. TLC **2007**, *20* (6), 483–486.
29. Podgorna, M. Application of topological index and the R_F parameter to the estimation of lipophilic properties of selected porphyrins. J. Liq. Chromatogr. Relat. Technol. **2008**, *31* (10), 1458–1464.
30. Niestroj, A. Use of RP-TLC to investigate the solubility in water of fatty acids, hydroxyl fatty acids and their esters. J. Planar Chromatogr. Mod. TLC **2006**, *19* (3), 208–211.

Topological Indices: Use in HPLC

Alina Pyka
Department of Analytical Chemistry, Medical University of Silesia, Sosnowiec, Poland

Abstract
This entry is an assessment of the possibility of using topological indices with the high-performance liquid chromatography (HPLC) technique. Every quoted work is a new aspect of the use of topological indices. Data from the scientific literature indicate that the discussed topological indices can be used to predict and describe retention and lipophilic parameters obtained by HPLC for the different classes of organic compounds. The results of the studies presented here indicate that the topological indices have significance in analytical and physicochemical investigations of organic compounds.

INTRODUCTION

A tendency in chemical investigations is to predict physicochemical and biological properties of chemical compounds from their structural parameters. The fundamental establishment of these investigations is based on the fact that the structure of a molecule determines its properties. The prediction of physicochemical and toxicological properties of organic compounds with selected topological indices has been reviewed in monographs and dedicated entries. The first topological indices used for the prediction of selected physicochemical properties (boiling point, heat of formation, heat of vaporization, molar volume, and molar refraction) were the Wiener index, polarity number, and Platt's index. The Wiener index has been continuously modified.

MOLECULAR STRUCTURE AND PROPERTIES

Only quantum mechanics completely describes the structure of a molecule, characterizing its geometric and electronic structures. In many cases, the structural description of a molecule is shown by type and order of the connections of atoms, and by the form and size of a molecule. The topological indices, which are derived from graph theory, are the simplest means of describing the structure of a molecule. The topological indices encode the structural information of a molecule. The topological index characterizes a molecule by a single number.[1–3]

The applications of the topological indices in investigations—quantitative structure–activity relationship (QSAR), quantitative structure–property relationship (QSPR), and quantitative structure–retention relationship (QSRR)—for organic compounds have been described in the scientific literature. The compounds investigated were homologous series or mixtures of compounds from different classes of organic compounds. The topological indices have been applied in chromatographic investigations. The short distance traveled by a solute on a chromatographic column is the reason for the limited application of topological high-performance liquid chromatography (HPLC).

The range and field of application of topological indices are limited.[1,2] The topological indices can be applied as a descriptor, only when the correlated property is primarily dependent on the structure of a molecule. Often, the monoparametric and multiparametric equations have low values for correlation coefficients. In such circumstances, the authors introduce the correlation or modification in the way of the topological indices calculation. Such procedures lead to correlation equations with high values of correlation coefficients.[1–3]

The application of the topological indices is an important field in theoretical chromatography. Topological indices open a new field of investigation in chromatographic science. Many scientists have reported the application of topological indices for the prediction of the retention data for different groups of organic compounds. The extent of this application in recent years has been unexpectedly large and includes the application of the topological indices in liquid chromatography [thin-layer chromatography (TLC) and HPLC].

In previous work, Pyka[3] described the possibility of using topological indices in TLC. The objectives of this review are to describe the use of topological indices in HPLC investigations reported in scientific literature and to discuss the significance of such works.

PRESENTATION AND DISCUSSION

The investigation of chromatographic retention is one of the most active areas for the QSRR studies using various topological indices. Many papers have been written on this important area of analytical chemistry.[1–30] The first

topological indices used for the prediction of retention parameters or lipophilic parameters were the Randić indices (molecular connectivity indices), the Wiener index, and the Balaban (I_B) index. Selected applications of topological indices for the prediction of retention parameters of compounds separated by HPLC are covered later in this entry.

Jinno and Kawasaki[4] correlated log k' with the connectivity index χ of 26 polycyclic aromatic hydrocarbons (PAHs) separated on phenyl ($r = 0.9926$), ethyl ($r = 0.9905$), octyl ($r = 0.9944$), and octadecyl ($r = 0.9912$) columns. Hurtubise, Allen, and Silver[5] separated 34 PAHs by reversed-phase(RP)-HPLC and correlated their log k' with the connectivity index χ:

$$\log k' = -0.55\chi + 0.30,\ r = 0.97 \tag{1}$$

Jinno and Kawasaki[6] also obtained the best correlations between log k' and the topological index χ, van der Waals volume (V_w), and hydrophobic parameter (log P) for alkylbenzenes separated on RP C_2, C_8, and C_{18} columns by HPLC ($r > 0.94$). In addition, Smith[7] presented the relationships between log k' and connectivity index χ for alkylbenzenes and *n*-alkylbenzenes separated by RP-HPLC on SAS-Hypersil and ODS-Hypersil columns ($r > 0.97$).

Burda et al.[8] separated 54 alkanes (C_5–C_{11}), with different degrees of branching, by RP-HPLC on an octadecyl-silica Lichrosorb R18 column, by using a mixture of methanol and water (80:20) as mobile phase. The connectivity index χ was used to correlate the structures of investigated alkanes with their obtained retention parameter log k'.

Wells, Clark, and Patterson[9] investigated 16 C_1–C_5 *n*-alkylbenzamides by RP-HPLC on a Partisil ODS column using methanol and water, as well as acetonitrile and water, in different volume compositions as mobile phases. The values of log k' and log k'_w were correlated with topological indices ${}^m\chi_t$ and ${}^m\chi_t{}^\nu$ values. The highest correlations were obtained with the connectivity data that describe molecular bulk, branching in the hydrocarbon portion of the molecule. For example, for log k'_w values for 0%, acetonitrile in mobile phase on Partisil ODS-2 and Ultrasphere ODS, the following correlation equations were obtained:

1) For Partisil ODS-2:

$$\begin{aligned}\log k'_w = {} & 0.070(\pm 0.013)({}^5\chi^v_{pc})^2 \\ & + 20.930(\pm 0.917)({}^6\chi^\nu_p)^2 \\ & + 2.154(\pm 0.082),\ r = 0.9885\end{aligned} \tag{2}$$

2) For Ultrasphere ODS:

$$\begin{aligned}\log k'_w = {} & 0.834(\pm 0.026)({}^o\chi^v) \\ & + 0.326(\pm 0.031)({}^6\chi^v_{pc})^{-1} \\ & - 3.991(\pm 0.267),\ r = 0.995\end{aligned} \tag{3}$$

Adler, Babic, and Trinajstic[10] applied the Wiener index for calculating HPLC parameters for polycyclic hydrocarbons. Retention index (I) was correlated with the Wiener index for 10 PAHs:

$$\log I = 0.225(\pm 0.026)W^{(0.460\pm 0.019)} \tag{4}$$

Siwek and Sliwiok[11] applied connectivity, Wiener index, and Balaban index to evaluate hydrophobicities (log k'_w) of selected isomer ketones, by using an RP-HPLC technique. Topological indices do not correlate well with log k'_w for a large group of compounds[11]:

$$\log k'_w = 0.015W + 0.50,\ n = 10;\ r = 0.804 \tag{5}$$

$$\log k'_w = 1.62\chi + 1.0,\ n = 10;\ r = 0.787 \tag{6}$$

$$\log k'_w = -0.28I_B + 3.41,\ n = 10;\ r = 0.616 \tag{7}$$

However, they can be used successfully for qualitative comparisons of hydrophobicity within the field of isomer pairs.

Kakoulidou and Rekker[12] predicted capacity factors (k') for 14 selected alkyl-substituted benzophenones and four halogen-substituted benzophenones (separated by RP-HPLC) based on connectivity indices ${}^o\chi^\nu$ and ${}^4\chi^\nu_{pc}$:

For alkyl-substituted benzophenones:

$$\begin{aligned}\log k' = {} & 0.215(\pm 0.022)({}^o\chi^v) \\ & - 0.223(\pm 0.091)\left({}^4\chi^v_{pc}\right) \\ & - 1.458(\pm 0.143),\ n = 14; \\ & r = 0.9939;\ s = 0.037;\ F = 483\end{aligned} \tag{8}$$

For halogen-substituted benzophenones:

$$\begin{aligned}\log k' = {} & 0.491(\pm 0.085)({}^o\chi^v) \\ & - 0.695(\pm 0.231),\ n = 4; \\ & r = 0.9965;\ s = 0.051;\ F = 281\end{aligned} \tag{9}$$

Wells, Clark, and Patterson[13] investigated a series of twenty-three 5,5-dialkylbarbituric acid derivatives by RP-HPLC on Partisil ODS and Partisil ODS-2 columns using mixtures of methanol and water in volume compositions 30:70 and 50:50. The same three molecular connectivity indices were selected: ${}^1\chi$, ${}^3\chi_p$, and ${}^3\chi^\nu_p$ in the chromatographic process at both 30% and 50% v/v methanol in water and on two different columns:

For Partisil ODS:

$$\begin{aligned}\log k'_{30\%MeOH} = {} & 0.033(\pm 0.002)\left({}^1\chi\right)^2 \\ & - 0.059(\pm 0.004)\left({}^3\chi_p\right)^2 \\ & + 0.708(\pm 0.040)\left({}^3\chi^v_p\right) \\ & + 1.294(\pm 0.085),\ r = 0.990\end{aligned} \tag{10}$$

$$\log k'_{50\%\text{MeOH}} = 0.018(\pm 0.001)\left({}^{1}\chi\right)^{2} - 0.036(\pm 0.002)\left({}^{3}\chi_{\text{p}}\right)^{2} + 0.431(\pm 0.020)\left({}^{3}\chi_{\text{p}}^{v}\right) - 0.886(\pm 0.042),\ r = 0.991 \quad (11)$$

For Partisil ODS-2:

$$\log k'_{50\%\text{MeOH}} = 0.034(\pm 0.002)\left({}^{1}\chi_{\text{p}}\right)^{2} - 0.064(\pm 0.004)\left({}^{3}\chi_{\text{p}}\right)^{2} + 0.773(\pm 0.035)\left({}^{3}\chi_{\text{p}}^{v}\right) + 1.526(\pm 0.075),\ r = 0.992 \quad (12)$$

This implies that the topological indices ${}^{1}\chi$, ${}^{3}\chi_{\text{p}}$, and ${}^{3}\chi_{\text{p}}^{\nu}$ define those molecular features that govern the RP-HPLC retention of barbiturates. The topological index ${}^{1}\chi$ decreased with increased branching of an alkyl group. The topological indices ${}^{3}\chi_{\text{p}}$ and ${}^{3}\chi_{\text{p}}^{\nu}$ described the exact position of branching for the investigated barbiturates.[13]

Wells, Clark, and Patterson[14] also used the combination of topological indices ${}^{0}\chi$, ${}^{0}\chi^{\nu}$, ${}^{4}\chi_{\text{pc}}$, and ${}^{4}\chi_{\text{pc}}^{\nu}$ to predict retention of the hydrocarbons on various C_{18} stationary phases in aqueous methanol and acetonitrile.

Lehtonen[15–17] used molecular connectivity indices to correlate chromatographic parameters with molecular structure for *n*-ethylbenzamides, amines, and dansylamines separated by HPLC. The best regression equation for 22 isolated amines from wines is[15]

$$\log k' = -22.1\left({}^{1}\chi^{v}\right)^{-2} - 5.08\left({}^{4}\chi_{\text{pc}}^{v}\right)^{-2} - 0.049\left({}^{6}\chi_{\text{pc}}\right) + 2.61,\ r = 0.991 \quad (13)$$

For example, the regression equation for 16 dansyl derivatives of amines (dansylamides) separated on a Nucleosil 5 C_{18} column using the mobile phase at 39% of propanol in water is[16]

$$\log k' = 0.00894\left({}^{1}\chi^{v}\right)^{2} + 0.604\left({}^{\text{o}}\chi^{v}\right)^{2} - 2.138,\ r = 0.9910 \quad (14)$$

Lehtonen[17] also calculated molecular connectivity indices to the third order, and a high degree of correlation was observed between the measured log k' and the topological indices for 16 *n*-ethylbenzamides:

For Spherisorb S5 ODS-2 column:

$$\log k' = 1.207(\pm 0.039)\left({}^{1}\chi^{v}\right) - 0.550(\pm 0.066)\left({}^{1}\chi\right) - 1.406(\pm 0.072),\ r = 0.9935 \quad (15)$$

For μBondapak C_{18} column:

$$\log k' = 1.074(\pm 0.086)\left({}^{1}\chi^{v}\right) - 0.482(\pm 0.059)\left({}^{1}\chi\right) - 1.173(\pm 0.064),\ r = 0.9937 \quad (16)$$

The selected pesticides, monolinuron, chlortoluron, diuron, isoproturon, linuron, dimefuron, diflubenzuron, teflubenzuron, and lufenuron were separated by an isocratic RP-HPLC technique using methanol and water as mobile phase, in which the proportional content of methanol was from 45% to 90%. *n*-Hexane was selected for determining the retention time of an unretained compound. The topological indices based on connectivity Gutman (M, M^{ν}) and Randić (${}^{0}\chi$, ${}^{1}\chi$, ${}^{2}\chi$, ${}^{0}\chi^{\nu}$, ${}^{1}\chi^{\nu}$, ${}^{2}\chi^{\nu}$) were calculated for the investigated compounds. The log k values obtained for the all investigated urea pesticides were extrapolated to pure water (to 0% v/v of methanol in mobile) according to the equations of Soczewinski and Wachtmeister. The obtained parameters of lipophilicity log k_{w} and $\varphi_{\text{o(HPLC)}}$ were correlated with topological indices. Only the Gutman index M^{ν} from among all topological indices was useful in the QSAR analysis of studied urea pesticides:[18]

$$\log k_{\text{w}} = 1.0383(\pm 0.3290) + 0.005267(\pm 0.000750)\ M^{v},\ n = 9;\ r = 0.9358;\ s = 0.463;\ F = 49.33;\ P < 0.0005$$

The Gutman index M^{ν} correlates worse with $\varphi_{\text{o(HPLC)}}$ ($r = 0.8861$) in comparison with log k_{w}.

Amic, Davidovic-Amic, and Trinajstic[19] developed a simple relationship between experimental retention time by HPLC and the Wiener index (W), polarity number (p), and number of OH groups (n_{OH}) in flavyliums:

$$t_{\text{R}} = a\left[\frac{W}{(pn_{\text{OH}})}\right] + b \quad (18)$$

where a and b are statistical parameters to be determined by least squares regression. Three groups of flavyliums were investigated and three correlation equations were obtained:

For anthocyanins:

$$t_{\text{R}} = 7.1794(\pm 0.1870)\left[\frac{W}{(pn_{\text{OH}})}\right] - 17.7954(\pm 0.7309),\ n = 6;\ r = 0.9986;\ F = 1474.6;\ s = 0.32 \quad (19)$$

For anthocyanin 3-glucosides:

$$t_{\text{R}} = 19.1354(\pm 0.7039)\left[\frac{W}{(pn_{\text{OH}})}\right] - 41.7504(\pm 4.6820),\ n = 10;\ r = 0.9946;\ F = 739.1;\ s = 4.25 \quad (20)$$

For anthocyanin 3,5-diglucosides:

$$t_R = 13.6883(\pm 0.5346)\left[\frac{W}{(pn_{OH})}\right] - 41.6262(\pm 3.7626),\ n = 10;\quad r = 0.9940;\ F = 655.6;\ s = 2.66 \tag{21}$$

Amic, Davidovic-Amic, and Trinajstic[19] also correlated the Schultz index [molecular topological index (MTI)] for anthocyanins. They suggest that the QSRR with MTI index should be identical to those with the Wiener index.

Martorell et al.[20] separated a series of twenty-two 6-fluoroquinolones by ion-pair RP-HPLC. The multiple linear correlation that best fits the experimental data is

$$\log k' = 6.8448(\pm 1.3184)QX_{24} - 0.2249(\pm 0.0933)DM - 4.0366(\pm 2.1135)DIF^3\chi_c + 5.0421,\ n = 22;\ r = 0.8543 \tag{22}$$

where QX_{24} is the negative net charge associated with the heteroatom X situated at position 4 of the heterocyclic aliphatic ring that functionalizes position C_7, DM is the dipolar moment, and $DIF^3\chi_c$ is the difference between the molecular connectivity index of valency and the nonvalency of the order 3 cluster.

In recent years, topological indices have become prominent on several different fronts. Many new topological indices were described after 1990.[1,2] Some among them were also applied in QSRR analyses of compounds investigated by the HPLC technique.[1,18,19,21–30]

De Julian-Ortiz et al.[21] calculated connectivity indices to the fourth order and proposed charge indices (G_k, J_k) for racemic hydantoins, racemic α-amino acids, and racemic arylamides. The best correlation equation for racemic hydantoins separated on β-cyclodextrin column using 10% methanol as a mobile phase is[21]

$$\log k' = -1.314 + 1.280\left({}^4\chi_p^v\right) - 0.185G_3^v,\ n = 17;\ r = 0.9426;\ F = 55.76;\ P < 0.001 \tag{23}$$

The best correlation equation for racemic α-amino acids separated on α-cyclodextrin column using 1% triethylamine acetate (pH = 5.1) as a mobile phase is[21]

$$k' = -8.262 + 0.2935G_2 - 12.187G_4 + 13.701G_4^v,\ n = 15;\ r = 0.9702;\ s = 0.62;\ F = 58.70;\ P < 0.001 \tag{24}$$

The best correlation equation for racemic arylamides separated on 1-(α-naphthyl)ethylamine column using *n*-hexane-tetrahydrofuran (75:25, v/v) as a mobile phase is[21]

$$\log k' = 3.264 - 0.209\ Pr_0 + 1.289\left({}^1\chi - {}^1\chi^v\right) - 1.943\frac{{}^4\chi_{pc}}{{}^4\chi_{pv}^v},\ n = 14;\ r = 0.9554;\ s = 0.12;\ F = 38.3;\ P < 0.001 \tag{25}$$

where Pr_0 is the number of vertices showing topological valence equal to 4.

Pyka[22] separated six selected steroids (corticosterone acetate, 11-dehydrocorticosterone acetate, corticosterone, 11-dehydrocorticosterone, hydrocortisone, and cortisone) by RP-HPLC on Separon Six C_{18} column. Column void time was determined using the peak derived from a solution of sodium nitrite in methanol. The mobile phase was prepared from analytical grade methanol and redistilled water (3:2, v/v). The Randić ($^0\chi$, $^0\chi^v$, $^1\chi$, $^1\chi^v$), Wiener (W), Balaban (I_B), and Pyka (A, ^0B) indices were calculated for the investigated compounds. The chromatographic data, log k', and partition coefficient log P values, of the compounds have been correlated with the numerical values of topological indices. The most accurate predictions of the log k' and log P values of the selected steroids were achieved by using monoparametric equations employing the topological indices ^0B:

$$\log k' = 18.5859(\pm 2.2622) - 7.0362(\pm 0.8882)^0B,\ n = 6;\quad r = -0.9696;\ s = 0.053;\ F = 62.75;\ P = 0.0014 \tag{26}$$

$$\log P = 106.454(\pm 3.332) - 41.464(\pm 1.308)^0B,\ n = 6;\quad r = -0.9980;\ s = 0.078;\ F = 1004.23;\ P = 0.0000 \tag{27}$$

Pyka and Sliwiok[23]separated six esters of nicotinic acids: methyl nicotinate, ethyl nicotinate, isopropyl nicotinate, butyl nicotinate, hexyl nicotinate, and benzyl nicotinate by adsorption HPLC on a LiChrospher Si 60 column. The mixtures containing benzene and methanol in volume proportions (0 + 10, 1 + 9, 2 + 8, 3 + 7, 4 + 6, and 5 + 5) were used as the mobile phases. The t_R (min) values of esters investigated have been correlated with the dipole moments (μ_{mph}) of the mobile phases applied, with numerical values of one topological index from among those based on the distance matrix (A, W, ^0B, ^1B, ^2B) or the adjacency matrix ($^0\chi^v$, $^1\chi^v$, $^2\chi^v$) with electrotopological states SaaCH, aaN, aasC, dO, ssO, and dssC, and structural descriptors based on information theory (I_{AC} and $\bar{I}_{AC}$). Dipole moments were used to characterize mobile phases. The correlation equations that enable the calculation of t_R

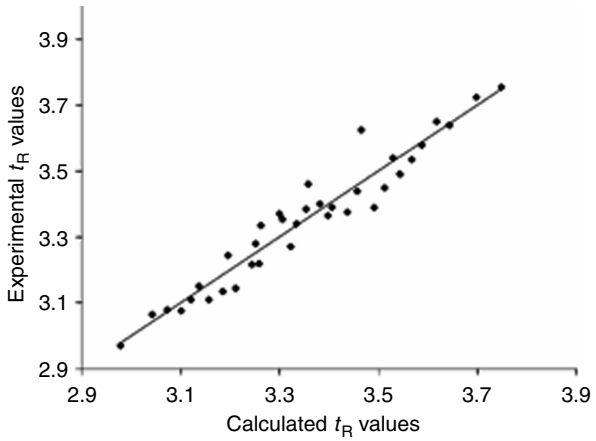

Fig. 1 Relationship between the experimental t_R (min) values of nicotinic acid esters and the t_R values calculated using Eq. 29. **Source:** From Use of traditional structural descriptors in QSRR analysis of nicotinic acid esters, in J. Liq. Chromatogr. Relat. Technol.[23]

values were obtained with topological indices based on adjacency matrices ${}^0\chi^\nu$ and ${}^1\chi^\nu$, with indices based on distance matrices ${}^1B$ and ${}^2B$, with index based on information theory (I_{AC} and $\bar{I}_{AC}$), and with electrotopological state aaN. All the equations are characterized by determination coefficients $R^2 > 90\%$. The best correlation equations were obtained with topological indices based on information theory I_{AC} and $\bar{I}_{AC}$, as well as based on distance matrices ${}^1B$ and ${}^2B$. For example,

$$t_R = -0.766(\pm 0.165) + 0.546(\pm 0.043)\mu_{mph} + 2.179(\pm 0.100)\bar{I}_{AC},\ n = 36;$$
$$R^2 = 95.08\%;\ F = 318.6;\ s = 0.046;\ P < 0.0001 \quad (28)$$

$$t_R = 1.838(\pm 0.082) + 0.546(\pm 0.050)\mu_{mph} + 1.600(\pm 0.087){}^1B,\ n = 36;$$
$$R^2 = 93.30\%;\ F = 230.0;\ s = 0.053;\ P < 0.0001 \quad (29)$$

The correlation equations (Eqs. 28 and 29) can be used to calculate t_R values of investigated esters. For example, the relationship between t_R (min) values measured experimentally and values calculated using Eq. 29 is shown in Fig. 1.

Eqs. 28 and 29 can also be used to predict the t_R values of the esters of nicotinic acid, whose measurement points have not been taken into consideration in the equation. A test was performed on Eqs. 28 and 29 to determine how well they predict t_R values of points not included in the training set. Three values were removed from the training sets (Eqs. 28 and 29). Isopropyl nicotinate (separated in benzene:methanol, 5:5, v/v) and ethyl nicotinate (separated in benzene:methanol, 4:6, and 0:10, v/v) from Eqs. 28 and 29 were removed. This subset of two parametric equations was recalculated as

$$t_R = -0.753(\pm 0.175) + 0.533(\pm 0.048)\mu_{mph} + 2.183(\pm 0.105)\bar{I}_{AC},\ n = 33;$$
$$R^2 = 94.85\%;\ F = 276.2;\ s = 0.047;\ P < 0.0001 \quad (30)$$

$$t_R = 1.872(\pm 0.090) + 0.522(\pm 0.056)\mu_{mph} + 1.604(\pm 0.090){}^1B,\ n = 33;$$
$$R^2 = 93.07\%;\ F = 201.6;\ s = 0.055;\ P < 0.0001 \quad (31)$$

The t_R values for esters of nicotinic acids, omitted during the derivation of Eqs. 30 and 31 and subsequently predicted using these equations, are listed in Table 1.

These equations are statistically significant and can be used for a reasonably good prediction of t_R values of the investigated esters of nicotinic acid. The high compatibility between experimental and predicted t_R values for esters omitted in the considered correlation equations was stated.

Djakovic-Sekulic, Perišic-Janjic, and Pyka[24] separated eight anilides of 2,2-dimethylpropanoic acid, nine anilides of benzoic acid, and nine anilides of α-phenyl acetic acid by RP-18 HPLC using mixtures containing methanol and water in volume proportions 6 + 4, 6.5 + 3.5, and 7 + 3 as the mobile phases. The log k values of investigated anilides have been correlated with the dipole moments (μ_{mph}) or permittivities (ε_{mph}) of the mobile phases applied, with numerical values of one topological index from among those based on the distance matrix (R, W, A, ${}^0B$, ${}^1B$, ${}^2B$) or on the adjacency matrix (M, M^ν, ${}^0\chi$, ${}^1\chi$, ${}^2\chi$, ${}^0\chi^\nu$, ${}^1\chi^\nu$, ${}^2\chi^\nu$), with partition coefficient by Rekker (log P_{Rek}), or with the number of hydrogen acceptors (HA), or with the solubility (log S), or with the molecular weight (M_w). Authors found 77 multiparametric equations with $R^2 > 90\%$. The best

Table 1 The t_R values (min) of nicotinic acid esters omitted from Eqs. 30 and 31, and predicted by these equations.

	t_R				
Omitted point	**Experimental**	**Predicted by Eq. 30**	**$\lvert\Delta t_R\rvert$**	**Predicted by Eq. 31**	**$\lvert\Delta t_R\rvert$**
isopropyl nicotinate (benzene:methanol, 5:5, v/v)	3.220	3.226	0.006	3.266	0.046
ethyl nicotinate (benzene:methanol, 4:6, v/v)	3.365	3.406	0.041	3.402	0.037
ethyl nicotinate (benzene:methanol, 0:10, v/v)	3.650	3.621	0.029	3.614	0.036

Source: From Use of traditional structural descriptors in QSRR analysis of nicotinic acid esters, in J. Liq. Chromatogr. Relat. Technol.[23]

equations for these groups of investigated anilides are as follows:

For anilides of 2,2-dimethyl propanoic acid:

$$\begin{aligned}\log k_{\mathrm{p}} &= -46.7031(\pm 2.5201) \\ &\quad + 25.7452(\pm 1.4278)\mu_{\mathrm{mph}} \\ &\quad + 0.002877(\pm 0.000467)M_W \\ &\quad + 0.2711(\pm 0.0230)\log P_{\mathrm{Rek}},\ n = 24; \\ R^2 &= 97.31\%;\ F = 240.8;\ s = 0.0471;\ P < 0.0001 \end{aligned} \quad (32)$$

For anilides of benzoic acid:

$$\begin{aligned}\log k_{\mathrm{b}} &= -6.7551(\pm 0.5235) \\ &\quad + 0.09581(\pm 0.00874)\varepsilon_{\mathrm{mph}} \\ &\quad + 0.007500(\pm 0.00164)M \\ &\quad + 0.4211(\pm 0.0344)\log P_{\mathrm{Rek}}, \\ n &= 27;\ R^2 = 92.16\%;\ F = 90.1; \\ s &= 0.0848;\ P < 0.0001 \end{aligned} \quad (33)$$

For anilides of α-phenyl acetic acid:

$$\begin{aligned}\log k_{\mathrm{ph}} &= -46.9896(\pm 2.2419) \\ &\quad + 25.6156(\pm 1.2646)\mu_{\mathrm{mph}} \\ &\quad + 0.004629(\pm 0.001086)M \\ &\quad + 0.3965(\pm 0.0208)\log \mathrm{P}_{\mathrm{Rek}},\ n = 27; \\ R^2 &= 97.36\%;\ F = 283.1;\ s = 0.0443;\ P < 0.0001 \end{aligned} \quad (34)$$

For all anilides investigated:

$$\begin{aligned}\log k_{\mathrm{all}} &= -52.7102(\pm 1.8869) \\ &\quad + 25.9835(\pm 1.0372)\mu_{\mathrm{mph}} \\ &\quad + 0.07725(\pm 0.01892)\left({}^2\chi^v\right) \\ &\quad + 2.2767(\pm 0.1816)^0B \\ &\quad + 0.002736(\pm 0.000360)M \\ &\quad + 0.3222(\pm 0.0142)\log P_{\mathrm{Rek}},\ n = 78; \\ R^2 &= 95.06\%;\ F = 277.6;\ s = 0.0671;\ P < 0.0001 \end{aligned} \quad (35)$$

Eqs. 32–35 can also be used for log k value prediction of anilides investigated, whose measurement points have not been taken into consideration in the equation. Four of the tests of predictive equations, such as 32–35, show how well they predict values of points not included in the training set.

From Eq. 32, log k for $(CH_3)_3C$–CO–NH–C_6H_4–CF_3 [separated with methanol and water, 7 + 3 (v/v)] was omitted, and the best subset equation using three parameters was recalculated as follows:

$$\begin{aligned}\log k_{\mathrm{p}} &= -46.3329(\pm 2.6616) \\ &\quad + 25.5281(\pm 1.5118)\mu_{\mathrm{mph}} \\ &\quad + 0.00290007(\pm 0.000480)M_{\mathrm{W}} \\ &\quad + 0.2738(\pm 0.0240)\log P_{\mathrm{Rek}}, \\ n &= 23;\ R^2 = 97.34\%;\ F = 231.4; \\ s &= 0.0480;\ P < 0.0001. \end{aligned} \quad (36)$$

From Eq. 33, log k for C_6H_5–CO–NH–C_6H_4–F [separated with methanol and water, 6 + 4 (v/v)] was omitted, and the best subset equation using three parameters was recalculated as follows:

$$\begin{aligned}\log k_{\mathrm{b}} &= -6.7834(\pm 0.5360) \\ &\quad + 0.09685(\pm 0.00917)\varepsilon_{\mathrm{mph}} \\ &\quad + 0.007390(\pm 0.00169)M \\ &\quad + 0.4199(\pm 0.0351)\log P_{\mathrm{Rek}},\ n = 26; \\ R^2 &= 92.19\%;\ F = 86.5;\ s = 0.086;\ P < 0.0001 \end{aligned} \quad (37)$$

From Eq. 34, log k for C_6H_5–CH_2–CO–NH–C_6H_4–F [separated with methanol and water, 7 + 3 (v/v)] was omitted, and the best subset equation using three parameters was recalculated as follows:

$$\begin{aligned}\log k_{\mathrm{ph}} &= -46.6855(\pm 2.3584) \\ &\quad + 25.4532(\pm 1.3258)\mu_{\mathrm{mph}} \\ &\quad + 0.004548(\pm 0.001116)M \\ &\quad + 0.3954(\pm 0.0213)\log P_{\mathrm{Rek}}, \\ n &= 26;\ R^2 = 97.26\%;\ F = 260.5; \\ s &= 0.0450;\ P < 0.0001 \end{aligned} \quad (38)$$

From Eq. 35, log k values for C_6H_5–CH_2–CO–NH–C_6H_4–CH_3, C_6H_5–CH_2–CO–NH–C_6H_4–CN, $(CH_3)_3C$–CO–NH–C_6H_4–$COCH_3$ [separated with methanol and water, 7 + 3 (v/v)], C_6H_5–CO–NH–C_6H_4–Cl, $(CH_3)_3C$–CO–NH–C_6H_4–Br [separated with methanol and water, 6.5 + 3.5 (v/v)], and $(CH_3)_3C$–CO–NH–C_6H_4–CF_3 [separated with methanol and water, 6 + 4 (v/v)] were omitted, and the best subset equation using five parameters was recalculated as follows:

$$\begin{aligned}\log k_{\mathrm{p}} &= -52.6507(\pm 2.0879) \\ &\quad + 25.9692(\pm 1.1317)\mu_{\mathrm{mph}} \\ &\quad + 0.07771(\pm 0.02096)\left({}^2\chi^v\right) \\ &\quad + 2.2620(\pm 0.2002)^0B \\ &\quad + 0.002742(\pm 0.000385)M \\ &\quad + 0.3213(\pm 0.0156)\log P_{\mathrm{Rek}},\ n = 72; \\ R^2 &= 94.32\%;\ F = 219.1;\ s = 0.0644;\ P < 0.0001 \end{aligned} \quad (39)$$

The experimental and predicted log k values calculated by 36–39 are presented in Tables 2 and 3. The differences

Table 2 The log k values of anilides omitted (experimental) from 36–38, and predicted by these equations.

Anilide	log k_p			log k_b			log k_{ph}		
	Experimental (methanol + water, 7+3, v/v)	Predicted by Eq. 36	$\lvert\Delta \log k_p\rvert$	Experimental (methanol + water, 6 + 4, v/v)	Predicted by Eq. 37	$\lvert k_b\rvert$	Experimental (methanol + water, 7 + 3, v/v)	Predicted by Eq. 38	$\lvert\Delta\log k_{ph}\rvert$
$(CH_3)_3C–CO–NH–C_6H_4–CF_3$	0.176	0.206	0.030	—	—	—	—	—	—
$C_6H_5–CO–NH–C_6H_4–F$	—	—	—	0.288	0.329	0.041	—	—	—
$C_6H_5–CH_2–CO–NH–C_6H_4–F$	—	—	—	—	—	—	–0.112	–0.088	–0.024

Source: From Correlation or retention of anilides and some molecular descriptors. Application of topological indexes for prediction of log k values, in Chromatographia.[24]

Table 3 The log k_{all} values of anilides omitted from Eq. 39 and predicted by this equation.

Anilides	log k_{all}		
	Experimental	Predicted by Eq. 39	$\lvert\Delta \log k_{all}\rvert$
C_6H_5–CH_2–CO–NH–C_6H_4–CH_3	–0.002[a]	–0.003	0.001
C_6H_5–CH_2–CO–NH–C_6H_4–CN	–0.208[a]	–0.207	0.001
C_6H_5–CO–NH–C_6H_4–Cl	0.358[b]	0.334	0.024
$(CH_3)_3C$–CO–NH–C_6H_4–CF_3	0.689[c]	0.705	0.016
$(CH_3)_3C$–CO–NH–C_6H_4–Br	0.406[b]	0.397	0.009
$(CH_3)_3C$–CO–NH–C_6H_4–$COCH_3$	–0.292[a]	–0.287	0.005

[a]With methanol + water, 7 + 3, v/v as mobile phase.
[b]With methanol + water, 6.5 + 3.5, v/v as mobile phase.
[c]With methanol + water, 6 + 4, v/v as mobile phase.
Source: From Correlation or retention of anilides and some molecular descriptors. Application of topological indexes for prediction of log *k* values, in Chromatographia.[24]

between experimental and predicted values $|\Delta \log k|$ were small.

Pyka[25] separated 16 PAHs (naphthalene, acenaphthylene, acenaphthene, fluorene, phenanthrene, anthracene, fluoranthene, pyrene, benzo[*a*]anthracene, chrysene, benzo[*b*]fluoranthene, benzo[*k*]fluoranthene, benzo[*a*]pyrene, dibenzo[*a,h*]anthracene, benzo[*g,h,i*]perylene, and indeno[1,2,3-*cd*]pyrene) according to the Environmental Protection Agency (EPA) by gradient HPLC on a LiChrospher® PAH column using acetonitrile and water as mobile phases. Retention times tr (sec) of investigated PAHs were correlated with topological indices based on the adjacency matrix (M, ${}^0\chi^\nu$, ${}^1\chi^\nu$, ${}^2\chi^\nu$, χ_{012}) and the distance matrix (W, A, C, D), and correlation equations were obtained, as follows (Table 4):

$$t_R = -564.65(\pm 75.78) + 8.649(\pm 0.379)M^\nu \quad (40)$$

$$t_R = -822.91(\pm 92.82) + 209.86(\pm 9.84)^0\chi^\nu \quad (41)$$

$$t_R = -866.18(\pm 105.10) + 335.35(\pm 17.43)^1\chi^\nu \quad (42)$$

$$t_R = -660.57(\pm 115.41) + 391.63(\pm 24.82)^2\chi^\nu \quad (43)$$

$$t_R = -308.08(\pm 62.44) + 2.413(\pm 0.166)W \quad (44)$$

$$t_R = -155.71(\pm 68.04) + 6.074(\pm 0.395)A \quad (45)$$

$$t_R = -400.5(\pm 105.6) + 116.03(\pm 7.81)C \quad (46)$$

$$t_R = -16.497(\pm 62.750) + 28.61(\pm 1.53)D \quad (47)$$

$$t_R = -792.9(\pm 97.2) + 304.1(\pm 14.7)\chi_{012} \quad (48)$$

The equations with the highest statistical parameters were obtained with topological indices based on the adjacency matrix. The relationship between t_R values and Gutman M^ν index according to Eq. 40 is presented in Fig. 2.

Pyka and Sliwiok[26] separated α-tocopherols, β-tocopherols, γ-tocopherols, and δ-tocopherols by normal-phase (NP)-HPLC and RP-C_{18}-HPLC. The selected topological indices based on connectivity (M^ν, ${}^1\chi^\nu$), distance matrix (W, ${}^0B$, MTI), and information theory (I_{AC}, $\bar{I}_{AC}$) were

Table 4 Relationships between retention time (t_R, sec) and selected topological indices for 16 PAHs separated by HPLC.

Correlation equation	*r*	*F*	*s*
Eq. 40	0.9868	520	78.0
Eq. 41	0.9850	455	83.3
Eq. 42	0.9816	370	92.0
Eq. 43	0.9730	248.9	111.2
Eq. 44	0.9686	212.5	111.9
Eq. 45	0.9717	236.8	113.9
Eq. 46	0.9697	220.7	117.8
Eq. 47	0.9807	351.5	94.4
Eq. 48	0.9841	428.9	85.7

[a]For 40–48: $n = 6$ and $p < 0.0001$.
Source: Pyka, A. Unpublished data.[25]

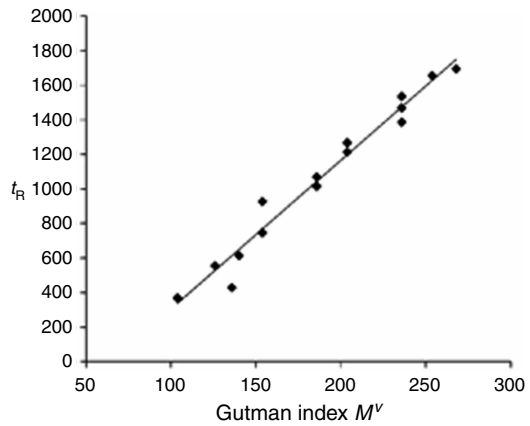

Fig. 2 Relationship between the t_R (sec) values and the Gutman index M^v for 16 PAHs according to Eq. 40.
Source: Pyka, A. Unpublished data.[25]

calculated for these tocopherols. As presented in Table 5, the topological indices clearly show that β-tocopherols and γ-tocopherols, as positional isomers, possess the same numerical values of topological indices $^1\chi^v$, M, I_{AC}, and $\bar{I}_{AC}$. In addition, the retention times have the same values for β-tocopherols and γ-tocopherols investigated by RP-C_{18}-HPLC. Instead, the numerical values of the topological indices W and MTI for α-tocopherols, γ-tocopherols, β-tocopherols, and δ-tocopherols in the given sequence grow smaller (decrease). Only the numerical values of the topological indices ^0B grow smaller (decrease) in the following order: α-tocopherols, β-tocopherols, γ-tocopherols, and δ-tocopherols. But the difference between the numerical values of the topological index ^0B is very small for β-tocopherols and γ-tocopherols. The definite dependence between the numerical values of topological index ^0B and the chromatographic separation of the investigated tocopherols was obtained. In the given sequence, grow retention times of tocopherols were investigated by NP-HPLC.[26]

Luhua et al.[27] separated by RP-HPLC and performance liquid chromatography–mass spectrometry chromatography (HPLC–MS) (–)-ephedrine and (+)-pseudoephedrine. The topological indices based on connectivity and distance matrix A, W, and $^h\chi^v$ were calculated. The structures particularly of (–)-ephedrine and (+)-pseudoephedrine were described by topological indices $^h\chi^v$, which were applied to interpret the chromatographic separations.

Lee et al.[28] separated 18 L-amino acids by RP-HPLC. Binding energy (E_b), hydrophobicity (log P), molecular refractivity (MR), polarizability (α), total energy (E_t), water solubility (log S), connectivity index (χ) of different orders and Wiener index (W) were also theoretically calculated. The retention factors with various physicochemical and structural properties of L-amino acids were represented. After investigating the effect of descriptors on the retention factors, the five major ones were found to be E_b, MR, E_t, $^1\chi$, and W. The correlation coefficient was more than 0.95.

The Wiener index (W) was also used for calculating the HPLC retention time of PAHs,[29] n-alkanes, and cycloalkanes.[30]

CONCLUSIONS

Topological index is indirectly connected with the structures of chemical compounds. Topological indices, as well as retention parameters, are most important for physicochemical characteristics of organic compounds. Chromatography is applied to the separation of chemical compounds both for analytical and for preparative aims. Correlation of retention parameters of organic compounds with selected topological indices (with structures of compounds studied) permits assignment of definite rules, which enable the prediction of chromatographic separations.

This work is an assessment of the possibility of using topological indices with the HPLC technique. Every quoted work is a new aspect of the use of topological indices. Data from the scientific literature indicate that the discussed topological indices can be used to predict and describe retention and lipophilic parameters obtained by HPLC for the different classes of organic compounds.

The results of the studies presented here indicate that the topological indices have significance in analytical and physicochemical investigations of organic compounds. These results indicate the capacity of molecular topology to identify and predict different structural features that determine HPLC data for a variety of organic compounds. The application of topological indices in the physicochemical investigation of organic compounds is constantly

Table 5 Retention times (t_R) obtained by NP-HPLC and RP-HPLC and numerical values of topological indices for the tocopherols investigated.

	Retention time (t_R) obtained (min)		Topological indices						
Compound	NP-HPLC	RP-HPLC	$^1\chi^v$	M	W	^0B	MTI	I_{AC} (bit)	$\bar{I}_{AC}$(bit)
α-Tocopherol	2.80	17.66	13.0432	252	3165.14	2.2070	15433.13	88.45	1.092
β-Tocopherol	3.86	13.98	12.6205	244	2944.79	2.1769	14554.13	85.58	1.097
γ-Tocopherol	4.88	13.98	12.6205	244	2945.96	2.1764	14560.14	85.58	1.097
δ-Tocopherol	5.60	10.80	12.1979	236	2728.94	2.1479	13692.47	82.70	1.103

Source: From Chromatographic separation of tocopherols, in J. Chromatogr. A.[26]

increasing. One reason for this is, among others, the use of computer programs to calculate topological indices.[1]

This review indicates that further investigations on the application of topological indices in HPLC are warranted.

ACKNOWLEDGMENT

This research was financed by the Ministry of Science and Information Society Technologies by resources reserved for science in the years 2005–2008 as research project No. 3 T09A 155 29.

REFERENCES

1. Devillers, J.; Balaban, A.T. *Topological Indices and Related Descriptors in QSAR and QSPR*; Gordon and Breach Science Publishers: The Netherlands, 1999.
2. Pyka, A. Topological indices and their significance in chromatographic investigations, Part II. Wiad. Chem. **1998**, 52, 727–754 (in Polish).
3. Pyka, A. The application of topological indexes in TLC. JPC, J. Planar Chromatogr. Mod. TLC **2001**, *14* (3), 152–159.
4. Jinno, K.; Kawasaki, K. Correlations between the retention data of polycyclic aromatic hydrocarbons and several descriptors in reversed-phase HPLC. Chromatographia **1983**, *17* (8), 445–449.
5. Hurtubise, R.J.; Allen, T.W.; Silver, H.F. Comparison of molecular connectivity and a chromatographic correlation factor in reversed-phase high-performance liquid chromatography for polycyclic aromatic hydrocarbons. J. Chromatogr. **1982**, *235*, 517–522.
6. Jinno, K.; Kawasaki, K. Correlations between retention data of isomeric alkylbenzenes and physical parameters in reversed-phase micro high-performance liquid chromatography. Chromatographia **1983**, *17* (6), 337–340.
7. Smith, R.M. Reversed-phase liquid chromatography of isomeric alkylbenzenes, J. Chromatogr. **1981**, *209*, 1–6.
8. Burda, J.; Kuraš, M.; Křiž, J.; Vodička, L. Relationship between retention behaviour and molecular structure of alkanes in reversed-phase high-performance liquid chromatography. Fresenius Z. Anal. Chem. **1985**, *321*, 549–552.
9. Wells, M.J.; Clark, C.R.; Patterson, R.M. Investigation of *n*-alkylbenzamides by reversed-phase liquid chromatography: III. Correlation of chromatographic parameters with molecular connectivity indices for the C_1–C_5 *n*-alkylbenzamides. J. Chromatogr. **1982**, *235*, 61–74.
10. Adler, N.; Babic, D.; Trinajstic, N. On the calculation of the HPLC parameters for polycyclic aromatic hydrocarbons, Fresenius Z. Anal. Chem. **1985**, *322*, 426–429.
11. Siwek, A.; Sliwiok, J. Reversed-phase high-performance liquid chromatography in the investigation of the hydrophobicity of selected ketones. J. Chromatogr. **1990**, *506*, 109–118.
12. Kakoulidou, A.; Rekker, R.F. A critical appraisal of log *P* fragmental procedures and connectivity indexing for reversed-phase thin-layer chromatographic and high-performance liquid chromatographic data obtained for a series of benzophenones. J. Chromatogr. **1984**, *295*, 341–353.
13. Wells, M.J.M.; Clark, C.R.; Patterson, R.M. Correlation of reversed-phase capacity factors for barbiturates with biological activities, partition coefficients, and molecular connectivity indices. J. Chromatogr. Sci. **1981**, *19*, 573–582.
14. Wells, M.J.; Clark, C.R.; Patterson, R.M. Structure–retention relationship analysis for some mono- and polycyclic aromatic hydrocarbons in reversed-phase liquid chromatography using molecular connectivity. Anal. Chem. **1986**, *58*, 1625–1633.
15. Lehtonen, P. Isolation and HPLC determination of amines in wine. Z. Lebensm.-Unters. Forsch. **1986**, *183*, 177–181.
16. Lehtonen, P. Use of molecular connectivity indices to predict LC retention of dansylamides in six different eluent systems. Chromatographia **1984**, *19*, 316–321.
17. Lehtonen, P. Reversed-phase liquid chromatographic elution characteristics of substituted *n*-ethylbenzamides. J. Chromatogr. A, **1983**, *267*, 277–284.
18. Pyka, A.; Miszczyk, M. Chromatographic evaluation of the lipophilic properties of selected pesticides. Chromatographia **2005**, *61* (1/2), 37–42.
19. Amic, D.; Davidovic-Amic, D.; Trinajstic, N. Application of topological indices to chromatographic data. Calculation of the retention indices of anthocyanins. J. Chromatogr. A, **1993**, *653*, 115–121.
20. Martorell, C.; Calpena, A.C.; Escribano, E.; Poblet, J.M.; Freixas, J. Influence of the chromatographic capacity factor ($\log k'$) as an index of lipophilicity in the antibacterial activity of a series of 6-fluoroquinolones. Relationship between physico-chemical and structural properties and their hydrophobicity. J. Chromatogr. A, **1993**, *655*, 177–184.
21. De Julian-Ortiz, J.V.; Garcia-Domenech, R.; Galvez-Alvarez, J.; Soler-Roca, R.; Garcia-March, F.J.; Anton-Fos, G.M. Use of topological descriptors in chromatographic chiral separations. J. Chromatogr. A, **1996**, *719*, 37–44.
22. Pyka, A. Chromatographic data–topological index dependence for selected steroids. J. Liq. Chromatogr. Rel. Technol. **2001**, *24* (4), 453–460.
23. Pyka, A.; Sliwiok, J. Use of traditional structural descriptors in QSRR analysis of nicotinic acid esters. J. Liq. Chromatogr. Relat. Technol. **2004**, *27* (5), 785–798.
24. Djakovic-Sekulic, T.; Perišic-Janjic, N.; Pyka, A. Correlation or retention of anilides and some molecular descriptors. Application of topological indexes for prediction of log *k* values. Chromatographia **2003**, *58* (1/2), 47–51.
25. Pyka, A. Unpublished data.
26. Pyka, A.; Sliwiok, J. Chromatographic separation of tocopherols. J. Chromatogr. A, **2001**, *935*, 71–76.
27. Luhua, Z.; Fang, Y.; Lili, Y.; Bingren, X. Chromatographic separation of (–)-ephedrine and (+)-pseudoephedrine in the traditional Chinese medicinal preparation Jiketing granule. Chem. Pharm. Bull. **2005**, *53* (11), 1494–1497.
28. Lee, S.K.; Polyakova, V.; Row, K.H. Interrelation of retention factor of amino acids by QSPR and linear regression. Bull. Okrean Chem. Soc. **2003**, *24* (12), 1757–1762.
29. Adler, N.; Babic, D.; Trinajstic, N. On the calculation of the HPLC parameters for polycyclic aromatic hydrocarbons. Fresenius' J. Anal. Chem. **1985**, *322* (4), 426–429.
30. Adler, N.; Rak, N.; Sertic-Bionda, K. The correlation between HPLC parameters and topological indices of alkanes. Fresenius' J. Anal. Chem. **1989**, *324* (2), 1432–1130.

Trace Enrichment

Fred M. Rabel
EMD Chemicals, Inc., Gibbstown, New Jersey, U.S.A.

INTRODUCTION

Very few chromatographic determinations using high-performance liquid chromatography (HPLC) can be done without first cleaning up the sample or sample solution in some way. The cleanup accomplishes many things, including removing extraneous matrix components and concentrating many of the components of interest so that they can more easily be detected. Many of these cleanup techniques are done off-line, which can increase analysis time by 50% or more.

Trace enrichment (TE) is a sample preparation technique using a minicolumn filled with a packing selected for its properties of attracting wanted components while eliminating unwanted ones. It is connected to the valve ahead of the analytical column, which traditionally is used only for sample injection. The sample solution is pumped (with a second pump) onto the TE column in one mobile phase, and usually washed with a second mobile phase to elute some unwanted components. Then, with a change in the flow path, it is backflushed to place the sample at the head of the analytical column, where separation begins. This speeds up the complete analysis, avoids many interferences for unwanted impurities, and when automated, runs unattended.

DESCRIPTION OF METHOD

Trace enrichment is a sample precleaning procedure that is performed prior to sample analysis. The purpose of any sample preparation procedure is twofold. First, such a procedure must selectively collect and concentrate the components of interest. Second, the method should eliminate any other components that would interfere with the analysis or would contaminate an analytical gas chromatography (GC) or HPLC column to shorten its useful analytical life.

There are many sample preparation techniques listed in texts, from simple filtration or centrifugation to many other kinds of extraction procedures, including both liquid–liquid and solid-phase extraction (SPE). When any type of sample preparation is used, it often is done manually if only a few samples are involved. If a large number of samples are to be analyzed, the entire procedure should lend itself to automation. Regardless of the number of samples, most sample preparation is done off-line; that is, the samples are prepared first with one of the methods listed, and then placed into an automated sample injection system for sequential analysis of all samples.

Trace enrichment is a sample preparation procedure that is performed by passing a "crude" sample through a special "collection" column, but with a couple of added features. It is often done online, one at a time, just prior to the analytical procedure. It usually involves a minicolumn very similar to the familiar off-line SPE tube, but packed into a stainless steel column and attached to the injection valve. This is called a "trace enrichment" column in many published procedures. Another name that is often given to this technique in the title or keywords of published entries is "column switching." This is because this technique involves valves that must be switched from one solvent flow path to another. The valve, in its initial position, allows the "crude" sample to be passed through the TE column with pump 1, whereas the mobile phase is passed only through the analytical column with pump 2 (Fig. 1). After the TE column has collected the sample components of interest, these components are backflushed onto the analytical column by switching the valve to its alternative position (Fig. 2).

The complete procedure for using a TE column is as follows:

1. The TE column is equilibrated with a minimum of two solvent combinations. The first solvent is strong, to wash the TE column free of impurities it may have accumulated from a previous sample (remember, this column is used over and over, so this step is critical so that there is no sample carry-over). This solvent is probably pure methanol or acetonitrile if using a bonded reversed-phase packing filled TE column. The second solvent is not strong; it is used to bring the TE column to equilibrium to accept the sample components of interest. Again, if a bonded reversed-phase packing filled TE column is used, this could even be pure water. The valving would be as shown in Fig. 1.
2. The "crude" sample is injected (if a small volume) or pumped (if a larger volume) onto the TE column. (*Note*: Even a "crude" sample requires membrane filtration and/or centrifugation to prevent shortened column life of the TE column.) The TE column attracts the components of interest, depending on the nature of the bonded phase packing in the TE column, the solvent in which the sample is dissolved,

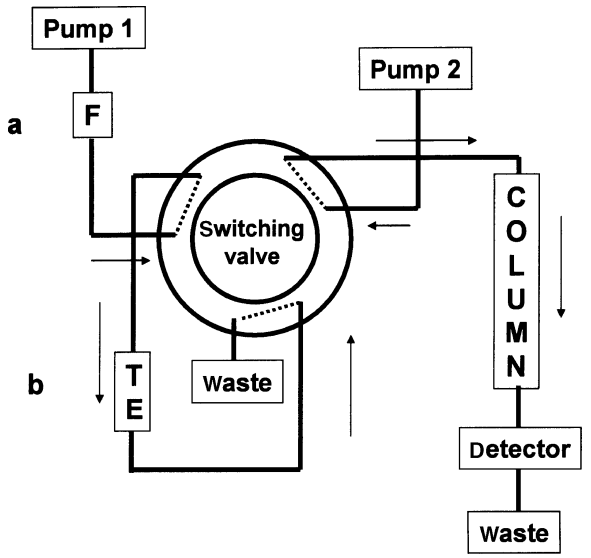

Fig. 1 Trace enrichment valving for the collection of the sample components. a, In-line filter (F) to increase the life of the TE column; b, trace enrichment column (TE). Note that the solvent from pump 2 is equilibrating the analytical column on the right while the TE column is being loaded with sample.

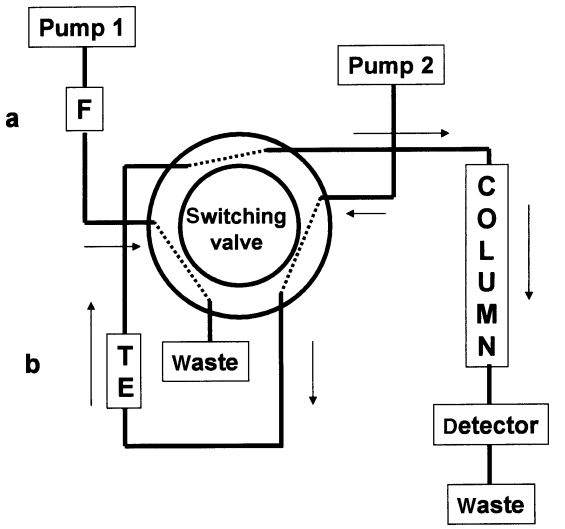

Fig. 2 Trace enrichment valving for the transfer of the prepared sample to the analytical column. a, In-line filter (F) to increase the life of the TE column; b, trace enrichment column (TE). Note that the sample is backflushed onto the analytical column. After a few seconds, the valve can be turned to the position in Fig. 1. The TE column is washed with a cleaning mobile phase, then conditioned back to the collection mobile phase, and another sample put on. See text for complete details.

and the solvent with which the TE column has been equilibrated. The TE column, most likely, will remove more than the components of interest and, thus, might need an additional solvent wash sequence to remove other unwanted collected impurities. This would be done before the final step described below. The valving would continue to be in the position shown in Fig. 1.

3. Finally, when the entire sample has been passed through the TE column, the valve is switched so that the final solvent mixture is passed, with reversed flow direction, through the TE column. This is usually a stronger eluting solvent combination that elutes the collected components to be chromatographed from the TE column. It is often the chromatographic mobile phase, which will also perform the actual analysis on the HPLC analytical column. Once the components are on the analytical column, the separation begins. This valving is shown in Fig. 2. After 5–10 sec, the valving can be set as in Fig. 1, repeat the sample preparation step for the second sample on the TE column while the separation of the first sample is proceeding on the analytical column.

Again, a strong solvent wash of the TE column and then the equilibrium sample wash precede injection of the second sample onto this column. The TE process on the minicolumn is usually accomplished within 2–3 min, and the actual separation might take 10 min. Thus, the time-limiting factor is the actual analysis, not the TE process itself. Shortening the analysis time with a shorter, more efficient HPLC column would lead to greater productivity as long as the actual analysis time is at least 1 min longer than the TE step.

The TE column ideally collects only the components of interest, permitting all unwanted impurities to pass through it. As mentioned, this is seldom completely true in practice, so the details of the entire TE have to be experimentally determined. These details involve determining which minicolumn packing to use and, perhaps, up to three solvent combinations. The first of these combinations is a solvent (or group of solvents) that dissolves the sample so that it carries the sample onto the TE column and simultaneously allows capture of the desired components. With solvent experiments, this first solvent combination can be designed to simultaneously remove some unwanted components as the components of interest are being sorbed onto the TE packing.

A second solvent combination is used to wash more of the remaining impurities out of the minicolumn. Finally, the third solvent combination is used to backflush the captured components from the TE column onto the analytical column. As mentioned, this is often the mobile phase used for the separation and is polar enough to also elute the collected compounds from the TE column.

When beginning the development of a TE column procedure, an excellent source of SPE information may be found in SPE device manufacturers' literature (or on their websites). Most manufacturers offer at least 25 years

of literature references on their products. Their procedures often provide useful information about compound types and the SPE chemistry used and the solvents for cleanup and elution. The same packing material may be used in the TE column, either the same size (usually 40–63 μm for SPE tubes) or a 5 or 10 μm version of it. Buying the TE packing material from the company that makes the SPE tubes allows the SPE solvent information previously determined to be used with the online work. Other bonded-phase chemistries from other manufacturers give *different* capture capacities and efficiencies, so the solvent to capture or elute would be completely different. If in doubt about the equivalency of the chemistries, again, manufacturers are a good source of information.

Some of the most difficult types of sample cleanup are those derived from serum, plasma, urine, or other plant or animal matrices. Proteins or other high-molecular-weight biopolymers quickly contaminate a HPLC column if they are not removed from samples. Such off-line procedures might involve multiple steps. However, another type of packing with special bonding has been used for this type of sample cleanup. It is called *restricted access material*, or RAM. This packing material has an outer surface diol-bonded phase and an internal bonded reversed phase. Biopolymers cannot penetrate into the smaller pores and are repelled by the diol phase and, thus, pass completely through the TE column. However, the components of interest, which are usually much lower-molecular-weight drug substances, are able to pass into the inner pores and attach themselves to the reversed phase. As mentioned earlier, it is still necessary to filter and centrifuge the sample before it is introduced onto the TE column, but these columns can often handle up to two thousand 50 μl injections before having to be replaced. They are available with different internal chemistries—C4, C8, C18, and ion exchangers—to allow different selectivities based on hydrophobic and ion-exchange interactions.

If biological samples are being purified, studies should also be conducted to see under what conditions any compounds of interest are released from the proteins being eluted from the typical RAM column mentioned above. This is due to the strong binding experienced with many compounds onto proteins. If 50% remains bound to the protein as it is washed away, there is 50% less compound collected for making a measurement. One might never achieve 100% release, but an extra 10–20% might be helpful in trace work.

The size of the TE column can be as small as 2–3 mm × 10–25 mm. It simply has to have sufficient capacity to capture all, or a major percentage, of the components of interest. It should be remembered that a TE column usually captures structurally related compounds and, perhaps, some impurities; hence, it might be assumed that only 15–25% of the capacity is taken up by the compound(s) of interest. Because a relatively strong mobile phase is used for backflushing, band broadening is not generally a problem in a TE method, regardless of the size of the column.

The way most TE columns are used with a valve-loop injector is that the sample solution first flows in one direction for capture, and then is backflushed onto the analytical column. This process of backflushing can also push particles captured on the inlet frit back onto the analytical column; therefore, this is another reason for filtration/centrifugation of samples before introducing them onto the TE column. Any in-line filter can also prevent particulates from migrating to places in the HPLC system where they can cause problems.

CONCLUSIONS

Trace enrichment is a valuable tool to use to simplify any laborious sample preparation technique. It is basically automation of the well-known SPE method of sample preparation. As such, it saves the analyst time, money, and solvent, and all but eliminates sources of analytical error. In addition to the traditional bonded reversed phase and ion exchange packings, newer packings have been developed with different surface and inner pore bonded phases. These RAMs have polar outer surfaces that repel biopolymers and non-polar or ionic inner surfaces that collect drugs and other smaller-molecular-weight components.

Although it takes some thought, experimentation, and additional equipment (a special valve and an additional pump), it can be a way of increasing productivity in the analytical laboratory and removing sample preparation errors.

BIBLIOGRAPHY

1. Boos, K.-S.; Grimm, C.H. HPLC integrated SPE in bioanalysis using restricted access precolumn packings. Trends Anal. Chem. **1999**, *18*, 175.
2. Majors, R.; Boos, K.-S.; Grimm, C.-H.; Lubda, D. Practical guidelines for integrated sample preparation using column switching. LC/GC Mag. **1996**, *14*, 554.
3. Schaefer, C.; Lubda, D. Alkyl diol silica: Restricted access precolumn packing for fast LC-integrated sample preparation of biological fluids. J. Chromatogr. A, **2001**, *909*, 73.
4. Yu, Z.; Westerlund, D.; Boos, K.-S. Evaluation of LC behavior of RAM precolumns in the course of direct injection of large volumes of plasma samples in column switching systems. J. Chromatogr. **1997**, *704*, 53.

Two-Dimensional TLC

Simion Gocan
Department of Analytical Chemistry, Babes-Bolyai University, Cluj-Napoca, Romania

INTRODUCTION

The two-dimensional (2-D) thin-layer chromatography (TLC) technique is one of the more versatile methods of TLC development. The first application of the 2-D chromatographic method to paper chromatography was reported in 1944 by Consden, Gordon, and Martin.[1] Since that time, this method has been mostly used for the separation of a large number of compounds that cannot be separated in a one-dimensional (1-D) TLC experiment. In 2-D TLC, separation is on one surface spread along the entire area of the plate. The resolving power of the 2-D TLC method has great application, especially in the areas of biochemistry, biology, natural products, pharmaceuticals, and environmental analysis.

TWO-DIMENSIONAL DEVELOPMENT

Two-dimensional TLC is performed by spotting the sample in one corner of a square thin-layer plate and developing in the usual manner with the first eluent. The chromatographic plate is then removed from the developing chamber and the solvent is allowed to evaporate from the layer. Then, the plate is placed in the second eluent so that development can take place in a second direction which is perpendicular to that of the first direction of development. In 2-D TLC, usually, the layer is of continuous composition, but two different eluents must be employed to obtain a better separation of a mixture. The success of the separation will depend on the ability to modify the selectivity of the second eluent compared to the selectivity of the first eluent. Fig. 1 shows the scheme of spot distribution on a 2-D TLC plate, following two developments for a theoretical case. In 2-D TLC, any spot can be identified by a pair of x_i and y_i coordinates or $R_{f,i1}$ and $R_{f,i2}$, respectively, where x_i divided by $Z_{f,1}$ is equal to $R_{f,i1}$ for the first eluent and $y_i/Z_{f,2}$ is equal $R_{f,i2}$ for the second eluent. The final position of the spot can be determined by the coordinates (x_i,y_i), in which $R_{f,i2\text{-}D}$ can be expressed as $(R_{f,i1},R_{f,i2})$.

A very good method for selection of the appropriate mobile phase for 2-D TLC separations is with the use of the "Prisma" system.[2]

The indole group of compounds is conveniently divided into the so-called "simple" indole derivatives and the indole alkaloids, which often have complicated structures, and indole dyes. Thus it was demonstrated that not all compounds are completely separated by either the basic eluent, methyl acetate–isopropanol–25% ammonia (45 : 35 : 20, v/v), or the acidic eluent, chloroform–96% acetic acid (95 : 5, v/v). Therefore one combines the effects of both of these eluent systems in the 2-D TLC method; in this way, 14 simple indole derivatives and anthranilic acid can be separated. Compounds are separated into groups according to their polarities.[3]

The 2-D TLC was successfully applied to the separation of amino acids as early as the beginning of TLC. Separation efficiency is, by far, best with chloroform–methanol–17% ammonium hydroxide (40 : 40 : 20, v/v), *n*-butanol–glacial acetic acid–water (80 : 20 : 20, v/v) in combination with phenol–water (75 : 25, g/g).[4] A novel 2-D TLC method has been elaborated and found suitable for the chromatographic identification of 52 amino acids. This method is based on three 2-D TLC developments on cellulose (CMN 300; 50 μ) using the same solvent system I for the first dimension and three different systems (II–IV) of suitable properties for the second dimension. System I: *n*-butanol–acetone –diethylamine–water (10 : 10 : 2 : 5, v/v); system II: 2-propanol–formic acid–water (40 : 2 : 10, v/v); system III: *sec*-butanol–methyl ethyl ketone–dicyclohexylamine–water (10 : 10 : 2 : 5, v/v); and system IV: phenol–water (75 : 25, g/g) (+ 7.5 mg Na-cyanide) with 3% ammonia. With this technique, all amino acids can be differentiated and characterized by their fixed positions and also by some color reactions. Moreover, the relative merits of cellulose and silica gel are discussed in relation to separation efficiency, reproducibility, and detection sensitivity.[5] Two-dimensional TLC separation of a performic acid oxidized mixture of 20 protein amino acids plus β-alanine and γ-amino-*n*-butyric acid was performed in the first direction with chloroform–methanol–ammonia (17%) (40 : 40 : 20, v/v) and in the second direction with phenol–water (75 : 25, g/g). Detection was performed via ninhydrin reagent spray.[6]

The TLC method was developed for amino acids; therefore, in principle, it is equally applicable to peptides. Peptides, such as amino acids, are generally hydrophilic. There are, however, limits to this analogy. Dinitrophenylamino acid derivatives (DNP amino acids) and phenylthiohydantoin derivatives (PTH amino acids) are obtained when reaction of peptides or proteins with dinitrofluorobenzene or phenyl mustards are properly degraded.[7,8] Their separation from reaction mixtures and their identification are considerable practical importance because they constitute essential steps

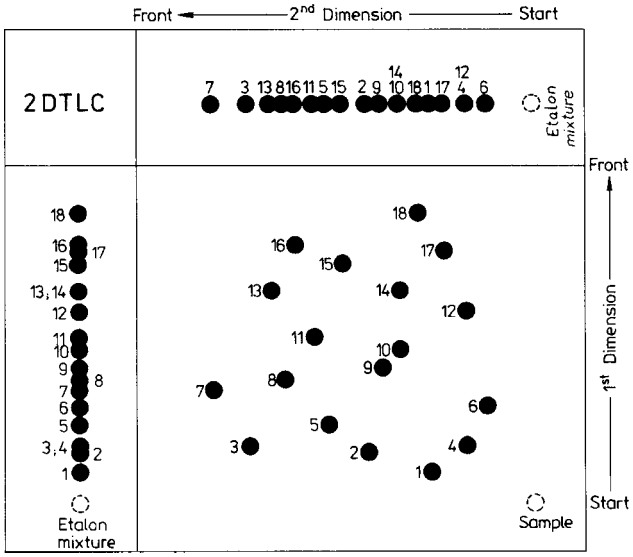

Fig. 1 Scheme of spot distribution on a 2-D TLC plate.

in the process of sequential analysis of peptide and protein structures. Generally, the run in the first direction is carried out in a toluene system. For the run in the second direction, there are many eluent systems that may be selected. Two-dimensional TLC was used to perform separation of DNP amino acids, using toluene as eluent for first direction and chloroform–benzylalcohol–glacial acetic acid (70 : 30 : 3, v/v),[9] chloroform–methanol–glacial acetic acid (95 :75 : 1, v/v), or benzene–pyridine–glacial acetic acid (80 : 20 : 2, v/v) as eluent for the second direction.[10] The majority of DNP amino acids are colored yellow.

The 2-D TLC separation of PTH amino acids may be performed with chloroform–methanol (90 : 10, v/v) and with chloroform-formic acid (100 : 5, v/v) as eluents in the first and the second developments, respectively.[11] There are many other systems of eluents that can be used to obtain good resolution. The chlorine/tolidine reagent is very useful for detection of PTH amino acids. An alternative is offered by fluorescence quenching.

A very complex mononucleotide mixture can be separated by 2-D TLC on poly(ethyleneimine)-cellulose anionexchange thin layers. After applying the nucleotide solution at the starting point, the chromatogram is developed in a closed rectangular jar by stepwise elution with LiCl solution of 0.2, 1.0, and, finally, 1.6 *M*. In order to remove LiCl, the plate is placed in a flat dish filled with anhydrous methanol. Then, the chromatogram is developed in the second direction with formic acid–sodium formate buffers, pH 3–4, by a stepwise elution with buffers of 0.5, 2.0, and 4.0 *M*. The complete resolution of a model mixture containing DPA, TPN, six nucleotide sugars, and 14 common nucleoside-5′-mono-, di-, and triphosphates takes less than 3 hr.[12]

The separation and identification of plant phospholipids and glycolipids was performed by 2-D TLC silica gel using chloroform–methanol–water (65 : 25 : 4, v/v) and diisobutyl ketone–acetic acid–water (80 : 50 : 10, v/v) as eluents for the first and the second dimensions, respectively.[13]

Amino-modified high-performance TLC (HPTLC) silica gel layers (NH_2 F_{254s} HPTLC) was used for identification of 13 amphetamine derivatives by unidimensional multiple development (UDM) in the 2-D TLC mode. The mobile phases used were ethanol–triethylamine–*n*-hexane (15 : 9 : 76, v/v) and acetone–triethylamine–*n*-hexane (23 : 9 : 68, v/v) in the first and the second directions, respectively. Because 1-D HP-TLC was not effective, UDM with the same solvent system and development distance and with two development steps was investigated. The resolution of separation was higher in the low hR_f compared to that predicted by the UDM theory.[14]

In the first direction, the development is isocratic; in the second direction, it is automated multiple development (AMD). The instrumental chromatographic method, AMD, provides a mean of normal-phase gradient developed in HPTLC. A maximum of 25 steps can be used to form an AMD gradient. The development distances increase as the solvent polarity is reduced. The plates are dried by vacuum between consecutive steps. The bands on the plate will be compressed by repeated developments, resulting in increased sensitivity and resolution. For the functional principle of the AMD device, one should consult Ref.[15] The developed distance was 8 cm. Isocratic TLC was performed with one typical eluent as the mobile phase in normal chambers previously equilibrated with the mobile phase. The AMD system was performed in a Camag device (Muttenz, Switzerland), but the gradient systems must have a different selectivity compared to isocratic development. The number of compounds separated by this method was greater than with isocratic TLC or with 1-D AMD.[16] The use of 2-D AMD with two gradients of different selectivities is a powerful method that can improve the separation of samples containing an unknown number of constituents in hydroalcoholic plant extracts.[17] The plant extract "fingerprint" is better for authenticity certification of the respective extract.

Two-dimensional TLC is a simple method that makes possible the rapid recognition of changes in individual components of a mixture. For this purpose, separations must be carried out in both directions, under exactly identical conditions. In such circumstances, a slight increase in resolution might occur because of an increase by a significant factor of the distance of migration of the zone which is a diagonal line ($Z_{f,2}$). However, this method of development indicates alterations of compounds during chromatography if the resulting spots do not lie on a diagonal line bisecting the plate. Between the first and the second developments, the compounds that suffer several structural transformations under physical agent (action of radiation) or from chemical reaction can be detected. This method can be used in photochemistry and stability control.[4]

TWO-DIMENSIONAL DEVELOPMENT ON BILAYERS

There are many reports concerning the placement of two adsorbents on the same plate.

An apparatus for simultaneously coating a plate with two adjacent layers of different adsorbents was accomplished by placing a plastic insert into a commercial spreader, thus forming two independent chambers. For this reason, combinations of two adsorbents, such as cellulose, silica gel, alumina, charcoal, silicic acid, magnesium silicate, etc. as a function of the sample were used. Then, the two eluents systems were optimized for the two development directions, e.g., 2-D separation of some ketones on a bilayer (charcoal/silicic acid) with benzene–ether–acetic acid (82:9:9, v/v) in the first direction (on charcoal) and with benzene–ether (85:15, v/v) in the second direction (on silicic acid).[18] In another paper,[19] the first adsorbent was silica gel (air-dried) and the second adsorbent was deactivated aluminum oxide. The same solvent system, toluene–ethyl acetate (3:1, v/v), was used in the two directions. In this condition, a mixture of 2,4-dinitrophenylhydrazine derivatives of hydroxycarbonyl compounds was resolved.

Silver nitrate-impregnated silica gel has also been used successfully in the separation of some classes of compounds that contain double bonds in their structures. Thus it was used in the separation of glycerides and isomers of unsaturated fatty acid esters. The 2-D TLC on adjacent layers of silica gel G and silica G impregnated with 5% of silver nitrate was used for development. The silica gel G layer covered a surface of 3×20 cm and the difference of the surface of 17×20 cm was covered with silica gel G impregnated with 5% $AgNO_3$. The first direction was performed on silica gel G with petroleum ether–diethyl ether (9:1, v/v) as eluent. The second direction was carried out on the impregnated silica gel G and developed twice with the same eluent as in the first direction. After the first direction, the mixture was fractioned into four groups of compounds (trialkyl glyceryl ethers, dialkoxy glycerides, alkoxy diglycerides, and triglycerides). After the second direction, each group was fractioned for another period into three or four compounds.[20] Thus the efficiency of the impregnated layer was demonstrated.

A method for the complete structural analysis of complex mixtures of methyl esters of saturated and unsaturated fatty acids has been performed by 2-D TLC. Adsorbent silica gel impregnated with a 10% solution of dodecane was used for the first direction with acetonitrile–acetone (1:1, v/v) as eluent. The silica gel for the second direction was impregnated with a 20% $AgNO_3$ and dipropyl ether–hexane (2:3, v/v) was used as eluent. In this way, complete separation of a standard mixture of the methyl esters of six saturated, nine monoethylenic, and three polyenic esters were achieved.[21]

The 2-D TLC on bilayers, silica gel for normal-phase (NP) and reversed-phase (RP), offer the special possibility to carry out two different separation processes on the same plate. Normal-phase chromatography can be performed in the first direction on silica gel; after the evaporation of the solvent, the plate was impregnated with paraffin oil dissolved in petroleum ether. After removal of the excess solvent, the plate was reversed phase developed in the second direction.

Another approach may also be performed by transferring the spots from one plate to another plate.[18] In such circumstances, the development in the first direction was carried out on a narrow 2 cm strip. After drying, it was clipped face to face to a 20×20 or 10×10 cm plate for development in the second direction. Close contact has to be maintained between the two layers for a proper development. In this case, the first plate can be used with a silica gel layer and the second plate can be used with a silica gel RP-C_{18} or vice versa.[22] In this way, the analysis of saponins in *Silene vulgaris* Gracke was carried out in the first direction on RP-18W HPTLC plates with 1.0% aqueous formic acid–methanol (30:70, v/v) as mobile phase and in the second, perpendicular, direction on silica gel Si 60 HPTLC with chloroform–methanol–formic acid–water (100:40:10:10, v/v) as mobile phase. With the use of 2-D TLC bilayers, the saponin mixture could be separated into 18 components, while conventional TLC could separate the mixture into nine components only.[23]

TWO-DIMENSIONAL SEPARATION BY TLC/ELECTROPHORESIS

Peptide maps of the tryptic digest of myosin have been performed on thin-layer plates (20×20 cm) by successive TLC and electrophoresis. In the first-dimension TLC with chloroform–methanol–ammonium hydroxide 34% (40:40:20, v/v) as eluent, the time was as long as 60 min. The second-dimension electrophoresis with pyridine–glacial acetic acid–water (1:10:489, v/v) buffer and 980 V, 30 mA current, the time was 1 hr. The peptide mixture is applied in amounts of 0.05 to 0.5 mg per peptide map.[24] In another paper,[25] electrophoresis was applied in one direction on buffered adsorbents, followed by chromatography in the second dimension. Here, phosphate esters were separated by TLC development twice with *n*-propanol–ammonium hydroxide–water (60:30:1, v/v), and electrophoresis was carried out in 0.28 *M* acetate buffer (pH 3.6), 1000 V, 35 mA, and 16 min.

CHROMATOGRAM EVALUATION

The best 2-D TLC separation is when all the components are separated and distributed on the entire surface of the chromatographic plate. The estimation of this separation can be made by an objective function. Generally, a good

agreement between visual evaluation of a chromatogram and computer evaluation using these objective functions was noticed.[26] On the other hand, a function is needed which can predict R_f value of the one-component function of the composition from the mobile phase.

There are programs for simulated chromatograms which are comparable to that obtained with experimental chromatograms.[26] Other details concerning the strategy of optimization of the mobile phase can be found in Ref.[22]

CONCLUSIONS

In conclusion, for difficulty separation problems the application of 2-D TLC is necessary because the power of 1-D TLC is often inadequate for complete separation of the complex samples with a high number of compounds. The main advantage of 2-D TLC separation process is that compounds are distributed widely over two-dimensional space with high zone (peak) capacity (~1500). The separation efficiency of 2-D TLC can be substantially increased in the future by a combination of the stationary and mobile phases of different polarity with automated multiple development.

REFERENCES

1. Consden, R.; Gordon, A.H.; Martin, A.J.P. Parition chromatography with paper. Biochem. J. **1944**, *38*, 224.
2. Nyiredy, Sz.; Dallenbach-Tölke, K.; Sticher, O. The "PRISMA" optimization system in planar chromatography. J. Planar Chromatogr. **1988**, *1*, 336.
3. Stahl, E.; Kaldewey, H. Hoppe-Seyler's. Z. Physiol. Chem. **1961**, *323*, 182.
4. Stahl, E. *Thin-Layer Chromatography*; Springer-Verlag: Berlin, 1965; Vol. 36, 403.
5. von Arx, E.; Neher, R. Eine Multidimensionale technik zur chromatographischen identifizierung von aminosäuren. J. Chromatogr. **1963**, *12*, 329.
6. Hirs, C.H.W. The oxidation of ribonuclease with perfornic acid. J. Biol. Chem. **1956**, *219*, 611.
7. Biserte, G.; Holleman, J.W.; Holleman-Dehove, J.; Sautière, P. Chromatographie sur papier des dinitrophénylaminoacides. J. Chromatogr. **1959**, *2*, 225.
8. Biserte, G.; Holleman, J.W.; Holleman-Dehove, J.; Sautière, P. Chromatographie sur papier des dinitrophénylaminoacides. J. Chromatogr. **1960**, *3*, 85.
9. Brenner, M.; Pataki, G. Experientia **1961**, *17*, 145.
10. Brenner, M.; Niederwieser, A. Experientia **1961**, *17*, 237.
11. Pataki, G. *Thesis*; Basel University: Basel, Switzerland, 1962.
12. Randerath, E.; Randerath, K. Resolution of complex nucleotide mixtures by two-dimensional anion-exchange thin-layer chromatography. J. Chromatogr. **1964**, *16*, 126.
13. Lepage, M. The separation and identification of plant phospholipids and glycolipids by two-dimensional thin-layer chromatography. J. Chromatogr. **1964**, *13*, 99.
14. Fatér, Z.S.; Tasi, G.; Szabady, B.; Nyiredy, Sz. J. Planar Chromatogr. **1998**, *11*, 225.
15. Cazes, J., Ed.; *Encyclopedia of Chromatography*; Taylor & Francis, New York, 2001; 533.
16. Muresan, L. *Thesis*; Babes-Bolyai University: Cluj-Napoca, 1998.
17. Olah, N.-K.; Muresan, L.; Cîmpan, G.; Gocan, S. Normal-phase high-performance thin-layer chromatography and automated multiple development of hydroalcoholic extracts of Artemisia abrotanum Artemisia absinthium, Artemisia vulgaris and Artemisia cinia. J. Planar Chromatogr. **1998**, *11*, 361.
18. Kirchner, J.G. *Thin-Layer Chromatography,* 2nd Ed.; John Wiley & Sons: New York, 1978; 136–137.
19. Anet, E.F.L.J. Thin-layer chromatography of 2,4-dinitrophenylhydrazine derivatives of hydroxycarbonyl compounds. J. Chromatogr. **1962**, *9*, 291.
20. Schmid, H.H.O.; Baumann, W.J.; Cubero, J.M.; Mangold, H.K. Fractionation of lipids by successive adsorption and argentation chromatography of adjacent layers. Biochim. Biophys. Acta **1966**, *125*, 189.
21. Bergelson, D.; Dyatlovitskaya, E.V.; Voronkova, V.V. Complete structural analysis of fatty acid mixtures by thin-layer chromatography. J. Chromatogr. **1964**, *15*, 191.
22. Nyredy, Sz., Ed.; *Planar Chromatography. A Retrospective View for the Third Millennium*; Springer: Budapest, 2001; 103–119.
23. Glensk, M.; Cisowski, W. J. Planar Chromatogr. **2000**, *13*, 9.
24. Ritschard, W.J. Thin-layer techniques for making peptide maps. J. Chomatogr. **1964**, *16*, 327.
25. Bieleski, R.L. Separation of phosphate esters by thin-layer chromatography and electrophoresis. Anal. Biochem. **1965**, *12*, 230.
26. Grinberg, N., Ed.; *Modern Thin-Layer Chromatography*; Marcel Dekker, Inc: New York, 1990; 361–368.

Two-Phase Solvent Systems, Aqueous: CCC

Jean-Michel Menet
Aventis Pharma, Vitry-sur-Seine, France

INTRODUCTION

Aqueous two-phase solvent (ATPS) systems are made of two aqueous liquid phases containing various polymers. Such systems are gentle toward biological materials and they can be used for the partition of biomolecules, membrane vesicles, cellular organites, and whole cells. They are characterized by a high content of water in each phase, by very close densities and refraction indices of the two phases, by a very low interfacial tension, and by high viscosities of the phases. As a result, settling times are particularly long and may last up to 1 hr or longer.

The partition of a substance between the two phases depends on many factors. Theoretical studies have been carried out in order to better understand the reasons for the separation in two aqueous phases, thanks to the introduction of various polymers, and the role of various factors on the partition of the substances. However, no global theory is available to predict the observed behaviors. Hopefully, some empirical knowledge has been acquired which will help in the use of these unique solvent systems.

Various devices have been used for the partition of substances in ATPS systems. Countercurrent chromatography (CCC) has again revealed its unique features, because it has enabled the use of such very viscous systems at relatively high flow rates while obtaining a satisfactory efficiency and a good resolution for the separation. Many applications have been described in the literature for the use of ATPS systems with CCC devices.

ATPS SYSTEMS

For further information on ATPS systems and the partitioning, we strongly recommend the books by Albertson[1] and Walter et al.,[2] as reference books in this area.

Polymers Used for ATPS Systems

Many ATPS systems contain a polymer which is sugar based and a second one that is of hydrocarbon ether type. Sugar-based polymers include dextran (Dx), hydroxy propyl dextran (HPDx), Ficoll (Fi) (a polysaccharide), methyl cellulose (MC), or ethylhydroxyethyl cellulose (EHEC). Hydrocarbon ether-type polymers include poly(ethylene glycol) (PEG), poly(propylene glycol) (PPG), or the copolymer of PEG and PPG. Derivatized polymers can also be useful, such as PEG-fatty acids or di-ethylaminoethyl-dextran (Dx-DEAE).

Dextran, or α-1,6-glucose, is available in a mass range from 10,000 to 2,000,000. Dx T500 fractions, also called Dx 48 from Pharmacia (Uppsala, Sweden), are among the best known: their weight-average molecular weight (M_w) varies from 450,000 to 500,000. These white powders contain about 5–10% of water. PEG is a linear synthetic polymer which is available in many molecular weights, the most common being between 300 and 20,000.

Physical Properties of the ATPS Phases

Common characteristics of ATPS phases are their high content of water for both phases, typically 85–99% by weight and very close densities and refraction indices for the two phases. Moreover, both phases are viscous and the interfacial tension is low, from 0.1 to 0.001 dynes/cm. The settling times in the Earth's gravitational field range from 5 min to 1 hr.

PRACTICAL USE OF ATPS

Because ATPS systems are particularly suited for protein separations, many research workers have worked in this area and have tried to model their behavior when varying the composition of these systems. However, there are still no theoretical models to calculate, a priori, the partition coefficient of a protein for a wide range of molecular weights of polymers and concentrations in salts and polymers. However, it remains possible to have qualitative explanations of the role of key factors on the partition of the substances.

CHOICE OF THE ATPS SYSTEM

The general principle for designing an ATPS system is to try various systems, either made from two phases containing polymers or from one phase containing a polymer and the other component a salt. The nature of the substances to

be separated shall be taken into account: Fragile solutes may be denaturated by a too high interfacial tension, as encountered in aqueous polymer–salt systems. Some substances may even aggregate in an irreversible way, or be altered in other ways by their contact with some polymers or salts. Moreover, some substances can require the specific use of given salts, or pH, or temperature. When all the previous considerations have been taken into account, the partition coefficients can then be determined in test-tube experiments. Afterward, the composition of the phases can be adjusted.

Systems Suited for the Separation of Molecules

A simple way consists in testing two ATPS systems, dextran 40/PEG-8000 and dextran 500/PEG-8000, which lead to a relatively quick settling and allow reproducible results. For charged macromolecules, the two key parameters are the pH with regard to the isoelectric point of the product and the nature and concentration of the chosen salt. The composition in polymer has a smaller influence, except for some neutral compounds.

Systems Suited for the Separation of Cells and Particles

The main parameter for such separations is the difference of concentrations of each polymer between the two phases. If the concentrations in polymer are quite high, particles tend to adsorb at the interface of the two phases, without any specificity. For instance, all human erythrocytes adsorb at the interface of the dextran 500/PEG-8000 systems with respective concentrations higher than 7.0% and 4.4% (w/w).

The goal is to find a system close to the critical point (in the phase diagram) to achieve the separation, as the partition coefficients all become close to one. However, this requires increased attention to the experimental conditions in order to obtain reproducible results. If necessary, a change in the molecular weight of one of the polymers allows one to choose the aqueous phase in which the particle tends to accumulate. For instance, most mammalian cells partition between the interface and the upper-phase rich in PEG in dextran 500/PEG-8000 systems, whereas they partition between the interface and the lower phase rich in dextran 40/PEG-8000 systems.

ADJUSTMENT OF THE PARTITION COEFFICIENT

We note that the partition coefficient K is defined as the ratio of the concentration of the substance in the upper phase to its concentration in the lower phase. As cells and particles tend to partition between one phase and the interface, only molecules, such as proteins, are the subject of this section.

First, the partition coefficient of the substance should be determined in a standard system, such as dextran 500 (7.0%, w/w)/PEG-8000 (5.0%, w/w) with 5–10 mM of buffer added. Then, the following empirical laws can be used for the adjustment:

1. K is increased by diminishing the molecular weight of the polymer which is predominant in the upper phase (e.g., PEG) or by increasing the molecular weight of the polymer which is predominant in the lower phase (e.g., dextran). Reversing these changes decreases K.
2. K is significantly different than the unit value only if the concentrations of the polymers are high. K tends to the unit value when the concentrations of the polymers are decreased.
3. K can be adjusted by the addition of a salt, as long as the proteins are not close to their isoelectric points. For a negatively charged protein, K is decreased by following the series: phosphate $<$ sulfate $<$ acetate $<$ chloride $<$ thiocyanate $<$ perchlorate and lithium $<$ ammonium $<$ sodium $<$ potassium (for instance, lithium decreases K by a smaller amount than sodium). The influence of the nature of the salt may be amplified by an increase of the pH, which increases the negative net charge of the molecule. Positively charged proteins exhibit the opposite behavior. All these rules apply only for low concentrations of salts. Higher concentrations could, however, be used to favor the partition of the molecules in the upper phase.
4. Charged polymers can also be used; their influence is greater than that of the salts. The most common include charged polymers derived from PEG, such as PEG–TMA (trimethylamino) or PEG–S (sulfonate). Dextran can also be modified.
5. The derivatization by hydrophobic groups can also facilitate the extraction of molecules containing hydrophobic sites. The most common polymer is PEG–P (PEG–palmitate).

K depends on the temperature, but in a complex way, so that its use is difficult for common cases.

Optimization of the Selectivity

Some general rules apply to proteins in PEG/dextran systems and are summarized as follows:

1. The concentration of the polymer is important: Decreasing the concentrations brings the system closer to the critical point (in the phase diagram), smoothing K values toward the unit value and finally decreasing the selectivity.

2. The nature of the salt is important. The most important effects are encountered for $NaClO_4$, which extracts positively charged molecules in the upper phase, and tetrabutyl ammonium phosphate, which extracts negatively charged proteins in the upper phase.

APPLICATIONS

These aqueous two-phase solvent systems are more difficult to handle than organic-based solvent systems, so that the number of applications in the literature is quite small as compared to the other systems. However, these applications are really specific, quite often striking in their separation power, and they truly reveal some unique features of counter current chromatography (CCC).

Former applications of ATPS systems on CCC devices were gathered by Sutherland et al.[3] For instance, both toroidal and type J [also called a high-speed countercurrent chromatography (HSCCC)] CCC were successfully applied for the fractionation of subcellular particles. Using standard rat liver homogenates, plasma membranes, lysosomes, and endoplasmic reticulum were separated by a 3.3% (w/w) dextran T500, 5.4% PEG-6000, 10 m*M* sodium phosphate–phosphoric acid buffer (pH 7.4), 0.26 *M* sucrose, 0.05 m*M* Na_2EDTA, and 1 m*M* ethanol. Purification of torpedo electroplax membranes were also carried out, and the separation of various bacterial cells were also described, including the purification of different strains of *Escherichia coli* and the separation of *Salmonella typhirum* cells, using PEG–dextran ATPS systems. Moreover, these CCC devices were also applied to larger cells, such as the separation of various species of red blood cells.

In the same way, the separation of cytochrome-*c* and lysozyme was achieved in 1988 by Ito and Oka[4] using the type J (or HSCCC) device. The chosen ATPS system consisted of 12.5% (w/w) PEG-1000 and 12.5% (w/w) dibasic potassium phosphate in water. The two peaks were resolved in 5 hr using a 1 ml/min flow rate, but the retention of the stationary phase was as low as 26%. The limitation of this type of apparatus is definitely the low retention of the stationary phase for ATPS systems.

Several ATPS systems were also used with a centrifugal partition chromatograph (also called Sanki-type from the name of its unique manufacturer). Foucault and Nakanishi[5] tested PEG-1000/ammonium sulfate, PEG-8000/dextran, and other PEG-8000/hydoxypropylated starch on a test separation of crude albumin using a model LLN centrifugal partition chromatography (CPC) containing six partition cartridges. They demonstrated that the systems could be used with the CPC apparatus, but the efficiency was particularly low (due to very poor mass transfer) and the flow rate was quickly limited by a strong decrease in the retention of the stationary phase (and not by the back-pressure). Afterward, CPC was then not considered as really suited for ATPS systems.

The third type, which is close in principle to the type J high-speed countercurrent chromatography, was designed in the early 1980s and is named "cross-axis coil planet centrifuge." Such a new design has led to successful results with highly viscous polymer phase systems.[6] Indeed, it allows satisfactory retention of the stationary phase of ATPS systems, either in the polymer–salt form or the polymer–polymer form. Such an apparatus eliminates the main drawback of the previous CCC devices, as it allows one to maintain a good retention of the stationary phase with a sufficient flow rate to ensure an acceptable separation or purification time. Using such solvent systems, it has been applied to the separation and purification of various protein samples:

- Mixture of cytochrome-*c*, myoglobin, ovalbumin, and hemoglobin.[7]
- Histones and serum proteins.[8]
- Recombinant uridine phosphorylase from *E. coli* lysate.[9]
- Human lipoproteins from serum.[10]
- Lactic acid dehydrogenase from a crude bovine heat extract.[11]
- Profilin–actin complex from *Acanthamoeba* extract.[12]
- Lyzozyme, ovalbumin, and ovotransferrin from chicken egg white.[13]
- Acidic fibroblast growth factor from *E. coli* lysate.[14]

The cross-axis coil planet centrifuge, consequently, has been demonstrated to be particularly suited for the use of ATPS systems, leading to satisfactory retention of the stationary phase while keeping a sufficient flow rate of the mobile phase to limit the duration of the experiments.

REFERENCES

1. Albertson, P.-A. *Partition of Cell Particles and Macromolecules,* 3rd ed.; John Wiley & Sons: New York, 1986.
2. Walter, H.; Brooks, D.E.; Fisher, D. *Partitioning in Aqueous Two-Phase Systems*; Academic Press: New York, 1985.
3. Sutherland, I.A.; Heywood-Waddington, D.; Ito, Y. Counter-current chromatography: Applications to the separation of biopolymers, organelles and cells using either aqueous-organic or aqueous-aqueous phase systems. J. Chromatogr. **1987**, *384*, 197.
4. Ito, Y.; Oka, H. Horizontal flow-through coil planet centrifuge equipped with a set of multilayer coils around the column holder: Counter-current chromatography of proteins with a polymer-phase system. J. Chromatogr. **1988**, *457*, 393.

5. Foucault, A.P.; Nakanishi, K. Comparison of several aqueous two phase solvent systems (ATPS) for the fractionation of biopolymers by centrifugal partition chromatography (CPC). J. Liq. Chromatogr. **1990**, *13* (12), 2421.
6. Bhatnagar, M.; Oka, H.; Ito, Y. Improved cross-axis synchronous flow-through coil planet centrifuge for performing counter-current chromatography: II. Studies on retention of stationary phase in short coils and preparative separations in multilayer coils. J. Chromatogr. **1989**, *463*, 317.
7. Shibusawa, Y.; Ito, Y. Protein separation with aqueous-aqueous polymer systems by two types of counter-current chromatographs. J. Chromatogr. **1991**, *550*, 695.
8. Shibusawa, Y.; Ito, Y. Countercurrent chromatography of proteins with polyethylene glycol-dextran polymer phase systems using type-XLLL cross-axis coil planet centrifuge. J. Liq. Chromatogr. **1992**, *15*, 2787.
9. Lee, Y.W.; Shibusawa, Y.; Chen, F.T.; Myers, J.; Schooler, J.M.; Ito, Y. Purification of uridine phosphorylase from crude extracts of *Escherichia coli* employing high-speed countercurrent chromatography with an aqueous two-phase solvent system. J. Liq. Chromatogr. **1992**, *15*, 2831.
10. Shibusawa, Y.; Ito, Y.; Ikewaki, K.; Rader, D.J.; Bryan Brewer, J., Jr. Counter-current chromatography of lipoproteins with a polymer phase system using the cross-axis synchronous coil planet centrifuge. J. Chromatogr. **1992**, *596*, 118.
11. Shibusawa, Y.; Eriguchi, Y.; Ito, Y. Purification of lactic acid dehydrogenase from bovine heart crude extract by counter-current chromatography. J. Chromatogr. B, **1997**, *696*, 25.
12. Shibusawa, Y.; Ito, Y. Am. Biotechnol. Lab. **1997**, *15*, 8.
13. Shibusawa, Y.; Kihira, S.; Ito, Y. One-step purification of proteins from chicken egg white using counter-current chromatography. J. Chromatogr. B, **1998**, *709*, 301.
14. Menet, J.M. Thèse de Doctorat de l'Université Paris 6; 1995.

Two-Phase Solvent Systems: Settling Time in CCC

Jean-Michel Menet
Aventis Pharma, Vitry-sur-Seine, France

INTRODUCTION

Countercurrent chromatography (CCC) is based on the use of two-phase liquid solvent systems. One of the characteristics of a two-phase system is its settling time, which is the time required for the mixture of both phases to be completely separated into two layers, usually in the Earth's gravitational field. The measurement of the settling time itself is helpful in preparing the experiment, for instance, when preparing the mobile and stationary phases in the same vessel. However, it is also intrinsically linked to the hydrodynamic behavior of the two-phase system and, therefore, to its physical parameters such as densities, viscosities, and interfacial tension. It was, therefore, used as a parameter for predicting the hydrodynamic behavior of various solvent systems in J-type CCC devices.

HOW TO MEASURE THE SETTLING TIME

The settling time depends not only on the nature of the solvent system but also on the experimental environment. As its definition is the time needed for the two phases to completely separate into two layers, the worker has to precisely choose the experimental conditions for the measurement. For instance, Ito[1] chose the following:

- Equilibrate the two-phase solvent system in a separatory funnel at room temperature.
- Separate the two phases.
- Take an aliquot of each phase.
- Put each aliquot in a graduated cylinder, which is then sealed with a glass stopper.
- Gently mix the two-phase system by inverting the cylinder five times.
- Place the cylinder immediately on a flat table in an upright position.
- Measure the time required for the two phases to settle.
- Repeat the experiment several times and take the mean time.

It is necessary to perform several experiments, as significant differences in the values are observed. A second set of tests may be performed by vigorously shaking the graduated cylinder five times and then averaging the times measured on several experiments.

The described experimental environment can be summarized as a 1 : 1 ratio of both phases, the choice of a graduated cylinder, room temperature, five-time inversion of the cylinder in a gentle or a vigorous manner, and the Earth's gravitational field. This should be only considered as an example of measuring the settling time, but what is important is to remain with a single definition in order to then use the resultant values in a comparative way.

VALUES OF SETTLING TIMES FOR USUAL CCC SOLVENT SYSTEMS

Ito has carried out the experiments, as described earlier, for 15 solvent systems. All mean values for gentle mixing and for vigorous mixing are gathered in Table 1 in the T and T' columns, respectively.[1]

The T and T' values are close; thus, they both can be considered as reliable measurements of the settling time for each solvent system. The values range from a few seconds (i.e., 3–5 sec) to about 1 min.

Other types of solvent system can be used in CCC. For instance, aqueous two-phase polymer systems (discussed elsewhere in this volume) are made of two aqueous liquid phases containing various polymers. Such systems are gentle toward biological materials and they can be used for the partition of biomolecules, membrane vesicles, cellular organites, and whole cells. They are characterized by a high content of water in each phase, very close densities, very low interfacial tension, and high viscosities of the phases. Settling times are particularly long and may last up to 1 hr. We refer the reader to the ATPS entry (see *Two-Phase Solvent Systems, Aqueous: CCC*, p. 2368) for further information on these systems.

HYDRODYNAMIC BEHAVIOR AND SETTLING TIME

The true purpose of Ito's study was to build a classification among the 15 solvent systems, based on their hydrodynamic behavior inside the column, measured through the retention of the stationary phase for various experimental conditions, on a J-type CCC device.

The first three solvent systems of Table 1 define the "hydrophobic" group, because they require the same

Table 1 Values of the settling times for 15 solvent systems.

Two-phase solvent system	Volume ratio	Settling time	
		T (sec)	T' (sec)
Hexane-water	1 : 1	<1	8
Ethyl acetate-water	1 : 1	15.5	21
Chloroform-water	1:1	3.5	5.5
Hexane-methanol		5.5	6
Ethyl acetate-acetic acid-water	4 : 1 : 4	15	16
Chloroform-acetic acid-water	2 : 2 : 1	29	27.5
Butanol-1-water	1 : 1	18	14
Butanol-1-0.1 *M* NaCl	1 : 1	16	14.5
Butanol-1-1 *M* NaCl	1 : 1	23.5	21.5
Butanol-1-acetic acid-water	4 : 1 : 5	38.5	37.5
Butanol-1-acetic acid-0.1 *M* NaCl	4 : 1 : 5	32	30.5
Butanol-1-acetic acid-1 *M* NaCl	4 : 1 : 5	26.5	24.5
Butanol-2-water	1 : 1	57	58
Butanol-2-0.1 *M* NaCl	1 : 1	46.5	49.5
Butanol-2-1 *M* NaCl	1 : 1	34	33.5

Note: T is the average value after five gentle mixings, and T' stands for five vigorous mixings.
Source: From Principles and instrumentation of CCC, in *Countercurrent Chromatography–Theory and Practice*.[1]

given combination of two experimental parameters [choice of a lighter or heavier phase as stationary one, and choice of the pumping direction (i.e., from the head to the tail of the column or vice versa)] to achieve a good retention of the stationary phase and because their organic phase is hydrophobic. The last six solvent systems define the "hydrophilic" group, based on the same combination of two experimental conditions, which are reversed as compared to "hydrophobic" systems, because their organic phase can be considered as hydrophilic. There remains six solvent systems whose hydrodynamic behavior is more complicated, as it depends on the ratio of the radius of the coil on the rotation radius of the apparatus. They define the "intermediate" group.

Table 1 reveals that the classification may be defined from the values of the settling times. Indeed, the settling times of the hydrophobic solvent systems are the shortest ones, ranging from 1 to 20 sec, whereas those of hydrophilic systems are in the 25–60 sec range. Solvent systems belonging to the intermediate group exhibit moderate settling times, ranging from 6 to 30 sec.

Consequently, the measurement of the settling time for a solvent system which is different from the 15 studied is a simple way of roughly classifying it among the 3 groups defined by Ito and then to know the best experimental combinations to obtain the highest retention of the stationary phase on a J-type device.

Increasing the temperature or the concentration of a salt in the aqueous phase are known ways of reducing the settling time. This is interesting, as systems with low settling times are easier to handle and are characterized by a "hydrophobic" hydrodynamic behavior in J-type CCC devices, which leads to high values of the retention of the stationary phase.

HYDRODYNAMICS AND SETTLING TIME

Three theoretical parameters were introduced by Menet et al. in order to better understand the hydrodynamic behaviors of two-phase solvent systems.[2] We will not discuss, here, the capillary wavelength, as it only enables the description of the formation of droplets of one liquid in another liquid. The two other parameters were introduced because it appeared interesting to introduce other "theoretical" parameters to better describe the dynamic phenomena occurring inside a CCC column (i.e., after the formation of the droplet described by the capillary wavelength). Two of these are presented here, namely V_{low} for the fall of a droplet of the heavier liquid phase (lower) in the continuous lighter one (upper) and V_{up} for the rise of a droplet of the lighter liquid phase in the continuous heavier one, and are defined as follows:

$$V_{low} = \gamma \left(\eta_{up} \frac{2 + 3(\eta_{low}/\eta_{up})}{3 + 3(\eta_{low}/\eta_{up})} \right)^{-1} \quad \text{and}$$

$$V_{up} = \gamma \left(\eta_{low} \frac{2 + 3(\eta_{up}/\eta_{low})}{3 + 3(\eta_{up}/\eta_{low})} \right)^{-1}$$

with γ the interfacial tension between the two liquid phases, η_{up} the dynamic viscosity of the lighter phase, and η_{low} the dynamic viscosity of the heavier phase.

It is interesting to note that as neither V_{up} nor V_{low} depend on g, these velocities do not depend on the selected angular velocity of rotation. This is because the field intensity influences in the same way the size of the capillary wavelength and the sedimentation velocity of the droplet.

Menet et al. have computed the V_{low} and V_{up} values for the 15 solvent systems studied by Ito, along with 6 not previously studied [i.e., dimethyl sulfoxide (DMSO)–heptane (1:1, v/v), dimethyl formamide (DMF)–heptane (1:1, v/v), toluene–water (1:1, v/v), *O*-xylene–water (1:1, v/v), heptane–acetic acid–methanol (1:1:1, v/v) and chloroform–ethyl acetate–water–methanol (2:2:2:3, v/v)]. All the results have allowed them to define ranges of settling velocities linked to the hydrophobic, intermediate, or hydrophilic behavior of the solvent system. They have demonstrated the most reliable scale was that based on V_{up}, which is the description of the rise of a droplet of the lighter phase in a continuous heavier one.

It was further demonstrated that this theoretical parameter was the right one to use, as Menet et al. have carried out experiments on the evolution of the hydrodynamic behavior of the butanol-1–water system with the temperature.[3] They showed that the observed change in behavior was explained by an increase in the V_{up} settling velocity with the temperature, and, thus, a decrease of the settling time, explaining the "hydrophobic" behavior of the solvent system.

As a conclusion, the research worker can use the settling time for both purposes. One is the knowledge of the solvent system, mainly its ease of use, as long settling times complicate the use of the solvent system. The other one is to roughly predict the hydrodynamic behavior inside a J-type CCC device, in order to know the best combinations of some experimental conditions to obtain the highest retention of the stationary phase. For this purpose, the research worker may also use the theoretical settling velocity of a droplet of a lighter phase inside the heavier continuous liquid phase. It was demonstrated to be the better way of predicting the hydrodynamic behavior and, consequently, the best combination of experimental parameters for the highest retention of the stationary phase.

REFERENCES

1. Ito, Y. Principles and instrumentation of CCC. In *Countercurrent Chromatography—Theory and Practice*; Mandava, N.B., Ito, Y., Eds.; Marcel Dekker, Inc.: New York, 1988.
2. Menet, J.M.; Thiébaut, D.; Rosset, R.; Wesfreid, J.-E.; Martin, M. Classification of countercurrent chromatography solvent systems on the basis of the capillary wavelength. Anal. Chem. **1994**, *66*, 168–176.
3. Menet, J.-M.; Rolet-Menet, M.C. Characterization of the solvent systems used in countercurrent chromatography. In *Countercurrent Chromatography*; Menet, J.M., Thiébaut, D., Eds.; Marcel Dekker, Inc.: New York, 1999.

Ultrathin-Layer Gel Electrophoresis

András Guttman
Diversa Company, San Diego, California, U.S.A.

Csaba Barta
Árpád Gerstner
Novartis Agricultural Discovery Institute, Inc., San Diego, California, U.S.A.

Huba Kalász
Mária Sasvári-Székely
Department of Pharmacology and Pharmacotherapy, Semmelweis University of Medicine, Budapest, Hungary

INTRODUCTION

Electrophoretic separation of double-stranded DNA (dsDNA) molecules, such as RFLP fragments or polymerase chain reaction (PCR) products, is usually accomplished in agarose, polyacrylamide, or composite agarose–polyacrylamide gels.[1] Agarose gels are extensively used to analyze DNA fragments from hundreds of base pairs (bp) to tens of thousands of bp, and polyacrylamide gels are regularly used for high-resolution DNA fragment analysis from several bp up to a thousand bp. In spite of numerous refinements in electrophoresis techniques during the past decade, agarose gel electrophoresis is still not efficient enough. The existing methodology requires multiple steps, such as gel casting, sample loading, staining, and imaging/documentation/data evaluation, making it very tedious and time-consuming because these tasks are not readily integrated and automated for highthroughput applications. Although several attempts have been made for automation, dsDNA fragment analysis in most laboratories is still done in a very conventional way: using submarine format agarose gel electrophoresis separation with ethidium bromide staining.[2] Some of the large, automated DNA sequencing systems are recently reported to be used for genotyping and STR profiling using cross-linked polyacrylamide gels and fluorescently labeled primers, and the configuration of these devices does not accommodate the use of agarose gels as separation medium.

DISCUSSION

Attempts to discover higher-resolution and faster electrophoresis separation techniques and media started in the 1960s, when miniaturized methods[3] were described as microelectrophoresis, but imaging technologies were not yet quite as adequate to be able to capture separations on such a minute scale. Later, polyacrylamide gels contained in glass capillaries were employed in order to separate both DNA and RNA molecules, but this progress was ultimately hampered by the inability to control extra-Joule heat. Recently emerging capillary-electrophoresis (CE) based methods are much less susceptible to the effects of Joule heat, due to the ability to dissipate heat via the large surface-to-volume ratios typical of narrow-bore capillary columns. Obtaining similarly high surface-to-volume ratios in planar-format electrophoretic systems require very thin layers, preferably reaching thickness in the capillary dimension (i.e., no greater than 0.25 mm).

The most recent advances in the electrophoretic separation of nucleic acids come from exploration of new separation matrices. Linear, non-cross-linked polymers, such as polyacrylamide, derivatized celluloses, and polyethylene oxides, have all been demonstrated to be effective in the size separation of biopolymers.[4] The advantages of these non-cross-linked polymers were proven almost entirely in high-performance CE applications;[5] however, it has been shown that very high-concentration non-cross-linked polymers can also be used in planar slab–gel format[6] for the separation of dsDNA molecules. Chemically modified agarose gels or composite agarose–non-cross-linked polymer gels capable of resolving differences of merely a few bases in DNA fragments of several hundreds of bases in length have also been developed.[7] The use of highly concentrated non-cross-linked polymers for DNA fragment analysis applications may be advantageous in several respects. First, it has been shown that non-cross-linked polymers may be supplied in a dessicated, dry form, providing a long shelf life.[8] Second, planar-form non-cross-linked polymer gels can be rehydrated to any of the range of final gel concentrations, buffer compositions, and/or ionic strengths. In addition to that, lower viscosity non-cross-linked polymers can be easily replaced in the separation platform; therefore,

cassettes supporting repetitive work with non-cross-linked polymers can be readily used with these matrices.

Visualization by covalent labeling of nucleic acids with fluorescent tags, such as fluorescein, tetramethylrodamine, Texas Red, and so forth, has been practiced for years.[9] This approach can be used for high-sensitivity DNA fragment analysis provided that the analyte is labeled by the appropriate fluorophore prior to the separation step. The approach reported in this work uses affinity binding (e.g., intercalation) dyes for *in migratio* labeling of the dsDNA fragments during the course of their electrophoretic separation. This method is beneficial in two aspects. First, unlabeled DNA fragments can be readily analyzed, because they become labeled during the separation process. Second, the complexation phenomenon usually increases the separation selectivity, resulting in a higher resolution.[10]

Large-scale, high-resolution DNA fragment analysis (e.g., mapping) requires an affordable, fully automated high-throughput agarose gel-electrophoresis based separation device that enables rapid, high-performance separations in a wide molecular-weight range. Here, we describe a system that greatly enhances the productivity of DNA fragment analysis by automating the current manual procedure and also reducing the separation time and human intervention from sample loading to data analysis.

SEPARATION PLATFORM

Fig. 1 shows the block diagram of the automated ultrathin-layer agarose gel electrophoresis system consisting of a high-voltage power supply (1); platinum electrodes (2 and 3); ultrathin layer separation platform with built-in buffer reservoirs (4), and a fiber-optic-bundle-based detection system (5). A lens set (7) connected to the illumination/detection system via the fiber-optic bundle, scans across the gel by means of a translation stage (6). A 532 nm frequency doubled Nd:YAG laser excitation source (8) and an avalanche photodiode detector (9) are connected to the central excitation fiber and the surrounding collecting fibers of the fiber-optic bundle, respectively. Interface electronics (10) is used to digitize the analog output of the detector and to connect the system to a personal computer. The separation platform also includes a positional heat sink holding the gel-filled cassette in horizontal position. This heat sink also eliminates local heat-spot-generated separation irregularities by means of homogenous dissipation of any extra heat over the gel surface during the separation. Three heating cartridges and a high-speed fan control the temperature (above ambient) of the separation platform at a preprogrammed level. The preheated (40–45°C) separation cassettes (18 cm × 7.5 cm × 190 mm) are filled with melted 2% agarose. After a few minutes of cooling/solidification, the gel-filled cartridge is ready to be used. The effective separation length of the agarose-gel-filled ultrathin-layer cartridge is 6 cm. The applied separation voltage is 750 V, generating 5–7 mA of current.

REUSABLE GEL CASSETTES AND MEMBRANE-MEDIATED SAMPLE LOADING

The reusable separation cassette has a flat bottom and top plate joined and secured in parallel, spaced 190 μm apart,

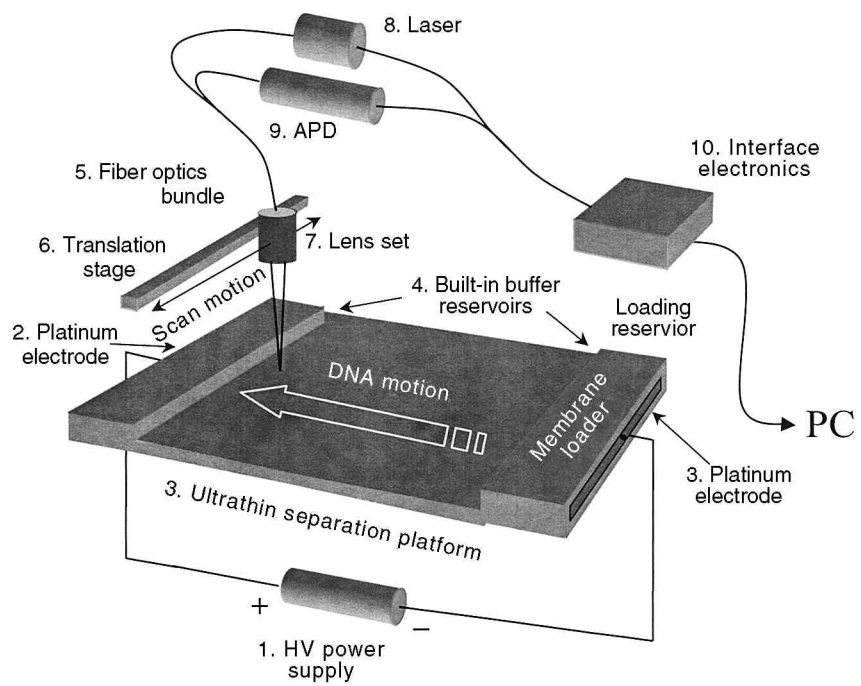

Fig. 1 Block diagram of the automated ultrathin-layer agarose gel electrophoresis system.

with buffer reservoirs permanently fixed to both ends. Two spacers run along the innerface edges of the plates to assure consistent distance between the glass plates (see the cassette in Fig. 1). For filling the cassette, a pump (e.g., large syringe) is used with a sealing applicator nozzle that matches to the top of the buffer reservoirs. To introduce the melted agarose gel into the cassette, the gel nozzle is placed at the top of one of the reservoirs, and the gel is pumped into the platform. The cassette should be preheated to approximately 40–45°C prior to the introduction of the melted agarose gel, in order to prevent premature solidification of the separation matrix. An appropriate amount of DNA staining dye [e.g., ethidium bromide (10–50 n*M*)] should be added to the melted agarose solution just before filling into the cassette.

Membrane-mediated sample loading provides a rugged, easy loading mechanism for ultrathin-layer electrophoresis gels, conveniently applicable for both vertical and horizontal formats.[11] The samples are spotted manually or automatically (robots) onto the surface of the loading membrane tabs, outside of the separation platform.The sample spotted membrane is then placed into the injection (cathode) side of the separation cassette, in intimate contact with the gel edge. By the application of the electric field, the sample components migrate into the gel. There is no need to form individual injection wells in the separation gel and loading is accomplished easily on the bench top. This novel sample injection method could be readily applied to most high-throughput gel electrophoresis based DNA analysis applications.

IN MIGRATIO FLUORESCENT LABELING

The use of fluorophore labeling of DNA fragments in gel electrophoresis expands the detection sensitivity and separation potential. Complex formation with fluorophores enables *in migratio* labeling [i.e., the migrating DNA fragments (negatively charged) complex with the countermigrating fluorophore intercalator dye (positively charged) which is dissolved in the separation matrix]. Using this method, high-sensitivity detection of the migrating DNA fragments as well as the high resolution of closely migrating components can be simultaneously obtained in a broad molecular-weight range. The appropriate concentration and type of the fluorophore complexing dye should be optimized for the wavelength of the excitation laser used in the illumination/detection system. For a 532-nm laser, ethidium bromide provides a good match (EX_{max} = 512 nm), but other high sensitivity dyes can also be used.[12]

AGAROSE-BASED REPLACEABLE SEPARATION MATRIX

In the ultrathin-layer slab–gel format described in this entry, dsDNA fragment analysis was accomplished using 2% agarose gel, filled into the separation cassette at 60°C and used for electrophoresis separation at room temperature. The advantage of employing liquefied agarose above its gelling temperature is that the gel can be easily replaced in the separation platform by simply pumping fresh melted gel into the cassette (i.e., it can be easily filled, rinsed, and refilled). The inner surface of the separation platform was coated with linear polyacrylamide in order to avoid the formation of an electric double layer and concomitant electro-osmotic-flow generation.[13]

MUTATION SCREENING BY ULTRATHIN-LAYER AGAROSE ELECTROPHORESIS

Screening of 10 patients for the dopamine D_4 receptor (D4DR) gene polymorphism was used as a model system to demonstrate the capability of this device.[14] D4DR is the major receptor type in the limbic system. Its gene contains a 48-base-pair sequence repeat in exon 3 with a variable (twofold to eightfold) repeat number in individuals. This polymorphism is believed to be associated with personality characteristics, such as novelty seeking and extravertation/introvertation. The fragment containing the polymorphic site was amplified by PCR using two primers that anneal upstream and downstream of this region, resulting in products different in length (359 and 475 bp) which were then separated by ultrathin-layer agarose gel electrophoresis (Fig. 2).

CONCLUSIONS

In this entry, we reported the use of an automated, high-performance DNA fragment analyzer for high-throughput applications, employing replaceable agarose gels in

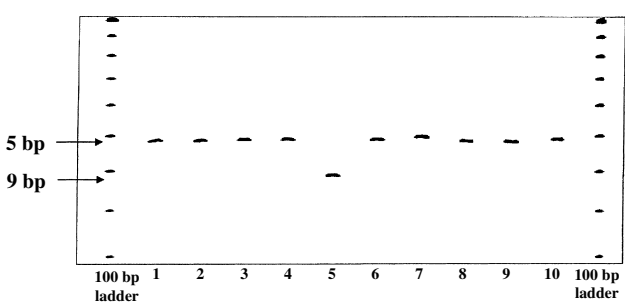

Fig. 2 Real-time electrophoretic image of the screening of 10 patients for the dopamine D_4 receptor (D4DR) gene polymorphism. Lanes 1–4 and 6–10 exhibit the 475-bp PCR product representing the common fourfold repeat alelle in homozygous form, whereas lane 5 shows a 359-bp fragment representing a patient homozygous for the twofold repeat polymorphism. [PCR was done in 35 cycles (95°C/min, 60°C/min, 72°C/min) using primers P1: 5′-GCG ACT ACG TGG TCT ACT CG-3′ and P2: 5′-AGG ACC CTC ATG GCC TTG-3′].

conjunction with a reusable ultrathin-layer separation cassette format in horizontal configuration. Sample loading onto the ultrathin separation platform was accomplished by membrane-mediated loading technology, which also enabled robotic spotting of multiple samples.[15] The sample loading membranes also allow bar coding for identification and cataloging purposes and can be stored for several days between spotting and analysis. The analyte DNA fragments were stained during the separation process by *in migratio* complexation with appropriate fluorophore intercalator dyes and detected by a scanning fiber-optic-bundle-based integrated laser-induced fluorescence–avalanche photodiode imaging system.

Cost-effectiveness for high-throughput applications was assured by simple replacement of the separation matrix by pumping fresh melted gel composition into the cassette for each consequent analysis. After a few minutes of solidification, the gel-filled cassette was ready to be used again. When compared to regular submarine agarose gel electrophoresis, the separation performance and detection sensitivity of this new method utilizing the ultrathin-layer electrophoresis platform were found to be far superior, allowing significantly faster and higher-resolution analysis (more than 10-fold). With full system integration and automation, a high-throughput automated dsDNA analysis system can be developed by simply coupling DNA sample preparation, PCR amplification, restriction digestion, sample loading, electrophoresis separation, data analysis, and map construction.

ACKNOWLEDGMENTS

The authors gratefully acknowledge the technical help of Doug Evans, Loi Nguyen, Swarna Ramanjulu, Nick Wilder, and Greg Theriault. This work was supported by the U.S.–Hungarian Joint Fund (J.F.No.654/96) and by the Hungarian funds FKFP 0658/1999, OTKA T022608.

REFERENCES

1. Chrambach, A. *Practice of Quantitative Gel Electrophoresis*; VCH: Deerfield Beach, FL, 1985.
2. Sambrook, F.; Fritch, E.F.; Maniatis, T. *Molecular Cloning,* 2nd Ed.; Cold Spring Harbor Laboratory Press: Plainview, NY, 1987.
3. Andrews, T. *Electrophoresis,* 2nd Ed.; Clarendon Press: Oxford, 1986.
4. Shieh, P.; Cooke, N.; Guttman, A. *High Performance Capillary Electrophoresis*; Khaledi, M.G., Ed.; John Wiley and Sons: New York, 1998; Chap. 5.
5. Guttman, A. *Handbook of Capillary Electrophoresis*; Landers, J.P., Ed.; CRC Press: Boca Raton, FL, 1994.
6. Bode, H.J. *Electrophoresis '79*; Walter de Gruyter & Co.: New York, 1980; 39.
7. Soto, D.; Sukumar, S. Improved detection of mutations in the p53 Gene in human tumors as single-stranded conformation polymorphs and double-stranded heteroduplex DNA. PCR Methods Applic. **1992**, *2*, 96.
8. Schwartz, H.; Guttman, A. *Separation of DNA by Capillary Electrophoresis*; Beckman Instruments: Fullerton, CA, 1995.
9. Smith, L.M.; Sanders, J.Z.; Kaiser, R.J.; Hughes, P.; Dodd, C.; Connell, C.R.; Heiner, C.; Kent, S.B.H.; Hood, L.E. Fluorescence detection in automated DNA sequence analysis. Nature **1986**, *321*, 674.
10. Guttman, A.; Cooke, N. Capillary gel affinity electrophoresis of DNA fragments. Anal. Chem. **1991**, *63*, 2038.
11. Cassel, S.; Guttman, A. Membrane-mediated sample loading for automated DNA sequencing. Electrophoresis **1998**, *19*, 1341.
12. Haugland, R.P.H. *Handbook of Fluorescent Probes and Research Chemicals*; Spence, M.T.Z., Ed.; Molecular Probes, Inc.: Eugene, OR, 1996; Chap. 8.
13. Hjerten, S. High-performance electrophoresis: Elimination of electroendosmosis and solute adsorption. J. Chromatogr. **1985**, *347*, 191.
14. Szoke, M.; Sasvari-Szekely, M.; Barta, Cs.; Guttman, A. Human dopamine D4 receptor allele genotyping by ultrathin agarose gel electrophoresis with to-Pro-3 complexation. Electrophoresis **1999**, *20*, 497.
15. Stanchfield, J.E.; Batey, D.W. *Genome Mapping and Sequencing Symposium*; 1998; 214.

Unified Chromatography

Fernando M. Lanças
Institute of Chemistry of São Carlos (USP), University of São Paulo, São Carlos, Brazil

INTRODUCTION

Gas chromatography (GC) was the first instrumental chromatographic mode to be demonstrated, back in the beginning of the 1950s.[1] Golay[2] proposed, in the same decade, the miniaturization of the technique by introducing the so-called capillary gas chromatography (CGC). It took almost two decades (1960s and 1970s) to spread out worldwide, particularly due to the problems in handling fragile glass columns, however in the 1980s and 1990s, CGC became the preferred GC mode using wall-coated open-tubular (WCOT) columns.

Supercritical fluid chromatography (SFC) was first demonstrated in the 1960s,[3] but became popular only after the 1980s. Two different approaches were developed: one using packed columns of large inner diameter (I.D.) similar to those used in liquid chromatography (LC), and the other one using non-packed or open-tubular capillary columns similar to those used in CGC. Although open-tubular columns offer the same advantages over packed columns already perceived in CGC, packed columns are still, by far, used more than open-tubular columns in SFC.

LC was the first chromatographic mode to be developed almost one century ago.[4] Its instrumental version [usually referred as high-performance liquid chromatography (HPLC)] was developed during the end of the 1960s. Although its miniaturization has been discussed since then, its development has not followed the same successful route as CGC. The first step in the miniaturization of LC was the development of 1.0 mm I.D. columns,[5] nowadays usually termed "microbore columns." The next attempt in this direction was the introduction of capillary LC with columns of inner diameter smaller than 0.5 mm.[6] This approach is still far from being developed to a satisfactory extent in order to become as widely accepted routine technique as its GC counterpart (CGC). Although slower to develop as than it should, the miniaturization of chromatographic techniques is mandatory for the development of unified chromatography.

THE CONCEPT OF UNIFIED CHROMATOGRAPHY

Although the chromatographic techniques—namely GC, LC, and SFC—have been developed in a completely independent way, there are no theoretical boundaries between these techniques, as pointed out by Giddings in 1965.[7] Based on this concept Ishii later proposed and demonstrated in practice the idea of unified chromatography.[8] According to him,[8] it is possible to demonstrate different-mode separations (viz. LC, SFC, and GC separation) using a single chromatographic system. Further, the separation mode could be selected, changing the column temperature and pressure.[8] Shortly after the early experiments on unified chromatography by Ishii and coworkers, Yang proposed that the practice of GC, SFC, and microcolumn HPLC become more similar as the column diameter becomes smaller.[9] He also proposed that in this case, the injector, column, and detector may all be the same. In the same year, Bartle and coworkers pointed out that unified microcolumn chromatography allows high-resolution separations that make use of the same chromatographic components (injector, column, and detector) for capillary GC, microcolumn SFC, and HPLC.[10]

A few reviews on unified chromatography have been published since its initial development.[11–13] To those readers interested in these techniques, it is highly recommended to consult the pioneer work described in these reviews because there is also, in the literature, some confusion about unified chromatography and multidimensional chromatography, as will be discussed next.

UNIFIED CHROMATOGRAPHY OR MULTIDIMENSIONAL CHROMATOGRAPHY?

As discussed in the previous section, the concept of unified chromatography as agreed upon by the pioneers of this technique includes the use of the same chromatographic components (injector, column, and detector) performing GC, SFC, and LC separations. Because it is very common from the beginning, unified chromatography allows several combinations of chromatographic techniques, such as GC combined with LC, GC combined with SFC, SFC combined with GC, and so on. In this case, the separation is performed in such a way that the sample is introduced into the column and a fraction of it is eluted using one of the chromatographic modes (for instance, GC). After that, the conditions (in the single-substance mobile-phase mode) or the chemical nature (in the multisubstance mobile-phase mode) of the mobile phase is changed in order to perform another chromatographic mode to elute the analytes still retained in the column (for instance, using SFC).

In this example, the first step will allow the elution of the more volatile compounds in the GC mode while the less volatile will be eluted in the SFC mode. If these two modes

were not enough to elute all analytes, it would have been possible to later perform a LC separation using the same instrument with a fraction of the sample still in the column. This is the original concept of unified chromatography. This concept has been confused with multidimensional chromatography that uses different columns to perform the separation. In this case, several publications deal with techniques such as GC/GC, LC/LC, SFC/SFC, GC/SFC, LC/GC, and so on. In this approach, either the total or a fraction of the analytes leaving a chromatographic column is transferred to a second column in order to obtain another dimension of analysis (thus the name "multidimensional chromatography"). In unified chromatography, there is no column transfer (switch) and the second dimension of the separation is provided by the change in the mobile-phase characteristics.

TERMINOLOGY OF UNIFIED CHROMATOGRAPHY

Several terms have been used to identify this technique, including the following:

- Unified Approach to Chromatography
- Unified Capillary Chromatography
- Unified Microcolumn Chromatography
- Unified GC and SFC
- Unified Chromatography for GC, SFC, and LC
- Unified Chromatography

The last term is more general and appropriate to the actual stage of the technique.

INSTRUMENTATION

The instrumentation used in unified chromatography is based on the ones used for GC, LC, and SFC with minor modifications.

SINGLE-SUBSTANCE MOBILE-PHASE APPROACH

Using a single substance as the mobile phase makes the instrumentation much easier than a multisubstance approach. In this case, the instrument could be a simple modification of HPLC equipment to also deal with a supercritical fluid, as used originally by Ishii. In this case, simply adjusting the mobile-phase pressure and temperature in order to be either in the SFC or LC mode can make the selection of the chromatographic mode (LC or SFC). This is the easiest way to perform unified chromatography but also the more limited one because it is difficult to find a single substance that presents good behavior as a chromatographic mobile phase in the GC mode as well as in the HPLC mode.

MULTISUBSTANCE MOBILE-PHASE APPROACH

In this approach, the mobile-phase chemical nature is changed during the analysis when going from one chromatographic mode to the other. The elution of the sample components can start in the GC mode by introducing the mobile phase (usually a gas) into the column and providing the elution of the volatile compounds. After finishing this step the mobile-phase supply is interrupted and a second eluent (for instance, a supercritical fluid or a liquid) is introduced into the column in order to perform the second separation step. If a third mode is intended, the second eluent is interrupted and the third one is introduced into the column. As a consequence of this approach, a more complex and expensive instrument will have to be built, but results will be more interesting because each one of the modes will have the mobile phase optimized independently. While the first approach can be used for simple procedures, the multisubstance mobile-phase approach might be necessary for more demanding and complex ones.

SELECTED APPLICATIONS

Although unified chromatography still has to find its own applications niche, it has already been used for the analysis of a wide variety of samples from aromatic hydrocarbons, styrene, esters, phthalates, crude oil, amines, household wax, pesticides in vegetable oils and many others.[11,14–16] Its major application in the near future will certainly be centered in the analysis of complex samples such as environmental samples, biological fluids, forensic chemistry, and so forth. In this case, there is a need for more than one separation mode because the sample might contain volatile, semivolatile, and nonvolatile compounds of interest, thus requiring different chromatographic conditions.

PROJECTED ENLARGEMENT OF THE UNIFIED CHROMATOGRAPHY CONCEPT

When unified chromatography was first proposed, the chromatographic techniques were divided into GC, SFC, and LC. Nowadays, there has been a general acceptance that GC and LC are extreme mobile-phase conditions and that several intermediate conditions are possible. This includes solvated GC enhanced LC, and subcritical fluid chromatography, among other possibilities. Considering

this fact, we can expect that in the near future, all these modes will be performed in the same instrument designed for unified chromatography. This will not only enlarge the theoretical concept of this technique but will also broaden its application range.

LIMITATIONS

The major limitation of unified chromatography is that there is no commercial instrument currently available to those interested in the techniques. The few existing instruments are basically located in universities and are built in-house to attend to the purpose of the investigator. Another considerable limitation of the techniques is the difficulty in making columns that can show good performance in more than two chromatographic modes. WCOT columns made for SFC can usually operate well in the capillary GC mode; packed columns for SFC can operate in the LC modes. However, a column that operates in an optimized way in the GC and LC mode is still to be developed. Although some attempts have been made in research laboratories, they are not commercially available. Another difficulty is related to the identification mode. Nowadays, mass spectrometry (MS) is the most powerful detector for all chromatographic modes. However, the interfaces for GC/MS and LC/MS (the extreme modes used in unified chromatography) are completely different. More research has to be developed in this field in order to fulfill this gap in the identification of the peaks eluted in unified chromatography.

CONCLUSIONS

Unified chromatography is an infant technique that combines all chromatographic modes in just one instrument. Although it is fascinating from the theoretical point of view, in practice it still presents several limitations. A major one is the absence of commercial instruments, which hinders the development of further applications. It is expected that in the near future, the technique will be fully developed and the frontiers within the chromatographic world will be removed.

ACKNOWLEDGMENTS

Professor Lanças wishes to acknowledge FAPESP (Fundação de Apoio à Pesquisa do Estado de São Paulo) and CNPq (Conselho Nacional de Desenvolvimento Científico e Tecnológico) for the financial support to his laboratory.

REFERENCES

1. James, A.T.; Martin, A.J.P. Gas-liquid partition chromatography: The separation and micro-estimation of volatile fatty acids from formic acid to dodecanoic acid. Biochem. J. **1952**, *50*, 679.
2. Golay, M.E. Brief report on gas chromatography theory. In *Gas Chromatography (1960 Eidinburg Symposium)*; Scott, R.P., Ed.; Butterworths: London, 1960; 139.
3. Klesper, E.; Corwin, A.H.; Turner, D.A. High pressure gas chromatography above critical temperatures. J. Org. Chem. **1962**, *27* (2), 700.
4. Tsett, M. Ber. Deut. Botan. Soc. **1906**, *24*, 316.
5. Horváth, C.G.; Preiss, B.A.; Lipsky, S.R. Fast liquid chromatography: An investigation of operating parameters and the separation of nucleotides on pellicular ion exchangers. Anal. Chem. **1967**, *39*, 1422.
6. Ishii, D.; Asai, K.; Hibi, K.; Jonokuchi, T.; Nagaya, M. A study of micro-high-performance liquid chromatography: I. Development of technique for the miniaturisation of high-performance liquid chromatography. J. Chromatogr. **1977**, *144*, 157.
7. Giddings, J.C. *Dynamics of Chromatography*; Marcel Dekker, Inc.: New York, 1965.
8. Ishii, D.; Niwa, T.; Ohta, K.; Takeuchi, T. Unified capillary chromatography. J. High Resolut. Chromatogr. **1988**, *11* (11), 800–801.
9. Yang, F.J. *Microbore Column Chromatography*; Marcel Dekker, Inc.: New York, 1989.
10. Bartle, K.D.; Davies, I.L.; Raynor, M.W.; Clifford, A.A.; Kithinji, J.P. Unified multidimensional microcolumn chromatography. J. Microcol. Separ. **1989**, *1* (2), 63–70.
11. Tong, D.; Bartle, K.D.; Clifford, A.A. Principles and applications of unified chromatography. J. Chromatogr. **1995**, *703* (1–2), 17–35.
12. Chester, T.L. Chromatography from the mobile-phase perspective. Anal. Chem. **1997**, *69*, 165A.
13. Lanças, F.M. GC × SFC × LC: Towards unified chromatography. Proc. VIth Latin American Congress on Chromatography, COLACRO VI, Caracas, Venezuela; Intevep, Ed.; 1996, 25–P1.
14. Liu, Y.; Yang, F.Y. Unified high-pressure gas and supercritical fluid chromatography with microbore packed columns. Anal. Chem. **1991**, *63*, 926.
15. Davies, I.L.; Yang, F.J. Unified open tubular column gas and supercritical fluid chromatography. Anal. Chem. **1991**, *63*, 1242.
16. Tong, D.; Bartle, K.; Clifford, A.A.; Robinson, R. Unified chromatograph for gas chromatography, supercritical fluid chromatography and micro-liquid chromatography. Analyst. **1995**, *120* (10), 2461.

Uremic Toxins in Biofluids: HPLC Analysis

Ioannis N. Papadoyannis
Victoria F. Samanidou
Laboratory of Analytical Chemistry, Chemistry Department, Aristotle University of Thessaloniki, Thessaloniki, Greece

INTRODUCTION

During the 1960s, target substances for removal in the blood of uremic patients were *small molecules*, such as urea, creatinine, and guanidine compounds. In the 1970s, "middle molecular substances," i.e., substances with molecular weights ranging from 300 to 5000 Da, were also included in the list of substances that have to be removed. Hemodiafiltration was developed as a more efficient method for removing middle molecular toxins, and separation and identification of such substances in uremic serum were actively attempted by many researchers worldwide.

UREMIA

The term "uremia" was initially proposed by Piorry and L'Heritier in 1840 to mean "urine in the blood." *Uremia*, or azotemia, is a condition resulting from advanced stages of kidney failure, in which urea and other nitrogen-containing wastes are found in the blood. Lethargy, mental depression, loss of appetite, and edema are some of the early signs of uremia, while subsequent symptoms include diarrhea, anemia, convulsions, coma, and a gray-brown coloration.

Treatment of uremia is usually performed with dialysis and/or renal transplantation. Since 1840, more than 2000 toxic substances were reported in uremic blood.[1,2]

UREMIC TOXINS

Uremic toxins are chemicals and waste products normally excreted by the kidneys; they are responsible for many of the signs of kidney disease. Blood urea nitrogen (BUN) is one of those substances, but it is not the only one. Early definitions (in 1978) proposed the following as minimal for the identification of uremic toxins:

1. They should be chemically identifiable and quantifiable in biological fluids.
2. The concentration in uremic subjects should exceed that in non-uremic subjects.
3. The concentration should correlate with specific uremic symptoms that disappear at the normal concentration.
4. Toxic effects in a test system should be demonstrable at the concentration found in uremic subjects.

Nowadays, this definition can be considered as classical. Because all of these criteria are rarely met simultaneously, the concept of uremic toxins has changed. In the new concept, substances that damage normal physiological functions, or interfere with physiological defense mechanisms in renal failure, have also been recognized as "uremic toxins." Some may play a role in the progression of renal disease, inducing uremic symptoms, and may contribute to dialysis-related complications.

As already mentioned, one way to treat uremia is through dialysis. Uremic toxins and excess fluid are removed by hemodialysis, which is accomplished by using a dialyzer. This is a convenient configuration, incorporating a semipermeable dialysis membrane with provisions for the flow of blood and dialysate on either side of the membrane. Blood is removed for purification from the patient's body via the blood access, pumped by the blood pump through blood tubing into the dialyzer, and is then pumped back to the patient. Dialysate of the desired chemical composition is prepared through the dialysate delivery system, by mixing water and concentrate in the appropriate ratio. Dialysate is pumped through the dialyzer to remove toxins and fluid crossing over from blood. An anticoagulant, such as heparin, is infused into the extracorporeal blood circuit to prevent blood clotting by a pump. Patients usually receive hemodialysis three times weekly for 4 hr each time.

Table 1 summarizes substances considered as possible uremic toxins. Fig. 1 illustrates the chemical structures of some of the most important uremic toxins that are determined by high-performance liquid chromatography (HPLC). In this entry, some of the most important uremic toxins are discussed (concerning their chromatographic determination).

DETERMINATION BY HPLC

Creatine–Creatinine

Molecules serving as effective biomarkers in clinical fluids are often low-molecular-mass metabolic end products. These small molecules can often be directly determined

Table 1 Possible uremic toxins.

Small water-soluble compounds
Guanidines
Asymmetric dimethylarginine
Creatinine
Purines
Oxalate
Phosphorus
Urea
Middle, large molecules
Advanced glycosylated end products
Parathyroid hormone
Oxidation products
Peptides (beta-endorphin, methionine-enkephalin, beta-lipotropin, granulocyte inhibiting proteins I and II, degranulation-inhibiting protein, adrenomedullin)
Beta 2-microglobulin
Complement factor D
Protein-bound compounds
Indoles
3-Carboxy-4-methyl-5-propyl-2-furanpropionic acid
Hippuric acid
Homocysteine
Indoxyl sulfate
p-cresol
Polyamines

in urine; however, their determination in plasma or serum often requires some form of protein removal. Creatinine is the most widely used clinical marker to assess renal function.

The reliable determination of uremic toxins, creatine, and creatinine in biofluids is a matter of great importance in clinical chemistry.

Creatine is present in muscle, brain, and blood and, although not present in large amounts in normal urine from adults, it is abundantly present in the urine of adults who have recently ingested creatine supplements. Ingestion of a creatine supplement has been shown to increase the level of phosphocreatine, and this has become extremely popular in recent years with many athletes who want to increase muscular power and to enhance their performance. Because of this, analysis for creatine has become more important in the clinical setting. Additionally, elevated serum concentrations of creatine can be observed in some cases of muscle catabolism such as primary myopathy, myositis, and muskelatrophie, as well as in the case of hyperthyroidism.

Creatinine is the end product of creatine catabolism. It is found in muscle tissue, blood, and urine as it is formed from the breakdown of muscle creatinine, and is proportional to the muscle mass. It results from the irreversible non-enzymatic dehydration and loss of phosphate from phosphocreatine, as shown in Fig. 2. Creatinine concentrations are very useful indices for evaluating glomerular filtration rate and, in general, are an important clinical marker of renal function.

Although creatinine concentration should be stable from day to day, it is a function of the amount of creatinine entering the blood from muscle, its volume of distribution, and its rate of excretion. Because the first two are usually constant, changes in the serum creatinine level would usually be a result of a change in the glomerular filtration rate (GFR). Abrupt cessation of glomerular filtration causes the serum creatinine to rise by 1–3 mg/dl daily. The blood urea nitrogen also rises with renal dysfunction, but is influenced by extrarenal factors as well.

Urine creatinine is used to adjust the values of urinary biological indicators; for example, creatinine measurements are necessary for correction of vanilmandelic and homovanillic acids, which indicate neuroblastoma and pheochromocytoma, when excreted in urine in abnormally increased concentrations. Ratios of vanilmandelic and homovanillic acids to creatinine have been utilized as a diagnostic index of these diseases.

Measurement of creatinine in serum and urine is routinely performed by photometric methods such as the Jaffé reaction, which is widely accepted and involves the formation of an adduct of creatinine with picric acid in alkaline solution, whose absorbance is measured at 500 nm. However, this method is unspecific and subject to perturbation by many interfering substances from endogenous and exogenous origins.

Therefore great efforts were undertaken to improve existing methods or to develop new measurement principles, using enzymatic and HPLC-based methods. Chromatographic techniques are attractive for clinical analysis because of their inherent ability to analyze multiple component biofluids and determine the analytes of interest with minimal interference from other species. Chemical methods give higher values because of the presence of endogenous and exogenous substances. HPLC methods for the determination of creatinine that can be found in literature involve ion exchange, ion-pairing, and reversed phase (RP). Most of these require deproteinization before analysis, but direct analysis of serum reatinine can also be achieved by column switching liquid chromatography (LC). Liquid–liquid extraction (LLE) for isolation of creatinine among other compounds has been reported. Capillary electrophoretic methods are also reported for the determination of creatine and creatinine.[3–9]

PURINE METABOLITES

Oxypurines: Allantoin, Uric Acid, Hypoxanthine, and Xanthine

Purines are metabolized in a series of reactions involving hypoxanthine, xanthine, uric acid, and allantoin as end products that are subsequently excreted in urine. Fig. 3 shows the metabolic pathways for xanthine. Measurement of urinary excretion of purine metabolites,

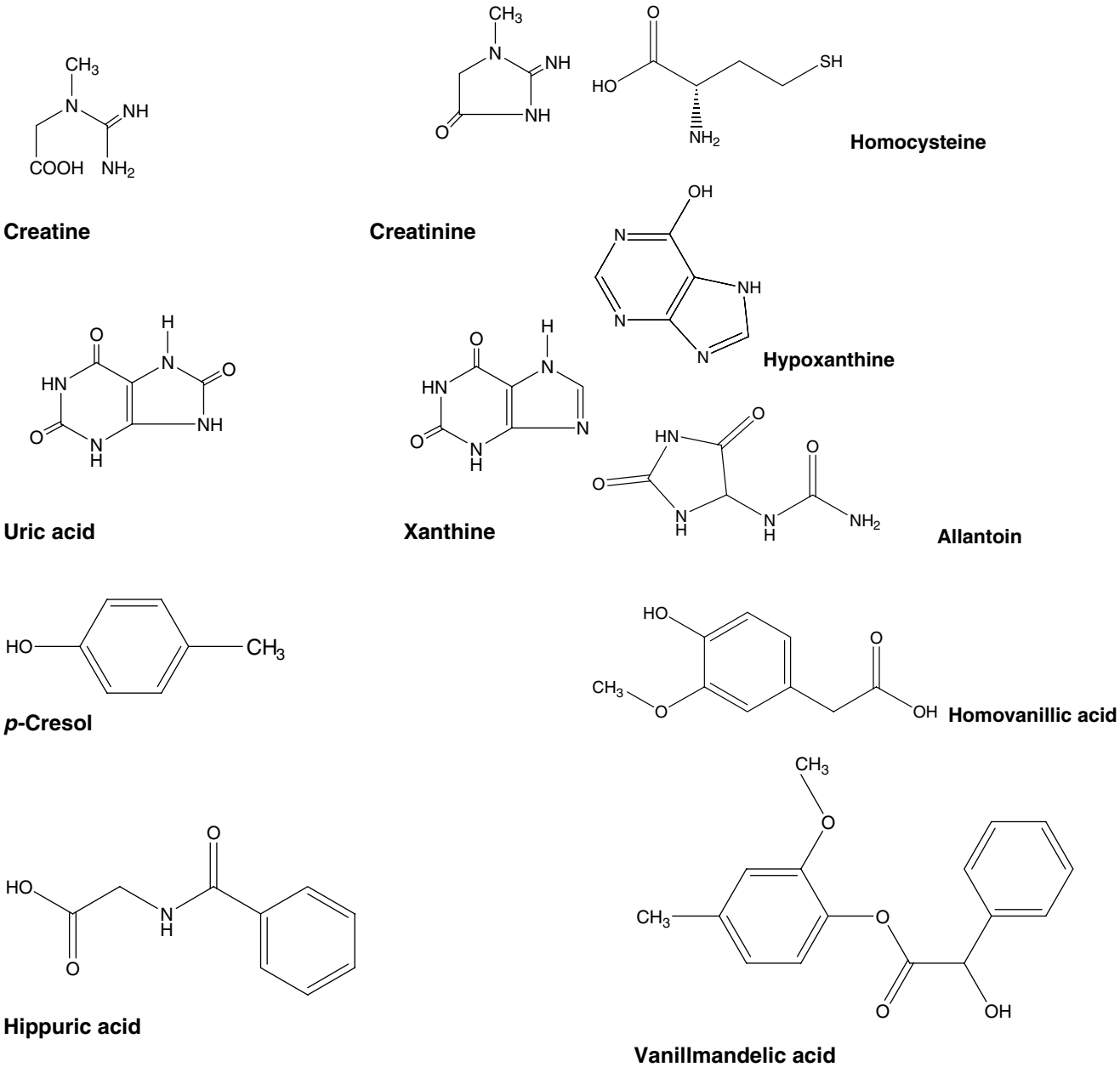

Fig. 1 Chemical structures of possible uremic toxins that are determined by HPLC.

primarily allantoin or, additionally, uric acid, xanthine, and hypoxanthine, has been proposed as a marker for microbial protein synthesis. The problem of non-specificity of the colorimetric assay for purine metabolites can be overcome by using a multitude of methods, with or without derivatization. HPLC determination of these compounds can be performed in urine samples directly after dilution.

Uric acid is a primary end product of urine metabolism in the kidney. Uric acid levels in human urine are like creatinine as an important parameter of renal function and a marker for renal failure as well as toxicity. As shown in Fig. 3, uric acid is the final product of catabolization of the purine nucleosides, adenosine, and guanosine.[10]

Xanthines, e.g., hypoxanthine and xanthine, are intermediates of the metabolism of adenine and guanine to uric acid and are, therefore, important analytes for diagnosis of certain types of metabolic disease.

Uric acid and xanthines are markers for metabolic disorders such as gout, Lesch–Nyman syndrome, and xanthinuria. Measurements of urinary excretion of purine metabolites, among them uric acid and xanthine, have been proposed as a marker for microbial protein synthesis. Their simultaneous determination is useful for diagnosis and treatment of hyperuricemia. In addition to xanthine and hypoxanthine, notable members of the xanthine class include caffeine, theophylline, and theobromine.[11–15]

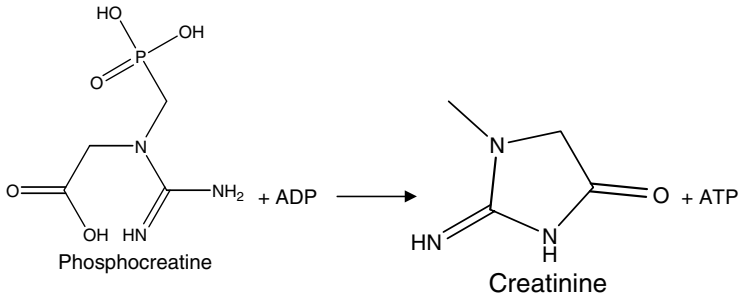

Fig. 2 Phosphocreatine metabolism.

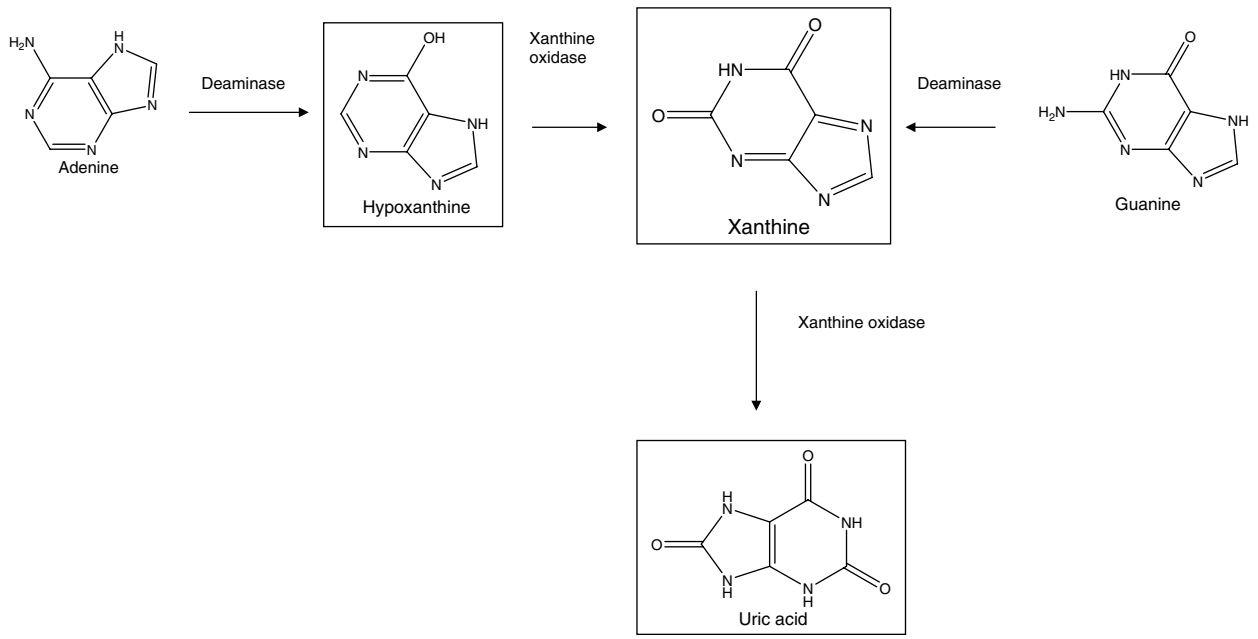

Fig. 3 Xanthine metabolic pathways.

Clearly, the determination of such compounds is crucial for diagnosis and monitoring of renal disease and metabolic disorders. The concentration of oxypurines in blood serum is among the most important parameters in biochemistry and clinical chemistry. Determination of uric acid is performed by enzymatic methods or colorimetrically by reduction of phosphotungstate.

The combination of HPLC RP C_8 columns with monitoring of the effluent at 205 nm provides an acceptable analytical tool for quantification of purine metabolites in the urine. Detection at short ultraviolet (UV) wavelengths up to 215 nm results in compromised method selectivity and, therefore, longer and more specific detection wavelengths were applied in recent methods. The combination of the direct separation and determination using a RP HPLC system, coupled with photodiode array detection, is found to be accurate and more precise and selective than previously published methods for the determination of purine metabolites in urine.

HPLC methods for the determination of uric acid found in literature include ion exchange, ion-pairing, RP, and size exclusion. Most of these require deproteinization before analysis, but direct analysis of serumuric acid was also successful by column switching LC.

In recent years, a number of methods based on HPLC, isocratic or gradient, have been reported for the quantification of allantoin and purine metabolites in biological fluids.

Various analytical methods for determining purine metabolites in biological samples, such as urine or blood plasma, have been described. These procedures are based mainly on separation by HPLC methods using RP C_{18} columns and monitoring at wavelengths ranging from 200 to 218 nm, or at 254 nm for compounds other than allantoin. The main advantage of these methods is that urine samples are analyzed directly, while the plasma samples only need acid deproteinization. Unfortunately, UV detection at short wavelengths (i.e., up to 218 nm) is not selective enough. Because allantoin is poorly retained on a C_8 column and has a very low molar absorptivity at wavelengths above 220 nm, allantoin may be converted to a derivative containing a chromophore group (Rimini–Schryver reaction). Some research groups removed the

Table 2 Chromatographic and sample preparation conditions for the simultaneous determination of creatine, creatinine uric acid and xanthine.

Chromatographic conditions
Mobile phase: 10 mmol/L KH_2PO_4
Analytical column: Kromasil C_8, 250 × 4 mm (I.D.), 5 μm
Pressure: 110–120 kg/cm^2
Flow rate: 0.8 ml/min
Detection: 200 nm

Sample preparation
Serum samples
1) 500 μl serum sample +1 ml acetonitrile to precipitate proteins
2) Centrifugation at 3500 rpm for 15 min
3) Evaporation of acetonitrile
4) Dilution of residual 10–20 times with deionized water
5) Direct analysis or spiking with stock solutions to apply standard addition technique

Human urine samples
1) Collection from healthy volunteers and storage at −20°C until analysis
2) Filtration through 0.2 μm membrane filters to remove cells and other particulate matter
3) Dilution, 400–500 times with deionized water
4) Direct analysis or spiking with stock solutions to apply standard addition technique

Source: From http://www.embbs.com/cr/rf/rf3.htm[1]

uric acid prior to the derivatization of allantoin; however, these methods are time-consuming and labor-intensive.

Simultaneous Determination of Creatine, Creatinine, Uric Acid, and Xanthine

Although several papers can be found in the literature dealing with the determination of single analytes or simultaneous determination of creatinine and uric acid, only a few have reported on the simultaneous determination of creatine, creatinine, uric acid, and xanthine in human biofluids. One of them reports about an HPLC method with UV detection permitting the analysis of human serum and urine for the determination of these substances in a single run. Low-wavelength UV detection is achieved at 200 nm using 10 mmol/L KH_2PO_4, as mobile phase, at a flow rate 0.8 ml/min and a Kromasil C_8, 250 × 4 mm, analytical column. Analysis is completed within approximately 8 min. Table 2 summarizes the chromatography and the sample preparation conditions. Fig. 4 shows a typical chromatogram obtained under the described chromatographic conditions.[16]

The limits of detection obtained by this method are 4 pg for creatine and creatinine, 20 pg for uric acid, and 6 pg for xanthine, while the limits of quantitation are 10 pg for creatine and creatinine, 60 pg for uric acid, and 20 pg for xanthine, when 20 μl are injected onto the column. A rectilinear relationship is observed up to 2 ng/μl for

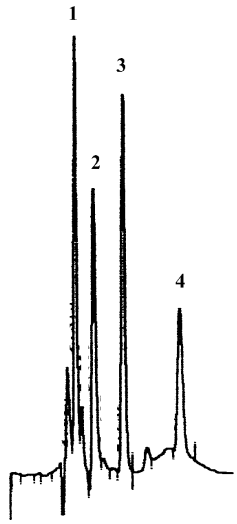

Fig. 4 High-performance liquid chromatogram of standard solution containing: 1) creatine, 2.631 min; 2) creatinine, 3.400 min; 3) uric acid, 4.645 min; and 4) xanthine, 7.014 min. Chromatographic conditions are described in Table 2.
Source: From http://www.embbs.com/cr/rf/rf3.htm[1]

creatine and creatinine, 12 ng/μl for uric acid and 5 ng/μl for xanthine.

The statistical evaluation of the method was examined by performing day-to-day ($n = 8$) and within-day ($n = 8$) calibration and was found to be satisfactory with high accuracy and precision results. Relative Standard Deviation (RSD) values were in the range of 0.4–4.3% for within-day measurements and 3.5–7.4% for day-to-day precision measurements.

This method was applied to serum and urine, simply after dilution. A typical chromatogram of creatine, creatinine, uric acid, and xanthine in serum and urine are

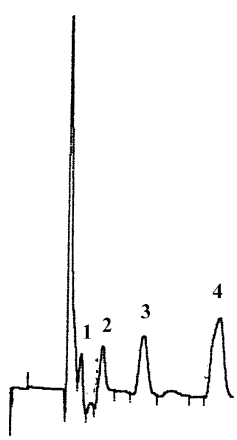

Fig. 5 High-performance liquid chromatogram of spiked human blood serum sample (after 20-fold dilution) containing: 1) creatine, 2.760 min; 2) creatinine, 3.615 min; 3) uric acid, 5.232 min; and 4) xanthine, 7.488 min. Chromatographic conditions are described in Table 2.
Source: From http://www.embbs.com/cr/rf/rf3.htm[1]

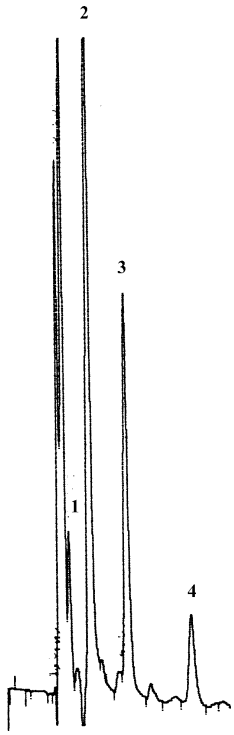

Fig. 6 High-performance liquid chromatogram of urine sample (after 400-fold dilution) containing: 1) creatine, 2.774 min; 2) creatinine, 3.675 min; 3) uric acid, 5.365 min; and 4) xanthine, 7.494 min. Chromatographic conditions are described in Table 2. **Source:** From http://www.embbs.com/cr/rf/rf3.htm[1]

shown in Figs. 5 and 6, respectively. The sensitivity of this method was high enough to determine the concentration of creatinine and uric acid in diluted serum (10- to 20-fold dilution) and urine (400- to 500-fold dilution) samples. Percentage recovery of analytes in spiked samples was in the range 91–105%. No interference was observed from endogenous compounds of human serum and urine. Correlation of analyzed samples using the developed method and conventional routine methods for creatinine and uric acid gave significantly similar results. The method appears to be a very useful tool for routine analysis of clinical samples, for simultaneous determination of creatinine, creatine, uric acid, and xanthine levels in serum and urine.

Phenol and Cresols

Urinary phenol, cresols, *p*-nitrophenol, and *p*-aminophenol are biological indicators of human exposure to aromatic hydrocarbons. Fig. 7 illustrates the scheme of phase 1 and phase 2 metabolism of inhaled benzene and toluene vapors, while Fig. 8 shows the metabolism of inhaled xylene and ethyl benzene vapors.

The determination of urinary cresols, particularly *O*-cresol, has been proposed as a biological monitoring method for toluene, as a fraction of the inhaled vapor is oxidized at the aromatic ring with the production of cresols.[17–19]

p-Cresol and hippuric acid are included among uremic toxins. *p*-Cresol (4-methylphenol) is a volatile, low-molecular-weight phenolic compound that is largely protein-bound, mainly to albumin, with partial lipophilic properties. It is related to several biochemical, biological, and physiological functions at concentrations currently observed in uremia.

p-Cresol can be considered as a prototype of protein-bound uremic retention solutes, with a protein binding of >99% in healthy subjects and approximately 90% in uremic patients. Several recent studies suggest that *p*-cresol interferes with various biochemical and physiological functions at concentrations currently observed in uremia. Concentrations of phenol and *p*-cresol in uremic serum are significantly higher than those in normal serum.

The present concept of dialysis focuses mainly on the removal of small water-soluble compounds, and the currently applied kinetic parameters of dialysis adequacy are also based on the behavior of water-soluble compounds. Nevertheless, many of the currently known biological effects in uremia are attributable to compounds with different physicochemical characteristics and, among these, protein-bound solutes may play an important role. Hippuric acid, homocysteine, and *p*-cresol are considered.[20]

Phenol and *p*-cresol noticeably accumulate in the serum of undialyzed and dialyzed uremic patients; they play a role in the development of uremic coma and defective platelet aggregation. They are synthesized in the small intestine from phenylalanine and tyrosine through 4-hydroxybenzoic acid and 4-hydroxyphenylacetic acid, respectively, by intestinal bacteria, as shown in Fig. 9. Aerobic bacteria tend to produce phenol from tyrosine, whereas anaerobic bacteria produce *p*-cresol. These phenols are absorbed from intestine and normally excreted into urine. In uremia, renal clearance of the phenols is impaired, leading to accumulation of the phenols in the blood. Compared to healthy controls, the serum *p*-cresol levels are 7–10 times higher in continuous ambulatory peritoneal dialysis patients, uremic outpatients, and hemodialysis patients.[21]

Only a few methods are available for the determination of *p*-cresol concentration in serum. In addition, these methods have only been used for the determination of total *p*-cresol. In particular, the evolution of free (non-protein-bound) *p*-cresol is of concern because, conceivably, this is the biologically active fraction. However, the concentration of free *p*-cresol is markedly lower than that of total *p*-cresol, in view of its important protein binding. Methods enabling the measurement of total and free *p*-cresol concentration in the serum of

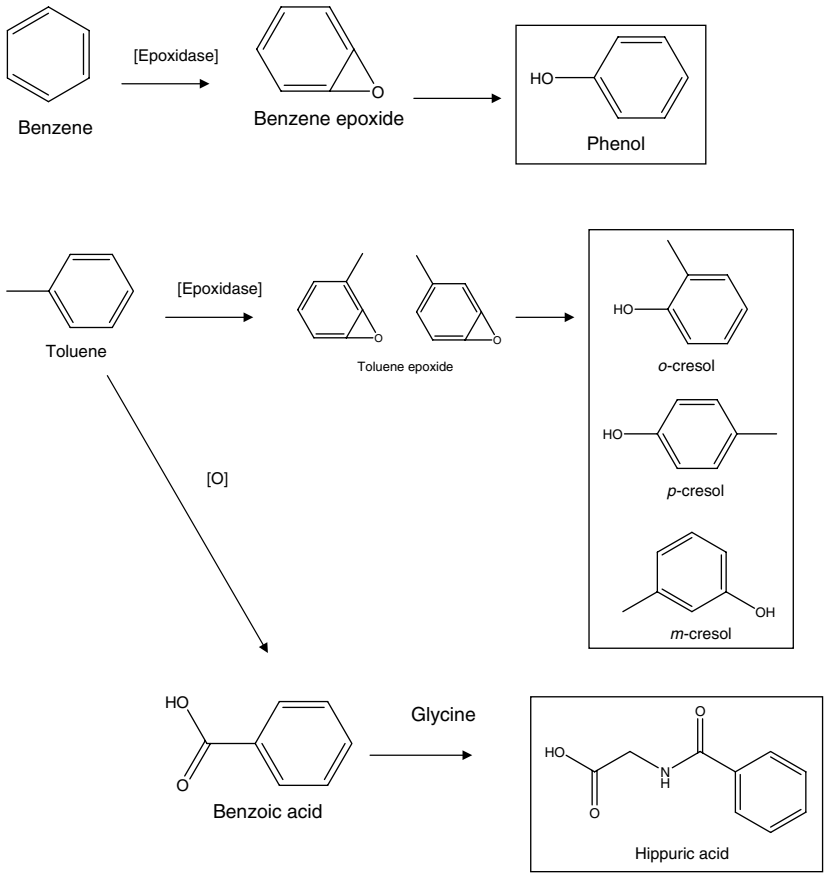

Fig. 7 Scheme of phase 1 and phase 2 metabolism of inhaled benzene and toluene vapors.

healthy controls and uremic patients are also reported in literature.

Deproteinization, extraction, and HPLC procedures are efficient, without interference of other protein bound ligands and/or precursors of *p*-cresol or phenol, via spiking experiments, and measurement of the UV absorbance over the 200–400 nm wavelength range.

HPLC methods can use fluorescence as a detector for quantifying serum phenol and *p*-cresol in uremic patients on hemodialysis.

Fluorescence detection at 284/310 nm (extinction/emission wavelengths) leads to a detection limit of 1.3 mmol/L (0.14 mg/ml for *p*-cresol). Identification of phenol and *p*-cresol may be confirmed by LC/MS. Because HPLC methods require only simple extraction, e.g., by ethyl acetate, and do not require further steps such as derivatization, they are simple and rapid compared with GC or GC/MS. Such methods are useful for monitoring serum phenols in dialyzed patients as an index of hemodialysis adequacy. However, the separation of the three isomers of cresol can only be performed by adding β-cyclodextrin to the liquid phase.

Hippuric Acid

Toluene and *o*-, *m*-, and *p*-xylene have been widely used, separately and as mixtures, as organic solvents, ingredients of thinners, and in the synthesis of chemicals. Toluene is widely used in industry as a replacement for the carcinogenic benzene, but toluene also exhibits considerable toxicity. In vivo, toluene is oxidized; the main metabolite in man is benzoic acid, which is then conjugated with glycine and excreted in urine as hippuric acid. Although hippuric acid is an endogenous metabolite commonly found in human urine, on exposure to toluene, the level is enhanced.[19–21] The three isomers of xylene in a mixture are commonly called "xylol." In vivo, these isomers are oxidized to isomeric toluic acids, then conjugated with glycine and excreted in urine as *o*-, *m*-, and *p*-methylhippuric acid.

Hippuric acid has been recognized as a potential marker of uremic toxicity in chronic renal failure. Additionally, hippuric acid and *o*-, *m*-, and *p*-methylhippuric acids are used as biological markers in studies of occupational exposure to diesel industrial solvents, because they show a good correlation with the level of exposure to toluene and xylenes. In urinary biological monitoring, expressing the amount of urinary metabolite per gram of creatinine has been used for spot samples of urine. This correction is thought to be particularly applicable for very concentrated and dilute samples. Therefore the biological exposure indices of urinary hippuric acid in toluene exposure, methylhippuric acid in xylene exposure, and mandelic acid in styrene exposure are expressed as metabolite concentrations in urine, corrected for creatinine.

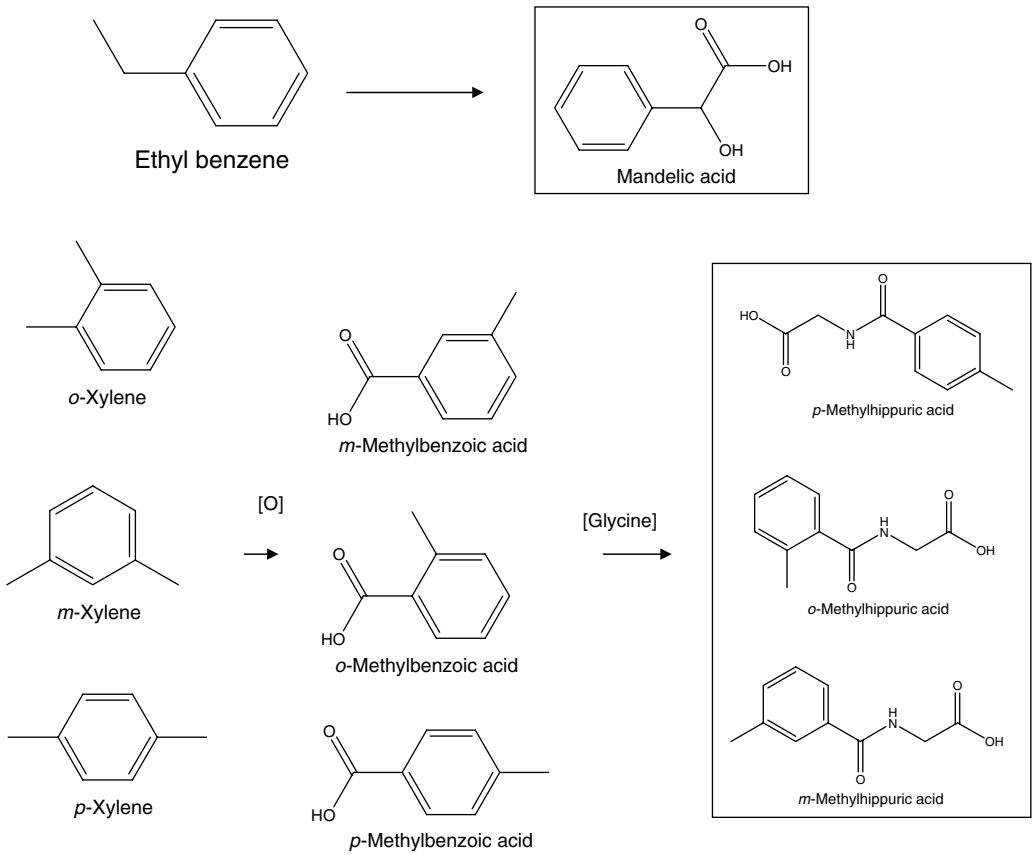

Fig. 8 Scheme of phase 1 and phase 2 metabolism of inhaled xylene and ethylbenzene vapors.

For the simultaneous determination of metabolite concentrations in the urine of workers exposed to aromatic solvents, HPLC has been widely used to obtain accurate and reliable results. Also, GC has been used for the determination of metabolite concentrations.

HPLC methods are considered by the National Institute for Occupational Safety and Health (NIOSH) to be the reference methods (e.g., NIOSH #8301). However, these methods cannot separately quantify each isomer of hippuric acid and methylhippuric acids.

GC methods are considered to be specific for determination of hippuric acid and methylhippuric acid, although they require a derivatization procedure with various reagents; for example, several investigators have used diazomethane; others have used trimethyl–silyl derivatives.

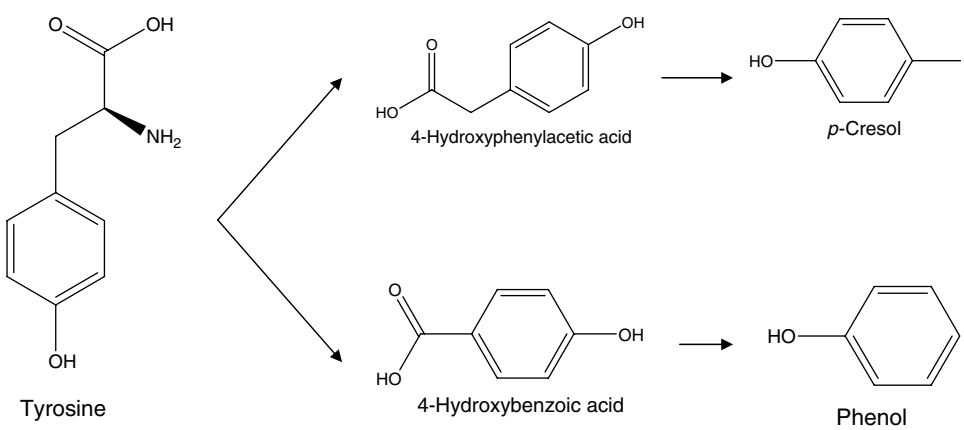

Fig. 9 Tyrosine metabolism.

RP–HPLC has been used without derivatization with ultraviolet or electrochemical detection. Liquid–liquid extraction can be performed, as well as solid-phase extraction (SPE), for sample preparation after acidification with HCl 1 mol/L (pH 1). Removal of the homovanillic acid from the variable salt concentration of the sample enhances the control of the ion exchange step. This is accomplished by SPE using a C_8 cartridge. This first stage also helps to reduce the number of anionic compounds from the matrix that will be loaded onto the strong anion exchange cartridge.[22] Recently, high-performance capillary electrophoresis (HPCE) has developed into a powerful analytical technique in diverse fields, and shows a high separation power with a short analysis time. In the field of occupational health, there are not many HPCE methods for the determination of metabolites in the urine of workers exposed to aromatic solvents, although HPCE methods have been used for hippuric acid (HA) in human urine and human serum, and for creatinine and uric acid.

Protein-bound uremic solutes play a role in the inhibition of drug protein binding. Substantial changes in protein binding of drugs occur during the progression of renal insufficiency. It has been suggested that hippuric acid in uremic ultrafiltrate is an inhibitor of theophylline protein binding. The inhibitory effect on theophylline protein binding of the deproteinized uremic serum has been shown to be higher than with ultrafiltrate ($p < 0.05$).[23]

Dose–response curves with the characterized compounds revealed that the most important role in binding inhibition could be attributed to hippuric acid. The identified uremic compounds are not entirely representative for the decreased protein binding of theophylline, indicating that additional factors than those identified in this study affect the protein binding as well.

Homocysteine

The absence of a chromophore for sensitive detection is a problem which is met with HPLC determination of these thiol analytes. However, two approaches are possible to resolve this point: 1) direct detection using electrochemistry, either amperometry on gold/mercury amalgamated electrodes or coulometry on porous graphite electrodes; 2) derivatization coupled with UV or spectrofluorometric detection. The derivatization reactions, either precolumn or postcolumn, involve different thiol selective reagents: ammonium 7-fluorobenzo-2-oxa-l,3-diazole-4-sulphonate (SBD-F), *O*-phthalaldehyde (OPA), etc.

RP–HPLC with fluorescence detection, after derivatization of plasma thiols with ammonium 7-fluorobenzo-2-oxa-l,3-diazole-4-sulphonate (SBD-F), is the most widely used method to determine total plasma amino thiols (cysteine, cysteinylglycine, and homocysteine). The time required for sample preparation (thiolic reduction, deproteinization, and precolumn derivatization with SBD-F) and for thiol derivatives separation is nearly 2 hr per sample.

Catecholamine Metabolites: Homovanillic and Vanillylmandelic Acid

Homovanillic and vanillylmandelic acids, the major metabolites of catecholamines, are often tested in urine for neurological diagnosis and for monitoring the response to therapy in diseases such as phaeochromocytoma and neuroblastoma.

Various HPLC methods have been described, mainly employing ion-pair RP chromatography, with electrochemical or fluorimetric detection, most of them including sample pretreatment with solid-phase or liquid extraction.

The determination of catecholamines requires a highly sensitive and selective assay procedure capable of measuring very low levels of catecholamines that may be present. In past years, a number of methods have been reported for measurement of catecholamines in both plasma and body tissues. A few of these papers have reported simultaneous measurement of more than two catecholamine analytes. One of them utilized lised UV for end-point detection and the samples were chromatographed on a RP phenyl analytical column. The procedure was slow and cumbersome because ofdue to the use of a complicated liquid–liquid extraction and each chromatographic run lasted more than 25 min with a detection limit of 5–10 ng on-column. Other sensitive HPLC methods reported in the literature use electrochemical detection with detection limits 12, 6, 12, 18, and 12 pg for noradrenaline, dopamine, serotonin, 5-hydroxyindoleacetic acid, and homovanillic acid, respectively. The method used very a complicated mobile phase in terms of its composition whilewhilst the low pH of 3.1 used might jeopardize the chemical stability of the column. Analysis time was approximately 30 min. Recently reported HPLC methods utilize amperometric end-point detection.[22,24]

CONCLUSIONS

Uremic toxins are chemicals and waste products normally excreted by the kidneys and are responsible for many of the signs of kidney disease. Since 1840, more than 2000 toxic substances were reported in uremic blood. Obviously, the determination of such compounds is crucial for diagnosis and monitoring of renal disease and metabolic disorders. The concentrations of several uremic toxins in blood serum and urine are among the most important parameters in biochemistry and clinical chemistry.

REFERENCES

1. http://www.embbs.com/cr/rf/rf3.htm
2. http://www.outilinemed.com/demo/nephrol/11244.htm
3. Shingfield, K.J.; Offer, N.W. Simultaneous determination of purine metabolites, creatinine and pseudouridine in

ruminant urine by reversed phase HPLC. J. Chromatogr. B, **1999**, *723*, 81–94.
4. Kochansky, C.; Strein, T. Determination of uremic toxins in biofluids: creatinine, creatine, uric acid and xanthines. J. Chromatogr. B. **2000**, *747*, 217–227.
5. Czauderna, M.; Kowalczyk, J. Simultaneous measurement of allantoin, uric acid, xanthine and hypoxanthine in blood by high-performance liquid chromatography. J. Chromatogr. B, **1997**, *704*, 89–98.
6. Seki, T.; Orita, Y.; Yamaji, K.; Shinoda, A. Simultaneous determination of uric acid and creatinine in biological fluids by column-switching liquid chromatography with ultraviolet detection. J. Pharm. Biomed. Anal. **1997**, *15*, 1621–1626.
7. Eiteman, M.A.; Gordillo Cabrera, M.L. Analysis of oxonic acid, uric acid, creatine, allantoin, xanthine and hypoxanthine in poultry litter by reverse phase HPLC. Fresenius J. Anal. Chem. **1994**, *348*, 680–683.
8. Shirao, M.; Suzuki, S.; Kobayashi, J.; Nakazawa, H.; Mochizuki, E. Analysis of creatinine, vanilmandelic acid, homovanillic acid and uric acid by micellar electrokinetic chromatography. J. Chromatogr. B, **1997**, *693*, 463–467.
9. Resines, J.A.; Arin, M.J.; Diez, M.T.; Garcia del Moral, P. Ion-pair reversed HPLC determination of creatine in urine. J. Liq. Chromatogr. Relat. Technol. **1999**, *22* (16), 2503–2510.
10. Seki, T.; Yamaji, K.; Orita, Y.; Moriguchi, S.; Shinoda, A. Simultaneous determination of uric acid and creatinine in biological fluids by column-switching liquid chromatography with ultraviolet detection. J. Chromatogr. A, **1996**, *730*, 139–145.
11. Czauderna, M.; Kowalczyk, J. Quantification of allantoin, uric acid, xanthine and hypoxanthine in ovine urine by high-performance liquid chromatography and photodiode array detection. J. Chromatogr. B, **2000**, *744*, 129–138.
12. Schoots, A.C.; Homan, H.R.; Gladdines, M.M.; Cramers, C.A.; de Smet, R.; Ringoir, S.M. Screening of UV absorbing solutes in uremic serum by reversed phase HPLC change of blood levels in different therapies. Clin. Chim. Acta, Int. J. Clin. Chem. **1985**, *146* (1), 37–51.
13. de Smet, R.; Vogeleere, P.; van Kaer, J.; Lameire, N.; Vanholder, R. Study by means of high-performance liquid chromatography of solutes that decrease theophylline/protein binding in the serum of uremic patients. J. Chromatogr. A, **1999**, *847*, 141–153.
14. Georga, K.A.; Samanidou, V.F.; Papadoyannis, I.N. Improved micro-method for the HPLC analysis of caffeine and its demethylated metabolites in human biological fluids after SPE. J. Liq. Chromatogr. Relat. Technol. **2000**, *23* (10), 2975–2990.
15. Georga, K.A.; Samanidou, V.F.; Papadoyannis, I.N. Use of novel solid-phase extraction sorbent materials for high-performance liquid chromatography quantitation of caffeine metabolism products methylxanthines and methyluric acids in samples of biological origin. J. Chromatogr. B, **2001**, *759*, 209–218.
16. Samanidou, V.F.; Metaxa, A.S.; Papadoyannis, I.N. Direct simultaneous determination of uremic toxins: Creatine, creatinine, uric acid, and xanthine in human biofluids by HPLC. J. Liq. Chromatogr. Relat. Technol. **2002**, *25* (1), 43–57.
17. Abreo, K.; Gautreaux, S.; de Smet, R.; Vogeleere, P.; Ringoir, S.; van Holdre, R. *p*-Cresol, a urinary compound, enhances the uptake of aluminum in hepatocytes. J. Am. Soc. Nephrol. **1997**, *8* (6), 935–942.
18. DeSmet, R.; David, F.; Sandra, P.; VanKaer, J.; Lesaffer, G.; Dhondt, A.; Lameire, N.; van Holder, R. A sensitive HPLC method for the quantitation of free and total *p*-cresol in patients with chronic renal failure. Clin. Chim. Acta **1998**, *278*, 1–21.
19. Fujii, T.; Kawabe, S.; Horike, T.; Taguchi, T.; Ogata, M. Simultaneous determination of the urinary metabolites of toluene, xylenes and styrene using high-performance capillary electrophoresis. Comparison with high-performance liquid chromatography. J. Chromatogr. B, **1999**, *730*, 41–47.
20. Garcia, A.J.; Apitz-Castro, R. Plasma total homocysteine quantitation: an improvement of the classical high-performance liquid chromatographic method with fluorescence detection of the thiol-SBD derivatives. J. Chromatogr. B, **2002**, *779*, 359–363.
21. Laurens, J.B.; Mbianda, X.Y.; Spies, J.H.; Ubbink, J.B.; Vermaak, W.J.H. Validated method for quantitation of biomarkers for benzene and its alkylated analogues in urine. J. Chromatogr. B, **2002**, *774*, 173–185.
22. Garcia, A.; Heinanen, M.; Jimenez, L.M.; Barbas, C. Direct measurement of homovanillic, vanillylmandelic and 5-hydroxyindole acetic acids in urine by capillary electrophoresis. J. Chromatogr. A, **2000**, *871*, 341–350.
23. Vanholder, R.; de Smet, R.; Lameire, N. Protein bound uremic solutes: the forgotten toxins. Kidney Inter., Suppl. **2001**, *78*, S266–S270.
24. Chi, J.D.; Odontiadis, J.; Franklin, M. Simultaneous determination of catecholamines in rat brain tissue by HPLC. J. Chromatogr. B, **1999**, *731*, 361–367.

UV-Visible Detection Including Multiple Wavelengths

José Almiro da Paixão
Department of Nutrition, Center of Health Sciences,
Federal University of Pernambuco, Recife, Brazil

Abstract
This entry covers the principles of UV detection coupled with high-performance liquid chromatography (HPLC) as a separation and detection technique that combines specific parameters in order to meet suitable applications involving UV–Visible and fluorescence detectors. The main subtopics deal with the specific chemical and physical properties of compounds for ideal separation by identification and quantification procedures using UV–Visible in combination with HPLC, through single and program wavelength in distinct standards and matrices. In order to choose a detector system, the compatibility of selected compounds with a detection system emphasizing molecule benzoic acid (single λ) and fat-soluble vitamins (program wavelength) is evaluated. If the compound does not absorb roughly UV–Visible and non-fluorescent light without sufficient chromophore units, other properties should be chosen. The detection of UV–Visible can be performed using single λ, optimized through various channels or using program wavelength for chemical compounds with any similarity. The closest association between detection and quantification systems to complete the quantification procedure is also indicated. The outcomes of the principles of detection by UV–HPLC are outlined and discussed, especially those involving standards and complex matrices. Contemporary means of achieving complete validation are identified and discussed. UV–Visible detection always requires concise steps to ensure complete transferability between complex matrices.

INTRODUCTION

UV detection coupled with high-performance liquid chromatography (HPLC) is a separation technique that combines specific mobile and stationary phases to meet the requirements of a suitably selective, non-destructive detection system. Recent techniques of this kind have utilized the properties of both organic and inorganic compounds, thereby providing sufficient characterization for appropriate identification and quantification procedures. In order to improve the current performance of the separation technique and to provide compatible alternative procedures at specific stationary phases, further knowledge is needed about molecular mass, clearly established chromophore units, polarity, ionic or non-ionic charges, and the solubility index. In addition, parameters should be followed in analytical separation, such as capacity factor (k) between 1 and 10, resolution (R_s) greater than 1.5, separation factor (α) greater than 1.5, and symmetry factor ideally not more than 1.2.[1]

Of the non-destructive detectors, UV–Visible, fluorescence, light scattering and refractive index are frequently used for various biochemical, chemical, clinical, pharmaceutical, and nutritional applications, as well as in the analysis of supplements and functional ingredients. Of these detectors, candidates of universal grade but still poorly understood are refractive index and light scattering, which exhibit responses that vary according to assay conditions, chiefly those involving temperature conditions. On the other hand, detectors most commonly used in combination with HPLC are UV–Visible and fluorescence. HPLC coupled with mass spectrometry is sufficient for obtaining identification and quantification procedures, which simultaneously uses appropriate fragmentation rules.[1–4] However, care should be taken, especially in the case of quantification procedures, because HPLC is a destructive system. Nevertheless, it is worth completing the characterization of chemical compounds using HPLC.[1–4]

As far as UV–Visible detection is concerned, this system involves orientation (M $\Leftrightarrow$ M*) that indicates the level of energy (in electron volts, ergs, joules, or calories) certain isolated chemical compounds require to bring about excitation, resulting 1) in a spectrum (determining the maximum wavelength) when results have been obtained using spectrometry and 2) in peaks found using single λ and program wavelength (if multiple λ) when results have been obtained using chromatography, obeyed accurate correlation between concentration and units of absorbance.[1–4]

This entry deals with the chemical and physical properties of compounds that help in accomplishing ideal separation through identification and quantification procedures

particularly using UV–Visible in combination with HPLC and involving single λ and program wavelength in distinct standards and matrices—which are some of the subjects discussed in this encyclopedia.

CHOOSING A DETECTOR SYSTEM

To meet the requirements of ideal separation, identification, and subsequent quantification procedures, the compatibility between selected compounds and a detection system should be checked.

Whether a detector linked to an HPLC system is suitable is determined by the properties of compounds. If the compound does not absorb UV–Visible and non-fluorescent light, other properties should be chosen in combination with mobile-phase properties, such as refractive index and light scattering.[1–3] Alternatively, if the compound absorbs UV–Visible and fluorescent light, both properties can be measured using tandem detection.[1–4]

The detection system involves measuring different properties of the mobile phase or, alternatively, compound properties, such as differences in maximum wavelength at a particular molar extinction coefficient. The molecular and normal absorptivities thus serve as complementary criteria for identification and quantification using both HPLC and spectrophotometric techniques.[1–4] One specific disadvantage of this system is that various organic compounds absorb at similar λ values. If the compounds are soluble in an organic solvent and exhibit good compatibility, then specific mobile and stationary phases are usually recommended. On the other hand, if the compounds are volatile and do not absorb UV, then scatter radiation is recommended.[1,3,4]

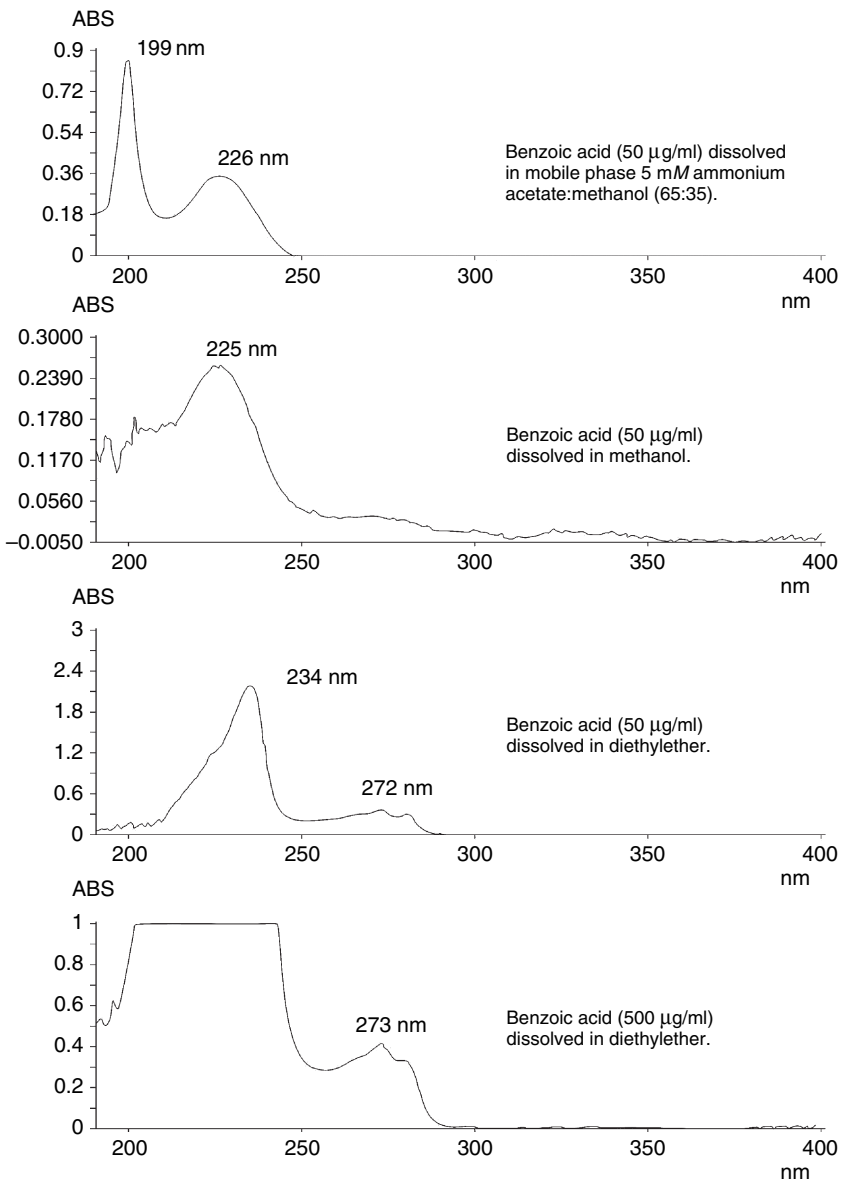

Fig. 1 Adjusting maximum λ wavelength through spectrophotometric assay before HPLC analysis.

If there is a real difficulty in selecting λ because of erroneous results in the literature or unreported results, operational conditions should be provided in such a way so as to set a maximum wavelength, taking into consideration the solubility of the compound in the mobile phase, a UV–Visible spectrum, and a particular composition of solvents as a point of reference. To demonstrate this, our research group conducted an experiment using benzoic acid (C_6H_5COOH), an ionic model compound that absorbs UV. Benzoic acid was well dissolved in an alcohol, diethyl ether, and alcohol-buffered media, whereas the mobile phase most recommended is methanol:ammonium acetate buffer 5 m*M* (65:35) in which solubility occurs easily.

The results of this experiment are shown in Fig. 1, which depicts how benzoic acid with the same concentration (50 μg/ml) performs well in particular solvent systems. It was, of course, to be expected that each solvent interferes with absorption, suggesting that it is also a good test for estimating the solubility index when for each solvent maximum wavelength varies with units of absorbance.

The detection of UV–Visible can be performed using single λ optimized through various channels (usually of 2–8) or, alternatively, using program wavelength (if multiple λ) for chemical compounds with any similarity, according to the functional group, such as benzene compounds with aldehydes, acids, alcohols, olefins, hydrocarbon chain, and others. If fluorescence is used, particularly for compounds derived from a reaction or originated directly from structural clusters, a different λ excitation or λ emission can be programed over time using the appropriate channel. Therefore, programing wavelength for UV–Visible and fluorescent light detection can alternatively be combined with pumps to achieve better performance of the mobile phase using reversed-phase and normal-phase HPLC. This removes specific effects of the mobile phase by carrying out baseline correction for each detection system.[1–4]

To select the ideal λ, chromophore units of a particular compound need to be well recognized, such as conjugated dienes coupled to an acid group ($\sigma \rightarrow \sigma^*$ and $\pi \rightarrow \pi^*$, respectively), since these are associated with electron valences C=C, C–C, C=O, particularly those involved in the benzoic acid molecule.[1,3,5,6]

For comparative measurements, the spectral index for UV–Visible accompanied by the Merck solubility index data needs to be established. If these values cannot be found in the literature, it is usually recommended to take a spectrum using a spectrophotometer or, alternatively, using an HPLC–diode array detector. There are two ways of combining this information to achieve a better quantification system by adjusting distinct channels: single λ is recommended when only one compound is used, and program wavelength is recommended for any series of chemical compounds with certain similarities, requiring multiple channels.[1–3,5–7]

PRINCIPLES OF UV–VISIBLE DETECTION

The relationship between energy (E, electron volts) and λ, $E = h\nu/\eta\lambda$, produces a response to the detection criteria, giving an direct relationship between energy and frequency (ν) associated with the particular spectral refractive index of solution (n) resolving main bands around maximum wavelength and absorption coefficient. These two criteria are used as detection principles for obtaining identification and quantification procedures by way of a linear response range, using any mode of regression (linear and non-linear effects) analysis coupled with spectrophotometric and HPLC assays. As compounds dissolve easily below a concentration of 10 m*M*, they are particularly suitable for chemicals with a molecular mass of less than 2000 Da.[1,3,4]

The chromophore units consist of a series of chemical compounds that produce molecular excitement at an appropriate energy level (electron volts) and a certain frequency (ν), causing the excitation of the molecule from a base level (M) to an excited level ($M + h\nu \Rightarrow M^*$). Returning of the molecule to the same energy level ($M^* \Rightarrow M$) is demonstrated in the form of spectral bands in which chemical groups roughly correspond to the spectral plots of wavelength vs. units of absorbance. Because this system produces heat, there is no need for any relaxation mechanism as required for the fluorescence detector.[1,3,4]

Various types of chemical changes at the valence stage of molecules that occur in the spectral mode involving the UV–Visible spectrum are as follows: η (non-ligands), σ, and π linkages that cause excitation; heteroatom carbon chains (–C≡O–); carbon–carbon chains (–C–C–); and unsaturated carbon chains, such as conjugated dienes (–C≡C–) and trienes (–C≡C–), plus amidines (–C≡N–) and nitriles (–C≡N–). The main transitions usually involve *d* and *f* orbitals and electron charge transfer. Therefore, the level of absorption of various chromophore units is suitable for defining structural properties using conjugated series of units. The UV–Visible detection is the most commonly used method, although a sufficiently accurate chemical characterization has not yet been achieved mainly because of the poorly defined rules that link most organic compounds that absorb at 190–800 nm.[1,3,4]

The maximum wavelength criterion can be adequately defined as the level of energy that excites molecular orbits, bringing the electron valences to a transitional level and returning to the same baseline energy level, in turn giving rise to particular spectral bands between 190 and 400 nm (if UV mode) and between 400 and 800 nm (if visible mode). This allows for the characterization of both organic and inorganic chemical

compounds. An adequate identification requires other techniques to confirm the result, such as infrared (0.8–300 μm), scatter light, and nuclear magnetic resonance, which are comparatively non-destructive methods that produce an accurate characterization of distinct chemical compounds.[1–4]

HPLC coupled with a mass detector has been shown to be suitable for determining minor differences in molecular masses, and thus can satisfactorily replace the UV–Visible detection method. In this destructive detection system, ideal separation (resolution below 1.5) is not required for completing the validation of identification and quantification procedures. However, the HPLC–mass-mass technique is not cost-effective and is more suitable for research centers. However, at present, the HPLC–UV technique is easily affordable in both developed and developing countries.

Maximum wavelength is a suitable criterion for quantification because the main response, concentration vs. units of absorbance, depends on chromophore units and the molecular absorption coefficient. The HPLC equipment is usually linked to software that programs various channels of signal output in order to select the best maximum wavelength, which is usually not known. However, if it is well known then various channels can be used for evaluation of the absorbance ratio, which is an additional criterion for the identification procedure involving comparative measurements using ultrapure analytical standards and real samples. This topic is discussed in detail below in the section on "Identification and Quantification Procedures Using Distinct Standards."

Fig. 2 demonstrates the main changes brought about by the absorbance ratio at $\lambda = 226$ nm (Channel A), $\lambda = 235$ nm (Channel B), and other λ for a single-compound detection system. Therefore the response of standard maximum wavelength using an HPLC technique is provided if is confirmed by a suitable spectrophotometric assay for adjusting maximum value. In this experiment, the benzoic acid standard gives an absorbance ratio of about 1.15, rendering maximum wavelength = 226 nm. This value is appropriate for use in comparing results of complex matrices, such as foods, animal feed, and drugs, and has been established as a specific reference value for unknown samples and analytical standards.[2,5–10]

The multipoint concentration varying from nano- to micrograms in quantities allows for the determination of a concentration range that lies within the minimum limits of detection (LOD) and maximum limits of quantification (LOQ)—both detection and quantification being performed using the HPLC assays. The compounds with low molar absorption (below 100 moles/L/cm) produce a narrow range of quantification, while those with medium-to-high absorption (100–1000 moles/L/cm) give better results. Besides, higher concentrations (more than 10 m*M*) usually produce overloaded peaks, reflecting the extra-polation of the column capacity (k) and hence non-ideal conditions for adequate quantification. An example of this case, particularly concerning partial validation, is depicted in Fig. 2.[1–4]

Any quantitative experiment at a particular λ (obtained from an HPLC technique and confirmed by a spectrophotometer) and absorbance ratio should be confirmed after a blank run of the mobile phase; this is illustrated in Fig. 3. Non-ideal blanks always exhibit accentuated baseline drift. This requirement is sufficient to provide analytical reliability in terms of the basic criteria for the determination of LOD and LOQ in order to validate the procedure. In addition, increase in units of absorbance from 1 to 2000 milliunits depends on an isolated threshold. If the solubility of the solvents involved in the mobile phase is good, then care should be taken with maximum wavelength when minor changes are performed using both HPLC and spectrophotometric assays.

Fig. 4 shows that benzoic acid depends on the pH of the ammonium acetate/methanol buffer (pH 4.4–5.1), providing effective reduction for a particular separation (retention time decreased from 8.0 to 3.4 min) in addition to decrease in asymmetry (2.32 to 1.81). The main effect on absorption, including that affecting the separation property, is as yet unknown. The probable explanation is that the absorption coefficient tends to decrease during the ionic phase and that the intrinsic relationship is demonstrated by the pH of the medium. The mobile and stationary phases for ideal separation that provide the best characterization of interaction are as yet unknown, mainly because the asymmetry is too large, as can be seen in Fig. 4. It has been assumed that a particular composition of the mobile phase interferes with both the absorption coefficient and the adjusted retention time (k).

When a spectral plot is not available, the absorbance ratio method is a satisfactory method for characterizing a real sample, using both spectrophotometric and HPLC assays. In addition, better performance needs to be achieved in carrying out advanced experiments, such as solid-phase extraction and other purification techniques coupled with HPLC quantification, in order to improve the separation properties.[1,3,4]

To improve any quantification system, it should be established that all points on the standard curve are injected in a similar loop according to rising or random order, and at least five points should be traced between minimum (LOD) and maximum (LOQ) concentrations. After defining the linear range response for particular compounds, a comparative analysis should be carried out for a similar group of samples and products in accordance with the regression analysis ($R^2 \geq 0.99$). For example, foods and animal feed having differences in lipid and water content and samples exploiting natural differences should arrive differently at this single identification and quantification procedure.[1–9]

An analytical approach has been developed that determines fat-soluble vitamins[2,7–10] in order to satisfy the ideal

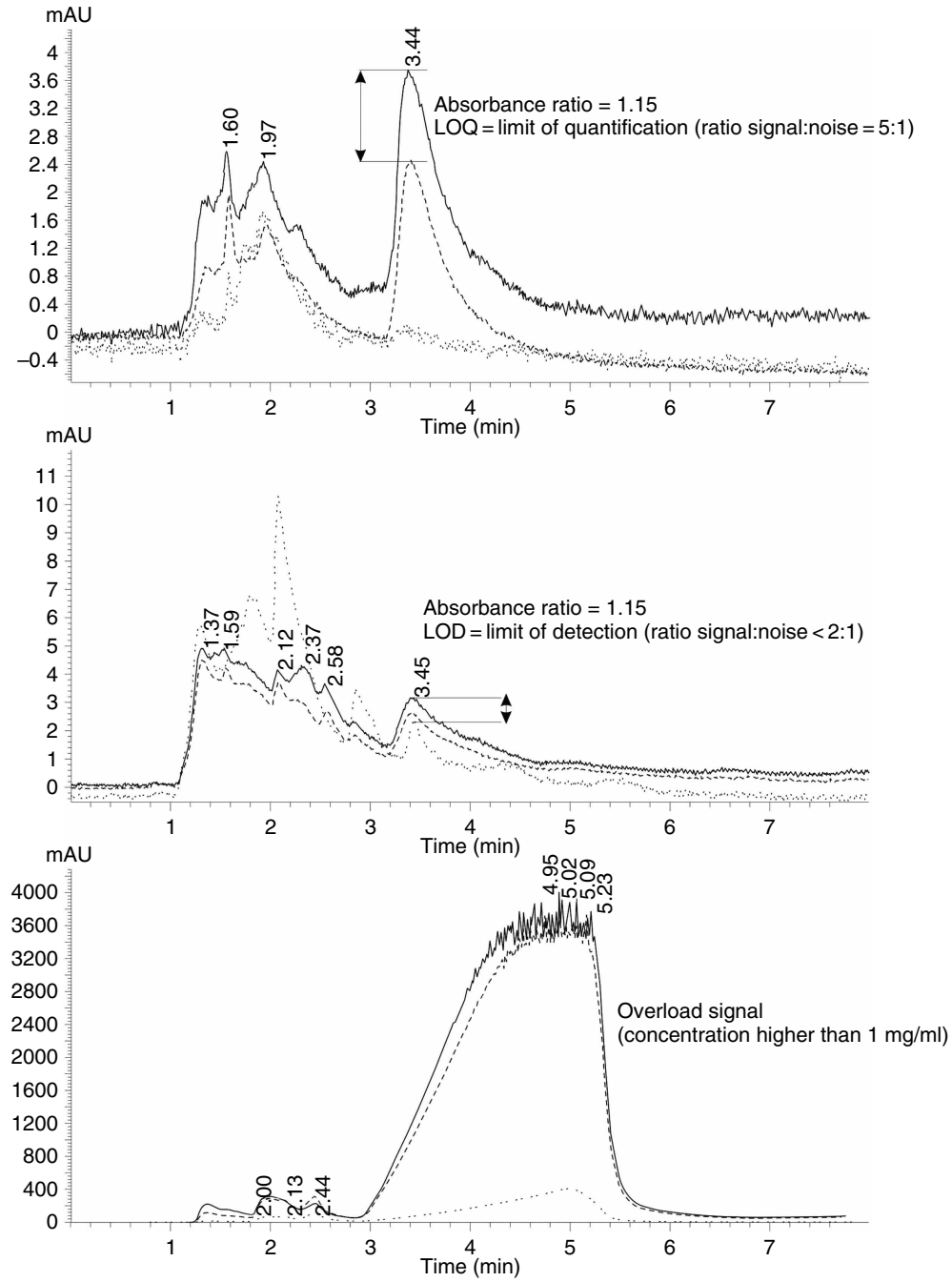

Fig. 2 Adjusting detection conditions of benzoic acid at different λ. Column: SPHERISORB ODS-2, 150 × 3.2 mm, 5 μm; mobile phase: 5 m*M* ammonium acetate:methanol (65:35); flow rate: 0.5 ml/min. Key: $\lambda = 226$ nm, —; $\lambda = 235$ nm, - - - -; $\lambda = 280$ nm, ...

requirements for using UV detection directly through programing wavelength. This has been concluded from numerous experiments using the new protocol for extraction in combination with maximum wavelength for each vitamin compound, which has adequately provided complete validation for individual groups of foods.[2,7–9]

To maximize the analytical performance of HPLC–UV methods, detection programing of various compounds that exhibit a fat-soluble vitamin function can be carried out. Improvements have recently been made to specific methods and other steps involved in optimizing the saponification conditions, thereby making it possible to separate, using the reversed-phase HPLC, majority of compounds that contain fat-soluble vitamins. And following the saponification procedure, only a minority of compounds can be detected. Irrespective of whether they use saponification or

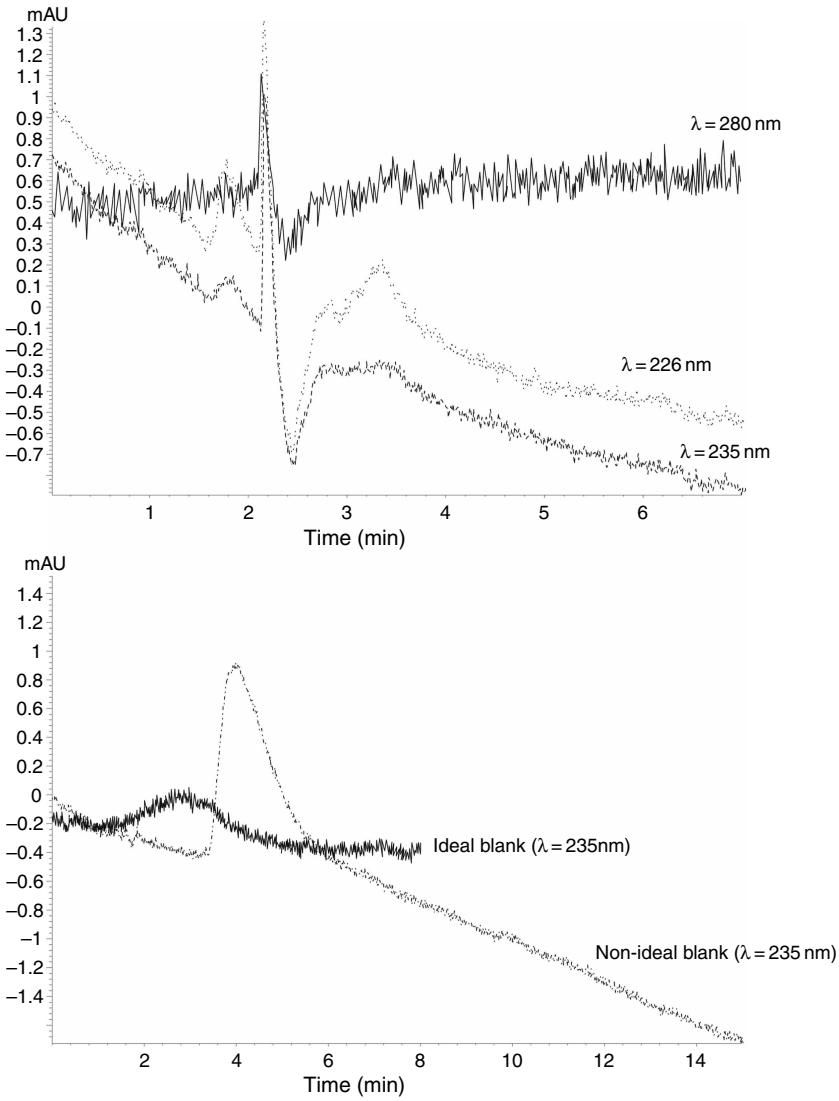

Fig. 3 Adjusting blank conditions of a particular mobile phase at different λ. Column: SPHERISORB ODS-2, 150 × 3.2 mm, 5 μm; mobile phase: 5 m*M* ammonium acetate:methanol (65:35); flow rate: 0.5 ml/min. Key: $\lambda = 226$ nm, —; $\lambda = 235$ nm, - - - - .

not, these methods may provide an estimate of the real quantities of fat-soluble vitamins. Chemical compounds containing fat-soluble vitamins belong to distinct groups of chemicals, such as alcohols, olefins, steroids, and quinones. Alcohol forms of vitamins A and E and their respective esterified forms are separate and can be quantified using an extraction procedure without saponification (Fig. 5A), while non-esterified vitamins A and E, D_2, D_3, and K_1, produce a good resolution of the vitamin value once the saponification procedure has been optimized[7–10] (Fig. 5B).

An improvement in identification and quantification procedures for fat-soluble vitamins in milk can be achieved through microcolumn associated with solid-phase extraction,[11] which, when coupled with the mass-mass–HPLC by chemical ionization at atmospheric pressure, can improve the resolution of D_2 and D_3 in the presence of vitamins A and E.[12] By contrast, if the vitamin is an ionic compound such as water-soluble vitamins, electrospray ionization is recommended.[13] Studies using a scattering radiation detector have proved to be less selective and to have poor resolution when compared to UV detection performed on isomers α- and γ-tocopherols.[14]

Since UV–Visible and fluorescence detection can determine the valence electrons of particular compounds, there is a particular λ for each compound. If detection using various channels is suggested, it is likewise recommended that maximum wavelength should be adjusted before program wavelength is being defined. This recommendation should be applied only to specific channels.

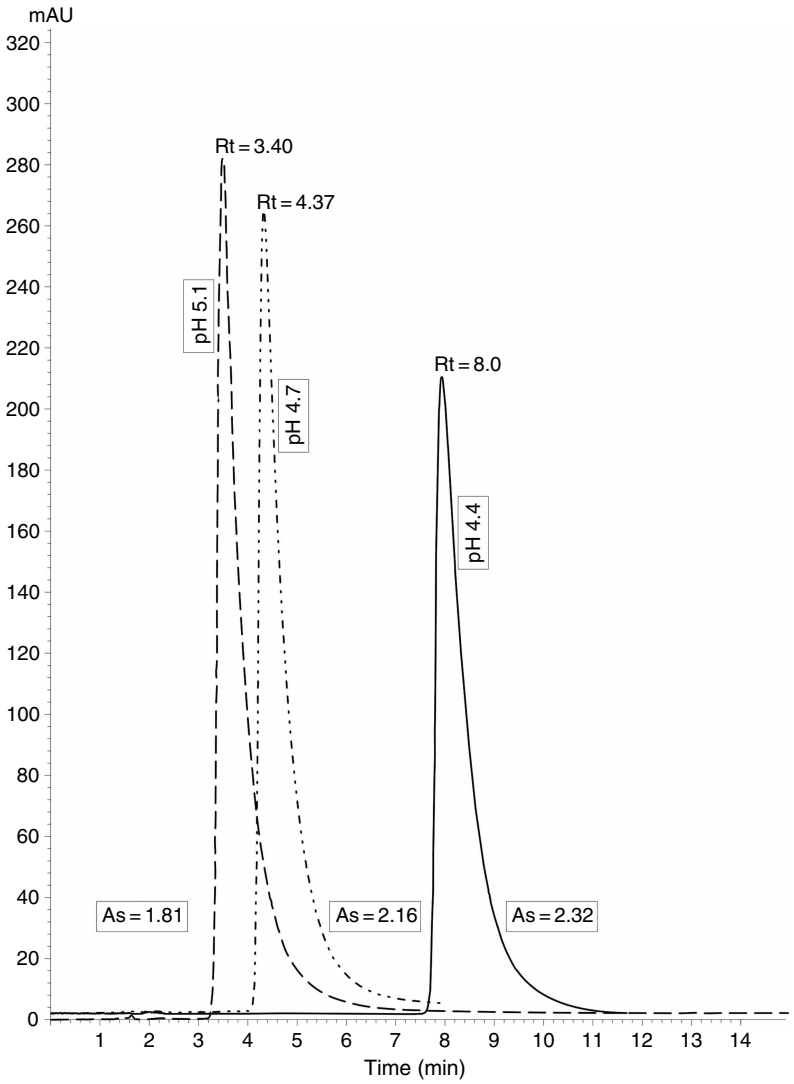

Fig. 4 Influence of pH mobile phase on k (adjusted retention time) of benzoic acid at λ = 226 nm. Column: ODS-2: 150 × 3.2 mm, 5 μm; mobile phase: 5 m*M* ammonium acetate:methanol (65:35); flow rate: 0.5 ml/min. Key: As = Asymmetry, Rt = Retention time.

SINGLE AND PROGRAM WAVELENGTH USING A COMPLEX MATRIX

The main problems regarding the baseline drift result instead are resulting from an incoherent signal that can be related to a particular mobile-phase composition, such as acid, acid buffer, acidified water, ionization agent, air bubbles, unidentified compounds, a failure of the reference material, excessive signal noise, and the natural difficulty of most biological materials to be free of compounds that absorb UV, among other factors.[1–4] Therefore, particular attention should be paid to sensitivity while using the units of absorbance described in the original method (that firstly described maximum wavelength). When developing a new protocol for the selection of a better mobile phase, efforts should be made to ensure that analytical standards are appropriately quantified using a blank run, in which the mobile phase passes through the column, in order to correct troubleshoot by monitoring baseline drift at a different threshold.

In this case, experiments were carried out and ideal and non-ideal conditions were outlined in order to initiate quantitative experiments, as shown in Fig. 6. Depending on the threshold selected (about 1 mAU), one blank run was carried out under ideal conditions for quantification of LOD and LOQ by way of a linear response range. The principal effects on the separation of vitamins A and E led to doubts regarding some chromatograms because of the non-ideal drift. The accommodation effect on the column may be an explanation for this.

An appropriate calibration of blank experiments has been performed using biological materials free of analytical compounds, such non-fatty milk, thereby making it necessary to certify these values by contrasting to reference materials too.[1,2] This is commonly found in the case of feedstuffs and pharmaceuticals, while it is less frequent in clinical chemistry, biological fluids, and other materials such as foods. Suitable and selective reference materials are required to simultaneously

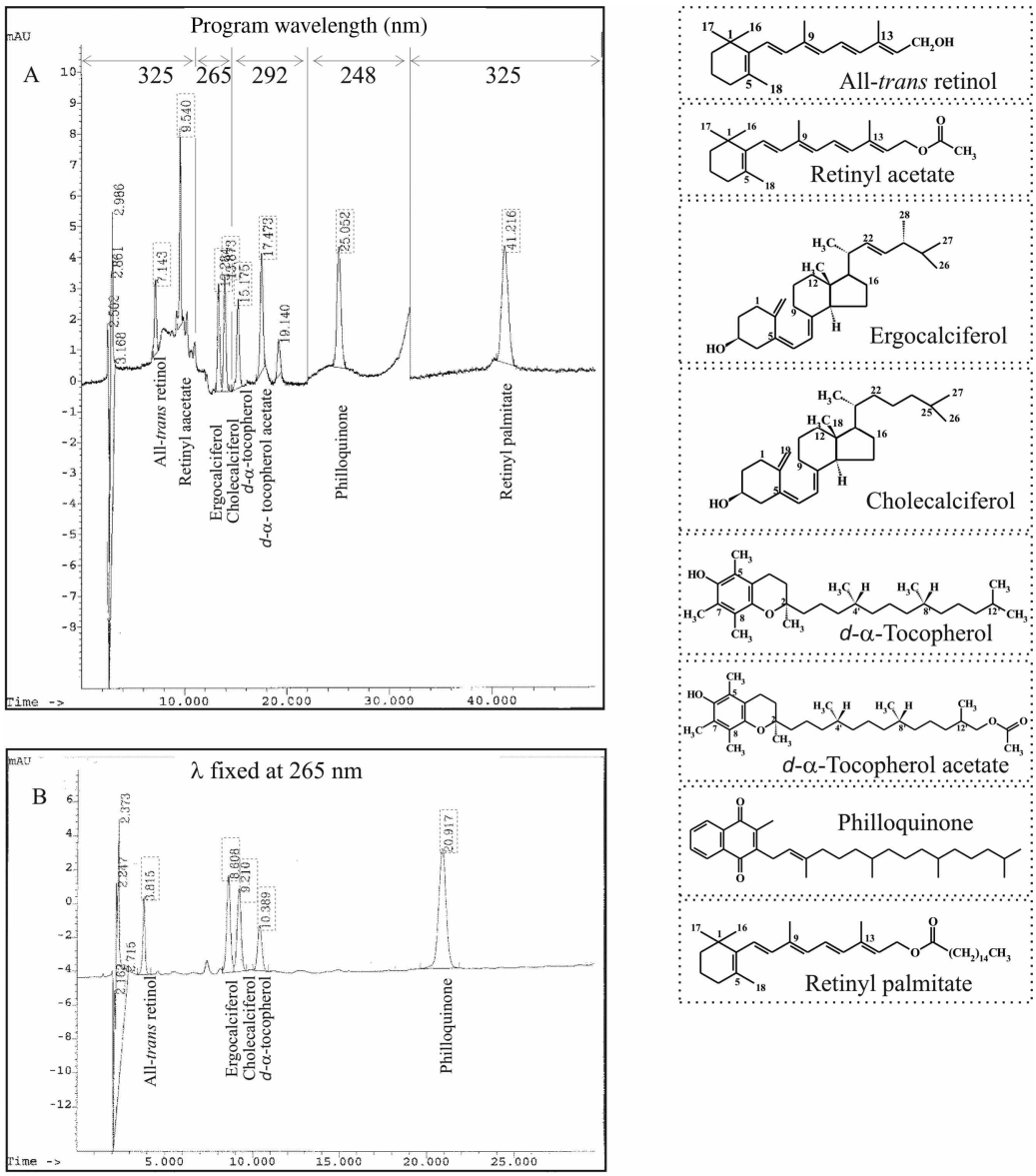

Fig. 5 Adjusted program wavelength in order to obtain detection of fat-soluble vitamins. A, Included esterified chemical forms (flow rate: 1.1 ml/min); B, Only non-esterified chemical forms (flow rate: 1.4 ml/min). Column: SPHERISORB ODS-2, 250 × 4.6 mm, 5 μm; mobile phase: methanol:water (99:1).

determine precision and accuracy. In addition, precision can be defined for particular groups of products. However, disappointing results have been obtained with certain biological materials, particularly those that are more heterogeneous than analytical standards required for some stages in the preparation of samples, such as dissolution, chemical reactions to remove interference, and chemical reactions needed to achieve a good level of purification.[1,5,6]

Different samples or matrices require suitable adaptation to the quantification system, such as fat-soluble vitamin determination in serum,[15,16] human milk,[16–18] nutritional supplements,[18] and infant formulas,[19] using external and internal standards. In fact, the complexity of matrices reveals innumerable compounds that differ in terms of modes of spread and linkage, such as liquid, semiliquid, and solid materials.[19–22] For example, liquid samples have shown high oxi-reduction potential compared to solid samples, while both have shown cross-linkage of heterogeneous compounds. Good dissolution in the mobile phase is always linked to an ideal separation technique when it is subjected to liquid–liquid and solid–liquid extraction, both of which are recommended to account for differences between matrices. When simultaneously linked to reversed-phase and normal-phase HPLC, from ideal analytical separation, both the

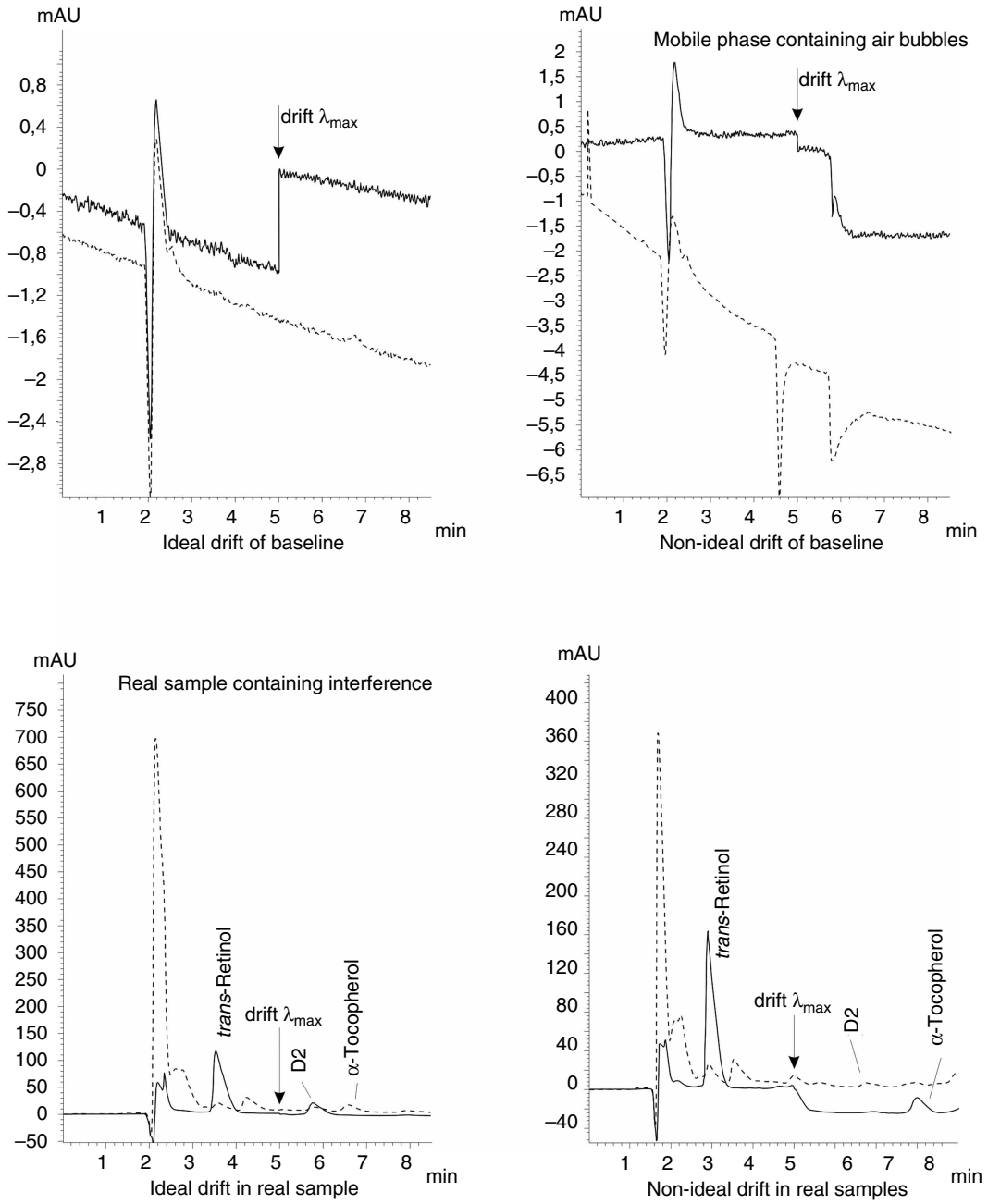

Fig. 6 Adjusted detection conditions in two channels (if multiple λ). Column: SPHERISORB ODS-2, 150 × 3.2 mm, 5 μm; mobile phase: methanol; flow rate: 0.5 ml/min. Key: Program wavelength = 325 nm until 5 min; from 5.01 min, λ = 292 nm, —; λ fixed at 265 nm, - - - -.

extraction methods have been shown to be compatible with the quantification, which is recommended as an additional criterion for accuracy studies.[1–4,22–25]

Interferences such as air bubbles, a mobile-phase composition, and a poorly conditioned column should be corrected before removing matrix interference, which subsequently helps in developing an appropriate procedure for extraction. It is worth considering the favorable conditions for detection: proper λ adjustment to mobile-phase interference.[1–4]

A few articles claim that chemical derivations are easy and must be done prior to the analytical separation procedure. In particular, there is a need for complete knowledge of the steps in the chemical reactions (i.e., the interaction between reagents and products) that helps in monitoring the characterization of compounds through a specific separation procedure. In the case of particular applications using HPLC techniques, unsatisfactory outcomes occur because unstable products (reduced or oxidized, neutralized or poorly dissociated

near pK_a) increase the capacity of buffering and dissociation,[1–6] thus affecting the separation properties.

To verify the suitability of an approach that ensures transferability through recovery rates for complete validation of the extraction and quantification steps, high levels of accuracy should always be accompanied by ideal repeatability in different samples combining precision and accuracy. Good recovery rates (higher than 80%) usually provide a rough indication of accuracy, and may therefore be distinguished in particular matrices, at least at two distinct points (low and high level). A reference material is also an additional criterion for complementary accuracy studies, providing complete validation.[1–3,22–25]

An extensive analytical approach can be developed using applications for distinct matrices. Earlier validation

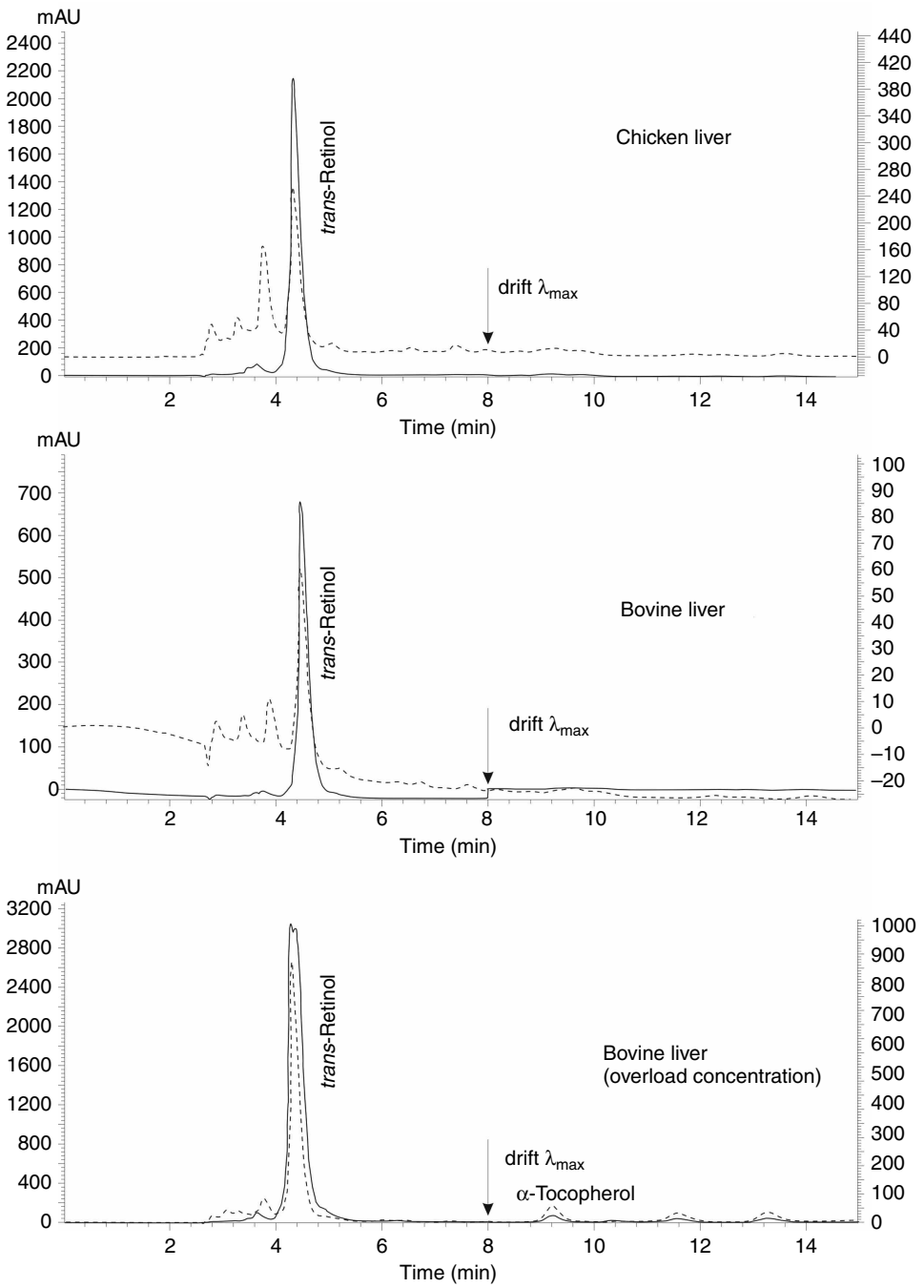

Fig. 7 Typical chromatograms of different complex matrices. Column: SPHERISORB ODS-2, 250 × 4.6 mm, 5 μm; mobile phase: methanol; flow rate: 1.0 ml/min. Key: Program wavelength = 325 nm until 8 min; from 8.01 min, λ = 292 nm, —; λ fixed at 265 nm, - - - -.

experiments can be used to ascertain the extent of transferability of a particular extraction, involving a complex matrix such as animal liver (see Fig. 7) and human milk, using fat-soluble vitamins as reference.[2,8–10,16,18–22] Recent studies in our laboratory that examined different stages of human lactation have shown that fat-soluble vitamins vary during transition of colostrums to mature milk,[22] as can be seen in Fig. 8. In this case representing a few obstacles to the quantitative analysis, which simultaneously evaluated the absorbance ratio (Table 1) and adjusted retention time (Table 2), confirming suitable transferability involving extraction and quantification steps. Therefore, it is beneficial to use a particular extraction method, initially developed for lacteal matrices and now extended to other matrices, as recommended by publications on infant formulae and fortified milk,[19] cheese and salami,[20] cooked meals and milk products,[21] and transition of colostrums to mature human milk.[22]

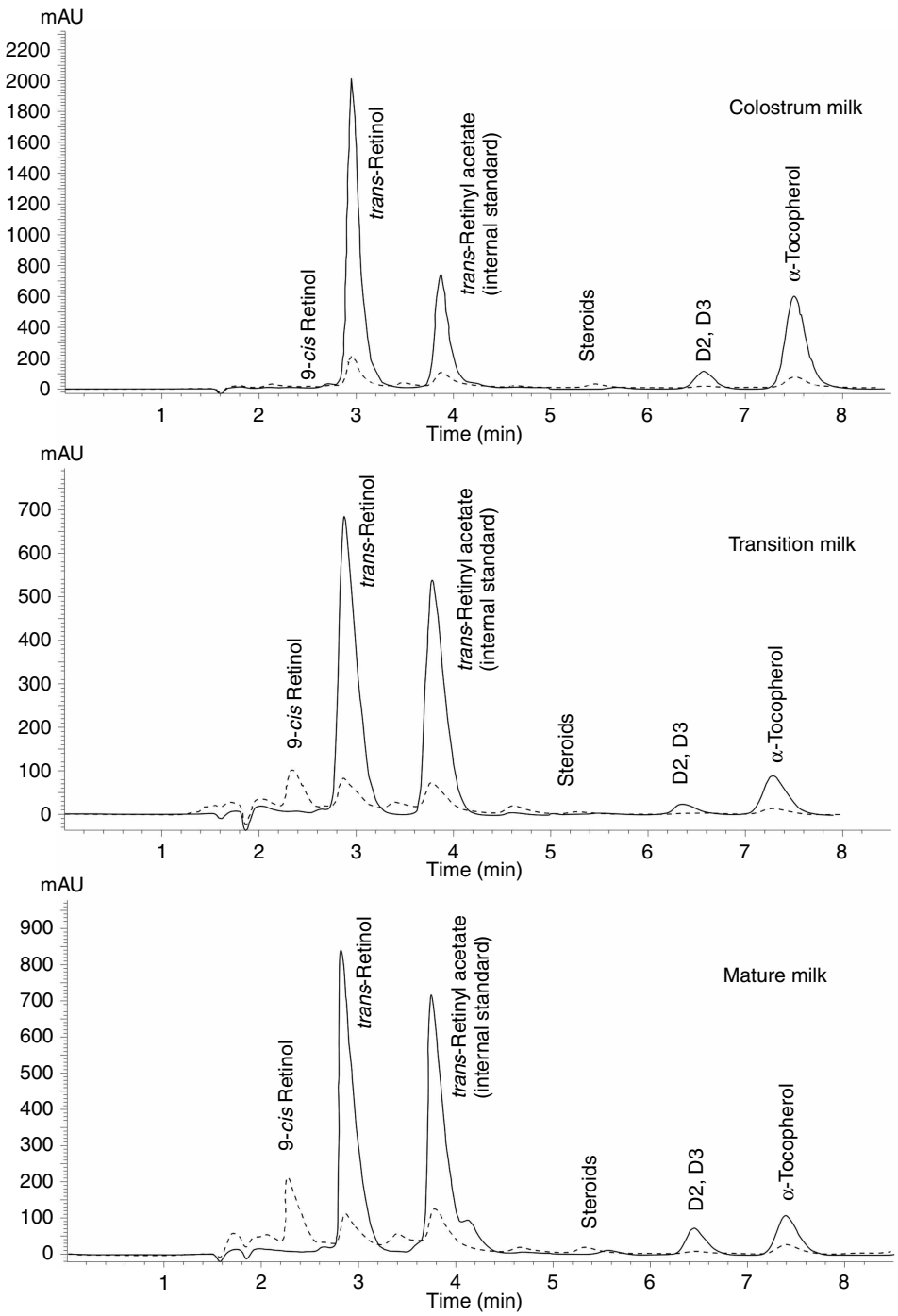

Fig. 8 Typical chromatograms of fat-soluble vitamins from different phases of lactation obtained from primiparous mothers. Column: ODS-2, 150 × 3.2 mm, 5 μm; mobile phase: methanol; flow rate: 0.5 ml/min. Key: Program wavelength = 325 nm until 5 min; from 5.01 min, λ = 292 nm, —; λ fixed at 265 nm - - - -.

Table 1 Absorbance ratio as a criterion for separation and identification of vitamins A and E at maximum wavelength 325 and 292 nm, respectively.

Treatment of standards/samples	λ_{max} (nm)	Mean ± SD	Min – max	Mode	Median
All standards ($N = 36$)	325	10.26 ± 0.69	6.93 – 11.93	10.00	10.00
	292	6.68 ± 1.54	4.00 – 10.42	7.50	7.00
Primiparous mothers ($N = 27$)	325	9.85 ± 0.89	7.63 – 11.93	9.80	9.85
	292	6.99 ± 1.35	4.23 – 9.00	7.50	7.43
Multiparous mothers ($N = 27$)	325	10.18 ± 0.47	8.66 – 10.97	10.25	10.17
	292	7.98 ± 1.03	6.00 – 10.42	8.04	8.07

All standards and samples were injected in triplicate.

IDENTIFICATION AND QUANTIFICATION PROCEDURES USING DISTINCT STANDARDS

Recent advances in the HPLC technique are highly recommended for identification. These include infrared spectroscopy coupled with Fourier transform,[1,3] light scattering,[14] or electrochemical detectors.[1,3,4] It is of particular interest that detector systems cover most organic and inorganic compounds. They require an extremely stable power supply, but without exhaustive chemical derivation requirements. The most useful non-destructive detectors are UV–Visible and fluorescence, while UV is less selective. It should be pointed out that a close association between detection and quantification systems suggests that it would be appropriate to combine these systems with accurate rules.[1,2,4]

Usually more than two channels are required to determine the ideal quantification procedure, and the use of external and internal standards is the most highly recommended way of producing the calibration curve. The particular example of benzoic acid was taken to demonstrate how LOD was determined (analytical signal-to-noise ratio $\leq$2:1; Fig. 2) in combination with the low variability observed between replicate analyses. Fig. 2 also clearly illustrates the establishment of minimum and maximum concentrations in order to define the response linear range for each compound using the UV detection system involving single λ. Comparative measurements were taken to complete quantitative experiments exhibited in Figs. 3–5, using single and program wavelength.

Given the complexity of the biological matrix, all experiments that are recommended for primary validation[23–24] and system suitability[25] should be carried out. In addition to criteria for suitable transferability, absorbance ratio is a complementary criterion that has been suggested for comparative measurements of distinct matrices using statistical parameters. Therefore the absorbance ratio taken directly from the peak (Table 1) and adjusted retention time (Table 2) measured at maximum wavelength have worked as complementary criteria for the identification procedure. When the absorbance ratio is clearly established, it is recommended that recovery rates should be determined.[23–25] The choice of matrix should have specific criteria according to the complexity, such as lipid and water content and nutrient content of a sample, as validated in our experiments using lacteal matrices of different chemical compositions.[2,7–10,22–25] Values of different samples should approximate to those established for distinct standards as shown in Tables 1 and 2.

In addition, the absorbance ratio has been shown to be a satisfactory substitute for the diode array detector because it monitors the intrinsic variability of methods, allowing for the development of a new protocol for distinct matrices. It should be borne in mind that minor variations required in the λ obviously depend on grooves originating from a prism or comb, which are the principal determining factors

Table 2 Adjusted retention time (k) as a criterion for separation and identification of vitamins A and E at maximum wavelength 325 and 292 nm, respectively.

Treatment of standards/samples	λ_{max} (nm)	Mean ± SD	Min – max	Mode	Median
All standards ($N = 36$)	325	0.64 ± 0.03	0.57 – 0.80	0.66	0.65
	292	3.14 ± 0.20	2.70 – 3.64	2.87	3.21
Primiparous mothers ($N = 27$)	325	0.62 ± 0.03	0.57 – 0.69	0.61	0.62
	292	3.00 ± 0.22	2.70 – 3.45	3.00	2.92
Multiparous mothers ($N = 27$)	325	0.63 ± 0.03	0.57 – 0.68	0.68	0.65
	292	3.13 ± 0.18	2.82 – 3.41	3.12	3.12

All standards and samples were injected in triplicate.

Table 3 Measurements of linear regression analysis obtaining different quantification methods involving external (ES) and internal standards (IS).

Pooled calibration curve	λ_{max} (nm)	Correlation coefficient *R*	Angular coefficient *B*	Linear coefficient *A*
Random order (ES)	325	0.9998	317.91650	138.28900
	292	0.9998	17.24770	75.96220
Rising order (ES)	325	0.9997	313.43390	101.04920
	292	0.9998	16.81200	64.65770
Internal standard (IS)	325	0.9991	0.05436	0.02564
	292	0.9992	0.00295	0.01388

for the variability achieved when quantitative procedures are used.[1–4,7,8] Lower resolution for maximum wavelength can be achieved using spectrophotometer-type filter optics in contrast in order to get maximum efficiency make use of a diffraction comb (usually with more than 2000 grooves), leading to an appropriate increase in the resolution of wavelength.[1,3,4]

Our recent research, in which multiparous and primiparous donors were compared during the initial phase (up to the 30th day) of human lactation, the quantities of fat-soluble vitamins were determined in colostrums, transition milk, and mature milk.[10,22] It was not possible to trace the recovery rate, because biological material was obtained in minimal quantities, especially at the colostrum phase. In addition, such complexity was bypassed to the absorbance ratio and adjusted retention time (k), both being used as complementary criteria for identification.

Table 1 shows similar variations in the absorbance ratio measured at maximum wavelength for vitamins A (325 nm) and E (292 nm), with the alternative λ set at 265 nm. Minor differences were also observed when real samples were compared to analytical standards using similar statistical parameters (such as mean, mode, and median), thereby providing sufficient transferability for a new matrix. Table 2 shows that the adjusted retention time (k) measured at maximum wavelength for vitamins A (325 nm) and E (292 nm) were sufficient to distinguish different materials. Minor differences were registered using statistical parameters, suggesting good transferability.

Standardization of areas at different peaks or a single normalization is the oldest technique. It differs greatly from the use of the external standard, although both require minimum disturbance of the baseline and reliable resolution of maximum wavelength. On the other hand, the internal standard requires the addition of particular compounds and it is usually difficult to determine what kind of compound is most appropriate and which steps should be added. It is therefore worth choosing the best procedure before determining which quantification system should be applied.[23–25]

Table 3 provides measurements of the regression analysis, allowing for the selection of the best procedure when comparing injection order, either random or rising order, using external and internal standards. However, no significant differences were registered in any of the modes evaluated. In this case, it was expected that the residual effect on the column would mask the particular way of constructing the calibration curve, especially when compared to the random injection order, because of the effect on the k value.

The addition of a standard is less used because it is difficult to achieve a matrix free of analytical compounds that absorb UV–Visible whereas any extraction procedure steps usually containing distinct chromophores that increase and modify parameters of absorption.

CONCLUSIONS

The outcomes of the principles of the UV–HPLC detection have been outlined and discussed, mainly those involving interferences of standards and complex matrices.

The single λ (maximum, or other set) and programed maximum wavelength criteria are the main ways of improving the performance of UV detection, particularly when linked to the absorbance ratio, recommended for use when coupled with a spectrophotometer or an HPLC.

Contemporary ways of achieving complete validation have been identified and discussed: programed maximum wavelength, absorption coefficient, adjusted retention time, and absorbance ratio measured at different λ.

Operational problems, such as baseline shift, and different ways of building up and injecting the standards and different matrices have also been discussed.

UV–Visible detection always requires small steps to complete validation, such as using complementary criteria for suitable identification and quantification coupled with the HPLC technique.

ACKNOWLEDGMENT

I express my gratitude to the Central Analítica, Departamento de Química Fundamental, Universidade Federal de Pernambuco, for the use of the HPLC equipment (Agilent Technologies, Inc., California, U.S.A.).

REFERENCES

1. Snyder, L.R.; Kirkland, J.J.; Glajch, J.L. *Practical HPLC Method Development*, 2nd Ed.; John Wiley & Sons: New York, 1997.
2. Paixão, J.A.; Stamford, T.L.M. Vitaminas lipossolúveis em alimentos—uma abordagem analítica. Química Nova **2004**, *27* (1), 96–105.
3. Christian, G.D. *Analytical Chemistry*, 5th Ed.; John Wiley & Sons: New York, 1994.
4. Skoog, D.A.; Leary, J.J. *Principles of Instrumental Analysis*, 4th Ed.; Harcourt Brace College Publisher: New York, 1992.
5. Ferreira, I.M.P.L.V.O.; Mendes, E.; Brito, P.; Ferreira, M. Simultaneous determination of benzoic acid and sorbic acids in quince jam by HPLC. Food Res. Int. **2000**, *33*, 113–117.
6. Mota, F.J.M.; Ferreira, I.M.P.L.V.O.; Cunha, S.C.; Oliveira, M.B.P.P. Optimisation of extraction procedures for analysis of benzoic and sorbic acids in foodstuffs. Food Chem. **2003**, *82*, 469–473.
7. Paixão, J.A. *Desenvolvimento de uma metodologia analítica para extração e quantificação de vitaminas lipossolúveis em matrizes lácteas*. Tese de Doutorado, Universidade Federal de Pernambuco, Departamento de Nutrição, Programa de Pós-Graduação em Nutrição, 2002; 80 pp.
8. Paixão, J.A.; Campos, J.M. Determination of fat soluble vitamins by reversed-phase HPLC coupled with UV detection: A guide to the explanation of intrinsic variability. J. Liq. Chromatogr. Relat. Technol. **2003**, *26* (4), 627–650.
9. Paixão, J.A.; Stamford, T.L.M. Lacteal matrices: A single guide for extraction and quantification of fat soluble vitamins. J. Liq. Chromatogr. Relat. Technol. **2002**, *25* (2), 217–239.
10. Campos, J.M. *Perfil dos níveis de vitaminas A e E em leites de doadoras primíparas e multíparas em bancos de leite humano*. Dissertação de mestrado, Universidade Federal de Pernambuco, Departamento de Nutrição, Programa de Pós Graduação em Nutrição, 2005; 73 pp.
11. Gomis, D.B.; Fernandez, M.P.; Alvarez, M.D.G. Simultaneous determination of fat-soluble vitamins and provitamins in milk by microcolumn liquid chromatography. J. Chromatogr. A, **2000**, *891*, 109–114.
12. Heudi, O.; Trisconi, M.-J.; Blake, C.-J. Simultaneous quantification of vitamins A, D_3 and E in fortified infant formulae by liquid chromatography–mass spectrometry. J. Chromatogr. A, **2004**, *1022*, 115–123.
13. Mittermayr, R.; Kalman, A.; Trisconi, M.-J.; Heudi, O. Determination of vitamin B_5 in a range of fortified food products by reversed-phase liquid chromatography–mass spectrometry with electrospray ionization. J. Chromatogr. A, **2004**, *1032*, 1–6.
14. Romeu-Nadal, M.; Morera-Pons, S.; Castellote, A.I.; López-Sabater, M.C. Determination of γ- and α-tocopherols in human milk by a direct high performance liquid chromatographic method with UV–Vis detection and comparison with evaporative light scattering detection. J. Chromatogr. A, **2006**, *1114*, 132–137.
15. Quesada, J.M.; Mata-Granados, J.M.; Luque de Castro, M.D. Automated method for the determination of fat soluble vitamins in serum. J. Steroid Biochem. Mol. Biol. **2004**, *89–90*, 473–477.
16. Schweigert, F.J.; Bathe, K.; Chen, F.; Buscher, U.; Dudenhausen, J. Effect of the stage of lactation in humans on carotenoids levels in milk, blood plasma and plasma lipoprotein fractions. Eur. J. Nutr. **2004**, *43*, 39–44.
17. Macias, C.; Schweigert, F.J. Changes in the concentration of carotenoids, vitamin A, α-tocopherol and total lipids in human milk throughout early lactation. Ann. Nutr. Metabol. **2001**, *45*, 82–85.
18. Iwase, H. Simultaneous sample preparation for high performance liquid chromatographic determination of vitamin A and β-carotene in emulsified nutritional supplements after solid phase extraction. Anal. Chim. Acta **2002**, *463*, 21–29.
19. Perales, S.; Delgado, M.M.; Alegria, A.; Barberá, R.; Farré, R. Liquid chromatography determination of vitamin D_3 in infant formulas and fortified milk. Anal. Chim. Acta **2005**, *543*, 58–63.
20. Perreti, G.; Marconi, O.; Montanari, L.; Fantozzi, P. Rapid determination of total fats and fat-soluble vitamins in Parmigiano cheese and salami by SFE. Lebensm. Wissen. und Technol. **2004**, *37*, 87–92.
21. Escrivá, A.; Esteve, M.J.; Farré, R.; Frígola, A. Determination of liposoluble vitamins in cooked meals, milk and milk products. J. Chromatogr. A, **2002**, *947*, 313–318.
22. Campos, J.M.; Paixão, J.A.; Ferraz, C. Fat-soluble vitamins in human lactation. Int. J. Vitam. Nutr. Res. **2007**, *77* (5), 303–310.
23. Jenke, H.E. Chromatographic method validation: A review of current practices and procedures. I. General concepts and guidelines. J. Liq. Chromatogr. Relat. Technol. **1996**, *19* (5), 719–736.
24. Jenke, H.E. Chromatographic method validation: A review of current practices and procedures. II. Guidelines for primary validation parameters. J. Liq. Chromatogr. Relat. Technol. **1996**, *19* (5), 737–757.
25. Jenke, H.E. Chromatographic method validation: A review of current practices and procedures. III. Ruggedness, revalidation and system suitability. J. Liq. Chromatogr. Relat. Technol. **1996**, *19* (5), 1837–1857.

van't Hoff Curves

Raymond P.W. Scott
Scientific Detectors Ltd., Banbury, Oxfordshire, U.K.

INTRODUCTION

van't Hoff curves are strictly graphs of log[distribution coefficient (K)] against the reciprocal of the absolute temperature, but, in practice, log[capacity factor (k')] or log [corrected retention volume (V')] are used as alternatives (see *Plate Theory*, p. 1829). van't Hoff curves can be very informative and explain both the nature of the separation and the importance of temperature in achieving an adequate resolution. An example of two van't Hoff curves relating log(V') against $1/T$ for two different types of distribution system are shown in Fig. 1. The two curves are highly exaggerated for the sake of emphasis and clarity.

DISCUSSION

It is seen that distribution system A has a large enthalpy value ($\Delta H_0/RT$) and a low-entropy contribution [($\Delta S_0/R$)-V_S]$_A$ The large value of ($\Delta H_0/RT$)$_A$ means that the distribution is *predominantly controlled by molecular forces*. The solute is preferentially distributed in the stationary phase as a result of the interactive forces between the solute molecules and those of the stationary phase being much greater than the interactive forces between the solute molecules and those of the mobile phase. Because the change in enthalpy is the major contribution to the change in free energy, *the distribution, in thermodynamic terms, is said to be "energy driven."*

In contrast, it is seen that for distribution system B, there is only a small enthalpy change ($\Delta H_0/RT$)$_B$, but in this case, a high-entropy contribution [($\Delta S_0/R$)-V_S]$_B$. This means that the distribution is *not* predominantly controlled by molecular forces. The entropy change reflects the degree of randomness that a solute molecule experiences in a particular phase. The more random and "more free" the solute molecule is to move in a particular phase, the greater its entropy. A large entropy change means that the solute molecules are more restricted or less random in the stationary phase in system B. This loss of freedom is responsible for the greater distribution of the solute in the stationary phase and, thus, greater solute retention. Because the change in entropy in system B is the major contribution to the change in free energy, *the distribution, in thermodynamic terms, is said to be "entropically driven."*

Separations dominated by size exclusion are examples of entropically driven systems. Chromatographic separation need not be exclusively "energetically driven" or "entropically driven"; in fact, very few are. In most cases, retention has both "energetic" and "entropic" components, which, by careful adjustment, can be made to achieve very difficult and subtle separations.

It is very rare, if at all, in GC that two solutes have identical standard free energies. Even when considering enantiomeric pairs, they will have differing standard free enthalpies and standard free entropies and, consequently, differing standard free energies. Accepting these facts, the van't Hoff curve provides critical information for the chromatographer. If two solutes (e.g., a pair of enantiomers) have different standard free enthalpies, then the linear van't Hoff curves must have different slopes and, therefore, they must intersect. As a consequence, there must be a temperature where the two curves intersect and there will be a specific temperature at which the two solutes must coelute. The coelution temperature may, or may not, be in the practical operating range of the chromatographic system, but it is clear that temperature is an essential operating variable. Temperature does not merely control the elution rate and allow the analysis to be achieved more rapidly, but also critically determines the column selectivity for closely eluting peaks. In fact, this is also true for LC.

There are some examples in the literature that purport to show non-linear van't Hoff curves. Taking an example from LC, a graph relating log(V_r') against $1/T$ for solutes eluted by a mixed solvent from a reverse bonded phase will often be non-linear. However, it must be emphasized that graphs relating log(V_r') against $1/T$ can only be termed van't Hoff curves, and be treated as such if they apply to an *established distribution system*, where the nature of *both* phases does not change with *temperature*. If a mixed-solvent system is employed as the mobile phase, the *solvents themselves* are distributed between the two phases *as well* as the solute. Depending on the actual concentration of solvent, as the temperature changes, so may the relative amount of solvent adsorbed on the stationary-phase surface, and so the nature of the distribution system will also change. Consequently, the curves relating log(V_r') against $1/T$ may not be linear and, as the distribution system is varying, will not constitute van't Hoff curves. This effect has been known for many years and an early example is afforded in some early work carried out by Scott and Lawrence,[1] who investigated the effect of water vapor

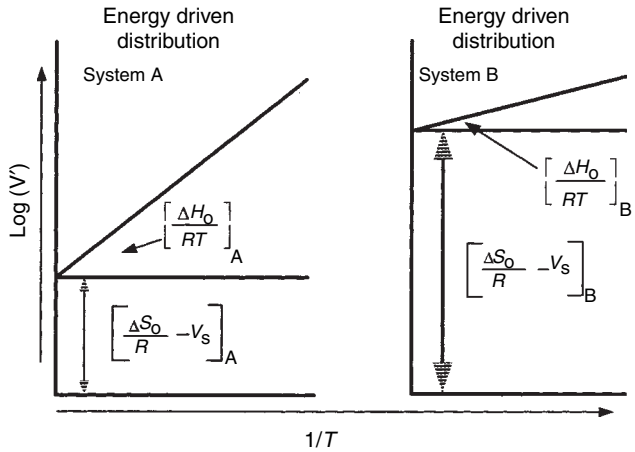

Fig. 1 van't Hoff curves for two distribution systems.

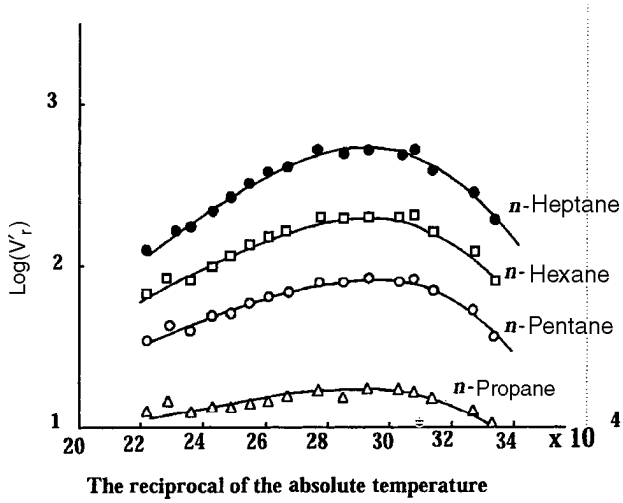

Fig. 2 Graphs of $\log(V_r')$ against $1/T$ for some *n*-alkanes separated on water-vapor-moderated alumina.

as a moderator on the surface of alumina in some gas–solid separations of some *n*-alkanes. Examples of the results obtained by those authors are shown in Fig. 2. The alumina column was moderated by a constant concentration of water vapor in the carrier gas. As the temperature of the distribution system was increased, less of the water moderator was adsorbed on the surface. As a consequence, the alumina became more active and the distribution system changed. Thus, initially, as the temperature was raised, the retention volume of each solute increased. When all the water was desorbed and the alumina surface assumed a constant interactive character and the distribution system also remained the same, the retention volume began to fall again in the expected manner and this part of the curve would then be a van't Hoff curve.

REFERENCE

1. Scott, R.P.W.; Lawrence, J.G. Effect of temperature and moderator concentration on efficiency and resolution of liquid chromatography columns. J. Chromatogr. Sci. **1969**, *7* (2), 65.

BIBLIOGRAPHY

1. Scott, R.P.W. *Techniques of Chromatography*; Marcel Dekker, Inc.: New York, 1995.
2. Scott, R.P.W. *Introduction to Analytical Gas Chromatography*; Marcel Dekker, Inc.: New York, 1998.

Vinyl Pyrrolidone Homopolymer and Copolymers: SEC Analysis

Chi-san Wu
Larry Senak
International Specialty Products, Wayne, New Jersey, U.S.A.

James Curry
Senior Scientist, Research and Development, R.P. Scherer North America, St. Petersburg, Florida, U.S.A.

Edward Malawer
International Specialty Products, Wayne, New Jersey, U.S.A.

INTRODUCTION

Polyvinylpyrrolidone (PVP) is a synthetic polymer derived from the Reppe chemistry and is widely used in the pharmaceutical, personal care, cosmetic, agriculture, beverage, and many industrial applications. PVP is a polar and amorphous polymer which is soluble in water and some organic solvents, such as alcohols, chlorinated hydrocarbons, dimethyl formamide, dimethyl acetamide, and *N*-methyl pyrrolidone.

Non-ionic, anionic, and cationic VP copolymers are all available commercially to enhance the hydrophilic, hydrophobic, and ionic properties of PVP for specific applications. Important comonomers include vinyl acetate (VA), acrylic acid (AA), vinyl alcohol, dimethylaminoethylmethacrylate (DMAEMA), styrene, maleic anhydride, acrylamide, methyl methacrylate, lauryl methacrylate (LM), α–olefins, methacrylamidopropyltrimethyl ammonium chloride (MAPTAC), vinyl caprolactam (VCL), and dimethylaminopropylmethacrylamide (DMAPMA).

MOLECULAR WEIGHT AND MOLECULAR DISTRIBUTION OF PVP BY SIZE-EXCLUSION CHROMATOGRAPHY

Commercial PVP are available in five grades, K-15, K-30, K-60, K-90, and K-120 with the respective range of M_W 7000–12,000, 40,000–65,000, 350,000–450,000, 900,000–1,500,000 and 2,000,000–3,000,000. Interactions between PVP and columns, such as adsorption, partition, and electrostatic interactions, have to be eliminated by prudent choice of column and mobile phase in order to obtain true separation by size and 100% recovery.

Belenkii et al. reported in 1975[1] the size-exclusion chromatography (SEC) of PVP using Pharmacia Sephadex G-75 and G-100 columns and 0.3% sodium chloride solution as the mobile phase. Hashimoto et al. reported in 1978[2] the SEC of PVP K-30 and K-90 using TSK-PW 3000 and two 5000 columns and 0.08 *M* Tris-HCl buffer (pH = 7.94) as the mobile phase.

By using an E. Merck LiChrospher SI300 column, modified with an amide group (–NH–CO–CH_3) chemically bonded to the surface, Englehardt and Mathesn reported in 1979[3] the SEC of PVP. Herman et al. synthesized monomeric diol onto E. Merck Lichrospher SI-500 and reported in 1981[4] the SEC of PVP. Mori reported in 1983[5] the SEC of PVP K-15 to K-90 using two Shodex AD-80M/S columns with DMF and 0.01 *M* LiBr as the eluent at 60°C. Domard and Rinaudo grafted quaternized ammonium groups onto silica gels with pore diameters of 150, 300, 600, 1250, and 2000 Å and reported in 1984[6] the SEC of PVP.

Malawer et al.[7] reported in 1984 the SEC of PVP K-15, K-30, K-60, and K-90 using diol-derivatized silica gel column sets and aqueous mobile phase modified with various polar organic solvents. Senak et al. reported in 1987[8] the determination of the absolute molecular weight and molecular-weight distribution of PVP by SEC–LALLS and SEC with universal calibration. The column set used consists of TSK-PW 6000, 5000, 3000, and 2000 columns and a mobile phase of water-methanol (50:50, v/v) with 0.1 *M* $LiNO_3$. One hundred percent recovery was reported. The results showed good agreement in M_w from SEC–LALLS and from SEC with universal calibration for PVP K-30, K-60, and K-90.

Size-exclusion chromatography of PVP K-15, K-30, K-60, K-90, and K-120 using linear aqueous columns such as the Showa Denko Shodex OH pack, Toyo Soda TSK-PW, and Waters Ultrahydrogel has been reported in 1995 by Wu et al.[9] Using single linear columns also greatly reduces analysis time and solvent consumption, making SEC a practical method for quality assurance. A comparison of four commercial linear aqueous columns and four sets of commercial PEO standards for SEC of PVP K-15, K30, K-60, K-90, and K-120 was reported by Wu et al. in 1999.[10] In recent years, SEC–MALLS has also been applied in this laboratory to PVP. Fig. 1 shows an overlay of SEC–MALLS chromatograms of all commercial grades of PVP using a linear aqueous column. The excellent overlap of absolute M_w vs. retention volume plots for all commercial grades of PVP in Fig. 1 demonstrates that there is no significant difference in branching among all

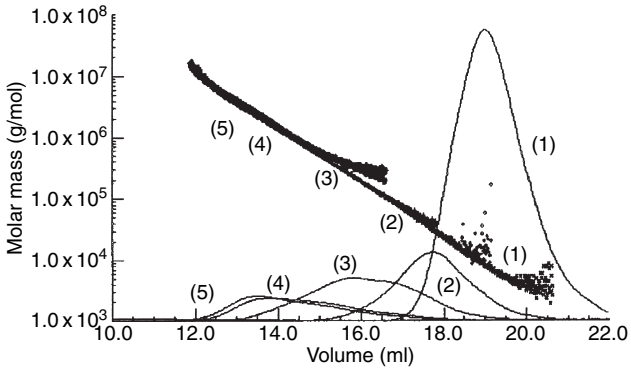

Fig. 1 Overlay of SEC chromatograms and M_w vs. retention volume plots by MALLS for PVP grades: (1) K-15; (2) K-30; (3) K-60; (4) K-90; (5) K-120.

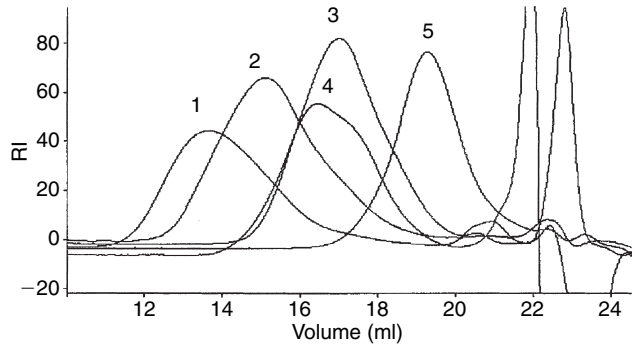

Fig. 2 Overlay of SEC chromatograms of VP-based copolymers in water–methanol (50:50) with 0.1 *M* lithium nitrate: 1, VP–DMAPMA; 2, VP–DMAPMA–AA–LM; 3, VP–VCL–DMAPMA; 4, VP–AA–LM; 5, VP–VA.

commercial grades of PVP, despite the different methods used to make them.

Finally, the following SEC columns, which have been introduced in recent years, have been demonstrated by the vendors to be successful with PVP: Jordi DVB Glucose BR linear column [in dimethyl sulfoxide (DMSO)], PL aquagel-OH column (in 0.1 *M*–0.3 *M* salt-buffer with 20% methanol); PSS Suprema column (in 0.1 *M* Tris pH 7 buffer), and PSS SDV column (in DMAC, 0.1% LiBr).[11–13]

MOLECULAR WEIGHTS AND MOLECULAR-WEIGHT DISTRIBUTIONS OF VP-BASED COPOLYMERS BY SEC

Wu et al. reported in 1991[14] the SEC of a non-ionic copolymer, such as copolymers of vinyl pyrrolidone and vinyl acetate (VP–VA) with different mole ratios and molecular weights, and a terpolymer of vinyl pyrrolidone, dimethylaminoethyl methacrylate and vinyl caprolactam (VP–DMAEMA–VC) in both aqueous and non-aqueous systems. For the aqueous system the column set used consisted of four Waters Ultrahydrogel columns of pore sizes 120, 500, 1000, and 2000 Å, and the mobile phase was water–methanol (1:1, v/v) with 0.1 *M* $LiNO_3$. For the non-aqueous system, the column sets were Shodex KD-80M plus Ultrahydrogel 120 Å, Shodex KD-80M plus PL gel 100 Å, and PL gel 10^4 Å plus 500 Å and the mobile phase was DMF with 0.1 *M* $LiNO_3$. However, it is the aqueous system that showed the best separation at the low-molecular-weight end. Fig. 2 shows the overlay of SEC chromatograms of VP-based copolymers in water–methanol (50:50) with 0.1 *M* lithium nitrate and a linear Shodex OHPAK column.

Wu and Senak reported in 1990[15] absolute molecular-weights and molecular-weight distributions of a quaternized copolymer of vinyl pyrrolidone and dimethylaminoethylmethacrylate (PVP–DMAEMA) by SEC–LALLS and SEC with universal calibration using Waters Ultrahydrogel 120, 500, 1000, and 2000 Å columns and a 0.1 *M* Tris, pH 7 buffer with 0.5 *M* $LiNO_3$ as the mobile phase. Due to the cationic charges on the molecules, a much higher salt content (0.5 *M* $LiNO_3$) is needed in the SEC mobile phase to improve the separation and recovery of the polymer.The water–methanol (1:1, v/v) mobile phase with 0.4 *M* lithium nitrate has also been used in this laboratory for SEC of this cationic copolymers with the Shodex OH pak or Ultrahydrogel linear columns with good results. Fig. 3 shows the overlay of SEC chromatograms of this cationic copolymers in a pH 7 buffer and a linear Shodex OH-PAK column.

Wu et al. reported in 1991[14] the SEC of anionic copolymers, vinyl pyrrolidone and acrylic acid (VP–AA) with different mole ratios and molecular weights, using a 0.1 *M* pH 9 Tris-buffer with 0.2 *M* $LiNO_3$ as the mobile phase and the Ultrahydrogel 120, 500, 1000, and 2000 Å column set. Fig. 4 shows overlay of SEC chromatograms of anionic copolymers in a pH 9 buffer and a linear Shodex OH–PAK column.

Copolymers and grafted copolymers of vinyl pyrrolidone and α–olefins, with α–olefins' contents higher than 60%, are not soluble in water or the water–methanol mixture. They should be analyzed in tetrahydrofuran using cross-linked

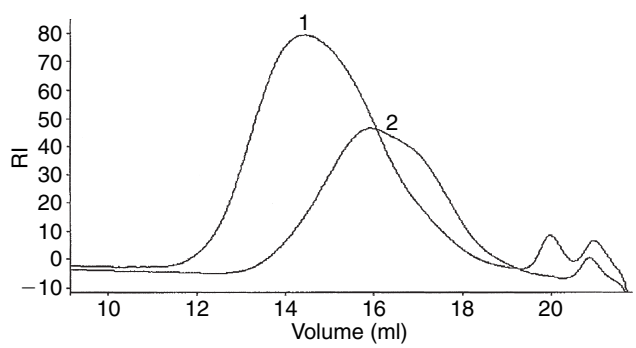

Fig. 3 Overlay of SEC chromatograms of VP-based copolymers in a pH 7 buffer: 1, high–MW VP–DMAEMA cationic copolymer; 2, medium MW VP–DMAEMA cationic copolymer.

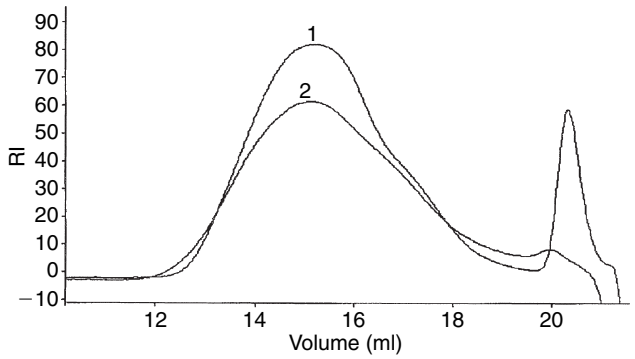

Fig. 4 Overlay of SEC chromatograms of VP–based copolymers in a pH 9 buffer: 1, VP–AA anionic copolymer; 2, VP–AA–LM anionic copolymer.

polystyrene columns. However, copolymers and grafted copolymers of vinylpyrrolidone and α–olefins, with only 10% aolefins, can be analyzed in the water–methanol mixture (50:50) with 0.1 *M* lithium nitrate.

CONCLUSIONS

With a proper choice of mobile phase (aqueous or non-aqueous), many commercially columns are available for SEC of PVP and VP-based copolymers. Mobile-phase modifiers (such as methanol, salt, and buffer) are normally required to eliminate interactions with columns. A single linear or mixed-bed column has been found to provide good separation of PVP and VP–based copolymers with a molecular weight range of from a few thousands to several millions. In general, the aqueous SEC system has better long-term stability and provides better separation than the non-aqueous SEC system, especially at the low-molecular-weight end. Hydroxylated methyl-methacrylate-type columns and water–methanol mobile phase (50:50, with salt) is a good first choice for SEC of PVP and many VP–based copolymers. New columns have been introduced to the marketplace in recent years; hopefully, they will offer better separation, solvent compatibility, stability, and minimal interactions.

REFERENCES

1. Belenkii, B.G.; Vilenchik, L.Z.; Nesterov, V.V.; Kolegov, V.J.; Frenkel, S.Y.A. Peculiarities in gel permeation chromatography of flexible-chain polymers on macroporous swelling sorbents. J. Chromatogr. A, **1975**, *109*, 223.
2. Hashimoto, T.; Sasaki, H.; Aiura, M.; Kato, Y. High-speed aqueous gel-permeation chromatography. J. Polym. Sci. Polym. Phys. Ed. **1978**, *16* (10), 1789.
3. Engelhardt, H.; Mathes, D. High-performance exclusion chromatography of water-soluble polymers with chemically bonded stationary phases. J. Chromatogr. **1979**, *185*, 305.
4. Herman, D.P.; Field, L.R. Calibration of size exclusion chromatography columns for molecular weight determination of polyacrylonitrile and poly(vinylpyrrolidone) in N,N-dimethylformamide. J. Chromatogr. Sci. **1981**, *19*, 470.
5. Mori, S. Calibration of size exclusion chromatography columns for molecular weight determination of polyacrylonitrile and poly(vinylpyrrolidone) in N,N-dimethylformamide. Anal. Chem. **1983**, *55*, 2414.
6. Domard, A.; Rinaudo, M. Gel permeation chromatography of cationic polymer on cationic porous silica gels. Polym. Commun. **1984**, *25*, 55.
7. Malawer, E.G.; De Vasto, J.K.; Frankoski, S.P. Size exclusion chromatography of poly(vinylpyrrolidone): I. The chromatographic method. J. Liq. Chromatogr. Relat. Technol. **1984**, *7* (3), 441.
8. Senak, L.; Wu, C.S.; Malawer, E.G. Size Exclusion Chromatography of Poly(vinylpyrrolidone): II. Absolute Molecular Weight Distribution by SEC/LALLS and SEC with Universal Calibration. J. Liq. Chromatogr. Relat. Technol. **1987**, *10* (6), 1127.
9. Wu, C.; Curry, J.F.; Malawer, E.G.; Senak, L. *Handbook of Size Exclusion Chromatography*; Wu, C., Ed.; Marcel Dekker, Inc.: New York, 1995; 311–330.
10. Wu, C.; Senak, L.; Osborne, D.; Cheng, T. *Column Handbook for Size Exclusion Chromatography*; Wu, C., Ed.; Academic Press: New York, 1999; 499–529.
11. Jordi, H. *Column Handbook for Size Exclusion Chromatography*; Wu, C., Ed.; Academic Press: New York, 1999; 367–425.
12. Meehan, E. *Column Handbook for Size Exclusion Chromatography*; Wu, C., Ed.; Academic Press: New York, 1999; Chap. 12.
13. Kilz, P. *Column Handbook for Size Exclusion Chromatography*; Wu, C., Ed.; Academic Press: New York, 1999; Chap. 9.
14. Wu, C.S.; Curry, J.; Senak, L. Size-exclusion chromatography of nonionic and anionic copolymers of vinylpyrrolidone. J. Liq. Chromatogr. **1991**, *14* (18), 3331.
15. Wu, C.S.; Senak, L. Size exclusion chromatography of quaternized poly(vinlpyrrolidone-co-dimethyl amino ethyl methacrylate) copolymer (PVPDMAEMA): Absolute molecular weights and molecular weight distributions by low angle laser light scattering and universal calibration. J. Liq. Chromatogr. Relat. Technol. **1990**, *13* (5), 851.

Viscometric Detection in GPC/SEC

James Lesec
National Center for Scientific Research (CNRS), City of Paris Industrial Physics and Chemistry Higher Educational Institution (ESPCI), Paris, France

INTRODUCTION

At the beginning of gel permeation chromatography (GPC), in the early 1960s, there was only one detector at the outlet of GPC columns, generally a differential refractometer, to continuously measure the concentration of eluents. This detection provided a chromatographic peak corresponding, roughly, to the mass distribution. In addition, it was possible to build a calibration curve corresponding to the response of the column set $\log(M) = F(V_e)$ (M being the molecular weight and V_e being the elution volume), which was roughly linear, by multiple injections of narrow standards with known molecular weights and very narrow molecular-weight distributions. At each increment of elution volume, the slice concentration C_i was calculated using the polymer peak intensity and the slice molecular weight M_i, using the calibration curve. Then, it was possible to calculate, by integration

$$\frac{\sum C_i}{\sum (C_i/M_i)} = M_n$$
$$\frac{\sum C_i M_i}{\sum C_i} = M_w$$
$$\left(\frac{\sum C_i {M_i}^a}{\sum C_i}\right)^{1/a} = M_v$$
$$\frac{\sum C_i {M_i}^2}{\sum C_i M_i} = M_z$$

[a being the viscosity-law (Mark–Houwink) exponent], the different average molecular weights (in number, M_n; in viscosity, M_v; in weight, M_w; in z, M_z), in a single experiment.

The use of the GPC technique spread very quickly but, very soon, it became obvious that this method was imperfect. Every polymer has its own calibration curve which differs from one polymer to another. Moreover, for copolymers or branched polymers, the molecular weight calibration curve does not work correctly.

In 1966, the "universal calibration" method was established at the University of Strasbourg, France.[1] It used, as a parameter, not molecular weight M, but the hydrodynamic volume represented by the product $[\eta]M$, $[\eta]$ being the intrinsic viscosity. This universal calibration curve $\log([\eta]M) = F(V_e)$ was supposed to be applied to every polymer and copolymer, linear or branched, as a unique calibration curve; it worked very well.

From that point, the necessity of continuously measuring viscosity, in addition to polymer concentration, became obvious. Several attempts were made to adapt existing viscometers as GPC detectors, but the problem of internal volume was critical. Ouano[2] published the first design of a single-capillary viscometer which was based on pressure measurement. Several similar designs[3–9] were published and a commercially available instrument, the Waters Model 150CV (Waters Associates, Milford, Massachusetts, U.S.A.), based on a design described in Ref.[4], became commercially available.

SINGLE-CAPILLARY VISCOMETER

The single-capillary viscometer (SCV) is represented in Fig. 1a. Its design is a direct extrapolation of classical viscometry measurement. It is composed of a small capillary, through which the solvent flows at a constant flow rate, and a differential pressure transducer (DPT), which measures the pressure drop across the capillary. SCV obeys Poiseuille's law and the pressure drop ΔP across the capillary depends on the geometry of the capillary, on flow rate Q, and on viscosity of the fluid η according to

$$\Delta P = \left(\frac{8}{\pi}\right)\left(\frac{l}{r^4}\right)\eta Q$$

where l and r are the length and radius of the capillary, respectively.

Classical viscometers maintain ΔP constant and calculate h by measuring the variations of flow rate Q. By contrast, the SCV uses the advantage of GPC, which already has a constant flow rate Q and allows the calculation of η by measuring the pressure drop variations ΔP across the capillary. At constant flow rate Q, the pressure drop is proportional to viscosity η, and at constant viscosity η, the pressure drop is proportional to flow rate Q. Consequently, in order to use the SCV as an accurate viscometer, the flow rate must be maintained absolutely constant during the GPC experiment. Conversely, SCV allows perfect control of flow rate and can also be used as a very accurate flow meter when only pure solvent

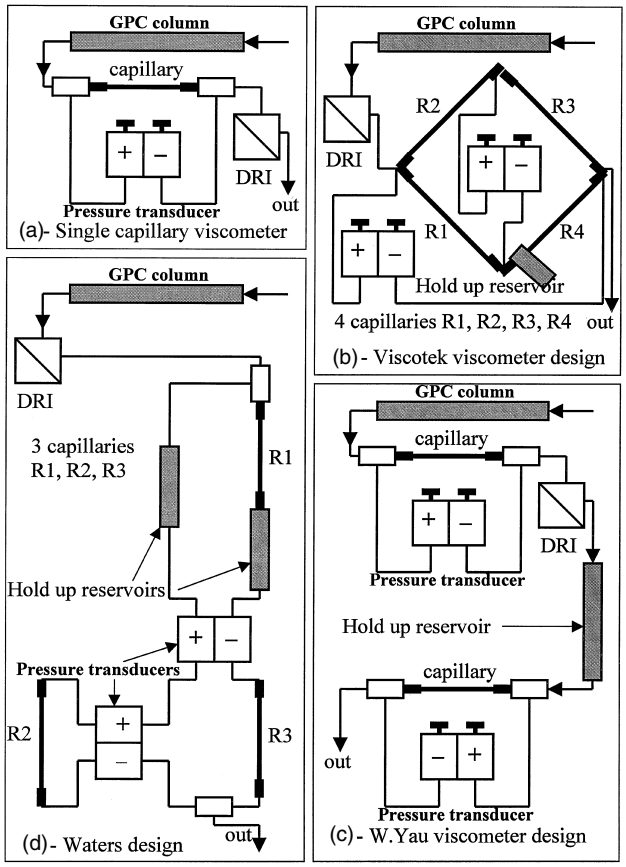

Fig. 1 Various designs of viscometric detection.

comes out of columns. At the outlet of the GPC columns, the polymer concentration is very small and the increase of solvent viscosity η is very small as well. When measuring ΔP proportional to ηQ, Q should be maintained extremely constant; this requires pulse dampeners in the flow system to smooth small flow variations due the pumping system design.

For that reason, some other, more complicated, viscometers, which are insensitive to small flow variations, were designed using multiple capillaries and pressure transducers.

MULTIPLE-CAPILLARY VISCOMETERS

The general purpose of multiple-capillary viscometers is to simultaneously measure the polymer solution in one part of the detector and pure solvent in a second part of the detector. In order to have these two parts at the same time, it is necessary to include a holdup reservoir to delay the polymer passing through the second part of the detector. One needs to wait until the delayed polymer comes out of the detector before reinjecting another sample. The basic principle is that one part of the detector measures polymer plus flow and the other part measures only flow. By obtaining the difference, the result is a signal which is proportional to polymer viscosity and insensitive to flow rate variations.

The first multiple-capillary viscometer was designed by the Viscotek Company (Houston, TX, U.S.A.).[11] It is represented in Fig. 1b. It is composed of four identical capillaries, assembled as a bridge. Here, the difference is generated by the bridge itself as a differential viscometer. The central DPT provides a differential viscosity signal DP and the second, DPT, provides inlet pressure IP. The intrinsic viscosity $[\eta]$ can be calculated by the formula

$$[\eta] = \frac{1}{C}\left(\frac{4\mathrm{DP}}{\mathrm{IP} - 2\mathrm{DP}}\right)$$

Another design was described by the Dupont Company.[12] It is represented in Fig. 1c. It is composed of two single-capillary viscometers. The first one (measure) is located as a normal SCV (Fig. 1a) and measures polymer plus flow. The second one (reference), identical to the first one, is located after a holdup reservoir which is connected after the refractometer and measures only the flow with pure solvent. It is just necessary to obtain the difference between the two signals to obtain the polymer signal with no flow contribution.

The last differential viscometer design is the Waters Corporation detector,[13] which is in the Alliance GPCV2000 high-temperature instrument. It is composed of three capillaries, two differential pressure transducers, and two holdup reservoirs; it is represented in Fig. 1d. The pressure transducers are connected flow-through; this eliminates the need for frequent purges. This detector provides, at the same time, "relative viscosity information" and "relative flow information." This design does not require a perfect matching of the capillaries.

THE USE OF VISCOMETRIC DETECTION

The first purpose of viscometric detection in GPC is to use a "universal calibration curve." At every slice, the concentration C_i is obtained through refractometric data, intrinsic viscosity $[\eta]_i$ is obtained through refractometric and viscometric data, and hydrodynamic volume $[\eta]M_i$ is obtained from the universal calibration curve. It is just necessary to divide $[\eta]M_i$ by $[\eta]_i$ to get M_i and obtain the couple C_iM_i that is necessary to calculate the various average molecular weights, as shown at the beginning of this entry, independently of the chemical nature of the sample and the standards used for calibration.

The secondary use of viscometric detection is for the determination of long-chain branching. At the same

molecular weight, a long-chain branched polymer has a more compact molecular structure than the linear one; consequently, it also has a smaller intrinsic viscosity. Therefore, it is eluted at a higher elution volume with a linear polymer of smaller molecular weight. That means that at a given elution volume, there is a mixture of polymers with different molecular weights and different degrees of branching eluting from the GPC column.

As intrinsic viscosity is affected by long-chain branching, viscometric detection provides branching information, just by comparing polymer viscosity laws. Fig. 2a represents the viscosity-law plot of a linear polymer, polyethylene (NBS1475), with a linear viscosity law and an exponent of 0.71. Conversely, Fig. 2b represents the viscosity-law plot of a branched polymer, polyethylene (NBS1476), with a curved viscosity law, under the linear polymer law (linear viscosity law). At every molecular weight, the branching distribution g_i' is calculated by

$$g_i' = \frac{[\eta]\mathrm{br}_i}{[\eta]\mathrm{lin}_i}$$

where $[\eta]\mathrm{br}_i$ and $[\eta]\mathrm{lin}_i$ are the slice intrinsic viscosities of the branched and the linear polymer, respectively.

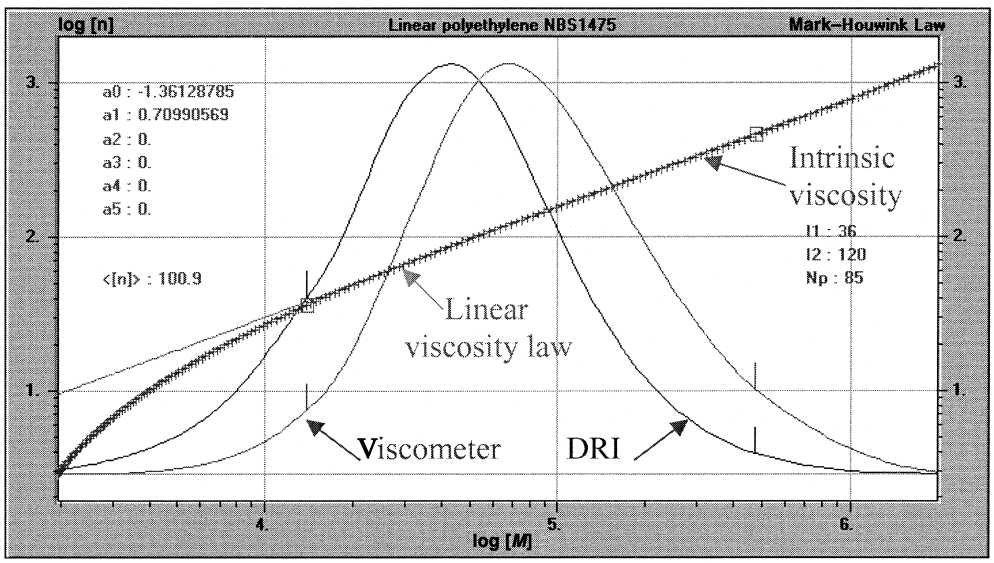

a

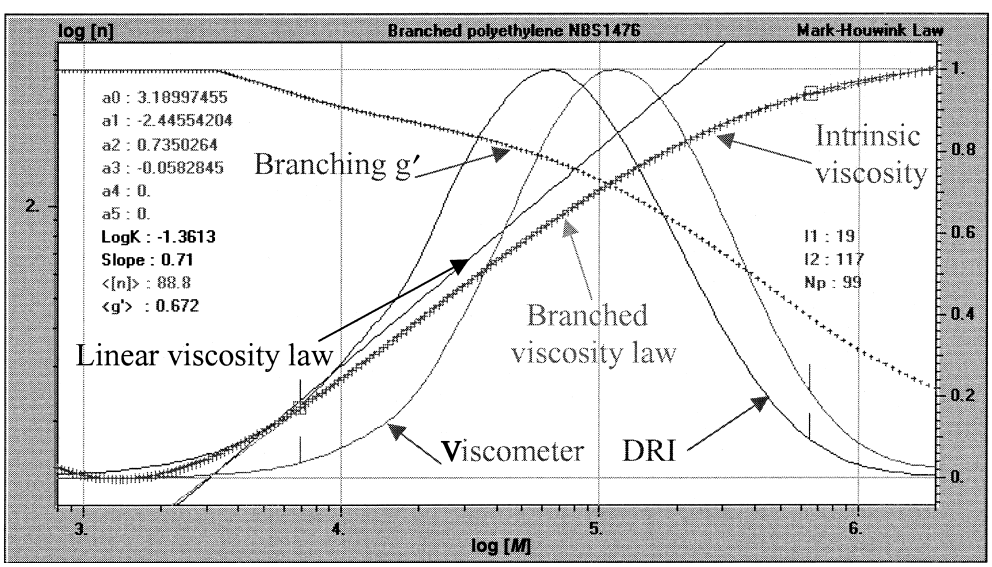

b

Fig. 2 (a) Mark–Houwink plot for linear polyethylene NBS1475. (b) Mark–Houwink plot for branched polyethylene NBS1476.

CONCLUSIONS

Viscometric detection in GPC–SEC is extremely useful. It allows continuous viscosity measurements, which, in turn, permits the use of a unique calibration curve for all polymers (universal calibration). In addition, the viscosity law is determined for linear polymers and long-chain-branching information can be obtained for branched polymers.

REFERENCES

1. Benoit, H.; Grubisic, Z.; Rempp, P.; Dekker, D.; Zilliox, G. J. Chim. Phys. **1966**, *63*, 1507.
2. Ouano, A.C. Gel-permeation chromatography. VII. Molecular weight detection of GPC effluents. J. Polym. Sci. A1 **1972**, *10* (7), 2169–2180.
3. Lesec, J.; Quivoron, C. Analysis **1976**, *4*, 399.
4. Letot, L.; Lesec, J.; Quivoron, C. J. Liquid Chromatogr. **1982**, *3*, 407.
5. Lecacheux, D.; Lesec, J.; Quivoron, C. J. Appl. Polym. Sci. **1982**, *27*, 4867.
6. Lecacheux, D.; Lesec, J.; Prechner, R. French Patent 2402324.6 (1982); U.S. Patent 4478071 (1984).
7. Malihi, F.B.; Kuo, C.; Kohler, M.E.; Provder, T.; Kah, A.F. ACS Symp. Ser. **1984**, *245*, 281.
8. Kuo, C.; Provder, T.; Kohler, M.E.; Kah, A.F. ACS Symp. Ser. **1987**, *352*, 130.
9. Lesec, J.; Lecacheux, D.; Marot, G. J. Liquid Chromatogr. **1988**, *11*, 2571.
10. Lesec, J.; Marot, G. J. Liquid Chromatogr. **1988**, *11*, 3305.
11. Haney, M.A. The differential viscometer. II. On-line viscositydetector for size-exclusion chromatography. J. Appl. Polym. Sci. **1985**, *30*, 3037.
12. Abbot, S.D.; Yau, W.W. (to Dupont). Differential pressure capillary viscometer for measuring viscosity independent of flow rate and temperature fluctuations. U.S. Patent 4627271, 1985.
13. de Corral, J.L. (to Waters Corp.). Three capillary flow-through viscometer. U.S. Patent 5637790, 1997.

Vitamins, Hydrophobic: TLC Analysis

Alina Pyka
Department of Analytical Chemistry, Medical University of Silesia, Sosnowiec, Poland

Abstract
The use of thin-layer chromatography (TLC) in the investigation of hydrophobic vitamins has been discussed. The use of TLC as a separation method allows for the qualitative and quantitative investigation of hydrophobic vitamins. The use of TLC technique together with densitometry gives precise and sensitive quantification of vitamins A, D, E, and K compounds on TLC plates. It was proven that TLC is an important investigative technique for the analysis of hydrophobic vitamins. This entry shows the progress of investigations of hydrophobic vitamins.

INTRODUCTION

Vitamins are biologically active organic compounds, controlling agents that are essential for an organism's normal health and growth, not synthesized within the organism, available in the diet in small amounts, and carried in the circulatory system in low concentrations to act on target organs or tissues. Vitamins are classified according to their solubility in water and in fats. Hydrophobic vitamins include vitamins A, D, E, and K. Chromatography is useful for the identification and determination of vitamins in pharmaceutical preparations, the identification and determination of vitamins and related substances in natural materials and foodstuffs, and the chemical and biochemical determination of vitamins and their metabolites in fats and tissues. The isolation of the vitamins, their metabolites, and related substances from natural material is the most difficult task.[1–3] The aim of this entry is to present selected works that describe the analytical investigations of hydrophobic vitamins by means of thin-layer chromatography (TLC).

VITAMIN A

Physiological forms of vitamin A include retinol (vitamin A_1) and its esters, 3-dehydroretinol (vitamin A_2) and its esters, retinal (retinene, vitamin A aldehyde), 3-dehydroretinal (retine-2), retinoic acid, neovitamin A, and neo-b-vitamin A_1. Active analogues and related compounds, known as vitamins A are α-, β-, and γ-carotene, neo-β-carotene B, cryptoxanthine, myxoxanthine, torularhodin, aphanicin, and echinenone. Foods of plant origin do not contain vitamin A, but are rich sources of previtamin A. About 50 of the 500 known carotenoids can be converted to vitamin A. β-Carotene is the most important of all the carotenoids that occur in nature. β-Carotene (provitamin A), precursor of vitamin A, is found in plants.

Sliwiok, Podgorny, and Siwek[4] used TLC and high-performance liquid chromatography (HPLC) to compare the hydrophobicity of vitamin A derivatives (all-*trans* retinic acid, all-*trans* retinal, vitamin A acetate, and vitamin A palmitate). TLC was performed on RP-2 F_{254} and Kieselguhr F_{254} (impregnated with 10% paraffin oil in cyclohexane) with methanol–water (95:5, v/v). Chromatographic data for vitamin A derivatives are listed in Table 1. The separations of the vitamin A derivatives on the paraffin oil-impregnated plates were better than those on the RP-2 plates. Log *P* values from fragmental constants for the all-*trans* retinic acid, all-*trans* retinal, vitamin A acetate, and vitamin A palmitate were calculated (log *P* 4.85, 6.48, 7.92, 15.30, respectively). The relationship obtained by the authors confirms the following sequence of increasing hydrophobicity: all-*trans* retinic acid < all-*trans* retinal < vitamin A acetate < vitamin A palmitate.

Perisic-Janjic, Petrovic, and Hadzić[5] described a method for the quantitative separation of vitamin A acetate and A palmitate by thin-layer chromatography on starch, cellulose, and talc impregnated with paraffin oil using acetone-concentrated acetic acid (3:2, v/v) as the mobile phase (Table 1).

Small amounts of intensely colored pigments can be detected in ultraviolet (UV) light and also in visible light; the limit of detection is 0.01 μg for carotenoids. Retinal (0.02–0.03 μg) can be detected after spraying with rhodanine (orange-red spot of retinal). Many vitamin A compounds fluoresce yellow-green in light at 365 nm (limit of detection 0.05 μg). Vitamin A compounds can be detected with antimony(III) chloride (Carr-Price reagent) and antimony(V) chloride (blue spots), with concentrated sulfuric acid (blue color of spot),[10] with molybdophosphoric acid (green-blue spots), and with potassium dichromate in sulfuric acid (limits of detection 0.1–0.3 μg). The limit of detection of retinol isomers converted to 2,4-dinitrophenylhydrazones of retinals is 1 μg.[1,2,5] Bromophenol blue was also used for detection of vitamin A (3 μg) after adsorption TLC.[11]

Table 1 R_F values of hydrophobic vitamins and metabolites of vitamin D_3 separated in different chromatographic conditions.

	Chromatographic conditions														
Substance	**I**	**II**	**III**	**IV**	**V**	**VI**	**VII**	**VIII**	**IX**	**X**	**XI**	**XII**	**XIII**	**XIV**	**XV**
All-*trans* Retinic acid	0.8	0.97	—	—	—	—	—	—	—	—	—	—	—	—	—
All-*trans* Retinal	0.76	0.87	—	—	—	—	—	—	—	—	—	—	—	—	—
Vitamin A Acetate	0.7	0.62	—	—	—	—	—	—	—	—	—	0.86	0.82[a]	0.85[a]	0.86[a]
Vitamin A Palmitate	0.45	0.06	—	—	—	—	—	—	—	—	—	—	0.25[a]	0.33[a]	0.27[a]
Vitamin D_2	—	—	0.56	0.5	0.38	—	—	—	—	—	—	—	0.79[a]	0.82[a]	0.83[a]
Vitamin D_3	—	—	0.48	0.41	0.29	—	—	—	0.69	0.56	0.65	0.62	0.79[a]	0.82[a]	0.83[a]
1-OH-D_3	—	—	—	—	—	—	—	—	0.35	0.39	0.4	—	—	—	—
25-OH-D_3	—	—	—	—	—	—	—	—	0.56	0.43	0.57	—	—	—	—
1,25-$(OH)_2$-D_3	—	—	—	—	—	—	—	—	0.2	0.15	0.33	—	—	—	—
24,25-$(OH)_2$-D_3	—	—	—	—	—	—	—	—	0.41	0.26	0.51	—	—	—	—
25,26-$(OH)_2$-D_3	—	—	—	—	—	—	—	—	0.3	0.17	0.35	—	—	—	—
α-Tocopherol	—	—	—	—	—	0.49	0.31	0.18	—	—	—	—	—	—	—
β-Tocopherol	—	—	—	—	—	0.53	0.37	0.2	—	—	—	—	—	—	—
γ-Tocopherol	—	—	—	—	—	0.57	0.41	0.22	—	—	—	—	—	—	—
δ-Tocopherol	—	—	—	—	—	0.63	0.47	0.24	—	—	—	—	—	—	—
Vitamin E	—	—	—	—	—	—	—	—	—	—	—	0.8	0.63[a]	0.72[a]	0.67[a]
Vitamin E-acetate	—	—	—	—	—	—	—	—	—	—	—	0.8	0.52[a]	0.63[a]	0.56[a]
Vitamin K_1	—	—	—	—	—	—	—	—	—	—	—	—	0.40[a]	0.53[a]	0.45[a]
Vitamin K_3	—	—	—	—	—	—	—	—	—	—	—	—	0.45[b]	0.57[b]	0.60[c]
Vitamin K_4	—	—	—	—	—	—	—	—	—	—	—	—	0.84[b]	0.77[b]	0.47[c]
Vitamin K_5	—	—	—	—	—	—	—	—	—	—	—	—	0.26[b]	0.18[b]	0.09[c]

Chromatographic conditions (stationary phase and mobile phase): **I** = RP2-plates and methanol–water (9:1, v/v); **II** = Kieselguhr F_{254} impregnated with 10% paraffin oil in cyclohexane, and methanol–water (9:1, v/v); **III**= Kieselguhr F_{254} impregnated with 10% paraffin oil in benzene and methanol–water (9.5:0.5, v/v); **IV**= Kieselguhr F_{254} impregnated with 10% paraffin oil in benzene and acetonitrile–water (9.5:0.5, v/v); **V**= Kieselguhr F_{254} impregnated with 10% paraffin oil in benzene and acetonitrile–water (9:1, v/v); **VI**= RP-18 plates and ethanol–water (10:0, v/v); **VII**= RP-18 plates and ethanol–water (9.5:0.5, v/v); **VIII**= RP-18 plates and ethanol–water (9:1, v/v); **IX**= Kieselgel 60 F_{254} (E. Merck, Germany) and chloroform–ethanol–water (183:16:1, v/v); **X**= Silufol UV 254 (Kavalier, Sazava, Czech Republic) and chloroform–ethanol–water (183:16:1, v/v); **XI**= silica gel 6061 (Eastman, Kodak, Rochester, U.S.A.) and chloroform–ethanol–water (183:16:1, v/v); **XII**=RP-18 plates and acetonitrile–benzene–chloroform (10:10:1, v/v/v); **XIII**[a]=starch plates impregnated with paraffin oil and acetone-concentrated acetic acid (3:2, v/v); **XIII**[b]=starch plates impregnated with paraffin oil and water–dioxane–acetone–formaldehyde (85:20:15:25, v/v/v/v); **XIV**[a]=cellulose plates impregnated with paraffin oil and acetone-concentrated acetic acid (3:2, v/v); **XIV**[b]=cellulose plates impregnated with paraffin oil and water–dioxane–acetone–formaldehyde (85:20:15:25, v/v/v/v); **XV**[a]=talk plates impregnated with paraffin oil and acetone-concentrated acetic acid (3:2, v/v); **XV**[c]=talk plates unimpregnated and water–dioxane–acetone–formaldehyde (85:20:15:25, v/v/v/v).

Adapted from Sliwiok, Podgorny, & Siwek,[4] Perisic-Janjic, Petrovic, & Hadzić,[5] Kocjan & Śliwiok,[6] Justova & Starka,[7] Pyka & Sliwiok[8] and Baranowska & Kądziolka.[9]

VITAMIN D

Physiological forms of vitamin D include vitamin D_2 (calciferol, ergocalciferol), vitamin D_3 (cholecalciferol), phosphate esters of D_2, D_3, 25-hydroxycholecalciferol, 1,25-dihydroxycholecalciferol, and 5,25-dihydroxycholecalciferol. Vitamins D_2 and D_3 are 9,10-secosteroids that differ structurally in the degree of saturation of an isoprenoid side chain. The biological activity of vitamin D_3 is greater than that of vitamin D_2. Vitamin D_2 is of vegetable origin, whereas D_3 is formed in the skin of humans and animals. From the chemical standpoint, ergocalciferol (vitamin D_2) is a relatively stable vitamin. Vitamins D_2 and D_3 are precursors of hormones. Vitamin D_3, which has little biological activity, is converted to biologically active metabolites by oxidation.

Kocjan and Sliwiok[6] determined the hydrophobicities of vitamins D_2 and D_3 by reversed-phase thin-layer chromatography (RPTLC), thin-layer adsorption chromatography, and infra red (IR) spectrometry. Partition TLC separations of vitamins D_2 and D_3 were done on TLC plates precoated with Kieselguhr $F_{254,}$ impregnated with 10% paraffin oil in benzene and developed to 10 cm with binary mixtures of methanol–water and acetonitrile–water. The R_F values of the best separation of vitamins are listed in Table 1. Adsorption TLC was done on glass plates precoated with activated silica gel 60 F_{254}, with a mobile phase of benzene–methanol (9:1, v/v). Measurement of the surfaces of the chromatographic spots obtained by adsorption TLC gave hydrophobicity coefficients (h_f 6.09 and 9.05 for vitamins D_2 and D_3, respectively). The results indicate that the hydrophobicity of vitamin D_3 is greater than that of vitamin D_2. This conclusion was proved by the lower R_F values for vitamin D_3 obtained by partition chromatography, the higher values of the respective hydrophobicity coefficients, and by the greater relative decreases in the ratio of free to bonded OH groups (obtained by spectrometric measurement).

Justova and Starka[7] described TLC separations of vitamin D_3 and its hydroxymetabolites. They tested three stationary phases (three commercial silica gel sorbents, namely, Kieselgel 60 F_{254}, Silufol UV 254, and silica gel 6061, and one relatively polar mobile phase (chloroform–ethanol–water, 183:16:1, v/v). R_F values of vitamin D_3 and its functional hydroxymetabolites are listed in Table 1. The optimal separation was achieved on Kieselgel 60 F_{254} foils produced by E. Merck, Germany. In biological samples, the vitamin D_3 hydroxymetabolite contents are at nanogram levels, which is below the limit of sensitivity of the applied visualization methods (UV light and the anisaldehyde reagent). Therefore, the hydroxycholecalciferols were localized with corresponding metabolites used as markers. Vitamin D_3 and 25-OH–D_3 were then scraped off the plate and extracted with ethanol; eluates were examined for radioactivity. The recovery of the markers in five replicate determinations was 97.8 ± 2.9% for vitamin D_3 and 98.7 ± 1.5% for 25-OH–D_3, respectively, when the effect of elution was verified. The effect of the complete chromatographic procedure was characterized by the accuracy and precision of the determination. These methods of TLC separation and determination of vitamin D_3 and its hydroxymetabolites are accurate and precise.[7]

Spots of vitamin D derivatives can be inspected in short-wavelength UV light (limit of detection 0.025–0.500 μg). The mono- and dihydroxycholecalciferols can be visualized under UV light at 254 nm or by spraying the foil with a solution of anisaldehyde in sulfuric acid (2%, w/v) mixed with glacial acetic acid (1:10, v/v) at 40°C. Vitamins D_2 and D_3 can be detected with antimony(III) chloride (Carr-Price reagent) and antimony(V) chloride (gray-blue and orange-red spots, respectively; limit of detection 0.025–0.300 μg), with concentrated sulfuric acid (brown and green spots, respectively, of vitamins D_2 and D_3; limit of detection 30 μg), with tungstophosphoric acid (gray-brown spots; limit of detection 0.2 μg), with molybdophosphoric acid (gray-blue spots; limit of detection 0.3 μg),and with trichloroacetic and trifluoroacetic acids (limit of detection 0.1–0.2 μg).[1–3,10] Vitamins D_2 and D_3 separated by adsorption TLC were visualized with 0.005% aqueous new fuchsine solution.[6] Vitamin D_3 was also detected with sodium hydroxide (yellow and orange spots in visible and UV light, respectively; limit of detection 1–8 μg), with iron(III) chloride (brown-red spot in visible light; limit of detection 8 μg), with iodoplatinate (black and brown spots in visible and UV light, respectively; limit of detection 1–8 μg), and with phosphomolybdate (pinkish brown spot in visible light; limit of detection 8 μg).[1–3] Bromocresol green, bromothymol blue, and helasol green can be used for detection of vitamins D_2 and D_3 after adsorption TLC (limit of detection 5 μg) and partition TLC (limit of detection 50 μg), respectively.[11] Jork et al.[10] obtained the fluorescence scan (λ_{exc} = 436 nm and λ_{fl} > 560 nm) of a chromatogram track with 50 ng vitamin D_3 per chromatogram zone after its separation on high-performance thin-layer chromatography (HPTLC) Kieselgel 60 (E. Merck) plates using cyclohexane–diethylether (40:20, v/v).

VITAMIN E

In nature, vitamin E occurs in eight different forms (α-, β-, γ-, and δ-tocopherols and α-, β-, γ-, and δ-tocotrienols), with varying biological activities. The biological properties of α-tocopherol are of particular importance. Of these eight compounds, α-tocopherol has the highest biological activity. The relative affinity (%) is 100, 38.1 ± 9.3, 8.9 ± 0.6, and 1.6 ± 0.3, respectively, for α-, β-, γ-, and δ-tocopherols.[8] Tocopherol possesses three asymmetric carbon atoms, and there are eight possible stereoisomeric tocopherols. Natural α-tocopherol occurs as the enantiomer about the configuration 2R, 4′R, and 8′R. Semisynthetic α-tocopherol is a mixture of the diasteroisomers about the configuration 2R/S, 4′R, and 8′R. The antioxidative effect of the different tocopherols may not be identical. It has been shown in antioxidation tests with foodstuffs that the antioxidative activity of the tocopherols increases in the order γ-, δ-, β-, and α-tocopherols. Vitamin E occurs principally in wheat germ, vegetable oil, and vegetables.

Tocopherols, α-, β-, γ-, and δ-, were separated (R_M values 0.438, 0.037, 0.008, and –0.275, respectively) on Kieselguhr G plates impregnated with a 10% solution paraffin oil in hexane with a mobile phase of methanol–water (9.5:0.5, v/v) by Sliwiok and Kocjan.[12] They correlated their results with those of quantum-mechanical

calculations and respective steric effects, and observed steric effects' influence on hydrophobic properties and biological activity of tocopherols. The percentage portion of $-CH_3$ groups in the chroman ring is 10.47, 7.21, 7.21, and 3.73, respectively, for α-, β-, γ-, and δ-tocopherols. Steric effects of the OH groups in α-, β-, γ-, and δ-tocopherols were earlier presented.[2,12] Hydrophobic constants (h_f values 20.5, 17.2, 16.6, and 14.8, respectively, for α-, β-, γ-, and δ-tocopherols) were determined by adsorption TLC (Kieselgel G plates and benzene–acetone, 9:1, v/v, as the mobile phase) and the partition coefficient by Rekker (log P 12.37, 11.86, 11.86, and 11.35, respectively, for α-, β-, γ-, and δ-tocopherols) were calculated for investigated tocopherols. It was established that the investigated tocopherols can be arranged with respect to their hydrophobic properties in the order α-tocopherol > β-tocopherol > γ-tocopherol > δ-tocopherol.[12]

However, enantiomers of DL-α-tocopherol were separated on Chiralplates (Machery–Nagel, Germany) with 2-propanol–water–methanol (17:2:1, v/v) as the mobile phase.[13] Under these conditions, two bands were generated with R_F values of 0.72 and 0.62.

Tocopherols, α-, β-, γ-, and δ-, were separated by reversed-phase high-performance thin-layer chromatography (RP-C_{18}-HPTLC), normal-phase high-performance liquid chromatography (NPHPLC), reversed-phase high-performance liquid chromatography (RP-C_{18}-HPLC), and gas chromatography (GC).[8] R_F values of the α-, β-, γ-, and δ-tocopherols separated by RP-C_{18}-HPTLC, using ethanol–water as the mobile phase, are shown in Table 1. The chromatographic conditions used allowed for the separation of the four tocopherols in various biological samples. The selected topological indices based on the connectivity–adjacency matrix (M^{ν},$^{1}\chi^{\nu}$), on distance matrix (W, ^{o}B, MTI), and on information theory (I_{AC},I_{AC}) were calculated for these tocopherols. The observed chromatographic separations of investigated tocopherols were compared. The comparison indicated that RP-C_{18}-HPTLC, HPLC, and GC are the best techniques for the separation of these tocopherols. Topological index ^{o}B was the most significant. A definite dependence between the numerical values of the topological index ^{o}B and the chromatographic separation of the investigated tocopherols was obtained.[8]

Pyka and Niestroj applied the dipole moments (or permittivity) of mobile phases and the topological indices to predict the R_M values of α-, β-, γ-, and δ-tocopherols separated on RP-C_{18}-HPTLC plates using methanol, ethanol, *n*-propanol, and mixtures containing ethanol and water, and *n*-propanol and water in the volume proportions 9.5 + 0.5, and 9 + 1 as mobile phases. The best regression equations were obtained using one topological index from among the topological indices $^{2}\chi^{\nu}$, ^{o}B, or C.[14]

Hachuła and Buhl[15] described analytical methods to determine α-tocopherol in Vitaminum E capsules (Polfa, Poznan, Poland) and soybean oil. Determination of α-tocopherol (after extraction of samples) has been performed by TLC on silica gel plates with benzene–ethanol (99:1, v/v) as the mobile phase. Levels of α-tocopherol in Vitaminum E capsules and in soybean oil were earlier presented.[2,15] The results obtained by authors indicate that they were in good agreement with those expected, and the precision of the measurements was satisfactory.

Densitometry was used for quantitative determination of α-tocopherol acetate in Vitaminum E oral fluid (Medana, Poland). The sample of Vitaminum E was prepared in absolute ethanol. Chromatography was performed on glass TLC plates with layers of silica gel 60 F_{254} (E. Merck, #1.05715) and using toluene as the mobile phase. The quantitative densitometric analysis on Camag TLC Scanner 3 was performed using analytical curve. On the basis of densitometric analysis, it was shown that the R_F value of α-tocopherol acetate is equal to 0.46 and the band characterized by absorption maximum of α-tocopherol acetate is placed at $\lambda_{max} = 203$ nm. The second densitometric band occurs on the chromatogram and has an R_F value equal to 0.33 and the band is characterized by absorption maximum at 200 nm; it is a chromatographic band of contraries that occurs in Vitaminum E preparation. It was stated that the contents of α-tocopherol acetate is equal to 104.5% in relation to the content declared by the Medana producer of Vitaminum E oral fluid. The presented method is accurate, selective, and precise, and can be used for routine quality control analysis and quantitative determination of α-tocopherol acetate in Vitaminum E preparation.[16]

Vitamin E compounds can be visualized (about 20 μg) as dark spots in UV light. They appear violet, and detection is more sensitive (0.02 μg) on layers that contain 0.02% sodium-fluorescein. Moreover, these are visible in daylight as red spots (limit of detection 2 μg). Spraying with fluorescein or dichlorofluorescein reagent produces the same effect. Non-specific visualization procedures for tocopherols and tocotrienols are based on spraying with sulfuric acid, molybdophosphoric acid, antimony(V) chloride, dipyridyl-iron reagent, nitric acid, copper(II) sulfate–phosphoric acid, or bathophenanthroline. α-Tocopherol was also visualized by a coupled redox-complexation reaction with iron(III) chloride, phenanthroline, and bromophenol blue.[1–3,10] Aniline blue, alkaline blue, and bromothymol blue can also be used for detection of vitamin E (1 μg) after adsorption TLC.[11] When β-carotene was used as a TLC spray reagent, tocopherols (10 μg) appeared as yellow spots against a white background.[1–3,10] The densitogram of D-α-tocopherol after spraying dipyridyl-iron reagent was given by Jork et al.[10] They obtained the reflectance scan ($\lambda = 520$ nm) of a chromatogram track with 200 ng D-α-tocopherol after its separation on HPTLC Kieselgel 60 (E. Merck) plates with the use of toluene–chloroform (10:10, v/v).

Six dyes as new visualizing reagents: gentian violet, methylene violet, methylene blue, methyl green, malachite green, and Janus blue, have been used to detect (±)-α-

tocopherol, and (+)-α-tocopherol acetate on silica gel 60.[17] Rhodamine B and 2,2′-bipyridine–iron(III) chloride reagent were used as the comparative visualizing reagents. The limit of detection (detectability), detection index, broadening index, modified contrast index, densitometric visualizing index, and linearity range were determined for (±)-α-tocopherol, and (+)-α-tocopherol acetate following the use of these visualizing reagents (Tables 2 and 3).[17] Among all the new visualizing reagents studied, methylene violet and methyl green are the best for detecting (±)-α-tocopherol. The densitometric bands of (±)-α-tocopherol after detection with methylene violet and methyl green are compacted (β are equal to 8° and 9°, respectively) and linearity ranges are from 0.75 to 5.76 μg. Methylene violet and methyl green are better visualizing reagents in comparison with universally applied Rhodamine and 2,2′-dipirydyl–iron(III) chloride reagent to detect (±)-α-tocopherol. The densitometric band of (±)-α-tocopherol after detection with Rhodamine has β equal to 12°; however, densitometric band of (±)-α-tocopherol after detection with 2,2′-dipirydyl–iron(III) chloride reagent is compact (β is equal to 9°), but the limit of detection of (±)-α-tocopherol is then equal to only 2.08 μg, whereas densitometric limit of detection of (±)-α-tocopherol after the use of methylene violet, methyl green, and Rhodamine B is equal to 0.30 μg. Densitometric analysis of (±)-α-tocopherol without using a visualizing reagent can also be recommended, because the limit of detection is equal to 0.45 μg; however, the linearity range is from 3.46 to 20.00 μg. The densitograms of 25.00 μg (±)-α-tocopherol without using a visualizing reagent and after detection with 2,2′-dipirydyl–iron(III) chloride reagent are presented in Fig. 1a and b, respectively. The densitograms of 25.00 μg (±)-α-tocopherol after detection with Rhodamine B and methylene violet are presented in Fig. 2a and b, respectively.[17]

The best way for detecting (+)-α-tocopherol acetate is the densitometric method without using a visualizing reagent. However, the densitometric limit of detection of (+)-α-tocopherol acetate is equal to 0.30 μg, and the linearity range is from 0.75 to 20.00 μg. However, among all studied new visualizing reagents, gentian violet, methyl green, and Janus blue are the best for detection of (+)-α-tocopherol acetate. These visualizing reagents have detection properties similar to (+)-α-tocopherol acetate in relation to Rhodamine B. The densitograms of 25.00 μg (+)-α-tocopherol acetate without using a visualizing reagent and after detection with methyl green are presented in Fig. 3a and b, respectively. The densitograms of 25.00 μg (+)-α-tocopherol acetate after detection with Rhodamine B and gentian violet are presented in Fig. 4a and b, respectively.[17]

It was stated that it was possible to obtain a linear dependence between the area of the densitometric band and the quantity of spotted (±)-α-tocopherol or (+)-α-tocopherol acetate by all apllied ways of detection. The range of linearity is different for different visualizing reagents and also depends on the detected compound.[17]

VITAMIN K

Physiological forms of vitamin K are vitamin K_1 (phylloquinone, phytonadione) and vitamin K_2 (farnoquinone). Active analogues and related compounds, known as vitamin K, are menadiol diphosphate, menadione (vitamin K_3), menadione bisulfite, phthiocol, synkayvite, menadiol (vitamin K_4), menaquinone-*n* (MK-*n*), ubiquinone (Q-*n*), and plastoquinone (PQ-*n*). Phylloquinone (K_1), and menaquinone-4 (MK-4) are natural K vitamins and are often used as medicines to prevent intracranial hemorrhage in the newborn. Vitamin K contributes to the formation and regulation of numerous proteins in the body, but most significantly to prothrombin, a protein essential for blood clotting. Vitamin K is also necessary for converting prothrombin to thrombin, which is also required for blood clotting.

Argentation TLC (on silver nitrate-impregnated silica gel plates) and hexane–ethyl acetate–di-isopropyl ether (2:2:1, v/v) as the mobile phase were used to separate vitamins K_1, K_2 K_3, ubiquinone-6, ubiquinone-9, and ubiquinone-10 (R_F values 0.71, 0.63, 0.57, 0.42, 0.21, and 0.28, respectively).[18]

Perisic-Janjic, Petrovic, and Hadzić[5] described a method for the quantitative analysis of hydrophobic vitamins K_3, K_4, and K_5 by thin-layer chromatography on starch, cellulose impregnated with paraffin oil, and talc (unimpregnated) using a mixture of water–dioxane–acetone–formaldehyde (85:20:15:25, v/v/v/v) as the mobile phase (Table 1).

Hachuła[19] developed a sensitive spectrophotometric method for the determination of vitamin K_4 in drugs (Styptobion, E. Merck) after chromatographic separation on silica gel with benzene–acetone (9:1, v/v) as the mobile phase. Beer's law was obeyed for 0.3–1.0 μg/ml vitamin K_4 ($\varepsilon = 196{,}000$). No detection limit was given. The results obtained from the proposed analytical procedure were in good agreement with those expected and the precision of the measurement was satisfactory. The proposed method is rapid and involves rather low analysis costs.

All lipoquinones at levels of 0.5 μg or more are visible as dark spots on layers containing inorganic fluorescent material when illuminated with UV light, after adding sodium-fluorescein or rhodamine B or 6G to the adsorbent, or by spraying the chromatographed layer with fluorescein or dichlorofluorescein reagent. These compounds can be detected in daylight and, with high sensitivity, in UV light. Vitamin K compounds can be detected with iodine vapor (brown spots), with concentrated sulfuric acid followed by heating (violet spots, limit of detection 3 μg), with molybdophosphoric acid (gray-blue spots, limit of detection 0.5 μg), and with potassium hexaiodoplatinate reagent. Long- and short-wave UV light were used to detect vitamin K; under shortwave UV light, vitamin K showed an intense

Table 2 Fundamental absorption band, broadening index, detection index and characteristic of densitometric band, modified contrast index, densitometric limit of detection, densitometric visualizing index, and linearity range of (±)-α-tocopherol on silica gel 60.

Detection way	Fundamental absorption band λ_{max} (nm)	Broadening index [μg/(AU)]	Detection index [μg/(AU)]	Densitometric band characteristic of 25 μg (±)-α-tocopherol			Modified contrast index (AU/deg)	Limit of detection (μg)	Densitometric visualizing index [AU/(μg.deg)]	Linearity range (μg/spot) (*r*, correlation coefficient)
				Area (AU)	Height (AU)	β (deg)				
Without using visualizing reagent	270	0.724	0.45/3,100	34,519	459	16	28.69	0.45	0.479	3.46 ÷ 20.00 ($r = 0.9894$)
2,2′-Bipyridine–iron(III) chloride	524	0.413	2.08/8,915	60,474	698	9	77.56	2.08	0.323	5.76 ÷ 30.00 ($r = 0.9927$)
Rhodamine B	270	0.814	0.30/1,658	30,712	483	12	40.25	0.30	0.853	0.75 ÷ 9.60 ($r = 0.9914$)
Gentian violet	270	0.990	0.75/3,359	25,254	409	10	40.90	0.75	0.337	1.25 ÷ 9.60 ($r = 0.9952$)
Methylene violet	270	0.618	0.30/3,456	40,426	636	8	79.50	0.30	1.684	0.75 ÷ 5.76 ($r = 0.9949$)
Methylene blue	203	1.196	2.08/1,670	20,895	458	8	57.25	2.08	0.126	5.76 ÷ 25.00 ($r = 0.9948$)
Methyl green	270	0.672	0.30/1,564	37,196	576	9	64.00	0.30	1.378	0.75 ÷ 5.76 ($r = 0.9863$)
Malachite green	270	0.765	0.45/2,860	32,691	529	11	48.09	0.45	0.660	0.75 ÷ 20.00 ($r = 0.9912$)
Janus blue	270	1.106	0.60/1,300	22,608	414	10	41.40	0.60	0.377	1.25 ÷ 9.60 ($r = 0.9935$)

Source: From Analytical evaluation of visualizing reagents used to detect tocopherol and tocopherol acetate on thin layer, in J. Liq. Chromatogr. Relat. Technol.[17]

Table 3 Fundamental absorption band, broadening index, detection index and characteristic of densitometric band, modified contrast index, densitometric limit of detection, densitometric visualizing index, and linearity range of (+)-α-tocopherol acetate on silica gel 60.

Detection way	Fundamental absorption band λ_{max} (nm)	Broadening index (μg/AU)	Detection index (μg/AU)	Densitometric band characteristic of 25 μg (+)-α-tocopherol acetate			Modified contrast index (AU/deg)	Limit of detection (μg)	Densitometric visualizing index (AU/ μg.deg)	Linearity range (μg/ spot) (*r*, correlation coefficient)
				Area (AU)	Height (AU)	β (deg)				
Without using visualizing reagent	203	0.740	0.30/1,100	33,796	591	11	53.73	0.30	1.024	0.75 ÷ 20.00 (r = 0.9978)
2,2′-Bipyridine–iron(III) chloride	—	—	—	—	—	—	—	—	—	—
Rhodamine B	203	0.960	0.45/1,511	26,031	455	15	30.33	0.45	0.386	1.25 ÷ 16.00 ($r = 0.9936$)
Gentian violet	203	0.849	0.75/1,884	29,441	545	10	54.50	0.75	0.392	2.08 ÷ 25.00 ($r = 0.9908$)
Methylene violet	203	0.874	0.75/2,514	28,604	481	13	37.00	0.75	0.293	1.25 ÷ 25.00 ($r = 0.9938$)
Methylene blue	203	1.170	0.75/2,100	21,369	412	13	31.69	0.75	0.219	3.46 ÷ 20.00 ($r = 0.9927$)
Methyl green	203	0.827	0.75/3,911	30,226	564	11	51.27	0.75	0.366	1.25 ÷ 25.00 ($r = 0.9943$)
Malachite green	203	0.848	0.75/2,429	29,491	507	12	42.25	0.75	0.328	1.25 ÷ 25.00 ($r = 0.9945$)
Janus blue	203	0.830	0.75/3,750	30,125	565	11	51.36	0.75	0.365	1.25 ÷ 25.00 ($r = 0.9938$)

Source: From Analytical evaluation of visualizing reagents used to detect tocopherol and tocopherol acetate on thin layer, in J. Liq. Chromatogr. Relat. Technol.[17]

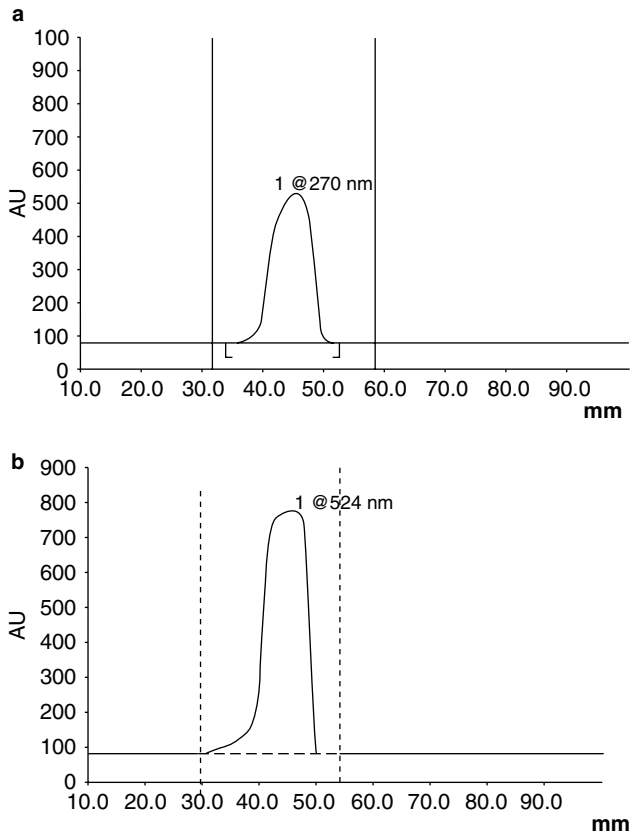

Fig. 1 Densitograms of 25.00 μg (±)-α-tocopherol (a) without using a visualizing reagent; (b) after detection with 2,2′-dipirydyl–iron(III) chloride reagent.
Source: From Analytical evaluation of visualizing reagents used to detect tocopherol and tocopherol acetate on thin layer, in J. Liq. Chromatogr. Relat. Technol.[17]

purple color. Vitamin K_1 was also detected with antimony(III) chloride (pink spots in visible light, limit of detection 8 μg), with iron(III) chloride (blue spot in visible light; limit of detection 8 μg), with sulfuric acid (green-brown spot in visible light; limit of detection 8 μg), with iodoplatinate (yellow and brown spots in visible and UV light, respectively; limit of detection 1–8 μg), and with phosphomolybdate (black spot in visible light; limit of detection 8 μg).[1–3,10]

SEPARATION OF MIXTURES OF HYDROPHOBIC VITAMINS AND OF HYDROPHOBIC VITAMINS FROM OTHER COMPOUNDS

Perisic-Janjic, Petrovic, and Hadzić[5] described a method for the quantitative analysis of a mixture of hydrophobic vitamins (vitamins A acetate, A palmitate, K_1, DL-α-tocopherol, DL-α-tocopherol acetate, D_2, D_3, K_3, K_4, and K_5) by TLC on starch, cellulose, talc impregnated with paraffin oil, and on unimpregnated talc. Vitamins A acetate, A palmitate, K_1, DL-α-tocopherol, DL-α-tocopherol acetate, D_2, and D_3 were separated on starch, cellulose, talc impregnated with paraffin oil using acetone-concentrated acetic acid (3:2, v/v) (Table 1), while vitamins K_3, K_4, and K_5 migrated with the front. Differences between the R_F values were satisfactory (except for vitamin A acetate and vitamins D_2 and D_3) and allowed for accurate identification. Vitamins K_3, K_4, and K_5 can be separated on starch impregnated with paraffin oil using a mixture of water–dioxane–acetone–formaldehyde (85:20:15:25, v/v/v/v) as the mobile phase, whereas all the others remain at the start position of the chromatographic plate. Separation is good on all three supports. It is necessary to point out that vitamins K_3, K_4, and K_5 were separated on the unimpregnated talc thin layer (Table 1).

Most of the prenyl lipids, such as chlorophylls, carotenoids, and prenylquinones, as well as tocopherols and vitamin K_1, which occur in plant lipid extracts, can be separated by TLC using silica gel plates or special mixtures of silica gel with other adsorbents.[18] But, the compounds with one double bond per isoprene and others with a partially or fully unsaturated isoprenoid chain can be separated efficiently by argentation TLC.

Chromatographic systems have been developed for RPTLC separation of hydrophobic vitamins on RP-18 as the stationary phase by Baranowska and Kadziolka.[9] A mixture of hydrophobic vitamins (A acetate, E, E acetate, and D_3) was separated using acetonitrile–benzene–chloroform (10:10:1, v/v) as the mobile phase (Table 1). Applied chromatographic conditions do not permit the separation of vitamin E and vitamin E acetate. Derivative spectrometry was used to determine vitamin A acetate in mixtures with other hydrophobic or water-soluble vitamins. Spectrodensitometric analysis of hydrophobic vitamins enables determination of vitamin A-acetate in the presence of vitamins E, E-acetate, and D_3 as well as lso of C, B_1, and nicotinamide, as earlier presented.[2,9]

Wardas and Pyka[11] separated vitamins D_2, D_3, acid of vitamin A, and DL-α-tocopherol by NPTLC and RPTLC. Vitamins D_2 and D_3 could not be separated by NPTLC and RPTLC. Eleven visualizing agents were used for detection of vitamins on TLC plates. In adsorption TLC, the limits of detection found for the vitamins followed the pattern: DL-α-tocopherol > acid of vitamin A > vitamin D_2 and D_3. After separation using adsorption TLC, the best results were obtained with aniline blue, alkaline blue, phenol red, bromocresol green, brilliant cresyl blue, and bromophenol blue. After separation using partition TLC, the best results were obtained with bromothymol blue and helasol green. The R_F values and limits of detection (μg) were earlier presented.[2,11] The color formation of vitamins D_2, D_3, acid of vitamin A, and DL-α-tocopherol with these visualizing agents were presented in earlier work.[1] The spectrodensitograms of α-tocopherol acetate, α-tocopherol, and cholecalciferol, without using the visualizing reagent,

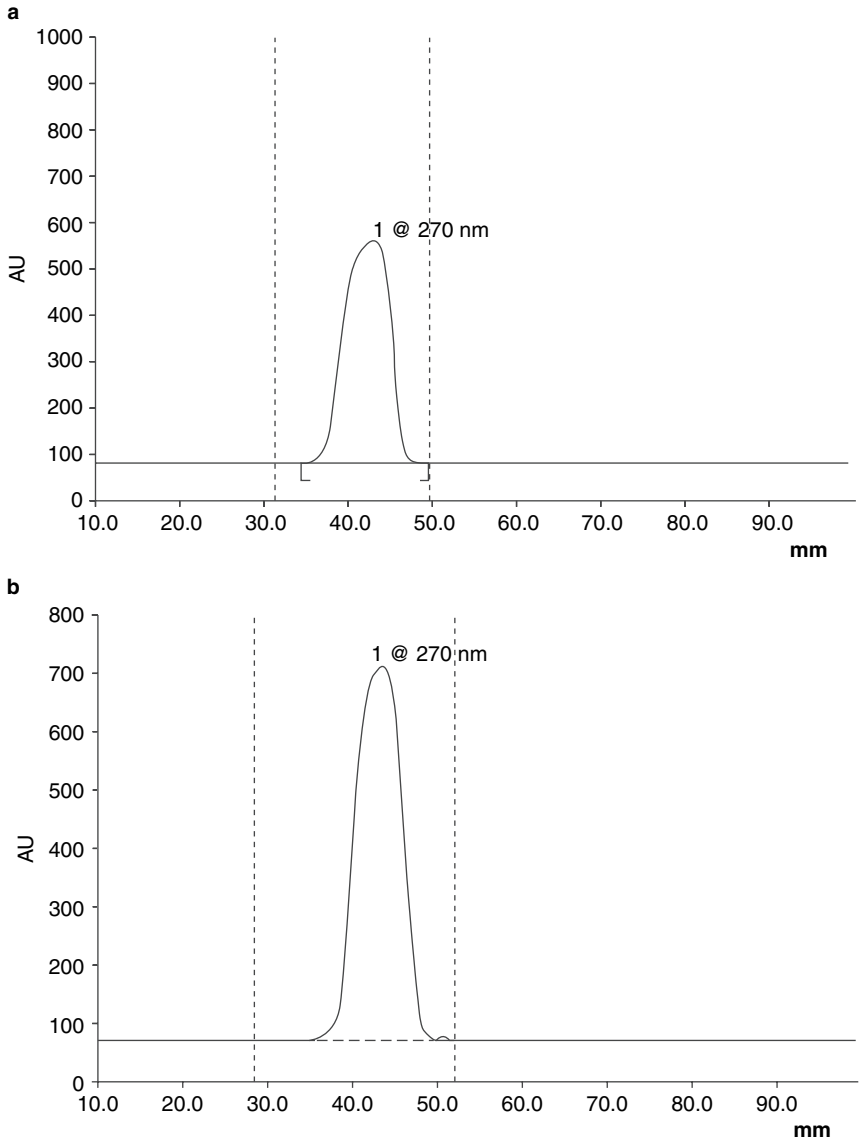

Fig. 2 Densitograms of 25.00 μg (±)-α-tocopherol after detection with (a) Rhodamine B; (b) methylene violet.
Source: From Analytical evaluation of visualizing reagents used to detect tocopherol and tocopherol acetate on thin layer, in J. Liq. Chromatogr. Relat. Technol.[17]

on different chromatographic sorbents (silica gel 60, silica gel 60 $F_{254,}$ mixture of silica gel 60 and Kieselguhr $F_{254,}$ neutral aluminum oxide $60F_{254,}$ neutral aluminum oxide $150F_{254,}$ and RP-18W) were compared.[20] The resultant spectrodensitograms of the studied compounds indicate that applied sorbents have an influence on the wavelength of the obtained fundamental absorption band (λ_{max}) and the additional absorption bands, as well as on their intensity values (AU). This fact indicates the need for standardization of the spectrodensitometric investigations regarding the applied chromatographic conditions.[20]

COMPARISON OF LIPOPHILIC PROPERTIES OF HYDROPHOBIC VITAMINS

The fat-soluble vitamins, namely, vitamin A (retinol, retinol acetate, retinol palmitate), vitamin D_2 (ergocalciferol), vitamin D_3 (cholecalciferol), vitamin E [(±)-α-tocopherol and tocopherol acetate], vitamin K_1 (phytonadione), and vitamin K_3 (menadione) were investigated by RPTLC on $RP8F_{254s}$ and $RP\text{-}18F_{254}$ plates with methanol–water mixtures of different volume compositions as the mobile phases. Linear relationships were obtained between the R_M values of the fat-soluble vitamins and the volume fraction of methanol in the mobile phase. Retention values, R_M, were extrapolated to zero methanol content and the lipophilicity values $R_{MW(RP8)}$ and $R_{MW(RP18)}$ obtained were compared with measured partition coefficients ($\log P_{exp}$) and partition coefficients ($A\log P_s$, $AC\log P$, AB/$\log P$, COSMOFRAG, milog$P$, KOWWIN, $x\log P$) were calculated using seven different software products.[21] The lipophilicity values $R_{MW(RP8)}$ and $R_{MW(RP18)}$ obtained indicate that menadione has the lowest lipophilicity. Retinol and retinol acetate have intermediate lipophilicity. However,

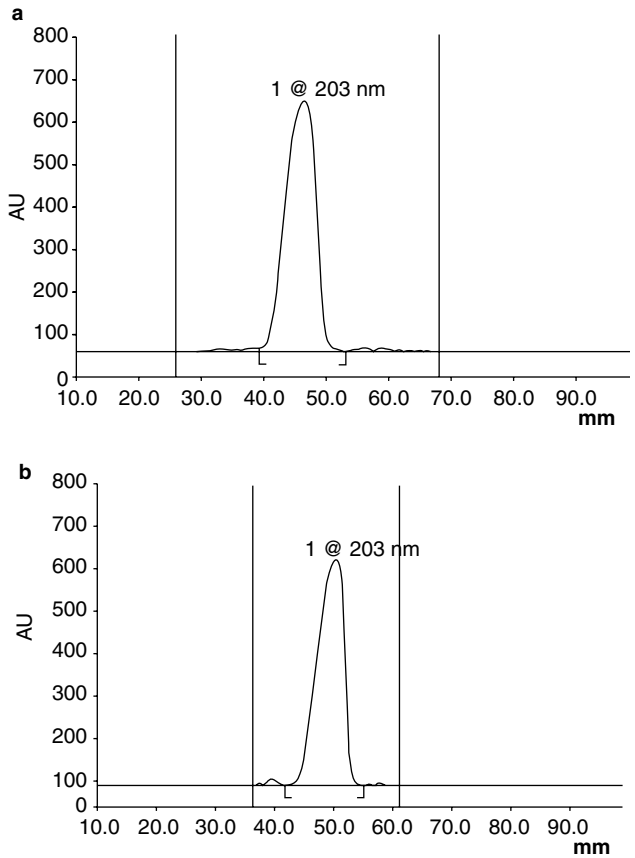

Fig. 3 Densitograms of 25.00 μg (+)-α-tocopherol acetate (a) without use a visualizing reagent; (b) after detection with methyl green.
Source: From Analytical evaluation of visualizing reagents used to detect tocopherol and tocopherol acetate on thin layer, in J. Liq. Chromatogr. Relat. Technol.[17]

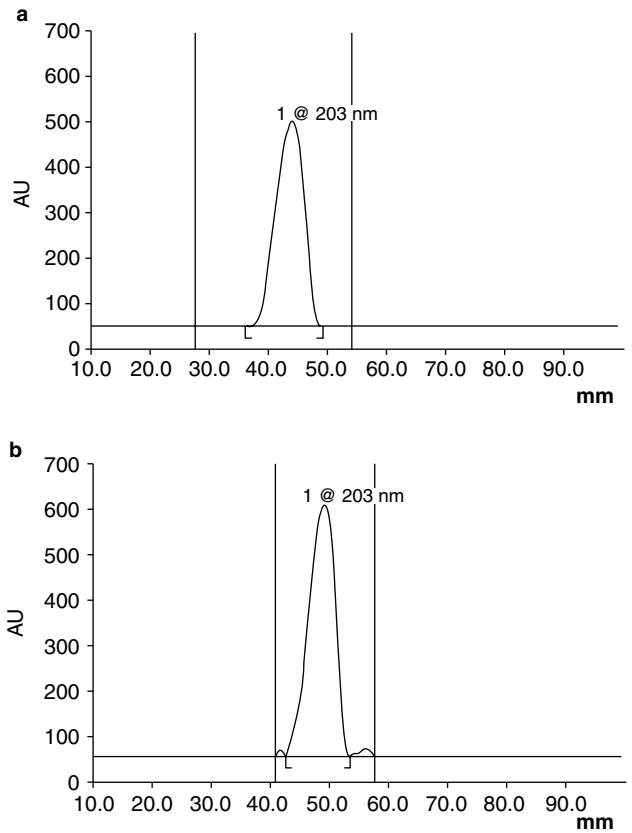

Fig. 4 Densitograms of 25.00 μg (+)-α-tocopherol acetate after detection with (a) Rhodamine B; (b) gentian violet.
Source*:* From Analytical evaluation of visualizing reagents used to detect tocopherol and tocopherol acetate on thin layer, in J. Liq. Chromatogr. Relat. Technol.[17]

ergocalciferol and cholecalciferol have higher lipophilicity and tocopherol, tocopherol acetate, phytonadione, and retinol palmitate have the highest lipophilicity. Cluster analysis was also applied for the comparison of the theoretical partition coefficients with the chromatographic lipophilicity ($R_{MW(RP8)}$ and $R_{MW(RP18)}$) of the fat-soluble vitamins. It was stated that the lipophilicity value $R_{MW(RP8)}$ shows the largest similarity to *AC*log*P*; however, $R_{MW(RP18)}$ shows the largest similarity to the theoretical partition coefficient KOWWIN. $R_{MW(RP8)}$ and $R_{MW(RP18)}$ values (i.e., values obtained on RP8F_{254s} and RP-18F_{254s} plates) well describe the lipophilic properties of fat-soluble vitamins.[21]

CONCLUSIONS

This entry has discussed the use of TLC in the investigation of hydrophobic vitamins. In earlier articles, Pyka referenced the full scientific literature for analysis of hydrophobic vitamins investigated by the TLC technique.[1–3] The use of TLC as a separation method allows for the qualitative and quantitative investigation of hydrophobic vitamins. The use of TLC techniques, together with densitometry, gives precise and sensitive quantification of vitamins A, D, E, and K compounds on TLC plates. Thin-layer chromatography is an important investigative technique for the analysis of hydrophobic vitamins.

ACKNOWLEDGMENT

This research was financed by the Medical University of Silesia as part of statutory research project KNW-1-012/08.

REFERENCES

1. Pyka, A. Lipophilic vitamins: TLC Analysis. In *Encyclopedia of Chromatography*, 3rd Ed.; Cazes, J., Ed.; Taylor & Francis: New York, 2010; 1389–1399.

2. Pyka, A. Vitamins, hydrophobic, analysis by thin layer chromatography. In *On-line Supplement of Encyclopedia of Chromatograph*, 2nd Ed.; Cazes, J., Ed.; Taylor & Francis, Inc.: New York, 2006; 1:1, 1–9. DOI:10.1081/E-ECHR-120042974; http://dx.doi.org/10.1081/E-ECHR-120042974 (accessed April 2007).
3. Pyka, A. Lipophilic vitamins. In *Handbook of Thin-Layer Chromatography: Third* Edition, *Revised and Expanded*; Sherma, J., Fried, B., Eds.; Marcel Dekker, Inc.: New York, 2003; 671–696.
4. Sliwiok, J.; Podgorny, A.; Siwek, A. Chromatographic comparison of the hydrophobicity of vitamin A derivatives. J. Planar Chromatogr. Mod. TLC **1990**, *3*, 429–430.
5. Perisic-Janjic, N.; Petrovic, S.; Hadzić, P. Separation of fat-soluble vitamins by thin-layer chromatography. Chromatographia **1976**, *9*, 130–132.
6. Kocjan, B.; Śliwiok, J. Chromatographic and spectroscopic comparison of the hydrophobicity of vitamins D_2 and D_3. J. Planar Chromatogr. Mod. TLC **1994**, *7*, 327–328.
7. Justova, V; Starka, L. Separation of functional hydroxymetabolites of vitamin D_3 by thin-layer chromatography. J. Chromatogr. **1981**, *209*, 337–340.
8. Pyka, A.; Sliwiok, J. Chromatographic separation of tocopherols. J. Chromatogr. A, **2001**, *935*, 71–77.
9. Baranowska, I.; Kądziolka, A. RPTLC and derivative spectrophotometry for the analysis of selected vitamins. Acta Chromatogr. **1996**, *6*, 61–71.
10. Jork, H.; Funk, W.; Fischer, W.; Wimmer, H. *Dünnschicht-Chromatographie, Reagenzien und Nachweismethoden*, *Physicalische ind Chemische Nachweismethoden: Grundlagen, Reagenzien I*; VCH: Weinheim, Germany, 1989; Vol. 1a; 206, 208, 216, 217, 218, 342, 402, 418.
11. Wardas, W.; Pyka, A. New visualizing agents for fatty vitamins in TLC. Chem. Anal. Warsaw **1995**, *40*, 67–72.
12. Sliwiok, J.; Kocjan, B. Chromatographische Untersuchungen der hydrophoben Eigenschaften von Tocopherolen. Fat. Sci. Technol. **1992**, *94*, 157–159.
13. Sliwiok, J.; Kocjan, B.; Labe, B.; Kozera, A.; Zalejska, J. Chromatographic studies of tocopherols. J. Planar Chromatogr. Mod. TLC **1993**, *6*, 492–494.
14. Pyka, A.; Niestrój, A. The application of topological indexes for prediction of the R_M values for tocopherols in RP-TLC. J. Liq. Chromatogr. Relat. Technol. **2001**, *24* (16), 2399–2413.
15. Hachuła, U.; Buhl, F. Determination of α-tocopherol in capsules and soybean oil after chromatographic separation. J. Planar Chromatogr. Mod. TLC **1991**, *4* (5), 416.
16. Pyka, A. Unpublished data.
17. Pyka, A. Analytical evaluation of visualizing reagents used to detect tocopherol and tocopherol acetate on thin layer. J. Liq. Chromatogr. Relat. Technol. **2009**, *32*, 312–330.
18. Lichtenthaler, H.K.; Börner, K.; Liljenberg, C. Separation of prenylquinones, prenylvitamins and prenols on thin-layer plates impregnated with silver nitrate. J. Chromatogr. **1982**, *242*, 196–201.
19. Hachuła, U. Determination of vitamin K_4 and B_1 in pharmaceutical preparations after chromatographic separation. J. Planar Chromatogr. Mod. TLC **1997**, *10*, 131–132.
20. Pyka, A.; Babuska, M.; Dziadek, A.; Gurak, D. Comparison of spectrodensitograms of the selected drugs on different chromatographic sorbents. J. Liq. Chromatogr. Relat. Technol. **2007**, *30*, 1385–1400.
21. Pyka, A. Evaluation of the lipophilicity of fat-soluble vitamins. J. Planar Chromatogr. Mod. TLC **2009**, *22*, 211–215.

Vitamins: CCC Separation by Cross-Axis Coil Planet Centrifuge

Kazufusa Shinomiya
College of Pharmacy, Nihon University, Chiba, Japan

Yoichiro Ito
National Heart, Lung, and Blood Institute (NHLBI), National Institutes of Health (NIH), Bethesda, Maryland, U.S.A.

INTRODUCTION

Cross-axis coil planet centrifuges (cross-axis CPC), which have been widely used in the separation of natural and synthetic products, are some of the most useful models among various types of countercurrent chromatographic (CCC) apparatuses.[1–3] It produces a unique mode of planetary motion such that the column holder rotates about its horizontal axis while revolving around the vertical axis of the centrifuge.[4–5] The centrifugal force field produced by the planetary motion provides stable retention of the stationary phase for polar two-phase solvent systems such as aqueous–aqueous polymer phase systems with extremely low-interfacial tension and high viscosity. Our previous studies demonstrated that cross-axis CPC, equipped with either a multilayer coil or eccentric coil assembly in the off-center position of the column holder, can be effectively applied for the separation of proteins[6–8] and sugars.[9]

This entry illustrates the CCC separation of various vitamins by means of cross-axis CPC equipped with eccentric coil assemblies.[10–11]

APPARATUS AND SEPARATION COLUMNS

All existing cross-axis CPCs are classified according to their relative column position on the rotary frame, e.g., *X*,[4–5] *XL*,[12] *XLL*,[13] and *XLLL*,[14] where *X* is the distance from the column holder axis to the central axis of the centrifuge, and *L* is the distance between the holder and the middle point of the rotary shaft. Increasing the ratio *L*/*X* improves the retention of the stationary phase by moderating phase mixing. The separations of vitamins described below were performed using the $X - 1.5L$ cross-axis CPC, which holds the separation column at $X = 10$ cm and $L = 15$ cm.

The separation column was prepared by means of a pair of eccentric coil assemblies, which were made by winding a single piece of 1 mm I.D. polytetrafluoroethylene (PTFE) tubing onto 7.6 cm long, 5 mm O.D. nylon pipes forming 20 units of serially connected left-handed coils. Then, a set of these coil units was arranged around the holder with their axes parallel to the holder axis. A pair of identical coil assemblies was connected in series to obtain a total column capacity of 26.5 ml.

CCC SEPARATION OF WATER-SOLUBLE VITAMINS

In CCC, the partition coefficient (K) is an important parameter which is used for selecting the optimal solvent system because it predicts the retention time of each component. Table 1 shows the K values of various water-soluble vitamins in the 1-butanol/aqueous 0.15 *M* monobasic potassium phosphate system. Most of the water-soluble vitamins were partitioned, almost unilaterally, into the aqueous phase in this solvent system, except that riboflavin and nicotinamide were distributed significantly into the organic phase ($K = 0.54$–1.84). Adding ethanol to the two-phase solvent system significantly increased the

Table 1 Partition coefficients of water-soluble vitamins in 1-butanol/aqueous 0.15 *M* monobasic potassium phosphate two-phase solvent systems.

1-Butanol	1	4	8
Ethanol	0	1	3
0.15 *M* KH_2PO_4	1	4	8
Thiamine nitrate (M.W. 327.36)	0.03	0.05	0.11
Thiamine hydrochloride (M.W. 327.27)	0.14	0.05	0.17
Riboflavin (M.W. 376.37)	0.54	0.83	1.08
Riboflavin sodium phosphate (M.W. 478.33)	0.11	0.18	0.34
Pyridoxine hydrochloride (M.W. 205.64)	0.23	0.43	0.59
Cyanocobalamin (M.W. 1355.38)	0.04	0.12	0.24
L-Ascorbic acid (M.W. 176.12)	0.07	0.11	0.15
Nicotinamide (M.W. 122.13)	1.84	1.41	1.34

Partition coefficients were calculated from the absorbance of the upper phase divided by that of lower phase at 260 nm.

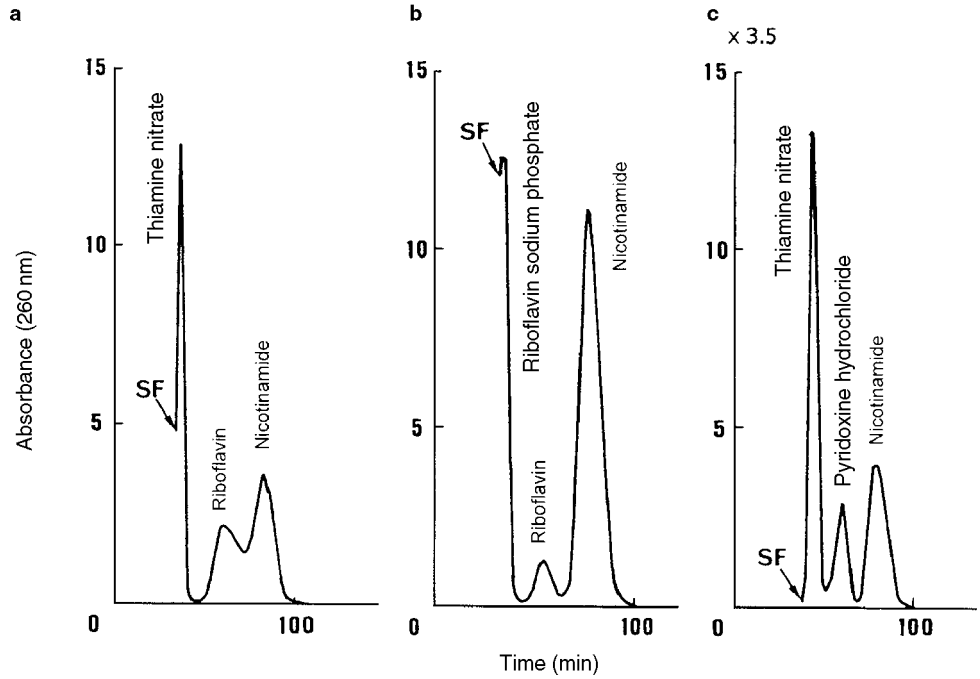

Fig. 1 CCC separation of water-soluble vitamins by cross-axis CPC. Experimental conditions: apparatus, cross-axis CPC equipped with a pair of eccentric coil assemblies, 1 mm I.D. and 26.5 ml capacity; sample. a, Thiamine nitrate (2.5 mg) + riboflavin (1.5 mg) + nicotinamide (2.5 mg). b, Riboflavin sodium phosphate (2.5 mg) + nicotinamide (2.5 mg). c, Thiamine nitrate (2.8 mg) + pyridoxine hydrochloride (4.0 mg) + nicotinamide (3.0 mg); solvent system: (a) and (b) 1-butanol/aqueous 0.15 *M* monobasic potassium phosphate (1:1) and (c) 1-butanol/ethanol/aqueous 0.15 *M* monobasic potassium phosphate (8:3:8); mobile phase: lower phase; flow rate: 0.4 ml/min; revolution: 800 rpm. SF = solvent front.

partition coefficients of riboflavin and pyridoxine hydrochloride.

Fig. 1a illustrates the CCC separation of thiamine nitrate, riboflavin, and nicotinamide by cross-axis CPC, with the 1-butanol/aqueous 0.15 *M* monobasic potassium phosphate (1:1) system. Riboflavin sodium phosphate is also resolved from riboflavin with the same solvent system (Fig. 1b). When a more polar solvent system consisting of 1-butanol/ethanol/aqueous 0.15 *M* monobasic potassium phosphate (8:3:8) is used, thiamine nitrate, pyridoxine hydrochloride, and nicotinamide are well resolved from each other, as shown in Fig. 1c.

In order to improve the separation of each water-soluble vitamin by cross-axis CPC, three ion-pair

Table 2 Effect of ion-pair reagents on partition coefficients of water-soluble vitamins in 1-butanol/aqueous 0.15 *M* KH_2PO_4 solvent systems.

	1-Butane sulfonic acid		1-Pentane sulfonic acid		1-Octane sulfonic acid
Ion-pair reagent concentration (%)	**1.5**	**2.5**	**1.5**	**2.5**	**1.5**
Thiamine nitrate (M.W. 327.36)	0.18	0.29	0.76	1.01	2.45
Thiamine hydrochloride (M.W. 327.27)	0.17	0.25	0.73	0.97	2.42
Riboflavin (M.W. 376.37)	0.58	0.70	0.57	0.95	1.07
Riboflavin sodium phosphate (M.W. 478.33)	0.04	0.29	0.08	0.20	0.13
Pyridoxine hydrochloride (M.W. 205.64)	0.57	0.73	0.77	0.86	1.63
Cyanocobalamin (M.W. 1355.38)	0.08	0.44	0.37	0.35	0.47
L-Ascorbic acid (M.W. 176.12)	0.04	0.13	0.09	0.09	0.09
Nicotinamide (M.W. 122.13)	1.32	0.78	1.46	1.39	1.49

Partition coefficients were calculated from the absorbance of the upper phase divided by that of lower phase at 260 nm.

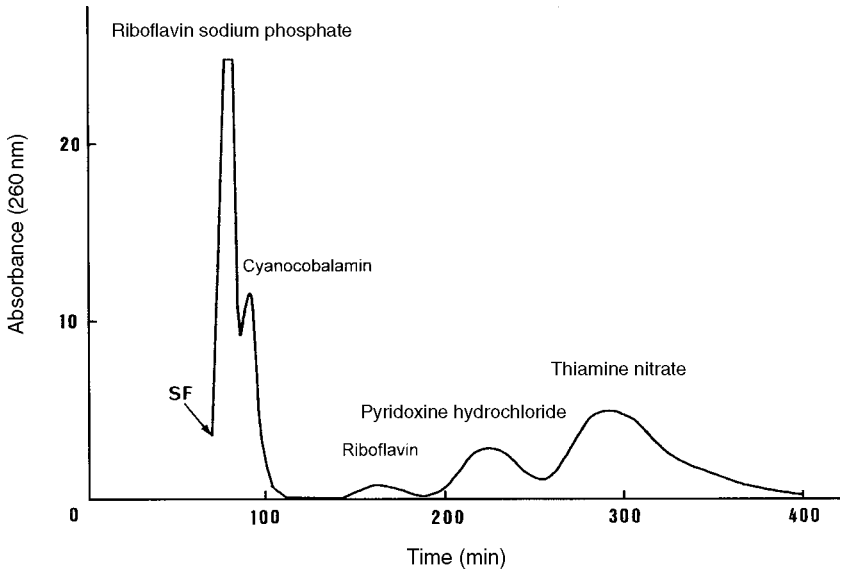

Fig. 2 CCC separation of water-soluble vitamins by cross-axis CPC. Experimental conditions: sample, riboflavin sodium phosphate (2.5 mg) + cyanocobalamin (2.5 mg) + pyridoxine hydrochloride (2.5 mg) + thiamine nitrate (2.5 mg); solvent system, 1-butanol and aqueous 0.15 *M* monobasic potassium phosphate containing 1.5% of 1-octanesulfonic acid sodium salt; mobile phase, lower phase; flow rate, 0.2 ml/min. For other experimental conditions, see Fig. 1 caption. SF = solvent front.

reagents were added to the 1-butanol/aqueous 0.15 *M* monobasic potassium phosphate system. The *K* values of the vitamins in this solvent system are summarized in Table 2. Most of the *K* values increased by increasing the concentration and carbon number of ion-pairing reagents added in the two-phase solvent system. Among these ion-pairing reagents, 1-octanesulfonic acid sodium salt was found to be most suitable and was selected for the separation of water-soluble vitamins by cross-axis CPC.

Fig. 2 illustrates the CCC chromatogram of water-soluble vitamins obtained with the above solvent system, which comprise 1-butanol and aqueous 0.15 *M* monobasic potassium phosphate, including 1.5% of 1-octanesulfonic acid sodium salt. Riboflavin sodium phosphate, cyanocobalamin, riboflavin, pyridoxine hydrochloride, and thiamine nitrate were separated using the lower phase as the mobile phase. Riboflavin was found as an impurity contained in the riboflavin sodium phosphate sample.

CCC SEPARATION OF FAT-SOLUBLE VITAMINS

The *K* values of fat-soluble vitamins obtained with four different kinds of solvent systems are summarized in Table 3. The most suitable solvent system was found to be the 2,2,4-trimethyl pentane (iso-octane)/methanol binary system.

Fig. 3a illustrates the CCC separation of fat-soluble vitamins using the cross-axis CPC equipped with eccentric coil assemblies. Calciferol, vitamin A acetate, and (±)-α-tocopherol acetate were well resolved from each other and eluted within 2.5 hr. Vitamin K_3 and Vitamin K_1 were also completely resolved with the same solvent system, as shown in Fig. 3b.

CONCLUSIONS

As described above, the cross-axis CPC, equipped with eccentric coil assemblies, can be used for the separation of both water-soluble and fat-soluble vitamins by selecting suitable two-phase solvent systems.

Table 3 Partition coefficients of fat-soluble vitamins in four different two-phase solvent systems.

	n-Hexane/aqueous 90% acetonitrile (1:1)	*n*-Hexane/ acetonitrile (1:1)	2,2,4-Trimethyl pentane/methanol (1:1)	*n*-Hexane/ethyl acetate/methanol/water (1:1:1:1)
Vitamin A acetate	5.34	1.69	1.34	130
Calciferol (M.W. 396.66)	8.14	3.29	0.83	71.2
(±)-α-Tocopherol acetate (M.W. 472.25)	48.5	10.1	3.11	62.6
Vitamin K_1 (M.W. 450.71)	61.6	5.79	3.92	9.23
Vitamin K_3 (M.W. 172.19)	0.31	0.22	0.35	2.40

Partition coefficients were calculated from the absorbance of the upper phase divided by that of lower phase at 280 nm.

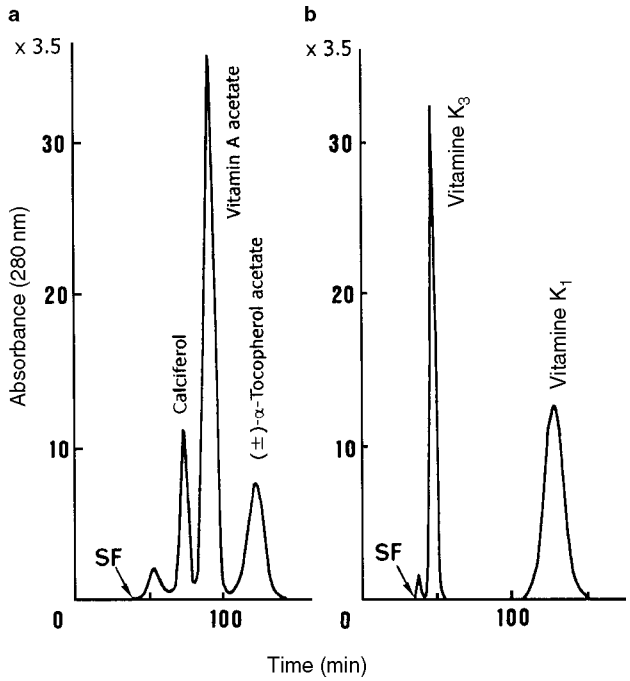

Fig. 3 CCC separation of fat-soluble vitamins by cross-axis CPC. Experimental conditions: sample, (a) calciferol (3 mg) + vitamin A acetate (30 mg) + (±)-α-tocopherol acetate (40 mg) and (b) vitamin K_3 (3 mg) + vitamin K_1 (10 mg); solvent system, 2,2,4-trimethyl pentane/methanol (1:1); mobile phase, lower phase. For other experimental conditions, see Fig. 1 caption. SF = solvent front.

REFERENCES

1. Mandava, N.B., Ito, Y., Eds.; *Countercurrent Chromatography: Theory and Practice*; Marcel Dekker, Inc.: New York, 1988; 79.
2. Conway, W.D. *Countercurrent Chromatography: Apparatus, Theory and Applications*; VCH: New York, 1990; 37.
3. Ito, Y., Conway, W.D., Eds.; *High Speed Countercurrent Chromatography*; Wiley-Interscience: New York, 1996; 3.
4. Ito, Y. Cross-axis synchronous flow-through coil planet centrifuge free of rotary seals for preparative counter-current chromatography. Part I: Apparatus and analysis of acceleration. Sep. Sci. Technol. **1987**, *22*, 1971.
5. Ito, Y. Cross-axis synchronous flow-through coil planet centrifuge free of rotary seals for preparative counter-current chromatography. Part II: Studies on phase distribution and partition efficiency in coaxial coils. Sep. Sci. Technol. **1987**, *22*, 1989.
6. Shinomiya, K.; Menet, J.-M.; Fales, H.M.; Ito, Y. Studies on a new cross-axis coil planet centrifuge for performing counter-current chromatography. I. Design of the apparatus, retention of the stationary phase, and efficiency in the separation of proteins with polymer phase systems. J. Chromatogr. **1993**, *644*, 215.
7. Shinomiya, K.; Inokuchi, N.; Gnabre, J.N.; Muto, M.; Kabasawa, Y.; Fales, H.M.; Ito, Y. Countercurrent chromatographic analysis of ovalbumin obtained from various sources using the cross-axis coil planet centrifuge. J. Chromatogr. A, **1996**, *724*, 179.
8. Shinomiya, K.; Muto, M.; Kabasawa, Y.; Fales, H.M.; Ito, Y. Protein separation by improved cross-axis coil planet centrifuge with eccentric coil assemblies. J. Liq. Chromatogr. Relat. Technol. **1996**, *19*, 415.
9. Shinomiya, K.; Kabasawa, Y.; Ito, Y. Countercurrent chromatographic separation of sugars and their *p*-nitrophenyl derivatives by cross-axis coil planet centrifuge of stationary phase. J. Liq. Chromatogr. Relat. Technol. **1999**, *22*, 579.
10. Shinomiya, K.; Komatsu, T.; Murata, T.; Kabasawa, Y.; Ito, Y. Countercurrent chromatographic separation of vitamins by cross-axis coil planet centrifuge with eccentric coil assemblies. J. Liq. Chromatogr. Relat. Technol. **2000**, *23*, 1403.
11. Shinomiya, K.; Yoshida, K.; Kabasawa, Y.; Ito, Y. Countercurrent chromatographic separation of water-soluble vitamins by cross-axis coil planet centrifuge using an ion-pair reagent with polar two-phase solvent system. J. Liq. Chromatogr. Relat. Technol. **2001**, *24*, 2615.
12. Ito, Y.; Oka, H.; Slemp, J. Improved cross-axis synchronous flow-through coil planet centrifuge for perfoming counter-current chromatography. I. Design of the apparatus and analysis of acceleration. J. Chromatogr. **1989**, *463*, 305.
13. Ito, Y.; Kitazume, E.; Bhatnagar, M.; Trimble, F. Cross-axis synchronous flow-through coil planet centrifuge (Type XLL). I. Design of the apparatus and studies on retention of stationary phase. J. Chromatogr. **1991**, *538*, 59.
14. Shibusawa, Y.; Ito, Y. Countercurrent chromatography of proteins with polyethylene glycol-dextran polymer phase systems using type-XLLL cross-axis coil planet centrifuge. J. Liq. Chromatogr. **1992**, *15*, 2787.

Void Volume in LC

Kiyokatsu Jinno
Department of Materials Science, Toyohashi University, Toyohashi, Japan

INTRODUCTION

The column dead volume can be defined as the space in the column which is not working for the chromatographic separations (i.e., not occupied by the stationary phase and its support). Its value is generally determined by an elution time or elution volume of a non-retained solute in the chromatographic system. If the column dead volume is measured by a retention time of a non-retained solute, one can refer to this as a *column dead time* t_0.

DISCUSSION

The accurate determination of the column void time, t_0, is of fundamental importance in chromatography.[1] This is explained by the fact that a reliable estimation of this quantity is essential for the correct calculation of the retention factors (some refer to this as the *capacity factor*), k, which serves as the fundamental parameter for the comparison of retention data and for the interpretation of the physicochemical phenomena taking place within a chromatographic column. However, the determination of this parameter is very sensitive to the estimated value of the column void time, as can be seen from the equation

$$k = \frac{t_r - t_0}{t_0} \tag{1}$$

where t_r is the solute retention time and t_0 is the column dead time (Fig. 1). A precise knowledge of t_0 is also essential for the proper optimization of the chromatographic system.[2] In contrast to gas chromatography (GC), where the problem of column dead-time determination has been satisfactory solved,[3] determination of the true column void time in liquid chromatography (LC) presents both theoretical and practical difficulties and still remains an open question.

Controversial opinions exist among scientists regarding the meaning of "column dead time" in liquid chromatography (LC).[4] In its broad sense, the term "column dead time" refers to the elution volume of an unretained and unexcluded solute, but it is not easy to establish which solute (if any) can be treated as both unretained and unexcluded. In LC practice, quite a large number of solutes[5] (e.g., mobile-phase components, isotopically labeled mobile-phase components, ionic and nonionic species) had been used as void time markers. The most popular method used in reversed-phase (RP) LC is to use sodium nitrate or sodium nitrite as the probe, but the use of such compounds as the marker was termed clearly dangerous by Berendsen et al.[6] Use of small ionic species such as sodium nitrate as a void time marker was found to have the drawback that there exists a possibility of exclusion of the ionic species and, when used in small concentrations, they serve as the marker for ionic exclusion volume instead of column dead volume (Donan exclusion). Even to use higher concentrations of ionic species is now rarely utilized due to obvious shortcomings by the Donan exclusion effect. Other existing experimental methods for the determination of LC column dead time also represent a serious contradiction of opinions among scientists and, at this moment, there are no definitive methods to determine column t_0.

One promising approach to experimentally determine t_0 is the linearization method,[6] although there are opinions against this method as "undesirable," pointing out some shortcomings. The linearization approach uses the homolog series of compounds, which have various alkyl chains; their retention times are plotted against their chain lengths. Then, the resultant linear curve is extrapolated to zero chain length for the t_0 value. Some people proposed various solutes in homolog series for this purpose, but there is no confirmation

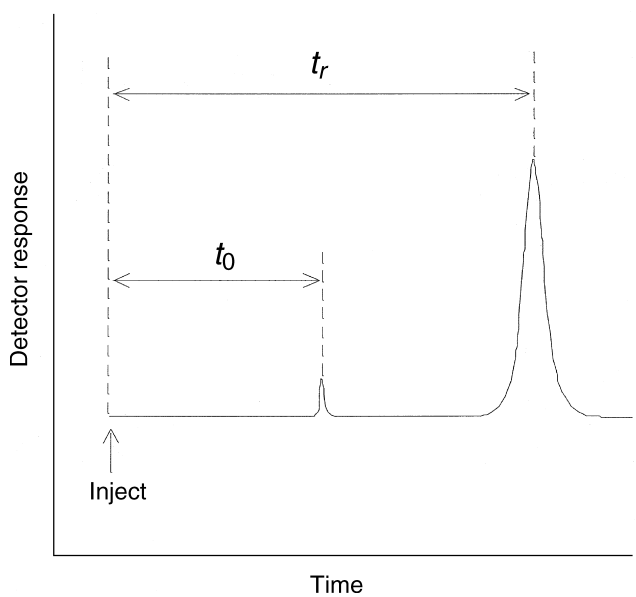

Fig. 1 Void volume determination.

concerning the accuracy of the measured t_0 value and, therefore, the opinions against on this method have also appeared in many publications. On the other hand, static methods[7] have been found to represent the upper limit of column porosity, and not the column dead volume proper.

Although the above discussions have appeared numerous times in many publications, workers always need to determine the retention factor, k, in LC separations. In order to determine t_0 experimentally, one has to state what kind of method was used to determine t_0 in his experiments. This is the only best way at this moment to recommend to all chromatographers concerning column void time, although, in the near future, the "best, reliable, theoretically well-interpreted" methods will be adopted.

REFERENCES

1. Krstulovic, A.M.; Colin, H.; Guiochon, G. Comparison of methods used for the determination of void volume in reversed-phase liquid chromatography. Anal. Chem. **1982**, *54*, 2438.
2. Alhedai, A.; Martire, D.E.; Scott, R.P.W. Column "dead volume" in liquid chromatography. Analyst **1989**, *114*, 869.
3. Ettre, L.S. Chromatographia **1980**, *13*, 73.
4. Knox, J.H.; Kaliszan, R. Theory of solvent disturbance peaks and experimental determination of thermodynamic dead-volume in column liquid chromatography. J. Chromatogr. **1985**, *349*, 211.
5. Malik, A.; Jinno, K. Determination of void/dead volume of liquid chromatographic columns containing β-cyclodextrin as the stationary phase—a survey of literature. Chromatographia **1990**, *30*, 135.
6. Berendsen, G.E.; Schoenmakers, P.J.; de Galan, L.; Vigh, G.; Varga-Puchnoy, Z.; Inczedy, J. On the determination of the hold-up time in reversed phase liquid chromatography. J. Liq. Chromatogr. Relat. Technol. **1980**, *3* (11), 1669.
7. Slaats, E.H.; Kraak, J.C.; Brugman, W.J.T.; Poppe, H. Study of the influence of competition and solvent interaction on retention in liquid-solid chromatography by measurement of activity coefficients in the mobile phase. J. Chromatogr. **1978**, *149*, 255.

Wheat Proteins: FFF

Susan G. Stevenson
N.M. Edwards
K.R. Preston
Grain Research Laboratory, Canadian Grain Commission, Winnipeg, Manitoba, Canada

INTRODUCTION

The technique of flow field-flow fractionation (FFF) has been used for size fractionation and analysis of wheat protein extracts since the mid-1990s. Since that time its application has been facilitated by improvements to instrumentation and new extraction methods allowing accurate quantification of size distribution. In addition, hyphenation of FFF systems with equipment such as refractive index (RI) and multiangle laser light-scattering (MALLS) detectors has enabled direct determination of molecular weight and radius of gyration (R_g), thus allowing estimates of protein shape. All these advances now provide the researcher with a tool that permits the quantitative and qualitative analysis of wheat proteins, and in particular, those larger polymeric proteins previously excluded in the void volume using traditional size fractionation techniques such as size exclusion HPLC (SE-HPLC), gel filtration, and sodium dodecyl sulfate-polyacrylamide gel electrophoresis (SDS–PAGE).

WHEAT PROTEINS

The storage proteins of wheat, collectively referred to as gluten, cover a wide molecular size range and include some of the largest known naturally occurring biological proteins.[1] The monomeric storage proteins (gliadins), as well as the salt soluble albumins and globulins, normally have molecular weights of $<$100,000. The polymeric storage proteins (glutenin) have molecular weights that extend into the millions. The size distribution of the gluten proteins, in particular, the polymeric wheat proteins, is closely related to the dough processing characteristics and quality of wheat based products.[2] Size fractionation techniques such as SE-HPLC, gel filtration, and SDS–PAGE are commonly used to characterize these proteins. These methods normally provide fractionation ranges up to molecular weights of $0.5–1 \times 10^6$ or slightly higher. However, many of the larger polymeric glutenin proteins appear in the void volume with SE-HPLC and gel filtration and are not resolved.[3] Flow FFF provides a newer tool to examine the polymeric wheat proteins, especially those constituting the highest molecular weight glutenin fraction, since its resolution is not impeded by an exclusion limit.[3]

FLOW FFF

Flow FFF is one of a family of techniques that allows fractionation of macromolecules based on size related parameters. A detailed explanation of the mechanism and theory appears elsewhere in this entry. Fractionation is achieved by the application of a field (cross-flow) perpendicular to the channel flow.[4] Components showing greater response to the force exerted by the field are displaced further from the center of the channel flow and toward the channel wall. Laminar flow through the channel produces a parabolic flow profile; therefore, the elution order of components is determined by their relative displacement. Size fractionation range, resolution, and run time can be adjusted by manipulating both the channel flow and the strength of the field. In symmetrical flow FFF, the eluent crossflow is introduced through a porous frit on one side of the channel (depletion) wall and exits through a semipermeable membrane and frit that form the other (accumulation) wall. With asymmetrical flow FFF, the upper channel wall is solid, and crossflow is generated by directing a portion of the channel flow through the accumulation wall. In both methods, components must be "relaxed" or equilibrated within the channel prior to elution. For symmetrical FFF, this is accomplished through a process referred to as "stop–flow" wherein the channel flow is "stopped" by diverting it around the channel leaving sample components exposed solely to crossflow forces. Component separation into layers within the channel occurs as equilibration is reached between crossflow and diffusion forces. In the case of asymmetrical FFF, sample focusing/relaxation is achieved through the use of switching valves to reverse the direction of flow at the channel outlet just prior to injection for the requisite focusing/relaxation period.[5] In conventional mode flow FFF, separation of macromolecules up to approximately 1 μm is based upon their diffusion coefficient.

Particles larger than 1 μm are separated in steric or hyperlayer mode and elute in reversed order (larger to

This entry is a contribution (no. M302) of the Canadian Grain Commission, Grain Research Laboratory, Canada.

smaller). In conventional mode, diffusion coefficients and the related Stokes' diameters (d_s) of separated species can be directly calculated based on elution time and channel characteristics for both symmetrical and asymmetrical flow FFF.[4]

APPLICATION OF FFF TO WHEAT PROTEIN ANALYSIS

Initial Studies

The first two reports on the use of flow FFF for separating wheat proteins appeared in the literature in 1996 when researchers from two independent laboratories reported characterization of wheat proteins from different varieties extracted by different methods and analyzed on two different types of flow FFF apparatus. Wahlund et al.[6] used asymmetrical flow FFF to examine proteins extracted from two bread wheat varieties of different protein content using sequential extraction with increasing concentrations of dilute hydrochloric acid (HCl). Stevenson and Preston[3] used symmetrical flow FFF to examine proteins extracted from Katepwa, a high quality bread wheat variety, using a modification of the traditional Osborne extraction procedure. Results from both studies showed that d_s for the monomeric gliadin-type fractions ranged in size from 8 to 10 nm while those of the polymeric glutenin fractions ranged from 15 to 35 nm in size.[3,6] Calculation of molecular weights based on hydrodynamic diameter transformations (lower limit defined by flexible random coil and upper limit by spherical protein) for the larger glutenin components resulted in values consistent with those reported in the literature for glutenins (440,000–11 million).[6]

Refinements to Equipment and FFF Techniques

A number of refinements to equipment design and techniques have been introduced since publication of the original wheat protein studies. Incorporation in the flow FFF channel of a frit inlet (FI), a small piece of permeable frit material equipped with a separate FI embedded in the depletion wall of the channel just past the sample inlet, has permitted the use of hydrodynamic relaxation as a replacement for stop–flow relaxation, thus eliminating pressure fluctuations associated with the latter.[7] FI also reduces sample adhesion to the membrane on the accumulation wall, thereby reducing the likelihood of baseline drift and artifacts. Incorporation of a frit outlet (FO) located at the depletion wall of the channel just before the channel outlet has facilitated the removal/recirculation of a high proportion of eluent buffer. The remaining eluent buffer containing the sample components is eluted in the channel outlet flow at much higher (up to 10 times)[7,8] effective concentrations resulting in much higher detector signal to noise ratios thereby eliminating the need for extremely sensitive detection methods. Recirculation of the FO flow back through the FI and that of the crossflow back through the upper frit leads to further baseline stability.[9]

Stevenson, Ueno, and Preston[9] used these refinements in channel architecture and techniques in the development of the first automated FFF procedure by using a frit inlet/frit outlet (FIFO) flow FFF channel with recirculating frit and crossflows. In addition to much higher throughput, analysis of wheat protein fractions produced by the same Osbome fractionation method and from the same flour as used for previous stop–flow studies[3] showed improved separation with more well-resolved peaks, particularly with the two polymeric glutenin protein fractions [acetic acid (HAc) extractable and sonicated HAc extractable]. As can be seen in Fig. 1a and b, the major peaks for albumins and globulins and for gliadins indicate molecular sizes <10 nm. The HAc extractable proteins (Fig. 1c) show major peaks at d_s 8 and 11 nm plus significant tailing in the 20–35 nm area, indicating the presence of some larger polymeric glutenin. The molecular size distribution in the sonicated fraction (Fig. 1d) covers a very broad range ($d_s = 12–50 + $ nm). Examination of all four fractograms (Fig. 1a–d) demonstrates that the bulk of the large polymeric material is extracted with sonication. The automated FIFO system also allows much more precise quantification of fractogram peak areas and/or size ranges. Average coefficients of variability of peak areas for six standard molecular size marker proteins were $<2\%$ while wheat protein size fractions showed values $<5\%$. The automated FFF procedure was exploited in conjunction with a simplified sequential extraction technique[10] employing dilute HAc without, then with, sonication to extract monomeric rich and polymeric rich wheat protein fractions to study the relationship of size distribution to dough strength properties. The proportion of total flour protein in the polymeric fraction and that of the larger sized (d_s) polymeric protein above 20 nm were highly correlated to dough mixing time. An extraction efficiency of about 97% compared favorably with that obtained using the same extraction protocol with 2% SDS in 0.05 *M* phosphate buffer, the buffer commonly used for polymeric wheat protein extraction. Added potential advantages of using HAc rather than SDS based buffers include easier removal from extracted protein where additional studies are to be conducted and less disruption of the secondary protein structure.

More recently, direct coupling (hyphenation) of MALLS and RI detectors to flow FFF channel has been used to provide direct, accurate determination of molecular weights, R_g and conformation of polymeric wheat proteins.[11–13] Problems such as overloading the FFF channel in order to provide sufficient signal for RI/MALLS have been addressed for both asymmetrical[11] and symmetrical[12] FFF.

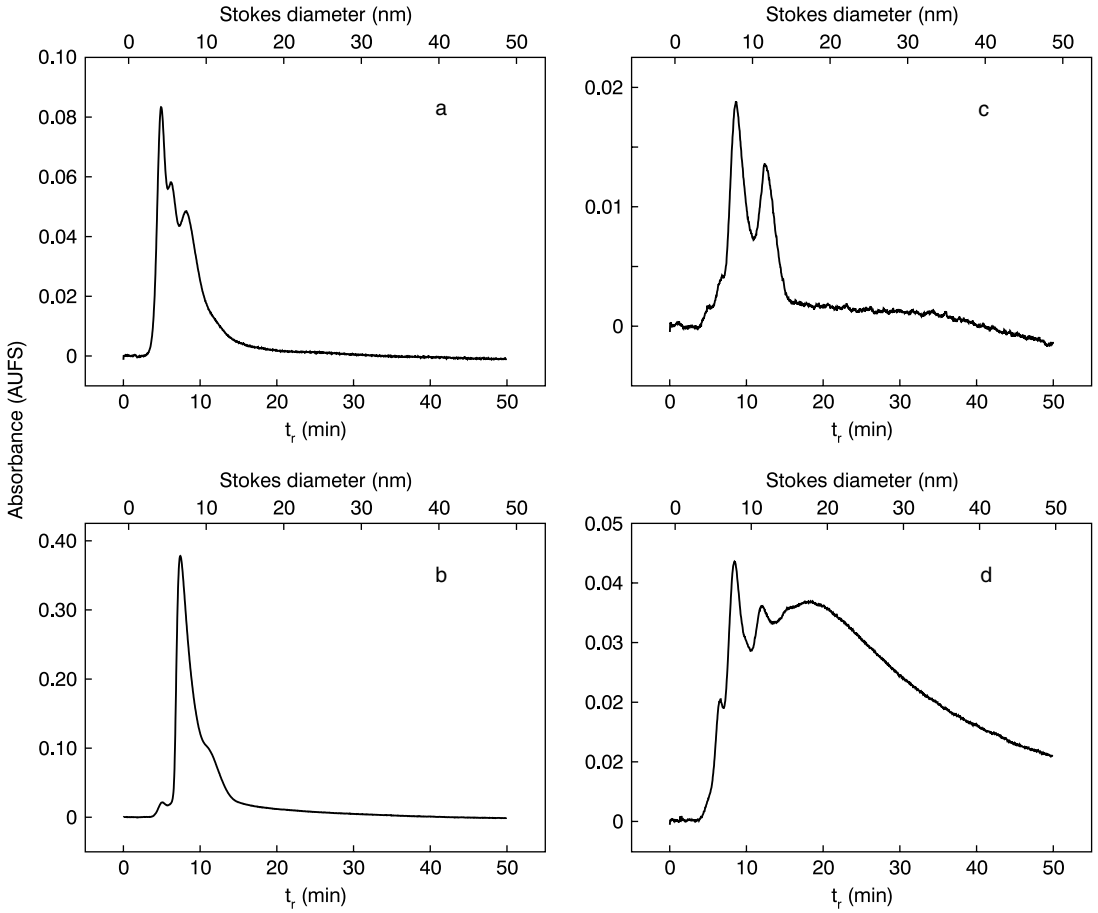

Fig. 1 Elution profiles for (a) albumin and globulin, (b) gliadin, (c) glutenin, and (d) sonicated acetic acid extractable fractions run on FIFO automated FFF channel. Normal operating conditions are $V_s = 0.2$, $V_f = 1.4$, and $V_c = 5$ ml/min.

The use of symmetrical flow FFF hyphenated with RI and MALLS detectors to assess the size and shape of sequentially dilute HAc extracted monomeric rich and sonicated HAc extracted polymeric rich wheat proteins was reported by Stevenson et al.[12] M_w values at peak for the monomeric extract varied from 31,000 to 33,000 and increased to approximately 110,000 at later elution times. Results for all five varieties of wheat included in this study were similar for the monomeric wheat protein extracts. The M_w profiles of polymeric extracts for the five wheat samples ranged from 225,000 to 300,000 at peak and increased to approximately 7×10^6 after 60 min of elution as shown in Fig. 2. R_g values for the polymeric protein fraction showed relatively small changes with increasing elution time (M_w), suggesting that the larger M_w polymeric proteins tend toward a more compact structure than the lower M_w polymeric proteins.

An asymmetrical FFF channel coupled to RI and MALLS detectors was used by Arfvidsson and Wahlund[11] to investigate the retention behavior of freeze dried HCl extractable glutenin resuspended by stirring or sonication in SDS buffer. Although sonication provided a rapid and efficient method for glutenin protein dissolution, there was evidence of physical breakdown of the largest glutenin proteins. For analysis of these proteins, the use of gentle stirring for long periods of time was preferable[11] since the average M_w increased to 2×10^7 compared to 5×10^6 with sonication.

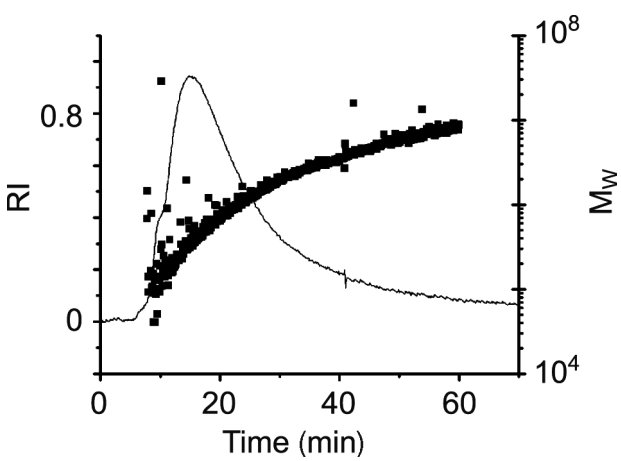

Fig. 2 Flow field-flow fractionation fractogram and MALLS M_w profile of polymeric protein fraction for the variety Katepwa.

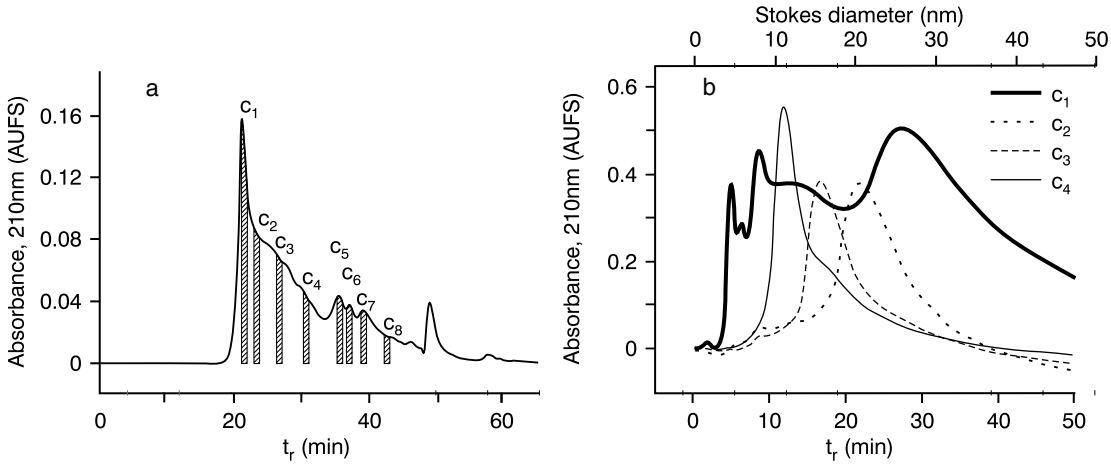

Fig. 3 Flow field-flow fractionation (flow FFF) analysis of size-exclusion HPLC subfractions from Katepwa wheat flour. a, SE-HPLC subfractions c_{1-8}; b, flow FFF profiles of SE-HPLC subfractions c_{1-4}.
Source: From A simplified dilute acetic acid based extraction procedure for the preparation of polymeric wheat flour protein for SE-HPLC and flow FFF analysis, in Cereal Chem.[10]

Measuring/Monitoring Changes in Molecular Size Distribution

Field-flow fractionation has shown to be useful for systematically monitoring changes in molecular size distribution of wheat proteins, for example, those caused by treatment with oxidants or reductants. Reduction of the polymeric glutenin fractions with dithiothreitol[3] or 2-mercaptoethanol[6] produced shifts in peak positions to <10 nm, indicating release of their interchain disulfide bonded constituent subunits. Stevenson, Ueno, and Preston[9] showed that treatment of a polymeric protein extract with hydrogen peroxide resulted in an increase in the size of the polymers. Several groups[14–16] have used FFF to measure the size distribution of glutenin polymers produced through oxidation of glutenin subunits. Beasley, Blanchard, and Bekes[14] followed the oxidation of purified high- and low-molecular-weight subunits by FFF and confirmed the formation of polymeric proteins. Veraverbeke et al.[15,16] compared the size distribution of glutenin produced by polymerization of high molecular weight glutenin subunits using different oxidation protocols. Field-flow fractionation showed changes in the size distributions of the polymeric proteins over a wide oxidation range, while no significant change in distribution was evident at higher oxidation levels using SE-HPLC and multilayer SDS–PAGE. The failure to see these changes with the latter methods was attributed to their much lower exclusion limit. These researchers[15,16] also showed that the size distribution of the polymers produced by oxidation differed from one oxidant to another.

Of additional significance to wheat protein research was the separation, using flow FFF, of a wheat polymeric protein extract sample collected from the void volume of a typical SE-HPLC run.[10] Size distribution of this sample (Fig. 3) reconfirmed the presence of very large proteins (d_s 50 + nm) in the SE-HPLC void volume and also showed the presence of smaller proteins (4–12 nm), suggesting that these proteins form stable complexes with the larger proteins or among themselves. This implies that the amount of larger polymeric proteins, previously reported in samples based on SE-HPLC areas, is overestimated.[10]

CONCLUSIONS

Continued improvements in FFF instrumentation, refinements in technique and hyphenation with detectors such as MALLS have broadened the application of this method and effectively elevated it from the status of "possibly useful technique" to a reliable "applied research tool" for assessing the size and shape of wheat proteins. For additional reading concerning FFF theory, principles, and applications, the reader is referred to other sections of this encyclopedia as well as to *Field-Flow Fractionation Handbook* edited by Schimpf et al.[17] A review of the application of FFF to wheat protein analysis can also be found in Preston and Stevenson.[5]

REFERENCES

1. Wrigley, C.W. Giant proteins with flour power. Nature **1996**, *381*, 738–739.
2. MacRitchie, F. Physicochemical properties of wheat proteins in relation to functionality. Adv. Food Nutr. Res. **1992**, *36*, 1–87.

3. Stevenson, S.G.; Preston, K.R. Flow field-flow fractionation of wheat proteins. J. Cereal Sci. **1996**, *23* (2), 121–131.
4. Giddings, J.C. Field-flow fractionation: Analysis of macromolecular, colloidal, and particulate materials. Science **1993**, *260*, 1456–1465.
5. Preston, K.R.; Stevenson, S.G. Size exclusion chromatography and flow field-flow fractionation of wheat proteins. In *Wheat Gluten Protein Analysis*; Shewry, P.R., Lookhart, G.L., Eds.; AACC: St. Paul, MN, 2003; 115–136.
6. Wahlund, K.-G.; Gustavsson, M.; MacRitchie, F.; Nylander, T.; Wannerberger, L. Size characterisation of wheat proteins, particularly glutenin, by asymmetrical flow field-flow fractionation. J. Cereal Sci. **1996**, *23*, 113–119.
7. Giddings, J.C. Hydrodynamic relaxation and sample concentration in field-flow fractionation using permeable wall elements. Anal. Chem. **1990**, *62*, 2306–2312.
8. Li, P.; Hansen, M.; Giddings, J.C. Advances in frit-inlet and frit-outlet flow field flow fractionation. J. Microcol. Sep. **1998**, *10* (1), 7–18.
9. Stevenson, S.G.; Ueno, T.; Preston, K.R. Automated frit inlet/frit outlet flow field-flow fractionation for protein characterization with emphasis on polymeric wheat proteins. Anal. Chem. **1999**, *71* (1), 8–14.
10. Ueno, T.; Stevenson, S.G.; Preston, K.R.; Nightingale, M.J.; Marchylo, B.M. A simplified dilute acetic acid based extraction procedure for the preparation of polymeric wheat flour protein for SE-HPLC and flow FFF analysis. Cereal Chem. **2002**, *70* (1), 155–161.
11. Arfvidsson, C.; Wahlund, K.-G. Mass overloading in the flow field-flow fractionation channel studied by the behaviour of the ultra-large wheat protein glutenin. J. Chromatogr. A. **2003**, *1011* (1–2), 99–109.
12. Stevenson, S.G.; You, S.G.; Izydorczyk, M.S.; Preston, K.R. Characterization of polymeric wheat proteins by flow field-flow fractionation/MALLS. J. Liq. Chromatogr. Relat. Technol. **2003**, *26* (17), 2771–2781.
13. Arfvidsson, C.; Wahlund, K.-G.; Eliasson, A.-C. Direct molecular weight determination in the evaluation of dissolution methods for unreduced glutenin. J. Cereal Sci. **2004**, *39* (1), 1–8.
14. Beasley, H.L.; Blanchard, C.L.; Bekes, F. Preparative method for in vitro production of functional polymers from glutenin subunits of wheat. Cereal Chem. **2001**, *78* (4), 464–470.
15. Veraverbeke, W.S.; Larroque, O.R.; Bekes, F.; Delcour, J.A. In vitro polymerization of wheat glutenin subunits with inorganic oxidizing agents. I. Comparison of single-step and stepwise oxidations of high molecular weight glutenin subunits. Cereal Chem. **2000**, *77* (5), 582–588.
16. Veraverbeke, W.S.; Larroque, O.R.; Bekes, F.; Delcour, J.A. In vitro polymerization of wheat glutenin subunits with inorganic oxidizing agents. II. Stepwise oxidation of low molecular weight glutenin subunits and a mixture of high and low molecular weight glutenin subunits. Cereal Chem. **2000**, *77* (5), 589–594.
17. Schimpf, M.E.; Caldwell, K.; Giddings, J.C. *Field-Flow Fractionation Handbook*; John Wiley & Sons, Inc.: New York, 2000.

Whey Proteins: Anion-Exchange Separation

Kyung Ho Row
Du Young Choi
Center for Advanced Bioseparation Technology and Department of Chemical Engineering, Inha University, Incheon, South Korea

INTRODUCTION

Three strong anion exchange membranes (CIM QA, Q100, and HiTrap Q) and reversed-phase high-performance liquid chromatography (RP-HPLC; 15 μm particle with a pore size of 300 μm) were investigated for the separation of major proteins, which are contained in whey, such as α-lactalbumin, bovine serum albumin (BSA), and β-lactoglobulin. Experiments were performed to determine the optimum mobile phase composition for separating the whey proteins using standard reagents for the proteins. For strong anion exchange membranes, the mobile phases were buffer A (20 mm piperazine–HCl, pH 6.4) and buffer B (buffer A + 1 *M* NaCl), with a linear gradient elution change of salt concentration applied. For RP-HPLC, the mobile phase consisted of a linear gradient of the two mixtures of 0.1% trifluoroacetic acid (TFA) in water and 0.1% TFA in acetonitrile (ACN). Standard protein reagents were used to investigate optimal mobile phase compositions with the three anion exchange membranes. From the experimental results, it was found that HiTrap Q was the most effective in separating whey proteins.

SEPARATION OF WHEY PROTEINS

Milk proteins are the most important source of bioactive peptides. The primary components of bovine milk are water, fat, lactose, and minerals; up to 6% of the mass consists of proteins and peptides, among them a number of high-value substances.[1] Particularly, milk contains two major protein groups (i.e., caseins and whey proteins), which differ greatly with respect to their physicochemical and biological properties. Normal milk contains 30–35 g/L proteins, approximately 80% of which are caseins, with the remainder being whey proteins.[2] Whey proteins can be acquired as a by-product in cheese manufacturing. The required long-term stability in functional performance of these proteins is often lacking. Although the two major proteins are scientifically significant materials, the study of the functional properties of whey proteins has attracted scientific interest for more than 20 years.[3] In general, whey is a dilute liquid composed of lactose, and a variety of proteins, minerals, vitamins, and fat. Whey contains about 6% solids, of which 70% or more is lactose and about 0.7% is proteins.[4] Whey protein components are α-lactalbumin, β-lactoglobulin, immunoglobulin A (IgA), immunoglobulin M (IgM), immunoglobulin G (IgG), BSA, lactoferrin, and lactoperoxidase. β-Lactoglobulin is the major whey protein in bovine milk. β-Lactoglobulin has a molecular mass of 18.4 kDa, possesses 162 amino acid residues, and has a concentration of 2–4 g/L. α-Lactalbumin is an albumin that has 123 amino acid residues. It possesses a molecular mass of 14.2 kDa and its concentration in milk is 0.6–1.7 g/L.[5] Bovine whey proteins have potential applications in veterinary medicine, food industries, and as supplements for cell culture media. IgG, IgA, lactoferrin, and lactoperoxidase, present in bovine whey, have high pharmaceutical value.[6] α-Lactalbumin can be used in infant formula and as a nutraceutical because of its high tryptophan content. β-Lactoglobulin is used in the production of confections.[7] Oral administration of bovine IgG is known to be an effective treatment of various infections of newborn infants.[8] Lactoferrin and lactoperoxidase are known to act as antimicrobial factors.[9] Therefore the whey proteins are used to replace other proteins, or to improve the functional properties of baby food, luncheon meat, soft drinks and milk-based drinks, ice cream, bakery, and convenience products.[10]

Traditionally, separation and purification are frequently achieved by RP-HPLC, although other HPLC methods such as ion exchange chromatography (IEC), hydrophobic interaction chromatography (HIC), size exclusion chromatography (SEC), and various types of affinity chromatography (AC) have also been used.[11] With the development of DNA recombinant techniques, HPLC has become an important tool in both quality control and process control in the production of recombinant proteins of pharmacological interest. This has contributed significantly to the development of RP-HPLC methods that can be used to carry out very rapid analyses for proteins with minimum complexity in both instrumentation and operating conditions.[12] Given the low diffusivity of biopolymers, the need to achieve fast separation of proteins by RP-HPLC has led to the development of different types of packing materials, such as non-porous microparticles (dp <5 μm) or wide-pore materials[13,14] that solve mass transfer problems in the stationary phase, allowing good separations within a reasonable time. The particles used in RP-HPLC have a porous structure of 300 μm.

Separation of whey proteins using ion exchange membranes has been investigated by many researchers and several methods have been reported.[15,16] Ion exchange separations take advantage of electrostatic interaction between surface charges of biomolecules, such as amino acids or proteins, and clusters of charged groups on a membrane. Adsorbing biomolecules displace counterions associated with the surface, discharging a complementary buffer salt in the process. Adequate buffering is required to shield native protein structures from changes in pH adjacent to exchange surfaces (Donnan effect) and pH effects induced by sorption. Selection of an appropriate buffer is critical to the success of ion exchange membranes.[17] Large molecules (>1,000,000 M_w) such as plasmid DNA are able to access charged groups, which envelope large pores of membrane adsorbers, although they would commonly be excluded from cellulose-based ion exchangers. Mobile phases and buffers employed in ion exchange bioseparations are non-denaturing to hydrophilic proteins. Elution and recovery of biologicals using ion exchange on performance are considered, as well as effects of additives and flow rate. The mobile phase composition is adjusted in the linear gradient along with NaCl concentration.

This work focused on the comparison of the separation characteristics of whey proteins using three strong anion exchange membranes (CIM QA, Q100, and HiTrap Q). In an analytical column (3.9 × 300 mm), the experiments were performed at a particle size of 15 μm with large pore sizes of 300 μm. The mobile phase was a binary system of water with 0.1% of TFA and ACN with 0.1% of TFA.

EXPERIMENTAL

Chemicals

The whey powder (from bovine milk) used in this experiment was purchased from Sigma Chemical Co. (St. Louis, Missouri, U.S.A.). The chemical composition of whey protein is shown in Table 1. Samples were prepared by diluting the appropriate amount of whey powder with water. The concentration of the samples remained at approximately 200,000 ppm. The standard chemicals of α-lactalbumin (Type III: deplete, form bovine milk, approximately 85%), β-lactoglobulin (form bovine milk, approximately 90%), and BSA were purchased from Sigma Chemical Co. Standard protein solutions were prepared in water. Standard solutions were made for each protein of 10 mg dissolved in 1 L with water. The water was filtered with HA 0.5 μm membranes (Division of Millipore, Waters Co., Milford, Massachusetts, U.S.A.) and deionized prior to use. The extra pure grade solvent of ACN was purchased from Duksan Pure Chemicals Company (Incheon, Korea). TFA was purchased from Sigma Chemical Co. The sample for injection was filtered with 0.45 μm polyvinylidene fluoride (PVDF) (Waters Co.). Sodium chloride and hydrochloric acid were purchased from Duksan Pure Chemicals Company. Piperazine was purchased from Sigma Chemical Co. For the anion exchange membrane, buffer A was 20 mm piperazine–HCl, pH 6.4, and buffer B was made by addition of 1 *M* NaCl to buffer A. The mobile phases for RP-HPLC were as follows: buffer A, 0.1% TFA in water; and buffer B, 0.1% TFA in ACN.

Table 1 Molecular masses and isoelectric points for whey proteins.

Protein	Molecular weights	Isoelectric points (p*I*)
α-Lactalbumin	14,000	4.2–4.5
β-Lactoglobulin	18,300	5.35–5.49
BSA	69,000	5.13

Equipment

The analytical column was a stainless steel μ-Bondapak™ C_{18}. The size of the analytical column was 3.9 × 300 mm, and it was packed in-house with RP-C_{18} (15 μm Merck Co.) by high-pressure pumping with solvent. The strong anion exchange membranes used in this experiment were CIM QA (BIA Separation Co.), Q100 (Sartorius), and HiTrap Q (Pharmacia). The Monolithic Convective Interaction Media (CIM) QA disk has a diameter of 16 mm and a thickness of 3 μm. The base material of CIM QA is a macroporous glycidyl methacrylate-co-ethylene dimethacrylate (GMA-EDMA) polymer matrix and the CIM QA disk bears a quaternary amine. The membrane material of Q100 is cellulose. The adsorption area of Q100 is 100 cm^2 and the binding capacity of protein is 100 μg/Q100 unit. The ion exchange media packed in HiTrap ion exchange columns are based on Sepharose high-performance material. The column volume of HiTrap Q is 1 ml. In RP-HPLC, the sample solution was passed through an Amicon 8400 (USA; maximum pressure, 75 psi) as an ultrafiltration kit and the UF membrane of cellulose discs [30,000 molecular weight cutoff (MWCO)] was utilized to extract lactose.

The analytical HPLC system was a Waters Model 600S liquid chromatography system (Waters Associates, Milford, Massachusetts, U.S.A.) equipped with a Waters 515 Multisolvent Delivery System with a 486 Tunable Absorbance Analytical Detector, and a Rheodyne injector (50 μl sample loop). The data acquisition system was a Chromate (Ver. 3.0; Interface Engineering, South Korea) installed in a PC. The flow rate of mobile phase was fixed at 4, 2, and 1 ml/min with CIM QA, Q100, and HiTrap Q, respectively. The wavelength was fixed at 260 and 280 nm and the injection volume was fixed at 20 μl. The experiment was performed at room temperature.

RESULTS AND DISCUSSION

Linear change or step change in mobile phase composition may produce differential migration of concentrated solutes. The average velocity of each desorbed solute is proportional to its fractional equilibrium mobile phase concentration. Therefore gradient elution has been normally used to remove adsorbed components from membranes. Gradient elution is convenient because it is difficult to determine, a priori, the modifier concentration required to selectively elute just the desired species.

The whey proteins α-lactalbumin and β-lactoglobulin from bovine milk were separated by RP-HPLC at room temperature using a silica-based, wide-pore C_{18} (300 μm) column and a linear binary gradient of ACN/water/0.1% TFA. However, it was observed that because of the small structural differences between α-lactalbumin and β-lactoglobulin, the desirable resolution of these proteins at the baseline was difficult to achieve. Several gradients of water–ACN, containing TFA (0.1%), were used. Fig. 1 shows the comparison of separation of the two standards of α-lactalbumin and β-lactoglobulin (dotted line) and the real whey proteins (solid line) after ultrafiltration (MWCO 30,000). The gradient condition consisted of a two-step linear binary gradient: buffer A/buffer B = 70/30–35/65 (vol.%), gradient time of 15 min.

For the anion exchanger experiment, a gradient mode with change in NaCl concentration was used to separate whey proteins of α-lactalbumin, β-lactoglobulin, and BSA. The protein standards were used and the strong anion exchange membranes used in this experiment were CIM QA (BIA Separation Co.), Q100 (Sartorius), and HiTrap Q (Pharmacia). The mobile phases were buffer A (20 mm piperazine–HCl, pH 6.4) and buffer B (buffer A + 1 *M* NaCl). In this experiment, the sample of whey was injected only with filtered 0.45 μm PVDF, without

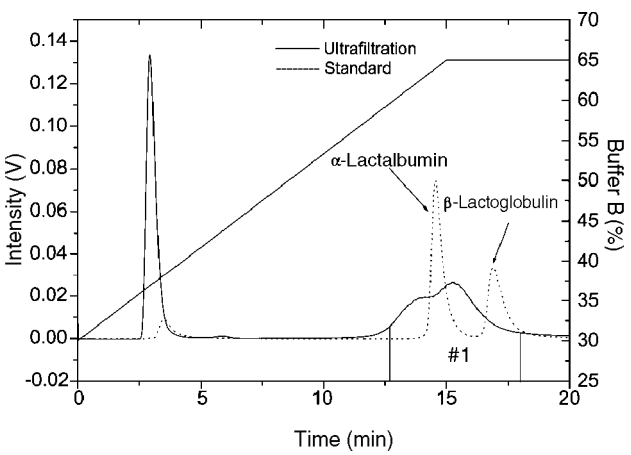

Fig. 1 Comparison of the two standard chemicals of α-lactalbumin and β-lactoglobulin and whey proteins after ultrafiltration (MWCO 30,000) by RP-HPLC (buffer A/buffer B = 70/30–35/65 vol.%, gradient time of 15 min).

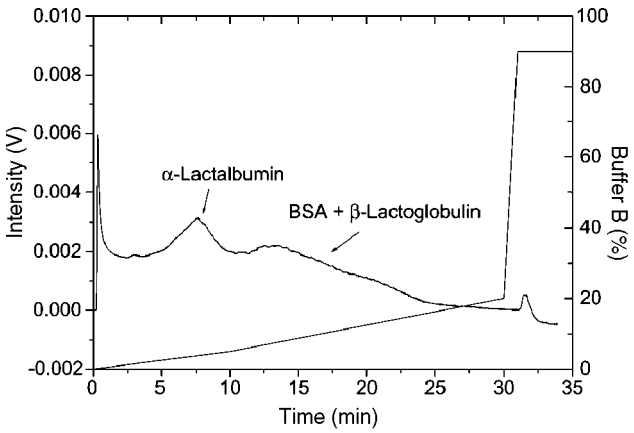

Fig. 2 Separation of standard chemicals of whey proteins using CIM QA [buffer A/buffer B: 100/0–95/5 (0–10 min), 95/5–80/20 (10–30 min), and 80/20–10/90 (30–31 min), CIM QA (BIA Separation Co.), 4 ml/min, 20 μm, 260 nm].

further pretreatment by ultrafiltration. Generally, the retention times of proteins were shorter with increasing amounts of NaCl in buffer B. The elution order of the proteins was α-lactalbumin, BSA, β-lactoglobulin B, and β-lactoglobulin A. β-Lactoglobulin was composed of β-lactoglobulin A and β-lactoglobulin B. In Fig. 2, CIM QA was used to separate whey proteins. In this case, the ratio of the volume of buffer A to the volume of buffer B in the mobile phase (buffer A/buffer B) was changed as follows: 100/0–95/5 (0–10 min), 95/5–80/20 (10–30 min), and 80/20–10/90 (30–31 min), and the flow rate of mobile phase was 4 ml/min. Although only α-lactalbumin was resolved from the other proteins, the resolution was not very good. The coeluted peak of BSA and β-lactoglobulin followed.

Fig. 3 shows the separation of whey proteins by Q100. The buffer A/buffer B ratio was changed as follows: 100/0–85/15 (0–30 min), 85/15 (30–40 min), 85/15–75/25 (40–60 min), and 75/25–10/90 (60–61 min), and the flow

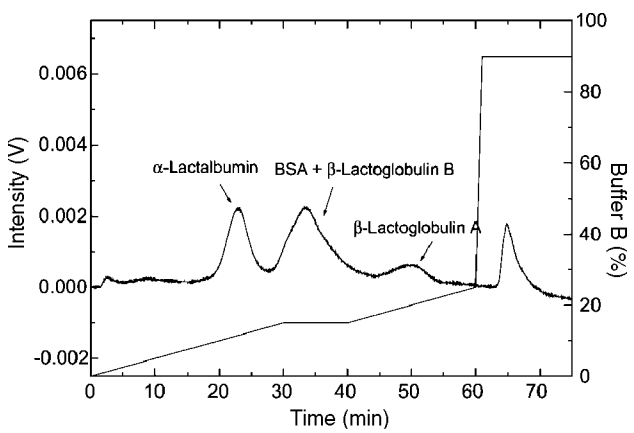

Fig. 3 Separation of standard chemicals of whey proteins using Q 100 [buffer A/buffer B: 100/0–85/15 (0–30 min), 85/15 (30–40 min), 85/15–75/25 (40–60 min), and 75/25–10/90 (60–61 min), Q100 (Sartorius), 2 ml/min].

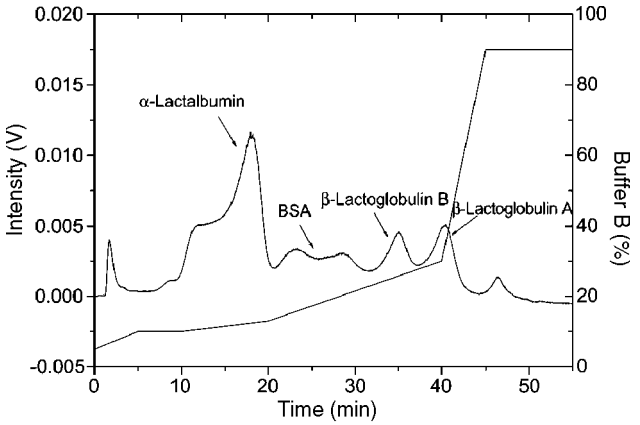

Fig. 4 Separation of standard chemicals of whey proteins using HiTrap Q [buffer A/buffer B: 95/5–90/10 (0–5 min), 90/10 (5–10 min), 90/10–87/13 (10–20 min), 87/13–70/30 (20–40 min), and 70/30–10/90 (40–45 min), HiTrap Q (Pharmacia), 1 ml/min].

rate was 2 ml/min. The resolution of α-lactalbumin was better than that using CIM QA; β-lactoglobulin A was also resolved, but BSA and β-lactoglobulin B coeluted.

The separation of whey proteins by HiTrap Q is shown in Fig. 4. The buffer A/buffer B ratio was changed as follows: 95/5–90/10 (0–5 min), 90/10 (5–10 min), 90/10–87/13 (10–20 min), 87/13–70/30 (20–40 min), and 70/30–10/90 (40–45 min), and the flow rate was 1 ml/min. The resolutions for whey proteins were quite excellent.

Real whey proteins were separated by the change of mobile phase composition obtained from Fig. 5. The injection volume was increased to 50 μl and the change of mobile phase composition was slightly modified to accommodate the larger injection volume and to improve the resolution of whey proteins. This result is shown Fig. 5.

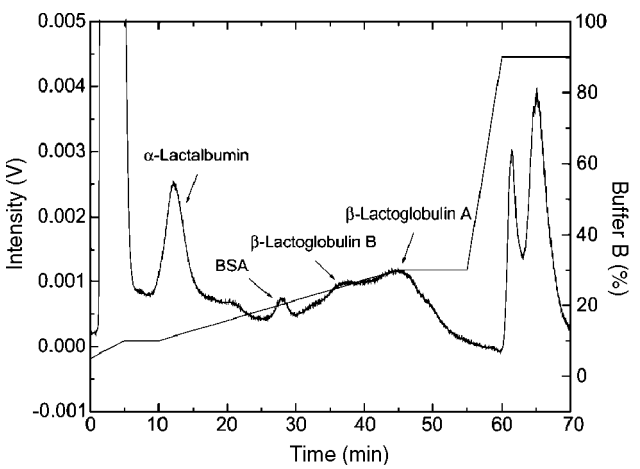

Fig. 5 Separation of the proteins contained in whey using HiTrap Q [buffer A/buffer B: 95/5–90/10 (0–5 min), 90/10 (5–10 min), 90/10–87/13 (10–20 min), 87/13–70/30 (20–40 min), and 70/30–10/90 (40–45 min), HiTrap Q (Pharmacia), 50 μm, 1 ml/min].

Although β-lactoglobulin A and β-lactoglobulin B were not satisfactorily separated, the other whey proteins were well resolved. The buffer A/buffer B ratio was changed as follows: 95/5–90/10 (0–5 min), 90/10 (5–10 min), 90/10–70/30 (10–45 min), 70/30 (45–55 min), and 70/30–10/90 (55–60 min).

In this work, three strong anion exchange membranes and RP-HPLC were used to separate whey proteins. From the result, it was found that anion exchanger and RP-HPLC were of similar separation efficiencies; in addition, HiTrap Q (Pharmacia) was the most effective anion exchange membrane for separation of whey proteins.

CONCLUSIONS

The separation characteristics of whey proteins of α-lactalbumin, BSA, and β-lactoglobulin were investigated with strong anion exchange membranes and RP-HPLC in a gradient mode. In RP-HPLC, the optimum experimental conditions of the mobile phase compositions and gradient conditions were experimentally determined to separate α-lactalbumin and β-lactoglobulins A and B contained in whey. The concentration of NaCl and the numbers of linear gradient steps were adjusted to find the optimum mobile phase with the commercially available anion exchange membranes. It was experimentally confirmed that HiTrap Q was the most effective in resolving the whey proteins. The described RP-HPLC method may be applicable to the wide application in the routine analysis of whey, fractionated whey streams, and whey protein powders produced by dairy industries.

ACKNOWLEDGMENTS

The authors gratefully acknowledge the financial support of the Center for Advanced Bioseparation Technology. This work was performed in the High-Purity Separation Laboratory of Inha University (Incheon, Korea).

REFERENCES

1. Amigo, L.; Recio, I.; Ramos, M. Genetic polymorphism of bovine milk proteins: Its influence on technological properties of milk—A review. Int. Dairy J. **2000**, *10* (3), 135–149.
2. Korhonen, H.; Pihlanto-Leppäla, A.; Rantamäki, P.; Tupasela, T. Impact of processing on bioactive proteins and peptides. Trends Food Sci. Technol. **1998**, *9* (8–9), 307–319.
3. Lieske, B.; Konrad, G. Physico-chemical and functional properties of whey protein as affected by limited papain proteolysis and selective ultrafiltration. Int. Dairy J. **1996**, *6* (1), 13–31.

4. Gerberding, S.J.; Byers, C.H. Preparative ion-exchange chromatography of proteins from dairy whey. J. Chromatogr. A, **1998**, *808* (1–2), 141–151.
5. Choi, D.Y.; Row, K.H. Separation of proteins in whey by strong anion-exchange membrane of Q Sepharose. Hwahak Konghak **2002**, *40* (4), 461–466.
6. Hahn, R.; Schulz, P.M.; Schaupp, C.; Jungbauer, A. Bovine whey fractionation based on cation-exchange chromatography. J. Chromatogr. A, **1998**, *795* (2), 277–287.
7. Zydney, A.L. Protein separations using membrane filtration: New opportunities for whey fractionation. Int. Dairy J. **1998**, *8* (3), 243–250.
8. Hutchens, T.W.; Magnuson, J.S.; Yip, T.T. Secretory IgA, IgG, and IgM immunoglobulins isolated simultaneously from colostral whey by selective thiophilic adsorption. J. Immunol. Methods **1990**, *128* (1), 89–99.
9. Strange, E.D.; Malin, E.L.; Van Hekken, D.L.; Basch, J.J. Chromatographic and electrophoretic methods used for analysis of milk proteins. J. Chromatogr. A, **1992**, *624* (1–2), 81–102.
10. Kim, J.I.; Choi, D.Y.; Row, K.H. Separation of whey proteins by anion-exchange membranes. Korean J. Chem. Eng. **2003**, *20* (3), 538–541.
11. Torre, M.; Cohen, M.E.; Corzo, N.; Rodriguez, M.A.; Diez-Masa, J.C. Perfusion liquid chromatography of whey proteins. J. Chromatogr. A, **1996**, *729* (1–2), 99–111.
12. Nadler, T.K.; Paliwal, S.K.; Regnier, F.E. Rapid, automated, two-dimensional high-performance liquid chromatographic analysis of immunoglobulin G and its multimers. J. Chromatogr. A, **1994**, *676* (2), 331–335.
13. Kalghatgi, K.; Horvath, C. Rapid peptide mapping by high-performance liquid chromatography. J. Chromatogr. A, **1988**, *443* (29), 343–354.
14. Lloyd, L.L.; Warner, F.P. Preparative high-performance liquid chromatography on a unique high-speed macroporous resin. J. Chromatogr. A, **1990**, *512* (20), 365–376.
15. Gerberding, S.J.; Byers, C.H. Preparative ion-exchange chromatography of proteins from dairy whey. J. Chromatogr. A, **1998**, *808* (1–2), 141–151.
16. Hong, S.B.; Row, K.H. Separation characteristics of whey protein by high performance membrane chromatography. Korean J. Chem. Eng. **2001**, *16* (6), 314–537.
17. Keith, D.R.; Edwin, N.L. Separation of biomolecules using adsorptive membranes. J. Chromatogr. A, **1995**, *702* (1–2), 3–26.

Zeta-Potential

Jetse C. Reijenga
Department of Chemical Engineering and Chemistry, Eindhoven University of Technology, Eindhoven, The Netherlands

INTRODUCTION

When an insulator is in contact with an aqueous solution of buffer components, the solid surface has a non-zero electric potential that decreases exponentially as a function of distance from that surface, to become zero at infinity.

DISCUSSION

Taking silica (bulk composition silicium oxide SiO_2), from which capillary material in capillary electrophoresis (CE) is manufactured, as an example, one can readily understand this when taking into account that on the silica surface, there are silicium hydroxide groups that are subject to an acid–base equilibrium according to

$$R{-}SiOH + H_2O \Leftrightarrow R{-}SiO^- + H_3O^+$$

indicating that the negative surface charge of the silica wall is pH dependent and becomes more negative as the buffer pH increases. At pH 2 or lower, the zeta-potential is virtually zero, as the above equilibrium is largely forced to the left due to an abundance of hydrogen ions. As the magnitude of the zeta-potential directly determines the electro-osmotic mobility, it is of importance to understand the effect of different buffer constituents on the zeta-potential and, hence, on the electro-osmotic flow (EOF). The electro-osmotic mobility μ_{EOF} is defined as

$$\mu_{EOF} = -\frac{\zeta\varepsilon}{\eta}$$

in which ζ is the zeta-potential, ε is the dielectric constant of the liquid, and η is the viscosity of the liquid at the plane of shear. The electro-osmotic velocity v_{EOF} is now

$$v_{EOF} = \mu_{EOF}E = -\frac{\zeta\varepsilon E}{\eta}$$

in which E is the electric field strength. Taking a more detailed look at the zeta-potential, one must realize that this potential is not really the value on the negatively charged silica surface, but rather the value on the plane of shear (i.e., at the interface between the stagnant layer of solvent molecules directly at the silica surface and the volume element that is subject to flow, caused by, for example, a longitudinal pressure drop). The combination of these is called the electric double layer.

There are several ways to dynamically change the zeta-potential and, thus, electro-osmosis. Adding a surfactant at a low concentration [generally smaller than the critical micelle concentration (CMC)] will alter the wall charge and zeta-potential due to selective adsorption on the capillary surface: sodium dodecyl sulfate (SDS) will make the zeta-potential more negative (and EOF more pronounced) and may even mask the pH dependence mentioned earlier. Cetyltrimethyl ammonium bromide (CTAB) can neutralize the wall charge, making the zeta-potential close to zero and, thus, eliminating EOF at a concentration of 5×10^{-5} *M*. A higher CTAB concentration will make the zeta-potential positive and reverse the EOF. Other additives merely decrease the zeta-potential exponentially to zero or to a small nagative value; they include polymers such as poly(vinyl alcohol), hydroxy-propylmethylcellulose, and others. Changing the liquid viscosity near the electric double layer is a usual side effect of these additives, another cause of EOF suppression. Polymers like those mentioned and many others have also been used successfully for chemical modification of the capillary surface, so that addition to the buffer (so-called dynamic coating) is not necessary.

EFFECT ON MIGRATION TIME

In uncoated fused-silica capillaries, surface charge and zeta-potential (and, consequently, EOF) can have a significant effect on migration time of anions, especially at higher pH values. As anions and EOF move in opposite directions, longer migration times are more sensitive to zeta-potential changes. This can be seen from the equation for migration time t_m:

$$t_m = \frac{L_d L_t}{(\mu_{cff} + \mu_{EOF})V}$$

where, because of opposite signs for μ_{cff} and μ_{EOF}, the denominator can be quite small. Consequently, migration time can be sensitive to slight EOF changes.

In the example in Fig. 1, a mixture of anions is analyzed in a Tris-acetate buffer of pH 8. A 2% change in zeta-potential, from −50 to −51 mV, results in a dramatic shift in migration time of peaks with longer migration times.

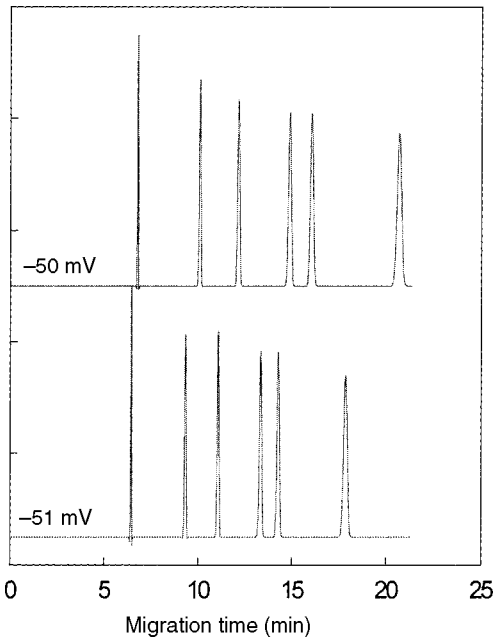

Fig. 1 Effect of capillary zeta-potential on the analysis of a mixture and anions in an uncoated fused-silica capillary in a 10 m*M* Tris-acetate buffer of pH 8. Normal zeta-potentials are around 50 mV at this pH.

BIBLIOGRAPHY

1. Beckers, J.L. Isotachophoresis, some fundamental aspects. In *Thesis*; Eindhoven University of Technology, 1973.
2. Boček, P.; Deml, M.; Gebauer, P.; Dolník, V. *Analytical Isotachophoresis*; VCH: Weinheim, 1988.
3. Everaerts, F.M.; Beckers, J.L.; Verheggen, Th.P.E.M. *Isotachophoresis: Theory, Instrumentation and Applications*; Elsevier: Amsterdam, 1976.
4. Hjertén, S. Free zone electrophoresis. Chromatogr. Rev. **1967**, *9*, 122.
5. Jorgenson, J.W.; Lucaks, K.D. Capillary zone electrophoresis. Science **1983**, *222*, 266.
6. Kenndler, E. Effect of electroosmotic flow on selectivity, efficiency, and resolution in capillary zone electrophoresis expressed by the dimensionless reduced mobility. J. Capillary Electrophoresis **1996**, *3* (4), 191.
7. Li, S.F.Y. *Capillary Electrophoresis—Principles, Practice and Applications*; Elsevier: Amsterdam, 1992.
8. VanOrman, B.B.; Liversidge, G.G.; McIntire, G.L.; Olefirowicz, T.M.; Ewing, A.G. Effects of buffer composition on electroosmotic flow in capillary electrophoresis. J. Microcol. Separ. **1990**, *2* (4), 176–180.

Zirconia–Silica Stationary Phases for HPLC

R. Andrew Shalliker
Sindy Kayillo
Center for Biostructural and Biomolecular Research, University of Western Sydney, Sydney, New South Wales, Australia

INTRODUCTION

This review details the development of zirconia–silica stationary phases in liquid chromatography (LC). Zirconia–silica stationary phases are just one member of a group of mixed oxide materials that have recently been studied in LC. Other members of this group include alumina–silica, magnesia–silica, and titania–silica.[1,2] Each of these mixed oxide composites contains silica, which is the most widely employed stationary phase material in modern high-performance liquid chromatography (HPLC). The dominance of silica in the chromatographic industry reflects the many desirable properties that silica affords the chromatographer. Silica can be prepared in a wide variety of pore size and particle size materials, and can be easily modified to yield stationary phases with a wide range of differing selectivities. For instance, the C_{18} column displays vastly different retention behavior to that of native silica and is the most widely employed reversed-phase (RP) chromatography column. Other types of modified silica stationary phases include, but are not limited to, the C_8 column for intermediate retention of non-polar compounds in RP LC, the C_4 column for protein work, and the phenyl, nitrile, and amino columns. Silica also has a high mechanical strength, making it suitable for the preparation of columns under high pressure; when operated under suitable conditions, these columns have a long life span. Collectively, each of these attributes has made silica the material of choice as a stationary phase or stationary phase support. In many respects, the high efficiency of today's chromatography column owes much to the properties of silica. However, as a chromatographic stationary phase, silica has some limitations. The siloxane linkage is the Achilles heel in any silica-based material, being easily hydrolyzed at low pH. Furthermore, silica has a high solubility in an alkaline environment, especially at higher temperatures, leading to a loss in column bed integrity. This, in general, limits the use of silica and modified silica to pH regions between 2 and 8. Another limitation of silica is the strong and often irreversible adsorption of basic species, occurring as a consequence of the hydrogen bonding between the solute and the surface silanol groups. This belies one of the most desirable features of a stationary phase; that being good adsorption and good desorption characteristics. Many modified silica-based stationary phases are consequently subjected to rigorous procedures that attempt to protect the solute from the residual hydroxyl groups through processes such as end capping.

BACKGROUND

Resolution (R_s) in a chromatographic system is a function of three essentially independent variables: the capacity factor (k') (defined generally by the solvent strength), the number of theoretical plates (N), and the selectivity (α) according to the well-known equation given below:

$$R_s = \frac{1}{4}\sqrt{N}\left(\frac{k'}{1+k'}\right)(\alpha - 1)$$

Of these three variables, changes in the selectivity very often yield the most substantial gain in resolution, albeit with results that are often unpredictable. One of the driving forces in the development of new stationary phases is the change in selectivity to yield improvements in separation. A second driving force is developing materials that overcome the limitations of silica as noted above. One of the more successful stationary phase materials that have been developed is that of zirconia and zirconia-based stationary phases, which are now commercially available as a high-grade chromatographic product. As a stationary phase, zirconia has several important attributes. Zirconia is a highly rigid support able to withstand the rigors of conventional column-packing processes. Zirconia is temperature-stable and is insoluble in alkaline and acidic solvents, allowing mobile phases with pHs between 1 and 14 to be employed as eluents. This is particularly useful for protein work, allowing "dirty" columns to be cleaned with strong base such as NaOH. The surface of zirconia is, however, heterogeneous, containing Lewis acid, Bronsted acid, and Bronsted base sites, which leads to a multitude of retention mechanisms that may complicate the elution process.[3] However, because zirconia is highly resistant to solvent attack, virtually any mobile phase modifying agent can be employed to control any unwanted interactions. Consequently, the highly functionalized zirconia surface can be fully utilized to maximize

selectivity. Zirconia can also be synthesized in a variety of particle size and pore size materials, in much the same manner as silica. Furthermore, zirconia can be modified to yield a variety of stationary phases with different selectivities. Nawrocki et al.[3] published an excellent review on zirconia for chromatographic use, and hence a detailed discussion on zirconia is not warranted in this text.

Recent studies in stationary phase development have lead chromatographers to explore the concept of mixed oxide chromatographic supports and materials for use in LC. These include alumina–silica, magnesia–silica, titania–silica, and zirconia–silica.[1,2] The driving force behind the development of these mixed oxide supports comes from the possibility of attaining a surface with properties that exploit the best attributes of both components in the mixed oxide. For example, the band tailing of basic species on magnesia–silica columns is substantially reduced compared to silica columns due to the reduced concentration of acid sites on the surface of the magnesia–silica composite.[1] In the current text, we present an overview on the development of zirconia–silica composites as stationary phase supports and then detail some applications for which this support has been employed.

PREPARATION OF ZIRCONIA–SILICA MIXED OXIDE SUPPORTS

The demand for mixed oxide chromatographic-quality stationary phase materials is small and only a few methods that detail their preparation are available in the literature. There are, however, numerous examples of the preparation of zircon powders and Ref.[4] is an example of such a process. In general, these types of powders are unsuitable for chromatographic stationary phases because their particle sizes are in the submicron range with very broad distributions. The synthesis of mixed oxide supports for chromatographic applications can essentially be divided into two types: coprecipitation methods and coating methods.

Coprecipitation Methods

Kaneko et al.[1,2] employed a coprecipitation method, which involved a base-catalyzed procedure that precipitated irregular particles of zirconia–silica mixed oxides. Specifically, a zirconium salt (zirconyl chloride octahydrate) was added to an acidified solution of sodium metasilicate ennehydrate. The solution was made alkaline (pH 7–9) to allow the precipitation of the mixed oxide gel. The gel was aged for 10 hr, collected by filtration and washed to remove residual chloride ions. The gel was dried at 110°C and then ground to an appropriate mesh size. The resulting precipitate was regarded as an intimate mixture of silica and metal oxide gel (in this case, zirconia). The silica framework was partly occupied with a widely spread metal oxide, hence decreasing the surface area of the silica gel itself.[1,2] In this procedure, the gel was not subjected to thermal treatment above 110°C.

Zhang, Feng, and Da[5] improved on the method of Kaneko et al.[1,2] by employing an oil emulsion sol–gel procedure, resulting in the formation of mixed oxide spherical particles (spherical particles being a desirable property of a modern LC packing). In their method, sodium metasilicate pentahydrate was hydrolyzed in an acidic aqueous solution and zirconyl chloride octahydrate was added with stirring. The resulting mixture was suspended in a surfactant-stabilized oil and homogenized for 10 min at a speed calibrated to yield 5 μm spherical particles. Precipitation of the gel was initiated by the slow addition of base. The resulting hydrogel was collected and washed to remove residual solvent and dried at 120°C for 2 hr, after which the material was calcined at 600°C for 1 hr.

Coating Processes

Coating processes have been used by a number of researchers. Chicz, Shi, and Regnier[6] coated commercially available 15–20 μm Vydac silica particles with zirconia. The surface coating was obtained by reacting a combination of 2,4-pentanedione, zirconium isopropoxide, and toluene (1 : 3 : 3) (v/w/v) with silica for 1 hr. The zirconyl-clad silica was then vacuum-dried overnight and calcined at 500°C for 8 hr, after which the material was washed with 2-propanol and then vacuum-dried. The zirconyl-clad silica was further modified with polyethyleneimine (PEI) to produce an ion-exchange surface that was tested for retention of proteins. The pore diameter of the resulting zirconyl-clad silica (22.6 nm) was approximately 75% of the original Vydac silica (300 nm), while the surface area decreased marginally (~10%).

Peixoto, Gushiken, and Baccan[7] employed a similar coating process to prepare zirconized silica. Silica particles were added to a solution of $ZrCl_4$ in anhydrous ethanol. The mixture was refluxed for 8 hr under a nitrogen atmosphere. The zirconized silica was then collected and dried at approximately 125°C, before being hydrolyzed and washed in water to remove the residual chloride ions. The final product was dried at 120°C for 5 hr. The resulting zirconized silica had a 3.25% ZrO_2 surface coverage. Melo et al.[8,9] modified the method of Peixoto et al. and coated 10 μm silica particles with zirconia by reacting the silica with zirconium(IV) butoxide in toluene according to the following reaction process:[8]

$$n\text{SiOH} + \text{Zr(OBu)}_4 \rightarrow (\text{SiO})_n\text{Zr(OBu)}_{4-n} + n\text{BuOH}$$
$$(\text{SiO})_n\text{Zr(OBu)}_{4-n} + (4-n)\text{H}_2\text{O} \rightarrow (\text{SiO})_n\text{Zr(OH)}_{4-n} + (4-n)\text{BuOH}$$

where SiOH stands for silanol groups on the silica surface. Following hydrolysis, the zirconized silica contained 15.3% Zr on the surface.

More recently, a similar procedure for the preparation of zirconia-coated silica microspheres was employed by Tsurita and Nogami,[10] who coated 3 μm silica spheres with zirconia derived from zirconyl chloride octahydrate. The resulting zirconia–silica spheres were subjected to thermal treatment in order to bring about crystallization and the subsequent development of the porous structure within the material.

A coating process was also employed by Shalliker et al.[11] where zirconia–silica mixed oxide supports were prepared by coating preformed zirconia microspheres with silica, the reverse process to the methods of Chicz et al.,[6] Peixoto et al.,[7] Melo et al.,[8,9] and Tsurita and Nogami.[10] In this method,[11] zirconia microspheres were first formed using a sol–gel method. The resulting spherical zirconia hydrogels were suspended in water and a solution of hydrolyzed sodium metasilicate pentahydrate was added. The quantity of sodium metasilicate pentahydrate varied depending upon the desired Zr/Si ratio in the final composite. The solution (~200 ml) containing the zirconia microspheres and the hydrolyzed sodium metasilicate pentahydrate was heated to 60°C, allowing the slow evaporation of water to a final volume of 15% of the original amount. The microspheres were collected by filtration and then washed. Calcination of the material followed, which influenced the crystallization and resulting surface properties of the support.[11–15] Extended calcination at 1300°C resulted in the complete homogenization of the support, yielding zircon.[11]

PROPERTIES OF ZIRCONIA–SILICA MIXED OXIDE SUPPORTS

Crystallization

The crystalline nature of zirconia microspheres prepared for chromatographic purposes is dependent upon the thermal history of the zirconia. A detailed discussion on the porous nature of zirconia and silica is not warranted in this text but is covered in detail in a review by Nawrocki et al.[3] It is perhaps important to note that zirconia is amorphous until subjected to temperatures that exceed the phase transition temperature required to form the tetragonal phase (usually between 440°C and 470°C depending on the procedure used to prepare the zirconia). Once thermal treatment exceeds this phase transition temperature, a metastable tetragonal phase predominates—where, after cooling, zirconia slowly transforms to the stable monoclinic form. As thermal treatment of the zirconia is required to obtain a suitable pore-structured stationary phase, most zirconias prepared for chromatographic purposes are predominantly monoclinic, or perhaps more correctly polymorphous.[3] Complete conversion from the amorphous phase to the monoclinic phase requires a substantial degree of thermal treatment and then time to allow the tetragonal phase to form the monoclinic phase. In contrast, the most common form of silica as a stationary phase material is usually the amorphous form,[16] but, on occasion, Cristobalite has been reported.[10] Silica doping of the zirconia, however, has been shown to have a marked effect on the crystallization of the zirconia phase.[4,5,11–15] As the concentration of silica increased, the phase transition temperature from the amorphous phase to the metastable tetragonal phase increased.[12] This was independent of whether the material was prepared through a coprecipitation process[5] or by a coating process.[11] For example, the relationship between the phase transition temperature and the percentage weight of silica in the zirconia–silica composite is shown in Fig. 1. As the concentration of silica doping increased, the phase transition temperature increased monotonically and was linear until 700°C.[11] Furthermore, the addition of the silica stabilized the metastable tetragonal phase, which delayed the transformation to the monoclinic phase.[11] In general, increased silica content decreased the apparent crystallinity. Studies by Tsurita and Nogami[10] on zirconia-coated silica microspheres support the findings described above. In their work, as the concentration of Zr doping increased (or, in other words, the relative concentration of Si decreased), there was a corresponding increase in the concentration of tetragonal zirconia. Furthermore, increasing concentrations of ZrO_2 suppressed the crystallization of silica gel.

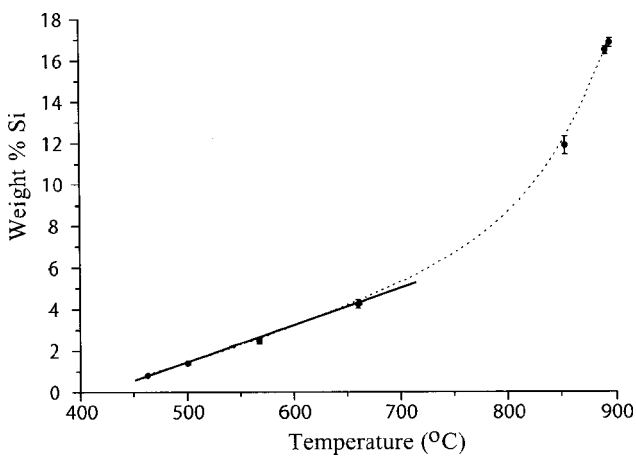

Fig. 1 Plot showing the relationship between the phase transition temperature from the amorphous to the tetragonal state and the composition of silica in the composite material.
Source: From The analysis of zirconia–silica composites using differential thermal analysis, Fourier transform–Raman spectroscopy and X-ray scattering/scanning electron microscopy, in Powder Technol.[12]

Pore Structures

Many of the most important properties of a chromatographic stationary phase relate to the pore structure, which provides a high surface area and pore volume for solute interaction for the chromatographic retention process to occur. As such, the pores should be of a suitable size to allow the solutes of interest to have unimpeded entry and exit to and from the pores. Microporous materials are of little interest in the chromatographic industry. They provide a high surface area, but one that is inaccessible to the vast majority of solutes. Mesoporous materials are the most sought after, with pore sizes between 2 and 50 nm, although macroporous materials find specialized use in the separation of macromolecules, e.g., Ref.,[16] but at the cost of a reduced surface area. Ideally, the pore shape should represent that of a cylinder and should be described by a type IV nitrogen sorption isotherm[17] as depicted in Fig. 2a. These types of isotherms are common in many industrial adsorbents with mesoporous structures. The hysteresis loop in the type IV isotherm is usually associated with capillary condensation in a mesoporous structure. These hysteresis loops can form several shapes; however, from a chromatographic aspect, the most important type of hysteresis loop is the type H1 (Fig. 2b), which represents pores that are uniform in shape and with a narrow size distribution. Many chromatographic surfaces display type H2 or intermediate H1–H2 hysteresis loops, which in a simplified form represents surfaces that have pore structures with wide bellies and narrow necks ("ink bottle" pores).[17]

In general, the pore size and subsequent surface area of zirconia-containing supports is a function of the thermal history, i.e., the crystalline nature. Calcination of the material at high temperatures leads to an increase in the pore size and a reduction in the surface area, as a consequence of particle sintering and crystallization.[3] Kaneko et al.[1] measured the physical properties (pore size distributions, specific surface areas, and pore volumes) of their stationary phases using nitrogen adsorption isotherms. The surface area and pore diameter of their stationary phase material reflected the absence of calcination at temperatures high enough to induce crystallization. Their stationary phase material was predominantly microporous, with a high surface area (122 m^2/g). No mention was made with regard to the pore shape.

In comparison, the stationary phases prepared using the coprecipitation process of Zhang, Feng, and Da[5] with thermal treatment at 600°C were mesoporous. The mean pore diameters were 8.6 nm for a composite containing 3.4% Si and 5.9 nm for a composite containing 15.8% Si. These stationary phase materials had surface areas of 29 and 76 m^2/g, respectively. It is of interest to note that the surface area for the composite containing the higher silica content was greater than the surface area for the composite with the lower silica content. The average pore diameter of the material with the low-silica content was greater than the average pore diameter of the composite with higher silica content. This reflects the decrease in crystallinity associated with an increase in the concentration of silica doping,[5] and the change in density due to the different zirconia concentrations. The composite materials prepared by Zhang, Feng, and Da[5] were reported as being type IV isotherms with H1 hysteresis loops, making them ideally suited as chromatographic adsorbents.

The pore structures of zirconia–silica composites prepared by Shalliker et al.[11–15] via a coating procedure were substantially different to those reported by Zhang, Feng, and Da.[5] In studies by Shalliker et al.[13–15] the pore characteristics were determined using inverse size-exclusion

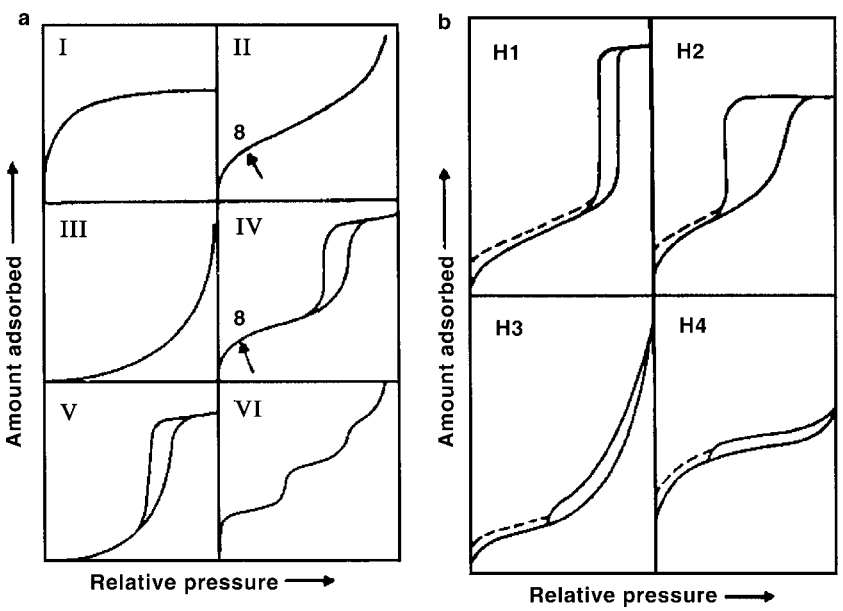

Fig. 2 (a) Types of physisorption isotherms. (b) Types of hysteresis loops.
Source: From Reporting physisorption data for gas/solid systems with special reference to the determination of surface area and porosity, in Pure Appl. Chem.[17]

chromatography (SEC) and nitrogen sorption. The inverse size exclusion technique was employed to measure the chromatographically available pore surface, while the nitrogen sorption measurements were carried out for comparative purposes with information already available in the literature. A range of composites were prepared with either 5 or 10 mol% silicon.[14,15] These composites were calcined for 1 hr at either 700°C or 810°C. Calcination of these materials at 810°C or 700°C yielded composites that were either predominantly amorphous or tetragonal depending on the concentration of the silicon doping. The increase in the phase transition temperature compared to that of native zirconia was consistent with the degree of silicon doping. For a composite material containing 10 mol% Si and calcined for 1 hr at 810°C, a type IV nitrogen sorption isotherm with an H3 hysteresis loop was obtained.[15] The type H3 hysteresis loop extended from the high relative pressure region to P/P_o approximately 0.42, indicating that the surface had a broad pore size distribution. The close proximity of the adsorption and desorption branches indicated that the entrances of the pores offered little restriction to the pore body. This type of hysteresis loop was consistent with a surface containing slit-like pores. The BET-specific surface area of the composite was 2.7 m^2/g and the pore size distribution was very broad and skewed significantly to the macroporous region, with a maximum at 3.4 nm.[15] The specific pore volume of this material was very low (0.0056 ml/g), consistent with a macroporous material. In comparison, the specific pore volume of the stationary phases prepared by Zhang, Feng, and Da[5] were 0.062 and 0.112 ml/g for the 3.4% Si and 15.8% Si composites, respectively. The specific pore volume of the stationary phase prepared by Kaneko et al.[1] was 0.17 ml/g.

The size exclusion curve for polystyrenes that eluted from a column prepared from the 10 mol% silicon composite of Shalliker et al.[14] also indicated that the material had a broad pore size distribution that extended well into the macroporous region. No exclusion limit was determined despite the elution of polymers with molecular weights in excess of 1.8 million Da. The mean pore diameter determined from the inverse size exclusion method was 56.2 nm (essentially a macroporous support) and the specific surface area agreed remarkably well with the BET-specific surface area (2.75 compared to 2.7 m^2/g). Reducing the calcination temperature from 810°C to 700°C, which was below the phase crystallization temperature for the same 10 mol% silicon phase, yielded an amorphous material. The mean pore diameter was 8.9 nm and there was a significant microporous contribution. Because of the microporous nature of this amorphous material, the surface area was almost 20-fold greater with a pore volume almost threefold higher than the predominantly tetragonal phase material obtained following calcination at 810°C.[14] Reducing the concentration of silicon to 5 mol% and calcining at 700°C yielded a very similar material to the one containing

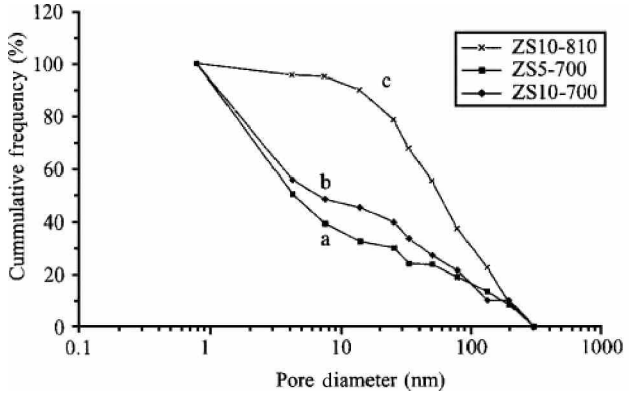

Fig. 3 Cumulative pore frequency plots of composite zirconia–silica stationary phases. a, ZS5-700; b, ZS10-700; and c, ZS10-810.
Source: From The development of stationary phase supports for liquid chromatography: I. Examination of the pore structure of zirconia–silica composites using size exclusion chromatography, in J. Liq. Chromatogr. Relat. Technol.[14]

10 mol% silicon, which was also calcined at 700°C. However, there was a significant concentration of the tetragonal phase in the 5 mol% silicon material, which was not the case for the 10 mol% silicon phase calcined at 700°C. The phase transition temperature of 5 mol% silicon support was approximately 700°C, hence the presence of the tetragonal phase. Fig. 3 illustrates the cumulative pore volumes of these three supports. This figure depicts the change in porosity as a function of the silica doping concentration and the thermal treatment of the support. For instance, for both phases calcined at 700°C, approximately 50% of the pores were less than 4 nm in diameter, whereas there were essentially no pores of this diameter for the material calcined at 810°C. The authors concluded in their study that because of the unfavorable pore shape, such supports would be unsuitable for chromatographic purposes.

Several researchers have investigated the inclusion of high melting point salts during the calcination processes in the synthesis of silica,[10,18] zirconia,[19] and zirconia–silica composites.[10,13–15] The function of the salt is to improve the pore structure of the material. The pores are homogeneously filled with a salt solution (typically sodium chloride), which is allowed to evaporate to dryness leaving behind salt deposited in the pores. Upon sufficient heating, both the salt and the stationary phase material partially liquefy and phase separation occurs.[18] The size and shape of the pores depend on the nature of the salt and on the calcination conditions. The stationary phase and salt solidify when cooled, and residual salt can be removed by washing, leaving behind widened pores. In the case of silica, this procedure has been used to prepare wide pore (>1000 nm) materials designed for bioseparations.[18] The surface structure of a LiChrosphere Si100 stationary phase that has been subjected to pore widening using a salt

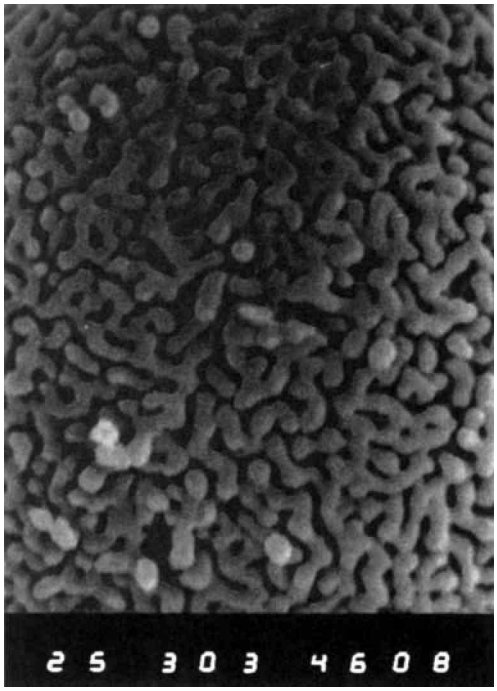

Fig. 4 Scanning electron micrograph of LiChrosphere Si100 soaked in NaCl solution and dried, heated to 800°C for 1 hr, washed out with water, and dried.
Source: From Structural inhomogeneities in wide-pore silica gels, in J. Chromatogr. A.[18]

impregnation process is illustrated in Fig. 4. Salt impregnation during calcination transformed mesoporous zirconia with surfaces that had type IV nitrogen isotherms with H1–H2 hysteresis loops to surfaces with type H1 hysteresis loops. No substantial increase in the overall pore diameter was observed although the salt transformed "ink bottle"-shaped pores to cylindrical-shaped pores.[19] Salt impregnation of zirconia–silica composites resulted in materials that had type H3 hysteresis loops being transformed to materials with intermediate type H1–H2 hysteresis loops.[15] The addition of salt resulted in a more than 15-fold increase in the pore volume and a greater than sixfold increase in the surface area (measured by the BET method).[15] The pore size distribution changed from being a very broad distribution for a zirconia–silica composite calcined without salt to one being mesoporous when calcined with salt. Even with the aid of salt impregnation, evaluation of the nitrogen sorption isotherms showed evidence of pores with hindered access. The mean pore radius was 21.0 nm when measured from the adsorption branch and 10.0 nm mean pore radius when measured from the desorption branch of a nitrogen sorption isotherm. The difference between the two mean pore radii determined from the adsorption and desorption branches indicated that the pores contain wider bellies with some degree of restriction near the pore entrance. Hence, the authors' concluded that these surfaces contained a significant degree of type H2 hysteresis and the hindered pore access limited their chromatographic suitability.[15]

Surface Acidity

The surface of zirconia is known to be basic, with a pK_a of between 10.5 and 12.8. The acidity of silica is dependent upon the state of hydrolysis, typically imparting a slight acidic nature to the surface.[3] Very little information has been published with respect to the acid/base properties of zirconia–silica composites and this is not surprising given the limited experience chromatographers have with these types of stationary phases. Zhang, Feng, and Da[5] determined that the acidity of their zirconia–silica composite increased as the concentration of silica increased. This finding was consistent with an increase in the concentration of acidic hydroxyl groups associated with the increase in silica content. In contrast, Kaneko et al. measured the acid/base properties of zirconia–silica mixed oxide supports via an amine titration method.[1] They found that in a comparison between the acidity of the four mixed oxides (alumina–silica, titania–silica, magnesia–silica, and zirconia–silica), only the zirconia–silica composite contained strong acid sites—despite the fact that both alumina and silica are more acidic than zirconia.[3] All four mixed oxides exhibited stronger acidity than native silica, which is somewhat surprising given the findings of Zhang, Feng, and Da.[5] This may indicate that routine preparation of these mixed oxide supports is sensitive to the process employed including thermal treatment, dehydroxylation, and rehydroxylation.

Surface Modification

Two excellent reviews that detail procedures for the preparation of bonded phase supports have recently been published by Leonard[16] and Buchmeiser.[20] One of the most popular methods of surface chemical modification involves the use of organosilanes. These organosilanes react with the surface metal hydroxyl groups and form a surface, which may be represented as M–O–R, where R represents an alkyl chain and M represents the metal (i.e., silica, zirconia, titania, etc.). One important factor that must be stated, however, is that the order of stability of M–O–R bonds increases in the order of $M = Si > Zr > Ti > Al$.[16] Improvements in the hydrolytic stability can be achieved by shielding the siloxane bond with, for instance, polymeric phases or an intensive multivalent attachment of the bonded layer.[16]

As zirconia–silica composites are relatively new surfaces in chromatography, few studies have detailed methods that modify the surface. One research group, however, has reported the preparation of RP zirconia–silica stationary phases.[8,9] In studies by Melo et al.,[8,9] a C_8 stationary phase material was prepared by grafting

poly(methyloctasiloxane) (PMOS) to the zirconia–silica composite followed by a gamma irradiation immobilization procedure. Surface modification was achieved by drying the zirconia–silica particles in air at 120°C for 24 hr. PMOS was dissolved in dichloromethane at a concentration to yield 1 g PMOS + support per 12 ml dichloromethane, resulting in a packing material with 50% w/w PMOS. The mixture (PMOS + zirconia–silica particles + dichloromethane) was stirred for 3 hr at room temperature after which the solvent was allowed to evaporate. The PMOS-sorbed zirconia–silica microspheres were then subjected to gamma irradiation at either 80 or 120 kGy using a Co-60 source. Columns prepared from the grafted and gamma-immobilized PMOS were tested for performance and compared to PMOS-sorbed silica and PMOS-sorbed zirconia–silica stationary phases that were not subjected to gamma irradiation. The authors concluded that the gamma irradiation of the PMOS-sorbed zirconia–silica composite improved the chromatographic performance for neutral and basic species. Furthermore, the gamma-irradiated PMOS-sorbed zirconia–silica stationary phase was shown to have superior chromatographic performance following alkaline stability trials when compared to PMOS-sorbed silica or zirconia–silica stationary phases that were not subjected to gamma irradiation. This was despite there being an apparent loss in sorbed PMOS (as indicated by a reduction in the capacity factor) following washing in very basic (pH 10) solvents. No retention information was presented on the performance of gamma-irradiated PMOS-sorbed silica in comparison to gamma-irradiated PMOS-sorbed zirconia–silica.

An inorganic anion-exchange resin based on a zirconia–silica support was prepared by Chicz, Shi, and Regnier.[6] The Lewis acid sites were employed as adsorption sites that permanently retained a PEI coating which then acted as an anion-exchange ligand. In this study, a continuous film of cross-linked PEI was achieved. These surfaces were then tested for the analysis of ovabumin and bovine serum albumin.

Through chance discovery, Shalliker et al.[13,21] prepared a surface-modified normal phase zirconia–silica composite. In studies designed to optimize the pore structure of zirconia–silica composites, sodium iodide was used as a salt for pore widening experiments. However, following calcination and subsequent washing to remove residual salt, the stationary phase was left with a permanent brown-yellow discoloration, indicating the presence of iodide remaining on the surface. Elemental analysis confirmed this to be so. Consequently, the authors considered that the presence of iodide may protect the solute from the Lewis acid sites on the surface of the support.[21] Normal phase retention studies showed a reduction in the degree of retention of basic solutes together with an improvement in the peak shape of basic compounds such as pyridine and aniline.

Alkaline Stability

One of the advantages of zirconia–silica composite stationary phases is supposedly a reduction in the solubility of the surface in alkaline solvents. However, only a limited amount of information detailing the alkaline stability of the surface is currently available. Chicz, Shi, and Regnier[6] demonstrated that a zirconia–silica composite that was coated with a PEI coating was stable in boiling alkaline solvent (1 *M* KOH) for 24 hr with no visual change in the stationary phase material. In contrast, a silica phase coated with PEI dissolved within 30 min in boiling 1 *M* KOH. As mentioned above, Melo et al.[8,9] also observed stability in their RP modified support following passage of 5000 column volumes of mobile phase (NH_4^+/NH_3 buffer) at pH 10. A reduction in retention was observed, but the column efficiency and resolution remained essentially constant.

APPLICATIONS

Commercially, zirconia–silica composites have, at present, found limited use in LC due to the popularity and dominance of silica and silica-based supports. The highly competitive market and the drive to satisfy consumer demand has ensured manufacturers of silica-based supports to investigate methods that overcome or limit the shortfalls of the surface, particularly with respect to the solubility of silica in aqueous and basic solvents. The synthesis of the new generation hybrid silica (XTerra) is an example of these developments.[20] Surface protection of the silica surface, with appropriate care being taken during the dehydroxylation and rehydroxylation of the surface also improves the behavior of basic solutes. There is, at present, very limited commercial interest in developing zirconia–silica composites and, consequently, applications on these surfaces are limited to researchers who prepare their own packing materials. Nevertheless, studies that have been published so far detail differences in selectivities between silica or zirconia and zirconia–silica composites. The employment of basic test substances such as pyridine and aniline in normal phase chromatography serves as a useful indicator of selectivity and secondary adsorption effects. This is particularly true for surfaces such as zirconia as these basic compounds display strong affinity toward Lewis acid sites and are also sensitive to the presence of hydroxyl groups. With that in mind, Kaneko et al.[1] used a mixture of benzene, dimethyl phthlate, and pyridine to observe the retention characteristics of four mixed oxide supports in a hexane (99%)/methanol (1%) mobile phase. Pyridine was not observed to elute from either the column packed with silica or from the column packed with the zirconia–silica composite. The column prepared from a silica–magnesia stationary phase gave the best separation, while extreme band tailing of the pyridine was observed on columns

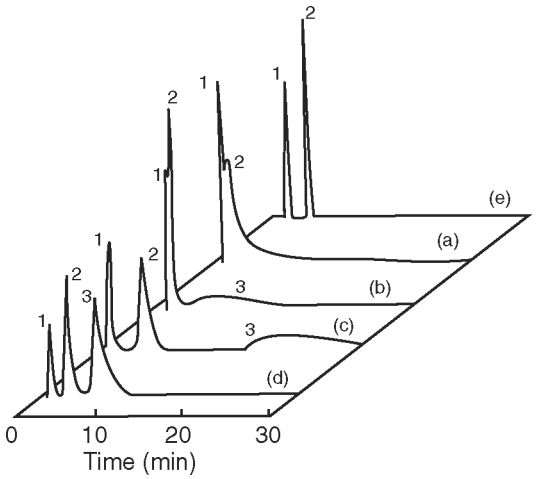

Fig. 5 Chromatograms obtained on four mixed oxide packing materials. Solute: 1 = benzene; 2 = dimethyl phthalate; 3 = pyridine. Column packing material: (a) silica–zirconia; (b) silica–alumina; (c) silica–titania; (d) silica–magnesia; (e) silica gel. Mobile phase, *n*-hexane containing 1% methanol: flow rate, 1 ml/min; column temperature, ambient; detection, UV 254 nm.
Source: From Separation behaviour of silica-containing mixed oxides as column packing materials for liquid chromatography, in J. Chromatogr. A.[1]

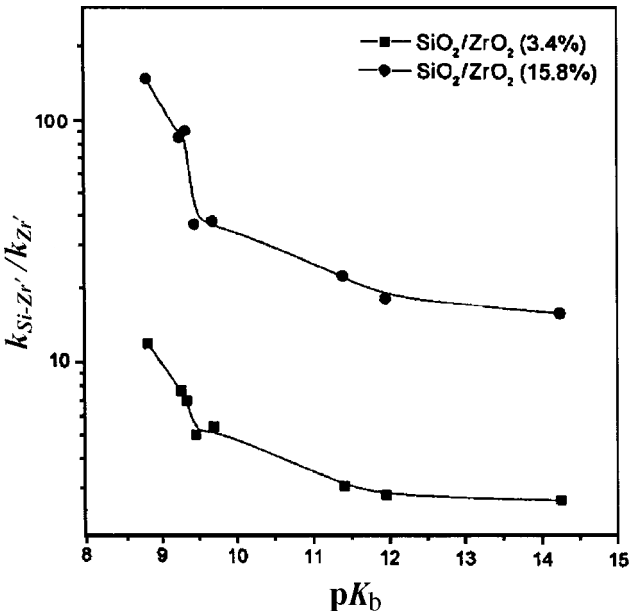

Fig. 6 Relationship between the k_{Si-Zr}'/k_{Zr}' and the pK_b of basic compounds.
Source: From The development of stationary phase supports for liquid chromatography: I. Examination of the pore structure of zirconia–silica composites using size exclusion chromatography, in J. Liq. Chromatogr. Relat. Technol.[14]

prepared from silica–alumina and silica–titania. Fig. 5 illustrates the results that were obtained. The authors concluded that because their zirconia–silica composite contained the highest concentration of strong acid sites, pyridine could not be eluted, whereas a broad tailing pyridine band was observed for the silica–titania and silica–alumina columns, both of which had a slightly lower concentration of strong acid sites than the zirconia–silica stationary phase. The silica–magnesia stationary phase with only weak acid sites gave the best separation and a symmetrical peak for pyridine.

In contrast, pyridine and other basic test solutes in normal phase conditions were observed to elute from zirconia–silica composites prepared by Zhang, Feng, and Da.[5] The retention of the basic solutes was greater on the zirconia–silica composite stationary phase than on a native zirconia stationary phase. The ratio k_{Si-Zr}'/k_{Zr}', where k_{Si-Zr}' and k_{Zr}' are measures of the capacity factor on the zirconia–silica stationary phase and the zirconia phase, respectively, decreased with an increase in the pK_b of the test solute, as illustrated in Fig. 6. Retention was also greater on the stationary phase containing the greater concentration of zirconia. However, the elution order of the aniline and *p*-nitroaniline was reversed when the surface concentration of zirconia increased from 3.4% to 15.3% and this was attributed to the stronger acid properties of the 15.8% zirconia–silica composite. Neutral compounds (PAHs) were also shown to be retained on the surface of the zirconia–silica composites and zirconia, and this was attributed to interactions between π electrons and Lewis acid sites.[5] The retention of acidic compounds was also studied by Zhang, Feng, and Da[5] and they suggested that the crystal structure of the support may be a factor in determining the extent of retention. In their study, retention of acidic compounds increased in the order of zirconia–silica (3.4% Zr) < zirconia < zirconia–silica (15.8%). The addition of silica to the zirconia improved the peak asymmetry.

Shalliker et al.[21] used pyridine and aniline as test solutes in normal phase chromatography. Strong retention of pyridine was observed on a native silica column ($k' = 9.5$), while the sample was only weakly retained on a native zirconia column ($k' \sim 1$). Even less retention was observed for pyridine on a zirconia–silica column ($k' = 0.86$). All pyridine bands were severely tailed with asymmetry factors as high as 2.4 for pyridine eluting from the silica column. However, elution of pyridine from a sodium iodide impregnated zirconia–silica column occurred with a capacity factor of 0.26, but most importantly, the peak tailing decreased substantially, as shown in Table 1. Similar results were observed for the elution of aniline. However, selectivity differences resulted in the elution order of pyridine and aniline being reversed between the sodium iodide impregnated zirconia–silica column and the unmodified zirconia–silica column.

Table 1 Capacity factor and asymmetry factors for pyridine in a normal phase separation on various silica and zirconia stationary phases.

Stationary phase	Capacity factor	Asymmetry factor
Silica	9.50	2.450
Zirconia	0.99	1.840
Zirconia–silica	0.86	1.795
NaI impregnated zirconia–silica	0.24	1.330

Source: From Retention behaviour of basic solutes on zirconia–silica composite stationary phase supports in normal phase liquid chromatography, in J. Liq. Chromatogr. Relat. Technol.[21]

In general, iodide impregnation decreased retention, and improved peak shape.

The ion-exchange properties of zirconia–silica surfaces were utilized in a study by Peixoto, Gushiken, and Baccan.[7] In this study, zirconica–silica microcolumns were employed for the selective extraction and enrichment of chromium(VI) in a flow injection system. The hydrated zirconia–silica surface adsorbed cations or anions depending on the pH. At low pH, the surface behaved as anion exchanger by a mechanism in which OH^- was displaced from the surface according to:[7]

$$ZrOH + H^+ + Cr_2O_7^{2-} \rightarrow Zr^+Cr_2O_7^{2-} + H_2O$$

They showed that the method was suitable for the analysis of Cr(VI) in natural waters with little interference from common ions normally found in these water samples.

The ion-exchange properties of zirconia–silica surfaces were also evaluated by Chicz, Shi, and Regnier;[6] however, their study was conducted on surfaces modified with a layer of PEI. A number of different stationary phase base support materials were employed in their study including zirconia–silica. They found that retention was dependent on the amount of PEI bound to the surface, leading them to suggest that base materials with similar charge density, surface area, and pore diameter (in other words, materials with the same capacity to adsorb the PEI coating) should behave in much the same manner. The advantage of the zirconia–silica base support over silica was that the zirconia–silica phase was stable in alkaline solvents whereas the silica phase rapidly dissolved.

Only one research group has illustrated the RP retention behavior of solutes on zirconia–silica modified surfaces. In the study by Melo et al.[8,9] on PMOS gamma-irradiated modified surfaces, the RP retention behavior of a test mixture containing acetone, benzonitrile, benzene, toluene, and naphthalene was evaluated. The authors

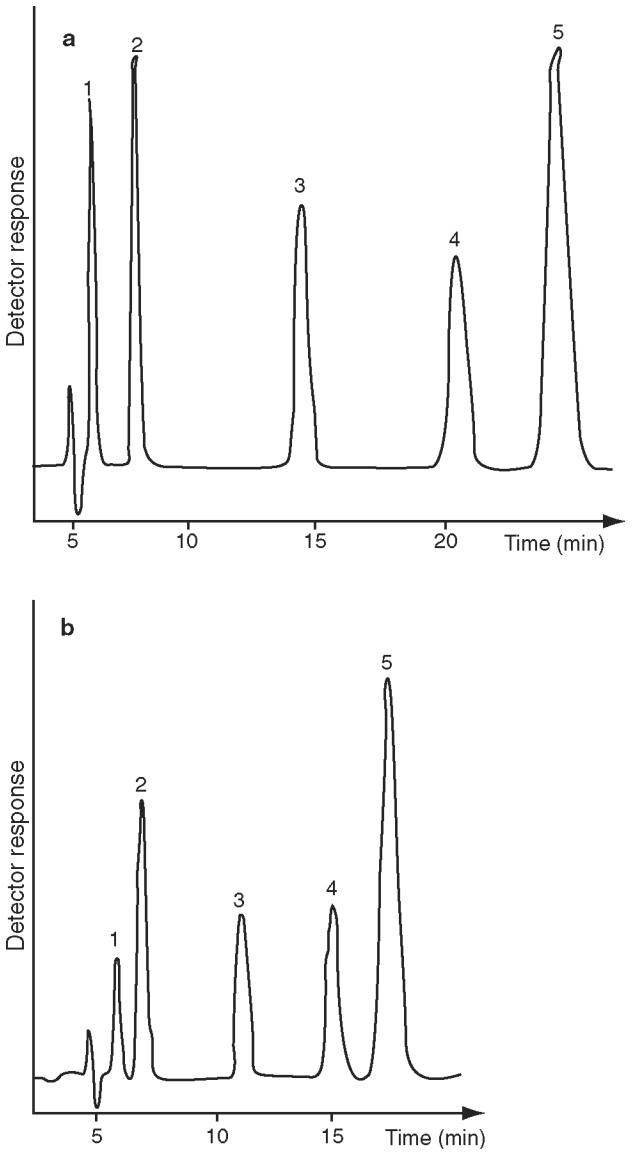

Fig. 7 Chromatograms of a mixture of acetone (1), benzonitrile (2), benzene (3), toluene (4), and naphthalene (5), obtained from a zirconized silica column with a radiation-immobilized PMOS coating (a) before initiating the stability test and (b) after completing the stability test with 5000 column volumes each of neutral and alkaline (pH 10) mobile phases.
Source: From Stability of high performance liquid chromatography columns packed with poly(methyloctylsiloxane) sorbed and radiation-immobilized onto porous silica, and zirconized silica in J. Chromatogr. A.[8]

illustrated good resolution of the five-component text mixture as shown in Fig. 7. Retention, however, decreased after the stationary phase was washed with 5000 column volumes of base (pH 10). Despite the base washing, uniform peak shape was maintained, with only a slight reduction in resolution as discussed in "Alkaline Stability" above.

CONCLUSIONS

In searching for new separation processes, the chromatographer develops new types of stationary phase materials in order to gain improvements in selectivity. The development of zirconia–silica composites is an example which—although, at present, applications on these surfaces are limited to their development—typifies the ongoing search. Whether the separations achieved on the zirconia–silica composites are better or worse than those achieved on either zirconia or silica is immaterial to the fundamental process of discovery. The important factor is that the separation is different and, therefore, an alternative separation strategy may be employed. In addition to the differences in selectivity that may be found when new surfaces are developed, beneficial surface properties may also be realized. These may be related to aspects such as the pore structure, the acidic or basic properties, or the solubility of the support.

In the specific case of zirconia–silica composites, the stationary phase could be prepared through relatively simple processes using either coprecipitation or coating methods. The addition of silica to the zirconia matrix increases the phase transition temperature from the amorphous phase to the tetragonal phase, which in turn stabilizes the tetragonal phase. The pore structure can be controlled through processes similar to those employed in the preparation of zirconia. However, the type of pore structure obtained appears to be dependent on the method of preparation. Calcination in the presence of salts improves the pore shapes. Zirconia–silica phases can also be surface-modified and C_8 and ion-exchange media have been prepared. Composite zirconia–silica stationary phases coated with PEI were shown to have a lower solubility in alkaline solvents than silica modified in the same manner. The ion-exchange properties of zirconia–silica stationary phases were utilized in the analysis of natural waters, where the concentration of chromium(VI) was enriched in a flow injection system that incorporated a microcolumn packed with zirconia–silica stationary phase. Several studies have shown the elution behavior of basic solutes on these composites, and one study illustrated that modifying the surface with a Lewis base could minimize peak tailing.

Future work in stationary phase design will probably continue to include studies on mixed oxide composites although these will continue to constitute only a small fraction of the stationary phase materials made for general purpose use. Many of the mixed oxide supports will be custom-made for specific applications, and at least in the short term, these types of stationary phases will be made by individual research groups.

REFERENCES

1. Kaneko, S.; Mitsuzawa, T.; Ohmori, S.; Nakamura, M.; Nobuhara, K.; Masatani, M. Separation behaviour of silica-containing mixed oxides as column packing materials for liquid chromatography. J. Chromatogr. A, **1994**, *669*, 1–7.
2. Kaneko, S.; Mitsuzawa, T.; Ohmori, S.; Nakamura, M.; Nobuhara, K.; Masatani, M. Silica-containing mixed oxides gels prepared by a coprecipitation method as novel packing materials for liquid chromatography. Chem. Lett. **1993**, 1275–1278.
3. Nawrocki, J.; Rigney, M.P.; McCormick, A.; Carr, P.W. Chemistry of zirconia and its use in chromatography. J. Chromatogr. A, **1993**, *657*, 229–282.
4. Kanno, Y. Thermodynamic and crystallographic discussion of the formation and dissociation of zircon. J. Mater. Sci. **1989**, *24*, 2415–2420.
5. Zhang, Q.-H.; Feng, Y.-Q.; Da, S.-L. Preparation and characterization of silica–zirconia supports for normal phase liquid chromatography. J. Liq. Chromatogr. Relat. Technol. **2000**, *23* (10), 1461–1475.
6. Chicz, R.M.; Shi, Z.; Regnier, F.E. Preparation and evaluation of inorganic anion-exchange sorbents not based on silica. J. Chromatogr. **1986**, *359*, 121–130.
7. Peixoto, C.R.M.; Gushiken, Y.; Baccan, N. Selective spectrophotometric determination of trace amounts of chromium(VI) using a flow injection system with a microcolumn of zirconium(IV) oxide modified silica gel. Analyst **1992**, *117*, 1029–1032.
8. Melo, L.F.C.; Collins, C.H.; Collins, K.E.; Jardin, I.C.S.F. Stability of high performance liquid chromatography columns packed with poly(methyloctylsiloxane) sorbed and radiation-immobilized onto porous silica and zirconized silica. J. Chromatogr. A, **2000**, *869*, 129–135.
9. Melo, L.F.C.; Jardin, I.C.S.F. Development of C_8 stationary phases immobilized by γ-radiation on zirconized silica for high-performance liquid chromatographic applications. J. Chromatogr. A, **2000**, *845*, 423–431.
10. Tsurita, Y.; Nogami, M. Preparation of porous supports in the SiO_2–ZrO_2–Na_2O system from microspherical silica gels. J. Mater. Sci. **2001**, *36*, 4365–4375.
11. Shalliker, R.A.; Rintoul, L.; Douglas, G.K.; Russell, S.C. A sol–gel preparation of silica coated zirconia microspheres as chromatographic support materials. J. Mater. Sci. **1997**, *32*, 2949–2955.
12. Shalliker, R.A.; Douglas, G.K.; Rintoul, L.; Russell, S.C. The analysis of zirconia–silica composites using differential thermal analysis, Fourier transform–Raman spectroscopy and X-ray scattering/scanning electron microscopy. Powder Technol. **1998**, *98*, 109–112.
13. Shalliker, R.A.; Douglas, G.K.; Rintoul, L.; Comino, P.R.; Kavanagh, P.E. The measurement of pore size distributions, surface areas, and pore volumes of zirconia and zirconia–silica mixed oxide stationary phases using size exclusion chromatography. J. Liq. Chromatogr. Relat. Technol. **1997**, *20* (10), 1471–1488.
14. Shalliker, R.A.; Douglas, G.K. The development of stationary phase supports for liquid chromatography: I. Examination of the pore structure of zirconia–silica

composites using size exclusion chromatography. J. Liq. Chromatogr. Relat. Technol. **1998**, *21* (12), 1749–1765.
15. Shalliker, R.A.; Douglas, G.K.; Elms, F.M. The development of stationary phase supports for liquid chromatography: II. Examination of the pore structure of zirconia–silica composites using nitrogen sorption. J. Liq. Chromatogr. Relat. Technol. **1998**, *21* (12), 1767–1781.
16. Leonard, M. New packing materials for protein chromatography. J. Chromatogr. B. Biomed. Sci. Appl. **1997**, *669*, 3–27.
17. Sing, K.S.W.; Everett, D.H.; Haul, R.A.W.; Moscou, L.; Pierotti, R.A.; Rouquerol, J.; Siemieniewska, T. Reporting physisorption data for gas/solid systems with special reference to the determination of surface area and porosity. Pure Appl. Chem. **1985**, *57*, 603–619.
18. Novak, I.; Berek, D. Structural inhomogeneities in wide-pore silica gels. J. Chromatogr. A, **1994**, *665*, 33–36, and references cited therein.
19. Shalliker, R.A.; Douglas, G.K.; Comino, P.R.; Kavanagh, P.E. Examination of various size zirconias for potential chromatographic applications. Powder Technol. **1997**, *91*, 17–23.
20. Buchmeiser, M.R. New synthetic ways for the preparation of high performance liquid chromatography supports. J. Chromatogr. A, **2001**, *918*, 233–266.
21. Shalliker, R.A.; Rizk, M.; Stocksiek, C.; Sweeney, A.P. Retention behaviour of basic solutes on zirconia–silica composite stationary phase supports in normal phase liquid chromatography. J. Liq. Chromatogr. Relat. Technol. **2002**, *25* (4), 561–572.

Zone Dispersion in FFF

Josef Janca
Department of Chemistry, University of La Rochelle, La Rochelle, France

INTRODUCTION

All separation processes are inherently accompanied by zone broadening, which is due to the dynamic spreading processes dispersing the concentration distribution achieved by the separation.[1] As long as the relative contributions of these dispersive processes decrease, the efficiency of the separation increases. A conventional empirical parameter describing, quantitatively, the efficiency of any separation system is the number of theoretical plates per separation unit, N, or the height equivalent to a theoretical plate (the theoretical plate height) H defined by

$$N = \left(\frac{V_R}{\sigma_V}\right)^2, \quad H = \frac{L}{N} \tag{1}$$

where V_R is the retention volume, σ_V is the standard deviation of the elution curve (fractogram) of a uniform retained sample, expressed at the same retention volume units, and L is the length of the separation unit; in the case of the field-flow fractionation (FFF), it is the length of the fractionation channel. Fig. 1a shows a model fractogram and the method of graphical determination of the efficiency of the involved separation system. A more accurate procedure for the determination of the efficiency of the separation system from the experimental fractogram consists in the numerical calculation of the statistical moments of the fractogram (viz. of the first statistical moment, which corresponds to the maximum of the fractogram and, thus, to the retention volume):

$$V_R = \frac{\Sigma V_i h_i}{\Sigma h_i} \tag{2}$$

where h_i are the heights of the fractogram at the corresponding retention volumes V_i. The square root of the second central moment corresponds to the standard deviation of the fractogram and, thus, to its width:

$$\sigma_V = \left(\frac{\Sigma (V_i - V_R)^2 h_i}{\Sigma h_i}\right)^{1/2} \tag{3}$$

It must be stressed that the terms band or zone broadening, spreading, and dispersion used here are equivalent from the viewpoint of their physical meanings.

PROCESSES CONTRIBUTING TO ZONE BROADENING

Several dispersive processes contribute to zone broadening: longitudinal diffusion, non-equilibrium and relaxation processes, spreading due to the external parts of the whole separation system, such as the injector, detector, connecting capillaries, and so forth. It has theoretically been found[2] that the resulting efficiency of the FFF, characterized by the height equivalent to a theoretical plate, can very accurately be described by

$$H = \frac{2D}{R\langle v(x)\rangle} + \frac{\chi^{w^2}\langle v(x)\rangle}{D} + \sum H_{\text{ext}} \tag{4}$$

where D is the diffusion coefficient of the retained species, R is the retention ratio, $\langle v(x)\rangle$ is the average linear velocity of the carrier liquid, w is the thickness of the fractionation channel, x is the dimensionless parameter defined later, and ΣH_{ext} is the sum of all contributions to the zone broadening from the external parts of the separation channel (injector, detector cell, and connecting capillaries).

The retention ratio R is defined as

$$R = \frac{V_0}{V_R} \tag{5}$$

where V_0 and V_R are the retention volumes of the unretained and retained species, respectively. Graphical representation of the particular spreading processes, as a function of the average linear velocity of the carrier liquid and of their sum, which results in a curve exhibiting a minimum, are shown in Fig. 1b. At very low linear velocities of the carrier liquid, the longitudinal diffusion, represented by the first term on the righthand side of the Eq. 4, plays a dominant role of all zone-spreading processes. The relaxation and non-equilibrium processes, represented by the second term on the right-hand side of the Eq. 4, become more important when increasing the velocity. The result is that H passes through the above-mentioned minimum. As the diffusion coefficients of the macromolecules and particles are relatively low, the contribution of the longitudinal diffusion is almost negligible and the optimal efficiency (the minimum on the resulting curve) appears at a very low flow velocity. The zone spreading due to the external elements of the fractionation channel can be minimized by reducing their volume.

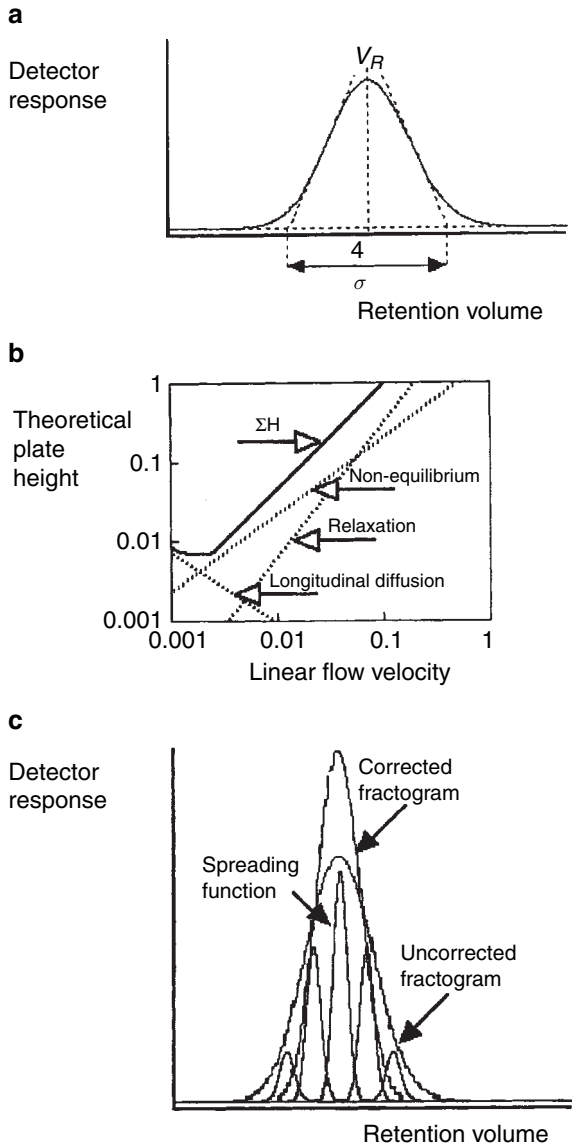

Fig. 1 Zone broadening and its correction. a, Schematic demonstration of the evaluation of the efficiency of the separation system of FFF; b, dependence of the theoretical plate height on the linear flow velocity; and c, schematic demonstration of the application of the correction for the zone broadening on a model fractogram.

The dimensionless parameter χ is a complex function of the retention parameter λ which, itself, can be approximated by the relationship

$$\lim_{\lambda \to 0} R = 6\lambda \tag{6}$$

Another approximate relationship holds between χ and λ:

$$\lim_{\lambda \to 0} \chi = 24\lambda^3 \tag{7}$$

Eq. 7 is a very important relationship because, with respect to Eq. 4, it indicates that in the most practical range of the linear flow velocities, above the optimal flow, the efficiency of the separation in FFF increases very rapidly with the retention ratio. This is rather an exceptional case among separation methods and the importance of this behavior has to be regarded with respect to the fact that the FFF methods and techniques are especially convenient for the fractionation of large and polydisperse species, such as macromolecules and particles. As the retention usually increases with the molar mass or particle size in polarization FFF, the efficiency is higher in the high molar mass or large particle size domain. This is one of the reasons why the FFF methods are particularly competitive in this field of application.

Nevertheless, the difficulty to separate the large polydisperse species enough, independently of the method or technique used, impose the necessity to introduce, and apply the powerful numerical methods, which are able to evaluate the amplitude of the zone broadening contribution to the apparent molar mass distribution (MMD) or particle size distribution (PSD), calculated by a simple data treatment of the experimental fractograms, and to correct, casually, the MMD and PSD data for zone broadening. Whenever the zone spreading attains a level not acceptable from the point of view of the analytical results obtained by a simple data treatment of the raw fractograms, a correction for the zone broadening must be applied.

RELAXATION

Relaxation represents an important contribution to the zone broadening and merits mention in particular, especially because it can be reduced by an appropriate experimental procedure.[3] The concentration distribution of the fractionated sample across the channel established immediately after the injection is far from the steady state, which is formed progressively during the elution. This leads to additional zone broadening. However, if the flow is stopped after the injection for a time necessary to achieve a steady state, the shift of the retention volume and the zone spreading can substantially be reduced. So-called secondary relaxation broadening can occur when the intensity of the field varies rapidly during the elution (e.g., by programming).

CORRECTION FOR THE ZONE BROADENING

The fractogram of a polydisperse sample is a superposition of the separation and of the zone broadening. This is shown in Fig. 1c, where the spread zones of the discrete species are overlapped and the fractogram is, in fact, a convolution of all individual zones. Whenever the zone spreading is important, the accurate MMD or PSD can be calculated from the experimental fractograms only by using a correction procedure. An efficient correction method applicable

in FFF[4] was derived from well-known correction procedures used in SEC.[5]

A raw fractogram $h(V)$ is a convolution of the fractogram corrected for the zone broadening $g(Y)$ and the spreading function $G(V, Y)$ which is a detector response to a uniform species having the elution volume Y:

$$h(V) = \int_0^\infty g(Y)G(V - Y)dY \tag{8}$$

The spreading function can be approximated by

$$G(V, Y) = \left(\frac{1}{2\pi\sigma_S{}^2}\right)^{1/2} \exp\left(-\frac{(V - Y)}{2\sigma_S{}^2}\right) \tag{9}$$

where the standard deviation should be independent of the elution volume. This independence is valid in FFF only within a not very wide range of the elution volumes. Eq. 9 can correctly be applied to the fractograms of the samples with a narrow MMD or PSD only. On the other hand, whenever a non-uniform spreading function with the dependent on the retention has to be used, the correction to be applied is

$$h(V) = \int_0^\infty g(Y)\left[\frac{1}{[2\pi(\sigma_S(Y)]^2}\right]^{1/2} \times \exp\left(-\frac{(V - Y)^2}{[2(\sigma_S Y)]^2}\right)dY \tag{10}$$

which is convenient for samples exhibiting wide MMD or PSD. Eq. 10 can be numerically solved. The graphical representation of a model result of the application of the described correction procedure is shown in Fig. 1c.

Practical utility of the described correction procedure of the experimental fractograms was demonstrated first by applying it to the real fractograms of a polymer latex obtained from sedimentation FFF[4] and was subsequently confirmed.[6–8]

REFERENCES

1. Giddings, J.C. *Dynamics of Chromatography*; Marcel Dekker, Inc.: New York, 1965.
2. Hovingh, M.E.; Thompson, G.H.; Giddings, J.C. Column parameters in thermal field-flow fractionation. Anal. Chem. **1970**, *42*, 195.
3. Janča, J. *Field-Flow Fractionation: Analysis of Macromolecules and Particles*; Marcel Dekker, Inc.: New York, 1988.
4. Jáhnová, V.; Matulík, F.; Janča, J. Correction for zone spreading in sedimentation field-flow fractionation. Anal. Chem. **1987**, *59*, 1039.
5. Hamielec, A.E. *Steric Exclusion Chromatography of Polymers*; Janča, J., Ed.; Marcel Dekker, Inc.: New York, 1984.
6. Schure, M.R.; Barman, B.N.; Giddings, J.C. Deconvolution of nonequilibrium band broadening effects for accurate particle size distributions by sedimentation field-flow fractionation. Anal. Chem. **1989**, *61*, 2735.
7. Mori, Y.; Kimura, K.; Tanigaki, M. Spec. Publ. Roy. Soc. Chem. **1992**, *102*, 290.
8. Vauthier, J.-C.; Williams, P.S. Numerical simulation of band-broadening during hydrodynamic relaxation in frit-inlet field-flow fractionation channels. J. Chromatogr. **1998**, *805*, 149.